

ENCYCLOPEDIA — OF — SEPARATION SCIENCE



ACADEMIC PRESS

Editors

Michael Cooke

Royal Holloway, University of London, Centre for Chemical Sciences
Egham Hill, Egham, Surrey TW20 0EX, UK

Colin F. Poole

Wayne State University, Department of Chemistry, Detroit MI 48202, USA

Editor-in-Chief

Ian D. Wilson

AstraZeneca Pharmaceuticals Limited, Mereside, Alderley Park, Macclesfield, Cheshire SK10 4TG, UK

Managing Technical Editor

Edward R. Adlard

Formerly of Shell Research Limited, Thornton Research Centre, PO Box 1, Chester CH1 3SH, UK

Editorial Advisory Board

Richard W. Baker

Membrane Technology & Research Inc (MTR)
1360 Willow Road, Suite 103
Menlo Park
CA 94025, USA

Kenneth L. Busch

Kennesaw State University
Office of Sponsored Programs
1000 Chastain Road
Kennesaw
GA 30144, USA

Howard A. Chase

University of Cambridge
Department of Chemical Engineering
Pembroke Street
Cambridge CB2 3RA, UK

Jan Cilliers

University of Science and Technology in Manchester
Department of Chemical Engineering
PO Box 880
Manchester M60 1QD, UK

Alan Dyer

University of Salford
School of Sciences, Cockcroft Building
Salford M5 4WT, UK

Heinz Engelhardt

Universität des Saarlandes
Instrumentelle Analytik/Umweltanalytik
Postfach 15 11 50
66041 Saarbrücken, Germany

William F. Furter

Royal Military College of Canada
Department of Chemical Engineering
Kingston
Ontario K7K 5L0, Canada

Josef Janca

Université de La Rochelle
Pole Sciences et Technologie
Equipe de Physico-Chimie Macromoléculaire
Avenue Michel Crepeau – 17042 La Rochelle, France

Walt Jennings

J&W Scientific Incorporated
91 Blue Ravine Road
Folsom CA 95630, USA

Kenneth Jones

Affinity Chromatography Limited
Freeport
Ballsalla
Isle of Man, UK

Chris Lowe

University of Cambridge
Institute of Biotechnology
Tennis Court Road
Cambridge, UK

David Perrett

St Bartholomew's and the Royal London School
of Medicine and Dentistry
St Bartholomew's Hospital, Department of Medicine
West Smithfield
London EC1A 7BE, UK

Douglas E. Raynie

The Procter and Gamble Company
Miami Valley Laboratories
PO Box 538707
Cincinnati
OH 45253-8707, USA

Peter Schoenmakers

Shell Research and Technology Centre Amsterdam
(SRTCA) and University of Amsterdam
Postbus 38000
1030 BN Amsterdam, The Netherlands

Darrell N. Taulbee

University of Kentucky-Center for Applied Energy
Research (UK-CAER)
2540 Research Park Drive
Lexington
KY 40511, USA

Gerda M. van Rosmalen

Delft University of Technology
Laboratory for Process Equipment
Leeghwaterstraat 44
2628 CA Delft, The Netherlands

Edward Woodburn[†]

University of Science and Technology in Manchester
Department of Chemical Engineering
PO Box 880
Manchester M60 1QD, UK

[†]deceased

Foreword

Separation science was first recognized as a distinct area of physical and analytical chemistry in the 1960s. The term was first coined, I believe, by the late J. Calvin Giddings, Research Professor at the University of Utah. Calvin Giddings recognized that the same basic physical principles governed a wide range of separation techniques, and that much could be learnt by applying our understanding of one such technique to others. This was especially true for his first loves, chromatography and electrophoresis and latterly field flow fractionation. Of course there are many separation techniques other than chromatography, many with a history at least as long, or indeed longer, than that of chromatography: distillation, crystallization, centrifugation, extraction, flotation and particle separation, spring to mind. Other separation techniques have emerged more recently: affinity separations, membrane separations and mass spectrometry. Most people, a few years ago, would not have classed mass spectrometry as a separation technique at all. However, with modern ionization methods, which minimize fragmentation, mixtures of compounds can first of all be separated and then each component identified through fragmentation by secondary ion-molecule collisions and further mass spectrometry. With the scale of mass spectrometry now matching that of microseparation methods such as capillary electrophoresis and capillary electrochromatography, combinations of orthogonal methods can now provide extremely powerful separation and identification platforms for characterizing complex mixtures.

Basically, all separation techniques rely on thermodynamic differences between components to discriminate one component from another, while kinetic factors determine the speed at which separation can be achieved. This applies most obviously to distillation, chromatography and electrophoresis, but is also obvious in most of the other techniques; even particle size separation by sieving can be classified in this way. The thermodynamic aspect is, of course, trivial being represented by the different sizes of the particles, as indeed it is for the size exclusion chromatography of polymers. However, the kinetic aspects are far from trivial. Anyone who has tried to sieve particles will have asked the question: is it better to fill the sieve nearly to the top and sieve for a long time, or is it better to dribble the material slowly into the sieve and just remove the heavies from time to time? One might further ask: how does one devise a continuous sieving process where large particles emerge from one port of the equipment, and small ones emerge from the other port? And how does one optimize throughput and minimize unit cost?

The publication of this *Encyclopedia of Separation Science* is a landmark for this area of science at the start of the third millennium. It will undoubtedly be of enormous value to practitioners of separation science looking for an overview and for guidance as to which method to select for a new problem, as well as to those who are at an early stage, simply dipping their toes into the waters, and trying to find out just what it is all about. Most important of all, by providing a comprehensive picture, it advances the whole field of separation science and stimulates further work on its development and application. The publishers, their editors and their authors are to be congratulated on a splendid effort.



John H. Knox
Edinburgh
8 March 2000

Preface

The ability to perform separations for the analysis, concentration or isolation of substances present in mixtures (of varying degrees of complexity) is arguably fundamental to the maintenance of our technological civilization. Separations can also be rather difficult to define, and over the course of a number of debates where we tried to ‘separate the wheat from the chaff’, we defined separations for the purposes of this work as ‘*processes of any scale by which the components of a mixture are separated from each other without substantial chemical modification*’. Of course some of the processes that are used in separations have a very long history, and the terms used to describe them are in widespread general use. So, we talk about how it is possible to distil wisdom, precipitate an argument, extract meaning and crystallize an idea and who can predict the future uses of the word chromatography? Whilst separations have been practised as an *art* for millennia, the last hundred years or so has seen the elucidation of the fundamentals that lie behind many of these processes. Thus, although separations are most widely used for achieving some practical objective, a firm theoretical understanding has been put into place that does allow the use of the term *separation science*. We have tried here to reflect the theoretical and practical aspects of the topics in this encyclopedia, and have attempted to achieve a blend of theory, practice and applications that will enable someone knowledgeable in a field to go directly to a relevant article; whilst the novice can begin with an overview and gradually iterate towards the practical application.

One thing is clear, separations cover such a wide range of topics that no single individual can be knowledgeable, let alone expert, in them all. It is against this background that we decided that an encyclopedia designed to cover this science would be of value as a single source of reference that would provide access to the whole field of separations.

For the purposes of defining the scope and coverage of the encyclopedia we have divided the area of separations into 12 families, or topic areas, using separation principles based on affinity, centrifugation, chromatography, crystallization, distillation, electrophoresis, extraction, flotation, ion exchange, mass spectrometry, membranes and particle size. Whilst there is no doubt that different editors might have grouped these slightly differently, they did not seem to us to be capable of further reduction. Taken together, we believe that they provide coverage of the whole field.

In preparing this multi-author and multi-volume work, all of the editors have been conscious of the gaps in their own expertise and the debt which they and the publishers owe to the Editorial Advisory Board, who to a large degree have compensated for the deficiencies in our own knowledge. Their help has been invaluable, as without them we would not have been able to achieve the necessary balance and it was, therefore, a source of particular sadness that one of them, Ted Woodburn, died prior to publication. Without Ted it is quite clear that the topic area of flotation would not have been so well covered, and we would like to think that he would have been well pleased with the finished work. We also hope that the masterly overview which he contributed to the encyclopedia, will be a lasting memorial to him. We are grateful to Jan Cilliers for stepping into the role of Editorial Board Advisor on flotation at short notice. We would also like to acknowledge the valuable input of G. J. Arkenbout at the beginning of this project, who was able to work with us for a short period of time before his death.

Assembling this knowledgeable and enthusiastic group of experts was a difficult task, and the editors would also wish to acknowledge the role of the Major Reference Works development team at Academic Press in this whole area, as well as thanking them for their assistance and patience throughout the project, from the initial planning to its final publication.

Finally, of course, we must acknowledge the contributions of the authors whose expertise constitutes this encyclopedia. Some of them have become firm friends in the period between the inception of this project and its completion. After all, separation science separates things but brings people together.

Ian D. Wilson, Edward R. Adlard, Michael Cooke, Colin F. Poole
Editors

Introduction

The need for separations as a means for performing the isolation, purification or analysis of substances, at scales ranging from tonnage quantities down to picograms or less, is an important feature of modern life. Such separations underpin virtually all aspects of research and commerce and indeed a vast industry has arisen to provide the equipment and instrumentation to perform and control these essential processes; indeed it is impossible to envisage our world without ready access to separations. To provide these capabilities a whole family of techniques has evolved to exploit differences in the physical or chemical properties of the compounds of interest, and to accommodate the scales on which the separations are performed. After all, a separation that works on the picogram scale based perhaps on capillary electrophoresis, may not easily be transferred to the gram scale and will be utterly impossible on the kilogram scale. In such instances an alternative type of separation, based on a totally different principle must be sought. And therein lies the problem—most scientists are specialists and while having an excellent knowledge of their own, often narrow, sphere of expertise are generally possessed of a much more hazy view of the capabilities and attributes of techniques outside that area. Even worse, such ignorance may persuade them to adopt an approach that is quite unsuited to the solution of the problem in hand.

The large number of articles in this encyclopedia, and the wide variety of the subject matter described in them, represents an attempt to provide separation scientists with a single authoritative source covering the broad range of separation methods currently available. Inevitably there is some overlap in places between articles dealing with closely related topics. However, in a work such as this where each article is meant to be a self-contained source of information, some overlap is unavoidable and not wholly undesirable in the context of ensuring full coverage of a topic.

The articles in the *Encyclopedia of Separation Science* fall into three categories as follows: ‘Level I’, which provides overviews of a particular separation area, e.g. flotation, distillation, crystallization, etc., written by acknowledged experts in the particular fields. These articles are presented with the aim of providing a wide ranging introduction to the topic from which the reader can then, if it seems appropriate, move on to ‘Level II’ articles.

Level II articles cover the theory, development, instrumentation and practice of the various techniques contained within each broad classification. For example the Level I article on chromatography is supported in Level II by descriptions of gas, liquid and supercritical fluid chromatography, together with information on instrumentation. Separations are, however, often of interest to practitioners because of their applications and Level II serves as an introduction to ‘Level III’.

Level III provides detailed descriptions of the use of the various methods described in Levels I and II for solving real problems. These might include articles on the various methods for extraction of pesticides or drugs from a matrix, with other articles on the chromatographic or electrophoretic techniques that could be used for their subsequent analysis. The extensive cross-referencing and exhaustive indexing for all of the articles in the work should enable the reader to obtain easily and rapidly all the relevant information in the encyclopedia. In addition, each article at whatever level contains a brief but carefully selected bibliography of key books, review articles and important papers. In this way the encyclopedia provides the reader with an invaluable ‘gateway’ into the separation science literature on a topic.

Lastly, because the importance of separation science lies in its value as an applied technique, we have commissioned a number of ‘essential guides’ to method development, in a limited number of key areas such as the isolation and purification of proteins and enzymes, etc., or the development of chromatographic separations.

While the techniques described in these volumes can in many cases be used as the basis of analytical methods, the emphasis of this work is on the methods of separation of mixtures, rather than their determination. For a treatise devoted to Analytical Science the reader is referred to the *Encyclopedia of Analytical Science*, also published by Academic Press, which can be considered to be complementary to the present work, in that it deals in depth with analysis rather than the application of separations.

The reader faced with the need to perform a separation, requiring information on a type of detector, or the use of a technique for a particular class of compound, etc., should therefore be able to look into the encyclopedia for information on that topic. Even where there is no information that is directly relevant to

the problem, it should still be possible to begin at Level I in order to determine the potential of a technique to solve the problem and then progress down through the levels until a solution begins to emerge.

The editors believe that, taken as a whole, this encyclopedia and its electronic version should provide a valuable source of knowledge and expertise for both those already skilled in the art of some aspect of separations and also for the novice. That, at least, is our hope.

This encyclopedia is a guide providing general information concerning its subject matter; it is not a procedure manual. The readers should consult current procedural manuals for state-of-the-art instructions and applicable government safety regulations. The publisher and the authors do not accept responsibility for any misuse of this encyclopedia, including its use as a procedural manual or as a source of specific instructions.

AFFINITY SEPARATION



K. Jones, Affinity Chromatography Ltd, Freeport,
Ballsalla, Isle of Man, UK

Copyright © 2000 Academic Press

Introduction

Of the collection of separation technologies known as 'affinity', affinity chromatography is by far the most widely used variant. Affinity chromatography is becoming increasingly important as the speed of the revolution taking place in biotechnology processing increases. The concept of an 'affinity' separation results from a naturally occurring phenomenon existing within all biological macromolecules. Each biological macromolecule contains a unique set of intermolecular binding forces, existing throughout its internal and external structure. When alignment occurs between a specific site of these forces in one molecule with the site of a set of forces existing in another (different) molecule, an interaction can take place between them. This recognition is highly specific to the pair of molecules involved. The interactive mechanism can be converted into a universal mutual binding system, where one of the binding pair is attached to an inert matrix, packed into a column and used exclusively to capture the other matching molecule. When used in this (affinity) mode, the technique is probably the simplest of all chromatographic methods. It is, however, restricted almost exclusively to the separation and purification of biological macromolecules, and is unsuitable for small molecules.

Affinity chromatography or bioselective adsorption chromatography was first used in 1910, but it was only in the 1960s that affinity chromatography as practised today was developed as a purification technique. By the late 1970s the emergence of recombinant DNA technology for the manufacture of protein pharmaceuticals provided a new impetus for this highly specific chromatographic method, implemented by the demand for ever-increasing product purity implicit in regulatory frameworks devised by (amongst others) the USA's Food and Drug Administration (FDA). Finally, the need to reduce the cost of drugs is under constant scrutiny by many Governments, particularly those with controlled health schemes funded by revenue raised by taxation. These mutually incompatible pressures indicate the need for more efficient separation systems; the affinity technique provides the promise of meeting all necessary requirements.

Separation and purification methods for biological macromolecules vary from the very simple to the esoteric. The type of technique adopted is basically a function of source, the fragility of the molecule and the purity required. Traditionally, high purity protein pharmaceuticals have used multistage processing, but this is very inefficient as measured by the well-documented fact that 50–80% of total production costs are incurred at the separation/purification stage. In contrast, the highly selective indigenous properties of the affinity method offer the alternative of very elegant single-step purification strategies. The inherent simplicity and universality of the method has already generated a wide range of separation technologies, mostly based upon immobilized naturally occurring proteinaceous ligands. By comparing the 'old' technologies of 'natural' ligands or multistage processing with the 'new', exemplified by synthetic designed ligands, the most recent advances in affinity processing can be described.

Biological Recognition

As nature evolved, life forms had to develop a protective mechanism against invading microorganisms if they were to survive. Thus there is a constant battle between the cell's defence mechanism and the attacking microorganisms, a battle resolved by the cells generating antibodies (the immunoglobulins) able to recognize the protein coat of attacking microorganisms and signal killer cells to destroy the invaders before they cause harm to the host. Equally, if microorganisms were to survive, they had continually to mutate and change their protein coats to avoid detection by existing antibodies. The 'attack and destroy' process is a function of changes in the molecular structure in a specific part of the protein, with only the most minute of changes occurring at the surface of the protein. Evolution has thus designed a system where every protein has a very precise structure, but one which will always be recognized by another. One element of the interacting pair can be covalently bonded onto an inert matrix. The resulting chromatographic medium can then be packed into a column, and used to separate exclusively its matching partner from an impure mixture when added as a solution to the top of the column. This fact can be stated as follows – *for every protein separation problem there is always an affinity solution*. The process of producing a satisfactory medium is quite difficult.

The matching pair must be identified, and one of them isolated in a pure form. Covalent bonding onto an inert matrix in a stable manner must always allow the 'docking' surface of the protein to be positioned to make it available to the target protein. The whole also has to be achieved at an acceptable cost.

This technique has resulted in many successful applications, often using antibodies as the affinity medium (immunoaffinity chromatography), but large scale separations using these 'natural' ligands are largely restricted by cost and regulatory reasons. Although immunoaffinity chromatography is still widely practised, in recent years the evolution of design technologies has provided powerful new approaches to mimic protein structures, resulting in the development of synthetic ligands able to work in harsh operational environments and at low cost.

The Affinity Process

The affinity method is critically dependent upon the 'biological recognition' existing between species. By permanently bonding onto an inert matrix a molecule (the ligand) that specifically recognizes the molecule of interest, the target molecule (the ligate) can be separated. The technique can be applied to any biological entity capable of forming a dissociable complex with another species. The dissociation constant (K_d) for the interaction reflects the complementarity between ligand and ligate. The optimal range of K_d for affinity chromatography lies between 10^{-4} and 10^{-8} mol L⁻¹. Most biological ligands can be used for affinity purposes providing they can be immobilized, and once immobilized continue to interact successfully with their respective ligates. The ligand can be naturally occurring, an engineered macromolecule or a synthetic molecule. Table 1 provides some examples of immobilized ligands used to purify classified proteins. The

affinity method is not restricted to protein separations; nucleic acids and whole cells can also be separated.

The simplicity of the chromatographic process is shown in Figure 1. The ligand of interest, covalently bonded onto the inert matrix, is contained in the column, and a solution containing the target (the ligate) is passed through the bed. The ligand recognizes the ligate to the exclusion of all other molecules, with the unwanted materials passing through the column packing while the ligate is retained. Once the bed is saturated with the target molecule (as measured by the breakthrough point), contaminating species are washed through, followed by collection of the target molecule as a very pure fraction using an eluting buffer solution. Finally, the column is cleansed from any strongly adsorbed trace materials, usually by regeneration with a strong alkali or acid, making it available for many more repeat runs. An outstanding advantage of the affinity process is an ability to concentrate very dilute solutions while stabilizing the captured protein once adsorbed onto the column. Many of the in-demand proteins manufactured by genetically engineered microorganisms are labile, allowing only minute quantities to be present in the fermentation mix before they begin to deteriorate. An ability to capture these very small quantities while stabilizing them in the adsorbant phase results in maximization of yield, making massive savings in total production costs.

Although the technical processing advantages are clear there is a major difficulty in the application of affinity chromatography as understood by most practitioners today. Most ligands described in Table 1 suffer from two primary disadvantages: a lack of stability during use; and high cost. Fortunately these problems have now been overcome, and affinity chromatography is now accepted as the major separations technology for proteins.

Table 1 Affinity ligands and purified proteins

<i>Immobilized ligand</i>	<i>Purified protein</i>
Divalent and trivalent metal ion	Proteins with an abundance of his, try and cys residues
Lectins	Glycoproteins, cells
Carbohydrates	Lectins
Reactive dyes	Most proteins, particularly nucleotide-binding proteins
Nucleic acids	Exo and endonucleases, polymerases, other nucleic acid-binding proteins
Amino acids (e.g. lys, arg)	Proteases
Nucleotides, cofactors substrates and inhibitors	Enzymes
Proteins A and G	Immunoglobulins
Hormones, drugs	Receptors
Antibodies	Antigens
Antigens	Antibodies

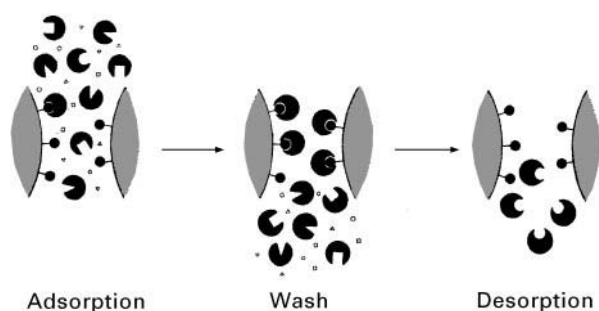


Figure 1 Schematic diagram of affinity chromatography.

Matrices

By definition matrices must be inert and play no part in the separation. In practice most play a (usually) negative role in the separation process. To minimize these disadvantages matrices have to be selected with great care. There is a theoretically perfect matrix, defined as consisting of monodispersed perfectly shaped spheres ranging from 5 to 500 μm in diameter, of high mechanical strength, zero nonspecific adsorption and with a range of selectable pore sizes from 10–500 nm, a very narrow pore size distribution and low cost. This idealized matrix would then provide the most efficient separation under all experimental conditions. As always, a compromise has to be reached, the usual approach being to accentuate the most attractive characteristics while minimizing the limitations, usually by manipulating the experimental conditions most likely to provide the optimum result.

The relative molecular masses of proteins vary from the low thousands to tens of millions, making pore size the most important single characteristic of the selected matrix. Very large molecules need very open and highly porous networks to allow rapid and easy penetration into the core of the particle. Structures of this type must therefore have very large pores, but this in turn indicates low surface areas per unit volume, suggesting relatively low numbers of surface groups to which ligands can be covalently attached. The matrix must also be biologically and chemically inert. A special characteristic demanded from biological macromolecular separations media is an ability to be sanitized on a routine basis without damage. This requires resistance to attack by cleansing reagents such as molar concentrations of strong alkali, acids and chaotropes. In contrast to analytical separations, where silica-based supports are inevitably used, silica cannot meet these requirements and is generally not favoured for protein separations. Table 2 contains examples of support matrices used in affinity separations.

The beaded agaroses have captured over 85% of the total market for biological macromolecule separations, and are regarded as the industry standard to which all other supports are compared. They have achieved this position by providing many of the desirable characteristics needed, and are also relatively inexpensive. Beaded agaroses do have one severe limitation – poor mechanical stability. For analytical applications speed and sensitivity are essential, demanding mechanically strong, very small particles. Beaded agaroses are thus of limited use analytically, a gap filled by high performance liquid chromatography (HPLC) using silica matrices. For preparative and large scale operations other factors are more important than speed and sensitivity. For example, mass transfer between stationary phase and mobile phase is much less important when compared to the contribution from the chemical kinetics of the binding reaction between stationary phase and protein. Band spreading is also not a serious problem. When combined with the highly selective nature of the affinity mechanism, these factors favour the common use of large sized, low mechanical strength particles.

In recent years synthetic polymeric matrices have been marketed as alternatives. Although nonbiodegradable, physically and chemically stable, with good permeabilities up to molecular weights greater than 10^7 Da, the advantages provided are generally offset by other quite serious disadvantages, exemplified by high nonspecific adsorption. Inorganic matrices have also been used for large scale protein separations, notably reversed-phase silica for large scale recombinant human insulin manufacture (molecular weight approximately 6000 Da), but are generally not preferred for larger molecular weight products. A very slow adoption of synthetic matrices is

Table 2 Support matrices

<i>Support matrix</i>	<i>Operational pH range</i>
Agarose	2–14
Cellulose	1–14
Dextran	2–14
Silica	< 8
Glass	< 8
Polyacrylamides	3–10
Polyhydroxymethacrylates	2–12
Oxirane–acrylic copolymers	0–12
Styrene–divinylbenzene copolymers	1–13
Polyvinyl alcohols	1–14
<i>N</i> -Acryloyl-2-amino-2-hydroxy-1, 2-propane	1–11
PTFE	Unaffected

PTFE, polytetrafluoroethylene.

indicated as improvements are made to current materials and the prices of synthetics begin to approach those of agarose beads. Other factors resist any significant movement towards synthetic matrices. Most installed processing units are designed for low performance applications. Higher performance matrices would need reinstallation of new, much higher cost high performance plant; plant operators would need retraining; operating manuals would need rewriting; and plant and factory would need reregistration with the FDA. In combination, the implication is that penetration of high performance systems for large scale applications will be slow, and agarose beads will continue to dominate the market for protein separations.

Covalent Bonding

A basic requirement of all chromatographic media is the need for absolute stability under all operational conditions through many cycles of use. Consequently all ligands must be covalently bonded onto the matrix, and various chemistries are available to achieve this.

A number of factors are involved:

1. The performance of both ligand and matrix are not impaired as a result of the coupling process.
2. Most of the coupled ligand is easily accessible to the ligate.
3. Charged or hydrophobic groups are not generated on the matrix, so reducing nonspecific adsorption.
4. The immobilized ligand concentration is optimal for ligate bonding.
5. There is no leakage of immobilized ligand from the matrix.

Some ligands are intrinsically reactive (or can be designed to be so) and contain groups that can be

coupled directly to the matrix, but most require coupling via a previously activated matrix. The affinity matrix selected must have an adequate number of appropriate surface groups onto which the ligand can be bonded. The most common surface group is hydroxyl. The majority of coupling methods involve the activation of this group by reacting with entities containing halogens, epoxy or carbonyl functional groups. These surface residues are then coupled to ligands through primary amines, hydroxyls or thiol groups, listed in **Table 3**.

Polysaccharides, represented by agarose, have a high density of surface hydroxyl groups. Tradition still dictates that this surface is activated by cyanogen bromide, but it is well established that this reagent forms pH-unstable iso-urea linkages, resulting in a poorly performing product. Furthermore CNBr-activated agarose needs harsh coupling conditions if high yields of final media are to be obtained, suggesting high wastage of often expensive ligands. This factor is particularly evident with fragile entities such as the very-expensive-to-produce antibodies, and yet many workers simply read previous literature and make no attempt to examine alternative far superior coupling methods. The advantages of mild coupling regimes are demonstrated in **Figure 2**, where the use of a triazine-activated agarose is compared to CNBr-activated agarose. Yield is significantly increased, largely by coupling under acidic rather than alkaline conditions.

Intermolecular Binding Forces

Almost all chromatographic separations rely upon the interaction of the target molecule with either a liquid phase or a covalently bonded molecule on the solid phase, the exceptions being those relying upon molecular size, e.g. molecular sieves and gel filtration. In affinity separations ligates are inevitably

Table 3 Activation materials

<i>Activating reagent</i>	<i>Bonding group on ligand</i>
Cyanogen bromide	Primary amines
Tresyl chloride	Primary amines, thiols
Tosyl chloride	Primary amines, thiols
Epichlorohydrin	Primary amines, hydroxyls, thiols
1,4-Butanediol diglycidyl ether	Primary amines, hydroxyls, thiols
1,1'-Carbonyldiimidazole	Primary amines, hydroxyls
Cyanuric chloride	Primary amines, hydroxyls
Divinylsulfone	Primary amines, hydroxyls
2-Fluoro-1-methylpyriinium-toluene-4-sulfonate	Primary amines, thiols
Sodium periodate	Primary amines
Glutaraldehyde	Primary amines

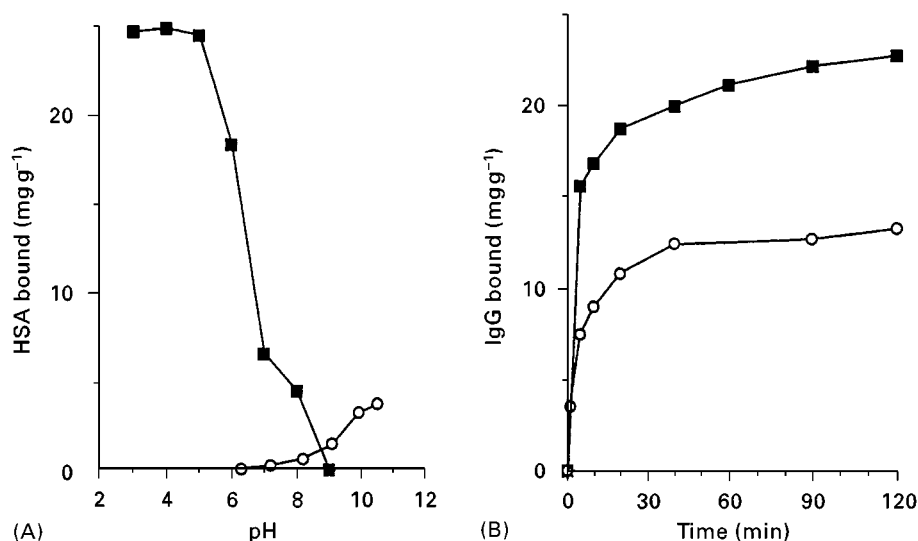


Figure 2 Triazine coupling. (A) Coupling of human serum albumin (HSA) to ready-activated supports as a function of pH. (B) Time course of coupling of human IgG to ready-activated supports at 4°C. ○, CNBr-activated agarose 4XL; ■, triazine-activated agarose 4XL.

complex biological macromolecules or assemblies, mostly or exclusively consisting of amino acids entities linked together in a specific manner. This complexity of structure provides many opportunities to exploit the physicochemical differences between the target molecule and the ligand to be used. Each structure contains the four basic intermolecular binding forces – electrostatic, hydrogen bonding, hydrophobic and van der Waals interactions – spread throughout the structure in an exactly defined spatial manner. The degree of accessibility and spatial presentation within the pore of the medium, and the strength of each force relative to each other, dictate whether these forces are utilized to effect the separation. The biological recognition between species is a reflection of the sum of the various molecular interactions existing between them, and this summation is fixed for the ligate. However, various ligands may be found that emulate some or all of the available binding forces to various degrees.

Affinity adsorbents are therefore assigned to one of three broad ligand categories: nonspecific, group specific or highly specific. Nonspecific ligands have only a superficial likeness to biological ligands and binding is usually effected by just one of the four binding processes described above. Although ion exchange materials can be used in a similar manner to affinity adsorbents, they only exhibit the single force of electrostatic binding. They are thus limited to relatively indiscriminate binding. In this case the only criterion for binding is that of an overall charge.

Fortunately there are a vast number of biological ligands that can interact with more than one macromolecule and consequently group-specific ligands are commonplace. Since group-specific adsorbents retain a range of ligates with similar binding requirements, a single adsorbent may be used to purify a number of ligates. Group-specific ligates can be used when the desired ligate is present in high concentration, but this implies that some preprocessing has taken place and a concentration step interposed. The use of non/group-specific adsorbents can only offer partial separations. This results in having to apply several stages in series, each only capable of removing a proportion of the impurities. In contrast a highly selective ligand can exclusively remove the target in one step, but often the resulting complexes are very tightly bound, have low binding capacities, are easily denatured and are expensive to produce. Until recently these adsorbents were restricted to technically difficult isolations. Today the use of computer-assisted molecular modelling systems provides opportunities to investigate relationships between designed ligands and relevant protein structures. For the first time logical design approaches can be applied and consequently stable inexpensive ligands have now become available.

Analytical Scale-Up

Modern biotechnology uses two different types of chromatography. Analytical separations require that run time is minimized, while resolution and

sensitivity are maximized. In contrast, for preparative and process applications, the objective is to maximize purity, yield and economy. These techniques have developed separately, simply because biological macromolecules pose unique difficulties, making them unsuitable for 'standardized' analysis. A major influence on this division has been that scale-up usually occurs very much earlier in the development of a process, causing biochemists to turn to the traditional low performance methods of ion exchange (IE), hydrophobic interaction (HI) and gel permeation chromatography (GPC). The highly efficient affinity chromatography method was generally ignored, primarily because of the difficulty of having to develop a unique ligand for each separation rather than having 'off-the shelf' column packings immediately available from external suppliers. For analytical purposes high performance affinity liquid chromatography (HPALC) is a rarity, a function of the limited availability of suitable matrices (Table 2) and the affinity process itself.

Where quantifiable high speed chromatography is required, reversed-phase HPLC (RP-HPLC) has no equal. Unfortunately there is no general purpose method for biomolecules to parallel the inherent power of RP-HPLC. The success of RP-HPLC for analysis can be judged from the large number of published applications developed for the 'first wave' of protein pharmaceuticals manufactured by genetically engineered microorganisms. These extracellular (relatively) low molecular weight proteins include human insulin, human growth hormone and the interferons. However, as molecular size and fragility increase, so difficulties in using HPLC increase, a primary reason why much analysis is still conducted on low performance systems. Low performance systems are easily scaled up; RP-HPLC is not.

Biological separation systems must be aseptically clean throughout the process. The mixtures are inevitably complex and usually contain many contaminating similarly structured species. Such species can adsorb very strongly onto the medium, demanding post-use washing with very powerful reagents to sterilize and simultaneously clean the column. Silica-based matrices cannot survive this type of treatment, hence scale-up of analytical procedures is generally precluded. The first wave of commercial protein pharmaceuticals have generally proved to be relatively stable under high stress conditions. On the other hand intracellular proteins, often of high molecular weight, are unstable. Analysis by high performance RP-HPLC methods then becomes problematic. Demand for fast, high resolution, analytical methods will continue to increase for on-line monitoring and process validation. Such techniques have already been

used to determine degradation of the target protein (for example deamidated and oxidized elements); to identify previously unidentified components; to establish the chromatographic identity between recombinant and natural materials; to develop orthogonal methods for the identification of unresolved impurities; and for many other demanding analytical approaches.

Affinity versus Traditional Media

When projects are transferred from research to development two sets of chromatographic techniques are carried forward: analysis, usually based on RP-HPLC; and larger scale serialized separation steps, often incorporating traditional methods of ion exchange, hydrophobic interaction and gel permeation chromatography. Major decisions have to be taken at this juncture – to scale up the separation processes developed during the research phase or to investigate alternatives. Regulatory demand and shortened patent lifetimes compel managements to 'fast track' new products. Commercial pressure is at a maximum. Being first to market has the highest priority in terms of technical and commercial reward. Very little time is left to explore other separation strategies. It is known that serial application of IE, HI and GPC inevitably leads to very high manufacturing costs, but which comes first? Most often the decision is taken to begin manufacture using unoptimized separations as defined in research reports. It is only in retrospect that very high production costs become apparent. By then it is too late – regulatory systems are firmly in place.

There is an alternative. If researchers were more aware of process economics and the consequences of regulatory demand, selection of superior separation processes could then result. Although most researchers are fully aware of the advantages of single-step affinity methods, paradoxically the high selectivity advantage of affinity chromatography is also a weakness. Suitable off-the-shelf affinity adsorbents are often unavailable, in which case an adsorbent has to be custom synthesized. Since the majority of biochemists have no desire (or time) to undertake elaborate chemical synthesis, antibody-based adsorbents are commonly used. However, raising suitable antibodies and purifying them before immobilization onto a preactivated support matrix is an extremely laborious procedure. In addition, proteins are so often tightly bound to the antibody that subsequent elution involves some degree of denaturation and/or loss of activity. Ideal media require the incorporation of elements of both nonselective and selective adsorbents to provide adsorbents with a general applicabil-

ity. If stable, highly selective and inexpensive affinity ligands were available, then opportunities would exist for researchers to develop efficient high yield separations even in the earliest phases of investigation. These systems could then be passed forward to production with the knowledge that optimally efficient separations are immediately achievable.

Production costs of any pure material reflect the absolute purity level required and the difficulty of achieving it. Therapeutic proteins have high purity requirements and the larger the administered dose, the purer it has to be. Since many protein pharmaceuticals will be used at high dose levels, purities need to exceed 99%, occasionally up to 99.999%. That these purities can be met by traditional methods is possible, but it is widely documented that the application of such methods massively increases production costs. Between 50 and 80% of total production costs of therapeutic proteins are incurred at the purification stage. The manufacturing cost of a product is directly related to its concentration in the mother liquor; the more dilute it is, the higher the cost of recovery. Since traditional purification processes on their own cannot selectively concentrate a target protein to the exclusion of all others, they have to be used in series. The number of stages required can vary between four and 15. Each step represents a yield loss, and incurs a processing cost. Yields of less than 20% are not uncommon. **Figure 3** shows an enzyme purified in multiple stages and by a one-step affinity process.

It was these limitations that caused biochemists to examine highly selective ligands. Almost any compound can be used as an affinity ligand provided it can be chemically bonded onto a support matrix and, once immobilized, it retains its ability to interact with the protein to be purified. The ligand can be

a simple synthesized entity or a high molecular weight protein. The affinity technique is theoretically of universal application and any protein can be separated whatever its structure and origin. As always, there are major limitations. The most effective affinity ligands are other proteins. Unfortunately such proteins are difficult to find, identify, isolate and purify. This results in high costs. An even greater deterrent is that most proteins are chemically, catalytically and enzymically unstable, a particularly unattractive feature if they are to be used for the manufacture of therapeutic substances; and regulatory authorities generally reject applications using proteinaceous ligands.

In anticipating that one day stable inexpensive affinity media would be in demand, a team led by C.R. Lowe began an investigation into which synthetic ligand structures offered the greatest possibility of developing inexpensive stable ligands. It was concluded that structures that could be manipulated into specific spatial geometries and to which intermolecular binding forces could easily be added offered the highest chance of success. Model compounds were already available; the textile dyes.

Synthetic Ligands

Textile dyes had already proved to be suitable ligands for protein separations. Blood proteins, dehydrogenases, kinases, oxidases, proteases, nucleases, transferases and ligases can be purified by a wide variety of dyes. However, they did not prove to be the breakthrough so eagerly awaited. An essential feature of all chromatographic processes is exact repeatability from column to column, year after year. Textile dyes are bulk chemicals, most of which contain many by-products, co-produced at every stage of the dye

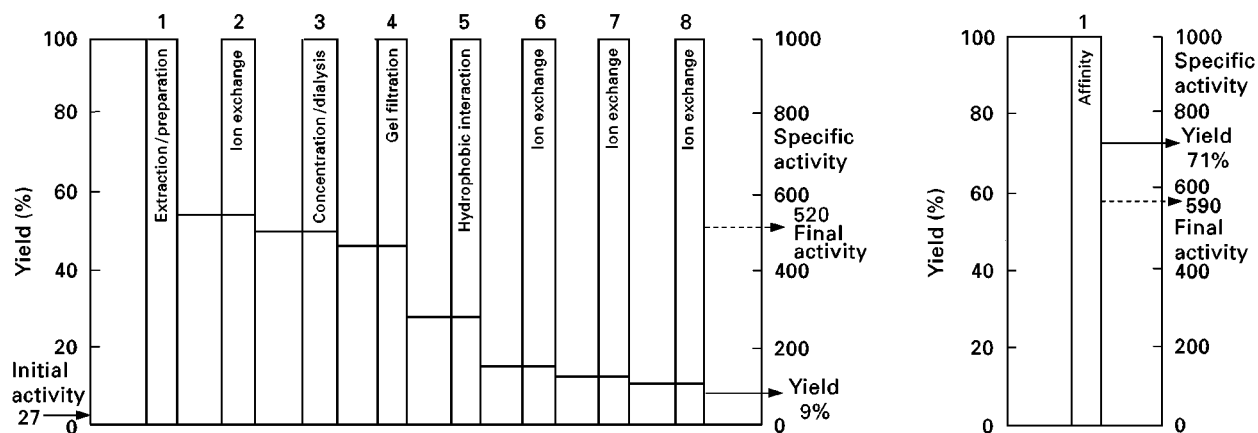


Figure 3 Comparison of multistep versus affinity separation.

manufacturing process. This fact alone makes reproducibility problematic. Furthermore, the bonding process between dye and matrix was poorly researched. This resulted in extensive leakage. All commercially available textile dye products leak extensively, especially under depyrogenating conditions (Figure 4). Despite these limitations, it was recognized that dye-like structures had a powerful underlying ability to separate a very diverse range of proteins. Their relatively complex chemical structures allow spatial manipulation of their basic skeletons into an infinite variety of shapes and configurations. Proteins are complex three-dimensional (3-D) structures and folds are present throughout all protein structures. An effective ligand needs to be shaped in such a manner that it allows deep insertion into a suitable surface fissure existing within the 3-D structure (Figure 5). In contrast, if the ligand only interacts with groups existing on external surfaces, then nonspecific binding results and proteins other than the target are also adsorbed. A much more selective approach is to attempt to insert a ligand into an appropriate fold of the protein, and add binding groups to correspond with those present in a fold of the protein. If all four of the basic intermolecular forces (Figure 5: W, electrostatic; X, hydrogen bond-

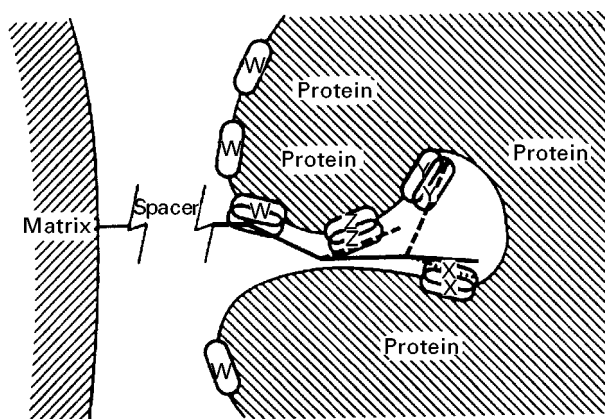


Figure 5 Schematic representation of ligand-protein interaction. W, electrostatic interaction; X, hydrogen bonding; Y, van der Waals interaction; Z, hydrophobic interaction. —, original backbone; ---, new structure added; ···, original backbone move; O, fields of interaction.

ing; Y, van der Waals; Z, hydrophobic) align with the binding areas in the protein fold, idealized affinity reagents result. The use of spacer arms minimizes steric hindrance between the carrying matrix and protein.

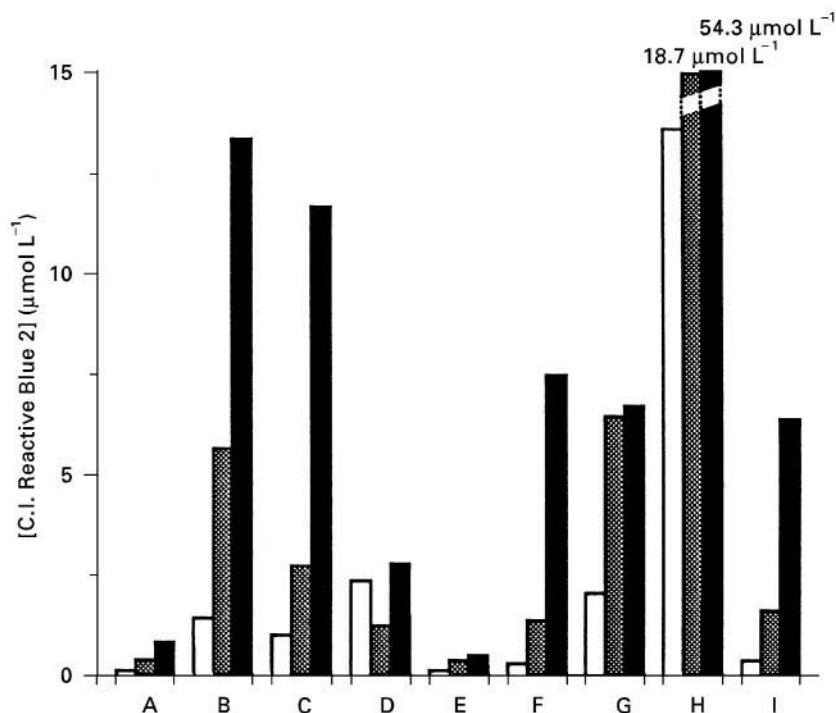


Figure 4 Leakage of blue dye from various commercial products. □, 0.1 mol L⁻¹ NaOH; ▨, 0.25 mol L⁻¹ NaOH; ■, 1 mol L⁻¹ NaOH. Key: A, Mimetic Blue 1 A6XL (affinity chromatography); B, Affi-Gel Blue (Bio-Rad); C, Blue Trisacryl-M (IBF); D, Fractogel TSK AF-Blue (Merck); E, C.I. Reactive Blue 2 polyvinyl alcohol-coated perfluoropolymer support; F, Blue Sepharose CL-6B (Pharmacia); G, immobilized Cibacron Blue F3G-A (Pierce); H, Cibacron Blue F3G-A = Si500 (Serva); I, Reactive Blue 2-Sepharose CL-6B (Sigma).

The final step is to design appropriate bonding technologies to minimize potential leakage. Until recently this type of modelling was a purely theoretical exercise. It was only the introduction of computer-assisted molecular modelling techniques that allowed the theory to be tested. Before the arrival of logical modelling the discovery of selective ligands was entirely based upon empirical observation, later followed by a combination of observation, experience and limited assistance from early computer generated models. Although several novel structures evolved during this period, a general approach to the design of new structures remained elusive. At this time only very few 3-D protein structures were available, again greatly restricting application of rational design approaches. As more sophisticated programmes, simulation techniques, protein fragment data and many more protein structures were released, logical design methods were revolutionized. However, many millions of proteins are involved in life processes, and it is clear that many years will elapse before the majority of these will be fully described by accurate models. Consequently intuition and experience will continue to play a major role in the design of suitable ligands. Of available rationally designed synthetic molecules, the Mimetic™ range can currently separate over 50% of a randomly selected range of proteins. Stability under depyrogenating conditions has been demonstrated for these products (Figure 6). This results in minimal contamination from ligand and matrix im-

purities, substantial increases in column lifetime, and improvements in batch-to-batch reproducibility.

Rational Design of Affinity Ligands

Modification of Existing Structures

The first example of a rational design of new biomimetic dyes used the interaction between horse liver alcohol dehydrogenase (ADH) and analogues of the textile dye Cibacron Blue F3G-A (Figure 7). It had been established that the parent dye binds in the NAD^+ -binding site of the enzyme, with the anthraquinone, diaminobenzene sulfonate and triazine rings (rings A, B and C, respectively, in Figure 7) apparently adopting similar positions to those of the adenine adenosine ribose and pyrophosphate groups of NAD^+ . The anthraquinone ring (A) binds in a wide apolar fold that constitutes, at one end, the adenine bridging site, while the bridging ring (B) is positioned such that its sulfonate group interacts with the guanidinium side chain of Arg271 (Figure 8). Ring C binds close to where the pyrophosphate bridge of the coenzyme binds with the reactive triazinyl chlorine adjacent to the nicotinamide ribose-binding site. The terminal ring (D) appears to be bound in a fold between the catalytic and coenzyme binding domains, with a possible interaction of the sulfonate with the side chain of Arg369. The binding of dye to horse liver ADH resembles ADP binding but differs significantly at the nicotinamide end of the molecule with the mid-point position of ring D displaced from the mid-point position of the nicotinamide ring of NAD^+ by about 1 nm. Consequently a number of terminal-ring analogues of the dye were synthesized and characterized in an attempt to improve the specificity of dye binding to the enzyme. Table 4 lists some of the analogues made by substituting -R in the D ring (Figure 7), together with their dissociation constants. These data show that small substituents bind more tightly than bulkier groups, especially if substituted in the *o*- or *m*-positions with a neutral or anionic group. Further inspection of the computer model given as Figure 8 showed that the dye analogues were too short and rigid to bind to horse liver ADH in an identical manner to the natural coenzyme, NAD^+ . Consequently analogues of the parent dye were designed and synthesized with central spacer functionalities to increase the length and flexibility of the molecule (Figure 9). This product proved to be some 10 times superior to any previously synthesized compound. This work provided the first proof that rationally designed molecules could be converted into stable, inexpensive, chromatographic media, while providing the most remarkable separations.

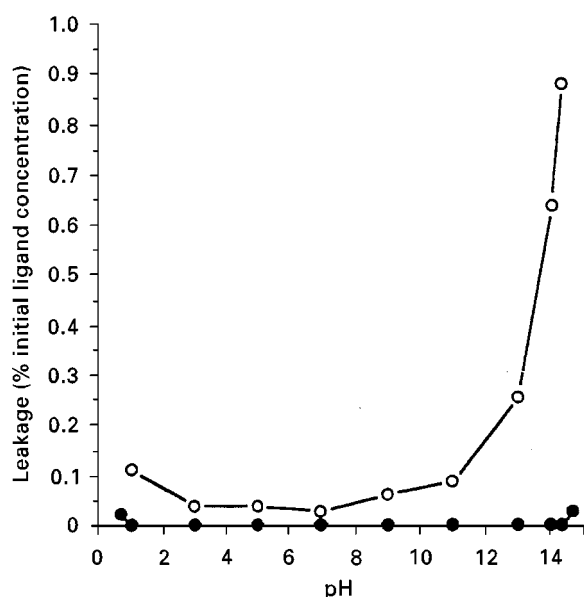


Figure 6 Comparison of ligand leakage from mimetic ligand affinity adsorbent A6XL (●) and conventional textile dye agarose (○).

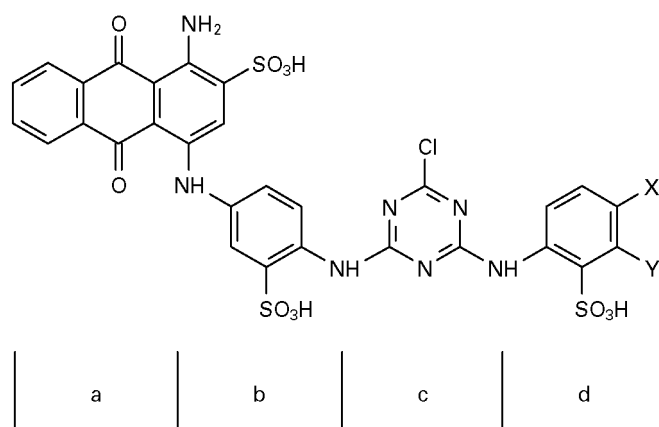


Figure 7 Principal structural elements of the anthraquinone dye, Cibacron Blue F3G-A.

De Novo Design

Most early efforts in proving the rational design technology was based upon dye structures. To date all dyes considered have been anionic, presumably because the charged chromophores of these ligands

mimic the binding of naturally occurring anionic heterocycles such as NAD^+ , NAPD^+ , ATP, coenzyme A, folate, pyridoxal phosphate, oligonucleotides and polynucleotides. However, some proteins, particularly proteolytic enzymes, interact with cationic substrates. The trypsin-like family of enzymes forms

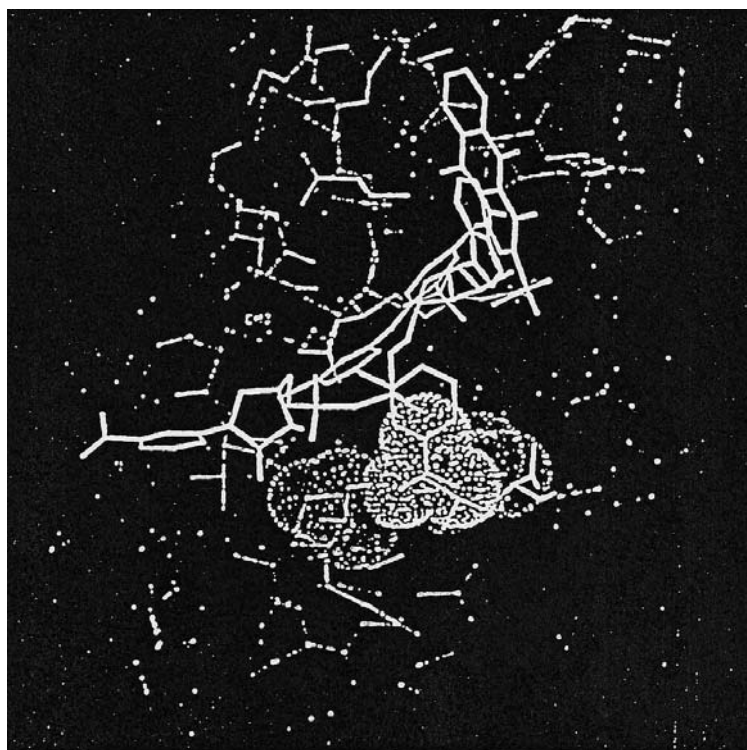
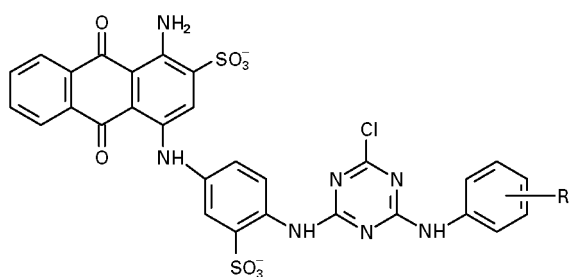


Figure 8 Putative binding pocket for the terminal-ring analogue ($m\text{-COO}^-$) of Cibacron Blue F3G-A in the coenzyme binding site of horse liver alcohol dehydrogenase (ADH). The site lies lateral to the main coenzyme binding site and comprises the side chains of two juxtaposed cationic residues Arg47 and His51.

Table 4 Apparent affinities of terminal-ring analogues of anthraquinone dyes for horse liver alcohol dehydrogenase (ADH)

R	Apparent K_d ($\mu\text{mol L}^{-1}$)
<i>m</i> -COO ⁻	0.06
H	0.2
<i>o</i> -COO ⁻	0.2
<i>o</i> -SO ₃ ⁻	0.4
<i>m</i> -SO ₃ ⁻	1.6
<i>m</i> -CH ₂ OH	4.5
<i>m</i> -CONH ₂	5.7
<i>p</i> -COO ⁻	5.9
<i>p</i> -SO ₃ ⁻	9.3
<i>p</i> -PO ₃ ²⁻	10.5
<i>p</i> -N ⁺ (CH ₃) ₃	172.0

one of the largest groups of enzymes requiring cationic substrates and includes enzymes involved in digestion (trypsin); blood clotting (kallikrein, thrombin, Factor Xa); fibrinolysis (urokinase, tissue plasminogen activator) and complement fixation. These enzymes possess similar catalytic mechanisms and bind the side chains of lysine or arginine in a primary pocket proximal to the reactive serine (Ser195), with specificity being determined partly by the side chain of Asp189 lying at the bottom of the pocket, and partly by the ability of the individual enzymes to form secondary interactions with the side chains of other nearneighbouring substrate amino acids. For example, tissue kallikrein differs from pancreatic trypsin in that it displays a marked preference for phenylalanine in the secondary site, probably because the phenyl ring on the phenylalanine residue neatly slips into a hydrophobic wedge-shaped pocket between the aromatic side chains of residues Trp215 and Tyr99 (Figure 10). Specificity for the secondary amino acid residue is less stringent in trypsin since Tyr99 is replaced by Ala99 and the hydrophobic pocket cannot be formed. By designing a mimic for the Ph-Arg dipeptide should result in a specificity for kallikrein. Figure 11 uses *p*-aminobenzamidine and phenethylamine functions substituted on a monochlorotriazine moiety. However, the active site of pancreatic kallikrein lies in a depression in the surface of the enzyme. The expected steric hindrance is eliminated

by insertion of a hexamethylene spacer arm between the designed ligand and the matrix. After synthesis of this medium it was demonstrated that purified pancreatic kallikrein was strongly bound, with over 90% of activity being recovered on elution with 4-aminobenzamidine, whereas trypsin appeared largely in the void of the column. This medium was able to purify kallikrein 110-fold from a crude pancreatic acetone powder in a single step.

There is an alternative to the rational design approach – the use of combinatorial libraries.

Combinatorial Libraries

The driving force behind the development of combinatorial libraries has been the many failed attempts to design therapeutic substances using theoretical knowledge allied to rational design; very few such approaches succeeded. In contrast, combinatorial library design is now thought by some to provide the best opportunity of discovering new novel peptides and small molecule structures for pharmaceutical application. A quite natural extension of the concept is to use combinatorial libraries to discover ligands capable of achieving highly efficient protein separations. When directed at drug discovery the earliest workers built libraries from peptides. For ligands libraries will generally utilize simple chemical molecules and occasionally smaller peptides. To distinguish this subsection from the earlier methods a convenient designation is the term Chemical Combinatorial Library (CCL)TM.

Although procedures for rationally designed ligands are well established, the newness of CCL suggests that CCL design of affinity ligands should be regarded as embryonic rather than immediately available for commercial application. There are thus two diametrically opposed systems – the rational design process, based on logic, experience and knowledge; and CCL which is illogical and completely random. One description of CCL is ‘a method of increasing the size of the haystack in which to find your needle’. A very recent approach is to combine both rational and CCL techniques, a process termed ‘intelligent’ combinatorial design. At the time of writing there are no published examples of ligands derived from CCL, although patents have been filed in this area.

Regulations and Drug Master Files

For researchers the relevance of regulations often seems remote, and yet the decisions taken in even the earliest stages of research can take on a great significance if the target product becomes a commercial

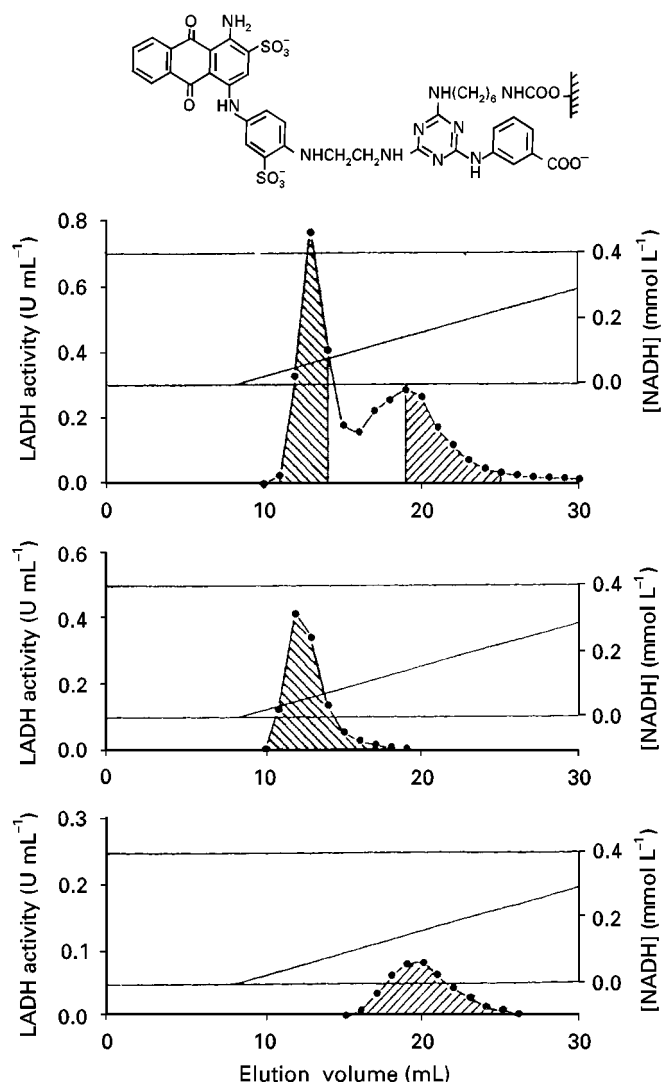


Figure 9 Horse liver alcohol dehydrogenase separation. Using the modified Cibacron Blue F3G-A (Figure 7) structure given above, the selectivity is greatly enhanced making it possible to separate the isoenzymes.

reality. It is regrettable that many researchers slavishly follow previously published data on a given separation problem without giving thought to the longer-term implications of their decisions. Sections above describe the adverse economic effects of multi-stage processing, but an equally important factor is regulatory issues. The most widely used regulations are those defined by the USA's Food and Drug Administration (FDA). Any company wishing to import products relevant to regulations existing in the USA must conform exactly to FDA requirements; drugs in particular are very strictly controlled. Detailed descriptions of any plant and process used in drug manufacture have to be lodged in documented form with the FDA, wherein every aspect of process description is given. This must include raw material

definition and suppliers, stability data for every step of the process, formulation methods, packaging, labelling, toxicity data and so on. The documentation has to be revised annually and any changes notified. Furthermore plant and process is open to inspection at all times for full audit of procedure. There is one large anomaly within the regulations. The largest volume of material in contact with a drug during manufacture is water, solvents and salts, all of which are exactly defined in terms of their physicochemical characteristics. The next largest is chromatographic media; ambiguously media do not have to be described in the same detail.

The outstanding stability of the synthetic chromatography media provides an excellent opportunity to develop and register Drug Master Files

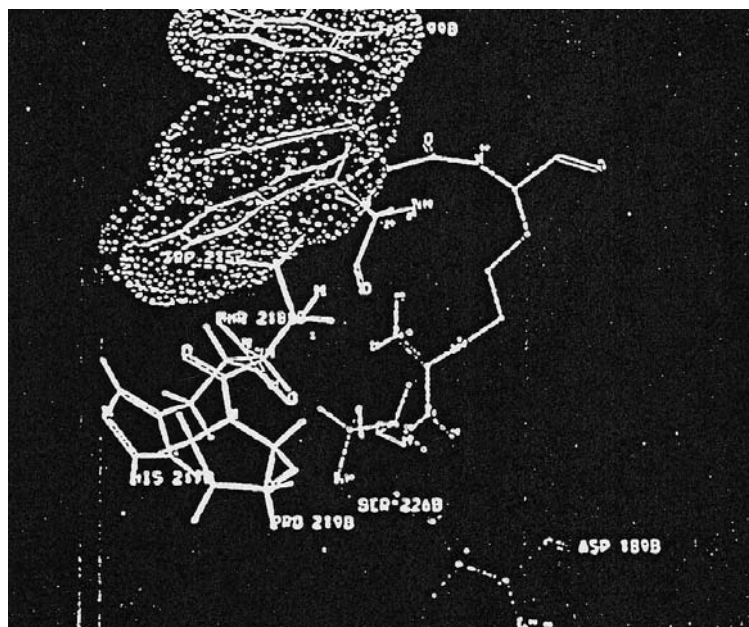


Figure 10 Model of the Phe-Arg dipeptidyl substrate bound in the active site of porcine pancreatic kallikrein. The illustration shows Asp189 at the bottom of the primary binding pocket as well as the side chains of Tyr99 and Trp215, which form the secondary binding pocket, with the phenyl ring of the Phe residue sandwiched between the hydrophobic side chains of these residues.

(DMFs) with the FDA. DMFs allows companies to use synthesized ligands for very high purity protein pharmaceuticals with total confidence. New Drug Applications (NDA) and Investigational New Drugs (IND) documents incorporating such stable affinity media can now be submitted to the FDA, safe in the knowledge that all appropriate information is on file. The effective guarantee of minimum quality

standards and Good Manufacturing Practice (GMP) is an integral part of a DMF. Few researchers selecting a specific medium consider the long-term implications of stability under depyrogenating conditions, the number of cycles that can be achieved (lifetime in use), its availability in bulk, whether it is manufactured under aseptic conditions and the price when supplied in bulk. If the researcher makes a good initial selection, the research data produced can be utilized in development phases with confidence. 'Fast tracking' is facilitated, with minimum aggravation, maximum efficiency and minimum purification costs.

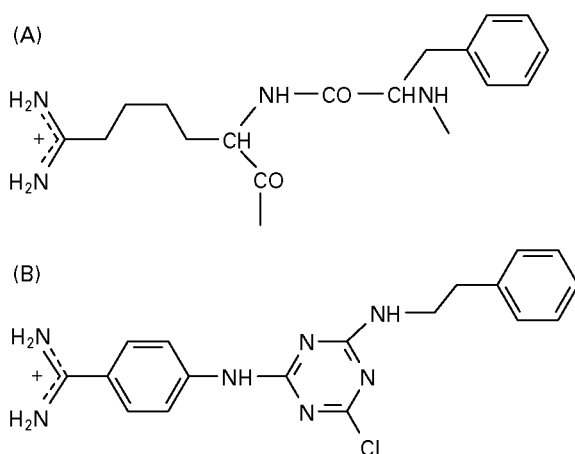


Figure 11 Comparison of the structures of (A) the Phe-Arg dipeptide, and (B) the 'biomimetic' ligand designed to bind at the active site of the porcine pancreatic kallikrein.

Alternative Affinity Approaches

Aqueous two-phase systems have been extensively applied to bimolecular purifications, by attaching affinity ligands to one of a pair of phase-forming polymers, a method known as *affinity partitioning*. Although a substantial body of research literature is available, few systems appear to have been adopted for commercial purposes. Reactive dyes, with their simple and well-defined coupling chemistries, have generally been favoured as the active ligand. The advantage of affinity partitioning is that the process is less diffusion-controlled, binding capacities

are high and the recovery of bound proteins is easier, created by the process operating with fewer theoretical plates than those generated by chromatography columns. This technique has also been combined with *affinity precipitation*, where a homobifunctional ligand composed of two ligand entities connected by a spacer (for example a bis-dye) is used. However, even in combination this approach suffers from considerable nonspecific binding and relatively low purification factors. A review of this combination suggests that it is more suited to large scale, low purity products. In contrast, perfluorocarbon emulsion chemistry utilizing mixer-settlers may offer more promise. By using a series of mixer-settlers connected in a loop a continuous process has been developed. A ligand (usually a reactive dye) is covalently bonded to a high density perfluorocarbon emulsion and contacted with the crude protein solution. After settling in the first tank the emulsion is pumped to a second settler and washed before passing to the third settler for elution. The emulsion is regenerated in the fourth settler. The supernatants from each settler, still containing some unbound target protein, are normally discarded. Although reasonable recoveries and yields are obtained, significant development is needed for this type of system to become competitive with conventional chromatography column methods.

Another favoured research approach to improving efficiency is to use *expanded beds*. Various techniques have been tried, with the primary objective of eliminating the 'solid bed' effect, where the bed acts as a filter, trapping insolubles and creating significant back-pressure. By partially removing the normal constraints of upper and lower retaining frits, which pack the particles tightly in the bed, the particles can expand, thereby releasing trapped solid impurities. Consequently longer operational cycles and higher flows result. One limitation of the expanded bed system is that adsorption can only be carried out in one stage, resulting in a less efficient process.

Expanded beds are only an intermediate stage towards *fluidized beds*. Several variations of fluidized bed technology have been adopted to evaluate them for affinity processing. One example is the use of perfluorocarbon emulsions in a countercurrent contactor. The affinity perfluorocarbon emulsion is loaded with crude source material into the base of a column in a similar manner to that of an expanded bed. The adsorbent is then removed from the base of the bed and carried forward through four identical contactors where washing, elution and regeneration are carried out successively. This process is claimed to improve significantly removal of target proteins compared to an expanded bed system.

Affinity Membranes

Ultrafiltration membranes are commonly employed as a 'polishing' stage of multistage separation processes for several commercially important proteins. Consequently attaching standard affinity ligands to create affinity membranes has become an actively researched area. The most obvious advantage of a membrane structure is the high rate of transport of the medium through the porous structure by filtration, thus minimizing the normally encountered diffusion limitations of mass transfer. High adsorption rates are achieved, especially if long distance electrostatic interactions are involved in the binding mechanism. However, in contrast to ion exchange membranes, similar high transport effects are not observed when used in the affinity mode, eliminating much of the initial attraction of this form of device. Other theoretically attractive features included: an inherent ability to control pore size across a very wide range, offering an opportunity to increase capacity of a given system; and ability to operate in either batch mode or filtration mode. In both cases experimental data have not confirmed these assumed advantages; a 10-fold change in the pore size resulted in only a two-fold capacity increase and when in filtration mode, although adsorption is fast, severe peak broadening on elution is experienced.

The chemistry relevant to particulate media is identical to that required for membranes, in effect making the systems compatible and allowing an easy technology interchange. The covalent bonding of affinity ligands to the surface of a membrane follows exactly the same chemistry as that applied to particulate media, and the same adsorption/desorption principles apply to both. Consequently the only difference between membrane systems and those of conventional chromatography is the exploitation of the characteristics of the membrane matrix compared with a particulate bed. Although the high mechanical strength of membranes is one major advantage, plus the scale-up is claimed to be very easy by stacking membranes (although scaling affinity columns is also very straightforward), it has been discovered that if the pressure drop across the membrane is too high sealing problems occur; the mobile phase then flows beyond the edges and past the membranes. Furthermore affinity membranes should be capable of use with unclarified extracts, but it has been generally observed that membrane capacity and lifetime are progressively reduced with time of use. Even with clarified broths, membrane fouling regularly occurs. This is almost certainly the reason why affinity membranes have not found favour in large scale processing.

Conclusion

Protein separations can be achieved by a variety of affinity techniques, but separations in the chromatography mode are by far the most widely used. Nature defined an appropriate pathway to highly efficient separation – utilization of the phenomenon of the automatic recognition mechanism existing between a given protein and at least one other. By covalently bonding one of the pair onto an inert matrix a theoretically simple separation process can be devised. Although these immunoaffinity separations are widely practised today, severe limitations exist, not least of which are cost and instability of the affinity medium when in use. As modern design aids have become commonplace, in conjunction with newer techniques such as the development of combinatorial library arrays, it has proved possible to mimic nature and replace immunoaffinity matrices by specifically designed synthetic ligands. These new ligands not only accurately emulate the exquisite precision of the natural protein–protein interaction mechanisms, but also provide the opportunity to manipulate the ligand structures, thus offering far more efficient separations than any previously achieved. For a given protein, from whatever source and at any dilution, it is now possible virtually to guarantee that a highly cost-effective and highly efficient separation process can be developed for eventual commercial use.

Designed ligand processes have already been adopted for several very large biotechnology projects scheduled to manufacture bulk protein pharmaceut-

icals. A mandatory part of any new protein pharmaceutical process is the acceptance by regulatory authorities of the separation process involved. That synthesized affinity ligand separation processes have now been fully accepted by the foremost regulatory authority, the USA's Food and Drug Administration, confirms a worldwide acceptance of the power of ligand design technologies.

See Colour Plate 1.

Further Reading

- Briefs K-G and Kula M-R (1900) Fast protein chromatography on analytical and preparative scale using modified micro-porous membranes. *Chemical Engineering Science* 47: 141–149.
- Burton SJ, Stead CV and Lowe CR (1988) Design and applications of biomimetic anthraquinone dyes. *Journal of Chromatography* 455: 201–216.
- Chase HA (1994) Purification of proteins using expanded beds. *Trends in Biotechnology* 12: 296–305.
- Dean PDG, Johnson WS and Middle FA (1985) *Affinity Chromatography: A Practical Approach*. Oxford: IRL Press.
- Jones K (1990) A review of affinity chromatography. *Chromatographia* 32: 469–480.
- Kenny A and Fowell S (1990) *Methods in Molecular Biology: Practical Protein Chemistry*. New York: Humana Press.
- Kopperschlager G (1994) Affinity extraction with dye-ligands. *Methods in Enzymology* 228: 121–129.
- Walker JM and Gaastra W (1987) *Techniques in Molecular Biology*. London: Croom Helm.

CENTRIFUGATION



D. N. Taulbee and M. Mercedes Maroto-Valer,
University of Kentucky-Center for Applied Energy
Research, Lexington, KY, USA

Copyright © 2000 Academic Press

Introduction

Centrifugation is a mechanical process that utilizes an applied centrifugal force field to separate the components of a mixture according to density and/or particle size. The principles that govern particle behaviour during centrifugation are intuitively comprehensible. This may, in part, explain why centrifugation is seldom a part of post-secondary science curricula despite the broad range of scientific, medical and industrial applications in which this technique

has been employed for well over 100 years. Applications that range from the mundane, industrial-scale dewatering of coal fines to the provision of an invaluable tool for biomedical research.

The first scientific studies conducted by Knight in 1806 reported the differences in orientation of roots and stems of seedlings when placed in a rotating wheel. However, it was not until some 60 years later that centrifuges were first used in industrial applications. The first *continuous* centrifuge, designed in 1878 by the Swedish inventor De Laval to separate cream from milk, opened the door to a broad range of industrial applications. About this same time, the first centrifuges containing small test tubes appeared. These were modest, hand-operated units that attained speeds up to 3000 rpm. The first electrically driven

centrifuges were introduced in 1910, further accelerating centrifuge development. Svedberg's invention of the analytical ultracentrifuge in 1923, operating at 10 000 rpm and equipped with transparent observation windows, marked another milestone in centrifuge technology. In the 1940s, the isolation of the first subcellular components by centrifugal techniques not only served to revolutionize our knowledge of the structure, composition and function of intracellular components, but demonstrated the potential of centrifugal methods for biomedical research. Although temporarily abandoned in 1943 in favour of a gaseous diffusion process, industrial-scale gas centrifuges were rapidly developed during World War II in an effort to enrich or separate uranium isotopes. In 1943, Pickels was the first to employ a sucrose-based density gradient to measure particle sedimentation rates. Density gradient centrifugation was further refined in the 1950s by Brakke, who applied the concept to purification and characterization of viruses, and by Anderson and co-workers at Oak Ridge National Laboratory, who designed a series of zonal centrifuge rotors for separation of subcellular particles and viruses. More recent advances have been characterized by significant improvements in materials and equipment and a broadening range of applications.

Today, centrifuges are routinely used in a variety of disciplines ranging from large-scale commercial applications to laboratory-scale scientific research. The number of centrifuge designs and configurations used in the mineral, petrochemical, chemical, medical, pharmaceutical, municipal/industrial waste, dairy, food, polymer, energy and agricultural industries (to name a few) seem almost as numerous as the applications themselves. An in-depth description of centrifuge designs and applications is, therefore, well beyond the scope of this treatise. Instead, this article will present the reader with an introduction to the theory of centrifugation, an overview of the various types of centrifugal separations, and a description of selected rotor/centrifuge designs and their more common applications.

Theory

Sedimentation by Gravity

A particle suspended in a liquid medium of lesser density tends to sediment downward due to the force of gravity, F_g . Newton showed that an object is accelerated by the gravitational force according to the relation:

$$F_g = mg = m \times 980 \text{ cm s}^{-2} \quad [1]$$

where m is the mass of the object and g is the acceleration due to gravity.

In an idealized case of a free-falling object being accelerated by gravity in a vacuum, the velocity of the object would exhibit a uniform rate of increase. However, for a real-world case of an object falling through air, or more appropriately for our purposes, settling in a liquid medium, there are two forces that oppose the gravitational force; the *buoyancy force*, F_b , and the *frictional force*, F_f .

Buoyancy force The buoyancy force was first noted by Archimedes, who showed that a particle suspended in a fluid experiences an upwards force that is equivalent to the weight of the fluid displaced:

$$F_b = m_M g = V_p \rho_M g \quad [2]$$

where m_M is the mass of the fluid medium displaced, V_p is the volume of the particle (=volume of the displaced fluid), and ρ_M is the density of the displaced fluid.

At pressures up to several bars (1 bar = 10^5 Pa), the buoyancy force in air or other gaseous media can be neglected to a first approximation with respect to the net gravitational acceleration experienced by solids or liquids. However, in a liquid medium, the buoyancy force is substantial. Since the volume of the settling material is equal to the volume of the fluid being displaced, the net gravitational force experienced by the particle is proportional to the difference between the mass of the particle and that of the displaced medium. Thus, assuming gravity sedimentation of a spherical particle with radius r and volume of $\frac{4}{3}\pi r^3$, eqn [1] can be rewritten to show the net gravitational effect, $F_{g\text{-net}}$:

$$F_{g\text{-net}} = \frac{4}{3}\pi r^3 (\rho_p - \rho_M) g = \frac{4}{3}\pi r^3 (\rho_p - \rho_M) \times 980 \text{ cm s}^{-2} \quad [3]$$

where ρ_M is the density of the medium (g cm^{-3}); ρ_p is the particle density (g cm^{-3}); and r is the particle radius (cm).

For those instances in which the medium density is greater than the density of the material in suspension, the net effect is negative, that is, particles would experience a net upward force in such instances and would tend to rise through the medium.

Frictional force, F_f In addition to the buoyancy force, the movement of a particle through a fluid medium is hindered by the viscosity of the medium, η , as described for a spherical particle by Stokes' equation:

$$F_f = 6\pi\eta r(dx/dt) \quad [4]$$

where η is the viscosity of the medium in poise, P ($\text{g cm}^{-1} \text{s}^{-1}$); r is the radius of the particle (cm); and (dx/dt) is the velocity of the moving particle (cm s^{-1}).

Eqn [4] shows that the frictional force is proportional to the particle velocity and its diameter. At low velocities and pressures, the frictional force is again negligible in a gas. However, at higher velocities, even in gases, this force becomes substantial, combining with the buoyancy force eventually to exactly oppose the gravitational force, resulting in no further acceleration of the particle. This condition is known as the limiting or *terminal velocity*. Mathematically, the conditions for attaining terminal velocity are met when:

$$F_g = F_b + F_f \quad [5]$$

The above discussion would imply that with sufficient time completely pure phases can be obtained by gravity sedimentation alone. While this may be true for the sedimentation of large particles in a medium with a significantly higher or lower density than the particle, this is not the case for smaller particles, which are impacted by diffusional forces that ultimately limit the separation efficiency as well as to other nonideality effects (see below).

Diffusion Random Brownian motion results in the net movement of solute or suspended particles from regions of higher concentration to regions of lower concentration, a process called diffusion. Thus, diffusion works in opposition to centrifugal sedimentation, which tends to concentrate particles. The rate of diffusion of a particle is given by Fick's law:

$$dP/dt = -DA(dP/dx) \quad [6]$$

where D is the diffusion coefficient which varies for each solute and particle; A is the cross-sectional area through which the particle diffuses; and dP/dx is the particle concentration gradient.

The precise impact of diffusion can be difficult and cumbersome to calculate for complex systems. It is often sufficient to keep in mind that the rate of diffusion is generally more pronounced for smaller particles than for larger ones, it increases with temperature, and its effects are lessened by higher centrifugal forces.

Aside from theoretical considerations, in a more practical sense, the time required for the settling of small to medium size particles in a gravitational field is often prohibitive. Additional obstacles to obtaining pure phases during gravity settling can also arise from

attractive forces between the particles being separated and/or the medium in which they are suspended. Often, gravitational force alone is insufficient to provide the minimum force necessary to disrupt such attractions. The use of centrifugal settling addresses the shortcomings of gravity settling by shortening the time required for sample recovery at a given purity, providing a greater force for disrupting particle/particle or particle/media interactions and, within limits, lessening the detrimental effects of diffusion.

Sedimentation in a Centrifugal Field

A particle moving in a circular path continuously experiences a *centrifugal force*, F_c . This force acts in the plane described by the circular path and is directed away from the axis of rotation. The centrifugal force may be expressed as:

$$F_c = ma = m\omega^2x \quad [7]$$

where m is the particle mass (g); a is the acceleration (cm s^{-2}); ω is the angular velocity ($\text{radians s}^{-1} = 2\pi \text{rpm}/60$); and x is the radial distance from the axis of rotation to the particle (cm).

Thus, centrifugal force is proportional to the square of the angular velocity and to the radial distance from the axis of rotation. The force generated during centrifugation can be compared to the gravitational force by the *relative centrifugal force*, RCF, often referred to as the *g* force:

$$\text{RCF} = F_c/F_g = (m\omega^2x)/(mg) = (\omega^2x)/g \quad [8]$$

Converting ω to rpm and substituting values for the acceleration due to gravity, eqn [8] can be rewritten in a more convenient form as:

$$\text{RCF} = 1.119 \times 10^{-5}(\text{rpm})^2x \quad [9]$$

While RCF is a ratio, and therefore unitless, it is frequently expressed in units of *g* to indicate the number of times that the force of the applied centrifugal field is greater than the force of gravity.

The forces acting on a particle suspended in a liquid medium in a centrifugal field are illustrated in **Figure 1**. Within the centrifugal plane, the centrifugal force acts to move particles away from the axis of rotation, while the buoyancy and frictional forces oppose this movement. The effect of the Earth's gravity can generally be regarded as negligible. Analogous to the conditions for attaining terminal velocity in a gravitational field (eqn [5]), the particle will reach a limiting or terminal velocity in a centrifugal field when the sum of the frictional and buoyancy

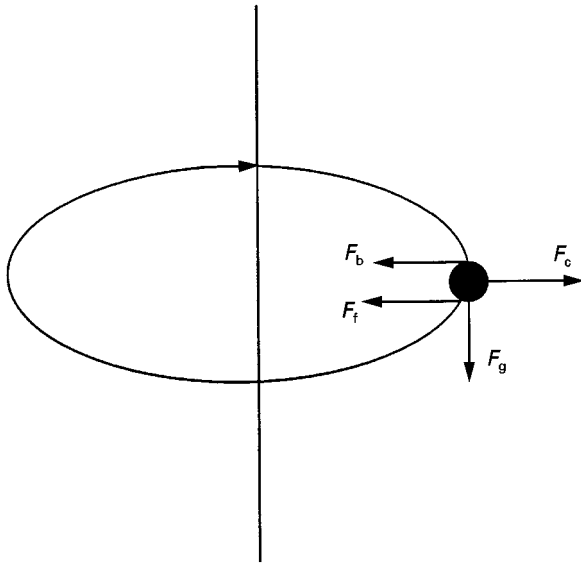


Figure 1 Forces acting on a particle in a centrifugal field: F_b , buoyancy; F_f , frictional; F_c , centrifugal; and F_g , gravitational.

forces equals the centrifugal force:

$$F_c = F_b + F_f \quad [10]$$

Substituting eqns [2], [4] and [7] into eqn [10] gives:

$$m\omega^2 x = V_p \rho_M \omega^2 x + 6\pi\eta r(dx/dt) \quad [11]$$

Assuming a spherical particle and substituting $\frac{4}{3}\pi r^3$ for volume gives:

$$(\frac{4}{3}\pi r^3)\rho_P \omega^2 x = (\frac{4}{3}\pi r^3)\rho_M \omega^2 x + 6\pi\eta r(dx/dt) \quad [12]$$

Then solving for dx/dt :

$$dx/dt = [2r^2(\rho_P - \rho_M)\omega^2 x]/9\eta \quad [13]$$

Eqn [13] is more commonly expressed in terms of particle velocity, v , and particle diameter, d :

$$v = (d^2(\rho_P - \rho_M)\omega^2 x)/18\eta \quad [14]$$

Eqn [14] may be integrated to determine the time required for a particle to traverse a radial distance from x_0 to x_1 :

$$t = [18\eta/(d^2(\rho_P - \rho_M)\omega^2)] \ln(x_1/x_0) \quad [15]$$

where x_0 is the initial position of the particle and x_1 is the final position of the particle.

While modifications can be made to eqns [13]–[15] to account for specific rotor design, liquid–liquid, density-gradient separations, etc., these equations describe the relative impact of the more significant para-

eters that govern settling velocity. They show that the sedimentation rate (i.e. limiting velocity) of a particle in a centrifugal field:

- increases as the square of the particle diameter and rotor speed, i.e. doubling the speed or particle diameter will lessen the run time by a factor of four;
- increases proportionally with distance from the axis or rotation; and
- is inversely related to the viscosity of the carrier medium.

These are the fundamental premises that a practitioner must know in order to develop a rational approach to centrifugal separation.

Sedimentation Coefficient

Since the terms r , ρ_P , ρ_M and η as given in eqns [13]–[15] are constant for a given particle in a homogeneous medium, the sedimentation rate, dx/dt , is proportional to $\omega^2 x$. This proportionality is often expressed in terms of the sedimentation coefficient, S , which is simply a measure of the sedimentation velocity per unit of centrifugal force. For a given set of run conditions, the sedimentation coefficient, S_r , may be calculated as:

$$S_r = (dx/dt)/(\omega^2 x) = 2r^2(\rho_P - \rho_M)/9\eta \quad [16]$$

The sedimentation coefficient, S , has the dimensions of seconds and is expressed in Svedberg units equal to 10^{-13} s. Its value is dependent on the particle being separated, the centrifugal force and the properties of the sedimentation medium. While adequate for a given set of run conditions, it is sometimes useful to compare sedimentation coefficients obtained under differing conditions and/or sedimentation media by reference to the behaviour of the particle in water at 20°C, $S_{20,w}$:

$$S_{20,w} = S_{T,M}\eta_{T,M}(\rho_P - \rho_{20,w})/\eta_{20,w}(\rho_P - \rho_{T,M}) \quad [17]$$

where the subscripts T and M denote the experimental temperature and medium, respectively.

Rotor Efficiency

The time required for a particle to traverse a rotor is known as the pelleting efficiency or *k-factor*. The *k*- or clearing factor, which is calculated at the maximum rated rotor speed, is a function of rotor design and is a constant for a given rotor. *k*-Factors provide a convenient means of determining the minimum residence time required to pellet a particle in a given

rotor and are useful for comparing sedimentation times for different rotors. The k -factor is derived from the equation:

$$k = \ln(r_{\max} - r_{\min}) \times 10^{13} / (3600\omega^2) \\ = 2.53 \times 10^{11} \times \ln(r_{\max} - r_{\min}) / \text{rpm}^2 \quad [18]$$

where r_{\max} and r_{\min} are the maximum and minimum distances from the centrifugal axis, respectively.

Eqn [18] shows that the lower the k -factor, the shorter the time required for pelleting. If the sedimentation coefficient of a particle is known, then the rotor k -factor can also be calculated from the relation:

$$k = TS \quad [19]$$

where T is the time in hours required for pelleting and S is the sedimentation coefficient in Svedberg units.

When k is known (normally provided by the manufacturer), then eqn [19] may be rearranged to calculate the minimum run time required for particle pelleting.

For runs conducted at less than the maximum rated rotor speed, the k -factor may be adjusted according to:

$$k_{\text{adj}} = k(\text{rpm}_{\max} / \text{rpm}_{\text{act}})^2 \quad [20]$$

where rpm_{\max} and rpm_{act} are the maximum rated rotor speed and actual run speed, respectively.

k -Factors are also useful when switching from a rotor with a known pelleting time, t_1 , to a second rotor of differing geometry by solving for t_2 in the relation:

$$t_1/t_2 = k_1/k_2 \quad [21]$$

where t_1 , t_2 , k_1 and k_2 are the pelleting times and k -factors for rotors 1 and 2, respectively.

Deviation from Ideal Behaviour

Eqns [13] and [14] showed the relative impact on settling velocity of the more important and controllable experimental parameters. However, there are other effects that are more difficult to characterize and which can result in significant deviations from the settling velocities predicted by these equations. The most common of these effects occurs when the particles are nonspherical, as these equations are derived from Stokes' equation assuming spherical particles. For nonspherical particles, eqns [13] and [14] may be modified with a correction

term, θ . In Stokes' equation, the term $6\pi\eta r$ describes the *frictional coefficient*, f_0 , for a spherical particle. The correction term, θ , is calculated as the ratio of the frictional resistance, f , encountered by a particle of nonspherical geometry to that encountered by a sphere of the same volume, or:

$$\theta = f/f_0 = f/6\pi\eta r \quad [22]$$

The equation describing the terminal velocity for nonspherical particles in a centrifugal field may be rewritten as:

$$dx/dt = [d_e^2(\rho_p - \rho_m)\omega^2 x] / 18\eta\theta \quad [23]$$

where d_e is the diameter of a sphere whose volume equals that of the sedimenting particle ($d_e/2$ is the Stokes radius).

The net result of this modification is that nonspherical particles are predicted to sediment more slowly, which is a more accurate depiction of their real-world behaviour.

In addition to deviations from spherical-particle geometry, there are other effects that can lead to departure from predicted behaviour (nonideality) during sedimentation. For example, many biological particles interact with the medium via hydration, the extreme case being for those particles with osmotic properties, which can result in drastic changes in particle density and, in turn, sedimentation coefficients. Interparticle attractions, e.g. charge or hydrophobic effects, may increase the effective viscosity of the medium. In more severe cases such attractions can lead to poor separations where the centrifugal energy is insufficient to disrupt the attractions between particles that are targeted for separation. This latter effect is aggravated by the fact that the larger or denser particle will lead as the particle pair migrates toward the rotor wall while the smaller or lighter attached particle follows in its wake, and therefore experiences less frictional drag. Particles may also concentrate locally to increase the effective medium density, or form aggregates that yield complicated sedimentation patterns. Because of such deviations from ideal behaviour, equivalent sedimentation coefficients, S^* , defined as the sedimentation coefficient of an ideal spherical particle, are often reported for a given set of experimental conditions.

Filtration

A mathematical description of liquid drainage from a packed bed by centrifugal forces is essentially the same as that used to describe more conventional gravity or differential-pressure filtration, the primary differences being that the centrifugal force

or the pressure generated by the centrifugal force is substituted for the gravitational or differential-pressure terms. As filtration is an extensively characterized field of study, a description of which is beyond the scope of this article, it is recommended that the reader refer to the literature for an in-depth mathematical discussion of both conventional and centrifugal filtration. However, a brief summary of some of the more important parameters that govern flow velocity and pressure drop during centrifugal filtration follow. A simple basket centrifuge is shown schematically in Figure 2. Assuming a constant height of liquid within the basket, the velocity of the filtrate, u , through a given cake thickness, dl , is given by the relation:

$$u = [1/(2\pi r' H)] dV/dt = [1/a\mu](-dP'/dl) \quad [24]$$

where H is the basket height or length ($2\pi r' H$ is the cross-sectional area of the filter); r' is the distance from the axis of rotation to the inner cake surface; dV/dt is the volume of filtrate passing in time dt ; a is the specific resistance of the cake; μ is the viscosity of the filtrate; dP' is the pressure drop across a given thickness of filter cake; and dl is a given cake thickness.

The velocity of the filtrate through the cake and underlying filter is thus proportional to the volume of filtrate flow or the pressure differential across the filter cake, and inversely related to the surface area of the filter, filtrate viscosity and cake resistance. Eqn [24] may be rearranged and integrated to determine the total pressure drop across the cake at time t :

$$-\Delta P' = (a\mu/2\pi H) dV/dt \ln(r/r') \quad [25]$$

where r is the distance from the axis of rotation to the outer cake surface.

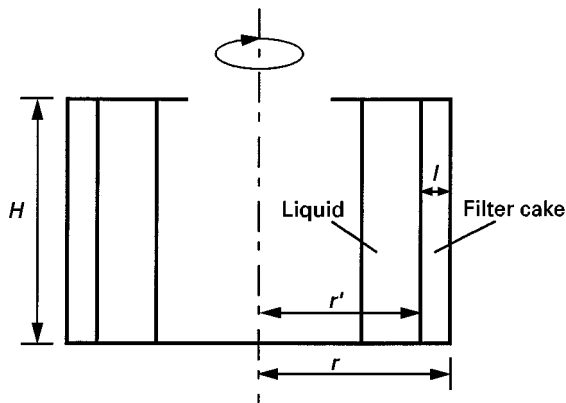


Figure 2 Basket filtration centrifuge.

If the resistance of the filter is negligible, $\Delta P'$ is equivalent to the centrifugal pressure. A parameter that is widely used to characterize the performance of filtration equipment is the drainage number:

$$\text{Drainage number} = \bar{d}(G)^{1/2}/\mu \quad [26]$$

where \bar{d} is the mean particle diameter (μm); G is the centrifugal force ($=\omega^2 r/g$), where r is the largest radius for a variable radius screen; and μ is the filtrate viscosity ($\text{m}^2 \text{s}^{-1}$). Higher drainage numbers correspond to more rapid drainage.

Types of Separation

One approach to classify centrifugal separations is according to the phase of the medium and the phase of the material to be purified, e.g. gas-gas, liquid-liquid or liquid-solid. Centrifugal separations of gas-phase materials are conducted in continuous mode only, while liquid-liquid and liquid-solid may be conducted in batch, semi-batch, or continuous modes. Gas-phase separations are very important in certain applications, particularly uranium isotope enrichment, but are highly specialized and not widely used. For space considerations, gas-phase separations are omitted from this discussion. Likewise, while liquid-liquid and even liquid-liquid-solid separations are common, discussion of the separation of immiscible liquids is, for the most part, limited to the discussion of centrifuge types in subsequent sections. Suffice it to say that the principles and approaches discussed in relation to liquid-solid separations generally apply to liquid-liquid separations. That is, small droplets of a liquid dispersed in a second, immiscible liquid will behave like solid particles settling through a liquid medium until the droplets sediment and coalesce, after which the methods to remove the separated liquids from the centrifuge usually differ from those used for solids removal.

Centrifugal separations may also be classified according to the method by which purified fractions are recovered. Three modes are used: (1) batch mode, in which the total sample to be separated is processed and then recovered at the conclusion of the run by decanting the supernatant and scraping the pellet from the rotor wall; (2) semi-batch mode, in which the sample mix is continuously fed to a spinning rotor as the supernatant is continuously discharged and the pellet is permitted to accumulate for post-run removal; and (3) continuous mode, in which the sample mixture is fed continuously, the supernatant is continuously discharged, and denser liquid or solid materials are either intermittently or continuously discharged while the run is in progress.

The types of separation to be discussed focus on the separation of solids from liquid media using any of the recovery modes described above. Discussion of simpler batch-mode operation is emphasized for simplicity. Three primary types of centrifugal separations are discussed: differential sedimentation, density gradient and filtration, with density gradient being further divided into rate-zonal and isopycnic (in isopycnic separations, particles sediment until they attain a position in the gradient at which the medium density is equal to their own).

Differential Sedimentation

As previously shown by the equations describing sedimentation (eqns [13] and [14]), larger and/or denser particles will sediment more rapidly in a centrifugal force field and will thus pellet onto the outer wall of the rotor faster than smaller or lighter particles. Most applications are based on this difference in behaviour, referred to as differential sedimentation or *pelleting*. In a simple batch-mode pelleting separation, a sample mixture called the homogenate (immiscible liquids or solid suspensions) is placed into a centrifuge container or rotor, and separated into two fractions as depicted in Figure 3. The unsedimented material is termed the *supernatant* and the sedimented material is the *pellet*. This approach works well when the objective is to pellet all the solid particles or to clarify the liquid. Such separations are also commonly used in the laboratory for 'quick and dirty' separations or where the objective is to enrich or clarify materials for subsequent analysis.

Obtaining high purity separations by differential sedimentation is more difficult. With respect

to separating particles of similar density according to size (classification), an approximate order of magnitude difference in mass between the particles is needed for differential sedimentation to be effective. The main disadvantage of separating a homogenate in batch mode is that the centrifugal field required to pellet the larger or denser particles that are initially nearer the axis of rotation is capable of pelleting smaller or lighter particles initially closer to the outer wall (Figure 3). Product purity or recovery may be improved by either recentrifuging the supernatant to obtain more pellet, or by resuspending the pellet and recentrifuging to obtain higher purity. When purity is the primary concern, this approach can still be used as a preparatory step to provide an enriched fraction for subsequent purification. However, a more efficient one-step approach is to layer the sample mixture on top of the preloaded medium. Stopping the run before the lighter or smaller contaminant particles reach the rotor wall allows them to be decanted with the supernatant. An alternative is to use a continuous-feed rotor in which the sample mixture is introduced near the axis of rotation and the supernatant, containing the smaller or lighter unsedimented particles, is continuously discharged. A more efficient approach is to layer or feed the sample to the top of a preloaded density gradient (see below).

Density Gradient Centrifugation (DGC)

DGC, developed in the 1950s, also relies on differential sedimentation behaviour to separate sample components, but compensates for some of the disadvantages of homogeneous media and also allows for the simultaneous separation of multicomponent mixtures. This is accomplished by the use of a density gradient, i.e. a liquid medium that increases in density from the layers nearest the axis of rotation to those farthest away. As will be discussed, this is achieved through variation in the concentration of an aqueous solute, or other gradient material, across the rotor. With minimal precautions, density gradients are surprisingly stable for extended periods, even with the rotor stopped. DGC separations are more extensively used for smaller-scale research applications in contrast to large-scale pelleting separations that are more common to industrial applications. DGC may be conducted as either rate or isopycnic separations.

Rate-zonal separations This technique, also called classification, is used to separate particles of similar density according to size. For batch separations, the sample mixture is layered on top of a preloaded medium, as shown in Figure 4. During a rate-zonal

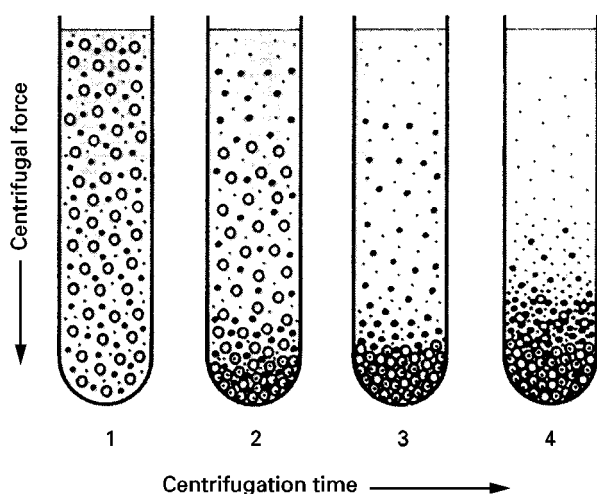


Figure 3 Differential sedimentation or pelleting. (Courtesy of Beckman Instruments, Inc.)

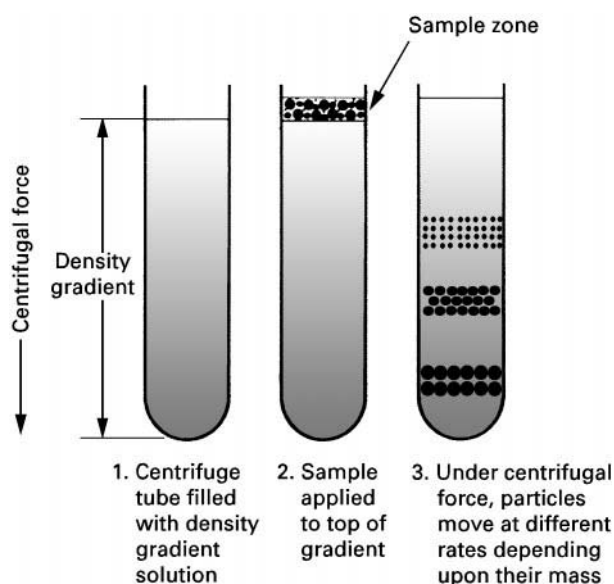


Figure 4 Rate-zonal separation in a swinging-bucket rotor. (Courtesy of Beckman Instruments, Inc.)

separation, larger particles sediment more rapidly, just as in a pelleting run. Also similar to a pelleting run, the maximum medium density is lower than the density of the particles being processed. However, unlike pelleting runs, the run must be stopped before particles reach the bottom of the tube or rotor wall, otherwise all sample components will simply sediment to the pellet.

Rate or *setting velocity* separations may be conducted with a homogeneous medium in batch or semi-batch mode. However, the use of density-gradient media offers several advantages. The steep gradient beneath the layer of sample suppresses premature sedimentation as well as convection currents in the liquid column, both of which lower the separation efficiency. In addition, the continuous increase in density, often accompanied by an increase in viscosity across the rotor, serves to slow the faster-moving particles and provide better resolution in the sample component *bands*. Increasing-viscosity gradients also lessen diffusional effects, though this advantage may be offset by an increase in the required run time. Rate-zonal separations are well suited for mixtures of particles of similar density that exhibit two or more well-defined modes of size distribution. However, owing to the additional steps and equipment required for DGC as opposed to pelleting, DGC separations are more commonly used to separate particle mixtures based on a parameter other than size, e.g. density.

Isopycnic separations These separations, which are based on differences in particle densities, are

conducted in a density gradient. The density range of the gradient often spans the full range of particle densities so that particles never reach the rotor wall, regardless of run time. Instead, particles move through the gradient until they reach a position in which the medium density is the same as their own (Figure 5). As governed by the settling velocity equations (eqns [13] and [14]), particles introduced to the top of a performed gradient sediment relatively quickly at first, with movement slowing as the difference in density between particles and gradient lessens and essentially stopping once the particles reach a position in the rotor where the density of the medium is equal to their own. Particles remain in this terminal position even after the rotor is stopped; this allows them to be recovered as density fractions. Differences in particle size only affect their rate of movement, though this may ultimately dictate the required run time. When the range of particle densities exceeds the range of the density gradient, then a mixture of pelleting and isopycnic separations will occur as some particles fully traverse the rotor and pellet while others attain their isopycnic position and remain suspended. While most density gradients are formed by the loading of solutions of successively higher density to the rotor, it is possible to form such gradients *in situ* from a homogeneous solution at high

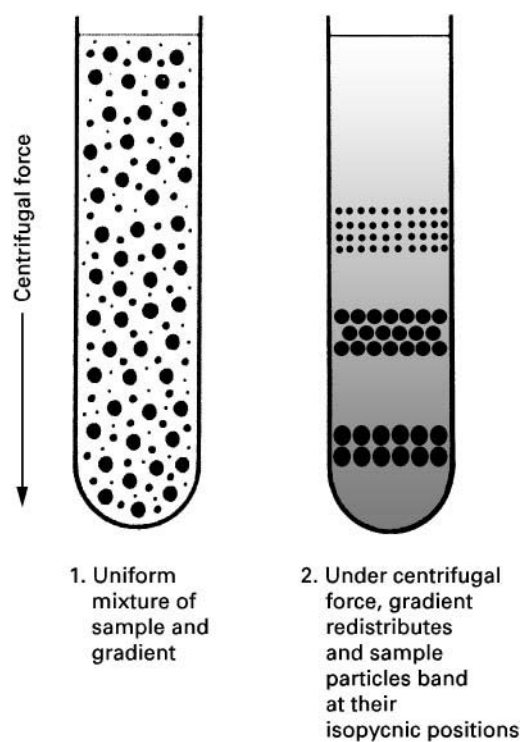


Figure 5 Isopycnic separation with a self-generating gradient. (Courtesy of Beckman Instruments, Inc.)

centrifugal speeds. This is achieved by routing the solutions to the rotor wall through veins in the central core. When such *self-generating* gradients are used, it is not necessary that the sample be layered on top of the solution but instead it may be mixed with the medium prior to loading (Figure 5). While self-generating gradients offer greater simplicity, they often require a significant increase in run time. For instance, though the advent of vertical tubes, faster centrifugal speeds, and overspeeding techniques have reduced run times to about one-third of those required only a few years ago, runs of 3 to 12 h are still typical for DNA banding experiments.

Isopycnic separation is a more powerful separation tool than rate-zonal separation in the sense that a generally greater number of particle types can be resolved. However, rate runs may still be preferred for separating large and/or fragile particles, since shorter run times and lower centrifugal forces are used. Run duration is crucial for a rate separation, whereas isopycnic runs simply require a minimum time for the particles to reach a stationary state. It is sometimes useful to conduct a two-dimensional separation in which, for instance, a rate-zonal run generates fractions of particles with similar *S* values that are further fractionated according to density in an isopycnic separation. The reverse process can also be performed to yield particles of similar density but different particle size distributions.

Gradient materials The selection of an appropriate gradient material is an important consideration as the gradient properties must be compatible with the separation objectives. The desired properties of an ideal gradient material, as set forth by Griffith and by Ridge, are summarized below.

The ideal gradient material should:

- span a density range sufficient to permit separation of the particles of interest without overstressing the rotor;

- be stable in solution;
- be inert towards the fractionated materials, including biological activity;
- exert the minimum osmotic effect, ionic strength and pH;
- be removable from the product;
- be readily available and either inexpensive or easily recyclable;
- be sterilizable.

It should not:

- generate a prohibitively high viscosity;
- interfere with the assay technique (e.g. absorb UV or visible light);
- be corrosive; or
- generate flammable or toxic aerosols.

From this list of properties, it is apparent that no single ideal gradient material exists, as each separation problem imposes its own set of requirements. Rather, selection can only be made after a careful evaluation of the gradient properties with respect to the requirements imposed by the separation to be conducted. The list of materials that have been used for gradient formation is extensive with examples of the more commonly used materials along with selected properties listed in **Table 1**.

With respect to biological inertness and low viscosity, the ideal aqueous gradient material is deuterium oxide (D_2O). However, D_2O is expensive and has a relatively low maximum density (1.11 g cm^{-3}).

Sucrose was used in the pioneering density-gradient work of Brakke and, due to its low cost, transparency, ready availability and nontoxic nature, is still the most widely used. Densities to 1.33 g cm^{-3} can be achieved, which is sufficient for separating most cells and intracellular organelles. However, sucrose solutions are not completely physiologically inactive and often contain UV-absorbing components. Mannitol and sorbitol can be used as substitutes to

Table 1 Physical properties of gradient materials in aqueous solutions at 20°C (from Sheeler, 1981)

Gradient material	Tradename	Maximum solution concentration			20% w/w solution	
		Concentration (% w/w)	Density (g cm^{-3})	Viscosity (cP)	Density (g cm^{-3})	Viscosity (cP)
Sucrose		65	1.33	182	1.08	2
Sucrose polymer	Ficoll	43	1.17	600	1.07	27
Colloidal silica	Ludox-SM	–	1.40	–	1.13	2
Colloidal silica	Percoll	23	1.13	10	1.11	8
Metrizamide		56	1.44	58	1.12	2
CsCl		65	1.91	1.3	1.17	0.9
Polytungstate salt	LST	85	2.89	14	1.20	–
Polytungstate salt	SPT	85	2.89	26	1.20	2

compensate for these deficiencies, but use of these sugars has disadvantages including higher viscosity and lower maximum densities. Polysaccharides also have a low osmotic pressure, but again are more viscous than sucrose solutions of equal density and may induce aggregation of the suspended sample via charge interactions.

Silica sols (e.g. Ludox™ and Percoll™), also called colloidal silica, are prepared from small silica particles in mildly alkaline solution. They provide low viscosities and osmotic pressures, even at high densities, and are transparent and inexpensive. Silica sols provide densities to 1.40 g cm^{-3} . Their disadvantages include a tendency to gel at $\text{pH} < 7$ and problems in complete removal from the sample. Percoll™, prepared by coating the silica particles with a polymer, eliminates the gelling problem and provides low viscosity, low osmotic pressure solutions, greater stability at low pH, and densities to 1.21 g cm^{-3} . However, this material is relatively expensive and removal from the sample can be a problem.

Salts are used to generate very high density aqueous solutions. Cesium chloride is by far the most widely used of this class. CsCl solutions can reach densities of $\sim 1.9 \text{ g cm}^{-3}$ at saturation while providing a very low viscosity at lower concentrations. Although expensive, CsCl can be readily recovered and purified. CsCl solutions also have a high osmotic pressure and are corrosive, though the titanium rotors generally used with this solute are relatively resistant. CsCl gradients are commonly used in applications ranging from the separation of viruses and dense cellular macromolecules such as DNA, to geological polymers found in coal or oil shale. Other salts that have been used to produce high density gradients include sodium bromide, sodium iodide, cesium bromide, cesium sulfate, cesium formate, cesium trifluoroacetate, rubidium bromide and rubidium chloride. Though expensive, tungstate polymers such as sodium polytungstate (SPT) and lithium heteropolytungstate (LST) have recently been used to generate aqueous gradients well over 2.5 g cm^{-3} . Applications

for these materials include the separation of graphitic carbon and mineral components from fly ash. When using such high density salt solutions, the user should be aware that at high concentration, salts may precipitate on the rotor wall, thereby generating high point densities and the potential for catastrophic rotor failure.

For nonaqueous gradients, organic liquids such as toluene, methanol or kerosene may be blended to attain gradient densities lower than that of water (1.0 g cm^{-3}). Of these, methanol presents an additional advantage of being water-soluble, thereby allowing gradients to be formed from a combination of the two. On the other end of the density scale, halogenated liquids such as diodomethane, bromoform and tetrabromoethane can be used to prepare very dense solutions over 2.8 g cm^{-3} . Problems associated with flammability, toxicity and attack of transfer lines and seals must be considered when using these materials.

Gradient formation and shape Gradient shape refers to the density profile across the tube or rotor as a function of gradient volume (Figure 6). Its choice is important as it governs the sedimentation rate in both rate and isopycnic experiments as well as the terminal position in isopycnic runs.

Gradients may be classified as *step* or *continuous*, as defined by the method of preparation. Step (discontinuous) gradients are prepared by the stepwise addition of solutions of successively higher density to the outer wall or bottom of the rotor. Steps gradients have the advantages that they may be formed without the need for a gradient generator. These gradients may also be readily *tailored* to provide larger volumes of separation media in the ranges that correspond to the density profile of the particles to be separated, thereby, permitting higher sample loadings. For continuous gradients, including the self-generating variety, the medium density varies in a continuous manner across the rotor or tube. Continuous gradients are classified as linear, exponential or isokinetic.

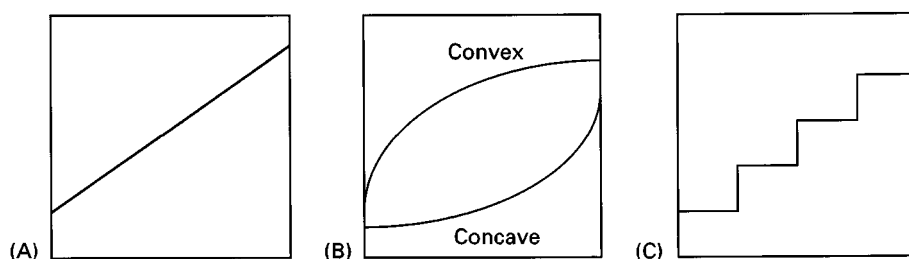


Figure 6 Gradient shapes: (A) linear; (B) exponential; and (C) isokinetic.

In a linear gradient, density increases linearly with distance from the axis of rotation (Figure 6A), and for cylindrical swing-out rotors, with increasing gradient volume as well. In an exponential gradient, the density increases or decreases exponentially across the rotor, producing convex or concave shapes, respectively, when plotted as a function of radial distance (Figure 6B). Isokinetic gradients are designed to produce a uniform sedimentation velocity throughout the gradient by counterbalancing the increase in centrifugal force particles experience as they traverse the gradient with an increase in the density and viscosity of the medium. Such gradients are often used in analytical rotors to study sedimentation behaviour. Simple linear sucrose gradients loaded in a swinging rotor provide a near isokinetic gradient.

Various methods are used to form gradients. The simplest approach is to form the gradient *in situ*, i.e. self-generating, by mixing the sample with a single-density medium prior to loading, then forming the gradient at high centrifugal speeds. While this is the simplest approach, higher speeds and longer run times are often required. Step gradients are also easily formed by simply pumping targeted volumes of successively denser solutions to the rotor wall. Inexpensive peristaltic pumps provide the simplest means of loading step gradients. The simplest liner-gradient generators consist of two equivalent cross-section cylinders that contain an initial and a limiting solution, respectively. The chambers are interconnected at the base with liquid from the limiting solution being drawn into and mixed with the initial solution as material from the initial-solution chamber is loaded. Exponential gradient generators are similar except that the cross-sectional area of one of the chambers changes in a predetermined manner as the chambers are depleted, thereby changing the relative volume contributed from the two chambers with time. More sophisticated gradient pumps are available including mechanical pumps that use cams to mix variable amounts of low and a high density solution prior to loading or programmable pumps, e.g. a liquid chromatograph pump, to generate the targeted gradient curve shape.

Several approaches are used to analyse and/or fractionate the rotor effluent. The simplest is to split the gradient into fractions according to volume, then subsequently analyse each fraction by chemical (density, absorbance, refractive index, fluorescence) or scintillation methods. However, this approach may be somewhat limited in resolution if the collected fractions are large, and thus represent a wider range in density. An alternative approach is to route the effluent through one or more in-line, low volume flow cells to monitor the gradient properties. Auto-

mated fractionators that select cut points and automatically switch collection vessels rely on such in-line detectors.

Analytical Centrifugation

This is the only type of centrifugal separation in which the primary objective is not to purify or de-water one or more of the feed components. Rather, this method is used to monitor particle sedimentation behaviour. Analytical centrifugation is used to characterize particle properties such as molecular weight, diffusion and sedimentation coefficients, buoyancy density, etc. The critical component in this technique is the addition of a transparent window, e.g. quartz or sapphire, to the centrifuge rotor to permit *in situ* optical measurements. Sample movement is typically monitored by UV absorption or refractive index during high speed separations in ultracentrifuges. Experiments are conducted in batch mode using very small sample volumes, as low as 5 μL for some rotors. Two classes of experiments are conducted in an analytical ultracentrifugation – sedimentation velocity and sedimentation equilibrium – analogous to rate and isopycnic experiments in preparative ultracentrifugation. Of these, sedimentation velocity is the more common. Analytical centrifugation is less common today than in the 1950s when this was the principal method for molecular weight determinations (1–10 kDa). However, the method is still used, primarily in biological applications, for studying phenomena such as interactions between macromolecules and ligand-induced binding events. More recently, this technique has experienced somewhat of a renaissance in drug discovery applications.

Continuous Centrifugation

These separations are similar to those previously discussed in the sense that separations are based on size or density differences. However, unlike batch-mode separation, in continuous centrifugation the sample mixture is introduced continuously to a spinning rotor as the supernatant stream continuously exits. For pelleting separations, the denser product may either accumulate on the rotor wall from where it is recovered after the rotor capacity is reached (semi-batch) or continuously discharged as the rotor spins (continuous mode). Continuous-feed centrifuges may be used for rate, pelleting, filtration, or isopycnic banding separations. They are best suited for applications in which large volumes of sample must be processed, the stream to be recovered is at low concentration, the particle sedimentation coefficient is high (less than about 50 S), or long acceleration/deceleration times are required.

The parameters of primary concern for continuous separations are centrifugal force and flow rate. These parameters must be carefully controlled to provide sufficient time for solid or denser liquids to sediment before being carried out with the supernatant, but not so long as effectively to under utilize the throughput capacity of the rotor. The parameters controlling particle sedimentation are the same in continuous-flow as in batch-mode separations. Therefore, the maximum flow rate that can be utilized in a specific rotor at a given speed may be estimated by using eqn [15] to determine the time required for a given particle to traverse the radial distance from the rotor exit, r_e , and to the outer rotor wall, r_{\max} . With information on liquid volume within the rotor and assuming laminar flow of liquid from the entry to the exit port(s), the flow rate can then be adjusted to provide this minimum residence time. The calculation of the minimum residence time is simpler if the rotor k -factor and the particle sedimentation coefficient are known, in which case the minimum residence time required for pelleting can be calculated from eqn [18] (i.e. $T = k/S$, where T is in hours).

Continuous centrifugation is used extensively in industrial applications, where large sample throughput and recovery is more common. However, laboratory-scale continuous-feed applications are also common, particularly in semi-batch mode where the component to be isolated is present at low concentrations. Owing to the variety of continuous-flow configurations that are available, further discussion of this approach is to be found in the section on centrifugal equipment below.

Filtration

Filtration is a mechanical means of separating solids from a liquid suspension via a porous medium or screen that permits the liquid to pass while retaining the solids. Similar to conventional filtration, achieved via a differential pressure across a filter, centrifugal filtration is driven by the pressure exerted by a liquid medium within a centrifugal force field. Opposing the centrifugal pressure is the combined resistance of the porous medium and filter cake. Centrifugal filters are commonly used to remove or recover coarse and crystalline solids from a fluid slurry, often followed by a rinse cycle to purify the solids and remove the residual mother liquor. In this technique, a sample slurry is fed to the rotor with the centrifugal pressure forcing the carrier liquid through a cylindrical screen or other permeable medium positioned around the outer wall to retain the solids or *filter cake*. The filter cake may be dried by shutting off the slurry feed and spinning the solids to attain resid-

ual moisture contents lower than generally provided by filter presses or vacuum filters. Most centrifugal filtration applications are typically conducted in continuous or semi-batch mode in which the liquids passing the filter are continuously discharged and the filter cake is continuously discharged or recovered post run. Perhaps the most widely used example of centrifugal filtration is the spin cycle in domestic washing machines.

Centrifugal filtration is a complex process that is dependent on a number of parameters including liquid viscosity, cake thickness, centrifugal force, screen area and, importantly, the size and packing characteristics of the particles themselves. Centrifugal filtration may be conducted in batch, semi-batch or continuous mode. While traditional industrial applications commonly use centrifugal filtration to recover solid materials with reduced moisture contents, many laboratory-scale spin filters, particularly in a test-tube configuration, are available. This technique is generally not amenable to broad generalizations and is, therefore, best approached on a case-by-case basis.

Centrifugal Equipment

Centrifuges and rotors are commercially available in literally hundreds of shapes, sizes and configurations. They range from small laboratory-scale units equipped with capillary tubes, operating at speeds in excess of 100 000 rpm or forces approaching 1 000 000 g to large industrial decanters that may continuously process up to 300 000 L h⁻¹. The primary rotor or centrifuge selection criteria must centre on the objective for conducting the separation. Parameters such as batch versus continuous; required centrifugal force and purity; throughput; the number of components to be recovered; sample toxicity/corrosiveness; time; cost; available space; noise tolerances, and so forth must be considered when selecting the appropriate centrifuge/rotor for a given application.

Early rotors were often manufactured of steel or brass, but are now more commonly constructed of aluminium and titanium. Newer carbon composites are also gaining acceptance, with plastics commonly used for small-scale applications and stainless steel for industrial-scale units. Though somewhat more expensive, titanium is particularly suitable as it has both a higher strength-to-density ratio and a high resistance to corrosion and erosion. Selected properties for steel, aluminium and titanium are shown in Table 2.

Centrifuge bottles and tubes are also constructed from a variety of materials. Early tubes were usually glass or stainless steel, but these have largely been replaced by plastics, e.g. polycarbonate, nylon,

Table 2 Strength data for commonly used rotor construction materials (from Sheeler, 1981)

Material	Density ($g\ cm^{-3}$)	Ultimate strength ($g\ cm^{-3}$)	Strength: density ratio
Aluminium	2.79	2159	774
Titanium	4.84	6088	1258
Steel	7.99	7915	991

cellulose nitrate and cellulose acetate, etc. Polycarbonate is one of the more popular materials owing to its transparency and strength. The choice of material is generally dictated by the properties of the particles to be fractionated and, in high speed separations, by the maximum rated g force.

An exhaustive discussion of the many equipment options along with their advantages and disadvantages is beyond the scope of this article. Rather, a brief overview is offered of the more common centrifuge designs together with typical applications. Much of the discussion will assume batch operation, though in most cases rotors are available or may be adapted for batch, semi-batch or continuous-mode operation. However, since continuous-mode centrifuges are so widely used in industrial applications and their analogues are often unavailable in laboratory-scale units, a section describing the more common or innovative continuous-flow configurations is included.

Bottle Centrifuges

The most common laboratory centrifuge is the bottle centrifuge. Bottle centrifuges consist of a motor-driven vertical spindle to which a horizontal rotor, machined with an even number of sample positions (2–36), is attached. The harness and rotors are covered with a safety shield, which may also serve to reduce air friction and facilitate temperature control. Such units are normally equipped with a timer, tachometer, and manual or automatic braking. Samples may be mixed with the medium prior to loading, or layered on top of a homogeneous medium or density gradient. Bottle centrifuges are usually bench-top units that may operate at speeds up to 30 000 rpm and g_{\max} of 65 000, but are also available as larger, free-standing units that generate centrifugal forces in excess of 100 000 g . Sample capacities range from capillary tube to 1 L bottles (4 L total capacity).

Bottle-centrifuge rotors classified as swinging-bucket, fixed-angle, and vertical (Figure 7). In the *swinging-bucket* type, the bottles are in a vertical position at rest but swing outward to a horizontal

orientation as the rotor speed increases. In this orientation, the centrifugal force is applied along the length of the tube, making them suitable for rate separations. They may also be used for batch separation of immiscible liquids with some rotors specifically designed to hold separatory funnels to facilitate post-run recovery. However, their high k -factors make them generally unsuitable for differential pelleting, though some rotors constructed to hold short, large-diameter bottles, are designed for such purposes. *Fixed-angle* rotors are loaded and operated in a similar manner except that, as the name implies, the tube remains at a fixed angle both at rest and during the run. The fixed angle is typically 20–45° from the vertical, though *near-vertical* rotors are less than 10° from the vertical. The fixed-angle design provides a shorter pathlength (Figure 7) with a corresponding reduction in run time (lower k -factor). Particles that reach the outer wall of the tube during the run aggregate and quickly slide down the tube wall to form a pellet in the bottom. This makes the fixed-angle rotor useful for both pelleting (Figure 3) or isopycnic banding (Figure 4). *Vertical* rotors can be considered as an extension of fixed-angle rotors in which the angle of repose is 0° from the vertical. In this design, the maximum pathlength is equal to tube diameter, thereby providing the lowest k -factors for a given tube size. Vertical tube rotors are commonly used for isopycnic banding where short run times are important, as compared to near-vertical rotors, which provide short pathlengths yet permit pellet accumulation.

The tubes loaded into both vertical and fixed-angle rotors must be sealed during the run to prevent the contents from escaping as the medium moves up the outer wall at speed. O-ring sealing systems or heat sealing are commonly used. If the volume is kept sufficiently low, this step may not be necessary except to prevent the escape of hazardous aerosols, in which case a plastic screw or push-on cap may suffice.

For pelleting runs, sample recovery entails decanting the supernatant from the top and scrapping or washing the pellet into a recovery vessel or filter. For density-gradient runs, the sample may be unloaded from either the top or bottom of the tube with a pump, a Pasteur pipette, syringe, displacement liquid, etc., or by using soft plastic tubes that may be pierced to facilitate recovery of a targeted central band.

Zonal Rotors

While bottle centrifuges can be, and are, effectively used for density-gradient centrifugation, their

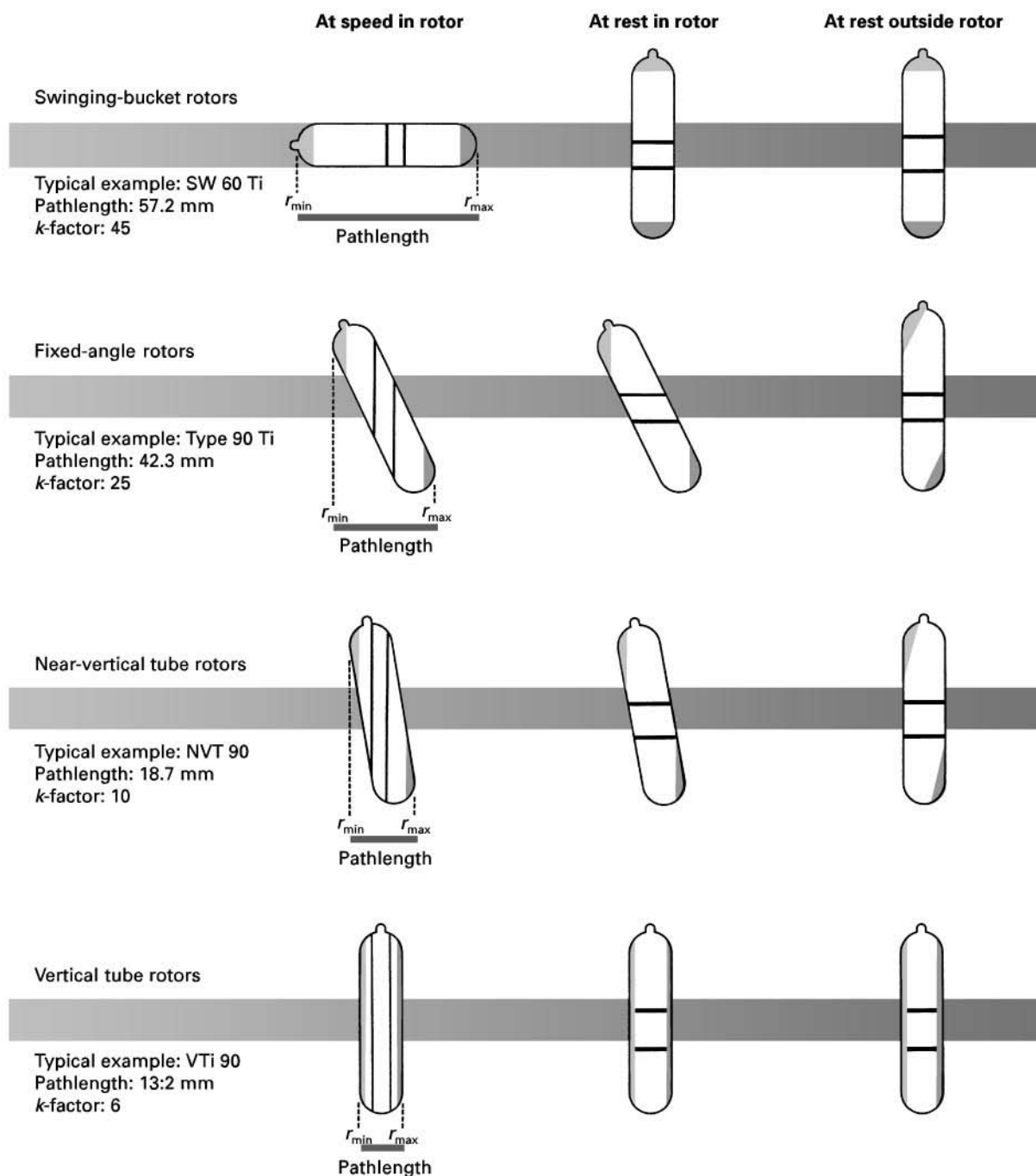


Figure 7 Particle separation in swinging-bucket, fixed-angle and vertical-tube rotors. Dark shading represents pelleted material, light shading in floating components, and band are indicated by black lines. (Courtesy of Beckman Instruments, Inc.)

capacity may be insufficient for certain applications. This obstacle may be addressed with zonal rotors, which provide a larger internal volume for a given radius. Zonal rotors are bowls or cylindrical cavities equipped with a central core and attached vanes or septa that divide the rotor into four or more sector-shaped compartments. Zonal rotors present additional advantages over bottle centrifuges such

as minimal wall effects, maximum particle and gradient resolution during sedimentation and recovery, rapid gradient formation, and high rotation speeds. Due to their higher efficiency and capacity, zonal rotors are widely utilized in applications ranging from separation/purification of proteins, viruses and subcellular components to the concentration of coal or kerogen macerals. Zonal centrifuges

can be operated in batch, semi-batch, or continuous modes and may be loaded or unloaded with the rotor stopped (*static*) or with the rotor spinning (*dynamic*).

Statically loaded and unloaded zonal rotors are also called reorienting gradient rotors. In this method, the gradient is loaded with the rotor at rest then slowly accelerated to permit the gradient to reorient from a horizontal to a vertical configuration, as illustrated in **Figure 8**. Solutions of increasing density are loaded to the bottom with the sample solution layered on top after the rotor is filled. When the rotor is accelerated, the gradient reorients to a vertical position with the lighter fractions and sample in the centre of the rotor. After centrifugation, the rotor is slowly decelerated and the gradient returns to a horizontal orientation. The heavier fractions may be removed first by displacement with air or the rotor lid removed and the gradient pumped out. Alternatively, the gradient may be displaced with a denser liquid that forces the lighter fractions out first. The advantages of the reorienting gradient technique are simplicity and the avoidance of rotating seals that may leak or fail during dynamic loading/unloading. The major disadvantage is the tendency of the gradient to swirl as it reorients, leading to a loss in resolution.

Dynamic loading and unloading, also known as 'rotating seal', is conducted as the rotor spins, as illustrated in **Figure 9**. The gradient is pumped through a rotating seal in the centre of the rotor lid into passages machined into the rotor core, which channel the solutions to the outer wall. The lighter-density solutions are loaded first, forming a vertical layer that is displaced inward by the ensuing denser solutions. An optional high density liquid *cushion* may be added last if a reduction in the effective rotor volume is desired. The sample is introduced to the centre of the rotor by reversing the feed/exit lines. The rotor is accelerated to the operating speed for a targeted time, then decelerated to the initial loading speed. In centre unloading, a high density immiscible liquid, such as Fluorinert™, may be routed to the outer wall, forcing the gradient from the rotor, lighter fractions first. Edge unloading is similar, only a light liquid is pumped to the centre, displacing the heavier fractions first. The gradient may be fractionated as it exits by routing the effluent through a programmable fractionator that automatically switches collection vessels, or manually by selecting cutoff points with a density meter, refractometer or UV absorption cell, or by collecting predetermined volumes. While somewhat more cumbersome, dynamic loading generally provides better resolution than static loading/unloading.

Ultracentrifuges

'Ultracentrifuge' is an ill-defined term applied to centrifuges with rated speeds greater than about 25 000 rpm, regardless of the medium or rotor design. While speed was historically used to designate ultracentrifugation, some manufactures now reserve this term for centrifuges that operate at sufficient speeds to require a vacuum to reduce frictional drag and/or rotor heating. Most such units are also equipped with refrigerant capability for the same purpose.

Ultracentrifuges are classified as preparative or analytical. Preparative ultracentrifuges are used to separate and recover purified sample components at speeds ranging up to 150 000 rpm and forces to 900 000*g*. The rotor configuration may be any of the types described in this section – bottle, zonal, or continuous – with fixed-angle and vertical-bottle centrifuges providing the highest speeds and titanium being the most common material of construction.

Analytical ultracentrifuges, originally developed by Svedberg, are used to study the behaviour of particles during sedimentation. While analytical rotors are available in various shapes and sizes, their defining feature is a transparent window, typically constructed of quartz or sapphire, that permits the sedimenting particles to be monitored optically during the run. UV absorption and/or refractive index measurements are the most common monitoring techniques. The required sample volume is low, ranging down to 5 µL, making this a useful technique when sample availability may otherwise be a limiting factor. Sample recovery is generally a secondary consideration, if conducted at all. Analytical ultracentrifuges are available at speeds up to 70 000 rpm and centrifugal forces in excess of 350 000*g*.

Continuous Centrifuges

Conventional batch separations are generally unsuitable for many industrial and certain laboratory-scale separations. Continuous-flow centrifugation offers certain advantages when large quantities of sample must be processed, the stream to be recovered is at low concentration, or long acceleration/deceleration times are required. Such units may be used for rate, pelleting, filtration, or isopycnic banding separations. In continuous-flow centrifugation, the sample mixture is introduced continuously to a spinning rotor as the supernatant stream continuously exits. The denser product may either accumulate on the rotor wall, from where it is recovered by stopping the run when the rotor capacity is reached (semi-batch mode), or continuously discharged during the run (continuous mode).

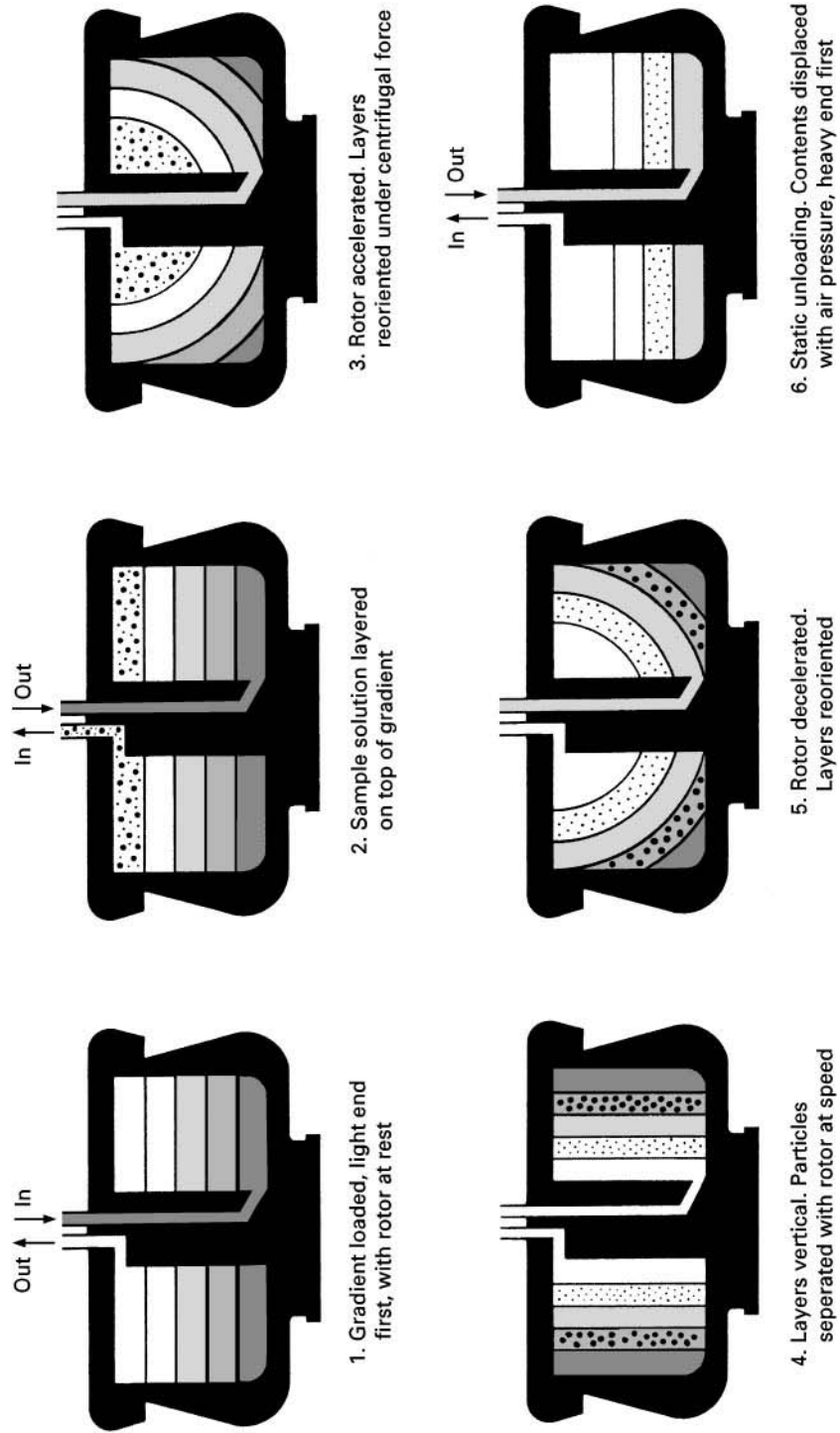


Figure 8 Static loading and unloading of a zonal rotor with a reorienting gradient core. (Courtesy of Beckman Instruments, Inc.)

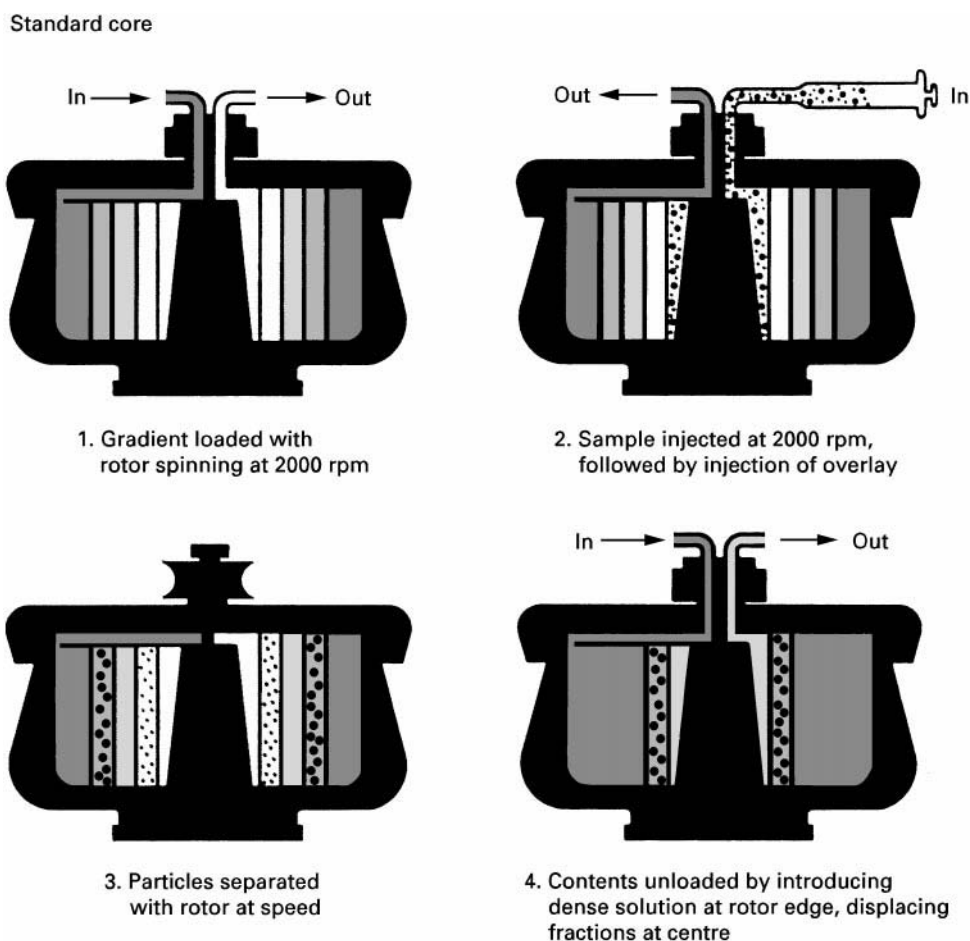


Figure 9 Dynamic loading and unloading of a zonal rotor. (Courtesy of Beckman Instruments, Inc.)

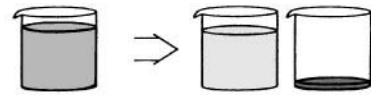
The rotors previously described can be, and often are, adapted for continuous-flow separations. However, the following discussion focuses on rotors that are designed specifically for continuous operation, particularly for industrial applications such as those depicted in **Figure 10**.

Disc centrifuges Disc centrifuges operate on the principle of differential sedimentation and are used for two-phase (liquid–solid or liquid–liquid) and three-phase (liquid–liquid–solid) separations. These are highly efficient units with some industrial-scale units generating forces of 10 000*g* and pelleting of particles as small as 0.1 μm . Disc centrifuges are essentially a rotating bowl equipped with an internal set of conical settling plates or discs mounted at an angle to the axis of rotation (typically 30–40°). The discs serve to decrease the sedimentation pathlength and increase the sedimentation surface area, i.e. capacity factor. Denser materials sediment onto and slide across the plate surfaces before accumulating on the bowl wall (**Figure 11**) as the clarified supernatant

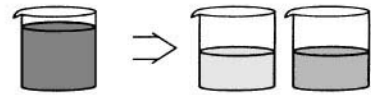
continuously exits. In addition to the parameters of centrifugal force and flow rate, the capacity and performance of disc centrifuges are also dependent on the number, spacing and diameter of the plates. Sample mixtures may be introduced to either the interior or outside of the disc stack, depending on the nature and concentration of solids, with most units configured for liquid–liquid or liquid–liquid–solid mixtures being centre fed.

Three variations of disc centrifuges, as distinguished by their solids-handling capability, are commonly used: solids-retaining, intermittent solids-ejecting and continuous solids-ejecting (**Figure 11**). Solids-retaining designs (**Figure 11A**) are appropriate for liquid–solid or liquid–liquid separations where the solids content is less than about 1% by volume. For liquid–solid separations, the solids that accumulate on the bowl wall are recovered when the rotor capacity is reached and the centrifuge is stopped. Removable baskets are incorporated into some designs to facilitate solids removal. Recovery of two liquid streams can be achieved by positioning exit

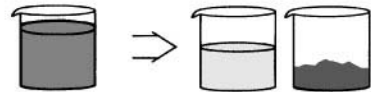
Clarification Separate suspended particles from a liquid



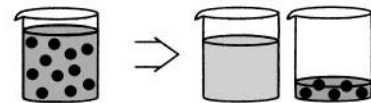
Purification Separate immiscible liquids (even with solids present)



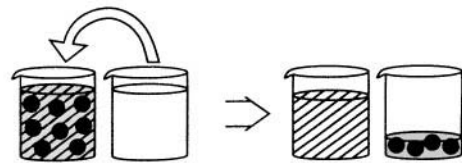
Dewatering Concentrate a slurry



Classification To split a suspension into two streams with different particle size distributions



Washing Countercurrent washing or dissolving of impurities in suspended, crystallized or amorphous solids



Extraction To mix a liquid containing a mineral or extract with a liquid agent, and then separate out the agent, which contains the extract or mineral

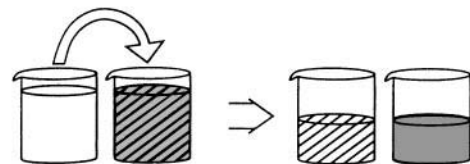


Figure 10 Major industrial applications for continuous centrifuges. (Courtesy of Alfa Laval Separations.)

ports at different radial distances as dictated by the relative concentration of the liquids. Commercial units are available with liquid throughput capacities of $60 \text{ m}^3 \text{ h}^{-1}$ and holding capacities of 30 L. A variation on the solids-retaining disc centrifuge is the cylindrical-bowl design shown in **Figure 12**, which incorporates a series of concentric cylindrical retainers for processing liquid–solid mixtures. Unlike the disc centrifuge, in which the feed stream is split and makes a single pass through the disc stack, in the cylindrical-bowl design the liquid stream is routed through each chamber in succession, resulting in a longer residence time, more efficient recovery, and generally greater capacity (to 70 L). Applications of solids-retaining centrifuges of the stacked-disc or cylindrical-bowl design include separation of cream from milk, organic waste from water, purification of lubricating oils, or removal of water and solids from jet fuel.

Solids-ejecting stacked-disc centrifuges (**Figure 11B**) are more suitable for processing samples with solids contents to about 15% by volume. These units operate similarly to the solids-retaining design, only solids or sludge that accumulate on the bowl wall are intermittently discharged through a hydraulically activated, peripheral opening. Laboratory models to 18 cm diameter and industrial units to 60 cm are available, with the latter capable of throughputs in excess of $100 \text{ m}^3 \text{ h}^{-1}$. Applications for these units include catalyst recovery, clarification of paints and varnishes, treatment of radioactive waste water, and copper extraction.

Continuous solids-discharge disc centrifuges, also called nozzle bowl separators (**Figure 11C**), are used to process samples with solids contents ranging from 5 to 30% by volume. In this design, solids are continuously discharged via backward-facing orifices, i.e. nozzles, closely spaced around the outer periphery of

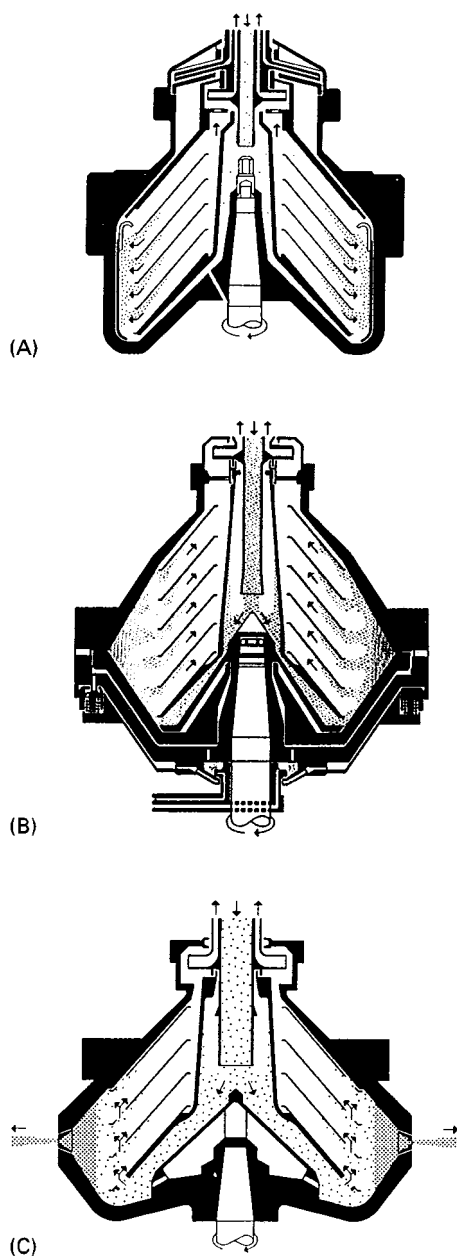


Figure 11 Disc centrifuge configurations: (A) solids-retaining; (B) intermittent solids-ejecting; and (C) continuous solids-ejecting. (Courtesy of Alfa Laval Separations.)

the bowl. Due to the high discharge velocities resulting from the centrifugal pressures, nozzle erosion can occur. Thus, the materials used for nozzle construction and the ease of replacement of eroded components should be considered. Newer designs discharge to an internal chamber where the discharge is pumped out as a product stream. Industrial units are available to $200 \text{ m}^3 \text{ h}^{-1}$ throughput capacity, elevated temperature ($\leq 200^\circ\text{C}$) or pressure (7 bar) capability, and particle removal to $0.1 \mu\text{m}$. Applica-

tions for continuous-discharge disc centrifuges include production of baker's yeast, dewatering of kaolin clay, titanium dioxide classification, and coal-tar and tar-sand clarification.

Continuous conveyor discharge These centrifuge types integrate an active mechanical solids discharge mechanism in an imperforate bowl for the continuous processing of larger sample volumes. The bowl shape is tubular, having a length-to-diameter ratio of 1.5–5.2, and may operate in either a horizontal or vertical configuration. The vertical configuration is generally preferred for reduced or elevated temperature and/or pressure applications owing to fewer mechanical problems with seals and heat expansion. The solids-discharge mechanism is most commonly, a helical screw turning at a slightly slower rate than the rotor, though pistons or conveyer belts are also used. **Figure 13** illustrates a helical-screw configuration used for three-phase separations (liquid–liquid–solid). Solid–liquid and liquid–liquid configurations with either concurrent or countercurrent flow regimes are commercially available. Such mechanical discharge units typically operate at lower centrifugal forces (to $5000g$) than disc centrifuges. However, they are capable of very high throughput, up to $300\,000 \text{ L h}^{-1}$, and can be used to process feed streams containing up to 50% solids by volume. While a limited number of industrial units operate on materials smaller than $1 \mu\text{m}$, particles smaller than about $2 \mu\text{m}$ are usually not collected in such units, a characteristic that is used to advantage for particle classification. Continuous conveyor centrifuges are widely used in the chemical, mining, pharmaceutical,

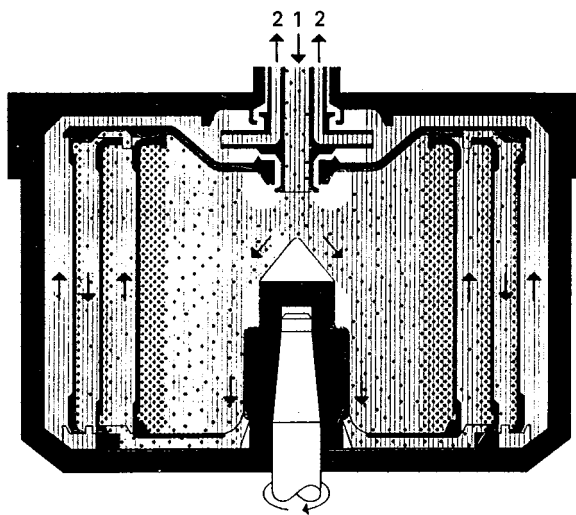


Figure 12 Schematic of a cylindrical-bowl centrifuge. (Courtesy of Alfa Laval Separations.)

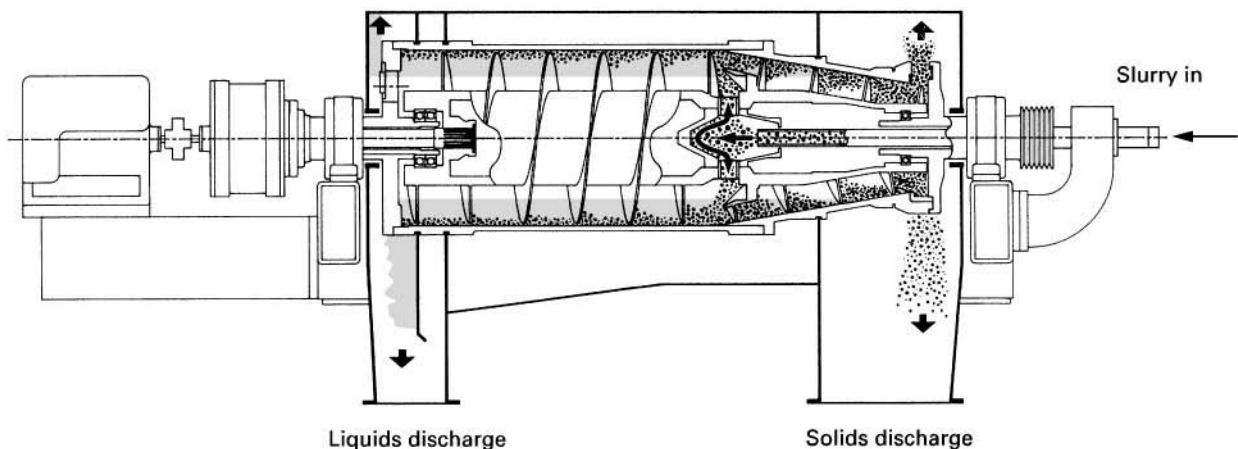


Figure 13 Schematic of a horizontal continuous-conveyor centrifuge. (Courtesy of Alfa Laval Separations.)

biotechnology and food sectors for clarifying, classifying, dewatering and thickening applications.

Tubular centrifuges These centrifuges utilize a vertically mounted, imperforate cylindrical-bowl design to process feed streams with a low solids content. Liquid(s) is discharged continuously and solids are manually recovered after the rotor capacity is reach-

ed. One configuration, designed for recovery of two immiscible liquids and a solid product, is shown in **Figure 14**. Other configurations for processing solid-liquid or liquid-liquid mixtures are also widely used. Industrial models are available with diameters up to 1.8 m, holding capacities up to 12 kg, throughput rates of $250 \text{ m}^3 \text{ h}^{-1}$, and forces ranging up to $20\,000g$. Laboratory models are available with

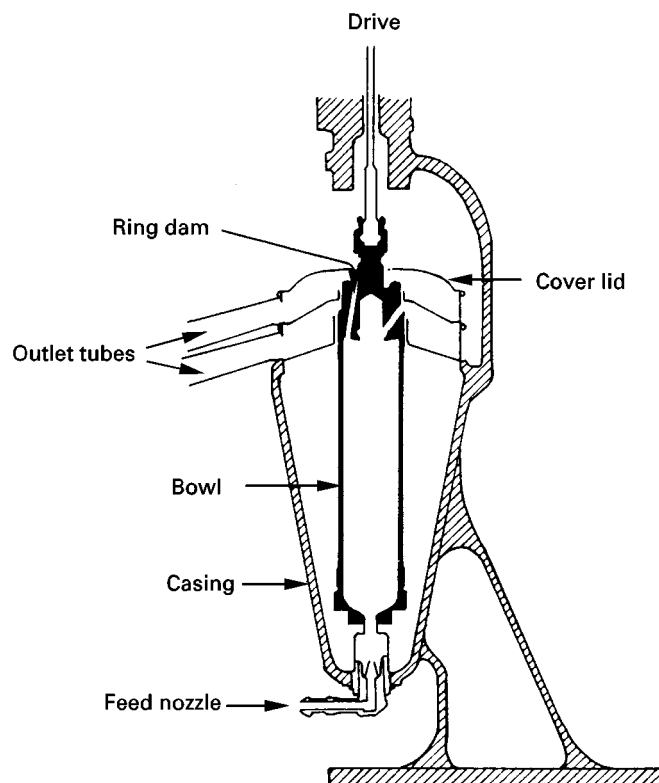


Figure 14 A tubular centrifuge configured for recovery of two liquids and one solids stream. (Courtesy of Alfa Laval Separations.)

diameters of 4.5 cm, throughput rates of 150 L h^{-1} , and centrifugal forces ranging up to $62\,000g$. Because of their high speed and short settling path, tubular centrifuges are well suited for the pelleting of ultrafine particles, liquid clarification, and separation of difficult-to-separate immiscible liquids. In addition to the standard electric motor used for most laboratory centrifuges, laboratory-scale tubular centrifuges are available with turbine drives. Tubular centrifuges were refined for the separation of penicillin during World War II but since then have largely been replaced by disc centrifuges because of their limited holding capacity. However, they are still widely used for applications that involve the efficient recovery of high value products at high purity, especially in the pharmaceutical and chemical industries. Typical applications include recovery of *Escherichia coli* cells and flu viruses, removal of colloidal carbon and moisture from transformer oils, removal of small particles from lubricating oils, blood fractionation, and de-inking.

Continuous zonal rotors Zonal rotors are often used for smaller scale, semi-batch separations. Operation is similar to that previously described for batch separation only a larger diameter core with a different flow pattern is inserted as illustrated in **Figure 15**. Continuous-feed separations in zonal centrifuges are best suited for low concentration, high volume samples. Such separations may be conducted with a homogeneous medium for sample pelleting, or with a density gradient for materials that may be adversely affected by pelleting (e.g. viruses that may lose their activity) or if simultaneous isolation of two or more materials is desired. Applications include purification of viruses from tissue-culture media, harvesting bacteria, or separating fine clay particles in water pollution studies.

Elutriation rotors Another type of laboratory-scale continuous-flow centrifugation is elutriation or counterstreaming, used to separate particles with differing sedimentation rates (rate separation). A schematic of the elutriation process is shown in **Figure 16**. Conical or funnel-shaped rotors are used with the small end positioned farthest from the axis of rotation. The rotor is initially filled with a buffer solution followed by the sample mixture, introduced at a constant rate to the small end of the spinning rotor, where particles experience the opposing forces of the centrifugal field and the flowing medium. Initially, the frictional force of the carrier medium is greater than the centrifugal force and all particles are swept inward by the flowing carrier. However, as the entrained particles migrate toward the large end of

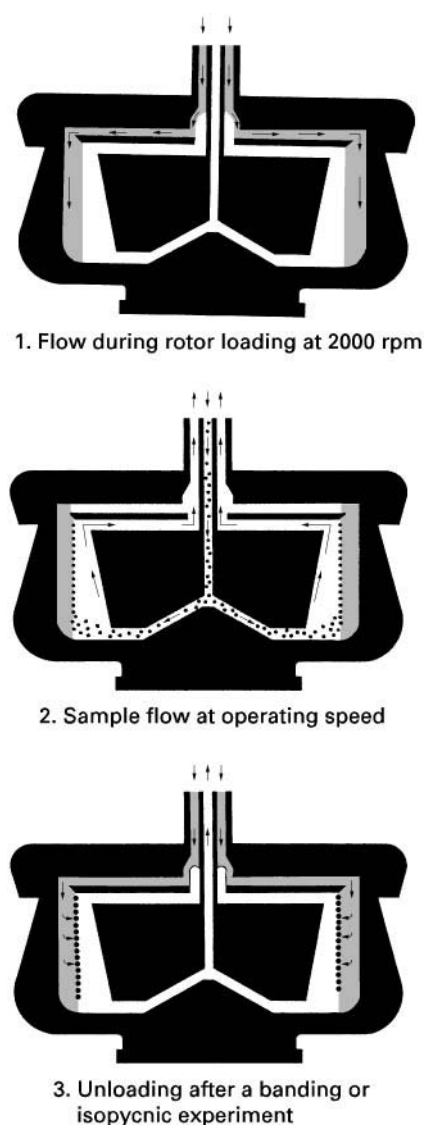


Figure 15 Flow regimes in a continuous-flow zonal rotor. (Courtesy of Beckman Instruments, Inc.)

the chamber, the linear velocity of the carrier decreases as the cross-sectional area of the rotor increases. Due to the greater sedimentation rates for larger particles in a centrifugal force field, smaller particles continue to migrate toward the centre of the rotor while larger particles remain suspended or move more slowly, resulting in particle classification. Such separations are semi-batch since, as the concentration of larger particles in the rotor increases to capacity, sample feed must be stopped so that these particles may be eluted with a higher velocity rinse solution. Elutriation rotors typically operate at lower centrifugal forces ($10\,000g$) with throughputs to 400 mL min^{-1} . A common application is the isolation of specific cell types.

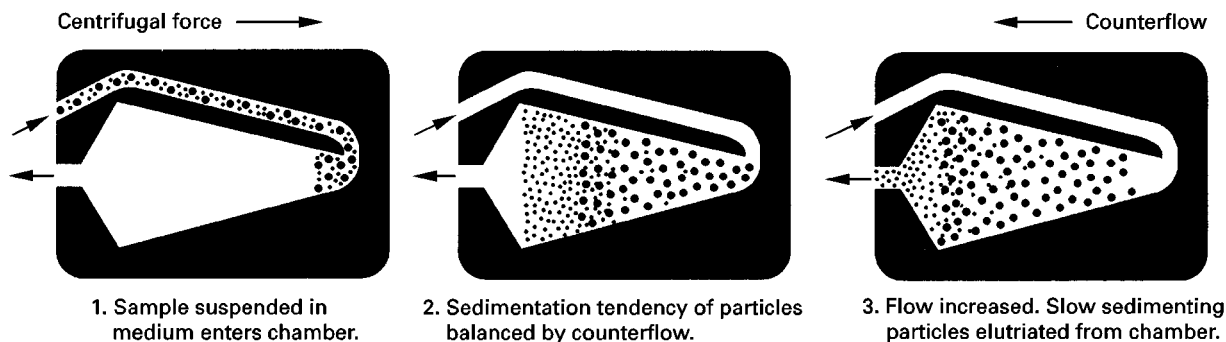


Figure 16 The elutriation process. (Courtesy of Beckman Instruments, Inc.)

Centrifugal Filtration Equipment

In centrifugal filtration, centrifugal force is used to press a solids suspension against a filter medium that permits the mother liquor to pass while retaining the solid particles. Such centrifuges are used for the separation of solids from liquid slurries, chiefly in industrial applications, and are usually characterized in terms of the final moisture content, drainage time and centrifugal force. In addition to the centrifugal field, the drain or screen area and cake thickness are the primary controllable parameters that govern performance. Filtration centrifuges are available in numerous configurations with units often designed or modified for a specific application. Three of the more common designs are batch/semi-batch basket centrifuges, continuous push-type and continuous conical centrifuges.

Basket centrifuges The simplest and most common centrifugal filtration units are basket centrifuges. They are particularly useful when the nature or concentration of the solids varies substantially with time or for the recovery of small or difficult-to-filter particles. Basket centrifuges incorporate a perforated cylindrical bowl that is lined with a filtration medium, usually a fabric or metal screen. Industrial units generally spin at relatively low rates (<4000 rpm), are available with bowl diameters ranging from 0.3 m to 2.4 m, and may be operated at elevated temperatures (350°C) and/or pressures (1 MPa). The slurry is fed to the centre of the basket with the mother liquor passing and the cake accumulating against the filtration medium. When the accumulated cake volume is sufficient either to retard further filtration or unbalance the centrifuge, the solids must be discharged. This is achieved in one of three ways: (1) the centrifuge is stopped and the cake is manually scraped, useful for smaller batches when production does not warrant the additional costs of automation,

for processing different materials in a single unit, or when the equipment must be sterilized between batches; (2) the cake is mechanically unloaded at reduced speed by using a single or multiple plow; or (3) the cake is continuously removed at speed with a hydraulic *knife* in a *peeler* centrifuge, most useful for moderate production rates and for materials that drain freely. Other basket centrifuges, termed *inverting filter* centrifuges, have flexible filters that may be inverted to discharge the accumulated solids.

Continuous centrifugal filters are more useful for higher volume processing of fast-draining solids in applications that do not require a low level of moisture in the recovered product. They can be further divided into push-type (cylindrical) and conical filters.

Push-type centrifugal filters These units consist of a rotating cylindrical drum that incorporates a feed funnel that rotates with the drum. The slurry is introduced via the feed funnel where it is accelerated before being deposited to one end of the drum. Liquids pass through a cylindrical screen under centrifugal pressure as the solids accumulate to form a cake. The cake is then pushed by a reciprocating piston toward the exit located at the opposite end of the drum. Push-type filters may be single or multiple stage, with the latter incorporating a cylindrical screen with two to six variable-diameter steps. The diagram of a multistage push-type filter in **Figure 17** illustrates the integration of filtration and rinse cycles in a continuous operation.

Conical centrifugal filters In a conical centrifugal filter, the slurry is introduced to the small end of a conical drum, which supports the filtration medium. Liquids drain through the drum filter as the solids are either mechanically or self-discharged through the large end. The movement of the solids from the small end of the cone to the larger-diameter end results in a thinning of the cake that facilitates

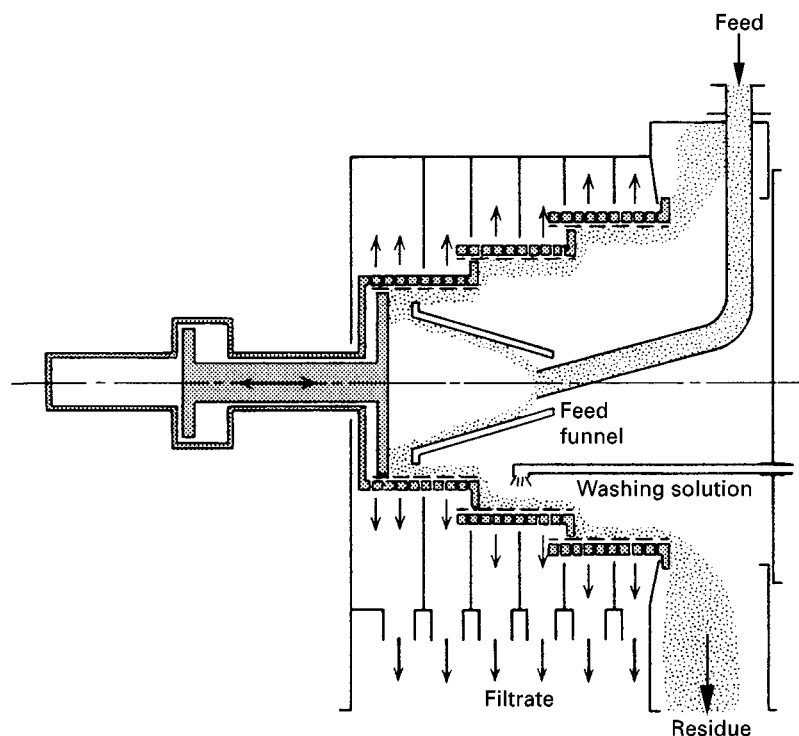


Figure 17 Multistage push-type centrifugal filter. (Courtesy of Alfa Laval Separations.)

drainage. Some designs incorporate a lower cone angle at the small end, where most of the drainage occurs, and a higher angle on the large end, to increase the solids-holding capacity and provide additional drainage time.

Three methods of solids removal are commonly used for conical filtration: screw conveyor, self-discharging or vibratory. Screw conveyers consist of a vertical or horizontal conical bowl with an internal helical screw rotating slightly faster than the conical drum. In this configuration, solids are continually moved from the small end of the cone and discharged from the larger end. Screw-conveyer units have cone angles that generally range from 10–20°, feed capacities of 1–15 m³ h⁻¹, and centrifugal forces to 3500*g*. Applications include the dewatering of crystalline solids and the extraction of solids from fruit and vegetable pulps. Self-discharging filters are similar to screw conveyers, only the cone angle is larger (20–35°) than the angle of repose of the cake. At these greater angles, the solids slide down the tapered walls and exit the large end of the conical drum without the need for mechanical assistance. Vibratory-discharge filters are also similar in design to screw-conveyer units, but in this case solids discharge is accomplished by applying a vibratory or oscillatory motion to the bowl or casing. Such units are typically operated at low speeds (300–500 rpm) and used to process larger particles (0.25–30 mm) than screw-conveyer or self-

discharging designs. The cone angle is 13 to 18° with throughput capacities of 25–150 t h⁻¹. Their most common application is for the dewatering of coal fines.

Acknowledgements

The authors wish to express their appreciation to Dr Allen Furst (Beckman Inst., Inc.) and Mr John McKenna (Alfa-Laval Sharples) for their helpful comments and timely review of this manuscript and to Ms Kimberly Neumann (Alfa-Laval Sharples) and Ms Joyce Pederson (Beckman Inst., Inc.) for provision of several portions of the reprinted artwork. We would also like to acknowledge the support of the University of Kentucky Center for Applied Energy Research.

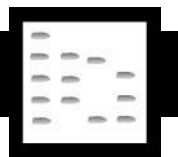
See Colour Plate 2.

Further Reading

- Birnie GD and Rickwood D (eds) *Centrifugal Separation in Molecular and Cell Biology*. London: Butterworths.
- Brakke MK (1952) Density gradient centrifugation: a new separation technique. *Journal of the American Chemical Society* 73: 1847–1848.
- Coulson JM, Richardson JF, Backhurst JR and Harker JH (1978) In: *Chemical Engineering*, 3rd edn, vol. 2: *Unit Operations*. Oxford: Pergamon Press.

- Griffith OM (1986) *Techniques of Preparative, Zonal, and Continuous Flow Ultracentrifugation*; DS-468H. Palo Alto, CA: Spinco Division of Beckman Instruments.
- Hsu HW (1981) In: Perry ES (ed.) *Techniques of Chemistry*, vol. XVI: *Separations by Centrifugal Phenomena*. New York: Wiley.
- Lavanchy AC and Keith EW (1979) Centrifugal separation. In: Grayson M and Eckroth D (eds) *Encyclopedia of Chemical Technology*, 3rd edn, vol. 5, pp. 194–233. New York: J Wiley.
- Letki A, Moll RT and Shapiro L (1997) Centrifugal separation. In: Ruthven DM (ed.) *Encyclopedia of Separation Technology*, pp. 251–299. New York: J Wiley.
- Price CA (1982) *Centrifugation in Density Gradients*. New York: Academic Press.
- Sheeler P (1981) *Centrifugation in Biology and Medical Science*. New York: J Wiley.
- Svedberg T and Peterson KO (1940) *The Ultracentrifuge*. Oxford: Clarendon Press.

CHROMATOGRAPHY



C. F. Poole, Wayne State University, Detroit, MI, USA

Copyright © 2000 Academic Press

Introduction

Chromatography is the most widely used separation technique in chemical laboratories, where it is used in analysis, isolation and purification, and it is commonly used in the chemical process industry as a component of small and large-scale production. In terms of scale, at one extreme minute quantities of less than a nanogram are separated and identified during analysis, while at the other, hundreds of kilograms of material per hour are processed into refined products. It is the versatility of chromatography in its many variants that is behind its ubiquitous status in separation science, coupled with simplicity of approach and a reasonably well-developed framework in which the different chromatographic techniques operate.

Chromatography is essentially a physical method of separation in which the components of a mixture are separated by their distribution between two phases; one of these phases in the form of a porous bed, bulk liquid, layer or film is generally immobile (stationary phase), while the other is a fluid (mobile phase) that percolates through or over the stationary phase. A separation results from repeated sorption/desorption events during the movement of the sample components along the stationary phase in the general direction of mobile-phase migration. Useful separations require an adequate difference in the strength of the physical interactions for the sample components in the two phases, combined with a favourable contribution from system transport properties that control sample movement within and between phases. Several key factors are responsible, therefore, or act together, to produce an acceptable

separation. Individual compounds are distinguished by their ability to participate in common intermolecular interactions in the two phases, which can generally be characterized by an equilibrium constant, and is thus a property predicted from chemical thermodynamics. Interactions are mainly physical in type or involve weak chemical bonds, for example dipole-dipole, hydrogen bond formation, charge transfer, etc., and reversible, since useful separations only result if the compound spends some time in both phases. During transport through or over the stationary phase, differential transport phenomena, such as diffusion and flow anisotropy (complex phenomena discussed later), result in dispersion of solute molecules around an average value, such that they occupy a finite distance along the stationary phase in the direction of migration. The extent of dispersion restricts the capacity of the chromatographic system to separate and, independent of favourable thermodynamic contributions to the separation, there is a finite number of dispersed zones that can be accommodated in the separation. Consequently, the optimization of a chromatographic separation depends on achieving favourable kinetic features if success is to be obtained.

The Family of Chromatographic Techniques

A convenient classification of the chromatographic techniques can be made in terms of the phases employed for the separation (**Figure 1**), with a further subdivision possible by the distribution process employed. In addition, for practical utility transport processes in at least one phase must be reasonably fast; for example, solid–solid chromatography, which may occur over geological time spans, is impractical in the laboratory because of the slow migration of

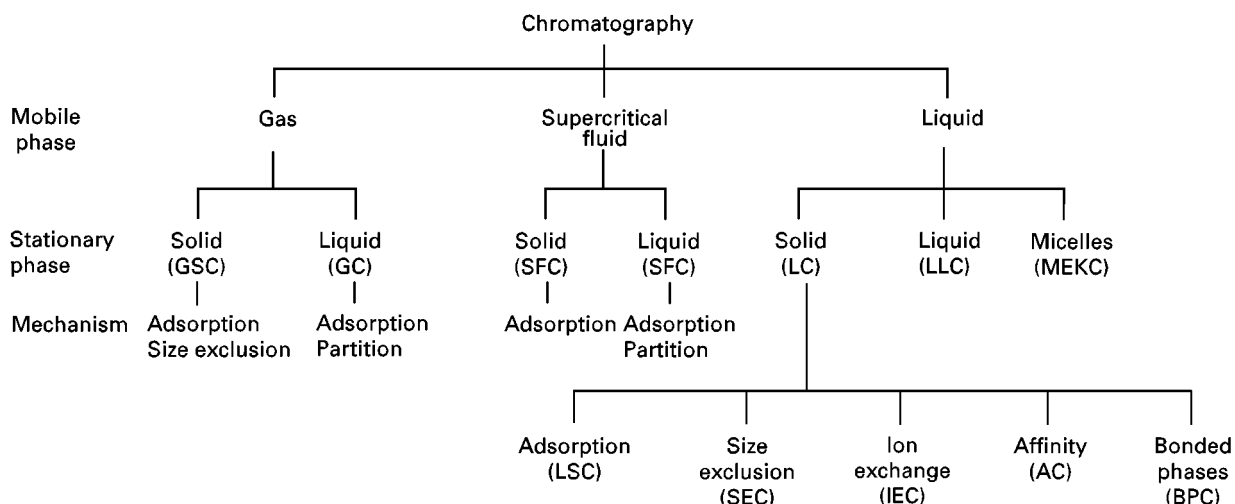


Figure 1 Family tree of chromatographic methods.

solutes through the crystal lattice. Two distinct phases are required to set up the distribution component of the separation mechanism, which explains why gas-gas chromatography does not exist and liquid-liquid separations are restricted to immiscible solvents. When the mobile phase is a gas the stationary phase can be a liquid or a solid and the separation techniques are called gas-liquid chromatography (GLC) and gas-solid chromatography (GSC). The simple term GC encompasses both techniques but, unless otherwise specified, it usually means GLC since this is the most common arrangement. Separations in GLC occur because of differences in gas-liquid partitioning and interfacial adsorption. In GSC the retention mechanism is governed by interfacial adsorption or size exclusion, if a solid of controlled pore size, such as a zeolite, is used as the stationary phase. When the mobile phase is a supercritical fluid (SFC) the stationary phase can be a liquid or a solid, and the distribution process may be interfacial adsorption or absorption.

When the mobile phase is a liquid the stationary phase can be a solid (liquid-solid chromatography, LSC) with interfacial adsorption as the dominant distribution process; a solid of controlled pore size (size exclusion chromatography, SEC), in which the distribution constant is characteristic of the ratio of the solute size to the dimensions of the stationary phase pore sizes; a solid with immobilized ionic groups accessible to solutes in the mobile phase with electrostatic interactions as the dominant distribution process (ion exchange chromatography or ion chromatography, IEC or IC); a solid with immobilized molecular recognition sites accessible to the analyte in the mobile phase (affinity chromatography, AC) in which the dominant distribution process

is the three-dimensional specificity of the molecular interactions between the receptor and the analyte (a technique used in biotechnology); a porous solid coated with a film of immiscible liquid (liquid-liquid chromatography, LLC) in which the dominant distribution process is partitioning; or a solid with a surface containing organic groups attached to it by chemical bonds (bonded-phase chromatography, BPC) in which the dominant distribution processes are interfacial adsorption and partitioning.

Bonded phases in liquid chromatography are widely used to tailor solid phases for different applications, including LSC, SEC, IEC, IC and AC (Figure 2). Reversed-phase chromatography (RPC) is a particular form of bonded-phase chromatography in which the mobile phase is more polar than the stationary phase (for most practical applications the mobile phase is an aqueous solution). It is the most popular form of liquid chromatography because of its broad applicability to neutral compounds of wide polarity. In addition, by exploiting secondary chemical equilibria weak acids and bases can be separated by pH control (ion suppression chromatography, ISC); ionic compounds by using ion pairing with an additive of opposite charge (ion pair chromatography, IPC); and metal ions by the formation of neutral complexes (metal-complexation chromatography, MCC). By adding a surfactant to the mobile phase, micelles can be used to modify the overall distribution constant (micellar liquid chromatography, MLC), and a totally aqueous buffered mobile phase and a decreasing ionic strength gradient can be used to separate biopolymers with minimal disruption of conformational structure (hydrophobic interaction chromatography, HIC). Bonded-phase chemistry is also commonly employed to prepare stationary

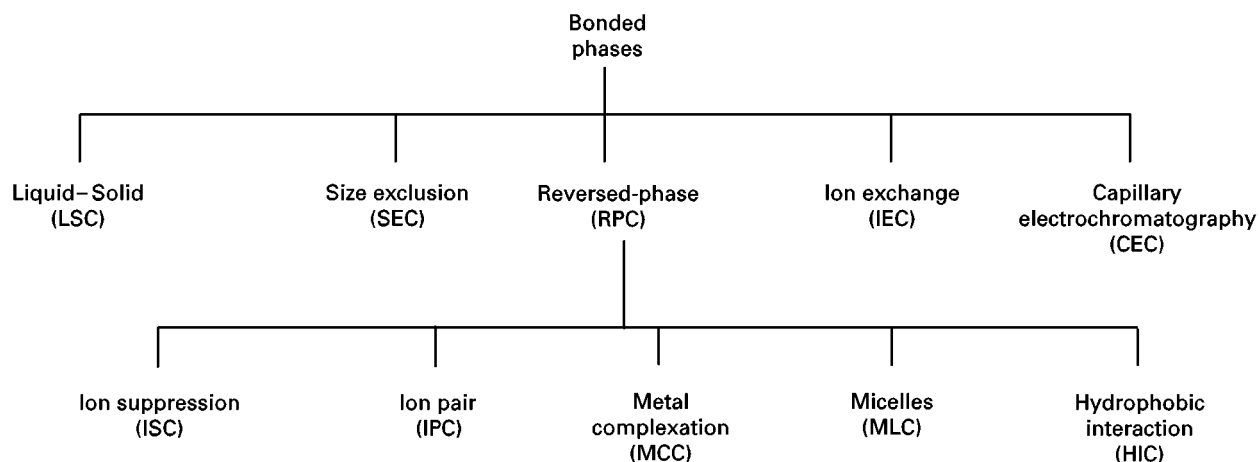


Figure 2 Applications of bonded phases in LC.

phases with immobilized enantiomer-selective groups for the resolution of racemates by chiral chromatography.

The mobile phase can be transported through or over the stationary phase by application of external pressure when the stationary phase is enclosed in a rigid container, or column. This is the ordinary mode of gas, supercritical fluid and liquid chromatography. If the stationary phase is distributed as a thin layer on a (usually) flat support, such as a sheet of glass or plastic, and the mobile phase is allowed to ascend through the layer by capillary forces, then this method is referred to as planar or thin-layer chromatography (TLC). The fundamental basis of the distribution mechanism between the mobile phase and the stationary phase is identical to that described for column liquid chromatography, only the separation format and transport mechanism for the mobile phase are different. TLC has largely superseded paper chromatography (PC) in contemporary practice. PC is mechanistically identical to TLC but, with a few exceptions, provides poorer separation characteristics. Bulk flow of liquid mobile phases containing an electrolyte can also be transported through a column by an electric field, through the process known as electroosmosis. When a column packed with a stationary phase is used this is called electrochromatography, or since columns of capillary dimensions are essential for this technique, capillary electrochromatography (CEC). The distribution process for neutral solutes is independent of the transport process, and separations occur by the mechanisms indicated for liquid chromatography. Ionic surfactants can form micelles as a continuous phase dispersed throughout a buffer. In an electric field these charged micelles move with a different velocity or direction to the flow of bulk electrolyte. Neutral

solutes can be separated, if their distribution constant between the micelles and buffer are different, by micellar electrokinetic chromatography (MEKC). The stationary phase in this case is referred to as a pseudo-stationary phase, since it is not stationary, but moves with a different velocity to the mobile phase. Ionic solutes in CEC and MEKC are influenced by the presence of the electric field and are separated by a combination of chromatography and electrophoresis.

Mode of Zone Displacement

In nearly all chromatographic systems, transport of solute zones occurs entirely in the mobile phase. Transport is an essential component of the chromatographic system since the most common arrangement for the experiment employs a sample inlet and a detector at opposite ends of the column, with sample introduction and detection occurring in the mobile phase (GC, SFC, LC, MEKC). In planar chromatographic systems (TLC, PC), sample introduction and detection is performed in the stationary phase, but the detection is of solute zones that have been transported different distances by the mobile phase. In GC the movement of solute molecules from the stationary to the mobile phase is controlled by the vapour pressure of the solutes in the column, and is usually manipulated by varying temperature. At an optimum temperature sample molecules will spend some of their time in the mobile phase, where they will be transported through the column, and some time in the stationary phase, where they are differentiated by their capacity for intermolecular interactions with the stationary phase. Displacement of solute zones can be achieved in three distinct ways: frontal analysis, elution and displacement (Figure 3).

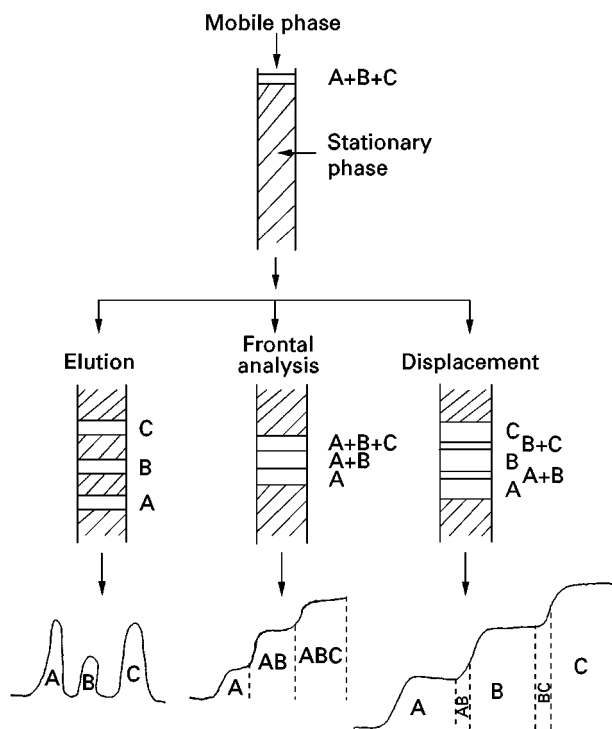


Figure 3 Mode of zone displacement in chromatography.

In frontal analysis, the mobile phase introduces the sample continuously onto the column (or the sample is the mobile phase) until eventually the column is saturated with the sample and the component with the lowest affinity for the stationary phase is displaced from the column by sample components of greater affinity. When the zone of pure component has completely exited the column it is followed by a mixture containing the next component, and so on. Frontal analysis can be used to obtain thermodynamic data from chromatographic measurements and to isolate a less strongly retained trace component from a major component. However, quantitation for each component in a mixture is difficult, and at the end of the experiment the column is contaminated by the sample so that reuse requires stripping the sample from the column.

In displacement chromatography the sample is applied to the column as a discrete band and a substance (or mobile-phase component) with a higher affinity for the stationary phase than any of the sample components is continuously passed through the column. The displacer pushes sample components down the column and, if the column is long enough, a steady state is reached. A succession of rectangular bands of pure components then exits the column. Each component displaces the component ahead of it, with the last and most strongly retained component

being forced along by the displacer. At the end of the separation the displacer must be stripped from the column if the column is to be reused. Displacement chromatography is used mainly in preparative and process chromatography, where high throughputs of pure compounds can be obtained (note that the contact boundary between zones may not be discrete and the collection of pure compounds may be restricted to the central region of the displaced zones).

In elution chromatography the sample is applied to the column as a discrete band and sample components are successively eluted from the column diluted by mobile phase. The stationary and mobile phases are normally at equilibrium prior to sample introduction. The mobile phase must compete with the stationary phase for the sample components; separation will only occur if the distribution constants for the various components, resulting from the competition, are different. Elution chromatography is the most convenient method for analysis and is the most common method of separation in GC, SFC, LC and MEKC. Development, a modification of the elution mode, is used in planar chromatography. Samples are applied to the dry layer as compact spots or bands and the layer subsequently contacted by the mobile phase, which ascends and moves the sample components to positions higher up the layer in the direction of mobile-phase flow. The separation is (usually) stopped before the mobile phase reaches the opposite edge of the layer and neither the eluent nor the sample components exit the layer. The two processes can be compared; all components travel the same distance and are separated in time using the elution mode in column chromatography, whereas all components have the same separation time and are separated in space (migration position) in planar chromatography using the development mode.

Chromatogram

The information obtained from a chromatographic experiment is contained in the chromatogram. When the elution mode is used this consists of a plot of the concentration or mass profile of the sample components as a function of the flow of the mobile phase or as a function of time. Typically the y-axis will be detector response and the x-axis time or volume of mobile phase in column chromatography or migration distance in planar chromatography. The position of each peak in the chromatogram is characteristic of the identity of the compound and the area under the peak is a function of the concentration or amount of each compound. Peak widths in the chromatogram are controlled by solute-dependent kinetic factors, which in turn can be used to deduce values for

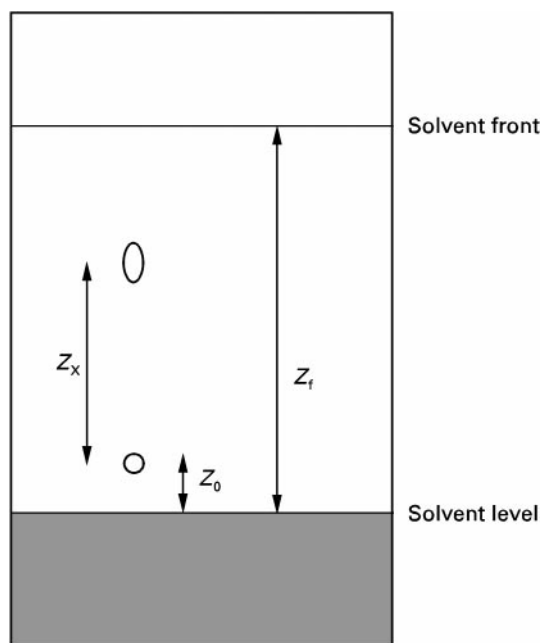


Figure 4 Calculation of the R_F value in planar chromatography. Z_x distance moved by the sample from the sample origin; Z_0 distance between the solvent entry position and the sample origin; Z_f distance between the solvent entry position and the solvent front.

characteristic physical properties of either the solute or the mobile and stationary phases.

The position of a peak in the chromatogram is made up of two contributions: (1) the time (or volume of mobile phase) required by a compound that does not interact with the stationary phase to reach the detector from the sample inlet, called the column hold-up time or dead time; and (2) the time that individual compounds spend in the stationary phase (all compounds spend the same time in the mobile phase). The column hold-up time is a feature of the experimental system and is not fundamentally related to solute properties. Because of this, retention time is not a useful parameter for column comparisons. A more useful term is the retention factor (previously known as the capacity factor), k , defined as the ratio of the time the solute spends in the stationary phase to the time it spends in the mobile phase. The ratio of the retention factors for two solutes is called the separation factor, α , which by convention is always expressed with the larger retention factor in the numerator ($\alpha \geq 1$). The separation factor expresses the ease with which the chromatographic system can separate two compounds, and is directly related to the difference in free energy for the interactions of the two compounds in the chromatographic system. It is a major optimization parameter, as we shall see later. In planar chromatography retention is usually expressed as the retardation factor, R_F , equivalent

to the ratio of the distance migrated by the solute zone, Z_x , to the distance moved by the solvent front, $Z_f - Z_0$, measured from the sample application position, ($1 \geq R_F \geq 0$), as illustrated in **Figure 4**. The planar chromatographic retardation factor and the column retention factor are simply related by $k = (1 - R_F)/R_F$.

Peak Shape Models

For an ideal separation the peaks in the chromatogram are usually considered to be Gaussian. This is a convenient, if not always accurate, model and peak asymmetry can arise from a variety of instrumental and chromatographic sources. The most common types of peak distortion are skewness (the peak front is sharper than the rear) and tailing (the rear of the peak is elongated compared to the front). Although instrumental sources of peak asymmetry should, of course, be minimized, chromatographic sources cannot always be avoided. Curve fitting by computer offers the possibility of deconvoluting chromatographic peak profiles into their individual contributions. The exponentially modified Gaussian function, obtained by the combination of a Gaussian function with an exponential decay function (that provides for the asymmetry in the peak profile), is often an acceptable description of chromatographic peaks in analytical applications.

Chromatographic sources of peak asymmetry result from mechanical effects, for example the formation of voids in the stationary-phase bed and excessive extra-column volumes, and from isotherm characteristics. Most of the theory of analytical chromatographic separations is based on a linear isotherm model where the compositions in the stationary and mobile phases are proportional and characterized by a distribution constant that is independent of sample size and composition (**Figure 5**). The peaks resulting from a linear chromatography model are symmetrical and can be characterized by a normal distribution. The width of the chromatographic zone is proportional to retention and can be obtained directly from peak shape considerations. The extent to which the properties of the chromatographic system contribute to zone broadening (peak widths) is given by the number of theoretical plates, N . For a normal distribution this is equivalent to $(t_R/\sigma_t)^2$, where t_R is the retention time and σ_t is the peak standard deviation in time units. Simple algebraic manipulation of this formula permits calculation of N from the peak width at base or half-height, etc. For column comparison purposes the height equivalent to a theoretical plate, H , equivalent to the column length divided by N , is generally used.

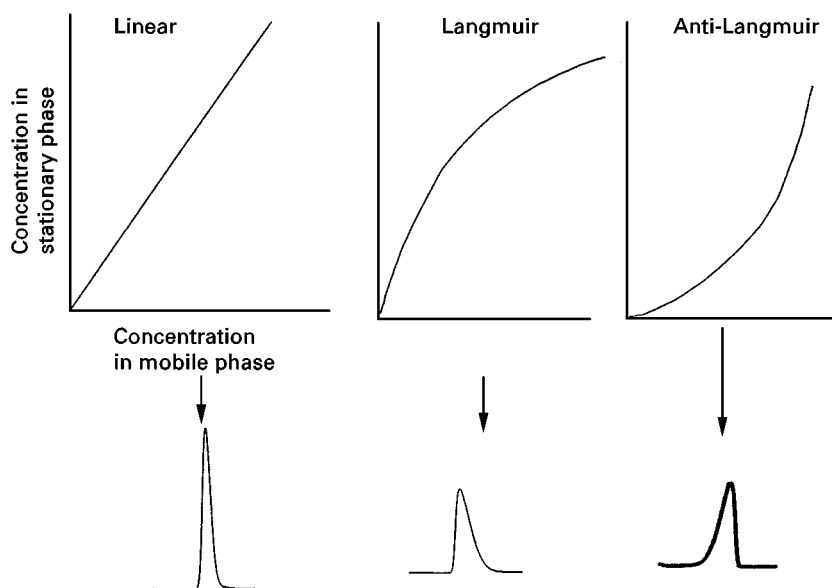


Figure 5 Influence of isotherm type on peak shapes.

Nonlinear isotherms (nonlinear chromatography) result in the production of asymmetric peaks. Langmuir isotherms are frequently observed for adsorption interactions on surfaces with an energetically heterogeneous distribution of adsorption sites with incompatible association/dissociation rate constants. For sorbents with monolayer coverage, Langmuir-type isotherms result when solute-stationary phase interactions are strong compared with solute-solute interactions. Because the interactions between solutes are comparatively weak, the extent of sorption decreases following monolayer formation, even though the concentration in the mobile phase is increasing. In this case the concentration of the component in the stationary phase at equilibrium is no longer proportional to its concentration in the mobile phase and the peak shape and retention time will depend on the sample composition and amount. Anti-Langmuir type isotherms are more common in partition systems when solute-stationary phase interactions are relatively weak compared with solute-solute interactions, or where column overload results from the introduction of large sample amounts. Such conditions are common in preparative chromatography, where economic considerations dictate that separations are optimized for production rate and to minimize mobile phase consumption and operating costs.

Flow through Porous Media

For an understanding of zone dispersion in chromatography, an appreciation of the mobile-phase linear velocity through different porous media is im-

portant. Gases are highly compressible and an average linear velocity for the column is used. Liquids can be considered incompressible and the average and outlet velocity should be about the same. Supercritical fluids are often assumed to be incompressible for the purpose of calculation, more for convenience than reality, with local velocity changes reflecting changes in density along the column. For packed columns containing porous particles with fluid mobile phases, the flow of mobile phase occurs predominantly through the interstitial spaces between the packing particles and the mobile phase occupying the particle pore volume is largely stagnant. Slow solute diffusion through this stagnant volume of mobile phase is a significant cause of zone broadening for condensed phases. The mobile-phase velocity for a chromatographic system may be determined by dividing the column length by the retention time of an unretained and unexcluded solute from the pore volume (average velocity) or the retention time of an unretained and excluded solute (interstitial velocity).

The mobile-phase flow profile and changes in local velocity are products of the driving force used to induce bulk flow of mobile phase through the separation system. These driving forces can be identified as capillary, pneumatic or electroosmotic forces. Capillary forces are responsible for the transport of the mobile phase in planar chromatography (PC and TLC). These forces are generally weak and result in a mobile-phase velocity that decreases with migration distance from the solvent starting position (**Figure 6**). Capillary forces are incapable of providing a sufficiently high velocity

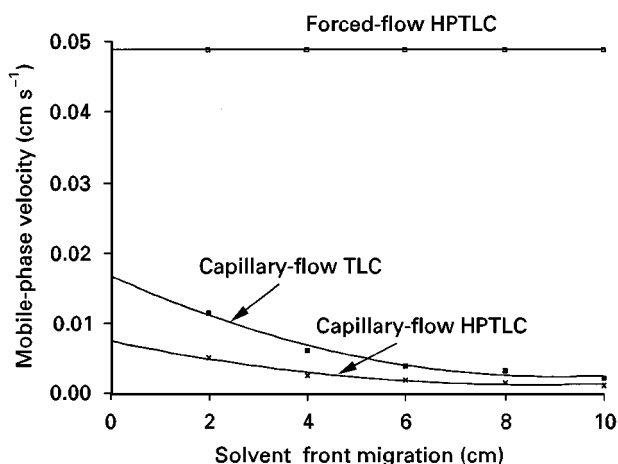


Figure 6 Relationship between mobile-phase velocity and migration distance for capillary-controlled and forced-flow development in planar chromatography. (Reproduced with permission from Poole CF and Wilson ID (1997) *Journal of Planar Chromatography* 10: 332, copyright © Research Institute for Medicinal Plants).

to minimize zone broadening. This has a number of consequences: zone broadening is largely dominated by diffusion; the useful development length for PC is set by the range of acceptable mobile-phase velocities; separation times are increased; and the separation potential of PC is less than that predicted for a constant and optimum mobile-phase velocity.

Pneumatic transport of the mobile phase is commonly employed in column chromatography. The mobile phase is pressurized externally to the column (a simple high pressure cylinder with regulator in the case of a gas, or a mechanical pump for liquids). The pressure gradient across the column provides the driving force to overcome the resistance to flow pre-

sented by the stationary phase and the rest of the system. In LC, Darcy's law relates the properties of the mobile phase, characteristic features of the column, and the external pressure required to obtain a useful mobile-phase velocity. This law can be stated as:

$$u = \Delta P K_0 d_p^2 / \eta L \quad [1]$$

where u is the mobile phase velocity, ΔP is the pressure drop across the column, K_0 is the column permeability, d_p is the average particle diameter, η is the mobile phase viscosity, and L is the column length. Since a minimum value for u is required for acceptable column performance and separation times, and the available column pressure drop is constrained to an upper limit by material and safety considerations, then there is a finite limit to the range of permissible d_p^2/L values that can be used. Thus a compromise must be accepted between separation time and efficiency, which results in an upper limit to the number of theoretical plates that can be obtained for fast separations or the use of long separation times when very large numbers of theoretical plates are required for a separation.

Bulk liquid flow under electrophoretic conditions occurs by electroosmosis. At the column wall or particle surface (packed columns) an electrical double layer results from the adsorption of ions from the mobile phase or dissociation of surface functional groups. An excess of counterions is present in the double layer in comparison with the bulk liquid and in the presence of an electric field shearing of the solution occurs only within the very thin diffuse part of the double layer, transporting the mobile phase through the column with a nearly perfect plug profile (Figure 7). The velocity of the bulk liquid flow

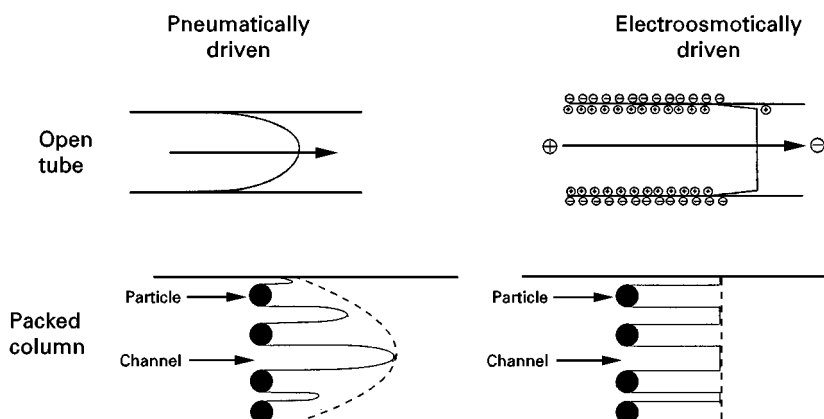


Figure 7 Flow profile for an open tube and a packed column using pneumatic and electroosmotic driving forces.

is given by:

$$u = \varepsilon \zeta E / 4\pi\eta \quad [2]$$

where ε is the solution dielectric constant, ζ is the zeta potential (potential at the boundary between the charged surface and the start of the diffuse part of the double layer), and E is the electric field strength. Note that there is no explicit dependence on the particle size and column length, which limit the total efficiency of columns when the flow is pneumatically driven. The column length and column internal diameter, however, cannot be treated as independent variables in MEKC and CEC, but are related through Joule heating of the electrolyte and its effect on the mobile-phase flow profile. Heat is generated homogeneously throughout the electrolyte but the temperature variation across the column diameter is parabolic. Radial temperature gradients between the centre of the tube and the column wall cause zone broadening resulting from sample diffusion and solvent density and viscosity differences in the direction of flow.

Zone Broadening

Rate theory attempts to explain the kinetic contribution to zone broadening in column chromatography as the sum of three main contributions: flow anisotropy (eddy diffusion), axial diffusion (longitudinal diffusion), and resistance to mass transfer. Flow anisotropy is illustrated in Figure 8. When a sample band migrates through a packed bed, the individual flow paths must diverge to navigate around the particles such that individual flow streams are of unequal lengths. These variations in flow direction and rate lead to zone broadening that should depend only on the particle size and homogeneity of the column packing. Flow anisotropy can be

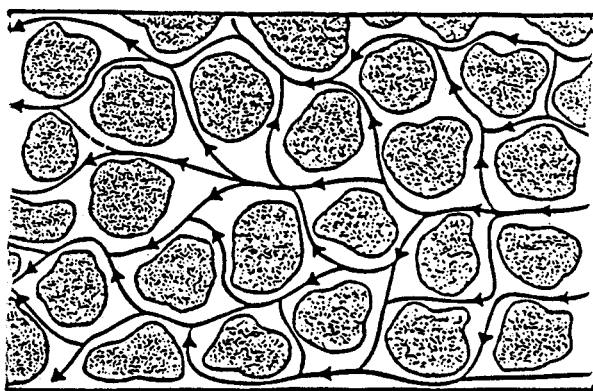


Figure 8 Representation of flow anisotropy in a packed column.

minimized by using particles of small diameter with a narrow particle size distribution in columns with a high and homogeneous packing density. For open-tubular columns, flow anisotropy is not a contributing factor since the streamlines have no obstacles in their way to cause disruption of the sample profile.

Axial diffusion is the natural tendency of solute molecules in the mobile phase to redistribute themselves by diffusion from a region of high concentration to one of lower concentration. Its contribution to zone broadening depends on the solute diffusion coefficient in the mobile phase and the column residence time. Diffusion of solute molecules occurs in all directions but only the components in the plane of mobile-phase migration contributes to the peak profile observed in the chromatogram.

Resistance to mass transfer in either the stationary or mobile phases is a consequence of the fact that mass transfer in the chromatographic system is not instantaneous and equilibrium may not be achieved under normal separation conditions. Consequently, the solute concentration profile in the stationary phase is always slightly behind the equilibrium position and the mobile-phase profile is similarly slightly in advance of the equilibrium position (Figure 9). The

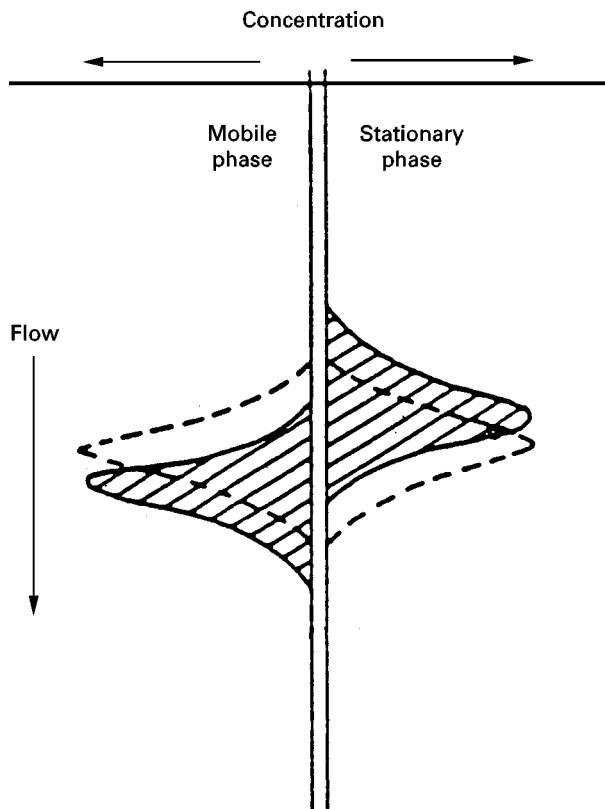


Figure 9 Representation of resistance to mass transfer in the mobile and stationary phases. The dashed line represents the equilibrium position and the solid line the actual position of the solute zones.

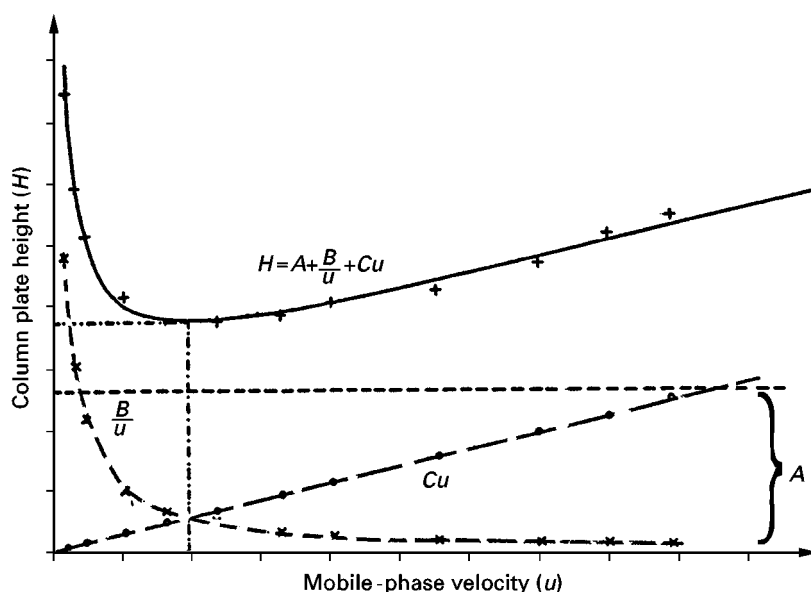


Figure 10 van Deemter plot of the column plate height as a function of the mobile-phase velocity. The solid line represents the experimental results and the broken lines the theoretical contribution from flow anisotropy (A), axial diffusion (B/u) and resistance to mass transfer (Cu).

resultant peak observed at the column exit is broadened about its zone centre, which is located where it would have been for instantaneous equilibrium, provided that the degree of nonequilibrium is small. Contributions from resistance to mass transfer are rather complicated but depend on the column residence time, mobile-phase velocity, stationary-phase film thickness, the particle size for packed columns, the solute diffusion coefficients in the mobile and stationary phases, and the column internal diameter.

The relationship between zone broadening (column plate height) and the mobile-phase velocity is given by the hyperbolic plot known as a van Deemter curve (Figure 10). The solid line represents the experimentally observed results and the dotted lines the contributions from flow anisotropy (A term), axial diffusion (B/u) and resistance to mass transfer (Cu). In this generic plot we see that there is an optimum velocity at which a particular chromatographic system provides maximum efficiency (a minimum column plate height). The position of this optimum velocity and the general curvature of the plot strongly depend on the characteristics of the chromatographic system, as shown by the values given in Table 1.

Gas Chromatography

Gases of low viscosity with favourable solute diffusivity, such as hydrogen and helium, are commonly used as mobile phases in GC. For these gases the

minimum in the plate height occurs at a high optimum mobile-phase velocity, resulting in efficient and fast separations. At these high mobile-phase velocities the contribution from axial diffusion to the column plate height is minimized. For thin-film columns, resistance to mass transfer in the mobile phase is the main cause of zone broadening, while for thick-film columns resistance to mass transfer in the stationary phase is equally important. Since diffusion in gases is relatively favourable, the column internal diameters required to maintain an acceptable contribution from resistance to mass transfer in the mobile phase offer little difficulty in practice. For supercritical fluids, solute diffusivity is not as favourable as for gases and in the case of liquids must be considered unfavourable. The unfavourable slow optimum mobile-phase velocity in SFC (in practice open-tubular columns are operated at 10 or more times the optimum velocity to obtain an acceptable separation time) requires significantly smaller internal diameter capillary columns than those needed for GC to minimize resistance to mass transfer in the mobile phase. At mobile-phase velocities used in practice the contribution of axial diffusion to the column plate height is negligible compared with the contribution of resistance to mass transfer in the mobile and stationary phases. For fast, high efficiency separations, column internal diameters $< 100 \mu\text{m}$ are required and much smaller diameters are preferred. As densities and solute diffusivity become more liquid-like, column dimensions for reasonable

Table 1 Characteristic values for column parameters related to zone broadening

Parameter	Mobile phase		
	Gas	Supercritical fluid	Liquid
Diffusion coefficient ($\text{m}^2 \text{s}^{-1}$)	10^{-1}	10^{-4} – 10^{-3}	10^{-5}
Density (g cm^{-3})	10^{-3}	0.3–0.8	1
Viscosity (P)	10^{-4}	10^{-4} – 10^{-3}	10^{-2}
Column length (m)			
Packed	1–5	0.1–1	0.05–1
Open-tubular	10–100	5–25	
Column internal diameter (mm)			
Packed	2–4	0.3–5	0.3–5
Open-tubular	0.1–0.7	0.02–0.1	< 0.01
Average particle diameter (μm)	100–200	3–20	3–10
Column inlet pressure (atm)	< 10	< 600	< 400
Optimum velocity (cm s^{-1})			
Packed	5–15	0.4–0.8	0.1–0.3
Open-tubular	10–100	0.1–0.5	
Minimum plate height (mm)			
Packed	0.5–2	0.1–0.6	0.06–0.30
Open-tubular	0.03–0.8	0.01–0.05	> 0.02
Typical system efficiency (N)			
Packed	10^3 – 10^4	10^4 – 8×10^4	5×10^3 – 5×10^4
Open-tubular	10^4 – 10^6	10^4 – 10^5	
Phase ratio			
Packed	4–200		
Open-tubular	15–500		

performance start to approach values similar to those for LC and are not easily attained experimentally. Slow diffusion in liquids means that axial diffusion is generally insignificant but mass transfer in the mobile phase is also reduced, requiring columns of very small internal diameter, preferably < 10 μm , which are impractical for general laboratory use. Packed columns dominate the practice of LC while open-tubular columns are equally dominant in the practice of GC, with both column types used in SFC.

Packed columns in GC are prepared from comparatively coarse particles of a narrow size distribution and coated with a thin homogeneous film of liquid for high performance. The relatively large particle size and short column lengths are dictated by the limited pressure drop employed for column operation. For thin-film columns, resistance to mass transfer in the mobile and stationary phases is the main cause of zone broadening with a contribution from flow anisotropy. For thick-film columns, resistance to mass transfer in the stationary phase tends to dominate. The intrinsic efficiencies of open-tubular columns and packed columns of similar phase ratio are comparable, but because the two column types differ greatly in their relative permeability at a fixed column pressure drop, much longer open-tubular columns can be used. Thus, packed GC columns are

seldom more than 5 m long while columns with lengths from 10 to 100 m are commonly used in open-tubular column GC, resulting in a 100-fold increase in the total number of theoretical plates available. In general, packed columns are used in GC for those applications that are not easily performed by open-tubular columns, for example separations that require a large amount of stationary phase for the analysis of very volatile mixtures, or where stationary phases are incompatible with column fabrication, preparative and process-scale GC, etc.

Liquid Chromatography

The intrinsic efficiency per unit length of packed columns in LC increases as the particle diameter is reduced. It can also be increased by using solvents of low viscosity, which result in smaller contributions to the column plate height from resistance to mass transfer and flow anisotropy. Operation at low mobile-phase velocities compared to GC further minimizes the contributions from resistance to mass transfer in the mobile phase at the expense of longer separation times. The pressure drop required to maintain a constant mobile-phase velocity is proportional to the ratio of the column length to the particle diameter squared. Since the available operating pressure is finite, the column length must be reduced as the

particle diameter is decreased. Consequently, most separations in LC are performed with a total of about 5000–20 000 theoretical plates that is largely independent of the particle size. However, since the retention time at a constant (optimum) mobile-phase velocity is proportional to the column length, this arbitrary fixed number of plates is made available in a shorter time for shorter columns packed with smaller diameter particles. Thus the principal virtue of using particles of a small diameter is that they permit a reduction in the separation time for those separations that do not require a large number of theoretical plates.

Conventional column diameters in analytical LC at 3–5 mm are comparatively large so as to minimize zone broadening from extracolumn effects in earlier instrument designs and have become the *de facto* standard dimensions, even though instrument capabilities have improved over time. Smaller diameter columns have been explored to reduce mobile-phase consumption (which is proportional to the square of the column radius) and to enhance mass detection through reduction in peak volumes, but offer no improvement in the intrinsic column efficiency, except perhaps for columns with a low column diameter-to-particle size ratio. Capillary columns of 0.1 to 0.5 mm internal diameter packed with 3–10 μm particles can be used in relatively long lengths for the separation of complex mixtures, where a large number of theoretical plates is required. Such columns probably minimize the contribution from flow anisotropy while at the same time providing a better mechanism for the dissipation of heat caused by the viscous drag of the mobile phase moving through the packed bed. The operation of these columns is still pressure-limited and separation times an order of magnitude greater than for GC have to be accepted as the price for high efficiency.

The enhancement of intraparticle mass transport is particularly important for the rapid separation of biopolymers, whose diffusion coefficients are perhaps 100-fold smaller than those of low molecular weight compounds in typical mobile phases used in LC. Also, the high surface area porous packings used for small molecules may be too retentive for biopolymers with a significant capacity for multisite interactions. For these compounds short columns packed with 1.5 and 2 μm pellicular or porous particles are used for fast separations. Longer columns containing perfusive particles of a large size with large diameter through-pores to promote convective transport can also be used for fast separations. Perfusive particles are also used for the preparative-scale separation of biopolymers.

Supercritical Fluid Chromatography

In SFC, mobile-phase modification of the stationary phase and its dependence on fluid density, together with the variation of fluid density along the length of the column, result in additional sources of zone broadening that cannot be treated in an exact way. Packed columns used in SFC are identical in type to those used in LC. When separations can be achieved with a modest number of theoretical plates (up to about 80 000), then packed columns provide much faster separations, perhaps up to an order of magnitude, than open-tubular columns, which are generally preferred when very large numbers of theoretical plates are required.

Systems with Electroosmotic Flow

Plug flow in CEC results in a smaller contribution to the plate height from flow anisotropy and transaxial diffusion compared with pressure-driven column liquid chromatography, while contributions to the plate height that are flow-profile-independent are the same. The absence of a pressure drop in electroosmotically driven systems provides the necessary conditions to achieve a larger total number of theoretical plates in CEC in a reasonable time through the use of smaller particles and longer columns (see **Table 2** and **Figure 11**). Under normal operating conditions CEC columns have the potential to provide column plate numbers 5–10 times higher than LC columns. Ultimately the performance in CEC is limited by Joule heating, which causes additional zone broadening and restricts applications of CEC to the use of microcolumns, since columns with a small internal diameter (<100 μm) are required for efficient heat dissipation. The dominant cause of zone broadening in MEKC is axial diffusion, with significant contributions from slow sorption-desorption kinetics between the analyte and micelles and electrophoretic dispersion arising from the polydispersity

Table 2 Achievable theoretical plate numbers in HPLC and CEC

Particle size (μm)	HPLC		CEC	
	Length (cm)	Plates/ column	Length (cm)	Plates/ column
5	5	55 000	50	115 000
3	25	45 000	50	170 000
1.5	10	30 000	50	250 000

Column pressure drop = 400 atm for HPLC and the field strength < 30 kV in CEC for operation at the minimum point in the van Deemter plot.

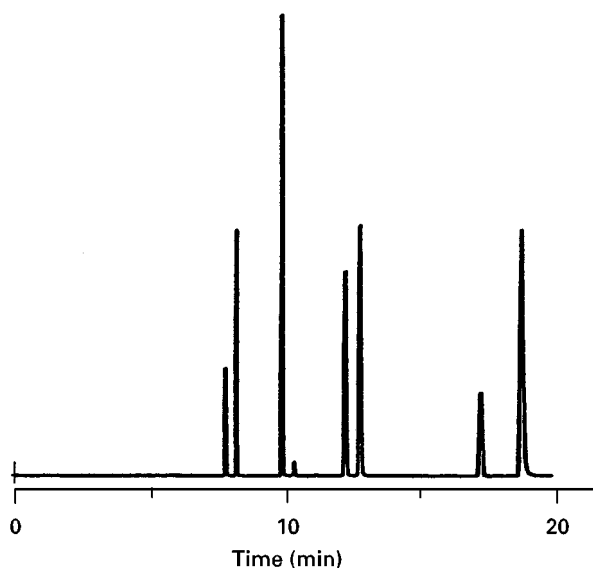


Figure 11 Separation of aromatic compounds by CEC on a 50 cm \times 50 μ m i.d. fused silica capillary column packed with 1.5 μ m spherical octadecylsiloxane-bonded silica gel with 70% (v/v) acetonitrile buffer as mobile phase, temperature 25°C, and field strength 30 kV.

of micelle sizes. Resistance to mass transfer in the mobile phase is minimized by the capillary dimensions of the column and the small size and homogeneous distribution of the micelles throughout the mobile phase combined with the near-perfect plug flow of the mobile phase. Thermal dispersion, as described for CEC, is an additional potential source of zone

broadening resulting from radial temperature gradients. Separations in MEKC are typically carried out with between 100 000 and 500 000 theoretical plates. Adsorption of solutes on the column wall can greatly reduce the potential column efficiency and experimental conditions should be optimized to minimize these contributions whenever possible.

Planar Chromatography

The consequence of the suboptimal mobile-phase velocity in planar chromatography obtained by capillary-controlled flow is that zone broadening is dominated by diffusion. Since the mobile-phase velocity varies approximately quadratically with migration distance, solutes are forced to migrate through regions of different local efficiency and the plate height for the layer must be expressed by an average value (Figure 12). Each solute in the chromatogram experiences only those theoretical plates over which it migrates, with solutes close to the sample application point experiencing very few theoretical plates and those close to the solvent front experiencing up to an upper limit of about 5000. High performance layers, with a nominal average particle size of about 5 μ m, provide more compact zones than coarser particles, provided that the solvent front migration distance does not exceed about 5–6 cm; beyond this point zone broadening exceeds the rate of zone centre separation. When the development length is optimized the separation performance of conventional layers (average particle size about 10 μ m) is not very

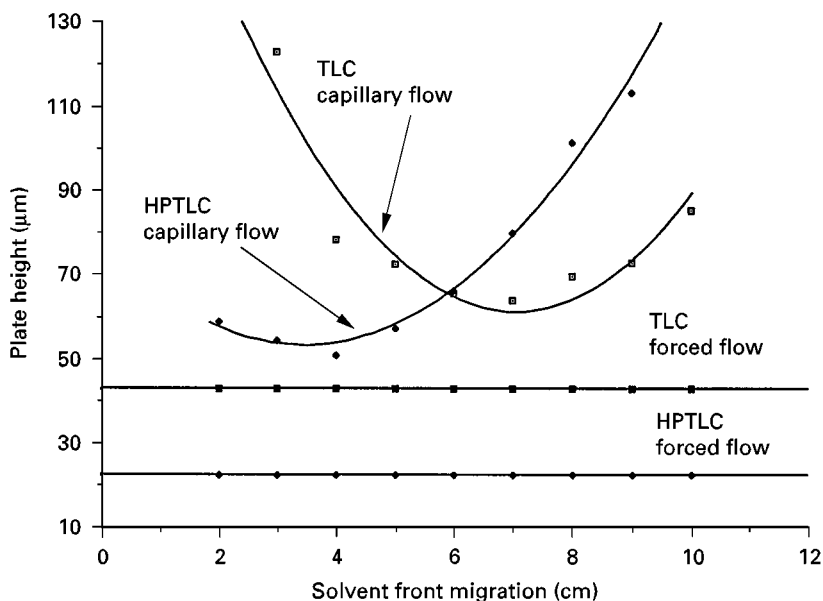


Figure 12 Variation of the average plate height as a function of the solvent front migration distance for conventional and high performance silica gel layers with capillary-controlled and forced-flow development. (Reproduced with permission from Poole CF and Poole SK (1997) *Journal of Chromatography A* 703: 573, copyright © Elsevier Science B.V.)

different from that of the high performance layers; the primary virtue of the latter is that a shorter migration distance is required to achieve a given efficiency, resulting in faster separations and more compact zones that are easier to detect by scanning densitometry. The minimum in the average plate height under capillary-controlled conditions is always greater than the minimum observed for forced-flow development, indicating that under capillary-controlled flow conditions the optimum potential performance is currently never realized in full. Under forced-flow conditions the minimum in the plate height is both higher and moved to a lower velocity compared with values anticipated for a column in LC, (Figure 13). Also, at increasing values of the mobile-phase velocity, the plate height for the layer increases more rapidly than is observed for a column. At the higher mobile-phase velocities obtainable by forced-flow development, resistance to mass transfer is an order of magnitude more significant for layers than for columns. The large value for resistance to mass transfer for the layers may be due to restricted diffusion within the porous particles or is a product of heterogeneous kinetic sorption on the sorbent and the binder added to layers to stabilize their structure. The consequences for forced-flow TLC are that separations will be slower than for columns and fast separations at high flow rates will be much less effi-

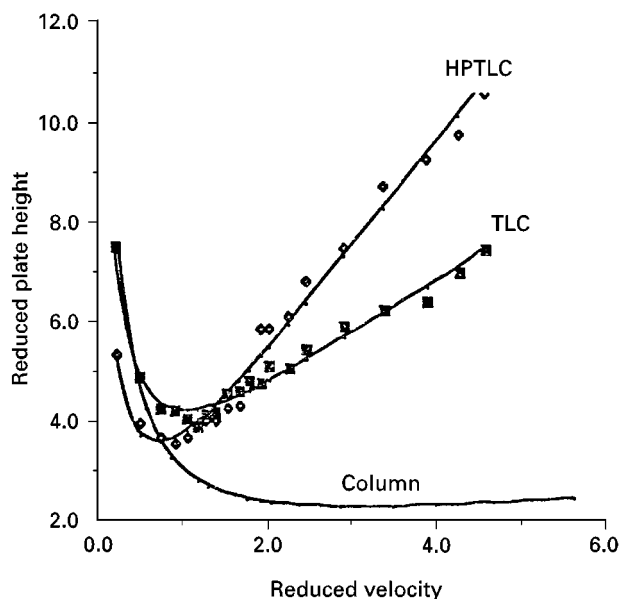


Figure 13 Plot of the reduced plate height (H/d_p) against the reduced mobile-phase velocity ($u d_p / D_m$) for a high performance and a conventional TLC layer using forced-flow development superimposed on a curve for an ideal LC column. (Reproduced with permission from Fernando WPN and Poole CF (1991) *Journal of Planar Chromatography* 4: 278, copyright © Research Institute for Medicinal Plants.)

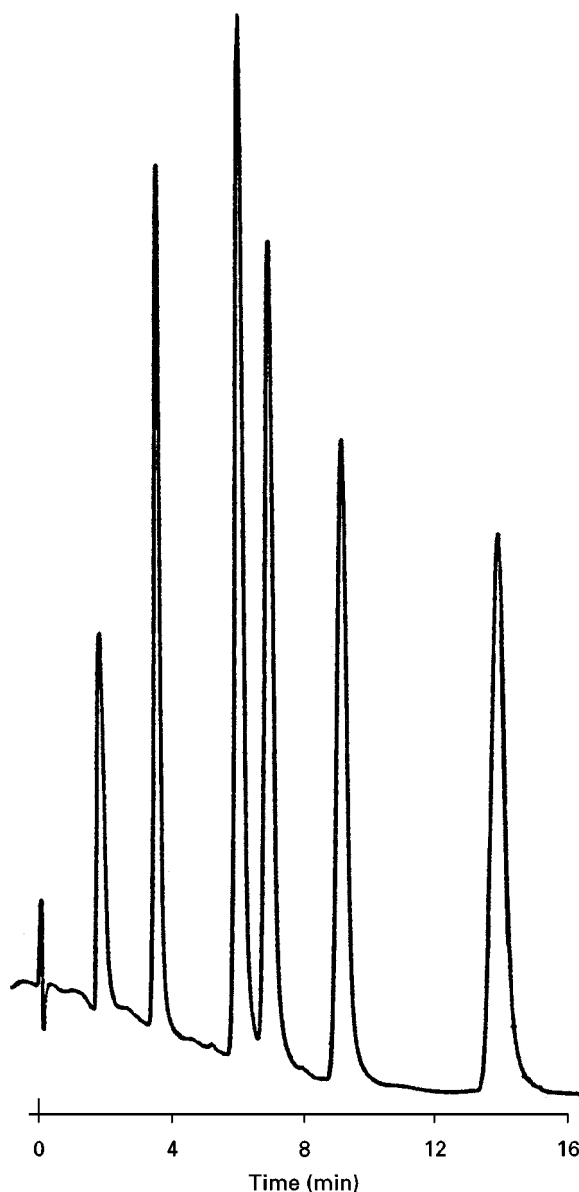


Figure 14 Separation of polycyclic aromatic hydrocarbons by forced-flow TLC with online detection (elution mode). A silica gel high performance layer, migration distance 18 cm, with hexane as the mobile phase (0.07 cm s^{-1}) was used for the separation. (Reproduced with permission from Poole CF and Poole SK (1994) *Analytical Chemistry* 66: 27A, copyright © American Chemical Society).

cient than for columns, although in terms of total efficiency and separation speed the possibilities for forced-flow development are significantly better than those of capillary-controlled separations (Figure 14).

Separation Quality

The general object of a chromatographic separation is to obtain an acceptable separation (resolution)

between all components of interest in a mixture within the shortest possible time. The resolution between two peaks in a chromatogram depends on how well the peak maxima are separated and how wide the two peaks are. This can be expressed numerically by the ratio of the separation of the two peak maxima divided by the average peak widths at their base. Baseline separation of the peaks is achieved at a resolution of about 1.5 but a value of 1.0, representing about 94% peak separation, is taken as an adequate goal for components that are difficult to separate. Resolution is also simply related to the properties of the chromatographic system. For this purpose it is convenient to consider a simple model of a three-component mixture in which the optimum column length is dictated by the number of theoretical plates required to separate the two components that are most difficult to separate, and the total separation time is dictated by the time required for the last peak to elute from the column. The resolution of the two peaks that are most difficult to separate is then related to the column variables by:

$$R_S = (\sqrt{N/2}) \times [(\alpha - 1)/(\alpha + 1)] \times k_{AV}/(1 + k_{AV}) \quad [3]$$

where k_{AV} is the average value of the retention factor for the two peaks, or in an approximate form by:

$$R_S = (\sqrt{N/4}) \times [(\alpha - 1)/\alpha] \times k_2/(1 + k_2) \quad [4]$$

for peaks with approximately equal base widths in which the elution order of the peaks is $k_2 > k_1$.

Column Chromatography

To a reasonable approximation, the three contributions to resolution (efficiency, selectivity and time) can be treated independently and optimized separately. Resolution increases only as the square root of N , so although the influence of efficiency is the most predictable parameter in the resolution equation, it is also the most limited. In practice all separations have to be made in the range $N = 10^3$ – 10^6 (Table 1). For GC this full range is available, so that increasing the column length or, better, reducing the column internal diameter of an open-tubular column at a constant length (separation time is proportional to column length), is often an effective strategy. For LC only a modest number of theoretical plates can be obtained in a reasonable time. In this case the general approach is to use the maximum available value for N and optimize resolution by changing the other variables. SFC is an intermediate case in which the general strategy depends on whether the fluid is more gas-like or liquid-like.

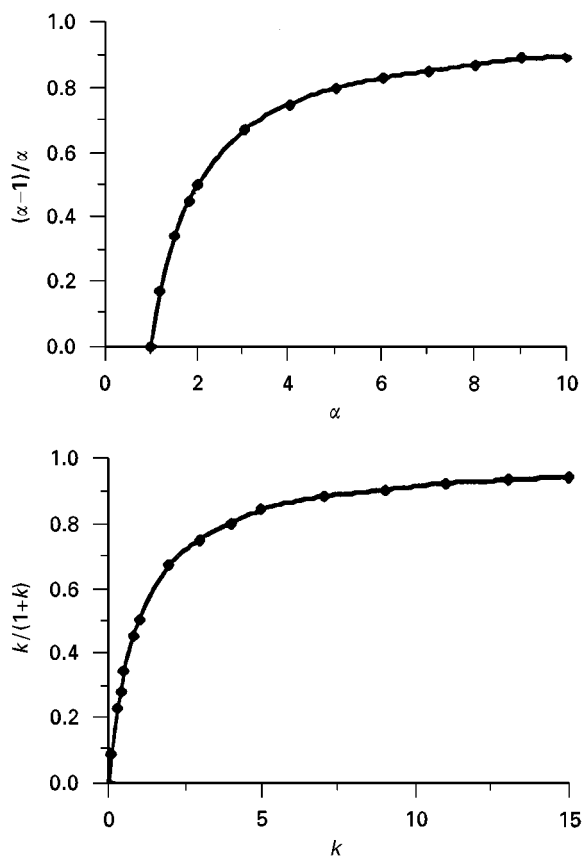


Figure 15 Influence of the separation factor (α) and the retention factor (k) on the resolution of two closely eluting peaks in column chromatography. (Reproduced with permission from Poole CF and Poole SK (1991) *Chromatography Today*, p. 31, copyright © Elsevier Science B.V.)

The separation factor determines the ability of the chromatographic system to differentiate between the two components based on the difference in their thermodynamic interactions with the mobile and stationary phases. When $\alpha = 1$ a separation is impossible but, as can be seen from Figure 15, only a small increase in α above unity is required to improve resolution considerably. At comparatively large values of α , resolution is little influenced by further changes; indeed, separations in which $\alpha > 2$ are easy to achieve. Selectivity optimization is the general approach to improve resolution in LC, where a wide range of mobile and stationary phases are available to choose from and a wide range of different retention mechanisms can be employed. Empirical or statistically based experimental approaches to selectivity optimization are often used because of a lack of formal knowledge of exact retention mechanisms for computer-aided calculations. Although powerful, selectivity optimization in LC can be a time-consuming process. The ease of achieving a separation by selectivity optimization can be

Table 3 Factors affecting resolution in column chromatography

Value of N needed for $R_s = 1$ at $k = 3$ for different values of α		Value of N needed for $R_s = 1$ at different k values for $\alpha = 1.05$ and 1.10		
α	N	k	$\alpha = 1.05$	$\alpha = 1.10$
1.005	1 150 000	0.1	853 780	234 260
1.01	290 000	0.2	254 020	69 700
1.02	74 000	0.5	63 500	17 420
1.05	12 500	1.0	28 220	7 740
1.10	3 400	2.0	15 880	4 360
1.20	1 020	5.0	10 160	2 790
1.50	260	10.0	8 540	2 340
2.00	110	20.0	7 780	2 130

illustrated by the data in Table 3, which indicate the number of theoretical plates required for a separation. These data can be compared to the data in Table 1, which indicates the number of theoretical plates available for different chromatographic systems. This is a clear indication of the need for selectivity optimization in LC and SFC, and the more relaxed constraints for GC.

Resolution will initially increase rapidly with retention, starting at $k = 0$, as shown in Figure 15. By the time k reaches a value around 5, further increases in retention result in only small changes in resolution. The optimum resolution range for most separations occurs for k between 2 and 10. Higher values of k result in long separation times with little concomitant improvement in resolution, but they may be necessary to provide sufficient separation space to contain all the peaks in the chromatogram.

The separation time is given by:

$$t_R = (H/u) \times 16R_s^2 \times [\alpha/(\alpha - 1)^2] \times (k_2 + 1)^3/k_2^2 \quad [5]$$

If the separation time (t_R) is to be minimized, then the acceptable resolution should not be set too high ($R_s = 1$); the separation factor should be maximized for the most difficult pair to separate; the retention factor should be minimized ($k = 1-5$) for the most difficult pair to separate; and the column should be operated at the minimum value for the plate height corresponding to the optimum mobile-phase velocity.

Micellar Electrokinetic Chromatography

The resolution equation for MEKC is identical to eqns [3] and [4] but contains an additional term, $(t_M/t_{MC})/[1 + (t_M/t_{MC})k_1]$, to account for the limited elution range (all solutes must elute between the retention time of an unretained solute, t_M , and a solute

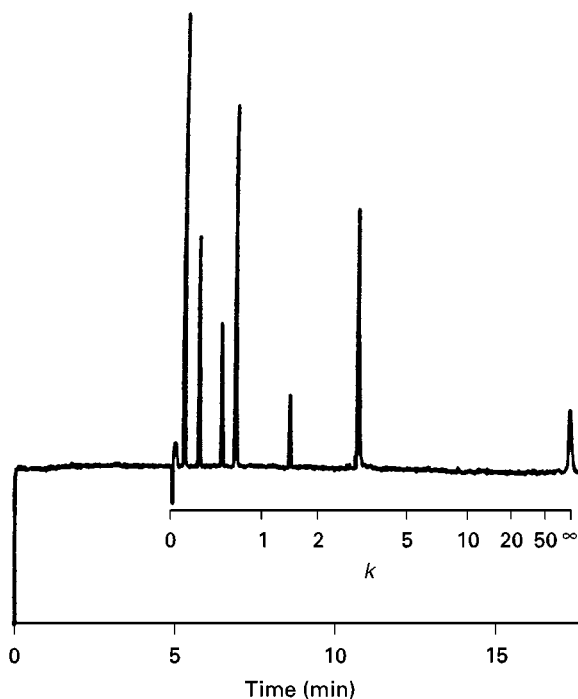


Figure 16 Separation of aromatic compounds by MEKC using a 65 cm (effective length 50 cm) \times 50 μ m i.d. fused silica capillary and a mobile phase containing 30 mmol L⁻¹ sodium dodecyl sulfate and 50 mmol L⁻¹ sodium phosphate/100 mmol L⁻¹ sodium borate buffer (pH = 7) at a field strength of 15 kV. (Reproduced with permission from Terabe S (1989) *Trends in Analytical Chemistry* 8: 129, copyright © Elsevier Science B.V.)

totally retained by the micelles, t_{MC} ; see Figure 16). The intrinsic efficiency of MEKC is much higher than column liquid chromatography, and optimization of the separation factor depends on a different set of parameters (changing surfactant type, use of additives, etc). Large values of the retention factor are unfavourable for obtaining high resolution since the additional term added to the resolution equation tends to zero at high k values. The optimum value of k for maximum resolution is around 0.8–5, corresponding to $(t_M/t_{MC})^{1/2}$. The retention factor is usually optimized by changing the surfactant concentration.

Planar Chromatography

For a single development under capillary-controlled flow conditions the TLC analogue of the general resolution equation for column chromatography can be expressed in approximate form as:

$$R_s = [(N_1 R_{F2})^{1/2}/4] \times [(k_1/k_2) - 1] \times (1 - R_{F2}) \quad [6]$$

where N_1 is the maximum number of theoretical plates available corresponding to the solvent front position. The use of $N_1 R_{F2}$ is only a rough

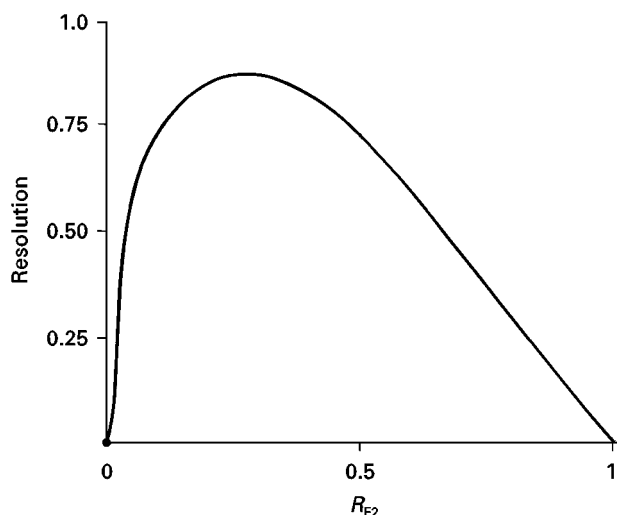


Figure 17 Variation of the resolution of two closely migrating zones as a function of the R_F value for the faster moving zone. (Reproduced with permission from Poole CF and Poole SK (1991) *Chromatography Today*, p. 669, copyright © Elsevier Science B.V.)

approximation for the number of theoretical plates that a particular zone has migrated across. Relatively small changes in selectivity have enormous impact on the ease of obtaining a given separation in TLC, since the total number of theoretical plates available for a separation is never very large. Separations in TLC are fairly easy when $R_{F2} - R_{F1} > 0.1$ and very difficult or impossible for $R_{F2} - R_{F1} \leq 0.05$ in the region of the optimum R_F value for the separation. Maximum resolution is obtained at an R_F value of about 0.3 and does not change much in the R_F range of 0.2 to 0.5, as can be seen in **Figure 17**. Resolution is zero for compounds that are retained at the origin or migrate with the solvent front.

General Elution Problem

Constant separation conditions, for example isothermal operation in GC and isocratic elution in LC, are unsuitable for separating samples containing components with a wide retention range. Employing average separation conditions will result in a poor separation of early-eluting peaks, poor detectability of late-eluting peaks, and excessively long separation times. In GC there is an approximately exponential relationship between retention time and solute boiling point under isothermal conditions. For mixtures with a boiling point range $> c. 100^\circ\text{C}$ it is impossible to identify a compromise temperature that will provide an acceptable separation. The solution in this case is to use temperature programming, flow programming, or both. Temperature programming is the most common and usually involves a continuous linear increase in temperature with time, although other programme profiles are possible, including segmented programmes incorporating isothermal periods. The reduction in separation time, increase in peak capacity, and nearly constant peak widths obtained are illustrated by the separation in **Figure 18**. The general elution problem in LC is solved using solvent-strength gradients. Here, the composition of the mobile phase is changed as a function of time. Binary or ternary solvent mixtures are commonly used as the mobile phase in which the relative composition of the strong solvent (that solvent with the capability of reducing retention the most) is increased over time. In SFC it is usual to programme the density, mobile-phase composition or temperature as a single factor, but it is also possible for some combination of parameters to be changed simultaneously. The goal remains the same, as indicated by the

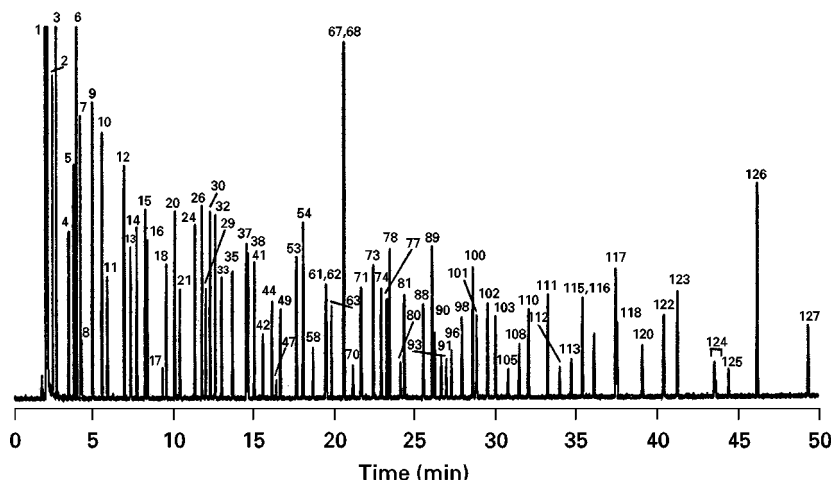


Figure 18 Temperature programmed separation of fragrance compounds by GC on a 30 m \times 0.25 mm i.d. fused silica open-tubular column coated with DB-1, film thickness 0.25 μm , helium carrier gas 25 cm s^{-1} and temperature program 40°C (1 min isothermal) then $40\text{--}290^\circ\text{C}$ at 5°C min^{-1} . (Reproduced with permission from J&W, copyright © J&W Scientific Inc.)

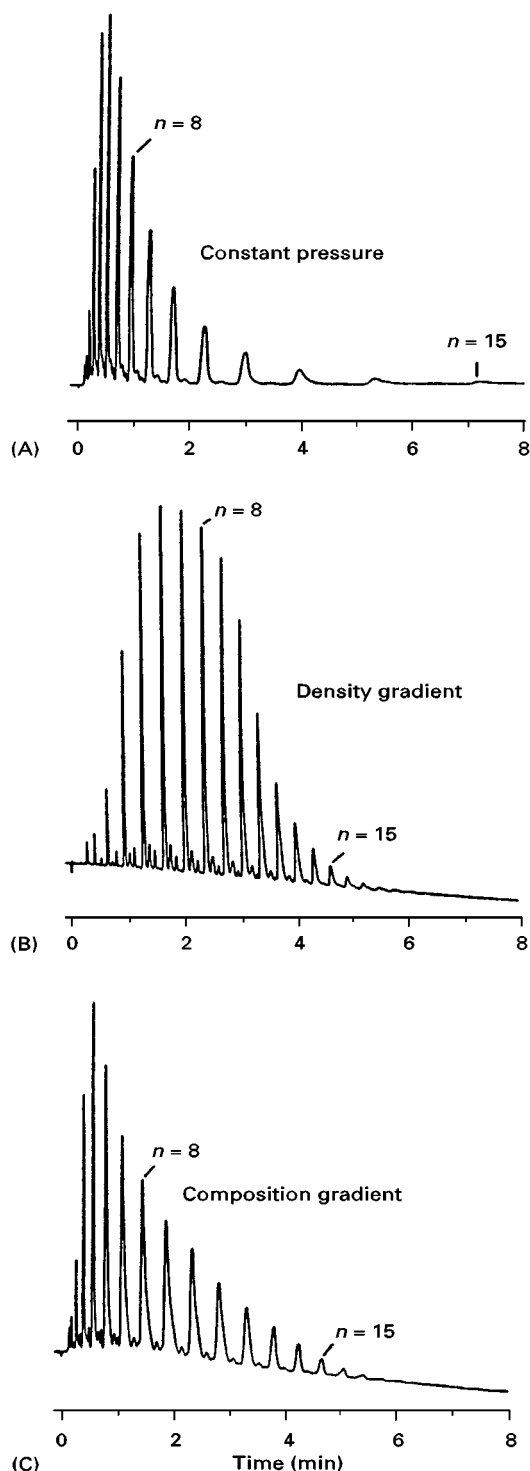


Figure 19 Separation of Triton X-114 by SFC using programmed elution on a 10 cm \times 2 mm i.d. column packed with 3 μ m octadecylsiloxane-bonded silica gel at 170°C with UV detection. (A) Carbon dioxide/methanol (2 + 0.125) mL min⁻¹ at 210 bar; (B) as for (A) with pressure programmed from 130 to 375 bar over 8 min; and (C) using a mobile-phase composition gradient from 0.025 to 0.4 mL min⁻¹ methanol over 8 min at 210 bar. (Reproduced with permission from Giorgetti A, Pericles N, Widmer HM, Anton K and Datwyler P (1989) *Journal of Chromatographic Science* 27: 318, copyright © Preston Publications, Inc.)

density- and composition-programmed separation of oligomers in **Figure 19**.

Solvent-strength gradients in TLC are usually discontinuous and achieved through the use of uni-dimensional multiple development. This is accompanied by zone refocusing resulting in a larger zone capacity and easier-to-detect separated zones. All uni-dimensional multiple development techniques employ successive repeated development of the layer in the same direction with removal of the mobile phase between developments. Each time the solvent front traverses the sample zone it compresses the zone in the direction of development because the mobile phase contacts the bottom edge of the sample zone first where the sample molecules then start to move forward before those molecules ahead of the solvent front. Once the solvent front has reached beyond the zone, the refocused zone migrates and is broadened by diffusion in the usual way. When optimized, it is possible to migrate a zone a considerable distance without significant zone broadening beyond that observed for the first development. If the solvent composition is varied for all, or some, of the development steps during multiple development, then solvent strength gradients of different shapes can be produced. With increasing solvent-strength gradients it is usually necessary to scan the separation at a number of intermediate development steps corresponding to the development at which different components of interest are separated, since in later developments these zones may be merged again because of the limited zone capacity in TLC. Alternatively,

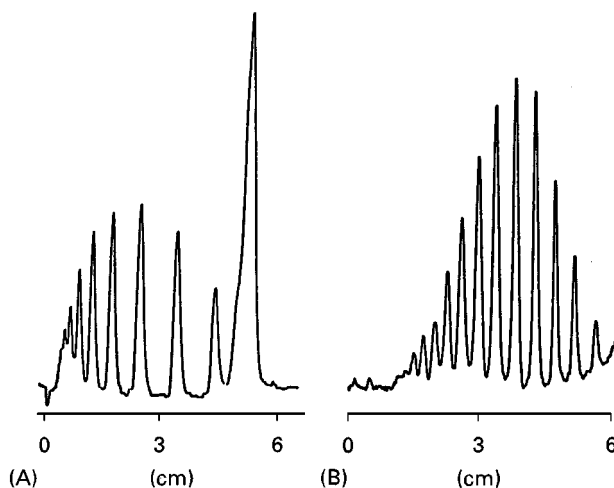


Figure 20 Separation of the 3,5-dinitrobenzoyl esters of poly(ethylene glycol) 400 by (A) a single conventional development and (B) by incremental multiple development with a step-wise gradient of methanol, acetonitrile and dichloromethane over 15 developments (Reproduced with permission from Poole CF, Poole SK and Belay MT (1993) *Journal of Planar Chromatography* 6: 438, copyright © Research Institute for Medicinal Plants.)

incremental multiple development can be used with a decreasing solvent-strength gradient. In this case, the first development distance is the shortest and employs the strongest solvent composition, while subsequent developments are longer and employ mobile-phase compositions of decreasing solvent strength. The final development step is the longest and usually corresponds to the maximum useful development length for the layer and employs the weakest mobile phase. In this way sample components migrate in each development until the strength of the mobile phase declines to a level at which some of the sample zones are immobile, while less retained zones continue to be separated in subsequent development steps, affording the separation of the mixture as a single chromatogram (Figure 20). Incremental multiple development with a decreasing solvent-strength gradient is easily automated.

Multidimensional and Multimodal Chromatography

The analysis of complex mixtures requires a very large peak capacity since the probability of peak overlap increases with the number of compounds requiring separation. Multidimensional and multimodal chromatographic systems provide a better route to achieving high peak capacities than is possible with single-column systems. The necessary characteristic of these systems is that the dominant retention mechanism should be different for each dimension. Other uses of multidimensional and multimodal chromatography include trace enrichment, matrix simplification, increased sample throughput, and as an alternative to gradient elution in LC.

Multidimensional column chromatography involves the separation of a sample by using two or more columns in series where the individual columns differ in their capacity and/or selectivity. Multimodal separations involve two or more chromatographic methods in series, for example, the online coupling of LC and GC (LC-GC) or SFC and GC (SFC-GC). Both methods involve the transfer of the whole or part of the eluent from the first column to another via some suitable interface. The function of the interface is to ensure compatibility in terms of flow, solvent strength and column capacity. The design requirements and ease of coupling differ significantly for the different chromatographic modes. Coupling GC-GC, SFC-GC, SFC-SFC, LC-LC, LC-GC and LC-TLC are routine and other combinations such as SFC-TLC, SFC-LC and GC-TLC have been described in the literature. Trace enrich-

ment and sample clean-up on short pre-columns is finding increasing use in the automated determinations of drugs in biological fluids and crop protection agents in water by LC-LC. Figure 21 illustrates the separation of a mixture of deoxyribonucleosides and their 5'-monophosphate esters using LC-LC with an anion exchange column and a reversed-phase column connected in series by a microvolume valve interface. The neutral deoxyribonucleosides are switched as a single peak for separation on the reversed-phase column while the phosphate esters are resolved by the anion exchange column. The separation time remains acceptable since both separations are performed almost simultaneously. TLC-TLC is commonly called two-dimensional TLC and is a widely used qualitative method of analysis. It is very easily performed by placing a sample at the corner of the layer and developing the plate in the normal way, evaporating the solvent, turning the plate through a right angle and developing the plate a second time at 90° to the first development. If adequately optimized this is a very

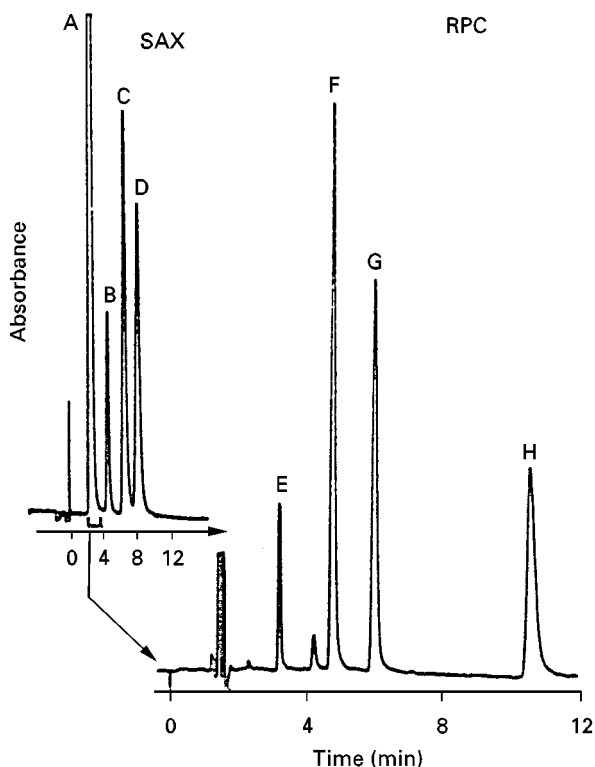


Figure 21 Separation of the major deoxyribonucleosides and their 5'-monophosphate esters by multidimensional LC-LC. The first column is a strong anion exchange column and the second a reversed-phase column. The unseparated nucleosides, A, are switched to the second column after which the 5'-monophosphate esters, B to D are separated on the IEC column and the parent deoxyribonucleosides, E to H, are separated on the RPC column. (Reproduced with permission from Sagliano N, Hsu SH, Floyd TR, Raglione TV and Hartwick RA (1985) *Journal of Chromatographic Science* 23: 238, copyright © Preston Publication, Inc.)

powerful separation method, but more frequently than not, solvents of different composition are used for the two developments employing retention mechanisms that differ in intensity rather than kind, and the zones are only dispersed around the diagonal between the two development directions and not uniformly over the whole layer.

Mode Selection

Chromatography provides many different approaches for the separation of mixtures. There are many instances where the same mixture can be adequately separated by more than one approach. In this section we will take a mechanistic look at how solutes are separated by the common chromatographic techniques to provide some guidelines for method suitability.

If the only consideration were efficiency and speed, then GC would be the preferred technique. In practice, GC is restricted to thermally stable compounds with a significant vapour pressure at the temperature required for their separation. The upper temperature limit for common GC stationary phases is 200–400°C. Few compounds with a molecular weight greater than 1000 Da have sufficient vapour pressure to be separated in this temperature range, and many low molecular weight compounds are known to be labile at temperatures required for their vaporization. Derivatization techniques extend the scope of GC to otherwise labile compounds by forming thermally stable derivatives, often with increased volatility, and by tagging compounds with specific groups that simplify trace analysis using one of the selective and sensitive group or element-selective detectors available for GC.

Under typical conditions the mobile phase in GC behaves essentially as an ideal gas and does not contribute to selectivity. To vary selectivity either the temperature is changed or a new stationary phase (column) is employed for the separation. Temperature and separation time are closely connected in GC. The range over which temperature can be varied is usually short and will likely provide only a small change in selectivity, but because of the large number of theoretical plates available for a separation in GC, this may be sufficient to provide adequate resolution. Provided that stationary phases that differ in their relative capacity for intermolecular interactions are selected, then larger changes in selectivity can be anticipated by stationary-phase optimization. In modern column technology the most versatile group of stationary phases are the poly(siloxanes), which can be represented by the basic structure $-(R_2SiO)_n-$, in which the type and relative amount of

individual substituents can be varied to create the desired variation in selectivity (R = methyl, phenyl, 3,3,3-trifluoropropyl, cyanoethyl, fluorine-containing alcohol, etc.) Special phases in which R contains a chiral centre or a liquid-crystalline unit are used to separate enantiomers and geometric isomers. Other common stationary phase include hydrocarbons, poly(phenyl ethers), poly(esters) and poly(ethylene glycols), although many of these phases are restricted to packed column applications because of difficulties in either coating or immobilizing them on the walls of fused-silica capillaries, favoured for the manufacture of open-tubular columns. The solvation parameter model provides a reliable systematized approach for selectivity optimization and the prediction of retention in GLC. For GSC the stationary phase is usually silica, alumina, graphitized carbon, organic polymer or zeolite porous particles (packed columns); or a thin layer dispersed over the inner surface of a capillary column with an open passageway down the centre (porous layer open-tubular column, or PLOT column). These materials are used to separate inorganic gases, volatile halocarbon compounds, low molecular weight hydrocarbons and, in particular, geometric and isotopic isomers.

LC and GC should be considered as complementary techniques. Since the only sample requirement for LC is that the sample has reasonable solubility in some solvent suitable for the separation, and since separations by LC are commonly carried out close to room temperature, thermal stability is not generally an issue. The large number of separation mechanisms easily exploited in the liquid phase provides a high level of flexibility for selectivity optimization. In general, many applications of LC can be categorized as those for which GC is unsuited and includes applications to high molecular weight synthetic polymers, biopolymers, ionic compounds and many thermally labile compounds of chemical interest.

Mode selection within LC is quite complicated because of the number of possible separation mechanisms that can be exploited, as illustrated in **Figure 22**. Preliminary information on the molecular weight range of the sample, relative solubility in organic solvents and water, and whether or not the sample is ionic, can be used as a starting point to arrive at a suitable retention mechanism for a separation. The molecular weight cutoff at 2000 indicated in **Figure 22** is quite arbitrary and reflects the fact that size exclusion packings are readily available for the separation of higher molecular weight solutes, although size exclusion is not used exclusively to separate high molecular weight compounds because of its limited peak capacity. Wide-pore packing materials allow polymers with a molecular weight

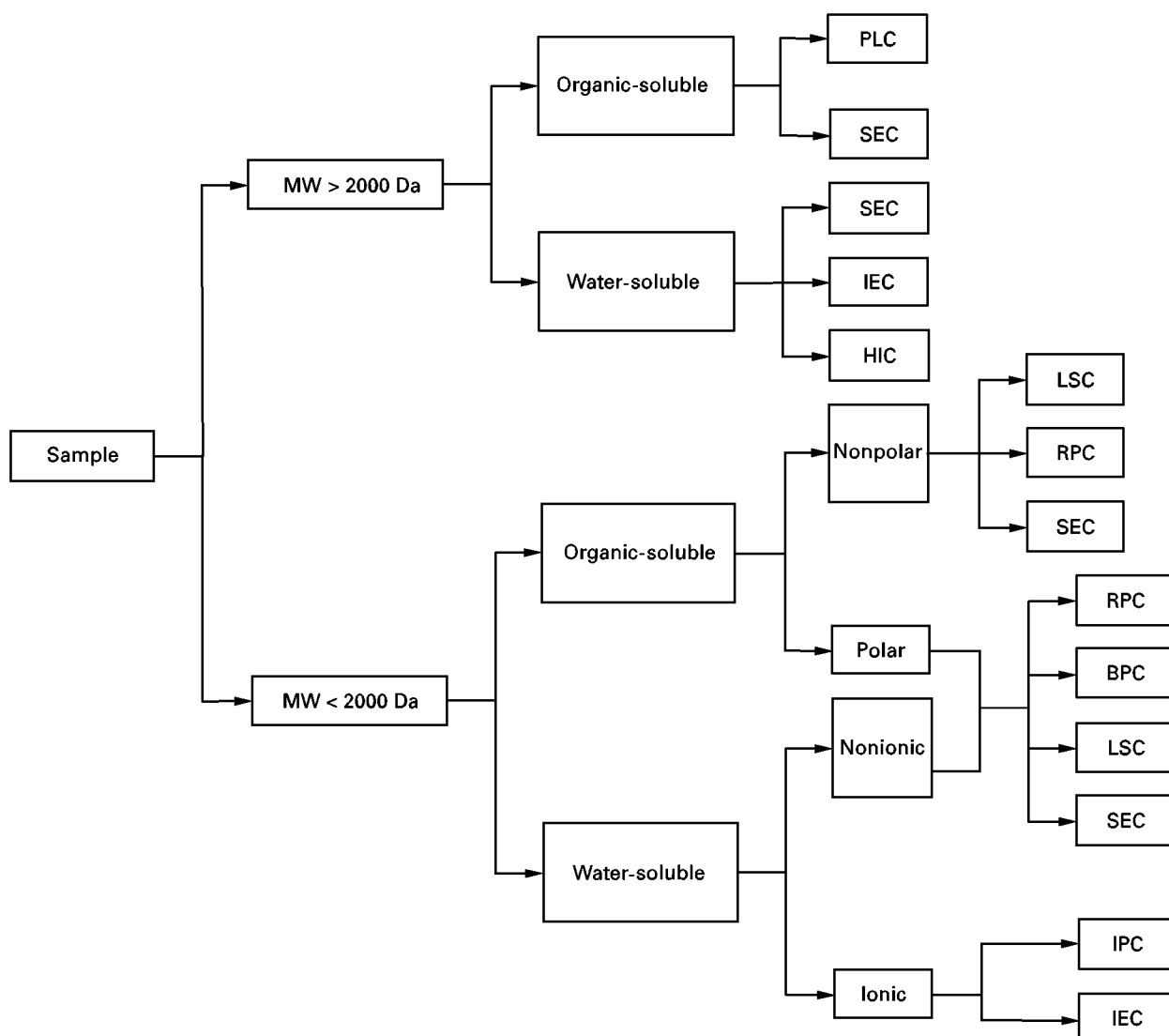


Figure 22 Selection of the separation mechanism in LC based on the criteria of sample molecular weight, solubility and conductivity. (Reproduced with permission from Poole CF and Poole SK (1991) *Chromatography Today*, p. 455, copyright © Elsevier Science B.V.)

exceeding 2000 to be separated by conventional sorption and ion exchange mechanisms.

Liquid-solid chromatography (LSC) is characterized by the use of an inorganic oxide or chemically bonded stationary phase with polar functional groups and a nonaqueous mobile phase consisting of one or more polar organic solvents diluted to the desired solvent strength with a weak solvent, such as hexane. A characteristic of these systems is the formation of an adsorbed layer of mobile-phase molecules at the surface of the stationary phase with a composition that is related to the mobile-phase composition but generally not identical to it. Retention is essentially determined by the balance of interactions the solute experiences in the mobile phase and its competition with mobile-phase molecules for adsorption sites at

the surface of the stationary phase. The position and type of polar functional groups and their availability for interaction with discrete immobile adsorption sites is responsible for selectivity differences when silica or alumina are used as stationary phases. The ability of LSC to separate geometric isomers has been attributed to the lock-key type steric fitting of solute molecules with the discrete adsorption sites on the silica surface.

Reversed-phase liquid chromatography (RPC) is characterized by the use of a stationary phase that is less polar than the mobile phase. A chemically bonded sorbent or a porous polymer could be used as this stationary phase, while for most practical applications the mobile phase contains water as one of its major components. RPC is ideally suited to the

separation of polar molecules that are either insoluble in organic solvents or bind too strongly to inorganic oxide adsorbents for normal elution. RPC employing acidic, low ionic strength eluents is a widely established technique for the purification and characterization of biopolymers. Other favourable attributes include the possibility of simultaneous separation of neutral and ionic solutes; rapid equilibrium between phases facilitating the use of gradient elution; and the manipulation of secondary chemical equilibria in the mobile phase (e.g. ion suppression, ion pair formation, metal complexation and micelle formation) to optimize separation selectivity in addition to variation in solvent type and composition of the mobile phase. A large number of chemically bonded stationary phases of different chain length, polarity and bonding density are available to complement mobile-phase optimization strategies. About 70% of all separations performed in modern LC are by RPC, which gives an indication of its flexibility, applicability and ease of use. The main driving force for retention in RPC is solute size because of the high cohesive energy of the mobile phase compared to the stationary phase, with solute polar interactions, particularly solute hydrogen bond basicity, reducing retention. These findings strongly reflect the properties of water, which is the most cohesive of the solvents normally used in LC, as well as a strong hydrogen bond acid.

Ion exchange chromatography (IEC) is used for the separation of ions or substances easily ionized by manipulation of pH. Stationary phases are characterized as weak or strong ion exchangers based on the extent of ionization of the immobile ionic centres, and as anion or cation exchangers based on the charge type associated with the ionic centres. Thus, sulfonic acid groups are strong, and carboxylic acid groups are weak, cation exchangers. Most of the metal cations in the Periodic Table have been separated by IEC with acids or complexing agents as eluents. In clinical laboratories ion exchange has long been employed as the basis for the routine, automated separation of amino acids and other physiologically important amines involved in metabolic disorders and to sequence the structure of biopolymers. Soft, nondenaturing, ion exchange gels are widely used in the large-scale isolation, purification and separation of peptides, proteins, nucleosides and other biological polymers. Metal-loaded ion exchangers and anion exchange chromatography of complexed carbohydrates are well-established separation techniques in carbohydrate chemistry. The combination of pellicular ion exchange columns of low capacity, low concentration eluents with a high affinity for the ion exchange packing, and universal, online detection with a flow-through conductivity detector revolution-

ized the analysis of inorganic and organic ions in industrial and environmental laboratories. As well as electrostatic interactions, retention in IEC is influenced by hydrophobic sorptive interactions between the sample and stationary phase similar to those in RPC, and size and ionic exclusion effects. Resolution is optimized by choice of the mobile-phase counterion, the ionic strength, pH, temperature, flow rate, and addition of organic modifiers.

In size exclusion chromatography (SEC) retention differences are controlled by the extent to which sample components can diffuse through the pore structure of the stationary phase, as indicated by the ratio of sample molecular dimensions to the distribution of stationary-phase pore size diameters. Since no separation will result under conditions where the sample is completely excluded from the pore volume or can completely permeate the pore volume, the zone capacity of SEC is small compared with that of the other LC techniques. The separation time is predictable for all separations, corresponding (ideally) to a volume of eluent equivalent to the column void volume. No solvent optimization beyond finding a solvent for the sample that is compatible with the stationary phase is required. For synthetic polymers this can result in the use of exotic solvents and high temperatures. SEC is a powerful exploratory method for the separation of unknown samples, since it provides an overall view of sample composition within a predictable time, and is also commonly employed in sample fractionation to isolate components belonging to a defined molecular size range. Analytical separations employ small particles of rigid, polymeric or silica-based gels of controlled pore size to separate samples of different molecular size and to obtain average molecular weights and molecular weight distribution information for polymers.

Fundamentally the retention mechanisms for LC and TLC are identical. TLC is selected over LC when advantage can be taken of the attributes of employing a planar format for the separation. Examples include when a large number of samples requiring minimum sample preparation are to be separated, when post-chromatographic reactions are usually required for detection, or if sample integrity is in question. The use of a disposable stationary phase for TLC allows sample clean-up and separation to be performed simultaneously. Reasons for preferring LC over TLC are its greater separation capacity for mixtures containing more components than can be adequately resolved by TLC; a wider range of stationary phases are available for methods development; a wider selection of detection techniques exist; and automation for unattended operation is more straightforward.

The retention mechanism for MEKC strongly resembles that of RPC with two important differences. Surfactants used to generate the pseudo-stationary phases provide a different type of sorption environment to solvated chemically bonded phases and, therefore, different selectivity. The intrinsic efficiency of MEKC is significantly greater than that of LC and enhances resolution, although the peak capacity is lower owing to the finite migration window for MEKC. A significant number of RPC-type applications are now performed by MEKC, indicating that the method can compete favourably with RPC for some separations. MEKC is inherently a microcolumn technique, providing advantages in coupling to other chromatographic systems and for the analysis of samples only available in small amounts. Disadvantages include sample introduction problems, limited dynamic sample concentration range, and poor limits of detection for trace analysis (because of the very small sample sizes involved). Selectivity optimization is determined largely by the choice of surfactant and the use of mobile- and stationary-phase additives.

Supercritical fluids have solvating properties that are intermediate between those of gases and liquids. In addition, supercritical fluids are compressible so that their density and solvating power can be varied by changing external parameters, such as pressure and temperature. This feature is unique to supercritical fluids and represents a major approach to selectivity optimization. Temperature not only affects density, but may also influence the vapour pressure of low molecular weight solutes, promoting some GC-like character to the retention mechanism. The most common mobile phase is carbon dioxide, a relatively nonpolar fluid. More-polar fluids, such as water, ammonia or methanol, tend to have unfavourable critical constants or are highly corrosive to column or instrument components, limiting their use. Mixed mobile phases can be used to vary selectivity, such as carbon dioxide-methanol mixtures, but miscibility problems and high critical constants for the mixed mobile phases may restrict the range of properties available. SFC can provide faster separations than LC, but it is more restricted than LC in the choice of mobile phases and retention mechanisms to vary selectivity. SFC is compatible with most detection options available for both GC and LC. All practical applications of SFC occur significantly above ambient temperature, which is unsuitable for the separation of some thermally labile compounds and most biopolymers. Supercritical fluids such as carbon dioxide are unable to mask active sites on typical column packings, resulting in unsatisfactory separations of polar compounds owing to adsorption, which pro-

duces unacceptable peak shapes and poor resolution. However, SFC finds applications in many areas where GC and LC are unsatisfactory, for example in the separation of middle molecular weight compounds, low molecular weight synthetic polymers, fats and oils, enantiomers, and organometallic compounds.

Instrumentation

Modern chromatographic methods are instrumental techniques in which the optimal conditions for the separation are set and varied by electromechanical devices controlled by a computer external to the column or layer. Separations are largely automated with important features of the instrumentation being control of the flow and composition of the mobile phase, provision of an inlet system for sample introduction, column temperature control, online detection to monitor the separation, and display and archiving of the results. Instrument requirements differ significantly according to the needs of the method employed. Unattended operation is usually possible by automated sample storage or preparation devices for time-sequenced sample introduction.

Gas Chromatography

For GC a supply of gases in the form of pressurized cylinders is required for the carrier gas and perhaps also for the detector, for operating pneumatic valves, and for providing automatic cool-down by opening the oven door. To minimize contamination, high purity gases are used combined with additional purification devices. Each cylinder is fitted with a two-stage pressure regulator for coarse pressure and flow control. Fine tuning is achieved using metering valves or by electronic pressure control combining electromechanical devices with sensors to compensate automatically for changes in ambient conditions. The column oven is generally a forced air circulation thermostat heated resistively and capable of maintaining a constant temperature or of being programmed over time. The detector and sample inlet are generally thermostated separately in insulated metal blocks heated by cartridge heaters. The most common method of introducing samples into a GC inlet is by means of a microsyringe (pyrolysis, headspace and thermal desorption devices can be considered specialized sample inlets). For packed-column injection a small portion of (liquid) sample is introduced by microsyringe through a silicone septum into a glass liner or the front portion of the column, which is heated and continuously swept by carrier gas. The low sample capacity and carrier gas flow

rates characteristic of narrow-bore open-tubular columns require more sophisticated sample-introduction techniques based on sample splitting or solvent elimination and refocusing mechanisms.

The principal methods of detection are varied, conveniently grouped under the headings of gas-phase ionization devices, bulk physical property detectors, optical detection and electrochemical devices. Further classification is possible based on the nature of the detector response – universal, selective or specific. The flame ionization detector and thermal conductivity detector are examples of (near) universal detectors; the flame photometric detector, thermionic ionization detector and atomic emission detector are element-selective detectors; and the photoionization detector and electron capture detector are structure-selective detectors. GC coupling to mass spectrometry and IR spectroscopy is straightforward and widely utilized for automated structure identification as well as detection. Detection in the gas phase is a favourable process and GC detectors are among the most sensitive and versatile by virtue of the range of mechanisms that can be exploited.

Liquid Chromatography

Modern LC employs columns with small particle sizes and high packing density requiring high pressures for operation at useful mobile-phase velocities. Syringe-type or single- or multiple-head reciprocating piston pumps are commonly used to provide the operating pressures needed in configurations that depend on the design of the solvent-delivery system. A single pump is sufficient for isocratic operation. A single pump and electronically operated proportioning valves can be used for continuous variation of the mobile-phase composition (gradient elution) or, alternatively, independent pumps in parallel (commonly two) are used to pump different solvents into a mixing chamber. Between the pump and sample inlet may be a series of devices (check valves, pulse dampers, mixing chambers, flow controllers, pressure transducers, etc.) that correct or monitor pump output to ensure that a homogeneous, pulseless liquid flow is delivered to the column at a known pressure and volumetric flow rate. These devices may be operated independently of the pump or in a feedback network that continuously updates the pump output. Mobile-phase components are stored in reservoir bottles with provision for solvent degassing, if this is required for normal pump and detector operation. Loop-injection valves situated close to the head of the column are universally used for sample introduction. This allows a known volume of sample to be

withdrawn at ambient conditions, equivalent to the volume of the injection loop, and then inserted into the fully pressurized mobile-phase flow by a simple rotation of the valve to change the mobile-phase flow paths. Although most separations are performed at room temperature, either the column alone or the whole solvent-delivery system may be thermostated to a higher temperature when this is desirable or required for the separation. The separation is monitored continuously on the low pressure side of the column using several bulk physical property, photometric, or electrochemical detectors fitted with microvolume flow cells.

Common detection principles are UV absorbance, fluorescence, refractive index and amperometry. Coupling to MS and IR spectroscopy is becoming more common, as is online coupling to nuclear magnetic resonance (NMR) spectrometers. Detection is a more difficult aspect in the condensed phase and neither the variety nor operating characteristics of LC detectors compare favourably with GC detectors, although they allow a wide range of sample types to be analysed routinely. Special materials are used in the fabrication of biocompatible and corrosion-resistant instruments for the separation of biopolymers and for ion chromatography. Individual pumps can handle solvent delivery requirements over a decade range or so of flow rates. The diversity of column diameters used in modern LC for analysis and preparative-scale applications demands flow rates that vary from a few μL per minute to tens of litres per minute. Consequently, instruments are designed for efficient operation within a particular application range and are not universal with respect to column selection. Furthermore, analytical detectors tend to be designed with sensitivity as the main concern and preparative-scale detectors for capacity, such that the two are generally not interchangeable even when the same detection principle is employed. For preparative-scale work some form of automated sample fraction collection is necessary and economy of operation may dictate incorporation of an integrated mobile-phase recycle feature.

Supercritical Fluid Chromatography

Instrumentation for SFC is a hybrid of components used in GC and LC modified to meet the requirements of operation with a compressible fluid. The mobile phase is typically carbon dioxide (with or without modifier) contained in a pressurized cylinder and delivered to the pump in liquid form. Syringe pumps or cooled reciprocating piston pumps modified for pressure control are commonly used. A high precision

pressure transducer is installed between the pump and sample inlet for programming the inlet pressure or fluid density during the course of a separation. Simultaneous measurement of the column temperature and pressure control allows constant density or density programming under computer control if the appropriate isotherms are known or can be approximated. Two pumps are generally used to generate mobile-phase composition gradients comprising liquid carbon dioxide and an organic solvent. Loop-injection valves similar to LC are the most convenient devices for sample introduction. The column oven is usually a forced air circulation thermostat similar to those used in GC. The full range of flame-based detectors used in GC can be used with only slight reoptimization as well as the main optical detectors used in LC, after modification for high pressure operation. A unique feature of the chromatograph is a restrictor required to maintain constant density along the column and to control the linear velocity of the fluid through the column. Orifice-type restrictors are usually placed between the column and detector for flame-based detectors and back-pressure regulators after the detector flow cell for optical detectors.

MEKC and CEC

MEKC and CEC employ the same instruments as used for capillary electrophoresis with the addition of overpressure capability for the buffer reservoirs when used for CEC. The separation capillary is terminated in two buffer reservoirs containing the high voltage electrodes that provide the electric field to generate the flow of mobile phase. The buffer reservoirs can be moved into place pneumatically and sequenced automatically to introduce a sample vial for sample introduction or a run buffer vial for separation. The column area is thermostated to maintain a constant temperature. A miniaturized optical detector positioned between the buffer reservoirs is commonly used for on-column detection. Some form of interlock mechanism is used to prevent operator exposure to the high voltages, up to 30–50 kV, typically used. A high level of automation is achieved under computer control and unattended operation is generally possible.

Planar Chromatography

The total automation of sample application, chromatogram development and *in situ* quantitation in planar chromatography has proved difficult. Instead the individual procedures are automated, requiring operator intervention to move the layer from one operation to the next. Samples are typically ap-

plied to the layer as spots or narrow bands using low volume dosimeters or spray-on techniques. Application volume, method, location and sample sequence are automated for unattended operation. The chromatogram is obtained by manual development in a number of development chambers of different design, or can be automated such that the conditioning of the layer, the selected solvents for the development, and the development length are preselected and controlled through the use of sensors. For multiple-development techniques the layer can be alternately developed, dried, new solvent introduced and the process repeated with changes in the development length and mobile-phase composition for any or all the programmed development steps. Apparatus for forced-flow development is also available and resembles a liquid chromatograph with the column replaced by the layer sandwiched between a rigid support and a polymeric membrane in an overpressure development chamber to allow external pressure to be used to create the desired mobile-phase velocity.

After development the chromatogram is recorded using scanning or video densitometry. The unique feature compared with detection in column chromatography is that the separation is recorded in space rather than time while in the presence of the stationary phase. The common forms of detection are optical methods based on UV-visible absorption and fluorescence. In mechanical scanning the layer is moved on a translation stage under a slit projecting the image of the monochromatic light source on the layer surface and the light reflected from the surface monitored continuously with a photodiode or similar device. Substances that absorb the light produce a proportional decrease in the intensity of the reflected light that can be related to the amount of sample present (for fluorescence there is a proportionate increase in the amount of light emitted at a wavelength that is longer than the absorbed wavelength). Electronic scanning is not as well developed but involves uniformly illuminating the whole layer and imaging the plate surface onto a video camera, or similar device, to capture and integrate the static image of the absorbing zones.

Conclusion

Many of the important developments in chromatography have already been made, yet the technique continues to evolve by the introduction of new materials that extend the scope of existing methods and through finding new applications. General applications are dominated by the techniques of gas chromatography and column liquid chromatography,

which are the most mature in terms of their evolutionary development, although it is widely recognized that column liquid chromatography still lacks a sensitive and universal detector for general applications. This void may be filled by mass spectrometry, which has made great strides in the last few years towards this goal based on particle-beam interfaces and atmospheric ionization techniques coupled with the development of low cost mass separators. By comparison, thin-layer chromatography and supercritical fluid chromatography have become recognized as techniques with niche applications and are unlikely to supplant gas and column liquid chromatography as the dominant chromatographic methods used in analytical laboratories. The microcolumn techniques of capillary electrophoresis, micellar electrokinetic chromatography, and capillary electrochromatography have quickly established themselves as useful laboratory methods and are likely to become of increasing importance as they complete their evolutionary cycle. In particular, the infant capillary electrochromatography has the potential to replace column liquid chromatography from many of its traditional separation roles, but has yet to reach a state of development to be considered as a routine laboratory technique.

The only thing that is certain about science is uncertainty. Although chromatographic methods are likely to dominate separation science for the first part of the twenty-first century, it would be a foolish person who predicts their form, continuing development, and main applications. Throughout the history of chromatography general approaches have had to adapt to changing needs brought about by dramatic shifts in the focus on different types of applications, and this has a significant impact on the relative importance of the various techniques. However, chromatography should be considered as an holistic

approach to separations, and will be better understood and correctly employed if we abandon the current trend to compartmentalize the technique based on specialization in individual subject areas.

See Colour Plate 3.

Further Reading

- Berger TA (1995) *Packed Column Supercritical Fluid Chromatography*. Cambridge: Royal Society of Chemistry.
- Braithwaite A and Smith FJ (1996) *Chromatographic Methods*. London: Blackie Academic & Professional.
- Giddings JC (1991) *Unified Separation Science*. New York: Wiley-Interscience.
- Guiochon G and Guilleman CL (1988) *Quantitative Gas Chromatography for Laboratory Analysis and On-Line Process Control*. Amsterdam: Elsevier.
- Guiochon G, Shirazi SG and Katti AM (1994) *Fundamentals of Preparative and Nonlinear Chromatography*. Boston: Academic Press.
- Heftmann E (1992) *Chromatography*, Parts A and B. Amsterdam: Elsevier.
- Jennings W, Mittlefehldt E and Stremple P (1997) *Analytical Gas Chromatography*. San Diego: Academic Press.
- Lee ML, Yang FJ and Bartle KD (1984) *Open Tubular Column Gas Chromatography. Theory and Practice*. New York: Wiley-Interscience.
- Li SFY (1992) *Capillary Electrophoresis. Principles, Practice and Applications*. Amsterdam: Elsevier.
- Poole CF and Poole SK (1991) *Chromatography Today*. Amsterdam: Elsevier.
- Robards K, Haddad PR and Jackson PE (1994) *Principles and Practice of Modern Chromatographic Methods*. London: Academic Press.
- Sherma J and Fried B (1997) *Handbook of Thin-Layer Chromatography*. New York: Marcel Dekker.
- Snyder LR, Kirkland JJ and Glajch JL (1997) *Practical HPLC Method Development*. New York: J Wiley.

CRYSTALLIZATION



H. J. M. Kramer and G. M. van Rosmalen,
Delft University of Technology, Delft, The Netherlands
Copyright © 2000 Academic Press

Introduction

Crystallization from solution is a separation technique where a solid phase is separated from a mother liquor. In contrast to other separation processes,

however, the dispersed phase consisting of numerous solid particles also forms the final product, that has to meet the required product specifications. Crystallization can thus also be seen as a technique to obtain solid products, where the crystallization process has to be carefully controlled in order to meet the ever-increasing demands of the customer on particle properties like particle size distribution, crystal shape, degree of agglomeration, caking behaviour and purity. Since the particles must also be easily

separated from the mother liquor, additional demands on filterability and washability can be formulated.

Because of the mostly rigid structure of the solid phase, the formation of solid particles is a rather slow process, and to reach an acceptable production rate large vessels are generally needed. This rigid structure on the other hand impedes the incorporation of foreign substances or solvent molecules, and in only one separation step a pure solid product is obtained.

Crystallization is often used as a generic term for evaporative or cooling crystallization, precipitation and melt crystallization. There are, however, considerable differences between the three types of crystallization as far as the processing method and the corresponding equipment are concerned. In precipitation the drop-out of the solid phase is achieved by mixing two feed streams that are either two reactants or a solvent containing the solute and an antisolvent. The hydrodynamics of the process therefore play a predominant role in precipitation with regard to the properties of the obtained product.

In melt crystallization the potential of crystallization to produce a pure product is mainly utilized, and the solid phase is remolten to obtain the final product. The applications are mainly in the ultrapurification of organic compounds or to produce pure water as a concentration technique.

An upcoming technique in crystallization is supercritical crystallization, mostly with condensed CO₂, because of its benign properties compared to organic solvents. Condensed CO₂ can be used either as a solvent or as an antisolvent, and specifically adapted processes and equipment have been developed for these high pressure crystallization techniques.

Also the crystallization of proteins requires its own dedicated approach, because large, sometimes easily degradable molecules require carefully designed processes.

Because 70% of the products sold by the process industry and the pharmaceutical industry – as bulk products, intermediates, fine chemicals, biochemicals, food additives and pharmaceutical products – are solids, crystallization in its widest definition is the largest separation process after distillation.

Although this chapter will primarily focus on evaporative and cooling crystallization, the energy, mass and population balances treated here as well as the kinetic rate expressions for the physical processes such as nucleation, growth and agglomeration and the characterization of the particles can equally be applied to the other types of crystallization.

Several books on the diverse aspects of crystallization have been published over the last 10 years. These books that can be recommended for a wide overview

in this field contain an abundance of references. The authors of these books are Mersmann (1995), Mullin (1993), Randolph and Larsen (1987), Myerson (1993), Nývlt (1992), Tavare (1995) and Hurlé (1993). Söhnel and Garside (1992) have written a book on precipitation and Arkenbout (1995) a book on melt crystallization.

This article reviews industrial evaporation and cooling crystallization processes. A basic modelling approach is presented which enables the analysis and design of industrial crystallization processes, either by analytical calculations or by making use of modern computational tools.

Crystallization Methods and Supersaturation

Crystallization only occurs when supersaturation is created that acts as the driving force for crystallization. The crystallization method is mainly chosen on the basis of the thermodynamic and physical properties of the compound and the solvent, as well as on the required purity of the product. There are several ways to represent the phase diagram, depending on the mode of crystallization. For evaporative and cooling crystallization a solubility diagram is mostly used, in which the solubility of the compound is expressed as a function of temperature. In precipitation the solubility is always very low, and the solubility product at the operating temperature is needed. In antisolvent precipitation, the solubility diagram mostly has to be determined for the particular three-phase system. In melt cooling crystallization T - x diagrams are used, while for melt pressure crystallization pT - x diagrams are needed.

A decision scheme for the selection of the appropriate crystallization method is presented in **Figure 1**. For a high purity product or when the use of a solvent poses environmental or safety problems, melt crystallization is chosen. A melt temperature lying between 0 and 100°C is preferred, since at higher temperatures many organic compounds become unstable, while at temperatures below 0°C operating the process becomes more difficult, although not impossible. A high viscosity of the melt hampers the operation.

At solubilities below about 1 mass %, the process is designed as a precipitation process to obtain a reasonable production rate. The supersaturation that is generated by the mixing of reactants often reaches high values. Also in antisolvent crystallization, low solubility of the solute and high supersaturation are reached by mixing two solvents.

Finally, for the more easily soluble substances the choice between cooling and evaporative crystallization

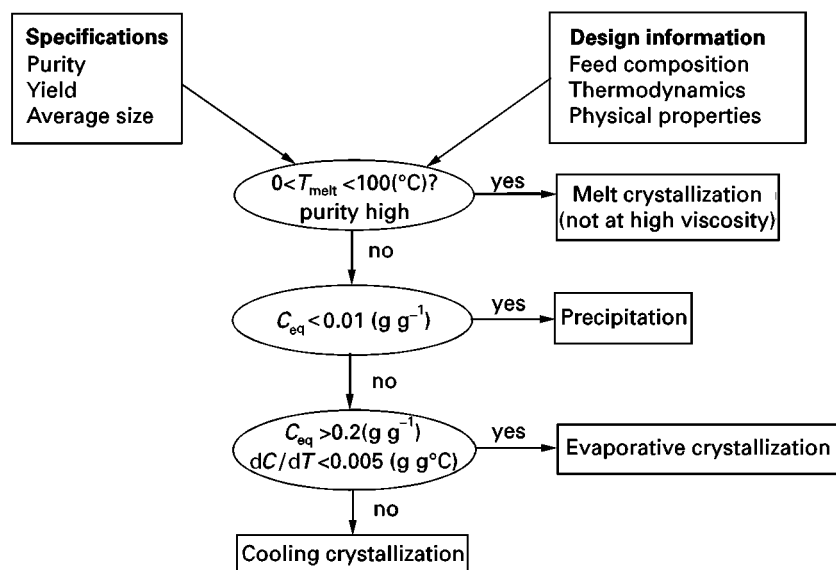


Figure 1 Decision diagram for choosing the method of crystallization.

is made on the basis of the solubility curve, and the prevailing supersaturations are generally low. Especially where water is the solvent, cooling crystallization is more favourable than evaporative crystallization, except for highly soluble substances. Therefore, multi-effect flash evaporation where the vapour is used for heating next crystallizer or the feed stream is frequently applied to reduce the energy costs, if evaporative crystallization is applied.

In cooling crystallization direct cooling, flash cooling or indirect cooling can be applied. Where indirect cooling is used encrustation on the cooling surfaces must be minimized. In flash cooling this problem is largely avoided at the expense of a more complicated installation. Also direct cooling uses an inert cooling medium or refrigerant that is bubbled directly into the solution and evaporates does not suffer from abundant incrustation, but needs recompression of the cooling medium.

So, in these various methods of crystallization, supersaturation is created by cooling, by evaporation of solvent or by a combination of the two in the case of flash evaporation or flash cooling, or by mixing two reactants or solvents. In all these cases the actual concentration is higher than the equilibrium concentration, and a driving force for crystallization is achieved.

From a thermodynamic point of view this driving force is reflected by the difference in chemical potential of the solute in the liquid and in the solid phase at temperature T :

$$\Delta\mu = \mu_L(T) - \mu_S(T) \quad [1]$$

For cooling crystallization from the melt or the solution, eqn [1] can be transformed into:

$$\Delta\mu = \frac{\Delta H_{eq}}{T^*} \cdot \Delta T \quad [2]$$

For melt pressure crystallization:

$$\Delta\mu = \Delta V_{molar} \Delta P = \frac{\Delta\rho}{\rho_{melt}\rho_{solid}} \cdot \Delta P \quad [3]$$

For practical reasons the supersaturation in cooling is mostly indicated by:

$$\Delta T = T - T^* \quad [4]$$

and can also be translated via the solubility curve into a concentration difference:

$$\Delta c = c - c^* \quad [5]$$

Other frequently used expressions are the dimensionless saturation ratio:

$$S = \frac{c}{c^*} \quad [6]$$

or the relative supersaturation:

$$\sigma = \frac{c - c^*}{c^*} = \frac{\Delta c}{c^*} = S - 1 \quad [7]$$

Here c can be expressed by kg solute per kg or m^3 of the solvent or solution, but an expression in kg solute per m^3 solution (=liquid) phase is generally used in mass balances (=mass fraction, w).

For evaporative crystallization, eqn [1] can be transformed into:

$$\Delta\mu = RT \ln\left(\frac{a}{a_{\text{eq}}}\right) = RT \ln\left(\frac{\gamma c}{\gamma_{\text{eq}} c^*}\right) \quad [8]$$

Given the relatively low supersaturations, σ , that often lie between 0.001 and 0.01 with more easily soluble substances, eqn [8] simplifies into:

$$\Delta\mu = RT \frac{\Delta c}{c^*} = RT\sigma \quad [9]$$

For two or more A and B ions in solution that react to form crystal c , the expression for $\Delta\mu$ becomes:

$$\Delta\mu = RT \ln \frac{\prod_i a_i^{\nu_i}}{K_{\text{sp}}} \quad [10]$$

and for stoichiometric solutions equals:

$$\Delta\mu = RT\nu \ln S \approx RT\nu\sigma \quad [11]$$

In practice the supersaturation is often indicated by eqn [5].

For flash cooling or evaporation two terms contribute to the driving force (ΔT and Δc).

For precipitation, no simplifications are allowed, owing to the high supersaturation values ($\sigma \gg 1$), and either eqn [8] or eqn [10] is used. For antisolvent precipitation the value of c depends on the actual concentration of the solute in the original solvent and, like c^* , on the degree of dilution by the antisolvent.

Mass and Heat Balances

Traditional design of an industrial crystallizer is based on only mass and enthalpy balances. The production rate determines to a large extent the dimensions of the crystallizer as well as the energy consumption. It also determines the mode of operation, which means batchwise or continuous, single or multistage operation. In the next section the balance equations are given for an evaporative and for a cooling crystallizer.

Evaporative Crystallizers

Consider an ideally mixed vessel. The composition of the product stream is kept similar to that of the

content of the crystallizer. The volume, V , of the crystallizer is often assumed to be constant in eqns [12–19]. However, by making V and the feed streams time-dependent, dynamic effects can be taken into account, and thus also batch processes. The mass balance is given by:

$$\begin{aligned} \frac{dM_{\text{total}}}{dt} = & \phi_{v,\text{feed}}(\varepsilon_{\text{feed}}\rho_{\text{feed,liquid}} + (1 - \varepsilon_{\text{feed}})\rho_{\text{crystal}}) \\ & - \phi_{v,\text{prod}}(\varepsilon\rho_{\text{liquid}} + (1 - \varepsilon)\rho_{\text{crys}}) - \phi_{v,\text{vapour}}\rho_{\text{vapour}} \end{aligned} \quad [12]$$

The component balances are given by:

$$\begin{aligned} \frac{dM_i}{dt} = & \phi_{v,\text{feed}}\left(\varepsilon_{\text{feed}}\rho_{\text{feed,liquid}}w_{\text{feed,liquid},i} + (1 - \varepsilon_{\text{feed}})\rho_{\text{crystal}}w_{\text{feed,crystal},i}\right) \\ & - \phi_{v,\text{prod}}(\varepsilon\rho_{\text{liquid}}w_{\text{liquid},i} + (1 - \varepsilon)\rho_{\text{crystal}}w_{\text{crystal},i}) \end{aligned} \quad [13]$$

($i = 1, N_{\text{comp}}$)

with:

$$M_i = V(\varepsilon\rho_{\text{liquid}}w_{\text{liquid},i} + (1 - \varepsilon)\rho_{\text{crystal}}w_{\text{crystal},i}) \quad [14]$$

where component $i = 1$ is the main compound to be crystallized, and components $i = 2, 3, \dots, N_{\text{comp}}$ are the impurities present.

The distribution coefficients relate the impurity uptake by the solid and the concentration of the impurity in the liquid phase:

$$k_{\text{distr},i} = \frac{w_{\text{crystal},i}}{w_{\text{liquid},i}} \quad (i = 2, \dots, N_{\text{comp}}) \quad [15]$$

Instead of substituting all component balances into the total mass balance given by eqn [12] to solve the mass balance of the total system, it is more convenient to combine the solvent mass balance together with the component balances:

$$\begin{aligned} \frac{dV\varepsilon\rho_{\text{liquid}}w_{\text{liquid,solvent}}}{dt} = & \phi_{v,\text{feed}}(\varepsilon_{\text{feed}}\rho_{\text{feed,liquid}}w_{\text{feed,solvent}}) \\ & - \phi_{v,\text{prod}}(\varepsilon\rho_{\text{liquid}}w_{\text{liquid,solvent}}) \\ & - \phi_{v,\text{vapour}}\rho_{\text{vapour}} \end{aligned} \quad [16]$$

Finally, the sum of the mass fractions in both the liquid and the solid phase must equal one:

$$w_{\text{liquid,solvent}} + \sum_i w_{\text{liquid},i} = 1 \quad [17]$$

$$\sum_i w_{\text{crystal},i} = 1 \quad [18]$$

The enthalpy balance with the production rate or solids production, P , is given by:

$$\frac{dH}{dt} = \phi_{H,feed} - \phi_{H,prod} - \phi_{H,vapour} + Q_{heat} + P\Delta H_{cr} \quad [19]$$

The total enthalpy and the enthalpy of the streams are defined as:

$$\begin{aligned} H &= V(\varepsilon\rho_{liquid}C_{p,liquid} + (1 - \varepsilon)\rho_{crystal}C_{p,crystal})T \\ \phi_{H,feed} &= \phi_{v,feed}(\varepsilon_{feed}\rho_{feed,liquid}C_{p,liquid} \\ &\quad + (1 - \varepsilon_{feed})\rho_{crystal}C_{p,crystal})T_{feed} \\ \phi_{H,prod} &= \phi_{v,prod}(\varepsilon\rho_{liquid}C_{p,liquid} + (1 - \varepsilon)\rho_{crystal}C_{p,crystal})T \\ \phi_{H,vapour} &= \phi_{v,vapour}(\rho_{vapour}C_{p,vapour}T + \rho_{vapour}\Delta H_{evap}) \end{aligned} \quad [20]$$

The crystal free volume fraction ε should be as low as possible to reduce the crystallizer volume.

The liquid mass fraction $w_{liquid,1}$ of the main component must be determined or can be approximated by the saturation concentration, especially for soluble compounds with a low σ value.

With the production rate, P , as a design parameter, the volumetric product flow rate can be deduced for the chosen ε value from:

$$P = \phi_{v,prod}(1 - \varepsilon)\rho_{crystal} = \phi_{v,prod}M_T \quad [21]$$

From the product flow rate so obtained and the mean residence time that is needed to grow sufficiently large crystals, the necessary suspension volume for the crystallizer can be calculated from:

$$\phi_{v,prod} = \frac{V}{\tau} \quad [22]$$

$$\tau = \frac{L_{mean}}{4G_{mean}} \quad [23]$$

Here, for the desired L_{mean} , a reasonable value must be chosen, that is related to its solubility and the mean growth rate, G_{mean} , can be estimated from a correlation (Mersmann, 1988; Kind and Mersmann 1990) or determined by laboratory experiments.

From the crystallizer suspension volume, V , the needed vapour head, the process streams and the heat duty that has to be accommodated, the crystallizer dimensions can now be determined. Constraints for the design are a height/diameter ratio of about 3 : 2, and a cross-sectional area for evaporation that is large enough to avoid entrainment of liquid droplets

into the condensor. For the design of the heat exchanger see Sinnott (1998).

Cooling Crystallizers

In cooling crystallization the warm feed stream is cooled to the process temperature. In principle the same set of mass and heat balance equations can be used, except that no vapour flow exists. Furthermore, the process temperature cannot freely be chosen, because it is determined for a given production rate, crystal free fraction, ε , residence time, τ and liquid mass fraction, $w_{liquid,1}$. This latter liquid mass fraction of the main component will depend on the process temperature, so a temperature-dependent equation for $w_{liquid,1}$ must be added. The degrees of freedom for the crystallizer design are therefore more limited.

The Population Balance

The Crystal Length-based Population Balance Equation

In crystallization as a separation process, the separability of the particles from the mother liquor by, for example, filtration are of utmost importance, as well as their washability and drying. The efficiency of these processes is directly related to the crystal size distribution (CSD) of the solid, and as soon as the CSD of the solid phase becomes an interesting product specification, the population balance equation (PBE) must be introduced. The PBE describes how the size distribution develops in time as a result of various kinetic processes. The concept of the PBE was introduced to crystallization by Randolph. A general form of the PBE is as follows:

$$\begin{aligned} \frac{\partial(n(L)V)}{\partial t} &= -V\frac{\partial(G_L(L)n(L))}{\partial L} + B(L)V - D(L)V \\ &\quad + \sum_{j=1}^m \phi_{v,in,j}n_{in,j}(L) - \sum_{k=1}^n \phi_{v,out,k}h_{out,k}(L)n(L) \end{aligned} \quad [24]$$

where the amount and the size of the crystals (or particles) are expressed in terms of number density $n(L)$ ($\#/(m^3m)$) and crystal (or particle) length L (m) respectively (Figure 2A).

All the variables in this equation are in principle also time-dependent. For the sake of simplicity, the t dependence is omitted here.

In other representations of the PBE, the amount of particles may also be expressed in terms of volume density $\nu(L)$ ($m^3/(m^3m^1)$) or mass density $m(L)$ ($kg/(m^3m^1)$, where the size is represented by the

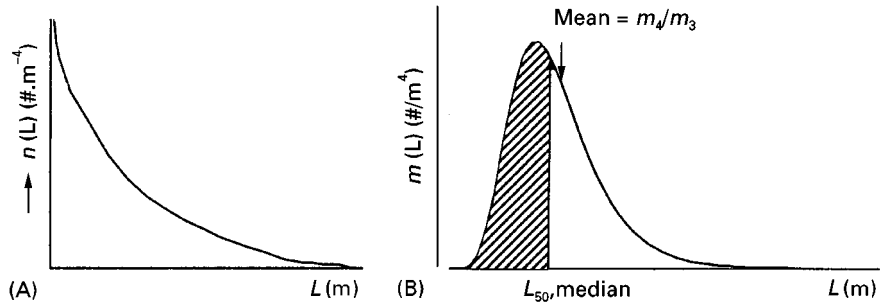


Figure 2 (A) Number and (B) mass distribution of a crystal population.

length L (Figure 2B). Figure 2 also shows two often-used values which characterize the crystal size distribution, the mean crystal size and the volume-based median size (the size at which the integral over the $m(L)$ curve from zero to L_{50} equals half of the integral over the entire curve).

For particle sizes given in terms of volume, the corresponding number density becomes $n(v)$ instead of $n(L)$. The latter representation becomes more convenient if agglomeration of crystals plays an important role.

In eqn [24] V is the suspension volume in the crystallizer with m streams entering and n streams leaving the crystallizer with volumetric flow rates ϕ_v .

$G_L(L)$ is the linear size-dependent growth rate (m s^{-1}), and $B(L)$ and $D(L)$ are birth and death terms

respectively ($\# \text{m}^{-3} \text{m}^{-1}$). Birth and death events can be caused by agglomeration and disruption of earlier agglomerated particles, but also by breakage of crystals and by the birth of small crystals, called nuclei. Breakage of crystals will not happen under normal operating conditions.

The classification function $h(L)$ describes the relation between the CSD in the crystallizer and that on an outlet stream.

The processes on the right-hand side of eqn [24] that lead to the crystal population in a certain size interval, dL , are depicted in Figure 3. In the PBE given by eqn [24] all operation modes are represented. The difference between batch and continuous processes only influences the in- and outflow terms on the right-hand side of the PBE.

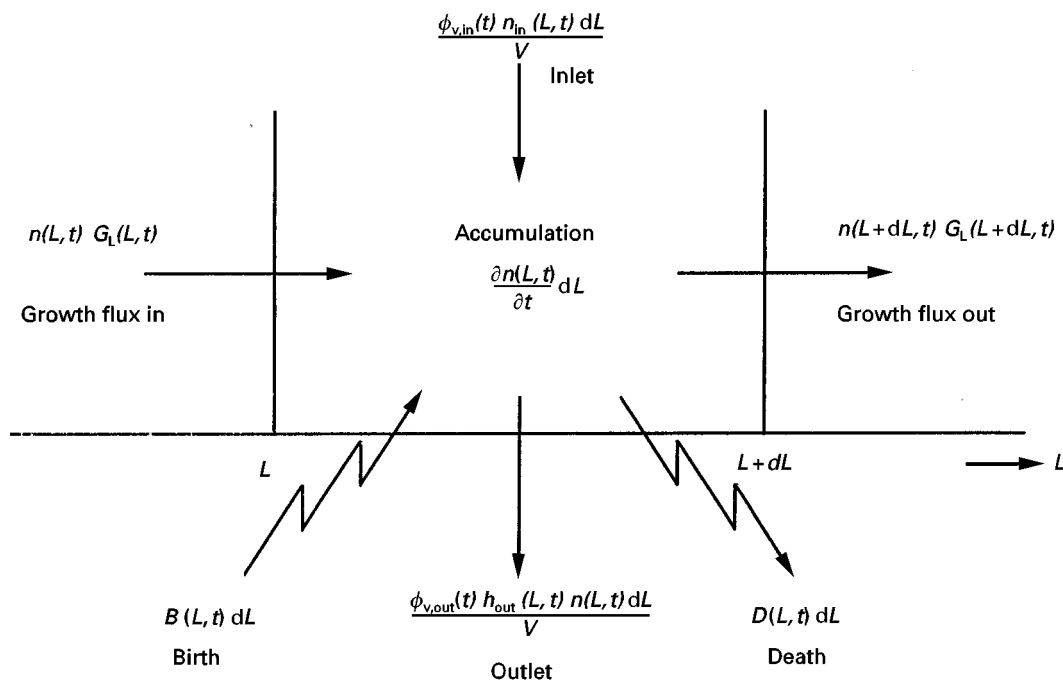


Figure 3 Schematic depiction of the processes affecting the CSD. In an infinitesimally small size range from L to $L + dL$, crystals may enter and leave due to growth, aggregation, attrition, breakage and volumetric input and output flow streams.

As the PBE is a partial differential equation with respect to time t and crystal length L , two boundary conditions are needed to solve it analytically:

$$n(0, t) = \frac{B_0}{G_L(0)} \quad [25]$$

$$n(L, 0) = \text{initial distribution} \quad [26]$$

As primary and secondary nucleation typically involve the birth of small crystals, nucleation is often presented as the birth of nuclei at zero size. Instead of a birth term in the PBE for the nucleation event $B(L)$ that happens over a size range $0 \leq L \leq y$, the birth rate B_0 given by the boundary eqn [25] is used. These two are related by:

$$B_0 = \int_0^y B(L) dL \quad [27]$$

For the second boundary condition, a seed population or a population formed by the outgrowth of primary nuclei can be substituted.

Population Balance Equation for Stationary Operation

For continuous crystallization the PBE can be simplified by assuming that:

1. a steady state is reached
2. there is one crystal-free inlet stream
3. nucleation only occurs at zero size and is given by the boundary condition at $L = 0$ (eqn [25])
4. growth is size-independent, $G_L(L) = G_L$
5. the crystallizer volume is constant in t
6. there is no agglomeration or breakage

This results in:

$$VG_L \frac{\partial n(L)}{\partial L} + \sum_{k=1}^n \phi_{v, \text{out}, k} h_{\text{out}, k}(L) n(L) = 0 \quad [28]$$

If the crystallizer content is also well mixed, and there is only one nonclassified outflow, i.e. $h(L) = 1$, this equation becomes:

$$VG_L \frac{\partial n(L)}{\partial L} + \phi_{v, \text{out}} n(L) = 0 \quad [29]$$

Such a crystallizer is named a mixed suspension mixed product removal (MSMPR) crystallizer.

Integration of eqn [29] leads to:

$$n(L) = n(0) \exp\left(-\frac{L}{G_L \tau}\right) \quad [30]$$

By plotting $\ln(n(L))$ versus L , the kinetic growth rate G_L can be derived from the slope of the straight line, and the nucleation rate B_0 from the intercept with the y axis.

The number of process parameters that can be varied for a specific crystallizer in order to shift the CSD and in particular the mean crystal size is usually very limited. Typical process actuators are fines removal and product classification. Their influence on the CSD can be analytically solved by introducing more classified outflow streams, which cause different residence times for the mother liquor and the fine, medium and large crystals in the crystallizer. A generic numeric solution is achieved more easily, as will be addressed later.

Moment Equations for Stationary and In-Stationary Operation

Analytical solutions of the PBE for in-stationary crystallizers hardly exist. By transforming the PBE into a moment form, however, analytical solutions are attained that allow us to describe the dynamical behaviour of crystallizers in terms of the moments of the distribution. The moments are defined as:

$$m_i = \int_0^\infty n(x) x^i dx \quad [31]$$

and the first five moments are related to measurable physical properties of the distribution, as shown in **Table 1**. The shape factors k_a and k_v relate the crystal length to its surface area and volume respectively.

For a continuously operated system with a constant V , a size-independent growth rate, no agglomeration, nucleation at zero size, one crystal-free inlet stream, and a nonclassified product stream, the PBE presented in eqn [24] transforms into:

$$\frac{\partial n(L)}{\partial t} = -G_L \frac{\partial n(L)}{\partial L} - \frac{n(L)}{\tau} \quad [32]$$

Table 1 Physical properties of the moments of the distribution

Property	Symbol	Moment equation
Total number	N_T	m_0
Total length	L_T	m_1
Total surface area	A_T	$k_a m_2$
Total volume	V_T	$k_v m_3$
Total mass	M_T	$\rho k_v m_3$

with similar boundary conditions. This equation can be reduced to a set of ordinary differential equations by means of the moment transformation:

$$\frac{dm_j}{dt} = jG_L m_{j-1} - \frac{m_j}{\tau} + B_0 L_0^j \quad [33]$$

where L_0 , the size of the nuclei, is here zero. Only the first four moment equations ($j = 0-3$) have to be solved to obtain all the information about the lumped properties of the CSD.

Population Balance Equation for Batch Operation

For batch operation, the PBE (eqn [24]) can be simplified by assuming that:

1. the inlet stream is crystal-free
2. nucleation only occurs at zero size, and is reflected by the boundary condition at $L = 0$ (eqn [25])
3. growth is size-independent
4. there is no agglomeration or disruption

This results in:

$$\frac{\partial n(L)V}{\partial t} = -VG_L \frac{\partial n(L)}{\partial L} \quad [34]$$

Since batch operation is inherently ‘in-stationary’, a moment transformation is needed to obtain analytical solutions to the PBE. This leads to

$$d \frac{d(Vm_j)}{dt} = jG_L m_{j-1} V + B_0 L_0^j V \quad [35]$$

where the size of the nuclei, L_0 , is zero. Again ordinary differential equations ($j = 0-3$) have to be solved to attain the lumped properties of the CSD.

To improve the CSD, a controlled cooling or evaporation trajectory can be imposed.

The Crystal Volume-Based Population Balance Equation

When a crystallizing system depends purely on nucleation and growth processes, it is favourable to use a PBE with length as the crystal size co-ordinate. For kinetic processes where the volume of particles are combined or split up, like in agglomeration and disruption, a PBE with the particle volume as crystal size coordinate is preferred. This leads to:

$$\begin{aligned} \frac{\partial(n(v)V)}{\partial t} = & -V \frac{\partial(G_v(v)n(v))}{\partial v} + B(v)V - D(v)V \\ & + \sum_{j=1}^m \phi_{v,in,j} n_{in,j}(v) - \sum_{k=1}^n \phi_{v,out,k} b_{out,k}(v)n(v) \end{aligned} \quad [36]$$

A volumetric growth rate is then required. Crystal growth rates are, however, available in length-based rates, so $G(v)$ has to be calculated from:

$$G_v(v) = \frac{dv}{dL} G_L = 3k_v L^2 G_L \quad [37]$$

This expression prohibits the introduction of zero-sized nuclei as a boundary condition, and nucleation has to be modelled as birth within a certain size interval.

The number of particles in a certain size interval must be the same, regardless of whether the bounds of that interval are expressed in terms of length of volume. This implies that:

$$n(L) dL = n(v) dv \quad [38]$$

and, after some rewriting, the following transformation equations:

$$n(L) = 3k_v L^2 n(v)$$

$$n(v) = \frac{1}{3\sqrt[3]{k_v v^2}} n(L) \quad [39]$$

Agglomeration and Disruption

To solve the PBE where there is agglomeration and disruption of earlier agglomerated particles, the birth and death terms for these processes must be derived.

The rate of agglomeration, r , is given by:

$$r(v_1, v_2) = \beta(v_1, v_2, \sigma, \varepsilon) n(v_1) n(v_2) \quad [40]$$

The rate constant, β , commonly called the agglomeration kernel, depends on the particle sizes v_1 and v_2 , the supersaturation σ and the turbulence level, represented by the power input ε . The birth and death terms associated with the agglomeration of two particles, resulting in the birth of a new one and the death of the original two, are:

$$B(v) = \frac{1}{2} \int_0^v \beta(u, v-u) n(u) n(v-u) du \quad [41]$$

$$D(v) = n(v) \int_0^\infty \beta(u, v) n(u) du \quad [42]$$

The factor $\frac{1}{2}$ is needed to avoid double-counting, since the integral takes each interaction twice. The dependency of β on σ and ε has been omitted here for notation simplicity.

There is also disruption of earlier agglomerated particles with a corresponding disruption rate. This disruption process of earlier agglomerated particles

can be described in the PBE by an additional death term for the disrupted particles, and an additional birth term for the newly formed particles:

$$D(v) = S(v, \varepsilon) \cdot n(v) \quad [43]$$

$$B(v) = \int_v^\infty b(v, u) S(u, \varepsilon) n(u) du \quad [44]$$

where $S(v)$ is a selection function that describes the rate at which particles fall apart, and b is a breakage function that describes how many particles of size v are formed on disruption of a particle of size u .

Often, the disruption terms are loaded into the agglomeration kernel β , which then represents the effective agglomeration kernel. In that case terms expressed by the eqns [43] and [44] can be left out and only eqns [41] and [42] are needed for substitution in the PBE. The main disadvantage of this lumped description of the whole agglomeration process is that prediction of the agglomeration behaviour for different hydrodynamic conditions (and thus for different scales and geometries) becomes virtually impossible because β and σ have a different dependency on ε .

The PBE with agglomeration and disruption terms can rarely be solved analytically. A moment transformation is again required with the moments defined as:

$$m_i = \int_0^\infty n(v) v^i dv \quad [45]$$

where v represents crystal size volume v . The zero moment is again the total number of particles, but the first moment of the volume-based CSD already equals the third moment of the length-based CSD.

Substitution of the above expressions into the PBE (eqn [36]) for a system with agglomeration and growth and no nucleation, with a constant crystallizer volume, only one crystal-free inlet stream and a nonclassified product stream, results after a moment transformation in:

$$\frac{dm_i}{dt} = -\frac{m_i}{\tau} + jG_v m_{i-1} + \overline{B_{\text{aggl},j}} - \overline{D_{\text{aggl},j}} \quad [46]$$

where the moment forms of B and D due to agglomeration are defined as:

$$\overline{B_{\text{aggl},j}} = \int_0^\infty v^j B dv \quad [47]$$

$$\overline{D_{\text{aggl},j}} = \int_0^\infty v^j D dv \quad [48]$$

A solution is only obtained for a size-independent kernel β_0 . For a batch-agglomerating system (without growth), only solutions for m_0 and m_1 (which is equal to the m_3 in size coordinates) are obtained:

$$\frac{dm_0}{dt} = -\frac{1}{2}\beta_0 m_0^2 \quad [49]$$

$$\frac{dm_1}{dt} = 0 \quad [50]$$

The numerical solution of the population balance for cases where nucleation, growth and agglomeration is present often imposes a problem, because no analytical solution exists and the generation of numerical solutions is not easy. It is essential to divide the size axis into proper size intervals to obtain reliable results and to transform the population balance, a partial differential equation, into a set of ordinary differential equations. Hounslow *et al.* presented a numerical scheme based on a geometrical discretization of the size axis in which for each size interval the ratio between the upper and lower boundary r is exactly equal to $\sqrt[3]{2}$. Although accurate results are obtained in the absence of crystal growth and nucleation, the method is in general not accurate enough in the presence of these crystallization phenomena and gives rise to an overestimation of the higher moments. An improved finite-element technique has been introduced to solve the steady-state solution of the population balance for nucleation, growth and agglomeration.

Kinetic Expressions

In order to solve the population balance equation, kinetic expressions are needed to represent the physical processes that take place in the crystallizer, such as nucleation, growth and agglomeration. Their mechanisms and the corresponding equations will be treated here.

Nucleation

Two different nucleation mechanisms can be distinguished: primary and secondary nucleation.

Primary nucleation is new phase formation from a clear liquid or solution. It can be subdivided into homogeneous and heterogeneous nucleation. In the latter case a foreign substrate of tiny invisible particles, e.g. dust or dirt particles, is present in the solution on which nucleation starts. In homogeneous nucleation such a substrate is absent and nuclei are formed by statistical fluctuations of solute entities that cluster together.

Secondary nucleation is the breeding of nuclei from crystals of the crystallizing material that are already present in the solution. These nuclei are in general attrition fragments, and result from collisions of the larger crystals with the hardware of the crystallizer, in particular with the blades of impellers and pumps. At high solid densities in the crystallizer collisions between the larger crystals can create fragments that act as secondary nuclei.

During the start-up phase of evaporative or cooling crystallization of moderately to very soluble compounds, primary nucleation takes place. After their outgrowth to larger crystals, secondary nucleation takes over, and becomes the most important source of nuclei at low supersaturation values. For precipitation of slightly soluble compounds the process generally remains dominated by primary nucleation for two reasons. Supersaturation remains high enough, especially at the inlet points of the feed streams, to produce primary nuclei, and the often agglomerated crystals remain too small to be prone to attrition.

Homogeneous primary nucleation Local fluctuations in concentration induce the formation of numerous clusters that can fall apart again. In under- or just saturated solutions, cluster formation and cluster decay are in equilibrium; it is a reversible process. In supersaturated solutions, however, clusters of a critical size are formed that either fall apart or grow out. In the classical nucleation theory of Volmer, Becker and Döring, these clusters are formed by the attachment and detachment of single solute entities. Although clusters can also grow by the collision of clusters, their concentration is always so much lower than that of single solute entities that this process of cluster enlargement can be ignored.

The critical size of a cluster that is represented by its critical radius, r^* , is given by:

$$r^* = 2\gamma \frac{V_{\text{molar}}}{\Delta\mu} \quad [51]$$

and is thus related to the supersaturation via $\Delta\mu$, and to the interfacial tension γ .

For the homogeneous nucleation rate, J_{homo} ($\#m^{-3}$), the following equation can be derived after some simplifications:

$$J_{\text{homo}} = AS \exp\left(\frac{16\pi\gamma^3 V_{\text{molar}}^2}{3k^3 T^3 (\ln S)^2}\right) \quad [52]$$

In this Arrhenius type of expression, changes in the supersaturation ratio S in the pre-exponential factors $A \cdot S$ are of minor influence compared to changes in S in the exponential term. Various authors use dif-

ferent expressions for A and this can cause considerable differences in the attained values of J (Merzmann, 1995; Söhnel and Garside, 1992; Kashchiev, 2000).

Heterogeneous primary nucleation The occurrence of homogeneous nucleation is rare, in practice since nucleation on a foreign substrate will substantially reduce the nucleation barrier. For this type of nucleation, a similar rate equation can be used:

$$J_{\text{hetero}} = A_{\text{hetero}} S \exp\left(\frac{16\pi\gamma^3 V_{\text{molar}}^2}{3k^3 T^3 (\ln S)^2}\right) \quad [53]$$

where the interfacial tension γ is replaced by a much lower γ_{eff} . Although A_{hetero} is lower than A , the effect of the exponential term dominates up to very high supersaturation values, that are rarely met in practice (Figure 4).

Secondary nucleation The classic expression for the secondary nucleation rate in a suspension of growing crystals, B_0 , is the empirical power law, based on three experimentally accessible parameters that were recognized already early on to be important:

$$B_0 = k_N G^i N^h M_T^j \quad [54]$$

Since the growth rate is directly related to the supersaturation σ , and the rotational speed to the power input, the power law can also be written as:

$$B_0 = k_N^1 \sigma^b \varepsilon^k M_T^j \quad [55]$$

Frequently measured values for b , k and j under steady-state conditions are $1 < b < 3$, $0.6 < k < 0.7$ and $j = 1$ or 2 . For nucleation dominated by crystal-impeller collisions $j = 2$, while for nucleation ruled by crystal-crystal collisions, $j = 2$.

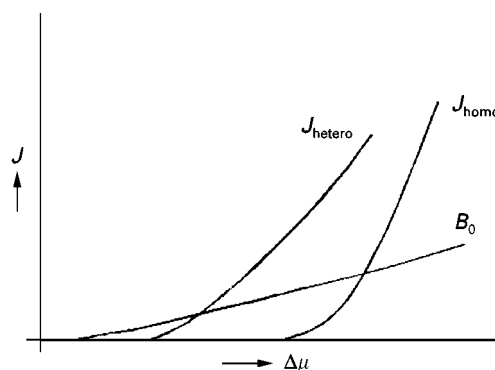


Figure 4 Nucleation rate as a function of the supersaturation ($\Delta\mu$). J_{homo} and J_{hetero} , homogeneous and heterogeneous nucleation rate; B_0 , secondary nucleation rate.

Also the crystallizer geometry-like type of stirrers or pumps, and number of blades, as well as the scale of operation influence the attrition rate of the crystals. These effects were supposed to be included in k_N of k_N^1 , that could only be established experimentally. The power law with its four parameters, used together with other kinetic parameters (e.g. those related to the growth of the crystals) seems to be perfectly adequate to describe the steady-state median crystal size in continuous crystallization processes.

The power law, however, fails to describe the dynamics of a crystallization process. If, for example, the median crystal size is plotted versus time from immediately after the start-up, often an oscillating behaviour is observed that dampens out until finally a steady-state value is reached (Figure 5). This oscillating behaviour can be explained by the observation that only crystals above a certain size breed secondary nuclei by attrition. The first nuclei are created by primary nucleation and grow out, which causes the supersaturation to decrease. When the mean size has reached its first peak, more of the larger crystals are withdrawn with the product than are grown into the larger crystal sizes by outgrowth of secondary nuclei. This happens because at the early stages no large crystals are available for breeding.

Some groups have tried to account for this phenomenon by adding a target efficiency to the power law that is a function of the crystal size. One author, Eek, allowed only crystals above a certain size to breed. This improved the simulations, although none of them was fully successful.

An attrition function for the crystals, was introduced by O'Meadhra based on the approach of Mersmann. He distributed the attrited volume over the small crystal sizes. In this way a birth function $B(L)$ was calculated from the volumetric attrition rate. A disadvantage of this modelling, in common with the power law, is that it has no predictive value, since

the attrition function also must be determined experimentally for the particular crystallizer.

Gahn and Mersmann were the first to derive a secondary nucleation rate model based on physical attrition properties. Their approach comprises three consecutive steps and calculates the secondary nucleation rate of crystals that collide with the blades of an impeller.

1. A simplified flow pattern based on geometric considerations as presented by Ploss *et al.* is used to calculate the impact velocity and the chance of crystals from size class i to collide with an impeller segment j .
2. Subsequently a model was developed to calculate the volume of attrition fragments produced during a single collision of a crystal corner represented by a cone, and a hard flat surface of the impeller. The model relates the attrited volume of crystal i and segment j to the impact energy of the crystal collision via its relevant mechanical properties, such as the Vickers hardness, the fracture resistance of the substance and the shear modulus. The model assumes that the circulation time is sufficient to heal the damaged crystal corner before a subsequent collision of the same corner takes place. This assumption is often not valid for crystallizers up to 100 L. A minimum impact energy required to cause fracture can also be derived, and thus the minimum crystal size for a given velocity profile is prone to attrition. The model also provides a normalized number density function of the fragments formed at each collision of crystal i with impeller segment j . In general, the size distribution of fragments lies in the range from 2 to 100 μm .
3. In the third step the rate of secondary nucleation is linked to the rate of formation of attrition fragments. The amount of stress remaining in the fragments limits the number that grows into the population, because stress increases their chemical potential. Their real saturation concentration c^* becomes:

$$c_{\text{real}}^* = c^* \exp\left(\frac{\Gamma_K}{KTL_{\text{fragment}}}\right) \quad [56]$$

The stress content of the fragments is directly related to their length, and the value of Γ_K has to be determined experimentally, for example from experiments where the fines of a crystallizer are withdrawn, and allowed to grow out in a growth cell.

The formed fragments with size L_{fragment} can now be distributed with their respective length and stress content. A number of fragments will dissolve, and the

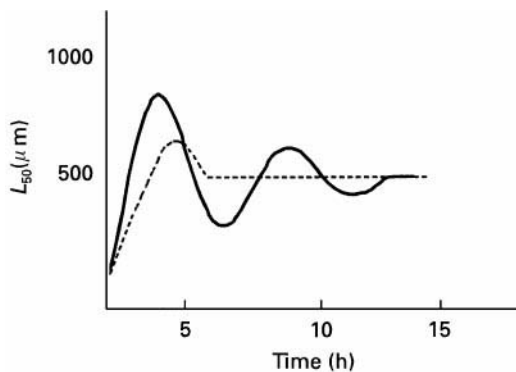


Figure 5 Dynamic behaviour of the CSD. Continuous line, measured; dashed line, modelled with the power law.

rest will grow into the population with a size-dependent growth rate.

This model does not deliver a secondary nucleation rate, B_0 , with nuclei born at zero size or a birth term, $B(L)$, for the distribution of secondary nuclei, but calculates from the number of collisions, and from the surviving fragments per collision, the number of new developing crystals. Since for this calculation an initial CSD is needed, iteration loops are always needed if this nucleation model is used as a predictive tool for secondary nucleation.

Both this model and that of O'Meadhra are able to describe the dynamic behaviour of crystallization processes.

Crystal Growth

Definitions of growth rate The growth rates of the crystallographically different faces ($h k l$) of a crystal can vary considerably. The growth rates of the crystal faces determine the shape of the crystal and, together with the growth mechanisms, also the crystal surface structure.

The growth rate of a particular crystal face ($h k l$) is mostly defined by its linear growth rate R_{lin} ($m s^{-1}$), which refers to the growth rate of that face along the normal direction. An overall linear growth rate \bar{R}_{lin} averaged over all different ($h k l$) faces can be defined in several ways. One definition which is often used relates \bar{R}_{lin} to the increase of the crystal mass in time:

$$\frac{1}{A} \frac{dm}{dt} = \frac{\rho k_v}{k_a L^2} \frac{dL^3}{dt} = 3 \frac{k_v}{k_a} \rho G_L = 6 \frac{k_v}{k_a} \rho \bar{R}_{lin} \quad [57]$$

For spheres and cubes (or for crystals where L is based on the diameter of a sphere with the same volume), $k_a/k_v = 6$, and:

$$\frac{1}{A} \frac{dm}{dt} = \frac{1}{2} \rho G_L = \rho \bar{R}_{lin} \quad [58]$$

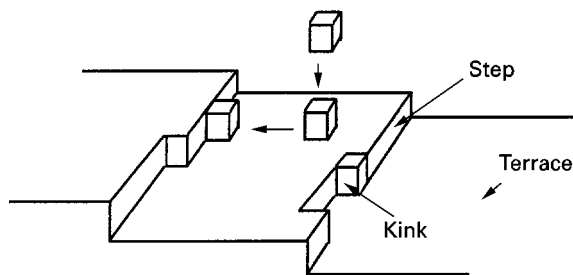


Figure 6 Diffusion of a growth unit towards and integration into the crystal surface layer.

Note that $G = dL/dt = 2 \bar{R}_{lin}$ for substitution of the linear rate equations in the population balance equation.

Crystal growth mechanisms For growth from solution the crystal growth processes can be roughly divided into two steps (Figure 6):

1. (volume) diffusion of growth units towards the crystal-solution interface
2. subsequent integration of these growth units into the crystal surface

The concentration profile perpendicular to the crystal surface is given in Figure 7, where the concentrations in the bulk at the crystal-solution interface and the equilibrium concentration at the growth site are indicated by c_b , c_i and c^* respectively.

For very soluble compounds, the growth rate is only limited by diffusion through the stagnant layer with thickness δ at the interface, with $c_b - c^*$ as the driving force for diffusion. For poorly soluble compounds the surface integration step is growth-limiting, and the driving force for the integration equals $c_b - c^*$. For most compounds, however, both steps must be taken into account. For growth from the melt the transport of the heat of crystallization becomes a third rate-limiting step. This is also the case for very concentrated solutions. In the following, first the surface integration and volume diffusion growth mechanisms and the related growth rate

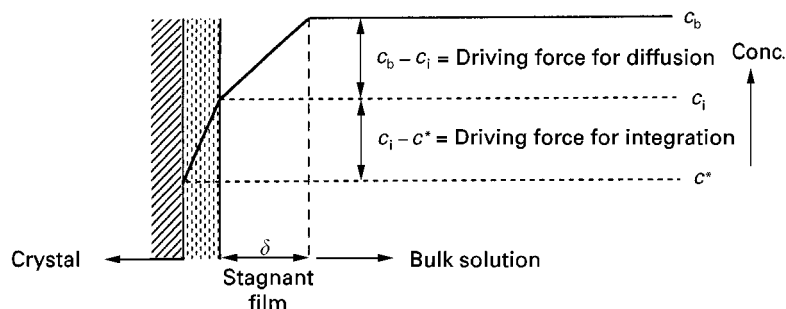


Figure 7 Concentration profile perpendicular to the crystal surface during growth.

expressions will be given, as well as the growth rate expressions for a combination of both steps. The expressions for heat transfer-controlled growth and for simultaneous heat and mass transfer will not be discussed here.

Surface integration controlled growth

Rough surfaces The structure of a growing surface at a molecular level is influenced by several factors: first, by the binding energies between the atoms, ions or molecules in the crystal surface layer. Also the solvent, temperature and driving force can play an important role. Depending on these factors, surfaces can become roughened. For a given compound and a selected solvent, either thermal or kinetic roughening may occur.

Each crystal face has a critical temperature above which the surface becomes rough. For ionic compounds these temperatures are very high, and always above the normal operating conditions. For organic compounds, however, roughening temperatures can even be close to room temperature, as with paraffin crystals growing from hexane. For rough growth the crystal faces tend to become rounded, especially at the edges, and nicely faceted crystals are no longer formed.

Kinetic roughening is caused by growth at too high supersaturation, and also happens for ionic substances. Rough growth always affects the crystal quality in a negative way, in particular the crystal purity, since impurities or solvent molecules are more easily incorporated.

It is not surprising that for rough growth the linear growth rate depends linearly on the supersaturation, because all surface sites can act as growth sites, and the rate constant k_r is proportional to the solubility of the compound. The solubility reflects the number of growth units that potentially impinges on the crystal surface, and thus contributes to its growth. The linear growth rate is given by:

$$R_{\text{lin}} = k_r \sigma \quad [59]$$

Smooth surfaces For growth of smooth crystal faces, as normally happens under moderate operating conditions, an orderly deposition of subsequent growth layers is needed. This can be realized by the propagation of growth steps along the crystal surface (Figure 6). Two sources can be identified for the generation of steps, and the two mechanisms of layered crystal growth are named after these sources: the 'birth and spread' or two-dimensional (2D) nucleation and growth model or the spiral growth model.

In the birth and spread model the steps are generated by the formation of 2D nuclei on the crystal surface that grow into islands by spreading laterally along the crystal surface. New nuclei can be formed on the original surface as well as on top of the already growing island. 2D nuclei can only be formed if the supersaturation is high enough to overcome the 2D nucleation barrier. The linear growth rate is given by:

$$R_{\text{lin}} = k_r (S - 1)^{2/3} S^{1/3} \exp\left(-\frac{B_{2D}}{3 \ln S}\right) \quad [60]$$

where $S = \sigma + 1$.

At low supersaturations, where 2D nuclei are not yet formed, screw dislocations that are present as lattice defects in the crystals and emerge on the crystal surface will act as step sources. The steps will curve around the defect emerging point, and spiral hillocks are formed.

The linear growth rate, also known as the parabolic growth law, equals:

$$R_{\text{lin}} = k_r \sigma^2 \quad [61]$$

In both eqns [60] and [61] k_r is directly proportional to the solubility of the compound. This solubility dependence is clearly seen in plots of the growth rates and the mean crystal sizes of many salts versus the supersaturation, as given by Mersmann. So, at the low supersaturations generally prevailing in evaporative and cooling crystallization, the surface integration growth step mostly obeys the parabolic law. At higher supersaturations, 2D nucleation and growth take over. If, at very high supersaturations, the size of the 2D nuclei approaches that of one growth unit, rough growth occurs (Figure 8).

Volume diffusion controlled growth Because diffusion through the stagnant boundary layer at the crystal surface is the rate-limiting step, this

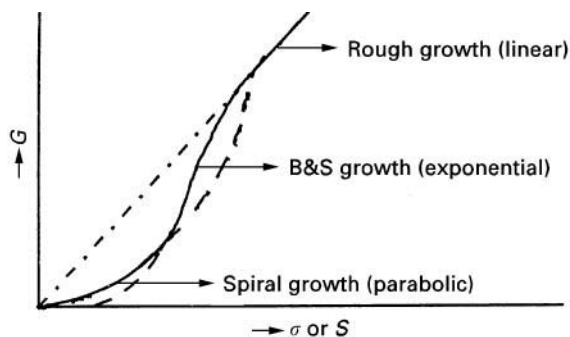


Figure 8 Growth curves for spiral, birth and spread (B&S) and rough growth.

growth model is also called the diffusion layer model. Even for rather concentrated solutions the simplified Fick's law can be applied, and the increase in crystal mass is given by:

$$\frac{dm}{dt} = \frac{D}{\delta} A(c_b - c^*) = k_d A(c_b - c^*) \quad [62]$$

The mass transfer coefficient k_d follows in its simplest form from $Sh = k_d L/D$, where for Sh several correlations provided in literature can be used. The values for Sh generally lie between 2 and 10. For concentrated solutions the Maxwell–Stefan equation is used

$$\frac{dm}{dt} = \frac{k_d}{(1-w)} A(c_b - c^*) \quad [63]$$

with w = mass fraction of the solute.

So, for most cases the linear growth rate is given by:

$$\bar{R}_{lin} = \frac{k_a k_d}{6k_v \rho} c^* \sigma \quad [64]$$

The dependency of \bar{R}_{lin} on σ is first order, and \bar{R}_{lin} is directly related to the solubility. It always limits the maximal growth rate by which a crystal can grow at a given supersaturation in Figure 8.

Volume diffusion and surface integration controlled growth For combined volume diffusion and rough growth as growth rate-determining steps, the growth process can be described by:

$$\frac{1}{A} \frac{dm}{dt} = \frac{k_d k_r}{k_d + k_r} (c_b - c^*) \quad [65]$$

while for combined volume diffusion and spiral growth surface integration the growth rate becomes:

$$\frac{1}{A} \frac{dm}{dt} = k_d(c_b - c^*) + \frac{k_d^2}{2k_r} - \left[\frac{k_d^4}{4k_r^2} + \frac{k_d^3(c_b - c^*)}{k_r} \right]^{1/2} \quad [66]$$

With eqn [57] either \bar{R}_{lin} or G can be calculated.

The temperature dependence of k_r and k_d is given by an Arrhenius-type equation, where the corresponding Arrhenius activation energies are typically of the order of 40–60 kJ mol⁻¹ for surface integration and 10–20 kJ mol⁻¹ for the volume diffusion step.

For easily soluble compounds generally linear growth rates of 10⁻⁷ m s⁻¹ are permissible in order to

obtain smoothly grown crystals at σ values of 0.001 to 0.01, while for slightly soluble substances growth rates of 10⁻⁹ to 10⁻⁸ m s⁻¹ are commonly encountered at σ values of 10–100. Their corresponding mean sizes vary from 600 μ m to 10 μ m respectively.

Growth rate dispersion Small crystals, regardless whether they are born by primary or secondary nucleation, grow slower than their parent crystals. This is attributed to a certain content of stress in the small crystals. During the growth of the nuclei, the outer layers of the crystals lose some of the stress – a process called healing. Although the stress content of individual small crystals of the same size can differ, and thus their growth rate – a phenomenon named growth rate dispersion – the overall effect of stress on the growth rate of a large number of small crystals can equally be described by a size-dependent growth function. The equilibrium concentration then becomes a size-dependent function analogous to eqn [56].

$$G(L) = kg \left(\sigma - \frac{W_i(L)}{kT} \right)^g \quad [67]$$

where $W_i(L) = \Gamma_k/L_{fragment}$ and $g = 1$ for volume diffusion-dominated growth, and 2 for spiral growth. The value of Γ_k is, as mentioned before, a fitting parameter that has to be determined experimentally.

Dissolution of Crystals

Only at very low undersaturations or for extremely insoluble substances such as BaSO₄, the dissolution process proceeds by the disappearance of subsequent layers, and a smooth surface is maintained. Normally surface disintegration occurs at the crystal edges and at etch pits, and the surface becomes easily roughened. So the dissolution rate is either given by an expression where only volume diffusion is rate controlling:

$$-\frac{1}{A} \frac{dm}{dt} = k_d(c^* - c_b) \quad [68]$$

or by a combined volume diffusion and surface disintegration rate, as given by eqn [65] and, more rarely, by eqn [66], but now with a negative value for the change in mass, and a decreasing A .

Agglomeration

The agglomeration process consists of the transportation and collision of particles, and the attachment of the particles, followed by either disruption or cemen-

Table 2 Predominant agglomeration models for the possible transport mechanism as a function of particle size L and the Kolmogorov length scale η

Transport mechanism	Particle size L	Collision mechanism
Brownian motion	$L < 0.5 \mu\text{m}$	Perikinetic
Laminar flow	$L < 6 \eta$	Orthokinetic
Laminar flow	$L > 25 \eta$	Inertial
Turbulent flow	$L < 6 \eta$	Orthokinetic
Turbulent flow	$L > 25 \eta$	Inertial
Relative particle settling	$L < 6 \eta$	Inertial

tation of the attached particles. The cemented particles are agglomerates. If the supersaturation is zero, no cementation occurs and all loosely agglomerated particles fall apart again. Since in practice only the combined result of disruption and cementing can be observed, an effective agglomeration rate is generally defined.

The main transport mechanisms by which particles can collide are Brownian motion, laminar or turbulent flow or relative particle setting. Depending on the particle size and the Kolmogorov length scale of the different flow regimes, different collision mechanisms can be distinguished (Table 2).

In case of orthokinetic collisions the effective agglomeration rate constant or agglomeration kernel can be described as a product of the collision rate constant and an efficiency factor:

$$\beta = \psi(\varepsilon, \sigma)\beta_{\text{coll}} \quad [69]$$

β_{coll} increases linearly with the shear rate γ , that equals $\sqrt{\varepsilon/\nu}$ in a stirred vessel, whereas the efficiency factor ψ decreases strongly with γ in this high shear region, and thus β also decreases after having reached a maximal value at a rather low shear rate value. Although β should be size-dependent, experimental agglomeration data can often be fitted with a size-independent kernel. Hounslow and co-workers recently introduced a dependence of β_{coll} on the mean particle size. The efficiency factor includes the supersaturation dependence that is needed for the cementation of the particles. The supersaturation-dependent cementation explains why, for large crystallizers with a sufficiently large circulation time between two subsequent collisions with the impeller blades, abundant agglomeration may occur, while hardly any agglomeration is noticed for small scale crystallizers.

It must also be kept in mind that agglomeration is a kinetic process that depends on collisions, and thus on the local turbulence or power input ε . Averaging the power input ε for the calculation of β might

therefore lead to a wrong estimation of the degree of agglomeration.

Industrial Crystallizers

Several types of crystallizers are commercially available. The choice of crystallizer depends on the material to be crystallized and the solvent, the method of crystallization, the product specifications, in particular the crystal size distribution, and the flexibility of the design in cases where products of various coarseness (L_{50}) must be crystallized on demand in the same equipment.

Here only three large scale evaporative and cooling crystallizers will be discussed. These examples mainly serve to illustrate that in practice and in particular for a large scale crystallizer several compartments can be distinguished, where different processes may dominate.

Forced Circulation Crystallizer

The forced circulation (FC) crystallizer is the most widely used crystallizer. It is most common in multi-stage flash evaporative crystallization of salts with a flat solubility curve. It is the least expensive vacuum crystallizer, especially for evaporation of substantial amounts of water. The crystallizer as depicted in Figure 9 comprises two separate bodies that can be designed separately for evaporation and crystallization and for heat input.

The boiling zone with often a tangential inlet of the incoming flow should be large enough for vapour

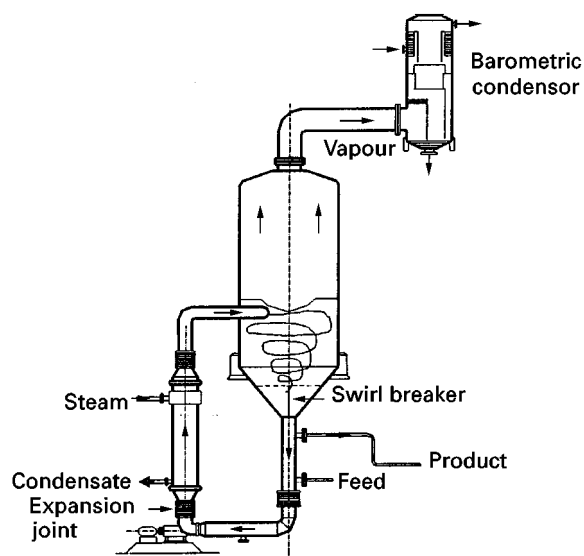


Figure 9 Forced circulation crystallizer with a tangential inlet (Swenson type). Reproduced with permission from Bennett (1993).

release, while the vessel bulk zone should maintain a sufficiently large volume to retain the growing crystals until the supersaturation is consumed. A slurry pump circulates the crystal slurry through the tubes of the heat exchanger, that can act as an internal fines dissolver, back into the boiling zone. This pump also creates most of the attrition fragments that may grow out as secondary nuclei, although usually an (axial-type) centrifugal pump is applied to minimize the attrition in order to get a sufficiently large mean crystal size. Because the forced circulation causes good mixing, the FC crystallizer is often modelled as a one compartment or MSMPR crystallizer in spite of its various zones.

The supersaturation and the turbulence may however differ locally.

Draft Tube Baffled Crystallizer

In this draft tube baffled (DTB) crystallizer with an external heat exchanger, as depicted in Figure 10, the heat duty is also separated from the crystallizer body. Fines removal has been realized by installing a skirt baffle that creates a settling or annular zone. The flow in the draft tube thus has to be upwards: this is effected by the impeller that also creates most of the attrition fragments. The fines flow can be diluted or heated to partly or totally dissolve

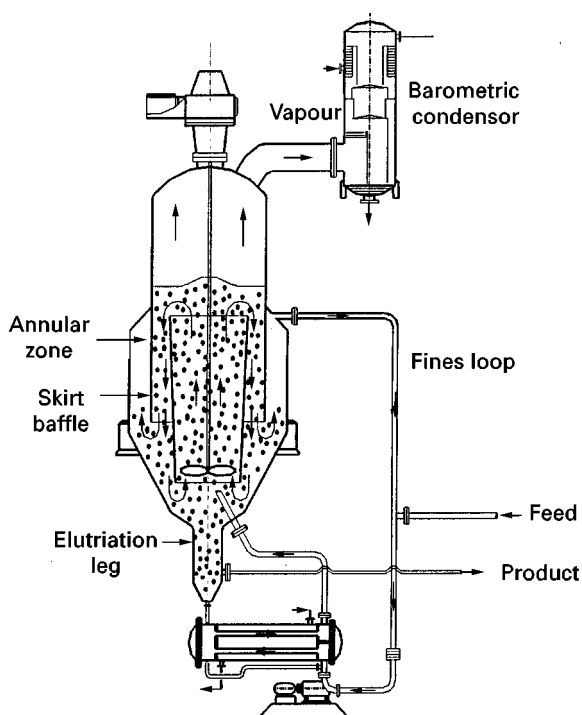


Figure 10 Stirred draft tube baffled (DTB) crystallizer with an external heat exchanger and fines destruction (Swenson type). Reproduced with permission from Bennett (1993).

the fines. An increase in fines flow increases the number of fines that are removed from the crystallizer, but also the cut size of the fines. The fines loop in this way serves as an actuator that can be applied for control of the mean crystal size, although the variation in mean crystal size that can be achieved is limited.

The addition of an elutriation leg at the bottom of the crystallizer or the addition of another type of classifier allows classification of the product flow, and thus also serves as an actuator to influence the CSD of the product.

Obviously the various zones of the DTB crystallizer have different functions, and different supersaturation and turbulence values can be expected, in particular for large scale crystallizers.

The DTB crystallizer can also be applied as cooling crystallizer by using the heat exchangers as a cooling system.

Fluidized Bed Crystallizer

A fluidized bed crystallizer (Figure 11) is especially designed to produce large and uniformly sized crystals. The heat duty and the crystallizer body are again separated. At the top of the bed the crystals are settled, and only the fines leave the crystallizer with the exhausted mother liquor to be circulated through the heat exchanger after mixing with the feed stream. The hot circulated flow enters the vaporizer head, where the solvent is flashed off. The supersaturated solution leaves the vaporizer through the downcomer, and enters the densely packed fluidized bed at the bottom of the crystallizer. The supersaturation is consumed on its way up, and a coarse product leaves the crystallizer at the bottom.

Secondary nucleation here results from crystal-crystal collisions. Also for this crystallizer several functions can be identified that are restricted to various zones in the crystallizer. The supersaturation and the turbulence are also not evenly distributed.

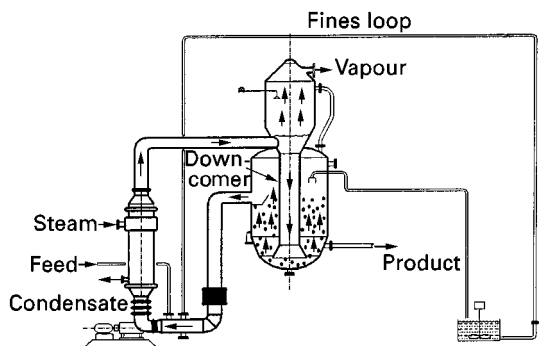


Figure 11 Fluidized bed crystallizer (Swenson type). Reproduced with permission from Bennett (1993).

Since the residence time of the crystals can be considerably increased, this type of crystallizer is commonly used to produce large crystals.

This crystallizer can also be used for cooling crystallization. No vapour chamber is then needed. Other well-known cooling crystallizers are: first, a Swenson type where the suspension is circulated through a heat exchanger; second, a direct cooling crystallizer, where a refrigerant is introduced directly into a draft tube crystallizer; and third, a cooling disc crystallizer, that can be regarded as a compact cascade of cooling crystallizers with various cooling elements that are scraped by rotating wipers.

Compartmental Modelling

In an industrial crystallizer various zones with different functions can be identified, as has been illustrated in the former section. The supersaturation (Kramer *et al.* 1999) and the turbulence (Derksen and van den Akker, 1999) in a crystallizer are therefore not necessarily evenly distributed. Their local values depend on the geometry and scale of the crystallizer,

on the flow pattern, as well as on the rates of the kinetic processes and the production rate of the specific crystallizing compound. In particular, the nonlinear kinetic processes such as nucleation and agglomeration are strongly dependent on these local values. It also has to be established whether locally the supersaturation does not exceed a maximum beyond which value rough growth occurs or too many solvent inclusions are incorporated in the crystals.

As the conventional modelling techniques use geometrically lumped descriptions (i.e. MSMPR) of the physical processes inside a crystallizer vessel (Randolph, 1998; Mersmann, 1995; Eek, 1995; O'Meadhra, 1996), they do not account for the variations in the local process conditions and have therefore seldom proven to be reliable for scale-up purposes. A reliable tool for modelling of crystallizers requires the separation of kinetics and hydrodynamics. A well-known technique for this purpose is compartmental modelling. This technique, which is frequently applied for standard reactor engineering problems, has been applied within crystallization for a number of years (Kramer, 1999).

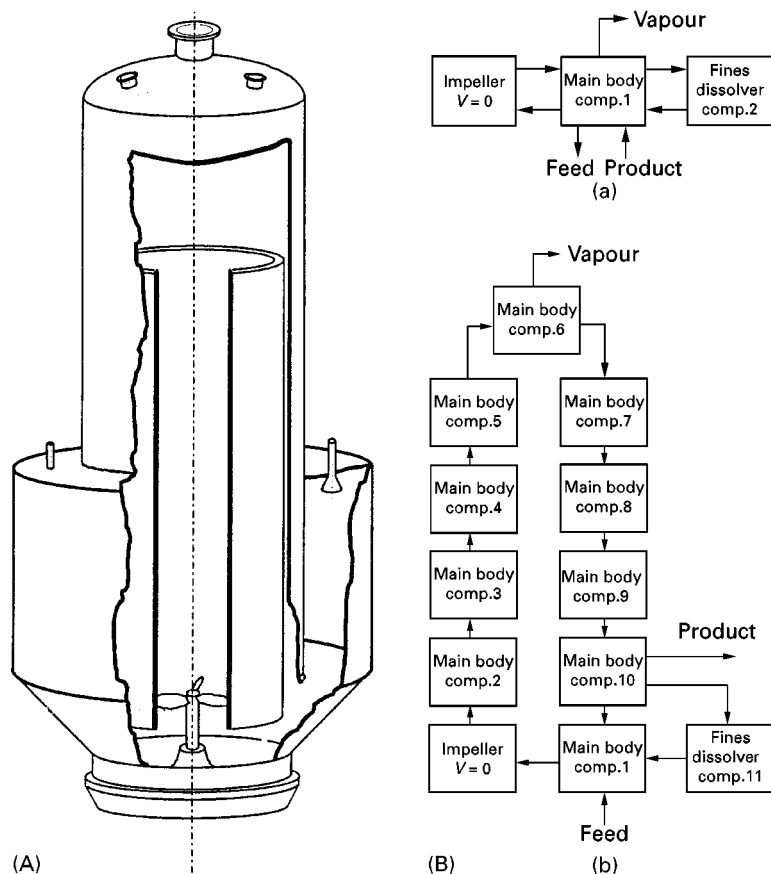


Figure 12 (A) A DTB crystallizer and (B: a,b) two compartment structures.

Here an example will be presented to illustrate the design of a compartment model for a 360 m³ DTB crystallizer, with the main crystallizer body modelled as a one- or as a multicompartment vessel.

The subdivision of the crystallizer into multiple compartments is performed on the basis of crystallizer geometry, hydrodynamic analysis and characteristic times of the crystallization kinetics (Kramer 1999). In compartmental modelling, process conditions may differ between compartments but not within compartments, because the individual compartments are modelled as well-mixed vessels. A three-step approach is used to define the size and location of the compartments as well as the exchange flow rates between them:

1. Set up a rough compartment structure on the basis of the crystallizer geometry, e.g. an inlet compartment, a propeller compartment, a boiling zone compartment, etc.
2. Compare the characteristic time of supersaturation depletion due to crystal growth with the residence time in each compartment to check the constant supersaturation assumption. If necessary, the compartment structure may be refined.
3. Use computational fluid dynamic (CFD) results to refine further the compartment structure, specifically with respect to the exchange flow rates and the constant energy dissipation assumption in each compartment.

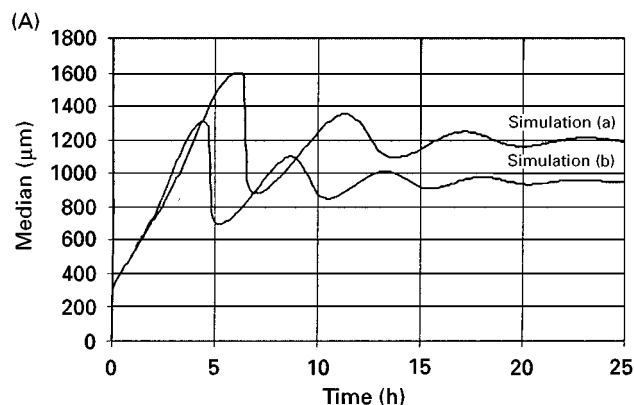
The importance of compartmental modelling is illustrated for a 360 m³ DTB crystallizer (Figure 12)

with ammonium sulfate and water as the model system. This crystallization system is dominated by secondary nucleation and growth. The model framework of Gahn and Mersmann (see section on secondary nucleation, above) is the most sophisticated for such systems and is hence used in this example. Figure 12 also contains two compartment structures for this DTB crystallizer. The first compartment structure (Figure 12B a) describes a MSMPR crystallizer with fines removal and fines dissolution. The second structure (Figure 12B b) was created using the three-step approach presented in the previous paragraph.

Both compartment structures will now be used to describe the behaviour of the 360 m³ DTB crystallizer operating with a residence time of 75 min, an impeller frequency of 45 rpm and a fines withdrawal rate of 157 m³ min⁻¹. Additional information regarding the equipment, operating conditions and simulation details can be found in Bermingham *et al.* (1999).

Results of simulations with both compartment structures are depicted in Figure 13. Taking the spatial distribution of the supersaturation into account clearly has a large influence on the predicted crystal size distribution. The lower median size of simulation (b) is most probably related to the higher supersaturation of the withdrawn fines flow, i.e. 1.78 as opposed to 1.38 kg m⁻³. Furthermore, it is interesting to note that a large majority of the crystal mass is produced in only half the crystallizer volume.

This example clearly illustrates the effect of varying process conditions in different zones of an industrial crystallizer on the CSD of the produced



(B)		
	Crystal mass production (kg m ⁻³ s ⁻¹)	Supersaturation, c-c* (kg m ⁻³)
Simulation (a)		
MB-C1	0.0434	1.38
FD-C2	-0.0478	-4.03
Simulation (b)		
MB-C1	0.0008	0.23
MB-C2	0.0007	0.24
MB-C3	0.0007	0.23
MB-C4	0.0007	0.23
MB-C5	0.0007	0.23
MB-C6	0.1118	2.66
MB-C7	0.0964	2.41
MB-C8	0.0834	2.18
MB-C9	0.0725	2.00
MB-C10	0.0799	1.78
FD-C11	-0.0512	-3.60

Figure 13 (A) Dynamic trend of the median crystal size and (B) steady-state crystal mass production and supersaturation for simulations (a) and (b).

crystals. Compartmental modelling is therefore an important or even essential tool in the design of industrial crystallizers to predict the influence of crystallizer geometry, scale, operating conditions and process actuators on the process behaviour and product quality.

Only using this approach can a reasonable prediction can be obtained for the composition of the bleed and/or product streams, and of the filterability and washability of the product, which determine the efficiency of this separation process.

Product Properties Related to the Process Conditions

In order to apply crystallization as an adequate separation process, the solid phase has to fulfil a number of requirements. The crystal size distribution as well as the shape of the crystals should meet the demands of a good filterability and washability of the product, as is needed for a good separation. The surface roughness of the crystals may also play a role, because a rough surface leads to attrition, and the attrited fragments may hamper the downstream processes.

The crystals should be formed under process conditions that minimize the uptake of impurities or mother liquor inclusions in the crystals. This can happen when the (local) supersaturation is too high. A too high local turbulence should be avoided, this causes attrition of especially the corners or edges of the crystals. Although healing of the crystals will occur particularly in the regions of the highest supersaturations, this healing process is never perfect, and always leads to the uptake of solvent inclusions. That crystals are prone to attrition beyond a certain size that also depends on the degree of turbulence can be seen from Figure 14.

Agglomeration should in general be prevented, since liquid incorporation between the primary par-

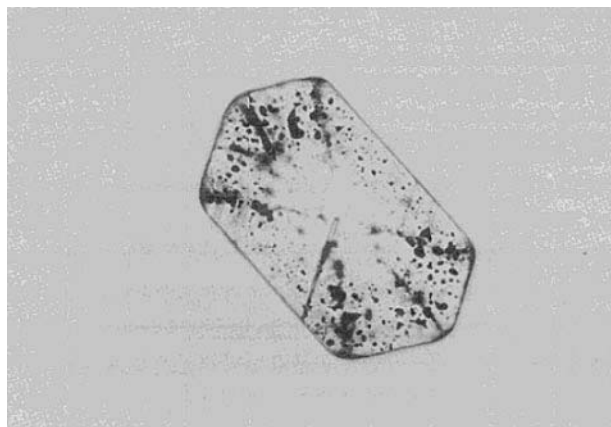


Figure 14 Liquid inclusions in $(\text{NH}_4)_2\text{SO}_4$ crystal embedded in a liquid of similar refractive index.

ticles of an agglomerate is unavoidable. Only if, as often happens in precipitation processes, the primary particles are too small for filtration, agglomeration should just be promoted. In that event the solute concentration in the mother liquor is extremely low and some incorporation of it in the solid phase hardly affects the separation process.

Final Remarks

To summarize, it can be said that the design of a good evaporative or cooling crystallization process is based on heat, mass and population balances, kinetic processes of nucleation, growth and agglomeration of the particles, as well as on the hydrodynamics that exist in the crystallizer of a given geometry and scale. However, as the prevailing process conditions are not evenly distributed in industrial crystallizers, local descriptions of the crystallization phenomena are needed to calculate the local variations in the process conditions, their effect on the process performance and to predict their dependence of the scale and geometry of the crystallizer. It has been shown that by taking all these balances and processes into account in a compartmental modelling tool, the efficiency of the separation process as well as the quality of the crystalline product and the process performance can be properly predicted.

Symbols

a	activity	J mol^{-1}
A	primary nucleation factor	$\# \text{m}^{-3} \text{s}^{-1}$
A_T	total crystal surface area per unit crystallizer volume	$\text{m}^2 \text{m}^{-3}$
$B(\varepsilon, \nu)$	breakage function	$\# \text{m}^{-1}$
B_0	birth rate	$\# \text{m}^{-3} \text{s}^{-1}$
$B(L)$	birth rate (size-based)	$\# \text{m}^{-3} \text{m}^{-1} \text{s}^{-1}$
$B(\nu)$	birth rate (volume-based)	$\# \text{m}^{-3} \text{m}^{-3} \text{s}^{-1}$
c	concentration	kg m^{-3}
C_p	specific heat	$\text{J kg}^{-1} \text{K}^{-1}$
$D(L, t)$	death rate	$\# \text{m}^{-3} \text{m}^{-1} \text{s}^{-1}$
$D(\nu, t)$	death rate	$\# \text{m}^{-3} \text{m}^{-3} \text{s}^{-1}$
G_L or G	linear growth rate	m s^{-1}
G_V	volumetric growth rate	$\text{m}^3 \text{s}^{-1}$
H	enthalpy	—
$H(L)$	classification function	—
J	primary nucleation rate	$\# \text{m}^{-3}$
k	Boltzmann constant	J K^{-1}
k_a, k_v	surface, volume shape factor	—
k_n or k_v^*	nucleation rate constant	—
k_{distr}	distribution constant impurity uptake	—

L	particle length	m
L_D	dominant crystal size	m
L_T	total crystal length per unit crystallizer volume	m m^{-3}
m_j	j th moment of a distribution	...
M_T	total crystal mass per unit crystallizer volume	kg m^{-3}
$m(L)$	mass density	$\text{kg m}^{-3} \text{ m}^{-1}$
$m(v)$	mass density	$\text{kg m}^{-3} \text{ m}^{-3}$
$n(L)$	number density	$\# \text{ m}^{-3} \text{ m}^{-1}$
$n(v)$	number density	$\# \text{ m}^{-3} \text{ m}^{-3}$
N_T	total number of crystals	$\# \text{ m}^{-3}$
P	production rate	kg s^{-1}
r	radius	m
$r(\nu_1, \nu_2)$	rate of aggregation	$\# \text{ m}^{-9} \text{ s}^{-1}$
R	gas constant	$\text{J mol}^{-1} \text{ K}^{-1}$
R_{lin}	linear growth rate of a crystal face	m s^{-1}
S	supersaturation ratio	—
$S(v)$	selection function	s^{-1}
t	time	s
T	temperature	K
u	particle volume	m^3
v	particle volume	m^3
V	crystallizer volume	m^3
V_T	total crystal volume per unit crystallizer volume	$\text{m}^3 \text{ m}^{-3}$
V_{molar}	molar volume	$\text{m}^3 \text{ mol}^{-1}$
w	mass fraction	—
W_i	stress energy crystals	J
β	aggregation kernel	$\text{m}^3 \text{ s}^{-1}$
γ	interfacial free energy, activity coefficient	J m^{-2} , —
ε	specific power input impeller	W m^{-3}
η	Kolmogorof length scale	m
ϕ_v	volumetric flow rates	$\text{m}^3 \text{ s}^{-1}$
μ	chemical potential	J mol^{-1}
ρ	material density	kg m^{-3}
σ	relative supersaturation	—
τ	residence time	s
ψ	efficiency factor for agglomeration	—
Γ_k	surface-related stress	Jm

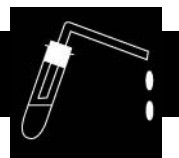
See Colour Plate 4.

Further Reading

- Arkenbout GF (1995) *Melt Crystallization Technology*. Lancaster, USA: Technomic.
- Becker R and Göring W (1935) Kinetische Behandlung der Keimbildung in übersättigten Dämpfen. *Ann Physik* 24: 719–752.
- Bennema P (1993) Growth and morphology of crystals. In: Hurle DTJ (ed.) *Handbook of Crystal Growth*, vol. 1A, pp. 477–583. Amsterdam: Elsevier Science.
- Bennett RC (1993) Crystalliser selection and design. In: Meyerson A (ed.) *Handbook of Industrial Crystallisation*, pp. 103–130. Boston: Butterworth Heinemann.
- Birmingham SK, Neumann AM, Kramer HJM *et al.* (1999) A design procedure and predictive models for solution crystallisation processes. In: *Proceedings of Fifth International Conference on Foundations of Computer Aided Process Design, FOCAPD'99*, Breckenridge, USA, paper I21.
- Derksen J and van den Akker HEA (1999) Large eddy simulations on the flow driven by a rushton turbine. *AIChE Journal* 45: 209–221.
- Eek RA, Dijkstra SJ and van Rosmalen GM (1995) Dynamic modelling of suspension crystallisers, using experimental data. *AIChE Journal* 41: 571–584.
- Gahn C and Mersmann A (1997) Theoretical prediction and experimental determination of attrition rates. *Transactions IChemE* 75(A): 125–131.
- Gahn C and Mersmann A (1999) Brittle fracture in crystallisation processes. Part A. Attrition and abration of brittle solids. *AIChE Journal* 54: 1273–1282.
- Gahn C and Mersmann A (1999b) Brittle fracture in crystallisation processes. Part B. Growth of fragments and scale up of suspensions crystallisers. *AIChE Journal* 54: 1283–1292.
- Hounslow MJ (1998) The population balance as a tool for understanding particle rate processes. *KONA* 16: 179–193.
- Hounslow MJ, Mumtaz HS, Collier AP, Barrick JP and Bramley AS (1999) Aggregation during precipitation – putting the pieces of the puzzle together. *Proceedings of the 14th International Symposium on Industrial Crystallization*, CD ROM.
- Hurle D (1993) *Handbook of Crystal Growth*. Amsterdam: Elsevier Science.
- Ilievski D and Hounslow MJ (1995) Tracer studies of agglomeration during precipitation. Part II: Quantitative analysis of tracer data and identification of mechanism. *AIChE Journal* 41: 525–535.
- Kashchiev D (2000) *Nucleation: Theory and Application*. Oxford: Butterworth Heinemann.
- Kind M and Mersmann A (1990) On supersaturation during mass crystallisation form solution. *Chemical Engineering Technology* 13: 50–62.
- Kramer HJM, Dijkstra JW, Neumann AM *et al.* (1996) Modelling of industrial crystallizers, a compartmental approach using a dynamic flow-sheet tool. *Journal of Crystal Growth* 166: 1084–1088.
- Kramer HJM, Birmingham SK and van Rosmalen GM (1999) Design of industrial crystallisers for a required product quality. *Journal of Crystal Growth* 198/199: 729–737.
- Litster, JD, Smit DJ and Hounslow MJ (1995) Adjustable discretized population balance for growth and aggregation. *AIChE Journal* 41: 591–603.

- Mersmann A (1988) Design of crystallisers. *Chemical Engineering Process* 23: 213–228.
- Mersmann A (1995) *Crystallisation Technology Handbook*. New York: Marcel Dekker.
- Meyerson AS (1993) *Handbook of Industrial Crystallisation*. Boston: Butterworth Heinemann.
- Mullin JW (1993) *Crystallisation*. Boston: Butterworth Heinemann.
- Mumtaz HS, Hounslow, MJ, Seaton NA and Paterson WR (1997) Orthokinetic aggregation during precipitation: a computational model for calcium oxalate. *Transactions of the IChemE* 75: 152–159.
- Mutaftschiev B (1993) Nucleation theory. In: Hurle DTJ (ed.) *Handbook of Crystal Growth*, vol. 1A, pp. 187–247. Amsterdam: Elsevier.
- Nicmanis M and Hounslow MJ (1998) Finite-element methods for steady-state population balance equations. *AIChE Journal* 44: 2258–2272.
- Nyvelt J (1992) *Design of Crystallisers*. Boca Raton, FL: CRC Press.
- Ó Meadhra R, Kramer HJM and van Rosmalen GM (1996) A model for secondary nucleation in a suspension crystalliser. *AIChE Journal* 42: 973–982.
- Ottens EPK, Janse AH and De Jong EJ (1972) Secondary nucleation in a stirred vessel cooling crystalliser. *Journal of Crystal Growth* 13/14: 500–505.
- Ploß R, Tengler T and Mersmann A (1989) A new model of the effect of stirring intensity on the rate of secondary nucleation. *Chemical Engineering Technology* 12: 137–146.
- Randolph AD and Larson MA (1988) *Theory of Particulate Processes*. 2nd edn. New York: Academic Press.
- Sinnott RK (1998) In: *Chemical Engineering Design*, vol. 6. (Coulson JM and Richardson JF eds.), Oxford: Butterworth Heinemann.
- Söhnle O and Garside J (1992) *Precipitation*. Oxford: Butterworth Heinemann.
- van der Eerden JP (1993) Crystal growth mechanisms: In: Hurle DTJ (ed.) *Handbook of Crystal Growth*, vol. 1A, pp. 307–477. Amsterdam: Elsevier Science.
- van der Heijden AEDM, van der Eerden JP and van Rosmalen GM (1994) The secondary nucleation rate; a physical model. *Chemical Engineering Science* 3103–3113.
- Volmer M (1939) *Kinetik der Phasenbildung*. Dresden: Steinkopf.

DISTILLATION



R. Smith and M. Jobson, Department of Process Integration, UMIST, Manchester, UK

Copyright © 2000 Academic Press

Introduction

Distillation is the most commonly used method for the separation of homogeneous fluid mixtures. Separation exploits differences in boiling point, or volatility, between the components in the mixture. Repeated vaporization and condensation of the mixture allows virtually complete separation of most homogeneous fluid mixtures. The vaporization requires the input of energy. This is the principal disadvantage of distillation: its high energy usage. However, distillation has three principle advantages over alternative methods for the separation of homogeneous fluid mixtures:

1. The ability to handle a wide range of feed flow rates. Many of the alternative processes for the separation of fluid mixtures can only handle low flow rates, whereas distillation can be designed for the separation of extremely high or extremely low flow rates.

2. The ability to separate feeds with a wide range of feed concentrations. Many of the alternatives to distillation can only separate feeds that are already relatively pure.
3. The ability to produce high product purity. Many of the alternatives to distillation only carry out a partial separation and cannot produce pure products.

It is no accident that distillation is the most common method for the separation of homogeneous mixtures. It is a versatile, robust and well-understood technique. We shall start explaining distillation by a single-stage separation, before understanding how to set up a cascade of separation stages, which is distillation.

Single-Stage Separation

Consider the liquid mixture illustrated in **Figure 1**. If this liquid mixture is partially vaporized then the vapour becomes richer in the more volatile components (i.e. those with the lower boiling points) than the liquid phase. The liquid becomes richer in the less volatile components (i.e. those with the higher boiling points). If we allow the system in **Figure 1** to come to equilibrium conditions, then the distribution of the components between the vapour and liquid phases is

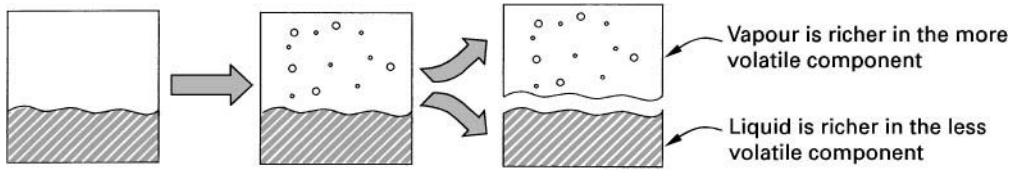


Figure 1 Partial vaporization of a liquid mixture creates a separation.

dictated by thermodynamic vapour–liquid equilibrium considerations. All components can appear in both phases. However, involatile components will tend to stay in the liquid phase.

Rather than partially vaporize a liquid, as shown in Figure 1, we could have started with a mixture of components in the vapour phase and partially condensed the vapour. We would still have had a separation, as the liquid which was formed would be richer in the less volatile components, while the vapour would have become depleted in the less volatile components. Again, the distribution of components between the vapour and liquid is dictated by thermodynamic vapour–liquid equilibrium considerations if we allow the system to come to equilibrium. Any noncondensable components present in the vapour will tend to stay in the vapour phase.

For each component in the mixture, thermodynamic equilibrium is given by the condition when the vapour and liquid fugacities are equal:

$$f_i^v = f_i^L \quad [1]$$

Fugacity is a thermodynamic pressure which, when substituted for pressure in thermodynamic expressions for ideal systems, allows them to be used for nonideal systems. It can be thought of as an escaping tendency. Defining the vapour phase fugacity coefficient ϕ_i^v :

$$f_i^v = y_i \phi_i^v P \quad [2]$$

Defining the liquid-phase fugacity coefficient ϕ_i^L and activity coefficient γ_i :

$$f_i^L = x_i \phi_i^L P \quad [3]$$

or:

$$f_i^L = x_i \gamma_i f_i^0 \quad [4]$$

For moderate pressures f_i^0 is usually taken to be the saturated vapour pressure P_i^{SAT} :

$$f_i^L = x_i \gamma_i P_i^{\text{SAT}} \quad [5]$$

These equations can be combined to give an expression for the constant, K :

$$K_i = \frac{y_i}{x_i} = \frac{\phi_i^L}{\phi_i^v} \quad [6]$$

This expression provides the basis for vapour–liquid equilibrium calculations based on equations of state (e.g. Peng–Robinson equation). Alternatively:

$$K_i = \frac{y_i}{x_i} = \frac{\gamma_i P_i^{\text{SAT}}}{\phi_i^v P} \quad [7]$$

This expression provides the basis for vapour–liquid equilibrium calculations based on liquid-phase activity coefficient models (e.g. Wilson equation). At moderate pressures:

$$K_i = \frac{y_i}{x_i} = \frac{\gamma_i P_i^{\text{SAT}}}{P} \quad [8]$$

When the liquid phase behaves as an ideal solution, this expression simplifies to:

$$K_i = \frac{y_i}{x_i} = \frac{P_i^{\text{SAT}}}{P} \quad [9]$$

which is Raoult's law. Correlations are available to relate component vapour pressure to temperature (e.g. the Antoine equation), activity coefficients to composition and temperature (e.g. the Wilson equation) and fugacity coefficient to mixture, pressure and temperature (e.g. from the Peng–Robinson equation of state). Regression analysis of experimental data provides the adjustable parameters used in the various models.

The ratio of equilibrium constants for two components measures their relative volatility:

$$\alpha_{ij} = \frac{K_i}{K_j} \quad [10]$$

where α_{ij} is the relative volatility between components i and j .

Figure 2 shows the vapour–liquid equilibrium behaviour for a binary mixture of benzene and toluene.

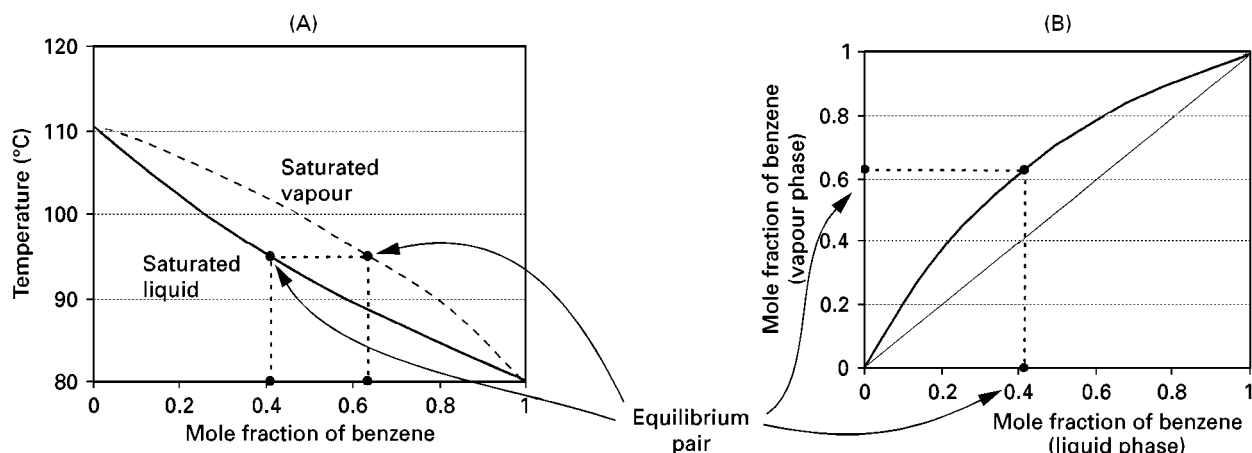


Figure 2 Vapour-liquid equilibrium for a binary mixture of benzene and toluene at a pressure of 1 atm.

Figure 2A shows the behaviour of the temperature of the saturated liquid and saturated vapour as the mole fraction of benzene is varied (the balance being toluene).

Figure 2A also shows a typical vapour-liquid equilibrium pair where the mole fraction of benzene in the liquid phase is 0.4 and that in the vapour phase is 0.62. Shown in Figure 2B is an alternative way of representing the vapour-liquid equilibrium behaviour (x - y diagram). This plots the mole fraction of benzene in the vapour versus mole fraction of benzene in the liquid. A diagonal line across this diagram would represent a situation where the concentration in the vapour and the liquid are equal. The phase equilibrium behaviour, however, shows a curve above the diagonal line. This indicates that the benzene has a higher concentration in the vapour phase than the toluene, i.e. the benzene is the more volatile component in this case. Figure 2B shows the same vapour-liquid equilibrium pair as that shown in Figure 2A with a mole fraction of benzene in the liquid phase of 0.4 versus a mole fraction in the vapour phase of 0.62.

Figure 3 shows a single equilibrium stage. Liquid is fed with composition x_0 and vapour is fed with com-

position y_2 . Contact between the vapour and the liquid streams makes the vapour richer in the more volatile components and the liquid richer in the less volatile components. Once the feed conditions and compositions, the system pressure and the relative flow rates of the vapour and liquid have been fixed, then the temperature and compositions of the exit streams are unique. Let us also, initially, make a simplifying assumption that the molar flow rates of the liquid L and molar flow rates of the vapour V are constant for the stage. This assumption is known as constant molar overflow and is true if sensible heat effects are small, molar latent heats of vaporization of the components are equal, heat of mixing is negligible and there are no heat losses or gains. Let us now carry out a mass balance around the equilibrium stage shown in Figure 3. First we assume constant molar overflow:

$$L_0 = L_1 = L \quad [11]$$

$$V_2 = V_1 = V \quad [12]$$

A component mass balance gives:

$$Lx_{0,A} + Vy_{2,A} = Lx_{1,A} + Vy_{1,A} \quad [13]$$

which can be rearranged to give:

$$y_{1,A} = -\frac{L}{V}x_{1,A} + \frac{Lx_{0,A} + Vy_{2,A}}{V} \quad [14]$$

This equation can be plotted on an x - y diagram, as shown in Figure 4. The mass balance line is a straight line which depends on the liquid and vapour flow rates and the feed compositions of liquid and vapour. In Figure 4 the liquid and vapour feeds are not in equilibrium. Following the mass balance line until it

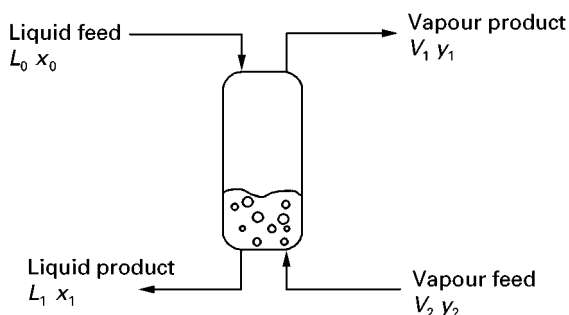


Figure 3 Separation in a single equilibrium stage.

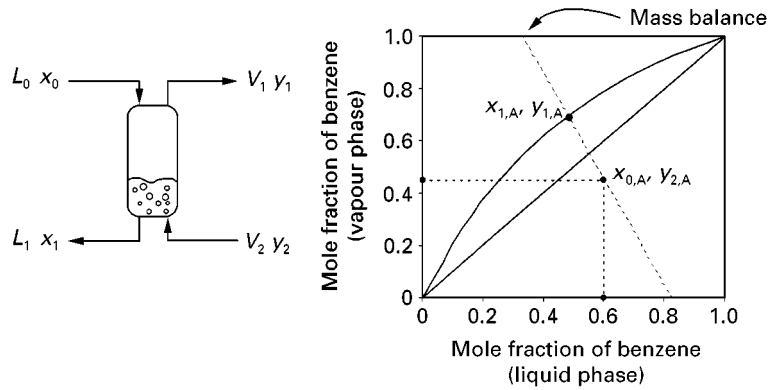


Figure 4 Single-stage separation for a binary mixture.

crosses the equilibrium line allows us to predict the vapour and liquid composition at the exit of the stage. We can now see quantitatively the separation carried out by the single equilibrium stage. However, the separation which is achieved on a single equilibrium stage is limited. We now need to consider how we can extend the idea to carry out further separation.

Cascade of Separation Stages

We have seen that a single equilibrium stage can only achieve a limited amount of separation. To extend the amount of separation we can make a cascade of stages, as shown in **Figure 5**. It is assumed in the cascade that streams leaving each stage are in equilibrium. Using a cascade of stages in this way allows the more volatile components to be transferred to the vapour phase, the less volatile components to be transferred to the liquid phase and a greater degree of separation to be achieved than for a single stage.

Figure 6 shows the liquid and vapour flows connecting the stages in a countercurrent cascade. As before, we assume constant molar overflow:

$$L_0 = L_m = \dots = L_N; V_1 = V_m = \dots = V_{N+1} \quad [15]$$

We can write an overall mass balance for component i across the cascade:

$$L_0 x_{0,i} + V_{N+1} y_{N+1,i} = L_N x_{N,i} + V_1 y_{1,i} \quad [16]$$

We can also write a mass balance around the envelope shown in **Figure 6** over m stages:

$$L_0 x_{0,i} + V_{m+1} y_{m+1,i} = L_m x_{m,i} + V_1 y_{1,i} \quad [17]$$

This equation can be rearranged to give:

$$y_{m+1} = \frac{L}{V} \cdot x_m + \frac{Vy_1 - Lx_0}{V} \quad [18]$$

This operating line relates the composition streams after m stages.

Figure 7 shows the cascade in terms of a more conventional representation in a distillation column. At the top of the column we need liquid to feed the cascade. This is produced by condensing and returning some of the vapour which leaves the top stage. We also need vapour to feed the cascade at the bottom of the column. This is produced by vaporizing

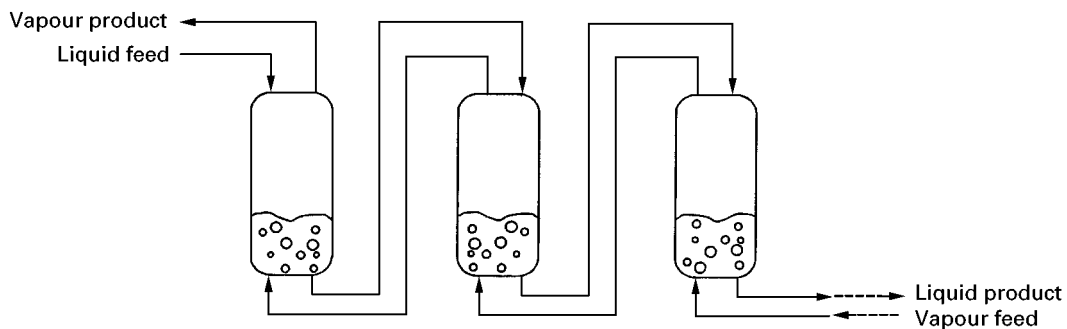


Figure 5 A cascade of separation stages.

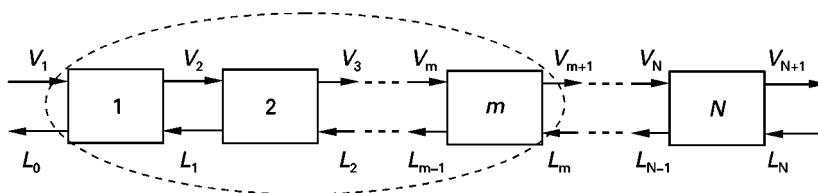


Figure 6 Mass balance on a countercurrent cascade.

and returning some of the liquid leaving the bottom stage. The feed to the process is introduced at an intermediate stage; products are removed from the condenser and the reboiler (vaporizer).

The method by which the vapour and liquid are contacted with each other in distillation columns falls into two broad categories. **Figure 8** shows a plate or tray column. Liquid enters the first tray at the top of the column and flows across what is shown in **Figure 8** as a perforated plate. Liquid is prevented from weeping through the holes in the plate by the upflowing vapour. In this way the vapour and liquid are contacted. The liquid from the first tray flows over a weir and down a downcomer, to the next stage and

so on. The design of stage used in **Figure 8** involving a plate with simple holes is known as a sieve tray. Many other designs of tray are available involving, for example, valve arrangements for the holes in the trays. In practice, the column will need more trays than the number of equilibrium stages as mass transfer limitations prevent equilibrium being achieved on a tray.

The other broad class of contacting arrangement is that of packed columns. Here the column is filled with a solid material which has a high voidage. Liquid trickles across the surfaces of the packing and vapour flows upward through the voids in the packing, contacting the liquid on its way up the column. Many different designs of packing are available.

The design of a distillation column like the one shown in **Figure 8** involves a number of steps:

1. Set the product specifications.
2. Set the operating pressure.
3. Determine the number of theoretical stages required and the energy requirements.
4. Determine the actual number of trays or height of packing needed and the column diameter.
5. Design the column internals, which involves determining the specific dimensions of the trays, packing, liquid and vapour distribution systems, etc.
6. Carry out the mechanical design to determine wall thicknesses, internal fittings, etc.

Let us start by considering the simplest case of binary distillation.

Binary Distillation

Consider the mass balance on a simple distillation column. By simple column, we mean that the column has one feed, two products, one reboiler and one condenser. Such a column is shown in **Figure 9**, together with the feed and product flow rates and compositions. We can write an overall mass balance as:

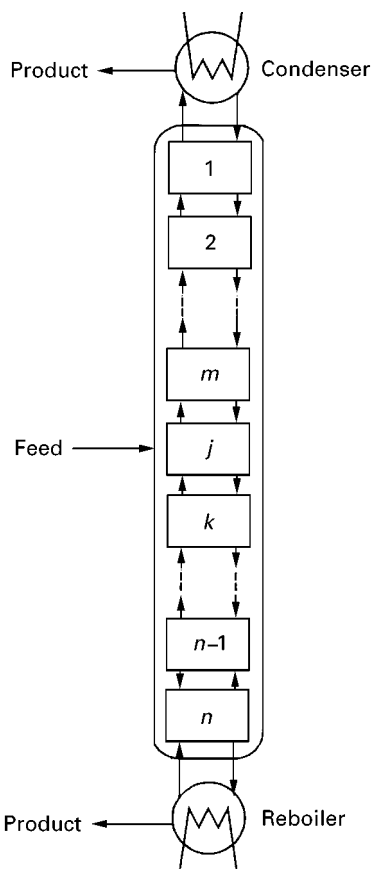


Figure 7 Refluxing and reboiling.

$$F = D + B$$

[19]

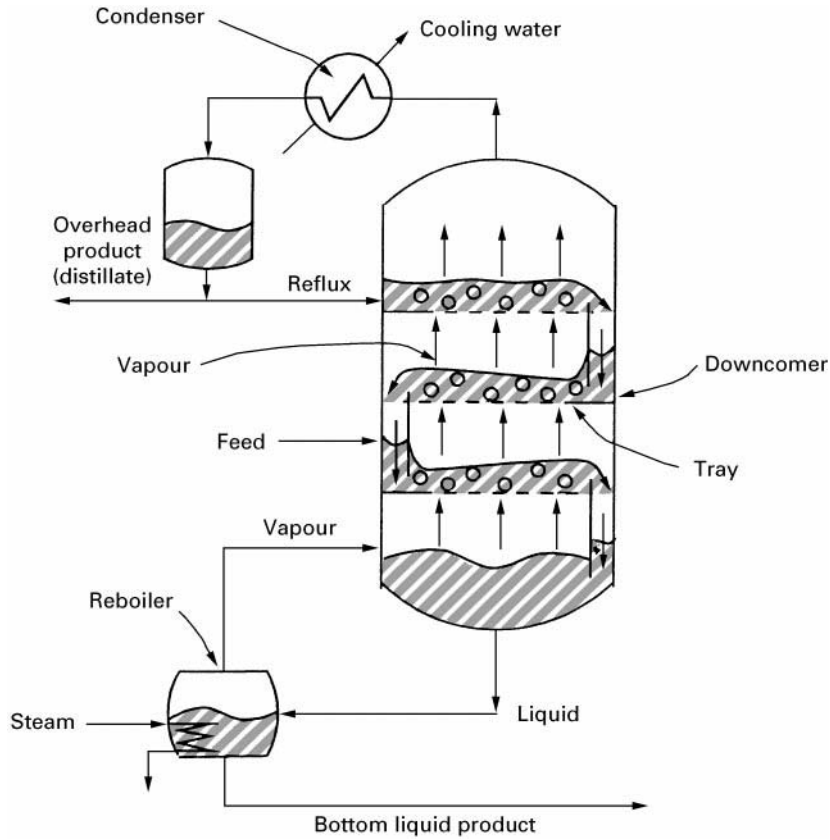


Figure 8 The distillation column.

We can also write a component balance as follows:

$$Fz_i = x_{D,i}D + x_{B,i}B \quad [20]$$

Given the reflux ratio, we can express the vapour flow in terms of R :

$$V = (R + 1) D \quad [24]$$

However, to understand the design of the column more fully, we must be able to follow the mass balance throughout the column. Let us start by considering the mass balance for the part of the column above the feed – the rectifying section. **Figure 10** shows the rectifying section of a column and the flows and compositions of the liquid and vapour in the rectifying section. First we write an overall balance for the rectifying section:

$$V_{n+1} = L_n + D \quad [21]$$

We can also write a component balance:

$$V_{n+1}y_{n+1,i} = L_nx_{n,i} + Dx_{D,i} \quad [22]$$

We assume constant molar overflow (L and V are constant) and define the reflux ratio, R , to be:

$$R = L/D \quad [23]$$

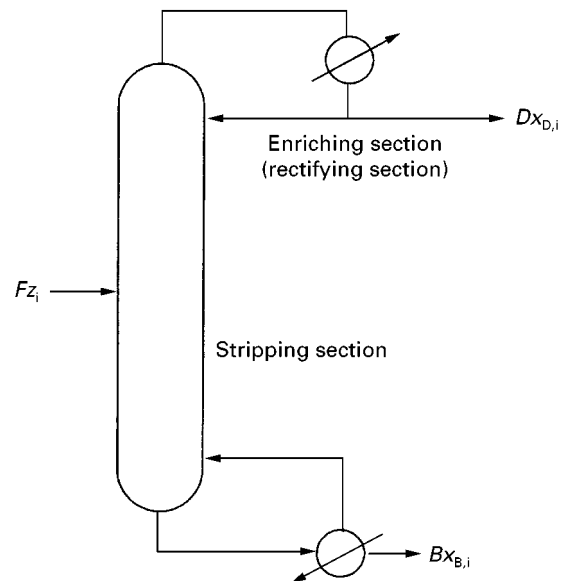


Figure 9 Mass balance on a simple distillation column.

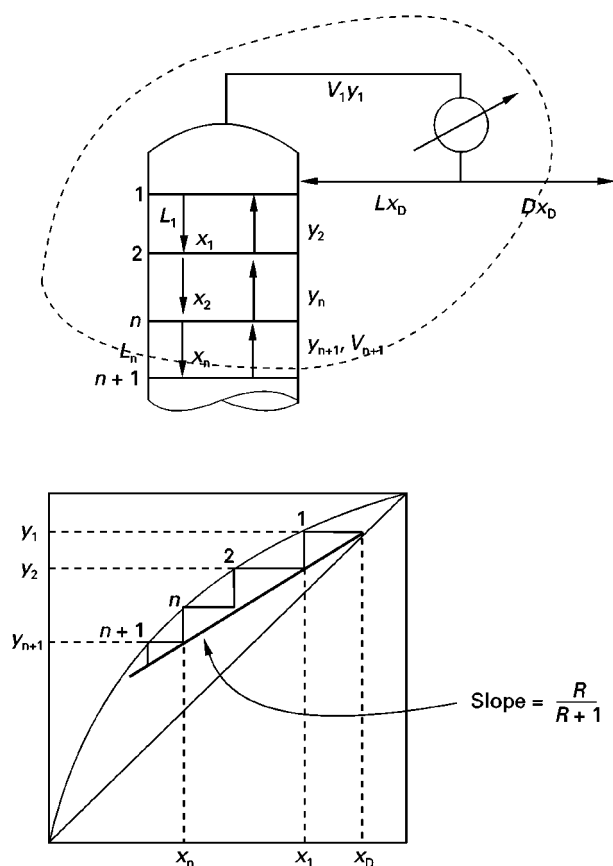


Figure 10 Mass balance on the rectifying section.

These expressions can be combined to give an equation which relates the vapour entering and liquid flows leaving stage n :

$$y_{n+1,i} = \frac{R}{R+1} x_{n,i} + \frac{1}{R+1} x_{D,i} \quad [25]$$

On an x - y diagram for component i , this is a straight line starting at the distillate composition with slope $R/(R+1)$ and which intersects the diagonal line at $x_{D,i}$.

Starting at the distillate composition x_D in Figure 10, a horizontal line across to the equilibrium line takes us to the composition of the vapour in equilibrium with the distillate, y_1 . A vertical step down takes us to the liquid composition leaving stage 1, x_1 . Another horizontal line across to the equilibrium line gives us the composition of the vapour leaving stage 2, y_2 . A vertical line to the operating line gives us the composition of the liquid leaving stage 2, x_2 , and so on. Thus, as we step between the operating line and equilibrium line in Figure 10, we follow the change in vapour and liquid composition through the rectifying section of the column.

Now consider the corresponding mass balance for the column below the feed, the stripping section. Figure 11A shows the vapour and liquid flows and compositions through the stripping section of a column. An overall mass balance for the stripping section around stage m gives:

$$L_m = V_{m+1} + B \quad [26]$$

A component balance gives:

$$L_m x_{m,i} = V_{m+1} y_{m+1,i} + B x_{B,i} \quad [27]$$

Again, assuming constant molar overflow (L and V are constant), these expressions can be combined to give an equation relating the vapour entering and the liquid leaving stage m :

$$y_{m+1,i} = \frac{L}{V} x_{m,i} - \frac{B}{V} x_{B,i} \quad [28]$$

We can plot this line in our x - y plot, as shown in Figure 11B. It is a straight line with slope L/V which intersects the diagonal line at x_B . Starting from the

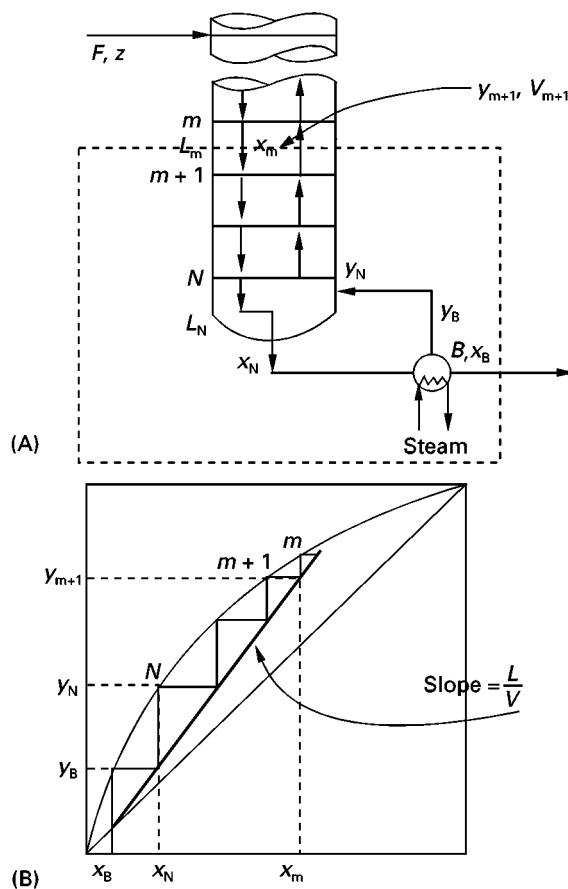


Figure 11 Mass balance on the stripping section.

bottom composition, x_B , a vertical line to the equilibrium line gives the composition of the vapour leaving the reboiler, y_B . A horizontal line across to the operating line gives the composition of the liquid leaving stage N , x_N . A vertical line to the equilibrium line then gives the vapour leaving stage N , y_N , and so on.

Let us now bring together the rectifying and stripping sections at the feed stage. Consider the point of intersection of the operating lines for the rectifying and stripping sections. From eqns [22] and [27]:

$$V_{n+1}y_i = L_nx_i + Dx_{D,i} \quad [29]$$

$$V_{m+1}y_i = L_mx_i - Bx_{B,i} \quad [30]$$

where y_i and x_i are the intersection of the operating lines. Subtracting eqns [29] and [30] gives:

$$(V_{n+1} - V_{m+1})y_i = (L_n - L_m)x_i + Dx_{D,i} + Bx_{B,i} \quad [31]$$

Substituting the overall mass balance, eqn [20], gives:

$$(V_{n+1} - V_{m+1})y_i = (L_n - L_m)x_i + Fz_i \quad [32]$$

Now we need to know how the vapour and liquid flow rates change at the feed stage.

What happens here depends on the condition of the feed, whether it is sub-cooled, saturated liquid, partially vaporized, saturated vapour or superheated vapour. To define the condition of the feed, we introduce the variable q , defined as:

$$q = \frac{\text{heat required to vaporize 1 mol of feed}}{\text{molar latent heat of vaporization of feed}} \quad [33]$$

For a saturated liquid feed $q = 1$ and for a saturated vapour feed $q = 0$. The flow rate of feed entering the column as liquid is $q \cdot F$. The flow rate of feed entering the column as vapour is $(1 - q) \cdot F$. **Figure 12A** shows a schematic representation of the feed stage. An overall mass balance on the feed stage for the vapour gives:

$$V_n = V_m + (1 - q)F \quad [34]$$

An overall mass balance for the liquid on the feed stage gives:

$$L_m = L_n + qF \quad [35]$$

Combining eqns [32], [34] and [35] gives a relationship between the compositions of the feed and the

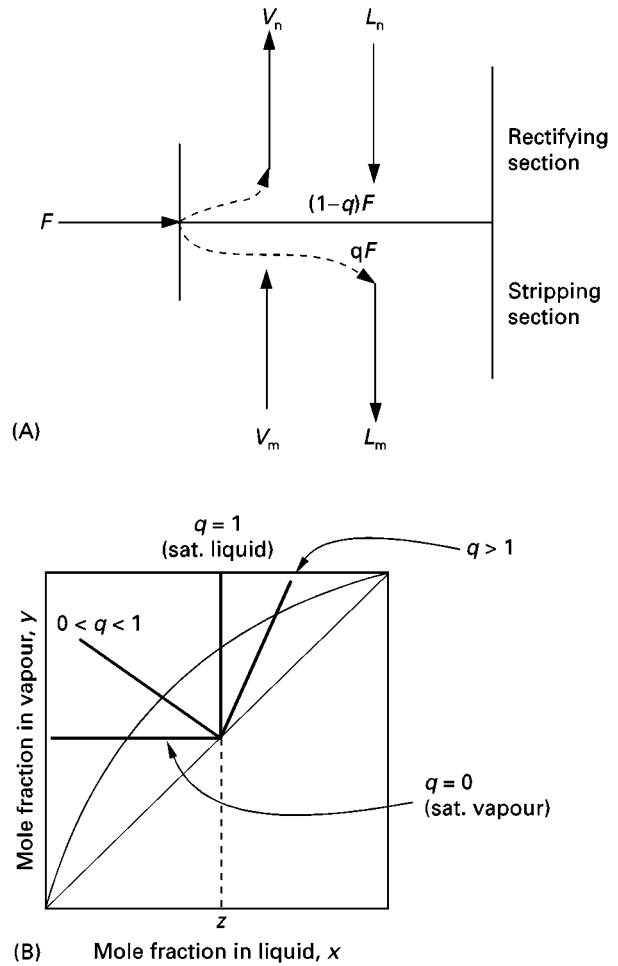


Figure 12 Mass balance for the feed stage.

vapour and liquid leaving the feed tray:

$$y_i = \frac{q}{q-1} \cdot x_i - \frac{1}{q-1} \cdot z_i \quad [36]$$

This equation is known as the q -line. On the x - y plot, it is a straight line with slope $q/(q-1)$ and intersects the diagonal line at z_i . It is plotted in Figure 12B for various values of q .

We are now in a position to bring together the mass balance for the rectifying and stripping sections. **Figure 13** shows the complete design. The construction is started by plotting the operating lines for the rectifying and stripping sections. The q -line intersects the operating lines at their intersection. The intersection of the operating lines is the correct feed stage, i.e. the feed stage necessary to minimize the overall number of theoretical stages. The construction steps off between the operating lines and the equilibrium lines. The construction can be started either from the overhead composition working down or from the bottom composition working up. The

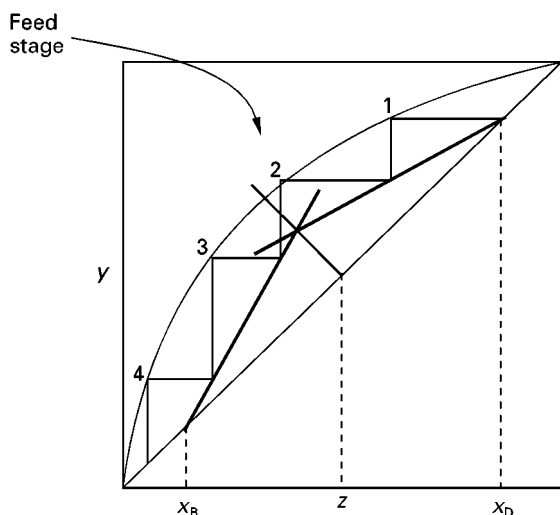


Figure 13 Combining the rectifying and stripping sections.

stepping procedure changes from one operating line to the other at the intersection with the q -line. We should also note that a partial reboiler represents a separation stage and a partial condenser (as opposed to a total condenser) also represents a separation stage.

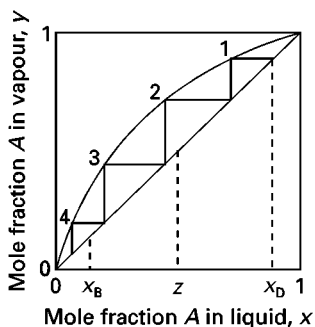
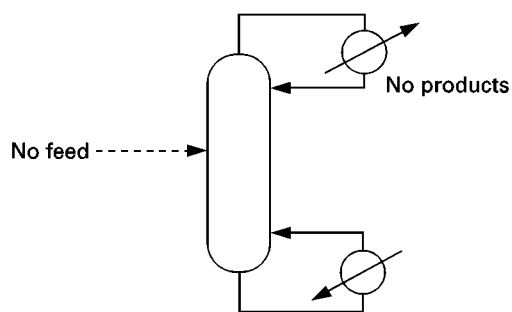
There are two important limits that we need to consider for distillation. The first is illustrated in **Figure 14A**. This is total reflux in which no products are taken and there is no feed. All of the overhead

vapour is refluxed and all of the bottom liquid re-boiled. Figure 14A also shows total reflux on an x - y plot. This corresponds with the smallest number of stages required for the separation. The other limiting case, shown in Figure 14B, is where the reflux ratio is chosen such that the operating lines intersect at the equilibrium line. As this stepping procedure approaches the q -line from both ends, an infinite number of steps are required to approach the q -line. This is the minimum reflux condition, and we term the condition at the feed stage to be a pinch.

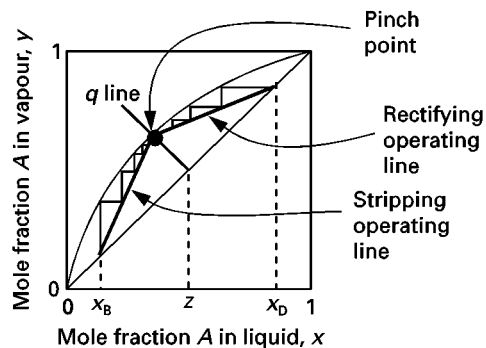
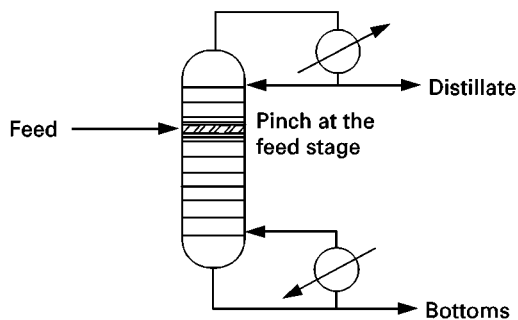
This method of design for binary distillation is known as the McCabe–Thiele method. It is restricted in its application because it only applies to binary systems and involves the simplifying assumption of constant molar overflow. However, it is an important method to understand as it gives important conceptual insights into distillation, which cannot be obtained in any other way.

Multicomponent Distillation

Before a multicomponent distillation column can be designed, a decision must be made as to the two key components between which it is desired to make the separation. The light key component will be the one we wish to keep out of the bottom product. The heavy key component will be the one we wish to keep out of the top product. The recovery of the light key or the concentration of the light key in the overhead



(A)



(B)

Figure 14 (A) Total and (B) minimum reflux in binary distillation.

product must be specified, as must the recovery of the heavy key or the concentration of the heavy key in the bottom product. Intermediate boiling components will distribute between the products.

A number of short-cut methods are available for the design of multicomponent distillation columns. Each considers different aspects of the design of multicomponent columns. Each of the short-cut methods involves some simplifying assumptions and the designer must be fully aware of these assumptions when applying these methods. One simplifying assumption, which all the methods have in common, is the assumption of constant relative volatility. The relative volatility for the feed composition can be calculated, but this might not be characteristic of the overall column. By making some assumption of the product compositions, the relative volatility at the top and bottom of the column can be calculated and a mean taken:

$$(\alpha_{i,j})_{\text{mean}} = \sqrt{(\alpha_{i,j})_{\text{top}} \cdot (\alpha_i^j)_{\text{bottom}}} \quad [37]$$

Fenske Equation

The Fenske equation is used to estimate the minimum number of stages, N_{\min} . This is at total reflux and the flows of component i and a reference component, r , are related by:

$$\frac{d_i}{d_r} = \alpha_{i,r}^{N_{\min}} \cdot \frac{b_i}{b_r} \quad \text{or} \quad \frac{x_{D,i}}{x_{D,r}} = \alpha_{i,r}^{N_{\min}} \cdot \frac{x_{B,i}}{x_{B,r}} \quad [38]$$

When component i is the light key component L , and r is the heavy key component, H , we can write:

$$N_{\min} = \frac{\log \left[\frac{d_L}{d_H} \cdot \frac{b_H}{b_L} \right]}{\log \alpha_{L,H}} \quad [39]$$

$$N_{\min} = \frac{\log \left[\frac{x_{D,L}}{x_{D,H}} \cdot \frac{x_{B,H}}{x_{B,L}} \right]}{\log \alpha_{L,H}} \quad [40]$$

$$N_{\min} = \frac{\log \left[\frac{r_{D,L}}{1 - r_{D,L}} \cdot \frac{r_{B,H}}{1 - r_{B,H}} \right]}{\log \alpha_{L,H}} \quad [41]$$

Hengstebeck–Geddes Equation

The Hengstebeck–Geddes equation is used to estimate the composition of the products. The Fenske equation can be written in the form:

$$\log \left[\frac{d_i}{b_i} \right] = A + C \log \alpha_{i,r} \quad [42]$$

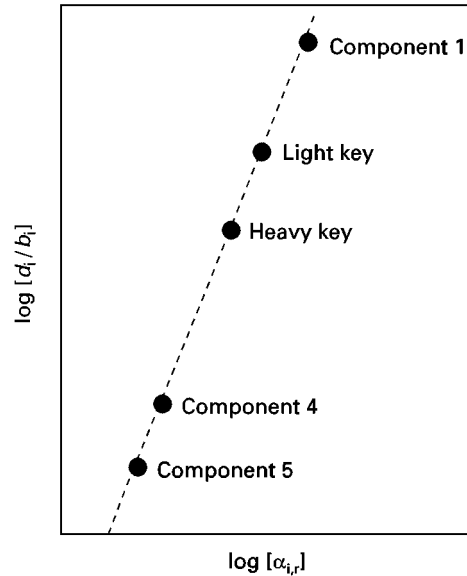


Figure 15 The Hengstebeck–Geddes method.

The parameters A and C are obtained by applying the relationship to the light and heavy key components. This allows the compositions of the non-key components to be estimated. This is illustrated in **Figure 15**. Having specified the distribution of the light and heavy key components, knowing the relative volatilities for the other components allows their compositions to be estimated. The method is based on total reflux conditions. It assumes that the component distributions do not depend on reflux ratio.

The Underwood Equations

The Underwood equations are used to estimate minimum reflux ratio. There are two equations. The first is given by:

$$\sum_{i=1}^n \frac{\alpha_i x_{i,F}}{\alpha_i - \theta} = 1 - q \quad [43]$$

This equation must be solved for the root θ . This root will have a value between the relative volatilities of the light and heavy key components. Having obtained the value θ , this is then substituted into the second equation to determine the minimum reflux ratio, R_{\min} :

$$R_{\min} + 1 = \sum_{i=1}^n \frac{\alpha_i x_{i,D}}{\alpha_i - \theta} \quad [44]$$

The Gilliland Correlation

The Gilliland correlation is an empirical relationship used to determine the number of stages, given the minimum reflux ratio R_{\min} and minimum number of stages N_{\min} . The original correlation was presented in

graphical form. Two parameters were used to correlate the experimental data:

$$Y = \frac{N - N_{\min}}{N + 1}, \quad X = \frac{R - R_{\min}}{R + 1} \quad [45]$$

Various attempts have been made to represent the correlation algebraically. For example:

$$Y = 0.2788 - 1.3154X + 0.4114X^{0.2910} + 0.8268 \cdot \ln X + 0.9020 \ln\left(X + \frac{1}{X}\right) \quad [46]$$

The Kirkbride Equation

The Kirkbride equation is used to estimate the most appropriate feed point for the column. It is given in the form:

$$\log \frac{N_r}{N_s} = 0.206 \log \left[\frac{z_H}{z_L} \cdot \frac{B}{D} \cdot \left(\frac{x_{B,L}}{x_{D,H}} \right)^2 \right] \quad [47]$$

Rigorous Methods

All of the above equations are approximate in some way. To develop a completely rigorous approach to distillation design, consider **Figure 16**. This shows a general stage in the distillation column. Vapour and liquid enter this stage. A liquid side-stream can be taken, as can a vapour side-stream. Feed can enter

and heat can be transferred to or from the stage. This is a general stage and allows for many design options other than simple columns with one feed and two products. By using a general representation of a stage, as shown in **Figure 16**, designs with multiple feeds, multiple products and intermediate heat exchange are possible. We can write rigorous equations to describe the material and energy balance.

1. Material balance (N_{comp} equations for each stage):

$$L_{j-1}x_{i,j-1} + V_{j+1}y_{i,j+1} + F_jz_{i,j} - (L_j + U_j)x_{i,j} - (V_j + W_j)y_{i,j} = 0 \quad [48]$$

2. Equilibrium relation for each component (N_{comp} equations for each stage):

$$y_{i,j} - K_{i,j}x_{i,j} = 0 \quad [49]$$

3. Summation equations (one for each stage):

$$\sum_{i=1}^{N_{\text{comp}}} y_{i,j} - 1.0 = 0 \quad \sum_{i=1}^{N_{\text{comp}}} x_{i,j} - 1.0 = 0 \quad [50]$$

4. Energy balance (one for each stage):

$$L_{j-1}H_{j-1}^L + V_{j+1}H_{j+1}^V + F_jH^F - (L_j + U_j)H_j^L - (V_j + W_j)H_j^V - Q_j = 0 \quad [51]$$

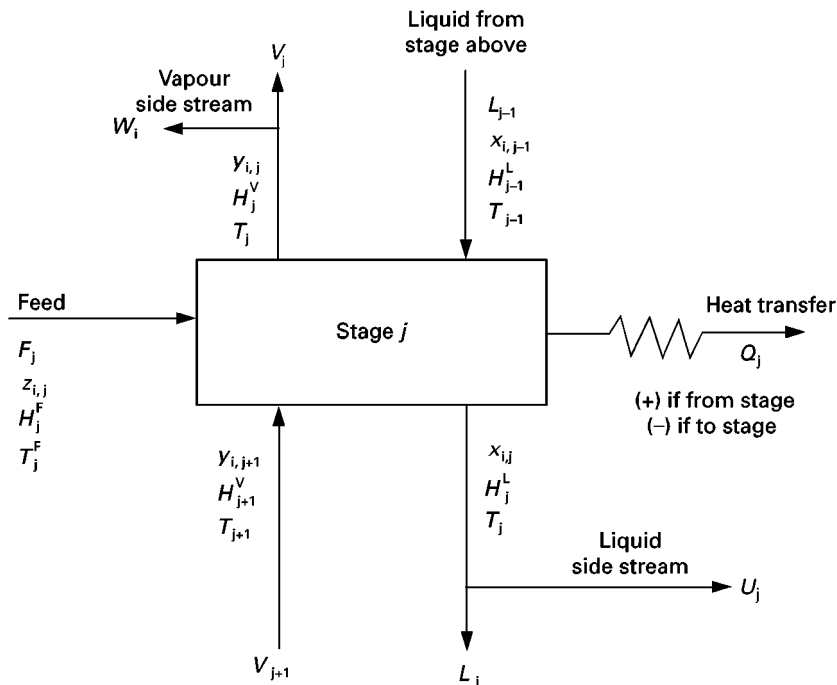


Figure 16 A general stage for rigorous methods in multicomponent distillation.

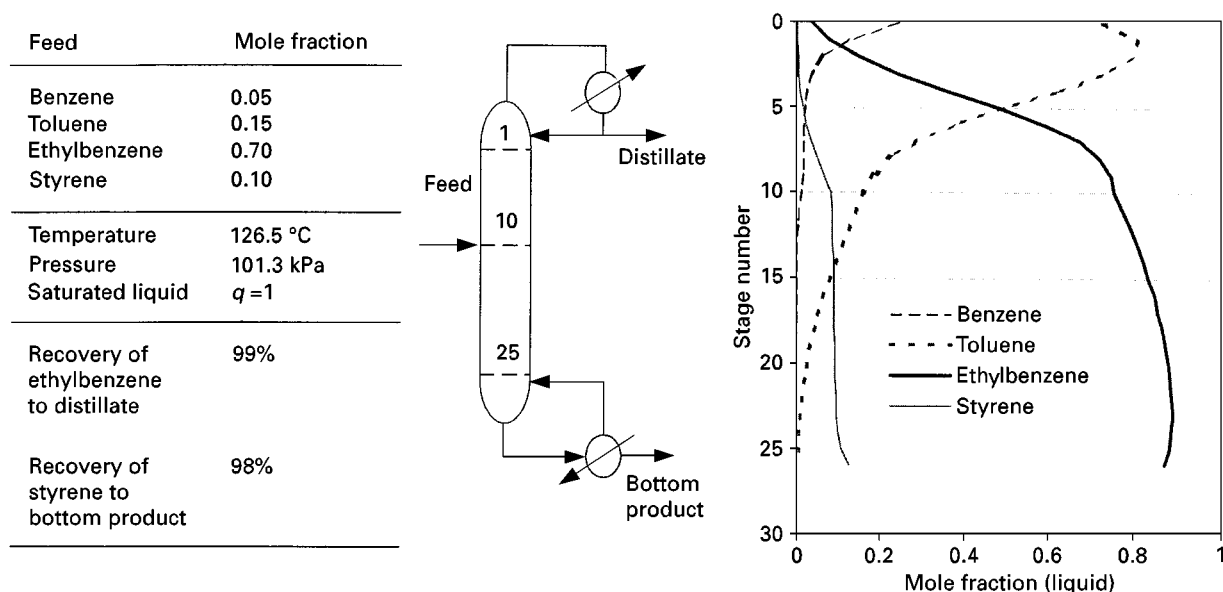


Figure 17 Simulation results for multicomponent distillation.

This set of equations must be solved iteratively and the calculations are complex. Many methods are available and in practice designers use commercial simulation packages.

Figure 17 shows a typical result for the rigorous simulation of a distillation column with a feed mixture containing benzene, toluene, ethylbenzene and styrene. Because such simulations are numerically complex and time-consuming, short-cut calculations are used to explore the various design parameters before setting up a rigorous simulation.

Choice of Operating Parameters

The feed composition and flow rate are usually fixed. Also, the product specifications are usually given in the statement of the design problem. These may be

expressed in terms of product purities or recoveries of certain components. The operating parameters to be selected by the designer include:

1. operating pressure
2. reflux ratio
3. feed condition
4. feed stage location
5. type of condenser

Pressure

Once the products have been specified, the pressure must be specified before the design can proceed. Pressure has an important effect on all aspects of the distillation column design. Figure 18 shows the trends of various properties of the distillation as

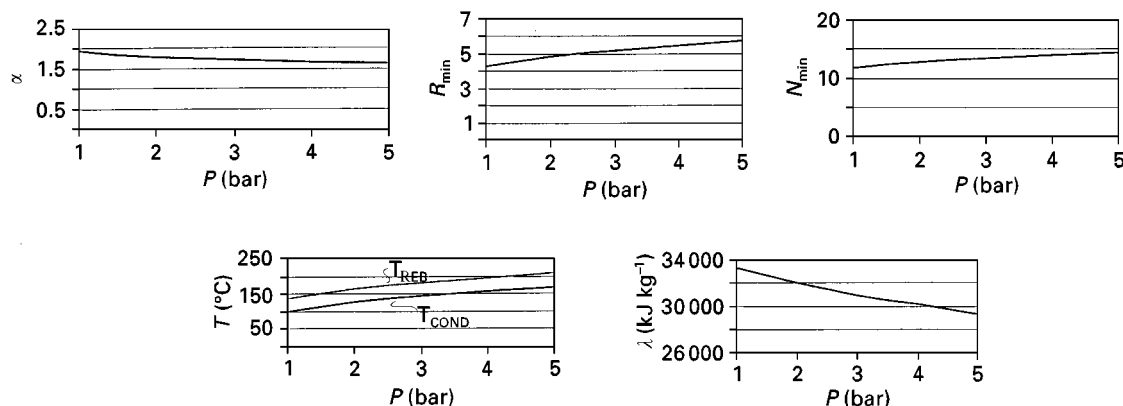


Figure 18 Effect of pressure on the distillation of a mixture of benzene, toluene, ethylbenzene and styrene.

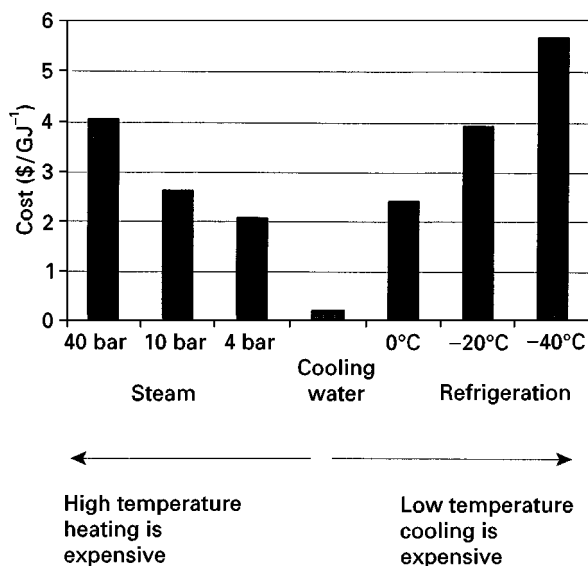


Figure 19 Effect of temperature on utility costs.

pressure increases. As pressure increases, the relative volatility decreases, making separation more difficult. Minimum reflux ratio also increases with increasing pressure, as does the minimum number of stages. All of these trends point to operating the distillation columns at a pressure as low as possible. However, the latent heat decreases with increasing pressure; this would have the effect of decreasing the reboiler duty as pressure increases. Finally, Figure 18 also shows the trend of condenser and the reboiler temperature as pressure increases; both increase with increasing pressure.

The temperature of the condenser and reboiler, as shown in Figure 18, dictate the choice of utilities to supply heating and cooling. Figure 19 shows the trend for the variation in utility costs for heating and cooling at different temperatures. Figure 19 shows that extreme temperatures for heating and cooling require more expensive utilities. Matching the distillation condenser and reboiler against cheap utilities is usually the dominant issue when choosing the operating pressure of the distillation column.

When starting a distillation design, we usually choose to operate at atmospheric pressure unless this leads to thermal degradation of products in the reboiler because of high temperatures, or requires refrigeration in the condenser. If product degradation is a problem, then we would operate the column under vacuum conditions to decrease the temperatures of the distillation. If refrigeration is required in the condenser, then we might choose to increase the column pressure until cooling water can be used for the condenser (which means the overhead condenser temperature must be 30–40°C or higher), unless very high pressures are required for the distillation.

Choice of Reflux Ratio

Figure 20 shows the variation of the number of stages required versus the reflux ratio. Starting from minimum reflux, we require an infinite number of stages. As the reflux ratio is increased, the number of stages becomes finite and decreases towards the minimum number of stages at total reflux. Actual reflux ratios will lie somewhere between the two extremes.

Figure 21 shows a plot of annual cost versus reflux ratio. At minimum reflux ratio there is the requirement for an infinite number of stages and the annual capital cost is correspondingly infinite. However, as the reflux ratio is increased the capital cost diminishes. On the other hand, as reflux ratio is increased from the minimum, the utility costs increase steadily. Combining the annual capital costs with the annual utility costs gives a total annualized cost which shows a minimum at the optimum reflux ratio. This optimum is usually fairly flat for a significant range of reflux ratios and an initial setting of 1.1 times the minimum reflux ratio is often assumed.

Choice of Feed Condition

The feed condition affects vapour and liquid flow rates in the column, and in turn:

1. reflux ratio, heating and cooling duties
2. column diameter
3. most appropriate location of the feed stage

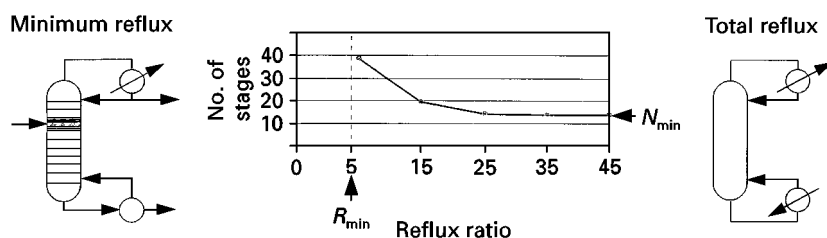


Figure 20 Range of reflux ratios.

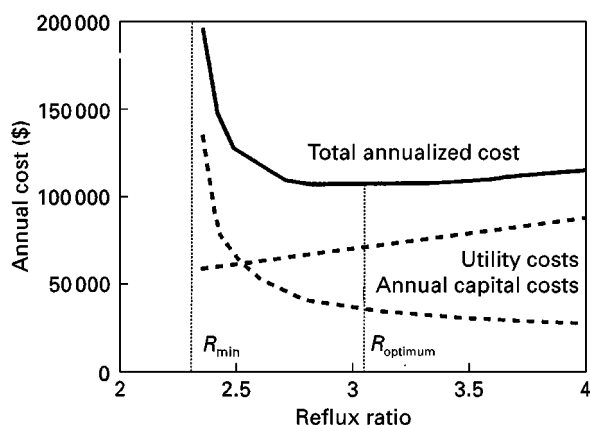


Figure 21 Capital–energy trade-offs determine the optimum reflux ratio.

The feed temperature usually lies between the extreme temperatures of the column (condenser and reboiler temperatures).

Cooling the feed:

1. decreases the number of stages in the rectifying section but increases the number of stages in the stripping section
2. requires more heat in the reboiler but decreases the cooling duty of the condenser

Heating the feed:

1. increases the number of stages in the rectifying section but decreases the number of stages in the stripping section
2. decreases the heat requirement of the reboiler but increases the cooling duty of the condenser

Heating or cooling the feed can reduce energy costs. If heat is added to the feed and saves heating in the reboiler, the heating of the feed can be carried out at a lower temperature than would be required in the reboiler. Cooling the feed can be carried out at a lower temperature than cooling in the condenser. In both cases heating or cooling the feed is done at more moderate temperatures and, in principle, with a cheaper utility.

Choice of Feed Stage Location

When choosing the feed stage location, our objective is to find a stage in the column for which the composition matches as closely as possible that of the feed. For binary distillation it is, in theory, possible to find an exact match between the composition on a stage and the composition of the feed. In practice, because there is a finite change from stage to stage, even for

a binary system, an exact match may not be possible. In multicomponent systems it is highly unlikely that the composition of all of the components can be matched. Mismatches between the composition on the feed stage and that of the feed create inefficiencies in the distillation. These inefficiencies lead to an increase in the number of stages required for the same separation, or more reflux, which means increased energy requirements, or a combination of both.

Distillation Equipment

Let us now turn our attention to the equipment used for distillation operations. As pointed out previously, there are two broad classes of internals used for distillation: trays and packing.

Trays

Figure 22A shows a conventional tray arrangement. Liquid flows down a downcomer across a tray in which the upflowing vapour contacts the liquid flowing across the tray. The liquid flows down the next downcomer to the following tray, and so on. The perforated plate used in Figure 22A, known as a sieve tray, is the most common arrangement used. It is cheap, simple, and well understood in terms of its performance. There are many other designs of tray which are used. Many use simple valve arrangements in the holes to improve the performance and the flexibility of operation to be able to cope with a wider variety of liquid and vapour flow rates in the column. One particular disadvantage of the conventional tray in Figure 22A is that the downcomer arrangement makes a significant proportion of the area within the column shell not available for contacting liquid and vapour. In an attempt to overcome this, high capacity trays, with increased active area, have been developed. Figure 22B illustrates the concept. Again, many different designs are available for high capacity trays.

When designing a column to use trays, we need to know the tray efficiency to convert from

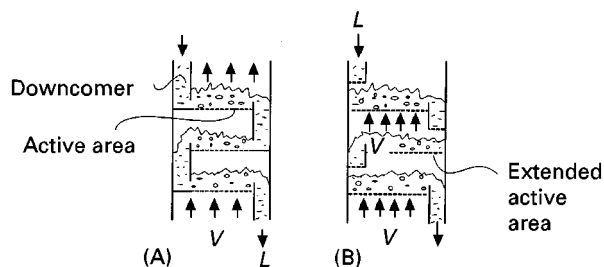


Figure 22 Distillation trays. (A) Conventional tray; (B) high capacity tray.

theoretical stages to real trays. The difference between the performance of an ideal stage and a real tray results from the fact that equilibrium is not achieved on a real tray because of mass transfer limitations. We therefore define an efficiency to convert from the theoretical stages to real trays. Three different efficiencies can be defined:

1. Overall tray efficiency, E_o :

$$E_o = \frac{\text{number of theoretical stages}}{\text{number of real stages}} \quad [52]$$

E_o depends on the design of the tray and the mixture being distilled and typically varies between 60% and 90% for distillation.

2. Murphree tray efficiency, E_M . This characterizes the performance of individual trays rather than having an overall measure as defined by E_o . This is because efficiencies can vary throughout the column. The Murphree tray efficiency for stage j is defined as:

$$E_M = \frac{y_j - y_{j+1}}{y_j^* - y_{j+1}} \quad [53]$$

The Murphree tray efficiency measures the change in concentration of the vapour phase for an actual tray relative to that for an ideal stage.

3. Point efficiency, E_{MP} . This measures the efficiency not only of an individual tray but at a local point on a tray. It is defined in the same way as the Murphree tray efficiency, but at a point on the tray. It is defined as:

$$E_{MP} = \frac{y_{j,\text{local}} - y_{j+1,\text{local}}}{y_{j,\text{local}}^* - y_{j+1,\text{local}}} \quad [54]$$

E_{MP} varies across the tray and must be integrated across the tray to obtain E_M . The result will depend on the mixing pattern on the tray. For example, if the tray is perfectly mixed then $E_M = E_{MP}$.

Correlations are available to predict E_o , E_M and E_{MP} .

Trays have a range within which they can operate satisfactorily in terms of the hydraulic design. For example, Figure 23 shows the range of operation of a sieve tray. Using a sieve tray, internal flows in the distillation column are limited by:

1. flooding, in which liquid cannot flow down the column
2. entrainment, in which liquid drops are carried up the column by the vapour flow

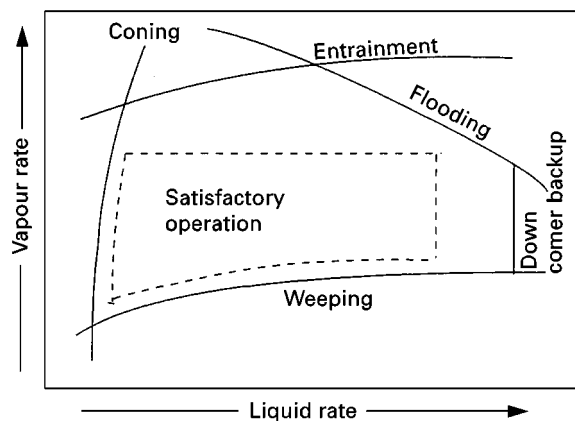


Figure 23 Sieve tray performance.

3. downcomer backup, in which liquid backs up in the downcomers
4. weeping, in which vapour flow is too low to maintain liquid on the tray
5. coning, in which poor vapour-liquid contact occurs due to the vapour forming jets

Packing

Figure 24A shows a traditional design of packing, which is random or dumped packing. The random or dumped packing is pieces of ceramic, metal or plastic which, when dumped in the column, produce a body with a high voidage. The liquid trickles down over the surfaces of the packing and the vapour is in contact with the liquid as it flows up through the voids in the packing.

Figure 24B shows structured packing. This is manufactured by sheets of metal being preformed

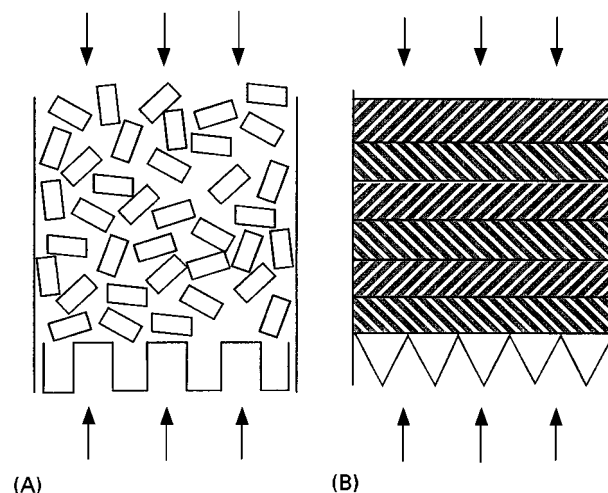


Figure 24 Distillation packing. (A) Random or dumped packing; (B) structured packing.

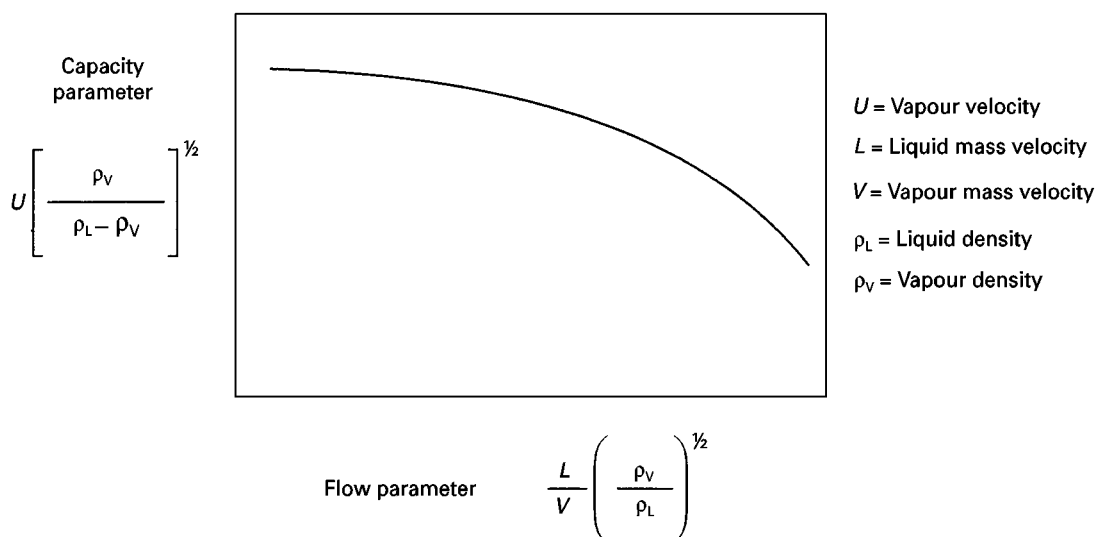


Figure 25 Flood point correlation for packing.

with corrugations and holes and then joined together to produce a preformed packing with a high voidage. This is manufactured in slabs and built up in layers within the column.

Many types of both random and structured packing are available. We need to be able to calculate the height of packing required by relating to the theoretical stages to the height of packing. For this we need the height equivalent of a theoretical plate, HETP. Thus, the packing height is simply the product of the number of theoretical stages and the HETP. Correlations are available for HETP.

As with the hydraulic design of trays, packing has a limited range over which the hydraulic design is acceptable. At very low vapour velocities through the packing, liquid flows are not influenced by the vapour flow. As the vapour velocity increases, the vapour starts to hinder the downward flow of liquid. This is the loading point. A limit is reached at a high vapour velocity, characterized by heavy entrainment of liquid and a sharp rise in the pressure drop across the packing. This is the flood point. Correlations are used to determine the flood point and a typical correlation is shown in **Figure 25**. We usually design the packing for a vapour velocity to be some proportion of the flooding velocity (e.g. 80%).

Complex Distillation Arrangements

All of the distillation arrangements which we have considered so far have involved one feed, produced two products, have a reboiler and condenser, and operation has been assumed to be continuous. Distillation designs have been adapted to suit different purposes, as discussed below.

Batch Distillation

In batch distillation, the feed is charged as a batch to the base of the distillation column. Once the feed has been charged, it is subjected to continuous vaporization. This vapour would then flow upwards through trays or packing to the condenser and reflux would be returned as with continuous distillation. However, unlike continuous distillation, the overhead product will change with time. The first material to be distilled will be the more volatile components. As the vaporization proceeds and product is withdrawn overhead, the product will become gradually richer in the less volatile components. Thus, batch distillation allows different fractions to be taken from the same feed. The batch distillation strategy depends on both the feed mixture and the products required from the distillation. By careful control of the reflux, it is possible to hold the composition of the distillate constant for a time until the required reflux ratio becomes intolerably large, as illustrated in **Figure 26**.

Azeotropic Distillation

Figure 27 shows an x - y diagram in which the equilibrium curve crosses the diagonal line. At the point where the equilibrium curve crosses the diagonal, the vapour and liquid have the same composition; this is an azeotrope. A mixture in which the vapour and liquid have the same composition cannot be separated by conventional distillation. There are two means by which a mixture such as that shown in **Figure 27** can be separated. The first uses two columns operating at different pressures and takes advantage of the fact that the composition of the azeotrope might change significantly with a change in

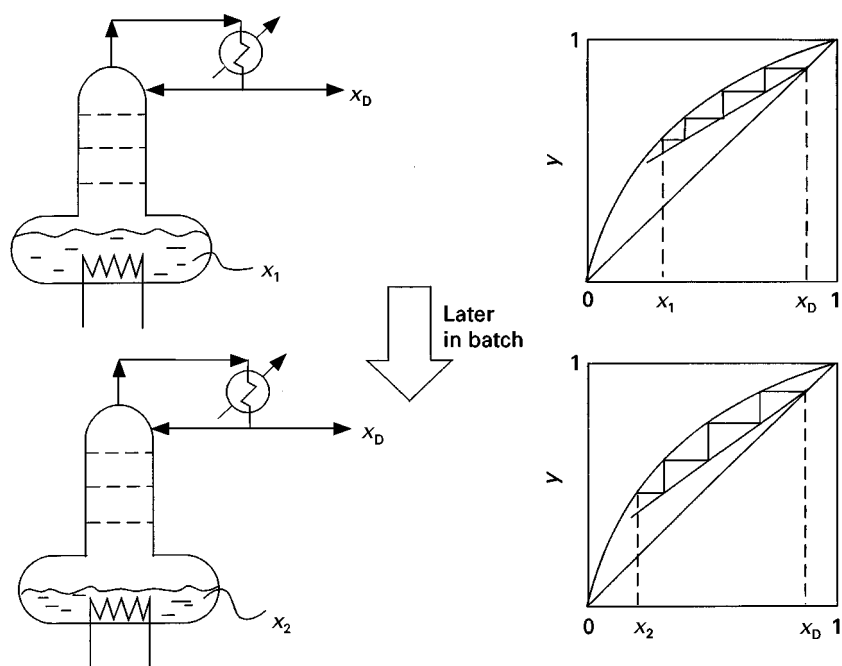


Figure 26 Reflux ratio can be varied in batch distillation to maintain overhead product purity.

pressure. The second method is to add a mass separation agent (known as an entrainer or a solvent). The mass separating agent must change the relative volatility of the original mixture in a way which allows the separation to be achieved.

Steam Stripping

Sometimes live steam is added at the base of the distillation column. When steam is used in this way, for example for the separation of hydrocarbon mix-

tures, the steam acts as an inert carrier, the presence of which decreases the partial pressure of the components in the vapour phase. This is like operating the distillation column at a lower pressure as far as the separation is concerned. However, the use of stripping steam is not quite the same as reducing the operating pressure.

Intermediate Reboiling and Condensing

Rather than use a single reboiler at the bottom of the column and a single condenser at the top of the column, it is possible to add or reject heat at intermediate points within the column. Below the feed but above the base of the column, liquid can be withdrawn from one of the stages into an intermediate reboiler to be vaporized and the vapour returned to the column. This inter-reboiling substitutes part of the reboiling at the base of the column. The advantage of inter-reboiling is that the heat can be supplied at a lower temperature in the inter-reboiler, compared with the temperature required for the reboiler at the base of the column.

Similarly, vapour can be withdrawn from the column above the feed but below the top of the column, condensed and the liquid returned to the column. Cooling in the intercondenser substitutes cooling in the overhead condenser. Because the cooling in the intercondenser is carried out at a higher temperature than the overhead condenser, this can have advantages in terms of the utility costs. In practice, it is difficult to extract part of the vapour flowing up

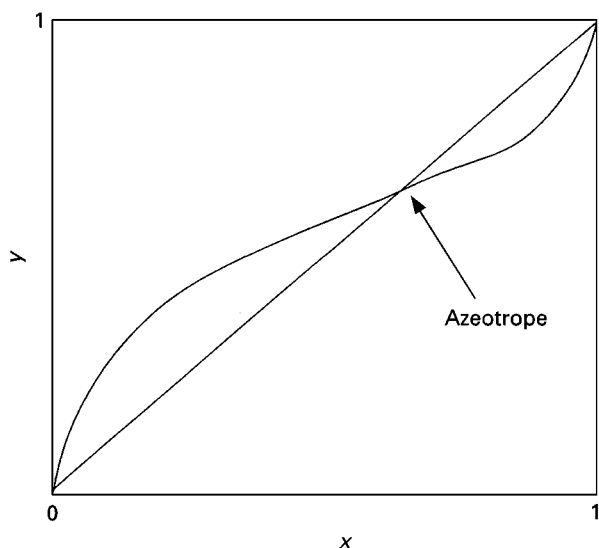


Figure 27 Azeotropic behaviour.

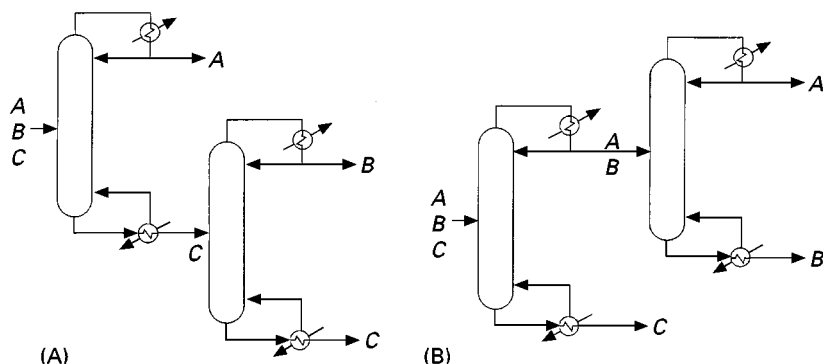


Figure 28 Sequencing simple distillation columns. (A) Direct sequence; (B) indirect sequence.

the column into an intercondenser. Because of this, it is more usual to take a liquid side-stream from the column, sub-cool the liquid and return the sub-cooled liquid to the column. The sub-cooled liquid provides condensation directly. Such arrangements are known as pump-arounds or pump-backs.

Multiple Feeds

Sometimes it is necessary to separate two or more streams with the same components but with different compositions. If this is the case, it is wrong to mix the streams with different compositions to produce a single feed for the distillation column. This is because we would mix streams only to separate them later and this is thermodynamically inefficient. If we have several streams with the same components but significantly different compositions, then it is better to feed them to the distillation column at different points, trying as much as possible to match the composition of each feed with that of one of the stages in the column.

Multiple Products

It is sometimes possible to withdraw more than two products from the same column. Part of the liquid flowing down the column or part of the vapour flow-

ing up the column can sometimes be taken as a side-stream to form a third product. Such side-stream column designs are only possible under special circumstances.

Column Sequences

If a feed mixture needs to be separated into more than two products, then more than one distillation column will usually be required. Figure 28 illustrates the options for the separation of a mixture of three products. In the first arrangement, the lightest component is taken overhead first and the two heavier products are separated in the second column. In the second arrangement, the heaviest product is separated first and then the two lightest products are separated in the second column. For a three-product separation, there are two possible sequences, as shown in Figure 28. As the number of products in the mixture increases, the number of possible distillation sequences increases significantly. For example, if we have six products, then there are 42 possible sequences of columns.

Thermal Coupling

Figure 28 showed different arrangements of simple distillation columns for the separation of a three-product mixture. Each column had one feed,

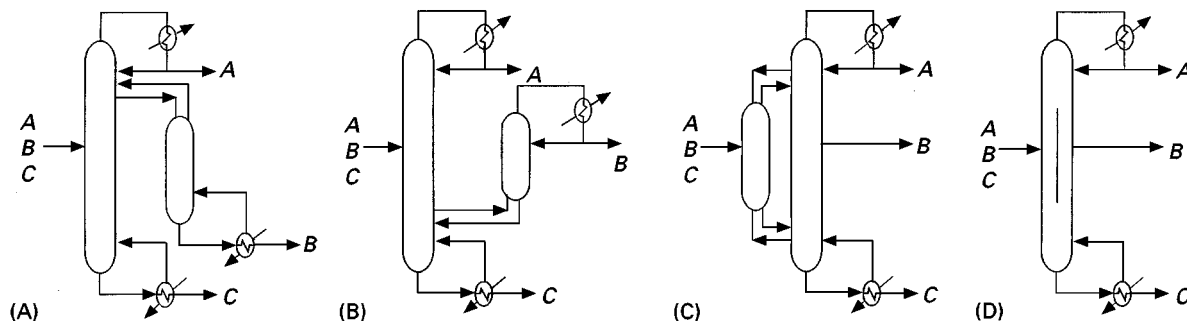


Figure 29 Thermally coupled columns. (A) Side-stripper, (B) side-rectifier; (C) fully thermally coupled (Petlyuk) column; (D) dividing wall column.

Table 1 Cases not suited to separation by distillation

<i>Case</i>	<i>Problem</i>	<i>Possible solutions</i>
Separate materials of low molecular mass	Low condensation temperature	Absorption, adsorption, membranes
Separate heat-sensitive materials of high molecular mass	Thermal degradation of products	Vacuum distillation
Separate components present in low concentrations	High flow rates in columns	Absorption, adsorption
Separate classes of components (e.g. aromatics from aliphatics)	Boiling temperatures/volatilities of components in a class are not adjacent	Liquid-liquid extraction
Separate components with similar relative volatilities	Difficult separation: high operating and capital costs	Add mass separating agent and employ extractive or heterogeneous distillation or liquid-liquid extraction, crystallization
Separate components which form an azeotrope	Azeotrope limits product composition	Add mass separating agent and employ extractive or heterogeneous distillation or liquid-liquid extraction, crystallization
Separate volatile and involatile components	Distillation requires that all components are mobile for countercurrent flow	Evaporation, drying, nanofiltration
Separate condensible and noncondensable components	Only partial condenser can be used overhead	Use single-stage separation (flash)

two products and had a reboiler and a condenser. Sometimes, it is desirable to exchange heat between columns directly using thermal coupling connections. Figure 29 shows some thermally coupled distillation designs for the separation of a three product mixture. Figure 29A shows a side-stripper and Figure 29B a side-rectifier. Figure 29C shows a fully thermally coupled arrangement, sometimes known as a Petlyuk column. Figure 29D shows what is known as a dividing wall column. This is the same arrangement as the Petlyuk column but the arrangement is built in a single shell with a dividing wall down the middle of the column. The arrangements in Figure 29C and 29D are both equivalent thermodynamically, if there is no heat transfer across the dividing wall in Figure 29D.

Summary

Distillation is a versatile, robust and well-understood technique and is the most commonly used method for the separation of homogeneous fluid mixtures. There are cases for the separation of homogeneous fluid mixtures for which distillation is not well suited. Table 1 presents a summary of these cases, along with possible solutions. It should be noted, however, that even though distillation is not well suited to the separation duties in Table 1, distillation is still used in some form for many of these problematic cases.

Symbols

b_i bottoms flow rate of component i
 B molar bottoms flow rate
 d_i distillate flow rate of component i
 D molar distillate flow rate
 E_M Murphree tray efficiency

E_{MP} point efficiency
 E_o overall tray efficiency
 f_i^L fugacity of component i in the liquid phase
 f_i^V standard-state fugacity of component at the temperature of the system
 f_i^0 fugacity of component i in the vapour phase
 F molar feed flow rate
 H molar enthalpy
 K_i equilibrium constant for component i
 L molar flow of liquid
 N_{min} minimum number of stages
 N number of stages
 N_{comp} number of components
 P system pressure
 P_i^{SAT} saturated vapour pressure of component i at the system temperature
 q feed condition
 Q heat duty
 R reflux ratio
 r recovery
 R_{min} minimum reflux ratio
 T temperature
 U vapour velocity
 V molar flow of vapour
 x_i mole fraction of i in the liquid phase
 y_i mole fraction of i in the vapour phase
 y_i^* mole fraction of vapour that would be in equilibrium with liquid leaving stage j
 $y_{j,local}^*$ mole fraction of vapour that would be in equilibrium with the local concentration on stage j
 z_i feed composition of component i
 α_{ij} relative volatility between components i and j
 ρ density
 ϕ_i^L liquid-phase fugacity coefficient for component i

ϕ_i^V vapour-phase fugacity coefficient for component i
 γ_i activity coefficient for component i

See Colour Plate 5.

Further Reading

Geankoplis CJ (1993) *Transport Processes and Unit Operations*. New Jersey: PTR Prentice Hall.

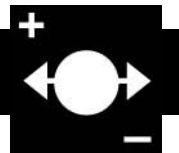
King CJ (1980) *Separation Processes*. New York: McGraw-Hill.

Kister HZ (1992) *Distillation Design*. New York: McGraw-Hill.

Seader JD and Henley EJ (1998) *Separation Process Principles*. New York: John Wiley.

Stichlmair JG and Fair JR (1998) *Distillation Principles and Practice*. New York: Wiley-VCH.

ELECTROPHORESIS



D. Perrett, St Bartholomew's and the Royal London School of Medicine and Dentistry, St Bartholomew's Hospital, London, UK

Copyright © 2000 Academic Press

An Outline of the Historical Background to Electrophoretic Separations

The movement of charged particles under the influence of an electric field was observed as long ago as 1807 by Ferdinand Frederic Reuss. In 1909, the term, electrophoresis, was introduced by Michaelis as a description of this phenomenon and is derived from the Greek word *elektron* meaning amber (i.e. electric) and *phore* meaning bearer. Yet it was not until the 1930s that electrophoresis, as we know it today, developed from the work of Tiselius, who, in 1948, was awarded the Nobel Prize for this development. Table 1 charts the development of the technique over the last century. By the 1950s electrophoresis was a common laboratory technique equivalent in usefulness to planar chromatography techniques such as paper and thin layer. However, with the advent of high-performance liquid chromatography (HPLC) in the 1970s, analytical electrophoresis became something of a 'Cinderella' technique. Only in biochemical and clinical laboratories did electrophoresis continue in use as a qualitative separation technique for macromolecules, such as proteins and DNA.

It has been claimed that currently at least half of all separations are performed by electrophoresis since separations of blood proteins and DNA digests are routinely performed by the technique. The technique is now so routine in biomedicine and related disciplines that it is rarely referred to in the abstracts and titles of papers where it is a core technology, for example DNA sequencing. Even so, it is mentioned by name in almost as many papers as is chromatography (Table 2). However, with the development of

capillary electrophoresis after 1981 electrophoresis has returned as a substantial topic of interest to mainstream analytical chemistry.

Fundamentals of Electrophoresis

Unlike chromatography, there is no formal International Union of Pure and Applied Chemistry (IUPAC) definition of electrophoresis, although one is being developed at the time of writing. However, through teaching the subject over the past 10 years, I have developed the following definition:

'Electrophoresis is a mainly analytical method in which separations are based on the differing mobilities (i.e. speed plus direction of movement) of two or more charged analytes (ionic compounds) or particles held in a conducting medium under the influence of an applied direct current electric field' (Figure 1).

Electrophoresis therefore contrasts to chromatography which is defined as a method used primarily for the separation of two or more components of a mixture, in which the components are distributed between two phases, one of which is stationary while the other moves. Another difference is that in chromatography the modelling of the separation from first principles is complex, difficult and imprecise whereas a relatively simple theoretical background to electrophoresis has been developed and is reproduced below. For a more complete discussion of electrophoretic theory see Mosher *et al.* (1992).

In electrophoresis the movement is towards the electrode of opposite charge to that of the particle or ion being separated. Cations are positively charged ions and move towards the negative electrode (the cathode). Anions are negatively charged ions and move to the positive electrode (the anode). It is important to note that neutral species do not move under the influence of the electric field, although they

Table 1 An outline history of electrophoresis

Date	Researcher(s)	Development
1807	Reuss	Observed movement of colloids in an electric field – the discovery of electrophoresis
1886	Lodge	H ⁺ migration in a tube of phenolphthalein 'jelly' (i.e. zone electrophoresis)
1892	Picton and Lindner	Invention of boundary electrophoresis
1892	Smirnow	Electrofractionation of diphtheria toxin solution
1893	Whetham	'Moving boundary' separation of solution of coloured ions in vertical tubes
1899	Hardy	Globulin movement in U-tube with electric current
1904	Romer	Diphtheria toxin solution separation via U-tubes
1905	Hardy	Detailed study of globulins with various U-tube designs
1907	Field and Teague	Toxin/antitoxin separated via agar tube bridges between beakers of sample and water
1912	Ikeda and Suzuki	Isoelectric focusing (IEF) first observed during studies on amino acid electrophoresis
1914	Schwerin	Patent describing electrophoresis of colloidal systems
1923	Kendall and Crittenden	Preparative separation of isotopes in agar U-tube
1930	Tiselius	Moving boundary studies of proteins in solution
1937	Tiselius	Improved apparatus for moving boundary studies including ultraviolet detection of proteins
1939	Coolidge	Electrophoretic separation of serum proteins in tubes of glass wool
1946	Consden <i>et al.</i>	'Ionophoresis' of amino acids and peptides in silica gel slab; first 'blotting' experiments
1948	Wieland and Fischer	Filter paper electrophoresis
1950	Hagland and Tiselius	Electrophoresis in a glass powder column
1952	Tiselius	Electrophoresis in filter paper and other media
1954	Kolin	Introduced artificial pH gradients for IEF
1954	Strain and Sato	Introduction of 'electrochromatography'
1956	Porath	Column electrophoresis using cellulose powder
1959	Raymond and Weintraub	Introduced polyacrylamide gels (PAGE)
1964	Ornstein and Davis	Design of apparatus for tube 'disc' electrophoresis
1965	Tiselius <i>et al.</i>	'Free zone' electrophoresis of virus particles in 3 mm internal diameter rotating capillary
1965	Hjerten <i>et al.</i>	'Particle sieving' electrophoresis of ribosomes in polyacrylamide gel electrophoresis (PAGE) tube gels
1965 +	Many continued developments in microcapillary tube gel electrophoresis and isotachopheresis	
1967	Shapiro <i>et al.</i>	Sodium dodecyl sulfate (SDS)/PAGE technique for the determination of the molecular weight of proteins
1975	O'Farrell and Klose	Independently introduced two-dimensional IEF/SDS-PAGE
1979	Mikkers <i>et al.</i>	High-performance electrophoresis in polymer capillaries
1981	Jörgenson and Lukacs	Theoretical/experimental studies on high-resolution electrophoresis in glass capillaries (CZE)
1984	Terabe	Micellar electrokinetic capillary chromatography (MEKC) introduced
1987	Microphoretics	First commercial capillary electrophoresis system

may diffuse from the load position or be carried by electroosmotic flow.

The rate of migration (velocity) of any charged particle in an electric field can, at its simplest, be

considered to be the vector sum of a driving force (the electrical force) and any resisting or aiding forces.

Any ion, compound or body carrying an overall charge at a given pH value will move in solution

Table 2 Separation techniques in biomedicine and related areas

Separation mode	Type	Total number of papers
Electrophoresis	All modes	150 000
	Simple planar	13 800
	Sodium dodecyl sulfate–polyacrylamide gel electrophoresis (SDS–PAGE)	78 000
	Immuno	19 700
	Isoelectric focusing	14 400
	Pulsed field	1 600
	Two-dimensional PAGE	4 800
	Capillary electrophoresis	6 700
Chromatography	All modes	250 000
	Planar	52 000
	Column	98 000
	High-performance liquid chromatography	62 500
	Gas chromatography	32 000

Papers in Medline and on the author's database from 1976 to 1999.

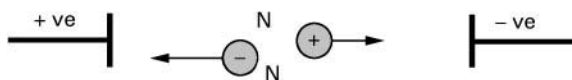


Figure 1 The basic principle of all electrophoretic separations is that charged ions attempt to move in an electric field towards the electrode of opposite polarity. Neutral compounds do not move.

under appropriate conditions. In simple solutions, ions will move freely toward the electrode of opposite charge and the product of the charge on the ion and the applied electric field (E) gives the electric force experienced by the ion. However, since even a simple ion can be considered as a particle this movement is opposed by a frictional drag given by Stokes' law.

The driving force is represented by the potential gradient along which the charged particle moves and is given by the electric field strength (E):

$$E = \frac{\text{applied voltage}}{\text{distance between electrodes}} = \frac{V}{D} \quad [1]$$

The applied field (F_{ef}):

$$F_{\text{ef}} = qE \quad [2]$$

where q is the total charge on the ion.

The friction (F_{fr}) drag is given by:

$$F_{\text{fr}} = 6\pi r v \eta \quad [3]$$

where η is the viscosity of the media, r is the 'radius' of the molecule and v is the velocity.

On applying a voltage there is a rapid acceleration of all the molecules and equilibrium is achieved in a few microseconds. A vector diagram at equilibrium for movement in an electric field is shown in **Figure 2**, and under such circumstances the following equilibrium conditions apply:

- at equilibrium:

$$F_{\text{ef}} = F_{\text{fr}} \quad [4]$$

- therefore:

$$qE = 6\pi r v \eta \quad [5]$$

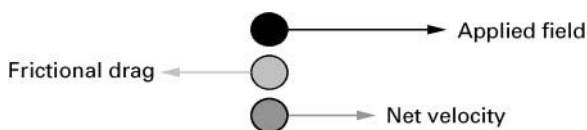


Figure 2 A vector diagram for movement in an electric field at equilibrium.

- so the velocity is given by:

$$v = \frac{qE}{6\pi r \eta} \quad [6]$$

Mobility (μ) is defined as the average velocity with which an ion moves under unit applied electric field under defined conditions:

$$\mu = \frac{\text{average migration velocity}}{\text{electric field strength}} = \frac{v}{E} \quad [7]$$

Substituting for v from eqn [3]:

$$\mu = \frac{q}{6\pi r \eta} \quad [8]$$

Mobility can therefore be interpreted as proportional to a charge-to-size ratio for a molecule in a given buffer at a set pH. Absolute mobility is the apparent or measured mobility corrected by any other effects adding to or subtracting from the absolute mobility (an example is electroosmotic drift). Sometimes, the term relative mobility is used when the apparent mobility of one compound is calculated in relation to another compound.

The units of μ are cm s^{-1} divided by V cm^{-1} and are therefore $\text{cm}^2 \text{V}^{-1} \text{s}^{-1}$. The magnitude of μ for typical small ions is of the order of $10^{-6} \text{cm}^2 \text{V}^{-1} \text{s}^{-1}$, e.g. for the sodium ion, $\mu = 5 \times 10^{-6} \text{cm}^2 \text{V}^{-1} \text{s}^{-1}$ or for the protein albumin, $\mu = -1.5 \times 10^{-4} \text{cm}^2 \text{V}^{-1} \text{s}^{-1}$. Note the difference in the sign of the mobility and hence the direction of movement.

A small, highly charged species, for example, an ion, will have a high mobility and a large ionizable compound, such as a protein, will have a low mobility. It is clear that electrophoresis can readily separate large and small ionic species. Then, for two or more closely related ionic species, if the basic descriptors used in eqn [6] are known, it should be a simple matter to calculate the separation conditions and the degree of resolution that can be achieved. The charge on an ionizable molecule, such as an amino acid, is determined by the pH of the electrophoretic medium. The viscosity of the medium at a given temperature will also be known precisely. The difficulty from a theoretical predictive standpoint is to determine the radius of a molecule. Many attempts have been made to calculate this value from first principles and these are discussed later. It is also clear that the distance moved is proportional to the applied voltage and the time period over which the voltage is applied.

The above analysis of the movement is a further simplification in that the resisting forces are not just

due to simple frictional drag but can also include effects such as:

- size and shape of the molecule;
- electrolyte concentration;
- solubility;
- adsorption to surfaces;
- complexation with species in the electrolyte solution.

The two basic electrical equations that govern electrophoresis are first Ohm's law which states that $V = iR$, where i is the current and R is the resistance. Secondly, power, that is the product of current and voltage or, alternatively, the heat generated is given by $i^2R = W$ where W is power measured in watts. This heating effect is termed Joule heating. The quantity of heat generated is, of course, time dependent. The development of heat and then temperature gradients in electrophoresis leads to:

- convection currents;
- diffusional/thermal broadening;
- evaporation;
- viscosity changes;
- pH variations;
- thermal degradation of analytes especially proteins and matrices.

These changes all result in band broadening and the lower resolution of separated analytes. Heat can also lead to gels drying, buffers boiling and in extreme situations even fires.

The effect of heating processes on electrophoretic separations is complex and often variable. Traditionally, workers have countered these effects by using buffers that generate low currents, for example dilute buffer solutions, low conductivity buffers, by operating at low voltages (100–500 V), operating in constant current or constant power modes and, of course, using external cooling systems, such as circulating cold water around the instrument.

Electroosmosis

The second important effect in electrophoresis is electroosmotic flow (EOF) or electroosmosis. If ionized groups cannot migrate in an electrical field (e.g. when part of a static support medium) then the liquid adjacent must move in order to maintain thermodynamic equilibrium. This EOF is seen as a bulk movement of liquid over a solid surface. In the case of silica or the carboxyl residues on a sheet of paper, the water will move in the direction of the cathode with a characteristic mobility (μ_{eof}) depending on pH. The

μ_{eof} is related to the zeta-potential of the solid surface and the dielectric constant of the electrolyte. As with mobility of an ion, μ_{eof} also varies with the viscosity of the electrolyte. The magnitude of the EOF is pH dependent. EOF leads to diffusional broadening of separated bands in slab electrophoresis but is used to good effect in capillary electrophoresis (see later section).

The Modes of Electrophoresis

There are four fundamental modes of electrophoresis, at least, in the traditional planar formats, namely moving boundary electrophoresis, zone electrophoresis, isoelectric focusing and isotachopheresis.

Moving Boundary Electrophoresis

This was the method that was studied by Tiselius in his detailed development of electrophoresis.

In this system the sample plus buffer are placed in the appropriate sample reservoir (electrolyte chamber). Tiselius used a U-tube containing the sample mixed with the buffer and the electrodes were dipped into each end. A single buffer solution therefore connects the two electrodes by way of the separation matrix. When the potential is applied, the analytes in the sample separate according to their differing mobilities. In the situation shown in **Figure 3** the cation of highest mobility moves ahead of the rest such that its front is resolved from the others. However, only the fastest analyte and, possibly, the slowest are truly separated and then only partly. The resolution of the components from others then diminishes. Tiselius observed the separated analytes via changes in their refractive index using Schlieren optics. Today such a separation mode is of little practical use except possibly in a preparative mode.

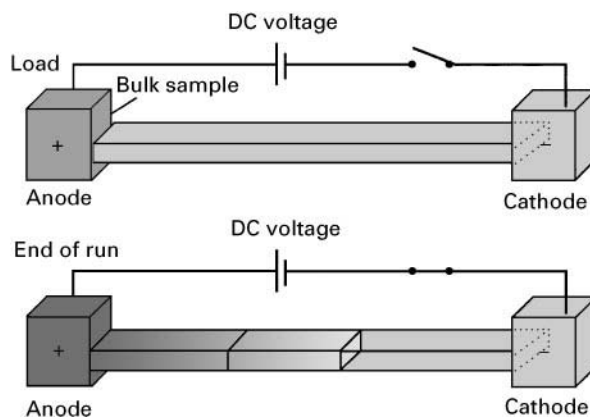


Figure 3 (See Colour Plate 6) The principle of moving boundary electrophoresis.

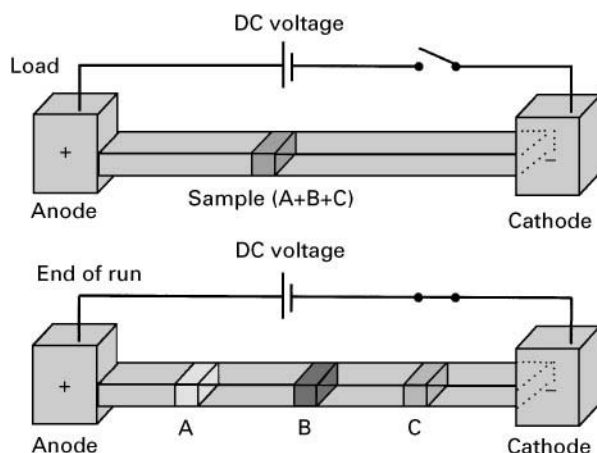


Figure 4 (See Colour Plate 7) The principle of zone electrophoresis.

Zone Electrophoresis

This is probably the most common form of electrophoresis in both slab and capillary formats (see **Figure 4**). The sample is loaded as a discrete plug or zone into a buffered electrolyte filled media such as a gel. The load point is somewhere between the electrodes in the middle if the charge on the analytes is not known or nearer to one than the other if the ionic nature of the analytes is known. The two electrode chambers and the matrix contain the same buffer. On application of the voltage, which in traditional systems is 100–500 V DC, the components of the sample migrate at different speeds and possibly in differing directions due to their differing

mobilities and their respective charges. So, after an appropriate time period, they will have separated into (hopefully) distinct zones. Turning off the voltage terminates the separation. The degree of separation will depend on the voltage applied, the distance over which the sample separates and the time as well as the nature of the analytes and the buffer. The resultant zones will most often be of a distribution that is broader than the original loading zone due to the thermal mixing and so on that will have occurred during the separation process. With few exceptions some means of revealing the zones such as staining will be necessary.

The major factor controlling the mobility of the analytes in zone electrophoresis is the pH of the buffering electrolyte. For most ionic species the buffer controls the degree of ionization via the relationship expressed in the following equation (Henderson–Hasselbach equation):

$$\text{pH} = \text{pK}_a + \log(1/\alpha - 1) \text{ for anions,} \\ -\log(1/\alpha - 1) \text{ for cations} \quad [9]$$

For analytes such as peptides or proteins which contain a number of independently ionizable groups, the overall charge on the molecule is given by summing the contribution from each group at the pH in question:

$$\mu_{\text{eff}} = \sum \alpha_i m_i \quad [10]$$

where $m_i = \mu_i$ of each completely ionized form and α_i is the degree of ionization of each ionized form. An example of the change in charge for a number of different peptides is shown in **Figure 5**.

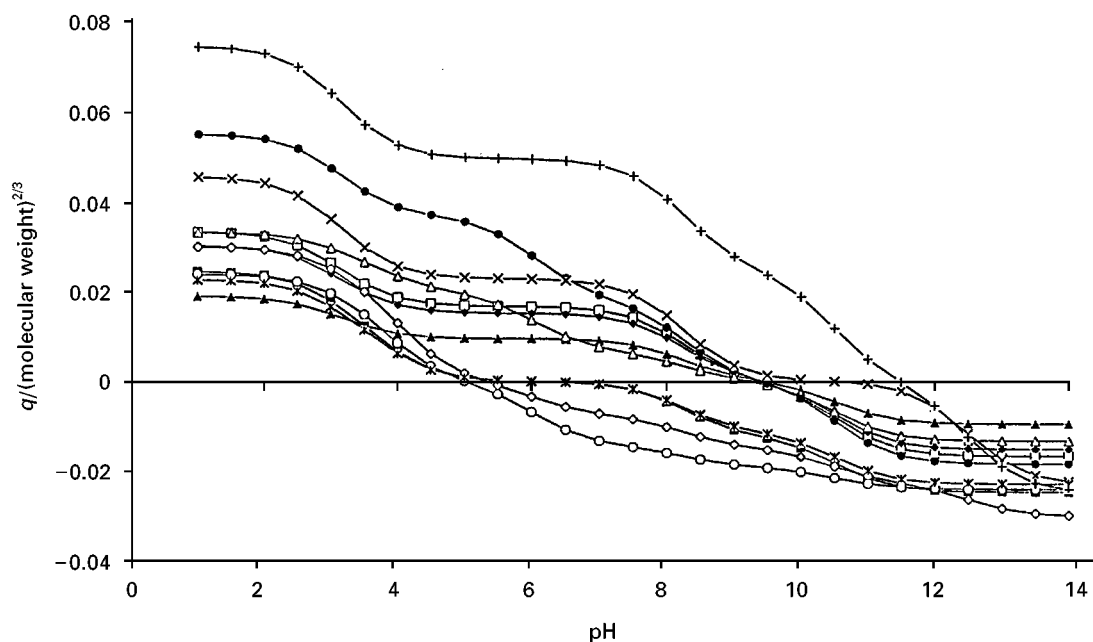


Figure 5 An example of the change in charge for a number of different peptides. ■, AT1; □, AT2; ◆, AT3; ◇, AT4; ▲, AT5, △, AT6; ●, AT7; ○, AT9; ×, AT10; ×, AT11; |, AT14.

Since the mobility of an ion is a charge-to-size ratio (eqn [8]), one way to modify this for macromolecules is to change the size and shape of the molecules. For proteins this may be brought about by configuration changes due to changes in the pH, and in the case of DNA by incorporating an intercalating agent such as ethidium bromide. It is less simple to change the size and shape of small molecules, but one possible technique is complexation. For example, sugars will complex with borate ions in borate buffers and metal ions can complex with both peptides and nucleotides.

Equation [8] also indicates that mobility is dependent on the frictional drag exerted by the background electrolyte; in other words its viscosity. Adding agents such as polyethylene glycol (PEG) or cellulose derivatives to the buffer can increase viscosity and hence change the separation achieved.

Isoelectric Focusing

Isoelectric focusing (IEF) is steady-state electrophoresis in a pH gradient. Ionic compounds migrate to the point in the gradient where they have zero overall charge and therefore zero net mobility. For proteins this means that they migrate to their isoelectric point (pI value). The pH gradients used can be linear or nonlinear and cover either wide pH ranges, for example, 2–10 or narrow ranges (< 2 pH units). The pH gradient is formed by the application of a voltage to a mixture of amphoteric compounds (ampholytes) with closely spaced pIs encompassing a chosen pH range. A mix of at least 200 individual ampholyte species is required to establish a pH gradient of 4–10. Typically, the protein mixture is mixed with ampholytes and the resultant mixture is placed between the electrodes (Figure 6). The synthesis of such carrier ampholytes by attaching carboxylic acid moieties to polyvalent amines was perfected by Vesterberg in the

Karolinska Institute in 1964. Even the first application showed the remarkable resolving power of IEF when two myoglobin molecules differing in pI by only 0.05 pH units were resolved.

The resolving power of IEF is very high and is described by the following equation:

$$\Delta pI = \left(\frac{D(dpH/dx)}{-E(d\mu/dpH)} \right) \quad [11]$$

where D is the diffusion coefficient, E is the electric field strength and μ is the mobility of the proteins. Good resolution between analytes is therefore favoured first by low diffusion coefficients (i.e. ideal for proteins) and a steep mobility profile through their pI, and secondly by high field strengths and a shallow pH gradient.

Once a protein has reached its pI position in the pH gradient, effects such as diffusion and EOF will cause some drift from the focused zone. This drift is countered by the fact that the protein will develop a small amount of ionization and migrate back to its pI position in the pH gradient and so become re-focused. Focusing takes time, depending on the voltage used and the nature of the analytes: electrophoresis may need several hours before a steady-state is reached. Proteins are therefore resolved into narrow concentrated bands. In fact this concentrating effect is such that solubility problems can occur.

IEF was commercialized by LKB and the carrier ampholytes marketed under the tradename of Ampholine. The use of polyacrylamide gels was introduced to simplify the IEF methodologies. Although commercialized, the early ampholyte systems were in simple solution but separations tended to be irreproducible due to drifting towards the electrodes due to EOF effects. Modern IEF uses immobilized ampholytes that were developed by Righetti and co-workers in 1982. In such systems the ampholytes are immobilized to a gel matrix usually contained in a thin cylinder and so giving stable pH gradients in an easy to use format. The resolving power of these new gels with immobilized pH gradients (IPG) was much improved and permitted resolution to 0.001 pH units. More recent systems, such as the Pharmacia IPGphor, use ampholytes immobilized on flexible plastic strips. Once focused, the strips can be easily transferred to a second dimension or even used as the target in mass spectrometry.

Isotachopheresis

Isotachopheresis (ITP) is a form of steady-state electrophoresis in which a voltage gradient generated by

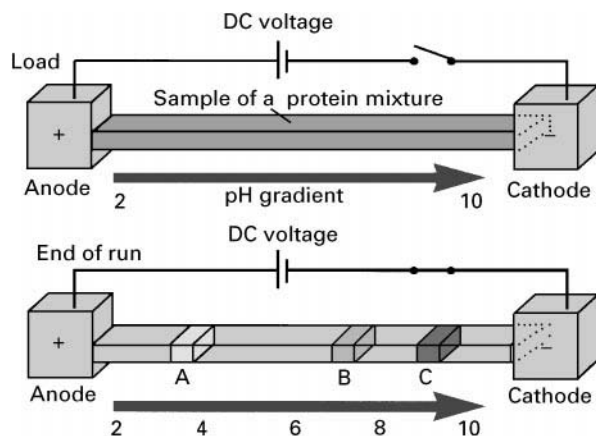


Figure 6 (See Colour Plate 8) The principle of isoelectric focusing.

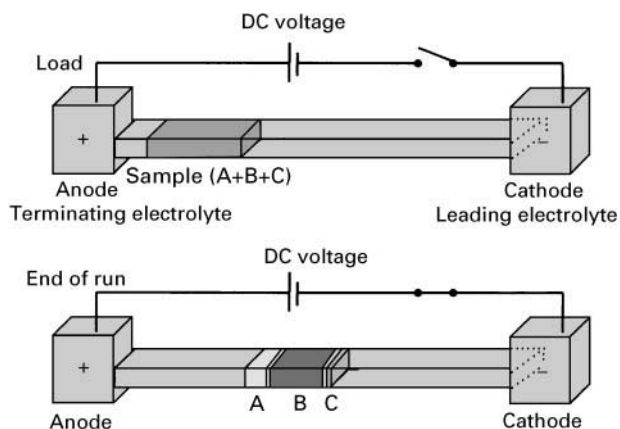


Figure 7 (See Colour Plate 9) The principle of isotachopheresis.

using buffers of differing mobility at constant current is used. It is therefore a discontinuous system. Electrophoresis proceeds until all ionic analytes are migrating with the same (*iso*) speed (*tacho*) (Figure 7). The theory is dependent on the Kohlraush regulatory function (1897), which defines the conditions at the boundary between two different ions A and L such that

$$[A] = [L] \times \text{a constant}$$

For ITP to occur, an unbuffered sample should be placed between a leading electrolyte whose $\mu_{\text{buffer ion}} \gg \mu_{\text{sample}}$ and a terminating electrolyte with a $\mu_{\text{buffer ion}} \ll \mu_{\text{sample}}$. Leading electrolytes are usually small ions such as chloride and the terminating electrolytes are larger buffer ions such as histidine.

Applying the voltage causes the analytes to separate into zones according to their mobilities, but they must remain adjacent in order for the current to be carried. From Ohm's law all zones including the terminating and leading electrolytes must carry the same current so R and V must increase. When a steady-state is obtained all bands have the same ionic concentration because they must have the same R so they will be of differing lengths. Zones must therefore increase in concentration to match the concentration of the leading electrolyte. The resultant output is usually observed as a series of steps in a conductivity trace in which the length of each band is proportional to the amount of analyte. Since analysts are usually happier looking at peaks, these traces are often differentiated in order to generate a profile with peaks so that the distance between the peaks can be measured. The development time is proportional to the amount of sample injected and to the differences in μ of the sample components.

LKB devoted considerable sums of money to develop a commercial ITP system (the Tachophore) in the late 1970s but this was a commercial failure. Commercial systems are still available from Japan (Shimadzu) and the Czech Republic (Villa Labco). Although ITP is little used today as an analytical tool, it is commonly encountered in many zone electrophoresis protocols when the loading of samples in solutions differing from the BGE is recommended. ITP will often occur transiently in the loading band leading to a concentration of some analytes at the front or rear of the loading band.

Electrophoretic Separation Media

Electrophoresis can be performed in free solution, but thermal and diffusional mixing are usually too great to give satisfactory resolution of the components. It has long been recognized that it is usually necessary to use some type of static support in order to contain the background electrolyte, contain the sample and limit diffusion. The primary function of the stabilized support media is to limit the dispersion that results from convective disturbances. The stabilization should not change the mobility of the ions significantly provided that neither absorption onto the support occurs nor do large analytes become physically trapped.

Over the years a large number of supports have been used as stabilizing media, but relatively few satisfy all the criteria for the ideal support (Figure 8). These criteria are a reproducible structure, good mechanical strength, ease of formation into appropriate shapes, chemically inert to both the electrolyte and the analytes, no thermal degradation and minimal background in the detection processes. The earliest support was probably cellulose in the form of sheets of laboratory filter paper. Kunkel and Tiselius published the classic study on paper electrophoresis in 1951. Cellulose acetate membranes have large pores and do not retain proteins either chemically or physically. It is the preferred membrane for serum protein separations.

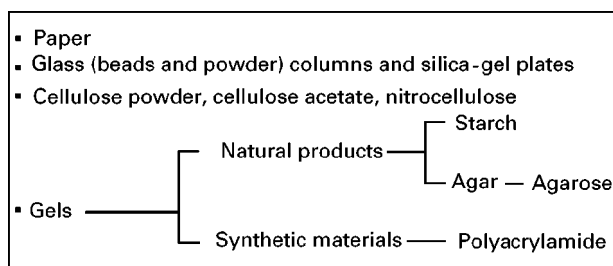


Figure 8 Common stabilized media used in electrophoresis.

Slab Gel Electrophoresis

Subsequently naturally occurring gels were investigated particularly for the separation of plasma proteins. Agar gels, especially in the form of the highly purified subunit agarose, are still a popular medium for protein separations. Agar forms gels at relatively low concentrations, but due to its high number of sulfate and carboxylic groups it generates a significant EOF. The sulfate and carboxylic fraction can be removed chemically to leave agarose, which has much reduced EOF and gives a better resolution of proteins. The gels are formed as slabs by pouring a liquid gel into a mould and letting it set before placing in an electrophoresis system.

In 1955 Smithies, modifying an earlier method, introduced the technique of starch gel electrophoresis and its superior resolving power for proteins was immediately apparent. The starch was derived from hydrolysed potato starch and poured to a thickness of 5–10 mm. In addition, the pores in the starch gel matrix are close to the molecular size of proteins so that in this form electrophoretic movement is accompanied by some molecular sieving, but the effect was irreproducible.

In 1955 Raymond and Weintraub introduced a synthetic polymer gel made from the monomer polyacrylamide, as a replacement for starch. Polyacrylamide gels have many advantages over starch being tougher, more flexible, naturally clearer and chemically inert. Acrylamide gels are formed by the polymerization of the monomer acrylamide in the presence of an *N,N'*-methylenebisacrylamide (BIS). The reaction requires initiators and a catalyst (cross-linking reagent). Commonly used catalysts are ammonium or potassium persulfate (for chemical polymerization) or light and riboflavin (for photopolymerization). A common initiator is *N,N,N',N'*-tetramethylethyldiamine (TEMED). The polymerization should be performed at above 20°C to prevent incomplete polymerization. The reaction takes place via vinyl polymerization and gives a randomly coiled gel structure. The concentration of polyacrylamide can be varied over a wide range without making the gels unmanageable. The pore size can also be controlled exactly by varying the amount of BIS used in the polymerization (Table 3) so the precision of the molecular sieving is enhanced.

The use of such gels for electrophoresis is commonly referred to as polyacrylamide gel electrophoresis (PAGE). In addition to the tight control of pore size other advantages of polyacrylamide gels compared to starch gels are that the adsorption of macromolecules to polyacrylamide is negligible, there is little EOF associated with polyacrylamide and strong,

Table 3 Effect of cross-linking on pore size of acrylamide gels

Percentage of <i>N,N'</i> -methylenebisacrylamide (BIS)	Molecular weight range resolved
5	50 000–300 000
10	10 000–100 000
15	~ 5 000

but thin, transparent gels can be cast permitting faster separation. A disadvantage is that the monomers are toxic and need to be handled with caution.

Development of the gel system followed rapidly. In 1964 Ornstein and Davis simultaneously introduced discontinuous (DISC) electrophoresis, which improved both the solubility of the proteins in the gel as well as improving the resolution. In DISC electrophoresis the gel is formed in two sections, a stacking gel and a resolving gel. The resolving gel has small pores filled with a buffer of pH 8.8 high mobility buffer (e.g. 2-amino-2-hydroxymethylpropane-1,3-diol-hydrochloric acid (TRIS-HCl)) and a large pore stacking gel contains a buffer of about pH 6.8. The sample is loaded at approximately pH 8.8. These conditions induce the proteins to migrate according to isotachopheresis through the stacking gel, then stacked at the interface with the resolving gel before slowly destacking and resolving as they pass through that gel.

The size and shape of macromolecules complicates their separation, so special buffer/electrolyte conditions are employed. Non-dissociating (native) buffer systems, as described earlier for DISC electrophoresis, are used to separate the native forms of proteins and double-stranded DNA. Dissociating (denaturing) buffer systems can also be used, for example, double-stranded DNA is denatured using urea, formamide, sodium hydroxide or intercalating agents such as ethidium bromide prior to application to the gel.

Although it is appreciated that the use of gels not only aided the electrophoretic separation, for macromolecules it also introduced a size-sieving effect equivalent to gel filtration in chromatography. This can be used to 'size' molecules, particularly proteins. So if the conditions are correct and if the pores are of the appropriate dimensions could PAGE also be used to determine the molecular weight of proteins?

Sodium Dodecyl Sulfate–Polyacrylamide Gel Electrophoresis (SDS–PAGE)

Unlike DNA, proteins exhibit considerable differences in their overall charge-to-mass ratios.

Depending on pH, their charge can range from basic to anionic and from hydrophobic to hydrophilic, and their shapes can vary from globular to linear with varying degrees of cross-linking. Shapiro introduced electrophoresis in the presence of sodium dodecyl sulfate (SDS) which is an anionic surfactant that is used to solubilize proteins. Proteins are first denatured with SDS which binds to the hydrophobic backbone of proteins in a regular fashion. Almost regardless of the type of protein, 1.4 g of SDS binds to 1 g of protein and solubilizes it. In addition, the charge on the SDS overwhelms the charges on the protein. The degree and type of denaturing can also be enhanced by using SDS solutions which also contain urea and/or a thiol such as dithiothreitol (DTT). The complex is now more or less linear with an overall negative charge so all proteins migrate in a single direction. The denatured unknown proteins are then electrophoresed by PAGE in a buffer system incorporating 0.1% SDS. By running a series of known standards in a parallel lane, the technique can be used to derive molecular weight information since there is a fixed relationship between the relative migration distance of SDS-protein complex and the molecular weight of the native protein.

Pulsed Field for DNA

Agarose gel electrophoresis is the method of choice to resolve DNA restriction fragments provided the fragments are between 1000 and 23 000 bp in size. For larger fragments, Schwartz and Cantor developed the technique of pulsed field gel electrophoresis (PFGE) in 1984. In PFG DNA fragments greater than 23 kbp are forced to change their structure during electrophoresis by pulsing the applied field so causing the molecules to relax and expand regularly and thereby interact with the gel pores. DNA molecules up to the size of chromosomes can be electrophoresed in this manner, but the separation can take many hours or even days.

Basic Instrumentation for Electrophoresis

Instrumentation for performing electrophoresis is both cheap and simple. It consists of a means of generating a DC voltage, a buffer tank which also has some means of holding the separation media between the two electrodes. A schematic diagram of such a horizontal tank is shown in **Figure 9**. Such an apparatus needs to be levelled in order to prevent the electrolyte from siphoning from one end to the other and so disturbing the electrophoretic resolution. The

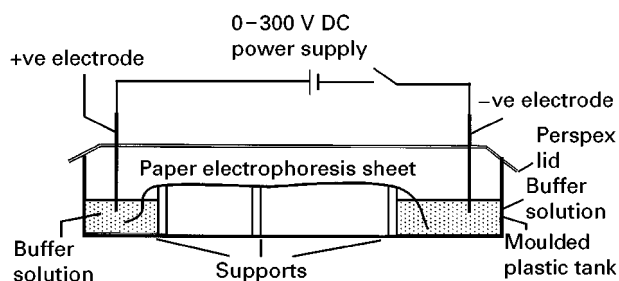


Figure 9 Schematic diagram for a paper or membrane electrophoresis system.

power supply can be as simple as a 12 V battery, but is usually a mains electricity transformer delivering 100–500 V DC. The required voltage is selected by a digital potentiostat combined with a polarity switch, the run time can also be selected digitally. Usually there are controls to select constant voltage, constant current and constant power modes of operation. If the instrument's designed maxima in any of these modes are exceeded there is a cut-off (safety) trip. Electrical power is usually taken to the electrophoresis tank via a pair of suitably rated copper cables. The tank itself is typically made of a waterproof and electrically insulated plastic material covered with a lid to prevent evaporation and contamination of the system. The size of the tank will depend on the type of separation being undertaken and can range from as small as 100 mm square to as large as 500 mm × 300 mm. The tank is divisible into a number of compartments with plastic spaces. The outer two hold the electrodes. The electrodes are usually made of fine platinum wire connected through the tank wall to the leads from the power supply. Suitable safety devices are included in the tank to prevent operator accidents, for example the power is cut-off if the lid is removed.

With the development of gel electrophoresis system new forms of apparatus were developed. It is necessary to mount and support the gel between the two electrode chambers so that the only electrical connection is via the gel. Electrical contact between the gel and the electrolyte is made either directly or by a wick of some description. Gels can be of many sizes depending on the separation distance required. Tubes of gel with an internal diameter of 1–5 mm and 50–250 mm in length can be prepared, but slab gels, either used vertically or horizontally, are much more common. Vertical slab gels are cast by pouring liquid gel into the space between a pair of glass plates separated by thin spacer strips positioned at the edges and bottom. The plates are clamped to prevent leakage. The thickness of the gel depends on the thickness of the spacers, which can be from 50 µm to 5 mm

depending on the application. At the top, a sample well comb is used to create indentations into which samples can be placed. Following the setting and/or polymerization of the gel, the comb is carefully removed and sample(s) (5–10 μL) are loaded into each well. Molecular weight markers, known proteins or DNA fragments, are usually applied to one or both of the two outer lanes. The upper and lower buffer chambers are then filled and the system is connected to the power supply. Appropriate voltages are selected and the power is turned on for the appropriate time. In order to monitor the progress of the separation it is common practice to include a marker dye in the sample. When the dye reaches the end of the gel (normally after some hours) the power is disconnected. The buffer is drained and the gel removed from between the plates prior to staining or blotting (Figure 10).

As well as vertical formats it is also possible to run horizontal slab gels either completely immersed in electrolyte solution (so-called submarine gels) or with suitable wetted connectors.

Although it is relatively easy to construct your own low-voltage electrophoresis system, especially the tanks, systems are available from a large number of suppliers, such as Amersham-Pharmacia, Bio-Rad, Hoeffer, and so on. The cost of commercial systems range from a few hundred pounds to about £5000 depending on size, configuration, maximum voltage and whether or not cooling systems are included. Today, even the preparation of gels can be simplified. Premixed reagents are available to simplify the production of reproducible gels and it is

now possible to buy precast gels which only need to be mounted in a suitable holder.

Detection Methods in Electrophoresis

At the end of an electrophoretic run the analytes are distributed over a two-dimensional surface or included within a thin three-dimensional gel. With only a few exceptions, the majority of analytes will not be visible to the naked eye and many methods for both the detection, localization and quantitation of separated bands and spots have been developed.

Direct optical methods can be applied in some cases. For example, the bands of haemoglobin separated by electrophoresis on a nitrocellulose membrane can be observed directly. In some cases placing the paper or gel on a ultraviolet (UV) lightbox or under a UV lamp can reveal UV absorbing bands, UV fluorescence bands and sometimes bands that quench the background UV fluorescence.

Since the analytes are often trapped within a fragile gel, then some means of extracting them from that matrix often is necessary before a visualization method can be applied. For this purpose, one of the blotting techniques is applied. Blotting involves the transfer of the sample bands or spots from a gel to a sensitized membrane using either physical or electrical mechanisms. Nitrocellulose, Nylon or polyvinylidene difluoride (PVDF) are the most common membranes because they provide hydrophobic surfaces on which proteins readily adhere, as well as being physically strong. In 1975 Professor Ed Southern described the first of these procedures, which is commonly called Southern blotting, for use with DNA. In this method, diffusion of DNA from a continuously wetted electrophoresis gel to a membrane is achieved by pressure applied to a sandwich of wetted wick-gel-membrane-stack of blotting paper (Figure 11). The DNA in the gel is carried into the membrane that binds the DNA giving a faithful image of the original gel. The process takes up to 24 h but can be speeded by using a vacuum to draw the buffer through the gel.

The same procedure when applied to RNA is playfully, but consistently, called a Northern blot. In the same vein a Western blot is any procedure for the transfer of proteins from a gel to a membrane. Although with proteins this usually involves their electromigration linked to immunodetection with appropriate antibodies. Transfer using electrophoretic techniques applied across the thickness of the gel is generally faster than capillary action. The gel, containing protein or DNA, clamped next to the blotting membrane in a cassette, is then immersed in a buffer solution between two electrodes.

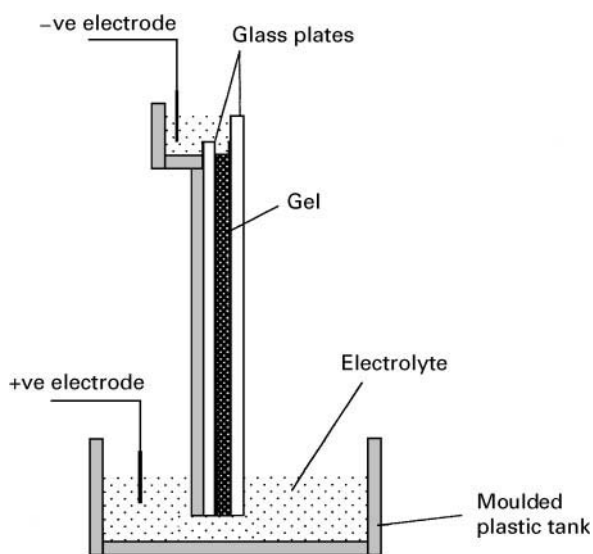


Figure 10 Schematic diagram of a vertical gel electrophoresis system.

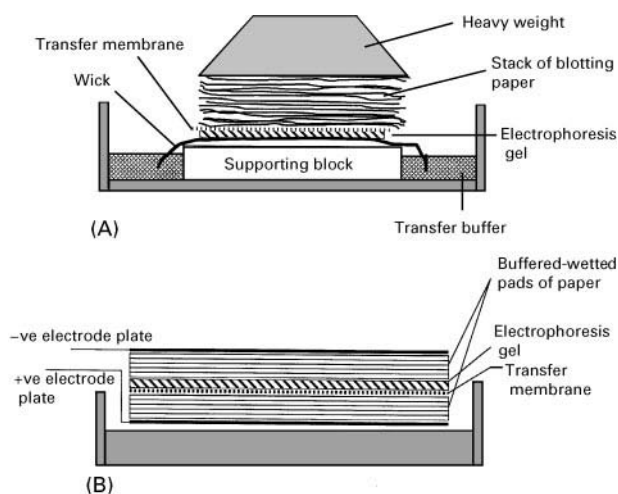


Figure 11 The principles of two types of blotting: (A) Southern blotting and (B) semi-dry Western blotting.

Applying a voltage causes the proteins/DNA to migrate to the membrane. If filter papers wetted with buffer are used instead of buffer, then this is called semi-dry blotting. Once the analytes have been stabilized on the membrane they then can be probed in order to detect the analytes (this is discussed further below).

If separations were performed on sheets or have been blotted, then the position of the analytes can be determined by the following methods. If radioactivity has been incorporated in the analytes prior to electrophoresis, then the position of the analytes on the membrane can be determined by autoradiography. The membrane is placed with the gel in contact with photographic film and left to expose (hours to weeks) in the dark and possibly the cold. The film is developed and the position of the analytes is revealed by the exposed parts of the negative. If required, the original membrane or gel can then be overlaid on the negative and the radioactive spots obtained by cutting-up the gel followed by elution and scintillation counting.

It is often necessary to reveal analytes of interest using some form of derivatization. This may mean spraying the blot or membrane with a specific reagent that chemically reacts with the analyte to give a coloured product, for example, ninhydrin gives a purple product with amino acids, peptides and some proteins. For macromolecules it is more common to refer to this process as staining using either appropriate dyes or other reagents. Proteins can be detected in gels with a large number of dyes of which the most common is Coomassie brilliant blue which can detect as little as 0.3 μg of protein in a spot. DNA is usually detected using the fluorescent intercalating dye ethidium bromide. The process involves staining fol-

lowed by destaining to remove unbound dye and then fixing of the image. Both proteins and DNA can react with silver ions to form black silver precipitates. This method is some 100 times more sensitive than the current dye methods and can detect as little as 2 ng of some proteins.

The above methods are relatively non-selective, although for simple mixture comparisons against standards they may be sufficient to identify proteins. More specific methods of detection include zymography and immunoelectrophoresis. Early methods include immunodiffusion in which an antiserum is allowed to diffuse into a gel so generating precipitin bands and rocket electrophoresis. Today the most common application of immunotechniques is in Western blotting with immunodetection; this is so common that many workers believe it is Western blotting. After blotting, the immobilized proteins are probed with primary antibodies specific for the protein(s) of interest. This is followed by an enzyme-linked second antibody directed against the first antibody, for example sheep anti-mouse immunoglobulin G (IgG). The enzyme is usually a peroxidase or alkaline phosphatase. The blotted membrane is first soaked in a solution to block non-specific binding sites followed by incubation with a suitably diluted solution of the first antibody for up to 1 h. The antibody solution is then washed off before incubating with the secondary antibody complex. Again, following washing, the proteins are revealed by incubation with an appropriate visualization reagent. Depending on the antibodies available such methods can be very selective and also very sensitive.

Finally, the most modern methods of both detection and protein characterization involve mass spectrometry and are dealt with below.

Quantitation

The above methods are usually indirect and qualitative, so if you wish to obtain quantitative analytical data from electrophoretic separations or blots it is necessary to determine the area of the separated bands. The amount of analyte present is related to the area of the spot or band when compared to standard solutions. The areas of bands can be obtained using densitometry or digital image analysis to scan the gels or blots. However, even modern densitometry is only semi-quantitative with coefficients of variation of 10–20% at best.

Two-dimensional Separations

Since traditional electrophoresis is usually planar, more than one separation dimension can easily be

combined. The use of orthogonal techniques increases the resolution of the systems in proportion to the product of the resolution of each dimension assuming the two modes are truly orthogonal. For example, separations that each give 10 bands in a single direction/mode will theoretically give 100 spots if combined. The sacrifice is, of course, speed, it will take twice as long, and increases the number of manipulations involved.

Early work such as peptide mapping often used high-voltage electrophoresis in the first dimension and then chromatography in the second. For a decade or more this was the standard method for generating tryptic maps for studies on such areas as haemoglobin variant analysis. However, each sample would take nearly two days to run, a day for each dimension.

The most popular two-dimensional electrophoretic method is the combination of IEF with SDS-PAGE. O'Farrell and Klose independently introduced this system in 1975. In O'Farrell's original system isoelectric focusing in ampholytes was used in the first dimension and the resulting tube gel was then carefully attached to a slab gel followed by running in the SDS-PAGE mode. This method was able to separate up to 1000 protein spots from a protein extract of a tissue. However, the system required considerable expertise to use due to the variation in the IEF step; many workers found it irreproducible. With the development of immobilized IPGs the ease of operation of the IEF component was, as already discussed, greatly improved and relatively simple two-dimensional systems are now available commercially. For gels of 250 mm × 250 mm up to 3000–4000 protein spots can be revealed by silver staining from extracts of tissues such as liver. In this mode electrophoresis is probably the separation technique with the highest resolution available to the modern researcher.

Proteome analysis (proteomics) is a major new field of biomedical research. The proteome is defined as the total complement of proteins found within an organism, cell, tissue or biofluid. While the human genetic code will soon be known, its relationship to cell function will only be ascertained by advances within proteomics. For example, DNA sequences are not predictive of post-translational modifications such as glycosylation within the encoded proteins. Proteomics is the method of qualitatively determining this large number of proteins. It combines the high-resolution two-dimensional electrophoretic techniques mentioned above with digital image analysis, some elements of HPLC and modern mass spectrometry plus on-line bioinformatics to search databases. For example, two-dimensional proteome maps can be produced for a tissue such as liver and then digitally compared with the same tissue taken

from a diseased subject. The differences in the complex pattern, which may contain 1000+ spots, can be highlighted automatically and then mass spectrometry either of the MALDI-ToF and/or electrospray variety can be used to identify the variant proteins. By using such approaches it is now possible to identify known proteins using bioinformatic tools over the Internet in a matter of minutes, and to determine the structure of an unknown protein may only take a day or two.

Fields of Application

Although almost every class of molecule, especially those of a biochemical nature, has been separated by planar electrophoretic methods few are now done so. Early textbooks on electrophoresis detail separations of amino acids, sugars, purines and pyrimidines, nucleotides, some drugs, carboxylic acids, vitamins, and so on, but today's analyst would now use HPLC or capillary electrophoresis for such quantitative studies. Only for protein and DNA molecules is planar electrophoresis still the method of choice? Electrophoretic methods are used for qualitative and quantitative separation of proteins in clinical samples, biotechnological production and quality control, genomic and proteomic studies.

Traditional Planar Electrophoresis – Conclusions

This is still a basic tool in biochemistry and biomedicine since it is simple and often very cheap, parallel analyses are usual and so although any one run is slow, the many bands can be run at the same time so overall throughput is reasonably high. With the appropriate detection techniques, selectivity and sensitivity can be very good. By using thick media electrophoresis the technique can be made at least semi-preparative. Finally, in two-dimensional formats (IEF-SDS-PAGE) electrophoresis probably gives the highest resolution known in separation science.

However, perceived disadvantages are that it offers only low resolution in one-dimensional separations and the results are at best only semi-quantitative. Since it is difficult to use high voltages, it is seen as a slow technique made slower by the fact that detection is nearly always off-line.

Nevertheless there is a wealth of experience with the hundreds of available methods and probably millions of analytes are separated every day using traditional electrophoretic methods. Many of these analyses go unnoticed, for example the routine examination of serum proteins in clinical biochemistry laboratories throughout the world and the hundreds of daily runs sequencing DNA and so on in molecular

biology laboratories. However, research still continues into the technology and ultra-thin gels for DNA sequencing are giving excellent results and automated equipment for use with proteomics both in the electrophoresis stage and the sample isolation stage is being developed. Even after 100 and more years there is still much life in this technology.

Capillary Electrophoresis (CE)

For 40 years it had been appreciated that the excessive Joule heating that developed when high voltages were used to speed-up electrophoresis caused many of the technique's disadvantages. These disadvantages ranged from simply boiling the buffer solutions through to instrument fires and even electrocution. Many attempts were made to overcome the physico-chemical problems that degraded the separations. For a time in the 1960s and 1970s high-voltage electrophoresis systems operating at up to 10 kV were available. They were usually very large pieces of equipment that used large sheets of chromatography paper for the separations and required substantial pumped water cooling systems to remove the heat generated. Other equally complex systems with rotating Pyrex tubes to equalize the heating effects were also developed.

As with many problems, the solution when it came was very simple. In 1981 Jørgenson rationalized the problem to one of increasing the rate of cooling by substantially increasing the surface-to-volume ratio of the electrophoresis buffer. This, he showed, was readily achieved by performing the electrophoresis in small-bore capillaries. In a classic series of papers in that year Jørgenson and Lukacs described spectacular separations of peptides using zone electrophoresis in glass capillaries of 75 μm internal diameter using voltages of up to 30 kV with electrokinetic injection and fluorescence detection. This format enabled the Joule heating that normally degrades the resolution by thermal mixing to be efficiently dissipated. In addition, this new format used the significant electroosmotic (EOF) flow of the background electrolyte in the capillaries to separate cation, anions and uncharged molecules simultaneously with all analytes usually going towards the cathode where a single on-line detector was placed.

This discovery led to the development of a new form of analytical separation instruments that was very equivalent in its operation to HPLC. Most of the major HPLC instrument manufacturers had by the end of the 1980s introduced CE systems with varying degrees of sophistication. There was also considerable optimism that CE was going to replace HPLC for analytical separations. Ten years later only three

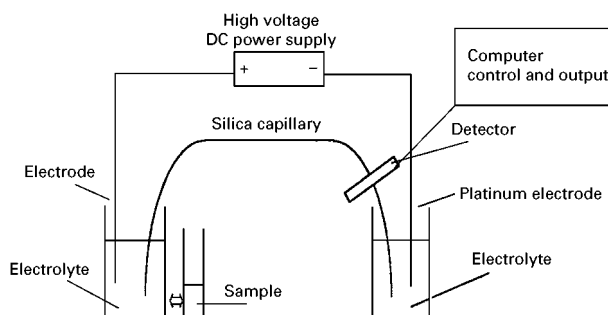


Figure 12 The configuration of a simple capillary electrophoresis (CE) instrument.

companies are still marketing complete CE instruments.

Today CE is characterized by its ability to resolve, using applied DC voltages giving field strengths up to $500 \text{ V}^{-1} \text{ cm}^{-1}$, the components of complex aqueous samples with very high resolution ($N > 250\,000$) analysing less than 10 nL of sample with analytical precision. To maintain efficiency, detection (UV, fluorescence) is nearly always on-line, i.e. across a window burnt into the polyimide coating of a silica capillary. Detection at the end of capillary can be achieved using electrochemical detectors or more usefully mass spectrometry.

A typical CE instrument consists of a capillary, detector, high-voltage power supply, recording device (**Figure 12**). The capillary used is made of fused silica and externally coated with a thin layer of polyimide, to make the capillary flexible. The capillary is usually about 375 μm outside diameter and 10–150 μm inside diameter with 50 and 75 μm the more usual. There is no set capillary length, although in commercial instruments there are minimum lengths which can be used, and this is usually dependent on the position of the detector. To allow detection a small section of polyimide coating has to be removed making a weak point in the capillary.

In CE electroosmotic flow (EOF) is a positive benefit, unlike in traditional electrophoresis systems. The silanol groups on the inner surface of the silica capillary are negatively charged above approximately pH 3 so cations build up near the silanol groups to maintain the charge balance. When the potential difference is applied to the capillary these cations are attracted towards the cathode, and they drag the bulk solution along with them (**Figure 13**).

The magnitude of the EOF is dependent on the surface charge of the capillary silanol groups, which varies with pH so that the EOF velocity increases with increasing pH. The flow profile of the EOF is different to the solvent flow profile found in HPLC. The laminar or parabolic flow produced by

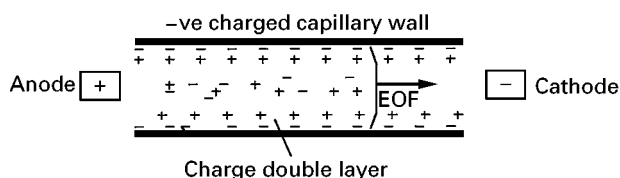


Figure 13 The electroosmotic flow (EOF) profile in a silica capillary electrophoresis (CE) capillary.

a liquid chromatography pump is due to the shear force at the capillary walls. In CE there is no pressure drop and therefore a flat flow profile is produced giving very much sharper peaks. In addition, at $\text{pH} > 6$ the EOF will be of sufficient magnitude to carry all the analytes regardless of their change in the same direction, this will only happen if the magnitude of the EOF is greater than the electrophoretic mobilities of the anions. The EOF will also carry neutral molecules along, although it cannot separate them. Since everything is moving in one direction an on-line detector can be placed at the cathodic end of the capillary. The output from a CE system is therefore very similar to that from HPLC systems – a series of peaks with baselines drawn in (if required) and areas of peaks calculated.

The present generation of commercial CE instruments is capable of unattended operation and features auto-injection using a variety of modes, integration and spectral analysis in a manner analogous to HPLC. CE has become widely available and the technology is now included in a number of other instruments such as a clinical protein analyser (Beckman Paragon) and in a DNA sequencer (PE-ABI 3700). In both of these instruments a large number of capillaries are operated in parallel in order to increase sample throughput, but the end users buys an instrument dedicated to a specific application not a CE instrument.

Modes of operation for CE CE is generally recognized as the description appropriate for the whole field of this separation science. CZE stands for capillary zone electrophoresis, in which ions are separated according to their mobility in free solution. This is the most frequently used separation mode option available within CE. A subtype of CZE is capillary ion analysis (CIA), which is used to determine simple ion species in aqueous solution rapidly. The other forms of electrophoresis described earlier such as isoelectric focusing and isotachopheresis can also be performed in a capillary format and are called cIEF and cITP, respectively. MEKC, sometimes called MECC – micellar electrokinetic capillary chromatography – is a separation mode introduced in 1984 by Terabe which allows the separation of neutral molecules by

their differential partition into charged micelles formed from detergents incorporated into the CE electrolyte. MECC can also be viewed as a subclass of CE methods involving complexation and inclusion using additives to the background electrolyte. Another separation mode is capillary gel electrophoresis (CGE), which was introduced by Cohen and Karger in 1988. This offers DNA and SDS-PAGE separations in a capillary, but with advantages in terms of speed, quantitation and ease of automation. The filling of capillaries with gels has now been supplanted by the use of entangled viscous polymer solutions to separate DNA. A recent development is the use of EOF to drive eluent through a capillary packed with HPLC stationary phase. This is termed capillary electrochromatography (CEC) and some very high efficiencies for neutral compounds have been demonstrated using this technique. CEC is performed on standard CE instrumentation, but has the added advantage that the eluents used are more readily interfaced to MS than is CE.

There has been a great deal of debate about the benefits and disadvantages of CE and it is worth touching on a few points here. The immediate attraction of CE for many analyses is its high efficiency giving the resolution needed to analyse complex samples and mixtures of biomolecules. CE can readily achieve separation efficiencies of orders of magnitude greater than those obtained by HPLC. From 100 000 to 250 000 theoretical plates per capillary is common, while up to 30 million have been reported for the CGE of oligonucleotides. Such efficiencies mean that 'isocratic' CE is capable of improving on the resolution obtained by both isocratic and gradient HPLC. **Figure 14** shows the separation of the complex array of metabolites and exogenous compounds excreted in normal human urine. A simple MEKC separation is shown resolving over 60 peaks in about 10 min. CE separations are simpler both in operation and equipment, and potentially much faster and quantitative. Thirty per cent more peaks have been observed resolved by CE compared to gradient HPLC under similar sample detection conditions. By using a high potential in short, narrow capillaries very fast assays using CE are possible. Many small ions can be resolved in only a few minutes. So-called short-end injection is also useful for high-speed separations. Such runs combined with minimal sample preparation means that some assays can take less than 1 min by CE. Mass sensitivity in CE is superb, as proved in the many elegant experiments that have determined various components in a single living cell. However, the concentration sensitivity is about one order of magnitude lower than in HPLC for the same detector. This is because the probed volumes

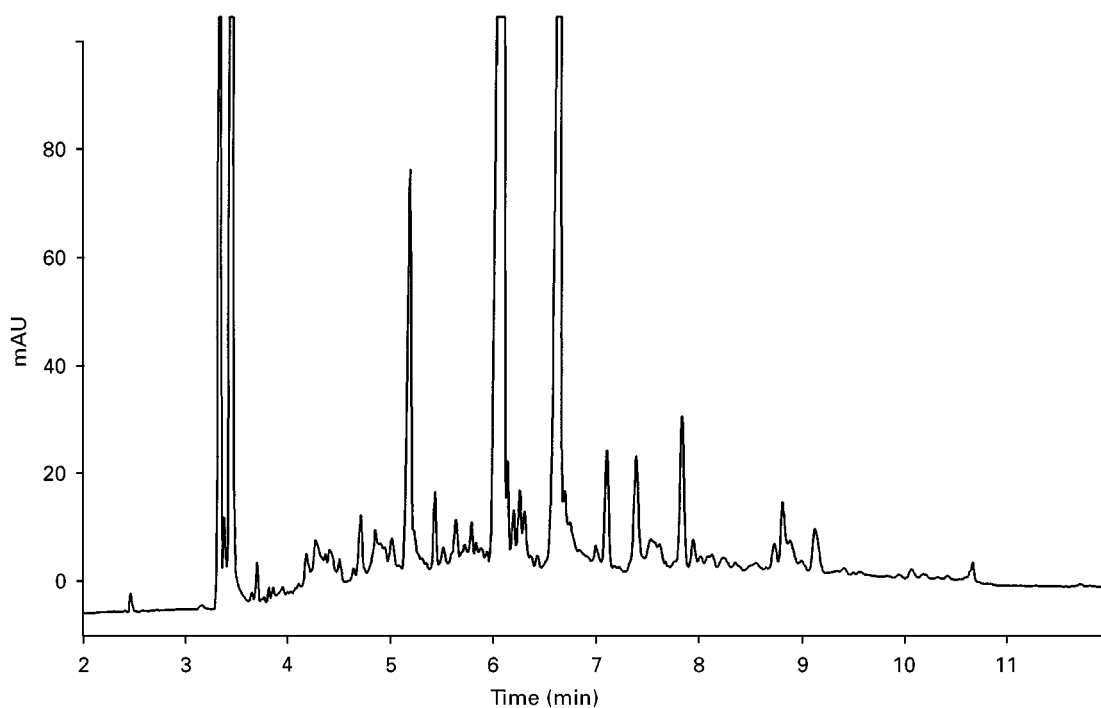


Figure 14 High-resolution separation of UV absorbing components of human urine separated by MEKC with detection at 195 nm.

are correspondingly lower, e.g. UV detection samples across a 50 μm capillary in CE compared to 10 mm in HPLC. There is much activity in detector development to address the problem of sensitivity. Laser-induced fluorescence (LIF) has been studied widely and promises to bring detection limits down to the single molecule level for appropriate fluorophores. LIF detection is now commercially available. CE-MS with electrospray ionization has proved to be a powerful technique with applications to structural studies of large biomolecules as well as small ions, and there is good concentration sensitivity using capillary isotachopheresis as the separation mode.

Applications Clearly CE is very good for separating charged species whether small molecules or macromolecules. It is necessary to operate in MECC mode to separate neutral molecules such as drugs. There are now some 5000 publications describing separations of some 10 000 compounds by CE. Charged and neutral compounds are all easily separated but there are too many examples in the literature to even attempt to describe them here. The high resolving power of CE is such that it can readily resolve enantiomeric compounds. The most commonly employed method is to include cyclodextrins into the electrolyte. β -Cyclodextrin is the most readily available compound, but recently sulfated derivatives of β -cyclodextrin have been shown to give separation of chiral compounds with spectacular resolution between the enantiomers. Oligonucleotides have pro-

ved to be readily separated using entangled polymeric additives such as hydroxyethylcellulose in the electrolyte to increase its viscosity and therefore gel-filtration effects. While the potential for quantitation shows enormous promise for proteins, there are several problems which remain to be overcome. Wall interactions degrade resolution and at worst lead to total adhesion of proteins to negatively charged sites on the silica capillary. Strategies to minimize this include covalent bonding to give coverage of the surface by hydrophobic groups, and dynamic coating using solution-phase additives.

In comparison to HPLC, CE achieves better resolution than both isocratic and gradient HPLC using simpler instrumentation. CE is not a preparative technique, although it has been used as a micropreparative system to isolate very small amounts of protein for sequencing. It is less sensitive than HPLC by about an order of magnitude. There is little difference in terms of quantitative data and analytical precision. Sample preparation probably needs to be better controlled and understood than for HPLC. At present, CE instrumentation is more expensive than HPLC, although running costs are considerably lower. CE uses much less sample and reagents than HPLC. Waste disposal problems are considerably reduced.

CE has now found a role in many laboratories and offers useful complementary separations to HPLC. It is clearly an established technique with a long-term future in the separation sciences.

See Colour Plates 6, 7, 8, 9.

Further Reading

- Andrews AT (1986) *Electrophoresis Theory, Techniques and Biochemical and Clinical Applications*, 2nd edn Oxford: Oxford University Press.
- Camilleri P (1997) *Capillary Electrophoresis: Theory and Practice*, 2nd edn. Boca Raton, FL: CRC Press.
- Dunn MJ (1993) *Gel Electrophoresis of Proteins*. Oxford: Bios.
- Everaerts FM, Beckers JL and Verheggen TP (1976) *Isotachopheresis: Theory, Instrumentation and Applications*. New York: Elsevier.

- Landers JP (ed.) (1994) *Handbook of Capillary Electrophoresis*. Boca Raton, FL: CRC Press.
- Mosher RA, Saville DA and Thormann W (1992) *The Dynamics of Electrophoresis*. Weinheim: VCH.
- Smith I (1968) *Chromatography and Electrophoresis*, vol. II. *Zone Electrophoresis*. London: Heinemann.
- Vindeogel J and Sandra P (1992) *Introduction to Micellar Electrokinetic Chromatography*. Heidelberg: Hüthig.
- Weinberger R (1993) *Practical Capillary Electrophoresis*. New York: Academic Press.
- Westmerier R (1997) *Electrophoresis in Practice*, 2nd edn. Weinheim: VCH.
- Zweig G and Whitaker JR (1967) *Paper Chromatography and Electrophoresis*, vol. 1. *Electrophoresis in Stabilizing Media*. New York: Academic Press.

EXTRACTION



D. E. Raynie, The Procter & Gamble Company, Cincinnati, OH, USA

Copyright © 2000 Academic Press

Introduction

Extractions are common in the world around us. Each time we brew a cup of tea or a pot of coffee, and each time we launder our clothes, we're performing a chemical extraction process. Perhaps because of this familiarity, extraction processes in chemical laboratories are often not fully appreciated, or fully understood. Quite simply, an extraction is the process of moving one or more compounds from one phase to another. Yet behind this simple definition lies a great deal of subtlety: separations are contrary to thermodynamic intuition, because entropy is gained through mixing, not separation; extraction methods are developed based on a drive towards equilibrium, yet the kinetics of mass transfer cannot be ignored. Such a list of physical chemical nuances provides the basis for this chapter on the fundamentals of chemical extractions.

Extractions are carried out for a variety of reasons, for example when distillation is either impractical (e.g., distillations are favourable when the relative volatility of the compounds to be separated is greater than about 1.2) or is too expensive, to isolate material for characterization, to purify compounds for subsequent processing, etc. Extractions can be classified according to a number of schemes:

- analytical versus preparative (depending on the quantity of pure compound to be separated);

- batch versus continuous (depending on the mode of feeding the material to be separated into the extraction apparatus);
- based on the physical principles involved (is the extraction strictly based on partitioning, or are adsorption or other processes involved?);
- based on the types of phases involved (so called liquid-liquid extraction, gas-solid extraction, supercritical fluid extraction, etc.).

Perhaps the biggest recent advances in the field of chemical extractions have taken place in the petroleum, nuclear, and pharmaceutical industries. The understanding and practise of extraction lies at the crossroads of analytical, inorganic, organic, and physical chemistry, with theoretical and applied chemical engineering. Yet the fundamental physico-chemical principles involved are the same. Because of the author's background, this chapter presents a description of the fundamental basis for chemical extractions and an overview of extraction techniques with a slant, or emphasis, towards the analytical chemists' perspective.

In general, the extraction process occurs as a series of steps. First the extracting phase is brought into intimate contact with the sample phase, usually by a diffusion process. Then the compound of interest partitions into or is solubilized by the extracting solvent. With liquid samples this step is generally not problematic. However with solid samples, for the compound being extracted to go into the extracting solvent the energy of interaction between the compound of interest and the sample substrate must be overcome. That is, the material's affinity for the extracting solvent must be greater than its affinity

Table 1 Summary of selected extraction techniques by phases involved and the basis for separation

Extraction technique	Sample phase	Extracting phase	Basis for separation
Liquid-liquid extraction	Liquid	Liquid	Partitioning
Solid-phase extraction (and microextraction)	Gas, liquid	Liquid or solid stationary phase	Partitioning or adsorption
Leaching	Solid	Liquid	Partitioning
Soxhlet extraction	Solid	Liquid	Partitioning (with applied heat)
Sonication	Solid	Liquid	Partitioning (with applied ultrasound energy)
Accelerated solvent extraction	Solid	Liquid	Partitioning (with applied heat)
Microwave-assisted extraction	Solid	Liquid	Partitioning (with applied microwave irradiation)
Supercritical fluid extraction	Solid, liquid	Supercritical fluid	Partitioning (with applied heat)
Purge-and-trap	Solid, liquid	Gas	Partitioning
Thermal desorption	Solid, liquid	Gas	Partitioning (with applied heat)

for the sample. Finally the extracting phase (containing the compound of interest) must diffuse back through the sample, separate into a distinct phase, and be removed for subsequent processing. With proper selection of the extracting solvent this final step is generally not difficult, though the formation of emulsions must be avoided with liquid samples.

As previously mentioned, extractions (and other separation processes) are contrary to the principles of thermodynamics and work must be applied to overcome these thermodynamic constraints. Perhaps this has been expressed most eloquently by Giddings:

It seems enigmatic that we often struggle so hard to achieve desired separations when the basic concept of moving one component away from another is inherently so simple. Much of the difficulty arises because separation flies in the face of the second law of thermodynamics. Entropy is gained in mixing, not in separation. Therefore it is the process of mixing that occurs spontaneously. To combat this and achieve separation, one must apply and manipulate external work and allow diffusion in a thermodynamically consistent way.

This external work is often applied as heat (temperature), which results in faster kinetics, decreased solvent viscosity and surface tension, increased solute solubility and diffusivity, and aids in overcoming interactions between the solute and the sample. A general analytical chemistry textbook (Peters, Hayes, and Hieftje (1974) *Chemical Separations and Measurements: Theory and Practice of Analytical Chemistry*. Philadelphia: Saunders) further describes the extraction process and areas for improvement:

If two compounds are to be separated, we must, somewhere along the line, get them into two dif-

ferent and separable phases ... At the heart of any chemical separation are the processes of (1) phase contact and equilibrium and (2) phase separation. These steps occur in all separation techniques, and a key in understanding a given method is the identification and classification of the steps according to the nature of the phases involved and the mechanism of phase contact and separation. Similarly, if a particular method of separation is to be improved, these are the only processes worth adjusting.

Using this discussion as a framework we can classify various extraction techniques according to the phases and applied work (or the basis of separation), as shown in **Table 1** for several selected extraction techniques.

The progress of an extraction is graphically depicted in **Figure 1**, which is a plot of the extraction yield (e.g. mass extracted) versus the progress of an extraction (e.g. solvent volume, time, equilibrium stages, etc.). This plot is generally asymptotic and consists of two regions. The initial, more steeply sloped region is the equilibrium region. This is the area where the effects of solute partitioning and solubility exist.

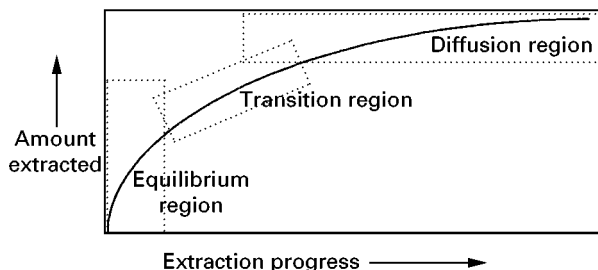


Figure 1 Plot of the relative amount (mass) extracted as a function of extraction progress (e.g. solvent volume, time, etc.). Three regions are defined: an equilibrium region dominated by solute partitioning, a diffusion region controlled by solute diffusion, and a transitional region.

As the extraction progresses it transitions into a region predominated by solute diffusion as well as the necessity for the solute to overcome effects such as solute-sample matrix interactions.

Preliminary Requirements

Chemical samples requiring extraction are composed of the compound of interest and the sample matrix, which may contain interfering species. Prior to choosing an extraction method, knowledge must be gained about the structure (including functional group arrangement), molecular mass, polarity, solubility, pK_a , and other physical properties of both the species of interest and potential interfering compounds. Constraints specific to the sample and the solvent must be considered, and the resulting concentration and desired degree of purification must be taken into account. This section discusses these preliminary considerations. Solvent-specific considerations and the roles of solute solubility, partitioning, and diffusion will subsequently be addressed.

Terminology

In discussing the fundamental processes in extraction, it is important to keep the appropriate terminology in mind. Extractions occur by the distribution of a compound between two immiscible phases. The mixture containing the component(s) to be separated is called the *feed* or *sample*. The extracted compounds of interest are described by several terms, including *solute* or *analyte*, while the phase left from the feed after being contacted by the extracting phase is the *raffinate* (generally used for liquids) or *residue* (solids). The *solvent* is the immiscible extracting fluid added to the process for the purpose of extracting solutes from the feed. One key feature is the lack of mutual solubility between the feed and the extracting solvent. Usually less than 10% solubility of the solvent in the feed is desired. Because phase separation is a defining parameter in chemical extractions, fluid flow is important for transporting the solute both through the sample (facilitating diffusional mass transfer by maintaining a concentration gradient at the interface between the phases) and through the system. Thus the solvent must be a gas, liquid, or supercritical fluid. (Solid extracting phases do not serve to move the extracted material through the system. In extraction techniques such as solid-phase extraction or matrix-solid-phase dispersion the solid phase assists in removing the solute from the feed, but fluid solvents are required to remove the solute from the solid phase.) During an extraction process, each equilibrium event is termed a *stage*; hence a theoret-

ical (or equilibrium) stage is a mechanism, or extraction region, where the immiscible phases are brought under equilibrium conditions then physically separated. The placement of the extraction stage can help define the extraction process. For example, a *cross-current* extraction is composed of a cascading series of states where the raffinate is brought into a subsequent stage and contacted with fresh solvent. In a *countercurrent* extraction, the solvent and feed enter from opposite ends of the system, and these two immiscible phases pass each other in opposing streams.

Batch and Continuous Extraction Modes

One means of classifying extractions is based on the mode of operation, batch or continuous and static or dynamic. The terms batch and continuous refer to how the sample (feed) is placed into the system. In batch extraction processes the entire material to be extracted is loaded into the extraction device. In the case of continuous extractions the feed is continuously introduced into the extraction device. Static and dynamic describe the exposure of the two phases. In the static mode the extracting solvent and the feed are brought into contact and allowed to commingle for a prescribed period before the phases are separated, while dynamic extractions occur by continuously passing clean (whether fresh or recycled) extracting solvent through the sample.

Most analytical extractions are performed using a batch-wise process. This mode is used when the distribution ratio (i.e., the ratio of the solute between the two phases) is high, favouring the extraction solvent. With batch extractions few stages are needed to achieve quantitative results, though phase separation has to occur before the extraction is complete. Batch extractions can occur in static or dynamic modes, or in some combination. For example, the familiar Soxhlet technique for extracting solid samples, depicted in Figure 2A, is considered a batch process with discontinuous solvent infusion, that is involving both static and dynamic modes.

Similar extractors for laboratory-scale liquid-liquid extraction, again shown in Figure 2, are also based on distilling the extracting solvent with subsequent condensation. The condensed solvent passes through the sample solution to be extracted, phase separation occurs, and the extracting solvent flows back into the receiving flask for redistillation. Design considerations account for the solvent density. The glassware shown in Figure 2B is representative of aqueous-organic extractions using heavier-than-water solvents, while Figure 2C illustrates an apparatus for use with lighter-than-water solvents.

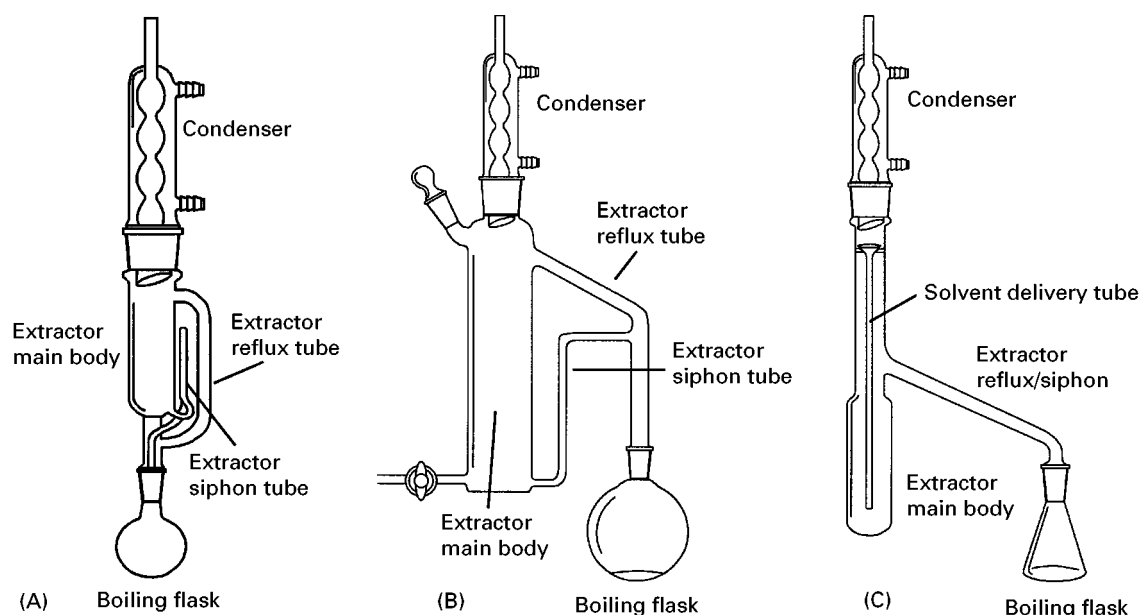


Figure 2 Laboratory glassware for performing (A) Soxhlet extraction, (B) liquid-liquid extraction with extracting solvents more dense than the liquid solvent, and (C) liquid-liquid extraction with extracting solvents less dense than the liquid sample.

When batch-wise extraction procedures are used for studying physical chemical properties, such as solubility or distribution ratios, special care must be taken, especially when aqueous phases are involved. Volume changes due to mutual solubility of the phases should be noted for precise measurements. Both the extraction and sampling must take place at the same temperature, since the values of many properties change as a function of temperature.

When distribution ratios are small, and also in many production-scale systems, continuous extraction processes are used. Continuous extractions are by definition also dynamic, since the two phases are continuously passed through each other. High efficiency continuous extractions depend on the viscosity of the two phases, the equilibrium rates, distribution ratios, solvent volumes, and the surface/contact area between the phases.

Countercurrent Extraction

A continuous extraction approach (though sometimes performed in a batch-wise manner) is countercurrent extraction. In countercurrent extraction both phases are continuously added (or changed) and flow in opposite directions as the extraction progresses. (When only one phase is continuously added, the procedure becomes a crosscurrent extraction.) In the case of both countercurrent and crosscurrent extractions, the feed is repeatedly (continuously) contacted or washed with extracting solvent. The number of theoretical stages is maximized by using solvents with favourable distribution coefficients (see sub-

sequent discussion) or by increasing the solvent-to-feed ratio. Commonly, these processes employ up to eight theoretical stages. Although they have been replaced by chromatographic methods in many cases, countercurrent extractions are useful in that they use solvent only, without sorbents, and relatively mild conditions. They are favoured when the distribution coefficient is small. However, countercurrent extractions use large volumes of solvent and are not advantageous when large amounts of solute are to be isolated. The Craig countercurrent device, popularly used to study partition chromatography, is a discontinuous, differential migration process, since the extraction stages are performed step-wise rather than as continuous extractions.

Solvent Considerations

The requisite immiscibility and viscosity of the extracting fluid have been discussed.

Several other solvent properties that are important to the extraction process are listed here.

- Selectivity, i.e. the ability to extract the material of interest in preference to other, interfering material. Solvent selectivity can be supplemented through the use of adsorbents and secondary solvents, and by other means.
- High distribution coefficient to minimize the solvent-to-feed ratio.
- Solute solubility, which is usually related to polarity differences between the two phases, leading to low solubility in the raffinate.

- Ability to recover the extracted material. Thus the formation of emulsions and other deleterious events must be minimized.
- Capacity, the ability to load a high amount of solute per unit of solvent.
- Density, as density differentials are needed for countercurrent flow. The solvent density is related to solubility in supercritical fluid extracting solvents.
- Low interfacial tension to facilitate mass transfer across the phase boundary. Interfacial tension tends to decrease with increasing solute solubility and as solute concentration increases. In liquid-liquid extraction low interfacial tension allows the disruption of solvent droplets (entrained in the feed solution) with low agitation.
- Low relative toxicity.
- Nonreactive. In some instances, such as ion-exchange extractions, known reactivity in the extracting fluid is used. In addition to being nonreactive with the feed, the solvent should be nonreactive with the extraction system (e.g., non-corrosive) and should be stable.
- Inexpensive. Cost considerations should emphasize the energy costs of an extraction procedure, since, for a given extraction method, capital costs are relatively constant.

Solubility

Of the solvent properties necessary for extraction, solubility of the solute into the solvent is of fundamental importance. The general understanding of 'like dissolves like' is handy in the preliminary choice of extraction solvents. Solvent classification schemes are often helpful, especially if the selectivity of solvents is of interest. The Snyder selectivity triangle results in eight classifications of solvents according to proton donor, proton acceptor, and dipole interaction properties. Another solvent classification scheme is as follows.

- Class 1 solvents: capable of forming three-dimensional networks of strong hydrogen bonds.
- Class 2 solvents: have active hydrogen atoms and donor atoms, but do not form three-dimensional networks.
- Class 3 solvents: contain donor atoms, but not active hydrogen atoms.
- Class 4 solvents: contain active hydrogen atoms, but not donor atoms.
- Class 5 solvents: do not have hydrogen-bonding capability or donor atoms.

Comparisons of solubility values can give approximations for the partitioning of a solute between two

solvents. Although experimentally generated solubility data is preferred, relative solubility scales can be used for estimation purposes. However, it is important to remember that no scale has been developed that completely accounts for all of the intermolecular interactions influencing solubility.

The most common relative solubility scale is the Hildebrand solubility parameter scale. The Hildebrand solubility parameter, δ , is a measure of the cohesion (interaction) energy of the solvent-solute mixture and is defined by $\delta = (\Delta E_v/V)^{1/2}$, where E_v is the heat (energy) of vaporization necessary for volume V . Thus, the ratio $\Delta E_v/V$ is the cohesive energy density. The 'total' Hildebrand solubility parameter (δ_t) is related to the hydrogen-bonding ability (δ_h), the dispersion coefficient (δ_d), and the polarity (δ_p) by $\delta_t^2 = \delta_h^2 + \delta_d^2 + \delta_p^2$. Consequently, there is a strong correlation between the Hildebrand solubility parameter value and the polarity. For extraction purposes, it is preferable to use solvents that have δ values similar to those of the solutes of interest. Several references provide detailed development of the Hildebrand solubility parameter, and similar scales, and these values are tabulated for several solvents.

When supercritical fluids are used in place of liquids, modified versions of the Hildebrand solubility parameter are used in which $\delta = 1.25P_c^{1/2}(\rho/\rho_{liq})$ or $\delta = \delta_{liq}(\rho/\rho_{liq})$, where P_c is the critical pressure, ρ is the density, and δ_{liq} and ρ_{liq} are the Hildebrand value and density at liquid conditions. This modification for supercritical fluids, while only approximate, provides for reference to liquid values of polarity and other 'chemical' properties, and for the relationship between supercritical density and solubility.

Solvent Removal Methods

Once the solute is extracted into the extraction solvent, it generally must be isolated from the solvent. Thus, the chosen solvent should facilitate this procedure. Most simply, this is done by evaporation or distillation of the solvent from the solute. Distillation procedures can be quite efficient. Other solvent removal methods include precipitation, adsorption, and back-extraction. Precipitation of the solute and subsequent decanting or filtering usually results in low yields. Where appropriate, these yields can be moderately improved by converting the (ionic) solute to the salt. Adsorption onto a suitable stationary phase is especially desirable if additional solute purification is needed. Back-extraction also results in additional purification. This secondary extraction can use a third solvent or can be an extraction back into the original feed solvent (for liquid systems) through changes in the distribution ratio by adjusting parameters such as pH. For example, with ionizable

compounds and an aqueous phase the fraction ionized into the aqueous phase is approximated by the Henderson–Hasselbach equation (i.e., $\log \text{ionized} (\alpha) / \log \text{nonionized} (1 - \alpha) = \text{pH} - \text{p}K_a$). So in this example, the ionic form of 99% of the solute can be changed by adjusting the pH by two units from the $\text{p}K_a$.

Extraction of Ions

The extraction of ionic species, especially from aqueous phases into organic phases, often requires somewhat specialized treatment, generally ion-exchange or ion-pairing extraction. In ion-exchange extraction the ionic compound is covalently bonded to a compound of opposite charge, resulting in a neutral species. The more common ion-pairing extraction is based on formation of a neutral ion pair through the interaction of the ionic species of interest with a counterion. The resulting neutral ion pair is soluble in organic solvents. Usually solubility is greater in polar solvents. The solubility in the organic solvent is usually increased by selecting an ion-pair reagent containing a nonpolar portion in addition to the charged moiety. Counterions used are generally soft acids or bases possessing large ionic radii. In addition to selection of the counterion, experimental parameters that can influence ion-pair extractions include pH, ionic strength (i.e., the total concentration of all ionic species in the sample), organic solvent, and flow rate.

Solute Distribution

Chemical extractions proceed by a drive towards equilibrium. Consequently, knowledge of the equilibrium distribution of the solute between the phases is useful. Berthelot and Jungfleisch studied phase distribution in 1871 and twenty years later, in 1891, Nernst developed his distribution law in which $K_D = (\text{concentration of solute in phase 1}) / (\text{concentration of solute in phase 2})$, where K_D is the *distribution coefficient*. However, the simple ratio of solute concentrations is not thermodynamically rigorous, since it does not account for association or dissociation in either phase. The IUPAC (International Union of Pure and Applied Chemistry) definition of the *distribution ratio*, K' , includes all species of the same component and is used when the solute does not chemically react in either phase. This definition discusses the ratio, in organic–aqueous systems, as ‘the total analytical concentration of the substance in the organic phase to its total analytical concentration in the aqueous phase, usually measured at equilibrium’. This relationship follows from Gibbs’ phase rule in which: $P + V = C + 2$, where P is the number of phases, V is

the number of degrees of freedom (independent system variables), and C is the number of components. So for the example of a simple extraction with two immiscible phases and a single solute of interest, $P = 2$ and $C = 3$. At constant temperature and pressure, the number of degrees of freedom is one, meaning the solute concentration in each phase is fixed. (Note that while activities and concentrations are not strictly equivalent, they can generally be treated equally over practical concentration ranges.)

Distribution ratios cannot be determined from the relative solubility data for several reasons: (1) the extraction may not be at equilibrium, (2) mutual solubility of the phases, and (3) solubility differences, for example between hydrated and anhydrous forms of the solute. Therefore the ratio of solubilities is not the same as the distribution ratio for these same reasons. However, if solvation is properly considered, the relationship between solubility and extractability can be determined, especially for liquid–liquid systems. Assuming equilibrium and phase immiscibility, the fraction of solute extracted, E , can be determined for a given phase ratio, V or V_1/V_2 , by the expressions:

$$E = C_1 V_1 / (C_1 V_1 + C_2 V_2) = K_D V / (1 + K_D V)$$

$$E = 1 - [1 / (1 + K_D V)]^n$$

$$\%E = 100 K_D / (K_D + V_2 / V_1)$$

where C is the solute concentration, n is the number of extractions (assuming the extracted phases are pooled), and subscripts 1 and 2 represent the two phases. A practical application of the use of distribution ratios is shown in Figure 3, which illustrates the need for a series of extraction stages, rather than simply, an increase in the volume of extraction

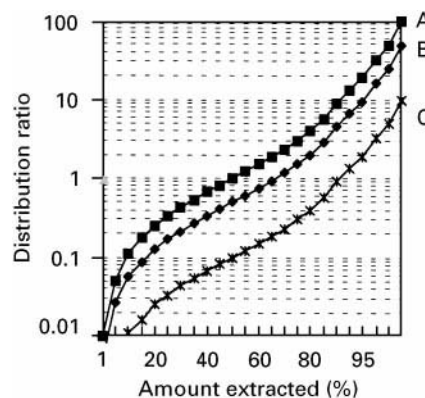


Figure 3 Relationship between distribution ratio and amount (percent) of solute extracted for (A) phase ratio of one, (B) phase ratio of two, and (C) phase ratio of ten.

Table 2 Solute distribution between phases in multistage extraction

	Stage				Distribution of solute
	0	1	2	3	
Initial equilibrated sample	<i>a</i>				
	<i>b</i>				
First transfer	0	<i>a</i>			
	<i>b</i>	0			
Amount of solute in each stage	<i>a</i>	<i>b</i>			<i>a + b</i>
Second transfer	0	<i>ab</i>	<i>a</i> ²		
	<i>b</i> ²	<i>ba</i>	0		
Amount of solute in each stage	<i>b</i> ²	<i>2ab</i>	<i>a</i> ²		<i>(a + b)</i> ²
Third transfer	0	<i>ab</i> ²	<i>2ba</i> ²	<i>a</i> ³	
	<i>b</i> ³	<i>2b</i> ² <i>a</i>	<i>ba</i> ²	0	
Amount of solute in each stage	<i>b</i> ³	<i>3b</i> ² <i>a</i>	<i>3a</i> ² <i>b</i>	<i>a</i> ³	<i>(a + b)</i> ³
Amount of solute in each stage upon subsequent transfers					<i>(a + b)</i> ^{<i>n</i>}

solvent. In this example, assuming a constant distribution ratio of 1, a doubling of the extraction volume (from phase ratio = 1 to phase ratio = 2, where the phase ratio is the simple ratio of the extraction solvent volume to the sample volume) only increases the amount extracted in a single stage from about 50% to about 66%. A ten-fold increase in solvent volume only increases the amount extracted from about 50% to about 90%. As additional stages are added, the solute distributes itself in each phase. This is similar to the distribution studied by Craig and shown in Table 2. In this case, a solute distributes itself between the two phases in the ratio of a/b and the amount of solute in each stage can be determined. In practice, however, the stages are combined to maximize solute yield and recovery.

Diffusion

In addition to the roles of solubility and distribution ratios during the equilibrium portion of an extraction, diffusion is the largest factor influencing the extraction of solutes. Diffusion is that spontaneous, irreversible process by which a compound moves from an area of high concentration to an area of lower concentration, resulting in a concentration equilibrium within a single phase. More rigorously, the diffusional flow, J , of a compound is defined as the mass of the material of interest passing through a reference surface during a specified time, and laws of diffusion can correlate this diffusional flow with the concentration gradient responsible for the flow. If the rate of mass flow per unit area, or the

diffusion flow, J , is in $\text{g cm}^{-2} \text{s}^{-1}$ and concentration is in mol cm^{-3} , Fick's first law of diffusion provides a correlation with the concentration gradient such that $J = -D(\Delta c/\Delta x)$, where D is the diffusion coefficient (given in $\text{cm}^2 \text{s}^{-1}$) and $\Delta c/\Delta x$ is the concentration gradient (in g cm^{-4} , concentration c is in g cm^{-3} and area x is in cm^2). Thus, Fick's first law defines a diffusion coefficient that is independent of solute concentration and is unique to every solute-solvent pair at constant temperature. Generally, this diffusion coefficient, D , is in the range 10^{-5} – $10^{-6} \text{cm}^2 \text{s}^{-1}$ in liquid solutions, whether aqueous or organic. When a steady state cannot be assumed, the concentration change with time must be considered, leading to Fick's second law of diffusion, $\Delta c/\Delta t = D(\Delta^2 c/\Delta x^2) = DV_{\text{mol}}^2 c$, where t is time (s) and V_{mol} is molar volume. Thus in non-steady-state conditions the temporal rate of concentration change is proportional to the spatial rate of concentration change in the direction of the concentration gradient.

Diffusion in Liquids

In liquid systems, with small or medium-sized molecules in dilute solution, diffusion is highly dependent on viscosity, η , and consequently on temperature, T . Assuming a spherical particle, diffusion in liquids can be expressed by the Stokes-Einstein equation, $D = (10^{-7} T/\eta V_{\text{mol}}^{1/3})$.

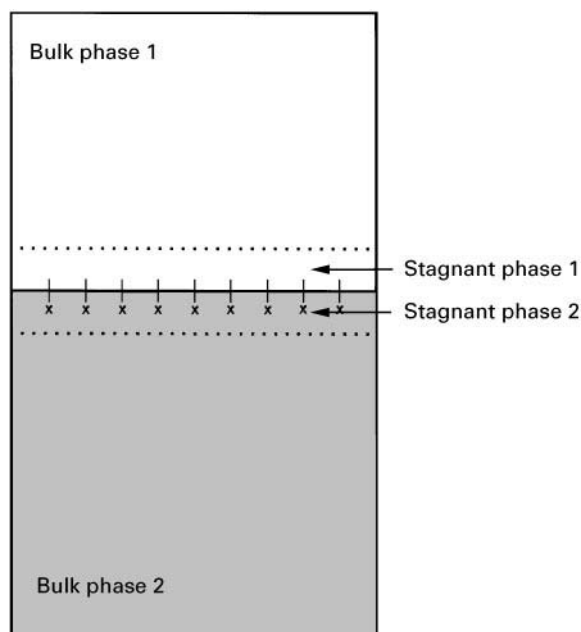


Figure 4 Schematic diagram of the role of interfacial diffusion in liquid-liquid extraction. Each stagnant layer is about 10^{-2} – 10^{-4}cm . In this depiction, the molecules diffusing through the liquid-liquid interface contain a moiety (\times) with an affinity toward phase 2 and a moiety ($-$) with an affinity toward phase 1.

For the purposes of extraction, the rate of diffusion across the liquid–liquid boundary layer is of primary importance. This diffusion rate is dependent on solute shape and size and on solvent viscosity. Agitation or turbulence at the liquid–liquid interface can enhance the rate of diffusion across the phase boundary, but there is a practical limit to the degree of agitation in an extraction mixture. **Figure 4** depicts the liquid–liquid system, including the stagnant films on either side of the phase boundary. In practical extraction examples the bulk phases are adequately stirred so that diffusion in the bulk phases can be neglected. However, the interfacial stagnant layers are about 10^{-2} – 10^{-4} cm (compared with diffusion coefficients in the range 10^{-5} – 10^{-6} cm² s⁻¹) and must be considered as controlling the overall extraction kinetics. Moderate shaking or agitation can reduce the thickness of the stagnant, or stationary, films. If agitation is too vigorous, solutes in the mixture are given a high translational motion without an increase in the rate of solute movement to the phase interface. As phase dispersion increases, the relative velocity of the two phases decreases, until the limiting case of an emulsion (in which relative velocity becomes zero) is reached.

Diffusion in Solids

When extracting solutes from solid samples, one must not only overcome the solute–sample attraction, but

the solute must diffuse with the solvent back out of the porous solid sample. This diffusion through the pores of a solid sample is influenced by the geometry or tortuosity of the pore structure (e.g. the diffusion path length). Diffusion in solids, assuming weak solute–sample sorption (i.e., a linear isotherm), is expressed by $D_{\text{eff}} = (\phi D)/\gamma(K_D + 1)$, where D_{eff} is the effective (or apparent) diffusivity, ϕ is the fraction of space available to the extracting solvent, K_D is the distribution coefficient (expressed as the ratio of solute concentration in the solid volume to solute concentration in the solvent volume), D is the (true) diffusivity in the bulk solvent, and γ is a tortuosity factor. With ionic solutes, if the pore wall carries an electric charge, diffusion is also affected by the electrical potential gradient.

This knowledge of diffusion through porous solids can provide an understanding of practical extractions. **Figure 5** represents an overview of the processes occurring when extracting solutes from solids. This understanding is described in the ‘hot-ball model’ advocated by Professors Keith Bartle and Tony Clifford at Leeds University. For example, with small quantities of extractable compounds that diffuse out of the homogeneous spherical particle into the extraction solvent, the extracted compounds are infinitely dilute. The extraction rate is obtained through the expression for the ratio of the mass, m , of

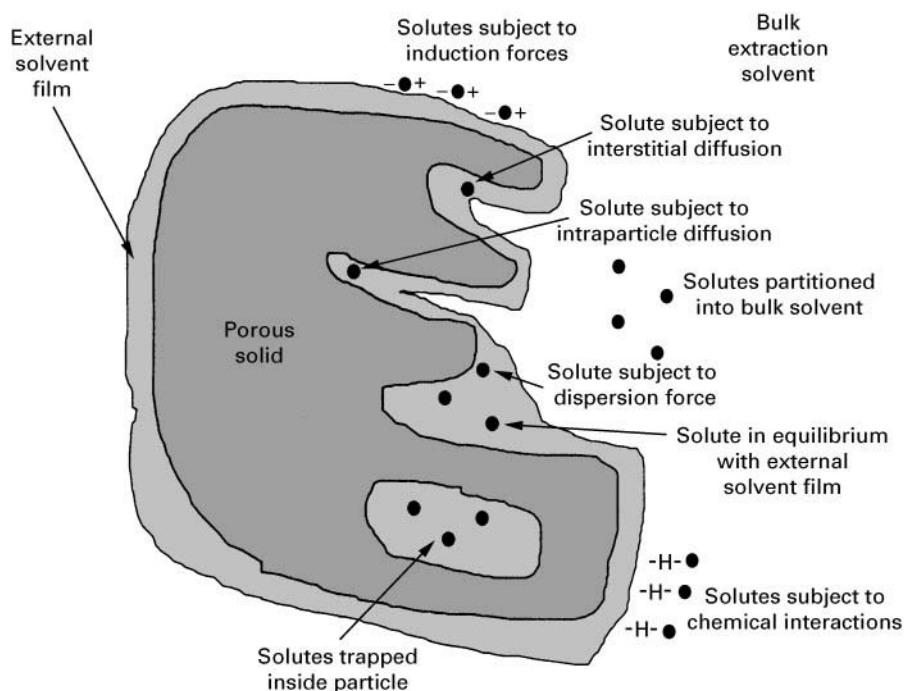


Figure 5 Schematic diagram of major physical/chemical processes that may occur during the extraction of solutes from a solid sample particle.

extractable material remaining after time t to the initial mass of extractable material, m_0 , where $m/m_0 = (6/\pi^2)\Sigma(1/n^2)\exp(-n^2\pi^2Dt/r^2)$, where n is an integer, D is the diffusion coefficient of the material in the sample matrix, and r is the radius of the spherical sample. This equation reduces to a sum of exponential decays, and a plot of $\ln(m/m_0)$ versus time eventually becomes linear. The physical explanation for the model is that, during the initial phases of an extraction, there is a concentration gradient at the surface of the sphere and diffusion from the sphere is rapid. This corresponds to the 'equilibrium' region (see Figure 1). When the concentration across the entire sphere becomes even and the rate of diffusion (and, hence, extraction) is a simple exponential decay, the 'diffusion' region of the extraction process (shown in Figure 1) is reached. Extrapolation of this linear portion of the plot of $\ln(m/m_0)$ versus time can be used to determine the time (or amount of solvent) necessary to achieve quantitative extraction recoveries.

Extraction Techniques

The previous sections described, in a practical way, the theory and the physical chemical basis for extraction. The importance of the phase interface was noted, and it was emphasized that mass transfer is a function of several properties, such as diffusion, viscosity, density, interfacial tension, turbulence, etc. Extractions are more practically a function of those experimental parameters that affect diffusion, viscosity, etc. For example, temperature plays one of the largest roles in improving extraction yields (though selectivity may suffer), as does the particle size of solid samples. The geometry of the extraction system must also be considered.

Chemical extractions can take on a number of embodiments. This section will provide a brief overview of these (mostly analytical) extraction techniques. The most important, and/or newly developed, are discussed in detail in other articles. While the methods discussed here are categorized as 'liquid' or 'solid' methods, there is some degree of exchange and methods used predominantly for solids can also be adopted for liquids in many cases, for example.

Extraction from Liquids

Liquid-liquid extraction (LLE) During LLE the solute partitions between two immiscible liquid phases. The devices shown in Figure 2, as well as the common separatory funnel, are simple laboratory methods for performing LLEs. The extraction solvents are chosen based on solubility differences

with the sample solvent. For example, with neutral, acidic, or basic aqueous samples, organic solvents such as hydrocarbons, ethers, halocarbons, and aliphatic alcohols or ketones are commonly used. LLE can be performed in batch or continuous mode, can accommodate unattended operation, is suitable for systems with low distribution ratios, and uses relatively low solvent volumes. If solvent reflux is used care must be taken to avoid loss of volatile solutes and thermal degradation of the sample or the solute. In all LLEs the formation of emulsions should be avoided.

Solid-phase extraction (SPE) In SPE, a solid, or a liquid phase adhered onto a solid support, is used to selectively (and reversibly) retain sample components as the sample solution passes through the extraction device, usually configured as a packed bed or disk. The solute is then removed from ('washed off') the sorbent phase with the extracting solvent. In essence, this extraction procedure can be thought of as a crude chromatographic method and many of the same principles, and stationary phases, apply. SPE is especially useful for improving the selectivity of an extraction for instance to 'clean up' dirty samples for analysis. The selective stationary phases can retain solutes based on ionic or hydrogen bonding, or dipole-dipole, dipole-induced dipole, or dispersion forces. The primary advantages of the technique, in addition to selectivity, include speed, efficiency, reproducibility, economics, and safety.

Another, specialized, version of SPE is solid-phase microextraction (SPME). With SPME, the sorbent phase is coated on a small fibre which then comes in contact with the sample. The extracted solutes are eluted from the fibre, in most cases directly by the chromatographic inlet system. The advantage of this technique is that the extraction is coupled directly with the analytical chromatography (so that all of the solute is introduced into the chromatographic system) so that the system can be 'solvent-free'.

Extraction from Solids

It is estimated that 40% of all analytical samples are solids. This significant portion of the analytical sample load represents the most difficult extraction challenge, since solute interactions with the sample matrix must be overcome and the solute must then diffuse through the solid sample. As a result, the development of extraction methods for solids has focused on improving the diffusion issues.

Leaching Leaching simply involves soaking the sample in the extraction solvent for a prescribed period, and is a batch process. Because of the adsorp-

tive properties of the sample and the slow diffusion through a solid, leaching is not a very efficient extraction method. Improvements to simple leaching can be made by placing the extraction vessel on a heat source (such as a heating plate or steam bath). Agitation, as in shake-filter methods, and a decrease in the sample particle size can also improve recoveries. An adaptation of leaching is forced-flow leaching. In this case the sample is placed in a tube and solvent flow is forced (under pressure) through the tube. In many instances the solvent is heated to near its boiling point and forced-flow leaching can be a continuous process.

Soxhlet extraction This common procedure, which uses the device shown in Figure 2A, was developed nearly 100 years ago and is still in routine use. The sample is placed into a porous container (called a thimble) and the volatile extraction solvent is continuously refluxed and condensed through the sample. Although the method can be slow (12–24 h Soxhlet methods are not uncommon), the apparatus can be left unattended with multiple extractions being performed by a bank of Soxhlet extractors. As with any technique using applied heat, loss of volatile compounds and thermal degradation are concerns. Because of its routine use in established analytical procedures, Soxhlet extraction is undoubtedly the extraction method to which other methods for extracting solids are compared.

New developments in Soxhlet extraction include a high pressure system, developed by J & W Scientific, which allows liquid carbon dioxide to be used as the extraction solvent, and an automated version. The automated Soxhlet extractor allows the thimble to be immersed in the boiling extraction solvent for a prescribed period, before the extraction is completed in the more traditional Soxhlet approach. This two-step process can be 4–10 times faster than conventional Soxhlet extractions and use about half of the solvent volume.

Sonication Sonication or ultrasound extractions can be considered a development of leaching, in which ultrasonic energy is applied to disrupt solute-sample interactions and facilitate solute diffusion. The use of ultrasonic probes can be quite efficient.

Accelerated solvent extraction (ASE) (also called pressurized fluid extraction) This technique, developed by the Dionex Corporation, is commonly discussed using the trademarked name, accelerated solvent extraction. However, the more generic term pressurized fluid extraction is becoming more widely used. In this technique the sample is placed into a sealed container and solvent is pumped through this extraction vessel. Because a modest pressure is

applied, temperatures much greater than the atmospheric boiling point can be used with liquid extraction solvents. The technique is automated. This application of temperature greatly enhances solute solubility, diffusion, and viscosity, resulting in extractions that are qualitatively and quantitatively equivalent to Soxhlet in minutes instead of hours, and with significantly less solvent.

Microwave-assisted extractions In some respects microwave extractions can be thought of as a form of leaching with the addition of microwave irradiation. The microwave irradiation, when absorbed by materials with a permanent dipole, leads to heating. In a closed system, the approach is like ASE in the respect that temperatures greater than the atmospheric boiling point of the solvent can be achieved. This form of the technique is generally used with polar solvents (which absorb microwave energy). Open-cell approaches are generally used with non-absorbing solvents and samples with a high water content (or that otherwise possess a high dielectric constant). In this case localized heating in the sample allows extraction efficiencies to be improved.

Supercritical fluid extraction (SFE) SFE employs solvents, generally carbon dioxide (neat or with added co-solvents), at temperatures and pressures near or above the critical point. These high-temperature, high-pressure solvents have gas-like diffusion, liquid-like solvation properties, and do not possess surface tension. Hence, SFE can be quite rapid. With the use of carbon dioxide, the deleterious effects (e.g. cost, health and environment concerns, etc.) of organic solvents can be minimized. Another advantage of SFE is that solvating properties can be modified as a function of temperature and pressure, adding a selectivity advantage to the technique. In SFE the sample is placed in an extraction vessel and the supercritical fluid passes through the vessel in a series of static and dynamic steps. Upon depressurization of the extracting fluid the extracted solute remains in a solute collection region.

Gas-phase methods When volatile compounds are being extracted they can often be forced from the solid into the gas phase and subsequently trapped. In static methods the volatile compounds above the sample (often after heating) are simply trapped. Dynamic methods are exemplified by the purge-and-trap technique. In purge-and-trap, a continuous purge of the sample with an inert gas takes place and the volatile solutes are trapped onto a solid support. Thermal desorption is similar to the purge-and-trap technique, except the sample is heated ballistically to

higher, controlled temperatures to force the solutes into the gas phase. Each of these gas-phase methods have been modified for use with the SPME approach to solute trapping.

Future Directions

Chemical extractions are thought to be a mature science. However, progress is still being made. The key influences driving these advances include the need for faster and more selective extractions and extractions that use smaller (if any) amounts of organic solvents. Better predictive models to aid the design and scale-up of extraction processes will also continue to be of great interest.

Further Reading

Barton AFM (ed.) (1990) *Handbook of Polymer-Liquid Interaction Parameters and Solubility Parameters*. Boca Raton: CRC Press.

Dean JR (1990) *Extraction Methods for Environmental Analysis*. New York: John Wiley & Sons.

Giddings JC (1991) *Unified Separation Science*. New York: John Wiley & Sons.

Handley AJ (ed.) (1999) *Extraction Methods in Organic Analysis*. Sheffield: Sheffield Academic Press.

Karger BL, Snyder LR and Horvath C (1973) *An Introduction to Separation Science*. New York: John Wiley & Sons.

Lide DR (ed.) (1994) *Handbook of Organic Solvents*. Boca Raton: CRC Press.

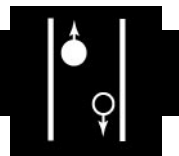
Morrison GH and Freiser H (1957) *Solvent Extraction in Analytical Chemistry*. New York: John Wiley & Sons.

Perry RH and Green DW (eds) (1997) *Perry's Chemical Engineer's Handbook*, 7th edn. New York: McGraw-Hill.

Rydberg J, Musikas C and Choppin GR (eds) (1992) *Principles and Practice of Solvent Extraction*. New York: Marcel-Dekker.

Wolf FJ (1969) *Separation Methods in Organic Chemistry and Biochemistry*. New York: Academic Press.

FLOTATION



E. Woodburn, UMIST, Manchester, UK

Copyright © 2000 Academic Press

Introduction

Overview of the Essential Elements of Separations Based on Froth Flotation

The objective of a flotation separation operation is to remove small hydrophobic particles from an aqueous suspension (pulp) by causing them to collide with, and to attach to, air bubbles. The bubble-particle aggregates rise through the suspension forming a froth at the upper surface of the pulp. The froth, which consists of the bubble-particle aggregates with inter-bubble water containing both hydrophobic and hydrophilic particles, forms a second phase where further enhancement of the hydrophobic/hydrophilic particle separation occurs, by water draining back to the pulp. The final product in which the hydrophobic particles are concentrated is removed as a froth overflow.

The science of the separation is primarily concerned with improving the selectivity of the hydrophobic particle attachment in the pulp through the addition of surface active chemicals. In addition, the hydrodynamics of the bubble-particle collision in the aerated suspension is important, as is the regulation

of the drainage of water-containing hydrophilic particles from the froth by controlling its structure, also with surfactants.

It is probably fair to say that the industrial practice of flotation is effective even in the absence of a complete understanding of its scientific basis. The successful application of flotation separations in industry can be classified into three areas.

Mineral Processing

Froth flotation is a widely used technique in the mineral processing industry as an early step in the process of concentrating a valuable material from an ore. It is preceded by crushing and grinding and may be followed by leaching/(ion exchange) electrowinning or smelting. In data cited by Merrill and Pennington from a US Bureau of Mines survey for 1960 nearly 200 million tons of raw material were processed annually by flotation in the USA from which 20 million tons of concentrates were recovered. These consisted of 34 different commodities which, although principally metallic and non-metallic ores and coal, also currently reflects an increasing interest in recycling waste material.

More recent data supplied by Bowes, courtesy of the Anglo-American Research Laboratories in Crown Mines South Africa, is given in **Table 1**. These figures are estimates and should be used with caution, as the

Table 1 World-wide flotation tonnages (millions of tons), 1991–7

	1991	1992	1993	1994	1995	1996	1997
Copper	950	960	960	960	1000	1000	1080
Lead	93.3	91.4	79.2	78.4	78.4	84.3	87.5
Zinc	119.8	121.5	111.9	110.6	114.2	118.9	119.8
Nickel and cobalt	19.6	19.4	18.9	19.9	23.9	25.6	27.2
Iron	125	126	124	123	129	136	139
Phosphate	378	382	374	371	389	412	420
Industrial minerals	52	52	51	51	53	56	57
Coal	54	54	53	53	55	59	60
Totals	1791.7	1808.3	1772.0	1766.9	1842.5	1951.8	1990.5

Calculated based on the tonnages of pure metal produced; the mine production of ores are based on the following data:

Copper: average grade 0.8% Cu mined, at a processing recovery of 90%

Lead: average grade 3.0% Pb mined, at a processing recovery of 95%

Zinc: average grade 5.7% Zn mined, at a processing recovery of 82%

Nickel: average grade 1.6% Ni mined, at a processing recovery of 85%.

Source: Bowes (1997) Personal communication, Anglo-American Research Laboratories, Crown Mines, South Africa.

processing recovery refers to the flotation operation only. Where other recovery techniques are used such as leaching of nickel laterites and the recovery by leaching and solvent extraction of by-product cobalt from copper mining, these figures have not been included. Lead and zinc are often mined together and the separate tonnages reported for flotation processing may be overstated. The figures given for iron, phosphate, industrial minerals and coal are based on the percentages of the total tonnages. It is felt that particularly for iron and phosphate the figures may be excessive.

Overall the total ores processed annually using froth flotation given in Table 1 are consistent with the figure of 2 billion tons given by Fuerstenau in 1996. It is expected that significant growth will be seen in the next decade with flotation processing of copper ores rising to 1.6 billion tons per annum which represents 55% of the total tonnage anticipated.

Froth flotation has proved itself to be an important process in the mineral industry and will only become more important in the future.

Non-mineral Processing Recycling

This includes deinking wastepaper, separating individual components from plastic wastes, and effluent treatment of textile and smelter wastes.

Wastepaper deinking The growth of production has increased rapidly in recent years from 5.9 million tons per year in 1981 to 17.6 million tons per year in 1991. It is estimated that by 2001 the production of deinked waste will have increased to 31 million tons/year.

The objective of wastepaper deinking is to rid the grey repulped waste stock of unwanted particulates, usually inks. The reflectance of sheets of paper produced from the retreated waste pulp to light at 457 nm gives a measure of the brightness. However, changes in brightness are themselves not necessarily a complete description of the effectiveness of the separation of ink, as brightness changes are also associated with the presence of white inorganic fillers.

Prior to flotation the wastepaper is repulped in water at about a 15% suspension of fibre in water, in the presence of either a sodium soap or an anionic surfactant such as sodium dodecyl sulfate (SDS). These provide detergency, liberating the ink particles from their associated fibres. In some deinking plants this pulp is diluted to about a 1% fibre suspension, before being fed to a flotation separator in which the grey pulp suspension is aerated using cell designs similar to those in the mineral industry. The product stream from these cells is an inky foam, which is the reject, and a non-floated fibre suspension below the froth level which is the deinked product.

Although this process has some resemblance to minerals flotation there are significant differences. Specifically these relate to the properties of the fibre suspension. Their settling rate is low in any event, but as flocculated agglomerates they can trap small bubbles which give them a buoyancy that makes them easily entrainable in the water associated with the air bubbles forming the foam. This can result in the reject stream being as much as 10% of the feed, although the ink and its associated print vehicle oil will only account for between 1 and 2% of the feed fibre. Of this 1–2% only 10–20% is cellulose the rest being the oil/vehicle required for printing.

The mass of the reject stream is a serious environmental problem with land-fill costs rising sharply. There is also little information relating to the brightness increase of the deinked pulp as the removal of talc filler with the reject stream will seriously reduce the brightness of the final paper. It is clear that while deinking by flotation is potentially a valuable technique much fundamental work needs to be done before it reaches an acceptable level of separation.

Separation of plastic components from solid waste It has been said that of the 16.2 million tons of plastic waste generated annually in the USA only 2.4% is recycled with the rest being discarded to land-fill. As

mentioned earlier, this is becoming an increasingly expensive option and a scheme is envisaged where the individual components, polyethylene terephthalate (PET), polyethylene (PE), polyvinyl chloride (PVC) and polypropylene (PP), can be separated and hence become reusable.

PVC and PET can be separated from the others by gravity separation and by using 190 ppm of a surfactant, methyl iso-butyl carbinol (MIBC), at pH 11 in a 1% suspension of the solids, the PVC can be removed in a flotation froth giving high recoveries and purities, leaving pure PET in the unfloated tailings. This process, although at an early stage, offers a promising recycling opportunity.

Recovery of metals from refinery effluents It is possible that these may also respond to the use of froth flotation in transforming environmentally hazardous discharges into economically attractive sources of raw materials.

It is clear that considerable development work will be required in all the new applications and while it is sensible to make use of the extensive knowledge of the minerals industry of this separation technique, solving the special problems associated with each new application will most profitably be done by application of scientific fundamentals.

Water and Waste Treatment

Removal of contaminants from domestic water The technique of dissolved air flotation (DAF) is used as an alternative to sedimentation after flocculation in the preparation of water for domestic consumption. The bubbles are generated by first saturating a fraction of the treated raw water with air under pressure and then depressurizing in the total water. After depressurization the bubbles rise through the bulk solution, where they will be entrapped by the flocculated impurities. The bubble-floc aggregates rise to an overflow where they are removed. DAF differs from mineral flotation in that the bubbles are very small and are not stabilized by added surfactants, and there is no selective attachment. The justification for its use is that the aerated flocs rise faster than the settling rate of ordinary flocs whose density is close to that of water and whose structure favours a high resistance to settling flow.

Separation of dispersed oil from production water The processing of oil from offshore wells involves the removal of suspended solids from the oil and the separation of an oil-water mixture. Both the solid particles and the dispersed oil droplets are very fine; in the region of 10–50 μm . The processing involves

the concentration of oil from a 5–50% by volume in water to 95–100% oil. This may involve a multistage operation particularly for very wet crudes, with a second concentrator stage treating the oil-rich product from the first stage to achieve the desired final oil purity.

If there is a second stage its water-rich waste stream is recycled to the first stage feed. The waste product from the first stage is water containing up to 0.1% oil by volume dispersed as ultrafine droplets. Before this water can be discharged, its oil content has to be reduced to comply with strict environmental standards both with respect to its oil content and the biological oxygen demand (BOD). Froth flotation has been used particularly in final clean-up units because of the small droplet size. DAF has been used as the bubbles coming out of solution following a reduction in pressure are thought to nucleate directly on the droplets. Unfortunately, the rise velocity of these air-droplet aggregates is so slow that extremely large cells are required. Their operation is in turn adversely affected by the pitching motions of floating rigs. Induced gas flotation (IGF) has also been used when the air is added to the feed stream at the throat of a Venturi nozzle. These have higher recovery rates but lower oil removal efficiencies than the DAF units. These reasons, together with the perceived high chemical costs, have favoured the use of liquid-liquid hydrocyclones in these situations.

Quantitative Measure of Flotation Performance

The performance of any separation unit is usually defined in terms of the fractional recovery (removal) R of the valuable product (contaminant) and its purity (concentration) in the product (waste) stream G .

Grade-Recovery Curves for Mineral Beneficiation

To characterize the flotation step in the beneficiation of a mineral ore, it is necessary to postulate that the mixture consists of at least two distinct particle populations, one largely valuable and the other principally waste (gangue). The gangue will invariably consist of several different mineral types, the presence of each being undesirable in the valuable mineral. Each population is characterized by a size distribution, and the amount of undesired material it contains. The fraction of misplaced material in a particular population can almost invariably be reduced by a sequence of size reducing steps usually consisting of primary and secondary crushing followed by fine grinding.

Increasing the fineness of grinding is said to liberate the valuable species from its associated waste

component. This will result in increasing the fraction of the desired component in the valuable mineral recovered and reducing its amount in the gangue. While liberation of the valuable component is clearly desirable, overgrinding will increase the power consumption of the mills, and as observed by Klimpel, also possibly introducing difficulties into the flotation process and subsequent downstream processing.

It is important to have a measure of the effectiveness of separation before an optimal solution can be identified. From a systems viewpoint, the flotation operation in mineral processing will separate a feed stream, F , into two product streams, a concentrate stream, C , containing an increased fraction of the valuable component and a tailings stream, T , containing a reduced amount of the valuable component. The following overall mass balance will apply:

$$Fx_F = Cx_C + Tx_T \quad [1]$$

where x_F , x_C and x_T are the mass fractions of the valuable component in the feed, concentrate and tailings, respectively. The performance measurement is characterized by two parameters. The fractional recovery R of the valuable component in the concentrate:

$$R = \frac{Cx_C}{Fx_F} \quad [2]$$

and its purity (grade) in the concentrate stream. The grade may simply be the mass fraction x_C or can be normalized between 0 and 1:

$$G = 1 - \frac{1 - x_C}{1 - x_F} \quad [3]$$

The upper limit, $G = 1$, clearly follows from the concentrate mass fraction of valuables, $x_C = 1$, while the lower limit, $G = 0$, presumes that the worst system performance is associated with no upgrading of the valuable mass fraction in the concentrate with respect to its concentration in the feed, although negative grades are mathematically possible.

Attainable Regions

The grade–recovery curve divides the grade–recovery space, $0 \leq G, R \leq 1.0$, into attainable and non-attainable regions. The grade–recovery curve is a function of a set of operational controls of which the fineness of grind of the feed is one. The others are actions that affect the selective attachment of the valuable component to air bubbles and the preferential drainage of the waste material back from the

froth. The optimal performance of the flotation operation is defined in terms of the minimum cost of achieving a particular grade–recovery target.

Pulp Microprocesses

Wetting of the Particles' Surfaces

The particles are always dispersed in water and the nature of the wetting of their surfaces is critical for the effectiveness of the flotation separation.

Figure 1 shows the concept of an attached water film in which water dipoles are held by van der Waals forces together with ions held by electrostatic interaction with charges on the particle surfaces.

The stability of the adsorbed water film on the solid surfaces is clearly fundamental to the selective attachment of bubbles. Qualitatively for hydrophilic particles the water film is strongly bound to the solid, and hence is stable; conversely for hydrophobic solids the water film is weakly bound and will fail more readily.

The attachment of hydrophobic particles to bubbles is usually considered to consist of two sequential stages. First, the particle must collide with (intercept) the bubble. The second stage after interception has two components: (a) a bubble–particle contact time and (b) an induction time which is that required for the water film between the particle and bubble to thin to a point of failure at which point attachment is presumed to occur.

The selectivity of the separation is commonly enhanced by the adsorption of surface active chemicals onto the surfaces of the solid particles. These reagents have a molecular structure which has a polar and

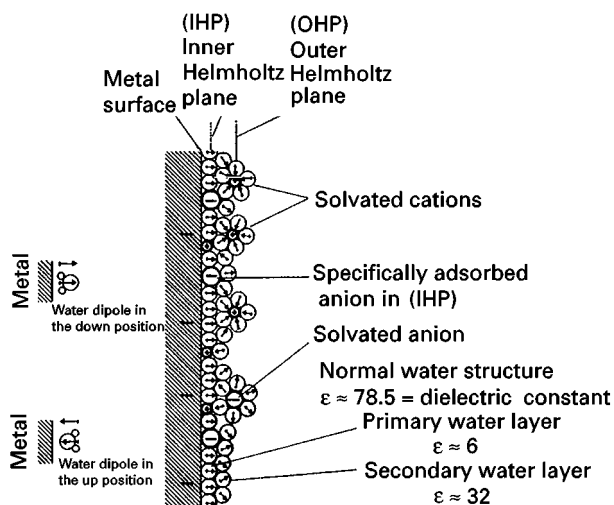


Figure 1 Model of a metal electrolyte interface showing film of water dipoles. Reproduced with permission from Leja J (1982) *Surface Chemistry of Froth Flotation*. New York: Plenum Press.

a non-polar end. Ideally, they will strongly attach to the valuable particles through their polar ends, with their non-polar ends confer an increased hydrophobicity. For the waste particles no attachment is considered to take place and consequently no hydrophobic increase will occur.

Clearly the choice of a suitable reagent is critical and is highly specific to a particular separation. Although the choice of reagent(s) for a particular separation usually has evolved with experience, the search for ever more effective reagent mixtures is an area of continuing research and development. A sound basis for these investigations is to develop an understanding of the free energy changes at the solid–water and bubble–water interfaces, consequent on changes of the reagent types and conditioning procedures.

Particle Surface Hydrophobicity

Theoretical basis for estimation To describe bubble–particle attachment after interception mathematically it is necessary briefly to review the nature and magnitude of the forces acting across the various interfaces.

After the initial interception, the particle and bubble will be separated by a water film. The film will become thin because of the forces of attraction between particle and bubble. The rate of thinning is determined by the dissipation of the kinetic energy of the particle on impact, associated with a resultant of long-range London–van der Waals molecular attraction (dispersion forces), capillary forces generated by the distortion of the bubble surface during the impact, electrostatic interactions between the uncompensated surface charges on the solid and those in the adjacent water layer, and as has been shown by Xu and Yoon, an additional force of attraction which appears to exist between two hydrophobic surfaces.

If the film thins to a critical value, failure will occur that will result in a successful attachment event. Both the thinning process and the critical thickness of the film must clearly depend on the interaction energy of the particle–water interface.

For the van der Waals forces of attraction, a treatment of the dispersion energy between a single gaseous atom and a slab of infinite extent is outlined by Adamson as:

$$\varepsilon(h_x)|_{\text{atom-slab}} = -\frac{\pi}{6}nC_1 \frac{1}{h_x^3} \quad [4]$$

where $C_1 = \frac{3}{4}h\nu_0\alpha^2$ and $\varepsilon(h_x)|_{\text{atom-slab}}$ is the potential energy of interaction in ergs/molecule at a separation distance h_x (cm), N_0 is the Avogadro number (6.02×10^{23} molecules/g mol wt) for water from

Adamson, $h\nu_0 = 18 \text{ eV} (= 18 \times 10^{-12} \text{ ergs})$, α (polarizability) $= 1.46 \times 10^{-24} \text{ cm}^3$. Since ρ_w density of liquid water g cm^{-3} and $n = N_0\rho_w/18 = 3.34 \times 10^{22}$ molecules/cm³ using these figures $C_1 = 28.8 \times 10^{-60}$ ergs cm⁶.

The dispersion energy between two infinite flat surfaces after integration is:

$$\varepsilon(h_x)|_{\text{slab-slab}} = -\left(\frac{\pi}{12}\right)\frac{(n^2C_1)}{h_x^2} \quad [5]$$

where $\varepsilon(h_x)|_{\text{slab-slab}}$ is in ergs cm⁻².

Fowkes has equated $\varepsilon(h_x)$ of eqn [5] to γ_s^d , the dispersion component of the total energy for water. As will be shown later, he has linked this dispersion energy with the physical adhesion energy at the interface between two different phases.

The dispersion energy for liquid water, γ_w^d , is calculated from eqn [5] to be $35.8 \text{ ergs cm}^{-2}$ using the values given above and a value of 2.76 \AA for the average intermolecular distance. This is somewhat higher than the experimentally determined value of $21.8 \text{ ergs cm}^{-2}$ from contact angle measurements, but nevertheless it is valuable as it gives a theoretical basis for the forces of attraction at the interface between two immiscible phase surfaces. This is relevant to studies where the adsorption of a surfactant (collector) on a solid surface is used to modify the surface's hydrophobicity.

Eqn [5] is usually written in terms of, A , the Hamaker constant, which is specific for a given separation; for water $A = \pi^2 n^2 C_1 = 0.3 \times 10^{-12}$, and on average is of the order of 10^{-12} ergs:

$$\varepsilon(h_x)|_{\text{slab-slab}} = -\left(\frac{1}{12\pi}\right)\frac{A}{h_x^2} \quad [6]$$

The attraction stress between the two surfaces is:

$$\frac{\partial \varepsilon(h_x)|_{\text{slab-slab}}}{\partial h_x} = \frac{A}{6\pi h_x^3} \text{ (dynes cm}^{-2}\text{)}$$

For a condensed system involving different phases the potential energy of interaction is still given by eqn [6] but with a modified Hamaker constant.

Consider a particle, 1, and an adjacent bubble, 2, in a water medium, 3. The particle and the bubble surfaces will be associated with water molecules. In the simplest case the film on the particle will consist of OH⁻ ions as well as molecular water dipoles and will be of the order of a monolayer in thickness,

which is the effective range of the van der Waals attractive forces. The bubble will have a layer of surfactant on its surface which will be orientated with its polar end in the water and the hydrophobic end in the air.

The interaction energy is expressed in terms of a net Hamaker constant, A_{132} , which is approximated by Adamson as a simple linear relationship:

$$A_{132} = A_{12} - (A_{13} + A_{23} - A_{33}) \quad [7]$$

The binary Hamaker constants expressed above refer to two-surface interactions only. Some of these are physically difficult to interpret, but are nevertheless useful in formulating a conceptual understanding. With these reservations, A_{12} is the interfacial energy between a solid particle and a bubble separated by a vacuum and A_{33} is the interaction energy between water molecules.

A_{13} and A_{23} are the Hamaker constants representing the particle–water and bubble–water interaction energies. If these energies are low with respect to the mutual interaction energy of the water molecules then A_{132} will be greater than the interaction A_{12} . The enhanced attraction between the particle and the air bubble in the presence of water reflects *hydrophobic bonding*.

Leja quotes interaction energy potentials and London dispersion forces for various configurations following integration of atom–atom interaction energies. The dispersion force of attraction between two spheres of radius R_1 and R_2 , for example, is given by:

$$\text{at } h_x \ll R_1, R_2, \quad F = \frac{AR_1R_2}{6b_x^2(R_1 + R_2)} \quad [8]$$

Experimental characterization of hydrophobicity – contact angle Interfacial energies for liquids may be measured by surface tension, while those for solid–liquid interfaces may be inferred from contact angle measurements.

If a liquid is placed on a solid surface it will form a droplet (Figure 2). The droplet will have a definite angle of contact, θ , with the surface. The change in the free energy ΔG^0 of the three-phase contact surface if the area of contact, ΔA_s , between the droplet and the surface were to change slightly is:

$$\Delta G^0 = \Delta A_s[(\gamma_{SL} - \gamma_{SV}^0) + \gamma_{LV} \cos(\theta - \Delta\theta)] \quad [9]$$

where γ_{SL} , γ_{LV} and γ_{SV}^0 are the interfacial energies for solid–liquid, liquid–vapour and solid–saturated vapour. At equilibrium this leads to the Young

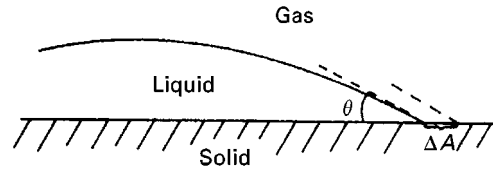


Figure 2 Contact angle θ of liquid droplet on a solid surface.

equation:

$$\lim_{\Delta A_s} \frac{\Delta G^0}{\Delta A_s} = 0, \quad \gamma_{SL} - \gamma_{SV}^0 + \gamma_{LV} \cos \theta = 0 \quad [10]$$

Bangham and Razouk observed that as γ_{SV}^0 represented the energy of a surface in contact with a saturated vapour of partial pressure p^0 , there must be present on the surface a film of condensed vapour with its own surface energy π^0 . The total surface energy of the solid is thus:

$$\gamma_S = \gamma_{SV}^0 + \pi^0 \quad [11]$$

Substituting for γ_{SV}^0 in eqn [10] gives:

$$\gamma_{LV} \cos \theta = \gamma_S - \gamma_{SL} - \pi^0 \quad [12]$$

The interfacial energy of the solid–liquid interface γ_{SL} , can also be expressed as the sum of the surface energies of the individual phases separately, where γ_S is the surface energy of the solid, and γ_{LV} is the surface energy of the liquid in contact with vapour, and w_{SLV} is the work of adhesion which has to be subtracted:

$$\gamma_{SL} = \gamma_S + \gamma_{LV} - w_{SLV} \quad [13]$$

The work of adhesion for the three-phase contact is then obtained from the Young equation after substituting for γ_{SL} from eqn [12] into eqn [13]:

$$w_{SLV} = \gamma_{LV}(1 + \cos \theta) + \pi^0 \quad [14]$$

Equation [14] is a form of the Dupré equation that relates an increasing contact angle to a reduction in the adhesion energy between the solid surface and water, or alternatively to an increase in the hydrophobicity of the solid surface.

Fowkes modified the Girifalco–Good equation for the work of adhesion and suggested that it was due to the London–van der Waals dispersive forces in each phase rather than the total intermolecular energies. Equation [15] describes the resulting expression for the interface energy between a solid

and liquid:

$$\gamma_{SL} = \gamma_S + \gamma_{LV} - 2\Phi\sqrt{(\gamma_S^d\gamma_L^d)} \quad [15]$$

(Φ is commonly taken as unity).

Fowkes applied eqn [15] to eqn [12], to express a relationship between the contact angle and the dispersive energy of the solid surface, γ_S^d , this being considered to be a parameter most characteristic of the influence of the nature of the surface on the interface phenomena important in flotation:

$$\begin{aligned} \gamma_{LV} \cos \theta &= -\gamma_{LV} + 2\sqrt{(\gamma_S^d\gamma_L^d)} - \pi^0 \\ \cos \theta &= -1 + 2\sqrt{\gamma_S^d} \left[\frac{\sqrt{\gamma_L^d}}{\gamma_{LV}} \right] - \frac{\pi^0}{\gamma_{LV}} \end{aligned} \quad [16]$$

The dispersion forces in a particular solid, γ_S^d , can therefore be estimated by using contact angle measurements with different liquids obviously of known surface dispersion γ_L^d . Linear plots of $\cos \theta$ against the ratio of dispersive energies of the liquids confirm the validity of eqn [16] and the slope of the line gives $\sqrt{\gamma_S^d}$.

Experimental characterization of interfacial energies – adsorption studies Adsorption data may be used to estimate π which reflects changes in interfacial energies. These require knowledge of the adsorption isotherm, relating Γ , the mols of vapour adsorbed per square centimetre of solid surface with p , the partial pressure of the solute in the gas.

Bangham and Razouk derived an expression for π by integrating the Gibbs equation. This states that:

$$d\gamma = -\Gamma RT d \ln p$$

from which:

$$\begin{aligned} \pi &= - \int d\gamma = RT \int \Gamma d \ln p \\ \pi &= \gamma_S - \gamma_{SV} = RT \int_0^p \Gamma d \ln p \\ \pi^0 &= \gamma_S - \gamma_{SV}^0 = RT \int_0^{p^0} \Gamma d \ln p \end{aligned} \quad [17]$$

Harkins by defining γ_{SV} as being equal to $\gamma_{SL} + \gamma_{LV}$ related the energy π of the adsorbed liquid film to the

surface activities:

$$\pi = \gamma_S - (\gamma_{LV} + \gamma_{SL}) \quad [18]$$

By substituting for γ_{SL} from eqn [15], Fowkes obtained an expression which links γ_S^d with π as determined from adsorption studies:

$$\pi = 2\sqrt{(\gamma_S^d\gamma_L^d)} - 2\gamma_{LV} \quad [19]$$

The derivation assumes that the adsorption of vapour is determined solely by dispersion forces (physical adsorption):

$$\gamma_S^d = \frac{(\pi + 2\gamma_{LV})^2}{4\gamma_L^d} \quad [20]$$

It is clearly of interest to compare the surface free energies γ_S^d determined from gaseous adsorption studies with those obtained from contact angle measurements. Fowkes quotes an average value of 122 ergs cm^{-2} for the dispersive energy of a graphite surface, γ_S^d , from the adsorption of N_2 and n-heptane, which compares well with the value of 109 ergs cm^{-2} from contact angle measurements of a water droplet on a graphite surface ($\theta = 85.7^\circ$ and $\pi^0 = 19$ ergs cm^{-2}).

The surface free energies can also be experimentally determined from heats of immersion ΔH_i since:

$$\begin{aligned} \gamma_{SL} - \gamma_S &= \gamma_{LV} - 2\sqrt{(\gamma_S^d\gamma_L^d)} \\ \Delta H_i &= (\gamma_{SL} - \gamma_S) - T \left(\frac{d\gamma_{SL}}{dT} \right) \\ \Delta H_i &= \gamma_{LV} - 2\sqrt{\gamma_S^d\gamma_L^d} \\ &\quad - T \left[\frac{d\gamma_{LV}}{dT} - 2\sqrt{\gamma_{LV}^d} \frac{d\sqrt{\gamma_S^d}}{dT} - 2\sqrt{\gamma_S^d} \frac{d\sqrt{\gamma_{LV}^d}}{dT} \right] \end{aligned} \quad [21]$$

Experimental characterization of interfacial energies – heat of immersion Equation [21] can be used with heats of immersion measured calorimetrically to determine the contribution of polar interactions between the solid and the liquid into which it has been immersed. If dispersion forces only were significant at the interface, then the equality of eqn [19] should hold. Deviations from the equality of eqn [19] referred to as the excess by Fowkes are a measure of the strength of the polar interaction:

$$\text{the excess} = (\pi + \gamma_{LV}) - 2\Phi\sqrt{(\gamma_S^d\gamma_L^d)} \quad [22]$$

Table 2 Polar interfacial interactions at solid-liquid interfaces

<i>Solid</i>	<i>Liquid</i>	$2\sqrt{(\gamma_S^d, \gamma_L^d)}$ (<i>ergs cm⁻²</i>)	$\pi + 2\gamma_{LV}$ (<i>ergs cm⁻²</i>)	<i>Excess</i> (<i>ergs cm⁻²</i>)
Graphite	n-Heptane	96	96	0
	Benzene	114	134	20
Silica	n-Heptane	100	100	0
	Benzene	118	138	20
	Acetone	98	156	58
	n-Propanol	98	182	84
	Water	94	462	368

Reproduced with permission from Fowkes FM (1964) The Interface Symposium. *Industrial and Engineering Chemistry* 56(12), 40–52, Table IX.

Table 2 shows polar interactions at some solid-liquid interfaces in terms of the excess.

From the limited data reproduced in table it can be seen that the adsorption of hydrocarbons both on graphite and silica is principally through dispersion forces while that of n-propanol and water on silica show significant polar interactive forces. Clearly, the presence of these strong attractive forces will result in very stable films.

The Forces Between a Charged Particle Surface and an Ionic Solution

Origin of particle surface charge The attraction between a charged surface and a concentration of counterions in the diffuse double layer adjacent to the particle surface will be the source of increased interaction energies. The charge density on the surface of the solid particles, and hence the potential gradients in the diffuse double layers, is determined by the degree to which the intermolecular forces at the crystal surface are non-compensated. These are related to the structure of the crystal lattice and to the orientation of the cleavage planes at the surface.

As a consequence of a surface charge, to a greater or lesser extent hydrated ions will be adsorbed, the energy of attachment being related to the charge density on the particle surface. As both orthorhombic sulfur and graphite exhibit comparatively weak residual surface forces with strong non-polar bonds being localized within the unit cells of the crystal lattice, the attachment energy of hydroxyl and hydrated ions will be low giving the surfaces their hydrophobic character.

On the other hand, for ionic crystals the uncompensated electrostatic forces at the surface may be high and can lead to strong attachment of water. As the electrostatic forces operate over significantly longer distances than do the London-van der Waals

forces they will give hydrated layer thicknesses of the order 20–60 Å. According to Klassen and Mokrousov who quote Derjaguin and Derjaguin, Karasiev and Zorin, the hydrated layer has an increased viscosity over that of the bulk water and the change in viscosity is discontinuous.

Diffuse boundary layer To illustrate the previous observations consider a plane surface with a uniform charge density σ_0 in contact with water with a bulk ionic concentration n_0 . If the solid-water interface has a positive electrical potential, ψ_0 , the potential in the solution will decrease to 0 as one proceeds in a normal direction away from the surface into the solution. Close to the positively charged surface, however, there will be an excess of negative ions. If n^+ and n^- are the concentrations of the positive and negative ions, of equal and opposite charge, $+z$ and $-z$, respectively, at a point in the solution then the net charge density ρ at that point in the solution will be:

$$\rho = ze(n^+ - n^-) \quad [23]$$

Using the Boltzmann factor, the ionic concentrations can be linked to the local potential at a point in the solution:

$$n^- = n_0 \exp\left(\frac{ze\psi}{kT}\right)$$

and:

$$n^+ = n_0 \exp\left(-\frac{ze\psi}{kT}\right)$$

from which:

$$\rho = -2n_0ze \sinh\left(\frac{ze\psi}{kT}\right) \quad [24]$$

The integral of ρ to infinity will give the total excess charge in the solution per unit cross-sectional area which is equal to but opposite in sign to the charge density on the surface σ . The situation is that of a double layer of charge, the one localized on the solid surface and the other in the diffuse region.

To link the potential in the solution with the normal distance x from the surface the Debye-Hückel treatment may be followed. This uses Poisson's equation which relates the divergence of the gradient of the electrical potential at a given point to the charge

density at that point:

$$\nabla^2 \psi = -\frac{4\pi\rho}{D}$$

$$\nabla^2 \psi = \frac{8\pi n_0 z e}{D} \sinh\left(\frac{ze\psi}{kT}\right) \quad [25]$$

where ∇^2 is the Laplace operator and D is the dielectric constant of the medium (for water = 78). For small values of $ze\psi$ with respect to kT , eqn [25] can be expressed as:

$$\nabla^2 \psi = \kappa^2 \psi$$

$$\kappa^2 = \frac{8\pi n_0 z^2 e^2}{DkT} \quad [26]$$

The treatment for a plane charged surface is due to Gouy and Chapman (after defining):

$$y = \frac{ze\psi}{kT} \quad \text{and} \quad y_0 = \frac{ze\psi_0}{kT} \quad [27]$$

Eqn [26] can be written as:

$$\frac{d^2 y}{dx^2} = \kappa^2 \sinh y$$

with the boundary conditions at:

$$x = \infty, y = 0 \quad \text{and} \quad \frac{dy}{dx} = 0 \quad [28]$$

For the case where y_0 is small, for example for univalent ions at room temperature, $\psi_0 < 25$ mV, the

solution of eqn [28] reduces to:

$$\psi = \psi_0 \exp -\kappa h_x \quad [29]$$

setting $x = h_x$ as the separation distance.

The quantity $1/\kappa$ is the distance from the surface where the potential in the solution reaches $1/e$ ($= 0.3679$) of its value at the surface; the plane $1/\kappa$ is used to represent the thickness of the diffuse layer adjacent to the surface. The charge density of the solid surface can be obtained from a knowledge of $\psi(x)$ vs x since:

$$\sigma_0 = - \int_0^\infty \rho \, dx = \frac{D}{4\pi} \int_0^\infty \frac{d^2 \psi}{dx^2} dx$$

$$= - \left(\frac{D}{4\pi} \right) \left(\frac{d\psi}{dx} \right) \Big|_{x=0} \quad [30]$$

For small potentials, the diffuse double layer can be likened to an electrical condenser of charge density σ_0 and a plate separation of $1/\kappa$.

Figure 3 shows very interesting relations between $\psi(x)$ and x and between σ_0 and ψ . Figure 3(A) shows the exponential decay in the solution potential for a surface whose potential ψ_0 is 25 mV, while Figure 3(B) shows that increasing the concentration of the bulk solution of univalent ions, from 0.001 to 0.01 M significantly reduces the dispersion layer thickness from almost 200 to less than 40 Å.

Figure 3(C) shows a reduction of dispersion layer thickness of similar magnitude to that reported in Figure 3(B) following the replacement of a 0.001 M univalent solution by a 0.001 M divalent solution. Figure 3(D) and (E) show the relation between the

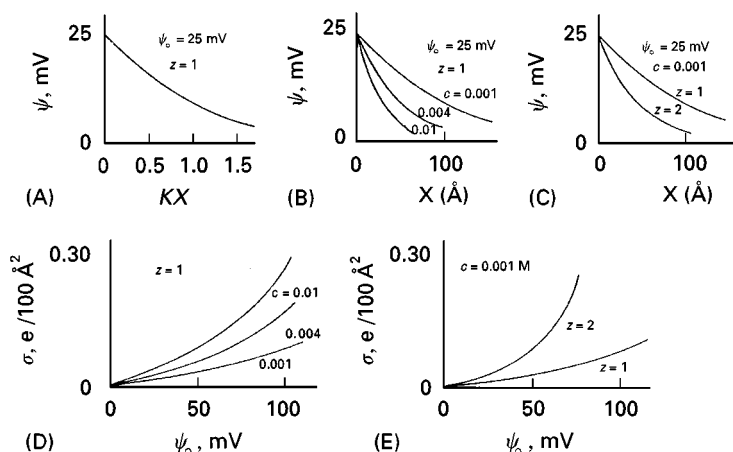


Figure 3 The diffuse double layer. Reproduced with permission from Adamson AW (1982) *Physical Chemistry of Surfaces*, 4th edn. New York: John Wiley.

surface charge density ($e/100 \text{ \AA}^2$) and the surface potential ψ_0 .

Conversion to SI units requires a conversion constant, the permittivity (of vacuum), $\epsilon^0 = 8.859 \times 10^{-12}$ coulombs/(metre volt). The conversion in cgs/esu to SI units of the potential ψ and the charge e is given in eqn [31]:

$$\psi_{\text{cgs/esu}} = \psi_{\text{SI}} \times (4\pi\epsilon^0)^{1/2} \quad \text{and} \quad e_{\text{cgs/esu}} = \frac{e_{\text{SI}}}{(4\pi\epsilon^0)^{1/2}} \quad [31]$$

To illustrate the use of the conversion constant, the interchange energies between two charged surfaces, as given by Coulomb's law, are:

$$\begin{aligned} \text{in CGS units} \quad \epsilon(\text{ergs}) &= \frac{q_1 q_2}{h_x D} \\ \text{in S.I. units} \quad \epsilon(\text{Joules}) &= \frac{q_1 q_2}{4\pi\epsilon^0 h_x D} \end{aligned} \quad [32]$$

The equivalent equation in SI units to eqn [26] then becomes:

$$\nabla^2 \psi = \frac{2n_0 z^2 e^2}{\epsilon^0 D k T} \psi = \kappa^2 \psi \quad [33]$$

To illustrate the magnitude of κ , consider a 1 mM solution in water of a uni-univalent solute. In this case the number of molecules, n_0 , of solute per cubic metre is just the Avogadro number, $N_0 = 6.02 \times 10^{23}$. Note also that $\epsilon^0 D$, sometimes written only as D , is $= 6.91 \times 10^{-10}$ coulombs/(volt metre). Substituting parameters for this case in the relationship for κ implied in eqn [33], a value for κ of $1.0 \times 10^8 \text{ m}^{-1}$ is obtained, or $1/\kappa = 10 \text{ nm}$.

The Stern treatment of the electrical double layer
The Gouy–Chapman treatment gives absurd answers for small values of κh_x when ψ_0 is large. Adamson illustrates this point with the example for $\psi_0 = 300 \text{ mV}$:

$$y_0 = \frac{300}{25.69} = 12 \quad [34]$$

if $n_0 = 0.001 \text{ M}$ then $n^- = 0.001 \times e^{12} = 160 \text{ moles/litre!}$ This is due to the treatment of the charges as point sources by neglecting the ionic diameters.

Stern suggested that the region in the liquid adjacent to the surface be divided into two parts, an inner compact layer consisting of ions or hydrated

molecules which are firmly attached to the surface, and an outer diffuse layer in which the ions were less firmly bound. The key to his analysis is the estimation of the extent to which solute molecules will enter the compact layer, which requires them to displace water dipoles, in particular.

If S_0 is the number of occupiable sites on the surface then the maximum charge density for the compact layer is $\sigma_0 = zeS_0$. In the presence of a dilute solute phase, however, the ratio of the sites occupied by the solute to those potentially occupiable is proportional to, N_s , the mole fraction of solute. In dilute solution, Stern linked this fraction and the potential ψ_δ at the outer surface of the compact layer to a charge density σ_s in the compact layer, with ϕ allowing for any additional chemical adsorption potential. This approximates to:

$$\frac{\sigma_s}{\sigma_0} = \frac{N_s \exp[-(ze\psi_\delta + \phi)/\kappa T]}{1 + N_s \exp[-(ze\psi_\delta + \phi)/\kappa T]} \quad [35]$$

This suggests that the charge σ_s in the compact layer can be linked to the potential at its outer boundary ψ_δ , using eqn [30] with the approximation:

$$-\left. \frac{d\psi}{dx} \right|_0 \approx \frac{\psi_0 - \psi_\delta}{\delta} \quad \text{hence} \quad \sigma_s \approx \frac{D'}{4\pi\delta} (\psi_0 - \psi_\delta) \quad [36]$$

where δ is its thickness and D' is an apparent dielectric constant for the layer.

In the diffuse layer as one proceeds outwards from the surface a potential at position x can be calculated using eqn [29] with ψ_δ replacing ψ_0 . The ions are mobile in this layer and the layer is characterized by a thickness $= 1/\kappa$.

The electrodynamic potential (ζ) A charged surface experiences a force in an applied electric field. As it moves the boundary of the water moving with it is the shear plane of thickness $1/\kappa$, which has a potential $\psi(1/\kappa)$, commonly referred to as the zeta-potential (ζ).

The potential of the shear plane can be experimentally determined by electrophoresis. If for a spherical particle of radius R_p , the charge density of the diffuse layer up to the shear plane is σ_D , the force exerted on it in an electric field of $F_s (\text{V m}^{-1})$ will be:

$$f_E = \sigma_D \times F_s \times 4\pi R_p^2 \text{ (newtons)} \quad [37]$$

this will cause it to move at a velocity at which the viscous drag is equal to the applied electrical force. From Stokes' law the shear resistance f_s , of a particle

of radius R_p , moving at a velocity v is given by:

$$f_s = 6\pi\mu R_p v \quad \text{which gives} \quad v = \frac{2\sigma_D F_s R_p}{3\mu} \quad [38]$$

The relation between the charge density, σ_D , of the diffuse layer and the potential at the shear plane treated as a parallel plate condenser with plates $1/\kappa$ apart in SI units is:

$$\sigma_D = \varepsilon^0 D \zeta \kappa \quad (\text{coulombs m}^{-2}) \quad [39]$$

If the ζ -potential of a spherical particle, of radius $1\mu\text{m}$ moving in an external field of 1V cm^{-1} is 25mV , then the velocity calculated from eqns [38] and [39] is $1.15 \times 10^{-6}\text{ m s}^{-1}$. Data quoted by an equipment manufacturer gives a velocity $v = 2.0 \times 10^{-6}\text{ m s}^{-1}$, for the same conditions.

The charge density σ_D of the diffuse layer follows from the ζ -potentials measurements. The charge density of the surface, σ_0 , follows as the sum of the charge densities of the compact layer σ_s and σ_D .

Collectors

General A collector is a surface-active chemical which has a polar and a non-polar group. The work of adhesion of a collector to a solid surface has been separated into three components by Leja:

$$w_{SLV} = w^d + w^b + w^i \quad [40]$$

where w^d is the dispersive component, w^b is the energy associated with polar adsorption of water at non-ionic sites and w^i is the contribution through electrostatic interactions with the Stern layer associated with the solid surface (Figure 4).

The collector molecule must be firmly attached to the solid surface through its polar group and must be able to confer sufficient hydrophobicity to the surface through the non-polar component to facilitate bubble attachment. It appears that for effective attachment, multilayer adsorption is required. Fuerstenau and Fuerstenau have suggested that the multilayer arise from the dispersive interactions between the non-polar parts of the molecules; they have referred to the resulting structure of the adsorbed layer as hemimicelles.

The attachment of a bubble to the solid ultimately involves an interaction between the polar groups adsorbed on the bubble surface and the multilayered collector on the particle's surface. As the science of the interactions is still imperfectly understood it is

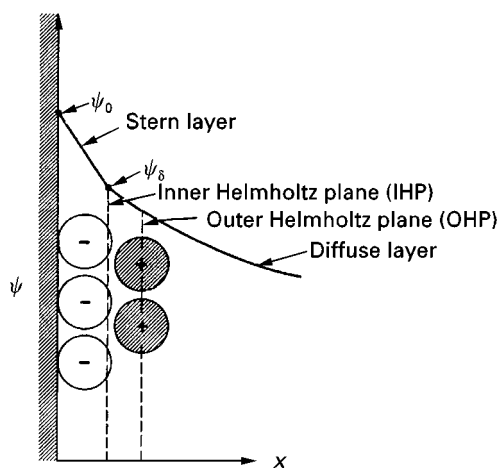


Figure 4 The Stern layer. Reproduced with permission from Adamson AW (1982) *Physical Chemistry of Surfaces*, 4th edn. New York: John Wiley.

necessary briefly to review the nature of the collector in specific separations.

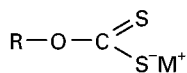
Thiol collectors The discovery of xanthates in the 1920s caused a rapid increase in the flotation process generally, but specifically with nearly all the sulfide ores. While they confer hydrophobicity on sulfide minerals, they do not affect the flotation of silicates, aluminosilicates, oxides or mineral salts. However, to achieve selective separation between sulfides within the same ore-body careful choice of reagent and control of operating conditions is required.

Although there appears to be a wide range of these sulfur-bearing compounds, they are derived from a restricted number of oxygen-bearing compounds through the substitution of sulfur for the oxygen. The great majority are derived from carbonic, carbamic and phosphoric acids, urea and the alcohols. They are usually surface-active with respect to the liquid-solid interface, but less so at the bubble-liquid surface. Some of the most important of these sulfhydryl collectors are discussed below, with their structures given in Figure 5(A). In all cases R denotes a non-polar group.

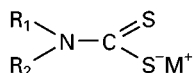
Alkyl dithiocarbonates or xanthates ($R-O-CS_2^- M^+$) Potassium ethyl xanthate (KETX) is used for the selective flotation of Cu-Zn, Pb-Zn and Cu-Pb-Zn sulfides. The effective recovery of the sulfide increases with the length of the alkyl group R; n- and iso-propyl and butyl giving increased recovery over the ethyl homologue but with a reduced selectivity. These conflicting trends increase up to amyl and hexyl. All the xanthates mentioned are soluble in water and are restricted to a pH range of 8–13 as they undergo hydrolysis under more acid conditions.

(A) Sulfhydryl collectors

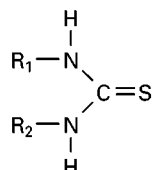
Alkyl dithiocarbonate K^+ xanthates,
R denotes a non-polar group



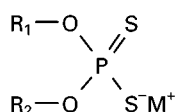
Dialkyl dithiocarbamate, $(R_1, R_2)N-CS_2^-M^+$



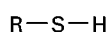
Dialkyl thiourea, $(R_1NH-, R_2NH-)C=S$



Dialkyl and diaryl thiophosphates
 $(R_1-O-, R_2-O-)PS_2^-M^+$

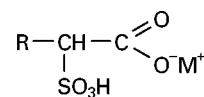


Alkyl mercaptans, $R-S-H$

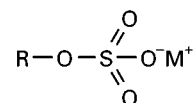


(B) Anionic collectors

Sulfonated carboxylic acids



Alkyl sulfuric acid and salts



Alkyl phosphoric acid and salts

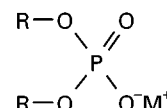


Figure 5 Industrial flotation reagents.

Dialkyl dithiocarbamate $(R_1, R_2)N-CS_2^-M^+$ These are selective collectors for Cu or Cu-activated Zn from FeS_2 . They are sparingly soluble and are used as emulsions in the pH range 4–9. The non-polar group R_1 is usually CH_3 or C_2H_5 while R_2 is either propyl or butyl.

Dialkyl thiourea $(R_1NH-, R_2NH-)C=S$ These are selective collectors for Cu, Pb and Ag ores and have been used in the flotation of complex Cu–Pb–Zn ores. They are not water soluble and have to be used as dispersions in water.

Dialkyl and diaryl thiophosphates $(R_1-O-, R_2-O-)PS_2^-M^+$ The di-ethyl and di-sec-butyl derivatives are used as collectors for Au, Ag and Cu. The dicresyl derivative is used for Ag, Cu, Pb and Zn. Generally, the dithiophosphates (DTP) reagents are more selective than the xanthates particularly in preventing the flotation of iron sulfides. The alkyl derivatives are water-soluble and are used in 5–20% solutions over the pH range 4–12. The most common alkyl homologues are diethyl and dibutyl. The alkyl derivatives are essentially non-frothing.

The aryl derivatives are dicresyl and exhibit frothing behaviour. They are not water soluble and are used undiluted.

Alkyl mercaptans $R-S-H$ Only homologues higher than C_{12} have been used. Dodecyl mercaptan is a powerful non-selective collector particularly for Cu. The mercaptans are not water soluble and are

used either in an organic solution or as a liquid emulsion.

Xanthate derivatives $R-O-S_2^-M^+$ These are used mainly in Cu flotation. They are water insoluble and are used either as an aqueous emulsion or as an organic solution. They are effective over a wide pH range.

Anionic collectors These are ionizable non-thio compounds derived from carbonic, sulfuric, phosphoric, phosphonic and arsonic acids (Figure 5(B)). They are anionic, depending on the pH of the flotation pulp and are used to collect a wide range of oxide, silicate and salt-type minerals. These minerals usually have positive ζ -potentials and consequently bind OH^- ions giving them a hydrophilic character. For the adsorbed surface to become hydrophobic the non-polar part of the anionic collector molecules must have longer carbon chains than those of the thiols. Their attachment is primarily through electrostatic interactions between the polar group of the collector and the particle surface while dispersive interactions between the non-polar groups of adjacent collector molecules increase the hydrophobicity of the surface by producing multilayered adsorbed films.

Fatty acid salts $R-COO^-M^+$ The cation M^+ is either Na^+ or K^+ , with very few exceptions they operate at high pHs where they are highly dissociated.

The non-polar radical R most used lies in the C_{16} – C_{18} range, typically oleic, linoleic and linolenic.

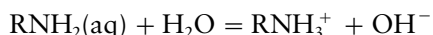
Unsaturated molecules are preferred. At alkaline pH the metal salts are soluble in water. They are used for the flotation of apatite, calcite, fluor spar and barite. Because of the electrostatic nature of their adsorption they are very powerful collectors for surfaces with positive ζ -potentials but selectivity is difficult to effect and requires careful control of the chemical environment which usually requires the use of depressants.

Alkyl sulfuric acid and salts $R-O-SO_3^- M^+$ These are stronger acids than the fatty acids and exist in an ionized water-soluble form above pH 1–2; the alkyl radical is usually C_{12} and saturated. Organic sulfates and sulfonates are used to float oxides and silicates such as iron ores, chromite, garnet, beryl and zircon. As the bonding with the solid surface is primarily electrostatic, pH control is critical, especially for the shorter chain length alkyl groups, as it affects their intermolecular dispersive bonding.

Alkyl and aryl sulfonic acid and salts $R-SO_3^- M^+$ A typical collector of this type is sodium dodecyl benzene sulfonate $C_{12}H_{25}-C_6H_4-SO_3^-O^-Na^+$ which is a strong acid and will operate in pulps with pH values above 2.

Alkyl phosphoric acid and salts $(R_1O-, R_2O-)PO_2^- M^+$ R_1 and R_2 can be either aliphatic or aromatic. Dialkyls are more strongly frothing than the monoalkyls. They are used in separations from quartz gangue, in particular for the separation of heavy minerals from glass sands. They have also been used in flotation of tungsten, uranium and phosphate ores. They are not selective in the presence of apatite, calcite, fluor spar or barite.

Cationic collectors This group consist of amines which below ceratin pH values exist in the cationic form, RNH_2 , R_1R_2NH , $R_1(R_2)_2N$. The amines are insoluble in the free base form but are treated by acids such as acetic or hydrochloric to solubilize them. They ionize in aqueous solutions as follows:



Typical collectors of this type are a primary aliphatic amine, n-amylamine ($C_5H_{11}NH_2$), a primary aromatic amine, aniline ($C_6H_5NH_2$), and pyridine (NC_5H_5), nitrogen in a benzene-like nucleus.

Particularly important are the quaternary ammonium salts, $R_1(R_2)_3N^+X^-$, which ionize strongly and are water soluble. The collecting action of this group is based on being strongly attached to surfaces with negative ζ -potentials and are consequently rarely selective but are effective over a wide pH

range. Important collectors of this type include alkyl propylenediamine, $(RNH_2(CH_3)_3NH_3)^{2+} 2X^-$, and tetradecyltrimethylammonium bromide (TTAB), $CH_3(CH_2)_{13}-(CH_3)_3-N^+ Br^-$.

Cationic collectors are used to separate sylvite (KCl) from halite (NaCl) in brine and are also used in the separation of silica from phosphate and in the flotation of zinc carbonates and silicates.

The Mechanism Associated with the Flotation of Some Important Ores

Sulfides – recovery of galena – effect of collectors

Most data are associated with the flotation of the lead ore galena PbS , which has been studied extensively. Although the tonnage of lead ore processed is only a tenth of the amount of the copper ores processed (Table 1), the fact that it exists in only one valence state simplifies data interpretation. The overall mechanism for copper sulfide ore processing is accepted as being similar to that of lead despite the copper valence change under oxidizing conditions. Both copper and lead are floated with sulfhydryl collectors and it is of interest to review the concepts associated with the collector action. It is often the case that, despite the high selectivity of the sulfhydryl collectors for sulfides in the presence of oxide and silicate gangues, that further selectivity between different sulfide minerals is required. It is consequently not necessarily sufficient to determine optimum recovery for a specific collector, but it is also necessary to investigate its effect on the simultaneous recovery of an undesired sulfide mineral.

The effect of oxygen on the ζ -potential and KETX adsorption on a galena surface In the absence of oxygen the adsorption density of ethyl xanthate is independent of pH and remains constant at a level of 2×10^{-6} g moles/g of galena, which corresponds to effectively a coverage of a monolayer assuming one xanthate ion adsorbed at one lead site on the surface. The area occupied by an anion of amyl xanthate disposed perpendicularly to the surface of a mineral is given by Klassen and Mokrousov to be 28 \AA^2 . This adsorption area should be independent of the length of the hydrocarbon chains of normal xanthates.

However, the adsorption density does fall as the length of the alkyl chain increases to about half the monolayer adsorption density with octyl xanthate. Additionally, in the absence of both oxygen and xanthate, the ζ -potential vs pH curve for galena, falls from +20 mV at pH 2 to –40 mV at pH 12. The pH at which the ζ -potential is zero is called the point of zero charge (PZC) which is a useful characterizing parameter.

In the presence of 1×10^{-3} molar ethyl xanthate the ζ -potential remains steady at -40 mV over the pH range of 4–12.

This seems to indicate that the attachment is due to the chemisorption of the alkyl part of the xanthate molecule on the galena surface, presumably after displacing H_3O^+ or OH^- ions. The unchanged outer negatively charged compact surface layer is associated with the polar end of the molecule.

In the presence of oxygen, but without xanthate, the ζ -potential vs pH differs significantly from the previous case. Over the pH range from 4 to 6 the ζ -potential vs pH curve is convex upwards with a maximum of just under $+20$ mV at pH 6. At increasing pHs the ζ -potential falls to 0 at pH 6.9, the PZC; from 6.9 to 12 it falls from 0 to -40 mV. It should be noted that for the previous case of no oxygen and no xanthate the pH at the PZC is 2.6.

In the presence of 1×10^{-4} mol L^{-1} ethyl xanthate and oxygen, the ζ -potential–pH curve is again electronegative over the range 4–12, as with the case for xanthate without oxygen, but is no longer constant, falling from -20 mV at pH 4 to -40 mV at pH 12.

There are conflicting explanations for the effect of oxygen on the galena surface. One plausible theory is that, in the presence of oxygen, the surface is oxidized to thiosulfate and sulfate. As air also contains CO_2 , lead carbonates may also form displacing the sulfates. Some of these surface compounds may move into the inner compact layer in the solution. In the presence of xanthates, a significant xanthate fraction may react directly at the surface, possibly with the sulfates, forming a strong bond with the lead mineral. The rest of the xanthate will displace the sulfate from the inner to the outer compact layer, causing the potential at the outer compact layer ψ_δ to remain electronegative.

It is further postulated that with excess xanthate, metathetic replacement of the sulfate will occur producing uncharged hydrophobic, insoluble lead ethyl xanthate. This process is clearly kinetic requiring diffusion of the unreacted sulfate at the surface through the compact layer. Multiple layers of the insoluble lead ethyl xanthate will confer increased flotability on the galena. Finkelstein, Allison, Lovell and Stewart reported improved flotation recoveries for galena using ethyl xanthate in terms of the thickness of the lead ethyl xanthate layers expressed as monolayers. The recovery increased from zero with no ethyl xanthate to 70% for a single monolayer increasing to 95% with five monolayers.

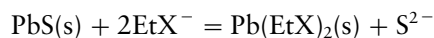
Selective flotation of galena – effect of depressants
Reagents which, to a greater or lesser degree depress

recoveries of sulfides (depressants), include OH^- , S^{2-} and chromate.

Fuerstenau in 1982 reported 100% recovery of galena, using 1×10^{-5} mol L^{-1} ethyl xanthate in the presence of oxygen, over the pH range 2–10. However, if the lead content (grade) of the concentrate is required to be low in the presence of other sulfides, which are themselves being floated by the 1×10^{-5} mol L^{-1} ethyl xanthate, this requires a reduction (depression) of the galena recovery simultaneously with a smaller reduction in the recovery of the desired sulfide.

Depression of galena using hydroxyl is effected at pH values greater than 11, due to the formation of HPbO_2 , which is the unhydrated form of $\text{Pb}(\text{OH})_3^-$, in the Stern compact layer, this causes the galena surface to become hydrophilic with consequent reduction in lead recovery.

The depression of galena using sodium sulfide is much greater than that of all other sulfide minerals. Additions of sodium sulfide to a galena suspension in xanthates will cause an insoluble hydrophilic lead sulfide rather than lead xanthate to form at the solid surface according to the reaction:



In the presence of chromate the adsorption of xanthates does not decrease, but when lead chromate forms on the surface, the hydration of the chromate is so strong that the collector hydrophobicity is significantly reduced.

Grade-recovery of copper ores In view of the economic importance of chalcocite (Cu_2S) and chalcopyrite (CuFeS_2) their selective recovery from ores containing undesired pyrites will be briefly reviewed.

Depression of pyrite – Effect of pH. Flotation of pyrite will be possible with short-chain xanthates such as potassium ethyl xanthate at pHs below 11. At addition rates of 2×10^{-4} mol L^{-1} of KETX , 100% recovery is possible. The recovery is thought to be due to the adsorption of dixanthogen on the surface. However, at high pH values xanthate oxidation to dixanthogen does not occur according to the reaction shown below, thus depressing the pyrite recovery:



Effect of CN^- . Pyrite is significantly depressed by KCN . In the absence of KCN pyrite recoveries of 100% are obtained at pH below 7, using 1×10^{-4} mol L^{-1} KETX . Significant amounts of

pyrite are still present in the concentrate even up to pH 10. However, with a KCN addition of $6.0 \times 10^{-3} \text{ mol L}^{-1}$, recovery is significantly depressed at pH 4 and completely depressed above pH 7.

Effect of pyrite depressants on copper recovery
To assess the selective separation of copper ores from pyrite it is necessary to see how the copper floats under conditions identical to those reported for pyrite depression.

Chalcocite will float completely at up to pH 10 using 5.0×10^{-5} ethyl xanthate. The mechanism of flotation in the presence of amyl xanthate is similar to that of galena, with a chemisorbed cuprous amyl xanthate after which further xanthate additions form multilayers of cuprous xanthate in the compact layer, increasing the overall hydrophobicity.

At pHs between 8 and 10, the addition of sodium sulfide will depress pyrite without significantly altering the chalcocite recovery. The most effective depressant for this separation does however appear to be potassium cyanide which hardly affects the chalcocite recovery between pH 8 and 12 while virtually completely suppressing the pyrite over this range.

Chalcopyrite will float at 100% recovery over the pH range 2–12 both with $1 \times 10^{-5} \text{ mol L}^{-1}$ ethyl xanthate and $1.3 \times 10^{-5} \text{ mol L}^{-1}$ dioxanthogen. No depression in recovery is observed up to pH 13. From this it may be inferred that at these high pHs it is the stability of the cuprous ethyl xanthate which effects flotation.

As chalcopyrite contains iron it is to be expected that it will to some extent be affected by the pyrite depressants but will be less sensitive to NaCN additions than the pyrite. For example, in a system where 60.9% pyrite recovery was achieved simultaneously with 90.5% chalcopyrite recovery with no depressant at pH 8.8, the addition of 0.04 kg ton^{-1} NaCN changed these figures to 26.1% pyrite recovery and 84.2% chalcopyrite recovery. Further additions of cyanide reduced the pyrite recovery to 15.6%, but also cut the chalcopyrite recovery to 31.0%.

Finally, it should be noted that sodium sulfide will depress chalcopyrite more than pyrite. This is due to the preferential formation of cupric sulfide over that of cuprous ethyl xanthate.

Flotation of oxides and silicates Oxides and silicates are the most abundant minerals in the earth's crust. Their flotation behaviour is important both because of their inherent value and because they act as gangue in the flotation of other minerals. Once again only a sample of the separations of interest can be discussed. Consider firstly the separation of quartz from haematite in iron ore processing.

Fuerstenau and Healy have suggested six possible procedures, four of which have been successfully employed in industry. These are based on the ζ -potential for haematite being positive in the pH range 2–4 with a PZC in the region of pH 6, while for quartz over the same range the ζ -potential is negative with a PZC at pH 2.

These procedures are:

- Flotation of haematite using an anionic sulfonate collector, for example sodium dodecyl benzene sulfonate which will adsorb on the positively charged haematite surface but not on the negatively charged quartz.
- Flotation of the haematite by the chemisorption of a fatty acid collector at pH 6–8. Chemisorption on the quartz will not occur because of its large negative ζ -potential at this pH.
- Reverse flotation of quartz at pH 6–7 using a cationic collector, for example, amylamine which will adsorb on the highly negatively charged quartz but not on the essentially uncharged haematite.
- Reverse flotation of quartz activated with calcium ions, with a long-chain fatty acid collector and the haematite depressed through the addition of starch. The hydrophilic starch molecules will chemisorb on the haematite through their carboxyl groups. Without the starch the haematite would also float under these conditions.

The successful implementation of these separations is clearly consistent with the electrostatic theory of collector adsorption.

Further thoughts on the electrostatic model of flotation. For collectors to function through physical interactions they must be present as counterions in the compact layer. Under these conditions the net charge on the outer boundary of the diffuse layer is reduced and hydrophobic interactions with the non-polar surfactants on the bubble surface can occur. Iwasaki *et al.* reported very interesting results relating to the flotation of goethite (FeOOH). Goethite has a PZC at pH 6.7 and they measured flotation recoveries, in a laboratory Hallimond tube, as a function of pH using $1.0 \times 10^{-3} \text{ mol L}^{-1}$ of the anionic collectors sodium dodecyl sulfate and sodium dodecyl sulfonate and the cationic collector dodecyl ammonium chloride. They achieved effectively 100% recoveries up to pH 6.0 using the anionic collectors with the recovery falling effectively to zero above pH 7.0.

The recovery of goethite vs pH using the $1.0 \times 10^{-3} \text{ mol L}^{-1}$ cationic dodecylammonium chloride was the inverse of this with virtually no recovery up to pH 6.0 and 100% recovery between

pH 8 and 12.2 when the recovery fell to zero because the quaternary ammonium salt hydrolysed to the parent amine.

The increased flotation response at lower pHs with the anionic collectors is associated with an increased charge density σ_s in the compact layer which causes larger amounts of collector to be present as counterions. The increased concentration of their non-polar groups in the compact layer will increase the particle's hydrophobicity.

Modi and Fuerstenau reported tests on corundum (Al_2O_3), which has a PZC at pH 9, at four different pH values using an anionic collector, sodium dodecyl sulfate, at concentrations ranging between 10^{-7} and 10^{-1} mol L $^{-1}$.

At pH 4.0, 100% recovery was achieved with 0.5×10^{-4} mol L $^{-1}$, but it required 10 times that concentration for 100% recovery at pH 6.0, while at pH values of 9.3 and 11.0 the highest recovery achieved was only 30% at a reagent concentration of 10^{-3} mol L $^{-1}$.

Effect of the length of the hydrocarbon chain on the collector performance. Data have been reported for the flotation of quartz (PZC at pH 2.0) at pH 6–7, using the cationic alkylammonium acetates, with the alkyl chain length varying between C_4 and C_{18} . Incipient flotation occurs from about 10^{-8} mol L $^{-1}$ for C_{18} to 10^{-1} for C_4 . Similarly high rates are observed at 10^{-6} mol L $^{-1}$ for C_{18} to 0.5 mol L $^{-1}$ for the C_4 . The onset of the high flotation rates are equated to the onset of hemimicelle formation.

Frothers

Chemical types A frother is a surface-active chemical whose principal function is to increase significantly the dispersion of air at a given aeration rate in the pulp phase of a flotation machine by producing small bubbles; this is done through the reduction of the surface tension at the air–water interface. If the pressure of the dispersed air is p_0 and the hydraulic pressure in the liquid at the aerator is p_b then the bubble radius R_b will be:

$$R_b \approx \frac{2\gamma}{(p_0 - p_b)} \quad [41]$$

Laskowski has reviewed the mechanism of the action of surface-active reagents in flotation. He said that frother molecules have an uneven distribution of polar and non-polar groups which cause them preferentially to orientate at the air–water interface with the polar groups forming a liquid film around the bubble by hydrogen bonding with the water and the non-polar groups forming a gaseous film within

the bubble. They may be classified into five groups:

1. Aliphatic alcohols with a single hydroxy group R–OH, where R is either a straight-chain alkyl group with five to eight carbon atoms or a branched chain with six to sixteen carbon atoms. Typical of the branched alcohols are methyl iso-butyl carbinol (MIBC), di-acetone alcohol and 2-ethyl hexanol. These frothers produce fine-textured, fairly selective froths.
2. Cyclic alcohols. These are represented by pine and eucalyptus oils of which the active components are the terpene alcohols typically α -terpineol. These are traditional frothers and are still used usually in combination with other frothers and collectors in 30% of the world's copper concentrators.
3. Phenols of which cresylic acid a mixture of cresols and xylenols, is the most commonly used.
4. Alkoxyparaffins of which the most successful is 1,1,3-triethoxybutane, have come into use in sulfide flotation as they seem also to have collector specificity.
5. Finally the polyglycols, particularly polypropylene glycol, these are available as commercial products with the general formula $\text{R}(\text{X})_n\text{OH}$, where R is either H or $\text{C}_m\text{H}_{2m+1}$ and X is either ethylene oxide (EO) $-\text{CH}_2\text{CH}_2\text{O}-$, propylene oxide (PO) $-\text{CH}_2\text{CH}(\text{CH}_3)-\text{O}-$ or butylene oxide (BO) $-\text{CH}_2\text{CH}_2\text{CH}(\text{CH}_3)-\text{O}-$. In the PO and BO frothers the propylene and butylene groups are hydrophobic and the ether oxygen and the hydroxyls are hydrophilic. Varying the relative length of the hydrophobic to hydrophilic groups in the molecule permits tailoring the molecule to a specific application.

Bubble stability in pulp The crucial property of a bubble in an aerated flotation cell relates to its ability to survive the collision and attachment of a particle without bursting. Although it is possible to observe that the addition of frothers does increase the stability of a single bubble, a coherent quantitative stability model does not exist. This will need to relate to the ability of its water film surrounding the bubble to withstand local disturbances. This ability is thought to be related to dynamic changes in surface tensions in the film following the local decreases in frother concentration after distortion has occurred following impact with a particle.

The effect of frother concentration on the surface energy of the solution has been used by Laskowski to characterize the surface activity of various frothers as related to their molecular structure. This is based on the application of the Gibbs adsorption isotherm, where Γ is the surface excess of the surface-active

agent, a its activity in the bulk solution and γ_{LV} is the bubble-liquid interface energy:

$$\Gamma = -\frac{a}{RT} \times \frac{\partial \gamma_{LV}}{\partial a} \quad [42]$$

This implies that a decrease in a , the surfactant activity, at the gas-liquid interface following local surface increases, will be associated with a very sensitive surface tension γ increase.

Bubble-Particle Collision Dynamics

Interception efficiency – single bubble – particle collision Flint and Howarth observed that for a rational basis for flotation cell design to be achieved it is necessary that methods for the prediction of bubble-particle collision and subsequent adhesion be available.

For a single particle falling under gravity in the path of a single rising bubble, they provided a general definition of collision efficiency E , as the ratio of the number of particles which collide with the bubble to the number that would have collided if the liquid streamlines had not been diverted by the bubble. Their analysis is based on calculating the trajectories of single particles, initially remote from the bubble, and which are a distance δ from the centreline of the path of the rising bubble (Figure 6). Although all the liquid will pass around the bubble, particles on streamlines which pass closer to the bubble than the radius of the particle, are deemed to have come into contact with the bubble.

Calculation of single particle trajectories The bubble and particle are both assumed to be spherical, with the bubble of radius R_b rising vertically at a velocity U , and the particle of radius R_p falling under gravity. The trajectory calculation begins at a point where the lateral components of the flow field ahead

of the rising bubble begin to induce a sideways motion of the particle. At this point the particle is considered to be offset by a distance, δ , from the centreline of the rising bubble.

The consequence of the flow field assumed by the authors is that the trajectory is defined by the initial δ . A grazing trajectory is defined where for particles with an initial offset δ_0 , the trajectory passes at a distance R_p from the bubble shell on its horizontal diameter. For particles at smaller offsets, contact will be made at some point on the bubble shell, while those with $\delta > \delta_0$ will make no contact.

The collision efficiency then follows:

$$E = \frac{\delta_0^2}{(R_b + R_p)^2} \quad [43]$$

The particle trajectories under the influence of gravity and the flow pattern ahead of the rising bubble can be computed by integrating eqn [44] with the initial offset δ as a boundary condition. The liquid flow field ahead of the rising bubble is described in two dimensions, y (vertical) and x (horizontal), by its local velocity components u_y and u_x (assuming axisymmetric flow) using either the Stokes' or the potential flow stream functions. As the particles are very small ($R_p < 100 \mu\text{m}$) consideration of the interaction between the flow fields of particle and fluid is not necessary. The motion of the particle is described by its velocity components v_y and v_x .

The velocity components are normalized by dividing by U and setting the dimensionless time $t^* = tU/R_b$. The equations can then be expressed in terms of the dimensionless parameters K and G , where $K = (2\rho_p R_p^2 U)/(9\mu_f R_b)$ which is directly related to the ratio of inertial to drag forces on the particle while $G = (2[\rho_p - \rho_f]R_p^2 g)/(9\mu_f U)$ represents the terminal settling velocity of the particle in an undisturbed fluid:

$$K \frac{\partial v_x^*}{\partial t^*} = u_x^* - v_x^* \quad [44]$$

$$K \frac{\partial v_y^*}{\partial t^*} = -G - u_y^* + v_y^*$$

Although this treatment greatly oversimplifies the flow processes in a highly aerated well-stirred suspension of particles in water, it does make interesting statements about the effects of bubble size on the efficiency of collection of a single particle of a given size and density.

Flint and Howarth report the fractional collision efficiency, E , as a function of the parameters K and G . For K values less than 0.1 E is a function of G only

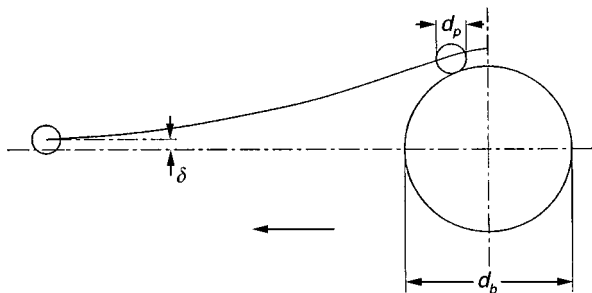


Figure 6 Single particle trajectory in the region of a rising bubble. Reproduced with permission from Flint and Howarth (1971) The collision efficiency of small particles with spherical air bubbles. *Chemical Engineering Science* 26, 1155-1168.

according to:

$$E = \frac{G}{G + 1} \quad [45]$$

The upper limit of $K = 0.1$ corresponds for example to a situation of 20 μm particles in an aerated suspension of 0.2 mm bubbles. Bubbles of this size will rise through still water at $U = 5 \text{ cm s}^{-1}$. K for silica, chalcopryrite and galena under these conditions is respectively 0.06, 0.095 and 0.17; the corresponding G values are 0.028, 0.055 and 0.11.

Using eqn [45], the respective collision efficiencies are 0.027, 0.052 and 0.10. If the bubbles in the aerated suspension were larger, the collision efficiencies would drop. For example for 0.4 mm bubbles whose rise velocity $U = 10 \text{ cm s}^{-1}$, the K values would fall further below 0.1 and the G values would also fall to 0.014, 0.027 and 0.055 with corresponding E values of 0.014, 0.026 and 0.052.

Thus, while 0.4 mm bubbles are probably satisfactory for floating chalcopryrite and galena, it might be necessary to generate smaller bubbles to float silica selectively. However, 60 μm silica particles will be efficiently floated with 1 mm bubbles. The bubble size required for the effective flotation of 60 μm chalcopryrite and galena need be no smaller than 5 mm.

These observations are obviously of both technical and economic importance, as while it is unnecessary to generate small bubbles for medium-size sulfide mineral particles, for light silicate mineral particles it may be necessary for selective separation to aerate the pulp suspension down to 100 μm microbubbles.

Bubble-particle contact time – general Following initial interception of the particle by the bubble, two possible modes of contact have been proposed.

First, the bubble shell is considered to deform elastically and for the particle either to attach to the bubble, or ultimately to be expelled from the shell under the elastic forces. The contact time is that lapsing between the moment of initial contact when the surface begins to deform, to the time when it first regains its original undistorted shape, subsequent oscillations being ignored.

In the second technique the particle after collision with the bubble is assumed to remain in contact with an undeformed surface, while being swept around from the point where it initially made contact, until it approaches the bubble's wake, where it is detached from the shell. The contact time according to this method is the time lapsed between the original contact to that when it first enters the bubble's wake.

Contact time assuming bubble – shell deformation Ye and Miller developed a model based on estimating the penetration distance $h(t)$ of a particle into the bubble shell. **Figure 7** shows their concept of defining $h(t)$ for the special case when contact is made on the line of centres. The deformed area increase is approximated in terms of $h(t)$ as:

$$A(t) = \pi h(t)^2 \quad [46]$$

The force resisting the motion of the particle after collision is described in terms of the increase in the surface free energy of the deforming bubble surface:

$$dG_A = \gamma dA(t) = 2\pi\gamma h(t)dh(t) \text{ and the resisting force}$$

$$F(t) = \frac{dG_A}{dh(t)} = 2\pi\gamma h(t) \quad [47]$$

The particle and the bubble approach each other at a relative velocity v^* . The position of the initial point of contact by the particle at the bubble surface is defined by an angle α between the contact point and the bubble centre and the centreline of the rising bubble.

The deformation is presumed to occur along the radial angle α at a relative velocity v_b^* . After impact the motion of the particle is resisted by the deforming bubble surface and is decelerated to zero. It is then accelerated in the reverse direction by the shell tension until it reaches the local bubble velocity, at which time it is presumed to lose contact with the

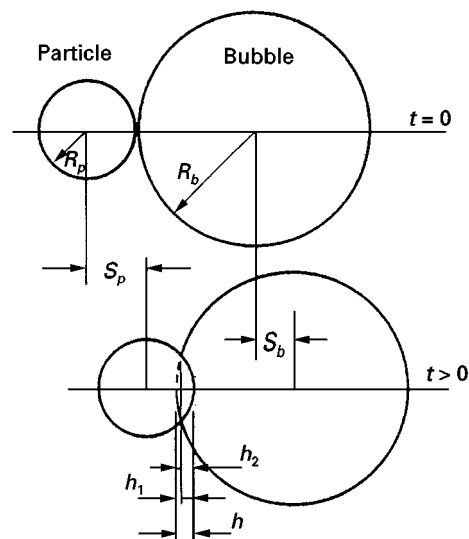


Figure 7 Bubble-particle contact time. Reproduced with permission from Ye and Miller (1988) Bubble/particle contact time in the analysis of coal flotation. *Coal Preparation* 5, 147–166.

bubble. If, however, the water film between the particle and the bubble during the deformation is thinned to the point of rupture then attachment will follow.

By assuming an average touching angle of $\sin^{-1}(2/3)$ they quote, for the overall contact time τ in seconds:

$$\tau = 13.5 \times \sqrt{\left(\frac{\pi \bar{m}_b m_p}{\gamma(\bar{m}_b + m_p)} \right)} \quad [48]$$

Figure 8 shows contact times calculated using eqn [48] for a particle with a specific gravity of 2.6. It can be seen that if the particle mass is very much greater than the effective bubble mass then the contact time depends only on the bubble size.

Contact time assuming sliding contact Dobby and Finch have developed a model to predict contact time following an initial particle–bubble shell contact, at an angle α_n with respect to the centre of the bubble. The particle is pressed against the shell surface by its settling velocity $v_T \cos \alpha$ in the inward direction to the bubble centre while it is also being driven tangentially by the liquid moving in close contact with the bubble shell, at a velocity u_x . It leaves the shell at an angle α_m at which point its inward radial motion is equal the outward radial component of the surface liquid. The particle contact time t_s follows from the length of

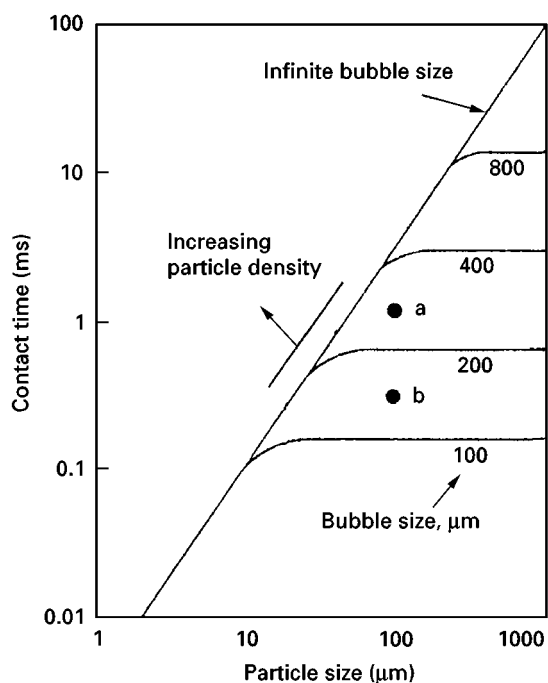


Figure 8 Particle bubble contact times. Reproduced with permission from Ye and Miller (1989) The significance of bubble/particle contact time in the analysis of coal flotation. *International Journal of Mineral Processing* 25, 199–219.

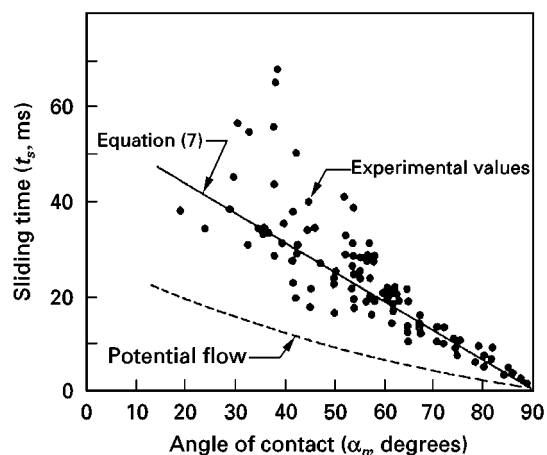


Figure 9 Particle bubble sliding contact times. Reproduced with permission from Dobby and Finch (1985) A model for particle sliding time for flotation size bubbles. *Journal of Colloid and Interface Science* 109(2), 493–498.

the arc between α_n and α_m divided by its tangential velocity $v_{p,x}$:

$$t_s = \int_{\alpha_n}^{\alpha_m} \frac{\pi(d_b + d_p)}{v_{p,x}} d\alpha \quad [49]$$

This gives a sliding contact time in terms of an average $v_{p,x}$ which is computed using an average vorticity $\zeta_{s,avr}$ and an average value for $\sin \alpha$, with α in degrees:

$$t_s = \frac{(\alpha_m - \alpha_n)}{360} \times \frac{\pi(d_b + d_p)}{\bar{v}_{p,x}} \quad [50]$$

Figure 9 shows sliding times computed for a 160 μm particle, of density $\rho_p = 2.5 \text{ g cm}^{-3}$ with a terminal settling velocity $v_T = 1.58 \text{ cm s}^{-1}$, on 3 mm bubbles rising at $v_b = 8.42 \text{ cm s}^{-1}$ giving an approach velocity of 10 cm s^{-1} . These times show a linear dependency on the angle of contact decreasing from 40 ms at $\alpha_n = 20^\circ$ to 0 when $\alpha_n = \alpha_m = 90^\circ$.

Thinning of the Water Film Attachment

Induction time–critical thickness Li, Fitzpatrick and Slattery have developed a mathematical model from which the attachment between the bubble and the particle can be characterized. The model relates to an initially spherical bubble approaching a stationary spherical particle. As the bubble–particle separation reduces, the water film separating them will thin and possibly reach a *critical thickness* at which it will rupture.

The *induction time* is the time between the initial contact, defined by the formation of a dimple on the bubble surface, and the final rupture of the separating film. Restating the previous sentence, a condition for attachment is for the *induction time* to be shorter than the *contact time*.

The model is defined in axisymmetric cylindrical coordinates with the z -axis coinciding with the line of approach of the bubble and particle centres. The particle is assumed to be spherical of radius R_p and the bubble away from the neighbourhood of close approach is also to be assumed spherical with a radius R_b . The origin of the system is taken as the centre of the spherical particle, the frame of reference being stationary with reference to the particle.

Figure 10 shows the bubble–film interface $z = h_1(r, t)$ and the surface of the solid $z = h_2(r)$. The surface of the bubble is dimpled on the nearest point of approach to the particle on the line of centres, the rim of the dimple is located at a radius $R(t)$ from the line of centres.

It has been assumed that the initial time of the bubble–particle contact $t = 0$ occurs when the thinning rate in the film becomes dependent on radial position.

The film thickness between the two surfaces $h_x(r, t)$ is given by the difference:

$$\begin{aligned} h_x(r, t) &= h_1(r, t) - h_2(r) \\ h_0 &= h_x(r, 0) \quad \text{and} \quad R_0 = R(0) \end{aligned} \quad [51]$$

For the spherical solid particle:

$$h_2(r) = (R_p^2 - r^2)^{1/2} \quad [52]$$

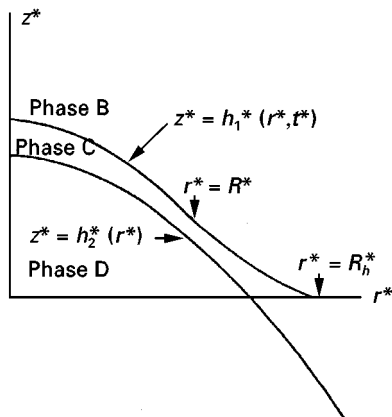


Figure 10 Thin liquid film formed as a small bubble approaches a small solid particle. Reproduced with permission from Li, Fitzpatrick and Slattery (1990) Rate of collection of particles by flotation. *Industrial Engineering Chemistry Research* 29, 955–957.

The thinning of the film is due to the pressure in the film $P(r, t)$ being greater than the hydraulic pressure p_b remote from the line of centres; at this point $r = R_b$. The pressure inside the bubble p_0 is linked to the hydraulic pressure p_b by:

$$p_b = p_0 - 2 \frac{\gamma}{R_b} \quad [53]$$

Components of the thinning pressure in the film

The local total film pressure $P(r, t)$ has three components: (a) the London–van der Waals interactive pressure π_v , (b) the electrostatic π_{el} pressure due to the charges on the solid and the bubble surfaces, and (c) a pressure π_{cap} caused by the deformation of the bubble surface from that of a sphere to $z = h_1(r, t)$, in the neighbourhood of the solid particle.

For the van der Waals component, π_v , for a film of thickness h_x the following is considered:

$$\pi_v = \frac{B}{h_x^m} \quad [54]$$

When the film thickness was greater than 400 Å, $m = 4$ and $B = 10^{-19}$ erg cm, but when the film thickness was less than 120 Å the corresponding values were taken as $m = 3$ and $B = 10^{-14}$ erg.

These values are consistent with those quoted earlier for the Hamaker constant A . When B is positive the London–van der Waals forces between liquid–gas and the solid–liquid interfaces are mutually attractive.

The electrostatic interaction potential π_{el} between the particle–water and the water–bubble surfaces is given by:

$$\pi_{el} = \Delta \exp(-\kappa h_x) \quad [55]$$

where:

$$\kappa^2 = \frac{8\pi n z_i^2 e^2}{DkT}$$

$$\Delta = 64nkT \tanh\left[\frac{z_i e \psi_{s-w}}{4kT}\right] \tanh\left[\frac{z_i e \psi_{w-g}}{4kT}\right]$$

where ψ_{s-w} and ψ_{w-g} are the electrostatic potentials at the bounding interfaces. When the interfaces have the same sign, Δ is positive and the surfaces are mutually repulsive and when the signs are different, Δ is negative and the surfaces are mutually attractive.

As deformation of the bubble surface occurs, the capillary pressure in the film $\pi_{cap}(r, t)$ is a function of

the mean curvature H_1 and the bubble pressure:

$$\pi_{\text{cap}}(r, t) = p_0 - 2H_1\gamma \quad [56]$$

where γ is the surface tension of the distorted film:

$$\pi_{\text{cap}}(r, t) = p_0 - \frac{\gamma}{r} \frac{\partial}{\partial r} r \frac{\partial z_1(r, t)}{\partial r}$$

A lateral pressure gradient will develop in the water film normal to the separation distance h_x . Under this pressure gradient water will move to the bulk liquid, causing thinning:

$$\frac{\partial P(r, t)}{\partial r} = \frac{\partial}{\partial r} \left(\frac{B}{h^m} - \Delta e^{-\kappa h} - 2\gamma H_1 \right) \quad [57]$$

assuming that the van der Waals and the electrostatic disjoining pressures are attractive. To calculate the induction time it is necessary to obtain values for the velocity components of the water in the flowing film $v_r(r, z, t)$ and $v_z(r, z, t)$ in terms of the pressure gradient. For an incompressible Newtonian fluid with constant viscosity, the momentum balance equation for creeping flow for radial symmetry $v_\theta = 0$ and for negligible pressure variation in the z -direction reduces to:

$$\frac{\partial P}{\partial r} = \mu \frac{\partial^2 v_r}{\partial z^2} \quad [58]$$

A solution for $v_r(z, r)$ at time t is obtained for both a mobile and an immobile bubble–water interface:

$$v_r(r, z) = \frac{1}{\mu} \frac{\partial P}{\partial r} \left[\frac{(z - h_2)^2}{2} - \frac{h}{n} (z - h_2) \right] \quad [59]$$

where $n = 1$ for a mobile interface and $n = 2$ for an immobile interface. This, when substituted into the equation of continuity gives v_z , which together with v_r , gives a solution for the configuration of the bubble–water interface $z = h_1(r, t)t$. From this the change in film thickness at radial position r , with time follows:

$$\frac{\partial h_x}{\partial t} = \frac{1}{\mu} \frac{3-n}{2n} \left[\frac{1}{3} h_x^3 \left(\frac{\partial^2 P}{\partial r^2} + \frac{1}{r} \frac{\partial P}{\partial r} \right) + h_x^2 \frac{\partial h_x}{\partial r} \frac{\partial P}{\partial r} \right] \quad [60]$$

A radial position R_b is estimated, as the smallest value of R where the local bubble curvature is the same as that of the undeformed bubble. The force

acting on the water film at the particles surface is then computed to be:

$$F(t) = 2\pi \int_0^{R_b(t)} (P(r, t) - p_0) dr \quad [61]$$

The induction time is that when $F(t_{\text{ind}})$ is deemed just to have exceeded the adhesion energy of the solid–water interface. For the case where the effects of the electrostatic double layer can be neglected, the numerical integration shows an inverse power dependence of the induction time on the van der Waals parameter.

These conclusions have been tested against the experimental data reported by Ye and Miller whose observations were based on forcing a bubble through a solution on to a bed of particles for a predetermined time and recording as the induction time the time at which 50% of the events resulted in attachment.

The theoretical treatment predicts that when the particle radius R_p is very much smaller than the bubble radius R_b , $\log t_{\text{ind}}$ will be a linear function of $\log R_p$. This is consistent with the experimental data of Ye and Miller, although the predicted slopes are slightly lower than those reported.

When the electrostatic effects are allowed for the predictions have to be graphical as a general equation cannot be derived; there are also no experimental data available for checking. From **Figure 11** and **Table 3** it is, however, clear that these electrostatic effects are very significant.

Li, Fitzpatrick and Slattery have reported values for Δ and κ reproduced here as Table 3 which they used in conjunction with their derived relationships.

The data in the table are given for univalent ions and the surface potentials are given as equal on each surface, but both cases can be easily adapted. When the sign of the surface charges are opposite and the surfaces are consequently mutually attractive, Δ is negative.

The authors report induction times for a system corresponding to that of Ye and Miller although no direct comparisons with experimental data could be made. Figure 11 is typical of the predictions made.

For electrostatic interactive forces on a 100 μm particle in a 10^{-3} molar solution the induction times vary from 10 ms for $\pi_{el} = -80$ mV to more than a second for $\pi_{el} > +20$ mV.

As the solution molarity falls to 10^{-4} mV the induction time for $\pi_{el} = -80$ mV remains at 10 ms but falls to 100 ms for $\pi_{el} = +20$ mV.

The effect of particle size is also interesting; for a 10^{-3} molar solution and $\pi_{el} = -80$ mV the induction time is less than 1 ms for a 10 μm particle rising

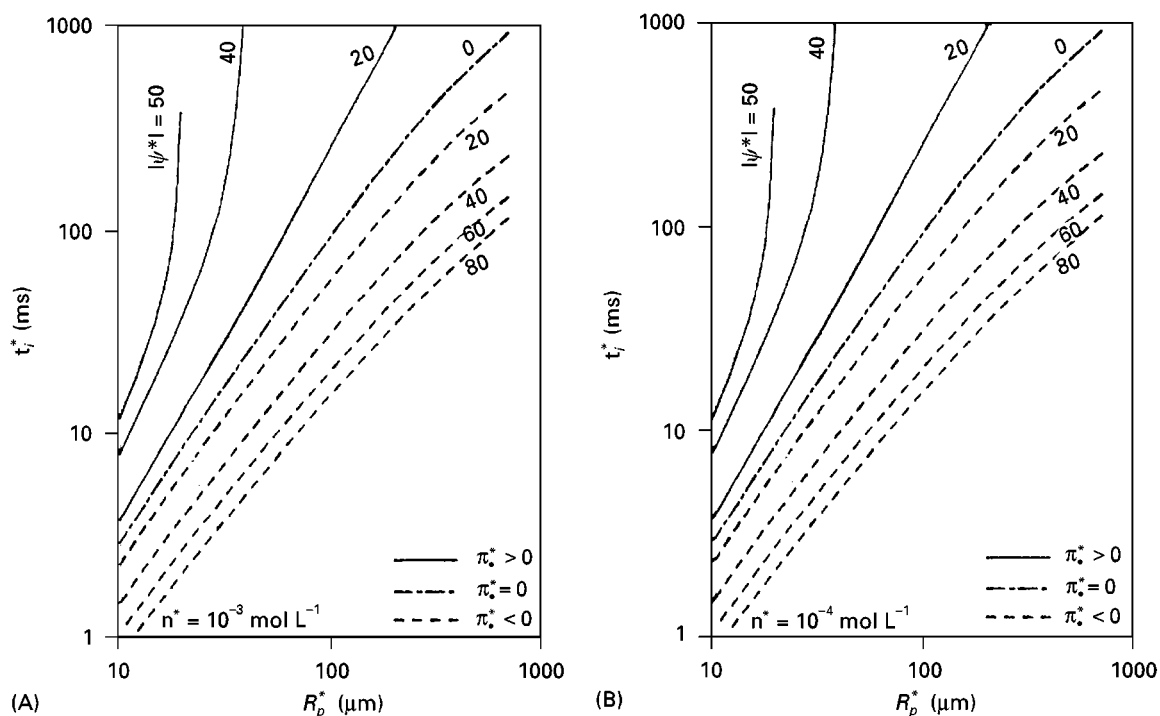


Figure 11 Induction times as a function of the charge density on particle and bubble surfaces, which are assumed equal but of similar or opposite signs, and the particle radius. (A) $n = 10^{-3}$ and (B) $n = 10^{-4}$ mol L $^{-1}$. Reproduced with permission from Li, Fitzpatrick and Slaterry (1990) Rate of collection of particles by flotation. *Industrial Engineering Chemistry Research* 29, 955–957.

to 100 ms for a 1000 μm particle. The effect of a reduction in solution molarity to 10^{-4} does not, however, change the induction times significantly as it does in the previous case.

Although the model refers only to single bubble–single particle contact and the experimental data are similarly idealized, it is nevertheless valuable

as it predicts induction times in fundamental terms which surely provides a sound basis for the experimental use of them as a characterizing parameter, for the development of reagent addition strategies for industrial separations.

Transfer across the Pulp–Froth Interface

The bubble structure at the top of the pulp is shown for two-phase foams in **Figure 12**. It can be shown that the rate at which bubbles are required to cross through a volume at the top of the pulp, described by the surface area of the cell multiplied by one bubble diameter, is determined by the overall aeration rate to the cell and the bubble size produced by the agitator or sparger.

The free rise velocity of a single bubble of a typical size produced in this way has a residence time significantly smaller than that calculated by dividing the liquid volume in the cell by the aeration rate. The dispersed bubble hold-up in the pulp is thus considerably less than that the bubble hold-up in the close-packed foam structure, producing a sharp discontinuity in the bubble volumetric fraction at the pulp–froth interface.

If, at the bottom of the foam layer the bubbles remain spherical in a closest-packed rhombohedral

Table 3 Showing values of Δ and κ as functions of surface potentials ψ_s, ψ_f at various solution molarities: $10^{-6}, 10^{-4}, 10^{-2}$ for univalent ions $z = 1$

$\pm \psi_s$ (mV)	$\pm \psi_L$ (mV)	$\pm \Delta$ at M (mols/litre)		
		10^{-6} (molar)	10^{-4} (molar)	10^{-2} (molar)
20	20	58.6	5.86×10^3	5.86×10^5
40	40	217.9	2.179×10^4	2.179×10^6
50	50	323.3	3.233×10^4	3.233×10^6
60	60	437.9	4.379×10^4	4.379×10^6
80	80	673.8	6.738×10^4	6.738×10^6
100	100	892.2	8.922×10^4	8.922×10^4
κ (cm $^{-1}$)		3.257×10^4	3.257×10^5	3.257×10^6

Reproduced with permission from Li D, Fitzpatrick JA, Slaterry JC (1990) Rate of collection of particles by flotation. *Industrial Engineering Chemistry Research* 29, 962, Table II.

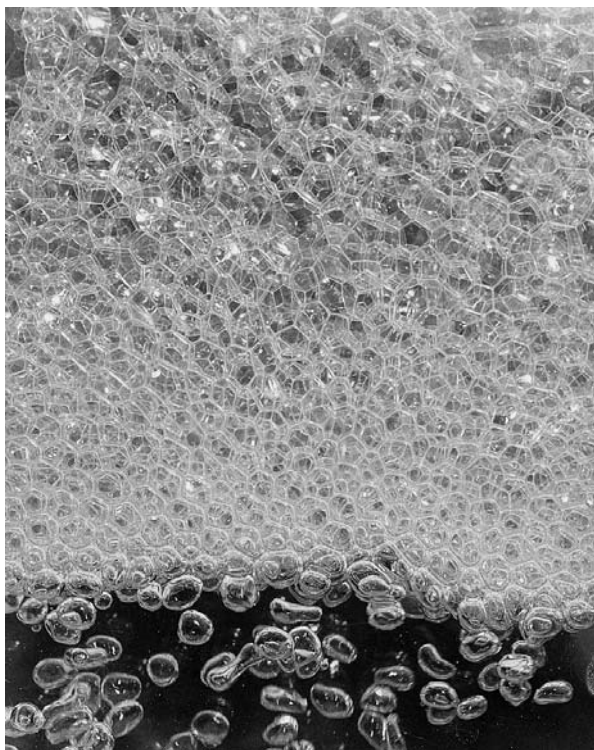


Figure 12 The structure of the interface between bubbles dispersed in water containing surfactant and the froth. No particles are present in this system.

structure, the volume fraction occupied by inter-bubble water will be $\varepsilon = 0.26$.

This means that solids transfer from the pulp to the froth in two ways. In the first the valuable particles are selectively attached to the bubble surface, while in the second the particles will be non-selectively entrained in the inter-bubble water. This entrainment will adversely affect the selectivity of the separation, but will apparently improve the total particle recovery.

Froth Microprocesses

Grade Enhancing – General

For the froth to perform a grade-enhancing (cleaning) function it is clearly necessary to reduce the entrainment of undesired solids.

The froth which forms at the pulp–froth interface is a close-packed structure of spherical bubbles (*kugelschaum*), which it will have a volumetric water fraction of about 30%. The solids content of this water will not have been selectively separated. To reduce the amount of entrained solids at the froth overflow it is necessary either to reduce the water content by drainage or to displace the solids in the inter-bubble water by adding external wash water at the upper froth surface.

Removal of Entrained Solids

Coalescence Froths with high water contents are mobile and overflow at high rates giving good recoveries at the expense of low grades. These froths occur when the bubbles on their upward passage from the pulp–froth interface through the froth to the overflow, retain their shape and do not coalesce.

It is theoretically possible that selective drainage of solids within the entrained water may occur, giving some grade improvements without a reduction in water content. However, the settling path within the froth is down the plateau borders and even with heavy minerals and low-density gangue, the differential settling rates are usually small and significant upgrading from this effect is uncommon.

The volume fraction of water in the *kugelschaum* can be reduced by allowing the close-packed spherical bubbles to coalesce to form a polyhedral structure (*polyederschaum*). The lower water content of this structure is related to the thinness of the water lamellae separating the flat polygonal sides of the bubbles.

The point at which three bubbles meet is called a plateau border. Drainage occurs down a network of these borders. At the plateau border the curvature of the bubble surfaces is relatively high. The difference between the curvature of the bubble surfaces at the plateau border and that of the flat sides, generates a capillary pressure which causes the lamellar water to flow towards the plateau border. This causes them to thin further to a point where they may rupture causing further coalescence.

The reduction of the froth water content by drainage is directly dependent on the degree of bubble coalescence which occurs during their passage upwards through the froth. This in turn depends on the stability of the inter-bubble lamellae of the *polyederschaum*.

The coalescence may possibly cause some rejection of the valuable solids into the draining inter-bubble water, and may also be associated with an increased bursting rate of the froth bubbles, which will also cause valuable solids to be rejected into the drainage water.

This suggests a linkage between the appearance of the overflowing froth and the cell performance. Regulation of the degree of coalescence which occurs in the froth is achieved by varying the addition of the frother. Woodburn, Austin and Stockton have reported experimental studies, carried out in a 1 litre laboratory Denver cell, relating to the removal of ash-forming mineral from a low-rank British coal. In these the demineralized coal is the valuable product and the ash-forming mineral the waste product. The tests relate on-line visual images to cell performance as characterized by grade-recovery curves

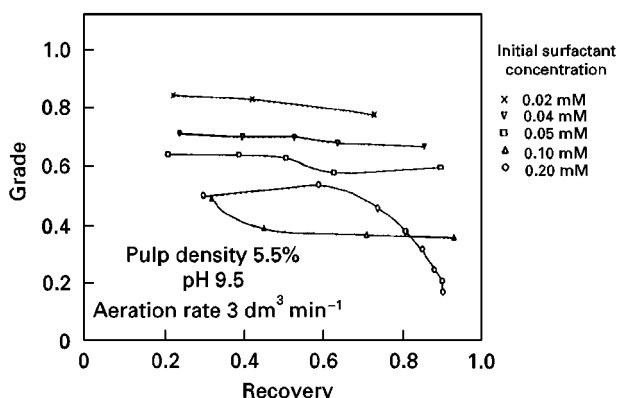


Figure 13 Grade recovery trajectories of batch coal flotation tests with varying initial single additions of the anionic collector/frother sodium dodecyl sulfate. Reproduced with permission from Woodburn ET, Austin LG and Stockton JB (1994) A froth based flotation kinetic model. *Chemical Engineering Research and Design* 72(A2), 211–226.

(Figure 13). There is a limiting achievable grade which reflects perfect separation. This is because, that even after fine grinding there is a residual inherent mineral content of the fine coal. This material which is determined in this case, by the ash content of the float fraction in a heavy medium (specific gravity of 1.4) centrifugal separation, is referred to as being unliberated.

Figure 13 shows a progressive reduction of grade with increasing recovery for a single test, and an overall grade reduction and recovery increase over all the tests, with increased addition of the frother/collector sodium dodecyl sulfate (SDS).

Each grade–recovery curve, with the partial exception of the run with 0.10 mM SDS initial addition, completely encloses all runs with higher initial additions. This run was done on a different coal sample from the same pit. Tables 4–7 show that for the coal froths the average concentration of SDS in the concentrate increases as expected with increases in the initial dose, but does not change significantly over a run despite the observed increased coalescence.

In all the tests the concentrate was free-flowing and then terminated when the froth would no longer flow, and had a high bubble bursting rate. Both effects are consistent with lamellae thinning to below a thickness where lateral flow to the plateau border stops. The reduction of grade with time and increased coalescence, during the course of a single test, is however not consistent with the simple entrainment model.

A possible explanation for the grade reduction despite the increased coalescence, is that there may be a competitive adsorption of valuable and waste material on the bubble surface rather than perfect selectivity. As a batch test proceeds there is an increasing fraction of waste solids in the pulp, which may consequently cause a corresponding increase in the waste solid attachment to the bubble surface. The increasing waste solid concentration may also contribute to the decreased lamella stability, despite the presence of SDS, because of the lower repulsion between two closely adjacent bubble surfaces, rather than that between the two surfaces with a higher fraction of coal. These observations must be treated as speculative.

Figure 14 shows for the same series of tests the percentage of solids in the overflowing concentrates as a function of time. From this it can be seen that the water content of the concentrate increases with increased SDS addition. Comparison with the grade–recovery curves of Figure 13 clearly relates decreases in grade and increase in recovery with the concentrate water content. It is also interesting to note that the time of a single test increased with increased surfactant reflecting the increased stability of the bubbles in the froth. For the run with 0.2 mM initial SDS addition, the solids content in the overflowing froth towards the end of the run was about that of the pulp solids, which indicates almost complete entrainment.

Figures 15 and 16 show the appearance of the top surface of the froth for the runs with initial SDS additions of 0.04 and 0.05 mM L⁻¹, respectively.

Table 4 The effect of froth structures on flotation kinetics and selectivity

Time (s)	Dry solids in sample (g)	Water in sample (g)	Ash (%w/w)	Mean bubble size (mm)	Sodium dodecyl sulfate concentration in water (μmolar)	Particle size d_{50} (μm)
46.0	9.9	19.39	2.06	8.31	12.9	55.0
64.0	8.57	18.39	2.14	11.60	7.93	65.0
90.0	13.9	23.59	2.83	17.40	7.57	63.0
Tailings	12.77		37.6		0.64	45.0

Feed mass 49.5 g coal, feed ash 12.7%, total water 850.6 g, sodium dodecyl sulfate 0.02 mM. Reproduced with permission from Stockton J (1989) PhD thesis, UMIST, Manchester.

Table 5 The effect of froth structures on flotation kinetics and selectivity

Time (s)	Dry solids in sample (g)	Water in sample (g)	Cum ash (%w/w)	Mean bubble size (mm)	Sodium dodecyl sulfate concentration in water (μ molar)	Particle size d_{90} (μ m)
7.0	10.93	51.37	3.64	3.07	24.06	67.0
30.0	7.11	37.19	3.78	4.29	23.7	60.0
47.0	5.92	23.98	3.81	5.12	38.6	63.0
62.0	4.63	15.62	4.10	4.67	45.0	62.0
105.0	10.23	14.07	4.23	–	68.4	70.0
Tailings	6.63	–	63.0	–	4.74	34.5

Feed mass 49.5 g coal, feed ash 12.7%, total water 850.6 g, sodium dodecyl sulfate 0.04 mM. Reproduced with permission from Stockton J (1989) PhD thesis, UMIST, Manchester.

Table 4 reports for the 0.04 mM run, an increase in the mean bubble size from 3.07 mm at 17 s to 4.67 mm at 62 s, while for the 0.05 mM run the mean bubble size varied from 1.7 mm at 23 s to 3.6 mm at 77 s.

The smaller bubbles of the 0.05 mM run corresponded with poorer grades and lower concentrate solids content than those observed in the 0.04 mM run. It can be seen that in both runs the mean bubble size as viewed from above increased with time of the test.

Figure 17 shows the junction of three bubbles after coalescence. The plateau border can be seen, as can be the plane liquid lamella separating two adjacent bubbles. The presence of solids on the bubble surfaces can also be seen. These show incomplete surface coverage.

Displacement washing The structure of a column flotation cell is quite different from that of the mechanical (sub-aeration) cells which have by implication formed the basis of this presentation. In both, air bubbles are dispersed through a suspension of solids in water, but while in mechanical cell this is done with an aerating agitator, in column cells air is disper-

sed from the bottom of the pulp through a sparger. In mechanical cells the aspect ratio is such that the cross-section is of the same order as the height of the cell while in column cells the depth of the collection/bubbling zone (pulp) is much greater than the cross-section. For instance Yianatos, Finch and Laplante quote for the molybdenum column cleaner and recleaner cells, at the Noranda Mines, Gaspé in Quebec, cross-sections which are respectively 0.91 and 0.47 m square with overall heights of 12 m for both.

In the column cell the feed suspension is added near the top of the bubbling zone and the particles are free to settle. While they are settling they encounter the rising bubbles in a physical situation which is closer to that envisaged in the model of Flint and Howarth, than that in the strongly turbulent mechanical cells. The flow pattern of the rising gas bubbles and the settling solids approximates to plug flow whereas that in the mechanical cells is closer to perfectly mixed.

As with the subaeration/mechanical cells a froth phase forms above the aerated pulp/collection zone into which entrainment of water containing non-selectively separated solids occurs. In column cells, the inter-bubble water containing the unwanted

Table 6 The effect of froth structures on flotation kinetics and selectivity

Time (s)	Dry solids in sample (g)	Water in sample (g)	Cum ash (%w/w)	Mean bubble size (mm)	Sodium dodecyl sulfate concentration in water (μ molar)	Particle size d_{90} (μ m)
23.0	9.7	56.9	4.62	1.7	36.9	64.0
39.0	8.11	43.1	4.55	2.4	31.2	64.0
57.0	5.17	27.7	4.67	3.2	37.7	66.0
77.0	5.69	24.7	5.28	3.6	53.8	63.0
180.0	12.09	14.2	5.07	10.00	122.7	54.0
Tailings	6.76	–	57.6	–	6.69	35.0

Feed mass 49.5 g coal, feed ash 12.7%, total water 850.6 g, sodium dodecyl sulfate 0.05 mM. Reproduced with permission from Stockton J (1989) PhD thesis, UMIST, Manchester.

Table 7 The effect of froth structures on flotation kinetics and selectivity

Time (s)	Dry solids in sample (g)	Water in sample (g)	Ash (%w/w)	Mean bubble size (mm)	Sodium dodecyl sulfate concentration in water (μmolar)	Particle size d_{90} (μm)
20.0	14.0	108.0	6.37	0.76	153.0	52.0
30.0	13.1	78.6	5.8	1.16	78.0	49.5
45.0	7.3	99.3	6.9	1.63	133.0	44.0
60.0	3.6	85.9	7.85	1.86	128.0	47.0
80.0	2.4	79.4	8.7	1.83	125.0	40.0
100.0	1.65	71.9	9.5	2.39	109.0	41.0
130.0	1.00	55.1	10.09	3.0	115.0	43.0
300.0	0.6	50.8	10.54	5.0	134.0	33.0
Tailings	1.4	–	68.82	–	51.0	34.5

Feed mass 49.5 g coal, feed ash 12.7%, total water 850.6 g, sodium dodecyl sulfate 0.02 mM. Reproduced with permission from Stockton J (1989) PhD thesis, UMIST, Manchester.

solids is displaced by spraying solids-free wash water on to the upper froth surface.

Yianatos, Finch and Laplante reported laboratory and plant studies relating to the effectiveness of the displacement washing. For the plant tests these involved a broad step pulse injection of 200–600 g of LiCl tracer dissolved in 5 L of water into the feedbox. The feedbox was 35 cm below the collection zone/froth interface. Tracer concentrations were measured 100 cm below the injection point, 10 cm into the froth above the interface, from the overflowing concentrate at the top of the froth and from the tailings stream at the base of the cell.

In the 0.91 m² cross-section cell, a froth zone varying between 45 and 130 cm depth was reported while in the 0.45 m² cross-section cell the froth depth varied between 110 and 140 cm.

For all the runs reported virtually no tracer was detected in the overflowing concentrate, although at

high superficial gas rates of 2 cm s⁻¹ tracer was detected in the froth up to 70 cm above the interface. The tracer residence time distributions (RTD) after the pulse injection, at 35 cm below the froth interface, indicated significant mixing in the water between the

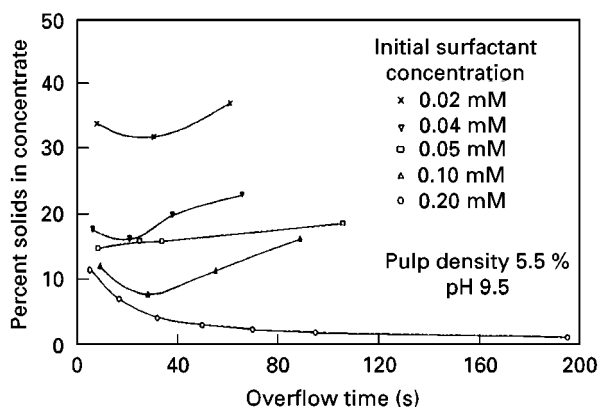


Figure 14 Percentage of coal solids in the overflowing concentrate at varying times during an individual test. The data are taken from the same tests reported in Figure 13. Reproduced with permission from Woodburn ET, Austin LG and Stockton JB (1994) A froth based flotation kinetic model. *Chemical Engineering Research and Design* 72(A2), 211–226.

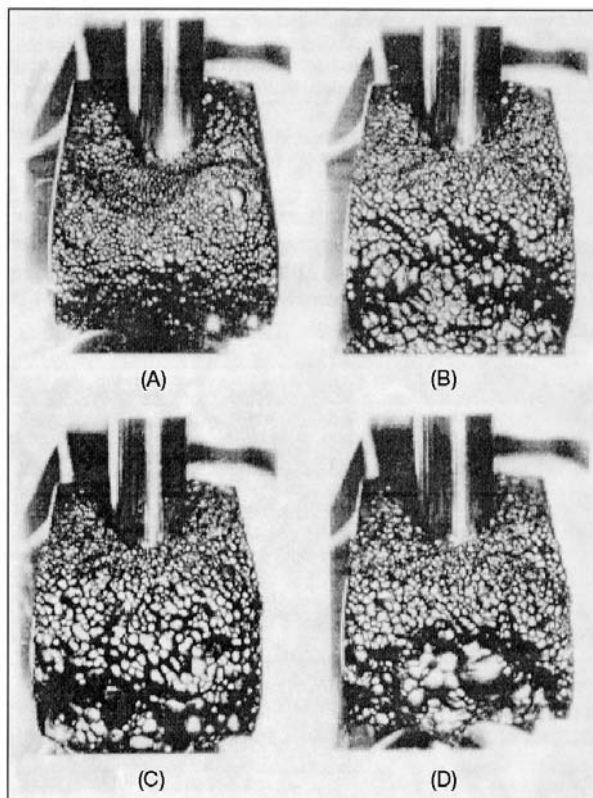


Figure 15 Photographs of overflowing coal concentrates. Single initial addition of 0.04 mmol L⁻¹ sodium dedecyl sulfate: (A) after 24 s – first concentrate, (B) after 43 s – second concentrate, (C) after 55 s – third concentrate, (D) after 81 s – fourth concentrate. Reproduced with permission from Woodburn ET, Austin LG and Stockton JB (1994) A froth based flotation kinetic model. *Chemical Engineering Research and Design* 72(A2), 211–226.

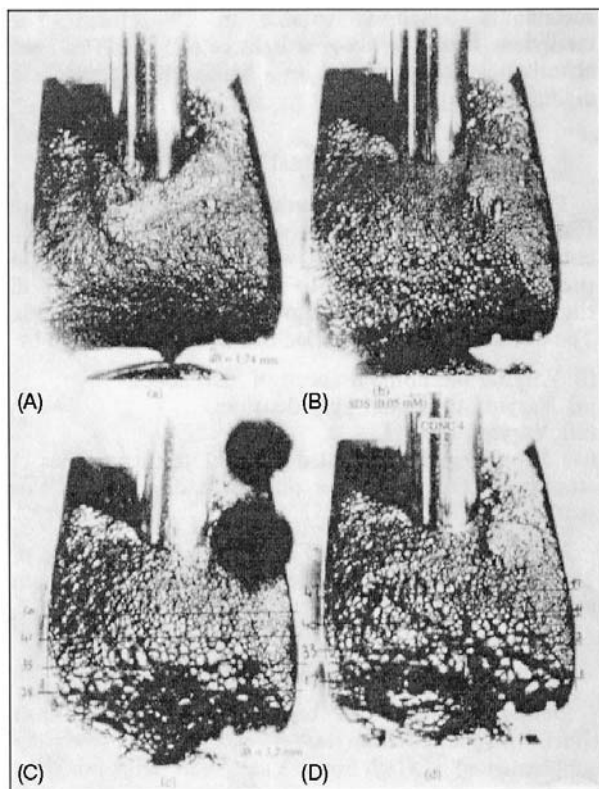


Figure 16 Photographs of overflowing coal concentrates. Single initial addition of 0.05 mmol L^{-1} sodium dedecyl sulfate: (A) after 31 s – first concentrate, average bubble diameter 1.74 mm; (B) after 50 s – second concentrate, average bubble diameter 2.35 mm; (C) after 66 s – third concentrate, average bubble diameter 3.2 mm; note 154 features identified on four lines; (D) after 92 s – fourth concentrate; note 137 features identified on four lines. Each line is 122 mm long. Reproduced with permission from Woodburn ET, Austin LG and Stockton JB (1994) A froth based flotation kinetic model. *Chemical Engineering Research and Design* 72(A2), 211–226.

feed point and the froth interface. Similarly, the tracer RTDs in the tailings stream showed significant axial mixing in the collection zone below the feed point.

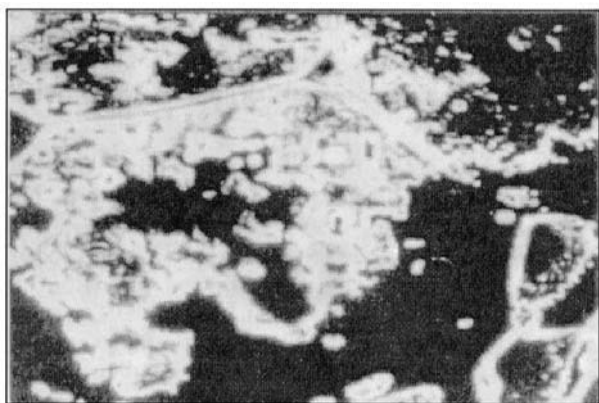


Figure 17 Image of the upper surface of coal-laden bubbles. Note the inter-bubble lamellae and plateau border.

For both cells the mean residence time of the tracer in the collection zone was approximately 10.0 min.

From these tests it seems that froth depths up to 100 cm may be needed to ensure complete removal of entrained solids from the final concentrate. These tracer studies are consistent with the high grades which are achieved in these cells.

There is a question relating to the capacity of column cells. The rate of flotation in both types of cell depends on the effectiveness of the bubble–particle collision and attachment processes. A key factor in the evaluation of these is the velocity of approach of the particle and the bubble. In the mechanical cells high approach velocities are achieved through the turbulence in the pulp. In column cells the approach velocity is determined by the bubble rise and particle settling velocities. For small particles, and hence small bubbles, these velocities are so low, that the collection zone must be impractically high if the necessary frequency of bubble–particle encounters is to be achieved. In industrial practice the column cells are most effective where high grades at low throughputs are required. This is particularly the case where previously produced concentrates have to be cleaned and re-cleaned.

Sam, Gomez and Finch have shown that the bubble rise velocity is reduced in the presence of surfactants over that in distilled water and further that the surfactant adsorption is a rate process. This retardation of the rising bubble appears to be a function of the surface immobility which in turn should improve attachment after a successful interception, by increasing the contact time with individual particles.

Tuteja, Spottiswood and Misra in reporting the reverse flotation of undesired talc from a gold-bearing pyrite ore, have shown that there is virtually no grade change with height in the collection zone but that there is a dramatic increase in the percentage of talc in the froth solids, increasing from 3% at the base of the froth to 50% at the concentrate overflow. At the same time the presence of an arsenic contaminant fell from 3750 ppm in the pulp solids to 750 ppm in the concentrate overflow.

Cell Design and Control

Outline of the Factors Influencing Single Cell Design

In general, the contractor is responsible for the engineering design of the cell, while the customer is responsible for the design of the separation system. This involves the selection of both chemical collectors, depressants and frothers and also the solution pH. The principles underlying these have been thoroughly discussed earlier.

In addition, the degree of pretreatment required to liberate the desired component from the waste, prior to the flotation separation, has to be decided. Obviously the two parties to the project have to interact and this is done in the first instance through laboratory and pilot plant trials, followed if possible by a large-scale plant trial.

The contractor's responsibility is to provide, within economic constraints, equipment in which dispersed bubbles of a specified size will be generated in the pulp, to achieve efficient bubble interception with particles of a specified density and size distribution. The fundamental considerations underlying this have been discussed earlier. There are two main types of equipment, which employ very different techniques for bubble-particle contact.

Mechanical sub-aeration cells In these cells the pulp is stirred vigorously by a centrally located agitator, on of whose functions is simply to prevent solids settling. In most cells the central agitator also induces air down an annulus surrounding its shaft and disperses the air radially as bubbles into the pulp. The intense turbulence generated by the agitator favours a high rate of bubble-particle collision, but also if the turbulent intensity is too high then previously attached particles may detach from the bubble surface.

The flow pattern in these cells divides into an intense inner region in the vicinity of the impeller, and a much larger less turbulent outer region in the bulk of the cell. In the relatively quiescent outer region the bubble-particle aggregates rise to form a froth. The cell design provides a sufficient depth between the pulp/froth interface and the overflow weir to permit drainage of some entrained solids. In commercial cells the froth can be removed by mechanical scrapers so froth mobility at the overflow is not usually a serious concern.

Finally, a class of cells should be mentioned in which specific attention is paid to achieving a high degree of bubble-particle contact without subsequent detachment. One example of this class of intensive cell, pumps the feed through a venturi nozzle which induces air under pressure into the low pressure region at the venturi throat. This causes bubbles to form which appear to nucleate on the solid particles.

Column cells In these cells particle-bubble interception occurs under low turbulent conditions essentially through particles settling under gravity meeting rising bubbles. The bubbles are introduced at the bottom of the collection zone through a sparger, and the feed particle suspension near the top of the collection zone. The low approach velocities of fine particles

settling slowly and bubbles rising against down-flowing water reduce the interception rates, thus requiring more possible contacting opportunities, leading to very deep collection zones.

At the top of the collection zone a froth bed forms, which itself may be deep with bed depths of over 1 m being reported. The column cells produce very high purity products, achieved largely by the displacement of entrained water after adding wash water to the upper froth surface.

Multiple Cell Circuits

Circuit configuration In industrial operation it is necessary to have many cells in operation if the desired upgrading of large quantities of low-grade feed is required. The cells are operated in banks in which the tailings stream from one cell moves in sequence to the next. However, the concentrates are withdrawn from each individual cell into a concentrate launder which runs parallel to the cell bank.

Each bank then produces a single concentrate and a single tailings stream. These streams may in their turn be reprocessed. Typically, the first bank in a circuit would be called the rougher. The tailings stream from the rougher is then fed to the scavenger bank whose function is to recover any residual valuable material which may not have been floated in the rougher.

The concentrate stream from the rougher is fed to the cleaner bank whose function is to improve its grade. Finally, it may be necessary further to upgrade the cleaner concentrate by sending it to a recleaner bank. The circuit is completed by internal recycling. The final product of the circuit is the cleaner (recleaner) concentrate and the scavenger tailings.

The chemical environment of a particular bank of cells is determined by the addition of chemicals and pH regulators to the feedbox of the first cell of the bank.

Kinetic modelling For the design of circuits, a description of the kinetics of particle removal of any given cell to the concentrate overflow is required. Attempts to develop such a model have centred on the transfer rate in terms of the local concentration of a solid class in the pulp. This requires a matrix of deterministic single rate constants characterizing each solid species and particle size class within that species. These parameters can be determined either from batch cell tests or from the performance of a single continuously operating cell. Even with a large dimension matrix of rate constants, the ability of the model to predict accurately circuit performances of operating plant, is limited. The fundamental weakness of this approach is that it treats the pulp and the froth as

one, ignoring the very different subprocesses affecting separation in each of the phases.

On-line control The difficulty of implementing on-line control is the necessity for off-line analysis of solid grades and to a certain extent off-line measurements of the mass flow of solids and water at different points in the circuit.

Informal operational control is performed by experienced operators following subjective comparisons of the appearance of overflowing froths, with a desired structure. The advantage of this approach is that the structure of the overflowing froth is easily observable and corrective actions can be rapidly implemented.

Currently several groups of academic workers are working on quantifying the froth characterization using on-line image analysis, with promising results. This is, of course, only a first step in the development of a feedback control system by which optimum operation can be effected.

This is an exciting development which can be anticipated with some confidence to lead to implement optimal control strategies.

See Colour Plates 10, 11.

Further Reading

Adamson AW (1982) *Physical Chemistry of Surfaces*, 4th edn. New York: John Wiley.
 American Institute of Chemical Engineers (1975) *Natural and Induced Hydrophobicity in Sulfide Mineral Systems*. AIChE Symposium Series, Vol. 71, No. 150. New York: AIChE.

Fuerstenau DW (ed.) (1962) *Froth Flotation, 50th Anniversary Volume*. New York: American Institute of Mining Metallurgical and Petroleum Engineers.

Fuerstenau DW and Healey TW (1972) *Adsorptive Bubble Separation Techniques*, Chap. 6. New York: Academic Press.

Fuerstenau MC (ed.) (1976) *Flotation. AM Gaudin Memorial Volumes I and II*. New York: American Institute of Mining Metallurgical and Petroleum Engineers.

King RP (ed.) (1982) *Principles of Flotation*, Monograph Series No. 3. Fuerstenau MC. *The Flotation of Oxide and Silicate Minerals*; Fuerstenau MC and Fuerstenau DW. *Sulphide Mineral Flotation*; Lovell VM. *Industrial Flotation Reagents*: (a) *Structural Models of Sulphydryl Collectors*, (b) *Structural Models of Anionic Collectors*, (c) *Structural Models of Frothers*. Johannesburg: South African Institute of Mining and Metallurgy.

Klassen VI and Mokrousov VA (1963) *An Introduction to the Theory of Flotation*. London: Butterworths.

The Interface Symposium (1964) *Attractive Forces at Interfaces. Industrial and Engineering Chemistry* Vol. 56, No. 12.

Laskowski JS (1989) *Frothing in Flotation: A Volume in Honor of Jan Leja*. New York: Gordon & Breach.

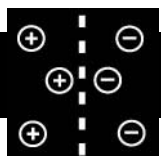
Laskowski JS (1993) *Frothers and Flotation Froths. Mineral Processing and Extractive Metallurgy Review*, Vol. 12. New York: Gordon & Breach.

Laskowski JS and Woodburn ET (eds) (1998) *Frothing in Flotation II*. Amsterdam: Gordon & Breach.

Leja J (1982) *Surface Chemistry of Froth Flotation*. New York: Plenum Press.

Sebba F (1987) *Foams and Biliquid Foams – Aphrons*. New York: John Wiley.

ION EXCHANGE



A. Dyer, University of Salford, Salford, UK

Copyright © 2000 Academic Press

Introduction

Ion exchange has been described as the oldest scientific phenomenon known to humanity. This claim arises from descriptions that occur in the Bible and in the writings of Aristotle, but the first truly scientific allusion to ion exchange is attributed to two English agricultural chemists in 1850. These were J. T. Way and H. S. Thompson, who independently observed the replacement of calcium in soils by ammonium ions. This discovery was the precursor to the study of inorganic materials capable of 'base' exchange, and in 1858 C. H. Eichorn showed that natural zeolite minerals (chabazite and natrolite) could reversibly exchange

cations. The importance of this property in water softening was recognized by H. Gans who, at the turn of the century, patented a series of synthetic amorphous aluminosilicates for this purpose. He called them 'permutites', and they were widely used to soften industrial and domestic water supplies until recent times, as well as being employed in nuclear waste treatment. Permutites had low ion exchange capacities and were both chemically and mechanically unstable.

This early work has generated some myths commonly stated in elementary texts, namely that zeolite minerals are responsible for the 'base' exchange in soils and that permutites are synthetic zeolites. The presence of clay minerals in soils accounts for the majority of their exchange capacity, and zeolites by definition must be crystalline. Both these topics will arise later in this article.

The emphasis started to change in the 1930s when the Permutit Company marketed organic ion exchange materials based on sulfonated coals, which had been known from about 1900. These were sold as 'Zeo-Karb' exchangers and, despite their low capacities and instability, were still available in the 1970s.

Ion exchanger production was radically altered by the discovery of synthetic resin exchangers by B. A. Adams and E. L. Holmes in 1935. They used a condensation polymerization reaction to create a granular material able to be used in columns and until very recently the majority of ion exchange has been carried out on resin-based materials. Sophisticated developments of novel resin exchangers (and inorganic materials), together with improvements in properties of commercial products, continue to be heightened by the extensive area that modern ion exchange interests cover. The process governs ion separations important to analytical techniques, large-scale industrial water purification, pharmaceutical production, protein chemistry, wastewater treatment (including nuclear waste) and metals recovery (hydrometallurgy). In addition it has a critical role in life processes, soil chemistry, sugar refining, catalysis and in membrane technology.

This article will attempt a modern overview of inorganic and organic ion exchange materials, including their properties and the development of new substrates. It will consider the theory of ion exchange together with its industrial and analytical importance. Its wider role in the other aspects mentioned above will also be briefly discussed.

What Is Ion Exchange?

Some Definitions

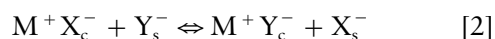
A broad definition of ion exchange is that it is the transfer of ions across a boundary; this would then cover movement of ions from one liquid phase to another. This is too broad a base for the purpose of this article, which will restrict itself to those exchanges of ions that occur between a liquid phase and a solid (organic or inorganic) that is insoluble in that liquid. A simple representation of the process when univalent cations are being transferred is given in the chemical equation [1] below:



Here $M^-A_c^+$ represents a solid carrying a negative charge ('solid anion', sometimes described as a 'fixed ion') neutralized by the A^+ ions inside its structure. The A^+ ions are replaced by B^+ originally in the solution phase (normally aqueous). The subscripts 'c' and 's' refer to the solid and solution phase, respec-

tively. The process must be totally reversible to fit the strict definition of ion exchange. However, in practice interference from other nonreversible events may occur. Examples of disruptive influences that may have to be faced are the imbibition of salt molecules, precipitation reactions, chelating effects, phase changes and surface sorption. Some of these will be mentioned later.

An equivalent stoichiometric equation can be written for the anion exchange process, as in eqn [2]:



Now M carries a positive charge ('solid cation' or 'fixed ion') and X and Y are exchanging anions moving reversibly between solid and liquid phases. The ion pairs, A , B and X , Y are called 'counterions'. An ion which is mobile and has the same charge as that of the solid exchanger is called a 'co-ion'.

The extent to which an exchanger can take up ions is called its 'capacity'. In the case of an organic resin exchanger, this can be related to the number of fixed groupings that have been introduced into the polymer as part of its synthesis to create ion exchange properties. These are known as 'ionogenic' groups and are either ionized, or capable of dissociation into fixed ions and mobile counterions. In an inorganic exchanger the ionogenic nature of the solid matrix arises from the presence of positive or negative charges on the solid (usually on an oxygen ion). These charges are a consequence of metal cations in the exchanger that are in nonexchangeable sites. Examples of these will be discussed later.

Recent workshops on ion exchange nomenclature have suggested that the ion exchange capacity is expressed as the concentration of ionizable (ionogenic) groups, or exchange sites of unit charge, per gram of dry exchanger. The units of concentration should be millimoles or milliequivalents per gram. This definition can be taken as the theoretical capacity – Q_0 .

The workshops also prefer the term 'loading' to describe the capacity experienced under the specific experimental conditions at which the ion uptake is being observed. This can be higher or lower than the theoretical capacity. Higher capacities can arise from electrolyte imbibition or surface precipitation, and lower capacities often arise in inorganic exchangers when all the sites of unit charge are not accessible to the ingoing ion. These circumstances will be considered later.

The suggested definition of loading is the total amount of ions taken up per unit mass, or unit volume, of the exchanger under clearly defined experimental conditions. The concentrations again should be given in millimoles or milliequivalents, but with

the option to relate this to mass *or* volume. An appropriate symbol would be Q_L .

It should be noted that this is a new approach, differing from the IUPAC recommendations of 1972, and is felt necessary because of the new interest in inorganic exchangers whose properties do not fit the IUPAC concepts.

The definition of capacity associated with column use remains unchanged. The 'breakthrough capacity' (Q_B) of a column is still best defined according to the IUPAC definition as the practical capacity of an ion exchanger bed under specified experimental conditions. It can be estimated by passing a solution containing the ion to be taken up through the column and observing the first appearance of that ion in the column (bed) effluent, or when its concentration in the effluent reaches a convenient, arbitrarily defined, value. Q_B can be expressed in units of millimoles, or milliequivalents, of wet, or dry, exchanger using volumes or mass as appropriate.

General Properties of Exchange Media

An ideal ion exchange medium is one that fulfils the following criteria:

1. a regular and reproducible composition and structure;
2. high exchange capacity;
3. a rapid rate of exchange (i.e. an open porous structure);
4. chemical and thermal stability and resistance to 'poisoning' as well as radiation stability when used in the nuclear industry;
5. mechanical strength stability and attrition resistance;
6. consistency in particle size, and compatibility with the demands of the use of large columns in industry.

In addition some applications demand the ability to exchange a specific ion(s) selectively from high concentrations of other ions. This is particularly true for aqueous nuclear waste treatment and in hydrometallurgy. In some of these applications ion exchangers with lower capacities can be effective.

The Theory of Ion Exchange

Ion Exchange Equilibria

When an ion exchange solid is allowed to reach equilibrium (checked by a prior kinetic experiment) with a solution containing two counterions, generally one ion will be taken up preferentially into the solid. The solid is then said to be exhibiting *selectivity* for the preferred ion. Selectivity can be quantified by the experimental construction of an ion exchange iso-

therm. At a fixed temperature solutions containing counterions A and B in varying proportions are allowed to equilibrate with known, equal, weights of exchanger in, say, the MA form. The total ionic concentration of the ions A and B in the respective solutions is kept constant, i.e. each solution has the same normality (N) but, as the concentration of B increases it is compensated by a decrease in concentration of A. At equilibrium the solids and liquids are separated and *both* phases analysed for A and B.

This enables an isotherm to be plotted that records the equilibrium distributions of one of the ions between the two phases. Examples of typical isotherms are shown in Figure 1. The selectivity shown by an isotherm can be quantified; a general example of cation exchange will be used to illustrate this. First eqn [1] will be rewritten for an exchange involving cations (A, B) of any charge, as in eqn [3]:



where $Z_{A,B}$ are the valences of the ions and the bar represents the ions inside the solid phase.

The axes of the isotherm record the equivalent fraction of the ingoing cation (A) in solution (A_s) against its equivalent fraction in the exchanger (A_z). These quantities are defined in eqns [4] and [5] below:

$$A_s = Z_A m_A / (Z_A m_A + Z_B m_B) \quad [4]$$

and:

$$\bar{A}_z = Z_A M_A / (Z_A M_A + Z_B M_B) \quad [5]$$

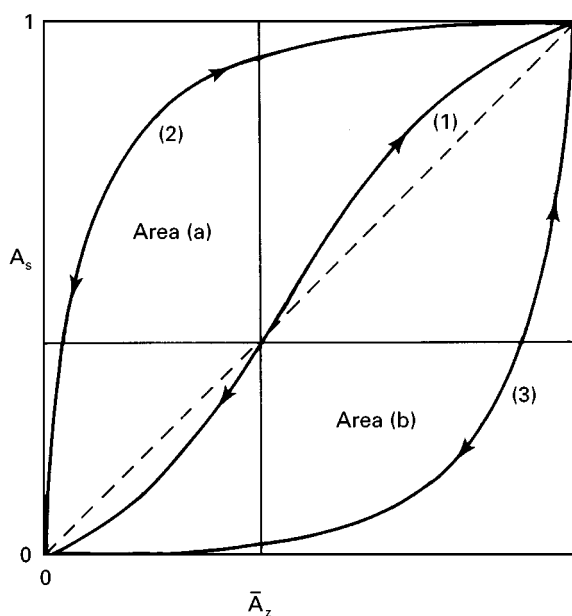


Figure 1 Idealized ion exchange isotherms (see text for details).

where $m_{A,B}$ and $M_{A,B}$ are the ion concentrations in mol dm^{-3} in solution and solid, respectively.

On Figure 1 the dashed line shows the case where the solid has an equal selectivity for ions A and B. The isotherm (3) describes the circumstance when A is selectively taken up, while isotherm (2) describes the circumstances when B is favoured by the exchanger.

A simple quantitative expression of the selectivity is via the selectivity factor (α) defined in eqn [6]:

$$\alpha = \bar{A}_C m_B / \bar{B}_C m_A \quad [6]$$

where by definition:

$$\bar{B}_C = 1 - \bar{A}_C \quad [7]$$

In Figure 1 α can be calculated from area (a) divided by area (b), illustrated for a typical isotherm (1).

Not all isotherms in the literature are constructed in the formal way described above. Often they arise from solutions containing only the ingoing ion placed in contact with the exchanger, only one ion is analysed in one phase, and various units of concentration are used. These simple approaches are still valid comparisons of *practical* selectivities, but when isotherms are needed to generate thermodynamic data the more rigorous experimental methodology must be followed. It is also necessary to demonstrate that the exchange being studied is fully reversible to allow the laws of mass action to be applied. When inorganic exchangers are involved it may be appropriate not to dry the solid before the reverse leg of the isotherm is constructed, as heating the solid can change the number of cation sites partaking in the exchange. This is particularly so for the zeolite minerals. In cases where organic resin exchangers are examined, the resin is used preswollen (fully hydrated) to avoid discrepancies caused by the resin expanding on initial contact with the solution phase.

Distribution Coefficients

Each point on an isotherm (simply or rigorously constructed) represents the distribution of ions between the solid and liquid phases. At each point a *distribution coefficient* (D_A) can be defined for the ion A as follows. D_A = concentration of A per unit weight of dry exchanger/concentration of A per unit volume of external solution.

The distribution coefficient is widely used as a convenient check of selectivity at fixed, pre-determined, experimental parameters. Equilibrium must have been achieved for this assessment to be valid.

Analysis of Isotherms to Provide Thermodynamic Data

For a fully reversible isotherm a mass action quotient (K_m) can be used to defined the process, as with any other reversible chemical process, namely:

$$K_m = A_Z^{Z_B} m_B^{Z_A} / B_Z^{Z_A} m_A^{Z_B} \quad [8]$$

From this the thermodynamic constant (K_a) can be determined using eqn [6]:

$$K_a = K_m \Gamma (f_A^{Z_B} / f_B^{Z_A}) \quad [9]$$

where:

$$\Gamma = \gamma_B^{Z_A} / \gamma_A^{Z_B} \quad [10]$$

γ_A and γ_B are the single ion activity coefficients of A^{Z_A} and B^{Z_B} , respectively, in solution, and $f_{A,B}$ are the activity coefficients of the same ions in the solid phase.

K_a can be determined by graphical integration of a plot of $\ln K_m \Gamma$ against \bar{A}_Z (or by an analytical integration of the polynomial that gives the computed best fit to the experimental data).

The quantity $K_m \Gamma$ can be described as:

$$K_c = K_m \Gamma \quad [11]$$

where K_c is the Kielland coefficient related to K_a by the simplified Gaines and Thomas equation:

$$\ln K_a = (Z_B - Z_A) + \int_0^1 \ln K_c dA_Z \quad [12]$$

Values for $\gamma_{A,B}$ cannot be determined, but Γ is available from the mean stoichiometric activity coefficients in mixed salt solutions via eqn [10]:

$$\Gamma = \gamma_B^{Z_A} / \gamma_A^{Z_B} = ([\gamma_{\pm BX}^{(AX)}]^{Z_A(Z_B + Z_X)} / [\gamma_{\pm AX}^{(BX)}]^{Z_B(Z_A - Z_X)})^{1/Z_X} \quad [13]$$

In eqn [13], Z_X is the charge on the common anion $\gamma_{\pm BX}^{(AX)}$, and $\gamma_{\pm AX}^{(BX)}$ can be calculated from $\gamma_{\pm BX}$ and $\gamma_{\pm AX}$ using the method of Glueckauf. $f_{A,B}$ values are available from the Gibbs-Duhem equation.

Having obtained K_a , a value of ΔG^θ can be gained from:

$$\Delta G^\theta = - (RT \ln K_a) / Z_A Z_B \quad [14]$$

where R and T have their usual meanings, and ΔG^θ is the standard free energy per equivalent of charge.

The standard states of the exchanger relate to the respective homoionic forms of the exchanger immersed in an infinitely dilute solution of the corresponding ion. This implies that the water activity in the solid phase in each standard state is equal to the water

activity in the ideal solution, and that the standard states in the solution phase are defined as the hypothetical ideal, molar (mol dm^{-3}) solutions or the pure salts according to the Henry Law definition of an ideal solution.

At this point it should be commented that this approach is based on a simplified Gaines and Thomas treatment. In the complete version of eqn [12] the LHS should be $\ln K_a - \Delta$, where Δ is a water activity term. For most selectivity studies the ΔG^θ values measured using the simplified treatment are adequate.

To obtain a *selectivity series*, isotherms should be constructed for a homoionic exchanger initially in, say, sodium form in contact with solutions of ingoing ions (for instance Li, K, Rb, Cs). This yields ΔG^θ values that, when arranged in order of decreasing negativity, provide an assessment of the affinity the exchanger has for the alkali metals.

Ion Exchange Kinetics

When an exchanger is in contact with a solution of exchanging ions the rate of exchange can be rate controlled by one of three steps:

1. *film diffusion* – controlled by the rate of progress of an ion through a film of water molecules, which by virtue of the surface charge on the exchanger can be regarded as ‘stagnant’ (the Nernst layer);
2. *particle diffusion* – controlled by the progress of ions inside the exchanger;
3. *chemical reaction* – controlled by bond formation. Examples of this process are not simple to define but the most often cited case is when chelating *ionogenic* groups, present in an ion exchange organic resin, are able to form strong bonds with, say, a transition metal ion to create a very specific extractant.

The three possible steps are illustrated in **Figure 2**.

Distinction between *film* and *particle* control can be made from the following criteria.

- *Film diffusion* is affected by the speed of stirring in a batch exchange (or the rate of passage of liquid through a column of exchanger). The rate of diffusion will directly depend upon the total concentration in the external solution.
- *Particle diffusion* has a rate that is dependent on the particle size, and is independent of both stirring speed and external solution concentration.

Kressman has devised a simple *interruption* test to distinguish between *film* and *particle* control. The exchange being studied is interrupted for a short

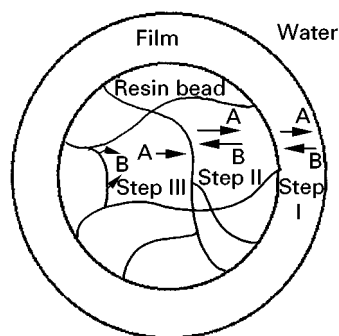


Figure 2 Possible rate-determining steps in an ion exchange process. Step I, diffusion of ions through a surface film. Step II, diffusion through the solid exchanger. Step III, formation of chelate bond at the ionogenic group.

period of time by separating the liquid and solid phases. The phases are then recombined to recommence the exchange. Provided that the exchange is remote from equilibrium at the time of interruption, diagnostic rate profiles will ensue. The *film*-driven process will have an undisturbed profile, whereas the *particle*-driven step will have attained a partial equilibrium even in the absence of an external driving force. The different profiles observed when fractional attainments of equilibrium with time are plotted are illustrated in **Figure 3**.

Rate Equations

When diffusion is the rate-controlling step, in principle an equation can be written to elucidate experimentally derived plots of the fractional attainment of equilibrium with time for an ion exchange process. In practice this is difficult to achieve because the movement of one counterion (A) is coupled to the other (B), and this must be taken into account in both *film*- and *particle*-controlled exchange. A further complication arises in that water fluxes can play a significant part in affecting rates of exchange, especially for cations in the solid phase.

Detailed discussions on the appropriateness of the many equations available for kinetic interpretation of ion exchange results is beyond the scope of this article, and interested readers should consult the sources provided in the Further Reading section for further information.

So far as column data are concerned, the usual experiment method is to obtain a breakthrough curve, like those shown in **Figure 4**, where the appearance of the ingoing ion in the effluent is plotted against the volume of solution passed through the column. The effectiveness of the exchange can then be simply quantified in terms of the number of ‘bed-volumes’ passed through the column before the ingoing ion is detected in the effluent. This

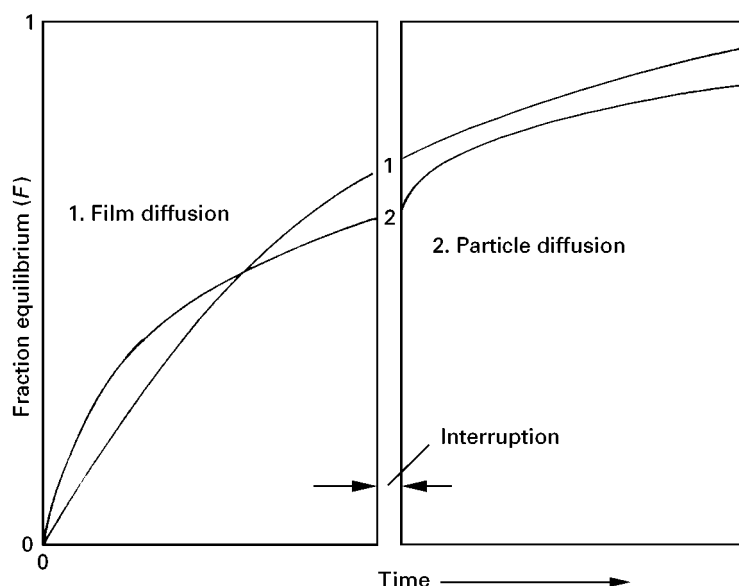


Figure 3 The effect on the shape of the ion exchange profile caused by interrupting the time of exchange. (Reproduced from Harland, 1994, with permission.)

requires that the profile is reasonably sharp so that the breakthrough point can be estimated. The shape of the profile is a function of the selectivity; when $K_A^B \gg 1$, $\alpha_A^B \gg 1$, the exchange front is sharp, and conversely when K_A^B , $\alpha_A^B \ll 1$ the front is more ill-defined (see Figure 4).

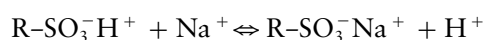
Ion Exchange Materials

Organic Resins

These are the most widely used of exchangers. They are made by addition polymerization processes to

produce resins capable of cation and anion exchange. There is much on-going research devoted to devising synthetic routes to new resins aimed at the refinement of their capabilities, but the bulk of commercial production follows well-established routes.

Polystyrene resins Ethenylbenzene (styrene) readily forms an addition polymer with divinylbenzene (DVB) when initiated by a benzoyl peroxide catalyst. The polymerization process can be controlled to produce resins with various degrees of cross-linking as robust, spherical, beads. The ability to vary the extent of cross-linking increases the range of possible applications by altering the physical and chemical nature of the beads. In addition the production process can be moderated to give beads of closely controlled particle size distribution, a requirement for the industrial use of resins in large columns. Subsequent treatment of the styrene-DVB copolymer beads can introduce ion exchange properties. If the beads are treated with hot sulfuric acid the aromatic ring systems will become sulfonated, thereby introducing the sulfonic acid functional group ($-\text{SO}_3\text{H}$) into the resin. When the treated resins are then washed with sodium hydroxide or sodium chloride, the sodium form of the resin (R) is produced, namely:



The sodium form is used as a strong acid cation exchanger, the sodium ion being the ion for which the resin has least selectivity.

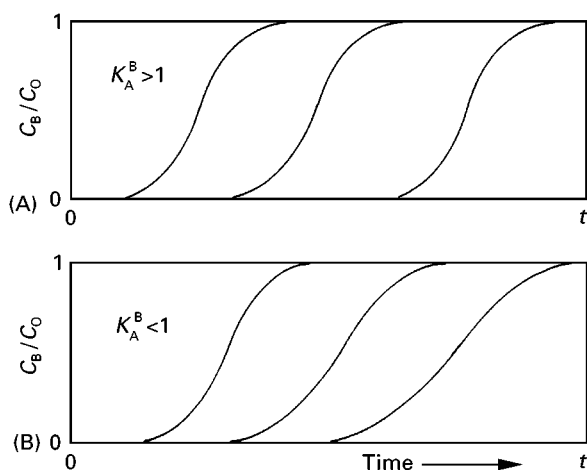


Figure 4 Breakthrough curves. (A) Favourable equilibrium, $K_A^B > 1$, shape of profile constant throughout the bed. (B) Unfavourable equilibrium, $K_A^B < 1$, edge of profile becomes more spread out with time. (Reproduced from Harland, 1994, with permission.)

Anion functionality can be introduced by a two-step process. The first step involves a chloromethylation using a Friedel–Crafts reaction between the copolymer and chloromethoxymethane with an aluminium chloride catalyst. The second step is to react the chloromethyl groups ($-\text{CH}_2\text{Cl}$), introduced into the styrene moieties, with an aliphatic amine. If this is trimethylamine, $(\text{CH}_3)_3\text{N}$, then the functional group produced on the resin is $\text{R}-\text{CH}_2\text{N}(\text{CH}_3)_3^+\text{Cl}^-$, and the resin is said to be a Type I strongly basic anion exchanger. The use of dimethylethanolamine $[(\text{CH}_3)_2(\text{C}_2\text{H}_4\text{OH})\text{N}]$ to react with the chloromethyl groups yields a resin with the functional group $\text{R}-\text{CH}_2\text{N}(\text{CH}_3)_2(\text{C}_2\text{H}_4\text{OH})^+\text{Cl}^-$, which is a Type II strong base anion exchanger. When methylamine, or dimethylamine, are used weakly basic resins are obtained, with the respective functional groups $\text{R}-\text{CH}_2\text{NH}(\text{CH}_3)$ and $\text{R}-\text{CH}_2\text{N}(\text{CH}_3)_2$.

Acrylic resins DVB forms polymers suited to ion exchange with materials other than styrene. The most commonly used are its copolymers with propenoic (acrylic) monomers. The use of methylpropenoic acid gives a weakly basic cation exchange resin ($\text{R}-\text{C}(\text{CH}_3)\text{COOH}$). Substituted propenoic acid monomers, propenenitriles (acetonitriles), and alkyl propenoates (acrylic esters) have all been used to make weakly basic resins. The acrylic matrix can also play host to anion functionality. Incorporation of dimethylaminopropylamine (DMAPA) produces a weak base resin, while the employment of a subsequent chloromethylation step converts this to a strong base functionality. Acrylic resins can be used to develop a material with simultaneous properties of a weak and strong base. These are called bifunctional anion exchangers. The equivalent bifunctional cation exchanger is not now commercially available, although products of this sort have been marketed in the past. The acrylic resins have advantageous kinetic and equilibrium properties over the styrene resins when organic ions are being exchanged.

Selective resins The resins described above have been developed as nonselective exchangers, where

the aim is to reduce the ionic content of an aqueous media to a minimum, such as is required in the ‘polishing’ of industrial boiler waters to reduce corrosion.

The flexibility offered by the skill of the synthetic organic chemist facilitates the introduction of specific groups into the polymer matrix to give the resulting exchanger the ability to take up an ion, or a group of ions, in preference to other ions. An example of this is the incorporation of the iminodiacetate group ($-\text{CH}_2\text{N}(\text{CH}_2\text{COO}^-)_2$) in a styrene-based matrix, which is then able to scavenge Fe, Ni, Cu, Co, Ca, Mg cations with the exclusion of other ions present. The iminodiacetate group is then described as a selective ionogenic group; further examples of these are given in Table 1.

Resins of this sort are continually being developed for specialist applications. The example in Table 1 of the use of a phenolic ionogenic group to pick up caesium has arisen from the nuclear industry. In this case a phenol-formaldehyde copolymer is used to meet the temperature and radiation stability needs of that industry.

The interaction between a selective ionogenic group and a cation probably will not be strictly ionic. Often there has been a deliberate intent to induce chelating effects to achieve the desired selectivity. If this has happened, then the rate-controlling step for progress of cations into the resin is likely to be the formation of a chemical bond, as mentioned earlier, rather than a diffusion process. When the cation would not be expected to form strong chelate bonds with the *ionogenic group*, such as the caesium cation mentioned above, then the nature of the rate-determining step is less clearly defined. If a thermodynamic approach to a specific exchange process is wanted these facts must be considered. Clearly a true chelating process will not be reversible and the theories of ion exchange, which are reliant on the application of reversible thermodynamics, cannot be invoked.

This introduces a grey area into the study of the uptake of ions onto a substrate supposedly capable of ion exchange. The problem often arises in the study of inorganic ion exchange materials – particularly oxides and hydroxides when uptake is pH-dependent,

Table 1 Examples of ionogenic groups and their selectivity

Matrix	Group	Selectivity
Styrene-DVB	Iminodiacetate $-\text{CH}_2-\text{N}(\text{CH}_2\text{COO}^-)_2$	Fe, Ni, Co, Cu, Ca, Mg
Styrene-DVB	Aminophosphonate $-\text{CH}_2-\text{NH}(\text{CH}_2\text{PO}_3)^{2-}$	Pb, Cu, Zn, UO_2^{2+} , Ca, Mg
Styrene-DVB	Thiol; thiocarbamide $-\text{SH}; -\text{CH}_2-\text{SC}(\text{NH})\text{NH}_2$	Pt, Pb, Au, Hg
Styrene-DVB	<i>N</i> -Methylglucamine $-\text{CH}_2\text{N}(\text{CH}_3)[(\text{CHOH})_4\text{CH}_2\text{OH}]$	B (as boric acid)
Styrene-DVB	Benzyltriethylammonium $-\text{C}_6\text{H}_4\text{N}(\text{C}_2\text{H}_5)_3^+$	NO_3^-
Phenol-formaldehyde	Phenol : phenol-methylenesulfonate $-\text{C}_6\text{H}_3(\text{OH}), -\text{C}_6\text{H}_2(\text{OH})\text{CH}_2\text{SO}_3^-$	Cs

and surface deposition of metal oxides and salts can occur. In many cases workers have found that the use of Freundlich isotherms (or similar treatments) can be successfully used to describe ion uptake.

Resin structures The traditional resins made as described above have internal structures created by the entanglement of their constituent polymer chains. The amount of entanglement can be varied by controlling the extent to which the chains are cross-linked. When water is present, the beads swell and the interior of the resin beads resembles a gel electrolyte, with the ingoing ion able to diffuse through regions of gel to reach the ionogenic groups. The ions migrate along pathways between the linked polymer chains that are close in dimension to the size of hydrated ions (cations or anions). This means that the porosity that they represent can be described as microporous. It is not visible even under a scanning electron microscope, as illustrated in **Figure 5**, and cannot be estimated by the standard methods of porosity determination, such as nitrogen BET or porosimeter measurements.

The tightly packed nature of these gel-type resins increases the chance of micropore blockage in applications where naturally occurring high molecular weight organic molecules (e.g. humic and fulvic acids) are present in water. This organic fouling was present in the earlier anion exchangers and led to the development of a new type of resin with more open internal structures. This was achieved by two routes, the sol and nonsol route.

In the sol method a solvent capable of solvating the copolymer is introduced into the polymerization pro-

cess. If the cross-linking is high (about 7–13%), pockets of solvent arise between regions of dense hydrocarbon chains. When the solvent is subsequently removed by distillation, these pockets are retained as distinct pores held by the rigidity arising from the cross-linking. In the nonsol method the organic solvent does not function as a solvent for the copolymer, but acts as a diluent causing localized regions of copolymer to form. These regions become porous when the diluent is removed.

These resins are termed macroporous, and the extent of their regions of porosity can be readily measured by porosity techniques and are visible in scanning electron micrographs (see **Figure 6**). Some literature describes them as macroreticulate because the pores they contain cover a much wider pore size distribution than the conventional International Union of Pure and Applied Chemistry (IUPAC) definition of a macroporous material. The IUPAC definition is traditionally related to inorganic materials where a macropore is one of greater than 50 nm in width. **Figure 7** illustrates the envisaged pore structure of a macroporous resin.

Macroporous resins are commercially available with acrylic and styrene skeletons, both cation and anion, carrying all types of functional groups. Their successful development has spawned two other major uses of acrylic and styrene resins that need highly porous media to function properly. These are the employment of resins as catalysts, and their use in the separation and purification of vitamins and antibiotics. Although these are of high industrial significance, they fall outside the intent of this article and will not be considered further.



Figure 5 Scanning electron micrograph of the internal surface of a gel resin. Magnification $\times 17000$. (University of Manchester Electron Microscopy Unit, courtesy of Hoechst Celanese Corporation.)

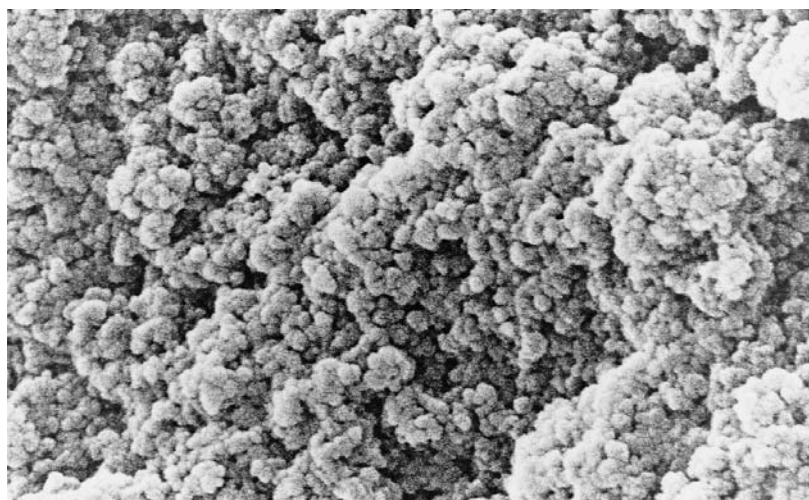


Figure 6 Scanning electron micrograph of the internal surface of a macroporous resin. Magnification $\times 17\,000$. (University of Manchester Electron Microscopy Unit, courtesy of Hoechst Celanese Corporation.)

Inorganic Ion Exchange Materials

Classification There are countless inorganic substances for which ion exchange properties have been claimed. Unfortunately a large number of these reports lack essential details of a reproducible synthesis, proper characterization and checks for reversibility. It is clear that many of the materials are amorphous and are often obtainable only as fine particles unsuited for column use. These pitfalls notwithstanding, there are many instances when inorganic exchangers are highly crystalline, well-characterized compounds, as well as instances when they can be made in a form appropriate for column use (even when amorphous). It also needs to be said that even a poorly defined ion exchanger may still be invaluable to scavenge toxic moieties from aqueous environments. This circumstance is valid in the treatment of aqueous nuclear waste and often drives the less rigorous studies mentioned earlier.

The traditional classification of inorganic ion exchange materials is:

- hydrous oxides
- acidic salts of polyvalent metals
- salts of heteropolyacids
- insoluble ferrocyanides
- aluminosilicates.

A more modern overview tends to blur some of these classes, but they still serve their purpose here with an addendum for the more recent materials of interest.

Hydrous oxides The compounds described in this section are 'oxides' precipitated from water. They retain OH groups on their surfaces and usually have loosely bound water molecules held in their structures. They can function either as anion exchangers, via replaceable OH^- groups, or as cation exchangers, when the OH groups ionize to release H^+ (H_3O^+) ions. The tendency to ionize depends on the basicity

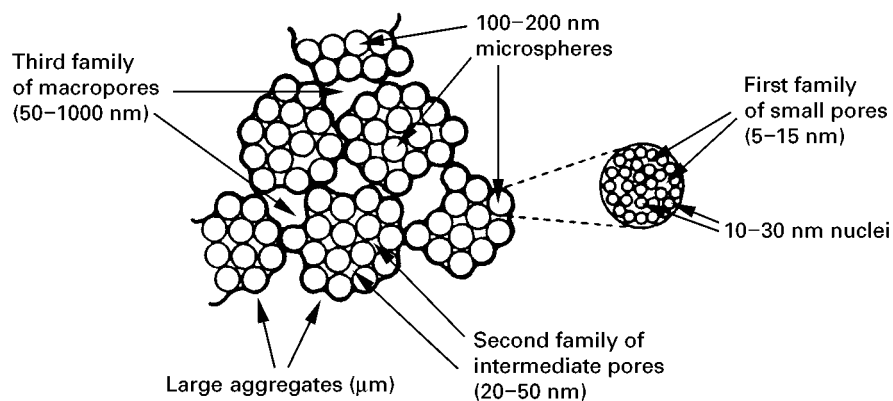


Figure 7 Schematic representation of the pores present in a macroporous resin. (Reproduced from Dyer *et al.*, 1997, with permission.)

of the metal atom attached to the OH group, and the strength of the metal-oxide bond relative to the O-H bond. Some materials are able to function as both anion and cation exchangers, depending upon solution pH, i.e. they are amphoteric. Capacities lie in the range 0.3–4.0 meq g⁻¹.

Hydrous oxides of the divalent metals Be, Mg, Zn have exchange properties, usually anionic, often in combination with similar materials derived from trivalent metals.

The most well-known trivalent hydrous oxides are those of iron and aluminium. Both produce more than one hydrous oxide. Examples of the iron oxides are the amorphous substances α -FeOOH (goethite), β -FeOOH, and γ -FeOOH (lepidocrocite). The similar compounds which can be prepared from aluminium are complex, and have been thoroughly researched because of their use as catalyst support materials and chromatographic substrates. Those that exhibit exchange are α -Al₂O₃, α -Al OOH and α -Al(OH)₃. Certain of the Fe and Al oxides are amphoteric; **Figure 8** demonstrates this via a pH titration. This is a common method of study for inorganic exchangers of this type, as well as those in the other classes which contain exchangeable protons. Other trivalent oxides with exchange properties are known for gallium, indium, manganese, chromium, bismuth, antimony and lanthanum.

Amphoteric exchange is known in the hydrous oxides of the tervalent ions of manganese, silica, tin, titanium, thorium and zirconium. Silica gel is particularly well studied because of its use as a chromatographic medium. It has weak cation exchange capacity (1.5 meq g⁻¹ K⁺ at pH 10.2) and can function as a weak anion exchanger at pH ~ 3. Zirconia and titania phases also have been the subject of much interest, particularly for nuclear waste treatment, and manganese dioxide is unique in its high capacity for strontium isotopes.

Hydrous oxides of elements of higher valency are known but only one has merited much study namely, antimony oxide (also called antimoninic acid and hydrated antimony pentoxide, or HAP). This exists in crystalline, amorphous and glassy forms and is an example of a material that is amenable to a reproducible synthesis. It can also be well characterized by, for example, X-ray diffraction and infrared spectroscopy. Many proposed applications have been suggested, especially based on the separations of metals that can be carried out on crystalline and other forms. An example of this is the ability of the crystalline phase selectively to take up the alkaline metals from nitric acid solution where the selectivity sequence is Na > Rb > Cs > K >> Li. HAP has the sequences Na > Rb = K > Cs in nitric acid, Na > Rb >

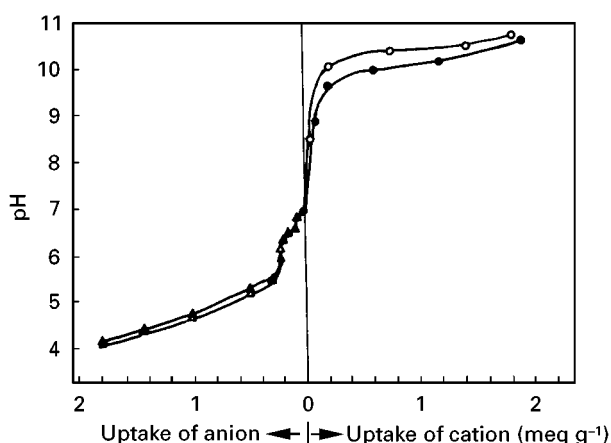


Figure 8 Titration curve for the titration of a commercial alumina with 0.02 mol L⁻¹: ○, LiOH; ●, KOH; △, HCl; ▲, HNO₃. (Reproduced from Clearfield, 1982, with permission.)

Cs > K in hydrochloric acid. This unique ability to selectively take up sodium finds wide use in neutron activation analysis where the presence of sodium isotopes is a constant hindrance to the γ -spectroscopy vital to the sensitivity of the technique. This is particularly important in environmental and clinical assays.

Acidic salts of polyvalent metals

Amorphous compounds The recognition that phosphates and arsenates of such metals as zirconium and titanium have ion exchange capabilities can be traced back to the 1950s. Around that time studies into the possible benefits of inorganic materials as scavengers of radioisotopes from aqueous nuclear waste were being initiated and amorphous zirconium phosphate gels were developed for that purpose, and used on a plant scale.

Later similar products of thorium, cerium, and uranium were studied, and also the analogous tungstates, molybdates, antimonates, vanadates and silicates. These compounds turn out to be of limited interest, and value because of the inherent difficulties in their sound characterization. In addition they often have a liability to hydrolyse, and these difficulties prompted the search for more crystalline phases of related compounds.

Polyvalent metal salts with enhanced crystallinity The most success in producing crystalline, reproducible and characterizable compounds has been in the layered phosphates exemplified by those of zirconium and, to a lesser extent, titanium.

Zirconium phosphates Extensive refluxing of zirconium phosphate gel in phosphoric acid, or direct precipitation from HF, yields a layered material

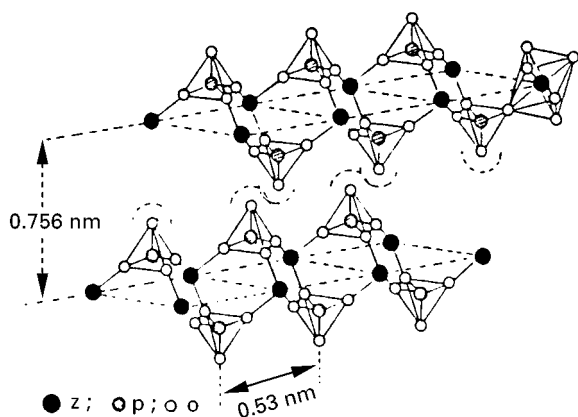


Figure 9 Schematic diagram of adjacent layers of α -ZrP; inter-layer water and protons not included. (Reproduced from Williams and Hudson, 1987, with permission.)

with a diagnostic X-ray diffraction pattern. Its stoichiometry corresponds to $\text{Zr}(\text{HPO}_4)_2 \cdot \text{H}_2\text{O}$ -zirconium bis(monohydrogen orthophosphate) monohydrate, with an exchange capacity of 6.64 meq g^{-1} . It has been designated as an α -phase and given the shorthand notation ' α -ZrP'. Its idealized structure is shown in **Figure 9**; the layers form a series of cavities in which reside protons and water molecules.

Potentiometric titration demonstrates that the structural unit shown above has two replaceable protons. Detailed studies of its cation exchange properties have been done, including determinations of the thermodynamic quantities for the exchange of the protons for most common metals—especially those of Groups 1 and 2. An interesting feature of these studies is the finding that the layer structure expands to accommodate monovalent ions, with the interlayer spacing being a function of ionic radius and water content. Intermediate 'half-full' phases are stable and well characterized. When the divalent ions of the alkaline earths are the ingoing ions a size restriction operates that is a complex function of the hydrated ion size and instability to shed water of hydration.

For these reasons calcium and strontium exchanges proceed, but magnesium and barium exchanges are very limited (if at all). If, however, α -ZrP is first converted to a half-exchanged sodium form, then Mg and Ba phases can be obtained.

Selectivity series have been constructed, with the half-exchanged Na phase (α -NaH ZrP $\cdot 5\text{H}_2\text{O}$) as the initial exchanger, for the alkali metals and the divalent cations of first row transitional elements. They are: $\text{K} > \text{Cs} > \text{Na} > \text{Li}$, and $\text{Cu} > \text{Zn}$, $\text{Mn} > \text{Fe} > \text{Co} > \text{Ni}$. Exchange into ZrP (amorphous and crystalline) from fused salts gives a selectivity series $\text{Li} \gg \text{Na} > \text{K}$.

A more hydrated phase of zirconium phosphate has been prepared with the formula $\text{Zr}(\text{HPO}_4)_2 \cdot 2\text{H}_2\text{O}$, designated γ -ZrP. It has a different arrangement of layers, with the phosphate groups being sited above each other rather than being staggered as in the α -phase (**Figure 9**). γ -ZrP also exchanges protons in two stages, creating half-exchanged materials; the replacement of the first proton takes place at about pH 2–3, and the second above pH 7.

Alkali metal ion selectivities are in the following order at low pH: $\text{K} > \text{Rb} > \text{Na} > \text{Cs} > \text{Li}$, but at high pH this becomes $\text{Li} > \text{Na} > \text{K} > \text{Rb}$. Recently a novel γ -phase containing mixed zirconium phosphate/phosphite layers has been synthesized. This has one replaceable proton, and hence a lower capacity for cation exchange (3.3 meq g^{-1}) than the other layered materials described in this section.

Other layer compounds Layered phosphate materials of the α type have been prepared for titanium, tin and hafnium. Arsenates of tin, titanium and zirconium with similar structures also are known. Only titanium and zirconium phosphates have γ -phases. **Table 2** illustrates the interlayer spacings of α - and γ -phases of tetravalent acid salts.

Intercalates A considerable body of work exists in which workers have shown that layered substances derived from salts of tetravalent acids can readily expand their layers to accommodate organic molecules capable of protonation. They include amines, alcohols, amino acids and metallocene derivative and they have large interlayer distances. **Figure 10** shows the formation of intercalation compounds of α -ZrP containing *n*-alkyl-monoamines.

Other salts of polyvalent acids Cerium phosphate readily precipitates as a fibrous material that can be formed into sheets. This material has attracted interest,

Table 2 Tetravalent acid salts with their interlayer distances

Compound	Interlayer distance (nm)
α-Salts	
Titanium phosphate	0.756
Zirconium phosphate	0.756
Hafnium phosphate	0.756
Germanium phosphate	0.760
Tin phosphate	0.776
Lead phosphate	0.780
Titanium arsenate	0.777
Zirconium arsenate	0.778
Tin arsenate	0.780
γ-Salts	
Zirconium phosphate	1.22
Titanium phosphate	1.16

both as an inorganic ion exchange paper and as a thin-layer material for the separation of inorganic ions. Cerium phosphate can also be prepared in robust granules for column use. Cerium phosphate is semicrystalline, as are the fibrous forms of thorium phosphate, titanium phosphate and titanium arsenate, which have also been prepared.

Salts of heteropolyacids These are the well-known salts of the parent 12-heteropolyacids, having the general formula $H_mXY_{12}O_{40} \cdot nH_2O$, where $m = 3-5$, $X = P, As, Si, Ge$ or B , and $Y = Mo, W, V$ (and others). Their structures have been known from the early days of X-ray single crystal analysis, and are examples of three-dimensional assemblages of linked $[XO_4]^{4-}$ tetrahedra and $[YO_6]^{6-}$ octahedra. The resulting frameworks contains voids large enough to contain replaceable cations.

The two most studied salts are the molybdophosphates and the tungstophosphates. Until recently it was thought that exchange was facilitated by the presence of water in the framework voids, but it now seems that ammonium molybdophosphate (AMP) is anhydrous and that any water noted as present 'as-synthesized' is contained in the solid by capillary condensation. This means that entering cations must be stripped of hydration water. AMP was one of the first inorganic materials to be used to scavenge radiocaesium from aqueous nuclear waste on a plant scale. Ammonium tungstophosphate (ATP) has a similar selectivity. A large number of organic salts of these acids have been synthesized, e.g. di-, tri- and tetramethylammonium 12-molybdophosphate and pyridinium 12-tungstophosphate.

Insoluble ferrocyanides A variety of compounds have been reported with metal cations held in a framework of linked $[FeCN_6]^{4-}$ octahedra. They include those with mixed metal hexacyano anions, and when cobalt is included in the composition a useful exchanger is obtained.

The product can be written as $K_{2(1-x)}Co_x[CoFe(CN)_6]_x \cdot \gamma H_2O$. When $x = 0.6-0.7$, a stable granular material results that has a high selectivity for caesium. It is used to scavenge caesium radioisotopes from waste emanating from the Lovissa Nuclear Power Plant, Finland.

Several other compounds of this type are being investigated for nuclear waste management, and include the potassium and sodium forms of nickel and copper hexacyanoferrates. In these hexacyanoferrates the exchange is restricted to the surface of the exchanger, but even this restriction still gives an adequate caesium capacity (0.35 mmol g^{-1}) and acceptable kinetics.

Aluminosilicates

Clay minerals These are another group of compounds whose structures have been studied since the earliest days of X-ray crystallography. Their structures are composed of layers of linked polyhedra, and a convenient subdivision of their structural types is into those with:

1. single layers;
2. nonexpandable double layers;
3. expandable double layers.

The most common single-layered clays are the kaolins. These have layers of $[SiO_4]^{4-}$ tetrahedra linked by three corners to create sheets. Between these layers are aluminium ions held to the fourth corners of the $[SiO_4]^{4-}$ tetrahedra that provide, on average, three hydroxyls from one layer and one hydroxyl plus two oxygens from the next layer. This results in another layer of hexagonally coordinated aluminium ions resembling those of gibbsite, a natural aluminium hydroxide mineral. In these clays ion exchange can take place at structural defects (broken bonds), or at exposed (edge) hydroxyls. The possibility also exists that a small amount of Al^{3+} , or Fe^{3+} , can isomorphously replace silicon from some tetrahedral

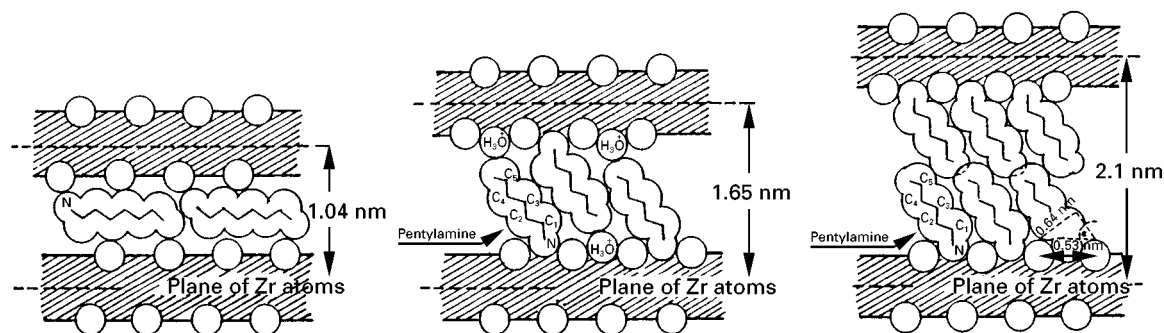


Figure 10 Arrangement of *n*-alkyl monoamines in α -ZrP, illustrating the change in interlayer spacing with increased loading. (Reproduced from Williams and Hudson, 1987, with permission.)

environments. The presence of $[\text{FeO}_4]^{5-}$ entities confers a negative charge on the silica layers, which can then be compensated by exchangeable cations sited between the layers.

Whatever the mechanisms whereby cations are accommodated into single-layer clays, their exchange capacities are low. The minerals can also exhibit a low anion capacity via labile hydroxyl groups.

In double-layered clays the element of structure is that of two sheets of tetrahedra separated by cations. The unexpandable double layer aluminosilicates, like the micas, have isomorphous substitution of aluminium for silicon in the double layers. This creates strong ionic bonding between the negatively charged layers and the interlayer cations. The cations are in an environment virtually water free so ion exchange is difficult, and confirmed mainly to defect and edge effects. The micas, and similar minerals, are examples of exchangers where the potential cation ion exchange capacity, expected from their stoichiometry, is not experimentally achieved. The need for the concept of loading is thereby illustrated.

In the expandable double-layered silicates hydrated cations are held in interlayer positions by weak electrostatic forces between their hydration shells and the silica sheets. Some isomorphous substitution in the tetrahedral layers is present but does not have a major effect on ion exchange behaviour. The loosely held cations are readily exchanged, and the interlayer distance changes as a function of hydrated cation size. Further ingress of solvent is easy. More water, or even organic molecules such as glycols, can penetrate the layers to further swell the structure. Montmorillonites are typical expanding double-layered clays. Examples of cation capacities for the clay minerals are listed in Table 3.

The ability of clays to act as exchangers is, of course, a major property of soils related to their ability to sustain plant nutrients. Incorporation of metals, such as copper and nickel, aids their use as catalysts. Their use as ion exchangers seems to be limited to wastewater treatment by glauconite (green sand), sometimes in manganese form, and often erroneously described as a zeolite.

Zeolites In these aluminosilicate minerals the constituent $[\text{SiO}_4]^{4-}$ and $[\text{AlO}_4]^{5-}$ share all corners to create a three-dimensional framework structure carrying a negative charge. This framework charge is balanced by the presence of cations contained in channels and cavities within the framework. Many zeolites are able to contain a large amount of water in these cavities and channels, which can have void volumes as high as 50% of their total volume. They are known both as natural species and as synthetic

Table 3 Examples of the cation exchange capacities of some clay minerals

<i>Mineral</i>	<i>Capacity (meq g)⁻¹</i>
Single layer	
Kaolinite	0.03–0.15
Halloysite	0.05–0.10
Double layer (nonexpanding)	
Muscovite (mica)	0.10
Illite	0.10–0.40
Glauconite	0.11–0.20
Pyrophyllite	0.40
Talc	0.01
Double layer (expanding)	
Montmorillonite	0.70–1.00
Vermiculite	1.00–1.50
Nontronite	0.57–0.64
Saponite	0.69–0.81

minerals capable of being manufactured on the tonnes scale.

Nearly 100 different frameworks have been crystallographically defined for zeolites, and related structures, each one having a unique molecular architecture. The internal dimensions of their channels and cavities are close to molecular dimensions and this has led to their employment as ‘molecular sieves’ and catalysts. Usually synthetic zeolites perform these functions and thereby make an incalculable contribution to the world economy, particularly in the oil industry. Examples of zeolite structures are provided in Figures 11 and 12.

Most zeolites readily exchange the cations from their voids. This facile process is vital to their utility as both molecular sieves and catalysts, and has been responsible for most of the literature describing their cation exchange properties. Because detailed crystallographic data is available for some zeolites (even including the positions of water molecules within their frameworks), they have been used to model theories of ion exchange kinetics and equilibria.

These minerals can exhibit very high selectivities, with high capacities, and have been extensively studied for use as such, while being restricted by their instability in acid environments. Examples where use can be made of cation exchange properties will be considered in a later section.

Zeolite cation capacities are a function of the extent of aluminium substitution into framework interstices; examples are listed in Table 4. As with the clays, the loading may not correspond to the cation content. The reasons why full exchange cannot be attained in some zeolites is a complex subject – sometimes framework charges are too low to strip hydration spheres, and the ingoing ions (bare, hydrated or even partially hydrated) may be too large to readily

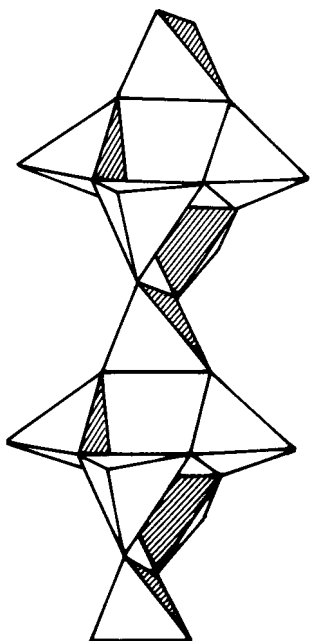


Figure 11 Linkage of Si, AlO_4 tetrahedra to form a chain structure that, when joined in three dimensions, forms the framework of the zeolite natrolite.

pass through the restricting dimensions in the channels. These effects contribute to the 'ion-sieve' effects noted in some zeolites.

Other framework structures Earlier the point was made that adherence to the traditional classifications of inorganic ion exchangers was not entirely appropriate. This has arisen for a number of reasons, a major one being the endless search for novel catalysts. The synthetic routes chosen frequently mimic those of zeolite synthesis with the aim to produce robust framework structures based on the assemblage of coordination polyhedra. Implicit in this is the likelihood that a microporous medium possessing ion exchange properties will result. To date very little attention has been given to the numerous substances appearing from this source in the context of ion exchange, so only a brief survey will be given.

Prominent in the novel frameworks produced by assemblage of tetrahedral units has been the incorporation of $[\text{TO}_4]$ units into zeolite-like structures. Numerous varieties with $\text{T} = \text{P}, \text{B}, \text{Co}, \text{Cu}, \text{Zn}, \text{Mn}, \text{Mg}, \text{Ga}, \text{Ge}, \text{Be}$ have been identified, and some have also been found in nature. The possibility has already been claimed that a new family of anion exchangers can be made with a framework in which an excess of $[\text{PO}_4]^{5-}$ over $[\text{Si}, \text{AlO}_4]^{n-}$ tetrahedra prevails, rendering the framework positively charged.

Discoveries like these have prompted a reassessment of the opportunities to make inorganic 'molecu-

larly ordered solids' (MOS) based on well-understood coordination polyhedra (tetrahedral and octahedral) formed by metals such as Ti, As, Zr, Hf, Nb, Mo, W, V, etc. They will prove a fruitful area in which to pursue the search for selective exchangers.

Other layer structures

Pillared materials Mention has already been made of the exchange of organic molecules into clays and layered phosphates/phosphites. Similar expansions can arise when a large inorganic ion is introduced between the layers. An early example of this was the exchange of a 'Keegin' ion, such as $[\text{Al}_{13}\text{O}_4(\text{OH})_{24}]^{7+}$, into expandable clays. Subsequent calcination leaves

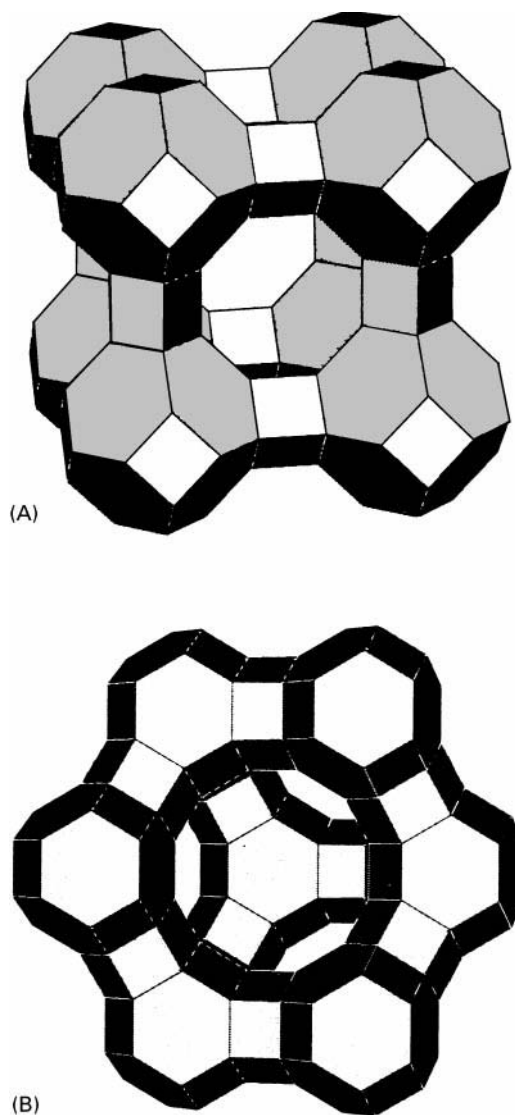


Figure 12 Structure of (A) synthetic zeolite A and (B) synthetic faujasite (zeolites X and Y) showing the internal cavities of molecular dimension. (Each line represents an oxygen and each junction a silicon or aluminium.)

Table 4 The cation exchange capacities of some zeolite minerals

<i>Zeolite</i>	<i>Capacity (meq g⁻¹)</i>
Natural	
Analcime	4.95
Chabazite	4.95
Phillipsite	4.67
Clinoptilolite	2.64
Mordenite	2.62
Synthetic	
A	4.95
X	6.34
Y	4.10

an alumina pillar propping open the layers to 1–2 nm. Again, the intention of this work was to develop wide-pored cracking catalysts. When ion exchange capacities were measured they proved to be orders of magnitude greater than the equivalent amount of alumina. No significant residual capacity arising from the clay was detected. Many similar pillared substances have now been made with a variety of different layered compounds (natural and synthetic) and inorganic pillars. Little is known of their ion exchange properties.

Hydrotalcites The natural mineral, hydrotalcite, is a layered compound of composition $\text{Mg}_6\text{Al}_2(\text{CO}_3)(\text{OH})_{16} \cdot 4\text{H}_2\text{O}$. Synthetic analogues can be obtained with other metals replacing magnesium and aluminium (Co, Ni, Fe for example). They are commercially available as anion exchangers.

Uses of Ion Exchange Materials

Resins

Water treatment The annual production of ion exchange resins has been estimated at 500 000 m³, of which at least 90% goes to industrial water treatment. The various end uses in this area will now be described.

Softening The removal of calcium and magnesium ions from water supplies is a requirement for many industries. Laundries, dye-houses and cleansing plants are examples of specific industries but the need can be generalized to many hot water circuits, heat exchangers and low pressure boilers. Strong sulfonate styrene gel cation resins, in sodium form with 8–12% cross-linking, are the usual choice, but macroporous resins may well be used when the process is demanding in terms of attrition, elevated temperatures or in the presence of oxidizing agents. An example of such

an aggressive environment is in the modern Chlor-Alkali membrane electrolysis cell for the production of chlorine gas and sodium hydroxide. This process also provides an example of the use of a chelating style resin (iminodiacetate, or aminophosphinate) to scavenge alkaline earth ions (see Table 1).

Dealkalization In dealkalization, weakly acidic carboxylic resins, in hydrogen form, are used to meet the limits of calcium and magnesium concentrations needed in feed water to medium pressure boilers. Hydrogen ions released are neutralized by the HCO_3^- and CO_3^{2-} anions present to give carbon dioxide, which remains in solution as carbonic acid. The softening is only partial and sometimes a sodium resin treatment, as above, is added. There may be an ancillary need to attain some demineralization as well which would involve an additional column treatment.

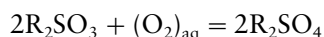
Single-stage dealkalization finds wide application in the treatment of cooling water and water used in the food and drinks industries. Desalination is a dealkalization process. Modern plants use membranes made from ion exchange resins in an electrodialysis cell.

Demineralization Demineralization involves the use of both cation and anion resins to produce 'de-ionized water'. This can be achieved by a two-stage process in which the raw water is first passed through a column containing a strong cation resin (H) form, and then through a strong anion resin (Type I or II). Some ion exchange plants use weak anion resins, and multistage processes or countercurrent variants are available as standard plant.

An alternative, and common, option is to use mixed beds that contain uniform mixtures of strong cation resins (H) and anion resins (OH). Variants of this approach are widely used to 'polish' water previously demineralized by strong cation/anion beds. Now the admixture of resins can be adjusted to cope with the expected load of residual ions from a specific process water, and so meet the heavy demands of water purity essential, for example, for high pressure steam production in power generation. This is the technology of 'condensate polishing' pervasive through this and similar industrial circumstances. It is appropriate to mention here the production of resins to meet the special needs of the nuclear industry. This manifests itself as 'nuclear grade' resins which are themselves of high purity to reduce potential problems that otherwise would arise from leaching of materials capable of being neutron-activated in reactor circuits. These add to the radiation fields in the reactor, create additional decontamination and waste disposal considerations, and do not help in the

general aim to inhibit corrosion. The nuclear power industry constantly strives to reduce potential corrosion in its steam/water circuits. In pressurized water reactors with 'recirculating steam generators' some operators have a target of low ng levels of ionic impurities per kg water used. These reactors use additions to the primary coolant of (a) boric acid to help moderate the fission process and control corrosion and (b) lithium hydroxide, also to inhibit corrosion. They depend on a sophisticated use of resin beds to achieve the desired coolant water chemistry. In the semiconductor manufacturing industry the demands for 'ultra pure' water are even more stringent with targets in the range $\mu\text{g kg}^{-1}$. (Note 'ultra pure water' is usually taken to mean water with less than $\mu\text{g kg}^{-1}$.) Water used in the production of pharmaceuticals also involves the use of high purity water.

In both dealkalization and demineralization the choice between a gel or macroporous resin is again conditioned by the relative aggressiveness of the feed. In some instances additional factors such as high column pressure differentials and the need for fast kinetics will lead to the use of macroporous materials. Additional treatment of demineralized water with a sulfite-based exchanger removes oxygen via the following route:



Removal of organics In this context 'organic' means the complex anions arising from decay products of organic matter and peaty soils. They are mainly derivatives of fulvic and humic acids and can be removed by employment of a macroporous strong anion resin. This was one of the main uses envisaged from the development of resins of this type. Typical waters requiring treatment contain a total organic carbon (TOC) of 2–20 mg of carbon per litre, which can be more than halved by resin exchange.

Nitrate removal The presence of nitrates in water intended as a potable supply, or for the food industry, is a major environmental concern, arising from the use of nitrate fertilizers. The suggested limit is $50 \text{ mg NO}_3^- \text{ L}^{-1}$, and the options open to attain this include microbiological, reverse electrodialysis using nitrate selective membranes, and traditional ion exchange methods.

Ion exchange is the cheapest and most reliable approach, not least because of the wealth of experience and established technology available. It makes use of nitrate-selective resins based on triethylammonium as functional groups. It is thought that the selectivity may arise from a size/shape exclusion effect that encourages the uptake of the small, flat,

nitrate anion in preference to the larger sulfate, and perhaps chloride, ions, with their spherical nature also being a factor.

Waste effluent treatment Prevention of the release into the environment of toxic metals arising from industrial processes has long been a useful application of ion exchange. Typical examples come in the metal finishing industries whereby wash solutions containing chromium and zinc, for example, can be rendered suitable for discharge. Many similar examples can be found in the photographic, paper and metal pickling industries. Some progress has been made in the employment of resins in the recovery of water from sewage treatment plants.

Another area of concern is in the treatment of aqueous nuclear wastes. The use of ion exchange offers the prospect of vastly reducing some problems by volume minimization of the waste form. Resins have high capacities for the trace quantities of hazardous isotopes arising from nuclear fuel production, reprocessing, reactor water circuits, decommissioning, and in 'pond' waters. The latter can be used as a major example where ion exchange materials can be used to scavenge the caesium and strontium radioisotopes that leak into the ponds in which spent fuel rods are stored prior to decladding and reprocessing (see Table 1).

In all nuclear applications the ultimate safe storage of the waste form is of prime importance. Previous practice has often been to store the highly radioactive resins in a concrete pit. Clearly this is undesirable, due to the limited radiation stability of the organic resins, and new approaches are now preferred, either by using inorganic exchangers or by encapsulating the spent resins in concrete. Even encapsulation should be regarded as temporary in the timescales recommended for nuclear waste disposal. The search for suitable inorganic materials has only been realized in a limited area because of reasons that will be considered later. The resin manufacturers are continuing to synthesize nuclear resins, and seek to provide products that can take up radioisotopes with high degrees of selectivity, often by chelating action. An example of this area of work is in the potential use of novel strong base polyvinylpyridine anion resins to remove americium and technetium from nuclear wastes.

Metal recovery Resins often form part of metal recovery processes, both in primary ore processing and from process waste streams. The second of these is becoming of increasing economic importance with the need to create efficient metal 'winning' from low grades ores, tailings, mine wastewater and

Table 5 Metals recovered and purified by ion exchange

Uranium
Thorium
Rare earths
Plutonium (and other trans-uranics such as neptunium and americium)
Gold
Silver
Platinum metals
Copper
Cobalt
Nickel
Zinc
Chromium
Rhenium
Molybdenum

mineral dumps. Ion exchange competes with liquid-liquid extraction in these areas, with varying success, and can be used in combination with this process in some instances. Macroporous resins are popular for these applications. Table 5 provides a list of metals that can be recovered on a commercial basis by ion exchange.

Note should be made of the essential role played by resins in aiding the separation of uranium from its ore in nuclear fuel production, whereby uranyl sulfate is loaded onto anion resins from which it is leached prior to solvent extraction to complete the separation process. Solvent extraction is the major separation technique in the process and the same is true of reprocessing, but both anion and cation resins are an essential part of the method whereby purified uranium and plutonium are obtained.

Other applications of ion exchange resins The reader is reminded of the wide use of resins in catalysis, and in the purification of antibiotics, vitamins, nucleotides, amino acids, proteins, enzymes and viruses that have been excluded from this review. One application in the purification of natural substances is the use of a finely sized cation resin to replace sodium and potassium ions by magnesium in sugar refining. Sodium and potassium promote the deleterious formation of molasses that has to be discarded.

Historically the best studied area of ion exchange application has been the use of exchange materials to perform separations to aid quantitative analysis. Originally, in the majority of cases the intent was either to remove interfering ions or to scavenge trace ions onto an exchanger so as to preconcentrate sufficient material for analysis. This work forms the basis of ion exchange chromatography, which has evolved into one of the most useful analytical techniques ever developed, namely high performance ion chromatography (HPIC). In HPIC low capacity ion exchange

materials are used in pellicular form on stable microspheres. Fast uptake of trace quantities of ions is guaranteed and differential elution provides an adequate separation so that individual ions can be recognized by their diagnostic column residence times. This presupposes that a suitable detector can monitor the column effluent to detect the ions in the eluent. Conductivity changes prove to be adequate for most purposes.

An important stage in the development of the technique was the use of suppressor columns that were able to remove the ions present as a consequence of the use of eluents by retaining them on suitable resins, thus greatly improving the detection sensitivity. Highly sophisticated instruments are now able to revolutionize the quantitative trace analysis of cations and anions, both organic and inorganic. The method is highly reproducible, rapid, and able to carry out routine analyses on a diverse range of analytes.

Inorganic Exchangers

Inorganic materials offer the possible advantages of increased thermal, and radiation, stability over their resin counterparts. In some cases, e.g. the zeolites, they can also compete in terms of capacity and in extremely selectivity exchange. These advantages have created great interest in their potential use for aqueous nuclear waste treatment. This is encouraged by the preferences stated by regulatory bodies that inorganic exchangers are preferred for incorporation into the accepted waste disposal forms for medium and intermediate level radioactive waste.

The main problems, some of which have been mentioned earlier, encountered in progress towards this ideal are:

1. the inherent difficulties in developing reliable characterization methods for many amorphous exchangers;
2. the fact that synthesis often results in products with small particle sizes inappropriate to column use;
3. the lack of materials compatible with direct treatment of the acid streams common in, for instance, reprocessing plants, and even the high pH (~ 11.4) encountered in fuel storage ponds;
4. the liability to hydrolytic damage, even under modest pH conditions.

These disadvantages clearly extend to many other non-nuclear areas of potential use where acid or alkaline media need to be treated. Despite these problems there have been some successful uses of inorganic exchangers, as will now be described.

Waste effluent treatment

Nuclear waste Reference has already been made to the earlier use of AMP and zirconium phosphate to scavenge Cs and Sr radio isotopes from nuclear waste streams. Other earlier processes made use of clays, green sand, and amorphous aluminosilicates. These latter materials, marketed as 'Zeolites', resembled the early 'permutites'. The zeolite minerals also were early candidates for use, but often resins took preference until the increased environmental considerations related to the safe disposal of highly active resins became of concern.

Initially studies in the US nuclear industry showed that the natural zeolites chabazite, mordenite and clinoptilolite had high selectivities for strontium and caesium fission isotopes, and these have been developed into modern plants. Examples of these are the use of clinoptilolite in the SIXEP process at BNF, Sellafield, UK, and chabazite at Oak Ridge, USA. A mixture of synthetic zeolite A and chabazite was the main agency used to scavenge caesium after the Three Mile Island accident, and clinoptilolite was extensively used at Chernobyl. Mention should be made of the use of clinoptilolite to reduce the body burden of fission isotopes in living hosts (including humans), and to reduce their presence in crops.

Work in progress on the treatment of high level waste (HLW) to encapsulate a wide range of isotopes, including α -emitters, includes tests on composite exchangers based on inorganic materials in polyacrylic resins. Considered also are ferrocyanides and silicotitanates with framework structures. Zeolites, zirconium phosphate and AMP have been used to obtain pure isotopes for commercial purposes.

Wastewater treatment The ubiquitous occurrence of clinoptilolite on the Earth's surface has created numerous publications describing its use to treat water from sewage plants. Several plants have been constructed to this end, e.g. Denver and Rosemount, USA and Budapest, Hungary. These make use of local supplies, and regeneration steps have been developed. Other areas of the world pursuing this application include Italy, Cuba, Japan and several locations in Eastern Europe. Eastern Europe has also been the major source of literature describing the employment of clinoptilolite to remove toxic metals from effluent streams. In these cases regeneration is not usually an option, that is the processes are 'once-through'. Recently clinoptilolite has been widely used to treat swimming pool water in circulatory systems, with regeneration.

Other areas

Detergency The need to remove hardness from washing water has long meant that a softener ('builder') has been a vital component of commercial deter-

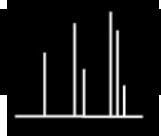
gents. Within the last 10–15 years there has been a move away from the phosphate builders traditionally used. The main agencies chosen to replace them have been synthetic zeolites. Currently the world annual production of synthetic zeolites for this purpose is approaching 1 million tonnes. This is largely as zeolite A, but a synthetic gismondine, zeolite MAP, is an alternative. Zeolites can be incorporated into both powder and liquid detergents, and natural zeolites have been used in cheaper powders.

Dialysis Amorphous zirconium phosphate is used in portable renal dialysis equipment. To remove urea from the dialysate it is first converted to ammonium carbonate by the enzyme urease. The ammonium ion is then taken up by ZrP. In some systems hydrous zirconia has been used to sorb phosphate ions released from the ZrP by hydrolysis.

Further Reading

- Clearfield A (1982) *Inorganic Ion Exchange Materials*. Boca Raton, FL: CRC Press.
- Dyer A, Hudson MJ and Williams PA (eds) (1993) *Ion Exchange Processes: Advances and Applications*. Cambridge: Royal Society of Chemistry.
- Dyer A, Hudson MJ and Williams PA (eds) (1997) *Progress in Ion Exchange: Advances and Applications*. Cambridge: Royal Society of Chemistry.
- Harland CE (1994) *Ion Exchange: Theory and Practice*, 2nd edn. Cambridge, UK: Royal Society of Chemistry.
- Helfferich F (1962) *Ion Exchange*. New York: McGraw-Hill.
- IAEA (1967) *Operation and Control of Ion Exchange Processes for the Treatment of Radioactive Wastes*, Technical Report Series no. 78. Vienna: IAEA.
- Marinsky JA and Marcus Y (eds) (1995) *Ion Exchange and Solvent Extraction*, vol.12. New York: Marcel Dekker (and earlier volumes in this series).
- Naden D and Streat M (eds) (1984) *Ion Exchange Technology*. Chichester: Ellis Horwood.
- Qureshi M and Varshney KG (1991) *Inorganic Ion Exchangers in Chemical Analysis*. Boca Raton, FL: CRC Press.
- Slater MJ (ed.) (1992) *Ion Exchange Advances*. London: Elsevier Applied Science.
- Streat M (ed.) (1988) *Ion Exchange for Industry*. Chichester: Ellis Horwood.
- Tsitsishvili GV, Andronikashvili TG, Kirov GN and Filizova LD (1992) *Natural Zeolites*. Chichester: Ellis Horwood.
- Williams PA and Hudson MJ (eds) (1987) *Recent Developments in Ion Exchange*. London: Elsevier Applied Science.
- Williams PA and Hudson MJ (eds) (1990) *Recent Developments in Ion Exchange-2*. London: Elsevier Applied Science.
- Tsitsishvili GV, Andronikashvili TG, Kirov GN and Filizova LD (1992) *Natural Zeolites*. Chichester: Ellis Horwood.

MASS SPECTROMETRY



K. L. Busch, Kennesaw State University,
Kennesaw, GA, USA

Copyright © 2000 Academic Press

Perspective of the Field

Despite the emphasis in this article on the combination of chromatography with mass spectrometry (MS), the first applications of MS in organic analysis used a direct insertion probe (from which only a crude sample mixture fractionation could be achieved), or a vapour inlet system in which the volatile samples from a glass bulb were introduced simultaneously into the ion source of the mass spectrometer. Before this, MS was not used for the analysis of organic compounds at all. Pioneers such as Aston (who won a Noble prize for the development of MS and associated instrumentation) and Dempster worked in the early part of the twentieth century on the determination of masses and relative abundances of isotopes. Preparative MS was used in the Manhattan project (carried out by the United States during World War II) to separate the isotopes of uranium, and accumulate enough fissionable material to create the first atomic bombs. A short description of the Calutrons that were used, which are based on sector instruments and still used for isotopic enrichment, is given later.

If each and every compound provided a unique retention time (or a unique set of retention times on different columns) when subjected to column chromatographic separation, only the most general detection method would be required, since the retention times alone would suffice to establish compound identity. Conversely, if MS provided a differentiating mass spectrum for each and every compound, then no separation of mixture components prior to spectral analysis would be required. Any measured mass spectrum could simply be deconvoluted as the sum of individual mass spectra. Reality destroys these idealistic dreams, as even simple mixtures can sometimes confound analytical methods used to characterize them. Approaches to mixture characterization are always based on many independent analytical data sources. The more complex the mixture, the greater the individual differentiating abilities of the methods applied must be, and the greater their independence should be. Modern column chromatography (meaning capillary column

gas chromatography, microcolumn liquid chromatography, and capillary electrophoresis) provides extraordinary separations for complex mixtures. There must still be a detector to trace the elution of separated components as they elute from the column, and a nonspecific detector would suffice if the separation were perfect and distinctive. But even with the capabilities of modern chromatography, given a completely random set of compounds in a mixture, overlaps in retention time can be expected for as few as 15–20 components. For a set of related compounds, the overlap could reasonably be expected to occur at a lower number of components. At this point, the analyst must turn to the results of measurements provided by the independent detector to provide some differentiation. Consider the various detectors used in gas chromatography (GC). The thermal conductivity detector, the flame ionization detector, the electron-capture detector, and the nitrogen/phosphorous photometric detectors represent a graduated series from the more general to the more specific. But use of these detectors in and of themselves does not provide the data needed to identify a compound that elutes at any given time. They provide information that is necessary, but not sufficient, for compound identification. GC coupled with infrared (IR) or nuclear magnetic resonance (NMR) spectroscopy provides more specific information. However, the highest degree of differentiating power, clear independence from chromatography, and the greatest ease of interfacing to the chromatographic column, is provided with the use of MS. The analytical authority of combined chromatography-mass spectrometry is reflected in the pervasiveness of the method and its standing in legal and regulatory venues. This article provides a rational overview of the analytical principles of these methods as a combined analytical tool.

Technology Overview

Technological secrets are the most fleeting of all, as both scientists and engineers are inquisitive about and insistent upon the latest analytical instrumentation. The ubiquity of combined chromatography-mass spectrometry results in a competitive commercial market for such instruments. Manufacturers strive continuously for both substantive and incremental improvements. Hardware/software configurations that do not compete effectively, or do not meet

the current analytical need, are soon relegated to obscurity. This rush to sophistication often obscures the history of instrumental/methods development. However, the end result of this evolving but continually renewed market is an installed base of instrumentation that can be described in broad brushstrokes, and that is the purpose of this section.

Separation Methods

This section begins with a brief overview of the aspects of separation methods that are of general concern in the interface to MS. Then each subsection covers traits that are specific to particular methods. As a sample introduction system, the purpose of the chromatography column is to transport single, separated components of the mixture efficiently and completely into the source of the mass spectrometer. The relevant questions are therefore simple. How much material is transported? How fast is it coming through? In what form are the sample components? How well is each component separated in time from other components of the mixture? To summarize, these issues are scale, flux, phase, and purity. Therefore, the descriptions that follow will not be comprehensive overviews of how the various chromatographic interfaces to the mass spectrometer were developed or how they are operated, but will concentrate on these four central issues.

Gas chromatography The characteristic of GC that makes the interface to MS (electron ionization (EI) and chemical ionization (CI)) especially straightforward is the fact that the sample molecules are already in the gas phase, and that they are transported into the source of the mass spectrometer by a carrier gas with substantially different physical characteristics from those of the sample molecules themselves. In packed column GC, the flow of helium carrier gas was so high under the conditions normally used for separation that an 'enrichment' device had to be used to remove most of the helium, and therefore increase the concentration of sample molecules in the gas flow entering the source. The higher diffusivity of helium gas formed the basis for most of these separators. As higher pumping speeds became available with improved vacuum technology, and as the use of capillary column GC cut the flux of helium into the source of the mass spectrometer by a factor of ten, it was found that the flow of helium gas (and entrained sample molecules) could be handled directly by the improved pumping in the source of the mass spectrometer, maintaining the pressure at 10^{-5} – 10^{-6} torr.

The helium was present in the source in excess, but the low mass of helium was an advantage in that most

mass spectra were recorded only to a lower mass limit of about m/z 45. So the ions from helium were not recorded, and neither were ions from nitrogen, oxygen, argon, water, and carbon dioxide, all of which constituted residual molecules in the vacuum system. As there was no separate enrichment device, the efficiency of sample transport into the source was 100%, and the sample molecules were in the gas phase. As packed columns were replaced by capillary columns in GC, the influx of sample molecules changed from nanogram–microgram levels of sample per peak to picogram–nanogram levels of sample per peak. Higher amounts of sample overloaded the capillary column, and compromised separation, but these picogram–nanogram amounts of sample material were still within the detection range of the mass spectrometer. As the widths of the peaks in capillary columns were decreased relative to the widths generated by packed column chromatography, the flux in terms of amount of material(s) was still similar, even though the total amount of material was reduced. Of course, with reduced peak widths and higher separation resolution, the chances of any given peak being completely resolved were also increased. Issues that remain relevant are the need to scan the mass analyzer fast enough that representative mass spectra of a narrow peak can be recorded, and the increased demands upon a data system that is called upon to record thousands of mass spectra for hundreds of resolved sample mixture components.

Liquid chromatography Interfaces for liquid chromatography–mass spectrometry (LC-MS) must deal with transport issues that are additionally complicated by the fact that the sample is a solute in the liquid phase, the transfer into the gas phase produces large volumes of solvent vapour, and the samples are likely to be those that are relatively nonvolatile in the first place (otherwise GC would be used). Although the separation resolution may not be as high as in the best capillary GC, peaks are usually still only a few seconds wide and the amount of sample to be transported is also in the picogram–nanogram range, so the flux of material into the source is similar to that in GC-MS. The purity of the sample assessed relative to other mixture components is also similar, with separations designed to produce clean, well-resolved peaks. However, the solvent is often a mixture (as in reversed-phase gradient LC) and buffers and additives may be added to the solvent system. There is a background signal contribution from these components, and this contribution may change during the course of a chromatographic separation. As detailed in the appropriate sections, EI and CI MS act upon sample molecules in the gas phase. This is not the

form in which the sample molecules are found in LC, and it is difficult to transfer nonvolatile sample molecules into the gas phase without thermal degradation. Several ionization processes have been developed that do not rely on the sample being in the gas phase. Thermospray ionization, continuous flow fast atom bombardment, and discharge ionization sources have been developed and optimized. However, the most widely used ionization method is electrospray ionization (ESI). In this technique, a combination of progressive desolvation and field-assisted ion extraction creates a series of multiply charged ions from the sample molecules, even if those sample molecules are 'nonvolatile' and thermally fragile. The flow and flux ranges accommodated by the ESI sources overlay the range of flow and flux in modern LC, endorsing the combination.

Capillary electrophoresis In capillary electrophoresis (CE) the movement of sample molecules (often charged, but neutral molecules move through the column as well) is induced by a combination of electrophoretic and electroosmotic flow. The small differences in mobility exhibited by molecules result in different retention times within the 0.5–1-m-long columns usually used. These columns have a small diameter (50 μm) capillary to efficiently dissipate the heat produced by the high potential difference (30 kV, for example) between the front and the back of the column. The flow profile in the column is not parabolic (as in pressure-driven systems) but is essentially flat, leading to very high resolution separation. There are few instances of overlapped peaks. The small column diameter limits the amount of material that can be loaded onto the column, with loadings 10–100 times lower than in LC. Peak widths are still a few seconds wide, so the instantaneous concentration of sample is lower than in GC or LC. A small volume of sample solution (picogram–nanogram levels of sample in 10 nL of solvent) is injected at the positive end of the capillary and the separated components are detected near the negative end of the capillary. Detection is accomplished with all of the same detectors as in LC, including mass spectrometers. However, the dynamic ranges of CE and MS are not as extensively overlapped as in GC or LC coupled with MS. Despite the general assumption that MS is the most sensitive detection method in use, laser-induced fluorescence detection provides lower limits of detection than MS, but not, of course, with the same specificity. As in LC, the sample molecules of interest are not amenable to evaporation, and so ESI is most often used with CE. In fact, the electrical requirements of the capillary electrophoretic separation often dovetail nicely with

the requirements for the ESI source (*vide infra*). As noted, sample peak purity is usually high because of the extraordinary resolution achievable with this method, and detection may be simplified so the solvent (often methanol) background contribution is simple and often suppressed relative to the signal from the sample.

Ionization Methods

The mass analysis step in MS requires the interaction of charged ions with magnetic or electrical fields, and therefore a means must be found either to create ions from neutral molecules, or to extract ions from a sample solution and transfer them to (or isolate them in) the gas phase. The ionization source in the mass spectrometer accomplishes this task. In mass spectrometers that interface to various methods for separation, particularly column chromatographic methods, only three ionization methods are used for the majority of applications, and will form the focus of the discussion here. EI dates back to the first developments of MS, and is the basis for the extensive mass spectral libraries available. CI was developed in the mid-1960s and is a powerful adjunct to EI. It is especially useful for the determination of molecular masses of compounds that fragment extensively under EI conditions. ESI is more recent in origin, and produces a different type of mass spectrum. Matrix-assisted laser desorption ionization (MALDI) is an even newer ionization method with special applications to high mass biomolecules. As separation methods are developed for separation of truly high mass biomolecules, and mixtures of such compounds, MALDI may become as common an ionization method as the others described in this section. Note that both EI and CI deal with sample molecules in the gas phase, while ESI brings charged species directly out of a liquid solution, and MALDI generates sample-related ions from a mixture of the solid sample and an energy-absorbing matrix.

Electron ionization EI was the first ionization method developed for MS, and it remains the most widely used. The term 'electron impact' is still also used, and the acronym EI covers both terms. Importantly, the most extensive mass spectral libraries assembled are those of EI mass spectra recorded under a 'standard' set of conditions (70 eV electron energy). The gas that flows into an EI source (helium from a gas chromatograph, for example) is confined so that the gas-phase sample molecules interact with the electrons emitted from a metal filament. A high conductance of un-ionized, neutral sample molecules out of the source must also be maintained to minimize cross-peak contamination. EI sources are maintained at

a temperature of about 200°C to prevent condensation of sample molecules on the source walls.

The ionization process is the direct result of the interaction of an energetic electron with the sample molecule. The electrons are emitted from a filament through which 3–4 A of current is passed to heat the filament to about 2000°C. Electrons are accelerated into the source by maintenance of the electron filament at a potential more negative than that of the source itself; a potential difference of 70 V (therefore 70 eV) is standard. Then electrons travel across the source to the trap where they are collected and the current is amplified. The trap is used as part of the feedback loop to maintain a constant emission of electrons from the filament. This current is usually about 100 μ A (about 6.25×10^{14} electrons per second). Only a small fraction of the electrons passing through the ion source participates in ionization of sample molecules, and only about 1% of the sample molecules are ionized in EI. The EI process can be written for the gas-phase sample molecule M:

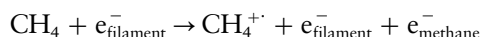


The molecular ion $\text{M}^{+\cdot}$ (the dot denotes an unpaired odd electron) may subsequently dissociate, since EI imparts more energy to the gas molecule M than is required for ionization alone. The excess energy can cause the dissociation of the molecular ion $\text{M}^{+\cdot}$, or it can be retained in the ion as excess internal energy. Since an electron is far too light to transfer kinetic energy to the sample molecule in a collisional process, the process of EI involves only electronic excitation of M. The molecular ion $\text{M}^{+\cdot}$ retains the original structure of the molecule M, at least for a short time after its formation. If dissociations of the molecular ion are prompt, therefore, we can assume that the dissociations represent those of the original molecule and not a structurally reorganized isomer. Some molecular ions formed will be stable enough to pass through the mass spectrometer and reach the detector. Their measured m/z ratio is a direct indication of the molecular mass of the sample molecule itself. For those molecular ions that dissociate, the fragment ions that form are produced from a structure that is a direct analogue of the molecular structure. Clues to the original structure can thus be obtained by piecing together or rationalizing the processes that lead to fragmentation.

Chemical ionization In EI, if too much energy is deposited into the $\text{M}^{+\cdot}$ ion during the ionization process, or if the molecule is especially prone to dissociate, fragment ions may be seen in the mass spectrum, but the $\text{M}^{+\cdot}$ may be reduced to such a low intensity that it is indistinguishable from the back-

ground signal level. Without the molecular ion, the determination of molecular mass is difficult. CI was developed to overcome this difficulty and provide molecular ions for such compounds. CI involves a collision and reaction between an ion and a gas-phase sample molecule. The ion is called the reagent ion and the molecule is the gas-phase neutral sample molecule. There is no common and standard set of operating conditions for measurement of CI mass spectra such as exists with the EI source. As a result, there is not a large CI spectral library, and interpretation of CI mass spectra depends more heavily on the skill and experience of the user.

The CI source is a variation of the standard EI source, with modifications required to achieve a higher source pressure (about 1 torr) while keeping the mass analyser pressure within acceptable limits. Methane is a common CI reagent gas, and the reagent ion CH_5^+ will transfer a proton to the gas-phase sample molecule to form $(\text{M} + \text{H})^+$. The protonated molecule is relatively stable, and can usually be observed in the mass spectrum of a compound for which the molecular ion $\text{M}^{+\cdot}$ formed by EI cannot be distinguished. The source filament is still heated to a high temperature so that electron emission occurs, but in CI the electron energy is usually 250–500 eV; the higher energy allows the electrons to penetrate through the high pressure in the source. The gas pressure caused by sample molecules is still about 10^{-5} – 10^{-6} torr, just as it was in the EI source. As the pressure of methane is 1 torr, in an equal source volume, the electron emitted from the filament is much more likely to encounter a methane molecule. When it does, an EI process occurs, namely:



The $\text{CH}_4^{+\cdot}$ ion does not travel far before it encounters a neutral gas molecule, and at 1 torr of methane and 10^{-6} torr of sample, the molecule it encounters will most likely be a methane molecule. The next reaction creates CH_5^+ and CH_3 . Several other reactions occur, and the final distribution of ions depends explicitly on the source temperature and pressure. The primary reactant ion for methane reagent gas is usually CH_5^+ , and this ion acts as a strong gas-phase acid that protonates anything more basic than methane. The sample molecules are sufficiently basic to accept a proton to form the protonated molecule. The protonated molecule then fragments in accordance with the amount of internal energy it contains. In most cases not all of the protonated molecules fragment, and since there is an observable signal for the protonated molecule in the mass spectrum, the molecular mass of the sample compound can be established. The

fragmentation processes in CI are different from those observed in the EI mass spectrum, since the $(M + H)^+$ ion is an even-electron rather than an odd-electron species. The pattern of fragment ions is still interpreted to support a structure for the sample molecule. Other reagent gases form ions that transfer protons to the neutral sample molecules, forming an ion of the same mass but with a different amount of internal energy. The protonated molecule therefore fragments to a different extent. The degree of fragmentation of the sample molecule can be 'tuned' by choice of the reagent gas, and this experiment can be useful in interpretation of CI mass spectra.

Electrospray ionization In GC, helium carrier gas that enters the source along with the vapours of the sample does not disrupt the EI or CI process. However, both LC and CE separate species in a solvent, and the sample enters the ionization source along with a continuous flow of solvent (aqueous or organic) that generates a tremendous amount of solvent vapour. If EI or CI are to be used, the bulk of the solvent must be removed without loss of the sample, as the great excess of solvent vapour will certainly affect the ionization process. Various means have been devised to accomplish this task, but the efficiency is low and the process cumbersome and subject to many complicating factors. ESI allows ions to be created directly from the sample solution, and conveniently at atmospheric pressure. In ESI, the mechanical need for solvent removal is greatly reduced, albeit at the cost of allowing only a small continuous flow of solution to enter the mass spectrometer.

In ESI the sample solution is passed from the LC column or CE column through a connection junction into a short length of stainless steel capillary. A high positive or negative electrical potential, typically 3–5 kV, is applied to this capillary. There is clearly a need for electrical isolation in the LC connection, and potential management in CE. As the solution is forced to flow through the capillary tip, the solution is nebulized into a spray of very small droplets. This spray is formed at atmospheric pressure. The mass spectrometer operates at a vacuum of 10^{-5} – 10^{-6} torr. The pressure must therefore be reduced before the droplets (and the sample species that they contain) enter the mass spectrometer. The spray of droplets is usually directed through a skimmer that provides a differential pressure aperture, and also acts as a momentum separator. As the droplets move through this region, neutral solvent molecules evaporate rapidly and the droplets become progressively smaller. As droplets leave the charged capillary needle, most of them retain an excess of positive or

negative electrical charge, corresponding to the potential applied to the capillary. This excess charge resides on the surface of the droplets. As the droplets get smaller, the electrical surface charge density increases until the natural repulsion between like charges causes ions as well as neutral molecules to be expelled from the droplets. This field-induced evaporation also forces the droplets to become progressively smaller. Note that ions themselves cannot evaporate from the droplet. However, if the charge density is high, a Coulomb-force-induced 'explosion' can expel them from the droplet. As solvent molecules evaporate from the droplets they diffuse in all directions, while the higher momentum, charged droplets are directed towards the first skimmer, and then (usually) through a second concentric skimmer that lowers the pressure even further, by a combination of momentum separation and steering potentials applied to the skimmers. In some ESI sources a drying gas (nitrogen) flows along and past the end of the capillary and skimmer to assist with evaporation of the solvent from the droplets. The end result of the electrospray and progressive desolvation process is a stream of ions that have been extracted directly from the solution in which they were originally found.

If sample ions are already present in the solution then it is clear that these ions can be sampled directly. Solvents used in LC and CE also have appreciable ion concentrations, especially as buffers and ionic modifiers are often present in the solutions. In most cases, there is a substantial free proton population. Protons will not evaporate from the droplet as it becomes smaller; the 'pH' rises inexorably as the droplet becomes smaller. During the last stages of solvent evaporation, the protons will be forced to associate with the most basic molecules remaining in the droplet. This is not necessarily an acid–base equilibrium situation, because the dynamics of desolvation and sampling play a large role. However, the situation can be considered as one in which a free proton (a strong acid) protonates the sample molecule, which is forced to act as a proton acceptor. Other Lewis acids (cations) present in the droplet act similarly. There is a transition from the lower concentrations of ionic species present in the bulk solution to the near 100% ionic population present in a nanodroplet. The 'pH' drops to such a low value that multiple protonation is common.

The unique nanodroplet environment from which ions are drawn in ESI provides a route to highly protonated, multiply charged ions. It is the formation of multiply charged ions that makes ESI valuable for examination of sample molecules of high molecular masses. In EI and CI, most ions are formed with a single positive or negative charge. The x-axis of the

mass spectrum is the m/z ratio, and z is one. Therefore the mass on the ' m/z ' axis is directly indicative of the sample molecular mass. In ESI, values of z greater than one are commonplace. ESI-derived positive ions are found as $[M + nH]^{n+}$, where n ranges from 2 to 30, and is sometimes as high as 100. Several factors contribute to the propensity of ESI to create multiply charged ions. The first is the strongly acidic environment of the nanodroplet. The second is the fact that higher molecular mass molecules are, quite naturally, large molecules, and larger molecules can accommodate a greater number of protons. For a protein, for example, a basic amino acid residue will be the site associated with the proton. Basic amino acid residues will be far enough apart in a typical protein that the protons add independently, and there is minimal Coulombic repulsion between the charged sites. The higher order structure of the protein will therefore determine what sites are accessible for protonation, and this characteristic is the basis for some of the most intriguing and revealing ESI experiments.

Suppose that M , the molecular mass of the sample molecule, is 10 000 Da. In ESI, the $(M + 20H)^{20+}$ ion may be formed. This ion has a mass-to-charge ratio of $(M + 20H)^{20+}$, and therefore $m/z = 10\,020/20 = 501$. This mass is well within the range of the mass spectrometer, and can be determined accurately. Usually several different forms of the multiply charged ions are found, namely $(M + nH)^{n+}$, with a distribution of intensities. Each successive molecular ion contains one more proton and therefore one more charge. The series is easy to identify, and the value of n need only be determined for any one ion for the entire ion series to fall into place. The value of n can be determined from the spacing of isotope peaks in the molecular ion isotopic envelope, and the derivation has now been fully automated. The mass spectrum that contains the array of multiply charged ions is plotted in terms of the m/z values of those ions. But M is the same for each of those ions, and each ion is a slightly different pointer to that value of M . Having determined the masses of each of the multiply charged ions, the series of equations can be solved to determine the value of M . The data can now be presented as a transformed spectrum with one molecular ion, M . If there is more than one sample molecule M , the m/z spectrum can appear extraordinarily complex, but the transformed mass spectrum clearly shows the presence of multiple components (although the relative intensities may not accurately reflect the solution concentrations of the sample molecules).

Matrix-assisted laser desorption ionization The title of this section reveals MALDI as the most 'matrix-

dependent' of the ionization methods discussed in this overview. This should not be surprising, as the ionization usually occurs from a solid-phase mixture of sample molecules in a large excess of energy-absorbing matrix molecules. Therefore, MALDI would appear to be the most ill-suited of the techniques discussed for interfacing to column chromatographic methods. However, effluents from LC separations have been deposited onto collection surfaces, and then the trail in space (along the x -dimension, for example) analysed by MALDI to provide the corresponding trace of sample elution in time. MALDI has also been applied to planar separation methods such as thin-layer chromatography (TLC) and gel electrophoresis. As interface technology improves, a miniaturized solid surface may be used to intercept effluents from columns. This may be a particularly attractive interface since MALDI, in conjunction with a time-of-flight mass analyser, has been shown to be a very capable ionization method for the production of simple mass spectra of very high mass biomolecules. Column chromatography will increasingly be used to perform separations of mixtures of such molecules, although not necessarily in the forms described previously in this section, and MALDI may be used increasingly in such applications.

Mass Analysis Methods

Each of the ionization methods discussed here has characteristics that affect the design and operation of the interface between chromatography and MS. Similarly, methods of mass determination affect the overall analysis, but not as directly. In most standard operating protocols, the data processing has assumed primary importance, and the details of the instrument on which the mass spectra were measured are hidden. This current state of affairs is in direct contrast to the situation 20 years ago, when there were distinct differences in mass spectra measured with quadrupole and sector instruments, and specific means were undertaken to normalize the mass spectra for purposes of library matching and identification. Similarly, scanning speed advantages of the quadrupole over the sector were an early boost for the former's incorporation into GC-MS instruments. Additionally, the high source potential of sector instruments made some of the early LC-sector MS designs problematic. Each of these technological hurdles has been overcome. With the introduction of the ion trap mass analyser, benchtop instruments for both GC-MS and LC-MS are becoming still smaller and even vehicle-portable. It is useful to briefly review attributes of each of the common methods of mass analysis. Simplified schematics for each of the mass analysers discussed are presented in Figure 1.

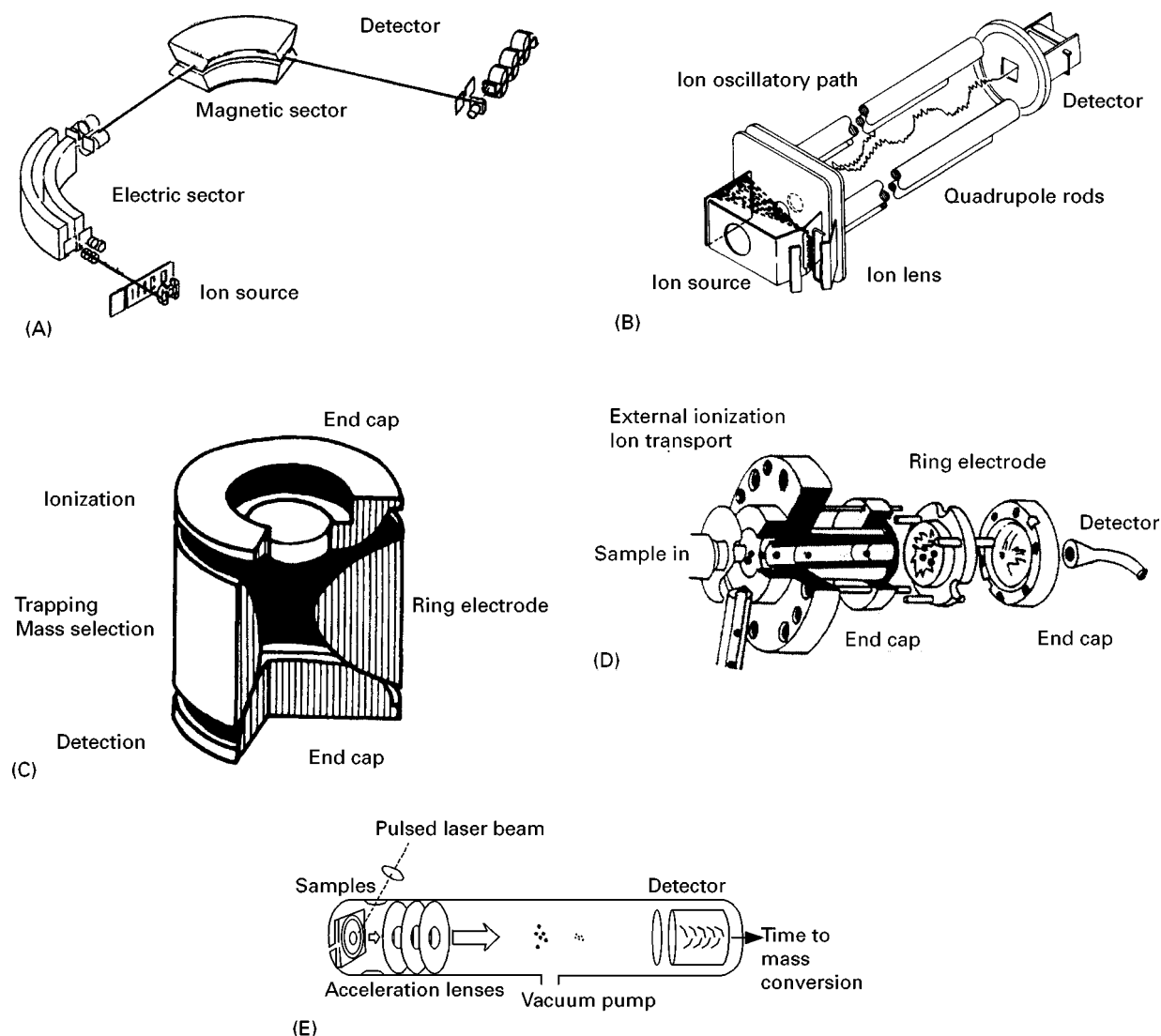


Figure 1 Simplified schematic drawings of (A) a sector mass spectrometer; (B) a quadrupole mass filter; (C) an ion trap; (D) an ion trap incorporated into a complete system; (E) a time-of-flight mass spectrometer.

Sector mass analysers The term 'sector' mass spectrometer refers to instruments in which the mass separation of the ions is accomplished by passage of the ion beam through a magnetic field directed perpendicular to the direction of ion motion. At any given magnetic field strength, ions of different mass follow trajectories of different radii. Given an equal kinetic energy for all ions, lower mass ions will trace a path of lower radius than higher mass ions. A narrow slit allows only those ions whose path follows a radius equal to that of the magnetic sector itself to pass through to the detector. Scanning the magnetic field strength passes ions of different mass to the detector. The scanning speeds of modern electromagnets are such that a mass range of 10–1000 Da is accomplished within about 0.3 s. Sev-

eral complete spectral scans are therefore recorded for a typical chromatographic peak. A double-focusing sector instrument (a magnetic sector used in combination with an energy-analysing electric sector) provides higher mass resolution, that is, the m/z values of the ions can be measured to an accuracy of several decimal places (e.g., 131.12 Da). Such information can be useful in unambiguous identification of compounds as they elute from a chromatographic column. Based as they are on 'sectors' of electromagnets, these mass spectrometers tend to be larger than other types of analysers, although a significant downsizing is apparent in the current generation of sector instruments. The larger size is reflected in the higher initial costs of such instruments, and therefore sector instruments are usually not the

instrument first acquired by an analytical laboratory for chromatography-mass spectrometry. In collection of data, scanning speed is not usually an issue except for very high resolution chromatography. In selected ion-monitoring experiments, a sector instrument takes some time to hop from mass to mass, whereas a quadrupole instrument (for example) makes the transition instantaneously. Again, this is only an issue in the most exacting of experiments.

Finally, the sector-based mass analyser is used as part of a beam instrument, that is, a device in which the ion beam physically moves through the instrument from ion source to ion detector. In certain geometries the sector instrument is configured such that, at any given magnetic field strength, ions of only one mass are able to pass through the detector slit and reach the ion detector. In this characteristic the sector-based instrument is similar to the quadrupole instrument, although the latter provides a lower resolution and abundance sensitivity, and provides no transport discrimination against neutral species. The fundamental difference from ion trap and time-of-flight mass analysers will become apparent as the principles of operation of those analysers are described. Since the sector-based instrument provides a physical separation of an ion beam of one mass from an ion beam of a different mass, it can be used for the separation and collection and subsequent enrichment of that mass-selected isotopic species. The Calutron is a physically large magnetic-field mass spectrometer built to separate isotopes, with a mass throughput orders of magnitude greater than in a conventional analytical instrument. Preparative-scale MS was used at Oak Ridge as part of the Manhattan project during World War II. Several of these mass spectrometers were constructed and operated in parallel, with production reaching 200 g per day of 88% enriched ^{235}U . Two stages of enrichment were carried out on two different series of 180° sector preparative mass spectrometers, called the alpha and beta series, arranged in racetracks. These instruments maintained beam currents a billion times more intense than those in modern analytical mass spectrometers. More recently, electromagnetic isotope separation was at the cornerstone of an Iraqi programme to develop nuclear weapons. Estimates are that between five and ten billion US dollars was spent on this programme between 1981 and 1991 at Tuwaitha and Tarmiya. Initial devices used for electromagnetic isotope separation could develop a 0.5 mA beam of U^+ ions at 35 keV energy. Production devices were designed to operate with a 150 mA beam current through 1-m-radius magnets. Such uses represent exploitation of the same basic principles used for organic analysis using chromatography-mass spectro-

metry, with an emphasis on production of isotopes rather than production of analytical information.

Quadrupole mass filters A quadrupole mass analyser (more accurately a mass filter) consists of four rigorously parallel rods of hyperbolic or circular cross-sections, and lengths of about 20–25 cm. The ions pass through this rod structure. Opposite pairs of rods are connected electrically. A voltage composed of a direct current (DC) component and a radio-frequency (RF) component is applied to the rods. Relatively slow-moving ions (kinetic energies of 10–50 eV) move from the source into the quadrupole. They are attracted first to one rod, and then to the adjacent rod as the voltages applied to the rods change (the RF frequency). This induced oscillation in the ions results in a spiral trajectory of increasing xy magnitude as the ions move through the rods in the z direction. At a given ratio between the DC and RF voltages ions of only one mass pass completely through the quadrupole rod structure to the detector, while ions of all other masses follow trajectories that result in their collision with the rods. Scanning the magnitude of the DC and RF voltages, while keeping the ratio of the DC and RF voltages constant, allows the mass range to be scanned at a constant mass resolution.

Both the resolution and the scanning speed of the quadrupole mass filter are controlled electronically (rather than physically as with sector instruments) and can be changed quickly. In the 1970s, the much faster scanning speed of quadrupole mass filters compared with the sector instruments catalysed the development of the first viable commercial GC-MS instruments. Since that time, quadrupoles of ever increasing performance have been developed, and many entry-level instruments are based on their use.

Ion traps The ion trap consists of two end caps and a ring electrode to which DC and RF voltages are applied. Ions are formed during a short ionization pulse, after which they are forced to oscillate in stable orbits in the interior volume of the trap. The ions are kept near the centre of the trap by repeated collisions with a low pressure of helium 'buffer' gas, which removes any excess energy and relaxes the ions into stable orbits. Ion traps can be used to trap ions for extended periods of time for various purposes, including ultra high resolution accurate mass measurement. In an ion trap used in a chromatography-mass spectrometry instrument, however, the ions are trapped for only a short period of time. To scan the mass spectrum, the ions are forced out of their stable orbits to a detector by increasing the amplitude of the RF. Ions of appropriate mass (e.g. orbits of a matched

frequency) reasonably absorb that energy. These ions become 'unstable', and trace an orbital trajectory of increasing radius until they are ejected into the detector located just outside the ion trap. As with the quadrupole mass filter, resolution and scan speed (and ion excitation for other experiments) are adjusted electronically. The ion trap itself is very small (contained within a 10 cm × 10 cm × 10 cm volume), and its associated vacuum and hardware components are assembled into a compact, low-cost benchtop unit.

Time-of-flight mass analysers The time-of-flight mass analyser is a racetrack for ions. In its most simple linear form, it is a tube approximately 1 m long. The ions are formed in a short pulse and then accelerated into the flight tube with a potential drop of a few thousand volts. Given equal kinetic energy, ions of different mass will travel at different velocities. The lighter ions are speedy, while the heavier ions lag behind. Ion arrival time at the detector is converted into a mass value by a simple equation. The resolution is relatively low because of spreads in ion velocity (and therefore flight time) derived from other sources, but the mass analyser is exceedingly simple and robust, and provides a complete mass spectrum with every pulse of the ionization source. There is no scanning involved. While other mass analysers (sectors, quadrupole mass filters, and ion traps) are used with every form of column chromatography, the time-of-flight mass analyser is used almost exclusively with MALDI and therefore has been used mostly with planar chromatographic methods of separation.

Data Processing in Chromatography–Mass Spectrometry

A chromatography–mass spectrometry file contains far more data than is usually extracted and displayed to solve a specific analytical problem. However, the specific analytical problem may be restructured, or additional questions may be asked based on the answer to the first question. It is not uncommon for a data set to be interrogated several times. Further, there may be good laboratory practice or regulatory issues that require data storage for extended periods of time. The analyst usually expends far more time in data processing than in data acquisition, especially as the latter may be automated, and the former should never be. Therefore, the focus here is on elements of data processing and interpretation that are affected by the conjunction of chromatography and MS, and in how the information derived from one augments the other.

Synergism in a Hyphenated Method

The result of the linkage between two independent procedures in a hyphenated method can be treated rigorously through information theory. In essence, both methods provide a means to characterize the components in a mixture, but the information provided by one method is independent of that provided by the other. In GC-MS, for example, the retention time of a particular component does not determine the distribution of ions in the mass spectrum. There are special traits that characterize the combination of chromatography with MS, many of which will become apparent in the following discussion. Oddly, the nomenclature for hyphenated methods sometimes includes the solidus rather than the hyphen, so one finds 'GC/MS' rather than GC-MS. The end user seldom redesigns instrumentation, makes any fundamental changes in standard operating procedures, or argues the correctness of nomenclature. The end user spends most effort gathering, analysing, and interpreting data.

Time Basis of Mass Spectral Data

Column-based chromatographic methods continuously elute sample into the ionization source of the mass spectrometer. For the most part, ionization sources also operate in a continuous fashion, generating an uninterrupted stream of ions for mass analysis. However, most mass analysers do not provide continuously measured mass dispersion. The mass range selected by the user is scanned. Usually, the mass analyser scans from a high mass to a low mass. At any given instant, ions of only one mass-to-charge ratio are passed through the mass analyser to the detector, which registers the arrival of the mass-selected ion as an electrical signal. Ions that do not possess the 'correct' mass-to-charge ratio at that particular instant follow a flight path that brings them into collision with some part of the instrument. The ions that are not selected are neutralized at the surface, and the deposited material eventually desorbs from the surface, diffuses through the vacuum, and is removed from the instrument by the vacuum pumps. The consequence of analyser scanning is that only a small fraction of the molecules that are ionized in the source proceed successfully through the mass analyser to the detector to produce a measured signal. It is the extraordinarily high gain (10^6 – 10^8) available with modern electron multiplier detectors that compensates for the inherent 'transmission inefficiency' associated with a scanning mass analyser.

Therefore, in a hyphenated chromatography–mass spectrometry method, the time behaviour of the data as established by the chromatography is convoluted

with the time behaviour of the data as established by the operation of the mass spectrometer. The latter is usually determined by scanning, but in the past was sometimes delineated by how fast the data could be captured and stored. In the ideal analytical design, the chromatography time base would predominate, and the time evolution of the data would be biased at least 100 : 1 in favour of the chromatographic determinant. In practice, the ratio is much closer to 10 : 1, and the time bases for operation of the mass spectrometer should be of constant concern in analysis of the data.

Procedures for Data Processing in Chromatography–Mass Spectrometry

A data set acquired with a GC-MS device will be used as the base to describe the common procedures of data processing in chromatography–MS. In GC-MS, samples are eluted into the source of the mass spectrometer at their characteristic retention times. For a Gaussian-shaped peak, the concentration of the sample in the source starts at a low value, increases to its maximum value, and then decreases symmetrically. Part of the challenge of MS is to record a characteristic mass spectrum for this sample of constantly changing concentration, given that a certain amount of time is required to scan the mass filter across its mass range. Modern mass spectrometers (considered here to be quadrupole, sector, or ion trap mass spectrometers) scan across the usual mass range in a short time. The instrument specifications for a sector instrument may show that the scan speed of the mass analyser can be as fast as $0.1 \text{ s decade}^{-1}$. In this context a decade is the mass range between 10 and 100 Da, or similarly between 100 and 1000 Da. In a sector instrument the scanned parameter is the magnetic field strength, and the ion m/z passing through the instrument varies with the square of this value. In a quadrupole or ion trap instrument, the scan parameter is linearly proportional to the mass of the ion in the analyser.

Approximately ten scans of the mass analyser are required to characterize any GC peak. This requirement stands regardless of the width of the GC peak, and, as the peaks in GC narrow with the achievement of higher separation resolutions, the requirements on the scan speed of the mass analyser become more onerous. Changing concentration of the sample in the source will distort the true intensities of the ions observed in the measured mass spectrum in each individual scan, so mass spectra recorded across the entire width of the peak are averaged together to create a mass spectrum that contains more accurate ion intensities. To ease the burden, the mass analyser can be forced to scan faster and faster, but eventually

a fundamental hardware constraint limits the scan speed. Faced with these limits, the analyst can narrow the mass range across which the analyser must scan, or choose to monitor only certain significant ions from within the mass range. In either case, the analyst risks losing the ability to accurately identify unexpected compounds in a complex mixture.

The discussion that follows is software-independent. Each computer system will handle the operations described in its own unique fashion, and there may be specialized procedures beyond those that are described here. It is expected that the analyst will understand the general principles involved, and then take the time to explicitly explore these functions on the particular instrument to be used for analysis.

Background subtraction Resolution in chromatography is established by the time between adjacent peaks in which no sample components are eluting into the source of the mass spectrometer. Generally, the higher the chromatographic resolution, the more ‘empty’ space there is in the chromatogram. The mass spectrometer is recording mass spectral data even during the times when nothing is eluting from the chromatograph. These scans become the mass spectra of the background. The background mass spectrum is not constant. During a GC-MS run the background changes because of increased bleed from the column at increased temperatures encountered during a temperature ramp, low-level, highly retained components, and the continual desorption of organic compounds and contaminants absorbed throughout the system. As background is not constant, the details of background subtraction are not constant, although the correct procedure is generally accepted.

There is no error-free method of arbitrarily reducing the contributions of background in a mass spectrum to zero. However, based on the assumption that the sample background and ionization is independent of the elution and ionization of the sample component itself, then the number of scans averaged together to create a background mass spectrum should be equal to the number of scans averaged together to provide the mass spectrum of the sample. Simplistically, if ten mass spectral scans are necessary to completely characterize a peak, and these ten scans will be averaged together, then the ‘background’ mass spectrum should also be the average of ten scans. The scans taken for the background should be taken from as close before the peak elution, and from as close after the peak elution, as practical. There is no guarantee that the intensities of background ions in the mass spectrum will be reduced to zero, but they

will be minimized relative to those ions that are derived from the sample component. Simple mathematical subtraction may lead to negative relative intensities for some ions; these are arbitrarily set to zero.

When two sample components elute very close to one another, it is not possible to follow the before/after procedure just outlined. In the simple identification of a background mass spectrum, advantage is taken of the fact that the background does not change rapidly. The portion of the chromatogram from which the background mass spectrum is taken is simply the first encountered as one moves to a point in the chromatogram when it is assumed that there is no contribution from the eluting compound. A more enlightened use of background subtraction involves creating a high quality mass spectrum from each of two closely eluting or even overlapped components. In this case advantage is taken of the fact that peak intensities that are reduced in intensity to zero do not distort the mass spectrum, and that the probabilities that ion masses overlap are small. In the case described, one can enter as background mass spectra those scans that are clearly from the second of two components with the assurance that the ions from this component will be effectively removed from the mass spectrum of the first.

The intensity behaviours of ions that belong to the background and those that belong to an eluting peak are different. This difference can be highlighted mathematically. The first derivative of the values for ion intensities that are changing will have a nonzero value. However, the first derivative of the ion intensities in an eluting peak will be characteristic in crossing zero at the retention time. This difference in behaviour can be used to identify ions from the sample as opposed to ions from the background. The mathematical result is an 'enhanced' mass spectrum. Note that the first derivatives for different ions will cross zero at slightly different times, depending on the rate of scan of the mass analyser.

Data averaging In the perfect chromatographic separation, the peak has a Gaussian shape. In the perfect spectroscopic detection system, the signal can thus be plotted as a convoluted function of mass analyser scan time and the number of scans across the peak profile, and the assumed constant level of noise recorded in the mass spectrum, from either chemical or electronic sources. None of these ideal assumptions is true. To increase the signal-to-noise (S/N) ratio of the mass spectrum recorded for a chromatographic peak, it is common practice, as described, to sum or average all of the mass spectra gathered as the peak elutes.

The need for data averaging is most apparent when the scan time is a significant fraction of the peak

width. Given that ten scans across a peak are needed to establish the elution profile, the example described here is for just such a situation. Further, we will make the assumption that (as is commonly the case) the analyser scan is from high mass to low mass. The first scans across a peak are recorded as the concentration of the sample in the source is increasing. There is a bias in ion intensities towards the low-mass end of the mass spectrum. If a steady state sample concentration is reached, a mass spectrum with accurate and true ion intensities is recorded. However, such a situation is unlikely. After the instantaneous maximum in sample concentration is reached, the amount of sample in the source starts to decrease, and the remaining scans are recorded as the concentration of the sample is decreasing. The trailing scans will also be biased in that the ion intensities at the higher mass end of the spectrum will be too high relative to their low-mass counterparts. If the peak is symmetrical, and there are enough scans on either side of the peak maximum, the bias can be muted by simply averaging all the spectra together. This processed mass spectrum should be approximately the same as if the sample concentration in the source was constant, and it can therefore be searched against a mass spectral library.

Intuitively, the analyst wants to average all the mass spectra that are recorded for an eluting peak, even at the leading and trailing edges of the peak where the signal is first and last discernible against background. Even though a simple summation is the most common practice, it is not optimal in terms of providing the maximum S/N ratio in the processed mass spectrum. Recent work by Chang shows that only the mass spectra for which the ions are at least 38% of the maximum recorded ion abundance should be included in the summation. Furthermore, the use of a matched filter (such as used in NMR experiments) provides an additional increment in S/N ratio, provided that the shape of the matched filter parallels that of the chromatographic peak itself. The data processing applies to any combination of chromatography and detection, but is demonstrated specifically with the combination of LC and MS. The widespread use of processed mass spectrometric data to provide enhanced chromatographic resolution, based on the independence of the mass spectrometric data, makes this study particularly worthwhile. It is revealing that background subtraction has been used in mass spectral data processing for decades, and essential elements of its character are still being deduced.

Reconstructed ion chromatograms A peak eluting from a chromatographic column exhibits a characteristic retention time. When using MS as a detection

technique, that retention time is determined by the point at which all the ion intensities in the mass spectrum reach their maximum value. As described previously, the first derivative of the ion intensities crosses zero. That statement was carefully crafted to differ from the statement that the retention time is the point at which the total ion current (TIC) trace reaches a maximum. The TIC summed intensity is derived from both sample-related and background ions. The two statements are usually, but not always, identical in meaning. Using the more accurate description also provides the underlying basis for introduction of the reconstructed ion chromatogram (RIC) procedure.

A data file contains mass spectra recorded as a function of time; the mass spectrum is a table of m/z values and intensities. Therefore the data file is a collection of intensities of all of the m/z channels recorded as a function of time. Any m/z value can be specified, and the intensity data can be extracted from the data set and plotted as a function of time. In the elution of a sample peak from a column into the mass spectrometer, all of the sample-related ions should follow a similar time profile as the concentration rises. It is assumed that if an ion properly 'belongs' in the mass spectrum, then its intensity profile should track in time all of the other sample-related ions. Therefore, the converse should hold. If an ion intensity trace follows the same profile as ions that are known to be in the mass spectrum, then it 'belongs' in the mass spectrum. More powerfully, if it does not follow that trace exactly, then it does not belong. The RIC is nothing but an independent series of intensity versus time traces that graphically establish spectral propriety, and provide hints when something is amiss. The plots are independently calculated, and the absolute intensity of the ion is normalized. The graphical appearance of correctness is striking in the alignment of peak maxima and in the duplication of peak shape on both leading and trailing edges. When there is an unresolved peak component, ions that belong in that mass spectra show a strikingly different trace. A peak that belongs in the background will show a slowly changing trace with multiple maxima.

If the sample analysed by GC-MS is a mixture of closely related compounds, the mass spectra of each member of that compound class will generally contain characteristic ions of the same mass. As the analyst recognizes that a correspondence exists between the ion mass and the compound class, the entire data set can be interrogated for those characteristic ions. The RIC trace should exhibit multiple maxima that correspond to the retention times of each of the individual compounds in that class. The

relative areas or peak heights for each trace do not directly represent the quantitative distribution of those class members, since they reflect the relative intensity of that mass-specific ion in the mass spectrum. However, the power of the RIC in highlighting compounds within a homologous series is evident.

Selected ion monitoring Selected ion monitoring (SIM) is a procedure used in data acquisition and processing in which the mass analyser is not scanned over a mass range, but instead hops rapidly between several preselected m/z values (this is called peak hopping). For example, instead of scanning the mass range from 35 to 1000 Da in 0.2 s, the analyser will spend some time at m/z 77, some time at m/z 91, some time on the ion at m/z 135, and finally some time at m/z 180. Usually, all of these ions are those that belong in the mass spectrum of the targeted sample component. In the scanning experiment the analyser will spend $0.2 \text{ s}/965 = 2.07 \times 10^{-4} \text{ s}$ recording the signal in each nominal mass channel. In the SIM experiment the same 0.2 s (ignoring the short time that it takes to hop between peaks) is spent monitoring the ion signal in four ion channels. The detector is integrating a signal for a period that is 242 times as long in the SIM experiment. If this is indeed where the signal is to be found, then an increase in the sensitivity of the mass spectrometric analysis can be attained simply by virtue of the fact that a longer time is spent recording the signal. S/N ratios for each individual ion trace are appropriately increased as well, since this value scales with the number of independent measurements taken. Various values for the increase in sensitivity attained with the use of SIM are found in the literature. These values range from 10 to 100 fold, and depend on the width of the ion mass window monitored, and the intensity of the ions to be found within that window. Unfortunately, ions chosen for SIM are often only those that are found in the mass spectrum of the targeted sample component. It is wise to include in the selected ions a m/z value that represents a nonsample ion, so that the true S/N ratio for the experiment can be determined.

The analyst should be clear about what is gained and what is lost in the SIM experiment. Clearly there is a gain in sensitivity. The resolution of the mass analysis is not changed, so there is no tradeoff here. What is lost is the generality of the mass spectrometric detection. In short, the analyst must already know the identity of the target compound, for example, and the masses of the ions to be monitored. These are established in separate experiments that precede the selection of the SIM experiment. If a large amount of an unexpected sample is eluted from the GC during the SIM experiment, and this unexpected

adulterant does not produce ions at the monitored masses, and there is no matrix effect as a result of its presence, it will simply go undetected, even if it elutes at exactly the same time as the targeted component. Loss of such 'insurance' capability should always be carefully considered when setting up a SIM protocol.

The output of a RIC looks identical to the output of a SIM experiment. However, in this case the RIC graphical output is the result of a data processing routine. During the data acquisition process, the mass analyser is scanned across the full mass range, and each scan is a complete mass spectrum in the stored computer file. A full data set can be interrogated repeatedly with different selected ions. A SIM experiment contains ion intensities only for those ions that were selected. The RIC provides an increase in confidence of spectral propriety, but no increase in sensitivity.

Advanced computer processing The combination of chromatography with MS would not exist today were it not for the capabilities of computers in instrument control, data acquisition, data processing, and spectral manipulation and display. Advances in computer capabilities have provided more precise control, faster and more accurate data acquisition, faster and more sophisticated data processing, and higher content and more striking visual displays of chromatographic and mass spectral data. Computational power has always been applied to the interpretation of mass spectral data, and computer-assisted interpretation of mass spectral data, specifically in the area of structure/spectral relationships, continues. Computer-aided interpretation, originally applied exclusively to EI mass spectra, is now used with success in the interpretation of CI, ESI, and MS-MS data. It is analytically compelling to support this expansion, as it is unlikely that libraries of these types of mass spectral data will grow to the size of the current libraries of EI mass spectral data. The precepts behind computer applications in the interpretation of mass spectral data have been described (Karjalainen). More recent applications have increased the speed and expanded the scope of applications, but no matter what, the progress the fundamental principles continue to apply. Pattern recognition programs can be used to recognize similarities in groups of mass spectra data. Calibration, especially in isotope ratio measurements, often involves sophisticated computer-performed mathematical algorithms. Pyrolysis MS often involves searches for similarities and differences in complex mass spectra through computer algorithms. Correlation analysis is used in many different areas of MS.

The growth in computer-assisted evaluation of chromatography-mass spectrometry data has been slower. This is surprising given the sophistication of computer hardware and software, and the proliferation of chromatography-mass spectrometry instruments. The quantitative information content of GC-MS has been described using latent variables in the context of multivariate analysis. Regression and least squares methods have been used to specifically model quantitative results obtained for GC-MS of closely eluting compounds. Procrustes analyses have been used to determine the number of significant masses in GC-MS, where significant masses represent the ions in the mass spectrum that differentiate one compound from the other. Each of these recent studies suggests that there is more information to be obtained from GC-MS than we have yet mined. The promise is that the general informational methods described will be adopted seamlessly into LC-MS and CE-MS as well.

Data Storage in Chromatography-Mass Spectrometry

Regulatory issues and requirements for good laboratory practice affect all users of analytical methods such as chromatography-mass spectrometry. Details and procedures for each user, company, or institution become part of the proper way of conducting scientific business for that organization, defined by tradition and regulation. Here, the causes and impacts of several overarching data storage and archiving issues are discussed. GC-MS is again used as the example, but of course the general issues apply to any form of chromatography-mass spectrometry.

The product of a GC-MS analysis is data. There is no collection of vials that represents a collection of compounds separated from a complex mixture. The sample aliquot analysed by the instrument is destroyed, leaving only measurement data as residue. Often, only a small fraction of that data appears in hard copy form for perusal by the analyst, who may receive a paper copy of a TIC trace, print-outs of a few selected mass spectra, and tabulated results of an automatic library search for each of these mass spectra. Each of these outputs is calculated as needed from the original data set, which is preserved within the data system, along with relevant parameters of instrument operation, calibration, and certification. Often there are several layers of safeguards that prevent post-analysis changes to the original data set. Further, in some instances a duplicate copy of the master data set is recorded remotely, while all post-run processing occurs from a local copy of the data. The backup of the data occurs automatically without

operator intervention. The rapid growth of GC-MS, coupled with the more rapid growth of regulation, implies that the sheer volume of this form of data will predictably overwhelm attempts to logically archive or access it.

Hardware Overview

GC-MS could not have been developed without the advent of the computerized data system. Conversely, the computerized data system makes it possible to exploit all the synergistic powers of the hyphenated method. It is revealing to return to early published forays into the method and read the concerns of the practitioners regarding the sheer volume of data that was available and recorded. In retrospect, the first data systems were primitive beasts. Processing speeds were very slow, and they were matched by the speed of the analogue-to-digital conversions. Data storage initially used magnetic tapes, similar to those still available today but with lower capacities. The early high-capacity data storage devices were removable platter drives. Generically, they were known as Winchester drives. The term Winchester comes from an early type of disk drive developed by IBM in 1973 that stored 30 MB and had a 30 ms access time. It was called a Winchester in honour of the 0.30-calibre rifle of the same name. For the mainframe data systems that controlled mass spectrometers, the platters (encased in cassettes with diameters of about 40 cm and thicknesses of about 5 cm) had a capacity of 10 MB. In GC-MS each platter filled up quickly; the full disk was removed from the drive, and an empty platter inserted. Winchester hard disk drives were not available for personal computers (PCs) until 1980. The PCs of today are more powerful than the mainframes used in the early days of GC-MS. Commercial systems are controlled by PCs, which is one reason that they have dropped in price. Storage capacities of 20 GBs on a single platter are available today.

Data records have a much longer life than does the original sample itself. There are rules that govern how long a sample or sample extract can be stored, at what temperature, and in what form. Outside of that time limit, that sample cannot be used for analysis. These rules exist as a result of concerns about sample degradation. In general, analysts do not worry about data degradation, although the long-term stability of magnetic-based recording media has been a topic of discussion. The relevant lifetime of data records depends on the availability of a software system that can access and manipulate the data. Analogies with commonplace computer software can be drawn readily, as each new iteration of software makes obsolete some fraction of the installed software base and its associated data. The problem is exacerbated by

a competitive marketplace and manufacturers that disappear or are eager to make older systems obsolete.

Data processing and manipulation routines are manufacturer-specific and sometimes proprietary. The computer for a mass spectrometer may remain in the laboratory past the time when the mass spectrometer itself is removed so that the system can be used as required to read and process old data files. Clearly this is neither a desirable nor an efficient approach to data archival management. Manufacturers of commercial mass spectrometers have become much more cognizant of this fact over the past few years, and analytical data interchange efforts have been undertaken. The issue of backwards data compatibility is significant, and should be considered as part of the yearly performance assessment of an analytical laboratory using chromatography-mass spectrometry. Hardware capabilities are not the only issue. The preferences and habits of individual analysts also affect the manner in which data are presented and interpreted. Individuals are shuttled into and out of laboratories regularly, and a record of individual proclivities needs to be maintained and understood, especially in systems as complex as chromatography-mass spectrometry. The proper time to determine whether archived data can be located, read, processed and re-evaluated is not in the midst of crisis or urgency. If the data are worth saving, it is worth going through an exercise to test one's ability to retrieve those data. If the exercise shows that retrieval and reuse is not feasible, the data should not be saved. Previously the criterion for saving the data was the amount of storage capacity that was available, as GC-MS files were 'large', and it was considered impossible to physically save all of the data that could be recorded. The files are still indeed 'large', but storage capacities have increased by a factor of 1000 over the past 20 years, while the files have increased in size by only a factor of 2-3 (the laboratory time frame has not changed in its perception, and the resolution of the recorded data has increased only slightly). Storage capacity is no longer a relevant issue. Meaningful retrieval has become the determinant factor.

Regulatory and Legal Issues

The very public disputations over drug testing of athletes is emblematic of many of the same issues that arise in defining and documenting the impact of chromatography-mass spectrometry. GC-MS, LC-MS, and CE-MS underlie analytical results in environmental testing, drug testing, pharmaceutical analysis, and forensic investigations, in addition to being core techniques in exploratory and discovery

research. Laboratory accreditation requires strict adherence to issues of sample handling, instrument calibration and operation, and data processing and archiving. Many commercial laboratories offer such services. This section touches on the broad perspectives of the field in this area.

It is important to remember that many analyses involving chromatography-mass spectrometry are protocol-driven. This means that the exact procedures and the instrumental means of analysis are prescribed in specific detail. Deviation results in an invalidation of the results. Such protocols may not represent the 'best' way of performing the analysis. Quality attributes such as fastest, cheapest, most sensitive, most accurate, or least prone to interference are comparative. Analytical laboratories are usually paid to produce results, not to provide comparisons. Regulations are prescriptive of what methodology can be used and proscriptive of anything else. Regulations most certainly lag behind state-of-the-art capabilities. A general rule is that regulations will not change until the approved methodology lags behind current methodology by a factor of 10. Further, that factor of 10 must be meaningful. A 10-fold lowering in the limit of detection is irrelevant if the current limit of detection suffices for practical needs.

The variability in legal treatment of analytical data from court-to-court and country-to-country suggests that any justification for preemptive consistency is weak. A chromatography-mass spectrometry approach generally recognized as valid by experts is a good basis on which to build an argument, and the 'value imputed by scientific consensus' argument is accepted in many legal systems. Analytical details have to be in conformance, and good laboratory practice helps to ensure this. In the final analysis, an explanation of the results of an analysis by chromatography-mass spectrometry will be presented to a jury or a judge with a minimum of scientific background. Here, clear and focused explanations of the basic principles of the analyses are of highest value; such explanations are the purpose of this overview.

Conclusions

It is dangerous to predict that all of the essential technical innovations that allow the linkage between chromatography and mass spectrometry are in place. It would be equally foolish to try and identify any combination for which the interface technology has not already been demonstrated, at least in a primitive sense. Certainly one major area of future innovation will be in the continued reduction in the size of the instruments. However, although gas chromato-

graphic and capillary electrophoretic separations on a chip level have been demonstrated, such devices have not swamped the marketplace. There is a realistic laboratory scale for the physical dimensions of instrumentation, and the sizes of a computer keyboard and a computer monitor are quintessential examples of that scale. Further reductions in physical size may be possible, but are not in concordance with human operation. It is not unrealistic to predict that GC-MS units will soon be the size of a PC, and may be moved about and reconfigured as easily. This reduction in physical size by a factor of about two from present day instruments will require clever packaging and insightful engineering, but does not depend on the development of fundamentally new technologies. As long as the analysis of samples occurs in a single instrumental channel (serial analysis), such scale is appropriate.

What would happen if mass spectrometers could be reduced in physical scale to the chip size (xyz dimensions of a few centimetres) and interfaced to some form of miniaturized chromatographic separation? Assuming that the performance of each individual combination was the same, the serial analysis has the potential to become a parallel analysis. The analytical results would be the same no matter which channel of analytical instrumentation is specified. Therefore parallel analysis allows many similar analyses to be run simultaneously, with special data acquisition and processing programs designed to zero identical results (results identical to each other or to a standard result) and highlight differences. Alternatively, adjacent channels of analysis may sample a system in which a variable (temperature, pressure, time, light, reactant concentration) is systematically varied. The possibilities for such miniature analytical instrument arrays are diverse and exciting.

What technological impediments stand between the present and, as an example, miniaturized laser ionization, time-of-flight mass spectrometers? The ions themselves are small, lasers and filaments can be small, and flight tubes are nothing but channels that can be folded into compressed S shapes. Electron multiplier detectors can also be made very small, subject only to space charge effects that limit the entire system. Electrical connections to the outside world are entirely manageable on a micrometre scale. There are two other physical connections to the outside world that have to be managed. The first is the introduction of the sample to the mass spectrometer. Assuming that the sample is eluted from the column, the problem is transformed into loading the sample onto the column. Miniaturized robotic injectors or microfluidics are already available for this task. The second physical connection is the attainment and

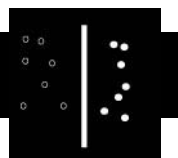
maintenance of a vacuum. Vacuum pumps are, in general, not amenable to miniaturization, since they must possess the physical means to transport molecules from inside the system to the outside environment. The only restriction is the insistence on maintaining vacuum, with the assumption that many samples will be analysed by the same mass spectrometer. If a miniaturized mass spectrometer has a total evacuated volume of 1 mL (not outside the reasonable scale), then a vacuum reservoir of 100 mL suffices for pumping by virtue of expansion. Essentially the vacuum is a rechargeable resource. Removing of the vacuum hardware as a physical limitation to the size of the mass spectrometer will be a genuine innovation in the field. Hopefully, this same overview written ten years from now will document the applications of new miniaturized chromatography-mass spectrometry systems.

See Colour Plate 12.

Further Reading

- Brakstad F (1995) *Chemometrics and Intelligent Laboratory Systems* 29(2): 157–176.
- Cole RB (ed.) (1997) *Electrospray Ionization Mass Spectrometry: Fundamentals, Instrumentation, and Applications*. New York: Wiley-Interscience.
- Demir C and Brereton RG (1997) Calibration of gas chromatography-mass spectrometry of two-component mixtures using univariate regression and two- and three-way partial least squares. *Analyst* 122: 631–638.
- Demir C, Hindmarch R and Brereton RG (1996) Procrustes analysis for the determination of number of significant masses in gas chromatography-mass spectrometry. *Analyst* 121: 1443–1449.
- Harrison AG (1992) *Chemical Ionization Mass Spectrometry*, 2nd edn. Boca Raton: CRC Press.
- Hillenkamp F, Karas M, Beavis RC and Chair BT (1991) Matrix-assisted laser desorption/ionization mass spectrometry of biopolymers. *Analytical Chemistry* 63: 1193A–1203A.
- Karjalainen EJ and Karjalainen UP (1996) *Data Analysis for Hyphenated Techniques*. Amsterdam: Elsevier Science.
- Martinsen DP and Song BH (1985) *Mass Spectrometry Reviews* 4(4): 461–490.
- Owens KG (1992) *Applied Spectroscopy Reviews* 27(1): 1–49.
- Smith RD, Olivares JA, Nguyen NT and Udseth HR (1998) *Analytical Chemistry* 40: 436–441.
- Vairamani M, Mirza UA and Srinivas R (1990) *Mass Spectrometry Reviews* 9(2): 235–258.
- Van der Greef J and Niessen WMA (1992) *Int. J. Mass Spectrom. Ion Proc.* 118–119: 857–873.
- Zenobi R and Knochenmuss R (1999) *Mass Spectrometry Reviews* 17: 337–336.
- Zhang Z and McElvain JS (1999) Optimizing spectroscopic signal-to-noise ratio in analysis of data collected by a chromatographic/spectroscopic system. *Analytical Chemistry* 71(1): 39–45.

MEMBRANE SEPARATION



R. W. Baker, Membrane Technology & Research Inc. (MTR), Menlo Park, CA, USA

Copyright © 2000 Academic Press

Introduction

Since the 1970s industrial membrane separation technology has developed into a US\$1–2 billion per year business. The market is fragmented, but can be divided into six principal industrial process areas: microfiltration, ultrafiltration, reverse osmosis, electrodialysis, gas separation and pervaporation. Dialysis, another membrane separation technique, is limited to two biomedical processes, haemodialysis (artificial kidneys) and blood oxygenators (artificial lungs). The market for these two biomedical applications is another US\$2 × 10⁹ per year. Further membrane separation applications, including membrane contactors, membrane reactors and coupled and facilitated transport, are under development. Although

similar membranes and membrane module designs are used in all of these process areas, the ways by which the separations are performed and the process applications are very different. A brief overview of each process is given here; more detailed descriptions of the individual processes are given elsewhere in the encyclopedia.

History

The concept of the ideal semipermeable membrane able to separate two species with the theoretical minimum work has been used by thermodynamicists for more than 150 years, but attempts to use membranes for practical separations did not begin until the 1900s, when Bechhold devised a technique for preparing nitrocellulose membranes of graded pore size. Later workers, particularly Zsigmondy, Bachmann, Elford and Ferry, refined these preparative techniques and membranes were used to separate a variety of laboratory solutions by dialysis and microfiltration.

By the 1930s, microporous membranes were produced commercially on a small scale. The first ion exchange membranes were made at about the same time; these were used by Teorell, Meyer and Seivers to develop their theory of ion transport. This work led eventually to the development of electrodialysis.

By the 1960s, therefore, the elements of modern membrane science had been developed, but membranes were only used in laboratories and in a few small, specialized industrial applications. There was no significant membrane industry, and total sales for all applications probably did not exceed US\$10 million. Membrane processes suffered from three problems that prohibited their widespread use: they were too slow, too expensive and too unselective. Partial solutions to each of these problems have since been developed, and sales of membranes and membrane separation equipment have grown several hundred-fold. Currently, several tens of millions of square metres of membranes are produced each year, and a membrane industry has been created.

The problem of slow permeation rates through membranes was largely overcome in the late 1960s and early 1970s by the development of imperfection-free ultrathin membranes. These membranes are anisotropic structures and consist of a thin selective surface film supported by a much thicker microporous substrate to provide mechanical strength. Because the selective surface film is very thin, these membranes have high fluxes.

The problem of packing a large membrane area into a low-cost module has also been solved since the 1980s. The earliest module designs were plate-and-frame or tubular units similar to conventional heat exchangers. These designs are still used in some processes, such as ultrafiltration, in which the ability to clean fouling deposits from the membrane surface is important. However, the cost of both designs is relatively high, and in most processes they have been displaced by capillary, hollow-fine-fibre and spiral-wound module designs.

The problem of low selectivity remains one of the principal limitations of membrane processes. No general solution has been found, although substantial improvements have been made since the 1950s.

Ultrathin Membranes

The first useful ultrathin membranes were cellulose acetate reverse osmosis membranes produced by Loeb and Sourirajan, two researchers at the University of California at Los Angeles. The development of these thin, and hence high flux, membranes led to the reverse osmosis industry in the 1960s. In the Loeb–Sourirajan technique, a solution containing ap-

proximately 20% polymer is cast as a thin film on a nonwoven fabric web and is then precipitated by immersion in a bath of water. The water very rapidly precipitates the top surface of the cast film, forming the selective skin. This skin then slows down the entry of water into the underlying polymer solution, which precipitates much more slowly, forming a more porous substructure. A scanning electron micrograph showing the porous substructure and the selective skin of a Loeb–Sourirajan membrane is shown in **Figure 1**. The selective layer thickness is typically less than 0.2 μm .

About one-third of the reverse osmosis and almost all ultrafiltration membranes currently produced are made by the Loeb–Sourirajan technique. This type of membrane is also widely used in gas separation processes.

In recent years, new approaches have been developed to produce anisotropic membranes with even thinner selective layers than those made by the Loeb–Sourirajan method. Selective layers only a few tens of nanometers in thickness, and effectively free of imperfections, have been claimed for these so-called thin-film composite membranes. Thin-film composite membranes can be made by a number of methods, of which two are particularly important: coating with a dilute polymer solution and interfacial polymerization. In the coating method, which was developed first, a very dilute solution of the polymer is prepared in a volatile solvent, such as hexane. A thin film of this polymer solution is deposited on the microporous support surface by immersing and then slowly withdrawing the support from the solution. As the solvent evaporates, an extremely thin polymer film is left behind. This technique is used to manufacture ultrathin membranes for gas separation and pervaporation.

The second important method for preparing composite membranes is interfacial polymerization. In this method, an aqueous solution of a reactive monomer, such as a diamine, is deposited in the pores of a microporous support membrane. The membrane is then immersed in a water-immiscible solvent solution containing a multivalent reactant, such as a triacid chloride in hexane, which causes the monomer to polymerize and cross-link. Polymerization is confined to the interface of the two immiscible solutions, so a thin, highly selective layer is formed. The procedure is illustrated in **Figure 2**. The interfacial polymerization technique is used to produce most of today's reverse osmosis membranes.

Membrane Modules

The principal module designs – plate-and-frame, tubular, hollow-fibre and spiral-wound – are illustrated

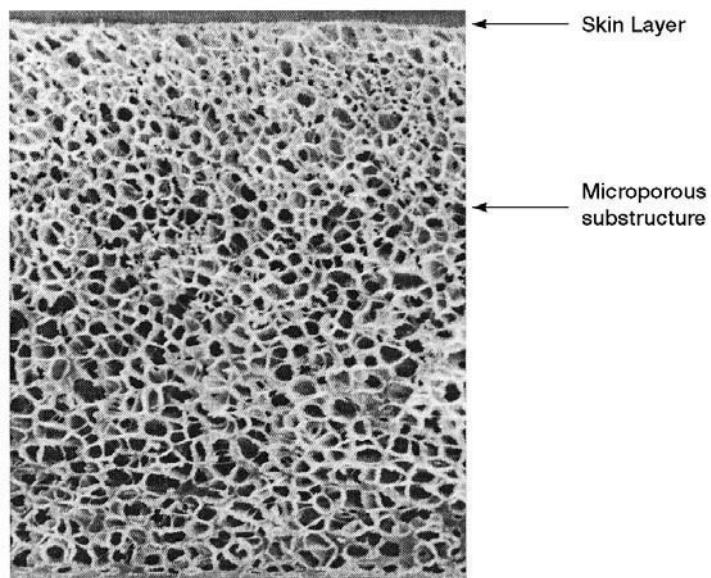


Figure 1 Scanning electron micrograph of the cross-section of a Loeb-Sourirajan reverse osmosis membrane. The development of this type of anisotropic membrane was a critical breakthrough in the development of membrane technology.

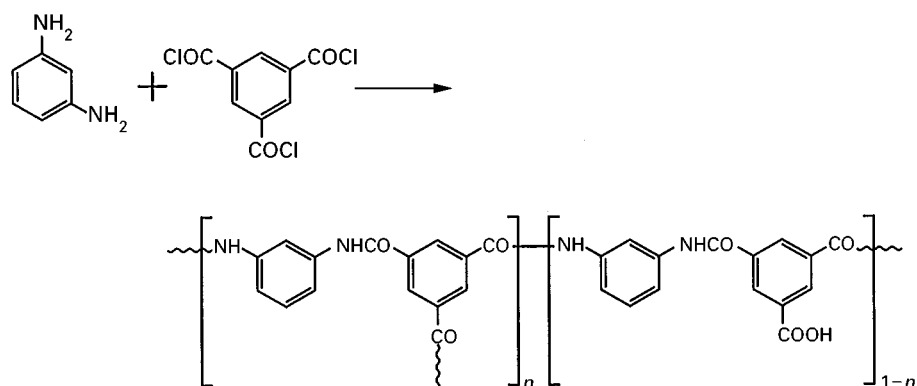
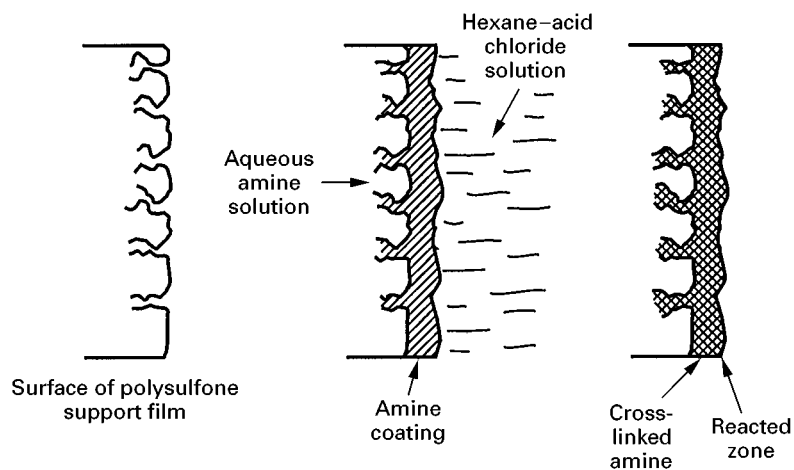


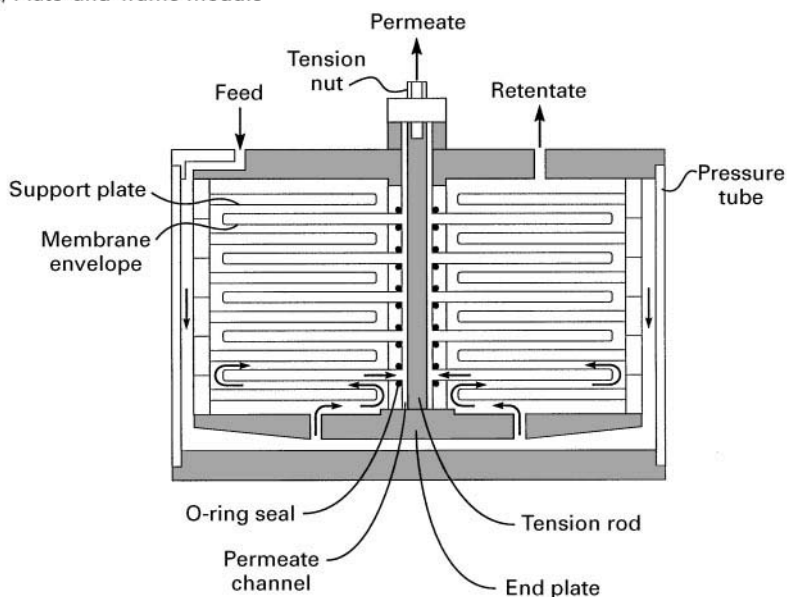
Figure 2 Preparation of ultrathin composite membranes by reaction of an amine dissolved in water and an acid chloride dissolved in hexane. The chemistry shown is widely used to prepare seawater desalination reverse osmosis membranes. (Reproduced with permission from Roselle LT *et al.* (1977). In: Sourirajan (ed.) *Reverse Osmosis and Synthetic Membranes*.)

in Figures 3 and 4. In the plate-and-frame design shown in Figure 3A a series of membrane discs separated by spacers and support plates are held between two end plates connected by a tension rod. The geometry of the plates is such that solution entering one end of the module passes sequentially over all the membrane area. Solution that permeates the membrane is collected in a permeate collection channel. Tubular modules shown in Figure 3B consist of a porous support tube, which is coated on the inside surface with the selective membrane. The porous support tube nests inside steel or strong plastic tubes that

can support the applied pressure. Each tube is between 0.5 and 2 cm in diameter and up to five tubes can be housed in a single support tube. Tubular modules are now only used in ultrafiltration applications for which good flow distribution across the membrane surface with no stagnant areas is required to control membrane fouling. In this application up to 20 tubes are connected in series as shown in Figure 3B.

Plate-and-frame and tubular membranes were widely used in the early days of the modern membrane era, but by the 1980s had been largely displaced by hollow-fibre, capillary or spiral-wound membrane

(A) Plate-and-frame module



(B) Tubular module

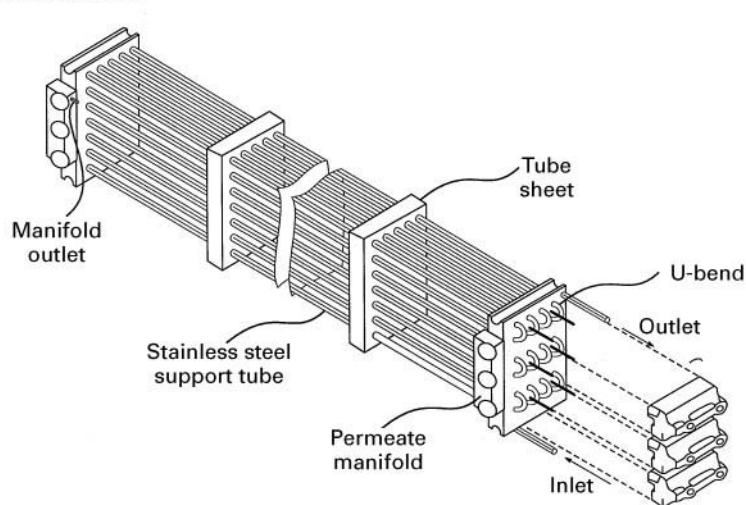
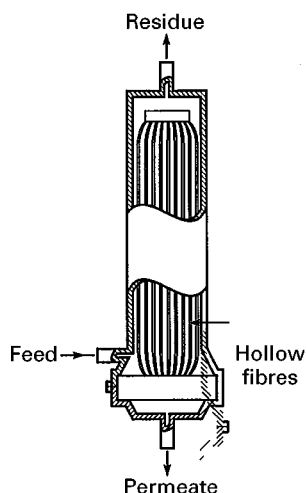


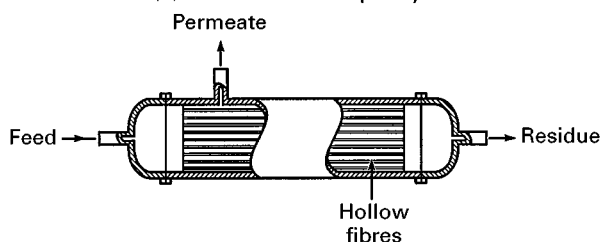
Figure 3 Schematic of a reverse osmosis plate-and-frame module (A) and a tubular ultrafiltration membrane module (B). These two module designs were used in the first large industrial membrane systems but are now limited to a few niche applications.

(A) Hollow-fibre module

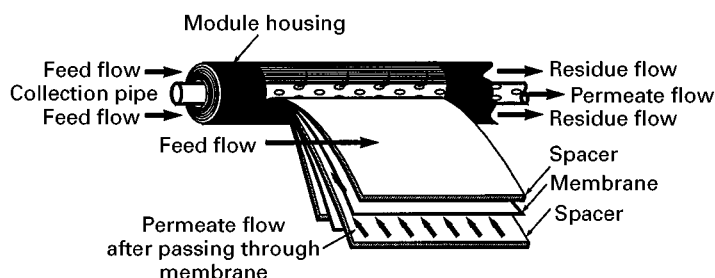
(i) Shell-side feed hollow fine fibre modules



(ii) Bore-side feed capillary module



(B) Spiral-wound module



Spiral-wound module cross-section

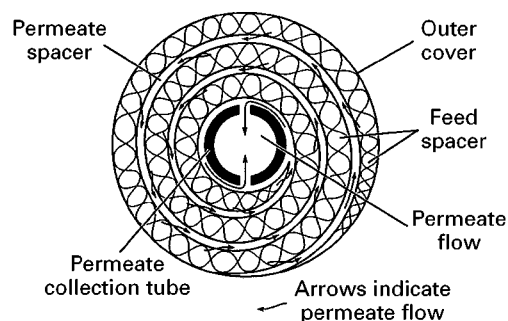


Figure 4 Schematic illustrating hollow-fibre (A) and spiral-wound (B) membrane modules. Most large-scale membrane processes use one of the designs shown.

modules, which are much less expensive to produce per square metre of membrane area. Capillary and hollow-fine-fibre membranes are quite similar, differing principally in the diameter of the fibre used. Both types are produced by a spinning process much like conventional fibre spinning. As a result, the cost of producing the membrane per square metre is quite low. Most of the cost of producing hollow-fibres is incurred in the fibre potting operation when fibres are mounted inside the module shell. Currently, in capillary modules, the feed fluid circulates through the fibre lumen (bore side) as shown in Figure 4A. In hollow-fibre modules, the feed fluid circulates around the outer surface (shell side) of the fibres as shown in Figure 4B.

Spiral-wound modules were originally developed for reverse osmosis applications but are now used in ultrafiltration and gas separation processes as well. This work, carried out by Fluid Systems Inc. under sponsorship of the Office of Saline Water

(later the Office of Water Research and Technology), resulted in a number of spiral-wound module designs. The design shown in Figure 4 is the most common, consisting of a membrane envelope wound around a perforated central collection tube. The module is placed inside a pressure vessel, and feed solution is circulated axially down the module across the membrane envelope. A portion of the feed permeates into the membrane envelope, spirals towards the centre of the module and exits through the collection tube.

The flat-sheet membranes used in spiral-wound modules usually have higher fluxes than capillary and hollow-fibre membranes made from the same material. This is because it is difficult to make hollow-fibre selective skins as thin as flat-sheet skins. For this reason, although spiral-wound modules are usually two to five times more expensive on a square metre basis than hollow-fibre membranes, they are competitive in many applications.

Membrane Selectivity

Improving membrane selectivity is still an area of active research. In some applications such as desalination of water, progress has been made, and membranes have the required selectivity to compete with other processes such as distillation. The first reverse osmosis membranes had salt rejections of approximately 96–97% and could only produce potable water from low concentration brackish water feeds. The best current membranes have salt rejections of up to 99.7% and can produce potable water from seawater. Further improvements in membrane selectivity are not required in this application.

In other applications, the low selectivity of membranes remains a problem. Ultrafiltration membranes, for example, cannot separate dissolved macromolecules, such as albumin (M_r 60 000) and γ -globulin (M_r 150 000). Therefore, ultrafiltration is limited to the separation of very large molecules from very small ones, such as macromolecules from dissolved micro-ions. Selectivity problems also exist in electrodialysis, gas separation and pervaporation.

Mechanism of Membrane Separation

The property of membranes used in separation processes is their ability to control the permeation of different species. Most membranes fall into one of the two broad categories illustrated in **Figure 5**. In microporous membranes, permeants are separated by pressure-driven flow through tiny pores. A separation is achieved between different permeants because one of the permeants is excluded (filtered) from some of the pores through which the smaller permeants move. In solution-diffusion membranes the membrane material is a dense polymer layer and contains no fixed pores. Permeants dissolve in the membrane material as in a liquid and then diffuse through the membrane down a concentration gradient. Separation of different permeants oc-

curs because of differences in the solubility of the permeant in the membrane material and the rate at which the permeant diffuses through the membrane.

The difference between the pore-flow and the solution-diffusion mechanisms lies in the relative size and lifetime of pores in the membrane. In dense polymeric solution-diffusion membranes, no permanent pores exist. However, tiny free volume elements, a few tenths of a nanometre in diameter, exist between the polymer chains from which the membrane is made. These free-volume elements are present as statistical fluctuations that appear and disappear on a timescale only slightly slower than the motion of molecules traversing the membrane. Permeating molecules diffuse from free-volume element to free-volume element at a rate determined by the thermal motion of the polymer chains from which the membrane is made. In contrast, in a pore-flow membrane the pores are fixed and do not fluctuate in position or size on the timescale of molecular motion. The larger the individual free-volume elements are, the more likely they are to be present long enough to produce pore-flow characteristics in the membrane. As a rule of thumb the transition between permanent (pore-flow) and transient (solution-diffusion) pores appears to be in the range 0.5–1.0 nm diameter. This means that the processes of gas separation, reverse osmosis and pervaporation, all of which involve separation of permeants with molecular weights of less than 200, use solution-diffusion membranes. On the other hand, microfiltration and ultrafiltration, which involve separation of macromolecular or colloidal material, use finely microporous pore-flow membranes.

Commercial Membrane Separation Processes

The current status of membrane separation technology is summarized in **Table 1**. There are seven commercial membrane separation processes. Of these, the first five – microfiltration, ultrafiltration, reverse osmosis, electrodialysis and dialysis – are all well-established technologies with a market served by several experienced companies. Although incremental improvements in membranes and membrane systems for these technologies are expected, no major breakthroughs appear imminent. The remaining two technologies – gas separation and pervaporation – are developing technologies for which the market size, application area, and process design are still changing. Finally, several processes not shown in **Table 1**, including coupled and facilitated transport, membrane contactors and membrane reactors, are still in

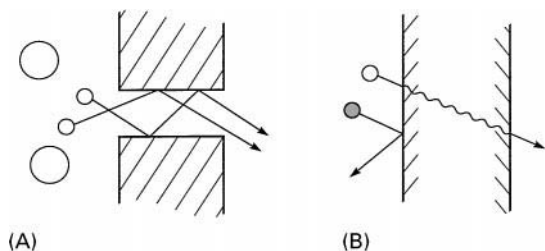


Figure 5 Schematic illustrating the two principal types of membrane separation mechanisms. (A) Microporous membranes separate by molecular filtration. (B) Dense solution-diffusion membranes separate because of differences in the solubility and mobility of permeant in the membrane material.

Table 1 Summary of the established membrane separation technologies

<i>Process</i>	<i>Type of membrane</i>	<i>Material passed</i>	<i>Material retained</i>	<i>Driving force</i>	<i>Status – typical application</i>
Microfiltration	Finely microporous 0.1–10 μm	Water, dissolved solutes	Suspended solids, bacteria	Pressure difference 5–50 psi	Developed (\sim US\$700 million per year). Removal of suspended solids, bacteria in pharmaceutical, electronics industries
Ultrafiltration	Finely microporous 1–100 nm	Water, dissolved salts	Macromolecules, colloids	Pressure difference 20–100 psi	Developed (\sim US\$150 million per year). Removal of colloidal material from wastewater, food process streams
Reverse osmosis	Dense solution-diffusion	Water	Dissolved salts	Pressure difference 100–1000 psi	Developed (\sim US\$200 million per year). Drinking water from sea, brackish or groundwater; production of ultra-pure water for electronics and pharmaceutical industries
Electrodialysis	Electrically charged films	Water	Ions	Voltage difference 1–2 V	Developed (\sim US\$200 million per year). Drinking water from brackish water; some industrial applications too
Dialysis	Finely microporous 10–100 nm	Dissolved salts, dissolved gases	Blood	Concentration differences	Developed (\sim US\$1.3 billion per year for artificial kidney; US\$500 million per year for artificial lung)
Gas separation	Dense, solution-diffusion	Permeable gases and vapours	Impermeable gases and vapors	Pressure difference 100–1000 psi	Developing (\sim US\$150 million per year). Nitrogen from air, hydrogen from petrochemical/refinery vents, carbon dioxide from natural gas, propylene and VOCs from petrochemical vents
Pervaporation	Dense, solution-diffusion	Permeable micro-solutes and solvents	Impermeable micro-solutes and solvents	Vapour pressure 1–10 psi	Developing (\sim US\$10 million per year). Dehydration of solvents (especially ethanol)

the laboratory or early commercial stage. In the following sections each of these membrane technology areas is described briefly. More detailed descriptions of the more important processes are given elsewhere in the encyclopedia.

Microfiltration

The process Microfiltration, ultrafiltration and reverse osmosis are related membrane processes differing in the size of the material retained by the membrane. As shown in **Figure 6**, reverse osmosis membranes can generally separate dissolved micro-solutes with a molecular weight below 500 by a solution-diffusion mechanism. When the molecular weight of the solute exceeds 500, the separation mechanism of the membrane is molecular filtration, in which separation characteristics are determined by the size of the particles in the mixture and the diameter of the pores in the membrane. By convention, membranes having pore sizes up to approximately 0.1 μm in diameter are considered to be ultrafiltration membranes. Microfiltration membranes are those with pore diameters in the range of 0.1 to 10 μm .

Above 10 μm the separation medium is considered to be a conventional filter.

Ultrafiltration/microfiltration membranes fall into two broad categories: screen membrane and depth membrane filters, as shown in **Figure 7**. Screen filters are anisotropic with small surface pores on a more open substructure. The surface pores in screen membrane filters are uniform and show a sharp cutoff between material that is completely retained by the membrane and material that penetrates the membrane. Retained material accumulates on the membrane surface. Depth membrane filters have a much wider distribution of pore sizes and usually have a more diffuse cutoff than screen membrane filters. Very large particulates are retained on the surface of the membrane, but smaller particulates entering the membrane are trapped at constrictions or adsorbed onto the membrane surface. Screen filters are usually used in ultrafiltration applications (see next section). The membrane pores are normally very small, on the order of 5–50 nm in diameter. Particulates and colloidal matter retained at the membrane surface are removed by a tangential flow of the feed solution. In this type of process, 80–90 vol% of the

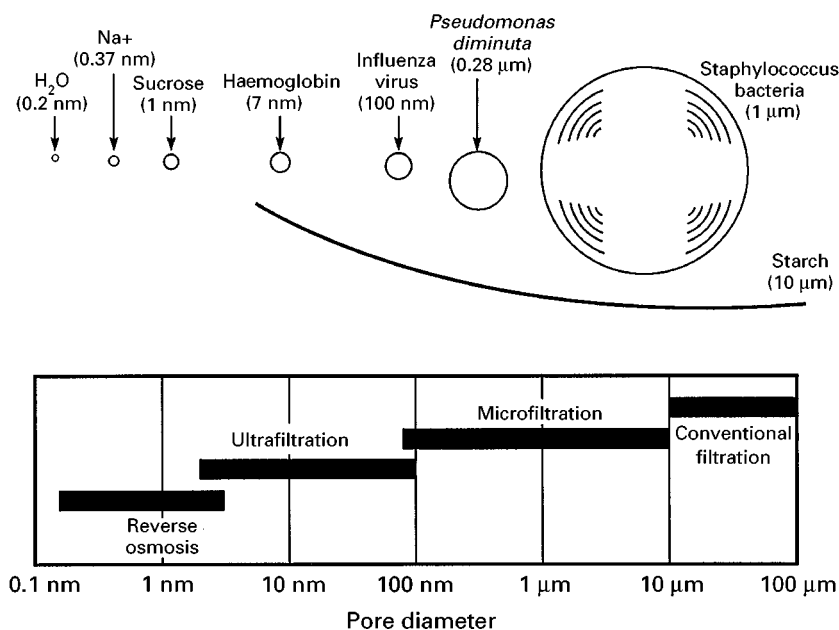


Figure 6 Pore sizes of reverse osmosis, ultrafiltration, microfiltration and conventional filtration membranes.

feed solution permeates the membrane as a clean filtrate. The remaining solution containing the rejected material is collected as a concentrated residue.

Depth filters are usually used in microfiltration applications. The surface membrane pores can be quite large, on the order of 1–10 μm in diameter, but many smaller restrictions occur in the interior of the membrane. This means that bacteria or virus particles as small as 0.2 μm in diameter are completely prevented from penetrating the membrane. Microfiltration membranes are usually used as an in-line filter. All of the feed solution is forced through the membrane by an applied pressure. Retained particles are collected on or in the membrane.

The lifetime of microfiltration membranes is often improved by using a more open prefilter membrane

directly before the final membrane. Prefilters are not absolute filters, but trap most of the very large particulates and many of the smaller ones before the feed solution reaches the finer membrane filter. This reduces the particle load that the finer membrane must handle, and thus increases its useful life.

Applications The primary market for microfiltration membranes is disposable cartridges for sterile filtration of water for the pharmaceutical industry and final point-of-use polishing of ultrapure water for the electronics industry. The cost of microfiltration compared with the value of the products is small. Cold sterilization of beer, wine and other beverages is another emerging market area. In these processes the microfiltration cartridge removes all yeast and

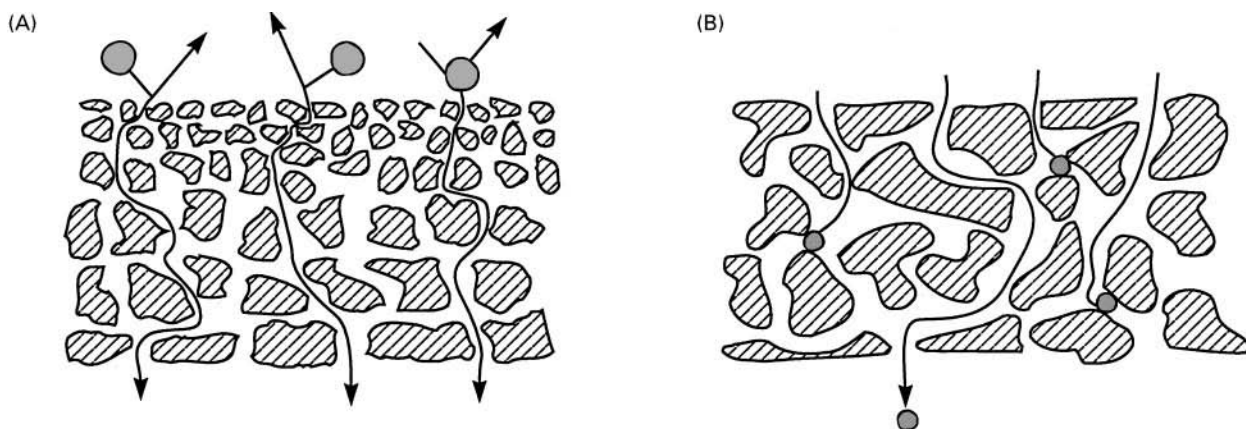


Figure 7 Separation of particulates can take place at the membrane surface according to a screen filtration mechanism (A) or in the interior of the membrane by a capture mechanism as in depth filtration (B).

bacteria from the filtrate. This process was introduced on a commercial scale in the 1960s. Although not generally accepted at that time, the process has become common in recent years.

Ultrafiltration

The process Ultrafiltration is intermediate between microfiltration and reverse osmosis. The most retentive ultrafiltration membrane has a substantial rejection to microsolute, such as raffinose (M_r 504), while the most open ultrafiltration membrane will be just able to retain a molecule of relative molecular mass one million. In practice, the distinction between ultrafiltration, reverse osmosis and microfiltration is vague, and it is possible to prepare membranes covering the entire range of reverse osmosis, ultrafiltration and microfiltration by making small changes in membrane preparation procedures.

Essentially all ultrafiltration membranes are screen filtration membranes and separate the retained material because of the small pores in their top surface layer (see Figure 7A). Membranes are characterized by their molecular weight cutoff, which is usually defined as the molecular weight at which the membrane retains more than 95% of the test solute. The definition is ambiguous, because flexible-backboned, linear molecules can penetrate membranes more easily than rigid, globular molecules, such as dissolved proteins. In addition, despite the claims of the manufacturers, no ultrafiltration membrane has a perfectly sharp molecular weight cutoff. All membranes contain a range of pore sizes and the passage of molecules through the pores is completely unhindered only for very small molecules. Typical molecular weight cutoff curves for a series of commercial membranes are shown in Figure 8.

Ultrafiltration systems generally operate at pressures of 20–100 psi (140–690 kPa). Osmotic pressure effects are not significant in ultrafiltration, and high operating pressures are not required to produce high fluxes. Moreover, because of their porous structure, ultrafiltration membranes compact under pressures above 100 psi (690 kPa).

The most important problem associated with ultrafiltration membranes is surface fouling. The problem is illustrated in Figure 9. Material unable to pass through the membrane accumulates at the surface, forming a solid gel-like film that acts as a barrier to the flow of permeate through the membrane. The thickness of the fouling film is controlled by the sweeping action of the feed solution past the membrane surface. This circulating flow of solution hydrodynamically scrubs the membrane surface, continuously removing the surface film. Thus a balance is

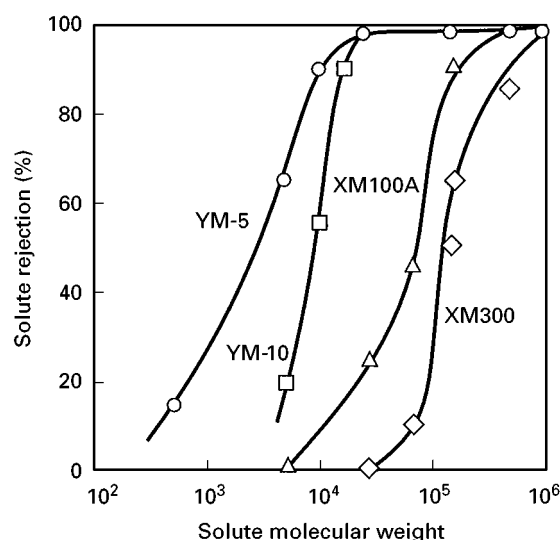


Figure 8 Molecular weight cutoff curves of various ultrafiltration membranes. (Amicon Corporation trade literature.)

achieved between circulation of solution past the membrane surface, which removes the gelled material, and the flux of permeate through the membrane, which brings fresh material to the membrane surface. Therefore, in ultrafiltration, only a portion of the feed

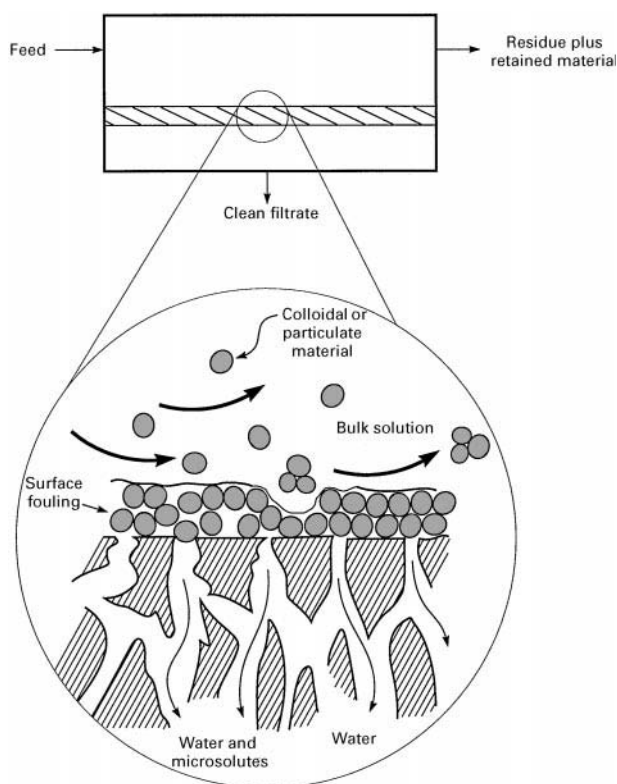


Figure 9 Schematic of ultrafiltration illustrating the dynamic process of deposition and removal of particulate and colloidal material from the surface of the membrane.

solution permeates the membrane; the remaining solution, containing the retained material, is removed as a concentrated residue stream.

If the feed solution circulation rate across the membrane surface is increased, the thickness of the fouling layer on the membrane surface decreases, and higher permeate fluxes through the membrane are obtained. However, at some point the increased energy cost involved in recirculating the feed solution offsets the savings produced by the higher membrane fluxes. With highly fouling solutions, energy consumption of 30–100 kWh per 1000 gallons (30–100 MJ m⁻³) of permeate produced is typical. The resulting electric energy expense represents a large fraction of the operating cost of an ultrafiltration plant. Increasing the operating pressure of the membrane system to force more permeate through the membrane is not a viable method of increasing the membrane flux because this only produces a thicker gel layer on the membrane surface so that the flux remains constant or even declines.

Even when most of the layer of deposited material on the membrane surface is continuously removed, a portion remains and gradually densifies. This results in decreased permeate flux through the membrane with time. Periodically, ultrafiltration membrane modules are cleaned by washing with a membrane-cleaning solution. This restores the flux to almost its original value, after which the flux begins to decline again. The process is illustrated in **Figure 10**. Unfortunately, cleaning of badly fouled membranes does not completely restore the flux to the starting value so that a proportion of the membrane flux is permanent-

ly lost. This permanent loss results from deposits of fouling material inside the membrane, which cannot be removed even by vigorous cleaning. The fouling material gradually accumulates until even the flux of a freshly cleaned membrane is less than 50% of the original value. At this time, the membrane is due for replacement. A typical ultrafiltration membrane life-time is 1–3 years.

Because of membrane fouling, the flux of ultrafiltration membranes depends highly on the composition of the feed solution and the process operating conditions. In the removal of trace particulates for the preparation of ultrapure water, the feed solution is already clean, and fluxes higher than 50–100 gal per ft² per day (85–170 L per m² per day) are achieved. With more concentrated and contaminated solutions, such as food processing streams, industrial wastewaters, or electrocoat paint wastes, typical fluxes are 10–30 gal per ft² per day (17–50 L per m² per day).

Applications Ultrafiltration membranes were originally developed for the laboratory market and found an application in the concentration and desalting of protein solutions. Later, Abcor and Romicon developed the industrial ultrafiltration market. The first major application was the ultrafiltration of electrocoat paint. The process is illustrated in **Figure 11**. In electrocoat paint operations metal parts are immersed in a tank containing 15–20% of the paint emulsion. After coating, the piece is removed from the tank and rinsed to remove excess paint. The ultrafiltration system removes ionic impurities from the paint tank carried over from earlier operations and provides clean rinse water for the countercurrent rinsing operation. The concentrated paint emulsion is recirculated back to the tank. Tubular and capillary fibre membrane modules are generally used in these plants because the feed solution easily fouls the membrane. Other large applications of ultrafiltration are the concentration of milk whey in the food industry to recover milk proteins and to remove lactose and salts in the membrane filtrate, and the concentration of oil emulsions in the metal finishing industry. Although some ultrafiltration plants treat industrial waste streams, this is not a common application because the process is expensive. The preparation of ultrapure water by ultrafiltration for the electronics industry is a newer, but growing, application. Biotechnology applications are, as yet, small.

The problem of membrane fouling in ultrafiltration systems requires expensive, energy-consuming pumps to recirculate the feed solution. Costs of ultrafiltration systems are on the order of US\$5–10 per 1000 gal of permeate, precluding its use in large, low-value applications such as wastewater treatment.

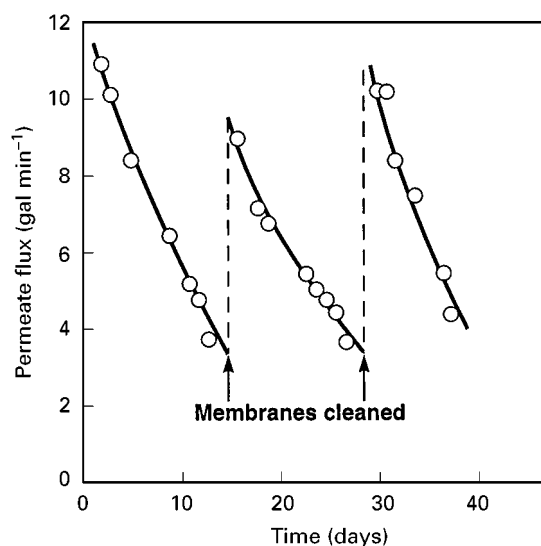


Figure 10 Ultrafiltration flux as a function of time for an electrocoat paint latex solution. Fouling causes flux decline in a matter of days. Periodic cleaning is required to maintain high fluxes.

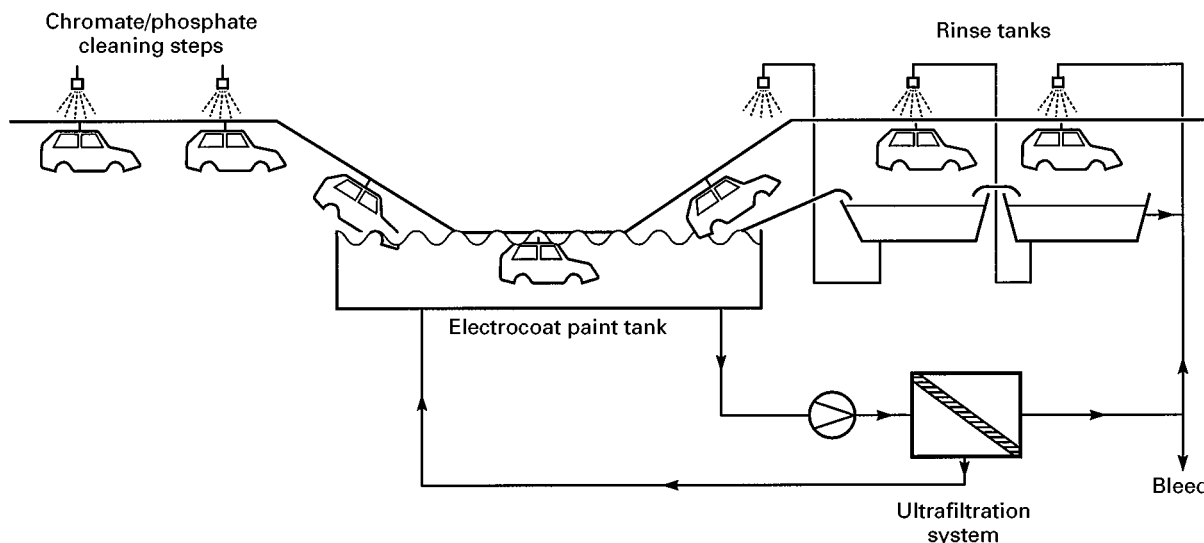


Figure 11 Flow schematic of an electrocoat paint ultrafiltration system. The ultrafiltration system removes ionic impurities from the paint tank carried over from the chromate/phosphate cleaning steps and provides clean rinse water for the countercurrent rinsing operation.

Therefore, ultrafiltration is limited to the type of high-value streams listed above. Development of more fouling-resistant membranes and better module designs could allow wider use of the process.

Reverse Osmosis

The process The processes of osmosis and reverse osmosis are illustrated in **Figure 12**. In normal osmosis, a membrane is used to separate water from a salt solution. If the membrane is semipermeable, that is, it allows the passage of water but does not pass salt, the small difference in water concentration (salt solution) will cause water to flow into the salt side of the membrane. This flow will continue until the hydrostatic pressure head on the salt solution exactly balances the flow of water across the membrane. This balance is known as osmotic equilibrium. In reverse

osmosis, a pressure is applied to the salt solution that is even higher than the osmotic pressure of the solution. This applied pressure reverses the osmotic water flow, and water flows from the salt solution to the pure water side of the membrane. Therefore, reverse osmosis is a method of desalting saltwater solutions. Equilibrium osmotic pressures are directly proportional to salt concentration and are surprisingly large. For example, the osmotic pressure for sodium chloride is approximately 100 psi (690 kPa) for a 1% salt solution.

Two parameters affect the performance of reverse osmosis membranes. The first is the flux or flow per unit area per time, J , of water through the membrane, usually described by the equation:

$$J = A(\Delta P - \Delta \pi) \quad [1]$$

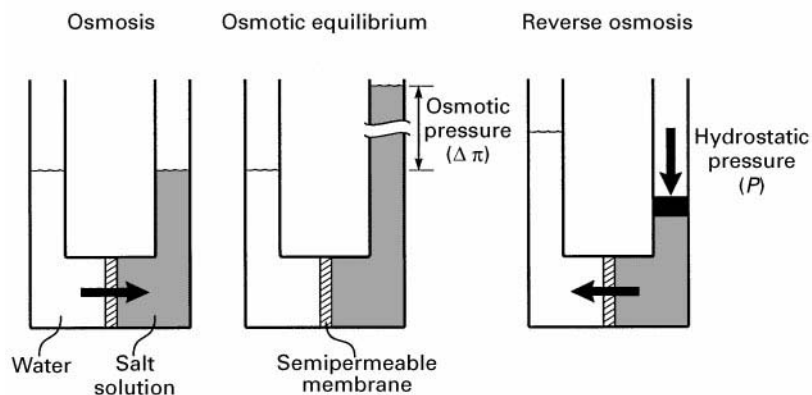


Figure 12 Osmotic effects across a semipermeable membrane. (Reprinted with permission from Roper and Lightfoot (1995) *Journal of Chromatography* 702: 3–26, with permission from Elsevier Science.)

where A is the hydrodynamic water permeability parameter, ΔP is the pressure difference across the membrane, and $\Delta\pi$ is the osmotic pressure difference across the membrane. Thus, once the osmotic pressure of the salt solution has been overcome, the water flux increases linearly with applied pressure. The salt flux through reverse osmosis membranes, J_s , is proportional to the salt concentration differences (ΔC) across the membrane, but is independent of the applied pressure. Thus:

$$J_s = B(\Delta C) \quad [2]$$

where B is the salt permeability factor. This means that the performance of reverse osmosis membranes, as measured by the salt rejection, improves as the applied pressure increases. Therefore, reverse osmosis membranes are usually operated at high pressures to obtain the maximum throughput commensurate with reasonable capital and energy costs. With current membranes, operating pressures are usually between 200 (1380) and 800 psi (5520 kPa).

The second parameter that affects membrane performance is the salt passage through the membrane. Ideally, the membrane should be completely selective for salt. This is never the case, and a small fraction of the salt passes through the membrane. The fraction that appears in the product is usually measured in terms of the rejection coefficient of the membrane, defined as:

$$R = \frac{[\text{salt concentration in feed} - \text{salt concentration in product}]}{\text{salt concentration in feed}} \times 100\% \quad [3]$$

Thus, a completely selective membrane has a rejection of 100%, whereas a completely nonselective membrane has a rejection of 0%. A typical plot of flux and rejection versus operating pressure is shown in Figure 13.

The first successful reverse osmosis membranes were made by Loeb and Sourirajan and had rejections in the range 97–98%. These membranes produced potable water (less than 500 ppm salt) from feed water containing up to 1% salt. This salt concentration is typical of many brackish groundwaters, so these membranes found an immediate application in the desalination of such waters. However, production of potable water from seawater requires a membrane with a salt rejection of greater than 99%. Loeb–Sourirajan cellulose acetate membranes can be modified to obtain this rejection, but only by reducing membrane flux to uneconomically low values. In the mid-1970s, Du Pont produced improved polyamide hollow-fibre membranes (the B10 Permeator) which had greater than 99% rejection. At about the same

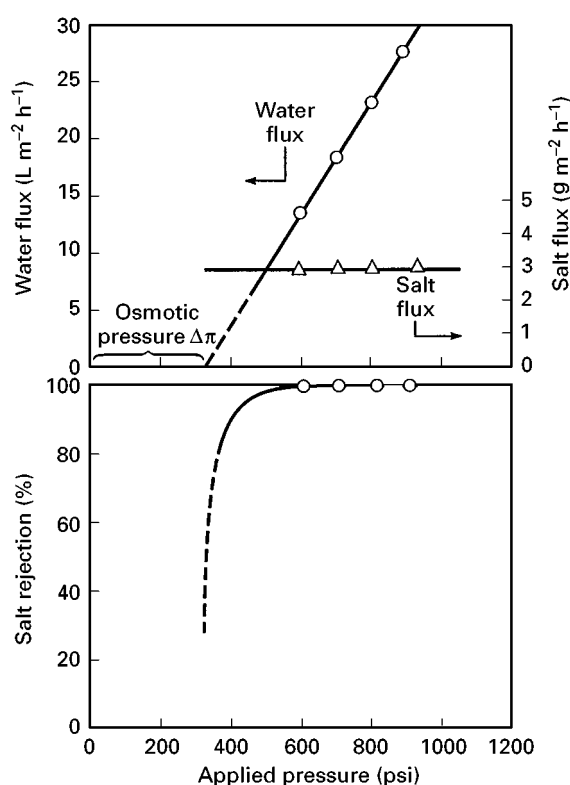


Figure 13 Flux and rejection data for a model seawater solution (3.5% sodium chloride) in a good quality reverse osmosis membrane (FilmTec Corp. FT 30 membrane) as a function of pressure. The salt flux, in accordance with eqn [2], is essentially constant and independent of pressure. The water flux, in accordance with eqn [1], increases with pressure, and, at zero flux, meets the pressure axis at the osmotic pressure of seawater ~ 350 psi. (Reprinted from Wijmans JG and Baker RW (1995) The solution-diffusion model: a review. *Journal of Membrane Science* 107: 1–21, with permission of Elsevier Science.)

time, interfacial polymerization composite membranes were produced by Cadotte at North Star Research. These composite membranes had salt rejections greater than 99%, and subsequent improvements have raised these rejections to 99.5–99.8%. Interfacial composite membranes have now become the industry standard; three-quarters of current reverse osmosis membranes are of this type.

Reverse osmosis membranes are produced in several module configurations. Most of the modules used are of the spiral-wound type, which has 80% of the market. Hollow-fibre membrane modules are generally limited to seawater reverse osmosis plants. A few plate-and-frame and tubular modules are used in food processing and the treatment of industrial wastewater, which usually contain high levels of suspended solids and require this type of nonfouling module.

Applications Approximately half of the reverse osmosis systems currently installed are desalinating

brackish water or seawater. Another 40% are used to produce ultrapure water for electronics, pharmaceuticals and power generation. The remainder are used in small niche applications such as pollution control and food processing.

Brackish water desalination The salinity of brackish groundwater is usually between 1500 and 5000 mg L⁻¹. The World Health Organization recommends that drinking water should contain less than 500 mg L⁻¹ salt, so up to 90% of the salt must be removed from these waters. This is easily achieved by reverse osmosis. A typical process flow scheme is shown in **Figure 14**. Frequently brackish water is contaminated with suspended solids, so flocculation, sand filtration, and a final cartridge filter are used to remove these components first. Adjustment of pH and addition of antiscalants may also be necessary to prevent calcium, magnesium or silica precipitating on the membrane as water is removed and the feed becomes more concentrated. The water may also be sterilized by addition of chlorine to prevent bacterial growth on the membrane. Even when these elaborate and costly feed water pretreatment steps are used, some fouling of the membrane still occurs. Therefore, periodically the plant is taken off-line and the membranes are cleaned by circulating a hot cleaning solution. Typical operating pressures for these systems are in the 200–300 psig range. Plant capital costs are in the range US\$1.00–2.00 per gal per day (plant) capacity, and operating costs are about

US\$1–2 per 1000 gal of treated water produced. Well-maintained plants have useful membrane lifetimes of 3–5 years.

Seawater desalination Seawater contains about 3.5% dissolved salt, which means membranes with salt rejections above 99.3% are required to produce potable water. Today's membranes can easily meet these targets, and many seawater desalination plants are now operating. Because of the high osmotic pressure of seawater (~ 350 psi (2415 kPa)) these plants operate at pressures of 800–1000 psi (5520–6900 kPa). Typical seawater reverse osmosis plants have a capital cost of US\$4–5 gal per day capacity and produce desalted water for a cost of about US\$5 per 1000 gal of product. These costs mean the process is most competitive for systems below 10 million gal per day capacity. Above this range economies of scale tend to favour multi-effect evaporation plants often built to use the waste heat from electric power stations.

Ultrapure water With the development of the electronics industry, a large market has emerged for reverse osmosis plants to produce ultrapure water containing < 1 ppb total ions from water normally containing 50–100 ppm total ions. Typical operating pressures for the reverse osmosis systems used in these plants are low, on the order of 100–150 psi (690–1035 kPa). The reverse osmosis plant removes 98–99% of the salts and dissolved particles in the feed

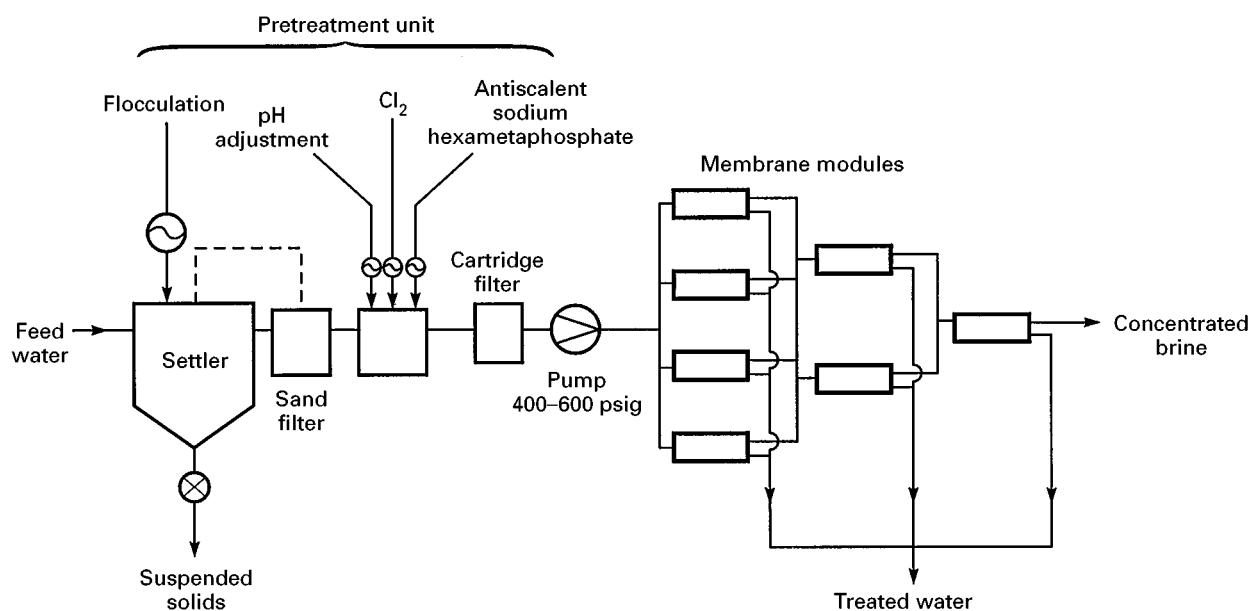


Figure 14 Flow schematic of a brackish water reverse osmosis plant. The plant contains seven pressure vessels each containing six membrane modules. The pressure vessels are arranged in a Christmas tree array to maintain a high feed velocity through the modules as treated water is removed in the permeate.

water. Carbon adsorption and ion exchange units are used to remove the remaining contaminants.

Electrodialysis

The process Electrodialysis is a process in which electrically charged membranes are used to separate ions from aqueous solutions under the driving force of an electrical potential difference. The process, illustrated in **Figure 15**, utilizes an electrodialysis stack built on the filter press principle. The stack consists of 200–400 alternate cationic and anionic membranes between two electrodes; the aqueous feed solution flows through the cells between each pair of membranes. When an electrical potential difference is applied between the two electrodes, positively charged cations in the feed solution move toward the cathode. These ions easily pass through the negatively charged cation exchange membranes, but are retained by the positively charged anion exchange membranes. Similarly, negatively charged anions migrate towards the anode, pass through the anion exchange membrane and are retained by the cation exchange membrane. Because of the arrangement of ion-selective

membranes, the migrating ions become concentrated in each alternate cell in the stack. Thus, ions removed from the aqueous feed solution are concentrated into two separate streams.

Applications

Brackish water Brackish water desalination is the largest application of electrodialysis. The competitive technologies are ion exchange for very dilute solutions (below 500 ppm) and reverse osmosis for solutions above 2000 ppm salt. In the 500–2000 ppm range, electrodialysis is almost always the lowest cost process. One advantage of electrodialysis when applied to brackish water desalination is that a large fraction, typically 80–95% of the brackish feed, is recovered as potable water. However, these high recoveries mean that the concentrated brine stream produced is 5–20 times more concentrated than the feed. Precipitation of insoluble salts in the brine can limit the water recovery.

Since the first electrodialysis plants were produced in the early 1950s, several thousand brackish water

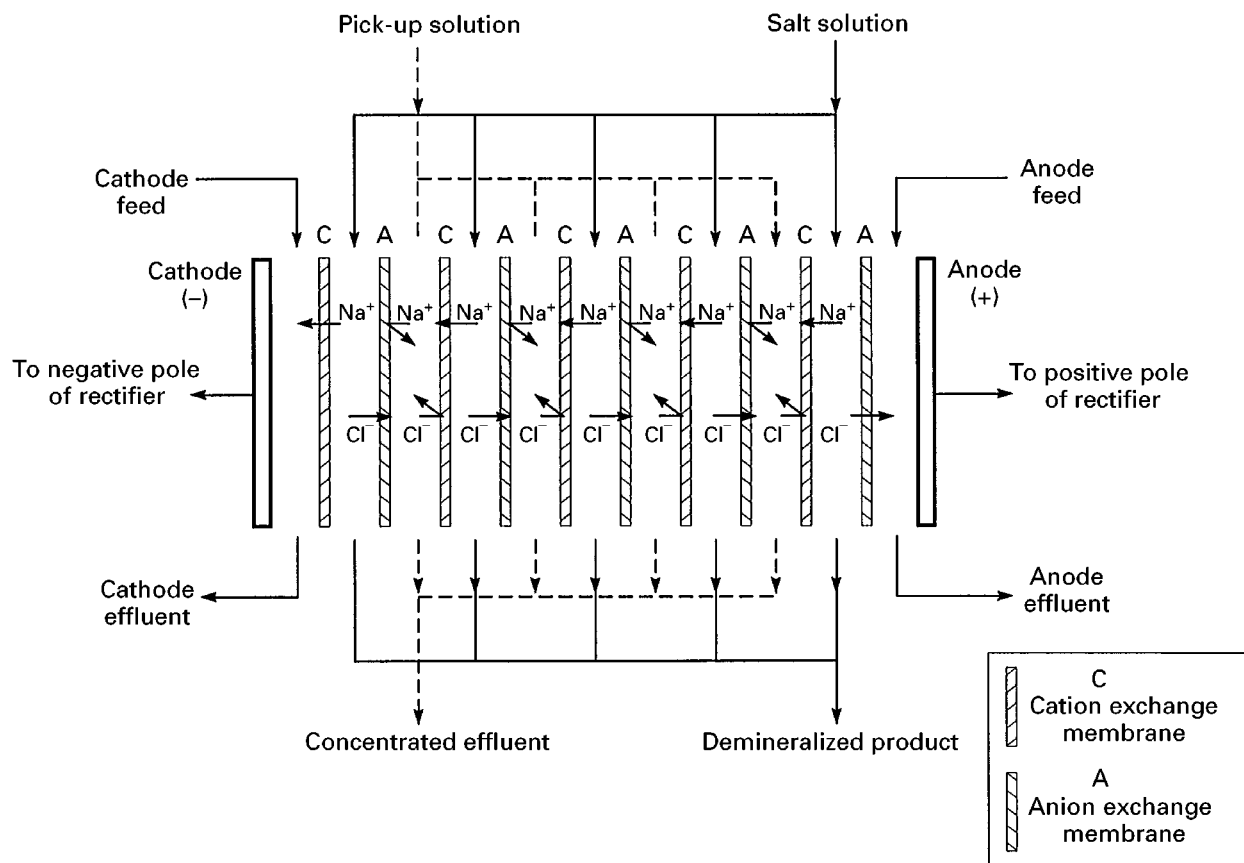


Figure 15 Schematic diagram of a plate-and-frame electrodialysis stack. Alternating cation- and anion-permeable membranes are arranged in a stack of up to 100 cell pairs.

electrodialysis plants have been installed around the world. Modern electrodialysis units are generally fully automated and require only periodic operator attention. This has encouraged installation of many small trailer-mounted plants. However, a number of very large plants with production rates of 10 million gal per day or more have also been produced.

The power consumption of an electrodialysis plant is directly proportional to the salt concentration in the feed water, and varies from 4 kWh per 1000 gal (4 MJ m^{-3}) for 1000 ppm feed water to 10–15 kWh per 1000 gal ($10\text{--}15 \text{ MJ m}^{-3}$) for 5000 ppm feed water. About one-quarter to one-third of this power is used to drive the feed water recirculation pumps.

Seawater A second major application of electrodialysis is the production of table salt by concentration of seawater. This process is only practised in Japan, which has no other domestic salt supply. The process is heavily subsidized by the government. Total production is approximately 1.2 million tons per year of salt, with more than 500 000 m² of membrane used in the plants.

A flow scheme for one such seawater salt-production plant is shown in Figure 16. A cogeneration power plant produces the power required for the electrodialysis operation, which concentrates the salt in seawater to about 18–20 wt%. Waste steam from

the power plant is then used to concentrate the salt further by evaporation.

Gas Separation

The process The study of gas permeation through membranes has a long history dating back to the work of Thomas Graham in the mid-nineteenth century. However, the first systematic studies with polymers of the type used today did not begin until 100 years later.

The mechanism of gas permeation developed in the 1950s and 1960s was the solution-diffusion model. In this model, the rate of diffusion through the polymer membrane is governed by Fick's law of diffusion. For simple gases, it can be shown that Fick's law leads to the expression

$$J = \frac{Dk\Delta p}{l} \quad [4]$$

where J is the membrane flux ($\text{cm}^3(\text{STP})/\text{cm}^2 \text{ s}$), k is the Henry's law sorption coefficient linking the concentration of gas in the membrane material to the pressure of the adjacent gas ($\text{cm}^3(\text{STP})/\text{cm Hg}$), Δp is the partial difference across the membrane, l is the membrane thickness (cm), and D is the permeant diffusion coefficient ($\text{cm}^2 \text{ s}^{-1}$), a measure of the permeant's mobility in the membrane. This expression can be further simplified to

$$J = \frac{P\Delta p}{l} \quad [5]$$

where P is a permeability, equal to the product Dk , and is a measure of the rate at which a particular gas moves through the membrane of a standard thickness (1 cm) under a standard driving pressure (1 cm Hg). The permeability unit, $1 \times 10^{-10} \text{ cm}^3 (\text{STP}) \text{ cm}/\text{cm}^2 \text{ s cm Hg}$, is called a Barrer, after R.M. Barrer, a pioneer in membrane permeation studies.

A measure of the ability of a membrane to separate two gases (1) and (2) is the ratio of their permeabilities, called the membrane selectivity, α :

$$\alpha_{1,2} = \frac{P_1}{P_2} = \frac{D_1}{D_2} \times \frac{k_1}{k_2} \quad [6]$$

The factors that determine membrane permeability can best be understood by considering the component terms D and k . For simple gases, the diffusion coefficient tends to decrease with increasing permeant diameter, because large molecules interact with more segments of the polymer chains and are thus less mobile. On the other hand, the sorption

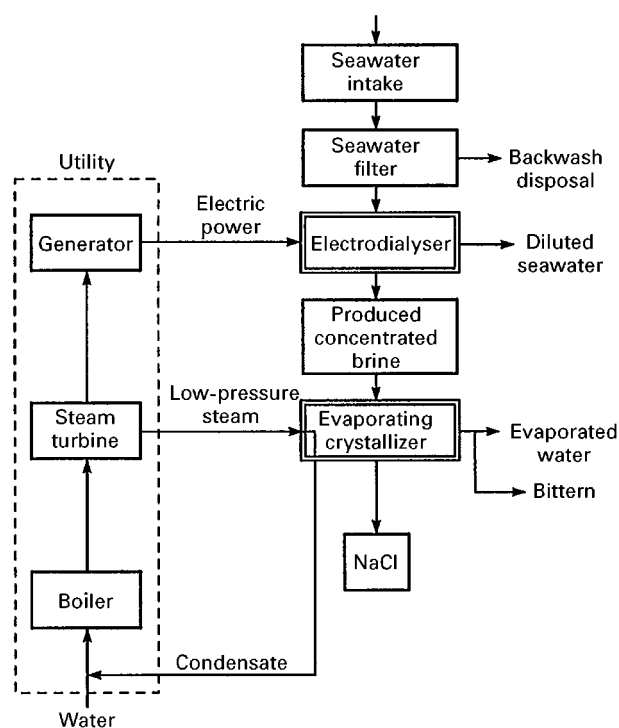


Figure 16 Flow scheme of a typical electrodialysis process used in a seawater salt concentration plant.

coefficient of gases increases with the condensability of the gas. Normally, the sorption coefficient also correlates with molecular diameter, larger molecules being more condensable than smaller molecules, and the Henry's law sorption coefficient increases with increasing permeant diameter. Thus, the effect of increasing permeant size on permeability is a balance between the opposing effects of diffusion coefficient, which decreases with increasing size, and solubility, which increases with increasing size. This balance determines the selectivity of a membrane for any pair of gases and is a function of the membrane material.

In glassy, rigid polymers such as polysulfone or polyimides, permeant diffusion coefficients are most important. Therefore, these polymers preferentially permeate the small, noncondensable gases, hydrogen, nitrogen and methane, over the larger, condensable gases, propane and butane. On the other hand, in rubbery polymer such as silicone rubber (polydimethylsiloxane), permeant solubility coefficients are most important. Therefore, these polymers preferentially permeate the larger, more condensable gases, propane and butane, over the smaller, noncondensable gases, hydrogen, nitrogen and methane.

Applications The principal developed gas separation processes are listed in Table 2. The first large-scale commercial application of gas separation was the separation of hydrogen from nitrogen in ammonia purge gas streams. The process, launched in 1980 by Permea, then a Division of Monsanto, was followed by a number of similar applications, such as hydrogen/methane separation in refinery off-gases and hydrogen/carbon monoxide adjustment in oxo-chemical synthetic plants.

Following Permea's success, several US companies produced membrane systems to treat natural gas streams, particularly to remove carbon dioxide. The goal is to produce a stream containing less than 2% carbon dioxide to meet the national pipeline specifications and a permeate enriched in carbon dioxide

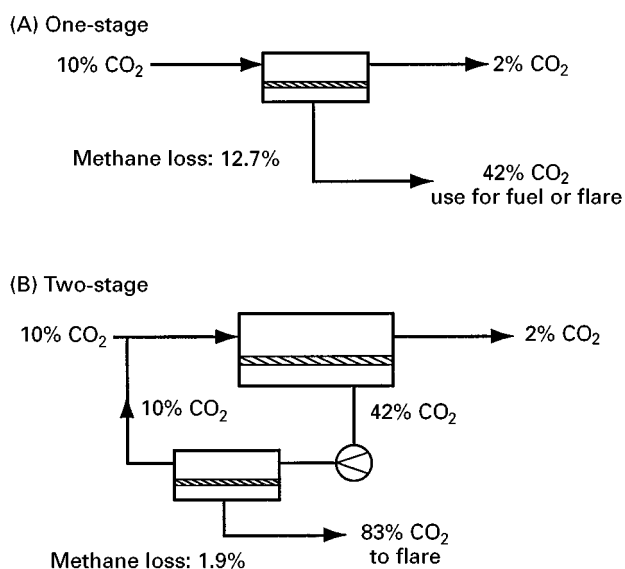


Figure 17 Flow scheme of (A) a one-stage and (B) a two-stage membrane gas separation system for the separation of carbon dioxide from natural gas.

to be flared or reinjected into the ground. Currently, cellulose acetate is the most widely used membrane material for this separation, but because the carbon dioxide/methane selectivity of cellulose acetate is only 15–20, two-stage systems are often required to achieve a sufficient separation. More selective polyimide membranes are beginning to replace cellulose acetate membranes in this application. Flow schemes for a one-stage (A) and a two-stage (B) cellulose acetate membrane system for carbon dioxide/natural gas separations are shown in Figure 17. The single-stage system has a low capital cost, but 12.7% of the methane in the gas is lost with the carbon dioxide. This loss becomes unacceptable for large systems, so a two-stage unit is used. The methane loss is reduced to less than 2% but at the expense of more membrane area and a large compressor. The membrane process is generally best suited to relatively small streams in the 5–20 MMscfd range, but the economics of the process have slowly improved over

Table 2 Membrane gas separation applications

Separation	Status
H ₂ /N ₂ , CO, CH ₄ , etc.	~500 units installed. Various hydrogen recovery applications in refineries, petrochemical and ammonia plants
CO ₂ /CH ₄	~200 units installed, some very large (5000–50 000 scfm) to separate carbon dioxide from natural gas
N ₂ /air	~5000 units installed, most small in the 50–500 scfm range (98–99.5% nitrogen)
Organic solvent vapour/air, N ₂	~100 units installed. Diverse applications include gasoline vapour recovery at oil terminals, recovery of monomers from reactor vents
H ₂ O/air	Many thousands of small modules sold for drying compressed air

the years and more than 200 natural gas treatment plants have now been installed – some quite large.

By far the largest gas separation process in current use is the production of nitrogen from air. The first membranes used for this process were based on polysulfone, poly(trimethylpentane) and ethyl cellulose. These polymer materials had oxygen/nitrogen selectivities of 4 to 5, and the economics of the process were marginal. The second-generation materials now used have selectivities in the range 6 to 7. With these membranes, the economics of nitrogen production from air are very favourable, especially for small plants producing 50–500 scfm of nitrogen; 5000 of these small systems are now in operation. In this range, membranes are the low-cost process, and most new nitrogen plants use membrane systems.

A growing application of membrane systems is the removal of condensable organic vapours from air and other streams. Unlike the process described above, organic vapour separation uses rubbery membranes, which are more permeable to the organic vapour. More than 100 organic vapour recovery plants have been installed. In Europe, most of the plants recover gasoline vapours from air vented during transfer operations; in the USA, most plants recover chlorinated and fluorinated hydrocarbons from refrigeration or chemical processing streams. Separation of propylene from nitrogen in polyolefin plants is an emerging application worldwide.

Pervaporation

The process Pervaporation is a membrane process used to separate liquid mixtures. The feed liquid contacts one side of a membrane, which selectively permeates one of the feed components, as shown in Figure 18. The permeate, enriched in this component, is removed as a vapour from the other side of the membrane. The driving force for the process is the low vapour pressure on the permeate side of the membrane, which is generated by cooling and condensing the permeate vapour. The separation achieved is proportional to the differences in rates of permeation of the components of the mixture through the membrane.

Pervaporation offers the possibility of separating solutions, mixtures of components with close boiling points, or azeotropes that are difficult to separate by distillation or other means. An illustration of the ability of pervaporation membranes to break azeotropes is shown in Figure 19 for the separation of benzene/cyclohexane mixtures. The vapour–liquid equilibrium for the mixture shows that benzene/cyclohexane mixtures form an azeotrope at approximately 50% benzene. Distillation is unable to

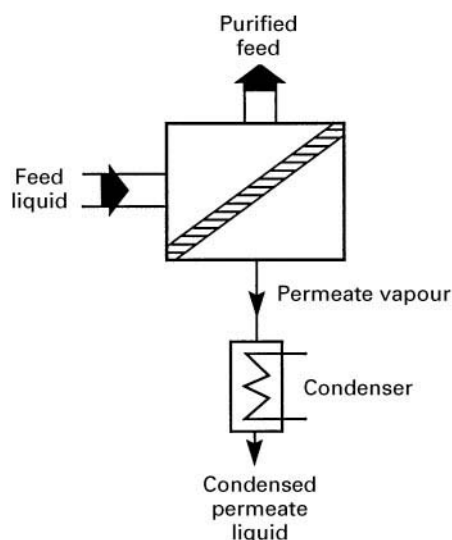


Figure 18 In the pervaporation process, a liquid contacts the membrane, which preferentially permeates one of the liquid components as a vapour. The vapour, enriched in the more permeable component, is cooled and condensed, spontaneously generating a vacuum that drives the process.

separate a feed stream of this composition. However, pervaporation treatment of this mixture produces a vapour permeate containing more than 95% benzene.

The first systematic work on pervaporation was done by Binning and co-workers at American Oil in the 1950s. The process was not commercialized at that time and remained a mild academic curiosity until 1982, when GFT (Gesellschaft für Trenntechnik

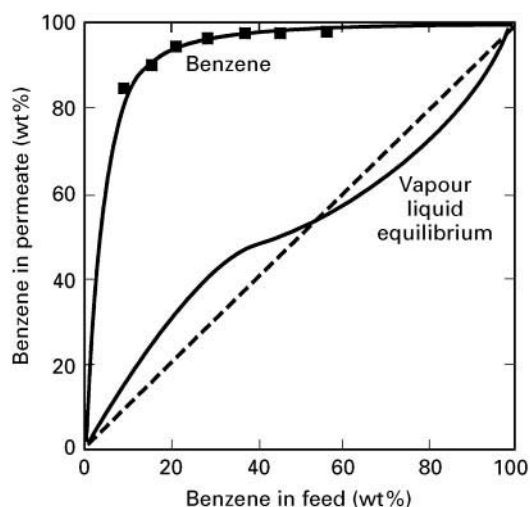


Figure 19 Fraction of benzene in permeate as a function of feed mixture composition for pervaporation at the reflux temperature of a binary benzene/cyclohexane mixture. (Reprinted with permission from *Industrial and Engineering Chemical Research* 22 (1983) 313. Copyright 1983 American Chemical Society.)

GmbH, Germany) installed the first commercial pervaporation plant. That plant separated water from concentrated alcohol solutions; GFT has since installed more than 50 such plants. The ethanol feed to the membrane generally contains $\sim 10\%$ water. The pervaporation process removes the water as the permeate, producing pure ethanol with less than 1% water, and avoiding all the problems of azeotropic distillation.

Spurred on by this success, a great deal of effort is being made to apply pervaporation to other difficult separations. Exxon, for example, pursued the separation of hydrocarbon mixtures containing aromatics and aliphatics, a major separation problem in refineries. Another application is the separation of dissolved volatile organic compounds (VOCs) from water, developed by Membrane Technology and Research, Inc.

Applications To date, the largest application of pervaporation is the dehydration of ethanol or isopropanol. This process has been pioneered by GFT, now a division of Sulzar, using polyvinyl alcohol composite membranes that are far more permeable to water than alcohol. A flow scheme of a GFT plant combining distillation and pervaporation to produce dry alcohol is shown in Figure 20. The distillation column produces an ethanol overhead stream containing 85–90% ethanol which is fed to the pervaporation system. To maximize the vapour pressure driving force across the membrane the pervaporation module usually operates at a temperature of 105–130°C, corresponding to a feed stream vapour pressure of 2–6 atm. The permeate vapour is cooled and condensed at 0 to -10°C . The permeate contains 40–50% ethanol which is recycled to the distillation column; the residue stream is better than 99.5 wt% ethanol. Most of the installed solvent de-

hydration systems have been for ethanol dehydration, but applications to other solvents, including isopropanol, glycols, acetone and methylene chloride, have also been studied.

The only other commercial pervaporation application is the separation of dissolved VOCs from water. Relatively hydrophobic composite membranes, such as silicone rubber coated on a microporous polyimide support membrane, are used. Extremely high separation factors can be obtained for the more hydrophobic VOCs such as toluene, benzene, chlorinated solvents, esters and ethers. Frequently the VOC in the condensed permeate is enriched 100- to 1000-fold over the feed. Target applications include removal of VOCs from industrial wastewater streams and the recovery of volatile flavour and aroma components in the food processing industry. The GC traces in Figure 21 illustrate the concentration and recovery of orange juice flavours from the water evaporated from orange juice obtained by pervaporation.

The current commercial pervaporation processes involve the separation of organics and water. This separation is relatively easy, because organic solvents and water have very different polarity and exhibit distinct membrane permeation properties. No commercial pervaporation systems have yet been developed for the separation of organic/organic mixtures. However, current technology now makes development of pervaporation for these applications possible, and the process is being actively developed by a number of companies. The first pilot-plant results for an organic–organic application – the separation of methanol from methyl *t*-butyl ether/isobutene mixtures – was reported by Separex in 1988. This is a particularly favourable application, and available cellulose acetate membranes achieve a good separation. More recently, Exxon started a pervaporation pilot plant for the separation of

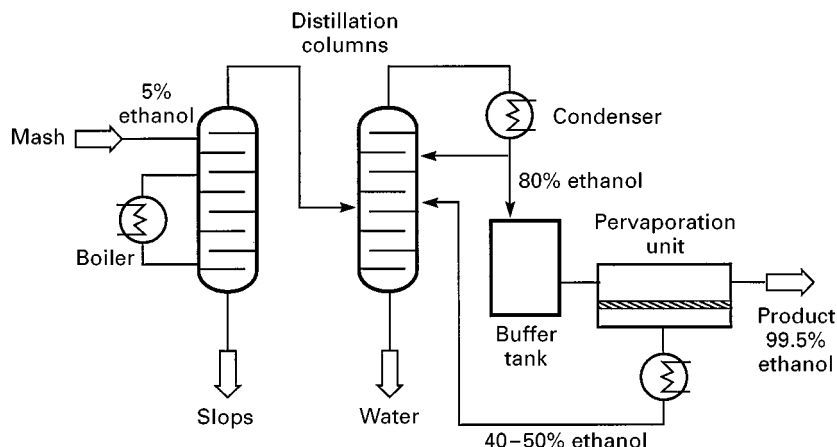


Figure 20 Flow scheme of an integrated distillation/pervaporation plant for ethanol recovery from fermentors.

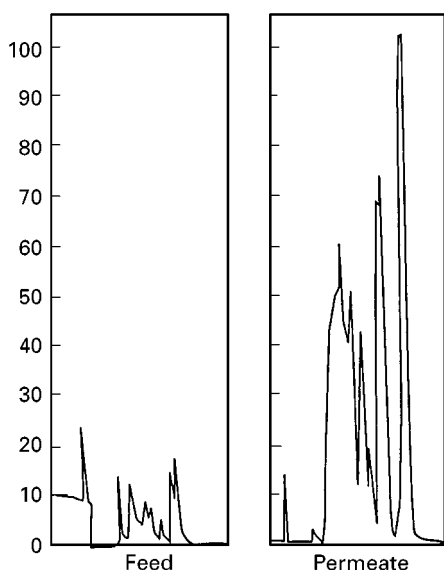


Figure 21 HPLC traces showing recovery of flavour and aroma components from orange juice evaporation condensate by pervaporation.

aromatic/aliphatic mixtures, using polyimide/polyurethane block copolymer membranes.

Dialysis

The process Dialysis was the first membrane process to be used on an industrial scale with the development of the Cerini dialyser in Italy. The production of rayon from cellulose expanded rapidly in the 1930s, and a need arose to recover sodium hydroxide from hemicellulose/sodium hydroxide solution by-product streams formed in the process. A finely microporous membrane was used to separate the concentrated hemicellulose solution from water. The smaller sodium hydroxide molecules diffuse across the membrane down a concentration gradient to produce an uncontaminated product stream, as shown in **Figure 22**.

With the development of ultrafiltration and microfiltration membranes in the 1960s and 1970s, industrial applications of dialysis largely disappeared because dialysis membranes were slow and unselective compared to the newer technologies. However, in the medical area, two very large applications have been

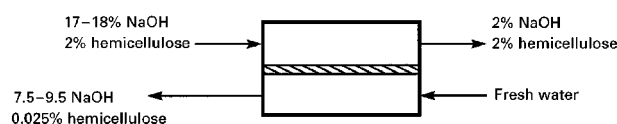


Figure 22 The separation of sodium hydroxide from hemicellulose by dialysis. This separation became important in the production of rayon in the 1930s and 1940s.

developed, namely the dialysis of blood – haemodialysis – in the artificial kidney, and the related process used to exchange oxygen and carbon dioxide in blood in the artificial lung. Both processes use the low-pressure, mild conditions of dialysis.

Applications

Haemodialysis (artificial kidney) The kidney is a key component in the body's waste disposal and acid-base regulation mechanism. Approximately 1 in every 10 000 persons will suffer irreversible kidney failure, which before 1960 was invariably fatal. Now a number of treatments, of which haemodialysis is by far the most important, can maintain these patients. As many as 800 000 patients worldwide are treated by haemodialysis devices. Each patient is dialysed two to three times per week with a dialyser that contains about one square metre of membrane area. Economies of scale allow the membrane modules to be produced at about US\$15 each. The devices are generally disposed of after one or two uses. As a result the market is about US\$1.3 × 10⁹ per year, making this the largest membrane separation process in terms of sales per year and membrane area used.

The first successful artificial kidney was constructed by Kolf and Berk in Holland in 1945. Over the next 20 years Kolf and others developed a number of improved devices, and by the 1960s the process began to be widely used. Early dialysers used coiled tubes or plate-and-frame designs. The development of hollow-fibre dialysers reduced costs considerably, making widespread use of the process possible. Each fibre dialyser contains 0.5–2.0 m² of membrane formed as fibres 0.1–0.2 mm in diameter. A typical dialyser module (**Figure 23**) contains several thousand fibres in a 2 in (5 cm) diameter tube 1–2 ft (30–60 cm) long. Blood flows down the bore of the fibre, and an isotonic saline solution is circulated around the outside. Urea, creatinin and other metabolites in the blood diffuse through the membrane to the dialysate solution. The process must be carried out

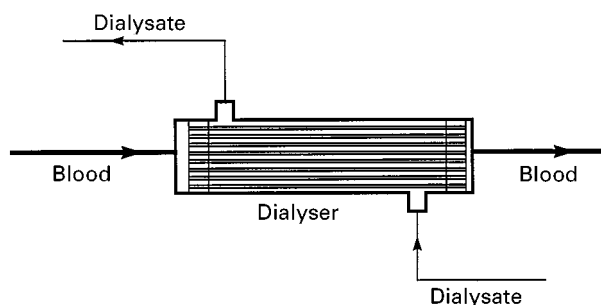


Figure 23 Schematic of a hollow-fibre haemodialyser.

slowly to avoid shock to the patient; typically 2–4 h are required to eliminate all of the accumulated toxins.

Blood oxygenators (artificial lungs) Blood oxygenators are used during heart surgery. Until the early 1980s direct oxygenation of blood was used to maintain patients during surgery. Rotating discs or small countercurrent contacting towers delivered oxygen to the blood and removed carbon dioxide. This procedure required a large volume of blood to prime the units and damaged the blood during long surgeries. The introduction of hollow-fibre membrane contactors largely solved both of these problems and was one reason for the dramatic expansion of open-heart surgery in the 1980s. Currently, about one million procedures are performed annually world-wide. A successful heart-lung must normally deliver about 250 cm³(STP) per min of oxygen and remove about 200 cm³(STP) per min of carbon dioxide. Microporous polyolefin hollow-fibre membrane modules with a membrane area of 2–10 m² are generally used.

Other Membrane Separation Processes

The seven processes described above represent the majority of commercial membrane separation technologies. However, a number of processes are still in the laboratory or early commercial stage and may yet become important. These processes are described briefly below.

Carrier-Assisted Transport

Carrier-assisted transport usually employs liquid membranes containing a complexing or carrier agent. The carrier agent reacts with one permeating component on the feed side of the membrane and then diffuses across the membrane to release the permeant on the product side of the membrane. The carrier agent is then reformed and diffuses back to the feed side of the membrane. Thus, the carrier agent acts as a shuttle to transport selectively one component from the feed to the product side of the membrane.

Facilitated transport membranes can be used to separate gases; membrane transport is then driven by a difference in the gas partial pressure across the membrane. In the example shown in Figure 24, the carrier is haemoglobin, used to transport oxygen. On the upstream side of the membrane, haemoglobin reacts with oxygen to form oxyhaemoglobin, which then diffuses to the downstream membrane in-

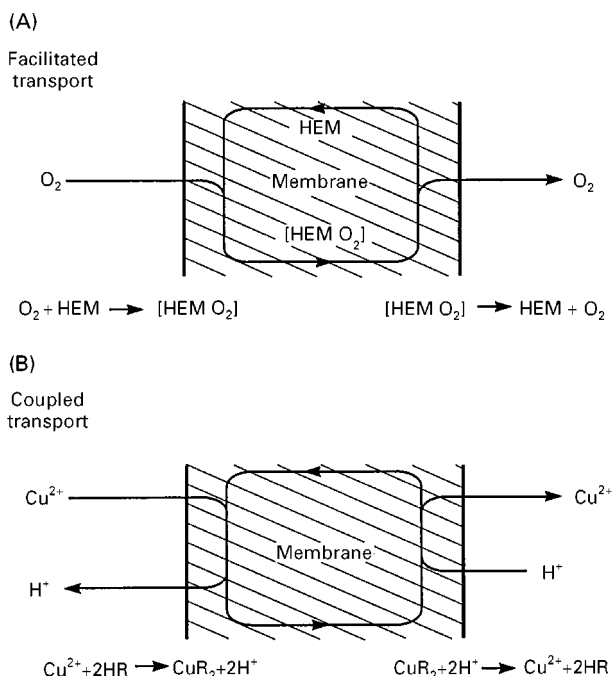


Figure 24 Schematic examples of (A) facilitated and (B) coupled transport of gas and ions. The facilitated transport example shows the transport of oxygen across a membrane using haemoglobin as the carrier. The coupled transport example shows the transport of copper ions across the membrane using a liquid ion exchange reagent as the carrier.

terface. There, the reaction is reversed – oxygen is liberated to the permeate gas and haemoglobin is reformed. The haemoglobin then diffuses back to the feed side of the membrane to pick up more oxygen. In this process haemoglobin acts as the shuttle, transporting oxygen selectively through the membrane. Other gases, such as nitrogen, which do not react with the carrier, are left behind.

Coupled transport is similar to facilitated transport and also incorporates a carrier agent in the membrane. However, in coupled transport the carrier agent couples the flow of two species. Because of this coupling, one of the species can be moved against its concentration gradient, provided the concentration gradient of the second coupled species is sufficiently large. In the example shown in Figure 24, the carrier is an oxime that forms an organic-soluble complex with copper ions. The reaction is reversed by hydrogen ions. On the feed side of the membrane, two oxime carrier molecules pick up a copper ion, liberating two hydrogen ions to the feed solution. The copper–oxime complex then diffuses to the downstream membrane interface, where the reaction is reversed because of the higher concentration of hydrogen ions in the permeate solution. The copper ion is liberated to the permeate solution and two

hydrogen ions are picked up. The reformed oxime molecules diffuse back to the feed side of the membrane. Metal ions can also be selectively transported across a membrane, driven by a flow of hydrogen or hydroxyl ions in the other direction.

Because the facilitated and active transport processes employ a reactive carrier species, very high membrane selectivities can be achieved – often far larger than those achieved by other membrane processes. This has maintained interest in facilitated transport since the 1980s, yet no significant commercial applications exist or are likely to exist in the immediate future. The principal limitations are the physical instability of the liquid membrane and the chemical instability of the carrier agent.

Membrane Reactors

In membrane reactors, the membrane is used to shift a chemical equilibrium or separate the products of a reaction. A wide variety of processes have been suggested, and a few have reached the commercial stage. A simple example is shown in Figure 25 – the reaction of *n*-butane to butadiene and hydrogen:

$$\text{C}_4\text{H}_{10} \rightleftharpoons \text{C}_4\text{H}_6 + 2\text{H}_2$$

This is an equilibrium reaction and in a conventional process a mixture of components is withdrawn from the reactor, separated, and the unreacted *n*-butane recirculated to the feed. In the membrane reactor, hydrogen is removed through the membrane so that the chemical equilibrium in the reactor is shifted to the right and the conversion of *n*-butane to butadiene is increased. Essentially pure butadiene leaves the reactor. This type of process is the subject of a considerable research effort, mostly using ceramic membranes operating at high temperatures. The development of these devices for the production of syngas (a mixture of carbon monoxide and hydrogen) is the focus of very large research programmes at Air Products and Standard Oil. Promising results have been obtained in the laboratory, but scale-up to an economical process is still far off.

Membrane Contactors

In the membrane separation processes discussed so far, the membrane acts as a selective barrier allowing

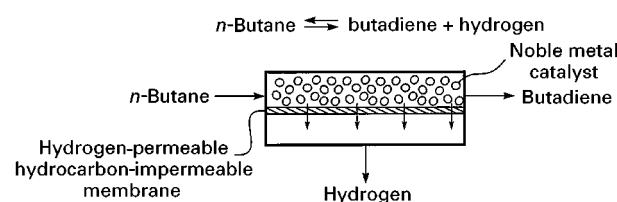


Figure 25 Schematic of a membrane reactor to separate butadiene from *n*-butane.

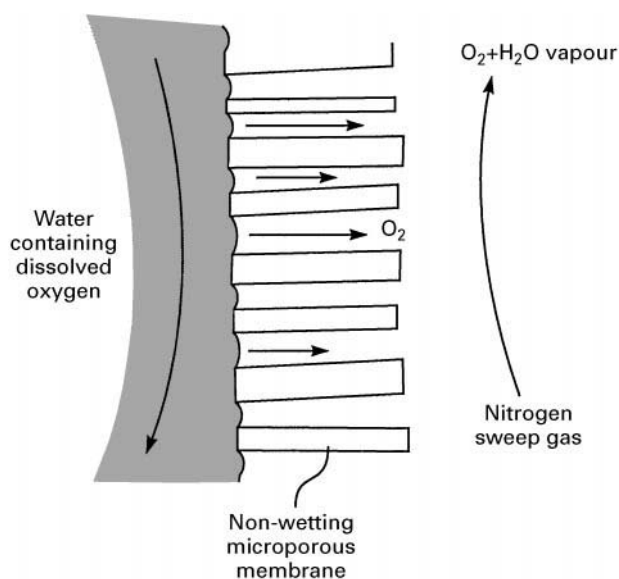


Figure 26 Schematic showing application of a membrane contactor to remove dissolved oxygen from water. This process is used to prepare power plant boiler feed water.

relatively free passage of one component while retaining another. In membrane contactors the membrane function is to provide an interface between two phases but not to control the rate of passage of permeants across the membrane. An example of this technology, in which the membrane is used in a process to deoxygenate water, is shown in Figure 26.

A hollow-fibre microporous membrane separates the oxygen-containing water from the nitrogen sweep gas. Even though the dissolved oxygen concentration in the water is very low, its equilibrium concentration in the gas phase in contact with the water is several thousand times higher. This means that oxygen permeation through the membrane down the concentration gradient to the nitrogen sweep gas is high. The membrane provides a large surface contact area between the water and nitrogen sweep gas but does not affect the relative permeabilities of oxygen and water vapour through the membrane. In this type of application, the membrane serves as a contactor or phase separator. Exactly the same separation could be achieved by running the water and nitrogen countercurrent to each other in a packed tower, but membrane contactors are much more compact. Membrane contactors are typically shell- and tube-devices containing microporous capillary hollow-fibre membranes. The membrane pores are made sufficiently small that capillary forces prevent direct mixing of the two phases on either side of the membrane.

A small market has already developed for membrane contactors to degas ultrapure water for the electronics industry and boiler feed water for power

plants. The long-term goal of the process is to replace packed towers in conventional absorber–stripper operations. Practical problems related to membrane fouling and lifetime are the principal limitations.

The Future

Since the 1970s there has been a period of very rapid growth for the membrane separation industry. Total sales for all membrane applications have grown approximately 400-fold to the US\$3–4 × 10⁹ per year level. In the areas of microfiltration, ultrafiltration, reverse osmosis, electrodialysis and dialysis, the technology is relatively mature. Significant growth is still occurring, however, as membranes continue to displace more conventional separation techniques. The most rapidly expanding area is gas separation, which has grown to a US\$150 × 10⁶ per year business in just a few years. Gas separation is poised to grow a further two- or three-fold as the technology is used more widely in the refinery, petrochemical and natural gas processing areas. If the development of ceramic oxygen-permeable membranes for syngas membrane reactors is successful, a membrane process that could change the basis of the chemical industry would then be available.

Further Reading

Amjad Z (1993) *Reverse Osmosis*. New York: Van Nostrand-Reinhold.

- Baker RW, Cussler EL, Eykamp W *et al.* (1991) *Membrane Separation Systems*. Park Ridge, NJ: Noyes Data Corp.
- Bakish R (ed.) (1991) *Proceedings of the International Conference on Pervaporation Processes in the Chemical Industry*, Heidelberg. Englewood, NJ: Bakish Materials Corp.
- Bakish R (ed.) (1992) *Proceedings of the International Conference on Pervaporation Processes in the Chemical Industry*, Ottawa. Englewood, NJ: Bakish Materials Corp.
- Bakish R (ed.) (1995) *Proceedings of the International Conference on Pervaporation Processes in the Chemical Industry*, Reno, NV. Englewood, NJ: Bakish Materials Corp.
- Brock TD (1983) *Membrane Filtration*. Madison, WI: Sci. Tech. Inc.
- Cheryan M (1986) *Ultrafiltration Handbook*. Lancaster, PA: Technomic Pub. Company.
- Crespo JG and Bøddeker KW (eds) (1994) *Membrane Processes in Separation and Purification*. Dordrecht: Kluwer Academic.
- Ho WS and Sirkar KK (eds) (1992) *Membrane Handbook*. New York: Van Nostrand Reinhold.
- Mulder M (1991) *Basic Principles of Membrane Technology*. Dordrecht: Kluwer Academic.
- Parekh BS (ed.) (1988) *Reverse Osmosis Technology*. New York: Marcel Dekker.
- Paul DR and Yampol'skii YP (eds) (1994) *Polymeric Gas Separation Membranes*. Boca Raton, FL: CRC Press.
- Porter MC (ed.) (1990) *Handbook of Industrial Membrane Technology*. Park Ridge, NJ: Noyes Publications.
- Rautenbach R and Albrecht R (1989) *Membrane Processes*, Chichester: John Wiley & Sons.
- Toshima N (ed.) (1992) *Polymers for Gas Separation*. New York: VCH.

PARTICLE SIZE SEPARATIONS



J. Janča, Université de La Rochelle, La Rochelle, France

Copyright © 2000 Academic Press

Historical Development

In 1556, an extraordinary book entitled *De Re Metallica, Libri XII* appeared in Basel. The author was a German physician, naturalist and mineralogist, calling himself Georgius Agricola (originally called Georg Bauer), living in Jáchymov, Bohemia, from 1494 to 1555. Agricola described, in a fascinating manner, the contemporary advances in metals and

minerals recovery and gave us a very detailed report on the sophisticated technologies of his epoch. This late medieval period saw a true expansion of science and technology in Europe. Winston Churchill once said: ‘... from this date, 1492, a new era in the history of mankind takes its beginning’. As many metal recovery processes used at that time were based on various separations of particulate matter and *De Re Metallica, Libri XII* seems to be the first printed review of separation technologies, it is fitting to acknowledge Agricola’s publication priority in this field and to consider his book as the beginning of a modern scientific approach to particle size separations.

The reproduction of a rendering in **Figure 1** taken from Agricola’s book shows a surprisingly sophisticated device for gold (and other metals) recovery by ‘panning’ or ‘sluicing’ which used gravity and

¹This article does not deal with the important particle separation techniques of filtration, flotation and the use of membranes which are dealt with elsewhere in the Encyclopedia.



Figure 1 Mediaeval device for the recovery of gold particles and minerals from sand, clay, and soil blends by combining the sedimentation and quasi-horizontal stream of water, accompanied by vigorous manual stirring of the mud cake. (Bottom) The author of the book *De Re Metallica, Libri XII*, Georgius Agricola.

a stream of running water to separate gold particles from other solid material (soil, clay, sand, etc.). Astonishingly, this technology dates back to at least 4000 to 5000 BC.

Original scientific discoveries, outstanding inventions and innovations in technology representing the

important achievements at a given moment reflect continuity of imagination throughout the long history of civilization. When looking for the background and genesis of modern and powerful separation methodologies and technologies, very often natural analogies can be found at a macroscopic level. An image of a river meandering through the countryside and removing soil, clay, sand, and stones from a river bank, carrying them off in the stream, and depositing them later at other places, is one such example. On the other hand, although ancient technologies can have essentially the same goal (separation), in a manner similar to that in which 'cat's cradle' is equivalent to a sophisticated electronic computer game, the intellectual progress is evident.

Dry and wet sieving, sedimentation, and filtration are probably the most ancient, intelligently applied, separation processes on which the foundations of modern separation science stand. These processes were originally exploited for the separations of disintegrated matter whose average 'particle' size was somewhere between millimetre and centimetre fractions, sometimes even bigger. Slowly, the need to separate smaller and smaller particle size material became apparent. The old-fashioned but transformed methods still afforded positive answers to questions which appeared in relation to the new separation problems. However, these transformations gave rise to newer methods which, together with the discovery and invention of completely new principles, symbolize the state of the art of particle separation.

Particles, Sizes, and Methods

In order to make clear what this article deals with, the useful and necessary terms, limits and conditions must be defined. *Particles*, within the frames of this text, is an ensemble of single subjects of disintegrated matter which is dispersed in a continuum fluid or *in vacuo*. One particle, regardless of its size, is usually not identical with one molecule but with a large number of molecules aggregated by physical forces. In the case of polymeric matter, however, one macromolecule can be identified with one particle, under certain conditions. The second important attribute which defines one particle is that, physically, it represents a subject delimited in three-dimensional space by a phase discontinuity. The particles, representing one discontinuous phase which can be solid or liquid, are dispersed in a second continuous phase which is gaseous or liquid.

As concerns the *sizes* of the particles, a strict definition is less easy, because the effective dimension(s) (independently of the physical shape of each individual particle) can vary as a function of the

chemical character of the surrounding dispersing fluid but also of the imposed physical conditions: obvious ones, such as, e.g., the temperature, and less obvious as, e.g., the electric charge, etc. Moreover, it has to be taken into account that the results of the measurements of the particle size can strongly depend on the method of its determination. As a result, the questions are not only what the size that we obtain from a particular measuring method means and whether the result corresponds to a true size, but also what kind of effective size we measure by applying any particular method. Not only one but many effective sizes obtained by different measuring methods can correspond to the physical reality (they all can be 'true'). This is due to the fact that the measured data can contain various information on the particle-dispersing fluid and particle-particle interactions, on the size fluctuations in time, on the transport behaviour of the particles in the dispersing fluid, etc. Although all these phenomena can complicate the determination of a definite particle size, they provide much useful information on the whole dispersed particulate system. Having in mind these complications, we can define the range of particle sizes of practical interest as lying within the range from a diameter of few nanometres to thousands of micrometres.

The definition and limitation of the particles and the particle size ranges, as outlined, determine the relevant separation *methods*. Those methods can be considered relevant that are directly related to the separation according to differences in particle size or concerned indirectly due to the fact that they can provide complementary information necessary to an accurate interpretation of the experimental data obtained from particle size-based separations.

Objectives and Methods

The aim of any separation, including particle size separation, is either analytical or preparative. *Analytical separations* are generally used to increase the sensitivity or selectivity of the subsequent analytical measurement, or to obtain more specific information about the analysed sample. Very often, the original sample is a complicated mixture making the analysis possible only with a prior separation step. Hence, the original multicomponent sample to be analysed must first be separated into more or less pure fractions. Whenever the samples are of particulate character and/or of biochemical or biological origin, direct analysis without preliminary separation is often impossible. An accurate analytical result can be obtained from any analytical separation method by employing an appropriate treatment and interpretation of the experimental data. Separation is usually based on the differences in extensive properties, such as

the mass or size of the particles, or according to intensive properties, such as density, electrophoretic mobility, etc. If the relationship between the separation parameters and the size of the separated particles is known or can be predetermined by using an appropriate calibration procedure, the characteristics of an unknown analysed sample can be evaluated quantitatively. The particle size distributions of the analysed samples are determined conveniently from the record of a coupled detector: a fractogram. Detailed information concerning the associated properties of the separated and characterized particles and/or composition of the analysed system which can be extracted from the fractogram represents more sophisticated application of a particular separation method.

Preparative separations are aimed at obtaining a significant quantity of the separated fractions from the original sample. The fractions are subsequently used for research or technological purposes, for detailed analysis of various effective sizes, for the determination of the structure or chemical composition of the particles of a given size, etc. The practical preparative separations can range from laboratory microscale, which cannot be experimentally distinguished from analytical separations, up to industrial macroseparation units.

Analytical and preparative separations are fundamentally identical so that, consequently, we do not distinguish between them and all separation methods are described and discussed from the point of view of the principles involved by making comments on their specific applications only if the discussed technique exhibits particular characteristics predetermining it for a special analytical or preparative purpose.

The most suitable and widespread methodologies for particle size separations described below, starting from the most versatile to more specific ones, are:

- field-flow fractionation
- size-exclusion chromatography
- hydrodynamic chromatography
- centrifugation
- electrophoresis

Besides these modern techniques, some classical procedures mentioned above such as wet or dry sieving, filtration, etc., should not be forgotten.

Field-Flow Fractionation

Field-flow fractionation (FFF) is a relatively new but important and versatile method suitable for the separation and characterization of particles in the submicron and micron ranges. It has been developed over the last three decades into a complex of specific methods and techniques.

Principle of Separation

Separation in FFF is based on the action of effective physical or chemical forces across the separation channel in which the particles are transported due to the flow of a carrier liquid. The field interacts with the particles, separating and concentrating them at the appropriate positions inside the channel. The concentration gradient so formed induces an opposition diffusion flux. When equilibrium is reached, a stable concentration distribution of the particles across the channel is established. Simultaneously, a flow velocity profile is formed across the channel in the longitudinal flow of the carrier liquid. As a result, the particles are transported longitudinally at different velocities depending on the transverse positions of their zones and are thus separated. This principle is shown in Figure 2. The carrier liquid is pumped through the sample injector to the fractionation channel. The detector connected at the end allows the recording of the fractogram.

Separation Mechanisms

Two particular mechanisms, *polarization* and *focusing*, can govern the separation. The components of the fractionated sample can be differently compressed to the accumulation wall of the channel or focused at different levels. Polarization and focusing FFF have many common characteristics such as the experimental procedures, instrumentation, data treatment, and the range of potential applications. The separation is carried out in one liquid phase. The absence of a stationary phase of large surface area can be of fundamental importance for the fractionation of biological particles whose stability against degradation can be sensitive to interactions with the surfaces. The strength of the field can be easily controlled to manipulate the retention. Many operational variables can be programmed.

The *polarization* FFF methods are classified with regard to the character of the applied field, while the

focusing FFF methods are classified according to the combination of various fields and gradients. Although some earlier separation methods are also based on the coupled action of field forces and hydrodynamic flow, the beginning of FFF proper can be attributed to Giddings who in 1966 described the general concept of polarization FFF. Focusing FFF was originally described in 1982.

Polarization FFF methods make use of the formation of an exponential concentration distribution of each sample component across the channel with the maximum concentration at the accumulation wall which is a consequence of constant and position-independent velocity of transversal migration of the affected species due to the field forces. This concentration distribution is combined with the velocity profile formed in the flowing liquid.

Focusing FFF methods make use of transversal migration of each sample component under the effect of driving forces that vary across the channel. The particles are focused at the levels where the intensity of the effective forces is zero and are transported longitudinally according to their positions within the established flow velocity profile. The concentration distribution within a zone of a focused sample component can be described by a nearly Gaussian distribution function.

Retention

The retention ratio R is defined as the average velocity of a retained sample component divided by the average velocity of the carrier liquid which is equal to the average velocity of an unretained sample component:

$$R = \frac{v_{r,ave}}{\langle v(x) \rangle}$$

FFF is usually carried out in channels of simple geometry allowing calculation of the rigorous relationship between the retention ratio and the size of the separated particles. If this relationship is difficult to determine, a calibration can be applied. The particle size distribution (PSD) in both cases is determined from the fractogram.

Zone Dispersion

The separation process is accompanied by the zone spreading which has a tendency to disperse the concentration distribution already achieved by the separation. The conventional parameter describing the efficiency of the separation is the height equivalent to a theoretical plate H :

$$H = L \left(\frac{\sigma}{V_R} \right)^2$$

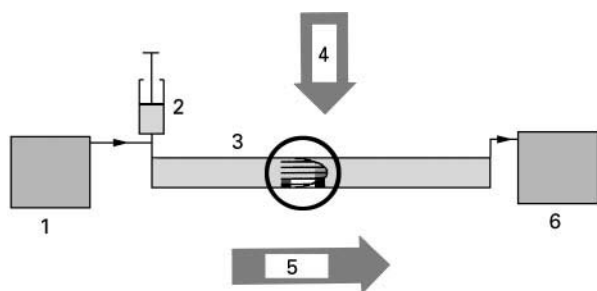


Figure 2 Schematic representation of the general principle and experimental arrangement of field-flow fractionation: (1) pump; (2) injector; (3) separation channel; (4) external field; (5) hydrodynamic flow; (6) detector.

where V_R is the retention volume and σ is the standard deviation of the elution curve. The width of the elution curve reflects several contributions: longitudinal diffusion, nonequilibrium and relaxation processes, and spreading due to the external parts of the whole separation system such as injector, detector, connecting capillaries, etc. The sum of all contributions results in a curve shown in Figure 3 which exhibits a minimum. As the diffusion coefficients of the particles are very low, the longitudinal diffusion is practically negligible and the optimal efficiency (the minimum on the resulting curve) is situated at very low flow velocity. The instrumental and relaxation spreading can be minimized by optimizing the experimental conditions.

Applications of Polarization FFF

The character of the applied field determines the particular methods of polarization FFF. The most important of them are:

- sedimentation FFF
- flow FFF
- electric FFF
- thermal FFF

Sedimentation FFF is based on the action of gravitational or centrifugal forces on the suspended particles. The sedimentation velocity is proportional to the product of the effective volume and density difference between the suspended particles and the carrier liquid. The channel is placed inside a centrifuge rotor, as shown in Figure 4. The technique can be used for the separation, analysis and characteriza-

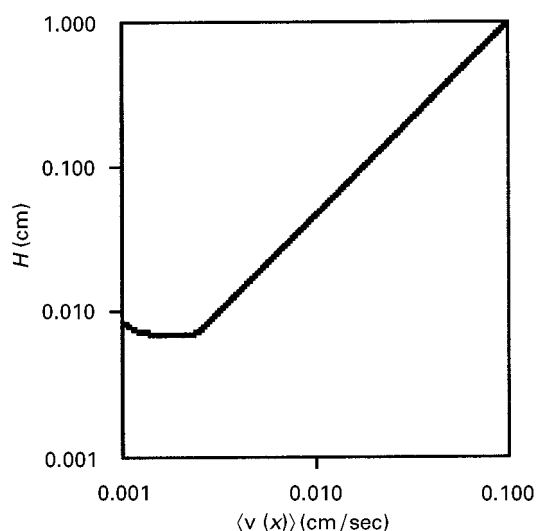


Figure 3 Dependence of the efficiency of FFF, expressed as the height equivalent to a theoretical plate H , on the average linear velocity of the carrier liquid $\langle v(x) \rangle$.

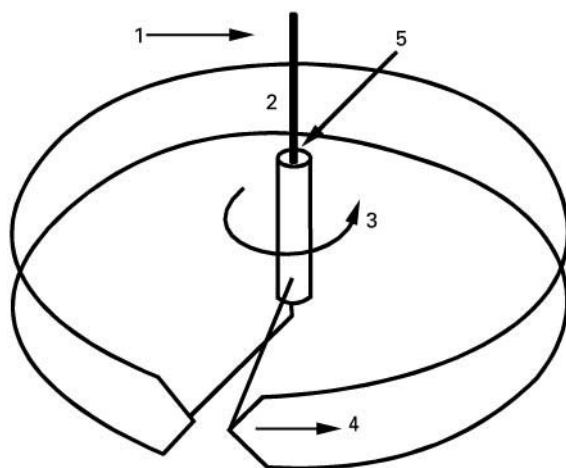


Figure 4 Design of sedimentation FFF channel: (1) flow in; (2) channel; (3) rotation; (4) flow; (5) flow out.

tion of polymer latex particles, inorganic particles, emulsions, etc. The fractionation of colloidal particles in river water, diesel exhaust soot, and of the nuclear energy-related materials, are typical examples of the use of sedimentation FFF in the investigation of environmental samples. Droplets of liquid emulsions can also be separated and analysed. Biopolymers and particles of biological origin (cells) belong to the most interesting group of objects to be separated by sedimentation FFF. The performance of sedimentation FFF is superior to, or as good as, those of other separation methods. A complication in interpreting the experimental data is due to the fact that the retention is proportional to the product of particle size and density. When performing the fractionation in one carrier liquid only, the density must be assumed constant for all particles. However, it is possible to determine the size and density of the particles independently if the fractionations are performed in carrier liquids of various densities.

An example of a typical application of sedimentation FFF shown in Figure 5 allowed detection of a bimodal PSD in a sample of a polymer latex. The order of the elution from the small to the large diameter particles corresponds to the polarization mechanism. Figure 6 shows a rapid, high resolution sedimentation FFF of the polymer latex particles. In this case, the mechanism of steric FFF dominates, and the order of the elution is inverted.

Flow FFF is a universal method because different size particles exhibit differences in diffusion coefficients which determine the separation. The cross-flow, perpendicular to the flow of the carrier liquid along the channel, creates an external hydrodynamic field which acts on all particles uniformly. The channel, schematically demonstrated in Figure 7, is formed between two parallel semipermeable

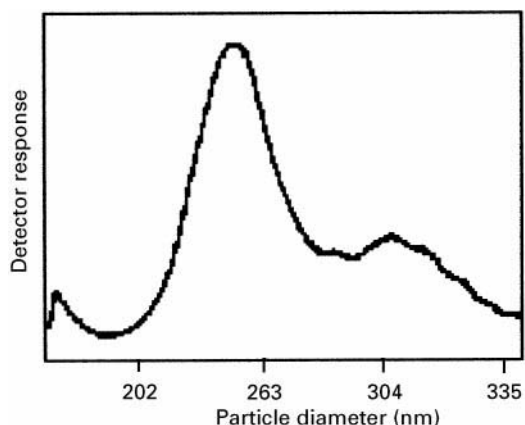


Figure 5 Fractogram of poly(glycidyl methacrylate) latex showing a bimodal character of the PSD.

membranes fixed on porous supports. The carrier liquid can permeate through the membranes but the separated particles cannot. Separations of various kinds of particles such as proteins, biological cells, colloidal silica, polymer latexes, etc., have been described.

Electric FFF uses an electric potential drop across the channel to generate the flux of the charged particles. The walls of the channel are formed by semipermeable membranes as in flow FFF. The particles exhibiting only small difference in electrophoretic mobilities but PSD and, consequently, important differences in diffusion coefficients, can be determined. The advantage of electric FFF compared with electrophoretic separations, e.g., with capillary electrophoresis, is that high electric field strength can be achieved at low absolute values

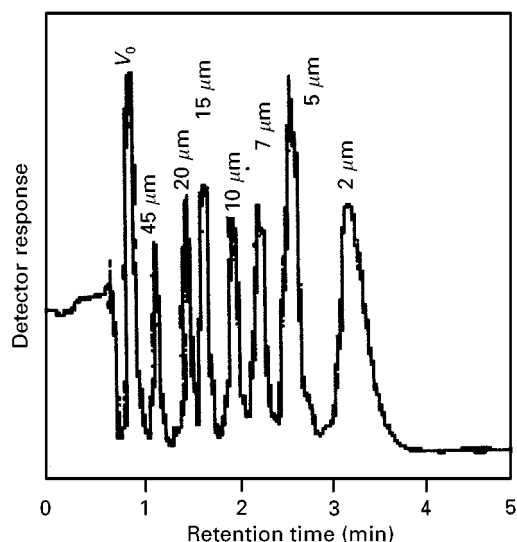


Figure 6 Fractogram of high-speed high resolution sedimentation FFF of latex beads.

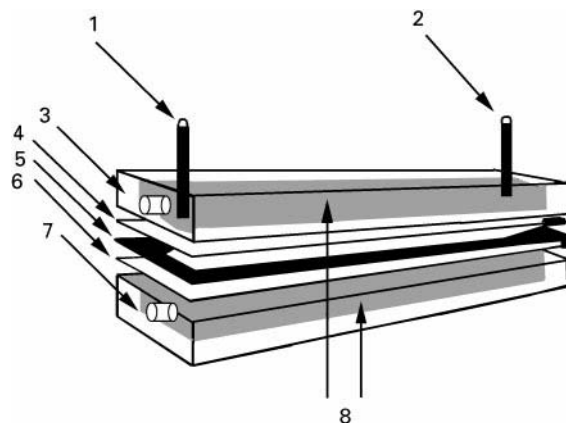


Figure 7 Design of flow FFF channel: (1) flow in; (2) flow out; (3) cross-flow input; (4) membrane; (5) spacer; (6) membrane; (7) cross-flow output; (8) porous supports.

of the electric potential due to the small distance between the walls of the channel. Electric FFF is especially suited to the separation of biological cells as well as to charged polymer latexes and other colloidal particles. The fractionation of the charged particles represents a vast application field for exploration.

Thermal FFF was the first experimentally implemented technique, introduced several years ago. Until now, it has been used mostly for the fractionation of macromolecules. Only very recently have attempts been made to apply this method to the fractionation of particles. The potential of thermal FFF justifies a description here, regardless of its recent limited use in particle separations. The temperature difference between two metallic bars, forming channel walls with highly polished surfaces and separated by a spacer in which the channel proper is cut, produces a flux in the sample components, known as the Soret effect, usually towards the cold wall. The particle sizes can be evaluated from an experimental fractogram by using an empirical calibration curve constructed with a series of samples of known sizes. This calibration can be used to determine the characteristics of an unknown sample of the same chemical composition and structure, with the same temperature gradient applied. The pressurized separation systems permit operation above the normal boiling point of the solvent used. The fractionations can be achieved in few minutes or seconds. The performance parameters favour thermal FFF over competitive methods.

Applications of Focusing FFF

Focusing FFF methods can be classified according to various combinations of the driving field forces

and gradients. The gradients proposed and exploited are:

- effective property gradient of the carrier liquid
- cross-flow velocity gradient
- lift forces
- shear stress
- gradient of the nonhomogeneous field action

Focusing can appear due to the *effective property gradient of the carrier liquid* in the direction across the channel combined with the primary or secondary transversal field. The density gradient in sedimentation–flotation focusing field-flow fractionation (SFFFF) or the pH gradient in isoelectric focusing field-flow fractionation (IEFFFF) has already been implemented for separation of polystyrene latex particles and of biological samples. Separation by SFFFF is carried out according to the density difference of the latex particles. An electric field can be applied to generate the density gradient in a suspension of charged silica particles. The separation by IEFFFF is carried out according to the isoelectric point differences by using the electric field to generate the pH gradient and to focus the sample components. A simple design of a channel for SFFFF is shown in Figure 8 and an example of the separation of two latex particles according to small density difference is demonstrated in Figure 9. The separation is very rapid and much less expensive when compared to isopycnic centrifugation.

The effective property gradient of the carrier liquid, e.g., the density gradient, can be preformed at the beginning of the channel and combined with the primary or secondary field forces. A step density gradient is formed in such cases but the preforming is not limited to a density gradient.

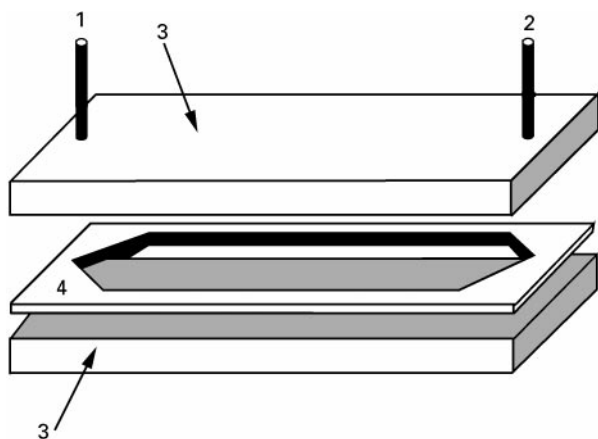


Figure 8 Schematic representation of the channel for focusing FFF in coupled electric and gravitational fields: (1) flow in; (2) flow out; (3) channel walls forming electrodes; (4) spacer.

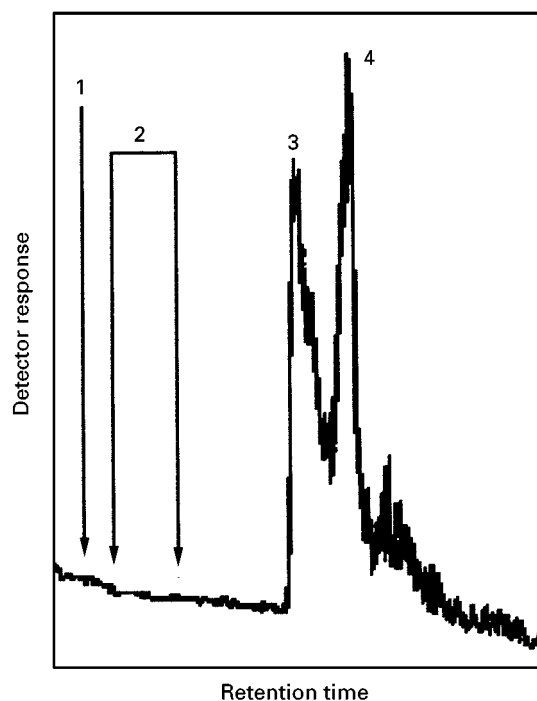


Figure 9 Fractogram of two samples of polystyrene latex particles showing a good resolution obtained by focusing FFF while no detectable resolution was achieved under static conditions: (1) injection; (2) stop-flow period; peaks corresponding to particle diameters of 9.87 μm (3) and 40.1 μm (4).

The focusing appears in the *gradient of transverse flow velocity* of the carrier liquid which opposes the action of the field. The longitudinal flow of the liquid is imposed simultaneously. This elutriation focusing field-flow fractionation (EFFFF) method has been investigated experimentally by using a trapezoidal cross-section channel to fractionate micrometre-size polystyrene latex particles but the use of the rectangular cross-section channel is possible.

The *hydrodynamic lift forces* that appear at high flow rates of the carrier liquid combined with the primary field are able to concentrate the suspended particles into the focused layers. The retention of the particles under the simultaneous effect of the primary field and lift forces generated by the high longitudinal flow rate can vary with the nature of the various applied primary field forces.

The *high shear gradient in a carrier liquid* can lead to the deformation of the soft particles. The established entropy gradient generates the driving forces that displace the particles into a low shear zone. At a position where all the driving forces are balanced, the focusing of the sample components can appear. Although this method was originally proposed by applying a temperature gradient acting as a primary field and generating the thermal diffusion flux of the macromolecules which opposes the flux due to the

entropy changes generated motion, it should be applicable to soft particles as well.

A *nonhomogeneous high-gradient magnetic field* can be used to separate various paramagnetic and diamagnetic particles of biological origin by a mechanism of focusing FFF. A concentration of paramagnetic particles near the centre of a cylindrical capillary and the focusing of diamagnetic particles in a free volume of the capillary should occur. No experimental results have yet been published.

Other gradients and a variety of the fields can be combined to produce the focusing and to apply these phenomena for PSD analysis. This review of the mechanisms used in focusing FFF should give an idea of their potential.

Size-Exclusion Chromatography

Size-exclusion chromatography (SEC) is utilized for the fractionation and analytical characterization of macromolecules but also for the separation of particles. The term gel-permeation chromatography (GPC) is used simultaneously in the literature with almost equal frequency. Other terms employed to describe this separation method are steric-exclusion liquid chromatography, steric-exclusion chromatography, gel filtration, gel-filtration chromatography, gel chromatography, gel-exclusion chromatography, and molecular-sieve chromatography. Each reflects an effort to express the basic mechanism governing the separation but the appropriate choice is more a question of individual preference.

The historical origins of SEC date from the late 1950s and early 1960s. Using cross-linked dextran gels swollen in aqueous media, Porath and Flodin separated various proteins according to their sizes. The 'soft gel' column packing used in these experiments was applicable only at low pressure and, consequently, at low flow rates resulting in very long separation times. The first successful separation of a synthetic polymer by SEC was described by Vaughan who succeeded in separating low molar mass polystyrene in benzene on a weakly cross-linked polystyrene gel. Some years later, Moore described the separation of polymers on moderately cross-linked polystyrene gel column packings.

The first rigid macroporous packing, suited also for the separation of particles, was porous silica introduced in 1966 by De Vries and co-workers. This packing was fully compatible with both aqueous and organic solvents, exhibited a very good mechanical stability, but its use was restricted by strong nonsteric exclusion interactions between the silica surface and a number of separated species. In 1974, the appearance of the packings of small porous particles with

a typical diameter around 10 μm , instead of 50–100 μm particle diameter used in conventional SEC columns, resulted in an important technological improvement in SEC. The high pressure technology, the lowering of the column volume due to the use of small particle diameter packings and the high efficiency of the columns allowed the separation time to be reduced from hours to minutes. Other porous silica microparticle packings, introduced by Kirkland, Unger, and others, were resistant to the high pressure and compatible with the quasi-totality of the solvents. The undesired interactions were suppressed by organic grafting or by organic coating of the porous silica.

Principle of Separation

The separation mechanism can be explained on the basis of a specific distribution of the separated particles between the eluent outside the porous particles of the column packing (mobile phase) and the solvent filling the pores (stationary phase). This distribution is due to the steric exclusion of the separated particles from a part of the pores according to the ratio of their size to the size of the pores. The particles whose sizes are larger than the size of the largest pores cannot permeate the pores, passing only through the interstitial volume, i.e., through the void volume between the particles of the column packing, whereas very small particles may permeate all the pores. Particles of intermediate size are, to a greater or lesser extent, excluded from the pores. Hence, the elution proceeds from the largest particles to the smallest ones. This mechanism is schematically demonstrated in Figure 10.

The total volume of a packed chromatographic column, V_t , is given by the sum of the total volume of the pores, V_p , the volume of the matrix proper of the porous particles, V_m , and the interstitial or void volume, V_o , between the porous particles:

$$V_t = V_p + V_m + V_o$$

The retention volumes, V_R , of the separated particles lie within V_o and $V_o + V_p$. V_R of a uniform particle size fraction of the sample is defined as a volume of the eluent that passes through the column from the moment of the sample injection to the moment when the given particles leave the separation system at their maximal concentration. The retention can alternatively be expressed in time units as the retention time t_R . The particles permeating the pores are excluded from some of the pores and partially permeate the accessible pores. The retention volume of a given species can be written as:

$$V_R = V_o + K_{\text{sec}} V_p$$

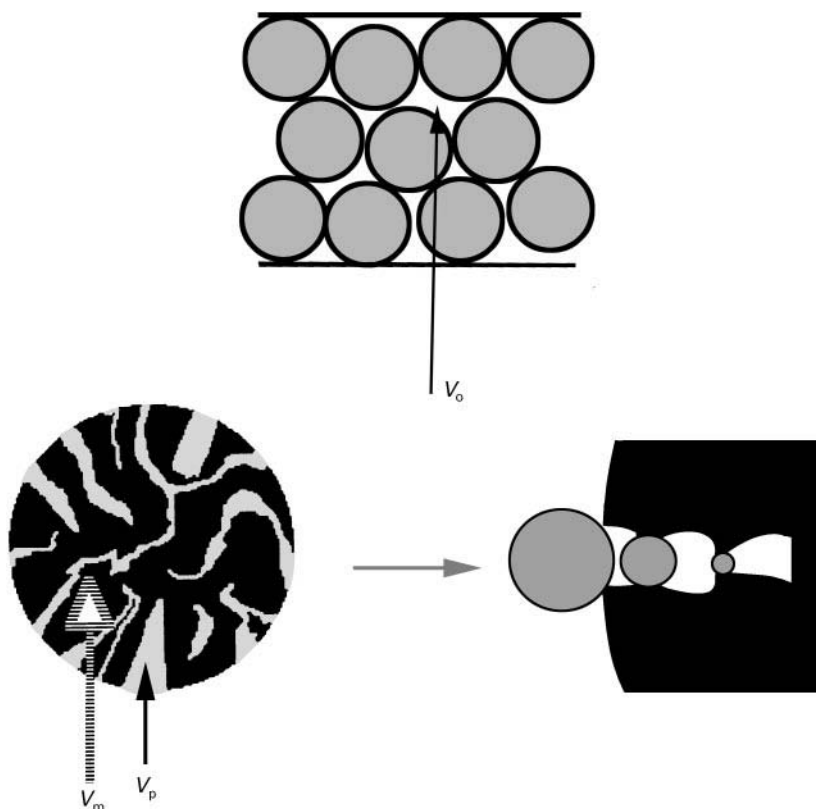


Figure 10 Schematic representation of the chromatographic column for SEC. Column with the void volume between the spherical particles of the column packing, the structure of one porous particle with the pore and matrix volumes, and the imaginary shape of one pore allowing the total permeation of smallest separated particles, partial permeation of intermediate size particles, and exclusion of largest particles.

where K_{sec} is the formal analogue of the distribution coefficient between the mobile and stationary phases.

Separation Mechanisms

Many attempts have been made to explain the mechanism of separation in SEC but steric exclusion (or size exclusion) is accepted to be the main process governing the separation. This mechanism is based on a thermodynamic equilibrium between stationary and mobile phases. As the nature of the solvent is the same in both phases, the question is to explain the dependence of the distribution coefficient K_{sec} on the size of the separated species. One of the simplest approaches uses the above-mentioned geometrical models; nevertheless, the retention volume is determined not only by the accessibility of a part of the volume of the individual pores but also by the size distribution of the entire system of pores in the column packing material. The distribution coefficient for an individual pore depends on the ratio of the pore size to the size of the separated particles and can be expressed by:

$$K_{\text{sec}} = \frac{c_p}{c_o}$$

where the concentrations c_p and c_o refer to the pores and the interstitial volume. If the pore size distribution of the column packing particles is taken into consideration, the retention volume is given by:

$$V_R = V_o + \int_R^{r_{\text{max}}} K(R, r)_{\text{sec}} \phi(r) dr$$

where $\phi(r)dr$ is the total volume of the pores whose radii lie within r and $r + dr$, and R is an equivalent radius of the retained particles. Hence, the retention volume of a given particulate species is determined coincidentally by the accessibility of a part of the volume of the individual pores and by the size distribution of the entire system of pores inside the column packing particles. Although different column packings exhibit almost identical dependences of V_R on separated particles size, porosimetric measurements indicate various pore size distributions. This means that the relationship between the pore size distribution and the retention volume of the separated species is not so straightforward.

An interesting model of separation by flow was proposed by Di Marzio and Guttman. The porous

structure of the SEC column packing is approximated by a system of cylindrical capillaries. The separated species move down the pores by the action of the flow but cannot get nearer to the pore wall than a distance determined by their radius. Consequently, they move at a velocity higher than the average velocity of the liquid flow due to a parabolic flow-velocity profile established in an imaginary cylindrical pore. Hence, the retention is determined by the ratio of the pore to the particle diameter. There are several factors that militate against this separation mechanism. The model assumes that the liquid can flow through the pores, which will not be true in most cases with polymeric gel particles used as column packing materials. Moreover, even in those cases when the pores are open to through flow, their diameter in comparison with the size of the interstitial voids cannot allow the flow rate to be high enough to explain the real values of the retention volumes. For the same reason, the frequently used explanation of the SEC mechanism of separation by an oversimplified model of molecular sieving is not accurate. This model, however, explains quite well the separation of large particles in hydrodynamic chromatography where either very large open pores are present in the particles of column packing or the packing particles are not porous and the separation by flow is performed in the interstitial volume only.

More complicated mechanisms based on the interactions between the separated species and the stationary phase may occur in an SEC column in addition to the steric exclusion mechanism: adsorption, liquid-liquid partition, electrostatic repulsions between the separated particles and the packing material, etc. The pure SEC separation mechanism can be operating only if the column packing material and the solvent are chosen to suppress these secondary effects. If the distribution coefficient K_{sec} is larger than 1, it is certain that other interactions, e.g., adsorption, beside the steric exclusion mechanism come into play and increase the retention. Unfortunately, if K_{sec} lies between 0 and 1, it does not mean that secondary interactions are definitely not interfering. Although such interactions are secondary, they can either improve or worsen the resulting separation. From the thermodynamic point of view, the separation is carried out near equilibrium conditions and the distribution coefficient can be described by:

$$K_{\text{sec}} = \exp\left(\frac{-\Delta H^\circ}{RT}\right) \exp\left(\frac{\Delta S^\circ}{R}\right)$$

Dawkins and Hemming considered the enthalpic term on the right-hand side of this equation as a distribution coefficient, the value of which is unity,

provided that size exclusion is the only effective mechanism. In such a case, the entropic term represents the pure size-exclusion mechanism. If other attractive interactions come into play ΔH° becomes negative and, if some repulsive interactions are involved, ΔH° is positive.

Other mechanisms explaining the separation in SEC have been proposed but most of them apply exclusively to the separation of macromolecules. The details can be found in the specialized literature. The above-presented approaches give an accurate basic idea of the separation of particles by SEC.

Applications of SEC

SEC allows, with respect to the basic separation mechanism, separation of particles according to differences in their effective sizes. Its application to the separation of particles in the submicron size range is limited only by the availability of column packing materials having sufficiently large pore size diameters. In order to cover as large a range of sizes of commonly fractionated particles as possible, the column packing material should have the pore size distribution from a few tenths of nanometres to hundreds of nanometres. For technical reasons, it is only possible to prepare the packings with a limited range of pore sizes and the SEC separation system is composed of an assembly of several columns in series, packed with several particle packing materials of different porosities, or another possibility is to use only one column packed with a mixture of several different packing materials with various porosities. The selectivity and the resolution of such a separation system is, however, lower than a system with a more homogeneous distribution of the pore dimensions.

Besides standard particle size separations, SEC has been successfully applied to the analytical characterization of micelles and submicron particles. Under the appropriate experimental conditions it can be used for separations in organic solvents as well as in water, at elevated temperatures, etc. An interesting application of SEC is so-called *inverse SEC*. The difference, as compared to conventional SEC, lies in the column packing particles being analysed from the viewpoint of the pore size distribution or average pore size dimensions, using a series of well-characterized size standards.

The analytical application of SEC for the determination of PSD is related to the use of either any calibration procedure and/or to the coupling of the separation system with the detector, the response of which is proportional to the size-related property of the analysed particles such as, e.g., the intensity of the

scattered light. The coupling of the concentration-sensitive detector and a size-sensitive detector, together with the use of an appropriate calibration procedure for the separation system, allows extraction of more information on PSD and other structural parameters of the particles under study.

Hydrodynamic Chromatography

Hydrodynamic chromatography (HC), as a new method for the separation of the particles of submicrometre sizes, was described by Small in 1974. HC is not a variant of SEC although some processes can participate in the separation mechanisms of both methods. It is not a subtechnique of FFF although the hydrodynamic phenomena can actively participate in the separation mechanism of FFF whose fundamental characteristic is the selective migration of the separated species due to an effective field. Formally, HC could be considered as a limiting case of FFF when the intensity of an effective external field is zero.

Principle of Separation

The name of the method designates the principal mechanism governing the separation: hydrodynamic phenomena appearing in fluids flowing through porous media or in capillaries. The separation in HC is performed in a carrier liquid flowing either through the void volume of a packed column or inside an open capillary of small diameter. The separated particles are carried by the flow with a velocity higher than the average velocity of the carrier liquid due to the tendency of the particles to concentrate in a radial position where the streamline velocity is higher compared with the average velocity of the liquid. Such a radial position corresponds to an energy minimum of the particles migrating within the field of shear forces. The driving forces which cause the radial flux of the separated particles can be of very diverse character. Another phenomenon participating in the separation processes can be the steric exclusion of the particles from a part of the volume within which the carrier liquid can flow near the column packing surface or near the wall of an open capillary. The velocity of the carrier liquid decreases to zero toward these surfaces and only small separated particles which can approach the surface of the column packing or capillary wall can elute with slow velocity in the vicinity of these surfaces. This situation is demonstrated in **Figure 11** for a model case of the HC carried out in an open capillary.

Separation Mechanisms

According to Small, the separation in HC is governed by three contributing effects: hydrodynamic forces,

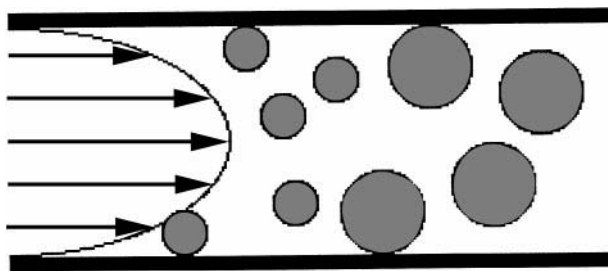


Figure 11 Schematic representation of the HC separation principle. Larger particles are excluded from the wall and can freely migrate only in a part of the volume of the capillary column. As a result, their elution times are shorter compared with the elution times of smaller particles.

electrostatic repulsions, and Van der Waals forces. The density of the separated particles influences only their mobility and rotational moments. Soft particles can be deformed due to the high shear stress and this effect can influence their retention volumes.

A model of the separation by flow was originally proposed by DiMarzio and Guttman to explain retention in SEC. Their model approximates the structure of a packed chromatographic column to a complex system of capillaries in which the separation is caused by the same steric exclusion phenomenon as shown in **Figure 11**. The average velocity of the carrier liquid in a cylindrical capillary is given by:

$$\langle v(r) \rangle = \frac{\Delta P R^2}{8\mu L}$$

where ΔP is the pressure drop along the capillary of the length L and the radius R , μ is the viscosity of the carrier liquid and r is the radial coordinate. The average velocity of uniform-sized particles is given by:

$$v_{\text{ave}} = \frac{\Delta P}{4\mu L} \left[R^2 - \frac{(R-a)^2}{2} - \gamma a \right]$$

where a is the radius of the separated particles. The last term of the equation represents the rotational moment of the particles which reduces the velocity of their axial migration. The resulting retention is defined, similarly as in FFF, by the ratio of both velocities:

$$R = \frac{v_{\text{ave}}}{\langle v(r) \rangle}$$

Whenever HC is carried out in an open capillary, the separation is clearly dominated by this mechanism. Many authors consider that particles do not move within all the sterically accessible volume but in an

annular volume which is determined by the radial forces generated by the flow of the carrier liquid. The particles carried by the flow undergo the effect of the radial force which concentrates them within the annular volume. This force is due to the combination of the rotational and translational movements of the particles and is analogous to the Magnuson effect.

The electrostatic double layer on the surface of the separated particles influences their effective sizes. The electrostatic double layer, on the surface of the chromatographic packing or of the wall of the capillary column, reduces the accessible volume of the column due to the repulsion of separated particles of the same charge. The increased concentration of ions (ionic force) in the carrier liquid causes the screening of the surface electric charges and, consequently, reduces all electrostatic interactions. On the other hand, the reduced repulsions allow the separated particles to approach within a small distance at which the attractive Van der Waals force become effective. As a result, the hydrodynamic phenomena and electrostatic repulsions dominate the separation mechanism at a low ionic force of the carrier liquid, while at a high ionic force, the separation is dominated by hydrodynamic forces and adsorption phenomena. The order of the elution can be inverted, the particles can form aggregates, and the separation can be completely perturbed by these effects.

Applications of HC

HC is widely used for the separations of particles of very different character, starting from inorganic particles, polymer latexes, and biological cells, to synthetic and natural molecules, oil emulsions, etc. Modern short capillary columns allow substantial reduction in the separation time and an increase in the efficiency and resolution. Although HC was originally developed for the separations of micrometre-sized particles, the size range of applications has recently been lowered to tens of nanometres. The example in **Figure 12** shows the chromatogram of three polymer latex size standards separated on an open capillary column. The separation was accomplished in one minute.

Centrifugation

Starting in the early 1920s with the famous work of Svedberg, centrifugation became probably the most popular method for separation of particles. Based on extensive knowledge and experience of the sedimentation of particles in a natural gravitational field, centrifugation, using more intense inertial forces gen-

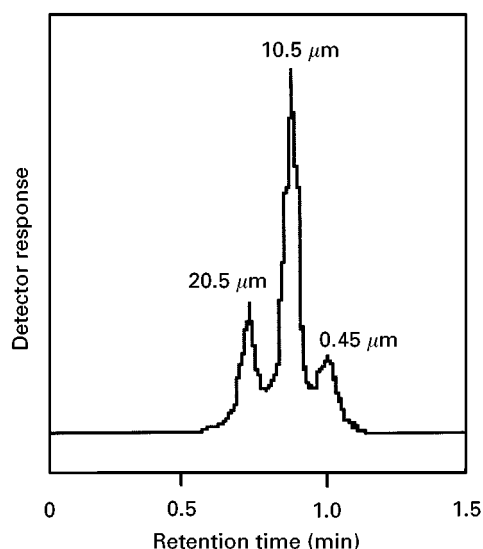


Figure 12 Separation of different size polymer latexes by HC.

erated at slow rotational speeds, allowed the separations of relatively small particles. The invention of the ultracentrifuge (which uses extremely high speeds of rotation, allowing a reduction in the size limits of the separated species) and of new coupled detectors, upgraded a simple sedimentation fractionation technique into powerful separation methodology applicable to preparative separations as well as for analytical characterization of particles and macromolecules. The impressive progress in theory, methodology, techniques and applications was of a long-lasting nature, from the 1920s to the 1970s. Thereafter, some stagnation appeared but the beginning of the 1990 represented a renaissance era for analytical and preparative ultracentrifugation and derived techniques.

Principle of Separation

A particle suspended in a fluid settles under the effect of gravitational or inertial centrifugal force which is proportional to the effective mass of the particle, i.e., the difference between its true mass m and the mass of the same volume V of the suspending liquid, according to Archimedes principle:

$$F_1 = (mg - \rho Vg)$$

where g is the acceleration due to the gravitational or centrifugal field forces and ρ is the density of the suspending liquid. Force F_1 is opposed by the force of friction F_2 which is proportional to the velocity of sedimentation U with a constant of proportionality f , called the friction coefficient:

$$F_2 = fU$$

With the exception of the initial short period of time during which the sedimentation velocity of the particle increases until the steady state is reached at which both forces are equal, the velocity of sedimentation in a homogeneous liquid is constant. Stokes calculated the friction coefficient of hard spherical particles and obtained:

$$f = 6\pi\eta r$$

for a particle of the radius r sedimenting in a liquid of the viscosity η . Einstein derived the relationship between the friction and diffusion coefficients:

$$D = kT/f$$

It is evident that the sedimentation processes in homogeneous suspending liquids separate the particles according to their effective masses and if the particles are uniform with respect to their densities, the separation proceeds strictly according to the differences in particle size. The analysis of PSD can be realized on the basis of the measurement of the sedimentation velocity during the sedimentation process or from the equilibrium concentration distribution. Nevertheless, it has to be stressed that although centrifugation is, in principle, the separation method, the size-based separation of the particles can be rather complicated because various size particles sediment together and form a complex, superposed concentration gradient in which all size particles are always present in various relative proportions. On the other hand, if the separated particles exhibit nonuniformity in both size and density, size separation can be a rather difficult task.

Sedimentation processes can generate the formation of a density gradient in a complex, multicomponent suspending liquid. The particles suspended in such a density-gradient forming liquid can undergo focusing phenomena and, as a result, they can be separated according to differences in densities. Recent theoretical and experimental findings demonstrate that the size polydispersity in such cases influences the width of the focused zones. Evidently, therefore, if the particles exhibit polydispersity in size and density, the separation is complicated.

Modern theoretical approaches as well as the experimental results demonstrate that sedimentation and focusing can appear together even in a simple suspending liquid because the size polydispersity of the separated particles is itself able to generate the isoperichoric (from Greek: *isos* = equal and *perichoron* = environment) focusing phenomena. It can complicate the use of centrifugation as a simple tool for particle size separation. On the other hand,

although not yet fully mastered and understood, these new approaches offer a challenge for fundamental research and development.

Separation Mechanisms

Sedimentation processes lead to the formation of a concentration gradient. Fickian diffusion, Brownian motion, general entropic tendency and repulsive interactions counterbalance the concentration gradient formed. The sedimentation of an ensemble of particles progresses until an equilibrium concentration distribution is achieved due to the opposed sedimentation and dispersive fluxes. The equilibrium can be described by the differential transport equation:

$$-D \frac{dc}{dx} - Uc = 0$$

where c is the concentration of the sedimenting particles and dc/dx is the concentration gradient formed in the direction of the sedimentation. There exist some limits to the validity of this equation but the details are beyond the scope of this review. The thermodynamic approach defines the equilibrium on the basis of the chemical potential of the sedimenting species μ_i :

$$m_i(1 - v_i\rho(x))\omega^2 x dx - \sum_k \frac{\partial \mu_i}{\partial c_k} dc_k = 0$$

where v_i is the molar volume of the sedimenting species and ω is the angular velocity of the centrifuge rotor. The concentration distribution of uniform-size particles at equilibrium in a homogeneous liquid is exponential. When different but uniform-size colloidal particles sediment separately by forming the exponential concentration distributions, the larger size particles are compressed close to the bottom of the sedimentation cell. This situation is demonstrated in **Figure 13**. On the other hand, the sedimentation of the colloidal particles exhibiting some PSD can lead to very different equilibrium concentration distributions of the particles of different sizes. Larger size particles can be compressed closer to the bottom of the sedimentation cell but they can form focused zones at higher levels as well. These two situations are demonstrated in **Figure 14**.

In the first case shown in **Figure 14**, two exponential concentration distributions corresponding to two different size particulate species are superposed. The lower part of the sedimentation cell contains a higher proportion of larger particles compared with the original mixture and vice versa for the upper part

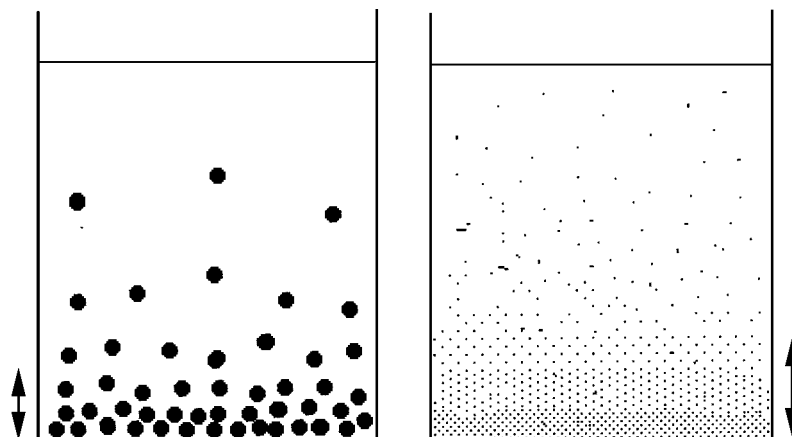


Figure 13 Schematic representation of the sedimentation of different size particles. Concentration distribution is more compressed to the bottom of the sedimentation cell for larger size particles (left) and centre of gravity of the concentration distribution is closer to the bottom compared with smaller size particles (right).

of the sedimentation cell, and thus size fractionation exists. It is impossible, in principle, to achieve more complete size separation of particles by simple centrifugation.

In the second case shown in Figure 14, larger particles are focused in the density gradient due to the equilibrium exponential concentration distribution of smaller particles. The concentration distribution of larger focused particles approaches a Gaussian distribution function.

The two imaginary cases shown in Figure 14 demonstrate two limit situations which can appear in actual centrifugation experiments in a homogeneous suspending liquid. The focusing phenomenon is, of

course, actively exploited in isopycnic (or more generally isoperichoric) focusing separations of particles. In such cases, a two- or multicomponent liquid is used to form the density gradient and larger particles are separated according to density differences.

The particle-particle interactions which limit the degree of freedom of the particle movements, and whose importance increases with increasing concentration, are the major factors imposing the particular concentration distribution of each sedimenting species of a polydisperse colloidal sample. Consequently, the results of the particle separation performed by any centrifugation method must be carefully evaluated.

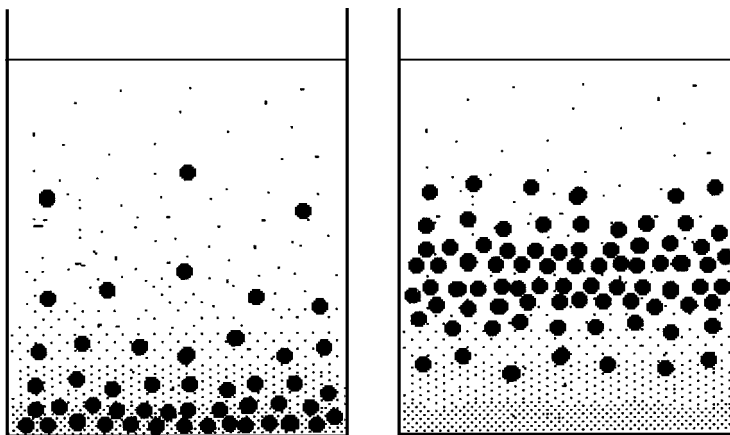


Figure 14 Schematic representation of the sedimentation of a mixture of different size particles. The exponential concentration distribution of larger and smaller size particles can be either superposed (left) or larger size particles can be focused within the density gradient formed by the exponential concentration distribution of smaller particles (right).

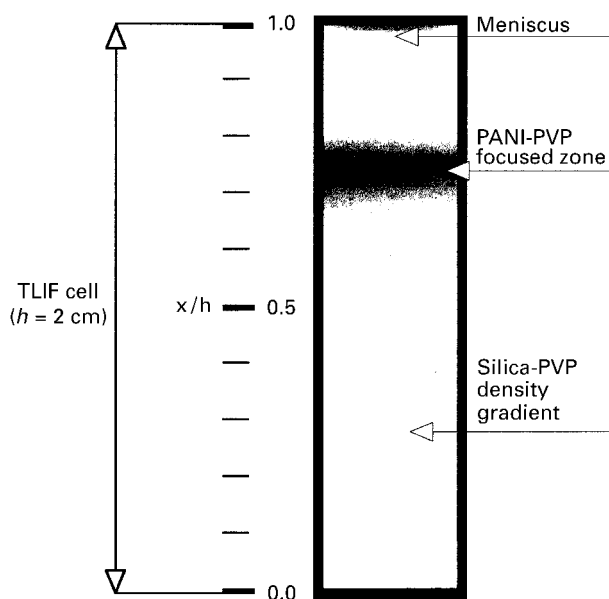


Figure 15 Isoperichoric focusing of coloured polyaniline particles in the density gradient formed by colourless silica particles in thin-layer isoperichoric focusing (TLIF) cell in a centrifugation experiment.

Applications of Centrifugation

When taking into account the potential and limitations of sedimentation processes, centrifugation can be successfully applied and, in reality, is widely used for the separation of colloidal particles of very different character: inorganic, polymer and biological, and also for the separations of macromolecules. An example of the use of centrifugation is in **Figure 15** which shows the zone of the coloured polyaniline particles focused from a bidisperse mixture with colourless silica particles. This focusing experiment was, indeed, intended not to separate the polyaniline particles from the silica particles of comparable size but to prove the existence of the focusing phenomenon under the given experimental conditions. However, the size separation of the particles using this phenomenon is real.

Electrophoresis

Electrophoresis is a separation technique based on differential transport of electrically charged species. The discovery of electricity was paralleled with an understanding of electrophoretic phenomena and consequently, this separation technique can be considered as classical.

Over the last two decades, all electrophoretic techniques have undergone an explosive growth, especially as concerns the analytical applications of the capillary version of electrophoresis. Nevertheless,

there are only few publications describing the applications of this technique to the separation of charged particles. This can be explained by the fact that separation in electrophoresis is primarily based on differences in electric charge density which is inherently related to the size of the separated particles. As described in the section on HC, the effective size of the particles includes the thickness of the electric double layer which varies with the ionic force of the suspending liquid. This means that whenever the size separation concerns the particles in their natural environment, their effective size includes the electrostatic double layer and separation can be carried out by using electrophoretic transport processes. As the electric charge contains information on the nature of the particle surface, separation by electrophoresis is certainly a useful technique when used appropriately.

The general theory of electrophoretic separations applies to particle separations as well. This has been discussed above in respect to electric FFF. As the applications of electrophoretic techniques to particle separations are still very limited, it is impossible to review this technique as fully as for the other separation methods. Only one recent example, an interesting separation of polyaniline and silica particles, is shown in **Figure 16**.

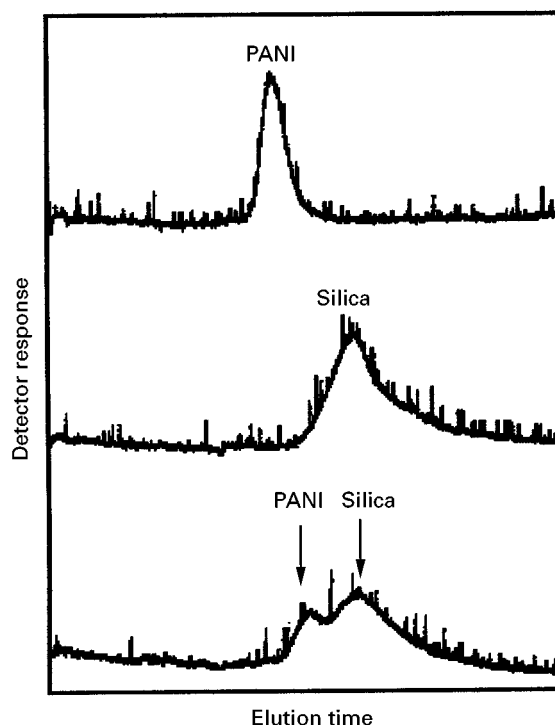


Figure 16 Electropherograms of the individual polyaniline (PANI) and silica composite particles and of the separated mixture of both obtained by capillary electrophoresis.

Future Development

A search for the historical origins of a scientific discovery is often a difficult task but, with regard to the rapid advances in separation science in general, and of particle size separations in particular, the long-term prediction of progress is almost a 'mission impossible'. However, cautious examination of the state of the art and of potential exigencies concerning particle size separations, allows a few statements about what is likely to happen in the near future to be made.

Further increases in efficiency, resolution and selectivity represent a permanent challenge in particle size separations. An ideal is to separate two particulate species differing by a minimal increment in terms of a 'construction' unit, e.g., one molecule or atom, and not only in terms of 'size increment' which is a rather arbitrary choice.

Increase of the separation speed can be an important factor whenever the separated particles exhibit an evolution in time and it is necessary to capture information on the actual PSD at a given moment. Many biological concepts are approached in this way. The ways to be explored lead to more extensive use of supercritical fluids allowing substantial increase of transport coefficients.

Most recent methods and techniques of particle size separations exploit simple physical and physicochemical principles single driving forces leading to the separation. Coupling of two or more physical fields and field gradients as selective driving forces and their combinations with nonselective transport due to the carrier fluid flow seems to be a recently emerging approach.

Large-scale particle size separations represent important parts of many industrial technologies. The performance of a large-scale separation is often lower in comparison with an essentially identical technique applied under analytical-scale conditions. The optimization of large-scale separation processes in order to approach the performances comparable with analytical-scale conditions. The optimization of large-scale separation processes in order to approach the performances comparable with analytical-scale separations has a potentially important economic impact.

The permanent search for noninvasive conditions in particle size separations is an important field of activity related to fundamental research in the life sciences and also to many important biotechnologies.

These directions of potential future progress in the domain of particle size separations are certainly not exhaustive but they represent an overview of, probably, the most important activities in research and development.

Further Reading

- Agricolae D (1556) *De Re Metallica, Libri XII*. Basileae.
- Barth HG (ed.) (1984) *Modern Methods of Particle Size Analysis*. New York: John Wiley.
- Belenkii BG and Vilenchik LZ (1983) *Modern Liquid Chromatography of Macromolecules*. Amsterdam: Elsevier.
- Dawkins JV (1978) In: Epton RE (ed.) *Chromatography of Synthetic and Biological Polymers*, vol. 1. Chichester: Ellis Horwood.
- Dawkins JV (ed.) (1983) *Developments in Polymer Characterization-4*. London: Applied Science.
- Dawkins JV (1989) Size exclusion chromatography. In: Booth C and Price C (eds) *Comprehensive Polymer Science*, vol. 10 Oxford: Pergamon Press.
- Grossman PD and Colburn JC (eds) (1992) *Capillary Electrophoresis: Theory and Practice*. New York: Academic Press.
- Janča J (ed.) (1984) *Steric Exclusion Liquid Chromatography of Polymers*. New York: Marcel Dekker.
- Janča J (1987) *Field-flow Fractionation: Analysis of Macromolecules and Particles*. New York: Marcel Dekker.
- Janča J (1995) Isoperichoric focusing field-flow fractionation based on coupling of primary and secondary field action. In: Provder T, Barth HG and Urban MW (eds) *Chromatographic Characterization of Polymers, Hyphenated and Multidimensional Techniques*. Advances in Chemistry Series 247. Washington DC: American Chemical Society.
- Kolin A (1977) Reminiscences about the genesis of isoelectric focusing and generalization of the idea. In: Radola BJ and Graesslin D (eds) *Electrofocusing and Isoelectrophoresis*. Berlin: de Gruyter.
- Orr C and Groves MJ (eds) (1978) *Particle Size Analysis*. London: Heyden.
- Silebi CA and McHugh AJ (1978) In: Becker P and Yundfreund MN (eds). *Emulsions, Lattices, and Dispersions*. New York: Marcel Dekker.
- Small H (1974) Hydrodynamic chromatography: A technique for size analysis of colloidal particles. *Journal of Colloid and Interface Science* 48: 147-161.
- Yau WW, Kirkland JJ and Bly DD (1979) *Modern Size Exclusion Chromatography*. New York: Wiley Interscience.

AFFINITY SEPARATION



Affinity Membranes

K. Haupt, Lund University, Lund, Sweden

S. M. A. Bueno, Universidade Estadual de Campinas, Brazil

Copyright © 2000 Academic Press

The rapid development in biotechnology and the large potential of biomolecules for applications in medicine, food industry and other areas, result in an increasing demand for efficient and reliable tools for the purification of proteins, peptides, nucleic acids and other biological substances. This situation is being additionally enforced by the increasing number of recombinant gene products that have arrived on the market or that are currently being investigated, such as insulin, erythropoietin and interferons. The recovery of fragile biomolecules from their host environments requires their particular characteristics to be taken into account for the development of any extraction or separation process. On the other hand, there is a demand for techniques that can easily be scaled up from laboratory to industrial production level.

In this context, the use of affinity methods has the advantage that coarse and fine purification steps are united through the introduction of a specific recognition phenomenon into the separation process. The most widely used method for preparative affinity separation of biomolecules is liquid chromatography on beaded resins (soft gels). Despite the commercial availability of many affinity ligands immobilized on to gel beads for use in column chromatography, there are some drawbacks in a large scale application of these supports. Flow rates and thus performance are limited by the compressibility of the resins and pore diffusion. Because of these intrinsic limitations, other chromatographic techniques, such as perfusion chromatography, or different separation techniques, such as affinity precipitation and affinity phase partitioning, have been suggested as possible alternatives. Another technique that is gaining increasing importance is membrane-based separation. Adsorptive membrane chromatography was introduced as a purification method in the mid 1980s. Microporous membranes have been successfully coupled with biological or biomimetic ligands, yielding affinity membrane chromatography supports. Several of them, with for

example protein A and G, dye or metal chelate ligands, are commercially available. Affinity membrane chromatography is in fact a hybrid technique combining affinity gel chromatography and membrane filtration, with the advantages of the two technologies.

The purpose of the present review is to discuss relevant aspects and developments that are important for the design of an affinity membrane chromatography process, including the choice of the membrane material, coupling chemistry, affinity ligands, membrane configurations, operation modes and scale-up. In a wider sense, membrane-based affinity fractionation also comprises affinity filtration methods where the target molecule binds to an affinity ligand coupled to nanoparticles, which can then be separated by filtration through a membrane. However, this application will not be discussed here in detail.

General Characteristics of Membrane Chromatography

In contrast to chromatographic supports based on beaded resins with dead end pores, membrane chromatographic supports have through-pores and lack interstitial space. Mass transfer is mainly governed by forced convection and pore diffusion is negligible. The observed back-pressures are normally quite low, and high flow rates and thus high throughputs and fast separations become possible without the need for high pressure pumps or equipment. As the association time for an antibody-antigen complex is typically about 1 s or less, but the diffusion of a protein molecule to the centre of a 50 μm porous bead takes tens of seconds, in a membrane support, the low diffusional limitation leads to faster adsorption kinetics and higher throughput efficiency. Little deterioration of the separation efficiency occurs even at elevated flow rates. On the other hand, with affinity membranes the formation of the affinity complex can become the rate-limiting process at high flow rates.

A problem often encountered in membrane chromatography is extra-cartridge back-mixing, which can severely degrade membrane performance. This phenomenon is due to dead volumes outside the membrane, in tubing, fittings and valves, and leads to peak broadening and dilution. It is more pronounced

in membrane chromatography systems compared to conventional columns packed with beaded supports, owing to the larger throughput/bed volume ratio.

Although the specific surface area of membranes is typically only 1% of that of conventional chromatographic resins, microporous membrane systems have high internal surface areas and reasonably high capacities. The open-pore structure of membranes increases the accessibility of affinity ligands and reduces steric hindrance compared to small-pore adsorbents.

Membrane Geometry

Just like filtration membranes in general, affinity membranes can be produced in different configurations, and membrane modules of various geometries are commercially available or have been manufactured in research laboratories (Figure 1).

Flat sheet or disc membranes can be mounted as individual membranes in specially designed cartridges or in commercial ultrafiltration units for use in dead-end filtration mode. This allows for the production of inexpensive single- or multiple-use devices for the rapid adsorption of a target molecule from dilute samples in batch or continuous recycling mode. Car-

tridges are also available that allow for operation in cross-flow filtration mode.

Stacks of flat membrane discs have been employed for affinity membrane chromatography in column-like devices, the main purpose being to increase the adsorption capacity. Another configuration is continuous rod-type membranes which can be directly cast in a chromatographic column. Both types of membrane columns are compatible with conventional high performance liquid chromatography or fast protein liquid chromatography systems and have advantages over columns packed with beaded resins, as described above. Being highly porous with a mean pore diameter of 0.1–10 μm , they allow for efficient separations even at high flow rates.

If the target molecule is to be recovered from complex feed solutions such as cell homogenates or blood plasma, or from solutions containing high molecular mass additives such as antifoam agents or even particulate material, the use of membranes in dead-end filtration mode is often impossible due to membrane fouling. A remedy to this problem is the operation in cross-flow filtration mode where the build-up of a polarization layer at the membrane surface is avoided or diminished. Hollow-fibre membranes are well adapted for such applications. They are usually

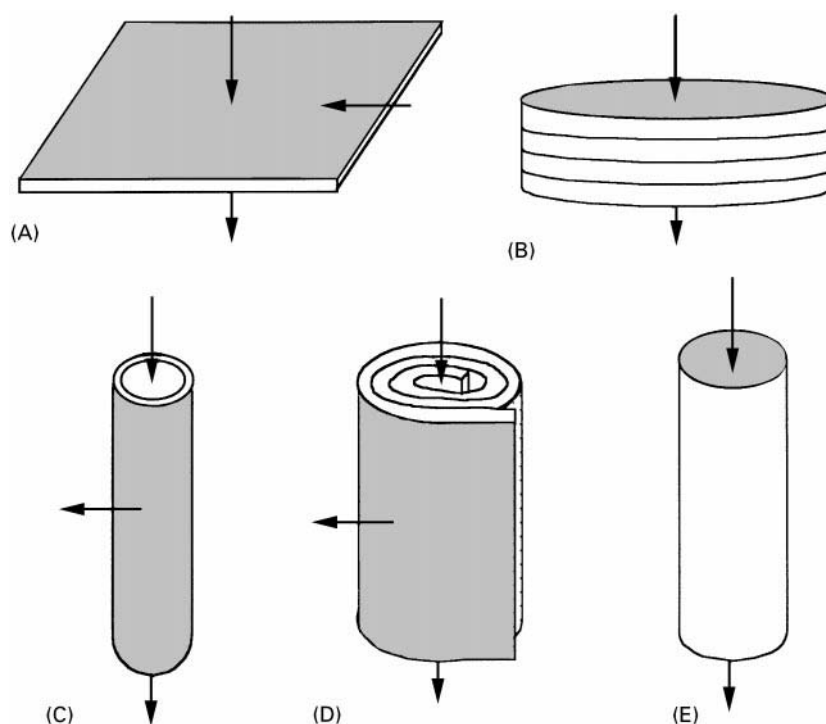


Figure 1 Different geometries of affinity membranes. (A) Flat sheet; (B) stack of flat discs; (C) hollow fibre; (D) spiral-wound flat sheet; (E) continuous rod. The arrows indicate flow directions. (Adapted from *Journal of Chromatography* 702, Roper DK and Lightfoot EN, Separation of biomolecules using adsorptive membranes, pp. 3–26, Copyright 1995, with permission from Elsevier Science.)

mounted as bundles in tubular cartridges. Another configuration are flat-sheet membranes that are spiral-wound around a cylindrical core. Both systems have the advantage of high surface area/cartridge volume ratios and high operational capacities.

Membrane Material, Activation and Ligand Coupling

Membrane Material

Due to the specific properties of biomolecules, the membrane materials to be used for their separation should ideally possess the following characteristics:

- **Macroporosity:** This will allow biomolecules to cross the membrane and to access the affinity sites.
- **Hydrophilicity:** Using hydrophilic supports, non-specific adsorption by hydrophobic interactions and denaturation of biomolecules can be avoided.
- **Presence of functional groups:** These are required for the coupling of an affinity ligand.
- **Chemical and physical stability:** The material has to withstand the sometimes harsh conditions during derivatization, operation and regeneration.
- **Biocompatibility:** This is particularly important if the membranes are used in extracorporeal devices, for example for blood treatment.
- **Large surface area relative to membrane volume:** This will allow for the construction of small, integrated devices with high operational capacities.

Cellulose and cellulose acetate were among the first materials that have been used for affinity membrane preparation. They are hydrophilic and biocompatible, and due to the presence of hydroxyl groups, ligand coupling can be easily achieved using for example CNBr or carbonyldiimidazole activation. In order to improve the mechanical and chemical stability of cellulose membranes, chemical cross-linking with epichlorohydrin is sometimes carried out. Cellulose membranes normally have a rather small pore size, resulting in a high pressure drop. Attempts to produce membranes with larger pores using coarse cellulose fibres have resulted in a less uniform membrane structure.

Polysulfone is another suitable membrane material which has good film-forming properties. It is of sufficient physical, chemical and biological stability, and ligands can be coupled after chloromethylation-amination or acrylation-amination.

Microporous polyamide (nylon) membranes have also been used for the preparation of affinity

membranes. This material is mechanically stable and has a rather narrow pore size distribution. It contains only a small number of terminal amino groups for ligand coupling, which can, however, be increased by partial hydrolysis of the amide functions.

A suitable membrane material is polyvinyl alcohol, in particular because of its hydrophilicity and biocompatibility. Poly(ethylene-co-vinyl alcohol), which has a somewhat higher chemical stability, has also been used. Both materials contain hydroxyl groups and can be activated by the CNBr method, allowing immobilization of affinity ligands having an amino function. Ligands can also be coupled using epichlorohydrine or butanediol diglycidyl ether-activation.

Other materials that have been used for affinity membranes are poly(methyl methacrylate), poly(hydroxyethyl dimethacrylate), polycaprolactam, poly(vinylidene difluoride), poly(ether-urethane-urea) and silica glass. Table 1 shows a list of membrane materials and the appropriate ligand-coupling chemistries.

Composite Membranes

The main difficulty when choosing a membrane for affinity separation of biomolecules is sometimes to find a material that fulfils several or all of the above-mentioned requirements. For example, a chemically stable material might be too hydrophobic and lead to nonspecific and irreversible adsorption of the protein to be separated, whereas a hydrophilic material that is compatible with the fragile protein molecules might not withstand the conditions required for ligand coupling and for regeneration and sterilization of the membrane. Therefore, the choice of a membrane material will sometimes be a compromise. The use of a composite membrane consisting of two or more different materials may often be the only solution to a particular separation problem. This approach consists of the grafting of hydrophilic polymers on to a chemically and mechanically stable microporous membrane. The result is an increased biocompatibility as well as the introduction of suitable functional groups for ligand coupling. One example is the radiation-induced graft polymerization of 2-hydroxyethyl methacrylate or glycidyl methacrylate on to a polyethylene hollow fibre membrane. This increases the hydrophilicity of the material and introduces active hydroxyl groups or reactive epoxy groups.

Activation and Ligand Coupling

From a practical point of view, apart from the chemical compatibility of the membrane material with the activation and coupling solutions, an important

Table 1 Membrane materials and possible chemistries for ligand coupling

<i>Membrane material</i>	<i>Coupling chemistries</i>	<i>Ligand functional group</i>
Cellulose, cellulose diacetate	Epichlorohydrin, butanediol diglycidyl ether	Amino, (hydroxyl)
	Carbonyldiimidazole	Amino, hydroxyl
	CNBr	Amino
	Anhydride	Amino
	Hydrazide	Amino
Polysulfone	Acrylation-amination, chloromethylation-amination	Cl ⁻ (aromatic)
Polyamide	Ethylene glycol diglycidyl ether	Amino, (hydroxyl)
	Glutaraldehyde (Schiff base)	Amino, amido
	Divinyl sulfone	Hydroxyl
	2-Fluoro-1-methylpyridinium toluene-4-sulfonate	Primary amino
	Butanediol diglycidyl ether	Amino, (hydroxyl)
Poly(vinyl alcohol), poly(ethylene vinyl alcohol) Electrostatically spun poly(ether-urethane-urea)	Formaldehyde	Hydroxyl
	Epichlorohydrin, butanediol diglycidyl ether	Amino, (hydroxyl)
	Carbonyldiimidazole	Amino, hydroxyl
	CNBr	Amino
	Carbonyldiimidazole	Amino, hydroxyl
Glass	Glycidyloxypropyl trimethoxysilane	Amino, (hydroxyl)
	Aminopropyltrimethoxysilane	Carboxyl

aspect is that these solutions need to access the pores of the membrane. In many cases it will therefore be necessary to do the activation in dynamic mode, that is, by forced convection. This is especially important if the membrane material is hydrophilic and the activation and coupling solutions are based on nonpolar solvents, since in that case the wettability of the membrane by the solutions will be low.

Spacer Arms

Occasionally, affinity membranes may show poor performance if the ligand, and in particular a small ligand, is coupled directly to the membrane. This is often due to a low steric availability of the ligand, a problem that can be overcome by the use of a suitable spacer arm. In that way, the ligand accessibility for the molecule to be separated is improved, resulting in an increase in membrane-binding capacity. For example, 1,6-diminohehexane or 6-aminohehexanoic acid are often used as spacers. In other cases, the coupling method itself provides a spacer, as is the case with butanediol diglycidyl ether. If composite membranes with crafted flexible copolymer chains are used, spacer arms are not normally required.

Affinity Ligands

Biological Ligands

Just like other affinity separation techniques, affinity membrane technology uses biomolecules as the affinity ligands, thus taking advantage of the specificity of biological recognition. One of the most

common applications is the use of immobilized monoclonal antibodies against natural or recombinant proteins as the ligand for immunoaffinity separation. Another important example are membranes with covalently coupled protein A or protein G for immunoglobulin purification from plasma, serum or cell culture supernatants. Immobilized lectines have been used for the purification of glycoproteins. The use of inhibitors or coenzymes for the purification of enzymes is also possible. Although biomolecules are widely used as ligands for their selectivity, they do have drawbacks. Their poor stability and sometimes high price can make them problematic for use in large scale affinity separation. Drastic conditions are often necessary for elution of the ligate, for example with high affinity antibody-antigen interactions. This can lead to partial inactivation of the molecule to be purified. Ligand denaturation and inactivation, in particular with protein ligands, can occur during regeneration and sterilization of the membrane. Another important issue is the possible leaching of the affinity ligand, leading to a contamination of the final product, which is particularly problematic if the product is to be used in medical applications.

Pseudobiospecific Ligands

An alternative approach involves the use of biomimetic or pseudobiospecific affinity ligands. These are usually smaller and simpler molecules with higher chemical and physical stability than biomolecules. The working principle of pseudobiospecific ligands relies on the complementarity of

structural features of ligand and ligate rather than on a biological function, whereas biomimetic ligands have a certain structural resemblance with a biological ligand. For example, textile dyes can be used for the separation of proteins, and in particular Cibacron Blue F3GA has been employed as ligand in affinity membranes for the purification of dehydrogenases, since it often binds specifically to the nucleotide-binding site. Other dyes may adsorb proteins less specifically, but by selection of the right dye (a large number of different dyes is currently available) and the appropriate adsorption and elution conditions, highly efficient separations can be obtained.

Proteins carrying accessible histidine residues on their surface have been shown to have affinity for transition metal-chelate ligands. Typical examples are the iminodiacetate-copper(II) complex (IDA-Cu(II)) and the nitrilotriacetate-nickel (NTA-Ni(II)) ligand widely used for purification of recombinant proteins with genetically attached poly-His tails.

A third group are amino acids such as phenylalanine, tryptophane and histidine. Being the least selective, they have nevertheless been successfully employed for protein purification. However, fine-tuned adsorption and elution conditions are necessary to achieve efficient separation. Mention should also be made of the thiophilic affinity system that has been used with affinity membranes. It is based on the salt-promoted adsorption of proteins via thiophilic regions (containing aromatic amino acids) on to sulfone or thioether-containing heteroaliphatic or aromatic ligands.

Molecularly Imprinted Membranes

A completely different approach for the preparation of affinity membranes is the use of molecularly imprinted polymeric materials. These are produced by polymerization of functional and cross-linking monomers in the presence of the target molecule (the molecule to be separated later), which acts as a molecular template. In this way, binding sites are introduced in the polymer that are complementary in shape and functionality to the target molecule, and that often have specificities comparable to those of antibodies. At the same time, the cross-linked polymeric material provides a porous, chemically and physically very stable support. Even though the technology is in principle applicable to larger biomolecules such as proteins, it has mainly been used for the separation of small molecules like amino acids and peptides. The molecular imprinting technique is reviewed in more detail elsewhere.

Scale-up

Process scale-up tends to be rather easy in adsorptive membrane chromatography, at least compared to the use of conventional beaded resins as the chromatographic support. It has been demonstrated that the diameter of a stack of disc membranes can be increased by up to one order of magnitude and more, with the dynamic capacity remaining constant. This allows for the processing of considerably larger sample volumes at higher flow rates. With radial flow membranes, when both the height and diameter of the cartridge were increased and the flow rate adjusted proportionally to the increased cartridge volume, the apparent specific capacity decreased only slightly.

Applications

Several different applications of affinity membranes have been described. Typical examples of their use for the separation and purification of biomolecules are shown in Table 2.

The most common application is the separation and purification of biomolecules and especially proteins for large scale production. A common example is the separation of immunoglobulins from blood serum or plasma or from cell culture supernatants. Hollow-fibre cartridges with immobilized protein A or pseudobiospecific ligands have been used for this purpose. Figure 2 shows a chromatogram from a case study of immunoglobulin G separation from human plasma using a small, developmental-scale (28 cm² surface area) poly(ethylene-co-vinyl alcohol) hollow-fibre membrane cartridge. The pseudobiospecific affinity ligand histidine was immobilized on to the membrane after activation with butanediol diglycidyl ether, thus introducing a spacer arm. Serum was injected 10-fold diluted in cross-flow filtration mode. Weakly retained and entrapped proteins were then removed by washing the lumen and the outer shell of the fibres, as well as the pores in back-flushing mode. Adsorbed immunoglobulins were subsequently eluted with a buffered solution of 0.4 mol L⁻¹ NaCl in back-flushing mode. The eluted fraction contained 93% immunoglobulins (82% IgG, 10.8% IgM). The dynamic binding capacity of the membrane for immunoglobulin G was determined to be 1.9 g m⁻². The process could then be scaled up by using a cartridge with 1 m² membrane surface area.

A related application is the final polishing of an already pure product. For example, the removal of bacterial endotoxins from contaminated solutions of monoclonal antibodies has been demonstrated using membrane-bound pseudobiospecific ligands.

Table 2 Examples for the use of affinity membranes for isolation and purification of biomolecules

<i>Isolated substance</i>	<i>Affinity ligand</i>	<i>Membrane material</i>	<i>Configuration</i>	<i>Application</i>
Human serum amyloid protein	Anti-hSAP Ab (polyclonal)	Cellulose	Flat sheets	Extracorporeal circuit, removal of amyloid from blood
Heparin	Poly-L-lysine	Cellulose diacetate poly(ethylene-co-vinyl alcohol), coated polyethylene	Hollow fibres	Extracorporeal circuit, removal of heparin from blood
Human IgG	Recombinant protein A	Poly(caprolactam) Modified poly(caprolactam) Polysulfone-coated hydroxyethyl cellulose	Hollow fibres Hollow fibres, flat sheet Hollow fibres	Purification
Recombinant protein G	Human IgG	Glycidyl methacrylate-co-ethylene dimethacrylate	Discs	Purification
Trypsin (porcine)	Soybean trypsin inhibitor	Modified cellulose	Spiral wound sheet (radial flow)	Purification
Glucose-6-phosphate dehydrogenase	Cibacron blue	Nylon	Stack of flat sheets	Purification from clarified yeast homogenate
Human IgG	Histidine	Poly(ethylene-co-vinyl alcohol)	Hollow fibres	Purification from blood plasma and serum
Autoantibodies				Removal from blood plasma in extracorporeal circuit
Lysozyme, cytochrome c, ribonuclease A	IDA-Cu ²⁺	Glass	Hollow fibres	Purification

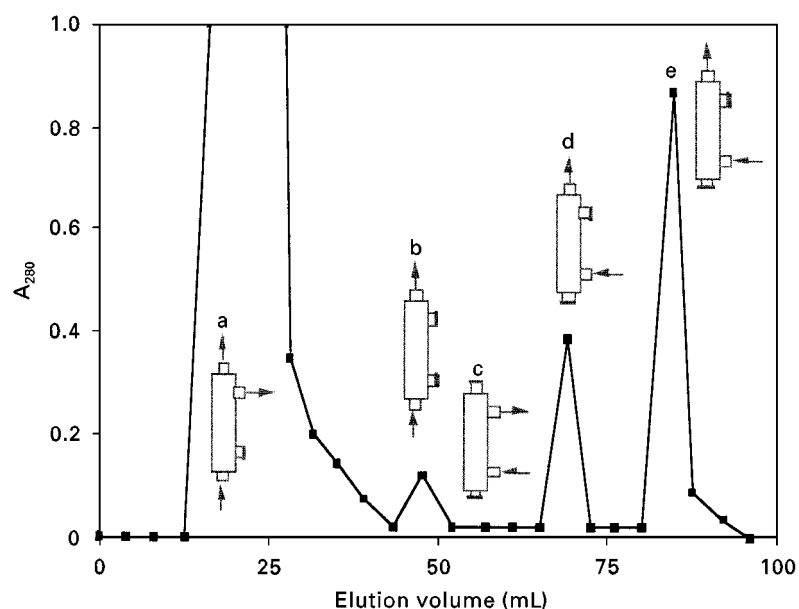


Figure 2 Separation of immunoglobulins from human serum using a poly(ethylene-co-vinyl alcohol) hollow-fibre cartridge with immobilized L-histidine. (a) Immunoglobulin adsorption in cross-flow filtration mode; (b) lumen wash; (c) shell wash; (d) back-flush wash; (e) back-flush elution. (Adapted from *Journal of Membrane Science* 117, Bueno SMA, Legallais C, Haupt K and Vijayalakshmi MA, Experimental kinetic aspects of hollow-fiber membrane-based pseudobioaffinity filtration: Process for IgG separation from human plasma, pp. 45–56, Copyright 1996, with permission from Elsevier Science.)

Affinity membranes have also been suggested for use in extracorporeal circuits, for the removal of toxic substances such as certain metabolites or antibodies from blood. For example, exogenous human serum amyloid P component, a substance associated with Alzheimer's disease, has been removed from whole rat blood in an extracorporeal circulation system. This model system used a polyclonal antibody coupled to cellulose flat-sheet membranes. The biocompatibility of the membrane was also demonstrated. A similar application is the removal of autoantibodies from human plasma, using membrane-bound affinity ligands in extracorporeal circuits.

Apart from preparative applications, small cartridges with membrane discs or continuous membrane rods should be useful for analytical-scale separations and affinity solid-phase extraction, for example for immunoextraction.

Conclusions

Affinity membrane separation techniques combine the specificity of affinity adsorption with the unique hydrodynamic characteristics of porous membranes. They provide low pressure separation systems which are easy to scale up and ideal for the processing of large volumes of potentially viscous feed solutions (e.g. microbial broth, bacterial cell extract, conditioned media) often involved in the production of recombinant proteins. The additional microfiltration effect of membranes allows for the processing even of unclarified, particle-containing feed solutions. The high performance of this separation technique is due to the presence of throughpores and the absence of diffusional limitations; mass transfer is mainly governed by forced convection. Affinity membranes are used in applications such as purification of biomolecules, final product polishing, removal of unwanted substances from patients' blood in extracorporeal circuits, but also

for smaller scale analytical separations. Biological affinity ligands and biomimetic or pseudobiospecific ligands are currently employed, as well as different membrane configurations such as flat sheets, hollow fibres or continuous rods. The technology is now in the process of being adapted more and more for large scale industrial separation and purification.

See also: I/Affinity Separation. Membrane Separations. II/Affinity Separation: Dye Ligands; Immunoaffinity Chromatography; Imprint Polymers; Rational Design, Synthesis and Evaluation: Affinity Ligands; Chromatography: Liquid: Large-Scale Liquid Chromatography. Membrane Separations: Filtration. III/Immunoaffinity Extraction. Appendix 1/Essential Guides for Isolation/Purification of Enzymes and Properties. Essential Guides for Isolation/Purification of Immunoglobulins. Appendix 2/Essential Guides to Method Development in Affinity Chromatography.

Further Reading

- Brandt S, Goffe RA, Kessler SB, O'Connor JL and Zale SE (1988) Membrane-based affinity technology for commercial scale purifications. *Bio/Technology* 6: 779.
- Charcosset C (1998) Purification of proteins by membrane chromatography. *Journal of Chemical Technology and Biotechnology* 71: 95.
- Klein E (ed.) (1991) *Affinity Membranes: Their Chemistry and Performance in Adsorptive Separation Processes*. New York: John Wiley.
- Roper DK and Lightfoot EN (1995) Separation of biomolecules using adsorptive membranes. *Journal of Chromatography* 702: 3.
- Suen S-J and Etzel MR (1992) A mathematical model of affinity membrane bioseparations. *Chemical Engineering Science* 47: 1355.
- Thömmes J and Kula MR (1995) Membrane chromatography – an integrative concept in the downstream processing of proteins. *Biotechnology Progress* 11: 357.

Affinity Partitioning in Aqueous Two-Phase Systems

G. Johansson, Center for Chemistry and Chemical Engineering, Lund University, Lund, Sweden

Copyright © 2000 Academic Press

Aqueous Two-phase Systems in General

The division of water into non-miscible liquid layers (phases) by addition of two polymers has led to the

remarkable possibility of being able to partition proteins and other cell components between phases of nearly the same hydrophilicity. Proteins can be separated by partitioning if they have unequal distribution between the phases, i.e. when their partition coefficients, K (the concentration in top phase divided by the concentration in bottom phase), differ. Usually the difference in the K value of many proteins is not very large and then repeated extractions have to be carried out to get a reasonable

purification. If, however, the protein of interest (the target protein) has a very high K value and is mainly in the upper phase and all the contaminating proteins have very low K values so that they are in the bottom phase, an effective and selective extraction can be obtained in a single or a few partitioning steps. This type of partitioning has been made possible by using affinity ligands restricted to the upper phase.

The composition of the phases when two polymers like dextran and polyethylene glycol (PEG) are dissolved together in water depends on the amount of the polymers and their molecular weights. The concentration of the polymers in two phases of a given system can be found in the phase diagram for the temperature being used. A typical phase diagram is shown in Figure 1.

The line that connects the points in the diagram representing the compositions of the top and bottom phases of a system is called the tie-line. Each system with a total composition (percentage of each polymer) belonging to the same tie-line will have the same phase compositions. The smaller the tie-line, the more similar are the two phases in their composition. The greatest difference in composition of the top and bottom phases is therefore obtained by using high polymer concentrations.

The partitioning of proteins and also of membranes and particles depends on the polymer concentration of the system. The K value of a protein will be the same for all systems belonging to the same tie-line.

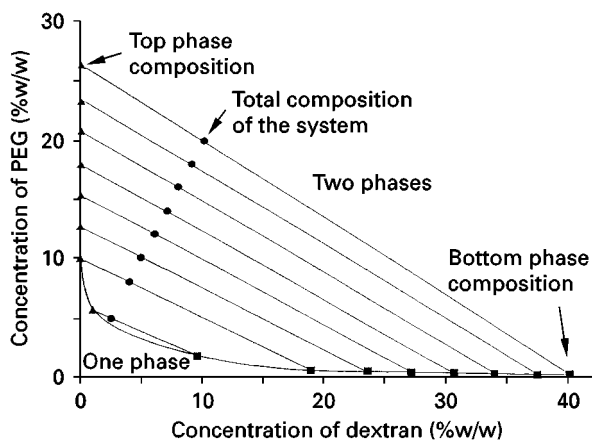
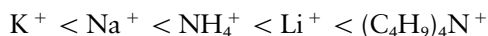
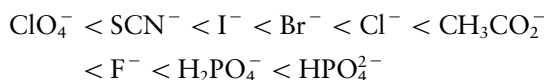


Figure 1 Phase diagram for the system dextran 500 (500 000 Da), PEG 8000 (8000 Da), and water at 23°C. Polymer compositions above the curved line (bimodal curve) give two liquid phases. All two-phase systems with their total composition on the same straight line (tie-line) have the same composition of top phase (▲) and bottom phase (■). The systems differ in phase volume ratio depending on their position on the tie-line. The indicated total compositions (●) give systems with more top phase (three to five times) than bottom phase.

The partition coefficient will, in most cases, decrease with the length of the tie-line, i.e. by using higher concentrations of the two polymers the material will accumulate more in the lower phase. Another way to affect the partitioning of proteins is by addition of salts to the system. Their effect depends on the type of cation and anion introduced with the salt. Negatively charged proteins show increasing K values when the cation is changed in the series:



For the anion the partition coefficient increases in the following order:



The highest K value of negatively charged proteins will then be obtained with the salt tetrabutylammonium hydrogenphosphate and the lowest K value with potassium perchlorate. Proteins with zero net charge (at their isoelectric points) are not affected by salts while positively charged proteins behave in an opposite manner to the negatively charged ones. For a number of proteins the log K values are nearly a linear function of their net charge (Figure 2).

Affinity Partitioning

The principle of affinity partitioning is to localize an affinity ligand in one phase to make it attract ligand-binding proteins. Since the phase-forming polymers are in each phase, either one can be used as ligand carrier. The standard system for affinity partitioning has been the one composed of dextran, PEG and water. Dextran is then used for localizing the ligand in the bottom phase while PEG can be used to concentrate the ligand to the top phase. PEG has often been chosen as ligand carrier because bulk proteins can be effectively partitioned into the dextran-rich lower phase by using high concentrations of polymers and a suitable salt. Thus, the target protein is extracted towards the upper phase leaving contaminating proteins in the bottom phase. PEG has two reactive groups (the terminal hydroxyl groups) which can be used as points of ligand attachment. In many cases only one ligand molecule is attached per PEG molecule. If the ligand is a large molecule (e.g. an antibody protein) several PEG chains may be attached to the one ligand molecule. Normally, only a fraction (1–10%) of the PEG in the two-phase system has to carry the ligand to reach maximal extraction efficiency. The more extreme the partitioning of a ligand-polymer is toward a phase the more effective it will be in extracting a ligand-binding protein into this phase. The partitioning of

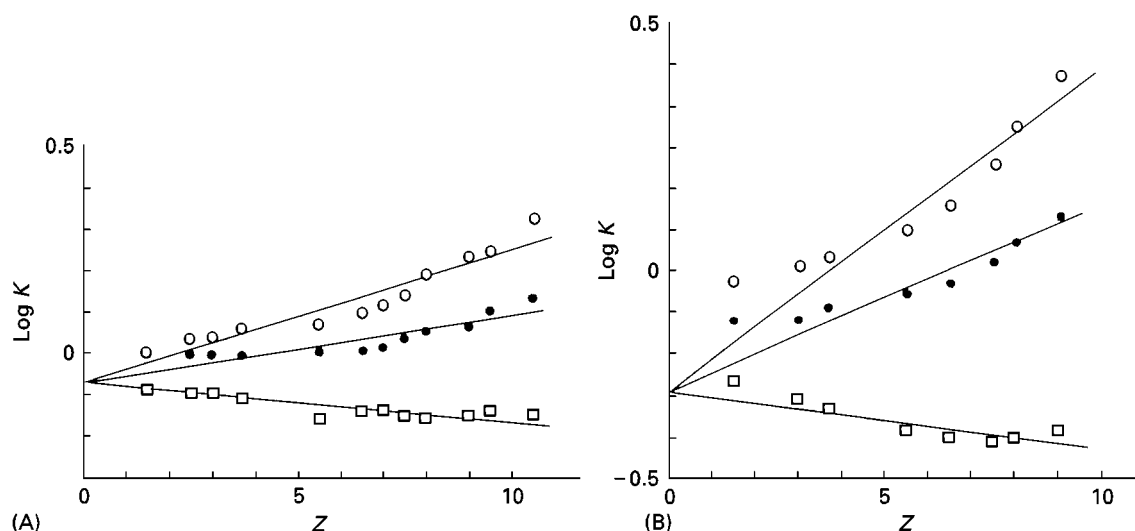


Figure 2 Log K of the protein ribonuclease-A as function of its net charge, Z , in a two-phase systems containing KSCN (\circ , 100 mM), KCl (\bullet , 100 mM), or K_2SO_4 (\square , 50 mM). System compositions: (A) 6.2%w/w dextran 500 and 4.4%w/w PEG 8000; (B) 9.8%w/w dextran 500 and 7.0%w/w PEG 8000. Protein concentration, 2 g L^{-1} . Temperature, 20°C . (Reprinted from Johansson G (1984) *Molecular Cell Biochemistry* 4: 169–180, with permission from Elsevier Science.)

the ligand–polymer should be in the same range as the non-derivatized polymer but it may, in some cases, be more extreme. The higher the polymer concentrations are in the system, i.e. the longer the tie-line of the system, the more extreme is the partitioning of PEG to the top phase and dextran to the bottom phase. This can be expressed by the partition coefficients of the two polymers:

$$K_{\text{PEG}} = \frac{c_{\text{PEG,top}}}{c_{\text{PEG,bottom}}} \quad \text{and} \quad K_{\text{dextran}} = \frac{c_{\text{dextran,top}}}{c_{\text{dextran,bottom}}}$$

where c is the respective polymer concentration in top or bottom phase. Table 1 shows the K_{PEG} and K_{dextran} values for systems containing PEG 8000 and dextran 500. Dextran has a more extreme value of K than PEG, i.e. $K_{\text{PEG}} < 1/K_{\text{dextran}}$. Dextran should therefore, in principle, be a better ligand carrier than PEG. The concentration ratio for dextran is roughly the square of the ratio for PEG in the same system.

A Simple Theory for Affinity Partitioning

A basic theory for affinity partitioning was elaborated by Flanagan and Barondes in 1975. They analysed the combined binding and partition equilibria taking place in and between the two phases, respectively (Figure 3).

In this scheme the ligand–PEG(L), the free protein (P) and the two complexes (PL and PL_2) have each their own partition coefficient (K_L , K_P , K_{PL} and K_{PL_2}). Furthermore, in both phases association between protein and ligand–PEG takes place which can be described by the association constants:

$$K_1 = [PL]/([P][L]) \quad \text{and} \quad K_2 = [PL_2]/([PL][L])$$

one set for each phase.

A total association constant for the equilibrium:



can also be used: $K_{\text{tot}} = K_1 K_2$.

Table 1 Partition coefficients of PEG (K_{PEG}) and dextran (K_{dextran}) and their logarithmic values (log) at various tie-line lengths of the system in Figure 1

Tie-line length (polymer concentration scale)	K_{PEG}	K_{dextran}	$\log K_{\text{PEG}}$	$\log K_{\text{dextran}}$
8.0	1.9	0.25	0.28	− 0.60
14.2	6.7	0.023	0.83	− 1.64
17.4	12	0.0088	1.08	− 2.06
25.6	35	0.0022	1.54	− 2.66
31	46	0.0004	1.66	− 3.4
35	61	0.0001	1.79	− 4.0

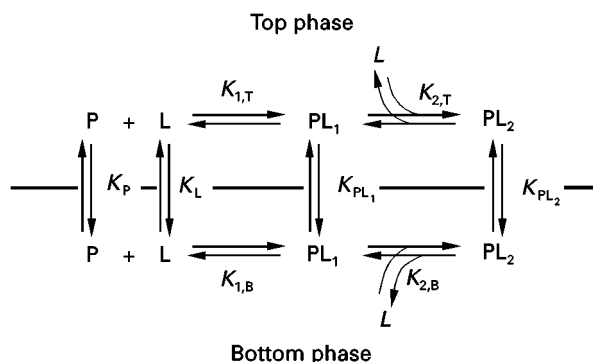


Figure 3 Scheme for affinity partitioning of a protein (P) with two binding sites for a ligand attached to PEG (L). The complexes between protein and ligand-PEG are PL and PL₂, respectively.

The association constants, K_{tot} , K_1 and K_2 may differ between the two phases. According to Flanagan and Barondes, the measured $\log K$ value of a protein, $\log K_{\text{protein}}$, will, theoretically, give rise to a saturation curve when plotted versus the concentration of polymer-bound ligand in the system (compare Figure 4).

The $\log K_{\text{protein}}$ value reaches a plateau when the concentration of L-PEG is so high that practically all the protein is present as the fully saturated complex PL₂. The protein molecule is then surrounded by two PEG chains and outwardly shows a PEG atmosphere.

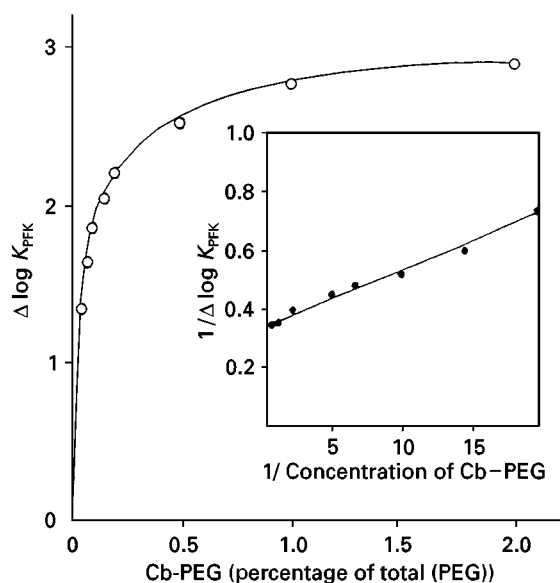


Figure 4 Increase in the logarithmic partition coefficient of phosphofructokinase (PFK) from bakers' yeast as function of the concentration of Cibacron blue F3G-A PEG (Cb-PEG). System composition: 7%w/w dextran 500, 5%w/w PEG 8000 including Cb-PEG, 50 mM sodium phosphate buffer pH 7.0, 0.5 mM EDTA, 5 mM 2-mercaptoethanol and 4 nkat g⁻¹ enzyme. Temperature, 0°C. The inverse plot inserted is used to determine the $\Delta \log K_{\text{max}}$.

The maximum partition coefficient of protein, $\hat{K}_{\text{protein}} (= K_{\text{PL}_2})$, is related to K_p , K_L and the K values via the following equations:

$$\hat{K}_{\text{protein}} = K_p K_L^2 \frac{K_{1,T} K_{2,T}}{K_{1,B} K_{2,B}}$$

or:

$$\hat{K}_{\text{protein}} = K_p K_L^2 \frac{K_{\text{tot},T}}{K_{\text{tot},B}}$$

The maximum increase in the logarithmic partition coefficient, $\Delta \log K_{\text{max}}$, is consequently given by:

$$\begin{aligned} \Delta \log K_{\text{max}} &= \log \frac{\hat{K}_{\text{protein}}}{K_p} \\ &= 2 \log K_L + \log K_{\text{tot},T} - \log K_{\text{tot},B} \end{aligned}$$

If $K_{\text{tot},T} = K_{\text{tot},B}$ then $\Delta \log K_{\text{max}} = 2 \log K_L$.

From the values in Table 1 it may therefore be assumed that for proteins with two binding sites $\Delta \log K_{\text{max}}$ can be as high as 3.57 (an increase of 3700 times in K) when PEG is used as ligand carrier with $K_L = 61$. If dextran is used as carrier, in the same system, the $\Delta \log K_{\text{max}}$ should theoretically be around -8 corresponding to a one hundred million times increase in the affinity of the protein for the lower phase if K_L is 0.0001. A higher number of binding sites (n) should then give strongly increasing $\Delta \log K_{\text{max}}$ values with $\Delta \log K_{\text{max}} = n \log K_L$. However, the affinity extraction effect may be reduced by a reduction of individual binding strengths.

Experimental Results

The extraction curves of a protein, here exemplified with phosphofructokinase (PFK) from baker's yeast, using Cibacron Blue F3G-A PEG, closely follows the predicted behaviour (Figure 4). The inverse plot makes it possible to estimate the value of $\Delta \log K_{\text{max}}$.

The dependence of $\Delta \log K_{\text{max}}$ of PFK on the polymer concentration is shown in Figure 5. Increasing concentration of polymers corresponds to longer tie-line length (and greater K_L value) and this makes the affinity partitioning, measured as $\Delta \log K_{\text{max}}$, more efficient.

In addition to the concentration of polymers and ligand-PEG the actual K_{protein} obtained also depends on pH value, the salt added to the system and the temperature. Two salts which have little or no effect on the affinity partitioning are phosphates and acetates in concentrations up to 50 mM. In the case of PEG the $\Delta \log K_{\text{max}}$ is reduced with increasing temperature.

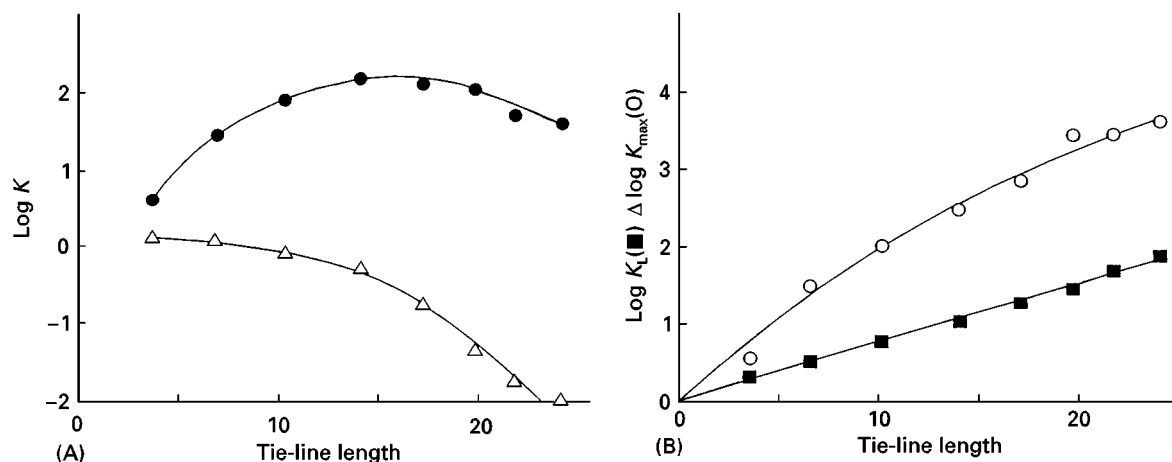


Figure 5 (A) $\log K$ of phosphofructokinase from bakers' yeast as function of the tie-line length, expressed in the polymer concentration scale, in systems with an excess of Cibacron blue F3G-A PEG (Cb-PEG) (●), 3% of total PEG; or without Cb-PEG (Δ). (B) $\Delta \log K_{\max}$ (○) and $\log K_L$ (■) as function of the tie-line length. System composition: dextran 500 and PEG 8000 (including Cb-PEG) in weight ratio 1.5:1, 50 mM sodium phosphate buffer pH 7.0, 0.5 mM EDTA, 5 mM 2-mercaptoethanol, and 4 nkat g^{-1} enzyme. Temperature, 0°C.

The detachment of ligand from the enzyme can be achieved either by using a high concentration of salt or by the addition of an excess of free ligand. For PFK the addition of adenosine triphosphate (ATP) to the

system containing ligand-PEG strongly reduces the partition coefficient of the enzyme (Figure 6).

Types of Affinity Ligands Used

A number of affinity ligands have been used and some are presented in Table 2. The attachment of ligand to polymers and the purification of the ligand-polymer differs from case to case. Some ligands such as reactive textile dyes can be bound directly to PEG and to dextran in water solution of high pH. Other ligands are introduced by reactions in organic solvent, such as the attachment of acyl groups to PEG by reaction with acyl chloride in toluene. PEG may also be transformed into a more reactive form such as bromo-PEG, tosyl-PEG or tresyl-PEG. Some reaction pathways are shown in Figure 7. A number

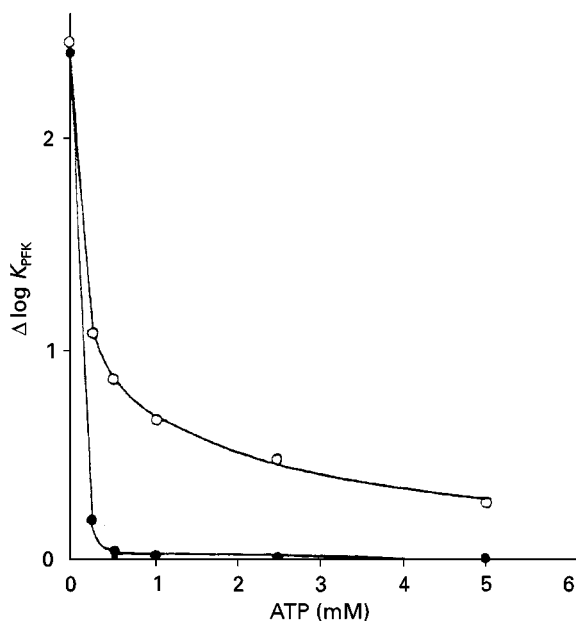


Figure 6 The effect of adenosine triphosphate (ATP) and of ATP + Mg^{2+} on the partitioning of phosphofructokinase from bakers' yeast in a system containing Cibacron blue F3G-A PEG (Cb-PEG). $\Delta \log K$ of enzyme as function of concentration of ATP. Without addition of Mg^{2+} (○); and with 10 mM MgCl_2 (●). System composition: 7% w/w dextran 500 and 5% w/w PEG 8000 including 0.5% Cb-PEG (of total PEG). 50 mM sodium phosphate buffer pH 7.0, 0.5 mM EDTA, 5 mM 2-mercaptoethanol, and 4 nkat g^{-1} enzyme. Temperature, 0°C.

Table 2 Examples of affinity partitioning

Partitioned substance	Ligand
Colipase	Lecithin
Dehydrogenases and kinase	Textile dyes
α -Fetoprotein	Remazol yellow
Haemoglobin and phosphovitin	Cu(II)-chelate
Liver plasma membranes	Lectin
Myeloma protein	Dinitrophenol
Nucleic acids	Dyes
Oxosteroid isomerase	Oestradiol
Red blood cells	Antibodies
Serum albumins, histones and lactalbumin	Fatty acids
Synaptic membranes	Opiates and antagonists
Trypsin	<i>p</i> -Aminobenzamidine

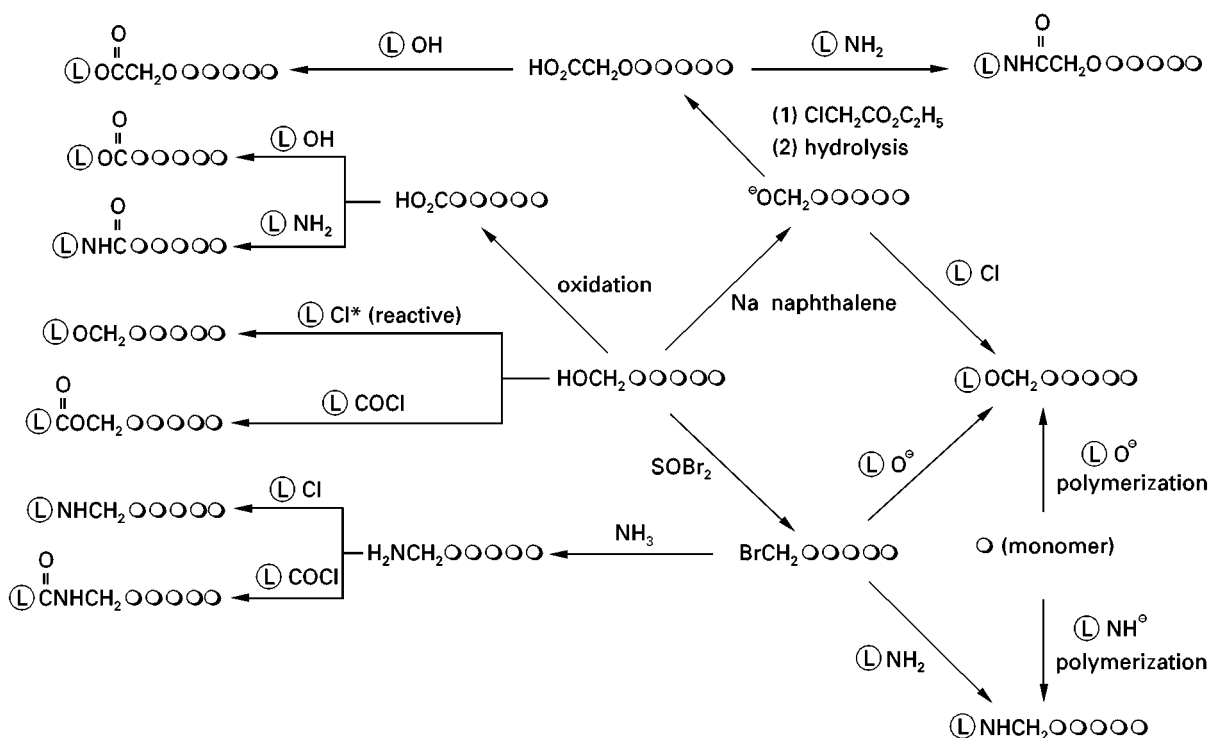


Figure 7 Some reactions used for the covalent linkage of ligands to polymers, preferentially to PEG. The encircled 'L' represents the ligand and the open circles the polymer chain.

of methods to synthesize polymer derivatives have been published by Harris.

Preparative Extractions

The following steps may be useful for a high degree of purification by affinity partitioning.

1. Pre-extraction in a system without ligand-PEG to remove proteins with relatively high partition coefficients. The target protein stays in the bottom phase by adjusting the choice of polymer concentration, salt and pH.
2. Affinity partitioning is carried out by changing the top phase for one containing ligand-PEG. The target protein will now be in the top phase.
3. Washing the top phase with bottom phase to remove co-extracted proteins.
4. 'Stripping' of protein from the affinity ligand by addition of highly concentrated phosphate solution (50%w/w) to the separated upper phase. This generates a PEG-salt two-phase system with PEG and ligand-PEG in the top phase and target protein in the salt-rich bottom phase. An alternative stripping procedure can be carried out by adding a new pure dextran phase to the recovered top phase and supplying the system with free

ligand. In this case the target protein will be collected in the lower phase.

For each step the number of extractions and the most suitable volume ratios for yield and purity can be optimized. The procedure is summarized in **Figure 8**.

The yield in the top phase, Y_T , can be calculated from the K value of target protein and the volumes of top and bottom phase, V_T and V_B , respectively, using the following equation:

$$Y_T (\%) = \frac{100}{1 + V_B/(V_T K)}$$

and the yield in the bottom phase, Y_B

$$Y_B (\%) = \frac{100}{1 + V_T K/V_B}$$

A considerable concentration of the target protein, in addition to purification, can be achieved by choosing an extreme volume ratio with a small collecting phase.

An example of preparative extraction of an enzyme by applying the method given in **Figure 8** is the purification of lactate dehydrogenase (LDH) using a PEG-bound textile dye. Crude extract of pig muscle,

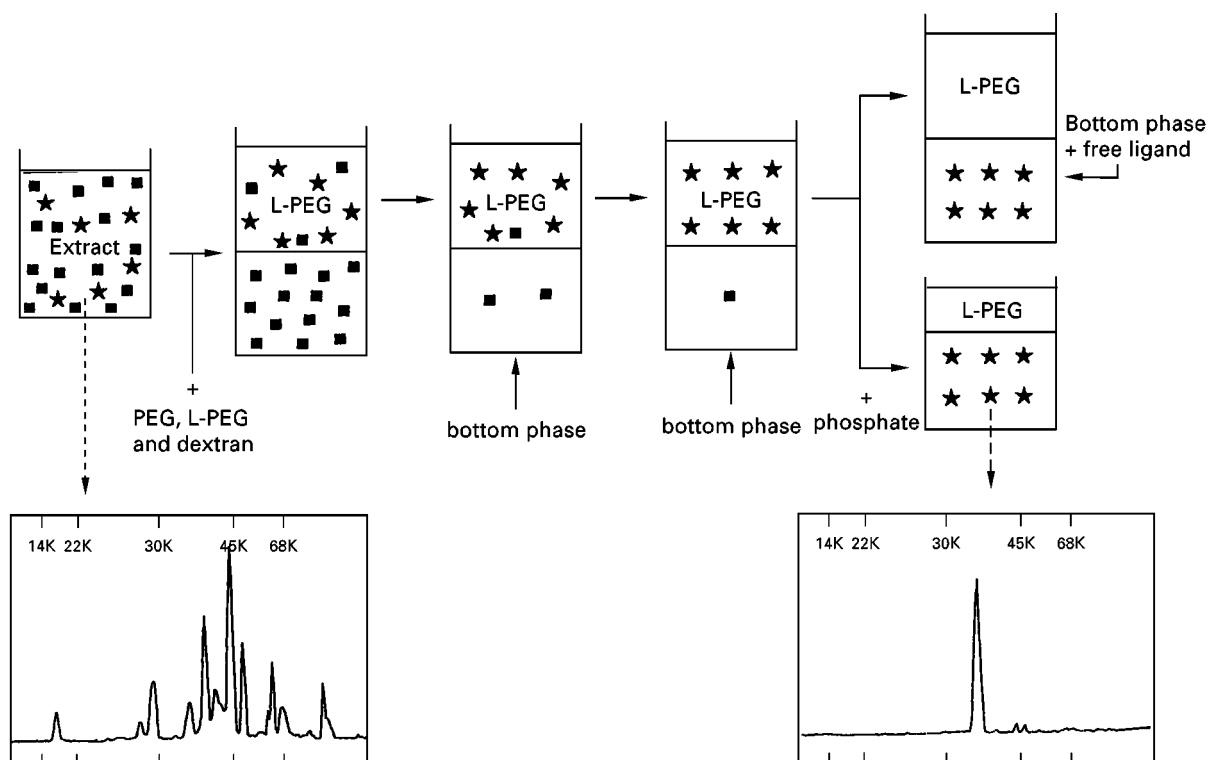


Figure 8 Scheme for the purification of an enzyme (★) from contaminating proteins (■) by using four partitioning steps and PEG-dextran two-phase systems with PEG-bound ligand. This approach has been used for the purification of lactate dehydrogenase (LDH) from meat juice by affinity partitioning with Procion yellow HE-3G PEG. The inserted SDS-PAGE patterns of the original meat extract and the final product (obtained in the phosphate-rich phase) show the removal of contaminating proteins. Recovery of enzyme = 79%. System composition: 10% w/w dextran 500 and 7.1% w/w PEG 8000 including 1% Procion yellow HE-3G PEG (of total PEG), 50 mM sodium phosphate buffer pH 7.9, and 25% w/w muscle extract. Temperature, 0°C. (Reprinted from Johansson G and Joelsson M (1986) *Applied Biochemistry Biotechnology* 13: 15–27, with permission from Elsevier Science.)

cleared by centrifugation, is mixed with PEG, dextran and Procion yellow HE-3G PEG. After the first partitioning the top phase is washed twice with pure lower phases and then it is mixed with a 50% w/w salt solution (25% NaH_2PO_4 + 25% $\text{Na}_2\text{HPO}_4 \cdot \text{H}_2\text{O}$). The protein content of the final product in the salt-rich phase compared with that of the initial extract is demonstrated by the polypeptide pattern in sodium dodecyl sulfate-polyacryl amide gel electrophoresis (SDS-PAGE) shown in Figure 8. The

L-PEG (and PEG) recovered in the final top phase is $\geq 95\%$ of the initially introduced amount.

Purification of PFK in combination with a precipitation step with PEG before the affinity partitioning step greatly reduces the original volume of enzyme solution. The extraction included both pre-extraction and washing steps. The final polishing of the enzyme was made by ion exchanger and desalting with gel chromatography. The results can be seen in Table 3.

Table 3 Purification of phosphofructokinase from 1 kg (wet weight) bakers' yeast

Purification step	Volume (ml)	Total activity (U)	Total protein (mg)	Specific activity (U/mg)	Purification factor	Yield (%)	Proteolytic activity ^a (%)
Homogenate	1370	5400	13 170	0.41	1	100	100
Fractional precipitation with PEG	120	4810	1836	2.62	6.4	89	18
Affinity partitioning	120	3610	153	23.6	58	67	0.9
DEAE-cellulose treatment	40	2520	63	40	98	47	0.4
Gel filtration	4	1625	28	58	142	30	0.05

^aIn the presence of the protease inhibitor phenylmethylsulfonyl fluoride.

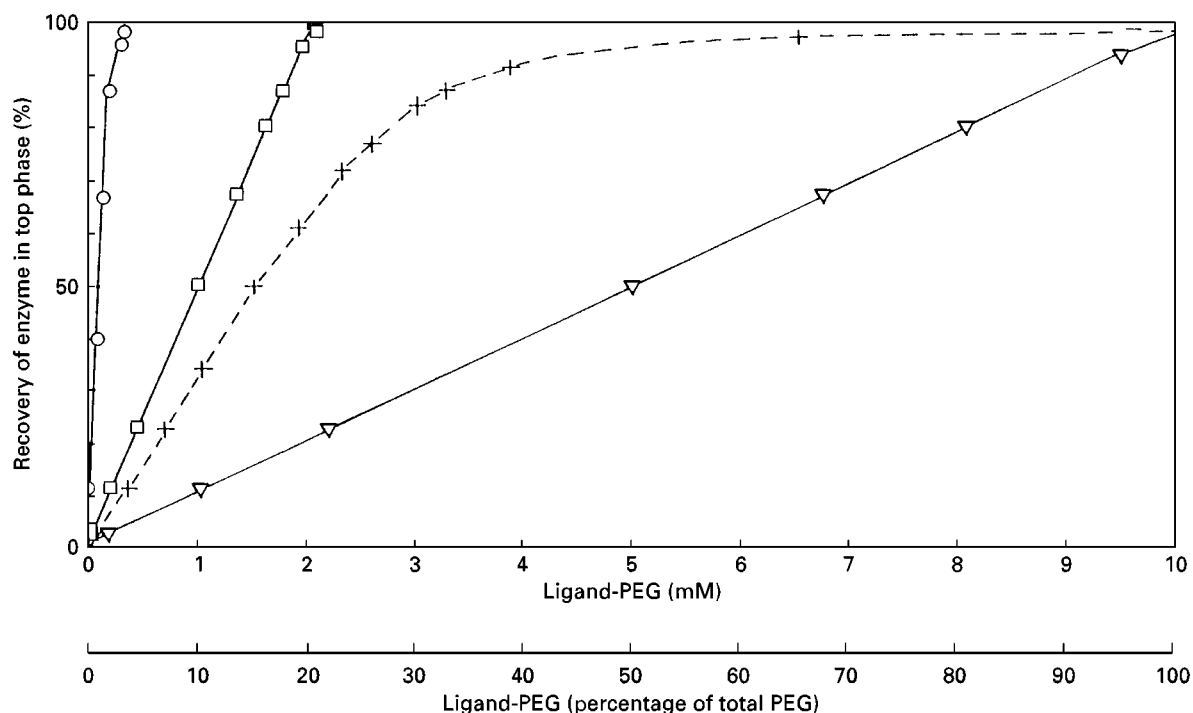


Figure 9 Affinity extraction into the top phase, by using increasing amount of PEG-bound ligand, calculated for an enzyme with the mole mass $100\,000\text{ g mol}^{-1}$, containing two binding sites for the ligand, and with $K_p = 0.01$. The value for the partition coefficient, K_L , of the ligand is 100. The association constant, K , for each site is 10^{-6} M^{-1} (○, □) or 10^{-4} M^{-1} (+). The concentration of enzyme: 10 (○), 100 (□, +) and 500 g L^{-1} (Δ).

The effectiveness of affinity partitioning depends on the binding strength between ligand and protein. Good extraction is obtained with association constants of 10^4 M^{-1} or more (Figure 9). The capacity, based on the amount of ligand in the system, is in the range of several hundred grams of protein per kilogram of system. Affinity extractions with 150 g of protein per kilogram of system have been carried out, and in these cases the two-phase systems strongly change the phase volume ratio while the bulk protein acts as a phase-forming component. In systems with high protein concentration the amount of dextran can be reduced or even excluded.

Countercurrent Distribution

A convenient way of multiextraction is countercurrent distribution (CCD). Here a number of top phases are sequentially moved over a set of bottom phases and equilibration takes place after each transfer. The process can be seen as a step-wise chromatography. The original two-phase system, number 0, contains the sample and after that a number (n) of transfers have been carried out $n + 1$ systems are obtained and the various proteins in the sample are distributed along the CCD train. The CCD process is visualized in Figure 10(A).

The distribution of a pure substance can be calculated from the K value of the substance and the volumes of the phases, V_T and V_B . Assuming that all of the top phase volume is mobile and all bottom phase stationary, the fractional amount, $T_{n,i}$, in tube number i (i goes from 0 to n) after n transfers will be given by:

$$T_{n,i} = \frac{n!}{i! (n-i)!} \frac{G^i}{(1+G)^n}$$

This makes it possible to calculate the theoretical curve for a substance and to make comparisons with the experimental distribution curve. Such an analysis may reveal the presence of several components even if they are not separated into discrete peaks. Figure 10(B) shows an example of a CCD of a yeast extract using PEG-bound affinity ligands. The distribution of a number of enzyme activities has been traced.

Use of Dextran as a Ligand Carrier

Dextrans of the molecular weights normally used (40 000 and 500 000 Da) contain many thousands of reactive hydroxyl groups per molecule. The affinity partitioning effect achieved by introducing

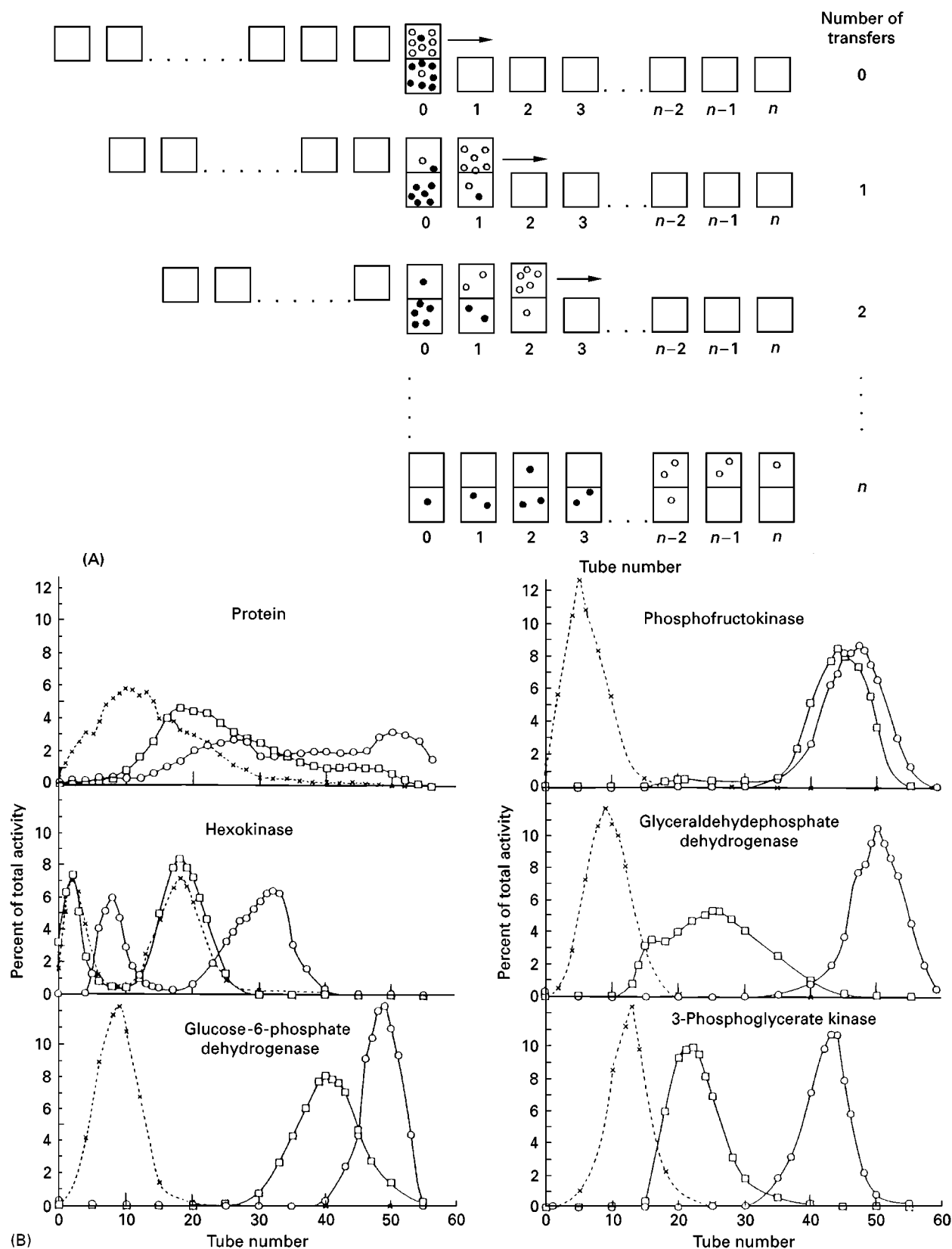


Figure 10 (A) Scheme of the countercurrent distribution (CCD) process. (Reprinted from Johansson G, Andersson M and Akevaland HE (1984) *Journal of Chromatography* 298: 485–495. With permission from Elsevier Science.) (B) Distribution of protein and some glycolytic enzymes after CCD of an extract of bakers' yeast using 55 transfers. Without ligand-PEG (\times); with Procion Olive MX-3G PEG, 1% of total PEG (\square); and with Procion yellow HE-3G PEG, 1% of total PEG (\circ). System composition: 7% w/w dextran 500 and 5% w/w PEG 8000 including ligand-PEG, 50 mM sodium phosphate buffer pH 7.0, 0.2 mM EDTA, and 5 mM 2-mercaptoethanol. Temperature, 3°C. Systems in chamber 0–2 were initially loaded with yeast extract.

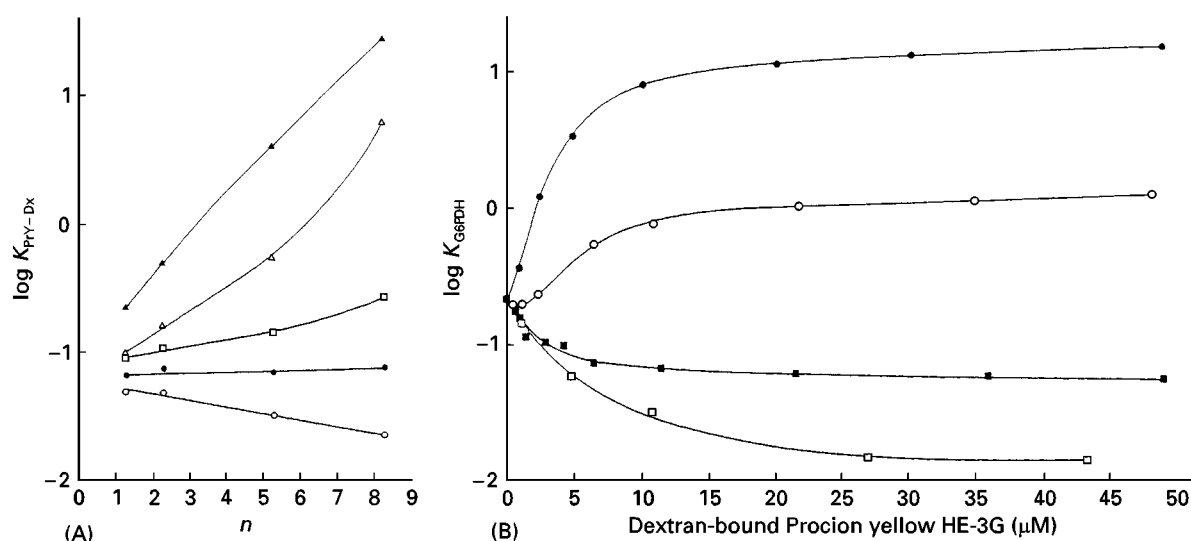


Figure 11 (A) Partitioning of Procion yellow HE-3G dextran 70 (PrY-Dx) depending on the degree of substitution, n (expressed in molecules of dye bound per molecule of dextran), in systems containing 50 mM sodium phosphate buffer (\blacktriangle); 10 mM sodium sulfate (\triangle); 100 mM sodium acetate (\square); 100 mM KCl and 5 mM sodium phosphate buffer (\bullet); or 100 mM $KClO_4$ (\circ), at pH 7.9. Arrow indicates K of unsubstituted dextran. System composition: 8% w/w dextran 70 and 4.5% w/w PEG 8000 including PrY-Dx (50 μM bound dye), and indicated salt. Temperature, 22°C and pH of system adjusted to 7.9. (Reprinted from Johansson G and Joelsson M (1987) *Journal of Chromatography* 411: 161–166. With permission from Elsevier Science.) (B) Effect of the concentration of PrY-Dx on the partitioning of the enzyme glucose-6-phosphate dehydrogenase (G6PDH) using PrY-Dx with n equal to 1.3, \square ; 2.3, \blacksquare ; 5.3, \bullet ; and 8.3, \circ . System as in (A) with 50 mM sodium phosphate buffer.

one or just a few dye ligands is shown in Figure 11. Since the dye ligands used here carries seven to ten charged groups per molecule they also add a considerable (negative) net charge to the ligand dextran. Its partitioning will then be sensitive to the presence of salt and the choice of salt. The ligand–dextran can be directed either to the bottom phase or the top phase. This steering is more effective the greater the number of ligands per dextran molecule.

The effect of ligand–dextran on the partitioning of an enzyme, glucose-6-phosphate dehydrogenase, is shown in Figure 11. There is also a tendency towards affinity precipitation when the concentration of ligand molecules is equal to the concentration of enzyme binding sites in the system. This is seen as a shallow dip in the extraction curve.

Use of a Third Polymer as Ligand Carrier

The ligand can be bound to a third polymer chosen in such a way that it will be mainly concentrated in one phase. Alternatively, if it is carrying enough charged groups, it may be steered to one phase by using salts. The efficiency, measured as $\Delta \log K / \log K_L$, equal to the apparent number of binding sites of the protein, has in several cases showed that the most effective polymer for carrying the ligand is neither of the two phase-forming polymers. The effect of a dye ligand, bound to various polymers, on the partitioning of lactate dehydrogenase in a dextran–PEG system is presented in Table 4.

Table 4 The effect of ligand carrier on its efficiency in producing affinity partitioning

Ligand carrying polymer	$\Delta \log K_{LDH}$	$\log K_{L-polymer}$	$n_{app} = \Delta \log K_{LDH} / \log K_{L-polymer}$
Ficoll	2.11	0.90	2.3
Hydroxypropylstarch	0.59	0.32	1.8
Poly(ethylene glycol)	2.23	1.50	1.5
Dextran (D.S. = 8.3)	2.31	1.60	1.4
Ethylhydroxyethyl cellulose	2.06	1.63	1.3

Lactate dehydrogenase (LDH) was partitioned in systems containing 7% (w/w) dextran 500, 5% w/w PEG 8000, 25 mM sodium phosphate buffer, pH 7.5, and Procion yellow HE-3G polymer of dye concentration of 42 μM . Temperature, 22°C. (Reprinted from Johansson and Joelsson M (1984) *Journal of Chromatography* 411: 161–166. With permission from Elsevier Science.)

Chiral Affinity Partitioning

For separation of low molecular weight substances into their enantiomeric forms a system may be used where one of the phases contains a high molecular weight substance which binds one of the enantiomers. Bovine serum albumin as well as cyclodextrin have been used for this purpose.

Analytical Uses

Besides the preparative use of aqueous two-phase systems, they have been applied to a number of analytical studies of the properties of biological macromolecules and particles. Some of these uses are binding studies, conformational changes, studies of antibodies, and homogeneity studies of protein, nucleic acids, membranes, organelles and cells.

Multiphase Systems

By using more than two polymers, multiphase systems can be obtained. In principle, the number of phases can be as many as the kinds of polymers used. A three-phase system of PEG, Ficoll, and dextran has been used with two ligands (in different phases) for directing the partitioning of blood serum proteins.

Semi-organic Systems

Part of the water in a two-phase system may be replaced by certain solvents. Often dextran cannot be used because of low solubility but it may be replaced by Ficoll. The log K of a protein may change drastically by introducing the organic solvent. Also the $\Delta \log K$ may in some cases be reduced while in other cases has been found to remain relatively unaffected.

Affinity Partitioning of Nucleic Acids and Bioparticles

Affinity partitioning in aqueous two-phase systems is not restricted to proteins, but has been also used for purification of DNA, using base-pair specific ligands, membrane fragments, and cells, such as erythrocytes. Some examples of such affinity extractions are found in Table 2.

Future Prospects

More specific ligands will certainly come into use for affinity partitioning and systems with much lar-

ger partition coefficients will be developed. This will allow not only specific extraction of biomaterials but also their many-fold concentration. Effective recycling processes of ligand-polymers will make it economically feasible to use affinity partitioning for extraction of enzymes on a technical scale. Successive extraction of several components from one and the same source by using a number of ligands in series extraction can be foreseen.

Conclusions

Affinity partitioning is a method of selective liquid-liquid extraction for purification and studies of proteins and other 'water stable' cell constituents. The scaling up of this process is uncomplicated and the recovery of ligand polymer reduces the cost.

See also: I/Affinity Separation. II/Affinity Separation: Dye Ligands; Rational Design, Synthesis and Evaluation: Affinity Ligands. III/Nucleic Acids: Extraction. Proteins: Electrophoresis; High-Speed Countercurrent Chromatography; Ion Exchange. Appendix 1/Essential Guides for Isolation/Purification of Cells. Essential Guides for Isolation/Purification of Enzymes and Proteins. Essential Guides for Isolation/Purification of Nucleic Acids.

Further Reading

- Albertsson PA (1986) *Partition of Cell Particles and Macromolecules*, 3rd edn, pp. 334–340. New York: John Wiley.
- Albertsson PA and Birkenmeier G (1988) Affinity separation of proteins in aqueous three-phase systems. *Analytical Biochemistry* 175: 154–161.
- Flanagan SD and Barondes SH (1975) Affinity partitioning – a method for purification of proteins using specific polymer-ligands in aqueous polymer two-phase systems. *Journal of Biological Chemistry* 250: 1484–1489.
- Harris JM (1985) Laboratory synthesis of polyethylene glycol derivatives. *Journal of Macromolecular Science. Reviews of Polymer Chemistry and Physics*. C25: 325–373.
- Johansson G (1995) Multistage countercurrent distribution. In: Townshend A (ed.) *The Encyclopedia of Analytical Science*, pp. 4709–4716. London: Academic Press.
- Johansson G and Joelsson M (1987) Affinity partitioning of enzymes using dextran-bound Procion yellow HE-3G. Influence of dye-ligand density. *Journal of Chromatography* 393: 195–208.

- Johansson G, Kopperschlager G and Albertsson PA (1983) Affinity partitioning of phosphofructokinase from baker's yeast using polymer-bound Cibacron blue F3G-A. *European Journal of Biochemistry* 131: 589–594.
- Kopperschlager G and Birkenmeier G (1990) Affinity partitioning and extraction of proteins. *Bioseparation* 1: 235–254.
- Tjerneld F, Johansson G and Joelsson M (1987) Affinity liquid–liquid extraction of lactate dehydrogenase on a large scale. *Biotechnology and Bioengineering* 30: 809–816.
- Walter H and Johansson G (eds) (1974) *Methods in Enzymology*, Vol. 228, *Aqueous Two-phase Systems*. San Diego, CA: Academic Press.

Aqueous Two-Phase Systems

See II/AFFINITY SEPARATION/Affinity Partitioning in Aqueous Two-Phase Systems

Biochemical Engineering Aspects of Affinity Separations

H. A. Chase, University of Cambridge,
Cambridge, UK

Copyright © 2000 Academic Press

Introduction

Affinity separations are popular methods for the purification of biological molecules and other biological entities. They can readily be implemented on the laboratory scale but a number of additional factors have to be considered when these techniques are to be used for production purposes. Under these circumstances it is necessary to apply biochemical engineering principles to the design, scale-up and optimization of affinity separations. These topics are the subject of this article.

Selective interactions are exploited in affinity separations in order to achieve greater adsorbent selectivity for the desired molecule. Subtle differences in physical properties such as charge, size and hydrophobicity are often found to be insufficient for the required degree of purification in many separations of biological compounds. Many separations require the isolation of a minority component from a highly complex feedstock which may contain large amounts of similar compounds. As a consequence, it has been necessary to devise recovery flow sheets that consist of an extensive sequence of different steps – a sequence that may result in low overall yields and excessive costs. Hence affinity separations have been developed as alternatives to the more widely used separations based on ion exchange, hydrophobic interaction and size exclusion methods. Provided

a ligand can be obtained which is truly selective for the desired component, it is possible to recover that component from a complex feedstock to a high degree of purity and in high yield. Typically the ligand is used in heterogeneous phase separations in which it is immobilized on to the surfaces of a porous solid-phase matrix material and employed in chromatographic and other adsorption techniques. Other approaches including the use of affinity ligands in selective precipitation and in modifying the phase selectivities in aqueous two-phase separations (ATPS) have been reported, but are not considered further here.

A variety of ligands with a wide range of molecular complexities have been developed for use in affinity separations and these are reviewed extensively elsewhere in this work. In many examples, duplication of the selective interactions that occur during the normal function of biomolecules have been exploited during such affinity separations; the affinity ligand is frequently one of the components of a recognition interaction. Examples include the recognition between an enzyme and its inhibitor or co-factor, or the highly specific interaction between an antigen and an antibody raised against it. Biomimetic molecules have been developed to mimic the recognition sites of more complex molecules, either by exploiting fortuitous interactions shown by readily available compounds (e.g. textile dyes) or as a result of the identification of new compounds either by studying the detailed three-dimensional structure of the target, or by the techniques of combinatorial synthesis. Selective molecular recognition can also be achieved without mimicking any naturally occurring

biological interactions. A typical example would be in the use of immobilized metal ion affinity chromatography in the purification of proteins and peptides containing poly-histidyl sequences.

Although affinity separations are frequently considered to be highly selective, they are not always good at selecting between closely related variants of essentially the same compound, e.g. when changes have occurred that do not result in elimination of the molecular recognition of the ligand. For proteins, such changes include minor amino acid variations during synthesis, partial misfoldings, and the formation of dimers and higher oligomers. Under these circumstances, separations that exploit differences in the size or subtle differences in the surface characteristics of the molecules are called for; affinity interactions are not sufficient.

Affinity separations are mainly used in preparative techniques where the adsorbent is chosen to interact selectively with the desired product and hence to be used as a tool for its purification. An equivalent approach can be used in analytical techniques if the goal of the analysis is determination of the level of one or a group of closely related compounds. However, such an approach is comparatively rare as other, less selective, techniques when operated

in a manner suited to the resolution of multiple components are able to yield, simultaneously, quantitative information about a larger number of components, even though such separations would not have sufficient throughput for use for preparative purposes. The approach that is adopted in this contribution is to introduce the considerations that are needed when affinity separations are to be used for preparative purposes at scales greater than that encountered in the laboratory (Table 1). Traditionally the approach and input of biochemical engineering to the optimization of bioprocesses is not considered important or necessary at the laboratory scale, where equipment and consumable costs are modest, and considerations such as yields, throughputs and batch cycle times are less important. The latter considerations become of much greater importance as the scale is increased through pilot to production procedures. However, much of what will be said is also applicable to the optimization of laboratory-scale procedures. The scale-up and optimization of affinity separations are characterized by features many of which are also of prime importance in the scale-up of other chromatographic methods and these should be considered in addition to the approach adopted here.

Table 1 Biochemical engineering aspects of affinity separations

<i>Criterion</i>	<i>Pertinent aspects</i>	<i>Implications</i>
Choice of affinity ligand	Selectivity Strength of binding Chemical identity and origin	Purification achieved Elution conditions Adsorbent longevity Cost Regulatory implications
Choice of immobilization material	Surface area Mass transfer characteristics	Contactor configuration and volume Separation time
Position in process flow sheet	Reduction in overall number of steps Feedstock composition Feedstock volume	Process economics Adsorbent longevity CIP procedures Contactor design Bed volume Adsorbent kinetics
Process design	Optimization of separation performance Choice of liquid-phase compositions, flow rates and stage durations	Laboratory-scale process development Computer modelling
Scale-up	Preservation of separation performance	Design heuristics and computer modelling
Monitoring and control	Measurement of levels of target molecule Detection of fault conditions	Online process optimization Improved yield and productivity Manufacture to GMP standards
Process validation	Manufacture to GMP standards	Equipment installation and commissioning Process reproducibility and robustness
Economic	Minimization of costs Competitiveness with alternative separation procedures	Adsorbent choice and longevity Liquid-phase selection Waste minimization, disposal and recycling

Position in Process Flow Sheet – Direct Recovery

One of the most important initial decisions regarding the adoption of an affinity separation technique in a recovery flow sheet is the selection of the point when that step should occur. Considerations of the expense and fragility of affinity ligands have often resulted in affinity separations being reserved for the later stages of a separation procedure, where, in general, the feedstocks are cleaner and the volume of liquid to be processed is less. Under such circumstances, affinity adsorbents would be expected to be able to be used for more cycles of operation, and each cycle of operation could be conducted in a smaller bed. Both these features would reduce process costs. However, this conservatism often results in underutilization of the potential resolving power of the affinity separation technique. The possibility of using a highly selective adsorbent for the capture and purification of an adsorbate from a very crude feedstock logically dictates that such a technique should be used at a very early stage in a separation protocol, thus eliminating the need for a series of less selective separation steps, each involving additional expense and a reduction of overall yield. However, the early stages of a separation protocol often involve feedstocks that contain particulates, including whole cells, pieces of broken cells and subcellular structures. The application of such feedstocks directly to packed beds results in the clogging of the bed arising from the capture of the particulates within the bed voids. Such feedstocks are typically pre-clarified by centrifugation or microfiltration, i.e. the use of techniques that not only may have expensive capital and running costs, but also may result in significant reductions in product yields. Recent advances in biochemical engineering have led to the development of a new technique to overcome the need for pre-clarification of the feed before application to an adsorbent bed. Expanded bed adsorption involves the use of beds with greater void volumes created by fluidizing the adsorbent beads in a stable manner as a result of upwards flow of liquid through the bed. Affinity ligands have been used with success in expanded bed adsorption techniques in order to achieve capture, concentration, clarification and purification in a single stage process.

Choice of an Appropriate Affinity Ligand and Immobilization to a Support

There are a number of factors that have to be considered when choosing an appropriate affinity ligand for use in affinity separations. One critical

consideration is the selection of a ligand with appropriate affinity and selectivity towards the target molecule. Although the selection of ligands that form complexes with very low dissociation constants improves capture of adsorbate from feedstocks at low concentrations and permits extensive washing of the adsorbed complex to remove less tightly adsorbed impurities, it may prove difficult to achieve dissociation of the complex during the subsequent elution phase. Elution may need to be achieved as a result of major changes to the physical conditions of the irrigating buffer (e.g. pH, ionic strength) with the possibility of subsequent denaturation of the adsorbate and/or the ligand. In addition, there is the possibility that dissociation of the adsorbed complex will be slow as a result of low values of the rate constant of this step. When being used on a large scale, the cost of the affinity ligand and the number of cycles in which it can be used are also important considerations. Problems and costs associated with the manufacture of ligand in the quantities required to prepare large amounts of affinity adsorbents may become significant, together with any implications that the nature and the source of the ligand may have on the validation of the process. It may prove impossible to find ligand immobilization chemistries that totally prevent low levels of ligand leakage from the affinity adsorbent during all phases of the purification cycle. The use of affinity separations in the production of therapeutic products dictates the need for these processes to be operated in a manner that can be fully validated to comply with good manufacturing practice (GMP). The need for thorough sanitation as part of the inherent clean-in-place (CIP) procedures may necessitate exposure of the affinity ligand to harsh reagents or sterilization protocols not previously encountered during use of the technique in the laboratory, with a consequent increase in the likelihood of deterioration of the affinity adsorbent.

Once a suitable affinity ligand has been chosen, it has to be immobilized on to a suitable support in order to generate an affinity adsorbent. Considerations in the choice of a suitable support are common to those that would be used in other adsorption and chromatographic procedures. In general the use of porous particles has been the most popular in large-scale separations, although the benefits of using membrane materials in achieving fast mass transfer have been demonstrated in some small-scale systems. Important properties of a suitable support include:

- High surface area accessible by the target molecule per unit volume of matrix, to minimize the volume of the adsorbent needed for the separation.

- Spherical particle shape and narrow particle size distribution to facilitate packing the bed to obtain optimal flow characteristics.
- Good mechanical properties of the matrix to resist compression and compaction in tall beds operated at high flow rates at high pressure drops and to resist attrition should removal of the adsorbent from the bed be necessary periodically for thorough sanitation procedures.

A wide variety of matrices, designed specifically for use in process-scale separations, are commercially available. In some cases, they may be purchased with popular, widely used, affinity ligands already covalently immobilized on their surface. Alternatively, base matrices may be available in a chemical form which facilitates customized covalent immobilization of more specialized ligands.

Operating Protocols, Equipment, Monitoring and Control

Affinity separations are carried out using equipment that is suitable for use in other adsorption and chromatographic procedures. In almost all cases this will involve the use of a packed bed of adsorbent, although the benefits of using expanded bed adsorption technology when processing particulate-containing liquids are also rapidly becoming apparent. These affinity procedures are operated in a batch mode with a number of sequential stages during each cycle of operation (adsorption, washing, elution, cleaning, re-equilibration). Reasons for the choice of such methods include the ease of automation and improved quality assurance over stirred tank adsorption procedures. Valves can be employed to ensure that the appropriate process solutions (feedstocks, buffers, eluents, etc.) are pumped on to the bed and that liquid fractions from the bed are diverted to appropriate vessels for collection. Typically these actions are under the control of an automated system which either follows a pre-programmed time sequence, or responds interactively to the features of the separation by exploiting information being received from sensors and monitors installed in the process.

In order to run an affinity separation optimally, it is necessary to be able to monitor the success of the separation as it is proceeding. Ideally, information is required on the levels of key components that accurately reflect the state of the separation. In affinity separations such components will include the adsorbate itself, the level of total protein and possibly the levels of key contaminants. The on-going development of biosensors able to provide continuous

measurement of particular compounds will be of crucial importance in this area. Meanwhile, use is beginning to be made of techniques such as flow injection analysis, surface plasmon resonance sensors and rapid liquid chromatographic monitoring. These techniques yield much more specific information than is available from traditional flow measurement techniques such as spectroscopy (mainly used to measure the general level of protein) and pH and conductivity measurements whose contribution is restricted to monitoring the physical properties of the liquids flowing into and out of the column. The ability to be able to monitor online the levels of particular compounds enables optimization of the duration of the adsorption stage of the separation, terminating it when the level of the target compound begins to break through the bed without being captured. Such monitoring can also participate in the location of the target in the flow from the bed during elution.

Scale-up and Validation

One of the principal biochemical engineering considerations associated with affinity separations is to transform a successful laboratory separation procedure into a viable industrial unit operation. Packed bed separation procedures can be successfully scaled up to almost any extent provided certain rules are maintained and scale-up of affinity separations can also be achieved in a rational manner without difficulty. A suggested approach is:

- Ensure that the same adsorbent (including the chosen particle size) is used in both laboratory and large-scale procedures.
- Conduct investigations to determine the approximate dynamic capacity of the affinity adsorbent for the desired product and estimate the volume of the bed that will be needed to process the scaled-up batch size.
- Select a bed height of adsorbent that is compatible with the above volume. This will depend to a large extent on the diameters of commercially available columns, paying due regard to manufacturers' recommendations concerning minimum bed height to diameter ratios to achieve satisfactory flow distribution across the bed and maximum bed heights recommended to avoid excessive pressure drops and resultant bed compression.
- Optimize all stages of the separation in laboratory experiments using narrow columns of the same height as chosen for the full sized bed.
- Maintain the linear flow velocities and durations of each stage of the optimized laboratory process in the scaled-up procedure.

Adherence to these procedures should ensure that the characteristics of the separation and cycle time of the separation are maintained.

Before any downstream purification process can be used in the production of therapeutic agents it must be validated as part of the procedure to ensure compliance with GMP. For affinity separations, the issues are similar to those pertaining to any adsorption or chromatographic procedure. However, quality assurance issues associated with the source and origin of the affinity ligands may be of additional importance especially if these are molecules isolated from natural sources. Issues such as installation qualification and operational qualification and the associated documentation are dealt with in depth by Sofer and Hagel (see Further Reading).

Optimization

Two approaches to the optimization of affinity separations can be identified. The first 'practical' approach makes use of information and experience gained from experimentation, typically at the laboratory scale. Such an approach may be expensive and time consuming and may require the availability of substantial amounts of the target biomolecule, a situation that may be highly undesirable in the early stages of the development of a product with possible therapeutic value. The second 'theoretical modelling' approach is based on the philosophy that a complete understanding of the events that occur during an affinity separation can lead to optimization being achieved by computer-based methods. Such a situation is potentially cheaper and quicker, but requires confidence that the modelling approach adopted accurately describes the true situation. Sometimes it is necessary to combine the two approaches.

In addition to optimization of the choice of affinity ligand and the materials and methods for its immobilization, which have already been described above, a number of factors have to be considered when optimizing an affinity separation. These factors, which will have an influence on each other, include:

- Choice of flow rates. It is necessary to adopt a suitable compromise between fast rates to minimize purification time and slow rates to allow mass transfer and kinetic processes to occur. The nature of the matrix material chosen for the process and its resultant mass transfer characteristics strongly influence this consideration;
- Choice of irrigating liquid. The success of washing and elution procedures depends critically on the influence the liquid has on the strength of the

adsorbent/adsorbate complex, particularly in relation to its effect on complexes of other compounds adsorbed specifically or non-specifically.

- Cutting the eluted peak. Most affinity separations achieve resolution and purification in the adsorption stage resulting from the specificity of the affinity ligand. However the use of 'group-specific' ligands may result in the adsorption of compounds other than the desired target. Under these circumstances attempts may be made to resolve the adsorbed species by use of a series of step changes in eluent composition and/or the use of a continuous gradient, and it is necessary to identify the portion of eluent containing the target compound. The cut may be made as a compromise between the yield and the degree of purification required.

Theoretical Modelling

A number of approaches have been adopted for the modelling of adsorption and chromatography operations in computer-aided process engineering. Some of these describe the features of the separation in gross, overall terms and essentially describe the mass balance over the process. Alternatively, other attempts have involved a detailed consideration of the details of such processes. One approach towards understanding the features that dictate the success and characteristics of an affinity separation has involved a detailed study of the nature and characteristics of the equilibrium and mass transfer processes for the adsorption/desorption of the adsorbate, and in some cases other key components in the separation. The nature of adsorbents adopted for use in practical affinity separations results in a totally thorough approach to modelling being complicated and impractical. Accurate analysis is frustrated by the presence of a distribution of particle diameters and pore characteristics, in addition to a non-homogeneous distribution of immobilized ligand throughout the interstices of the adsorbent. It has often been necessary to use approximate methods that overlook the latter complications. In general, the modelling of preparative chromatography is also difficult as a result of the need to consider the simultaneous adsorption of multiple species. However, the fact that affinity separations often involve the adsorption of only one or a few components can simplify the task. It must be remembered that although the selection and subsequent solution of a set of algebraic equations which describe the characteristics of an adsorption system can often be undertaken, it is also essential to obtain values for the parameters used in such equations which apply to the actual separation under

Table 2 Strategies for optimizing the stages of affinity separations

Stage	Criteria of efficiency	Achieved by
Adsorption	Sharp breakthrough curves	Adsorbents with good kinetic properties (small particles, adsorption to outer surfaces) Low flow rates High inlet concentrations of adsorbate
Washing	Selectivity Maximum removal of contaminants, minimum removal of adsorbate	Appropriate choice of ligand Appropriate choice of buffers
Elution (gradient)	Maximum concentration of product	Reversed flow direction Strong eluents Low flow rates
Elution (step)	Minimum denaturation of product	Weak eluents High flow rates

consideration. Commercial packages are now available which are reported to be effective for scale-up and optimization of affinity separations, although substantial improvements to a process can also be made on the basis of a qualitative understanding of the basic features of an affinity separation (Table 2).

It has already been pointed out that resolution in affinity separations is almost always achieved during the adsorption process and is less likely to be necessary during elution unless the specificity of the affinity ligand is low and multiple species have been adsorbed. Hence the majority of effort has been expended towards understanding the events that occur during the adsorption stage of the separation and is thus directed towards optimizing the duration of the adsorption stage to ensure that the potential adsorption capacity of the bed is utilized as far as possible, i.e. full use has been made of the costly immobilized ligand. Of particular importance is the correct assessment of the amount of adsorbate that can be removed from the feedstock during a cycle of operation. This requires knowledge of not only the maximum capacity of the adsorbent (q_m) but also the dissociation constant (K_d) of the adsorbed species. It is important to remember that the capacity of the adsorbent is governed by the nature of the adsorption isotherm, even when kinetic limitations allow the adsorbent to become loaded to equilibrium with the feedstock. In many cases, the equilibrium characteristics have been shown to be adequately described by a simple Langmuir isotherm, although the situation is certainly more complicated where more than one component can bind to the adsorbent. The shape of the adsorption isotherm is in most cases hyperbolic, with characteristics described by:

$$q = \frac{q_m c_A}{K_d + c_A}$$

Only in situations where the concentration of adsorbate in the feedstock, c_A , is of greater magnitude than the value of the dissociation constant of the adsorbed species (K_d) will the affinity adsorbent show equilibrium binding capacities as great as the maximum adsorption capacity (q_m). Indeed for values of c_A smaller than K_d , the equilibrium capacity of the adsorbent (q) decreases linearly with decreasing c_A and is given by

$$q = \frac{q_m c_A}{K_d}$$

This simple consequence of the law of mass action often accounts for the apparently low adsorption capacities that are observed during the development of affinity separations which are frequently mistakenly identified as a malfunction of the adsorbent. This point shows the importance of knowing the value of K_d of the selected ligand, but also the need to select an affinity ligand where the dissociation constant of the adsorbed complex with adsorbate is sufficiently low to ensure satisfactory capture of adsorbate from feedstock, particularly if attempts are being made to capture an adsorbate present at low concentrations.

Economic Considerations

Evaluation of the economics of the separation requires consideration of the fixed costs of the equipment (columns, reservoirs, pumps, valves, monitors, control system), and the running costs including the cost of the adsorbent, the chemicals used (including the need for large volumes of high quality water) and labour charges.

Although much attention is appropriately paid to the cost and longevity of the affinity adsorbent and its attached ligands, concentrating particularly on the number of cycles in which the adsorbent can be

used, due consideration must also be paid to the costs of all stages of the separation procedure. Such consideration should cover not only the basic costs of the chemicals employed, but also all costs associated with disposal and/or recycling of those chemicals after use. Some affinity procedures may involve specific eluents (e.g. enzyme co-factors) whose expense is greater than that of the simple strategies of changes in pH, ionic strength or dielectric constant used to elute many adsorbates. These economic considerations become of much greater importance in the design of process-scale procedures and are often overlooked at the laboratory scale.

Conclusions and Future Prospects

There are no technical barriers preventing the use of affinity separations in the production of biological molecules and entities. The biochemical engineering principles associated with the scale-up and optimization of affinity separations are well developed and the resultant conclusions are readily implemented. The conservatism surrounding their current use stems from the widespread lack of suitable affinity ligands. It is anticipated that novel molecules emerging from new techniques such as phage display technology and combinatorial chemistry will be excellent candidates for use of ligands in affinity separations. Affinity separations will be used in the purification of soluble biomolecules and also in the isolation of more complex species such as viruses, cells and other products for use in gene therapy. Affinity separations will therefore play an essential part in the preparation of future generations of therapeutic biotechnological products. Their adoption will result in the simplification and improvement of downstream processing flow sheets and will enable a rapid transition between discovery and utilization of these products.

See also: I/Affinity Separation: Covalent Chromatography; Dye Ligands; Rational Design, Synthesis and Evaluation: Affinity Ligands; Theory and Development of Affinity Chromatography.

Further Reading

- Chase HA (1984) Prediction of the performance of macropreparative affinity chromatography. *Journal of Chromatography* 297:179.
- Chase HA (1988) Optimisation and scale-up of affinity chromatography. In Jennissen HP and Müller W (eds) *Macromolecular Symposia* 17. Basel: Hüthig & Wepf Verlag.
- Chase HA (1988) Adsorption separation processes for protein purification. In Mizrahi (ed.) *Downstream Processes: Equipment and Techniques*. New York: Alan R. Liss.
- Chase HA (1994) Purification of proteins from feedstocks containing particulate material by adsorption chromatography in expanded beds. *Trends in Biotechnology* 12: 296.
- Dean PDG, Johnson WS and Middle FA (eds) (1985) *Affinity Chromatography: A Practical Approach*. Oxford: IRL Press.
- Harrison RG (ed.) (1994) *Protein Purification Process Engineering*. New York: M. Dekker.
- Janson JC and Rydén L (eds) (1997) *Protein Purification: Principles, High Resolution Methods, and Application*. New York: Wiley.
- Kline T (ed.) (1993) *Handbook of Affinity Chromatography*. New York: Dekker.
- Ladisch MR (ed.) (1990) *Protein Purification: From Molecular Mechanisms to Large-scale Processes*. Washington, DC: American Chemical Society.
- Scopes RK (1994) *Protein Purification: Principles and Practice*. New York: Springer-Verlag.
- Sofer GK and Hagel L (1997) *Handbook of Process Chromatography: A Guide to Optimization, Scale-up, and Validation*. San Diego: Academic Press.
- Subramanian G (ed.) (1995) *Process Scale Liquid Chromatography*. New York: VCH.
- Wheelwright SM (1991) *Protein Purification: Design and Scale-up of Downstream Processing*. Munich: Hanser Publishers.

Covalent Chromatography

K. Brocklehurst, University of London, London, UK

Copyright © 2000 Academic Press

Introduction

Conventional affinity chromatography involves specific recognition of biomolecules such as antibodies and enzymes by immobilized ligands (antigens and

inhibitors) usually by a multiplicity of non-covalent interactions. By contrast, the separation process in covalent chromatography does not require specific adsorptive binding and thus does not require knowledge of the structural determinants of the binding area of the component to be isolated. Instead, specificity relies on the nature of the chemical reaction of the chromatographic material with one or more components of a mixture. When complete specificity is

achieved in the bonding step, only one of the components reacts. The other components are removed by washing and the bonded component is then released by another chemical reaction. Ideally this leaves the chromatographic material in a form that is readily regenerated. When several components react with the chromatographic material, specific isolation of individual components needs to be achieved subsequently, e.g. in the elution step (sequential elution covalent chromatography). A recent extension of covalent chromatography involves derivatization specifically of thiol-containing components by reaction

with a dithiopyridyl polyethyleneglycol (PEG) reagent. This provides charge shielding effects and facilitates separation of the derivatized proteins by ion exchange chromatography.

The development of covalent chromatography is discussed below and is summarized in **Table 1** in which key papers and reviews are identified. Those key papers not listed in the Further Reading section may be found in one or more of the reviews. Widespread application of the technique began after 1973, when covalent chromatography by thiol–disulfide interchange using the 2-mercaptopyridine leaving

Table 1 Milestones in the development of covalent chromatography and some key publications

1963	<i>Fundamental paper</i> reports the synthesis of an 'organomercurial polysaccharide' for the isolation of thiol-containing proteins and the first example of covalent chromatography (Eldjarn and Jellum).
1970	<i>Fundamental paper</i> reports unusual high reactivity of the thiol group of papain towards 2,2'-dipyridyl disulfide (2-Py-S-S-2-Py; 2PDS) at pH 4 which provided the basis for covalent chromatography by thiol–disulfide interchange with provision for selectivity for low pK_a thiol groups (Brocklehurst and Little).
1972	<i>Fundamental paper</i> reports an early example of covalent affinity chromatography (a combination of covalent and conventional affinity chromatographies) in which penicillin-binding proteins are isolated by reaction with the β -lactam ring of immobilized 6-aminopenicillamic acid and released by reaction with hydroxylamine (Blumberg and Strominger).
1973	<i>Fundamental paper</i> introduces covalent chromatography by thiol–disulfide interchange for the isolation of fully active papain using a Sepharose-(glutathione-2-pyridyl disulfide) gel (Brocklehurst, Carlsson, Kierstan and Crook; marketed by Pharmacia).
1975	<i>Fundamental paper</i> reports the synthesis and use of a more highly substituted gel with an electrically neutral and less sterically demanding spacer, the Sepharose 2-hydroxypropyl-2'-pyridyl disulfide gel (Axén, Drevin and Carlsson; marketed by Pharmacia).
1978	<i>Fundamental paper</i> reports the introduction of <i>N</i> -succinimidyl-3-(2'-pyridyl disulfany)l propanoate which readily permits the introduction of auxiliary thiol groups into non-thiol-containing proteins to widen the scope of targets for reversible immobilization by thiol–disulfide interchange (Carlsson, Drevin and Axén).
1980	<i>Review</i> cites approx. 150 papers on covalent chromatography published between 1973 and 1978; although most publications are concerned with thiol-containing proteins, there are some references to covalent chromatography involving serine, methionine and tryptophan side chains and to the isolation of nucleic acids and membrane fragments (Lozinskii and Rogozhin).
1981	<i>Fundamental paper</i> reports development of sequential elution covalent chromatography to separate protein disulfide isomerase and glutathione insulin transhydrogenase (Hillson).
1982	<i>Review</i> discusses selectivity by proton-activated covalent chromatography using 2-pyridyl disulfide gels in acidic media as a logical extension of the more general use of soluble disulfides containing the 2-mercaptopyridine leaving group in protein chemistry and enzymology as enzyme active centre titrants, reactivity probes, delivery vehicles for spectroscopic reporter groups and heterobifunctional crosslinking reagents (Brocklehurst).
1983	<i>Fundamental paper</i> reports the use of (Gly-Phe-Phe) ₂ -cystamine immobilized on Affi-Gel10 (BioRad) for the isolation of cathepsin B; this is an example of an extension of the general method of covalent chromatography by thiol–disulfide interchange by provision of recognition sites to create a covalent affinity gel (Evans and Shaw).
1985	<i>Review</i> discusses covalent chromatography and its applications in biochemistry and biotechnology; extensive detailed descriptions are given of the synthesis, characteristics and commercial sources of activated support materials (Brocklehurst, Carlsson and Kierstan).
1995	<i>Fundamental paper</i> reports examples of selectivity in covalent chromatography by thiol–disulfide interchange determined by steric and electrostatic restrictions (Thomas, Verma, Boyd and Brocklehurst).
1996	<i>Review</i> summarizes applications of covalent chromatography by thiol–disulfide interchange with references also to the use of some other types of thiol-specific chromatography: organomercurials, isothiocyanates and 4-aminophenylarsenoxide-agarose for the selective isolation of molecules containing vicinal thiol groups (Brocklehurst).
1996	<i>Fundamental paper</i> discusses an example of a development of covalent chromatography whereby monomethoxypolyoxy-(ethylene glycol) (mPEG)-(glutaryl)-S-S-2-Py is used to derivatize components of a mixture of thiol-containing enzymes to facilitate their separation by ion exchange chromatography (Azarkan, Maes, Bouckaert, Thi, Wyns and Looze).

Table 2 Applications of covalent chromatography by thiol–disulfide interchange using 2-pyridyl disulfide-containing gels or 2-pyridyl disulfide derivatives of the target protein or peptide

Applications	Comments
Fractionation and specific isolation of thiol-containing proteins and peptides	Purification of a wide range of enzymes and other proteins by the various versions of the technique has been reported
Isolation and sequencing of thiol-containing peptides	Facilitates purification of thiol-containing peptides which is often difficult from proteolytic digests. Two versions: (i) immobilization of the protein by reaction with the disulfide gel followed by proteolysis; (ii) derivatization of the protein by reaction with 2PDS, proteolysis in solution and isolation by reaction with the thiolate gel
Removal of prematurely terminated peptides during solid-phase peptide synthesis	Premature chain termination of the peptide by blocking of the free terminal amino group results in unwanted by-products in solid-phase peptide synthesis. These are readily separated from non-terminated peptides by addition of Cys-Met to the free amino group of the non-terminated peptide prior to cleavage from the solid-phase matrix in preparation for covalent chromatography
Reversible immobilization of enzymes with associated purification	This method contrasts with most methods of immobilization which are irreversible. An additional advantage is that eventual release of the enzyme by thiolysis can produce purified enzyme if the preparation applied was not fully active
Synthesis of specific adsorbents for conventional affinity chromatography	Thiol–disulfide interchange provides a convenient method of attaching ligands containing specific recognition features to insoluble matrices

group was introduced by Brocklehurst *et al.*, initially for the specific isolation of the fully active form of the cysteine proteinase, papain.

Various approaches developed subsequently are discussed including the range of gel types, the reactions involved in attachment, elution and gel reactivation and brief discussion of specific covalent attachment via groups other than thiol groups. The range of applications of covalent chromatography by thiol–disulfide interchange is summarized in Table 2.

Development of the Technique

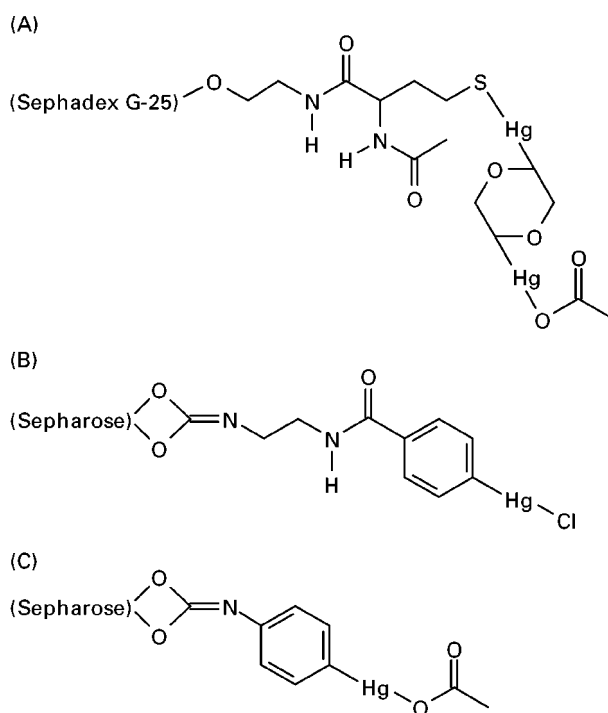
Scope

Most of the published papers on covalent chromatography relate to proteins and peptides. The emphasis has been on thiol-containing molecules but immobilization procedures via the side chains of serine, methionine and tryptophan have been devised. In addition the use of covalent chromatography for the isolation of polynucleotides, low M_r co-factors, and gene fragments has been reported.

The Pre-Pyridyl Disulfide Era

The first example of covalent chromatography dates from 1963 when Eldjarn and Jellum reported the use of an organomercurial dextran based on Sephadex G-25 (Figure 1A) for the isolation of thiol-containing proteins which are released from the gel by treatment

with low M_r mercaptans. Simpler and more effective products using a better support material (agarose) were developed subsequently, e.g. by Cuatrecasas

**Figure 1** Some organomercurial gels. (A) Due to Eldjarn and Jellum, 1963. (B) Due to Cuatrecasas, 1970. (C) Due to Sluyterman and Wijdenes, 1970.

(Figure 1B) and by Sluyterman and Wijdenes (Figure 1C) both in 1970. Some solid phase organomercurials are available commercially but as Lozinskii and Rogozhin pointed out in their review in 1980 (Table 1) relatively little interest was shown in the technique of covalent chromatography until the introduction of the version involving thiol–disulfide interchange using a solid phase 2-pyridyl disulfide gel in 1973 (Table 1). Problems with organomercurial gels include gradual loss of the metal with consequent contamination of the purified protein, lack of absolute specificity for thiol groups and lack of provision both for designed selectivity and of a means of spectral monitoring of occupancy of gel sites by the target protein.

Covalent Chromatography by Thiol–Disulfide Interchange Using 2-Pyridyl Disulfide Gels

The reactions involved in attachment, elution and gel reactivation Covalent chromatography using insoluble mixed disulfides containing the 2-mercaptopyridine leaving group (Gel-spacer-S-S-2-Py) was devised by Brocklehurst *et al.* in 1973 as a logical extension to the use of 2,2'-dipyridyl disulfide (2PDS or 2-Py-S-S-2-Py) as a thiol titrant with selectivity in acidic media for intact catalytic sites in the cysteine proteinase papain. In 1970 Brocklehurst and Little had observed unusually high reactivity of the thiol group of Cys25 in papain towards 2PDS which has its origin in the coexistence of the catalytic site ion pair motif, (Cys25)-S⁻/(His159)-Im⁺H, and the activated, protonated form of the disulfide, 2-Py-S-S-2-Py⁺H. The coexistence of significant concentrations of these reactants arises from the low pK_a value for ion pair formation (3.3) and its relationship to the pK_a value of the 2-Py-S-S-2-Py⁺H cation (2.45). Soluble reagents of the general type R-S-S-2-Py (reviewed by Brocklehurst in 1982; see Table 1) have proved useful in the study of thiol-containing proteins, e.g. as enzyme active centre titrants, reactivity probes, delivery vehicles for spectroscopic reporter groups and crosslinking reagents. 2,2'-Dipyridyl disulfide and simple alkyl-2-pyridyl disulfides successfully titrate intact catalytic sites in cysteine proteinases even in the presence of low M_r mercaptans or denatured enzyme that still retains its thiol group but with the ion pair disrupted. It was as part of a programme designed to exploit the two-protonic-state nature of reagents of the type R-S-S-2-Py⁺H/R-S-S-2-Py where the protonated forms possess reactivities *c.* × 1000 greater than those of the unprotonated forms that covalent chromatography was originally devised. Thus selectivity of attachment in favour of low pK_a thiol groups may be achieved by carrying out

the attachment procedure at pH *c.* 4 where reaction is with the protonated gel (Gel-spacer-S-S-2-Py⁺H (see Figure 2A) and reaction of thiol groups with 'normal' pK_a values (8–10) will not occur because these will exist in the non-nucleophilic RSH forms. The technique is more generally applied in weakly alkaline media (pH 8) where reaction with the unprotonated gel (Gel-spacer-S-S-2-Py) (see Figure 2B) would be expected to occur readily with most thiol-containing compounds. Thus when covalent chromatography using a Sepharose-spacer-2-pyridyl disulfide gel is applied to the isolation of thiol-enzymes at pH 8, thiol-containing protein is freed from irreversibly oxidized and hence inactivated enzyme containing sulfinic acid (–SO₂H) groups in place of thiol groups. When applied, e.g. to cysteine proteinases at pH 4, attachment is specifically by reaction of the catalytically active form of the enzyme containing the essential (Cys)-S⁻/(His)-Im⁺H ion pair generated by protonic dissociation with pK_a of about 3.

Reaction of the thiol-containing protein with either protonation state of the gel may be quantified by spectral analysis of the chromophoric pyridine-2-thione released in the thiol–disulfide interchange (λ_{max} 343 nm, $\epsilon_{343} = 8080 \text{ M}^{-1} \text{ cm}^{-1}$). This provides a measure of the practical capacity of the gel for a particular protein. The theoretical capacity may be determined by reaction of the 2-pyridyl disulfide sites in the gel with a low molecular weight mercaptan such as 2-mercaptoethanol and spectral analysis of the pyridine-2-thione released into solution. The practical capacity is usually less than the theoretical capacity due to the inaccessibility of some sites to macromolecules. After removal of unreactive components by washing, the thiol-containing protein is released from the gel by elution with a reducing agent, usually a low molecular weight mercaptan (Figure 2C). During elution the gel is left in the non-activated, thiolated state (Gel-spacer-SH) and may be reactivated by reaction with 2PDS (Figure 2D).

An alternative version of this type of covalent chromatography involves derivatization of the thiol-containing protein (PSH) by reaction with 2PDS and attachment by reaction of P-S-S-2-Py so produced to a non-activated thiolated gel (Figure 2E). Other disulfide gels have been used subsequently for covalent chromatography, such as those prepared by reaction of thiol groups in gels with 5,5'-dithiobis-(2-nitrobenzoate). Such gels lack the ability to increase their reactivity by protonation at low pH and thus do not offer the possibility of selectivity that 2-pyridyl disulfide gels provide.

Support materials and spacers As in other separation techniques the solid support for the reactive

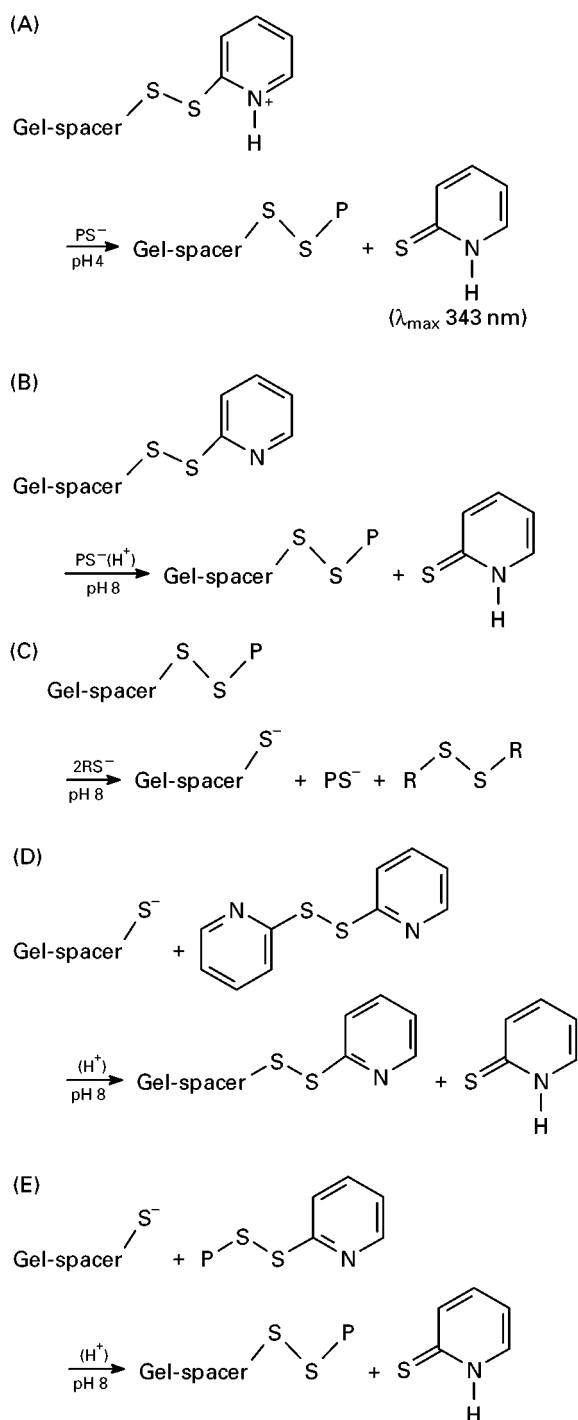


Figure 2 Reactions involved in covalent chromatography by thiol-disulfide interchange. (A) Selective attachment of a thiol-containing protein (PSH) containing a low pK_a thiol group by reaction with the protonated gel sites at pH values *c.* 4. (B) More general attachment of a thiol-containing protein containing a thiol group with a 'normal' pK_a value (8–10) by reaction with the unprotonated gel sites in weakly alkaline media (e.g. pH 8). (C) Elution of the thiol-containing protein by reaction with a low molecular weight mercaptan (RSH). (D) Reactivation of the thiolated gel by reaction with 2PDS. (E) Covalent chromatography using a non-activated thiolated gel and a protein-S-S-2-Py mixed disulfide prepared by reaction of the protein (PSH) with 2PDS.

groups in covalent chromatography must have sufficient mechanical, chemical and biological stability to resist degradation during the chromatographic process. It needs to be sufficiently permeable to permit access of macromolecules to reactive groups within the support material and sufficiently inert so as not to denature the molecules to be isolated. Spherical beads provide good column packing and flow properties. The support must allow opportunities to introduce the chemically reactive groups required for the immobilization process without serious perturbation of the other properties mentioned above. The support that has been most widely used in covalent chromatography is the polysaccharide, agarose. Beaded agarose is available, e.g. as Sepharose 2B, 4B and 6B and as crosslinked products with increased mechanical stability such as the CL-Sepharoses. The original (1973) version of covalent chromatography by thiol-disulfide interchange utilized the gel shown in **Figure 3A**, prepared by reaction of cyanogen-bromide-activated agarose with the amino group of glutathione followed by reaction of the thiol group with 2PDS. Use of the 5-nitro derivative of 2PDS provides an activated gel that releases a coloured thione (λ_{max} 386 nm) during the attachment of a thiol-protein. Spacers other than glutathione (e.g. cysteine, cysteamine and ethane) have been attached to agarose but the activated gel shown in **Figure 3B**, reported in 1975 by Axén *et al.* (**Table 1**) is particularly noteworthy. Whereas the glutathione gel (**Figure 3A**) is negatively charged, the hydroxypropyl gel (**Figure 3B**) is electrically neutral and, in addition, is more highly substituted and less sterically demanding. The difference in these characteristics accounts for the different selectivities exhibited by the two gels demonstrated in 1995 by Thomas *et al.* in connection with studies on the highly negatively charged enzyme actinidin and on chymopapain M, an enzyme that rejects all but the smallest ligands in one of its recognition sites. The activated glutathione gel bonds to all of the cysteine proteinases in *Carica papaya* except chymopapain M (for steric reasons) and fails to bond with actinidin because of electrostatic repulsions. More generally, the spacer between the gel and the reactive attachment site should not be long and hydrophobic in order to minimize non-specific hydrophobic effects. Neither should it possess substantial ion exchange properties. These requirements of course are common to any separation technique that relies on specific reaction or interaction with particular sites engineered into the gel. Other support materials that fulfil some or all of the requirements for a satisfactory chromatographic material include crosslinked polyacrylamide and inorganic materials such as porous

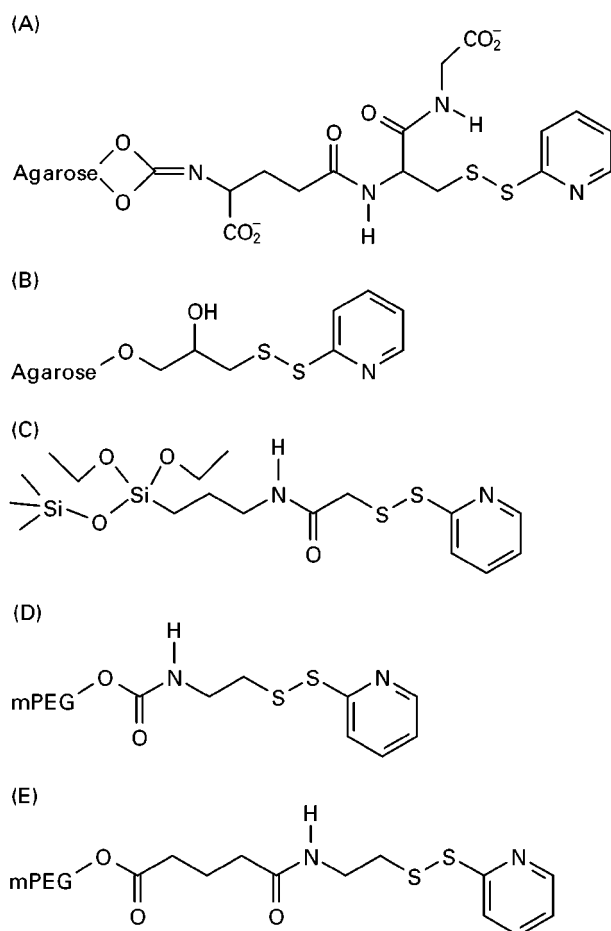


Figure 3 Some activated gels used in covalent chromatography by thiol-disulfide interchange. (A) The original (1973) Sepharose–glutathione-2-pyridyl disulfide gel. (B) The more highly substituted, electrically neutral, less sterically demanding (1975) Sepharose–hydroxypropyl-2-pyridyl disulfide gel. (C) A macroporous silicon oxide derivative (1979). (D) and (E) Two soluble mPEG derivatives used to modify the surface properties of thiol-enzymes by interactions with the monomethoxypolyethylene glycol (mPEG) 5 kD chains (1995/96).

glass coated with hydrophilic polymers. An example of an inorganic material that has been used in covalent chromatography is the macroporous silicon oxide derivative (Figure 3C) reported by Lozinskii *et al.* in 1979.

Sequential elution covalent chromatography This extension to the technique was introduced by Hillson in 1981. A mixture containing different thiol-containing proteins is applied to a 2-pyridyl disulfide gel and in most cases all would be expected to react. Separation is achieved in this case in the elution step. Elution either with different concentrations of a given mercaptan or with a series of mercaptans each of different redox potential results in the

sequential elution of each component with consequent separation.

Use of mPEG–Enzyme Mixed Disulfides in Conjunction with Ion Exchange Chromatography

During the mid-1990s Looze and co-workers introduced the use of soluble mixed disulfides containing the usual 2-mercaptopyridine leaving group and derivatives of monomethoxypolyethylene glycol (mPEG; nominal molecular mass 5 kDa) (Figures 3D and 3E) for the isolation of thiol-containing enzymes by ion exchange chromatography. The chromatographic behaviour of the enzymes appears to be modified by the charge shielding effects of the PEG chain. This approach provides another means of separating components of mixtures of thiol-enzymes as an alternative to sequential elution covalent chromatography.

Other Types of Covalent Chromatography

Attachment via thiol groups Substitution of the 2-mercaptopyridine leaving group by other aromatic mercapto groups results in the loss of selectivity at low pH and does not appear to offer substantive advantage. The intramolecular agarose thiolsulfonates introduced by Carlsson and his colleagues in the mid-1990s provide an alternative to the mixed agarose–aromatic disulfide gels discussed above. Thiolated agarose is subjected to mild oxidation by potassium ferricyanide to produce disulfide groups followed by further oxidation to thiolsulfonate groups by a stoichiometric amount of magnesium monoperoxyphthalate. These gels also lack the opportunity to provide selectivity for low pK_a thiol groups at low pH. They do not require external leaving groups but because of that do not offer the possibility of measurement of reactive site content by thiolysis and spectral analysis. An example of covalent affinity chromatography using a substrate-like symmetrical disulfide (Gly-Phe-Phe)₂-cystamine immobilized by amide bond formation on Affi-Gel 10 was reported by Evans and Shaw in 1983. In this type of approach specific binding interactions align the nucleophilic (thiolate) and electrophilic (disulfide) reactants for the covalent bonding process.

In some applications thiol groups exist as part of the support material and one example involving reaction of thiol-agarose gels with thiol-proteins derivatized as mixed disulfides by reaction with 2PDS (Figure 2E) constitutes one of the alternative versions of covalent chromatography by thiol-disulfide interchange. A different application of thiol-agarose gels is in studies on nucleic acids. Cytosine and uracil residues in polynucleotides can be mercurated

without appreciable change in function. These derivatives form mercaptides by reaction with thiol-agarose and are eluted subsequently by treatment with a low molecular weight mercaptan.

Attachment by reaction of thiol groups is not restricted to reaction at electrophilic sulfur. The higher reactivity of arylisothiocyanates towards thiol groups than towards amines permits their use in thiol-selective covalent chromatography. An immobilized trivalent organoarsenical, 4-aminophenylarsenoxide-agarose, has been used for the selective isolation of molecules and assemblies containing vicinal thiol groups (lipoic acid and the 2-oxoglutarate dehydrogenase multienzyme complex of which lipoic acid is a covalently bonded co-factor). Attachment involves cyclic dithioarsenite formation. Elution by 2,3-dimercaptopropane-1-sulfonic acid releases the reduced (dimercaptan) form of lipoic acid.

Attachment via seryl hydroxy groups Organophosphate agarose derivatives are an obvious choice for isolation of proteins with highly reactive seryl hydroxy groups such as the serine hydrolases. Coupling of 2-aminoethyl 4-nitrophenyl methyl phosphonate to succinylated aminoagarose produced a material that reacted specifically with serine hydrolases such as acetylcholine esterase and chymotrypsin. The problem with these gels is the very slow release of the enzymes even by good nucleophiles that provide reactivation in analogous soluble systems.

Attachment via methionyl thioether groups The known selectivity of alkylating agents for methionyl residues in acidic media to produce sulfonium derivatives and the possibility of regeneration by sulfur nucleophiles led Schechter *et al.* in 1977 to produce a chloroacetamidoethyl polyacrylamide derivative for the isolation of proteins via methionyl side chains. The relatively severe conditions required for attachment (low pH and long reaction times) limit the applications of this method. The methionyl residue cannot be at the C-terminus because such residues are converted to homoserine residues and attachment is not achieved. Regeneration of the covalent chromatography material is not provided for in this method.

Attachment via tryptophanyl side chains Arylsulfonyl chlorides and sulfur monochloride (S_2Cl_2) selectively modify tryptophan residues in acidic media to form 2-arylsulfonyl tryptophan and 2-mercaptotryptophan moieties respectively. Rubinstein *et al.* used this knowledge in 1976 to prepare polyacrylamide derivatives that react covalently with tryptophan-containing peptides which are released in modified

forms by treatment with a low molecular weight mercaptan. The tryptophan side chain is converted to a 2-mercaptotryptophan side chain in the process. The method could find application in protein sequencing but is of limited use for protein isolation not only because of the necessary introduction of the mercapto group but also because of the requirement for acid stability of the protein.

Applications of Covalent Chromatography

The range of applications of covalent chromatography is illustrated in Table 2 by reference to methods that utilize thiol-disulfide interchange. Examples of these applications can be found in one or more of the reviews listed in the Further Reading section.

Concluding Comments

The ease with which specificity and selectivity can be provided in covalent chromatography involving attachment via thiol groups, together with the advantages due to the mild conditions required for attachment, elution and reactivation of the gel, account for the outstanding success of versions of the technique involving thiol-disulfide interchange, particularly those using 2-pyridyl disulfide sites. Attachments via other protein side chains are generally less satisfactory in these respects and have been used only to a limited extent. Often covalent chromatography has been used at a relatively late stage in the purification process but the successful isolation of bovine mercaptalbumin from crude extracts reported by Carlsson and Svenson in 1974 suggests that this approach should be considered in other cases. Some of the applications listed in Table 2 can be applied to non-thiol-containing proteins by the introduction of an auxiliary thiol group, e.g. by use of the valuable heterobifunctional reagent, *N*-succinimidyl-3-(2'-pyridyl disulfanyl) propanoate, introduced by Carlsson, Drevin and Axén in 1978 or by site-directed mutagenesis.

Further Reading

- Axén R, Drevin H and Carlsson J (1975) Preparation of modified agarose gels containing thiol groups. *Acta Chemica Scandinavica* B27: 471-474.
- Azarkan M, Maes D, Bouckaert J, Thi M-HD, Wyns L and Looze Y (1996) Thiol pegylation facilitates purification of chymopapain leading to diffraction studies at 1.4 Å resolution. *Journal of Chromatography A* 749: 69-72.

- Brocklehurst K (1982) Two-protonic state electrophiles as probes of enzyme mechanism. *Methods in Enzymology* 87C: 427–469.
- Brocklehurst K (1996) Covalent chromatography by thiol–disulfide interchange using solid-phase alkyl 2-pyridyl disulfides. In Price NC (ed.) *Protein Labfax*. pp. 65–71. Oxford, UK: Bios; San Diego, USA: Academic Press.
- Brocklehurst K, Carlsson J, Kierstan MPJ and Crook EM (1974) Covalent chromatography by thiol–disulphide interchange. *Methods in Enzymology* 34: 531–544.
- Brocklehurst K, Carlsson J and Kierstan MPJ (1985) Covalent chromatography in biochemistry and biotechnology. *Topics in Enzyme and Fermentation Biotechnology* 10: 146–188.
- Eldjarn L and Jellum E (1963) Organomercurial polysaccharide – a chromatographic material for the separation and isolation of SH-proteins. *Acta Chemica Scandinavica* 17: 2610–2621.
- Evans B and Shaw E (1983) Inactivation of cathepsin B by active-site directed disulfide exchange. Application in covalent affinity chromatography. *Journal of Biological Chemistry* 258: 10227–10232.
- Hillson DA (1981) Resolution of thiol-containing proteins by sequential-elution covalent chromatography. *Journal of Biochemical and Biophysical Methods* 4: 101–111.
- Lozinskii VI and Rogozhin SV (1980) Chemospecific (covalent) chromatography of biopolymers. *Russian Chemical Reviews* 49: 460–472.

Dye Ligands

Y. D. Clonis, Laboratory Enzyme Technology,
Department of Agricultural Biotechnology,
Agricultural University of Athens, Athens, Greece

Copyright © 2000 Academic Press

Introduction

Dyes employed in protein and enzyme purification are synthetic hydrophilic molecules bearing a reactive, usually a chlorotriazine, moiety by which they can easily be attached to various polymeric supports. Among the various known reactive dye ligands, Cibacron Blue 3GA or F3GA (CB3GA, **Figure 1A**), an *ortho*-isomer of CI Reactive Blue 2, has attracted most attention from biotechnologists in protein purification. The foundations of the important role of CB3GA may well be attributed to pure historical accident; an anomalous gel permeation chromatography run of pyruvate kinase when using blue dextran as a void volume marker. It was later found that the blue chromophore, CB3GA, was responsible for binding the enzyme thus leading to co-elution of enzyme and blue dextran. As with many critical but unexpected discoveries, the importance and breadth of applications were hardly appreciated in those early days. Since then, CB3GA and other triazinyl dyes have been immobilized on to various supports and used in the affinity purification of many proteins and enzymes.

Development of Dye Ligands and Dye Affinity Adsorbents

The originally exploited dyes were commercial textile chlorotriazine aromatic polysulfonated molecules

which when attached to appropriate supports, usually bearing hydroxyl groups, yield dye affinity adsorbents. The range of shades of commercial dyes derives primarily from anthraquinone, azo and phthalocyanine chromophores bonded to suitable reactive functions such as triazinyl and other mainly polyhalogenated heterocyclics. Anthraquinone dyes produce blue and the phthalocyanines turquoise shades. Green dyes contain mixed anthraquinone–stilbene, anthraquinone–azo or phthalocyanine–azo structures, whereas most other shades are derived from the azo class.

Unlike most biological affinity adsorbents, the stability of dye affinity adsorbents is usually limited only by the support itself. Dyes offer clear advantages over biological ligands, in terms of economy, ease of immobilization, safety, stability and adsorbent capacity. The main drawback of textile dyes is their moderate selectivity during the protein-binding process. In spite of this, the overall size, shape and distribution of ionic and hydrophobic groups enable dyes to interact with the binding sites(s) of proteins sometimes fairly specifically, as for example, with the nucleotide-binding site of several dehydrogenases, kinases, and several nucleotide-recognizing enzymes. The dye–protein interaction should not be compared to a simple ion exchange type since binding is frequently possible at pHs greater than the *pI* of the targeted protein. Furthermore, dissociation of the dye–protein complex is often achieved specifically by competing ligands, suggesting interaction with the protein at discrete sites. The view is supported by chromatographic, kinetic, inactivation, affinity labelling and spectra difference studies.

The last few years have seen a novel approach for tackling the problem of dye selectivity, signalling the

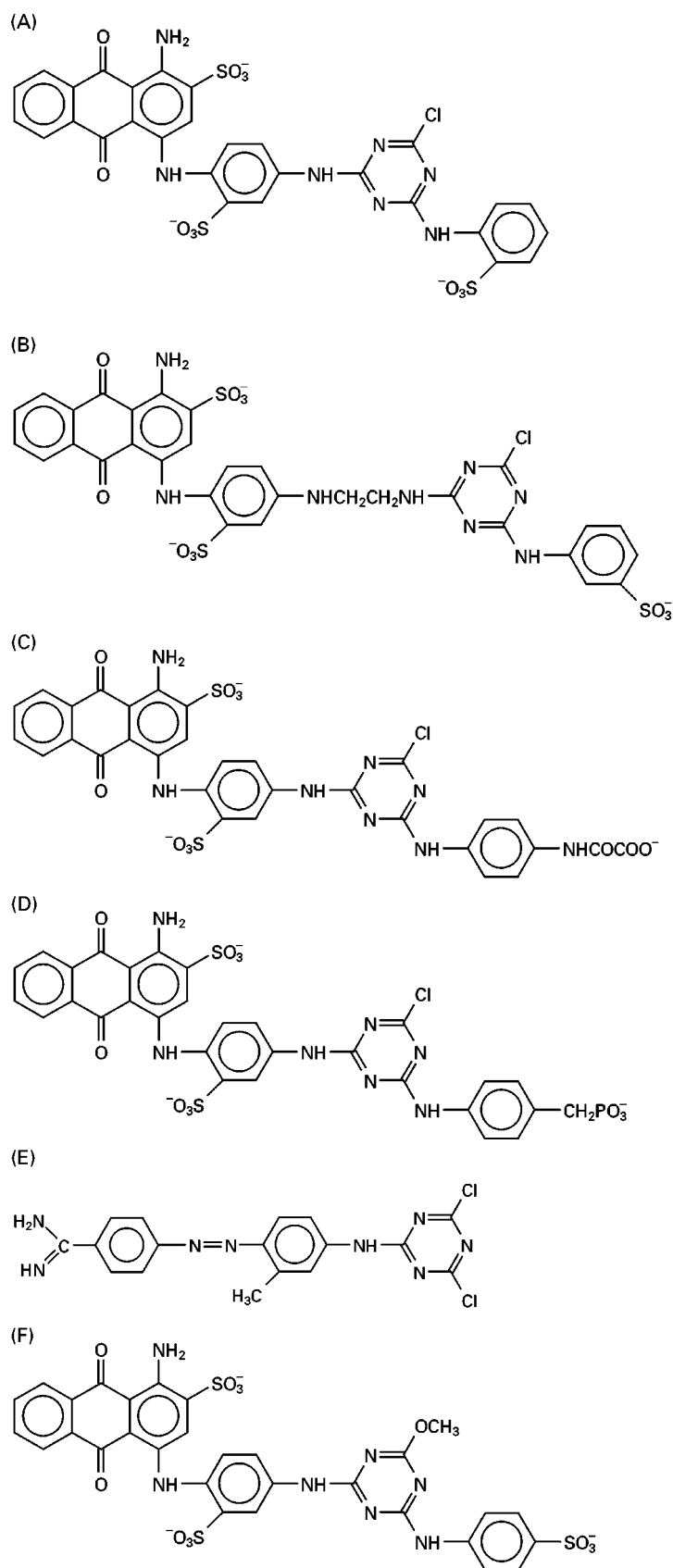


Figure 1 Structures of the parent textile dye Cibacron Blue 3GA (CB3GA), (A) the three blue (B)–(D) and one yellow (E) biomimetic dyes, and the blue dye (F) for selective LDH precipitation.

beginning of a new era in affinity bioseparation. This approach is based on a generation of the so-called biomimetic dyes. By employing molecular modelling techniques, it is possible to redesign the parent dye (e.g. CB3GA) or design *de novo* a new dye in such a way that the resulting biomimetic dye mimics naturally occurring biological ligands, thus displaying increased selectivity for the targeted enzyme. Figure 1 shows the structures of the parent dye CB3GA (A) and four biomimetic dyes (B–E). For the case of the NAD^+ -dependent enzyme alcohol dehydrogenase (ADH), having used molecular modelling to compare the conformations that NAD^+ and CB3GA adopt during binding to the enzyme, it was possible to propose the biomimetic structure of Figure 1(B) that exhibits increased affinity for ADH as compared to CB3GA. Recently a family of anthraquinone biomimetic dyes has been designed specifically for (keto)carboxyl-group-recognizing enzymes. Each member of this dye family is composed of two enzyme-recognition moieties (e.g. Figure 1C). The terminal biomimetic moiety bears a (keto)carboxyl structure linked to the triazine ring, thus mimicking substrates of the targeted enzyme, e.g. L-malate dehydrogenase (MDH). The chromophore anthraquinone moiety remains unchanged and the same as that of the parent dye (Figure 1A), recognizing the nucleotide-binding site of MDH. Members of this dye family show increased affinity for the targeted enzymes and have been designed for other enzymes as well, e.g. L-lactate dehydrogenase (LDH). In the case of the orthophosphate ester hydrolase alkaline phosphatase, a biomimetic dye was designed by substituting the terminal 2-aminobenzene sulfonate of CB3GA for a 4-aminobenzene phosphonate ring (Figure 1D). The corresponding dye adsorbent offers an impressive purification of calf intestinal alkaline phosphatase of over 300-fold in a single chromatography step. The biomimetic structure of Figure 1(E) is a benzamidino-cationic yellow dye designed for a different application. The cationic dye bears a guanidino group, the same as the potent trypsin inhibitor benzamidine. When the dye is immobilized, it is able to separate the two main proteolytic constituents of crude pancreatic extract, trypsin and chymotrypsin, since only the former enzyme is adsorbed. The use of biomimetic dyes is expected to increase and help towards simplifying enzyme purification problems.

Development of the Techniques

Dyes, whether conventional or biomimetic, have been exploited by different affinity bioseparation

techniques for protein and enzyme purification, as described below.

Affinity Chromatography

Reactive chlorotriazinyl dyes are easily and safely immobilized on agarose and other polyhydroxylic supports (e.g. cellulose, polyacrylates) or, less often, on amino-group-bearing supports, after nucleophilic substitution in alkaline environment. Alternatively, a diaminoalkane (e.g. 1,6-diaminohexane) spacer molecule can be chemically attached to the chlorotriazine ring of the dye, before the resulting conjugate is immobilized on various pre-activated polyhydroxylic supports. Although chemical immobilization of reactive dyes on polyhydroxylic supports is the most straightforward and widely used technique, perhaps the most unusual one is immobilization via adsorption. For example, it is possible, first, to chemically attach to the reactive dye a hydrophobic 1H,1H-pentadecafluorooctylamine tail by nucleophilic substitution. Then, the dye–tail conjugate can be physically adsorbed on to hydrophobic fluorocarbon particles. Hydrophobic fluorocarbon supports can be transformed into surface-hydrophilic materials. In this case, hydrophobic perfluorocarbon tails are chemically attached to hydrophilic polyvinylalcohol (PVA). Afterwards, the PVA–tail conjugate is physically adsorbed on to the hydrophobic surface of Teflon® particles. Therefore, the transformed Teflon® surface is hydrophilic and rich in hydroxyl groups through which reactive dyes can be immobilized.

At the end of the immobilization reaction, the coloured adsorbent is washed to remove free dye, packed in a chromatography column, and equilibrated with the appropriate buffer for protein purification. The sample is applied and nonadsorbed proteins are washed off, before the desired protein is desorbed (eluted) by changing the composition of the buffer eluent. This is realized either by non-specific desorption techniques (i.e. change of the ionic strength or pH) or by specific desorption techniques, for example, introducing competing substances (i.e. substrates, inhibitors, metal chelators) in order to selectively perturb the enzyme–dye complex on the column.

In the development of a protein purification protocol, some form of adsorbent screening exercise should be performed as the first step. The adsorbent exhibiting the highest purification factor and recovery for the targeted protein on the one hand, and on the other hand the adsorbent showing no adsorption of the protein of interest but good total protein adsorption, are promising candidates for employment in

positive and negative affinity chromatography, respectively.

Although beaded porous polyhydroxylic supports have been used for decades in biochromatography, rapid mass transfer has only been achieved recently thanks to two novel chromatography supports. The 'flow-through particles', which are exploited in perfusion chromatography, have pores wide enough (0.6–0.8 μm) to allow convective flow through them. Smaller diffusive pores along the throughpore channels of these particles provide a high adsorption area with diffusion path lengths less than 1 μm . These particles reduce process time by improving mass transfer. An alternative for the same purpose is offered by hyperdiffusion chromatography; this uses rigid particles with their entire pore volume filled by a homogeneous flexible soft hydrogel where the affinity ligands are immobilized. The proteins can diffuse freely through the hydrogel network and interact with the ligand.

High Performance Affinity Chromatography

When the support is made of noncompressible, spherical particles of small diameter (e.g. 5–20 μm) and narrow size distribution (e.g. 0.2–2.0 μm) the technique is termed high performance affinity chromatography (HPAC). Silica-based supports have been used with dyes for HPAC, although silica has serious drawbacks: poor chemical stability in an alkaline environment; the need for derivatization with organofunctional silanes prior to dye immobilization; and relatively small pore size. In spite of its problems, silica is still used in HPAC mainly on an analytical scale. Synthetic high performance polyhydroxylic particles probably offer a better alternative to silica for HPAC. The chemistry of support activation and dye immobilization is generally the same as that for softer materials, as described earlier.

A different concept for column packings was introduced by the following two materials: deformed nonporous high performance agarose; and nonporous fibres. The former support consists of 12–15 μm diameter nonporous beads which, when compressed, are claimed to result in superior resolution at high flow rates. The latter support consists of nonporous fibre-form quartz material of mean diameter 0.5 μm . This material has first to be silylated prior to proceeding with ligand immobilization. The above materials are potentially suitable for use with dye ligands.

Centrifugal Affinity Chromatography

Centrifugal affinity chromatography combines the high flow rate, created by centrifugation force, with the specificity of affinity chromatography. It

is an alternative to closed column chromatography (i.e. columns with adapters at their ends minimizing dead volumes) which usually but not always requires elaborate instrumentation. This technique has demonstrated its usefulness in the removal of albumin from human serum using immobilized CB3GA, and in the rapid screening of a large number of immobilized dyes for binding goat IgG.

Heterobifunctional Ligand Affinity Chromatography

The principle of heterobifunctional affinity ligand chromatography requires that a soluble heterobifunctional affinity ligand possessing two different affinity moieties is available. This alone may be a drawback for the technique, when considering factors such as labour and cost. One moiety is destined to interact in solution with the targeted protein for purification, while the second moiety should be able to recognize and bind to a suitable affinity adsorbent. A model system based on this principle has been developed for purifying lactate dehydrogenase (LDH). In this case, the soluble heterobifunctional ligand consisted of the dye CB3GA chemically linked to soya bean trypsin inhibitor, whereas immobilized trypsin is used in an affinity column for binding the soluble complex trypsin inhibitor·CB3GA-LDH.

Continuous Affinity Recycle Extraction

In continuous affinity recycle extraction, instead of packing affinity adsorbent particles in a fixed bed, adsorbent/liquid contact is performed in well-mixed tanks. The adsorbent is continuously circulated between two tanks. Each tank consists of two concentric cylindrical vessels. The wall of the interior vessel is made of a supported filter. The filter porosity is such that it does not allow passage of the adsorbent but only of the liquid stream and its soluble contents, so they can flow through freely. The affinity adsorbent is placed in the space between the concentric cylinders and is continuously recirculated between the two tanks. In one tank there is continuous adsorption of protein to the affinity adsorbent, whereas unbound materials pass through the filter to waste or recycle. In the second tank there is continuous desorption of product from the adsorbent, through the filter, to the collection apparatus. This technique can be applied to dye affinity adsorbents, particularly on a large scale.

Aqueous Two-phase Affinity Partitioning

Affinity partitioning is an inexpensive alternative to affinity chromatography-based purification

technologies, and it is also suitable for large scale application. When aqueous solutions of two high molecular weight polymers, e.g. dextran and polyethylene glycol (PEG), are mixed and then left to settle, depending on the relative molecular mass of the polymers, their concentration and temperature, two phases may be formed: an upper PEG-rich phase and a bottom dextran-rich phase. Under appropriate conditions, many proteins partition to the bottom dextran-rich phase. However, when some of the PEG of the upper phase is replaced by a suitable dye-PEG conjugate, the targeted protein may bind to the dye-PEG conjugate and selectively partition to the upper PEG-rich phase, thus, leading to some purification. An important advantage of affinity partitioning is that the technique can be exploited at the first stage of a purification process, immediately after cell disintegration, without need of centrifugation for prior debris removal. Dye-PEG conjugates have been employed in two-phase affinity systems for partial purification of numerous enzymes, especially those recognizing nucleotides.

Membrane Affinity Filtration

Chemical attachment of the affinity ligand to a filtration membrane provides the principle of the membrane affinity filtration technique. The role of the filter component can be taken by a hollow-fibre microporous membrane where the ligand is chemically attached. The feed stream moves along the interior of the fibre whose pores are large enough (0.5–1.0 μm) to permit convective flow through its body. While binding of the targeted protein to the immobilized ligand occurs without diffusion limitations, unbound substances pass through the fibre body to its outer surface. The main advantage offered by this technique, which is important to industrial-scale purification, is that there is no need for solids removal from the feed stream after cell disintegration. In fact, liquid-solid separation and affinity purification are combined and performed simultaneously when using this technique. Affinity membranes permit rapid processing of large volumes, sometimes even immediately after cell harvesting or disintegration, thus eliminating concentration and partial purification stages. Membrane systems other than hollow fibres have been developed, for example membrane discs and modules of flat membrane sheets bearing immobilized dyes. Such materials are effective tools in protein downstream processing.

Affinity Cross-flow Ultrafiltration

The availability of an affinity macroligand capable of reversible and selective binding of the

targeted protein is essential for applying the technique of affinity cross-flow ultrafiltration. A macroporous membrane is also required which allows passage of the unwanted substances and the targeted protein, but not of the affinity macroligand. When the sample is filtered in the presence of the macroligand, the protein of interest is retained by adsorbing on to the macroligand. During the washing step the targeted protein is desorbed, passes through the membrane and is collected. However, the macroligand will remain retained by the membrane and can therefore be recycled and reconditioned. As with membrane affinity filtration, affinity cross-flow ultrafiltration offers rapid mass transfer, high throughput, and is capable of processing unclarified and viscous materials.

Affinity Precipitation

Affinity precipitation is a bioseparation technique whereby an insoluble network is formed by cross-linking a multifunctional affinity ligand with the protein of interest, thus resulting in selective precipitation of the targeted protein from solution. In principle, such a ligand should be composed of three recognition sites which are able to bind the protein simultaneously. Furthermore, the targeted protein should possess enough ligand-binding sites for the formation of a network. This technique offers certain advantages which are particularly important for large scale purification: no need for solid supports, high ligand utilization, low capital cost, and the possibility of sequential precipitation. True affinity precipitation has been demonstrated for only a few purification cases. An impressive example is the dye structure of **Figure 1(F)**. This nonreactive molecule selectively precipitates and purifies lactate dehydrogenase to homogeneity from crude extract of rabbit muscle. Affinity precipitation has been claimed to occur also with bis-Cibacron Blue 3GA but this technique has not found the anticipated attention.

Instrumentation

Of the techniques described above, dye affinity chromatography and high performance dye affinity chromatography are the main ones employing sophisticated instrumentation. Closed columns (i.e. columns with adapters at both ends) packed with affinity adsorbents can be run and studied with the highest possible precision on automated and computerized chromatography instruments. Such instruments are, for example, the FPLC® System of Pharmacia Biotechnology, and the Waters 650E Advanced

Protein Purification System. Of course, the systems can be used also with nonaffinity chromatography materials. The FPLC® system (pressure limit 4 MPa/580 psi, flow rate range 0.02–8.3 mL min⁻¹) is composed, typically, of a chromatography controller, which offers the facility for connecting to a computer, and controls the rest of the system components: two dual-syringe high precision pumps; a mixing device; an injection motor valve; a sampling loop device to introduce, without dilution, volumes of up to 50 mL; an absorbance detector system with a recorder to monitor column effluents; and a fraction collector with a solenoid valve. Additional motor valves can be used for selecting different liquid phases and columns. The same company also manufactures the BioPilot® system, made especially for exploiting large column beds and processing large sample volumes; it has the similar basic philosophy as the FPLC®. The system offers a flow rate range 0.5–100 mL min⁻¹ at pressures up to 2 MPa/290 psi, and sample volumes up to 150 mL introduced via a loop device. A money-saving alternative to FPLC® offered by Pharmacia Biotechnology, is the GradiFrac™ which incorporates, in a one piece instrument, a fraction collector and a gradient maker. It requires additionally a peristaltic pump, an absorbance monitor, an injection valve, a mixing device, a solenoid valve to form the gradient, and a fraction collector with a solenoid valve. The Waters system is also a nonmetallic liquid chromatograph, operating at flow rate ranges of 0.1–45 mL min⁻¹ or 0.5–80 mL min⁻¹, depending on the pump heads used, having a pressure limit of 750 psi. It is composed of a chromatography and gradient controller which offers the facility for connecting to a computer, a high precision two-head pump, a solenoid four-solvent delivery valve for solvent selection and mixing, a sample injection valve, and an absorbance detector to monitor column effluents. In contrast to the FPLC®, in the 650E system the liquid phase gradient is made at low pressure and prior to entering the pump.

Dye affinity adsorbents based on conventional supports result in low back pressures, when packed in short, wide columns to minimize particle deformation, can be run using peristaltic or other appropriate types of pumps. In contrast, adsorbents composed of small size particles suitable for HPAC (e.g. 5–10 µm) usually need to be run on high pressure instruments, such as those employed in HPLC applications. In this latter case, it is most advisable that titanium pump heads and tubings be used to prevent metal corrosion. However, small size particles with narrow size distribution (e.g. Monobeads®) can be run on

medium pressure instruments (e.g. FPLC® and Waters 650E).

Introduction to Applications

Dyes were originally introduced as cheap alternatives to costly nucleotide ligands for enzyme purification. Given the advantages of dyes over biological ligands, their broad protein-binding spectrum, and also the possibility of improving their selectivity for targeted proteins via molecular modelling, it is no surprise that these colourful tools are finding increasing application in various affinity-based bioseparation techniques. The literature abounds with examples where dye ligands have been employed to purify individual proteins and enzymes: albumin, antibodies, blood-clotting factors, plasminogen activator, proteolytic activities, growth factors, interferons, cellulolytic and lipolytic enzymes, collagenases, restriction endonucleases, and numerous nucleotide-binding proteins and enzymes, to name some examples. It is no exaggeration to claim that for almost every protein purification problem, a dye ligand can be found to help towards its solution.

See also: I/Affinity Separation. II/Affinity Separation: Affinity Membranes; Affinity Partitioning in Aqueous Two-Phase Systems; Rational Design, Synthesis and Evaluation: Affinity Ligands. Membrane Separations: Membrane Bioseparations; Ultrafiltration. III/Enzymes: Liquid Chromatography. Proteins: Capillary Electrophoresis; Centrifugation; Electrophoresis. Pressurised Fluid Extraction: Non-Environmental Applications. Appendix 1/Essential Guides for Isolation/Purification of Enzymes and Proteins; Appendix 2/Essential Guides to Method Development in Affinity Chromatography.

Further Reading

- Clonis YD (1991) Preparative dye-ligand chromatography. In: Hearn MTW (ed.) *HPLC of Proteins, Peptides and Polynucleotides*, pp. 453–468. New York: VCH Publishers.
- Clonis YD, Atkinson A, Bruton CJ and Lowe CR (eds) (1987) *Reactive Dyes in Protein and Enzyme Technology*. Basingstoke: Macmillan.
- Labrou NE and Clonis YD (1994) The affinity technology in downstream processing. *Journal of Biotechnology* 36: 95–119.
- Labrou NE, Eliopoulos E and Clonis YD (1996) Molecular modelling for the design of chimeric biomimetic dye-ligands and their interaction with bovine heart mitochondrial malate dehydrogenase. *Biochemical Journal* 315: 695–703.

- Labrou NE, Eliopoulos E and Clonis YD (1999) Molecular modeling for the design of a Biomimetic chimeric ligand. Application to the purification of bovine heart L-lactate dehydrogenase. *Biotechnology and Bioengineering* 63: 321–331.
- Lowe CR (1984) Applications of reactive dyes in biotechnology. In: Wiseman A (ed.) *Topics in Enzyme and Fermentation Biotechnology*, vol. 9. Chichester: Ellis Horwood.
- Lowe CR, Burton S, Pearson J, Clonis YD and Stead CV (1986) The design and applications of biomimetic dyes in biotechnology. *Journal of Chromatography* 376: 121–130.
- Lowe CR, Burton SJ, Burton NP, Alderton WK, Pitts JM and Thomas JA (1992) Designer dyes: 'biomimetic' ligands for the purification of pharmaceutical proteins by affinity chromatography. *Trends in Biotechnology* 10: 442–448.

Hydrophobic Interaction Chromatography

H. P. Jennissen, Institut für Physiologische Chemie, Universität-GHS-Essen, Essen, Germany

Copyright © 2000 Academic Press

Introduction

According to J.N. Israelachvili (1985), hydrophobic interactions constitute 'the unusually strong attraction between nonpolar molecules and surfaces in water'. For two contacting methane molecules, the attraction energy is about sixfold higher in water than the van der Waals interaction energy in a vacuum. This energy, which has been estimated to be about -8.5 kJ mol^{-1} for two methane molecules is due to the extrusion of ordered water on two adjacent hydrophobic surfaces into less-ordered bulk water with a concomitant increase in entropy. This entropy-driven attraction between nonpolar groups in water is the basis for hydrophobic interaction chromatography.

The chromatographic separation of proteins depends on the differential accumulation of molecules at certain sites within a chromatographic system. Two principal types of chromatographic systems employing hydrophobic media have been described: (a) reversed-phase and (b) hydrophobic interaction chromatography. The principle of reversed-phase chromatography is based on a hydrophobic, e.g., silica, support of very high hydrophobicity which is capable of retaining nonpolar liquid phases (stationary liquid phase) when applied as the less polar phase in a solvent system. In this classical system the solutes are absorbed and separated (partitioned) in the apolar stationary liquid phase (i.e., a three-dimensional system) and not on the solid phase. In hydrophobic interaction chromatography the solutes (proteins) are adsorbed and separated on the apolar stationary solid phase (i.e., a two-dimensional system) carrying

immobilized hydrophobic groups. Because of the very different scopes and methodological details, reversed-phase chromatography will not be treated here. The same holds for other forms of liquid–liquid partition chromatography. A differentiation will also not be made between classical chromatographic systems and HPLC since, in essence, it is only the bead or particle size which leads to the higher performance (e.g. throughput, resolution) in the latter method.

Discovery and Development of Hydrophobic Interaction Chromatography

The chromatographic purification of proteins on specifically synthesized hydrophobic solid supports was first reported independently by Yon and Shaltiel in 1972. In both cases the hydrophobic matrix consisted of agarose to which aminoalkane derivatives have been coupled by the CNBr method. Yon synthesized mixed hydrophobic-charged gels (aminodecyl-, or N-3-carboxypropionyl)aminodecyl-agarose) with an alkyl residue to charge ratio of at least 1 : 1 for the adsorption of lipophilic proteins such as bovine serum albumin or aspartate transcarbamoylase. These proteins were adsorbed at low ionic strength at the isoelectric point and eluted at acidic or alkaline pH by charge repulsion. The surprising result in Shaltiel's experiments was that a very normal hydrophilic enzyme, phosphorylase *b*, could be purified on hydrocarbon-coated agaroses to near homogeneity in one step, implicitly questioning the general doctrine of the time that all hydrophobic amino acids are buried in the interior of proteins. Phosphorylase was adsorbed at low ionic strength on immobilized butyl residues which had no resemblance to the substrates of the enzyme (excluding affinity chromatography) and was eluted by a 'deforming buffer' which imposed a limited conformational change on the enzyme. Taken together with Shaltiel's systematic approach of grading the hydrophobicity of the gels via an immobilized homologous hydrocarbon series, the immediate

impression was that here was a novel method applicable not only to hydrophobic or lipophilic but also to hydrophilic, possibly to all proteins. The name 'hydrophobic chromatography' coined by Shaltiel therefore soon came to widespread use. Only a few months after Shaltiel's first paper, B.H.J. Hofstee published a series of papers leading to similar results.

As stated above, all of these hydrophobic gels were synthesized by the simple CNBr method. Some criticism however arose that positive charges, introduced by a side reaction into the matrix by the CNBr procedure, were influencing the chromatographic results on hydrocarbon-coated agaroses. A rational approach and solution to this problem proved difficult since the chemical mechanism of the CNBr coupling reaction was conclusively clarified only some time later by M. Wilchek in 1981. Wilchek found that the number of charges introduced into the matrix depended on the pH of the washing solution and the length of the washing procedure after CNBr activation of the agarose, since intermediate cyanate esters were selectively hydrolysed in alkali in contrast to the imidocarbonates which were hydrolysed in acid. Thus pure charged isourea gels, pure uncharged imidocarbonate/carbamate gels or mixed ionic-hydrophobic gels can be obtained by the CNBr procedure. In a later paper, Shaltiel conclusively showed that under his conditions the influence of charges in his hydrocarbon-coated agaroses had been small. In addition it was shown by various other groups that salts also effectively quenched the charges introduced by the CNBr method.

Fully uncharged hydrophobic gels were therefore synthesized in 1973 by Porath's group who reacted benzyl chloride with agarose at high temperatures. The synthesis of a graded homologous series of hydrocarbon-coated agaroses was however not possible by this method. In addition Porath demonstrated the inverse salt behaviour of proteins adsorbed on such gels. In contrast to ion exchangers, proteins were applied to these gels at *high salt concentrations* and eluted by decreasing the ionic strength (negative salt gradients). Interestingly the protein cytochrome *c* was adsorbed when 1–3 M NaCl was included in the buffer, a salt which in itself had very little salting-out potential. A similar salt behaviour of protein binding on hydrophobic gels synthesized by the CNBr procedure was reported later by Hjerten who demonstrated that Shaltiel-type gels showed similar properties as the Porath-type gels. Hjerten also suggested the term 'hydrophobic interaction chromatography' which is now popularly accepted. In 1974 Hjerten described a novel preparation of uncharged hydrophobic gels of broad potential by

coupling alkyl and aryl groups via the glycidyl ether method.

In retrospect, although there is no doubt that fully uncharged hydrophobic gels are, by virtue of displaying a single (pure) type of noncovalent interaction, superior to the CNBr-prepared gels, it appears that all groups involved in the development of hydrophobic (interaction) chromatography observed the binding and fractionation of proteins by predominantly hydrophobic interactions. Both terms, 'hydrophobic chromatography' and 'hydrophobic interaction chromatography' can be used synonymously, the shorter term 'hydrophobic chromatography' being no more a misnomer than 'affinity chromatography'.

Fundamentals of Hydrophobic Interaction Chromatography

The Chain Length Parameter

A general systematic approach to the purification of proteins via hydrophobic interactions was initiated by Shaltiel who introduced the principle of variation of the immobilized alkyl chain length in the form of the homologous series of hydrocarbon-coated agaroses (Seph-C_{*n*}, *n* = 1–10). The major conclusion of his experimental result was that an increase of the chain length by –CH₂– units concomitantly increased the strength of protein binding from retardation to reversible binding up to very tight binding ('irreversible' binding). In addition to this variation in binding affinity with the chain length, the gels also changed their specificity towards the adsorbed protein. Thus it was suggested that the properties of hydrophobic agaroses for protein purification could be optimized by variation of the immobilized alkyl chain length.

The Surface Concentration of Parameter

Critical surface concentration of immobilized residues In 1975 we showed that a second parameter is of equal if not greater importance than the alkyl chain length. If, instead of the chain-length, the density (surface concentration) of immobilized alkyl groups is varied, protein adsorption is a sigmoidal function of the surface concentration of immobilized alkyl residues (**Figure 1**) (i.e., surface concentration series). Here also the strength of binding increased from retardation to very tight binding as in the homologous series of Shaltiel. Figure 1 also illustrates the effect of chain elongation in a homologous series which leads to a leftward shift of the sigmoidal curves and to a loss of sigmoidal shape. Another important finding was that a threshold value of the alkyl surface

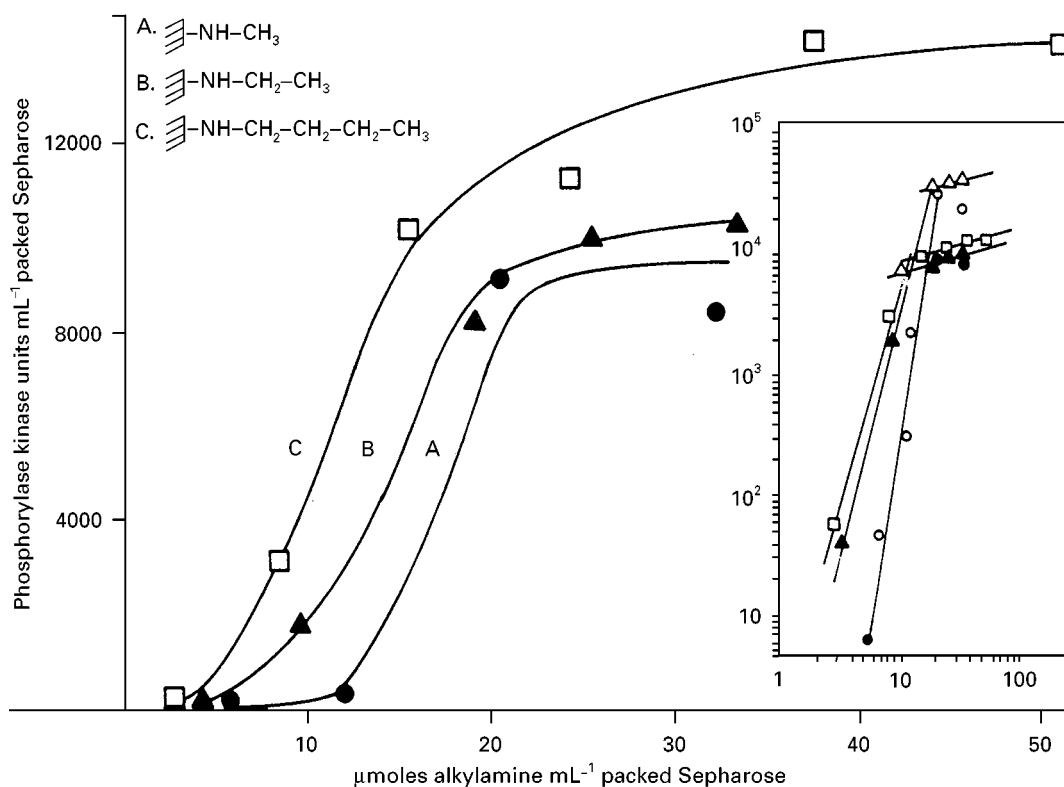


Figure 1 Dependence of the adsorption of phosphorylase kinase on the chain-length and surface concentration parameters of a homologous series of alkyl-Sepharoses at low ionic strength. The amount of adsorbed enzyme activity per mL packed Sepharose was calculated from the difference between the total amount of applied units and the amount excluded from the gel. The crude rabbit muscle extract or purified phosphorylase kinase was applied to columns containing ca. 10 mL packed gel. The alkyl agaroses were synthesized by the CNBr method. The ratio of alkyl residues to positive charges was ca. 10 : 1. Inset: Double logarithmic plots of adsorbed phosphorylase kinase as a function of the degree of substitution. Experiments with purified phosphorylase kinase are included. A, Seph-C₁: (●) crude extract; (○) purified phosphorylase kinase. B, Seph-C₂: (▲) crude extract; (△) purified phosphorylase kinase; C, Seph-C₄: (□) crude extract. For further details see the text and Jennissen HP and Heilmeyer Jr LMG (1975) General aspects of hydrophobic chromatography. Adsorption and elution characteristics of some skeletal muscle enzymes. *Biochemistry* 14: 754–760.

concentration, a 'critical hydrophobicity', had to be reached before a protein adsorbed. With a ratio of alkyl residues to positive charges in the gels of about 10 : 1, the predominance of hydrophobic interactions as the basis for adsorption was strongly indicated. Thus sigmoidal adsorption curves and critical hydrophobicities could also be obtained in the presence of high salt concentrations (see Figure 2) excluding the argument that the sigmoidal shape was due to the action of charges. Finally, the same sigmoidal behaviour of protein adsorption was found on uncharged hydrophobic gels at low ionic strength and an example will be shown in this article.

Cooperative interaction of multiple immobilized residues with the protein A straightforward interpretation of the sigmoidal curves (Figures 1 and 2) was provided by the concept of multivalence and cooperativity of protein adsorption. It became clear

that the sigmoidicity and the 'critical hydrophobicity' were due to the multivalence of the interaction (i.e., the necessity for a simultaneous interaction of more than one alkyl residue with the protein moiety). The term 'multivalence' is to be preferred to other terms such as 'multiple contacts' since the latter does not differentiate between the binding of a protein to separate alkyl residues or to different segments of one and the same alkyl residue. At high salt concentrations, protein binding displays a positive temperature coefficient in agreement with hydrophobic interactions (see Figure 2). A mathematical model of cooperative protein binding to an immobilized alkyl residue lattice was also developed allowing an estimation of the minimum number of alkyl residues (see Figure 2B) interacting with the protein. The model of multivalence was confirmed by equilibrium binding studies of phosphorylase *b* with alkylamines at high salt concentrations.

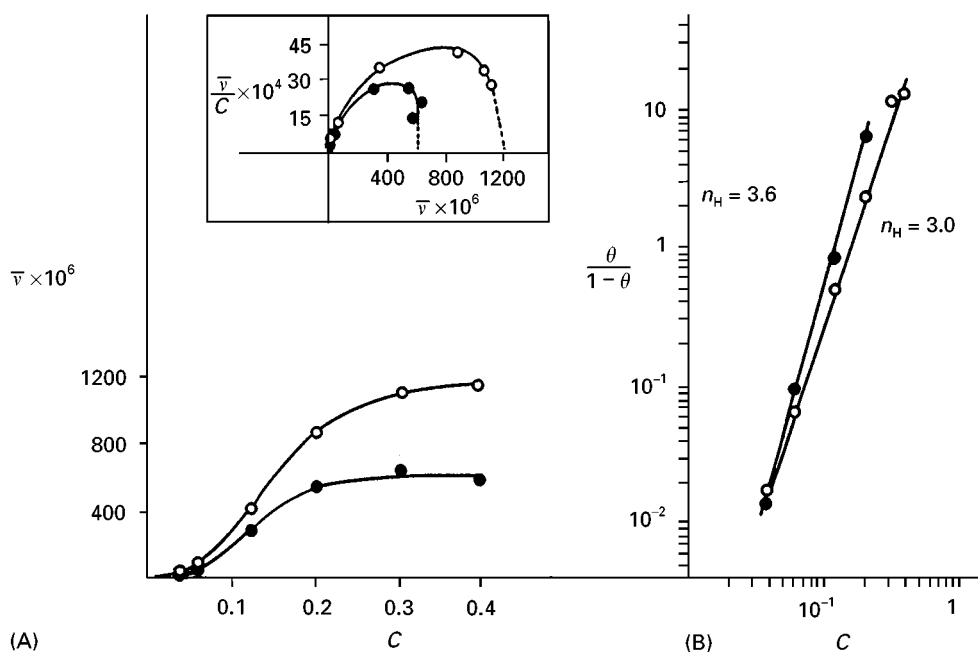


Figure 2 Dependence of the adsorption of phosphorylase *b* on the surface concentration parameter of Seph-C₄ at 5°C and 34°C at high ionic strength. The adsorbed amount of phosphorylase in the presence of 1.1 M ammonium sulfate was calculated from adsorption isotherms measured at each point at an apparent equilibrium concentration of free bulk protein of 0.07 mg mL⁻¹. The adsorbed amount of enzyme (\bar{v}) is expressed in relation to the anhydrodisaccharide content of agarose in mol⁻¹ anhydrodisaccharide. Similarly C indicates the immobilized butyl residue concentration in relation to the anhydrodisaccharide content of agarose in moles of alkyl residue per mole of anhydrodisaccharide. A monomer molecular mass of 10⁵ was employed for phosphorylase *b*. The alkyl agaroses were synthesized by the CNBr method. (A) Adsorption isotherms ('lattice site binding function') of phosphorylase *b* in Cartesian coordinates. Inset: Scatchard plots of the sigmoidal binding curves with extrapolation of fractional saturation of 610 (5°C) and 1220 (34°C) μ moles enzyme per mole of anhydrodisaccharide (corresponding to 6.2 and 13.4 mg mL⁻¹ packed gel respectively). The broken lines indicate the mode of extrapolation. (●) 5°C; (○) 34°C. (B) Hill plots of the sigmoidal binding curves. θ the fractional saturation was calculated from the extrapolated saturation values of the Scatchard plot (A). The Hill coefficients n_H are given in the graph. The apparent dissociation constants of half-maximal saturation ($K'_{D,0.5}$) are 0.137 and 0.167 mole butyl residue per mole of anhydrodisaccharide at 5°C and 34°C respectively (which corresponds to 14.0 and 17.0 μ mole butyl residues per ml packed gel, respectively). (●) 5°C; (○) 34°C. For further details see the text and for the source see Jennissen HP (2000) *Hydrophobic (interaction) chromatography*. In: Vijayalakshmi MA (ed.). *Theory and Practice of Biochromatography*. Amsterdam: Harwood Academic Publishers.

Adsorption hysteresis An important consequence of cooperative multivalent protein binding on alkyl-substituted surfaces is protein adsorption hysteresis. Protein adsorption hysteresis implies that the adsorption isotherm is not retraced by the desorption isotherm, due to an increase in binding affinity after the protein is adsorbed. The binding affinity increase can be attributed to an increase in the number of interactions (multivalence) which can either be due to a reorientation of the protein on the surface or to a conformational change in which buried hydrophobic contact sites (valences) are exposed due to the surface binding strain on the adsorbed protein. Adsorption hysteresis provides evidence for the concept that protein adsorption to multivalent surfaces in general is thermodynamically irreversible ($\Delta_r S > 0$) and that a true equilibrium has not been reached. Another conclusion from this concept is that protein adsorption in hysteretic systems is, moreover, not thermodynamically but kinetically controlled. Thus

adsorption hysteresis has a strong influence on hydrophobic interaction chromatography by leading to nonlinearity and skewed elution peaks in zonal chromatography and to 'irreversibility' in adsorption chromatography. Hysteresis can, however, be easily reduced by decreasing the surface concentration of immobilized alkyl residues.

The Salt Parameter

Salting-out and salting-in on hydrophobically substituted hydrophilic gels The enhancement of hydrophobic interactions by high salt concentrations was first shown by Porath on uncharged benzyl ether agarose and termed a 'salting-out phenomenon'. Trypsin inhibitor could be purified 25-fold after being adsorbed at 3 M NaCl followed by elution in buffer without salt. Proof as to the mechanism and principle underlying these salt effects came in simultaneous, independent reports that the effect of

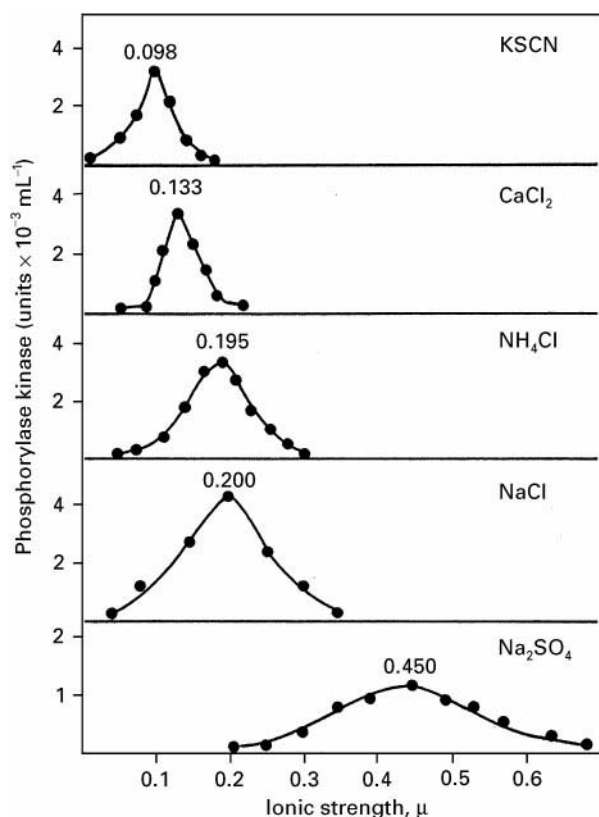


Figure 3 Influence of the salt parameter on the desorption (salting-in) of purified phosphorylase kinase from Seph-C₂ (25 $\mu\text{mol mL}^{-1}$ packed gel) with salt gradients of different ionic composition. Each column with 5 mL of the above gel (CNBr method) was loaded with ca. 11 mg of the enzyme. The gradients were produced from 100 mL low ionic strength adsorption buffer and 100 mL salt containing buffer. The number at the maximum of the elution profiles indicates the ionic strength of the peak fraction. For further details see the text and for the source see Jennissen HP and Heilmeyer Jr LMG (1975) General aspects of hydrophobic chromatography. Adsorption and elution characteristics of some skeletal muscle enzymes. *Biochemistry* 14: 754–760.

salts on the adsorption and elution of proteins on alkyl agaroses indeed followed the Hofmeister series of salts. It could be shown that phosphorylase kinase was eluted ('salted-in') from a Seph-C₂-column by increasing salt gradients. The ionic strength of the peak fractions eluted, was inversely related to the salting-in power of the anions in the gradient in agreement with the Hofmeister series of salts (see **Figure 3**). Similarly proteins could also be eluted (salted-in) from uncharged octyl-Sepharose by an increasing salt gradient of MgCl_2 as shown by Raymond. The opposite effect, namely, the salting-out of phosphorylase *b* by ammonium sulfate on a Seph-C₁-column is shown in **Figure 4B**. The salted-out, i.e. adsorbed enzyme is eluted by omission of this salt from the buffer. Finally Pahlman showed that the salting-out power of anions, for the adsorp-

tion of human serum albumin (HSA) on uncharged Seph-C₅, also followed the order of the Hofmeister series of salts. All of these experiments clearly indicate that the action of the ions was not due to an electrostatic but to a lyotropic effect.

Theories of salt effects One of the earliest approaches to a theory of salt effects was based on the action of chaotropic ions on the solubility of proteins. The general conclusion of this work, with consideration of electrostatic and dispersion forces, was that chaotropes interacted indirectly with solutes (e.g. proteins) mainly through their effect on

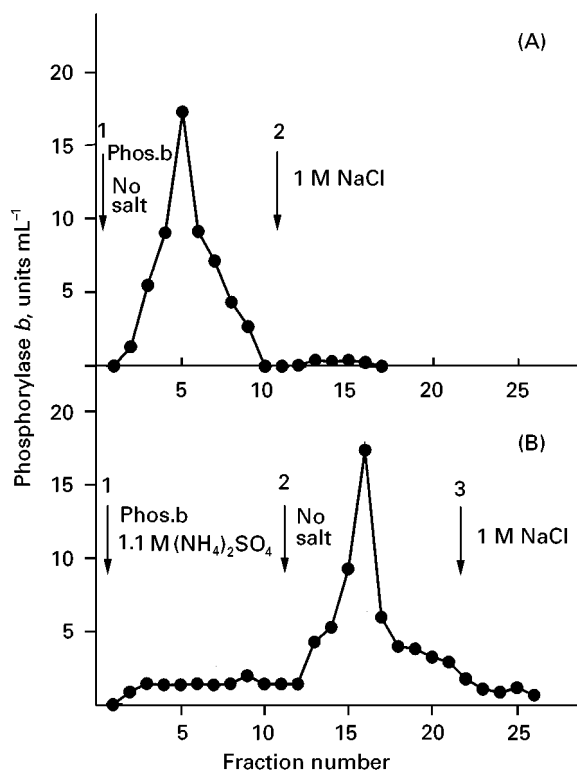


Figure 4 Influence of the salt parameter on the adsorption (salting-out) of purified phosphorylase *b* on Seph-C₁ (30 $\mu\text{mol mL}^{-1}$ packed gel). The equilibration buffer contained 10 mM sodium β -glycerophosphate, 20 mM mercaptoethanol, 2 mM EDTA, 20% sucrose, 0.5 μM PMSF, pH 7.0 (buffer B) to which either 1.1 M ammonium sulfate or NaCl was added. 6 mg per 3 mL phosphorylase *b* was added to 20 mL Seph-C₁ in a 2 cm i.d. \times 17 cm column. Fractions of 6.5 mL were collected. The gel was prepared by the CNBr procedure. (A) Application of enzyme to a column equilibrated with buffer without $(\text{NH}_4)_2\text{SO}_4$ or NaCl: (1) application of phosphorylase *b* in buffer B; (2) elution with buffer B + 1 M NaCl. (B) Application of enzyme to a column equilibrated with buffer with $(\text{NH}_4)_2\text{SO}_4$: (1) application of phosphorylase *b* in buffer B + 1.1 M ammonium sulfate; (2) elution with buffer B; (3) elution with buffer B + NaCl. For further details see the text and for the source see Jennissen HP (2000) Hydrophobic (interaction) chromatography. In: Vijayalakshmi MA (ed.). *Theory and Practice of Biochromatography*. Amsterdam: Harwood Academic Publishers.

water structure. In the solvophobic approach of Horváth the surface tension of water was also of central importance. The energy necessary for bringing a solute into solution was equated with the energy needed for forming a corresponding cavity in water against the surface tension with a reduction in free volume. The net free energy involved in the association of two molecules was thus related to a reduction of the cavity size. Salting-in and salting-out were explained on the basis of the respective surface tension-decreasing/-increasing effect of the salt which was applicable to reversed-phase chromatography as well as to hydrophobic interaction chromatography. Finally, according to Arakawa (1984, 1991) there also do appear to be specific salt effects resulting from a direct binding of salt ions (e.g. of MgCl_2) to the protein.

Irrespective of the mechanism, the applicability of the Hofmeister (lyotropic) series of salts expanded by the chaotropic series, to hydrophobic interaction chromatography has been verified by many groups and these salts are important tools in controlling the adsorption and elution of proteins on these resins. The individuality of each protein in its quantitative interactions in such a system especially when in the native state should, however, not be underestimated.

Optimization of Hydrophobic Chromatographic Systems

Twenty years after the introduction of hydrophobic interaction chromatography, the method has not gained the same foothold in the methodological repertoire of protein chemistry as has affinity chromatography. Although a large number of proteins have been successfully purified by this method a recent paper by Oscarsson *et al.* comes to the conclusion that certain 'classical' commercial hydrophobic adsorbents are inadequate for ideal downstream processing because of their high hydrophobicity. The criticism of these authors is essentially correct. The major problem encountered on such hydrophobic gels is that proteins can be very effectively adsorbed but elution in the native state is often impossible. Although a similar problem can be encountered in affinity chromatography, it appears to be the major handicap in hydrophobic interaction chromatography and must be taken into account in any general optimization procedure.

The Homologous Series Method

Shaltiel's homologous series method of synthesizing hydrocarbon-coated agaroses was supplemented by

the so-called exploratory kit, for choosing the most appropriate column and for optimizing resolution. This analytical kit, which was commercially available for some years, contained a homologous series of small columns from Seph-C₁ to Seph-C₁₀ with two control columns. The principle was to determine the lowest member of the homologous series capable of retaining the desired enzyme or protein. This column was then selected for the purification of the desired protein. In a second step it was attempted to increase resolution by optimizing the elution procedure which ranged from mild salting-in procedures to reversible denaturation steps. This procedure or variants thereof are still the method of choice for most groups. However as illustrated by Oscarsson *et al.*, the number of failures is probably very high.

The Critical-Hydrophobicity Method

As stated above there are two methods for the synthesis of controlled hydrophobicity gels (a) via the homologous series of hydrocarbon-coated Sepharoses (variation of alkyl chain length) or (b) via the concentration series (variation of the alkyl surface concentration). The importance of the latter series has been underestimated. Both gel series essentially correspond to members of 'hydrophobicity gradients'. Although the decisive importance of the immobilized alkyl residue concentration for the hydrophobic adsorption of proteins (critical hydrophobicity) has been stressed for many years, no hydrophobicity gradient gel series has ever been produced commercially. Against the background of obvious problems in hydrophobic interaction chromatography, a novel rational basis for the optimization and design of such chromatographic systems has been suggested.

High yields in hydrophobic interaction chromatography can only be obtained if the protein to be purified is fully excluded from the gel under elution conditions as near as possible to physiological conditions, i.e., at low ionic strength. This means that the gel should be fully non-adsorbing under these conditions. On the other hand, since a purification is only possible if the protein is adsorbed to the gel, the matrix should be constructed in a way that adsorption can be easily induced by other means without denaturing the protein. Thus working at, or near to the critical hydrophobicity point, could solve both problems. In the synthesis of such critical-hydrophobicity gels the charge-free immobilized residues should be restricted to alkane derivatives, to ensure a 'purity' of hydrophobic interactions. NaCl, centrally located in the Hofmeister series, appears to be ideal. The procedure involves three steps: (i) selection

of an appropriate alkyl chain length, (ii) determination of the critical surface concentration of alkyl residues (critical hydrophobicity), and (iii) determination of the minimal salt concentration (NaCl) necessary for the complete adsorption of the protein. The three parameters are determined by a form of quantitative hydrophobic interaction chromatography utilizing primarily the high-affinity adsorption sites.

Selection of the appropriate alkyl chain length In the first step, an experimental setup similar to the homologous series method of Shaltiel is employed to gain information on the general hydrophobic binding properties of the protein and columns. However it is essential that a quantification of the immobilized surface concentration has taken place at this stage. Gels of $20\text{--}25\ \mu\text{mol mL}^{-1}$ packed gel appear optimal. In general a constant amount of protein (ca. $0.5\ \text{mg mL}^{-1}$ packed gel, which can be 100% adsorbed on the column of highest hydrophobicity) is applied at low or physiological salt concentration to each column (1–2 mL packed gel). One then determines the gel in the homologous series which adsorbs ca. 50% of the applied protein. In the case of the example below, ca. 50% of the applied fibrinogen was adsorbed on an uncharged Seph-C₅ gel containing $22\ \mu\text{mol mL}^{-1}$ packed gel.

Determination of the critical hydrophobicity As previously defined, the critical hydrophobicity is that degree of substitution at which adsorption of a protein begins. As shown in Figure 5 a strongly sigmoidal adsorption curve of fibrinogen is obtained on the concentration series of uncharged Seph-C₅ gels at a physiological NaCl concentration. The aim is to get as close as possible to the critical hydrophobicity point with a minimum of adsorbed protein. Since there was no measurable adsorption of fibrinogen at $12\ \mu\text{mol mL}^{-1}$ packed gel and only ca. 2% was adsorbed at $13.6\ \mu\text{mol mL}^{-1}$ packed gel (critical hydrophobicity), the ideal juxtacritical hydrophobicity range for fibrinogen was taken as $12\text{--}14\ \mu\text{mol mL}^{-1}$ packed gel.

Determination of the minimal salt concentration (NaCl) necessary for adsorption In experiments with NaCl concentrations between 0.5 and 5 M, it was found that all of the applied purified fibrinogen was adsorbed on Seph-C₅ of a residue surface concentration of $13.6\ \mu\text{mol mL}^{-1}$ packed gel at a salt concentration of 1.5–1.6 M NaCl. The salt concentration necessary for half-maximal adsorption was ca. 0.75 M NaCl. Since no (i.e., 2%) fibrinogen was

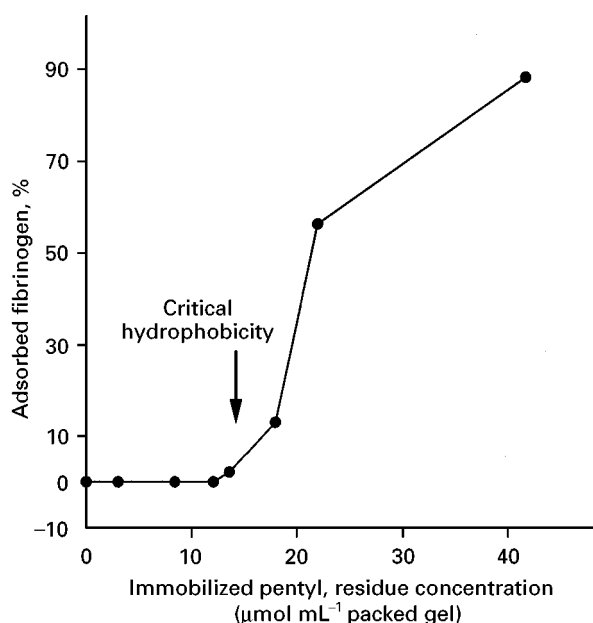


Figure 5 Determination of the critical surface concentration (critical hydrophobicity) of Seph-C₅ for the adsorption of purified fibrinogen. The uncharged pentyl agaroses were synthesized by the carbonyldiimidazole method. Purified human fibrinogen (1 mg) was applied in 1 mL to a column (0.9 cm i.d. \times 12 cm) containing 2 mL packed gel in 50 mM Tris/HCl, 150 mM NaCl, 1 mM EGTA, pH 7.4. Fractions of 1.5 mL were collected. The column was washed with 15 mL buffer followed by elution either with 7.5 M urea or, at high hydrophobicity of the gel, with 1% SDS for the determination of the amount of protein bound. 100% equals 1 mg fibrinogen adsorbed to 2 mL packed gel of Seph-C₅. The total amount of adsorbed fibrinogen, corrected for the amount adsorbed to unsubstituted control Sepharose 4B, is shown. For further details see the text and for the source see Jennissen HP (2000) Hydrophobic (interaction) chromatography. In: Vijayalakshmi MA (ed.). *Theory and Practice of Biochromatography*. Amsterdam: Harwood Academic Publishers.

adsorbed to this pentyl Sepharose at low ionic strength, a complete recovery of fibrinogen adsorbed under these conditions is now possible by decreasing the salt concentration. Thus the critical hydrophobicity gel together with NaCl constitutes a fully reversible hydrophobic adsorption system for fibrinogen.

One-step purification of native fibrinogen from human blood plasma Employing Seph-C₅ of critical hydrophobicity equilibrated with 1.5 M NaCl it is possible to purify fibrinogen from human plasma in a single step (Figure 6). The procedure is so robust that fibrinogen can be purified from human blood plasma directly (no dialysis) in spite of a temporary decrease in NaCl concentration (fractions 5–9) during the run. After extensive washing with 1.5 M NaCl ca. 20-fold purified pure fibrinogen

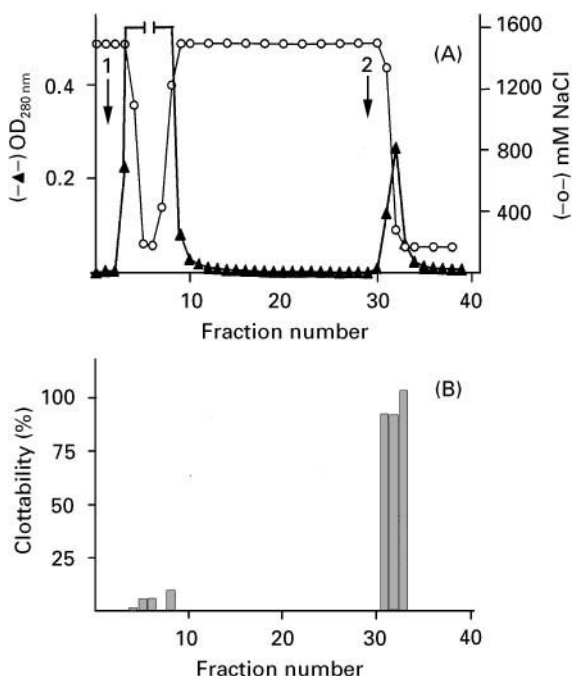


Figure 6 One-step purification of fibrinogen from human blood plasma by hydrophobic interaction chromatography at the critical hydrophobicity point of Seph-C₅. (A) 19 mL fresh unclotted human blood plasma was applied (arrow 1) to 20 mL packed Seph-C₅ (13.6 $\mu\text{mol mL}^{-1}$ packed gel in a column 1.4 cm i.d. \times 13 cm) equilibrated with 50 mM Tris/HCl, 1.5 M NaCl, pH 7.4 at a flow rate of 70 mL h⁻¹ and a fraction volume of 6 mL. The nonadsorbed protein was washed out with 200 mL equilibration buffer. Elution (arrow 2) was facilitated by equilibration buffer containing a tenfold lower salt concentration of 150 mM NaCl. (B) The fractions 30–32 contain pure fibrinogen with a clottability of 93–100% with a total yield of 25%. For further details see the text and legend to Figure 5 and for the source see Jennissen HP (2000) Hydrophobic (interaction) chromatography. In: Vijayalakshmi MA (ed.). *Theory and Practice of Biochromatography*. Amsterdam: Harwood Academic Publishers.

(clottability 93–99%; Figure 5) is eluted by a negative step gradient from 1.5 to 0.15 M NaCl. The total yield is 25% with some loss in the run-through. Yields of fibrinogen of up to 60% have been obtained. If blood plasma equilibrated with 1.5 M NaCl is applied to the gel and eluted by a negative salt gradient, a clottability of 80% is obtained (Figure 6).

Conclusions

From the foregoing it can be concluded that hydrophobic interaction chromatography is one of the very basic separation methods in classical biochemistry. A great deal of information on the mechanisms involved in the method has been obtained and it appears that the critical hydrophobicity method

for the optimization of hydrophobic supports offers a rational approach to the purification of proteins. The only drawback is that such hydrophobic gel series are not commercially available so that the application of this method necessitates experience in the synthesis of alkyl agaroses and the quantification of immobilized residues. Methodological investments of this types thus pose the 'high-energy barrier' to a more widespread and successful application of hydrophobic interaction chromatography in enzymology and protein chemistry.

See also: I/Affinity Separation. III/Affinity Separation: Liquid Chromatography. **Glycoproteins:** Liquid Chromatography. **pH-Zone Refining Countercurrent Chromatography:** High Speed Countercurrent Chromatography. **Polymers:** Field Flow Fractionation. **Appendix 1/Essential Guides for Isolation/Purification of Enzymes and Proteins.**

Further Reading

- Hanstein WG (1979) Chaotropic ions and their interactions with proteins. *Journal of Solid-Phase Biochemistry* 4: 189–206.
- Hjerten S (1981) Hydrophobic interaction chromatography of proteins, nucleic acids, viruses, and cells on noncharged amphiphilic gels. *Methods of Biochemical Analyses* 27: 89–108.
- Jennissen HP and Heilmeyer Jr LMG (1975) General aspects of hydrophobic chromatography. Adsorption and elution characteristics of some skeletal muscle enzymes. *Biochemistry* 14: 754–760.
- Jennissen HP (1988) General aspects of protein adsorption. *Makromolecular Chemistry, Macromolecular Symposia* 17: 111–134.
- Jennissen HP (2000) Hydrophobic (interaction) chromatography. In: Vijayalakshmi MA (ed.). *Theory and Practice of Biochromatography*. Amsterdam: Harwood Academic Publishers. In press.
- Oscarsson S, Angulo-Tatis D, Chaga G and Porath J (1995) Amphiphilic agarose-based adsorbents for chromatography. Comparative study of adsorption capacities and desorption efficiencies. *Journal of Chromatography A* 689: 3–12.
- Porath J, Sundberg L, Fornstedt N and Olsson I. (1973) Salting-out in amphiphilic gels as a new approach to hydrophobic adsorption. *Nature* 245: 465–466.
- Shaltiel S (1974) Hydrophobic chromatography. *Methods in Enzymology* 34: 126–140.
- Shaltiel S (1984) Hydrophobic chromatography. *Methods in Enzymology* 104: 69–96.
- Yon RJ (1977) Recent developments in protein chromatography involving hydrophobic interactions. *International Journal of Biochemistry* 9: 373–379.

Immobilized Boronates/Lectins

W. H. Scouten, Utah State University,
Logan, UT, USA

Copyright © 2000 Academic Press

Lectins and boronates have affinity for very similar biological compounds. They are both useful for separating glycoproteins, glycolipids, and other glycosylated compounds as well as for the separation of sugars and, in the case of boronates, other compounds containing appropriate 1,2 or 1,3 diols. There is, however, a fundamental difference between lectins and boronates. Lectins bind to glycosylated molecules because of a natural biological interaction between the lectin and the sugar moiety of the glycosylated compound. Lectins have biological purposes and functions related to this sugar-lectin interaction. On the other hand, boronates have no biological function but serve as a compound which, by chemi-selection, binds to 1,2 or 1,3 vicinal, co-planar, diols. Since many sugars contain such diols, boronates are very useful functioning as a 'chemical lection'. However, lectins have a much higher degree of binding specificity, as would be expected from the fact that biological interactions depend on multiple binding sites and intricate interactions with complex stereochemistry. Thus, any given lectin may bind to a specific sugar; or in other cases, may bind to an array of sugars. Thus, there exists a broad repertoire of lectins that are capable of binding to various types of glycosylated biomolecules. Fortunately, a sufficient number of lectins are available commercially to provide essentially the entire array of binding sites and, certainly, that array which is needed for biological separations of glycosylated biomolecules.

The corollary to this is that while boronates have a fairly low degree of specificity, they have a much higher stability than lectins. Thus an immobilized boronate, such as a boronate chromatography matrix, can be stored for years, whereas a lectin may have limited storage and operational stability.

Finally, in lectin affinity chromatography it should be understood that lectins are purified by affinity chromatography on a variety of immobilized sugars. Such 'reverse' lectin chromatography is beyond the scope of this discussion but does provide a methodology for identifying and isolating lectins that have a unique specificity for a particular rare combination of one or more sugar molecules.

Applications

None of these can be considered *the* application for lectin or boronated chromatography. By far the largest application of both is in the separation of glycosylated haemoglobin from non-glycosylated haemoglobin for diagnosis of diabetes (see below).

Other diagnostic applications for both lectins and boronates have been proposed. In particular, lectins have been used to bind proteins associated with specific forms of cancer. These have the potential to be developed into useful diagnostic procedures.

In addition, both lectins and boronates have the potential to be used in large-scale purification of various glycosylated proteins and other glycosylated biomolecules for commercial purposes. Since most extracellular mammalian proteins are glycosylated, and since many of these have useful commercial value, boronate chromatography is likely to develop into a significant tool for commercial purification.

Basic research also utilizes affinity chromatography based on lectins and boronates. Lectins are far more commonly utilized when the goal is to identify different glycosylated isoforms of particular proteins or to determine which oligosaccharides are present on the surface of the cells and organelles. Utilizing successive chromatography with a bank of lectins of various specificities, coupled with glycosylases with distinct and varied specificities, the entire sequential composition of oligosaccharides can be readily determined.

Other uses, of course, exist for lectin and boronate chromatography; for example, the purification of specific organelles or cells utilizing the sugar moieties of glycosylated proteins forming the membrane surface of the organelle and/or cell.

Problems or Pitfalls

There are numerous difficulties with any type of chromatography. Perhaps the foremost is the expectation from a method containing the word 'specific' that one will obtain a highly purified material in a single chromatographic step. Occasionally this can be true, but far more commonly either lectin or boronate chromatography is just one of several steps needed to obtain a reasonably pure product. The true advantage of these two chromatographic methods, however, is that they complement standard chromatographic methods such as ion exchange, gel permeation and hydrophobic chromatography.

Among the other problems associated with boronate and affinity chromatography is that the binding of molecules to a particular lectin or boronate can only be determined by trial and error. This calls for a fairly large pilot study which employs various lectins and/or boronate derivatives bound to various matrices and at several ligand concentrations. Without this information, it is difficult to optimize the separation; nevertheless, simple separations are sometimes done by taking a commercial immobilized lectin off the shelf and attempting a full chromatographic separation. In most cases, this is done with a concanavilin A stationary phase, since Con A is relatively inexpensive, fairly stable, and has a broad specificity for a number of saccharide moieties. Thus it has a high probability of effecting a reasonable separation of glycosylated molecules from nonglycosylated molecules or from molecules which are glycosylated in significantly different ways. Con A has a primary binding to glucose or mannose moieties which are, fortunately, very common terminal sugars in glycosylated proteins.

An additional problem found in affinity chromatography is nonspecific binding. Both the lectin itself and the alkyl portion of the boronate can be the source of nonspecific binding.

One final problem with lectin chromatography is the high toxicity of some lectins. The reader should be warned that some lectins are highly toxic and must be handled with extreme caution, although others have little or no toxicity.

Applications of Boronate Chromatography

The interaction of boronate with low molecular weight compounds has been known since the mid-nineteenth century when it was first observed by Biot. Since then this interaction has been employed for the separation of many biologically important vicinal diols, particularly monosaccharides, polysaccharides and various glycosylated macromolecules. The earliest applications involved the separations of various sugars. Boronate forms a charged complex with a sugar diol and, occasionally, a bridge compound in which two sugar molecules are bridged by a single boronate. These complexes can be separated from one another and from unchanged molecules by ion exchange chromatography. Boronate in elution media converts normally neutral sugar molecules into an ionic component in which the charge eventually is dependent upon the structure and stability of the boronate-sugar complex.

A variation of this is boronate affinity chromatography, in which a boronic acid is coupled by

means of a spacer organic molecule to an appropriate matrix. The most widely used is *m*-aminophenylboronic acid, which has been coupled with agarose, polyacrylamide gel and beaded cellulose, among other matrices. In this case, the sugar will bind to the boronate matrix and can be eluted using appropriate elution conditions. Binding is generally aided by an alkaline pH at a fairly high ionic strength, since the resulting complex between the bound sugar and the immobilized boronate is negatively charged and high ionic strength stabilizes the charged spacer. Elution can be readily effected using mildly acidic or neutral pH and a low ionic strength eluent.

Separation of sugars on boronate affinity matrices has been little utilized and is of only minor importance. On the other hand, the separation of many biological macromolecules containing sugars is of extreme significance. Nucleosides, nucleotides, catecholamines and tRNA are among the more important compounds which have been separated by this method.

The most important separations that have been performed on boronated affinity chromatography are those of glycosylated proteins, including glycosylated enzymes. Most proteins exported from cells are glycosylated prior to their secretion. This glycosylation has been observed to be of significance in determining the lifetime of, for example, a serum protein, as glycosylases remove the sugar residues until a nearly sugar-free molecule is recognized by liver cells and removed from the blood stream by phagocytosis.

Many proteins which are naturally glycosylated in mammalian tissue are produced in recombinant microorganisms in a nonglycosylated form. While many of these have utility in a research laboratory, there is considerable reluctance to utilize human proteins without normal glycosylation as therapeutic materials; therefore, many of these mammalian proteins are now produced by recombinant systems in organisms which glycosylate the proteins in a way that mimics their natural glycosylated state. For this reason, determination of the oligosaccharide structure of glycosylated residues is very important. As will be seen in the following section, this is done chiefly using lectin chromatography. Boronate chromatography, on the other hand, provides a general way in which glycosylated proteins can be purified and separated from nonglycosylated proteins and often other glycoproteins. The interactions between the matrix and the glycosylated proteins need to be minimized, while the chemi-selective adsorption of the sugar diols to form diesters with the boronate needs to be maximized. To do this, the chromatography must be done under conditions in which the pH is reasonably high, usually above the pK of the boronate, and, at the same time, the ionic

strength must be high enough to suppress the ion exchange properties of the naturally charged boronate residues. At the same time, too high ionic strength will increase hydrophobic interactions between the protein to be purified and the matrix on which the boronate residue is bound or the organic molecule which bears the boronate, for example the phenyl portion of the *m*-aminophenylboronic acid. To accomplish both of these goals simultaneously, normally a cation such as magnesium is employed. Magnesium is effective at suppressing the boronate charge at relatively low concentrations, which do not significantly promote hydrophobic binding of the protein to the matrix. Many glycosylated proteins and enzymes can be separated from their nonglycosylated counterparts in a single chromatographic step, which, while not always producing a homogeneous protein, effects considerable purification and selection.

By far the most important boronate separation is the separation of glycosylated haemoglobin from its nonglycosylated counterpart. Glycosylated haemoglobin is created in a very different fashion from the biological glycosylation of secreted proteins. Haemoglobin produced within the red blood cell is not glycosylated; however, in a nonenzymatic process, amine residues of the haemoglobin react with glucose and form a transient Schiff's base. This Schiff's base then undergoes a rearrangement (the Amadori rearrangement) to produce a stable fructosamine derivative of the haemoglobin molecule. The rate at which this reaction occurs and thus the percentage of haemoglobin which is glycosylated, is totally dependent upon the concentration of glucose in the blood stream. Since the haemoglobin molecule has a half-life of approximately 60 days in the blood stream, the percentage of glycosylated haemoglobin provides a good measure of the long-term average blood glucose concentration. By separating the glycosylated haemoglobin from nonglycosylated haemoglobin, the physician has a diagnostic tool for the diabetic management of patients. Diabetic patients notoriously mis-report their exercise and adherence to dietary prescriptions of the physician. By taking a small sample of blood and separating the diabetic, or glycosylated, haemoglobin from nondiabetic, or nonglycosylated, haemoglobin, a reasonable measure of the history of the patient's serum glucose levels can be achieved. This is a very widely used test of great significance in the control of this important disease. Proteins, other than haemoglobin, could be utilized for this assay, since other serum proteins such as serum albumin undergo nonenzymatic glycosylation. Glycosylated haemoglobin is the most readily measured in a reliable fashion and has, to date, provided the physician with the best diagnostic methodology.

In addition to the diabetic analysis, boronate chromatography has the potential to form the basis of other significant diagnostic assays, such as assays for catecholamines, as well as for various differences in protein composition and nucleoside concentrations in various tumours. This potential has not yet been fully realized.

Lectin Chromatography

Immobilized lectins are true complements to boronate chromatographic materials. Lectins do not have the stability that boronates possess, but they possess a considerably higher and broader range of specificity. While there are several immobilized commercial boronate materials available for boronate affinity chromatography, there are a much greater number of different types of immobilized lectins. For example, one commercial firm offers 19 different lectins immobilized by several different methods, chiefly to agarose. The same firm offers approximately 60 purified lectins in a nonimmobilized state, any one of which could be immobilized by a researcher for his or her own specific purposes. Since the specificity of lectins can vary from relatively narrow specificity to those which have very broad specificities, and since the specificities between lectins are so varied, they offer a very powerful tool for separating many glycoproteins. An idealized purification scheme utilizes boronate affinity chromatography in an initial purification step, which allows one to obtain first the glycosylated protein fraction as a whole, followed by lectin affinity chromatography to separate the glycosylated proteins.

Lectins are obtained from either plant or animal materials and have various biological functions. Originally, lectins were also termed phytohaemagglutinins because they were isolated from plant sources (phyto) and were used to classify blood cells by their agglutinating property (haemagglutinins). The agglutination occurs because lectins are multimeric proteins with multiple sugar binding sites which can crosslink red blood cells, thus aggregating them.

There are two basic approaches to lectin affinity chromatography. At the present time, the easiest approach, and the one most commonly used, is to survey the commercially available lectins, preferably those which are already immobilized, for their ability to bind the target protein. It is helpful if the terminal sugar of the glycosylated protein is already known, since that makes the choice of lectin much easier. On the other hand, it is also relatively simple to carry out a trial and error procedure to determine which immobilized lectin is best in the purification of a particular

protein. It is also possible to immobilize an appropriate lectin from among the many commercial lectins that are available if the terminal sugars of the glycoconjugate to be purified are known.

The second approach is to determine the terminal sugar of the glycoconjugate to be purified and then to purify, *de novo*, a new lectin, by immobilization of the desired terminal sugar to a matrix, such as agarose, by means of a spacer arm. This allows the screening of numerous potential lectin sources to find as many lectins as possible that will bind to the target sugar. This methodology was used for many years prior to the present significant commercial availability of purified lectins.

After the lectin has been chosen and obtained in an immobilized form, or is immobilized by one of many simple procedures, for example agarose or cyanogenbromide-activated agarose, or Affi-gel 10, adsorption/desorption, method conditions need to be defined. The binding of glycoproteins to lectins is generally easier than their elution. The factors in binding are generally temperature and salt concentration, as well as the density of coverage of the lectin immobilized on the matrix. High densities of lectins are not desirable in most instances. Although high ligand density may yield a marginal increase in capacity, it significantly increases the difficulty of eluting the target protein. The use of a moderate salt concentration is often helpful during binding of the glycoprotein target to the immobilized ligand. In many instances, it is necessary to be certain that the required metal ions are included in the sample wash and elution buffers in order to prevent deforming and/or denaturation of the lectin. Once the protein binding conditions have been determined, elution conditions need to be investigated. If one wants to have the highest purity product and to be certain that binding the protein to the immobilized lectin is through the biologically significant, sugar-protein interaction, then elution should be done by a high concentration of the free sugar. This will bind competitively to the lectin, displacing the glycoconjugate and thus eluting it. The sugar concentration during elution must be high enough to compete effectively with the lectin for the glycoconjugate, particularly when the density of the immobilized lectin is high.

Nonspecific elution of the glycoprotein from the lectin is frequently used. Changes in pH, temperature and salt can affect elution by decreasing the affinity of the lectin for the glycoconjugate. If elution were either with free sugar or by changing binding conditions, for example pH, a good yield is not obtained. It is also possible to apply an eluent to the column and stop the flow, thus allowing equilib-

rium to be reached in the free solution. This may or may not be necessary, however, and frequently a simple clean elution can be obtained by a proper choice of conditions.

One of the more interesting applications of immobilized lectins is the determination of the structure of sugar residues bound to the glycoconjugate. For example, a protein will be applied to a specific immobilized lectin and found to bind to that lectin. If the lectin has a rather broad specificity, the investigator cannot be certain which sugar is the terminal sugar on the oligosaccharide moiety of the glycoprotein. However, by using various glycoses to remove the terminal sugar, the investigator can determine which glycase yields a derivative that will no longer bind to the immobilized lectin used. The glycase specificity indicates the identity of the terminal sugar. This procedure can be done repetitively and from the results a reasonable understanding of the structure of the oligosaccharide of the glycosylated protein can be determined.

Conclusion

Both boronate chromatography and lectin affinity chromatography have considerable potential for future use in biotechnology. Proteins with proper glycosylation are becoming more and more important because it is perceived to be desirable to have proper glycosylation for therapeutic purposes. In addition, researchers are becoming more and more aware that the structures of oligosaccharides bound to glycosylated proteins contain valuable information on the biological system from which the protein was isolated. It appears that both boronate and affinity chromatography will be valuable in basic research and in commercial protein purification and undoubtedly for other applications as yet unknown.

See also: III/Immobilised Boronic Acids: Extraction.

Further Reading

- Adamek V, Liu X-C, Zhang YA, Adamkova K and Scouten WH (1992) New aliphatic boronate ligands for affinity chromatography. *Journal of Chromatography* 625: 91-99.
- Beneš M, Štambergova A and Scouten WH (1993) In: Ngo T (ed.) *Affinity chromatography with immobilized benzenboronates. Molecular Interactions in Bioseparations*, pp. 313-321. New York: Plenum Press.
- Bergold A. and Scouten WH (1983) In: Scouten WH (ed.) *Boronate chromatography. Solid Phase Biochemistry*, pp. 149-188. New York: Wiley.

- Freeze NH (1995) Lectin affinity chromatography. *Protocols in Protein Chemistry*, pp. 901–919. New York: Wiley.
- Gerard C (1990) Purification of glycoproteins. In: Deutscher MP (ed.) *Guide to Protein Purification, Methods in Enzymology*, vol. 182. New York: Academic Press.
- Liu X-C and Scouten WH (1994) New ligands for boronate affinity chromatography. *Journal of Chromatography A*, 687: 61–69.
- Liu X-C and Scouten WH (1996) Studies on oriented and reversible immobilization of glycoprotein using novel boronate affinity gel. *Journal of Molecular Recognition*, 9: 462–467.
- West I and Goldring O (1996) Lectin affinity chromatography. In: Doonan S (ed.) *Methods in Molecular Biology, Protein Purification Protocols*, vol. 59, pp. 177–185. New Jersey: Humana Press.

Immobilized Metal Ion Chromatography

D. P. Blowers, AstraZeneca Pharmaceuticals,
Alderley Park, Macclesfield, Cheshire, UK

Copyright © 2000 Academic Press

Introduction

Since its introduction by Porath in 1975, immobilized metal ion affinity chromatography (IMAC) has developed into a robust and versatile tool. The number of uses is large and includes the isolation of metal-binding compounds from sea water, separation of enantiomeric forms of amino acids, tetracycline removal from animal products and protein purification. This article will focus on its application to protein purification, where it relies on the ability of certain amino acid side chains to form coordinative interactions with immobilized metal ion chelate complexes. As a chromatographic method it falls somewhere between biospecific affinity chromatography and ion exchange chromatography. The evolution of the technique, current tools and some specific technical details are discussed.

Background

Knowledge of the interaction of metal ions with proteins and the potential utility of immobilized metal chelators began during 1940–50, although it was not until 1974 that the method was first used to isolate a metalloprotein. The general use of IMAC was initiated in 1975 with a *Nature* publication from Porath. A summary of key milestones in the history of IMAC is presented in Table 1.

In the late 1970s and 1980s there were numerous publications on the choice of metals and investigations on the precise nature of the interactions that take place with proteins. It was assumed that surface-exposed residues were coordinating with the immobilized metal ions. Studies using free amino acids, peptides, and eventually engineered recombinant proteins, revealed the importance of certain amino acids


– in particular histidine. Additionally, depending on the metal and chelating ligand employed, the spatial arrangement of the amino acids within the peptide or protein was also found to influence binding. This led to studies using model peptides with a wide range of histidine-containing sequences and in 1988 the first use of six consecutive histidine-residues as a purification tag (6His tag). In parallel with this 1987 saw the introduction of a metal–chelate complex with a high degree of selectivity for adjacent histidine residues (Ni^{2+} –NTA). Proteins purified using the 6His tag have been found to retain biological activity and their structures have also been solved by both X-ray and NMR – illustrating that, in the absence of metal ions, the tag has no defined secondary structure. Despite the enormous utility of the 6His tag the use of metal chelating ligand/metal combinations still has a role to play in the isolation of nontagged proteins from a wide variety of sources. The literature contains many examples of using IMAC as a one-step process to isolate native proteins, e.g. α -lactalbumin from milk and factor IX from blood. In addition, immobilized Fe^{3+} has been successfully used to separate phosphoproteins and immobilized Ca^{2+} to purify calcium-binding proteins.

The potential exists for even wider application to the separation of protein mixtures, with new chelators being introduced (e.g. TACN, see below).

Table 1 Key dates in the history of immobilized metal ion affinity chromatography

1974	First use of immobilized chelators to isolate metalloproteins
1975	First description of general technique (IMAC) using IDA
1983	Introduction of high performance on silica based media
1986	Use of Fe^{3+} chelates to purify phosphoproteins
1987	Introduction of NTA
1988	Introduction of genetically engineered His tags
1992	Introduction of TREN
1998	Introduction of TACN

Table 2 Abbreviations, names and functional structures of chelators

Name	Full name	Dentation	Structure
IDA	Iminodiacetic acid	3	$\sim \text{N}(\text{CH}_2\text{COOH})_2$
TACN	1,4,7-Triazacyclonane	3	$\sim \text{N}(\text{CH}_2\text{CH}_2\text{NHCH}_2\text{CH}_2)$ 
NTA	Nitrilotriacetic acid	4	$\sim \text{CH}(\text{COOH})\text{N}(\text{CH}_2\text{COOH})_2$
TREN	Tris(2-aminoethyl)amine	4	$\sim \text{NHCH}_2\text{CH}_2\text{N}(\text{CH}_2\text{CH}_2\text{NH}_2)_2$
Talon	Proprietary	4	Proprietary
TED	Tris(carboxymethyl)ethylenediamine	5	$\sim \text{N}(\text{CH}_2\text{COOH})\text{CH}_2\text{CH}_2\text{N}(\text{CH}_2\text{COOH})_2$

~ Indicates chosen form of linkage to a chromatographic support, usually with a suitable spacer.

– Indicates atoms involved in metal ion coordination.

Whether purifying proteins using native exposed histidines, post-translation modifications with phosphate or via an engineered 6His tag, IMAC provides a versatile and relatively gentle method with the potential to provide greater than 90% purity in a single chromatographic step.

Components

Metal Ions

A search of the literature on IMAC reveals a bewildering array of metal ions that have been used in this technique (e.g. Ag^+ , Al^{3+} , Ca^{2+} , Co^{2+} , Cr^{3+} , Cu^{2+} , Eu^{3+} , Fe^{3+} , Hg^{2+} , La^{3+} , Mn^{2+} , Nd^{3+} , Ni^{2+} , Yb^{3+} , Zn^{3+}). The reason for this is that the nature of the metal ion (and indeed its chelator) influences the selectivity and affinity of the protein interaction. The most commonly used metals can be grouped into the 'hard' and 'soft' types – reflecting their electron orbital configuration and ability to act as electron acceptors. In free solution the metal ions exist with a shell of water molecules. Upon chelator or protein binding the water is displaced and a coordination bond to the metal ion is formed by the donation of free electron pairs from atoms in the chelator or in the amino acids (e.g. N, O and potentially S) of the protein. As such the atoms behave as monodentate ligands with the affinity estimated to be in the micromolar range. Both the protein and the immobilized chelator have the potential to be polydentate. For protein binding the 'soft' metal ions (e.g. Cu^{2+} , Co^{2+} , Zn^{2+} , Ni^{2+}) show a preference for coordination with nitrogen-containing functional groups such as the imidazole of histidine (either δ or ϵ nitrogens). The 'hard' metal ions (e.g. Al^{3+} , Ca^{2+} , Fe^{3+}) show a preference for oxygen-containing groups such as carboxyls or phosphates found in phosphorylated proteins. These preferences are exploited in the nature and types of proteins purified with particular

combinations of chelator and metal ion, and, to a certain extent, with the choice of buffer conditions. Within the 'soft' metal group a rank order of affinity for histidine residues has been established. In increasing strength of binding this order is $\text{Co}^{2+} \approx \text{Zn}^{2+} < \text{Ni}^{2+} < \text{Cu}^{2+}$. Histidine is relatively rare, representing only 2.2% of the amino acids across all proteins with many containing none or none accessible on their surface. This provides a built-in selectivity for certain native proteins. The use of genetic engineering to introduce a 6His tag further exploits the selectivity for histidine. The preferred use of Ni^{2+} in IMAC with 6His tagged proteins is in part due to its higher coordination number ($\text{Cu}^{2+} = 4$, $\text{Ni}^{2+} = 6$) and the fact that the weaker binding potential of the Ni^{2+} is compensated for by the tag, thus providing an even greater degree of selectivity over other proteins from the recombinant host.

Chelating Ligands

Metal chelators bound to chromatographic media fix the metal ion to a solid support, enabling the separation process to take place. They modulate the affinity and selectivity of the chromatographic matrix as well as its capacity for proteins. A relatively large number of such ligands exists in the literature, although only a subset of these have found routine use in IMAC. This discussion limits itself to the most common chelating ligands and new developments in the area. Table 2 presents a summary of the properties for a selection of chelating ligands.

During the design of chelating ligands several factors have been taken into consideration. Increasing the dentation number of the chelator will increase its affinity and reduce unwanted metal ion leakage from the column. Counterbalanced with this is the need to provide free coordination sites for the protein with binding capacity and affinity increasing as the number of these sites increases. In addition, metal ion transfer must be avoided, i.e. the chelating ligand

must bind the metal ion sufficiently tightly so as not to be stripped by proteins in the mixture to be purified.

As a consequence of the above considerations, several chelating ligands have been developed and successfully used in IMAC. **Figure 1** shows a schematic representation of the octahedral coordination of a metal ion (e.g. Ni^{2+}) with the chelators IDA, NTA and TED, illustrating the decrease in available protein-binding sites as the dentation of the chelator increases. IDA was the chelating ligand used by Porath in the first publication on IMAC in 1975. While adequate for the purpose, and still used today, this ligand is only tridentate and metal ion leakage can be a problem. When complexed with Cu^{2+} only one coordination site remains for protein binding. With Ni^{2+} , while three free coordination sites are available for protein binding, the metal binding is

often too weak for practical use. For these reasons NTA was developed by Hochuli as an alternative to IDA. As shown in **Figure 2** the structure of NTA is closely related to that of IDA. NTA chelate with the oxygens of three carboxyl groups and a nitrogen, while IDA uses just two carboxyl groups and a nitrogen. The tetradentate nature of NTA means that metals other than Cu^{2+} must be used. When complexed with Ni^{2+} , two coordination sites are available for protein binding. The increased stability and coordination potential of NTA-based matrices has provided remarkable selectivity, especially when combined with recombinant proteins with engineered histidine tags. This combination was first introduced commercially by Qiagen.

To further address the issues of stability, selectivity and capacity, several alternative tetradentate

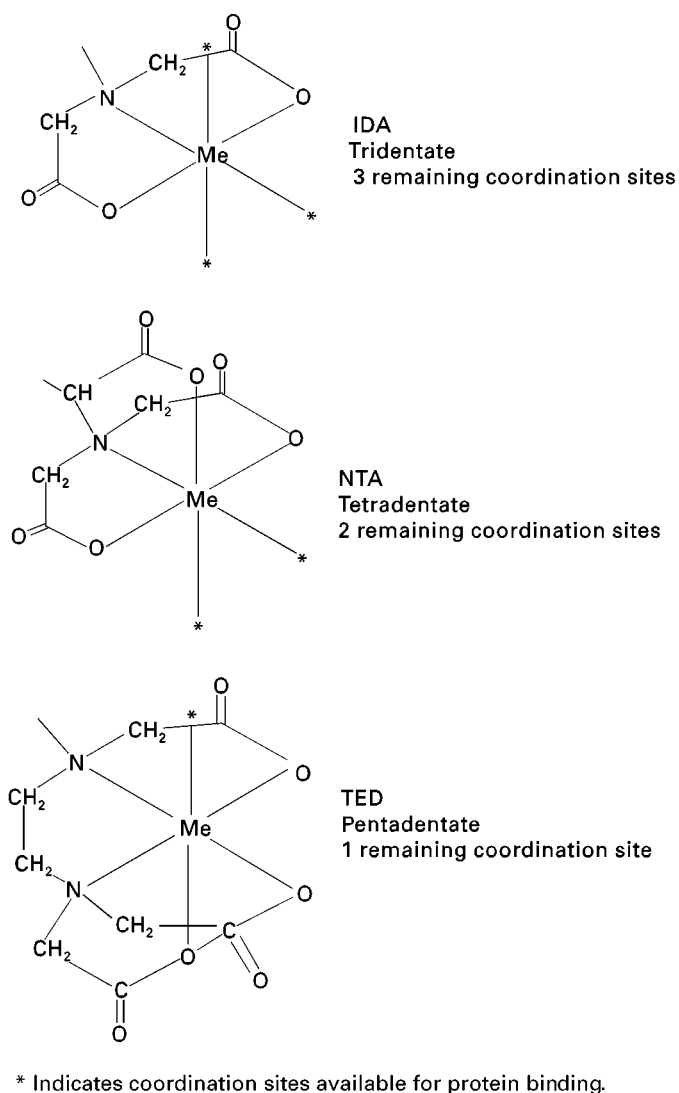


Figure 1 Schematic representation of IDA and NTA metal chelation.

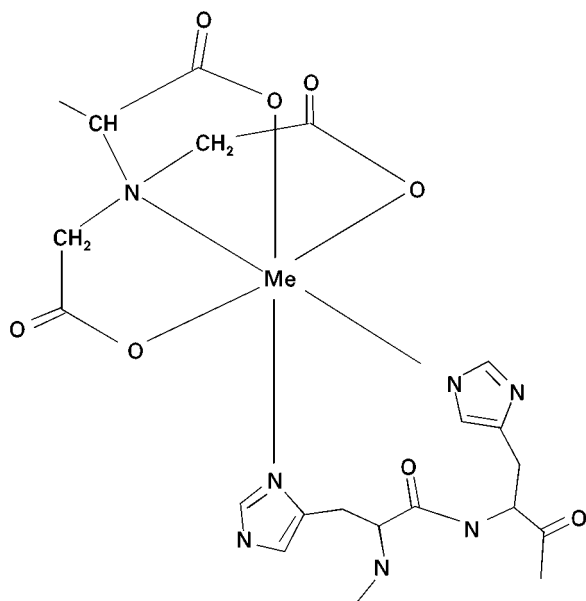


Figure 2 Ni^{2+} -NTA chelation and binding of consecutive histidine residues.

chelating ligands have also been developed and used successfully, e.g. TREN coupled to a high capacity matrix (Novarose-Inovata AB) for the rapid purification of goat immunoglobulins and Talon (Clontech) as a Co^{2+} loaded support which claims even higher selectivity in the isolation of 6His tagged proteins. TACN has recently been introduced and used with a range of 'soft' metal ions. This chelator exhibits remarkable metal-binding stability at low pH, where other chelators would exhibit loss of the metal. This extended pH range could be used to gain further selectivity. The pentadentate TED offers very tight metal ion binding and highly selective protein binding. In addition, the strength of metal ion binding to TED can be exploited as a second column to remove potentially leached metal ions from other IMAC eluates.

Media

The first commercially available IMAC medium was IDA-Sepharose (AP Biotech). Today, many IDA-chelating media are available, including modified forms of Sepharose (AP Biotech), agarose, polystyrene, polystyrene/divinylbenzene (Poros-Perseptive Biosystems), poly(alkalhydroxy-methacrylate), silica and even magnetic polystyrene beads (Dynabeads, Dynal Inc.). Among these types most are available as loose media and prepacked columns for either low pressure or high performance liquid chromatography. The commercially available NTA medium (Qiagen) and Talon (Clontech) are based on Sepharose CL-6B. At the time of writing, commercial media for TACN,

TED and TREN are not available, although they can be made relatively easily using the chelator and commercially available activated media. In addition, membrane-based media can also be purchased (e.g. Sartobind IDA-Sartorius) or created via coupling of ligands to activated membranes.

Practical Considerations

The use of metal chelate chromatography should be relatively straightforward, i.e. charge with metal ions, wash, load with protein, wash and elute. However, as with most chromatographic processes there are a few points that may need close attention. In addition, the use of metal chelate chromatography has now gone beyond just the purification of proteins from crude mixtures to applications in protein folding, protein-protein interactions (footprinting) and immobilization of enzyme activities.

Protein Purification

Equipment Needs here can range from batch adsorption and elution, through very simple gravity-driven columns, to sophisticated pumping and control equipment for high performance methods. Since precise gradient mixing is not generally required, and many media present few problems with back pressure, IMAC is a relatively 'low-tech' process.

Buffers and loading conditions IMAC columns are compatible with a wide range of buffers, although those with the potential to act as chelators (e.g. citrate, Tricine) should be avoided. For the isolation of phosphoproteins on immobilized Fe^{3+} the use of phosphate buffers should be avoided. It should also be noted that phosphate buffers are not compatible with certain metals (e.g. Ca^{2+}) due to the formation of insoluble salts. The pH of the buffer will clearly be application dependent, although exposure of most columns to low pH (< 5) should be avoided since it will lead to loss of chelated metal ions due to protonation of the chelating groups. Any solutions containing imidazole should have the pH checked since imidazole can markedly alter the pH of 'buffered' solutions. Inclusion of a relatively high level of salt (e.g. 500 mM NaCl) is common practice in IMAC, serving to reduce nonspecific ionic interactions between the protein and the metal chelate complex. However, inclusion of such high levels of salt will also tend to increase nonspecific hydrophobic interactions with the column matrix. It is frequently best to ascertain the most suitable salt concentration on a case-by-case basis. The use of other chelating agents (e.g. EDTA, EGTA), often added as protease inhibitors, is also best avoided although separations

may be possible in the presence of ~ 1 mM concentrations if the load volume is relatively small compared to that of the column and/or the residence time is short. Reducing agents can also present a problem due to reduction of the metal ions, although low (10 mM) concentrations of β -mercapto ethanol may be tolerated by Ni^{2+} -NTA. Nonionic surfactants, low levels of organic solvents, 8 M urea and 6 M guanidine hydrochloride are generally compatible with IMAC. Temperature has little effect on the capacity of IMAC media.

When working with small volumes of load material or recombinant protein with a low accumulation level, the load volume/bed volume ratio becomes important. Deliberately overloading the column in such instances can improve the purity of the eluted material. In overloading the column the desired product, which binds with relatively higher affinity, will actively compete with weaker nonspecific interactions.

Certain components in common load materials from recombinant sources can introduce difficulties or potential contaminants. Insect cell media frequently contain high concentrations of histidine as a nutrient and can prevent the binding of 6His-tagged proteins being purified directly from the culture supernatant. Dialysis or dilution is required prior to loading. There is also a growing list of *Escherichia coli* proteins that regularly turn up as contaminants when purifying 6His-tagged proteins. These proteins include: chloramphenicol acetyl transferase from resistance selection; aspartate carbamoyl transferase; 30S ribosomal protein, rotamase and peptidyl prolyl *cis-trans* isomerase.

Washing Having loaded the media, in either batch or column mode, it is necessary to wash away unbound protein. This is generally achieved by washing with several bed volumes of loading buffer until the protein content of the wash material has reached an acceptable level. Low concentrations of eluting agents (e.g. imidazole) in the wash can help to improve the purity of the final product by eluting those components with relatively weak affinity. Inversely, the procedure of 'titration loading' can also be employed wherein weak binders are prevented from binding to the column by the inclusion of a low level of eluting agent in the loading buffer. Including a wash step with reduced salt can also serve to remove those potential contaminants bound to the medium via hydrophobic interactions. Proteins exhibiting such hydrophobic interaction include *E. coli*-derived proteases which, when concentrated along with target protein on the medium, can lead to severe degradation of the target. A low salt wash step can alleviate this problem.

Elution There are three potential ways of eluting protein from IMAC media:

1. Adding chelating agents that compete with the chelating ligand and the protein for metal ions.
2. Lowering the pH to protonate both the protein and the chelating groups on the chelating ligand, thus preventing metal ion chelation.
3. Introducing chelating agents that will compete with the protein for coordination to immobilized metal ion.

All three methods require further clean-up of the eluted material to remove unwanted components. Of the three methods, probably the least favourable is method 2 since this may lead to metal ion contamination of the eluted protein and retention of activity may not be compatible with low pH. Method 1 also strips the medium of metal ions, although in this instance they will be complexed with the added chelator. Method 3 is probably the most gentle form of elution. Imidazole mimics the coordination of histidine residues in the protein and can lead to effective elution when used in the tens to hundreds of millimolar range (Figure 3 shows an example purification). For phosphoproteins immobilized on Fe^{3+} it is normal to use phosphate in the elution buffer and concentrations as low as 10 mM may be effective. The minimum concentration required should be determined on a case-by-case basis and cannot be simply predicted. Even for 6His-tagged proteins the minimum concentration of imidazole required for elution can vary by an order of magnitude depending on the target protein. In some instances a sharper elution profile can be obtained by inversion of the column prior to elution. Care should be taken regarding the potential effects of imidazole on the activity of the target protein (e.g. some protein kinases will appear to be inactive until the imidazole is removed). Additionally, protein precipitation can occur during removal of > 100 mM imidazole and upon thawing frozen samples.

Protein refolding The compatibility of IMAC with 8 M urea and 6 M guanidine hydrochloride has led to its use (primarily with 6His-tagged proteins) in refolding studies on immobilized protein. The potential advantage is that the protein is anchored to a solid support, thereby reducing aggregation that may be observed in even dilute solution refolding experiments. While no generic method is available this method has been successfully used to refold a growing number of proteins. In essence washing the immobilized protein on the IMAC column replaces conventional dialysis. With the protein immobilized in the presence of a strong denaturant, the level of

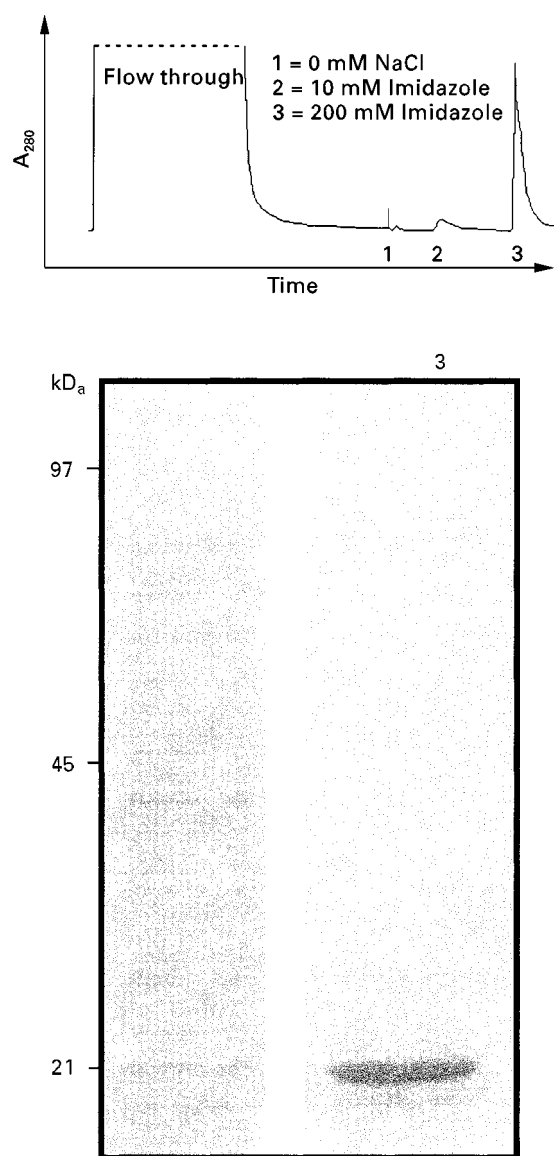


Figure 3 A 6His tagged fragment encoding residues 1–117 of human mdm2 (mdm2(1–177)-6His) was expressed in *E. coli* at ~1% total cell protein. Clarified lysate (L) was loaded on to a Ni^{2+} -NTA column in lysis buffer (50 mM Tris HCl, pH 8.0, 0.5 M NaCl, 10 mM β -mercapto ethanol, 1 mM PMSF, $1 \mu\text{g mL}^{-1}$ leupeptin, $1 \mu\text{g mL}^{-1}$ aprotinin, $1 \mu\text{g mL}^{-1}$ pepstatin). After loading, the column was washed to baseline absorbance in the same buffer. Two washes were then performed: (1) 50 mM Tris HCl pH 7 and (2) as for (1) with 10 mM imidazole. Protein was then eluted by increasing the imidazole to 200 mM (3). The SDS-PAGE indicates that > 90% purity is obtained in this single chromatographic step.

denaturant is modulated in either a stepwise or gradient fashion. The refolded protein can then be eluted in a conveniently small volume.

Standard refolding protocols frequently employ dilute protein solutions and IMAC also provides a suitable method for concentrating the proteins during

such processes. However, it should be noted that not all denaturants are compatible with IMAC (e.g. 400 mM arginine employed in arginine-assisted refolding interferes with binding of 6His-tagged proteins to Ni^{2+} -NTA).

Protein–protein interactions The binding of proteins to IMAC columns can also be used to study protein–protein interactions. Having bound one protein to the column, and washed away any excess, it is possible then to expose that protein to other proteins or mixtures to detect binding. This method can be used to ‘footprint’ a specific binding interaction or to detect binding partners in a complex mixture. If weak binders are of particular interest then it is also possible to minimize post-binding wash steps and directly run the SDS-treated beads on polyacrylamide gel electrophoresis.

Conclusion

The purification of proteins on immobilized metal ions is both effective and versatile. As well as a long standing role in the isolation of proteins with naturally available histidine residues, it has now become an everyday method for the isolation of 6His-tagged recombinant proteins. Recent reviews on the separation of phosphoproteins on immobilized Fe^{3+} indicate continued interest in such applications and no doubt additional uses will be found in the future.

See also: I/Affinity Separation. II/Affinity Separation: Theory and Development of Affinity Chromatography. III/Enzymes: Liquid Chromatography; Proteins: High-Speed Countercurrent Chromatography. **Appendix 1/ Essential Guides for Isolation/Purification of Enzymes and Proteins.**

Acknowledgements

Thanks to everyone in Protein Science within AstraZeneca Pharmaceuticals for providing details under ‘Practical considerations’. The author is particularly grateful to Rick Davies, Richard Mott and Mark Abbott.

Further Reading

- Anspach FB (1994) Silica based metal chelate affinity sorbents II. Adsorption and elution behaviour of proteins on iminodiacetic acid affinity sorbents prepared via different immobilisation techniques. *Journal of Chromatography* 676: 249–266.
- Benson Chandra V (ed.) (1995) Current Protocols in Protein Science, Section 9.4. New York: Wiley.

- Hermanson GT, Krishna Mallia A and Smith PK (eds) (1992) *Immobilised Affinity Ligand Techniques*, Section 3.1.5, pp 179–183. San Diego, USA: Academic Press.
- Hochuli E, Dobeli H and Schacher A (1987) New metal chelate adsorbent selective for proteins and peptides containing neighbouring histidine residues. *Journal of Chromatography* 411: 177–184.
- Hochuli E, Barnwarth W, Dobeli R, Gentz R and Stuber D (1988) Genetic approach to facilitate purification of recombinant proteins with a novel metal chelate absorbent. *Bio/Technology* 6(11): 1321–1325.
- Holmes LD and Schiller MR (1997) Immobilized iron(III) metal affinity chromatography for the separation of phosphorylated macromolecules: Ligands and applications. *Journal of Liquid Chromatography and Related Technologies* 20(1): 123–142.
- Linder P, Guth B, Wulfig C, Krebber C, Steipe B, Muller F and Pluckthun A (1992) Purification of native proteins from the cytoplasm and periplasm of *Escherichia coli* using IMAC and histidine tails: a comparison of proteins and protocols, *METHODS: A Companion to Methods in Enzymology* 4: 41–56.
- Porath J (1992) Immobilised metal ion affinity chromatography. *Protein Expression and Purification* 3(4): 263–281.
- Porath J, Carlsson J, Olsson I and Greta B (1975) Metal chelate affinity chromatography a new approach to protein-fractionation. *Nature (London)* 258(5536): 598–599.
- Winzerling JJ, Berna P and Porath J (1992) How to use immobilised metal ion affinity chromatography. *METHODS: A Companion to Methods in Enzymology* 4: 4–13.
- Wong JW, Albright RL and Wang N-HL (1991) Immobilized metal ion affinity chromatography (IMAC): chemistry and bioseparation applications. *Separation and Purification Methods* 20(1): 49–106.
- Yip T-T and Hutchens TW (1994) Immobilized metal ion affinity chromatography. *Molecular Biotechnology* 1: 151–164.

Immunoaffinity Chromatography

I. D. Wilson, AstraZeneca Pharmaceuticals,
Mereside, Alderley Park, Macclesfield, Cheshire,
UK

D. Stevenson, University of Surrey,
Guildford, UK

Copyright © 2000 Academic Press

Introduction

Immunoaffinity chromatography is a general term that covers a range of techniques the use of which is now widespread. Often these are based upon the use of antibodies to a specific target molecule or macromolecule immobilized on some form of support (Figure 1). This is then used to separate or isolate the target molecule (or molecules of a similar structure) from a matrix in order to purify it for some subsequent purpose. Alternatively, immunoaffinity chromatography can be used to isolate antibodies by immobilizing the antigen, and indeed the first example of the use of the technique can be traced back to the pioneering work of Campbell *et al.* who, in 1951, immobilized bovine serum albumin to a derivatized cellulose in order to purify antibodies that had been raised to it (Figure 2). These immunologically-based methods include in addition immunoaffinity precipitation, immunoaffinity adsorption and immunoaffinity extraction. Indeed the use of the term ‘chromatography’ is perhaps something of a misnomer as the technique often corresponds more to the online extraction of the target molecule onto the

sorbent. Following extraction, a wash step is used to remove unwanted material followed by the recovery of the desired molecule with a strong eluent. It could thus be argued that in many applications immunoaffinity chromatography is simply immunoaffinity extraction in a column format. The term ‘immunoaffinity chromatography’ is however, widely used and understood by its practitioners.

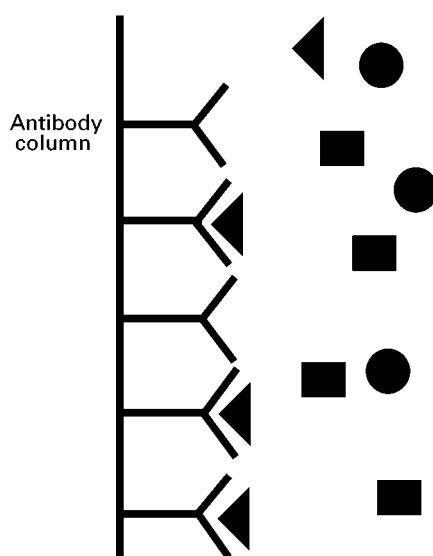


Figure 1 Stationary phase with antibodies bound, only the antigen to which the antibodies were raised is retained. Other molecules pass through with little or no retention.

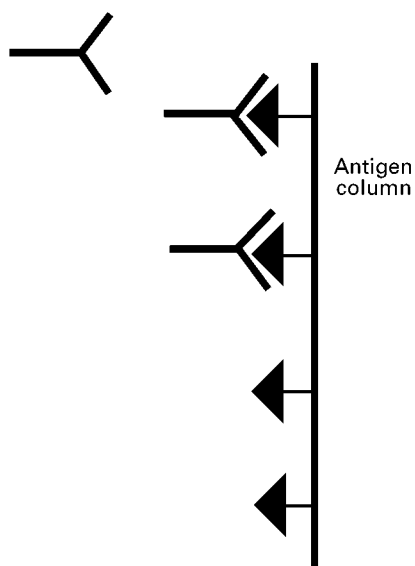


Figure 2 Stationary phase with antigen bound. Only antibodies to the antigen are retained.

Two, essentially different, types of applications of affinity chromatography can be distinguished. Thus there are those applications where isolation is with the intention of analysis (e.g. pesticides from water or drugs from blood plasma). Alternatively, immunoaffinity chromatography is used for preparative purposes and the latter is often used for the isolation of high-value proteins in the biotechnology industry.

Antibodies

The most important reagent in immunoaffinity chromatography is the antibody. These are produced by the immune system in response to foreign compounds. They are of large molecular mass (150 000–900 000). Most small molecular mass compounds such as drugs and pesticides will not provoke an immune response. The usual approach is to bind the analyte (or a structural analogue) to a carrier protein and to immunize the test species with this over a period of up to one year. Blood samples are taken and assessed for the presence of antibodies. One of the disadvantages of this type of work is that it is not certain that antibodies of suitable quality will be produced. If they are produced they are purified by techniques such as ion-exchange chromatography. Although much work is carried out on mice and rabbits, sheep are preferred as much greater volumes of antisera are produced. The antibodies produced contain a heterogeneous population of antibodies known as ‘polyclonal’. These will only be produced for the lifetime of the animal. Monoclonal antibodies contain a homogeneous population and can be

produced by the fusion of myeloma cells with the secreting cells of immunized animals to produce a hybridoma cell. In theory, these can be produced for an infinite length of time.

In the case of techniques where the antibody is immobilized to the support, both polyclonal and monoclonal antibodies can and have been used. However, with the development of methods for the production of monoclonal antibodies, these have been preferred because they offer advantages of reproducibility and a more defined specificity. In addition to the whole antibody, fragments can also be used, and these may confer advantages in terms of attaching them to the support (see below).

Immunoaffinity Supports

A considerable number of different materials have been used as supports for immunoaffinity chromatography. Traditionally, these have generally employed materials such as agarose or cellulose or synthetic polymers such as acrylamide or polymethacrylate-based materials. These provide stationary phases that can be operated under gravity flow but are less suited to systems generating high pressures or flow rates because of limited stability. The main disadvantage of such phases is that they have slow mass transfer properties and thus have a relatively low performance.

Supports based on more rigid materials such as glass and silica, or certain organic polymers such as azalactone beads or polystyrene have been produced which, because of their higher mechanical stability and efficiency, enable higher back pressures and flow rates to be used which may be important in some applications. Because of the increased performance of these materials the term ‘high performance immunoaffinity chromatography’ (HPIAC) has been coined for methods based on the use of these materials.

There are also many methods for attaching the antibody to the support. A common method is simply to covalently attach the antibody directly to the support. One method of achieving this attachment is by reacting free amino groups on the antibody with supports that are activated with e.g. *N,N'*-carbonyl diimidazole, *N*-hydroxysuccinamide, or cyanogen bromide, etc., or to supports sporting reactive epoxide or aldehyde groups. Although technically undemanding and readily achieved, such methods of attaching the antibodies to the support bring with them the problem that the random orientation of the antibodies can interfere with their subsequent ability to interact with the antigen.

Antibodies (or fragments) can also be attached to the support via rather more selective means using, e.g.

free sulfhydryls produced in the production of Fab fragments or by coupling through the carbohydrate residues of the antibody rather than amino groups. A number of sulfhydryl-reactive supports are available, e.g. maleimide, divinylsulfone, etc., for the coupling of the Fab fragments. Coupling via the carbohydrate moiety of the antibody is facilitated by mild oxidation (periodate or enzymic) to yield aldehydes. Once formed, the aldehyde can then be reacted with amine or hydrazide-derivatized supports to bond the antibody. Such immobilized antibodies are believed to provide greater accessibility for the antigen to the antibody binding site and thus provide immunoaffinity supports with higher binding capacity relative to less selective methods. However, it should be noted that this is not always the case, and some workers have compared such 'site-directed' methods with 'random coupling' using monoclonal antibodies (Mabs). These experiments used murine Mabs to either Factor IX or protein C (human plasma proteins) which were immobilized at low density to agarose matrices. The results for this study showed that the site-directed hydrazide-coupled immunosorbents had lower binding capacity for Factor IX and higher capacity for protein C than the equivalent cyanogen bromide-coupled materials.

It has also been demonstrated that the masking of the Fab regions of the antibody with a synthetic antigen prior to covalent immobilization can result in improved immunosorbent efficiency. Thus masking of a murine Mab to protein C with water-soluble adducts of poly(2-methyloxazoline) polymers and a synthetic peptide epitope was performed followed by the immobilization of the antibody complex and then the removal of the Fab-masking antigen (FMA). The procedure resulted in significantly improved antigen binding and accessibility of the Fab domain for protein C, with the best results obtained using the largest FMA employed. Whilst this work was performed on a membrane support rather than beaded material, there seems no *a priori* reason why the approach should not work in immunoaffinity chromatography as well.

There are also a variety of indirect methods of noncovalently attaching the antibody to a support. Thus the aldehyde-containing antibodies generated above can also be reacted with biotin hydrazide, which can then be attached to a streptavidin support. Alternatively, the antibody can be adsorbed onto the bacterial proteins 'protein A' or 'protein G' attached to a support. These proteins will bind to the Fc (stem) region of the antibody reasonably strongly under physiological conditions but this can be reversed by changing the pH, etc. Whilst this does not produce

particularly robust immunoaffinity supports, it can be useful in that the antibody can be replaced should the need arise, enabling the column to be regenerated. It should also be noted that protein A does not recognize all the subclasses of IgG, and has varying avidity for the IgGs of different species.

Retention and Elution in Immunoaffinity Chromatography

Retention

Retention of the compounds of interest, be they low-molecular-mass compounds or macromolecules is effected by the appropriate combination of buffer concentration and pH. Typically a pH of 7.0–8.0 would be used to promote binding to the antibody. It is also quite common to add a small percentage of sodium chloride to the buffer. Phosphate-buffered saline is the most common retention buffer quoted. In addition, in some cases, binding to the antibody depends on metal ions. For example, in the case of protein C, binding only occurs in the absence of calcium ions.

Elution

Having retained the compound or macromolecule of interest on the immobilized antibody, elution can be accomplished by a variety of methods. If the antibody is covalently bound to the support, relatively strong eluotropic conditions can be used including organic solvents such as ethanol, changes in buffer concentration and/or pH, or the use of chaotropic reagents. For speed and sharp elution profiles of the analyte/product, a rapid change in eluent composition from conditions promoting retention to those favouring elution can and are used, i.e. a simple step gradient. However, gradient elution can be used if less aggressive conditions need to be employed and the dilution of the target molecule, relative to step gradient elution, can be accommodated. A further method of elution that can be used where antibodies with relatively weak affinities are used is competitive displacement using another molecule that has an affinity for the antibody (this technique has been termed 'weak affinity chromatography'). In addition, as described below in greater detail, peptides (against which the antibodies were raised) that correspond to a particular region of the target proteins can be used to promote desorption.

Furthermore, as noted above, certain proteins binding to the antibody is metal ion dependent. Thus the protein C bound in the absence of calcium ions was eluted from the immunosorbent using a calcium chloride-containing buffer.

'Analytical' Applications of Immunoaffinity Chromatography

Immunoaffinity chromatography in essentially analytical applications can be considered under a number of headings. These include clinical analysis of endogenous macromolecules for the diagnosis and monitoring of disease, drug analysis in biological fluids (clinical, pharmaceutical and toxicological) and environmental monitoring (e.g. for pesticides in water, etc.). In such methods, a variety of analytical end points are possible ranging from the direct detection of the analyte following elution from the immunoaffinity column. Alternatively, many systems have been developed where the immunoaffinity column is placed in series with an analytical chromatography column and appropriate detector. Whatever the ultimate configuration of the system, the matrix containing the analytes passes through the immunoaffinity column which selectively extracts it allowing contaminants to pass through unretained. The analyte is then eluted from the immunoaffinity support for quantification.

Macromolecules

There are a considerable number of immunoaffinity chromatography-based methods in the literature for clinical analysis. Analytes include anti-idiotypic antibodies, fibrinogen, granulocyte colony-stimulating factor (GCSF), immunoglobulin G and E antibodies, transferrin and interferon, etc. These methods have been demonstrated to compare well with other techniques such as for example, electrophoresis or immunoassay. In such assays the columns seem to be stable up to several hundred sample applications.

Drugs

Immunoaffinity has been used for the measurement of several drugs and endogenous compounds, including anabolic steroids, betamethasone, bufuralol, clenbuterol, corticosteroids, dexamethasone, fluoroquinones, leukotrienes, LSD, morphine, *S*-phenylmercapturic acid, salbutamol, sulphathiazole, tetracyclines, and the thromboxanes TxB1 and TxB2. Matrices include blood, plasma, urine, faeces, liver, milk and honey. In the case of immunoaffinity extraction, this has been used offline (as a form of solid-phase extraction) and in HPLC column-switching mode, with the immunoaffinity column as the first column. In some instances, the immunoaffinity column was used directly on diluted urine or plasma as the only sample preparation; in others, it was used in combination with other sample pretreatment steps such as liquid-liquid extraction or protein precipitation.

Even with these most challenging samples, immunoaffinity chromatography was able to produce clean chromatographic traces.

Environmental Samples

A number of pesticides and other trace organics of environmental interest have also been determined by methods incorporating immunoaffinity chromatography. Examples include aflatoxins, algal toxins, atrazine and triazines generally, carbendazim, chlorotoluron, isoproturon and other phenylurea herbicides, mycotoxins, ochratoxin A, polyaromatic hydrocarbons, and TCDD. Matrices have included nuts, milk, shellfish, water, cereals, coffee, beer, wheat, sludge, sediment, tissue, soil, potatoes, carrots, peas, serum, and fruit juice. One of the most popular examples of the use of immunoaffinity chromatography is for the determination of pesticides in water. The antibodies bind the analyte very tightly so large volumes of water can be passed through an immunoaffinity column to facilitate trace enrichment and clean-up in one step.

Immunoaffinity chromatography has also been proposed as a simple inexpensive device for monitoring chlortoluron in water. Antibodies were bonded to a column and water passed through. Reagents to give a colour stain, the length of which would give a semiquantitative measure of pesticide concentration provided a simple rapid test.

Protein Purification by Immunoaffinity Chromatography

The purification of high-value products from complex biological matrices such as fermentation broths or extracts still represents a considerable challenge. In such preparative applications there is clearly a requirement to deal with large quantities of biological matrices (either fermentation broths or e.g. plasma after varying degrees of preliminary clean-up) compared to the analytical examples cited above. The use of larger columns also means that larger quantities of antibody are required in order to prepare sufficient immunosorbent resulting in considerable expense, which can effectively limit the range of applications. A further consequence of the high cost of the columns is the need to protect them from contamination or mechanical damage which might shorten the lifetime of the column. In addition, where the purified proteins from immunoaffinity chromatography are designed for use in the clinic it is important to ensure that the antibody does not contaminate the product due to leakage from the sorbent as it may itself produce an immune response in the patient. The cost of

the antibody has led to a considerable amount of work aimed at optimizing the capacity of the sorbents, as well as the optimization of flow rates, pressure limits and mechanical stability. It seems to be generally accepted that the typical operational life of such a column is about fifty uses without significant loss of purification capacity, depending upon matrix and process conditions.

An illustrative example of the use of immunoaffinity chromatography for the purification of a protein is provided by studies on protein C, a vitamin K-dependent glycoprotein. This protein has a molecular weight of 62 000 Da, comprising a light chain of 21 000 Da and a heavy chain of 41 000 Da and contains some 23% as carbohydrate. Protein C has potent anticoagulant properties and it is envisaged that there may be potential for its use therapeutically for patients with protein C deficiency, abnormal clotting problems or in victims of heart attacks, etc. In this study a murine monoclonal antibody (Mab 8861) to human protein C was bonded to a variety of support materials and their comparative performance assessed. Columns prepared with these materials were equilibrated with an adsorption/wash buffer (consisting of 0.02 mol L^{-1} sodium citrate, 0.08 mol L^{-1} sodium chloride) at a pH of 6.0 (chosen to increase the stability of the load material). The sample containing protein C was then loaded on to the column which was then left for 30 min to ensure sufficient time for the protein to interact with the antibody. The column was then washed for a further 30–40 min (4–5 column volumes) after which the elution solvent (0.1 mol L^{-1} sodium carbonate, 0.15 mol L^{-1} sodium chloride pH 10) was applied to the column to recover the protein C. The eluent containing the protein C was then immediately taken to pH 7.5 with HCl. However, as described above the binding of protein C can also be dependent on the absence of calcium ions, and in an alternative protocol, using the murine antibody 7D7B10-Mab to human protein C (bound to either agarose or cellulose) this property was exploited. Thus feedstock from the recombinant protein (pre-centrifuged transgenic pig milk whey containing 50 mmol L^{-1} EDTA) was diluted with buffer (1.0 mol L^{-1} sodium chloride, 0.05 mol L^{-1} Tris, 0.025 mol L^{-1} EDTA at pH 7.0) (3 parts buffer to 1 part whey). After centrifugation, the sample was applied to the immunosorbent, and the columns then washed with 18 volumes of buffer. Elution was accomplished with the same buffer with the addition of 25 mmol L^{-1} calcium chloride. Following elution the columns were then regenerated with successive washes of 4 mol L^{-1} sodium chloride, 2 mol L^{-1} sodium thiocyanate and then the application buffer (with 5 mmol L^{-1} EDTA).

Obviously one problem that afflicts all immunoaffinity-based methods is that an antibody to the target protein must first be raised, which may be difficult if the target protein is not available in sufficient quantity or purity. It has now been demonstrated that, for example, peptides to the C-terminal regions of chimeric α -amylase, recombinant CD2 and the insulin β -chain can be used to obtain antibodies. These rabbit antibodies had sufficient affinities to the target proteins to be suitable for use on immunosorbents. The peptide to which the antibody has been raised can then be used as a mobile-phase additive in the eluent in order to displace the target protein from the antibody. Thus, when processed fermentation broths containing the target protein mentioned above were applied to the column they could be recovered either using non-specific eluents (e.g. 2.5 mol L^{-1} sodium thiocyanate, 5 mmol L^{-1} calcium chloride, pH 5.0 for the amylase), or by eluents containing the appropriate peptide in a sodium acetate (50 mmol L^{-1})–calcium chloride (5 mmol L^{-1}) buffer at pH 5.0. For the amylase example, concentrations of the peptide in the eluent of 0.153 or 0.48 mg mL^{-1} produced similar elution profiles, with recoveries of 50–60% of the adsorbed protein (similar to the recoveries with the nonspecific eluent). To regenerate the immunoaffinity column the peptide was then eluted with 0.1 mol L^{-1} HCl. This process of protein purification is interesting as it avoids the use of chaotropic reagents, and also resulted in high-purity products. Post-elution from the column, the proteins and eluting peptides could be separated by ultrafiltration or gel permeation chromatography.

As these examples show, immunoaffinity chromatography for protein purification is a well established and effective method for obtaining high-value proteins, with a continuing high level of innovation.

Conclusions

Immunoaffinity chromatography is a widely used, and useful, family of techniques for the isolation or analysis of both macromolecules and low-molecular-mass compounds for either preparative or analytical purposes. Continuing advances in the production of antibodies and immunoaffinity phases by the use of improved supports and coupling chemistries will result in higher capacities and longer-lived materials. These advances will undoubtedly result in the increased use of immunoaffinity methods in analytical chemistry and in biotechnological applications.

See also: I/Affinity Separation. II/Chromatography: Polymer Separation by Size Exclusion Chromatography;

Membrane Separations: Ultrafiltration. III/ Immunoaffinity Extraction. Pesticides: Extraction from Water. Appendix 1/Essential Guides for Isolation/Purification of Enzymes and Proteins. Essential Guides for Isolation/ Purification of Immunoglobulins. Appendix 2/Essential Guides to Method Development in Affinity Chromatography.

Further Reading

- Godfrey MAJ (1998) Immunoaffinity extraction in veterinary residue analysis – a regulatory viewpoint. *Analyst* 123: 2501–2506.
- Hage DS (1998) Survey of recent advances in analytical applications of immunoaffinity chromatography. *Journal of Chromatography B* 715: 3–28.
- Hermanson GT, Mallia AK and Smith PK (eds) (1992) *Immobilized Affinity Ligand Techniques*. New York: Academic Press.
- Katmeh MF, Aherne GW, Godfrey AJM and Stevenson D (1997) Enzyme immunoaffinity chromatography – a rapid semi-quantitative immunoassay technique for screening the presence of isoproturon in water samples. *Analyst* 121: 481–486.
- Katoh S, Terashima M and Shiomi N (1998) Utilization of antipeptide antibodies as affinity ligands in immuno-

- affinity purification. *Journal of Chromatography B* 715: 147–152.
- Kang K, Ryu D, Drohan WN and Orthner CL (1992) Effect of matrices on affinity purification of protein C. *Biotechnology and Bioengineering* 39: 1086–1096.
- Kaster JA, de Oliveira W, Glasser WG and Velander WH (1993) Optimization of pressure–flow limits, strength, interparticle transport and dynamic capacity by hydrogel solids content and bead size in cellulose immunosorbents. *Journal of Chromatography* 648: 79–90.
- Orthner CL, Highsmith FA, Tharakan J *et al.* (1991) Comparison of the performance of immunosorbents prepared by site-directed or random coupling of monoclonal antibodies. *Journal of Chromatography* 558: 55–70.
- Phillips TM (1989) High-performance immunoaffinity chromatography. *Advances in Chromatography* 29: 133–173.
- Ubrich N, Rivat C, Vigneron C and Maincent P (1998) Microporous particles designed as stable immunosorbents. *Biotechnology and Bioengineering* 58: 581–586.
- Velander WH, Subramanian A, Madurawe RD and Orthner CL (1992) The use of Fab-masking antigens to enhance the activity of immobilised antibodies. *Biotechnology and Bioengineering* 39: 1013–1023.

Imprint Polymers

P. A. G. Cormack, K. Haupt and K. Mosbach, Lund University, Lund, Sweden

Copyright © 2000 Academic Press

Introduction

Molecular imprinting is now recognized as one of the most rapid and powerful methods for creating tailor-made synthetic receptors with strong, yet selective, affinities for a diverse selection of analytes. The imprinting of small organic compounds, metal ions and peptides is well developed and almost routine, and the imprinting of much larger analytes, such as proteins and cells, has also now been demonstrated. The impressive molecular recognition characteristics of molecularly imprinted materials, allied to their highly robust physical nature, makes them ideally suited for numerous applications in affinity separation. This article will outline the general principles behind molecular imprinting and the generic approaches to the preparation of imprinted materials. Particular emphasis will be placed on their role as affinity materials in separation science.

The Imprinting Principle

Molecular imprinting has been demonstrated in silica and in synthetic organic polymers, but it is organic polymers that have found the most favour and indeed probably have the most to offer to the affinity separation area. The rest of this article will therefore deal exclusively with molecular imprinting in the latter medium.

The technique of molecular imprinting in organic polymers is a polymerization process in which a rigid, and insoluble, macroporous polymer network is formed around an analyte (template) of interest (**Figure 1**). In a typical imprinting experiment the analyte is initially allowed to form, in solution, an assembly with one or more functional monomers, which interact with the analyte via either covalent or non-covalent bonds. Once the assembly has been generated, copolymerization with an excess of cross-linking monomer (usually >50 mol%) is initiated, and the insoluble polymeric product phase separates from solution as the polymerization proceeds. The analyte functions as a template during the

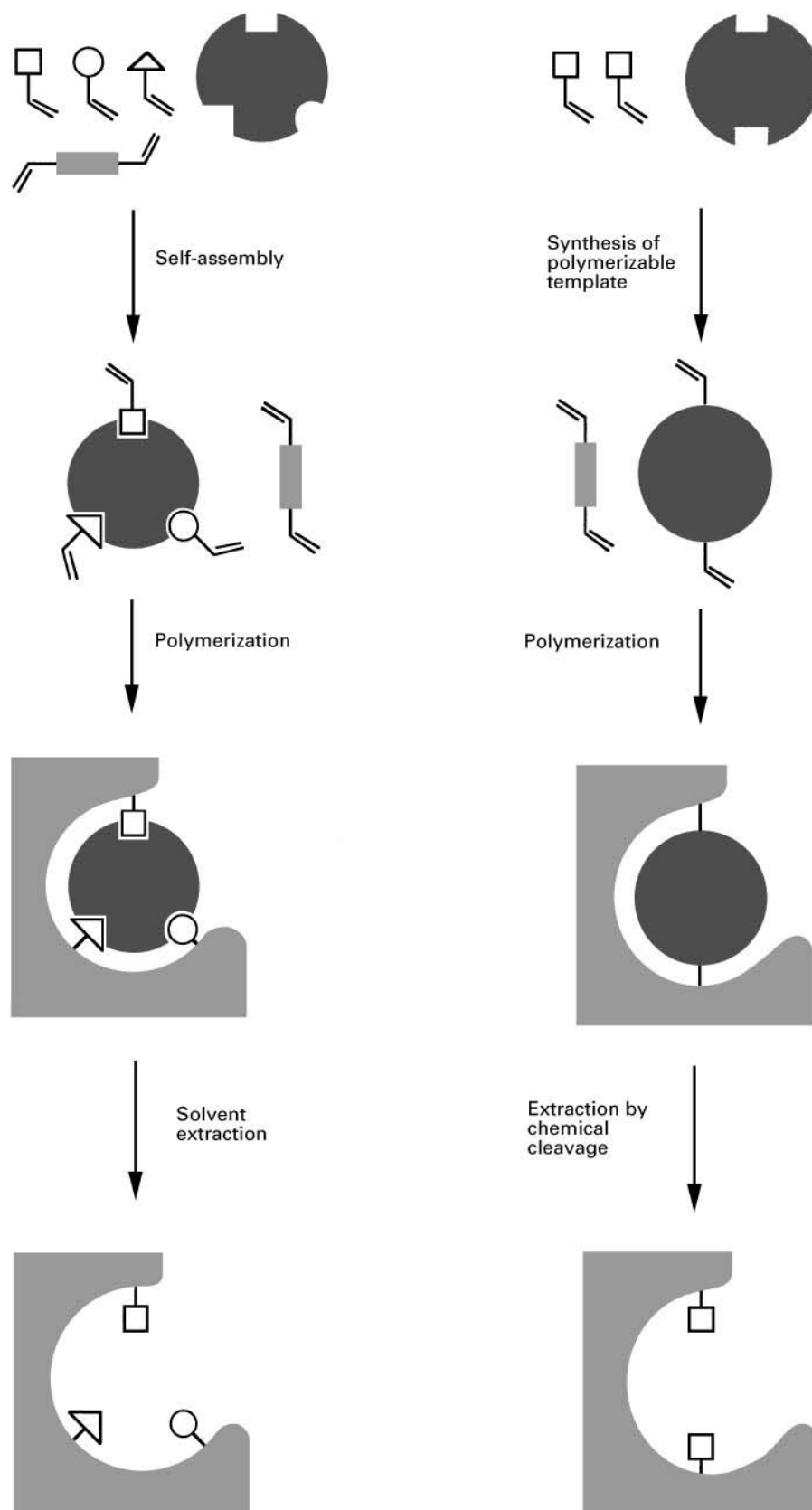


Figure 1 Schematic representation of the molecular imprinting principle. Non-covalent approach (left) and covalent approach (right).

polymerization process, controlling the chemical functionality of the polymer network which forms around it, and since the polymer network is macroporous and the interactions between the analyte and the polymer are quite labile, the analyte can subsequently be extracted from the network via either a simple solvent washing step or by relatively mild chemical treatment. The extraction process reveals binding sites within the polymer network which are complementary to the analyte in terms of their size, shape and functionality, and the polymer can therefore specifically rebind the analyte in these cavities. It is this ability to specifically rebind an analyte which can be taken advantage of in affinity separations.

Numerous analytes have now been successfully imprinted, the majority of which are small, organic compounds, such as drugs, amino acids, sugars and pesticides (Table 1). Metal ions and larger organic compounds (e.g. peptides) have also been imprinted. Although the imprinting of much larger analytes, for example proteins and cells, is in principle and in practice somewhat more difficult to achieve, this has now been demonstrated also.

As mentioned already, there are two distinct imprinting approaches that one can follow. The first is the so-called covalent approach (pre-organized approach) in which the interactions between the analyte and the functional monomers in the pre-polymerization assembly are covalent in nature (this classification generally also includes metal-coordinated analytes). Extraction of the analyte from the network requires these covalent bonds to be cleaved, but they are reformed upon subsequent analyte rebinding. In contrast, non-covalent bonds (e.g. hydrogen bonding, ion pairs and π - π interactions) exist between the analyte and the functional monomers in the pre-polymerization assembly in the non-covalent (self-

assembly) approach. Rebinding of the analyte to the polymer is also non-covalent in nature.

Both imprinting approaches have their own merits and drawbacks, but what can be said in general is that the covalent approach yields binding sites that are better defined. However, it does require chemical derivatization of the analyte prior to polymerization, which is not always easy or practical. The non-covalent method, on the other hand, requires no chemical derivatization step, and is therefore much more general in nature and applicable to a considerably wider range of analytes. Rebinding kinetics are also much more favourable. Indeed, because of its inherent simplicity, the non-covalent approach tends to be the method of choice, although the overall quality of the binding sites tends to be somewhat poorer.

As for the binding sites themselves, the strength and the selectivity of analyte rebinding has been shown in some cases to be on a par with those of natural receptors such as antibodies. This is quite remarkable in itself. In a typical imprinted polymer, however, there is usually a variety of binding sites with different affinities for the analyte, and it is only those sites with the strongest affinities which are comparable to the binding affinities of antibodies. In analogy with antibody terminology, such polymers are usually termed polyclonal to describe their heterogeneous populations of binding sites. There is, needless to say, considerable effort being made to prepare imprinted polymers with homogeneous binding sites, i.e. monoclonal materials.

Besides their impressive molecular recognition properties, molecularly imprinted polymers have several other attractive features. They are exceedingly robust, and can be utilized under conditions which would be disastrous for enzymes or antibodies. They are stable at elevated temperatures and pressures, they are resistant to many chemical environments and can be used in both aqueous and non-aqueous media. Furthermore they are of low cost, have good shelf-lives and can be re-used time and time again without significant detriment to their properties.

In terms of potential applications for imprinted polymers, several avenues are being explored. Imprinted polymers are showing promise as molecular recognition elements in *biomimetic sensors*, as *antibody binding mimics* ('plastic antibodies'), as *catalysts* ('plastic enzymes') and in the *screening of chemical libraries*, but it is in the *affinity separation* area where they are attracting the greatest attention. Indeed, they have already shown their value in chromatography, solid-phase extraction, capillary electrophoresis and membrane separations. Before moving on to consider these applications in greater

Table 1 A selection of analytes that have been imprinted

<i>Analytes imprinted</i>	<i>Examples</i>
Drugs	Propanolol, diazepam, pentamidine, nicotine
Hormones	Enkephalin
Steroids	Steroidal ketones, cholesterol, testosterone
Amino acids	Various free and derivatized amino acids
Peptides	Various small peptides
Carbohydrates	Various sugar derivatives
Proteins	RNase A, transferrin, haemoglobin
Co-enzymes	Pyridoxal derivative
Nucleotides	NAD ⁺
Nucleotide bases	9-Ethyladenine
Pesticides	2,4-D, atrazine, triazine
Dyes	Rhodanile blue, Safranin O
Metal ions	Ca ²⁺ , Cu ²⁺ , Hg ²⁺ , Eu ³⁺
Bacteria	<i>Listeria monocytogenes</i>

detail, the chemical constitution of molecularly imprinted polymers and general methods for their preparation will be briefly described.

The Preparation of Molecularly Imprinted Polymers

Success in the preparation and application of molecularly imprinted polymers relies upon a good understanding of both the principles and practicalities behind the imprinting process. Although a complete, in-depth guide to the preparation of good quality imprints for all analytes is far beyond the scope of this article, there are some general guidelines which provide a good basis for success. The generalities are covered here. The specific details can be found elsewhere.

Nature of the Analyte

The majority of analytes imprinted to date have been low molecular weight organic compounds of molecular mass 200–300 Da, but with appropriate modification of the imprinting conditions much larger analytes can also be imprinted. Various chemical and physical properties of the analyte are of considerable importance; besides having a suitable chemical handle for interaction with a functional monomer, an analyte must be compatible with the functional monomers and crosslinkers used, it must be soluble in the solvent(s) used for imprinting, and it must be stable and inert under the polymerization conditions employed.

Functional Monomers

Functional monomers are selected based on their ability to bind reversibly, via either covalent or non-covalent bonds, to the analyte. In covalent imprinting approaches, the covalent bonds linking the functional monomers to the analyte need to be reasonably labile to allow removal of the analyte from the polymer matrix under relatively mild conditions. This requirement is somewhat limiting, and only metal-chelates, boronic acid esters, disulfides and Schiff bases have been developed to any great extent. The non-covalent approach is much less restricting in this respect, and numerous vinyl-based monomers have been successfully employed (Table 2).

In non-covalent imprinting protocols, the analyte–functional monomer assembly is dynamic in that the functional monomers exist in both the free and the complexed state, and indeed are free to move from one state to another. To push the equilibrium towards assembly formation, it is not unusual to use an excess of functional monomer in the polymerization mixture (typically two-fold or greater). This

does have the side effect of increasing the level of non-specific rebinding of the analyte to the polymer, but at the same time it increases the number of good binding sites, so it is a compromise.

Cross-linking Monomers

Copolymerization of the functional monomers with an excess of cross linking monomer (usually >50 mol%) yields an insoluble polymer matrix which phase separates from solution as the polymerization proceeds. High ratios of crosslinking monomers are generally required to give the polymer matrix the rigidity necessary to retain the integrity of the binding sites. Usually analyte rebinding is enhanced considerably as the crosslinking ratio is increased up to 80 or 90 mol%. The improvements in recognition thereafter are much less spectacular. Many different crosslinking monomers have been used, including some which act simultaneously as functional monomers, but the three which have found the most favour are ethyleneglycol dimethacrylate (EGDMA), divinylbenzene (DVB) and trimethylolpropane trimethacrylate (TRIM) (Table 3).

Solvents

The solvent, besides acting as the medium in which the polymerization is performed, has an important secondary role as a porogen. It controls the porous structure of the polymer matrix to a large extent, and a good porogen is essential if one wants the porous structure in the polymer to be well developed. Sometimes, however, a good porogenic solvent can be a bad solvent for the analyte, so once again a compromise is sometimes required. Common imprinting solvents include toluene, chloroform and acetonitrile.

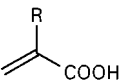
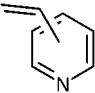
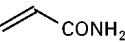
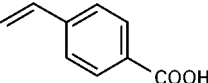
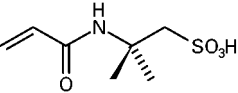
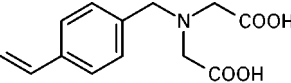
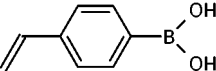
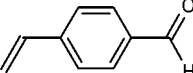
In non-covalent imprinting, there is one further solvent effect which is of great importance. Polar solvents destabilize the analyte–functional monomer assembly and it is therefore better to use non-polar solvents, whenever possible, to maximize the concentration of the assembly in the pre-polymerization mixture. The same argument applies for analyte rebinding. In spite of this, non-covalent imprints have in some cases still shown good recognition properties in aqueous buffers, which are of course highly polar.

One final point of note, which applies to both covalent and non-covalent approaches, is that the best recognition is generally observed when the solvent used for both the polymerization and analyte rebinding is the same.

Initiators and Polymerization Conditions

Classical free radical initiators such as 2,2'-azobisisobutyronitrile (AIBN) are commonly used to

Table 2 A selection of functional monomers commonly used in molecular imprinting

Functional monomer(s)	Structure	Approach
Acrylic acids	 $R = H, CH_3, CF_3 \text{ etc.}$	Non-covalent
Vinylpyridines		Non-covalent
Acrylamide		Non-covalent
Vinylbenzoic acids		Non-covalent
Acrylamido-sulfonic acids		Non-covalent
Vinyl-iminoacetic acids		Metal coordination
Vinylboronic acids (for boronate esters)		Covalent
Vinylbenzaldehydes (for Schiff bases)		Covalent

initiate the polymerization under either thermal or photochemical conditions. Thermal conditions may be preferred in some cases due to limited analyte solubility at lower temperatures, but photochemical initiation at these lower temperatures has certainly been shown to give better results in non-covalent imprinting.

Physical Form of Imprinted Polymers

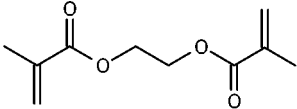
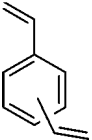
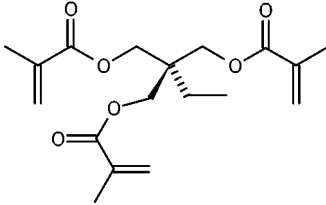
Molecularly imprinted polymers can be prepared in a variety of forms to suit the final application desired. The most common, and indeed the crudest, method for preparing molecularly imprinted polymers is via solution polymerization followed by mechanical or manual grinding of the monolithic block generated, to give small, molecularly imprinted particles. If required, sizing of the particles through sieving and/or sedimentation can then be performed. Besides being

time consuming and wasteful, this method produces particles of irregular shape which are not ideal for chromatographic applications. The grinding process may also destroy a few of the binding sites. Improved polymerization methods which obviate the need for grinding are therefore being investigated.

One seemingly general method which has been developed, and which overcomes the grinding problem completely, involves the suspension polymerization of imprinting mixtures in liquid perfluorocarbon continuous phases. Spherical beads of controlled, regular diameters (down to ca. 5 μm) can be prepared reproducibly by this technique, and are isolated simply by filtration. In the same way, imprinted beads can also be obtained via emulsion, seeded emulsion or precipitation polymerization methodologies.

For chromatographic applications, another solution to the grinding problem is to perform the polymerization directly inside the chromatographic column,

Table 3 Crosslinkers commonly used in molecular imprinting

Cross-linker	Structure
Ethyleneglycol dimethacrylate (EGDMA)	
Divinylbenzene (DVB)	 Usually a mixture of isomers
Trimethylolpropane trimethacrylate (TRIM)	

i.e. *in-situ* polymerization. This approach is particularly attractive for capillary electrophoresis applications, where filling of the capillary can often be problematic.

One final format, which is finding increasing interest, involves imprinted membranes. Generally they are composed either of crosslinked polymers which have been prepared in the standard way, or of linear polymers which have been precipitated in the presence of the analyte. They can be either free-standing or supported.

Applications in Separation Technology

As mentioned earlier, the application of imprinted polymers that has been the most extensively explored

is separation and isolation. *Chiral separations* have been a major area of investigation, and indeed molecularly imprinted materials have been employed as chiral matrices in several different separation techniques. A characteristic of imprinted chiral separation matrices is the pre-determined migration or elution order of the enantiomers, which depends only on which enantiomer is used as the template molecule. For instance, when the *R*-enantiomer is used as the template, it will be retained more by the polymer than the *S*-enantiomer, and vice versa (Figure 2). The discrimination of enantiomers is often very efficient with molecularly imprinted materials. Highly selective, chirally discriminating recognition sites have been prepared using covalent or non-covalent imprinting protocols, and large separation factors between the enantiomers have been recorded.

For analytes containing two chiral centres, all four stereoisomers may be selectively recognized by the imprinted materials. Thus, for a polymer imprinted against the dipeptide Ac-L-Phe-L-Trp-OMe, the LL-form can be selectively distinguished from the DD-, the DL- and the LD-isomers. In systems where more than two chiral centres are involved, such as carbohydrates, these properties of molecularly imprinted materials become even more significant. For example, in a study where polymers were imprinted against a glucose derivative, very high selectivities between the various stereoisomers and anomers were recorded.

Apart from the separation of enantiomers, imprinted polymers are also very useful for the separation of other compounds with closely related structures. An overview of the different separation techniques in which molecularly imprinted polymers have been employed is given below.

Liquid Chromatography

The use of imprinted polymers as stationary phases for HPLC is by far the most studied application. This

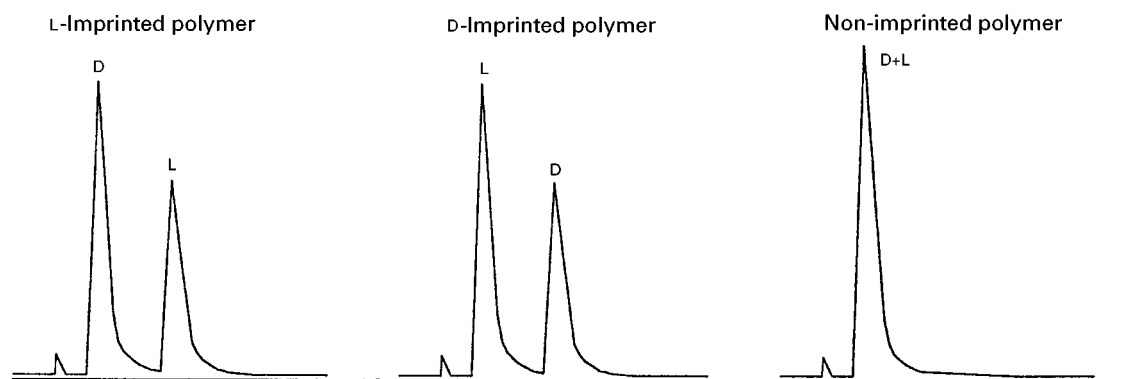


Figure 2 Typical chromatograms of an enantiomeric mixture using a polymer imprinted with the L-enantiomer, a polymer imprinted with the D-enantiomer and a non-imprinted polymer as column packing material.

is partly for historical reasons, because liquid chromatography is a convenient method for assessing the quality of an imprint, particularly during the optimization of an imprinting protocol.

Most research has concentrated on chiral resolution, and molecularly imprinted chiral stationary phases have been prepared for a wide range of compounds. Many of the early investigations employed amino acid derivatives as model substances. In recent years, however, a great deal of emphasis has also been put on the chiral discrimination of drug compounds. Several studies involving the separation of physiologically active compounds, e.g. naproxen (a non-steroidal anti-inflammatory drug), ephedrine (an adrenergic agent) and timolol (a β -adrenergic antagonist) have been described. Typically, separation factors of between 1.5 and 5 are obtained with imprinted polymers, which is relatively high when compared with other chiral stationary phases. In consequence, excellent separations should be possible to achieve in theory, but in practice several factors often lead to rather modest results, especially in terms of resolution. The heterogeneity in the binding site affinities and accessibilities in non-covalently imprinted polymers often leads to band broadening and peak tailing, and thus to a poor column efficiency. Even for non-retained compounds, low plate numbers ($2000\text{--}5000\text{ m}^{-1}$) are usually obtained. One factor which has a deleterious effect on the separation is the unfavourable shape and size distribution of particles, which leads to poor flow characteristics and low functional capacities. A good strategy to improve the performance of imprinted stationary phases should therefore take into account the following aspects:

- *Optimization of particle size and shape.* This can be achieved by using suspension polymerization procedures for instance, which can generate uniformly sized spherical beads of controlled dimension.
- *Optimization of the column packing.*
- *Optimization of the mobile phase.* In many cases, the addition of competitors can improve peak shapes, and carefully designed gradient elution protocols can minimize tailing, especially of the more retained peak.
- *Increasing the capacity of the imprinted stationary phase.* This can be realized by optimizing the polymer recipe. It has been shown that substituting trimethylolpropane trimethacrylate for ethylene-glycol dimethacrylate as the crosslinker leads to higher load capacities, since a lower degree of crosslinking is necessary and more functional monomer can be accommodated in the polymer,

i.e. the number of theoretical binding sites is increased.

By these means, improved separation and resolution can already be expected. However, the most important issue is certainly the binding site heterogeneity, which is undesirable and has to be addressed. In order to obtain a more homogeneous population of binding sites in an imprinted polymer, the pre-polymerization complex between the template and the functional monomers has to be stabilized. Certainly, covalent bonds should give the best results in this respect, but even stronger or multiple non-covalent interactions between monomer and template will afford a more stable complex. For example, acrylamide or trifluoromethylacrylic acid can in some cases be substituted for methacrylic acid, resulting in a considerably improved separation which can be attributed to the stronger noncovalent bonds formed by these monomers as compared to methacrylic acid.

Thin Layer Chromatography

Finely ground imprinted polymer coated on to an inert support has been suggested for use in chiral TLC. Although only a limited amount of work has been done in this area, it has been shown that the racemates of a number of amino acids can be resolved. Problems were encountered due to band broadening, which led to the formation of zones rather than small spots or thin bands. This in turn led to band overlap and poor resolution, and measurements of R_f values were also made more difficult. However, this method may nevertheless be attractive for the determination of the enantiomeric purity of compounds such as a chiral drugs, owing to its simplicity, its speed and the possibility of running multiple parallel samples. Optimization of particle shape, size and porosity, similarly HPLC, will probably result in considerably improved shape of the bands.

Capillary Electrophoresis

The feasibility of using imprinted polymers as selective matrices for affinity capillary electrophoresis and capillary electrochromatography has been demonstrated. Owing to the difficulty in packing ground polymer particles or polymer beads into microbore capillaries, an *in-situ* polymerization seems better suited for this application. Imprinted capillaries have been prepared by *in-situ* synthesis of a macroporous polymer monolith within the capillary, which can be covalently attached to the capillary wall. Ideally, the polymerization is carried out in such a way that

the capillary is not completely filled with polymer and an axial flow-pore is obtained, which allows the solvent to be exchanged easily. Entrapping imprinted polymer particles in a polyacrylamide gel formed *in-situ* in the capillary has been suggested as an alternative way of preparing imprinted capillaries. However, this approach seems to be somewhat less practical since the solvent cannot be exchanged easily and because the lifetime of such capillaries may be rather short due to problems with air bubble formation during operation.

Enantioselective imprinted columns for capillary electrochromatography could be very useful, especially because considerably higher efficiencies can be obtained ($>100\,000$ plates m^{-1}) than with HPLC columns. Chiral separations of drugs such as the β -adrenergic antagonist propranolol have been achieved within 2 min, and an enantiomeric mixture containing as little as 1% *S*-enantiomer could be resolved. Since imprinted capillaries can be prepared quickly and easily, and are normally very stable in use over a period of several months, this represents a highly promising development for analytical chiral separations.

Membrane-based Separation

Chromatographic separation techniques are well established and widely used, however they do have some limitations, especially in the scale-up of separation processes. For larger-scale separations, they are therefore often replaced by membrane-based techniques, since membranes can be used in continuous mode unlike the batch-wise operation in chromatography.

Polymeric membranes can be made specific for certain target molecules by molecular imprinting. Imprinted membranes have been prepared in different ways; they can be cast directly as a thin layer on a flat surface or between two surfaces, and may or may not contain a stabilizing matrix. Alternatively they can be prepared by a phase inversion precipitation technique. Although imprinted membranes have great potential for applications in separation, especially chiral separation (enantiomeric polishing), they have until now merely been used in model studies and as recognition elements in biomimetic sensors. As an example, molecularly imprinted polymer membranes have been shown to be capable of distinguishing between enantiomers or otherwise closely related molecules. Usually, such membranes facilitate the diffusion of the compound which was imprinted relative to other closely related molecules. Thus, a membrane imprinted with 9-ethyladenine showed faster transport of adenosine

than of guanosine. In other applications, selective retention by the membrane of the compound which was imprinted has been observed. For example, chiral discrimination was possible for D,L-phenylalanine, with the passage of the imprinted enantiomer being retarded.

Solid-phase Extraction

Owing to their ability to bind antigens specifically, antibodies have been used in immunoaffinity chromatography and immunoextraction protocols specifically to enrich an analyte prior to its quantification in, for example, medical, food and environmental analysis. Furthermore, it has been demonstrated that the natural receptors can be successfully replaced by imprinted polymers. The use of imprinted polymers for sample concentration and clean-up by solid-phase extraction is attractive due to their high specificity and stability, and also their compatibility with both aqueous and organic solvents. Often the work-up of samples in routine analysis involves a solvent extraction step or a solid-phase extraction step with a more general adsorbent, e.g. an ion exchange or hydrophobic resin. This could be replaced by solid-phase extraction with an imprinted polymer. The advantages are an increased selectivity of the extraction step, and a reduced solvent consumption.

The applicability of this method for analysis has been demonstrated on a number of model compounds such as drugs and herbicides, which can be selectively extracted even from complex samples like beef liver extract, blood serum, urine and bile. For example, the analgesic drug sameridine could be extracted from blood plasma at a concentration of 20 nmol L^{-1} , and subsequently quantified by GC. In this way, much cleaner chromatograms were obtained as compared to the standard liquid-liquid extraction method (Figure 3), since fewer contaminants were co-extracted with sameridine by the imprinted polymer-based method.

In analytical applications, problems may be encountered due to small amounts of template remaining in the polymer even after very thorough solvent extraction. This may falsify the results of the analyte quantification following the solid-phase extraction step if traces of the template are released into the sample. A possible solution to this problem is to use, as the template, a molecule with a structure very closely related to the target analyte, rather than the analyte itself. In such a case, the polymer may still bind the target analyte specifically, whereas traces of template liberated during the extraction procedure can be separated from the target analyte upon sub-

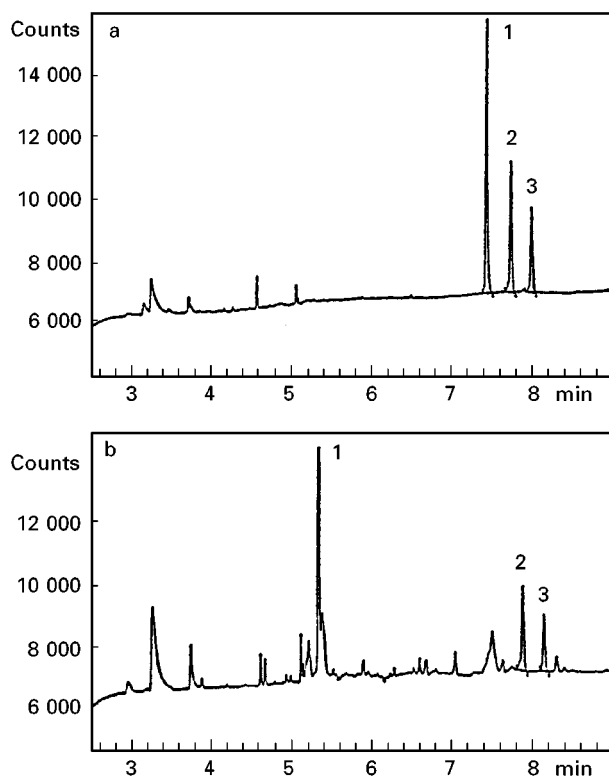


Figure 3 GC traces of human plasma samples spiked with sameridine and an internal standard, and subjected to (a) solid-phase extraction with an imprinted polymer, and (b) standard liquid-liquid extraction. The peaks are the template molecule (1) (a close structural analogue of sameridine), the analyte sameridine (2) and the internal standard (3). (Adapted with permission from *Chromatographia* (1997) 46, 57).

sequent analysis. This approach was demonstrated very nicely for the sameridine case described above, where a close structural analogue of sameridine was imprinted. The polymer displayed a high affinity for sameridine as well as for the analogue, but the two compounds could be readily separated by GC and the sameridine quantified.

Apart from analytical applications, imprinted polymers may also be used for preparative separations, e.g. for product recovery during chemical and enzymatic syntheses, or from fermentation broths or production waste streams. However, for the time being at least, the low binding capacity of imprinted polymers might limit these applications.

It should also be mentioned here that imprinted polymer particles or beads can be made magnetic, which can be advantageous in both analytical and preparative applications since it enables easy removal of the polymer from the extracted medium.

Conclusions

In summary, molecularly imprinted polymers have much to offer to the area of affinity separation. Their highly attractive physico-chemical properties allied to their impressive molecular recognition properties make them particularly well suited for application in a number of important areas, including chromatography, solid-phase extraction, capillary electrophoresis and membrane separations. The period of hitherto unknown expansion, which the molecular imprinting field is currently enjoying, bodes well for the future, and molecularly imprinted polymers will surely play an ever increasing part in affinity separation as the molecular imprinting field matures further.

See also: **II/Extraction:** Solid-Phase Extractions. **III/Chiral Separations:** Molecular Imprints as Stationary phases; Thin-Layer (Planar) Chromatography.

Further Reading

- Ansell RJ, Ramström O and Mosbach K (1996) Towards artificial antibodies prepared by molecular imprinting. *Clinical Chemistry* 42: 1506.
- Bartsch RA and Maeda M (eds) (1998) *Molecular and Ionic Recognition with Imprinted Polymers*. A.C.S. Symposium Series 703, American Chemical Society, Washington, DC.
- Mayes AG and Mosbach K (1997) Molecularly imprinted polymers: useful materials for analytical chemistry? *Trends in Analytical Chemistry* 16: 321.
- Mosbach K and Ramström O (1996) The emerging technique of molecular imprinting and its future impact on biotechnology. *Bio/Technology* 14: 163.
- Sellergren B (1997) Non-covalent molecular imprinting: antibody-like molecular recognition in polymeric network materials. *Trends in Analytical Chemistry* 16: 310.
- Wulff G (1995) Molecular imprinting in cross-linked materials with the aid of molecular templates – a way towards artificial antibodies. *Angew. Chem. Int. Ed. Engl.* 34: 1812.

Molecular Imprint Polymers

See **II/AFFINITY SEPARATION/Imprint Polymers**

Rational Design, Synthesis and Evaluation: Affinity Ligands

G. Gupta and C. R. Lowe,

Institute of Biotechnology, University of Cambridge,
Cambridge, UK

Copyright © 2000 Academic Press

Introduction

For years, the structure, function and dynamics of proteins have intrigued biochemists and chemists and inspired the design of targeted low molecular weight drugs. Today, as biotechnology progresses, proteins are themselves being used in the treatment of several diseases. Almost every gene can now be cloned and its protein product produced in any expression system depending on the desired folding, stability, post-translational modification, cost of production and ease of recovery. An increase in the isolation of large volumes of recombinant proteins such as antibodies, antivirals, cytokines, enzymes, clotting factors and vaccines for therapeutic, diagnostic and research purposes has made efficient protein purification the most important step in the recovery of efficacious and fully active biopharmaceuticals.

All steps in the production of biopharmaceuticals need to be compliant with the safety guidelines laid out by regulatory authorities such as the US Food and Drug Administration and the equivalent European authority. The final product should be a 'well characterized biologic' with defined major impurities, if any, very low levels of DNA and viruses (less than 10 pg per dose), pyrogens (less than 300 endotoxin units per dose) and leachates from the separation matrices. **Table 1** highlights some of the quality control requirements imposed by the regulatory authorities on proteins used for clinical applications. Commonly purified end products are mixtures of isoforms of proteins with variations in post-translational modifications such as glycosylation, oxidation, end terminal alterations, misfolding, incorrect disulfide bridging and nicked or truncated variants. Thus, techniques such as high performance liquid chromatography (HPLC), peptide mapping, capillary electrophoresis, isoelectric focusing, circular dichroism and mass spectrometry are also gaining an impetus in thorough characterization of the potency, purity and safety of protein drugs.

The increasing demand for peptides, nucleotides, low molecular weight synthetic molecules and biomimetic ligands for protein purification has inspired chemists to generate focused and general combinatorial libraries of diverse compounds. Rational ligand

or drug design can provide directionality and help increase the possibility of success, even with a small library of compounds. In this article we have tried to give the reader an overview about sophisticated technologies and alternatives to peptides and nucleotides for protein purification and the art of ligand design for focused combinatorial synthesis.

Affinity Chromatography

The choice of purification strategy is largely contingent on its performance and economics, which is related to the effectiveness of the separation strategy employed and its robustness. Conventional purification techniques based on precipitation with salts, temperature, pH and high molecular weight polymers are now being substituted by highly selective and sophisticated strategies based on affinity chromatography. This highly selective technique simulates natural processes such as biorecognition. Molecular recognition encompasses interactions such as those between enzyme and substrates, antigens and antibodies, ligands and receptors, DNA and protein interactions, viral proteins and cell surface glycoproteins, hormones and transmitters that generate a cascade of events to carry out important biological activities. Exploitation of this affinity for interaction between target proteins and their complementary ligands or binding partners is the essence of all affinity techniques. The concept can be traced back to 1910 when Starkenstein first reported the isolation of α -amylase by adsorption onto insoluble starch, and was subsequently followed by several remarkable examples. Only in the second half of the 20th century did the use of the technique gain momentum and the technique was termed affinity chromatography in 1968 by Cuatrecasas. **Table 2** outlines the historical perspectives in the development of affinity chromatography. Ever since, techniques in affinity chromatography

Table 1 Quality concerns of purified recombinant protein products

Purity, efficacy, potency, stability, pharmacokinetics and pharmacodynamics
Toxicity and immunogenicity
Presence of contaminants such as nucleic acids, pyrogens, viruses, residual host cell proteins, cell culture media contaminants, leachates from separation media and unknown impurities
Post-translational modifications; mainly glycosylation and proteolytic processing
Protein folding and aggregation

Table 2 Important dates and achievements in the history of affinity techniques

1910	Starkenstein purified α -amylase on insoluble starch
1923	Lipase enrichment on powdered stearic acid
1951	Immunoaffinity chromatography
1967	Cyanogen bromide activation, <i>Staphylococcus</i> nuclease purified
1968	Term affinity chromatography coined by Cuatrecasas, biospecific adsorbents; a new era of modern affinity chromatography begins
1970	Group-specific adsorbents (coenzymes, lectins, nucleic acids)
1972	Boronates in affinity chromatography
1978	Textile dyes
1979	High performance liquid affinity chromatography (HPLAC)
1984	Biomimetic dyes
1985	Phage display
1986	Purification tags
1990	<i>De novo</i> ligand design

have been considerably refined for compliance with present-day strict quality control demands such as end product purity, safety, potency and stability. The choice of a stable and efficient solid support, activation and coupling chemistry and selection of a ligand have been investigated in detail since they contribute to efficient recoveries of the target protein.

The most commonly employed adsorbents in affinity chromatography are based on biomolecules such as monoclonal antibodies that offer selectivity and specificity. However, these adsorbents, besides being expensive, are prone to chemical and biological degradation, and themselves need purification prior to immobilization on a solid support and may have issues such as viruses and nucleic acids associated with them. Although biologicals have high selectivity, they have low capacities, a limited life cycle and a low scale-up potential. To counteract these problems, more durable and controllable peptides, peptidomimetics and synthetic ligands were introduced.

Peptide-based Ligands

In the last few years, peptide libraries have been a major area of development for the selection of biologically active peptides. These libraries offer the opportunity to study interactions between proteins and their natural ligand and are being used as potential drugs, antimicrobials and enzyme inhibitors, as bioactive peptides and as ligands for protein purification. Peptide libraries can be generated either by phage display or synthetic solid- or solution-phase chemical approaches. One of the most widespread and commonly used peptide-based technologies, phage display was conceived in 1985 by Smith and has been revolutionary in the synthesis, diversity and application of random peptide libraries in the search for novel protein-binding ligands for purification, structural and functional studies.

Random peptides are displayed on the surface of a filamentous bacteriophage (M13 or related bacteriophages) by fusion of the desired DNA sequence with either the minor (gIII) or major (gVIII) coat proteins of the bacteriophage. Multiple copies (five to thousands) of the peptide are then expressed on the bacteriophage surface owing to the presence of several copies of the coat proteins. Preparation of a large number of random oligonucleotides helps generate a combinatorial library of several millions of peptides. Selection of the phage particles expressing the peptide sequence with the desired activity and selectivity is performed through a process termed 'bio-panning'. The desired receptor for the peptides is immobilized on a solid support and the peptide-phage particles are loaded. The peptide-phage assemblies that do not bind wash off and the ones bound are eluted and amplified in *Escherichia coli*. The entire process is repeated 2–3 times to wash away any nonspecifically or weakly bound assemblies. The sequence of the selected peptide is determined by sequencing the coding region of the viral DNA.

The criteria for evaluation of peptide libraries includes generation of all possible combinations (millions) and numbers of peptide sequences to give the maximum probability of finding success. This aspect highlights the importance of rapid and efficient high-throughput screening for analysis of thousands or hundreds of millions of peptide candidates. The length of the sequences should be such that they include equimolar amounts of the tetramers and hexamers and the library should incorporate natural L-amino acids, their D-counterparts and unnatural amino acids.

In comparison with synthetic peptide synthesis, phage display is less labour-intensive and does not involve the painstaking synthesis of limited numbers of peptides. The peptide libraries can help localize

epitopes on the surfaces of antibodies (monoclonal or polyclonal), act as enzyme inhibitors, mimic cytokines, and DNA binding proteins may be used in the design of novel ligands for peptide receptors. The ability to identify regions in a protein that interact with certain peptides without dependence on structural data and other pre-existing data is remarkable. The opportunities in drug and ligand discovery are substantiated by a number of remarkable applications in the literature.

Oligonucleotide-based Ligands

Oligonucleotide (DNA or RNA)-based combinatorial chemistry has been exploited in a technology called SELEX (systemic evolution of ligand by exponential enrichment) to identify and isolate high affinity ligands directed for proteins, nucleic acids and low molecular weight targets such as peptides. The K_d values for such types of ligands are between 10^{-9} and 10^{-12} mol L⁻¹ for proteins and between 10^{-6} and 10^{-9} mol L⁻¹ for low molecular weight targets. The methodology involves random condensation of a mixture of activated monomers for generation of a combinatorial array of nucleic acid sequences that are assessed for binding towards any target (protein, nucleic acid, peptide or low molecular weight compound). The sequences are amplified by polymerase chain reaction, and the ones that show positive activity are selected and reamplified. The numbers of sequences that can be generated by commercially available synthesizers have been reported to be 10^{14} – 10^{15} in literature. The multiple rounds of selection exponentially enrich the group of oligonucleotide ligands with high affinity for the target.

Synthetic Ligands

Low molecular weight ligands that mimic the action of biologics have gained popularity not only in drug discovery and enzyme inhibition but also in several protein purification applications. The use of synthetic chemistry for the generation of compounds bound to a solid support (resin beads, silica surfaces or plastic pins) or in solution (for latter derivatization) is a fundamental yet powerful tool. However, nonspecific binding is a major disadvantage and has prompted the emergence of rationally designed ligands or biomimetics. These biomimetics have endearing properties such as high stability, defined chemical structure and toxicity, resistance to degradation, inexpensiveness and sterilizability *in situ*. They mimic the action of natural counterparts of proteins and can selectively extract the protein of interest. The devel-

opment of such synthetic molecules has been inspired and aided by the increasing availability of protein structural data and knowledge about protein–ligand complexes.

Synthetic combinatorial libraries comprising several hundreds to tens of millions of compounds are potential sources for drugs, enzyme inhibitors and antimicrobials. Peptidomimetic and organic libraries are yielding compounds to replace biomolecules for easier manipulation of the physical, chemical and biological properties and to address issues related to cost and availability. Oligomeric *N*-substituted glycines (NSG) or peptoids are novel polymers that are also being widely used for generation of vast chemical libraries. They are achiral, protease-resistant, inexpensive and are hydrolytically and enzymatically stable.

Design Rationale

A valuable approach in biotechnology involves the marriage of several technologies for the production of commercially viable diagnostics and therapeutics. The process of exploiting structural analysis, chemical synthesis and advanced computational tools when combined with rational design makes the technology more powerful, faster and logical. Structure elucidation of proteins by X-ray crystallographic and nuclear magnetic resonance (NMR) studies and improvement in software algorithms to generate homology models form the basis for rational ligand or drug design. Software programs provide us with an opportunity to calculate, visualize, formulate and hypothesize about the properties of molecules in terms of energy and orientation in their functionally active three-dimensional state and in complex with putative ligands.

The research strategy for the identification of key ligands typically involves obtaining structural information about the protein of interest, such as crystallographic, NMR or homology data. A target ligand-binding site is then identified on the protein; this may be an active site, a solvent-exposed region or motif on the protein surface or a site involved in binding the natural ligand. A combination of sophisticated modelling software packages and organic synthesis followed by activity analysis helps select a lead ligand. The optimum performance of the ligand is assessed by subjecting it to a range of experimental conditions and/or by constructing a library of near-neighbour ligands and selecting the one with desired key features. A general affinity (K_d) of 10^{-4} – 10^{-8} mol L⁻¹ between the immobilized ligand and the target protein proves satisfactory.

Design Tools

Modelling software can be used to probe properties of the three-dimensional structure of a protein such as charge distribution, key electrostatic interactions, hydrophobicity, hydrogen-bonding sites, extent of surface or solvent exposure of epitopes on the protein surface and identification of cavities, pockets and active sites. This information is essential for the site-directed *de novo* design of the ligand or drug candidates that may form novel leads. However, it is important to remember that proteins are elastic molecules that can bend and twist and even change their conformation upon ligand binding.

With an exponential increase in the availability of protein structures from the Brookhaven database (over 7000 protein entries), several sophisticated programs have emerged for modelling and visualization of molecules in three dimensions. SWISS-PROT, SCOP and the University College London (UCL) protein database (adapted from Protein Data Bank (PDB) files) are further sources for protein structures, with additional features such as LIGPLOTS of protein-ligand complexes. Homology models of proteins can be displayed with programs such as MODELLER that uses probability maps and COMPOSER that first defines the conserved regions, then the variations in structure such as loops and finally the side chains. Automated docking programs like DOCK and LUDI help predict the structure, mode and the binding free energy of the ligand-protein complexes. These programs work in conjunction with chemical structure databases such as the Cambridge Structural Database (Cambridge Crystallographic Data Centre with 110 000 compounds) or the Available Chemicals Database (100 000 compounds). HOOK is another program that generates putative ligands based on the chemical and steric complementarity between the ligand and the binding site on the protein. Calculation of molecular parameters is performed by force fields, with CHARMM, MM2, MM3 and AMBER being the commonly used programs. Force fields give information in terms of classical and mechanical potential energy functions rather than quantum mechanics.

The introduction of combinatorial synthesis has given us the capacity for multiple choices and alternatives. It is imperative not to be misled by the technique and synthesize a whole library of compounds that show no activity and cost money and time to synthesize. There are programs such as PRO-SELECT (SELECT = systematic elaboration of libraries enhanced by computational techniques) that help limit the size of a combinatorial library by using structural constraints on the protein target. Compact

molecular modelling software packages such as QUANTA, SYBYL, MACROMODEL and INSIGHT can be commercially obtained with a choice of energy minimization, autodocking and homology programs. Although there is a jungle of information and programs on drug and ligand design, these algorithms can only provide a certain rationale to rather serendipitous discoveries.

Designer Dyes

In 1968 Haeckel and others observed during gel filtration that Cibacron Blue F3G-A, the textile dye part of blue dextran, bound to pyruvate kinase. This observation subsequently led to the purification of a whole series of proteins and opened a new chapter in the role of textile dyes in protein purification. Dyes usually contain polyaromatic ring systems with electron withdrawing or donating groups and proteins contain a variety of hydrophobic and ionic residues. This complementarity assists in dye-protein interactions. Chlorotriazine dyes are inexpensive, easily synthesized and immobilized on solid support matrices and display a high capacity for proteins. The binding action mimics the binding of natural anionic heterocyclic substrates such as nucleotides, nucleic acids, adenosine triphosphate and coenzymes with enzymes. However, proteins (factor X, thrombin and kallikrein) that bind to cationic substrates have also been reported to bind nonspecifically to anionic dyes. Synthetic dyes have several advantages over biologics, although they can lack specificity. This prompted the *de novo* design and synthesis of biomimetic ligands aimed at specific sites on target proteins.

De Novo Ligand Design and Synthesis

Trypsin-like Family of Enzymes

The trypsin-like family of enzymes requires cationic substrates for their enzymatic action. Common examples are tissue plasminogen factor, factor Xa, thrombin kallikrein and urokinase. These enzymes are known to bind to the side chains of lysine or arginine at a site (primary binding pocket) proximal to the reactive Ser195. The specificity is introduced mainly by the side chain of Asp189 present at the bottom of the primary binding pocket. Secondary interactions formed by amino acids binding adjacent to the primary pocket also confer specificity to individual members of the enzyme family.

Tissue kallikrein, that has kininogen as the natural substrate, shows a marked preference for arginine in the primary binding pocket and phenylalanine on

the secondary site (Figure 1). The phenyl ring of phenylalanine is believed to form hydrophobic interactions with Trp215 and Tyr99. In contrast, trypsin demands less specificity from the secondary site residue. Thus, Burton and Lowe (1992) hypothesized that a structure based on the Phe-Arg dipeptidyl template should be designed and synthesized. The biomimetic ligand consisted of phenethylamine and *p*-aminobenamidine oriented on a triazine scaffold (Figure 2). Since the primary binding pocket of kallikrein lies in a depression, a hexamethylene spacer was introduced between the ligand and solid support to counteract any steric hindrance from the matrix backbone. On performing affinity chromatography with a crude pancreatic acetone powder, the designed synthetic ligand was able to purify kallikrein selectively with 110-fold purification factor. This efficiency compares well with the natural substrate ligands.

Artificial Protein A

Antibodies are used extensively in diagnostics, immunoassays, therapeutics and purifications, and can

be used as probes for labelling and imaging. Monoclonal antibodies, single chain and humanized antibodies have found innumerable applications in most areas of protein chemistry, biochemistry and molecular biology. However, the availability of antibodies in their highly pure form has largely limited their range of application. Immunoglobulins are routinely purified by immobilized staphylococcal protein A (SpA) or by conventional protein purification procedures. The high clinical value of immunoglobulins and disadvantages of using potentially toxic biologics in their purification initiated a remarkable study combining the powerful tools of rational computer-aided modelling and organic synthesis to generate an artificial protein A.

The crystal structure of the Fc domain of IgG and fragment B (Fb) of SpA (Figure 3) shows involvement of a total of 32 amino acid residues over an intersurface area corresponding to 400 nm². The primary forces holding the complex together are hydrophobic, hydrogen bonding and two salt bridges. The hydrophobic stacking is mainly provided by residues

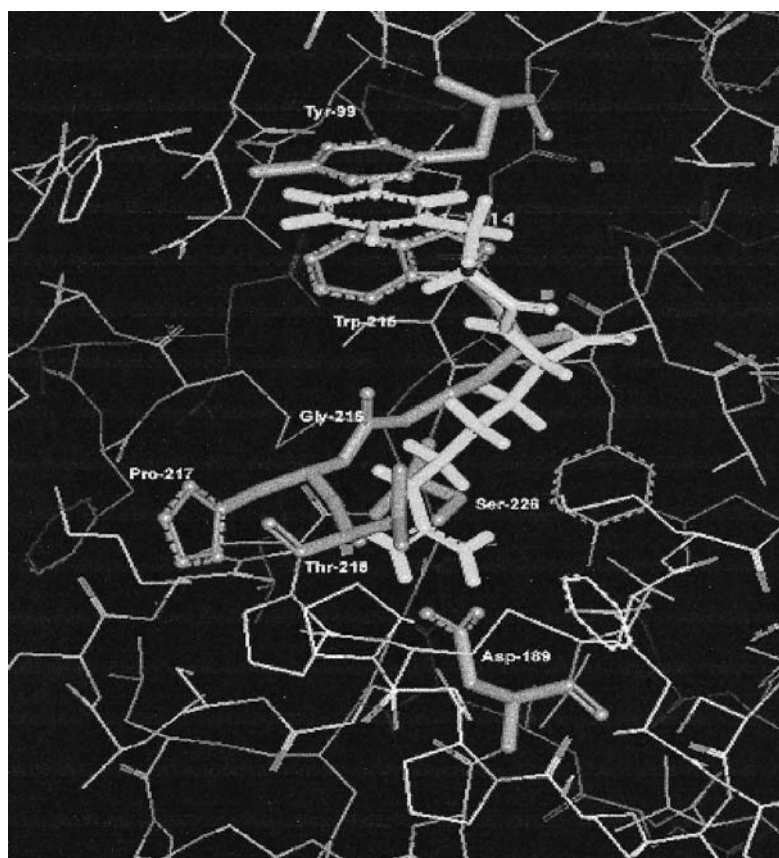


Figure 1 (See Colour Plate 15) Illustration of the molecular model of porcine pancreatic kallikrein with the dipeptidyl motif Arg-Phe occurring in the natural kallikrein substrate, kininogen. The model was generated by manipulating the BPTI-pancreatic kallikrein complex using Quanta 97. The residues in the BPTI inhibitor not involved in the complex were deleted, leaving residues Lys-15 and Cys-14, which were substituted with arginine and phenylalanine respectively. The dipeptide was energy-minimized and its side chains were adjusted to interact with the primary and secondary binding sites, as the Lys-Cys dipeptide does in the BPTI-pancreatic kallikrein complex.

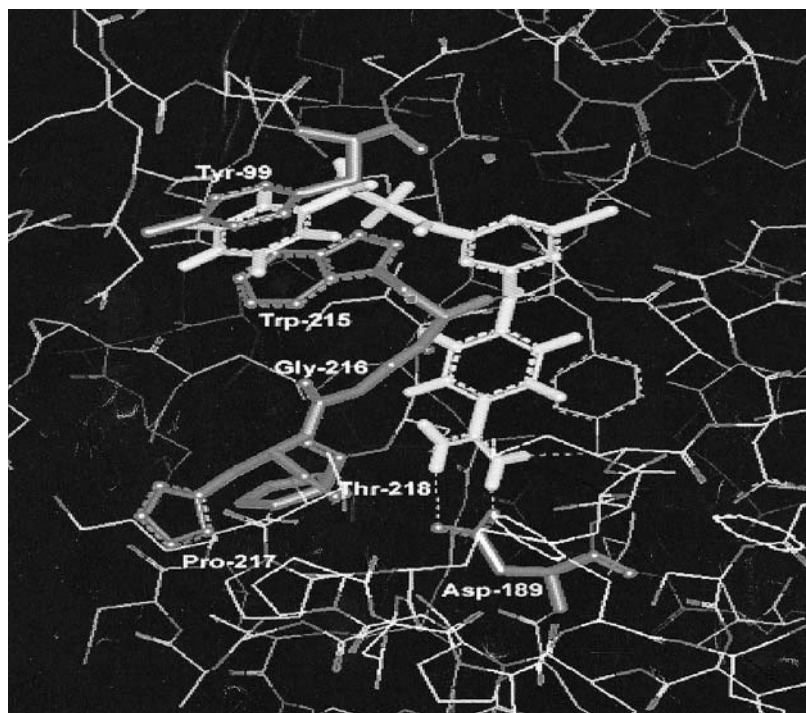


Figure 2 (See Colour Plate 16) Illustration of the synthetic ligand docked in the substrate-binding site of porcine pancreatic kallikrein. The ligand is an analogue of the Arg-Phe dipeptide that occurs in the natural substrate of kallikrein, kininogen, and is responsible for the enzyme-substrate complex. The benzamidine and phenethylamine moieties substituted on a triazine framework mimic the Arg-Phe dipeptide. The ligand was designed and energy-minimized in Quanta 97 and moved in the vicinity of the substrate-binding site, whence the side chains were adjusted to fit in the primary and secondary binding sites in porcine kallikrein. The aromatic ring of phenethylamine stacks in the primary binding site between Tyr-99 and Trp-215 and the benzamidine group forms several interactions with Asp-189, Ser-226, Gly-216, Pro-217 and Thr-218, forming the secondary binding site.

Phe124, Phe132, Tyr133, Leu136, Ile150 and the side chain of Lys154 on SpA and Ile 253 in IgG. Four hydrogen bonds can be identified between the ϵ^2 -amido group of Gln128 (SpA) and the γ -hydroxyl group of Ser254 (IgG), the δ^2 -amido group of Asn130 (SpA) and the δ^1 -carbonyl oxygen of Asn434 (IgG), the η -hydroxyl of Tyr133 (SpA) and the carbonyl oxygen of Leu432 (IgG), ϵ^2 -amido group of Gln311 (SpA) and the δ^1 -carbonyl oxygen of Asn147 (IgG). Salt bridges are formed between the δ -guanidino group of Arg146 (SpA) and the γ -carboxyl group of Asp315 (IgG) and between the ϵ -amino group of Lys154 and a sulfate ion in solution. The hydrophobic core dipeptide Phe132-Tyr133 on a helical twist of the SpA Fb region is oriented to interact with a shallow groove on IgG, comprising residues Leu251, Ile253, His310, Gln311, Glu430, Leu432, Asn434 and His435. This Phe-Tyr dipeptidyl motif is found in four highly conserved regions of SpA and each is capable of interacting with IgG from different species. If the binding pocket in IgG is made more hydrophilic by replacing the His435 with an Arg, the binding with SpA weakens, suggesting the importance of hydrophobic residues in the complex.

Li and co-workers (1998) noticed that this formed an exceptional basis for the design and synthesis of a ligand for the purification of IgG.

The biomimetic ligand (ApA) is comprised of anilino and tyramino substituents, mimicking the binding action of the Phe-Tyr dipeptidyl unit, spatially oriented on a triazine framework acting like the helical twist of SpA (Figure 4). A diethylamino spacer was used to immobilize the ligand on a solid support. This ligand proved to be complementary to the SpA binding site and had an affinity constant of 10^4 mol L^{-1} for IgG. ApA could purify 98% IgG from human plasma and also inhibit the binding between SpA and IgG on enzyme-linked immunosorbent assay. Immobilized ApA showed a capacity of 20 mg IgG per gram moist weight gel. This biomimetic ligand could be further optimized to increase selectivity, capacity and the use of milder experimental conditions. Thus, a combinatorial library comprising 88 adsorbents was constructed for lead optimization of ligand ApA. The synthesis was inspired by the 'mix and split' procedure on a triazine scaffold and was intended to mimic the binding mechanism of ApA with improved features.

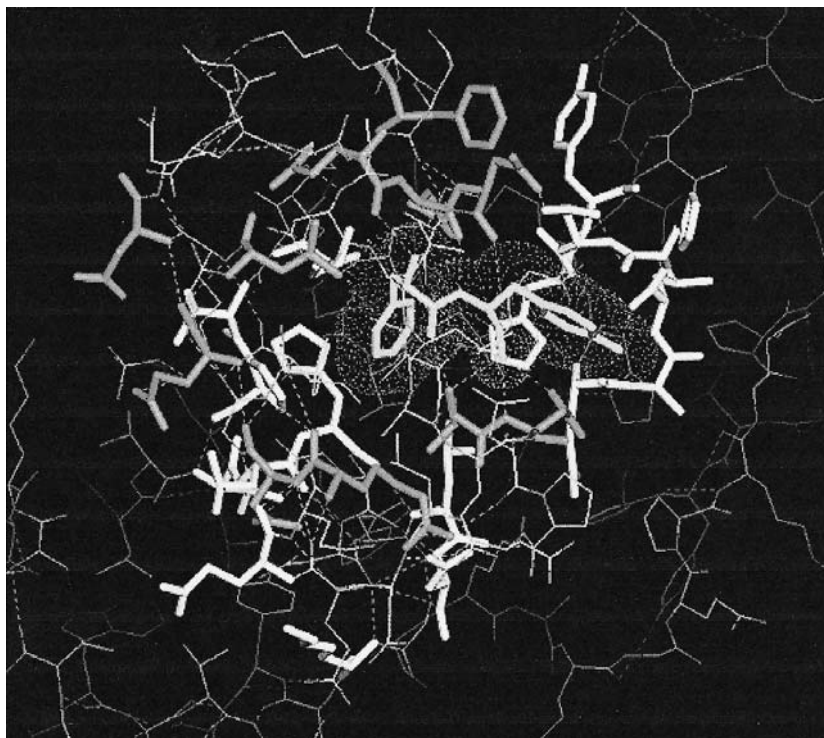


Figure 3 (See Colour Plate 17) The complex between the Fb fragment of SpA and the Fc fragment of IgG. The residues in pink represent amino acids in SpA interacting with the residues in yellow in IgG. The residues in green represent the Phe-Tyr dipeptide, key residues in holding the complex. The dotted lines represent inter- and intramolecular hydrogen bonding. The interaction involves a total of 32 amino acids spanning and intersurface area corresponding to 40 nm². The interaction is predominantly characterized by hydrophobic interactions as well as some hydrogen bonding and two salt bridges.

Combinatorial solid-phase synthesis and activity analysis suggested that a biomimetic (22/8) with 3-aminophenol and 4-amino-1-naphthol substituted on a triazinyl scaffold was able to purify IgG selectively from diluted human plasma and eluted more than 99% of bound IgG.

A similar approach was employed to design highly specific ligands for other industrially and clinically important recombinant proteins such as factor VIII and insulin. These designer ligands proved to be highly successful and were able to isolate target proteins from crude fermentation broth with high specific activities and purification factor.

Protein Structural Isoforms

Protein synthesis is accompanied by some important events, termed post-translational modifications, that convert the information carried by a two-dimensional polypeptide into a complex, biologically active three-dimensional protein. These modifications encompass events such as protein folding and phosphorylation, glycosylation, sulfation and myristoylation. Variations in post-translational modifications lead to variants of a protein that are products of the same

gene but may vary in structure, function, pharmacokinetics and pharmacodynamics. Glycosylation, the most important event during protein synthesis, has received much attention in the last few years due to its influence on the clinical and therapeutic properties of proteins. Most biopharmaceuticals produced by recombinant DNA technology, such as erythropoietin and tissue-plasminogen activator for *in vivo* administration, are glycosylated. These may suffer from glycoform heterogeneity due to variations in the carbohydrate sequence or due to variable site occupancy of the sugar moieties on the protein. Consequently, it is important to isolate, resolve and analyse recombinant glycoforms with defined glycosylation and biological properties prior to clinical prescription.

The strategy for the resolution of glycoforms involves generation of synthetic ligands that display affinity and selectivity for the sugar moieties on glycoproteins but have no interaction with the protein *per se*. A detailed assessment of native protein-carbohydrate interactions using molecular modelling tools formed the basis for the synthesis of carbohydrate-binding ligands. The ligands were synthesized on a solid phase and assessed for their sugar-binding ability with glycoenzymes. Chromatography

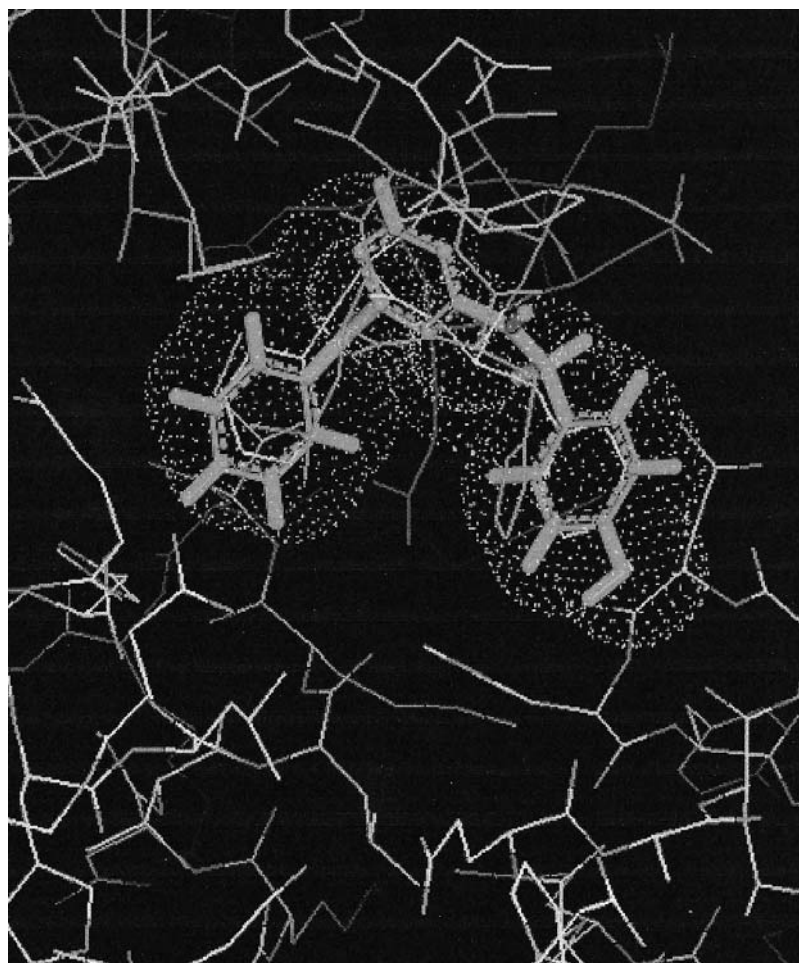


Figure 4 (See Colour Plate 18) Molecular model between the Fc fragment of IgG and the synthetic ligand ApA. The ligand, in red, is a mimic of the key dipeptide Phe-Tyr, in green, in SpA and comprises anilino and tyramino moieties substituted on a triazinyl framework. ApA is located at the putative binding site among the amino acid residues involved in the interaction between the Fc part of IgG and Fb fragment of SpA.

with partially and completely deglycosylated enzymes, elution of glycoproteins with sugars and inhibition of glycoproteins for the synthetic receptor in the presence of free sugars helped to assess the selectivity of the ligands for the sugars. Palanisamy and co-workers (1999) observed that triazine-based ligands display selectivity for the glycomoiety on glycoproteins and identified mannose-binding synthetic ligands.

Applications

Readers can put their imagination to the test and list innumerable applications for this technology. Reliable and robust synthetic affinity ligands are being used for the purification of several therapeutically and industrially important recombinant proteins for clinical, diagnostic or research purposes. The opportunity to use efficient, nontoxic and highly characterized synthetic compounds is lucrative not only in protein purification but also in localization

(probes) and tagging of macromolecules. A major application is in the removal of contaminants such as endotoxins, misfolded protein conformations, nucleic acids and viruses during recombinant protein production.

The applications of these synthetic low molecular weight ligands as drugs are forthcoming and these highly specific, nontoxic, characterized, inexpensive, easy-to-synthesize and nonlabile compounds could prove to be blockbuster therapeutics. The direct use of these ligands as drugs in diseases such as cancer stems from the fact that during infection there is an increased vasculature for nutrient supply. This is aided by overexpression of certain proteins that, if blocked from interacting with their complementary receptors, could help circumvent tumours.

Application of peptides and oligonucleotides as drugs, high affinity ligands or potent inhibitors is still in its infancy. The problems of low oral activities and susceptibility to hydrolysis has initiated tagging

the products with conjugates such lipophilic agents and polymers that not only reduce degradation but may enable efficient uptake by cells. However, a putative application is in identifying epitopes on proteins for receptor-binding studies, drug design and inhibition of proteases, proteins and oncogenes. In fact, the technology could complement rational ligand design when structural data for proteins are absent.

Bioprocess monitoring is another application that stems from requirements for optimizing cultivation conditions and harvesting times for recombinant protein products in fermentors. Modern bioprocessing demands control of several processing parameters with engineering ingenuity to obtain online monitoring to reduce labour, cost and analysis time. The ability to measure specific macromolecules in a fermentor in the presence of a soup of nutrients, host cell proteins, media components and other impurities requires highly selective and efficient ligands that can also be sterilized *in situ*. The selective biorecognition system, when incorporated with a sensitive transducer for interpreting the biorecognition signal into a comprehensible electric signal, generates a reliable biosensor for online measurements.

Conclusions and Future Prospects

Success in biotechnology and biochemistry is well attributed to developments in analytical techniques and instrumentation. The production of several high value therapeutics would not have gone to completion if it were not for efficient methods in protein purification. Conventional purification techniques are becoming outdated for industrial applications, and technologies based on proteins, peptides and oligonucleotides have gained an impetus, although they are prone to enzymatic and chemical degradation and have short *in vivo* and *in vitro* lifetimes. Peptides and oligonucleotides make undesirable drug candidates owing to poor oral activities. Furthermore, peptides have a large number of conformations that may be highly flexible and which can make attainment of the most favourable conformation and orientation difficult and lead to low affinity ligand-protein complexes.

The current focus is on compounds that lack the repetitive backbone units linked by facile bonds prone to chemical and biological (proteases and nucleases) cleavage. Thus, large number of alternative methodologies have been proposed to replace the peptide bond (peptidomimetics) with the use of peptoids, carbamates, sulfones, alkenes, urea, phosphodiesteres and sulfonamides.

Sophisticated organic synthesis has inspired chemists to synthesize receptors, drugs, peptides, nucleo-

tides and their mimetics to identify epitopes on surfaces of proteins for therapeutic, diagnostic, inhibitory and purification purposes. A combinatorial approach has become the choice of several chemists to maximize the possibility of success for lead generation, optimization and development of candidate drugs or ligands. However, it is very expensive and laborious to produce, screen and manage data for all these compounds. Some direction and rationale is essential. Information about structure-activity relationship lends that extra information that can help in pre-selection.

The availability of fast and sophisticated computer modelling software packages and the marriage of rationale and serendipity makes the design and synthesis a successful venture for investigation. A prerequisite in *de novo* design of biomimetics ligands is the availability of protein structural data and information on protein-ligand complexes. With the advances in proteomics, protein structural availability is hardly a limiting issue. In the coming years, there will be an explosion of protein structural data. The completion of the Human Genome Project will unveil countless new proteins, challenging methodologies such as random screening, rational design, combinatorial chemistry and high-throughput screening to become rapid, inexpensive and fully automated with the incorporation of robotics. Simultaneous developments in data management, proteomics and bioinformatics will integrate the technology and reduce time, cost and labour. The challenge to mimic the action of natural biological recognition is ongoing, and, as nature uses only a repertoire of 20 amino acids to generate an endless combinatorial list of proteins, the challenge for rational ligand design continues.

See Colour Plates 15, 16, 17, 18.

See also: II/Affinity Separation: Affinity Membranes; Biochemical Engineering Aspects; Covalent Chromatography; Dye Ligands; Imprint Polymers; Theory and Development of Affinity Chromatography. **Appendix 2/Essential Guides to Method Development in Affinity Chromatography.**

Further Reading

- Burton NP and Lowe CR (1992) Design of novel affinity adsorbents for the purification of trypsin-like proteases. *Journal of Molecular Recognition* 5: 55.
- Cuatrecasas P and Anfinsen CB (1971) Affinity chromatography. *Annual Reviews in Biochemistry* 40: 259.
- Haeckel R, Hess B, Lauterborn W and Wuster KH (1968) Purification and allosteric properties of yeast pyruvate kinase. *Hoppe Seylers Zeitschrift für Physiological Chemistry* 349(5): 699
- Li R, Dowd V, Stewart DJ *et al.* (1998) Design, synthesis, and application of a protein A mimetic. *Nature Biotechnology* 16: 190.

- Lowe CR, Burton SJ, Burton NP *et al.* (1992) Designer dyes: 'biomimetic' ligands for the purification of pharmaceutical proteins by affinity chromatography. *TIBTECH* 10: 442.
- Palanisamy UD, Hussain A, Iqbal S *et al.* (1999) Design, synthesis and characterisation of affinity ligands for glycoproteins. *Journal of Molecular Recognition* 12: 57.
- Smith GP (1985) Filamentous fusion phage: Novel expression vectors that display cloned antigens on the virion surface. *Science* 228: 1315.
- Starkenstein EV (1910) Über fermentenwirkung und deren beeinflussung durch neutralisalz. *Biochemische Zeitschrift* 24: 14.
- Teng SF, Sproule K, Hussain A and Lowe CR (1999) A strategy for the generation of biomimetic ligands for affinity chromatography. Combinatorial; synthesis and biological evaluation of an IgG binding ligand. *Journal of Molecular Recognition* 12: 67.
- Tuerk C and Gold L (1990) Systematic evolution of ligands by exponential enrichment: RNA ligands to bacteriophage T4 DNA polymerase. *Science* 249: 505.

Theory and Development of Affinity Chromatography

R. Scopes, La Trobe University, Bundoora, Melbourne, Australia

Copyright © 2000 Academic Press

Introduction

The term affinity chromatography began to be used extensively in the 1960s to describe protein separation methods that made use of the specific biological interaction of the desired protein with some ligand that was immobilized on an adsorbent matrix. Since most proteins, and all enzymes, bind to some compound very specifically, this immediately promised to solve most protein purification problems. But, as with all good ideas, there were many cases when it did not work as expected; the general concept of affinity chromatography for purifying proteins found its niche, but was no panacea. More recently, it has found a fairly widespread application in purifying recombinant proteins, using very standardized procedures.

Although most applications have been for proteins, it is not so limited in theory, since other biological macromolecules have specific interactions which can be exploited, especially nucleic acids. But, for the purposes of this article, the principles will be expounded with proteins as the prime target. We should consider the definition(s) of affinity chromatography carefully, since it does not mean the same to everyone. First, the word affinity. Any two components that are attracted to each other can be said to have an affinity, but if we took that as a definition, the term would be too broad to be useful – for instance, it could include all types of chromatography. It is better to limit the definition of affinity to a biologically significant interaction such as between a hormone and its receptor, an enzyme and its substrate, or an antibody and its antigen. Unfortunately, there are well-established uses of the term, such as immobilized metal affinity chromatography, in which

the interaction is not biologically relevant, though it too can be highly specific. Perhaps a better definition could imply simply a high specificity and selectivity of the interaction, though that can exclude some examples of true biological affinity.

The other word, chromatography, strictly means that process in which components are adsorbed and desorbed continuously as they move down a column, or through some other medium, resulting in a multi-stage separation of different components according to their partitioning between the stationary and mobile phases. But affinity methods are usually treated in an 'on-off' fashion in which, after total adsorption of the desired component, a stepwise change in the buffer mobile phase results in its complete elution, and true chromatography is not carried out. Nevertheless, the word chromatography is used more widely than its strict definition, to encompass any use of an adsorbent, even in this 'on-off' fashion.

And so we come up with a definition of affinity chromatography as a chromatographic procedure utilizing an adsorbent involving an immobilized ligand which has a high specificity for binding the desired component, preferably to the exclusion of all others. This binding can be loosened by a change in buffer conditions, to elute the desired component relatively free of contaminants. If the ligand is the natural biological ligand of the desired component, then the more precise term bioaffinity chromatography can be used. On the other hand, when the interaction is specific, but the ligand is unnatural, terms such as pseudo-affinity chromatography and biomimetic chromatography have been adopted.

Early Developments in Affinity Chromatography

The first protein to be purified by affinity chromatography was amylase in 1910, for which a column

packed with starch was used. Presumably the column disintegrated during the process! Attempts were made in the 1950s to link antigens to cellulose columns for the purification of antibodies, but these were not very successful because of the low capacity of the cellulose matrix. Unless the particles used to pack the column are permeable to the proteins, only the surface of the particles is available for attachment. The more successful applications commenced when suitable protein-permeable particulate materials were developed, together with reliable chemical methods that could be used for attaching specific ligands to these materials. Much of the original work was based on the use of cyanogen bromide as a method for activating the matrix, and the use of agarose beads as the support material. Agarose has almost ideal properties, in that the gel formation of the beads has pores permeable to most proteins, so that the internal volume of the beads is all available for attachment, as well as the outside surface. Moreover, agarose in itself has virtually no affinity for any protein (other than agarases), so nonspecific binding is rarely observed. It is still the matrix of choice for most affinity chromatography, though there are now many competing materials, both polysaccharide-based and synthetic.

Activation of the matrix involves treating the material with a chemical that introduces a group (normally reacting with hydroxyls on polysaccharide matrices) which itself will then react with something, usually an amine, in the ligand to be used. All such activating chemicals are extremely reactive and dangerous to handle, especially those that are volatile. Cyanogen bromide reacts to introduce several forms of cyanate derivatives, of which the cyanate ester is the most important. This ester will couple to a primary amine, such as a lysine residue in a protein, to produce the isourea-linked ligand (Figure 1).

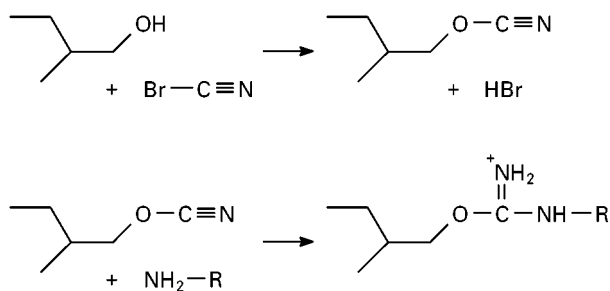


Figure 1 Activation of a carbohydrate matrix with cyanogen bromide. The major product is the cyanate ester after reaction with a primary hydroxyl group. This rapidly couples with an amine to produce the isourea structure, which is positively charged at neutral pH.

Cyanogen bromide activation is still widely used, and the dangerous chemistry is overcome by having the already-activated agarose available as a commercial product. However, it does have some disadvantages compared with other methods outlined below—in particular, the instability of the isourea linkage.

Many other activation methods have been developed, and a brief summary of these is given in Table 1. Several of these incorporate a bifunctional reagent, one end of which combines with the matrix, and the other with the ligand. These may cause some cross-linking within the matrix, but this can be advantageous for matrix stability. Bifunctional reagents also introduce a spacer arm (see below) of various lengths depending on the reagent. The activated matrix then reacts with a nucleophile such as an amine, or in some cases a sulfhydryl group in the ligand being coupled (Figure 2A).

The ligands exploited at first were mainly enzyme substrates. In particular, so-called group-specific ligands were developed which could be used for a variety of different enzymes having the same

Table 1 A selection of activation methods, and the properties of the spacer arms introduced after coupling with amino-reactive ligand. A positive charge can result in some nonspecific anion exchange behaviour at low ionic strengths. Cleaning of protein adsorbents is best carried out with alkali, but many linkages are alkali-labile

Reagent	Spacer arm length, atoms	Type of linkage	Charge at pH 7	Alkali lability
Cyanogen bromide	1	Isourea	+	Yes
Carbodiimide	1	Amide	0	Yes
Epichlorohydrin	3	Secondary amine	+	No
Bisoxirane	11	Secondary amine	+	No
Divinyl sulfone	5	Secondary amine	+	Yes
Tosyl/tresyl	0	Secondary amine	+	No
Hydroxy-succinimide	8 ^a	Amide	0	Yes
Cyanuric chloride	4	Aromatic amine	0	No

^aDepends on activation reagents.

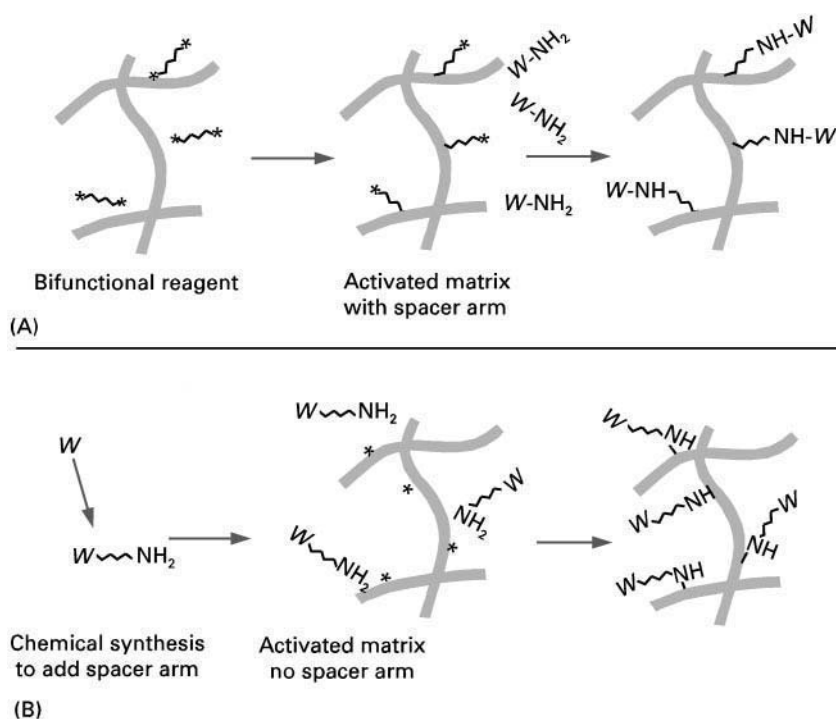


Figure 2 (A) Activation of a matrix with a bifunctional reagent, which provides a spacer arm. (B) Coupling of a ligand containing a built-in spacer arm to an activated matrix.

substrate – more particularly, a common cofactor. Thus we had, and can still purchase, adsorbents containing nucleotide cofactors such as ATP and NAD, lectins for glycoproteins and nucleic acids for binding either other nucleic acids or enzymes involved in nucleic acid metabolism. The use of affinity chromatography which exploits the interaction between an antibody and its antigen has been extensively developed, and is described in detail elsewhere.

The main problems associated with affinity chromatography soon appeared. These can be summarized as:

1. It took a long time to develop an adsorbent that does the job.
2. Once made, the adsorbent is expensive and has a limited useful life.
3. There is nonspecific binding of unwanted proteins.
4. There is a need for spacer arms.
5. There are difficulties in satisfactory elution.

Many of these problems have now been solved, with a clearer understanding of the important factors involved. It is now not often that a completely new adsorbent has to be developed. The expense parameter is less important on a research scale, but is a major consideration in large scale commercial purification. The related problems of nonspecific binding and spacer arms can usually be overcome by judicious

process design, and elution procedures for the more difficult tasks such as antibody–antigen interactions are now better established. Even so, there are many cases in which a workable true affinity method cannot be established, usually because the natural affinity may be very specific, but quantitatively weak.

Spacer Arms

The need for spacer arms was realized early on, since placing the ligand directly adjacent to the matrix might sterically hinder the interaction with the protein (Figure 3). But it has been shown that, as most spacer arms are hydrophobic, they can interact with other parts of the protein in a relatively nonspecific way. This has both advantages and disadvantages: the advantage, as described below, is that these nonspecific hydrophobic interactions can add to the binding strength of otherwise weak, though highly specific, interactions between a protein and its natural ligand. When inert, i.e. hydrophilic, spacer arms were introduced, many previously successful affinity methods did not work because the binding of the desired component was now too weak. The disadvantage of the use of spacer arms is that hydrophobic interactions with unwanted proteins may be so strong that these proteins may be bound as well.

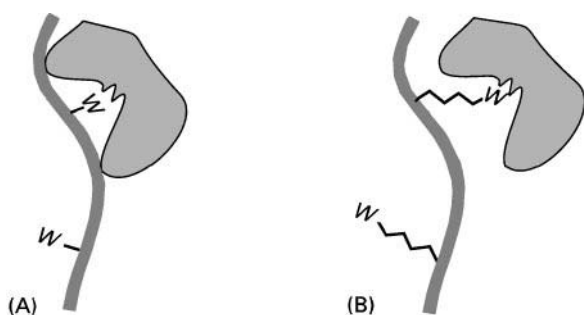


Figure 3 Demonstration of the role of a spacer arm in keeping the bound protein away from the matrix backbone. Without the arm, it may be impossible for the protein to interact with the ligand, *W*.

Spacer arms can either be introduced as part of the activation process (see **Table 1**), or added afterwards in a multi-step process of creating the adsorbent. Sometimes it is beneficial to synthesize chemically a suitable spacer arm (ending with an amine) attached to the ligand itself, when the ligand does not have a suitable active nucleophile for direct coupling (Figure 2B).

Thus, spacer arms have two possible functions in a successful affinity adsorbent. First, they place the ligand away from the matrix to avoid physical interference from the matrix backbone. Second, they can provide some weak nonspecific interactions that increase the overall binding energy so that adsorption is more complete.

Some Quantitative Parameters

For a protein to bind to an adsorbent in a column, it must have sufficient affinity (in the broadest sense) to partition to the solid phase. It need not be an absolute adsorption; the protein can be in a dynamic state between being adsorbed and in solution. An equilibrium can be established provided that the flow rate is not too great, and an equilibrium constant defined between the matrix binding sites and the protein itself. We can call this the affinity constant, equal to the association constant between the protein and the adsorbent. If the protein is to bind to the adsorbent, it must spend most of its time ($> 90\%$) in the adsorbed state so that its progress down the column is greatly delayed. We can calculate that, for strong binding the affinity constant will typically need to be at least in the range 10^{-5} – 10^6 mol L $^{-1}$. Alternatively, the reciprocal of this value may be expressed as a dissociation constants – 10 μ mol L $^{-1}$. It is useful to use dissociation constants, since they can be related to an enzyme's Michaelis constant value, which is easily determined from the enzyme's activity at different substrate

concentrations. The value of the required affinity constant depends very much on the effective concentration of binding sites in the matrix. Although the concentration of ligand attached to the matrix may be quite high, for steric reasons it is usually the case that only a small percentage are actually available for binding.

Since many enzymes do not bind their substrates with micromolar affinities, it appears that true affinity chromatography is often not possible. Nevertheless, it was soon discovered that strong binding could be obtained despite relatively high dissociation constants (i.e. weak binding) for the free ligand and the protein, and successful procedures could be developed. This was because nonspecific binding, mainly due to spacer arm interactions, increased the overall adsorption.

If we define a binding free energy for the biospecific interaction as ΔG_s^0 , and for nonspecific interactions as ΔG_n^0 , then the total binding energy is the *sum* of ΔG_s^0 and ΔG_n^0 . But the effective dissociation constant is equal to the *product* of K_{ds} and K_{dn} , the constants for the specific and nonspecific interactions. A very weak nonspecific interaction in addition to the biospecific one can tip the balance between adsorption and nonadsorption.

This theory describing an affinity constant is rather simplistic, because in fact any adsorbent will have a range of affinity constants according to the accessibility of the individual ligands. There will be some tight-binding sites which are occupied first, and weaker ones will be occupied as more sample is applied. There may be some bleeding of protein from the weakest sites as the column is washed. A further complication is the possibility of multi-point attachment, in which an enzyme made up of two or more subunits, each with a binding site, may be held by two or more ligands. Such binding would be very strong, only likely at high matrix ligand concentrations (> 20 μ mol mL $^{-1}$). All such theoretical treatments assume that equilibrium conditions exist: this is only an approximation at the flow rates that are commonly employed, and some diffusional processes are so slow that the equilibrium assumption is far from valid.

In order to elute the protein from the column, the binding must be weakened. In most cases, a decrease of ΔG_s^0 is sufficient, and this can be done by either nonspecific buffer changes such as increased salt concentration, or by specific methods (see below).

Types of Ligand

In theory, any molecule can be used as a ligand in affinity chromatography, from small ones like

amino acids to large proteins and even supramolecular fragments such as membranes or whole cells. It must be possible to immobilize the ligand in such a way that it is still recognized by its biological partner. Thus, a random attachment of an antibody through lysines will allow only a small proportion of the antibody molecules to be oriented in an appropriate way to bind with their antigen, but a more directed attachment, for instance through the carbohydrate moiety on the Fc fragment, can increase this proportion significantly. Attachment of a ligand through an amine that is part of the biological recognition site will not produce a satisfactory affinity adsorbent, and some subtle chemistry may be needed to synthesize a ligand derivative that attaches elsewhere.

Highly specific adsorbents which are expected to interact with only one protein are the ideal, but may need to be synthesized individually (antibodies are a good example of this). On the other hand, group ligands which are expected to interact with a range of different proteins will obviously be less specific, but can be used for a wide range of different purifications. Not surprisingly, it is the latter which tend to be available commercially. An example is AMP-agarose, which interacts with enzymes that have ATP or NAD^+ as substrates. Despite the fact that AMP itself binds very weakly to most such enzymes, the additional nonspecific hydrophobic interactions with the hexyl spacer arm create sufficient binding energy. Lectins, such as concanavalin A which specifically binds to mannose residues in glycoproteins, have been extensively employed. Pseudo-affinity group adsorbents such as dye ligands have many advantages, including simplicity of synthesis.

Possibly the best known types of affinity adsorbents are antibodies, for purification of antigens; protein A and protein G for purification of antibodies; and an increasing range of affinity and pseudo-affinity materials for purification of recombinant fusion proteins. This last group will be discussed below, and antibodies (immunoaffinity chromatography) are described elsewhere.

The Matrix

The vast majority of affinity chromatography adsorbents have made use of agarose as the base material, or matrix. Beads of diameters between 40 and 150 μm have been the most popular, and the agarose cross-linked to provide increased rigidity and temperature stability. But there are several propriety matrices, mostly synthetic materials, that are available as alternatives. These have mainly been developed as

high resolution, high performance adsorbents as ion exchangers, and have the desirable properties such as fast flow rates, uniform bead diameters and rigidity under high pressure conditions. These are properties that are not often relevant to affinity methods, and at least on a large scale the extra cost of these materials compared with agarose may not be justified. It is always important that there should be a minimum of adsorption of proteins on the matrix itself, and carbohydrates such as agarose satisfy that requirement better than most other materials. Although we usually talk about affinity columns, there are several other ways of using an affinity adsorbent apart from in a column. Batchwise processing can be very successful if the affinity interaction is sufficiently strong, and other configurations include stacks of membranes as matrix, with the sample being forced through the membranes under pressure.

The Elution Step

General Elution

Having bound the desired protein to the affinity column, it must now be eluted. The standard way with simple ligands is to increase the salt concentration, or use a radical shift in buffer pH. This normally interferes with natural bonding between protein and ligand, thereby weakening the affinity constant between the two. But there are many cases in which increasing salt concentration is not appropriate, especially with antibody-antigen interactions. If the adsorption has a high hydrophobic contribution, then increasing salt concentration may increase the strength of binding. In that case elution may be achievable by a very low ionic strength buffer, in combination with a slightly alkaline pH. Nonionic detergents may also assist. With immuno-adsorbents the elution is carried out by partially denaturing the antibody at low (2) or high (10) pH, or by chaotropic (structure-destabilizing) agents such as guanidine hydrochloride or sodium thiocyanate. The antigen is released, but if it is a protein, it might be denatured under these conditions.

Complete elution of all the protein from the column is fine if the adsorption has been specific, and only the desired component has been bound. But if unwanted proteins are bound in addition to the target component, then a more selective method is appropriate. The buffer conditions are adjusted so that the desired component is not quite eluted, but other proteins are, giving a preliminary clean-up. Then the conditions are adjusted again so that the desired component is just eluted, but other proteins remain on the

column. Sometimes this can be useful, but it is far preferable to use affinity techniques at the elution stage as well as at the adsorption stage.

Affinity Elution

Although it is hoped that only the desired component will bind to an affinity column, in many cases this is not so. For example, when a group adsorbent such as a nucleotide is used, there are likely to be many different enzymes with an affinity for that nucleotide which will bind to the column, and pseudo-affinity adsorbents such as dyes bind many proteins nonspecifically. Because of this, use of an affinity procedure during the elution can be highly beneficial. The principle is simple: free ligand is included in the elution buffer, and displaces the adsorbed protein from the immobilized ligand (Figure 4). The technique is called affinity elution, or biospecific elution. The displacement may occur at different pHs, different ligand concentrations, or salt concentration for each specifically bound protein that is on the column, since each is likely to have a different affinity constant. Thus, it is possible to elute the desired protein under conditions when few, if any, of the others accompany it. By applying affinity concepts at both the adsorption and the elution stages, a high degree of purification is obtained. The concentration of ligand used in the elution buffer must be sufficient to compete with the immobilized concentration, and generally at least 10 times the natural dissociation constant should be used. This can be quite costly on a large scale with some ligands.

Affinity elution is also valuable when the adsorption stage has been even less specific. The general concept of adding the ligand to the elution buffer so as to cause the desired protein to come off does not in itself dictate how the protein was bound in the first place. In fact, affinity elution has been very successful even with ion exchange adsorbents.

The best examples are with cation exchangers, when binding of a negatively charged ligand decreases the strength of binding of the positively charged protein to the adsorbent. But the most generally used adsorbents in which affinity elution is applied are the pseudo-affinity dye adsorbents.

Affinity Chromatography of Recombinant Proteins

During the last few years the use of affinity chromatography has become very widespread due to the ability, using molecular biology techniques, to modify proteins so that they can bind to specific adsorbents. The basic principle is illustrated in Figure 5. The gene encoding the protein is fused to DNA which encodes either a complete protein or a polypeptide that is to be used in the affinity process. The expressed protein is then readily purified from the host proteins by passing through the appropriate affinity adsorbent. Since only one adsorbent is needed for each particular system, one laboratory may use the same adsorbent for all its protein purifications. A brief list of some of the combinations of fusion/adsorbent is given in Table 2. These are all commercial products, and there is considerable competition, with new ones being introduced all the time. A popular term for the system is affinity tagging, with the tag being the fusion part. No one system is ideal for all proteins. In particular, the level of expression obtained can be dependent on the fusion type, and the maximum possible expression is required to optimize the overall process.

The end-product of the purification is not the original protein, but a fusion with the added protein or polypeptide. For many purposes this product is good enough, but there are methods of removing the fusion portion, generally by proteolysis. Vectors for creating fusion proteins include an amino acid sequence that is

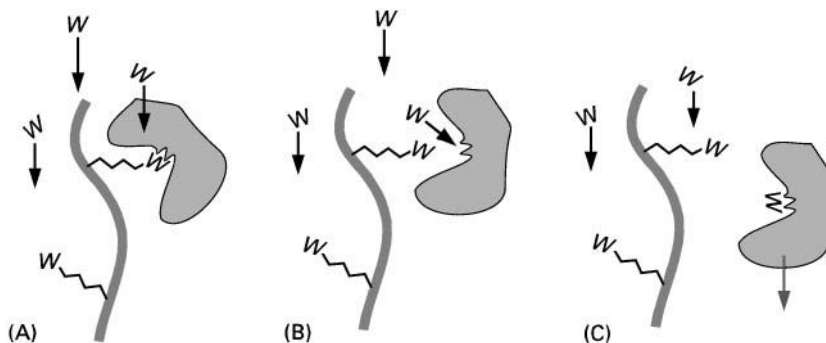


Figure 4 Principles of affinity elution. The specifically bound protein is displaced by binding preferentially with the free ligand, W , present in the elution buffer. Other proteins which may be adsorbed nonspecifically do not interact with ligand W , and so remain on the column.

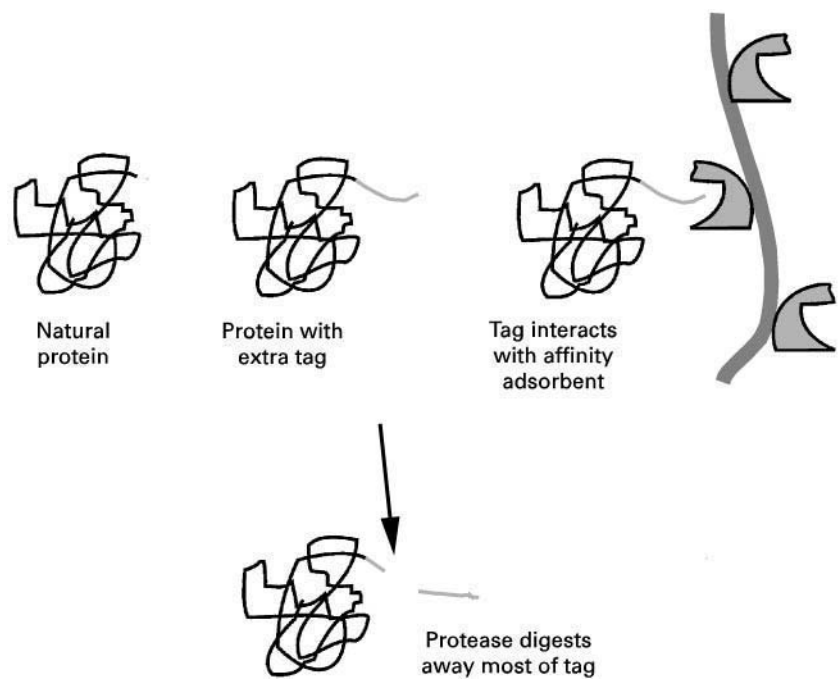


Figure 5 Principle of affinity tagging. The protein is expressed in recombinant form with an extra polypeptide tag. This may be a few amino acids, or may be a complete protein. The affinity adsorbent recognizes the tag, whereas untagged proteins are not adsorbed. The tag may be removed with a protease, either while still on the column, or after elution.

recognized by a highly selective proteolytic enzyme such as a blood-clotting factor. Treatment with this enzyme, either before or after the fusion protein has been eluted from the affinity column, releases the original protein, though still with a few extra amino acids in most cases.

Future Developments

We may assume that current trends will continue. As the number of gene sequences continues to expand, with the completion of the human genome project not far off, not to mention the many other genomes being sequenced, there will be more demand to ex-

press and purify these gene products. In many cases the actual nature of the protein will be unknown, with no assay available. By having a reliable fusion system, as outlined above, gene products can be isolated without knowing what their biological function is. So the use of standard affinity materials will be a major item in protein purifications in the near future. But there will still be a need for the more personal affinity system, for studying and isolating components of protein-protein or protein-DNA interactions. For this, the researcher needs a reliable activated matrix (such as those that have been commercially available for many years), to which to add the protein or DNA and get instant attachment.

Table 2 A selection of affinity tagging systems available commercially. Most tags are placed at the N-terminus of the expressing protein, but some, notably the hexahistidine, can be placed at either end

<i>System: fusion protein</i>	<i>Affinity adsorbent</i>	<i>Size of fusion (kDa)</i>
Hexahistidine	Immobilized metal: Ni or Co	1–2
Glutathione S-transferase	Glutathione	26
Maltose-binding protein	Amylose	38
Cellulose-binding domain	Cellulose	35
T7 Polymerase (peptide)	Monoclonal antibody	1
Protein A (partial)	IgG	14
Biotinylation site	Streptavidin	1
Various epitopes	Monoclonal antibodies	1 +

See also: I/Affinity Separation. II/Affinity Separation: Affinity Membranes; Affinity Partitioning in Aqueous Two-Phase Systems; Aqueous Two-Phase Systems; Biochemical Engineering Aspects; Covalent Chromatography; Dye Ligands; Hydrophobic Interaction Chromatography; Immobilized Boronates and Lectins; Immobilized Metal Ion Chromatography; Immunoaffinity Chromatography; Imprint Polymers; Rational Design, Synthesis and Evaluation: Affinity Ligands. **Appendix 1/Essential Guides for Isolation/Purification of Enzymes and Proteins. Essential Guides for Isolation/ Purification of Immunoglobulins. Appendix 2/Essential Guides to Method Development in Affinity Chromatography.**

Further Reading

Coligan J, Dunn B, Ploegh H *et al.* (eds) (1995) *Current Protocols in Protein Science*. New York: John Wiley.

Harris ELV and Angal S (eds) (1990) *Protein Purification Applications; A Practical Approach*. Oxford: IRL Press.

Hermanson GT, Mallia AK and Smith PK (1992) *Immobilized Affinity Ligand Techniques*. New York: Academic Press.

Kenny A and Fowell S (eds) (1992) *Practical Protein Chromatography*. New Jersey: Humana Press.

Matejtschuk P (ed.) (1997) *Affinity Separations: A Practical Approach*. Oxford: IRL Press.

Ostrove S (1990) Affinity Chromatography. *Methods in Enzymology* 182: 357–379.

Scopes RK (1993) *Protein Purification, Principles and Practice*, 3rd edn. New York: Springer-Verlag.

Scopes RK (1997) Protein purification in the nineties. *Biotechnology and Applied Biochemistry* 23: 197–204.

Turkova J (1993) *Bioaffinity Chromatography*. Journal of Chromatography Library, vol. 55. Amsterdam: Elsevier.

CENTRIFUGATION



Analytical Ultracentrifugation

J. L. Cole, Merck Research Laboratories, West Point, PA, USA

Copyright © 2000 Academic Press

Analytical ultracentrifugation (AUC) involves the measurement of the radial concentration gradients of molecules created by the application of centrifugal force. In contrast to preparative centrifugation, which is used to fractionate mixtures, AUC is a purely analytical technique. Since the pioneering work of Svedberg and associates in the 1920s, AUC has been employed to characterize the mass, size, shape and association properties of macromolecules in solution. The technique has been broadly applied to research problems in biochemistry, molecular biology and polymer sciences and has also found practical applications in the pharmaceutical and biotechnology industries. Some of the most attractive features of AUC are:

1. Versatility: a wide variety of samples can be examined by AUC, including molecules ranging in size from sucrose to virus particles.
2. Rigor: AUC experiments are directly interpreted in the context of thermodynamic and hydrodynamic theory, so it is not necessary to run standards to calibrate each experiment.

Also, because the experiments are performed in free solution there are no complications due to interactions with matrices or surfaces that can complicate interpretation of other types of measurements.

3. Convenience: recently, new instrumentation (Beckman Coulter XL-A and XL-I) and data analysis methods have made AUC much more convenient and accessible to the general biochemistry and polymer science communities. In contrast to earlier instruments, experiments are easy to set up and centrifugation parameters and data acquisition are all under computer control. In addition, powerful desktop computers and new software have greatly accelerated the data analysis process and have also extended the capabilities of AUC.

A complete treatment of the theory and applications of AUC is beyond the scope of this article, and the interested reader is referred to the Further Reading section.

Theoretical Background

The analytical ultracentrifuge is used to perform two different types of experiments, referred to as sedimentation velocity and sedimentation equilibrium. Sedimentation velocity is a hydrodynamic technique and is sensitive to both the mass and shape of a macromolecule. It can be used qualitatively to

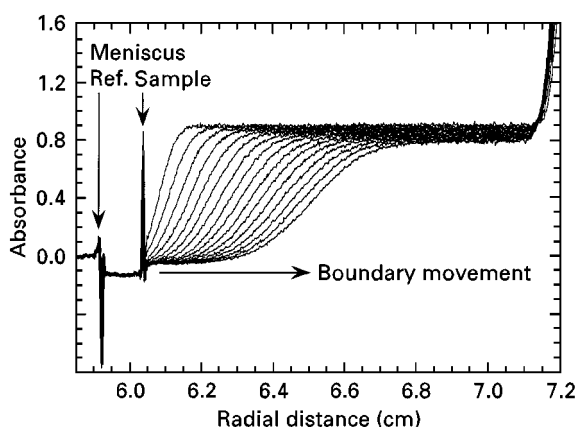


Figure 1 Sedimentation velocity of HIV-1 integrase catalytic core domain. Protein concentration 5.4 mg mL^{-1} in 20 mmol L^{-1} Tris, pH 7.5, 500 mmol L^{-1} NaCl, 1 mmol L^{-1} EDTA, 5 mmol L^{-1} DTT. Data obtained at 4°C at a rotor speed of $50\,000 \text{ rpm}$. Radial absorption scans are recorded at 250 nm at 5 min intervals. The rate of movement of the boundary is determined by the sedimentation coefficient, s , and the spreading of the boundary reflects the diffusion constant, D .

characterize sample homogeneity and quantitatively to define mass and shape parameters of the molecular species present in a sample. The experiments are based on simple physical principles. Application of a strong centrifugal field (high rotational velocity) leads to the net movement of solute molecules away from the air-solvent interface (the meniscus) and towards the bottom of the cell, giving rise to a moving boundary (Figure 1). Radial scans are recorded at regular time intervals, and the data are analysed to determine both the rate of movement and broadening of the boundary as a function of time. For a homogeneous sample, a single boundary forms; for mixtures, either a single or multiple boundaries may be resolved. In quantitative terms, the rate of sedimentation of a macromolecule, $v = dr/dt$, is proportional to the force $\omega^2 r$, where r is the radial distance from the centre of rotation, t is time, ω is the rotational velocity. The ratio $v/\omega^2 r$ is defined as the sedimentation coefficient, s . The sedimentation coefficient has the units of time, and is expressed in Svedberg (S) units ($1 \text{ S} = 10^{-13} \text{ s}$). The sedimentation coefficient may depend on concentration so it is customary to extrapolate s to zero concentration, to give s^0 . In addition, to allow comparison of sedimentation coefficients obtained in different solvents and at different temperatures, s^0 is usually corrected to standard conditions (pure water at 20°C) using the following equation:

$$s_{20,w}^0 = s^0 \left(\frac{(1 - \bar{v}\rho)_{20,w}}{(1 - \bar{v}\rho)_{T,b}} \right) \left(\frac{\eta_{T,b}}{\eta_{20,w}} \right) \quad [1]$$

where \bar{v} is the partial specific volume of the solute, ρ is the density of the solvent and η is the viscosity of the solvent. The subscript 20,w refers to properties measured at 20°C in water, and subscript T,b refers to properties measured at temperature T in a buffer solution b .

The sedimentation coefficient is related to molecular properties according to the following equation:

$$s = \frac{M(1 - \bar{v}\rho)}{N_0 f} \quad [2]$$

where M is the molecular mass, f is the frictional coefficient (which is related to macromolecular shape and size), and N_0 is Avogadro's number. The solvent parameters ρ and η are experimentally measurable or can be calculated from the solvent composition using tabulated data. For proteins, \bar{v} can be calculated with reasonable accuracy from the amino acid composition. Any further interpretation of the sedimentation coefficient requires an independent way to measure either M or f . Fortunately, the frictional coefficient is available from the sedimentation velocity data itself. During a velocity run the boundary not only moves towards the cell bottom but also becomes broader due to diffusion. Thus, in addition to measurement of the sedimentation coefficient, s , sedimentation velocity data can also be analysed to obtain the diffusion constant, D . According to the Einstein relationship, the diffusion constant is inversely proportional to the frictional coefficient:

$$D = \frac{kT}{f} \quad [3]$$

where k is the Boltzmann constant and T is the absolute temperature. Combining eqns [3] and [4] one obtains the Svedberg equation:

$$\frac{s}{D} = \frac{M(1 - \bar{v}\rho)}{RT} \quad [4]$$

where R is the gas constant. Thus, measurement of both s and D for a homogeneous sample in a sedimentation velocity experiment provides an independent method of obtaining the molecular mass. Given the mass, the frictional coefficient contains information about the shape and hydration of the molecule. Traditionally, frictional properties have been interpreted by modelling a macromolecule as a hydrated ellipsoid. However, more detailed, structure-based hydrodynamic calculations of frictional properties can now be readily performed using bead models.

In contrast, to sedimentation velocity, sedimentation equilibrium is a thermodynamic technique that is

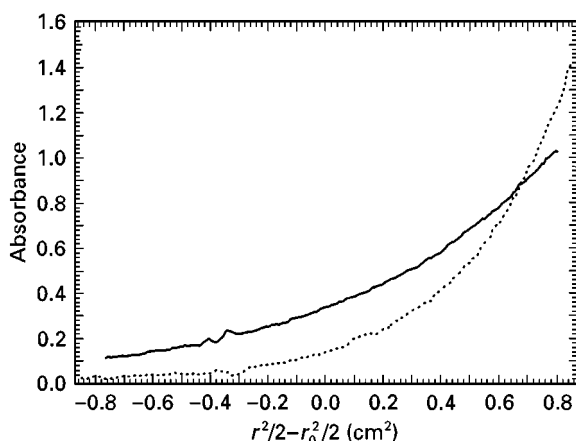


Figure 2 Sedimentation equilibrium of a 13 base pair DNA sequence. Continuous line, single-stranded; dotted line, double-stranded. 10 mmol L⁻¹ Tris, pH 7.5, 50 mmol L⁻¹ NaCl, 15 mmol L⁻¹ KCl, 0.1 mmol L⁻¹ EDTA, 2 mmol L⁻¹ Spermidine. Data obtained at 4°C at a rotor speed of 40 000 rpm. Radial absorption scans recorded at 260 nm. The molecular mass of the duplex DNA is twice that of the single-stranded form.

sensitive to the mass but not the size or shape of a macromolecule. Equilibrium sedimentation is a rigorous and very accurate method of determining the molecule mass and association state of macromolecules. It is also one of the best methods of defining reversible interactions of macromolecules in solution. Sedimentation equilibrium is performed at lower rotor speeds than sedimentation velocity experiments. When the centrifugal force is sufficiently small, the process of diffusion significantly opposes the process of sedimentation and a stable, smooth, equilibrium concentration distribution of macromolecules will eventually be obtained throughout the cell (**Figure 2**). For an ideal, homogeneous macromolecule, the radial equilibrium distribution is a simple exponential function of the buoyant mass of the macromolecule, $M(1 - \bar{v}\rho)$:

$$c(r) = c_0 \exp[M(1 - \bar{v}\rho)\omega^2(r^2 - r_0^2)/2RT] \quad [5]$$

where $c(r)$ is the sample concentration at radial position r and c_0 is the sample concentration at an arbitrary reference radial distance r_0 . Deviations from the simple exponential behaviour described by eqn [5] can result from the presence in the sample of either multiple noninteracting or interacting macromolecular species, or thermodynamic nonideality. For heterogeneous, polymeric systems, various molecular weight averages (M_n , M_w and M_z) are obtained by appropriate transformations of the data and are used to assess polydispersity and self-association behaviour. In the context of protein biochemistry, the data are usually analysed in terms of discrete oligomeric species, and equilibrium AUC is an excellent method

to determine the native association state of proteins. In the case where discrete oligomeric species are in reversible equilibrium, the stoichiometries (N), equilibrium constants (K_{eq}) and even the thermodynamic parameters (ΔH , ΔS) that define the interactions can be obtained using appropriate data analysis methods.

Instrumentation and Experimental Considerations

In addition to the drive system common to all ultracentrifuges, the analytical ultracentrifuge contains optical detection systems capable of directly measuring the sample concentration inside the centrifuge cell as a function of radial distance during sedimentation (**Figure 3**). The data can be viewed, or even analysed, in real time as the experiment progresses. The Beckman Coulter XL-A uses an absorbance optical system based on a xenon flashlamp and a scanning monochromator that allows measurement of sample concentration at wavelengths ranging from 200 to 800 nm (**Figure 3A**). More recently, Rayleigh interference optics were added, creating an analytical ultracentrifuge, the XL-I, that can simultaneously record data using both optical systems (**Figure 3B**). The Rayleigh interference optical system measures sample concentration based on refractive index changes. Each optical system has certain advantages and disadvantages. Absorption optics are particularly sensitive for detection of macromolecules containing a strong chromophore. Also, for samples containing two or more components with different absorption spectra (i.e. protein and nucleic acids), data can be obtained at multiple wavelengths during the same experiment to selectively monitor each chromophore. The Rayleigh interference optical system is used to analyse macromolecules lacking convenient chromophores (e.g. polysaccharides), as well as samples that contain strongly absorbing buffer components. It is also the optical system of choice for characterizing very concentrated samples. The data from each cell are acquired simultaneously on a CCD camera by the interference optical system, and the resulting rapid collection of large amounts of data is especially useful for certain types of sedimentation velocity experiments (see below). Interference optics are also useful for sedimentation equilibrium experiments that require a higher radial resolution than is provided by the absorbance optical system.

In AUC, the samples are contained in specialized cells which consist of a centrepiece containing channels to hold sample and reference solutions sandwiched between two quartz or sapphire optical windows. The optical pathlength is determined by the thickness of the centrepiece, and is typically 1.2 or

0.3 cm. Sample requirements are fairly modest and preparation is straightforward. It is a nondestructive technique, so the sample can be recovered following the experiment. For sedimentation velocity experiments a two-channel centrepiece is typically used (Figure 4A) and sample volumes of $\sim 420 \mu\text{L}$ are required. For sedimentation equilibrium experiments, the time to achieve equilibrium is inversely proportional to the square of the height of the sample column, and it is advantageous to use shorter columns. A commonly used centrepiece for this experiment contains three pairs of sample and reference channels requiring about $110 \mu\text{L}$ to produce a 3 mm column

(Figure 4B). The sample concentrations used depend on the nature of the macromolecule that is being examined, the sensitivity of the optical system and the analysis method. For charged macromolecules, the ionic strength should be at least 50 mmol L^{-1} to avoid nonideality due to charge effects. Samples should be equilibrated with buffer using either dialysis or gel filtration, and the equilibration buffer should be loaded into the reference sector. Analytical centrifuge rotors are available that hold either three or seven cells together with a reference cell used for radial calibration purposes (four-hole and eight-hole rotors, respectively).

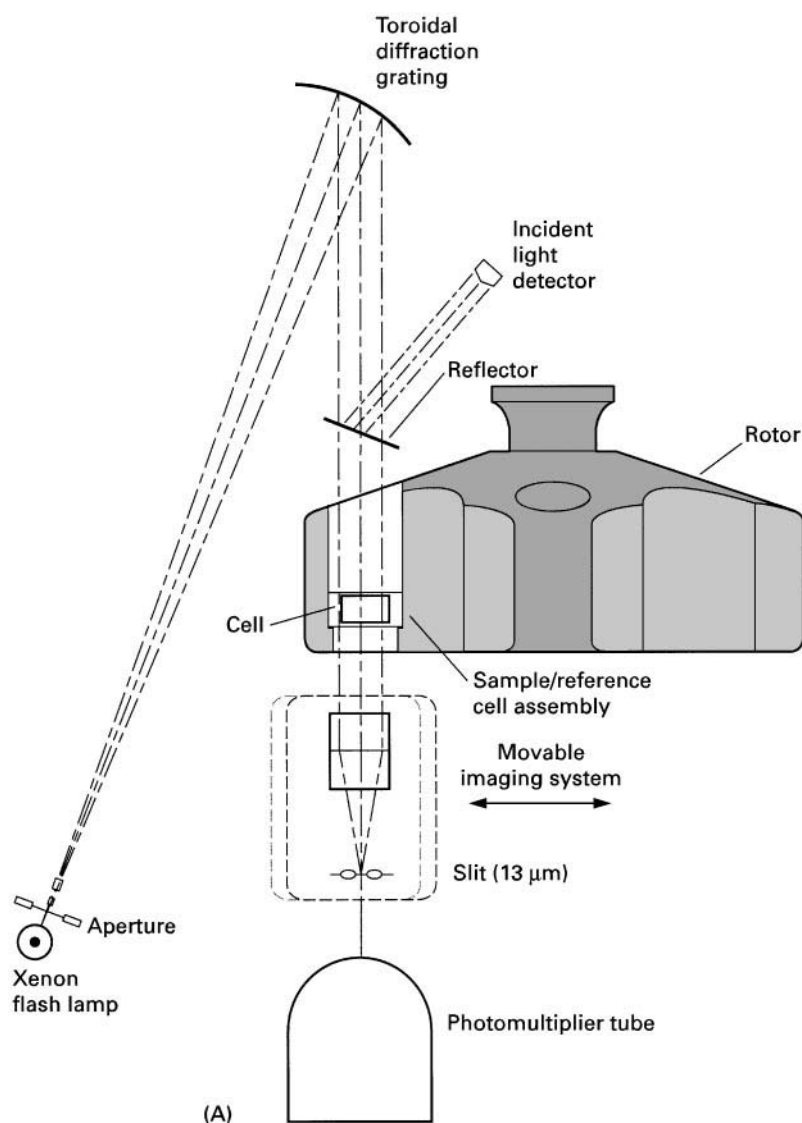


Figure 3 Optical systems in the Beckman XL-I analytical ultracentrifuge. (A) Absorption system. Light from a xenon flash lamp passes through a grating monochromator and is directed on to a sample/reference cell assembly. The transmitted light passes through a movable slit assembly and is detected with a photomultiplier tube. (B) Interference system. 675 nm light from a laser passes through a pair of slits and on to the sample and reference sectors. A series of lenses and mirrors combine the image of the sample and reference sectors to produce a fringe pattern which is imaged on a CCD camera. Refractive index changes result in vertical displacement of the fringe pattern.

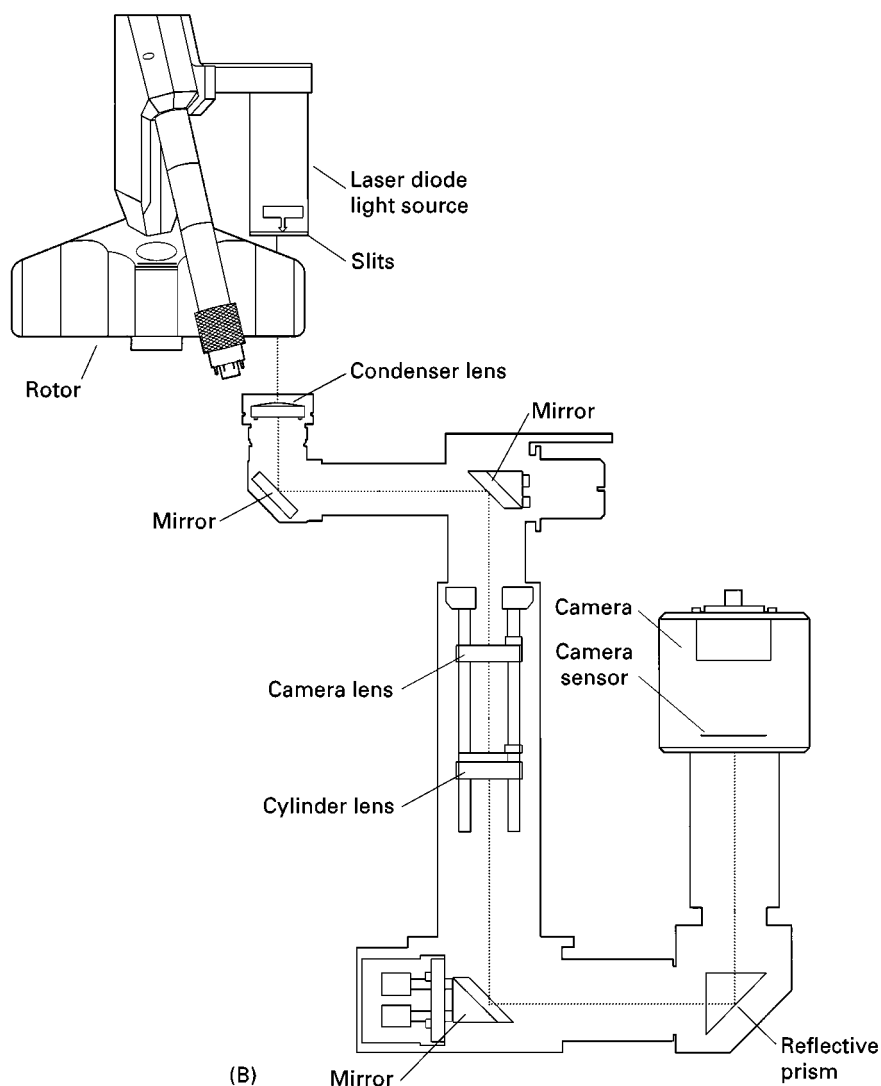


Figure 3 *Continued*

Data Analysis Methods

In order to extract the rich information that is available from AUC experiments it is necessary to use the appropriate data analysis methods. In recent years, new approaches have been developed for the analysis of both sedimentation velocity and equilibrium data. Many of these methods are implemented in software that can be downloaded over the Internet or in commercially available packages. Although much of the analysis software is deceptively simple to use, the fitting algorithms are often complicated. In order to obtain physically meaningful parameters from analysis of AUC data it is important for the user to have a good understanding of the underlying principles along with an appreciation of the limitations in the fitting procedures.

Sedimentation Velocity

In the case of a simple, homogeneous macromolecule, analysis of sedimentation velocity data provides s , the sedimentation coefficient, and D , the diffusion constant. Under favourable conditions, it is possible to extract s and D for mixtures of non-interacting macromolecular species, provided that boundaries for each species can be resolved or deconvoluted. The situation is more complicated for reversibly associating mixtures, since it is generally not possible to assign individual boundaries to discrete species.

A traditional method for analysis of sedimentation velocity experiments is to plot the natural logarithm of the boundary position versus time. The slope of this line is proportional to $\omega^2 s^*$ where s^* represents

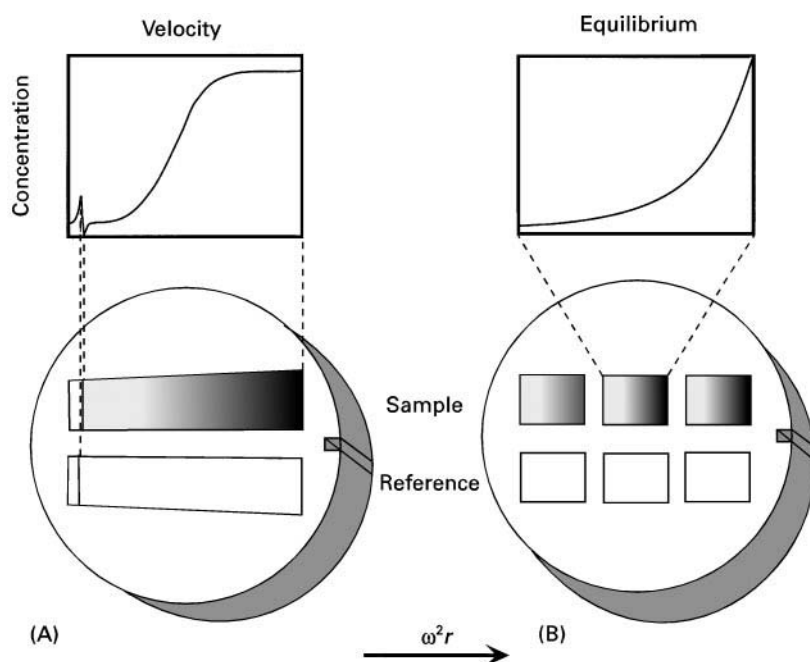


Figure 4 Sedimentation velocity and equilibrium cell designs. (A) Two-sector velocity cell. Sample is loaded into the upper sector and reference solution (buffer) is loaded into the bottom sector. The sample is centrifuged at high rotational velocity, generating a boundary that moves towards the bottom of the cell. (B) Six-channel equilibrium cell. Three sample reference pairs are loaded into the cell, which is centrifuged at moderate rotational velocity, resulting in equilibrium concentration gradients in each sample channel.

an apparent average sedimentation coefficient. This approach does not provide information about the homogeneity of the sample or the diffusion constant. Consequently, a number of analysis methods have been developed that involve analysis of the entire boundary region. In 1978, van Holde and Weischet described a transformation procedure for removing the effect of diffusion from the boundary. It is particularly useful to determine homogeneity and to detect nonideal behaviour. More recently, Stafford described a time-derivative method for analysis of velocity data in which the time-invariant noise is removed by a subtraction procedure, resulting in a great increase in the signal-to-noise ratio. This approach is particularly useful in the analysis of data obtained with the interference optics, making it feasible to work at very low protein concentrations (e.g. $10\text{--}100\ \mu\text{g mL}^{-1}$). Finally, there are methods for analysis of velocity experiments that involve directly fitting the scan data using either approximate or numerical solutions to the Lamm equation to determine both s and D . The Lamm equation is the partial differential equation that describes transport of solute(s) in the sector-shaped cells used in sedimentation velocity experiments. This approach can be used to fit data using single or multiple species models. Recently, Schuck has described a fitting algorithm which removes the radially-invariant and time-invariant noise contribution from the data, which makes

this method particularly useful for data obtained with the interference optics.

Sedimentation Equilibrium

As in the case of sedimentation velocity, methods for analysis of sedimentation equilibrium data can be divided into model-independent and model-dependent approaches. Model-independent methods are most useful to survey sample properties qualitatively, or for analysis of complex samples, i.e. polymeric mixtures, that cannot easily be described in a model-dependent analysis. In contrast, model-dependent analysis involves direct fitting of the sedimentation equilibrium concentration gradients to relevant physical models (e.g. single ideal species, noninteracting mixtures or a reversible association). This method provides the best-fit values and the associated statistical uncertainties in the fitting parameters (e.g. molecular mass, oligomer stoichiometry and association constants) and a statistical basis to discriminate among alternative physical models.

The simplest model-independent approach to obtain the molecular mass, M , is to plot $\ln c$ versus r^2 . According to eqn [5], the slope of this line is equal to $M(1 - \bar{v}\rho)\omega^2/2RT$. Although linearity of this plot has been taken as evidence that a sample contains a single ideal species, this method can be quite insensitive to heterogeneity, particularly if the concentration

gradient is shallow. Additionally, $d(\ln c)/dr^2$ can be calculated on a point-by-point basis to create a plot of the apparent weight-average molecular weight ($M_{w,app}$) versus concentration. For a homogeneous sample, $M_{w,app}$ will be constant as a function of concentration. An increase in $M_{w,app}$ with concentration indicates mass action-driven association. In this case, it is useful to overlay on the same plot data obtained from several samples over a range of loading concentrations and/or rotor speeds. For a reversibly self-associating system, all of the data will lie on a smooth curve, whereas for a noninteracting or slowly equilibrating system, the data will give rise to a family of nonsuperimposable curves. Other molecular weight averages (M_n , M_z) can also be obtained and can be useful in the analysis of associating systems or polymeric mixtures.

In model-dependent methods, a single experiment concentration gradient, or preferably, multiple concentration gradients, are fit to a physically relevant model using a nonlinear least-squares algorithm. In the simplest case of a single ideal species, data are fit to eqn [5]. For samples where there are more than one species in solution, or if thermodynamic nonideality is appreciable, it is necessary to fit the data to functions containing additional terms to incorporate sample heterogeneity, equilibrium association reactions or virial coefficients. Often it is difficult to distinguish between several models that fit the data equally well. In these cases, it is often useful to employ global methods in which multiple data sets that are collected over a wide range of sample loading concentrations and rotor speeds are simultaneously fit to a specific model. This global fitting approach helps to ensure that a unique solution is obtained and greatly reduces the statistical uncertainty in the parameters. Global nonlinear least-squares fitting of sedimentation equilibrium data was originally implemented in the NONLIN algorithm, and now several programs are available. In addition, equilibrium data are often fit using models programmed by the user within a general-purpose data analysis package.

Conclusions

AUC is a robust and widely accepted analytical method to characterize the molecular mass, size, shape and association of molecules in solution. It has been used extensively by biochemists and molecular biologists to define properties of biological macromolecules and has also found applications within the polymer science community. Experiments are performed using specialized centrifuge cells in an analytical ultracentrifuge capable of measuring radial

concentration gradients using absorption or refractometric optics. In sedimentation velocity experiments a moving boundary forms upon application of a high centrifugal force. The rate of movement of the boundary is determined by the sedimentation coefficient and the broadening of the boundary with time occurs because of diffusion. The sedimentation coefficient is a function of a molecule's mass and frictional properties whereas the diffusion constant is only determined by the frictional properties. Sedimentation equilibrium measurements are performed at lower rotation velocities where the sedimentation force is balanced by diffusion. The shape of the concentration gradient is determined by the molecular weight of the species present in the sample. A variety of computer data analysis methods have been developed for both sedimentation velocity and equilibrium data.

Further Reading

- Cantor CR and Schimmel PR (1980) *Biophysical Chemistry*. San Francisco: WH Freeman.
- Cole JL and Hansen JC (1999) Analytical ultracentrifugation as a contemporary biomolecular research tool. *Journal of Biomolecular Techniques* 10: 163–176.
- Fujita H (1975) *Foundations of Ultracentrifugal Analysis*. New York: Wiley.
- Harding SE, Rowe AJ and Horton JC (eds) (1992) *Analytical Ultracentrifugation in Biochemistry and Polymer Science*. Cambridge, UK: Royal Society of Chemistry.
- Laue TM (1996) *Choosing which optical system of the optima XL-I analytical centrifuge to use*. Beckman Coulter Application Information, number A-1821-A.
- Laue TM and Stafford WF (1999) Modern applications of analytical ultracentrifugation. *Annual Review of Biophysics and Biomolecular Structure* 28: 75–100.
- McRorie DK and Voelker PJ (1993) *Self-associating Systems in the Analytical Ultracentrifuge*. Fullerton, CA: Beckman Instruments.
- Ralston G (1993) *Introduction to Analytical Ultracentrifugation*. Fullerton, CA: Beckman Instruments.
- Schachman HK (1959) *Ultracentrifugation in Biochemistry*. New York: Academic Press.
- Schuster TM and Laue TM (eds) (1994) *Modern Analytical Ultracentrifugation*. Boston: Birkhauser.
- Tanford C (1961) *Physical Chemistry of Macromolecules*. New York: John Wiley.
- van Holde KE (1975) Sedimentation analysis of proteins. In: Neurath H and Hill RH (eds) *The Proteins*, vol. I, pp. 225–291. New York: Academic Press.
- van Holde KE and Hansen JC (1998) Analytical ultracentrifugation from 1924 to the present: a remarkable history. *Chemtracts – Biochemistry and Molecular Biology* 11: 933–943.

Large-Scale Centrifugation

T. Beveridge, Agriculture and Agri-Food Canada,
Pacific Agri-Food Research Centre, Summerland,
BC, Canada

Copyright © 2000 Minister of Public Works and
Government Services Canada

Introduction

Industrially, centrifuges are used for a variety of purposes related to separation of materials on the basis of density. This separation usually involves separation of insoluble particulates from supernatant liquids, but can also include extraction of dissolved substances from one immiscible liquid to another of different density, separating the mixed liquids centrifugally. The blending of the liquids, transfer of the solute and separation of the immiscible phases are sequentially carried out in the same machine at high speed.

Generally, centrifuges are used throughout many manufacturing industries (Table 1), to separate suspended solids from liquid utilizing the centrifugal acceleration of the suspended particles directed outward from the axis of rotation. This force initiates the particle movement to the centrifuge periphery where it is trapped or contained by the wall of the rotating body. Alternatively, a density difference between two immiscible liquids is exploited to accelerate separation of the liquids (i.e. fat separation in dairies for cream or butter manufacture). A specialized use involves separation of water from fresh-cut vegetables before modified atmosphere packaging.

Much experience and information related to industrial-scale centrifugation exists within companies manufacturing the centrifugal machinery and these sources should not be overlooked when seeking information. Table 2 lists a representative selection of companies involved in the manufacture of centrifuges and their Internet addresses current at the time of writing. The Internet itself should not be overlooked as a source of information: simply typing the word 'centrifuges' in the request space of one search engine provided over 25 000 items for perusal.

Centrifugation is treated as a separation unit operation in chemical engineering and the article in Dahlstrom *et al.* (1997) by Leung on centrifuges should be consulted for an engineering perspective (see Further Reading). For a comprehensive treatment of industrial centrifugation technology, Leung's book on industrial centrifugation technology should be consulted.

Over the past 10–15 years the growing uses for centrifuges industrially has resulted in a plethora of special centrifuges designed and adapted to particular uses. However, the machines may, in general, be characterized according to the classification of Table 3. Centrifuges fall into two general classifications, termed sedimentation centrifuges and filter centrifuges. In sedimentation centrifuges, solids are transported to the periphery wall of the rotating machine bowl and collected against this surface; liquid is removed from the solids by the close packing of the individual particulates. In filter centrifuges the solids are transported to the surface of a filter element and the solids trapped on this filter, while the liquid drains through the particulates and exits through the filter surface. The mechanism of solids drying is thus quite different between the two types of machine and the types of material each would be expected to treat most efficiently also differ considerably. The other important parameter is whether or not the machines are fed continuously or in batch mode. Generally, batch-mode machines are often considered obsolete for large scale separations, with the important exceptions of the continuing use of batch-mode basket centrifuges for the last recovery stages for white sugar and in the fresh-cut vegetable industry. Other exceptions also exist.

The approximate capabilities of several centrifuge types are indicated in Figure 1. The list is not exhaustive but examples of most types of centrifuge,

Table 1 Industrial use of centrifugal technologies

Food and agri-business

Sugar crystal recovery
Dewatering of fresh-cut salad and vegetables
Milk processing, bacterial removal, cream separation
Pulp-free orange juice
Formation of fruit and vegetable juices
Frying oil clean-up

Pharmaceutical/biotechnology

Recovery of valuable isolates
Recovery of cells (yeast and bacteria, plant and animal cells)
Clarification of fermentation broths

Environmental industries

Sewage solids recovery
Wastewater treatment
Removal of metal cuttings from industrial cutting lubricants

Chemical industries

Black coal separation from slurries
Isolation of synthetic products
Gas-phase isotope separation

Table 2 Companies manufacturing centrifugal equipment which may be contacted through the Internet^a

Alfa Laval Sharples	http://www.als.thomasregister.com
Barrett Centrifugals	http://www.barrettinc.com
Bird Machine	http://www.bakerhughes.com/bird/birdhome.htm
Carr Separations	http://www.carrsep.com
Dorr-Oliver	http://www.dorroliver.thomasregister.com
Eillert Veg. Proc. Mach. ^b	http://www.eillert.nl
Rousselet Centrifugation	http://www.rousselet.com
Tema Systems ^c	http://www.tema1-usa.com/corp.htm
Westfalia Separator	http://www.westfalia.com/default.htm

^aThe list is representative, not exhaustive. ^bFresh cut vegetable processing. ^cManufactures under licence from Siebtechnik (Germany).

along with an estimate of the range of *g* forces available from each machine type, is provided for purposes of illustration and estimation of requirements. Basket centrifuges are normally of low speed and provide maximum *g* forces in the 1500–2000 range.

Sedimentation Centrifuges

Centrifuges in this group (Table 3) collect particles against the centrifuge bowl wall. The centrifugal force exerted on a particle which causes particle movement to the wall is often expressed as the number of earth gravities (*g*) which a machine is capable

Table 3 Classification of centrifuges for industrial use according to general principles of operation

Sedimentation centrifuges

Continuous feed

Solid bowl decanter (scroll-type centrifuge)

Tricanter

Disk centrifuges (separators)

Intermittent discharge

Nozzle discharge

Hydrocyclones

Batch feed

Imperforate basket (generally considered obsolete, replaced by decanter)

Solid bowl

Tubular

Filter centrifuges

Continuous feed

Pusher centrifuge (single- or double-stage)

Screen/scroll

Screen bowl decanter

Batch feed

Vertical basket (particularly for sugar industry and fresh-cut produce)

Peeler

of developing (Figure 1). Particles sediment in the centrifugal field at a rate which increases with the centrifugal speed, increased particle size, increased density difference between liquid and solid phases, increased centrifuge radius and decreased fluid viscosity. The physical size, shape, design and construction of the centrifuge, in part, determine machine performance, but other factors affecting the properties of the feedstock are also important. Good separations of solid and liquid usually equate to high sedimentation velocity since large scale separations are usually carried out in a production plant where time is important, or in continuous-flow equipment where sedimentation velocity affects throughput rates.

Machine performance criteria are usually dependent on the purpose of centrifugation and can be measured by the purity of the separated liquid phase or the completeness of the removal of the solid phase. Performance may also be measured by several other criteria, some of which are listed in Table 4. A particularly effective method of enhancing separation performance is through increasing the diameter of the particles sedimented. This can be done by careful selection of conditions or addition of coagulants or flocculants. The purpose of coagulation or flocculation is to destabilize particles, inducing them to come together and agglomerate to form larger aggregates. This can be accomplished by modifying the surface charge characteristics, by modifying the hydrophobic/hydrophilic character of the particles, or by using surfactants to reduce water-binding characteristics. Alternatively, charge repulsion by individual particles is reduced by adding polyvalent cations such as aluminium or ferric ions. The materials and methods used to effect flocculation/coagulation are listed in Table 5. A wide array of commercially available materials are marketed carrying a wide range of molecular sizes. The flocculant/coagulant choice can be partially made on the basis of chemical knowledge of the particles to be sedimented, but the flocculant manufacturer's recommendations should also be considered in combination with empirical screening tests. Flocculant manufacturers can be particularly useful sources of information and again the Internet should not be overlooked as a source.

Sedimentation velocity is particularly important for continuous centrifuges where rapid sedimentation increases separation efficiencies and machine capacities. Particle removal from sewage particularly makes use of flocculant technology. Flocculant usage in food-processing applications is severely restricted because of health and safety regulations, and the need to provide food to consumers as free of additives as

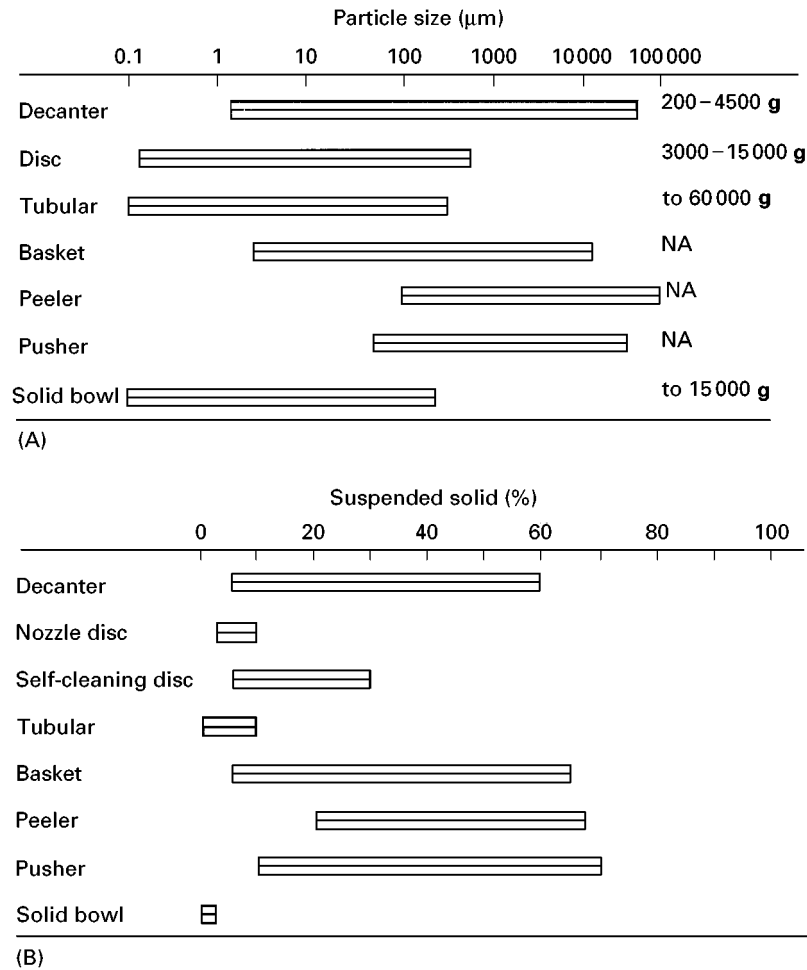


Figure 1 (A) and (B) Approximate capabilities of various centrifuge forms to sediment/separate particles and levels of suspended solids applicable. NA, Not applicable or not relevant (generally less than 1500 g). Adapted with permission from (<http://www.tema1-usa.com/centrifug.htm>) and Brunner and Hemfort (1988).

possible limits the acceptable flocculants. Downstream processing of fermentation broths or biotechnologically derived natural products for removal of particulate from a liquid stream provides another application of these flocculant materials. When used prior to unit operations such as chromatography or adsorption, these materials can help provide a clean, particle-free feed which will not block the columns

and adsorbent beds used for these purposes. Increasing the density difference between the liquid and solid phases is possible in certain applications by dilution prior to centrifugation if this is compatible with subsequent manufacturing steps, or by treatment with enzymes to hydrolyse viscous polymers and create denser core particles, which are more easily deposited. Apple juice manufacture by centrifugal means makes use of this latter mechanism. In this case, particle density is increased and the viscosity of the suspending liquid is reduced, both facilitating particle sedimentation. Another way of reducing the viscosity of the suspending liquid is to increase temperature. Increasing temperature decreases viscosity exponentially, improving sedimentation rates, thus sedimentation should be carried out at the highest temperatures compatible with preservation of any desirable properties of the material separated (supernatant or particulate), and the economics of the process being considered.

Table 4 Selected performance criteria for centrifuges according to functional definitions

Cake dryness or cake moisture content
Total solids recovery
Polymer dosage (flocculent concentration)
Yield
Volumetric or solids throughput
Purity of isolate of interest (either fluid stream or solids discharged)
Power consumption
Maintenance requirement

Table 5 Coagulants and flocculants. Adjustment of conditions or addition of specific chemicals achieves required increase in particle size

Metal salts, especially of aluminium or ferric iron ($\text{Al}_2(\text{SO}_4)_3 \cdot 16\text{H}_2\text{O}$; $\text{Fe}_2(\text{SO}_4)_3 \cdot 9\text{H}_2\text{O}$)
Natural flocculants
Starch
Gums
Tannin
Alginic acid
Sugar/sugar acid polymers
Polyglucosamine (chitosan)
Synthetic flocculants
Polyacrylamides
Polyamines/imines
Cellulose derivatives (e.g. carboxymethyl cellulose)
Polydiallyldimethyl ammonium chloride
Chilling temperatures below 20°C, particularly yeast cells
pH adjustment in range 3–6
Concentration – increases particle concentration, increasing collision frequency

Adapted from Whittington (1990) with permission.

Decanter Centrifuges

A schematic diagram of a solid bowl decanter is shown in **Figure 2**. The machine consists of a horizontally oriented cylindrical bowl with one end tapered to form a cone. Within this cylindrical/conical section is a conveying scroll, with the same profile as the cylindrical/conical bowl. This scroll is rotated at a slightly different speed from the bowl through a gear system or via a separate drive. This arrangement fixes the differential speed, allows adjustment during operation, or accommodates automatic systems. Either method ensures that the scroll turns fast enough to avoid blockage by the solids which accumulate on the scroll faces, while allowing maximum solids retention times for good separations and dry ejecta. An automatic system allows the scroll speed to be adjusted to optimize the differential

speeds under operating conditions. The length of the cylindrical and conical sections and the conical angle may be varied, as can the scroll design, to accommodate diverse requirements of feedstock to achieve solids separations. Slurry to be separated is fed continuously through the centre pipe to be distributed evenly near the level of the conical taper and is accelerated to bowl speed. During acceleration, high shear forces are generated and this may result in considerable foam generation in some slurries such as food materials which contain protein or pectin capable of retaining air in suspension.

The depth of the liquid pool rotating against the bowl wall is determined by the positioning of the fluid discharge ports, dams or pick-up tubes. Solids settle through this pool to the bowl wall and are conveyed to the outlet ports at the distal conical end where they are ejected. The solids undergo a drying effect as they are dragged along the bowl wall and elevated to the exit ports as liquid drains back to the pool. Given the decanter configuration, there are four parameters which can be varied: scroll/bowl differential speed, pool depth, bowl rotational speed and feed rate. Fluid or supernatant is conveyed countercurrent to the solids, following the path of the scroll flights, to exit at a discharge port at the end of the cylindrical section. Centrifugal force can vary to over 4000 g depending on application and centrifuge.

The decanter's particular advantage is that it provides continuous separation of a wide variety of feedstocks with a broad range of solids concentrations. It is possible to configure a decanter to process feedstocks containing an aqueous phase, an oil phase and suspended solids, separating the three phases in the same machine. These machines are sometimes termed tricanter (**Table 3**) because of the three phase separations possible. Thus the decanter can be used to separate solid-liquid two-phase systems or solid-aqueous-oily three-phase systems. Separation

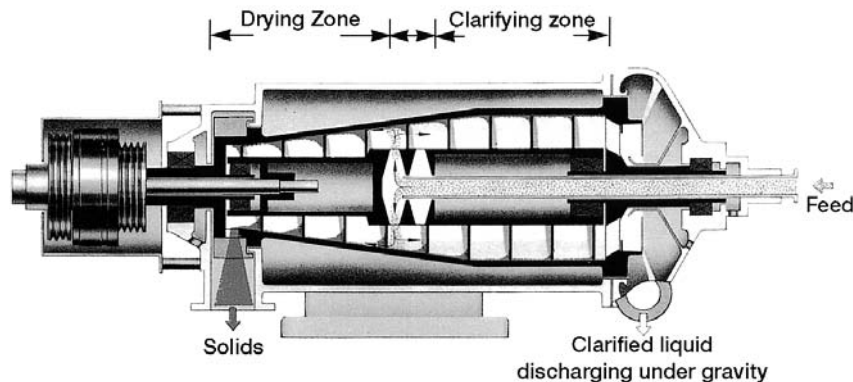


Figure 2 Schematic diagram of a decanter (scroll-bowl) centrifuge showing the major parts and indicating mode of operation. Reproduced with permission from Westfalia Separator AG, Oelde, Germany.

of two immiscible liquid phases is possible but is normally done in a disc-stack centrifuge specially designed for this purpose (i.e. cream separator). In the solid-liquid mode of operation, the ability to handle high solids content feed streams continuously, effectively and efficiently has made dewatering of municipal and industrial sewage a major use for decanter centrifuges. For similar reasons these machines have been used extensively for dewatering fine coal and for separation of mineral slurries in the mining and mineral-processing industries.

Decanters capable of separating three phases have been used to refine vegetable oils from complex feedstocks such as coconut, producing fat, milk and grated coconut solid fractions, recovery of animal fat from rendering operations and recovery of waste oil in petroleum refining. Watery oil derived from tank bottoms or trapped in containment lagoons which contain suspended solids may have this oil recovered using these machines. In each case value is added through the recovery of the oil phase as a saleable product. More recently, two-phase decanters have been adapted to replace presses in the extraction and further processing of a wide variety of fruit and vegetable juices. Separation in a tricanter of commercially exotic fruits such as sea buckthorn into pulp oil, juice and seed-enriched solid ejecta provides a potential future use of centrifugal technology. New, innovative uses for this versatile machine are still emerging.

The disadvantage of the machine is its inability to clarify liquid streams completely, as some suspended solids remain in the emerging stream. If complete clarity is required, another clarifying method must be used following decanter centrifugation. This may include equipment such as a disc centrifuge (clarifier) or filter system. For example, processes described for the extraction of fruit juices with a decanter replacing the press often have a clarifying disc stack centrifuge in the line following the decanter to provide the final solids removal and provide the brilliant clarity desired in many juice products. Alternatively, the clarifying centrifuge can be operated in such a way as to remove the particles larger than $0.5\ \mu\text{m}$ diameter to provide a stable juice opalescence.

Disc Stack Centrifuges

Originally designed as cream separators, these machines have achieved a high degree of sophistication and today represent a versatile group of centrifuges capable of achieving very high g factors, commonly ranging from 3000 to 15 000. The original application of cream separation is still performed as a specialized function in dairies where these machines

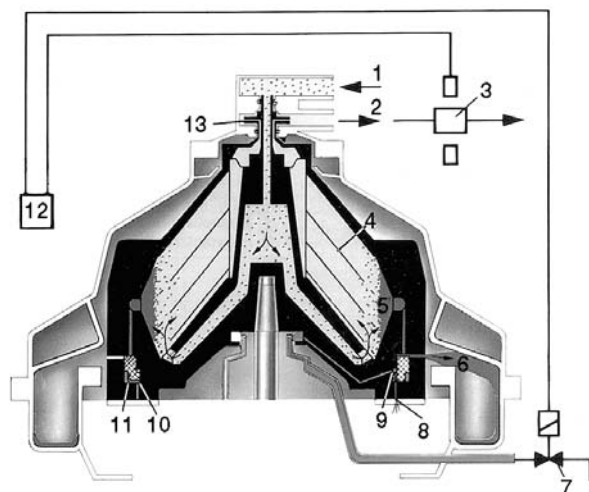


Figure 3 Bowl section of a self-cleaning disc stack centrifuge indicating direction of fluid flow and ejection of sedimented solids through passages controlled with hydraulically operated pistons. Discharge is intermittent. Nozzle machines allow for continuous discharge of solids through throttled nozzles while solid bowl machines without solid discharge mechanisms require manual cleaning from time to time depending upon feedstock solids. 1, Feed; 2, discharge; 3, photocell; 4, discs; 5, sediment holding space; 6, solids ejection ports; 7, operating water valve; 8, drain hole; 9, opening chamber; 10, closing chamber; 11, annular piston; 12, timing unit; 13, discharge pump. Reproduced with permission from Westfalia Separator AG, Oelde, Germany.

are also used for milk clarification and bacterial removal prior to high temperature-short time pasteurization. The disc stack centrifuge is a vertical-axis machine consisting of a series of conical spacers stacked within the centrifuge rotor (Figure 3). The centrifuge is arranged to allow continuous flow of feedstock into the lower part of the bowl. Fluid flows up through the channels formed by the stacked conical elements and particulates are sedimented to contact the inclined surface of a conical element. The particulates on the conical element are forced downward and outward until they underflow the cone to collect on the bowl wall. The effect of the angled conical element is to shorten the distance required for particle migration to a surface and reduce the turbulence produced by material flows within the centrifuge, resulting in rapid and complete clarification of the fluid stream. The number and spacing of the conical elements are important factors in the separation process.

These centrifuge types are for processing feedstocks with relatively low suspended solids in a feedstock requiring a high degree of clarification. They are also of use in situations requiring separation of two immiscible liquids – the separation of cream from milk is the most common example. However, extraction of biochemicals from aqueous substrates often makes

use of water-immiscible organic solvents and rapid separation of the two phases can be achieved in these machines. Removal/isolation of culture-grown bacterial or other cell is a useful function in the biochemical industries. In any role, consideration should be given to the need to seal the centrifuge against the dispersion of aerosols which may contain dangerous biochemicals, nonaqueous vapours or bacterial cells which may be toxic, flammable or explosive. Flushing with an inert gas such as nitrogen or carbon dioxide to avoid oxidation, and the need for temperature control of the centrifuge, feedstock and products should also be considered.

Disc stack centrifuges come in three basic configurations. In one configuration the sedimented solids are continuously ejected through carefully sized nozzles at the bowl periphery (nozzle discharge), allowing continuous operation of the machine with continuous discharge of solids. However, the degree of compaction of the solids is limited by the need to be free-flowing, and solids exit as a concentrate (~50%). In the second configuration, the bowl is equipped with the means to open a port at the periphery of the rotating bowl. This opening may be closed with a slide or piston which is hydraulically opened

according to a pre-set programme. The programme may be set by time or the centrifuge may be equipped with a monitoring device on the fluid exit side which monitors the light-scattering capability of the clarified output. Above set limits clarity deterioration triggers solid discharge. The centrifuge illustrated in Figure 3 is of this self-cleaning type. The third configuration is a solid-wall bowl which is primarily used for separation of liquid mixtures containing little or no solids. The bowl is cleaned manually, or with automatic removal machinery which requires process interruption, so it is advantageous for the sedimented solids content to be low since the machine operates in batch mode and machine capacity will be a function of the clean-out rate.

Solid Bowl and Tubular Centrifuges

Other batch-operated sedimenting centrifuges are the tubular centrifuge and the solid open-bowl centrifuge (without discs: Table 3 and Figure 4). Both machines are batch-operated because they do not incorporate the means for continually removing sedimented solids. The tubular centrifuge is configured with a long, small diameter tube capable of rapid rotation

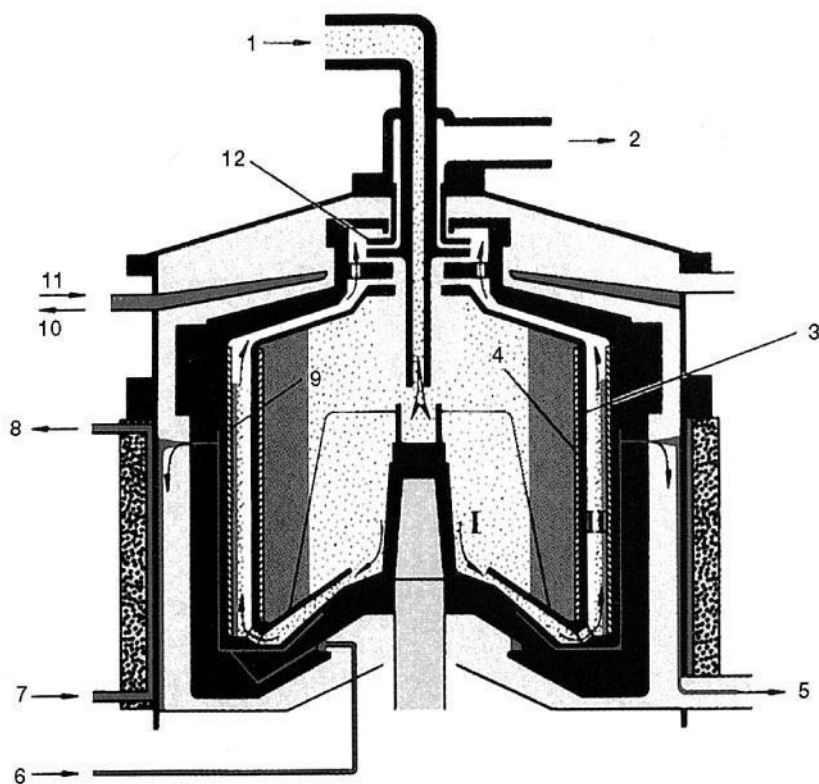


Figure 4 Solid-bowl separator for separating and collecting fine suspended solids in a liquid stream. 1, Product feed; 2, product discharge; 3, bowl insert; 4, removable liner; 5, coolant discharge (bowl); 6, coolant feed (bowl); 7, coolant feed and 8, coolant discharge (upper section of frame); 9, removable liner; 10, coolant discharge and 11, coolant feed (hood); 12, centripetal pump. Reproduced with permission from Westfalia Separator AG, Oelde, Germany.

and generating very high *g* forces to above 40 000 *g*, whereas the solid-bowl/chamber-bowl machines carry a larger diameter bowl and operate in the 5000–10 000 *g* range. The solid-bowl machines are often equipped with a removable liner to facilitate solid removal and centrifuge cleaning, to reduce down time between batches. The narrow tube means that the solid-retaining capacity of the tubular centrifuge is small but the high *g* force makes the machine useful for collecting small particulate or cell debris in biotechnological applications. They are particularly useful for collecting a valuable particulate present at low concentration which requires high relative centrifugal forces for its isolation. Final cleaning of a fluid stream is another application, particularly for the solid-bowl machine, if the solid to be removed is of a refractory type, which would impose extensive wear on the nozzles or solid ejection ports of a disc stack machine or where high compaction of the solids is of value. This latter condition can be very desirable for biotechnological applications where isolation of expensive precipitates is a key function.

Hydrocyclones

This device is particularly unique as it separates solids and liquids by centrifugal principles, but contains no moving parts. The principle of the machine is illustrated in Figure 5. The slurry or fluid to be separated is pumped at high speed and enters the conically shaped machine tangentially. The conical shape causes the flowing liquid to swirl or rotate within the cone, with the result that suspended solids move to the wall while clarified liquid remains in the centre of the cone. This clarified liquid is drawn off at the top of the cone while the separated solids move to the bottom of the chamber for removal. The degree of separation is generally coarse; however, hydrocyclones find use in applications such as removal of sand or grit from fruit mash streams intended for juice extraction, to protect expensive equipment such as decanter scrolls or disc stack deslugging mechanisms from premature wear. They find use in pulp mills for paper fibre removal from liquid streams. These units are used extensively to remove particles from gas streams such as flue gases and as a particle collection mechanism for spray driers used in the production of food powders of various kinds. While the medium of drying and particle conveyance is air, and the prefix 'hydro' does not strictly apply, the principle is the same. Hydrocyclones may precede in line with filtering centrifuges since they can be used to concentrate the centrifuge feed and increase the efficiency of the basket or filter centrifuge.

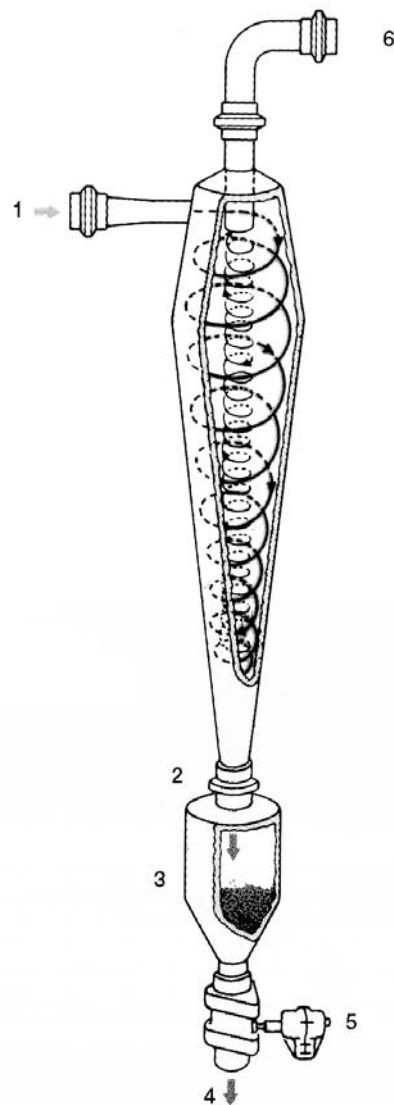


Figure 5 Schematic diagram of a hydrocyclone. 1, Feed; 2, apex nozzle; 3, grit pot; 4, outlet, solids; 5, valve; 6, discharge, clarified liquid. Reproduced with permission from Westfalia Separator AG, Oelde, Germany.

Filter Centrifuges

These machines are characterized by sedimenting particulate on to a screen which may consist of slots, holes, a porous membrane, or filter cloth, where the solids are retained while the liquid portion flows through the screen to be carried away (Figure 6). Generally, the solids should be free-draining and at least 100–200 μm in diameter. These properties allow filter centrifuges to handle high solid concentrations in the input stream (Figure 1b: basket, peeler, pusher). It is of advantage to feed the machine with a feedstock of high solid concentration, since this promotes frequent machine cycling. Solid concentrations can be enhanced by using hydrocyclones or

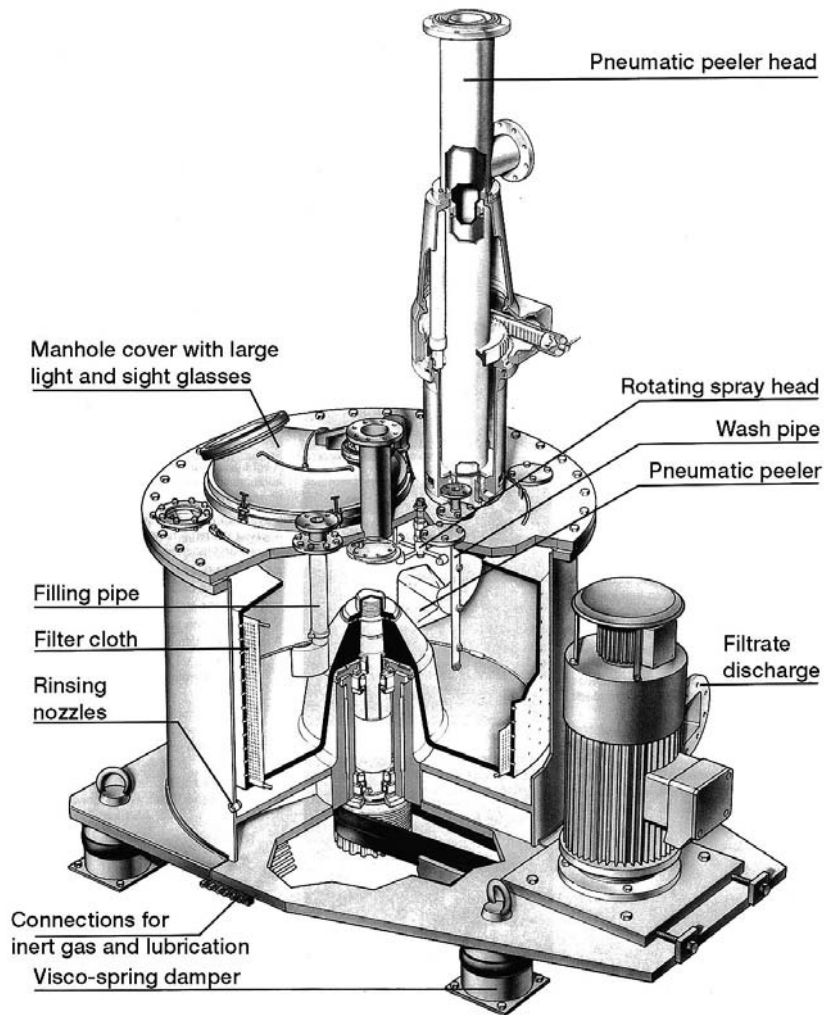


Figure 6 Vertical basket centrifuge with pneumatic top discharge. Reproduced with permission from Krauss Mofferi, Munich, Germany.

settling tanks as pretreatment concentrators. The revolving bowl may be driven either from above or below the rotating parts. The cycle of a variable-speed basket centrifuge consists of acceleration to medium speed, slurry feed and even distribution over the retaining filter surface, and acceleration to operational speed to remove the liquid portion. At this higher speed the dewatered cake may be washed if the centrifuge is equipped with interior washing nozzles, and dewatered for the final time. The rotor speed is decreased and the solids removed, usually by mechanical means using a knife or plow to release the cake from the centrifuge wall. Solids are either dropped through the centrifuge bottom in a vertical axis machine, or gravity-fed down a chute in a horizontally mounted machine. Batch machines offer flexibility in centrifugal conditions, allowing adjustments for feed rates or feed solid concentration; however, they are not widely used except in the white sugar industry

since the higher throughput capacity makes continuous centrifuges more attractive.

Basket centrifuges can be made continuous by incorporating the means of removal of solids while the machine operates. Machines mounted horizontally utilizing a knife to peel the solids from within the centrifuge bowl are termed Peeler-type basket centrifuges (Table 3). In this configuration the knife enters the centrifuge and unloads the cake while the machine operates at full speed. This overcomes the requirement for speed management and permits shorter cycles and higher throughput capacities than simpler batch basket centrifuges. Vertical pneumatic conveying (Figure 6) is another possibility. Pusher centrifuges also fulfil this requirement for continuous operation. A double-stage pusher centrifuge is shown in Figure 7. Multiple-stage machines are available.

The centrifuge consists of a rotating perforated basket with an open end. Feed is through a rotating

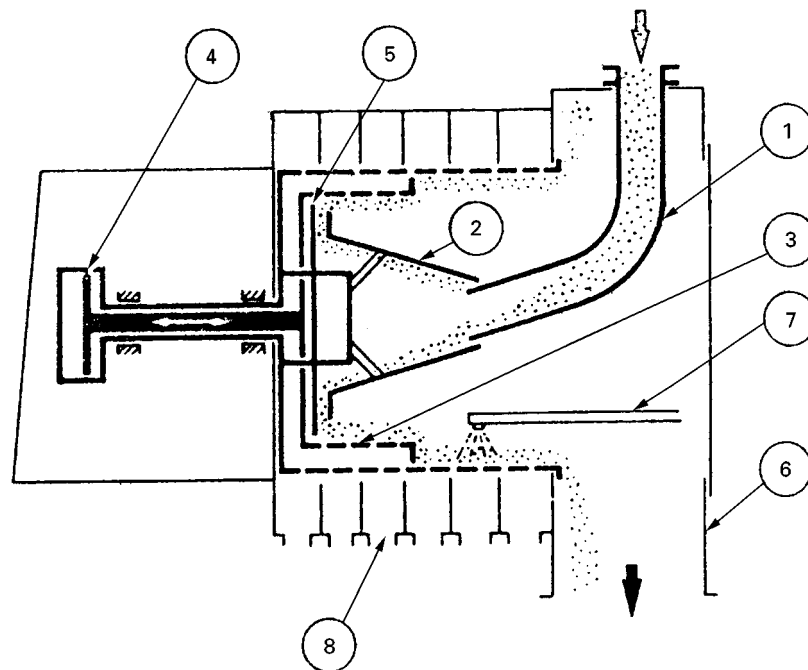


Figure 7 A two-stage pusher-type centrifuge. Feed enters at (1) and is accelerated while passing over the cone (2) and distributed on the first-stage basket (3). The first-stage basket (4) hydraulically reciprocates under a static pusher plate (5), which advances the filter cake to the second-stage basket on the back stroke. The forward stroke of the first basket pushes the second basket cake off into the collecting chute (6). The means to wash the filter cake (7) and collect mother liquor or wash fluids (8) is usually provided. Reproduced with permission from White (1979).

hollow tube to a solid distribution device which distributes the slurry evenly on the basket during the back stroke of the hydraulically driven distributing plate. On the forward stroke the distributing plate exerts a pressure on the deposited cake, causing it to overflow the open end of the basket. If required, the deposited cake may be washed before the return stroke causes overflow of the solids. The screen/scroll centrifuge is also horizontally oriented, but the basket is conical-shaped and transport of the deposited, centrifugally dried slurry is accomplished by a scroll or scrapper blades in a manner reminiscent of the decanter scroll. The transported solids overflow the open end of the basket and are removed from the machine. The screen-bowl decanter is of similar design to the solid-bowl decanter discussed earlier except for the addition of a cylindrical screen behind the conical section of the bowl. The scroll spans the entire length of the bowl including the screen and conforms to the profile of the bowl and screen. Solids retained on the screen are scraped by the scroll to an exit beyond the screen. The purpose of the machine is to combine the solid sedimenting centrifuge with a screen centrifuge in an attempt to obtain a drier cake. Washing of retained solids may be effected in the first portion of the screen, while dewatering taking place in the second part. Decanters such as this

may provide serious competition to the peeler and pusher centrifuges by facilitating continuous separations in a more compact, mechanically simpler package.

A special application which is of growing importance in the food industry is the use of low speed basket centrifuges to dewater or dry fresh-cut vegetables, especially salad greens, for later use in modified atmosphere packages (**Figure 8**). These machines are usually of lighter construction than the heavy-duty machines described above, are batch-operated, and often have reusable rotating perforated baskets, to facilitate rapid unloading and reloading of the centrifuge. The reusable baskets are usually of light construction, often plastic, to allow easy manual handling and economic replacement. Such materials have low tolerance for acceleration and deceleration forces but are well suited for undemanding applications.

Summary

This article has provided an overview of the use of centrifuges in various industries. The ubiquitous nature of the machine throughout the industrial spectrum is apparent. It appears in heavy industrial uses such as sugar and oil refining and in light industrial



Figure 8 Small industrial-scale centrifuge for dewatering fresh-cut produce. The machine is operated in batch mode, but use of insertable plastic bowl minimizes down time between loads. Reproduced with permission from Freshline Machines, Sydney, Australia.

separations such as dewatering of vegetables. Performance demands also vary widely, ranging from high g applications required in isolating and manufacturing the diverse products of biotechnology to dewatering hundreds of tons of municipal sewage per day using machines of relatively low g capability. This is made possible by the wide variety of machines available. The recent application of decanters as press replacements in the fruit and vegetable juice industry required the independent development and widespread use of pectin-digesting enzymes (pectinases) for routine juice production. The reduction in viscosity

and release of dense core particles from the fruit mash which is characteristic of the action of these enzymes is a necessary precondition for the successful use of decanters. The fruit-processing industry is increasingly interested in the production of products from new, unconventional fruits and vegetables. An example is sea buckthorn, a fruit which consists of a seed, pulp and pulp oil, a three-phase system which might be separated into an oil stream, a stable opalescent juice and a seed containing pulpy ejecta in a single operation using a three-phase decanter. From these two examples drawn from the author's experiences in this industry it appears that future innovations are likely to be applications, which will in turn drive further refinement and development of the centrifugal machinery.

See also: II/Centrifugation: Theory of Centrifugation.

Further Reading

- Beveridge T (1997) Juice extraction from apples and other fruits and vegetables. *Critical Review of Food Science and Nutrition* 37: 449–469.
- Brunner KH and Hemfort H (1988) Centrifugal separation in biotechnological processes. In: Mizrahi A (ed.) *Downstream Processes: Equipment and Techniques. Advances in Biotechnological Processes*, vol 8, pp. 1–50. New York: Alan R. Liss.
- Dahlstrom DA, Bennett RC, Emmett RC *et al.* (1997) Liquid–solid operations and equipment: centrifuges. In: Perry RH, Green DW and Maloney JO (eds) *Perry's Chemical Engineers' Handbook*, 7th edn, pp. 18–106. New York, NY: McGraw-Hill.
- Leung WW-F (1998) *Industrial Centrifugation Technology*. New York: McGraw-Hill.
- White WF (1979) Centrifuges. In: Bhatia MV and Cheremisinoff PN (eds) *Solids Separation and Mixing*. Process Equipment Series, vol. 1, p. 81. Westport CT: Technomic.
- Whittington PN (1990) Fermentation broth clarification techniques. *Applied Biochemistry and Biotechnology* 23: 91–121.

Macromolecular Interactions: Characterization by Analytical Ultracentrifugation

D. J. Winzor, Department of Biochemistry,
University of Queensland, Brisbane, Australia

Copyright © 2000 Academic Press

Analytical ultracentrifugation refers to the analysis of a macromolecular solution by its subjection to

gravitational forces up to 300 000-fold greater than gravity. From its inception by Svedberg in the mid-1920s, analytical ultracentrifugation has played a leading role in studies of macromolecular systems. One early success was its demonstration that proteins were polypeptides of discrete length rather than

polydisperse polymers of amino acid residues – the popular concept amongst colloid chemists at that time. This revolutionary finding was the seminal contribution that generated the present-day fields of protein chemistry and molecular biology. Indeed, for 40 years, the analytical ultracentrifuge was the primary source of information on the molecular mass and heterogeneity of proteins, as well as on the polydispersity of polymer preparations. At that stage, preparative ultracentrifugation, gel permeation (size exclusion) chromatography and gel electrophoresis were developed to take advantage of macromolecular separation on the basis of size and shape (as well as charge in some forms of gel electrophoresis). Meanwhile, the sedimentation equilibrium variant of analytical ultracentrifugation retained supremacy for many years as the benchmark standard of molecular mass measurement for a homogeneous protein – a role now being taken over by mass spectrometry. Furthermore, inroads into its status as the method of choice for determining molecular size distributions for polydisperse polymer preparations have now been made by light scattering as the means of analysing the column eluate in gel permeation chromatography. Nevertheless, such is the strength of analytical ultracentrifugation that it has survived those losses of traditional roles to become an invaluable tool for the characterization of reversible macromolecular interactions – a task which is beyond most of the techniques that have usurped its traditional roles.

Many proteins comprise a mixture of monomeric and polymeric states that coexist in rapid association equilibrium, whereupon the relative proportions of the two macromolecular states vary with total solute concentration in accordance with Le Chatelier's principle: the polymeric state is favoured by an increase in solute concentration whereas monomer is favoured by dilution. Analytical ultracentrifugation has great potential for characterizing the self-association equilibrium by virtue of these concentration-dependent changes in the average macromolecular state of the solute, and also for the characterization of rapid equilibria involving dissimilar reactants, for which similar considerations apply. The main emphasis in current analytical ultracentrifugation is thus the study of noncovalent macromolecular association equilibria: protein–protein interactions such as those involved in enzyme self-association or the binding of an antibody to its eliciting protein antigen; and protein–nucleic acid interactions such as those associated with regulation of the transcription of genetic information.

Sedimentation Velocity and Sedimentation Equilibrium

A complex in rapid association equilibrium with reactant species has no separate existence in the absence of the reactants. The characterization of such interactions requires methods that can accommodate the equilibrium coexistence of several species. This requirement is readily accommodated by either of the commonly used techniques in analytical ultracentrifugation – sedimentation velocity and sedimentation equilibrium. In the former, the centrifuge is operated at a sufficiently high angular velocity (speed) for the centrifugal force on a solute to dominate its migration. In sedimentation equilibrium the same instrument is operated at a much lower angular velocity to effect a balance between the radially outward flux of solute and the back-diffusional flow in response to the concentration gradient being generated. Before considering their application to the characterization of interacting systems, it is appropriate to describe the two techniques in relation to the information derived for a single noninteracting solute.

Measurement of a Sedimentation Coefficient

In sedimentation velocity, a solution is placed in a sector-shaped cell which allows unimpeded migration of solute molecules in a radially outward direction in response to the applied centrifugal field. At the commencement of the experiment, the solute concentration is uniform throughout the cell, but the application of a strong centrifugal field (typically 200 000–300 000 g operating at 50 000–60 000 rpm) leads to a progressive removal of solute from the inner region of the cell (**Figure 1**).

Migration of the resultant solute boundary is recorded optically and the sedimentation coefficient of the solute, s_A , is then determined from the rate of migration. Specifically:

$$s_A = (dr_p/dt)/\omega^2 r = (d \ln r_p/dt)/\omega^2 \quad [1]$$

where r_p denotes the radial position (cm) of the solute boundary after centrifugation at angular velocity ω (rad s⁻¹) for time t (s). Traditionally, the sedimentation coefficient has thus been determined from the slope ($\omega^2 s_A$) of the time dependence of $\ln r_p$. Despite being the rate of migration per unit field, s_A has the dimensions of time, but is usually reported in Svedberg units S (1 S = 10⁻¹³ s).

At the limit of zero solute concentration, the sedimentation coefficient, s_A^0 , is related to molecular

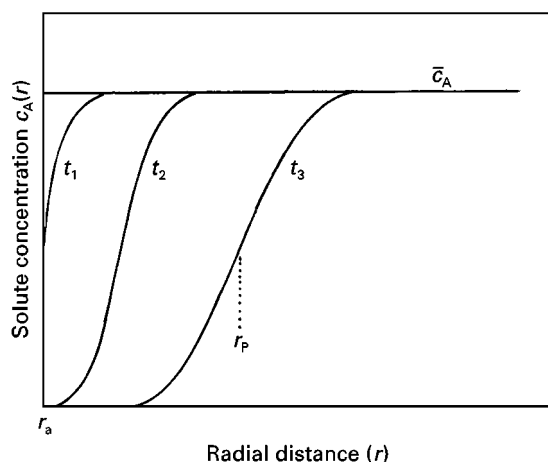


Figure 1 Schematic representation of migration in a sedimentation velocity experiment, showing the generation of a boundary between solvent and the solution subjected to centrifugation: r_p denotes the mean boundary position at time t_3 , and r_a the air–liquid meniscus (boundary position at zero time).

parameters by the expression:

$$s_A^0 = M_A(1 - \bar{v}_A\rho_s)/Nf_A \quad [2]$$

where f_A denotes the shape-dependent translational frictional coefficient of the solute with molecular mass M_A and partial specific volume \bar{v}_A ; ρ_s is the solvent density and N is Avogadro's number. Elimination of the frictional coefficient on the assumption of spherical geometry for the solute ($f_A = 6\pi\eta_s a_A$) leads to the relationship:

$$s_A^0 = M_A(1 - \bar{v}_A\rho_s)/(6\pi\eta_s a_A) \quad [3]$$

where η_s is the solvent density and a_A is the Stokes radius of the solute (radius of the equivalent hydrodynamic sphere). The sedimentation coefficient is thus a function of the size (shape) as well as the buoyant molecular mass, $M_A(1 - \bar{v}_A\rho_s)$, of the solute.

Experimental Aspects of Sedimentation Equilibrium

Unequivocal determination of the buoyant molecular mass by analytical ultracentrifugation is clearly conditional upon replacement of the frictional coefficient in eqn [2]. On the grounds that the translational diffusion coefficient, D_A^0 , is related to f_A by the expression:

$$D_A^0 = RT/(Nf_A) \quad [4]$$

where R and T refer to the universal gas constant and the absolute temperature (K), respectively,

the influence of f_A upon the separate magnitudes of the sedimentation and diffusion coefficients disappears from their ratio. Thus:

$$s_A^0/D_A^0 = M_A(1 - \bar{v}_A\rho_s)/(RT) \quad [5]$$

In sedimentation equilibrium, the solute distribution is governed by this ratio of s_A^0/D_A^0 . The parameter to emerge from the analysis of such distributions is the buoyant molecular mass of the solute, $M_A(1 - \bar{v}_A\rho_s)$. Its conversion to a molecular mass requires assignment of a magnitude to $(1 - \bar{v}_A\rho_s)$, which may be determined experimentally by density measurements and the relationship $(1 - \bar{v}_A\rho_s) \approx (\rho - \rho_s)/c_A$, where ρ is the density of a solute solution with weight concentration c_A .

Sedimentation equilibrium experiments are conducted in a double-sector cell. One sector contains the solution of macromolecular solute and the other the appropriate solvent, which for charged solutes is the buffer with which the solution of macro-ion is in dialysis equilibrium. As in sedimentation velocity, the solute concentration is initially uniform throughout the column of solution (Figure 2). Application of the centrifugal field then results in depletion of solute in the vicinity of the air–liquid meniscus (r_a) and its accumulation at the cell base (r_b). However, at the relatively low speeds of such experiments (say, 10 000 rpm for a 50 kDa protein), these tendencies are countered by back-diffusion in response to the concentration gradient being formed. The net result is a progression towards

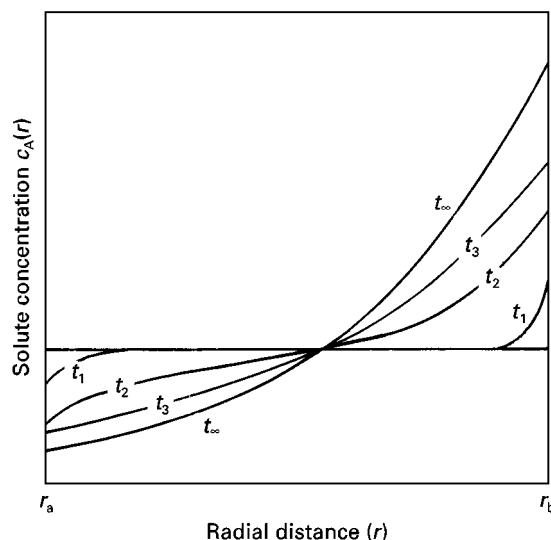


Figure 2 Schematic representation of the approach to a time-independent distribution in a sedimentation equilibrium experiment: the initially uniform concentration gradually changes into an exponential distribution described by eqn [7] for a single solute.

a time-independent exponential increase in solute concentration across the cell (Figure 2).

Because the time taken to attain sedimentation equilibrium varies inversely with the square of the column length, columns longer than 3 mm are rarely used. Whereas 3–4 weeks of centrifugation would be required to attain time independence of the solute distribution in a completely filled cell ($r_b - r_a \approx 1$ cm), effective sedimentation equilibrium can be reached within 16–36 h by decreasing the column length to 2–3 mm.

In the original treatise on analytical ultracentrifugation published by Svedberg and Pedersen in 1940, sedimentation equilibrium was considered in terms of the balance between the processes of sedimentation and diffusion. However, later consideration led to the realization that results from such experiments were amenable to rigorous thermodynamic analysis by expressing the diffusional flow in terms of the negative gradient of solute chemical potential. Consequently, even though the experimental record is in terms of solute concentration as a function of radial distance, the distribution of a single solute at sedimentation equilibrium is defined in terms of its thermodynamic activity:

$$z_A(r) = z_A(r_F) \exp[M_A(1 - \bar{v}_A \rho_s) \omega^2 (r^2 - r_F^2) / (2RT)] \quad [6]$$

which relates the thermodynamic activity of solute at any given radius, $z_A(r)$, to that at a chosen reference radial position, r_F . Although procedures have now been devised which make allowance for effects of thermodynamic nonideality, the situation is simplified for the present purpose by restricting consideration to ideal systems in which the two thermodynamic activities may be replaced by concentrations $c_A(r)$ and $c_A(r_F)$: eqn [6] thus becomes:

$$c_A(r) = c_A(r_F) \exp[M_A(1 - \bar{v}_A \rho_s) \omega^2 (r^2 - r_F^2) / (2RT)] \quad [7]$$

From the logarithmic form of eqn [7] namely:

$$\ln c_A(r) = \ln c_A(r_F) + M_A(1 - \bar{v}_A \rho_s) \omega^2 (r^2 - r_F^2) / (2RT) \quad [8]$$

it is evident that:

$$M_A(1 - \bar{v}_A \rho_s) = (2RT/\omega^2) d[\ln c_A(r)]/dr^2 \quad [9]$$

which allows an unequivocal estimate of the buoyant molecular mass to be obtained from the slope of $\ln c_A(r)$ versus the square of radial distance.

Ultracentrifuge Studies of Solute Self-association

The use of analytical ultracentrifugation in protein chemistry for molecular mass determination is now usually bypassed in favour of its calculation from the amino acid sequence or its measurement by mass spectrometry. However, because such molecular mass values refer only to the covalently linked polypeptides chain(s), they provide no information about the macromolecular state of the functional protein or enzyme. In the simplest current application of sedimentation equilibrium, molecular mass measurement is sometimes used to elucidate the nature of quaternary structure, which is an example of a self-association equilibrium displaced completely in favour of the polymeric state.

The aim of this section is to outline the basic principles of the use of analytical ultracentrifugation for the characterization of reversibly associating systems. Although more elaborate and intricate procedures are employed in practice, their description is beyond the scope of this introduction to the topic.

Characterization of Solute Self-association by Sedimentation Velocity

Because of the concentration-dependent variation in the average macromolecular state of a self-associating solute, the best approach in sedimentation velocity studies is to determine the dependence of the weight-average sedimentation coefficient, \bar{s}_A , upon total solute concentration, \bar{c}_A . Procedural details for the measurement of \bar{s}_A are as described above (eqn [1]), except that the asymmetric shape of the single reaction boundary that forms between solvent and the plateau region with concentration \bar{c}_A (Figure 1) necessitates the location of the boundary position, \bar{r}_p , as the square root of the second moment:

$$\bar{r}_p^2 = \left[\int_0^{\bar{c}_A} r^2 d\bar{c}_A \right] / \bar{c}_A \quad [10]$$

to make allowance for the effects of migration in a sector-shaped cell rather than one with uniform cross-sectional area.

For a two-state self-association involving monomer (species 1) and dimer (species 2) the weight-average sedimentation coefficient is given by the expression:

$$\bar{s}_A = \alpha_1 s_1 + (1 - \alpha_1) s_2 \quad [11]$$

where $\alpha_1 = c_1/\bar{c}_A$ is the weight fraction of monomer, and where the sedimentation coefficient of

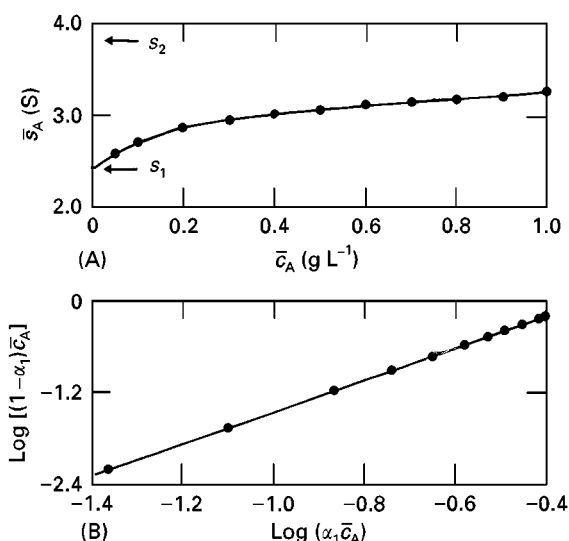


Figure 3 Studies of solute self-association by sedimentation velocity: (A) Concentration dependence of the weight-average sedimentation coefficient simulated (eqn [10]) for a monomer–dimer system where $K_2 = 3.5 \text{ L g}^{-1}$, $s_1 = 2.4 \text{ S}$ and $s_2 = 3.8 \text{ S}$. (B) Analysis of the data for the determination of K_2 by means of eqn [13].

monomer, s_1 , may be obtained by extrapolation of \bar{s}_A to zero solute concentration (Figure 3A). However, the evaluation of α_1 from eqn [11] also depends upon knowledge of s_2 , the sedimentation coefficient of dimer, which is not readily obtained experimentally. An estimate is therefore usually made on the basis of the relationship $s_2 = s_1(2^{2/3})$, which follows from eqn [3] and assumed spherical geometry for monomeric and dimeric species. Knowledge of s_2 then allows evaluation of the weight fraction of monomer from the following rearrangement of eqn [11]:

$$\alpha_1 = (s_2 - \bar{s}_A)/(s_2 - s_1) \quad [12]$$

whereupon the dimerization constant, $K_2 = (1 - \alpha_1)\bar{c}_A/(\alpha_1\bar{c}_A)^2$, may be determined.

Application of this approach to the data in Figure 3A, which have been simulated for a system with $s_1 = 2.4 \text{ S}$, $s_2 = 3.8 \text{ S}$ and $K_2 = 3.5 \text{ L g}^{-1}$, is illustrated in Figure 3B. From the logarithmic form of the expression for the dimerization constant ($K_2 = c_2/c_1^2$), namely:

$$\log[(1 - \alpha_1)\bar{c}_A] = \log K_2 + 2 \log(\alpha_1\bar{c}_A) \quad [13]$$

in present terminology, K_2 may be obtained as the ordinate intercept of the linear dependence of $\log[(1 - \alpha_1)\bar{c}_A]$ versus $\log(\alpha_1\bar{c}_A)$; this has a mandatory slope of 2 for a monomer–dimer equilibrium.

Characterization of Solute Self-association by Sedimentation Equilibrium

The above approach can be applied to the dependence of weight-average molecular mass \bar{M}_A upon total solute concentration \bar{c}_A by substituting molecular masses for the corresponding sedimentation coefficients in eqn [12]. Furthermore, there is no ambiguity about the magnitude of M_2 , which is twice the value of \bar{M}_A in the limit of zero solute concentration. Although this was indeed the original procedure used for characterizing solute self-association by sedimentation equilibrium, it has been superseded by a more accurate method involving direct analysis of the sedimentation equilibrium distribution(s).

Figure 4A presents simulated sedimentation equilibrium distributions at 15 000 and 25 000 rpm for a reversibly dimerizing protein with a buoyant molecular mass of 6.5 kDa for monomer ($M_1 \approx 25 \text{ kDa}$) and an equilibrium constant of 3.5 L g^{-1} . Because the

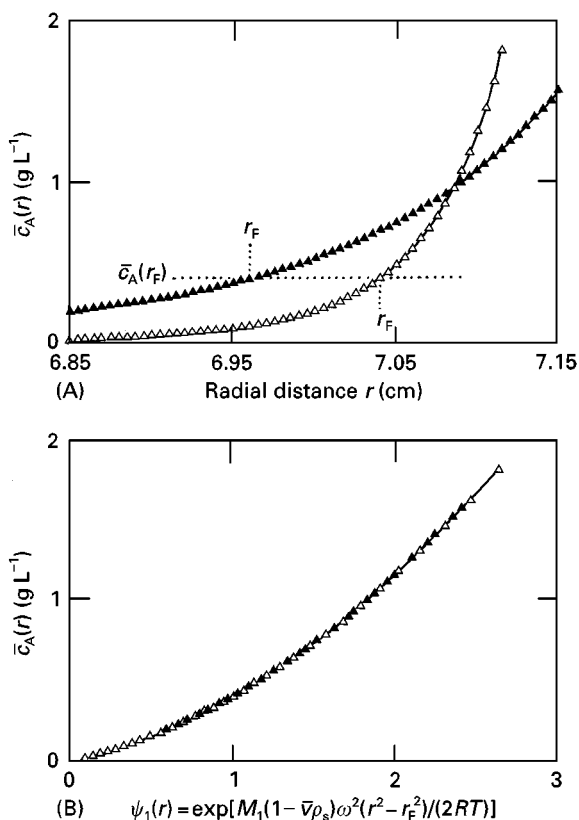


Figure 4 Studies of solute self-association by sedimentation equilibrium. (A) Simulated concentration distributions reflecting reversible dimerization of a monomer ($M_1 = 25 \text{ kDa}$) governed by an association equilibrium constant of 3.5 L g^{-1} in sedimentation equilibrium experiments at 15 000 (▲) and 25 000 (△) rev min⁻¹. (B) Plot of data in readiness for global analysis according to eqn [15] with a fixed value of 0.4 g L^{-1} for the total solute concentration $\bar{c}_A(r_F)$ at reference radial position r_F .

distributions are at chemical equilibrium, the total solute concentration at each radial distance may be expressed in terms of monomer concentration by the relationship:

$$\bar{c}_A(r) = c_1(r) + K_2[c_1(r)]^2 \quad [14]$$

On the other hand, the condition of sedimentation equilibrium dictates that the distribution of monomer be described by eqn [7]. Combination of these two requirements leads to the expression:

$$\bar{c}_A(r) = c_1(r_F)\psi_1(r) + K_2[c_1(r)\psi_1(r)]^2 \quad [15]$$

$$\psi_1(r) = \exp[M_1(1 - \bar{v}_A\rho_s)\omega^2(r^2 - r_F^2)/(2RT)] \quad [16]$$

The application of this approach is illustrated in **Figure 4B**, where global analysis of the two distributions from **Figure 4A** has been effected on the basis of a common $\bar{c}_A(r_F)$ value of 0.4 g L^{-1} , thereby ensuring a common value of $c_1(r_F)$. Magnitudes of $\psi_1(r)$ at 20°C have then been calculated on the basis of the appropriate r_F value, the buoyant molecular mass of monomer and the angular velocity. In as much as $c_1(r_F)$ and K_2 are both constants, their magnitudes are obtained by nonlinear curve-fitting of the combined $[\bar{c}_A(r), \psi_1(r)]$ data sets to the above quadratic expression in $\psi_1(r)$.

Interactions Between Dissimilar Reactants

Although interactions between dissimilar reactants far outnumber those entailing solute self-association in biology, the study of ligand binding by analytical ultracentrifugation has received far less attention – a situation being remedied to some extent now.

Studies of Ligand Binding by Sedimentation Velocity

In considering the quantification of acceptor–ligand interactions by sedimentation velocity, there are two situations to examine: one in which a macromolecule (acceptor, A) reacts with a small molecule (ligand, B); and the situation in which both acceptor and ligand are macromolecular. In the former, provided that the ligand is sufficiently small for the acceptor–ligand complex AB (or complexes AB_i for ligand binding to multiple acceptor sites) to co-migrate with acceptor ($s_{AB} \cong s_A > s_B$), the free ligand concentration is readily determined by sedimentation velocity. As depicted schematically in **Figure 5A**, the subsection of an equilibrium mixture to a high centrifugal field under those circumstances generates a biphasic boundary pattern

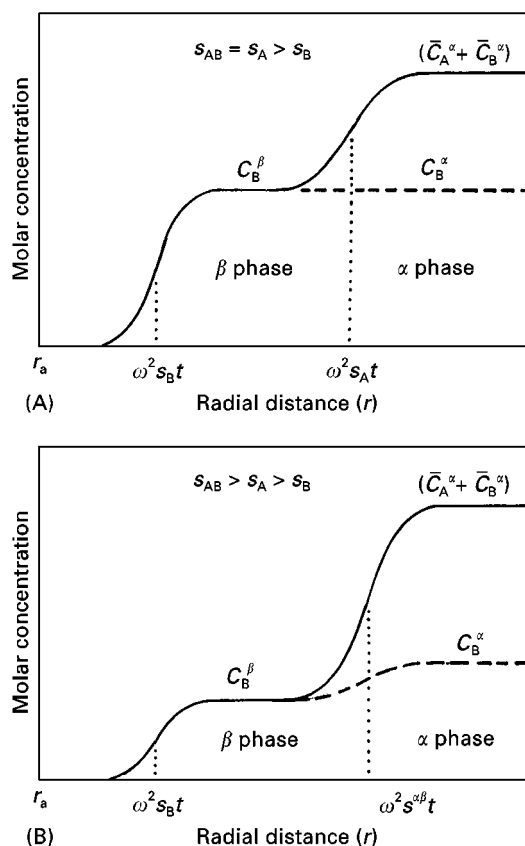


Figure 5 Schematic representations of boundary patterns encountered in sedimentation velocity studies of ligand binding. (A) Direct evaluation of the free ligand concentration (C_B^β) for a system where acceptor and acceptor–ligand complex(es) co-migrate. (B) The corresponding situation when acceptor and ligand are both macromolecular ($s_{AB} > s_A > s_B$).

in which the concentration in the slower-migrating (β) phase reflects free ligand at its equilibrium concentration in the mixture (α phase) with total molar concentrations \bar{C}_A^α and \bar{C}_B^α of acceptor and ligand, respectively. Results obtained are thus akin to conventional ligand-binding data obtained by (say) equilibrium dialysis; and may therefore be treated in an analogous fashion.

In the second case in which the ligand is also macromolecular, the sedimentation coefficient of the AB complex is likely to be greater than that of either reactant ($s_{AB} > s_A > s_B$). Under those circumstances, a biphasic boundary pattern is again generated, but the slower-migrating phase corresponds to the reactant in molar excess: the situation represented in **Figure 5B** reflects a molar excess of ligand. Although the concentration of pure ligand in the slower-migrating phase (C_B^β) can be measured, it does not equal the free ligand concentration (C_B^α) in the equilibrium mixture. However for a 1:1 interaction, the free concentration of the other reactant may be

determined from the expression:

$$C_A^\alpha = (\bar{C}_A^\alpha - \bar{C}_B^\alpha + C_B^\beta)(s^{\alpha\beta} - s_B)/(s_A - s_B) \quad [17]$$

where C_i again denotes a molar concentration, and where $s^{\alpha\beta}$ is the sedimentation coefficient of the reaction boundary between the pure solute phase and that corresponding to the original mixture. Combination of the consequent value of C_A^α with the composition of the mixture (\bar{C}_A^α , \bar{C}_B^α) then yields the binding constant K_{AB} on the grounds that:

$$K_{AB} = C_{AB}^\alpha / (C_A^\alpha C_B^\alpha) = (\bar{C}_A^\alpha - C_A^\alpha) / [C_A^\alpha (\bar{C}_B^\alpha - \bar{C}_A^\alpha + C_A^\alpha)] \quad [18]$$

For purposes of simplification, the above quantitative treatments assume migration in a rectangular cell under the influence of a homogeneous field. Sedimentation in a sector-shaped cell leads to radial dilution that slightly decreases the magnitudes of the various concentrations. However, the uncertainties inherent in the measurements of C_B^β and the various differences in sedimentation coefficients are usually sufficient to justify the approximations involved in such interpretation of sedimentation velocity patterns.

Studies of Ligand Binding by Sedimentation Equilibrium

For a reversible interacting between an acceptor A and a ligand B , there are only two independent sedimentation equilibrium distributions – one for the acceptor constituent which includes the acceptor contribution to AB complex(es) as well as free reactant; and the corresponding distribution for the ligand constituent. Thus:

$$\bar{C}_A(r) = C_A(r) + K_{AB}C_A(r)C_B(r) + \dots \quad [19]$$

$$\bar{C}_B(r) = C_B(r) + K_{AB}C_A(r)C_B(r) + \dots \quad [20]$$

Figure 6 presents sedimentation equilibrium distributions for the individual species in centrifugation of a 1 : 1 interacting system with $M_A(1 - \bar{v}_A\rho_s) = 12$ kDa, $M_B(1 - \bar{v}_B\rho_s) = 3$ kDa and $K_{AB} = 50\,000$ mol L⁻¹ at 15 000 rpm. Also shown are the constituent distributions.

Substituting the condition of sedimentation equilibrium (eqn [7]) for the individual reactants into the above expressions allows them to be rewritten in the form:

$$\bar{C}_A(r) = C_A(r_F)\psi_A(r) + K_{AB}C_A(r_F)C_B(r_F)\psi_A(r)\psi_B(r) + \dots \quad [21]$$

$$\bar{C}_B(r) = C_B(r_F)\psi_B(r) + K_{AB}C_A(r_F)C_B(r_F)\psi_A(r)\psi_B(r) + \dots \quad [22]$$

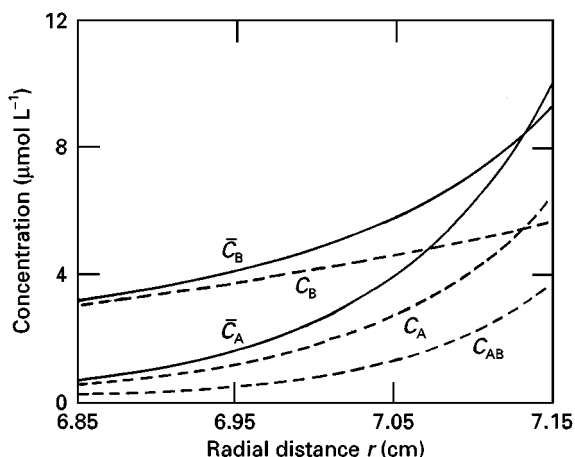


Figure 6 Simulated sedimentation equilibrium distributions for the individual species (---) resulting from centrifugation at 15 000 rpm of a mixture of acceptor with $M_A(1 - \bar{v}_A\rho_s) = 12$ kDa and ligand with $M_B(1 - \bar{v}_B\rho_s) = 3$ kDa undergoing reversible 1 : 1 interaction governed by a binding constant of $50\,000$ mol L⁻¹. The solid curves describe distributions in terms of the total concentrations of the separate constituents (\bar{C}_A , \bar{C}_B).

Furthermore, because $\psi_A(r) = [\psi_B(r)]^u$ where $u = [M_A(1 - \bar{v}_A\rho_s)]/[M_B(1 - \bar{v}_B\rho_s)]$, these expressions become discrete polynomials in terms of $\psi_B(r)$ and the constant parameters $C_A(r_F)$, $C_B(r_F)$ and K_{AB} . The problem of evaluating K_{AB} thus amounts to nonlinear regression analysis of the $[C_i, \psi_B(r)]$ distributions to obtain the three constants as curve-fitting parameters.

The extent to which advantage may be taken of this approach clearly depends upon the nature and number of sedimentation equilibrium distributions available for analysis. In that regard, the maximum potential for quantitative analysis pertains to the situation in which the optical system provides information on the separate concentrations of acceptor and ligand constituents. However, the optical system may well only monitor one constituent, or it may yield a single distribution related to the combined constituent concentrations, $\bar{C}_A(r) + \bar{C}_B(r)$. The latter situations are clearly less than optimal from the viewpoint of characterizing the interactions, but procedures (admittedly less accurate) have been devised to illustrate the feasibility of a quantitative analysis, even under these adverse circumstances.

Future Developments

Despite the fact that the characterization of macromolecular interactions by analytical ultracentrifugation has attracted the attention of physical biochemists for the past 50 years, its application is only now filtering through to the general biochemical community. Inasmuch as the required methodology is

largely in place, the stage seems set for an exciting revitalization of analytical ultracentrifugation as the cell biologists begin to tackle the characterization of the myriads on interactions detected during the past few decades of qualitative research.

See also: II/Centrifugation: Analytical Centrifugation, Theory.

Further Reading

- Fujita H (1962) *Mathematical Theory of Sedimentation Analysis*. New York: Academic Press.
- Harding SE and Winzor DJ (2000) Sedimentation velocity analytical ultracentrifugation as a probe for ligand binding. In: Harding SE and Chowdry PZ (eds). *Protein-Ligand Interactions: A Practical Approach*. Oxford: IRL Press.
- Harding SE, Rowe AJ and Horton JC (eds) (1992) *Analytical Ultracentrifugation in Biochemistry and Polymer Science*. Cambridge: Royal Society of Chemistry.

- Nichol LW and Winzor DJ (1972) *Migration of Interacting Systems*. Oxford: Clarendon Press.
- Schachman HK (1959) *Ultracentrifugation in Biochemistry*. New York: Academic Press.
- Schuster TM and Laue TM (eds) (1994) *Modern Analytical Ultracentrifugation: Acquisition and Interpretation of Data for Biological and Synthetic Polymer Systems*. Boston: Birkhäuser.
- Svedberg T and Pedersen KO (1940) *The Ultracentrifuge*. Oxford: Clarendon Press
- Williams JW (ed.) (1963) *Analytical Ultracentrifugation in Theory and Experiment*. New York: Academic Press.
- Wills PR, Jacobsen MP and Winzor DJ (1997) Direct analysis of sedimentation equilibrium distributions reflecting macromolecular interactions. *Progress in Colloid and Polymer Science* 107: 1–10.
- Winzor DJ and Harding SE (2000) Sedimentation equilibrium in the analytical ultracentrifuge as a probe of ligand binding. In: Harding SE and Chowdry PZ (eds) *Protein-Ligand Interactions: A Practical Approach*. Oxford: IRL Press.

Preparative Centrifugation

See II/CENTRIFUGATION/Large-Scale Centrifugation

Theory of Centrifugation

A. G. Letki, Alfa Laval, Warminster, PA, USA

Copyright © 2000 Academic Press

Introduction

Separation

Separation, as discussed here, is a mechanical means of the following:

- Separating immiscible liquids with different specific gravities (purification).
- Removing insoluble solids from a liquid (clarification if a liquid is the main product; dewatering if the solids are the chief product).
- Removing excess liquid from insoluble solids (thickening with the solids slurry in a more viscous form being the product).
- Some intermediate combination (degripping – removal of oversize particles; desliming – removal of fine particles; or some other form of classification – splitting the slurry into two generally liquid components with the solids being split based on particle size and/or density).

Centrifuges

Centrifuges are usually divided into two types, sedimenting and filtering. Sedimenting centrifuges are characterized by a solid bowl wall and include tubular bowl (Figure 1), disc stack (Figure 2) decanter (Figure 3) and imperforate basket centrifuges. Filtering centrifuges have perforated bowl walls, which support screens or cloth or both and include perforate basket centrifuges, peelers and pushers.

The ultracentrifuge and the gas centrifuge represent special cases that establish separations based on gradients on a molecular scale and are not included in this discussion.

Although centrifuges have been applied industrially for well over a century, centrifuge theory is not well developed. Centrifuges are not designed for specific applications using fundamental principles. Any discussion of centrifuge theory must also define the limitation of the theory. The best means of predicting the performance that will be obtained by processing a material through a centrifuge is to actually process the material through a centrifuge.

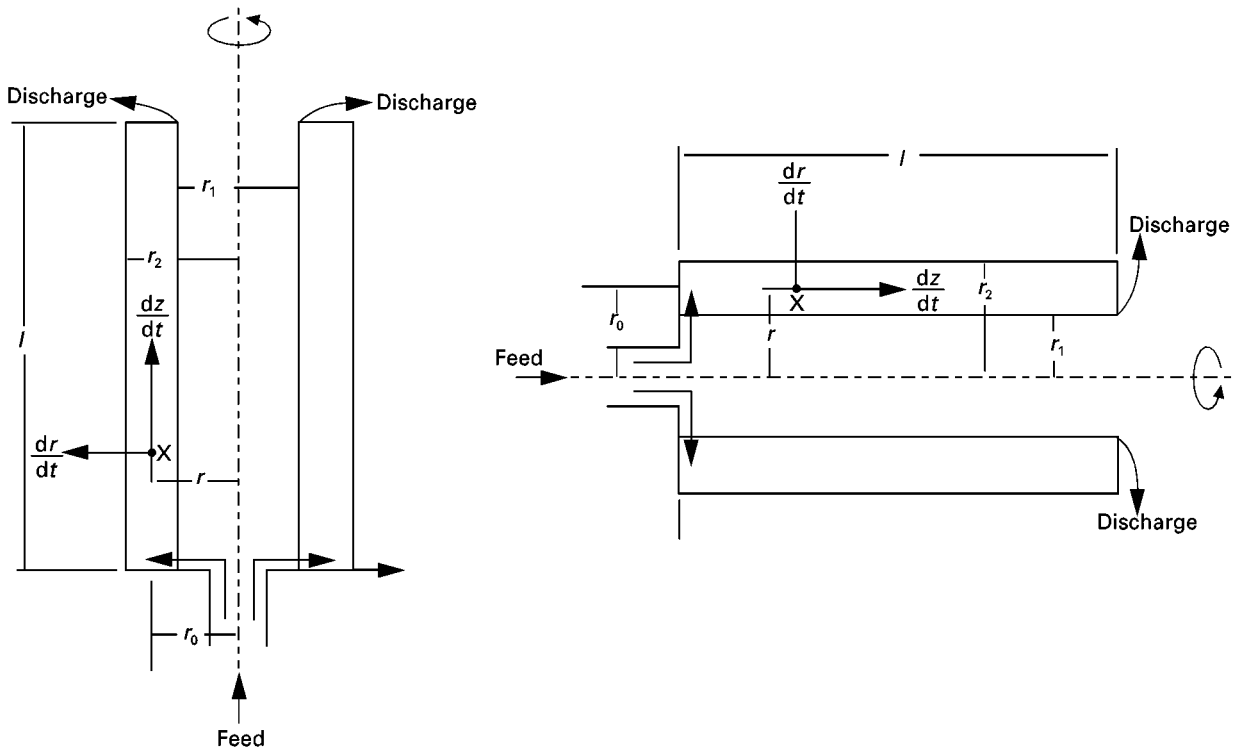


Figure 1 Tubular bowl (X represents the initial position). Centrifugal field is high enough that separating capacity of bowl is considered the same when rotating vertically or horizontally. Same sigma formula applies to tubular bowl, decanter and imperforate basket.

G-level

The fundamental characteristic of all centrifuges is that they contain a rotor that spins. A centrifugal field is used to augment separation. The magnitude of the enhancement is sometimes incorrectly described as the G-force. The relative centrifugal force (RCF) or G-level is not a force; it is a ratio, that of acceleration

of the centrifugal field to that of acceleration owing to the Earth's gravity. It has dimensionally no units:

$$G = \omega^2 r / g \left(\frac{1}{s^2} \times \text{cm} \right) / (\text{cm s}^{-2}) \quad [1]$$

This ratio may reach 60 000 on small laboratory units and 20 000 on small industrial scale units. This ratio tends to decrease as the size of the rotor increases. The ratio is normally large enough that a rotor rotating horizontally is considered to have the same separating capacity that it would have if it rotated

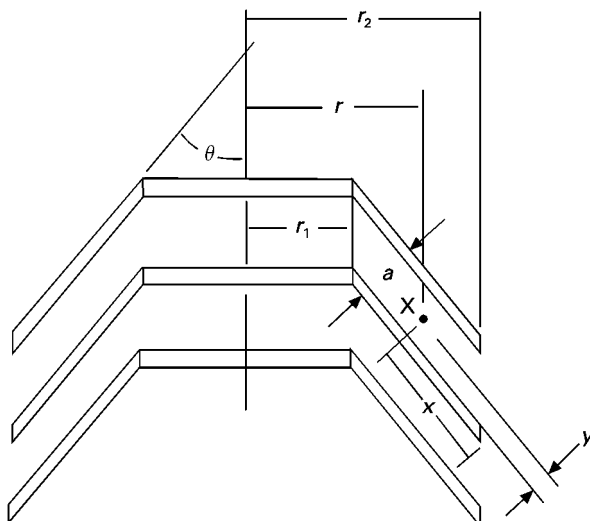


Figure 2 Disc centrifuge (X represents the initial position).

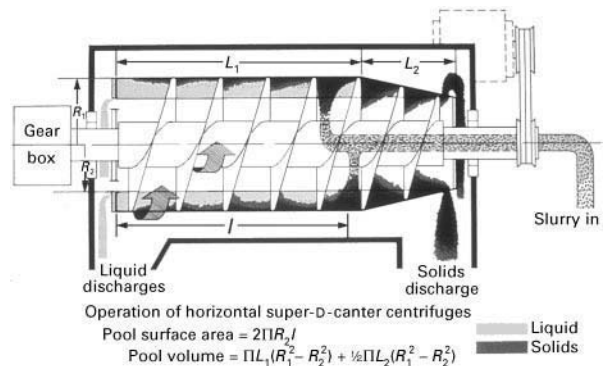


Figure 3 Decanter.

vertically, i.e. the influence of the Earth's gravitational field is negligible while the rotor is spinning.

Performance

Since centrifuges typically remove solids from one or more liquid streams, some measure of how well this is being performed is usually desirable. The recovery, sometimes (especially in the case of filtering centrifuges) referred to as yield, is defined as:

Recovery (%)

$$= \frac{\text{Collected insoluble solids}}{\text{Feed insoluble solids}} \times 100 \quad [2]$$

$$= \frac{\text{Cake insolubles (\%)} \times \text{Cake rate}}{\text{Feed insolubles (\%)} \times \text{Feed rate}} \times 100 \quad [3]$$

$$= \frac{cC}{fF} \times 100 \quad [4]$$

As a practical matter, cake rates are difficult to measure. This can be addressed by manipulating mass balances. Recovery can be defined in terms of insoluble (suspended) solids concentrations, which may be more accurately determined than cake rates.

The liquids balance:

$$F = C + E \quad [5]$$

or:

$$E = F - C \quad [6]$$

The solids balance:

$$fF = cC + eE \quad [7]$$

By substitution:

$$fF = cC + e(F - C) \quad [8]$$

$$= cC + eF - eC \quad [9]$$

$$F(f - e) = C(c - e) \quad [10]$$

$$C/F = (f - e)/(c - e) \quad [11]$$

$$\text{Recovery (\%)} = (c/f)((f - e)/(c - e)) \times 100 \quad [12]$$

Recovery then is also a function of feed solids concentration. Effluent quality is not the sole measure of recovery. High solids concentration in the effluent may simply mean that the feed solids are high. Conversely, lack of solids in the effluent may simply mean lack of solids in the feed, not a high level of recovery.

The use of overall percentage recovery may not be adequate to compare dissimilar centrifuges, especially

those on applications such as classification when recovery levels are kept low.

Centrifuges may have the effect of altering the particle-size distribution. Two different types of centrifuges, even if operating at the same overall recovery level, may split a slurry into components having significantly different particle-size distributions.

Sedimenting Centrifuges

Ideal System

Newton and Stokes have promulgated the laws describing the movement of particles. When a force is applied to a particle it is accelerated:

$$F = ma \quad [13]$$

In a static settling tank under the influence of the Earth's gravity, the particle settles along the radius of the earth. When g is the gravitational constant:

$$F = mg \quad [14]$$

In a centrifugal field, the acceleration, $\omega^2 r$, results in a force that acts normal to the axis of rotation (Figure 4):

$$F = m\omega^2 r \quad [15]$$

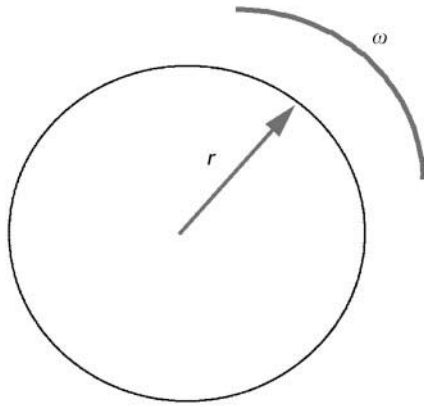
In a sedimenting centrifuge, a continuous liquid phase moves through the rotor. In order to accomplish a useful separation, the discontinuous phase – either the insoluble solids or immiscible liquids drops (or both) – must move in a direction different from the flow of the continuous liquid. Stokes' law is usually applied to describe the relationship. The effective force accelerating the particle in a centrifugal field is then described:

$$F_p = (m_p - m_1)\omega^2 r \quad [16]$$

where m_p is the mass of the particle and m_1 is the mass of the liquid displaced by the particle. If we define $\Delta\rho = (\rho_p - \rho_l)$, the difference in the density between the particle and the continuous liquid phase, then for a spherical particle of diameter, D :

$$F_p = (\Pi/6)\Delta\rho D^3 \omega^2 r \quad [17]$$

If the diameter is small, or the viscosity is high, the particle moves at a velocity below the turbulent range and Stokes' law defines the force of the liquid phase



Defined as:

$$\frac{\omega^2 r}{g}$$

where :

ω is rotational velocity (rad s⁻¹)
 r is radius of rotation in inches
 g is gravitational constant
 (32.2 in s⁻²)

Figure 4 G-level.

resisting the particle as:

$$F_l = 3\pi\eta Dv_s \quad [18]$$

If the particle settles long enough (reaches equilibrium), then $F_l = F_p$ and, in a centrifugal field:

$$v_s = (\Delta\rho D^2 \omega^2 r) / 18\eta \quad [19]$$

In the Earth's gravitational field:

$$V_g = (\Delta\rho D^2 g) / 18\eta \quad [20]$$

The difference between the velocity in the centrifugal field and in the Earth's gravitational field is twofold. The first difference is that the velocity in the centrifugal field may be three to four orders of magnitude higher. The second is that the velocity in a centrifugal field depends on the distance from the centre of rotation, so that the velocity increases as the particle moves outward from the centre of rotation. In the Earth's gravitational field, the velocity is considered independent of position.

Sigma Value

The most widely used method of quantifying capacity in sedimenting centrifuges is the sigma value which was introduced by Ambler in the 1950s. Sigma is used as an index of centrifuge size and typically has units of cm².

The sigma concept attempts to isolate the process system factors effecting separation from the centrifuge factors effecting separation (Figure 1). The tubular bowl was the first centrifuge to which sigma is applied. The tubular bowl is a rotating cylinder in which feed is introduced through the bottom end cap. The continuous fluid flows through the rotor and overflows the top of the bowl. If the solid particles having a specific gravity higher than the liquid are successfully separated, they accumulate on the inside of the rotor and are removed batchwise by manually cleaning the bowl. If the distance settled (x) is small, the velocity is constant, eqn [19] then can be expanded:

$$x = v_s t = [(\Delta\rho D^2 \omega^2 r) / 18\eta] (V/Q) \quad [21]$$

If we consider an ideal system, half of the particles of diameter D would be removed when:

$$x = s/2 \quad [22]$$

$$Q = [(\Delta\rho D^2) / 9\eta] (V\omega^2 r/s) \quad [23]$$

or:

$$Q = 2v_s \Sigma \quad [24]$$

where v_s characterizes the process system:

$$v_s = (\Delta\rho D^2 g) / 9\eta \quad [25]$$

and Σ characterizes the centrifuge:

$$\Sigma = (V\omega^2 r_e) / g s_e \quad [26]$$

with r_e and s_e being the effective radius and effective settling distance in the centrifuge.

The problem then is to define r_e and s_e . If the liquid layer is not thin, Ambler considered that:

$$r_e/s_e = 1/\ln(2r_2^2/r_1^2) \quad [27]$$

Ambler maximized the approximation for the tubular bowl as:

$$\Sigma = (2\pi l \omega^2 / g) (\frac{3}{4} r_2^2 + \frac{1}{4} r_1^2) \quad [28]$$

Svarovsky and Vesilind each use slightly different approximations for the effective radius.

Records argues that a second derivation assuming that all particles start on the surface instead of uniformly distributed throughout the annular space yields:

$$\Sigma = (2\pi l \omega^2 / g) (\frac{1}{2} r_2^2 + \frac{1}{2} r_1^2) \quad [29]$$

Clearly as the depth of liquid decreases $r_1 \rightarrow r_2$, the values for both estimates of Σ become equal.

The equivalent area of a decanter and a gravity settling tank is shown in Figure 3 and Figure 5, respectively.

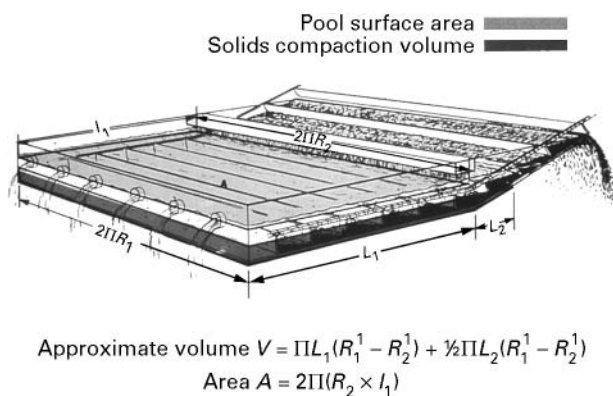


Figure 5 Gravity settling tank.

Sigma assumptions The assumptions can be divided as follows:

- **Stokes' law:** The particles or droplets are spherical and uniform in size. Settling of a particle is unhindered by the smaller particles ahead of it. The particles do not deaggregate, deflocculate, agglomerate, precipitate, dissolve, emulsify or flocculate. There is no change in viscosity or density (little or no temperature change).
- **Reynolds' number:** The value for the Reynolds' number, $(v_s \rho D)/\eta$, is less than one, so that the deviation from the Stokes settling velocity is relatively small.
- **Distribution:** The particles are evenly distributed in the continuous liquid phase. The feed is uniformly introduced into the full space available for its flow. The flow is streamlined. There is no displacement of flow of the continuous phase by the sedimented particle phase or the introduction of feed. There is no remixing of the continuous and discontinuous phases.

Sigma limitation: similarity of feed Since Σ is the index of the size of the centrifuge, traditionally the throughput (Q_1) of a centrifuge of a size (Σ_1) has been used to determine the throughput (Q_2) to a usually larger size (Σ_2) centrifuge. In the normal course of commerce, the performance of the test centrifuge with Σ_1 occurs at a time and place different from that in which the centrifuge with Σ_2 will operate. The small unit may be tested on lab batches, months or even years ahead of the construction of a full-scale plant. Eqn [24] can be restated as:

$$Q_1 = 2v_{s1}\Sigma_1 \quad [30]$$

and:

$$Q_2 = 2v_{s2}\Sigma_2. \quad [31]$$

It is important to remember that:

$$Q_2 = Q_1(\Sigma_2/\Sigma_1) \quad [32]$$

if and only if:

$$v_{s1} = v_{s2} \quad [33]$$

The process system parameters that allow v_{s1} must be duplicated to allow v_{s2} .

The feed stream and process system should be properly documented to ensure that the process system does not adversely effect the following properties described in eqn [25]:

$$v_s = (\Delta\rho D^2 g)/9\eta$$

It is generally assumed that increasing the sedimenting velocity (v_s) produces a better (more complete, faster, possibly more economical) separation. Therefore increasing v_s increases sedimentation capacity at constant Σ . Eqn [14] illustrates several important relationships:

- The larger the particle diameter, the greater the sedimentation rate.

Corollaries:

- A. Flocculation may enhance performance by increasing particle size.
 - B. Care should be taken in those process steps ahead of the centrifuge to limit particle-size degradation by either mechanical or biological means.
- The greater the difference in the density between the particle and the continuous phase, the greater the sedimentation rate.

Corollaries:

- A. Temperature is important. If the density differences are small, the percentage change in density of the continuous phase may be significant. The density of water is normally taken as unity, but actually changes by approximately 20% from 20°C to 30°C.
 - B. In certain systems, e.g. mineral oil and water, there may be no density difference at a given temperature, therefore separation would not be possible. Changing the temperature and thus the densities would make separation possible. In extreme cases, changing the temperature may invert the light and heavy immiscible phases.
- The lower the viscosity of the continuous phase, the greater the sedimentation rate.

Corollaries:

- A. Again, temperature is important. Warmer (not approaching the boiling point, and in the absence of significant increases in the solubility of the particles) is generally better than colder.

- B. Materials such as tar, that may be solid at room temperature, may be liquid with a low enough viscosity for processing at elevated temperature.

Parameters such as the speed of the feed tank agitator, the type of feed pump impeller, and ambient cooling owing to seasonal temperature fluctuations, may adversely impact the separation. In biologically active systems, factors such as differences in pH, alkalinity or volatile solids may indicate a difference in the feed stock to the separation system.

Sigma limitation: efficiency The sedimentation that the sigma value attempts to quantify is only a portion of the task to be accomplished. By assumption, sigma allows comparison of centrifuges which are geometrically and hydrodynamically similar. In practice, an efficiency factor is often introduced to extend the use of sigma to compare dissimilar centrifuges. Therefore we can expand eqn [21]:

$$Q_2 = Q_1(\Sigma_2/\Sigma_1)(e_2/e_1) \quad [34]$$

again, if and only if $v_{s1} = v_{s2}$.

If the two centrifuges are geometrically and hydrodynamically equal, the efficiency factors cancel. Axelsson has attempted to quantify the efficiency of the various types of sedimenting centrifuges and has provided the data in Table 1.

Scale-up The sigma formula for the various types of imperforate centrifuges are listed in Table 2.

When testing a new material for separability on a centrifuge, a bottle centrifuge (Figure 6) is usually used to estimate the G-level required. To estimate size from the bottle centrifuge:

$$Q_B/\Sigma_B = (2g/\omega^2 t) \ln(2r_c/(r_c + r_1)) \quad [35]$$

By adapting eqn [34], the full-scale centrifuge (Σ_L) for the full-scale flow (Q_L) can be determined:

$$(Q_L/Q_B) = (\Sigma_L/\Sigma_B)(e_L/e_B) \quad [36]$$

$$\Sigma_L = \Sigma_B(Q_L/Q_B)(e_B/e_L) \quad [37]$$

where $e_B = 1$ and e_L is between 0.5 and 0.9.

Table 1 Efficiency of various types of sedimenting centrifuges

Sedimenting centrifuge type	Efficiency factor (e)
Disc stack	45–73%
Decanter	54–67%
Tubular bowl	90–98%

Table 2 Sigma formula for the various types of imperforate centrifuges

Centrifuge type	Sigma formula
Bottle centrifuge	$\omega^2 V/2g[r_c/(r_c + r_1)]$
Imperforate bowls (tubular, decanter, basket)	$2\Pi/(\omega^2/g)(\frac{3}{2}r_2^2 + \frac{1}{4}r_1^2)$
Disc stack	$(2\Pi n\omega^2/3g)(\cot \Theta(r_2^3 - r_1^3))$

The sizing should then be confirmed by testing the selected centrifuge type.

The sigma concept indexes the size of centrifuges based solely on sedimentation performance. Other criteria and limitations must also be considered. These limitations most often involve the ability of the centrifuge to handle solids once they are sedimented. This may require knowledge of solids residence time, G-level, solids transportability (conveyability or flowability), compressibility and recognition of the limits on torque and solids loading.

Filtering Centrifuges

Ideal System

Filtration systems, centrifugal or otherwise, usually conform to the same fundamental relationship, which is defined as:

$$Q/A = P/R \quad [38]$$

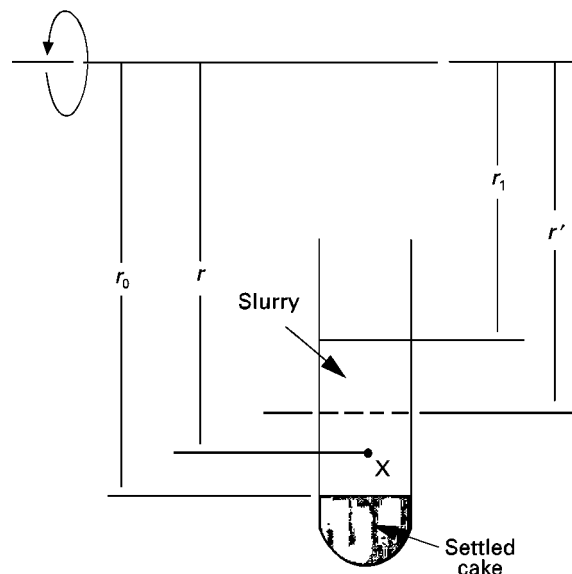


Figure 6 Bottle centrifuge (X represents the initial position).

where Q is the volumetric flow rate, and A is the cross-sectional area of the medium. P is the driving force, which is dependent on the equipment chosen. R is the resistance that depends on the materials being processed. Q/A , not surprisingly, is analogous to Q/Σ . The driving force (P) is proportional to the G-level. The bulk of the discussion revolves around how to determine the cake resistance (R).

Cake Drainage

The theory covering drainage in a packed bed is incomplete, especially when a centrifugal field is applied. It is an exceptional case when a theoretical solution might be applicable. Most of the work in this area involves numerical integration of experimental data if available, empirical rules, and simplifying assumptions. Liquid is held in the cake by various forces. Several flow mechanisms are proposed for liquid removal. In a centrifugal field, the acceleration is a function of radius from the centre of rotation which might cause changes in the packing of the bed and the acceleration of the liquid. The effective force on the particle is proportional to $(\rho_p - \rho_l)$, as the liquid in the bed drains $\rho_l \rightarrow 0$, so that the effective force on the particle changes. It is difficult to construct a useful theoretical model under these conditions that might be used in the absence of empirical data.

During cake deposition, a continuous head of liquid ranging in composition from that of the feed to an essentially clarified supernate may exist over the cake bed. If the cakes are slow draining a layer of clarified liquid may exist over the cake bed even after the feed is stopped. Draining under these conditions requires continuous flow through the cake. These interstitial spaces are assumed to be full. When a layer of free liquid no longer exists above the cake, the free liquid surface moves through the cake to an equilibrium position at the capillary height, leaving behind voids filled with gas or vapour. After bulk drainage of the larger voids, liquid still exists in the cake's upper portion in a film covering the surfaces of the solids and in partially filled voids having restricted outlets. Eventually, some of this liquid flows as a film to the continuous liquid layer at the capillary height. Typical drain time after the disappearance of a free liquid head above the cake is shown in Figure 7. Some essentially undrainable liquid exists within the body of each particle or in fine deep pores without free access to the surface except possibly by diffusion. This last type of liquid might be removed by evaporation or possibly by displacement with another liquid but cannot be removed mechanically by either

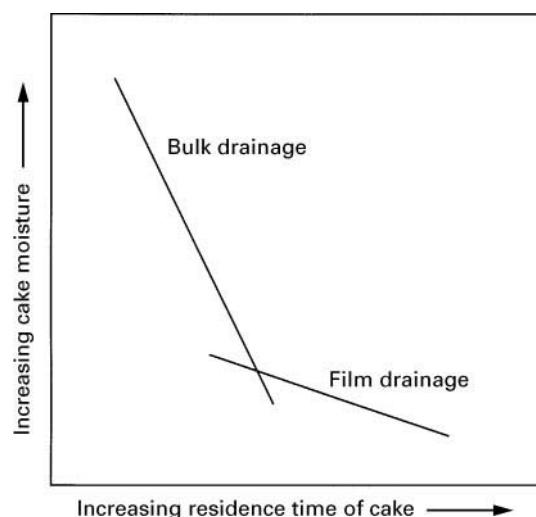


Figure 7 Typical drain time.

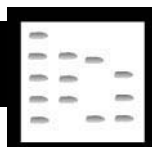
a gravitational or centrifugal field. Treatment of empirical data is discussed in the literature.

See also: II/Centrifugation: Large-Scale Centrifugation.

Further Reading

- Ambler CM (1952) *Chemical Engineering Progress* 48: 150.
- Ambler CM (1961) *Industrial & Engineering Chemistry* 53: 430–433.
- Axelsson H (1985) Centrifugation. In: Cooney CL and Humphrey AE (eds) *Comprehensive Biotechnology*, Vol. 2. *The Principles of Biotechnology: Engineering Considerations*, Chapter 25. Oxford: Pergamon Press.
- Batel W (1961) *Chemical Eng. Technology* 33: 541.
- Letki A, Moll R and Shapiro L (1997) Centrifugal separation. In *Kirk-Othmer Encyclopedia of Chemical Technology*, 4th edn, Vol. 21. New York: John Wiley.
- Nenninger Jr E and Storrow JA (1958) *AIChE J* 4: 305.
- Records FA (1977) Sedimenting centrifuges. In: Purchase DB (ed.) *Solid/Liquid Separation Equipment Scale-up*, Chapter 6. Croydon: Uplands Press.
- Storrow JA (1957) *AIChE J* 3: 528.
- Svarovsky L (1977) Separation by centrifugal sedimentation. In: Svarovsky L (ed.) *Solid-Liquid Separation*, 2nd edn. London: Butterworths.
- Tiller FM and Hysung NB (1990) *Comparison of Compacted Cakes in Sedimenting and Filtering Centrifuges*. Presented at the American Filtration Society, Third Annual Meeting, Washington DC.
- Vesilind PA (1979) *Treatment and Disposal of Wastewater Sludges*, revised edition. Ann Arbor, MI: Ann Arbor Science Publishers.

CHROMATOGRAPHY



Automation

E. Vérette, Gilson, Villiers-le-Bel, France

Copyright © 2000 Academic Press

The last 20 years have seen an important increase in published papers on chromatography, reporting fully automated systems or complete online techniques. This shows a strong interest in automation in chromatography to obtain faster, safer, more cost-effective and convenient analytical procedures, that satisfy regulatory compliance and good laboratory practice directives. Automation in chromatography takes place in the more general laboratory automation context, which is the application of computing, robotics, electronics and mechanical engineering technologies to laboratory problems for enhanced throughput, reproducibility and traceability. This has been made possible as a result of considerable improvements in equipment and techniques, from autosamplers, sample processors and reliable eluent delivery devices, to universal or more specific detectors, collectors, single point control software able to collect and handle accurate data (Figure 1) and, last but not least, laboratory information management systems.

The chromatographic techniques whose automation is principally discussed in this article are gas chromatography (GC), high performance liquid

chromatography (HPLC) and supercritical fluid chromatography (SFC). Other chromatographic methods such as planar chromatography can also be automated, but full automation is more difficult to achieve.

One of the most important aspects of automation is the introduction of interfaces between instruments and computers, and centralized user-friendly software for system control and data handling. The main qualities required for interfaces, designed to collect analog signals and digitize them to reflect detector output accurately, are good sampling rates and high resolution. Other important aspects of automation are directly related to the evolution of individual instruments, and the possibility of coupling them online. This article is not an exhaustive description of automation in chromatography, but highlights the principal trends in this field. It emphasizes sample preparation and application in chromatographic systems, multidimensionality and fully automated solutions widely used today such as high throughput screening and preparative chromatography.

Autosamplers

Not far behind computerized data acquisition and analysis, autosamplers are one of the biggest factors in automation, allowing long unattended series of analyses, therefore releasing the operator for other tasks. Autosamplers also give considerable improvement in reproducibility. Autoinjectors for HPLC, GC

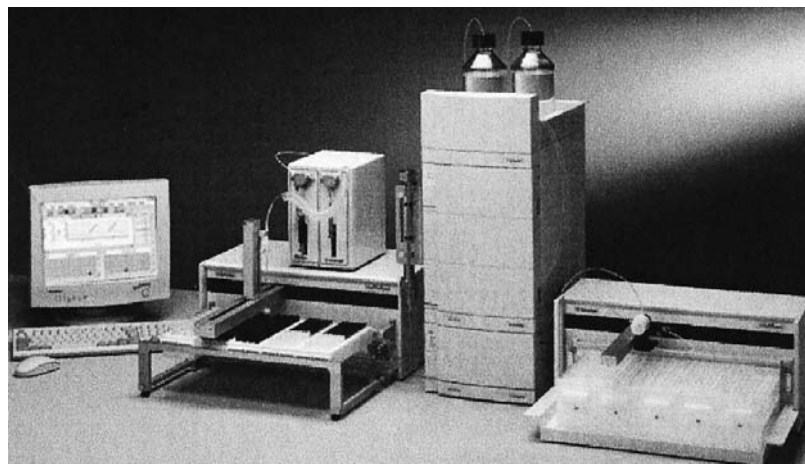


Figure 1 A fully automated HPLC system including an autoinjector, a pump, a detector and a collector controlled by centralized software.

and SFC are generally of Cartesian displacement or of carousel types.

High Performance Liquid Chromatography

HPLC is considered to be the major chromatographic technique available today for involatile or heat-sensitive substances. Sample injection is commonly performed using a switching valve via an external or internal sampling loop. Sample containers range from simple vials with a wide range of volumes to different types of microtitre plates (96 and 384 wells), with the option of temperature control. Using 384-well microtitre plates, some modern instruments can store and handle over 4600 samples unattended. Many autosamplers have three injection modes, total, partial and centred loop filling, depending on the sample volume limitations. In recent years the need for faster analysis has been a major consideration; therefore, the shortest time required between two injections (injector cycle time) appears to be an important criterion for autoinjectors, and may be less than 20 s in the fastest. Other important criteria are injection precision and the level of carryover, with typical values below 0.3% (relative standard deviation) and 0.02% respectively for the best instruments.

Gas Chromatography

Because of its extremely high separation efficiency, speed of analysis and wide range of sensitive detectors, GC and particularly capillary GC is an appropriate procedure for analysing many compounds in a great variety of applications, provided these compounds are volatile, thermally stable and with reasonable polarities to avoid problems encountered with derivatization procedures. However, until recently its major critical point was the injection of large volumes, especially when traces of organic compounds have to be analysed, and the suitability of the sample solvent. The injector influences accuracy, precision, resolution and analyte recovery. The use of new automatic injection devices has provided the means to enhance the limit of detection significantly. Five modes of operation (split, split-less, direct, cold on-column injection, and programmed temperature vaporizer) allow maximum injector flexibility. Among these, the programmed temperature vaporizer (PTV) is of major utility for the automated injection of large sample volumes (Figure 2). This technique is based on the selective elimination of the solvent, while simultaneously trapping the components with a much lower volatility. Liquid samples are introduced into a large capacity, sorbent-packed liner inserted in the injector head. By temperature-programming

the liner, the solvent is vented through the split exit while analytes are retained. The split valve is then closed and the injector is rapidly heated to transfer the analytes to the GC column. With such a technique, injection volumes in split-less capillary GC can be increased up to 1 mL and this procedure therefore brings enormous improvements in limits of detection.

Static or dynamic headspace sampling, is another interesting way of injecting volatile compounds from complex matrices into a GC. In this process, the vapour in equilibrium above a sample held at constant temperature in a sealed vial is drawn and analysed. Headspace GC is used to analyse a wide range of compounds in solid and liquid complex matrices, and fully automated devices are available today with computer-activated heating and pneumatic systems.

Sample Preparation

For a long time, sample preparation has been considered to be the bottleneck of the analysis. However, the advances of automation in this area have until recently been distinctly more modest compared with other areas. The move towards automation in sample preparation occurred for several reasons, including higher productivity, fewer and more skilled laboratory personnel, better analytical results and less hazardous conditions. Basically, there are two almost complementary types of equipment, anthropomorphic arms and Cartesian liquid handlers, used according to the nature and quantity of samples to be processed and the preparation complexity (Figure 3). Anthropomorphic arms are capable of grabbing objects and moving them from one place to another with high accuracy. They need a set of dedicated stations to carry out different operations such as grinding, homogenizing, drying, weighing, etc. The principal preparation steps used with Cartesian (XYZ) samplers are dilution, addition of reagents or internal standards and mixing. With additional equipment they can also perform temperature control, evaporation or filtration.

Solid-phase Extraction (SPE)

SPE has become a technique of choice for sample clean-up and trace enrichment in the fields of pharmaceutical, clinical, food and environmental analysis. Indeed, it offers better versatility and selectivity than other sample preparation techniques. Compared with liquid-liquid extraction, it is quicker, it requires much less solvent, it prevents possible formation of emulsions, sample volumes can be smaller, and it is

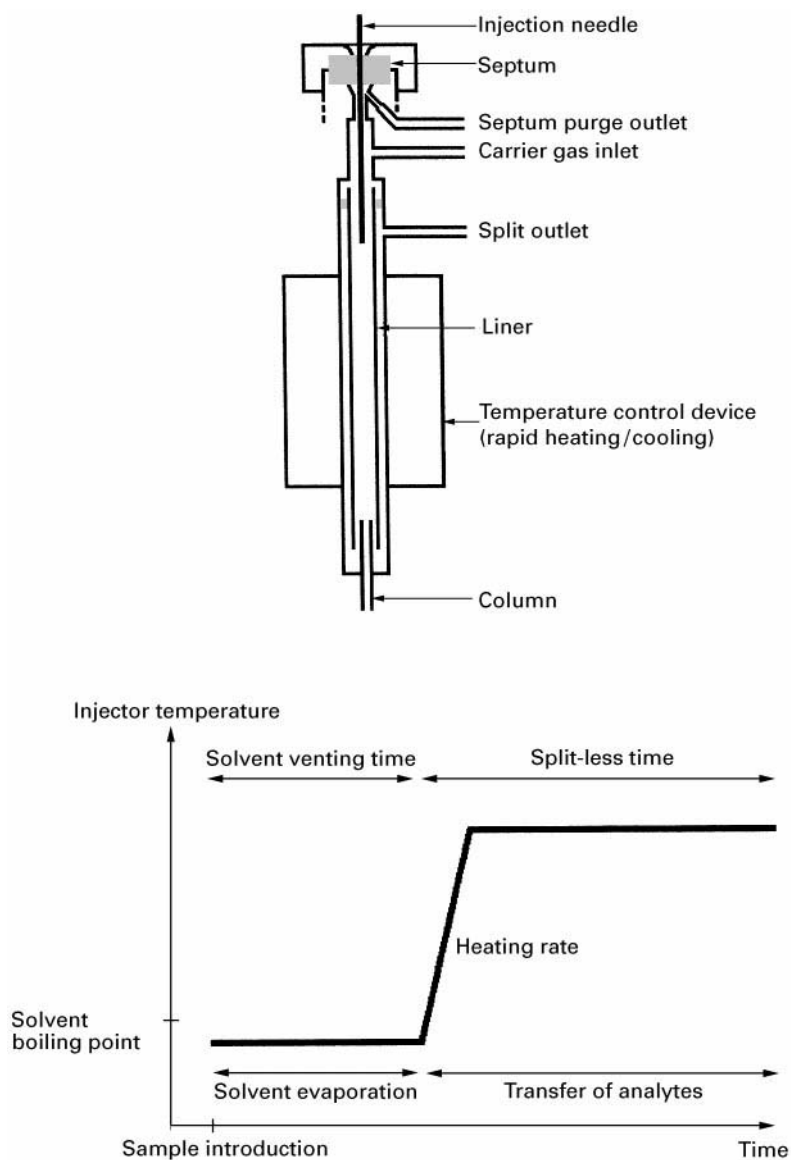


Figure 2 Schematic representation of a PTV injector and temperature profile of injection.

much more amenable to automation. The US Environmental Protection Agency has adopted more than 20 SPE methods as alternatives to liquid-liquid extraction. SPE formats range from traditional disposable extraction columns and membrane discs to 96-well plates and SPE pipette tip configurations. Today, a wide range of sorbents is available to increase selectivity and/or simplify the SPE procedure, from silica to polymer-based phases, including speciality phases with mixed-mode functionality.

An experimental SPE procedure typically follows four steps – conditioning, loading, washing and eluting. With offline systems using disposable columns, liquids go through the extraction columns

either by aspiration (vacuum manifolds), or by positive air pressure; the latter can be completely automated. **Figure 4** shows typical SPE automation, based on the mobility of a dedicated rack consisting of three parts. After elution and a final mixing step, the eluate can be automatically introduced into the chromatograph via an injection valve for analysis.

Fully automated offline SPE brings an easy transfer of manual methods, which results in a quick transposition of hundreds of existing protocols with little additional development. Since the introduction of the large volume GC injection with a PTV injector interface, automated SPE has been extended to numerous GC applications. Some SPE instruments

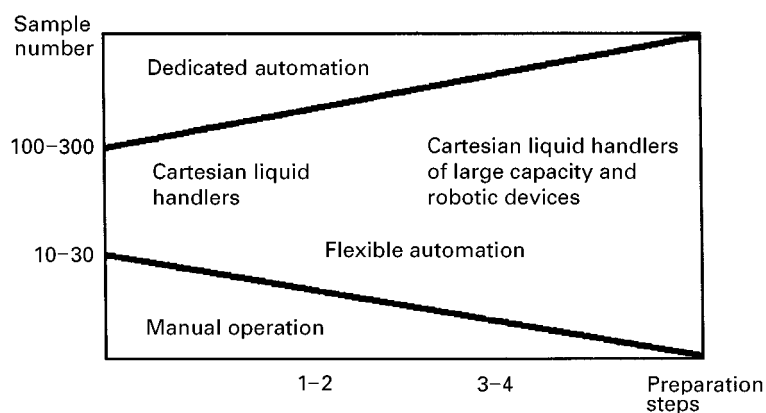


Figure 3 Diagram of estimated automation requirements according to sample number and preparation complexity.

propose a flexible process to develop new methods such as the possibility for multicollection, multi-modal SPE or column drying, and more recently the possibility of using 96-well SPE microplates with a multiple probe equipment.

In online configurations, an extraction cartridge is inserted as part of the chromatographic equipment, and is directly connected to the high pressure stream of the mobile phase. Such automated SPE equipment can use either the same cartridge for multiple extractions, or carry out automatic cartridge exchange. Online SPE processes are also known for pre-column concentration techniques, and may involve column switching or coupled-column procedures. The online approach provides high throughput and preserves the sample integrity, but the technique is still dependent on particular applications and the reproducibility of packing materials.

Solid-phase Microextraction (SPME)

SPME, introduced by Pawliszyn in the early 1990s, is a sample preparation and introduction method in which analytes migrate from a liquid, headspace or air sample on to a polymer (principally polydimethylsiloxane or polyacrylate) that is coated on a fused silica rod. The fibre is then displaced into a thermal or solvent desorption interface for analysis respectively by GC or HPLC. All these steps can be fully automated using autosamplers specifically adapted to SPME, such as the recent in-tube SPME device for HPLC. This technique, which is used repeatedly, provides fast, easy-to-use and inexpensive sampling, and eliminates organic solvents. Initially applied to the analysis of relatively volatile environmental pollutants in simple matrices, it now allows sampling of a broader range of analytes, including drugs in more complex media, with improved analytical performance.

Valve Switching Devices for Sample Preparation

Valve switching devices allow variable combinations of columns, mobile phases and/or detectors, which contribute to the overall system selectivity. When large numbers of substances are present in complex samples like biological fluids, and the compounds of interest are at very low concentrations, such devices are used sequentially to carry out sample clean-up and trace enrichment. Different set-ups are available depending on the type of application, permitting the transformation of offline multi-step methods to single-step procedures. The simplest configuration uses one pre-column between the sample injector and a six-port valve which rotates after venting the unwanted components to waste (straight-flush mode). A more powerful process can be achieved by operating in backflush mode, but necessitates additional equipment. In recent years, switching devices have regained interest due to the introduction of the bimodal restricted access sorbents. Designed for the deproteinization of biological samples, restricted access sorbents are characterized by a hydrophilic external surface incorporating reversed-phase coated pores. Interfering proteins are excluded from the pores by hydrophilic and size exclusion interactions, and low molecular analytes like drugs and metabolites are extracted and enriched on the bonded phase in the sorbent pores. This new type of separation medium is best used in the form of an extraction cartridge fitted to the six-port valve of a sampling injector, before analysis with a more conventional column.

A schematic diagram of a fully automated set-up including an auto-injector with two switching valves is shown on **Figure 5**, where a preliminary online filtration step is performed to extend the lifetime of the cartridge when analysing crude samples. After

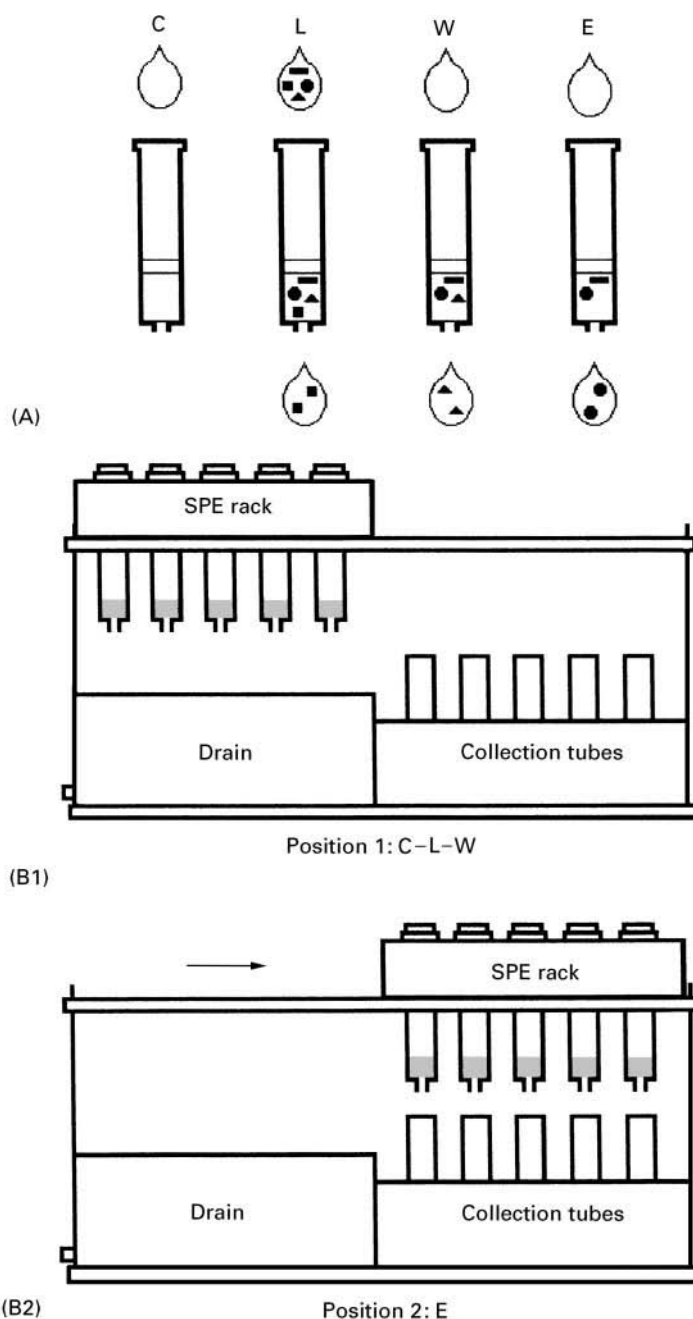


Figure 4 Automated solid-phase extraction based on ASPEC™ (Gilson) technology. (A) The four basic steps: conditioning (C), loading (L), washing (W) and eluting (E). (B1) Conditioning, loading and washing over the drain container. (B2) Eluting into the collection tubes.

injection the filtration device is regenerated with suitable solvents in backflush mode. Membrane-based sample clean-up such as dialysis, electrodialysis and ultrafiltration is another efficient and innovative way of discarding macromolecular and microparticulate matters before analysis. These devices can be automated and associated online with a chromatographic system, mostly HPLC, using switching valves.

Figure 6 shows a commercially available system automatically performing liquid transfer steps like addition of internal standards or derivatization, dialysis and trace enrichment from crude samples, for the online routine analysis of a large number of samples. This instrument consists of a XYZ autosampler, equipped with a dual-syringe pump, a flat-bed dialyser inserting a porous membrane and two six-port valves. After each analysis, the system is completely regenerated.

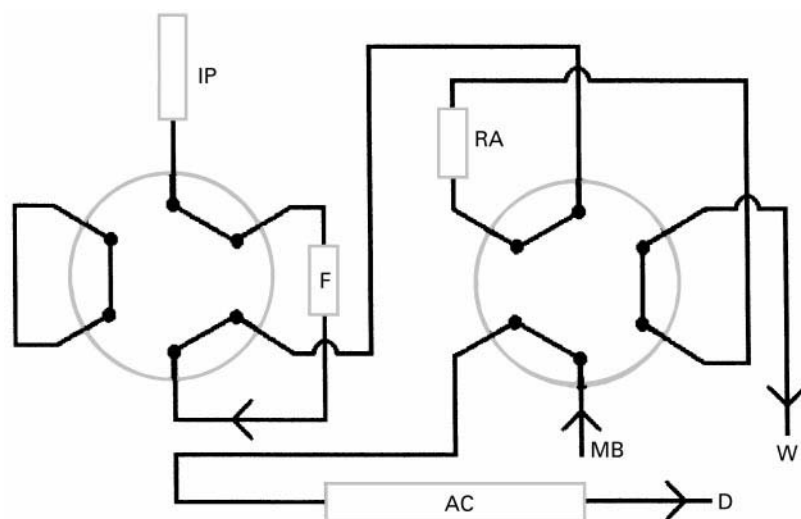


Figure 5 Online filtration and clean-up of biological fluid samples using valve-switching devices. AC, Analytical column; D, detector; F, filtration cartridge; IP, injection port; MB, mobile phase; RA, restricted-access sorbent cartridge; W, waste.

Supercritical Fluid Extraction (SFE)

Supercritical fluids have physical and chemical properties that make them particularly useful for extraction of analytes from solid and liquid matrices. Above their critical temperature, they can be compressed to increase their density and therefore their solvating power; moreover, they keep gas-like viscosity and diffusivity, and they can easily be evaporated by lowering the pressure. Because of these properties, SFE has received much attention as an alternative to

Soxhlet extraction. Automated SFE can be incorporated online with various analytical techniques such as HPLC, GC or SFC.

Multidimensionality

In the analysis of complex samples, a single analytical column combined with a selective detector does not always provide the required sensitivity and selectivity. Automated multidimensional chromatography has emerged as a convenient answer to these

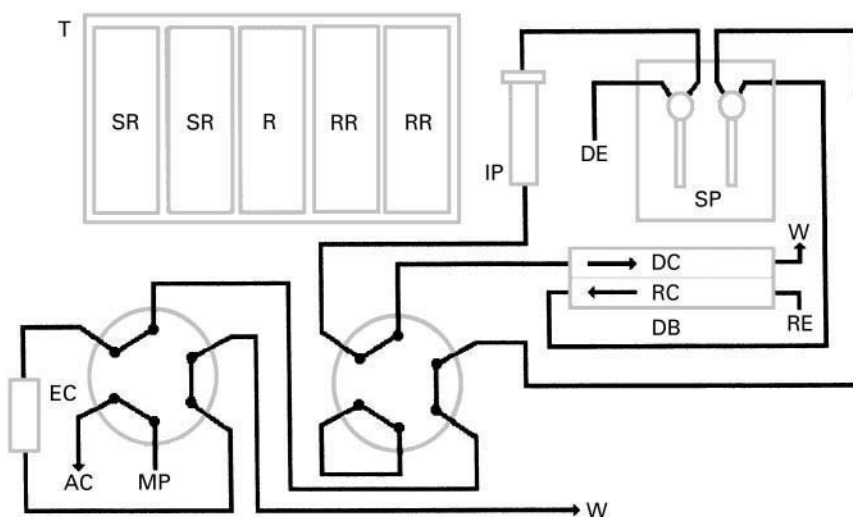


Figure 6 Online dialysis and trace enrichment of liquid samples using ASTED™ (Gilson) technology. AC, Analytical column; DB, dialyser block; DC, donor channel; DE, dilutor eluent; EC, enrichment cartridge; IP, injection port; MP, mobile phase; R, reagent rack; RC, recipient channel; RE, recipient eluent; RR, result rack; SP, dual-syringe pump; SR, sample rack; T, tray; W, waste.

problems. Multidimensional separation techniques constitute a powerful class of methods in which two or more independent steps are linked together. Roughly, multidimensionality includes two major branches: hyphenation and coupled-column techniques. A hyphenated instrument can be described as the combination of two (or more) instruments automated as a single integrated unit via a hardware interface whose function is to reconcile the output limitations of one instrument and the input limitations of the other.

Couplings of Chromatographs and Spectral Technique Devices

In recent years, numerous publications have described coupled techniques associating chromatographic instruments like HPLC, GC or SFC with sophisticated detectors or spectrometric devices, such as mass spectrometers (MS), MS coupled with diode array detector (DAD), MS-MS, Fourier transform infrared and nuclear magnetic resonance. However, for these online couplings, complete automation is generally required, and they are only feasible if suitable interfaces are available. Among these combinations, GC-MS and HPLC-MS are the most widely used in laboratories.

Gas Chromatography–Mass Spectrometry MS data provide the qualitative information for identification and characterization of sample components that is lacking in most other GC detectors. The availability of highly inert, durable and selective fused-silica columns and the ease of coupling GC systems with relatively low cost mass spectrometers make GC-MS a method of choice for numerous analyses, and this automated combination is now a routine analytical technique in many laboratories. The main restriction is that the analytes must be sufficiently volatile and thermostable for transfer to the vapour phase without decomposition, or that they can be derivatized to provide these properties.

High performance liquid chromatography–mass spectrometry Of all LC detectors, MS is a very powerful confirmatory tool for screening applications, and is widely used for impurity identification or quantification of drugs and metabolites in biological fluids. Nevertheless, no method of interfacing HPLC and MS exists that can be universally applied to all types of analyses. However, considerable progress has been made recently in the development of soft ionization techniques such as matrix-assisted laser desorption ionization, and also in sample introduc-

tion devices like particle beam, electrospray/ion spray or atmospheric pressure chemical ionization interfaces. When nonvolatile buffers like phosphates or ion-pairing agents are used, removal of these additives can be automatically performed, changing the phase system with additional equipment, using coupled-column and valve-switching techniques.

Couplings of Chromatographic Systems

These techniques are versatile and powerful, and are well suited to the separation of multicomponent mixtures. They include zone-cutting methods, in which fractions from one chromatographic column are usually transferred via a loop installed on a switching valve, to one (or more) secondary column(s) in series for additional separation(s), or to another chromatographic system. In LC-LC, a special area of interest of column-switching is the resolution of enantiomeric drugs in biological fluids, by coupling chiral systems to conventional reversed-phase columns. Other useful associations combine size exclusion or ion chromatography with reversed-phase chromatography. Parallel settings using switching valves are also possible for column and mobile-phase selection. Such systems have been reported for fully automated, rapid and easy method development to analyse different types of compounds, including enantiomers.

LC-GC is a very convenient combination which associates the selectivity of LC with the high efficiency capillary GC. Moreover, GC possesses many sensitive and specific detectors. Such a coupled technique enables the analysis of samples with complex matrices, and considerably prolongs the GC column lifetime. The first set-up was described by Majors in 1980; since then important improvements in development have been achieved. With this transfer technique, specific attention must be paid to interfaces. Several interfaces are available to couple the two systems online, such as on-column, loop-type and PTV interfaces which permit the transfer of large volume samples into the gas chromatograph. Insertion of a short trapping column between HPLC and GC also enables direct coupling from reversed-phase systems.

Fully Automated Dedicated Systems

The production of chemical compounds at the laboratory or plant scale requires fully automated and reliable separation techniques. This is true from discovery, through process control, to the final stage of purification and quality control of a new compound or drug. Numerous complete solutions exist today,

such as online systems available in biotechnology, which involve automated process monitoring for the determination of small organic molecules, and interactive controls of the physicochemical and biochemical growth conditions in culture media. In many fields, including combinatorial chemistry, preparative separations are certainly widely used and require the most complete online solutions.

Preparative Chromatography

The objective of preparative chromatography is to obtain sufficient quantities of compounds at the required purity, with the highest throughput and at the lowest price. Material to be purified can be simple or more complex, such as fermentation broths and natural products. In such instances, fully automated preparative HPLC on a laboratory scale (milligrams to grams) is one of the best separation techniques for this objective, and also because of its flexibility to accommodate frequent application changes and variable quantity ranges.

The requirements of a preparative HPLC system differ according to the quantity of product to be collected, and the nature and number of samples to be purified. However it should provide reliable and complete automation for unattended operations with error-handling methods, and total traceability of all events, including the collected fractions. Fraction collectors are key instruments in preparative HPLC, and should be selected according to their collection facilities and fractionation software. Devices exist that can perform peak collection with automatic

tracking of the baseline drift. With such instruments, collection is initiated if the detector signal is above user-set parameters in relation to threshold level and peak width. The graphic sample tracking which is feasible with some recent centralized software is also an important feature in preparative chromatography. Indeed, it can provide useful information to the user on sample identification, collection positions and associated chromatograms.

Since the introduction of independent programming of mobile-phase pressure, composition, and flow rate, SFC with packed columns has received considerable interest for several reasons, including its suitability and exceptional performances in preparative works. Consequently, this technique may become a serious competitor to preparative HPLC in the near future. **Figure 7** shows a completely automated system for analytical and preparative SFC. A versatile dual-valve autosampler of large capacity is used to perform both injection and collection. A solvent-less injection mode and a column-switching procedure are realized by two extra six-port valves. Such a system performs analytical development and switches easily and quickly to preparative chromatography for linear scale-up, and back to analytical for the purity check of the collected fractions. All these steps are automatically monitored by centralized software.

Analysis and Purification in Combinatorial Chemistry

Combinatorial chemistry appeared a few years ago in the pharmaceutical and biotechnological industries as

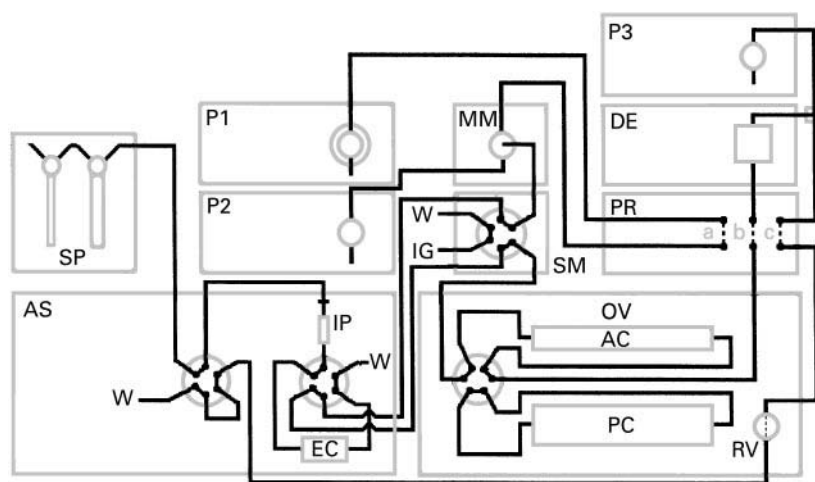


Figure 7 Automated analytical/preparative supercritical fluid chromatography on packed columns, with a solvent-less injection mode, based on Series SF3™ (Gilson) technology. AC, Analytical column; AS, dual-valve autosampler; DE, detector; EC, enrichment cartridge; IG, inert gas; IP, injection port; MM, mixing module; OV, oven; PC, preparative column; PR, pressure regulator (a, upstream pressure and pulse damper; b, heat exchanger; c, downstream pressure regulator); P1, liquid carbon dioxide pump; P2, modifier pump; P3, collection solvent pump; RV, pressure relief valve; SM, switching valve module; SP, dual-syringe pump; W, waste.

a novel approach to finding new drugs, and has undergone outstanding development since then. It is defined by a variety of automated high throughput synthesis techniques, to produce large numbers of small organic molecules, for screening these compounds against several biological targets for drug discovery. Combinatorial chemistry includes three basic steps – synthesis, candidate screening and library product purification – but chromatography is principally involved in the last two.

In drug candidate screening, library product verification can be performed with various analytical techniques. Among these, gradient reversed-phase HPLC with UV detection is widely used. Such a system, fitted with an autoinjector which accommodates microtitre plates, provides a robust and highly automated approach. Fast HPLC methods (generally of less than 5 min) generate up to 300 analyses per day per system and are required to produce libraries of products with widely differing polarity. These generic methods use short C_{18} columns with sharp slope gradients from acidified water to acidified organic solvents, high flow rates and UV detection set at 220 or 254 nm. Automated HPLC-MS, HPLC-DAD-MS and HPLC-MS-MS have also become important routine tools for the combinatorial chemist, because they provide structural information to identify the compounds which have been synthesized.

Automated purification to an extremely high level with sample quantities of up to 100 mg can be achieved with a preparative HPLC system equipped with an autoinjector and a fraction collector. The technique uses the same packing material and mobile phases as those used in analytical separation. Fast and easy clean-up can also be performed using SPE cartridges or microplates. Samples may therefore be processed in parallel with an automated device for optimum throughput. And last but not least, preparative SFC, although with limited applications so far, also provides a high productivity approach to purification, and in the near future should acquire a much bigger place in combinatorial chemistry.

Future Trends

Automation in chromatography has been a major preoccupation in recent years, mostly for pharmaceutical and clinical laboratories, and this will certainly be more intensive in the future, with concomitant developments in other fields like chemical, agrochemical, food or environmental analysis. The main goal is to provide more analyses giving the maximum and the most accurate information in the shortest time, at the lowest cost. This is the current situation in pharmaceutical and biomedical research

for high throughput screening in combinatorial chemistry, genomics or proteomics. Future trends in automation will surely follow the evolution of instruments, including mixed-mode techniques like capillary electrochromatography, more efficient interfaces, and more versatile and user-friendly software. They will also follow the progress in chromatographic media like restricted-access sorbents or advanced stationary phases with sub 3 μm particles for LC, and new materials for sample preparation such as 96-well SPE extraction plates.

Miniaturization in chromatography, including automated micro- and nano-techniques, is certainly an important step towards this goal, and a good example is given by the fast separation of complex mixtures with miniature gas chromatographs, which can now be performed in the field. Moreover, in addition to allowing the analysis of very limited volume samples with good sensitivity, and to reduce mobile-phase consumption, miniaturization tends to reduce work space, robot displacements and liquid transfers and consequently overall analysis time. The evidence of the release on the market of 384-well SPE extraction plates will obviously confirm this trend. Down-sizing even further, the use of 1536-well microtitre plates automated by sample processors equipped with distribution heads and chip format technology will certainly be expanded in the very near future. This goal involves refinement of the technique to carry out continuous separations with sub-second time resolution and attomole detection limits.

See also: II/Chromatography: Liquid Chromatography - Gas Chromatography. **Chromatography: Gas:** Historical Development; Detectors: Mass Spectrometry. **Chromatography: Liquid:** Detectors: Mass Spectrometry; Instrumentation; Large-Scale Liquid Chromatography. Multidimensional Chromatography. **Electrophoresis:** Capillary Electrophoresis. **Extraction:** Solid-Phase extraction; Solid-Phase Microextraction; Supercritical Fluid Extraction.

Further Reading

- Anton K and Berger C (eds) (1998) *Supercritical Fluid Chromatography with Packed Columns – Techniques and Applications*. Chromatographic Sciences series. New York: Marcel Dekker.
- Grob K (1995) Review: development of the transfer techniques for on-line high-performance liquid chromatography – capillary gas chromatography. *Journal of Chromatography A* 703: 265.
- Hills D (ed.) (1998) *Current Trends and Developments in Sample Preparation*. LC GC International. Chester, UK: Advanstar Communications.

Niessen WMA and Tinke AP (1995) Review: liquid chromatography-mass spectrometry. General principles and instrumentation. *Journal of Chromatography A* 703: 37.

Poole CF and Poole SK (1991) *Chromatography Today*. Amsterdam: Elsevier.

Prinzis S, Fraudeau C, Hutchinson G and Paulus M (1997) *Gilson Guide to SPE Automation*. Villiers-le-Bel, France: Gilson.

Stevenson D and Wilson ID (eds) (1994) *Sample Preparation for Biomedical and Environmental Analysis*. New York: Plenum Press.

Convective Transport in Chromatographic Media

A. E. Rodrigues, LSRE Faculty of Engineering,
University of Porto, Porto, Portugal

Copyright © 2000 Academic Press

New liquid chromatographic media have been developed in the last decade containing large pores for convective mass transport and smaller diffusive pores to provide adsorption capacity. These permeable packings are at the heart of perfusion chromatography, patented in 1991, leading to better column efficiency and speed of separation with applications in the rapid analysis of biological macromolecules and preparative scale purification of proteins. This improved column efficiency is based on the concept of augmented diffusivity by convection, available from parallel development in the chemical reaction engineering area.

The analysis of column performance requires an extended van Deemter equation for the HETP (height equivalent to a theoretical plate) as a function of the superficial velocity. A methodology for obtaining basic data for design of perfusive chromatography is suggested involving elution chromatography of proteins in nonretained and frontal chromatography experiments.

Permeable Chromatographic Media

Packing materials in bead form can be grouped into four classes: homogeneous cross-linked polysaccharides (e.g. agarose), macroporous polymers based on synthetic polymers (e.g. POROS particles used in perfusive chromatography with large pores of 600–800 nm and diffusive pores of 50–100 nm), tentacular adsorbents allowing faster interaction between proteins to be separated and functional groups and materials based on the concept of ‘soft gel in a rigid shell’ combining the good capacity of soft gels with the rigidity of composite materials.

In conventional packings, solutes are carried to sites on the particle surface by bulk convective flow of the mobile phase through the column and then diffuse to binding surfaces inside the particle. The intra-particle diffusion process can be quite slow for large molecules (proteins, peptides). In order to maximize capacity and resolution, interaction with as many sites as possible is required; however, this will be more difficult at high flow rates and therefore trade-offs between speed, resolution and capacity are needed. In permeable, flow-through particles used in perfusive chromatography the flow rate can be increased one order of magnitude compared with conventional packings because of the short diffusion path length inside the microspheres.

New materials aim to achieve higher sorption capacity and better sorption kinetics. Some developments consider new geometries: fibres, membranes or discs (cellulose, polymethacrylate) or continuous beds (rods, monoliths). In continuous rods of acrylamide-acrylate polymers, flow pores are of 3–4 µm diameter and in methacrylate-styrene polymers large pores of 0.5–2 µm and even 20 µm are obtained with microspheres of less than 0.5 µm. Similar developments on continuous silica rods are taking place. In continuous bed technology, channels are of 3–5 µm with microspheres of 0.5–1 µm, whilst in bead form, packings are typically of 3–50 µm with pore size of 0.1 µm. Also superagarose beads of 300–500 µm have been prepared with superpores of 30 µm as well as 3 mm thick membranes. Table 1 reports examples of convective chromatographic media.

The Concept of Augmented Diffusivity by Convection

The design of chromatographic media aims to eliminate or reduce the mass transfer resistance inside particles by coating a nonporous support with active species, decreasing the particle size or increasing par-

Table 1 Examples of convective chromatographic media

Base material	Trade name	Process	Producer
Polystyrene	PL4000	HPLC	Polymer Laboratories, UK
Polystyrene	POROS	HPLC	PE Biosystems, USA
Agarose	Sephacrose	Fast flow	Pharmacia, Sweden
Silica gel	Daisogel SP2705	HPLC	Daiso Co, Japan
Polymeric	TSK-PW	SEC	Toso-Haas, USA
Hydroxyapatite	Macro-Prep	Preparative chromatography	Bio-Rad, USA
Methacrylate copolymer	Macro-Prep	HPLC	Bio-Rad, USA
Alumina	Ceraflo	Membrane	Norton, UK
Cellulose	MemSep	MCLC	Millipore, USA
Polymer matrix	CIM	CBT IEX	BIA Separation, Slovenia
			JM Science, USA
Polymer matrix	UNO	CBT IEX	Bio-Rad, USA

CIM, Convective interaction media; MCLC, membrane convective liquid chromatography; CBT, continuous bed technology; IEX, ion exchange; SEC, size exclusion chromatography; HPLC, high performance liquid chromatography.

ticle permeability as in convective chromatographic media (Figure 1). The use of flow-through particles (Figure 2) has been increasing recently in relation to protein separation by HPLC with perfusive chromatography. Intraparticle forced convection is a mass transport mechanism which, in addition to diffusive transport, cannot be neglected in large pore materials. The key concept to be retained is the augmented diffusivity by convection, which explains why the efficiency of adsorptive processes is improved with convective chromatographic media.

The effect of intraparticle convective flow due to a total pressure gradient was quantified in 1982 by a group measuring effective diffusivities by chromatographic techniques. The analysis of experimental results was first made with a conventional model which included an apparent diffusion (lumping diffusion and convection) of tracer inside pores. The apparent diffusivity was found to increase with the superficial velocity. From the equivalence of the conventional model and a detailed model which allows for the separate contribution of diffusive and convective flow (Figure 3) the apparent diffusivity or augmented diffusivity by convection, \tilde{D}_e was calculated for an inert tracer as a function of the true effective diffusivity

D_e and the intraparticle mass Peclet number λ :

$$\tilde{D}_e = D_e \frac{1}{f(\lambda)} \quad [1]$$

where:

$$f(\lambda) = \frac{3}{\lambda} \left(\frac{1}{\tanh \lambda} - \frac{1}{\lambda} \right)$$

The intraparticle Peclet number, λ , is the ratio between the time constant for pore diffusion, τ_d , and the time constant for intraparticle convection, τ_c . For slab geometry, $\tau_d = \varepsilon_p \ell^2 / D_e$ and $\tau_c = \varepsilon_p \ell / v_0$ so $\lambda = v_0 \ell / D_e$ where ℓ is the half-thickness of the slab particle and v_0 is the intraparticle convective velocity inside large pores; for sphere geometry with particle radius R_p , the diffusion time constant is $\tau_d = \varepsilon_p R_p^2 / D_e = R_p^2 / D_p$ and $\lambda = v_0 R_p / 3 D_e$.

The enhancement of diffusivity by intraparticle convection is $1/f(\lambda) = \tilde{D}_e / D_e$ and so the apparent diffusion time constant $\tilde{\tau}_d = \tau_d f(\lambda)$. Figure 4 shows the enhancement factor \tilde{D}_e / D_e as a function of the intraparticle Peclet number λ . At low bed superficial velocities, u_0 , the convective velocity inside pores, v_0 , is also small; therefore $f(\lambda) = 1$ and $\tilde{D}_e = D_e$ (diffusion-controlled case); at high superficial velocities u_0 , and therefore high v_0 and high λ ,

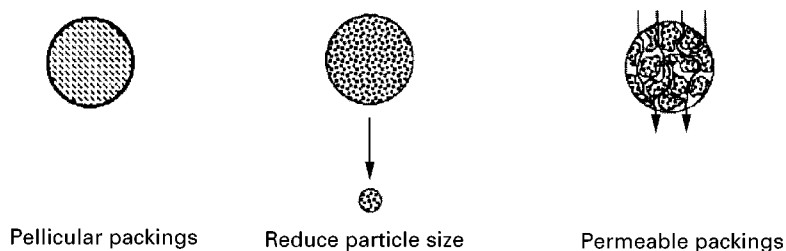


Figure 1 Strategies for eliminating or reducing intraparticle mass transfer resistances. (Reprinted from Rodrigues AE (1997) with permission from Elsevier Science.)

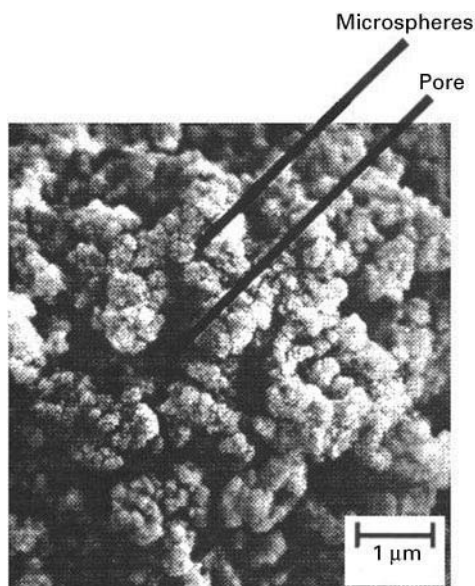


Figure 2 An example of permeable or flow-through chromatographic media with large pores and gel microspheres.

$f(\lambda) = 3/\lambda$; the augmented diffusivity is $\tilde{D}_e = v_0 \ell / 3$ for slab geometry and $\tilde{D}_e = v_0 R_p / 9$ for spheres (convection-controlled case), which depends only on the particle permeability, fluid viscosity and pressure drop across the particle.

Column Performance Using Convective Chromatographic Media

Conventional Packings

The column performance can be assessed in terms of HETP as a function of bed superficial velocity

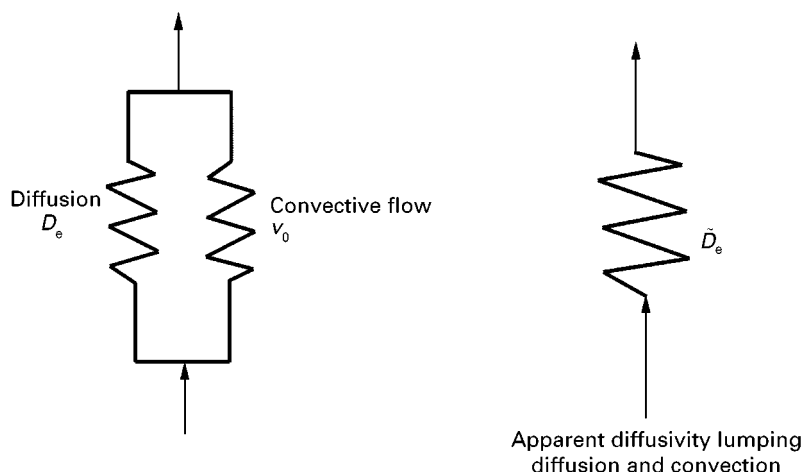


Figure 3 Analogues of mass transport mechanisms in chromatographic media – model equivalence.

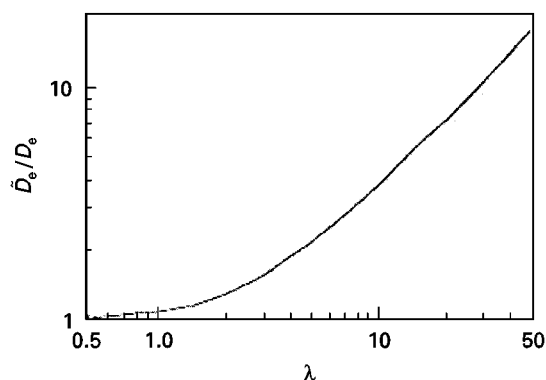


Figure 4 Enhancement factor \tilde{D}_e/D_e versus intraparticle Peclet number λ . (Reprinted from Rodrigues AE (1997) with permission from Elsevier Science.)

following the classic van Deemter analysis. The van Deemter equation for linearly retained species in conventional packings of sphere geometry is:

$$\text{HETP} = A + \frac{B}{u_0} + \frac{2}{15} \frac{\varepsilon_p(1 - \varepsilon_b)b^2}{[\varepsilon_b + \varepsilon_p(1 - \varepsilon_b)b]^2} \tau_d u_0 \quad [2]$$

where ε_p is the intraparticle porosity, ε_b is the bed porosity and $b = 1 + \{(1 - \varepsilon_p)/\varepsilon_p\}K$ is the adsorption equilibrium parameter for a linear isotherm with slope K . In a condensed form the van Deemter equation is:

$$\text{HETP} = A + \frac{B}{u_0} + C u_0$$

with:

$$C = \frac{2}{15} \frac{\varepsilon_p(1 - \varepsilon_b)b^2}{[\varepsilon_b + \varepsilon_p(1 - \varepsilon_b)b]^2} \tau_d$$

For protein separation the B term is negligible and the plot HETP versus u_0 in HPLC is a straight line in most of the domain when conventional supports are used. Moreover, the HETP increases with the square of the particle size.

Permeable Packings

For convective chromatographic media, since $\tilde{\tau}_d = \tau_d f(\lambda)$, the extended van Deemter equation (Rodrigues equation) is:

$$\text{HETP} = A + \frac{B}{u_0} + Cf(\lambda)u_0 \quad [3]$$

In the above equation one can notice that the last term pertaining to intraparticle mass transfer is reduced for permeable particles since $f(\lambda) < 1$. The van Deemter equation for conventional packings and Rodrigues equation for large pore supports are shown in Figure 5. At low velocities both equations lead to similar results. However, at high superficial velocities the last term in the Rodrigues equation becomes a constant since the intraparticle convective velocity v_0 is proportional to the superficial velocity u_0 . The HETP reaches a plateau which does not depend on the value of solute diffusivity but only on particle permeability and pressure gradient (convection-controlled limit). The column performance with permeable adsorbents is improved since HETP is reduced when compared with conventional packings and the speed of separation can be increased without losing column efficiency.

Bidisperse Chromatographic Media

In perfusive chromatography, packings contain both convective large pores and smaller diffusive

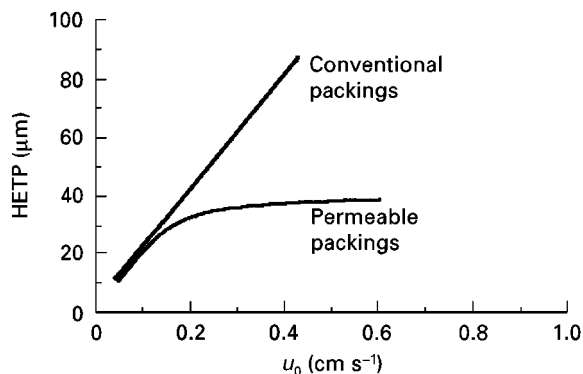


Figure 5 HETP versus superficial velocity u_0 (van Deemter equation for conventional packings and Rodrigues equation for large pore packings). (Reprinted from Rodrigues AE (1997) with permission from Elsevier Science.)

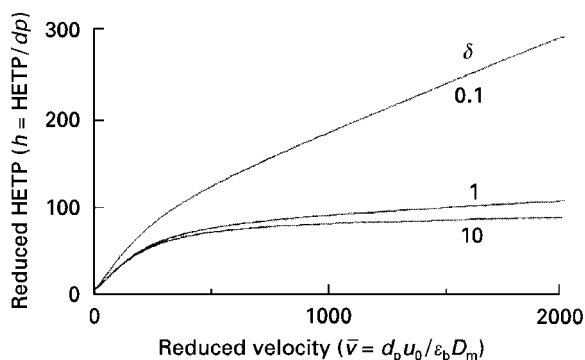


Figure 6 Influence of the ratio of time constants for diffusion in macropores and gel microspheres δ on the HETP versus u_0 plot for bidisperse permeable packings. (Reprinted from Carta G and Rodrigues AE (1993) with permission from Elsevier Science.)

pores. Carta and Rodrigues provided an equation for the column performance measured by HETP:

$$\text{HETP} = A + \frac{B}{u_0} + C \left\{ f(\lambda) + \frac{b-1}{b^2 \delta} \right\} u_0 \quad [4]$$

where $\delta = (D_c/r_c^2)/(D_p/R_p^2)$ is the ratio of time constants for diffusion in macropores and in microspheres with radius r_c . Figure 6 shows the effect of δ on the HETP versus u_0 plot when the fraction of flow permeating the packing is 1%. A criterion to determine when microparticle diffusion is the limiting step is given by:

$$\frac{b-1}{b^2 \delta} \gg f(\lambda)$$

Extension to Include Adsorption/Desorption Kinetics

In protein separation by high performance liquid chromatography (HPLC) with flow-through particles, the effect of convective flow inside pores (say, 1% of the total flow through the bed) is sufficiently important to enhance the low diffusion coefficient for proteins ($\approx 5 \times 10^{-7} \text{ cm}^2 \text{ s}^{-1}$) and intraparticle Peclet numbers λ of 30 are easily obtained. When the kinetics of adsorption/desorption is considered with rate $r_{\text{ads}} = k_a c_i' - k_d q_i'$ where c_i' and q_i' are the species concentrations in the fluid phase inside pores and in the adsorbed phase, respectively and k_a and k_d are the kinetic constants for adsorption and desorption, the extended van Deemter equation becomes:

$$\text{HETP} = A + \frac{B}{u_0} + C \left\{ f(\lambda) + \frac{5}{Bi_m} + \frac{3(b-1)}{b^2 \phi_d^2} \right\} u_0 \quad [5]$$

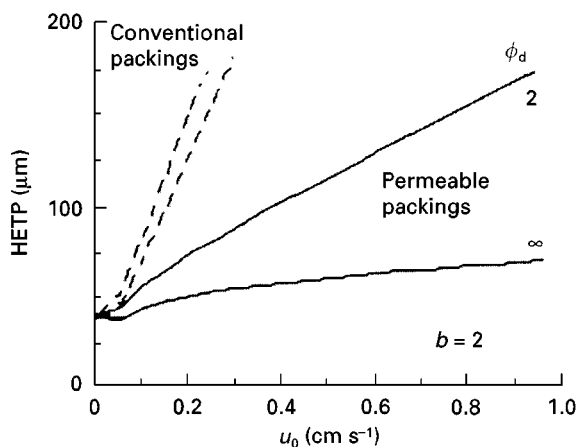


Figure 7 Effect of adsorption/desorption kinetics on HETP versus superficial velocity u_0 . (Reprinted from Rodrigues AE *et al.* (1992) Influence of adsorption/desorption kinetics on the performance of chromatographic processes using large-pore supports. *Chemical Engineering Science* 47: 4405–4413, with permission from Elsevier Science.)

Parameters are the Biot number $Bi_m = k_f R_p / D_e$, accounting for film mass transfer and the Thiele modulus $\phi_d = \sqrt{k_d \tau_d}$. Figure 7 shows the effect of ϕ_d on the HETP versus u_0 plot. The performance of permeable packings is still better than that of conventional materials; intraparticle convection enhances pore diffusivity but has no effect on the mechanism of adsorption/desorption. Adsorption/desorption kinetics have to be taken into account in process such as affinity chromatography.

Methodology for Design

Estimating Intraparticle Peclet Number λ

The importance of convective flow in permeable particles can be assessed by intraparticle Peclet number λ . The convective velocity v_0 inside pores can be calculated from the equality of pressure drops across the particle Δ_p/d_p and across the bed $\Delta P/L$; in laminar flow both for the bulk fluid phase and pore fluid as in HPLC we obtain:

$$v_0 = \frac{B_p}{B_b} u_0$$

where B_b and B_p are bed and particle permeability, respectively. The fraction of flow rate entering the column which goes through the macropores by convection is:

$$(1 - \varepsilon_b) \left(\frac{B_p}{B_b} \right)$$

Bed Permeability

The measurement of the bed pressure drop, ΔP , versus u_0 allows the calculation of bed permeability. In laminar flow, the pressure drop ΔP across a bed of length L packed with particles d_p is given by Darcy's law:

$$\frac{\Delta P}{L} = \frac{\eta u_0}{B_b}$$

where:

$$B_b = \frac{\varepsilon_b^3 d_p^2}{150(1 - \varepsilon_b)^2}$$

Bed permeabilities B_b are obtained from the slope of the plot $\Delta P/L$ versus u_0 and then the bed porosity ε_b can be calculated. As a typical example for a POROS Q/M (PE Biosystems, USA) column 4.6 mm i.d. \times 100 mm long with a bed volume of 1.7 mL filled with 20 μ m particles, the bed permeability is $B_b = 2.35 \times 10^{-9} \text{ cm}^2 \text{ s}^{-1}$ and $\varepsilon_b = 0.34$.

Elution Chromatography with Nonretained Proteins

Elution chromatography experiments under non-retained conditions ($b = 1$) allow the understanding of mass transport inside particles. Flow rates up to 10 mL min⁻¹ corresponding to superficial velocities of 1 cm s⁻¹ were used. The diffusivities of proteins myoglobin, ovalbumin and bovine serum albumin (BSA) in aqueous solution at 25°C are 16.1×10^{-7} , 6.4×10^{-7} and $1 \times 10^{-7} \text{ cm}^2 \text{ s}^{-1}$, respectively.

The HETP is calculated from the experimental chromatographic peaks by:

$$\text{HETP} = \frac{\sigma^2 L}{\mu_1^2}$$

where σ^2 is the peak variance, μ_1 is the first moment of the peak, μ_2 is the second moment and L is the column length. Figure 8 shows the experimentally measured reduced HETP $h = \text{HETP}/d_p$ as a function of the bed superficial velocity.

The efficiency of chromatographic columns can be characterized by the HETP; for columns packed with permeable packings, eqn [3] applies. The A term accounts for eddy dispersion effects and becomes a constant at high superficial velocities, $A = 2d_p$; $B = 2D_m$ and so the term B/u_0 can be neglected in the case of proteins. The simplified equation for HETP with permeable packings is $\text{HETP} \cong A + C f(\lambda) u_0$. In the low velocity region

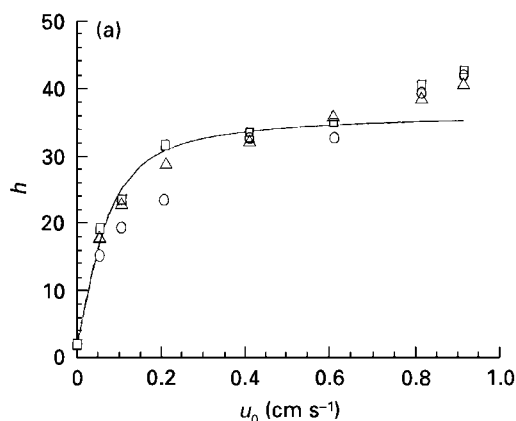


Figure 8 HETP versus superficial velocity u_0 for elution chromatography of proteins under unretained conditions in a POROS Q/M column. Solvents were TRIS-HCl 50 mmol L⁻¹, pH 8.6, mixed with NaCl 0.5 mol L⁻¹ at 22°C. Circles, myoglobin; squares, ovalbumin; triangles, bovine serum albumin; continuous line, Rodrigues' equation. (Reprinted from Rodrigues AE *et al.* (1996) Protein separation by liquid chromatography using POROS Q/M particles. *Chemical Engineering Journal* 61: 191–201, with permission from Elsevier Science.)

where pore diffusion is the controlling mechanism of mass transfer, the slope of HETP versus u_0 is

$$C = \frac{1}{30} \frac{v}{(1+v)^2} \frac{\varepsilon_p}{\varepsilon_b} \frac{d_p^2}{D_e}$$

At high flow rates a plateau is reached with:

$$H_{\text{plateau}} = A + \frac{3}{5} \frac{v}{(1+v)^2} \frac{\varepsilon_p}{\varepsilon_b} \frac{B_b}{B_p} d_p$$

where:

$$v = \frac{(1 - \varepsilon_b)}{\varepsilon_b} \varepsilon_p$$

When the particle structure characterized by the intraparticle porosity, ε_p , is known, the initial slope and the plateau values provide measured values of D_e and B_p .

The straight line at low flow rates crosses the plateau at critical point where

$$u_{0,c} = \frac{18D_e}{d_p} \frac{B_b}{B_p}$$

For POROS Q/M, $\varepsilon_p = 0.5$ and $B_p = 1.5 \times 10^{-11}$ cm² for an experimental h plateau of 36 (reduced HETP) and $D_e = 7 \times 10^{-8}$ cm² s⁻¹.

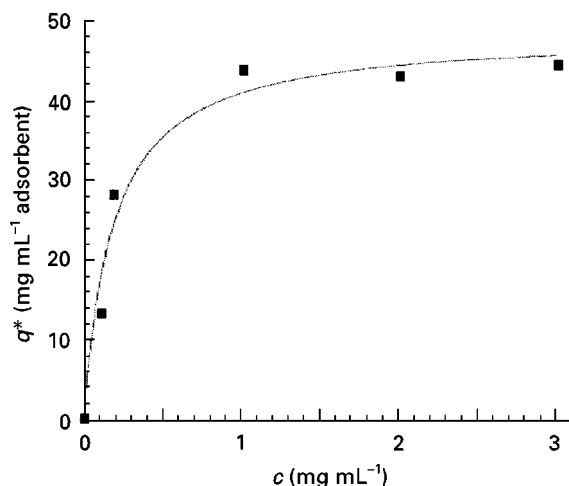


Figure 9 Adsorption equilibrium isotherm for bovine serum albumin on POROS Q/M packing. (Reprinted from Rodrigues AE *et al.* (1996) Protein separation by liquid chromatography using POROS Q/M particles. *Chemical Engineering Journal* 61: 191–201, with permission from Elsevier Science.)

Frontal Chromatography Experiments

In frontal chromatography experiments a solution of protein with concentration c_0 is continuously passed through the column under retained conditions. The breakthrough curve is measured from which the amount of protein retained in the adsorbent, q_0^* is calculated by mass balance leading to a point on the adsorption equilibrium isotherm. The adsorption equilibrium isotherm of BSA in POROS Q/M is shown in Figure 9 and follows the Langmuir equation. Breakthrough curves with BSA at feed concentration of 2 mg mL⁻¹ and various flow rates merge together when the outlet concentration is normalized by the feed concentration and the time is reduced by the stoichiometric time, as shown in Figure 10. Moreover, breakthrough curves are very sharp, indicating that the useful dynamic capacity approaches the total column capacity.

Future Developments

Convective chromatographic media have found applications in the preparative chromatography of peptides and proteins. The use of these materials in preparative and industrial scale simulated moving bed (SMB) technology for chromatographic processes will eventually occur in view of the trade-off between pressure drop and packing efficiency; the simplified design of the SMB unit with simple linear driving force models to describe intraparticle mass transfer is straightforward, using an apparent mass transfer coefficient $\tilde{k} = k/f(\lambda)$.

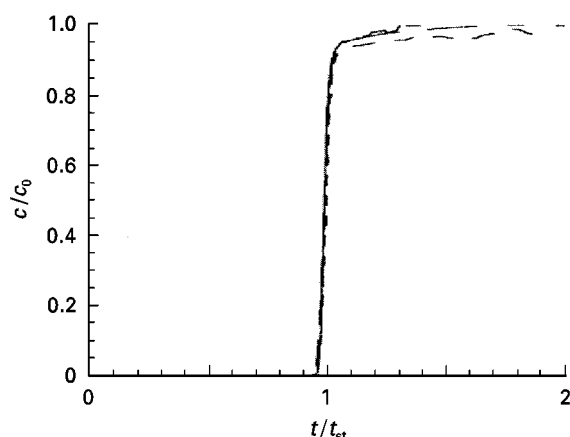


Figure 10 Normalized breakthrough curves for BSA 2 mg mL^{-1} , c/c_0 versus t/t_{st} , on POROS Q/M column at various flowrates. Continuous line, 2 mL min^{-1} ; dashed line, 5 mL min^{-1} ; dotted line, 7 mL min^{-1} . (Reprinted from Rodrigues AE *et al.* (1996) Protein separation by liquid chromatography using POROS Q/M particles. *Chemical Engineering Journal* 61: 191–201, with permission from Elsevier Science.)

Continuous bed technology is a promising area which allows convective flow in wider channels and at the same time smaller diffusion limitations in microspheres since they have a very small diameter.

See also: II/Chromatography: Size Exclusion Chromatography of Polymers. Chromatography: Liquid: Mechanisms: Size Exclusion Chromatography. III/Peptides and Proteins: Liquid Chromatography.

Further Reading

Afeyan N, Fulton S, Gordon N *et al.* (1990) Perfusion chromatography: an approach to purifying macromolecules. *Bio/technology* 8: 203.

Afeyan N, Gordon N, Mazsaroff I *et al.* (1990) Flow-through particles for the high-performance liquid chromatography separation of bio-molecules: perfusion chromatography. *Journal of Chromatography* 519: 1–29.

Afeyan N, Regnier F and Dean R Jr (1991) *Perfusive Chromatography*. US patent 5019270 May 28.

Carta G and Rodrigues AE (1993) Diffusion and convection in chromatographic processes using permeable bidisperse supports. *Chemical Engineering Science* 48: 3927–3935.

Frey D, Schwesenheim and Horváth C (1993) Effect of intraparticle convection on the chromatography of bio-macromolecules. *Biotechnology Progress* 9: 273.

Gustavsson PE and Larsson PO (1996) Superagarose: a new material for chromatography. *Journal of Chromatography A* 734: 231–240.

Lloyd L and Warner F (1990) Preparative HPLC on a unique high-speed macroporous resin. *Journal of Chromatography* 512: 365–376.

Potschka M (1993) Mechanism of size-exclusion chromatography I. Role of convection and obstructed diffusion in SEC. *Journal of Chromatography* 648: 41–69.

Rodrigues AE (1993) An extended van Deemter equation (Rodrigues equation) for performing chromatographic processes using large-pore, permeable particles. *LC-GC* 6: 20.

Rodrigues AE (1997) Permeable packings and perfusion chromatography in protein separation. *Journal of Chromatography B* 699: 47–61.

Rodrigues AE, Ahn B and Zoulalian A (1982) Intraparticle forced convection effect in catalyst diffusivity measurement and reactor design. *AIChEJ* 28: 541.

Rodrigues AE, Lu ZP and Loureiro J (1991) Residence time distribution of inert and linearly adsorbed species in fixed-bed containing large-pore supports: applications in separation engineering. *Chemical Engineering Science* 46: 2765.

Rodrigues AE, Lopes J, Lu ZP *et al.* (1992) The importance of intraparticle convection on the performance of chromatographic processes. *Journal of Chromatography A* 590: 93–100.

Svec F and Fréchet JM (1998) Molded rigid monolithic polymers: an inexpensive, efficient and versatile alternative to beads for the design of materials for numerous applications. *Industrial Engineering and Chemical Research* 38: 34.

Van Kreveland M and Van den Hoed N (1978) Mass transfer phenomena in gel permeation chromatography. *Journal of Chromatography* 149: 71–91.

Correlation Chromatography

H. C. Smit, University of Amsterdam, Amsterdam, The Netherlands

This article is reproduced from Encyclopedia of Analytical Science, Copyright © 1995 Academic Press

Principles

Correlation chromatography (CC, multiplex chromatography, multiple input chromatography)

belongs to the family of multiplex methods and is essentially statistical in nature. It is a typical example of an integrated product of chemometric principles and an analytical technique. A schematic set-up of a CC system is shown in Figure 1.

In conventional chromatography the sample is injected over a short time, and the response of the chromatographic system – the chromatogram – can be considered as an impulse response. In CC the input

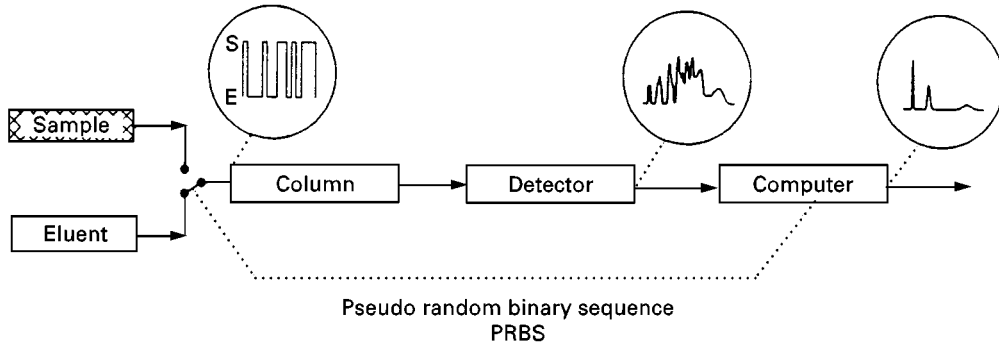


Figure 1 Mechanical valve-controlled correlation chromatography system: s and e correspond to sample and eluent injection, respectively.

flow of the column is rapidly switched between the sample and the eluent, according to a (pseudo) random pattern. A cross-correlation function (correlogram) of the random input signal and the resulting very complex detector signal is also identical to the impulse response (chromatogram) of the chromatographic system, if the input satisfies certain conditions. In other words, the correlogram is identical to a conventional chromatogram obtained by a pulse-shaped injection.

In CC the sample is usually injected according to a pseudo random binary sequence (PRBS) pattern $p(i)$, where i is the discrete time. A PRBS is a binary noise with a specific length M , the sequence length, of $2^n - 1$ periods (n is a positive integer) controlled by a clock; the only levels are $+1$ and -1 , or 1 and 0 . The M clock periods correspond to $I = 2^n - 1$ injections. The periodic nature of the PRBS input signals yields low estimate variance of the estimation of statistical quantities such as correlation functions if taken over an integer number of sequences.

The signal power of a PRBS, determining the final intensity of the detector response, is much higher than that of an impulse-like injection function with similar amplitude, and it is equally spread over the frequency range of the chromatographic system. This 'white noise' property is essential for the application of CC. In addition the levels can be used to control simple on/off valves, corresponding to injection of sample or mobile phase.

The detector signal y_i is built up of noise-free chromatograms $h(i)$ shifted in time, according to the PRBS pattern, plus detector noise $n(i)$:

$$y(i) = \sum_{j=0}^{M-1} [h(j), p(i-j)] + n(i) \quad [1]$$

The PRBS length is chosen to be equal to or longer than the time duration of the comparable chromatogram obtained from a single injection. The detector

signal becomes circular after one PRBS sequence, the so-called presequence. The calculation of a correlogram comparable with a similar chromatogram requires the inverse of the PRBS, defined as the function $p^{-1}(i)$, producing a Kronecker delta function $\Delta(i)$ after circularly cross-correlating with $p(i)$:

$$R_{p^{-1}p}(i) = \frac{1}{M} p^{-1}(j+i) \cdot p(j) = \Delta(i)$$

$$\Delta(i) = 1 \quad \text{for } i = 0$$

$$\Delta(i) = 0 \quad \text{for } i \neq 0. \quad [2]$$

Owing to the special properties of a PRBS, the inverse calculated from a PRBS with one point per period and levels 1 and 0 gives the same PRBS, but with levels $+M/I$ and $-M/I$ instead of $+1$ and 0 . Cross-correlating the detector signal $y(i)$ with the inverse $p^{-1}(i)$ results in a correlogram with a reduced noise level. In the calculations, non-correlated (white) noise is assumed:

$$\begin{aligned} R_{p^{-1}, y}(k) &= \frac{1}{M} \sum_{i=0}^{M-1} [p^{-1}(i+k) \cdot y(i)] \\ &= \frac{1}{M} \sum_{i=0}^{M-1} \left\{ p^{-1}(i+k) \cdot \left(\sum_{j=0}^{M-1} [h(j) \cdot p(i-j)] + n(i) \right) \right\} \\ &= \sum_{j=0}^{M-1} \left\{ h(j) \frac{1}{M} \sum_{i=0}^{M-1} [p^{-1}(i+k) \cdot p(i-j)] \right\} \\ &\quad + \frac{1}{M} \sum_{i=0}^{M-1} p^{-1}(i+k) \cdot n(i) \end{aligned} \quad [3]$$

Considering the levels $+M/I$ and $-M/I$ for $p^{-1}(i+k)$, $p^{-1}(i+k) \cdot n(i)$ can be replaced by

$(M/I) \cdot n(i, k):$

$$R_{p^{-1}, y}(k) = \sum_{j=0}^{M-1} [h(j)\Delta(k-j)] + \frac{1}{M} \sum_{i=0}^{M-1} \frac{M}{I} \cdot n(i, k) \quad [4]$$

Adding M noncorrelated points for every k results in noise with a standard deviation (SD) of $M^{1/2}$ times the original SD of the noise:

$$R_{p^{-1}, y}(k) = h(k) + \frac{M^{1/2}}{I} n(k) \approx h(k) + \sqrt{\frac{2}{I}} n(k) \quad [5]$$

With one point per period, the detector signal can also be cross-correlated with the original PRBS. This produces a comparable correlogram multiplied by a factor I/M .

A similar derivation can be made in the continuous time domain. It has been shown that the resulting cross-correlogram is identical to a chromatogram obtained from an injection with a profile equal to the autocorrelogram of the input sequence. For this reason this autocorrelogram is sometimes referred to as the 'virtual injection' profile. Sometimes a 'true' random binary sequence is used. In that case other deconvolution methods are necessary, such as deconvolution in the Fourier domain.

The correlation procedure can be continued for an arbitrary integer number of sequences. Theoretically, noise not correlated with the input pattern can be reduced to any desired level – but at the cost of time – assuming that the chromatographic system is stationary and that enough sample is available. The noise reduction in only one sequence is about a factor of 10 to 20.

Correlation techniques can be applied in different column separation methods, applications in gas chromatography (GC), liquid chromatography (LC) and capillary zone electrophoresis (CZE) are known. Particularly in LC and CZE, the detection limit can be a problem and correlation techniques in principle offer possibilities to increase the signal-to-noise ratio considerably without preconcentration of the sample. Another feature is the possibility of using CC for continuous monitoring; CC allows a fast and almost continuous updating of the value of the varying concentrations to be monitored. However, the moving average effect, typical for the correlation procedure, limits the highest frequency that can be monitored. CC permits to monitor a frequency about a factor of 2 higher than conventional chromatography. A considerable improvement is possible, if the multiple injection (PRBS) input is maintained, but the correlation procedure is replaced by non-linear fitting. The time-varying concentra-

tions are described as functions of the time and a number of parameters are optimized in the fitting procedure. A detector signal is calculated using the parameters, the known PRBS and known peak shapes; the squared differences with the real detector signal are minimized. The maximum frequency is not determined by the chromatogram length but by the peak width, orders of magnitude better.

Instrumental Requirements

The separation system, column, detector and separation conditions are similar in CC and in conventional chromatography. Nonlinearity of both the column and the detector, and poor stability, i.e. changing chromatographic conditions during the procedure, influence the correlation procedure, resulting in a disturbed baseline. Modern chromatographic systems fulfil the stringent demands of CC in this respect. An important modification is the special injection device required. Such a device has to meet several demanding requirements such as high reproducibility, absence of memory effects, high switching speeds, rugged design (no wear and tear problems) and controllability by a computer. Incorrect injection will cause disturbances (ghost peaks) are specific relative positions on the time axis, and in general cause so-called 'correlation noise' proportional to the amplitude of the real peaks. This therefore limits the determination of traces in the presence of the main components. Injection of sample for one clock period of the PRBS ideally results in an amount of sample transported to the column that is solely dependent on the value of the PRBS in the clock period concerned; 1 represents injection of sample and 0 represents no injection of sample. However, in general the injection is not ideal. After each 0 to 1 transition less than 100% of the ideal amount of sample is injected; and after each 1 to 0 transition a percentage of the sample is still fed into the column. This phenomenon gives rise to PRBSs shifted in time, resulting in the ghost peaks mentioned. Disturbances due to nonsymmetric and reproducible nonideal injection can be corrected. A reliable, accurate and simple injection system, meeting all demands of correlation LC, is obtainable. It is based on a common 8-port or 10-port LC valve, two equal sample loops and a valve actuator.

Computer Requirements

The appropriate hardware and software for injection control and data processing are essential in CC. Off-line data processing is possible, but a flexible and user-friendly program running on a microcomputer is to be preferred. The computer requirements

are modest: a standard PC with 640-kbyte memory is sufficient. A hardware card for controlling the valves, and an A/D converter (12 bits, minimum sampling frequency 10 Hz), including an anti-aliasing filter to prevent back-folding of high-frequency noise, are necessary. The software includes the generation of an arbitrary number of PRBSs, with selectable duration of the clock period and $2^n - 1$ clock periods in a sequence; n is integer number mostly between 5 and 12. The standard deviation of the smallest (first) peak and the desired resolution determine the clock period.

The data processing is relatively simple. Straight-forward cross-correlation may be replaced by the application of an off-line Hadamard transform procedure, speeding up the calculation. Display of the selected parameters (clock period, sequence length, number of sequences), the time varying detector signal, the on-line calculated correlogram, and possibly the injection PRBS are indispensable for application in practice.

Advantages and Disadvantages Compared with Conventional Chromatography.

The main advantage of CC is the improvement of the signal-to-noise ratio without preconcentration in a relatively short time. The resulting lower detection limit makes the technique very suitable for trace analysis. Another important advantage is that the compounds to be analysed remain on the average in their original chemical environment. This property of CC is particularly useful if compounds present in the sample degrade easily once isolated from their matrix. Another feature is the possibility of continuous monitoring of the varying concentrations encountered in process analysis. An interesting possibility is the strong reduction of effects due to nonlinear behaviour of the chromatographic system. When using CC, non-linear affected separations may improve drastically, although correlation noise may arise. Chromatographers need no special knowledge or skill to use CC in daily practice.

Possible disadvantages are the high demands on the chromatographic system, particularly the injection (reproducibility, wear and tear); the possible correlation noise, mainly due to injection errors; the extra sample required; and the extra time. In addition, the separation conditions are not exactly the same as in conventional chromatography, because of the continuous presence of sample throughout the column. The improvement of the signal-to-noise ratio is less than when the analytical signal itself is increased by a comparable preconcentration of the sample. How-

ever, preconcentration is often cumbersome or even undesirable, for example because of poor reproducibility.

The principles of CC are based on the assumption of stability of the system. Therefore, the application of gradient elution or programmed temperature techniques is out of the question in normal CC.

Modifications

Differential CC

The distortions of the correlogram caused by imperfect injection and nonlinearities are proportional to the concentration differences between the compounds in the sample and the eluent. CC can be used in a differential mode. The differences mentioned can be made much smaller by making the eluent almost equivalent to the sample by adding the (known) main components, present in the sample, to the eluent. Also, another sample – possibly modified for optimum separation conditions – can be used as eluent; only differences between the samples are measured, resulting in positive and negative peaks in the correlogram. This can be very useful in environmental analysis and trace analysis of samples with a relatively complex matrix.

Simultaneous CC (SCC)

In principle, it is possible to determine simultaneously n different samples on the same column, each injected according to its own mutual uncorrelated random pattern, using multiplex techniques. Completely uncorrelated (pseudo) random patterns in one sequence are impossible. However, the use of only one long PRBS for each sample, with a time shift equal to an integral number of chromatogram duration different for each sample, allows simultaneous CC. The correlation time is equal to $n + 1$ chromatogram lengths. This technique can be used for high precision chromatography. Unknown sample and calibration standards can be processed under exactly the same conditions, resulting in a very accurate calibration. The determination of pure compounds simultaneously with a complex sample gives the exact place and peak shape of these compounds in the correlogram. This can be used for optimization purposes, for optimum intensity estimation, and for resolving strongly overlapped peaks.

Single-Sequence CC (SSCC)

Single-sequence correlation chromatography is an intermediate between single-injection chromatography and CC. The injection volume is significantly enlarged in comparison to single-injection chromatog-

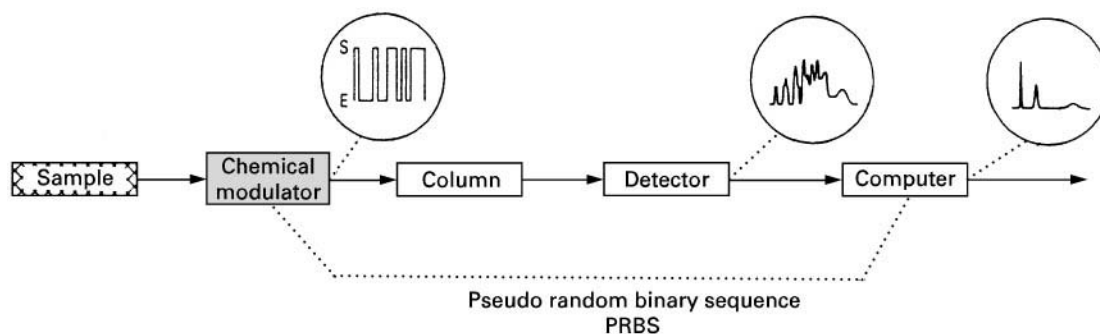


Figure 2 Chemical modulation correlation chromatography system.

raphy. However, the rectangular input function is modulated with a fine structure; one sequence of a PRBS. A deconvolution procedure allows the preservation of good peak resolution for fast-elution narrow peaks, while the other more broadened peaks are processed in a conventional way. In both cases the signal-to-noise ratio is improved. Gradient elution liquid chromatography (or programmed temperature GC) is still applicable, in contrast to conventional correlation and multiplex techniques.

Special attention has to be given to deconvolution errors due to the transient nature of the signals. Some noise frequencies may be amplified enormously if the number of points used for deconvolution is not optimally chosen.

Chemical Concentration Modulation CC

Chemical concentration modulators can be used in CC instead of mechanical injection valves. They can be considered as a chemical switch positioned at the head of the column. The eluent, which is continuously pumped through the system, contains the sample. In 'off' position of the switch nothing happens

and a constant sample concentration is introduced into the column. In the 'on' position a chemical reaction takes place in the cell, causing certain components to react, yielding reaction products with different chemical structures and different retention and detection characteristics. The chemical reaction may add selectivity to the method. Nonreacting components will not influence the correlogram, because of the different properties of CC. **Figure 2** shows a set-up of a chemical modulation CC system.

Several modulators in gas CC, both destructive and nondestructive, are known. Examples, particularly suited for trace analysis in air, are the hot-wire modulator, the spark modulator, and the thermal desorption modulator. In correlation LC, electrochemical concentration modulation has been tried successfully.

Illustrative Examples

The performance of correlation LC, compared with conventional LC, can be illustrated with a calibration graph as shown in **Figure 3(A)**. Phenol was measured

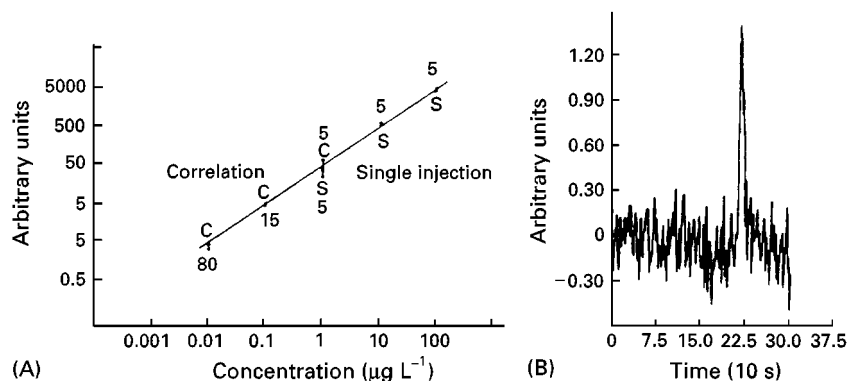


Figure 3 (A) Calibration graph with fluorimetric detection for five concentrations of phenol ($0.01 \mu\text{g L}^{-1}$ to $100 \mu\text{g L}^{-1}$); s and c indicate single injection and correlation, respectively. For each point the chromatogram length or the correlation time (min) is given. The bars indicate $\pm 3\sigma$ (standard deviation of the peak area). (B) Correlogram of a $0.01 \mu\text{g L}^{-1}$ phenol sample. The detection limit is about $0.001 \mu\text{g L}^{-1}$; 80 min correlation time.

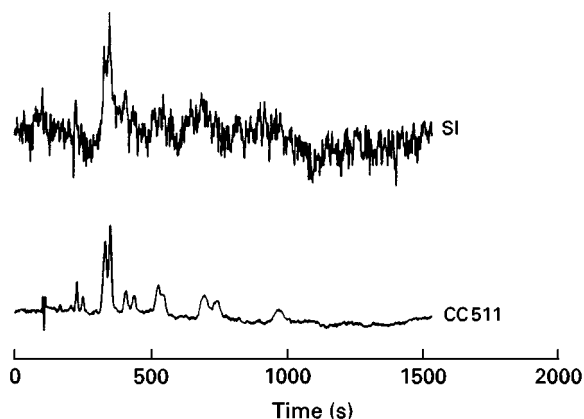


Figure 4 LC analysis of PAH samples by single-injection (SI) and correlation (CC 511 – the number of clock periods in the Pseudo Random Binary Sequence) chromatography under similar separation conditions.

at a five concentrations: 0.01 to 100 $\mu\text{g L}^{-1}$. The three higher concentrations (1–100 $\mu\text{g L}^{-1}$) were determined by conventional reversed-phase chromatography, the three lower concentrations (0.01–1 $\mu\text{g L}^{-1}$) by CLC. Measurements at the 1 $\mu\text{g L}^{-1}$ level were done by both techniques. The bars indicate the peak area $\pm 3\sigma_1$ (arbitrary units), where σ_1 is the standard deviation of the integrated noise. The correlation time is 1, 3 and 16 sequences or chromatogram lengths, corresponding to 5, 15 and 80 minutes, respectively.

Figure 3(B) shows the correlogram of a very low concentration of phenol for 80 minutes of correlation. The detection limit in this case is approximately 0.003 $\mu\text{g L}^{-1}$. For a comparison with conventional LC it must be noted that the injection volume injected in one clock period of the PRBS is 48 μL , a factor of 2.4 more than the 20 μL single injection.

Another example of the possibilities of CLC is shown in Figure 4. Here a diluted rather complex standard material was analysed, containing a number of compounds at different known concentrations. The separation is not optimal, but the condi-

Table 2 Concentrations of the compounds in the samples used in the SCC experiment

	Concentration (mg L^{-1})		
	Naphthalene	Anthracene	1,2-Benzanthracene
Sample 1	7.690	0.320	2.152
Sample 2	3.845	0.320	1.076
Sample 3	1.922	0.320	0.538

tions are effective for examining the behaviour of CC in the case of more complicated mixtures.

Table 1 gives the composition of the samples, consisting of a mixture of polynuclear aromatic hydrocarbons (PAHs), prepared from standard reference material SRM 1647 (National Bureau of Standards). The improvement by application of CC, particularly in case of the diluted sample, is considerable.

A typical application of simultaneous correlation chromatography (SCC) is accurate calibration in LC, as is shown in the following experiment. Three different samples, each composed of naphthalene, anthracene and 1,2-benzanthracene, were prepared (Table 2). The concentration of anthracene was kept constant. Anthracene was used as an internal standard to correct for variations in the injected volumes of the different samples. The samples were injected according to a PRBS of 127 clock periods; the starting points of the injection patterns of the different samples were shifted over one-third of the sequence length. The clock period was divided into three subperiods, one for the injection of each sample.

Figure 5 shows the simultaneous correlogram. The peak areas were determined and corrected for systematic errors with the internal standard anthracene. The calibration graph is shown in Figure 6; the calculated correlation coefficient of the linear fit was 0.999 97 – a very good fit.

In principle SCC allows excellent quantification. Deterministic disturbances and drift influence

Table 1 Composition of the PAH sample

Compound	Concentration ($\mu\text{g L}^{-1}$)	Compound	Concentration ($\mu\text{g L}^{-1}$)	Compound	Concentration ($\mu\text{g L}^{-1}$)
Naphthalene	18.0	Fluoranthene	8.08	Benzo[k]fluoranthene	4.02
Acenaphthylene	15.3	Pyrene	7.87	Benzo[a]pyrene	4.24
Acenaphthene	16.8	Benz[a]anthracene	4.02	Benzo[ghi]perylene	3.21
Fluorene	3.94	Chrysene	3.74	Dibenz[a,h]anthracene	2.94
Phenanthrene	4.05	Benzo[b]fluoranthene	4.09	Indeno[1,2,3-cd]pyrene	3.25
Anthracene	2.63				

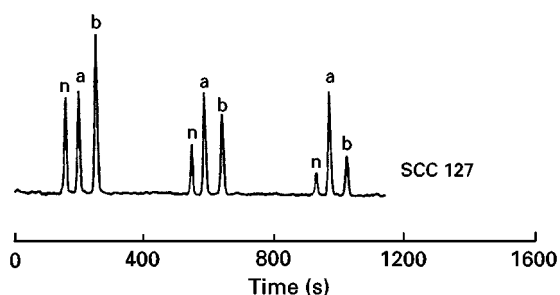


Figure 5 Simultaneous chromatogram of three samples of mixtures of naphthalene (n), anthracene (a), and 1,2-benzanthracene (b) with different concentration ratios.

measurement and calibration samples in exactly the same way. Also, the noise-reducing property of CC is maintained. A comparison with sequential calibration can be made by successively performing independent experiments. Each calibration experiment yields an almost perfectly fitting linear calibration plot, but the points for the same concentration, measured successively, are distributed with rather large standard deviations. The bars in Figure 6 indicate the standard deviations of the measurements.

An illustrative example of the application of chemical concentration modulation correlation chromatography is the selective determination of traces of phenol. An electrochemical modulation cell (EMC) and a fluorescence detector are used. This combination, together with a suitable column, is both selective and sensitive to phenol.

Figure 7 shows log-log calibration graphs for conventional loop injection and EMC-CC, respectively. The signal-to-noise enhancement of EMC-CC is a factor of 11 higher at the most, equal to the theoretically predicted value.

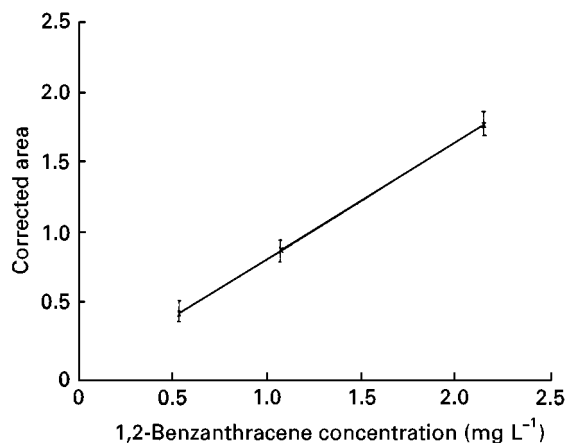
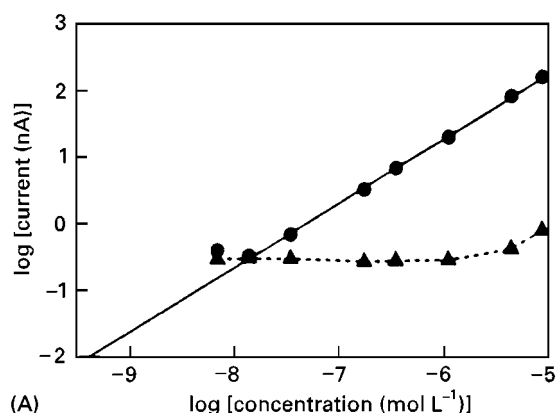
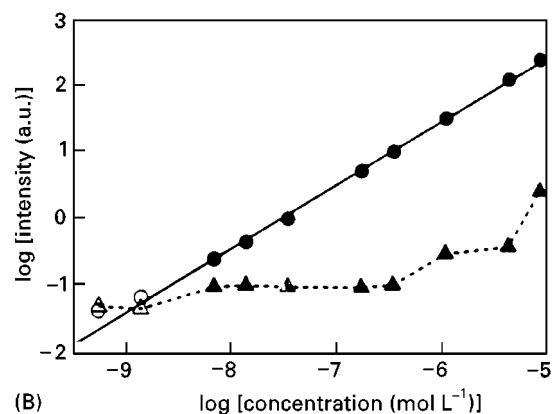


Figure 6 1,2-Benzanthracene calibration graph. The bars indicate the confidence interval for successive independent measurements.



(A)



(B)

Figure 7 Log-log calibration graphs (solid lines) using loop injection (A), and electrochemical concentration modulation CC (B), both with fluorescence detection. The dashed lines represent the $3\sigma_{\text{baseline noise}}$ curves. Solid symbols were from 63 clock period (cp) injection sequences (11 min); open symbols were from 511 cp sequences (80 min).

Correlation Capillary Zone Electrophoresis (CCZE) Micromachinery

CZE is known for its high detection limits. Correlation techniques, as used in chromatography, can be applied in CZE as well. The goal and basic principles are the same. The main problem is the high demand on the injection system, just as in CC. However, in CCZE the injection system can relatively easily be modified, because CZE is electrically – rather than pressure – driven.

Microchip technology is very well suited for application in CZE systems and particularly in correlation CZE. A high quality injection device on a microchip, connected to a fused silica capillary and particularly usable for correlation CZE, is reported. The speed of separation in a microchip CZE system can be increased due to higher accessible field strengths. Detection is the major problem, because of the smaller channel dimension. The application of

correlation techniques drastically reduces the high detection limit in a modest time.

See also: I/Chromatography. II/Chromatography: **Liquid:** Theory of Liquid Chromatography. **Electrophoresis:** Capillary Electrophoresis.

Further Reading

- Engelsma M, Kok WT and Smit HC (1990) Selective determination of trace levels of phenol in river water using electrochemical concentration modulation. *Journal of Chromatography* 506: 201–210.
- Fister JC, Jacobson C and Ramsey M (1999) Ultra sensitive cross correlation electrophoresis on microdevices. *Analytical Chemistry* 71: 4460–4464.
- Kaljurand M and Küllik E (1989) *Computerized Multiple Input Chromatography*. Chichester: Ellis Horwood.
- Laeven JM, Smit HC and Kraak JC (1987) Differential cross-correlation high performance liquid chromatography, a method of establishing small concentration differences in samples of similar origin. *Analytica Chimica Acta* 194: 11–24.

- Louwerse DJ, Boelens HFM and Smit HC (1992) Single-sequence correlation chromatography. A novel technique to decrease detection limits. *Analytica Chimica Acta* 156: 349–359.
- Louwerse DJ, Smit HC and Kaljurand M (1997) Monitoring time-varying concentrations in sample streams by multiple input chromatography. *Analytica Chimica Acta* 346: 285–297.
- Mars C and Smit HC (1990) Sample introduction in correlation chromatography. Application, properties and working conditions for a novel injection system. *Analytica Chimica Acta* 220: 193–208.
- Smit HC, Mars C and Kraak JC (1986) Simultaneous correlation chromatography, a new technique applied to calibration in high performance liquid chromatography. *Analytica Chimica Acta* 181: 37–49.
- van der Moolen JN, Louwerse DJ, Poppe H and Smit HC (1995). Correlation capillary zone electrophoresis, a novel technique to decrease detection limits. *Chromatographia*, 40: 368.
- van der Moolen JN, Poppe H and Smit HC (1997) A micro machined injection device for CZE, Application to Correlation CZE. *Analytical Chemistry* 69: 4220–4225.

Countercurrent Chromatography and High Speed Countercurrent Chromatography: Instrumentation

W. D. Conway, School of Pharmacy, State University of New York at Buffalo, Buffalo, NY, USA
Copyright © 2000 Academic Press

Introduction

This article presents a brief overview of the most significant aspects of the history, apparatus, theory and practice of countercurrent chromatography (CCC). CCC is primarily a preparative technique for the isolation and purification of chemicals on a milligram to multigram scale. It has been broadly applied to natural products, pharmaceuticals and other synthetic organic and inorganic chemicals.

What is Countercurrent Chromatography?

Countercurrent chromatography can be broadly characterized as a form of liquid–liquid chromatography (LLC) in which two mutually saturated immiscible liquids are employed. One phase is retained in the chromatograph as a long continuous or segmented stationary bed without the use of an absorptive matrix; the second phase passes through

the stationary bed and is efficiently equilibrated with it by means of either hydrodynamic or turbulent mixing.

In earlier forms of liquid–liquid partition chromatography introduced by Martin and Synge, where one phase is retained in a porous matrix such as diatomaceous earth or cellulose, significant peak tailing is often seen and some analytes are lost by irreversible adsorption on the supporting matrix. In CCC, the stationary phase is retained by gravitational, inertial or capillary forces and adsorption is precluded by construction of the apparatus from polytetrafluoroethylene (PTFE) or other inert, usually polymeric, material. Thus analyte migration in CCC is determined only by its partition coefficient in the two-phase system and peaks are typically quite symmetrical.

CCC differs from countercurrent distribution (CCD) of the type introduced by Craig in the 1940s in that CCD is a discontinuous process based on attainment of partition equilibrium prior to phase transfer, whereas CCC is a continuous dynamic or steady-state process which characterizes all forms of chromatography. Both CCC and CCD may employ the same solvent systems and both achieve separations based on the partition coefficient, but the apparatus

employed and the mathematical treatment of each process are quite different.

The term CCC was coined by analogy to the earlier CCD process and is considered a misnomer by some because, as usually practised, one phase is stationary in the apparatus. However, the terms are justified by the consideration that if the observer resided in either one of the phases, without reference to the stationary apparatus, it would appear that the phases move in countercurrent fashion. Indeed it is possible to actually move both phases in opposite directions but it is then necessary to refer to the process by a redundant term such as 'true' CCC or 'dual' CCC.

Apparatus

Devices that today might be called countercurrent chromatographs were described as early as the 1930s and were used to separate lipophilic substances such as oil-soluble vitamins. However, the modern era of CCC began in the mid-1960s when Yoichiro Ito observed that if two immiscible liquids were placed in opposite halves of a closed helical coil and the coil was rotated on its axis, the liquids flowed into one another in countercurrent fashion (Figure 1). When placed at the initial interface, the individual components of a soluble sample migrate at different rates determined by their relative partition coefficients, K , in the two-phase system. If K , for example, is defined as concentration in the shaded phase divided by concentration in the unshaded phase shown in Figure 1 then components with K higher than unity will migrate to the right, while those with K less than unity will migrate to the left, and those with K equal to one will concentrate in a band at the initial interface. Ito's first CCC apparatus produced true countercurrent flow and was demonstrated to separate soluble mixtures of dyes and proteins in organic-aqueous systems, and also erythrocytes as an example of particulates that partition in two-phase aqueous polymer systems.

When the ends of the coil are opened, the system resembles an Archimedes' screw pump and both phases migrate in the same direction towards what is called the head end of the helix. The actual direction of flow depends on the handedness, left or right, of the coil and its direction of rotation, and will be

towards the right side of the example shown in Figure 1. Now, if either one of the phases is pumped into the right end of the rotating coil in Figure 1, creating head-to-tail flow of the mobile phase, the other phase, attempting to flow towards the head, will be retarded by viscous forces and a very stable equilibrium will be established in which 40 to 60% of the unpumped phase will remain in the column as a stationary phase. Components of a sample introduced as a bolus in the mobile phase will partition between the mobile phase and the stationary phase and be eluted from the coil at the tail end in order of their partition coefficients. This process is exactly analogous to conventional column partition chromatography. As in other forms of chromatography, it is desirable to define the partition coefficient as

$$K = C_s/C_m$$

where C represents concentration in the stationary (C_s) and mobile (C_m) phases, respectively. Then substances with higher partition coefficients will be retained longer in the column.

Instrument geometries

Ito and colleagues have devised many ways in which a helical or modified helical coil of tubing can be rotated with respect to gravitational and inertial fields to achieve good retention of a stationary phase while minimizing band spreading and promoting efficient mass transfer of solutes. A few will be described here based on their historical or practical significance.

Horizontal flow-through coil planet centrifuge The behaviour just described in 'Apparatus' above is that produced by the horizontal flow through coil planet centrifuge (HFTCPC), first described in the late 1970s. Its characteristic motion is shown in Figure 2B. The device typically consisted of several single-layer helices formed by winding PTFE tubing, measuring a few millimetres internal diameter, on rods about 12 mm in diameter and about 40 cm long, and mounting several of these, connected in series, on a cylindrical column holder. The holder was geared to rotate on its own axis, twice in each orbit, as it revolved around a central or solar shaft. Separations

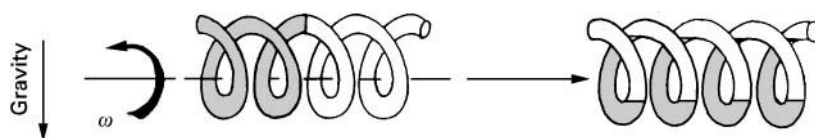


Figure 1 Countercurrent migration of immiscible liquids in a rotating helical tube with closed ends.

typically required 10 or more hours. The HFTCCP was not a commercial success at the time, but the configuration has reappeared as an optional column configuration in some recently described high-speed CCC apparatus.

Droplet countercurrent chromatography Earlier in the 1970s, Ito and colleagues described a simple non-centrifugal CCC technique called droplet countercurrent chromatography (DCCC). As illustrated in Figure 2A with a mobile heavy phase, it consisted of some 300 glass tubes, 1.8 mm i.d., connected in series with narrow-bore PTFE tubing. Either phase could be mobile. The technique, however, was limited to solvent systems that formed droplets. It relied on gravity for phase separation and was very slow, requiring 60 or more hours for a typical separation. In spite of these limitations, it was successfully marketed and was widely employed by natural product chemists; the technique is still available today.

Multilayer coil planet centrifuge The multilayer coil planet centrifuge (MLCPC) described by Ito and colleagues in the early 1980s is one of the most versatile and widely used instruments. Versions of it are available worldwide from several companies. It is shown schematically in Figure 2C, where the helical coil is seen to consist of several layers of tubing wound concentrically on the column holder, which again

rotates twice on its axis in each orbit. The forcefield acting on the coil is quite different here from that obtained in the eccentric configuration (Figure 2B) just described. The orbital radius, R , is typically about 10 cm and the orbital frequency is typically about 800 r.p.m. The coil consists of about 10 to 16 layers of PTFE tubing, 2–3 mm i.d., wound on a spool 5 or more cm wide, starting at a radius r of about 5 cm (half of R) to a maximum of 8 or 9 cm. The winding is not actually a spiral as shown in Figure 2C, but consists of the multiple back-and-forth helical layers typically obtained by winding flexible tubing on a spool. A spool 5 cm wide and 17 cm in diameter might contain about 130 m of tubing 1.68 cm with i.d., with a total volume of about 300 mL.

The forcefield obtained in the MLCPC produces a unique mixing pattern in which the phases in the outward portions of the coil are separated as concentric layers of moving phase and stationary phase, the heavier layer being outwardly directed. On the other hand, in a segment of the inner portion of the coil, comprising about one-third of the coil volume, the phases are quite vigorously mixed. This dynamic mixing pattern is independent of the mobile phase flow rate and since the entire coil rotates through the mixing zone some 13 times each second, very good solute mass transfer is obtained. Typical separations are obtained in from 2 to 6 hours in 300-mL coils and

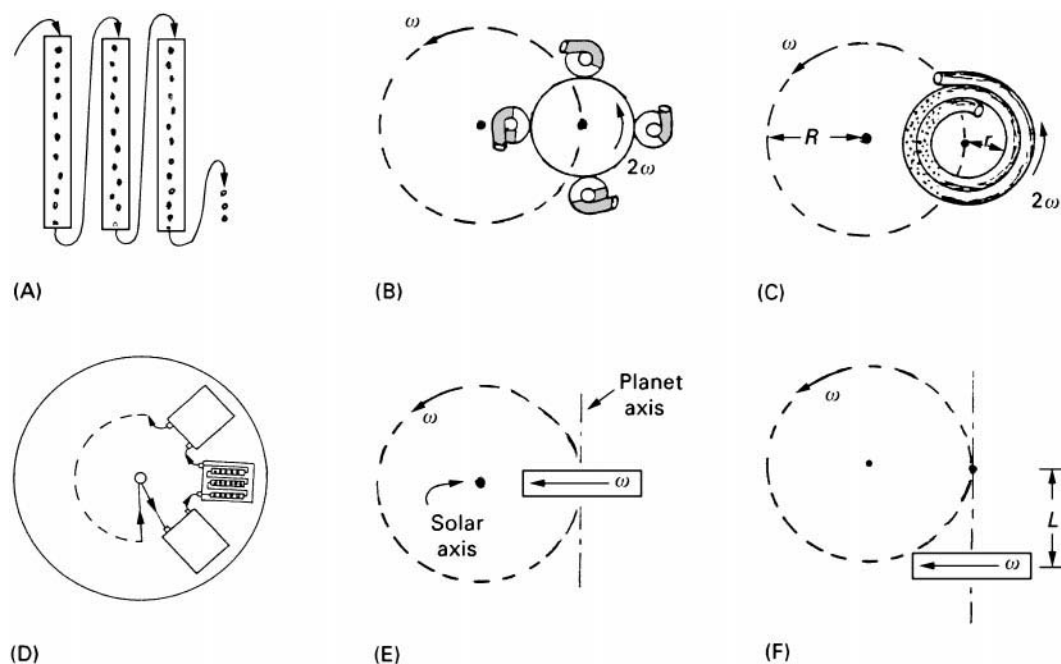


Figure 2 Schematic illustrations of (A) droplet countercurrent chromatography, (B) the horizontal flow-through coil planet centrifuge, (C) the multilayer coil planet centrifuge, (D) the centrifugal droplet countercurrent chromatograph or centrifugal partition chromatograph, (E) the cross-axis CCC and (F) the laterally displaced cross-axis CCC.

much faster separations are obtained, with some loss of resolution, in smaller coils. Resolution is enhanced in the MLCPC by its very high retention of stationary phase, often 80% of the coil volume. A unique feature of all Ito-style CCC apparatus developed since about 1980 is the lack of a rotating seal. Because of the gear systems employed to rotate the columns, influent and effluent streams convey liquids from the instrument exterior to the rotating coil using a so-called antitwisting scheme, which does not involve a rotating seal, thereby avoiding leakage, local heating and contamination associated with such seals. Apparatus is available containing one, two or three spools on a single rotor and in some instruments multiple coils are available in a single spool. These may be operated independently or in series making the MLCPC one of the most versatile types of CCC apparatus.

Centrifugal partition chromatography One of the few types of modern CCC instrumentation developed outside Ito's laboratory was designed by Murayama and colleagues at Sanki Engineering (Japan) and was introduced in the early 1980s. It was designated simply as a centrifugal countercurrent chromatograph and today is usually referred to as a centrifugal partition chromatograph (CPC). Some confusion results from use of the CPC acronym since it is widely used to represent the coil planet centrifuge in Ito-style chromatographs. Conceptually the technique has been described as centrifugal droplet countercurrent chromatography (CDCCC, see Figure 2D). This description is based on the early models of the apparatus, which consisted of a series of cartridges of fluoroplastic in which a series of drilled cylindrical chambers were connected by small grooves, superficially resembling the larger gravitational DCCC apparatus. Cartridges were connected in series and spun at high speed in a rotor, to which inlet and outlet lines were connected through rotating seals. The apparatus could be filled with one phase and, when rotated, the other phase could be pumped through. Either the heavy (descending mode) or lighter (ascending mode) phase could be pumped through. In later versions of the apparatus, the chambers and passageways are formed by etching them in the surface of a sandwiched stack of rotor plates. Although described as a form of droplet chromatograph, actual droplet formation may not play a major role in mass transfer since many solvent systems function well in the CPC that do not form droplets in the gravitational apparatus. The apparatus is sometimes characterized as a static system, as opposed to a dynamic system, since mixing and mass transfer are dependent on the chamber design and on the mobile phase flow rate; mixing

efficiency increases with increasing flow rate. An advantage of the CPC is that units of very large volume can be constructed since it is not subject to the problems of vibration associated with coil planet centrifuges.

Cross axis and laterally displaced cross axis CCC Since about 1989, Ito and colleagues have published many papers on chromatographs described as cross-axis, X-axis or laterally displaced cross-axis chromatographs (XL). It is difficult to illustrate these without three-dimensional models, but an attempt has been made to show them schematically in Figure 2E and F. In the X-axis unit, the coil axis is simply tilted 90° , or crossed with respect to the solar axis. In the earlier CCC units (Figure 2B and C), these axes are parallel. In the XL unit, the coil is further displaced a distance L along the planet axis from the central X position, where the solar axis lies in the rotational plane of the coil.

The effect of tilting the coil is to introduce a third dimensional component to the forcefield. In the parallel shaft units (Figure 2B and C), the forcefield vectors all lie in the two-dimensional plane of rotation of the coil. But the X and XL displacements introduce a force vector in the vertical or solar axis plane. These changes have a significant effect in improving phase mixing phenomena and column efficiency. This is particularly important for viscous solvent systems such as aqueous two-phase polymer systems of the polyethylene glycol-salt and polyethylene glycol-dextran type. These systems function poorly in the HFTCPC and even less well in the MLCPC systems. The aqueous two-phase polymer systems are important for the separation of proteins, enzymes and biological particulates. Unfortunately, the X and XL chromatographs are mechanically more complex than previous instruments and are not yet commercially available.

Monitors

Many CCC technicians simply collect fractions and monitor their composition by thin-layer chromatography (TLC). The column effluent can often be continuously monitored by UV absorption spectrophotometry. The main interference with monitoring is the tendency for droplets of stationary phase carried into the flow cell to cause noise spikes or to adhere to the cell windows. The problem is minimized by using a flow cell with a vertical flow path and by flowing a lighter mobile phase in the downward direction, and a heavier mobile phase in the upward direction. This tends to flush droplets of stationary phase through the cell quickly. Other methods used include warming the column effluent

just before it enters the monitor cell, or bleeding a stream of a miscible solvent, such as methanol, into the column effluent. Another approach uses a diode array detector to monitor the droplet noise in an area of the spectrum where the analyte does not absorb, such as the visible region, and to subtract the noise, on line, from the absorbance at the wavelength used for monitoring. Fluorescence may be used for monitoring and presents similar problems to absorptiometry.

Evaporative light-scattering detectors are excellent for monitoring compounds that lack chromophores and work with other compounds as well. The volatile solvents employed in CCC are quite compatible with evaporative light scattering as long as no non-volatile constituents like salts or buffers are incorporated into the solvent system. Several publications have appeared linking CCC with mass spectrometry and with nuclear magnetic resonance (NMR).

Theory

Countercurrent chromatography (CCC) is usually done by first filling the column at rest with stationary phase, then starting rotation and pumping in the mobile phase at a constant flow rate. The sample may be introduced at the head of the mobile phase stream or later. As it makes its initial pass through the coil, the mobile phase stream will displace a volume, V_{CO} , of stationary phase, which will be carried over into the collection vessel. Subsequently, the phase-volume ratio in the column is usually stable. This carryover volume is then a measure of the mobile-phase volume V_m and the stationary phase volume, V_s , can be estimated by subtracting V_{CO} from the known column volume V_C :

$$V_s = V_C - V_m = V_C - V_{CO}$$

Measuring the retention time of an unretained solute provides an alternative means for estimating V_m .

Because V_s is known in CCC, the chromatogram can be advantageously described in terms of the concentration partition coefficient K (defined earlier as $K = C_s/C_m$) of the analyte, rather than the quantity

distribution coefficient or retention factor, k , used in other forms of chromatography.

The countercurrent chromatogram can be succinctly perceived visually in terms of K and the fact that an analyte with $K = 1$ will *always* elute with a retention volume equal to the column volume, V_C . The column volume, or the time corresponding to it, is the focal point of the countercurrent chromatogram and the emergence of $K = 1$ at this point is independent of the phase volume ratio. Of course, analytes with $K = 0$ will not be retained and will emerge with the mobile phase front. Other analytes with integral values of K will elute at multiples of the stationary phase volume, or time, beyond $K = 1$ and the position of intermediate values can be determined by linear interpolation. Therefore, **Figure 3** presents a completely general picture of a countercurrent chromatogram of analytes with $K = 0, 1, 2, 3$ and it is apparent that the elution pattern is described by the equation:

$$V_R = V_m + KV_s$$

where V_R is the analyte retention volume.

Since flow rate is usually constant, a time scale can be added or imagined. For instance if **Figure 3** were obtained with a 300-mL column at a flow rate of 3 mL per min, $K = 1$ would emerge at 100 min and $K = 0$ at about 30 min. V_s then corresponds to 70 min and $K = 3$ emerges at about 240 min. An analyte with $K = 1.5$ could be expected to emerge at about 135 min. An example showing the separation of a series of phenylalkanols is shown in **Figure 4**.

Separation of the closely related compounds pacilitaxel and cephalomantine by a form of recycling CCC is shown in **Figure 5**. In this approach, the peak containing the mixture was separated from other extraneous material in the first cycle through the CCC by shunting the effluent containing it into a holding tube of the same diameter tubing used in the CCC column. The shunt was then reconnected to the CCC inlet and the material chromatographed a second time, and the shunting process was again repeated to obtain the separation shown in **Figure 5**.

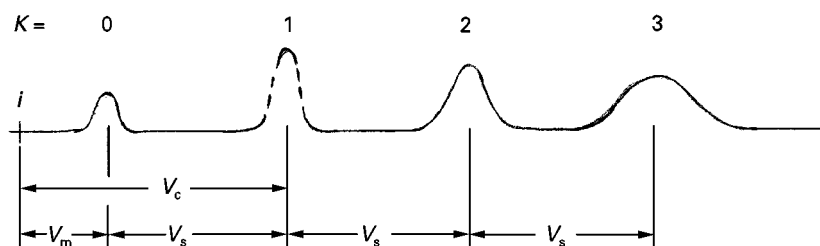


Figure 3 A generalized countercurrent chromatogram for solutes with partition coefficients, K , of 0, 1, 2 and 3.

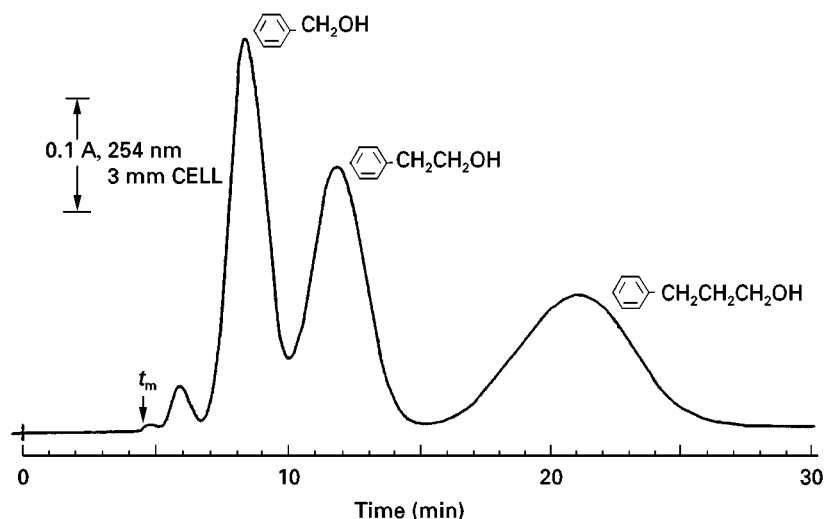


Figure 4 CCC separation of a mixture of 10 μ L each of benzyl alcohol, 2-phenylethanol and 3-phenylpropanol on a 24-m coil of 1.68-mm PTFE, 56 ml volume using heptane as stationary phase and a mobile phase of 25% 2-propanol in water flowing at 4 mL min^{-1} . Reproduced from Conway WD, Buchert EL, Sarlo AM and Chan CW (1998) with permission from Marcel Dekker.

Resolution

The effect of V_s on analyte resolution is also apparent from Figure 3. Experimental parameters that alter V_s , such as flow rate or rotational speed, will not affect the $K = 1$ point. But as flow rate is increased, more stationary phase will be carried over and the V_m distance will increase towards the right, decreasing V_s . The V_s distances beyond $K = 1$ will move to the left, thereby decreasing resolution between the peaks. In the extreme case of high flow rate, all stationary

phase will be forced from the column and all peaks will converge and be eluted at the column volume, or $K = 1$ point, which emphasizes the importance of the column volume or $K = 1$ point in the countercurrent chromatogram.

Direct measurement of the resolution, R_s , of two peaks on a chromatogram is based on the definition:

$$R_s = \frac{V_2 - V_1}{0.5(W_2 + W_1)}$$

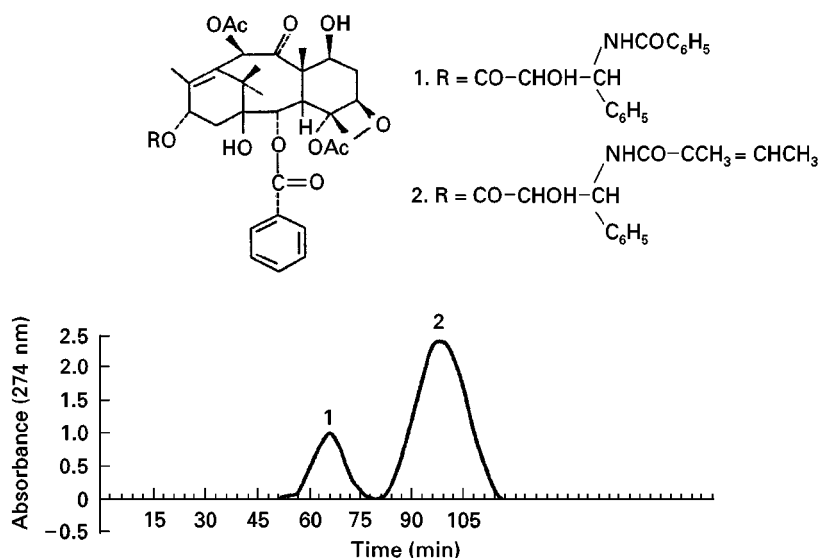


Figure 5 Separation of paclitaxel (1) and cephalomarine (2) by recycling CCC using the solvent system hexane/ethyl acetate/methanol/water – 6 : 4 : 5 : 5 (v/v/v/v) and a 230-mL column of 1.6 mm PTFE with a mobile aqueous phase flowing at 1.7 mL min^{-1} . Reproduced from Du Q-Z, Ke C-Q and Ito Y (1998) with permission from Marcel Dekker.

where V_2 and V_1 are the retention volumes of the second and first peaks to emerge and W_2 and W_1 are their 4-sigma base widths measured in the same units as V_2 and V_1 . With this definition an R_s value of 1.5 represents baseline resolution.

The contribution of other factors to resolution in CCC is summarized in the following general resolution equation:

$$R_s = 0.25(\alpha - 1)N^{0.5} \left[\frac{K_1}{0.5K_1(\alpha + 1) + (1 - S_F)/S_F} \right]$$

where K_1 is the partition coefficient of the first of a pair of chromatographic peaks to emerge and α , N and S_F are the separation factor, the column or coil efficiency, and the fraction of the column volume occupied by stationary phase, respectively.

The separation factor is defined as:

$$\alpha = K_2/K_1$$

where K_2 is the partition coefficient of the second peak of the pair to emerge and is always calculated to be greater than 1.

Efficiency in theoretical plates is defined in terms of the peak base width as:

$$N = 16 \left(\frac{V_R}{W_1} \right)^2$$

where W_1 is the 4-sigma base width of the peak and is measured in the same units as V_R .

S_F , the stationary phase fraction is:

$$S_F = V_s/V_C$$

and its expression in the denominator of the resolution equation is seen to represent the phase-volume ratio:

$$(1 - S_F)/S_F = V_m/V_s$$

The resolution equation confirms the visual observation from Figure 3 that increasing V_s will increase resolution.

The three terms in the resolution equation are usually called the separation factor term, the efficiency term and the large term in brackets is the partition coefficient term. Each can be evaluated independently from the countercurrent chromatogram.

The α term The separation factor term depends on the selectivity of the solvent system for one analyte versus another. It is often the dominant term leading to separation but it is not predictable and must be

determined by an empirical examination of various solvent systems. The search is best conducted by non-CCC means of measuring partition coefficients, such as high performance liquid chromatography (HPLC) or TLC or by using small-volume CCC columns. An advantage of CCC is that a very large number of solvent systems is available.

The efficiency term The square root dependence of N indicates that doubling resolution will require a four-fold increase in column length, which is often not practical because of the resultant increase in backpressure and separation time. CCC provides only a modest number of theoretical plates, usually in the range of 300 to 1000, unless narrow-bore columns are employed at low flow rate. It is comparable to flash-column chromatography in terms of N . However, resolution in CCC is frequently much better than might therefore be expected because of the greater contribution of α and because of the very high S_F , typically 0.7 or more, obtained with some solvent systems.

The partition coefficient term Changing the polarity of the solvent system to increase K_1 will increase resolution, but the benefit rapidly diminishes as K_1 increases. The magnitude of the effect depends on S_F , but when S_F is 0.4, 80% of the effect of increasing K_1 will be obtained when K_1 reaches about 4, at which retention time will be quite long, especially for K_2 .

If S_F is 0.8, 80% of the effect of increasing K will be obtained when K_1 is about 1, so it is more practical to arrange conditions so that S_F is as high as possible and then adjust K of the component of interest to the range of about 1 to 2.

Solvent Systems

A very wide range of two-phase solvent systems can be used in CCC. These include an aqueous phase with solvents ranging in polarity from hexane through chloroform, ethyl acetate and n-butanol. Partition coefficients can be modified by mixing the organic solvents with each other or by adding a miscible solvent such as methanol, 2-propanol or acetonitrile to the system. While these dissolve primarily in the aqueous phase, they partially dissolve in the organic phase, making the system more miscible and shifting the analyte partition coefficient towards 1. When systems become too miscible, the stationary phase is poorly retained. An example is 2-butanol, which when saturated contains about 40% water by weight. Some solvent systems that have been extensively employed in CCC are given in Table 1.

Table 1 Representative solvent systems for CCC

1. Hexane/ethyl acetate/methanol/water – 3 : 7 : 5 : 5 (v/v/v/v)
2. Chloroform/methanol/water – 7 : 13 : 8 (v/v/v)
3. Chloroform/methanol/water – 4 : 4 : 3 (v/v/v)
4. Chloroform/methanol/water – 5 : 5 : 3 (v/v/v)
5. Hexane/methanol – any ratio
6. Hexane/acetonitrile – any ratio
7. n-Butanol/water – any ratio

The first system given in Table 1 is useful for lipophilic materials; the chloroform systems are widely used for solutes of intermediate polarity and n-butanol/water is one of the most polar systems available. Systems 5 and 6 (Table 1) are non-aqueous systems and are particularly useful for very lipophilic materials with no solubility in water. Prior to its use in the CCC, the solvent system is always shaken in a separation funnel and allowed to separate to ensure mutual saturation of the two phases. Solvent systems are covered extensively in all of the reference works listed in Further Reading and are only discussed here very briefly.

Screening solvent systems

To use CCC successfully it is necessary to empirically search for suitable solvent systems using non-CCC methods initially. The first goal is to find a system that provides a K of 1 to 2 and that provides good sample solubility in *both* phases. This latter point is important because sample capacity will be limited by the phase in which the sample is least soluble. Two approaches to screening K values will be described here briefly.

Using TLC Prepare a small amount of the proposed bi-phasic solvent system and partition some sample between about 200 μL of each phase. Spot 20 μL of each of the phases side by side on a TLC plate and develop with a suitable TLC system. Visual examination, or better, scanning with a TLC densitometer, of the separated spots for the two phases will allow a judgement to be made as to which of the components have K values in the neighbourhood of 1.

Using HPLC Dissolve a small amount of sample in about 500 μL of aqueous phase. Chromatograph 20 μL in a suitable HPLC system. Then equilibrate the aqueous solution with the same volume of non-aqueous phase, discard the non-aqueous extract and again chromatograph 20 μL of the aqueous phase. From the respective peak heights, the partition coefficients in the CCC solvent system can be calculated.

Since CCC retention depends only on K , using the equation for V_R , or simply referring to Figure 3, the expected retention times of the sample components can be calculated.

Other Chromatographic Approaches

Substances with high K values that are not eluted, will be to some extent separated along the column and can be recovered by stopping the apparatus and pumping out the column contents. An alternative approach is to switch phases without stopping the chromatography. In the MLCPC, the appropriate directions for pumping the phases is head to tail for the heavy phase and tail to head for the lighter phase, so this approach involves switching the column inlet as well. For the CDCCC, the corresponding directions are downward for heavy phase and upward for lighter phase.

Yet another approach to manipulating CCC is to fill the column initially with a non-equilibrium ratio of phase volumes by simultaneously filling both phases at once. Retention of particular K values can be enhanced or diminished by choosing the appropriate phase-volume ratio. Gradients can also be used for a number of systems, particularly where the composition of the stationary phase changes very little as the polarity of the mobile phase is changed.

For acidic and basic substances, adjustment of pH or use of a pH gradient can be useful. The range of pH is not a limitation as far as the apparatus is concerned. Ion-pair formation and use of liquid-ion exchangers can also be exploited, and various chelating agents have been used for the separation of metals, particularly rare earths. Optical resolutions have been achieved by addition of chiral selectors predominantly soluble in one of the phases to the solvent system.

The above examples indicate a few of the many ways in which CCC apparatus can be manipulated to achieve separations by means other than straightforward chromatography.

pH-Zone Refining

The technique of pH-zone-refining CCC primarily developed by Weisz and Scher in collaboration with Ito, deserves special mention because it is unique to CCC. It is applicable to organic acids and bases and is clearly the technique of choice for obtaining highly purified dyes and samples of the impurities contained therein.

For a very brief explanation it is convenient to view the technique as a kind of two-phase acid–base titration carried out in a CCC column. To illustrate this, imagine a series of aromatic carboxylic acids that

differ slightly in pK_a as well as lipophilicity. Typically a simple solvent system such as methyl t-butyl ether (MTBE) and water is mutually saturated and the phases put in separate containers. The organic phase is acidified with trifluoroacetic acid (TFA) and the column is filled with it as the stationary phase. In practice, either phase can serve as the stationary phase but the organic phase is chosen in this example. The sample of mixed acids is dissolved, or suspended if incompletely soluble, in a portion of the acidified stationary phase and introduced at the column inlet. The aqueous phase is made basic with ammonia and pumped into the rotating column. The acidified sample will dissolve in a relatively small zone of acidified MTBE at the column inlet and as the basic mobile aqueous phase is introduced it will neutralize portions of the sample, which will then be extracted into the aqueous phase. However, on moving down the column, the zone will encounter more TFA, undergo re-acidification and again be transferred to the stationary organic phase. This neutralization and transfer will proceed, as in a titration, first with the acid of lowest pK_a , modified also by the lipophilicity of the particular acid, those with lowest pK_a and lowest lipophilicity migrating fastest.

Monitoring the eluent by UV absorption is usually not informative, but monitoring the pH shows a series of broad steps of increasing pH containing very pure samples of the individual acids with

impurities concentrated at the interfaces between the zones. Bases can be separated in a similar fashion. This technique provides a sample capacity of several grams.

An example showing the separation of two isomeric nitrochloromethoxybenzoic acids by pH-zone refining is presented in Figure 6. Monitoring the UV absorbance of the effluent yields only a flat trace, which does not indicate the separation. However, the effluent pH shows sharp steps at the start and end of the component zones. Using a 310 mL-column and a sample size of 20 g, the separation yielded 9 g of the pure 2-nitro compound, 5.3 g of the 6-nitro isomer and 2 g of a mixture of the two.

Conclusion

Modern CCC is a novel form of preparative LLC that offers more versatility in the choice of solvents, ranging from very lipophilic to moderately polar organic or aqueous systems. It provides predictable retention behaviour and complete recovery of sample since retention depends only on the solute partition coefficient and adsorption is precluded by the inert nature of the apparatus. Its separation capability is further enhanced by various technical manipulations of solvent composition and flow during chromatography, which cannot be reproduced in other types of chromatography. CCC has been widely employed by

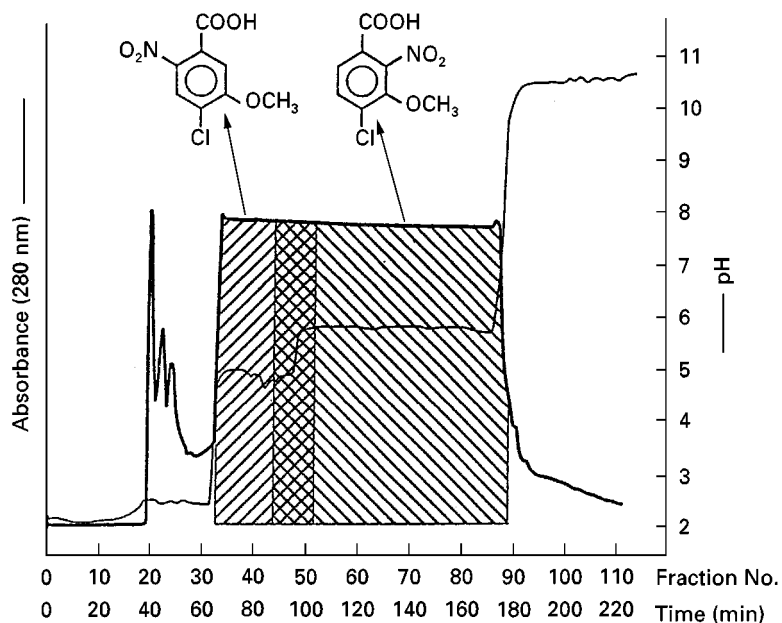


Figure 6 Separation of 2- and 6-nitro-4-chloro-3-methoxybenzoic acids by pH-zone-refining CCC. Initial stationary phase is 0.3% (12 mM) trifluoroacetic acid in the upper organic phase of a mixture of methyl t-butyl ether/acetonitrile/water – 4 : 1 : 5 (v/v/v). The mobile phase was 0.8% (100 mM) ammonia in the lower aqueous phase pumped at 3 mL min⁻¹. The column volume is 310 mL. Reproduced from Dudding T, Mekonnen B, Ito Y and Ziffer H (1998) with permission from Marcel Dekker.

natural product chemists for the isolation and purification of unstable bioactive materials from complex matrices. The technique deserves more attention from analytical chemists confronted with the separation of complex mixtures, synthetic chemists facing purification of non-crystalline products, diastereomers or optical resolution of racemates, and physical chemists seeking new approaches to the study of solvent interactions or the measurement of chemical properties such as partition coefficients or dissociation constants. Continuing study of new applications of CCC in several laboratories, as well as the commercial development of more reliable and user-friendly apparatus, promises to extend the use of CCC in the foreseeable future.

CCC Literature

References to CCC applications are found throughout the analytical and natural product literature and in the monographs cited below. A large number of references are found in *Journal of Chromatography* and in *Journal of Liquid Chromatography and Related Techniques*, many of which are collected in periodic special issues of these journals, the latest of which contains over 20 articles. A list of earlier special issues can be found in Conway (1995).

See also: **III/Alkaloids:** High-speed Countercurrent Chromatography. **Antibiotics:** High-speed Countercurrent Chromatography. **Chiral Separations:** Countercurrent Chromatography. **Dyes:** High-speed Countercurrent Chromatography. **Ion Analysis:** High-speed Countercurrent Chromatography. **Natural Products:** High-speed

Countercurrent Chromatography. **Proteins:** High-speed Countercurrent Chromatography.

Further Reading

- Conway WD (1990) *Countercurrent Chromatography, Apparatus Theory and Applications*. New York: VCH
- Conway WD and Petroski RJ (eds) (1995) *Modern Countercurrent Chromatography*. ACS Symposium Series 593. Washington, DC: American Chemical Society.
- Conway WD, Bachert EL, Sarlo AM and Chan CW (1998) Comparison of countercurrent chromatography with flash chromatography. *Journal of Liquid Chromatography and Related Technologies* 21: 53–63.
- Du Q-Z, Ke C-Q and Ito Y (1998) Recycling high-speed countercurrent chromatography for separation of taxol and cephalomannine. *Journal of Liquid Chromatography and Related Technologies* 21: 157–162.
- Dudding T, Mekonnen B, Ito Y and Ziffer H (1998) Use of pH-zone-refining countercurrent chromatography to separate 2- and 6-nitro-4-chloro-3-methoxybenzoic acid. *Journal of Liquid Chromatography and Related Technologies* 21: 195–201.
- Foucault AP (ed) (1995) *Centrifugal Partition Chromatography*. New York: Marcel Dekker.
- Ito Y and Conway WD (eds) (1996) *High-Speed Countercurrent Chromatography*. New York: John Wiley.
- Mandava NB (ed) (1998) Countercurrent chromatography. *Journal of Liquid Chromatography and Related Technologies* 21 (Special Issue Nos 1 & 2): 1–261.
- Mandava NB and Ito Y (eds) (1988) *Countercurrent Chromatography, Theory and Practice*. New York: Marcel Dekker.
- Menet J-M and Thiébaud D (eds) (1999) *Countercurrent Chromatography*, Chromatographic Science Series Vol 82. New York: Marcel Dekker.

Detectors: Laser Light Scattering

R. P. W. Scott, Avon, CT, USA

Copyright © 2000 Academic Press

Introduction

There are two types of light scattering detectors used in liquid chromatography, the evaporative light scattering detector and the liquid light scattering detector. The former evaporates the solvent from the column eluent in a gas stream and measures the light scattered by the residual solute particles; this type of detector is

described elsewhere in this encyclopedia. The second, the liquid light scattering detector, senses the actual solute molecules themselves by light scattering measurements. Liquids containing large molecules such as synthetic polymers, biopolymers, e.g. polypeptides, proteins and polysaccharides, scatter light and, providing the incident light is strong enough, the scattered light can be sensed and used to detect the presence of the solute. In practice the column eluent is allowed to flow through a cell through which passes a high intensity beam of light. The light source is usually a parallel beam laser (light amplification by

the stimulated emission of radiation) that generates light at an appropriate wavelength for measurement. The scattered light is viewed at a specific angle by a photosensor, the output of which is electronically modified and passed to a potentiometric recorder or, more probably, to a computer data acquisition system.

Alternative Light Scattering Detectors

Two basic types of liquid light scattering detectors have been developed and made commercially available, each having its unique advantages and disadvantages. The two forms of the detector: the low angle laser light scattering (LALLS) detector and the multiple angle laser light scattering (MALLS) detector. Both devices are used extensively in polymer analysis. The multiple angle laser light scattering detector is somewhat more versatile and, under the right conditions, can also provide molecular dimensions as well as molecular masses. As would be expected from its name, in the low angle laser light scattering detector, the intensity of the scattered light is measured at a very small angle to the path of the incident light (virtually 0°). Under these conditions, the signal can also receive light that has been scattered by contaminating particulate matter that is always present in the eluent. This extra light source can contribute considerable noise to the signal, which, in turn, will reduce the detector sensitivity. Discussions on these aspects of the different detectors have been given by, P.J. Wyatt and some early experimental results reported by D.T. Phillips.

From the work of Rayleigh, the ratio of the intensity of the light scattered at an angle (ϕ), (I_ϕ) to the intensity of the incident light (I_0), is given by the following equation:

$$\frac{I_\phi}{I_0} = \alpha \omega R_\phi \quad [1]$$

where α is the attenuation constant, ω is a function of the refractive index, and R_ϕ is Rayleigh's constant.

Thus, the Rayleigh constant can be extracted from the above equation giving:

$$R_\phi = \frac{I_\phi}{\alpha \omega I_0} \quad [2]$$

Now, the relative molecular mass (M_r) of the solute that is scattering the light is, in turn, related to the Rayleigh factor by the following expression:

$$M_r = \frac{R_\phi}{c(K - 2A_2R_\phi)} \quad [3]$$

where c is the concentration of the solute, A_2 is a function of polymer-polymer interactions, and K is the polymer optical constant.

Substituting for R_ϕ in eqns [3] from [2]:

$$M_r = \frac{I_\phi / \alpha \omega I_0}{c(K - 2B_2(I_\phi / \alpha \omega I_0))} = \frac{I_0}{c(\alpha \omega I_0 K - 2B_2 I_\phi)} \quad [4]$$

where:

$$K = \frac{2\pi^2 \eta^2}{\lambda^4 N (d\eta/dc)^2} \quad [5]$$

and η is the solvent refractive index, λ is the wavelength of the light in vacuum, and N is the Avogadro number.

Eqn [4] gives the basic relationship between the relative molecular mass of the scattering material, the intensity of the scattered light and the physical properties of the materials and equipment that are being employed. Unfortunately, eqn [4], includes a number of constants, the magnitude of which can be extremely difficult, if not impossible, to determine accurately. Consequently, an alternative procedure must be adopted to handle the data provided by the intensity of the scattered light and the angle at which it is measured. In practice, a simple graphical procedure is adopted to determine the relative molecular mass of the solute that avoids the need to determine all the pertinent constants.

Rearranging eqn [3]:

$$\frac{1}{M_r} = \frac{c(K - 2A_2R_\phi)}{R_\phi} = \frac{cK}{R_\phi} - 2cA_2$$

or:

$$\frac{cK}{R_\phi} = 2cA_2 + \frac{1}{M_r} \quad [6]$$

This arrangement provides a convenient linear relationship between the important variables that can be measured. Thus c , K and R_ϕ are either known or can all be calculated from known data and calibration light scattering measurements; consequently, by plotting (cK/R_ϕ) against c a straight line will be produced with the intercept being ($1/M_r$).

It follows that a value for the relative molecular mass of the eluted polymer can also be estimated.

Low Angle Laser Light Scattering Detector

The optical system of a commercial low angle laser light scattering detector is shown diagrammatically in

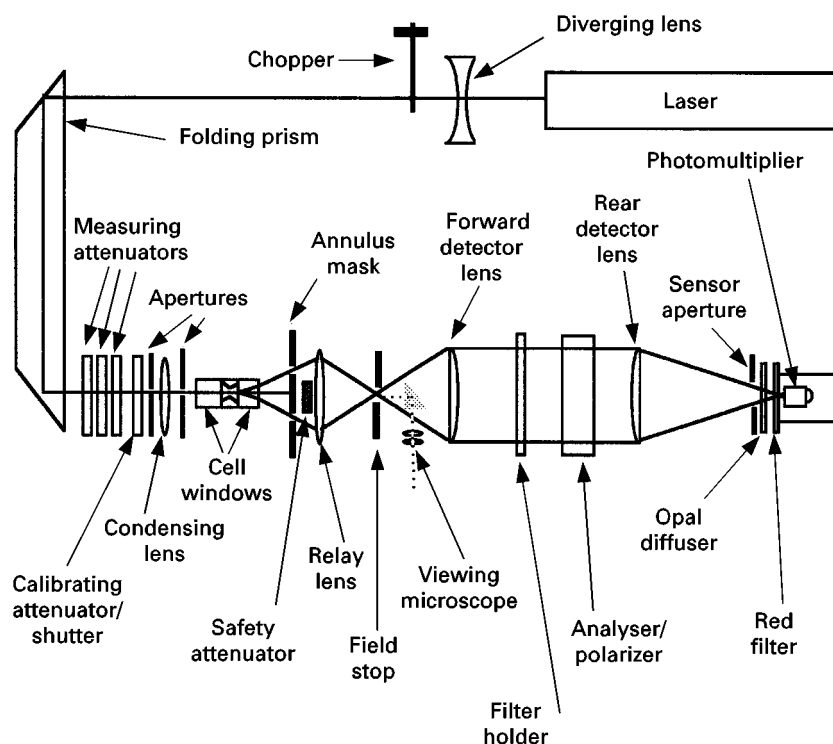


Figure 1 Optical diagram of a low angle laser light scattering detector (LALLS). (Reproduced by permission of LDC Analytical, Thermo Instruments Corporation.)

Figure 1. Owing to the length of the laser light generator, the instrument can become extremely bulky so certain optical space-saving arrangements need to be adopted. To conserve space and make the optical system compact, a folding prism system is used that allows the optical system to be contained to a reasonable size and still accommodate the length of the laser generator.

Light from the laser source passes through diverging lens, then through a chopper, and finally through the folding prism. The laser beam then passes out of the folding prism, through some measuring attenuators, then through a calibrating attenuator shutter and finally through the cell. Between the cell and the relay lens is placed an annular mask that only allows light scattered in the cell at a low angle to pass to the relay lens. Between the annular shutter and the relay lens is placed a safety attenuator that ensures that none of the laser light can reach the photomultiplier, which would cause severe damage. The scattered light is focused through a field stop onto the forward detector lens. For convenience, a prism is placed between the field stop and the forward detector lens, allowing the scattered light to be viewed through a microscope. A filter holder and an analyser/polarizer is placed between the forward detector lens and the rear detector lens. Finally, the scattered

light is focused through the sensor aperture on to an opal diffuser that spreads the scattered light through a red filter and onto the sensor plate of a photomultiplier. The device is conveniently operated in series with a refractive index detector in order to coincidentally measure the refractive index of the eluent.

It is clear from eqn [5] that in order to calculate K the refractive index of the solute must also be known. It is also seen from eqn [4] that an estimate of the relative molecular mass of a solute can be obtained from the intercept ($1/M_r$) of the graph relating (cK/R_ϕ) to the solute concentration c , as shown in **Figure 2**. The concentration is usually determined from the output of the refractive index detector from prior calibration.

The overall sensitivity (minimum detectable concentration) of the detector appears to be very similar to that of the refractive index detector (i.e. about $1 \times 10^{-6} \text{ g mL}^{-1}$ at a signal-to-noise ratio of 2) and would seem to have about the same linearity and linearity range (i.e. $0.97 > r > 1.03$ over a concentration range of 2–3 orders of magnitude). However, the most important characteristic of this detector is not its propensity for accurate quantitative analysis but its proficiency in providing relative molecular mass for extremely large molecules.

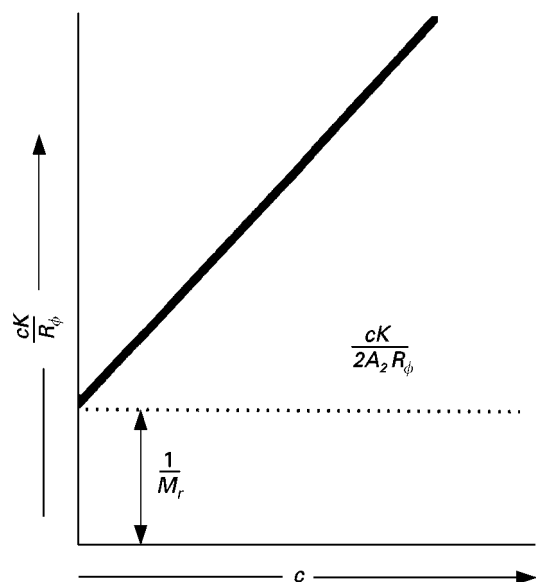


Figure 2 Determination of relative molecular mass from low angle light scattering measurements.

An example of the use of the low angle laser light scattering detector to monitor the separation of bovine serum albumin monomer, anti-bovine serum albumin and bovine serum albumin complex is shown in **Figure 3**. The relative molecular masses of the three components as measured by the LALLS detector were, bovine serum albumin monomer, 66 700 (literature value 66 000), anti-bovine serum albumin, 150 800 (literature value 150 000) and the bovine serum albumin complex 297 300. It is seen that fairly accurate estimates of relative molecular mass can be achieved by this type of detector. The column used was the G 3000 SWXL and the mobile phase a phosphate saline solution buffered at pH 7.1–7.2. The flow rate was 0.4 mL min⁻¹ and the sample volume was 100 µL. The UV detector was operated at 280 nm.

Multiple Angle Laser Light Scattering (MALLS) Detector

The multiple angle laser light scattering detector differs significantly from the low angle laser light scattering detector in that scattering measurements with this device are made at a number of different angles, none of which are close to the incident light. This reduces, in fact almost eliminates, the problem associated with scattering from particulate contaminants in the sample. In addition, measuring the scattered light simultaneously at a number of different angles allows the root-mean-square (rms) of the molecular radius $\langle r^2 \rangle^{1/2}$ of the polymer to be calculated in addition to its relative molecular mass.

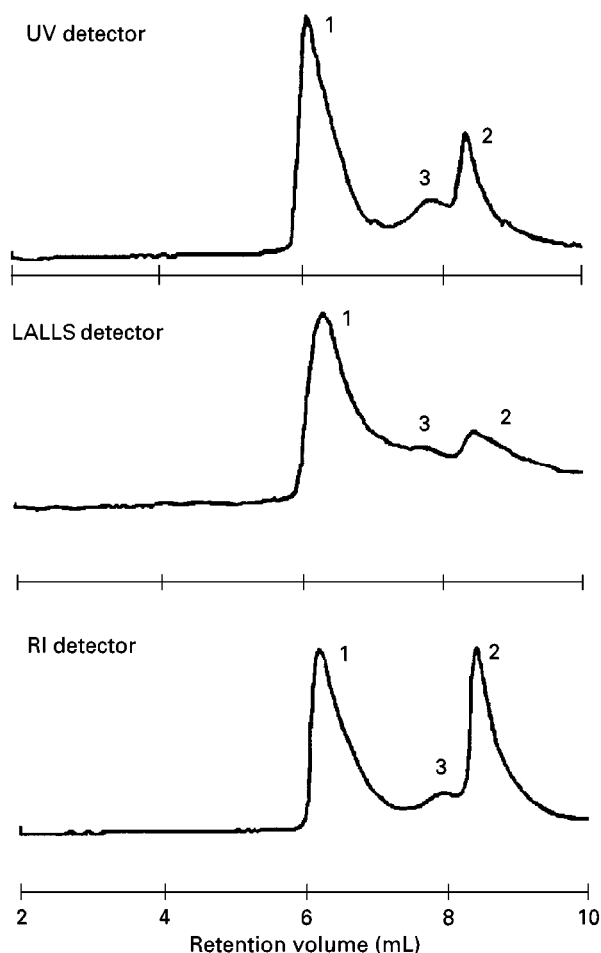


Figure 3 Separation of anti-bovine serum albumin and some bovine serum albumin complexes. Peaks: 1, anti-bovine serum albumin; 2, bovine serum albumin monomer; 3, bovine serum albumin complex. (Reproduced by permission of Qian RL, Mhatre R and Krull IS, 1997.)

The relationship that is used to process the data from this detector is as follows:

$$\frac{cK}{R_\phi} = a\langle r^2 \rangle^{1/2} \sin(\phi)^2 + bM_r \quad [7]$$

where the symbols have the meanings previously defined.

In fact, detailed examination of the theory of light scattering at larger angles can provide explicit functions for the constants a and b . However, in practice, values for these constants are usually obtained from measurements made on calibrating substances of known relative molecular mass and molecular radii. Furthermore, in any practical device each photocell (used to sense the light at the different scattered angles) will not have precisely the same response to light of low level intensity. Consequently, calibration

procedures are also necessary to take the different response of the individual sensors into account to provide appropriate correction factors.

The number of different angles at which the scattered light is measured differs widely with different instruments, and commercial equipment that measure the intensity of the scattered light at as many as 16 different angles are available. It is clear that the greater the number of data points taken at different angles, the more precise and accurate the results will be. A diagram of a relatively simple commercial (MALLS) detection system which measures the light scattered at only three different angles is shown in Figure 4. The device is very simple – it contains no mirrors, prisms or moving parts and is designed such that the light paths are direct and there is no need to use an optically ‘folded’ light system. It is seen Figure 4 that light passes from the laser (wavelength 690 nm) directly through a sensor cell. The scattered light passes from the centre of the cell through three narrow channels to three different photocells, set at 45° and 90° and 135° to the incident light. Thus, scattered light is continuously sampled at three different angles during the passage of the solute through the cell.

A continuous analogue output is provided from the 90° sensor for monitoring purposes and, in the particular system described, all the sensors are sampled every 2 s. The relative molecular mass range is claimed to extend from 10^3 to 10^6 and the rms radii from 10 to 50 nm. The total cell volume appears to be about 3 μL and the scattering volume is as little as 0.02 μL . The detector has a sensitivity, which is defined by the manufacturers, in terms of the minimum detectable excess Rayleigh ratio of $5 \times 10^{-8} \text{ cm}^{-1}$. This sensitivity is difficult to translate into normal concentration units but appears to be very similar to that of the refractive index detector, which is

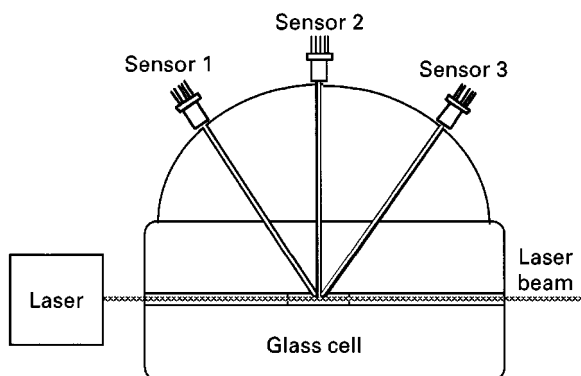


Figure 4 The multiple angle laser light scattering detector (miniDawn®). (Reproduced by permission of Wyatt Technology Corporation.)

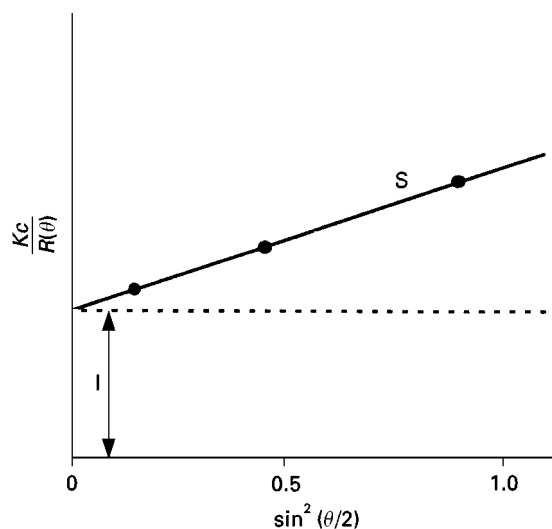


Figure 5 Calibration curves for the multi angle light scattering detector. Intercept (I) gives a value for the relative molecular mass; slope (S) give a value for the rms molecular radius.

equivalent to a minimum detectable concentration of about $10^{-6} \text{ g mL}^{-1}$.

The relationship between the intensity of the scattered light, the scattering angle and the molecular properties, are given by the following equation:

$$\frac{cK}{R_\phi} = 2cA_2 + \frac{1}{M_r P(\phi)}$$

where $P(\phi)$ describes the dependence of the scattered light on the angle of scatter and the other symbols have the meanings previously attributed to them.

In fact, the relationship between the angle of scattering, θ , the relative molecular mass and the rms molecular radius of the solute is obtained using eqn [7]. Employing appropriate reference materials, graphs of the form shown in Figure 5 can be constructed to evaluate constants a and b and thus permit the measurement of the relative molecular mass and molecular radius of unknown substances. This detecting system can be extremely valuable when dealing with unknown biopolymers where little or no evidence is available as to their mass or size and the use of the mass spectrometer is prohibited by either their mass or thermal instability.

The separation of bovine serum albumin (BSA), lysozyme, bradykinin and leucine enkephalin monitored by the multiangle light scattering detector and the refractive index detector in Figure 6. The high response of the multiangle light scattering detector to the high relative molecular mass BSA is clearly demonstrated. The relative molecular mass measurements made on the solutes are shown in

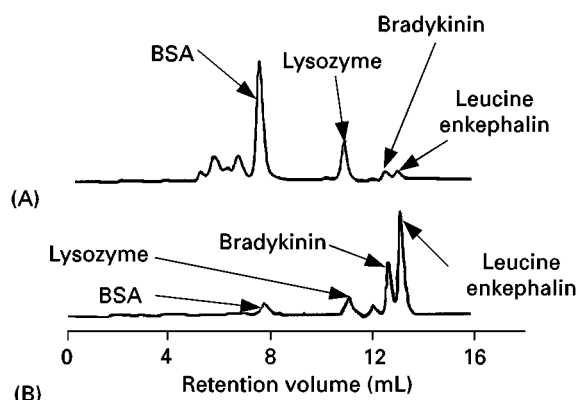


Figure 6 Chromatograms obtained simultaneously from the multiangle light scattering detector (A) and the refractive index detector (B).

Table 1 Peptide and protein mass values from the multiangle light scattering detector

Peak	Solute	M_r (sequencing)	M_r (measured)
1	BSA	67 000	64 300 \pm 700
2	Lysozyme	14 300	14 600 \pm 300
3	Bradykinin	1 060	1 090 \pm 10
4	Leucine-enkephalin	556	592 \pm 6

Table 1, which also includes relative molecular mass data obtained from sequencing the solutes.

It is seen that fairly accurate values for relative molecular mass can be obtained for the larger

molecules, which can be extremely useful when dealing with completely unknown biopolymers. The errors involved are significantly greater for the materials of smaller relative molecular mass because the response (the amount of light scattered) is much less, and the output signal is much closer to the noise level of the sensing system. Further discussion of these types of detector are furnished in references provided in the Further Reading section.

See also: II/Chromatography: Liquid:Detectors: Evaporative Light Scattering. **Chromatography: Protein Separation. Appendix 1/Essential Guides for Isolation/Purification of Drug Metabolites. Essential Guides for Isolation/Purification of Enzymes and Proteins.**

Further Reading

- Phillips DT (1969) *Nature* 221: 1257.
 Qian RL, Mhatre R and Krull IS (1997) Characterization of antigen-antibody complexes by size exclusion chromatography coupled with low-angle light scattering photometry and viscometry. *Journal of Chromatography* 787: 101-108.
 Scott RPW (1996) Liquid light scattering detectors. In: *Chromatography Detectors*, pp. 215-222. New York: Marcel Dekker.
 Wyatt PJ (1968) *Applied Optics* 7: 1879.
 Wyatt PJ (1993) Light scattering and the absolute characterization of macromolecules. *Analytica Chimica Acta* 272: 1-40.
 Wyatt PJ (1993) The mean square radius of molecules and secondary instrumental broadening. *Journal of Chromatography* 648: 27-32.

Hydrodynamic Chromatography

A. Revillon, Centre National de la Recherche Scientifique, BP 24, F-69390 Vernaison, France

Copyright © 2000 Academic Press

Summary

Hydrodynamic chromatography (HDC) is one of the many techniques for particle size determination in the micron range. It has some similarities with size exclusion chromatography and field flow fractionation, but needs only one phase and one field. The main advantages are the separation of species according to size only, rapidity of measurement in the untreated medium and ease of operation of equipment. Variation in operating parameters allows a considerable

range of possible applications. Disadvantages are low resolution, necessity for peak dispersion correction and calibration for signal intensity according to size. It has many applications in latex production and quality control.

Definition and General Features

Definitions

Particles may be separated according to their size by several techniques: HDC is one of them. This interesting rapid method (about 10 min) separates and sizes solutes or particulates in the micron range (0.030-60 μm) at a high dilution, without being

affected by their density. Particle size distributions (PSD) and their averages may be obtained. The separation takes place in packed (PHDC) or in open tubular capillary columns. Components are eluted in the order of decreasing size, as in size exclusion chromatography (SEC), a method which has many features in common with HDC. HDC appears as a complement, either to SEC, which is limited to small size and solute species, or to other fractionation processes based on the effect of an external field, e.g. field flow fractionation (FFF). They are all transport methods, but differ in order of elution and domain of separation. Resolution is examined below. Other techniques for size measurements are static ones and can be used to check the validity of the results from HDC. It is necessary to combine different measurement processes, according to the conditions and purposes required: to obtain a relative or absolute value, with or without separation, affecting or not the state of the sample, and depending on the size and resolution required.

In HDC the key value for a given particle of diameter D_p is called the separation factor R_F . This is the ratio of the highest elution volume (V_m) to that measured for this particle (V_p):

$$R_F = V_m/V_p \quad [1]$$

This factor is greater than one, the inverse of the situation in thin-layer chromatography (TLC), where the solvent migration is more rapid than that of solute. By plotting the graph of known D_p versus R_F a calibration curve is obtained. This allows interpolation of the diameter of an unknown sample (Figure 1A). Another presentation is similar to that of SEC, log D_p versus V_p (Figure 1B) or D_p versus ($V_m - V_p$).

Other terms, detailed below, have the same meaning as in general liquid chromatography. Despite interest in this method, there are only a few papers (around 200) in the literature, as compared to separation by other chromatographic principles. Those that do exist are related to theoretical as well as practical aspects. General presentation may be found in papers by Barth, Hamielec and Tijssen. Currently, effective applications and use are increasing.

Origin

The first fundamental work was published by Small in 1974. The term hydrodynamic refers to the main driving force for separation. Under certain conditions, the nonturbulent flow in the column can be considered to be Poiseuille flow. Laminar flow occurring at a Reynolds number less than 2000 ($Re = 2R\bar{u}\rho/\mu$, where R = tube radius, \bar{u} = velocity, μ = viscosity and ρ = density of medium), leads to a parabolic velocity profile in which the highest velocity is the centre of the tube (Figure 2A). For geometric reasons larger particles are statistically located preferentially in the axis of the capillary, whereas smaller ones are close to the walls. This difference in flow velocity is one of the separation mechanisms. Electrostatic effects must also be taken into account (Figure 2B).

The term separation by flow was initially proposed. Liquid exclusion chromatography has been used with porous packing. HDPC refers to a combined permeation and hydrodynamic process on small pore particles and porous hydrodynamic chromatography is used in packing with large pores. For capillary chromatography in more restricted conditions, another term has been used: tubular pinch chromatog-

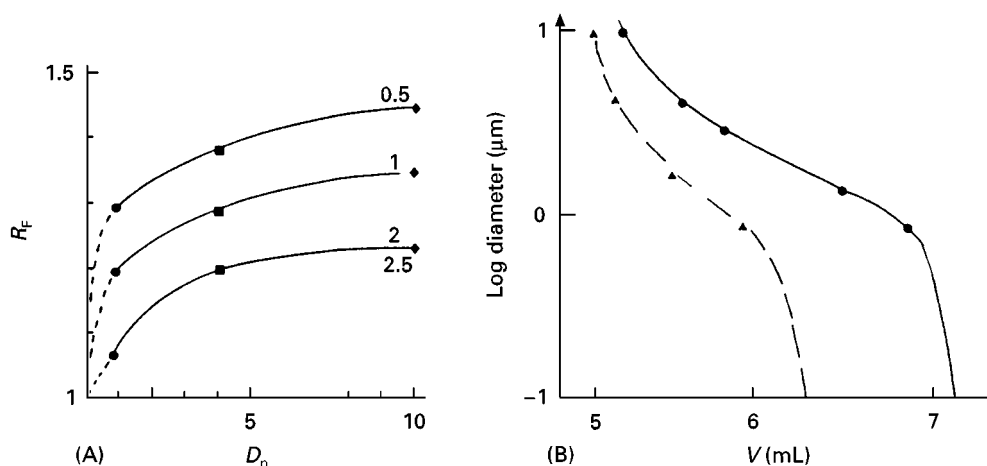


Figure 1 Calibration curves: (A) R_F versus sample diameter (D_p) at flow rates 0.5–2.5 mL min^{-1} and (B) log sample diameter versus elution volume (V). (Reproduced with permission from Revillon A and Boucher P (1989) Capillary hydrodynamic chromatography: Optimization study. *Journal of Applied Polymer Science: Applied Polymer Symposium* 43: 115.

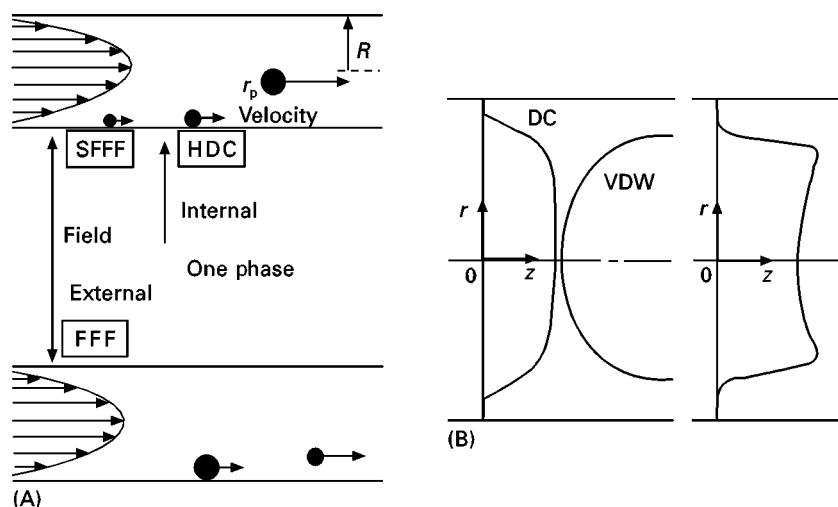


Figure 2 (A) Radial velocity in laminar Poiseuille flow (SFFF, steric FFF) and (B) concentration profile of particles under the effect of double-layer (DC) and van der Waals (VDW) forces (r , variable along radius of column; z , direction of flow). (Reproduced with permission from Revillon A (1996) *Chromatographie hydrodynamique à colonne capillaire et à colonne remplie*. In: Cavaille JY, Garcia-Ramirez M and Vigier G (eds) *Polymères: de la polymérisation aux propriétés*, pp. 167–174. Paris: Polytechnica.)

raphy. In slalom chromatography, the hydrodynamic effect in the interstices between particles leads to increasing elution volume with sample size.

A more frequently used alternative is hydrodynamic fractionation, since the process involved is not a classical chromatographic one of mass distribution equilibrium between two phases. In fact, there is only one phase, the mobile phase as an eluent, and only one field, the hydrodynamic one (Figure 2A). In FFF, a set of techniques for particle sizing, another external field is added. The intention is to modulate the intensity of the second field to inverse the elution order (e.g. in steric FFF). In HDC with packed columns, the nonporous stationary phase is theoretically inert. For porous packings, which allow the use of smaller capillaries, the SEC process operates simultaneously with HDC. Improvements on the original process are described in many papers and have been developed mainly at Lehigh University by Silebi and co-workers.

Advantages and Limitations

The main advantages of HDC are that it is a rapid and convenient method for the separation of particles. It allows one to obtain a fingerprint of the size distribution with an easy-to-operate instrument, similar to those used in liquid chromatography, at room temperature. Direct analysis of the original colloid medium and the use of high dilutions avoid modification of a sample which may be observed in a dry state (e.g. shrinking under the beam in transmission electron microscopy), and any effect of interactions.

Existence of a unique, universal calibration curve allows calculation of D_p and PSD for any sample, since there is no effect of sample nature, surface charge and density on elution volume. At low ionic strength, no effect has been found of the chemical nature of the sample for vinyl copolymer colloids, even for those of low glass transition temperature, T_g . On the other hand, at high ionic strength, sample chemistry may present an additional parameter for separation. With this technique, there are none of the limitations encountered in liquid chromatography (solvent nature, stability and availability of stationary phase and temperature range).

However, there are some difficulties related to the proper choice of operating variables. Elution has been shown to depend on size and porosity of packing beads, eluent flow rate, ionic strength, pH and additives such as surfactants. It is evident that column length and diameter play a role on plate numbers, resolution and domain of measurement. Particle size may affect the total recovery of material (with packed columns). Moreover, it may act on the detector response. In consequence, the PSD might be affected by the incomplete recovery of particles, due to adsorption effects, mainly for larger particles. For example, total recovery is observed up to 200 nm only with 20 μm packing.

Intrinsic limitations include a low plate number, N , and low resolution, R_s , so that generally the number of peaks (peak capacity p) in a chromatogram is low (about 5–10). Quantitative interpretation for determination of particle size distribution needs calibration in order to establish correspondence between

sample size and elution volume and the relationship between signal intensity and amount of particles. Moreover, band broadening, common to every chromatographic process, has a larger influence on PSD because of the low resolution. The interpretation of data assumes that particles are spherical, although an equivalence has been found for elongated structures (1 μm particles appear as spheres of 0.153 μm diameter). Finally, soft materials may be deformed under the high rate of shear in packed column and orientation in flow may affect the apparent size.

Applications

There is no limitation to the nature of the sample, but most studies are in the polymer field. In control and in research, particle characterization is a necessity and numerous chemical and physical data have to be determined, such as molecular weight distribution (MWD) and averages (\bar{M}) or PSD. These values are key parameters for determining rheological, mechanical, thermal and optical properties, storage stability, film-forming capability and the general behaviour of polymer materials. MWD and \bar{M} are commonly measured by SEC and particle size may be obtained by a variety of methods.

To reduce use of organic solvents in the production of polymers (by bulk and in organic solvent processes), free radical suspension and emulsion polymerization heterogeneous processes are used. The first process leads to larger bead sizes (around μm), which are not dealt with in HDC but HDC is typically suited for latex evaluation (around 100 nm) obtained by the second process. These polymer particles are used either largely in water-borne paints, inks and relatively low cost coatings, or as high value colloids for model compounds. For instance, they are used as standards for calibration (membranes) or in biochemistry for diagnostic aids and purification, or for packing chromatography columns. Much of the practical HDC work has been devoted to synthetic organic colloid separation and diameter measurements for quality control. Separation of natural products such as proteins is also of interest. The rapidity of the measurement is compatible with kinetic studies and monitoring during the polymerization process. Swelling of carboxylic latexes has been measured according to pH. The stability of mini-emulsions (50–500 nm) has been studied successfully. Flocculation of colloids in the presence of water-soluble ionic polymers or inorganic oxides has been observed by HDC in conjunction with other methods. Association of particulates under the effect of a thickener is clearly demonstrated, though it can be broken by intensive shear, and the same applies to aggregates.

Some authors have attempted to determine molecular weight or size for very large polymers, for instance water-soluble ones, like polyacrylamide, xanthane, polysaccharides and tobacco mosaic virus. The flow and dynamic behaviour of macromolecules in packed bed have been studied.

A variety of other compounds have been examined, such as carbon black, paper fibres, cement, clay, metals and oxides of Fe, Ti, Si, Al, silver halides and biomaterials such as milk or liposomes from egg yolk lecithin. Silica has been extensively used since it has the advantage of being a hard spherical model for HDC mechanism studies.

Moreover, HDC is of interest in the fundamental study of flow behaviour in tubing or pores which are encountered in transport technology of materials. Applications are also found in geology.

Equipment

Instrument

The instrument is similar to a liquid chromatograph: solvent source, pump, injection valve and column. Optical detection is spectrometry, refractometry, turbidimetry or light scattering.

Conditions to be satisfied are accurate flow rate control and high detection sensitivity. The first condition is due to the narrow elution domain and the second to the small injected volume of a very dilute sample.

Optical detection is more difficult since particle dimensions are in the range of the wavelength involved, λ . With a UV spectrometer, sensitivity is so high that as few as 25 particles in the detector cell give a noticeable signal. Sensitivity varies with wavelength, sample type and with sample size since the signal depends on absorption and scattering, which vary with sample diameter to the power a . The result is that quantitative interpretation needs preliminary signal calibration for each species.

A general formula in liquid chromatography for the instantaneous detector response H at each elution volume V is:

$$H = \sum N_i(V) D_i^a(V) K_i(V) \quad [2]$$

where K_i is the extinction coefficient for particles of diameter D_i and $a = 2$ in the Mie scattering regime for a turbidity detector. In the Rayleigh regime, valid for $\lambda/D_p < 0.3$, $a = 6$ for turbidity and 3 for refractometry. Hamielec observed a factor 6 in turbidimetry and a linear increase of signal with particle size in refractometry: there was a three times increase between 100 and 500 nm for polystyrene (PS) collo-

ids. For the same given weight of PS colloids, the UV signal is three times higher for 354 nm than for 88 nm particles. This also explains the effect of wavelength on signal shape and intensity. The peak separation is better with a refractometer, which may appear less sensitive than the turbidity detector. Generally, $\lambda = 254$ nm is chosen, but differences in relative sensitivity at $\lambda = 380, 254$ and 220 nm for PS colloids of 38 nm and 176 nm diameter have been found; this variation for larger PS colloids, 0.84 μm and 4 μm diameter, was also observed. A continuous and moderate increase in specific extinction coefficient at 254 nm and a higher and nonmonotonous increase at 220 nm have been measured. A low signal obtained for small particles may be enhanced by working at lower wavelength so that the apparent separation is increased. Difference in absorption may allow the apparent separation of PS/PVC. Intermediate values of a may correspond to a combination of a and $K(V)$. The value $a = 1$ holds for refractometry and spectrophotometry of polymers in SEC, so that the range 1–6 must be considered for a general data treatment.

Assuming the formulas for number and weight average diameters:

$$\overline{D}_n = \sum ND / \sum N \quad [3]$$

$$\overline{D}_w = \sum ND^4 / \sum ND^3 \quad [4]$$

and the simplified general relationship H proportional to ND^n , (K and a are independent of V), then:

$$\overline{D}_n = \sum (H/D^{n-1}) / \sum (H/D^n) \quad [5]$$

and:

$$\overline{D}_w = \sum (H/D^{n-4}) / \sum (H/D^{n-3}) \quad [6]$$

For all the investigated PS latexes, average diameters of the number and weight greatly decrease when n is increased (Figure 3). The best agreement with values measured with transmission electron microscopy is obtained for $n = 3$ –4, which is in agreement with theory since their diameters are in the range of the wavelength of detection (254 nm). Except for $n = 2$, the polydispersity index $P = \overline{D}_w / \overline{D}_n$ is not affected by n , and is the same for all samples. Nevertheless, these distributions do not correspond to true ones. The high polydispersity values compared to those determined by transmission electron microscopy (1.02) clearly show the necessity of a band-broadening correction.

A number of workers have built apparatus for HDC by putting together high performance liquid

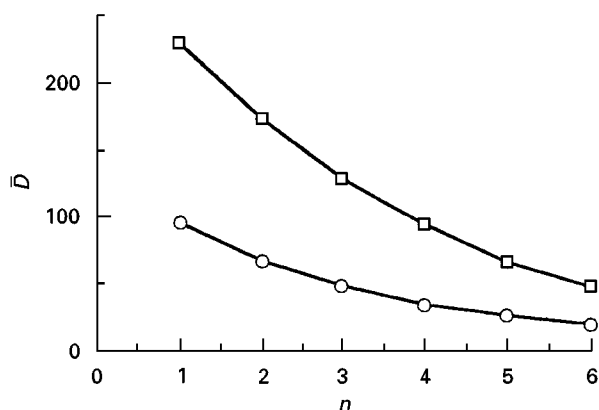


Figure 3 Effect of n value on average diameters: number (circles) and weight (squares) for standard PS latex 106 nm. (Reproduced with permission from Revillon A and Guillard JF (1990) Software for data acquisition and treatment: hydrodynamic chromatography (HDC) analysis. *Journal of Applied Polymer Science: Applied Polymer Symposium* 45: 125–137.

chromatography components. Matec Applied Scientific (Hopkington, MA, USA) currently markets a high resolution instrument CHDF-1100 with UV detection. Separation is operated in a narrow capillary (2.5 $\mu\text{m} \times 10$ m) enclosed in a cartridge. Careful choice of eluent components avoids blocking the column for long-term use. Control of temperature allows accurate flow rate. The signal resulting from absorption and scattering is treated with the help of Mie theory. A mixture of small size latexes is well separated in about 10 min. Length of column may be increased, and diameter may be changed to cover different particle sizes. The apparatus may be used in process control.

Improvements to enhance the accuracy of R_F and PSD, resolution, sensitivity of detection and rapidity of analysis include the following:

1. The injection valve may be replaced by a 12-port valve and a delay column, with two injection loops (Valco Europe, Vici, Switzerland). This allows the injection of two (identical or different) samples on one or two consecutive columns. One of the advantages is the accurate determination of R_F by the help of an internal standard, avoiding sample mixing or reaction, and peak interference. Moreover, the comparison of the signals of the sample passing through active and inert columns allows determination of percentage particle recovery.
2. An additional fine metering valve (Vernier Handle, 18/21Y, Hoke, Creskill, NJ, USA) may be placed before the packed column to divide the main flow into two parts, one entering directly

into the column and the other through the injection valve. This reduces peak asymmetry from 5 to 1.5 and increases plate number by a factor of two. The optimum effect is obtained when the flow is divided in two equal parts; the main flow is less diluted and the side flow entering the column, close to the injection point, prevents broadening of the liquid jet containing the sample.

3. Effort has been put into the reduction of void volume, by direct column injection, design of a detector with reduced connection and cell volumes, on-column detection, improved sensitivity and the use of micro-equipment similar to that used in liquid chromatography and SEC.
4. Recycling, as used in SEC, may improve resolution or R_F determination without changing or increasing the R_F value.
5. A diode array UV-visible spectrometer allows simultaneous determination of the signal at several wavelengths, which means either signal enhancement or decrease (masking of a component).
6. Laser light scattering is of high sensitivity and may also be used, combining photon correlation spectroscopy with integration of the signal, at one angle, during a low counting time (a few seconds). It may give directly both the instantaneous size and concentration of the sample. Low angle laser light scattering is the detector used to determine the molecular weight of polyacrylamide. Variants of this include the evaporative light-scattering detection and condensation nucleation light-scattering detection. To overcome a calibration problem and use of standards, online viscosity has been proposed as an alternative, but this method awaits the development of improved pressure transducers. Fluorometry has been suggested as a high sensitivity detector for tagged polymers. The approach in the author's laboratory is discontinuous measurements of sample size on eluted fractions by transmission electron microscopy, photo correlation spectroscopy and sedimentometry.

Dispersion Correction

Even with micro-equipment and enhanced resolution, selectivity generally appears low. Results must be corrected for band spreading, in order to get individual peaks and true distribution.

There are many approaches for solving the dispersion problem based on Tung's equation, which expresses the experimental chromatogram, $F(v)$, as the result of the true chromatogram, $W(y)$, times a dispersion function, $G(v - y)$:

$$F(v) = W(y) * G(v - y) \quad [7]$$

This equation has received integral and numerical solutions. It has been shown that skewed instrumental spreading functions derived from the plug flow dispersion model fit data for particle separations by HDC, where the spreading function is:

$$G(v, y) = \{4(\pi Pe^{-1}(v/y))\}^{-0.5} \times \exp\{- (v - y)^2/4Pe^{-1}(v/y)\} \quad [8]$$

(where the dispersion term or Peclet number, $Pe = UL/D'$ when U = superficial velocity, L = length of the packed bed, D' = empiric dispersion coefficient; v = elution volume and at the maximum of peak = y). Increasing Pe leads to narrower peaks.

$Pe = 100$ corresponds to no peak correction. With packed column, whatever the value of n , \overline{D}_n increases with Pe , the effect is stronger for higher exponent, n . On the other hand, \overline{D}_w increases or decreases with Pe , depending on n . A quasi-constant value corresponds to $n = 3-4$ (Figure 4).

In another representation of results for different Pe values, \overline{D}_w versus n curves for all samples have a common intercept between $n = 3$ and 4. A rapid change of D is noted up to $Pe = 500$, then \overline{D}_n and \overline{D}_w tend to converge slowly, independently of n .

Practically, considering the whole set of results with UV detection, n must be chosen as 3-4 and Pe 500, to get the best average and distribution values, as well as narrow peaks, which means enhanced resolution.

Experimental Parameters

Sample is put in the liquid used as the eluent; the eluent which must be filtered (e.g. 0.22 μ m: Millipore) to prevent contamination and ensure long-term reproducibility. No other specific treatment is needed. Weight concentration is in the range of 10^{-4} , depending on the detector. This concentration does not need to be known exactly. A small amount of this solution or suspension is transferred with a syringe into the loop of a six-port valve. Loop capacity is typically from 1 to 50 μ L. Samples are injected separately or in mixtures. It is necessary to ensure high accuracy in data acquisition, since the useful elution domain is narrow. Frequent flow rate calibration is also necessary, with the ability to correct small changes in elution volume. With most detectors, the signal increases linearly with concentration or injected volume, in a range useful for application. This means, that no interaction, adsorption or overloading occurs. Peak characteristics are not affected.

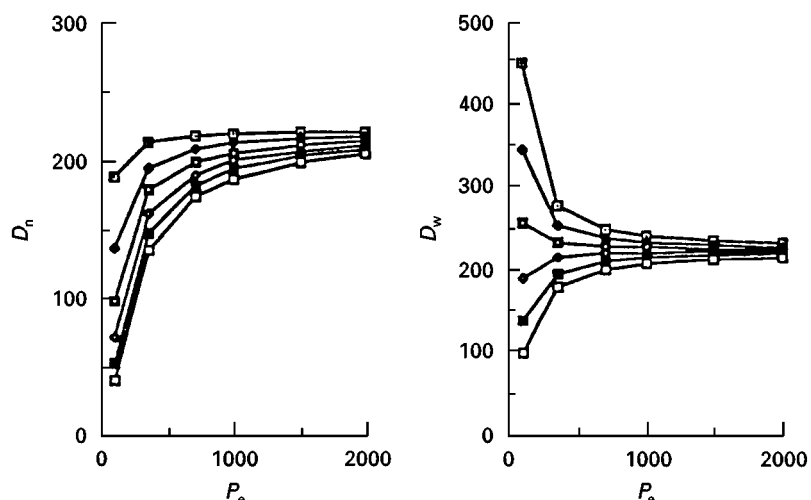


Figure 4 Effect of n and P_e values on average diameters: number and weight for standard PS latex 234 nm. (Reproduced with permission from Revillon A and Guillard JF (1990) Software for data acquisition and treatment: hydrodynamic chromatography (HDC) analysis. *Journal of Applied Polymer Science: Applied Polymer Symposium* 45: 125–137.

For packed columns, the usual eluent is deionized water with additives, such as traces of formaldehyde to prevent bacterial contamination. A variety of ionic (e.g. sodium lauryl sulfate, about 1 g L^{-1}) and nonionic (AOT/Rohm & Haas, Brij, Triton/American Cyanamid) surfactants may be used at a concentration of $1\text{--}10 \text{ mmol L}^{-1}$. Ionic strength is preferentially ensured by sodium nitrate (0.5 mmol L^{-1}). A buffer may be added. Organic solvents may have interesting thermodynamic features and have been used for some applications.

Column dimensions are $0.8\text{--}1.1 \text{ m}$ in length and even $15\text{--}50 \text{ cm}$, with inner diameter from 2 to 10 mm . Sometimes two shorter columns, which are easier to pack, are assembled in series. Glass may be the column material, but stainless steel is more common. Column packing diameter has decreased from $20\text{--}100$ to $5\text{--}10 \mu\text{m}$, so that the number of plates is about $30\,000$ for a 0.5 m column. $N = 42\,000$ is obtained with small particles of $1.4 \mu\text{m}$ and 15 cm length. Flow rate varies from 0.07 to 0.7 mL min^{-1} , but is generally about 1.5 mL min^{-1} .

With capillary columns, aqueous and organic eluents have been tested with various additives in the aqueous eluents similar to those described above. Organic eluents may be advantageous because of their physical properties (viscosity, refractive index, solvating power) but the preferred eluent is water. Flow rate varies from 0.1 to 3 and even 9 mL min^{-1} , but is generally about 1 mL min^{-1} .

The reference sample, used as marker for determination of maximum elution volume V_m , is generally $\text{Cr}_2\text{O}_7\text{K}_2$ or $\text{Cr}_2\text{O}_7\text{Na}_2$, giving a high intensity signal. Compounds such as salicylic acid with the fluorometer or tritiated water may also be used.

Reference materials for calibration are monodisperse PS latexes, prepared by emulsion polymerization in the laboratory or commercially available. Quantitative measurements on peaks are: height (H), base width (w), half-height width ($w_{1/2}$), skewing or asymmetry factor ($sk = a/b$, ratio of second to first part of the peak width at $h/10$), absolute (V_e) and relative (R_F) elution volumes.

Liquid Carrier

The effect of additives in water (surfactant, ionic strength and viscosifying agents) will be considered here.

Surfactant Colloids must be stabilized sterically and/or electrostatically. The surfactants are either bonded or adsorbed on the particles; in the latter case, a part passes in the dispersing phase when dilution takes place (for injection and during the elution) so that flocculation can occur. Moreover, experiments with packed columns have shown that surfactants play a role in elution. Silebi observed a decrease of R_F when concentration is increased, but no change in the slope of $\log D$ versus ΔV . This is shown in Figure 5, for R_F at various amounts of sodium dodecyl sulfate (mmol L^{-1}) in the presence of $0.2 \text{ mmol L}^{-1} \text{ NaCl}$.

Sodium dodecyl sulfate is frequently used below or above its critical micellar concentration (2.5 g L^{-1}). This agent provides wettability of beads and ensures a low ionic strength (0.01). This favours higher R_F , better elution and increased resolution. The effect is greater for larger particle sizes. Other work has found that nonionic surfactants lead to higher R_F than

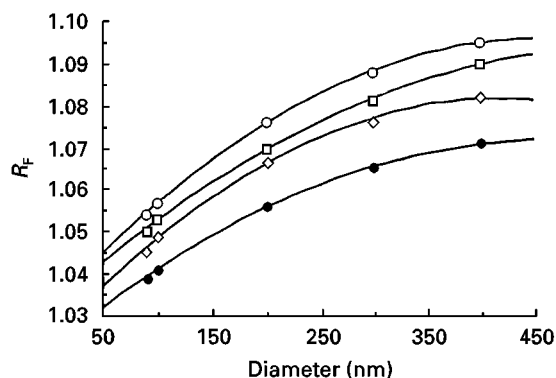


Figure 5 Effect of surfactant (SDS) on R_F , in the presence of NaCl 0.2 mmol L^{-1} . Open circles, 0.13 mmol L^{-1} ; open squares, 0.26 mmol L^{-1} ; open triangles, 0.52 mmol L^{-1} ; filled circles, 1.08 mmol L^{-1} . (Adapted with permission from results of Silebi CA and MacHugh J (1978) In: Becher P and Yudenfreund MN (eds) *Emulsions, Lattices and Dispersions*, pp. 155–173. New York: Dekker.

ionic ones, whereas stabilization by anionic surfactants is claimed to be considerably more effective than with nonionic ones. It is important to bear in mind that molecules of surfactant are in equilibrium with micelles above the critical micellar concentration. Depending on the amount and nature of surfactant in the sample, a new equilibrium between sample and eluent may explain the differences in observed results. It has been reported that SDS, tested from 0 to 4.8 g L^{-1} improves baseline, peak shape and reproducibility and increases R_F in capillary columns.

Ionic strength Electrolytes may have four effects:

1. on the limiting R_F value
2. on percentage recovery
3. on the size domain of interest
4. on sample chemical composition

Electrolytes greatly modify the critical micellar concentration of the surfactant and affect the repulsive electrostatic double layer around the particles. Basically, a low ionic strength I is necessary for screening charges. Recall that:

$$I = 0.5 \sum c_i Z_i^2 \quad [9]$$

where c_i = total concentration of species i , of valency Z_i .

1. Increasing the ionic strength, I , leads to a decrease in R_F (Figure 6). In the initial work, even the ionic marker was affected: a 3% change in V_m was observed when increasing NaCl concentrations by a factor of 1000. Initial results obtained with packed columns have been confirmed by several

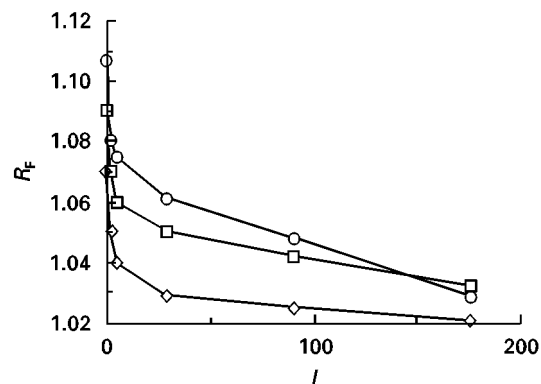


Figure 6 Effect of ionic strength I (Na_2HPO_4) on R_F for three PS latexes of diameter 100 nm (triangles), 200 nm (squares) and 300 nm (circles) in the presence of 2.67 mmol L^{-1} surfactant. (Adapted with permission from results of Silebi CA and Mac Hugh J (1978) In: Becher P and Yudenfreund MN (eds) *Emulsions, Lattices and Dispersions*, pp. 155–173. New York: Dekker.

authors, who observed a change in R_F with ionic strength I , due to competition mainly between van der Waals (attractive) and double-layer (repulsive) forces. At high ionic strength, elution is opposite to the normal mode. The reason could be that very strong van der Waals interactions dominate over the hydrodynamic effect. Some authors have observed a normal decrease in R_F when I increased, but no change in the slope of $\log D_p$ versus ΔV .

2. Percentage recovery is decreased for various colloids when I is increased on a $20 \mu\text{m}$ packing but is more constant for PS on large pore, large packings (63 – $125 \mu\text{m}$ Fractosil). A short column favours the recovery of large particles.
3. Change of I may make possible the separation or the elution of large particles (limit 850 nm instead of 500 nm), even if N or R_F is decreased.
4. In addition, the chemical composition of the sample can affect the elution, so that a mixture of polystyrene and poly(methylmethacrylate) (PMMA) latexes of identical size (240 nm) can be separated in the presence of 0.4 mol L^{-1} NaCl , on a 1 m column packed with $20 \mu\text{m}$ PS beads. On the other hand, there is no elution difference between latexes of PS and PMMA of diameters from 58 to 207 nm , when NaCl is varied from 4.44 to 15.6 mmol L^{-1} .

In capillary columns, no effect was observed for either NaNO_3 (0 – 28.6 g L^{-1}) or NaCl (0 – 48.7 g L^{-1}). Peak shape and elution volume of samples and marker were not modified – or only slightly – by variation in the salt concentration, but NaNO_3 has some absorption and affects the baseline.

Viscosity additives Some authors have observed a change in R_F mainly for larger particles, in the presence of ethylene glycol or sucrose. A small amount of ethylene glycol prevents aggregation. Theoretically, transverse motion must be decreased with decreased tailing and increase in R_F , when the viscosity is increased. In this respect, polymers have been used with some success. Neither increase in R_F nor shape improvement in peaks was observed in the range 0–6% ethylene glycol with capillary columns. The pressure is markedly increased, according to Darcy's law and a permeability coefficient, K_o , may be derived. For $L = 60$ m, a K_o value of $2.4 \times 10^{-8} \text{ m}^2$ is far lower than that of filtration membranes (10^{-12} m^2), which indicates the low separating power of a capillary column.

As a result of these observations, only the surfactant SDS at 3 g L^{-1} was used as an additive in capillary columns.

Flow rate, Q and nature of the eluent Flow rate may have two effects: one on N and one on the sample.

A high flow rate may induce polymer deformation or degradation. It was found that under 2.5 cm s^{-1} no deformation of soft polymer is expected from a calculation using a Deborah number.

Increase of resolution by a factor of 2 has been observed with a 10 times decrease of flow rate, but the effect is small if the packing is of very small particle size. It is known that, in general, low flow rates favour minimum equivalent plate height, H_e , according to the van Deemter equation:

$$H_e = L/N = a + b/v + cv \quad [10]$$

where v is linear velocity. Here, this general expression holds with zero as c value, since it represents the mass transfer term. In capillary HDC diffusion has been found to be $b = 7 \text{ cm}^4 \text{ min}^{-1}$ and $a = 10 \text{ cm}$ for longitudinal and eddy terms, respectively. These values, which are far higher than in liquid chromatography, mean a high sinuosity coefficient and large equivalent bead sizes.

In capillary columns, N , R_S and R_F vary differently with eluent (water) flow rate Q , depending on sample size. Number of plates was found to increase with flow rate, but R_F decreases for a $4 \mu\text{m}$ sample and the resolution is slightly affected. Some deformation of peaks was observed at low flow rates. For instance, the resolution between $0.84 \mu\text{m}$ particles and marker or $4 \mu\text{m}$ particles was unchanged, but was decreased between $4 \mu\text{m}$ and marker. The interpretation may be found in the tubular pinch effect, by taking account of the respective Reynolds numbers of the particles, Re_p (see above).

Their values correspond to very different flow rates so that a change in mechanism occurs in the investigated region.

These different results for R_S , N and R_F show that operating conditions are not rigid and they must be chosen as a function of the particular analysis. Depending on the objective, it may be required to obtain either rapid results in 1.5 min with medium resolution or higher resolution in 36 min. It is also interesting to note that the highest number of plates is obtained not only for the marker, but for the largest sample.

In methanol, the number of plates increased from a constant value for 0.84 and $4 \mu\text{m}$ particles and marker to a maximum for the $10 \mu\text{m}$ sample, when Q increased. The resolution, like R_F , decreased when flow rate, Q , was increased.

Tetrahydrofuran has low viscosity and is a good solvent for polymers. These characteristics may allow higher flow rates and the study of polymers in solution. In fact, although excellent baselines, very high number of plates and good chromatograms of cross-linked PS ($10 \mu\text{m}$) were obtained, the upper limit of R_F was decreased with this solvent. In tetrahydrofuran polybutadiene, polyisoprene and PS of nearly the same molecular weight ($300\,000$) were eluted according to their respective dimensions, $r_g = 28.9$, 26.6 and 25 nm on a packed column.

Water, being a more versatile eluent, and offering a good compromise between R_F and N values, is the main solvent at a flow rate of about 1 mL min^{-1} with a capillary column. This flow rate also corresponds to a compromise between higher R_F (Figure 1A) and lower resolution at the higher velocities. Table 1 summarizes the experimental conditions and results.

As an ancillary practical application, Poiseuille's law allows the determination of one of the parameters: flow rate Q , pressure P , length L , viscosity μ and capillary radius R :

$$\Delta P = 8\mu LQ/\pi R^4 \quad [11]$$

Table 1 Experimental conditions with capillary columns

Length (m)	30	60	120	120	60	120
Radius (μm)	125	125	125	125	250	125
Eluent	W	W	W	Meth	W	THF
Maximum R_F	1.4	1.45	1.45	1.45	1.6	1.26
N (m)	500	900	1900	7000	400 ^a	5300
Maximum N (m)	16.7	15	15.8	58.3	38.3	250

W, water; flow rate 1 mL min^{-1} , except ^a 5 mL min^{-1} ; Meth, Methanol; THF, tetrahydrofuran. Reproduced with permission from Revillon A and Boucher P (1989) *Journal of Applied Polymer Science: Applied Polymer Symposium* 43: 115–128.

Columns

Capillary columns for capillary HDC are used for larger particles, generally in the range from 1 to 60 μm . New capillary columns allow separation in the sub-micron range. Packed columns are effective for smaller particles, with diameters of 30–1000 nm. Since its introduction, HDC studies have been mainly devoted to separations with packed columns.

Packed columns Columns may be slurry- or dry-packed in the same way as for liquid or gas chromatography. Packings used include ion exchange resins, cross-linked poly(styrene-divinylbenzene), nonporous glass and silica gel among others. As an example, analysis has been performed with a slurry-packed column (cross-linked PS spheres of uniform diameter 20 μm ; 50 cm length, 0.78 cm internal diameter).

The main determining parameter is packing particle size. A general trend in liquid chromatography is an increase in plate number when particle diameter decreases (N is inversely proportional to the square of particle diameter). It has been shown in the initial work on HDC that resolution is increased by using packings of small monodisperse spheres; **Figure 7** shows this result. Moreover, resolution is also decreased when size increases (more than a factor of 2 between 20 and 40 μm). Whatever the size of the packing material, the elution region is very limited, defined by a maximum ratio R_F of 1.15 in most papers. By using 2 μm nonporous silica gel packing and tetrahydrofuran as eluent, a value of 1.21 is obtained for R_F , yet the chromatogram contains only five peaks: four for PS and one for toluene. R_F values as high as 1.3 have been obtained.

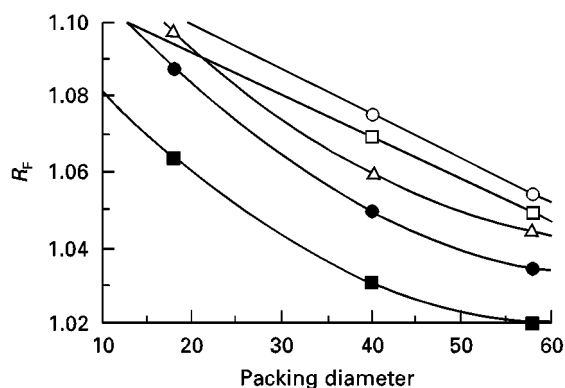


Figure 7 R_F versus packing diameter for five latexes. Open circles, 1000 nm; open squares, 800 nm; open triangles, 600 nm; filled circles, 400 nm; filled squares, 200 nm. (Adapted with permission from results of Small H (1974) *Journal of Colloid and Interface Science* 48: 147–161.

Large (125–180 μm) but porous particles are still used (at low flow rate: 2 cm min^{-1} , in the presence of 0.01 mmol L^{-1} NaCl) to take advantage of the pores as capillaries, with an R_F value of 1.16 or up to 1.39 in the measurement range 240–1230 nm. The equivalent capillary radius R is 2.8 μm , calculated according to the formula:

$$R = \frac{r_p}{1 - \sqrt{2 - R_F}} \quad [12]$$

By combining HDC and SEC, and using porous particles, the R_F may be increased by a factor 1.1–1.2 to a value of 2 or 2.2. The peak broadening decreases or increases, so that resolution is inferior to that obtained on nonporous packing. Moreover, small size porous packings in SEC (2 μm Hypersil or polymeric 3 μm packing with 5 or 15 nm pore radius) allows a high plate number in a 0.45 cm column to be obtained, with an expected peak number of 66. Considering a resolution of unity, constant with V , the peak capacity is:

$$p = 1 + (R_F - 1)N^{0.5}/4R_F \quad [13]$$

This leads to $p = 37$ in this case, and the number obtained is approximately 15, which is an excellent value. The authors of this work also used nonporous monodisperse particles, leading to the theoretical plate height minimum value (5 μm), with no dependence of flow rate in the range 3–7.5 cm min^{-1} . N is 42 000 for a 15 cm length column, with 1.4–2.7 μm silica particles so that a mixture of styrene polymers in the range of molecular weight 10^4 – 10^7 are well separated in 6 min, but shear degradation occurs for the higher molecular weight polymers.

Capillary columns With open capillary tubular columns, the resolution is poorer than with packed columns, but the R_F may be as high as 1.45, so that the peak capacity may be the same as that obtained with a packed column.

The main parameters are length and diameter. A systematic study of the length has been made with stainless-steel columns of 30, 60 and 120 m, and internal diameters of 0.25 and 0.5 mm. The 30 m column gave results of insufficient quality, so most of the work was done with the 60 m columns and finally optimized with 120 m length columns. By going from 60 to 120 m, the theoretical plate height was found to be unchanged and N increased from 380 to 800, for a 4 μm sample. A way to illustrate this increase in resolution is to consider the calibration as represented in SEC. A lesser slope (Figure 1B) allows a better separation.

Table 2 Characteristics of capillary hydrodynamic chromatography systems

Length (m)	Internal diameter (mm)	N (m)	Maximum R_F max
88–201	250–500	?	1.3
50	180–450	25	1.5
60–200	250–500	10	1.55
15	100	25–200	> 1.2
0.45–7	1000	6	1.5
0.15–0.2	1	250	1.1
0.7–3.3	1.2–10	105	1.05
91–168	250–500	16–100	1.4
12	15 000	?	1.15
30–120	250–500	16–250	1.5
2	4	2000	> 1.15
2	6.5	?	1.42
5	7	600	1.63
2.5	10	580	> 1.46

Reproduced with permission from Revillon A *et al.* (1991) *Journal of Applied Polymer Science: Applied Polymer Symposium* 48: 243–257.

The second characteristic of the column is its diameter. Table 2 summarizes conditions of separation and typical results (N , R_F). It can be seen that capillary diameter varies considerably, from 1 to 1000 (or even 15 000) μm . Most of the initial work has been done with 250–500 μm internal diameter column. The choice of tube diameter corresponds to the different ranges of sizes to be separated. The limit in R_F shows that over a certain sample size, no separation occurs. This limit of size may be related to the ratio of the average radius of the sample, r_p , to the tube radius, R . A third order law, relating r_p to R , may have a reasonable approximation in a linear one in agreement with Small's observations:

$$r_p = f + kR \text{ (}\mu\text{m)} \quad [14]$$

with $f = -7$ and $k = 0.1$ (R and r_p in μm). A column of diameter 500 μm may have a medium range of separation of 18 μm instead of 5 μm for the 250 μm one. Taking into account the published results, the ratio of R to r_p is about 100, and for a given diameter of column, the usable r_p/R range varies roughly from 10^{-3} to 10^{-1} . The interest in large diameter columns

is because of the decrease of rate of shear, γ , but the resolution is higher for narrow tubes.

To reduce extra-column band broadening, optimization of the injection-detection system has been attained with 50–100 μm capillaries judging by results obtained in capillary electrophoresis. With microcolumns, efficient separation has been obtained for PS samples with molecular weight of 10^3 – 10^6 Da. The chromatogram was similar to that of SEC, but with a limited R_F of 1.1 (instead of 2 in SEC) and a low number of plates ($N = 50$). Work by Tijssen shows a very high number of plates ($N = 10^5 \text{ m}^{-1}$), but a more limited R_F , of 1.05. The increase in N was not accompanied by an increase in R_F , so that the peak capacity remained low (less than 10). More recent work indicates higher values of R_F : 1.63 and rather good resolution between latex samples. Even with 4000 plates, the peak capacity is only about 7. Table 3 summarizes the conditions and results observed with capillary and packed column HDC.

Mechanism and Other Methods

Some of the difficulties for M or PSD determination may be solved using other types of chromatography: liquid, FFF – normal and steric (SFFF) – supercritical fluid, capillary electrophoresis, or combining with other methods (thermal FFF). Countercurrent chromatography or centrifugal partition chromatography is a potential tool for separating copolymers of different structure or nature, but currently there are few examples. These methods correspond to a large variety of separation mechanisms based on kinetics or thermodynamics, where surface, volume, active specific sites of materials and thermal, gravity, electric, magnetic applied fields bring their contribution. They are also called fractionation and have features in common with chromatography. One characteristic is the absence of the stationary phase, which avoids the problems of interfering phenomena such as adsorption, mass transport, column channelling, degradation and shear rate. This allows a greater choice of eluent.

Some other solutions are nonchromatographic methods, working with or without separation, such

Table 3 Comparison between capillary and packed columns for HDC

Column Type	Length (m)	Diameter (mm)	V (mL)	u (cm s ⁻¹)	Shear (s ⁻¹)	ΔP (bar)	N	N (m)	H (cm)	R_F max	Range (mm)
Capillary	120	0.25	5.9	34	10^{-4}	175	1500	12.5	8	1.45	0.8–20
packed	0.5	5	7.4	0.1	10^{-8}	35	7000	14 000	0.007	1.15	0.05–1

Reproduced with permission from Revillon *et al.* (1991) *Journal of Applied Polymer Science: Applied Polymer Symposium* 48: 243–257.

as dynamic light scattering (photocorrelation spectroscopy) and sedimentometry under centrifugation in a disc. In the presence of SDS, at low ionic strength, HDC results in the range of 200 nm are slightly higher but close to disc centrifuge values. The latter method is of high resolution, since the separation time is inversely proportional to the diameter squared. Analysis time is low in photocorrelation spectroscopy (1 min) and is similar for HDC and centrifugation in a disc. Photocorrelation spectroscopy operated with a proper choice of parameters, gives an excellent correlation with transmission electron microscopy values and an excellent resolution for the mixture of two latexes.

Mechanism of Separation Mode

Classical chromatographic separation occurs because of the differences in partition of compounds between mobile and stationary phases. More generally, separation is the result of local differences in distribution of the sample compounds in the mobile phase. The partition coefficient K is related to the thermodynamic relationship: $\ln K = \Delta G^\circ/RT$, which indicates the possible effects of three factors: enthalpy (ΔH) or entropy (ΔS) changes, and temperature T (Kelvin). Practically, separation is achieved under the effect of two forces (or fields) operating in one or two phases. One phase is necessary for transport and may have a physical or chemical role in the separation.

In HDC, separation results under the effect of one hydrodynamic field which is moving one mobile phase. The nature of the mobile phase is theoretically irrelevant, but differences in results obtained with different solvents have been observed. The separation is due to the existence of a flow-velocity profile in the channel, in which small particles tend to be closer to the external wall, where the flow is stagnant. If a packing is present, its only role is to decrease the capillary size. Voids between beads (diameter Φ_p) in packed columns play the role of small channels of continuously variable diameter similar to a set of capillaries. Bird proposed the equation:

$$R = \Phi_p \varepsilon / 3(1 - \varepsilon) \quad [15]$$

where ε is the ratio of interstitial volume to total column volume, i.e. about 0.35–0.40, so that R is around $\Phi_p/5$ –6. In consequence, the mechanism of HDC in packed or capillary columns may be described by the same parallel capillary model.

The velocity profile $u(r)$ is parabolic, obeying Poiseuille's equation:

$$u(r) = dP(R^2 - r^2)/4\mu dL \quad [16]$$

where dP and dL are increments of pressure and column length, R is the column radius, r is the particle radius and μ is the eluent viscosity. It is easy to see that $u(0)$ is a maximum when $u(R)$ is zero. The average fluid velocity, \bar{u} , is:

$$\bar{u} = \frac{\int_0^R u(r)r dr}{\int_0^R r dr} = \frac{R^2 dP}{8\mu dL} \quad [17]$$

which is half that of the maximum. A particle in the fluid is assumed to have the same velocity as the flow, in its gravity centre, and moving from the column to a distance $R - r$ of the wall:

$$\bar{u}_p = \frac{\int_0^{R-r} u(r)r dr}{\int_0^{R-r} r dr} = \bar{u} \left\{ 1 + \frac{2r_p}{R} - \left(\frac{r_p}{R} \right)^2 \right\} \quad [18]$$

Taking into account the definition of R_F , we derive:

$$R_F = \frac{\bar{u}_p}{\bar{u}} = 1 + 2\left(\frac{r_p}{R}\right) - \left(\frac{r_p}{R}\right)^2 \quad [19]$$

An additional term expresses the rotational motion, so that the velocity profile is:

$$\frac{\bar{u}_p}{\bar{u}} = 1 + 2\left(\frac{r_p}{R}\right) - \gamma\left(\frac{r_p}{R}\right)^2 \quad [20]$$

where γ is a wall effect parameter, the value of which depends upon the radial position of the particle (from about 1 to 60). In capillary HDC R_F must be independent of length L , but the coefficients of the equation are quite far from the theoretical values. This expresses the fact that R_F is higher than expected and that particles move far from the wall.

For small r_p/R (about 0.1), R_F is a linear function of r_p/R . In fact, the corresponding curve tends rapidly to a plateau value. This means that this equation is valid for one particle and is only the result of the hydrodynamic effect. If allowance is made for non-zero stagnant volume, another term is required to complete the above equation. It includes the fraction K of stagnant volume available for polymer and V_s and V_m , stagnant and mobile volumes, respectively:

$$u_p = \Delta P \{ (R^2 - (R - r_p)^2 - \gamma(r_p^2)) / \{ 8\mu L(1 + KV_s/V_m) \} \} \quad [21]$$

The concentration profile of particles, $C_p(r)$, resulting from Brownian diffusion and colloidal interactions, must also be taken into account:

$$\bar{u}_p = \frac{\int_0^{R-r} u_p(r) C_p(r) 2\pi r dr}{\int_0^{R-r} C_p(r) 2\pi r dr} \quad [22]$$

where:

$$C_p(r) = A \exp(-\phi(r)/K_B T) \quad [23]$$

after a sufficient diffusion in the column. K_B is the Boltzmann constant and $\phi(r)$ an energy term depending on packing and particle interactions. ϕ is the resulting sum of repulsive double-layer and attractive van der Waals forces (Born repulsive forces are of negligible effect). A graphical representation of the overall profile of particle concentration is shown in Figure 2B. Van der Waals forces depend on the Hamaker constant and double-layer forces depend on latex surface potential and dielectric constant of particles and packing. The result is:

$$\bar{u}_p = \frac{\int_0^{R-r} u_p(r) \exp\left(-\frac{\phi(r)}{K_B T}\right) r dr}{\int_0^{R-r} \exp\left(-\frac{\phi(r)}{K_B T}\right) r dr} \quad [24]$$

The exponential term may be corrected by another one accounting for the particle migration under inertial hydrodynamic force and electrokinetic lift effects. Many experiments have been carried out to fit elution (volume and peak width) results and equations, by adjusting these values. Listing of the results is more relevant to colloid chemistry than HDC.

Another effect must be considered, described as early as 1836 when Poiseuille observed a corpuscle-free region near the wall in blood vessels. More precisely, Taylor observed an uneven distribution of erythrocytes in flowing blood: there was low concentration not only near to the wall but also near to the centre, provided the velocity was large enough. Further studies concluded that radial forces tend to carry a rigid sphere to an equilibrium position at approximately $0.6R$, depending on the velocity and on the ratio r/R . This was called the tubular pinch effect. Experiments were done with large spheres (0.16–0.85 mm radius in a tube of radius 5.6 mm, at a velocity from 5 to 90 cm s⁻¹ and viscosity from 17 to 410 cP. Ploehn assumed that lateral migration of small particles is primarily due to diffusion, while large particles are focused by the inertial force at an equilibrium position, as observed in the tubular pinch experiment. This experiment may be responsible for separation in the capillary column (see above).

Resolution

We now turn to comparison of resolution (R_s) in the different fractionation processes: we shall examine R_s value and its variation with elution volume.

Table 4 Resolution of various fractionation methods

Parameter	Capillary HDC	HDC	DCP	TFFF	SFFF	SFC
R_s	0.15	0.15	1.5	0.7–2	2.2	1.2
R_t	0.025	0.025	0.15	0.2–0.02	0.07	0.03
t (min)	6	6	10	45–120	30	20–60
ϕ (μm)	> 1	< 1	< 60	< 1	< 2	0.05

Reprinted with permission from Revillon A (1994) *Journal of Liquid Chromatography* 17: 2991–3023. CHDC, Capillary HDC; DCP, centrifugation under disc; TFFF, Thermal FFF; SFFF, steric FFF; SFC, supercritical fluid chromatography.

Firstly, we define a specific resolution (R_{sp}) = R_s /ratio of the diameter of the species under consideration. Secondly, we define resolution per unit time (R_t) = R_{sp} /time of measurement, in order to compare different samples and different elution conditions, respectively. To obtain polymer dimensions in solution, molecular mass, M , is converted to diameter, applying the equation: diameter is proportional to $M^{0.6}$.

R_s depends on chemical or physical factors, packing size being one of them. As a general rule in chromatography, resolution increases when the particle size of the packing decreases. In HDC with packed columns, the R_F ratio is increased by using fine packings and resolution is increased. Pore size and pore volume, being the origin of molecular separation in SEC, strongly affect elution, whereas the effect of porosity is controversial in HDC, where the main phenomenon takes place essentially between – and not in the porous part of – the packing particles. Combined HDC and SEC action increases separation, in terms of sample mass and elution volume (see above).

For SEC, HDC, supercritical fluid chromatography and TFFF, theoretical plate height generally increases with flow rate according to the van Demter equation, so that resolution decreases. Sometimes R_t may increase, particularly if a gradient is used properly or when mass transfer does not play a role.

For all separations, it is possible to obtain an accurate molecular weight by using deconvolution to remove system dispersion.

Table 4 indicates meaningful values of R , R_s , R_t and analysis time with the various separation systems.

Conclusion

HDC is a complementary method for particle characterization in the micron size range. It is rapid, low cost, easy to carry out and very sensitive. It allows separation and size measurement of organic colloids,

soft and rigid polymers and various materials (spheric or elongated) in about 10 min, without special sample preparation. Moreover, it has been the subject of many theoretical studies, assuming different mechanism models and explaining the effect of parameters on separation. Effort has been directed to column design, detection sensitivity and fit of chromatogram for PSD. Some conditions must be obeyed to obtain reliable results, whatever columns are used. Firstly, there is the need for accurate calibration, with frequent adjustment of parameters and choice of a column set giving a low slope. Secondly, there is the need to adjust the detector response factor (exponent n of diameter) to the sample and to the chosen detector. Thirdly, axial dispersion must be corrected using a simple equation. As a consequence of the combined analysis of the effects of n and Pe , the proposed value for exponent n was 3.5 with UV detection and a Peclet number of 500. Results have been compared on eluted fractions with those of direct methods. With proper use of HDC interpretation parameters, PSD and average diameters are in agreement with those obtained by other methods, for instance photon correlation spectroscopy and sedimentometry, this last technique has high resolution as its main characteristic.

In packed columns, packing size, ionic strength, I , nature and amount of surfactant have very large effects on R_F and other elution parameters, such as percentage recovery, which decreases for large particles. R_F decreases when I or packing size or amount of surfactant increases. Porous packings may add a SEC separation effect, enhancing R_F . Improvements in packing material (5 μ m) and methodology tend to use a 0.5 m long column.

In capillary HDC, the effect of additives is low; surfactants are the most useful. The separation factor R_F is fairly constant in water but is strongly affected by flow rate in methanol. The high number of plates in tetrahydrofuran is not accompanied by a high maximum R_F value. This separation factor may be higher with a 60 m than with a 120 m column, but the resolution, R_S , is not so high. This emphasizes the fact that R_F , R_S and N may vary independently.

Micro-equipment (diameter of the capillary in the micron range, short column (10 m), on-column injection and detection) enhances resolution and R_F as it lowers axial dispersion. Peak capacity remains limited at about 10, but for rheological properties and size range, this is an interesting alternative to packed columns.

See also: I/Particle Size Separation. II/Chromatography: Liquid: Mechanisms: Size Exclusion Chromatography. Particle Size Separation: Electrostatic Precipitation;

Field Flow Fractionation: Thermal. III/Polymers: Field Flow Fractionation. Proteins: Field Flow Fractionation.

Further Reading

- Barth HG (ed.) (1984) *Modern Methods of Particle Size Analysis*. New York: John Wiley.
- Bird RB, Stewart WE and Lightfoot EN (1960) *Transport Phenomena*. New York: Wiley.
- Bos J and Tijssen R (1995) Hydrodynamic chromatography of polymers. In: Adlard ER (ed.) *Chromatography in the Petroleum Industry*, ch. 4. pp. 95–125. Amsterdam: Elsevier.
- Daniels CA, McDonald SA and Davidson JA (1978) Comparative particle size techniques for poly(vinyl chloride) and other lattices. In: Becher P and Yudenfreund MN (eds) *Emulsions, Lattices and Dispersions*, pp. 175–193. New York: Dekker.
- Dos Ramos JG (1998) High-resolution particle size characterization for quality control. *ACS Symposium Series* 693: 207–221.
- Gunderson JJ and Giddings JC (1989) Field-flow fractionation. In: Allen G and Bevington JC (eds) *Comprehensive Polymer Science*, vol. 1, ch. 14, p. 279. Oxford: Pergamon Press.
- Hamielec AE (1984) Detection systems for particle chromatography. In: Barth HG (ed.) *Modern Methods of Particle Size Analysis*, ch. 8, pp. 251–275. New York: John Wiley.
- Hoagland DA, Larson KA and Prud'homme RK (1984) Hydrodynamic chromatography of high molecular weight water-soluble polymers. In: Barth HG (ed.) *Modern Methods of Particle Size Analysis*, ch. 9, pp. 277–301. New York: John Wiley.
- Janca J (1988) *Field-Flow Fractionation. Analysis of Macromolecules and Particles*, Chromatography Science Series 39. New York: Dekker.
- Prud'homme RK and Hoagland DA (1983) Orientation of rigid macromolecules using HDC separations. *Separation Science and Technology* 18: 121–134.
- Silebi CA and MacHugh J (1978) Particle size distribution of colloidal latexes by HDC. In: Becher P and Yudenfreund MN (eds) *Emulsions, Lattices and Dispersions*, pp. 155–174. New York: Dekker.
- Small H (1974) HDC. A technique for size analysis of colloidal particles. *Journal of Colloid and Interface Science* 48: 147–161.
- Styring MG and Hamielec AE (1989) Hydrodynamic chromatography. In: Allen G and Bevington JC (eds) *Comprehensive Polymer Science*, vol. 1, ch. 13, pp. 259–278. Oxford: Pergamon Press.
- Tijssen R and Bos J (1992) Mechanisms of the separation and transport of polymer systems in chromatographic media. *NATO ASI Series, Series C, Theoretical Advancement in Chromatography and Related Separation Techniques*, pp. 397–441.
- Tung LH (1966) Method of calculating molecular-weight distribution functions from gel-permeation chromatography. *Journal of Applied Polymer Science* 10: 375–385.

Laser Light Scattering Detectors

See II/CHROMATOGRAPHY/Detectors: Laser Light Scattering

Liquid Chromatography–Gas Chromatography

K. Grob, Official Food Control Laboratory
of the Canton of Zürich, Zürich, Switzerland

Copyright © 2000 Academic Press

Introduction

On-line coupling of high performance liquid chromatography (HPLC) to capillary gas chromatography (GC) means that LC fractions comprising one or several peaks are directly transferred to the gas chromatograph, mostly in a fully automated mode.

The first coupled system, developed by R. Majors in 1980, involved splitless injection by means of a GC autosampler and merely transferred a small part of an LC peak. The first transfer of complete LC fractions was described in 1984. Full transfer is essential, first because of sensitivity (the sample capacity of LC is limited), and second, to obtain reliable quantitative results. The main obstacle to overcome was the introduction of 100–1000 μL volumes of LC eluent into a gas chromatograph.

LC-GC seldom corresponds to ordinary LC with GC added as a detector. Usually GC performs the main analysis and LC is specially designed for a kind of pre-separation or clean-up. The technique presupposes that the compounds to be analysed are amenable to GC, i.e. that they are of limited polarity and rather low molecular mass. For most applications, only normal-phase LC is suitable, either because the matrix material to be injected is not soluble in reversed-phase eluents (e.g. mineral or edible oils), the components are derivatized prior to LC, or the sample consists of an extract from an aqueous phase.

LC columns are kept small (mostly of 2 mm i.d.) in order to keep the fraction volumes below 1000 μL . For the isolation of wider fractions of compounds, solid-phase extraction-type cartridges of lower separation efficiency, yielding smaller fractions, may be more suitable.

In contrast to clean-up by solid-phase extraction (SPE) cartridges, HPLC columns are used over long periods of time. During GC analysis, they are reconditioned, commonly by backflush with a stronger solvent.

Purposes of Coupling LC to GC

Clean-Up

Much of LC-GC serves for the routine analysis of a single or a small group of trace components, i.e. for automated clean-up at high separation efficiency. The LC detector installed between the LC and the GC enables careful optimization of the LC pre-separation and accurate cuts of the window transferred to the GC. Optional 'peak detection' automatically compensates for shifts in LC retention times by the use of the up- and/or down-slope of a peak determined by the LC detector.

Often LC-GC is used for the elimination of time-consuming manual sample preparation. In other instances, only the separation efficiency of HPLC is adequate for the removal of disturbing material of similar characteristics. The determination of traces of ergosterol or $\Delta^8(14)$ -stigmastenol in edible oils, fats, or food extracts in the presence of far larger amounts of phytosterols are examples. A number of applications even involve two-dimensional LC with heart cutting or LC-GC with intermediate solvent evaporation.

Group-Type Separation

Characterization of complex mixtures often necessitates prior separation into classes of compounds. Examples are the LC fractionation of mineral oil and its products into aliphatics and aromatics of a given number of aromatic rings, the analysis of the pattern of the alkylidibenzothiophenes in mineral oil, the determination of sterol dehydration products for the detection of adulterated olive oils, or the determination of irradiation in fatty foods through olefins cleaved from the triacylglycerols.

Sample Enrichment

Large amounts of some samples can be injected into the LC under conditions that remove the matrix and enrich the components of interest. At least 10 mL of water can be injected, reconcentrating the organic material on, for example, a reversed-phase C_{18} column. Salts are removed and the organic material fractionated by a suitable mobile phase before transfer to the GC.

Transfer of LC Fractions

On-line transfer must be capable of introducing many hundreds of microlitres of LC eluent into the GC. While this has been routine for almost a decade for normal-phase LC eluents (typically based on pentane or hexane), transfer of water-containing eluents is still at an experimental stage, both as a result of technical difficulties, and because of limited applicability.

Routine transfer in on-line LC-GC is mostly achieved by on-column techniques. Usually an early vapour exit is used, releasing the solvent vapours through an outlet installed after a pre-column system. This protects the GC detector and accelerates the discharge of the large volume of vapours (increases the evaporation rate). An uncoated and/or a retaining pre-column is used. The uncoated pre-column serves to evaporate the eluent and reconcentrate the initial bands of higher boiling solutes by the retention gap effect. The coated pre-column retains the solutes during release of the solvent.

Distinction must be made between fully and partially concurrent solvent evaporation. Fully concurrent evaporation means that all the eluent is evaporated during introduction into the GC, i.e. no liquid accumulates in the pre-column system. Volumes of up to several millilitres can be transferred, but volatile components are lost. Partially concurrent evaporation leaves behind unevaporated solvent that must be retained by a relatively long uncoated pre-column and vaporized after the end of the transfer. It is used when solvent trapping is needed for the retention of the volatile components during release of the solvent vapours; components as volatile as heptane can be analysed quantitatively in pentane.

The most obvious alternative to on-column transfer, programmed temperature vaporizing (PTV) solvent splitting, has been proposed, but not described as a routine technique so far.

On-Column Interface

The on-column interface is used for the transfer by partially concurrent evaporation (see Figure 1).

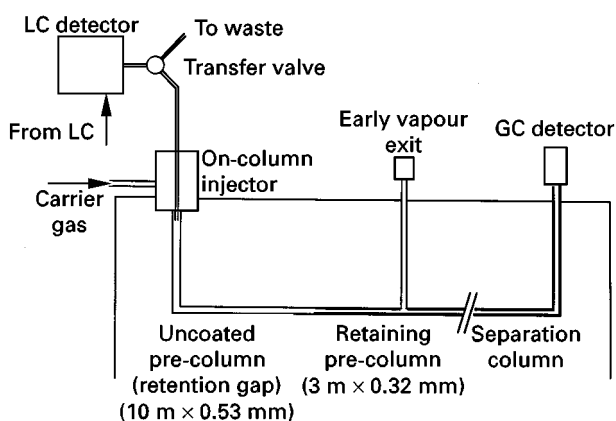


Figure 1 On-column interface for samples containing highly volatile solutes.

Transfer occurs by the same principles as on-column injection of large volumes (retention gap technique). The eluent from the LC passes through a valve for selecting the fraction to be introduced into the GC. It then enters an uncoated pre-column of typically 10 m \times 0.53 mm i.d., with a capacity of retaining 100–250 μ L of wetting liquid. Partially concurrent evaporation ensures that LC fractions with larger volumes do not overfill the uncoated pre-column. Mostly a retaining pre-column (2–3 m \times 0.32 mm i.d.) has been used, but if the early vapour exit is closed before the end of solvent evaporation, it is not really needed. The technique has been routinely used for fractions of up to 800 μ L volume.

Loop-Type Interface

Transfer through the loop-type interface (Figure 2) is used for fully concurrent evaporation and is suitable for the analysis of components eluted at oven temperatures above about 150°C. It is the technique most frequently used because of its simplicity: the introduction rate is self-adjusting and the end of the transfer

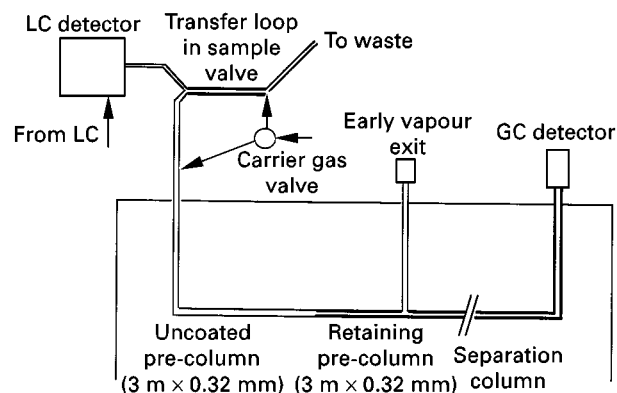


Figure 2 Loop-type interface for transfer by concurrent eluent evaporation.

can be detected automatically. The maximum volume transferred to date is 20 mL.

The LC eluent passes through a loop mounted in the sample valve with an internal volume chosen to match the volume of the LC window to be transferred. At the end of the fraction, as observed by the LC detector, the valve is switched and the carrier gas pushes the liquid from the loop into the GC pre-column. The temperature of the GC oven is above the solvent boiling point at the carrier gas pressure, which causes the liquid to be stopped as soon as it enters the oven-thermostatted pre-column. The vapours are discharged through the coated pre-column retaining the solutes, driven by the pressure of the carrier gas behind the plug of liquid to be transferred (overflow technique). A separate valve actuated simultaneously with the sample valve feeds the carrier gas either behind the liquid to be transferred or to a T-piece allowing purging of the sample valve during analysis.

Stop-Flow Introduction

In 1985, Cortes described LC-GC by a 'stop-flow' transfer technique. The interface used is shown in Figure 3. A valve either conducts the LC eluent to waste and supplies the carrier gas to the GC column, or transfers the LC fraction to the GC while the carrier gas flow is interrupted. The vapours are discharged by expansion during evaporation, driven by their own vapour pressure (also called 'overflow').

Vaporizer/Overflow Interface

The vaporizer/overflow interface (Figure 4) is a further development of the stop-flow technique. The transfer valve sends the LC eluent either to waste or into a vaporizer chamber typically thermostatted at around 300°C, replacing the uncoated pre-column. Actuated simultaneously, a separate valve (to avoid contact with solvent) stops the carrier gas supply during transfer. The vaporizer consists of 0.32 mm

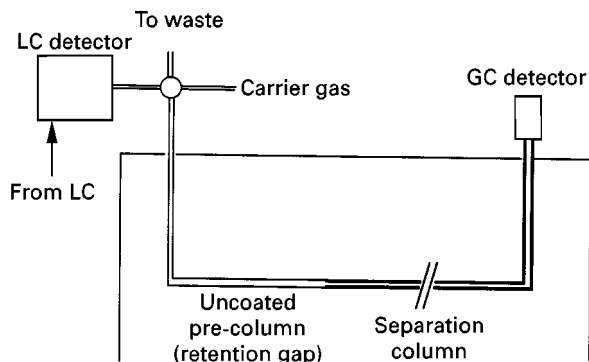


Figure 3 Stop-flow interface.

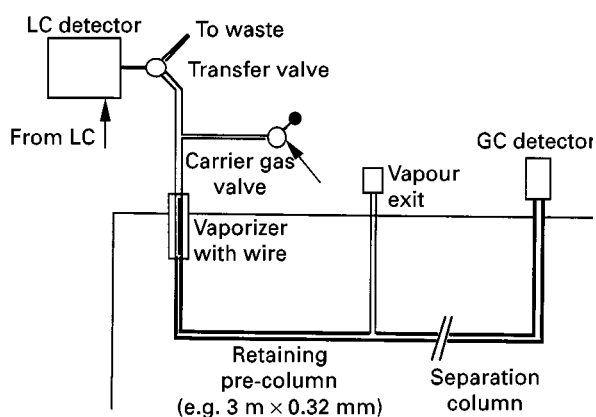


Figure 4 Vaporizer/overflow interface.

i.d. fused silica capillary with a piece of wire (bare metal or metal deactivated by the Silcosteel™ procedure) inserted to prevent liquid from shooting through the chamber. The oven temperature is selected to be near the minimum that avoids solvent recondensation, i.e. at, or slightly above, the boiling point at the pressure required to discharge the vapours (usually 5–15°C above the standard boiling point). A retaining pre-column (typically 2 m × 0.53 mm i.d.) connects to the T-piece of the vapour outlet. Compared with the loop-type interface, the technique improves the retention of the volatile solutes. However, no solvent trapping can be achieved.

Vaporizing Chamber Interface

For the transfer of water-containing eluents or LC fractions containing amounts of nonevaporating material disturbing on-column introduction, a vaporizing chamber is inserted between the on-column injector and the pre-column system (Figure 5). It consists of a packed liner of 1–2 mm i.d. and is thermostatted at a high temperature (around 300°C) in order to supply the large amount of heat consumed by solvent evaporation. Vapours are discharged by a carrier gas stream through the vapour exit. An uncoated pre-column is used for partial solvent recondensation if solvent trapping is required, but is of no utility for nonwetting water-containing eluents.

Applications

It is estimated that currently about 200 automated on-line LC-GC instruments are in use. More than half of the applications are in three fields. These were determined by the people involved rather than by particular suitability of the technique and should, therefore, not be understood as an indication that other applications would not be at least equally promising.

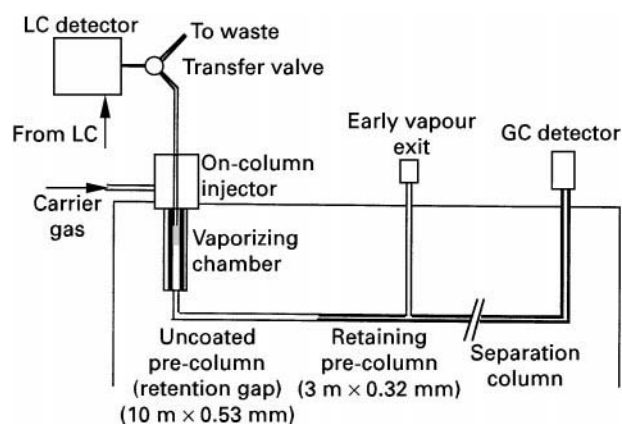


Figure 5 On-column interface with vaporizing chamber.

Mineral Oil Analysis

The petroleum industry has used LC-GC for the pre-separation of products into paraffins and aromatics, as well as for the separation of the highly

alkylated aromatics into classes of given ring number (using an amino column). Bartle used the same technique for analysing exhausts from diesel engines. Mineral oil products and their aromatic components have also been determined in foods.

Edible oil

Methods have been developed for the analysis of edible oils or fatty foods in order to achieve faster analysis (circumventing manual clean-up) and analyses of trace components that are difficult to analyse otherwise. They include the analysis of sterols (after transesterification of the oil), the minor components in the oil (after silylation), sterol dehydration products, volatile terpenes in cold-pressed oils, contamination by mineral oil or polyaromatic hydrocarbons, and organophosphorus insecticides.

Figure 6 demonstrates the extremely high resolution achievable by on-line LC-LC-GC-FID for the

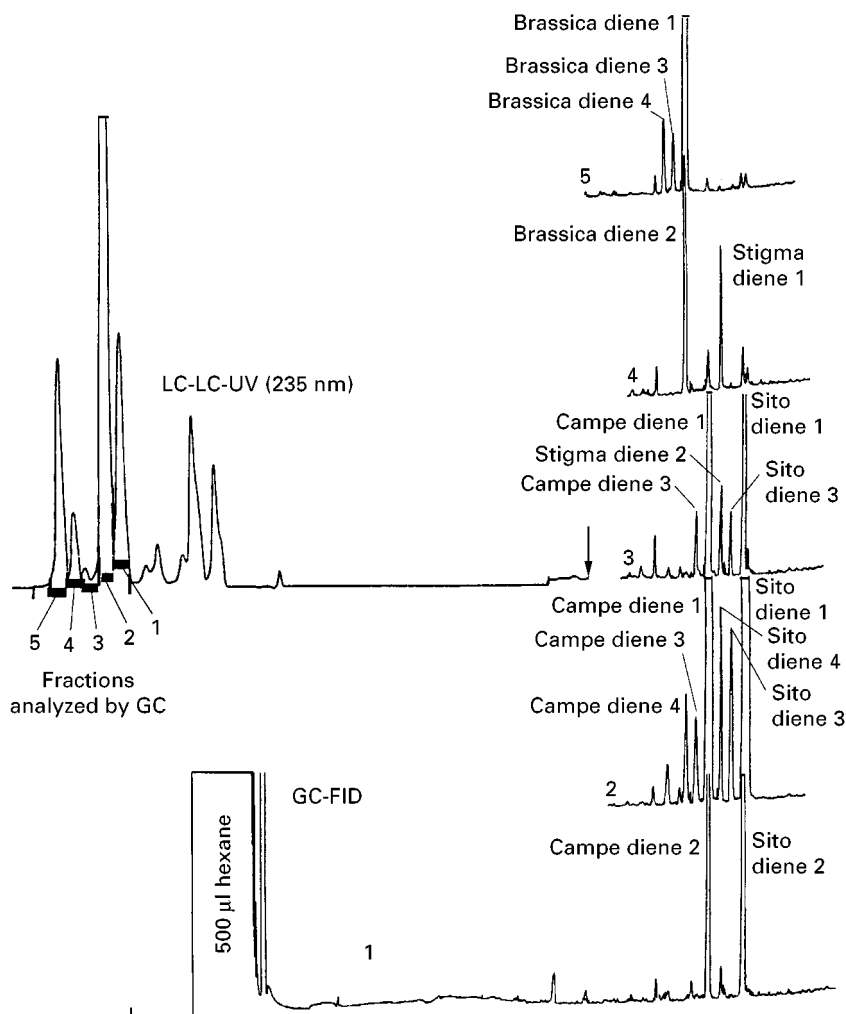


Figure 6 Liquid chromatogram and LC-LC-GC-FID chromatograms of the fractions marked: analysis of sterol dehydration products of rapeseed oil. (Reproduced with permission from Grob K, Biedermann M and Mariani C (1994) LC, GC and GC-MS of sterol dehydration products. *Riv. Ital. Sostanze Grasse* 71: 533-538.

analysis of sterol dehydration products from refined rapeseed oil (the composition of which is of interest for detecting adulteration of other oils, e.g. olive oil). Sample preparation consisted of preparing a 1:5 dilution of the oil. The first LC column isolated the hydrocarbons (with the column backflushed by a stronger eluent after each analysis), while the second one separated the products of interest into groups, such that the closely related compounds could be separated by GC. The fractions from LC-LC and the related gas chromatograms are numbered.

Water Analysis

Brinkman, Vreuls, Noij and others have worked on the enrichment of organic materials from water on LC cartridges, followed by on-line liquid or thermal desorption into a gas chromatograph. The aim is a permanent, fully automated analysis of pesticides and other critical contaminants in rivers or the supply lines of water works. A standard procedure consists in extraction of 1–10 mL of water on short polymer-packed LC columns, which are then washed with clean water and dried by a stream of nitrogen. After desorption with ethyl acetate, the sample is transferred through the on-column or loop-type interface.

Conclusion

On-line LC-GC techniques are extremely powerful with regard to selectivity, sensitivity (as a result of the excellent clean-up) and efficiency (as most manual sample preparation is integrated into the automated analysis). It seems, however, that currently they are too demanding for widespread routine use.

See also: III/Crude Oil: Liquid Chromatography. Terpenoids: Liquid Chromatography. Essential Oils: Gas Chromatography. Oils, Fats and Waxes: Supercritical Fluid Chromatography. Petroleum Products: Liquid Chromatography. Pesticides: Gas Chromatography.

Further Reading

- Beens J and Tijssen R (1995) An on-line coupled HPLC-HRGC system for the quantitative characterization of oil fractions in the middle distillate range. *Journal of Microcolumn Separations* 7: 345–354.
- Grob K (1991) *On-Line Coupled LC-GC*. Heidelberg: Hüthig.
- Grob K (1994) On-line normal phase LC-GC. Methods for routine applications. In: Riva del Garda Sandra P and Devos G (eds). *Proceedings of the 16th International Symposium on Capillary Chromatography*, pp. 1–9. Heidelberg: Hüthig.
- Grob K (1995) Development of the transfer techniques for on-line HPLC-capillary GC (Review). *Journal of Chromatography* 703: 265–276.
- Grob K and Mariani C (1994) LC-GC methods for the determination of adulterated edible oils and fats. In: Tyman JHP and Gordon MH (eds), *Development in the Analysis of Lipids*, p. 73. Cambridge: Royal Society of Chemistry.
- Kelly GW and Bartle KD (1994) The use of combined LC-GC for the analysis of fuel products: a review. *Journal of High Resolution Chromatography* 17: 390–397.
- Noij THM and van der Kooi MME (1995) Automated analysis of polar pesticides in water by on-line SPE and GC using the co-solvent effect. *Journal of High Resolution Chromatography* 18: 535–539.
- Vreuls JJ, de Jong GJ, Ghijsen RT and Brinkman UATH (1994) LC coupled on-line with GC: state of the art. *Journal of the American Organization of Analytical Chemist* 77: 306–327.

Paper Chromatography

I. D. Wilson, AstraZeneca Pharmaceuticals, Mereside, Alderley Park, Macclesfield, Cheshire, UK

Copyright © 2000 Academic Press

Introduction

The techniques of paper chromatography and paper electrophoresis are sufficiently intertwined as to be worth considering together, as indeed they often were in books and reviews at the height of their popularity.

Paper Chromatography

The origins of paper chromatography have been traced back by some authorities as far as Pliny (23–79 AD), who described the use of papyrus impregnated with an extract of gall nuts to detect ferrous sulfate. Further examples of the use of paper chromatography can be seen in the 19th-century work of the German chemist Runge who described in his book *Zur Farbenchemie* the use of this type of separation for the investigation of inorganic mixtures. Subsequently another book (*Der Bildungstrieb der Stoffe*) by

Runge appeared, containing examples of this work. Further work in this area was undertaken by Schonbein and his student Goepplshroeder, who investigated the technique of *Kapillaranalyse* (capillary analysis). However, these early studies seem to have stimulated little real interest and, although there appear to have been some limited further studies in the 1930s and 1940s, it was not until the seminal work of Consden, Gordon and Martin in 1944 on the analysis of amino acids in protein hydrolysates, and subsequent studies by Consden, Gordon, Martin and Synge, that paper chromatography made a major contribution to separations.

Paper chromatography is now obsolete, except perhaps as an inexpensive technique for teaching chromatography in schools and colleges. However the introduction of paper chromatography may truly be regarded as revolutionary, and was one of the innovations in partition chromatography that led ultimately to the award of the Nobel prize to Martin and Synge in 1952. One author stated, in a handbook on the topic, that 'By this stroke of genius, they changed the analysis of protein composition from a lifetimes' work to a 2–3-day simple technique that could be carried out in any laboratory'. So rapid was the adoption of the technique that a book on the subject published in 1954 contained nearly 4000 references to its use. Quotations from textbooks of the period contain statements such as 'Paper chromatography is so widely used that it is impossible to make more than a rough estimate of its application' or 'it can be stated that there is virtually no field of chemistry or biology in which paper chromatography has not made a substantial contribution to the furtherance of knowledge and understanding'.

However, despite its huge impact at the time, paper chromatography suffered from a range of problems that led to its rapid replacement by thin-layer chromatography (TLC), to which it was inferior in almost every respect. In particular, separations on paper were often very slow (often up to 10 or 20 h), and spots tended to be much more diffuse than, for example, separations on cellulose TLC plates.

The Practice of Paper Chromatography

Equipment

Probably the major advantage of paper chromatography, and one that ensured its rapid adoption, is the simplicity of the equipment required in order to perform it. Essentially this equipment is the same as that now used for TLC and all that is required is a suitable

type of paper to act as the stationary phase, a means of applying the sample, a developing tank and a solvent system. A typical set-up for descending paper chromatography is illustrated in **Figure 1** showing, in addition to the tank and solvent reservoir the anti-siphon rod used to prevent excessive solvent flow from flooding the paper. Tanks were normally operated with the atmosphere saturated with the vapours of the solvent used for development in order to ensure good and reproducible results.

Solvents

In general, the solvent systems used in paper chromatography were based on mixtures of one or more organic solvents with water. Acids (HCl, acetic, etc.) or bases (aqueous ammonia) were added to control the ionization of the analytes. Typical solvent mixtures for amino acids, for example, might be composed of butan-1-ol, acetic acid and water; butan-1-ol, pyridine and water or phenol and water. For sugars, solvents based on ethyl acetate, pyridine and water; ethyl acetate, propan-1-ol and water or ethyl acetate, acetic acid and water were popular. For inorganic ions, solvent systems such as acetone, concentrated HCl and water; pyridine and water or butan-1-ol and HCl mixtures were suitable. In the case of some of these solvents the mixtures suggested separated on standing into two phases. In such circumstances it was customary to separate the two phases and use the aqueous layer to saturate the atmosphere in the developing tank and the organic layer as the eluent for chromatography.

Papers

The media used for both paper chromatography and paper electrophoresis were based on filter paper, with Whatman no. 1 being perhaps the most widely used and no. 3 also popular. However, paper manufactured by other companies was also used and Schleicher & Schull 2043b paper was popular according to some sources. Paper suitable for use in paper chromatography was also manufactured by Munktell, Macherey Nagel, Eaton-Dikeman and D'Arches. Not surprisingly, the availability of a range of papers produced numerous studies comparing the relative merits of the different products, eliciting the somewhat jaundiced comment in one review of the subject that 'These workers are not always in agreement ... and it is probable that the differences introduced by their individual experimental methods are of a greater magnitude than the differences between the various grades of paper'. Some papers were available in slow, standard and fast grades with the speed of development controlled by the coarseness of the cellulose fibres and the packing

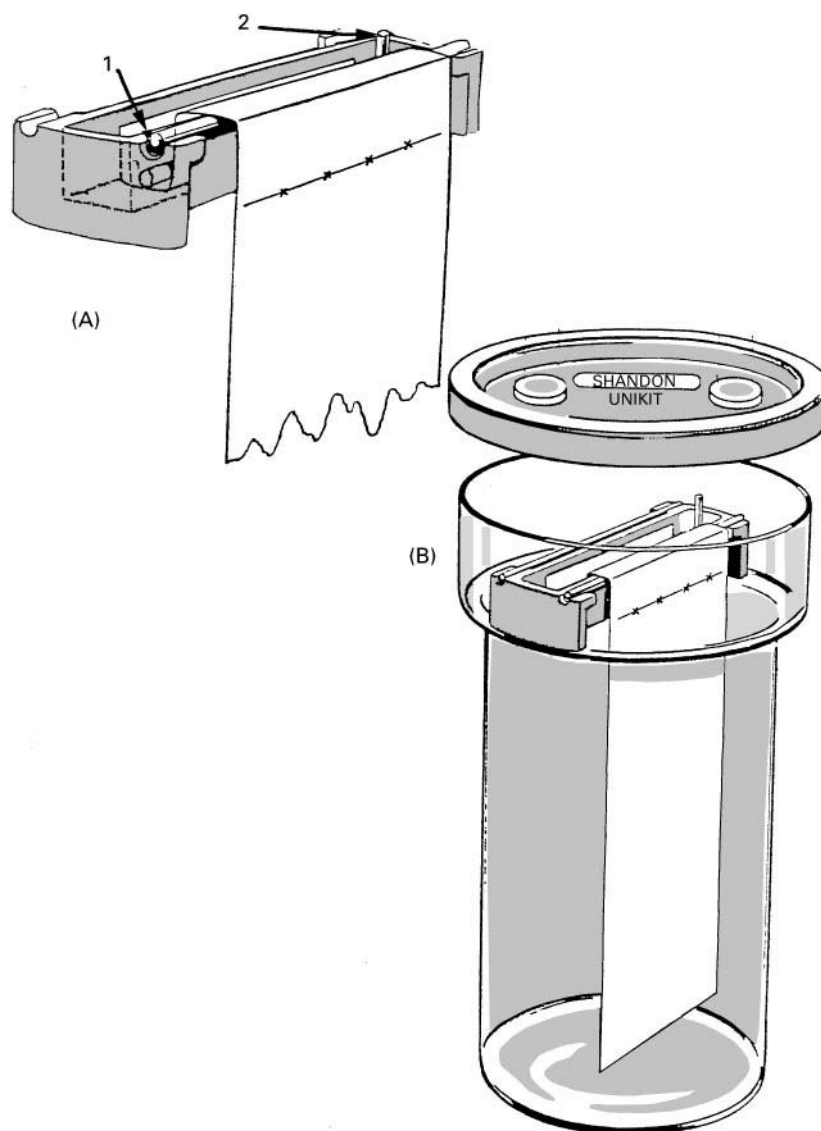


Figure 1 A typical commercial system (Shandon Unikit) for descending chromatography. (A) Set-up for hanging the paper, which hangs freely over the anti-siphon rod (1) and dips into the solvent reservoir where it is held in place with the anchor rod (2). (B) The assembled reservoir and paper in place in the developing tank. At this point the solvent would be added and the tank closed with the lid.

density. In general, the standard papers gave the best compromise between speed and resolution, with fast papers more suitable for simple separations and the slow papers used where the greatest resolution was required. Whilst suitable for analytical work, these papers were often replaced in preparative applications by more specialized materials such as Whatman no. 3 MM and 31ET or Schleicher & Schull 2071. In addition to pure cellulose, a variety of modified papers were also produced, including ion exchange materials, acetylated or benzoylated papers, silicone oil-impregnated papers, as well as silica and alumina-impregnated papers.

Modes of Paper Chromatography

In most of its practical aspects (e.g. sample application, equipment such as developing tanks and visualization procedures), paper chromatography somewhat resembles TLC. The most noticeable difference is that, as the paper is not rigid, it must either be suspended from an appropriate support during development or arranged in such a way as to be self-supporting. Only the major types of paper chromatography are described below, but it should be noted that there were many minor variants of the technique (e.g. centrifugal, continuous).

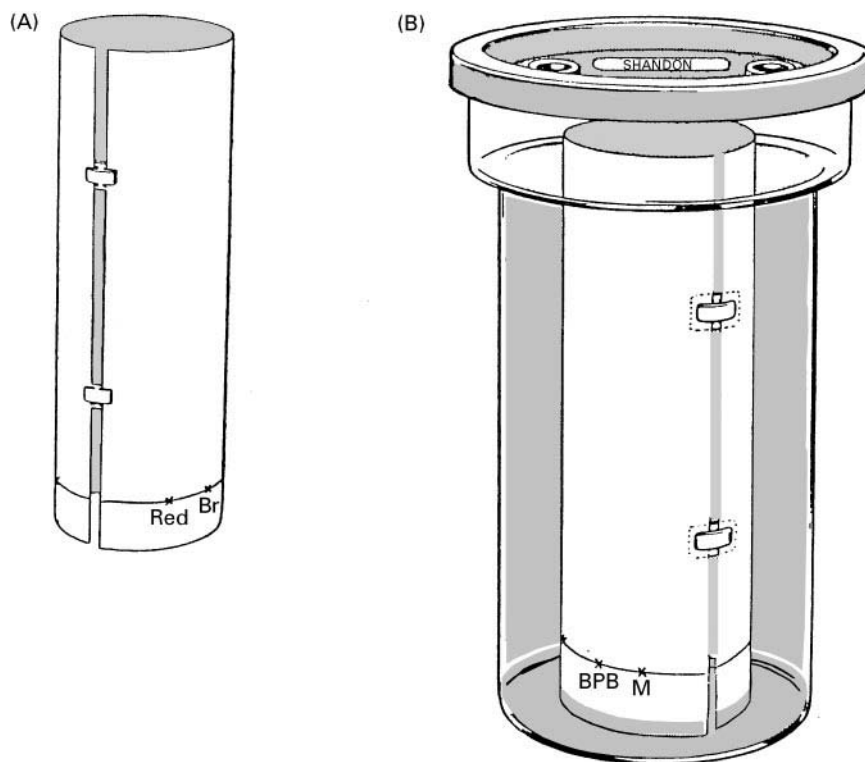


Figure 2 (A) One method of ascending chromatography involved the formation of a self-supporting cylinder, held together with tongued clips. The cylinder was then placed in a tank containing the solvent for development (B).

Ascending Paper Chromatography.

In the ascending mode of development the paper is suspended so that the lower edge is below the level of the solvent, and the solvent moves up via capillary action. An alternative to suspending the paper was to form a self-supporting cylinder from the paper. These arrangements are illustrated in Figure 2. As with TLC, multiple development, with either the same or different solvent, was used to improve resolution, although the time taken for each development must have made this especially tedious to perform.

Descending Paper Chromatography

The descending method of chromatogram development was that originally proposed by Martin and his co-workers. In descending paper chromatography the upper end of the paper is immersed in a solvent contained in a suspended trough so that the flow, initiated as in the ascending mode by capillary action, is sustained by gravity and will continue so long as there is solvent to feed it. This had the useful consequence that a sheet of any (practical) length could be used. In addition, the solvent could be allowed to run off the end of the paper, thus extending the chromatographic run if needed to improve resolution, or enabling compounds to be eluted from the paper

and collected for further experiments. The results obtained for a particular sample/solvent system combination run in either ascending or descending mode were usually similar; however, the latter was generally faster.

Two-dimensional Separations on Paper

Where separations were not achieved in a single development, it was often possible to achieve the desired result using a second solvent system of different composition and development in a second dimension at 90° to the original direction of chromatography. Two-dimensional paper chromatography was first described by Consden, Gordon and Martin for the separation of 20 amino acids, but was subsequently widely employed. An additional possibility was the use of paper chromatography in one direction with paper electrophoresis (both high and low voltage) in the second. Indeed, there are numerous examples in the literature of either chromatography followed by electrophoresis or electrophoresis followed by chromatography. A typical example of the type of result that could be obtained using two-dimensional paper chromatography is shown in Figure 3, whilst Figure 4 shows the combination of electrophoresis followed by chromatography in the second dimension for amino acids in fruit juice.

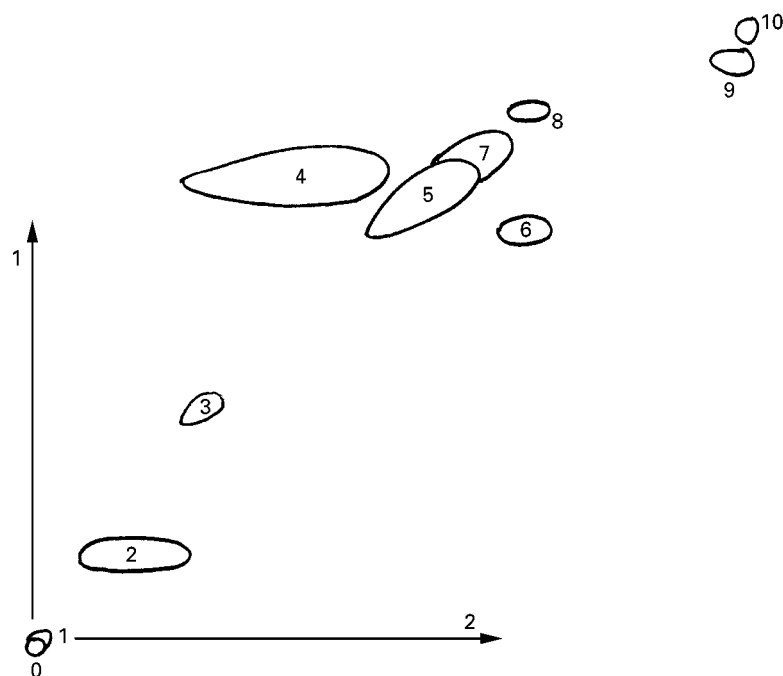


Figure 3 A two-dimensional separation of a mixture of black and brown ink using butan-1-ol-ethanol-2 mol L⁻¹ aqueous ammonia (6 : 2 : 2) for the first development and butan-1-ol-acetic acid-water (6 : 1.5 : 2.5) for the second dimension, on Whatman no. 1 paper. Key: 0, origin; 1, dark blue material remaining at or near the origin; 2, yellow pigment; 3, pink pigment; 4, diffuse brown pigment; 5, pink pigment; 6, yellow pigment; 7, scarlet pigment; 8, pink pigment; 9 and 10, faint spots of orange and yellow pigments respectively.

Horizontal or Circular Paper Chromatography

Horizontal (or circular) paper chromatography was performed in two ways. In the classical method, a spot of the sample to be analysed was placed at the centre of a circular filter paper. Then a short wick was made by making parallel incisions *c.* 2 mm apart from the edge of the filter paper to its centre. This wick was then cut to an appropriate size and bent so that it dipped into the solvent contained in a Petri dish. The general arrangement is shown in Figure 5A. Sub-

sequently, apparatus became available that eliminated the need for cutting the paper to form a wick, and one such is shown in Figure 5B.

Preparative Paper Chromatography

For a time preparative paper chromatography was an important method for the isolation of substances, leading to comments such as: 'These methods are so well developed today that some laboratories prefer them to the methods of column chromatography'. The simplest methods of preparative paper chromatography were essentially scaled-up versions of the analytical methodology using either several sheets of paper or custom-made preparative cardboards (e.g. Schleicher & Schull 2071). In addition, techniques were developed such as the Chromatopile (a number of discs of filter paper in a tightly compressed stack to form a column, with development by either ascending or descending chromatography), the Chromatopack (strips or sheets of paper pressed together to form a block which was then developed as if it were a single sheet) or rolls of filter paper wound over a core of polyethylene and inserted into a polyethylene column (sometimes these rolls were placed in a pressurized jacket). Using such techniques the preparation of milligram quantities of material was readily achieved.

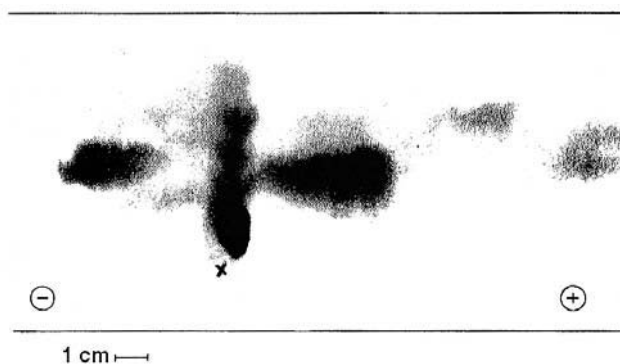


Figure 4 A typical two-dimensional separation of amino acids in orange juice effected by electrophoresis in pyridine-acetic acid followed by chromatography with butan-1-ol-acetic acid-water for the second. Detection with ninhydrin.

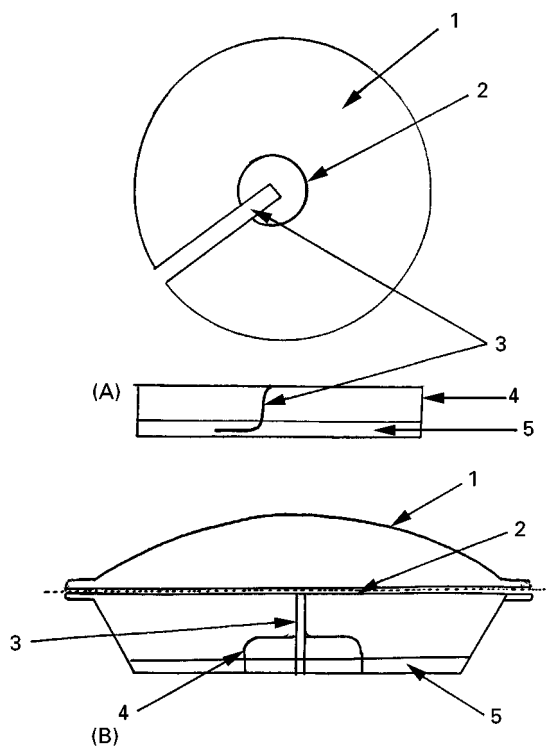


Figure 5 (A) Horizontal circular paper chromatography based on the method devised by Rutter. The upper part of this diagram shows 1, the paper; 2, the circle of sample applied to the paper (this could also be in the form of individual spots of different samples); and 3, the wick cut into the filter paper. The paper was supported on a Petri dish (4) containing the solvent (5) into which the wick was dipped in order to initiate development. Later the methodology was adapted by the introduction of a special development chamber which removed the need to cut a wick into the paper. One such, based on the apparatus devised by Kawerau, is shown in (B): 1, lid; 2, paper; 3, solvent capillary; 4, adjustable collar; 5, solvent.

Applications of Paper Chromatography

Given the importance of paper chromatography in its heyday, a list of its applications covers all types of analytes, including proteins, peptides, amino acids, poly-, oligo-, di- and monosaccharides, natural products, sterols, steroids, bile acids, pigment, dyes and inorganic species. A typical application to the separation of a series of inks is shown in Figure 6.

Paper Electrophoresis

It is possible to trace the development of paper electrophoresis back to the work of König, beginning in 1937 with a publication in Portuguese. However, this work attracted little interest at the time and it was the

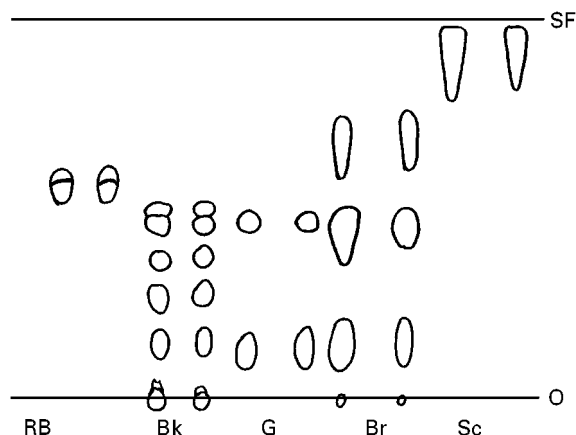


Figure 6 Separation, by ascending paper chromatography, of a series of ink samples (in duplicate). Key: RB, royal blue; Bk, black; G, green; Br, brown; Sc, scarlet; O, origin; SF, solvent front. Solvent system butan-1-ol-acetic acid-water (6:1.5:2.5) with Whatman no. 1 paper.

later work of Wieland and Fischer on amino acids in 1948 and Durram on serum proteins (1949, 1950) that attracted the attention of the scientific community. Some measure of the importance of the technique in its heyday may be gained from the observation in a volume on paper chromatography and electrophoresis published in 1957 that 'more than 2000 papers dealing with the subject of zone electrophoresis have appeared. Over 90% of these have dealt with paper electrophoresis'. Faced with such apparent success, it is possible to forgive the enthusiasm of the authors of a subsequent manual, published in 1977, on the subject who felt able to say that: 'In fact, it can be truly said that the history of paper electrophoresis still lies before it'. In fact, as with paper chromatography, this type of electrophoresis is now considered by most workers to be entirely obsolete.

The Practice of Paper Electrophoresis

Paper electrophoresis can be broadly divided into three main techniques: low voltage, high voltage and continuous. Of these, the low voltage (up to 1000 V) technique was probably the most widely used.

Low Voltage Paper Electrophoresis

Strips of paper arranged either vertically or horizontally and moistened with the buffer were used. The application of the voltage ($2\text{--}10\text{ V cm}^{-1}$) used to perform separations generated some heat, but this was generally carried away by evaporation when the open strip method was used. In the open strip technique the paper was suspended between the

electrodes in the saturated gaseous phase of the developing chamber. This suspension was accomplished in a wide variety of ways, with one review of the technique stating that: 'Paper has been arranged in this chamber in almost every conceivable configuration, but it is usually either pulled horizontally taut or allowed to hang free from a central support at the apex'. Both the horizontal and hanging strip methods were reported to provide excellent resolution, but the latter was claimed to give better reproducibility. Other configurations included the semi-closed strip, where the paper was supported on one side by a cooled glass surface to enable temperature control, and the closed-strip method where the paper was either held between two glass plates or submerged in a nonpolar immiscible liquid (e.g. heptane or carbon tetrachloride). With the former system, evaporation was not permitted and pressure could be applied so as to control the amount of electrolyte taken up by the paper. Using the nonpolar immiscible liquid method, some heat was removed from the paper by convection and conduction to a thermostatic bath. A simple commercial low voltage paper electrophoresis apparatus, of the open strip type, is illustrated in Figure 7.

As well as one-dimensional separations, two-dimensional paper electrophoresis was also performed when needed to improve particular separations.

High Voltage Paper Electrophoresis

The name high voltage electrophoresis was used to describe separations performed at voltages from 1 to 10 kV. The potential gradients used in high voltage systems were generally in the region of $50\text{--}100\text{ V cm}^{-1}$ and, as a consequence, one of the main problems encountered was heating. The apparatus used therefore required the presence of some form of heat exchanger to ensure that the heat was conducted away.

High voltage electrophoresis was considered to be best used for low molecular weight substances with many applications in amino acid analysis.

Continuous Electrophoresis

In continuous paper electrophoresis the sample was applied continuously to the paper (Figure 8), enabling a considerable volume to be applied over time, allowing preparative separations to be performed. The layout of the paper in this type of separation is shown in the diagram. Thus, the paper is suspended vertically (often referred to as a curtain) so that the buffer solution flowed downwards (as in descending chromatography). A field was then applied across the direction of the flow, causing the ionic substances to be separated, as indicated in the figure. The individual components of the mixture could be collected into appropriate receptacles as they eluted from the paper.

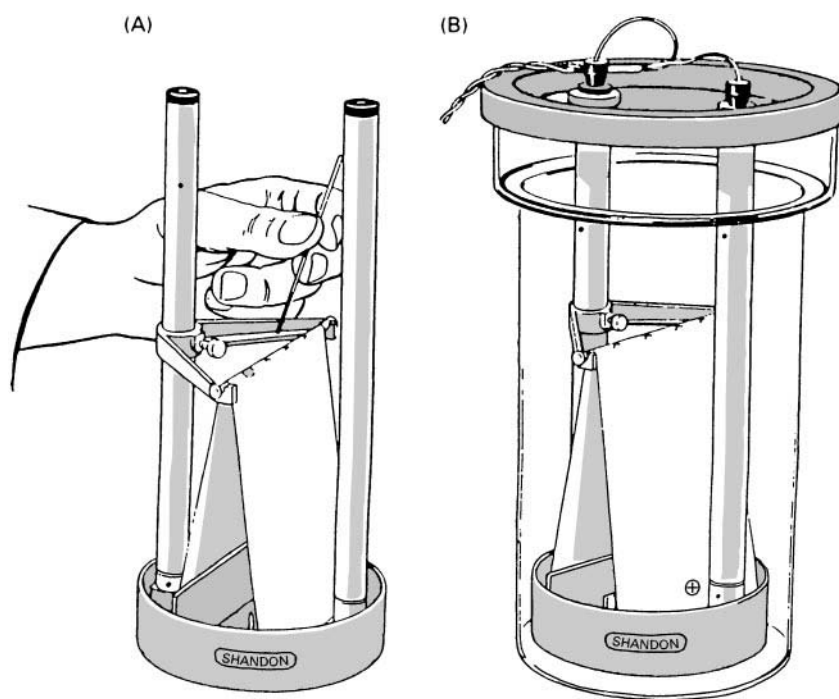


Figure 7 A simple commercial apparatus (Shandon Unikit) for paper electrophoresis. (A) The electrophoresis assembly showing the application of the samples to the paper which is suspended in a V shape via a glass rod. (B) Once prepared, the assembly is placed in the tank and the current switched on.

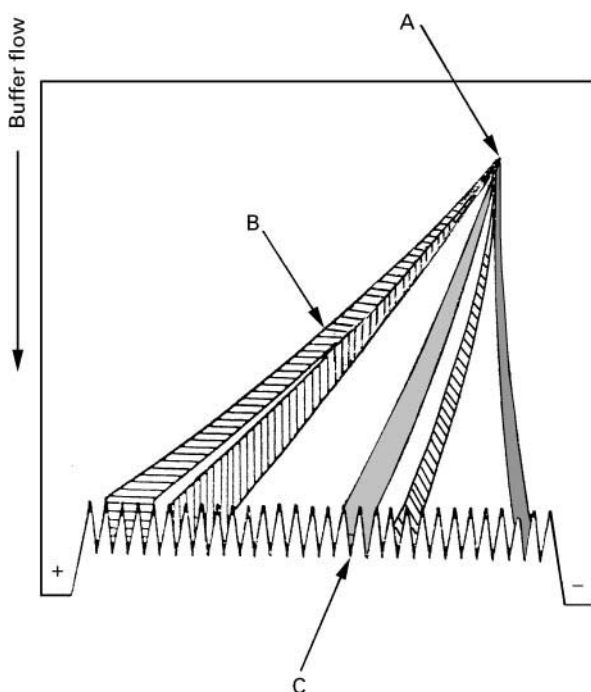


Figure 8 The arrangement for continuous electrophoresis. (A) Sample was applied continuously at this point and travelled down the paper under the influence of the flow of buffer. Current was applied at the point indicated by + and -, causing the components (e.g. B) to separate. They could then be collected into suitable receptacles as they eluted from the paper at C.

Applications of Paper Electrophoresis

As with paper chromatography, the applications of paper electrophoresis were legion and included amino acids, organic acids, natural products such as alkaloids, polysaccharides, nucleotides, proteins, peptides, pigments and inorganic species. The scope of the applications of paper electrophoresis is best appreciated by reference to the texts indicated in the section on Further Reading.

Detection and Quantification of Substances on Paper Chromatograms or Electropherograms

As in TLC, following separation the papers are removed from the developing chamber and dried. Coloured spots were visualized directly without difficulty, whilst those that fluoresce under UV irradiation were also detected relatively easily. In the case of colourless compounds, many of the visualization procedures, of varying degrees of specificity, currently used for this purpose in TLC were also used for detection after paper chromatographic separation, using either spraying or dipping. Although considered

primitive by comparison with modern methods, separations on paper were also used for quantitative assays in addition to qualitative work. As with other planar methods, varying degrees of sophistication were employed, from comparison of the size of spots compared to a standard, cutting out the bands/spots and eluting the analytes for subsequent spectroscopic determination (i.e. UV, visible or fluorescence measurements) all the way up to the use of densitometry (with accuracies of $\pm 5\%$).

Conclusions

Paper chromatography and electrophoresis were once techniques of considerable importance but this is no longer the case. Whilst still useful as an aid to teaching chromatography in schools and colleges, there are virtually no situations where separations originally developed for paper chromatographic methods cannot now be performed faster and better by TLC. The same comments apply to the relationship between paper electrophoresis and the modern slab gel technique.

Acknowledgement

Figures 1, 2, 4 and 7 are adapted from a Shandon Southern Product Manual and are reproduced with permission.

See also: I/Electrophoresis. II/Chromatography: Thin-Layer (Planar): Densitometry and Image Analysis; Historical Development; Spray Reagents.

Further Reading

- Block, RJ, Durrum, EL and Zweig G. (1958) *Paper Chromatography and Paper Electrophoresis*, 2nd edn. New York: Academic Press.
- Consden R, Gordon, AH and Martin AJP (1944) Qualitative analysis of proteins: a partition chromatographic method using paper. *Biochemistry Journal* 38: 224.
- Heftmann, E. (1961) *Chromatography*. New York: Reinhold.
- Lederer E and Lederer M (1953). *Chromatography*. Amsterdam: Elsevier.
- Morris CJOR and Morris P (1964) *Separation Methods in Biochemistry*. London: Pitman.
- Pucar Z (1960) Kontinuierliche electrophorese und zweidimensionale electrochromatographie. *Journal of Chromatography* 4: 261.
- Smith I and Feinberg JG (1977) *A Manual for Paper and Thin-layer Chromatography and Electrophoresis*, 2nd edn. Shandon Southern Products.
- Stock R and Rice CBE (1967). *Chromatographic Methods*, 2nd edn. Gateshead on Tyne: Northumberland Press.

Polymer Separation by Size Exclusion Chromatography

See II/CHROMATOGRAPHY/Size Exclusion Chromatography of Polymers

Protein Separation

R. K. Scopes, La Trobe University,
Melbourne, Victoria, Australia

Copyright © 2000 Academic Press

Introduction

Proteins are the essence of life processes. DNA contains the coded information for life, and is analogous to computer software, but it is the proteins that are analogous to the hardware, that actually carry out the job. Proteins have many roles, from catalysts (enzymes), through proteins that bind and interact with other molecules to control their behaviour, to structural and storage proteins which, although less functional, are nevertheless just as essential. Some proteins are 'solid', e.g. the proteins in our skin; others are soluble, such as those in our blood.

As with most separation procedures, those designed for proteins are designed to deal with a complex mixture of similar components, and separation often depends on slight and subtle differences between these components. Moreover, whereas some proteins may comprise a substantial proportion of the starting mixture, others may make up only a tiny fraction. The situation is very much like mining for minerals: first, select a source that is particularly enriched in the component you want, then work on removing all those you do not want. However, protein purifiers have one advantage over miners: nobody has succeeded in finding the philosopher's stone to turn base metals into gold, but molecular biologists do have the equivalent – the ability to greatly enrich the starting material with the desired protein. Consequently when talking about protein purification today, it is necessary to include a discussion of techniques for production of the protein by recombinant procedures. We also refer to the overall separation processes as 'purification', since the object is usually to obtain a homogeneous preparation of one single protein type, a 'pure' protein (even if this aim is not always quite achieved).

Separation procedures depend on differences in properties between the components, and fortunately proteins do come in a wide range of shapes and sizes. The properties that are exploited are solubility, ionic charge, size and shape, surface features and natural biological interactions. With recombinant techniques it is possible to modify the protein's structure so as to greatly simplify its purification.

The Starting Material

As indicated previously, the starting material should be rich in the protein of interest. That is not always possible, of course; the proteins may only come from a particular source, such as blood, mosquito larvae or potatoes (to name just a few possible sources). But even then it is possible to use molecular biology techniques to amplify the amount in either the natural source, or in an unnatural one, provided the gene (DNA) that encodes the protein, is known. Techniques for isolating the gene are outside the scope of this article, as are the details of the methods used for production of the recombinant protein, but both are becoming increasingly easy, and are often the first consideration when wanting to purify a protein. If the gene route is feasible, it will nearly always be the best way. Take the example of blood. Handling of human blood is now tightly controlled because of the dangers of viruses and because of ethical concerns, so if a blood protein can be produced in a fermentor full of yeast, or even in a cow's udder, these problems are circumvented. It is also much easier to produce a few grams of bacteria than a few grams of mosquito larvae.

Apart from simplifying and standardizing the raw material, the other two advantages of recombinant protein production are that (1) the amount of the desired protein, i.e. as a percentage of the protein in the starting material, will nearly always be much higher than in the natural source, and (2) simple techniques for modifying the protein by genetic means can make it very easy to separate from all the other proteins.

In most cases the desired protein will be soluble in aqueous media. If not, there are both advantages and disadvantages: the advantages include the ability to remove all the water-soluble proteins by simple extraction, which is a major separation process in itself. But the disadvantages include the problems of deciding what to do next, and how to separate the many insoluble proteins from each other. The answer is to get them into solution, and often this involves detergents, or other agents that may actually disrupt the natural biological state of the proteins. The natural state is called 'native' protein, whereas the disrupted state is called 'denatured'. It is sometimes possible to 'renature' a protein from the denatured state, and this may be necessary when recombinant expression of otherwise soluble proteins results in an insoluble, denatured product (inclusion bodies).

Solubility

Separation by solubility characteristics is the oldest technique in protein purification. Changes that result in proteins becoming less soluble in aqueous media include addition of salts, miscible organic solvents and organic polymers, and adjustment of pH. The aim is to make some proteins less soluble than others by varying these conditions, so the proteins can be separated from each other by centrifugation. It is not possible to predict which proteins will be affected, so it is essential to have a method for detecting the protein that is to be isolated, so that its position is known after any separation procedure. Typical precipitants include ammonium sulfate as a salt, ethyl alcohol and acetone as miscible solvents, polyethylene glycol as an organic polymer, and pH adjustment with a weak acid to about pH 5, which coagulates complex proteins.

After centrifuging the precipitate, it can be redissolved in a buffer that lacks the precipitant. **Table 1** illustrates an idealized analysis of the results of an ammonium sulfate fractionation of an extract containing an enzyme. Before the next separation procedure, it may be necessary to remove excess precipitant by dialysis or gel filtration.

Ionic Charge

All proteins have charges on them as a result of amino acid side chains such as aspartate, glutamate, histidine, lysine and arginine. The net charge on a given protein depends on its exact composition, and on the pH. Consequently at a given pH different proteins will have different net charges, and a shift in pH will change this value for each protein, though for all them it will become more negative for a higher pH, and more positive for a lower pH.

Although it is possible to exploit the charge differences by electrophoretic techniques, this has rarely been fully successful in preparative (as opposed to analytical) separations of proteins. The main problems have been in the design of reliable and safe equipment; there are some useful systems, but usually they will only be used when all else has failed. Ionic charge separations are carried out by ion exchange chromatography, which has been the most successful and widely used method of protein separation since its introduction some 40 years ago. Anion exchange columns have positive charges that attract negatively charged proteins, and at neutral pH most native proteins are negatively charged. For the minority of positively charged (high isoelectric point) proteins, cation exchangers are used. Samples are applied in a buffer that has low salt content (low ionic

Table 1 Results of a typical ammonium sulfate fractionation procedure in purifying an enzyme. Percentages are given as a percentage of saturation with ammonium sulfate. Specific activity is in units of enzyme activity per milligram of protein. Although the degree of purification is not high (2.1-fold), it is useful to note that much of the nonprotein material stays in the supernatant, and the precipitated fraction containing the enzyme can be dissolved in a much smaller volume than the starting extract. Results are also given for a second trial, in which recovery of activity has been sacrificed for a higher degree of purification

<i>Fraction</i>	<i>Volume (mL)</i>	<i>Amount of protein (mg)</i>	<i>Amount of enzyme (units)</i>	<i>Specific activity</i>	<i>Purification (x-fold)</i>	<i>Recovery (%)</i>
Extract	500	6000	380	0.063	1	100
0–50%	20	750	20			
50–60%	45	2400	310	0.130	2.1	82
60–70%	35	1600	70			
70% supernatant	540	1000	0			
0–55%	40	1500	90			
55–60%	35	1300	220	0.169	2.7	53
60% supernatant	535	3100	70			

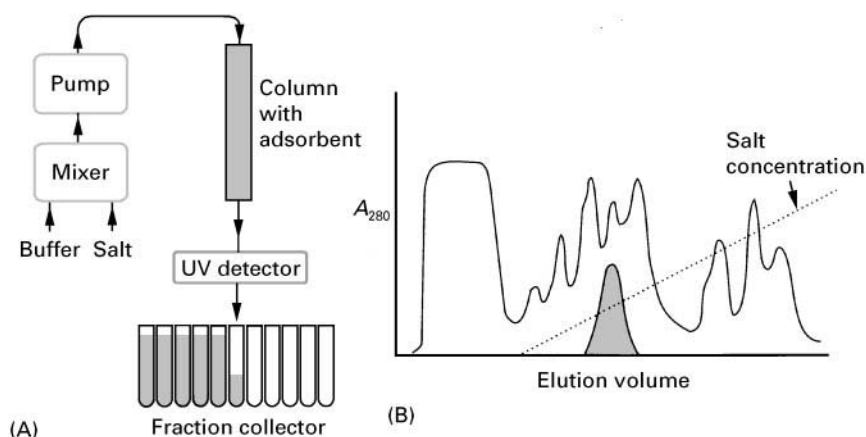


Figure 1 Example of protein separation using anion exchange chromatography. (A) A diagram of the basic principles of the equipment. The amount of protein emerging from the column is monitored by detecting the absorbance of light in the ultraviolet region (280 nm or 215 nm) due to proteins, and separate fractions are collected automatically. (B) The elution pattern. Some proteins did not bind to this adsorbent, being positively charged at this pH. The elution position of a specific protein is indicated by the shaded peak.

strength), and proteins of the opposite charge to the column are adsorbed. Proteins are generally eluted by increasing the ionic strength with gradual salt addition to the buffer, so that proteins of successive adsorbing strengths elute as the salt concentration goes up. This enables relatively high resolution of separate protein components, giving a high degree of purification. There are many commercial adsorbents and equipment to use them with. The type to be used will depend very much on the purpose; 'high performance' systems are expensive to operate and may not be suitable for commercial production of the protein, but most suited to research and development. Speed may be desirable, or may be of little concern; there are materials for all needs. An example of the separation of a fairly complex mixture of proteins on a 'moderate performance' adsorbent is shown in Figure 1.

Size and Shape

The sizes of protein molecules vary over a large range, but most have a molecular weight 20 000–200 000 Da (native protein). This translates to a size, assuming a perfect sphere, of roughly 3–8 nm in diameter. Many proteins are not spherical, however, so their longer dimensions will be greater than these figures. Separation by size is carried out by a process called gel filtration or size exclusion chromatography. The principle of gel filtration is shown in Figure 2. Beads that are porous, with pores of similar size to the proteins, are packed into a column. The largest proteins cannot penetrate the beads because the pores are too small, so they flow quickly around the outside of the beads, and emerge first.

They do not emerge until after a volume (the void volume, V_0) that is equivalent to the volume of liquid outside the beads has passed through the column. This volume is typically about 30% of the total column volume, V_t . The smallest proteins are able to penetrate the pores in the beads. While in the beads they are isolated from the flow of liquid (which cannot pass through the beads because of capillary forces), and so do not move down the column. However, they do spend some time outside the beads, and eventually, after a full column volume has passed through, they emerge from the column at V_t . The gel

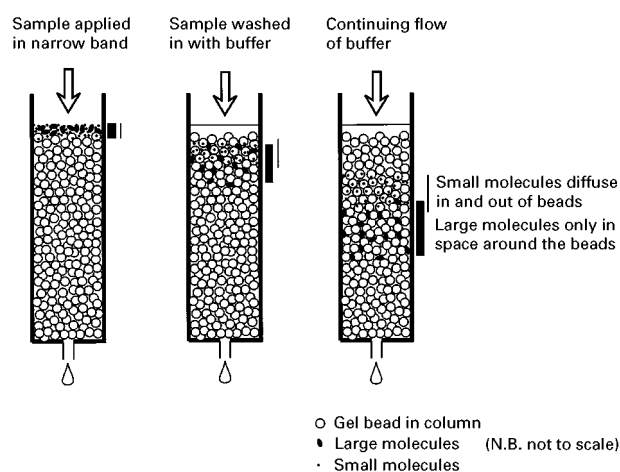


Figure 2 Principles of gel filtration. A mixture of proteins is applied to the column. Only the smallest molecules can penetrate the beads, while the larger molecules pass round the outside of the beads. Intermediate-sized molecules can partially penetrate the beads. As the separation continues, the larger molecules run out ahead of the smaller ones.

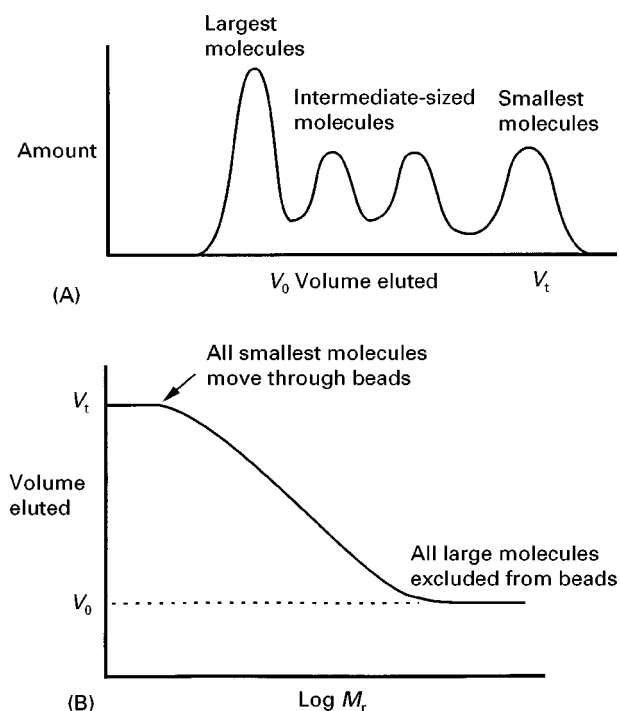


Figure 3 (A) The elution pattern of a mixture of proteins from a gel filtration column. (B) Plot of the 'elution volume' against the logarithm of the molecular weight. All small molecules emerge at V_t , all very large molecules earlier at V_0 , and the values for intermediate-sized molecules fall on a straight line over about a 10-fold increase in molecular weight range. By comparing the results with the elution volumes of proteins of known molecular weight, the molecular weight of an unknown protein can be determined.

beads have a range of pore sizes, so that intermediate-sized proteins can spend some time inside the beads, but not as much as the smallest proteins. Consequently the emergence volume of each protein is related to size, as shown in Figure 3.

This is also the principle used to separate large molecules from small molecules in general, and is very useful for removing salts from protein solutions. In this case the beads have pores so small that even the smallest proteins cannot penetrate the beads, but salts can.

Gel filtration is a very gentle method; the proteins remain in solution at all times, and need not be exposed to any extremes of pH or salt concentrations. Resolution depends on the relative sizes of the proteins in the starting mixture. Gel filtration will commonly be used at a later stage of purification, when the quantities of sample have been reduced.

There are also membranes available which have pores of suitable size to separate proteins. A force, such as gas pressure, is used to push the liquid, plus smaller molecules through the membrane. The largest molecules are retained, and concentrated

behind the membrane. This has application in the relatively crude separation of large proteins from small ones.

Separation by size is the commonest technique in the analysis of proteins, and is described in a later section. Using slab gels, which have pore sizes similar to the beads described previously, proteins are forced by electrophoresis to separate according to their size, the larger ones having more difficulty in finding their way through the gel, and so moving more slowly. This method has been applied preparatively, but only on a relatively small scale and mainly with unfolded, denatured proteins. Normally, one wants to isolate the protein in its native state, as not all proteins can be re-folded *in vitro*.

Other Surface Features of Proteins

The charged amino acids in a protein are responsible for the properties that allow separation on the basis of overall electrical charge. Other amino acids, especially those exposed on the surface of the molecule, confer other properties that can be exploited in separation methods. In particular, hydrophobic side chains would prefer not to be in contact with water. These amino acid side chains like to stick to each other, or to some surface that is also hydrophobic, and will do so in preference to being surrounded by water.

An adsorbent that consists of fat-like molecules attached to the insoluble beads is called a hydrophobic adsorbent, and will attract those proteins that have a larger proportion of hydrophobic side chains on their surface. Hydrophobic interactions are strengthened by inclusion in the solution of high concentrations of certain salts such as sulfates. A typical procedure would be to add up to 1 M sodium sulfate to the protein mixture, then run it through a column of hydrophobic adsorbent. Many proteins will not bind; these have few hydrophobic side chains. Then the salt concentration is gradually decreased, and proteins successively elute. The most hydrophobic proteins remain even a low salt concentration, and need other solutes such as chaotropic salts (e.g. thiocyanates), nonionic detergents, or high concentrations of glycols to elute them.

The most widely used method that exploits hydrophobic interactions is generally known as high performance liquid chromatography (HPLC). In this application proteins are adsorbed onto a material containing an aliphatic chain, such as C8 or C18, in conditions that result in partial unfolding of the native state of the protein so that internal hydrophobic regions are exposed. An increasing gradient of organic solvent then weakens the interactions between the protein and the adsorbent. Each protein is eluted

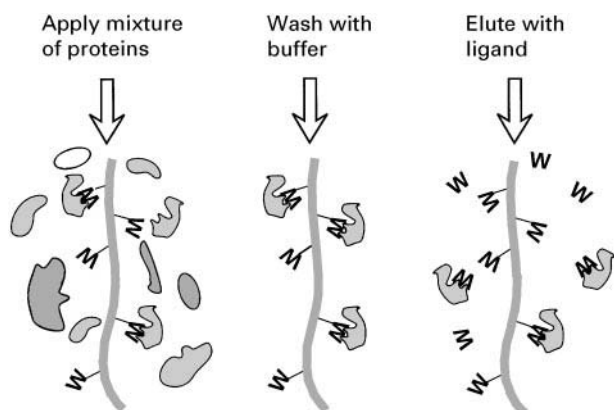


Figure 4 Principles of affinity chromatography. A ligand W that the desired protein binds to naturally is immobilized by attachment to column material. The protein mixture is applied, and the desired protein sticks to the immobilized ligand, while other proteins pass through and are washed away. Ideally only the proteins that bind to ligand W are left, though in practice there are usually others. Consequently a second 'affinity' step, involving washing the column with the natural, free ligand, is used to displace the specific proteins from the column.

in a narrow and very reproducible range of solvent concentrations, and provided that the proteins refold rapidly as they are eluted, this gives a very high resolution of components. This has been highly successful with small proteins and peptides, but is less useful for larger and more unstable protein components.

Bioaffinity

One surface feature that most proteins have is a binding site that corresponds to their natural physiological role. Enzymes, for example, bind to substrates known as ligands, which may be small molecules or parts of large ones. This binding is often very tight and specific, and can be made use of in separation procedures. The method is called 'affinity chromatography', and exploits the affinity of the protein for its natural ligand. The principle is illustrated in **Figure 4**. The adsorbent is designed so that it selects out only those proteins that bind to that particular ligand. The proteins may subsequently be eluted using some solute that disrupts the interaction, often just salt or more specifically with the natural ligand, free in solution.

Affinity Methods Associated with Recombinant Proteins

The most significant development in the past decade for purifying proteins has been the use of molecular

biology techniques not only to express the desired protein in large amounts, but also to modify it in a way that makes its purification easy. This is achieved by making the protein longer with extra amino acid residues (polypeptide) that can be recognized by an affinity column. The product is called a fusion protein. There are many systems available, and the process is made easy by commercially available expression systems that automatically add the desired polypeptide. In some cases, the addition may be fewer than ten amino acids. In other cases it is a whole extra protein, which folds into an active shape while linked to the desired protein being expressed. Often the overall expression level is even higher with these 'fusion products' than with the unmodified protein, because the expression of the fusion portion has been optimized in designing the vector.

After purifying the fusion protein, it may be necessary to remove the fusion portion. This can be done with selective proteases, though these usually still leave a few extra amino acids on the end. One system involving an intein, or self-splicing protein, enables release of exactly the desired protein with no gain or loss of amino acid.

Integrated Purification Schemes

Purification of proteins, even when using the highly selective affinity methods, usually requires more than one step, with the extra steps carried out sequentially. The starting material is the most bulky stage, the crudest and least pure sample of the desired protein, and the first separation step needs to be able to deal with such material. A traditional scheme is to use salt (ammonium sulfate) fractionation first, then an ion exchange column, followed by gel filtration. Each of these steps exploits a different property of the proteins, so when combined they give a good chance of high selectivity. Repeated use of one particular procedure, e.g. ion exchange chromatography, will produce diminishing returns in terms of separation and recovery of protein.

An alternative first stage is to use an adsorbent that acts as a pseudo-affinity material and selects out the desired protein (along with many others), allowing nonprotein material to be removed. Any such adsorbent must be cheap to produce, because the crude extract can cause changes to its properties after a few uses, such as clogging or degradation. Dye adsorbents have been used for this purpose: brightly-coloured columns bind certain proteins selectively, and these can be washed off, then put through other steps such as ion exchange and/or gel filtration.

Table 2 Purification of an enzyme using three different procedures: dye adsorbent chromatography exploiting surface characteristics; ion exchange chromatography exploiting charge differences; and gel filtration to separate by size. The enzyme was xylulokinase from a thermophilic *Bacillus* sp. (author's unpublished results). Specific activity is in units of enzyme activity per milligram of protein. Nearly 200-fold purification was achieved, and the final enzyme was judged to be about 95% pure. This implies that the xylulokinase enzyme made up just 0.5% of the total protein in the original extract.

Purification step	Volume (mL)	Amount of protein (mg)	Amount of enzyme (units)	Specific activity	Purification (x-fold)	Recovery (%)
Extract	50	650	290	0.45	1	100
Off dye adsorbent	29	36	208	5.8	13	72
Off anion exchange	15	7.5	150	20	44	52
(NH ₄) ₂ SO ₄ precipitated	0.65	2.2	150	66	147	52
Gel filtration	2.0	1.4	120	86	190	41

The final stage in a protein purification will often be a high resolution step such as HPLC. Any asymmetry of the final peak might indicate that impurities are still present.

A purification procedure ideally results in a good yield of a 'pure' protein. If the final product is an enzyme it is relatively easy to determine how much remains at the final stage, compared with the amount in the crude extract, by measuring its activity.

Sacrifices of recovery for purity (or vice versa) during the procedure will need to be made, depending on the relative importance of these two factors. Table 2 illustrates a typical purification of an enzyme, with a respectable recovery of activity and an end product that was analytically close to homogeneous.

Analytical Separations

At various stages, but more particularly at the end, one needs to know how close to purity the protein fraction is. Of many different analytical techniques that have been used, one is universally employed. This is known as SDS-PAGE, which stands for sodium dodecyl sulfate-polyacrylamide gel electrophoresis. The gel (polyacrylamide) has pores that are similar in size to the protein molecules, and the mixture of proteins is forced through the gel by an electric field. First the proteins are fully denatured by treatment with the anionic detergent sodium dodecyl sulfate, which binds to all the proteins and confers on them a negative charge proportional to their size. The smaller proteins move through the gel relatively easily, but the larger ones are retarded by the lack of pores large enough to move through. Consequently there is a separation of components according to size, in a logarithmic way similar to that observed for gel filtration (see Figure 3). The individual components remain in tight bands; as a consequence proteins that differ in size by only 3–5% can be completely separated. This sharp resolution is thus able to detect small amounts of impurity, and a judgement can be

made on the absolute purity of the sample. One further feature is that, as with gel filtration, the distance moved by an unknown protein can be compared with known standards and the unknown molecular weight determined to within about 5% accuracy. The amount of protein required is only about 1 µg or less, depending on the detection (staining) method. Capillary electrophoresis systems can be even more sensitive and accurate for analytical work.

See also: II/Affinity Separation. Theory and Development of Affinity Chromatography. Chromatography: Protein Separation. Chromatography: Liquid: Column Technology; Large-Scale Liquid Chromatography; Mechanisms: Ion Chromatography. Electrophoresis: One-dimensional Sodium Dodecyl Sulphate Polyacrylamide Gel Electrophoresis; Proteins, Detection of; Two-dimensional Polyacrylamide Gel Electrophoresis.

Further Reading

- Coligan J, Dunn B, Ploegh H, Speicher D and Wingfield P (eds) (1995) *Current Protocols in Protein Science*. New York: John Wiley.
- Deutscher MP (ed.) (1990) *Methods in Enzymology*, vol. 182: *Guide to Protein Purification*. San Diego: Academic Press.
- Harris ELV and Angal S (eds) (1990) *Protein Purification Applications; A Practical Approach*. Oxford: IRL Press.
- Janson J-C and Ryden L (eds) (1989) *Protein Purification: Principles, High Resolution Methods, and Applications*. New York: VCH Publishers.
- Kenney A and Fowell S (eds) (1992) *Practical Protein Chromatography*. New Jersey: Humana Press.
- Price NC (ed.) (1995) *Proteins Labfax*. Oxford: Bios Scientific Publishers. San Diego: Academic Press.
- Scopes RK (1993) *Protein Purification, Principles and Practice*, 3rd edn. New York: Springer-Verlag.
- Scopes RK (1997) Protein purification in the nineties. *Biotechnology and Applied Biochemistry* 23:197–204.
- Wheelwright SM (1991) *Protein Purification; Design and Scale up of Downstream Processing*. Munich: Carl Hanser Verlag.

Size Exclusion Chromatography of Polymers

B. Trathnigg, Karl-Franzens-University,
Graz, Austria

Copyright © 2000 Academic Press

Obviously, elution volumes in ideal SEC are always smaller than the void volume of the column:

$$V_i < V_e < V_0 = V_i + V_p$$

$$0 < K_{\text{SEC}} < 1$$

Introduction

In the characterization of polymers, size-exclusion chromatography (SEC) has become a standard technique for determining molar mass averages and molar mass distributions (MMD) of polymers. The principle of SEC is easily understood: owing to limited accessibility of the pore volume within the particles of the column packing, polymer molecules are separated according to their hydrodynamic volumes, which can be correlated to their molar mass. Unfortunately, this is not as easy and simple as it looks. There are numerous sources of error and pitfalls in the separation, in the detection and in the treatment of the raw chromatographic data.

Separation

In SEC, the separation should be solely governed by size exclusion, which need not always be the case. Let us first consider the ideal case, in which size exclusion does govern the separation.

Separation by Exclusion

Elution volumes in ideal SEC are limited to a narrow range (smaller than the column volume). It is clear, that no fraction of the sample can be eluted, before the interstitial volume V_i (i.e. the volume of the solvent outside the particles of the column packing) has passed the column.

- Large molecules, which have no access to the pores (exclusion limit), are eluted at V_i .
- Small molecules, which have access to the entire pore volume V_p , will appear at the void volume V_0 , which is the sum of the interstitial volume V_i and the pore volume V_p .
- Molecules of a size between these extremes have access only to a part of the pore volume, hence they will be eluted with an elution volume V_e between V_i and V_0 , which is determined by K_{SEC} , the equilibrium constant of a sample in ideal size exclusion chromatography:

$$V_e = V_i + K_{\text{SEC}} V_p$$

The relation between V_e and the molar mass of a polymer is determined by calibration, as will be discussed later.

Exclusion Versus Nonexclusion Effects

The equilibrium constant of a chromatographic separation can be correlated with thermodynamic parameters.

The driving force for a separation at the (absolute) temperature T is the change in Gibbs Free Energy ΔG , which results from the changes in enthalpy (ΔH) and entropy (ΔS), respectively:

$$\Delta G = \Delta H - T\Delta S = -RT \ln K$$

In ideal SEC, which should be governed solely by entropy, ΔH should equal zero, and the equilibrium constant K_{SEC} should be given by:

$$K_{\text{SEC}} = e^{\Delta S/R}$$

while the equilibrium constant of adsorption chromatography (in the absence of exclusion) is determined by the enthalpy (typically, K_{LAC} is much larger than unity):

$$K_{\text{LAC}} = e^{-\Delta H/RT}$$

However, adsorption effects cannot always be completely eliminated. The distribution coefficient will then be given by:

$$K = K_{\text{SEC}} K_{\text{LAC}}$$

Under certain conditions, entropic and enthalpic phenomena will compensate each other, and K will equal 1. In this case, which is called the critical point of adsorption, all chains of the same structure are eluted in a narrow peak and separation of groups different from the repeating unit (end groups, branching sites, etc.) can be achieved.

This effect can be used in the analysis of functional oligomers or block copolymers. Even in the absence of adsorption phenomena there may be

another effect, which is called secondary exclusion. It originates from (electrostatic) repulsion of polar groups and has nothing to do with molar mass. The equilibrium constant K can then be divided into contributions from ideal size exclusion and from repulsion:

$$K = K_{\text{SEC}}K_{\text{rep}}$$

If interactions with the stationary phase also occur, the elution volumes will depend on all three distribution coefficients:

$$V_e = V_i + V_p K_{\text{SEC}} K_{\text{rep}} K_{\text{LAC}}$$

In ideal SEC, repulsion and adsorption should be absent, hence K_{rep} as well as K_{LAC} should equal unity.

The column(s)

Unlike other modes of high-performance liquid chromatography (HPLC), separation efficiency comes only from the stationary phase, while the mobile phase should have no effect. The whole separation occurs within the volume of the pores, which typically equals approximately 40% of the total column volume. This means, that long columns, or often sets of several columns are required. Different types of SEC columns are available, which are either based on porous silica or on semi-rigid (highly cross-linked) organic gels, in most cases copolymers of styrene (St) and divinylbenzene (DVB).

Table 1 lists some commercially available column packings for nonaqueous SEC. In general, silica-based packings are quite rugged, while organic packings must be handled with care. Typically, the separation range of a column covers approximately two decades of molar mass (e.g. from 1×10^4 to 1×10^6). Most producers also offer mixed bed columns covering a much wider range.

Obviously, a good separation is only one part of a good analysis. Another crucial point is the detection of the fractionated sample leaving the column.

Detection

Among the numerous HPLC detectors, only a limited number can reasonably be applied in SEC. One has to distinguish between concentration detectors and molar mass detectors.

- The response of a *concentration detector* is determined by the concentration of the solute in the mobile phase.
- The response of a *molar mass detector* depends on molar mass of the solute, as well as on concentration.

At least one concentration-sensitive detector has to be used in an SEC system. In the analysis of copolymers, a second concentration-sensitive detector is required, the sensitivity of which towards the components of the polymer differs from that of the first detector.

Concentration-sensitive Detectors

The concentration detectors most frequently used in SEC of polymers are the UV and the RI detectors. Infrared (IR) detection suffers from problems with the absorption of the mobile phase. Two other detectors are useful in the analysis of non-UV absorbing polymers: the density detector and the evaporative light-scattering detector (ELSD).

The UV detector detects UV-absorbing groups in the polymer, which may be the repeating unit, the end groups, or both. Hence, one has to distinguish two situations. For polymers, in which the repeating units contain a chromophoric group, the response of the UV detector represents the mass eluted in a given volume interval; for polymers with chromophoric end groups, however, the response depends on the number of polymer molecules. Many chromatographers use this assumption, when they derivatize 'nonabsorbing' polymers with UV-active reagents. Detection wavelengths are in the range of 180–350 nm but many SEC solvents allow detection only above a wavelength of 250 nm. Diode array detectors allow the measurement of an entire UV-spectrum at any point of the chromatogram, which is useful in SEC of copolymers.

Table 1 Column packings for nonaqueous size exclusion chromatography

Producer	Packing	Material
Rockland Technologies	Zorbax PSM	Porous silica microspheres
Shodex	Asahipak GF HQ	Highly crosslinked polyvinyl alcohol
Macherey-Nagel	Nucleogel GPC	St-DVB copolymer
Merck	LiChrogel PS	St-DVB copolymer
Phenomenex	Phenogel	St-DVB copolymer
Polymer Laboratories	PL gel	St-DVB copolymer
Waters	Styragel HR, HT, MW, Ultrastayragel	St-DVB copolymer
Jordi	Jordi GPC	100% DVB polymer

The ELSD detects any nonvolatile components of a sample. In this instrument, the eluate is nebulized and the solvent evaporated from the aerosol. Each droplet containing nonvolatile material will form a particle, which scatters the light of a transversal light beam. The response of this instrument for copolymers is, however, unclear – it depends on various parameters and the nature of these dependencies is rather complex. Moreover, lower oligomers may be strongly underestimated.

The refractive index (RI) detector exists in various modifications. It is the most common instrument in SEC besides the UV detector.

The density detector, which has been developed in the author's group, uses the principle of the mechanical oscillator. The measuring cell of this instrument is an oscillating, U-shaped capillary, the period of which depends on its reduced mass, and thus on the density of its contents. The signal of the density detector is thus inherently digital, and its response is integrated over each measuring interval.

Molar Mass-sensitive Detectors

The response of such a detector depends on the concentration and also on the molar mass of the fraction, hence it has to be combined with a concentration-sensitive detector. The following types of molar mass-sensitive detectors are on the market: low angle light scattering detectors (LALLS); multi-angle light scattering detectors (MALLS); and differential viscosimeters.

From light-scattering detection, the absolute molar mass distribution (MMD) can be determined directly but no information is obtained on polymer conformation. However, SEC with viscosity detection yields the intrinsic viscosity distribution (IVD). Hence it makes sense to combine a light-scattering detector with a viscosimeter detector. In light-scattering detectors (LALLS, MALLS) the light of a laser beam is scattered by the dissolved polymer coils in the measuring cell and the intensity of the scattered light is measured at angles different from zero.

The (excess) intensity $R(\theta)$ of the scattered light at the angle θ is correlated to the weight average of molar mass M_w :

$$\frac{K^*c}{R(\theta)} = \frac{1}{M_w P(\theta)} + 2A_2c$$

where c is the concentration of the polymer, A_2 is the second virial coefficient, and $P(\theta)$ describes the scattered light's angular dependence. K^* is an

optical constant containing Avogadro's number N_A , the wavelength λ_0 refractive index n , and the refractive index increment dn/dc :

$$K^* = 4\pi^2(dn/dc)^2/(\lambda^4 N_A)$$

In a plot of $K^*c/R(\theta)$ versus $\sin^2(\theta/2)$, M_w can be obtained from the intercept and the radius of gyration from the slope. It must be mentioned, that dn/dc of copolymers may vary strongly with composition.

Viscosity detectors yield the intrinsic viscosity $[\eta]$, the so-called limiting viscosity number, which is defined as the limiting value of the ratio of specific viscosity ($\eta_{sp} = (\eta - \eta_0)/\eta_0$) and infinitely low concentration c :

$$[\eta] = \lim_{c \rightarrow 0} \frac{\eta - \eta_0}{\eta_0} = \lim_{c \rightarrow 0} \frac{\eta_{sp}}{c}$$

Since the concentrations in SEC are typically very low, $[\eta]$ can be approximated by η_{sp}/c . In viscosity detection, one has to determine the viscosity, η , of the sample solution as well as the viscosity, η_0 , of the pure mobile phase.

This is typically done by measuring the pressure drop across a capillary; the pressure drop is proportional to the viscosity of the streaming liquid (using a differential pressure transducer). The problems of single capillary viscometers (SCV) are obvious: the viscosity changes, $\Delta\eta = \eta - \eta_0$, will typically be very small compared to η_0 . Moreover, pressure differences due to pulsations of a reciprocating pump will be much larger than those resulting from the viscosity change caused by the eluted polymer.

A better, but still not perfect approach is the use of two capillaries in series, each of which is connected to a differential pressure transducer and a sufficiently large hold-up reservoir in between. Pulsations will be eliminated in this setup, because they appear in both transducers simultaneously.

A sophisticated approach is used in a differential viscometer, which is commercially available from Viscotek. In this instrument, four capillaries are arranged similar to a Wheatstone bridge. The detector measures the pressure difference ΔP at the differential pressure transducer between the inlets of the sample capillary and the reference capillary, which have a common outlet, and the overall pressure P at the inlet of the bridge. The specific viscosity, $\eta_{sp} = \Delta\eta/\eta$ is thus obtained from $\Delta P/P$.

Data Processing

Provided that the separation itself is reliable (which cannot always be taken for granted), the subsequent transformations are subject to errors:

- Elution time to elution volume: because of the logarithmic relation between molar mass and elution volume, small changes of the flow rate can cause large errors in molar mass.
- Elution volume to molar mass: the molar mass of a fraction can be obtained either from calibration or from a molar mass-sensitive detector (in addition to the concentration detector).
- Detector response to polymer concentration: this requires a sufficiently wide linear range, a well-defined response of the detector(s) along the entire peak (i.e. for all molar masses within the MMD) and, in the case of copolymers, a second concentration detector.

Determination of Elution Volumes

The absolute flow rate can be obtained by measuring the time to fill a calibrated flask or by weighing the solvent passing the system in a defined time.

The knowledge of the absolute flow rate is, however, not completely necessary as long as flow rate variations are compensated by using an internal standard. The corrected flow rate is obtained from the ratio of the elution times of this standard peak. Such a correction only works well, if the flow rate is sufficiently constant within the entire chromatogram.

Determination of Molar Mass

Unless a molar mass-sensitive detector is used, one has to determine the molar mass of a fraction eluting at the volume V_e from a calibration, which can be obtained in different ways.

Calibration with narrow standards If a series of standards with a narrow MMD is available, their elution volumes must be determined to establish a calibration from which the molar mass for a given elution volume may be obtained. In the early years of SEC, a linear relation between $\log M$ and V_e was assumed, which is, however, only a first approximation, the quality of which depends very strongly on the columns:

$$\log M = A + BV_e$$

where A and B are constants, which can be determined very easily by linear regression. For many columns, the calibration line is, however, sigmoidal rather than linear (Figure 1). In this case, a polynomial fit matches the experimental points much better:

$$\log M = A + BV_e + CV_e^2 + DV_e^3 + EV_e^4 + \dots$$

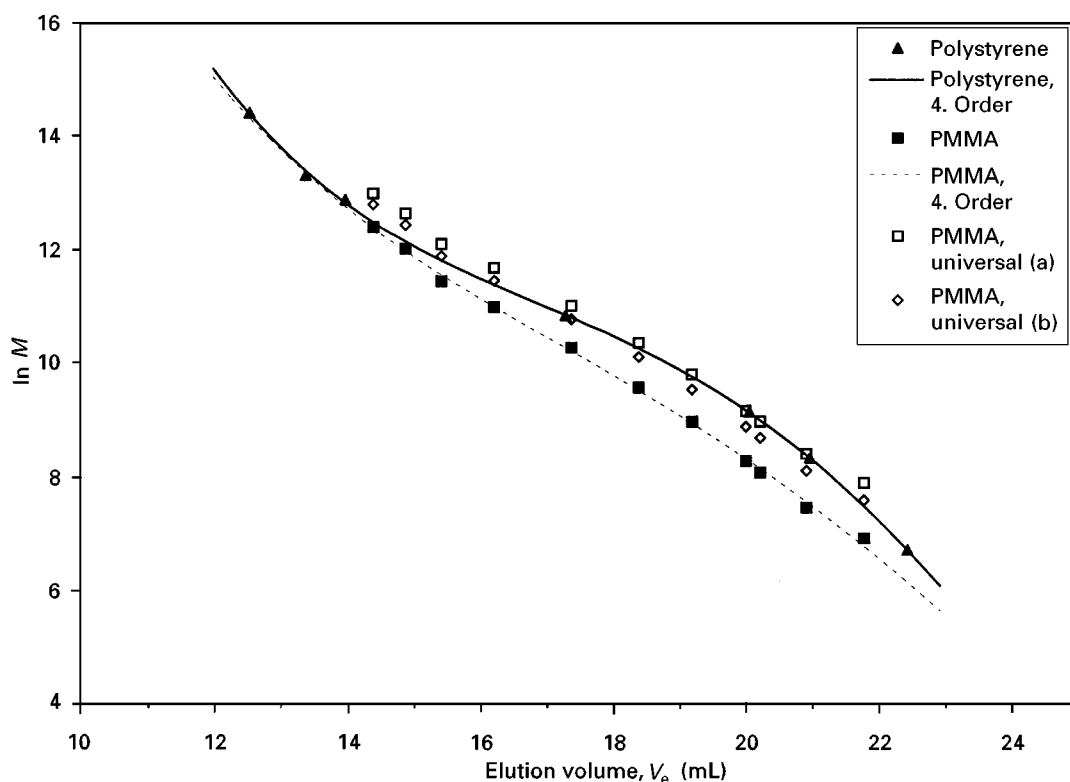


Figure 1 SEC calibration of a mixed bed column (Phenogel M, 7.8×600 mm) in 2-butanone at 25°C .

The order of the polynomial fit is, however, critical in some cases: if the number of data points (i.e. the number of standards) is too small, a fit of a too high order may produce an erroneous calibration line.

It must also be mentioned that there can be considerable differences between the calibration lines for different polymers on the same column in the same mobile phase.

This is especially important in the analysis of copolymers or polymer blends. Consequently, different molar masses will elute at the same volume, when a mixture of two homopolymers is analysed by SEC. The elution volume of a copolymer should be between the elution volumes of the homopolymers of the same molar mass.

If the composition of the copolymer at each point of the peak is known, a good approximation will be achieved by interpolation between the calibration lines. Calibration with narrow standards can be applied to many types of polymers, because appropriate standards have become commercially available for many polymers. In the low molecular range, additional data points can be taken from the maxima of oligomer peaks, which are at least partly resolved.

Different approaches have been described in the literature for the analysis of samples, for which no narrow MMD standards are available.

Calibration with broad standards If a well-characterized sample with broad MMD is available, different procedures may be used to establish a calibration fitting these averages.

The integral-MMD method can be applied if the entire MMD of the standard is known with high accuracy (which is, however, seldom the case). The method assumes, that the MMD of the sample can be described by the most probable distribution function and matches the calibration to this distribution. No assumptions on the shape of the calibration are made and the precision of the method is rather poor.

If only the molar mass averages of the sample are known from independent methods (light scattering or osmometry), linear calibration methods can be applied. The assumption of a linear calibration may, however, lead to erroneous results.

Universal calibration A very elegant approach is based on the fact, that in SEC the elution volume V_e of a polymer depends on its hydrodynamic volume, which is proportional to the product of its molar mass M and intrinsic viscosity $[\eta]$.

In a plot of $\log(M[\eta])$ versus V_e (obtained on the same column), identical calibration lines should be found for two polymers (1 and 2), which can be

considered as universal calibration:

$$M_1[\eta]_1 = M_2[\eta]_2$$

The intrinsic viscosity is a function of molar mass, which is described by the Mark-Houwink relationship, where K and a are constants for a given polymer in a given solvent at a given temperature:

$$[\eta] = KM^a$$

Combination of the equations above yields:

$$K_1 M_1^{a_1+1} = K_2 M_2^{a_2+1}$$

If a column has been calibrated with one polymer (1), the calibration line for another polymer (2) can be calculated, provided that the constants K and a are known for both polymers with sufficient accuracy:

$$\ln M_2 = \frac{1}{1+a_2} \ln \frac{K_1}{K_2} + \frac{1+a_1}{1+a_2} \ln M_1$$

The concept of universal calibration will also provide an appropriate calibration for polymers, for which no narrow standards exist.

The problem is, however, that the accuracy of K and a is limited even with polymers for which a sufficient number of well-defined standards exists: there are very large variations in the values reported in literature even in this case, as can be seen from Table 2.

Table 2 Mark-Houwink-Sakurada parameters from literature^a for common polymers in different solvents at 25°C

		K	a
CHCl ₃ , 25°C			
Polyethyleneglycol		0.20600	0.50
Poly(methyl methacrylate)	a	0.00581	0.79
	b	0.00480	0.80
	c	0.00340	0.83
Polystyrene	d	0.00716	0.76
	e	0.01120	0.73
2-Butanone, 25°C			
Poly(methyl methacrylate)	a	0.00680	0.720
	b	0.00710	0.720
	c	0.00680	0.830
	d	0.00939	0.680
Polystyrene	e	0.03900	0.580
	f	0.03050	0.600
	g	0.01950	0.635

^aKurata M, Tsunashima Y, Iwama M and Kamada K (1975) In: Brandrup J and Immergut E (eds), *Polymer Handbook*. New York: Wiley, p. IV-1.

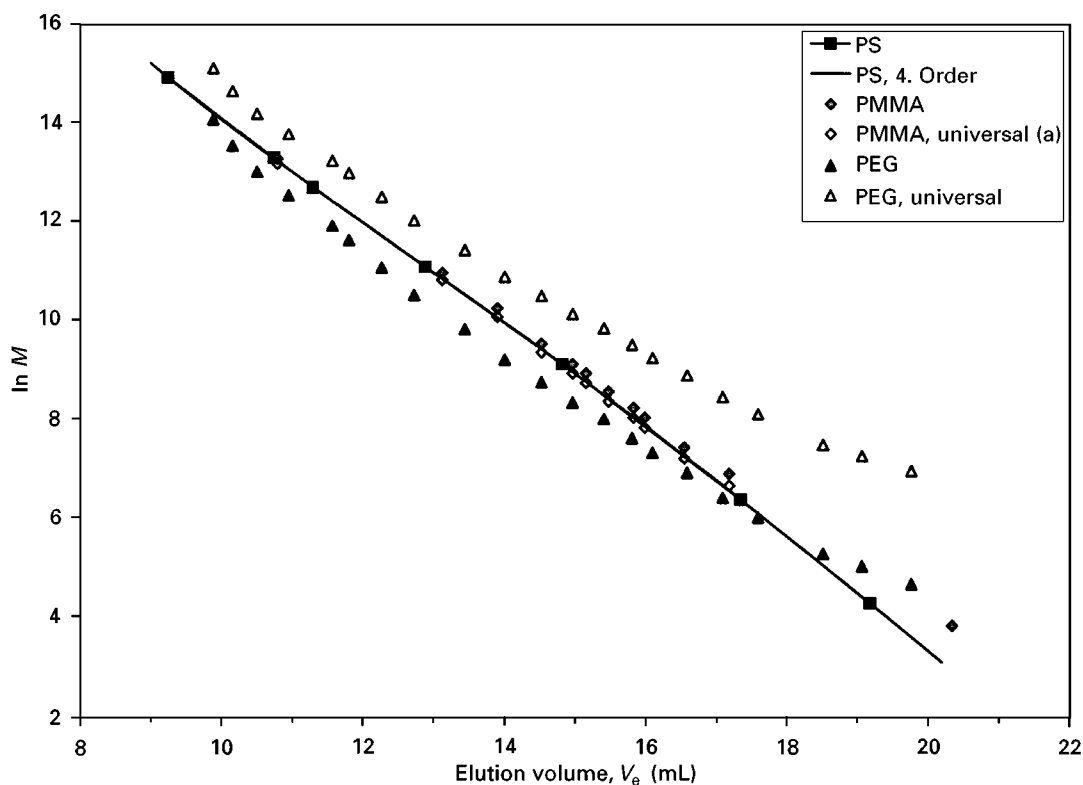


Figure 2 SEC calibration of a mixed bed column (PL Microgel M, 7.8×600 mm) in chloroform at 25°C .

The consequences can be dramatic, as is shown in Figures 1 and 2. In 2-butanone, the calibration functions obtained on a Phenogel MTM (Phenomenex) (mixed bed) column are quite different for polystyrene (PS) and poly(methyl methacrylate) (PMMA) (Figure 1). While the PS calibration is rather sigmoidal, a nearly linear calibration is found for PMMA. Using the MHS parameters from the literature (Table 2), both calibrations are closer, but there are still considerable differences.

In Figure 2, the calibrations of a PL Microgel MTM (Polymer Laboratories) (mixed bed) column are shown, which were obtained with PS, PMMA and PEG standards in chloroform. For PS and PMMA, very nice linear calibration functions are found, which almost coincide, while the attempt to establish a universal calibration for PEG with literature data makes the deviations even larger.

Quantification in SEC

After the first two transformations – time to volume and volume to molar mass – have been performed, there remains the third transformation – detector response to amount of polymer in a fraction – which can also be subject to errors, depending on the nature of the samples. In the following section, the particular

problems are referred to with respect to the type of polymer to be analysed.

Molar Mass Dependence of Response Factors

In chromatography of polymers, the most frequently used detectors are the UV and the RI detector. Recently, we have introduced the density detector, which is very useful in the analysis of non-UV absorbing polymers.

The UV-detector responds to UV-absorbing groups in the polymer, which may be the repeating unit, the end groups, or both.

RI and density detectors measure a property of the entire eluate, that means, they are sensitive to a specific property of the sample (the RI increment or the apparent specific volume, respectively). It is a well known fact, that specific properties are related to molar mass:

$$x_i = x_\infty + \frac{K}{M_i}$$

where x_i is the property of a polymer with the molecular weight M_i , x_∞ is the property of a polymer with infinite (or at least very high) molecular weight, and

K is a constant reflecting the influence of the end groups.

A similar relation holds for the response factors for RI and density detection:

$$f_i = f_\infty + \frac{K}{M_i}$$

In a plot of the response factor, f_i , versus the molecular weight, M_i of a polymer homologous series (with the same end groups) one will obtain a straight line with the intercept f_∞ (the response factor of a polymer with very high molecular weight, or the response factor of the repeating unit) and the slope K , which represents the influence of the end groups.

Once f_∞ and K have been determined, the response factors for each fraction eluting from the column can be calculated using this equation (with the molecular weight obtained from the SEC calibration).

One more problem concerns preferential solvation: when a polymer is dissolved in a mixed solvent, the composition of the latter within the coils can be different from outside because of different interactions of the polymer chain with the individual components of the solvent. When the sample is separated on the column from the zone where the solvent would elute, a system peak (vacancy peak) appears, which is due to the missing component of the mobile phase. Obviously, the missing amount of solvent in the system peak appears in the peak of the polymer, the area of which is now different from what it would be in absence of preferential solvation.

Although this effect has been known for a long time, it is often neglected by chromatographers because they consider their mobile phase to be a 'pure' solvent, which is, however, generally not the case: even HPLC-grade solvents are seldom more than 99.5% pure and, if so, they take up moisture from the air, form peroxides and so on. The content of a second component (e.g. water or a stabilizer) can thus be much higher than the concentration of the sample when it leaves the column and enters the detector.

If the polarity of the end groups of a polymer is considerably different from that of the repeating units, their contribution cannot be neglected, and preferential solvation depends on molar mass.

Copolymers and polymer blends In the analysis of copolymers, the use of multiple detectors is generally inevitable. If the response factors of the detectors for the components of the polymer are sufficiently different, the chemical composition along the MMD can be determined from the detector signals.

When multiple detection is used, one has to be aware of errors arising from peak spreading between the detectors and from inaccurate shift time (just as in combinations with molar mass detectors). Typically, a combination of UV and RI detection is used, but other detector combinations have also been described.

If the components of the copolymer have different UV-spectra, a diode array detector will be the instrument of choice. However, one has to keep in mind, that nonlinear detector responses may also occur with UV detection. In the case of non-UV absorbing polymers, a combination of RI and density detection yields the desired information on chemical composition. The ELSD is not equally suitable because of unclear response to copolymers.

The principle of dual detection is quite simple: when a mass m_i of a copolymer, which contains the weight fractions w_A and w_B ($w_B = 1 - w_A$) of the monomers A and B, is eluted in the slice i of the peak, it will cause a signal $x_{i,j}$ in the detectors, the magnitude of which depends on the corresponding response factors $f_{j,A}$ and $f_{j,B}$, where j denotes the individual detectors:

$$x_{i,j} = m_i(w_A f_{j,A} + w_B f_{j,B})$$

The weight fractions w_A and w_B of the monomers can be calculated using:

$$\frac{1}{w_A} = 1 - \frac{\left(\frac{x_1}{x_2} * f_{2,A} - f_{1,A}\right)}{\left(\frac{x_1}{x_2} * f_{2,B} - f_{1,B}\right)}$$

Once the weight fractions of the monomers are known, the correct mass of polymer in the slice can be calculated using:

$$m_i = \frac{x_i}{w_A * (f_{1,A} - f_{1,B}) + f_{1,B}}$$

and the molecular weight, M_C of the copolymer is obtained by interpolation between the calibration lines of the homopolymers:

$$M_C = M_B + w_A * (M_A - M_B)$$

wherein M_A and M_B are the molecular weights of the homopolymers, which would elute in this slice.

A typical example is given in **Figure 3**, which shows the MMD of a block copolymer of ethylene oxide (EO) and propylene oxide (PO), as obtained by SEC (in chloroform) with coupled density and

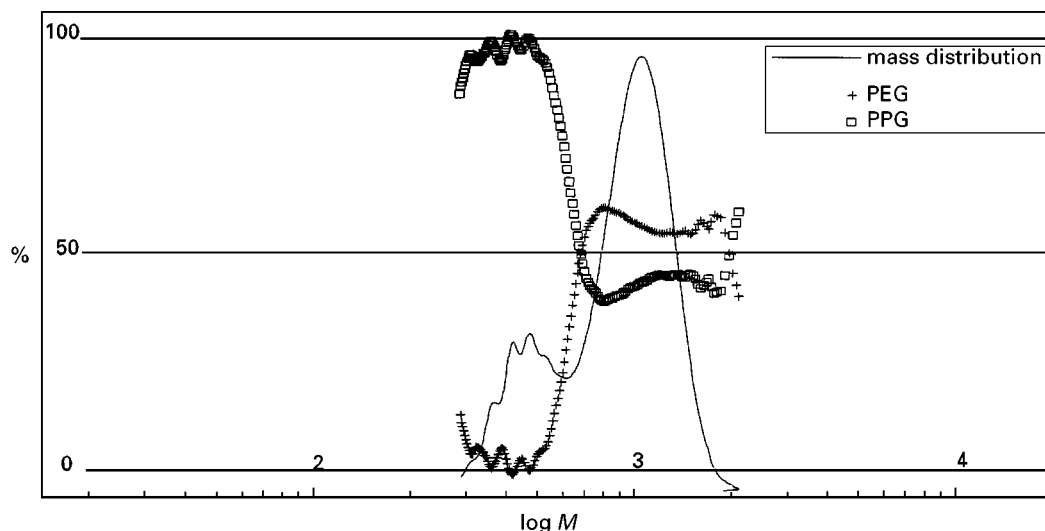


Figure 3 MMD and chemical composition of an EO-PO block copolymer (Figure 2), as determined by SEC in chloroform with density and RI detection. PEG + PPG.

RI detection. As can be clearly seen, this sample obviously contains polypropylene glycol as a by-product.

The interpolation between the calibration lines cannot be applied to mixtures of polymers (polymer blends): if the calibration lines of the homopolymers are different, different molecular weights of the homopolymers will elute at the same volume.

The universal calibration is not capable of eliminating the errors originating from the simultaneous elution of polymer fractions with the same hydrodynamic volume, but different composition and molar mass. Obviously it is feasible to use a combination of molar mass-sensitive detectors, such as a LALLS, MALLS and viscosity detector with two concentration detectors, from which the (average) composition for each fraction can be obtained, and thus the amount of polymer in the fraction. Nevertheless, discrimination of copolymers and polymer blends is impossible with one-dimensional chromatography.

Conclusion

The potential of SEC in polymer characterization is very great, especially when this technique is combined with other modes of liquid chromatography. Multiple detection is in most cases inevitable: combinations of different concentration detectors provide information on copolymer composition, and molar mass-sensitive detectors can eliminate errors with inadequate calibrations. For complex polymers (with distributions in molar mass, chemical composition,

functionality, etc.) one-dimensional techniques can, however, only provide part of the desired information. For these samples, multidimensional separations will be required. In most cases, one of the dimensions which will be SEC, while the other(s) could be gradient HPLC, or liquid chromatography at the critical point of adsorption (LCCC).

See also: II/Chromatography: Liquid: Derivatization; **Detectors:** Refractive Index Detectors; Evaporative Light Scattering Detectors in Liquid Chromatography. **Detectors:** Ultraviolet and Visible Detection; **III/Polymers:** Field Flow Fractionation.

Further Reading

- Pasch H and Trathnigg B (1997) *HPLC of Polymers*. Berlin: Springer.
- Provder T (ed.) (1987) *Detection and Data Analysis in Size Exclusion Chromatography*. Washington: American Chemical Society.
- Provder T (ed.) (1991) *Chromatography of Polymers - Characterization by SEC and FFF*. Washington: American Chemical Society.
- Trathnigg B and Jorde Ch (1987) *Journal of Chromatography* 385: 17-23.
- Trathnigg B and Leopold H (1980) *Makromolecular Chemistry, Rapid Communications* 1: 569.
- Vandermeeren P, Vanderdeelen J and Baert L (1992) Simulation of the Mass Response of the Evaporative Light-Scattering Detector. *Analytical Chemistry* 64: 1056-1062.
- Yau WW, Kirkland JJ and Bly DD (1979) *Modern Size Exclusion Chromatography*. New York: Wiley.

Universal Chromatography

D. Ishii, Kumamoto Institute of Technology,
Kumamoto, Japan

T. Takeuchi, Gifu University, Gifu,
Japan

Copyright © 2000 Academic Press

Chromatography is classified into gas chromatography (GC), supercritical fluid chromatography (SFC) and liquid chromatography (LC), depending on the physical properties of the mobile phase. Since the mobile phase in GC is a gas such as helium or nitrogen that does not have any interaction with analytes and carries them through the column, it is called a carrier gas. On the other hand, the mobile phase in LC dissolves analytes and will interact with them. Therefore, the mobile phase in LC significantly affects the selectivity of the separation. Although there are many options to improve the selectivity of the separation in LC, experience and knowledge are required for optimization. In SFC a high density gas is employed as the mobile phase, where the temperature and pressure in the column are higher than the critical values of the mobile phase employed. The mobile phase in SFC has intermediate properties between those in GC and in LC. **Table 1** compares physical properties of the mobile phase in three chromatographic modes. The density, viscosity and diffusion coefficients determine the solubility of analytes, permeability of the column and the speed of analysis, respectively.

The effect of temperature on retention behaviour in SFC on a thermodynamic basis has been discussed elsewhere, as well as thermodynamic retention behaviour in open tubular capillary SFC. It was found that LC-like or GC-like retention mechanisms were involved in the supercritical temperature region, depending on the column temperature and the inlet pressure.

Generally, separations in GC are performed using completely different systems from those in LC. The separation system in SFC is a hybrid between GC and LC. However, it should be noted that the

temperature and pressure can control the physical properties of the mobile phase. If these two parameters are controlled, separations can be obtained in any three chromatographic modes using a single chromatographic system. Both plunger and syringe pumps can be used for this purpose.

Instrumentation

When an LC-like detector such as a UV detector is used, a two-pump system is favoured. The two pumps are operated in the pressure control mode, and the inlet and the outlet pressures are controlled independently, so that the pressure drop across the column can be controlled.

When a GC-like detector such as a flame ionization detector (FID) is used, the two-pump system is not applicable and a single-pump system is used. A low dead-volume restrictor is generally employed in this case to maintain an appropriate pressure and to avoid additional dispersion of analytes.

The oven should be capable of negative as well as positive temperature programming. Negative temperature programming is useful in SFC, as shown below.

Open tubular capillary columns with various immobilized stationary phases are commercially available. The smallest diameter commercially available is around 50 μm . On the other hand, packing materials with 3–50 μm particle diameters for LC can be used for packed capillary columns, and fused silica tubing or glass-lined stainless-steel tubing are available. Conventional packed columns (1–5 mm i.d.) are still used most often in SFC, but they do not fit into the compromise that constitutes universal chromatography.

Temperature Effect

Figure 1 shows the effect of column temperature on retention behaviour using a packed column and carbon dioxide or methanol as the mobile phase. The relationships between the logarithm of the retention factor of aromatic hydrocarbons, $\log k$, and the recip-

Table 1 Comparison of physical properties of the mobile phase in three chromatographic modes

Chromatography	Density (g cm^{-3})	Viscosity ($\text{g cm}^{-1} \text{s}^{-1}$)	Diffusion coefficient ($\text{cm}^2 \text{s}^{-1}$)
Gas chromatography	10^{-3}	$(0.5\text{--}3.5) \times 10^{-4}$	0.01–1.0
Supercritical fluid chromatography	0.2–0.9	$(0.2\text{--}1.0) \times 10^{-3}$	$(0.1\text{--}3.3) \times 10^{-4}$
Liquid chromatography	0.8–1.0	$(0.3\text{--}2.4) \times 10^{-2}$	$(0.5\text{--}2.0) \times 10^{-5}$

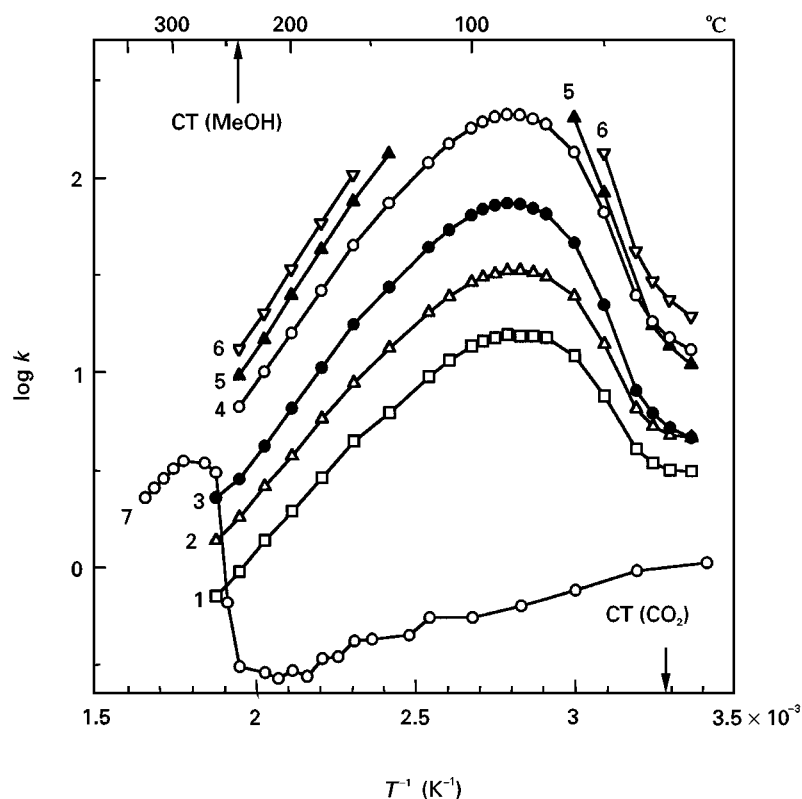


Figure 1 Relationships between the logarithm of the retention factor of aromatic hydrocarbons ($\log k$) and the reciprocal of absolute column temperature (T^{-1}). Columns: Develosil ODS-5 (5 μm ODS), 150 \times 0.5 mm i.d. (1–6) or 145 \times 0.3 mm i.d. (7). Mobile phase: carbon dioxide (1–6) or methanol (7). Inlet pressure: 12 MPa (1–6) or 9.0 MPa (7). CT, Critical temperature. Samples: 1 = biphenyl; 2 = fluorene; 3 = *o*-terphenyl; 4 = pyrene; 5 = 9-phenylanthracene; 6 = triphenylene; 7 = pyrene. Detector: UV.

reciprocal of absolute column temperature, $1/T$, are shown in the figure with an inlet pressure of 12 MPa for carbon dioxide and 9.0 MPa for methanol. It should be noted that the pressure in the column is higher than each critical pressure, e.g. 7.38 MPa for carbon dioxide and 7.95 MPa for methanol. The critical temperatures of carbon dioxide and methanol are denoted as CT in the figure. At each higher critical temperature region, the retention factor increases with decreasing column temperature, while at each lower critical temperature region it decreases with decreasing column temperature. When the mobile phase is liquid, i.e. at a temperature lower than the CT, the retention factor increases with decreasing column temperature, as shown in the case of the methanol mobile phase.

It should be noted that the density of the mobile phase decreases with increasing temperature. The density of carbon dioxide is shown in Figure 2.

It is possible to distinguish a region in which the retention factor decreases with decreasing column temperature (SFC region) from one in which it increases with decreasing column temperature (high pressure GC region). The former region appears at lower supercritical temperatures, in which solvation

of the analyte by the mobile phase is dominant, while the latter region appears at higher supercritical temperatures, in which the contribution of volatility is

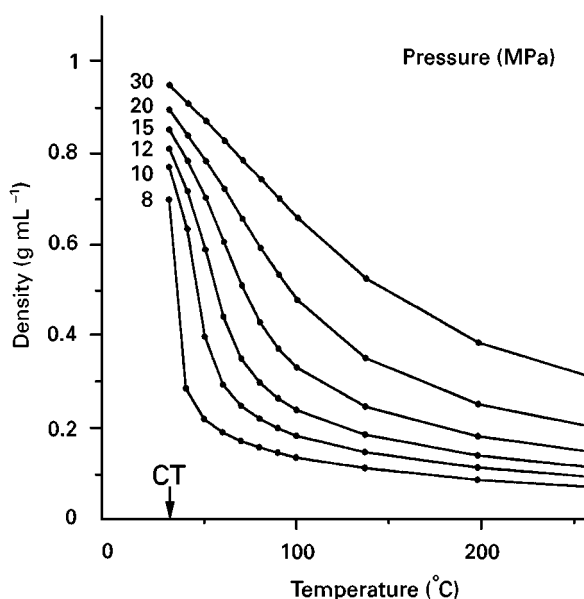


Figure 2 Density of carbon dioxide.

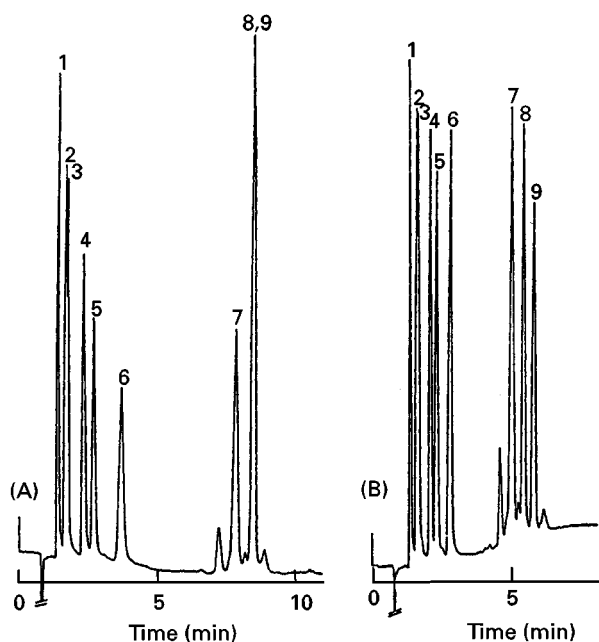


Figure 3 (A) Negative and (B) positive temperature programming of dialkyl phthalates on an SB-octyl-50 column. Column: SB-octyl-50 (5% *n*-octylmethylpolysiloxane), 10 m \times 50 μ m i.d. Mobile phase: carbon dioxide. Inlet pressure: 12 MPa. Samples: 1 = dimethyl; 2 = diethyl; 3 = diisobutyl; 4 = di-*n*-propyl; 5 = diisobutyl; 6 = di-*n*-butyl; 7 = diheptyl; 8 = di-2-ethylhexyl; 9 = dinonyl phthalate. Initial temperature: 130°C. Temperature programming: (A) $-10^{\circ}\text{C min}^{-1}$ for 4 min, and $-5^{\circ}\text{C min}^{-1}$ for the rest of the analysis; (B) $+10^{\circ}\text{C min}^{-1}$ for 2 min, $+20^{\circ}\text{C min}^{-1}$ for the next 4.5 min and kept at 240°C for the rest of the analysis. Wavelength of UV detection: 225 nm. (Reproduced with permission from Takeuchi *et al.* (1988). Temperature programming elution in capillary supercritical fluid chromatography. *Chromatographia* 25: 127.)

dominant. In the intermediate temperature region, both contributions are involved. In addition, non-volatile analytes cannot be eluted in the high pressure GC region, but they are eluted in the SFC and LC regions. It is clear that both SFC and high pressure GC separations can be demonstrated by changing the column temperature. Negative temperature programming is useful for the former, while positive temperature programming is useful for the latter mode.

Figure 3 demonstrates the separation of dialkyl phthalates using negative and positive temperature programming using an SB-octyl-50 open tubular capillary column and a UV detector. Both temperature programmes are started from the same temperature, i.e. 130°C. The programming rate is changed during the separation so that optimum resolution can be achieved in a reasonable time. The pressure is kept constant at 12 MPa during the separation. In Figure 3(A), SFC-like separation is demonstrated, while GC-like separation is demonstrated in Figure 3(B).

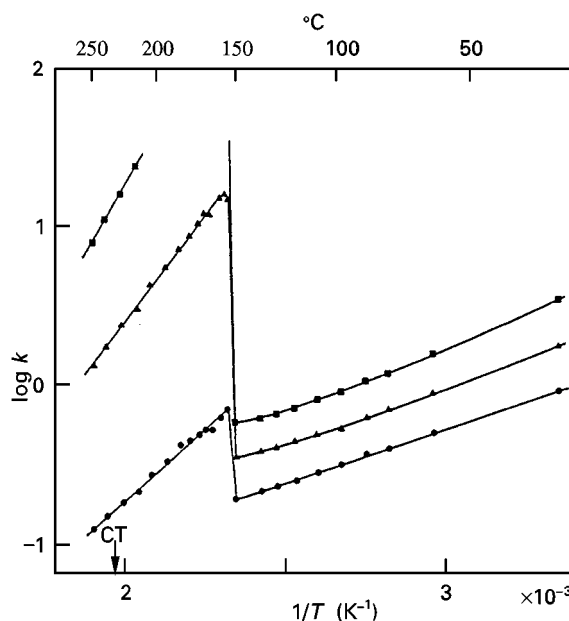


Figure 4 Log k versus $1/T$ for hexane mobile phase. Column: Develosil-60-10 (10 μ m silica gel), 300 \times 0.5 mm i.d. Mobile phase: hexane. Inlet pressure: 0.49 MPa. Outlet pressure: ambient pressure. CT, Critical temperature. Samples: \bullet = benzene; \blacktriangle = naphthalene; \blacksquare = anthracene. Wavelength of UV detection: 254 nm. (Reproduced with permission from Takeuchi *et al.* (1988). Micropacked column GC with vapor of organic substance as the mobile phase. *Chromatographia* 25: 994.)

GC Using an LC System

In GC permanent gases are usually employed as the carrier gas. The vapour of an organic substance can also be used as the mobile phase for GC when the pressure in the column is lower than the vapour pressure at the operating temperature. In contrast, when the pressure in the column is higher than the vapour pressure, analytes are subjected to LC-mode separation. By controlling the column temperature and pressure, it is possible to demonstrate both GC and LC using a single LC system. It is convenient to use a micro-LC system because the heat capacity of micropacked columns of 0.2–0.5 mm i.d. is small.

Figure 4 shows the relationships between the logarithm of the retention factor and the reciprocal of the absolute column temperature when hexane and silica gel are used as the mobile and stationary phases. In Figure 4 the inlet pressure is 0.49 MPa, while the outlet pressure is atmospheric. The mobile phase is liquid when passing through the flow cell of the UV detector. The critical temperature and pressure of hexane are 234°C and 3.0 MPa, respectively. The critical temperature of hexane is denoted as CT in the figure. It should be noted that the pressure in the column is lower than the critical pressure. At higher

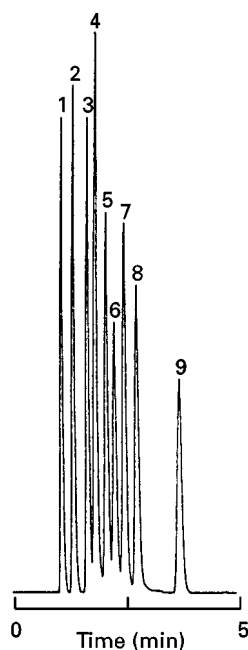


Figure 5 GC separation of alkylbenzenes at an inlet pressure of 0.49 MPa using hexane as a carrier gas. Column: Develosil-60-10 (10 μm silica gel), 300 \times 0.5 mm i.d. Mobile phase: hexane. Inlet pressure: 0.49 MPa. Outlet pressure: ambient pressure. Column temperature: 205°C. Peaks: 1 = benzene; 2 = toluene; 3 = naphthalene; 4 = *o*-xylene; 5 = *n*-propylbenzene; 6 = mesitylene; 7 = sec.-butylbenzene; 8 = *n*-butylbenzene; 9 = *n*-amylbenzene. Wavelength of UV detection: 254 nm. (Reproduced with permission from Takeuchi *et al.* (1988). Micropacked column GC with vapor of organic substance as the mobile phase. *Chromatographia* 25: 995.)

temperatures linear relationships between $\log k$ and $1/T$ are observed, where the GC separation mode is involved. Since the applied pressure is lower than the critical pressure, the hexane vaporizes at a temperature lower than the critical temperature. When the outlet pressure is higher than the vapour pressure at the operated temperature, the hexane is liquid in the column and analytes are separated in the normal-phase LC mode; almost linear relationships between two parameters are observed. At some intermediate temperature the retention factor drastically changes with column temperature, where the state of the hexane in the column changes from liquid to gas, and both liquid and gaseous hexane exist at the boundary region in the column.

Figure 5 demonstrates GC separation of alkylbenzenes using hexane vapour as the mobile phase. The analytes are monitored by a UV detector at 254 nm. The mobile phase is liquefied while passing through a 60 cm \times 70 μm i.d. capillary tube connecting the separation column and the flow cell of the detector. The capillary tubing is kept at ambient temperature.

GC Using LC Columns

Micropacked columns for LC can be applied to GC separation of hydrocarbons. When a glass-lined stainless-steel tube of 30 cm \times 0.3 mm i.d., packed with 5 μm alkyl-modified silica, is employed as the separation column, a microvalve injector for LC should be used because of the large pressure drop across the column.

Figure 6 demonstrates the separation of C_6 – C_{20} straight-chain hydrocarbons using carbon dioxide carrier gas, an octadecylsilica (ODS) column and an FID. The inlet pressure of carbon dioxide as the carrier gas is kept at 6.2 MPa. A volume of 0.02 μL of the sample dissolved in pentane is injected. The concentration is *c.* 2% (v/v) each, corresponding to *c.* 0.3 μg each of the injected amount. The column temperature is 35°C for the initial 5 min, programmed to 230°C at a rate of 5°C min^{-1} , and then held at 230°C. As far as alkyl-modified silica packings are employed, the SFC mode will be favoured for hydrocarbons with a carbon number larger than 15 because an increase in the background signal of the FID is observed at temperatures higher than 160°C.

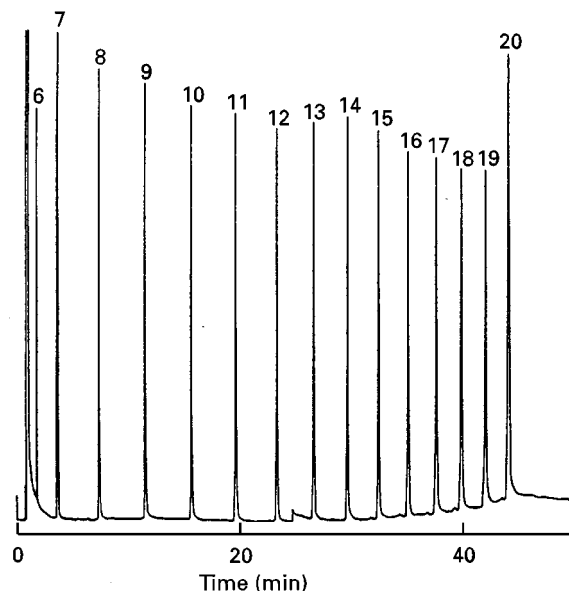


Figure 6 Separation of an artificial mixture of straight-chain hydrocarbons. Column: Capcell Pak C18 (5 μm ODS), 300 \times 0.3 mm i.d. Mobile phase: carbon dioxide. Inlet pressure: 6.2 MPa. Column temperature: 35°C for the initial 5 min, then programmed at 5°C min^{-1} , held at 230°C. Peaks: straight-chain hydrocarbons (the numbers refer to the carbon numbers of the corresponding straight-chain hydrocarbons), *c.* 2% (v/v) each dissolved in pentane is injected. Detector: FID. (Reproduced with permission from Takeuchi *et al.* (1989). New approach to the GC separation of hydrocarbons by using LC-like microcolumns. *Chromatographia* 27: 183.)

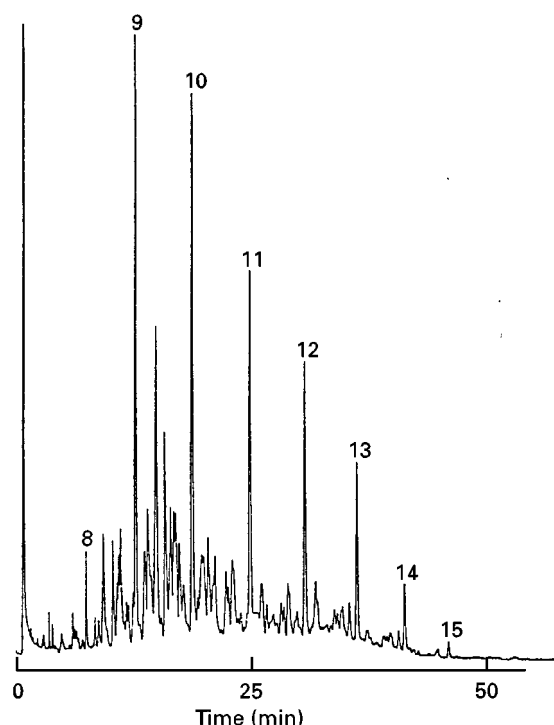


Figure 7 Separation of components of a kerosene. Operating conditions as in Figure 6, except for the sample and the temperature-programming rate. Column temperature: 35°C for the initial 5 min, then programmed at 3°C min⁻¹. Sample: kerosene diluted twice with pentane. (Reproduced with permission from Takeuchi *et al.* (1989). New approach to the GC separation of hydrocarbons by using LC-like microcolumns. *Chromatographia* 27: 184.)

Figure 7 demonstrates the separation of the components of a kerosene. The temperature-programming rate of the column is reduced to 3°C min⁻¹. The numbers in the figure correspond to the carbon numbers of straight-chain hydrocarbons. The results offer encouragement for the use of a micropacked column as a common separation column for GC, SFC and LC.

SFC Using LC Columns

Figure 8 demonstrates the pressure-programming separation of methylphenylsiloxane oligomers using diethyl ether as the supercritical fluid. The critical temperature, pressure and density are 194°C, 3.6 MPa and 0.264 g cm⁻³, respectively. The initial inlet pressure is 4.4 MPa and the pressure is programmed at 0.1 MPa min⁻¹ for 10 min, 0.05 MPa min⁻¹ for the next 10 min and 0.025 MPa min⁻¹ for the rest of the analysis. The pressure drop across the column is maintained at 0.49 MPa using a two-pump system. The temperature is kept constant at 225°C and the analytes are detected by UV at 215 nm.

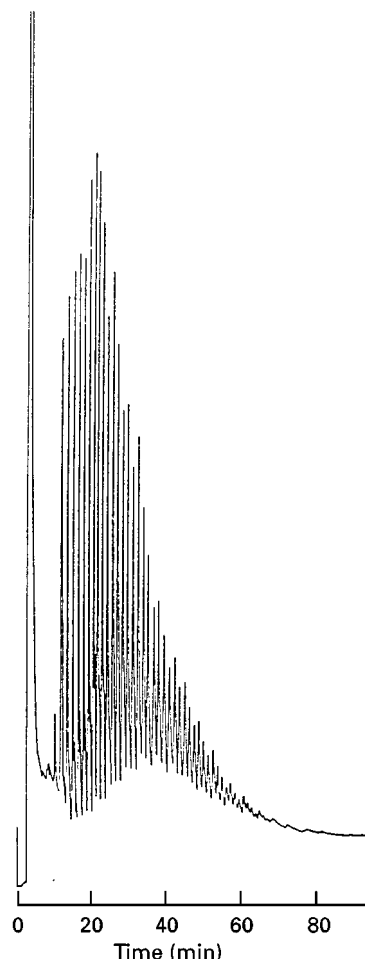


Figure 8 Pressure-programming SFC separation methylphenylsiloxane oligomers using diethyl ether as the mobile phase. Column: Develosil ODS-5 (5 µm ODS), 300 × 0.5 mm i.d. Mobile phase: diethyl ether. Initial inlet pressure: 4.4 MPa. Pressure programmed at 0.1 MPa min⁻¹ for 10 min, 0.05 MPa min⁻¹ for the next 10 min and 0.025 MPa min⁻¹ for the rest of the analysis. Pressure drop: 0.49 MPa. Temperature: 225°C. Sample: OV-17 dissolved in tetrahydrofuran. Detector: UV (215 nm). (Reproduced with permission from Takeuchi *et al.* (1987). Retention behaviour in liquid and supercritical fluid chromatography using methanol or diethyl as mobile phase. *Chromatographia* 23: 932.)

Ether is toxic and flammable. Even a small leakage of the mobile phase should be avoided for safety reasons.

Multi-mode Separations in a Single Chromatographic Run

Changing the column temperature and the pressure by using a single system allows different modes of separation to be carried out. Capillary columns, packed or open tubular, facilitate the demonstration

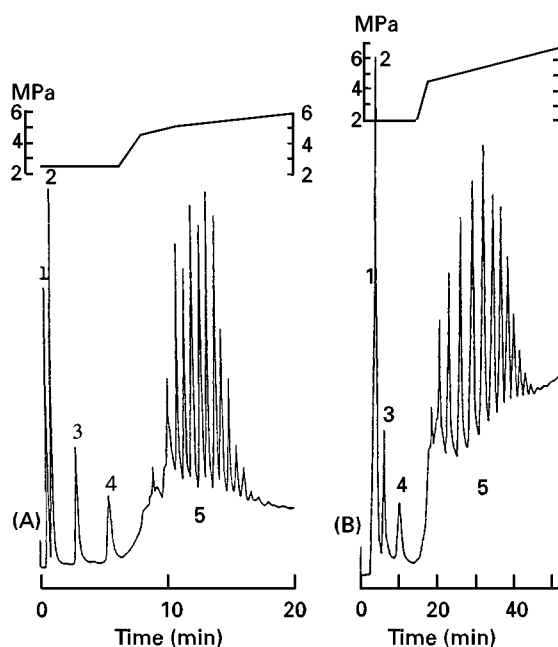


Figure 9 Multi-mode separation of aromatic hydrocarbons and styrene oligomers. Columns: (A) Develosil 100-5 (5 μm silica gel), 150 \times 0.5 mm i.d.; (B) 13 m \times 53 μm i.d., treated with 1 mol L⁻¹ sodium hydroxide at 55°C for 2 days. Mobile phase: diethyl ether. Initial inlet pressure: programmed as shown in the figure. Pressure drop: 0.49 MPa. Temperature: 220°C. Samples: 1 = benzene; 2 = naphthalene; 3 = anthracene; 4 = pyrene; 5 = polystyrene A-1000. Wavelength of UV detection: 220 nm. (Reproduced with permission from Ishii *et al.* (1988). Unified capillary chromatography. *Journal of High Resolution Chromatography & Chromatographic Communications* 11: 801.)

of these different modes of separation with a single chromatographic system. This is because the capillary column can achieve excellent column efficiencies. While universal chromatography allows a number of combinations to be used, it does offer more restrictions, e.g. in terms of permitted column diameters and flow rates, compared with three separate instruments.

Figure 9(A) demonstrates the separation of a prepared mixture of aromatic hydrocarbons and styrene oligomers on a silica gel packed column using the vapour of diethyl ether as the mobile phase. The analytes are isothermally separated at supercritical temperature, and the pressure is programmed so that the aromatic hydrocarbons can be separated in the GC mode prior to the SFC separation of the styrene oligomers. The pressure drop across the separation column is kept at 0.49 MPa by using a two-pump system. The inlet and outlet pressures are controlled by a microcomputer. The hydrocarbons are separated at subcritical pressure; the inlet and outlet pressures are kept at 2.45 and 1.96 MPa, respectively. The styrene oligomers are then separated by pressure-

programmed elution. The profile of the pressure programme is shown in the figure. This type of separation is of practical importance when the sample contains constituents with a wide range of volatility.

Figure 9(B) demonstrates the separation of the same mixture as in Figure 9(A) using an open tubular glass capillary column with 53 μm i.d. \times 13 m. The active surface is produced by treating soda-lime glass capillary tubing with 1 mol L⁻¹ sodium hydroxide aqueous solution at 55°C for 2 days. Nearly the same selectivity is observed between the open tubular and packed silica gel column.

Conclusion

Universal chromatography can perform the analysis of a variety of samples using a single chromatograph in which all separation modes can be selected. Universal chromatography also allows different modes of separation in series in a single run using a single chromatographic system. It allows the possibility of analysing a variety of samples with a wide range of volatilities in a single run by selecting multiple separation modes. For the more widespread use of universal chromatography appropriate detectors and stationary phases need to be developed.

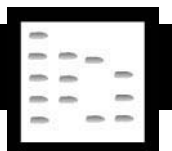
See also: I/Chromatography. II/Chromatography: Gas: Theory of Gas Chromatography. Chromatography: Liquid: Theory of Liquid Chromatography. Chromatography: Supercritical Fluid: Theory of Supercritical Fluid Chromatography.

Further Reading

- Chester TL and Innis DP (1985) Retention in capillary supercritical fluid chromatography. In: Sandra P and Bertsch W (eds) *Proceedings of the Sixth International Symposium on Capillary Chromatography*. Heidelberg: Huethig, p. 944.
- Ishii D and Takeuchi T (1989) Unified fluid chromatography. *Journal of Chromatographic Science* 27: 71.
- Ishii D, Niwa T, Ohta K and Takeuchi T (1988) Unified capillary chromatography. *Journal of High Resolution Chromatography & Chromatographic Communications* 11: 800.
- Pentoney SC Jr, Giorgetti A and Griffiths PR (1987) Combined gas and supercritical fluid chromatography for high-resolution separation of volatile and nonvolatile compounds. *Journal of Chromatographic Science* 25: 93.
- Takeuchi T, Hashimoto Y and Ishii D (1987) Temperature effect in packed microcolumn chromatography using a carbon dioxide mobile phase. *Journal of Chromatography* 402: 328.
- Takeuchi T, Hamanaka T and Ishii D (1988) Micropacked column GC with vapor of organic substance as the mobile phase. *Chromatographia* 25: 993.

- Takeuchi T, Ohta K and Ishii D (1988) Temperature programming elution in capillary supercritical fluid chromatography. *Chromatographia* 25: 125.
- Takeuchi T, Ohta K and Ishii D (1989) New approach to the GC separation of hydrocarbons by using LC-like microcolumns. *Chromatographia* 27: 182.
- Tong D, Bartle KD and Clifford AA (1995) Principles and applications of unified chromatography. *Journal of Chromatography A* 703: 17.
- Yonker CR, Wright BW, Petersen RC and Smith RD (1985) Temperature dependence of retention in supercritical fluid chromatography. *Journal of Physical Chemistry* 89: 5526.

CHROMATOGRAPHY: GAS



Column Technology

W. Jennings, J&W Scientific, Inc., Folsom, CA, USA

Copyright © 2000 Academic Press

Introduction

It is the role of the column to achieve separation of the components of injected mixtures. In many cases, it is also possible to accomplish *extra-column* 'separation', i.e. 'separation' by distinguishing between merged or co-eluting solutes. Selective detectors, such as the flame photometric detector, are useful in this regard, but our focus here will be directed toward separation as accomplished in the column.

The resolution equation is usually presented in one of two popular forms:

$$N_{\text{req}} = 16R_s^2[(k+1)/k]^2[\alpha/(\alpha-1)]^2 \quad [1]$$

or:

$$R_s = 1/4\sqrt{N[k/(k+1)](\alpha-1)/\alpha} \quad [2]$$

Equation [1] is used to estimate the number of theoretical plates that will be required (N_{req}) to separate any two solutes to some specified degree of resolution (R_s), as functions of the retention factor (k) of the second of those two solutes, and of their separation factor (α). These relationships will be utilized later.

Equation [2] emphasizes that resolution (i.e. the degree to which solutes are separated) is affected by only three parameters: (1) the number of theoretical plates (N); (2) solute retention factors (k); and (3) solute separation factors (α).

The number of theoretical plates is a function of the 'sharpness' of a peak, relative to the time that the solute spends in the column. The measurement is affected by the length of the solute band introduced into the column (it is assumed that this is infinitesimally small, which is never the case), the length (L) and radius (r_c) of the column, the retention factor (k) of the solute, and the average linear velocity (\bar{u}) of the carrier gas. It can also be affected by the thickness of the stationary phase film (d_f), and by solute diffusivity in the stationary phase (D_s). Small values of k yield disproportionately large values of N . This anomaly essentially disappears with values of $k \geq 5$.

The parameters affecting the solute retention factor (k) can be deduced from the inviolable relationship that must always exist between k , the distribution constant (K_c), and the column phase ratio (β):

$$K_c = \beta k \quad [3]$$

From this, it is evident that $k = K_c \times 1/\beta$, or (using the definitions in the Glossary):

$$k = c_s/c_M \times V_s/V_M \quad [4]$$

For a given solute, k varies directly with solubility of that solute in the stationary phase (e.g. the k value of pentane would, under similar conditions, be higher in a polydimethylsiloxane stationary phase than in a polyethylene glycol stationary phase). In a given stationary phase, k varies indirectly with temperature: as the temperature increases, c_s decreases and c_M increases, and k decreases in a manner that is essentially exponential.

Finally (as evidenced in eqns [3] and [4]), k varies inversely with the column phase ratio, β (or directly with $1/\beta$). In other words, solute retention factors (k) increase as the volume of column occupied by stationary phase (V_s) increases and/or the volume occupied by mobile phase (V_M) decreases. In packed columns, β is usually controlled by the stationary phase 'loading'; in the open-tubular column, β is controlled primarily through d_f , and to a smaller extent, through r_c . There are some practical limitations: where $d_f < 0.1 \mu\text{m}$, columns can exhibit excessive activity, as evidenced by 'tailing' (reversible and irreversible adsorption) of 'active' solutes. Where $d_f > 1.0 \mu\text{m}$ (or even less if $D_M < 10^{-7} \text{cm}^2 \text{s}^{-1}$), the mass transport term of the van Deemter equation (C_M) becomes limiting, and column efficiency (as reflected by N) decreases. Solute retention factors interrelate with determinations of N . Unless the gas velocity is so high that solutes can no longer undergo equilibrium partitioning (this would require extremely high velocities), k is independent of \bar{u} .

Comparisons of Packed and Open-Tubular Columns

One thousand plates per foot of column length, or approximately 3000-plates per metre, represents the best that can be expected from a packed column; although packed columns rarely achieve this value, it is often exceeded in the open-tubular system. The

length of the packed column is limited in practice to about 5 m, because the packing offers a much greater resistance to gas flow than does the open tube. As a result, the packed column can deliver a maximum of about 15 000 theoretical plates, which pales in comparison to the 150 000 to 500 000 theoretical plates that can be attained in the modern open-tubular columns. Some work has been reported using longer packed columns operated under extreme pressures, but these applications have not proven practical in a working environment.

In the open-tubular column, the theoretical maximum achievable efficiency can be estimated from the fact that:

$$H = L/N \quad [5]$$

and:

$$H_{\text{theor min}} = r_c \{[(11k^2) + 6k + 1]\}^{1/2} / [3(1 + k)^2] \quad [6]$$

It was mentioned in earlier discussions of k that small values of k exhibit disproportionately large values of N (or small values of H). If we use eqn [6] to calculate $H_{\text{theor min}}$ and $N_{\text{theor max}}$ for a 0.25 mm open-tubular column, we obtain the values shown in Table 1. A graph of these data (Figure 1) stresses the very large values of N that are obtained for small values of k . Note that this effect becomes negligible as $k \geq 5.0$.

For many years, packed columns offered a distinct advantage to the analyst concerned with the separation of highly volatile solutes, because the phase ratio (β) of the packed column is rarely greater than about 30, while the phase ratios of early wall-coated open-tubular columns were usually about 300. From eqn [3], it is evident that solute retention factors (k) will be some 10 times greater (300/30) on packed columns than on these early open-tubular columns, with all other conditions constant.

Table 1 Maximum theoretical values of the numbers of theoretical plates per metre of column length ($N \text{ m}^{-1}$) as a function of the retention factor (k) of the test solute. Values are calculated for a 0.25 mm column, and assume $D_M = 0.6 \text{ cm}^2 \text{ s}^{-1}$ and $D_S = 10^{-7} \text{ cm}^2 \text{ s}^{-1}$

k	$N (\text{m}^{-1})$, theoretical maximum
0.01	13 582
0.1	11 661
1	6 531
2.5	5 270
5	4 753
7	4 505
10	4 362

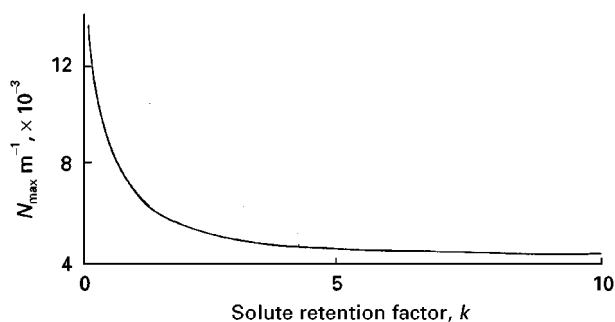


Figure 1 Graph of the data shown in Table 1, maximum theoretical values of the numbers of theoretical plates per metre of column length ($N \text{ m}^{-1}$) as a function of the retention factor (k) of the test solute. Values are calculated for a 0.25 mm column, and assume $D_M = 0.6 \text{ cm}^2 \text{ s}^{-1}$, and $D_S = 10^{-7} \text{ cm}^2 \text{ s}^{-1}$.

The number of theoretical plates that will be required to separate any two solutes is the product of three multipliers in eqn [1]: (1) the degree of resolution required [$16R_s^2$] (for baseline separation, $R_s \cong 1.5$, and this one multiplication factor becomes 36); a squared ratio of the separation factors $[\alpha/(\alpha - 1)]^2$, and a squared ratio of the retention factors $[(k + 1)/k]^2$. A highly volatile solute might exhibit $k = 0.01$ on one of these earlier open-tubular columns, and the $[(k + 1)/k]^2$ multiplier would therefore be $[101/1]^2 \cong 10\,000$. On the packed column, the phase ratio is lower, and the k of this solute (all other conditions constant) would increase by the factor $300/30 \times 0.01 \cong 0.1$. This results in the $[(k + 1)/k]^2$ multiplier becoming 121 instead of 10 000, and the number of theoretical plates required for the separation of this low- k solute has been decreased by two orders of magnitude.

Because of these relationships, the packed column user was more successful in attaining the separation of some highly volatile (low- k) mixtures that resisted separation on the wall-coated open-tubular columns of those times. The subsequent development of cross-linked and surface-bonded stationary phases permitted the manufacture of open-tubular columns with much thicker films of stationary phase – 3, 5 and 8 μm . In a 0.25 mm column, these give phase ratios of 20.8, 12.5 and 7.8, respectively, and this particular advantage of the packed column disappears. Alternatively, retention factors are usually significantly higher on porous-layer open-tubular (PLOT) columns that utilize the more retentive mode of gas–solid adsorption chromatography rather than gas–liquid partition chromatography. Even fixed gases such as argon, nitrogen, oxygen can be resolved on such columns.

Thick-film open-tubular columns suffer some distinct disadvantages, however. The exploration of this is facilitated by an examination of the van Deemter

equation. In its packed column form, this can be expressed as

$$H = A + B/\bar{u} + C\bar{u} \quad [7]$$

where A is the eddy diffusion or packing factor term, B is the longitudinal diffusion term and C is the resistance to mass transfer term. Because H is a function of $1/N$, the smaller the sum of these terms, the smaller H , and the more efficient the system. (Efficiency equations really represent the efficiency not of the column, but of the total system. A number of extra-column factors – the injection process, extra volume in the injector and detector, too low a split ratio or make-up gas flow, lag time in signal acquisition – detract from system efficiency, but efficiency equations attribute all of this to the column.) The open-tubular column has no packing, and the A term can be discarded to yield the Golay equation: $H = B/\bar{u} + C\bar{u}$. Some major differences between packed and open-tubular columns become more apparent if the C term is expanded to distinguish mass transfer from stationary phase to mobile phase (C_s) from mass transfer from mobile phase to stationary phase (C_M):

$$H = B/\bar{u} + \bar{u}[C_M + C_s] \quad [8]$$

In packed columns, most of the interior volume of the column is occupied by the particles of support material; each particle is covered with a relatively thick film of stationary phase, and there is a minuscule gas volume in the interstitial space between the particles. Hence the volume of stationary phase is large, the volume of mobile (gas) phase is small, and the packed column typically has a smaller phase ratio or β . In the packed column, the magnitude of the C term is largely a function of mass transfer from stationary to mobile phase (C_s). A solute molecule dissolved in stationary phase takes some time before it re-enters the mobile phase, where it must proceed only a minuscule distance through the carrier gas (C_M) before it again enters stationary phase. C_s is the *limiting factor* in the packed column, but C_M is trivial: hence, hydrogen, helium, nitrogen, argon-methane or carbon dioxide yield essentially the same efficiencies when used as the mobile phase in packed columns.

In the open-tubular column, a much thinner film of stationary phase is on the wall of a tube, which while usually of capillary dimension, requires solute molecules to traverse a much longer flow path through the mobile phase. Thus the transverse distance across the open-tubular column is significantly greater than the interparticle distance encountered in packed columns. As a consequence, column efficiency (and the

optimum average linear velocity of the carrier gas) varies directly with the diffusivity of the mobile phase. In the open-tubular column, C_M is the limiting factor and C_s is trivial – until we come to the thick-film open-tubular column. In this case, *both* C_s and C_M are significant; the major advantage of the open tubular column has been sacrificed, and column efficiency suffers.

An analogous limitation is encountered with low diffusivity stationary phases. In the polydimethylsiloxane stationary phase, D_s for a C_{12} compound at 150°C approximates to $1 \times 10^{-7} \text{ cm}^2 \text{ s}^{-1}$. At this value, columns yield about the same efficiencies when the stationary phase film (d_f) is varied from 0.1 to $0.4 \mu\text{m}$; at $d_f > 0.4 \mu\text{m}$, the efficiencies of columns coated with this stationary phase begin to decrease. Polysiloxanes are relatively permeable, and substitutions that increase the carbon/oxygen ratio (e.g. phenyl) have an adverse effect on that permeability. This lowers the value of D_s , and column efficiency – in terms of plates per metre – decreases, unless d_f is also decreased. As an example, smaller values of d_f are desirable on columns coated with polymethylsiloxanes containing phenyl, cyanopropyl and/or polyethylene glycol-type substituents, where a significant increase in efficiency is exhibited by $0.15 \mu\text{m}$ film columns as compared to $0.25 \mu\text{m}$ films. As the rate of diffusion through the stationary phase decreases (this is a function of D_s), the distance the solute must travel through that stationary phase (a function of d_f) becomes increasingly important.

Many investigators have contributed to our progress in stationary phase and column developments. While a thorough discussion of the interrelationships and significance of these contributions is beyond the scope of this article, the Further Reading section include some of the more salient efforts in column developments.

The Stationary Phase

Many of the disparate materials employed as ‘liquid phases’ on the earliest packed columns soon proved unsatisfactory for open-tubular columns. It was eventually realized that higher temperature stabilities in open-tubular columns required highly viscous phases whose viscosity endured at the operating temperatures. With this realization, the polysiloxanes attracted interest, because they could be cross-linked to produce a semisolid gum-like phase; the term ‘stationary phase’ soon replaced ‘liquid phase’ in common usage. Columns coated with these materials exhibited higher temperature tolerances and longer lifetimes. This is another area in which a multitude of individual investigators have contributed to progress.

As discussed earlier, packed columns are typically limited to lengths that can generate 10 000 to 15 000 theoretical plates because of their higher pressure drops. With this restriction on N , the separation factor, α , becomes more critical to the packed column (eqn [2]), and α is best controlled through the choice of stationary phase. While α values do respond to changes in temperature, the direction of any given response can be predicted only for solutes whose functionalities are similar. For example, in a series of methyl ketones or a series of paraffin hydrocarbons, α values vary inversely with temperature. But if the column temperature is decreased for a sample containing a mixture of methyl ketones and paraffin hydrocarbons, one can predict only that the α of any two hydrocarbons (and that of any two ketones) will increase. The α of a mixed pair – hydrocarbon and ketone – can increase or decrease as the temperature is lowered, and that effect will be reversed if the temperature is raised. In short, the effect of temperature on α cannot be predicted for two solutes of different functionality. Hence for any given group of mixed solutes, α values are controlled primarily through experience and observations on the probability of interactions between given solutes and a given stationary phase.

The limitation on N and the resultant increased reliance on α made stationary phase selectivity of major import to the packed column, and has been largely responsible for the proliferation of some 300 different stationary phases for packed columns. Because much higher numbers of theoretical plates are attainable in open-tubular columns, solute separation factors – α – were initially less critical to the user of open-tubular columns. However, the inexorable increase in the demands placed upon the analytical chemist ultimately necessitated the development of high- N columns coated with high- α phases.

Low-Bleed Columns

As the column temperature is increased, there is an increase in the steady-state baseline signal. The chemical bonds of the stationary phase are under increased thermal stress, degradation fragments are produced at an increased but constant rate, and the baseline signal rises and remains steady as long as that temperature is maintained. In polysiloxane stationary phases, the degradation fragments consist largely of cyclic siloxanes, dominated by trimers and tetramers of (–Si–O–) to which the methyl (or other) substituents occupying the remaining two bonds of the tetravalent silicon atom may remain attached, or may cleave. True column bleed does not generate peaks or

humps; a signal that rises and then falls must have a ‘point source’. Bleed signal is annoying with any bleed-sensitive detector, and can be the limiting factor in GC-MS, especially with the newer ion trap mass spectrometers (ITD). For a given quality of stationary phase under a given set of conditions (temperature, carrier gas flow), bleed is always a function of the mass of stationary phase in the flow path. Hence, shorter, smaller diameter, thinner film columns will exhibit lower bleed levels than longer, larger diameter, thicker film columns.

At the present time, column bleed is usually reported in terms of pA of FID (flame ionization detector) signal at a given temperature, but this is an imprecise specification. It would be better to report bleed as ‘pg carbon emitted per unit time’ as measured on a *calibrated* detector. Only where the same detector is used under the same conditions for both determinations can different columns be truly compared in terms of ‘pA of FID signal’. Bleed signal from polysiloxane columns is generally attributed to cyclic siloxanes that usually arise from thermal and/or oxidative degradation of the phase, but contaminants in the detector or in gas lines supplying that unit, materials outgassing from septa and ferrules, and contaminating oils from column installation also contribute to what is *perceived* as column bleed. The latter sources are usually (but not always) dwarfed by the former, but their significance increases in the case of low bleed columns. It should also be noted that at elevated temperatures, even a pristine FID *without any column* generates 1–2 pA signal.

Some years prior to the invention of gas chromatography, Sveda, a Du Pont chemist working on bulk polymers, filed two patents on silarylene-siloxane polymers. Shown in **Figure 2** are generic structures of (A) the conventional 95% dimethyl–5% diphenylpolysiloxane (in which the phenyl groups are pendant to the siloxane chain), and (B) Sveda’s poly(tetramethyl-1,4-silphenylene siloxane).

Not surprisingly, the two forms display somewhat different selectivities toward solutes. More than 40 years after Sveda’s work, several column manufacturers began offering proprietary ‘low-bleed’ columns that would appear to be based on the silarylene siloxanes. The lengthy delay may have been partly due to the fact that, until quite recently, bleed rates from high quality ‘conventional’ columns were not considered excessive in most applications. A more probable cause is that silarylene polymers are not yet commercially available, so that those wishing to utilize them must resort to a sequential series of in-house syntheses that are both materials and labour intensive, each step of which is usually characterized by low yields.

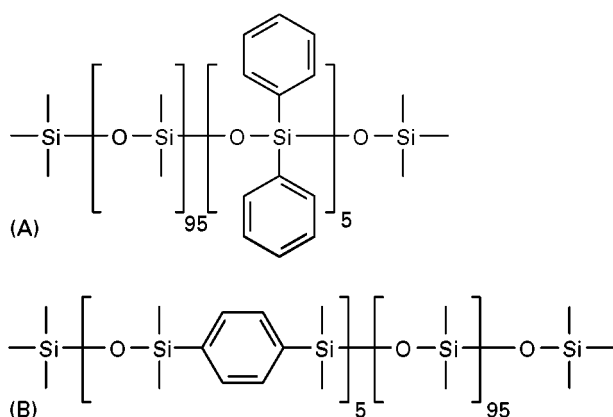


Figure 2 Generic structures of (A) the conventional 95% dimethyl – 5% diphenylsiloxane and (B) Sveda's poly (tetramethyl-1,4-silphenylene siloxane).

Several pathways have been postulated for the thermal degradation of siloxanes, some of which require a proximity of two normally separated groups that would require folding of the siloxane chain. It has been suggested that such reactions might be blocked

by the insertion of groups that would make the chain more rigid and restrict its flexibility. Such efforts have led to the introduction, by more than one manufacturer, of stationary phases that are characterized by the generation of lower bleed signals, even at elevated temperatures, e.g. 360°C.

Figure 3 contrasts the bleed profiles of examples of 'first generation' (a silphenylene siloxane) and 'second generation' (a silphenylene siloxane containing 'chain-stiffening' groups) low-bleed columns. Note that the latter not only exhibits a bleed level about half that of the former, but the bleed pattern is simpler, making the phase especially valuable for those utilizing bleed-sensitive detectors such as the ion trap mass spectrometer. It also possesses a unique selectivity that has excited great interest among those interested in a variety of problematic separations, including the polychlorinated biphenyl congeners.

Column performance is also influenced by the deactivation, or surface preparation treatment. The observation that thin-film columns often exhibit adsorption toward active solutes, and that thicker films of stationary phase result in more inert columns,

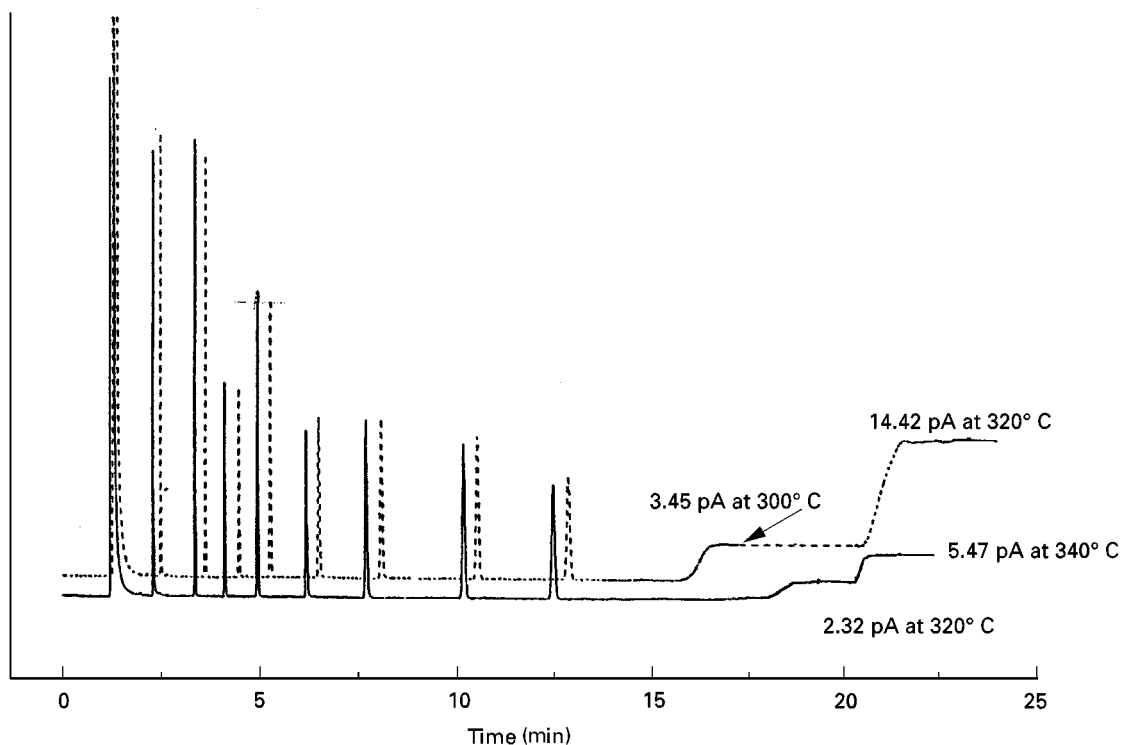


Figure 3 Chromatograms of a column test mixture on 30 m × 0.25 mm, d_i 0.25 μm columns. Test mixtures were run at 130°C isothermal, and columns ramped to higher temperatures to determine bleed profiles. Note that the 'delta bleed' is 2.32 pA at 320°C for the 'second generation' column, versus 14.42 pA for the 'conventional' column. This is essentially the 'maximum temperature' of the latter column, which has reached a point where bleed increases exponentially with temperature. The latter column is capable of still higher temperatures, however, and exhibits a bleed signal of 5.47 pA at 340°C. Key: ---, first generation 35% diphenylpolysiloxane column; —, second generation 35% phenyl low-bleed column.

suggests that activity sometimes depends on whether solutes 'see' the surface. As solute molecules migrate through the stationary phase toward the siliceous surface, the carrier flow sweeps the solute molecules in the gas phase downstream. To re-establish the distribution constant in that portion of the column, solute molecules in the stationary phase reverse direction and migrate toward the mobile phase. Whether this impetus to change the direction of migration occurs before or after the solute has reached the surface would, under a given set of conditions, depend on the thickness of the stationary phase film.

The affinity of the surface for polar stationary phases is sometimes estimated by measuring the surface energy of the prepared surface. While both

the nature and strength of surface-to-polymer interactions are important to column performance, they are not necessarily predictable. A given 'high energy' surface is not always suitable for the deposition of a 'high energy' polymer. Architectural 'tailoring' of the surface can be as difficult as tailoring stationary-phase selectivity. The concept of 'coating efficiency', used in Figure 4, ($CE = 100 \times H_{\text{theor min}}/[H_{\text{observed}}]$) is often used to measure the compatibility of a surface for a given stationary phase.

Figure 4 shows four dimensionally identical columns under the same operational conditions and coated with the same experimental high phenyl stationary phase; each column received a different deactivation treatment. Note the third example (C),

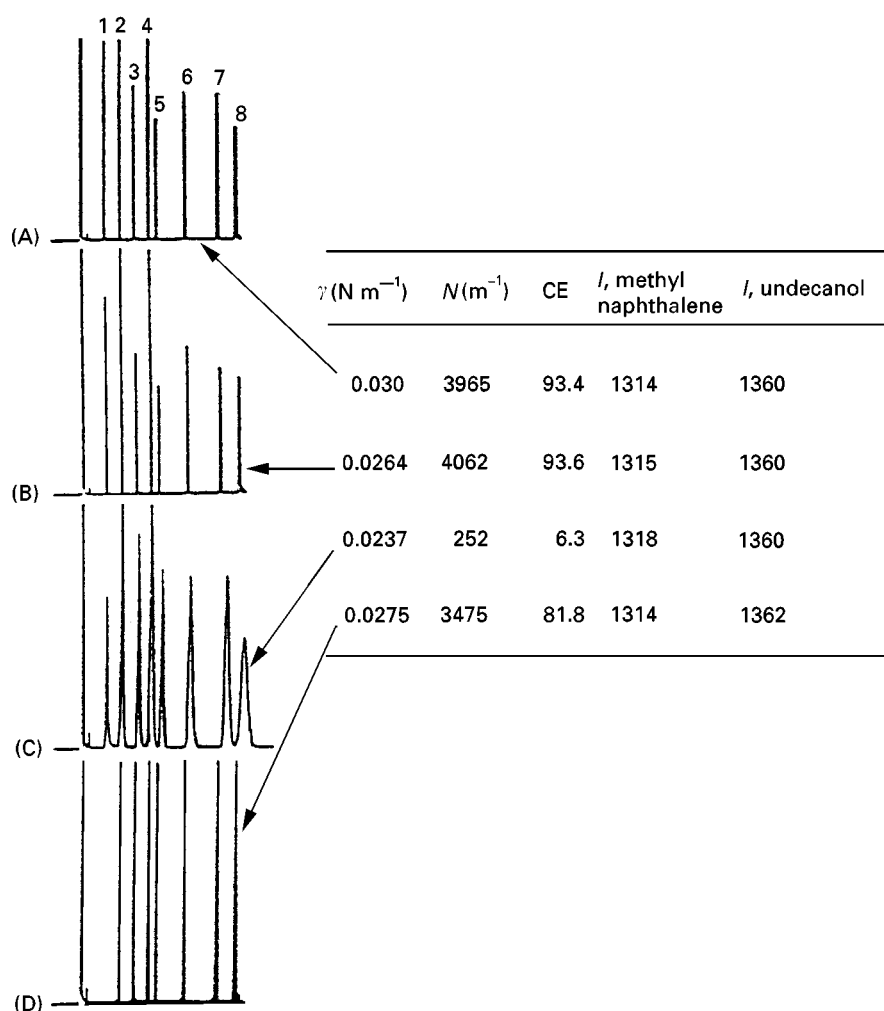


Figure 4 Chromatograms of a test mixture on four dimensionally identical columns, all coated with the same experimental high phenyl stationary phase, but subjected to different deactivation pretreatments. Note the disappearance of 2-ethylhexanoic acid in (D) and the intercolumn variations in retention indices (I) for methyl naphthalene and undecanol. See text for discussion of the effects of the surface energies (γ) on coating efficiencies (CE). Solutes in order of elution: 1, 2-ethylhexanoic acid (totally adsorbed in chromatogram D); 2, 1,6-hexanediol; 3, 4-chlorophenol; 4, tridecane; 5, 2-methylnaphthalene; 6, 1-undecanol; 7, tetradecane; and 8, dicyclohexylamine.

which has high surface energy but very poor coating efficiency. (A), (B) and (D) all are nonbeaded surfaces, but the coating efficiencies of (A) and (B) are significantly better than that of (D). The coating efficiencies of these three columns vary in the order $2 > 1 > 4$, while the surface energies vary in the order $1 > 4 > 2$. The column with the lowest surface energy of the coatable surfaces (column B), yields the highest coating efficiency. In column (D), the acid peak disappeared. In every case, there is almost surely at least a slight effect on selectivity. One of our better ways for estimating this quality is the duplicability of retention indices for polar and apolar compounds, and column-to-column variations in these comparisons imply that closely eluting solutes of different functionalities may exhibit a given elution order on the one column, and a different elution order on the other column. These data indicate that both the stationary phase (which may be proprietary) and column pretreatments (which are almost always proprietary and vary from manufacturer to manufacturer) affect retention factors, separation factors, and even the elution order. Surface pretreatments, including but not limited to deactivation, can, and often do, exert profound effects on overall column performance.

Conclusions

During its half century history, gas chromatography (GC) has evolved to become the world's most widely used analytical technique. The growth has accelerated with the commercial availability of columns, the quality of which has shown consistent improvements, and by the continuing development of compatible instrumentation and combined techniques (e.g. gas chromatography-spectrometry, GC-AED, etc.). Also important to that growth is the fact that the technique possesses separation powers so great that the unskilled analyst can abuse the technique and still generate useful data. Other analytical methods (e.g. capillary electrophoresis, capillary zone electrophoresis, liquid chromatography) have shown promise of greatly increased growth, but GC has not stagnated. Many of the elements necessary for 'fast' GC have been known for some time, but their application usually requires instrumental modification and adaptation beyond the purview of most practising analysts. Some cracks in this barrier have recently appeared. Developments in more selective stationary phases, electronic pneumatic controls, micropacked columns, and shorter columns of smaller diameter now permit some users to demonstrate improved separations while reducing analysis times. Appreciable time savings have been demonstrated merely through refinement of operational parameters (temperature,

program rates, gas velocity). By changing both operational and design parameters (e.g. column dimensions), analysis times using unmodified instrumentation have been reduced from 30 min to a few seconds. A greater utilization of these newer developments, however, will require honing the skills of the average analyst through continuing education.

See Colour Plates 19, 20.

See also: II/Chromatography: Gas: Detectors: General (Flame Ionization Detectors and Thermal Conductivity Detectors); Detectors: Mass Spectrometry; Detectors: Selective; Gas-Solid Gas Chromatography; Historical Development; Sampling Systems; Theory of Gas Chromatography. Appendix 2: Essential Guides to Method Development in Gas Chromatography.

Further Reading

- Blomberg L, Markides K and Wannman T (1980) *Journal of High Resolution Chromatography* 3: 527-528; (1982) 5: 520-533.
- Buijten JC, Blomberg L, Hoffmann S, Markides K and Wannman (1984) *Journal of Chromatography* 301: 265-269.
- Burns W and Hawkes SJ (1977) *Journal of Chromatographic Science* 15: 185-190.
- Dandenau R and Zerriner E (1979) *Journal of High Resolution Chromatography* 2: 351-356.
- Desty DH, Haresip JN and Whyman BHF (1960) *Analytical Chemistry* 32: 302-304.
- Dvornic PR, and Lenz RW (1990) *High Temperature Siloxane Elastomers*. Basel: Huethig & Wepf.
- Ettre LS (1993) Nomenclature for chromatography. *Pure and Applied Chemistry* 65: 819-872.
- Jennings W (1987) *Analytical Gas Chromatography*, 1st edn, pp. 11-18. San Diego, CA: Academic Press.
- Jennings W, Lautamo R and Reese S (1997) In Kaiser O and Kaiser RE (eds) *Chromatography: Celebrating Michael Tswett's 125th Birthday*, pp. 117-125. Dusseldorf: In Com.
- Jennings W, Mittlefehldt E and Stremple P (1997) *Analytical Gas Chromatography*, 2nd edn, pp. 332, 336-339.
- Kong JM and Hawkes SJ (1976) *Journal of Chromatographic Science* 14: 279-287.
- Wright BW, Lee ML, Graham SW, Phillips LV and Hercules DM (1980) *Journal of Chromatography* 199: 355-369.

Glossary

Based on the most recent recommendations of the International Union of Pure and Applied Chemistry (IUPAC), which appeared in *Pure and Applied Chemistry* 65: 819-872 (1993).

A Eddy diffusion, or packing factor term of the van Deemter (packed column) equation.

α Separation factor; the adjusted retention time of the more retained solute relative to that of the less retained solute.

- B** Longitudinal diffusion term of the van Deemter and Golay equations.
- β** Column phase ratio. The column volume occupied by mobile (gas) phase relative to the volume occupied by stationary phase. In open-tubular columns: $\beta = [r_c - 2d_f]/[2d_f] \cong r_c/2d_f$.
- c_M, c_S** Solute concentrations in mobile and stationary phases, respectively.
- C** Resistance to mass transfer (or mass transfer) in the van Deemter (or Golay) equations; C_M and C_S denote mass transfer from mobile to stationary and from stationary to mobile phases, respectively.
- d_c** Inner diameter of the column. Both mm and μm are commonly used. The latter, while consistent with the units used for d_f , implies three significant figures, which is rarely true.
- d_f** Thickness of the stationary phase film, usually in μm .
- D** Diffusivity; D_M and D_S denote solute diffusivities in the mobile and stationary phases, respectively; usually given in $\text{cm}^2 \text{s}^{-1}$.
- F** Volumetric flow of the mobile phase, usually in $\text{cm}^3 \text{min}^{-1}$. Many practical chromatographers assume equivalency with (and hence employ) mL min^{-1} .
- FID** Flame ionization detector.
- GC-MS** The combination of gas chromatography and mass spectrometry, usually a single integrated unit in which fractions separated by GC are sequentially introduced to the MS.
- H** Length equivalent to one theoretical plate (height equivalent to a theoretical plate): $H = L/N$. When measured at u_{opt} , the result is termed H_{min} .
- k** Solute retention factor (formerly partition ratio). Ratio of the amounts of a solute (or time spent) in stationary and mobile phases, respectively. Because all solutes spend t_M time in the mobile phase, $k = [t_R - t_M]/t_M$, and $k = t'_R/t_M$.
- K_c** Distribution constant. Formerly K_D . Ratio of solute concentrations in stationary and mobile phases, respectively: $K_c = c_S/c_M$.
- L** Length of the column, usually expressed in metres for column length, in cm for the determination of \bar{u} , and in mm for the determination of H .
- N** Theoretical plate number; $N = [t_R/\sigma]^2$, where σ is the standard deviation of the peak.
- N_{req}** Number of theoretical plates required to separate two solutes of a given alpha and given retention factors to a given degree of resolution: $N_{\text{req}} = 16R_s^2[(k+1)/k]^2[\alpha/(\alpha-1)]^2$.
- o.d.** Outer diameter of the column.
- r_c** Inside radius of the column.
- R_s** Peak resolution. A measure of separation as evidenced by both the distance between the peak maxima and by the peak widths. ASTM and IUPAC definitions are based on w_b (peak width at base) measurements, which require extrapolation. If peaks are assumed to be Gaussian, then $R_s = 1.18[t_{R(B)} - t_{R(A)}]/[w_{h(A)} + w_{h(B)}]$.
- σ** Standard deviation of a Gaussian peak.
- t_M** Gas hold-up time. The time (or distance) required for a nonretained substance (e.g. mobile phase) to transit the column.
- t_R** Retention time. The time (or distance) from the point of injection to the peak maximum.
- t'_R** Adjusted retention time. Equivalent to the residence time in stationary phase; difference of the solute retention time and the gas hold-up time: $t'_R = t_R - t_M$.
- \bar{u}** Average linear velocity of the mobile (gas) phase: $\bar{u} (\text{cm s}^{-1}) = L (\text{cm})/t (\text{s})$.
- V** Volume. V_M and V_S represent volumes of the mobile and stationary phases, respectively.
- w_b** Peak width at base. Determined by measuring the length of baseline defined by intercepts extrapolated from the points of inflection of the peak, and equivalent to four standard deviations in a Gaussian peak.
- w_h** Peak width at half-height. Measured across the peak halfway between baseline and peak maximum, this can be measured directly without extrapolation, and is equal to 2.35 standard deviations in a Gaussian peak.

Derivatization

P. Hušek, Institute of Endocrinology, Prague, Czech Republic

Copyright © 2000 Academic Press

Introduction

Gas chromatography (GC), the longest established instrumental chromatographic technique, dominated

the separation field from the early 1950s until the mid-1970s when high performance liquid chromatography (HPLC) became a competitive technique. During this 20-year period, considerable effort was expended in developing procedures to make compounds sufficiently volatile, more thermally stable and less polar so that they would be more amenable to GC analysis. Such efforts were aimed almost

exclusively at removal of active hydrogen atoms(s) from protonic functional groups by the action of a suitable reagent, giving rise to a derivative with the hydrogen atoms substituted by less active functional groups.

Development of a particular derivatization method requires a good knowledge of organic chemistry, taking into consideration as many reaction mechanisms as possible. This is particularly true for the derivatization of protein amino acids, where so many different chemical groups are involved, such that a remark has been made about having here 'the whole of Beilstein'. The history of their more or less successful derivatization can be found in the book *Amino Acid Analysis by Gas Chromatography* (see Further Reading).

In general, the nature of the compounds to be analysed and their chemical properties govern the choice of the particular chemical treatment. This does not mean, however, that the reactions used on a macro-scale by organic chemists can be automatically adopted to the scale of microlitre volumes. The recent discovery of chloroformate-induced esterification of carboxylic acids is a good example of this. Over time, many derivatization methods have become more or less obsolete as their original usefulness was determined by a lack of alternative methods for the determination of minute amounts of some analytes, especially those in biological fluids. Until the discovery of immunoassay (radioimmunoassay, RIA, and enzyme immunoassay, EIA) and the development of specific and sensitive HPLC detectors, the electron-capture detector (ECD) in GC was the only way to reach picomole concentration levels. At that time, therefore, there was considerable interest in the conversion of analytes into perhalogenated products with a correspondingly high ECD response. Some of these methods or principles still persist; others do not. A comprehensive list of various chemical treatments can be found in the *Handbook of Derivatives for Chromatography* by Blau and Halket (see Further Reading). Some of the older useful methods and recent novel discoveries will be discussed in more detail below (see also the reviews by Hušek and Wells listed in the Further Reading section).

Esterification

Carboxylic acid groups usually require treatment with a group-oriented reagent that will not react in most cases with any other protonic groups that may be present. The choice of treatment depends on what class of acidic compounds – with or without extra reactive groups in the molecule – is to be esterified and what kind of detection (ECD or flame ionization detection, FID) is required.

Esterification with Acidified Alcohols

For analytical work, esterification with methanol through to isoamyl alcohol is best done in the presence of a volatile catalyst such as hydrogen chloride, thionyl chloride or acetyl chloride, which can be readily removed together with any excess alcohol. Fatty acids are often methylated by a short boiling with BF_3 /methanol, and this catalyst has proved to be effective even for transesterification of acylglycerols (neutral lipids are, however, most easily saponified using sodium or potassium hydroxide in methanol). Higher alcohols, most often *n*-butanol and isobutanol, have been used for HCl-catalysed esterification of amino acids in two steps (with lower alcohols, evaporative losses of the lower mass members occur). For effective conversion, heating at or above 100°C is required.

Esterification via Pyrolytic Methylation

Strongly basic quaternary salts of ammonia, e.g. tetramethyl or trimethylphenylammonium hydroxide in methanol, when co-injected with fatty acids into the heated inlet of a GC, convert the acids into quaternary salts that are immediately pyrolysed into methyl esters and swept onto the analytical column. However, this rapid procedure is not recommended for polyunsaturated fatty acids because isomerization of the double bonds may occur owing to the high inlet temperature and alkalinity of the reagents. It has been reported that tetraalkylammonium fluorides, cyanides or acetates frequently offer considerable advantages over the hydroxides in terms of derivatization selectivity without compromising derivatization efficiency. Regarding on-column benzylation reagents, the 3,5-bis(trifluoromethyl)benzyltrimethylphenylammonium fluoride and some related compounds have been shown to be very useful new derivatization reagents with a variety of uses (see the review by Wells in the Further Reading section). Dimethylformamide dimethylacetal ($(\text{CH}_3)_2\text{NCH}(\text{OCH}_3)_2$) and its higher alkyl analogues have also been employed as hot inlet esterification agents. Hopes of being able to use them for one-step derivatization of amino acids have not been fulfilled, however.

Esterification with Diazoalkanes

Diazomethane, a yellow gas normally used as a solution in ether, readily esterifies fatty acids in the presence of methanol at room temperature and excess reagent can easily be removed by evaporation. However, the gas is highly carcinogenic and unstable, partially reacting with double bonds, carbonyl, phenolic and hydroxyl groups. This method, once popular, is now the exception. The same is true for the

higher analogues diazoethane and phenyldiazomethane (used to make benzyl esters). The recent use of commercially available trimethylsilyldiazomethane (solution in hexane) has proved to be useful in some applications.

Esterification via Carbodiimide-Induced Coupling

The carbodiimide-coupled esterification of carboxylic acids is a well-known reaction in organic chemistry. *N,N'*-Dialkylcarbodiimides act as water scavengers, promoting condensation of an acid with an alcohol while being transformed into an *N,N'*-dialkylurea (from $X-N=C=N-X$ to $X-NHCONH-X$, where X is an alkyl radical). For example, diisopropylcarbodiimide (DIC) was used for the esterification of some aromatic acids with hexafluoroisopropanol. A concentration of 0.1–0.15% DIC and the alcohol in hexane was found to be sufficient to esterify within 1 min.

Esterification with Alkyl Halides

Alkyl (aryl) iodides, bromides (less often chlorides) have been used for treatment of potassium, *t*-amines, tetraalkylammonium or 'crown' ether salts of acids in a suitable organic solvent such as acetonitrile, acetone or methanol. Corresponding alkyl/aryl esters are formed without heating the sample at optimum conditions in high yields. It has been reported by Wells and co-workers (see Further Reading) that macroporous quaternary ammonium anion exchange resins are a very effective support matrix for the methylation of strongly acidic organic analytes with methyl iodide in either supercritical carbon dioxide or acetonitrile. The isolation and determination of simple volatile aliphatic acids from urine by trapping on ion exchange resin followed by simultaneous derivatization with pentafluorobenzyl bromide (PFBBBr) and extraction with supercritical carbon dioxide has also been reported. The electron-capturing pentafluorobenzyl (PFB) esters have become increasingly popular for GC-ECD analysis of fatty acids regardless of chain length. Conversion to PFB esters has been reported to succeed in the presence of acetonitrile and diisopropylethylamine in 10 min.

Silylation

A wide range of highly reactive and specific reagents for nearly every application with a trimethylsilyl (TMS) or the increasingly popular *t*-butyldimethylsilyl (TBDMS) donor is now available. These reagents, which are of general utility, will be discussed in a separate section. Some of them can convert the carboxylic acid group into the TMS ester ($RCOO-Si(CH_3)_3$) practically instantaneously and

GC analysis can be done by direct injection of the reaction mixture. Reagents with a TBDMS donor require longer reaction times but provide hydrolytically more stable derivatives. Under controlled conditions, with mild silylating agents, e.g. hexamethyl disilazane (HMDS), only the carboxylic acid group will be esterified. Silylation is the preferred way for treating dicarboxylic acids or polycarboxylic compounds. Haloalkylsilylation reagents have been used for sensitive ECD detection but they are expensive and less popular than they once were.

Derivatization by Alcoholysis of the Intermediate Mixed Anhydrides

Haloalkyl anhydrides, especially the perfluorinated ones of acetic, propionic and butyric acids, are able to promote condensation reactions with an alcohol (see Table 1 for the reagents and abbreviations), when in a molar excess over the alcohol. TCE, TFE or HFIP in combination with TFA or HFBA have often been used to attain higher ECD response. Heating is usually employed without the catalytic presence of an organic base. This approach will be mentioned again in the next section.

At the beginning of the 1990s, chloroformates with the simplest alkyl groups, i.e. methyl and ethyl chloroformate (MCF and ECF), were shown to act as exceptionally rapid esterification reagents. The catalytic presence of pyridine has been found to be a prerequisite for ester formation; water can be, or for some applications should be, a constituent of the medium, together with an alcohol and commonly acetonitrile also. This promising treatment has a broader utility and will be discussed further. The reaction mechanism is based, as in the first case, on alcoholysis of a mixed anhydride intermediate. The advantageous use of this approach in comparison with the former can be seen from Table 2.

Acylation/Alkylation

Reagents treated in this section have proved to be especially suitable for handling the various nitrogen protic groups for which silylation with TMS donors is clearly inferior due to the lability of the N–Si bond. A comprehensive review on the derivatization of amines for GC analysis has been published by Kataoka (see Further Reading).

The perfluorinated anhydrides, despite their much higher molecular weight, yield derivatives of high volatility since interaction between the perfluoroalkane chain and a nonfluorinated stationary phase is substantially weakened. The retention of perfluoroalkyl(acyl) derivatives is, therefore, often markedly less

Table 1 Electrophoric reagents frequently used for esterification, acylation and alkylation

Haloalkyl(acyl) group	Matrix	Formula	b.p. (°C)	Abbreviation
2-Chloro-	Ethanol	$\text{ClCH}_2\text{CH}_2\text{OH}$	129	2CE
2,2,2-Trichloro-	Ethanol	$\text{CCl}_3\text{CH}_2\text{OH}$	151	TCE
	Ethyl chloroformate	$\text{CCl}_3\text{CH}_2\text{OCOCl}$	171	TCECF
2,2,2-Trifluoro-	Ethanol	$\text{CF}_3\text{CH}_2\text{OH}$	78	TFE
	Acetic anhydride	$(\text{CF}_3\text{CO})_2\text{O}$	40	TFAA
Chlorodifluoro-	Acetic anhydride	$(\text{CF}_2\text{ClCO})_2\text{O}$	96	CDFAA
1,1,1,3,3,3-Hexafluoro-	Isopropanol	$(\text{CF}_3)_2\text{CHOH}$	59	HFIP
2,2,3,3,3-Pentafluoro-	Propanol	$\text{C}_2\text{F}_5\text{CH}_2\text{OH}$	81	PFP
	Propionic anhydride	$(\text{C}_2\text{F}_5\text{CO})_2\text{O}$	96	PFPA
2,2,3,3,4,4,4-Heptafluoro-	Butanol	$\text{C}_3\text{F}_7\text{CH}_2\text{OH}$	96	HFB
	Butyric anhydride	$(\text{C}_3\text{F}_7\text{CO})_2\text{O}$	108	HFBA
	Butyryl chloride	$\text{C}_3\text{F}_7\text{COCl}$	39	HFB-Cl
Pentafluorobenzoyl	Chloride	$\text{C}_6\text{F}_5\text{CH}_2\text{COCl}$	158	PFB-Cl
Pentafluorobenzyl	Bromide	$\text{C}_6\text{F}_5\text{CH}_2\text{Br}$	174	PFBBr
	Chloroformate	$\text{C}_6\text{F}_5\text{CH}_2\text{OCOCl}$		PFB-Cl
	Hydroxylamine	$\text{C}_6\text{F}_5\text{CH}_2\text{ONH}_2$		PFBHA
	Aldehyde	$\text{C}_6\text{F}_5\text{CHO}$	165	PFBA

than that of their hydrocarbon analogues. Another reason for their popularity is the high sensitivity to ECD, which increases rapidly with increase in F substitution. The response can be further augmented by incorporation of Cl, Br or I atoms into the molecule but the volatility of such derivatives declines rapidly and reagents carrying more than three Cl atoms are unsuitable for derivatization of higher mass analytes.

Treatment of Amino and/or Hydroxyl Groups

Reactive anhydrides listed in Table 1 are frequently employed for this purpose. Acetic anhydride, which has the additional advantage of reacting in aqueous media, has proved its usefulness for esterification of phenolic hydroxyl groups. However, its lower reactivity and the lower volatility of the (per)acetylated forms prevents its wider use.

Acylation of amino acid butyl or isobutyl esters with TFA or HFBA carried out at 100°C or more, usually in the presence of a solvent such as dichloromethane after evaporation of the first esterification

medium, is one of the best-established procedures of the 1960s and 1970s. All protein amino acids, including arginine, which is the most difficult amino acid to derivatize and determine by GC, have been successfully analysed and quantitated. Experience gained in the derivatization of amines, alcohols and acids is valuable for procedures for amino acids. A study of these approaches affords a basic knowledge of commonly occurring derivatization problems.

Acid halides have been employed for acylation less often. Except for PFB-Cl, which has even been used for acylation of amino acid isobutyl esters, the use of other acid chlorides is rather rare. However, surprisingly good results have been reported for catecholamines treated with HFB-Cl, which results in ready acylation of the phenolic, amino and alcoholic groups of analytes in an aqueous buffer. Unlike other chlorides, which are almost explosively reactive with water, HFB-Cl appears to be more stable towards hydrolysis. Many applications, aimed at the trace analysis of amines, phenols and alcohols with ECD by acylation with haloanhydrides are outside the

Table 2 Comparison of the reaction conditions for HFBA- and the ECF-induced esterification of carboxylic acids

	HFBA-catalysed ^a		ECF-catalysed ^b	
Medium	Chloroform		Chloroform	Water-acetonitrile (1 : 1)
Alcohol	TCE (1–10%)	EtOH (20%)	EtOH (1%)	EtOH (30%)
Reagent	HFBA (six-fold volume)		ECF (1%)	ECF (5%)
Base	None	Pyridine (25%)	Pyridine (2%)	Pyridine (8%)
Reaction time	30 min	4 min (boiling)	Few seconds	
Yield	Not given		> 90%	
Extraction	Chloroform versus aq. HCl and NaOH		Hexane versus aq. NaHCO ₃	

^aEdman DC and Brooks JB (1983) Gas-liquid chromatography—frequency pulse-modulated electron-capture detection in the diagnosis of infectious diseases. *Journal of Chromatography* 274: 1–25.

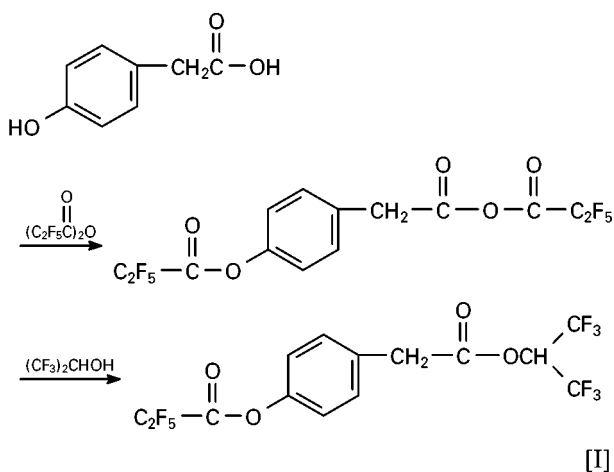
^bHušek P, Rijks JA, Leclercq PA and Cramers CA (1990) Fast esterification of fatty acids with alkyl chloroformates. Optimization and application in gas chromatography. *Journal of High Resolution Chromatography* 13: 633–638.

scope of this article; for details the reader should consult the Blau and Halket book or the papers by Poole (see Further Reading).

The amino group is best derivatized in aqueous media with chloroformates. Catecholamines are treated with MCF; if the alcoholic OH group is present it is silylated or acetylated in addition. During this step the MCF-alkylated phenolic hydroxyls reconvert to O-TMS or O-acetyl esters and only the amino group retains the alkyl group from the MCF. On well-deactivated capillaries the analysis succeeds even without this extra treatment. When tertiary amines are treated with chloroformates, the smallest alkyl group attached to the nitrogen undergoes a displacement and the amine is thus transformed to a carbamate. Hydrolysis of the latter yields a secondary amine, which is then exposed for further derivatization.

Concurrent Treatment Involving Carboxylic Groups

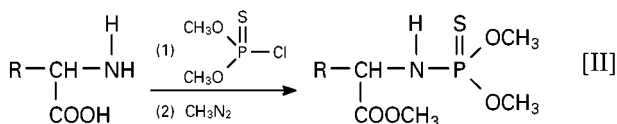
As already mentioned, the perfluorinated anhydrides TFAA, HFBA and less often the more expensive PFPA, can promote esterification of carboxylic groups provided that they are in a molar excess over the haloalcohol present. It is logical to suppose that even polyfunctional acids might be effectively treated, since side chain groups are acylated smoothly. This has been confirmed experimentally by treating hydroxyphenolic acids, bile acids and even amino acids, the carboxylic and side chain groups of which are esterified and acylated simultaneously. It is assumed that the reaction proceeds in two steps, i.e. by the formation of mixed anhydride intermediate that is subsequently alcoholysed to the ester, as shown by *p*-hydroxyphenylacetic acid treated with PFPA/HFIP (reaction [I]). Derivatization of a number of carboxylic acids has been achieved by treatment with TFAA and HFB or TFE in the presence of an organic base with heating to 60°C for 30–40 min.



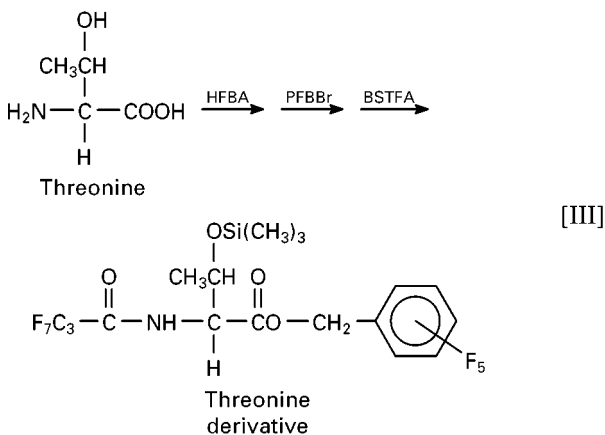
Alkylation Preceding the Carboxyl Treatment

This procedure deals with amino acids in the reverse order – first the amino group, including any side chains, is derivatized, and then the carboxyl group is methylated or silylated. The unique ability of chloroformates to react rapidly with analytes in aqueous media is utilized in a procedure employing isobutyl chloroformate (IBCF) followed by methylation with diazomethane. More than 50 amino acids (with the exception of arginine) have been analysed in this way as their *N*-isobutyloxycarbonyl (IBOC) methyl esters.

Alternatively, instead of methylation, the carboxylic group can be treated with a TBDMS donor and many amino acids have been analysed as *N*(O,S)-IBOC TBDMS esters. An ECD-oriented procedure was based on derivatization of the amino groups with dimethylchlorothiophosphate, followed by methylation (reaction [II]).

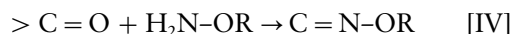


Likewise a three-stage treatment involving acylation of the amino groups with HFBA, extractive alkylation with PFBBR (for the carboxyl groups) followed by BSTFA silylation of aliphatic hydroxyl groups served the same purpose. The derivatization of threonine is an example of this procedure (reaction [III]). This scheme may seem unnecessarily complicated but the treatment is rapid and conditions are mild as each group undergoes its respective derivatization. In general the use of one reagent to react with different groups requires more drastic conditions.



Oximation of keto groups is one way to prevent isomerization (and/or enol formation) of keto acids before further derivatization by, for example, silylation. The keto group reacts with hydroxyl, methoxy

or ethoxyamine as follows:



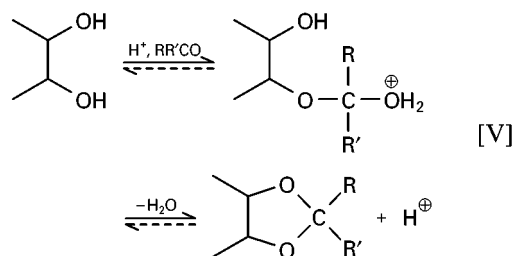
If one wishes to shift the derivatization products of simple aliphatic keto acids to products with greater retention times, then a correspondingly higher boiling reagent PFBHA (see Table 1) can be employed.

Cyclization

Some reagents selectively react with two protonic groups to form a heterocyclic compound with five, six or seven atoms, i.e. the groups to be treated are in positions 1,2, 1,3 or 1,4 on an aliphatic chain or 1,2 on an aromatic ring (see the review by Poole and Zlatkis listed in the Further Reading).

Acetals/ketals

This kind of cyclization is often used to provide protection for *cis*-diols and thiols. It is based on the reaction of aldehydes or ketones with 1,2-diols in the presence of an acid catalyst and proceeds via the formation of a hemiketal that is further rearranged to the dioxolane product (called acetonide or isopropylidene when acetone is used as the ketone; see reaction [V]).

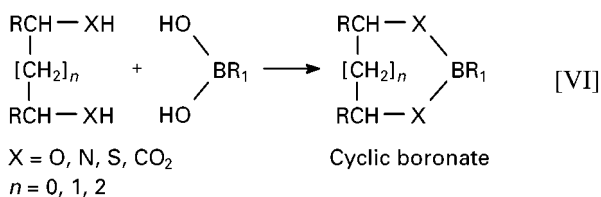


Acetonide derivatives are prepared, e.g. from α -monoacylglycerols (β -isomers do not react), and separated by GC. Corticosteroids with *cis*-C-20,21- or C-17,20-dihydroxy groups form acetonides under mild conditions and the products are suitable for GC analysis. The acetonide group is also stable under conditions of further treatment such as silylation or acetylation. The reaction is specific to *cis*-diols since the *trans*-C-20,21 diol does not form an acetonide. Siliconides are also formed by a similar mechanism when dimethylchlorosilane is used in pyridine, but multiproduct formation and instability of the derivatives has prevented wider use.

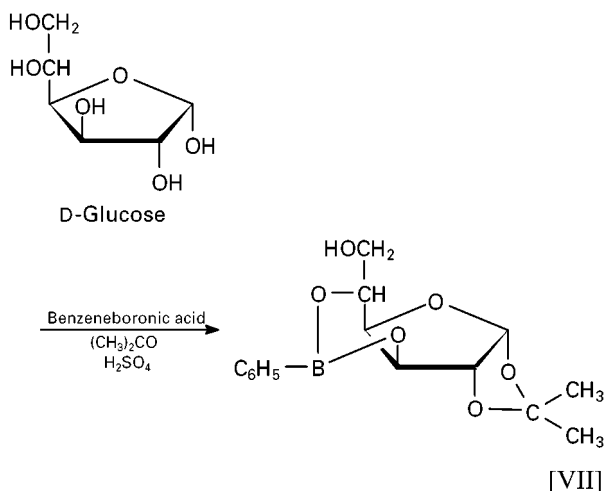
Boronates

Many diols are best handled with boronic acids. Alkyl boronates were used extensively in the 1970s

since they exhibit a broad ability to cyclize and are able to bridge diols up to a 1,4 position. The cyclic products (reaction [VI]) are stable enough to be analysed by GC and may even be made in the GC inlet.

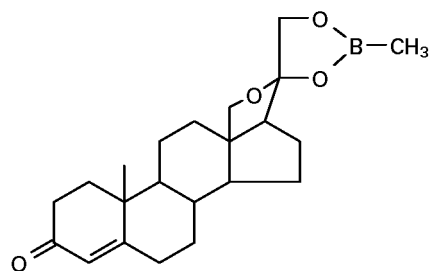


However, hydrolytic stability is not good and the products of reaction with a single OH group cannot be analysed. This can cause problems with, for example, steroids containing an additional alcohol group or groups next to the diol. The required additional treatment (acetylation, silylation) often results in unwanted by-products. Various alkyl groups, such as *t*-butyl, have been investigated with a view to improving the stability of the product, but the results have not always been as expected. The *n*-butaneboronates offer a convenient compromise between volatility and stability. For ECD, 2,4-dichloro- and 3,5-bis(trifluoromethyl)benzeneboronic acid have proved to be the best, since PFB-boronates are unstable to hydrolysis. Some useful applications include treatment of monosaccharides with benzeneboronic acid in acetone to give mixed acetonide-boronate products, as shown in reaction [VII]).

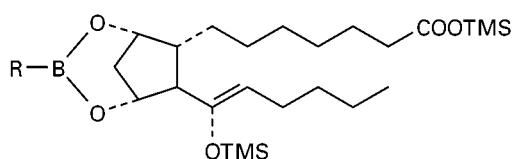


The action of methaneboronate on the corticosteroid (structure [VIII]) leads to an interesting rearrangement in the side chain and the selective reaction of the *cis*-diol group of prostaglandin F allows it to be distinguished (after silylation) from the structure with a *trans*-diol group, which does not react (structure [IX]). Boronates as reagents for GC analysis

are now rather ancient history but they do represent a considerable amount of successful past effort.



Methaneboronate of 18-hydroxy-11-deoxycorticosterone
[VIII]



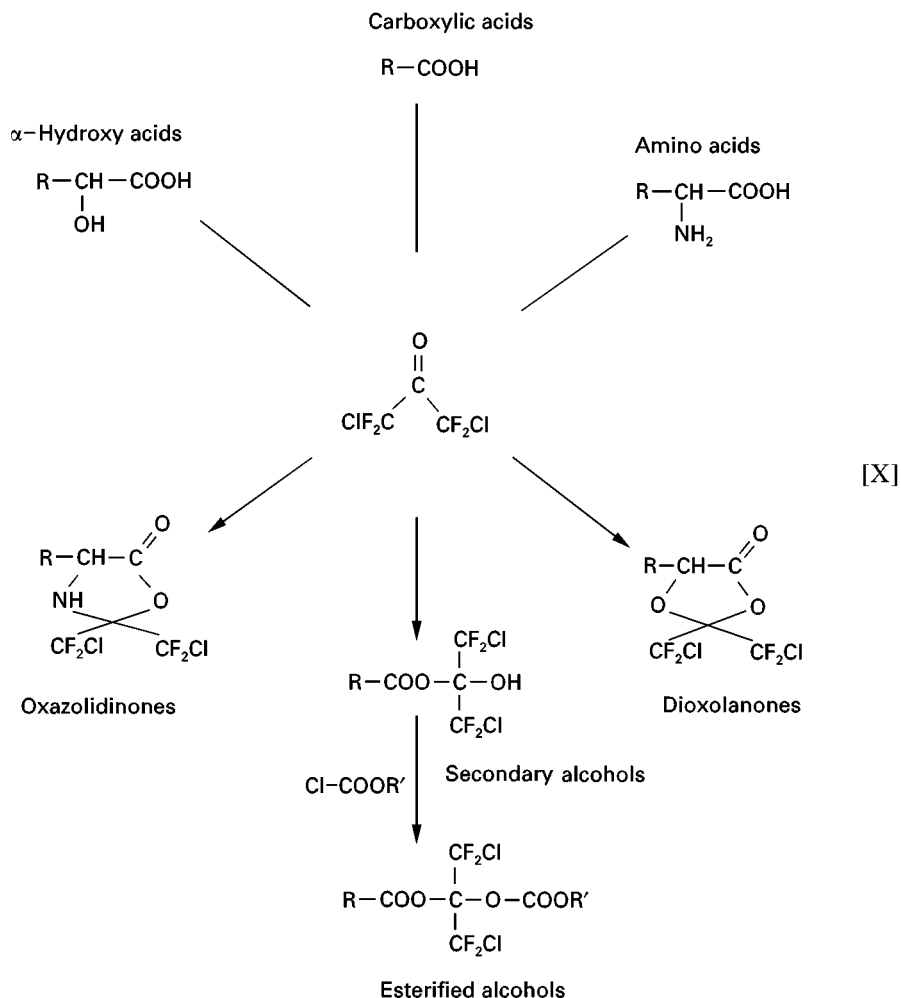
Prostaglandin F_{12} cyclic boronate TMS ether TMS ester
derivative
[IX]

Oxazolidones

The conditions for the condensation of amino acids with 1,3-dichlorotetrafluoroacetone (DCTFA) were established in the early 1980s, but before the method could establish its worth HPLC became the preferred technique and the reagent disappeared from the catalogues of all the major suppliers.

Substitution of halogens into the acetone molecule enhances the acidic character of the carbonyl group and promotes formation of stable adducts that are not otherwise obtained with aliphatic ketones. A scheme for some reactions with DCTFA is shown in scheme [X].

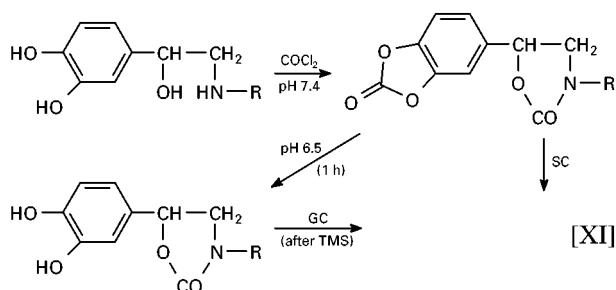
The double-step treatment with DCTFA followed by HFBA in the same aprotic medium, together with the subsequent analysis by capillary GC, gave the most rapid analysis of the protein amino acids, including arginine, at the time the method was developed. With an ECD, femtomole levels are easily attained. The method was originally developed for the derivatization of thyroid hormones with three to four iodine atoms in the molecule. The derivatized



thyroxine T_4 , with a molecular mass of over 1000 Da, is one of the largest compounds ever analysed by GC, the haloalkyl moiety providing relatively high volatility and high electron-capture response. However, the method came at a time when immunoassay was developed as an alternative and further applications of this derivatization method have not been pursued.

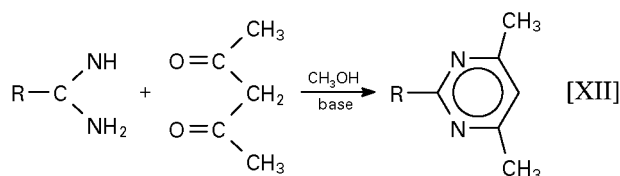
The potential of DCTFA to act as a reagent for detector-oriented derivatization has not been fully explored. As shown in the scheme in Figure 4, application to various classes of carboxylic acids still remain to be exploited.

Phosgene, dissolved in toluene or liberated from trichloromethyl (TCM) chloroformate or bis(TMC) carbonate, is able to cyclize adjacent groups of amino alcohols, aromatic diols, etc., as shown for catecholamines. The cyclic carbonate is not sufficiently stable and must be transformed to, for example, a TMS ester (reaction [XI]). Phosgene-induced cyclization to oxazolidones has been used for the GC analysis of enantiomers of pharmaceutically important amino alcohols. More details of the use of this reagent can be found in the review by Gyllenhaal and Vessman (see Further Reading).



Pyrimidines

Of the selective procedures for bifunctional compounds that result in cyclized products, the last to be described is that in which pyrimidines are formed by the action of acetylacetone or hexafluoroacetylacetone, or even malonaldehyde, on the guanidino group (reaction [XII]). This could represent a solution for the pre-treatment of arginine but the procedure is time-consuming and requires heating. For further information, see the review by Poole and Zlatkis listed in the Further Reading section.



Peralkylation

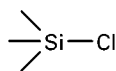
In addition to amino acid mixtures, another difficult class of compounds to deal with is the acidic metabolites of physiological fluids. Even when compounds with amino groups are not present (except in the case of glycine conjugates), the various classes of acids present – mono-, di- and tricarboxylic acids, keto and hydroxycarboxylic acids, aromatic acids with substituted chains, etc. – make sample preparation particularly challenging. There are one-step, one-reagent procedures that are able to derivatize most protic groups in such a mixture of analytes. These can be effective with alkylating or silylating reagents and also with chloroformates, under the active participation of a component in the reaction medium.

Alkylating Agents

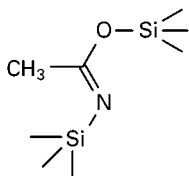
Isopropyl bromide has proved to be a useful reagent for amino acids dissolved in dimethylsulfoxide/sodium hydride, except for the determination of arginine. Methylation of acids with diazomethane has also been used for metabolic profiling despite the formation of artefacts. Resin-mediated methylation of polyfunctional acids found in fruit juices has also proved successful. Fumaric, succinic, malic, tartaric, isocitric and citric acids, isolated from fruit juices by trapping onto anionic ion exchange resins, can be efficiently converted to methyl esters by reaction with methyl iodide in both supercritical carbon dioxide and acetonitrile. To provide for the analysis of even short chain fatty acids in serum, a procedure has been developed with benzyl bromide. This has been successfully employed for serum and urine organic acid profiling. The method cannot be used for citric acid or sugar-related acids.

Silylating Agents

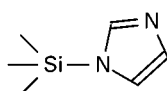
Silylation is the most widely used method for metabolic profiling, especially for urinary organic acids. On the other hand its use for amino acids has a number of disadvantages as already mentioned. For some applications, silylating agents are too powerful in that they are able to react with compounds which will not elute from the column. The most popular reagents are listed in Table 3 and many others are described in detail in the Fluka handbook edited by van Look (see Further Reading). For metabolic profiling the TMS donors are used much more frequently than the TBDMS donors although the latter are more convenient for treating amino groups in those applications where greater hydrolytic stability is required. Reactivity of functional groups towards silylation is as follows: alcohols > phenols > acids > amines > amides. Disadvantages include the need to operate under

Table 3 Reagents for silylation: (I) most common TMS donors; (II) a TBDMS donor; and (III, IV) reagents for special application**(I) Trimethylchlorosilane (TMCS)**

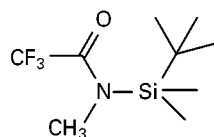
First silylation reagent prepared (1944)
Rarely used in analytical applications alone,
rather in mixtures with HMDS and pyridine

***N,O*-Bis(TMS)acetamide (BSA)**

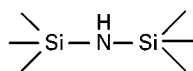
First reported in 1963
as a more potent TMS
donor;
usually in combination
with TMCS (1–20%)

TMSimidazole (TMSIM)

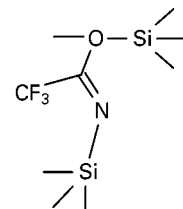
Prepared in 1965;
considered to be the
strongest reagent
available for silylation
of hydroxyl groups

**(II) *N*-Methyl-*N*-*t*-butyldimethylsilyl-
trifluoroacetamide (MTBSTFA)**

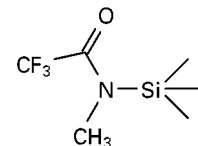
Alternative silyl
derivatives for enhanced
hydrolytic stability
(1975/1980)
increasingly popular,
suitable even for
amino acids

Hexamethyldisilazane (HMDS)

One of the earliest (1957)
Favorable solvating properties for many compounds
Not a strong silyl donor but more selective

***N,O*-Bis(TMS)trifluoroacetamide (BSTFA)**

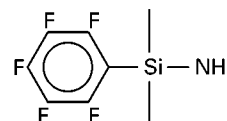
Most widely used for silylation
in general (prepared 1968)
Very versatile, reacting with
all the common protic sites in
organic material present;
more volatile by-products!

***N*-Methyl-*N*-TMS-trifluoroacetamide (MSTFA)**

Introduced in 1969, has become
one of the most important reagents;
can be used for all protic groups
and its by-products are more
volatile than BSTFA

**(III) Pentafluorophenyldimethylsilyl
(flopemesyl) reagents**

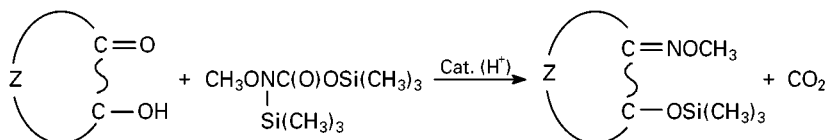
halogenated
reagents for
EC detection



(1975), particularly suitable for analysis
of sterols; silylation power:
flopemesylamine > flopemesylchloride

(IV) *N*-Methoxy-*N,O*-bistrimethylsilyl carbamate (BSMOC)

for simultaneous oximation & silylation at room temperature (reported 1986) as follows:

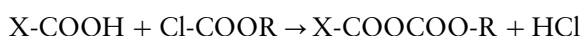


anhydrous conditions, to heat the sample and to inject a reactive mixture onto the column. This means that the compounds of interest have to be isolated, the extraction medium evaporated and the column replaced more frequently. For further information on profiling see the review by Sweetman.

Chloroformates

Chloroformates are known in organic chemistry for their ease of coupling to acids, resulting in the forma-

tion of so-called mixed anhydrides:



which are, in most cases, stable enough for GC analysis and potentially even reactive enough with amino acids to give peptides. Coupling with an acid is mostly successful in an organic solvent and in the presence of a strong base such as triethylamine (TEA). Considerable effort has been expended into finding reaction conditions to accelerate decarboxylation of the

mixed anhydride to the ester but with the exception of 2-keto acids the process was far from smooth. However, it was found fortuitously that on a micro-scale the presence of pyridine in a mixture with acetonitrile or water and alcohol results in immediate esterification. The alkyl chloroformates previously used for treating amines and phenols only suddenly became the general-purpose reagent.

The reaction mechanism is based on alcoholysis of the intermediate alkoxycarbonyl ester (the mixed anhydride). On the numerous applications published since 1990, the results for amino acids are especially impressive. It has been found that the alkyl group of the reagent and the alcohol need not be the same and different combinations lead to a variety of esters. In the field of metabolic profiling there is a report on simultaneous analysis of amino acids with other classes of compounds in serum without the need to isolate the analytes from the matrix. Profiling of urinary organic acids, for example, has been made possible after a simple sample pretreatment. Details are given in the review by Hušek (see Further Reading).

Conclusion

Silylating reagents were introduced in the 1960s and have been widely accepted as general purpose derivatizing reagents for GC, especially for polyfunctional compounds where derivatization is reduced to a one-step process. In the 1990s chloroformates were discovered as another family of powerful reagents which, in conjunction with a component of the medium, readily enable derivatization of many hydrogen-containing groups. They bring the additional advantage of derivatization in aqueous media, which often considerably simplifies the sample work-up. Last but not least, advanced alkylation/esterification procedures allow the simultaneous derivatization and extraction of analytes in sample matrices. The present

emphasis and future advances will focus on simplification and speed-up of sample preparation methods by process automation and combination of derivatization with work-up procedures.

See also: II/Chromatography: Gas: Detectors: Mass Spectrometry; Detectors: Selective. III/Acids: Gas Chromatography. **Amino Acids:** Gas Chromatography.

Further Reading

- Blau K and Halket JM (eds) (1993) *Handbook of Derivatives for Chromatography*, 2nd edn. Chichester: J. Wiley & Sons.
- Gyllenhaal O and Vessman J (1988) Phosgene as a derivatizing reagent prior to gas and liquid chromatography (review). *Journal of Chromatography* 435: 259–269.
- Hušek P (1998) Chloroformates in gas chromatography as general-purpose derivatizing agents. *Journal of Chromatography B* 717: 57–91.
- Kataoka H (1996) Derivatization reactions for the determination of amines by GC and their applications in environmental analysis (review). *Journal of Chromatography A* 733: 19–34.
- Poole CF and Poole SK (1987) Derivatization as an approach to trace analysis by GC with electron-capture detection. *Journal of Chromatographic Science* 25: 434–443.
- Poole CF and Zlatkis A (1980) Cyclic derivatives for the selective chromatographic analysis of bifunctional compounds (review). *Journal of Chromatography* 184: 99–183.
- Sweetman L (1991) In Hommes FA (ed.) *Techniques in Diagnostic Human Biochemical Laboratories: A Laboratory Manual*, p. 143. New York: Wiley-Liss.
- van Look G (1995) *Silylating Agents*. Buchs: Fluka.
- Wells RJ (1999) Recent advances in non-silylation derivatization techniques for gas chromatography. *Journal of Chromatography A* 843: 1–18.
- Zumwalt RD, Kuo KCT and Gehrke CW (eds) (1987) *Amino Acid Analysis by Gas Chromatography*, Vols I–III. Boca Raton, FL: CRC Press.

Detectors: General (Flame Ionization Detectors and Thermal Conductivity Detectors)

D. McMinn, Gonzaga University, Spokane, WA, USA

Copyright © 2000 Academic Press

The two most common detectors for use after separation by gas chromatography (GC) are the flame ionization detector (FID) and the thermal conductivity detector (TCD). They are considered general (non-selective) detectors since they respond to virtually all

components that they encounter. In a strict sense of course this is not true, especially for the FID which does not respond to fixed gases or to gases commonly used as carrier gases. None the less, it is responsive to most components of interest and is clearly not selective in comparison to an electron-capture or nitrogen-phosphorus detector.

It is sometimes useful to denote detectors as ionizing or nonionizing depending on their mode of

action. By their very nature, ionizing detectors are destructive and the sample is not available for additional analysis. On the other hand, nonionizing detectors do not destroy the sample. Thus, two detectors may be set up in series, with the sample first encountering the nonionizing detector, and then directed to the ionizing detector. Of all the detectors available for use following separation by GC, the FID and the TCD are the leading examples of each of these types. These general-purpose detectors are in wide use following both packed column and capillary separations.

The material which follows is directed mainly to applications after capillary column separation, although some reference to packed columns is necessary in order to complete the discussion. Further details regarding packed column applications can be found by consulting the Further Reading section.

The Flame Ionization Detector

The FID was developed in 1958 by McWilliam and Dewar in Australia and almost simultaneously by Harley, Nell and Pretorius in South Africa and quickly became the detector of choice in commercial instrumentation. As an ionization detector, the FID responds readily to compounds that contain carbon and hydrogen and to a lesser extent to some compounds containing only carbon. It is unresponsive to water, air and most carrier gases. Because of its broad applicability and relative ease of operation, it is probably the most common detector in GC systems. The FID responds quickly and can be constructed with a small internal volume, which makes it especially well suited for capillary GC.

Response of an FID is due to the sample being burned in a fuel-rich mixture and producing ions. In the same process, electrons are produced. Either ions or electrons are collected at an electrode and produce a small current. Since there are virtually no ions present in the absence of sample, the baseline is stable and the current is easily converted to a voltage and amplified to produce a signal. The response to most hydrocarbons is about 0.015 C g^{-1} carbon.

As shown in **Figure 1**, the most often used configuration has the jet tip at approximately 200 V relative to the collecting electrode. For use with capillary columns, a smaller jet tip (c. 0.3 mm i.d. rather than the 0.5 mm used with packed column configurations) is utilized in order to increase detector sensitivity. The capillary column is usually inserted through the ferrule and then a few centimetres are broken off and discarded. Ideally, the column is positioned within 1–2 mm of the jet tip and column effluent enters the detector and mixes with hydrogen (fuel) and make-up gas without undue contact with metal surfaces. This

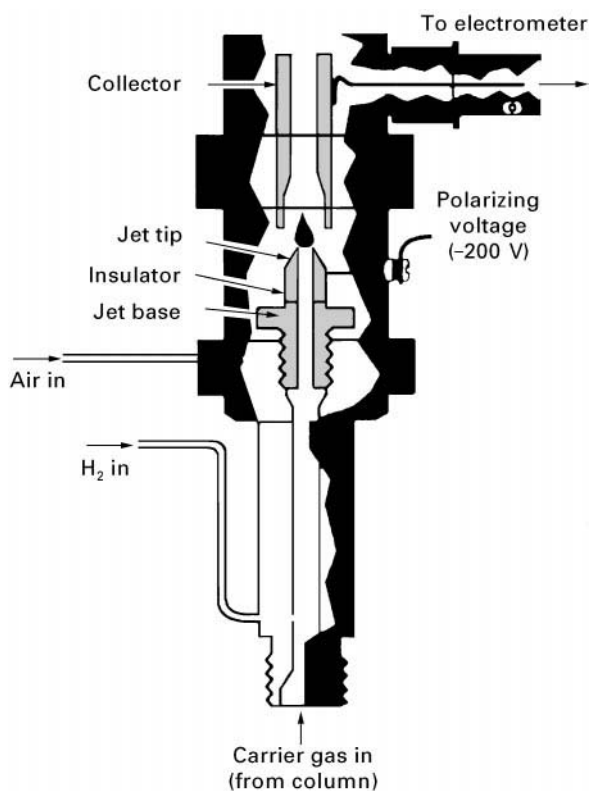


Figure 1 Cross-sectional diagram of a flame ionization detector.

mixture is combusted in an excess of air and the organic components are decomposed into ions. The ion chemistry of the diffusion flame has been studied by mass spectrometry. It appears that the ultimate positive charge carrier is H_3O^+ (or clusters of this with water molecules) resulting from charge transfer reactions from the initially formed ions (principally CHO^+). Thus the detector is often referred to as providing an 'equal per carbon response'.

This response to hydrocarbons allows one to quantify mixtures, for example from petroleum samples, without necessarily identifying each of the components individually present. With compounds other than hydrocarbons, the response is decreased when partially oxidized carbon atoms are present. This requires corrections to be made when the compounds contain, for example, oxygen, nitrogen or halogens. Either pure sample compounds or compounds of similar structure are used to establish appropriate response factors. Alternatively, the concept of effective carbon number has been updated to provide a model for the quantification of components in a complex organic mixture if they can be assigned to general functional group categories.

When used with narrow capillary columns, the FID usually requires a make-up gas for maximum sensitivity. The wider (530 μm) columns can be operated at

a higher carrier gas flow rate and may often be used without the additional make-up gas. For most operations the total flow rate (column + make-up) will be 20–60 mL min⁻¹. The fuel and air flow rates are maintained close to that recommended by the manufacturer – often 30–40 mL min⁻¹ for the hydrogen fuel and about 10-fold higher for the air. Under these conditions, the minimum detectable amount (MDA) of organic compounds is approximately 10–100 pg, depending on the structure. In addition, response is usually linear from the MDA to a concentration some 10⁷ times as great. (This higher limit is often beyond the loading capacity of narrow-bore capillary columns.) Flows to the detector can be adjusted while using standard samples containing the components of interest in order to obtain maximum response.

Water is a product of the combustion process producing the ions. Thus, the detector assembly must be kept hot in order to prevent condensation. A convenient guide is to have the detector 20–50° greater than the upper column temperature, but in no case lower than 150°C. Then water vapour, along with the other combustion gases, is swept out of the detector body. With most instruments, once the thermal environment of the detector has stabilized, temperature fluctuations are small and easily tolerated.

The FID is often described as a ‘forgiving’ detector since acceptable results are obtained even when the gas flows and other conditions are not optimized. None the less, some caution must be taken to avoid baseline drift, loss of sensitivity and the presence of spurious peaks. It is important to ensure that the gases employed are free from hydrocarbon impurities. Filters are available for this purpose. The flame itself is quite small and invisible, so checking for the presence of water vapour is the best approach to ensure that flame ignition has been successful. This can be done by holding a cold mirror above the outlet of the detector and observing condensation of the water vapour. Deterioration of performance of a properly operating FID is often the result of having used chlorinated solvents. Soot particles and the presence of HCl eventually lead to high and noisy baselines. The jet tip and collector electrode may have to be cleaned or, if badly corroded, replaced. Some spiking may be observed if portions of the polyimide coating are burned off the end of the capillary column.

The FID is mass flow-sensitive, meaning that the area response for a compound does not change as flow rate is varied. For quantitative work, appropriate response factors must be obtained, especially if a split injection mode is employed. When properly configured, a FID can respond to approximately 20 pg of each component eluting from a high resolution capillary column.

The Thermal Conductivity Detector

The TCD has long been a standby in packed column chromatography. It is a simple device, well suited to routine analyses where it is not necessary to detect low concentrations of components. It has been in use since the beginning of GC and has proven to be a rugged and dependable detector, in part because of the relatively simple electrical requirements. It is often encountered in less expensive instruments, and is the commonly used detector for the analysis of fixed gases. Until the introduction of the FID, it was by far the most common detector in use. Unlike the FID, no additional gases (beyond the carrier gas) are required, which makes it useful in situations where hydrogen gas would be hazardous or where additional gas supplies are not readily available. This may be important in field applications where portability is a factor.

For use with capillary columns, the TCD has been engineered down to a small volume in order to accommodate the need for a response time of the detector that is significantly less than the chromatographic peak width. Competing with this desire for small volume is the practical consideration that TC detectors become more sensitive to external effects as cell volume is decreased. A similar trade-off occurs when use of a make-up gas is warranted in order to help sweep the detector clear of sample, because the resultant sample dilution decreases the voltage difference responsible for the detector response. Currently, cell volumes are in the 100 µL range, suitable for use with 530 µm columns without make-up gas. At least one manufacturer offers a cell volume of less than 5 µL, but still recommends the use of make-up gas so that the total flow through the cell is 5 mL min⁻¹. Thus, the narrow-bore capillary columns can be accommodated, albeit with some loss of sensitivity resulting from the dilution.

The TCD responds to bulk properties of the effluent. It compares the conductivity of a filament exposed to the carrier gas to that of a filament exposed to sample components. The baseline is established by heating the filaments to a constant temperature with carrier gas flowing. Since the thermal conductivity of helium or hydrogen (often used as the carrier gas) is higher than virtually any other material likely to be encountered, the temperature of the filament increases when sample components are present in the effluent. The electronics of the TCD adjusts the current to maintain a constant temperature or allow the temperature to rise and respond to the difference in resistance. In either case the resulting voltage is used as the chromatographic signal based on the assumption that other thermal effects remain constant. The filament itself is constructed from tungsten

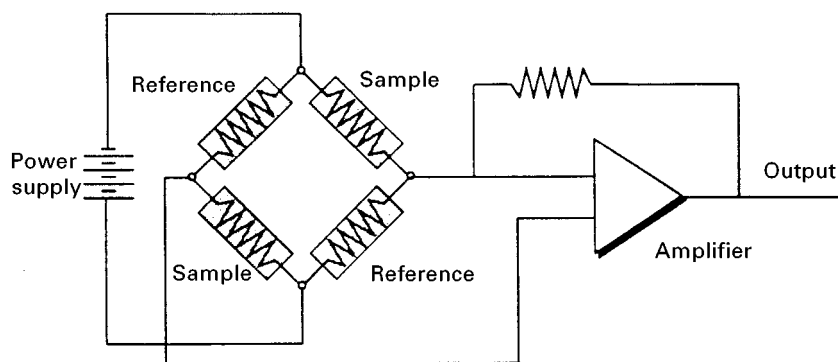


Figure 2 Schematic diagram of thermal conductivity detector electronics.

or tungsten–rhenium alloys to take advantage of the high resistance–temperature coefficient. TCD sensitivity increases as the temperature difference between the filament and the detector wall increases. This, coupled with the desire to have relatively low filament temperature (in order to increase lifetime), means that the detector body temperature should be set as low as possible while still preventing sample components from condensing.

Various detector designs incorporate geometries with as many as four filaments. These are often incorporated into a Wheatstone bridge circuit (Figure 2) and produce a voltage imbalance when an analyte passes through one side. In the HP 5890 series II TCD cell depicted in Figure 3 there is a single filament and a switching system so that the gas stream alternates every 200 ms. The response is due to the voltage difference of a filament exposed

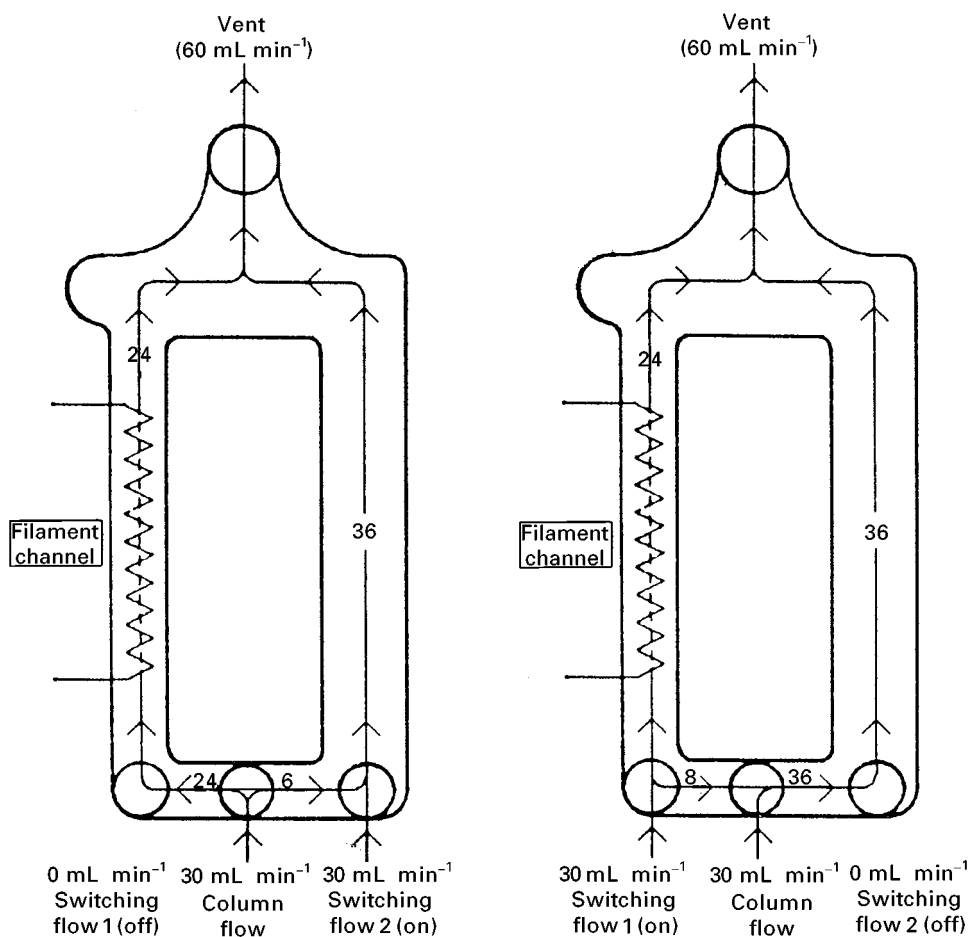


Figure 3 HP 5890 series II thermal conductivity cell.

alternatively to pure carrier gas and carrier gas plus sample.

As mentioned above, He and H₂ are commonly used as carrier gases when the TCD is involved. H₂ has a significantly higher thermal conductivity than does He, but is often not chosen because of its potential explosiveness and because it may reduce the oxide coating on the filament and thus cause changes in response factors. Most sample components have thermal conductivities well below that of either hydrogen or helium (Table 1), thus providing a detector with a universal response. Analysis of hydrogen requires special consideration. For instance, N₂ or Ar could be used as a carrier gas, but then sensitivity to other compounds would be much reduced. Alternatively, He can be used as a carrier gas, and the detector temperature kept relatively high.

The TCD is a concentration-dependent detector, so that the peak size is dependent on flow rates. The MDA is much higher than for the FID, corresponding to about 10 p.p.m. of C₉ in the cell. Although response factors cannot be calculated from thermal conductivities alone, they have been determined for many compounds and shown to vary only slightly within a homologous series. This makes the TCD useful for quantitative work. Organometallic compounds have somewhat low response factors, as do halogenated compounds. Some representative response values, relative to benzene, are shown in Table 1.

Operationally the TCD is quite simple, although the filament can be permanently damaged if current is left on without gas flow being maintained. Likewise,

Table 1 Thermal conductivities and TCD response values for selected compounds

Thermal conductivity of common gases (relative to He = 100) ^a	Molar response (in helium) (relative to benzene = 100)
H ₂	125.3
He	100
N ₂	18
Ar	12.8
CO ₂	12.7
Ethane	19.3
<i>n</i> -Butane	13.5
<i>n</i> -Nonane	10.8
<i>i</i> -Butane	14.0
Cyclohexane	10.1
Benzene	10.4
Acetone	9.9
Ethanol	12.5
Chloroform	5.9
Methyl iodide	4.5
Ethyl acetate	9.7111

^aTemperature 100°C.

exposure to traces of oxygen is damaging to the filament, so that the system must be leak-free. Use of plastic tubing such as nylon or polytetrafluoroethylene is discouraged since they are permeable to oxygen. Temperature variations in the detector will result in baseline fluctuations so careful control of heating elements is necessary. When properly operating, the noise level is only a few microvolts.

The design of these two detectors has not changed markedly since their introduction over three decades ago and they are firmly entrenched in chromatographic analyses. This will continue to be the case for systems in traditional laboratories. In addition, there has been recent progress in the development of miniature gas chromatographic systems and fast chromatography. This miniaturization has been driven by advances in field analyses and the concomitant need for portability. These systems take advantage of silicon micro machining and integrated circuit-processing techniques, including a microthermal conductivity detector. More information about this can be obtained from the publication by Etiope (see Further Reading).

See also: II/Chromatography: Gas: Column Technology; Detectors: Mass Spectrometry; Detectors: Selective; Historical Development; Theory of Gas Chromatography. III/Gas Analysis: Gas Chromatography.

Further Reading

- Etiope G (1997) *Journal of Chromatography (A)* 775: 243–249.
- Hinshaw JV (1990) Flame ionization detectors. *Liquid Chromatography–Gas Chromatography* 8(2): 104–114.
- Hinshaw JV (1990) Thermal conductivity detectors. *Liquid Chromatography–Gas Chromatography* 8(4): 296–300.
- Hinshaw JV and Ettre LS (1994) *Introduction to Open-tubular Column Gas Chromatography*. Cleveland, OH: Advanstar Communications.
- Jorgensen AD, Picel KC and Stamoudis VC (1990) Prediction of gas chromatography flame ionization detector response factors from molecular structures. *Analytical Chemistry* 62: 683–689.
- McMinn DG and Hill HH (1992) The flame ionization detector. In: Hill HH and McMinn DG (eds) *Detectors for Capillary Chromatography*, Ch. 2. New York: Wiley.
- Miller JM (1988) *Chromatography – Concepts and Contrasts*, pp. 121–129. New York, NY: Wiley Interscience.
- O'Brien MJ (1985) Detectors. In: Grob RL (ed.) *Modern Practice of Gas Chromatography*, 2nd edn pp. 211–248. New York, NY: John Wiley.
- Wilson M (1988) Detectors. Evaluation of a micro gas chromatographic technique for environmental analyses of CO₂ and C₁–C₆ alkanes. In: Hyver KJ (ed.) *High Resolution Gas Chromatography*, 3rd edn, pp. 4–16. Avondale: Hewlett-Packard.

Detectors: Mass Spectrometry

M. R. Clench and L. W. Tetler, School of Science and Mathematics, Sheffield Hallam University, Sheffield, UK

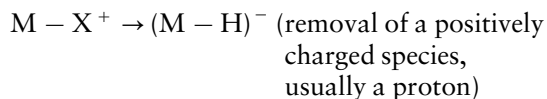
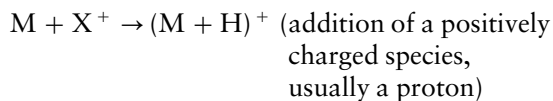
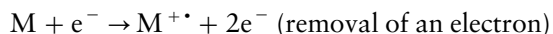
Copyright © 2000 Academic Press

Introduction

The mass spectrometer provides the most powerful detector available for gas chromatography. It is sensitive, selective and offers vastly superior qualitative information over conventional detectors such as the flame ionization detector (FID) or electron-capture detector (ECD). Modern instruments for gas chromatography-mass spectrometry (GC-MS) are small, reliable and much less expensive than formerly. In many laboratories small 'bench-top' GC-MS instruments have virtually replaced 'stand-alone' gas chromatographs for even routine applications. In this short paper we shall attempt to describe some of the basic principles of mass spectrometry and how they are applied in GC-MS. In order to illustrate some of the techniques available the determination of nitrated polycyclic aromatic hydrocarbons in diesel particulates will be utilized as a case study.

Ion Formation

Mass spectrometers are used to analyse ionized sample molecules. There are essentially four methods in which a neutral sample molecule (M) can be converted into an ionic species:



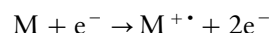
The *ion sources* used in GC-MS make use of each of these four processes in order to form positive or negative ions as appropriate.

Electron Ionization (EI)

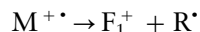
The most important method for the production of ions in GC-MS instruments uses the electron ioniza-

tion (EI) ion source. A schematic of a typical EI ion source is shown in **Figure 1**.

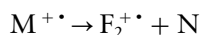
The filament, usually a simple coil of tungsten wire, is heated. On heating it produces electrons, which are then accelerated into the ion source chamber by applying a potential difference between the filament and the chamber. This potential difference is usually in the range 50–70 V, giving the electrons a kinetic energy (*the electron energy*) of 50–70 eV (where $1 \text{ eV} = 1.602 \times 10^{-19} \text{ J}$). Interaction of neutral sample molecules with the electrons causes ionization by removal of one electron:



This process creates the positively charged *molecular ion* of the sample molecule, i.e. a radical cation. However, the first ionization energy of most organic compounds is only of the order of 10 eV. Hence molecular ions formed in an EI ion source have excess internal energy and further fragmentation occurs in order to dissipate this energy. Fragmentation occurs via a variety of processes and leads to mass spectra containing a fingerprint of the molecule. The processes of fragmentation are shown below:



and/or:



(where F_1^+ represents an even electron fragment ion, R^\bullet a neutral radical, $F_2^{+\bullet}$ an odd electron fragment ion, often called a radical ion, and N a neutral species).

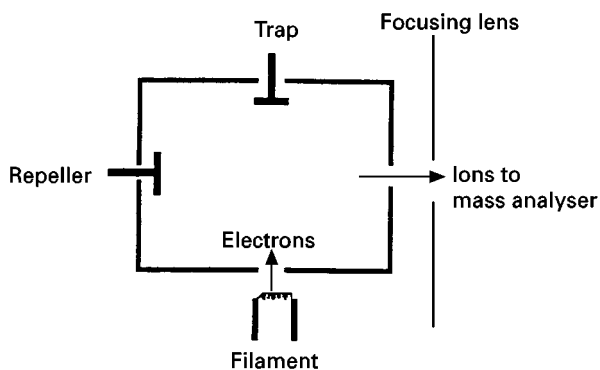
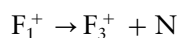
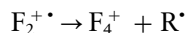


Figure 1 Schematic of an electron ionization (EI) ion source. Ions formed by interaction of the sample molecules with electrons emitted from the filament are extracted and focused into the mass analyser by the action of the repeller and the focusing lens.

Both types of initial *fragment ions* may also further fragment:



and/or:



Fragmentation will continue until the excess internal energy is dissipated. The appearance of EI mass spectra is a function of the compound under investigation, the electron energy used and the ion source temperature. For this reason it is usual to record EI mass spectra at an electron energy of 70 eV which gives good sensitivity, interpretable fragmentation and allows comparison to be made between spectra recorded on different instruments and with standard spectra stored in computerized libraries.

An EI mass spectrum of 2-nitrofluorene, a nitrated polycyclic aromatic hydrocarbon, is shown in Figure 2A. This mass spectrum illustrates some of the key features of EI spectra. A small molecular ion can be seen at m/z 211 along with fragment ions corresponding to the loss of $\cdot\text{OH}$ and NO_2 groups. The pattern of fragment ions, i.e. their intensity and distribution is characteristic of 2-nitrofluorene and library search, used where possible in combination with GC retention time (obtained from a standard sample), allows the sample to be easily identified.

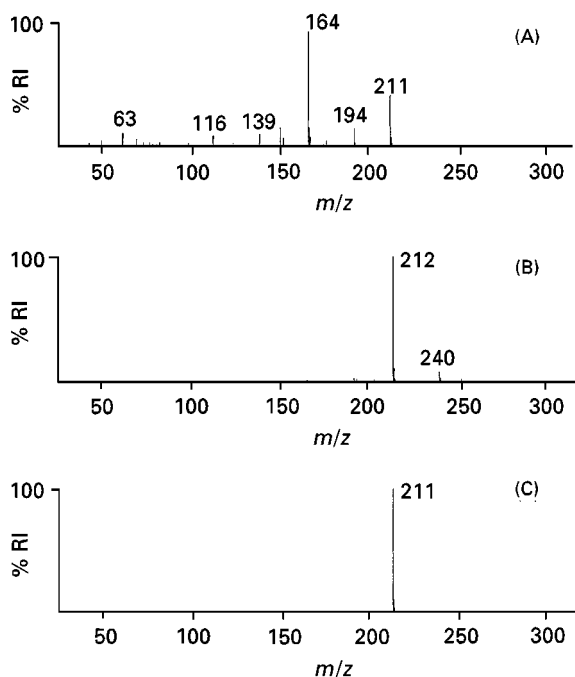
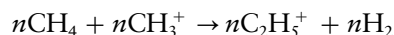
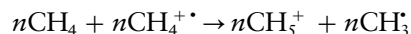
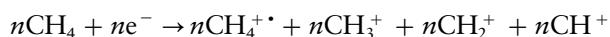


Figure 2 Comparison of (A) electron ionization, (B) positive chemical ionization and (C) negative chemical ionization mass spectra of 2-nitrofluorene. Note the higher degree of fragmentation in the EI mass spectrum.

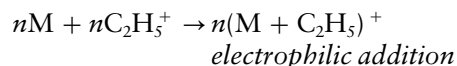
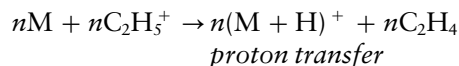
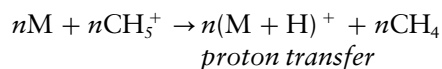
Electron ionization is the most widely used ionization technique for GC-MS. However, it has a number of limitations. The most important of these is caused by the excess internal energy of the initially formed molecular ions. For certain classes of compounds, they all fragment in the ion source and hence a molecular ion is not observed in the recorded mass spectrum. This removes one of the key pieces of information from the mass spectrum, i.e. the relative molecular mass of the compound under investigation. In order to overcome this, other ionization techniques are available to the mass spectroscopist, the most important of these being chemical ionization (CI).

Chemical Ionization (CI)

Positive ion chemical ionization In positive ion CI an ion source slightly modified from that shown in Figure 1 (by reduction of the size of the ion exit aperture) is filled with a *reagent* gas (e.g. methane, isobutane or ammonia) to a pressure of about 0.1–1.0 mbar. At this pressure ion–molecule reactions can occur between ions of the gas (created by EI processes) and neutral gas molecules. Taking as an example some of the processes that occur when methane is used as a reagent gas:



In a similar way when sample molecules are introduced into the ion source, ion molecule reactions between reagent gas ions and gaseous sample molecules can occur, to produce sample ions, i.e.



The formation of sample ions via these reactions is much less energetic than molecular ion formation via electron ionization. Hence the mass spectra obtained show less fragmentation than the corresponding EI mass spectra. When methane or isobutane are used as the reagent gas, proton transfer is the dominant reaction. Hence the relative molecular mass of the compound of interest can now be derived from the

$n(M + H)^+$ *protonated molecular species* with additional confirmation of the assignment being given by the presence of the $(M + C_2H_5)^+$ *adduct ion*. Where ammonia is used as the reagent gas electrophilic addition is often as important or the dominant process and in this case the $(M + NH_4)^+$ adduct ion may be used.

Figure 2B shows the positive ion chemical ionization mass spectrum of 2-nitrofluorene obtained using methane as reagent gas. Note the large $(M + H)^+$ peak at m/z 212 and the reduced fragmentation compared to the corresponding EI spectrum. Also visible is the adduct ion at m/z 240 corresponding to the $(M + C_2H_5)^+$ ion formed by the electrophilic addition process discussed earlier.

Negative ion chemical ionization (NCI) Chemical ionization is also a useful way of producing negatively charged species for mass spectrometry. There are two important mechanisms for ion formation in NCI. The first, which is analogous to the processes already described for positive CI, is proton transfer:



This type of reaction will occur when the relative proton affinity of the reagent gas anion (B^-) is high. It is a relatively low energy process and leads to mass spectra containing intense $(M - H)^-$ ions and little fragmentation.

However, a more important mechanism of ion formation in NCI, and one that has been widely utilized in GC-MS, is via an electron capture process. If a compound containing one or more suitable electronegative groups is introduced into the ion source in the presence of a high pressure (~ 1 mbar) of a *buffer gas* (e.g. methane) the following reaction can occur:



In the above equation the thermal electrons (e^{-th}) are produced from the electron ionization of the methane. The neutral methane molecules also act to collisionally stabilize the excited radical anion formed by associative resonance electron capture. This leads to the observation of a radical anion ($M^{\cdot-}$) in mass spectra recorded using this ionization method.

Electron capture is a very low energy process and the recorded mass spectra contain little or no fragmentation. The NCI mass spectrum of 2-nitrofluorene is shown in Figure 2C. This compound contains an electronegative nitro group, and is ionized via the electron capture process. An intense $M^{\cdot-}$ ion can be seen at m/z 211 with no evidence of fragmentation.

In a similar manner to the use of the electron-capture detector for gas chromatography, the use of electron capture NCI GC-MS can introduce sensitivity and specificity into an analysis. Whereas approximately 100 pg of sample are required to record a mass spectrum in EI mode, NCI spectra have been recorded from a little as 500 fg (for appropriate electron capturing compounds). This will be further illustrated below.

The Separation of Ions and Recording of Mass Spectra

There are many methods available for the separation of ions and recording of mass spectra. The ionization methods described above have been incorporated into all of the current commercial types of mass spectrometer. In this section only brief descriptions of these are offered. For a more complete discussion see either Chapman (1993) or Johnstone and Rose (1996).

The key parameters to take into account in the selection of a particular type of mass spectrometer for a GC-MS experiment are the masses of the compounds under consideration and the selectivity and sensitivity required for the analysis. Where the largest compounds to be encountered are likely to have a relative molecular mass of less than 1000 any of the types of mass spectrometer described below is useful.

The Quadrupole Mass Filter

The quadrupole mass filter is the most widely employed type of mass analyser in current use. It comprises four metal rods accurately aligned around a central axis. RF and DC voltages on the rods create a complex electrostatic field within the area bound by them. Ions entering this region are acted on by the electrostatic field and their motion through the rods can be likened to two superimposed sine waves. Under these conditions the forces acting on most ions cause the amplitude of the oscillations to increase and accelerate them into the quadrupole rods. However, some ions are not accelerated into the rods and undergo trajectories that traverse the full length of the rods. The parameters that govern the equations of motion of ions in a quadrupole mass filter are the mass to charge ratio of the ions, the spacing between the rods, the frequency of the RF voltage and the magnitude of the RF and DC voltages. Hence the RF and DC voltages may be selected such that ions of only one m/z value have 'stable' trajectories. By varying the RF and DC voltages but keeping the ratio between them the same a range of m/z values can be made to undergo stable trajectories, be brought to focus on the detector and a mass spectrum recorded.

The Ion Trap

The ion trap operates in a similar manner to a quadrupole mass filter. It comprises a doughnut-shaped ring electrode to which the RF voltage is applied and two end caps either earthed or with supplementary AC or DC voltages. Ions formed either in the trap, or externally to the trap and transported into it, are initially stored within the trap. Mass separation is then achieved by increasing the RF voltage such that ions are ejected from the trap in ascending m/z order.

The Double Focusing Magnetic Sector Mass Spectrometer

The double focusing magnetic sector mass spectrometer differs from those discussed so far in that the mass analyser comprises two distinct components, an electromagnet and an electrostatic analyser. The magnet acts as a momentum analyser and affects mass separation, while the addition of an electrostatic analyser corrects for some variations in the kinetic energy of ions of the same m/z value and allows them to be brought to focus on the detector at the same time. Hence the use of a double focusing arrangement as a mass analyser allows very high *resolution* to be achieved. In mass spectrometry resolution is defined as the ability of the mass spectrometer to separate ions of very similar m/z value.

Resolution is important in mass spectrometry since it may be used to introduce specificity into an experiment. An important application of high resolution arises in the determination of polychlorinated dibenzodioxins (PCDDs) and polychlorinated dibenzofurans (PCDFs) by GC-MS. These compounds are found ubiquitously in the environment and their determination is important owing to concern about their toxicity, mutagenicity and carcinogenicity. The only method that has been found to offer the appropriate degree of sensitivity and specificity for this analysis is GC followed by high resolution MS detection. High resolution is required since matrices which accumulate PCDDs and PCDFs are also likely to accumulate other polychlorinated aromatic hydrocarbons, e.g. polychlorinated biphenyls. These compounds, which may co-elute with the PCDDs and PCDFs of interest, contain fragment ions in their EI mass spectra which have the same integer m/z value as the molecular ions of PCDDs and PCDFs. However, by monitoring the accurate mass value of the PCDD and PCDF molecular ions (i.e. the exact mass value of their elemental composition), at an adequate resolution to separate them from likely interfering ions, specificity is introduced. GC-MS is used extensively in environmental analysis for a range of ap-

plications including dioxin analysis. For further details the interested reader is referred to Bruner (1993).

Interfacing Mass Spectrometers with Gas Chromatographs

There are several methods available for interfacing gas chromatographs with mass spectrometers. These include the use of jet separators for packed columns and a variety of ways of interfacing capillary columns. For packed columns the jet separator, a form of momentum separator, is required to remove the majority of the carrier gas. A 'solvent dump valve' is also incorporated into these devices in order that the injection solvent can be vented to waste rather than it passing into the mass spectrometer.

Although a number of interfaces for packed column GC-MS have been described in the past, capillary columns are currently almost exclusively used for GC-MS. The most widely used interface, in this case, is the direct interface, where the column is passed through a simple heated transfer line directly into an EI or CI ion source. The low (1 mL min^{-1}) carrier gas flow commonly used with capillary columns can readily be accommodated by the MS pumping system in order to maintain a good vacuum. **Figure 3** shows a complete instrument based around the use of a capillary column, a simple direct interface and a quadrupole mass spectrometer. For a more complete discussion of the full range of GC-MS interfaces see either Chapman (1993) or Johnstone and Rose (1996).

GC-MS Experiments

Full or Normal Scan

The standard GC-MS mode of operation is the full or normal scan mode. On injection of the sample into the GC, the mass spectrometer is set to repetitively scan over a preset mass range. Typically this would involve the mass spectrometer recording a mass spectrum over the scan range 35–500 Da once a second.

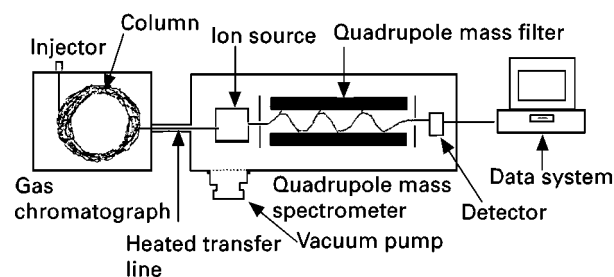


Figure 3 A quadrupole based GC-MS instrument employing a direct interface for connection between the GC and the MS.

The requirement for relatively fast acquisition rates is due to the fact that open tubular GC columns typically produce peaks of only about 10–15 s wide. Hence, in order to acquire a representative number of mass spectra from each peak, fast scan rates are required. A second consequence of these fast acquisition rates is the requirement for a data system on all GC-MS instruments. Each mass spectrum can then be stored in the data system for subsequent examination/data processing.

Full scan data are used by the data system to generate a total ion chromatogram (TIC). This is achieved by summing the intensity of the ions in each mass spectrum to create a value for the total ion intensity, as a number of ions or total number of analogue to digital converter bits. This number is then plotted against time/scan number to create a chromatogram. One of the great strengths of GC-MS using EI ionization is that the TIC generated by this method is then directly comparable with a chromatogram produced from the same sample using flame ionization detection.

Selected Ion Monitoring (SIM)

Selected ion monitoring (SIM) is a technique widely used for trace analysis. In this technique, rather than the mass spectrometer being set to scan over a pre-defined mass range and record full mass spectra it is set to monitor the intensity of specific m/z values. SIM is used to introduce selectivity into an analysis and improve sensitivity. Sensitivity is enhanced over the full scan mode experiment since in the full scan experiment a large proportion of the scan time is spent recording areas of the spectrum where no ions of interest occur. Ions are still being produced in the ion source but are lost in the mass analyser as it brings others into focus on the detector. In SIM, in a 1 s duty cycle, only a few, i.e. 1–10, ions are selected. Hence, the mass analyser transmits these ions for a longer percentage of the time in which they are being produced and therefore more of the ions of the particular m/z values of interest are recorded.

SIM may also be used to introduce selectivity into the experiment. This also has the effect of increasing sensitivity by decreasing the amount of 'chemical noise', i.e. real signal, but not from the compound of interest, observed when peaks of interest elute. The increase in selectivity may also be achieved by the use of a double focusing mass spectrometer and high resolution and this may be enhanced by, for example, the use of negative chemical ionization.

An example of the increase in selectivity obtained by the use of SIM combined with NCI from our own laboratory can be seen in the determination of nit-

rated polycyclic aromatic hydrocarbons (nitro-PAH) in vegetation extracts. Nitro-PAH are absorbed on to vegetation from anthropogenic emissions, however their determination is made complex by the large amount of other compounds extracted from the vegetation by the sample preparation procedure. Figures 4A and B show a comparison between the chromatogram obtained from an extract of bark from a maple tree in an urban region using an ECD and the individual mass chromatograms obtained from the same extract using GC-MS in NCI-SIM mode. The

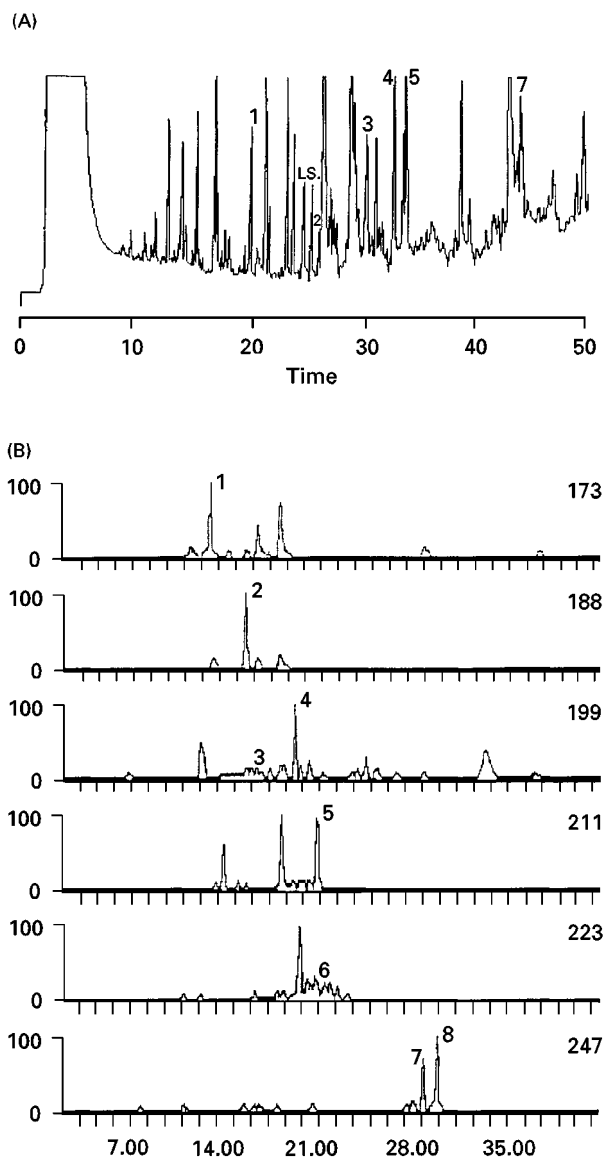


Figure 4 A comparison of the chromatograms obtained from the analysis of a complex extract containing nitrated polycyclic aromatic hydrocarbons by gas chromatography (A) using an electron-capture detector and (B) by GC-MS employing negative chemical ionization and selected ion monitoring. Note the increase in specificity afforded by the use of GC-MS under these conditions.

quadrupole mass spectrometer used in this case was set to monitor the M^+ ions obtained from 9 nitro-PAH. The complex chromatogram shown in Figure 4A does not allow simple identification of the peaks of interest and the possibility of interferences/peak overlap leads to difficulties when attempting quantification. This can be observed for peak 5 ($t_r = 34.1$ min) in Figure 4A. This peak arises from the presence of 2-nitrofluorene in the bark extract. As can be seen, accurate and precise integration of this peak is made difficult by the presence of peaks with very similar retention time. In contrast the peaks from the nitro-PAH monitored by NCI-SIM can be seen clearly in Figure 4B. Each chromatographic trace in this figure represents the ion current observed from monitoring the m/z value of the M^+ ion of a series of nitro-PAH. Peaks are readily integrated for quantification with the 2-nitrofluorene peak (peak 5) appearing well resolved on the m/z 211 trace.

One of many areas in which the use of resolution to introduce specificity into SIM experiments is important is the petroleum industry. Dibenzothiophenes (DBT) have been suggested as marker compounds for oil pollution. However, taking as an example dibenzothiophene itself, this has the same nominal molecular mass (184 Da) as the C_4 -alkylated naphthalenes which are also present in crude oil. Hence in order to specifically measure dibenzothiophene in crude oil it is necessary to monitor the accurate mass to charge ratio (m/z 184.0347) of its molecular ion at high resolution in a SIM experiment. Figure 5 compares the GC-MS-SIM analysis of dibenzothiophene in crude oil carried out using low and high resolution. As can be clearly seen the C_4 -naphthalenes are not observed in the high resolution data. The power of such analyses can be seen in Figure 6 which shows a comparison of the GC-HRMS-SIM data obtained from the analysis of methyl and C_2 substituted dibenzothiophenes for three different crude oils obtained from two North Sea oil fields. The different crude oils can be clearly distinguished with such data.

Other Techniques

Mass Spectrometry–Mass Spectrometry (MS-MS)

Mass spectrometry–mass spectrometry, also known as tandem mass spectrometry, is the term used to describe mass spectrometric methods employing instruments that contain more than one mass analyser. Such instruments may be used to increase the amount of structural information obtained or to introduce more specificity.

The simplest tandem mass spectrometer to consider is the triple quadrupole mass spectrometer. This com-

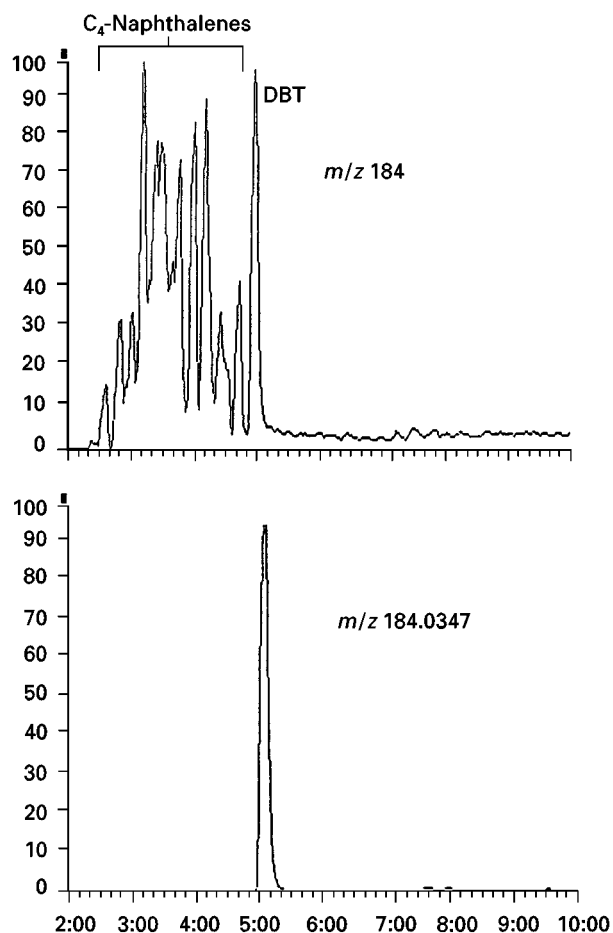


Figure 5 GC-MS analysis of dibenzothiophene (DBT) in a crude oil using low resolution (top) and high resolution (bottom) selected ion monitoring. (Reproduced from Tibbets and Large (1988) by kind permission of John Wiley and Sons.)

prises two quadrupole mass filters and a multipole collision cell and is shown schematically in Figure 7. In principle the operation of such an instrument follows the following sequence: ion selection in the first quadrupole mass filter, ion dissociation in the collision cell and separation of the products of ion dissociation in the second quadrupole mass filter. For illustration, Figure 2C, the NCI mass spectrum of 2-nitrofluorene, only contains the M^+ ion at m/z 211. Hence the only information contained in this mass spectrum is the relative molecular mass of the compound. In order to generate structural information a *product ion scan* could be carried out. To do this the first quadrupole mass filter would be set to transmit only m/z 211. This ion would then be subjected to collisions with a gas held in the collision cell (collisionally induced decomposition (CID)) and the resulting *product ions* recorded using the second quadrupole mass filter. The resulting *product ion spectrum* then shows only ions that have arisen

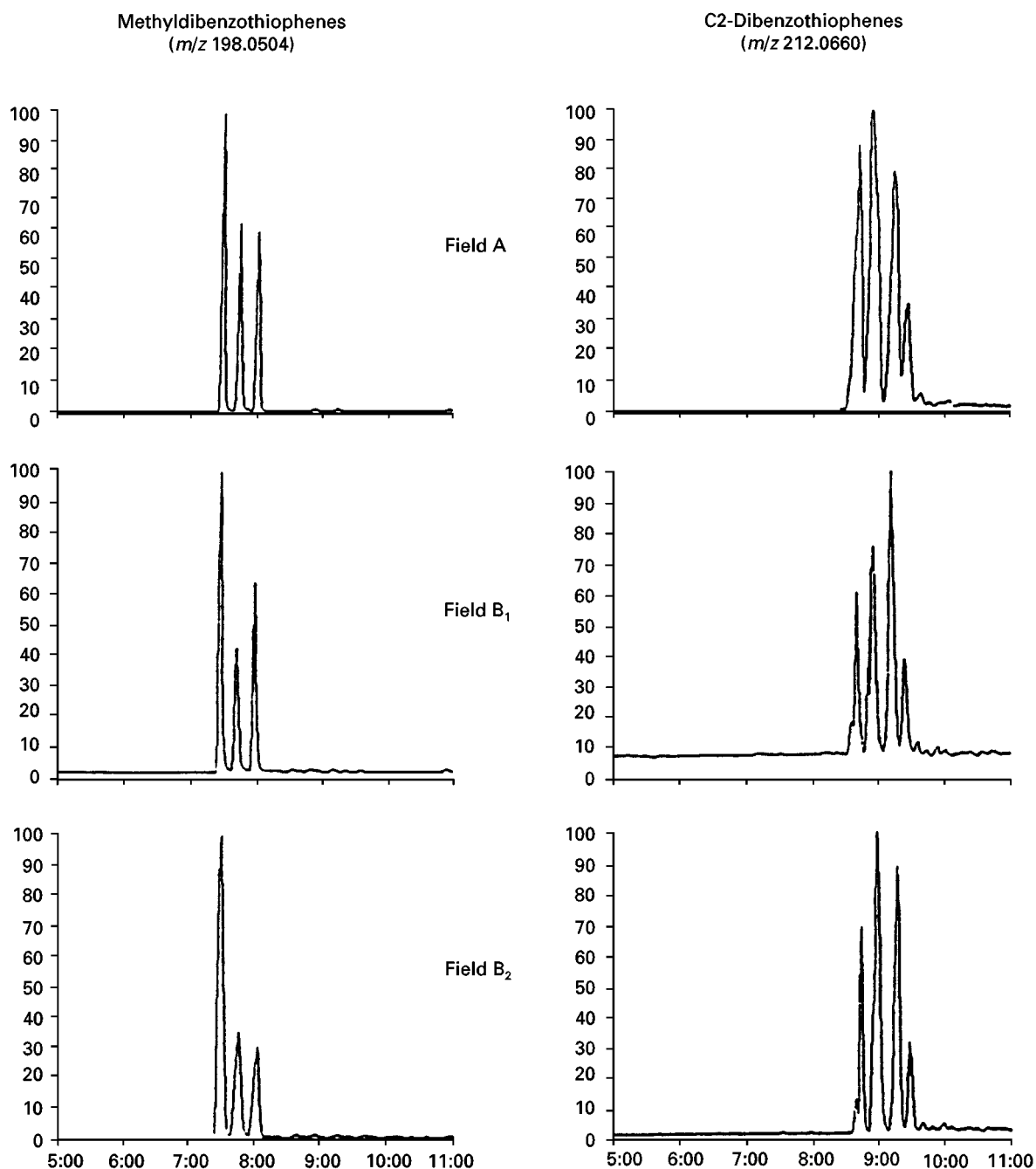


Figure 6 A comparison of the GC-HRMS-SIM fingerprints of methyldibenzothiophenes and C_2 -dibenzothiophenes in three crude oils from two North Sea fields. (Reproduced from Tibbets and Large (1988) by kind permission of John Wiley and Sons.)

directly from the fragmentation of m/z 211 and contains structural information. It can be seen that this method is also useful for clearing up ambiguities in the interpretation of EI spectra, since it allows *precursor/product ion* relationships to be clearly defined.

A second application of tandem mass spectrometry often used in conjunction with GC-MS utilizes a technique called *multiple reaction monitoring* (MRM). This technique, like high resolution SIM, is used to

increase the specificity of an analysis. After first recording product ion mass spectra of the analyte(s) of interest, one or more precursor/product ion relationships are chosen. The criteria for this are that the product ions selected are intense and characteristic of the specified analyte. Then in order to carry out the MRM experiment, the first quadrupole mass analyser is set up in SIM mode, to switch between the precursor ions of interest. The collision cell is operated in

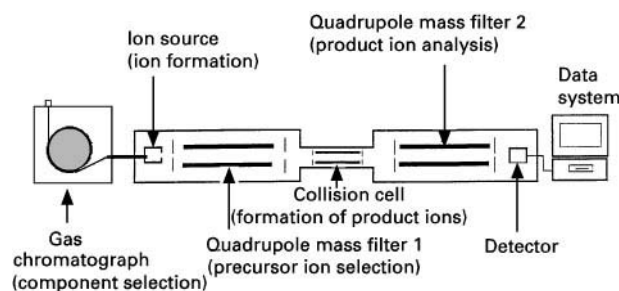


Figure 7 A triple quadrupole mass spectrometer. On leaving the GC column sample components are first ionized, then ions selected by the first quadrupole mass filter are fragmented in the collision cell for analysis by the second quadrupole mass filter. Such instruments may yield greater structural information than single stage instruments and allow further selectivity to be introduced into GC-MS experiments.

the normal way, and the second quadrupole mass filter is set up to switch between the characteristic product ions.

The output from such an experiment is chromatographic, producing one or more plots of signal intensity against time. Peaks are only observed in such chromatograms when an ionized compound yields an ion of the selected precursor ion m/z value, which also subsequently fragments, under CID, to give a product ion of the selected product ion m/z . The two stages of mass selection make this a highly selective technique and it has been proposed as a viable alternative to high resolution SIM for a variety of applications.

Recent advances in ion trap technology have meant that similar modes of operation also available on these compact, relatively low cost instruments. In this case ions other than the precursor ion of interest are selectively ejected from the trap. The selected precursor ion is then subjected to CID in the trap and a product ion mass spectrum may be recorded by ejecting these ions. For a fuller discussion of tandem mass spectrometry see Busch *et al.* (1988).

Conclusions

A developing field in GC-MS is the use of time of flight mass analysers with short capillary columns for very rapid analyses. We have described time of flight mass analysers and the advantages offered by their use for the acquisition of mass spectral data from narrow chromatographic/electrophoretic peaks in the companion paper to this one, on the use of mass spectrometry as a detector for liquid chromatography. The same arguments apply for fast GC-MS analyses and a number of manufacturers have recently launched instruments of this type. Specialist GC-MS instrumentation is also increasingly being used in the

clinical field in order to accurately determine isotope ratios, e.g. the presence of *Helicobacter pylori* in the gastric epithelium has been linked with gastritis, peptic ulcers and gastric cancer. The presence of *Helicobacter pylori* can be determined by measuring the $^{13}\text{C}/^{12}\text{C}$ isotope ratio in exhaled breath following ingestion of isotopically labelled urea. Gerhards *et al.* (1999) have examined the use of GC-MS in clinical analysis and Platzner (1997) provides a full discussion of modern isotope ratio mass spectrometry.

The future of mass spectrometry as the detector of choice for gas chromatography looks secure. In this paper we have illustrated some of the benefits of this happy marriage of techniques. Modern GC-MS instruments are compact, robust, sensitive, selective and give access to a range of information not possible when using conventional detectors, hence their importance in the modern GC laboratory.

See also: II/Chromatography: Gas: Detectors: Selective. Chromatography: Liquid: Detectors: Mass Spectrometry. Mass Spectrometry: Spectrometry - Mass Spectrometry Ion Mobility. III/Clinical Diagnosis: Chromatography. Geochemical Analysis: Gas Chromatography.

Further Reading

- Bruner F (1993) *Gas Chromatographic Environmental Analysis*. New York: VCH Publishers.
- Busch KL, Glish GL and McLuckey SA (1988) *Mass Spectrometry—Mass Spectrometry*. New York: VCH Publishers.
- Chapman JR (1993). *Practical Organic Mass Spectrometry*, 2nd edn. Chichester, UK: John Wiley.
- Davis R and Frearson M (1987) *Mass Spectrometry*. Analytical Chemistry by Open Learning Series. Chichester, UK: John Wiley.
- Evershed R. (1993) In: Baugh PJ (ed.) *Gas Chromatography – A Practical Approach*. Oxford, UK: Oxford University Press.
- Gaskell SJ (ed.) (1986) *Mass Spectrometry in Biomedical Research*. Chichester, UK: John Wiley.
- Gerhards P, Bons U and Sawazki J (1999) *GC/MS in Clinical Chemistry*. Chichester, UK: John Wiley.
- Johnstone RAW and Rose ME (1996) *Mass Spectrometry for Chemists and Biochemists* 2nd edn. Cambridge, UK: Cambridge University Press.
- Lee TA (1998) *A Beginners Guide to Mass Spectral Interpretation*. Chichester, UK: John Wiley.
- Oehme M (1998) *Practical Introduction to GC-MS Analysis with Quadrupoles*. Heidelberg: Hüthig Verlag.
- Platzner I (1997) *Modern Isotope Ratio Mass Spectrometry*. Chichester, UK: John Wiley.
- Smith RM and Busch KL (1999) *Understanding Mass Spectra. A Basic Approach*. New York: John Wiley.
- Tibbets PJC and Large R (1988) In Crump GB (ed.) *Petroanalysis '87*. Chichester, UK: John Wiley.

Detectors: Selective

E. R. Adlard, Burton, South Wirral, UK

Copyright © 2000 Academic Press

Introduction

The packed columns used in the early days of GC were inefficient by modern standards and so selective detectors that only gave a response to particular elements or compounds had obvious advantages when analysing complex mixtures. There was also a big incentive to develop more sensitive detectors and the detection of an organic vapour in an inert gas lent itself to the development of a host of devices, the majority of which have failed to make any lasting impact. Even today when the mass spectrometer is the selective detector *par excellence* there are still a number of other, more limited, detectors commercially available and this situation seems likely to continue. This paper describes some of these detectors; it should be noted that they are described as 'selective' rather than 'specific' since although they may give a large signal for one type of analyte they will also invariably give a small signal for others.

In general, selective detectors usually have more operating parameters than the two common universal detectors, the thermal conductivity detector (TCD) and the flame ionization detector (FID), and are more sensitive to small changes in these parameters. Some selective detectors are so temperamental that, having needed several days to set them up, they are then best left in continuous standby even when not in use.

Element-Selective Detectors

Although there are selective detectors for most elements, the common ones are those for sulfur, nitrogen, phosphorus and the halogens. These elements account for the great majority of published work because they are the ones most likely to be encountered in most real life applications.

Sulfur-Selective Detectors

Sulfur is an important element which turns up in many fields usually with deleterious effects; 0.1 ppm of a mercaptan in isopropyl alcohol would, for example, render it totally unfit for perfumery applications.

The flame photometric detector (FPD) monitors the light emitted by a hydrogen-rich 'cold' flame. Under these conditions sulfur (the S_2 species) has a band

spectrum with a maximum at 394 nm and phosphorus (HPO) has a band spectrum with a maximum at about 526 nm. Since these are band spectra they do not exhibit the very sharp emission lines of atomic spectra and are, therefore, only moderately selective. There are carbon band spectra, for example at 388 nm, that tend to interfere with the sulfur spectrum. The response is approximately equimolar for different sulfur compounds unless oxygen is also present in the molecule. Since it is an S_2 species being monitored in the flame the response is approximately proportional to the square root of the concentration. This disadvantage can be catered for by suitable electronics but there is always some doubt about whether the response follows the square root relationship accurately and calibration is essential for reliable quantitative results. Another severe disadvantage of the simple FPD is that co-eluted organic compounds not containing sulfur will 'quench' the sulfur emission and cause a drastic diminution of signal.

In spite of these disadvantages the FPD has proved a popular and important detector especially in the food and petroleum industries. For example, in the former it has been used for the detection of mercaptans in lager. In the latter it has been shown that a crude oil, so biodegraded that it can no longer be identified by its hydrocarbon fingerprint, can still be recognized by its sulfur fingerprint since the sulfur compounds are much more slowly degraded.

There have been a number of attempts over the years to improve the performance of the FPD. A dual-flame version oxidizes the sulfur compounds to SO_x in an ordinary oxidizing flame and the products of combustion are then taken to the hydrogen-rich cold flame. This gives a considerable reduction in the quenching effect of co-eluting compounds but at the cost of at least 10-fold loss in sensitivity from about 10^{-9} g s^{-1} for the single flame version. Another version, the pulsed FPD, developed by Amirav *et al.* in 1991, reduced the hydrogen flow rate so that the flame is extinguished and re-ignited about 2–4 times a second. The emission during each period of emission is scanned from the time of ignition and electronically time-gated. Under these conditions it is possible to discriminate on a time basis between carbon emissions taking place at 2–3 ms after ignition and sulfur emissions which take place at about 6 ms. Thus with this design there is both wavelength and time discrimination and the combined effect is a very high selectivity and a sub-picogram per second sensitivity. In spite of these advantages there are few publications on the use of the PFPD to date.

Most versions of the FPD can be used for phosphorus detection by changing the filter from 394 nm for S to 526 nm for P and a number of other elements such as Se, Sn, As and Ge have also been determined at various wavelengths and with varying degrees of selectivity and sensitivity. Simultaneous detection of two elements is also possible.

A different type of sulfur/nitrogen selective detector has been successfully developed in the last few years. In the sulfur chemiluminescence detector (SCD), the sulfur-containing compounds are combusted in an oxidizing flame or in later versions in a miniature ceramic furnace to SO_x which is then reacted with ozone in a low pressure chamber at about 10–15 Torr. Reaction with ozone raises the sulfur oxides to an excited state and as the molecules drop back to the ground state they emit light in the far blue end of the spectrum which is monitored by a photomultiplier tube after passing through an optical filter. Sub-picogram per second sensitivity is claimed for this detector with a linear response over five orders of magnitude, equimolar response for different sulfur compounds and no quenching effects. By replacing the optical filter for sulfur with one in the red region (610 nm) the detector can be used selectively for nitrogen. This is, in effect, similar to the so-called Thermal Energy AnalyserTM which was produced in the 1970s specifically for the analysis of nitrosamines in food but which never achieved wide popularity.

Figures 1A–D show chromatograms of a gas oil before and after a hydrotreater unit designed to reduce the total sulfur content of the fuel from about 220 ppm to 2 ppm. Figures 1A and B show the before and after FID traces where it is difficult to see any difference and Figures 1C and D show the before and after SCD chromatograms where the difference is clearly apparent.

Nitrogen-Selective Detectors

To a certain extent these have been covered in the section above but the commonest nitrogen-selective detector is the flame thermionic detector. This is abbreviated to FTD or NPD, since by operating under different conditions the detector can be made selective for nitrogen or phosphorus (but not both simultaneously). Like the FPD this detector has a long history of development originating in the observation that alkali metal compounds introduced into a flame gave a high response for halogens. Indeed, early detectors were made by modifying leak detectors used to monitor the escape of halogenated gases from refrigeration units. By operating under different conditions, selectivity for nitrogen and phosphorus could also be obtained. The next development was to use a small

flame as in an FID to impinge upon a pellet of an alkali metal salt; later versions had an alkali metal salt flame tip. All these versions suffered from the fact that, as the salt was gradually vaporized in the flame, the response of the detector altered and consequently required frequent calibration. The current version looks very similar to a conventional FID in construction but has a bead of rubidium glass that can be electrically heated to 600–800°C between the flame jet and the main collector electrode. This acts in a somewhat analogous manner to the grid in an electronic triode valve. Since the bead does not depend on a combustion flame for heating it is more stable and less susceptible to variations in response. For nitrogen the hydrogen gas supply to the detector is very small (about 4 mL min⁻¹) and the area of reaction is described as a hydrogen plasma rather than a flame. Increasing the hydrogen flow rate to the flame to about 30 mL min⁻¹ increases the sensitivity for phosphorus and reduces the nitrogen response. Typical performance characteristics for the NPD are shown in Table 1.

There is still considerable controversy about the mechanism of response of the NPD and for an in-depth discussion of this the reader should consult Patterson (see Further Reading).

The NPD is capable of giving excellent results if used by a skilled operator and it has been used in the nitrogen mode for a wide variety of samples. However, the difficulties in its use for routine analysis and the alternative detectors now available seem to indicate a decline in its use in the future.

Figure 2A shows an FID chromatogram of a sample containing 2 ng amounts of cocaine and heroin and Figure 2B shows the equivalent chromatogram obtained with an NPD. The improved sensitivity and selectivity of the NPD are clearly demonstrated.

Multi-Element Selective Detectors

There are at least two detectors commercially available that are capable of multi-element detection. The first of these is the electrolytic conductivity detector (ELCD), sometimes known as the Hall detector after its main developer and the second is the microwave plasma detector.

The Electrolytic Conductivity Detector (ELCD)

This detector can be used for halogens, nitrogen and sulfur but not for all three simultaneously. The principle of operation of the ELCD is extremely simple. The gases eluting from the column are passed with hydrogen through a small nickel furnace heated to

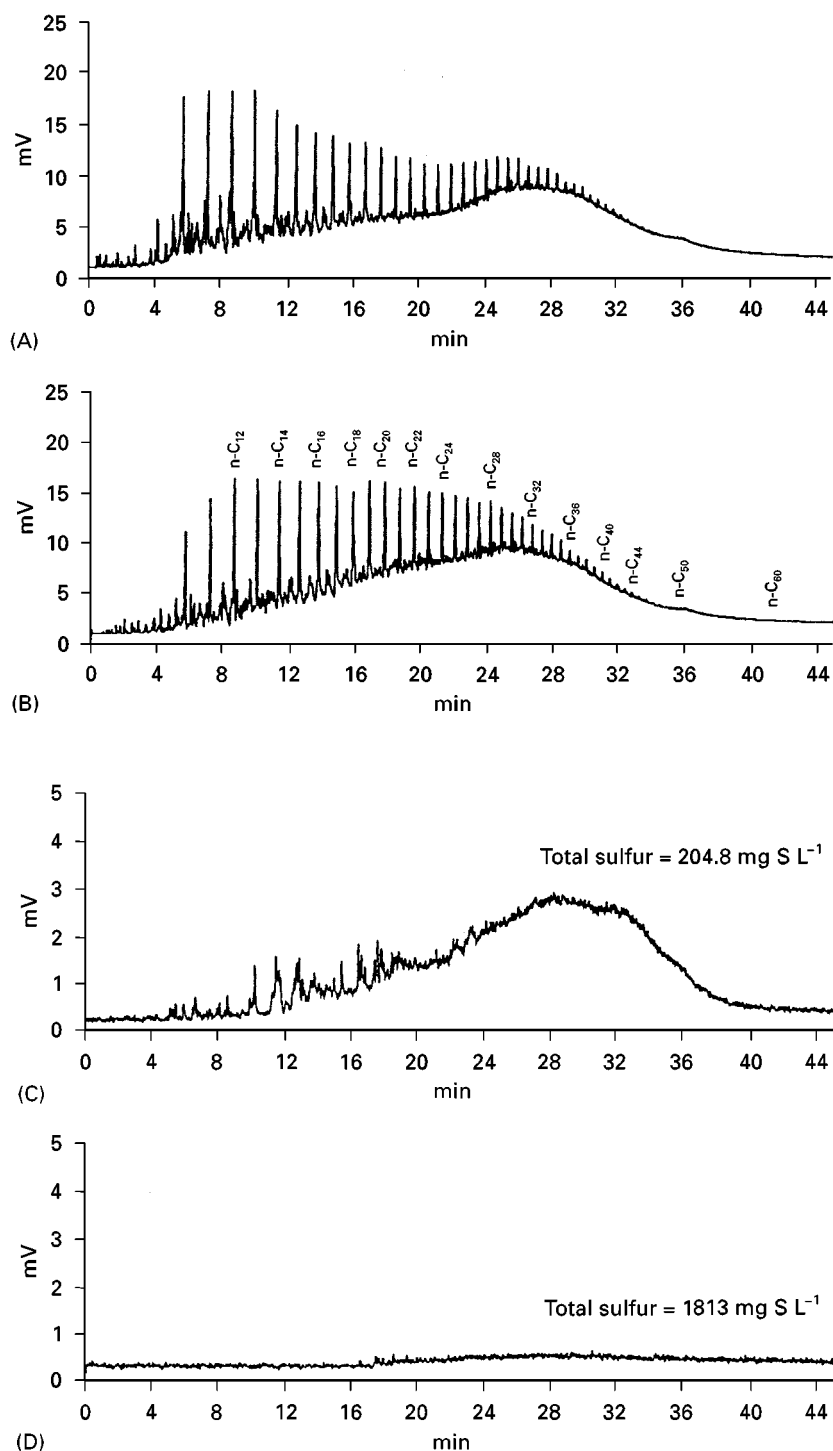


Figure 1 FID chromatograms of gas oil before (A) and after (B) hydrotreating. SCD chromatograms of gas oil before (C) and after (D) hydrotreating. (From Hutte RS. In *Chromatography in the Petroleum Industry* (1995) Adlard ER (ed.). Reproduced with permission of Elsevier Science.)

about 850–1000°C. Under these conditions halogen compounds are reduced to HX, nitrogen compounds to NH₃ and sulfur compounds to H₂S. These gases are all very soluble in water and if they are passed into a circulating water stream the electrical conductivity

will show major changes as the gases emerge. It is also possible to operate in an oxidizing mode so that sulfur goes to SO_x, halogens to HX and nitrogen to N₂.

In practice the equipment is complicated by the fact that the system outlined above would give an integral

Table 1 Typical performance characteristics for the NPD

Characteristic	Typical values
Sensitivity	$S_N = 0.1\text{--}1.0 \text{ A} \cdot \text{s/g N}$ $S_P = 1.0\text{--}10.0 \text{ A} \cdot \text{s/g P}$
Detectivity	$D_N = 5 \times 10^{-14}\text{--}2 \times 10^{-13} \text{ g N s}^{-1}$ $D_P = 1 \times 10^{-14}\text{--}2 \times 10^{-13} \text{ g P s}^{-1}$
Specificity	$S_N/S_C = 10^3\text{--}10^5 \text{ gC/gN}$ $S_P/S_C = 10^4\text{--}5 \times 10^5 \text{ gC/gP}$ $S_N/S_P = 0.1\text{--}0.5 \text{ gP/gN}$
Linear range	$10^3\text{--}10^5$

Source: From PL Patterson in *Detectors for Capillary Chromatography* (eds. HH Hill and DG McMinn). Reproduced courtesy of John Wiley and Sons Inc.

chromatogram rather than the more familiar differential chromatogram and this is overcome by circulating the electrolyte through ion exchange resins to constantly regenerate pure electrolyte. Selectivity for

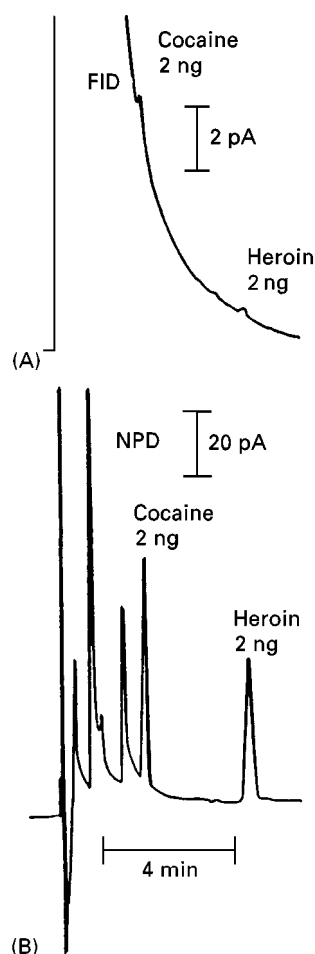


Figure 2 Comparison of FID and NPD chromatograms for a sample containing trace amounts of cocaine and heroin. (From Patterson PL. In *Detectors for Capillary Chromatography* (1992) Hill HH and McMinn DG (eds). Reproduced with permission of John Wiley & Sons, Inc.)

halogens co-emerging with nitrogen or sulfur compounds can be obtained by using other electrolytes rather than water (n-propanol is recommended since other reaction gases are not soluble in it). Another way to obtain selectivity is to use small scrubbers containing chemicals that will remove specific gases. For example an acidic scrubber removes ammonia but allow halogen acids to pass through.

Clearly there are number of opportunities for variation in the chemistries involved (material of reaction tube construction, reaction tube temperature, oxidation or reduction, electrolyte and scrubber) in order to obtain optimum sensitivity and selectivity. For halogens the sensitivity is in the low picogram range with a linearity of five orders of magnitude and a halogen/hydrocarbon selectivity of better than 10^6 . In spite of these impressive performance figures the main use of the ELCD has been in the determination of halogenated compounds in water where its use is specified in US Environmental Protection Agency Method 502.2. **Figure 3** shows a chromatogram obtained by purge and trap sampling of water with the ELCD in the halogen mode.

Like the NPD it seems probable that the application of this detector will decline in the future. As separations tend to become faster it is doubtful if the ELCD is capable of providing the rapid response and low dead volume required in such circumstances.

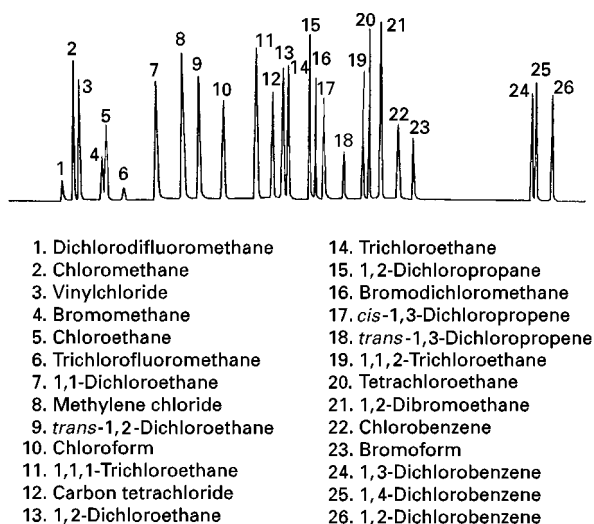


Figure 3 Chromatogram obtained by purge and trap sampling of water with the ELCD in the halogen mode. (From Hall RC. In *Detectors for Capillary Chromatography* (1992) Hill HH and McMinn DG (eds.). Reproduced with permission of John Wiley & Sons, Inc.) Column: Restek 502.2 FS 0.53 mm \times 105 M. Program: 35°C for 11 min, 5°C min⁻¹ to 160°C, 4-min final hold. Carrier: helium at 8 mL min⁻¹. ELCD conditions: reactor temperature, 960°C; electrolyte, 35 μ L min⁻¹ n-propyl alcohol; reaction gas, 100 mL min⁻¹ H₂.

The Atomic Emission Detector (AED)

Most of the detectors described above can be used selectively for several elements but this is normally carried out one element at a time, although the FPD, for example, can determine at least two elements (S and P) simultaneously if desired. One of the advantages of the AED is that theoretically it can detect a large number of elements simultaneously with high sensitivity and selectivity. In practice the number determined simultaneously is usually limited to four and, since one of these is normally a carbon channel, only three other elements can be determined.

In the AED, or microwave plasma detector, the compounds are subjected to a high energy microwave plasma so that the emitted spectra are line spectra which are of an extremely narrow wavelength, often only 0.1 Å wide. This results in (potentially) a much higher selectivity and sensitivity.

The AED had a long history of development. It first appeared commercially in the early 1970s. This detector was operated with a microwave plasma in pure helium at low pressure (10–100 mm) and made use of a nitrogen purge to remove carbon deposits from the wall of the silica discharge tube at the outlet of the column. The emission spectra were resolved with a conventional $\frac{3}{4}$ m optical spectrometer which resulted in a rather large and unwieldy apparatus which was also sensitive to movement, requiring fairly frequent realignment of the optics. One of the claimed advantages of this detector was that it was possible to obtain the carbon, hydrogen and other element contents of an unknown molecule and so calculate an empirical formula. In practice it was found to give an empirical formula for low molecular weight compounds that was accurate to about $\pm 10\%$ and the equipment was never really seriously used for this purpose. Sensitivity and selectivity varied considerably from one element to another. In favourable cases such as the halogens, picogram per second levels could be detected with a selectivity over carbon of about 10^3 but nitrogen and oxygen gave much poorer performance mainly due to the large background signal.

A new version was made commercially available in the 1980s. This version differs from the original in two main respects – firstly the microwave discharge takes place in a cavity at atmospheric pressure and secondly the optical spectrometer is replaced by a photodiode array. The result of these modifications is a detector that is much smaller and easier to operate although the actual performance in terms of sensitivity and selectivity is not greatly different from the original designs. The relative compactness and ease of operation have led to a resurgence of interest in this

detector but it is not cheap and as GC-MS systems come down in price they represent strong competition. The definitive account of the various forms of microwave plasma detector is given by de Wit and Beens (see Further Reading).

The Oxygen Selective Detector (O-FID)

The phasing out of lead antiknock compounds in gasoline and their replacement by ‘oxygenates’ – mainly alcohols and ethers such as methyl tertiary butyl ether (MTBE) – created a need for an oxygen-selective detector, easy to use with capillary columns. The O-FID was first proposed by Schneider in 1982 and is now commercially available. The principle of the detector is that the effluent from the GC column is first passed through a microfurnace made of platinum/rhodium alloy heated to about 1200°C where hydrocarbons are cracked to carbon (which is deposited on the Pt/Rh tubing) and hydrogen. Oxygenated compounds on the other hand form CO which is then passed to a second microreactor with a stream of hydrogen. The microreactor containing nickel deposited on alumina is heated to about 350°C and is small enough to fit into the body of a standard FID. Under these conditions each CO molecule is reduced to a methane molecule so that every oxygen atom in the original effluent peak produces one methane molecule. The whole arrangement sounds complex but it works remarkably well for samples up to 20 µg which is of course satisfactory for capillary columns. The detector is ideally suited for the purpose for which it was designed. **Figure 4** shows an O-FID chromatogram of a gasoline sample containing alcohols, water, ethers and acetone. It should be noted that the detector gives a quite respectable peak from the oxygen in the water.

The disadvantages of the detector are its relatively low concentration sensitivity and linearity compared to other selective detectors and the ordinary FID. The limit of concentration sensitivity is about 0.01%.

Other Element-Selective Detectors

A number of organometallic compounds such as those of tin, lead, arsenic and mercury are readily separated by GC and many more as chelate derivatives. Even such an unlikely element as iron can be dealt with as the volatile chloride, FeCl₃, although there are many better methods for such an analysis. For organometallic compounds, atomic absorption and emission spectrometers (AAS and AES), have been used with considerable success. In view of the fact that the vapour emerging from a GC column would appear to be in an ideal state for presentation

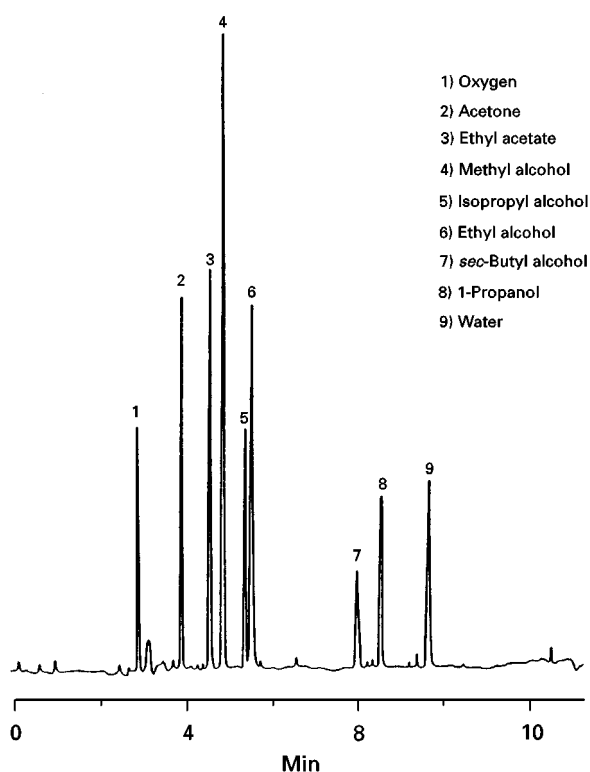


Figure 4 Detection of oxygenates in gasoline at 200 ppm level. (From Sironi, A and Verga, GR. In *Chromatography in the Petroleum Industry* (1995) Adlard, ER (ed.). Reproduced with permission of Elsevier Science Publishers.)

to an AAS it is a little surprising that the technique has not been used more frequently. It has the virtues of high sensitivity for many metals and high selectivity. It also gives information about the speciation of the organometallics which is very difficult to obtain in other ways.

In spite of these advantages relatively little has been published on the use of such detection systems, probably reflecting the relatively minor importance of the analysis of organometallics compared to ordinary organic compounds. Organometallics are, however, important in a number of fields, e.g. the determination of butyltin antifouling paint residues in the environment, and it seems likely that this niche area will remain but not expand significantly in the future.

Compound-Selective Detectors

This category refers to detectors that respond specifically to whole molecules or, more commonly, to various functional groups in a molecule.

An example of a detector responding to functional groups is the automatic titrimeter described by James and Martin in their earliest publications on the separation of the lower fatty acids. Although slow and

lacking in sensitivity by modern standards, this detector represented a major advance at the time. Attempts over the years to use microcoulometers as detectors for compounds capable of oxidation or reduction at suitable electrodes have virtually disappeared since, in general, they have slow response and the electrodes are subject of contamination.

Compared to element-selective detectors, there are very few compound-selective detectors and indeed in terms of modern commercially available equipment they can be limited to four – the electron-capture detector (ECD), the photoionization detector (PID) and two spectroscopic detectors, Fourier transform infrared (FTIR) and ultraviolet (UV) detectors. Trapping out polynuclear aromatic hydrocarbon fractions for further analysis by UV spectroscopy was reported many years ago but although there is now an online GC-UV instrument on the market, it is of limited application and will not be discussed further.

The Electron-Capture Detector (ECD)

The development of the ECD by Lovelock in the late 1950s led to its application in environmental studies and the discovery of the wide distribution of chlorinated pesticide residues such as DDT. This was followed by the discovery of the emission of methyl iodide from open ocean waters which again had great significance in the study of the Earth's ecosystem.

The ECD has evolved over many years into an instrument very different in detail from the original even though the principle of detection remains the same. The ionization cross-section detector used a small radioactive source to produce electrons in a cell with two electrodes with about 100 V between them. This caused a small current to flow in the cell as a result of ionization of carrier gas molecules by collision. Compounds eluting from the GC column were ionized to different amounts depending on the cross-section of ionization for each compound. The net result was a variation in the current flowing in the cell which could be recorded electronically. Lovelock modified this detector, firstly by using argon as the carrier gas and secondly by using a much higher voltage (≈ 1000 V) across the electrodes. Under these conditions, multiple ionization takes place via excited argon atoms so that there is a small standing current but a very much larger signal current than given by the cross-section detector. After the argon detector had been on the market for some time, anomalous results were reported especially for halogenated compounds. On investigation, Lovelock concluded that compounds with a strong electron affinity such as polyhalogenated compounds were capturing electrons and thereby reducing the signal

from the detector. He, therefore, maximized the electron capturing effect by using argon with 5–10% methane as carrier gas and about 50 V across the electrodes. Such a cell has a phenomenally high sensitivity for compounds such as CCl_4 and is capable of detecting femtogram quantities (10^{-15} g). Indeed the ECD has a higher sensitivity under favourable conditions than any other detector with the possible exception of radioactivity detectors.

Molecules that capture electrons form charged entities with a much lower mobility than the free electrons responsible for the standing current in the cell. Because of their lower mobility they lose their charge readily and hence cause a reduction in the standing current. The ECD is the only detector that measures a decrease in a large standing current; all other detectors measure an increase in a small standing current. Since the standing current can only be reduced to zero, the ECD can be easily overloaded and has, even in its modern versions, a relatively limited linear range of about 10^4 . Modern versions of the ECD pulse the voltage on the electrodes rather than using a steady DC potential. This allows equilibrium to be achieved between the electron flux and the gas mixture in the cell and is somewhat analogous to a distillation column under total reflux from which a small grab sample is removed from time to time. By changing the frequency of the pulses the current in the cell can be kept constant and the variation in frequency required to maintain a constant current is monitored rather than changes in the current itself. This is a very

simple arrangement electronically that is readily compatible with integrating circuits. The most recent modification to the ECD dispenses with the radioactive source and uses electrons produced by a helium discharge in an extension to the cell proper.

As indicated in the introduction to this section, the very high sensitivity of the ECD to polyhalogenated compounds made it extremely important for the analysis of trace pesticides in crops since many pesticides were compounds of this type. In addition to a very high sensitivity for some classes of compounds it has a negligible response for others such as paraffin hydrocarbons. Table 2 shows that the response to different classes of compounds varies over a range of at least 10^6 .

This response is not amenable to accurate prediction from the chemical structure of the compounds and even apparently small differences in structure can result in large differences in electron affinity. The ECD is not suitable for detection of an unknown mixture since large peaks may be from small amounts of compounds with high electron affinity or large amounts of compounds with a low electron affinity. In spite of its rather anomalous response and limited linear range, the ECD is an extremely important detector under favourable circumstances.

The Photoionization Detector (PID)

In the photoionization detector energy sufficient to ionize the compounds emerging from the GC is

Table 2 The electron absorption coefficients of various compounds and of classes of compound for thermal electrons

<i>Electron absorption coefficient^a</i>	<i>Compounds and classes</i>	<i>Electrophores</i>
1	Aliphatic saturated, ethenoid, ethinoid and diene hydrocarbons, benzene, and cyclopentadiene	None
1–10	Aliphatic ethers and esters, and naphthalene	None
10–100	Aliphatic alcohols, ketones, aldehydes, amines, nitriles, monofluoro and chloro compounds	•OH•NH ₂ •CO• •CN
100–1000	Enols, oxalate esters, stilbene, azobenzene, acetophenone, dichloro, hexafluoro and monobromo compounds	Halogens •CH:C•OH •CO•CO•
10 ³ –10 ⁴	Anthracene, anhydrides, benzaldehyde, trichloro compounds, acyl chlorides	Halogens CO•O•CO• Phenyl•CO•
10 ⁴ –10 ⁵	Azulene, cyclooctatetrene, cinnamaldehyde, benzophenone, moniodo, dibromo, tri, and tetrachloro compounds, mononitro compounds	Halogens NO ₂ Phenyl•CH:CH•CO•
10 ⁵ –10 ⁶	Quinones, 1,2-diketones, fumarate esters, pyruvate esters, diiodo, tribromo, polychloro, and polyfluoro compounds, dinitro compounds	•CO•CO• •CO•CH:CH•CO• Quinone structure Halogens NO ₂

Source: After Lovelock. ^aValues are relative to the absorption coefficient of chlorobenzene.

supplied by a small, cheap UV lamp which can be changed over a range of wavelengths to give a certain amount of selectivity. The first commercial detector was designed to operate with packed columns but the large amount of stationary phase bleed from these columns caused rapid fouling of the quartz window of the cell facing the UV lamp and consequent deterioration of performance. Relatively simple design modifications reduced the dead volume to about 40 μL which is adequate for capillary columns of about 0.25 mm i.d. or greater. Use of capillary columns minimizes the fouling from stationary phase and also results in much sharper peaks; since the PID is a concentration-dependent detector this gives a considerable improvement in sensitivity. The main drawback of the commercial PID lies in the UV lamp sources available. Only one gives a single pure wavelength and this is of such low intensity that it offers poor sensitivity. The 10.2 eV lamp emits two wavelengths with an average energy of 10.2 eV. The inhomogeneity of the source blurs the selectivity of the detector although there is no doubt that it gives up to two orders of magnitude greater sensitivity for aromatics over aliphatic compounds with olefins somewhere in between. The lamp of higher wavelength (11.7 eV) is sufficiently energetic to ionize most compounds indiscriminately so the detector fitted with this lamp becomes more or less universal in response. The ideal version of this detector would be one with a tunable laser source and such a detector might rival the mass spectrometer in qualitative information. Unfortunately, the current cost of a tunable laser would render the detector prohibitively expensive and development on these lines is unlikely in the near future.

The FTIR Detector

The main disadvantage of simple mass spectrometry detection is its inability to distinguish between many positional isomers. The technique ideally suited to give such information and the presence of functional groups such as CO and OH is IR spectroscopy. Conventional IR spectroscopy with a grating is too slow for GC purposes but FTIR has the required speed provided that sufficient computing power is available (the computing power required is considerably greater than that required for other techniques). Another disadvantage is that the spectra obtained are gas phase spectra whereas IR spectral libraries have been traditionally liquid phase spectra. The main disadvantages, however, are the wide variation in extinction coefficients, the rather poor sensitivity for many compounds (the upper nanogram range) and light pipe cells with a relatively large dead volume.

Since capillary GC seems to be moving in the direction of faster separations via short, very narrow bore capillaries it seems doubtful if GC-FTIR will ever find any great application except perhaps in niche application areas such as essential oil and perfumery analysis.

Conclusion

There still appears to be a place for selective detectors provided that they can offer specific advantages. Early versions of most of the detectors described appeared 30 or more years ago and have survived by constant modifications and improvement in design and performance. In the light of this and the fact that just about every conceivable property of gas mixtures has been exploited over the years it is difficult to envisage any great new advance.

Many detectors have specific advantages for particular applications. The PID only requires one gas supply which makes it suitable for portable equipment. A laboratory monitoring the amount of stenching agents in natural gas is hardly likely to abandon the simplest form of FPD for anything more sophisticated. The ECD reigns supreme in the field of polyhalogenated compounds and the O-FID is ideally suited for the purpose that it was designed for. As speed of analysis increases, detectors are required with very fast response time and low dead volume leading to devices such as time-of-flight mass spectrometers. It would appear that in spite of nearly 50 years of continuous development there is still room for further advances in detectors.

See also: II/Chromatography: Gas: Column Technology; Detectors: General (Flame Ionization Detectors and Thermal Conductivity Detectors); Detectors: Mass Spectrometry. III/Environmental Applications: Gas Chromatography – Mass Spectrometry. **Fungicides:** Gas Chromatography; **Herbicides:** Gas Chromatography; **Pesticides:** Gas Chromatography; **Petroleum Products:** Gas Chromatography. **Appendix 2: Essential Guides to Method Development in Gas Chromatography.**

Further Reading

- Adlard ER (1975) *Critical Reviews in Analytical Chemistry* 5(1): 13–36. (A review of selective detectors up to that date.)
- Adlard ER (1995) *Chromatography in the Petroleum Industry*. Amsterdam: Elsevier. (This contains definitive accounts to date on the microwave plasma detector (A de Wit and J Beens), the sulfur chemiluminescence detector (RS Hutte) and the O-FID (A Sironi and GR Verga).)

Brown RA and Searl TD (1979) In: Altgelt KH and Gouw TH (eds) *Chromatography in Petroleum Analysis*. Ch. 13. New York: Marcel Dekker. (An account of early work on offline GC-UV.)

Dressler M (1986) *Selective Gas Chromatography Detectors*. Amsterdam: Elsevier. (A literature survey of most of the selective detectors described up to about 1984. Mainly of historic interest.)

Eicman GA (1990) In: Clement RE (ed.) *Gas Chromatography, Biochemical, Biomedical and Clinical Applications*, Ch. 14. New York: Wiley Interscience. (An account of the GC of organometallic compounds.)

Hill HH and McMinn DG (eds) (1992) *Detectors for Capillary Chromatography*. New York: Wiley Interscience. (An excellent book with chapters on the ELCD (by Hall), the NPD (by Patterson) and GC-FTIR (by Gurka) in particular.)

Gas Chromatography-Infrared Spectrometry

P. R. Griffiths, University of Idaho, Moscow, ID, USA

This article is reproduced from *Encyclopedia of Analytical Science*, Copyright Academic Press 1995.

Knowing the identity of each component in a mixture is necessary for many analytical-scale separations, and simply measuring retention data for this purpose is often too ambiguous for the identification of molecules eluting from a capillary gas chromatography (GC) column, which has the capability of resolving several hundred components. Prior knowledge about the chemical structure of the components and spiking of the mixture with one or more reference standards may aid the identification process; however, a less ambiguous identification can be accomplished by interfacing the chromatograph to a sensitive, rapid-scanning spectrometer to obtain unique signatures of each component. This instrument should allow each component to be detected in real time without any loss in chromatographic resolution. Mass spectrometry (MS) is the most commonly applied technique for this purpose, but it has certain limitations, in particular for distinguishing between structural isomers, such as *ortho*-, *meta*- and *para*-xylene, whose electron-impact and chemical-ionization mass spectra are identical. For such molecules a technique complementary to MS is desired. Fourier transform infrared (FT-IR) spectrometry, which yields unique spectra for most structural isomers, has frequently been used as an alternative technique for this purpose.

Light-Pipe-Based GC-IR Instruments

Measurement of the Spectrum

The coupling of gas chromatographs and FT-IR spectrometers (GC-IR) has been accomplished by three approaches. In the first, and by far the simplest, the

GC column is connected directly to a heated flow-through cell. For capillary GC, this cell is usually fabricated from a 10-cm length of heated glass tubing with an internal diameter of ~ 1 mm. The inside bore of this tube is coated with a thick enough film of gold to be highly reflective to infrared (IR) radiation. IR-transparent windows (for example made of potassium bromide) are attached to both ends of the tube. IR radiation entering one window is multiply reflected down the gold-coated interior bore before emerging from the other window, giving rise to the name *light-pipe* for this device. The effluent from the GC column is passed into one end of the tube and out of the other via heated fused-silica transfer lines. The entire unit is held at a temperature between 250 and 300°C to preclude the condensation of semi-volatile materials.

Infrared radiation from an incandescent source, such as an SiC Globar, is collimated and passed through a rapid-scanning interferometer so that each wavelength in the spectrum is modulated at a different frequency. The beam of radiation is then focused onto the first window of the light-pipe and the infrared beam emerging from the second window is refocused onto a sensitive detector (typically a liquid-nitrogen-cooled mercury cadmium telluride (MCT) photoconductive detector). A typical system is illustrated schematically in **Figure 1**. The signal measured in this way is known as an *interferogram* and the Fourier transform of the interferogram yields a single-beam spectrum. By calculating the ratio of a single-beam spectrum measured when a component is present in the light-pipe to one measured when only the helium carrier gas is present, the transmittance spectrum, $T(\nu)$, of the component is obtained. The transmittance spectrum is usually immediately converted to an absorbance spectrum, $A(\nu)$, by the standard Beer's law operation, $A(\nu) = -\log_{10} T(\nu)$, as the relative intensities of bands in absorbance spectra are independent of the concentration of the analyte, thereby allowing spectral library searching to be

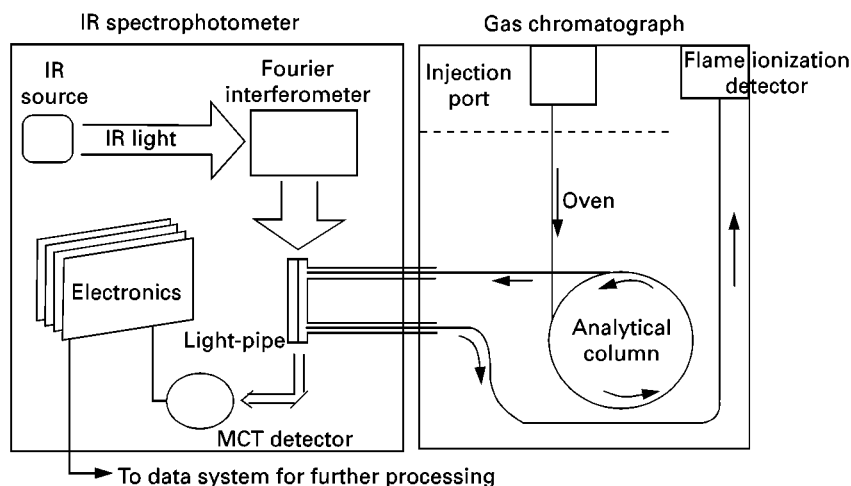


Figure 1 Schematic of typical light-pipe-based GC-FTIR interface (based on Hewlett Packard IRD).

performed. For light-pipe-based GC-IR systems, it is rarely necessary to measure spectra at high resolution, as the spectral bands are quite broad. Since most bands in the spectra of molecules in the vapour phase have a width of at least 10-cm^{-1} , the typical resolution at which GC-IR spectra are measured is 8 cm^{-1} .

When operated at their highest scan speeds, FT-IR spectrometers can measure between 5 and 20 interferograms per second that would yield spectra of this resolution. During a chromatographic analysis, interferograms are measured continuously. Thus for a 30-min-long chromatogram, it would be possible to measure tens of thousands of interferograms, giving rise to an amount of data that could exceed 100/MB and hence could exceed the capacity of the disk on a typical personal computer (PC). Fortunately, most GC peaks have a full-width at half-height (FWHH) of several seconds. Thus it is common practice to average blocks of interferograms for a period of time that is slightly less than the FWHH of the narrowest peak in the chromatogram (usually 1–2 s). The single-beam spectrum is then computed from this signal-averaged interferogram and ratioed against an appropriate background spectrum; finally, the resulting transmittance spectrum is converted to a linear absorbance format. On many fast PCs this entire sequence of operations is performed while the next block of interferograms is being acquired.

Reconstruction of Chromatograms

The end result of this process is that over 1000 absorbance spectra, corresponding to the contents of the light-pipe measured at approximately 1-s intervals throughout the entire chromatogram, are stored at the end of the run. Many of these spectra contain no useful information as they were measured when

no component was present in the light-pipe; thus the next step in a GC-IR analysis is to determine which of the stored spectra contain useful information. To achieve this, a chromatogram must be reconstructed from the spectroscopic data. This is usually achieved in two ways, the first of which is known as the *Gram-Schmidt* (GS) vector orthogonalization method. Here, short, information-rich regions of the interferograms are treated as vectors and the vector distance between this part of each interferogram measured during the chromatographic run and several interferograms that were acquired when nothing except the helium carrier gas was flowing through the light-pipe (known as the basis set) is calculated. When an analyte elutes from the column, the magnitude of the vector difference is approximately proportional to the quantity of this material in the light-pipe. Because only a short region of the interferogram is examined, calculation of the GS 'signal' can be achieved in a few milliseconds. Furthermore, since all compounds besides monatomic and homonuclear diatomic molecules have at least one band in their IR spectrum, GS chromatograms are very nonselective. Some compounds yield much stronger IR spectra than others, however. For example, the spectra of most nonpolar compounds are rather weak, whereas the spectra of very polar compounds are usually much stronger. As an example, the detection limits for GS chromatograms of polycyclic aromatic hydrocarbons (which have very low absorptivities over most of their IR spectra) are about 20 times greater than the corresponding values for the barbiturates (which are very polar and have several strong IR absorption bands in their spectra).

The other commonly used algorithm by which chromatograms are constructed from the IR data involves calculating the integrated absorbance in one

or more specified spectral regions. These regions are usually chosen to correspond to the characteristic absorption frequencies of functional groups present in the class(es) of molecules of interest. The chromatograms generated by this approach have been called by a variety of names including ChemigramsTM, functional group (FG) chromatograms and selective wavelength (SW) chromatograms. FG chromatograms are, of course, far more selective than GS chromatograms, but are rarely completely selective as many molecules have weak overtone and combination bands over much of the fingerprint region of the spectrum. For compounds with functional groups giving rise to intense absorption bands, such as the C=O stretching mode of carbonyl compounds, the limits of detection of FG chromatograms may be less than those of the corresponding GS chromatograms, but the two algorithms often have comparable sensitivity. A useful way to detect the presence of a particular functional group is to compare the relative heights of peaks in the GS and FG chromatograms. If the ratio of the peak heights in the FG and GS chromatograms is large, the presence of that functional group in that component is indicated: if the ratio is small, there is a much smaller probability that the analyte contains that functional group.

Spectral Searching

Once the chromatography has been completed, the spectra of those components of interest can be displayed. (In fact, several GC-IR software packages allow the spectra to be displayed while data acquisition is still in progress.) Each component generating a peak in the GS chromatogram with a signal-to-noise ratio greater than about 10 can usually be identified by comparing its spectrum to a library of vapour-phase reference spectra. The unknown and reference spectra are first scaled so that the most intense band in each spectrum has the same absorbance (usually 1.0). By treating the spectra as vectors, the Euclidean distance between the unknown and each reference spectrum is calculated. This distance is usually called the *hit quality index* (HQI); the smaller the HQI, the better is the spectral match. The highest probability for the identity of the unknown is that of the compound in the reference library yielding the smallest HQI. Some software scales the Euclidean distance and then subtracts it from, say, 1000 to give the HQI; in this case, of course, the larger the HQI, the better the spectral match. However unequivocal identifications cannot be made on this basis alone, for several reasons. The reference spectrum of the authentic analyte may not be present in the spectral library. If the spectrum of the unknown is noisy, the value of the

HQI may be determined more by noise than by the true absorption spectrum. The reference spectrum may have been measured with the sample at a different temperature from the light-pipe, measured at a slightly different resolution, or computed with a different apodization function. Finally, some members of homologous series can have very similar spectra, so it is not uncommon for compounds of the same type (e.g. methacrylate esters) to give similar HQI values.

It is always recommended that the user should make a side-by-side comparison of the GC-IR spectrum and the reference spectra of the top few 'hits' to get a good idea of the probability that the structure of the top hit, or by one of the other close hits, or whether there is enough similarity between the GC-IR spectrum and all of the closely matching reference spectra that unequivocal identification is impossible. In this case, the simultaneous application of MS may be necessary to yield an unequivocal identification.

Limits of Detection and Identification

The limit of detection (LOD) for an acceptable GC-IR response for most compounds is between about 1 and 20 ng (injected) per component, the actual value depending on the chemical nature of the analyte. The LOD is often defined with respect to the strongest band in the spectrum. Most bands in the IR spectra of nonpolar compounds are fairly weak and so these compounds tend to have the highest LODs, but even these compounds usually have at least one band in the spectrum with a high absorptivity. Examples include the C-H stretching bands of alkanes and the aromatic C-H out-of-plane deformation bands of polycyclic aromatic hydrocarbons. Detection limits also depend on the width of the GC peak; the wider the peak, the more dilute the analyte and the higher the LOD.

The amount of a given component that must be injected into the chromatograph to yield an identifiable spectrum, often known as the minimum identifiable quantity (MIQ), depends not on the *strongest* band, but on the signal-to-noise ratio of the *most characteristic bands* in the spectrum. For an analyte with a spectrum that is very different from any other spectra in the reference database, the MIQ may be only slightly higher than the LOD. On the other hand, there are often only very subtle differences between the spectra of members of this class of compounds. If the analyte is a member of a homologous series and several reference spectra of members of this series are contained in the library, the signal-to-noise ratio of the spectrum must be high, and hence the MIQ will be much greater than the LOD if the analyte is to be correctly identified.

If a minor peak is present in a chromatogram measured with a conventional GC detector such as a flame ionization detector (FID), but is not observable in the GS or FG chromatogram, it may be possible simply to inject a greater volume of the sample into the chromatograph. Even if the major components overload GC column in this case, the minor components will not. However, sometimes the major peaks will broaden to the point that they start to overlap a neighbouring minor peak. In this case, it may become necessary to subtract the spectrum of the major peak (linear in absorbance) from the spectrum measured in the region of the minor peak, to identify the minor component. This procedure is needed because of the relatively low sensitivity of light-pipe-based GC-IR instruments. Two other approaches that have led to increased sensitivity for GC-IR measurements are described here.

Matrix-Isolation GC-IR

In the first approach, argon is mixed with the helium mobile phase, either as a minor ($\sim 1\%$) component in the carrier gas or by addition at the end of the GC column. The column effluent is then sprayed from a heated fused-silica transfer line onto a rotating gold-plated disk that is maintained at a temperature of less than 15 K. Helium does not condense at this temperature but argon does. By locating the end of the transfer line an appropriate distance from the cooled disk, argon is deposited as a track approximately 300 μm in width. Any component emerging from the transfer line at the same time is trapped in the argon matrix. After the separation has been completed, the disk is rotated to a position where the focused beam from an FT-IR spectrometer is transmitted through the track of argon, reflects from the gold-coated disk, passes again through the argon and then is collected and focused on to an MCT detector, as shown in **Figure 2**. In principle, if the concentration of any analyte in the argon matrix is low enough, each analyte in the argon matrix is low enough, each analyte molecule will be isolated from similar molecules by the argon matrix. Despite the fact that the concentration is usually a little too high for true matrix isolation to be achieved in GC-IR measurements, this technique none the less is known as *matrix-isolation GC-IR*. By rotating the disk slowly, a series of spectra can be measured that is analogous to the series of spectra that is measured in real-time during a light-pipe-based GC-IR run and either GS or FG chromatograms can be constructed from these data. Each component may be identified by spectral library searching, but a special library of spectra of matrix-isolated standards is required.

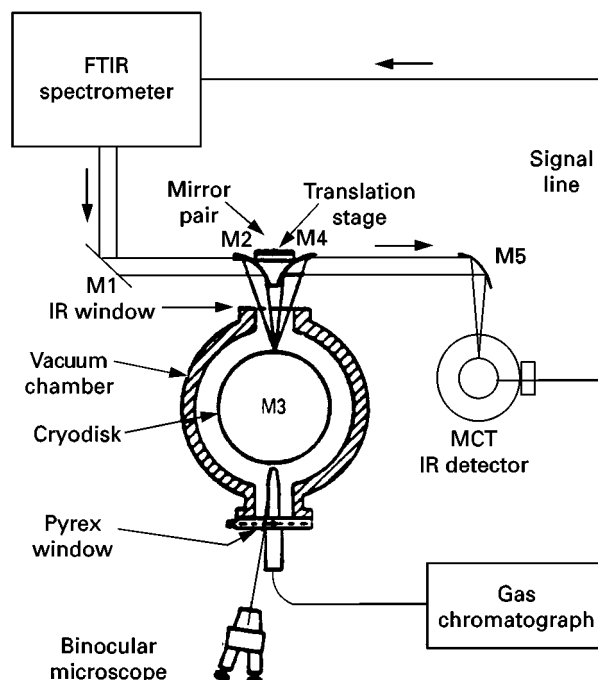


Figure 2 Schematic diagram of matrix-isolation GC-FTIR interface (based on Mattson Instruments Cryolect).

The advantages of matrix isolation are based on the following considerations. First, the width of the track is about 300 μm , compared with 1 mm for the diameter of a light-pipe. Thus the sample is more concentrated over the cross-sectional area of the IR beam and a given amount of sample will yield a spectrum with more intense absorption bands. Second, because each component is trapped on the disk, it is common practice when minor components are to be identified by matrix isolation GC-IR to signal-average interferograms for several minutes with the disk stationary, enabling a significant increase in sensitivity to be achieved over real-time measurements. A final advantage that has been claimed for matrix-isolation GC-IR measurements is the increase in the absorptivity at the peak of each band in the spectrum because of the decrease in bandwidth that occurs on matrix isolation (the band area remaining approximately constant). This is true for small molecules, but large molecules disrupt the crystal structure of the argon to such an extent that a certain amount of molecular motion is possible. As a result, the widths of many bands in the spectra of large asymmetric molecules prepared in this way are surprisingly similar to widths of corresponding bands in the spectra of the corresponding molecules prepared as KBr disks.

The exception to this behaviour is observed in the spectra of compounds that contain O-H or N-H groups. In the crystalline form of such compounds,

the O–H and N–H groups are strongly intermolecularly hydrogen bonded. As a consequence, the O–H and N–H stretching bands in their KBr-disk spectra are exceptionally broad, often having a width of several hundred wavenumbers. When these molecules are isolated in an argon matrix, however, no intermolecular hydrogen bonding takes place, and the O–H and N–H stretching bands appear as very narrow spectral features. Thus, when the spectra of matrix-isolated species such as alcohols, phenols or amines are measured at high resolution, excellent specificity is often gained by matrix-isolation GC-IR.

The major problem with this approach to GC-IR (which can to a certain extent be shared with vapour-phase measurements) is the lack of extensive libraries of appropriate reference spectra. This disadvantage has largely been overcome by the final type of GC-IR interface, which is described next.

Direct-Deposition GC-IR

In the remaining approach to GC-IR, the effluent from the column is directed at a slowly moving, cooled window mounted on a computer-controlled x - y stage. Zinc selenide cooled to the temperature of liquid nitrogen is the most commonly used substrate. Each eluting component is deposited on the window as a very narrow spot. In the commercially available form of this interface, shown in Figure 3, the typical width of each spot is about 100 μm . The stage moves so that each deposited component passes through the beam focus of an IR microspectrometer shortly after deposition. As for light-pipe-based GC-IR systems, spectra are measured continuously throughout the chromatographic run and GS and/or FG chromatograms can be output in real time. This *direct depos-*

ition approach for GC-IR has two important advantages over light-pipe or matrix isolation GC-IR systems – it yields higher sensitivity and the measured spectra are very similar to reference spectra of standards prepared as KBr disks. Let us first recognize the reason for the increased sensitivity of direct deposition GC-IR measurements.

As we saw in the previous section, the smaller the cross-sectional area of the sample, the greater the absorbance of all bands in the spectrum. Because the sample is contained in a 100- μm diameter spot rather than a 1-mm diameter light-pipe, its cross-sectional area is 100 times less, so that bands will be about 100 times more intense. To attain the optimal sensitivity, the diameter of the IR beam should be approximately equal to the width of the spot, i.e. about 100 μm , and a detector of the same size should also be used. Several other optical factors should be included in the comparison, but in general it is found that the signal-to-noise ratio of GC-IR spectra measured online using the direct deposition technique is about 50 times greater than the corresponding measurement made using a light-pipe system. The sensitivity advantage of direct-deposition GC-IR systems can be further increased by post-run signal averaging in a manner analogous to the matrix-isolation GC-IR system described previously. If each real-time spectrum is measured over 1-s blocks, post-run averaging for just 1 min will yield an improvement in sensitivity of almost a factor of eight.

As noted previously, the MIQ or direct-deposition GC-IR measurements varies with the polarity of the analyte. The LOD for real-time measurements of several analytes by this technique is about 50 pg. When very polar analytes are injected, this number can be further reduced. For example, the LOD for several barbiturates is found to be about 13 pg. Spectra of these barbiturates in the high-wavenumber region measured by a light-pipe-based GC-IR instrument (Hewlett Packard IRD) and a direct-deposition system (Bio-Rad/Digilab Tracer) are shown in Figure 4. Differences between the vapour-phase and condensed-phase spectra of molecules that can exhibit strong intermolecular hydrogen bonding are readily apparent in this figure. For example, the sharp bands absorbing near 3430 cm^{-1} in the vapour-phase spectra are due to the N–H stretching vibrations of isolated (non-hydrogen-bonded) molecules. In the corresponding condensed-phase spectra measured by direct deposition GC-IR, the N–H stretching modes of the intermolecularly hydrogen-bonded barbiturates are seen as broad bands near 3220 and 3110 cm^{-1} . Similar differences between vapour-phase and condensed-phase spectra of barbiturates are also seen in the spectral region between 2000 and 1000 cm^{-1} (see

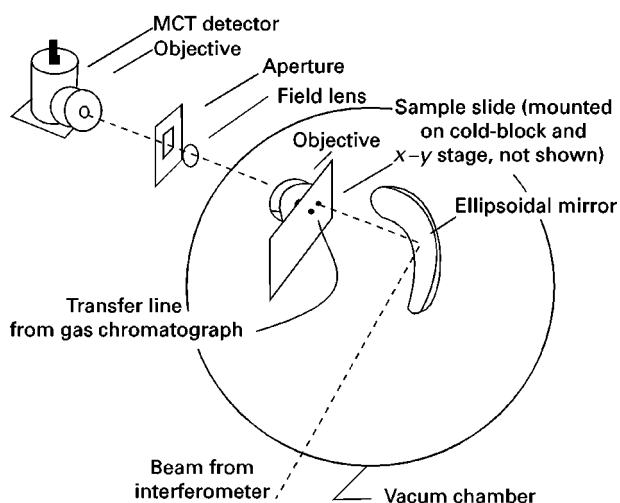


Figure 3 Schematic diagram of direct deposition GC-FTIR interface (based on Bio-Rad/Digilab Tracer).

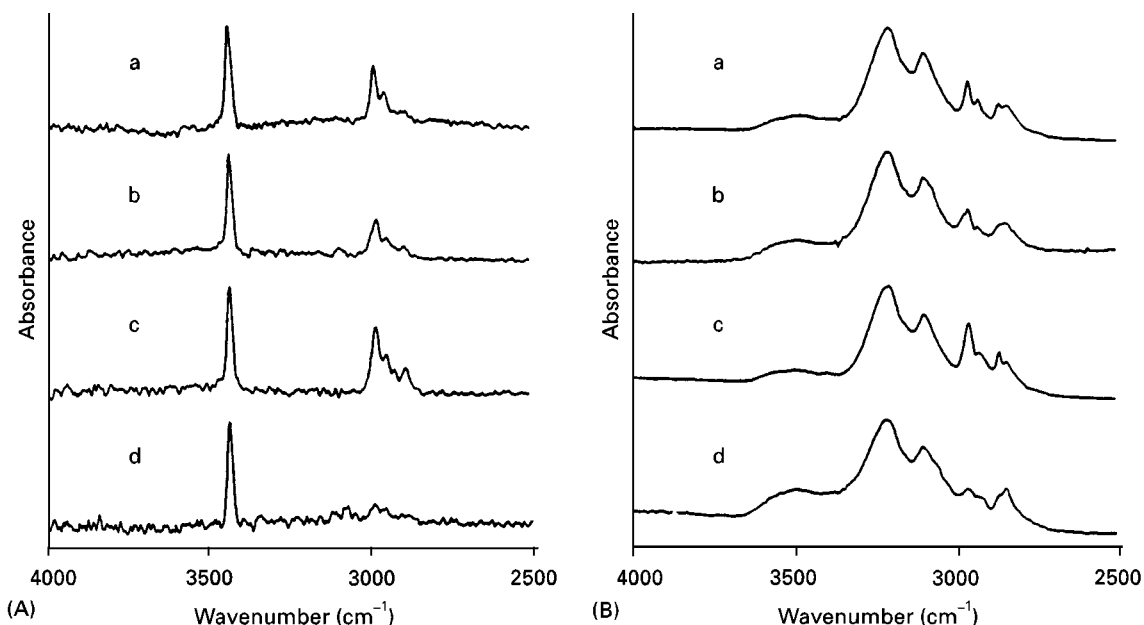


Figure 4 (A) Flow-cell and (B) direct-deposition GC-FTIR spectra of (a) barbital, (b) aprobarbital, (c) butabarbital and (d) phenobarbital from 4000 to 2500 cm^{-1} ; 12.5 ng and 375 pg of each component were injected for the light-pipe and direct-deposition spectra, respectively.

Figure 5). The difference between the sensitivity of the light-pipe and direct-deposition GC-IR measurements can be seen by comparing the noise levels of the spectra shown in Figure 4 and recognizing that it required 30 times more of each barbiturate to be injected for the spectra measured using a light-pipe than for those measured using direct deposition.

On deposition, the molecules of a given analyte form randomly oriented crystallites on the zinc selenide window. These crystallites are similar to the crystallites that are formed on grinding of solid samples during the preparation of KBr disks or mineral-oil mulls. Not surprisingly, therefore, the spectra of compounds obtained by direct-deposition GC-IR are

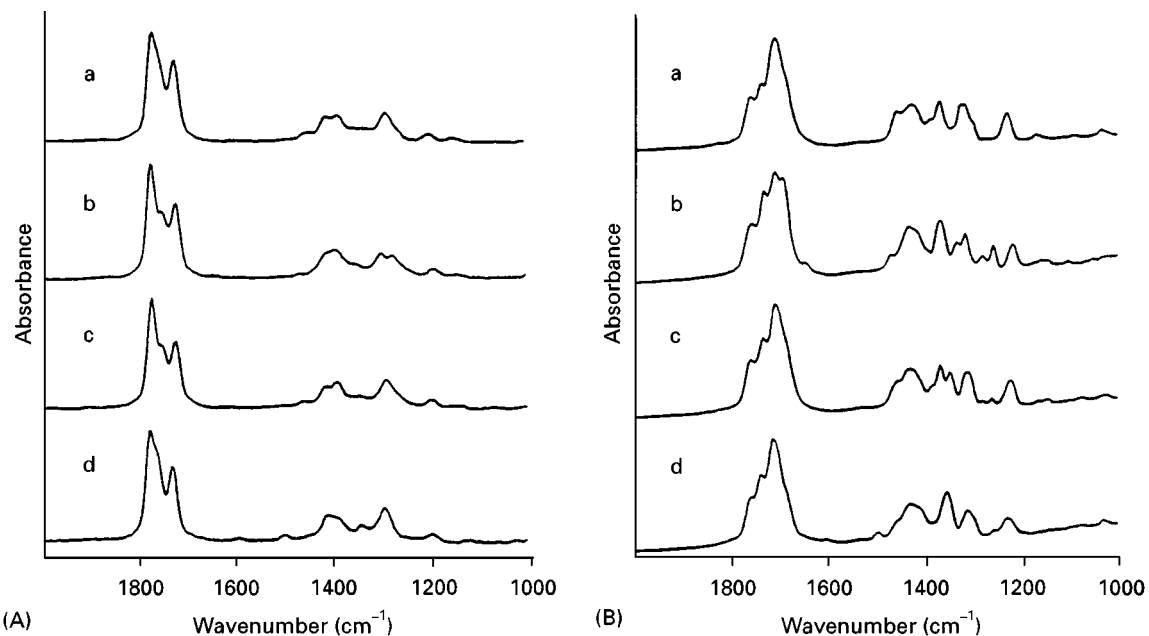


Figure 5 Low-wavenumber region of the spectra shown in Figure 4.

very similar to the KBr-disk spectra of the corresponding compounds. Extensive libraries (>150 000 entries) of reference spectra of standards prepared in this way are available commercially. The only compounds that cannot be readily identified in this manner are molecules with very strongly hydrogen-bonding groups or for analytes exhibiting polymorphism. For trace analytes containing O-H or N-H groups, the best results on library searching are usually found by examining only the spectral region below 2000 cm^{-1} and eliminating the region containing the strong, broad O-H and N-H stretching modes from the search.

Prognostication

Online IR spectrometry is proving to be an important way of identifying molecules eluting from a gas chromatograph. Light-pipe-based systems are the simplest, least expensive and most reliable, but often prove to have inadequate sensitivity for the identification of minor components. Of the two deposition-based techniques, the direct-deposition approach has LODs that rival those of benchtop GC-MS systems and has the great advantage of producing spectra that are directly comparable with KBr-disk reference spectra, of which there are over 150 000 available in digital form (i.e. suitable for computerized library searching). Thus one can forecast an increasing use of systems based on this principle in the future. It is also noteworthy that interfaces between FT-IR spectro-

meters and both supercritical-fluid and liquid chromatographs based on the same principle have been described.

See also: II/Chromatography: Gas: Detectors: General (Flame Ionization Detectors and Thermal Conductivity Detectors); Detectors: Mass Spectrometry; Detectors: Selective; Gas Chromatography-Ultraviolet.

Further Reading

- Bourne S, Haefner AM, Norton KL and Griffiths PR (1990) Performance characteristics of a real-time direct deposition GC/FT-IR system. *Analytical Chemistry* 62: 2448-2452.
- Griffiths PR and de Haseth JA (1986) *Fourier Transform Infrared Spectrometry*, ch. 18. New York: Wiley-Interscience.
- Herres W (1987) *HRGC-FTIR: Capillary Gas Chromatography - Fourier Transform Infrared Spectroscopy; Theory and Application*. Heidelberg: Huethig.
- Norton KL and Griffiths PR (1995) Comparison of direct deposition and flow-cell gas chromatography-Fourier transform infrared spectrometry of barbiturates. *Journal of Chromatography A* 703: 383-392.
- Reedy GT, Ettinger DG, Schneider JF and Bourne S (1985) High resolution gas chromatography/matrix isolation infrared spectrometry. *Analytical Chemistry* 57: 1602-1609.
- White R (1990) *Chromatography/Fourier Transform Infrared Spectroscopy and its Applications*. New York: Marcel Dekker.

Gas Chromatography-Mass Spectrometry

See II/CHROMATOGRAPHY: GAS/Detectors: Mass Spectrometry

Gas Chromatography-Ultraviolet

V. L. Lagesson and L. Lagesson-Andrasko,
GC-UV Center, Linköping, Sweden
Copyright © 2000 Academic Press

During recent decades much interest has been focused on hyphenated analytical techniques. Gas chromatography (GC), liquid chromatography (LC), mass spectrometry (MS) and Fourier transform infrared (FTIR) spectrophotometry have been arranged online, usually in a series. For example a GC separation directly combined with IR or MS is established and

widespread. The combination considerably increases the degree of selectivity and identification possibilities. This is also applicable for ultraviolet (UV) absorption spectrophotometry, but GC-UV has been largely overlooked. The interest concerning UV absorption spectrophotometry for analytical purposes has been directed towards the liquid phase for the vast majority of studies involving UV absorption because of its frequent use as a detector for high performance liquid chromatography (HPLC).

However, the first attempt to utilize UV absorption detection combined with GC was made by Kaye in

the early 1960s. He used a Beckman DK2 spectrophotometer and, in order to reach the far UV region, the instrument was purged by nitrogen. He recorded spectra of various substances in the vapour phase by means of a high speed mechanical scanner and a fast recorder in the wavelength range of 165–220 nm. His article from 1961 concerning analytical applications of UV spectroscopy includes a list of 256 references. The oldest reference was from 1932, but the first analytical application of UV absorption in the gas phase, which reported the determination of ammonia in nitrogen and in air, was from 1956.

At that time there were highly limited possibilities for handling large numbers of full scan data. Interest during this period was also increasingly focused on GC-MS and later also on GC-FTIR. These circumstances probably led to the lack of interest concerning the GC-UV hyphenation for a long time. Novotny published work on GC-UV in 1980 in connection with the introduction of Perkin Elmer GC-55 UV detector. The detection was carried out at various single wavelengths. This instrument was, for some reasons, withdrawn from the market shortly afterwards.

From about the mid-1980s there has been a gradual increase in interest in GC-UV. Most of the instrumental techniques described use commercially available spectrophotometers working in either a direct or remote configuration. With these conventional instruments there is no possibility of measuring at wavelengths shorter than 190 nm. A new instrument, GC-UV INSCAN 175 spectrophotometer, was introduced on the market in 1996. This instrument has been used for spectral recordings of reference substances and a spectral library of about 1000 gas-phase UV spectra in the wavelength region of 168–330 nm has been established for the first time.

Tables 1 and 2 present the development of GC-UV in terms of the spectrophotometric and chromatographic conditions and specifications found in the literature. The various subjects discussed in these works are, for example, the influence of temperature on the noise level and the signal-to-noise ratios at various wavelengths. A number of examples of analysis, applications and determinations of isomers have been published. No review articles or monographs have yet been written about GC-UV. However, there is a thesis, mainly dealing with this subject and its development until 1992, and a popular science article was published in 1996 (see Further Reading).

Gas-phase UV Spectrophotometry

The spectral region of the UV electromagnetic absorption of interest to the analytical chemists extends from about 160 to 330 nm. Molecules in which all

valence shell electrons are involved in single bonds, such as the straight chain saturated hydrocarbons, show absorption maxima in the region of 160–170 nm. Their spectra are observed only as ‘end absorptions’ because of instrumental limitations. The other groups of nonaromatic hydrocarbons are bathochromic-shifted and possess their absorption edges in the range of 190–200 nm. This is one aspect of the importance of measuring the absorption of the UV light in the gas phase because there is no solvent wavelength cutoff at 190–200 nm. The other important aspect is that the spectra are not influenced by solvent effects and therefore well defined. There are also no shifts in λ_{\max} values and the bands are sharp in comparison with the relatively broad bands observed in the liquid phase, where their shapes depend on the degree of interaction between solvent and solute. Furthermore, in liquids, it is only very rarely that separation of vibrational bands is possible because the solvent effect generally tends to obscure the vibrational structure. By measurements in the vapour phase, these drawbacks are eliminated, which makes the UV spectra in the gas phase highly suitable for computer-based identifications of unknowns against a spectrum reference library. An example of the reproducibility of spectral details is shown in Figure 1, where a spectrum, taken from an analysis of cigarette smoke, is normalized and overlaid on the reference spectrum of isoprene. The absorbance spectra as well as the first derivatives are plotted. Derivatives of absorption spectra are preferably used in order to enhance spectral details. Derivatives of spectra can also be utilized in order to make selective determination of specific functional groups.

A study of molecular UV absorption spectra between 168–330 nm in the gas phase, for about 1000 organic compounds has demonstrated the importance of the short UV wavelengths for analytical purposes. About 70% of the 1000 spectra registered have absorption maxima at wavelengths shorter than 190 nm and their intensities are up to 100 times higher than those of the absorption bands at longer wavelengths. In addition to the high sensitivity of detection, the lower wavelength region is the spectral range, where the amount of details used for identification purposes increases considerably. Moreover, most of the functional groups in compounds not considered UV-absorbing, such as alkanes, ethers, aldehydes and ketones, display detailed spectra in this region.

The influence of temperature on the shape of spectra has been studied in the range of 15–205°C. A slight broadening effect on spectral absorption bands (0.3 nm) and the vibrational structure (maximally 1.4 nm) with increased temperature was observed. These effects are however, considered to have

Table 1 The development of GC-UV: instrumental conditions

Author (year)	Instrument principle	Separation column	Separation conditions	Flow cell configuration
Kaye (1962)	Beckman DK-2, modified and N ₂ -purged	1.8 m, i.d. 3.2 mm, packed column	Injection volume: 30 µL Flow (He): 189 mL min ⁻¹	Path length: 1, 5, 10 cm Volume: 1.5–3 mL
Kaye (1964)	Beckman DU, modified and N ₂ -purged	1.8 m, i.d. 3.2 mm, packed column	Injection volume: 30 µL Flow (He): 123 mL min ⁻¹	Path length: 1 cm Volume: 1.5 mL
Novotny (1980)	Perkin-Elmer GC-55 variable wavelength monitor	30 m, i.d. 0.7 mm, UCON 50 HB2000, capillary column	Injection volume: 0.1 µL	Path length: 1.12 cm Volume: 50 µL
Adams (1984)	Tracor Model 970 in a remote configuration. 240 nm and 260 nm bandpass filters	2 m, i.d. 2 mm, packed column 3% OV101 on 100/120, Supelcoport	Injection volume: 5 µL Flow (N ₂): 30 mL min ⁻¹ 150°C, 2 min; 10°C min ⁻¹ , 250°C	Path length: 1.6 cm Volume: 200 µL
Lagesson (1984)	Varian Cary UV-Vis spectrophotometer	8 cm, i.d. 1.5 mm, packed column (10 µm particles), DDP, OV101	Injection volume: 1 µL Flow (N ₂): 10 mL min ⁻¹ ~ 90°C	Path length: 9.5 cm Volume: 170 µL
Kube (1985)	HP 8450A, photodiode array	1.8 m, i.d. 6 mm, packed column 5% SP-1200, 1.75%, Bentone-34	Injection volume: 0.2–0.5 µL Flow (He): 60 mL min ⁻¹	Path length: 12.5 cm Volume: 22 mL
Lagesson (1989)	HP 8452A, photodiode array, 324 diodes	8 cm, i.d. 1.5 mm, packed column (10 µm particles), DCQF1	Injection volume: 1 µL Flow (N ₂): 15 mL min ⁻¹ start 70°C, ramp 15°C min ⁻¹	Path length: 9.5 cm Volume: 170 µL
Bornhop (1991)	Rapid-scanning LC detector, Linear Instruments	30 m i.d. 0.53 mm, 1.0 µm, B-210, capillary column	Flow (He): 5 mL min ⁻¹	Path length: 1.2 cm Volume: 85 µL
Bornhop (1992)	Rapid-scanning LC detector, Linear Instruments	25 m i.d. 0.32 mm, 0.4 µm, SE-52, capillary column	Injection volume: 0.5 µL, 1 : 100 Flow (He)	Path length: 1.2 cm Volume: 85 µL
Hackett (1995)	Remote detection using fibreoptics 206HR detector, Linear Instruments	30 m, i.d. 0.32 mm, 0.25 µm, DB5, capillary column	Injection volume: 1 µL splitless Flow (He): 30 cm s ⁻¹	Path length: 1.2 cm Volume: 85 µL
Sanz-Vicente (1996)	HP 8451, photodiode array	4 m, i.d. 1/8 in, packed column, 5% SE-30, Chromosorb W HP	Injection volume: 30 µL	Path length: 1 cm Volume: 70 µL
Sanz-Vicente (1998)	HP 8451, photodiode array	4 m, i.d. 1/8 in, packed column, 5% SE-30, Chromosorb W HP	Injection volume: 50 µL	Path length: 1 cm Volume: 70 µL
Lagesson-Andrasko (1998)	INSCAN 175 GC-UV spectrophotometer, photodiode array, 1024 diodes, N ₂ -purged	8 cm, i.d. 1.5 mm, packed column	Injection volume: 1 µL Flow (N ₂): 15 mL min ⁻¹	Path length: 9.4 cm Volume: 170 µL
Lagesson (2000)	INSCAN 175 GC-UV spectrophotometer, photodiode array, 1024 diodes, N ₂ -purged	30 m, i.d. 0.32 mm, 0.25 µm, Hp-5, capillary column	Injection volume: 1 µL Flow (N ₂): 3 mL min ⁻¹ , make-up flow 7 mL min ⁻¹	Path length: 9.4 cm Volume: 170 µL

References:

- Kaye W (1962) *Analytical Chemistry* 34: 287–293.
 Kaye W and Waska F (1964) *Analytical Chemistry* 36: 2380–2381.
 Novotny M, Schwende FJ, Hartigan MJ and Purcell JE (1980) *Analytical Chemistry* 52: 736–740.
 Adams KA, Debra L, Van Engelen and Thomas LC (1984) *Journal of Chromatography* 303: 341–349.
 Lagesson V, Lagesson-Andrasko L (1984) *Analyst* 109: 867–870.
 Kube M, Tierney M and Lubman DM (1985) *Analytica Chimica Acta* 171: 375–379.
 Lagesson V (1989) *Analytical Chemistry* 61: 1249–1252.
 Bornhop DJ and Wangsgaard JG (1991) *Journal of High Resolution Chromatography* 14: 344–347.
 Bornhop DJ, Holousek L, Hackett M and Wang H (1992) *G.C., Rev. Sci. Instrum.* 63: 191–201.
 Hackett M, Wang H, Miller GC and Bornhop DJ (1995) *Journal of Chromatography A* 695: 243–257.
 Sanz-Vicente I, Cabredo S, Sanz-Vicente F and Galban J (1996) *Chromatographia* 42: 435–440.
 Sanz-Vicente I, Cabredo S and Galban J (1998) *Chromatographia* 48: 542–547.
 Lagesson-Andrasko L, Lagesson V and Andrasko J (1998) *Analytical Chemistry* 70: 819–826.
 Lagesson V, Lagesson-Andrasko L, Andrasko J and Baco F (2000) *Journal of Chromatography A* 867: 187–206.

Table 2 The development of GC-UV: instrumental specifications

<i>Author (year)</i>	<i>λ range (nm)</i>	<i>Bandwidth (nm)</i>	<i>Noise level</i>	<i>Detection limits</i>	<i>Data collection and handling</i>
Kaye (1962)	165–220	0.08	3×10^{-4} AU	10 ng naphthalene	Strip chart recorder
Kaye (1964)	160–210		3×10^{-4} AU	10 ng naphthalene	Sanborn Model 60-1300 dual-channel high speed recorder; scanning speed: 6 s
Novotny (1980)	Recordings at wavelengths: 205, 210, 220, 260 and 280	~ 20	1.6×10^{-4} AU	0.3 ng naphthalene	Strip chart recorder
Adams (1984)	Recordings at wavelengths: 240 and 260			43 ng naphthalene 8–94 ng polycyclic aromatics	Digital integrator
Lagesson (1984)	Single wavelength recordings Spectral scanning after carrier gas stop	0.25–3.5	5×10^{-4} AU	0.5 ng carbon disulfide	Strip chart recorder
Kube (1985)	226–350	2	2×10^{-4} AU	530 ng benzene	Printer
Lagesson (1989)	190–510	2	2×10^{-4} AU	80 pg mesitylene	PC data handling
Bornhop (1991)	195–360	5	2×10^{-5} AU		IBM model 50
Bornhop (1992)	192–360	5	2×10^{-5} AU	0.2 ng coumarin	IBM model 50
Hackett (1995)	192–360	2	2×10^{-5} AU	90 pg naphthalene	IBM model PS2 55 SX, 206 software, Linear Instruments
Sanz-Vicente (1996)	190–300	2	3×10^{-4} AU	15 ng mesitylene	Integration time: 0.5 s Data handling by means of a program in BASIC
Sanz-Vicente (1998)	190–250	2	3×10^{-4} AU	40 ng phenol	Integration time: 0.5 s Data interpretation by means of a program in BASIC
Lagesson-Andrasko (1998)	168–330	0.7 and 1.7	4×10^{-5} AU		Data collection: Instaspec II, Oriel Corp Data handling: Grams/386, Galactic Industries
Lagesson (2000)	168–330	1.7	4×10^{-5} AU	0.5–3 pg naphthalene	Data collection: Instaspec II, Oriel Corp Data handling: Grams/386, Galactic Industries

References: As shown in Table 1.

negligible influence on spectral searching for unknowns, especially if the reference spectrum and the unknown spectrum are registered at similar temperatures.

Instrumentation

The various parts of a GC-UV instrumental set-up are shown in Figure 2. This particular equipment consists of a remote configuration between the gas flow cell and a commercially available UV spectrophotometer (LC detector). For this arrangement fibre-optics were utilized.

The only commercial instrument, the GC-UV INSCAN 175 spectrophotometer, contains a purge gas flow system, which takes up the concept from Keye, in order to prevent oxygen and water vapour from entering the UV light path of the instrument. Nitro-

gen gas has a negligible absorption at wavelengths longer than 140 nm. Therefore dry and pure nitrogen can be used as the purge gas, which permits recordings at wavelengths shorter than 190 nm, which is the limit if air is present in the optical path. The lowest limit of the spectral scale (168 nm) is dependent on the quartz optics and the diode array. The additional available wavelength range of 168–190 nm is of considerable importance for the performance characteristics of the instrument. It places the GC-UV into a general method of analysis because all organic compounds and most of the inorganic gaseous molecules give rise to detailed spectra of high intensities in this range.

Light Pipes

From Table 1 it can be seen that the geometry of the gas flow cells used differs considerably, with path

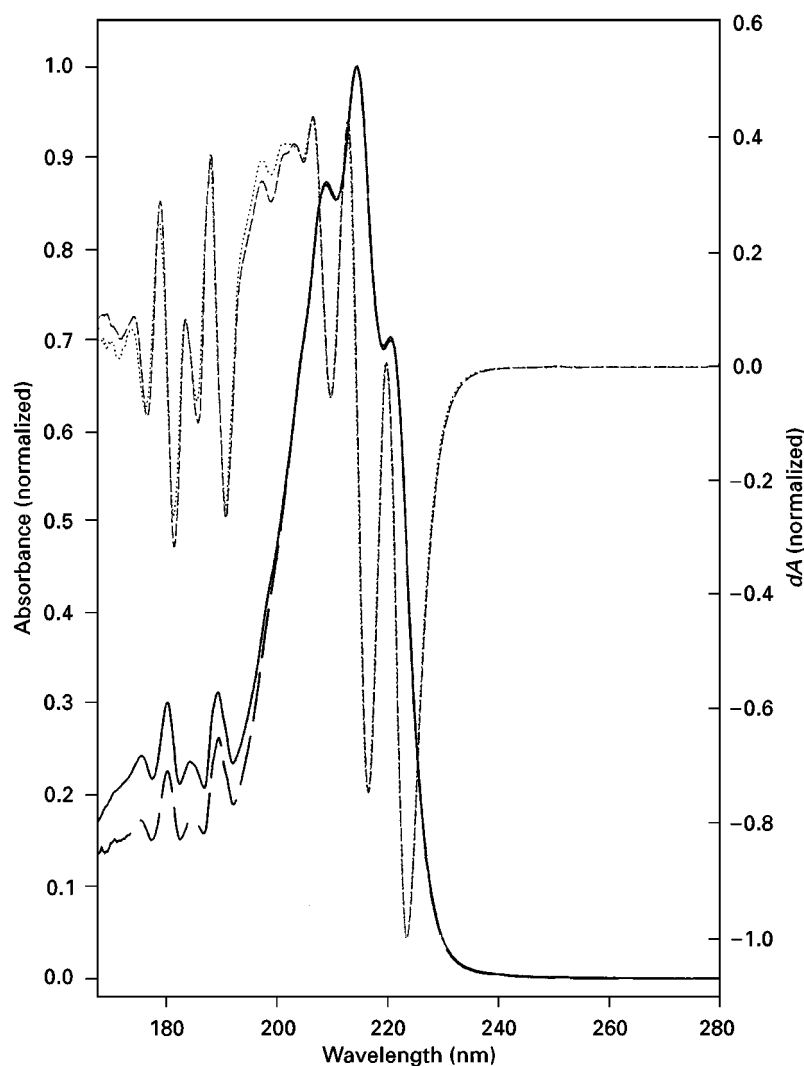


Figure 1 The reference spectrum for isoprene and a spectrum recorded at the analysis of 200 μL cigarette smoke. Both absorption spectra are normalized and overlaid together with their first derivatives. —, Unknown absorbance; --, reference absorbance;, unknown dA ;, reference dA .

lengths varying from 1 cm up to 12.5 cm and volumes ranging from 70 μL up to 22 mL. Optimization of the gas flow cell involves keeping a low volume for a good chromatographic resolution. At the same time, the path length and the light throughput should be maximized. These optimization factors are the same as for GC-FTIR, where an internally gold-coated gas flow cell is used. A total reflection is obtained at the gold-coated walls, leading to a high light throughput in gas flow cells about 10 cm long and with an internal diameter usually ~ 1 mm. Because of the use of internal reflection, these gas flow cells are called light pipes. For GC-UV it was realized, at an early stage, that an internal coating was not necessary and an ordinary glass tubing gave a high light throughput due to a total reflection of UV light on the internal glass walls.

A useful rule is that the optimum performance of a GC-UV system in terms of signal-to-noise and band dispersion is obtained from a light pipe with an effective volume equivalent to the volume of a 'typical' GC peak, described by the peak width at half the maximum amplitude. Typical light pipe volumes currently employed for GC-FTIR vary from 50 to 200 μL and these figures should also be valid for GC-UV light pipes.

Figure 3 shows a light pipe configuration that consists of a gas flow cell with a built in micro gas chromatograph together with the light pipe. In addition to the use of this internal micro GC, the cell can easily be linked to an external capillary GC by means of a heated transfer line, as shown in the figure. The 10 cm long gas chromatographic column, which can also be directly connected to a one-stage thermal

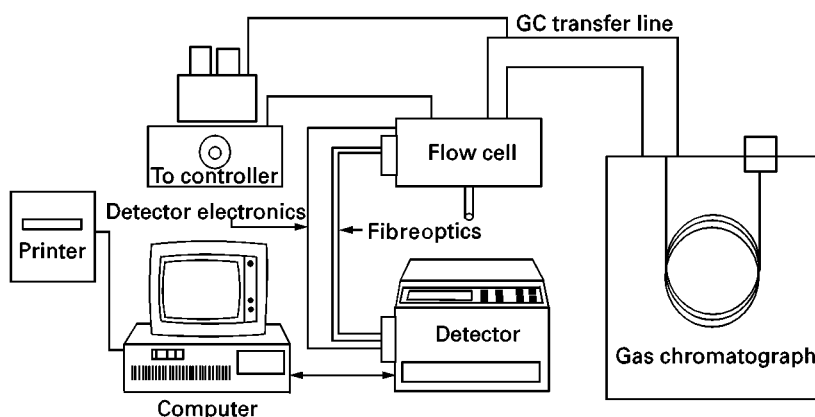


Figure 2 Block diagram for a GC-UV system. Reproduced from (1992) *Capillary gas chromatography. Rev. Sci. Instrum.* 63(1): 192.

desorption unit or to a gas loop injector, is preferably used for fast separations of gaseous and relatively volatile molecules.

Spectrophotometric Detection and Recording

Earlier work involved measurements at a single wavelength while recent spectrophotometric detection involves full spectral scans covering the whole chromatographic retention time scale. The results are obtained in three dimensions – wavelength, absorbance and retention time. Such a result is shown in **Figure 4**, where the wavelength scale follows the x -axis, the absorbance values the y -axis and the retention time goes along the z -axis. This particular sample is cigarette smoke injected by means of a loop injector (200 μL) on the micro gas chromatograph shown in **Figure 3**. UV spectra of compounds in the cigarette smoke are measured by means of an array of 1024 diodes, which cover a wavelength range from 168 to 330 nm. The spectrometer employed has a band width 1.7 nm or less in order to record the finer spectral details. The diode array detectors usually have a minimum exposure time of 0.02 s. The

measuring exposure time must be below a level where a saturation of the diodes occurs. Typically, the exposure time is ~ 0.1 s. A number of these exposure values are measured and their average is calculated. The absorbance values at any retention time are then calculated for every diode representing a wavelength. The number of the exposure values are chosen according to the desirable chromatographic resolution.

Data Acquisition and Handling

A full scan GC-UV analysis generates a considerable amount of data. These data, which are calculated as absorbance values, easily exceed 10^6 measuring points, when capillary column separation with spectral recording every 2 s is employed. However, the use of modern computer technology makes the handling of a large number of measuring values possible. Various calculations and mathematical functions can be applied to the measuring data. Besides the simple functions, interactive subtraction, baseline corrections, various orders of derivatives, rotation (90°), damping functions and cuts at selected wavelengths can be applied.

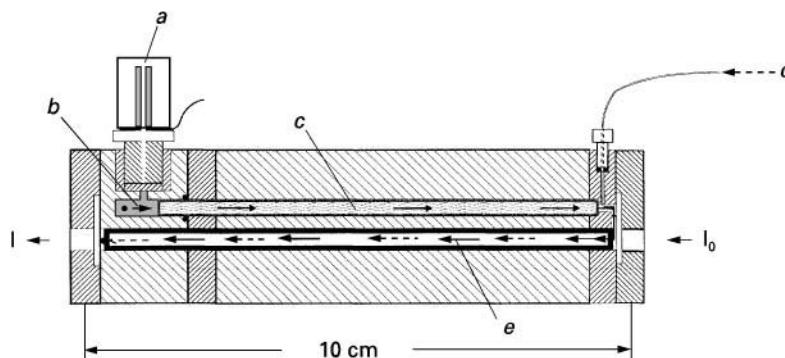


Figure 3 A 10 cm long gas flow cell for GC-UV measurements containing a built-in micro gas chromatograph and a light pipe *a*, Injector; *b*, injector chamber with carrier gas inlet; *c*, separation column; *d*, inlet from external GC; *e*, light pipe.

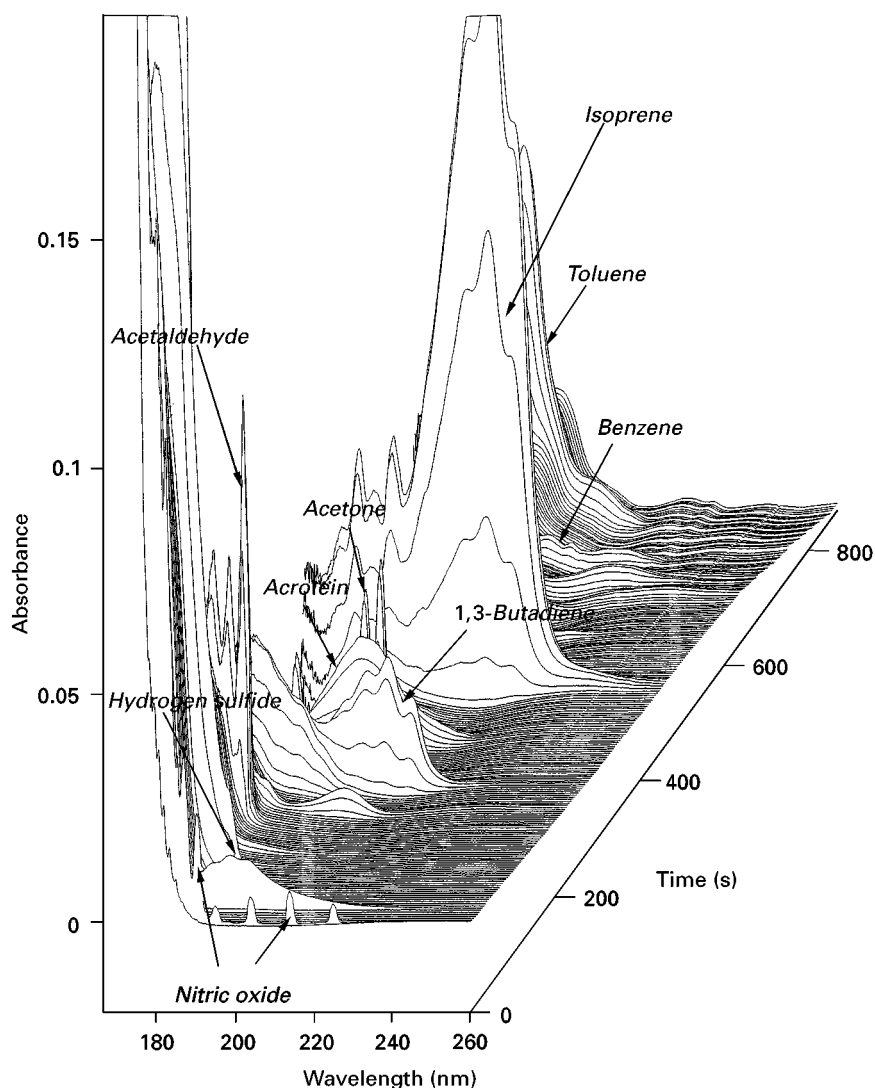


Figure 4 Results of cigarette smoke analysis obtained with the GC-UV method with the micro gas chromatograph, which is especially suitable for analysis of the most volatile compounds in cigarette smoke. The wavelength scale follows the *x*-axis, the absorbances the *y*-axis, and retention time the *z*-axes.

During an analysis the recording follows the axes shown in Figure 4 and, in order to monitor the chromatographic sequence, the data are turned 90° to get the retention time along the *x*-axes. Chromatograms can now be studied at any chosen wavelength, or for the average absorptions within a chosen wavelength region.

The gas-phase UV spectra are well defined and most of them contain a fine structure. In order to enhance the spectral details, derivatives of the absorption spectra are preferably utilized. When forming chromatograms the negative values obtained upon derivation are not convenient to handle and, to avoid this problem, the absolute values of the derivatives can be used. **Figure 5** shows the results from an analysis of a polychlorinated biphenyl (PCB, Arochlor

1248) sample. The presentation mode of the measured values is the same as for Figure 4, but the second derivatives with absolute values of the recorded absorption spectra are drawn for the retention times between 800 and 1600 s. The spectral details of the congeners and isomers concerning this group of related compounds appear quite clearly. Various types of graphical views can be carried out in order to suit certain presentations of results. One example of such a view is a contour plot, which is an effective way to treat the results. In **Figure 6** a contour plot is created from the analysis of a petroleum product. The advantage of these type of presentations is that compounds with close retention times appear as nonsymmetrical contour lines, which makes it possible to 'see' the hidden peaks. Another advantage is that

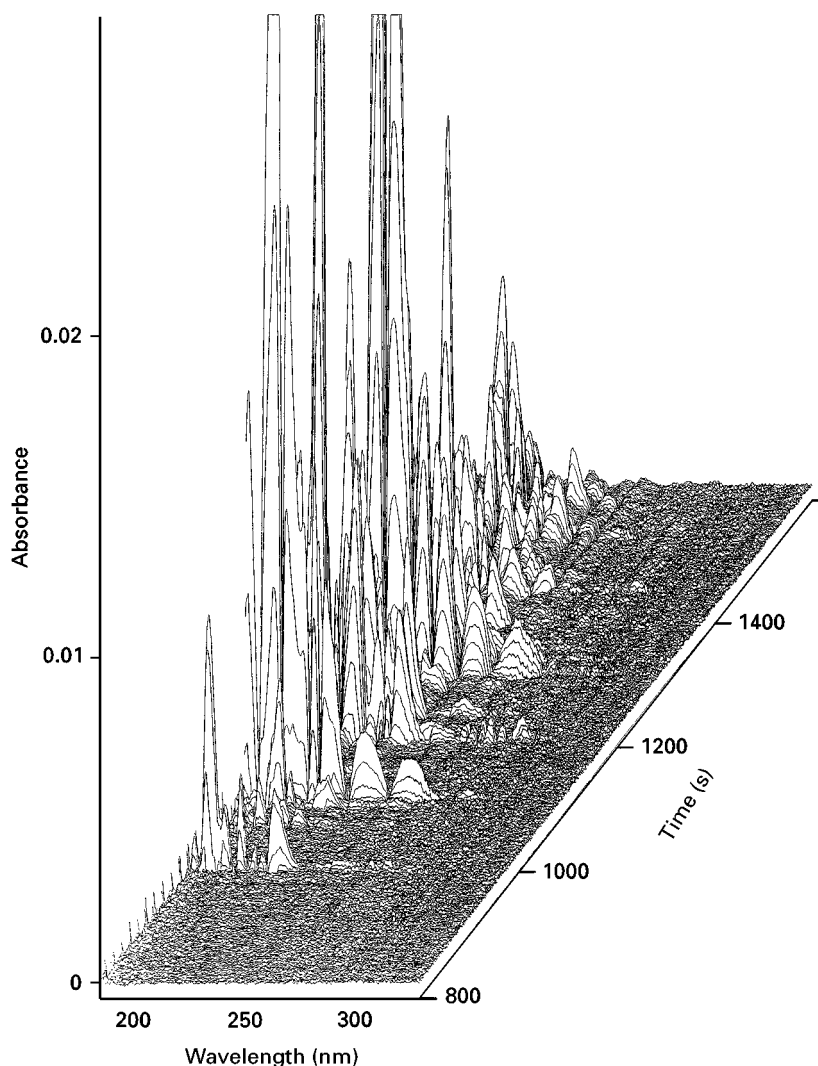


Figure 5 The result from a retention time of 800 s up to 1600 s is shown in a three-dimensional plot of the absolute values of second derivatives of absorption spectra collected at the analysis of a PCB sample.

compounds possessing the same functional group can often be directly shown.

Accuracy and Precision

To describe a position in the absorption spectrum the wavelength is used as the locating unit. This puts a high demand on the spectrophotometric measurements, especially accuracy, precision and reproducibility, of the wavelength. The weekly calibration of the wavelength scale of GC-UV INSCAN 175 spectrophotometer, using the spectral lines from a mercury-argon pen lamp, always gave the same wavelength values of the spectral lines measured in the region of 168–330 nm. The 1024 element photodiode array covers the scale from 166.7 to 330.0 nm. This gives a value of 0.16 nm per diode, which is to be considered as an ultimate limit of resolution. The reproducibility was measured for different bands of 1-hexene (λ_{\max} 178.7 nm), 1-hexadecene (λ_{\max}

177.9 nm) and 1-iodopropane (the band at λ : 177.6 nm, at λ_{\max} : 182.7 nm and the band at λ : 199.4 nm) for 1 year. The standard deviation values were in the range of 0.05–0.15 nm, i.e. all were lower than the distance between two diodes (0.16 nm).

Sensitivity and Detection Limits

The discrepancy in sensitivity of the GC-UV method, given by detection limits in Table 2, can primarily be derived from the differences in the geometry of the gas flow cell and from the separation columns (packed or capillary) used.

In comparison with the infrared wavelength region, the absorptivities are up to 1000 times higher in the UV wavelength region. Also, the fact that the noise level could be kept equal to or lower than for FTIR detectors ought to imply a considerably more favourable signal-to-noise ratio. The specification concerning the noise level, along the time scale, given

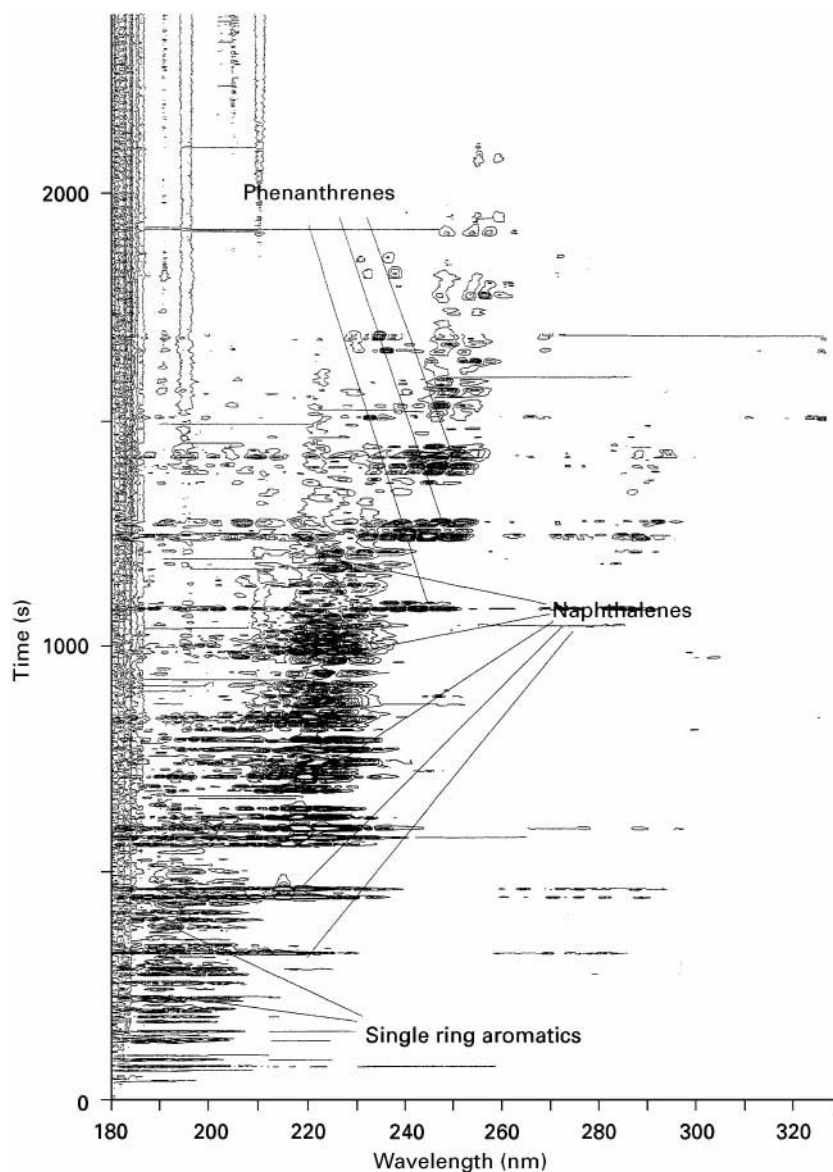


Figure 6 A contour plot showing the result obtained at the analysis of a petroleum product: the second derivatives are plotted and, as indicated, the single, double and polyaromatic compounds appear clearly.

for the GC-UV INSCAN 175 spectrophotometer, is about 0.5×10^{-4} peak to peak.

For a detection limit defined as the amount giving rise to an absorption of 1.5×10^{-4} AU, and expressed as the minimum amount of the compound per second that could be detected, the following values were calculated: perchloroethylene 55 pg s^{-1} , naphthalene 3.3 pg s^{-1} , mesitylene 8.9 pg s^{-1} , carbon disulfide 4.8 pg s^{-1} , acetone 49 pg s^{-1} and benzene 5.4 pg s^{-1} .

The noise level can be lowered by smoothing and by taking the average absorption values within a wavelength range. However, it has been shown that this noise reduction is most effectively obtained using average derivatives values. The derivatives are in these cases differentials with a rather large gap value

(2–6 nm) along the wavelength scale. The noise level obtained, using this mode, was $\sim 1 \times 10^{-5}$ AU peak to peak, which gives a calculated detection limit for naphthalene of $\sim 0.5 \text{ pg s}^{-1}$.

The limit of quantification (MIQ: minimum identification quantity) is usually defined as the lowest quantity when the hit rate of the unknown is still found among the first five proposals. This depends on the size of the spectrum library and, at this stage, the available reference spectrum library is probably not large enough to make any closer estimations. However, clear identifications can be made in the mid pg range, provided that the compound possesses a functional group with relatively high absorptivity values (e.g. aromatics). For the GC-UV method the

introduction of an additional sensitivity level, namely a minimum of classification quantity (MCQ), appears to be desirable. The suggestion is to define MCQ as the minimum quantity necessary for giving the right functional group at the first library search proposal.

Qualitative Analysis

The identification of an unknown is commonly carried out by comparison with a library of reference gas-phase spectra. The absorption process of an atom or a molecule in the gas phase is free from any influence, which reproduces not only the unique character of the electronic transitions, but also of the accompanying simultaneous changes in the vibrational states. This gives rise to spectral shapes which are strictly defined and, in most cases, accompanied by fine structures. Therefore the UV spectra are well suited for identification by means of a computer-based spectral search against a reference spectrum library. A spectrum library of ~ 1000 gas-phase UV spectra recorded in the wavelength region of 168–330 nm has been established. A commercially available IR search program has been used with success for identification. Because of the relatively small size of this library, the identification possibilities are limited. Nevertheless, identification of classes of compounds can most often be directly pointed out. The compounds containing the same functional group show a number of characteristic similarities, but at the same time clear differences between individuals within a group are observed. The exceptions are cases when various straight alkyl chains are involved. The spectra of acetophenone and propiophenone, for example, are hard to distinguish from each other.

Determination of Specific Functional Groups

The reference spectrum library mentioned above has made it possible to identify ~ 50 functional groups due to their characteristic spectral appearances. These characteristics allow the assignment of a specific functional group in a compound without access to any reference spectrum. The specific functional groups can, for example, be exposed in a contour plot shown in Figure 6, where the measuring data (second derivatives) for single, double and polyaromatic compounds are outlined quite clearly. Specific chromatograms can be obtained for these aromatic groups by taking the average absorption in appropriate wavelength ranges.

Another example of specific detection is shown in Figure 7, where 6 mg of a dust sample was analysed by means of GC-MS and GC-UV. In both cases the analysis involved a thermal desorption before the gas chromatographic separation and in both cases the same type of capillary column and the same temper-

ature programme were used. Figure 7A shows the chromatogram from the GC-MS total ion signal and Figure 7B–D shows the GC-UV chromatograms obtained at the wavelength ranges indicated. The chromatograms were calculated using the absolute values of the first derivatives of absorption spectra. Identifications were carried out by means of GC-MS for the peaks indicated 1–5 with following results: (1) hexanal; (2) heptanal; (3) octanal, (4) nonanal and (5) decanal. The nonaromatic straight chain aldehyde group has a characteristic sharp UV absorption edge at 187 nm. Therefore a specific detection of nonaromatic straight chain aldehydes can be made in the 187–190 nm wavelength range, as shown in the figure. The next GC-UV trace shows the chromatogram from the average values in the 187–220 nm range. This gives a less specific chromatogram. Naphthalene was identified at the indicated position (6) by means of a search against the gas-phase UV reference spectra library. The same library was used for the identifications of benzaldehyde at position (7) and 2-furaldehyde at position (8). The spectrum of 2-furaldehyde has a dominating absorption profile between 230 and 270 nm and, consequently, it only appears in the 238–244 nm wavelength trace.

The experiences of combining results from GC-MS and GC-UV have recently been explored and there are indications of valuable possibilities. The characteristic complementary qualities for GC-UV compared to GC-MS allow specific determinations – determinations of specific functional groups and also of structural isomers, which are difficult to distinguish by means of MS.

Isomers

There are numerous examples of structural isomers in chemistry and isomers of a certain compound have different physical and chemical as well as physiological properties. Thus, for example in the field of toxicology, some isomers possess toxicity which differ by several orders of magnitude.

Ninety-five groups of various isomeric compounds have been investigated and in all cases the GC-UV method was able to distinguish clearly between structural isomers. However, when the analysis involves various straight or branched alkyl chains the identification is complicated. For difficult identifications like these derivative functions can be applied in order to enhance differences in spectral details and thus distinguish between isomers not resolved by comparing the absorbance spectra alone. Some groups, like nonaromatic halogenated hydrocarbons and nonaromatic alcohols, show minimal differences. Nevertheless, they are still distinguishable and the first derivatives of their spectral curves give clear shifts of ~ 2 –3 nm in the absorption maxima and minima.

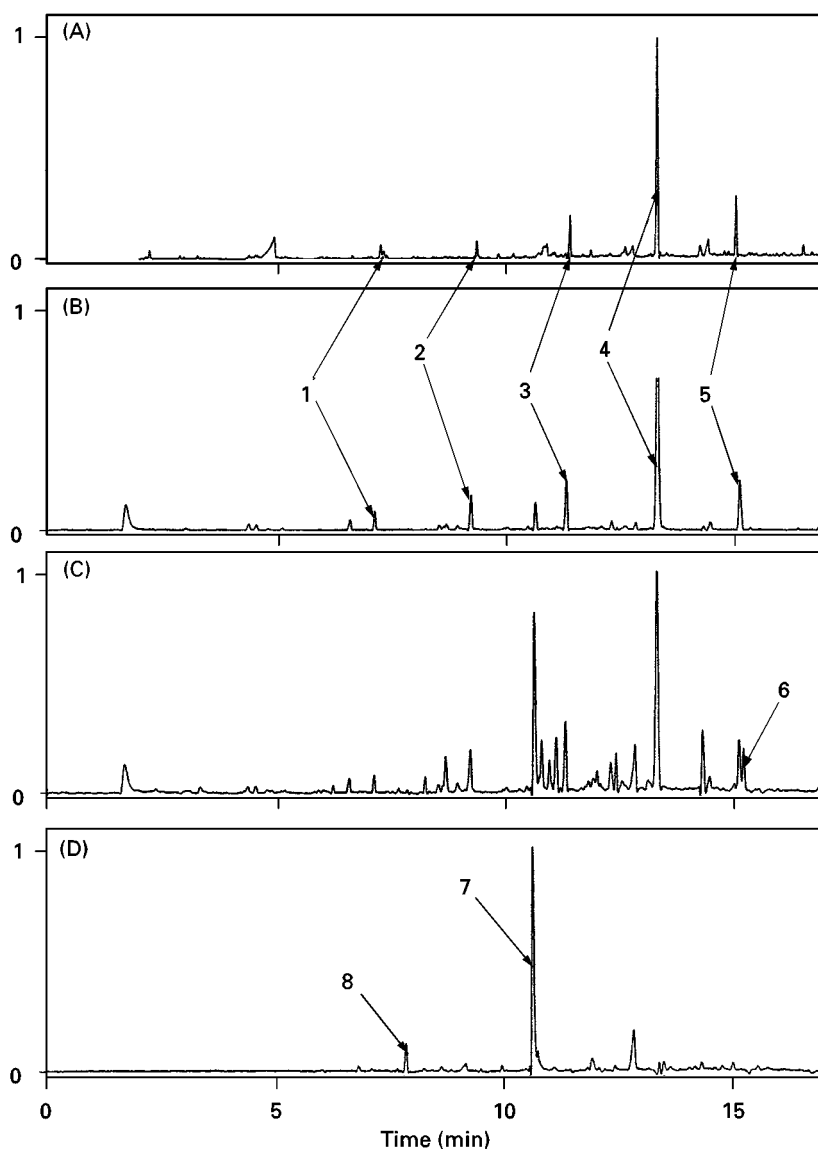


Figure 7 Four chromatograms after the analysis of a dust sample. (A) The upper trace shows the total ion current (TIC) obtained from the analysis of 10 mg dust by means of GC-MS linked to the thermal desorption unit. The next three traces show the chromatograms based on first derivatives for (B) 187–190 nm, (C) 187–220 nm and (D) 238–244 nm wavelength ranges from the analysis of 6 mg dust by means of GC-UV. The peaks indicated 1–5 were identified using GC-MS and the peaks indicated by 6–8 by GC-UV. The identification results are given in the text.

Quantitative Analysis

A linearity of detector response over a range of $\sim 10^4$ for aromatic hydrocarbons in the vapour phase has been reported. Similar linear responses were observed for more polar aromatic compounds (coumarin and phenols) and no deviations from Lambert–Beer’s law were found in the range of the mass loading limits imposed by the capillary column employed. Also the linearity for nitric oxide standards has been studied in the range of 10–1800 ng at the wavelength of 213.5 nm. The standards were prepared from a standard gas tube containing 99% nitric oxide. Standard concentrations in nitrogen were prepared

from the tube using Tedlar bags and gas-tight syringes. The standard curves were linear in the range studied.

Studies of day-to-day variation and repeatability have been carried out at a temperature of 110°C using a GC-UV INSCAN 175 spectrophotometer linked to a dynamic dilution system for the standard concentrations and a 200 μ L loop injection. The compounds determined were methanethiol and diethyl sulfide. The within-day relative standard deviations (RSD) were 2.3% ($n = 7$) for diethyl sulfide at a concentration of 82 p.p.m. and 3.0% ($n = 7$) for methanethiol at 79 p.p.m. The between-days deviations were measured for 3 months ($n = 36$). The RSD values were

determined for the slope of the standard curves, with concentrations between 80 and 2000 p.p.m.

These between-days RSD values were 4.0% for diethyl sulfide, and 5.0% for methanethiol. These results include the errors arising from the dynamic dilution system used. In this case a photo diode array type detector was employed, which has the advantage of having a low wavelength drift.

Applications

GC-UV is a general method of analysis with numerous possible application areas. So far, the method has been little used and most investigations have been concerned with the fundamentals of the analytical principle. Nevertheless, a number of works have been published, for example the determinations of nitric oxide adsorbed on mineral fibres and isoprene and acetone determinations in exhaled breath. A method, using GC-UV for the determination of alcohols, denoted as GC-GPMAS (gas chromatography with gas-phase molecular absorption spectrometry) has been reported. These are short reports concerning determinations of single, double and polyaromatics in petroleum products, volatile compounds at low concentrations in air, irritants adsorbed on dust particles, determinations of compounds present in cigarette smoke, identifications of compounds in flavour samples, analysis of methanethiol, diethyl sulfide and hydrogen sulfide in paper industry, and identifications of congenes and isomers of polychlorinated biphenyls (PCBs) and polychlorinated naphthalenes (PCNs).

Future Developments

UV absorption spectra are basically electronic spectra which arise from transitions between electronic states and are accompanied by simultaneous changes in the vibrational and rotational states. Thus, an absorption spectrum is a function of the whole structure of a molecule and an expression for its fundamental chemical properties. UV absorption spectra in the gas phase are very well defined and can be denoted as finger-

prints of organic as well as inorganic compounds. They have considerably higher absorptivities than their counterparts in the infrared wavelength region and are very well suited for computer-based spectral search systems. The size of reference spectra presently available is much smaller compared with that available for GC-FTIR and particularly for GC-MS. Future development of the GC-UV method will include continuous extension of the reference spectrum library.

One of the main advantages of UV gas-phase spectra might be to make detailed classification of functional groups. At present ~ 50 groups with characteristic features can be identified. However, this will certainly be extended and will also include a number of groups with mixed functionalities.

Concerning further instrumental development, recordings of spectra at lower wavelengths than 168 nm will probably be possible. Another instrumental development that can be expected is matrix isolation and direct deposition techniques similar to the ones developed for GC-FTIR measurements. Furthermore, the GC-UV spectrophotometer will, in the near future, be adapted to online measurements in industrial process monitoring and control.

See also: II/Chromatography: Gas: Derivatization; Detectors: Mass Spectrometry; Detectors: Selective; Gas Chromatography-Infrared.

Further Reading

- Brown RA and Pearl TD (1979) Chapter 15. In: Altgelt KH and Gouw H (eds) *Chromatography in Petroleum Analysis*. New York: Marcel Dekker.
- Lagesson V (1992) *Micro Gas Chromatographic Separation combined with UV- and IR-Spectrophotometric Detection/Identification with Applications within the Occupational Hygiene Field using Diffusive and Active Sampling followed by a Direct Thermal Desorption Technique*. PhD thesis, Department of Analytical and Marine Chemistry and Department of Occupational Medicine, Göteborg, 1992.
- Lagesson V and Lagesson-Andrasko L (1996) *Reaching New Peaks*. Analysis Europa.

Gas-Solid Gas Chromatography

J. de Zeeuw, Varian-Chrompack, Middelburg, The Netherlands

Copyright © 2000 Academic Press

Introduction

Gas-solid chromatography (GSC) has been used since the earliest days of gas chromatography and preceded

gas-liquid chromatography. Through this early work the limitations of GSC were well recognized and, although the advantages of GSC were also apparent, it was quite some time before reliable and reproducible GSC columns became commercially available. There are many methods in the literature describing the application of GSC to specific analyses, for example the UK Institute of Petroleum method

IP345/80 describes the use of a 3 m × 2.3 mm stainless-steel column containing Porapak R for the separation of nitrogen, oxygen and carbon dioxide and hydrocarbons up to C₈ in the gas above crude oil. The method requires programming the column from –50°C to 240°C, which is unattractive in that it requires a supply of coolant such as liquid nitrogen.

Although the superior separation characteristics of adsorption materials in porous-layer open-tubular (PLOT) columns were recognized, the main problem was that the preparation procedures for PLOT columns are complex and difficult to implement. However, with the introduction of new capillary column coating technology it is now possible to deposit stable layers of adsorbents on the inner wall of fused silica capillaries. These columns give better separations in a shorter time than the older packed columns.

Adsorption materials that are now commercially available in capillary columns are aluminium oxides, molecular sieves, activated carbon such as graphitized carbon black, porous polymers and silica. Besides fused silica capillary columns, the adsorbents are also deposited in metal columns, expanding the application of adsorbents in the area of process analysers and portable equipment.

Each adsorbent has its own specific application field, as summarized in **Table 1**. In general the application field of PLOT columns covers the permanent gases and volatile mixtures with boiling points up to c. 225°C.

Molecular Sieves

Molecular sieves are synthetic and naturally occurring zeolites with well-defined structures that have found extensive use for the separation of permanent (or fixed) gases. Molecular sieves have a pore size that is defined by the particular ion used in the preparation

of the material – calcium aluminium silicate gives a pore size of 0.5 nm, whereas sodium aluminium silicate gives a pore size of approximately 1 nm. These are the two commonest molecular sieves; other pore sizes are available but are less widely used. The separation on a molecular sieve is based on more than one retention mechanism. The first selection depends on size – molecules that are smaller than the pore size will diffuse inside the pores. Once inside the cavities, the small molecules can interact with a large surface area, which means that they will have relatively long retention times. Large molecules such as branched alkanes or sulfur hexafluoride (SF₆) are too big to enter the pores and these compounds will elute earlier. Compounds that are too large to enter the pores will only be retained by relatively weak adsorption on active sites on the outside of the particles, and thus give shorter retention times.

The retention of components with dipole interaction and hydrogen bond formation, like water and carbon dioxide, is very high. Carrier gas and samples should be as dry as possible. Water is absorbed by the molecular sieve and will cause a reduction of retention times. The water can be removed by heating for a few hours at 300°C. A molecular sieve of pore size 0.5 nm is an ideal adsorbent for the separation of permanent gases; this is also the main use of the column. Normally molecular sieves are not used for separations above C₂ except for hydrocarbon type analysis. Higher boiling compounds are strongly adsorbed and can only be eluted by using undesirably high temperatures (molecular sieves are good catalysts!), vicinal exchange coupled with backflush techniques or even destruction of the sieve with hydrogen fluoride. A typical separation of a permanent gas mixture is shown in **Figure 1**. The 0.53 mm fused silica column is usually coated with a 50 µm layer of 0.5 nm molecular sieve to generate sufficient retention to make a high resolution separation possible at temperatures above ambient. The separation of argon and oxygen is baseline. The 50 µm layer provides a relatively high retention for carbon dioxide. If the separation of argon–oxygen is not important, a 15 µm film can be used. For a comparison of the separations with 50 and 15 µm layers, see **Figures 1** and **2**. Several other applications have been reviewed. Molecular sieves are also successfully coated onto Ultimet capillary columns of 0.53 mm i.d. Applications of these columns are especially of interest for analyser systems where reliability is a major issue (see metal PLOT columns below).

Molecular sieves of the 13X type are also used. These materials have a lower absolute retention due to the larger pores. They are used in the petroleum

Table 1 General application fields of adsorbents

<i>Absorption material</i>	<i>Applications</i>
Molecular sieves	Permanent gases, hydrogen isotopes, CO, N ₂ O
Porous polymers	Volatile polar and nonpolar compounds; samples containing water; CFCs; solvents
Alumina	Hydrocarbon impurities in C ₁ –C ₅ hydrocarbons
Carbon	CO and CO ₂ in air; impurities in ethylene
Silica	C ₁ –C ₃ hydrocarbons, sulfur gases; hydrocarbon and semipolar impurities; samples containing water

CFC, chlorofluorocarbon.

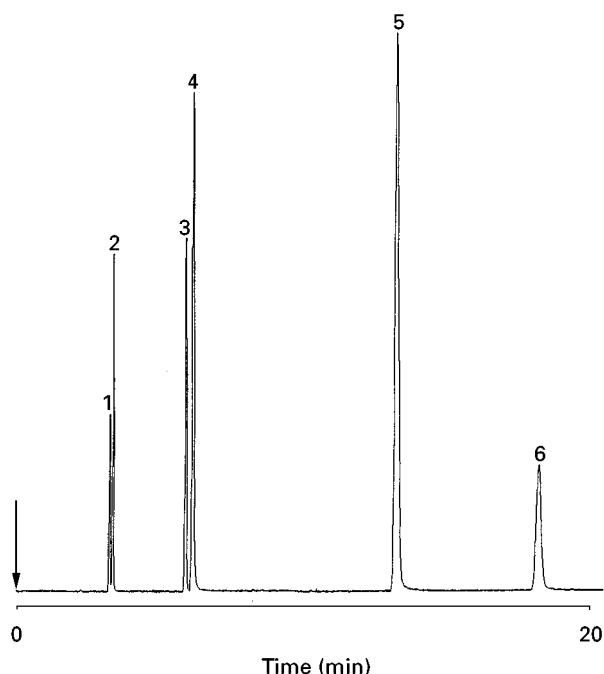


Figure 1 Permanent gases on a 50 μm Molsieve 0.5 nm PLOT column. Experimental details: column, 50 m \times 0.53 mm fused silica; oven, 30°C; carrier gas, hydrogen; injection, split; detection, TCD. Peaks: 1, helium; 2, neon; 3, argon; 4, oxygen; 5, nitrogen; 6, methane.

industry for the type separation of naphthenes from paraffins, olefins, naphthenes and aromatics (PONA analysis), mainly in packed column configurations.

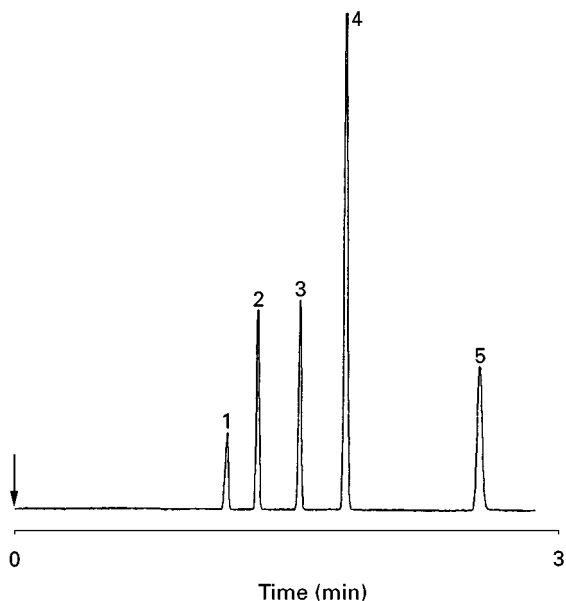


Figure 2 Fast separation of permanent gases on a 15 μm Molsieve 0.5 nm PLOT column. Experimental details: column, 30 m \times 0.53 mm fused silica, Molsieve 0.5 nm d_f = 15 μm ; oven, 50°C; carrier gas, hydrogen; injection, split; detection, TCD. Peaks: 1, helium + neon; 2, argon + oxygen; 3, nitrogen; 4, methane; 5, carbon monoxide.

Alumina Adsorbents

Alumina adsorbents in capillary columns were introduced as long ago as 1963 and were made commercially available in fused silica capillary columns in 1981. Alumina has a very high activity and will retain components as light as ethane. To make the highly active alumina work as stationary phase in GC, it has to be deactivated. Deactivation can be done in many ways, but the most practical and reproducible method is deactivation with inorganic salts.

Alumina deactivated with potassium chloride (KCl) provides a general nonpolar adsorbent that is widely used. Such a column will elute acetylene before butane (Figure 3). The alumina surface can be made more polar by deactivation with sodium sulfate instead of KCl. The resulting alumina layer will elute acetylene after the butane peaks, indicating the higher polarity.

The selectivity of alumina for hydrocarbons is very high. All C_1 – C_4 hydrocarbons can be baseline separated. The resolution between the different hydrocarbons is sufficient to be able to measure many trace amounts of C_1 – C_4 hydrocarbons in a main stream of any one of these hydrocarbons (Figures 4–6). For this reason alumina is one of the most widely used columns in petrochemistry for analysing hydrocarbon impurities in ethylene, propylene (Figure 5) and 1,3-butadiene (Figure 6).

Although alumina has unique separation characteristics, it also has limitations. The activity of the adsorbent is such that it will adsorb any moisture, carbon dioxide or other polar impurity in the sample. When

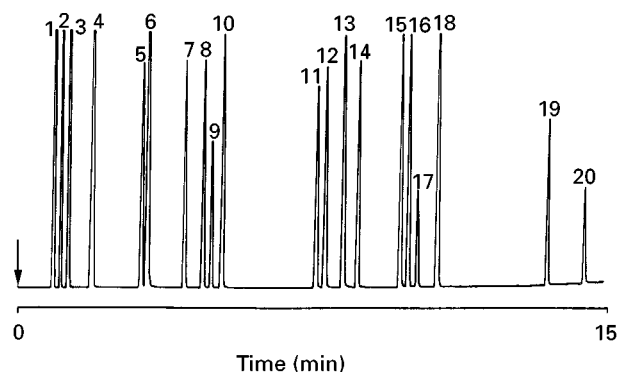


Figure 3 C_1 – C_6 hydrocarbons on an Al_2O_3 , KCl PLOT column. Experimental details: column, 50 m \times 0.32 mm fused silica, $\text{Al}_2\text{O}_3/\text{KCl}$, d_f = 5 μm ; oven, 70°C (4 min) \rightarrow 180°C, 10°C min^{-1} ; carrier gas, helium; injection, split; detection, flame ionization detection (FID). Peaks: 1, methane; 2, ethane; 3, ethylene; 4, propane; 5, cyclopropane; 6, propylene; 7, acetylene; 8, isobutane; 9, propadiene; 10, butane; 11, *trans*-2-butene; 12, 1-butene; 13, isobutene; 14, *cis*-2-butene; 15, isopentane; 16, methylacetylene; 17, pentane; 18, 1,3-butadiene; 19, ethylacetylene; 20, hexane.

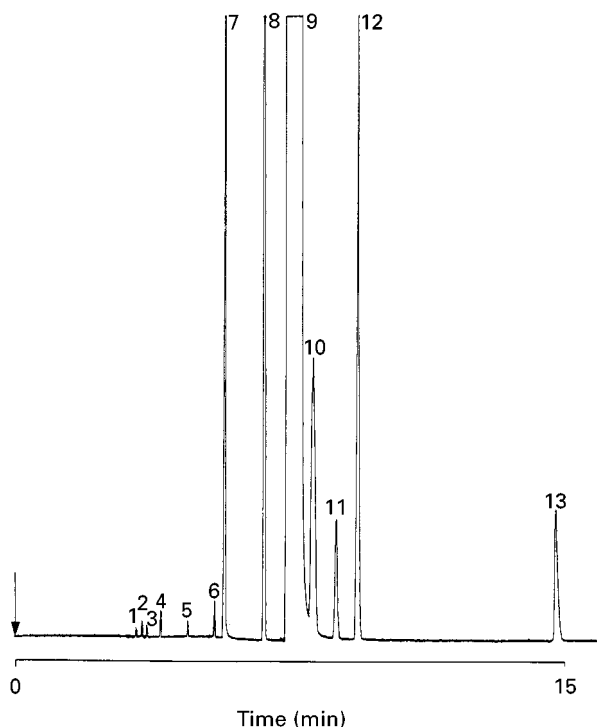


Figure 4 Impurities in *trans*-2-butene on an $\text{Al}_2\text{O}_3/\text{Na}_2\text{SO}_4$ adsorbent PLOT column. Experimental details: column, $50\text{ m} \times 0.32\text{ mm}$ fused silica, $\text{Al}_2\text{O}_3/\text{Na}_2\text{SO}_4$, $d_f = 5\text{ }\mu\text{m}$; oven, 110°C ; carrier gas, nitrogen; injection, split; detection, FID. Peaks: 1, methane; 2, ethane; 3, ethylene; 4, propane; 5, propylene; 6, isobutane; 7, butane; 8, cyclobutane; 9, *trans*-2-butene; 10, 1-butene; 11, isobutene; 12, *cis*-2-butene; 13, 1,3-butadiene.

alumina is exposed to water, the retention times for hydrocarbons are altered and resolution is degraded. The water will deactivate the surface and, as a consequence, the column will have lower retention. The water can simply be removed and the column performance regenerated by heating to 200°C for a short time. If an isothermal setup is required, a polar pre-column that retains the water can be employed. A polyethylene glycol-coated column with a $1.2\text{ }\mu\text{m}$ film works very well as the $\text{C}_1\text{--C}_6$ hydrocarbons will elute from this column before the water and by simple backflushing or a vent switch the water peak can be removed. For more polar impurities, regeneration may take longer, but it is possible. Alumina columns are difficult to destroy and oxygen in the carrier gas will not harm the column. It has been found that sulfur impurities present up to 2000 ppm do not seriously interfere with the retention characteristics of alumina. The maximum temperature of alumina columns should not exceed 200°C ; above this temperature recrystallization of the deactivating compound will occur, causing changes in selectivity. Alumina layers coated in Ultimet tubing are very stable and find wide application in hostile environments.

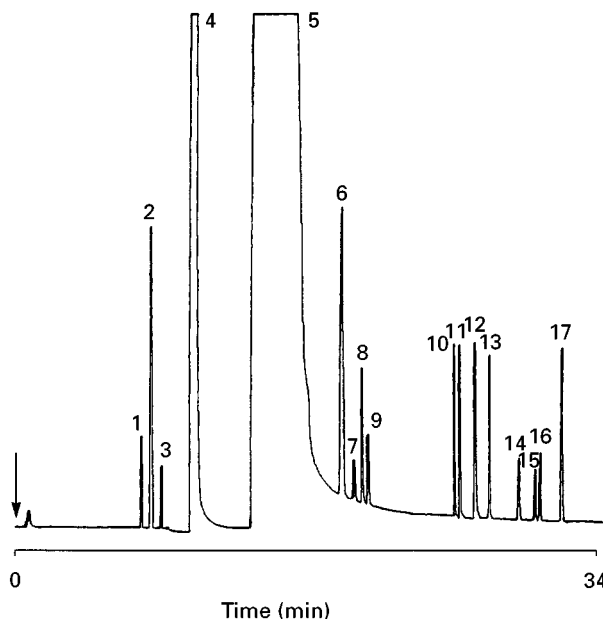


Figure 5 Impurities in propylene on an $\text{Al}_2\text{O}_3/\text{KCl}$ PLOT column. Experimental details: column, $50\text{ m} \times 0.53\text{ mm}$ fused silica, $\text{Al}_2\text{O}_3/\text{KCl}$, $d_f = 10\text{ }\mu\text{m}$; oven, 40°C (10 min) $\rightarrow 160^\circ\text{C}$, 5°C min^{-1} ; carrier gas, helium; injection, split; detection, FID. Peaks: 1, methane; 2, ethane; 3, ethylene; 4, propane; 5, propylene; 6, isobutane; 7, acetylene; 8, butane; 9, propadiene; 10, *trans*-2-butene; 11, 1-butene; 12, isobutene; 13, *cis*-2-butene; 14, isopentane; 15, methylacetylene; 16, pentane; 17, 1,3-butadiene.

Porous Polymers

The preparation of capillary columns with porous polymers synthesized *in situ* was described by Hollis in 1973. These columns were quite active and only worked well for hydrocarbons; polar compounds elute with severe tailing. Using new coating techniques, it has become possible to coat porous polymers very efficiently on fused silica capillary columns.

Porous polymers are prepared by the copolymerization of styrene and divinylbenzene or other related monomers. The pore size and specific surface area can be varied by the amount of monomer added to the polymer. Several types of porous polymers have become commercially available under different names, including GS-Q, PoraPLOT Q and Supel-Q. It should be noted that the selectivity of some porous polymers in capillary columns does deviate strongly from the original polymer consisting of 100% styrene-divinylbenzene.

In general the polymer-coated capillaries are highly efficient and inert. **Figure 7** shows the separation of a range of solvents with different functional groups; all the different types of compounds elute with good peak symmetry. A typical application for a porous polymer of the 'Q' type is shown in **Figure 8**, where

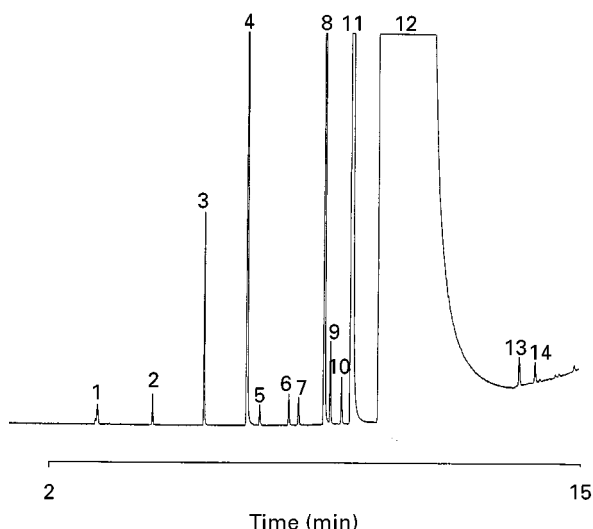


Figure 6 Impurities in 1,3-butadiene on an $\text{Al}_2\text{O}_3/\text{KCl}$ PLOT column. Experimental details: column, 50 m \times 0.25 mm fused silica, $\text{Al}_2\text{O}_3/\text{KCl}$, $d_i = 4 \mu\text{m}$; oven, 50°C (1 min) \rightarrow 200°C, 10°C min $^{-1}$; carrier gas, helium; injection, split; detection, FID. Peaks: 1, methane; 2, propane; 3, propylene; 4, isobutane; 5, butane; 6, cyclobutane; 7, unknown; 8, *trans*-2-butene; 9, 1-butene; 10, isobutene; 11, *cis*-2-butene; 12, 1,3-butadiene; 13, ethylacetylene; 14, hexane.

traces of acetaldehyde are measured in a hydrocarbon matrix.

Porous polymers are also available with different selectivities. By the incorporation of vinyl pyridine or methacrylate groups, the general selectivity can be changed and the polymer can be made much more polar.

Porous polymers have become very popular because of the high retention, the inertness and the selectivity that these materials provide. With porous polymers very volatile components can be separated at temperatures above ambient. In addition, one of the unique characteristics of porous polymers is their highly hydrophobic behaviour. The interaction with

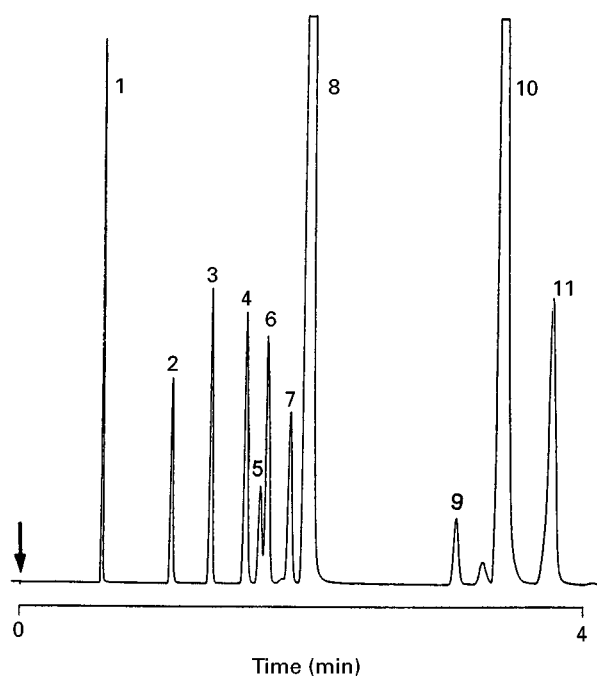


Figure 7 Solvents on a porous polymer PLOT column. Experimental details: column, 10 m \times 0.53 mm fused silica, PoraPLOT Q, $d_i = 20 \mu\text{m}$; oven, 100°C \rightarrow 200°C, 10°C min $^{-1}$; carrier gas, hydrogen; injection, split; detection, FID. Peaks: 1, methanol; 2, ethanol; 3, acetonitrile; 4, acetone; 5, isopropanol; 6, dichloromethane; 7, methylacetate; 8, pentane; 9, ethyl acetate; 10, hexane; 11, benzene.

water is very low, which results in a fast elution of water so that, for example, water elutes on a 100% styrene-divinylbenzene column before acetone and methanol.

The porous polymers are also recognized to be very inert, which makes them applicable for a wide range of compounds. A series of porous polymers of different selectivity has been commercialized and is nowadays available in 0.53, 0.32 and also 0.25 mm internal column diameter. Porous polymers have recently

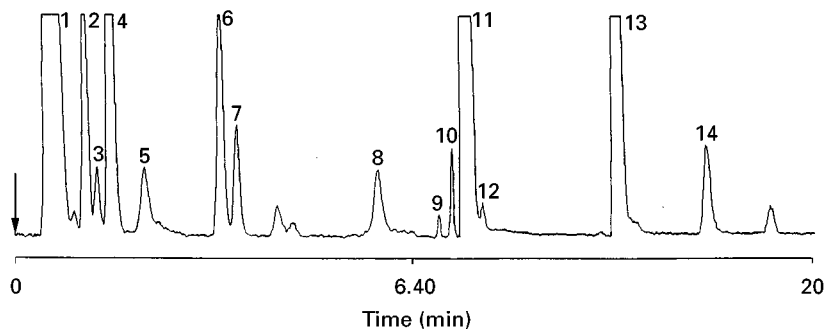


Figure 8 Trace acetaldehyde in a hydrocarbon matrix. Experimental details: column, 25 m \times 0.32 mm fused silica, PoraPLOT Q, $d_i = 10 \mu\text{m}$; oven, 140°C; carrier gas, helium; injection, split; detection, mass selective detection (MSD). Peaks: 1, air, argon and methane; 2, sulfur hexafluoride; 3, ethylene; 4, ethane; 5, water; 6, propylene; 7, propane; 8, acetaldehyde; 9, isobutane; 10, butane; 11, *cis*-2-butene; 12, acetone; 13, isopentane; 14, pentane.

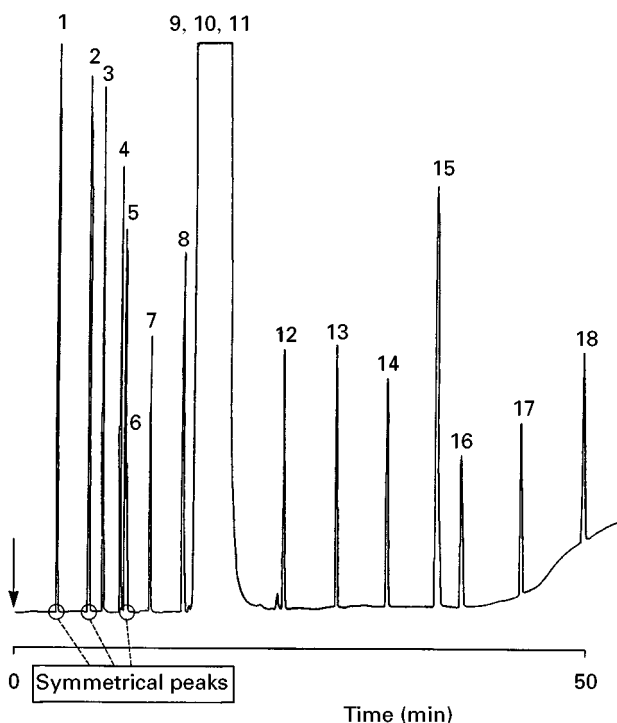


Figure 9 Solvents on a porous polymer PLOT column. Experimental details: column, 25 m \times 0.53 mm fused silica, PoraPLOT Q-HT, $d_i = 20 \mu\text{m}$; oven, $100^\circ\text{C} \rightarrow 250^\circ\text{C}$, 5°C min^{-1} ; carrier gas, hydrogen; injection, split; detection, FID. Peaks: 1, methanol; 2, ethanol; 3, acetonitrile; 4, acetone; 5, isopropanol; 6, dichloromethane; 7, pentane; 8, ethyl acetate; 9, hexane; 10, benzene; 11, cyclohexane; 12, toluene; 13, ethylbenzene; 14, propylbenzene; 15, decane; 16, butylbenzene; 17, undecane; 18, dodecane. Note the elution of volatile solvents.

become available in metal tubing, which has expanded their application even more as PLOT columns can now also be used in a process-type environment.

One of the latest developments is the improved stabilization of the 100% styrene-divinylbenzene porous polymers, which has resulted in the introduction of a high temperature material, called PoraPLOT Q-HT. This porous polymer can be used up to temperatures of 290°C , an increase of 40°C over the previously available material, and the bleed level of the polymer at lower temperatures has been reduced. The selectivity and inertness of the new polymer is not influenced by the stabilization process (Figure 9).

Carbon Adsorbents

Unique selectivity is found with the carbon adsorbents. This type of material has been used for many years in packed columns. One of the problems associated with the material available in the early days was its lack of reproducibility; the introduction of graphitized carbon black has improved this situation. The graphitized carbon adsorbent often has its separ-

ation properties modified by the incorporation of a small quantity of a stationary liquid such as Carbowax 20M. Two commercial materials currently available are known as Carbosieve and Carbo-pack. Much elegant work has been done on graphitized carbon black capillary columns by Bruner and his co-workers at the University of Urbino, who have demonstrated that such columns can give good separations of hydrocarbons and amines with short analysis times (see Further Reading). Their suggestion of the name GLOT (graphitized-layer open-tubular) columns has so far met with little recognition.

The Carboxene and CarboPLOT columns have comparable characteristics and are useful for the separation of carbon monoxide, carbon dioxide and air from C_1 and C_2 in coke oven gas (Figure 10). The main restriction to the application of carbon-coated PLOT columns is their limited temperature range. Carbon layers become extremely active on heating and application of these materials is limited to about

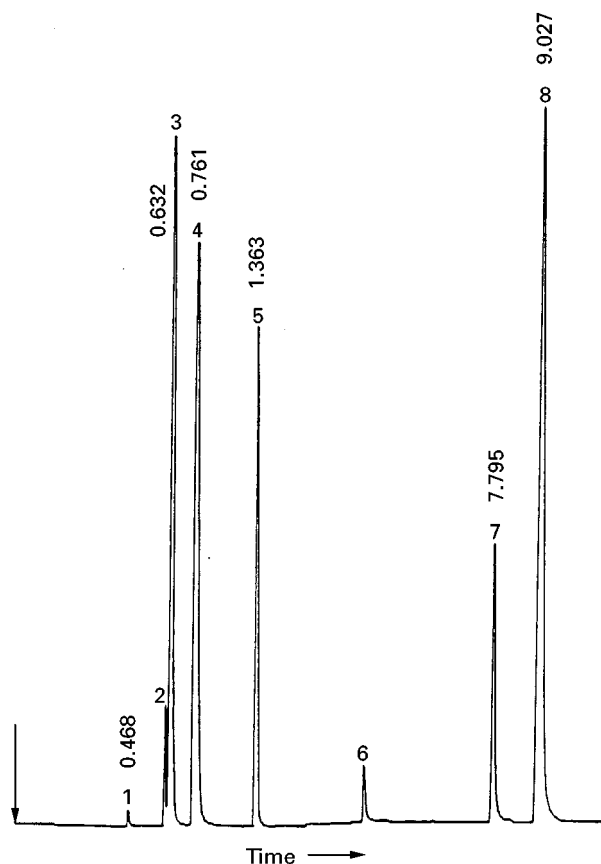


Figure 10 Coke oven gas on a carbon PLOT column. Experimental details: column, 25 m \times 0.53 mm fused silica CP-CarboPLOT P7, $d_i = 25 \mu\text{m}$; oven, $35^\circ\text{C} \rightarrow 115^\circ\text{C}$, $15^\circ\text{C min}^{-1}$; injection, split; detection, TCD/FID. Peaks: 1, hydrogen (51%); 2, oxygen (0.5%); 3, nitrogen (6%); 4, carbon monoxide (10%); 5, methane (25%); 6, carbon dioxide (2.5%); 7, ethylene (1%); 8, ethane (2%) (signal ethylene and ethane by FID).

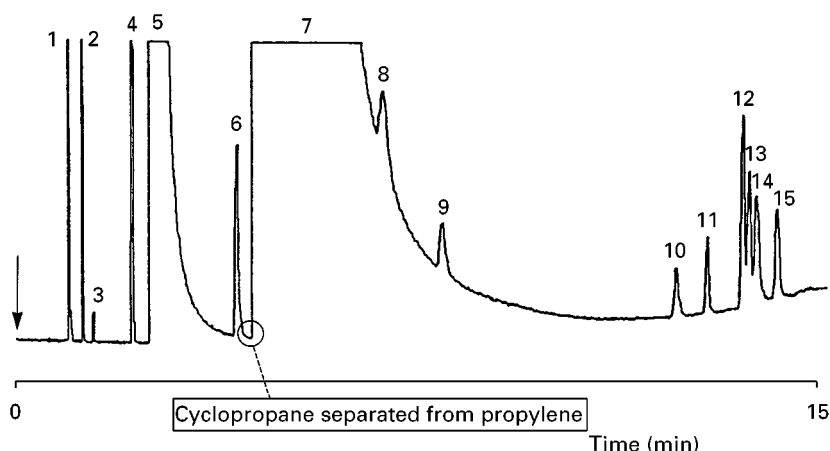


Figure 11 Impurities in propylene on a silica PLOT column. Experimental details: column, 30 m \times 0.32 mm fused silica CP-Silica-PLOT, $d_i = 4 \mu\text{m}$; oven, $50^\circ\text{C} \rightarrow 180^\circ\text{C}$, 5°C min^{-1} ; carrier gas, helium; injection, split; detection, FID. Peaks: 1, methane; 2, ethane; 3, ethylene; 4, acetylene; 5, propane; 6, cyclopropane; 7, propylene; 8, isobutane; 9, butane; 10, 1-butene; 11, methylacetylene; 12, 1,3-butadiene; 13, *trans*-2-butene; 14, isobutene; 15, *cis*-2-butene.

200°C . Higher temperatures may be possible but require specifically deactivated layers, which involves a risk of altering the selectivity.

Silica

The application of silica as adsorption material was established from the very earliest days of GSC. Later publications have shown the high separation and inertness of silica in PLOT columns but absolute retention and capacity were always the limiting factors in successfully applying silica as an adsorbent for these columns. The deposition of a layer of silica in a capillary column could not compete with the high selectivity and retention provided by alumina or the inertness and retention of porous polymers. Theoretically, silica should be a very interesting adsorbent because it has a very low catalytic activity.

The silica layer in a silica PLOT column is activated at 250°C and can be used for a wide variety of compounds such as C_1 to C_8 hydrocarbons, volatile sulfur compounds and halogenated compounds in the C_1 to C_6 range. The hydrocarbon selectivity of a silica PLOT column is shown in Figure 11. Note the high separation efficiency of the C_1 – C_3 compounds. Also cyclopropane elutes before propylene, making low level quantification in propylene possible.

Sulfur compounds are well separated from hydrocarbons and there is, therefore, no risk of quenching if a flame photometric detector is used. Silica adsorbents also produce very sharp peaks for sulfur compounds, making low level measurement possible. Determination of carbonyl sulfide and hydrogen sulfide in pure propylene is possible down to low ppb levels using sulfur selective detection as shown in Figure 12. Sulfur dioxide also elutes as a sharp peak.



Figure 12 Volatile sulfur impurities in propylene on a silica PLOT column. Experimental details: column, 30 m \times 0.32 mm fused silica CP-SilicaPLOT, $d_i = 4 \mu\text{m}$; oven, $50^\circ\text{C} \rightarrow 120^\circ\text{C}$, $10^\circ\text{C min}^{-1}$; carrier gas, helium; injection, valve, $375 \mu\text{L}$ propylene; detection, sulfur chemiluminescence detection. Peaks: 1, carbonyl sulfide (34 p.p.b.); 2, hydrogen sulfide (108 p.p.b.).

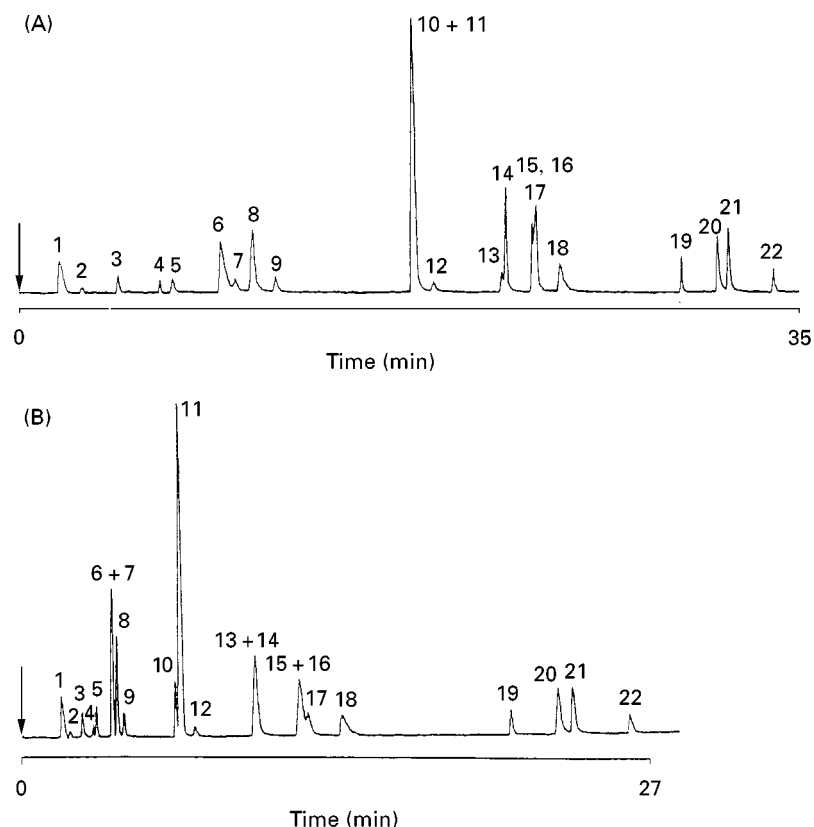


Figure 13 Chlorofluorocarbons on a silica PLOT column. Experimental details: column: 30 m \times 0.32 mm fused silica CP-Silica-PLOT, $d_i = 4 \mu\text{m}$; injection, split; detection, FID. Chromatogram (A): oven, 35°C, 12 min \rightarrow 150°C, 4°C min $^{-1}$; carrier gas, helium, 2.5 mL min $^{-1}$. Chromatogram (B): oven, 70°C, 12 min \rightarrow 150°C, 4°C min $^{-1}$; carrier gas, helium, 2.0 mL min $^{-1}$. Peaks: 1, nitrous oxide; 2, CFC-23; 3, CFC-13B1; 4, CFC-32; 5, CFC-115; 6, CFC-12; 7, CFC-125; 8, CFC-143a; 9, CFC-22; 10, CFC-134a; 11, chloromethane; 12, CFC-12B1; 13, CFC-114; 14, CFC 152a; 15, CFC-142b; 16, CFC-124; 17, bromomethane; 18, CFC-11; 19, dichloromethane; 20, CFC-141b; 21, CFC-123; 22, trichloromethane.

The selectivity of silica for separation of volatile halogenated hydrocarbons like the CFCs, is very specific. Unlike alumina, the CFCs do not decompose or react on silica, which makes their quantification possible at low levels (Figure 13). The low catalytic activity is also important for the analysis of pentadienes. On alumina these compounds polymerize due to the catalytic activity of the surface, while on silica these compounds elute as symmetrical peaks.

One of the key benefits of deactivated silica as an adsorbent is a more reproducible retention behaviour in the presence of water. Although water is retained by silica, the water will elute from the column and the influence on retention is small. Because of this, samples containing moisture can be analysed at lower temperatures. This is especially important if isothermal or fast analysis conditions are required, as in a plant analyser.

Metal PLOT Columns

The maximum temperature of polyimide-coated fused silica columns is limited to *c.* 350°C owing to

the stability of the polyimide protective outer coating. For higher temperatures a more stable tubing material is required. Metal capillary columns would be ideal but are very active. Several companies have been successful in deactivating metal to make it almost as inert as fused silica, and these deactivated metal columns have been successfully coated with alumina adsorbents, molecular sieves and 100% divinylbenzene porous polymers.

In comparison with fused silica columns, the metal column provides higher mechanical stability and offers, therefore, better mechanical reliability. Besides the high temperature capability, metal columns are especially applicable to process monitoring, on-line analysis and portable instrumentation.

Conclusion

Although it is likely that gas-solid chromatography will always represent something of a niche market in the gas chromatographic field as a whole, it is nevertheless of vital importance, particularly for gas analysis.

In the field of gas analysis, adsorbents offer the possibility of very selective separations that depend on the geometry of the molecules to be separated rather than the more generalized solubility mechanisms acting in gas-liquid chromatography. It should be theoretically possible to design adsorbents for particular separations. In the branch of liquid chromatography known as affinity chromatography, for example, it is already possible to manufacture stationary phases of exquisite specificity. An analogous approach might be possible in gas-solid chromatography and considerable work is in progress on the preparation and properties of molecular sieves with different dimensions to the well-established materials.

See also: II/Chromatography: Gas: Column Technology; Detectors: General (Flame Ionization Detectors and Thermal Conductivity Detectors); Historical Development; Theory of Gas Chromatography. *III/Gas Analysis: Gas Chromatography.*

Further Reading

- Berezkin V and de Zeeuw J (1996) *Capillary Gas Adsorption Chromatography*. Heidelberg: Hüthig.
 Bruner F, Attaran Rezai M and Lattanzi L (1995) *Chromatographia* 41 (7/8): 403–406.
 de Nijs RCM and de Zeeuw J (1983) *Journal of Chromatography* 279: 41–48.
 de Zeeuw J, de Nijs R, Buyten J. and Peene JA (1988) *Journal of High Resolution Chromatography and Chromatographic Communications* 11: 162.

Headspace Gas Chromatography

B. Kolb, Owingen, Germany

Copyright © 2000 Academic Press

Introduction

The term ‘headspace analysis’ was first applied to the analysis of gases in sealed cans and was later applied to the general analysis of vapours in contact with the sample from which they come. Gas chromatography was the technique of choice for this type of analysis; the combination is therefore called *headspace-gas chromatography* (HS-GC).

For quantitative analysis calibration of the volatiles in the vapour is necessary. This is achieved preferably, but not necessarily, in a state of equilibrium. To reach this state the sample is placed in a glass vial and thermostatted. When equilibrium is achieved, an aliquot of the gas phase above the sample is rapidly transferred onto the GC column. The term *equilibrium HS-GC* is commonly used for this sampling technique. However, since under certain circumstances calibration for quantitative analysis may also be performed in a nonequilibrium system, the term *static HS-GC* is more appropriate to distinguish this sampling technique from the so-called *dynamic HS-GC* techniques. In dynamic HS-GC analysis, the volatile compounds are stripped off completely from the sample by a continuous flow of an inert gas. This takes some time and the continuously delivered volatiles need to be concentrated in a trap, either by absorption or by cold trapping. The trapped compounds are released from the trap by thermal desorption and transferred to the gas chromatograph. This

technique, also known as *purge and trap*, is thus an off-line procedure, in contrast to the static headspace technique, where the headspace gas is transferred directly and on-line to the gas chromatograph. Thermal desorption is also used for sample transfer with a technique called *solid-phase microextraction* (SPME), where a thin rod or a small fibre, coated with a nonvolatile liquid phase, is inserted into a liquid sample or into the gas space of a headspace vial. The volatile compounds in the headspace are absorbed into the liquid-phase coating. After transfer into the heated injector of a gas chromatograph, the trapped compounds are released by thermal desorption. Off-line techniques, dynamic HS-GC and SPME are not discussed here, but all the important considerations regarding sample properties, such as matrix effects, necessary equilibration time, diffusion processes and sampling pretreatment, are common to all headspace techniques.

Fundamentals of Static HS-GC

The theory of static HS-GC is best explained using the example of a liquid sample present in a closed vial, as shown in **Figure 1**. The volatile analyte present in the liquid sample will evaporate into the gas phase until the concentration in both phases (C_s and C_g) remain constant. Equilibrium is achieved by diffusion from the sample into the gas phase and vice versa. The equilibrium constant is called the partition coefficient (K), and can be split into the mass ratio (k) and the phase ratio (β).

The aim of every quantitative analysis is the determination of the original concentration of the analyte (C_0) in the sample. The peak area (A) in a headspace

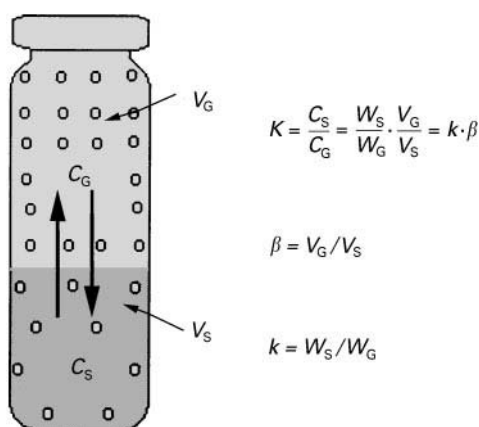


Figure 1 A headspace vial containing a liquid sample with a volatile analyte. Concentrations of the volatile analyte, C_G in the gas phase, C_S in the liquid phase; mass of the volatile analyte, W_G in the gas phase, W_S in the liquid phase; V_G , volume of the gas phase; V_S , volume of the liquid sample; K , partition coefficient; k , mass ratio; β , phase ratio.

chromatogram is proportional to the gas-phase concentration ($A \propto C_G$) and depends on the phase ratio (β). However, it depends not only on the sample volume (V_S), but also on the partition coefficient (K), as described by eqn [1]. This is the key relationship for static HS-GC:

$$C_G = \frac{C_0}{K + (V_G/V_S)} = \frac{C_0}{K + \beta} \quad [1]$$

The partition coefficient depends on both the temperature and volume. These two parameters strongly influence headspace sensitivity and are conditions that can easily be selected by the operator.

Sensitivity of Static HS-GC

Influence of Sample Volume and Temperature on Headspace Sensitivity

The sample volume (V_S) is included in the phase ratio (β) in eqn [1], but its influence on headspace sensitivity is not independent of the partition coefficient (K). The latter can vary widely from practically zero in the case of a gas sample up to several thousands, where the applicability of HS-GC ends. The phase ratio (β), and thus the influence of the sample volume, does not generally span such a wide range. For example, a 1 mL sample in a 10 mL vial has a phase ratio of 9, while with a sample volume of 5 mL the phase ratio decreases to 1.

Whether or not this causes an increase in the resulting gas concentration, and thus of the resulting peak area, depends mainly on the partition coefficient. In the case of a high partition coefficient ($K >$

100, e.g. ethanol in water), a change in the phase ratio from 1 to 5 will barely influence headspace sensitivity; in contrast, where the partition coefficient is very small the sensitivity increases in proportion to the sample volume (e.g. *n*-hexane in water at 50°C). This result may be surprising since it differs so much from normal GC analysis, where peak areas increase with increasing volumes of injected sample.

The vapour pressure of a compound increases exponentially with temperature. One would therefore expect a similar increase in the volatility, and thus enhanced sensitivity for a headspace compound. Again, however, there is a dependence on the partition coefficient. In the case of nonvolatile compound ($K \rightarrow \infty$), a higher temperature will not alter its nonvolatility. In the case of a highly volatile compound ($K \rightarrow 0$, already at room temperature), the temperature will not affect the headspace sensitivity either, because in this case nearly all of the compound is already present in the gas phase. Headspace samples generally fall between these two extremes. Table 1 gives typical values of partition coefficients at three temperatures for three compounds with a small (tetrachloroethylene), a medium (ethyl acetate) and a high (ethanol) partition coefficient.

Sensitivity Enhancement by Matrix Modification

The partition coefficient can be altered by modifying the sample matrix. A common technique is the use of the *salting-out* effect. For aqueous samples with a high partition coefficient (e.g. ethanol in water), the addition of salt may enhance the sensitivity by up to a factor of 10. Again, the result depends on the value of the partition coefficient. In the case of a highly volatile compound ($K \rightarrow 0$), where nearly all of the analyte is already present in the gas phase, the sensitivity will not improve.

A similar effect is achieved with a sample containing a nonpolar volatile compound dissolved in a water-miscible organic solvent, such as dimethylacetamide, dimethylformamide, etc. If water is added to this solution, the solubility of the nonpolar compound will decrease and its volatility will increase.

Table 1 Partition coefficients (K) in water–air equilibrium system

Compound	Temperature		
	40°C	60°C	80°C
Tetrachloroethylene	1.5	1.3	0.9
Ethyl acetate	62.4	29.3	17.5
Ethanol	1355	511	216

Sensitivity Enhancement by Modifying the Volatile Analyte

Polar compounds, particularly those with an active hydrogen (alcohols, phenols, acids, amines, etc.), usually have low volatility as a result of intermolecular interaction with the polar matrix through hydrogen bond formation. However the reactivity of the active hydrogen can be used to prepare less polar derivatives with better volatility and lower solubility. Simple reactions are preferred, such as esterification, transesterification, acetylation, etc., which are carried out in the headspace vial during the equilibrium time. An advantage of HS-GC is that the reaction products are less polar and more volatile, thus shifting the equilibrium of the chemical reaction towards completeness.

Instrumentation for Headspace Sampling

All the devices that are commonly used for gas sampling may be applied to headspace analysis, including gas-tight syringes and gas-sampling valves. A particular problem in HS-GC is the internal pressure in the headspace vial that is generated during thermostating at elevated temperature, represented by the sum of the partial vapour pressures of all the volatile compounds present, including water (since most samples contain some water). The vial must therefore be closed by a septum (preferably lined with polytetrafluoroethylene) (PTFE) and crimp-capped pressure-tight by an aluminium cap. This internal pressure may cause problems with sample loss during sample transfer with a gas syringe if it is not equipped with a pressure-tight valve. So that they can operate independently of the internal vial pressure, most automated headspace samplers surmount this problem by pressurizing the vial up to a certain pressure level

above the original pressure prior to sample transfer. Although it is not possible here to describe the various commercially available instruments in detail, the common principle is shown schematically in **Figure 2**.

Inert carrier gas enters the gas chromatograph through valve V and branches before the column. Part of the gas is directed to the sampling needle N. If this needle penetrates the septum, carrier gas flows into the vial and pressurizes it, usually up to the column head pressure, but any other pressure may be applied. Sample transfer is subsequently performed by closing valve V for a short time (usually few seconds), thus disconnecting the gas supply. The pressurized headspace gas in the vial expands either through the sample loop of a gas-sampling valve to atmosphere or directly onto the column. This on-column headspace sampling (also known as balanced pressure sampling) has the advantage that no headspace gas is wasted by unnecessary expansion to atmosphere, allowing the application of cryofocusing enrichment techniques. The actual volume of the headspace gas and the amount of analyte in it can be calculated from the transfer time (seconds) during which valve V is closed and from the volume flow rate (mL s^{-1}) at the column head.

The carrier gas flow rate in a capillary column is much lower than in a packed column, and therefore a much smaller volume of the headspace gas is introduced during the same sampling time. The resulting lower sensitivity can be circumvented by an increased sampling time, provided the accompanying band-broadening is suppressed by the technique of cryofocusing (also called cryogenic trapping or cold trapping). The normal admissible sample volume in a capillary column is about 50–200 μL , which is only 1% of the usually available volume of 5–20 mL headspace gas in the vial. With this technique of splitless on-column headspace sampling it is possible to

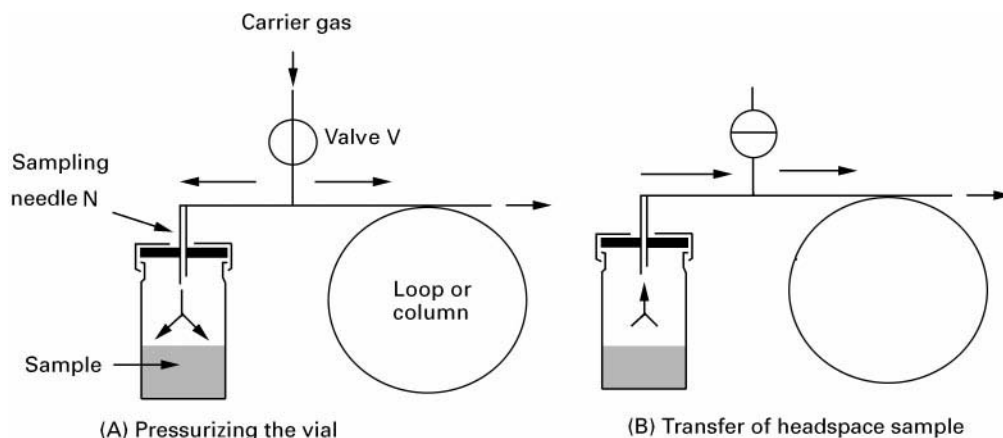


Figure 2 Principle of headspace sampling by either direct on-column sampling or by pressure/loop-filling with previous pressurization of the headspace vial.

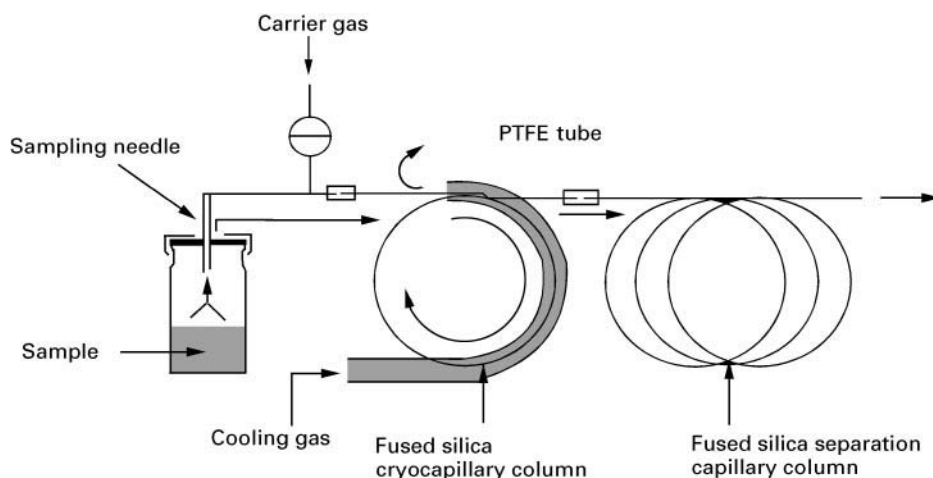


Figure 3 Principle of cryogenic headspace trapping with splitless on-column headspace sampling.

extend the sample transfer time from a few seconds up to several minutes with an accompanying increase in the headspace gas volume and sensitivity.

In the automated headspace sampler shown in **Figure 3** the cryotrap is placed in the oven of the gas chromatograph. The cryotrap is essentially a short piece of fused silica capillary column, either the first coil of the separation capillary or a corresponding short piece of a different capillary column. The latter, called here the cryocapillary column, is coated, preferably with dimethylsilicone, a substance with a glass transition temperature of -114°C . Dimethylsilicone works as a stationary phase even at that low temperature, dissolving the compound in the liquid phase rather than just trapping by condensation. This cryocapillary column may then be connected to any other type of a capillary column by a butt connector. The cryocapillary column is jacketed by a 0.5 m PTFE tube, through which cold nitrogen gas flows outside the capillary column but in the opposite direction to the flow of warm carrier gas inside. The volatile analytes are trapped along the resulting strong temperature gradient in the capillary column. When sample transfer is interrupted by opening valve V, the flow of cooling gas is also stopped. A very rapid desorption is then achieved with a sharp starting band profile, since the warm carrier gas inside the capillary now heats the low mass fused silica capillary rapidly up to the oven temperature. The nitrogen gas used for cooling is produced outside the gas chromatograph by passing the nitrogen through a metal coil in a cooling bath, for example through liquid nitrogen. The sampling time and thus the headspace gas volume is restricted to only a few minutes before ice forms from the water sample, causing a blockage. However, a remarkable improvement

of the sensitivity compared to the usual injection times of a few seconds is obtained. Injection times of up to 10 min can be obtained by placing in the sample transfer line a small trap containing lithium chloride on a solid support in a small tube. This water trap (optional and not shown in **Figure 3**) is regenerated after each analysis by heating to 200°C and backflushing the released water. The chromatogram in **Figure 4** gives an example of the headspace analysis of low ppb concentrations of volatile aromatic hydrocarbons (BTEX) in a water sample by cryo-HS-GC.

Quantitative Headspace Analysis

Any quantitative method used for HS-GC has to take into account the influence of the sample matrix. The neat matrix should be available to prepare calibration standards, except for gas samples or if the composition of the gas phase only has to be determined, as in aroma research. The calibration techniques of *standard addition* or *multiple headspace extraction* (MHE) do not need the pure sample matrix, as opposed to internal or external standard calibration, which do. A neat matrix is also not necessary if the volatiles are completely evaporated into the gas phase. This effect can be achieved by reducing the sample size in the vial to a very small amount – say 10–15 mg. The determination of phenols in a resin-coated copper wire is shown in **Figure 5** as an example for this technique, called *total vaporization* (TVT), or sometimes *full evaporation* (FET). The small amount of 10 mg in a 22.3 mL vial gives a phase ratio (β) of >2000 and thus a nearly exhaustive extraction, allowing calibration by an external vapour standard, prepared also by TVT.

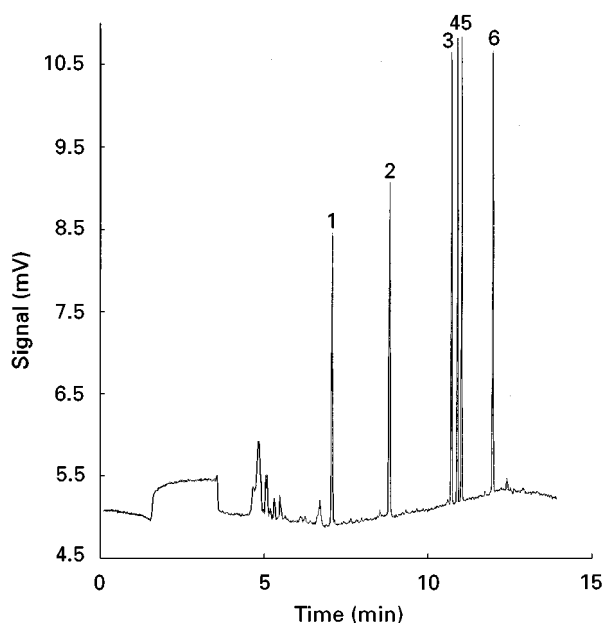


Figure 4 Determination of volatile aromatic hydrocarbons (BTX) in water by cryo-HS-GC with FID. Perkin-Elmer AutoSystem, HS40 Automatic Headspace Sampler with cryoaccessory and water trap; cryocolumn: 0.8 m \times 0.32 mm i.d. fused silica capillary, coated with immobilized dimethylsilicone, film thickness 1 μ m; separation column: 60 m \times 0.25 mm i.d., Stabilwax (Restek), film thickness 0.25 μ m; temperature program: 40°C (1 min), 20°C min⁻¹, 65°C (4 min), 10°C min⁻¹, 100°C (8 min); carrier gas: He, 210 kPa; sampling: splitless 3 min; sample: 10 mL, equilibrated 35 min with shaker at +80°C. Components: 1 μ g L⁻¹ each of: 1, benzene; 2, toluene; 3, ethylbenzene; 4, *p*-xylene; 5, *m*-xylene; 6, *o*-xylene.

Liquid samples are also accessible to this technique. In the case of solutions it is feasible to reduce the volume such that even the solvent evaporates completely at the appropriate temperature of the vial, without forming a condensed liquid phase, while nonvolatile sample constituents (e.g. salt in a wastewater sample or the polymer in the case of the polymer emulsion) remain as a dry residue in the vial. The admissible sample volume depends on the molar volume of the solvent and is typically about 15 μ L in a 20 mL headspace vial. The vial is used here just as the glass liner in a normal GC injector, which retains the nonvolatile residue. An automated headspace sampler is thus used in a similar manner to an autosampler but with disposable injectors. This technique is very useful for samples that do not need the highest sensitivity; time-consuming equilibration is not required here and the volatile fraction of the sample is completely present in the gas phase. No matrix influence has to be calibrated and the quantitative analysis therefore is as simple as in normal GC.

However, HS-GC is, in general, applied to determine the volatile fraction of a sample and, except for normalization (which makes hardly any sense here),

all other calibration methods may be applied. The principles behind these calibration methods for liquid samples are briefly discussed here; solid samples are treated below.

The use of an internal standard is the most popular calibration method in gas chromatography, but has some limitations for headspace analysis. A detector response factor must be determined, but if applied to HS-GC, matrix effects must also be included. A neat matrix must therefore be available to prepare a calibration standard. Such a calibration matrix may be prepared from the sample by stripping off all the volatiles first and spiking the remaining sample with the compounds to be analysed. Sometimes also an artificial matrix may be prepared (e.g. 11% ethanol in water, if flavour compounds in a wine sample are to be quantitated). If the sample is sufficiently concentrated it may be diluted with a (high boiling) solvent. This solvent then becomes a surrogate sample matrix because compounds below a concentration of about 1% usually have no measurable matrix effect. Sometimes an internal standard is added only to compensate for slight variations of the sample matrix. Since matrix effects are caused by intermolecular interaction, the internal standard should be of the same chemical nature as the compounds to be determined. For example, in blood alcohol analysis, another alcohol (*t*-butanol or *n*-propanol) is used. The main purpose of an internal standard calibration is to

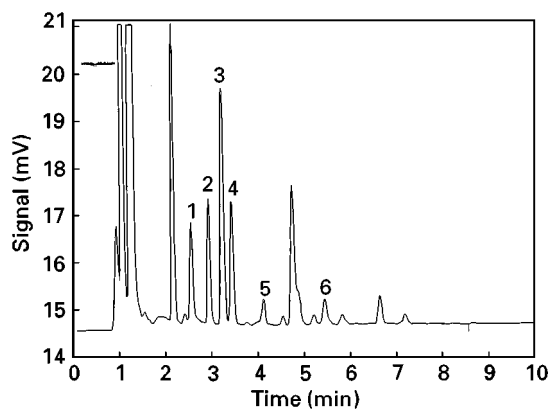


Figure 5 Determination of phenols from a resin-coated wire by TVT. Perkin-Elmer AutoSystem, HS40 Automatic Headspace Sampler; column: 25 m \times 0.32 mm i.d. fused silica capillary, coated with immobilized poly(14% cyanopropylphenyl/86% dimethylsiloxane), film thickness 1 μ m; temperature programme: 150°C (10 min), 10°C min⁻¹, 220°C; carrier gas: He, 118 kPa; split sampling: split flow 16 mL min⁻¹, sampling time: 0.08 min; detector: flame ionization (FID); headspace conditions: pressurizing gas (He), 145 kPa; needle and transfer line temperature, 200°C; sample, 10 mg, equilibrated 35 min at 210°C. Components: 1, phenol, 2.4% (w/w); 2, *o*-cresol; 3, 2,3-dimethylphenol; 4, *m*-cresol + *p*-cresol; 5, 2,4-dimethylphenol + 2,5-dimethylphenol; 6, 3,4-dimethylphenol.

compensate for poor sampling reproducibility. This may still be a problem with manual syringe injection, but not with autosamplers, whose sampling precision is in general <1%.

External standard calibration also requires the neat matrix for preparing a standard sample, but permits simpler sample handling since no additional compounds need to be added to each sample. The sample is placed in the vial, which is closed immediately. The vial remains closed until an aliquot is withdrawn for analysis, thus guaranteeing sample integrity. This is the most simple calibration technique.

If a neat matrix sample is not available, then the method of standard addition is the most universal calibration method. Calibration is carried out with each analyte and no response factor is necessary. The added compound suffers the same matrix effects as the original sample. Standard addition needs at least two analyses to be carried out for each sample, but the increased time required is less of a disadvantage if an automated headspace sampler is used. Several repeated determinations are necessary in any case if statistical confirmation of the analytical result is required, preferably by multilevel addition with linear regression calculation of the result.

Another technique that does not need the neat sample matrix uses repeated gas extractions. This is similar to the dynamic headspace technique, with the difference that the volatiles are removed by a stepwise gas extraction rather than continuously. This technique of multiple headspace extraction (MHE) can be carried out with the same instrumentation as used for static HS-GC. With the technique of direct on-column headspace sampling it is carried out in such a way that the vial is first pressurized as described above. When sample injection is stopped, the vial is pressurized again, but its gas phase subsequently vented to the atmosphere. Thus most of the headspace gas is removed, depending on the ratio of headspace pressure (P_H) to atmospheric pressure (P_A). The equilibrium is disturbed, since the gas-phase concentration (C_G) has dropped. The equilibrium has to be re-established by additional evaporation of the analyte and the next analysis now gives a smaller peak, the difference corresponding to the amount of the analyte vented.

This stepwise gas extraction analysis is repeated several times and a series of exponentially decreasing peak areas is obtained. The logarithm of the peak area is plotted against the number of extractions, to give a straight line that allows the application of linear regression to obtain the sum of the area values as the sum of a geometric progression. It is not necessary to proceed until exhaustive extraction is achieved, since a minimum of two area values allows

such a linear regression calculation. The total area obtained corresponds to the total amount of the analyte in the sample and this value is independent of the matrix influence. The resulting area total must be calibrated, but for this purpose the matrix is not required, and even a vapour standard, prepared very conveniently by the TVT technique, can be used as an external standard. In practice it is the gas phase concentrations in both vials that are compared. A correction for the sample volume is therefore necessary, since the volume of the gas phase in the vial containing the sample differs by the sample volume in comparison to the 'empty' calibration vial, and so does the corresponding concentration in the gas phase.

Classification of Sample Types

All of the calibration techniques described above may be applied to liquid samples with no particular problems. Sometimes it is necessary to dilute very viscous samples or to reduce long equilibration times by using a shaker. Liquid samples also show a wide range of linear relationships between concentration in the sample and peak area – the headspace linearity. Solid samples can also be analysed by HS-GC, but only if they behave as a partition system, similar to liquid samples, owing to inherent calibration problems. However, most solid samples behave as a nonlinear adsorbent. Additional problems are caused by slow diffusion in a solid matrix; size, porosity and specific surface of solid samples are therefore very important parameters. Bulky solid samples are not amenable to HS-GC at all unless they are pulverized, for example by freeze grinding, with loss of the volatiles avoided by chilling the sample with liquid nitrogen or dry ice. There are many problems to be taken into account and most techniques for solid samples try to establish a partition system, which can then be treated like a liquid sample.

Polymers and plastic materials often behave as partition systems if heated above the glass transition temperature. A classical example is the determination of vinyl chloride monomer in a polyvinyl chloride (PVC) resin above the glass transition temperature of 85°C. Such solid samples can be handled as a quasiliquid sample with all types of calibration techniques. Even the technique of standard addition may be applied, because the analyte may be added to the gas phase and not necessarily into the sample using the existing equilibrium system to achieve homogeneous partitioning from both directions. However, considering the variety of plastic materials – pure resins, preforms, copolymers, complex mixtures with all type of additives and finished products – any new solid sample has to be checked carefully for this

property. An example for a systematic approach to develop a suitable quantitative method for a solid sample is given below.

The most common procedure for headspace analysis of solids is the *solution approach*, where the sample is dissolved in an appropriate high boiling solvent, which is eluted late in the chromatogram and may be removed by column backflushing. The disadvantage is the reduced sensitivity due to the dissolution.

Insoluble samples can often be handled as a suspension in water or an organic solvent, using the displacement effect of the solvent. This *suspension approach* works well where the analytes are superficially adsorbed. It is obvious that the samples should be a powder rather than a bulky material, to provide the necessary large surface. Calibration in this case is straightforward by using an external standard in the same solvent. The insoluble solid sample remains as a slurry in the headspace vial and causes no matrix effect. A smaller amount of solvent is sufficient here to dissolve only the displaced volatiles, compared to the solution approach where the whole sample must be dissolved. But the resulting smaller dilution effect may be even further minimized by reducing the volume of the high boiling solvent such that only the surface of the sample is wetted by the solvent, which then works as a surface modifier. This *surface modification* technique provides a homoge-

neous surface with constant adsorptivity. In this way a much better sensitivity can be achieved owing to the smaller amount of such a liquid displacer. The absence of any residual adsorptivity, however, has to be confirmed, e.g. by the MHE technique. In this case the solid sample with its homogeneous surface behaves like a partition system, where the partition coefficient remains constant over a wide range.

Practical Example: Determination of Ethylene Oxide in a PVC Tube

From the foregoing discussion it is apparent that there are several possible ways to carry out a quantitative headspace analysis. A systematic approach to develop the most suitable calibration technique is therefore desirable. This is illustrated by the following example of the determination of ethylene oxide (EO) in a sterilized PVC tube. Ethylene oxide is widely used for sterilization, but due to its toxicity the residual concentration must be carefully controlled down to a safe limit (e.g. 1 ppm). This example covers several of the aspects discussed above. Since PVC tubing is a solid sample, the solution approach was naturally the first choice. The sample was dissolved in dimethylacetamide and calibration was by multilevel standard addition (see Figure 6), resulting in an EO concentration of 19.95 ppm with a precision as expressed by the correlation coefficient of 0.9961.

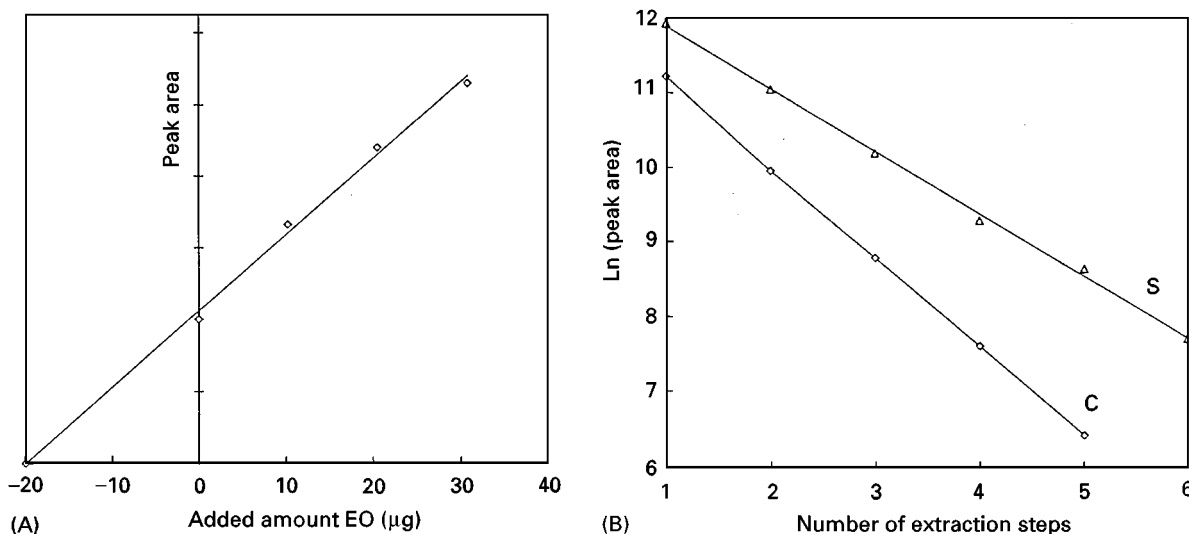


Figure 6 Determination of EO in a sterilized PVC tube by standard addition calibration (STA) and by multiple headspace extraction (MHE). Gas chromatographic conditions: Perkin-Elmer SIGMA 2000, HS100 Automatic Headspace Sampler; 2 m × 3.2 mm stainless steel column, packed with Chromosorb 101, 80/100 mesh; temperature programme: 100°C (7.5 min), 15°C min⁻¹, 200°C; detector: FID; carrier gas: He, 20 mL min⁻¹; calibration standard: aqueous solution of EO (10.3 µg µL⁻¹).

(A) STA. Sample preparation: 1 g PVC tube, dissolved in 2 mL dimethyl acetamide, equilibrated 90 min at 90°C; calibration by adding 10, 20 and 30 µL of the calibration standard; result: 19.95 µg g⁻¹ EO, regression coefficient $r = 0.9961$.

(B) MHE. Sample preparation: 1 g PVC tube, cut in pieces of 3 mm × 4 mm, 1 mm thick, equilibrated as above; calibration by external vapour standard, prepared by TVT of 8 µL; total area counts from sample analysis: 258 464, from calibration standard: 104 132; result: 19.53 µg g⁻¹ EO; regression coefficients: sample (S), $r = -0.99914$; calibration standard (C), $r = -0.99990$.

Due to problems with solvent impurities and also to achieve a better sensitivity, a solvent-free method was expected to be superior. A six-step MHE procedure with the sliced solid sample was calibrated with a five-step MHE of an external vapour standard (see Figure 6) and after the necessary volume correction a nearly identical concentration of 19.53 ppm was obtained, but now with a four-times higher sensitivity. Also the precision was better, as expressed by the linear regression coefficients of -0.99914 for the sample and -0.99990 for the calibration standard. This allowed reduction of the MHE procedure to three steps, but still with a linear regression calculation, and a two-step procedure is sufficient if the highest precision is not required.

From these good results some more conclusions may be drawn to simplify the analysis further. The good linearity over the whole working range indicated that the solid PVC matrix was behaving as a partition system; this conclusion allowed the application of standard addition calibration in the form of gas-phase addition. Even the use of an internal standard appears feasible, since from a successful gas-phase addition it can be concluded not only that EO partitions between both phases, but that any other compound will do the same, provided it is similar in its chemical properties (e.g. dimethyl ether). As discussed above, a calibration factor has to be determined first, which comprises not only the differences in the detector response but also the different solubilities (partition coefficients) in the PVC matrix. For this example it is no problem to obtain a PVC tube without any EO in it.

Taking into account all these possibilities, the final decision as to what is a suitable calibration technique may depend on other considerations such as the simplicity of sample handling or the sample throughput in an automated headspace sampler. For example, the standard addition calibration needs a series of vials to be subsequently analysed, thus occupying the corresponding number of places in the turntable of an autosampler, while for the MHE procedure the determinations are all carried out from the same vial and the sample throughput in an autosampler will therefore not be affected. On the other hand, the addition of an internal standard to every sample is tedious and prone to errors, particularly if pipettes are used to transfer solutions with highly volatile compounds.

Applications

Static HS-GC relies in general on a thermodynamically controlled equilibrium. It is natural therefore that it has been applied not only for analytical purposes, but also for the determination of physico-

Table 2 Selected analytical applications of static headspace gas chromatography

-
- Residual solvents in pharmaceuticals, food, packing material, aluminium and plastic films
 - Monomers in polymer resins, emulsions and finished products
 - Ethylene oxide in sterilized clinical material
 - Volatile aromatic and halogenated hydrocarbons in air, water and soil
 - Flavour compounds in beverages and spices
 - Odour compounds in foodstuffs, herbs, flowers and perfumes
 - Rancidity of fat and oil
 - Water content in any type of liquid and solid sample as an alternative to KF titration
 - Dithiocarbamates, degraded to CS₂, in vegetables, fruits and flowers
 - Analysis of beverages for diketones (in beer), sulfur compounds, alcohols, esters, aldehydes and acids
 - Ethanol in blood, food and beverages
 - Volatile fermentation products from anaerobic bacteria
-

chemical data such as vapour pressures, partition coefficients, activity coefficients and related mixing functions (energies and enthalpies of mixing), adsorption isotherms, and also for kinetic measurements such as the determination of reaction constants and the rate of release of volatile compounds from solid material. Table 2 lists some important analytical applications.

See also: II/Chromatography: Gas: Column Technology; Historical Developments; Sampling Systems; Theory of Gas Chromatography. III/Gas Analysis: Gas Chromatography.

Further Reading

- Hachenberg H and Beringer K (1996) *Die Headspace-Gaschromatographie als Analysen- und Meßmethode*. Braunschweig/Wiesbaden: Vieweg.
- Hachenberg H and Schmidt AP (1977) *Gas Chromatographic Headspace Analysis*. London: Heyden.
- Ioffe BV and Vitenberg AG (1984) *Headspace Analysis and Related Methods in Gas Chromatography*. New York: Wiley.
- Kolb B (ed.) (1980) *Applied Headspace Gas Chromatography*. London: Heyden; later New York: Wiley.
- Kolb B (1999) Headspace sampling with capillary columns. *Journal of Chromatography A* 842: 163–205.
- Kolb B and Ettre LS (1997) *Static Headspace-Gas Chromatography – Theory and Practice*. New York: Wiley.

High Temperature Gas Chromatography

P. Sandra, University of Ghent, Ghent, Belgium
F. David, Research Institute for Chromatography,
 Kortrijk, Belgium

Copyright © 2000 Academic Press

Introduction

Gas chromatography (GC) is generally believed to be restricted to the analysis of 'volatiles' and is less applicable to the analysis of so-called 'heavy' compounds. The introduction of persilylated glass and fused silica columns, of thermostable stationary phases and of non-discriminative injection devices in capillary GC (CGC) have made the definitions of 'volatile' and 'heavy' very flexible.

High temperature GC (HTCGC) was developed in the 1980s as a result of work carried out by Grob, Geeraert and Sandra, Trestianu *et al.*, Lipsky and Duffy, and Blum and Aichholz (see Further Reading). Although HTCGC was initially not accepted as a 'robust' analytical technique for the analysis of high molecular weight compounds, in recent years several research groups have demonstrated the capabilities of HTCGC for the analysis of hydrocarbons with carbon numbers in excess of 130 (simulated distillation), of lipid compounds, of emulsifiers, of detergents, of polymer additives, of oligosaccharides, of porphyrins and of many more solutes.

Defining a temperature in HTCGC is not straightforward but it is now generally accepted that 420°C is the maximum allowable column temperature limit in practice. Applications at higher column temperatures have been carried out but, with the exception of hydrocarbons, most organic compounds do not withstand temperatures higher than 420°C. Moreover, the maximum allowable operating temperatures (MAOT) of the stationary phases applied in HTCGC are all lower than 450°C. A prerequisite in HTCGC is that the solutes to be analysed are thermally stable and can be volatilized. The thermal stability of organic compounds depends not only on their nature, but also on the activity of the environment to which they are subjected and on the thermal stress given to the solutes. HTCGC is nowadays performed in a completely inert system, i.e. high purity carrier gas, dedicated and purified stationary phases, fused silica columns with less than 0.1 ppm trace metals and specially deactivated, etc. Moreover, thermal stress is reduced by applying cool on-column (COC) or programmed temperature vaporizing (PTV) injection. Lipids may serve as a good illustration. When oils or

fats are used in food preparation, they decompose (formation of volatiles) or polymerize (formation of dimers, trimers, etc.) as a function of time, which makes them no longer useful for cooking. These alterations are caused by the presence of water and oxygen. When heated under inert conditions, however, fats and oils are stable and evaporate. **Figure 1** shows the thermogravimetric profiles for triolein with a molecular mass of 886 Da under a stream of pure nitrogen (A) and of air (B).

In present state-of-the-art HTCGC, the systems are operated under the circumstances shown in curve A. Volatility, on the other hand, is related to the vapour pressure (boiling point) of the compounds. Polydimethylsiloxanes with molecular masses as high as 5000 Da are volatile enough to be analysed by HTCGC, whereas low molecular weight (oligo)saccharides, for example, are not volatile at all. This is because of the polarity of the functional groups. Derivatization is often employed to impart volatility and to yield a thermostable product, thereby also improving chromatographic performance and peak shapes. Silylation, alkylation and acylation are used to modify the active hydrogen in compounds containing -OH, -COOH, and -NH₂ functionalities.

HTCGC is a reliable analytical method if a number of prerequisites are fulfilled. The different aspects of the technique are discussed and the potential illustrated with a number of relevant applications.

Instrumentation for HTCGC

Columns and Stationary Phases

Different support materials have been applied in HTCGC. Leached and deactivated borosilicate glass provides an excellent surface for high temperature

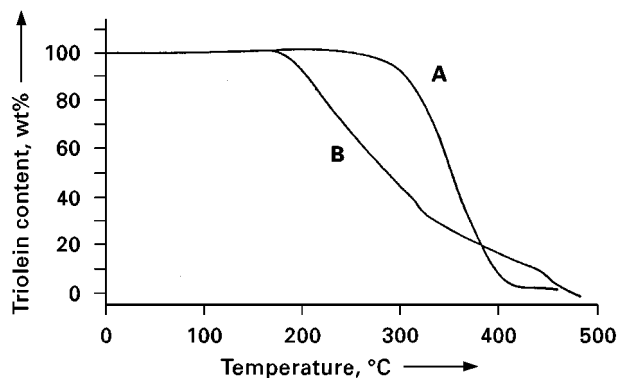


Figure 1 Thermogravimetric analysis of triolein. Ramp from 20 to 500°C at 5°C min⁻¹. (A) pure nitrogen, (B) air.

work. The surface can be coated with different high temperature phases for applications up to 450°C. Glass columns are, however, not really accepted for routine work as they break easily and are difficult to handle. Nevertheless, some laboratories still use glass columns because of their excellent performance for specific applications (Blum and Aichholz). Leached and persilylated fused silica is nowadays mostly applied. The outer polyimide coating of classical fused silica open tubular (FSOT) columns withstands temperatures up to 400°C, thus covering most of the applications of HTCGC. To increase the lifetime of the columns, they are often wrapped in aluminium foil to avoid contact with oxygen which initiates polyimide decomposition. Aluminium-clad fused silica columns have been introduced for applications up to 450°C. Because of the different expansion coefficients of fused silica and aluminium, the columns can become brittle under continuous heating and cooling conditions. An excellent alternative to glass, polyimide-coated fused silica and aluminium-clad fused silica columns are the recently introduced metal columns for which the active surface has been passivated, for example with a thin layer of fused silica. Silcosteel and Ultimet capillary columns for high temperature work are commercially available. The suppliers both make special columns to perform simulated distillation by GC according to ASTM method D 2887.

A large number of stationary phases have been synthesized for HTCGC. The group of W. Blum has been very active in this respect. Their HTCGC experiments, including the synthesis of the phases and the coating of capillary columns, are summarized in an excellent book. The three phases most often applied in HTCGC are methylsilicone, diphenyldimethylsilicone with phenyl contents varying between 5% and 65% and a carborane-modified methylsilicone. The main reason for this is that high temperature columns with these phases are commercially available. The phases are OH-terminated and immobilization by polycondensation takes place at high temperatures after coating. This increases thermal stability and makes the columns solvent resistant.

Inlet Systems

Different injection devices for CGC have been developed over the years, but only two are applicable in HTCGC, namely COC and PTV injection. With both devices the sample can be introduced at low temperatures avoiding solute alteration or discrimination. For cool on-column injection, an injector device with an elongated secondary cooling tube is advised because this enables high oven temperatures to be used. A hot injector such as a split/splitless injector, has

been used to analyse quaternary ammonium salts. At injection temperatures above 360°C the salts are demethylated and the resulting tertiary amines can be analysed by HTCGC. Standard deviations are, however, quite high.

Carrier Gas and Mode of Delivery

Carrier gases with fast diffusion properties, i.e. hydrogen and helium, should be used. When the viscosity is also taken into account, namely $1990 \times 10^{-7} \text{ g cm}^{-1} \text{ s}^{-1}$ for helium versus $840 \times 10^{-7} \text{ g cm}^{-1} \text{ s}^{-1}$ for hydrogen, the performance of the latter is much better because the H vs. u plot at high temperatures is relatively flat whereas the plot for helium is much steeper. If, for safety reasons, hydrogen cylinders are not allowed, a hydrogen generator can offer a solution. The use of electronic pneumatic control (EPC) allows column flow to be maintained constant or even increased during a temperature programmed run, reducing elution times and temperatures. The effective operating range is thereby extended compared to constant pressure operation.

The features of EPC are illustrated with the analysis of some polymer additives (Table 1). The sample mixtures include a wide range of additive types, including polar and labile compounds as well as high molecular weight components. Irganox 1010 (compound 24) with molecular mass 1176 Da is particularly important here as an indicator of HTCGC capabilities in polymer analysis. The sample was analysed on a $25 \text{ m} \times 0.32 \text{ mm}$ i.d. fused silica open tubular column coated with a $0.17 \mu\text{m}$ film of methylsilicone. Hydrogen, delivered at a constant pressure (50 kPa) or in the constant flow mode, was the carrier gas. The column temperature was programmed from 80°C to 380°C at $10^\circ\text{C min}^{-1}$. Cool on-column injection was carried out in the oven track mode, which means that the injector and the column are then programmed at the same rate, and the FID detector was set at 380°C. The analysis shown in Figure 2 was done under isobaric conditions. The peak shapes and resolution are good but Irganox 1010 could not be eluted at 380°C. For the $25 \text{ m} \times 0.32 \text{ mm}$ i.d. column, 50 kPa hydrogen corresponds to 58 cm s^{-1} carrier gas velocity at the initial oven temperature (80°C) but only to 39 cm s^{-1} at the end of the run (380°C). For the chromatogram shown in Figure 3, the analysis was carried out in the constant flow mode. In this operating mode, the pressure is automatically increased (from 50 to 112 kPa in this case) as oven temperature increases, to maintain the initial flow rate throughout the run. Under these conditions, Irganox 1010 elutes at 32 min. The use of cool on-column injection with electronic pneumatic control also provides excellent repeatability in retention

Table 1 List of polymer additives

No	Name	Empirical formula	MW	% RSD on t_R	% RSD on peak area
1	BHA	C ₁₁ H ₁₆ O ₂	180	0.04	0.42
2	Diethylphthalate	C ₁₂ H ₁₄ O ₄	222	0.02	0.29
3	Dibutylphthalate	C ₁₆ H ₂₂ O ₄	278	0.02	0.48
4	Tinuvin P	C ₁₃ H ₁₁ ON ₃	225	0.03	1.48
5	Triphenylphosphate	C ₁₈ H ₁₅ O ₄ P	326	0.02	1.77
6	Dicyclohexylphthalate	C ₂₀ H ₂₆ O ₄	330	0.02	0.55
7	Diethylphthalate	C ₂₄ H ₃₈ O ₄	390	0.02	0.24
8	Tinuvin 327	C ₂₀ H ₂₅ ON ₃ Cl	357	0.02	0.42
9	Benzophenone UV 531	C ₂₁ H ₂₆ O ₃	326	0.01	0.98
10	Erucamide	C ₂₂ H ₄₃ ON	337	0.02	1.74
11	Tinuvin 770	C ₂₈ H ₅₂ O ₄ N ₂	480	0.01	0.30
12	Irgaphos 168	C ₄₂ H ₆₃ O ₃ P	646	0.01	0.91
13	Irganox 1076	C ₃₅ H ₆₂ O ₃	530	0.01	1.48
14	Tinuvin 144	C ₄₂ H ₇₀ O ₅ N ₂	682	0.01	0.24
15	Irganox 245	C ₃₄ H ₅₀ O ₉	602	0.01	0.44
16	Irganox 259	C ₄₀ H ₆₂ O ₆	638	0.02	0.35
17	Irganox 1035	C ₃₈ H ₅₈ O ₆ S	642	0.01	0.58
18	Irganox 565	C ₃₈ H ₅₆ ON ₄ S ₂	588	0.02	0.50
19	Crodamide	C ₄₀ H ₇₆ O ₂ N	588	0.01	0.66
20	Irganox 1098	C ₄₀ H ₆₄ O ₄ N ₂	636	0.01	0.65
21	Irganox 3114	C ₄₈ H ₆₉ O ₆ N ₃	783	0.02	0.68
22	Irganox 1330	C ₅₄ H ₇₈ O ₃	774	0.01	0.29
23	Irganox PS802	C ₄₂ H ₈₂ O ₄ S	682	0.01	0.72
24	Irganox 1010	C ₇₃ H ₁₀₈ O ₁₂	1176	0.01	1.50

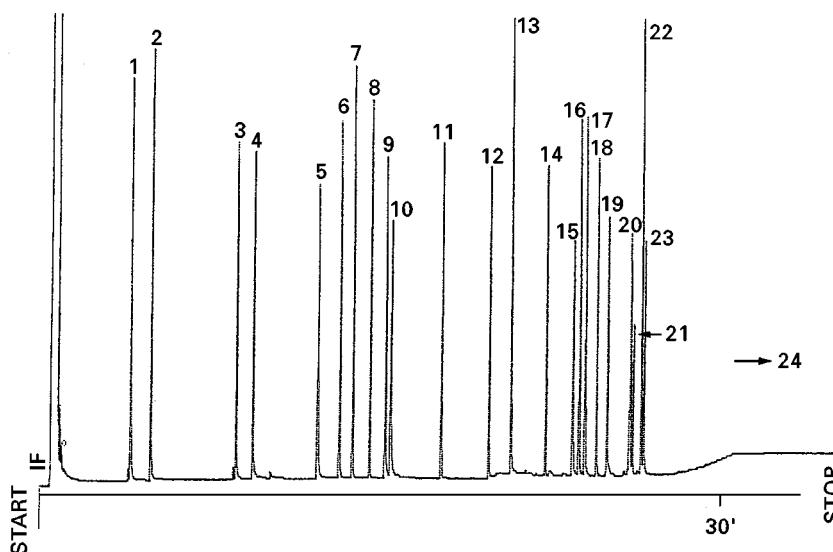
times and quantitation. Average retention times and absolute peak areas for five runs are shown in Table 1. Relative standard deviations are within 0.04% for the retention times and 2% for the raw peak areas, even for the polar compounds such as erucamide and Irgaphos 168. This illustrates the robustness of HTCGC.

The combination of CGC with mass spectrometry (CGCMS) can also be used successfully for the analysis of these polymer additives. Helium was the carrier

gas in the GCMS combination and this had some consequences on the selection of the column. The column length was reduced to 12 m, the i.d. to 0.2 mm and the film thickness to 0.11 μ m. With helium at an inlet pressure of 10 kPa and operated in the constant flow mode, Irganox 1010 eluted at 39.5 min.

Detectors

The use of the universal flame ionization detector (FID) or selective detectors such as nitrogen-phos-

**Figure 2** HTCGC analysis of the polymer additives using constant pressure mode. Peak identifications are given in Table 1.

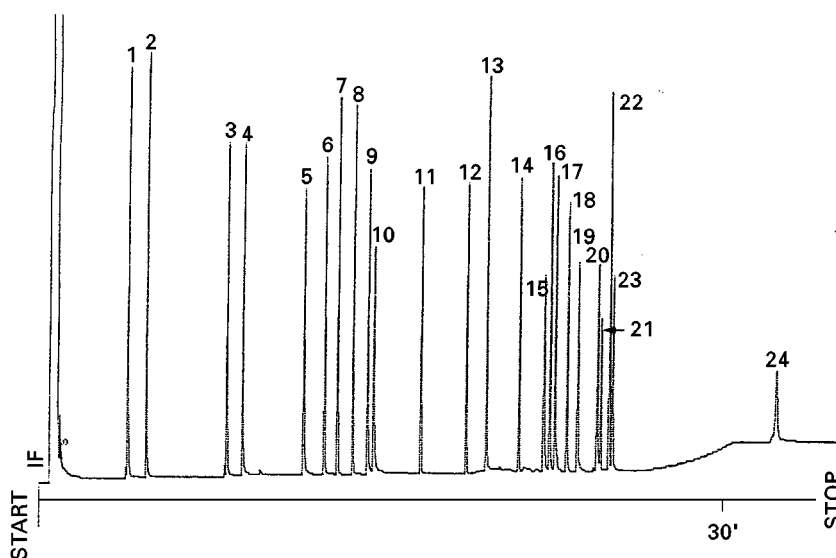


Figure 3 HTCGC analysis of the polymer additives using constant flow mode. Peak identifications are given in Table 1.

phorus detection (NPD) or electron-capture detection (ECD) does not pose any problem in HTCGC. Moreover, the spectroscopic techniques mass spectrometry (MS), atomic emission detection (AED) and inductively coupled plasma mass spectrometry (ICPMS) are compatible with HTCGC. As an illustration, Figure 4 shows the element-specific chromatograms for the phosphorus line at 178.1 nm (A) and the sulfur line at 181.4 nm (B) for the sample listed in Table 1 with the AED detector. The transfer line and cavity temperatures of the AED were set at 340°C. The other chromatographic conditions were very similar to those used for Figure 3.

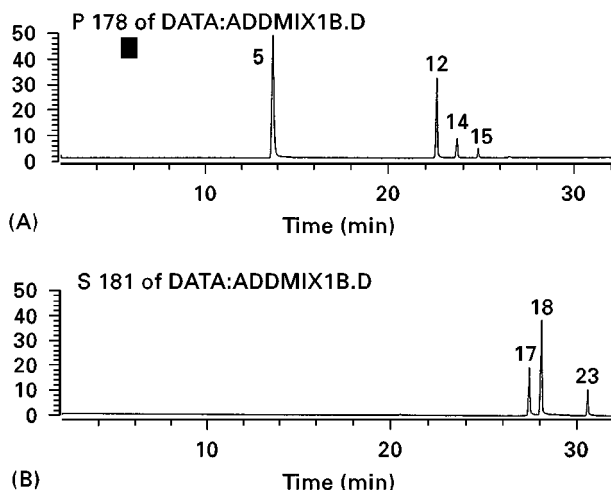


Figure 4 Element-specific chromatograms of the polymer additives recorded with atomic emission detection: (A) phosphorus line at 178.1 nm; (B) sulfur line at 181.4 nm.

Applications of HTCGC

In the framework of this contribution, it is impossible to review all applications of HTCGC. Some of the most relevant applications are detailed.

Hydrocarbons

HTCGC is nowadays intensively applied for the calculation of the true boiling point distribution of heavy petroleum products (simulated distillation or SIMDIS). In this type of analysis, high resolution is not wanted. The most desirable prerequisite the technique should fulfil is complete and quantitative elution. Hydrocarbons up to C_{130} elute quantitatively on short capillary columns coated with a thin film of methylsilicone.

Lipids

The qualitative and quantitative elucidation of glycerides is an important analysis in different fields, e.g. characterization of natural products, of food products, in lipid metabolism studies, bacterial identification, etc. A variety of techniques is routinely applied including liquid chromatography (LC), supercritical fluid chromatography (SFC) and HTCGC. Of these techniques, HTCGC provides the highest resolution in the shortest analysis time. The HTCGC analysis of a standard mixture of silylated mono-, di- and triglycerides is shown in Figure 5. The analysis was performed on a 12 m \times 0.32 mm i.d. \times 0.17 μ m methylsilicone column programmed from 80°C to 380°C at 15°C min. Hydrogen was the carrier gas at 65 cm s⁻¹ and both cool on-column and PTV injection could be applied.

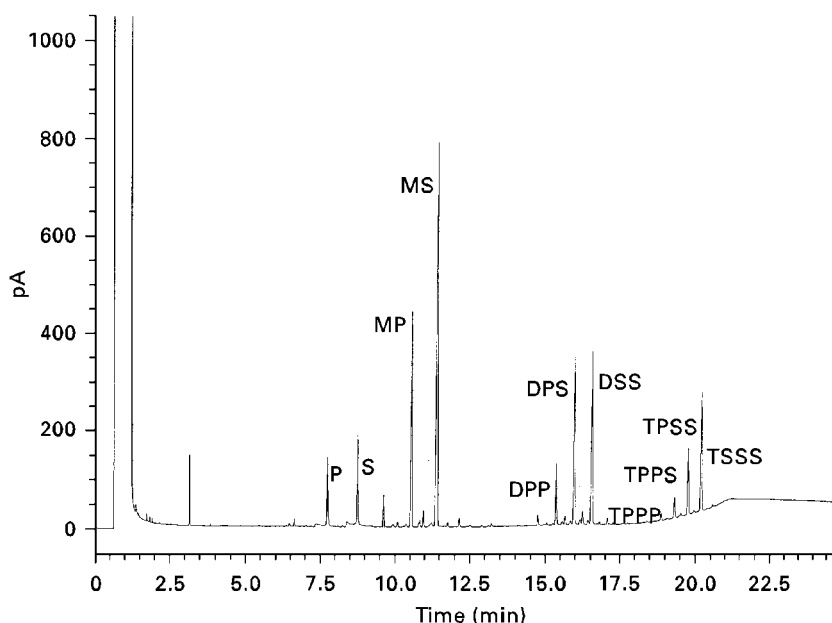


Figure 5 Analysis of silylated mono (M)-, di(D)- and tri(T)-glycerides. P, palmitic acid; S, stearic acid.

It is often claimed that HTCGC yields erratic quantitative results for triglycerides because of decomposition. Problems can indeed be encountered with oils containing large amounts of highly unsaturated triglycerides such as trilinolenin (LnLnLn), which tend to polymerize and not to decompose. For quantification of such lipids, calibration is necessary. Most of the oils and fats, however, can be analysed perfectly well by HTCGC. On apolar columns of the methylsilicone type, triglycerides are separated according to the carbon number. On polarizable diphenyl (50–65%) dimethylsilicone phases, besides a carbon number separation, lipids are also separated according to the different combinations of saturated and unsaturated fatty acids in the triglycerides. **Figure 6** shows the analysis in 3 min of the lipids in palm oil. The diglycerides with carbon numbers 32 to 36 and the triglycerides from C46 to C56 were separated on a 5 m × 0.25 mm i.d. × 0.1 µm methylsilicone in a temperature programmed run from 290°C to 350°C at 30°C min⁻¹ applying cool on-column injection and with hydrogen as carrier gas at 103 kPa. **Figure 7** shows the analysis of inter-esterified cocoa butter on a poly(dimethyldiphenylsiloxene) column 25 m × 0.2 mm i.d. × 0.1 µm film. The sample was introduced via a PTV injector. Besides a carbon number separation, the triglycerides on this phase are also separated according to degree of unsaturation.

HTCGC is nowadays the method of choice in the chocolate industry to control the natural origin of cocoa butter and to elucidate the addition of cocoa butter equivalents and/or nut oils.

Detergents and Surfactants

Most of the non-ionic surfactants can be analysed by HTCGC. This is illustrated in **Figure 8** with the analysis of trimethylsilylated Triton X-100, an alkyl-phenol polyethoxylate, on a 10 m × 0.32 mm i.d. × 0.1 µm diphenyl (5%) dimethylsilicone column.

The temperature was programmed from 65°C to 200°C at 40°C min⁻¹ and then to 390°C at 8°C min⁻¹. Cool on-column injection was used. Helium was the carrier gas at 70 kPa. The relative standard deviation of retention times was lower than 0.1% and on raw peak areas lower than 0.7%. Another type of non-ionic surfactant is the polyethylene glycols (PEGs). HTCGC is able to analyse samples containing PEGs up to 1300 Da (PEG 1000).

Oligosaccharides

Oligosaccharides are thermally unstable and have to be derivatized into the well-known oxime-trimethylsilyl derivatives. The limits of HTCGC are illustrated in **Figure 9**. An oligosaccharide sample, obtained by hydrolysis of insulin extracted from *Cichorium intybus*, with DPs ranging from DP1 to DP12 could be analysed in approximately 30 min on a 10 m × 0.53 mm i.d. × 0.1 µm methylsilicone column. The degree of polymerization (DP) is the number of sugar units in the oligosaccharides. Both the pressure (50–200 kPa) and the temperature (100–430°C) were programmed to elute the high DP numbers. The analysis was performed on an aluminium-clad column. In this application resolution is sacrificed for speed of elution.

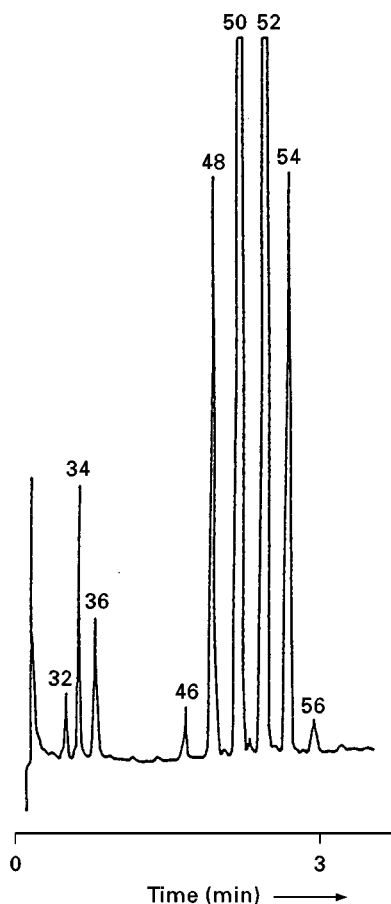


Figure 6 Fast carbon number separation of palm oil.

Emulsifiers

Organic substances added to food products to form emulsions are very complex mixtures. At present, there is no universal analytical method to elucidate the nature and origin of an emulsifier. Nevertheless,

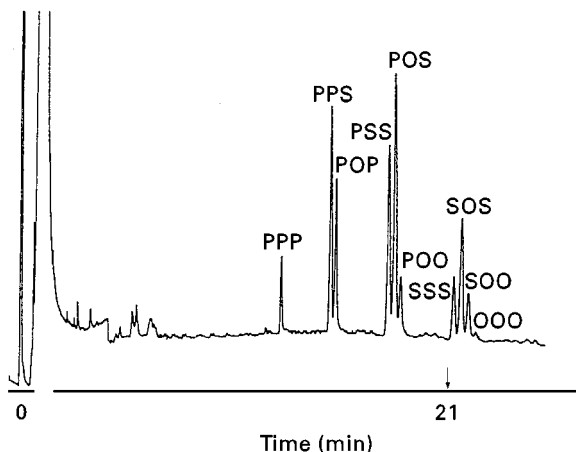


Figure 7 Analysis of inter-esterified cocoa butter. P, palmitic acid; S, stearic acid; O, oleic acid.

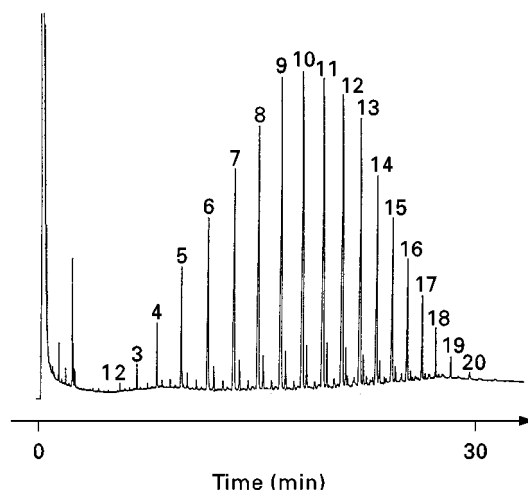


Figure 8 HTCGC analysis of Triton X-100 as trimethylsilyl derivatives. Numbering: ethylene oxide (EO) units.

HTCGC allows the characterization of a large number of emulsifying mixtures. This is illustrated with the analysis of two commercially available emulsifiers: one based on sorbitol (**Figure 10A**) and one on lactic acid (**Figure 10B**). Both samples were analysed on an automated HTCGC instrument (HP 6890) equipped with a 13 m \times 0.32 mm i.d. \times 0.1 μ m methylsilicone column and a cool on-column injector. The silylated samples were injected in the oven track mode with an oven temperature programme from 70 to 370°C at 15°C min⁻¹. Hydrogen was the carrier gas at 25 kPa.

Miscellaneous

This overview of applications of HTCGC is far from complete and could be extended with the analysis of metal porphyrins in crude oils (geomarkers), of tall oil components, of mycolic acids, of antifoam agents, of antibiotics, etc. The applied methodologies are, however, similar to those described for the other applications.

Conclusion

HTCGC is a powerful analytical method for the analysis of high molecular weight compounds. Instrumentation and columns are commercially available. For some applications, derivatization into stable volatile substances is required.

In HTCGC we cannot expect spectacular new developments because the thermal stability of the compounds being separated is the limiting factor. The MW range can be expanded a little by applying high speed columns, i.e. short lengths and small internal diameters. By reducing the residence time in the column, the thermal stress is reduced as well.

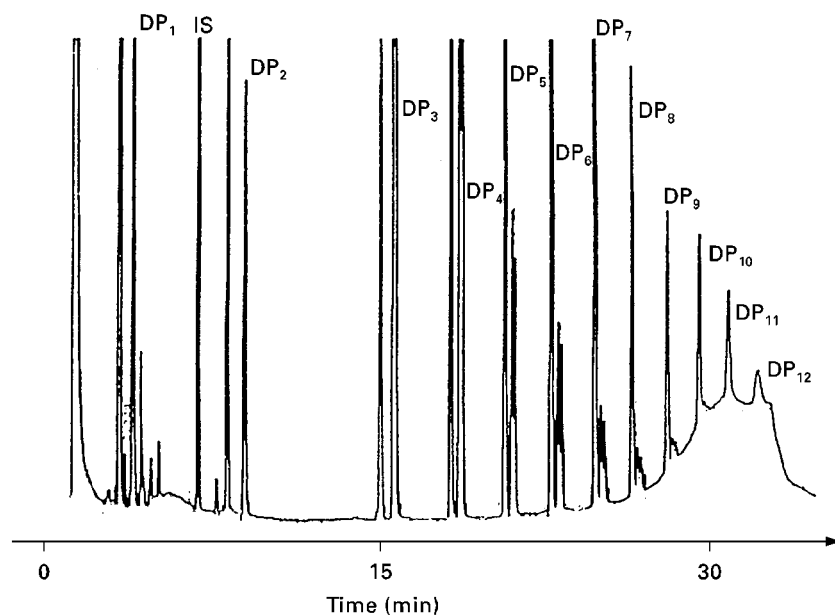


Figure 9 HTCGC analysis of an oligosaccharide sample using a temperature and pressure programme.

On the other hand, we will see more and more applications in the literature because CGC is always superior in terms of efficiency and speed of analysis compared

to the other separation methods. With state-of-the-art HTCGC a number of applications presently carried out with LC or SFC, can be done much better with GC.

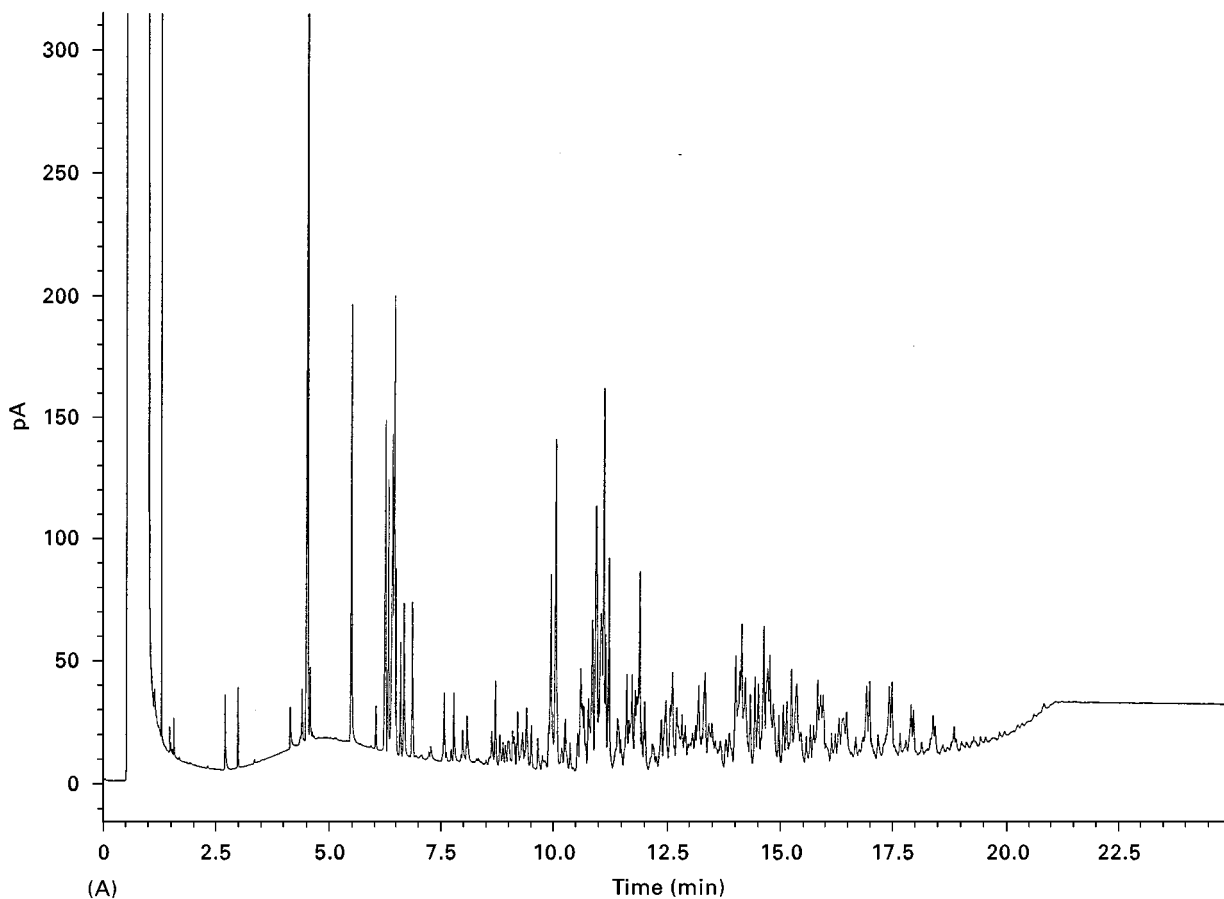


Figure 10 Analyses of emulsifiers based on sorbitol (A) and on lactic acid (B).

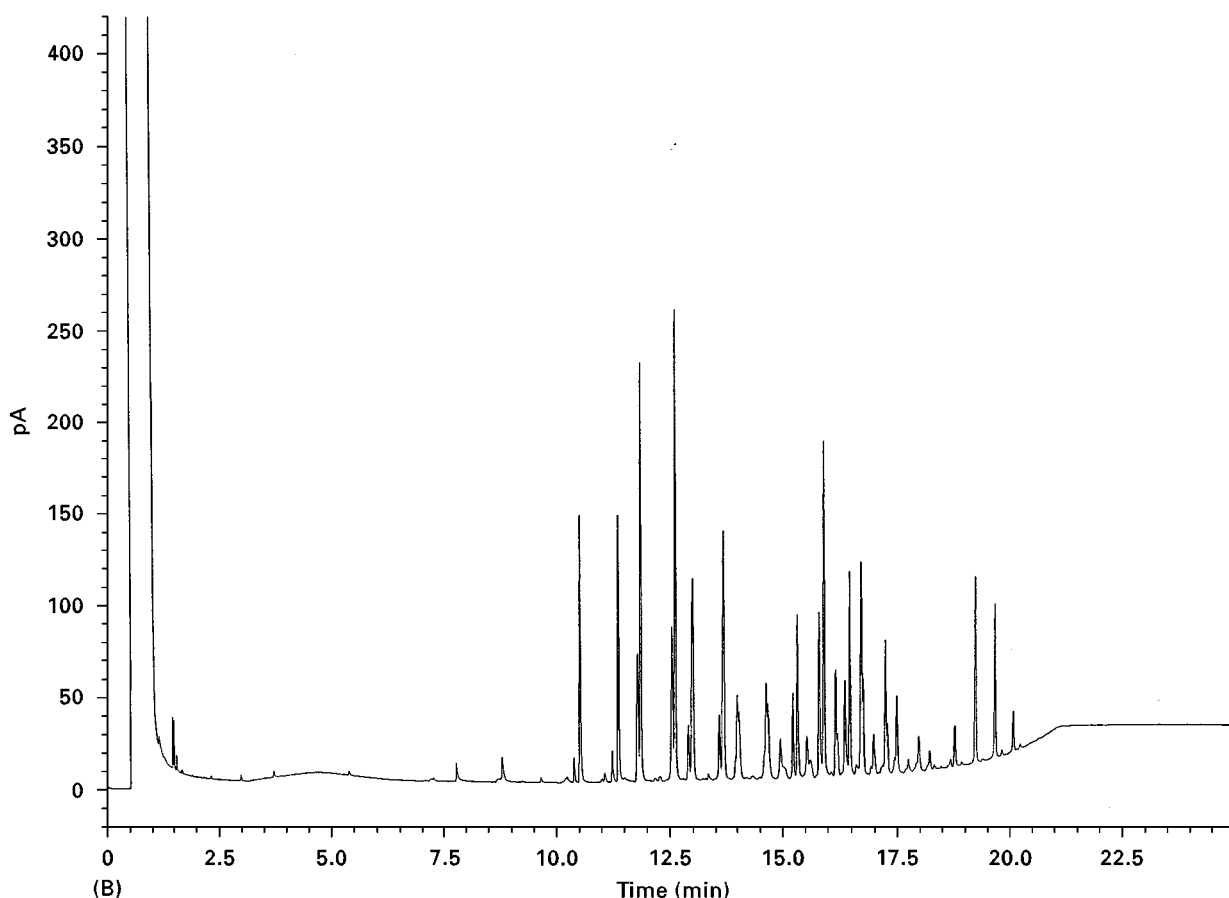


Figure 10 Continued

See also: **II/Chromatography:** Column Technology; Derivatization; Detectors: General (Flame Ionization Detectors and Thermal Conductivity Detectors); Detectors: Mass Spectrometry; Detectors: Selective; Sampling Systems. **III/Lipids:** Gas Chromatography. **Oils, Fats and Waxes:** Supercritical Fluid Chromatography. **Petroleum Products:** Gas Chromatography.

Further Reading

- Blum W and Aichholz R (1991) *Hochtemperatur Gas-Chromatographie*. Heidelberg: Hüthig Verlag.
- David F and Sandra P (1988) Analysis of aliphatic amines and quaternary ammonium salts by capillary supercritical-fluid chromatography. *Journal of High Resolution Chromatography* 11: 897-898.
- Geeraert E (1985) In Sandra P (ed.) *Sample Introduction in Capillary GC*, pp. 287. Heidelberg: Hüthig Verlag.
- Geeraert E and Sandra P (1987) Capillary GC of triglycerides in fats and oils using a high-temperature phenylmethylsilicone stationary phase. II. Analysis of chocolate fats. *Journal of American Oil Chemistry Society* 64: 100-105.
- Geeraert E, Sandra P and De Schepper D (1983) On-column injection in the capillary gas chromatographic analysis of fats and oils. *Journal of Chromatography* 279: 287-295.
- Grob K (1980) Gas-chromatographic stationary phases analysed by capillary gas chromatography. *Journal of Chromatography* 198: 176-179.
- Lipsky SR and Duffy ML (1986) High-temperature gas chromatography: development of new aluminium-clad flexible fused-silica glass capillary columns coated with thermostable non-polar phases. II. *Journal of High Resolution Chromatography* 9: 725-730.
- Termonia M, Munari F and Sandra P (1987) High oven temperature - cold on-column injection for the automated CGC (capillary gas-chromatographic) analysis of high-molecular-weight compounds such as triglycerides. *Journal of High Resolution Chromatography* 10: 263-268.
- Trestianu S, Zilioli G, Sironi A, Saravalle C, Munari F, Galli M, Gaspar G, Colin JM and Jovelín JL (1985) Automatic simulated distillation of heavy petroleum fractions up to 800°C TBP by capillary gas chromatography. I. *Journal of High Resolution Chromatography* 8: 771.

High-Speed Gas Chromatography

A. Andrews, Ohio University, Athens, OH, USA

Copyright © 2000 Academic Press

Introduction

High speed gas chromatography (GC) has been the subject of an increasing number of papers in both journals and at conferences in recent years. These articles have progressed from concept papers mainly detailing the necessary instrumental modifications to the potential applications of high speed GC.

This article is focused on reported applications of what may be regarded as traditional high speed GC, i.e. short, wall-coated open tubular columns (generally of internal diameter (i.d.) <0.32 mm) operated at a higher than optimal carrier gas flow rate. The total chromatographic separation time is required to be less than 3–4 min. This eliminates some work on polychlorinated biphenyl separations where run times are approximately six times faster than conventional GC, but still take around 10 min. Other areas in high speed GC, such as rapid packed column separations, porous layer open tubular columns and the newly emerging imaging technique of solvating GC using packed columns will not be addressed. In addition, only those articles which specifically relate to the use of high speed GC for a particular analysis have been considered. The separation of a large number of compounds by high speed GC has been demonstrated in many research articles, but many of the mixtures separated are not specific to any particular problem or truly relevant to real world analysis.

High speed GC is still mainly an academic research technique. The number of published applications is small and review articles or books detailing these applications are nonexistent. For this reason this article draws mainly on journal papers.

High speed GC is not a new analysis technique. The first true high speed separations involving capillary columns were carried out nearly four decades ago by Desty. Although this clearly demonstrated that separations in seconds were possible, the instrumental demands that high speed GC makes upon the gas chromatograph made it unsuitable for general use at that time. In the following years several notable research groups around the world have made excellent progress both in solving some of the instrumental problems and in clarifying the theoretical considerations involved with high speed GC. In particular, the major contributions of Annino and Guiochon to theoretical developments and the research groups of

both Cramers and Sacks for instrumental advances deserve specific mention.

There are several reasons for this slow transfer of high speed GC from the research laboratory to the analytical laboratory. One is the reluctance of application laboratories to substitute a new untried procedure for a known analytical method, even when the new procedure offers major time savings. New methods frequently encounter this hurdle and as more literature reports on high speed GC applications appear, this barrier should slowly crumble.

Another barrier, which will be harder to overcome, is the problem of sample preparation. The advantages of a very fast chromatographic separation are negated if the sample preparation step takes an order of magnitude or more longer than the separation. Further basic research is required in the sample preparation area to bring these two stages closer inline with each other. The workers who have pioneered high speed GC research in the last decade are already incorporating faster sample preparation steps into their research and it is likely that the coming years will see the progress needed in this area.

To date, most high speed GC applications have been in the analysis of volatile organic chemicals (VOCs) in either air or water. Other applications include chlorinated pesticides, polyaromatic hydrocarbons (PAHs), and the use of high speed GC to determine solvent purity. Each of these areas will be considered in more detail below.

Volatile Organic Chemicals

Air

Near real-time results may be particularly beneficial for a system where a centrally located high speed gas chromatograph is connected to a network of sampling lines. The high speed GC analysis of VOCs must be able to detect compounds at and below regulatory levels, such as the threshold limit value (TLV).

Original work utilized a valve loop system for sampling, but the use of mechanical valves may be a problem for an automated system. Valves may require periodic maintenance, or may change the sample through interaction with valve surfaces. In addition, changing the sample size requires either changing the loop or the use of several loop cycles. Ice formation which may plug the collection tube, resulting from water vapour in the air is another area of concern. However, studies to date have not shown this to be a problem.

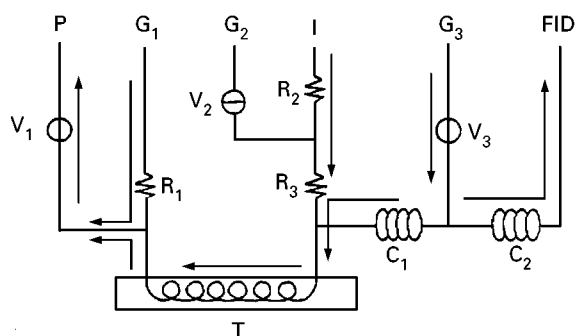


Figure 1 Complete high speed GC system with direct atmospheric sample collection. T, Cold trap system; V, valves; R, restrictors; P, vacuum pump; I, atmospheric pressure source; C, separation column; G, gas source. Arrows show flow directions during sample collection. (Reproduced with permission from Akard and Sacks, 1994.)

An alternative approach to achieve the detection limits required is a technique termed cryointegration. In this method, VOCs from an air sample, usually contained in a sampling loop, are cryofocused in a liquid nitrogen-cooled metal tube. Thus, dilute samples can be preconcentrated prior to high speed analysis. Resistive heating of the metal tube is used to ensure a narrow injection plug compatible with high speed GC requirements. This has been incorporated with a reversed-flow sample collection system. **Figure 1** shows the complete high speed GC system for an air monitor using this type of set-up.

The vacuum pump pulls sample and carrier gas through the cryotrap for the sample collection period. This time period can be adjusted to allow for more or less sample to be collected as required. After collection, the sample is introduced on to the separation column by heating the metal cryotrap tube.

The positioning of the sample near the column end of the cryotrap reduces band broadening and the potential for sample decomposition. The decreased bandwidth leads to narrower, taller peaks, which in turn improve the limit of detection (LOD). Although water vapour in the sample condensing in the cryotrap is not a problem, water vapour from the flame ionization detector (FID) is. For this reason, a gas source attached midway through the separation column has been used to prevent water vapour from the detector reaching the cryotrap.

Figure 2 shows representative chromatograms obtained using gasbag samples. The sampling flow rate is constant and about 0.3 mL min^{-1} once steady-state flow is achieved. There is, of course, a trade-off between reducing the LOD and loss of real-time data as the sampling time increases.

Tables 1 and **2** show the limit of detection values obtained using the conventional loop system and the

reverse-flow collection system respectively. It can be seen that, as the sampling time increases with the cryointegration system, the LOD values approach those obtained using a fixed 1 mL loop. One would expect that further increases in sampling time would reduce the LOD even further. The disadvantage with further increases in sampling time is the loss of real-time information. These LOD values are already below regulatory or guideline concentrations such as the TLV and a further reduction in LOD would seem unnecessary.

Water

The apparatus used for VOC analysis in water by high speed GC is essentially the same as that used for the air analysis work. This is because, as sample preparation is conducted by a static headspace equi-

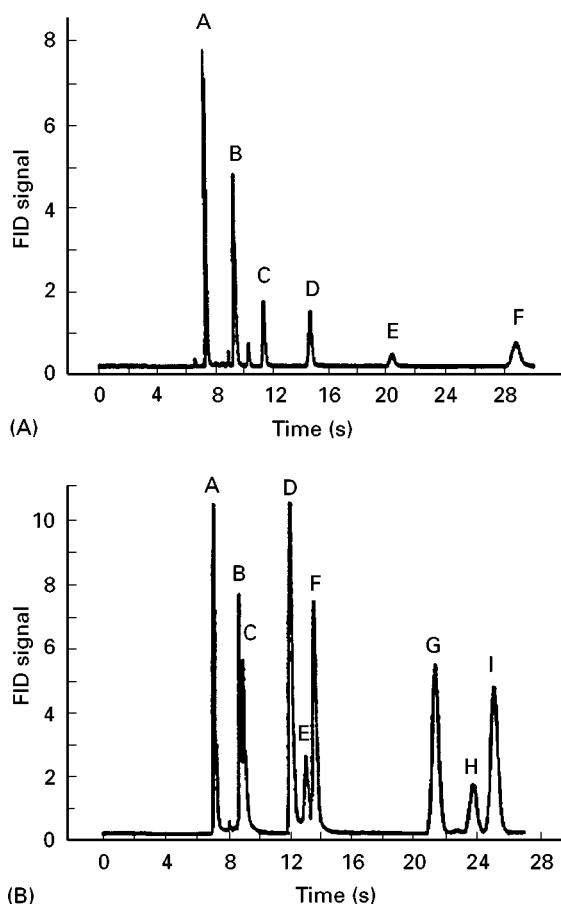


Figure 2 High speed chromatograms using gasbag samples and the reverse-flow collection instrument: (A) six-component mixture; (B) nine-component mixture. Peaks in (A) A, *n*-pentane; B, *n*-hexane; C, benzene; D, *n*-heptane; E, toluene; F, *n*-octane. Peaks in (B) A, *n*-hexane; B and C, isomers of 2-hexene; D, 1-heptene; E and F, isomers of 2-heptene; G, 1-octene; H and I, isomers of 2-octene. (Reproduced with permission from Akard and Sacks, 1994.)

Table 1 Limits of detection and quantitation measured for 13 common organic compounds

Compound	LOD (p.p.b.v.)	LOQ (p.p.b.v.)
Pentane	2	7
Hexane	3	10
Heptane	4	13
Octane	5	17
Benzene	8	27
Toluene	2	7
<i>o</i> -Xylene	50	170
<i>m</i> -Xylene	1	3
Dichloromethane	< 1	< 3
Chloroform	< 1	< 3
Tetrachloroethylene	< 1	< 3
1,1,2,2 Tetrachloroethane	2	7
1,2,3 Trichloropropane	< 1	< 3

All values are expressed in parts per billion by volume and are based on a sample volume of 1 mL. Values reported as <1 required extrapolation below sample volumes that were actually tested.

LOD, sample mass producing a peak height equal to a blank plus three standard deviations of the noise; LOQ, the sample mass producing a peak height equal to a blank plus 10 standard deviations of the noise. Reproduced with permission from Mouradian *et al.* (1991).

librium method, the actual sample analysed is an air sample.

Detection limits using an FID were found to be $<10 \mu\text{g L}^{-1}$ for benzene, toluene, ethylbenzene and the xylenes (BTEX compounds). Again, by increasing the injection loop volume, these detection limits could be reduced further. Real samples from ground water obtained near a leaking underground storage tank have been analysed and preliminary comparisons to more established methods made. Full validation of the high speed method has not been carried out.

Table 2 Statistical data for air analysis using reverse-flow sample collection with two different sampling periods

Component	Correlation coefficient	Log-log slope	LOD (p.p.b.)	
			20	110
Benzene	0.993	0.99	26	4.6
<i>n</i> -Heptane	0.997	1.04	37	6.9
Toluene	0.999	1.07	25	4.0
Octane	0.995	1.07	47	8.4
<i>p</i> -Xylene	0.999	1.09	29	4.4

Detection limits (LOD) for a signal-to-noise ratio of 3.0 for both the 20 s and the 110 s sampling times. Reproduced with permission from Akard and Sacks (1994).

An alternative method for aqueous sample analysis combines solid-phase microextraction (SPME) with fast GC. The SPME extraction is conducted on the headspace above a water sample in a sealed vial. The analytes are then rapidly desorbed in a specially made injection port into a commercially available portable gas chromatograph. Separation of the BTEX compounds is achieved in less than 30 s. The photoionization detector for this work was not optimized for fast separations. Modification of the detector internal volume is required to reduce band broadening and provide performance suitable for use with high speed GC without the use of make-up gas. As the headspace above a sample is extracted with the SPME fibre, the method is easily adapted to soil sample analysis for VOCs.

One reason for the lack of published applications dealing with VOC analysis in water may be the large disparity between chromatographic analysis time and sample preparation time. Having a chromatographic time scale of 20 s (Figure 3), as is the case with this

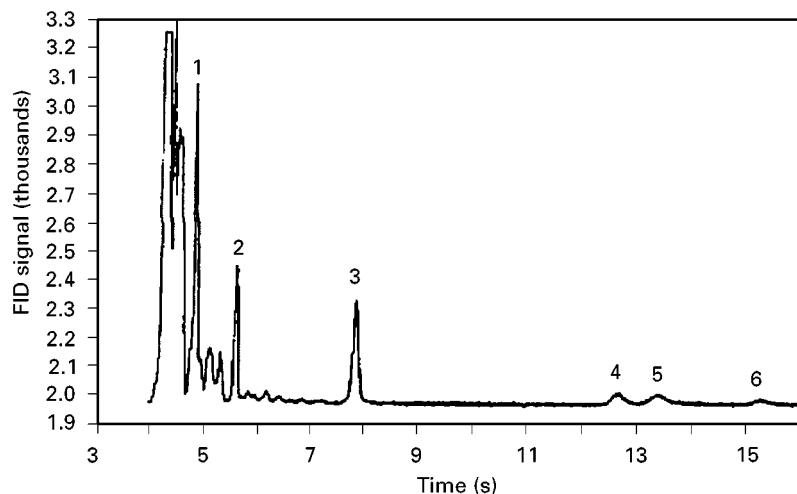


Figure 3 High speed chromatogram of the static headspace above a sample of gasoline-contaminated ground water. Peak identification. 1, methyl *t*-butyl ether ($2370 \mu\text{g L}^{-1}$); 2, benzene ($97 \mu\text{g L}^{-1}$); 3, toluene ($109 \mu\text{g L}^{-1}$); 4, ethylbenzene ($2 \mu\text{g L}^{-1}$); 5, co-eluting *m*- and *p*-xylenes ($12 \mu\text{g L}^{-1}$); 6, *o*-xylene ($<0.3 \mu\text{g L}^{-1}$). (Reproduced with permission from Wang *et al.*, 1991.)

BTEX analysis, has little advantage when the sample preparation time is between 20 and 60 min.

Pesticides

Due to concerns regarding adverse health effects resulting from pesticide residues in food or run-off from fields into the water supply, a large number of analytical methods have been published concerned with pesticide analysis. With the increase in studies linking pesticide residues to adverse human health effects comes a concurrent increase in the number of samples required to be analysed for pesticides.

Several approaches to speeding up pesticide analysis have been taken. One approach utilized the two-dimensional chromatographic approach for a comprehensive analysis of up to 17 pesticides. The two-dimensional approach has the advantage that if the two stationary phases have completely different retention mechanisms for the analytes then a truly orthogonal separation is achieved.

The instrumentation in the two-dimensional approach housed both GC columns (first column $2\text{ m} \times 250\text{ }\mu\text{m}$ i.d., second column $0.80\text{ m} \times 100\text{ }\mu\text{m}$ i.d.) in a single GC oven connected via a home-made thermal desorption modulator. The modulator collects the eluent from the first column and releases it on to the second column with a cycle time of 2.5 s. Thus, analysis in the first dimension is 4 min and 5 s in the second dimension. **Figure 4** shows the chro-

matogram obtained in the first dimension without any separation in the second dimension. Poor peak resolution is clearly seen.

Quantitation is achieved with one of two internal standards (IS). Using a FID, LOD values are between 1.8 and 3.8 pg of pesticide on-column and the relative standard deviation (RSD) of the response (in volume counts pg^{-1}) is less than 10% for all four pesticides reported.

This method has been used for a spiked human serum sample after supercritical fluid extraction. Although one of the IS peaks overlapped with a matrix component, quantitation was still possible using the other IS. This overlap can clearly be seen in **Figure 5**. The method allows for faster method development as rapid feedback on the performance of the extraction process is provided. This has been found to be very useful in this application as the supercritical fluid extraction method used only reliably extracted eight of the pesticides under investigation.

A second approach has been to use high speed GC as a screening tool for chlorinated pesticides in water samples. The rationale here is that many samples may contain pesticide residues at levels below those set as acceptable by regulatory agencies. By using a fast analysis method for screening, the number of samples requiring full analysis is reduced.

Using a conventional high speed GC system employing a cryotrap/thermodesorption system and a short $100\text{ }\mu\text{m}$ i.d. GC column, separation of 10

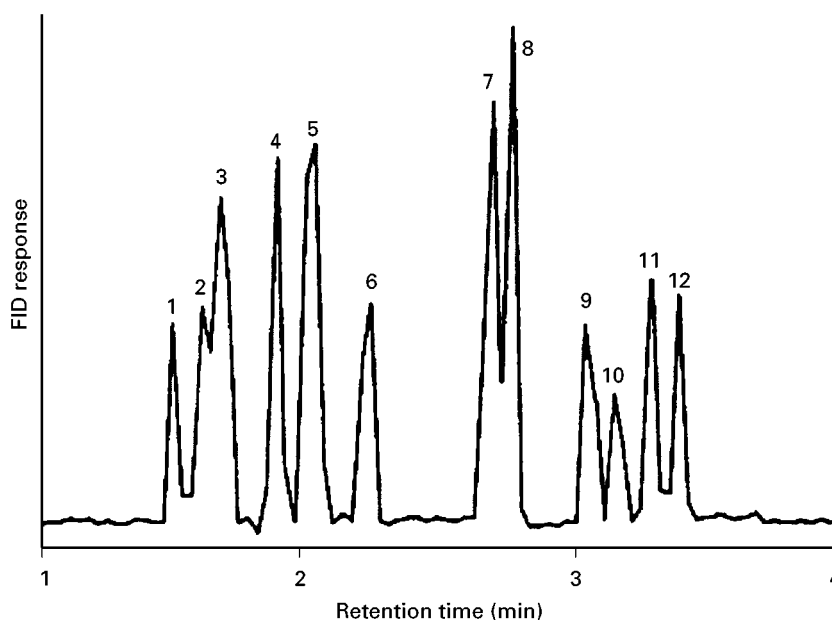


Figure 4 First-dimension chromatogram of a pesticide mixture. The GC oven was kept at 120°C for 0.3 min and then programmed at $15^{\circ}\text{C min}^{-1}$ to 180°C . The modulator chamber was kept at 150°C isothermal. Peak identification : 1, dicamba; 2, trifluralin; 3, dicloran and phorate; 4, atrazine; 5, fonofos and diazinon; 6, terbufos; 7, alachlor; 8, metalaxyl; 9, malathion; 10, DCPA; 11, captan; 12, folpet. (Reproduced with permission from Liu *et al.*, 1994.)

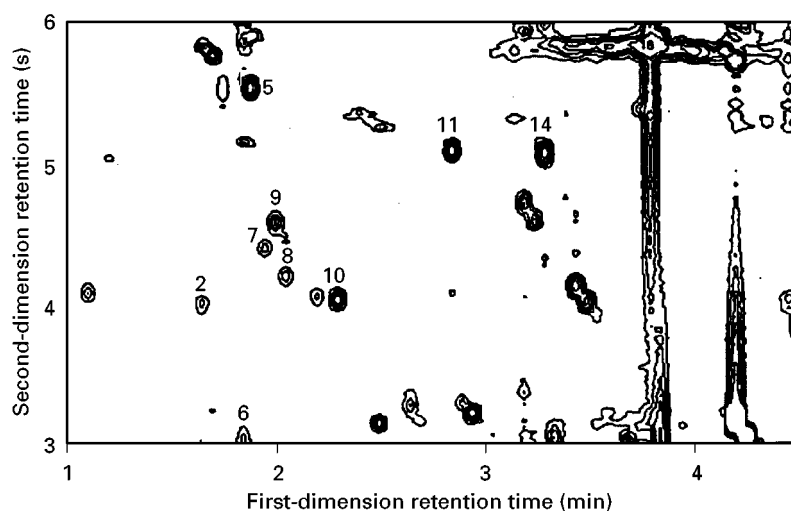


Figure 5 Two-dimensional gas chromatogram of a supercritical fluid extract of a spiked human serum sample. The GC oven was kept at 118°C for 0.5 min and then programmed at 15°C min⁻¹ to 200°C. Peak identifications are the same as in Figure 4. (Reproduced with permission from Liu *et al.*, 1994.)

chlorinated pesticides and an IS in under 2 min has been achieved.

The use of the pulsed-discharge detector operated in the electron capture mode gave on-column LOD values between 10 and 50 fg. This is an order of magnitude lower than that reported in previous work with high speed GC and a conventional radioactive electron-capture detector. These low LOD values allow reduced sample preparation and smaller sample volumes to be used prior to analysis.

The use of nonequilibrium solid-phase microextraction as the sample preparation method reduces the sample preparation time to just over 4 min per sample. The sample preparation step actually consists of a 2 min extraction stage and a 2 min desorption stage. LOD values for the complete method range

from 10 to 20 ng L⁻¹, which is below current regulatory levels set by the Environmental Protection Agency in the USA for these chlorinated pesticides in water. Table 3 shows the detection limits obtained with the fast screening method in comparison to other methods and regulatory levels.

Real river water samples spiked and analysed give good agreement between expected and actual values. Figure 6 shows representative chromatograms obtained from spiked water and blank river water samples together with the focusing of septum bleed. RSD values were found to be high (20%). This was attributed to the very short extraction time. Despite this, the method offers a relatively simple way of screening a large number of samples for chlorinated pesticides.

Table 3 Results of the calibration curve obtained by solid-phase microextraction over the range 10–400 ng L⁻¹

	r^2	LOD (ng L ⁻¹)	From literature ^a	From literature ^b	EPA 508
α -BHC	0.992	10	900	1	25
β -BHC	0.980	20	9000	1	10
δ -BHC	0.965	20	2000	2	10
<i>cis</i> -chlordane	0.978	5	N/A	N/A	1.5
<i>trans</i> -chlordane	0.969	5	N/A	N/A	1.5
<i>p, p'</i> -DDE	0.908	10	100	1	10
<i>p, p'</i> -DDD/endrin	0.969	10 + 10 ^c	60 + 200 ^c	0.1 + 1 ^c	2.5 + 15 ^c
Endosulfan sulfate	0.929	10	50	0.6	15
Endrin ketone	0.964	10	500	1	N/A

^a Solid-phase microextraction with GC-FID analysis.

^b Solid-phase microextraction with GC-mass spectrometry analysis.

^c Respective LODs for *p, p'*-DDD and endrin. Values obtained in this study are estimates based on co-eluted peaks obtained.

N/A, Not analysed.

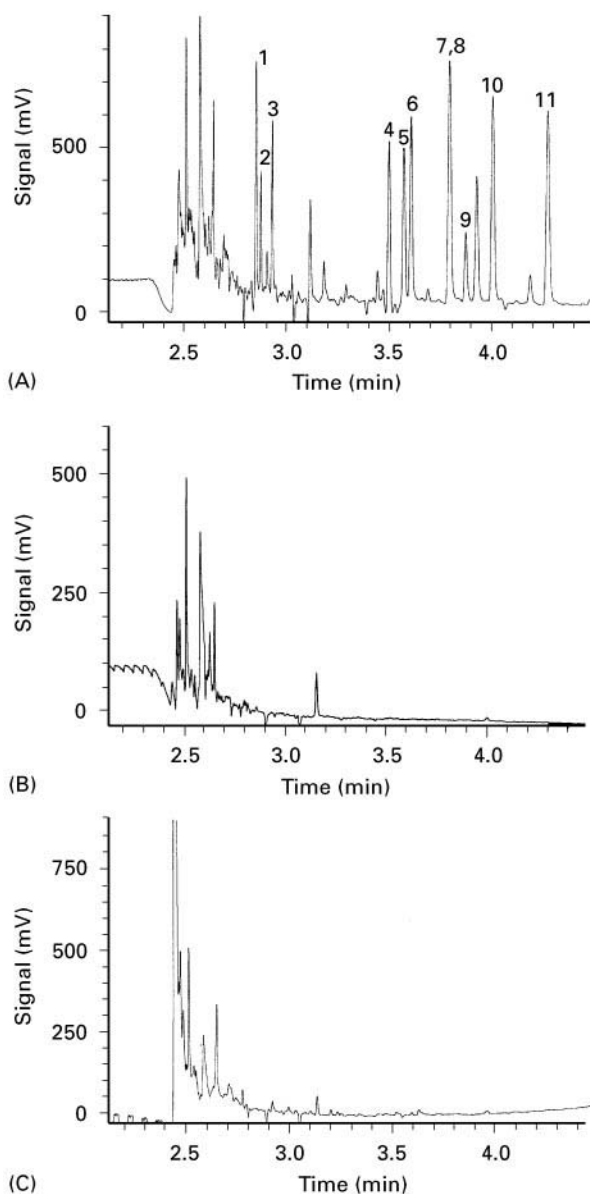


Figure 6 Chromatograms obtained after 2.3 min trapping at 60°C. (A) Solid-phase microextraction (SPME) fibre desorbed for 2 min after 2 min extraction of a 0.2 ng mL⁻¹ spiked water sample. Peaks: 1, α -BHC; 2, β -BHC; 3, δ -BHC; 4, *cis*-chlordane; 5, *trans*-chlordane; 6, *p,p'*-DDE; 7, *p,p'*-DDD; 8, endrin; 9, endrin aldehyde; 10, endosulfan sulfate; 11, endrin ketone. (B) Blank run showing the extraneous peaks caused by septum bleed being focused by the cryotrap. (C) SPME of Hocking river water; no pesticide peaks observed. (Reproduced with permission from Jackson and Andrews, 1998.)

PAHs

The use of high speed GC coupled with filter tape sampling and thermal desorption has been applied to the online assessment of PAHs in a combustion process.

Gas and particulate material are sampled directly from the emission stack using a null-type probe. A

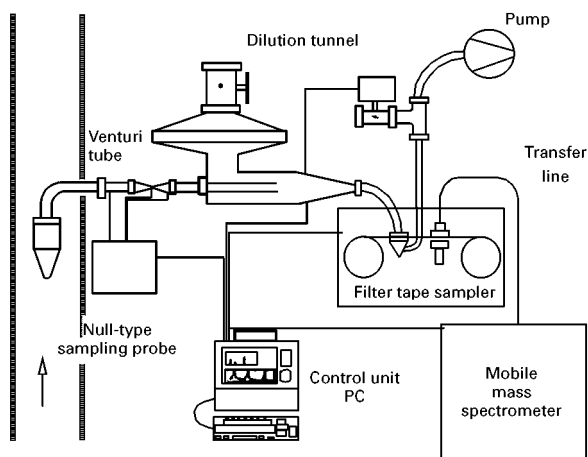


Figure 7 Overview of the sampling and analysis system for online measurement of PAHs in a combustion process. (Reproduced with permission from Munchmeyer *et al.*, 1996.)

dilution method is used to cool the gas stream to below 50°C so that condensation of the PAHs occurs on particulates in the gas stream. These particulates are then retained on a glassfibre filter. **Figure 7** shows the instrumental layout used for this work.

Once sampling is complete the PAHs are desorbed at 300°C by contact with a heated piston. The sample enters a short (1.6 m) metal capillary column, resistively heated, which allows for rapid cycling. The sample is detected using mass spectrometry. Complete separation of all PAH isomers is not achieved, although overlapping peaks of substances with different mass spectra can be resolved by correlation software. With a sample volume of 100 L the LOD values were found to be below the emission limits for carcinogenic compounds such as benzo[*a*]pyrene.

Solvent Purity

The analysis of impurities in high purity solvents is a very difficult task. By utilizing high speed GC instrumentation which has the ability to control the direction of carrier gas flow through the column this analysis can be greatly simplified.

The ability of dual-flow direction instrumentation allows for minor impurities in the solvent to be separated and identified by venting off the solvent peak only. After the majority of the solvent peak has passed off the column and into the detector, the carrier gas flow is reversed with subsequent refocusing of the residue left on the column in the cryotrap at the column head. This residue can then be reinjected.

This is well illustrated in **Figure 8**, which shows both 2-fluorotoluene and octane as impurities in toluene. Even with only 0.53 nL of sample on-column, the 2-fluorotoluene is still almost completely obscured in the

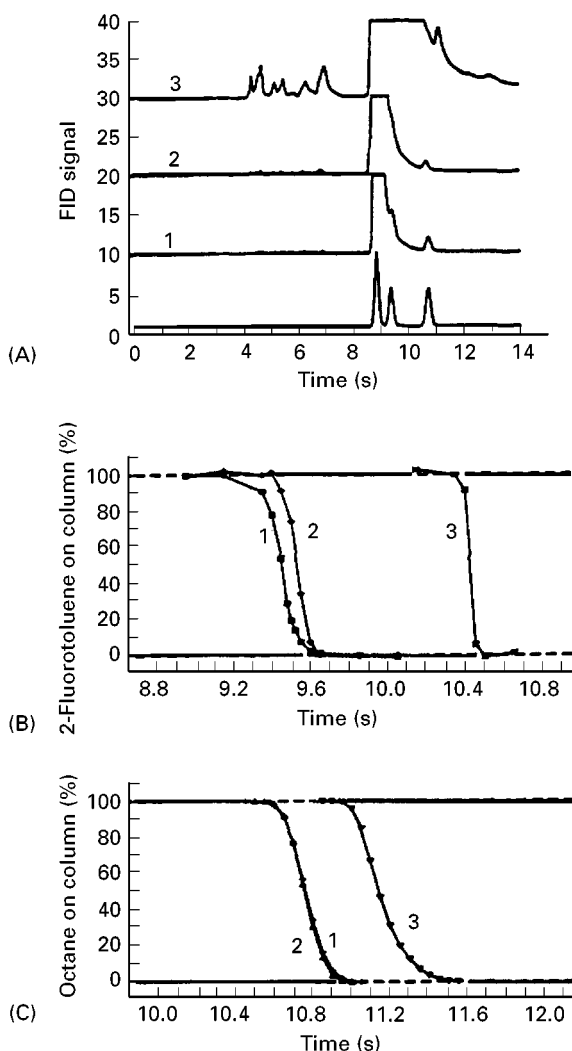


Figure 8 (A) Chromatograms showing the impurities in toluene. For plots 1, 2 and 3, 0.53, 2.67 and 13.3 nL of sample were collected in the cold trap. (B) and (C) show the percentage of impurity on column relative to time before refocusing commenced for plots 1, 2, and 3 from (A). This is the effect of solvent loading on the elution profiles of (B) 2-fluorotoluene and (C) octane in toluene. (Reproduced with permission from Klemp and Sacks, 1991.)

solvent peak. By venting the solvent and refocusing, the impurities can clearly be seen (Part (A), trace 1).

Stationary-phase film thickness is an important consideration in this type of fast analysis. Too thin a film will not sufficiently resolve impurities, which elute prior to the solvent peak. Too thick a film will degrade resolution of the peaks after the solvent peak, increase the size of the solvent tail and increase the total run time. An intermediate film thickness, such as 0.25 μm , is a satisfactory compromise between the two extremes.

Miscellaneous

One novel application of high speed GC has been in the rapid screening of soil gas samples for fuel-related

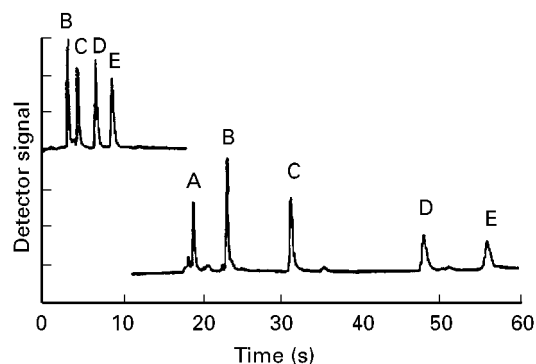


Figure 9 Comparison of high speed screening mode using the photoionization detector (top) and the advanced field analysis mode using the FID (bottom) for a test mixture containing; A, *n*-pentane; B, benzene; C, toluene; D, ethylbenzene; E, *o*-xylene. (Reproduced with permission from Sacks *et al.*, 1996.)

hydrocarbons. The gas samples are continuously generated from a cone penetrometer (CPT) equipped with a heated probe tip. The GC instrument is located in the CPT truck and connected to a heated gas transport line. The whole instrument is intended to provide high spatial resolution for contaminated soil site characterization.

The instrument can operate in two modes: either a high speed mode to detect BTEX compounds using a photoionization detector, or an advanced field mode using a FID to obtain a finger print-type chromatogram for fuel-type identification. The time frame for the separation in the two modes is 10–20 s and up to 200 s respectively. Figures 9 and 10 show representative chromatograms obtained in the two modes.

Another unusual application has been the coupling of multidimensional high speed GC with Fourier transform infrared (FTIR) detection. Using an offline interface solved the mismatch generated by the fast separation and the slow acquisition of the FTIR

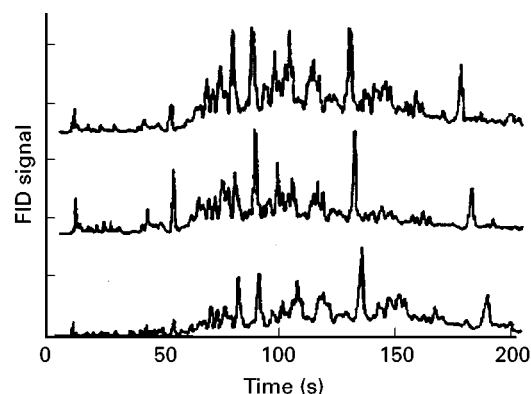


Figure 10 Advanced field analysis chromatograms of headspace from soil samples spiked with diesel fuel. (Top) Sand with 18% moisture; (middle) silty clay with 28% moisture; (bottom) silty loam with 38% moisture. (Reproduced with permission from Sacks *et al.*, 1996.)

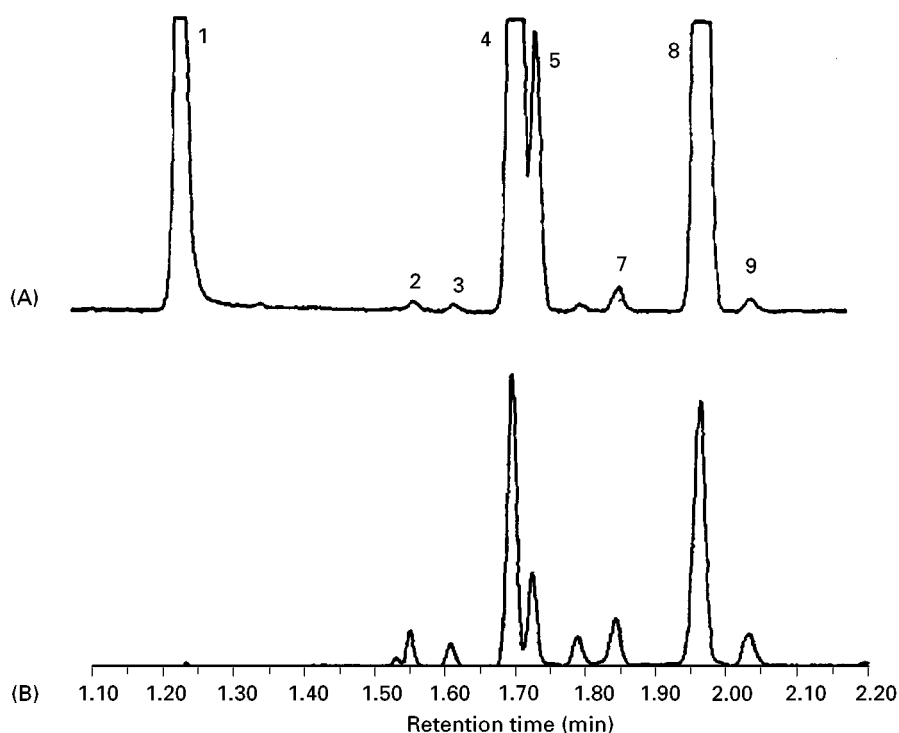


Figure 11 Secondary separation: (A) IR reconstructed chromatogram of a segment of a eucalyptus oil separation using a Rtx-1701 column and (B) FID trace. The secondary separation conditions were isothermal at 95°C with a linear carrier gas velocity of 90 cm s⁻¹. (Reproduced with permission from Ragunathan *et al.*, 1994.)

detector. The eluent from the fast GC column was deposited on to a cooled rotating collector disc and actual analysis of the disc with the FTIR was undertaken after completion of the GC run.

The system was applied to the heart-cut analysis of essential oils from cascarilla and eucalyptus. A chromatogram of the eucalyptus analysis is shown

in Figure 11. The use of FTIR detection provides structural information concerning the oil components, even the minor components present. Spectrum quality was found to be sufficient for component identification by library search methods. An infrared spectrum obtained from one of the components in Figure 11 is shown in Figure 12. One disadvantage is

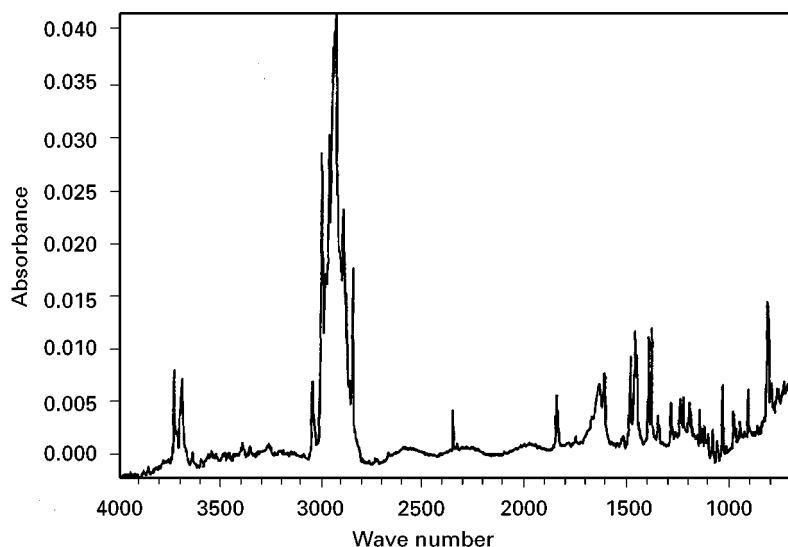


Figure 12 Infrared spectrum of the α -pinene peak (number 3 in Figure 11). The spectra acquisition conditions were 128 scans at 4 cm⁻¹ resolution with a mirror velocity of 1.27 cm s⁻¹. The time for acquiring this spectrum was 120 s. The bands at ~ 3700 and 1600 cm⁻¹ are due to water. (Reproduced with permission from Ragunathan *et al.*, 1994.)

that, for large sample sizes, some decomposition is seen from the reheating of the cryotrap region between the two columns.

Future Developments

High speed GC can probably be best described as currently being in an interim phase. It is in the process of moving from the research laboratory to the analysis laboratory. Most of the basic research demonstrating the feasibility of high speed GC and the instrumental modifications necessary for successful high speed analysis have been accomplished and the findings are well disseminated in the literature, yet the number of true applications remains small.

One technique, which has not been commented on in this article, is the combination of high speed GC with mass spectrometry (MS) as a detection method. The advent of fast scanning time-of-flight mass analysers has provided the data acquisition rates necessary for interfacing with high speed GC. Although the concept of coupling the two techniques together has been demonstrated, no real application articles using both techniques are currently available. Given the prominence of GC-MS analysis in many areas, this will surely change in the near future.

Other future developments will probably include the interfacing of other selective detectors with high speed GC and the subsequent expansion of high speed GC into the areas of analysis served by these selective detectors.

See also: II/Chromatography: Gas: Column Technology; Detectors: General (Flame Ionization Detectors and Thermal Conductivity Detectors); Detectors: Mass Spectrometry; Detectors: Selective; Historical Development; Multidimensional Gas Chromatography; Sampling Systems; Theory of Gas Chromatography.

Further Reading

Akard M and Sacks RD (1994) High-speed GC air monitor using cryointegration for sample collection. *Journal of Chromatographic Science* 32: 499–505.

Górecki T and Pawliszyn J (1997) *Field Analytical Chemistry and Technology* 1: 277–284.

Jackson GP and Andrews ARJ (1998) Field-portable solid-phase microextraction/fast GC system for trace analysis. *Analyst* 123: 1085–1090.

Klemp MA and Sacks RD (1991) New fast screening method for organochlorine pesticides in water by using a solid-phase microextraction with fast gas chromatography and a pulsed-discharge electron-capture detector. *Journal of Chromatographic Science* 29: 248–252.

Klemp MA, Peters A and Sacks RD (1994) High-speed GC analysis of VOCs: sample collection and inlet systems. *Environmental Science and Technology* 28: 369A–376A.

Liu Z, Sirlmanne SR, Patterson DG Jr *et al.* (1994) Comprehensive two-dimensional gas chromatography for the fast separation and determination of pesticides extracted from human serum. *Analytical Chemistry* 66: 3086–3092.

Mouradian RF, Levine SP, Ke H-Q and Alvord HH (1991) Measurement of volatile organics at part per billion concentrations using a cold trap inlet and high speed gas chromatography. *Air Waste Management Association Journal* 41: 1067–1072.

Munchmeyer W, Walte A and Matz G (1996) Online measurement of polycyclic aromatic hydrocarbons by fast GC/MS. *Polycyclic Aromatic Compounds* 9: 299–306.

Ragunathan N, Sasaki TA, Krock KA and Wilkins CL (1994) Multidimensional fast gas chromatography with matrix isolation infrared detection. *Analytical Chemistry* 66: 3751–3756.

Sacks R and Akard M (1994) High-speed GC analysis of VOCs: tunable selectivity and column selection. *Environmental Science and Technology* 28: 428A–433A.

Sacks R, Klemp M and Akard M (1996) High-speed capillary column GC for rapid screening of gasoline to diesel range organic compounds. *Field Analytical Chemistry and Technology* 1: 97–102.

Van Es A (1992) *High Speed Narrow Bore Capillary Gas Chromatography*. Heidelberg: Hüthig.

Wang S, Stuart JD, Ke H-Q and Levine SP (1991) Analysis of volatile aromatic compounds in gasoline-contaminated ground water samples by static headspace sampling and high speed gas chromatography. *Journal of High Resolution Chromatography* 14: 757–761.

Historical Development

E. R. Adlard, Burton, South Wirral, UK,
C. F. Poole, Wayne State University, Detroit, USA

Copyright © 2000 Academic Press

In 1941 Martin and Synge published their classic paper on liquid–liquid partition chromatography in

which they pointed out that there was no reason why the mobile phase should not be a gas. This suggestion was not followed up until 1952 when James and Martin published their paper on the separation of fatty acids by gas–liquid chromatography. This paper generated a frenzy of activity, particularly within the petroleum industry where the method represented an

enormous advance in the separation and analysis of hydrocarbon mixtures. Gas chromatography has now matured into the method of choice for the separation of volatile, thermally stable compounds with an upper molecular weight limit of about 1000 Da and is one of the most widely used laboratory methods today.

The development of gas chromatography was unique in many ways in particular the fact that, although workers in some academic establishments made notable contributions, the major impetus came from industry and from instrument companies. Another factor in its rapid development was the establishment of discussion groups in many countries dedicated to disseminating information on new advances. The Gas Chromatography Discussion Group (now the Chromatographic Society) was established in the UK in 1956 and similar bodies were formed in other parts of Europe and in North America soon afterwards. The history of gas chromatography has been described a number of times; the book by Zlatkis and Ettre gives the reminiscences of some of the early workers.

Four papers are identified in Table 1 that caused major advances in gas chromatography followed by periods of consolidation. These aspects are considered in more detail below.

Column Development

Packed Columns

For many years most gas chromatography was carried out with packed columns. Packed columns for analytical applications have internal diameters usually between 2 and 5 mm and lengths from 0.5 to 5 m, and contain particles around 100–250 μm in diameter with a range of $\pm 25 \mu\text{m}$, carrying the liquid phase. Packed columns have been constructed of various materials but the preferred materials are glass and stainless steel. The packing can be a solid adsorbent such as silica, alumina or graphitized carbon for gas–solid chromatography or a porous support coated with a high boiling liquid for gas–liquid chromatography. The usual support for the liquid phase is diatomaceous earth, a form of naturally occurring silica, with a surface area of about 0.5–4.0 $\text{m}^2 \text{g}^{-1}$ and a capacity to retain physically 5–30% (w/w) of liquid phase. Celite, a commercial diatomaceous earth, was used by Martin and James in their early experiments and is still a common support for packed columns. Polar compounds such as those found in the biomedical field give severe tailing, possible decomposition and

Table 1 Important advances in gas chromatography

1941	<i>Fundamental paper on partition chromatography</i> (Martin and Synge)
1952	<i>Fundamental paper introduces gas chromatography</i> (James and Martin)
1955	First commercial GC instrument (thermal conductivity detector)
1955–1960	Rapid period of technological growth <ul style="list-style-type: none"> Invention of ionization detectors (FID, ECD) Direct coupling to mass spectrometry Microsyringes Temperature programming
1958	<i>Fundamental paper describes open-tubular columns</i> (Golay)
1960–1970	Period of technical advancement <ul style="list-style-type: none"> Stainless steel open-tubular columns Transistors replace vacuum tubes Stable rubidium sources for AFID Improved FPD (several designs) Pulsed ECD
1970–1980	Period of consolidation and refinement <ul style="list-style-type: none"> Microprocessor-based instruments introduced Preparation of glass open-tubular columns mastered by some research groups
1979	<i>Fundamental paper describes fused silica open-tubular columns</i> (Dandeneau and Zerenner)
1980–1990	Period of technical advancement <ul style="list-style-type: none"> Gum and immobilized phases Thick-film open-tubular columns Wide-bore open-tubular columns On-column and PTV injection (greater understanding of the injection process) Large volume injection (LC-GC) Computing integrators for data handling Autosamplers
1990–Today	Period of consolidation and refinement <ul style="list-style-type: none"> Keyboard instrumentation (PC control of operation and data handling) Electronic pneumatic control Selectable elemental detection (AED) Sensitive and versatile spectroscopic detectors (MS, FTIR)

structural rearrangements or even complete adsorption on untreated diatomaceous earth. Acid and/or base washing to remove metallic impurities and silanization of surface silanol groups are widely used to minimize these effects. Fluorocarbon powders have been used occasionally in the separation of reactive compounds such as hydrogen chloride and organo-metallic compounds. Glass beads have also been used in theoretical studies, but have no practical application.

With packed columns the only way to make a radical alteration in the selectivity is by changing the liquid phase. This gave rise to a large number of stationary liquids, many with similar separation properties. Rohrschneider developed an empirical classification method based on the comparison of Retention Index (see below) differences for a number of standard compounds on the liquid phase to be characterized, relative to squalane as a reference phase. The scheme was extended by McReynolds and although it had no fundamental basis it did allow a list of preferred liquid phases to be drawn up. By employing the Rohrschneider-McReynolds classification the number of liquid phases can be drastically reduced and seven phases can be recognized as preferred choices for packed column gas-liquid chromatography (Table 2). If sample volatility is also considered then a poly(dimethylsiloxane) such as OV-1 would have to be substituted for squalane.

Another factor in the move towards rationalization of the choice of stationary phase was the introduction by Kováts in 1958 of the Retention Index system for expressing retention times (or volumes) relative to a series of standards. This was not a new idea, but Kováts proposed that the normal paraffins be taken as the standards for the scale of reference. The Retention Index system took rather a long time to be accepted since it was originally published in an over-complicated form in German and it was not until it was publicized by Ettre in *Analytical Chemistry* some years later that the system received wider acceptance.

Much work has been carried out on the relationship between structure and Retention Index and the concept has proved so useful that it has been transferred in a modified form to liquid chromatography.

Current uses of packed columns include large scale separations, physicochemical measurement of compounds used as stationary phases (inverse gas chromatography), separations employing stationary phases not easily immobilized on fused silica surfaces (see below) and the routine analysis of simple mixtures in a dirty matrix not tolerated by open-tubular columns.

Open-Tubular Columns

In 1958 Golay, wishing to simplify the mathematics of the flow of gas in a packed column with many tortuous paths, used a model consisting of a tube of capillary dimensions. He was able to demonstrate theoretically that such a capillary coated with a thin film of liquid would give columns with very high numbers of theoretical plates. The fundamental difference between packed and open-tubular columns is the much lower resistance to gas flow of the latter, which means that in practice very much longer columns can be used and very high efficiencies obtained. The reason for the need for a column of capillary dimensions can be understood from the equation derived by Golay stated in its modern form:

$$H = \frac{f_1[2D_{m,o}]}{u_o} + \frac{f_1[1 + 6k + 11k^2]d_c^2 u_o}{96(1 + k)^2 D_{m,o}} + \frac{f_2[2k]d_f^2 u_o}{3(1 + k)^2 D_s}$$

Here H is the height equivalent to a theoretical plate, f_1 and f_2 are pressure correction factors, k is the retention factor (frequently called the capacity factor), $D_{m,o}$ is the solute diffusion coefficient in the mobile phase at the column outlet pressure, D_s is the solute diffusion coefficient in the stationary phase, u_o is the velocity of the mobile phase at the column

Table 2 Selection of preferred stationary phases for method development at intermediate column temperatures

Representative phase	Solvent characteristics
Squalane	Low cohesion and minimal capacity for polar interactions
OV-17	Low cohesion with a weak capacity for dipole-type interactions and weak hydrogen-bond basicity
QF-1	Low cohesion and intermediate capacity for dipole-type interactions combined with low hydrogen-bond basicity
U50HB	Low cohesion and weak dipole-type interactions with interactions with intermediate hydrogen-bond basicity
CW 20M	Low cohesion and intermediate capacity for dipole-type interactions and intermediate hydrogen-bond basicity
QTS	Intermediate cohesion with a large capacity for dipole-type interactions and strong hydrogen-bond basicity
OV-275	Very cohesive solvent with a large capacity for dipole-type interactions and intermediate hydrogen-bond basicity

outlet, d_c is the column internal diameter and d_f is the thickness of the film of stationary phase.

The three additive components of the plate height represent the contributions of longitudinal diffusion, resistance to mass transfer in the mobile phase and resistance to mass transfer in the stationary phase, respectively. Open-tubular columns minimize the contribution from resistance to mass transfer in the mobile phase. The stationary phase mass transfer term becomes increasingly important as the liquid film thickness increases beyond about 1 μm .

Soon after his theoretical investigation, Golay was able to demonstrate successfully the practical application of the theory. An important factor in the development of open-tubular (capillary) columns was the discovery of the flame ionization detector capable of giving adequate signals for the small sample sizes required by these columns. These early advances gave some spectacular separations, especially for complex hydrocarbon mixtures, but the general use of open-tubular columns evolved only slowly because many difficult problems remained that required a further 20 years of development. Stainless steel capillaries gave satisfactory performance for hydrocarbon mixtures but for more polar compounds they gave tailing peaks and poor efficiencies, owing to adsorption. Desty and co-workers described a glass-drawing machine capable of producing long lengths of coiled glass capillary tubing as early as 1960 but it was soon found that it was difficult to obtain uniform and stable thin films on glass columns. The surface was too smooth to allow good adhesion by physical adsorption of many of the phases commonly employed at the time, and the many metals included in glass, although at relatively low concentrations, gave rise to adsorption of polar analytes. Considerable effort was expended to overcome these problems, particularly notable being the work of G. and K. Grob. Leaching with aqueous hydrochloric acid to remove some of the surface metal ions followed by treatment with silanes was one approach. Deposition of a layer of barium carbonate to retain the stationary liquid was another practical solution. Such treatments, although successful in skilled hands, were regarded by many as a black art and the resulting columns were fragile and easily destroyed. Figure 1 shows the separation of peppermint oil on three generations of Carbowax 20M columns up to 1980.

In addition to the work on true open-tubular columns, intermediate variants between these and packed columns were developed. These include micro-packed columns and support-coated open-tubular (SCOT) columns where a thin coating of a very fine diatomaceous support was deposited on the inner wall of a stainless steel capillary. Another

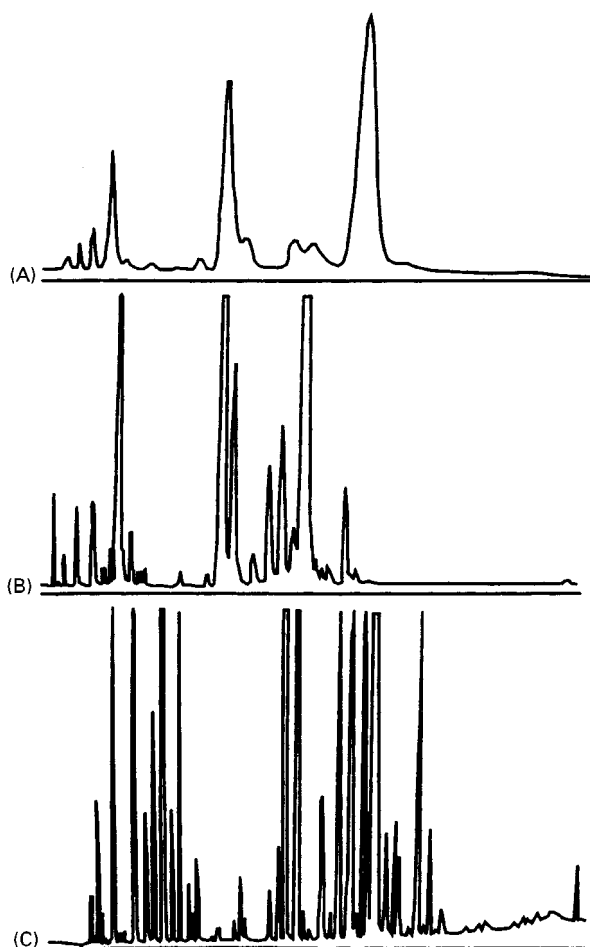


Figure 1 Three generations in gas chromatography. Peppermint oil separated on (A) 6 ft \times $\frac{1}{4}$ in. i.d. packed column, (B) 500 ft \times 0.03 in. i.d. stainless steel open-tubular column, and (C) 50 m \times 0.25 mm i.d. glass open-tubular column. All columns contained Carbowax 20 M stationary phase and were operated under optimized conditions. (Reproduced with permission from Jennings W (1979) The use of glass capillary columns for food and essential oil analysis. *Journal of Chromatographic Science* 17: 636–639, Copyright Preston Publication, Inc.)

variant was the porous-layer open-tubular (PLOT) column with a thin coating of an adsorbent on the inner wall of the capillary. PLOT columns still find application for the analysis of low boiling mixtures such as light hydrocarbon gases, but the other types are now no longer used.

The introduction of open-tubular columns made from fused silica in 1979 made glass capillaries obsolete almost overnight and also caused packed columns to be displaced as the dominant type. Currently the dimensions of commercially available open tubular columns range from 100 μm to 530 μm in inner diameter and from 5 m to 100 m in length.

Today nearly all open-tubular columns are prepared from either fused silica or metal capillaries

lined with fused silica. Fused silica is essentially pure silicon dioxide containing less than 1 ppm of metallic impurities. When drawn, these capillaries are very fragile and must be protected from moisture and surface imperfections by the application of an outer coating of a polymer or aluminium layer immediately on production. After such treatment the tubing is rugged and sufficiently flexible to be coiled into a circle of 10 cm diameter or less. Typical performance characteristics of modern wall-coated open-tubular (WCOT) columns are summarized in Table 3 and compared those of classical packed columns.

To achieve a high separation efficiency in any type of open-tubular column it is essential that the stationary phase be deposited as a smooth, thin and homogeneous film that maintains its integrity without forming droplets when the column temperature is varied. Phases showing little variation in viscosity with temperature are preferred for this purpose. Many of the stationary phases developed for packed columns are of limited use for WCOT columns and have been replaced by specially synthesized poly(siloxane)s or poly(ethylene glycol)s.

A great advance in column technology that took place about the same time as the introduction of fused silica columns was the immobilization of phases by reaction with the column wall and crosslinking to form a three-dimensional polymer to further stabilize the poly(siloxane) films without destroying their favourable solute diffusion properties. Thermal condensation of nonpolar and medium polar poly(siloxanes) at high temperature with silanol groups on the fused silica surface results in chemical

bonding of the phase to the surface to give columns suitable for use up to 400–425°C. High polarity phases are more difficult to bond; they require careful surface preparation to avoid film disruption during the bonding process and generally yield columns of lower thermal stability. The general approach for immobilization of stationary phases is by free-radical cross-linking of the polymer chains initiated with peroxides, azo compounds, or γ -radiation. With increasing substitution of methyl by bulky or polar functional groups the difficulty of obtaining complete immobilization increases, and moderately polar poly(siloxane) phases are prepared with various amounts of vinyl, tolyl, or octyl groups that increase the success of the cross-linking reaction. Cross-linking is also important in enabling columns to be prepared with thicker films ($> 0.5 \mu\text{m}$) than was possible with physically adsorbed stationary phases. Immobilization of polar phases remains a problem and so far cross-linking reactions are limited, in the main, to poly(siloxane)s and poly(ethyleneglycol)s, which limits the range of selective phases available for open tubular columns. The development of bonding and immobilization techniques facilitated large volume injection and online interfacing with liquid chromatography and supercritical fluid chromatography (or extraction), which require columns with a stationary phase resistant to solvent stripping.

Instrumentation

The essential elements of instrumentation were developed by the early 1960s, but the advent of the

Table 3 Chromatographic properties of commercially available columns

Column type	Length (m)	Internal diameter (mm)	Film thickness (μm)	Phase ratio ^a	H (mm)	N (column)	N/length
Classical	2	2.16	10% (w/w)	12	0.55	3640	1820
Packed	2	2.16	5% (w/w)	26	0.50	4000	2000
WCOT ^b	30	0.10	0.10	249	0.06	480 000	16 000
	30	0.10	0.25	99	0.08	368 550	12 285
	30	0.25	0.25	249	0.16	192 000	6400
	30	0.32	0.32	249	0.20	150 000	5000
	30	0.32	0.50	159	0.23	131 330	4380
	30	0.32	1.00	79	0.29	102 080	3400
	30	0.32	5.00	15	0.44	68 970	2300
	30	0.53	1.00	132	0.43	70 420	2340
	30	0.53	5.00	26	0.68	43 940	1470

^aPhase ratio = volume of gas phase/volume of liquid phase in the column (columns with a low phase ratio are more retentive).

^bSelecting a WCOT column: narrow-bore thin-film columns are used for high speed gas chromatography; columns with 0.25 and 0.32 mm internal diameters are used for general high performance applications; wide-bore columns with thicker films are used as replacements for packed columns; thin-film columns are employed for the separation of compounds of low volatility; and thick-film columns are used for separating volatile compounds and to obtain maximum sample loadability.

microprocessor has effected a radical change in design and use. Most gas chromatographs now have self-diagnostic software so that faults may be revealed and located. There has also been a revolution in the handling of the data produced (see below).

Column Heating

The column heater is generally a forced-circulation air oven, the temperature of which can be changed in a controlled manner with time for temperature programmed separations. Good temperature control is essential to obtain reproducible retention times. A low thermal mass for the oven is also important since it allows rapid cooling after temperature programming. Air circulation ovens give a very satisfactory performance but they do have some limitations. Liquid thermostat baths were frequently employed in early gas chromatography and are still necessary if extremely accurate temperature control is required, as in theoretical studies.

Sample Introduction

The most common method of sample introduction is by means of a microsyringe through a septum-sealed inlet. Microsyringes are useful for introducing liquid or gas samples, a technique developed by N.H. Ray in 1954. For quantitative work, gases are normally introduced by loop sampling valves, which are highly reproducible and readily automated. Solid samples may be introduced after dissolution in a suitable solvent. Direct introduction of solids is seldom used with open-tubular columns.

The limited sample capacity and low carrier gas flow rates associated with open-tubular columns makes sample introduction much more difficult than for packed columns. A thermostatted flash vaporization chamber in which the evaporated sample is mixed with carrier gas and divided between a stream entering the column (carrier gas flow) and a stream vented to waste (split flow) was the first practical solution to this problem. Split injection discriminates against high boiling compounds (bp > 250°C) owing to selective vaporization. Quantitative analysis of wide boiling range mixtures is difficult, and for the analysis of samples present in a dilute solution detectability is limited by the small amount of sample transferred to the column.

The so-called splitless injection technique was devised to overcome some of the deficiencies of split injection for the analysis of mixtures of compounds in a solvent (such as frequently occurs in environmental studies) through the transfer of relatively large volumes to the column. The gas flow through a splitless injector is relatively low, and the sample is introduced into the column over a comparatively long time

(30–60 s), relying on cold trapping and/or solvent effects to refocus the compounds at the head of the column. The importance of these refocusing mechanisms was not fully understood at first but splitless injection did demonstrate the possibility of performing trace analyses with open-tubular columns. It is also easy in practice to convert an injector from split to splitless operation by the operation of valves and minor hardware modifications.

The programmed-temperature vaporization (PTV) injector overcame many of the problems observed with the hot split and splitless injector. The PTV injector is designed to allow rapid heating and cooling and the sample is introduced at a low temperature. A rapid rise in temperature after introduction ensures rapid volatilization of the highest boiling sample components. The PTV injector may be used in both split and splitless modes and the accuracy and precision approach those obtained by cold on-column injection.

The production of wide-bore silica columns in the early 1980s allowed introduction of the syringe needle directly into the column and the use of immobilized phases eliminated the problem of removal of the stationary phase by large volumes of liquid sample. In cold on-column injection the sample is introduced as a liquid into the column inlet where it is subsequently vaporized. Discrimination based on volatility differences has been virtually eliminated and the risk of sample decomposition minimized. With secondary cooling of the injector, the oven temperature can be kept well above the boiling point of the solvent while maintaining the column inlet at a much lower temperature. This is important for using on-column injection in high temperature gas chromatography. Dirty samples present a problem owing to contamination of the sample introduction zone, which leads to poor chromatography and unreliable quantitation.

Detectors

The thermal conductivity detector (TCD) was used extensively in early work and is still used in a much improved form which makes it compatible with wide-bore open-tubular columns. The relatively poor sensitivity of the early TCD meant that it was largely displaced by the flame ionization detector (FID). The combustion of carbon-containing compounds in a small hydrogen/air diffusion flame produces ions that can be detected by applying a voltage between the flame jet and a collector electrode situated around the flame. The detector has a low dead volume, a high sensitivity for nearly all carbon-containing compounds and an extremely wide linear range of response. As already pointed out, the discovery of the FID played a crucial role in the development of open

tubular columns. The FID is rugged, reliable and relatively insensitive to operating variable so that it is now by far the most widely used of all detectors.

The TCD and the FID are universal detectors; that is, they give a response for all substances. This is not strictly true for the FID since it gives no response for the permanent gases and water (which makes it very suitable for the analysis of aqueous samples). Another universal detector, now becoming much more widely employed, is the mass spectrometer. Coupling to a mass spectrometer (GC-MS) dates almost from the beginning of gas chromatography, but in the early days the practical problems and high cost meant that the combination was confined to a few research laboratories. The advent of the silica open-tubular column, improved designs of mass spectrometers, the availability of computers to handle the large amount of data produced and a considerable reduction in cost have resulted in the GC-MS combination becoming very widely used. The great advantage of the mass spectrometer as a detector is its ability to identify the compounds being separated. It is not quite ideal in this respect since isomers sometimes give almost identical spectra, but techniques such as tandem mass spectrometry (MS-MS) and different methods of ionization can overcome some of these problems. Another advantage is that the mass spectrometer can also be used in a selective mode, often with greatly increased sensitivity.

Fourier transform infrared spectroscopy detectors for gas chromatography are also available; their range of application is not as wide as the GC-MS combination but to some extent they are complementary.

In addition to the universal detectors, a number of selective detectors are commercially available. The nitrogen and phosphorus detector (NPD) is similar in design to a conventional FID but has an electrically heated rubidium-glass bead situated between the flame jet and the collector electrode and (for nitrogen compounds) uses a very small hydrogen flow so that there is a heated plasma in the working zone rather than a flame. This detector is widely used for the analysis of drugs and pesticides in environmental and biological research. Other variants of the FID such as the hydrogen atmosphere FID, which gives a response to some gases, and the O-FID for the selective detection of oxygen-containing compounds, also exist.

The electron-capture detector has an outstandingly high response for polyhalogenated compounds and so has found extensive application in pesticide and environmental analysis. Indeed, the start of the concern for the distribution of compounds such as DDT in the environment can be attributed to the development of this detector in the early 1960s.

Other selective detectors include the microwave plasma emission detector, which can detect a number

of elements simultaneously. The photoionization detector gives a high response for environmentally important compounds such as benzene and vinyl chloride and finds use as a portable field instrument. The flame photometric detector and the chemiluminescence detector have a high response to sulfur and are used extensively in the petroleum industry. Chemiluminescence detection has also been used for the selective determination of nitrosamines in foodstuffs. The Hall detector catalytically decomposes the compounds emerging from the gas chromatography column into simple inorganic gases such as hydrogen chloride (for chlorine) and ammonia (for nitrogen), which are absorbed in a circulating stream of aqueous organic solvent followed by monitoring the electrical conductivity of the solution obtained.

Although selective detectors find extensive application for particular problems they are all more demanding in the control of operating parameters than the FID.

Data Handling

Data handling was originally by purely manual measurement of peak heights. It was recognized that peak area measurement was fundamentally better but areas could be obtained and approximately by measuring the peak height and the width at half height. Such an approach was satisfactory for simple mixtures but was totally impractical for mixtures containing perhaps 100 components in widely differing concentrations. Early integrators consisted of mechanical or electromechanical devices such as the ball and disk integrator and integrating amplifiers, but were very limited in range and speed of response. The mid-1960s saw the introduction of the first generation of electronic integrators and a little later the use of mainframe computers to handle data from a number of instruments simultaneously. The large amounts of data produced by open-tubular columns (especially when coupled to a mass spectrometer) can now be handled by a personal computer. The data can be acquired, manipulated and displayed in real time and can be stored electronically almost indefinitely for record purposes.

Future Developments

Looking to the future, it is reasonable to expect continued evolutionary development. In this context it is interesting to note that several new selective detectors have become available in the last few years. The use of GC-MS will become more widespread as the real cost of such instruments continues to fall and the performance of the mass spectrometry detector shows continuous improvement in sensitivity and resolving power.

The gas chromatograph will develop into a module for more complex analysers for automated sample processing and plant control. The separation time will continue to decrease; in the past there has been limited interest in fast separations but this could change as automated sample processing is developed. Increasing use of coupled techniques such as GC-GC, liquid chromatography-GC, and supercritical fluid chromatography-GC for the separation of complex mixtures will give resolution unachievable by single column operation.

Columns with immobilized phases of a wider range of selectivity than currently exist will be developed. New sorbent (PLOT) columns and hybrid columns with low loadings of liquid phases, special application phases for separating enantiomers and isomers, and columns better able to withstand aqueous samples can be expected.

Further Reading

Adlard ER (ed.) (1995) *Chromatography in the Petroleum Industry*. Amsterdam: Elsevier.

- Dyson N (1994) *Chromatographic Integration Methods*, 2nd edn. London: Royal Society of Chemistry.
- Ettre LS and Zlatkis A (eds) (1979) *75 Years of Chromatography – A Historical Dialogue*. Amsterdam: Elsevier.
- Grob K (1986) *Classical Split and Splitless Injection in Capillary Gas Chromatography*. Heidelberg: Hüthig.
- Grob K (1987) *On-Column Injection in Capillary Gas Chromatography*. Heidelberg: Hüthig.
- Guiochon G and Guilleman CL (1988) *Quantitative Gas Chromatography for Laboratory Analysis and On-line Process Control*. Amsterdam: Elsevier.
- Hill HH and McMinn DG (1992) *Detectors for Capillary Chromatography*. New York: Wiley.
- James AT and Martin AJP (1952) Gas-liquid partition chromatography: the separation of volatile fatty acids from formic acid to dodecanoic acid. *Biochemical Journal* 50: 679–690.
- Martin AJP and Synge RLM (1941) A new form of chromatogram employing two liquid phases. *Biochemical Journal* 35: 1358–1368.
- Poole CF and Poole SK (1991) *Chromatography Today*. Amsterdam: Elsevier.
- Rotzsche H (1991) *Stationary Phases in Gas Chromatography*. Amsterdam: Elsevier.

Ion Mobility Mass Spectrometry

D. Young and C. L. P. Thomas, UMIST,
Manchester, UK

Copyright © 2000 Academic Press

Introduction

J. J. Thompson made the first ion mobility measurements about a century ago. Modern ion mobility spectrometry (IMS), however, was first described in the early 1970s. The development of the electron-capture detector (ECD) had generated much interest with its impressive limits of detection, and this provoked thoughts of an ionization detector with an additional level of specificity that could operate as a stand-alone instrument. IMS was introduced initially as 'plasma chromatography', and sometimes as 'gaseous electrophoresis'. Such terms invited unrealistic comparisons between established separation techniques and IMS, with its modest resolving power. Superficial similarities to time-of-flight-mass spectrometry meant that IMS was also initially considered as an atmospheric pressure mass spectrometer, but poor mass-mobility correlations disproved this view too. Such unrealistic expectations arose from a lack of understanding of the principles of operation. Furthermore such misunderstandings confronted with com-

plex responses and memory effects observed in many investigations at that time resulted in disillusionment with the technique by many. IMS was generally dismissed as something of a curiosity.

By the late 1970s advances in sample handling (especially for trace levels) and better electronics led to renewed interest in IMS. Drift tubes were redesigned with heated components, which reduced memory effects, and sample introduction systems were re-evaluated, helping to avoid instrument overloads and allow quantitative work. Perhaps most importantly, IMS was evaluated on its own capabilities, rather than simply being compared with existing techniques.

The result was the appearance of the military chemical agent monitor (CAM) – a sensitive, highly selective, inexpensive, and fully portable instrument. The CAM also demonstrated that it was possible to produce IMS systems that could enable untrained personnel to make difficult chemical measurements in a hostile environment. The extent of the use of IMS in chemical agent monitoring is large. At the moment IMS instruments are issued at the platoon level across all the armies of the western alliance, thus making IMS arguably the most common trace VOC detection system in current use. Plans are underway to issue CAM devices to all military personnel.

The success of CAM encouraged further developments both at research and commercial levels, which are continuing with new applications and modifications constantly being suggested and investigated. Since the early 1980s the name 'ion mobility spectrometry' has been almost universally adopted, suggesting the analogy with mass spectrometry but emphasizing its unique operational basis.

IMS Theory and Instrumentation

Overview of Components and Signals

Figure 1 shows a generalized representation of an IMS system. Gas is brought into the reaction region, where ions are formed from the constituents of the gas. Ions of a selected polarity are moved down an electrical potential gradient and periodically

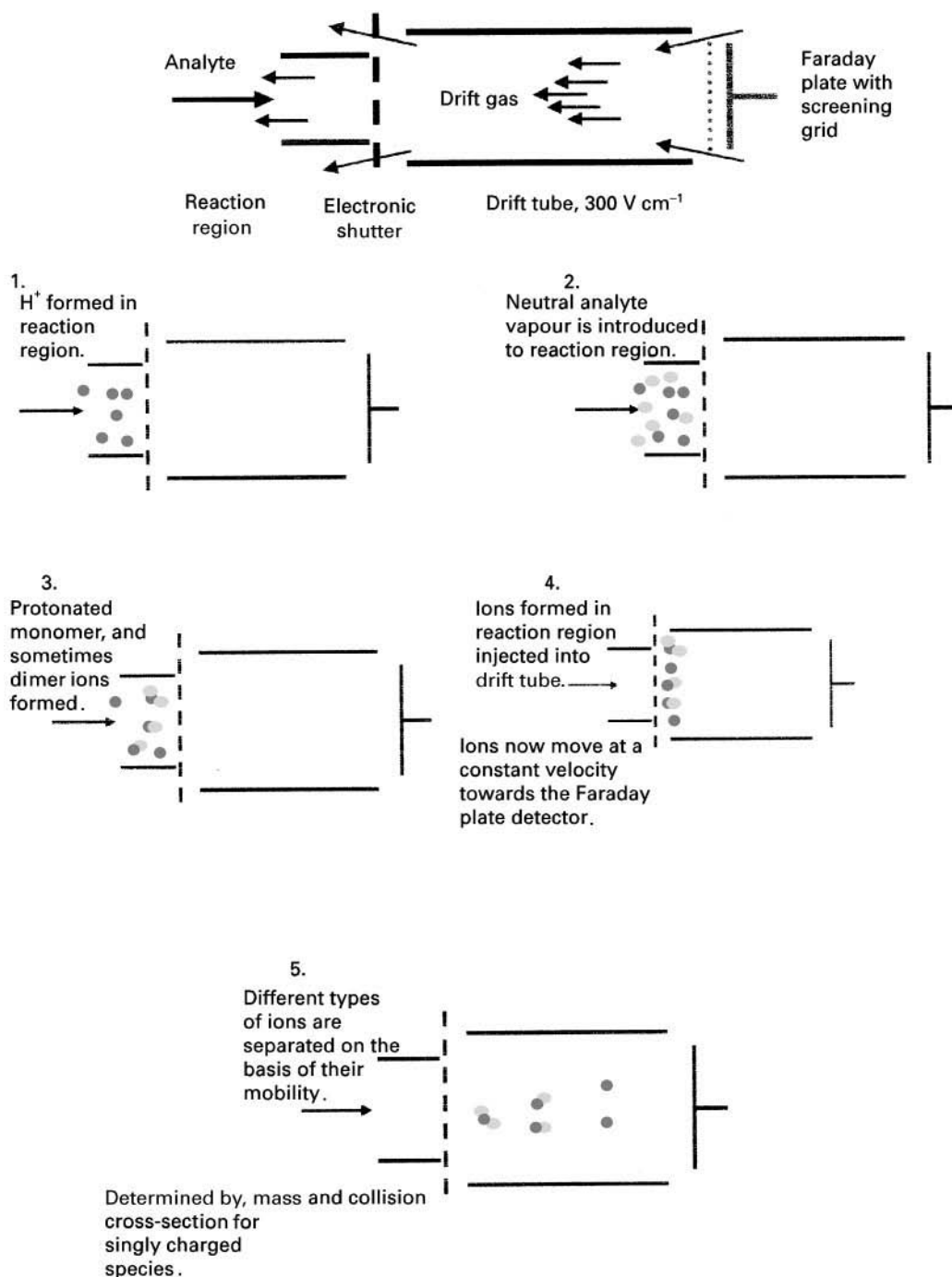


Figure 1 A schematic diagram showing the components and operation of IMS.

introduced into the drift region, where they are accelerated by an electric field and slowed by collisions with a countercurrent drift gas flow. Thus the ions attain an average velocity that is dependent, among other things, on the collision cross-section of the ions in the drift gas, the charge on the ion and its mass (see eqns [15]–[19] below). Consequently, different ions achieve different limiting velocities and thus can be separated. Detection is usually by a Faraday plate, leading to current spikes proportional to the number of ions arriving at different times. The resulting trace is referred to as an ion mobility spectrum.

A single mobility spectrum can be generated in the range of 3 to 25 ms, but the signal-to-noise ratio of the spectrum will be low, and small constituents of the spectrum will often be obscured. Thus, for most applications signal averaging is performed, and typically 1–5 s are required to yield an acceptable spectrum. Mobility spectra (Figure 2) are characterized by the position and area of the peaks produced by the arriving ion packets at the detector. Overall the response can be evaluated in terms of:

- the magnitude of the signal produced by the reactant ions (this is a measure of the amount of charge in the reaction region of the instrument, and the presence of all analytes in the system); and
- the responses associated with a known analyte (by integrating within a given drift time window).

Thus the amount of signal averaging required, and hence the speed of analysis, depends upon which part of the spectrum is relevant to the analysis and the concentrations of analyte in the sample.

Sample Introduction

As IMS is a vapour-phase analysis technique, it is most commonly used with gaseous or volatile

analytes, and analytes are introduced into the reaction region in a carrier gas. This is generally the same gas that is used for the drift flow, and consequently the sample inlet and drift gas flow rates are balanced so that analyte cannot be blown into the drift region.

The direct introduction of ambient air is not normally an effective sample introduction technique as the result is high levels of water and traces of ammonia in the reaction region. The high levels of water in ambient air can lead to formation of cluster ions and thus a loss of resolution in the mobility spectra, while ammonia can dominate the spectrum and prevent analyte response owing to its high proton affinity. Consequently a heated dimethylsilicone membrane is frequently used in the inlet. This excludes excessive amounts of water and ammonia from the reaction region but allows analytes to be sampled. This method works effectively with the military IMS units used for CAM. However, the use of a membrane in the inlet increases the response times of the instrument and reduces the sensitivity.

Not surprisingly, IMS has frequently been used with gas chromatography (GC). In fact the first reports of IMS described GC-IMS systems, and some workers still maintain that IMS cannot be effectively used without chromatography for the sample input. GC has been recognized as intrinsically compatible with IMS, as the carrier gas will not generate a response, samples are typically small enough to avoid saturation of the instrument, and pre-separation of analytes simplifies ionization procedures and responses. Interfacing the techniques is also relatively straightforward, although memory effects were initially found to be a problem. This was overcome by introducing the column effluent either laterally or axially after the ionization source (Figure 3), and allowing it to be carried back through the ionization region by the drift flow. These unidirectional flow configurations reduce IMS cell clearance times and significantly enhance the response of the instrument.

IMS has also been used for liquid samples. Membranes between the liquid sample and a flowing gas stream have enabled IMS to be used to detect chlorinated hydrocarbons and ammonia in water, for example. However, a recent and important development is the coupling of electrospray to IMS. This has been successfully used with IMS to analyse a wide variety of nonvolatile analytes and liquid samples. The electrospray needle is connected into the ionization region instead of the ^{63}Ni source, and the voltages are applied by a power supply independent of the drift voltage supply. Optimization is required in terms of cell and needle temperatures to improve resolution and avoid vaporization of samples before ionization. The electrospray needle is also insulated

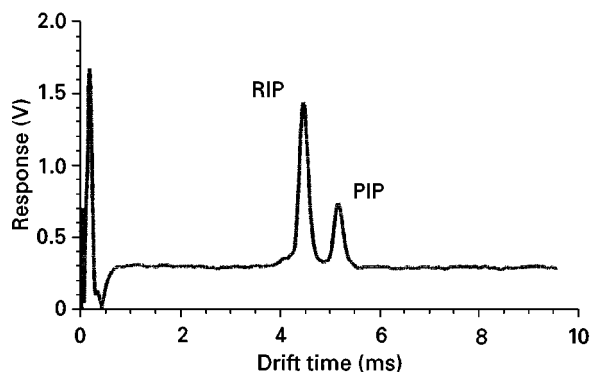


Figure 2 A typical mobility spectrum, showing the reactant ion peak (RIP) from clean air and a product ion peak (PIP) from 2,4-lutidine.

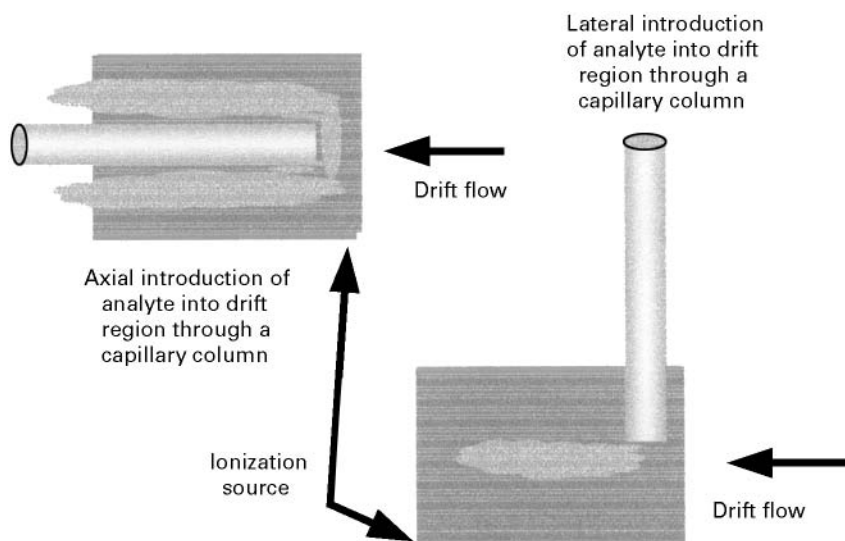


Figure 3 Methods for interfacing IMS to gas chromatography. Both these arrangements ensure that clear down times in the reaction region are rapid, while at the same time enabling the efficient production of product ions.

to avoid corona discharges. This coupling has been found to provide stable molecular ions and reproducible well-resolved ion mobility spectra.

Several major applications of IMS involve the detection of nonvolatile analytes at trace levels for example narcotics and explosives. In these applications the analysis of the analytes' headspace would not give a satisfactory response. However, thermal desorption of microparticulates of the analytes into a carrier gas stream and analysis with a heated IMS cell provides a highly sensitive and effective alternative that is the basis of several instrument systems used all over the world in support of police, customs, forensic and airline security applications.

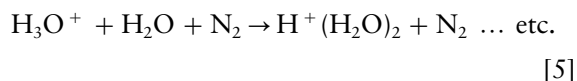
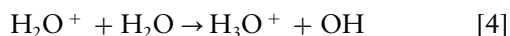
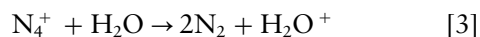
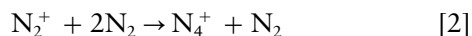
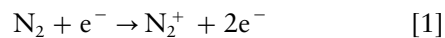
Ionization

Currently, the standard ionization source in IMS instrumentation is ^{63}Ni , favoured because it is stable and places no power demands on a portable instrument. A foil is typically used, often electroplated onto gold or platinum. Ionization principles based on this source are well understood, but there are powerful operational incentives to remove radioactive sources from what are primarily designed as portable instruments. Alternative methods include:

- electrospray ionization;
- photoionization using a UV lamp, which produces no reactant ions and limits the analytes which can be studied;
- laser ionization; and
- corona, with latterly, pulsed corona discharge sources that may be configured to behave in a similar manner to ^{63}Ni .

Currently the development of the pulsed corona discharge source appears to be the most promising alternative to radioactivity for general applications as it consumes little power, lasts a long time, operates in both positive and negative mode, and is already being incorporated into the next generation of miniaturized IMS instruments.

Ionization of the gases in the reaction region is perhaps usefully described in terms of ^{63}Ni , as this is the most widely studied and best-understood ionization source. The first step is direct ionization of the carrier gas by the β -particles emitted by the source, which triggers off a multistage reaction leading to the formation of stable reactant ion species. The following example is for the positive-mode ions in air, or nitrogen with low moisture content:



The dominant positive-mode reactant ions in clean air will thus be $(\text{H}_2\text{O})_n\text{H}^+$, where n will be dependent on the moisture content of the gas as well its pressure and temperature. Minor contributions are also generally seen from $(\text{H}_2\text{O})_n\text{NH}_4^+$ and $(\text{H}_2\text{O})_n\text{NO}^+$.

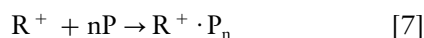
An analogous reaction scheme occurs for the negative ions, resulting in $(\text{H}_2\text{O})_n\text{O}_2^-$ and some $(\text{H}_2\text{O})_n\text{CO}_4^-$.

When analyte vapours are present in the source region, they may undergo collisional charge transfer reactions with the reactant ions to form product ions in atmospheric pressure chemical ionization (APCI) processes. In almost every case molecular ions are formed in IMS, as APCI causes little fragmentation. Some analyte fragmentation has been observed in IMS, although this has been attributed to thermal decomposition. Typical reaction pathways may be summarized as:

Proton transfer



Cluster formation



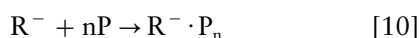
Electron capture



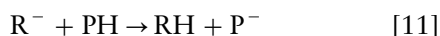
Dissociative electron capture



Cluster formation



Proton abstraction

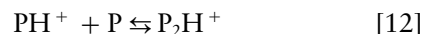


where R is the reactant ion species, P is the product ion species and M is a neutral fragment.

When any of these reactions occur, the mobility spectrum changes, the size of the reactant ion peak (RIP) reduces as the charge reservoir is depleted, and a new peak, the product ion peak (PIP), appears corresponding to the analyte ion (see Figure 2). These peaks will rise and fall in a synergistic relationship, and as charge is conserved in IMS, the summed peak areas of the mobility spectrum should remain constant throughout these changes.

As analyte concentration increases some polar compounds (e.g. esters and alcohols) form a second PIP, observed at longer drift time, which is due to an ion containing two analyte molecules. This is essentially a clustering reaction forming a proton bound dimer:

Dimer formation



A detailed discussion of the formation of proton bound dimers is beyond the scope of this article. Their appearance in a mobility spectrum is a function of the thermodynamics and kinetics associated with their formation along with their stability in the drift tube. The development of proton-bound dimers is usually associated with highly nonlinear responses associated with the monomer form of the PIP (Figure 4).

The formation of product ions occurs rapidly with one or two simple reactions, while the formation of reactant ions is a comparatively slow multi-step process. Once the analyte concentration rises above a critical level the rate of removal of the reactant ions will be faster than their production. This leads to rapid depletion of the charge reservoir in the reactant region, and no further increase in instrument response will be seen. This is referred to as saturation of the instrument, and sets a limit on the response behaviour.

Typical IMS response behaviour with analyte level is shown in Figure 4. The relationship between the instrument response and analyte level for a single-step reaction leading to a product ion may be simply expressed in terms of:

$$\text{RIP}_x = \text{RIP}_0 \times (e^{-\beta x}) \quad [13]$$

$$\text{PIP}_x = \text{RIP}_0 \times (1 - e^{-\beta x}) \quad [14]$$

where RIP_0 is the size of the charge reservoir (RIP peak area in the absence of analyte), RIP_x is the RIP area at analyte concentration x , PIP_x is the PIP area at analyte concentration x , β is the 'reactivity coefficient', a function of reaction time and rate constant and x is the analyte concentration.

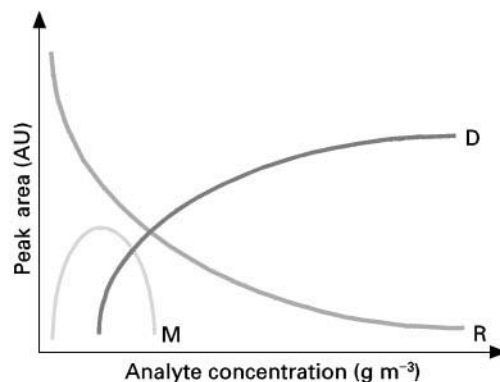


Figure 4 Schematic representation of the relationship between analyte concentration and three IMS peaks: R, reactant ions; M, monomer product ion; and D, dimer product ion.

Attempts to fit linear functions to IMS response trends have shown that linearity can only be approximated (with less than 5% errors) over the first 30–40% of the response range. Quantitative work in the literature suggests that the linear dynamic range of IMS is typically between 1 and 2 orders of magnitude of concentration. Beyond this range quantitation is undertaken on the basis of logarithmic relationships. Eventually, once the reactant ions are depleted, the instrument saturates to a population of product ions.

Working at or near saturation should be avoided. Peaks are frequently seen to broaden and/or their mobility vary as excess neutral analyte molecules cluster around the ions (forming new peaks), or further reactions occur in the drift region (broadening and smearing peaks). An excess of neutral analyte within the instrument also often leads to adsorption onto internal surfaces, such that spurious analyte peaks may be seen for a long time after the original analysis.

Proton or electron transfer can only take place if the proton, or electron, affinity of the neutral molecule is greater than that of the reactant ion. In the default case for positive mode air, the proton is held by water, which has a relatively low proton affinity. This suggests a method by which selectivity can be introduced into the ionization process. If a constant supply of suitably high concentration vapour is provided to the reaction region, then all the protons will be captured to form a new population of reactant ions. This is known as ‘doping’ the instrument. A dopant can be chosen to have a proton affinity just below that of the target analyte, so that the required response will still be generated but interferences from all compounds with proton affinity lower than the dopant will be prevented. This method has been successfully applied in many laboratory and field applications and has been found to reduce interferences and simplify responses to mixtures, and in some cases to enhance separation and sensitivity. For example acetone is used to dope CAM units, while nicotinamide is the dopant used for narcotics detection and chlorinated volatile organic compounds are used for explosives doping. However, not all compounds are suitable as dopants, for example pyridine-doped systems respond to all compounds (despite pyridine’s high proton affinity) and give distorted peaks. This is because clustering reactions rather than charge exchange reactions are occurring.

The concentration of dopant has also been found to be important, as too little does not impart full selectivity (i.e. some ‘old’ RIP still remains to react), while too much causes cluster formation due to excess neutrals. When doping conditions are optimized then

often no changes in PIP position or quantitative behaviour are observed between systems with different dopants.

IMS responses to mixtures can become complicated as components in a mixture compete for charge. The distribution of charge between them tends to be on the basis of concentration and ‘reactivity’ (e.g. proton or electron affinity). Thus peak areas for analytes in a mixture will not necessarily quantitatively reflect the proportions of each species present in the reaction region. A further problem with mixtures is that ‘mixed dimer’ ions can be formed, where molecules of two different analytes cluster together around a charge centre. This leads to the appearance of new peaks and more complicated spectra. In these terms the competitive ionization processes can be considered as a source of interferences, in much the same way as overlapping peaks in column chromatography.

In summary, the ionization processes are the cause of some of the major problems of IMS, for example the complicated and congested spectra obtained from mixtures and the limited linear range for many applications. However, they also provide some of the most useful features of the technique such as the spectacular detection limits due to the large number of collisions that occur at atmospheric pressure. Trace levels of analyte are ionized efficiently and the technique is able to respond to a large number of analytes.

Gating the Ions into the Drift Tube

This feature provides IMS with a time-resolved response as opposed to a change in a standing current. An ion shutter is pulsed open for, typically, *c.* 0.2 ms every 5–40 ms, depending on the experimental conditions. The duration that the gate is open is important, as the longer it is open the larger the response (more ions get through) but the broader the ion peaks (greater temporal distribution of identical ions), and hence the lower the resolution will be.

A most important advance has been control of the electric field at the point between the reaction and drift regions with an ion trap. This allows the accumulation of ions between injection pulses rather than their annihilation, with significantly increased sensitivity and much greater control of the ionization processes used to produce the mobility spectra (see Figure 5).

Drift Region and Ion Mobility

The drift region is a region of uniform electric field that moves the ions towards the detector with a flow of drift gas in the opposite direction to the ion

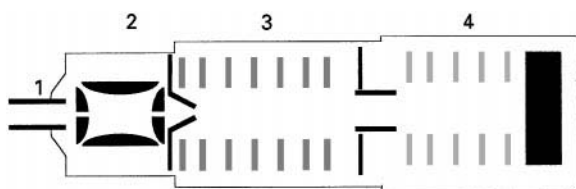


Figure 5 A schematic diagram showing the major systems for ion storage-ion mobility-time-of-flight mass spectrometry.

1. Analytes are ionized and introduced to an ion trap.
2. A tuned ion trap is used to collect ions of a specified mass-to-charge ratio (m/z).
3. The stored ions are injected into a drift tube where they are separated on the basis of their cross-sectional areas.
4. The ions are analysed and quantitated by time-of-flight mass spectrometry.

motion. The drift gas should be inert and free from contaminants, as reactions in the drift region change ion identities and move or broaden peaks. The drift gas also prevents neutrals from the reaction region entering the drift region and undergoing further reactions or clustering.

The electric field is generally provided by a series of conducting field-defining electrodes, and is typically in the range $50\text{--}250\text{ V cm}^{-1}$, which allows weak field approximations to be made with respect to mobility theory, although for many applications it has been shown that the actual value of the electric field is not as important as its homogeneity.

Analytes in IMS are characterized by the drift times of the ions that they form. The mobility of such ions is expressed as:

$$v = \frac{L}{t_d} \quad [15]$$

$$v = KE \quad [16]$$

where v is the ion velocity, L is the drift path length, t_d is the drift time, K is the mobility constant, and E is the electric field strength.

Ion mobility is also dependent on temperature and pressure, so these effects can be accounted for by normalizing to a reduced mobility, K_0 , enabling comparisons to be made between experiments:

$$K_0 = K \left(\frac{273}{T} \right) \left(\frac{P}{760} \right) \quad [17]$$

In practice differences in reduced mobility values are still observed due to variations in the internal instrument parameters used in different instruments. Thus the use of mobility standards has been proposed. Currently, 2,4-lutidine, with a K_0 of

$1.95\text{ cm}^2\text{ V}^{-1}\text{ s}^{-1}$, is widely used as it is considered to be relatively unaffected by temperature, clustering or relative humidity. However, dipropyleneglycol monomethylether ($\text{CH}_3\text{OC}_3\text{H}_6\text{OC}_3\text{H}_6\text{OH}$) has also been proposed for similar reasons. Whatever standard is used, reduced mobility values may be calculated as follows:

$$K_{0(\text{an})} = t_{d(\text{an})} \times \left(\frac{K_{0(\text{std})}}{t_{d(\text{std})}} \right) \quad [18]$$

where (std) refers to values for the standard and (an) refers to values for the analyte under investigation.

The mobility of an ion under weak field conditions is given by:

$$K = \frac{3e}{16N} \times \frac{2\pi^{1/2}}{\mu kT} \times \frac{1}{\Omega} \quad [19]$$

where e is the ion charge, N is the density of neutral molecules (drift gas), μ is the reduced mass of the ion neutral pair $mM/(m+M)$, k is the Boltzmann constant, T is the temperature of the ions and Ω is the collision cross-section.

Detection

The standard detector in IMS instruments is a simple Faraday plate. The vast majority of IMS instruments have an aperture grid placed *c.* 2 mm forward of the detector. While removal of this feature increases the total signal, it also causes broadening of the peaks, typically from *c.* 0.3 ms to *c.* 3 ms, and thus a loss of resolution. The aperture grid prevents incoming ions from inducing a current in the detector plate. Sensitivity may also be increased by increasing the electric field between the aperture grid and detector to a value significantly higher than that of the standard drift field.

The development of new methods and applications for IMS is greatly eased with the use of a mass spectrometer coupled to the drift cell. IMS-MS has been in routine use in research laboratories since the inception of the technique almost 30 years ago. The instruments are interfaced by using a pinhole aperture to the MS vacuum chamber in the Faraday plate of the ion mobility spectrometer. Such a system can be operated in several modes:

- Total ion monitoring yields the full IMS spectrum.
- Opening the shutters provides a full atmospheric pressure chemical ionization mass spectrometric characterization of the ions in the reaction region.
- Selective ion monitoring enables the contribution of specific species to the mobility spectra to be observed.

An exciting and important development has been the introduction of IMS to ion storage mass spectrometry (Figure 5). This combination of instruments has the potential to isolate selectively trace levels of volatile and nonvolatile materials from a wide range of matrices, identify and quantitate them in a time-scale of milliseconds to seconds. The separation speeds reported so far are of the order of greater than 10^6 theoretical plates per minute. Although the approach is still very much in its early stages of development, the potential for vastly increasing the speed of many analyses is considered by many in this field to be a very important factor in the future development of IMS.

Application Areas

Military and Security Applications

The use of IMS to detect chemical warfare agents has already been described. Following on from this application, government research establishments turned their attention to narcotics and explosives. Given the chemical properties of these materials it was not surprising that IMS was found to provide an effective solution to the problem of screening for such materials. Due to the low volatility and trace levels of the substances, these devices use thermal desorption sample introduction systems. The sample is obtained by wiping or vacuuming the surfaces associated with the suspected contamination (for example vehicle interiors, luggage, skin and clothing). Microscopic particles of the analytes are collected onto a filter and thermally desorbed off this medium into the instrument. The devices are installed with a library of spectra and will alarm and identify the substance if a sample produces a matching signal. This method has proven successful at detecting trace levels of a wide range of drugs and explosives materials from a variety of situations, and such devices have become commonplace in airports and at other security checkpoints.

Environmental and Process Monitoring

IMS responds to a vast range of volatile organic compounds as well as inorganic pollutants such as SO_2 , HF, NO_x and H_2S . Adaptations of military technology have been used successfully for applications designed to operate in remote and isolated environments (hydrazine monitoring during space shuttle missions, for example). However, the use of IMS as a presumptive monitoring technique for the supervision of pollution prevention measures has yet to be adopted, although research in Europe and the USA has already begun on the technology transfer from the military to the environmental arena.

IMS has also been applied to water monitoring. Solid-phase extraction, membrane thermal desorption and electrospray of environmental water samples have all been developed. No doubt solid phase micro-extraction will be reported soon as well.

Biological Analytes

The detection and enumeration of bacteria by monitoring for volatiles produced through enzyme-substrate reactions or pyrolysis has been applied to several types of bacteria of water and food hygiene interest (including *Escherichia coli* and *Listeria*). Water, urine and a range of foods have been studied in this way, with significant reduction in analysis times. Given the pedigree of IMS, it is not surprising that aerosol sampling-pyrolysis-GC-IMS systems have been developed for the detection of bacillus spores and other biological warfare agents.

Electrospray-IMS-MS techniques have also been developed for work with biopolymers. These techniques use low-pressure drift tubes (< 10 Torr N_2 , He or Ar) and a relatively weak electric field ($< 50 \text{ V cm}^{-1}$). An ion trap is most commonly used to inject and concentrate the ions. Although a recent development, this approach has already been used to great effect in the study of sequence and structure relationships. Biomolecular separations of complex mixtures, a protease digest for instance, have also been reported with some success. Variation of the potential used for ion injection has been demonstrated to fragment molecules, which enhances isomer identification and suggests a way to provide high speed sequencing information.

Chromatographic Detection

Combined with chromatography IMS provides an additional dimension to the analysis. It can often separate co-eluting components by mobility, the polarity of the drift tube or their proton or electron affinities. Selected drift time monitoring may be used in an exactly analogous way to selected ion monitoring in mass spectroscopy. Indeed, the development of GC-IMS systems by NASA to monitor continuously the air in the International Space Station has shown that GC-IMS has a near equivalent analytical capability to GC-MS – and one that can be achieved with significantly less complexity and cost. Similar developments are underway with HPLC separation, with sub-picogramme detection limits reported for many compounds. This area of activity is undergoing rapid development and it may be that IMS may come to be used as a general-purpose detection system for chromatography.

The Nature of Mobility Data

So far in this discussion the emphasis has been on assigning a feature in an ion mobility spectrum to the products of a specific ion–molecule reaction. However, there are other ways of using the information contained within a mobility spectrum.

It is possible to study gas-phase reactions and ion–molecule processes within the drift tube with a tuned mass spectrometer. Thus, equilibrium constants for clustering reactions, activation energies for ion–molecule reactants and molecular sizes have all been determined with IMS. The introduction of dopant to the drift region of the instrument enables the reaction kinetics of ion–molecule reactions to be studied and data derived so far from such studies have agreed closely with accepted literature values.

IMS data can also be used in a completely phenomenological-based manner. Complex but constant mixtures yield reproducible ion mobility spectra, although the interpretation and assignment of individual features in such spectra is not currently possible. The application of pattern recognition algorithms and standard chemometric tools enables IMS to be used to identify changes in composition or types of sample. So far identification of different types

of polymers, wood species, foodstuffs and pharmaceutical products has been demonstrated. This is an application area that undoubtedly has significant commercial potential.

The Future

Table 1 is a summary of current IMS research areas and applications. The future development of this technique can be seen to fall into three broad areas:

- *The development and improvement of IMS technology.* The problems of instrument saturation, nonlinear responses and complex ambiguous responses are difficult research challenges that will occupy many involved in IMS research and development. New ionization methods and better understanding of the fluid dynamics and kinetics of the ionization process are likely to be important development areas for some time.
- *Sampling interfaces and applications.* Improvements in sampling technology will enable IMS to be exploited in a wider range of contexts. Certainly the successful use of IMS in presumptive testing for narcotics and explosives has interesting possibilities when applied to a wide range of industrial, medical and environmental issues.

Table 1 A summary of current research and application activity in IMS

Analyte	Application area	Comment
Volatile organic compounds (VOC)	Environmental, process, clinical, and forensic analysis Workplace monitoring Chemical agent monitoring Space craft cabin atmosphere monitoring Extra-terrestrial VOC monitoring Kinetic and thermodynamic determinations of ion formations, lifetimes and stabilities	Established areas of operation for IMS. Commercial instruments available that are reliable, rugged and designed for use by the nonspecialist. Recent development offering rapid measurement techniques for characterizing gas-phase reactions. Not yet applied to larger molecules.
Surfaces, bulk materials	Contaminated soil analysis Surface characterization	Laser ablation and desorption techniques, developed recently, have significantly expanded the scope of applications that IMS may be applied to.
Pesticides	Environmental and process analysis	Electrospray ionization has expanded massively the types of analyte and analysis that may now be undertaken with IMS.
Peptides Sugars Proteins DNA and nucleotides	Life sciences Drug discovery Clinical analysis Foodstuffs characterization	Conformer and isomer separations now routinely achievable. Structure elucidation and fast separations of complex mixtures now a possibility.
Bacteria	Food safety Microbiology Biological warfare Clinical analysis	Pyrolysis techniques offer detection limits of 4 to 5 organisms dm ⁻³ , while ELISA approaches are offering fast and highly selective detection methodologies.

- **High speed separations.** The combination of mobility and mass spectrometric technologies described in Figure 5 offers analysis times in the regions of milliseconds to seconds per component. The development of this technology and its application to the life sciences is likely to be a major, perhaps the major, area of IMS development in the medium term. However, the performance of such instrument assemblies has to be offset against their significant capital costs. Miniaturization will play a vital role in this area, reducing the initial outlay required to operate such systems. The work by NASA and the production of GC-IMS databases will continue and it is likely that IMS-based detection systems will become commercially available as alternative approaches to GC-MS.

From the disappointments of the early work with IMS, recent research has yielded substantial advances in this technique. Perhaps the next few years will see the acceptance of IMS as a mainstream analytical approach. Certainly the recent developments in bio-separations have taken many by surprise, and consequently there is a general feeling that the near future will see a huge expansion in the use and application of IMS, particularly in the life sciences.

See also: **I/Mass Spectrometry. II/Chromatography: Gas:** Detectors: Mass Spectrometry; Detectors: Selective.

Mass Spectrometry: Spectrometry-Mass Spectrometry Ion Mobility.

Further Reading

- Carr TW (ed.) (1984) *Plasma Chromatography*. New York: Plenum Press.
- Eiceman GA and Karpas Z (1994) *Ion Mobility Spectrometry*. Boca Raton, FL: CRC Press.
- Hayhurst CJ, Watts P and Wilders A (1992) Studies on gas-phase negative ion/molecule reactions of relevance to ion mobility spectrometry: mass analysis and ion identification of the negative reactant ion peak in 'clean' air. *International Journal of Mass Spectrometry and Ion Processes* 121: 127–139.
- Liu Y, Valentine SJ, Counterman AE, Hoaglund CS and Clemmer DE (1997) Injected-ion mobility analysis of biomolecules. *Analytical Chemistry* 69: 728A–735A.
- Rokushika S, Hatano H, Baim MA and Hill Jr, HH (1985) Resolution measurement for ion mobility spectrometry. *Analytical Chemistry* 57: 1902–1907.
- St Louis RH and Hill HH (1990) *Critical Reviews in Analytical Chemistry* 5: 321–355.
- Watts P (1992) Studies on gas-phase negative ion/molecule reactions of relevance to ion mobility spectrometry: kinetic modelling of the reactions occurring in 'clean' air. *International Journal of Mass Spectrometry and Ion Processes* 121: 141–158.
- Zlatkis A and Poole CF (ed.) (1981) *Electron Capture: Theory and Practice in Chromatography*. Amsterdam: Elsevier Scientific.

Large-Scale Gas Chromatography

P. Jusforgues, Prochrom, Champigneulle, France

Copyright © 2000 Academic Press

Introduction

Large scale preparative gas chromatography (GC) is an old established technique: the idea of using a gas chromatographic process to produce pure fractions of a mixture dates back to the 1950s. It took a long time to transform the idea into an efficient and reliable tool for industrial production and, finally, during the 1970s, solutions were found to the crucial problems, and large scale preparative GC became commercially available. At the same time, models were developed to help optimize the separations and to understand the phenomena specific to chromatography at finite concentrations.

The questions raised by large scale preparative GC include the following:

1. What is it?
2. Why is it of interest?

3. How does it work?
4. At what scale?
5. What for (which applications)?
6. How much does it cost?

Principle

Large scale preparative GC uses the same chromatographic principle as analytical GC with packed columns: a carrier gas flows continuously through a column packed with the stationary phase. A pulse of a mixture is injected into the carrier gas at the column inlet and the different components of the mixture are eluted at the column outlet at different times, depending on their volatility and their affinity for the stationary phase. Preparative and analytical GC use the same carrier gases and stationary phases and the same types of detectors.

The goal of preparative GC is not to know the composition of the mixture as in analytical GC but to collect purified fractions for further use. Thus, in large scale preparative GC, for productivity reasons, injected pulses are as large as possible, column

capacity is enlarged (by increasing the diameter) and, at the column outlet, instead of discharging the various fractions to the atmosphere, they are directed to traps where they are condensed and separated from the carrier gas.

Two different categories of preparative GC exist which differ in both size and goal: laboratory-scale preparative GC and large scale preparative GC. Laboratory-scale preparative GC will not be described here since it is very similar to analytical GC. Its goal is to purify milligrams or hundreds of milligrams of compounds in order to identify them further: it is an analytical technique. The equipment used is similar to that used in analytical GC (except for column diameters that can be increased up to 10 mm) and the fraction collector is a simple device in which sample condensation is often not quantitative.

Large scale preparative GC, described below, is made for purification of kilograms and tonnage quantities of compounds.

Interesting Characteristics

The advantage of large scale preparative GC can be described in comparison with other well-known separation techniques such as distillation and liquid chromatography.

Selectivity

The very large selectivity range of packed column analytical GC is also available for preparative GC since the same stationary phases are used. The selectivity is based not only on the difference of volatility of the compounds (as in traditional distillation) but also on their relative affinity for the stationary phase. Thus, the choice of the stationary phase is a powerful tool to customize the separation (e.g. an impurity can be removed from a complex mixture without separating the other compounds).

Another advantage of preparative GC over distillation is the possibility of purifying azeotropic mixtures.

Efficiency

Very high separation efficiencies of several thousand theoretical plates can be obtained in preparative GC; this was one of the key technological points that had to be resolved before process could be commercialized. These high efficiencies allow high purities and/or high productivities of closely related compounds (e.g. *cis-trans* isomers) to be obtained.

Thermal Degradation

A limitation of the applicability of preparative GC is, as for distillation, the degradation of thermolabile

molecules that have to be vaporized. However, one advantage of preparative GC over distillation is the smaller residence time at high temperatures which reduces the thermal degradation.

Flexibility

Associated with the small residence times are the small hold-up volumes (no need for large boilers, no reflux). Thus, the start-up time and stop time of a large unit are smaller than with a large distillation column. It is also easier to clean and to change the application.

Absence of Solvent

The advantage of preparative GC compared with preparative liquid chromatography is its low cost. Indeed, the main drawback of preparative LC is the high cost associated with the large amounts of solvent used. In preparative GC, the equivalent of the solvent is the carrier gas, which is easily separated from the purified sample and can then be recycled at low cost. As a consequence, a large scale GC process costs from 10 to 100 times less than a preparative LC process and the purified sample is collected free of solvent.

Limitations

Despite its advantages preparative GC has a limited range of applications.

The first reason is technical: the processed compounds must be able to be vaporized without decomposition and, even for thermostable compounds, productivity considerations limit the application of preparative GC to compounds with normal boiling points under 250°C.

The second reason is economic: to separate compounds with relative volatilities greater than 1.2, distillation is often less expensive.

Implementation

Figure 1 shows a schematic flow diagram of a typical preparative GC. Typical values of temperatures and pressures are given at different points of the process. The range of operating temperatures and pressures used is given in Table 1.

Note that the pressure at the outlet condensers can be subatmospheric. This feature is used to increase the productivity of some separations when the vapour pressure of the sample at the operating temperature is too low. The use of vacuum raises a number of technical problems and should be avoided whenever possible.

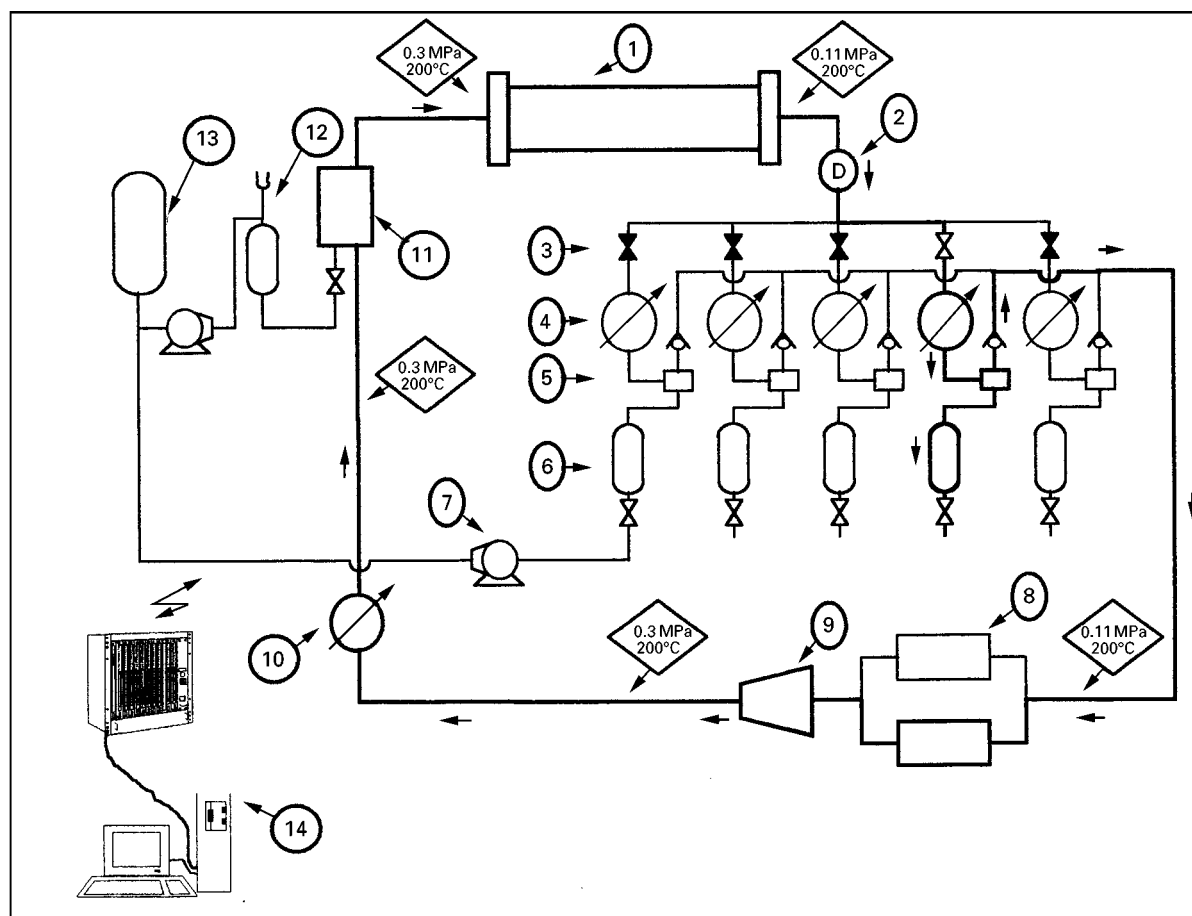


Figure 1 Schematic diagram of a large scale preparative GC. 1, Chromatographic column; 2, detector; 3, valves for trap selection; 4, condensers; 5, gas-liquid separators; 6, fraction collectors; 7, recycled fraction pump; 8, carrier gas cleaner; 9, compressor; 10, carrier gas pre-heater; 11, injector; 12, feed vaporizer; 13, feed reservoir; 14, automation.

Column

As in any chromatographic process, the column is one of the most important components of the system. It is heated to maintain the carrier gas and sample temperature constant. Small columns (up to 80 mm i.d.) are placed in an oven. Larger columns are heated by fluid circulating in a jacket. The column is made of stainless steel packed with a stationary phase. Both ends of the column are closed with metal frits.

Any type of stationary phase used in packed column analytical GC can be used for preparative pur-

pose. The only limitations are the cost and the availability of kilograms or tonnes of packing (e.g. a polymer of 2-6 diphenylparaphenylene oxide currently used in analytical GC is too expensive to be used on a tonne scale).

Most applications use a diatomaceous support coated with various liquid phases.

Packing the large diameter column is technologically difficult. Indeed, to be able to scale up results obtained during small scale experiments one must use 'similar' columns of any scale. 'Similar' columns means columns which have the same efficiency. This was the main difficulty encountered by the pioneers of preparative GC: their large diameter columns were inefficient compared to analytical columns and the separations obtained in the laboratory could not be reproduced for production. This problem has been solved empirically by filling the column with the stationary phase under a controlled vibration system. The packing procedure has not been published and is still the property of the column suppliers. Efficiencies

Table 1 Range of temperatures and pressures used in preparative GC

	Temperature (°C)	Pressure (MPa absolute)
Column inlet	+ 50 to + 300	0.1–0.5
Outlet condensers	– 20 to + 100	0.02–0.15

of 800–1000 plates per metre are now commonly obtained. Column life times are several years longer when treated correctly – no liquid flooding and no excessive temperature.

Detector

The function of the detector for preparative work is not to measure the quantity of compounds in the mixture but to help the operator (or an automated system) to determine when the various compounds are being eluted from the column and when the trap selection valves must be operated.

Any detector used in analytical GC can be used but the detector of choice is the thermal conductivity detector (TCD) because it is nondestructive and it can be used online in the full carrier gas flow. Other detectors can be installed on a small split line.

Trap Selection Valves

These valves are controlled by the automated control system. One, and only one, is opened at a given time.

As the compounds are eluted sequentially from the column at different times, they are directed to different traps so that the temporal separation is transformed into a spatial separation.

Condensers

In the condensers, the mixture of carrier gas and vaporized sample is cooled and the sample is condensed out of the carrier gas.

Phase Separators

Here the carrier gas is physically separated from the liquefied sample. The carrier gas is sent to the recycling line while the sample is directed to the fraction collector. The combination of condensers and phase separators is one of the technological key points of the system. It is theoretically easy to separate a liquid from a gas, but if the condensation is not performed properly the sample will condense in very small droplets (fog) which will be carried away with the gas phase. The solution to this problem depends on the nature of the sample and the size of the equipment.

Trapping yields of > 98% can reasonably be expected in practice.

Carrier Gas Cleaners

Separation of the carrier gas and the sample is not perfect and traces of sample may be recycled with the carrier gas, affecting the next cycle of the purification process. Thus, the carrier gas is cleaned by passing it through a bed of activated charcoal. Two beds are installed in parallel: one is used to clean the carrier gas while the other is being regenerated.

Compressor

The function of the compressor is to circulate the carrier gas through the system and to compensate for the pressure drops.

Carrier Gas Pre-heater

The pre-heater brings the carrier gas temperature to the chosen operating temperature.

Injector

The sample is vaporized and delivered to the injector where it is periodically mixed with the carrier gas.

Carrier Gas

Three carrier gases are used in preparative GC – hydrogen, helium or nitrogen. The influence of the chemical nature of the carrier gas on the selectivity is negligible, so the choice will depend on the physical properties of the gases and on the environment.

Two features influence the separation performance. Viscosity governs the pressure drop in the column and consequently the possible speed of the carrier gas and diffusivity influences the mass transfer of the sample in the column and consequently the efficiency.

Whenever possible, hydrogen is chosen because of its low viscosity, high diffusion coefficient and low cost. If, for safety reasons, it is not possible to use hydrogen then helium is the second choice.

Variants

Various working modes can be implemented in preparative GC. They include temperature gradients, multidimensional GC, moving bed or simulated moving bed GC. Although these techniques can theoretically be useful, they are not used in practice.

Temperature programming can be used for selectivity enhancement and/or elution time reduction when the feedstock components have a large range of retention factors but, due to the high thermal inertia of large systems, the time required to re-equilibrate the temperature between two injections is too long and overall productivity is affected. In such cases, the separation is made in several isothermal steps.

Multidimensional chromatography uses several columns online, packed with different stationary phases. One of the fractions eluted from the first column is directed to a second column, where it is further fractionated, while the second column is bypassed when the other fractions are eluted. The advantages of this configuration often fail to compensate for the increased complexity of the process and such separations are made in several steps.

Table 2 Examples of production scales

Column diameter (mm)	Column length (m)	Typical loading capacity (kg h ⁻¹) (tonnes year ⁻¹)		Carrier gas flow rate (Nm ³ h ⁻¹)
40	1–6	0.1	0.7	0.45
80	1–4	0.4	2.9	1.8
125	1 or 2	1.0	7.2	4.2
200	1 or 2	2.5	18	11.5
400	1 or 2	10.0	72	45
600	1 or 2	22.5	162	100

Moving bed GC (also named continuous counter-current chromatography) and its practical variant, simulated moving bed GC (SMB-GC) offer some of the theoretical advantages of the related technique SMB-high performance liquid chromatography (HPLC). In SMB-GC, the feed flow and fraction flow are continuous, thus the thermal control is easier in both vaporizer and condensers. The stationary phase is used more efficiently, thanks to the countercurrent process. However, in SMB-HPLC the complexity of the system is counterbalanced by savings on the mobile-phase consumption. This is not the case in SMB-GC because the carrier gas is already recycled.

Prep GC: What Scale?

Table 2 gives examples of production scales obtained with different column diameters. Of course, these are typical figures and, depending on the particular application, the actual figures may be five times bigger or smaller.

Preparative large scale GC can be used to purify hundreds of grams a week or hundreds of tonnes a year, as shown here.

6 g per injection on a 40 mm i.d. column
 × 4 injections per hour × 24 hrs per day
 × 4 days per week = 2.3 kg per week

1.5 kg per injection on a 600 mm i.d. column
 × 4 injections per hour × 24 hours per day
 × 300 days per year = 43 tonnes per year

Application examples

Over the last 20 years, preparative GC has been used in hundreds of applications, some of which are listed in Table 3.

cis-trans Pentanediene

In this example the *cis* and *trans* isomers of pentanediene with a purity greater than 99% needed to be recovered from a crude mixture (Figure 2). The preparative chromatogram and operating conditions are shown in Figure 2. One of the features of preparative chromatography compared to analytical chromatography can be seen: for productivity reasons, the column is overloaded and the peaks are not completely resolved. In spite of this, the high level of purity obtained for both isomers (99.8%) is a common feature of preparative GC.

Economy of Prep GC: Example

It is not possible to give an absolute purification cost of large scale preparative GC, since much depends on

Table 3 Examples of applications of preparative GC

Paraffins (C ₅ –C ₃₂), olefins	Methyl ionones
Dienes	Anethole (<i>cis-trans</i>)
Vinyl acetylene	Methyl esters of fatty acids (soya, oleic, linoleic, linolenic, stearic, palmitic)
Alkyl benzenes	Thiophenes (2-bromo, 3-bromo, 2-methyl, 3-methyl)
<i>m/p</i> bromobenzo trifluorides	Thenylamine
Benzyl alcohols, benzyl aldehydes	Chlorophyridines
α and β pinenes	Phosphines
Myrcene	Indoles
Camphene	Ylang-ylang
Limonene	Virginia pine oil
Caryophyllene (azeotrope with anethole)	Clove oil
α and β cedrenes	Fennel oil
Nerol, geraniol, citronellol, eugenol	Lemongrass oil
Farnesols (<i>cis-trans</i> , <i>trans-trans</i>)	Orange oil
Citral a and b	Lemon oil
Citronellal	

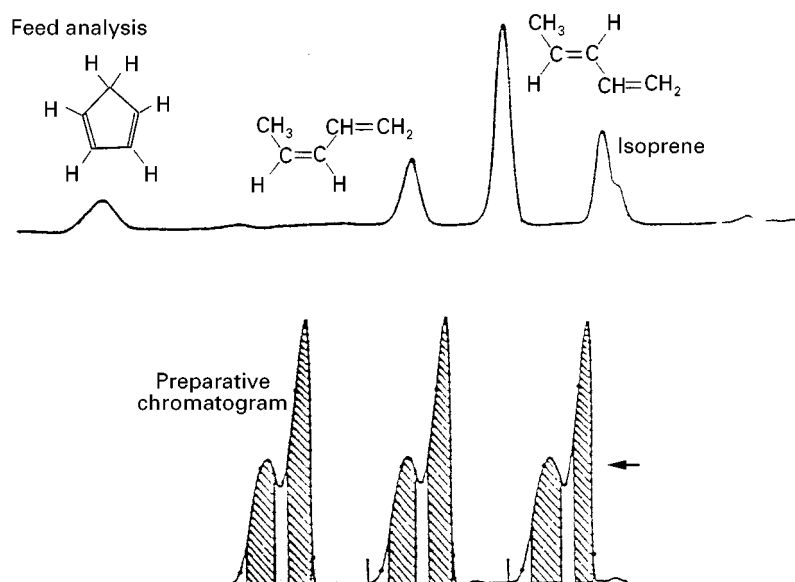


Figure 2 Purification of *cis* and *trans* pentadiene. Column: 40 mm i.d.; 4 m long; 20% w/w squalane on Chromosorb P. Carrier gas: helium at 5 cm s^{-1} ; 2.6 L min^{-1} ; 35°C . Injection: 4 mL of mixture injected per cycle; 1 cycle every 20 min. Purity: *cis* isomer = 99.8%; *trans* isomer = 99.8%.

the specific application and on the scale of the process.

The example described here is the purification of two heavy alcohols from a complex mixture.

The two alcohols to be collected are only 35% of the feedstock. **Figure 3** shows the analytical chromatogram of the feed and a preparative chromatogram.

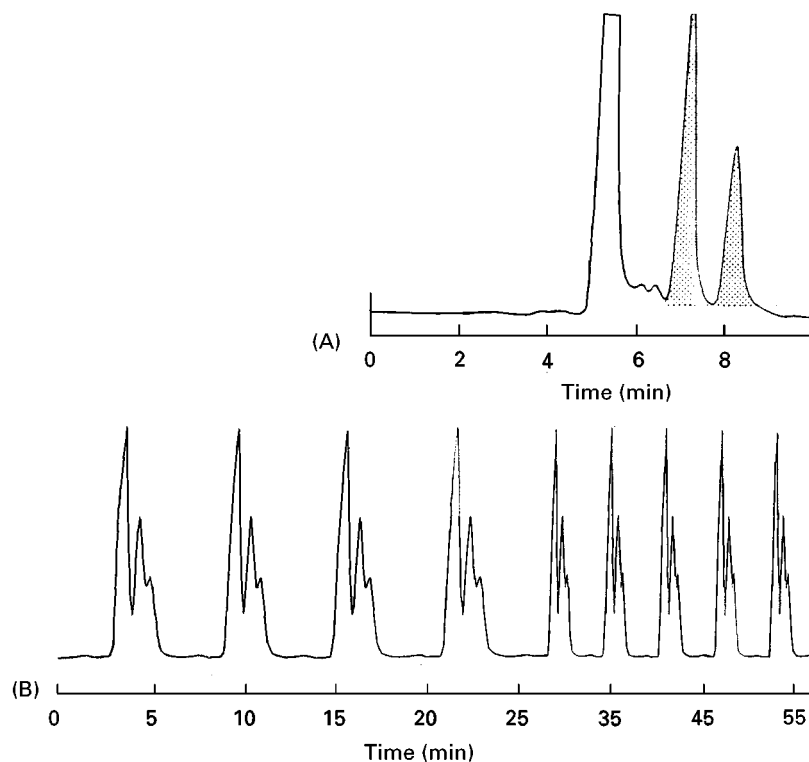


Figure 3 Purification of two heavy alcohols. (A) Analysis of the crude, showing the two alcohols to be recovered. (B) Successive preparative injections on an 80 mm i.d. column; one injection of 18 g every 10 min. Note: the recorder chart speed has been changed after the first four injections.

Table 4 Purification cost breakdown for a production of 36 tonnes per year of injected crude on a 400 mm i.d. column

<i>Operating costs</i>		<i>Annual cost (k\$ per year)</i>
Electricity: $1.44 \cdot 10^{12}$ J	Power	33
2000 h per year	Manpower	80
8000 m ³	Hydrogen make-up	11
5% of equipment cost	Maintenance	58
Replaced every 2 years	Stationary phase	62
(at half the cost of a new column)		
	Total	244 k\$ per year
	Total	6.8 \$ kg ⁻¹ of crude
		21.8 \$ kg ⁻¹ of pure product
<i>Investment costs</i>		<i>(k\$)</i>
	Chromatograph	1200
20% of equipment cost	Surroundings	240
Start-up and others	Miscellaneous	160
	Total	1600 k\$
Amortizement over 5 years	Total	320 k\$ per year
	Total	8.9 \$ kg ⁻¹ of crude
		28.6 \$ kg ⁻¹ of pure product
<i>Purification costs</i>		15.7 \$ kg ⁻¹ of crude
		50.4 \$ kg ⁻¹ of pure product

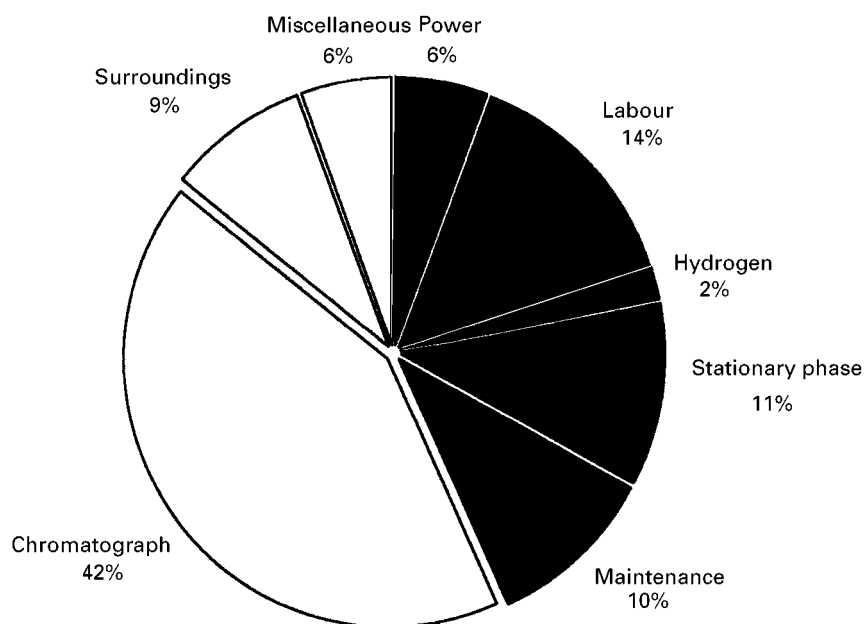
Optimizing the operating conditions has led to the production of 1 kg h⁻¹ for the first alcohol and 400 g h⁻¹ for the second on a column of 400 mm i.d. The yield of the two alcohols was 89% (mass of pure alcohol collected/mass of alcohol injected) and purity was > 95%.

The economics of the process are shown in Table 4 and Figure 4. The final purification cost is 15 \$ kg⁻¹ of injected feedstock. The normal purification costs

for an industrial process range between 10 and 100 \$ kg⁻¹.

Conclusion

Large scale preparative GC is a real purification tool. It is now reliable and economically viable for industrial production. Columns with internal diameter as large as 600 mm are available. The efficiencies

**Figure 4** Purification cost breakdown for a production of 36 tonnes per year of injected crude on a 400 mm i.d. column. Open segments, investment costs; shaded segments, operating costs.

obtained are between 800 and 1000 plates and the scale of production is between 20 and 200 tonnes per year.

Large scale GC can be used for the industrial production of ultrapure compounds or for the selective removal of impurities. For difficult separations, it is economically competitive with other techniques such as distillation. Whenever it is applicable, it is always competitive with preparative HPLC. Its applications are limited to compounds with normal boiling points under 250°C.

Preparative GC works well with a relatively simple technology; thus, over the last 10 years, technological improvements have been limited to automation in line with modern standards and to maintain simplicity. No major improvement is expected in future, except to adapt the process to specific cases (e.g. ultrapurification of gases for the electronics industry with an impurities level as low as 0.1 p.p.b. and simultaneous separation and reaction in a chromatographic column). The number of installations work-

ing throughout the world is limited to about 100, although the potential of the technique is much greater. The future is likely to see the development of some new very large scale applications.

Further Reading

- Bonmati R, Chapelet-Letourneux G and Guiochon G (1984) *Separation Science and Technology* 19 (2&3): 133–155.
- Jacob L and Guiochon G (1971) *Chromatography Review* 14: 77.
- Kovats E and Heilbronner E (1956) *Chimia* 10: 288.
- Rijnders GW (1966) In: Giddings JC and Keller RA (eds) *Advances in Chromatography*, p. 215. New York: Dekker.
- Roz B, Bonmati R, Hgenbach G *et al.* (1971) *Chromatographia* 4: 6.
- Valentin P and Guiochon G (1975) *Separation Science* 10: 245, 271, 289.
- Valentin P, Hgenbach G, Roz B and Guiochon G (1976) *Journal of Chromatographic Science* 14: 367.

Multidimensional Gas Chromatography

P. Marriott, RMIT University, Melbourne, Victoria, Australia

Copyright © 2000 Academic Press

Multidimensional Concepts

The multidimensional approach to solute separation involves the use of more than one column (almost always two columns) arranged in series, such that chosen components in a chromatogram, or selected sections of a chromatogram, are subjected to separation on each of the columns in the system.

Multidimensional methods may include interfacing of a chromatographic column with a multichannel detection system (mass spectrometry, atomic emission, Fourier transform infrared (FTIR), diode array detection and the like). This review will not extend into this area, focusing rather on multidimension gas chromatography (GC) separations. Within coupled separations, especially online and automated systems, simplification of the total sample analysis by incorporation of extraction steps such as solid-phase extraction, solid-phase microextraction, supercritical fluid extraction and other sampling approaches, combined with chromatographic separation, can be considered multidimensional analysis. These will also not be included here, and details on these methods should be sought elsewhere.

Why are multidimensional methods implemented for chromatographic analysis? The usual answer lies in the need for enhanced separation of closely eluting compounds – compounds with similar retention factor, k . Historically, chromatography has searched for better means to resolve compounds; as methods improve, we can separate compounds of closer chemical nature. Traditionally, chromatographers have improved column selectivity to provide a larger magnitude in differences of distribution constant, K (where $K = k\beta \propto t_R'$; therefore larger retention time differences results from increased K differences), or increased efficiency of the chromatographic process with narrower chromatographic bands giving better resolution. The former is achieved by using a stationary phase or separation mechanism with greater discrimination between the solutes to be separated, and the latter by employing narrower-bore columns, smaller particle packing sizes or other physical means to reduce peak dispersion. Very soon in the historical development of GC, it was recognized that one stationary phase would probably not resolve many compounds (hence the plethora of stationary phases that were produced), but also that a given mixture can contain a range of different classes of compounds that may best be separated on different phases. Thus, improved separation may require two columns for the one analysis. Two separate columns means that

the sample must be analysed twice, but when used in a coupled column arrangement the advantages of both columns can be utilized simultaneously. This is the genesis of multidimensional chromatography.

Effective implementation of multidimensional methods for improved solute separation depends on a number of critical parameters. Firstly, each dimension should separate according to different physical or chemical properties of the analytes and we look to specific selectivity differences towards a problem separation. Secondly, an efficient means of interfacing the (two) separation modes is also required. Switching valves or other methods will be needed to redirect the flow stream from one column to another. This may be combined with a method for peak compression or peak focusing between the two dimensions. Finally, the compatibility of the two separation modes must be taken into account. This will depend upon the carrier fluid (gas, liquid) that is used for each mode, and the mechanism by which solutes are retained on each dimension. For example, multidimensional high performance liquid chromatography (MDHPLC) combining strictly normal and reversed-phase modes will present a challenge because of the incompatibility of the mobile phases required by the two modes.

Basic Instrumental Requirements and Considerations

The main concern in implementing a multidimensional separation solution will be how to design the instrumental set-up. The greater the difference between the two dimensions, the greater the potential difficulty in their coupling, since there will be greater dissimilarity in the mechanisms of separation. The wide choice of column chromatography separation methods explains why the coupling or interfacing

may present a challenge. If the two dimensions are of the same chromatographic type – GC–GC, HPLC–HPLC, supercritical fluid chromatography (SFC)–SFC etc. – the task is not so problematic. Where different carrier phases are required for the two dimensions, chromatographic integrity must be maintained. Transferring a solution phase from HPLC to capillary GC or SFC requires an interface that can effectively introduce analyte into the narrow-bore column without compromising band dispersion, and whether analytical scale or large volume solvent injection is to be used determines the interface complexity.

Table 1 presents a summary of the potential successful multidimensional column chromatography methods. Some options will be generally incompatible, such as IC coupled with GC, since exclusion of the electrolyte carrier fluid from the GC system will be difficult, and ionic analytes for which IC is usually used will not be suited to GC analysis. The suitability of HPLC–GC and GPC–GC for volatile organics is the reason why these liquid-phase first-dimension separations are useful for sample differentiation prior to the GC step. **Table 2** further outlines various procedural aspects of selected multidimensional methods.

For multidimensional GC (MDGC) analysis, it is not a difficult task when dealing with relatively low boiling mixtures to couple two columns together, and to have gas-sampling valves or a flow-switching device to allow transfer of effluent. The classical Deans switch relies on pressure differences to pass carrier flow in different directions. **Figure 1** presents a schematic diagram of a typical commercial MDGC system, comprising one oven, two columns, two detectors, a midpoint restrictor at which point the diversion of column flow to either the first detector or the second column occurs. A cold trap focuses heart-cut

Table 1 Possible multidimensional coupling of separation dimensions in column chromatography

		<i>Second dimension</i>						
		<i>GC</i>	<i>NPHPLC</i>	<i>RPHPLC</i>	<i>IC</i>	<i>GPC</i>	<i>SFC</i>	<i>CE</i>
First dimension	GC	✓					✓	
	NPHPLC	✓	✓	✓	✓	✓	✓	✓
	RPHPLC	✓	✓	✓	✓	✓	✓	✓
	IC		✓	✓	✓			✓
	GPC	✓	✓	✓	✓	✓	✓	✓
	SFC	✓					✓	
	CE	✓	✓	✓	✓			✓

GC, Gas chromatography; NPHPLC, normal-phase high performance liquid chromatography; RPHPLC, reversed-phase high performance liquid chromatography; IC, ion chromatography; GPC, gel permeation chromatography; SFC, supercritical fluid chromatography; CE, capillary electrophoresis.

Table 2 Selected multidimensional (MD) chromatography modes and application areas

<i>Dimension 1</i>	<i>Dimension 2</i>	<i>Interface</i>	<i>Method</i>
Packed GC	Capillary GC	Heart-cut valve	Trace enrichment
Packed/capillary GC	Packed/capillary GC	Direct coupling; pressure tuning	Multi-chromatography
Capillary GC	Capillary GC	Heart-cut valve, with options (see Table 1)	Conventional high resolution MDGC
Capillary GC	Capillary GC	Continuous transfer; peak compression	Comprehensive 2D gas chromatography
HPLC	Capillary GC	Large volume injection	Multidimensional HPLC-GC
HPLC-GPC	Capillary GC	Large volume injection	Prior class separation before GC step

fractions, and a solenoid-controlled shut-off valve closes the flow through to the monitor detector and effects the transfer of the flow of column 1 to column 2.

Direct coupling of two or more columns, with all the effluent from one column passing wholly into the second column without hindrance (see later for variations on this theme), is normally not considered a MDGC analysis because MDGC methods should lead to greater *peak capacity* for the total system. Capacity may be thought of as the total available or achievable peak separation on a column. In simple terms, this is the total retention space divided by an average peak width parameter defining acceptable neighbouring peak resolution, i.e. the maximum number of peaks, resolved to a given extent, which can be produced by the system. Consider temperature-programming analysis. Assuming that the total chromatographic adjusted retention time is 90 min, and each peak basewidth is 10 s (peak widths may be approximately constant across the whole analysis, depending on the temperature ramp rate chosen), then a maximum of 540 baseline separated peaks could be recorded on this column. In practice, the actual number would be much smaller since the peaks are not eluted uniformly over the total time of the analysis.

Expanding System Capacity

Statistical methods have been employed to determine the ability of a column to resolve a complex mixture of compounds, assuming their distribution within the column to be entirely random. This theoretical analysis is informative, but typical complex mixtures must be treated on a case-by-case basis. The chromatographer must define the information required from an analysis; there may be no need to resolve every peak in a mixture if the required target solutes are only a small fraction of the total components. An optimized separation need focus only on those components which must be analysed. For example, the analysis of benzene and toluene in gasoline fractions, where only the resolution and quantification of these compounds

are required, means that the measurement of all other components is of less or even of no concern.

The capacity of the total system (or the restricted region about the target solutes) will be expanded in the multidimensional analysis. Specific regions of the effluent from the first column must be isolated and these small fractions transferred to the second column. These two columns may be referred to as the pre-column or first dimension, and the analytical column or second dimension.

Consider the above GC column with a capacity of 540 peaks. If this is coupled to a second column with capacity of, for example, 280 peaks, and if the two columns represent completely orthogonal separations, we would have a theoretical capacity of $540 \times 280 = 151\,200$ peaks. More generally:

$$n_{\text{tot}} = (\bar{n})^z$$

where n_{tot} is total peak capacity, \bar{n} is the average capacity on each column and z is the number of coupled columns.

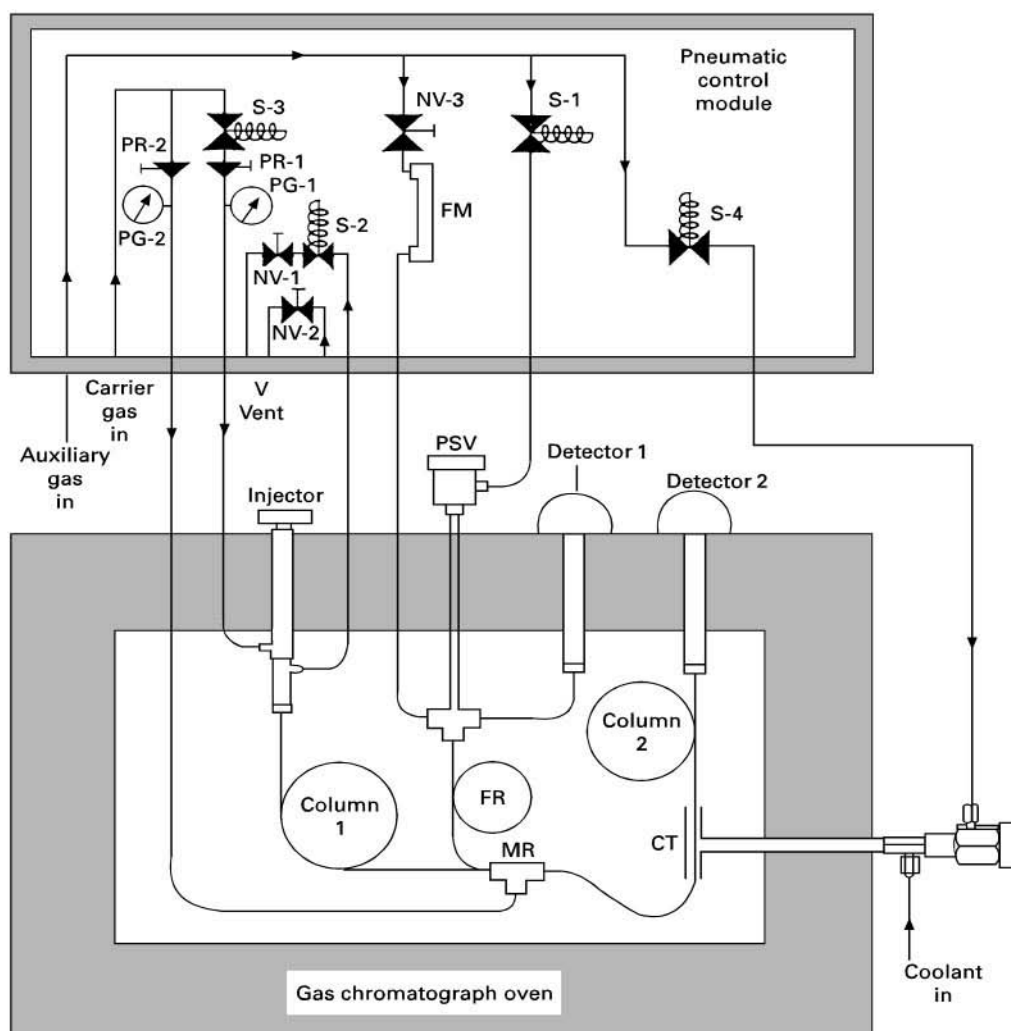
This can only be possible if the full capacity of each dimension can be achieved in the MDGC analysis. This is not normally so; it depends critically on the manner in which the column interfacing is performed, and how the transfer and subsequent second-dimension analysis is carried out. In fact, with selected heart-cut analysis, the total system capacity is better described as the summation, rather than the product, of the capacity of the two coupled columns:

$$n_{\text{tot}} = 2\bar{n}$$

or, more generally:

$$n_{\text{tot}} = \sum n_1 + n_2 + \dots n_z$$

Consider a first column with a small unresolved group of, say, five peaks each of 10 s basewidth, eluting over a period of 35 s which is transferred to the second column. The peak capacity of the first column in the region of interest is only 3.5. If the second column has the ability to separate these peaks

**Solenoid valves**

S-1 Controls pneumatic shut-off valve

S-2 Controls injection splitter and back-flush operation

S-3 Controls pre-column carrier gas input

S-4 Controls CO₂ or optional liquid nitrogen cold trap**Pressure regulators**

PR-1 Sets pre-column carrier gas input pressure

PR-2 Sets midpoint carrier gas pressure

Pressure gauges

PG-1 Monitors pre-column pressure

PG-2 Monitors midpoint pressure

Fixed restrictor

FR Deactivated transfer line from midpoint restrictor to monitor detector

Peripheral hardware

FM Flow meter

MR Midpoint restrictor

CT Cold trap

PSV Low dead volume pneumatically controlled shut-off valve

Needle valves

NV-1 Controls injector split flow

NV-2 Controls midpoint split flow for packed to capillary column operation

NV-3 Controls make-up gas flow rate

Figure 1 Multidimensional gas chromatography schematic diagram. Courtesy of SGE International.

just to basewidth, then its capacity towards the target solutes is 5. (If the peak separation is random, we will require a higher peak capacity in order to be assured that the five peaks will be separated.) In GC, solute boiling point plays a key part in the retention of compounds, and superposed on this primary retention parameter will be secondary properties such as polarity of the column and solutes, defining solute-

specific interactions. Since each column's retention depends in the first instance on the overall volatility of each component, then the heart-cut or transferred solutes cannot be distributed over the total elution space of the second column. Rather, it is restricted to the range that the combined effect of boiling point and polarity imposes on the compounds. A non-polar first column means close eluting solutes have similar

boiling points. A polar second column will enhance solute polarity differences to achieve separation. **Figure 2** shows examples of heart-cutting poorly resolved sections of one column to another column. If the solutes subsequently elute relatively close together, much of the theoretical capacity of the second column is not employed.

In many MDGC systems, a cryofocusing step is used at the start of the second column to collect heart-cut fractions as a narrow band, as shown in **Figure 2B** centre. When the cryogenic fluid is turned off, the solutes recommence their travel on the second column, starting at the same initial position and time. If unresolved compounds from the first column are

separated, the aim of the experiment is achieved. The use of a second oven, in which the second column is located, may require a cold trap since just keeping the second oven at a low temperature may not be sufficient to immobilize the solutes. If trapping is not required, the second oven may track the temperature of the first oven.

The need for a cryogenic trapping procedure requires further consideration. Since it will focus solutes at the start of the second column, it will also remix partially resolved compounds. Depending on whether the solutes reverse their relative retention on the two phases, the action of focusing the solutes may either improve or worsen the separation.

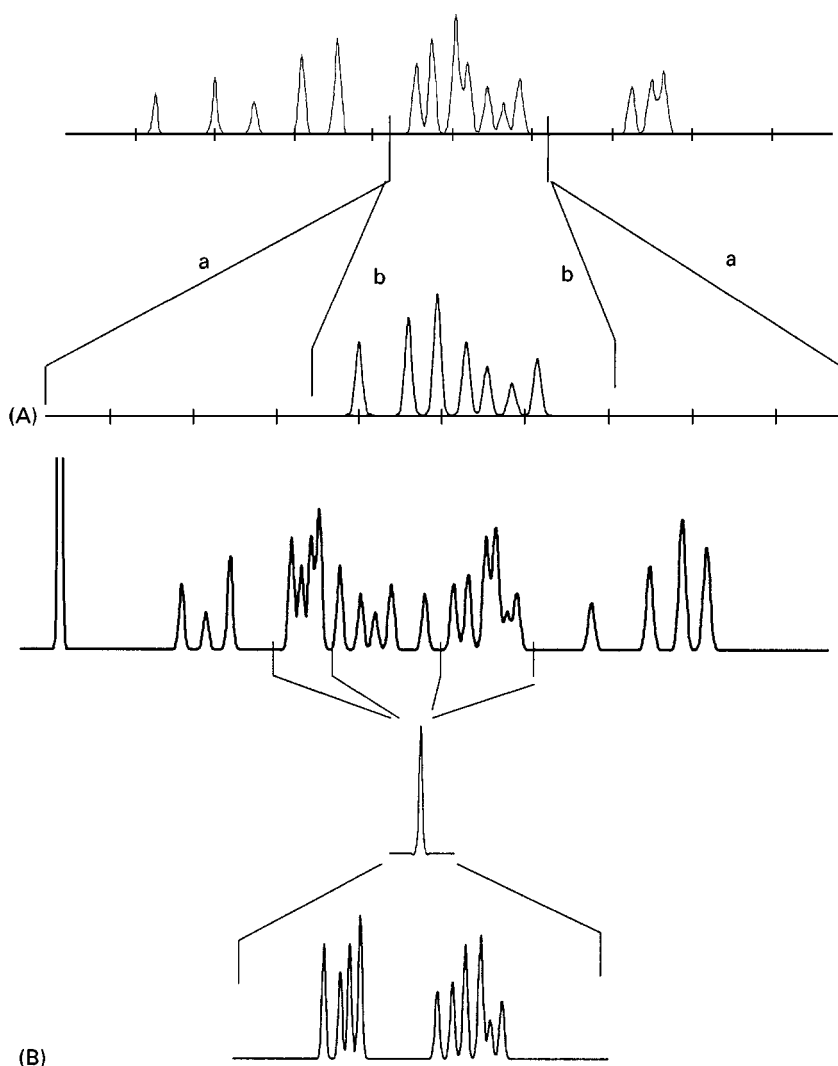


Figure 2 (A) Heart-cutting the poorly resolved section of the top column to the bottom column improves separation, but the full capacity of the second dimension may not be fully used. A second-dimension analysis, which only requires the space shown by lines labelled b, would be preferable to that shown by lines labelled a, where excess analysis time would result. (B) Two heart-cuts are performed on the first dimension (top). Both heart-cuts enter one cryogenic trap with all components recombined into one band (centre). The second-dimension analysis (bottom) is then used to provide greater selectivity difference for the range of solutes and enhanced separation of the components.

In summary, MDGC may be used in the following arrangements:

- single oven, with or without a cryotrap
- dual oven, with or without a cryotrap
- single or dual oven with multiple sorption/collection traps
- single oven with rapid second-dimension analysis and modulated transfer system – the so-called comprehensive 2D GC.

Figure 3 summarizes a number of different arrangements for performing multidimensional chromatography. Irrespective of the dimension types, the coupling must enable the flow stream to introduce solute into the second dimension. Direct coupling (or pressure tuning in GC) need only use a column connector, but other methods use multiple heart-cuts into one storage reservoir, as indicated by the circle shown in 3A (e.g. a single cryotrap in GC), or separate storage devices with discrete analysis of each, as shown in 3B, or a specially designed modulator to allow continual sampling/analysis of fractions from dimension 1, as in 3C (see later). In the case of method 3A, 2D will probably require a broad range of analysis conditions since collected fractions will have a wide volatility range. In 3B, each separate 2D analysis need only be performed over a limited range of conditions, selected according to volatility considerations.

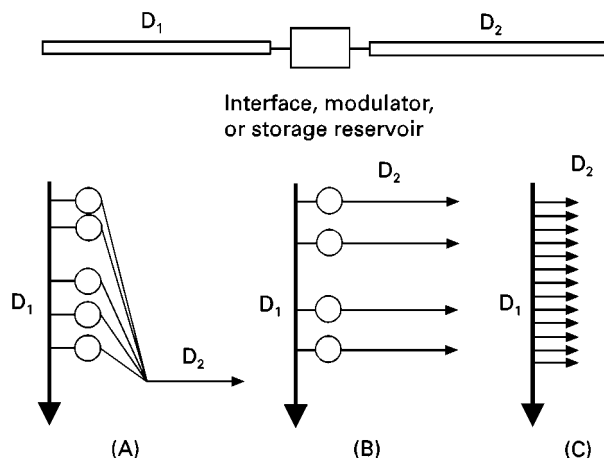


Figure 3 Coupling two dimensions, transferring selected bands and completing the second-dimension analysis can involve a range of procedures. (A) The second separation dimension can be a single chromatographic analysis, with selected dimension 1 (D₁) heart-cuts combined, e.g. in a cold trap, prior to dimension 2 (D₂). (B) A series of second-dimension analyses, each for an individual D₁ heart-cut, can be run with each heart-cut stored in a separate sample reservoir, e.g. sampling loops in HPLC or cold traps in GC. (C) By operating the second dimension in a rapid repetitive fashion, the comprehensive chromatography method is possible.

In regular MDGC, there will be a limited number of second-dimension analyses, or a limited number of heart-cut events. Conventionally, both dimensions will employ columns of reasonably normal types in respect of lengths, diameters and carrier gas flow rates.

In an offline system, or where fractions are collected in a storage section prior to introduction into the second dimension, such as a sampling loop in HPLC, the time between collection of heart-cut and second-dimension analysis might not strictly represent a continuous coupled analysis.

MDGC for Trace Enrichment

A capillary column has a limited sample capacity. Excessive amounts of sample lead to nonlinear conditions and broadened peaks are obtained. Such broadening can obscure small peaks of interest which elute with a similar retention factor to that of the large component, affecting quantification and identification of the trace solute. In MDGC, sample may be injected into a packed column which has a greater ability to maintain linear conditions at higher injected amounts. The zone of enriched trace component can then be heart-cut to a capillary column. Most of the major component will have to be excluded by the heart-cut event, and since now it does not overload the capillary column, there will be less probability that it overlaps the trace solute. Much more of the trace solute is passed to the capillary column than is otherwise possible. This application does not necessarily require different column phases on both the packed and capillary columns. The first column can be considered to be part of the sample introduction step into the second column.

Use of a Series of Parallel Heart-cut Reservoirs/Traps

Parallel traps are used to store successive heart-cut fractions prior to subsequent analysis. These might be liquid-phase loops (HPLC) or cryogenic traps (GC; Figure 3B). An array of packed cryogenically cooled traps may be used to collect selected fractions of heart-cut effluent from a capillary GC pre-column. The individual traps are then eluted into a second analytical capillary column, chosen for particular suitability to the required analysis. The effluent from the analytical column may then be split to different detectors, and the use of mass spectrometry/flame ionization detector and FTIR has been described, with FTIR receiving the larger flow due to its less favourable detection sensitivity. This procedure has been demonstrated with petroleum samples, where

FTIR is most advantageously used for isomers of compounds such as the xylenes. However, the complications arising from multiple trap management will reduce its attraction for many analysts.

Backflushing

In GC analyses where a sample consists of a wide boiling range of components, and where their prior separation is either difficult or troublesome, injection will introduce the low volatility components into the chromatographic column. If the target solutes are those that are eluted quickly, considerable time must be spent waiting for the high boiling point components to be eluted before the next analysis can be commenced. In MDGC, it is possible to reverse the flow in the pre-column (refer to column 1 in Figure 1) to back-flush the heavy constituents out of the column and vent them through the split vent line. This can be completed whilst the higher volatility components are being separated on the second column. This flow switching will be commenced when the desired solutes have passed the midpoint valve between the two columns (back-flushing is the oldest form of MDGC and has been employed since the earliest days of GC). Back-flushing can likewise be easily incorporated into other coupled separation systems such as MDHPLC.

Pressure Tuning

The technique of pressure tuning involves variation in the midpoint pressure between coupled columns to alter overall solute selectivity. This is not strictly an MDGC method, and has been given the term multi-chromatography in order to differentiate it from regular MDGC. However, pressure tuning is possible on regular MDGC systems, and some specific multi-dimensional results can be achieved on multi-chromatography pressure-tuned systems. The unified chromatography procedure, promoted by Bartle, alters the characteristics of the carrier phase during an analysis, for example progressing from GC to SFC conditions by applying a pressure programme to the carrier stream. Thus, one column is used, but different chromatography mechanisms are employed. This variation is again not strictly multidimensional. The pressure-tuning arrangement is shown in Figure 4.

Compounds are immediately presented to the second column as soon as they are eluted from the first column; their motion is not hindered by trapping or any other similar solute-focusing effect. Changing the midpoint pressure alters the relative flows in each column. Flow change by itself does not alter the capacity factor on either column (i.e. k is constant),

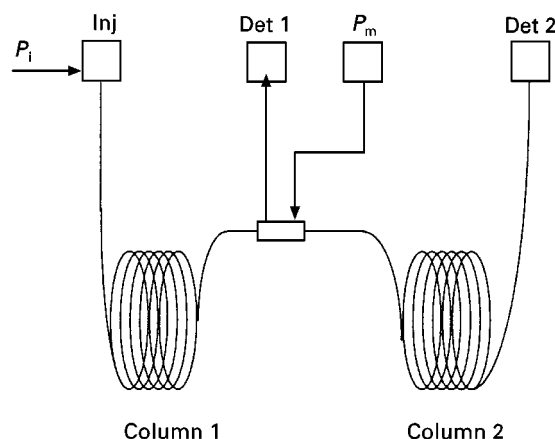


Figure 4 The pressure-tuning method involves a coupling between the two columns where additional pressure (P_m , midpoint pressure) can be applied above the natural pressure. P_i , inlet pressure; inj, injector; Det 1, Det 2, detectors 1 and 2.

although of course temperature change may affect relative k values. However, the overall k value may change dramatically with midpoint pressure changes. The contribution of each column in determining overall solute capacity on the system is varied, and so relative solute positions may change and best separation conditions may be determined. This procedure is essentially a continuously variable (at least over a given range) phase composition method, simulating column phases of selectable polarity based on the two phases comprising the coupled columns. It is possible to predict the effect of pressure on the overall separation, since individual retention factors on each column can be determined. The effect of carrier flow rate on each individual column's performance should still be considered. Figure 5 represents results which may be obtained, with the unretained peak time giving retention factors on each column. Peak overlap and exchange of relative retention of components are precisely what may be seen experimentally.

For a given column length, the total separation space does not increase in this method.

Comprehensive Multidimensional Chromatography

Comprehensive multidimensional chromatography is closest to a true continuous multidimensional column method since it subjects every emerging peak in the first dimension to second-dimension separation in almost continual fashion. Figure 3C is a representation of this approach. The term comprehensive chromatography is attributed to Bushey and Jorgenson, who demonstrated the advantages of the technique for coupled HPLC dimensions. Two major

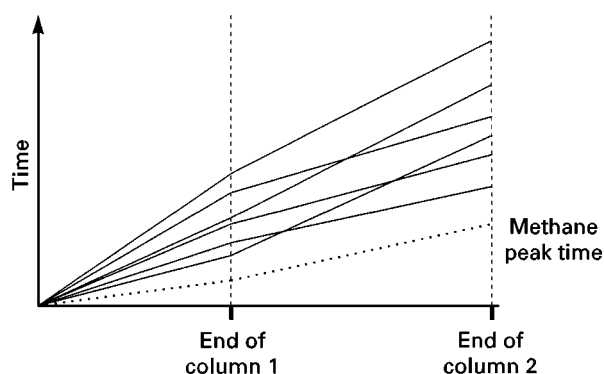


Figure 5 Pressure tuning allows retention factors to be determined on each separate column section provided t_R s of compounds (solid lines) and t_M (dotted line) are known on each dimension. After the midpoint, various solutes may swap position, possibly leading to better overall separation. The effect of the pressure tuning can be predicted by moving the right-hand vertical line along the horizontal axis.

variations depend on whether all the column flow or only a portion from the first column is transferred to the second column. These require different technical implementation of column coupling.

The second column elution time must be very short with respect to that on the first dimension – less than the frequency at which the first column effluent is sampled. This ensures that each second-dimension elution is completed before the subsequent band is introduced into the second column. Result presentation is best if the second-dimension analysis is rapid with respect to bandwidths on the first column, for example, a second-dimension analysis time about one-fifth of the peak width time on the first column. Given this requirement, first column performance leading to broad peaks may be required. The two columns chosen should ensure orthogonality. Retention of compounds in dimensions one and two can be defined as 1t_R and 2t_R respectively.

The final chromatogram will be a two-dimensional array of retentions, with a third dimension of peak height, leading to a contour plot chromatogram. Data presentation protocols and concepts such as retention indices, quantitative analysis considerations and relationships between peak position and phase polarities are only just being explored. Much further work is needed to evaluate these systems fully. **Figure 6** demonstrates how the three-dimensional data are presented in terms of a contour plot. The peak contour comprises a series of slices in the second dimension which is reconstructed as a peak with dispersion in both dimensions. The original first-dimension separation is shown.

In the comprehensive gas chromatography (C(GC)²) method, peak compression by a means of a focusing step between the two dimensions may be advantageous. This allows a very narrow band to be introduced to column 2 and allows the best peak capacity to be achieved on this column. Ideally, overlapping components in dimension 1 will be resolved on dimension 2. Peak compression of 20–50 times have been demonstrated, and this immediately translates into significant peak sensitivity enhancement with C(GC)².

In HPLC, the collected fraction of effluent would typically be analysed on a conventional column, so it would have a typical retention time in minutes.

Comprehensive Gas Chromatography

The (GC)² part of the abbreviation serves to indicate the multiplicative capacity of the system, and the term comprehensive reflects that the full suite of peaks from the first dimension is analysed.

The second dimension analysis time will be about 5 s or less, and the second dimension, comprising a short, high-phase ratio, narrow-bore open tubular column, might have a total peak capacity of only 10–20 peaks. C(GC)² uses first and second dimensions

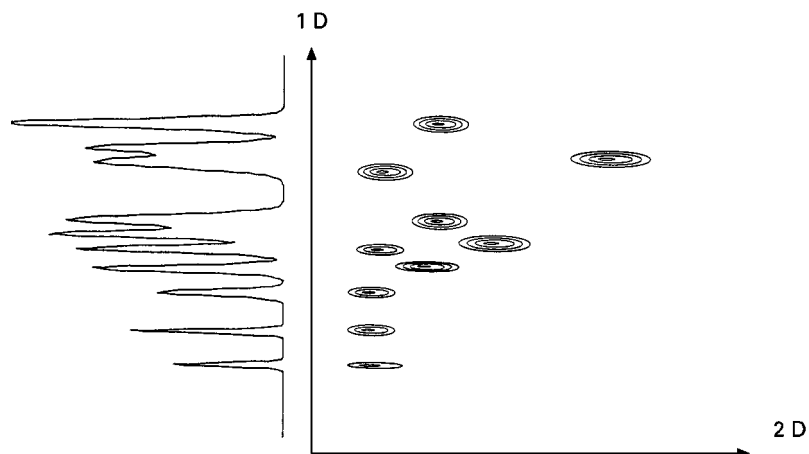


Figure 6 Peak contour representation of two-dimensional separation in comprehensive chromatography.

at the same oven temperature, allowing the second column effectively to resolve on the basis of polarity difference between the two columns. If adjusted properly, the full peak capacity on the second dimension should now be available for separation, and the total peak capacity should be the product of the first column capacity and the capacity available on the second column at any chosen operating temperature (the second column operates almost isothermally for each individual analysis).

Having a high peak capacity should not be too critical on the second column, but phase polarity or selectivity difference should be carefully chosen.

Peak compression, followed by fast second dimension analysis, results in improved sensitivity of detection; if a 5 s band of effluent from column 1 is compressed and leads to a detected peak width of 250 ms, a 20-fold sensitivity increase should result.

Technically, $C(GC)^2$ with compression in time requires novel procedures. Two systems have been described for $C(GC)^2$ employing band compression. One is based on a rotating elevated temperature modulator which passes closely over the junction between the two columns, incorporating a thick film accumulator section between the columns at the junction. An alternative device employs a longitudinal oscillating cryogenically cooled trap that can collect and focus solute from the first column, then pulse or remobilize the narrow band into the second column.

Given the need for very rapid analysis, rapidly recording detector systems are required.

Peak position in the two-dimension separation space will now be a complex function of volatility and polarity, determined by the individual mechanisms of the two columns chosen, and a full interpretation of the $C(GC)^2$ method is required in this respect. Possibilities for class separation demonstrate that the method has potential for multiresidue and screening applications, and characterization of petroleum products.

See also: II/Chromatography: Gas: Column Technology; Historical Development; Theory of Gas Chromatography. III/Gas Analysis: Gas Chromatography.

Further Reading

- Bushey MM and Jorgenson JW (1990) Automated instrumentation for comprehensive two-dimensional high-performance liquid chromatography of proteins. *Analytical Chemistry* 62: 161.
- Cortes H (ed.) (1990) *Multidimensional Chromatography: Techniques and Applications*. New York: Marcel Dekker.
- Cortes H (1992) Developments in multidimensional separation systems. *Journal of Chromatography* 626: 3.
- Davis JM (1994) Statistical theories of peak overlap in chromatography. *Advances in Chromatography*, 34: 109.
- de Gaus H-J, de Boer J and Brinkman UATH (1996) Multidimensionality in gas chromatography. *Trends in Analytical Chemistry* 15: 168.
- Giddings JC (1984) Two-dimensional separations: concept and promise. *Analytical Chemistry* 56: 1258A.
- Giddings JC (1987) Concepts and comparisons in multidimensional separations. *Journal of High Resolution Chromatography and Chromatography Communications* 10: 319.
- Giddings JC (1995) Sample dimensionality: a predictor of order-disorder in component peak distribution in multidimensional separation. *Journal of Chromatography A* 703: 3.
- Hinshaw JV and Ettre LS (1986) Selectivity tuning of serially connected open-tubular (capillary) columns in gas chromatography. Part I. Fundamental relationships. *Chromatographia* 21: 561.
- Mahler H, Maurer T and Mueller F (1995) Multicolumn systems in gas chromatography. In: Adlard ER (ed.) *Chromatography in the Petroleum Industry*. Amsterdam: Elsevier.
- Mondello L, Dugo G and Bartle KD (1996) On-line microbore high performance liquid chromatography-capillary gas chromatography for food and water analyses. A review. *Journal of Microcolumn Separations* 8: 275.
- Phillips JB and Xu JZ (1995) Comprehensive multidimensional gas chromatography. *Journal of Chromatography A* 703: 327.
- Schomburg G (1985) Multidimensional gas chromatography as a sampling technique. In: Sandra P (ed.) *Sample Introduction in Capillary Gas Chromatography*, vol. 1. Heidelberg: Dr Alfred Heuthig Verlag.
- Schomburg G (1995) Two-dimensional gas chromatography: principles, instrumentation, methods. *Journal of Chromatography A* 703: 309.

Pyrolysis Gas Chromatography

C. E. R. Jones, Redhill, Surrey, UK
Copyright © 2000 Academic Press

Introduction

The gas chromatographic process is wholly dependent upon solutes having significant vapour pressures

at the upper limiting operating temperature of the chosen solvent so that the partition of those solutes between the mobile and stationary phases affords viable separation.

Such a limitation prohibits the analysis of any intractable samples (i.e. potential solutes) unless the means to modify them are invoked.

In order to attain that goal, thermal fragmentation of such samples was proposed with the object of providing volatile products that would yield to conventional gas chromatographic separation. Having identified the resultant products and made the basic assumption that the fragmentation of the sample was complete, one then had to reassemble the jigsaw in order to elucidate the nature, even the identity, of the original sample. In any event, meaningful deduction must be implicit with the base assumption that one is considering primary degradation products, hence, pre-knowledge of the character and/or chemistry of a particular sample is often needed in order to arrive at a definitive conclusion.

Naturally, thermal degradation is a method that requires educated application in that resultant fragments must be of a molecular size that allows sensible interpretation. Obviously, a large number of small fragments are of little value since ultimately most organics will break down to very light hydrocarbons, both saturated and unsaturated, carbon oxides, water and a variety of inorganics of greater volatility, e.g. ammonia, hydrogen chloride, oxides of nitrogen or sulfur.

Although Davison, Slaney and Wragg are credited with the introduction of pyrolysis gas chromatography (PGC) in 1954, there is ample evidence that several workers were developing the method even earlier. It was immediately recognized that the technique was invaluable for the identification of synthetic polymers whose commercial viability depended on suppression of their chemical identities. Thus there was a good reason to conceal the fact that one could not only access competitors' products but learn as much or even more about a particular product than the manufacturer!

Whatever has been said and written about slow pyrolysis is very much open to question. Certain workers have long advocated the use of slow temperature ramps to reveal progressive transitions in the sample. It does not seem unreasonable to suggest that the approach is untenable as homogeneity of the sample is imperilled. Heat transfer within that sample and variable rates of diffusion of any products through unaffected, untransformed, undegraded, affected, transformed or degraded sample cannot be controlled and therefore leaves the question 'what is one actually looking at?' unanswered.

Terminology

It is now agreed that pyrolysis (alternatively, thermal breakdown, thermal cracking, thermal decomposition, thermal degradation or thermal fragmentation) is the transformation of a compound into another substance or substances through the agency of heat

alone. Indeed, most pyrolyses are thermal decompositions or fragmentations. Be warned that the formation of larger rather than smaller molecular weight substances is not only possible but, under certain conditions, highly probable (as the writer learnt to his cost very early in the development of the method).

A pyrogram is a chromatogram of a pyrolysate. It was originally used in the sense of a fingerprint and a tentative identity assigned after comparison with a library of known pyrograms which had been prepared under as near identical conditions as was then possible. With the advent of coupled gas chromatograph/mass spectrometer and discriminative mathematical treatments of vast quantities of data, the technique was promoted to a much higher plane but it should be remembered that statistical methods are, on occasion, far from infallible.

Modes of Pyrolysis

Many practitioners still prefer to fabricate their own pyrolysers without a true appreciation of the many factors that influence the results. Both inter- and intralaboratory reproducibilities are affected by introducing self-inflicted intangibles, inevitably reflected in differences of design and operating conditions.

The scale of these problems was highlighted by the outcome of the European PGC Correlation Trials arranged by the Gas Chromatography Discussion Group (now the Chromatographic Society) as long ago as 1968–1975; this was later duplicated on the same samples by Walker *et al.* in the USA. Gratifyingly, the two sets of results were encouragingly similar but, sadly, not identical.

However, despite serious efforts to introduce effective levels of standardization in both apparatus and practice, the technique fell into disrepute. This was principally due to a plethora of home-made pyrolysers, the conditions of their use and, finally, the total inability of inexperienced would-be practitioners to recognize the many pitfalls. Even worse, the method became stigmatized as 'dirty analysis' because of the damning evidence of tarry and/or carbonaceous residues remaining in the pyrolysis zone. The philosophy was that incomplete analysis has little credibility unless an experiment is focused on the observation of a unique independent event which is an indisputable marker of a specific situation.

The Furnace Pyrolyser

The furnace pyrolyser consists of a relatively small, electrically heated, isothermal chamber, preferably integral with the injection port of the chromatograph. Any connecting line should be similarly heated for as short a time as possible to minimize diffusion and

secondary reactions. The furnace itself must have a large thermal capacity to avoid any significant temperature sag upon introduction of the sample and its carrier. It must be so constructed as to allow the sample, contained in a miniature 'boat' or crucible to be introduced through a purged airlock by means of a suitable mechanism.

The most serious drawback is, of course, the presence of a significantly large dead volume where turbulence could cause the pyrolysis fragments to remain in the pyrolysis zone for a sufficient length of time to produce secondary fragments and thus confuse the picture.

The Filament or Platten Pyrolyser

The filament or platten pyrolyser is an electrically heated conductor having a relatively large usable surface area contained in a minimal volume. **Figure 1** shows a recent example of the device which has been fabricated from a piece of Pyrotenax topped by a suitable finned cooling cap carrying a socket accepting a two-pin plug. The filament itself is initially a 2.5 ohmic length of 22 wire gauge platinum, chromel-alumel, nichrome or other resistance wire tightly machine-coiled to an internal diameter of 1.0 mm, tensioned across the central conductor and an extension of the sheath to a 2 ohmic length and spot-welded in place.

Obviously the length of the Pyrotenax barrel must be tailored for a particular injection port and the port itself reamed out so that the annular space between the inner wall of the injection port and the Pyrotenax outer sheath is no wider than 0.2 mm. This is to combat the probability of a back-pressure pulse, for when the pyrolyser is fired at a temperature of, say,

700°C there is a large local carrier gas expansion. Due to the dynamic resistance of the chromatographic column this must be accommodated in the direction of the gas flow to prevent both diffusion and the risk of reverse flow that passes the pyrolysate through the pyrolysis zone a second time with the risk of further thermal modification. This is absolutely essential to observe the terms of good practice. It must also be taken into account that there is a temperature coefficient of resistance which must be accommodated and suitable measures taken to ensure reproducibility.

Temperature control is best achieved by making the filament or platten one arm of a Wheatstone Bridge circuit and adjusting the balance to control final temperature. The system is calibrated by inserting the pyrolyser in a dummy column maintained under the chosen chromatographic operating conditions and observing the melting points of a series of inorganic salts. It should be noted that the current density applied to the filament must be conducive to rapid heat-up for it is essential to attain the pyrolysis temperature in a few milliseconds (if not microseconds) and ensure a hold for, say, no more than 1–2 s by means of associated timer circuitry. In that time the pyrolysis products are on-column and being separated – ideally the thermal profile should be a square wave.

These instrument combinations and their operations, described above, have been tried and tested by the writer in many laboratories throughout the world over many years and have proved easy to handle by laboratory technicians. Pyrolyses themselves are eminently reproducible provided that the sampling

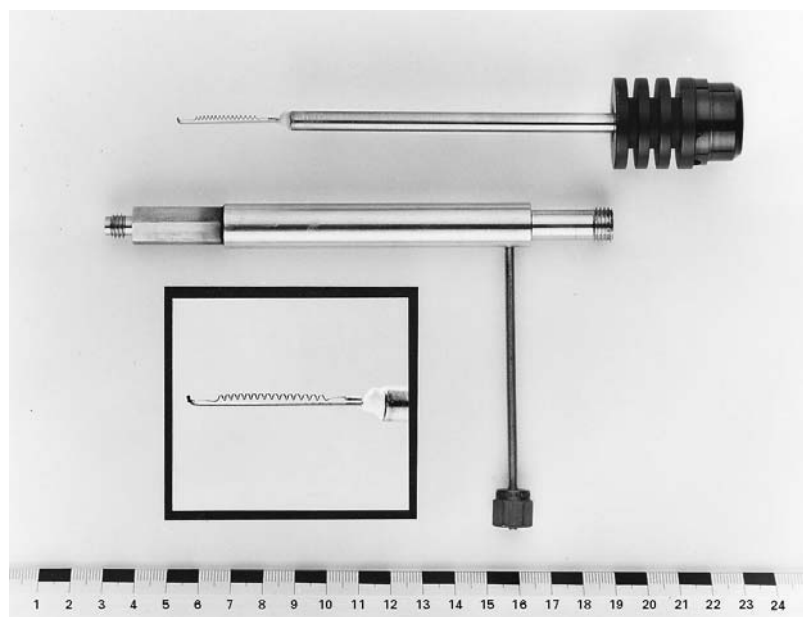


Figure 1 A modern filament pyrolyser together with its modified chromatographic injection port. Inset: detail of mounted filament.

procedure is standardized (see below) and equipment is maintained in as near-sterile conditions as reasonably possible.

At best, the pyrolyser should be cleaned by heating at a higher temperature in an inert atmosphere between every shot. This serves two purposes: first, it removes traces of any residues and second, if cleaned on-column, the completeness of the pyrolysis is verified. In the event that this process is too time-consuming it is better conducted externally or under back-flush conditions.

The possibility of the heating substrate acting as a catalyst has never been completely negated despite a series of standardized experiments conducted by Jones on a variety of metals, both before and after gold-plating. A second hazard is found in the build-up of carbon on the filament itself; this modifies the pyrolysis surface.

The Curie Point Pyrolyser

The adoption of inductive heating by Giacobbo and Simon in 1964 was very quickly recognized to possess many virtues. The most important is found in the fact that final skin temperature (the Curie Point) is a function of the composition of the ferromagnetic conductor when subjected to a given radiofrequency electromagnetic field. Additionally, the skin heating rate is constant for wires of identical cross-section. Moreover, there is no risk of cross-contamination as a 'virgin' wire can be used for each pyrolysis. Sterile storage and handling of new wires is the only precaution necessary.

Table 1 lists the constitutions and Curie Point temperatures of a range of ferromagnetic conductors.

It should be remembered that an energized radiofrequency coil generates an ellipsoid field. In consequence, the Curie wire should be located in such a position that the sample it carries is as near to the centre of the coil as is practically possible. In order to avoid any artefact introduced by an end effect, Jones pointed out that the use of a Helmholtz coil gave a stretched field uniform over a greater length of the coil and hence precise location of the sample became less critical.

A cross-sectional diagram of the built-in injection port receptor designed by Jones is pictured in Figure 2.

Figure 3 shows the Curie Point pyrolyser insert in cross-section. Obviously, a simpler, but dimensionally similar insert can be used for conventional liquid sampling so that the integrity of any comparative exercise is preserved.

Figure 4 details the cryogenic focusing unit contained in the oven necessary to counter the inevitable degradation of column performance by the unavoidable presence of an unusually large dead volume

Table 1 Metals and the composition of their alloys which give a usable range of Curie Point temperatures

<i>Metal or alloy (composition %w/w)</i>	<i>Curie temperature (°C)</i>
Fe/Ni (78.5% Ni)	200
Fe/Cu/Ni (9.0% Cu/36.0% Ni)	300
Ni	358 ^a
Fe/Al (16.0% Al)	400
Fe/Mo/Ni (4.0% Mo/79.0% Ni)	460
Fe/Ni (50.0% Ni)	500 ^a
Fe/Ni (68.0% Ni)	600 ^a
Fe/Co/Ni (7.0% Co/70.0% Ni)	650
Fe/Si (4.0% Si)	690
Fe/Co/Ni (25.0% Co/45.0% Ni)	715 ^a
Fe/Si (3.0% Si)	740
Fe	770 ^a
Fe/Co (50.0% Co)	980 ^a
Co	1130 ^a

^aThe metals or alloys most commonly available drawn as suitable wires. Warning: temperatures quoted are approximate because of impurities and the method of manufacture. Data from Bozorth RA (1951) *Ferromagnetism*. Toronto: Van Nostrand. The help of the British Library, Science, Technology and Business, in this matter is gratefully acknowledged.

which must encourage diffusion as well as other attendant difficulties. A timer/control unit triggers a solenoid valve to close a liquid nitrogen reservoir to build up pressure. A second solenoid valve opens a feed line to allow a jet of liquid nitrogen to play on the front end of the column for 2 s at the moment of pyrolysis. Warm-up of the chilled zone to column temperature to liberate the pyrolysate is near instantaneous by reason of the large thermal capacity of the oven/column assembly. Finally arrangement is made for pressure release in the liquid nitrogen vessel; the cycle is replicated for conventional liquid sampling.

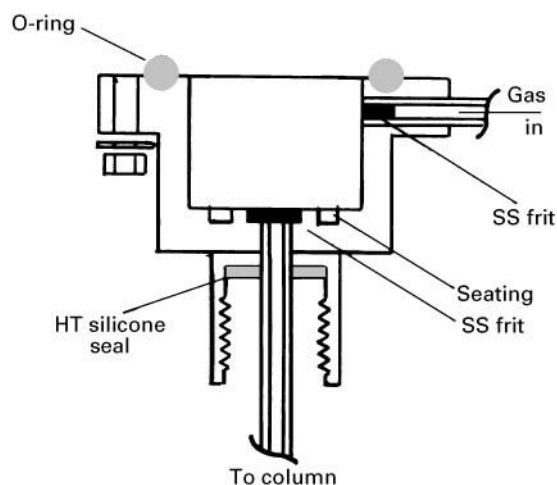


Figure 2 Cross-section of built-in replacement injection port which acts as a receptor for the several inserts (not to scale).

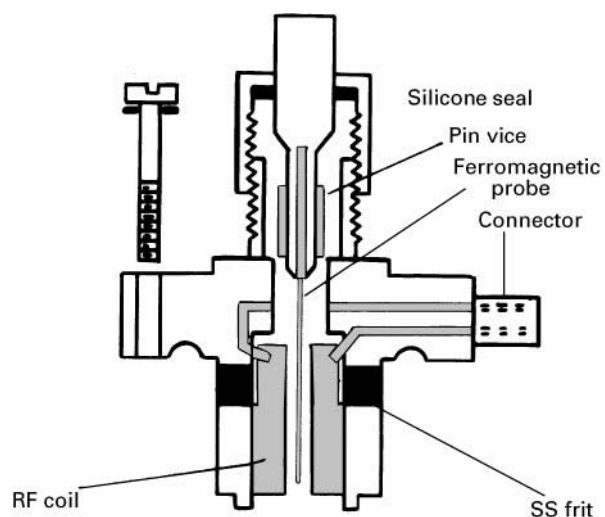


Figure 3 Cross-section of Curie Point pyrolyser insert (not to scale).

Laser Pyrolysis

Both ohmic and inductive pyrolyses are initiated by heating the back of the sample (which can be a serious disadvantage: see Sampling, below). In contrast, laser heating involves surface initiation of the degradation process. Table 2 compares the pertinent elements of the two processes.

One of the recommended sources of energy is a pulsed neodymium-YAG laser which is mounted in parallel with a neon laser aligned on an identical light path to afford a sight line to aid selection of the required target.

Very rapid heating requires a high thermal flux; perhaps the idea of a pulsed laser is far too simplistic when only the thermal aspects of laser-induced pyrolysis are considered, for the process involves a short, intensive photolysis which radically differs from our present understanding of the pyrolytic process.

A phase-coherent laser beam delivers packets of photons in a nanosecond pulse into the surface of the sample. It should be noted that if the sample is optically transparent, a pigment must be added to provide absorbing centres to promote the ionization of the molecules in the sample surface.

Table 2 Comparison of two heating processes

	<i>Ohmic inductive heating</i>	<i>Pulsed laser heating</i>
Substrate	Metal platten or coil, or ferromagnetic probe	Sample continuum (pigmented if necessary)
Sample	Solution or sonic dispersion	Solid chip or compacted powder
Heating geometry	Sample back	Sample front
Heating rate	10^3 K s^{-1}	10^7 K s^{-1}
Cooling rate	-10^3 K s^{-1}	-10^6 K s^{-1}
Pyrolysis condition	Both in an inert atmosphere	
Time	100–2000 ms	4–800 μs
Limitations	Possible catalytic effect(s). 'Blow-off' due to gaseous products at substrate causing molten undegraded sample to balloon and burst	Heat input/take-up indeterminant. Possibility of plasma reactions and photolysis. Transparent samples need pigmenting

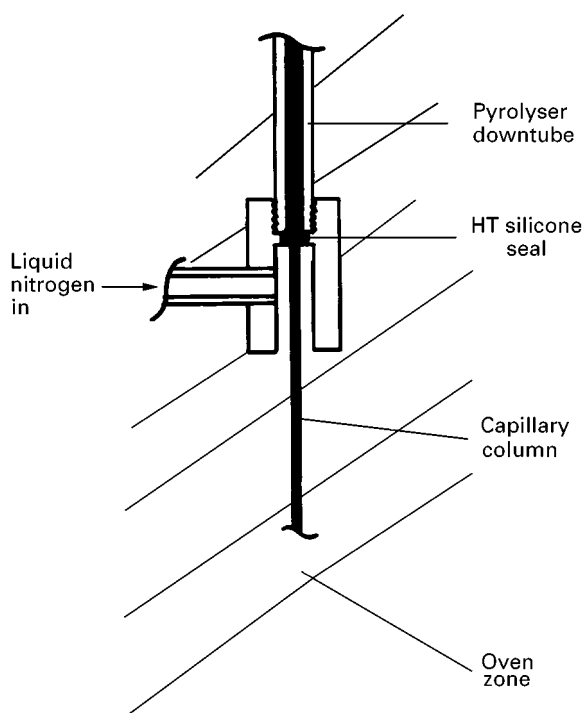


Figure 4 Diagrammatic cross-sectional representation of the pre-column concentration unit (not to scale).

The ionization process can be explained either by electron tunnelling or by multi-photon absorption. After initial ionization, photon energy is selectively absorbed by electrons above the sample surface and the hot electron cloud or laser plume collapses into the sample surface whereupon molecular fragments are pumped into the hot plasma. On termination of the pulse the system rapidly returns to ambient.

The plasma, consisting of unbound electrons, free atoms and those few radicals of unusual stability, is in kinetic equilibrium but when the unbound electrons return to their accustomed atomic states the resultant species quench directly from the plasma and provide an informative series of products. However, other species can arise from thermal scissoring within the solid sample and a further series of products can then result from interaction of those species with certain plasma components.

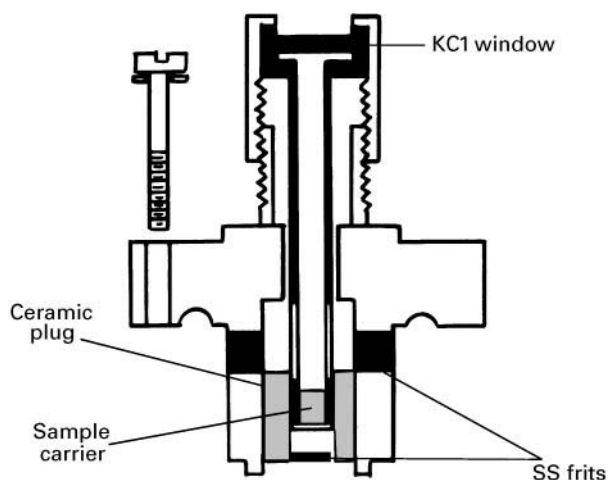


Figure 5 Cross-section of laser pyrolysis cell insert (not to scale).

A laser pyrolysis cell insert for the chromatographic injection port receptor (Figure 2) is shown in Figure 5.

UV Degradation

The only other energy source that has been used in the context of pyrolysis is the UV generator introduced by Juvet, who promulgated its use for stability studies.

The very slow reaction rates associated with time-dependent processes such as the weathering of synthetic coatings, adhesives, rubbers and textiles are in no way compatible with the fundamental concepts of pyrolysis as heretofore enunciated. Therefore the use of UV excitation has shown no advantage over traditional techniques and, in consequence, was abandoned.

Sampling

One of the foremost and, perhaps least appreciated of the initial problems is that of sampling. Sample size and distribution are critical because organics, which comprise the vast majority of potential samples, are invariably very poor conductors of heat.

Jones and Moyles enunciated the thin film concept in 1958. This is based on comparisons of strictly controlled pyrolytic events on the milligram, microgram and sub-microgram scales. Pyrograms of simple substances were demonstrated to be of ever-increasing complexity as sample size increased. The phenomenon was eventually shown to be due to diffusion of degradation products through partially degraded sample and longer residence times in the vicinity of the pyrolysis zone, which led to unwanted secondary reactions. For these reasons it is advisable to work on the nano- or even picogram scale whenever possible.

It should be realized that the most informative evidence leading to an unambiguous conclusion lies

in the certainty that all the scissive events viewed are primary reactions (notwithstanding the fact that most primary reactions must be the formation of free radicals which are themselves stabilized by recombination). Therefore it is imperative to regularize the situation as best as possible. That is, the fastest thermal gradient with respect to time within the body of the sample, a condition that is only satisfied by presenting the sample as a very thin film, ultimately as a uni-molecular layer. Unfortunately, the very nature of most samples submitted for pyrolysis prior to gas chromatography is that they are reluctant to form the uni-molecular layers that are theoretically essential. So a compromise has to be made and as thin a layer is distributed on the effective surface of the chosen pyrolyser as is practically possible.

When a sample is soluble in a volatile solvent the deposition problem is ameliorated but immediately poses further problems. What if the solvent lacks wetting power for metallic surfaces? Addition of an amount (e.g. up to 5% v/v) of tetrahydrofuran or dioxan as a wetting agent rarely affects solubilization and overcomes the beading that characterizes a non-wetting system.

After deposition of the sample, residual solvent is best removed in a vacuum oven at a temperature little above ambient. However should the sample be insoluble it is reduced to fine powder by slow freeze-grinding in order to minimize the risk of thermal degradation arising from localized heating due to mechanical friction. It is sonically mixed with a blend of a polar solvent and water containing 1% w/w of a refined natural gum or a purified poly(vinyl alcohol), and then stuck on the probe and dried in the manner already suggested. Conflicting pyrolytic fragments arising from breakdown of the adhesive used can be subtracted from the total pyrogram if deemed necessary; experience, however, has shown that there is little significance in any contribution from the presence of a relatively small amount of an alien material provided that the same routine is used in comparative exercises.

It cannot be emphasized enough that much depends on maintenance of strictly sterile conditions as always.

Applications

The universality of the application of PGC methods has long been a matter of dispute. Without doubt, most disagreement has come from those who have failed both to appreciate and then to observe the basic precepts outlined in this article.

Historically, the method found the greatest initial value in the identification of synthetic macromolecules, while subsequent work by Shin Tsuge in Nagoya led to the elucidation of polymeric microstructures.

There followed studies explaining mechanical strength, cold-drawing properties, film-forming capabilities, cohesion within films and their adhesion to a wide variety of substrates, pigment binding, and the mechanisms of cross-linking processes.

Reiner was the first to appreciate that the difference between a synthetic macromolecule and a biopolymer was merely that of environment. In consequence his work on microbacter and cellular transformations must now be considered to be the foundation for much of today's clinical and pathological practice.

The FOM Foundation group in Amsterdam, under the stewardship of Meuzelaar, expanded the field of application of PGC in parallel with their pioneering work in pyrolysis/mass spectrometry. There, their initial focus was on a broad spectrum of natural polymers.

Wheals, of the British Metropolitan Police Forensic Laboratory, introduced PGC in criminology and developed techniques that formed a basis for standard practice in forensic laboratories. Results are now generally accepted as evidence in many criminal jurisdictions.

The virtue of the very small samples needed for the vast majority of diagnoses has seen adoption of PGC, conducted under very carefully controlled conditions, for the preservation of many art gallery and museum exhibits. For example, deteriorating ancient varnishes and pigments have yielded their secrets and pictures may be cleaned and/or restored without further damage, which will benefit the generations still to come.

Environmental and ecological applications are now coming to the fore. The analysis of occlusions of harmful volatile organics on air-borne particulates has contributed much to our understanding of their significance in the context of respiratory problems.

Bracewell was among the first to develop PGC for the assessment of soil fertility. More recently, De Leeuw graphically demonstrated that reasonably volatile organics such as polycyclic and halogenated hydrocarbons could be excised from very complex matrices (e.g. soils or sediments) by flash evaporation by imposing a millisecond thermal ramp on the sample.

Jones and Vanderborgh employed PGC in conjunction with other pyrolytic studies in their elucidation

of coals. They demonstrated that their apparent heterogeneities were due to guest markers of the environments of both the initial debris and the maturation cycle then occluded in a formal cross-linked, spiral double-ladder polymer. An outcome of their work was a proposal for a 'down-hole' mole chromatograph containing a miniature laser pyrolysis cell designed to be lowered into a petroleum exploration, pilot drill hole for real-time *in situ* stratigraphic monitoring of hydrocarbons. Such an approach must certainly be quicker and cheaper than core extraction and subsequent off-site analysis.

In the light of the diversity of applications given here, it is more than apparent that PGC's potential is only limited by the wit and imagination of the educated user.

Conclusions

Despite the early stigma of unreliable and dirty analysis, PGC survived because of the dedication of a small handful of workers who were convinced that most practitioners were to blame for their failures rather than the tool they purported to use.

The method has re-emerged as an active member of the analytical chemist's armoury. This is handsomely substantiated by each successive issue of the *Journal of Analytical and Applied Pyrolysis*.

Material gain has resulted from the adoption of hyphenated instrumentation (e.g. coupling with high speed quadrupole mass spectrometry or Fourier transform infrared spectrophotometry) and has most certainly elevated the status of the technique.

See also: II/Chromatography: Gas: Detectors: Mass Spectrometry; Detectors: Selective. III/Archaeology: Uses of Chromatography in. Art Conservation: Use of Chromatography in. Humic Substances: Gas Chromatography. Space Exploration: Gas Chromatography.

Further Reading

Wampler TP (1995) *Applied Pyrolysis Handbook*. New York: Marcel Dekker.

Sampling Systems

I. W. Davies, Cambridge, UK

Copyright © 2000 Academic Press

Introduction

The term 'injection' encompasses techniques used to transfer samples of gases, liquids and solids on to the

column for the process of separation to take place. Sample components must be vaporized without decomposition and both major and trace components transferred quantitatively to the column, irrespective of volatility, polarity, etc. During this process, column efficiency must be preserved and band broadening arising from injection (dead space, adsorptive

sites) must be minimized. The operating conditions, e.g. column temperature and solvent used, should not influence injection, and retention times and peak areas should be reproducible.

Injectors for pyrolysis-GC and supercritical fluid chromatography will not be dealt with in this article.

Gas Samples

For accurate quantitative analysis gas samples are nearly always introduced by means of a valve fitted with an internal or external sample loop. Although the construction of gas-sampling valves takes a variety of forms, the principle of operation is common to all. In one configuration the gas passes through a loop ranging from approximately 0.1 to 10 mL in size while the carrier gas passes into the column. In the other configuration, the sample is isolated and the carrier gas stream sweeps the sample trapped in the loop onto the column. If care is taken to control the temperature and pressure of the gas, such valves offer very high reproducibility and all quantitative analysis can be performed by external calibration. They can also be readily automated for plant analysis. For further details see Gas analysis by gas chromatography. Gas samples can be injected on to columns by means of gas-tight syringes but the precision is much poorer than that with loop valves and their use is not recommended for accurate quantitative analysis.

Solid Samples

Solid samples are best dealt with by dissolving them in a suitable solvent and treating them as liquid samples. It is not always possible to find a suitable solvent or the 'sample' might be in a matrix such as soil or sand. For such materials packed columns have been fitted with capsule samplers where the capsule is dropped into a hot vaporizing zone and is withdrawn by a magnet after analysis.

Liquid Samples

The majority of samples analysed in the laboratory are in liquid form, as would be expected from the range of compounds likely to be amenable to GC. Most of this article is, therefore, concerned with the introduction of liquid samples onto packed and capillary columns.

Packed Columns

The equilibrium distribution of analyte between the two phases should be independent of sample size.

However, as sample size increases isotherms become nonlinear and peaks become broader and distorted, which leads to reduced resolution. A column is regarded as overloaded if its efficiency is reduced by 10%. The approximate maximum vapour volume (V_{\max}) of an individual solute not leading to detectable peak broadening can be calculated from:

$$V_{\max} = \frac{0.02 \times V_R}{\sqrt{N}} \quad [1]$$

where V_R is the retention volume and N is the number of theoretical plates.

For a component eluted with a retention volume of 150 mL (after 5 min at 30 mL min⁻¹) from a packed column of 3000 plates, V_{\max} is approximately 50 μ L, equivalent to 0.1 μ L liquid.

More empirically, initial bandwidth should be not more than a tenth of the width of the narrowest peak and the smaller the sample the better the chromatography. The analyst should inject microgram quantities. Since 0.1 μ L corresponds to 100 μ g for a liquid of unit density, dilute solutions are necessary if only a few micrograms are required.

Vaporizing Injector

Injection is usually performed with a syringe, through a replaceable, self-sealing plastic or rubber septum into an injector of approximately $\frac{1}{4}$ in i.d. (6 mm). The column is attached either to the base of the injector or inserted within it. In the former instance metal fittings are usually used. The injector is heated to facilitate rapid transfer of sample to the column ('flash vaporization'). To limit sample decomposition on hot metal surfaces, the injector usually contains a glass liner that can be replaced when dirty and can be regularly deactivated by silylation. The injector temperature should be high enough to vaporize the components of interest; as the temperature required to do this is rarely known, the temperature is usually set to *ca.* 50°C above the oven maximum.

The column inserted inside the injector usually reaches almost to the septum and the sample makes contact with the column only ('on-column' injection). Glass columns are installed with fittings incorporating ferrules of graphite or poly(tetrafluoroethylene) (PTFE) and these fittings must be leak-tested regularly. On-column injection can be used equally successfully for small injections of concentrated solutions or larger volumes of dilute solutions – initial band volume (of liquid) is unlikely to exceed 50 μ L. For high temperature chromatography the injector is heated and again the volume of vapour is important (unless the injector is heated after injection, when it should be confirmed that the heating rate matches that of the

column oven). The injector temperature should not exceed the maximum operating temperature of the stationary phase.

Injectors are rarely heated uniformly; the heating block encloses only part of the injector body and the rest is heated by conduction. Sometimes, to reduce septum decomposition and bleed, the injector is designed so that the septum nut is colder than the rest of the injector. Carrier gas enters the injector through an inlet in the jacket enclosing the injector liner. Usually it is warmed by passage through a coil of stainless-steel tubing wound round the injector heating block; this helps ensure that vaporized sample does not encounter cold carrier gas.

Syringes

Plunger-in-barrel (5–1000 μL) and plunger-in-needle (0.5 or 1 μL) syringes are widely available. The latter are used to dispense quantities up to 1 μL , although the 5 μL syringe can be used to dispense 0.3 μL with reasonable repeatability, especially if used on an autosampler, although the amount injected is not necessarily that indicated on the graduated scale. With the plunger-in-barrel syringe, needle volume is relevant if the injector temperature is above the solvent boiling point. When the plunger-in-needle syringe is used for vaporizing injection the needle temperature starts to increase when the needle penetrates the septum; the sample should, therefore, be partly withdrawn into the needle, otherwise part will be discharged into the septum.

It is difficult to determine the volume of sample remaining in the needle after vaporizing injection. Much will be forced from the syringe by explosive vaporization; this will cool the needle (passage of cold solution; absorption of latent heat of vaporization) and some sample will inevitably evaporate from inside the needle, depositing involatile residue. Such problems decrease in significance with increasing injection volume (but are immensely significant in capillary GC). Passage of sample through a hot steel needle can lead to decomposition of unstable sample components.

These considerations have led to the development of several different syringe-handling techniques.

Filled needle The plunger is moved quickly up and down to eject air and the syringe is removed from the sample with the plunger fully depressed. The sample is injected by pushing the syringe through the septum without moving the plunger. The needle volume only is injected, some sample is inevitably 'injected' into the septum, and much of the sample evaporates from the inner surface of the needle.

Cold needle The sample is withdrawn into the barrel and the syringe is inserted through the septum and the plunger depressed immediately. It is hoped that most of the sample passes through the needle in the liquid state with the needle still cold. Sample remaining in the needle, however, evaporates as the needle warms.

Hot needle Performed as above but the needle is left to warm in the injector for 3–4 s before rapid depression of the plunger. Much of the sample is rapidly ejected from the needle as a result of rapid explosive vaporization in the first stages of injection. The amount of sample evaporating from the inside of the needle is probably less than for cold needle injection.

Solvent flush A small volume (*c.* 1 μL) of solvent is withdrawn into the barrel, then the sample (possibly with an air barrier between the two to prevent mixing). Injection is performed by hot or cold needle injection. The sample can be sandwiched between two portions of solvent.

Air flush As above, but with air in place of solvent. However, the continuous introduction of oxygen into the column is not recommended for high temperature work because of the deleterious effect on the stationary phase.

Air and solvent As above, but with both air and solvent.

Sample Vaporization

It is not clear what happens to the sample inside the injector. Almost certainly it enters as liquid droplets. Although it is widely assumed that vaporization proceeds almost instantaneously, it is unlikely that enough energy is available, certainly in the carrier gas, to supply the latent heat required. If the liquid sample hits the wall of the injector, instant evaporation of the solvent in contact with the wall probably forces the sample away from the wall, i.e. the source of heat. Even if the sample is injected into a hot packing only a small amount of heat is available and the sample probably evaporates quite slowly.

Disadvantages

The vaporizing injector works well for packed-column injection but septa cause problems and must be changed frequently to avoid leaks. Septa also generate ghost peaks from plasticizers added for flexibility; decomposition products and delayed release of absorbed polar materials, especially if injection sizes are too large. The best solution to the problem is to

divert a small amount of carrier gas over the septum surface and to exhaust this stream to atmosphere.

Capillary Columns

Typical carrier gas flow rates for 0.3 mm i.d. wall-coated open-tubular (WCOT) columns are less than 2 mL min^{-1} . The vapour from $1 \mu\text{L}$ solvent occupies approximately 0.5 mL at 250°C . If the injector volume is 1.0 mL and flow of one injector volume of carrier gas sweeps all the vapour on to the column (no diffusion of sample with carrier gas), transfer time is $\geq 30 \text{ s}$ – considerably more than the 5 s peak widths typically encountered in capillary GC. In reality, sample concentration in the carrier gas decreases exponentially because carrier gas diffuses into the sample vapour cloud; this adds a tail to the band widths given above.

There is clearly a need for a different method of injection or a means of narrowing the band-width.

Split Injection

Split injection, or indirect sampling after vaporizing injection, was the earliest attempt to solve this problem. For many years it was the only technique available; it is still very popular.

Carrier flow through the injector is split; a small proportion is directed into the column and the remainder is vented. When the sample is vaporized a small proportion of the vapour cloud only is transferred to the column; this reduces the time during which sample is transferred into the column. The split ratio is:

$$\frac{\text{carrier flow to atmosphere}}{\text{flow through the column}}$$

Most of sample is lost so the technique is not suitable for trace analysis (sample components present at levels below 0.01%) but it is well suited for complex, relatively low-boiling mixtures, such as gasoline, containing many components in the range $0.01\text{--}10\%$.

Originally it was widely believed that the splitter eliminated the column overloading believed to be responsible for excessive bandwidths. This could have been achieved by diluting the sample. Although the capacities of capillary columns are well below those of packed columns, the effect of overloading on band broadening is negligible compared with the effect of slow sample transfer.

Using eqn [1] for a 0.32 mm i.d. column with $90\,000$ theoretical plates and a component for which V_R is 10 mL (elution after 5 min at 2 mL min^{-1})

shows that V_{max} is approximately $1 \mu\text{L}$ (equivalent to $0.002 \mu\text{L}$ liquid). This formula gives a pessimistic result for capillary columns and $15 \mu\text{L}$ is more realistic. Even so, to reduce 0.5 mL vapour to 0.015 mL requires a split ratio of $33:1$; to take account of sample diffusion in the carrier gas, practical split ratios must be considerably higher ($>100:1$).

Splitter Design Features

Splitting should be reproducible; reproducibility is, however, affected by many factors.

The sample must encounter inert surfaces only – the injector usually contains a glass liner. Splitting should be linear and nondiscriminatory, i.e. sample should be vaporized rapidly and pass the column inlet as a concentrated, homogeneous plug. Because of the limited heat available, the sample is unlikely to be vaporized instantaneously. Droplets can be carried into the column irreproducibly and evaporation of droplets in the injector leads to fractional distillation. Such behaviour can be overcome by using a mixing device, e.g. packing the liner with glass wool or glass beads. This can cause dilution of the sample (loss of sensitivity) and discrimination owing to adsorption, condensation and decomposition. Adsorption can be reduced by silylation *in situ* (because packing an injector with silylated glass wool results in fracture of the glass fibres and exposure of new active sites); condensation might be eliminated by increasing the temperature.

Packed injector liners were introduced as thermal reservoirs to encourage rapid vaporization. Calculations show, however, that except for volumes of *ca.* $0.5 \mu\text{L}$, the amount of heat available from carrier gas and liner packing is well below that required for vaporization. Heat is available from the injector wall, but when solvent droplets touch this they are instantly repelled by vaporization of the small amount of solvent in (instantaneous) contact with the wall. It is now accepted that the packing provides a surface that retains the entire sample during slow, controlled evaporation.

The carrier gas is heated so that at high split ratios the gas flow does not cool the injector, leading to variation in the split ratio or incomplete volatilization. If the vent flow is turned off after injection (to conserve carrier gas), ensure: (1) this does not affect column head pressure, hence carrier gas flow rate (back-pressure regulation is claimed to achieve this); (2) there is a small continuous flow from the injector to eliminate back diffusion of partially vented material; and (3) the injector septum is gently purged to atmosphere to eliminate ghost peaks from septum bleed.

It has been suggested that a buffer volume beyond the split point reduces pressure fluctuations that might lead to variations in carrier flow and split ratio; although such buffer volumes do indeed help dispel pressure waves, their benefits have been disputed.

Injection Technique

The most reproducible injections with least discrimination are given by the 'hot needle' (1.5–2 μL) and 'solvent flush' techniques. Needle-in-plunger syringes cannot be used because samples start to evaporate as soon as the syringe enters the injector, leading to fractionation and discrimination. Injector temperature should be near the boiling point of the sample's least volatile components or discrimination might arise even from a well-designed splitter, especially at low (<100:1) split ratios. If it is essential to use a low split ratio, e.g. in trace analysis, then a high temperature must be used. For unstable compounds a low injector temperature and high split ratio are desirable.

If the column temperature is below the solvent boiling point and the solvent vapour pressure is sufficiently high (depending on injection size and split ratio), sample can condense in the column. The resulting sudden drop in pressure leads to suction of material from the injector and the split ratio will vary. Similar effects might lead to condensation in gas lines control valves, etc., leading to ghost peaks later in the analysis as the material diffuses back into the injector.

The column should be mounted with its inlet at, or near, the injector base to minimize the volume from which back-diffusion might occur. For the largest signal, needle length should be such that sample is released at the column inlet (10 mm gap). The effect of needle length on response should be checked experimentally.

It is worth varying the split ratio over a wide range – a high split ratio might result in such rapid flow through the injector that the sample passes the column inlet while still in the form of a concentrated plug. The vapour cloud concentration can be optimized to prevent back-diffusion by use of an injector liner compatible with injection. For low split ratios (10:1–50:1) and 8 cm liner typical values are: a 1.5 mm i.d. liner for 0.4 μL injection, a 2.0 mm i.d. liner for 0.6 μL injection, and a 3.5 mm i.d. liner for 2.0 μL injection.

Advantages and Disadvantages

The advantages of the splitter are simplicity – for qualitative and semiquantitative work very little can go wrong. Its major disadvantage is discrimination: inhomogeneous mixing of carrier gas and sample and

different rates of evaporation and incomplete evaporation of components of different volatility inside the syringe needle and from droplets in the injector body. Other disadvantages include unsuitability for temperature-sensitive and involatile compounds and low sensitivity for trace analysis. Condensation of solvent inside the column, pressure surges on injection and changes in the volumes of carrier and sample gases on moving from injector to oven at different temperatures reduce reproducibility and mean that the actual split ratio is never that calculated from gas flow rates. To minimize errors from these effects, the operating conditions must be kept as constant as possible and internal standards should be used for quantitative analysis. Venting most of a sample to atmosphere may represent a safety hazard.

Reconcentration of Bands Broadened by Split Injection

Cold trapping If the difference between the column temperatures at injection and elution is $>45^\circ\text{C}$ (approx.), then material of low volatility is retained by the cold column and migrates only a small distance before transfer from the injector is complete; it starts to migrate only when the oven temperature is increased. The extent of reconcentration depends on the ratio of the migration rates of the volatile and involatile components. Because the migration speeds of most components are halved if the temperature is reduced by 15°C , there is a concentration factor of 2 for each 15°C difference between the column temperatures at injection and elution. A difference of 80°C will always render any band broadening resulting from injection undetectable and in normal circumstances a difference of 40 – 60°C will be sufficient.

Splitless Injection with Solvent Trapping

If solvent is injected by vaporizing injection into a column maintained at a temperature below the solvent boiling point, the vapour leaving the injector will, under certain conditions, condense in the column inlet. Splitless injection incorporating solvent trapping exploits this behaviour. The injector used is similar in design to some splitters (**Figure 1**), in that it has outlets to the column and splitter and a septum purge. During injection and for a short time afterwards (so-called 'splitless period') the injector and (often) septum purge vents are kept closed and the only exit from the injector is onto the column. At other times the vents remain open.

The injector vent is for rapid removal from the injector of material not reaching the column during

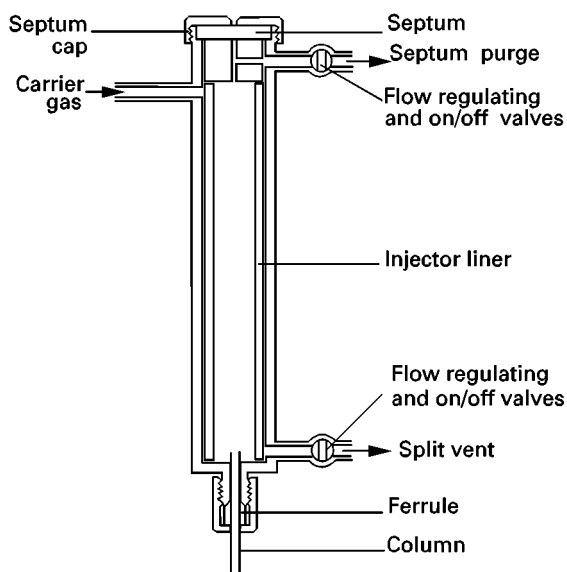


Figure 1 The split-splitless injector.

the splitless period. The vent flow is set to 20–100 mL min⁻¹. The purpose of the septum purge (1–2 mL min⁻¹) is as described above.

For injection, the oven temperature is set to $\leq 20^\circ\text{C}$ below the solvent boiling point (the optimum temperature is best determined experimentally), the vents are closed and the sample (1–2.5 μL) injected. After the splitless period (20–60 s) the vents are opened and chromatography initiated. The condensed solvent in the column acts as a thick layer of stationary phase, which dissolves the sample's components. Carrier gas passing over the film is rapidly saturated with solvent vapour so all solvent evaporation occurs at the rear of the film. As the length of the solvent film decreases, sample components remain in solution in the narrowing band of liquid. When the last trace of solvent evaporates, the sample components will have been concentrated into a narrow band from which to start chromatography.

Exploitation of solvent trapping is not limited to injection of liquids. If 2–3 μL solvent is condensed in the column inlet it can be used to trap volatile organic compounds injected as a vapour immediately afterwards (i.e. before the solvent has evaporated). This could be useful for headspace analysis.

Injection Technique

Initial vaporization of the sample is identical with that in split injection and so many of the factors described above are relevant. The text below covers points of special relevance to obtaining satisfactory solvent trapping.

The solvent boiling point should be 20°C below the column temperature at the start of chromatography.

Because, irrespective of oven temperature, the solvent will condense quantitatively only if its vapour pressure is sufficiently high, the amount of solvent injected must be adequate (1–2.5 μL is usually sufficient); excessive dilution of the sample vapour cloud with carrier gas should be eliminated by use of an injector liner of appropriate volume. If the solvent boiling point is too high the solvent peak might interfere with those of the sample components, although this might be overcome by choosing a solvent only sparingly soluble in the liquid phase and thus eluted quickly.

To reduce discrimination against less volatile sample components 90–95% of the sample must be transferred to the column. Because of dilution of sample in the injector, such transfer requires a splitless period four times that necessary to transfer undiluted sample; this could lead to excessive solvent tailing. In practice, the pressure drop caused by solvent condensation results in sample being sucked into the column faster than would otherwise occur; this offsets band broadening caused by sample dilution such that it is rarely a problem for sample volumes $< 4 \mu\text{L}$. The optimum splitless period should be determined experimentally, starting at *ca.* 20–30 s and increasing it for larger volumes and less volatile compounds. Optimum column position, needle length, etc., must also be determined experimentally.

If the injector has a separate septum purge and its flow is maintained sufficiently low, it may be possible to leave it open during injection without significant loss of sample, thus almost eliminating the effects of septum bleed.

Advantages and Disadvantages

The technique is reasonably simple, and applicable to dilute samples, trace analysis and to volatile and involatile compounds; it is reasonably good for quantitative analysis. Because the sample can be transferred to the column over a longer period than is possible for split injection, the injector can be maintained at a lower temperature, rendering the technique more suitable for the analysis of thermally unstable compounds.

In addition to the usual disadvantages of vaporizing injection (e.g. discrimination), solvent condensation leads to several extra problems including peak distortion and peak splitting. These can be overcome by employing a 'retention gap' (an uncoated pre-column) and by using solvents that wet the stationary phase (rather than forming droplets) and in which all the sample components are highly soluble; the volume injected should be as low as possible. Solvent condensation can lead to damage of very polar stationary phases (which are less well immobilized). The

solvent film can also result in variations in retention data, especially for different solvent volumes.

Cold On-Column Injection

This term denotes direct transfer of liquid sample into the column inlet, i.e. the sample is introduced to the column as a liquid rather than being evaporated from the syringe. Because the technique exploits solvent trapping, the column inlet must be kept cool, i.e. 10°C below the solvent boiling point (cf. 20°C below for splitless injection). In this way explosive evaporation of sample does not lead to its being flushed back into the cold injector where it might be lost completely or from where it might slowly drift back on to the column, leading to band broadening. The point of injection must, however, be positioned within the temperature control of the oven, usually 5–10 mm from the oven wall (a greater distance increases the chance of the needle being heated). The original design had the injector body only cooled. Later versions had the addition of secondary cooling so that during injection the section of column in the oven, and into which injection took place, could be cooled, thus increasing the range of temperatures over which the technique could be used. The injector body should be isolated from the hot insulating material of the oven top.

Injection is performed with a special syringe with a needle of o.d. 0.05 mm less than the column i.d. (so it does not plug the column and restrict carrier gas flow. The syringe is inserted into the column via a seal that prevents escape of carrier gas (column head pressure should be maintained). The carrier gas line to the injector should be through wide-bore tubing so that any slight leakage through the needle-seal does not affect the column head pressure. For borosilicate columns needle entry into the column is aided by chamfering the column inlet. This is not possible with fused silica because the column wall is too thin.

Injection speed depends on the injector. Better quantitative results are obtained by rapid injection, sending the sample well into the column to reduce the possibility of sample adhering to the needle and being removed when the syringe is withdrawn. Reproducible injection of 0.5–8 µL is possible. Smaller quantities are more difficult because they cannot be measured accurately with a 5 or 10 µL syringe and the speed at which the sample is ejected from a 0.5 or 1 µL syringe is insufficient to carry the sample well away from the syringe needle. If fast injection of these sample volumes is performed at oven temperatures near the solvent boiling point there are no problems with expanding clouds of solvent vapour being forced

back past the syringe needle (with consequent sample loss). At higher temperatures it is essential that the injector is fitted with secondary cooling so that sample is ejected into a cool section of the column. If secondary cooling is not available, it might be necessary to inject slowly at or about the solvent boiling point so that the vapour formed on evaporation from the column wall (not from the syringe needle) is carried away as it is formed. Some loss on the needle usually accompanies this technique, but losses are less than if the sample were to be forced explosively back into the injector body. Losses might be reduced by increasing the carrier flow and/or leaving the syringe in the injector for a few seconds after injection, to promote evaporation of the more volatile materials. However, this technique will lead to discrimination of another type, especially if the syringe needle becomes warm. Typical speeds for slow injection of different volumes of pentane are: 0.125 µL, 0.5 s; 0.5 µL, 1 s; 2 µL, 5 s; 8 µL, 20 s. If injections are much slower than this the solvent vapour pressure might be insufficient for condensation and no solvent trapping will occur. For volumes less than 0.2 µL rapid injection can be performed without secondary cooling, as the amount of vapour produced is insufficient to cause the sample to be expelled backwards.

In addition to cold trapping, which with on-column injection is effective for injections as small as 0.1 µL (cf. 0.5–1 µL for splitless injection), cold-trapping can also be exploited. Because cold trapping is less effective than solvent trapping the difference between elution and injection temperatures should be 80–120°C if effects are to be comparable.

Advantages

Quantitation and reproducibility are excellent and discrimination is negligible; the technique is ideal for heat-sensitive and low volatility materials that would not reach column if subjected to vaporizing injection. Vaporizing injectors perform very poorly with samples containing large amounts of involatile material, owing to irreproducible entrapment of volatile compounds.

Disadvantages

Insertion of the needle into the column can cause perturbations in carrier flow. The technique is susceptible to the peak splitting and solvent effects observed with splitless injection. Large amounts of solvent affect retention behaviour (cf. splitless injection) and can damage the column if an immobilized phase is not used (rare nowadays). The technique results in involatile sample components being deposited on the column; this can be overcome by washing the column

(the whole column if immobilized, the column inlet if not), removal of the column inlet, and/or use of a pre-column.

Programmed-Temperature Vaporizing Injector

Originally regarded as a means of injecting solids, the programmed-temperature vaporizing (PTV) injector is now seen as a means of overcoming problems associated with the hot needle in conventional vaporizing injectors. The sample is injected into a cooled injector body, which is then ballistically heated (at $10\text{--}30^\circ\text{C s}^{-1}$, possibly with several ramps and plateaux) to the required temperature (e.g. to 300°C in 20–30 s).

Design Features

The narrow (0.5–1.5 mm i.d., volume 15–150 μL), low thermal-mass injector liner ensures rapid heating and fast carrier flow. The insert is packed to retain sample droplets and, because the packing is fairly dense (for good thermal conduction), there is a seal between liner and injector body to ensure carrier passes through the liner. The packing can be glass fibre or beads for low retention (e.g. analysis of involatile materials), or porous materials such as Chromosorb (possibly coated with liquid phase) for greater retention. There is a facility for rapid cooling (e.g. by air flow) before injection, and the heater control can include a low temperature thermostating option for selective solvent removal. The septum is usually kept permanently cold, otherwise construction is similar to that of conventional vaporizers.

Advantages

This technique is useful for large volumes (10–50 μL , even 1 mL), especially if solvent vapours are vented to atmosphere before the remaining sample is directed on to the column. This is especially useful for analysis of high boiling solutes (sometimes called split-splitless injection or solvent-split injection), but results in loss of volatile compounds (possibly up to C_{20}). The vapour cloud from the solvent injected must not be so great that it flows back from the injector insert. To some extent this can be achieved by careful injector heating. Needle-in-plunger syringes can be used for small injections (injector not hot).

The PTV injector is useful for both split and splitless injection. Solvent trapping can be achieved with the latter but can often be avoided by adjusting the timing. Heating should be fast so that volatilization occurs quickly, especially if chromatographic migration starts immediately (i.e. no cold trapping

or solvent trapping), but this might cause thermal degradation.

The narrow liner means high carrier gas flow, so transfer to column is fast; retention by packing can be tolerated as carrier flow partially compensates (less likelihood of problematical matrix effects with dirty samples). Shorter transfer periods can be used for splitless injection; the use of lower column flow rates than for conventional split or splitless injection can still result in good transfer. The technique gives good precision because there is no aerosol formation and diffusion of quickly flowing carrier gas with sample means little recondensation of solvent in the column in split or solvent-splitless injection. There is no pressure wave, and less chance of matrix effects with dirty samples. Finally, there are no unwanted solvent effects with split or solvent-split injection.

Disadvantages

The rules for operation (e.g. injection speed, timing of heating and venting) are complicated and care is needed with timing of heating. Labile solutes, especially involatile materials requiring long transfer periods (high molecular weight triacylglycerols), are subject to thermal stress. The injector liner is too small for headspace samples. Transfer is by fractionation and any slight change in split ratio will result in components of different volatility being split by different ratios, probably irreproducibly.

Because of the small volume of the insert, the conventional PTV injector could not originally double as a split-splitless injector; this has been overcome by the introduction of an injector incorporating innovative heating technology that enables the size of the PTV to be increased to that of conventional vaporizing injectors. This injector can also be used for analysis of gases and solids. If the liner is packed with an adsorbent it can be used, either *in situ* or temporarily removed from the injector, to adsorb volatile organic compounds.

Cooled-Needle Vaporizing Injector

This injector was designed specifically to overcome problems associated with the hot syringe needle. It comprises a standard vaporizing injector with a glass insert. Between the septum and the upper region of the heated part of the injector body (and inserted into the upper region of the insert) is a gas-cooled jacket of length accommodating the needle of a standard syringe – when the needle is inserted only a millimetre protrudes into the heated region of the injector. After injection the syringe is removed and the cooling gas turned off. The base of the cooling jacket then heats

up so that material coming into contact with it might be vaporized. The technique should ensure minimization of discrimination caused by selective fractionation from the syringe needle. Published results seem to confirm that the technique gives highly precise quantitative results.

Conclusion

For many years the introduction of sample into the column represented the weak point for accurate quantitative analysis by capillary columns. In the last few years this has largely been remedied and good quantitation can be achieved by the use of one of the range of commercially available injectors. However, it was pointed out by Deans a number of years ago

that the only completely reliable method of sample introduction was in the vapour phase, i.e. handling all samples as gases. While this might be true, it is something of a council of perfection and it is likely that syringe injection through a septum will be with us for the foreseeable future.

See also: II/Chromatography: Gas: Column Technology; Historical Development. III/Gas Analysis: Gas Chromatography.

Further Reading

Grob K Jr (1987) *On-column Injection in Capillary Gas Chromatography*. Heidelberg: Hüthig.

Grob K Jr (1993) *Split and Splitless Injection in Capillary GC*. Heidelberg: Hüthig.

Theory of Gas Chromatography

P. A. Sewell, Ormskirk, Lancs, UK

Copyright © 2000 Academic Press

Introduction

Gas chromatography (GC) involves the separation of the components of a mixture by virtue of differences in the equilibrium distribution of the components between two phases; the gaseous (mobile) phase moves in a definite direction, while the other phase is stationary (stationary phase).

Stationary Phase

In gas-liquid chromatography (GLC) the stationary phase is a liquid coated onto a solid support, which may or may not contribute to the separation process, or onto the walls of an open tube. The liquid may also be chemically bonded to the solid or capillary tube (bonded phase) or immobilized on it, e.g. by *in situ* polymerization (cross-linking) after coating (immobilized phase). In gas-solid chromatography (GSC) the stationary phase is an active solid (e.g. silica, alumina or a polymer). Gas chromatography is always carried out within a tube and the combination of stationary phase and tube is referred to as the column (column chromatography). The stationary phase (liquid + support) may fill the whole inside volume of the tube (packed column) or be concentrated along the inside wall of the tube, leaving an unrestricted path for the mobile phase in the middle of the tube (open-tubular or capillary column).

In open-tubular columns, the liquid stationary phase can be coated onto the essentially unmodified

smooth inner wall of the tube (wall-coated open-tubular (WCOT) column). The inner wall may be made porous by etching the surface by chemical means or by depositing porous particles on the wall from a suspension, the porous layer acting as the stationary phase or as a support for a liquid (porous-layer open-tubular (PLOT) column); or the porous layer may consist of support particles deposited from suspension (support-coated open-tubular (SCOT) column). The term capillary column denotes a column (packed or open-tubular) having a small diameter.

With a solid stationary phase, separation is based mainly on adsorption affinities between the sample molecules and the surface of the active solid (adsorption chromatography). With a liquid stationary phase separation depends on the solubilities of the sample molecules (partition chromatography). In keeping with other partition processes, the sample molecules are often referred to as the solute and the stationary phase as the solvent. This terminology is acceptable in gas chromatography, but can cause confusion in liquid chromatography.

Mobile Phase

In GC at normal pressures (1–2 atm; $1\text{--}2 \times 10^5$ Pa) the mobile phase (usually called the carrier gas) plays little, if any, part in the separation, but only serves to carry the sample molecules through the column.

The time taken by a sample in passing through the column (the total elution/retention time, t_R) is a function of the carrier gas velocity, and the volume of carrier gas required to elute the component from the

column, the total retention volume (V_R), is given by: moves at the same velocity as the mobile phase:

$$V_R = F \times t_R$$

$$\bar{u} = L/t_M$$

where F is the volume flow rate of carrier gas measured at the column outlet at ambient temperature (T_a) and ambient pressure (p_a). If a water-containing flow meter (e.g. the soap bubble flow meter) is used, the measured flow rate must be corrected to dry gas conditions to give the mobile phase flow rate at ambient temperature (F_a):

$$F_a = F(1 - p_w/p_a)$$

where p_w is the partial pressure of water vapour at ambient temperature.

The mobile phase flow rate (F_c) at the column temperature (T_c , Kelvin) is:

$$F_c = F_a(T_c/T_a)$$

To achieve a flow rate through the column, the inlet pressure (p_i) of carrier gas must be greater than the outlet pressure (p_o), the difference being the pressure drop (Δp).

Gases are compressible fluids, and in order to correct for this flow rate measurements a correction, the mobile phase compressibility correction factor (j), has to be used. Thus:

$$j = \frac{3[(p_i/p_o)^2 - 1]}{2[(p_i/p_o)^3 - 1]}$$

It is easiest to measure the volume flow of the carrier gas through the column, but for many purposes the linear flow rate (\bar{u}) is required. The linear velocity across the average cross-section of the chromatographic column can be calculated from the flow rate at column temperature (F_c), the cross-sectional area of the column (A_c) and the interparticle porosity (ϵ):

$$\bar{u} = F_c/(\epsilon A_c)$$

where the interparticle porosity is the interparticle volume of a packed column per unit area. For an open-tubular column this term is equal to 1.

Since the flow rate at column temperature (F_c) is measured at the outlet, in GC the carrier gas velocity at column outlet (u_o) is frequently employed. Correcting this term for gas compressibility gives the average linear carrier gas velocity (\bar{u}) = $u_o j$.

In practice, the average linear carrier gas velocity is calculated by dividing the column length (L) by the retention time (t_M) of an unretained peak, i.e. one that

Methods of Chromatography

In most analytical applications of GC the mobile phase is continuously passed through the column and the sample is fed (or injected) into the system as a finite plug. This process is known as *elution chromatography*. If the conditions for the analysis are optimized the sample components can be separated completely from each other. If the sample is fed continuously onto the column with no added mobile phase, the process is known as *frontal analysis*. Only the first component to emerge from the column may be obtained pure, the other components being contaminated with earlier emerging components. A third technique, used occasionally in liquid chromatography (LC) but rarely in GC, is *displacement development*, which uses a strongly sorbed mobile phase to push (or displace) the components off the column. Each component can be obtained pure, but there is overlap between adjacent components placing a detector at the end of the column, which responds to some property of the sample molecules, produces a trace (the chromatogram) that is a plot of detector response against time.

The General Elution Problem

A typical chromatogram for the separation of a mixture of components is shown in **Figure 1**. This illustrates the characteristics of chromatography, often referred to as the 'general elution problem'. The properties illustrated by the chromatogram, which must be explained by any theory of chromatography, are:

- the components of the mixture elute from the column at different times (retention);
- peak widths increase with retention time (peak shape and broadening);
- the separation of pairs of peaks is not constant (column resolution).

Chromatographic Retention

Retention parameters are measured in terms of chart distances or times, mobile phase volumes or retention factors (k) (previously called capacity factors, k'). With a constant recorder speed, chart distances are directly proportional to times. Likewise if the flow rate is constant, the volumes are proportional to times, e.g. t_R (time) is analogous to V_R (volume). In GC with a compressible carrier gas, V_M , V_R and V'_R represent volumes under column outlet pressure.

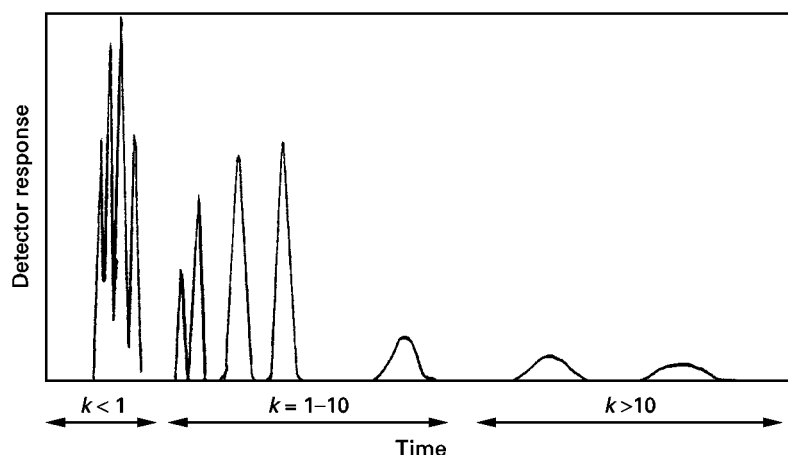


Figure 1 The general elution problem.

If F_c is used in their calculation these correspond to volumes at column temperature.

When a mixture is chromatographed, the time taken for a component to be eluted from the column, the (total) retention time (t_R), is measured from the moment of injection to the appearance of the peak maximum. This, together with the width of the peak measured at the baseline (w) or at half peak height (w_h), and the elution of an 'unretained peak', are important parameters in chromatography. These are illustrated in Figure 2, which represents the separation of a two-component mixture.

The retention volume (V_M) of an unretained peak (where $V_M = F \times t_M$) is also called the gas hold-up volume or dead volume, and is equal to the volume (both inter- and intra-particle) available to the mobile phase in the column. The corrected gas hold-up volume (V_M^0) is corrected for gas compressibility where $V_M^0 = V_M j$.

Injection techniques in GC, where the sample is held at the head of the column before it starts moving through the column, have necessitated the introduction of additional terms. These are the peak time/volume (t_R, V_R), where the time/volume is measured from the start of elution rather than time of injection, and the adjusted retention time/volume (t'_R/V'_R), which is the total elution time/volume minus the gas hold-up time/volume:

$$t'_R = t_R - t_M; \quad V'_R = V_R - V_M$$

The corrected retention time/volume (t_R^0/V_R^0) is the total retention time/volume corrected for carrier gas compressibility:

$$t_R^0 = t_R j = V_R j / F_c = V_R^0 / F_c; \quad V_R^0 = V_R j$$

The net retention time/volume (t_N, V_N) is the adjusted retention time/volume corrected for carrier gas

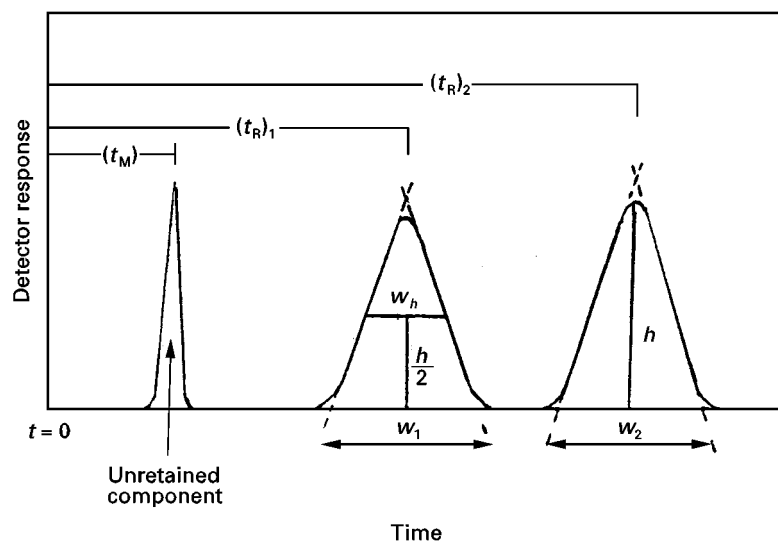


Figure 2 Separation of a two-component mixture showing retention parameters.

compressibility:

$$t_N = V'_R j / F_c = V_N / F_c; \quad V_N = V'_R j$$

The specific retention volume at column temperature θ (V_g^θ) normalizes the retention for the amount of stationary phase on the column (W_s):

$$V_g^\theta = V_N / W_s$$

Normalizing the specific retention volume to 0°C (273.15 K) gives rise to the specific retention volume at 0°C (V_g):

$$V_g = V_g^\theta \times \frac{273.15 \text{ K}}{T_c} = \frac{V_N}{W_s} \times \frac{273.15 \text{ K}}{T_c}$$

where T_c is the column temperature.

The unretained peak is given by a substance that has no affinity for the stationary phase and therefore passes through the column at the same speed as the mobile phase. A substance that shows affinity for the stationary phase moves through the column more slowly than the mobile phase and is said to be retained. The ratio of the two velocities is known as the retardation factor (R):

$$R = \frac{\text{rate of movement of retained peak}}{\text{rate of movement of mobile phase}}$$

A retained component spends time in both the mobile phase (t_M) and the stationary phase (t_s), and retention time t_R is given by:

$$t_R = t_M + t_s$$

The time spent in the stationary phase is dependent on the distribution coefficient (K_c) such that $t_s = K_c V_s$. If C_s and C_M are the concentrations of a component in the stationary phase and mobile phase, respectively, then the distribution constant is given by:

$$K_c = C_s / C_M$$

The rate of movement of a component through the column is inversely proportional to the distribution constant, i.e. a substance with a high concentration in the stationary phase (a high distribution coefficient) moves slowly through the column. Components of a mixture are, therefore, separated only if their distribution coefficients differ. Using volumes rather than times we can write:

$$V_R = V_M + K_c V_s \quad \text{or} \quad V'_R = K_c V_s$$

which is the fundamental equation for chromatography, neglecting the effects of nonlinearity of the sorption isotherm and band broadening.

Since, in general, migration of the solute through the chromatographic column depends upon the equilibrium distribution of the solute between the stationary and mobile phases, retention is controlled by those factors that affect the distribution. In GLC, the distribution is essentially that for a two-component system; the sample (or solute) and the stationary phase (or solvent) (or the adsorbate and adsorbent respectively in gas-solid chromatography). The distribution then is a result of the molecular forces between the sample and the stationary phase and the effect of temperature and pressure on these interactions, although at the pressures normally used in GC the effect of pressure is negligible. All such forces are electrostatic in origin and are based on Coulomb's laws of attraction and repulsion between charges. The major forces involve those between charged ions (e.g. in ion chromatography), i.e. dipole-dipole interactions, dipole-induced dipole interactions, dispersion forces and hydrogen bonding forces. Dispersion forces are present in all atoms and molecules, but the other interactions depend on structural features in the molecule, i.e. ions (e.g. Cl^-), polar functional groups (e.g. C-Cl, C-OH) and polarizable groups (e.g. aromatic and conjugated molecules).

In this case of GLC, assuming that the concentration of the sample (or solute) molecules in the mobile (gas) phase is very small, as is the case if small volume sample injections are made, then the solution of solute in the stationary phase may give rise to an 'ideal solution', and the vapour pressure (p) of the solute above the solution is given by Raoult's law:

$$p = p^\circ x$$

where p° is the vapour pressure of the pure liquid solute and x is the mole fraction of the solute in solution. To correct for the 'nonideality' of real solutions, Raoult's law must be written:

$$p = \gamma p^\circ x$$

where γ is the activity coefficient at infinite dilution. The distribution coefficient (K) for the sample in the stationary phase is given by:

$$K = \frac{RT_c}{M_s \gamma p^\circ}$$

where T_c is the column temperature and M_s the molecular weight of the stationary phase. For two solute

molecules (1, 2) with distribution coefficients K_1 and K_2 , activity coefficients γ_1 and γ_2 and vapour pressures p_1° and p_2° , we can write:

$$\frac{K_1}{K_2} = \frac{\gamma_2 p_2^\circ}{\gamma_1 p_1^\circ}$$

For solutions that approximate to ideal behaviour, $\gamma \sim 1$ and the separation depends on differences in the vapour pressures; this is the case with nonpolar solutes in a nonpolar stationary phase. The existence of polar interactions between the solute and stationary phase molecules introduces nonideality into the system and $\gamma \neq 1$. This can be made use of to provide a separation. A good example is the separation of benzene (C_6H_6) and cyclohexane (C_6H_{12}), which have boiling points of 353.2 and 353.8 K, respectively. In a nonpolar stationary phase the predominant molecular interactions, between benzene or cyclohexane and the stationary phase, will be dispersion forces, and the activity coefficients for both solutes are ~ 1 . Because the difference in the vapour pressures is small, little separation is observed and the solutes are eluted from the stationary phase in order of their boiling points, i.e. benzene is eluted before cyclohexane. If a polar stationary phase is used, cyclohexane, because of its saturated nature, still only exhibits dispersion interactions and $\gamma \sim 1$. However the π electrons in benzene cause it to undergo dipole-induced dipole interactions, leading to a decrease in γ and an increase in its distribution coefficient. Hence in a polar stationary phase benzene is eluted some time after cyclohexane.

The relationship between retention and molecular structure has long been used in GC as an aid to the assignment of chromatographic peaks. Many homologous series of compounds show a linear relationship between \log (retention) and boiling point or carbon number. Since different solute types (e.g. n -alkanes, n -alkyl alcohols, n -alkyl esters) give different linear relationships with different slopes, these plots can be used to assign a chromatographic peak to a particular class of compound and to determine its carbon number and boiling point. These relationships have also been used to provide data in the form of a Retention Index as an aid to peak identification. However, with the widespread use of mass spectrometer detectors these techniques are used less than formerly.

In adsorption chromatography the stationary phase volume is replaced by the surface area (A_s) of the stationary phase, and the distribution coefficient is replaced by the adsorption coefficient (K_A). In GC both V_R and V_M have to be corrected for gas compressibility.

An alternative expression (the retention factor, k) for the distribution of a sample component is in terms

of the relative number of moles (n) of a component in the stationary and mobile phases, such that:

$$k = n_s/n_M = K_c(V_s/V_M)$$

The ratio V_s/V_M is the phase ratio. Early literature will refer to the retention factor as the capacity ratio (k').

Since a sample molecule only migrates through the column when it is in the mobile phase, the retardation factor (R) may be written:

$$R = \frac{\text{amount of solute in the mobile phase}}{\text{amount of solute in mobile + stationary phases}}$$

or:

$$R = n_M/(n_M + n_s) = 1/(1 + k)$$

Substituting the retention factor into the equation:

$$V_R = V_M + K_c V_s$$

gives:

$$V_R = V_M(1 + k)$$

or using retention times:

$$t_R = t_M(1 + k)$$

and on rearrangement:

$$k = (t_R - t_M)/t_M$$

This last expression is widely used as a simple way of expressing retention from values easily measured from the chromatogram, and without the need to measure flow rates. Since:

$$t_M = L/\bar{u}_M$$

we can write:

$$t_R = \frac{L}{\bar{u}}(1 + k)$$

Hence the retention time is directly proportional to the column length and inversely proportional to the linear flow rate of the mobile phase.

Peak Shape and Broadening

The variation of solute concentration in the stationary phase with solute concentration in the mobile phase, at constant temperature, is known as the sorption isotherm. Simple chromatographic theory

assumes a linear isotherm relationship, i.e. the distribution coefficient is constant. Under these conditions the retention time is independent of sample concentration and the peak moves with a constant speed. Given a peak profile with plug-shape distribution on injection, this plug shape should be maintained as the peak passes through the column to emerge at the exit. However, because of longitudinal diffusion in the direction of flow, the peak takes on a Gaussian distribution. If the isotherm relationship is nonlinear (e.g. Langmuirian or anti-Langmuirian), the distribution coefficient is not constant but varies with solute concentration and there is a distribution of solute molecule velocities across the peak that is described as tailing or fronting. This relationship between isotherm shape and peak shape is illustrated in Figure 3.

The width of a chromatographic peak is a function of the column efficiency, expressed as the plate number (N), calculated from the following equations depending on the value used for the peak width (see Figure 2):

$$N = (V_R/\sigma)^2 = (t_R/\sigma)^2 = 16(t_R/w_b)^2 = 5.545(t_R/w_h)^2$$

where σ is the standard deviation of the Gaussian peak.

The column length divided by the plate number gives the plate height or height equivalent to one theoretical plate (H) and normalizes the plate number for column length:

$$H = L/N$$

The concept of 'plates' in chromatographic theory (the plate theory) is by analogy with the distillation process and represents the notional length of the column in which the solute molecules reach a distribution equilibrium. Thus a large number of theoretical plates corresponds to an efficient column.

Consideration of the chromatographic process as controlled by equilibrium gives a satisfactory explanation of chromatographic retention in term of the distribution coefficients. However when considering band broadening a different approach is required, known as the rate theory of chromatography. This was first applied by van Deemter, Klinkenberg and Zuiderweg to packed columns, but has been extended and modified to include open-tubular columns.

As the solute band passes through the column the bandwidth increases and the solute is diluted by the mobile phase. Although the process of fluid flow is complex, three main contributions to band broadening (i.e. to the variance (σ^2) of the Gaussian peak) may be recognized in GC: the multipath effect, A (formerly called eddy diffusion); molecular diffusion, B ; and mass transfer, C . These contributions have been combined by van Deemter and co-workers in the van Deemter equation, which expresses the broadening of a band in terms of the plate height, H , and the average linear velocity (\bar{u}) of the mobile phase:

$$H = A + B/\bar{u} + C_s\bar{u}$$

A plot of H versus \bar{u} is shown in Figure 4. The relationship highlights the importance of using the correct flow rate for minimum H values (maximum

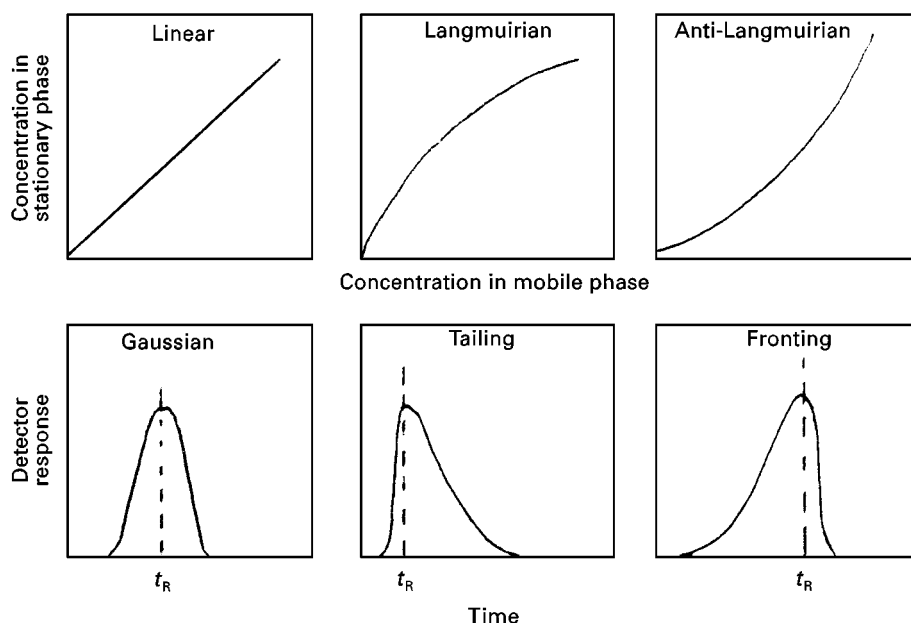


Figure 3 Isotherm shape and its effect on peak shape and retention times.

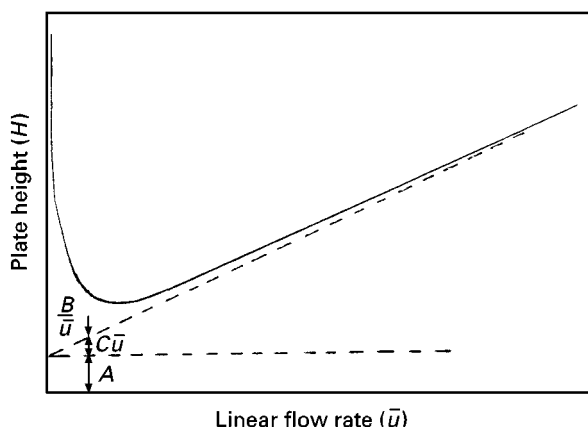


Figure 4 The 'van Deemter' plot and determination of the constants A , B and C_s .

N values) and allows values of A , B and C_s to be calculated as shown.

The multipath effect Molecules flowing through a packed bed of stationary phase will take paths of different lengths, resulting in a small difference in retention times. This has the effect of broadening the band by an amount dependent on the particle diameter (d_p), such that:

$$A = 2\lambda d_p$$

The packing constant (λ) is an empirical term depending on the shape (spherical or irregular) of the packing material and the packing efficiency, and reaches a minimum value $\cong 0.5$. For open-tubular column there is no 'A' term.

Longitudinal molecular diffusion Solute molecules diffuse in a longitudinal direction (i.e. along the column axis) according to Fick's law of diffusion. The amount of band spreading is directly proportional to the coefficient of diffusion (D_M) of the solute molecules in the mobile phase, and inversely proportional to the mobile phase flow rate. An obstruction factor (ψ) is introduced to account for the restricted diffusion in a packed bed. Hence:

$$B = 2\psi D_M / \bar{u}$$

Mass transfer In GC the only form of mass transfer that is significant involves the movement of the solute molecules in and out of the stationary phase (stationary phase mass transfer, C_s). At the head of the column the solute is distributed between the stationary and mobile phases according to the value of the distribution coefficient. As the band moves down the column, solute at the leading edge of the band is

continually meeting new stationary phase into which it dissolves. To maintain the equilibrium, solute will move from the trailing edge of the band, out of the stationary phase back into the mobile phase. Because this process is not instantaneous, the band is broadened. A fast-moving mobile phase sweeps the zone more rapidly through the column and accentuates the band broadening, as does a greater film thickness (d_f) of stationary phase. A higher rate of solute diffusion in the stationary phase (D_s) will decrease the band broadening, so that:

$$C_s = q \times \frac{k d_f^2 \bar{u}}{(1+k)^2 D_s}$$

where q is a configuration factor depending on the nature of the stationary phase. In adsorption chromatography the C_s term is expressed in terms of the adsorption/desorption kinetics of the solute molecules on the stationary phase.

van Deemter type plots using different carrier gases show that although nitrogen gives slightly lower H values, this is only achieved at relatively low flow rates ($\sim 15 \text{ cm s}^{-1}$), and as the flow rate increases the value of H increases rapidly. Hydrogen has a much flatter curve and is best for fast analysis with high flow rates (above 30 cm s^{-1}). Because of the inherent safety problems from hydrogen, helium is a good compromise and is used in most coupled techniques (e.g. gas chromatography-mass spectrometry, GC-MS).

A modernized version of the van Deemter equation includes the multipath term (A) in a more generalized term covering mass transfer in the mobile phase (C_M):

$$H = B/\bar{u} + C_s \bar{u} + C_M \bar{u}$$

where:

$$C_M = f(d_p^2, \bar{u})/D_M$$

Open-tubular columns are often evaluated by comparing the theoretical maximum number of plates with that of the actual calculated number of plates, where:

$$H(\text{min}) = r_o \frac{1 + 6k + 11k^2}{3(1+k)^2}$$

and r_o is the column radius.

Extra-column band broadening So far we have only considered band broadening processes within the chromatographic column itself, but in assessing the overall performance of the system the instrument as a whole is important. Thus the injection system,

detector and connecting tubing all contribute to the overall analysis. The objective for the injection is to vaporize the sample onto the column in as narrow a plug as possible; slow vaporization or the existence of zones unswept by mobile phase in the injector will lead to both band broadening and peak tailing. Large dead volumes in the detector can lead to remixing of components and deterioration of the separation as well as dilution of the sample peaks, thus reducing detection limits. Generally the design of gas chromatographs eliminates the need for long lengths of connecting tubing, often a major problem in liquid chromatographs.

Column Resolution

Chromatographic separation is only achieved when there is a difference in the distribution coefficients of two components, i.e. the molecular interactions (dispersion forces, dipole interactions and hydrogen bonding forces) between the sample molecules and the stationary phase are sufficiently different. More fundamentally it is the free energies of distribution $\Delta(\Delta G^\ominus)$ of the components of a mixture that must differ. It can be shown that:

$$\Delta(\Delta G^\ominus) = -RT \ln \alpha = -RT \ln [(K_c)_2/(K_c)_1]$$

A stationary phase that produces a large degree of separation is said to have a high selectivity. The separation of two components (1 and 2) is expressed by the relative retention (α):

$$\alpha = t'_{R(2)}/t'_{R(1)} = V'_{R(2)}/V'_{R(1)} = k_{(2)}/k_{(1)} = K_{C(2)}/K_{C(1)}$$

If one of the pair is a standard substance, the symbol used for relative retention is 'r'.

Having achieved a separation it is necessary to prevent remixing of the components. The ability to achieve this is a function of the column efficiency, as measured by the plate number. The combined effects of stationary phase selectivity and column efficiency is expressed in the peak resolution (R_s) of the column. (see Figure 2):

$$R_s = \frac{(t_R)_2 - (t_R)_1}{\frac{1}{2}(w_1 + w_2)}$$

A value of $R_s = 1.5$ is normally considered to represent baseline separation for Gaussian shaped peaks. To achieve the maximum peak resolution, both high selectivity and column efficiency (giving narrow bands) are required.

Increased resolution can always be achieved by an increase in column length since the peak separation (Δt_R) is proportional to the distance of migration down the column, but peak width is only propor-

tional to the square root of the migration distance. The penalty for this, however, is longer retention times and an increased inlet pressure of mobile phase.

The Purnell equation shows how peak resolution is related to the retention factor (k), the plate number (N) and the relative retention (α):

$$R_s = \frac{\sqrt{N_2}}{4} \times \frac{(\alpha - 1)}{\alpha} \times \frac{k_2}{1 + k_2}$$

where the subscript 2 refers to the second peak.

Conditions for obtaining maximum values of the plate number have already been discussed. The relative retention is mainly governed by the nature of the stationary phase, since in GC at normal pressures, only molecular interactions between the solute molecules and the stationary phase are involved. These interactions are maximized in the concept of 'like has an affinity for like'. Thus, for a sample that contains predominantly nonpolar species a nonpolar stationary phase will optimize the dispersion forces and, since polar interactions will be absent, solutes will elute according to their volatility with the most volatile (lowest boiling point) components eluting first. For polar samples a polar stationary phase is used to maximize both dipole-dipole interactions and dipole-induced dipole interactions. Because the effect of volatility is still present, it is much more difficult to predict elution behaviour in this latter case. Most naturally occurring mixtures contain species spanning a range of polarities, and in this case it is still better to use a polar stationary phase. At least a partial separation can be achieved with α values as low as 1.05, but values in the range 1.5–3.0 are preferable and above α values ~ 5.0 little additional resolution is achieved. Peak resolution increases rapidly with increasing k values, but at values >10 the term $k_2/(1 + k_2) \rightarrow 1$ and the term plays no further part in the resolution. The use of k values <1 gives very short retention times and poor resolution, so that the optimum range for k is between 1 and 10. The retention equation $t_R = L/\bar{u}(1 + k)$ shows that retention times are a function of both the mobile phase velocity (\bar{u}) and the retention factor.

In GC, k values are controlled by temperature. The van't Hoff equation describes the change in equilibrium constant with temperature and if the phase ratio (V_s/V_M) is independent of temperature we can also write for the retention factor:

$$\frac{d \ln k}{dT} = \frac{\Delta H}{RT^2}$$

where ΔH is the enthalpy of solution (or adsorption) from the mobile phase to the stationary phase.

Figure 1 for the general elution problem also shows values of k for different zones of the chromatogram. With low k values ($k < 1$) the peaks are eluted too rapidly and there is no time for separation. With high k values ($k > 10$) elution times are long, the peaks are broad and the peaks are overresolved. This problem can be corrected using the technique of temperature programming. Assuming that this chromatogram was obtained isothermally at 100°C it would be possible to choose a lower starting temperature (say 50°C) and then raise the temperature to say 150°C over a given period of time. This would have the effect of increasing the k values for the early peaks and decreasing the k values for the later peaks, the object being to get all peaks in the optimum region $1 < k < 10$. Modern computer-controlled gas chromatographs have the facility to use isothermal periods and linear and non-linear temperature programs with multiple ramps to give better control over k values.

The retention equation also indicates that a similar effect could be achieved using the analogous technique of flow-programming and changing the carrier gas flow rate. However, increase in carrier gas flow rate gives an approximately linear effect whereas temperature programming has a logarithmic effect. In spite of this, flow programming finds a use in the separation of labile and temperature-sensitive samples where high temperatures are to be avoided.

A satisfactory separation is achieved when all three terms in the Purnell equation are optimized.

Future Developments

The theory of gas chromatography is well established and it is unlikely that there will be any significant

new developments. A greater understanding of the interactions involving new stationary phases (e.g. chiral phases), and the preparation of stationary phases with better temperature stability would lead to an extension of its application. Developments in instrumentation with new coupled techniques is also a possibility. The most likely area for further development is in the area of data handling and instrument control using the newer breed of computers.

See also: II/Chromatography: Gas: Column Technology; Gas-Solid Gas Chromatography; Historical Development.

Further Reading

- Giddings JC (1965) *Dynamics of Chromatography*. New York: Marcel Dekker.
- Hawkes SJ (1983) *Journal of Chemical Education* 60: 393–398.
- Katsanos NA (1988) *Flow Perturbation Gas Chromatography*. New York: Marcel Dekker.
- Littlewood AB (1962) *Gas Chromatography*, pp. 1–202. London: Academic Press.
- Poole CF and Poole SK (1991) *Chromatography Today*. Amsterdam: Elsevier.
- Purnell H (1960) *Journal of the Chemical Society*: 1268.
- Purnell H (1962) *Gas Chromatography*, pp. 9–229. London: John Wiley & Sons.
- Robards K, Haddad PR and Jackson PE (eds) (1994) *Principles and Practice of Modern Chromatographic Methods*. London: Academic Press.
- van Deemter JJ, Zuiderweg FJ and Klinkenberg A (1956) *Chemical Engineering Science* 5: 271.

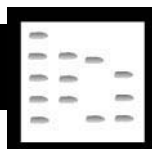
CHROMATOGRAPHY: LIQUID/Electron Spin Resonance Detectors in Liquid Chromatography

See II/CHROMATOGRAPHY: LIQUID/Detectors: Electron Spin Resonance

CHROMATOGRAPHY: LIQUID/Chiral Separations in Liquid Chromatography: Mechanisms

See II/CHROMATOGRAPHY: LIQUID/Mechanisms: Chiral

CHROMATOGRAPHY: LIQUID



Column Technology

P. Myers, Phase Separations Ltd, Deeside,
Flintshire, UK

Copyright © 2000 Academic Press

Introduction

Today, the main columns for high performance liquid chromatography (HPLC) are of tubular design, normally manufactured from high quality stainless steel and packed with spherical ceramic particles. Termination of the columns is via a metal frit held in place by an end fitting that can accept a 1/16 in (15.9 mm) male fitting to connect the column to the HPLC instrument.

Figure 1 shows a typical conventional HPLC column. This is now a mature design that has evolved over a period of 20 years. In that time, many variations have evolved, such as cartridge columns, removable end fitting columns, radial compression columns and nonmetal columns. Today, the most common analytical column has an inner diameter (i.d.) of 4.6 mm with an outer diameter of 1/4 in (63.5 mm). However, in recent years there has been a movement to smaller i.d. columns such as 3, 2, 1 and 0.5 mm. There has also been a development of packed capillary columns having i.d. of 0.32, 0.25 and 0.1 mm. Even newer columns with i.d. 0.05 mm have been developed for capillary electrochromatography (CEC). Columns are defined in Table 1 according to their internal diameters.

The most common length of an HPLC column is 25 cm but analytical columns are available in lengths down to 3 cm and guard columns are commonly 1 cm long.

The material packed into columns is mainly silica based, spherical in shape with a particle size of 5 μm . Material of diameter 10 μm has now virtually disappeared from analytical columns and 3 μm material, although introduced in the mid-1980s, is still not widely used. Newer, smaller-diameter particles of

2 and 1 μm are also available but at the time of writing occupy a niche market only.

The Conventional Column

Conventional analytical columns are 4.6 or 4 mm i.d., 1/4 in (63.5 mm) o.d. They are manufactured from high quality stainless steel such as 316 to withstand the high pressures that are used in packing (up to 10 000 psi; 69 000 kPa) and in operating the columns (around 2500 psi; 17 000 kPa). Manufacturers take particular care with the inner bores of these tubes; some use tubing 'as-drawn', while others use electropolished tubing. There have been reports of chemical modification with silanes to the inner surface.

The column packing material is held in the column with an end frit, which in turn is held in place by the column end fitting. The frit is normally made from a sintered metal, the porosity being determined by the size of the packing material used. For 5 μm materials, a 2 μm porosity frit is normally used, but for 3 μm and smaller, a 0.5 μm frit is common. The most common type of end fittings are those manufactured by Swagelok, Parker and Valco. Typical end fittings are shown in Figure 2.

Frits are held on the column by compression fittings; although it is possible to remove the end fitting to repair or top up the packed material (or to clean or repair a damaged frit), it is not generally recommended as it is not usually possible to regain good performance. Inserting and removing these classical columns from an HPLC instrument cannot be done without tools. In an attempt to make this into a simple 'no tools operation', and to reduce the amount of hardware used in the tube section of the column, the cartridge column was developed. The first successful commercial cartridge column was designed by Brownlee Labs and is today still known as the Brownlee system.

In this system, the column design is very simple in that the tubular column has the packing material held in place by frits that are pushed into the end of the tube. This packed tube is held in the cartridge column



Figure 1 Typical HPLC column.

Table 1 Definitions of columns

Column type	Internal diameter (mm)
Analytical	20–3
Microbore	2–0.5
Capillary	< 0.5



Figure 2 Typical end fittings.

held by hand-tight end nuts that are part of and free to rotate with the cartridge holder.

Since the Brownlee system was introduced, there have been many copies on this basic design and also developments into the finger-tight removable end fitting column (Figure 3). These columns, as shown in Figure 4, again have the frit pushed into the tube or held in place by a frit cap. This frit cap also contains a seal that allows the end fitting to be screwed down onto the frit. This design has many advantages. It allows easy removal of the frit to replace it or top up the column packing material, but more importantly,



Figure 3 Finger-tight end fitting column showing frit cap.



Figure 4 Removable end fitting column.

it allows columns to be coupled together with very low dead volumes.

Apart from the cartridge and removable end fitting columns, a different design approach was taken by Waters with their radial pack systems. As mentioned previously, high pressures are used to pack particles into column to obtain a well-packed bed. In packing columns, voids in the packing bed are produced if insufficient pressures are used; these voids are commonly along the axial direction. The idea of the radial packed column is to pack the material into a soft-walled tube. This tube is held in a device that can apply radial pressure, and so reduce the radial voids. Some examples are shown in Figure 5. This radial compression system has not been applied down to small i.d. tubes, but has been developed for semipreparative systems. In preparative systems, direct axial compression on to the top of the packing is also used.

Columns down to 3 mm i.d. can be used with what is commonly classed as conventional HPLC equipment, with detector flow cells in the order of 8 μ L.



Figure 5 (See Colour Plate 21) Radial compression column cartridge.

Table 2 Volumetric flow rates required to maintain a linear flow velocity of 1.5 mm s^{-1} in columns of different diameters

Column diameter (mm)	Flow rate (mL min^{-1})	Solvent consumption (mL h^{-1})
1.0	0.04	2.4
2.0	0.18	10.8
3.0	0.39	23.4
4.0	0.7	42.0
4.6	0.93	55.8
5.0	1.1	66.0
8.0	2.81	168.6

Reducing the column diameter below 3 mm requires detectors with smaller volumes to reduce detector band broadening. Pumps that can produce lower flow rates are also required. Table 2 gives the volumetric flow rates required to maintain a linear flow velocity of 1.5 mm s^{-1} .

Although microbore columns became commercially available in the mid-1980s, they have not displaced 4.6 mm i.d. columns. Many comparison reviews were written in the 1980s of 1 mm versus 4.6 mm i.d. columns. In general the conclusion was reached that solvent saving and packing material costs did not justify the capital expenditure in new equipment and that mass sensitivity enhancements were difficult to achieve. Since then much has improved, both in the instruments and especially in the column design, particularly in the end fittings used on $< 3 \text{ mm}$ i.d. columns.

From 1990 onward, further research was conducted and there was widespread discussion of the advantages of microbore columns, including increased resolution, decreased solvent consumption, lower heat capacity, increased mass sensitivity and, most importantly, the easier coupling of these columns to secondary systems and mass spectrometers. Columns with i.d. down to 1 mm are conventionally still manufactured from stainless steel, but as the i.d. is reduced so can the wall thickness be reduced. This allows the use of other materials, as the resulting pressure forces in the small i.d. tubes is also reduced. For 2 and 1 mm columns, glass-lined tubing has been used. This is in an attempt to give a very smooth inner surface, which in turn helps column packing and hence efficiency. Columns are now available manufactured from PEEK (poly(ether ether ketone), an ICI polymer). Columns of this material are produced in diameters down to 0.5 mm.

A conventional PEEK column is shown in Figure 6, and a 0.5 mm flexible PEEK column is shown in Figure 7. These columns have no wetted metal components and, since the 0.5 mm columns are flexible,

**Figure 6** PEEK column.

for the first time in HPLC it has become possible to consider a different design of instrument, in that there is no longer any need to have a fixed distance between the injector and detector. Another feature of these columns is that they can be cut to any length. If the

**Figure 7** PEEK-o-bore column.

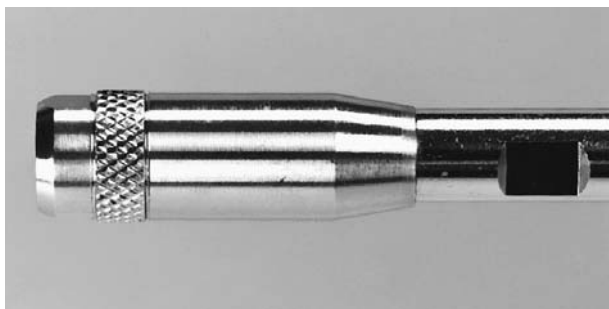


Figure 8 Integral guard column.

inlet blocks or becomes contaminated, then this part of the column can be cut off.

Capillary columns of less than 0.5 mm i.d. are almost exclusively manufactured from fused silica, in some cases with a metal outer case onto which the end fittings can be connected.

Guard Columns

As the name suggests, guard columns are used to protect the main analytical column. They are normally 1 cm in length, of the same diameter as the main column, and made of the same material. They are not extensively used in all application areas, possibly because they can reduce the total column efficiency and are not easy to install or replace. This is set to change with the development of removable end fitting columns. New designs, as shown in **Figure 8**, now allow easy connection and replacement of guard systems. However, manufacturers still only offer generic packings of either normal phase or reversed phase for these columns. **Figure 9** shows a guard column cartridge system that can be connected to any form of column.

Packing Materials

Porous silica is the most widely used adsorbent in HPLC, although extensive work has been conducted with alumina, zirconia and polymer supports. The majority of these supports are spherical and, for analytical applications with small molecules, have general physical parameters of pore size 10 nm, pore

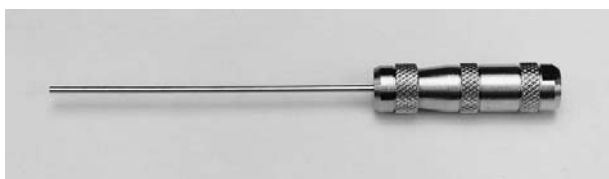


Figure 9 Stand-alone guard column.

volume 0.5 mL g^{-1} and surface area $250 \text{ m}^2 \text{ g}^{-1}$. The most common particle size used in columns is $5 \mu\text{m}$. Care must be taken when using the particle size given by a manufacturer. What is meant by $5 \mu\text{m}$ particles, is actually a $5 \mu\text{m}$ particle size distribution. Depending upon the type and mode of measuring instrument used by the manufacturer, there will be a particle size distribution based on number, area or volume.

In the number distribution the percentage of the particles in each size range is determined by dividing the number in each range by the total number of particles. In the area distribution, the percentage of the surface area in each size range is determined by dividing the surface area calculated for each size range by the total surface area of all the particles. This has the effect of emphasizing the larger particles more than the number distribution. For example, one particle of $10 \mu\text{m}$ diameter has the same surface area as 100 particles of $1 \mu\text{m}$ diameter. The volume distribution is calculated from the percentage of the volume of each particle size divided by the total volume of all the sizes. The volume distribution emphasizes the large particles even more than the area distribution, e.g. a $10 \mu\text{m}$ diameter particle has the same volume as 1000 particles of $1 \mu\text{m}$. Typical distributions (for a $5 \mu\text{m}$ Spherisorb) are given in **Figure 10**, showing the emphasis on the larger particle sizes in the distributions for area and volume.

Silica particles used for packing are commonly manufactured from a sol-gel type process, starting from a cation-based sol. This produces gels that are high in their cationic species, for example Spherisorb has a sodium content of 1500 ppm. Newer manufacturing methods introduced in recent years, use organic tetraethyl orthosilicate (TEOS) condensation systems that can produce exceptionally pure silicas.

In the sol-gel process, the size of the particles can be controlled by the viscosity of the mixture, the emulsification rate and the amount and type of surfactant used to stabilize the emulsion. However, none of the processes can produce monodispersed particles – they produce a particle size distribution and the required particle size is then obtained from this by air classification or elutriation.

The tighter the particle size distribution, the more uniform a column packing can be made. However, with very tight particle size distributions it becomes more difficult to pack the columns. Van Deemter curves demonstrating the effect of particle size on the column efficiency are shown in **Figure 11**.

The surface area, pore size and pore volume of packing material are determined either by nitrogen BET or mercury porosimetry. As with particle size distributions, care must be used in the interpretation of these data because different models are used by

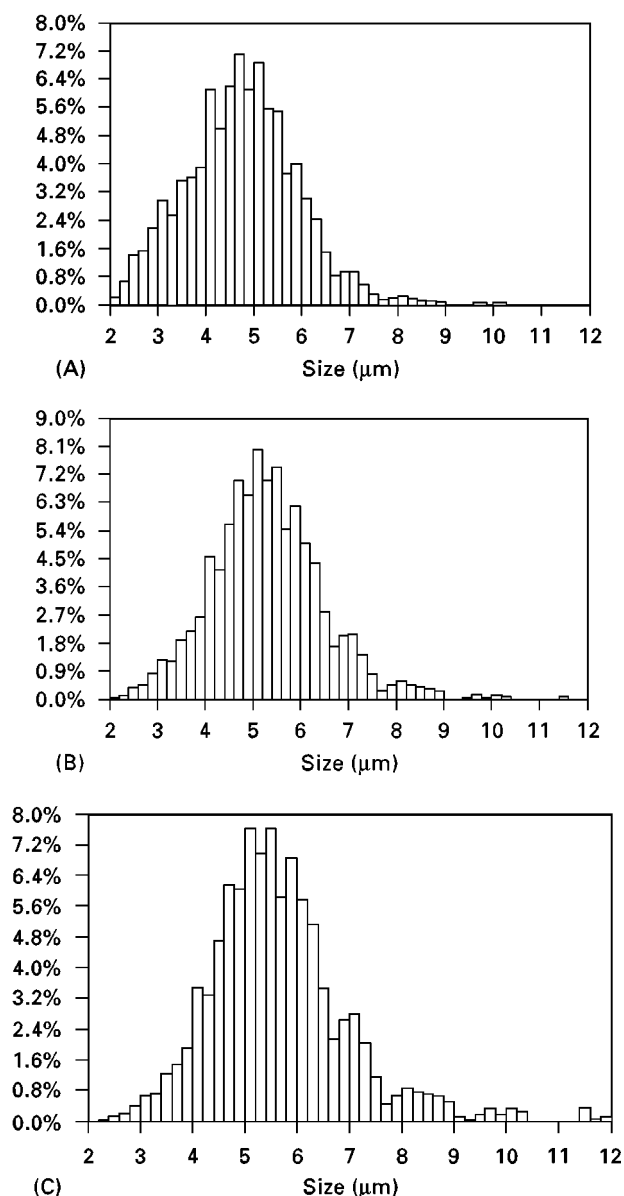


Figure 10 Particle size distributions for a 5 µm Spherisorb. (A) Number; (B) area; (C) volume.

different manufacturers, which can impose different interpretations on the type and shape of pores. In HPLC, an important factor is the absence of micropores and mesopores. Micropores are defined as having a diameter of less than 1 nm, while mesopores are less than 5 nm in diameter. If these pores are included

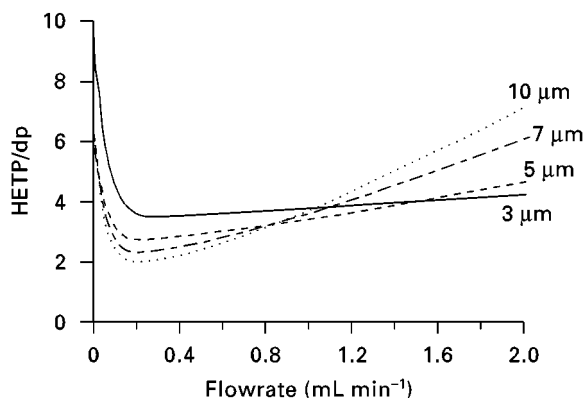


Figure 11 Van Deemter curves.

in the surface area calculations, then very large surface area values are obtained. However, most analyte molecules cannot penetrate into micropores and even if they could possibly penetrate into the mesopores, diffusion is very restricted by steric hindrance, which in turn affects mass transfer and hence efficiency.

Silica is a preferred adsorbent in HPLC as the surface characteristics can be modified by chemical reaction to change the hydrophilic silica surface into a hydrophobic surface suitable for reversed-phase chromatography, or to place an ionic exchange material on the surface for ion exchange chromatography.

A very broad range of functionality can be attached to the silica surface, through reaction with organosilanes, the most popular being C₁₈ or octadecylsilane. The linkage onto the silica is of the type Si-O-Si-R, where R is the functional group. Manufacturers use a variety of silanes, ranging from monochloro to trichlorosilanes to mono and tri methoxy and ethoxy silanes. Attachment of the monofunctional silane onto the surface of the silica leads to a monomeric phase, while the addition of small amounts of water into the bonding process can lead to polymeric phases.

Manufacturers normally give bonding figures as % carbon loadings. This is a very misleading figure as the percentage of carbon loading alone is not a relevant parameter because of differences in the surface area of the original silica, which result in different surface densities of the bonded alkyl groups. **Table 3**

Table 3 Column packing parameters

Description	Column volume (mL)	Si density (g mL ⁻¹)	Mass of packing (g)	Carbon load (%)	Amount of carbon in the column (g)
Nova-Pak C ₁₈	1.8	0.91	1.64	7	0.12
µBondapak C ₁₈	1.8	0.46	0.82	10	0.08

Table 4 Some commercially available bonded phases

<i>Phase name</i>	<i>Usage</i>	<i>Comments</i>
C ₁	Purification	
C ₄	Protein separations	
C ₆	Protein separations	
C ₈	General purpose	Almost 80% of all applications have been developed with C ₈ and C ₁₈ phases
C ₁₈ ODS	General purpose	Almost 80% of all applications have been developed with C ₈ and C ₁₈ phases
Phenyl	Separation of complex mixtures	Induced dipole interactions with polar analytes
Cyano CN	Broad spectrum of mixtures with different polarities	Can be used in both normal and reversed phase
Amino NH ₂	Sugar analysis and for aromatic compounds	Weak anion exchanger
Diol	Complex mixtures	Slightly polar adsorbent for normal phase
Ion exchange	Ionic species	
Chiral phases	Enantiomer separations	Four major types available: donor, polymer, cavity and exchange

ODS, octadecylsilica.

outlines this problem, showing the amount of carbon on a material against its percentage carbon loading.

Table 4 provides a broad summary of the bonded phases that are commercially available. It must be stressed that this is in no way an extensive list. There are many specialized phase-column combinations supplied by many manufacturers. In particular, these specialized phases tend to be in the chiral separation areas.

The term end-capping was introduced in the late 1970s to indicate that a secondary treatment had been applied to a bonded phase. This was an attempt to cover all available silanols. The most common end-capping agent is trimethylchlorosilane; this molecule is relatively small and so can penetrate into the pore system of the adsorbent. Generally end-capping leads to an improvement in the chromatography of basic compounds. However, even after the best end-capping, it is estimated that about 50% of all silanols are still unbonded.

A term that has recently been introduced into column packings is 'base-deactivated' reversed phases. This is a particularly unfortunate term since these packings are not deactivated with bases but have surface treatments or treatments of the silica that make them particularly useful for separating basic compounds. Amines, for example, tend to tail on conventional reversed-phase column packings because of the residual acidic silanols. These base-deactivated packings are normally manufactured from the new pure silicas and have a more uniform or reduced level of silanols.

A major problem with silica is the small pH range over which the adsorbent can be used. Above pH 8.5 the siloxane bridge is broken, leading to breakdown through solvation of the particle. Below pH 2.5, the bonded phase is hydrolysed from the surface of the silica. In an attempt to extend the pH range of silica, attempts have been made to manufacture pH-stable

bondings. These have normally been based on coating the silica with a polymer, such as polybutadiene or a grafted polysiloxane.

Other ceramics have been reported as packing materials. The most common are alumina, zirconia and titania. Although it is possible to attach hydrophobic groups onto all of these materials, with alumina the silane is very easily removed from the surface. To obtain a hydrophobic character for alumina, polybutadiene or grafted polysiloxane polymers are used. These types of bondings have been divided into two groups. The first comprises those polymers with siloxane bonds such as polymethyloctylsiloxane, polymethyloctadecylsiloxane and silica monomers, while the second is represented by purely organic monomers and oligomers such as polybutadiene.

Another support that has been developed and can be used under very aggressive conditions is porous graphitic carbon.

Polymer-based adsorbents are also used as a support material in HPLC columns. They are manufactured from synthetic cross-linked organic polymers. Their main application area is in size-exclusion chromatography and ion exchange chromatography. In normal-phase and reversed-phase HPLC they still have very few applications. A problem is that even though the new polymer packings are highly cross-linked and stable, they still carry the history of their precursors and they can swell with some solvents.

Conclusions

Much has changed over the last few years in both the manufacture of support materials and the design of columns. Manufacturers of supports now make more reproducible materials and very pure forms of support materials, especially in silica, where metal

impurity levels are now less than 5 ppm (the first silicas used had typical impurity levels of 1000–2000 ppm). In the silica support materials the latest developments have been towards base-deactivated materials and have tended to focus on the new very pure silicas. Particle size distributions have also become tighter around given means, leading to more stable and reproducible columns.

In column design, the move has been to cartridge type systems having smaller tube i.d. with smaller particles and shorter lengths.

The focus on development is now moving to micro systems. Future developments are likely to be systems with smaller and smaller column i.d., and even complete columns on microchips.

See Colour Plates 21, 22.

See also: II/Chromatography: Liquid: Mechanisms: Reversed Phases. III/Porous Graphitic Carbon: Liquid Chromatography. Porous Polymers: Liquid Chromatography.

Further Reading

Balke ST (1984) *Quantitative Column Liquid Chromatography*. Amsterdam: Elsevier.

Horvath C (ed.) (1980) *High Performance Liquid Chromatography, Advances and Perspectives*, vol. 1: *History of HPLC, Chemically Bonded Phases, Secondary Equilibria, Gradient Elution*. New York: Academic Press.

Horvath C (ed.) (1980) *High Performance Liquid Chromatography, Advances and Perspectives*, vol. 2: *Optimisation, Adsorption Chromatography, Reversed-Phase HPLC*. New York: Academic Press.

Kucera P (1984) *Microcolumn High Performance Liquid Chromatography*. Amsterdam: Elsevier.

Nawrocki J (1997) The silanol group and its role in liquid chromatography. *Journal of Chromatography A* 779: 29–71.

Neue UD (1997) *HPLC Columns. Theory, Technology, and Practice*. New York: Wiley-VCH.

Novotny M and Ishii D (eds) (1985) *Microcolumn Separations*. Amsterdam: Elsevier.

Scott RPW (1992) *Liquid Chromatography Column Theory*. New York: Wiley.

Scott RPW (ed.) (1984) *Small Bore Liquid Chromatography Columns: Their Properties and Their Uses*. New York: Wiley.

Unger KK (ed.) (1990) *Packings and Stationary Phases in Chromatographic Techniques*. New York: Marcel Dekker.

Countercurrent Liquid Chromatography

Yoichiro Ito, Lung and Blood Institute, NIH, Bethesda, MD, USA

Copyright © 2000 Academic Press

Introduction

Countercurrent chromatography (CCC) belongs to the family of liquid partition chromatography but with one distinct feature: the system totally eliminates the use of a solid support. Unlike liquid chromatography (LC), CCC utilizes two immiscible solvent phases. The partition process takes place in an open column where one phase (the mobile phase) continuously passes through the other (stationary phase), which is permanently retained in the column. To retain the stationary phase within the column, the system uses effective combinations of the column configuration and a force field (gravitational or centrifugal). Hence CCC instruments display a variety of forms that are quite different from those used in LC.

Because no solid support is used, CCC can eliminate all the complications arising from the use of a solid support such as adsorptive sample loss and denaturation, tailing of solute peaks and contamination.

The Two Basic CCC Systems

All existing CCC systems have been developed from two basic forms, the hydrostatic equilibrium system and the hydrodynamic equilibrium system (Figure 1).

The basic hydrostatic system (left) uses a stationary coiled tube. The coil is first filled with the stationary phase (either the lighter or the heavier phase of an equilibrated two-phase solvent system) and the mobile phase is introduced from one end of the coil. Owing to the action of gravity, the mobile phase percolates through the segment of the stationary phase in one side of the coil. This process continues until the mobile phase reaches the other end of the coil. Thereafter the mobile phase only displaces the same phase leaving the stationary phase in the coil. Consequently, solutes introduced at the inlet of the coil are partitioned between the two phases in each helical turn and separated according to their partition coefficients.

The basic hydrodynamic system (right) uses a similar arrangement except that the coil is rotated around its own axis. This simple motion produces a profound effect on the hydrodynamic process in the coil by generating an Archimedean screw force. All

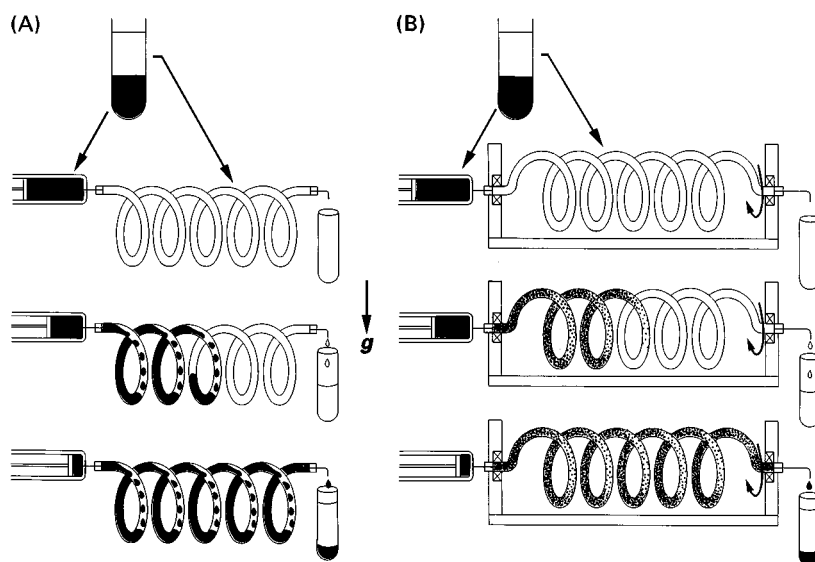


Figure 1 Two basic CCC systems. (A) Hydrostatic equilibrium system. (B) Hydrodynamic equilibrium system.

materials present in the coil that are either heavier or lighter than the suspending medium are driven toward one end of the coil. This end is conventionally called the head; the other end is called the tail.

Owing to the effect of this Archimedean screw force, the mobile phase introduced through the head end of the coil immediately interacts with the stationary phase to establish a hydrodynamic equilibrium. The two solvent phases are distributed fairly evenly in each helical turn where they are vigorously mixed by the rotation of the coil. After the entire coil reaches this equilibrium state, the mobile phase only displaces the same phase, leaving a large amount of the other phase stationary in the coil. Consequently, solutes introduced through the inlet of the coil are efficiently separated and eluted out in the order of their partition coefficients.

Each basic CCC system described above has its own merits. The hydrostatic system gives a stable retention of the stationary phase whereas the hydrodynamic system yields a higher partition efficiency by vigorous mixing of the two phases with the rotation of the coil. Several efficient CCC systems have been developed from each basic system.

Hydrostatic CCC Systems

During the early 1970s, hydrostatic CCC systems were rapidly developed because of their simplicity. Typical hydrostatic CCC systems are schematically illustrated in Figure 2. They are classified into gravitational and centrifugal schemes.

In the gravitational schemes, the basic hydrostatic equilibrium systems (HSES, shown in Figures 1 and 2, left) is modified as follows. One side of the coil,

which is entirely occupied by the mobile phase and therefore forms an inefficient dead space, is displaced with narrow bore transfer tubes, while the other side of the coil, which provides an efficient column space, is changed to large-bore straight tubes. In droplet CCC (DCCC, Figure 2A), the vertical column is first filled with the stationary phase and the mobile phase is introduced from one end. The mobile phase then forms multiple droplets, each occupying the space across the diameter of the column, thus dividing the column into a number of partition units. The system requires use of a proper solvent system for droplet

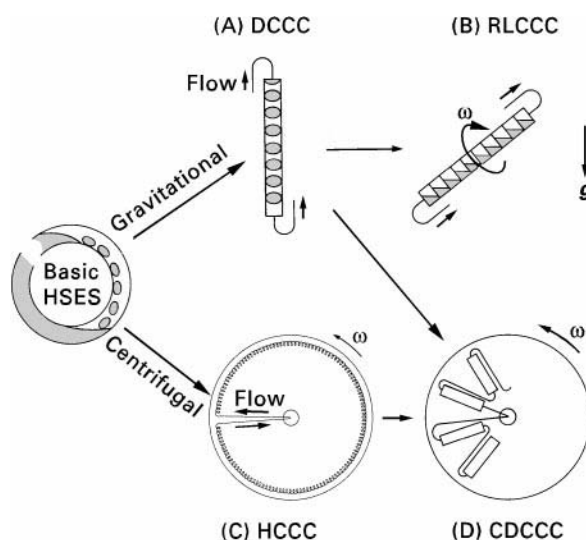


Figure 2 Development of hydrostatic CCC systems. These diagrams illustrate a variety of CCC schemes developed from the basic hydrostatic equilibrium system (HSES) shown in Figure 1, left. They are divided into the gravitational (upper) and centrifugal (lower) schemes.

formation. Rotation locular CCC (RLCCC, Figure 2B) utilizes a locular column prepared by the insertion of centrally perforated discs to divide the column space into multiple partition units called locules. This locular column is first filled with the stationary phase followed by introduction of the mobile phase at one end while the column is tilted and rotated about its own axis. When both column inclination and rotation speed are optimized, each locule holds a desired volume of the stationary phase, which is steadily mixed with the mobile phase by the rotation of the column.

In the centrifugal schemes, analytical helix CCC (HCCC) was developed by reducing the dimensions of the coil, which is then placed around the periphery of a centrifuge bowl (Figure 2C). Under a centrifugal force field the same partition process takes place in

each turn of the coil as observed in the basic hydrostatic system, but with a much higher efficiency due to the reduced column dimensions. Another centrifugal scheme called centrifugal droplet CCC (CDCCC) performs droplet CCC in a centrifugal force field (Figure 2D).

Hydrodynamic CCC Systems

Rotary-Seal-Free-Flow-Through Systems

The development of the hydrodynamic CCC systems was initiated by introduction of various flow-through centrifuge systems that can perform continuous elution without the use of conventional rotary seals. A series of such centrifuge systems is schematically illustrated in Figure 3. The diagrams show the

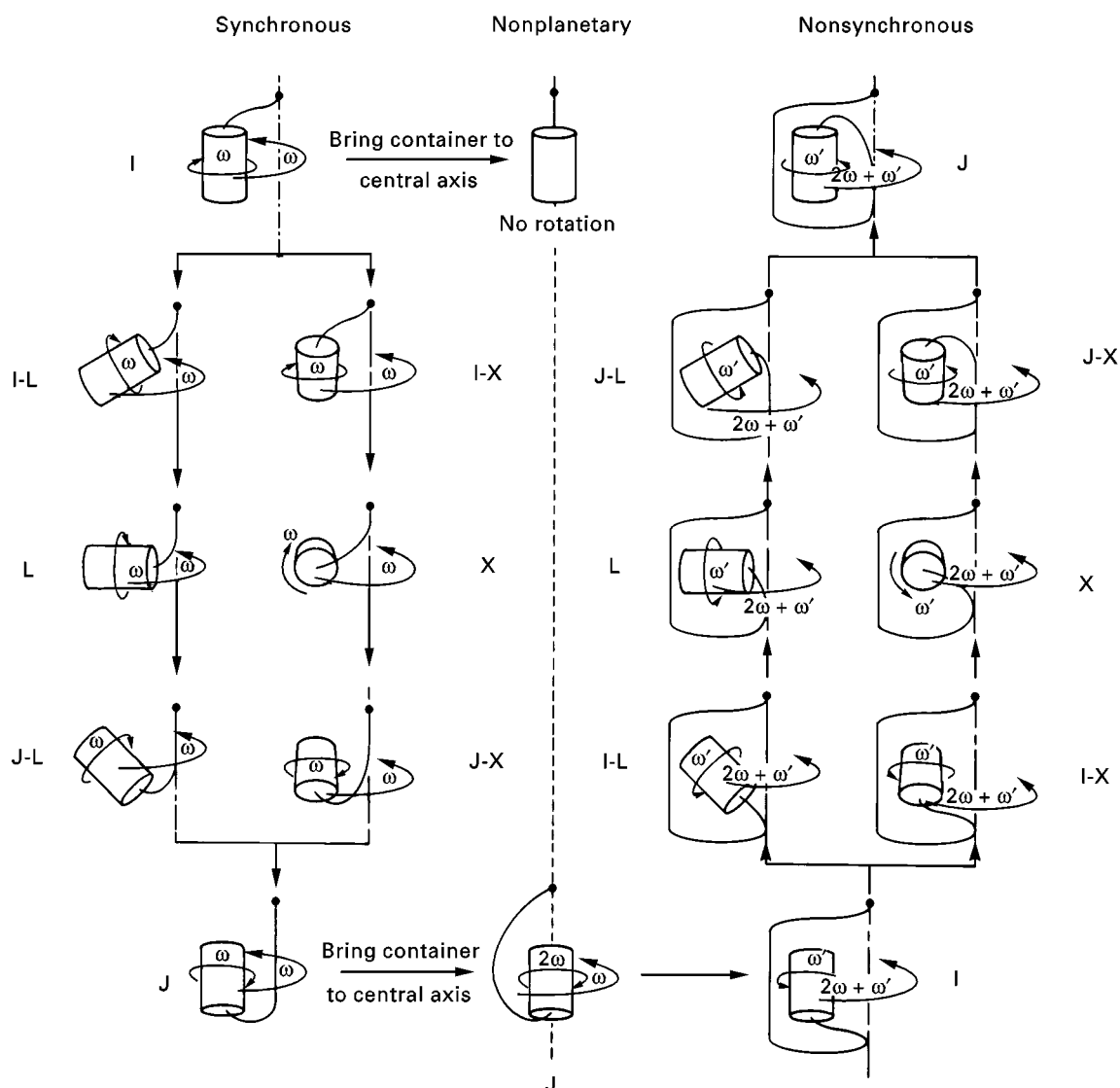


Figure 3 A series of flow-through centrifuge systems free of rotary seals.

orientation and motion of a cylindrical coil holder with a bundle of flow tubes, the end of which is supported on the centrifuge axis at the point marked with a black dot.

These centrifuge systems are classified in three groups according to their modes of planetary motion. The synchronous schemes (left column) produce a synchronous planetary motion of the coil holder, i.e. one rotation about its own axis during one revolution around the central axis of the centrifuge. In the nonsynchronous schemes (right column) the rates of rotation and revolution of the holder are independently adjustable. The nonplanetary scheme (middle column) produces simple rotation as in the conventional centrifuge system. In the Type I synchronous planetary motion (left, top) the holder revolves around the central axis of the centrifuge and synchronously rotates about its own axis in the opposite direction. This synchronous counterrotation of the holder steadily unwinds the twist of the tube bundle caused by revolution, thus eliminating the need for the rotary seal. This same principle can be applied to other synchronous schemes with tilted (Types I-L and I-X), horizontal (Types L and X), dipping (Types J-L and J-X) or even inverted (Type J) orientation of the holder. The Type J synchronous scheme is a transitional form to the nonplanetary scheme. When the holder of the Type J synchronous scheme is shifted to the central axis of the centrifuge, the rates of rotation (ω) and revolution (ω) of the holder are added and the holder rotates at an angular velocity of 2ω . In this case the tube bundle rotates around the holder at ω in the same direction as that of the holder to unwind the twist caused by the rotation of the holder. This nonplanetary scheme is further transformed to the nonsynchronous schemes. On the base of the nonplanetary scheme, the holder is again shifted towards the periphery of the centrifuge to perform a synchronous planetary motion. By selecting the holder orientation as specified in the synchronous schemes, the respective types of nonsynchronous schemes are produced.

Each scheme produces a specific pattern of the centrifugal force field that can be utilized for performing CCC. Among these, the Type J synchronous planetary motion is found to be most useful since it can perform high speed CCC that yields efficient separations in a short elution time.

Mechanism of High Speed CCC

The design of the Type J coil planet centrifuge is schematically illustrated in Figure 4. A cylindrical coil holder is equipped with a gear that is coupled to an identical stationary gear mounted at the central

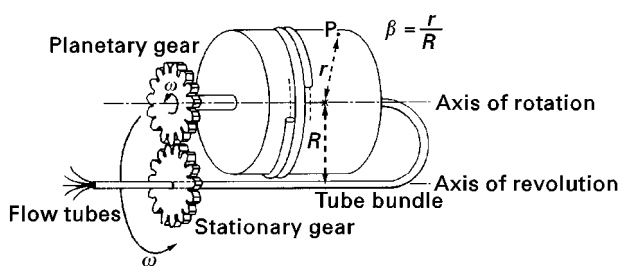


Figure 4 Design principle of Type J coil planet centrifuge.

axis of the centrifuge. This gear arrangement produces a synchronous planetary motion of the coil holder, i.e. revolution around the central axis of the centrifuge and rotation about its own axis, both at the same angular velocity and in the same direction as indicated by the arrows. As mentioned earlier, this planetary motion prevents the flow tubes from twisting and, therefore, the system permits continuous elution through the rotating column without the use of a conventional rotary seal device. The coil is directly wound around the holder as shown in the diagram. In practice, a long tube (usually over 100 m in length) is wound around a spool-shaped holder to form multiple coiled layers.

The mechanism of high speed CCC using this centrifuge design is illustrated in Figure 5, where all coils are shown as straight tubes for simplicity. When the coil is filled with two immiscible solvent phases and subjected to the planetary motion, the two phases are distributed in the coil in such a way that one phase (head phase) entirely occupies the head side and the other phase (tail phase) occupies the tail side (Figure 5A). This unilateral hydrodynamic distribution of

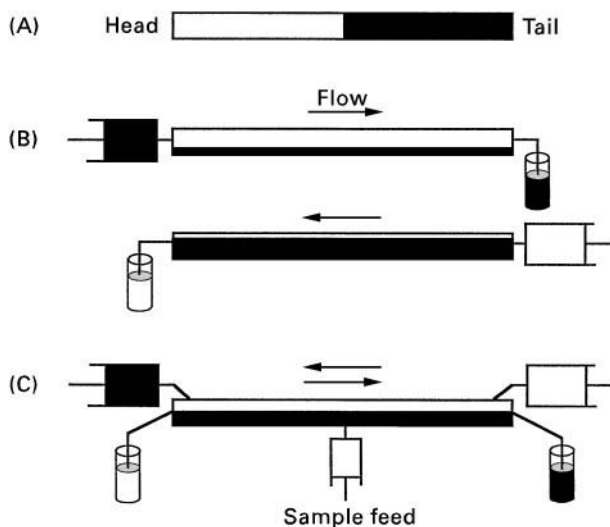


Figure 5 Mechanism of high-speed CCC. (A) Bilateral hydrodynamic equilibrium in a closed coil. (B) One-way elution modes. (C) Dual countercurrent system.

the two phases clearly indicates that the head phase (white), if introduced at the tail, would travel through the tail phase (black) toward the head, and similarly the tail phase, if introduced at the head, would travel through the head phase toward the tail. The above hydrodynamic trend can be efficiently utilized for performing CCC in two elution modes as shown in Figure 5B. The coil is first filled with the head phase (white) followed by elution with the tail phase (black) from the head toward the tail of the coil. Alternatively, the coil is filled with the tail phase followed by elution of the head phase from the tail toward the head of the coil. In either case, the mobile phase quickly flows through the coil and is collected from the other end, leaving a large volume of the stationary phase in the coil. Consequently, solutes locally introduced at the inlet of the coil are separated in a short period of time.

The system also permits simultaneous introduction of the two solvent phases through the respective terminals of the coil to induce a true countercurrent flow of the two phases. This dual CCC system requires an additional flow tube at each end of the coil to collect the effluent and, if desired, a sample injection tube at the middle portion of the coil as shown in Figure 5C. In addition to the liquid-liquid dual CCC, this system provides a unique application to foam separation. In the foam CCC system, gas and liquid phases undergo a true countercurrent flow through a long narrow coiled tube with the aid of the Type J synchronous planetary motion. When the liquid phase contains a surfactant, the above countercurrent process produces a foaming stream that moves with the gas phase toward the tail. The sample mixture introduced at the middle of the column is separated into its components according to their foam affinity; foam active components are quickly carried with the foaming stream toward the tail whereas the remainder is carried in the liquid stream in the opposite direction and collected at the head end of the coil. For samples with a strong foaming capacity such as proteins and peptides (bactracin), foam CCC can be performed without the use of the surfactant in the liquid phase.

In addition to the Type J planetary motion described above, some other synchronous planetary motions can produce the unilateral phase distribution (Figure 5A) that can be utilized for performing high speed CCC. Among these, the hybrid systems between Types X and L (see Figure 3) are extremely useful because they can retain a satisfactory volume of the stationary phase for viscous polymer phase systems that are used for partition of macromolecules and cell particles.

The hydrodynamic motion of the two solvent phases in the Type J high speed CCC system has been

observed under stroboscopic illumination. A spiral column was filled with the stationary phase and the coloured mobile phase was eluted through the column in a suitable elution mode. After the steady-state hydrodynamic equilibrium was reached, the spiral column showed two distinct zones. As shown in the upper diagram in Figure 6, vigorous mixing of the two solvent phases was observed in about one quarter of the column area near the centre of the centrifuge (mixing zone), while two phases are clearly separated into two layers in the rest of the area (settling zone). Because the location of the mixing zone is fixed with respect to the centrifuge system, while the spiral column rotates about its own axis, each mixing zone is travelling through the liquid like a wave of water over the sea, as shown in the bottom diagram in Figure 6. This highlights an important fact: at any given portion of the column the two solvent phases are subjected to a repetitive partition process of alternating mixing and settling at a high frequency of over 13 times per second at 800 rpm of column rotation.

This explains the high partition efficiency attained by high speed CCC. Figure 7 shows a typical separation of flavonoids from sea buckthorn (*Hippophae rhamnoides*) produced by the standard high speed CCC technique. Major components including isorhamnetin and quercetin are well resolved within 3 h at partition efficiencies ranging from 2000 to 3000 theoretical plates.

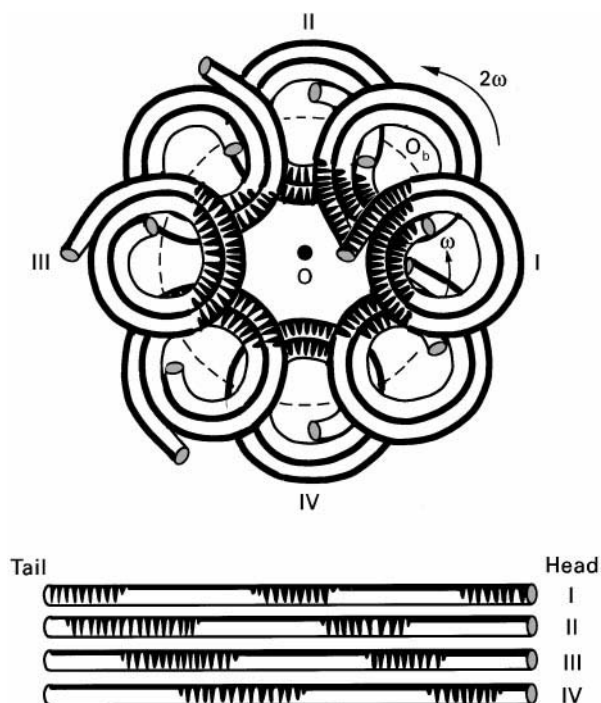


Figure 6 Hydrodynamic distribution of two solvent phases in a rotating spiral column.

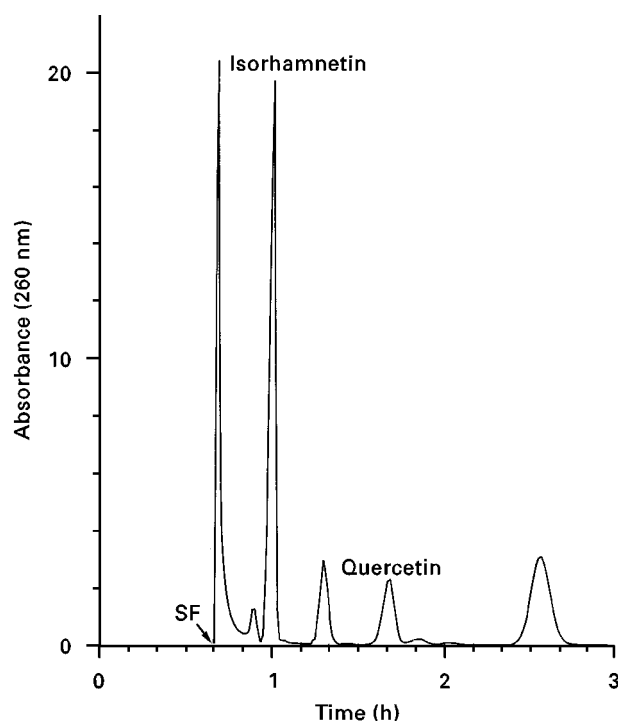


Figure 7 Separation of flavonoids from sea buckthorn by the standard high-speed CCC technique. SF, solvent front.

Standard Procedure of CCC

Selection of Two-Phase Solvent System

The first and most important step in CCC is to choose a proper solvent system that can satisfy the following requirements: the sample should be soluble and stable in the solvent system; the solvent system should provide a suitable partition coefficient for the target compounds; and it should produce a satisfactory retention of the stationary phase in the column. The partition coefficient and retention of the stationary phase are discussed below.

Partition coefficient CCC differs from other types of chromatography in that it uses two solvent phases and, therefore, the partition coefficient of the solute can be easily determined by a test tube experiment prior to the separation. In each measurement the sample is first partitioned between equilibrated two-solvent phases in a test tube, an aliquot of each phase is removed, and then the concentration of the solute in each aliquot is measured by ultraviolet or visual wavelength absorbance. Other methods of measurement such as radioactivity, enzymatic activity, etc., can be used. The partition coefficient, K , is the ratio between these two measurements and expressed in various ways such as $K(U/L) = C_U/C_L$ (solute concentration in the upper phase divided by that in the lower

phase), $K(S/M) = C_S/C_M$ (solute concentration in the stationary phase divided by that in the mobile phase), etc. When the sample is a mixture of multiple components, the partition coefficient of each component can be obtained by high performance liquid chromatography (HPLC), gas chromatography (GC) or thin-layer chromatography (TLC) analysis of each phase and by comparing the peak height or area of the corresponding peaks in the two chromatograms. In general the most suitable range of K value is $1 < K(S/M) < 2$ for the hydrostatic CCC systems and $0.5 < K(S/M) < 1$ for the hydrodynamic CCC systems. Once the K value has been determined, the retention volume of the solute can be computed from the following equation:

$$V_R = V_{SF} + K(S/M)(V_C - V_{SF})$$

where V_R is the retention volume of the solute, V_{SF} the retention volume of the solvent front (amount of the mobile phase in the column), and V_C the total column capacity.

Retention of stationary phase The retention of the stationary phase in the separation column is an important factor in determining the resolution of solute peaks in CCC. Generally, the greater the retention of the stationary phase, the better the separation. In hydrostatic systems, in which the phase mixing is not violent, the retention of the stationary phase is conveniently adjusted by varying the flow rate of the mobile phase and/or the rotation speed in the centrifugal CCC system. In hydrodynamic systems, which provide efficient mixing of the two phases, stationary phase retention requires more careful selection of the two-solvent system as well as the choice of the mobile phase and its elution mode. In high speed CCC using the Type J planetary motion, the settling time of the two solvent phases under gravity provides a useful measure for the stationary phase retention and the elution mode. The test is performed as follows: the two phases are preequilibrated in a separatory funnel and 2 mL of each phase is delivered into a 5 mL capacity graduated cylinder equipped with a stopper (an ordinary glass test tube, 13 mm o.d. and 10 cm long with a polyethylene cap can also be used). The contents are gently mixed by inverting the container five times and the time required to form two clear layers is measured. If this settling time is within 30 s, the solvent system can be used for separation by eluting the lower phase from the head toward the tail or the upper phase in the reversed mode. If the settling time exceeds 30 s, the above elution mode should be reversed while the retention of the stationary phase is usually considerably lower than an optimum range. However, this settling time test is not

applied to the cross-axis coil planet centrifuge systems based on the planetary motions of Type X, Type L and their hybrid systems (see Figure 3, left column). These centrifuge systems provide excellent retention of the stationary phase for almost all two-phase solvent systems including viscous polymer phase systems used for partition of macromolecules and cell particles.

The retention of the stationary phase in the hydrodynamic CCC systems has been extensively studied using various two-phase solvent systems. These results are summarized in a set of phase distribution diagrams that will provide a valuable guide for users of high speed CCC systems (see Further Reading).

Preparation of the Sample Solution

In CCC, the sample solution is usually prepared by dissolving the sample in the solvents used for the separation. If the amount of sample is small, it may be dissolved in the stationary phase. However, if the sample mixture contains multiple components with a wide range of polarity, it should be dissolved in both solvent phases. In this way, the volume of the sample solution is minimized and also the two-phase formation in the sample solution is ensured. Occasionally, a single phase is formed after dissolving a large amount of the sample, which would result in a detrimental loss of the stationary phase from the column. If this occurs, the sample solution should be diluted with the solvent until two phases are formed. Although CCC permits the loading of the sample solution containing undissolved particulates, the best results are obtained by filtering the sample solution before introduction into the column.

As in other forms of LC, the amount of sample and sample solution affects the separation. Usually, a typical semipreparative column with about 300 mL capacity will separate up to a few hundred milligrams of sample dissolved in 10 mL of the solvent mixture without significantly affecting the partition efficiency.

Elution Procedure

In both hydrostatic and hydrodynamic CCC, separation is initiated by filling the entire column with the stationary phase of a mutually equilibrated two-phase solvent system. This is followed by injection of the sample solution through the sample port. Then, the mobile phase is eluted through the column in the correct elution mode while the apparatus is rotated at a suitable speed (except for DCCC). Although sample injection may be made after the column had been equilibrated with the mobile phase (the routine procedure in HPLC), this practice does not usually improve the separation in CCC.

In hydrostatic CCC systems, the direction of eluting the mobile phase should be chosen in such a way that the upper phase is eluted against the acting force field (ascending mode), and the lower phase along the force field (descending mode). In hydrodynamic CCC systems, the direction of the Archimedean screw force also plays an important role in the retention of the stationary phase. Generally speaking, the lower phase should be eluted from the head toward the tail, and vice versa for the upper phase. For various polymer phase systems (such as polyethylene glycol/dextran) with a high viscosity, maximum retention of the stationary phase is usually obtained by using the less viscous phase as the mobile phase.

As in HPLC, CCC permits the use of gradient or stepwise elution. The method requires suitable selection of the solvent system so that the volume of the stationary phase in the column is not significantly altered by the mobile phase. Some examples are *n*-butanol/water with a concentration gradient of dichloroacetic acid or trifluoroacetic acid, and polymer phase systems with a pH gradient of sodium or potassium phosphate.

Detection

In the past, detection of the CCC effluent has been performed by adapting the UV/visible absorbance monitoring system used in HPLC. In this case, a straight vertical flow cell should be used. In order to avoid trapping the droplets of the stationary phase in the cell, the mobile lower phase should be introduced from the bottom of the flow cell upward and the mobile upper phase from the top of the flow cell downward. In addition to absorbance measurement, other monitoring methods may also be used which include post-column reaction, interfacing with a mass spectrometer or nuclear magnetic resonance (NMR), laser light scattering detection, pH or conductivity measurement, etc. Most of these methods are less sensitive to the carryover of the stationary phase droplets and therefore will produce better elution curves.

Variations of Countercurrent Chromatography

The standard CCC technique described above may be modified so that it is suitable for a particular type of separation. Many of these modified CCC schemes have their counterpart in LC, utilizing a solid support matrix. Table 1 summarizes the relationship between a variety of CCC techniques and their counterparts in LC.

Table 1 Variations of CCC with their counterparts in LC with solid support matrix

CCC	Description	Counterpart in LC
Normal mode	Organic phase mobile	Normal-phase LC
Reversed mode	Aqueous phase mobile	Reversed-phase LC
Dual mode	Both phases mobile	Moving-bed LC
Ion CCC	Ion exchanger in SP ^a	Ion LC
Affinity CCC	Affinity ligand in SP	Affinity LC
pH-Zone-refining CCC	Retainer in SP; eluter in MP ^b	Displacement LC
Chiral CCC	Chiral selector in SP	Chiral LC

^aSP, stationary phase.^bMP, mobile phase.

Ion CCC

Analogous to ion chromatography, CCC can separate both inorganic and organic ions according to their pK_a of affinity to the ionic ligand dissolved in the stationary phase. One example is illustrated in Figure 8, which shows separation of rare earth elements by pH gradient elution of a hydrochloric acid mobile phase through a hexane stationary phase containing a ligand, di-(2-ethylhexyl)phosphoric acid. Figure 9 is another example showing the separation of catecholamine. The left chromatogram, obtained with a ligand-free solvent system, shows no sign of separation (Figure 9A). When a basic ligand, triethylamine, is added to the stationary phase, all components are resolved (Figure 9B).

Chiral Countercurrent Chromatography

Enantiomers may be resolved by CCC if an appropriate chiral selector is present in the stationary phase. Figure 10 shows the separation of four enantiomeric

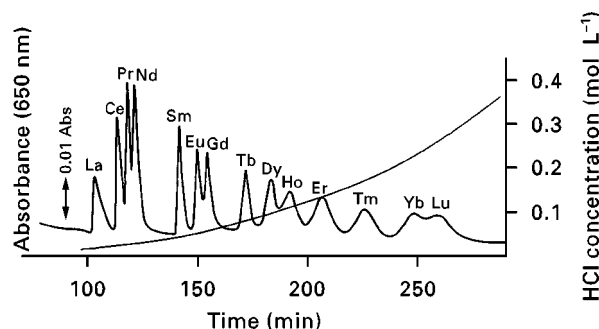


Figure 8 Analysis of rare earth elements by pH gradient elution with a ligand in the stationary phase. Apparatus, HS CCC centrifuge with 7.5 cm revolution radius; column, three multilayer coils, 1.1 mm i.d. \times 300 m, 270 mL capacity; stationary phase, 0.003 mol L⁻¹ di-(2-ethylhexyl)phosphoric acid in *n*-heptane; mobile phase, exponential gradient of 0–0.4 mol L⁻¹ HCl; sample, 0.001 mol L⁻¹ each of La, Ce, Pr, Nd, Sm, Eu, Gd, Tb, Dy, Ho, Er, Tm, Yb and Lu in 100 μ L; revolution, 900 rev min⁻¹; flow rate, 5 mL min⁻¹; pressure, 300 psi (\sim 2070 kPa).

pairs of dinitrobenzoyl amino acids using a chiral selector, *N*-dodecanoyl-L-proline-3,5-dimethylanilide in the stationary phase. When the separation is performed without the chiral selector, all components elute near the solvent front, resulting in poor separation (Figure 10A). The addition of the chiral selector to the stationary phase results in excellent separation with only one overlapping peak under otherwise identical experimental conditions (Figure 10B). Gram quantities of ionic enantiomers can be purified by means of the pH-zone-refining CCC technique described below.

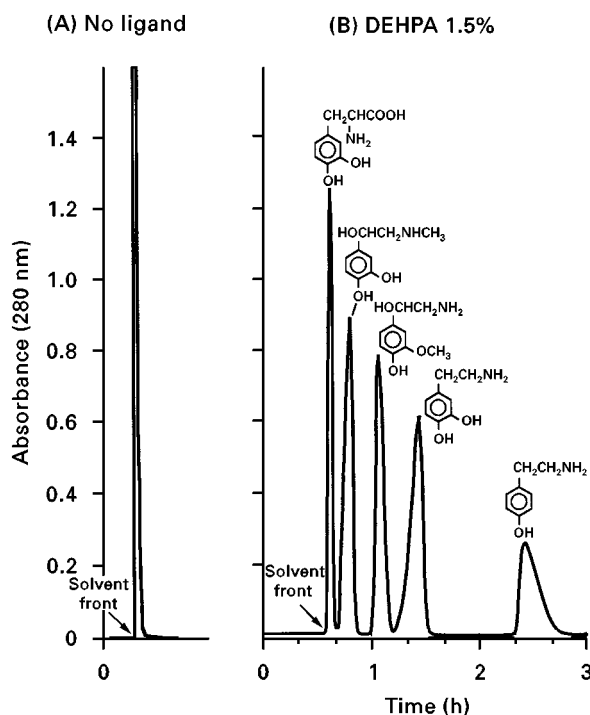


Figure 9 Separation of catecholamine and related compounds by high speed CCC using a ligand, triethylamine, in the stationary phase. The left chromatogram (A) obtained without ligand shows no evidence of separation. All components were completely resolved by introducing the ligand in the stationary phase, as shown in part (B).

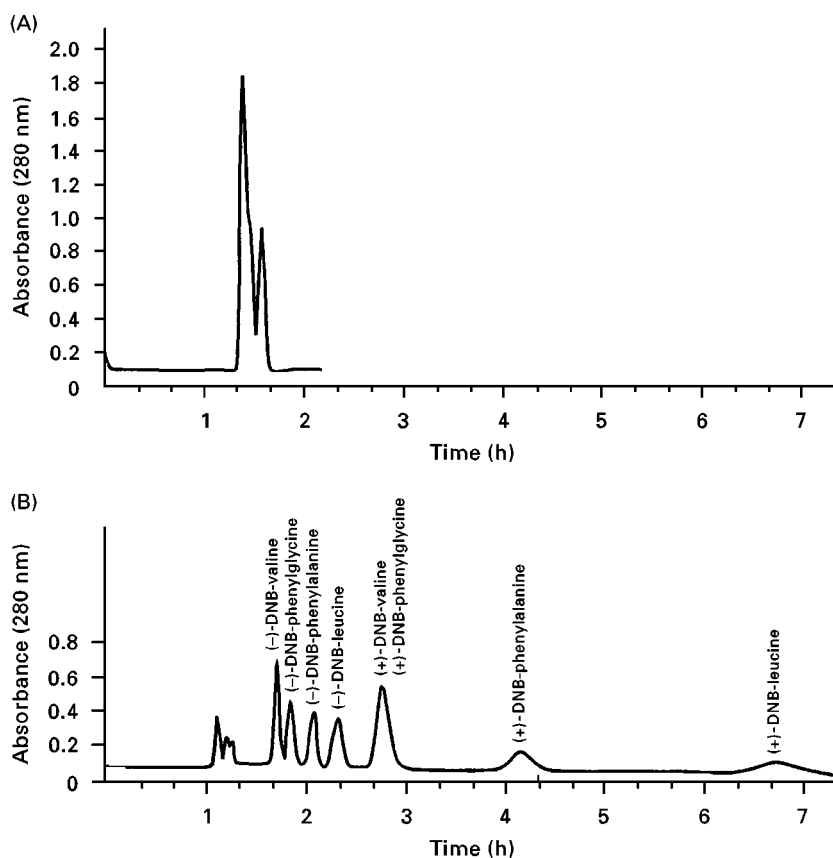


Figure 10 Separation of four enantiomeric dinitrobenzoyl (DNB) amino acids by high speed CCC, with (B), and without (A), a chiral selector, *N*-dodecanoyl-L-proline-3,5-dimethylanilide (DPA). In the upper chromatogram obtained without chiral selector, all components eluted near the solvent front with poor peak resolution. Introduction of 1.6 g of DPA in the stationary phase under otherwise identical experimental conditions resulted in a remarkable improvement in peak resolution.

pH-Zone-Refining CCC

This preparative CCC technique produces a train of highly concentrated rectangular peaks similar to those obtained in displacement chromatography. The method utilizes a retainer acid or base in the stationary phase and an eluter counterion in the mobile

phase. Interaction of ionic analytes forms a series of solute zones with sharp boundaries that move together through the column at the same rate (isotachic movement). Each zone consists of a single species, has its own specific pH and is arranged in the order of its pK_a and hydrophobicity. Charged minor components are concentrated at the boundaries of the major zone

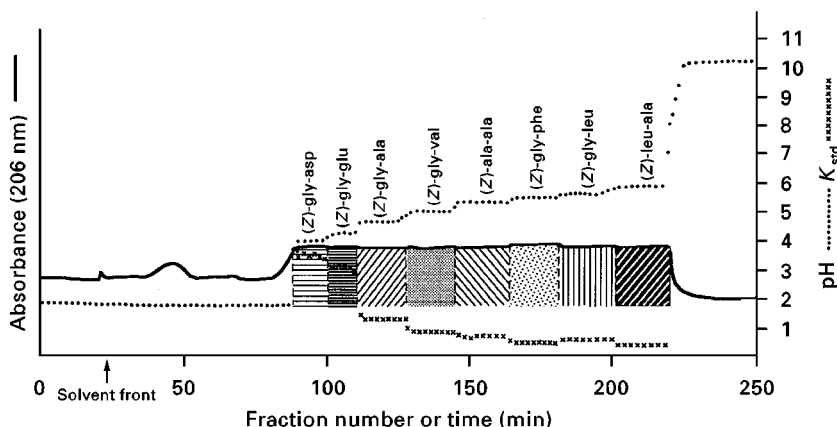


Figure 11 Separation of eight (Z)-(benzyloxycarbonyl) dipeptides by pH-zone-refining CCC.

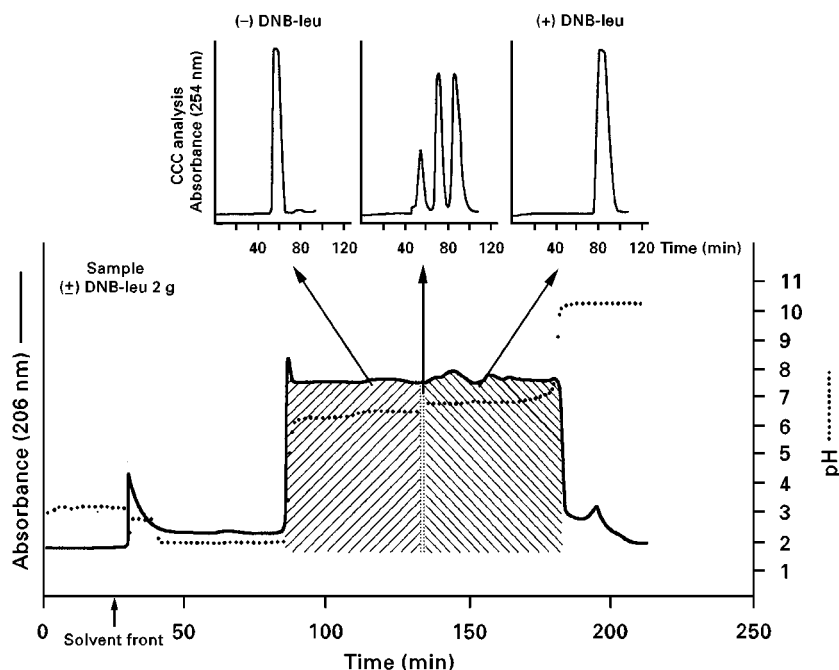


Figure 12 Separation of (±)-dinitrobenzoyl leucine ((±) DNB-leu) by pH-zone-refining CCC.

and are eluted as sharp peaks. **Figure 11** shows the separation of eight (Z)-(benzyl-oxycarbonyl) dipeptides by pH-zone-refining CCC. All components (100 mg of each) are well resolved with minimum mixing zones as evidenced by the sharp transitions of their partition coefficients (K_{std}) measured with a standard two-phase solvent system.

The method can also be applied to preparative-scale chiral separation using a chiral selector in the stationary phase. **Figure 12** illustrates separation of

2 g of (±)-dinitrobenzoyl leucine by pH-zone-refining CCC. pH-zone-refining CCC is described in detail in texts listed in Further Reading.

CCC with Polymer Phase Systems

Separation of proteins requires the use of aqueous–aqueous polymer phase systems to prevent denaturation of the analytes by organic solvents. **Figure 13** shows separation of four stable proteins by a polymer phase system composed of 12.5% (w/w) polyethylene glycol 1000 and 12.5% (w/w) dibasic potassium phosphate. The separation was performed by a cross-axis coil planet centrifuge (hybrid between Type L and X in Figure 2). The method has also been successfully applied for purification of recombinant enzymes.

Conclusions

Countercurrent chromatography covers a broad spectrum of samples ranging from small ions to macromolecules. The method provides various advantages over conventional liquid chromatographic techniques such as no sample loss and denaturation due to the solid support, high purity of fractions and high reproducibility. The CCC technique is particularly suitable for preparative separations of natural and synthetic compounds.

See also: II/Chromatography: Countercurrent Chromatography and High-Speed Countercurrent Chromatography:

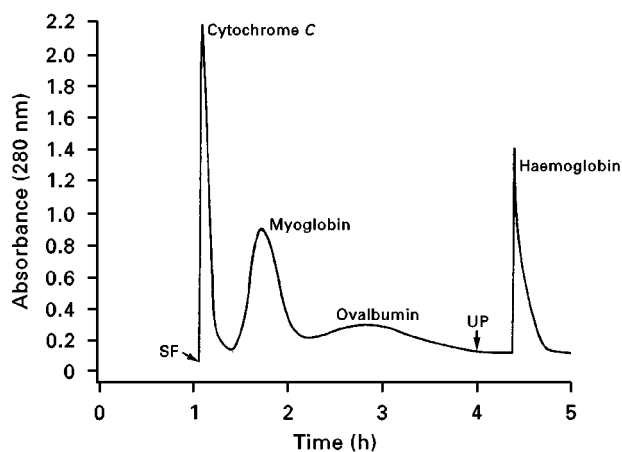


Figure 13 Protein separation with an aqueous–aqueous polymer phase system composed of 12.5% (w/w) polyethylene glycol 1000 and 12.5% (w/w) K_2HPO_4 in distilled water. The column was initially eluted with the lower phase. After point UP the column was eluted with the upper phase in the reverse direction to elute haemoglobin retained in the column SF, solvent front.

Instrumentation. **Chromatography: Liquid:** Partition Chromatography (Liquid–Liquid). **III/Chiral Separations:** Countercurrent Chromatography; Liquid Chromatography. **Foam Countercurrent Chromatography. Ion Analysis:** Liquid Chromatography; High-Speed Countercurrent Chromatography. **Liquid Chromatography. Medicinal Herb Compounds: High-Speed Countercurrent Chromatography. Natural Products:** High-Speed Countercurrent Chromatography; Liquid Chromatography. **Peptides and Proteins:** Liquid Chromatography. **Proteins:** High-Speed Countercurrent Chromatography.

Further Reading

Conway WD (1990) *Countercurrent Chromatography: Apparatus, Theory and Applications*. New York: VCH.
Conway WD and Petroski RJ (eds) (1995) *ACS Symposium Series Monograph on Modern Countercurrent Chromatography*. Washington, DC: American Chemical Society.

Ito Y (1981) Countercurrent chromatography (minireview). *Journal of Biochemical and Biophysical Methods* 5: 105–129.
Ito Y (1986) High-speed countercurrent chromatography. *CRC Critical Reviews in Analytical Chemistry* 17: 65–143.
Ito Y (1991) Countercurrent chromatography in *Chromatography V*, part A, chap. 2, pp. A69–A107. Amsterdam: Elsevier.
Ito Y (1996) Countercurrent chromatography. In: *Encyclopedia of Analytical Science*, pp. 910–916. London: Academic Press.
Ito Y (1996) pH-zone-refining countercurrent chromatography. *Journal of Chromatography A* 753: 1–30.
Ito Y and Conway WD (eds) (1996) *High-Speed Countercurrent Chromatography*. New York: Wiley-Interscience.
Mandava NB and Ito Y (1988) *Countercurrent Chromatography: Theory and Practice*. New York: Marcel Dekker.

Derivatization

I. S. Krull, Northeastern University, Boston, MA, USA
R. Strong, Repligen Corporation, Needham, MA, USA

Copyright © 2000 Academic Press

Introduction

Derivatization involves changing in some way the basic chemical or physical structure of a compound, usually to a single product, which may be more useful for the analysis of the original analyte in liquid chromatography (LC). Derivatization can be used for analytical or preparative scale LC. In the analytical mode, it can be used to improve the identification and quantitation of the analyte of interest. It may also be used to improve throughput and recovery in preparative scale LC purifications of large amounts of material. Changes in the basic structure of the analyte can also lead to improved peak shape, elution times, peak symmetry, efficiency, plate count, and other indicators of chromatographic performance. That is, elution times and retention factors, as well as resolution, separation factors, reduced plate heights, and other LC parameters of performance, can all be varied and improved by suitable, selective derivatization of the starting analyte.

The most general type of derivatization involves modifying the chemical structure of the starting compound by tagging or adding another reagent to it via a suitable functional group alteration (Figure 1). Thus, most simple derivatizations involve a derivatiz-

ing reagent, the substrate or analyte of interest, the desired derivative of the analyte, remaining excess reagent, and undesirable by-products coming from the excess derivatizing reagent reacting with solvent, water or thermally degrading (Figure 1). Ideally, only the desired derivative would remain at the end of the reaction period, without any remaining starting analyte, derivatizing reagent or by-products. However, this idealized situation is rarely observed and it is often necessary to separate prior to or during the LC analysis the desired derivative from all other possible compounds coming from the derivatization reaction and/or sample components and their possible derivatization products.

Though most derivatizations usually occur in a homogeneous solution between the analyte of interest and the reagent itself, it is possible to perform derivatizations on the analyte in solution with an immobilized or solid-phase reagent. Figure 2 illustrates a typical immobilized or solid-phase reagent that has been described in the literature for use with LC. It is also feasible to first immobilize the analyte on a solid support, such as silica gel, Immobilon™ membrane, poly(styrene-divinylbenzene), C₁₈ packing material, and others, and then perform the derivatization reaction on the now-immobilized analyte. Once the reaction is completed, the excess reagent is simply washed from the solid support still containing the derivative. The desired derivative is then eluted with a stronger solvent from the solid support, often in a disposable plastic tube (solid-phase extraction cartridge or Sep-Pak™), without any residual, unreacted starting

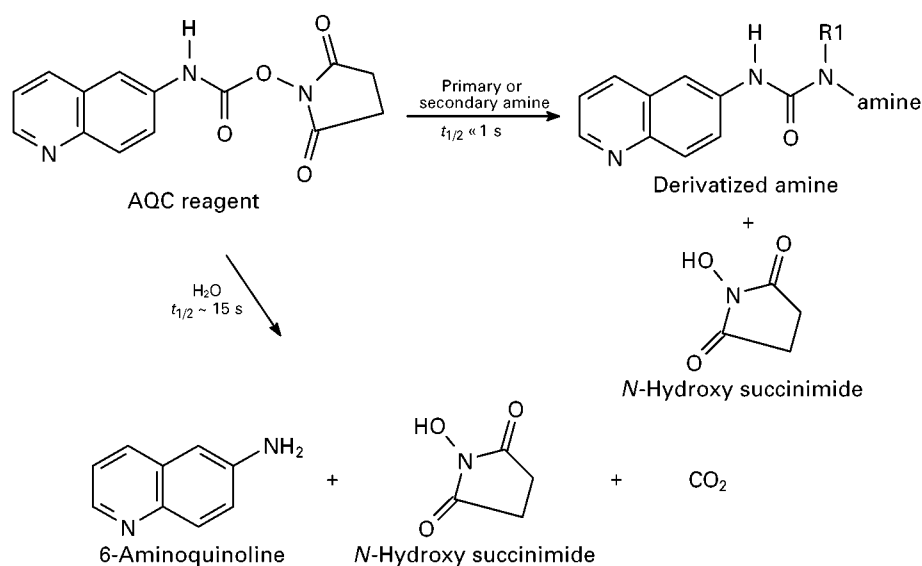


Figure 1 Chemical derivatization of an analyte using 6-aminoquinoyl-*N*-hydroxysuccinimide carbamate (6-AQC) reagent. This is a homogeneous reaction that occurs in solution. The 6-AQC degrades with water to form 6-aminoquinoline and *N*-hydroxysuccinimide, with the release of carbon dioxide.

analyte or by-products of the reagent, in a state suitable for direct LC injection.

Other approaches to derivatization involve the use of photochemical reactions, usually performed on-line after the separation occurs, which convert the starting analyte into one or more derivatives with improved detection properties (ultraviolet (UV), fluorescent (FL), electrochemical (EC), etc). This does not introduce excess derivatizing reagent, reagent by-products or hydrolysis products, since the reagent itself is light rather than a chemical. Such approaches have become popular in LC applications. It is also possible to utilize electrochemistry to perform de-

derivatizations in LC, as well as microwave digestion, immobilized enzyme reactors, pH alteration of the mobile phase after the separation, etc. **Table 1** summarizes the most commonly utilized derivatization techniques described in LC other than simple, chemical reactions.

General Approaches to Derivatization in Liquid Chromatography

Chemical derivatization in LC requires the optimization of several reaction or separation parameters. These include temperature, pH, solvent, time, ratio of

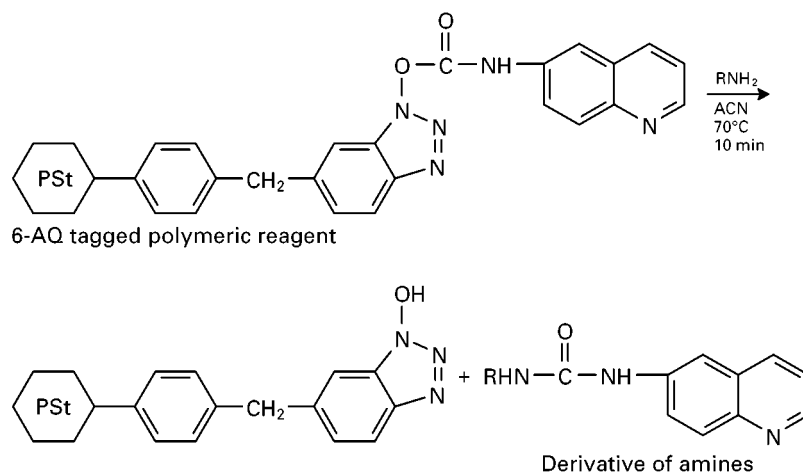


Figure 2 Typical immobilized or solid-phase reagent. The 6-AQ-tagged polymeric reagent reacts with amines (70°C, 10 min), producing a derivative free in solution, now 6-AQ derived. (6-AQ, 6-aminoquinoline; PSt, polystyrene.)

Table 1 Summary of common derivatization approaches, other than chemical reactions, used in LC

1. Photochemical conversions, photohydrolysis reactions, photocleavage or photoextrusion reactions, photobleaching, etc.
2. Electrochemical conversions (amperometric or coulometric), oxidative or reductive reactions to convert an electrochemically inactive analyte into an electrochemically active derivative.
3. Enzymatic conversions, enzyme–substrate reaction detection, used to detect enzymes post-column via their reaction with substrate and formation of the conversion product, which may then be UV, FL, EC and/or MS active. This is detection of enzymes first separated by LC.
4. Microwave digestion reactions, post-column, used to digest proteins/peptides, nucleic acids and other biopolymers, leading to monomeric species that are more easily detected (EC) and/or derivatized before final detection (e.g. proteins → amino acids + OPA → tagged amino acids; UV, FL, or EC active).
5. Immunodetection (ID), post-column in LC, used to tag an antigenic species with a FL or enzyme-tagged antibody, leading to indirect detection of the untagged antigen via its complex formation in a sandwich format. A primary antibody must be immobilized on the solid ID support to initially capture the antigen after separation by LC.
6. Enzymatic conversion of a substrate, post-column, to form the turnover product with improved UV, FL or EC detection properties. This is detection of enzyme substrates, first separated by LC, then detected post-column by addition of enzyme in solution or via an immobilized enzyme reactor column, pre-detection.

reagent to substrate, separation of derivative from sample components and reaction by-products, detector optimization for derivatives, chromatographic optimization of derivative peak shape, generation of standard derivative and structure confirmation, production of derivative calibration plot for quantitation, etc. The purity of the derivative peak in a sample must also be demonstrated by online photodiode array (PDA) or mass spectrometric (MS) methods. The derivatization reagent must be well characterized with regard to structure and its purity demonstrated. The reaction conditions need to be optimized to minimize reagent consumption, maximize derivative yield, and eliminate the formation or presence of reaction and reagent by-products that might interfere in the final separation and detection steps. It may even be necessary or desirable initially (pre-LC) to separate the excess reagent from the derivative and then introduce just the sample and the now-formed derivative into the analytical LC column.

Sometimes the reagents used have different detector properties from the final derivatives. The excess reagent at the end of the derivatization reaction

may then be transparent under the optimized detection conditions for the derivative. It may even coelute together with the derivative peak, yet not be observed under such detection conditions. This reduces the need for initial separation of excess, unreacted reagent from the derivative and sample, and/or optimization of LC conditions so that the derivative peak appears completely resolved from all the other peaks.

Large versus Small Analyte Molecules and Their Derivatizations

It is generally easier to derivatize small molecules than large ones, since the rates of chemical reactions of very large biomolecules are usually orders of magnitude slower than those of smaller species. This is a function of effective chemical collisions, the number of chemical collisions per unit time between reactive sites, conformational preferences of large biomolecules, and the number of active sites available in a biomolecule. That is not to say that biomolecules cannot be successfully derivatized – they often are and can be – but the efficiency of derivatization (percent derivatization per unit time) versus smaller reactive species is usually much less. Also, the energy of activation needed to derivatize a primary amino group in a large molecule is often much larger than that for a very small molecule having the same functionality. This is, of course, a function of the neighbouring groups, conformational preferences, conformations available, hydrogen bonding within the biomolecule, and other factors. A considerable danger with derivatizing large molecules (typically biopolymers) stems from the fact that, in most cases, such a polymer possesses a number of reactive groups, for reasons just specified, which may differ in their reactivity. The result may be the formation of a number of products bearing the same tag in different mole per mole ratios. Although in enzymatic amplification techniques the formation of multiple products helps identification, in the situation just described the formation of multiple derivatization products should be avoided. The separation of such mixtures is often difficult, usually resulting in broad peaks and low plate counts. Moreover, it may be difficult to trace back which derivative was derived from which solute present in the original sample.

Numerous chemical reactions have been used to derivatize different classes of biomolecules in LC, usually with a high degree of success. However, the overall enhancement is always dependent on the particular tags used. That is, derivatization reactions that tag a specific site within the biomolecule sometimes lead to a single, and sometimes several, tags incorporated into the derivative. As a function of the tag, there

will be improved detector response, but perhaps much smaller chromatographic changes than with small molecules if the derivatization is carried out pre-column. Derivatizations are therefore often performed post-column. An ideal derivatization scheme would generate many derivatives from the original biomolecule, such as via enzyme amplification. This is already used to detect intact enzymes, but is used much less to detect proteins, peptides, nucleic acids, etc. Thus, the scheme described using post-column, microwave digestion of proteins, followed by a second post-column solution reaction with a FL derivatizing reagent (e.g. *o*-phthaldialdehyde, OPA), leads to many amino acids now detectable by FL methods. This is, perhaps, an ideal example of a general approach that greatly improves detectability of large molecules, such as via enzyme amplification for enzymes.

Offline versus Online Arrangements

It is also necessary to differentiate between offline and online arrangements (Table 2). In the offline mode the reactions occur away from the high performance liquid chromatography (HPLC) system, although there may be some examples that could be defined as either offline or online (e.g. in a sample vial in a carousel as part of an automated derivatization-injection system in LC). In the online mode the reaction chemistry occurs as part of the HPLC system, integrated into the instrumentation and analysis, and is time constrained and controlled. Thus there are four different and distinct types of derivatization approaches, or modes, for LC: (1) online, pre-column; (2) online, post-column; (3) offline, pre-column; and (4) offline, post-column (Table 2).

Pre-column versus Post-column Arrangements

The derivatization can be carried out in the pre-column or post-column mode, i.e. before or after the separation has taken place. In the post-column approach the derivatization reaction does not have to yield a single, stable product, provided that the reactions are reproducible. There are several serious disadvantages associated with this technique: (1) excess

derivatization reagent must not interfere in the detection process; (2) reaction kinetics need to be rapid to allow real-time detection; (3) additional pumps are needed for a nonpulsating supply of derivatization reagent; (4) reaction solvents must be miscible with the separation mobile phase; and (5) an efficient mixing of derivatization reagent with the column effluent is required.

Pre-column derivatization is an alternative approach to post-column derivatization. One of its advantages is that derivatization is independent of the mobile phase and the reaction kinetics are not limited. Apart from an increase in detectability, pre-column derivatization can also improve the selectivity and chromatographic resolution of the overall method. Excess reagent present in the reaction mixture must be chromatographically resolved from the analyte derivative peaks, and/or be physically or chemically removed from the sample solution prior to injection. If several analytes yield the same derivative(s), then these would not be separable, and it would be impossible to determine which analyte was originally present in the sample. For example, the use of a substrate that could react with several enzymes, pre-column, would then lead to exactly the same product(s), preventing absolute identification of the enzyme actually present in the sample reaction mixture. More derivatizations have been performed online, post-column, as opposed to online, pre-column, or even offline, pre-column, for the above reasons, at least in LC areas. It is also possible to perform derivatizations *in situ*, or within the mobile phase. In this case derivatization reagent is placed in the solvents used for the LC separation. After separation has occurred, the eluent from the LC column can be heated to cause the reaction to occur, prior to the final detection stage. Unlike the online, post-column mode of operation, this does not require the addition of a mixing tee, heating coil, reagent pump, or ancillary tubing after the LC column.

Offline, Pre-column Derivatization

Offline, pre-column derivatizations have no extracolumn loss of efficiency and no solvent or kinetic limitations. Derivatization can be conducted under flexible reaction conditions or with harsh reagents. Offline derivatization can be optimized for high reaction yields and minimum by-products. Derivatization solvents need to be miscible with the chromatographic mobile phase. Otherwise, the derivatization solvents have to be evaporated and the residue of derivatives redissolved in a solvent compatible with the mobile phase. Offline derivatization does not need to give 100% theoretical yields, as long as there is good sample-to-sample reproducibility. However,

Table 2 Derivatization placement in LC

Mode	Reaction sequence
Pre-column, offline	Derivatization away from LC— injection—separation—detection
Pre-column, online	Derivatization on the LC— injection—separation—detection
Post-column, offline	Injection—separation— derivatization away from LC— detection
Post-column, online	Injection—separation— derivatization on the LC— detection

nonautomated offline pre-column derivatizations require operator attendance and manual manipulations.

Online, Pre-column Derivatization

Online, pre-column derivatization is accomplished by incorporation of a derivatization reagent into the flow scheme of the LC. Since all of the derivatized products are injected into the LC, this mode of derivatization does not have the solvent dilution problem observed in offline derivatization. There are several requirements for the conduction of online pre-column derivatization: (1) good chemical and/or pressure stability of derivatization reagents in organic solvent; (2) good solubility of derivatized products in the mobile phase; (3) no precipitate or gas generated in the derivatization; (4) compatibility of derivatization solvent with mobile phase; and (5) minimum volume of derivatization solvent or well packed solid-phase derivatization column. In online pre-column derivatization, the extraction and clean-up of complex samples often becomes part of the chromatographic operation, which can be automatically (computer/microprocessor interface) performed via switching of valves. Preliminary sample handling is minimized and automated derivatization procedures tend to provide better reproducibility.

Offline, Post-column Derivatization

This is perhaps the most unwieldy derivatization approach of all (Table 2). It involves separating the analyte of interest from the LC eluent prior to detection, performing a solution or solid-phase derivatization away from the instrumentation, manually or automatically, and then detecting the final derivatized solution. Automation is difficult, reproducibility is less than ideal, and even accuracy and precision falter, at times, because of a lack of total automatability. Thus, this mode receives the least emphasis in the literature and the lowest recommendation of application.

Online, Post-column Derivatization

In this approach (Table 2) injection-separation steps are followed by online derivatization, using automated, fully online instrumentation and methods. This technique utilizes post-column reactors (low dead volume mixing tees, knitted open-tubular reactors, low dead volume reaction coils, etc.) in which the chemical reagents are introduced to the LC eluent. A delay time is needed (reaction dependent) to convert the analyte to product(s), and the entire solution, along with excess reagent(s), is introduced into the detector. This approach also allows for online liquid-liquid extraction, ion suppression (dual column ion chromatography), pH adjustment, organic

solvent addition, basic hydrolysis reactions, additional chemical reactions modifying the solutes prior to the derivatization step (e.g. oxidation of imidazole ring in proline and hydroxyproline for their assay by the OPA reaction), enzyme addition, and the use of post-column, immobilized reagents or enzymes. There are many chemical reactions that have been employed post-column online: sequential reactions, solid-phase/catalytic enhanced reactions (e.g. carbamate detection), microwave digestion of proteins, photochemical reactions, etc. However, there are severe constraints or requirements on the nature of the reagent solvent and solution that can be mixed with the LC effluent, detector transparency of such solvents, prevention of analyte derivative precipitation before detection, mixing of reagents with analyte, lack of mixing noise, need for additional instrumentation, mixing tees, connecting joints, and extra tubing connections. Nevertheless, at least in LC areas, this particular mode has been the most widely employed and applied.

Specific Recommendations for Successful Application of Derivatization in Liquid Chromatography

It is clear that there are numerous approaches to successful derivatization possible in various modes of LC, including reversed-phase, ion exchange, normal phase and hydrophobic interaction. There are perhaps too many choices as to which specific reagent will prove applicable for a new analyte, or how to best optimize and apply any given reagent, much less what might prove the optimal LC conditions for the final derivatives. A rational approach to derivatization for all LC is called for. Such rational designs for method development, optimization and validation in HPLC are available from the literature. A rational approach to developing, optimizing and then validating a derivatization method for LC is described below.

1. Know the structure of the analyte(s), what functional groups are present for tagging, and what types of reactions might be employed. A good knowledge of organic chemistry is needed and available at this stage. Some of the existing texts on derivatizations for HPLC should be utilized.
2. What are the requirements of the final derivatization-LC method? It is necessary to decide what detection limits are needed, what sample matrices will be analysed, what limits of quantitation must be realized, what resolution (sample dependent) will be needed, and so forth.

3. What is known in the literature about the LC of the analyte of interest, as a standard pure compound (without regard to sample matrices yet)? Are conditions reported for underivatized analysis, and what conditions have been already described and optimized? Could these be eventually utilized for simple derivatives of the original analyte? What modifications might be needed to resolve the analyte derivatives? Are any tagging methods already reported for GC or thin-layer chromatography (TLC) that might prove applicable in LC? What types of reagents have been described? What were the specific reaction conditions already optimized for this derivatization scheme?
4. Perform simple, test tube reactions on a standard of the analyte offline, away from the LC instrument, to optimize reaction conditions and to demonstrate the nature of the products formed, their number, derivatization yield, ease of product work-up prior to LC, etc. Utilize TLC, gas chromatography (GC), LC, and whatever other analytical tools are available to determine which reagents will tag the analyte, the nature of the products formed. Follow the optimization steps described below.
5. Optimize the derivatization conditions in terms of the usual reaction parameters: time, solvent, pH, temperature, catalysts. This can be performed univariately or multivariately, even using computer algorithms (simplex/multiple routines) to realize surface maps of conditions leading to optimal formation of the desired derivative. Whatever the optimization routine used, the final conditions need to be compatible with pre- or post-column LC reaction requirements (instrumental, solvents, mixing). Optimize reaction conditions and demonstrate formation of the desired derivative *before* introduction into the LC instrument.
6. Demonstrate the formation of derivative, nature of the derivative (structure), purity of standard derivative, per cent derivatization (yield), etc., using standard organic chemistry methods (elemental analysis, mass spectrometry, Fourier transform infrared (FTIR) and nuclear magnetic resonance (NMR) spectroscopy). What is the nature of the derivative obtained from the analyte? What is its exact structure, solubility, stability to various LC solvents, detection properties (UV, FL, EC), etc.?
7. How does the final derivatization approach change the possible ionization states of the original analyte? What modifications to the separation conditions of the original, untagged analyte must now be made to accommodate the nature of the derivatized species (e.g. ion exchange chromatography (IEC) changes)? Will the new tag(s) induce additional charges on the original analyte that will then affect LC mobility, migration times, resolutions, etc.? Will the tags induce unwanted hydrophobic properties to the tagged species affecting solubility, migration tendencies, resolution, efficiency and peak shape? How do we then accommodate such structural and physical/chemical property changes, how do we know what those changes really are before any LC methods development is pursued? Will the newly tagged species still permit host-guest complexation, such as with cyclodextrins, crown ethers and other complexation additives to the LC buffer?
8. Now utilize the standard derivative to optimize the LC conditions, again consulting the literature to determine if this derivative or an analogous structure has already been described along with specific LC operating conditions. Utilize those conditions or slight variations to realize optimized LC conditions for your standard derivative. This may require optimization by univariate or multivariate methods, perhaps using computer algorithms, varying one parameter at a time to generate a surface map demonstrating optimized conditions. This is similar to resolution maps in LC via DryLab from LC Resources. There are other computer programs in the literature that might prove useful in this area of LC separation optimization for the standard derivative.
9. Demonstrate analytical figures of merit with standard derivative, based in part on original method/assay requirements, such as linearity of calibration plots possible (UV, FL, EC), detection limits, limit of quantitation, accuracy and precision of quantitations possible, robustness of the LC conditions to small operational changes (pH, temperature, solvent, ionic strength, voltage applied, sample introduction, etc.), time per analysis, cost per analysis, instrument/method preparation, etc. This is still all derived for standards of the derivative, and not yet with actual analyte or samples.
10. Demonstrate analytical figures of merit with standard analyte, exactly as above, but now introducing the actual derivatization steps required to convert the original standard analyte into the derivative.
11. Demonstrate analytical figures of merit with actual sample containing *known* levels of analyte, including all method requirements: limit of quan-

titration (LOQ), limit of detection (LOD), linearity of calibration plots, ruggedness, robustness, reproducibility, repeatability, accuracy/precision of quantitations, time per analysis, cost per analysis and sample preparation requirements.

12. Validate final, optimized method with known samples containing known levels of analyte using double-blind spiking, standard reference materials (if available), comparison with currently accepted method on split, spiked samples (known levels), and finally interlaboratory collaborative studies. Assemble all final data in terms of accuracy and precision, reproducibility from laboratory to laboratory, repeatability within one laboratory, ruggedness from laboratory to laboratory, robustness within any given laboratory, all in terms of qualitative identification of analyte present, and then final quantitative information in terms of accuracy and precision of such measurements.
13. Write up final procedure and protocols for performing the final, overall derivatization-LC method, including the necessary sample preparation steps, isolation of analyte from matrix (if required) before derivatization, possible derivatization of analyte in sample matrix followed by isolation of derivative, or derivatization of analyte in sample matrix with direct injection of crude mixture into LC with minimal (if any) sample preparation (dilute/shoot). Include all possible procedures and reagents, chemicals, solvents and instrumentation needed for another laboratory to reproduce, repeat, and obtain valid results using the newer method in their hands/laboratories.
14. Distribute the final protocols and procedures to all those laboratories that participated in the interlaboratory collaborative studies, so that they can validate and demonstrate reproducibility of the overall optimized methods involving derivatization-LC operations and conditions.

Problems and Pitfalls in Using Derivatization in Liquid Chromatography

There are some potential problems and pitfalls in the routine use of derivatizations in LC. Major amongst these is the need to remove the excess reagent and/or its hydrolysis and thermal degradation products from the final derivatization solution prior to detection. This can be accomplished by an initial sample clean-up offline, and/or by addition of a large amount of

another reactive compound to consume all of the excess reagent to form a single known derivative easily separated from the analyte's derivative. Sometimes the LC conditions themselves may resolve the excess reagent and any of its hydrolysis/by-products from the desired derivative. Other approaches utilize a derivatizing reagent that, together with its hydrolysis/by-products, does not appear in the final chromatogram because it has very different detector properties from those of the analyte's derivative.

Another possible problem in utilizing derivatization involves a low per cent conversion to the desired derivative. This can be improved by forcing the reaction conditions, working at elevated temperatures for longer periods of time, invoking a suitable catalyst and by increasing the concentrations of analyte and reagent. Sometimes isolating the analyte from the sample on a solid support, followed by reaction with the usual derivatization solution, can lead to a much faster and more efficient reaction and conversion. In general the higher the per cent conversion, the easier it is to detect trace levels of analyte in complex matrices, such as biofluids.

Another problematic area has to do with reactions from other components in the sample mixture, besides that of the desired analyte, leading to a complex mixture of derivatives difficult to resolve by LC and/or detection methods. This can be improved by selectively isolating the analyte of interest from the sample matrix prior to derivatization, followed by the desired reaction conditions and introduction of the derivative into the LC system. This can more easily be accomplished by combining affinity LC with another LC mode, such as reversed-phase, so that the affinity step isolates the analyte of interest. This is then followed by a derivatization on the affinity support with the analyte immobilized, or initial elution of the analyte from this support, solution reaction, and then introduction into the second LC system. A simple, solid-phase affinity extraction column can be used to isolate the desired analyte from the complex sample, and prepare it for the desired, homogeneous (solution) or heterogeneous (solid-phase) derivatization reaction.

Yet another possible pitfall has to do with the formation of several derivatives from the analyte, rather than the usual (desired) production of a single, homogeneously tagged derivative. It is usually desired to form a single, homogeneous derivative with good chromatographic and detector properties. However, if there are several possible reactive sites on the analyte, then it is always possible that more than one product will result. This can be avoided by using reaction conditions that force all sites to be tagged,

leading to a single product, or by preventing some of the sites from reacting by using suitable reaction conditions or protecting groups that will then leave only a single site left to react. In the case of protein or biopolymer derivatizations, multiple products are usually formed, leading to several LC peaks that then raise detection limits and make identification of the original protein and quantitation more difficult, especially at trace levels. In general, homogeneous (uniform) tagging of biopolymers is always problematic, though conditions are currently being developed that may eliminate such difficulties.

It is possible that the reaction conditions required for derivatization may cause the analyte itself to degrade, even as it reacts with the reagents. The degradation products can also react with the very same tagging reagent. This leads to a multiplicity of products, rather than a single homogeneous derivative, again making quantitation at trace levels and identification of the original analyte more difficult. However, this complex mixture of products can be forced to elute as a single, sharp peak by using suitable LC conditions. This can then function as a suitable peak for quantitation and identification of the analyte of interest.

Finally, there are the issues of reagent stability, purity, uniformity and shelf-life, all important areas when using a reagent over a long period of time for numerous analyses. Conditions must be found that provide a pure reagent with good shelf-life, long-term stability during the course of the reaction and storage, available from several commercial vendors at reasonable cost and amounts, and available in high purity and consistency. In most cases, such commercial reagents are indeed available for many LC applications today.

Conclusions and Summary

This article has provided an overview of derivatization for LC. It is clear that this approach has undergone significant developments over the past few decades, to the point where it is now a mature area of LC science. Numerous books and reviews have appeared in recent years, and the literature continues to grow. Several excellent primers are available on the use of derivatization in LC and other separation areas, such as capillary electrophoresis (CE). Derivatization serves several useful functions in LC, but can especially improve chromatographic performance and peak shape for the original analyte, improve detector response to permit trace determinations, and improve quantitation for the original analyte by improving signal-to-noise ratios in complex sample matrices.

Derivatization can also stabilize an otherwise reactive analyte by the formation of a more stable derivative. The formation of multiple derivatives, using either solution or solid-phase (mixed-bed) approaches, has enabled improved qualitative identification of an analyte, as well as confirmation of quantitation by providing two to three different peaks for such purposes, all from the same sample undergoing one or a series of tagging reactions. Automation of derivatization, both pre- and post-column and online or offline, has developed such that it has become virtually a routine part of LC analysis. It is quite common to perform derivatization of amino acids pre-column, offline or online, in order to improve the identification and quantitation of these species, for example in a protein hydrolysate or intravenous solution. Derivatization for trace level detection of many analytes has also become commonplace, particularly when combined with preconcentration as part of the sample preparation-derivatization-LC steps. These tagging approaches permit the trace analysis of many analytes in complex sample matrices that otherwise would not be detectable by direct LC analysis.

Derivatization has thus become very commonplace in much of LC analytical work and applications. A wide variety of suitable reagents are commercially available, providing enhanced detection in several modes (UV, FL, EC and MS). Derivatization approaches are being developed for proteins and peptides that would lead to directed fragmentation and/or improved ionization for lowered detection limits in various forms of mass spectrometry or LC-MS. These efforts to develop improved derivatization reagents for further LC-detector applications will undoubtedly continue for many years to come.

See also: II/Chromatography: Liquid: Detectors: Ultra-violet and Visible Detection. III/Peptides and Proteins: Liquid Chromatography.

Further Reading

- Blau K and Halket J (eds) (1993) *Handbook of Derivatives for Chromatography*, 2nd edn. New York: John Wiley & Sons.
- Frei RW and Zech K (eds) (1988, 1989) *Selective Sample Handling and Detection in High Performance Liquid Chromatography*, Parts A and B. Amsterdam: Elsevier.
- Knapp DR (1979) *Handbook of Analytical Derivatization Reactions*. New York: John Wiley & Sons.
- Krull IS (ed.) (1986) *Reaction Detection in Liquid Chromatography*. New York: Marcel Dekker.
- Krull IS, Deyl Z and Lingeman H (1994) General strategies and selection of derivatization reactions for liquid chromatography and capillary electrophoresis. *Journal of Chromatography B* 659: 1-17.

- Krull IS, Zhou F-X, Bourque AJ, Szulc M, Yu J and Strong R (1994) Solid-phase derivatization reactions for biomedical liquid chromatography. *Journal of Chromatography B* 659: 19–50.
- Krull IS, Mazzeo J, Szulc M, Stults J and Mhatre R (1996) Detection and identification in biochromatography. In: Katz E (ed.) *High Performance Liquid Chromatography: Principles and Methods in Biotechnology*, pp. 163–232. New York: John Wiley & Sons.
- Krull IS, Szulc ME and Dai J (1997) *Derivatizations in HPCE. A Primer*. Thermo Bioanalysis Corporation, San Jose, CA.
- Lawrence JF (1981) *Organic Trace Analysis by Liquid Chromatography*. New York: Academic Press.
- Lingeman H and Underberg WJM (eds) (1990) *Detection-Oriented Derivatization Techniques in Liquid Chromatography*. New York: Marcel Dekker.

Detectors: Electron Spin Resonance

K. Osterloh, Magnettech GmbH, Berlin, and Institute of Physiology, Freie Universität Berlin, Berlin, Germany
H.-H. Borchert, Institute of Pharmacy, Humboldt Universität zu Berlin, Berlin, Germany
C. Kroll, Hexal-Pharma GmbH, Magdeburg, Germany

Copyright © 2000 Academic Press

Introduction

The role of radicals in (bio-)chemical reactions is currently becoming increasingly significant. Free radicals may be generated by any kind of irradiation and contribute essentially to many aging processes in many materials, particularly in the presence of oxygen. They are even able to cause manifold organic damages as in lipid peroxidation or in inflammatory diseases. Organic reperfusion injuries after ischaemia are currently the subject of intensive research activities. On the other hand, stable free radicals are used practically in a number of applications in many fields, e.g. as additives in industrial processes such as polymerization or as analytical tools in research on membrane, emulsion and surface properties of materials or formulations. The utilization of such substances as protective additives, e.g. for process control or as research tools, has stimulated interest in the synthesis of new compounds of this class. The increasing search for radicals is paralleled with a rising demand for methods to detect, identify and quantify them. In the context of separation techniques, this means having a technique at hand to trace them in eluted fractions.

High chemical reactivity combined with low specificity is typical of the majority of radicals. As a consequence, solutions containing such substances are likely to alter their composition within a short time owing to the decreasing content of reactive components and to the accumulation of reaction products. This kind of change can easily be monitored by chromatographic methods. Having separated all the constituents at a given time, it may become necessary

to identify original or intermediate radicals to evaluate the particular stage of an ongoing reactive process. However, the detectors routinely used in HPLC cannot indicate directly any radical present in the separated fractions. The most advanced method suitable for this purpose is electron spin resonance spectroscopy (ESR), but most ESR spectrometers are currently installed as large and heavy instruments, not at all suitable as detectors for chromatographic methods. It will be shown here that this kind of spectroscopic method can be realized with devices of table-top size that can easily be integrated into any chromatographic separation line.

Electron spin resonance (or electron paramagnetic resonance, EPR) spectroscopy is the only direct method to measure radicals since it is based on the existence of unpaired electrons. Likewise, paramagnetic metal complexes are also sensitive to this spectroscopic method. A substantial advantage for the study of radical reactions would be the rapid analysis of a fraction directly upon separation to avoid changes caused by putative consecutive reactions. This can only be achievable by direct coupling of the separator (HPLC) with the specific detector (ESR) in the shortest possible way without any unnecessary dead volume (long tubing lines or valves). An absolute prerequisite for such an instrumental set-up is a spectrometer of a size that allows installation at the site of the sample separation, and not necessarily vice versa. The other problem is synchronization of sample separation and recording of a spectrum which requires a definite period of time. Both problems have been solved in the on-line coupling of HPLC and ESR spectroscopy described here.

ESR Spectroscopy as Detector

An introduction into the principles of ESR (or EPR) spectroscopy can be found in most textbooks on physical chemistry or in specialized monographs. Since this spectroscopic technique is rather uncommon

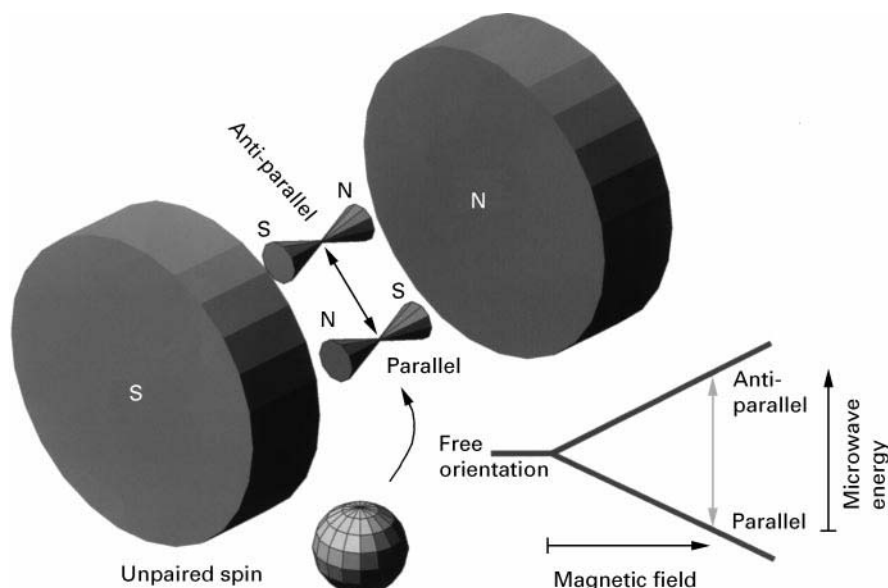


Figure 1 Alignment of an unpaired electron in a magnetic field.

in the field of separation sciences, a brief description of the principle is given here.

Electron spin resonance was detected by the Russian scientist Zavoisky in 1946 while researching the paramagnetic properties of matter. Radicals and metal complexes with an odd number of electrons in d-orbitals show paramagnetism since unpaired electrons generate local electromagnetic fields. They can be detected whenever they interact with an external magnetic field. This interaction can be understood in the way that the external field forces any unpaired electron to align (Figure 1).

Once in line with the parallel magnetic field, lines of a given strength the electrons are able to flip into the opposite direction while absorbing energy. The stimulating energy ($\Delta E = h\nu$, h is Planck's constant and ν is the frequency) to cause such a flip over must be of a frequency able to resonate with the unpaired electron tumbling in the magnetic field like a spinning top (Larmor frequency). This frequency again is linearly dependent on the applied magnetic field; in other words, the stronger the field, the higher must be the frequency of the energy to stimulate the flip over of a single electron. ($\Delta E = g\mu_B H$ where μ_B represents the Bohr magneton, H the external magnetic field and g is a dimensionless proportional factor, ~ 2 for a single electron, the so-called Landé factor. The whole term is part of the Hamiltonian operator which is used to describe the state of energy of a given system.)

In essence, the alignment of an unpaired electron in an external magnetic field can have two directions, either with the field (low-energy state) or against the field (high-energy state). This is the same kind of energy splitting (Zeeman splitting) as in nuclear mag-

netic resonance (NMR) spectroscopy. The transition between these two states needs energy in the range of high-frequency radio waves or microwaves, depending on the strength of the applied external magnetic field. Nowadays, it is quite common to use a microwave frequency between 9 and 10 GHz (within the so-called X-band) which requires a magnetic field in the range of 300–400 mT. To find the exact absorption energy of an unpaired electron, e.g. in a radical at a given strength of the applied magnetic field, two ways are possible in principle: either to scan the microwave at a fixed magnetic field, or vice versa, to scan the magnetic field at a fixed wavelength. Since it is technically much easier to vary the magnetic field rather than to tune a microwave source over a large range, ESR spectra are recorded by scanning the external magnetic field. They are commonly displayed as first derivatives which is different to all other spectroscopic techniques where absorption peaks are shown.

Interactions of unpaired electrons with surrounding paramagnetic nuclei result in additional splitting of energy levels (hyperfine splitting) that become visible as multiples of absorption lines. In some cases, different radical moieties can be identified by their individual hyperfine splitting structure.

Coupling between Radical Separation and Detection

The application of ESR spectroscopy as a detector in a separation technique like HPLC raises a number of problems which have been solved in the following way.

ESR Spectrometer Size

Common ESR spectrometers have a large magnet which makes the instruments rather heavy, up to half a ton in weight. However, newly developed ESR spectrometers have been reduced to a size comparable with commonly used diode array detectors.

Flow Conditions of HPLC Mobile Phases

Owing to the properties of the microwave, the sample size is geometrically restricted to a thickness of 0.3 mm, allowing only a total sample volume of some 50 μL (if the fluid phase contains water, the volume could be larger otherwise). The sample cuvette (a quartz flat cell) is located in a fixed position inside the instrument having open access from the bottom and top allowing tubing to be attached to fill the cuvette upwards and to flow out at the top of the instrument. This vertical flow direction of the mobile phase helps to avoid accidental trapping of gas bubbles that could spoil any spectral measurement. At a flow of 1 mL min^{-1} no turbulence occurs at any site within the sample cuvette ensuring homogeneous filling and flushing without any problem. The use of capillary tubing minimizes the dead volume between the common UV/visual light monitor and the ESR spectrometer and thus the flow delay between these two devices.

Tubing Material Required for Radical Detection

In all cases, non-metal tubing is used. It should be noted that steel capillaries can never be used in the vicinity of the magnetic field of the spectrometer. Moreover, it is advisable to avoid any metal surface at all when working on free radicals. Particularly if oxygen is present, even minute amounts of iron, for example, may be sufficient to catalyse the Fenton reaction.

Synchronization of Separation and Detection

A major problem to be solved is synchronization of the continuous sample flow from the chromatographic equipment and the scan time required for taking an ESR spectrum. This subject has already been tackled by a number of authors. However, problems regarding signal separation and measurement sensitivity remain. A typical ESR scanning time is one minute for a spectrum and this may be in conflict with the elution time of a single fraction from a HPLC column. Since complete chromatograms usually take some 8–15 min, single fractions are likely to take less than a minute to elute so no constant conditions can be expected in the sample cuvette while a spectrum is running. Simply stopping the flow for the time of recording a spectrum may result in local diffusion, causing a loss of resolution in the separation step, so

this approach is not recommended. Pulsed short-time spectra (FT-spectroscopy) are very sophisticated requiring a much more complicated instrumentation, so the 'cw' (continuous wave) technique still remains the current standard method.

Instrumental Arrangement and Operation

A practical solution that allows both continuous flow from the HPLC column and a resting period of a sample fraction in the ESR spectrometer cuvette is depicted in Figure 2. In principle, a shunt is provided to short-cut the passage through the ESR spectrometer. It is opened while an ESR spectrum is in progress and closed at any other time. This allows the cuvette to be filled with a fraction, to leave it for the time of scanning a spectrum, and to flush the sample upon completion. A disadvantage of this procedure is that it does not allow spectra of fractions running closely together to be obtained since the spectrum of the first sample is still being recorded while the second one is starting to elute from the column. In this case, it is necessary to repeat the chromatographic separation step for the second fraction of interest.

In order to control the flow either through or bypassing the ESR spectrometer, a T-connector is inserted into the tubing between the HPLC detector and the ESR spectrometer for branching off to the shunt. Both the outlet tubing from the spectrometer and the shunt are connected to a valve which alternately opens or closes either way. This arrangement has two major advantages: on the one hand, unnecessary and irregularly shaped dead volume that may disturb the sample flow from the HPLC device to the spectrometer is avoided by placing the control valve after both devices, and on the other hand, it is not possible to close off both paths by control error, thus minimizing the risk of accidentally building up destructive pressure in the tubing system. In a simple set-up, the valve can be operated by hand via an electrical switch. The delay time from the appearance of the peak of interest in the monitor system of the HPLC to the moment of filling the ESR cuvette with the corresponding fraction can be measured exactly and is highly reproducible. In more standardized or routine applications, automatic control is possible. This whole arrangement makes the ESR spectrometer truly an additional HPLC monitor that analyses radicals.

Supplementary Equipment

In some cases substances may turn into (short living) radicals after stimulation either by light irradiation or in the course of a reaction triggered by an added reagent. In other cases, reactive and short-lived radicals may be trapped in an adduct with a so-called

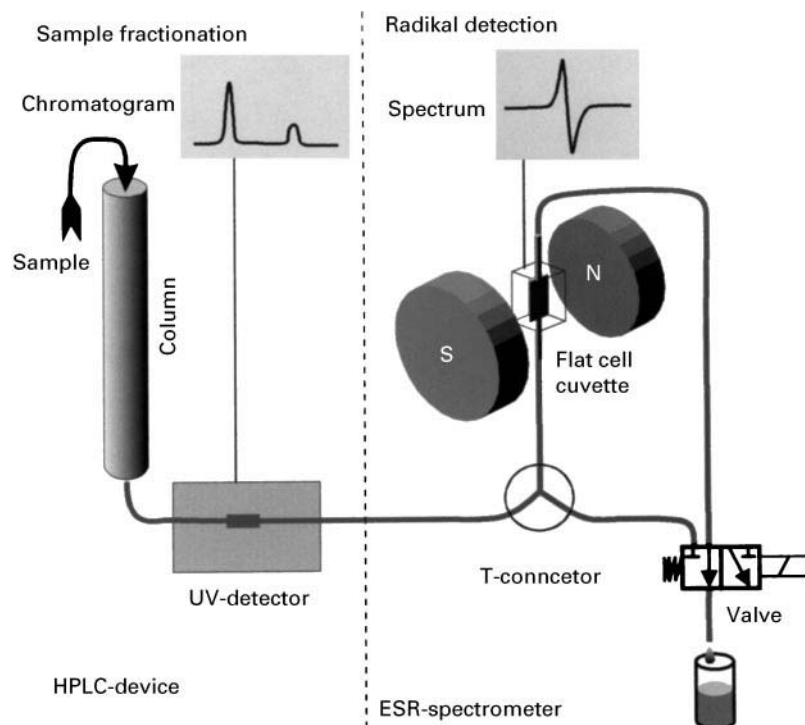


Figure 2 Instrumental set-up of synchronized online HPLC-X-band-ESR coupling (modified in accordance with Osterloh and Kroll (1998)).

‘spin-trap’. To provide the possibility for monitoring such reactions online with an eluted fraction, certain supplementary equipment may be added to the whole instrumental set-up as shown in Figure 3.

Application Examples

The following practical examples should demonstrate the advantages in detection of free radicals in HPLC

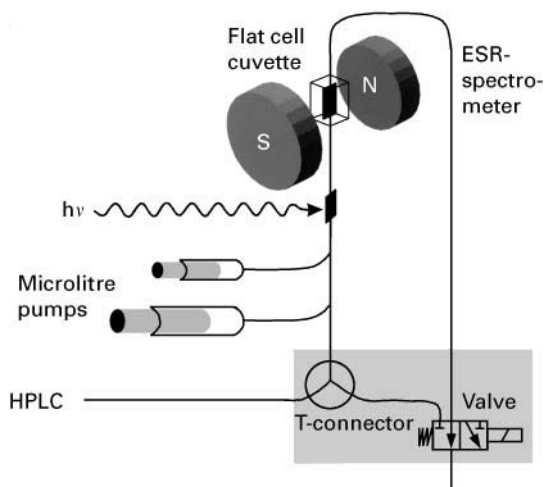


Figure 3 Attachment of supplementary equipment to the ESR spectrometer as radical detector.

direct and online by ESR. One deals with separation of a synthesized product, while the other deals with a reactive, short-lived radical species.

Synthesis of Stable Radicals

Stable radicals such as nitroxyl compounds become increasingly of interest for process control of radical reactions, e.g. polymerization. This practical example demonstrates both the complexity of sample composition after such a synthesis and the changes owing to the instability of a single component. The starting point here is a cleavable biradical which decomposes immediately in aqueous solution.

Chemicals: 3-PCA-anhydride [II] was synthesized by the method of Gallez *et al.* using PCA [I]; 3-carboxy-2,2,5,5-tetramethylpyrrolidine-1-oxyl and DCC (dicyclohexylcarbodiimide) (Figure 4).

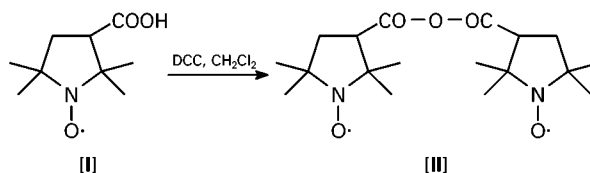


Figure 4 Synthesis scheme for PCA anhydride using DCC in purified methylenechloride.

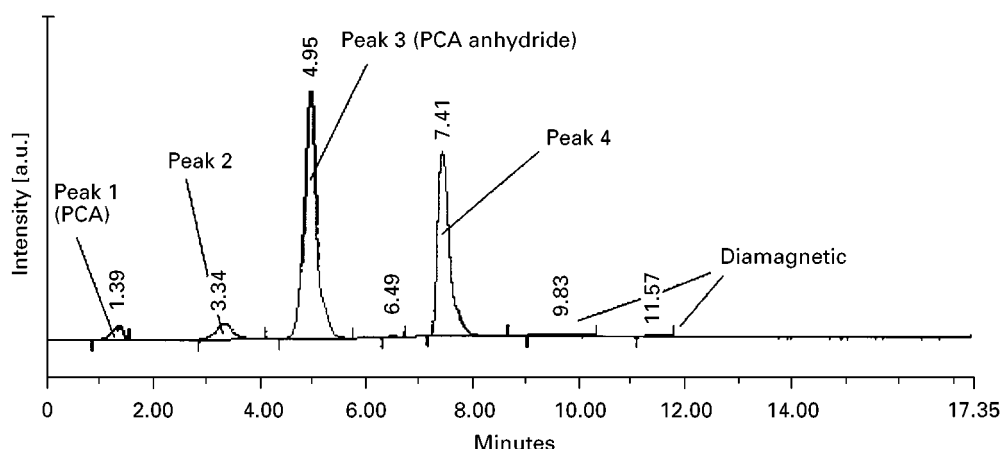


Figure 5 Chromatogram of synthesis product obtained by means of online coupled HPLC-ESR.

HPLC: Merck-Hitachi-HPLC with DAD (diode array detector), RP-18 (5 μ m) column (125/4 mm) and methanol-water solutions (flow rate 1 mL min⁻¹, pH 7, isocratic as well as gradient mode).

ESR: Miniscope MS-100 desk X-band spectrometer (Magnettech GmbH, Germany). GC-MS, IR and NMR-techniques were also used for the identification of unknown products.

In following the synthesis, mixtures of PCA anhydride [II] were investigated by online coupled HPLC-ESR. This anhydride in practice represents a suitable tool for the spin labelling of macromolecules such as albumin. The purified synthesis product was analysed. In contrast to the available

literature, the chromatogram obtained showed four ESR-active compounds after HPLC separation (Figure 5).

These were the PCA anhydride [II] (peak 3 with $t_R = 4.95$ min) and PCA [I] (peak 1 with $t_R = 1.39$ min) as expected as well as two new paramagnetic compounds with typical ¹⁴N-hyperfine coupling (peak 2 with $t_R = 3.34$ min and peak 4 with $t_R = 7.41$ min). Further, ¹H-NMR, IR and GC-MS experiments showed the compound with $t_R = 7.71$ min (peak 4) to be PCA dicyclohexylurea- amide. No other peaks gave an ESR signal.

Figure 6 represents the ESR spectra of the sample before and after chromatographic separations. Spectra of peak 1, 2 and 4 show a line triplet typical

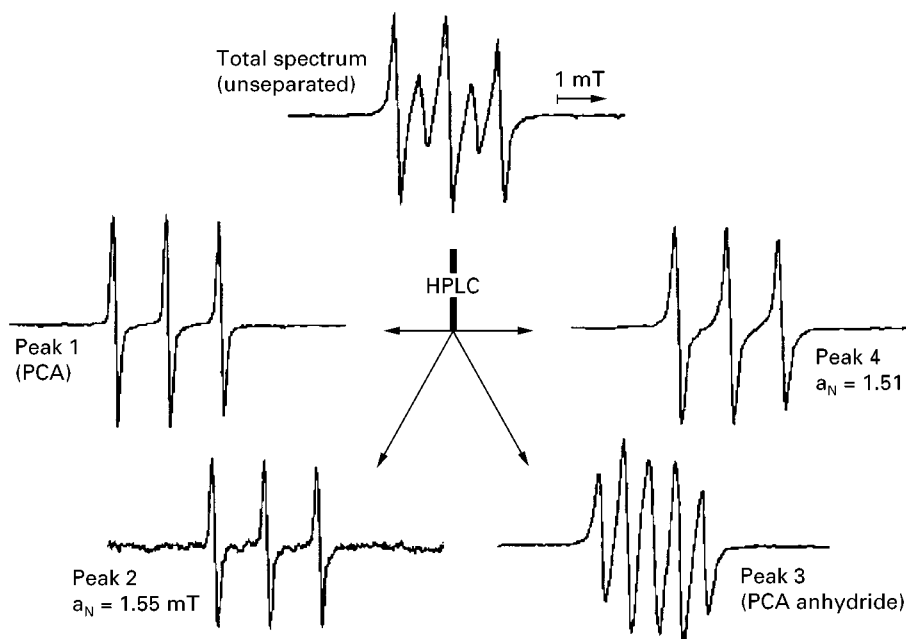


Figure 6 ESR spectra of the initial substance and four separated paramagnetic compounds.

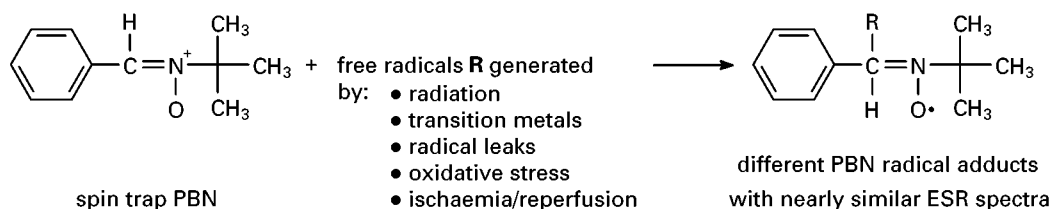


Figure 7 Scheme of formation of stable radicals in biological systems using PBN.

for nitroxyl radicals owing to the interaction between the unpaired electron and the nitrogen nucleus. The uneven number of protons and neutrons results in nuclear spin quantum numbers of -1 , 0 and $+1$, in equal distribution. Those nuclei with a spin different from 0 cause a magnetic field recognized by the unpaired electron in addition to that generated by the magnet of the spectrometer. The result is a hyperfine splitting into three spectral lines as shown in the respective spectra. Peak 3 comprises the biradical PCA anhydride [III] with two nitroxyl groups in close vicinity. The ESR spectrum is determined by additional interactions between these two radical moieties. All the single spectra of the separated peaks add to the composite one seen with the initial unseparated sample.

Common Radical Analysis

A typical characteristic of most radicals is their high reactivity so they normally have a short life. As a consequence, they may be present only in rather low concentrations so they may be difficult to analyse. Therefore, the spin-trapping technique was developed to detect short-lived radicals. **Figure 7** shows an example of this technique in which the reagent PBN (α -phenyl-*N*-*t*-butylnitron; not itself a radical)

forms a stable adduct with a reactive, short-lived radical. The highly reactive compounds analysed here are inherently linked to the aging process in living tissues.

The spectrum in **Figure 8** shows, in addition to the hyperfine splitting owing to the nitrogen nucleus (a_N), an additional one caused by the hydrogen nucleus in the β -position to the unpaired electron (a_H). This spin trap does not necessarily allow differentiation between radical species so combination of a separation step with the spin trapping reaction could provide this kind of information.

Conclusions

The simple and straightforward coupling of HPLC and ESR causes problems owing to the necessity to synchronize the chromatographic and the spectroscopic techniques. The first example presented shows that it is impossible to distinguish between more than two similar paramagnetic compounds with either technique alone. Therefore, the direct combination of both techniques requires additional equipment to solve the problems encountered. The second example demonstrates a tool to identify low concentrations, but highly reactive radicals, in separate fractions.

Our modified online HPLC–ESR coupling technique represents a suitable tool to solve such problems without any significant time lag with a high signal sensitivity comparable to conventional cw-ESR. Furthermore, the technique presented prevents severe problems that frequently occur in stop-flow chromatographic applications.

See also: II/Chromatography: Liquid: Detectors: Fluorescence Detection; Detectors: Infrared; Detectors: Mass Spectrometry; Detectors: Refractive Index Detection; Detectors: Ultraviolet and Visible Detection; Nuclear Magnetic Resonance Detectors.

Further Reading

Atkins P (1990) *Physikalische Chemie*. Weinheim: VCH.
Gallez B, Lacour V, Demeure R, Debuyst R, Dejeht F, DeKeyser JL and Dumont P (1994) Spin labelled arabinogalactan as MRI contrast agent. *Magnetic Resonance Imaging* 12 (1): 61–69.

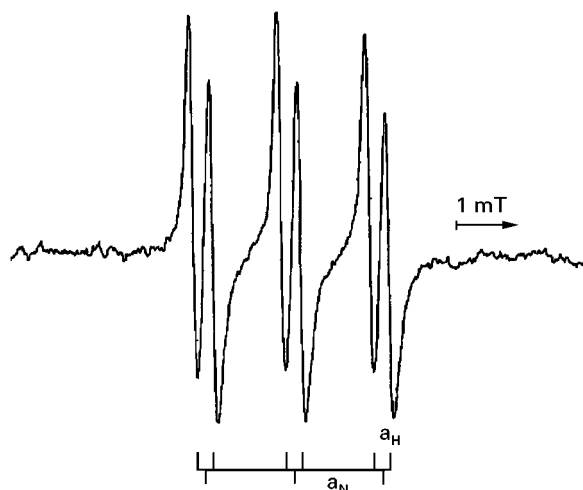


Figure 8 ESR spectra of a paramagnetic PBN adduct after HPLC separation measured by online HPLC–ESR coupling technique.

- Janzen EG and Blackburn BJ (1968) Detection and identification of short-lived free radicals by an electron spin resonance trapping technique. *Journal of the American Chemical Society* 90: 5909–5910.
- Kroll C, Osterloh K, Mäder K and Borchert H-H (1998) On-line coupled HPLC-ESR: Application for separation and characterization of organic radicals. *Archiv der Pharmazie – Pharmaceutical and Medicinal Chemistry* 331 (2): 40.
- Osterloh K, Kroll C, Mäder K, Borchert H-H, Sammler B and Kirmse C (1998) HPLC und Elektronenspinresonanz-Spektroskopie on-line gekoppelt [On-line Coupling of HPLC and Electron Spin Resonance Spectroscopy] (German). *GIT Labor-Fachzeitschrift* 42: 24–25.
- Poole CP (1983) *Electron Spin Resonance*, 2nd edn. New York: John Wiley.
- Poole CP and Farach HA (1994) *Handbook of Electron Spin Resonance: Data Sources, Computer Technology, Relaxation, and Endor*. Berlin: Springer.
- Sugata R, Iwahashi H, Ishii T and Kido R (1989) Separation of polyunsaturated fatty acid radicals by high-performance liquid chromatography with electron spin resonance and ultraviolet detection. *Journal of Chromatography* 487: 9–16.
- Suzuki S, Nakazawa H, Fujita M, Ono S, Suzuki M, Takitani S, Sonoda M and Sakagishi Y (1992) Flow analysis of UV-irradiated chemicals by chemiluminescence and electron spin resonance spectroscopy. *Analytica Chimica Acta* 261: 39–43.

Detectors: Evaporative Light Scattering

R. P. W. Scott, Avon, CT, USA

Copyright © 2000 Academic Press

The evaporative light-scattering detector evolved from the early work of Charleworth and MacRae. The device consists of a spray system that continuously atomizes the column eluent into small droplets. The droplets evaporate, leaving the solute as fine particulate matter suspended in the atomizing gas. In practice, the column eluent passes into a concentric nebulizer where it is nebulized in a hot stream of gas that may be air or, if so desired, an inert gas such as helium or argon. The suspended particulate matter is then made to pass through an intense light beam from a source such as a helium–neon laser. The light scattered by the particles is viewed at 45° to the incident beam by means, for example, of a pair of properly placed optical fibres. The scattered light that enters the fibres is transmitted to a photomultiplier, the output of which is electronically processed and passed either to a computer acquisition system or to a potentiometric recorder. The evaporative light-scattering detector might be considered to be a form of transport detector where the transport medium is the nebulizing gas. A diagram of the light-scattering detector is shown in **Figure 1**.

The column eluent enters the centre orifice of a dual, concentric jet nebulizer where it meets a heated stream of nebulizer gas from the surrounding annular orifice. The gas flow rate is adjusted to provide a jet velocity that is just above the speed of sound. The stream of droplets that are produced normally have a relatively wide range of size distribution and pass down a heated tube, called the drift

tube. In this tube the solvent evaporates, leaving the solute as residual solid particles still carried in the gas stream. It is clear that this type of detector cannot function effectively if solid involatile buffers are used in the mobile phase. After passing through the laser beam, the gas containing the solvent vapour and particles is aspirated through a simple water pump which safely disposes of both the solvent vapour and the solutes. The laser is employed as a convenient source of high intensity light and its coherence does not appear to confer any particular advantage on the detection system.

The amount of scattered light that is collected is related to the diameter of the particles, the wavelength of the incident light and the angle at which it is collected. It is not linearly related to the concentration of solute in the mobile phase, but varies as either the power or the exponent of the solute concentration. For a given set of operating conditions the droplet size will remain sensibly constant during the development of a chromatogram. Now the average diameter of the solid particles produced will be the average size of the droplets multiplied by the cube root of the solute concentration. Thus, if the solute has a concentration of $10^{-6} \text{ g mL}^{-1}$, the solute particles will be 100 times smaller than the size of the droplets and, assuming a common value for the mean diameter of the droplets of $20 \mu\text{m}$, the solute particles will be $0.2 \mu\text{m}$ in diameter. Thus the mean particle diameter is of approximately the same order of magnitude as the wavelength of the scattered light.

Physical Properties of the Nebulizer

The intensity of the scattered light will be determined, among other factors, by the diameter of the solid

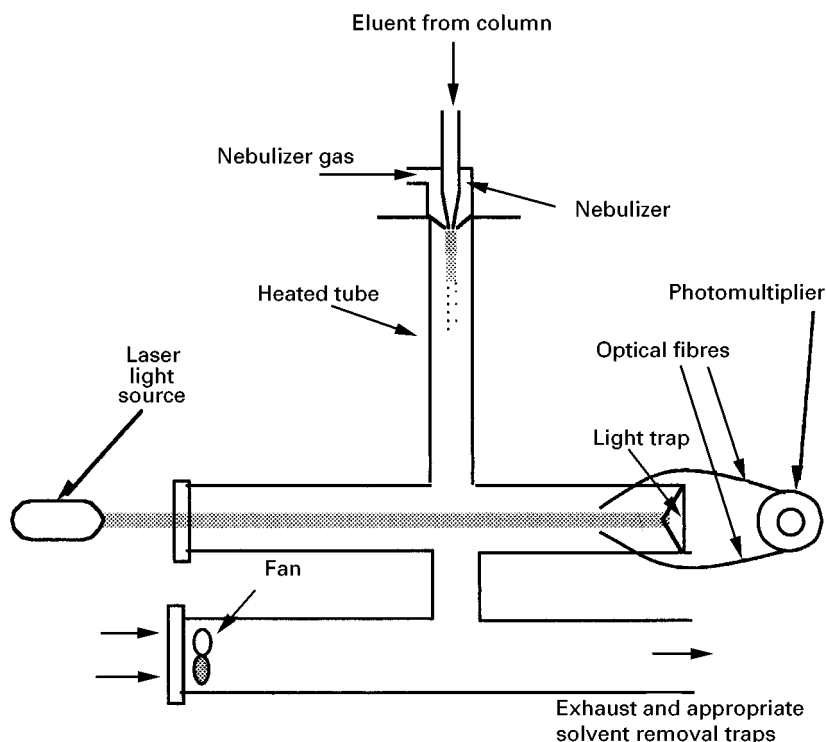


Figure 1 An evaporative light-scattering detector.

particles which in turn will be controlled by the size of the droplets generated by the nebulizer.

The average diameter of the droplets (D_0) in micron that is formed in a concentric nebulizer is given by the following equation:

$$D_0 = \frac{A\sigma_1^{1/2}}{u\rho_1^{1/2}} + B \left(\frac{\eta^1}{(\sigma_1\rho_1)^{1/2}} \right)^{0.45} \left(\frac{1000Q_1}{Q_g} \right)^{1.5} \quad [1]$$

where σ_1 is the surface tension of the mobile phase, ρ_1 is the density of the mobile phase, η_1 is the viscosity of the mobile phase, u is the relative velocity of the gas and liquid streams, Q_1 is the volume flow of mobile phase, Q_2 is the volume flow of the nebulizing gas and A and B are constants, taking values of 585 and 597.

The relationship between the mean solid particle diameter (D_s) and the mean droplet diameter (D_0) is given by:

$$D_s = D_0 \left(\frac{c}{\rho_2} \right)^{1/3} \quad [2]$$

where c is the concentration of solid solute in the eluent, and ρ_2 is the density of the solid solute. Thus:

$$D_s = \left(\frac{A\sigma_1^{1/2}}{u\rho_1^{1/2}} + B \left(\frac{\eta^1}{(\sigma_1\rho_1)^{1/2}} \right)^{0.45} \left(\frac{1000Q_1}{Q_g} \right)^{1.5} \right) \left(\frac{c}{\rho_2} \right)^{1/3} \quad [3]$$

Now it is the magnitude of D_s , the number of particles per unit volume and the wavelength of the laser light that determine the intensity of light scattered at a particular angle to the incident beam.

Intensity of the Scattered Light

There are two types of scattering that can take place, Mie scattering and Raleigh scattering, both of which can take place in the present design of light-scattering detector. Raleigh scattering occurs when the particle diameter is significantly less than the wavelength of light and Mie scattering occurs when the wavelength of the light is considerably less than the particle diameter. If the nebulizer is efficient, the major effect will be Raleigh scattering and thus only this type of scattering will be considered here.

One of the early scientists to examine scattered light was Tyndall, who showed that the scattered light from small particles was polarized. He found that light scattered at right angles to the incident beam was completely linearly polarized and demonstrated that the effect was independent of the nature of the scattering media and depended only on the particles being sufficiently small.

Lord Raleigh gave a simple explanation as to why light scattered at right angles to the incident beam is completely polarized. Consider a beam of unpolarized light travelling along the x -axis impinging

on a spherical particle located at the origin of a Cartesian coordinate system. The light can be resolved into two linearly polarized components that can each act independently of the other. If the particle is small compared with the wavelength of the light, then there is a uniform instantaneous electromagnetic field over the particle. As a consequence the particle will become polarized in the direction of the field. The net result is to produce a dipole that will oscillate synchronously and in the same direction as the vibrating electric field. The oscillating dipole will radiate electromagnetic energy and this scattered radiation will be polarized in the same sense as the dipole.

Assuming the scattering direction is taken from the origin through the point defined by the polar coordinates r , θ and ϕ , then:

$$x = r \sin \theta \cos \phi; \quad y = r \sin \theta \sin \phi; \quad z = r \cos \theta \quad [4]$$

If the angle measured from the scattering direction to the dipole is ϕ then the intensity of the scattered wave at a distance r from the particle will be:

$$I = \frac{16\pi^4 a^6}{r^2 \lambda^4} \left(\frac{\epsilon_1 - \epsilon_2}{\epsilon_1 + 2\epsilon_2} \right) \sin^2 \psi \quad [5]$$

which, from the Lorenz-Lorenz law becomes:

$$I = \frac{16\pi^4 a^6}{r^2 \lambda^4} \left(\frac{n^2 - 1}{n^2 + 2} \right) \sin^2 \psi \quad [6]$$

Furthermore, if ϕ is 45° then:

$$I = \frac{8\pi^4 a^6}{r^2 \lambda^4} \left(\frac{n^2 - 1}{n^2 + 2} \right) \quad [7]$$

It is seen that the light intensity varies inversely as the square of the distance from the particle, which would be expected from the inverse-square law. Not so obvious is the inverse dependence of the scattered light intensity on the fourth power of the wavelength of the incident light. In practice, the equation does not precisely predict the intensity of the scattered light as there are a significant number of particles present that are not greatly smaller than the wavelength of the incident light.

The Performance of the Light-scattering Detector

The evaporative light-scattering detector has two major advantages over many other liquid chromatography detectors. Firstly, like all transport detectors, its

function is almost completely independent of the solvent used for chromatographic development, with the one proviso that all the solvents used must be sufficiently volatile. This provides a wide range of solvent choice, allowing unique solvents to be used that would be impossible with other types of detectors. Its second advantage is its catholic response, which is similar to that of the refractive index detector. Moreover, as opposed to the refractive index detector, the evaporative light-scattering detector readily tolerates gradient elution development.

However, there are also certain disadvantages to this type of detector and certain precautions that need to be taken in its operation. One safeguard is to use a $0.45 \mu\text{m}$ filter in line with the nebulizing gas supply to remove any dust particles that may get caught up in the gas flow. Foreign particles in the nebulizing flow will contribute noise to the system and, as a consequence, reduce the sensitivity or increase the minimum detectable concentration. In addition, the nebulizer and drift tube will need to be cleaned regularly to remove accumulated sample deposits. This should be carried out every few weeks: failing to do this will not only result in significantly increased noise, but also adversely affect analytical reproducibility.

Occasionally the central jet of the nebulizer carrying the column eluent will become blocked, particularly if high solute concentrations or sticky solutions are nebulized. A blocked nebulizer tube will result in increased back-pressure and, if another detector is employed prior to the evaporative light-scattering detector, then the increased pressure can burst the sensor cell. A pressure sensor should be placed prior to the nebulizer so the back-pressure can be continuously monitored. If this pressure suddenly increases above the normal operating pressure, then the nebulizer will need to be disassembled and cleaned. A relief valve fitted behind the nebulizer will also protect any other detector that is being used from damage.

The nonlinear response of the evaporative light-scattering detector is a more serious problem as it renders quantitative analysis more involved. Furthermore, as the response varies between different solutes, calibration curves must be produced for each substance that is to be determined. The results are usually curve-fitted to an appropriate polynomial or power function which can then be used to modify the peak height or peak area measurements obtained in the actual analysis.

In general, the response of the detector can be fitted to the equation:

$$y = ac^b \quad [8]$$

where y is the detector response, c is the concentration of solute in the eluent, a and b are constants.

Consequently, the curve relating $\log y$ against $\log c$ will be linear and the slope will provide the value of b . In practice, b is usually found to be less than 2, which is the value it would be if only Raleigh scattering was taking place.

The two main disadvantages to the evaporative light-scattering detector are its relatively poor sensitivity (or high minimum detectable concentration) and its nonlinear response to the concentration of solute. There are a number of different commercial detectors of this type available and the consensus of opinion is that the sensitivity (or minimum detectable concentration) is similar to that of the refractive index detector, i.e. about $3 \times 10^{-6} \text{ g mL}^{-1}$. This sensitivity compares unfavourably with that of the fixed-wavelength UV detector, *c.* $5 \times 10^{-8} \text{ g mL}^{-1}$, the fluorescence detector, *c.* $1 \times 10^{-9} \text{ g mL}^{-1}$ and that of the modified moving ribbon transport detector, *c.* $8 \times 10^{-8} \text{ g mL}^{-1}$. Nevertheless, the sensitivity of $3 \times 10^{-6} \text{ g mL}^{-1}$ is quite practical for use in liquid chromatography and, due to its near universal response and its solvent independency, the detector is popular for lipid analysis and for other materials that do not fluoresce or have UV chromophores.

Applications of the Light-scattering Detector

Some examples of the use of the light-scattering detector to monitor the separation of materials that normally require gradient elution for resolution, but are sometimes difficult to sense by other types of detector, are lipids, fatty acids and phospholipids. An example of a chromatogram obtained from a sample containing a mixture of general lipid-class solutes and monitored by the light-scattering detector is shown in Figure 2 (Table 1).

The sample size is rather high for general quantitative liquid chromatographic analyses but the column does not appear to be overloaded. The minimum detectable mass estimated from this chromatogram appears to be about 10 ng of solute. To some extent, this detector provides an alternative to the conventional transport detector as it detects all substances irrespective of their optical or electrical properties. However, modern versions of the conventional wire or ribbon transport detector are reported to have significantly greater sensitivity.

Figure 3 depicts the separation of a mixture of fatty acids. The C_{18} -bonded silica column was 25 cm long, 2.1 mm i.d. and packed with particles of 3 μm diameter. The flow rate was 0.4 mL min^{-1} and the sol-

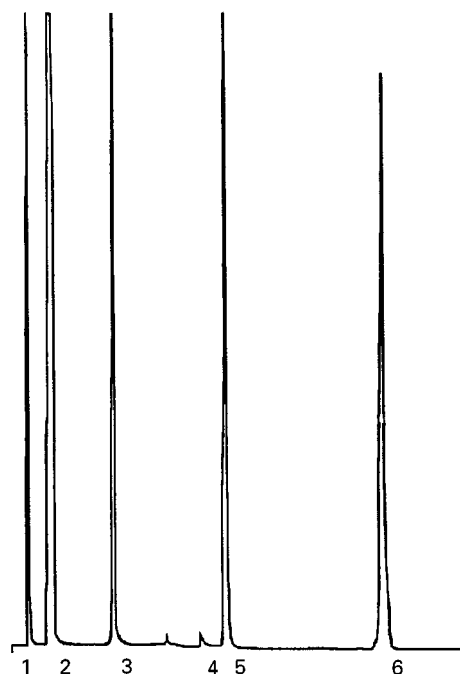


Figure 2 The separation of some lipid-class materials monitored by an evaporative light-scattering detector. For key, see Table 1.

vents used were water and acetonitrile. The gradient employed is shown in Table 2 and is typical for a reversed-phase column.

The solutes are initially retained by dispersive forces between the solutes and the stationary phase and are progressively eluted as the dispersive character of the mobile phase is increased with the greater concentration of acetonitrile. The weights quoted appear to be the concentration of each solute in the sample injected 20 μL of solvent. It is seen that an excellent response is obtained and the chromatogram is quite suitable for accurate quantitative analysis.

The separation of some phospholipids is shown in Figure 4. The column was 10 cm long, 4.6 mm i.d. and packed with particles of silica 3 μm in diameter.

Table 1 Key to Figure 2

Peak	Compound	Mass (μg)	Retention time (min)
1	Cholesterol ester	5	0.717
2	Triglyceride	18	1.746
3	Cholesterol	10	4.687
4	Unknown		8.860
5	Phosphatidyl choline	10	10.028
6	Phosphatidylethanolamine	10	17.390

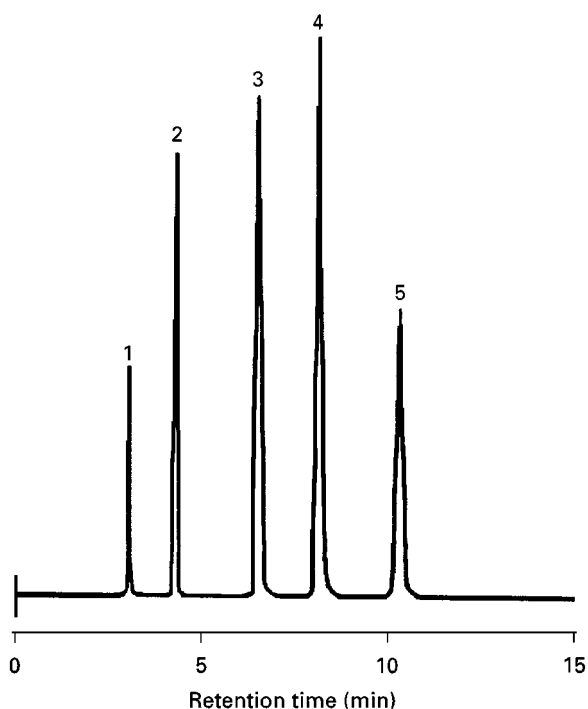


Figure 3 The separation of some fatty acids monitored by an evaporative light-scattering detector. Peaks: 1, capric acid (0.10 mg mL^{-1}); 2, lauric acid (0.03 mg mL^{-1}); 3, myristic acid (0.03 mg mL^{-1}); 4, pentadecanoic acid (0.02 mg mL^{-1}); 5, palmitic acid (0.03 mg mL^{-1}).

The flow rate was 1.25 mL min^{-1} and the solvents used were water, isopropanol and *n*-hexane. The gradient employed is shown in Table 3 and has obviously been specially developed for this type of separation on silica gel.

In this separation the solutes are largely retained by polar forces and are progressively eluted by increasing the proportion of isopropanol and water.

Table 2 Gradient for a typical reversed-phase column with solvents A (water) and B (acetonitrile)

	0 min	5 min	10 min	20 min
% B	77	80	90	95

Table 3 Gradient using solvents A (isopropanol), B (*n*-hexane) and C (water)

	0 min	7 min	15 min
% A	58	52	52
% B	40	40	40
% C	2	8	8

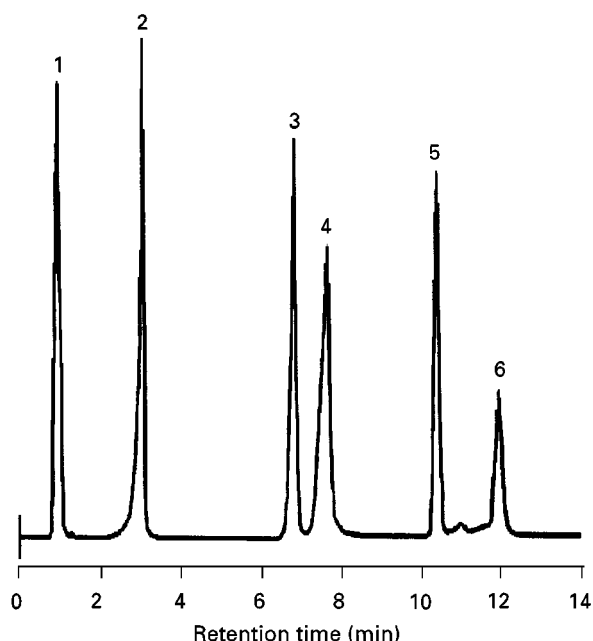


Figure 4 The separation of some phospholipids monitored by an evaporative light-scattering detector. Peaks: 1, cholesterol (0.15 mg mL^{-1}); 2, palmitic acid (0.25 mg mL^{-1}); 3, phosphatidylethanolamine (0.15 mg mL^{-1}); 4, phosphatidylserine (0.30 mg mL^{-1}); 5, phosphatidylcholine (0.15 mg mL^{-1}); 6, sphingomyelin (0.15 mg).

The strong polar solvents deactivate the stationary phase by preferential adsorption and this allows the strong dispersive forces between the solutes and the hexane to elute the solutes. Again, the weights quoted appear to be the concentration of each solute in the sample injected in $20 \mu\text{L}$ of solvent. It is clear that the detector is quite sensitive to these solutes and, again, the response and resolution are more than adequate for accurate quantitative analysis.

Conclusions

Although the evaporative light-scattering detector is mechanically somewhat clumsy, relatively expensive and has a nonlinear response and limited sensitivity, it still fills a need for an effective detector that can be used for certain classes of compounds that cannot be sensed by other detector types. In addition, as opposed to the refractive index detector that can also sense similar materials, it allows a free choice of solvent and easily tolerates solvent programming.

See also: II/Chromatography: Detectors: Laser Light Scattering. III/Lipids: Gas Chromatography; Liquid Chromatography; Thin-Layer (Planar) Chromatography.

Further Reading

- Charlesworth JM (1978) Evaporative analyzer as a mass detector for liquid chromatography. *Analytical Chemistry* 50: 1414.
- Kerker M (1969) *The Scattering of Light and other Electromagnetic Radiation*. New York: Academic Press.
- MacRae R and Dick J (1981) Analysis of carbohydrates using the mass detector. *Journal of Chromatography* 210: 138–145.
- Mourey TH and Oppenheimer LE (1984) Principles of operation of an evaporative light-scattering

- detector for liquid chromatography. *Analytical Chemistry* 56: 2427–2434.
- Oppenheimer LE and Mourey TH (1985) Examination of the concentration response of evaporative light-scattering mass detectors. *Journal of Chromatography* 323: 297–304.
- Stolyhwo A, Martin M and Guiochon G (1987) Analysis of liquid classes by HPLC with the evaporative light scattering detector. *Journal of Liquid Chromatography* 1243–1253.

Detectors: Fluorescence Detection

R. P. W. Scott, Avon, CT, USA

Copyright © 2000 Academic Press

The process whereby molecules are excited by electromagnetic radiation to produce luminescence is termed photoluminescence. If the release of energy is delayed, or persists after the removal of the exciting radiation, then the substance is said to be *phosphorescent*. Signal persistence (even with a short but significant lifetime) limits the use of phosphorescence for liquid chromatography (LC) detection, because signal continuance will produce apparent peak broadening and consequent loss of resolution. If the release of electromagnetic energy is immediate, or stops on the removal of the excitation radiation, the substance is said to be *fluorescent*. In contrast to phosphorescence, fluorescence has been shown to be extremely useful for LC detection, and has provided some of the highest sensitivities available.

When light is absorbed by a molecule, a transition to a higher electronic state takes place and this process is highly specific for each substance. This is because radiation of a particular wavelength, or energy, will be absorbed by specific molecular structures. If electrons are raised, due to absorption of light energy, to an upper excited singlet state, and the excess energy is not dissipated rapidly by collision with other molecules or by other means, the electron will return to the ground state with the emission of light at a lower frequency. Under such circumstances the substance is said to fluoresce. In reality, some energy is always lost before emission occurs and thus, in contrast to Raman scattering, the wavelength of the fluorescent light emitted is always greater than the incident light. For further information on the theory

of fluorescence the reviews by Guilbault, Udenfriend and Rhys-Williams are recommended (see Further Reading section).

With the exception of certain electrochemical detectors and the mass spectrometer, the fluorescence detector affords greater sensitivity to sample concentration than other devices. In addition, the fluorescence sensor is less sensitive to changes in ambient conditions, e.g. temperature and pressure. The high sensitivity that is achieved is also partly due to the very low background light level and the consequent low noise level. The low noise level of the fluorescent detector is in contrast to those detectors that involve light absorption measurements, where the signal is superimposed on a strong background signal with a high noise level. The major disadvantage of fluorescence detection is that relatively few compounds fluoresce in a practical range of wavelengths. However, the scope of fluorescence detection can be extended by forming derivatives. For example, the reagents fluoropa (*o*-phthalaldehyde) and fluorescamine (4-phenyl-spiro(furan-2-(3H),1'-phthalan)-3',3'-dione) are both commercially available derivatizing reagents that can react with primary amines to produce fluorescent derivatives. One other minor disadvantage is the effect of molecular oxygen which, if present in the mobile phase, can cause significant fluorescent quenching. It is essential, therefore, for maximum and constant response, to degas the solvents by helium sparging before use.

Most fluorescent detectors are configured so that the fluorescent light that is sensed is emitted at an angle (usually at right angles) to the direction of the exciting incident light beam. This arrangement minimizes the amount of incident light that may provide a background signal to the fluorescent sensor. It follows that the fluorescent signal is sensed against

a virtually black background and hence provides the maximum signal-to-noise ratio. If necessary, the background signal can be further reduced by the use of an appropriate filter to remove any stray scattered excitation light that might be received by the sensor.

The fluorescence signal (I_f) is given by

$$I_f = \phi I_0(1 - e^{-\epsilon cl})$$

where ϕ is the quantum yields (the ratio of the number of photons emitted and the number of photons absorbed), I_0 is the intensity of the incident light, c is the concentration of the solute, ϵ is the molar absorbance and l is the path length of the cell.

It is clear that the solute concentration is a somewhat complex function of the intensity of the emitted fluorescent light. As a consequence, the signal from the photocell must be electronically modified to produce an output that is linearly related to solute concentration.

Fluorescence detectors vary widely in complexity. The simplest consists of a single wavelength excitation source in conjunction with a sensor that responds to light at all wavelengths (UV and visible). For certain applications, this simple form of fluorescence detector can be very sensitive and inexpensive. However, by restricting the excitation light to a single wavelength, and with no means of selecting the emission wavelength, the system has limited versatility. At the other extreme is the fluorescence spectrometer that has been fitted with a sensor cell of appropriate dimensions. This comprehensive fluorescence monitoring system is highly complex and versatile and allows both the excitation and emission wave-

lengths to be chosen. Furthermore, excitation spectra can be obtained at any fixed emission wavelength, or an emission spectrum can be obtained for any fixed excitation wavelength.

The Fluorescence Detectors

The Single Wavelength Excitation Fluorescence Detector

With the exception of the electrochemical detector, the single wavelength excitation fluorescence detector is probably the most sensitive detector generally available to LC but, as already stated, it is so at the cost of limited versatility. A simple form of the fluorescence detector excited by light from a single wavelength UV source is shown in **Figure 1**.

The UV excitation source is usually a low pressure mercury lamp which is comparatively inexpensive and provides relatively high intensity UV light at 253.7 nm. Many substances that fluoresce will, to a lesser or greater extent, be excited by light at this wavelength. The excitation light is focused by a quartz lens, through the cell. Another lens situated normal to the incident light focuses the fluorescent light through a circular mask on to a photocell. Typically, a fixed wavelength fluorescence detector will have a minimum detectable concentration at an excitation wavelength of 254 nm of $c. 1 \times 10^{-9} \text{ g mL}^{-1}$ and a linear dynamic range of 1×10^{-9} – $5 \times 10^{-6} \text{ g mL}^{-1}$. One of the disadvantages of the fluorescence detector is this rather limited linear dynamic range.

Detectors have been designed as a compromise between the expensive fluorescence spectrometer and

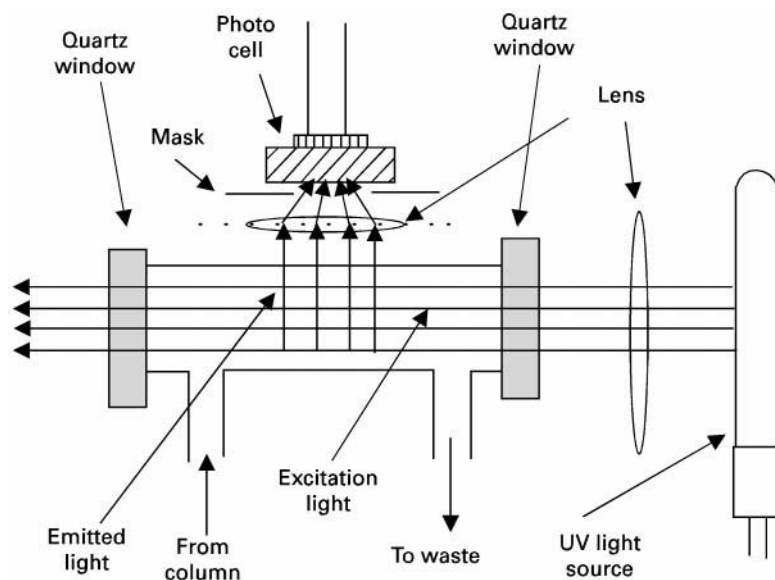


Figure 1 The single wavelength fluorescent detector.

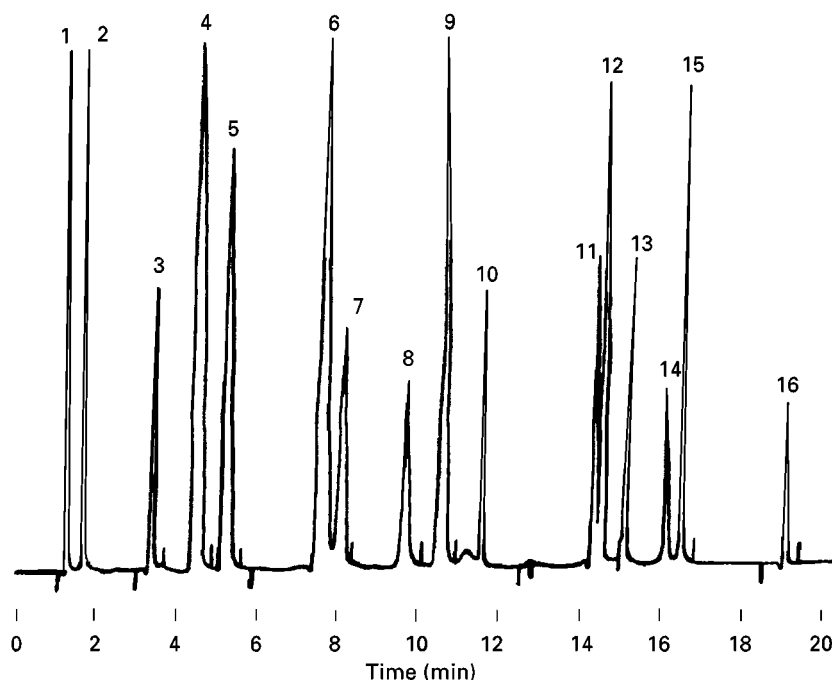


Figure 2 The separation of some amino acids by monitoring their *o*-phthalaldehyde derivatives with a fluorescence detector. Column: Supelcosil LC-18, 5 cm \times 4.6 mm, 5 μ m particles. Mobile phase: methanol-tetrahydrofuran-0.02 mol L⁻¹ sodium acetate (pH 5.9 with acetic acid) A, 22.5:2.5:77.5, B, 80:2.5:17.5. 2 min at 100% (A) to 100% (B) in 20 min. Flow rate: 2 mL min⁻¹. Sample: 50–100 pmol of each derivative in solvent A. Peak identification: 1, Aspartic acid; 2, glutamic acid; 3, asparagine; 4, serine; 5, glutamine; 6, glycine; 7, threonine; 8, arginine; 9, alanine; 10, tyrosine; 11, methionine; 12, valine; 13, phenylalanine; 14, isoleucine; 15, leucine; 16, lysine. (Courtesy of Supelco Inc.)

the fixed wavelength detector. A typical example of this compromise is the fluorescence detector that utilizes the monochromator of a dispersive UV spectrometer in conjunction with light filters. It consists of a UV dispersion spectrometer fitted with a special absorption cell having reduced dimensions.

The small sensor cell ensures that the narrow peaks produced by high efficiency LC columns can be monitored without loss of chromatographic resolution. The wavelength of the excitation light is selected by the monochromator which will be within the normal UV range of the spectrometer (*c.* 200–360 nm). The excitation light passes through the cell and the fluorescent light, emitted at right angles to the path of the excitation light, is focused on to a photocell. Up to this point, the sensor system is very similar to that of the fixed wavelength fluorescence.

In most of these types of compromise detectors, appropriate light filters can be inserted between the sensor cell and the lens that focuses the emitted fluorescent light on to the photocell. In this way, the wavelength of the light monitored by the sensor can be selected by the choice of an appropriate filter. This, in fact, is a rather primitive way of selecting the emission wavelength. Nevertheless, the arrangement can be quite effective, and certainly eliminates

the need for a second monochromator and the added cost. The use of this type of detector in monitoring the separation of the *o*-phthalaldehyde derivatives of some amino acids is shown in **Figure 2**. It is seen that a very high sensitivity is realized and the integrity of the chromatographic resolution is well maintained.

The Multi-wavelength Fluorescence Detector

One form of multi-wavelength fluorescence detector consists of two monochromators: the first selects the wavelength of the excitation light, and the second disperses the fluorescent light, and provides a fluorescence spectrum, or allows the separation to be monitored at a selected fluorescence wavelength. The multi-wavelength fluorescence detector is shown in **Figure 3**. The detector comprises a fluorescent spectrometer fitted with a suitable absorption cell that can be used with high efficiency LC columns without degrading the resolution of the column. The spectrometer involves two distinctly different light systems. The function of the detector is easier to understand if the different light systems and the respective light paths are considered separately. The detector

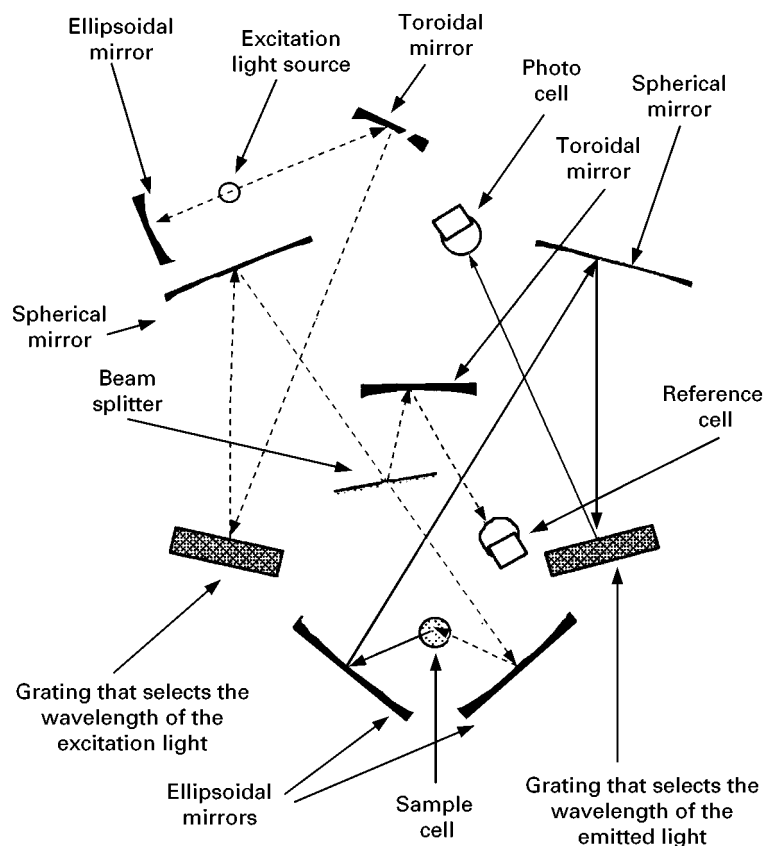


Figure 3 The fluorescence spectrometer detector. ---, excitation light; —, fluorescent light.

comprises an excitation light system and fluorescent light system.

The excitation source (emitting light over a wide wavelength range, such as a deuterium lamp) is situated at the focal point of an ellipsoidal mirror, shown at the top left-hand corner of the diagram. The parallel beam of light is collimated to fall on to a toroidal mirror, which then focuses it on to the grating, shown on the left-hand side of the diagram. This grating is used to select the wavelength of the excitation light or it can be used to scan the complete range of excitation wavelengths and provide a corresponding excitation spectrum that is monitored at a specific fluorescent wavelength. The selected wavelength then passes to a spherical mirror and then to an ellipsoidal mirror, shown at the base of the diagram, which focuses it on to the sample. The excitation light path is mostly depicted on the left-hand side of the diagram.

In the centre of the diagram, between the spherical mirror and the ellipsoidal mirror, is a beam splitter that diverts a portion of the incident light on to another toroidal mirror. This mirror focuses the light on to the reference photo cell. The reference photo cell provides an output that is proportional to the intensity of the excitation light. The path of the fluor-

escent light is depicted on the right-hand side of the diagram. Fluorescent light, emitted from the cell, is focused by an ellipsoidal mirror on to a spherical mirror at the top right-hand side of the diagram. This mirror focuses the light on to a grating which is situated at about centre right of the diagram. This grating selects a specific wavelength of the fluorescent light to monitor, or can scan the fluorescent light produced by excitation light of a given and selected wavelength, and provide a fluorescent spectrum. Fluorescent light from the grating passes to a photoelectric cell which monitors the intensity. The instrument is complex and relatively expensive; however, for measuring fluorescence, it is extremely versatile.

The optical system allows the wavelength of the excitation light and that of the fluorescent light to be chosen to provide the maximum selectivity for a given solute or its fluorescent derivative. The use of this optimization procedure is demonstrated by the high sensitivity detection of the fluoropa derivative of neomycin shown in **Figure 4**. It is an excellent example of the selection of a specific excitation light wavelength and the complementary emission light wavelength to provide maximum sensitivity.

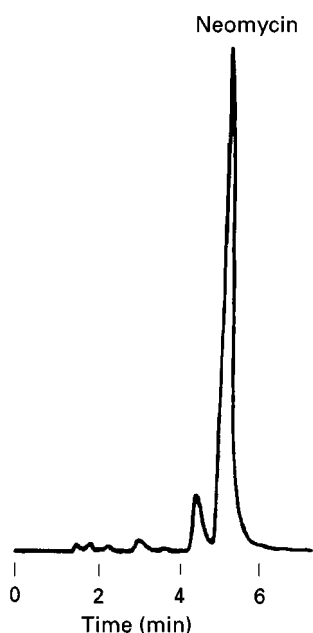


Figure 4 Detection of neomycin OPA derivative at an excitation wavelength of 365 nm and an emission wavelength of 418 nm. Column: Supelcosil LC-8, 15 cm \times 4.6 mm, 5 μ m particles. Mobile phase: tetrahydrofuran: 0.0056 mol L⁻¹ sodium sulfate–0.007 mol L⁻¹ acetic acid–0.01 mol L⁻¹ pentanesulfonate, 3:97. Flow rate: 1.75 mL min⁻¹. Post-column reagent: 1 L 0.4 mol L⁻¹ boric acid–0.38 mol L⁻¹ potassium hydroxide containing 6 mL 40% Brij-35, 4 mL mercaptoethanol, 0.8 g *o*-phthalaldehyde. Flow rate 0.4 mL min⁻¹. Mixer 5 cm \times 4.6 mm column packed with glass beads. Reactor 10 ft \times 0.5 mm knitted Teflon capillary tubing. Reaction temperature 40°C. Sample: 20 mL of a mobile-phase extract of a commercial sample. Excitation wavelength 365 nm; emission wavelength 418 nm. (Courtesy of Supelco Inc.)

The principle of optimizing excitation and emission light wavelengths to obtain maximum sensitivity for a multi-component mixture can be quite complex, as shown by the separation of some priority pollutants depicted in Figure 5. The separation was carried out on a column which was 25 cm long, 4.6 mm in diameter and packed with a C₁₈ reversed phase. The mobile phase was programmed from 93:7 acetonitrile–water to 99:1 acetonitrile–water over a period of 30 min. The gradient was linear and the flow rate was 1.3 mL min⁻¹. All the solutes were separated and the compounds, numbered from the left, are given in Table 1. The separation illustrates the clever use of wavelength programming to obtain the maximum sensitivity. The programme used is shown in Table 1.

The wavelength of the excitation light and that of the emission light was changed during chromatographic development to provide optimum fluorescent conditions, and thus maximum sensitivity, for each solute. This ensured that each solute, as it was eluted, was excited at the most energetic wavelength and then monitored at the strongest fluorescent wavelength.

It is seen that the analysis involves a somewhat elaborate wavelength programme; nevertheless, if the analysis is sufficiently important, it is readily justified. The system also provides fluorescence and excitation spectra, by arresting the flow of mobile phase when the solute resides in the detecting cell, and scanning the excitation and/or fluorescent light. (This is the

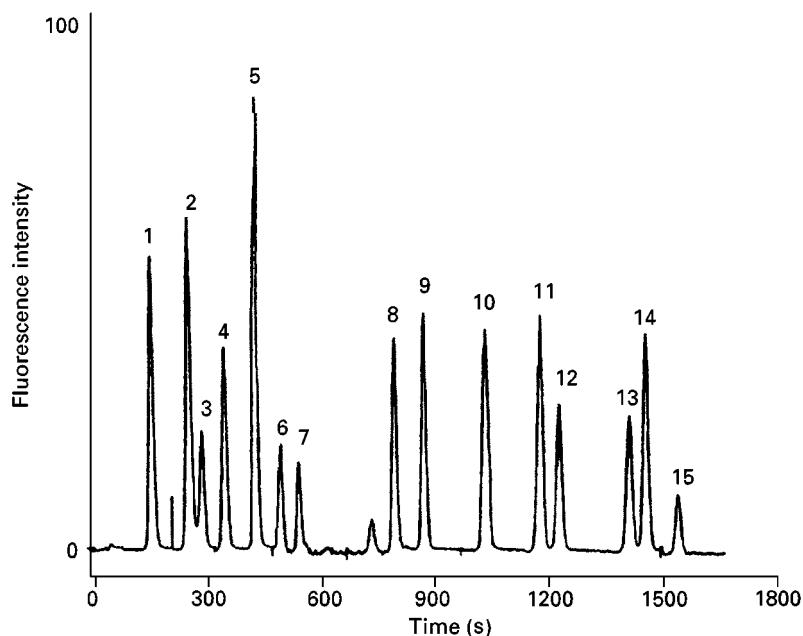


Figure 5 Separation of a series of priority pollutants with programmed fluorescence detection. 1, Naphthalene; 2, acenaphthene; 3, fluorene; 4, phenanthrene; 5, anthracene; 6, fluoranthene; 7, pyrene; 8, benz(a)anthracene; 9, chrysene; 10, benzo(b)fluoranthene; 11, benzo(k)fluoranthene; 12, benzo(a)pyrene; 13, dibenz(a,h)anthracene; 14, benzo(ghi)perylene; 15, indeno(123-cd)pyrene. (Courtesy of the Perkin Elmer Corporation.)

Table 1 Fluorescence detector programme

Time (s)	Wavelength of excitation light (nm)	Wavelength of emitted light (nm)
0	280	340
220	290	320
340	250	385
510	260	420
720	265	380
1050	290	430
1620	300	500

same technique as that used to provide UV spectra with the variable wavelength UV detector.) In this way, it is possible to obtain excitation spectra at any chosen fluorescent wavelength, or fluorescent spectra at any chosen excitation wavelength. Consequently, even with relatively poor spectroscopic resolution, many hundreds of spectra can be produced, any or all of which (despite many spectra being very similar) can be used to help confirm the identity of a compound.

The above spectrometric arrangement can be considerably simplified and much of the mechanical systems eliminated by employing a diode array sensing device for the fluorescent light. This allows the fluorescence spectrum to be recorded continuously throughout the development of the chromatogram. A specific excitation wavelength must be selected and this is achieved by employing the usual mechanical monochromator. Excitation spectra still need to be obtained by stopping the mobile-phase flow and scanning the excitation light.

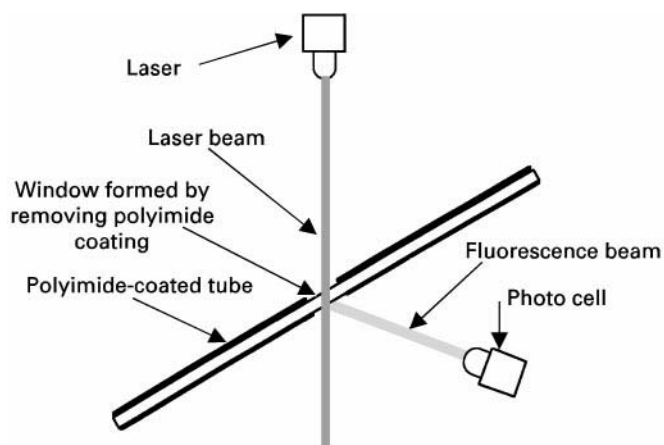
Due to the high sensitivities achieved by fluorescence detection, the technique has proved very useful as a detection system in capillary electrochromatog-

raphy and capillary electrophoresis. High sensitivity is achieved by employing a high energy excitation source such as a laser, emitting light at an appropriate wavelength. A typical optical system for fluorescent detection in capillary electrophoresis and capillary electrochromatography is shown in **Figure 6**. A window is opened in the quartz capillary tube, by removing the polyimide coating from about a millimetre length of capillary tube. The laser beam is arranged to pass through the window and the fluorescent light, emitted normal to the laser beam and the capillary tube, is focused on to a photoelectric cell or photodiode array. A filter can be interposed between the capillary window and the sensor measuring the fluorescent light, to eliminate scattered incident light. The signal from the photo cell is electronically modified in the same way as the normal LC fluorescence detector.

Unfortunately, lasers which have suitable wavelengths for this purpose are somewhat limited. However, lasers of various types are continuously being developed and this offers great promise for the future development of this type of detector.

An example of the use of fluorescence to monitor an electrophoretic separation of the AQC fluorescent derivatives of phenylalanine, methionine and serine are shown in **Figure 7**. In this separation vancomycin was used as the chiral additive. The separation was carried out on a 30.5 cm fused silica capillary, 50 μm i.d., containing 0.1 mol L^{-1} phosphate buffer and 5 mmol L^{-1} vancomycin. The pH of the buffer was 7.0 and the electrophoretic voltage 5 kV.

Fluorescence detection is the most popular high sensitivity detection method presently in use in LC, and will continue to be so for the foreseeable future. The system is basically simple, easy to use and provides at least an order more sensitivity than the generally popular UV detector.

**Figure 6** The laser system for fluorescence detection in capillary electrochromatography.

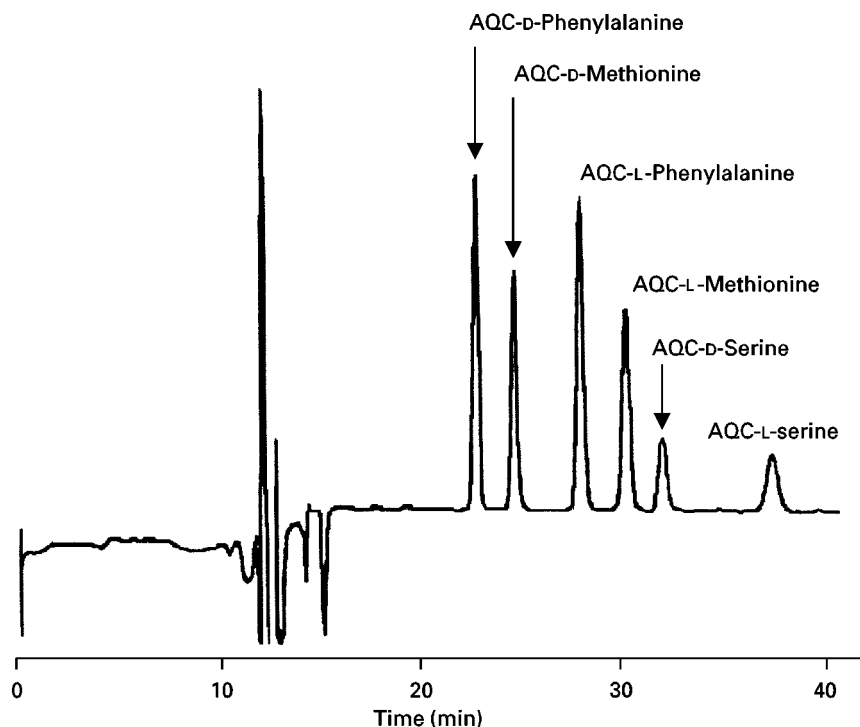


Figure 7 The separation of the enantiomers of the AQC fluorescent derivatives phenylalanine, methionine and serine. Courtesy of LC/GC. (T. L. Bereuer, *LC-GC*, Vol. 12 No. 10 (1994) 748).

Conclusion

Although relatively few substances are inherently fluorescent, most can be made to form fluorescent derivatives by relatively simple derivatization procedures. In addition, with the aid of a suitable laser, the natural high sensitivity of the device can be greatly enhanced. The main disadvantage of the fluorescence detector is its limited linear dynamic range but since in most LC analyses high sensitivity is usually required for trace analysis, in practice this limitation is not found to be so important.

See Colour Plate 22.

Further Reading

- Guilbault GG (1973) *Practical Fluorescence*. New York: Marcel Dekker.
- Kok WTh (1998) Principles of detection. In: Katz E (ed.) *Handbook of HPLC*, p. 143. Chichester: John Wiley.
- Rhys-Williams AT (1980) *Fluorescence Detection in Liquid Chromatography*. Beaconsfield: Perkin Elmer.
- Scott RPW (1996) *Chromatography Detectors*. New York: Marcel Dekker.
- Udenfriend S (1962) *Fluorescence Assay in Biology and Medicine*. New York: Academic Press.

Detectors: Infrared

R. P. W. Scott, Avon, CT, USA

Copyright © 2000 Academic Press

Introduction

Infrared (IR) light is the term given to electromagnetic radiation having a wavelength lying between 1 and 15 micron. In contrast to UV light, which is adsorbed when the light energy at a particular wavelength is equal to specific electronic transitions in the molecule, IR light is adsorbed when its energy is equal to

changes in the vibrational and/or rotational energy of a molecule. A molecule can be considered as being made from a number of spheres (atoms) joined by springs (chemical bonds) and thus can vibrate in a very complex manner. As a general rule, a polyatomic molecule containing (n) atoms will exhibit $(3n - 6)$ modes of vibration and a characteristic fundamental frequency (or wavelength) will be associated with each vibration mode. Both UV and IR spectra can be used for substance identification but, due to the many vibration modes that are possible,

there is considerably more fine structure in IR spectra and consequently, IR spectra are generally more useful and give less ambiguous identification.

In general, IR adsorption is much weaker than UV adsorption and thus much larger samples are required. In addition, most of the solvents that are used in liquid chromatography adsorb strongly in the IR region and thus there have been very few IR based LC detectors developed, and none sufficiently effective for general use. In practice, the liquid chromatograph is usually combined with an IR spectrometer as a tandem system to provide spectra of the eluted solutes for identification purposes and not primarily as a detector. The basic construction of the traditional IR spectrometer is similar to that of the UV spectrometer except that the optical components must be transparent to IR light and thus must be made of appropriate materials. In addition, due to relatively low sensitivity, the interface is usually some form of transport device that also concentrates the sample as well as removing any interfering solvent. There are two forms of IR spectrometer, the grating dispersion IR spectrometer and the Fourier transform IR spectrometer (FTIR). The dispersion instrument is rarely used today in conjunction with the modern liquid chromatograph and the FTIR-LC tandem instrument now dominates the LC/IR field. Consequently only the FTIR instrument will be briefly described.

The Fourier transform IR (FTIR) spectrometer involves relatively simple instrumentation but quite complicated data processing. Due to its basic design, the spectrometer monitors all the wavelengths coincidentally, and consequently, the FTIR spectrometer can scan samples much faster than the dispersive

instrument. This feature alone, makes the FTIR spectrometer highly suitable for tandem operation. A diagram of the basic system is shown in Figure 1.

Light from a broad band infrared source is collimated and passes into an optical system where it strikes a beam splitter consisting of a very thin film of germanium. 50% of the light passes through the film and is reflected back along its original path by a fixed mirror, where half of the light intensity (25% of the original light intensity) is reflected by the same beam splitter, through the sample cell, to the infrared sensor. The remaining 50% of the incident light is reflected at right angles to its incident path onto an axially movable mirror. Light from the moving mirror returns along its original path and again, half of the light intensity is transmitted through the beam splitter, through the sample cell, to the infrared sensor. As a result of this optical system, a quarter of the original collimated incident light from the source reaches the sensor from the fixed mirror and a quarter from the movable mirror. Because the path length of the two light beams striking the sensor will differ, there will be destructive and constructive interference, the system constituting a Michelson interferometer. As the movable mirror traverses its programmed path, it will produce a series of maxima and minima as all the different wavelengths generated by the source pass through conditions of constructive and destructive interference. These maxima and minima are continuously monitored by the sensor and recorded. It should be noted that the frequency of the waveform is controlled by the velocity of the moving mirror which will be selectable.

The interferometer actually takes a Fourier transform of the incoming signal. An example of an

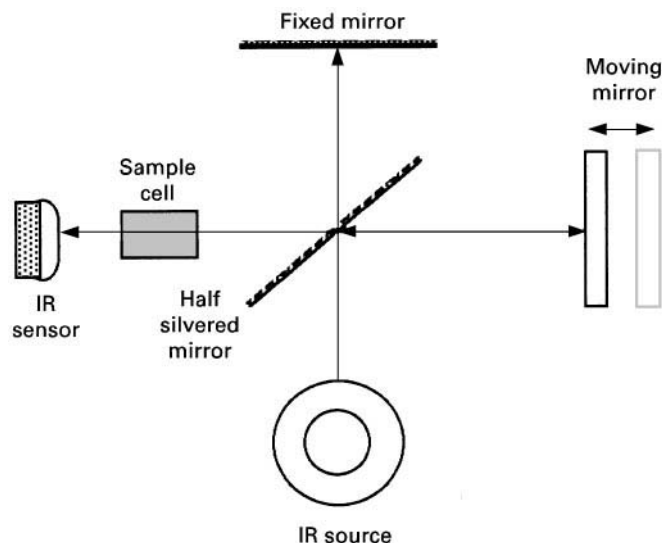


Figure 1 The elementary FTIR instrument. Courtesy of Nicolet Inc., Madison, Wisconsin, USA.

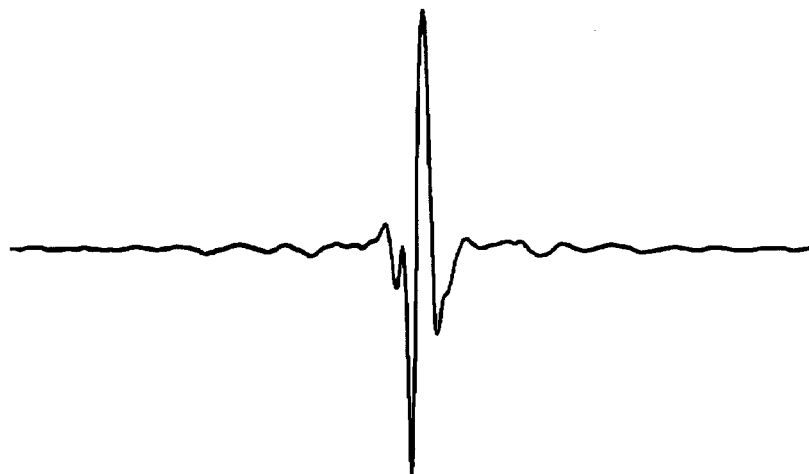


Figure 2 A typical interferogram. Courtesy of Nicolet Inc., Madison, Wisconsin, USA.

interferogram obtained from the FTIR is shown in Figure 2.

The resolution of the interferogram does not appear to be very good. However, this is misleading as a one second scan from an FTIR instrument gives equivalent resolution to that of a dispersive instrument scanning for 10 to 15 min. In any event, the FTIR resolution can be improved still further by using repetitive scans and processing the sum. The resolution is increased proportionally to the square root of the number of accumulated scans, e.g. 16 accumulated scans would increase the resolution by a factor of four. Spectra accumulation also increases sensitivity which is a distinct advantage in tandem systems, as the available sample may be severely limited. A single scan may take about a second, thus scanning for four seconds would double the sensitivity. Tandem systems involving IR measurements would not be successful without the introduction of the Fourier transform IR spectrometer.

LC/IR Transport Interfaces

The first transport system to be used as a liquid chromatograph-spectrometer interface was introduced by Scott *et al.* for a liquid chromatography/mass spectrometer tandem system. Eventually, the transport concept was extended to LC/IR tandem instruments and the most effective LC/FTIR interface commercially available incorporated a solvent transport interface. One of the first LC/IR transport systems was developed by Kuehl and Griffiths. Initially, moving ribbon devices were used in a similar manner to that of Scott *et al.*, but were eventually discarded in favour of a rather crude, but effective, rotating disc transport system. Their final model consisted of a cup carousel containing potassium chloride

that actually acted as a fraction collector and thus was hardly an in-line interface. Depending on the speed of the transport process, many transport interfaces could be considered as automated off-line monitoring devices. Fast moving transport systems such as a wire or belt transport however, give the impression of being in-line devices although in principle, they are not. The LC/IR carousel had 32 cups fitted with a fine mesh screen and filled with potassium chloride powder. Carousel position was controlled automatically in three positions, where specific sampling activities took place. In position (1) the eluent passed onto the potassium chloride until the halide powder was saturated with mobile phase. In position (2) a stream of air was drawn through the packing to evaporate the solvent. In position (3) infrared light was directed through the dry halide, and the spectrum was taken. The carousel interface concentrated the solute and increased the sensitivity of the LC/IR combination. Unfortunately, with modern LC columns, many peaks can be eluted in a few seconds and so intermittent sample collection is unsuitable. The carousel interface primarily acts as a chromatographic 'memory'; all the eluted solutes are stored as a 'physical' chromatogram as localized masses, deposited on the transport medium. The first chromatographic memory was introduced by Karmen, who used a wire transport detector to accumulate each eluted solute onto the wire surface, which was then stored on a reel. Subsequently, the wire was passed continuously through the flame of an FID, to produce a record of the separation. The most effective LC/IR interfaces are directly or indirectly based on this principle.

Jino and Fujimoto employed a potassium bromide plate as the transport system which was used as the sample holder for the IR measurement. Plate rotation

was actuated by the detector signal and, at the start of a peak, the plate was moved to a new collection position. The disc moved on when elution was complete so that the sample was isolated at a specific position on the plate perimeter. A small bore column was used (flow rate $5 \mu\text{L min}^{-1}$) so the eluent fell onto the plate and the solvent either evaporated under ambient conditions or with the aid of an infrared heater. After the separation was complete a spectrum was taken by measuring the light transmitted through the dry deposit in the usual manner. Obviously, because of the solubility of the halide in water, aqueous solvents could not be used.

Gagel and Bieman employed an aluminium disc, on top of which was cemented a circular glass mirror to form a transporter with a reflective surface; it was used in conjunction with a simple nebulizer that deposited the sample on the surface. Their basic apparatus is shown diagrammatically in Figure 3.

The disc rotated continuously during separation, leaving a spiral trail of solid deposits on the surface of the reflective plate. Evaporation was accomplished by the nebulizer. The column eluent passed into a T, one

limb of which carried a flow of nitrogen gas. The gas and eluent passed out *via* a narrow nozzle in the third limb, which directed the spray onto the disc surface. After separation, the disc was placed in a modified total reflectance IR accessory. The disc was rotated, the surface scanned by the IR spectrometer, and the reflectance-absorbance spectra continuously collected. This LC/FTIR interface appeared successful, and functioned without significant peak dispersion or loss of chromatographic resolution. The minimum mass needed to provide a satisfactory spectrum varied with the characteristic absorbance of the substances being monitored. However, it was shown that between 50 and 100 ng of sample could provide a recognizable spectrum.

Gagel and Bieman modified the nebulizer to improve the deposition, to make it amenable to aqueous solvents by reducing spreading, and to concentrate the material into a smaller area. The modified jet design involved the use of two nitrogen streams. The column eluent was mixed in a high pressure mixing T with nitrogen under pressure and directed through a syringe needle to the deposition surface. The needle

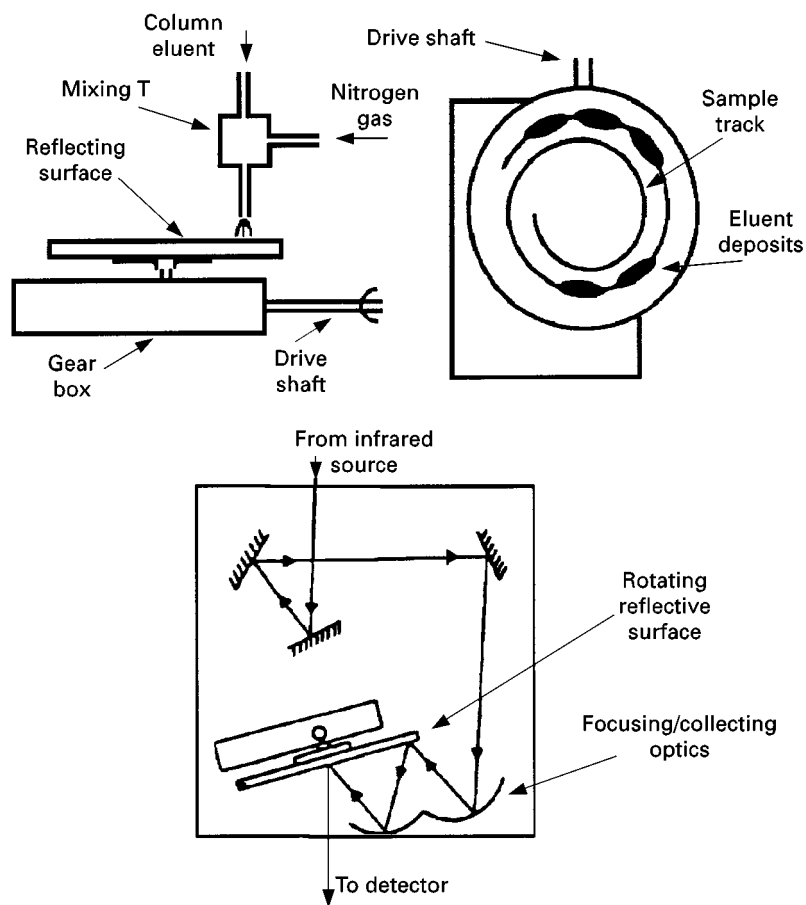


Figure 3 The layout of the transport LC/FTIR apparatus developed by Gagel and Bieman. (Reproduced with permission from Gagel and Bieman, 1986.)

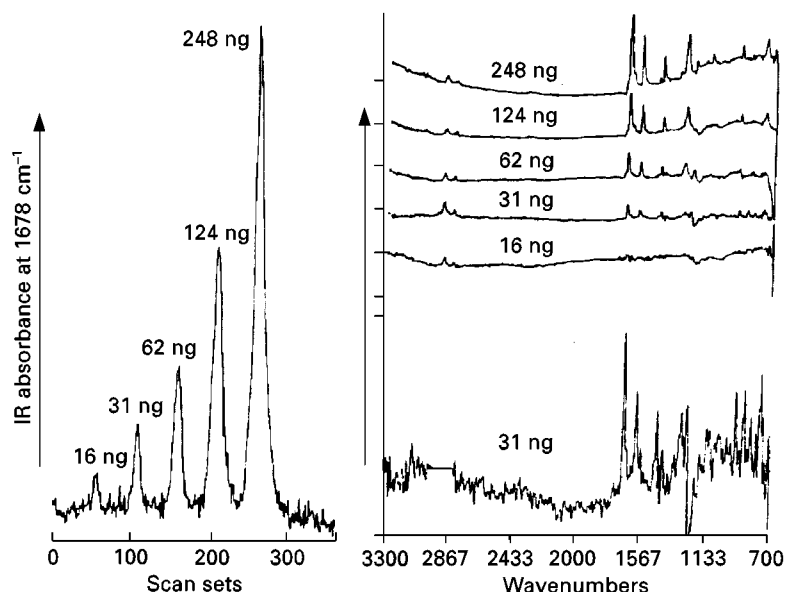


Figure 4 Results from the modified LC/FTIR interface demonstrating the overall sensitivity of the tandem instrument. (Reproduced with permission from Gagal JJ and Bieman K (1987) *Anal. Chem.*, 59(9): 1267.)

was situated inside another nozzle through which heated nitrogen was flowing. The new arrangement functioned well with aqueous solvent mixtures and the overall sensitivity of the apparatus was significantly increased. The sensitivity of the modified interface is demonstrated in **Figure 4**.

The peaks from the injection of different masses of phenanthraquinone are shown on the left. The peaks are curves relating the IR absorbance at 1678 cm^{-1} to scan number for samples deposited from 29% water in methanol. The ultimate sensitivity, defined as the mass of solute that would provide a signal to noise ratio of 2, was about 16 ng.

Solvent elimination is relatively easy with nonaqueous mobile phases but the majority of LC separations employ reversed phase columns and require mobile phases with a high water content. Poor volatility of such solvent mixtures, causes the deposits to be smeared into one another. This seriously impairs the separation. Water in the mobile phase also restricts the choice of the transport medium as it must be water resistant. A considerable amount of work has been carried out on nebulizer design to improve solute deposition and focus the material onto a smaller spot. Techniques that have been tried include thermospray and hydrodynamic focusing that employs a concentric gas flow to reduce the jet diameter by the Bernoulli effect. Different transport media have also been explored, including potassium chloride layers on the surface of a zinc-selenium metallic stage using diffuse transmission spectroscopy to obtain the spectrum of the deposited material. The deposition of

the eluent from a narrow bore reversed phase column, onto the surface of a linearly moving substrate, using a jet spray assembly as an interface, has also been developed. The immobilized chromatogram (actually a chromatographic memory) is analysed by moving the substrate linearly under an FT-IR microscope while collecting the spectra. Zinc selenide was found to be preferable to an aluminized reflective surface as a disc transport. An example of the disc system used to display a reversed-phase separation of some polynuclear hydrocarbons is shown in three-dimensional form in **Figure 5**. The sensitivity to pyrene at a signal to noise ratio of 2 was 13 ng.

The In-Line Flow Sensor

The alternative to a transport interface is an in-line flow-through cell, and in 1983 a micro IR cell, $3.2\text{ }\mu\text{L}$ in volume, that fitted directly into the IR spectrometer was described by Brown and Taylor. By using a small-bore column they achieved an overall increase in mass sensitivity of about two orders of magnitude, relative to that obtained from the standard 4.6 mm i.d. column. An FTIR spectrometer was used, but the actual sensitivity improvement was confused as the length of the small bore column differed significantly from that of the standard column. Consequently, the true sensitivity in terms of minimum sample mass that would provide an acceptable spectrum, could not be assessed accurately.

A different cell design cell for use with LC micro-bore columns interfaced with an FTIR spectrometer

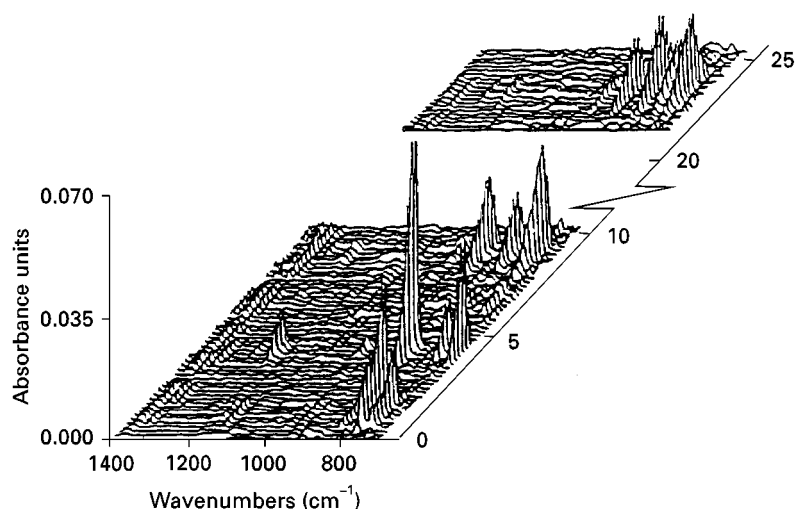


Figure 5 A three-dimensional reversed phase LC/IR plot of the separation of some polynuclear aromatic hydrocarbons. (Reproduced with permission from Conroy and Griffiths, 1984.)

was described by Johnson and Taylor. It was claimed that the cell would reduce the detection limit (the minimum mass required to produce a useful IR spectrum) to about 50 ng. The flow cell design is shown in Figure 6.

The cell was formed crystalline calcium fluoride or potassium bromide in the form of a block $10 \times 10 \times 6$ mm. A hole 0.75 mm i.d. was drilled through it to carry the mobile phase from the column through the block and out to waste. The collimated IR beam passed through the block, normal to the cylindrical aperture and, in doing so, transversed

a section of the exiting eluent. A beam condenser was used to reduce the focal diameter of the beam to that of the hole. It was noted that the maximum signal-to-noise was obtained by summing the spectra from scans taken across the peak, between $\pm 1.53 \sigma$ of the Gaussian profile, as it passed through the cell. As a practical point of interest, it was found easier to modify optically the size of the IR beam to match the flow cell, than to construct a cell that would accurately match the dimensions of the IR beam.

Sabo *et al.* developed an attenuated total reflectance cell for both normal- and reversed-phase

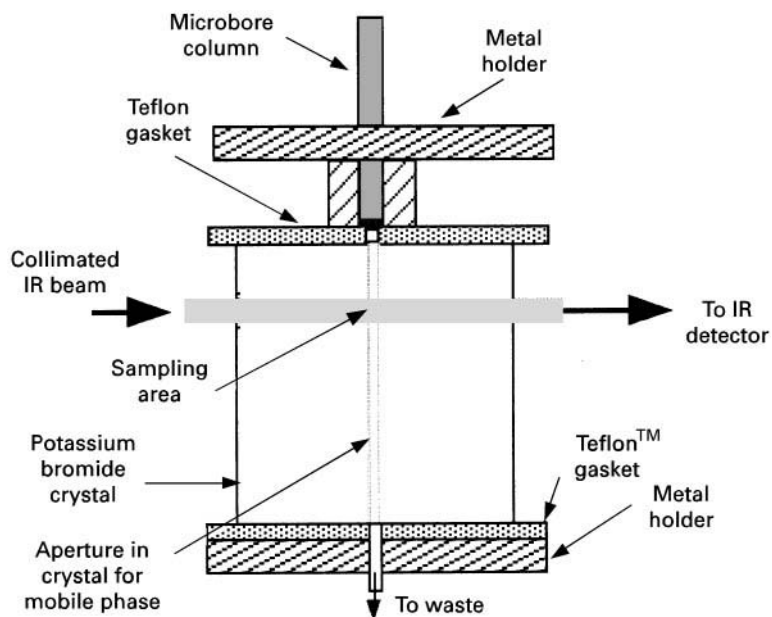


Figure 6 Zero dead volume micro IR cell.

chromatography. The cell was made with cone shaped ends, from a cylindrical shaped zinc selenide crystal, and mounted in stainless steel. The crystal was blazed at 45° and consequently gave ten reflections during passage of the IR beam down its length. The incident beam was focused onto the cone face and the radiation leaving the crystal was focused onto the IR sensor. The cell volume was large, ca. 24 μL and thus would adversely affect the resolution of a small-bore column. Clear, identifiable spectra were obtained from a 100 μL sample, containing 2% of acetophenone and ethyl benzoate and 1% of nitrobenzene from on-the-fly spectra. However, this was not a very sensitive device compared with other LC/FTIR systems.

A rather complicated solvent extraction system was developed by Conroy and Griffiths for use with an LC/FTIR tandem instrument. It involved a process that continually extracted the solute from the column eluent into dichloromethane. The solution is dichloromethane was concentrated and dispersed onto a plug of potassium chloride powder. The residual solvent was evaporated, the sample scanned and a spectrum taken. This process is somewhat clumsy but it introduces a new concept for constructing LC/IR interfaces. Employing the same basic principle Johnson *et al.* constructed a rather unique extraction cell for use with an LC/IR tandem system by introducing the technique of segmented flow. The aqueous eluent from a reversed phase column was mixed with chloroform (with which the column eluent was immiscible) producing segmented flow. The extraction solvent (chloroform) was then separated from the segmented flow by means of a 'hydrophobic' (dispersive) membrane. There were two pumps, one for the mobile phase and the other for the extraction solvent, which could be either chloroform or carbon tetrachloride. The two streams were mixed at a T junction (post column) and formed the segmented flow. The segmented flow then passed through an extraction coil and then to a separator. The separator was made of stainless steel with a membrane having pores about 0.2 μm in diameter dividing its length into half and its general layout is shown in Figure 7.

The volume on either side of the membrane was about 16 μL and the amount of solvent passing through the membrane was controlled by the differential pressure across the membrane. Obviously this device could cause serious peak dispersion and would be unsuitable for use with high-efficiency of small-bore columns. Samples containing at least 300 μg of material were necessary to produce a satisfactory spectrum, indicating a relatively poor sensitivity.

The segmented flow interface was developed further by Hellgeth and Taylor, who improved both the

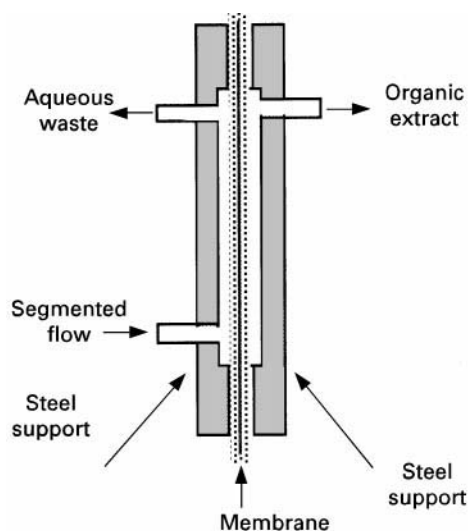


Figure 7 An extraction interface for LC/IR.

segmentation and the extraction efficiency. The segmented flow generator was made from 1/16 in. Swagelok T union, drilled out to contain 1/16 in. tubes the ends of which were only 0.45 mm apart and the general design is shown in Figure 8.

The column eluent and extraction solvent passed into the mixing T through tubes 0.020 in. i.d. The exiting segmented flow passed through an extraction conduit consisting of a TeflonTM tube, 75 cm long and 0.8 mm i.d. The membrane separator was constructed from two stainless steel plates with grooves in each surface, and a triple-layer membrane of Gore-TexTM sheet. The membrane was made from two materials. The inner layer comprised an unsupported 1 μm pore TeflonTM sheet which was sandwiched between two outer sheets of 1 μm pore TeflonTM. These sheets were supported by non-woven polypropylene membranes which were located on the outer surfaces. The infrared cell was a modified Spectra-Tech Inc. demountable flow cell fitted with windows of either calcium fluoride or zinc selenide. The system appeared to function reasonably well; satisfactory spectra were obtained from 100 μg of material. Although a considerable improvement, the sensitivity was still relatively poor compared with that obtained with the rotating disc transport interfaces.

Further work by Somsen *et al.* has resulted in a segmented flow concentrator with significantly reduced band dispersion. A conventional liquid chromatograph was employed. It included a pump, pulse damper, injection valve and column. The column eluent entered a T piece where it was joined by an immiscible extraction solvent, usually methylene dichloride, supplied from another pump and pulse damper.

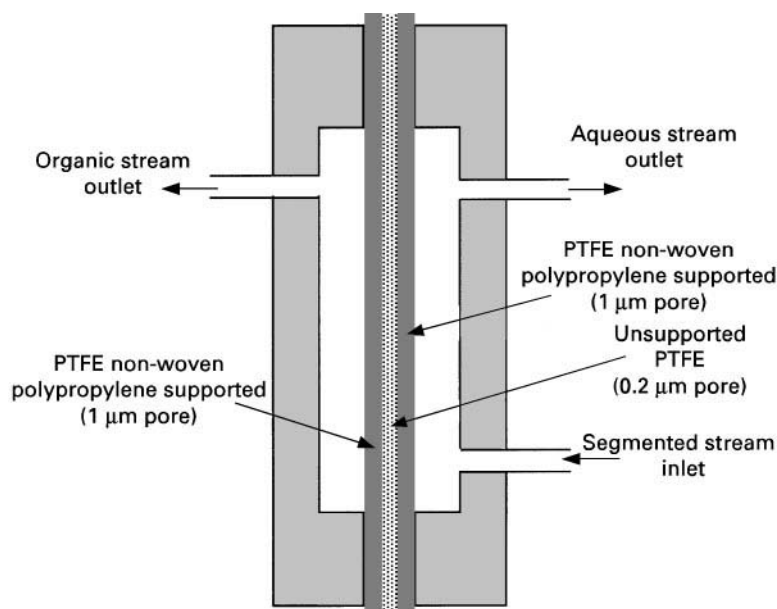


Figure 8 Diagram of a phase separator.

The extraction solvent flowed through a second column situated prior to the T piece to provide more pulse damping. The segmented mixture then passed through an extraction coil which provided the necessary time for the solutes to diffuse from the aqueous phase into the solvent. There is no parabolic velocity profile in segmented flow, and thus little or no peak dispersion can occur.

The segmented flow entered a phase separator and the separated solvent then passed through a UV absorption detector and into a spray jet assembly. Heated nitrogen was used in the spray jet assembly, to aid in the nebulization process. The chromatograms obtained indicate that very little peak dispersion occurs and that the column resolution is not significantly degraded. The finite volume of the extraction tube, however, produced a significant retention delay (about 3.5 min), which varied with both the flow rate and volume of the extraction system. Providing the solvents were reasonably volatile, they were completely removed in the nebulizing process. However, the percentage of organic solvent in the mobile phase must not be large enough to make it miscible with the methylene dichloride and prevent the formation of segmented flow. It follows that the choice of mobile phase was somewhat restricted.

Conclusion

Although considerable work has been applied to the development of LC/IR, it remains the least effective of all the LC tandem instruments. However, the IR

spectrum does provide unique information not readily available from other spectroscopic techniques and consequently, for the elucidation of certain molecular structures, can be extremely useful, if not essential. It would appear that, at this time, the transport interface will provide the highest sensitivity and the best spectra if sample availability is limited.

See also: II/Chromatography: Supercritical Fluid: Fourier Transform Infrared Spectrometry Detection.

Further Reading

- Brown RS and Taylor LT (1983) Microbore liquid chromatography with flow cell Fourier transform infrared spectrometric detection. *Analytical Chemistry* 55: 1492–1497.
- Conroy CM, Griffiths PR, Duff PJ and Azarraga LV (1984) Interface of a reversed-phase high-performance liquid chromatograph with a diffuse reflectance Fourier transform. *Analytical Chemistry* 56: 2636–2642.
- Gagel JJ and Bieman K (1986) Continuous recording of reflection-absorbance Fourier transform infrared spectra of the effluent of a microbore liquid chromatography. *Analytical Chemistry* 58: 2184–2189.
- Helgeth JW and Taylor LT (1987) Optimization of a flow cell interface for reversed-phase liquid chromatography/Fourier transform infrared spectrometry. *Analytical Chemistry* 59: 295–300.
- Jino K and Fujimoto C (1981) Combination of micro high performance liquid chromatography and Fourier transform infrared spectrometry using the potassium bromide crystal buffer memory technique. *Journal of High Resolution Chromatography* 4: 532–533.

- Johnson CC and Taylor LT (1984) Zero dead volume flow cell for microbore liquid chromatography with Fourier transform infrared spectrometric detection. *Analytical Chemistry* 56: 2642–2647.
- Johnson CC, Hellgeth JW and Taylor LT (1985) Reversed-phase liquid chromatography with Fourier transform infrared spectrometric detection using a flow cell interface. *Analytical Chemistry* 57: 610–615.
- Karmen A (1966) Flame ionization detector for liquid-liquid chromatography. *Analytical Chemistry* 38: 286–290.
- Kuehl D and Griffiths PR (1979) Novel approaches to interfacing a high performance liquid chromatograph with a Fourier transform infrared spectrometer. *Journal of Chromatographic Science* 17: 471–476.
- Raynor MW, Bartle KD, Davies IL, Williams A, Clifford AA, Chalmers JM and Cook DW (1988) Polymer additive characterization by capillary supercritical fluid chromatography/Fourier transform infrared microspectrometry. *Analytical Chemistry* 60: 427–433.
- Sabo M, Gross J, Wang J and Rosenberg IE (1985) On-line high-performance liquid chromatography/Fourier transform infrared spectrometry with normal and reverse phases using an attenuated total reflectance flow cell. *Analytical Chemistry* 57: 1822–1826.
- Scott RPW, Scott CG, Munroe M and Hess J Jr. (1974) A transport interface for LC/MS. *The Poisoned Patient: The Role of the Laboratory*, p. 395. New York: Elsevier.
- Somson GW, Hooijschuur EWJ, Goopijer C, Brinkman UATH and Velthorst NH (1996) Coupling of reversed-phase liquid column chromatography and Fourier transform infrared spectrometry using post column on-line extraction and solvent elimination. *Analytical Chemistry* 68: 746–752.

Detectors: Mass Spectrometry

M. R. Clench and L. W. Tetler,
Sheffield Hallam University, Sheffield, UK

Copyright © 2000 Academic Press

Introduction

Liquid chromatography (LC) can often separate complex mixtures but simple detectors (e.g. ultraviolet-visible UV/Vis) do not allow identification of the individual components. Comparison of retention data and spiking with known standards is normally required to provide evidence of composition but this may lead to erroneous results as absolute identification is not possible. Development of diode array detection has somewhat alleviated the problem but not removed it entirely. Absorbance requires the presence of a chromophore in the molecule and, as such, UV/vis spectra do not enable absolute identification but are frequently used to confirm identity through comparison of recorded spectra with reference spectra.

Mass spectrometry (MS) provides a unique means of determining the presence of a compound in a mixture by producing a mass spectrum which will aid or confirm its identification. The relative molar mass (RMM) and/or structurally important information may also be obtained from the mass spectrum.

The combination of a separation technique with MS provides a powerful instrumental method for the analytical scientist. Modern gas chromatography-mass spectrometry (GC-MS) instrumentation, having overcome the obstacles associated with coupling them to each other, has matured into an easy-to-use benchtop technique. The interfacing of high performance liquid chromatography (HPLC) with a mass

spectrometric detector (LC-MS) poses many problems, not least the different sample requirements of the respective instruments, i.e. liquid and vapour. The purpose of this article is to describe those interfaces that are most routinely used in LC-MS applications and, as such, will cover aspects of ionization methods and, to a lesser extent, mass analysers.

Background

The combination of HPLC and MS can be used as an offline technique, that is, fractions are collected and then a mass spectrum of each obtained. Much greater sensitivity, however, may be achieved by having an online interface, but this is much more difficult to achieve than with GC. The vapour flow in HPLC is much greater than in GC and there may be problems with electrical breakdown in high voltage instruments. HPLC may be operated in either normal or reversed-phase modes and the mobile-phase composition may be either isocratic or gradient. Different-sized columns are available (analytical, microbore and capillary), leading to a wide range of operational flow rates. The various possible configurations complicate the interfacing to MS.

The development of LC-MS has a history of more than 20 years and many interfaces have been reported, although only a small number have become commercially successful. Each method has its advantages and disadvantages (i.e. there is no universal interface). All facilitate the transition of analyte from solution into the gas phase with either simultaneous or sequential ionization. Those interfaces that have stood the test of time and are (or have been)

commercially available have relied on a particular ionization method and this presented limitations to the range of compounds that could be handled. Until the early 1980s, the mainstay ionization techniques were electron ionization (EI) and chemical ionization (CI), both of which required the sample to be in the vapour state. Development of LC-MS was slow, due to problems of matching vacuum requirements with liquid flow. Early interfaces utilized direct liquid introduction, usually after splitting the LC eluate. Thermal evaporation of the fraction of the liquid taken into the MS was followed by either EI or CI, with the reagent ions being generated from the solvent in the case of CI.

Of the many interfaces that have been reported, those most commonly employed in present applications are based on the following: particle beam (monodisperse aerosol generator interface for chromatography or MAGIC), continuous flow-fast atom bombardment (CF-FAB), thermospray and atmospheric pressure ionization.

Ion Formation

Particle Beam

The original particle beam interface was introduced by Willoughby and Browner in the mid-1980s using the acronym MAGIC. It relies on the nebulization of the chromatographic eluent followed by desolvation and then ionization of the resultant microparticles. A schematic of a typical particle beam interface is shown in Figure 1.

The initial nebulization of the eluent is accomplished with the aid of a dispersion gas (usually helium); thus a fine and homogeneous aerosol can be generated from mobile-phase flow rates ranging from 0.1 to 2.0 mL min⁻¹. Several designs of nebulizer are available, some utilizing heat or ultrasound in addition to a gas, to create the aerosol. The resultant mixture of gas and solvent droplets passes directly into a desolvation chamber where the droplets are converted into solvent-free particles before reaching the exit nozzle. To aid faster evaporation of solvent

molecules, the temperature of the chamber is maintained slightly above ambient. Momentum separation of the resultant stream of gas, solvent vapour and solute microparticles occurs between the desolvation chamber and the ion source. This is achieved by a series of skimmers placed in line with the nebulizer jet and exit nozzle. Differential pumping is effected in the regions between the skimmers. Expansion into the lower pressure regions leads to the formation of a high velocity jet of solute microparticles. Most of the helium and solvent vapours are removed in these lower pressure regions, leading to solute enrichment. The solid solute microparticles enter a conventional EI/CI ion source and are rapidly converted to the gas phase by flash vaporization upon contact with the heated walls of the source. Subsequent ionization by electron impact or chemical ionization follows.

The particle beam interface offers the advantage of producing library-searchable mass spectra but there are limitations of volatility and thermal stability for the analytes. In common with most LC interfaces for MS, the use of involatile buffers is best avoided, as is the use of mobile phases with a high water content. Disadvantages of the particle beam interface lie in the lack of sensitivity compared to other techniques which rely on 'soft ionization' methods, but careful optimization can lead to detection limits in the nanogram range for full scan acquisitions and use of selected ion monitoring can improve this to picograms. The development of particle beam interfaces capable of operating at lower flow rates would enable an increase in sensitivity to be achieved.

Continuous Flow-Fast Atom Bombardment

This technique relies on ionization of the sample by FAB. In a FAB ion source the sample is bombarded by a beam of energetic (usually 8 keV) atoms, resulting in the production of ions via the phenomenon of 'sputtering'. This process, although not fully understood, may be viewed as a series of impact cascades through the uppermost layers of the sample, resulting in the ejection of neutral and charged particles from the sample surface. Inert gases (Ar or Xe) are used to produce the atom beam but it is now more usual to employ a beam of fast ions, usually Cs⁺, with energies up to 30 keV. This latter method is also referred to as liquid secondary ionization mass spectrometry (LSIMS).

The sample material is deposited on the end of a direct inlet probe along with a viscous liquid (matrix). The matrix is necessary to prolong sample lifetime as mass spectra produced from solid samples are transient. Ideally the liquid matrix (e.g. glycerol, m-nitrobenzyl alcohol) should be capable of dissolving the sample molecules, be inert and have a low

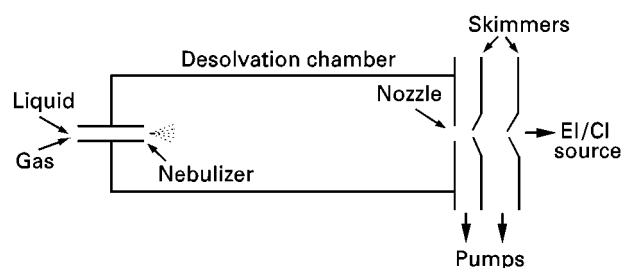


Figure 1 Simplified schematic of a particle beam interface.

vapour pressure. The ion source is normally operated at ambient temperatures and it is therefore possible to obtain mass spectra from thermally labile and/or involatile materials. Compounds of RMM up to 2 kDa are routinely analysed by FAB and it is possible to obtain mass spectra from larger molecules. FAB mass spectra generally show abundant ions of the type $(M + H)^+/(M - H)^-$, thus allowing RMM information. These even-electron species are relatively stable and there is not always sufficient fragmentation to be structurally informative. Chemical noise is often a problem in FAB mass spectra as it may obscure low intensity fragment ions, and peaks arising from the matrix may coincide with sample peaks, hindering interpretation.

CF-FAB (other variations are known as dynamic FAB or frit-FAB) employs either FAB or LSIMS to effect ionization. All rely on the introduction of liquid through a capillary that terminates at the end of a direct insertion probe (Figure 2). Different designs of probe tip have been developed but all require an even spread of liquid over the surface which allows the production of a stable sample ion current. The solution entering the ion source requires the presence of a matrix liquid, normally in the range 1–10% by volume, and this is usually introduced post-column for LC-MS applications. This reduction of the sample/matrix ratio may provide improved signal to chemical noise ratios and peaks associated with the matrix may be either absent or of low intensity. A reduction in the sample suppression effects observed in FAB may also result.

This is a very simple interface design and is applicable to many thermally labile and/or polar samples. The probe tip does require heating (up to 60–70°C) to maintain evaporation and prevent freezing due to latent heat of vaporisation. The prime disadvantage is the restriction imposed on flow rates which are in the

range 1–10 $\mu\text{L min}^{-1}$ and therefore a split in the column eluent is required for all but capillary columns. Splits may be achieved by a number of methods, involving the use of T-pieces, balanced columns and pneumatic splitters, either separately or in combination. Whatever method is employed, it should have low dead volume and provide a quick response to changes in solvent composition imposed by gradient elution.

Thermospray

Thermospray ionization is effected directly from a sample solution and may be readily interfaced with HPLC. The thermospray ion source, which was developed from direct liquid introduction interfaces, can accommodate a wide range of liquid flows (0.5–2.5 mL min^{-1}) but is limited to the use of volatile buffers. It is a soft ionization technique and produces mass spectra dominated by ions yielding RMM information, i.e. $(M + H)^+/(M - H)^-$, but modifications to the source have allowed a certain amount of controlled fragmentation to be induced.

The sample solution is carried into the source via a capillary tube which terminates in a heated block. This results in the formation of a supersonic jet of vapour which contains charged droplets, the charging of the droplets being aided by the presence of a volatile electrolyte (e.g. ammonium acetate). By a combination of ion evaporation and ion–molecule reactions, sample ions are formed and exit the source via a small sampling orifice. The excess solvent vapours are removed by a backing rotary pump. In those situations where it is not possible or desirable to add a volatile electrolyte to the mobile phase, ionization may be effected by a mechanism akin to CI. This is achieved either by use of an electron beam (often termed filament on) or by creating a plasma within the vapour-rich source, usually by a high voltage discharge from a needle – a technique sometimes referred to as a plasmaspray. A simple schematic of a thermospray source is shown in Figure 3.

A wide variety of compounds are amenable to thermospray but its ability to cope with large, non-volatile molecules is poor and the mass range appears to be limited for routine use to compounds below ~1500 Da. The operating temperatures of the source must satisfy the requirement of efficiently vaporizing the sample but without thermal degradation. Positive and negative ions are often formed with equal facility but, in general, basic compounds are best studied in the positive ion mode: negative ion operation is more sensitive for acidic molecules. Lack of knowledge with respect to proton affinities often means that the best ionization mode needs to be determined experimentally.

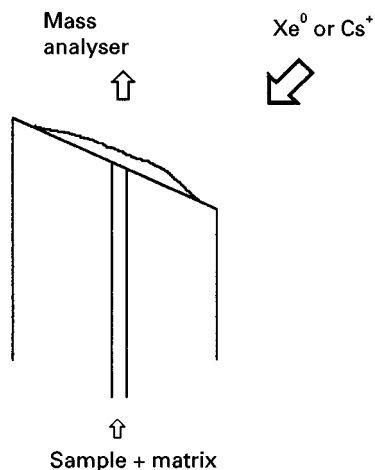


Figure 2 CF-FAB probe tip.

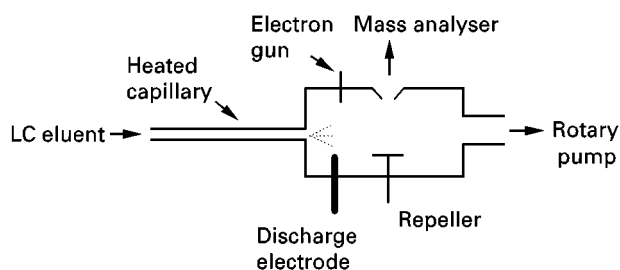


Figure 3 Simplified diagram of a thermospray ion source.

Lack of fragmentation is often observed in thermospray mass spectra but application of a higher voltage to a repeller electrode (located opposite the sampling cone) may be sufficient to induce the formation of fragment ions.

Criticisms of the technique have centred on the claims of poor reproducibility and compound dependence. The performance and optimization of the interface depend on the solution chemistry and solutions must be kept free of particulate matter that may lead to blockage of the capillary. Despite some disadvantages, many applications of thermospray have been described and it has been the mainstay for LC-MS development for a number of years. However, recent advances in alternative ionization methods may well see it superseded as the method of choice for LC-MS.

Atmospheric Pressure Ionization (API) Methods

In the sources so far described, ionization takes place in the vacuum region of the mass spectrometer, thus requiring removal, either through additional pumping or by a reduction in the flow rate of the mobile phase. The production of ions prior to entry to the MS high vacuum regions, i.e. at atmospheric pressure, would obviate these requirements. Development of atmospheric pressure ionization techniques has led to a rapid and exciting development in LC-MS instrumentation. Although API methods have been available for a number of years, it was not until the pioneering work of Fenn *et al.* that their potential was realized. The two variants normally employed in conjunction with HPLC are electrospray ionization (ESI) and atmospheric pressure chemical ionization (APCI).

Electrospray ionization ESI produces charged particles directly from solution at atmospheric pressure. Since its introduction in the mid-1980s it has developed into one of the most popular ionization techniques, especially for biomolecules. The source design is relatively simple and extraction of ions into the mass spectrometer is readily achieved. Although a variety of source designs have been developed and commercial instruments differ in this respect, the

basic processes of ion information and extraction are similar.

In its simplest form, ESI is realized from a sample solution (flow rate $2\text{--}10\ \mu\text{L min}^{-1}$) introduced through a capillary into the ion source, which is at atmospheric pressure. The emerging liquid is formed into a fine spray of charged droplets by the presence of a potential difference of $\pm 3\text{--}5\ \text{kV}$ applied between the capillary and a counter-electrode. The formation of gaseous ions from the sample solution occurs as a result of this droplet formation and subsequent desolvation. Formation of the charged droplets is reasonably well understood, but the process of ion formation from them is the subject of debate.

A typical source is shown in **Figure 4**.

The capillary delivering the liquid flow is contained, in a co-axial arrangement, within an outer stainless-steel capillary. A flow of gas through this outer capillary aids droplet formation and extends the usable flow rate up to $\sim 1.5\ \text{mL min}^{-1}$. Nitrogen is the usual nebulizing gas employed in this modification, sometimes referred to as ion spray. Beyond the counterelectrode is a sampling cone (or in some instruments this may be a short glass or steel capillary) which may be maintained at a low voltage ($\sim 30\text{--}250\ \text{V}$). Between this cone and the counterelectrode, a countercurrent flow of gas (usually nitrogen) is introduced. This gas, known as the drying or curtain gas, aids the desolvation process. Additionally, the source may be held at elevated temperatures ($\sim 60^\circ\text{C}$) as a further means of helping desolvation. Entry into the analyser region of the mass spectrometer proceeds via a skimmer held at ground potential. Stages of differential pumping (or cryopumping) reduce the source pressure (atmospheric) to that of the analyser ($\sim 10^{-5}\ \text{mmHg}$).

Electrospray is an extremely soft ionization technique and results in the formation of ions representa-

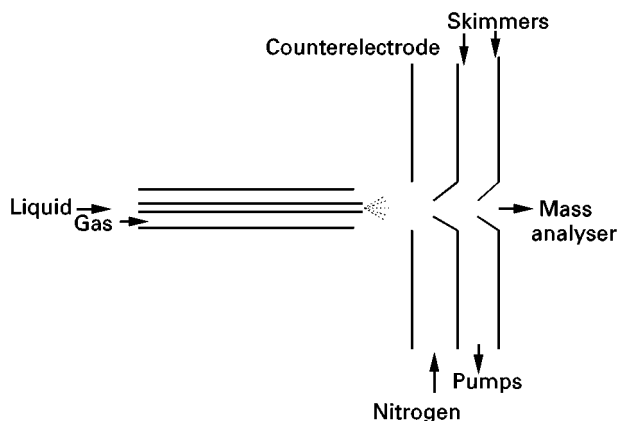


Figure 4 Ion source for electrospray ionization. For operation in APCI mode, a discharge needle would be placed between the inlet capillary and the counter-electrode.

tive of the intact molecule with virtually no fragmentation. For small molecules the mass spectra have a very simple appearance, generally showing just the protonated molecule ion and/or adduct ions, e.g. $(M + Na)^+$. The mass spectra of larger molecules, however, become more complicated because of the production of multiply charged ions. A series of molecule ions of the form $(M + nH^+)^{n+}$ is produced, where n varies according to the number of sites on the molecule which are able to accept a proton. The molecular mass of a compound is calculated from the ion series by a deconvolution algorithm contained in the instrument's software (though it can be done manually!). An example of a typical ESI spectrum and the result of deconvolution is shown in Figure 5.

Formation of negative ions occurs in electrospray, with both singly and multiply charged species being formed. The choice of ionization mode depends on the proton affinities of the analytes.

In addition to molecular weight information, ESI mass spectra may contain ions representative of both specific and nonspecific interactions that are noncovalent in nature. Fragmentation of intact molecule ions may be induced within the source region by manipulation of the cone voltage. The application of a voltage (up to 250 V) between the counter-electrode and the first sampling cone will lead to low energy collisions between sample ions and the curtain gas. Depending on the energy of these collisions, declustering and then fragmentation may occur.

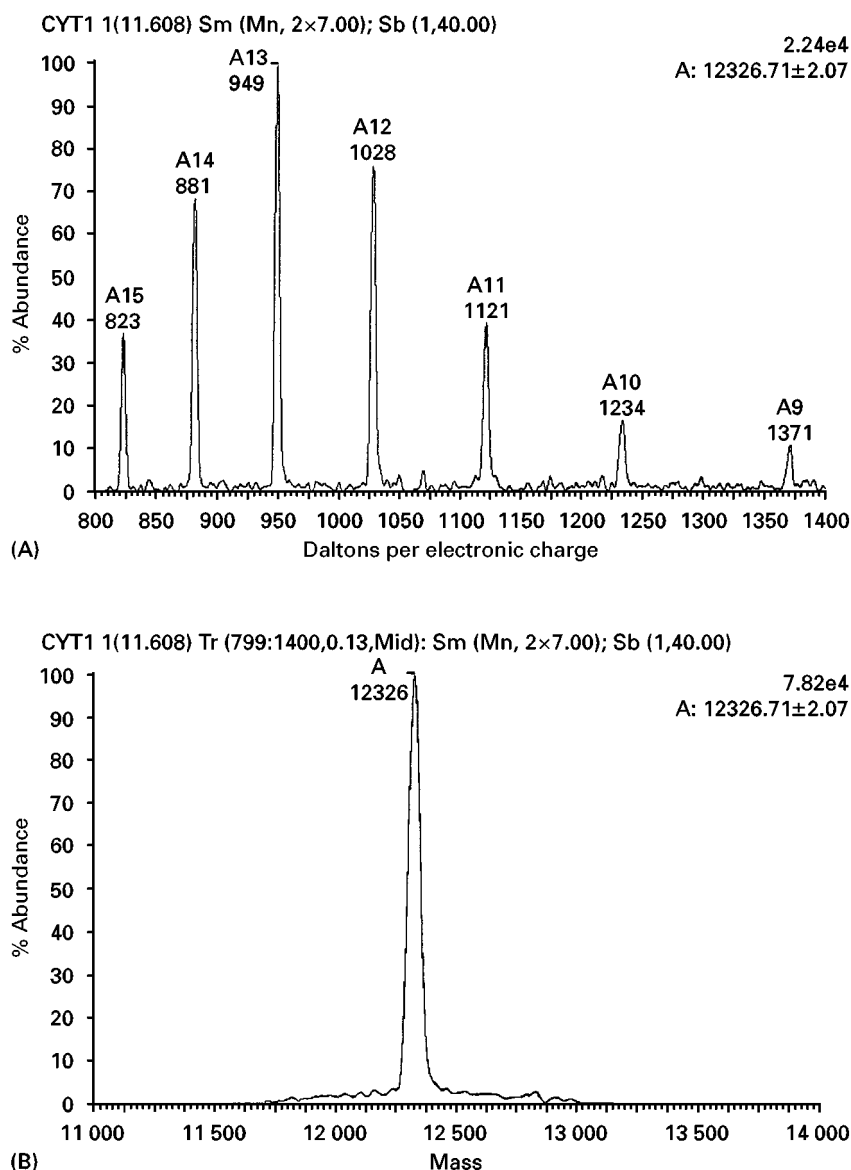


Figure 5 (A) ESI mass spectrum of cytochrome c; (B) deconvoluted mass spectrum of cytochrome c.

Since its introduction, ESI has undergone rapid development and has seen widespread application, especially in the biochemical field. Commercial instruments with dedicated ESI sources are readily available, ranging from simple benchtops to sophisticated tandem mass spectrometers.

The development of orthogonal sources has allowed the use of non-volatile buffers for LC-MS whereas 'in-line' sources are restricted to volatile buffers.

Atmospheric pressure chemical ionization An APCI source relies on the formation of reactant ions and their subsequent reaction with sample molecules. These reactant ions are formed at atmospheric pressure by a corona discharge achieved by maintaining a stainless-steel needle at a voltage of 3–6 kV. The source design for APCI, for LC-MS, is very similar to that of ESI, the major difference being the addition of the discharge needle in the region between inlet capillary and the counterelectrode. The LC eluent is converted into a fine droplet spray by a nebulizing gas and this is followed by vaporization in a heated region (up to 500°C, depending on the instrument) of the capillary. This rapid desolvation and vaporization minimizes any thermal decomposition. Chemical ionization of the sample is effected via ion molecule reactions: the reactant ions are formed from the LC mobile phase. Operation in either positive ion or negative ion mode is possible depending on the nature of the analyte. The use of a curtain gas aids declustering in a manner similar to electrospray. Molecular weight information is readily provided, but to obtain structural information the use of collision induced decomposition (CID) experiments is required.

Mobile phase flows from 0.1 to 2.0 mL min⁻¹ can be accommodated, eliminating the need for splitting. Both volatile and, with the advent of orthogonal sources, nonvolatile buffers are tolerated and mobile-phase compositions of up to 100% water are permitted.

Mass Analysis

All the above ionization techniques may be used in conjunction with different types of mass analyser, though the use of single or multistage quadrupoles is most common. The reader is referred to the chapter on GC-MS for a discussion of sector and quadrupole analysers.

Ion traps, time-of-flight and ion cyclotron resonance mass spectrometers have all been used in LC-MS instruments: a full treatment of them is beyond the scope of this article.

The ion trap is a device in which ions may be stored and consecutive experiments carried out upon them, i.e. mass spectrometry in time rather than space. Ions

may be produced directly in the trap, e.g. by EI (GC-MS) or they may be injected from an external source, e.g. ESI. Technological developments have ensured continued improvement to the mass range and resolution. The ability to undertake sequential CID experiments is a powerful feature of modern instruments. Dedicated LC-MS instruments employing ion traps in conjunction with ESI and APCI are now available.

Time-of-flight analysers are particularly well suited to pulsed ion sources, e.g. matrix-assisted laser desorption ionization (MALDI) and offer increased sensitivity over scanning instruments. Recently, pulsed orthogonal electrospray sources have been described in conjunction with time-of-flight.

The above method of mass analysis relies on the premise that, if ions of different masses leave the source at the same time, they will arrive at the detector separated in time. In practice, ions are accelerated into a field-free region (drift tube) with up to 20 keV energy. If all ions have the same kinetic energy then their velocity is dependent on their mass; thus, their time of arrival at the detector is different (light ions first). A pulse of ions is generated and the time taken for each ion to arrive at the detector is measured. Sophisticated electronics is required to measure these times accurately; in addition, a method of obtaining the start time is required. Ionization techniques capable of being pulsed are used, e.g. plasma desorption, laser desorption, atom/ion guns – these produce packets of ions with each pulse. Orthogonal instruments are now being developed which will allow the use of continuous ion sources such as electrospray (a simplified schematic is depicted in Figure 6). Traditionally, the resolution of time-of-flight analysers was considered to be low but modern instruments are capable of resolving powers up to 10 000. They have high transmission and are thus capable of high sensitivity; in addition they have a very high mass range. With the introduction of MALDI they have undergone a renaissance and continue to be developed. Commercial instruments interfaced to electrospray have recently been announced.

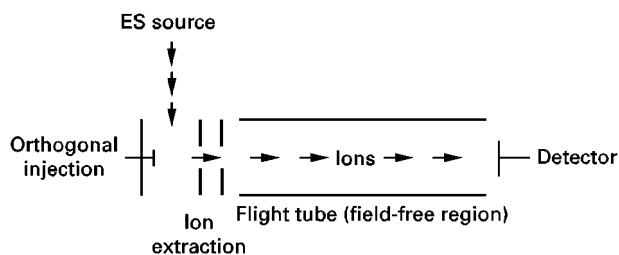


Figure 6 Schematic of a time-of-flight mass analyser with an orthogonal ESI source.

Instruments relying on ion cyclotron resonance (ICR) employ Fourier transform techniques and FT-ICR mass spectrometers are capable of achieving very high resolution. They require low pressures (\sim UHV) to operate effectively and the magnetic fields used are generated by super-conducting magnets. Ions, which may be formed directly within the ICR cell or injected from an external source (e.g. ESI, MALDI), are excited using a broad-band radiofrequency sweep and their cyclical motion induces an image current. This time domain signal is readily transformed to a mass spectrum by a Fourier transform. The very high resolution obtainable from this method of mass analysis enables separation of the isotopic peaks for each of the charge states resulting from ESI. This offers an advantage in the assignment of values of m and z in ESI mass spectra containing several masses.

Tandem Mass Spectrometry

Of the ionization techniques described, only the particle beam method produces sufficient fragmentation to give structural information. The softer ionization methods allow for RMM determination from either protonated molecule ions and/or adduct species, with little or no structural information being available owing to lack of fragmentation. It is possible to induce some degree of fragmentation in both thermospray and API sources by manipulating the source conditions. A more specific means of promoting fragmentation involves the use of sequential mass analysis, i.e. the isolation of a precursor ion followed by its interaction with a target gas to induce fragmentation by collisional activation, thus allowing a product ion mass spectrum to be recorded. This and other types of CID experiments can be carried out in time, in an ion storage device or in space using scanning or time-of-flight instruments. For a full discussion of the instruments and experiments possible, the reader is referred to the Further Reading section.

The most commonly used type of tandem mass spectrometer is the triple quadrupole, and benchtop instruments of this type with a dedicated LC interface are commercially available. They are relatively easy to use and offer a range of MS-MS scans. In addition to the product ion scan and the reaction monitoring scan (both MS1 and MS2 operate in selected ion mode), two other scan modes are available – precursor ion and constant neutral loss. In the former, MS1 is scanned whilst MS2 is set to pass a specific ion, thus yielding information as to the origins of a specific fragment ion. This may be employed to identify those components of a mixture which contain a common functional group, e.g. sulfonated compounds will typically fragment to give an ion at m/z 80 (SO_3^-) in negative ion mode; thus a precursor ion scan of this

ion should be specific for the presence of sulfonates. Neutral loss scans involve scanning both MS1 and MS2, but with the respective mass ranges offset by the mass of the neutral species.

Conclusion

This article has attempted to review the present situation with regards to the interfacing of LC to MS. LC-MS is now developing into a mature technique and modern instrumentation allows for routine and robust operation. Further developments will undoubtedly take place, with API and PB techniques to the forefront. The introduction of cheaper and easier-to-use benchtop instruments will promote continued expansion in the applications of this extremely powerful analytical method.

See also: III/Drugs and Metabolites: Liquid Chromatography–Mass Spectrometry. *Pharmaceuticals:* Chromatographic Separations.

Further Reading

- Bruins AP (1998) Mechanistic aspects of electrospray ionisation. *Journal of Chromatography A* 794: 345.
- Busch KL, Glish GL and McLuckey SA (1988) *Mass Spectrometry/Mass Spectrometry*. New York: VCH
- Cappiello A (1996) Is particle beam an up-to-date LC-MS interface. *Mass Spectrometry Reviews* 15: 283.
- Chapman JR (1993) *Practical Organic Mass Spectrometry* 2nd edn. Chichester: John Wiley.
- Chernushevich IV, Ens W and Standing KG (1999) Orthogonal-injection TOFMS for analysing biomolecules. *Analytical Chemistry* 71: 453A.
- Cole RB (ed.) (1997) *Electrospray Ionisation Mass Spectrometry: Fundamentals, Instrumentation and Applications*. New York: Wiley-Interscience.
- Fenn JB, Mann M, Meng CK and Wong SF (1990) Electrospray ionisation – principles and practice. *Mass Spectrometry Reviews* 9: 37.
- Matsuo T, Caprioli RM, Gross ML and Seyama Y (eds.) (1994) *Biological Mass Spectrometry: Present and Future*. Chichester: John Wiley.
- Niessen WMA (1998) Advances in instrumentation in liquid chromatography-mass spectrometry and related liquid-introduction Techniques. *Journal of Chromatography A* 794: 407.
- Niessen WMA, Tjaden UR and Van Der Greef J (1991) Strategies in developing interfaces for coupling liquid-chromatography and mass-spectrometry. *Journal of Chromatography* 554: 3.
- Willoughby RC and Browner RF (1984) Monodisperse aerosol generation interface for combining liquid-chromatography with mass spectroscopy. *Analytical Chemistry* 56: 2626.
- Willoughby R, Sheehan E and Mitrovich S (1998) *A Global View of LC-MS*. Pittsburgh: Global View.
- Yergey AL, Edmonds LG, Lewis IA and Vestal ML (1990) *Liquid Chromatography/Mass Spectrometry. Technique and Applications*. New York: Plenum Press.

Detectors: Refractive Index Detectors

R. P. W. Scott, Avon, CT, USA

Copyright © 2000 Academic Press

Introduction

The refractive index detector is a bulk property detector. A bulk property detector responds to some physical property of the total column eluent and not some specific property of the solute. Bulk property detectors have an inherently limited sensitivity, irrespective of the instrumental technique used. Consider a hypothetical bulk property detector that is to monitor the density of the column eluent. Assume it is required to detect the concentration of a dense material, such as carbon tetrachloride (specific gravity 1.595), at a level of $1 \mu\text{g mL}^{-1}$ in *n*-heptane (specific gravity 0.684).

This situation will be particularly favourable for this hypothetical detector, as the solute to be sensed exhibits a large difference in density from that of the solvent. Let the change in density resulting from the presence of the solute at a concentration of 10^{-6}g mL^{-1} be Δd . It follows that, to a first approximation:

$$\Delta d = \frac{X_s(d_1 - d_2)}{d_1} \quad [1]$$

where d_1 is the density of the solute, carbon tetrachloride, d_2 is the density of the mobile phase, *n*-heptane, and X_s is the concentration of the solute to be detected.

Thus, for the example given:

$$\Delta d = \frac{(1.595 - 0.684) \times 10^{-6}}{1.59} = 5.71 \times 10^{-7} \quad [2]$$

Now the coefficient of cubical expansion of *n*-heptane is approximately 1.6×10^{-3} per $^{\circ}\text{C}$. Thus, the temperature, ΔT , that would produce a change in density equivalent to the presence of carbon tetrachloride at a concentration of 10^{-6}g mL^{-1} can be calculated.

It follows that:

$$\begin{aligned} \Delta T &= \frac{5.71 \times 10^{-7}}{1.6 \times 10^{-3}} ^{\circ}\text{C} \\ &= 3.6 \times 10^{-4} ^{\circ}\text{C} \end{aligned} \quad [3]$$

Assuming that a concentration of one part per million carbon tetrachloride is just detectable (it provides a signal-to-noise ratio of 2), then the temperature fluctuations must be maintained below $1.8 \times 10^{-4} ^{\circ}\text{C}$ to achieve this sensitivity. In practice, such temperature stability would be extremely difficult to maintain and thus the temperature control can severely limit the sensitivity obtainable from such a detector. Even the heat of adsorption and desorption of the solute to and from the stationary phase can easily result in temperature changes of this order of magnitude. The density of the contents of the cell will also change with pressure and, if there is a significant pressure drop across the cell, with flow rate. These restrictions apply to all bulk property detectors and so all bulk property detectors will have a limited sensitivity determined by the stability of the ambient conditions. This limit of detection is probably around 10^{-6}g mL^{-1} .

The refractive index detector was one of the first online detectors to be developed and was described by Tiselius and Claesson in 1942. It was also one of the first online liquid chromatography (LC) detectors to be made commercially for general use. The refractive index detector is probably the least sensitive of the commonly used LC detectors. Its major disadvantage (as already discussed) is its sensitivity to changes in ambient conditions, such as temperature, pressure and flow rate. Another handicap is that it cannot be used for gradient elution, due to the continuous change in mobile-phase refractive index that results from the change in solvent composition. Nevertheless, as the refractive index detector has a universal response, it can be extremely useful for detecting those compounds that are nonionic, do not absorb in the UV and do not fluoresce (e.g. aliphatic alcohols, fatty acids, ethers, etc.).

When a monochromatic ray of light passes from one isotropic medium, A, to another, B, it changes its velocity and direction. The change in direction is called the refraction, and the relationship between the angle of incidence and the angle of refraction is given by Snell's law:

$$n'_B = \frac{n_B}{n_A} = \frac{\sin(i)}{\sin(r)} \quad [4]$$

where i is the angle of incident light in medium A, r is the angle of refractive light in medium B, n_A is the refractive index of medium A, n_B is the refractive index of medium B and n'_B is the refractive index of medium B relative to that of medium A.

Refractive index is a dimensionless constant that normally decreases with increasing temperature; values given in the literature are usually quoted at 20°C or 25°C, the actual measurement taken as the mean value for the two sodium lines. If a cell takes the form of a hollow prism through which the mobile phase flows, a ray of light passing through the prism will be deviated from its original path. If the light is focused on to a photocell the output will change as the refractive index of the mobile phase in the cell changes. This method of monitoring refractive index is called the angle of deviation method and has been used by a number of manufacturers in their detector design.

The modern refractive index detector is the result of considerable research which has been extended by the research and development laboratories of many instrument companies. A diagram of a simple refractive index detector based on the angle of deviation method measurement is shown in **Figure 1**. A beam of light from an incandescent lamp passes through an optical mask that confines the beam to the region of the cell. The lens collimates the light beam, which passes through both the sample and reference cells to a plane mirror. The mirror reflects the beam back through the sample and reference cells to a lens, which focuses it on to a photocell.

The location of the beam, rather than its intensity, is determined by the angular deflection of the beam caused by the difference in refractive index between the contents of the two cells. As the beam changes its position of focus on the photoelectric cell, the output changes and the resulting difference signal is electronically modified to provide a signal proportional to the concentration of solute in the sample cell.

An alternative method of refractive index measurement, the Fresnel method, has also been used in the design of commercially fabricated detectors. The two different systems provide comparable performance with respect to sensitivity and linearity, and mostly differ in the manufacturing techniques used to construct the instruments. The relationship between the reflectance from an interface between two transparent media, and their respective refractive indices, is given by Fresnel's equation:

$$R = \frac{1}{2} \left[\frac{\sin^2(i - r)}{\sin^2(i + r)} + \frac{\tan^2(i - r)}{\tan^2(i + r)} \right] \quad [5]$$

where R is the ratio of the intensity of the reflected light to that of the incident light and the other symbols have the meanings previously assigned to them. Now:

$$\frac{\sin(i)}{\sin(r)} = \frac{n_1}{n_2} \quad [6]$$

where n_1 is the refractive index of medium 1 and n_2 is the refractive index of medium 2.

Consequently, if medium 2 represents the liquid eluted from the column, then any change in n_2 will result in a change in R and thus the measurement of R could determine changes in n_2 resulting from the presence of a solute. Conlon utilized this principle to develop a practical refractive index detector. His device, now obsolete, illustrates the principle of the Fresnel method very simply (**Figure 2**).

The sensing element consists of a rod prism sealed into a tube through which the solvent flows. The rod prism is made from a glass rod 6.8 mm in diameter

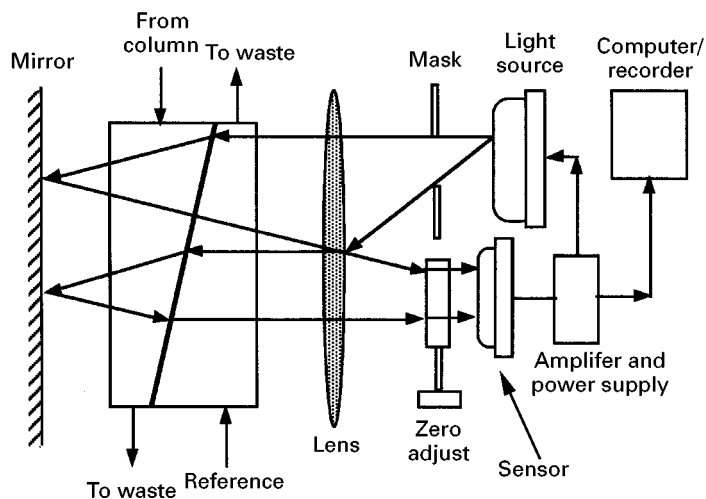


Figure 1 The refractive index detector based on the angle of deviation method of measurement. (Courtesy of Waters Chromatography.)

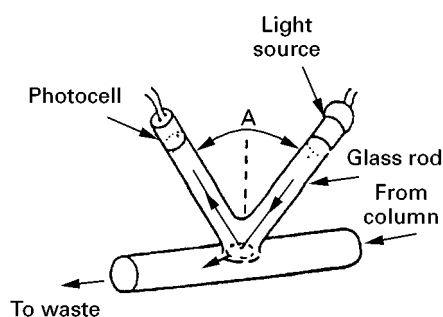


Figure 2 Early detector based on the Fresnel method of refractive index measurement.

and 10 cm long, bent to the correct optical angle (just a little less than the critical angle) and an optical flat is ground on the apex of the bend, as shown in Figure 2. The optical flat is then sealed into the window of a suitable tube that acts as a flow-through cell. The photocell is arranged to be one arm of a Wheatstone bridge and a reference photocell (not shown) monitoring light direct from the cell is situated in another arm of the bridge.

This detector was never manufactured as it had too large a cell volume and limited sensitivity. However, it was one of the first refractive index detectors to work on the Fresnel principle. A commercial refractive index detector that works on this principle is shown in Figure 3.

Light from a tungsten lamp is directed, through an infrared filter to prevent heating the cell, to a magnifying assembly that also splits the beam into two. The two beams are focused through the sample and reference cells respectively. Light refracted from the mobile phase/prism surface passes through the prism assembly and is then focused on two photocells. The

prism assembly also reflects light to a user port where the surface of the prism can be observed. The output from the two photocells is electronically processed and either passed to a potentiometric recorder or a computer data acquisition system.

The range of refractive index covered by the instrument for a given prism is limited and consequently three different prisms are made available to cover the refractive index ranges of 1.35–1.4, 1.41–1.44 and 1.40–1.55 respectively. An example of the separation of a series of polystyrene standards monitored by the detector is shown in Figure 4. The separation was carried out by size exclusion on a column packed with 5 μm particles operated at a flow rate of 0.8 mL min^{-1} .

The Christiansen Effect Detector

This method of measuring refractive index arose from the work of Christiansen on crystal filters. If a cell is packed with particulate material having the same refractive index as the mobile phase passing through it, light will be transmitted through the cell with little or no refraction or scattering. If, however, the refractive index of the mobile phase changes, there will be a refractive index difference between the mobile phase and that of the packing. This difference will result in light being refracted away from the incident beam and thus reduce the intensity of the transmitted light. If the transmitted light is focused on to a photocell, and the refractive index of the packing and mobile phase initially matched, then any change in refractive index resulting from the elution of a solute peak will cause light scattering. This scattering will reduce the intensity of the light falling on the sample photocell and thus provide a differential output relative to that of the reference cell.

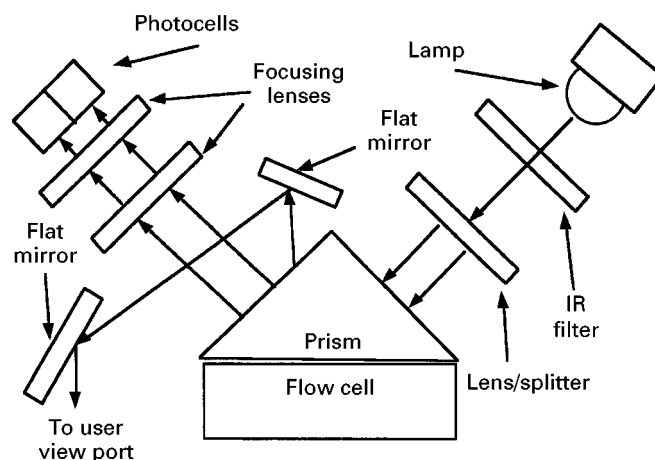


Figure 3 Diagram of the optical system of a refractive index detector operating on the Fresnel principle. (Courtesy of Perkin Elmer.)

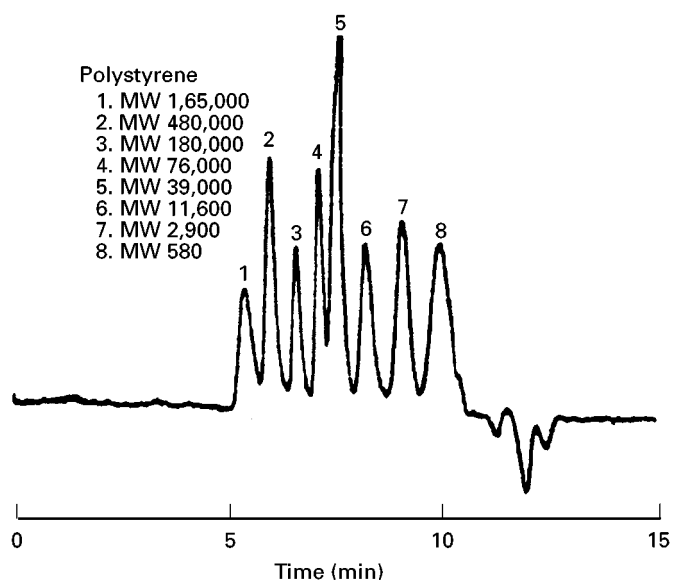


Figure 4 Separation of some polystyrene standards using a refractive index detector operating on the Fresnel principle. (Courtesy of Perkin Elmer.)

As the optical dispersions of the media are likely to differ, the refractive indices of the packing and the solvent will only match at one particular wavelength. Consequently, the fully transmitted light will be largely monochromatic. Light of other wavelengths will be proportionally dispersed depending on their difference from the wavelength at which the two media have the same optical dispersion. It follows that a change in refractive index of the mobile phase will change both the intensity of the transmitted light and its wavelength content.

A Christiansen detector is shown in **Figure 5**. The optical module contains a prefocused lamp, the voltage of which is adjustable to allow operation at low energy when the maximum sensitivity is not required. The condensing lens, aperture, achromat and beam-splitting prisms are mounted in a single tube to prevent contamination from dust and permit easy optical alignment. The system has two identical and interchangeable cells. The disadvantage of this detector is that the cells must be changed when alternative mobile phases are used in order to have a packing with

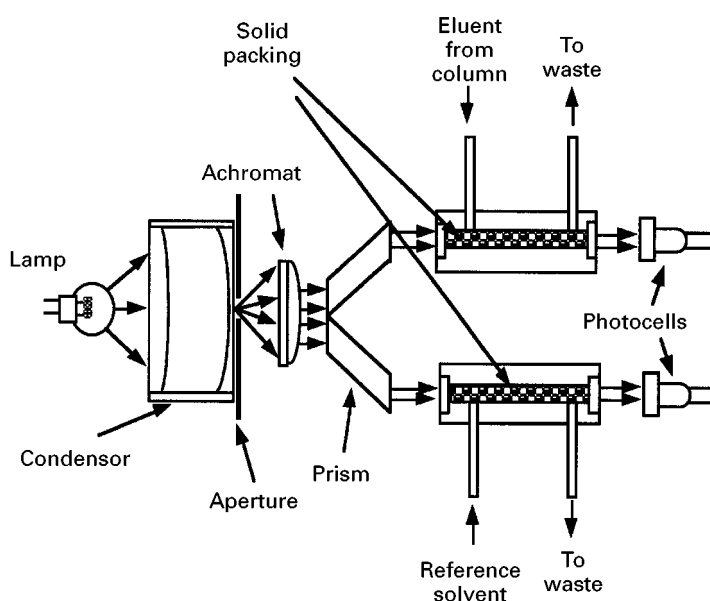


Figure 5 The Christiansen effect detector.

the appropriate refractive index. Close matching of the refractive indices of the cell packing and the mobile phase can be achieved by using mixed solvents.

Solvent mixing can usually be achieved without significantly affecting the chromatography distribution system, e.g. a small proportion of *n*-heptane in a mixture can be replaced with either *n*-hexane or *n*-octane either to increase or decrease the refractive index. The limitations inherent in this type of refractive index measurement, taken in combination with general disadvantages of the refractive index detector *per se*, have prevented this detector becoming very popular. This device has been claimed to have a sensitivity of 1×10^{-6} refractive index (RI) units. This would be equivalent to a sensitivity of 9×10^{-6} g mL⁻¹ of benzene (RI = 1.501) eluted in *n*-heptane (RI = 1.388). The cell was designed to have a minimum volume of 8 μ L, which is slightly large for modern sensors, but small enough to work well with normal 4.6 mm i.d. columns. Different cells packed with appropriate materials were necessary to cover the refractive index range of 1.31–1.60.

The Interferometer Detector

The interferometer detector was first developed by Bakken and Stenberg in 1971. The detector responds to the change in the effective path length of a beam of light passing through a cell, when the refractive index of its contents changes, due to the presence of an eluted solute. If the light transmitted through the cell is focused on a photocell coincident with a reference beam of light from the same source, interference fringes will be produced. These fringes will change, as the pathlength of one light beam changes with reference to the other. Consequently, as the concentration of solute increases in the sensor cell, a series of electrical pulses will be generated as each fringe passes the photocell.

The effective optical path length (d) depends on the change in refractive index (Δn), and the path length (l) of the sensor cell:

$$d = \Delta n l \quad [7]$$

It is possible to calculate the number of fringes (N : sensitivity) which move past a given point (or the number of cyclic changes of the central portion of the fringe pattern) in relation to the change in refractive index by the equation:

$$N = \frac{2\Delta n l}{\lambda} \quad [8]$$

where λ is the wavelength of the light employed.

As N increases for a given refractive index change, Δn , so will the detector sensitivity. Therefore l should be made as large as possible commensurate with the chromatographic properties of the system. The simple optical system originally employed by Bakken and Stenberg is shown in Figure 6. Light from a source strikes a half-silvered mirror and is divided into two paths. Part of the beam is reflected by a plane mirror back along the same path and on to a photocell. The other part of the beam passes through the sensor cell to a plane mirror, where it is reflected back again through the sensor cell to the half-silvered mirror that reflects it on to the photocell where interference takes place with the other half of the light beam.

The number of fringes that pass the sensor will be directly proportional to the total change in refractive index, which will be proportional to the total amount of solute present. Although it establishes the technical viability of the system, the apparatus has limited use, but it has been developed into a practical instrument and an example is that developed by Wyatt Technology. The optical system of the Optilab interference detector is shown in Figure 7.

Light from an appropriate source is linearly polarized at -45° to the horizontal plane. Horizontal and vertical polarized light beams are produced and, on passing through the Wollaston prism, one passes through the sample cell and the other through the reference cell. The beam passing through the sample cell is horizontally polarized and that through the reference cell is vertically polarized. After passing through the cells, the beams are focused on a second Wollaston prism and then through a quarter-wave plate which has its fast axis set -45° to the horizontal plane.

A beam that is linearly polarized in the fast-axis plane will, after passing through the plate, lead another linearly polarized, but orthogonal, beam by a quarter of a wavelength. The phase difference results in a circularly polarized beam. It can be assumed that each of the beams focused on the Wollaston prism consists of two such perpendicular beams which, after the quarter-wave plate, result in two circularly polarized beams of opposite rotation. These beams will interfere with each other to yield the original linearly polarized beam. A second polarizer is placed at an angle $(90 - \beta)$ to the first (for the significance of β , see below), allowing about 35% of the signal to reach the photocell. A filter-transmitting light at 546 nm precedes the photocell.

If the sample cell contains a higher concentration of solute than the reference cell, in general the refractive index will be higher and the interfering beams will be out of phase. The refractive index difference (Δn) and

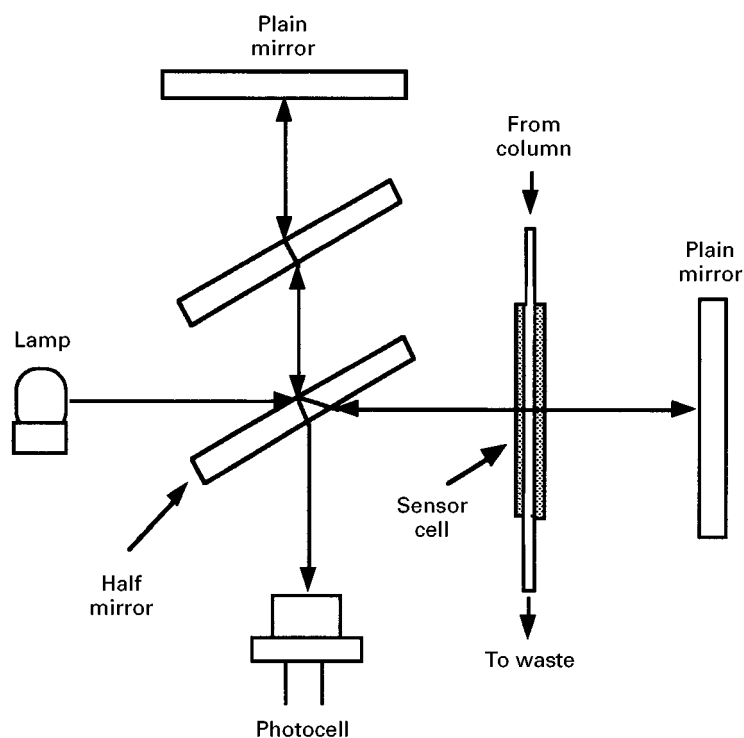


Figure 6 The original optical system used by Bakken and Stenberg in their interferometer detector.

the phase difference (Δp) are related by:

$$\Delta p = \frac{2\pi L \Delta n}{\lambda} \quad [9]$$

$\Delta p/2$ rad, and the amplitude of the light striking the photocell (A_p) will be given by:

$$A_p = A_0 \cos\left(90 - \beta - \frac{\Delta p}{2}\right) = A_0 \cos\left(\beta - \frac{\Delta p}{2}\right) \quad [10]$$

where L is the length of the cell and λ is the wavelength of the light.

The circularly polarized beams will interfere to yield a linearly polarized beam which is rotated

The smallest cell (1.4 μL : a cell volume that would be suitable for use with microbore columns) is re-

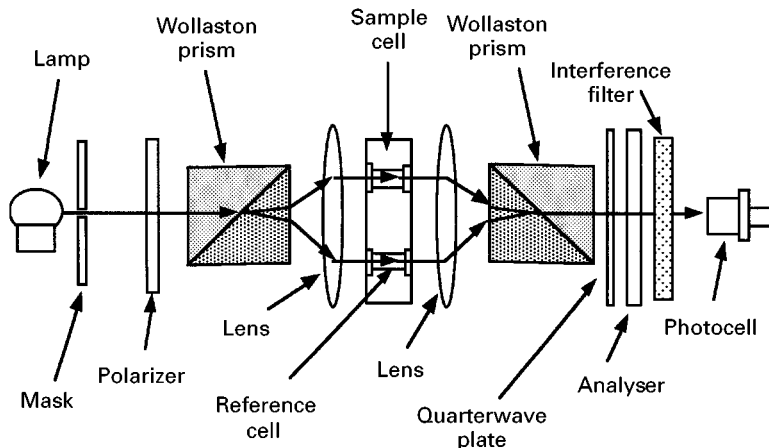


Figure 7 The Optilab interference refractometer detector.

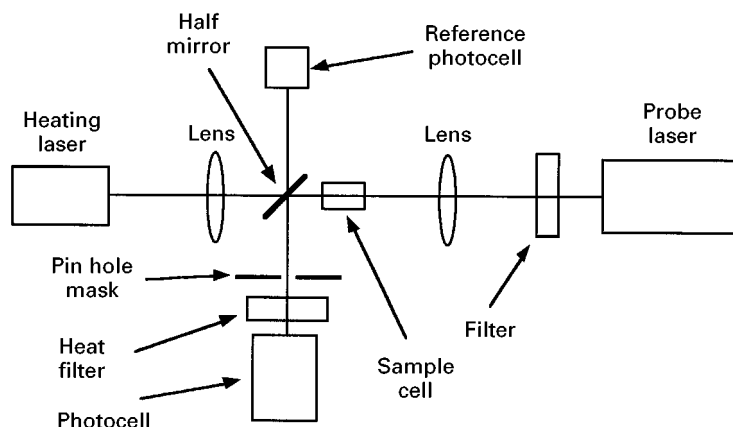


Figure 8 The layout of a thermal lens detector.

ported to give a sensitivity of about 2×10^{-7} RI units at a signal-to-noise ratio of 2. Consequently, for benzene (RI = 1.501) sensed as a solute in *n*-heptane (RI = 1.388), this sensitivity represents a minimum detectable concentration of $5.6 \times 10^{-5} \text{ g mL}^{-1}$. The alternative $7 \mu\text{L}$ cell would decrease the minimum detectable concentration to about $1 \times 10^{-6} \text{ g mL}^{-1}$, similar to that obtained for other refractive index detectors. However, this cell volume is slightly large for modern high efficiency columns.

The Thermal Lens Detector

There are a number of detectors that have been developed that are not classed as refractive index detectors, but their response is either based directly on refractive index measurement, or a function of some physical property of the mobile-phase system that is related to the refractive index. One such example of these is the thermal lens detector.

When a laser is focused on to an absorbing substance, the refractive index may be changed and modify the medium in such a way that it behaves as a lens. This phenomenon was first reported by Gorden *et al.* in 1964 and subsequently the effect has been examined by a number of workers. The formation of the thermal lens is caused by the absorption of laser light which may be extremely weak. The excited-state molecules subsequently decay to the ground state, with a resulting localized temperature increase in the sample. As the refractive index of the medium depends on the temperature, the spatial variation of the refractive index in the medium produces the phenomenon which appears to be equivalent to the formation of a lens within the medium. The temperature coefficient of refractive index is, for most liquids, negative; consequently, the insertion of a liquid in the laser beam produces a concave lens that results in beam divergence. The thermal lens effect has been used

by Buffet and Momis to develop a small volume detector. Their system is shown in **Figure 8**.

The device consists of a heating laser, from which light is passed directly through the sample via two lenses and a half mirror. Another laser, the probe laser, passes light in the opposite direction, through one lens, then through the sample to the half mirror where the light is reflected on to a photocell. Between the mirror and the photocell is a filter to remove the heating laser light and a small pinhole aperture. When an absorbing solute arrives in the cell, a thermal lens is produced which causes the probe light to diverge, and consequently the intensity of the light passing through the pinhole and on to the photocell is reduced. The cell can be made a few microlitres in volume and would thus be suitable for use with microbore columns. A sensitivity of 10^{-6} AU (the expected limiting sensitivity of a bulk property detector) was claimed for the detector and a linear dynamic range of about three orders of magnitude.

The use of two lasers adds significantly to the cost of the device. Basically, the thermal lens detector is a special form of the refractive index detector and as a consequence can be considered as a type of universal detector. However, it cannot be used with gradient elution or flow programming and its sensitivity is no better than other refractive index detectors.

Conclusion

Despite the refractive index detector being the oldest and least sensitive of all the LC detectors, its use survives, and will continue to survive, due to its universal response. All other LC detectors that are in use have sensors that only respond to certain types of solutes and therefore are restricted to specific sample types. At any time a new type of cathodic detecting system might be devised, but

after 30 years of detector development, only the evaporative light-scattering detector has offered any viable alternative. As a consequence, the future of the refractive index detector for specific applications still appears assured. In most applications an isocratic development procedure can be found that will provide satisfactory resolution of those solutes of interest, and so the problem of gradient elution can be circumvented. In addition, by using columns of 4.6 mm i.d. or more, the limited sensitivity of the refractive index detector can also be accommodated.

Further Reading

- Parriott D (1993) *A Practical Guide to HPLC Detection*. San Diego: Academic Press.
- Patonay G (1992) *HPLC Detector*. Newer Methods. New York: VCH.
- Scott RPW (1996) *Chromatography Detectors*. New York: Marcel Dekker.
- Vickrey TM (ed.) (1983) *Liquid Chromatography Detectors*. New York: Marcel Dekker.
- Yeung ES (ed.) (1986) *Detectors for Liquid Chromatography*. New York: Wiley.

Detectors: UV/Visible Detection

R. P. W. Scott, Avon, CT, USA

Copyright © 2000 Academic Press

The UV absorption detector, introduced in the early 1960s, was the first high sensitivity liquid chromatography detector to be developed. UV absorption detectors are considered to be those detectors that can sense substances that absorb light over the wavelength range 180–350 nm. Many compounds absorb light in this range, including those substances having one or more double bonds (π electrons) and those that have unshared (unbonded) electrons, e.g. all olefins, all aromatics and compounds, for example, containing $>C=O$, $>C=S$ and $-N=N-$ groups. As a result, providing the wavelength of the incident light can be selected, the UV detector tends to perform as a universal detector. There are exceptions: the UV detector will not readily detect hydrocarbons, aliphatic alcohols or other substances that do not have a UV chromophore that will absorb light in the wavelength range already defined.

The sensor cell consists of a short cylindrical tube having two terminating flat quartz windows and radial connections at either end for the column eluent to enter and to leave. To reduce band dispersion, the volume of the cell is usually limited to between 2 and 5 μ L. The UV light passes axially through the end windows and falls on a photoelectric cell (or array), the output from which is conveyed to an appropriate amplifier and thence to a recorder or data acquisition system.

The cell must be carefully designed to reduce peak dispersion that would result from the natural parabolic velocity profile of the mobile phase as it passes through the cell. A diagram of a typical UV absorption sensor cell is shown in Figure 1. The inlet and outlet conduits are designed to produce secondary flow and break up the parabolic velocity profile that

causes peak dispersion. Mobile phase enters the cell at an angle, and is directed at the cell window. As a consequence, the stream of mobile phase must virtually reverse its direction to pass through the cell, producing a strong radial flow which disrupts the Newtonian flow.

The same situation is arranged to occur at the exit end of the cell. The flow along the axis of the cell must reverse its direction to pass out of the port that is set at an angle to accomplish the same effect. By employing this type of cell geometry, dispersion in the cell resulting from viscous flow can be practically eliminated.

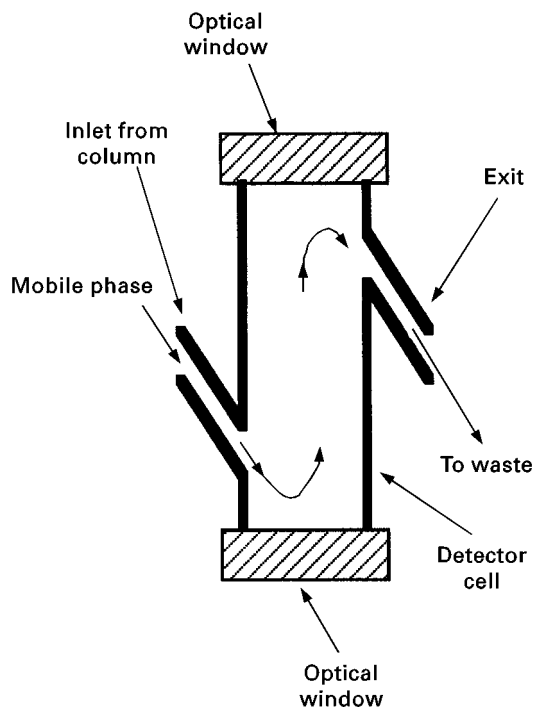


Figure 1 A simple UV detector sensor cell.

The relationship between the intensity of UV light transmitted through a cell (I_T) and the concentration of solute in it (c) is given by Beer's law:

$$I_T = I_0 e^{-\epsilon l c} \quad \text{or} \quad \ln(I_T) = \ln(I_0) - \epsilon c l \quad [1]$$

where I_0 is the intensity of the light entering the cell, l is the path length of the cell, and ϵ is the molar extinction coefficient of the solute for the specific wavelength of the UV light.

If eqn [1] is put in the form:

$$I_T = I_0 10^{-\epsilon l c} \quad [2]$$

The sensitivity of the detector is directly proportional to the value of the absorption coefficient and the path length of the cell. Thus, the sensitivity of the detector can be increased by increasing the path length. However, the volume of the cell must also be constrained to avoid more than a small fraction of a peak existing in the cell at any one time (this can cause peak dispersion and, at the extreme, when two peaks exist in the tube, peak merging). Consequently, as the length is increased, the radius must be reduced, which will increase the detector noise and cause a reduction in sensitivity. Thus, increasing the detector sensitivity by increasing the path length has limitations, and a well-designed cell involves a careful compromise between cell radius and length to provide the maximum sensitivity. Most modern UV detector sensors have path lengths that range between 1 and 10 mm and internal radii that range from about 0.25 to 1 mm.

From eqn [2]:

$$\log \frac{I_T}{I_0} = \epsilon l c = A \quad [3]$$

where A is termed the absorbance.

The term ΔA is often employed to define the detector sensitivity where the value of ΔA is the change in absorbance that provides a signal-to-noise ratio of 2, i.e.:

$$\Delta A = \epsilon l \Delta c \quad [4]$$

where (Δc) is the detector concentration sensitivity or minimum detectable concentration. Thus:

$$\Delta c = \frac{\Delta A}{l \epsilon} \quad [5]$$

It is clear that two detectors having the same sensitivity, defined as ΔA , will not necessarily have the same sensitivity with respect to solute concentration.

Two detectors having the same minimum detectable change in absorbance will only exhibit the same concentration sensitivity if the path lengths of the two sensors are identical.

UV detectors can be used with gradient elution providing the solvents do not absorb significantly over the wavelength range that is being used for detection. The solvents employed in reversed-phase chromatography are usually water, methanol, acetonitrile and tetrahydrofuran (THF), all of which are transparent to UV light over the wavelength range commonly used. In normal-phase operation, however, more care must be taken in solvent selection, as many solvents that would be appropriate for the separation absorb UV light very strongly. The *n*-paraffins, dichloromethane, and *n*-paraffins containing small quantities of aliphatic alcohols or THF are useful solvents that are transparent in UV, and can be used with normal distribution systems (e.g. with a polar stationary phase such as silica gel).

There are two types of UV detector: fixed-wavelength detector and multiple-wavelength detector.

Fixed-wavelength Detector

The fixed-wavelength detector functions with light of a single wavelength (or nearly so) generated by a specific type of discharge lamp. The most popular lamp for this purpose is the low pressure mercury vapour lamp, which generates most of its light at 254 nm. There are other lamps that are used with fixed-wavelength UV detectors: the low pressure cadmium lamp which generates light predominantly at 225 nm and the low pressure zinc lamp that emits light at 214 nm. None of the lamps are monochromatic and light of other wavelengths is always present but usually at a significantly lower intensity. The low pressure mercury light source (actual maximum emission wavelength 253.7 nm) is the lamp which is most frequently used in the fixed-wavelength detector.

The typical optical system of a fixed-wavelength UV detector is shown in **Figure 2**. Light from the UV source is collimated by a suitable lens through the sample cell and the reference cell, and then on to two photocells. The cells are cylindrical, with quartz windows at either end. The reference cell compensates for any absorption that the mobile phase might have at the sensing wavelength. The outputs from the two photocells are passed to a signal-modifying amplifier so that the output is linearly related to the concentration of solute being detected.

For reasons already discussed, modern sensor cells have angular conduits that form a Z shape to reduce dispersion. The UV detector can be fairly sensitive

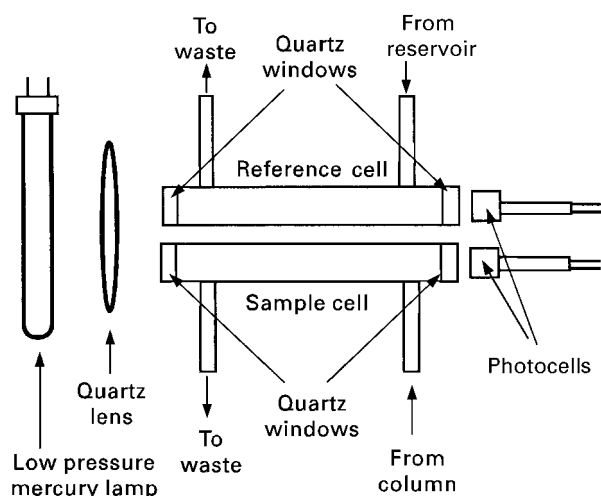


Figure 2 A fixed-wavelength UV detector.

to both flow rate and pressure changes but this instability can be greatly reduced if the sensor is well thermostatted. The fixed wavelength UV detector was once one of the most commonly used LC detectors; it is sensitive, linear and relatively inexpensive. However, today the diode array detector is the most popular, despite its much higher price. The sensitivity (minimum detectable concentration) of the fixed-wavelength detector to compounds with favourable detection properties is about $5 \times 10^{-8} \text{ g mL}^{-1}$, with a linear dynamic range of about three orders of magnitude.

Multiple-wavelength Detector

The multiple-wavelength detector requires a source that emits light over a wide range of wavelengths and, with the aid of a monochromator, light of a specific wavelength can be selected for detection purposes. Detector sensitivity can be improved by selecting light of a wavelength at which the solute has its maximum absorption. Alternatively, the emerging solution peak can be scanned over a range of wavelengths, and the absorption spectra of eluted substances can be used for identification purposes.

There are two basic types of multiple-wavelength detector: the dispersion detector and the diode array detector, the latter being the more popular. In fact, there are currently very few dispersion instruments commercially available but as there are many still in use, their characteristics will be discussed.

The two types of multiple-wavelength detectors have important differences. In the dispersive instrument, the light is dispersed before it enters the sensor cell, and thus virtually monochromatic light passes

through the cell. However, if the incident light can excite the solute and cause fluorescence at another wavelength, then the light falling on the photocell will contain that incident light that has been transmitted through the cell, together with any fluorescent light that may have been generated in the cell. Consequently, the light monitored by the photocell will not be solely monochromatic and light of another wavelength, if present, could impair the linear nature of the response. In most cases this effect is negligible, but with some substances it may be quite significant. The diode array detector operates in quite a different manner. Light of all wavelengths generated by the deuterium lamp is transmitted through the cell, and the transmitted light is then dispersed over an array of diodes. In this way, absorption at discrete groups of wavelengths is continuously monitored at each diode. However, the light falling on a discrete diode may not be solely that transmitted through the cell from the source, but may contain fluorescence light excited by light of a shorter wavelength. In this case, the situation is exacerbated by the fact that the cell contents are exposed to all the light emitted from the lamp, and so fluorescence is more likely. In general, this means that, under some circumstances, the transmitted light measured may also contain fluorescent light. As a consequence, the absorption spectrum obtained for a given substance may be degraded from the true absorption curve.

The ideal multiple-wavelength detector would be a combination of both the dispersion instrument and the diode array detector. This system would allow a monochromatic light beam to pass through the detector and then the transmitted beam would itself be dispersed again on to a diode array. Only that diode corresponding to the wavelength of the incident light would be used for monitoring the transmission. In this way any fluorescent light would strike other diodes, the true absorption would be measured and, if the incident light is scanned, accurate absorption spectra could be obtained.

The Multiple-wavelength Dispersive UV Detector

A conventional multiple-wavelength dispersive UV detector is shown in **Figure 3**. Light from the source is collimated by two curved mirrors on to a holographic diffraction grating. The dispersed light is then focused by means of a curved mirror on to a plane mirror and light of a specific wavelength is selected by appropriately positioning the angle of the plane mirror. Light of the selected wavelength is then focused by means of a lens through the flow cell and, consequently, through the column eluent. The exit beam from the cell is then focused by another lens on to a photocell which gives a response that is some func-

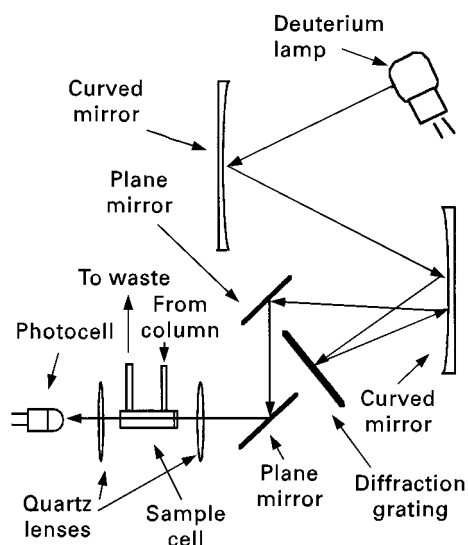


Figure 3 The multiple-wavelength dispersive UV detector. Courtesy of the Perkin Elmer Corporation.

tion of the intensity of the transmitted light. The detector is usually fitted with a scanning facility that, by arresting the flow of mobile phase, allows the spectrum of the solute contained in the cell to be obtained. Due to the limited information given by most UV spectra, and the similarity between UV spectra of widely different types of compounds, the UV spectrum is not usually very reliable for structure elucidation.

UV spectra are, however, useful for determining the homogeneity of a peak by obtaining spectra from a sample on both sides of the peak. The technique is to normalize both spectra, then either subtract one from the other and show that the difference is close to zero, or take the intensity ratio across the peak and show that it is constant throughout the peak.

A common use of the multiple-wavelength detector is to select a wavelength that is characteristically absorbed by a particular component or components of a mixture to enhance the sensitivity of the detector to those particular solutes. Alternatively, by choosing a characteristic absorption wavelength of the solute, the detector response can be made specific to the solute(s) and thus not respond significantly to other substances in the mixture that are of little interest.

The early multiple-wavelength, dispersive UV detector proved extremely useful, providing adequate sensitivity, versatility and a linear response. It was found, however, to be bulky (due to the need for a relatively large internal optical bench), required mechanically operated wavelength selection and a stop/flow procedure to obtain spectra 'on-the-fly'. The alternative diode array detector has all the ad-

vantages but none of the disadvantages and, as a result, has become the variable-wavelength UV detector of choice.

The Diode Array Detector

The diode array detector also utilizes a deuterium or xenon lamp that emits light over the UV spectrum range. Light from the lamp is focused by means of an achromatic lens through the sample cell and on to a holographic grating. The dispersed light from the grating is arranged to fall on a linear diode array.

The resolution of the detector ($\Delta\lambda$) will depend on the number of diodes (n) in the array, and also on the range of wavelengths covered ($\lambda_2 - \lambda_1$). Thus:

$$\Delta\lambda = \frac{\lambda_2 - \lambda_1}{n} \quad [6]$$

It is seen that the ultimate resolving power of the diode array detector will depend on the semiconductor manufacturer and on how narrow the individual photocells can be commercially fabricated.

A diode array detector is shown in **Figure 4**. Light from the broad emission source is collimated by an achromatic lens, so that the total light passes through the detector cell on to a holographic grating. In this way the sample is subjected to light of all wavelengths generated by the lamp. The dispersed light from the grating is then allowed to fall on to a diode array. The array may contain many hundreds of diodes, and the output from each diode is regularly sampled by a computer and stored on a hard disk. At the end of

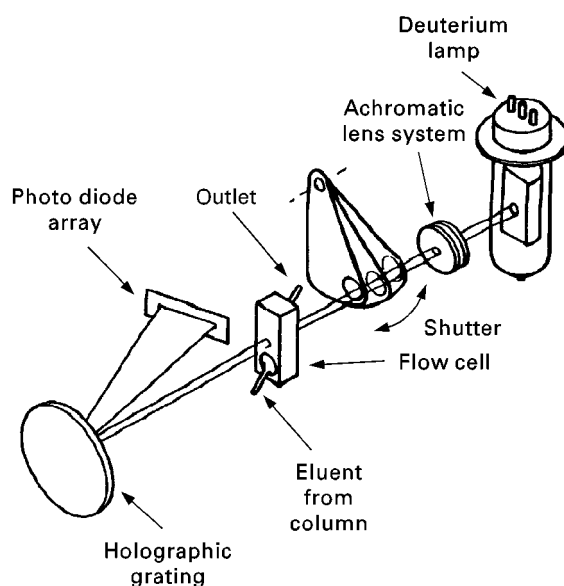


Figure 4 The diode array detector.

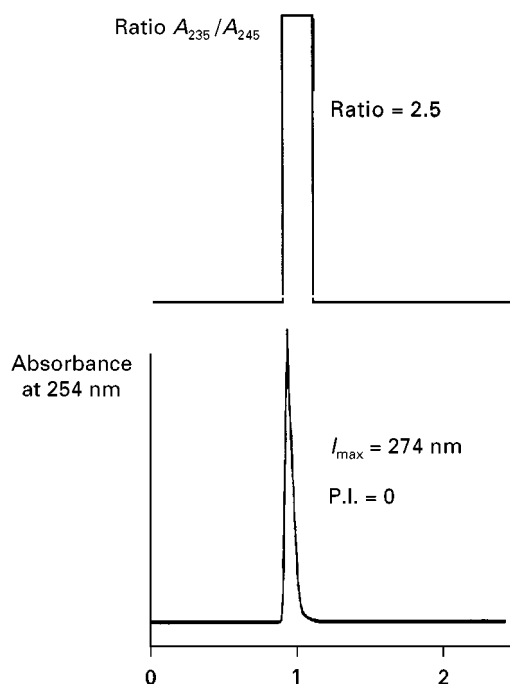


Figure 5 Dual-channel plot from a diode array detector confirming peak purity. Chlorthalidone was isolated from a sample of tablets and separated by a reversed-phase (C_{18}) column 4.6 mm i.d., 3.3 cm long, using a solvent mixture consisting of 35% methanol, 65% aqueous acetic acid solution (water containing 1% acetic acid). Flow rate: 2 mL min^{-1} . Courtesy of the Perkin Elmer Corporation.

the run, the output from any diode can be selected and a chromatogram produced using the UV wavelength that was falling on that particular diode.

Most instruments will allow at least one diode to be monitored in real time, so that a chromatogram can be generated as the separation develops. This system is ideal, as by noting the time of a particular peak, a spectrum of the solute can be obtained by recalling from memory the output of all the diodes at that particular time. This directly produces the spectrum of the solute. The diode array detector can be used in a number of unique ways: one example is to use it to verify the purity of a given solute, as shown in Figure 5. The chromatogram, monitored at 274 nm, is shown in the lower part of Figure 5. As a diode array detector was employed, it was possible to ratio the output from the detector at different wavelengths and plot the ratio simultaneously with the chromatogram monitored at 274 nm. Now, if the peak were pure and homogeneous, the ratio of the absorption at the two wavelengths (those selected being 225 and 245 nm) would remain constant throughout the elution of the entire peak.

The top part of Figure 5 shows this ratio plotted on the same time scale as the elution curve, and it is seen

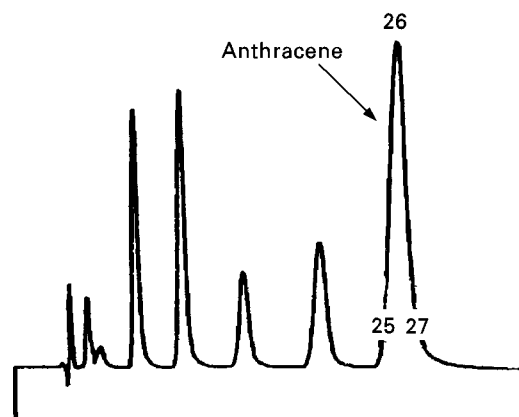


Figure 6 Separation of some aromatic hydrocarbons. Separation was carried out on a 3 cm long, 4.6 mm in diameter column packed with a $3 \mu\text{m}$ C_{18} sorbent. Courtesy of the Perkin Elmer Corporation.

that a clean rectangular peak is produced, confirming a constant absorption ratio at the two wavelengths. The wavelengths chosen to provide the confirming ratio will depend on the UV absorption characteristics of the substance concerned. Another interesting example of the use of the diode array detector to confirm the integrity of an eluted peak is afforded by the separation of the series of aromatic hydrocarbons shown in Figure 6.

It is seen that the separation appears to be satisfactory and, without further evidence, it would be reasonable to assume that all the peaks were pure. However, by plotting the absorption ratio, 250 nm/255 nm, for the anthracene peak it becomes evident that the tail of the peak contains an impurity as the clean rectangular shape of the ratio peak is not realized. The absorption ratio peaks are shown in Figure 7.

The presence of an impurity is confirmed unambiguously by the difference in the spectra obtained for

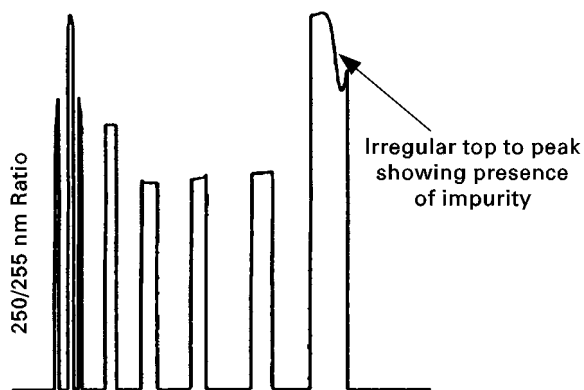


Figure 7 Curves relating the absorption ratio and elution time.

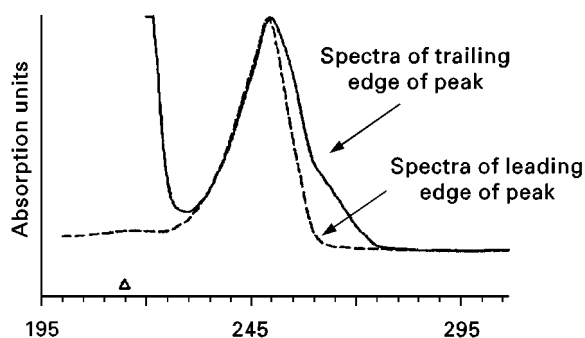


Figure 8 Superimposed spectra taken at the leading and trailing edges of the anthracene peak.

the leading and trailing edges of the peak. Spectra taken at the leading and trailing edge of the anthracene peak are shown superimposed in **Figure 8**. Further work identified the impurity to be 5% *t*-butylbenzene.

The diode array detector is now generally considered the most versatile and useful detector for everyday use in liquid chromatographic analyses. The performances of both types of multiple-wavelength detectors are very similar and typically have a sensitivity of about $1 \times 10^{-7} \text{ g mL}^{-1}$ and a linear dynamic range of about three orders of magnitude: 1×10^{-7} to $5 \times 10^{-4} \text{ g mL}^{-1}$. The device automatically records a spectrum at each sampling point and thus is extremely rapid. It is very suitable for use with fast separations completed in a few seconds.

The use of UV detection in capillary electrochromatography and for detection in capillary electrophoresis has enjoined a novel cell design. As the peaks are only a few nanolitres in volume, the sensor volume must be commensurately small. A practical detector has been constructed by removing the polyimide coating from the surface of a short length of quartz capillary tubing, as shown in **Figure 9**.

UV light from a suitable lamp traverses the tube window and falls on to a photocell. As the solutes migrate across the window they are detected by light absorption in the usual manner. Considering the expression given in eqn [1] for the output of the detector, it appears that, due to the very short pathlength of the cell (*c.* 300 μm), the detector would be very insensitive. However, the loss of sensitivity caused by the reduced pathlength is partly compensated by the relatively high solute concentration in the peaks resulting from the very high column efficiencies achieved in capillary electrochromatography (*c.* 10^5 theoretical plates). The electronic circuitry used with

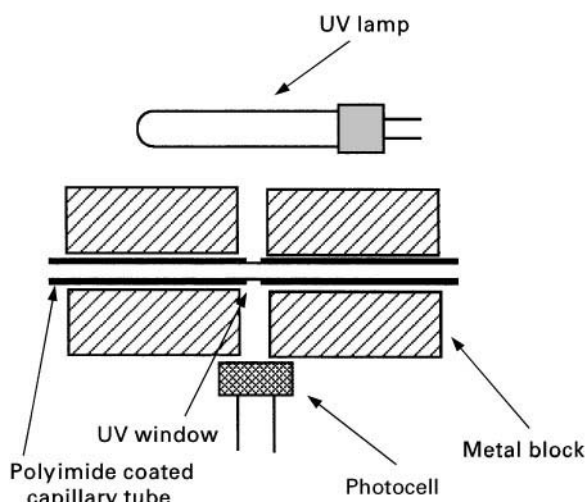


Figure 9 UV detector cell for capillary electrochromatography.

the microcell is basically the same as that used in the conventional larger cell detectors.

Conclusion

The design of the UV detector has changed little over the last decade and its performance has been only marginally improved. Radical changes do not appear likely in the future, although slow progress in improved sensitivity and cell design can be anticipated. The diode array detector is likely to continue as the 'workhorse' detector for liquid chromatography for many years to come. Further details on liquid chromatography detector design and performance can be found in the Further Reading section.

Further Reading

- Katz E and Scott RPW (1982) Liquid chromatography system for fast, accurate analysis. *Journal of Chromatography* 253: 159.
- Krull IS (ed.) (1986) *Reaction Detection in Liquid Chromatography*. New York: Marcel Dekker.
- Parriott D (ed.) (1993) *A Practical Guide to HPLC Detection*. San Diego: Academic Press.
- Scott RPW (1996) *Chromatography Detectors*. New York: Marcel Dekker.
- Sharaf MA (1997) Assessment of chromatographic peak purity. *Advances in Chromatography* 37: 1–28.
- Vickrey TM (ed.) (1983) *Liquid Chromatography Detectors*. New York: Marcel Dekker.
- Yeung ES (ed.) (1986) *Detectors for Liquid Chromatography*. New York: Wiley.

Electrochemically Modulated Liquid Chromatography

M. D. Porter and H. Takano, Iowa State University, Ames, Iowa, USA

Copyright © 2000 Academic Press

Introduction

Liquid chromatographic separations rely on subtle differences in the interactions of analytes between a mobile phase and a stationary phase. Examples include the separation of charged species using ion-exchange chromatography, enantiomeric compounds via chiral selective chromatography, and polymeric materials by size-exclusion chromatography. Each of these separations, however, requires a different stationary phase. Thus, a large number of such phases and mobile phase elution schemes are required to tackle the diversity of the separations routinely encountered in the analytical laboratory.

Recently, a technique has been developed that begins to address the need for a large number of stationary phases. The approach, which is termed 'electrochemically modulated liquid chromatography' (EMLC), is based on the transformation of a conductive stationary phase in a conventional liquid chromatographic system into the working electrode of a three-electrode electrochemical cell. With this arrangement, the column packing serves both as a stationary phase and as a working electrode. This dual-purpose function provides the ability to induce changes in the interfacial properties (e.g. donor-acceptor strength, solvophobicity, and oxidation state) of conductive stationary phases through alterations in applied potential which subsequently translate into changes in analyte retention. The column can therefore be viewed as a compositionally tunable stationary phase with retention characteristics that can be manipulated both prior to as well as during elution by changes in applied potential. The latter capability presents an approach whereby improvements in a separation can be realized through a dynamic alteration in the composition of a stationary phase that is conceptually, but not mechanistically, analogous to conventional solvent gradient elution techniques in liquid chromatography or to temperature-programming strategies in gas chromatography. With electrochemically modulated liquid chromatography, however, the changes in retention reflect a temporal gradient in the composition of a stationary phase.

The following discusses the emergence of this new separation strategy as a tool in the arsenal of liquid chromatography techniques. After examining issues

concerning the design and construction of the column, processes to control retention, illustrative applications demonstrating the versatility of the technique and issues related to improvements in column performance are presented.

Hardware

Column Development

The development of electrochemically modulated liquid chromatography can be traced back to the early 1950s and 1960s when concepts for the desalination of water and for the separation of metal ions explored a union of liquid chromatographic and electrochemical techniques. These and many subsequent investigations suffered from poor chromatographic efficiency ($10\text{--}200$ plates m^{-1}). As a consequence, interest in this technique has been limited until a few years ago. This limitation reflected the complexity in merging the design criteria necessary for both effective liquid chromatographic and electrochemical performance. In the case of the latter, a column must incorporate a reference electrode as a means to control precisely the potential applied to the stationary phase, and an auxiliary electrode as a means to complete the electrical circuit for current flow. In addition, the components of the column must be electrochemically as well as chemically inert and the mobile phase may need to be modified by the addition of an inert electrolyte to achieve the necessary solution conductivity; this modification is required to minimize the solution resistance of the mobile phase which, if not effectively manipulated, may degrade the ability to control the potential applied to the stationary phase.

Maintaining control over the applied potential is challenged, however, by the need for conductive stationary phases that have the characteristic size, shape, and surface area (e.g., $200\text{ m}^2\text{ g}^{-1}$) required for high separation efficiencies with packed columns. A critical design attribute for high performance chromatography is a large surface area to solution volume ratio for the stationary phase with respect to the mobile phase. As a consequence, the small voids between the particles and within the pores of the particles that often make up a stationary phase appear as highly resistive pathways in an equivalent electrical circuit model for a column under potential control. These high-resistance networks define the time required to charge the electrical double layer at the surface of the stationary phase, and therefore the

flow generated at the high surface area working electrode and as an inflexible container that defines the length and diameter of the column. The electrical circuit is completed by placing a reference electrode (e.g. Ag/AgCl(saturated NaCl)) inside a glass reservoir that surrounds the porous stainless-steel tubing and is filled with an aqueous electrolyte.

The ion-exchange membrane has three important functions in this design. It serves as:

- an insulating container that separates the stationary phase from the stainless-steel auxiliary electrode;
- an ionic bridge that completes the electrical connection between the stationary phase and auxiliary electrode; and
- a barrier that minimizes the loss of analyte through the porous stainless-steel cylinder as well as the possible contamination of the column by any electrolysis products generated at the auxiliary electrode.

With this design, the column equilibrates to alterations in applied potential on a time scale similar to that required for changes in mobile phase (~ 20 min), and performs at high chromatographic efficiencies (e.g., $15\,000$ plates m^{-1}).

Stationary Phases

Several types of conductive materials have been tested for use as packings in electrochemically modulated liquid chromatography. Some of the earlier examples investigated the utility of silver grains, mercury-coated platinum, uncoated graphitic particles, and various organic materials (e.g., conductive polymers) coated on graphitic particles. In general, the stationary phase material must meet the requirements in place for conventional liquid chromatography. These attributes include chemical inertness, high mechanical strength, high surface area, and small uniform size. To be effective as an electrode material, requirements including reasonable electrical conductivity ($\geq 0.01 \Omega\text{-cm}$) and stability over a wide range of applied voltage must be added to the list of attributes. For packings designed to undergo a formal change in oxidation state through an externally triggered electron-transfer process, the material must also be stable in both its oxidized and reduced forms.

Of the above materials, the greatest degree of success has been achieved to date using uncoated carbonaceous materials such as nonporous glassy carbon and porous graphitic carbon. These materials are stable both chemically (i.e. can be used in strongly

acidic and basic mobile phases) and electrochemically (i.e. can be used over a wide range of applied potentials), have a high mechanical strength, and are commercially available as micron-sized particles. The non-porous material, has a lower surface area ($\sim 1 \text{ m}^2 \text{ g}^{-1}$) and therefore a lower separation efficiency, whereas the porous material has a higher surface area ($\sim 200 \text{ m}^2 \text{ g}^{-1}$) and therefore a higher separation efficiency. The coated materials, especially those that undergo a formal change in oxidation state (see below), potentially offer an additional dimension in affecting a separation, but complications regarding stability and reliable coating procedures remain significant issues.

Ancillary Instrumentation

Other than the features described for the column, this technique uses standard analytical laboratory hardware. Commercially available liquid chromatographic systems (e.g. pump, injector, and detector) and electrochemical hardware (e.g. potentiostat) are all that are needed to perform separation using electrochemically modulated liquid chromatography. To minimize the time required to re-equilibrate the column to changes, the use of a potentiostat with a high output power (i.e. a few watts) is recommended.

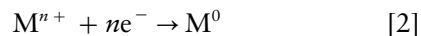
Retention Concepts

Conventional liquid chromatographic separations rely on a partitioning of an analyte between a mobile phase and stationary phase. This equilibrium is generally expressed as a distribution coefficient (K_d) where:

$$K_d = C_s/C_m \quad [1]$$

and C_s and C_m are the concentrations of an analyte in the stationary and mobile phases, respectively. Electrochemically modulated liquid chromatography therefore relies on the impact of the applied potential on the retention of an analyte through alterations in K_d .

Four principal formats have been used. The first format deals with an electrochemically induced reduction of metal ions (M^{n+}) onto a conductive stationary phase as M^0 . The generic form of this reaction can be written as:



where n represents the electron (e^-) stoichiometry of the reaction. The concentrations of the two species are then defined by the difference in the

standard reduction potential for the reaction (E^0) and the applied potential (E_{app}) through the Nernst equation:

$$E_{\text{app}} = E^0 + (0.059/n)(\log[M^0]/[M^{n+}]) \quad [3]$$

Substituting M^0 and M^{n+} into eqn [1] for C_s and C_m , respectively, and then combining eqns [1] and [3] yields:

$$\log K_d = (n/0.059)(E^0 - E_{\text{app}}) \quad [4]$$

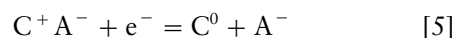
Eqn [4] shows that K_d changes by a factor of ten for every $0.059/n$ V alteration of the applied potential. However, while providing a means for the quantitative deposition of metal ions, the process suffers from poor selectivity. That is, metal ions with standard reduction potentials more positive than the applied potential are exhaustively deposited onto the column, whereas those with standard reduction potentials more negative than the applied potential pass through the column without being retained. Strategies that have been devised to address this limitation have been studied in a few specific applications.

The second format takes a notably different tactic in that the potential applied to a graphitic stationary phase is used to manipulate the chemical composition of a mobile phase. This strategy relies on the oxidation or reduction of water either to increase or decrease, respectively, the acidity of the mobile phase. This general tactic, though explored only briefly to manipulate the pH-dependent binding of metal ions to chelates immobilized onto the column packing, will undoubtedly be more extensively

exploited as interest in this new separation technique increases.

The third format, which has been the most used of the four, utilizes uncoated graphitic stationary phases. The basis of this format derives largely from the effect of the applied potential on the donor-acceptor properties (e.g. electrostatic and dipolar interactions) of the packing and is illustrated in Figure 2. Thus, as the applied potential becomes more positive, the carbonaceous packing becomes a stronger acceptor and analytes with a predominant donor character are more strongly retained. The retention of analytes with a predominant acceptor character, in contrast, increases as the applied potential becomes more negative. This approach has been employed, as discussed in the following section, to separate a wide ranges of samples, including, charged and neutral aromatic compounds, important pharmaceutical agents, and enantiomeric pairs.

The fourth format takes advantage of a different form of electrochemically modulated separation in which the composition of a column packed with an electroactive material is transformed by its oxidation/reduction. Eqn [5] depicts this process whereby a coating (C) is switched between its reduced and oxidized forms with the concomitant expulsion or uptake of anions (A^-). The analogous reaction:



can be written for coatings that involve cations as counterions. Thus, the charge density of the ion-exchange sites on a stationary phase can be tuned

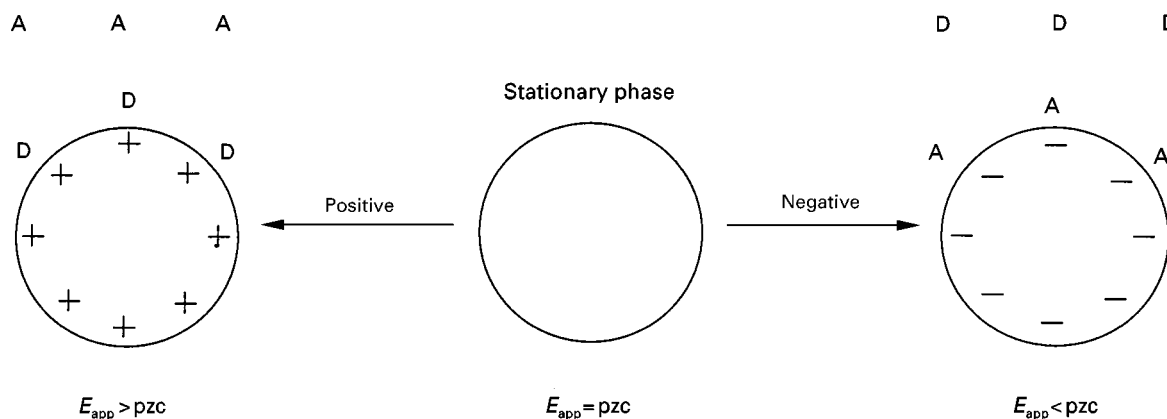


Figure 2 Idealized representations of the interactions of donor (D) and acceptor (A) analytes with a conductive stationary phase as a function of applied potential (E_{app}). Collectively, changes in applied potential alter the extent of the interaction of such analytes through a change in the surface charge of the stationary phase. At applied potential greater than the potential of zero charge (pzc), the stationary phase has a net positive surface charge and therefore a greater acceptor strength. This increase results in an increase in the attractive interaction between the stationary phase and a donor analyte. The converse applies as the applied potential becomes more negative than the pzc. In this case, the donor strength of the stationary phase increases, and the attractive interaction between the stationary phase and an acceptor analyte increases.

through changes in applied potential. Several intriguing features of this strategy have been described.

Electrochemically modulated liquid chromatography, therefore, presents a broad range of tactics that can, as demonstrated in the next section, be exploited in tackling the many separation challenges faced in the analytical laboratory.

Applications

This section presents a few examples of the capabilities of the technique, including the separation of aromatic compounds, pharmaceutical agents, and chiral compounds. The use in a concentration format is also described.

Aromatic Sulfonates

The earliest demonstration of the ability of electrochemically modulated liquid chromatography to separate complex mixtures at performance levels that rivaled conventional liquid chromatographic separations used porous graphitic carbon as the column packing and the aromatic sulfonates in Table 1 as analytes. Examples are presented in Figure 3. These results show that: (1) the retention for all of the analytes increases as the applied potential moves positive, (2) the retention of all the analytes (Figure 4) exhibit a linear dependence on applied potential, (3) the magnitude of the change in retention differs between analytes, and (4) all six analytes in the mixture are baseline resolved at +0.5 V. These results confirm that the analytical figures of merit (e.g. resolution and retention time) can be readily manipulated by changes in applied potential, and that the change in the surface charge of the stationary phase plays a key role in altering the extent of retention.

It is also possible to affect such separations by manipulating the applied potential during analyte elution, a strategy that parallels temperature pro-

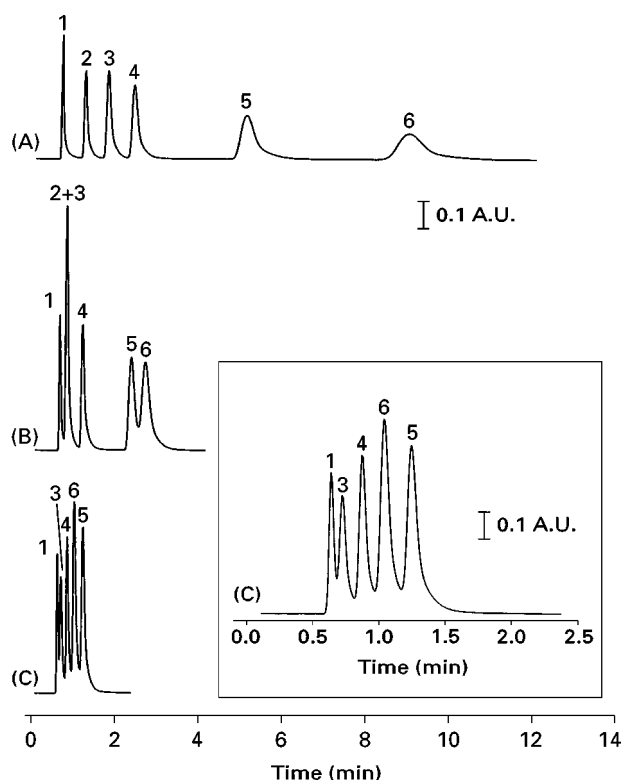
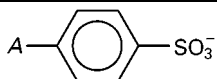


Figure 3 Separations of a mixture of aromatic sulfonates (see Table 1) using a porous graphitic carbon stationary phase at +0.50 V (A), open circuit (B), and -0.60 V (C). The mobile phase was water (0.1 M LiClO₄, 0.1% TFA) and acetonitrile (0.1 M LiClO₄) (88 : 12, v/v). The flow rate was 0.90 mL min⁻¹. (Reproduced with permission from Ting EY and Porter MD (1998) *Analytical Chemistry* 70: 94–99. Copyright ACS Publications.)

gramming in gas chromatography. Figure 5 demonstrates this possibility whereby a linear voltage ramp is imposed upon the stationary phase from +0.3 V to -1.0 V immediately upon sample injection. This strategy increases the resolution of the compounds that eluted early at the open circuit potential (i.e. the condition used in conventional liquid chromatography) by increasing their retention. At the same time, this waveform decreases the retention and narrows the bands for those compounds eluting much later in the open circuit separation. There is also a notable decrease in the time required to complete the separation (~4 min). Thus, a stationary phase gradient offers a pathway for the optimization of separations.

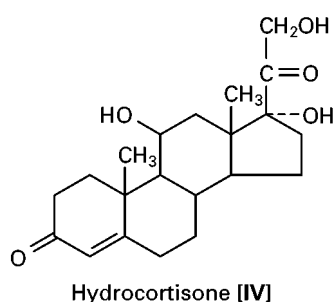
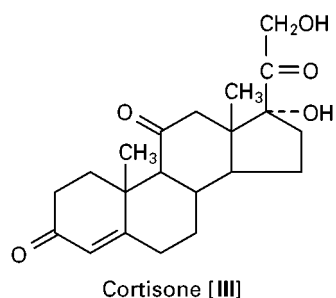
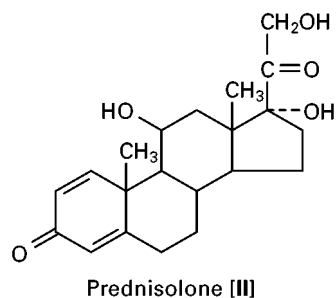
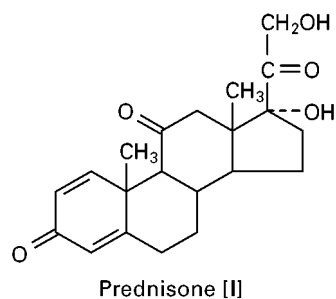
Table 1 Chemical structures and labelling schemes of the aromatic sulfonate derivatives

Compound	Acronym	A
1	ABS	NH ₂
2	HBS	OH
3	BS	H
4	TBS	CH ₃
5	CBS	Cl
6	BAS	COOH



Corticosteroids

Separations of structurally similar compounds can readily be fine tuned using electrochemically modulated liquid chromatography. The challenge presented by the separation of four corticosteroids, [I]–[IV], at a porous graphitic carbon stationary phase is a particularly intriguing example.



The complication with this mixture is the discrimination between structures containing differing numbers of double bonds (e.g. prednisone vs. cortisone) and/or small differences in the identity and number of substituents (e.g. cortisone vs. hydrocortisone). On bonded reversed phases, compounds with subtle differences in functionality generally exhibit greater differences in retention than those that differ by the number of double bonds. The converse is often more important for separations on porous graphitic carbon, which possesses π -electron sensitivity superimposed upon reversed phase characteristics. Thus,

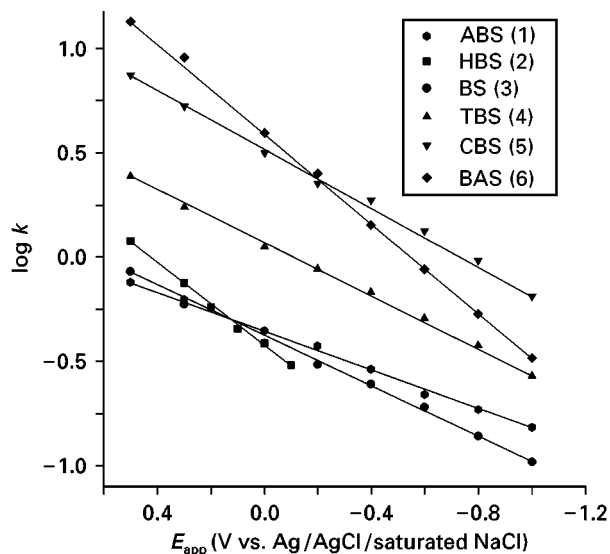


Figure 4 Plots of $\log k$ vs. applied potential (E_{app}) for the separations of the mixture of aromatic sulfonates (see Table 1) between +0.50 V and -1.00 V. Note that the values of HBS extend only from +0.50 V to -0.10 V because of its electroreduction which occurs at an E_{app} between -0.10 and -0.20 V. (Reproduced with permission from Ting EY and Porter MD (1998) *Analytical Chemistry* 70: 94-99. Copyright ACS Publications.)

strategies that would enhance the sensitivity of carbonaceous materials toward substituent differences, would improve their applicability as packings especially as they are more stable than many of the bonded phases when exposed to strongly acidic and strongly alkaline solutions.

The chromatograms in Figure 6 present the separations of the four compounds as a function of applied potential using a porous graphitic carbon stationary phase. At the open circuit potential, the separation is only marginally effective in resolving the four compounds. Changes in the applied potential, however, have a marked influence on the separation. Interestingly, the retention of prednisone and prednisolone increase as the applied potential becomes more negative, with that for prednisone becoming greater than that for prednisolone. This difference transposes the elution order for the two compounds. The same general dependencies for the retention of cortisone and hydrocortisone are observed. In contrast to the aromatic sulfonates, the supporting electrolyte can compete in some instances with the analyte for binding sites on the stationary phase, leading to retention dependencies that are nonlinear with respect to changes in applied potential. As a result of the combined effect of these dependencies, all four components are fully resolved at -700 mV, with a total elution time of ~ 10 min. Thus, separations based on manipulating the applied potential provide an effective and

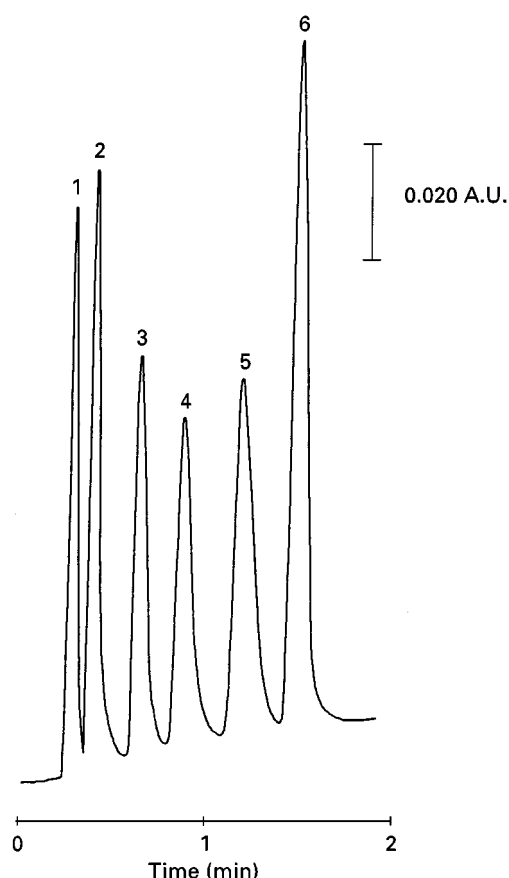


Figure 5 Separation of the six-component mixture of aromatic sulfonates (see Table 1) on a porous graphitic carbon stationary phase obtained by applying a linear voltage ramp from +0.30 V to -1.00 V. The voltage ramp was initiated immediately upon sample injection at 10 mV s^{-1} . The mobile phase consisted of aqueous 0.1 M LiClO_4 with 1.5% acetonitrile. The flow rate was 0.75 mL min^{-1} and the analyte concentrations were $\sim 200 \text{ ppm}$. The shift in the baseline reflects the gradual decrease in the interfacial concentration of the ClO_4^- anion of the supporting electrolyte in the mobile phase as the applied potential becomes more negative. The background baseline gradually returns to its initial value in $\sim 10 \text{ min}$. (Reproduced with permission from Deinhammer RS, Ting E and Porter MD (1993) *Journal of Electroanalytical Chemistry* 362 : 295–299. Copyright Elsevier Science SA.)

facile means to tackle the challenges posed by the strong structural similarity of these compounds.

Chiral Compounds

This technique can also be applied to separations of racemic mixtures. These separations, usually accomplished with a chiral selector either immobilized onto a stationary phase or as an additive to a mobile phase, are critical to pharmaceutical areas because therapeutic efficacy is often enantiomerically specific. However, the high level of structural discrimination required to separate optical isomers dictates the use

of a variety of stationary-mobile phase combinations. This separation can be realized by the reversible electrosorption of a chiral compound added to the mobile phase, a process that converts an achiral column into a chiral column. The concept is illustrated in Figure 7, using β -cyclodextrin as the chiral mobile phase additive. The choice of this additive reflects the notable enhancement of the interactions between hydroxyl functionalities and a carbonaceous packing as the applied potential becomes increasingly positive.

Results are presented in Figure 8 for the separations with and without the chiral selector present as a mobile phase additive at several different applied

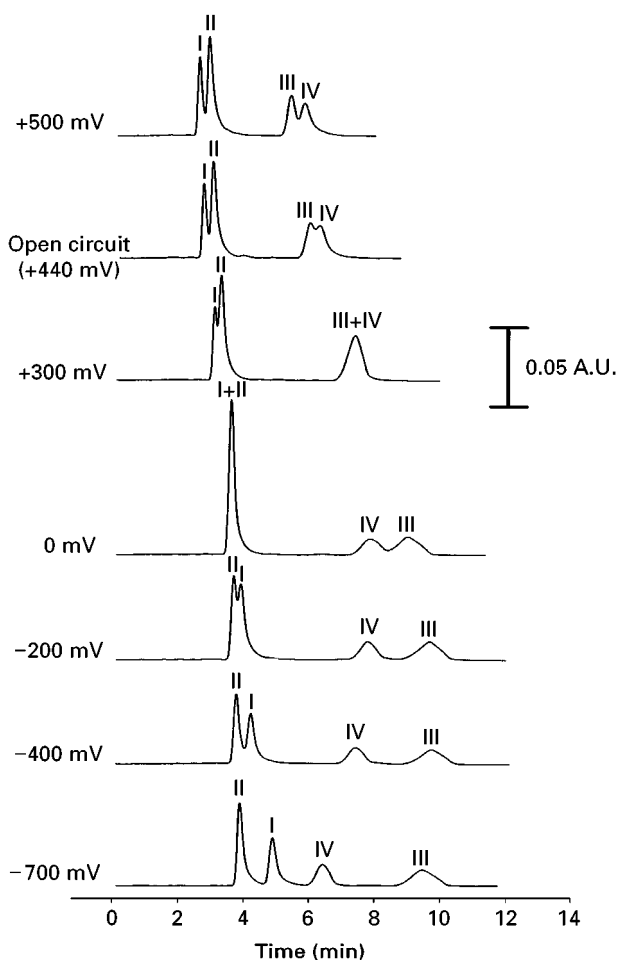


Figure 6 Separations using EMLC of a mixture of the mixture of prednisone [I], prednisolone [II], cortisone [III], and hydrocortisone [IV] at a porous graphite carbon stationary phase as a function of applied voltage: +500 mV, open circuit (i.e. +440 mV), +300 mV, 0 mV, -200 mV, -400 mV, -700 mV. All applied voltages are given with respect to an Ag/AgCl (saturated NaCl) electrode. The mobile phase was composed of two components: water (0.1 M HClO_4)/acetonitrile (0.1 M LiClO_4) 50:50 (v/v). The flow rate was 0.90 mL min^{-1} . (Reproduced with permission from Ting EY and Porter MD (1997) *Analytical Chemistry* 69: 675–678. Copyright ACS Publications.)

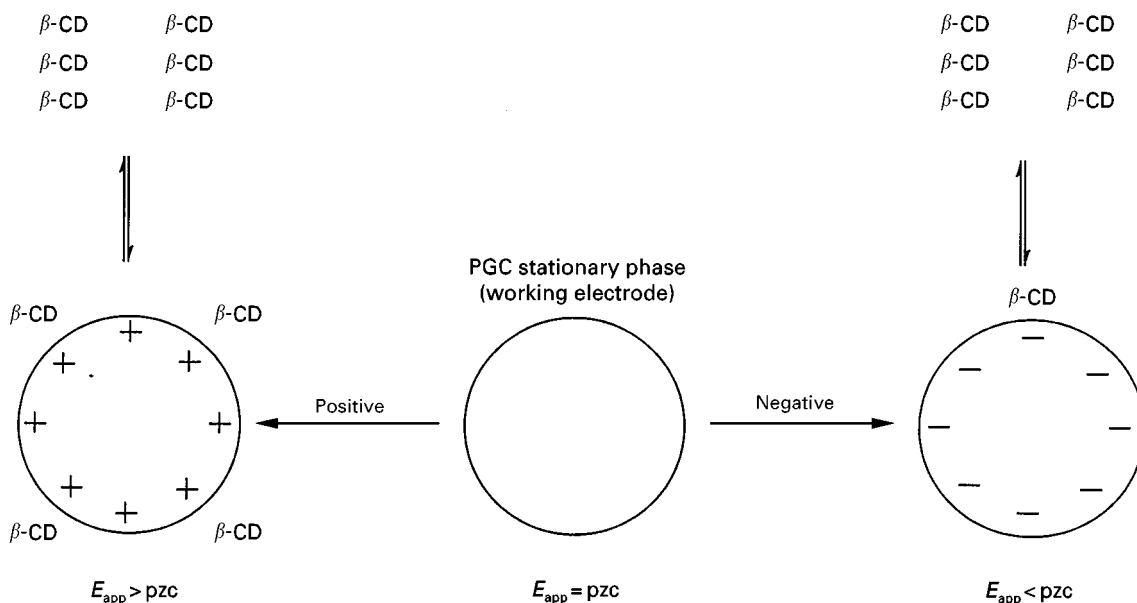


Figure 7 Idealized depiction of the electrosorption process of β -cyclodextrin (β -CD) onto porous graphite carbon (PGC). pzc , potential of zero charge.

potentials. The sedative hexobarbital is used as the chiral analyte. As expected for an achiral system, there is no detectable separation of enantiomers in Figure 8A. Furthermore, the retention of the sedative increases as the applied potential becomes more negative. This trend is consistent with the dominant acceptor character of this compound because of its protonation at the mobile phase ($pH \sim 2$).

Marked differences in the separations are found when β -cyclodextrin is added to the mobile phase. Figure 8B shows the results; the presence of the additive results in a separation of the hexobarbital enantiomers at several applied potentials. Enantiomeric separations are evident at -1.0 , 0.0 , and $+0.5$ V, with the highest resolution at $+0.5$ V. There is no observable enantiomeric separation for -0.5 V. Experiments in which an excess of one enantiomer was added to the mixture reveal the enantiomeric separation is controlled at the more negative applied potentials by interactions with the chiral additive in the mobile phase, and at the more positive applied potentials by interactions with the electro-sorbed chiral selector.

Experiments have also shown that the electrosorption-based modification of the porous graphitic carbon phase is reversible. This observation suggests that electrosorption may serve as a versatile means for altering the surface composition of conductive stationary phases whereby a chiral column for enantiomeric separations could, for example, be readily converted to a column with reversed phase character by the electrosorption of another mobile phase addi-

tive (e.g. a long alkyl chain alcohol). This intriguing strategy offers the possibility of requiring only one column for the separation of a wide range of complex mixtures.

Concentration

Another intriguing application of this technique is sample concentration. This approach takes advantage of the ability to modulate the capacity of a stationary phase, for example, by changes in the oxidation state of an electrochemically transformable stationary phase (e.g. eqn [5]). This strategy is similar to that employed in solid-phase extractions except that changes in applied potential rather than changes in solvent can be used to concentrate and then strip the analyte from the column.

An example of this strategy is the concentration of the dansylated amino acid tryptophan using a non-porous carbon stationary phase that is coated with a thin film of polypyrrole. Polypyrrole, which can be polymerized electrochemically onto a wide range of electrode materials, can be switched between its oxidized and reduced forms with the concomitant uptake or expulsion of anions, as represented in Figure 9. Thus, changes in applied potential transform the stationary phase between one devoid of ion-exchange sites to one with a large number of exchange sites. This transformation is evident in the cyclic voltammetric curve shown in Figure 10. This curve demonstrates the change of the coating from its neutrally charged (reduced) form at the more negative

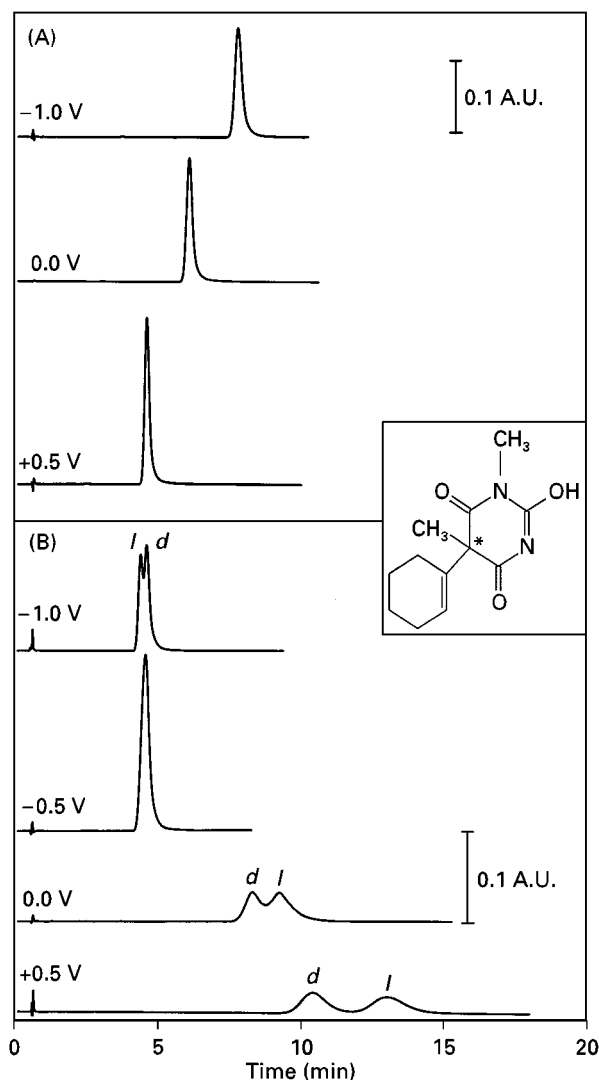


Figure 8 Separations of hexobarbital enantiomers (*d* and *l*), using a mobile phase of 20% acetonitrile and 80% water (0.1 M LiClO₄, 20 mM phosphate buffer (pH ~ 2)), a flow rate 0.9 mL min⁻¹, a detection wavelength of 220 nm, and an Ag/AgCl (saturated NaCl) reference electrode. (A) Separations in mobile phase devoid of β -cyclodextrin at -1.0 V, -0.5 V, 0.0 V and +0.5 V. (B) Separations with 15 mM β -cyclodextrin as a mobile phase additive at -1.0 V, -0.5 V, 0.0 V and +0.5 V. The concentration of hexobarbital is ~500 ppm, and the injection volume was 0.5 μ L. (Reproduced with permission from Ho MK, Wang S and Porter MD (1998) *Analytical Chemistry* 70: 4314–4319. Copyright ACS Publications.)

values of applied potential to its cationic (oxidized) form as the applied potential becomes increasingly positive.

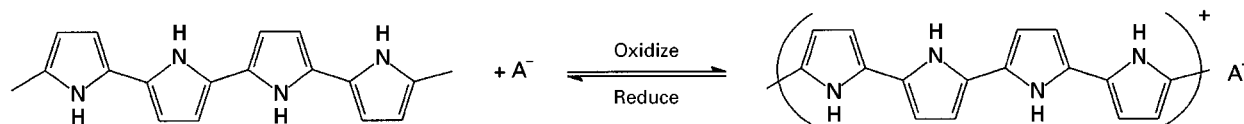


Figure 9 Electrochemical switching of polypyrrole between its oxidized and reduced forms showing the respective uptake or expulsion of an anion A⁻.

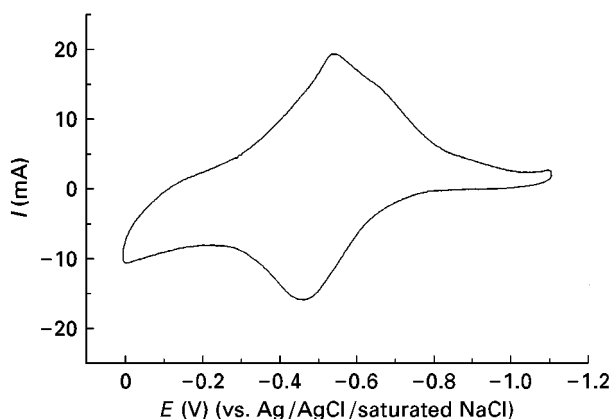


Figure 10 Cyclic voltammetric curve for a nonporous glassy carbon packing that has been coated with a thin film of polypyrrole in 0.10 M sodium benzoate. A silver wire is used as a quasi-reference electrode, and the scan rate was 5 mV s⁻¹. (Reproduced with permission from Deinhamer RS, Shimazu K and Porter MD (1995) *Journal of Electroanalytical Chemistry* 387: 35–46. Copyright Elsevier SA.)

Figure 11 presents the details of the experiment by showing the breakthrough curve for the concentration process. The experiment begins by passing a mobile phase containing dansylated tryptophan through the column continuously while the applied potential is held at -1.00 V. The applied potential is then stepped to and held at 0.00 V to oxidize the coating to its cationic form. Upon stepping potential to 0.00 V, the absorbance of the eluent rapidly decreases to the value of the acetate mobile phase, reflecting the exhaustive uptake of the amino acid by the coating. After ~67 min, the absorbance increases slowly to the value initially observed at -1.00 V.

This increase signals the saturation of the coating by the uptake of the amino acid from the highly dilute solution; the coating is fully saturated in 72.5 min. After saturation, the applied potential is stepped back to -1.00 V to reduce the coating to its neutral form, and strip the amino acid from the column in a narrow elution band. An analysis of the data gives a concentration factor of ~33 and a recovery of ~98%. Thus, this strategy offers an alternative approach to the solvent elution processes used in most other concentration techniques in that the stripping of an analyte from the column can be facilitated by a change in applied potential, opening the possibility of large reductions in the volumes of generated wastes.

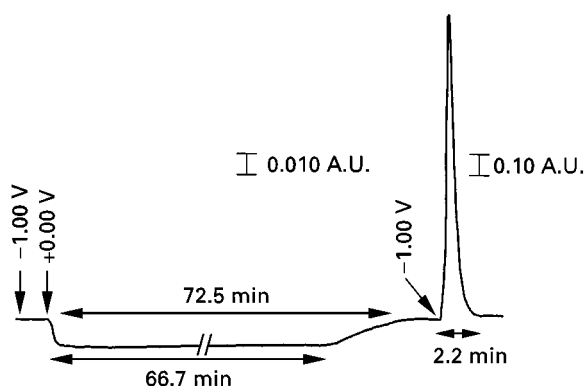


Figure 11 Breakthrough curve showing the concentration of a 1.6 ppm solution of dansylated tryptophan at a polypyrrole stationary phase. The applied potential was initially held at -1.00 V, stepped to 0.00 V for 72.5 min, and then stepped back to -1.00 V. The mobile phase consisted of 1.6 ppm dansylated amino acid tryptophan in 10 mM pH 6 acetate buffer. (Reproduced with permission from Deinhammer RS, Shimazu K and Porter MD (1995) *Journal of Electroanalytical Chemistry* 387: 35–46. Copyright Elsevier Science SA.)

Future Developments

Electrochemically modulated liquid chromatography is emerging as a valuable addition to the arsenal of liquid chromatographic techniques used in tackling the many challenges encountered in the day-to-day operations of the analytical laboratory. Advances in this area will continue with improvements in column design that reduce the equilibration time to changes in applied potential. Such developments will enhance the ability of the analyst to manipulate separations by dynamically altering the applied potential during analyte elution.

There are also several intriguing opportunities in the creation of separation formats using new types of stationary phases. Other types of conducting phases based, for example, on electrochemically transformable coatings offer pathways to manipulate separations by variations in the porosity of a coating which can be affected by the size of the dopant ion used in the electrochemical coating process. Variations in porosity may add size discrimination to the selectivity of the separation process. In addition, the incorporation of functional groups as substituents on the monomer precursors used for polymer formation can be exploited to design coating with hydrophobicity–hydrophilicity differences.

Another area of fruitful development lies in the coupling of this technique to other detector formats. Mass spectrometry, for instance, has proven invaluable as a detector in a wide range of chromatographic applications. The ability of electrochemically modulated liquid chromatography to address separations

that require the use of gradient-elution strategies may overcome the associated problems of a continuing changing background when using electrospray mass spectrometry. Enhancements may also be realized by electrochemically transforming an analyte to a form that improves not only its separation but also its response to conventional optical detection formats. These developments, coupled with systematic explorations of the interactions operative in the many retention mechanisms, promise to stimulate the widespread interest in this new mode of liquid chromatographic separations.

See also: III/**Steroids:** Liquid Chromatography and Thin-Layer (Planar) Chromatography. **Chiral Separations:** Cyclodextrins and Other Inclusion Complexation Approaches; Liquid Chromatography.

Further Reading

- Deinhammer RS, Ting EY and Porter MD (1993) Electrochemically modulated liquid chromatography (EMLC): a new approach to gradient elution separations. *Journal of Electroanalytical Chemistry* 362: 295–299.
- Deinhammer RS, Porter MD and Shimazu K (1995) Retention characteristics of polypyrrole as a stationary phase for the electrochemically modulated liquid chromatographic (EMLC) separations of dansyl amino acids. *Journal of Electroanalytical Chemistry* 387: 35–46.
- Fujinaga T and Kihara S (1977) Electrolytic chromatography and coulopotentiography – a rapid electrolysis at the column electrode used for the preparation, separation, concentration, and estimation of trace and/or unstable substances. *CRC Critical Reviews in Analytical Chemistry* 6: 223–253.
- Ge H and Wallace GG (1989) Characterization of conducting polymeric stationary phases and electrochemically controlled high-performance liquid chromatography. *Analytical Chemistry* 61: 2391–2394.
- Ge H, Teasdale PR and Wallace GG (1991) Electrochemical chromatography – packings, hardware, and mechanisms of interaction. *Journal of Chromatography* 544: 305–316.
- Ghatak-Roy AR and Martin CR (1986) Electromodulated ion exchange chromatography. *Analytical Chemistry* 58: 1574–1575.
- Hern JL and Strohl JH (1978) Modified graphites for chelation and ion exchange. *Analytical Chemistry* 50: 1955.
- Ho MK, Wang S and Porter MD (1998) Electrosorption-based modification of porous graphitic carbon: use of electrochemically modulated liquid chromatography to create a chiral stationary phase for enantiomeric separations. *Analytical Chemistry* 70: 4314–4319.
- Lam P, Elliker PR, Wnek GE and Przybycien TM (1995) Towards an electrochemically modulated chromatographic stationary phase. *Journal of Chromatography* 707: 29–33.

- Nagaoka T, Fujimoto M, Nakao H *et al.* (1994) Electrochemical separation of ionic compounds using a conductive stationary phase coated with polyaniline or polypyrrole film, and ion exchange properties of conductive polymers. *Journal of Electroanalytical Chemistry* 364: 179–189.
- Suzuki T, Noble RD and Koval CA (1997) Electrochemistry, stability, and alkene complexation chemistry for copper(I) triflate in aqueous solution. Potential for use in electrochemically modulated complexation-based separation processes. *Inorganic Chemistry* 36: 136–140.
- Ting EY and Porter MD (1997) Separations of corticosteroids using electrochemically modulated liquid chromatography: selectivity enhancements at a porous graphitic carbon stationary phase. *Analytical Chemistry* 69: 675–678.
- Ting EY and Porter MD (1998) Column design for electrochemically modulated liquid chromatography. *Analytical Chemistry* 70: 94–99.

Electrochromatography

N. Smith, Imperial College of Science,
Technology and Medicine, London, UK

Copyright © 2000 Academic Press

Introduction

High performance liquid chromatography (HPLC) is an established technique with a vast number of stationary phases available, but the efficiency is ultimately limited by the size of the particles used to pack the columns. Theory shows that for the highest efficiency the particles should be of a much smaller diameter than those in current use, but a significant move in this direction is constrained by the pressure required from the pumping system used to deliver the mobile phase. Capillary electrochromatography (CEC) uses an electric field rather than hydraulic pressure to drive the mobile phase through the packed bed of stationary phase. Since the resulting flow profile is plug-like rather than parabolic, very high efficiencies can be achieved.

Theory

The ability to drive a liquid through a packed capillary under the influence of an electric field was first described by Pretorius in 1974, but a lack of the necessary hardware at the time meant that his suggestion was not followed up. Pretorius showed that the linear velocity of a liquid (u) under electrical flow conditions was given by the equation:

$$u = \frac{\varepsilon E \zeta}{4\pi\eta} \quad [1]$$

where E is the applied electrical field in V cm^{-1} ; ε is the dielectric constant (dimensionless); ζ is the zeta potential in volts; and η is the viscosity of the liquid in $\text{kg m}^{-1} \text{s}^{-1}$.

Pretorius estimated from eqn [1] that, with voltages up to 1500 V cm^{-1} , it should be possible to

generate linear velocities of 0.1 to 1 cm s^{-1} , which are similar to those used in modern HPLC. He also noted that eqn [1] is independent of particle diameter, which means that the flow rate could be maintained in a column packed with very fine material. When the various contributions to column plate height are summed and plotted against linear velocity, it can be seen that the overall dispersion in an electrically driven system is approximately half that of a corresponding pressure-driven system. This is almost entirely due to a dramatic decrease in the contribution of the eddy diffusion term in the electrically driven system, as illustrated in **Figure 1**.

The driving force in electrochromatography results from the electrical double layer that exists at any liquid–solid interface. The electrical double layer inside a fused silica capillary filled with an electrolyte is shown in **Figure 2**.

Under alkaline conditions, the surface silanol groups of the fused silica become ionized, leading to a negatively charged surface. This surface will have a layer of positively charged ions in close proximity that is relatively immobile. This surface layer of ions is called the Stern layer. The remainder of the excess charge, constituting the Goüy layer, is solvated and has the characteristics of a typical solvated ion. This layer extends into the bulk of the liquid and is the so-called double layer. The concentration of ions in the double layer is relatively small compared to the total ion concentration and falls off exponentially from the capillary surface, as does the electrical potential, which is proportional to the charge density. The potential at the boundary between the Stern layer and the diffused Goüy double layer is known as the zeta potential, ζ , and ranges from 0 to 100 mV . As the charge density drops off with distance from the surface, so does the zeta potential. The distance from the immobile layer to a point in the bulk liquid at which the potential is 0.37 of that at the interface between the Stern layer and the diffuse layer is defined as the thickness of the double layer, denoted by δ . The

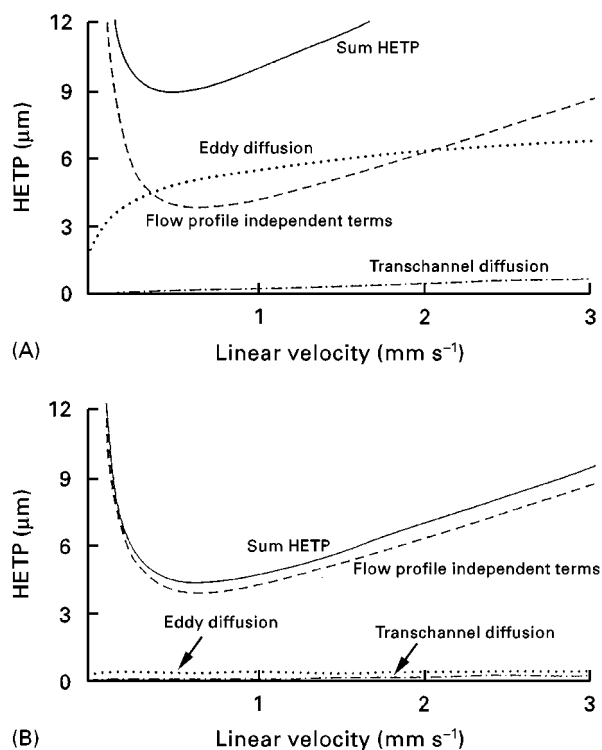


Figure 1 Contributions to plate height in (A) a pressure-driven system (HPLC) and (B) an electrically driven system (electrochromatography). HETP, height equivalent to one theoretical plate. (Reprinted from Dittmann MM and Rozing GP (1996) Capillary electrochromatography – a high efficiency micro-separation technique. *Journal of Chromatography A* 744: 63–74 with kind permission from Elsevier-NL.)

equation describing δ is as follows:

$$\delta = \frac{\varepsilon_r \varepsilon_0 R T^{1/2}}{2 c F^2} \quad [2]$$

where ε_r is the dielectric constant or relative permittivity of the medium; ε_0 is the permittivity of a vacuum ($8.85 \times 10^{-12} \text{ C}^2 \text{ N}^{-1} \text{ m}^2$); R is the gas constant ($8.314 \text{ J K}^{-1} \text{ mol}^{-1}$); T is the temperature in Kelvin; c is the molar concentration of the electrolyte; and F is the Faraday constant ($96\,500 \text{ C mol}^{-1}$).

Using the above equation with water ($\varepsilon_r = 80$), the thickness of the electrical double layer for a 1:1 electrolyte at a concentration of 0.001 mol L^{-1} in water would be 10 nm, while at a concentration of 0.01 mol L^{-1} it would be 1 nm.

Electroosmotic flow (EOF) in a capillary arises when an electric field is applied tangentially along the length of the column. This causes the ions in the diffuse (Gouy) layer that are not absorbed into the Stern layer to migrate towards the cathode. Shearing will occur within this region and electroosmosis will result because the core of liquid within this sheath

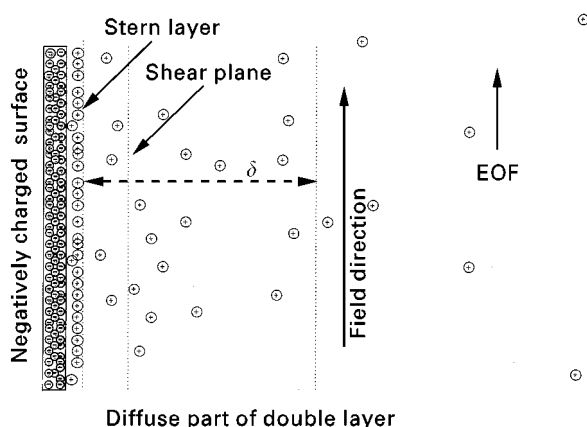


Figure 2 Electrical double layer. Origin of electroosmotic flow (EOF) in a fused silica capillary. (By permission of the author.)

will also be transported to the cathode. Because shearing only occurs within the diffuse layer, the resulting flow profile is plug-like and its velocity is independent of the capillary diameter (d), provided that $d \geq 10\delta$ (d is usually $> 20\delta$).

If d approaches δ , then double layer overlap will occur and the electroosmotic flow will be considerably reduced, taking on a parabolic profile. In the case of packed capillaries, the capillary diameter is replaced in the equation by the mean channel diameter. Thus for aqueous electrolytes between 0.001 mol L^{-1} and 0.01 mol L^{-1} there would be no double layer overlap as long as $d_p \geq 40\delta$.

If we assume a value of 10 nm for δ in a 0.001 mol L^{-1} aqueous solution, then $d_p = 0.4 \mu\text{m}$ and use of these small-diameter particles should give a dramatic increase in column efficiency. Since typical silica-based reversed-phase packing materials also contain silanol groups, these also contribute to the overall EOF, as illustrated in Figure 3.

Another important consideration in CEC is the relationship between the linear velocity and concentration of the electrolyte. Since u is directly propor-

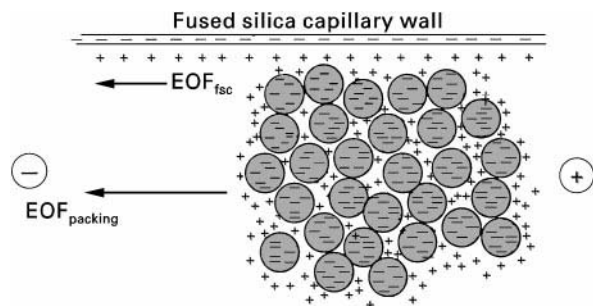


Figure 3 EOF at high pH in a capillary packed with standard HPLC material (e.g. C_{18} , C_8). (By permission of the author.)

tional to the zeta potential, which itself decreases with increasing electrolyte concentration, it is an important variable to consider during method development. The effect of electrolyte concentration on the zeta potential has been measured using 5 μm Hypersil ODS. The results showed that $10^{-4} \text{ mol L}^{-1} \text{ NaNO}_3$ had a zeta potential of $\sim 50 \text{ mV}$, while at $10^{-3} \text{ mol L}^{-1}$ the potential was $\sim 45 \text{ mV}$ and at $10^{-2} \text{ mol L}^{-1}$ it was $\sim 25 \text{ mV}$. When plate height and linear velocity were plotted against NaH_2PO_4 concentration, the reduced plate height was lowest at $10^{-3} \text{ mol L}^{-1}$ and the linear velocity altered little over the range $4 \times 10^{-5} \text{ mol L}^{-1}$ to $2 \times 10^{-2} \text{ mol L}^{-1}$. The best overall performance, i.e. the lowest values of plate height (H), at high EOF would be achieved at electrolyte concentrations of $c. 0.002 \text{ mol L}^{-1}$.

Experimental Considerations

If higher concentrations of buffer are used, particularly with high concentrations of organic solvent, then bubble formation can become a problem. This can be overcome by operating the whole capillary under pressure. Figure 4 is a schematic diagram showing such a pressurized apparatus.

The packing of small-diameter particles into narrow capillaries represents an enormous challenge. The initial stage is the formation of a suitable retaining frit, which must be capable of retaining particles of not more than $1 \mu\text{m}$ and also capable of withstanding pressures of the order of 10 000 psi (68 000 kPa). Outline details of how to form such frits can be found in the literature. The frits must have a good porosity if the packing process is to be successful; porosity can be tested with a conventional HPLC pump at 6000 psi (41 000 kPa) and a flow of water of

1 mL min^{-1} . For a good frit the pressure should rise to 6000 psi fairly rapidly and then stop due to the pressure cut-out. An ideal frit is one where the pressure decays to zero over a period of 10–20 s. If the pressure decay is much quicker then the frit has probably failed; if the decay is very slow then the frit is not porous enough for efficient column packing. Once a satisfactory frit has been formed, then the capillary can be slurry packed as outlined in Figure 5.

Although the packed capillary contains water it is not necessary to condition it with mobile phase since there is a sufficient EOF to allow the mobile phase to be pumped into the system. Once a steady current has been established the column is ready for use.

Applications

Figure 6 shows the separation of the steroid fluticasone propionate from two closely related impurities using micellar electrokinetic chromatography (MEKC) with sodium dodecyl sulfate (SDS) as the micelle while Figure 7 shows the corresponding HPLC trace using 3 μm Spherisorb ODS-1 stationary phase with gradient elution (impurity 3 was not present in the MEKC experiment).

If the sample is analysed by CEC with the same batch of 3 μm Spherisorb ODS-1, then the chromatogram shown in Figure 8 is obtained. Apart from a reversal in elution order from the MEKC/HPLC to the CEC the latter is extremely efficient with peak 3 in the CEC trace exhibiting an efficiency of almost $4 \times 10^5 \text{ plates m}^{-1}$ with a reduced plate height of 0.9.

If the electrolyte is changed from phosphate to borate and the organic content increased from 75 to 80%, then the chromatogram shown in Figure 9 is obtained. Although the capillary length has been increased, the analysis time has been reduced significantly. Also, a peak previously undetected has now shown up between peaks 1 and 2.

Increasing the organic content of the electrolyte can drastically reduce run times, but in order to maintain high efficiencies it is desirable to work at high buffer concentration. To meet this criterion it is necessary to work with so-called biological buffers since traditional inorganic buffers are insoluble in high concentrations of organic solvents. Figure 10 shows the fast, highly efficient analysis of the three impurity peaks from the parent steroid in less than 11 min using a mobile phase containing 0.1 mol L^{-1} Tris buffer (2-amino-2-hydroxymethylpropane-1,3-diol).

Figure 11 shows the chromatogram of a crude sample of a prostaglandin, GR63779X, obtained by using an unadjusted phosphate buffer on a 3 μm Spherisorb ODS-1 phase, while Figure 12 is the same

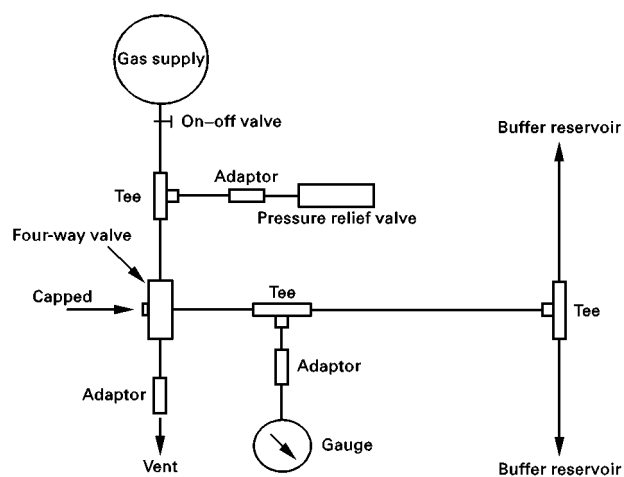


Figure 4 Schematic layout of the pressurization system for electrochromatography. (By permission of the author.)

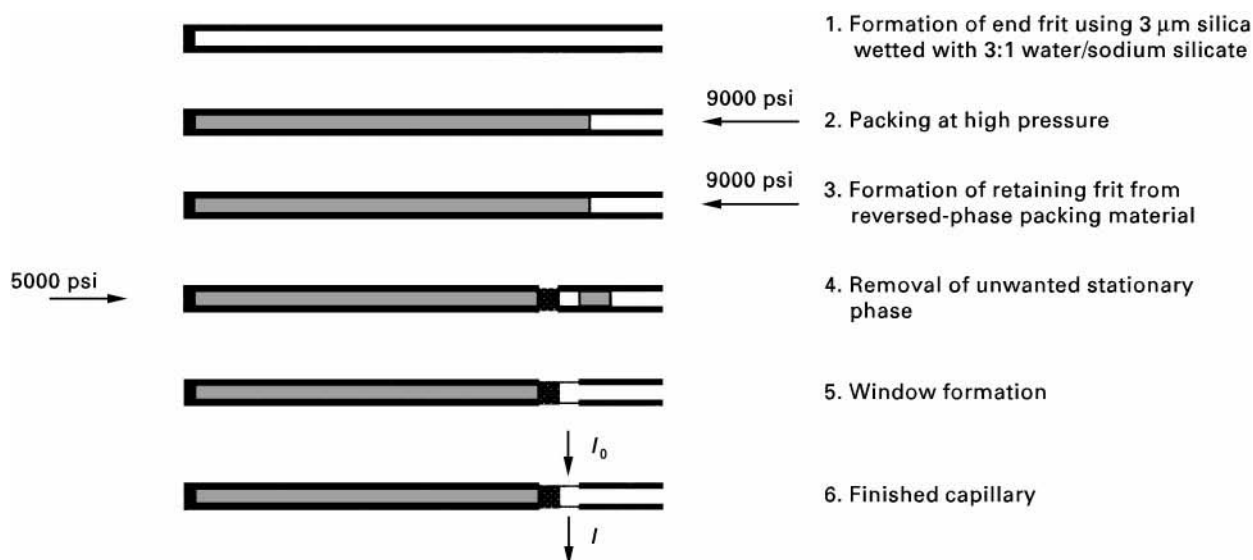


Figure 5 Capillary packing procedure. 5000 psi \approx 34 000 kPa; 9000 psi \approx 62 000 kPa.

sample run under identical conditions on a 1.5 μ m Zorbax C_8 column.

The expected increase in efficiency on going from 3 μ m to 1.5 μ m particles has not been realized. The efficiency for the peak eluting at 20 min on the smaller-particle Zorbax column is about 300 000 plates m^{-1} with a reduced plate height of 1.6. This is not as good as the figures for the 3 μ m column for two reasons: first, there is the difficulty in packing the smaller particles, and second, Zorbax itself is a difficult material to pack. However, for the two early

eluting peaks the 1.5 μ m Zorbax column gives much better peak shapes and slightly different selectivity. **Figure 13** shows a highly efficient separation of an angiotensin compound from 13 impurities. Apart from the two late emerging compounds, all the peaks are symmetrical with no apparent evidence of peak tailing. In contrast many of the compounds in this mixture gave tailing peaks when run on an HPLC column containing the same stationary phase. This may be due to the fact that the CEC separation was at high pH while the HPLC separation was at a pH less than 5. Experience has shown that it is possible to run columns under electrodrive conditions at a much higher pH than is possible in HPLC without any deterioration in performance and often with a considerable improvement in separation.

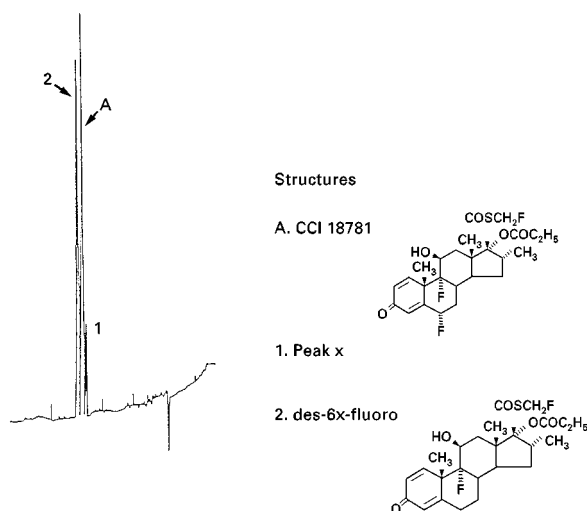


Figure 6 Separation of fluticasone from related compounds by MEKC. Capillary, 72 cm \times 75 μ m i.d.; detection at 238 nm with a range of 0.02 and rise time of 0.5 s; applied voltage, 30 kV; temperature, 60°C; carrier, 0.01 mol L^{-1} Na_2HPO_4 /0.006 mol L^{-1} $Na_2B_4O_7 \cdot 10H_2O$ /0.05 mol L^{-1} SDS in 20% methanol; injection, 1.0 s vacuum.

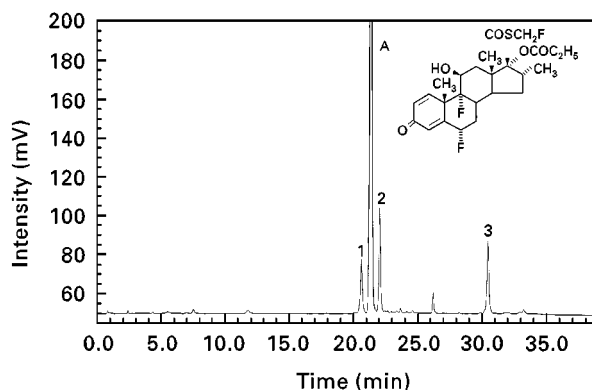


Figure 7 Separation of fluticasone from related compounds by HPLC. Column, 15 cm \times 4.6 mm i.d. packed with 3 μ m ODS-1; flow rate, 1.0 mL min^{-1} ; detection at 238 nm, 0.05 absorbance units full scale (aufs); gradient 40% acetonitrile/ H_2O \rightarrow 70% acetonitrile/ H_2O in 20 min. (By permission of the author.)

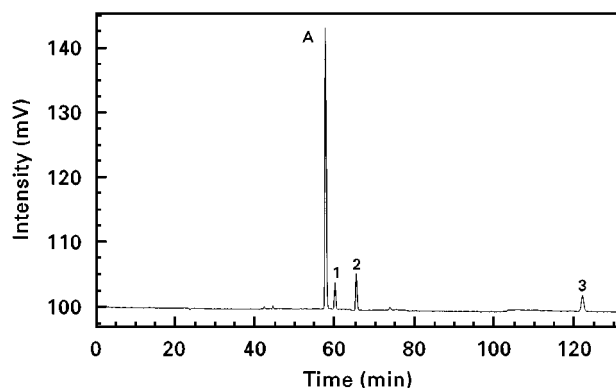


Figure 8 Separation of fluticasone from related compounds by capillary electrochromatography (CEC) with a phosphate buffer. Column, 40 cm \times 50 μ m i.d. packed with 3 μ m ODS-1; detection at 238 nm, 0.05 au/s; voltage, 30 kV; temperature, 30°C; carrier, 75% acetonitrile/H₂O; buffer 2 mmol L⁻¹ Na₂HPO₄, pH 8.3; injection, 0.4 min at 20 kV.

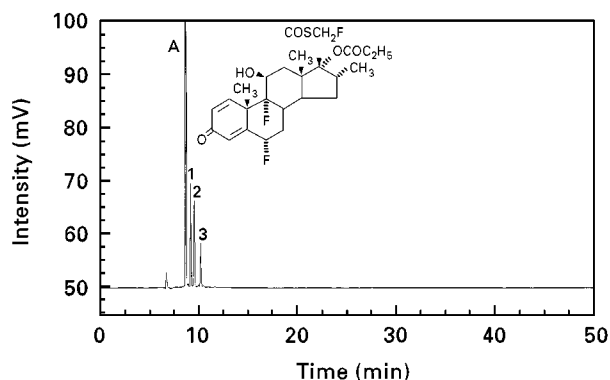


Figure 10 Rapid separation of fluticasone from related impurities by CEC with a Tris buffer. Column, 40 cm \times 50 μ m i.d. packed with 3 μ m ODS-1; detection at 238 nm, 0.05 au/s; voltage, 30 kV; temperature, 30°C; carrier, 90% acetonitrile/10% 0.1 mol L⁻¹ Tris; injection, 0.05 min at 10 kV.

Cephalosporins are a class of antibiotic compounds. As well as the chiral centre in the β -lactam ring, the compound shown in **Figure 14** possesses a chiral centre in the ester group on the adjacent six-membered ring, giving rise to a pair of diastereoisomers. In addition the oxime group can be in one of two positions – either the *syn* (*E*) or the *anti* (*Z*) – both of which give rise to isomers. Both pairs of diastereoisomers are readily resolved on the 3 μ m Spherisorb ODS-1 column with a length of 40 cm. The use of such a column length for HPLC would be impractical because the pressure requirements would be beyond the range of current instruments. Since there is no pressure drop in CEC, the use of long columns presents no practical problems.

If the extremely high efficiencies obtained with CEC for achiral compounds could be matched with

chiral compounds, then there would be less need to achieve high α values in order to separate the isomers. **Figures 15** and **16** show the separation of bendroflumethiazide and hexobarbital on an α -glycoprotein and a Cyclobond stationary phase, respectively. Although large α values are obtained with these columns, the overall efficiencies are extremely poor. This is possibly due to column overload, since these phases have a low sample capacity.

Nearly all CEC separations to date have been carried out on C₁₈ or C₈ phases. However, because EOF drops off substantially below pH 6, most studies have been carried out above pH 7 and as a result most CEC has been for neutral molecules. One way of promoting EOF at lower pH values is by the use of columns packed with a strong cation exchanger (SCX); such

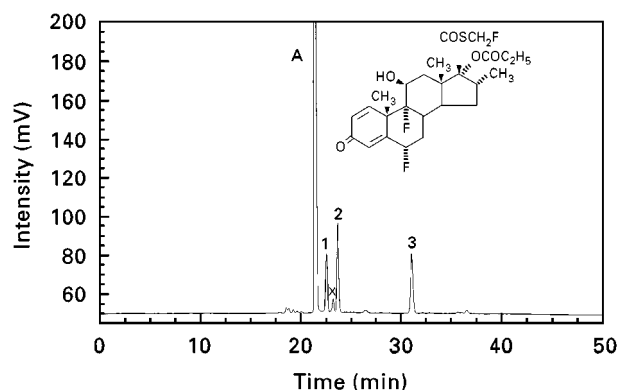


Figure 9 Separation of fluticasone from related compounds by CEC with a borate buffer. Column, 60 cm \times 50 μ m i.d. PC20 packed with 3 μ m ODS-1; detection at 238 nm, 0.05 au/s; voltage, 30 kV; temperature, 30°C; carrier, 80% acetonitrile/20% 5 mmol L⁻¹ borate, pH 9; injection, 0.4 min at 30 kV.

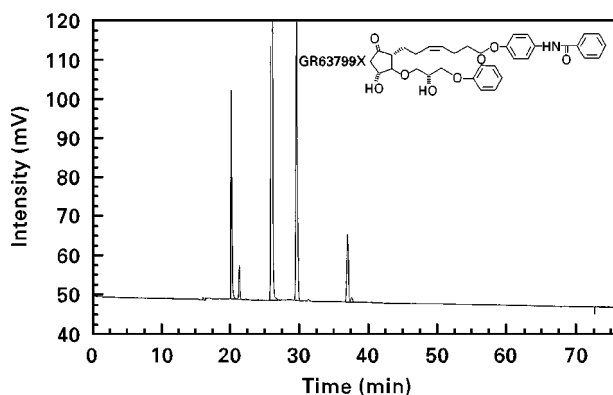


Figure 11 Separation of a prostaglandin from related impurities by CEC. Column, 60 cm \times 50 μ m i.d. packed with 3 μ m ODS-1; detection at 270 nm, 0.05 au/s; voltage, 30 kV; temperature, 35°C; carrier, 70% acetonitrile/30% 0.1 mol L⁻¹ Na₂HPO₄; injection, 0.04 min at 30 kV. (By permission of the author.)

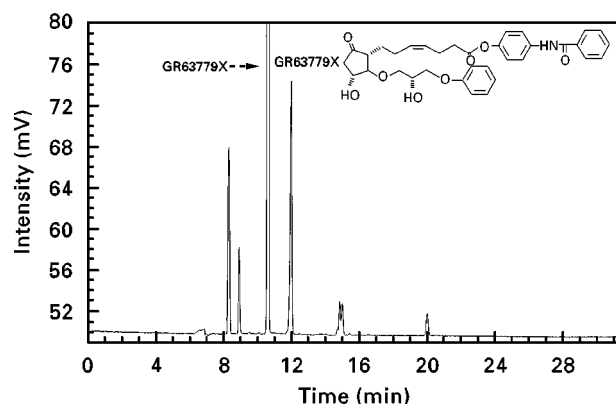


Figure 12 Separation of a prostaglandin from related impurities by CEC with a column packed with 1.5 μm C_8 silica. Column, 40 cm \times 50 μm i.d. packed with 1.5 μm Zorbax; detection at 270 nm, 0.05 a.u.; voltage, 30 kV; temperature, 30°C; carrier, 70% acetonitrile/30% 0.1 mol L⁻¹ Na₂HPO₄; injection, 0.04 min at 20 kV.

a material has been used for the CEC of neutral and charged analytes. The SCX used (manufactured by Phase Separations Ltd, Deeside, UK) had a sulfonic acid group linked to 3 μm silica via a propyl group to give a loading of 0.031 mEq g⁻¹.

Figure 17 shows the structures of a group of tricyclic antidepressants. Because of the highly basic nature of these compounds, with typical pK_a values of around 8, severe tailing is encountered with HPLC and even the new base-deactivated phases made from ultrapure silica still give some tailing.

When a test mixture containing bendroflumethiazide and four of the antidepressants was analysed on a Spherisorb ODS-1 capillary, only the neutral bendroflumethiazide eluted (Figure 18). However, CEC

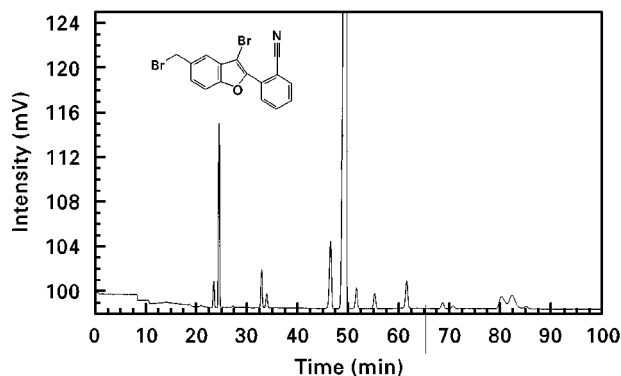


Figure 13 Separation of an angiotensin compound from impurities by CEC at a relatively high pH. Column, 30 cm \times 50 μm i.d. packed with 3 μm ODS-1; detection at 220 nm, 0.03 a.u.; voltage, 30 kV; temperature, 28°C; carrier, 76% acetonitrile/H₂O in 2 mmol L⁻¹ Na₂HPO₄ buffer, pH 7.3; injection, 0.4 min at 20 kV.

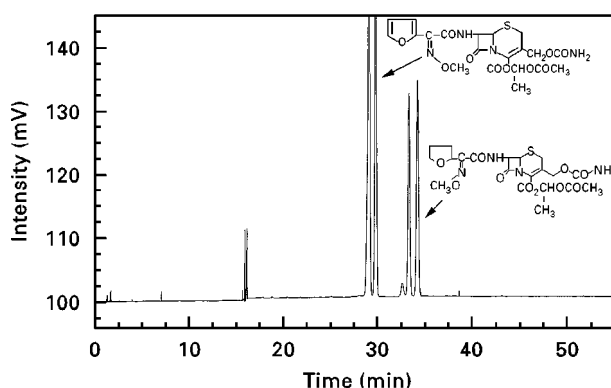


Figure 14 Separation of diastereoisomers by CEC. Column, 40 cm \times 50 μm i.d. packed with 3 μm ODS-1; detection at 276 nm, 0.03 a.u.; voltage, 30 kV; temperature, 30°C; carrier, 50% acetonitrile/50% 0.01 mol L⁻¹ Na₂HPO₄; injection 0.2 min at 20 kV.

analysis at low pH on the 3 μm SCX phase gave unexpectedly high efficiencies. Figure 19 shows the separation of three tricyclic antidepressants on the cation exchange phase at pH 3.5. It is noticeable in this chromatogram that the neutral compound bendroflumethiazide, despite eluting first, gives a significantly broader peak than the later eluting compounds. This suggests that some form of focusing effect is taking place. Plate numbers on this phase have been measured in excess of 8×10^7 , which is many orders of magnitude above that explicable by current theory.

Attempts to use a mixed-mode column with a C₁₈ ligand and a -SO₃H functional group attached to the same silica particle were not successful. When the antidepressant test mixture is injected onto the mixed-mode column at both pH 9.8 and pH 5.7, only

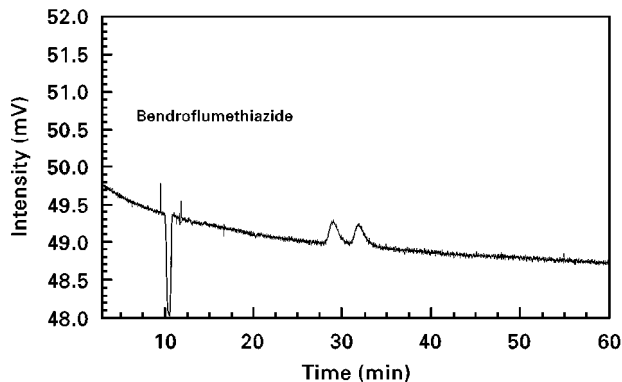


Figure 15 Chiral separation of bendroflumethiazide by CEC with an α -glycoprotein stationary phase. Column, 40 cm \times 50 μm i.d.; detection at 225 nm, 0.05 a.u.; voltage, 30 kV; temperature, 30°C; carrier, 10% IPA/0.01 mol L⁻¹ Na₂HPO₄ buffer, pH 7; injection, 0.4 min at 30 kV. (By permission of the author.)

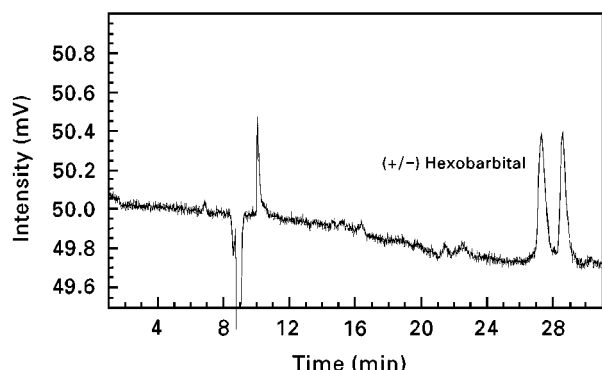


Figure 16 Chiral separation of hexobarbital by CEC with a Cyclobond 1 stationary phase. Detection at 210 nm, 0.05 aufs; carrier, 5% acetonitrile/95% Na_2HPO_4 , pH 7.1; injection, 0.3 min at 10 kV. (By permission of the author.)

the neutral bendroflumethiazide is eluted. Similar results were obtained with a mixed-mode phase with a C_6 chain. It is believed that the hydrophobic ligands

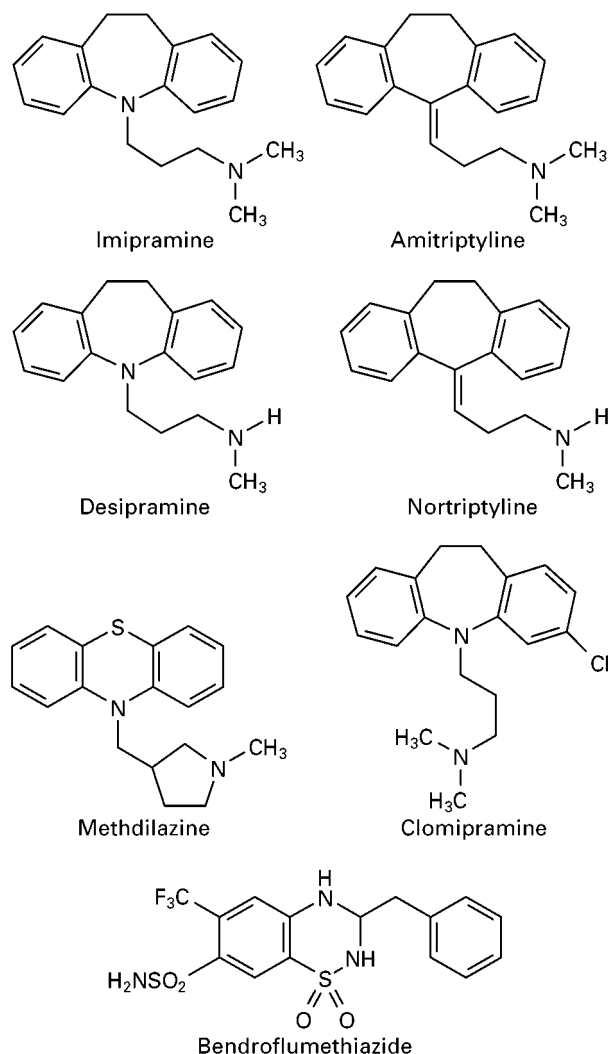


Figure 17 Structures of some tricyclic antidepressants separated by CEC.

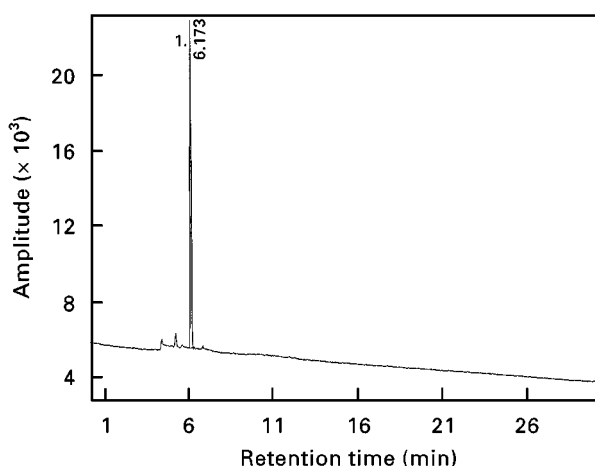


Figure 18 CEC of bendroflumethiazide and four tricyclic antidepressants by CEC on a $3\text{ }\mu\text{m}$ ODS-1 column. Detection at 210 nm, 0.05 aufs root temperature 0.2; voltage, 30 kV; temperature, 30°C ; carrier, 70% acetonitrile/30% 0.01 mol L^{-1} Na_2HPO_4 , pH 9.8 unadjusted; injection, 0.3 min at 3 kV. Peak 1 represents bendroflumethiazide. Nortriptyline, clomipramine, methdilazine and imipramine were not eluted.

collapse onto the $-\text{SO}_3\text{H}$ groups and shield them from participation in the focusing process. If a strong cation exchanger is produced, using a different link from the propyl group used for the original material, then the focusing effect returns. **Figure 20** shows the electrochromatogram of methdilazine, clomipramine and imipramine on a column containing a stationary phase where the sulfonic acid group is attached to the silica via a phenyl group. Once again, highly efficient separations are obtained. Methdilazine now elutes before clomipramine, whereas on the propyl $-\text{SO}_3\text{H}$ phase elution was the other way round.

Nonporous materials are used in HPLC for the analysis of highly hydrophobic compounds that

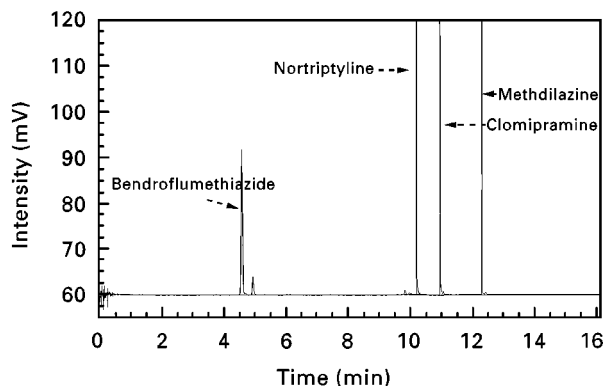


Figure 19 CEC of bendroflumethiazide and three tricyclic antidepressants on a $3\text{ }\mu\text{m}$ Spherisorb SCX column. Detection at 220 nm, 0.045 aufs; voltage, 30 kV; temperature, 30°C ; carrier, 70% acetonitrile/30% 0.05 mol L^{-1} Na_2HPO_4 , pH 3.5; injection, 0.5 min at 2 kV.

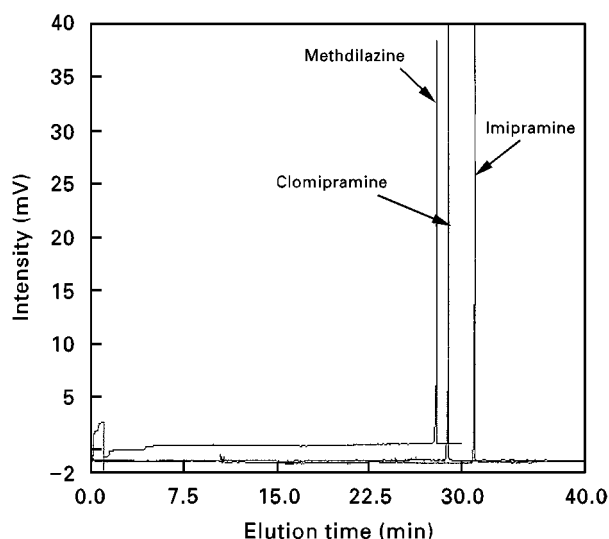


Figure 20 CEC separation of three tricyclic antidepressants on an SCX column with the SO_3H group attached to the silica via a phenyl group. Packed length = 40 cm, total length = 56 cm; voltage, 30 kV; detection at 210 nm; 0.02 aufs; carrier, 70% acetonitrile/30% $0.01 \text{ mol L}^{-1} \text{NaH}_2\text{PO}_4$, pH 2.3; injection, 0.4 min at 2 kV.

would normally be too strongly retained on conventional porous reversed-phase packings. Micropell C_{18} , made by Horváth (Yale, USA), has been used successfully for CEC with relatively small molecules even though there is little retention because of the very small surface area. **Figure 21** shows the separation of the neutral diol, GR5788X, from the dibenzyl compound, GR57994X, in less than 4 min on a 40 cm capillary packed with this $2 \mu\text{m}$ nonporous phase.

Conclusion

Capillary electrochromatography is a highly promising technique that couples the advantages associated with capillary electrophoresis with those of HPLC. Theory predicts a 2- to 3-fold increase in efficiency on going from an HPLC pressure-driven system to a CEC electrically driven system. Because there is no pressure drop across the capillary column in CEC, it is possible to use long columns that would require prohibitively high pressures if used in pressure-driven systems. Examples have been given of separations by CEC on 40 cm long capillaries giving efficiencies of $4 \times 10^5 \text{ plates m}^{-1}$. This is equivalent to 160 000 effective plates, which is a factor of about 15 times greater than that currently available in HPLC.

The development of stationary phases that allow CEC to be used over a wider pH range will allow the analysis of mixtures containing neutral and charged

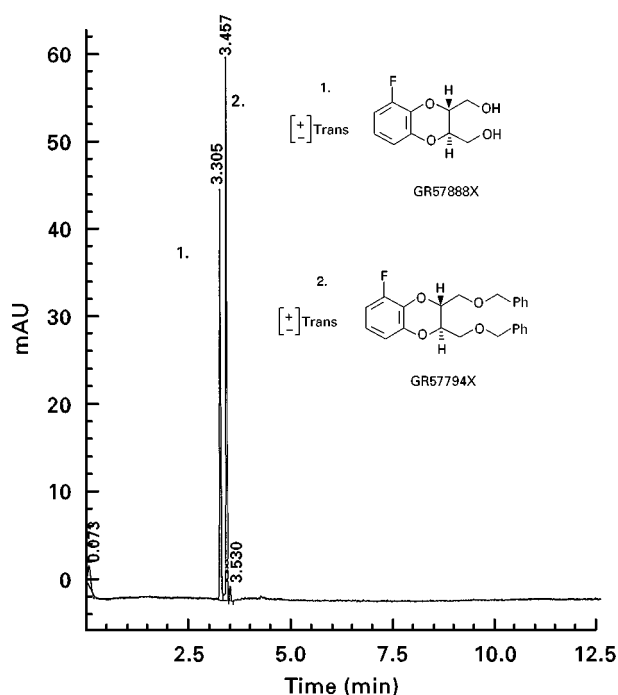


Figure 21 CEC separation on a nonporous phase, Micropell- C_{18} . Voltage, 30 kV; temperature, 30°C ; detection at 210 nm; carrier, 70% acetonitrile/30% $2 \text{ mmol L}^{-1} \text{Na}_2\text{HPO}_4$, pH 7.0; injection, 10 s at 2 kV.

species and will offer a viable complementary technique to HPLC and capillary electrophoresis.

See also: **II/Chromatography: Liquid:** Column Technology; Mechanisms: Reversed Phases; Detectors for Capillary Electrophoresis; Micellar Electrokinetic Chromatography. **III/Chiral Separations:** Capillary Electrophoresis.

Further Reading

- Dittman MM and Rosing GP (1996) Capillary electrochromatography – a high efficiency micro-separation technique. *Journal of Chromatography A* 744(1–2): 63–74.
- Knox JH and Grant IH (1987) Miniaturisation in pressure and electroosmotically driven liquid chromatography: some theoretical considerations. *Chromatographia* 24: 135–143.
- Knox JH and Grant IH (1991) Electrochromatography in packed tubes using 1.5 to $50 \mu\text{m}$ silica gels and ODS bonded silica gels. *Chromatographia* 32: 317–328.
- Pretorius V, Hopkins BJ and Schieke JD (1974) Electroosmosis – a new concept for high speed liquid chromatography. *Journal of Chromatography* 99: 23–30.
- Smith NW and Evans MB (1995) The efficient analysis of neutral and highly polar pharmaceutical compounds using reversed-phase and ion-exchange electrochromatography. *Chromatographia* 41: 197–203.

Enhanced Fluidity Liquid Chromatography

S. V. Olesik, Ohio State University,
Columbus, OH, USA

Copyright © 2000 Academic Press

Introduction

High performance liquid chromatography (HPLC) is often the method of choice for the separation of nonvolatile solutes. LC commonly exhibits longer analysis times, larger pressure drops and lower efficiency than either supercritical fluid chromatography (SFC) or gas chromatography (GC). The greater viscosities and lower diffusivities of liquids compared to those of supercritical fluids or gases are the primary cause of these differences in the three types of chromatography. The ideal mobile phase for a chromatographic separation of nonvolatile solutes would combine the positive attributes of liquids and supercritical fluids. That is, a solvent with low viscosity, high diffusivity and high solvent strength is desirable. Enhanced-fluidity liquid mixtures are solvents that have these attributes. These solvents are prepared by dissolving large proportions of liquefied gases, such as CO₂, in commonly associated liquid solvents such as methanol.

To date, enhanced-fluidity mixtures such as methanol-CO₂, methanol-CO₂-H₂O, tetrahydrofuran-CO₂, hexane-CO₂, methanol-fluoroform and methanol-fluoroform-H₂O have been used to improve the performance in a range of different types of liquid chromatographies.

Properties of Enhanced-Fluidity Liquid Mixtures

When a liquefied gas is added to an associated solvent, the viscosity of the resultant mixture decreases. For example, Figure 1 shows the variation in the viscosity of methanol-CO₂ and solute diffusivity as a function of the proportion of added CO₂ at 25°C. The addition of 50% v/v CO₂ causes the viscosity of the mixture to lower to a value that is approximately 70% of the viscosity of methanol. The viscosity, η , of a liquid is typically inversely related to the diffusion coefficient of a solute at infinite dilution, D_{12} , as described in eqn [1]:

$$D_{12}\eta^p = AT \quad [1]$$

where A and p are constants that are characteristic of the solute and T is the absolute temperature. There-

fore, Figure 1 shows that the addition of 50% v/v CO₂ causes the diffusion coefficient of benzene to increase by approximately a factor of 2.

If liquefied gas addition and temperature elevation are combined, improvements in mass transport are substantial. For example, at 58°C with a 0.49 : 0.21 : 0.30 mol fraction methanol-H₂O/CO₂ mixture, the diffusion coefficient of benzene increases ninefold relative to that in the same methanol-H₂O mixture at 26°C. Without temperature elevation, the diffusion coefficient of benzene increases by a factor of 2 by adding 0.30 mol fraction CO₂ to the 0.70 : 0.30 mol ratio methanol-H₂O mixture (Figure 2).

These improvements in the transport properties of the liquid mixtures are only advantageous if the solvent strength of the mixtures remains high when the liquefied gas is added. Figures 3 and 4 show the variation of the hydrogen bond acidity, hydrogen-bond basicity and dipolarity for methanol-CO₂ mixtures as measured by Kamlet-Taft α , β , and π^* solvent strength parameters. Clearly the hydrogen bond acidity and basicity of the methanol-CO₂ mixtures is similar to that of methanol, even with 70% added CO₂. The dipolarity of the mixture decreases faster than the hydrogen bond acidity or basicity with added CO₂. However, the dipolarity remains relatively high, even with 50% added CO₂. Data collected on a number of enhanced-fluidity mixtures have shown that often as much as 50% liquefied gas can be added to the organic solvent without significantly affecting the solvent strength.

Theory

To demonstrate the importance of mass transfer coefficients in liquid chromatography, the van Deemter equation (eqn [2]) is used to model the variation of the chromatographic band dispersion, H , in packed column as a function of linear velocity, u . A is a constant that measures the contribution to band dispersion caused by multiflow paths, B describes the band dispersion caused by longitudinal diffusion and C describes the band dispersion caused by nonequilibrium in both the stationary and mobile phases:

$$H = A + \frac{B}{u} + \sum C_i u \quad [2]$$

By taking the derivative of the van Deemter equation with respect to u , equating the derivative to zero, and substituting in appropriate definitions for A , B and C ,

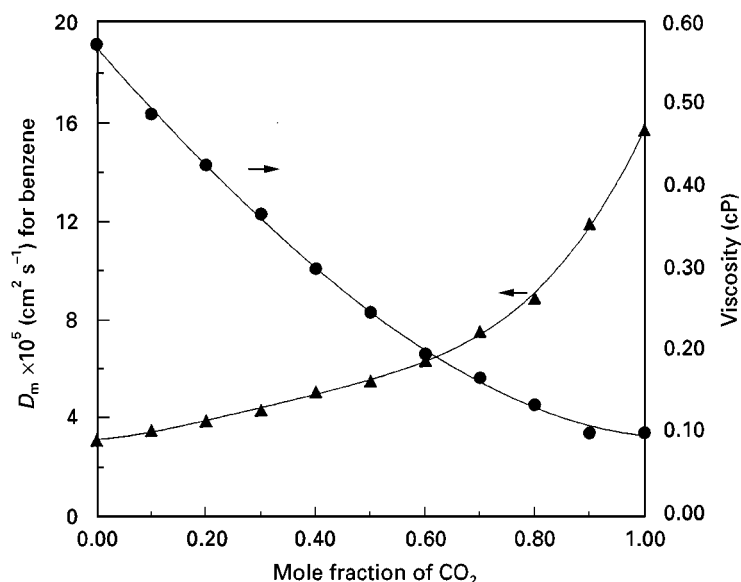


Figure 1 Variation of the viscosity (●) of methanol-CO₂ mixtures and the diffusion coefficient (▲) of benzene at 25°C and 170 atm as a function of mixture composition. (Reproduced with permission from Cui and Olesik (1991).)

the optimum velocity, u_{opt} , is described by eqn [3]: C_{stag} (eqn [4]):

$$u_{\text{opt}} \propto \frac{D_m}{\sqrt{f(k')}} \quad [3]$$

$$C_{\text{stag}} = \frac{f(k)}{D_m} \quad [4]$$

The use of enhanced-fluidity mobile phases is expected to increase the diffusion coefficients of the solute and therefore shift u_{opt} to larger values.

For most HPLC separations that involve packed columns containing porous particles and function at linear velocities greater than u_{opt} , the predominant contribution to band dispersion is the diffusion in the stagnant mobile phase inside the porous packing,

k is the retention factor and D_m is the diffusion coefficient of the solute in the mobile phase. Therefore, since solutes in enhanced-fluidity liquid mixtures have significantly higher diffusion coefficients than in the organic solvent, chromatographic band dispersion decreases (as will be illustrated later). In addition to higher diffusion rates in enhanced-fluidity solvents, the addition of the liquefied gas often lowers

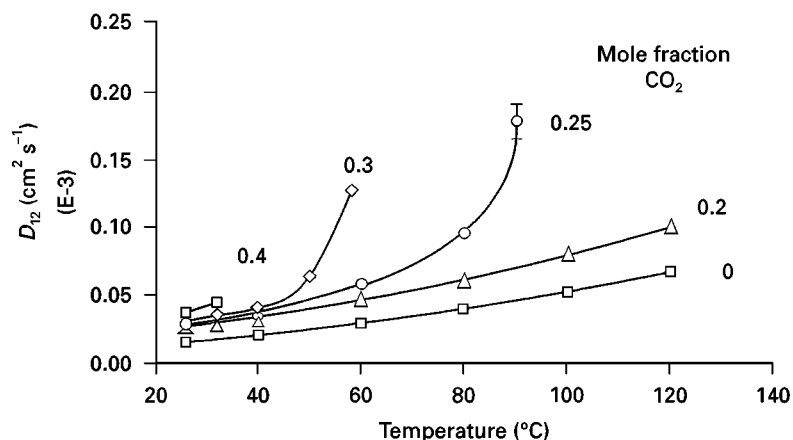


Figure 2 Variation in the diffusion coefficient of benzene for: squares, 0.70:30 mol fraction methanol-H₂O; triangles, 0.56:0.24:0.20 mol fraction methanol-H₂O-CO₂; circles, 0.49:0.21:0.30 mol fraction methanol-H₂O-CO₂; diamonds, 0.42:0.18:0.40 mol fraction methanol-H₂O-CO₂ as a function of temperature. (Reproduced with permission from Lee and Olesik (1994).)

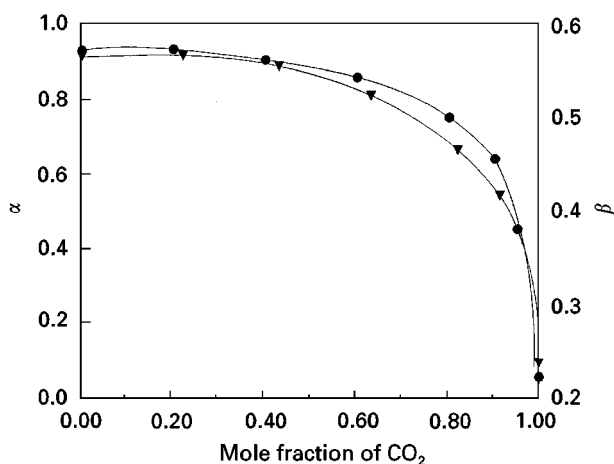


Figure 3 Variation of Kamlet-Taft α (●) and β (▼) parameter as a function of mixture composition for methanol-CO₂ mixtures at 25°C and 170 atm. (Reproduced with permission from Olesik (1991).)

the capacity factor of solutes in some liquid chromatographies. Significant improvements in efficiency can result from the combination of the two effects.

The separation time for a chromatographic analysis is proportional to the slope of a plot of H versus u . Therefore the separation time is also shortened when using enhanced-fluidity solvents. Finally, Darcy's law (eqn [5]) shows that the pressure drop across a packed chromatographic column is linearly related to the product of the linear velocity, u , and the mobile-phase viscosity, η :

$$\Delta P = \frac{u\eta\varepsilon L}{B^0} \quad [5]$$

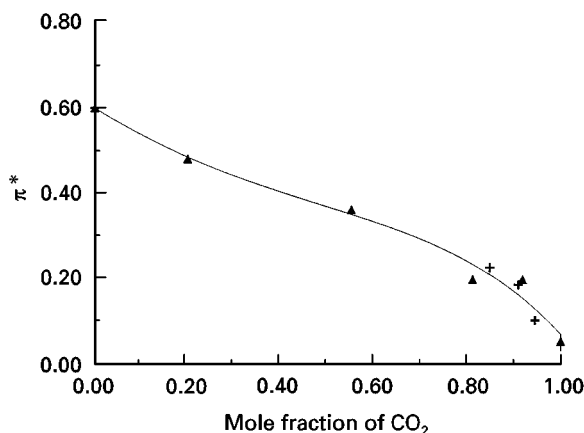


Figure 4 Variation of Kamlet-Taft π^* as a function of mixture composition for methanol-CO₂ mixtures at 25°C and 170 atm. (Reproduced with permission from Cui and Olesik (1991).)

where B^0 is the specific permeability, ΔP is the pressure drop across the column, ε is the interparticle porosity, η is the viscosity and L is the length of the column.

Experimental Methods and Instrumentation

The instrumentation required to do enhanced-fluidity liquid chromatography is very similar to a standard HPLC with two exceptions. Firstly, the components of the mobile phase (liquefied gas and associated liquid) are mixed under pressurized conditions. Therefore two pumps are required to make the mixtures. Either syringe pumps or reciprocating pumps may be used. Pumps that are commonly used for SFC are optimum for pumping the liquefied gases. Secondly, the outlet of the column must be pressurized to maintain single-phase conditions for the mobile-phase mixture at least until after the solutes are detected. Therefore a flow restrictor similar to those used in SFC is used in enhanced-fluidity LC. However, the problems which are often experienced in SFC with restrictor plugging do not occur in enhanced-fluidity LC because phase changes are not occurring in the restrictors and the solvent strength of the enhanced-fluidity liquids is greater than that of commonly used supercritical solvents. Finally, phase diagram information can be used to determine what the minimum operating pressure at the end of the column should be, to ensure that the mobile phase is operating under single-phase conditions. This information for the mixtures described herein is readily available in the literature.

Reversed-Phase Chromatography

When methanol-H₂O-CO₂ mixtures are used in reversed-phase separations with an octadecyl polysiloxane stationary phase, the efficiency of the separation increases significantly compared to the same conditions without the addition of CO₂. For example, the reduced plate height for naphthalene at a reduced velocity of 10 decreased from 11 to 4 for a mobile-phase composition change involving the addition of 0.50 mol fraction CO₂ to a 0.7 : 0.3 mol ratio methanol-H₂O mixture. The addition of 0.5 mol fraction CO₂ to the 0.7 : 0.3 mol ratio methanol-H₂O shortens the analysis time of a separation of polynuclear aromatic hydrocarbons by factors of 2.5 and 8 at linear velocities of 0.15 (reduced velocity = 5) and 0.35 (reduced velocity = 17) cm s⁻¹, respectively, compared to that for the methanol-water mixture at the same linear velocities.

Figure 5 shows the variation in the band dispersion of pyrene using the 0.70 : 0.30 mol ratio methanol-

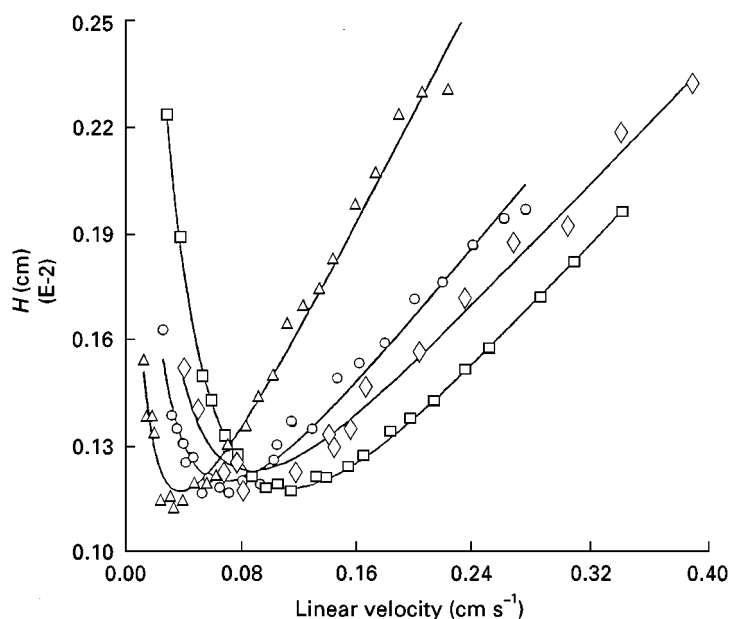


Figure 5 Variation of plate height with mobile-phase linear velocity for pyrene at 204 atm for different mobile-phase conditions: triangles, 0.70 : 0.30 mol ratio methanol-H₂O at 26°C, $k' = 3.77$; circles, 0.70 : 0.30 mol ratio methanol-H₂O at 60°C, $k' = 2.02$; diamonds, 0.49 : 0.21 : 0.30 mol ratio methanol-H₂O-CO₂ at 26°C, $k' = 1.82$; squares, 0.49 : 0.21 : 0.30 mol ratio methanol-H₂O-CO₂ at 60°C, $k' = 0.92$. (Reproduced with permission from Lee and Olesik (1994).)

H₂O mixture, with 0.30 mol fraction CO₂ added at room temperature and with 0.30 mol fraction CO₂ added at 60°C. As expected, the band dispersion decreased and the optimum linear velocity increased when CO₂ was added to the mobile phase. The increase in temperature also yields substantial gains in efficiency, especially at high linear velocities.

Figure 6 shows the improved separation time which is possible by adding CO₂ and increasing the temperature to 60°C at the same linear velocity for the separation of 16 polynuclear aromatic hydrocarbons. The separation required approximately 40 min with 0.70 : 0.30 methanol-H₂O approximately 15 min when 0.30 mol fraction CO₂ was added and less than 7 min when this mixture was heated to 60°C. However, when 30% CO₂ was present in the mobile phase and the temperature was 60°C, the selectivity of the separation degraded substantially.

Also, due to the low viscosity of the methanol-H₂O-CO₂ multiple columns can be placed in series to increase the overall efficiency of a chromatographic separation. For the same linear velocity, Figure 7 compares the separation of a coal tar sample using one and four ODS columns. Substantial gains in efficiency are obtained by placing the columns in series.

However, the addition of liquefied CO₂ is not optimal to improve the performance of every separation. When CO₂ is mixed with H₂O, carbonic acid is for-

med. The acidic nature of this mobile phase can have a significant impact on the retention factor of ionizable compounds. Also CO₂ and H₂O are not highly miscible at room temperature without the addition of a co-solvent. Even with the addition of co-solvent, the total amount of CO₂ that is miscible in the mixture is controlled by the amount of H₂O present. For example, a 0.70 : 0.30 mol ratio methanol-H₂O mixture is immiscible with more than 0.50 mol fraction CO₂. To eliminate many of these problems, other liquefied gases can also be used to modify the fluidity of the mixture.

Normal-Phase Chromatography

The addition of a liquefied gas is even beneficial when mixed with nonpolar solvents commonly used in normal-phase LC. For example, when 50 mol% CO₂ is combined with 50 mol% hexane, the efficiency increases by at least a factor of 2 across the entire range of linear velocities studied and the mobile phase viscosity also decreases by a factor of approximately 2. However, the addition of proportions of CO₂ greater than 50 mol% causes significant peak asymmetry and decreased efficiency.

Size Exclusion Chromatography

In size exclusion chromatography (SEC), the selectivity of the separation is not affected significantly by the

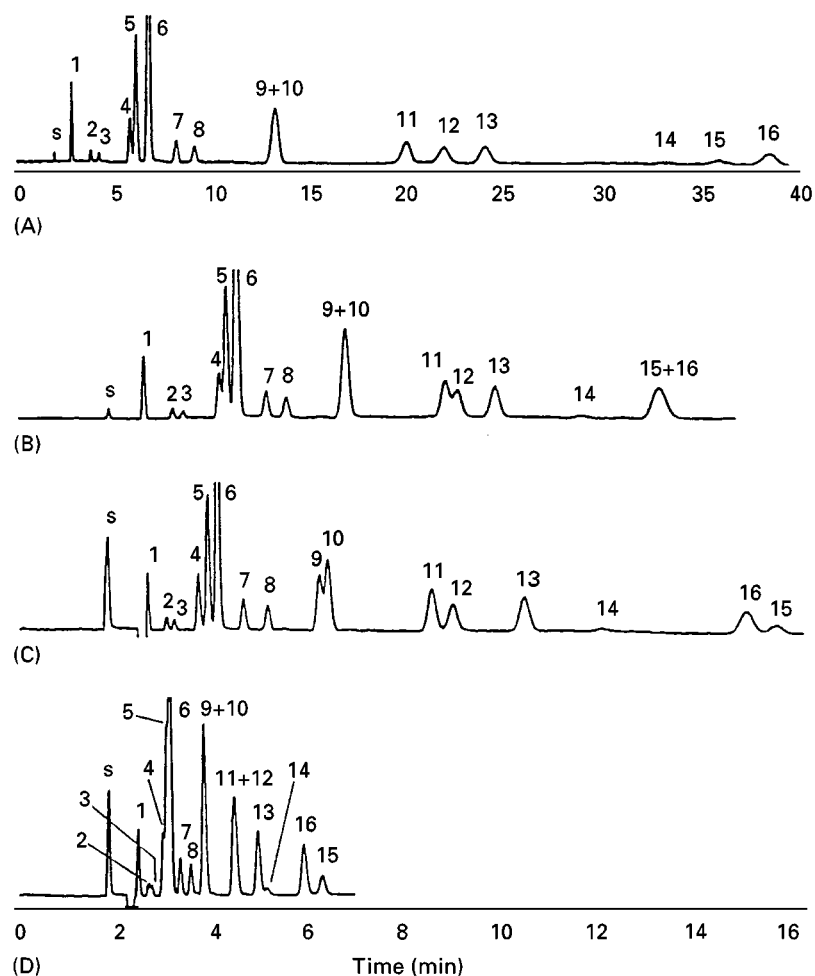


Figure 6 Chromatograms of 16 polynuclear aromatic hydrocarbons at 204 atm for different mobile-phase conditions: (A) 0.70 : 0.30 mol ratio methanol-H₂O at 26°C; (B) 0.70 : 0.30 mol ratio methanol-H₂O at 60°C; (C) 0.49 : 0.21 : 0.30 mol ratio methanol-H₂O-CO₂ at 26°C; (D) 0.49 : 0.21 : 0.30 mol ratio methanol-H₂O-CO₂ at 60°C. 1, Benzene; 2, naphthalene; 3, acenaphthalene; 4, fluorene; 5, phenanthrene; 6, anthracene; 7, fluoranthene; 8, pyrene; 9, benzo[a]anthracene; 10, chrysene; 11, benzo[b]fluoranthene; 12, benzo[k]fluoranthene; 13, benzo[a]pyrene; 14, dibenzo[a,h]anthracene; 15, benzo[ghi]perylene; 16, indeno[1,2,3-cd]pyrene. (Reproduced with permission from Lee and Olesik (1994).)

choice of mobile phase because the separation is based solely on the entropic partitioning of the solute between the bulk mobile phase and the stagnant solvent in the pores. Therefore, efficient separations are highly desirable in SEC. Often, to increase the total efficiency of a separation, analytical columns are connected in series until the maximum pressure of the chromatographic pumping system is approached. SEC is frequently used at elevated temperatures to improve the solubility of high MIC samples and this also lowers the mobile-phase viscosity and allows more columns to be linked together to increase the total efficiency of the separation.

Enhanced-fluidity liquid mixtures can improve the chromatographic performance of SEC without need-

ing to increase the temperature. When CO₂ was added to tetrahydrofuran (THF) for the separation of polystyrene standards, improved efficiency and decreased separation time resulted. For a mobile-phase velocity of approximately 0.8 cm s⁻¹, the reduced plate height for polystyrene (*M_w* 12 600) decreased by a factor of 2 by adding 0.40 mol% CO₂ to the THF. In addition, the 40 mol% CO₂ : 60 mol% THF mixture had a viscosity that was approximately 50% that of pure THF, which resulted in an approximate 50% decrease in the separation time for the separation. However, when greater proportions of CO₂ were added to the THF, the solvent strength diminished significantly, which caused adsorptive interactions to compete with the exclusion mechanism.

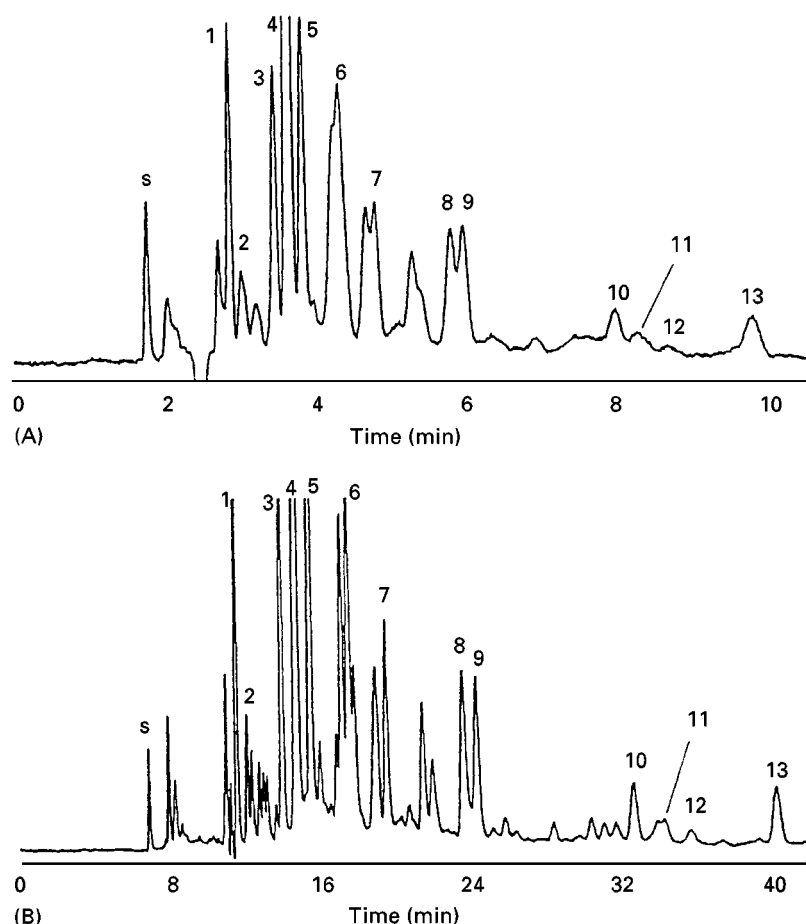


Figure 7 Chromatograms of the NIST SRM 1597 coal tar standard using 0.49 : 0.21 : 0.30 mol ratio methanol-H₂O-CO₂ at 26°C and 204 atm for (A) one and (B) four columns (A) $u = 0.143 \text{ cm s}^{-1}$; $\Delta P = 22.0 \text{ atm}$; (B) $u = 0.145 \text{ cm s}^{-1}$; $\Delta P = 127.5 \text{ atm}$. (Hypersil C₁₈ 150 × 1 mm packed with 5 μm diameter particles.) 1, Naphthalene; 2, acenaphthalene; 3, fluorene; 4, phenanthrene; 5, anthracene; 6, fluoranthene; 7, pyrene; 8, benz[a]anthracene; 9, chrysene; 10, benzo[b]fluoranthene; 11, benzo[k]fluoranthene; 12, perylene; 13, benzo[a]pyrene. (Reproduced with permission from Lee *et al.* (1995).)

Both enhanced-fluidity SEC and high temperature SEC have limits to the scope of their application. Enhanced-fluidity SEC is limited by the solvent strength of the high fluidity mixtures and high temperatures can cause decomposition of the polymer. Therefore the combination of increased temperature and use of enhanced-fluidity SEC might often be the best choice to improve the chromatographic performance in exclusion separations.

By adding 30 mol% CO₂ to THF and increasing the temperature from 24 to 80°C, the slope of a plot of reduced plate height versus linear velocity decreases substantially. For example, with styrene as the solute, the C coefficient in the van Deemter equation decreases to a value that is only 17% of the C value when THF at 24°C is the mobile phase (Figure 8). With such a flat slope, SEC separations can be accomplished at high velocities with minimal loss in efficiency.

Liquid Chromatography at Critical Condition

Liquid chromatography at the critical condition is a separation method that allows the analyst to decide what portion of the molecule will control the separation. For example, at the critical condition for polystyrene polymers, all polystyrene oligomers will elute at the same elution volume, while functionalized polystyrene will be separated based solely on the functionality distribution within the polymer. This method can also be used to make a component of a copolymer chromatographically invisible and then obtain separation based on the other components of the copolymer.

At the critical condition, the change in free energy associated with the transfer of the polymer (in this case, polystyrene) to the stationary phase is zero. That is, at the critical condition, the enthalpic interaction and the entropic interaction of the polymer with

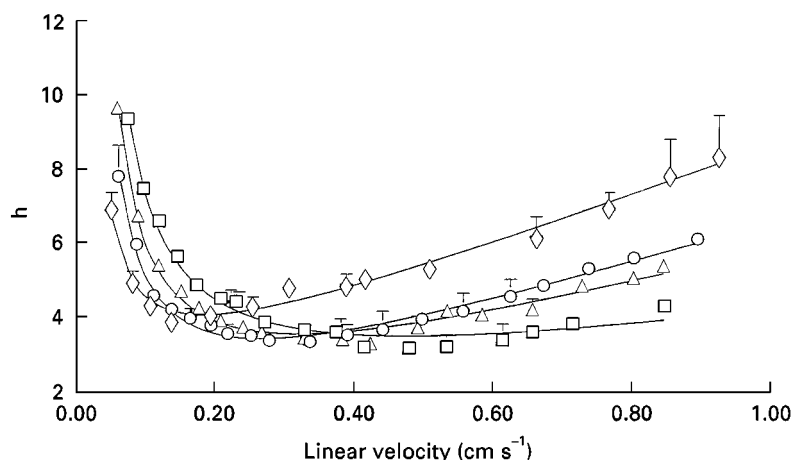


Figure 8 Variation of reduced plate height of styrene using a Betasil silica column with mobile-phase linear velocity using different mobile-phase compositions: diamonds, pure THF at 24°C; circles, 70 : 30 mol% THF-CO₂ at 24°C; triangles, pure THF at 80°C; squares, 70 : 30 mol% THF-CO₂ at 80°C. (Reproduced with permission from Yuan and Olesik (1997b).)

the stationary phase are exactly balanced. This chromatographic condition is typically found by carefully changing the mixture composition used as the mobile phase until this thermodynamic condition is met. This specific composition is sometimes difficult to determine experimentally.

Because the solvent strength of enhanced-fluidity liquid mixtures changes with varying pressure and,

temperature, as well as mixture composition, the critical condition is more readily found using these liquid mixtures than common liquids. **Figure 9** shows a molecular weight calibration plot for polystyrene polymers. With enhanced-fluidity liquid mixtures, by

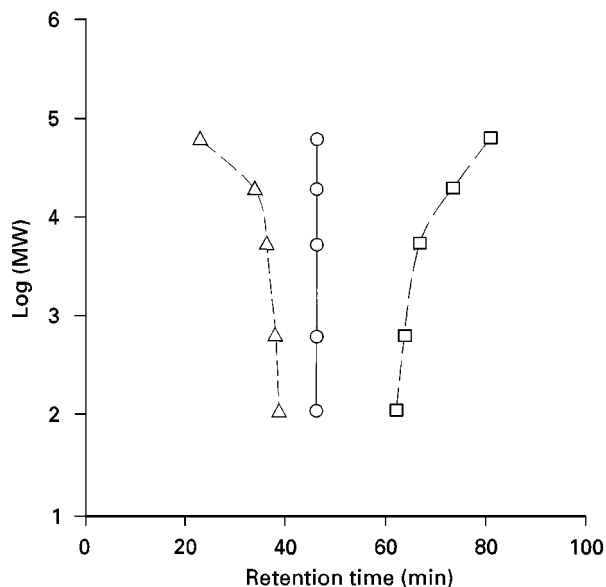


Figure 9 Plots of polystyrene molecular weight versus retention time at different mobile-phase conditions. Conditions: 1.8 m × 250 μm i.d. silica (20 nm pore size, 5 μm particle size) packed column, column pressure 260 atm: triangles, 50% CO₂ in THF; circles, 54% CO₂ in THF; squares 60% CO₂ in THF. (Reproduced with permission from Yuan and Olesik (1998a).)

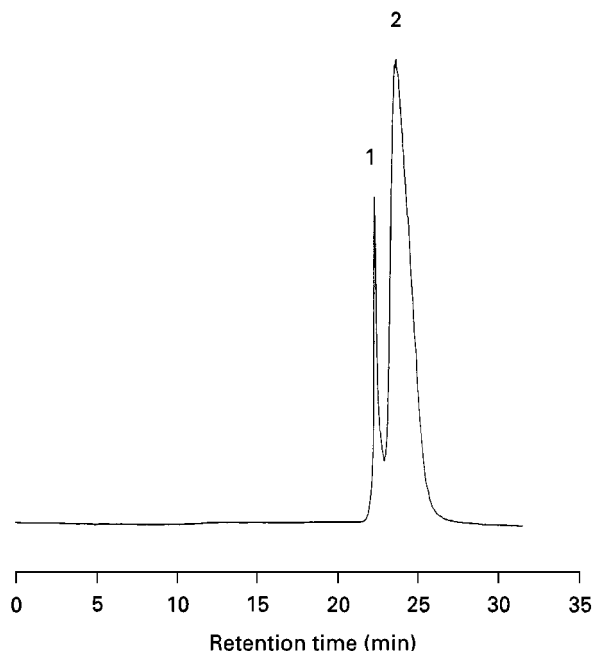


Figure 10 Chromatogram of polystyrenes with mono- and dicarboxylic terminal groups. Conditions: 1.8 m × 250 μm i.d. silica (20 nm pore size 5 μm particle size) packed column; 54% CO₂ in THF mobile phase at 260 atm; column at 70°C using evaporative light-scattering detection. Peaks: 1, polystyrene with dicarboxylic terminal groups, approximate MW 50 000; 2, polystyrene with monocarboxylic terminal group, approximate MW 50 000. (Reproduced with permission from Yuan and Olesik (1998a).)

changing the temperature and or pressure, all three modes of separation (size exclusion, critical chromatography and adsorption chromatography) of polystyrene polymers are possible using the same mixture as the mobile phase. Increased efficiency is also beneficial at the critical condition because only the weak interactions of the functionalities or of the other components of a copolymer control the separation. The low viscosity of enhanced-fluidity liquid mixtures allows significantly improved efficiency. Long (2 m) packed capillary columns have been produced that have efficiencies as high as 100 000 theoretical plates. Figure 10 shows an example of the critical condition separation of mono- and dicarboxy-terminated polystyrene polymers separated at the polystyrene backbone with a long packed capillary column.

Use of Alternative Liquefied Gases

While CO₂ was the first liquefied gas used for enhanced-fluidity liquid chromatography, other gases may also be useful to increase the fluidity of a liquid mixture. CO₂ is limited in its applications in that, when it is included in mixtures with water, carbonic acid is produced. Acidic buffer conditions can be generated for the reversed-phase separations but not basic buffers.

For a gas to be useful as a fluidity modifier, the gas must be highly miscible with the organic liquid solvent and have a low viscosity. Fluoroform is an example of a liquified gas that is highly soluble under similar pressure and temperature conditions to CO₂. Accordingly, the efficient separation of basic solutes using basic buffered mobile phases is possible when fluoroform is used to decrease the viscosity of the mobile-phase mixture instead of CO₂. For example, Figure 11 shows a comparison of the separation of some triazine herbicides and a common metabolite, hydroxyatrazine, using 64 : 36 mol% methanol–10 mmol L⁻¹ phosphate buffer (Figure 11A) with 51 : 29 : 20 mol% methanol–10 mmol L⁻¹ phosphate buffer–CO₂ (Figure 11B) and 51 : 29 : 20 mol% methanol–10 mmol L⁻¹ phosphate buffer–fluoroform (Figure 11C) as the mobile phase with the same flow restrictor. The addition of CO₂ clearly causes the co-elution of the more polar solutes. When the chromatogram using the methanol–buffer mixture is compared to that containing the same mole ratio methanol–buffer but with the addition of 0.20 mol fraction fluoroform, use of fluoroform is clearly optimal. The linear velocity and the efficiency increased with the addition of fluoroform. At constant linear velocity, the addition of 20 mol% fluoroform to the methanol–buffer solution increased the efficiency by approximately 30%.

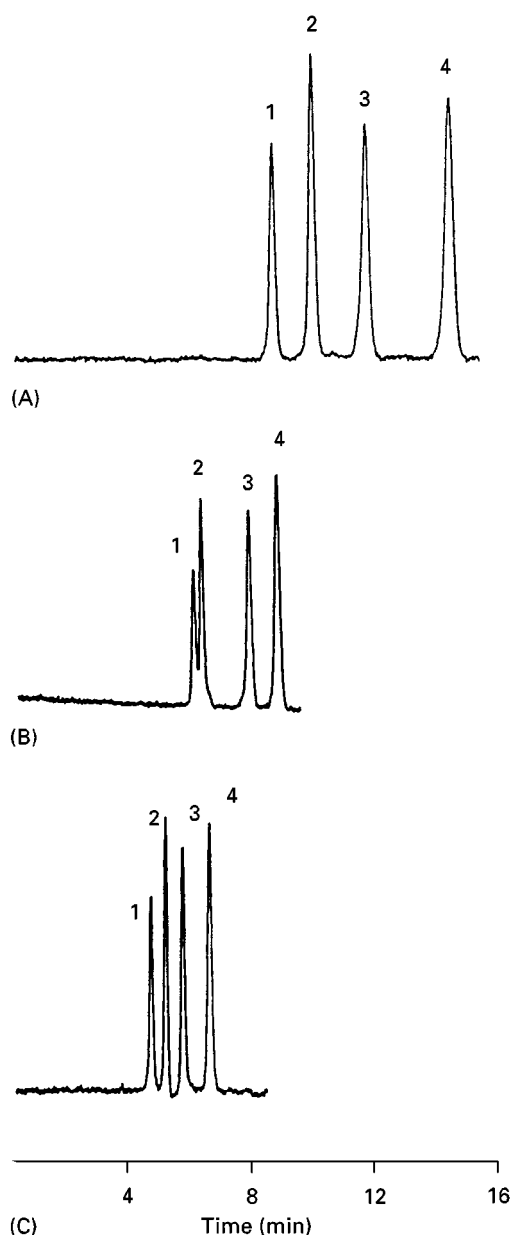


Figure 11 Chromatogram at same restrictor length and pressure drop of 16.3 atm with different mobile-phase conditions (A) 64 : 36 mol% methanol–10 mmol L⁻¹ phosphate buffer; (B) 51 : 29 : 20 methanol–10 mmol L⁻¹ phosphate buffer–CO₂; (C) 51 : 29 : 20 methanol–10 mmol L⁻¹ phosphate buffer–CHF₃. Peaks: 1, ammeline; 2, hydroxyatrazine; 3, atrazine; 4, terbutryne. (Reproduced with permission from Yuan and Olesik (1998b).)

Other Separations Using Enhanced-Fluidity Liquid Mixtures

The extraction of polar pollutants from very adsorptive matrices is a difficult task. A large range of polar pollutants can be effectively removed from adsorptive matrices such as dust and fly ash, by using enhanced-fluidity liquid mixtures. Solutes as polar as phenols,

triazine herbicides, and as large as 3–4 ring polynuclear aromatic hydrocarbons are effectively removed using enhanced-fluidity liquid mixtures, such as methanol–H₂O–CO₂ and methanol–H₂O and are superior to the use of other standard methods such as Soxhlet extraction.

Conclusions

Improved performance has been observed using enhanced-fluidity liquid mobile phases in every type of liquid chromatography studied to date. As mentioned earlier, typically as much as 50 mol% liquefied gas can be added to a polar solvent while still maintaining much of the solvent strength of the original organic solvent. As the solvent strength of the mixture decreases for mixtures containing more than 50 mol% liquefied gas, the chromatographic performance decreases. Extraction techniques for highly polar substances that would otherwise be very difficult to extract have been developed using enhanced-fluidity liquid mobile phases. The use of enhanced-fluidity liquids as mobile phases has also made viable a powerful technique termed critical chromatography. This separation method allows careful characterization of functionality distributions in polymers and oligomer distributions in copolymers. The precise control of solvent strength that is possible with enhanced-fluidity liquids will allow critical chromatography to be more thoroughly studied.

Reversed-phase liquid chromatography is presently the most commonly used HPLC method. pH variation is often used to control retention in reversed-phase HPLC. While the use of enhanced-fluidity mixtures significantly improves the chromatographic performance in reversed-phase HPLC, more information is needed on pH control in these mixtures to evaluate the potential of enhanced-fluidity liquid mixtures.

Chiral chromatography is another area of separation science where enhanced-fluidity liquid mixtures may find applications in the future. Increasingly, SFC is under consideration for chiral separations. However, solvent strength often limits the utility of SFC. Enhanced-fluidity liquid mixtures have high solvent strength and therefore may be applicable to separations that SFC cannot handle.

See also: II/Chromatography: Liquid: Mechanisms: Reversed Phases; Size Exclusion Chromatography; Theory of Liquid Chromatography. **Chromatography: Supercritical Fluids:** Theory of Supercritical Fluid Chromatography.

Further Reading

- Cui Y and Olesik SV (1991) High-performance liquid chromatography using mobile phases with enhanced fluidity. *Analytical Chemistry* 63: 1813.
- Cui Y and Olesik SV (1995) Reversed-phase high performance liquid chromatography using enhanced-fluidity liquid mobile phases. *Journal of Chromatography A* 691: 151.
- Lee ST and Olesik SV (1994) Reversed-phase high performance liquid chromatography using enhanced-fluidity mobile phases at room and elevated temperatures. *Analytical Chemistry* 66: 4498.
- Lee ST and Olesik SV (1995) Normal phase high performance liquid chromatography using enhanced-fluidity liquid mobile phases. *Journal of Chromatography A* 707: 217–224.
- Lee ST, Olesik SV and Fields S (1995) Application of reversed-phase high performance liquid chromatography using enhanced-fluidity liquid phases. *Journal of Microcolumn Separations* 7: 477–483.
- Souviguet I and Olesik SV (1997) Liquid chromatography at the critical condition using enhanced-fluidity liquid mobile phases. *Analytical Chemistry* 69: 66.
- Yuan H and Olesik SV (1997) High performance size exclusion chromatography using enhanced-fluidity liquid mobile phase. *Journal of Chromatographic Science* 35: 409.
- Yuan H and Olesik SV (1997) Comparison of the performance of enhanced-fluidity liquids and common-liquids as mobile phases for size exclusion chromatography at elevated temperatures. *Journal of Chromatography A* 785: 35.
- Yuan H and Olesik SV (1998) Comparison of reversed-phase HPLC separation using carbon dioxide and fluoroform for enhanced-fluidity liquid mobile phases. *Analytical Chemistry* 70: 1595.
- Yuan H and Olesik SV (1998) Improvements in polymer characterization by size exclusive chromatography and chromatography and liquid at the critical condition by using enhanced-fluidity liquid mobile phases with packed capillary columns. *Analytical Chemistry* 70: 3298.

Evaporative Light Scattering Detectors in Liquid Chromatography

See II/CHROMATOGRAPHY: LIQUID/Detectors: Evaporative Light-Scattering

Fluorescence Detectors in Liquid Chromatography

See II/CHROMATOGRAPHY: LIQUID/ Detectors: Fluorescence Detection

Historical Development

V. R. Meyer, EMPA, St. Gallen, Switzerland

Copyright © 2000 Academic Press

Tswett's papers on chromatography were published at the beginning of the 20th century but there was little interest in the technique for several decades. It was not until the 1930s that a growing number of researchers used liquid chromatography (LC) in open columns for the successful separation of complex mixtures of natural compounds, and it was only in the 1970s that LC found widespread use in its instrumentalized form. Over this time it developed:

- from a simple set-up to sophisticated instrumentation with computer assistance
- from the separation of coloured compounds which did not need an instrument for detection to an impressive variety of detectors which allow quantitation of analytes in the picomol range and lower
- from adsorption chromatography as the single option to a large number of varied separation principles (adsorption, reversed-phase, polar bonded phase, ion exchange, enantioselective, size exclusion and affinity chromatography)
- from trial-and-error to a deep understanding of theory, separation mechanisms and method development
- from open-column separations to high performance, closed-column chromatography
- from nonacceptance by the greatest scientists of the time to a method of the utmost importance.

It is difficult to name the most important participants in this development; exceptions are Martin and Synge, who published a paper in 1941 that can be looked upon as the beginning of modern chromatography. A large number of other scientists were responsible for various improvements in LC: **Table 1** lists the most important historical papers in the development of the technique.

The Beginning

Open-column LC was invented by Michael (Mikhail) Semenovich Tswett (1872–1919) at the beginning of

the 20th century and he was responsible for naming the method. Paper, thin-layer, closed-column liquid and gas chromatography were later invented by other scientists who varied the method set-up described by Tswett.

The father of chromatography was not a chemist but a botanist. Although born in Asti, Italy, and educated in Geneva, Switzerland, he was a Russian national. In 1896 he obtained a PhD from the University of Geneva. Later, when he was an assistant professor at the University of Warsaw, Poland, he needed a method to isolate plant pigments in pure form. At that time the standard technique for this purpose was the partition of plant extracts between immiscible organic solvents. However, Tswett was also interested in the problem of how the pigments are fixed, i.e. adsorbed, within the plant cell. He carried out numerous experiments with adsorbents and tested

Table 1 Important historical papers on liquid chromatography

- Tswett MS (1906) Adsorptionsanalyse und chromatographische Methode. Anwendung auf die Chemie des Chlorophylls. *Berichte der Deutschen Botanischen Gesellschaft* 24: 384
- Tswett MS (1910) *Khromofilly v Rastitel'nom i Zhivotnom Mire*. Warsaw: Karlasiakov
- Palmer LS and Eckles CH (1914) Carotin – the principal natural yellow pigment of milk fat: its relations to plant carotin and the carotin of the body fat, corpus luteum and blood serum. *Journal of Biological Chemistry* 17: 191
- Kuhn R, Winterstein A and Lederer E (1931) Zur Kenntnis der Xanthophylle. *Hoppe Seyer's Zeitschrift für Physiologische Chemie* 197: 141
- Martin AJP and Synge RLM (1941) A new form of chromatogram employing two liquid phases. *Biochemical Journal* 35: 1358
- Glueckauf E (1955) Theory of chromatography. IX. Theoretical plate concept in column separations. *Transactions of the Faraday Society* 51: 34
- Van Deemter JJ, Zuiderweg FJ and Klinkenberg A (1956) Longitudinal diffusion and resistance to mass transfer as causes of nonideality in chromatography. *Chemical Engineering Science* 5: 271
- Moore S, Sparkman DH and Stein WH (1958) Chromatography of amino acids on sulfonated polystyrene resins. An improved system. *Analytical Chemistry* 30: 1185
- Porath J and Flodin P (1959) Gel filtration: a method for desalting and group separation. *Nature (London)* 183: 1657

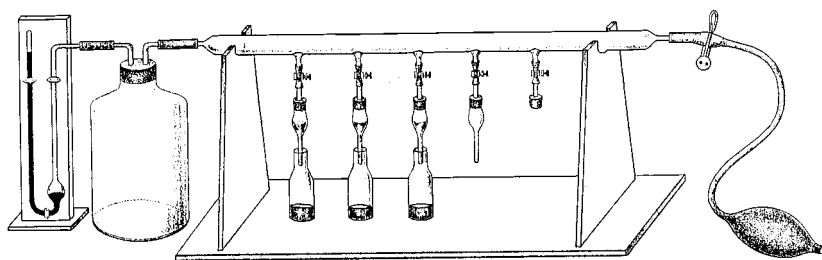


Figure 1 Tswett's chromatographic apparatus. (Reproduced from Tswett, 1906; see Table 1.) *Ber. Deutsch. Bot. Ges.* 24: 384.

more than 100 different powdered materials. Finally he found that inulin, sucrose and calcium carbonate were best suited for the separation of the pigments of green leaves – chlorophylls (two compounds) and xanthophylls.

Unfortunately the new method was only described in lectures, in a paper in a German botanical journal (1906) and in a book in the Russian language (1910). It is obvious that most chemists did not read either botanical journals or a Russian book published in Warsaw. Moreover, when reading these texts today, many details of the experimental set-up are missing. These facts, together with the outbreak of World War I in 1914 and Tswett's untimely death at the age of 47 in 1919, hindered the acceptance of the new method.

Tswett mainly used small glass columns of 2–3 mm diameter packed with adsorbent to a height of c. 30 mm. The plant extract was applied on top of the column and transported into the packing by a solvent – the mobile phase – which was added on top and sucked through the adsorbent by a slight vacuum or forced through with a slight pressure. The best eluents were found to be benzene and carbon disulfide; solvent mixtures and even gradients could also be

used. Several columns could be used in parallel (**Figure 1**).

Tswett did not publish more than three 'chromatograms'; one is shown in **Figure 2**. Experimental details of all these drawings are missing. The pigments were not eluted but the whole packing was pushed out of the glass tubing and the different zones were then cut apart with a knife. The pigments were extracted from the adsorbent by an appropriate solvent and identified by UV spectroscopy (which was a tedious and time-consuming method). **Figure 3** makes clear how similar the structures of chlorophylls a and b are and, from our current perspective, we get the impression that Tswett was a very skilled experimenter. It was difficult to reproduce his separations using only his descriptions.

The First Followers

A small handful of researchers used chromatography with great success despite the obstacles outlined above: Gottfried Kränzlin, Charles Dhéré and co-workers, and Leroy Sheldon Palmer. They were all able to isolate pure compounds from natural mixtures.

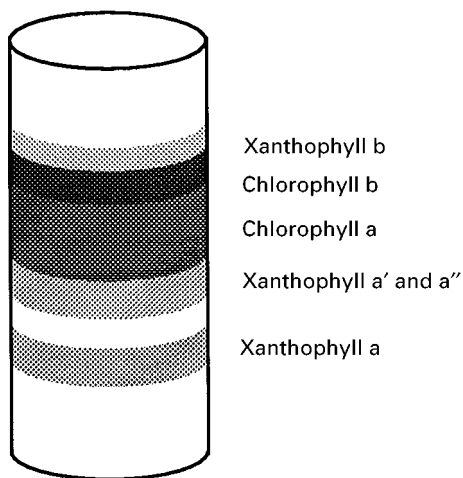


Figure 2 Separation of plant pigments as obtained by Tswett. (Redrawn after Tswett, 1906; see Table 1.)

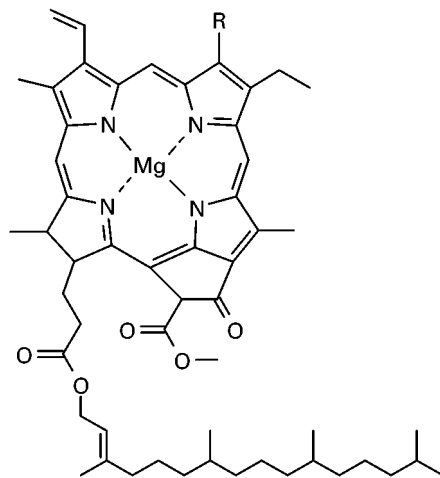


Figure 3 The structures of the chlorophylls separated by Tswett. Chlorophyll a: R = CH₃; chlorophyll b: R = CHO.

Kränzlin, at the Friedrich-Wilhelms University of Berlin, Germany, used Tswett's method in his PhD thesis work in the years 1906 and 1907 – just after Tswett's paper had been published. In a semiquantitative manner he determined the content of chlorophylls and carotenes in various plants from the width of the chromatographic bands. Dhéré was a professor of physiology at the University of Fribourg, Switzerland. In two PhD theses carried out under his guidance, chromatography was used to solve analytical problems: the spectroscopic investigation of the chlorophylls (Wladyslaw de Rogowski, 1914) and the isolation and characterization of invertebrate pigments (Guglielmo Vegezzi, 1916). Palmer, an agricultural chemist, used chromatography for his PhD thesis work at the University of Missouri, USA, in 1909–13. He investigated the pigment content in cattle food, i.e. grass, hay, and carrots, as well as in milk and butter. He proved that the carotene in cow's milk comes from the food plants and is not synthesized by the animal.

The work of these pioneers had only a minor influence on the later development of chromatography, perhaps because they were not chemists (or pure chemists) but were engaged in related fields. The great authorities of natural compound chemistry of the 1910s and later, most of all, the Nobel prize winner Richard Willstätter, were sceptical about the usefulness of chromatography.

The Renaissance

In fact, Willstätter had first-hand knowledge of chromatography because he owned a German translation of Tswett's book (the translator is unknown). Later the translated text came into the possession of Richard Kuhn, a professor of chemistry at the Kaiser Wilhelm Institute for Medical Research at Heidelberg, Germany; Kuhn was a former student of Willstätter. In 1930, Edgar Lederer joined Kuhn as a postdoctoral fellow. His task was to separate xanthophyll

(today called lutein) and zeaxanthin (Figure 4), and he was able to solve this problem after reading Tswett's book. Lederer used what we would call today preparative columns – glass tubes with a diameter of 7 cm. The results were published in three papers which appeared in leading German scientific journals in 1931. These articles mark the breakthrough and acceptance of chromatography. The method was successfully used in the laboratories of Nobel prize-winners Paul Karrer and Leopold Ruzicka (who received the award in 1937 and 1939, respectively; Kuhn was awarded it in 1938). All these scientists were active in the isolation and structure elucidation of natural compounds, and chromatography was an invaluable help to them.

The main problem in these years was how to find suitable stationary phases. Systematic tests and good luck were necessary to establish adsorbents such as alumina, magnesia and silica. Some researchers began to elute the chromatographic bands from the column instead of cutting the packing; however, it is not clear who used this technique first. It was proved that chromatography can be used on a large scale; Winterstein was able to obtain gram quantities of chlorophylls by using 12.5 cm i.d. columns.

The first application of chromatography to compounds other than organic molecules was done by Georg-Maria Schwab in Munich, Germany. In 1937 he separated inorganic cations on alumina. The first enantioselective separation was performed by Geoffrey M. Henderson and H. Gordon Rule, also in 1937. They were able to partially resolve (*R,S*)-phenylene-bis(iminocamphor) on lactose with petroleum-benzene 8 : 1 as the mobile phase.

From Empirism to Science

In 1940, Archer J. P. Martin and Richard L. M. Synge, two researchers at the Wool Industries Research Association in Leeds, England, were trying to separate the amino acids of wool proteins. They

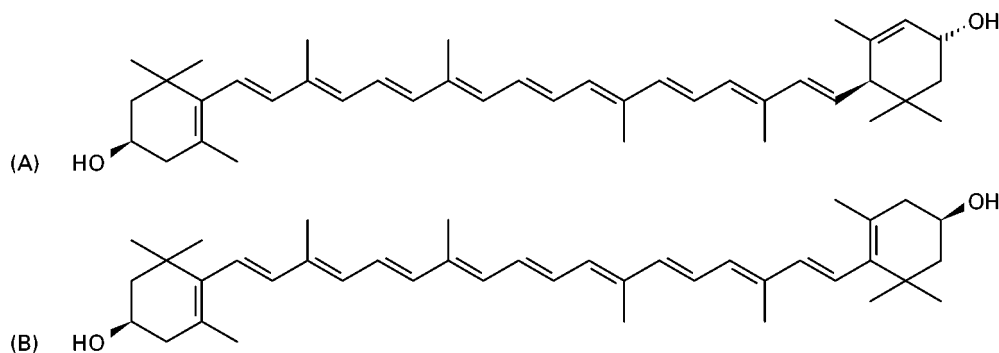


Figure 4 The structures of the carotenes separated by Lederer. (A) Lutein (xanthophyll); (B) zeaxanthin.

attempted to solve the problem by countercurrent extraction of the acetyl derivatives with water and chloroform. This process was time-consuming (one run took a week), tedious and required large volumes of solvents. With ingenuity they came upon a completely different procedure; they immobilized the water phase on silica, packed this material into columns and used the chloroform (with 1% *n*-butanol) as the mobile phase. Although this was chromatography, the technique was different to what had been done previously. It was not based on adsorption but on the partition between two liquid phases (water being the stationary phase). Martin and Synge had invented liquid-liquid partition chromatography.

In addition to the practical applications of liquid-liquid partition chromatography, Martin and Synge's paper also included:

- a theory of the chromatographic separation process which used the theoretical plate as a hypothetical compartment within the column where the solutes are equilibrated between the mobile and stationary phase (this concept was taken from the theory of distillation)
- the statement that a chromatographic process is governed by the diffusion coefficient of the analyte, which leads to specific problems for the separation of large molecules such as proteins
- the insight that there is an optimum flow rate for any chromatographic separation
- the prediction that the finer the particles of the stationary phase, the more efficient the column (this led to high performance liquid chromatography (HPLC) some 25–30 years later)
- the proposal that the mobile phase could also be a gas (this led to gas chromatography (GC), which was first successfully pursued by James and Martin some 10 years later).

In 1952 Martin and Synge were given the Nobel prize for their truly remarkable prescience.

The plate theory of chromatography was defined in the 1950s by Eugen Glueckauf (who worked for the UK Atomic Energy Authority) and others. It became clear how the separation performance can be influenced, i.e. which prerequisites are necessary for efficient chromatography. The prediction of Martin and Synge was quantified by Calvin Giddings: it would be necessary to use stationary-phase packings with particle diameters of 10 μm or less in order to get faster and better LC separations. In 1955, Jan J. van Deemter presented a rate theory approach to describe the chromatographic process and discussed the influence of mobile-phase velocity on the height of

a theoretical plate to give relationships known today as van Deemter curves. They show that there is an optimum mobile-phase flow rate for separations performed by gas, liquid or supercritical fluid chromatography.

A fruitful concept for the judgement and comparison of LC separations was introduced in 1977 by John H. Knox with reduced (dimensionless) expressions for theoretical plate height, mobile-phase velocity, pressure drop and overall efficiency. An excellent column should have a reduced plate height of not higher than 3, irrespective of its size, and the reduced flow velocity must not be smaller than 3, irrespective of the chemical natures of the phase system and the analytes.

Towards HPLC

The pre-HPLC era can be defined as the decades when particles of 20 μm and larger were used as stationary phases. High pressure was not necessary and the separations were usually performed with gravity flow or with moderate vacuum at the column outlet, i.e. without a pump. Hindered first by World War II and later, to a certain extent, by the impressive rise of GC, progress was slow but steady.

In the 1930s, the first ion exchange resins were synthesized and became commercially available in the next decade. They could be used not only for batch processes (e.g. desalting) but also as stationary phases, thus opening a new separation principle to LC. During World War II the ability to separate and identify the rare earth ions was of utmost importance in the research activities which led to the construction of nuclear bombs.

The first reversed-phase separations were performed in 1950 by Martin and Howard with a stationary phase of silylated kieselguhr and a

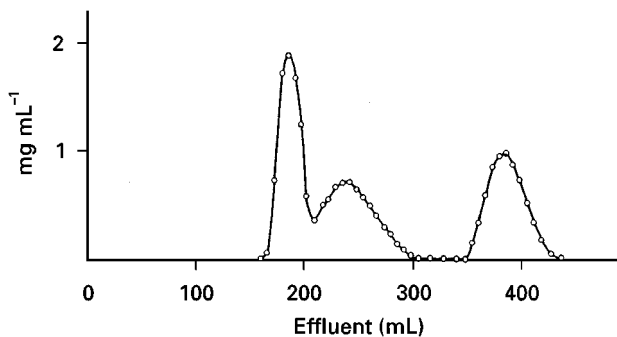


Figure 5 Size exclusion chromatogram of dextran (mol wt 20 000), dextran (mol wt 1000) and glucose as obtained by Porath and Flodin. Column: 36.5 \times 4.0 cm i.d.; stationary phase: dextran gel 100–200 mesh; mobile phase: water, 110 mL h⁻¹. (Reproduced from Porath and Flodin, 1959; see Table 1.)

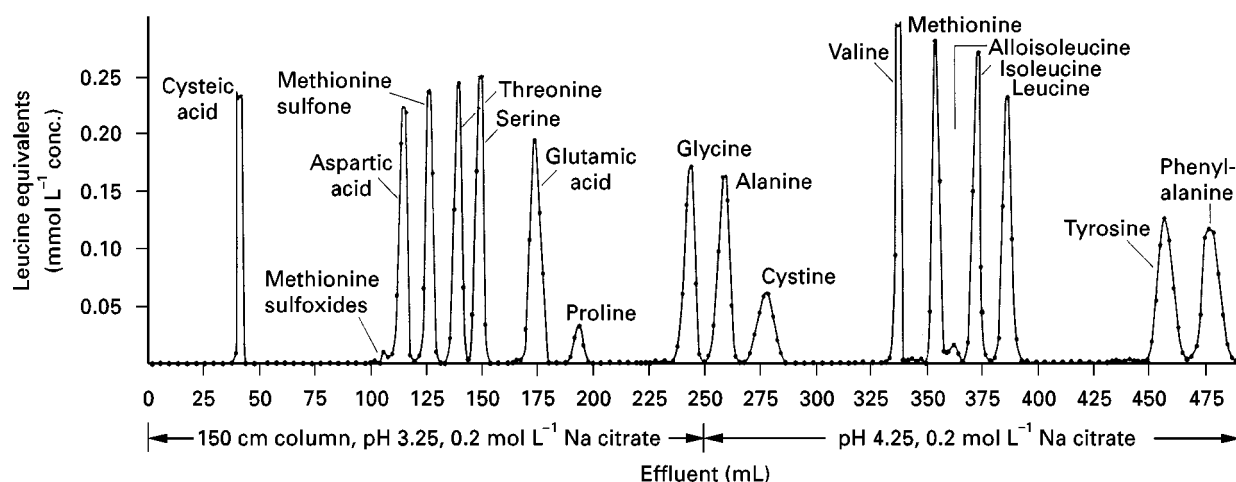


Figure 6 Separation of amino acids as obtained by Moore, Sparkman and Stein. Column: 150 × 0.9 cm i.d.; stationary phase: Amberlite Type III cation exchanger 400–600 mesh; mobile phase: citrate buffer pH 3.25 and pH 4.25, 12 mL h⁻¹. (Reproduced from Moore *et al.*, 1958; see Table 1.)

water-methanol-*n*-octane mobile phase. This system allowed the separation of fatty acids.

At Uppsala University, Sweden, Arne Tiselius introduced new chromatographic and electrophoretic techniques into biochemical research and invented flow-through refractive index detectors. (Previously, the effluent from a column had been collected as individual fractions which were analysed offline.) The first application of gradient elution chromatography was also made in the laboratories of Tiselius: mixtures of oligosaccharides were separated by a continuous increase of the ethanol content of the aqueous mobile phase. Also in Uppsala, size exclusion chromatography (as gel filtration with an aqueous mobile phase) was invented by Per Flodin and Jerker O. Porath (Figure 5). The stationary phase with well-defined pores was a cross-linked dextran.

Gel permeation chromatography, i.e. size exclusion in organic solvents, was introduced in 1964 with cross-linked polystyrenes by John C. Moore. For the convenient use of this analytical method an instrument was also built. In retrospect we can say that this was the first liquid chromatograph, in that it included all the necessary parts, from the pump to a refractive index detector. Several years before, in 1958, a specialized instrument, the automated amino acid analyser, had been introduced by Stanford Moore and William H. Stein. Although the separation of a complex mixture (with up to 50 amino acids and related compounds!) took several days (Figure 6), this analytical tool was of utmost value for biochemical research. It was a real breakthrough and a revolution. The separation was based on a polystyrene-type cation exchanger run with citrate or acetate buffers at elevated temperature.

Affinity chromatography, a highly selective bio-analytical technique, goes back to Jerker O. Porath and to Meir Wilcheck in 1967–68. This powerful method can be used for the isolation of proteins (e.g. insulin) or the quantitative analysis of bioactive compounds (e.g. aflatoxins).

High Performance Liquid Chromatography

The term HPLC is appropriate for separations of any size (from microanalytical to preparative) if the particles of the stationary phase are not larger than about 10 µm and if the reduced plate height (after Knox) is not larger than 5. This means that the pressure which is necessary in order to force the mobile phase through the column is a parameter of minor importance (the P in HPLC meant pressure when the abbreviation was first coined). It was a long way from pressure to performance with a wealth of technical improvements. Two obstacles needed to be overcome: it was not easy to pack columns with 5 µm particles, and the construction of pumps that can deliver a constant, pulse-free flow as low as e.g. 1 mL min⁻¹ at pressures up to 300 bar was demanding. Today we can choose from hundreds of packed column types and dozens of pumps.

Stimulated by the successful amino acid analyser and by the need of a separation method for molecules not suitable for GC, research activities towards an improved, instrumentalized LC began in the late 1960s. Although the available instruments were less sophisticated and less convenient than those available today and despite the fact that most users had to pack their own columns, it soon became clear that HPLC is

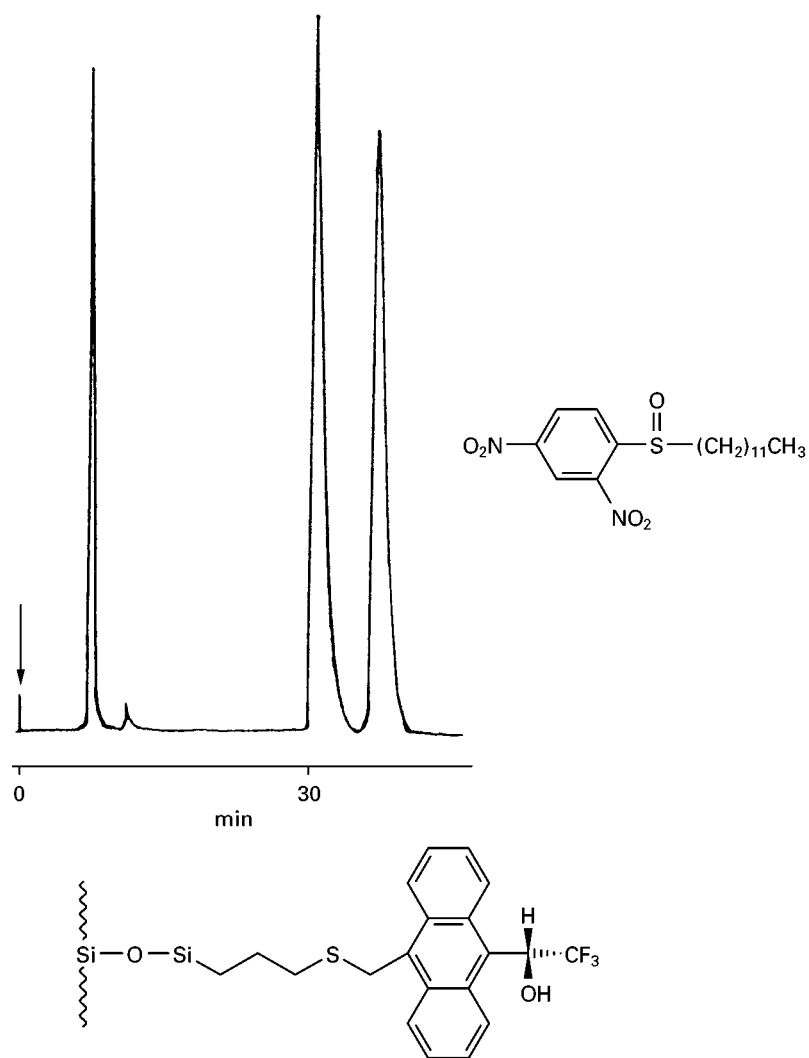


Figure 7 Separation of *(R,S)*-*n*-dodecyl-2,4-dinitrophenyl sulfoxide on a trifluoroantrhyryl ethanol chiral stationary phase as obtained by Pirkle and House. Column: 25.4 × 1 cm i.d.; mobile phase: hexane–2-propanol 4 : 1. (Reproduced with permission from Pirkle WH and House DW (1979) *Journal of Organic Chemistry* 44: 1957.)

a useful method for almost any type of sample. Much of the success of the new method was due to a number of excellent books which soon appeared; the most popular one was *Introduction to Modern Liquid Chromatography* by Lloyd R. Snyder and Jack J. Kirkland (first edition 1974), from which the first generation of users learnt the technique. In 1973, the first International Symposium on Column Liquid Chromatography took place in Interlaken, Switzerland.

Besides the techniques still in use today (adsorption, reversed-phase, ion exchange, size exclusion and affinity chromatography), in the early years of HPLC liquid–liquid partition chromatography was also used, following Martin and Synge's first paper. The stationary phase consisted of a liquid film held in place by a support, i.e. a special type of adsorbent. Although such a separation system can be highly

selective, it was inconvenient and temperature-sensitive. Classical liquid–liquid chromatography was abandoned with the rise of chemically bonded stationary phases of almost any polarity and selectivity.

The most important bonded phases are the C_8 and C_{18} reversed phases which are used with an aqueous eluent. The separation principle, first described by Martin and Howard (see above) gained in importance mainly due to the activities of Jack J. Kirkland and Istvan Halász. Today approximately half of all HPLC separations are performed in the reversed-phase mode. New developments in the field of stationary phases are nonporous particles of about 1 μm size; perfusive particles with large throughpores which allow the mobile phase to flow (not diffuse) through the body of the particle; and monolithic, rod-type chromatographic beds which are not built up from

particles but consist of one single, porous piece of stationary phase. All these concepts allow separation speed to increase markedly.

An important class of stationary phases which is now in widespread use are the chiral phases. Enantioselective chromatography can also be done with chiral additives in the mobile phase or with pre-column derivatization to diastereomers but the approach using chiral stationary phases (CSPs) was the most fruitful. Although not the first CSP, the trifluoroanthyrylethanol phase by William H. Pirkle opened the door to this new analytical field in 1979 (Figure 7). A large number of research groups found numerous other CSPs, including the cellulose and amylose derivatives of Yoshio Okamoto.

The introduction of materials for the separation of proteins and other biomolecules by Fred E. Regnier in 1976 and by William S. Hancock and Milton T. W. Hearn in 1978 marked an important breakthrough. The rise of industrial biotechnology was in fact only possible as HPLC was capable of identifying proteins or peptides exprimed by mutants, i.e. of guaranteeing the true identity of the isolated product (Figure 8).

Snyder's work on the interaction between stationary and mobile phase led to a better understanding of adsorption chromatography and to a scientific classification of solvents with regard to their dipole, proton donor and proton acceptor properties. Such classification is also important for reversed-phase separations and gives a sound background to the choice of methanol, acetonitrile or tetrahydrofuran in addition

to water or buffer as mobile-phase components. Several computer simulation programs have been developed which allow the prediction of separations based on the chemical structures of the analytes and to optimize the separations. It has been recognized how important temperature can be for most HPLC separations; therefore this parameter should be studied and optimized, too. High temperatures, even above the boiling point of the mobile phase, lead to fast separations; however, not all stationary phases are suited to such conditions, and a pressure restrictor at the detector outlet is necessary in order to prevent bubble formation in the cell.

With regard to instrumentation, continuous improvement in all parts of the HPLC system has taken place and is still going on. This concerns degassing systems, pumps, tubing, fittings, injection valves, autosamplers, columns (e.g. the cartridge principle), detectors and data handling. Authorities now demand that analyses are performed in accordance with Good Laboratory Practice or similar guidelines, therefore all aspects of the analysis, including data acquisition by computers and their manipulation by personnel, must be regulated. Concerning detectors, the refractive index principle was invented decades ago and UV and fluorescence detection were rather obvious. The diode array detector (Hewlett-Packard, 1979) was not obvious but it revolutionized the possibilities for analyte identification and peak purity judgement by UV/Vis spectroscopy. Of the less frequently used detectors, the electrochemical detector is

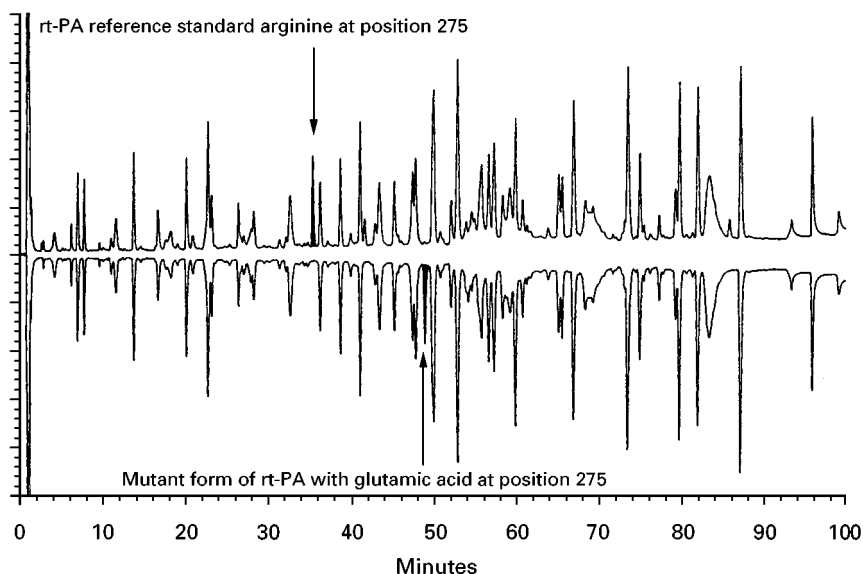


Figure 8 Separation of the tryptic hydrolysate of tissue-type plasminogen activator as obtained by Garnick, Solli and Papa. Top: normal protein with arginine at position 275; bottom: erroneous peptide with glutamic acid at position 275. Stationary phase: Nova Pak C18, 5 μm ; mobile phase: phosphate buffer pH 2.8/acetonitrile, step gradient, 1 mL min⁻¹; detector: UV 210 nm. (Reproduced with permission from Garnick RL, Solli NJ and Papa PA (1988) *The role of quality control in biotechnology: an analytical perspective. Analytical Chemistry* 60: 2546.)

an important one (Peter T. Kissinger, *c.* 1975): it can be used for analytes with readily oxidizable or reducible functional groups. An alternative to refractive index detection is the light-scattering detector for nonvolatile analytes. This instrument is able to detect all types of molecules irrespective of the presence or lack of functional groups; it does not respond to changes in eluent composition or temperature in the way that the refractive index detector does. LC-mass spectrometry (LC-MS) is no longer in its infancy and could become one of the most important detectors, even for routine analyses. LC-nuclear magnetic resonance (LC-NMR) has been developed into an excellent tool for structure elucidation. Depending on analyte concentration, NMR spectra can be obtained online or offline after storage of the relevant chromatographic peaks in loops.

Despite new techniques such as capillary electrophoresis, HPLC continues to be probably the most important analytical method, with more 100 000 instruments in daily use worldwide.

Further Reading

- Berezkin VG and Masson MR (eds) (1990) *Chromatographic Adsorption Analysis: Selected Work of Mikhail Semenovich Tswett*. Chichester: Ellis Horwood.
- Bussemas HH and Ettre LS (1994) Gottfried Kränzlin, the first follower of Tswett. *Chromatographia* 39: 369.
- Ettre LS (1980) Evolution of liquid chromatography: a historical overview. In: Horváth C (ed.) *High-performance Liquid Chromatography, Advances and Perspectives*, vol. 1, pp. 1–74. New York: Academic Press.
- Ettre LS and Sakodyskii KI (1993a) M.S. Tswett and the discovery of chromatography. I: early work (1899–1903). *Chromatographia* 35: 223.
- Ettre LS and Sakodyskii KI (1993b) M.S. Tswett and the discovery of chromatography. II: Completion of the development of chromatography (1903–1910). *Chromatographia* 35: 329.
- Ettre LS and Wixom RL (1993) Leroy Sheldon Palmer (1887–1944) and the beginning of chromatography in the United States of America. *Chromatographia* 37: 659.
- Ettre LS and Zlatkis A (eds) (1979) *75 years of Chromatography – A Historical Dialogue*. Amsterdam: Elsevier.
- Meyer VR and Ettre LS (1992) Early evolution of chromatography: the activities of Charles Dhéré. *Journal of Chromatography* 600: 3.
- Snyder LR (1997) Modern practice of liquid chromatography: before and after 1971. *Journal of Chemical Education* 74: 37.
- Wintermeyer U (1990) Historical review. In: Unger KK (ed.) *Packings and Stationary Phases in Chromatographic Techniques*, pp. 1–42. New York: Dekker.

Infrared Detectors in Liquid Chromatography

See II/CHROMATOGRAPHY: LIQUID/Detectors: Infrared

Instrumentation

W. R. LaCourse, University of Maryland, Baltimore, MD, USA

Copyright © 2000 Academic Press

The Instrumental Set-Up

Modern high performance liquid chromatography (HPLC) uses high pressure to force the mobile phase and an analyte through a closed column packed with micron-size particles, which constitute the stationary phase. HPLC instrumentation is made up typically of nine basic components: mobile phase/solvent reservoir; solvent delivery system; sample introduction device; column; post-column apparatus; detector; data collection and output system; post-detector

eluent processing; and connective tubing and fittings. All components except for the post-column apparatus are essential to performing HPLC. **Figure 1** shows a schematic diagram of a generic high performance liquid chromatography system.

Mobile-Phase Reservoir

The mobile-phase reservoir can be any clean, inert container. It usually contains from 0.5 to 2 L of solvent, and it should have a cap that allows for a tubing inlet line, which feeds mobile phase to the solvent-delivery system. The cap also serves to keep out dust, reduce solvent evaporation, allow for pressurization of the bottle, offer ports for additional inlet lines, and sparging (i.e. dispersing He or Ar into the

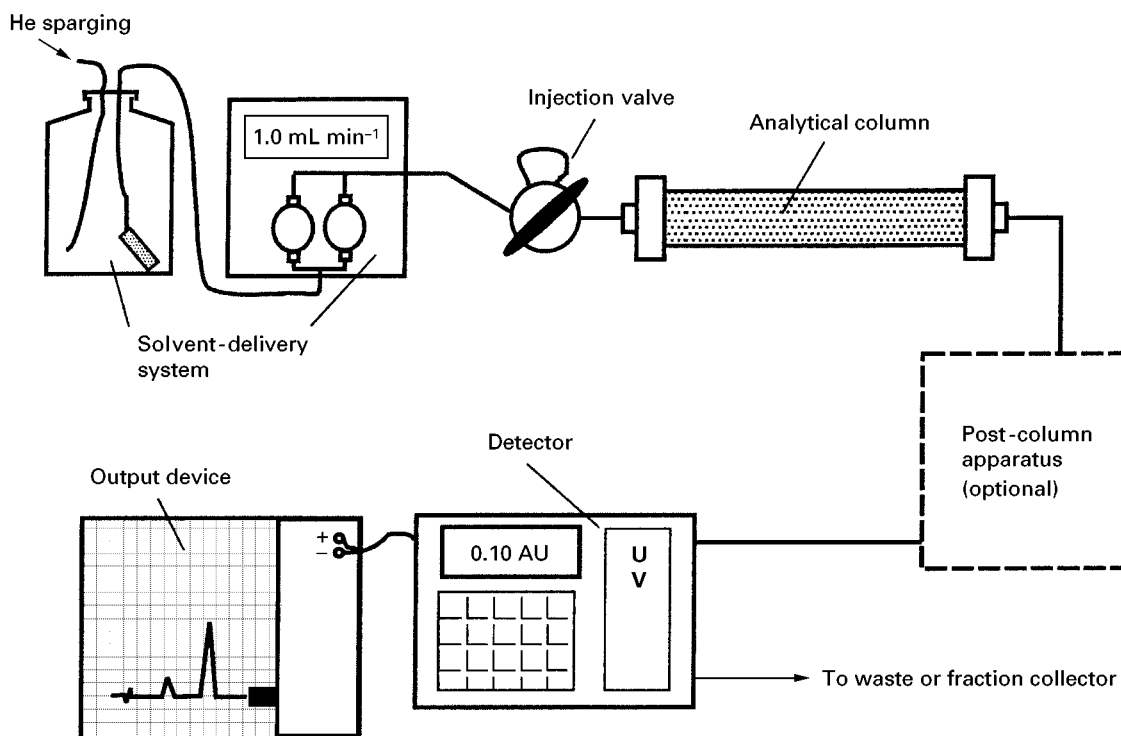


Figure 1 Generic HPLC system.

mobile phase to remove dissolved air). All mobile phases/solvents should be freshly filtered and preferably degassed. Online degassers, which are primarily used to remove small gas bubbles and reduce the amount of dissolved air, are now popular additions to many HPLC systems, and they eliminate the need to degas mobile phase offline. An additional filter is often placed at the end of the mobile-phase inlet line to remove any precipitants that may form in the mobile phase during its use. Sparging control and the ability to blanket the solvents with inert gases is highly recommended to eliminate carbonate formation in alkaline solvents and to maintain extremely low levels of dissolved oxygen, when performing electrochemical or fluorescence detection.

Solvent-Delivery System

The high-pressure pump can operate at pressures from 500 to 5000 psi. The purpose of the pump is to deliver a precise, accurate, reproducible, constant, and pulse-free flow of mobile phase to the column. Three major classes of HPLC pumps are currently in use: constant-pressure pumps; syringe-based or displacement pumps; and constant flow pumps. Neither constant pressure or syringe-based pumps are easily adapted to gradient solvent delivery; hence, constant-flow pumps are by far the most common.

The majority of commercial high-pressure pumps available today are designed around a simple recip-

rocating piston pump. The rotational energy of a motor is transferred into the reciprocal movement of the piston by an eccentric cam or gear. The piston is driven in and out of a solvent chamber in the pump head, which typically has a volume of 10 to 100 μ L. A pair of check valves control the direction of flow through the pump head. A piston seal keeps the mobile phase from leaking out of the pump head. On the intake stroke, the piston is withdrawn from the pump head, creating a low-pressure zone. The low pressure causes the inlet check valve (i.e. from the mobile-phase reservoir) to open and the outlet check valve (i.e. delivery to the column) to close, allowing the mobile phase to fill the pump head. On the delivery stroke, the piston moves into the solvent chamber, which increases the pressure. The high pressure closes the inlet check valve and opens the outlet check valve, allowing the mobile phase to flow to the column. In a single-head reciprocating pump, the solvent chamber is delivering mobile phase to the column only half the time. The other half of the time it is being used to fill the solvent chamber. With a twin-head reciprocating pump, two pump heads operate simultaneously but at 180° out of phase with each other. As a result, mobile phase flows to the column 100% of the time. The twin-head design gives essentially pulseless flow as compared to the single-head design.

Many separations can be done isocratically, which means that solvent composition being delivered to the

column is not changing in composition over the course of the separation. For more complex separations, gradient elution is required. Most commonly, gradient elution is performed by altering the proportion of the eluents over the course of the separation. In doing so, the early eluting compounds remain well resolved, while the more highly retained compounds elute quicker. Gradient elution is simply the programming, or changing of the solvent strength over the course of a separation. A gradient can be linear, convex, concave, stepped, or a complex sequence of each to achieve the desired separation. Computer-controlled pumping is required to generate a gradient flow. Three major approaches are used to produce a gradient flow: (i) controlled amounts of each eluent (up to four may be used) are metered into a mixing chamber before reaching the high-pressure pump; (ii) a proportioning valve, which is controlled by a microprocessor, regulates the amount of up to four eluents and the eluent mixture is sent to the high-pressure pump; and (iii) the outputs of multiple high-pressure pumps, which are controlled individually by a programming device, are mixed together in a high-pressure mixing chamber after the pump. Approaches (i) and (ii) are known as low-pressure mixing, and approach (iii) is high-pressure mixing. Low-pressure mixing is less expensive than high-pressure mixing since only one high-pressure pump is used versus the two or more required for high-pressure mixing, and the maintenance of one pump is much easier than the maintenance of two or more pumps. The main problem with low-pressure mixing is that it is more susceptible to bubble formation because the solvents are being mixed at atmospheric pressure. Hence, the common use of online degassers.

Sample-Introduction Device

In many instances, the limiting factor in the precision of an HPLC system lies in the reproducibility of the sample-introduction system. The sample-introduction device, also known as a 'sample injector', is used to introduce the sample into the HPLC system without depressurizing it. The most widely used method of sample injection is based upon a sample loop that can be placed in and out of the mobile phase flow path by merely switching a valve (Figure 2). When the valve is in the load position, the sample loop is filled at atmospheric pressure. Sample sizes often range from 5 to 500 μL . For best results, an excess of sample (i.e. two to five times the injection volume) is flushed through the loop to ensure that no trace of the previous sample remains. By turning the valve from the load to the inject position, the sample loop is connected to the high-pressure mobile-phase stream and the sample is then carried to the column.

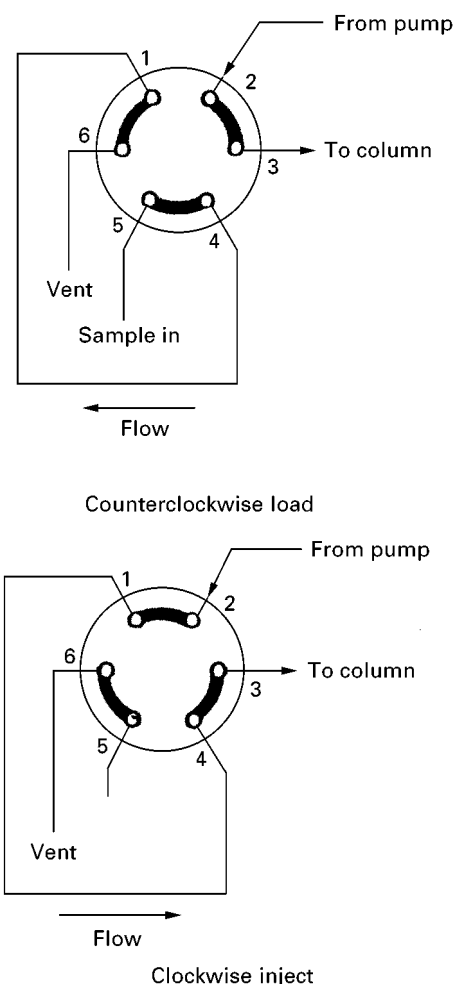


Figure 2 Generic high-pressure injection valve shown in the load and inject positions.

The valve-based sample-introduction system is easily automated using simple robotic technology. The use of auto-injectors not only improves injection reproducibility, but they allow for the continuous processing of numerous (i.e. tens to thousands) of samples at a time. Auto-injectors have also been used for the implementation of pre-column derivatization protocols, especially for amino acid analyses. Pre-column derivatization is used to improve the chromatographic and/or detection properties of analytes.

Column

The column is the part of the HPLC in which the separation occurs. HPLC columns are mainly constructed from smooth-bore stainless-steel tubing due to the high-pressure aspects of HPLC. Nowadays columns are sometimes constructed from heavy-walled glass, titanium, or plastic (e.g. PEEK®) to offer the analyst better performance for particular analytes. Common dimensions for analytical-scale

columns are in the range of 10 to 30 cm long and 4 to 10 mm inner diameter. The common particle sizes of packings are 3, 5, and 10 μm . Columns of these dimensions often have efficiencies of 40 000 to 60 000 plates per metre. The current trend has been the use of higher performance, high-speed columns, which have smaller dimensions than those described. Such columns have efficiencies of 100 000 plates per metre and have the advantage of speed and minimal solvent consumption. Hundreds of packed columns in differing size and packing material are available from numerous manufacturers.

It is important to read the manufacturers' literature relating to the maintenance, handling, and limitations of the column (e.g. silica-based columns are only compatible with pH values from 2 to 7). In addition to chemical limitations of the packing material, columns are easily degraded by the irreversible adsorption of impurities from samples and solvents. Hence, a small guard column is often used to protect the integrity of the analytical column, which is much more expensive. Also, for analytes, which may contain particulates, an inline filter can be placed between the injector and guard column. It should be noted that with the addition of each component after the injector, the efficiency of the separation is degraded. Hence, judicious use of inline devices is necessary.

For many applications, close control of column temperature is not necessary and HPLC separations are performed under ambient conditions. However, temperature control can enhance chromatographic reproducibility and afford opportunities to improve separation efficiency. Modern instruments can be equipped with column heaters/ovens that control column temperature to a few tenths of a degree from near ambient to 150°C.

Post-Column Apparatus

If post-column modification of the mobile phase or analyte is required, then the system will have a post-column apparatus in the flow path. Modification of the mobile phase (e.g. addition of buffers, changing the pH, and solvent strength) may be needed to enhance the compatibility of the mobile phase with the detector, while post-column derivatization of the analyte may be needed to improve the detection properties of the analytes after their separation. In either case, a post-column addition system consists simply of a reagent-delivery pump, a mixing-tee, and a mixing coil. Typically, a pressurized reservoir is commonly used to deliver a pulseless flow of the reagent. The vessel is usually fitted with a check valve to prevent reagent back-up. The major drawback of using a pressure-based delivery system is that it can-

not handle a great deal of system back-pressure. Hence, close attention must be paid to the minimization of post-column back-pressure sources. Any single-piston pump, even with extensive pulse dampening, is usually inadequate for high-sensitivity work.

Delivery of the post-column reagent to the chromatographic eluent flow is accomplished via a mixing tee. The mixing tee should be a low dead-volume fitting. Probably the most crucial component in the post-column system is the mixing coil, which connects the mixing tee to the detector. It is essential that the mixing coil produces a homogeneous solution in the most efficient manner, in other words, with minimal band-broadening. The best mixing is obtained with a woven/knitted reaction coil. The three-dimensional weave achieves efficient mixing and effectively reduces band-broadening effects by preventing laminar flow patterns. In addition, their open-tubular nature produces less back-pressure than packed-bed reactors, and woven reactors are easy to make using commercially available Teflon® tubing.

Detector

By passing the column effluent through the detector, some chemical or physical property of the analyte is transduced to an electrical signal, and the solutes are monitored as they are eluted from the column. The electrical signal, which can be amplified and manipulated by suitable electronics, is proportional to the level of some property of the mobile phase or solutes.

HPLC detectors are classified as either bulk-property detectors, which respond to a bulk property of the eluent such as refractive index or conductivity, or solute-property detectors, which respond to some property of the analyte such as UV absorbance. In either case, the response of the detector is modulated by the presence and amount of the analyte. Solute property detectors tend to be more sensitive than bulk property detectors (in the order of 1000 times or more).

Ideal characteristics of an HPLC detector are high sensitivity, good stability, linearity, short response time, reliability, non-destructiveness, ease of use, and low dead volume. Many types of analytical techniques have been applied to HPLC with varying degrees of success. It has been estimated that HPLC detection is divided as follows: 70% by UV absorption, 15% by fluorescence, 5% by refractive index, 5% by electrochemical methods, and 5% by other measurements. Table 1 lists some of the common HPLC detectors and their relevant properties. Only a brief review of the most common detectors is presented here.

Table 1 Performance characteristics of common HPLC detectors

Parameter	Detector				
	UV/vis absorption	Fluorescence	Electrochemical	Conductivity	Refractive index
Classification	Solute property	Solute property	Solute property	Bulk property	Bulk property
Response	Selective	Selective	Selective	Selective	Universal
Sensitivity	Nanogram	Picogram	Picogram	Nanogram	Microgram
Gradient compatibility	Yes	Yes	Limited	Yes (suppressed) No (nonsuppressed)	No
Flow sensitivity	No	No	Yes	Yes	Yes
Temperature sensitivity	No	No	Yes	Yes	Yes

UV/vis absorbance detectors In UV/vis detectors, the mobile phase is passed through a small flow cell, where the radiation beam of a UV/vis photometer or spectrophotometer is located. As a UV-absorbing solute passes through the flow cell, a signal is generated that is proportional to the solute concentration. Only UV-absorbing compounds, such as alkenes, aromatics, and compounds that have multiple bonds between C and O, N, or S are detected. The mobile-phase components should be selected carefully so that they absorb little or no radiation. Absorption of radiation is a function of concentration, c , as described by the Beer–Lambert law: $A = \epsilon bc$, where A absorbance, ϵ = molar extinction coefficient, and b = flow cell path length.

Three types of absorbance detectors are available: fixed wavelength; variable wavelength; and photodiode array. A fixed-wavelength detector uses a light source that emits maximum light intensity at one or several discrete wavelengths (e.g. 254, 280, and 365 nm for a mercury lamp) that are isolated by appropriate filters. A fixed-wavelength detector is the most sensitive and least expensive of the three. A variable-wavelength detector uses a relatively wide bandpass UV/vis spectrophotometer, and has the advantage of wavelength-selection flexibility. It is also more expensive than the fixed-wavelength detector. In order to generate a real-time spectrum for each peak as it is eluted, a photodiode array is used. Comparison of spectra generated chromatographically with a known spectrum is useful for solute identification. In addition, software has been designed to evaluate peak purity with diode array-generated data. The major disadvantage with scanning-wavelength technology is a loss in sensitivity.

Fluorescence detectors Fluorescent detectors exploit the ability of a compound to fluoresce upon irradiation. The emitted light, which is detected at right angles to the irradiation beam to minimize background noise, is then detected similarly to that of the

UV/vis detector. The major advantage of a fluorescent detector is selectivity and sensitivity for fluorescent solutes. Unfortunately, relatively few solutes fluoresce naturally, and analytes of interest must often be derivatized with a fluorescent entity. Because both the excitation and emission wavelengths can be varied, the detector can be made highly selective.

Electrochemical detectors Electrochemical detectors measure the current associated with the oxidation or reduction of solutes as they are eluted from the column. The suitability of electrochemical detection depends on the redox characteristics of the solute molecules in the environment of the mobile phase. Electrochemical detectors have the advantages of high sensitivity, high selectivity, and wide linear range. Most naturally occurring electroactive compounds have an aromatic substituent (e.g. catechols, quinines, and aryl amines). Polar aliphatic compounds (e.g. carbohydrates, amines, and thio compounds) can also be detected directly using pulsed electrochemical detection (PED). PED exploits electrocatalytic detection at noble metal electrodes by combining amperometric detection with pulsed potential cleaning to maintain uniform electrode activity.

Conductivity detectors Conductivity detectors are used primarily to detect ions in conjunction with ion chromatography (IC). This type of detector monitors the ability of the eluent to conduct electricity. In non-suppressed ion chromatography, the conductivity of the eluent is minimized via the careful selection of reagents and control of their concentration. Under these conditions, charged analyte ions are more conductive than the eluent and a signal is generated as they are pumped through the detector. In suppressed ion chromatography, the response of the background is neutralized using a post-column suppressor (e.g. eluent hydroxide ions in anion-exchange chromatography and eluent hydrogen ions in cation-exchange

chromatography are neutralized to water). Under these conditions, only the charged analyte ions are detected. Suppressed IC inherently, and in practice, has superior detection limits as compared to non-suppressed IC, despite having a larger dead volume.

Refractive index (RI) detectors Refractive index detectors monitor the difference in refractive index between the column eluent containing analyte and a reference stream containing mobile phase only. These detectors are the closest to universal detectors in HPLC because any solute can be detected as long as its refractive index is different from that of the mobile phase. Unfortunately, RI detection is limited by a number of significant drawbacks. The sensitivity of RI detection (Table 1) is poor owing to the small differences in the absolute refractive indices of many substances commonly analysed by HPLC. RI detection is sensitive to both temperature and pressure changes, and, as a consequence, strict temperature control of the detector and pulseless flow are mandatory. Since RI is a bulk property detector, it is sensitive to changes in the mobile-phase composition, as well as analyte concentration, and it is not amenable to gradient elution. Gradient elution can be performed with RI if the detector is configured with a working and a reference column and two flowing liquid streams – this is easier said than done.

Mass spectrometer Owing to innovations in LC-mass spectrometry (MS) interfacing, MS has become a very important HPLC detector because of its ability to generate structural and molecular weight information about the eluted solutes. The combination of HPLC and mass spectrometry allows for both separation and identification in the same step, an advantage few of the other detectors provide. Two major problems must be addressed when interfacing MS with HPLC. First, the flow rate in HPLC with conventional 4.6 mm i.d. columns is about 1 mL min^{-1} , which is much larger than the flow that can be taken by the conventional mass spectrometer vacuum systems. Second, MS has difficulty in vaporizing non-volatile and thermally labile molecules without degrading them.

Other detectors In addition to the highly popular detectors mentioned above, numerous other detectors have been used in HPLC including Fourier transform infrared (FTIR), radioactivity, element selective, and photoionization. Two detectors which have been gaining in popularity for specific applications are chiroptical for optically active compounds and evaporative light scattering for triglyceride analysis.

Data Collection and Output System

A data collection and output device (e.g. computer, integrator, or recorder) is connected to the electronic output of the detector. The data-collection device takes the electronic signal produced by the detector and outputs a plot of response versus time. This resulting chromatogram can then be evaluated for both qualitative and quantitative information. Recorders are rarely used today on their own. Both integrators and computers can integrate the peaks of a chromatogram and have the added advantage of being able to store chromatograms for post-collection processing. The data from computer-based collection systems can also be exported to other software programs and around the world by e-mail or over the Internet. In addition, the computer is typically able to communicate with and control the entire HPLC system. Hence, the majority of modern HPLC systems are fitted with computer control, data collection, and output systems.

Post-Detection Eluent Processing

After the eluent passes through the detector, it is often directed to a waste container. The waste container should be properly labelled for eventual disposal by environmentally acceptable means. If isocratic chromatography is being performed, a mobile-phase recycling device can be added after the detector. While the instrument is running and no injections are being made or during periods of the separation when no peaks are being eluted, the solvent-recycling device will direct clean mobile phase back to the mobile-phase reservoir.

If collection of the eluted peaks is needed, a fraction-collection device is added to the system after the detector. The collection of the peaks by the fraction collector can be done on the basis of a fixed interval of time or mobile-phase volume or via the output signal from the detector. Fraction collectors can also be under the control of an HPLC's computer for ease of use.

Connective Tubing and Fittings

The connective tubing in the HPLC system should be made of material inert to the solvents and constituents of the mobile phase. Often tubing is made of stainless steel or polymer-based materials (e.g. PEEK®, Teflon®, etc.). The connections between the tubings and HPLC components are made with fittings and unions designed to minimize excess volume, or dead volume. Zero dead volume (ZDV) and low dead-volume (LDV) fittings are necessary to reduce band-broadening effects. Also, great care should be used when assembling columns and fittings so that they match properly. Tubing should be cut flat and fit flush, and all fittings should be zero dead volume. Any

extra-column volume compromises separation efficiency. Polymer-based, or PEEK®, tubing and fittings throughout the chromatographic flow path are becoming very popular. PEEK tubing is available in a wide range of sizes, is colour-coded for ease of size selection, is easy to work with, is tolerant to a wide range of buffer and solvent conditions, and is impermeable to oxygen.

The effects of band-broadening are not important prior to injection; therefore, the inner diameter of the tubing from the pump to the injector/autosampler should be as large (i.e. typically 0.030 inch i.d.) as possible (i.e. to reduce system back-pressure) while maintaining high-pressure strength. From the injector to the column to the detector, all tubing should be as short as possible and of the narrowest diameter available to minimize extra-column effects. Post-injector tubing diameters are often 0.01–0.005 inch i.d.

Related HPLC Techniques

The HPLC system described above was based on the dimensions of a typical analytical system, otherwise known as ‘normal-bore chromatography’. The same basic components and designs are used in both micro- (i.e. column dimensions of 1–2 mm i.d.) and preparative systems, which have much larger column dimensions.

Microchromatographic techniques include micro-bore, nanobore, and capillary chromatography, which have column inner diameters of 2 to 1 mm, 1 to 0.3 mm, and less than 300 µm, respectively. Most importantly, microchromatographic systems require smaller extra-column volumes than normal-bore systems. Hence, great pains should be taken to use the smallest inner-diameter tubing available, zero dead-volume fittings, smaller injection volumes, and smaller detection cell volumes. Microchroma-

tographic systems are employed when sample volume is limited.

If compound purification or isolation is intended, preparative chromatography is used. Since a large quantity of material is to be injected in order to isolate a significant quantity of analyte, column capacity and, hence, column diameters are larger. Column diameters in preparative HPLC can be on the order of metres. The high flow rates needed for these large-scale systems require the use of special pumps and larger tubing throughout.

See also: II/Chromatography: Liquid: Derivatization; Detectors: Ultraviolet and Visible Detection; Mechanisms: Ion Chromatography.

Further Reading

- Karger BL, Snyder LR and Horváth C (1973) *An Introduction to Separation Science*. New York: John Wiley.
- Krull IS (ed.) (1986) *Reaction Detection in Liquid Chromatography*. New York: Marcel Dekker.
- LaCourse WR and Dasenbrock CO (1998) Column liquid chromatography: equipment and instrumentation. *Analytical Chemistry* 70: 37R–52R.
- Lough WJ and Wainer IW (ed.) (1996) *High Performance Liquid Chromatography: Fundamental Principles and Practice*. London: Academic and Professional.
- McMaster MC (1994) *HPLC: A Practical User's Guide*. New York: VCH.
- Snyder LR and Kirkland JJ (1979) *Introduction to Modern Liquid Chromatography*, 2nd edn. New York: John Wiley.
- Snyder LR, Glajch JL and Kirkland JJ (1988) *Practical HPLC Method Development*. New York: John Wiley.
- Swadesh J (ed.) (1997) *HPLC: Practical and Industrial Applications*. Boca Raton, FL: CRC Press.
- Willard HH, Merritt Jr., LL, Dean JA and Settle Jr FA. (1988) *Instrumental Methods of Analysis*, 7th edn. Wadsworth: Belmont.

Ion Chromatography: Mechanisms

See II/CHROMATOGRAPHY: LIQUID/Mechanisms: Ion Chromatography

Ion Pair Liquid Chromatography

J. Ståhlberg, Astra Zeneca, Tablet Production Sweden, Södertälje, Sweden

Copyright © 2000 Academic Press

Ion pair chromatography is a widely used reversed phase liquid chromatographic technique for the

separation of ionic analytes. Retention of ions in ion pair chromatography is determined by many experimental parameters and it therefore provides an effective tool for obtaining chromatographic separation between ionic analytes. A major part of this article discusses the influence of the most important

parameters on retention. A short presentation of the areas of application of ion pair chromatography, as well as some practical guidelines for its use, is also included.

Introduction to Ion Pair Chromatography

Ion pair chromatography (IPC) is an effective reversed-phase liquid chromatographic (RPLC) technique for separation of organic ions and partly ionized organic analytes. The technique utilizes the same types of stationary phases and mobile phases as RPLC; the main characteristic for IPC is that an ion pair reagent is added to the mobile phase. The ion pair reagent is usually an alkylsulfonate, an alkylsulfate or an alkylammonium salt. The high efficiency of RPC columns compared with columns used in ion exchange or ion chromatography also makes IPC a valuable alternative to these techniques.

The purpose of adding an ion pair reagent to the mobile phase is usually to change the retention time of ionic analytes. By varying the mobile phase concentration of the ion pair reagent, the retention factor for an oppositely mono-charged analyte can be continuously increased by a factor of 10–20 compared to the value with no added ion pair reagent. Correspondingly, it is possible to continuously reduce the retention factor for a similarly mono-charged analyte by a factor of 10–20. The retention factor for non-charged analytes is usually more or less unaffected by the presence of the ion pair reagent.

Ion pair extraction, i.e. extraction of ionized solutes into organic phases by adding an oppositely charged ion to the system, has been used for many decades. In this technique, the distribution of an ion into the organic phase is enhanced by the formation of an ion pair between the two oppositely charged ions. The pioneering work in IPC by Schill and co-workers in Uppsala was performed in the liquid–liquid partition mode. The extraction of an ion pair to the organic phase was considered to be the cause of retention, and the name ion pair chromatography originates from this early application. When covalently bonded non-polar stationary phases were introduced, important contributions to the further development of IPC were, among others, made by the research groups of Horváth, Knox, Schill and Haney.

IPC has been applied in almost all areas of analytical chemistry where chromatography is used. Since many drugs are basic or acidic, the driving force for the development of IPC came from the pharmaceutical industry where today it is used on a routine basis.

Of particular current interest is chiral separations of pharmaceutical compounds by using a chiral ion pair reagent. In IPC, water-rich mobile phases can be employed with a variety of buffers and ionic and non-ionic additives and the technique is therefore suitable for separation of important classes of biomolecules and specifically amino acids, peptides, proteins and nucleic acids. In the food industry, IPC is used for the analysis of water-soluble vitamins, caffeine, theobromine, amines, etc.

For the separation of inorganic cations and anions IPC is often used as an alternative to ion (exchange) chromatography and in these applications it is usually referred to as ion interaction chromatography. In ion interaction chromatography, the ion pair reagent is usually called the ion interaction reagent. The technique has been used, for example, in the area of environmental analysis for the separation and analysis of nitrate and nitrite. Another technique that is closely related to ion pair chromatography is micellar chromatography. Here the concentration of ion pair reagent in the mobile phase is so high that micelles are formed, i.e. the concentration of the ion pair reagent in the mobile phase is above the critical micelle concentration (CMC). Micellar chromatography is treated in a separate article.

When the analyte ion lacks properties that make it easily detectable by commonly used detectors, IPC in the indirect detection mode can be used. The basis of this method is that a constant concentration of a detectable ion pair reagent is added to the mobile phase. In the chromatographic zone, where the non-detectable analyte ion is present, a change from the otherwise constant concentration of the detectable ion pair reagent is induced by the analyte. Depending on the relative properties of the analyte and the ion pair reagent, the concentration of ion pair reagent in the analyte zone may be either higher or lower than in the mobile phase.

Retention and selectivity in reversed-phase IPC are influenced by a large number of experimental parameters. These parameters are given in **Table 1** together with a short description of their effect on retention. Briefly, for the separation of a particular set of analyte ions the parameters that are most important are type and concentration of ion pair reagent, type and concentration of organic modifier, and mobile phase pH. By varying these parameters while keeping the others constant within sensible ranges, an acceptable separation is usually obtained. A rational use of IPC is facilitated by a basic knowledge of the impact of the different parameters on retention. A more detailed analysis of the role of the most important parameters is presented below.

Table 1 Effect on retention of increasing the value of different chromatographic variables in reversed-phase ion pair chromatographic systems

Variable	Effect on k for oppositely charged solute	Effect on k for similarly charged solute
Increasing charge of analyte ion ($z_B = \pm 1, 2, \dots$)	Increases the slope of the $\ln k_{CB}$ vs $\ln c_A$ relation	Increases the absolute value of the slope of the $\ln k_{CB}$ vs $\ln c_A$ relation
Increasing charge of pairing ion ($z_A = \pm 1, 2, \dots$)	Slightly decreases the slope of the $\ln k_{CB}$ vs $\ln c_A$ relation	Slightly decreases the absolute value of the slope of the $\ln k_{CB}$ vs $\ln c_A$ relation
Increasing concentration of pairing ion (c_A)	Increases	Decreases
Increasing hydrophobicity of pairing ion (K_A)	Increases	Decreases
Increasing concentration of organic modifier (φ)	Decreases. The slope of the $\ln k_{CB}$ vs φ relationship becomes steeper compared with the regular RP slope	Decreases. The slope of the $\ln k_{CB}$ vs φ relationship becomes less steep compared with the regular RP slope
Increasing polarity of the organic modifier	The slope of the $\ln k_{CB}$ vs φ relationship decreases	The absolute value of the slope of the $\ln k_{CB}$ vs φ relationship increases
Increasing ionic strength (I)	Decreases	Increases
Type of stationary phase	A parallel shift of the $\ln k_{CB}$ vs $\ln c_A$ relationship occurs for both positively and negatively charged analytes when using different columns	
Eluent pH	Retention of the ionized form increases; it can become even larger than the regular RP retention of the non-ionized form	Retention of the ionized form decreases

Retention Theories for Ion Pair Chromatography

Stoichiometric Theories

In this article IPC means liquid chromatography performed on columns with covalently bonded non-polar stationary phases, in combination with polar mobile phases containing an ion pair reagent. The earliest retention theories for IPC were stoichiometric, i.e. the retention is assumed to be caused by the formation of a 1 : 1 stoichiometric complex between the ion pair reagent and the oppositely charged analyte ion. Depending on the particular theory, complex formation is considered to take place in the mobile phase or in the bonded phase. Other theories consider the ion pair reagent to be adsorbed to the stationary phase surface and describe retention as a result of a stoichiometric ion exchange process between the analyte ion and the counter ions to the ion pair reagent. In 1981 it was pointed out by Knox and Hartwick that many of the proposed stoichiometric retention theories are thermodynamically equivalent and that it is therefore not possible to distinguish them from each other by retention measurements alone.

The physicochemical cause of retention in ion pair chromatography has been a controversial issue. Because of this disagreement many alternative names

have been proposed for this technique. These include: dynamic ion exchange chromatography, ion-interaction chromatography, hetaeric chromatography, and soap chromatography. Correspondingly, many names have been used for the ion pair reagent.

Non-stoichiometric Theories

Modern retention theories recognize that the layer of the bonded phase is so thin that the surface area to bonded phase volume ratio is extremely high. As a consequence, the surface science view on adsorption of both the analyte and the ion pair reagent to the stationary phase can be applied. In these theories, the electrostatic interaction between the ion pair reagent and the analyte ion leads to a non-stoichiometric retention theory. The non-stoichiometry is a consequence of the fact that the electrostatic interaction is long ranged and therefore gives rise to a multibody interaction (Figure 1).

The common basis of modern retention theories is that a charged surface is created when the ion pair reagent adsorbs at the interface between the polar mobile phase and the hydrophobic stationary phase. The inorganic counterions to the ion pair reagent are territorially bound to the charged surface in a diffuse layer and a diffuse double layer is formed. Physically this results in a difference in electrostatic potential, $\Delta\Psi_0$, between the bulk of the mobile phase and the surface ($\Delta\Psi_0$ has the same physical origin as the more

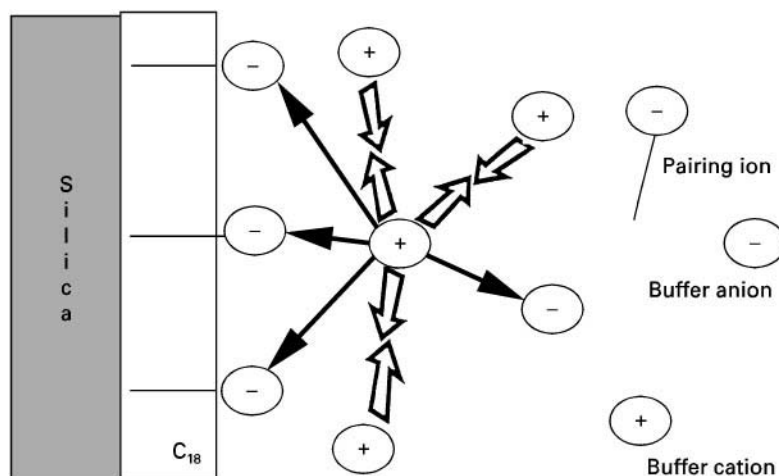


Figure 1 Schematic illustration of the long-range nature of electrostatic forces between ions in typical ion pair chromatographic systems. Open and full arrows represent electrostatic repulsion and attraction forces, respectively. (Reproduced with permission from Bartha Á and Ståhlberg J (1994) *Journal of Chromatography A* 668: 255.)

frequently encountered zeta-potential, although they may differ in their numerical value). For a positively charged ion pair reagent the numerical value for $\Delta\Psi_0$ is positive and for a negative reagent it is negative. Qualitatively, the charging of the stationary phase surface infers that the retention of analyte ions of opposite charge to the pairing ion increases due to electrostatic attraction. It also infers that the retention of analyte ions of similar charge to the

pairing ion decreases due to electrostatic repulsion (Figure 2).

Several non-stoichiometric theories have been proposed, which all use the difference in electrostatic potential between the mobile and stationary phase as a parameter that influences the retention of an ionic analyte. However, there are important differences between the theories in the physical description and also in the role that the electrostatic surface potential plays in retention. For example, in the theory proposed by Cantwell and co-workers, retention is considered to be due to a mixed ion exchange and electrostatic effect. The disagreement today among the proponents of non-stoichiometric theories seems to be on how retention is best described under conditions of high surface loadings of the ion pair reagent, i.e. when the electrostatic surface potential is higher than ± 60 mV. The disagreement is a consequence of the fact that under these conditions a number of different, not fully understood, physical phenomena may occur in the diffuse double layer.

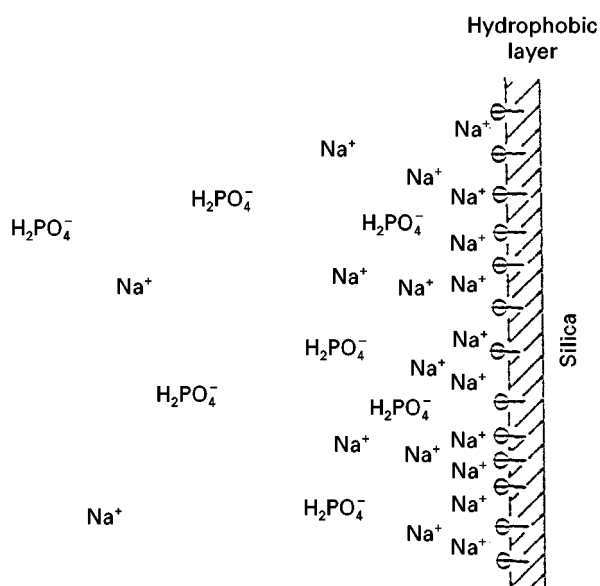


Figure 2 A schematic picture of the electrical double layer in reversed-phase ion pair chromatography. (Reproduced with permission from Bartha Á and Ståhlberg J (1994) *Journal of Chromatography A* 668: 255.)

Parameters Controlling the Retention factor in Ion Pair Chromatography

Theoretical Aspects

A simplified version of the surface adsorption double layer model for IPC provides a convenient framework for treating the influence of the various experimental parameters on the retention of medium-sized ($mw = 100\text{--}300$) mono- and di-charged organic ions. This is a non-stoichiometric theory developed for electrostatic surface potentials in the range 15–40 mV.

In this theory, the retention factor of an analyte ion in the absence of the ion pair reagent, k_{0B} , is related to its standard free energy of adsorption, ΔG_B^0 , according to:

$$k_{0B} = \phi \cdot \exp\left(-\frac{\Delta G_B^0}{RT}\right) \quad [1]$$

where the subscript zero denotes that the concentration of the ion pair concentration reagent is zero and ϕ is the column phase ratio. To a first approximation, the presence of the ion pair reagent on the surface does not change any property of the stationary phase other than its electrostatic potential. This infers that in the presence of the ion pair reagent the standard free energy of adsorption of the analyte changes to ΔG_t^0 where:

$$\Delta G_t^0 = \Delta G_B^0 + z_B F \Delta \Psi_0 \quad [2]$$

Here z_B is the charge of the analyte ion and F is the Faraday constant. ΔG_B^0 is usually referred to as the chemical part of the free energy of adsorption and $z_B F \Delta \Psi_0$ as the electrostatic part. Assuming that the retention of the analyte is due to adsorption to the stationary phase surface only, its retention factor, k_{cB} , in the presence of the ion pair reagent becomes:

$$\begin{aligned} k_{cB} &= \phi \cdot \exp\left(-\frac{\Delta G_B^0 + z_B F \Delta \Psi_0}{RT}\right) \\ &= k_{0B} \cdot \exp\left(-\frac{z_B F \Delta \Psi_0}{RT}\right) \end{aligned} \quad [3]$$

According to equation [3], the retention of an ionic analyte in IPC is determined by its retention in the absence of the ion pair reagent, the charge of the analyte ion and the electrostatic surface potential induced by the ion pair reagent. The influence of different experimental variables on the retention can for most cases be rationalized and quantitatively or semi-quantitatively described from eqn [3]. Deviations may occur, for example, when the value for k_{0B} is less than ≈ 0.5 , or when the surface concentration of the ion pair reagent is higher than 40–50% of the monolayer capacity of the surface.

The value for $\Delta \Psi_0$ is primarily a function of the surface concentration of the ion pair reagent and of the ionic strength of the mobile phase. The relationship between these variables can be obtained from solving the Poisson–Boltzmann equation for charged surfaces in contact with an electrolyte solution. When the electrostatic surface potential is below ± 25 mV the solution shows that there is a linear relation between the surface concentration of charges

and $\Delta \Psi_0$:

$$\Delta \Psi_0 = \frac{z_A n_A F}{\kappa \epsilon_0 \epsilon_r} \quad [4]$$

where n_A is the surface concentration of the ion pair reagent (mol m^{-2}), κ is the inverse Debye length ($1/\text{m}$), ϵ_0 is the permittivity of vacuum and ϵ_r is the dielectric constant of the mobile phase (dimensionless). The numerical value for κ is proportional to the square root of the ionic strength of the mobile phase.

In practice, it is not the surface concentration of the ion pair reagent but its mobile phase concentration that is experimentally controlled. The relationship between these two is determined by the adsorption isotherm of the ion pair reagent onto the stationary phase surface. In analogy with the discussion concerning the adsorption of the analyte ion, the free energy of adsorption of the ion pair reagent is divided into a chemical and an electrostatic part. Physically this means that the electrostatic surface potential created by the ion pair reagent must be included in its own adsorption isotherm. The simplest is the surface potential-modified linear adsorption isotherm:

$$n_A = n_0 K_A c_A \cdot \exp\left(-\frac{z_B F \Delta \Psi_0}{RT}\right) \quad [5]$$

where n_0 is the monolayer capacity of the surface, c_A is the mobile phase concentration of the ion pair reagent and K_A is its association constant to the stationary phase. The exponential term in the equation accounts for the electrostatic repulsion induced by the adsorbed ion pair reagent itself and it gives rise to a nonlinear adsorption isotherm. Equation [5] has been experimentally verified in many different reversed phase ion pair systems and can be used when n_A is less than $0.3n_0$.

After making some approximations it is possible to derive eqn [6] from eqns [3]–[5]

$$\begin{aligned} \ln k_{cB} &= \ln k_{0B} + \frac{-z_A z_B}{(z_A^2 + 1)} \left[\ln n_0 K_A + \ln c_A \right. \\ &\quad \left. - \frac{1}{2} \ln I + \text{const.} \right] \end{aligned} \quad [6]$$

where I is the mobile phase ionic strength. This equation in a convenient way separates the influence of the different experimental variables on retention. For oppositely mono-charged analyte and ion pair reagent, the equation is approximately valid in the interval 2–10 for the k_{cB}/k_{0B} ratio.

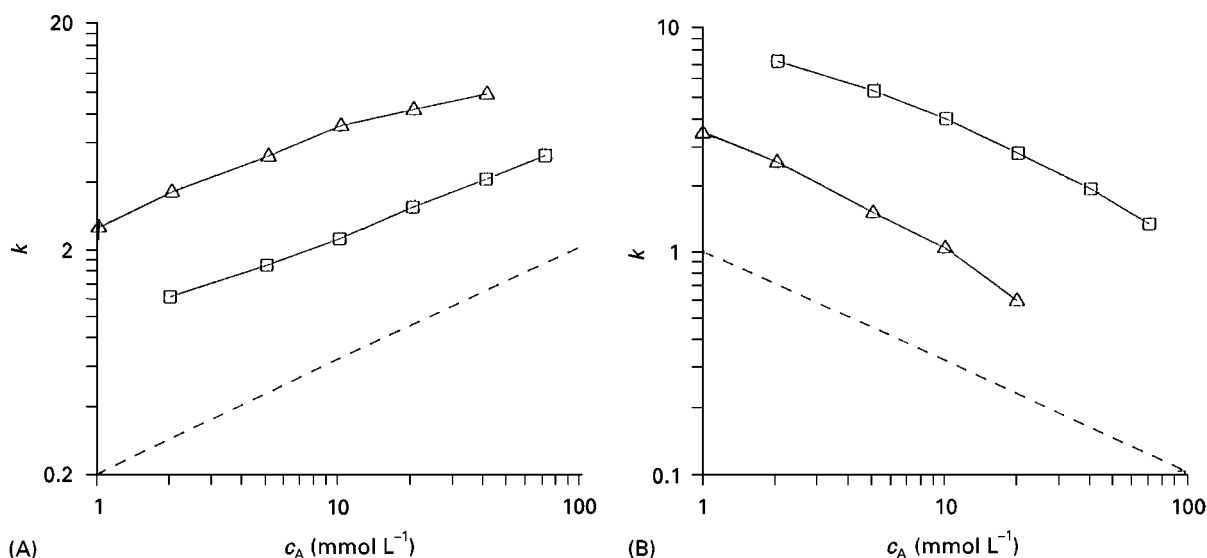


Figure 3 Retention factor for (A) dopamine and (B) naphthalenesulfonic acid as a function of the mobile phase concentration of sodium hexylsulfonate (\square) and octylsulfonate (\triangle) pairing ions. ---, Theoretical slope. Measurements were made in methanol–aqueous phosphate buffer (pH 2.1, 10 : 90 v/v). (Reproduced with permission from Bartha Á and Ståhlberg J (1994) *Journal of Chromatography A* 668: 255.)

Charge of the Analyte and Ion Pair Reagent Ion

The influence of the charge of the analyte ion on retention when the mobile phase concentration of the ion pair reagent varies can be understood from eqn [6]. When $z_A = +1$ and $z_B = -1$, the equation predicts that in a $\ln k_{CB}$ vs $\ln c_A$ plot the slope of the straight line is equal to $1/2$ and when $z_B = z_A = -1$ it is equal to $-1/2$. Examples of experimental data for these two cases are shown in Figure 3.

For multiple charged ion pair reagents, the non-linearity of the adsorption isotherm becomes more pronounced than for monocharged reagents. Quantitatively, this is described in eqns [4]–[6] through the value for z_A ; when $z_A = +2$ eqn [6] predicts that the slope of the $\ln k_{CB}$ vs $\ln c_A$ plot is $2/5$ for a negatively mono-charged analyte ion and $4/5$ for a di-charged ion. An example is shown in Figure 4 where the di-charged hexamethonium bromide ion is used as ion pair reagent. The solid lines in the figure corresponds to the theoretically predicted slope.

Type of Analyte Ion and Ion Pair Reagent

In a reversed phase chromatographic system, the ionized form of a molecule has a much lower retention factor than the corresponding non-ionized form. The main reason is that charged species have a lower energy in a medium of high dielectric constant (i.e. the mobile phase) than in a medium of low dielectric constant (i.e. the hydrophobic surface layer). Within a series of analyte ions of identical charge but differ-

ent hydrophobicity, the retention order follows the same rules as for non-ionized analytes, i.e. the more hydrophobic analyte is more retained. This property is reflected in eqns [3] and [6] by different k_{OB} values for different fully ionized analytes.

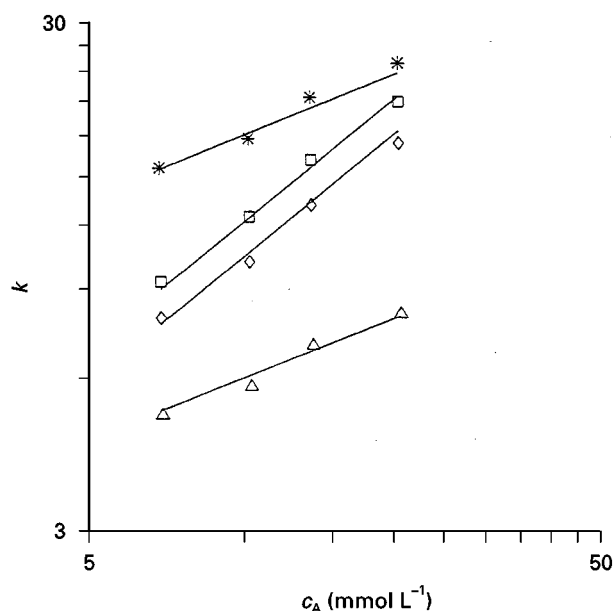


Figure 4 Retention factor data for mono-charged (\triangle , 1-naphthylamine-4-sulfonic acid; $*$, 6-naphthol-2-sulfonic acid) and double-charged sulfonic acids (\square , 2-naphthol-6,8-disulfonic acid; \diamond , naphthalene-2,7-disulfonic acid) as a function of eluent concentration (c_A) of the double-charged pairing ion, hexamethonium bromide ($z_A = +2$). (Reproduced with permission from Bartha Á and Ståhlberg J (1994) *Journal of Chromatography A* 668: 255.)

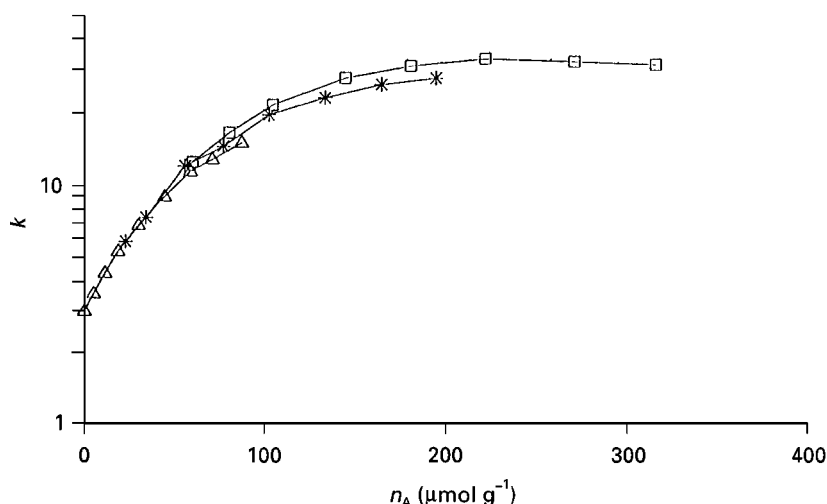


Figure 5 Retention factor of adrenaline as a function of the stationary phase surface concentration (n_A) of sodium butyl- (Δ), hexyl- ($*$) and octyl- (\square) sulfonate pairing ions measured at constant ionic strength (175 mM Na^+) of the phosphate buffer (pH 2.1) on an ODS-Hypersil column. (Reproduced with permission from Bartha Á and Ståhlberg J (1994) *Journal of Chromatography A* 668: 255.)

Under the condition of identical mobile phase concentration of two ion pair reagent ions of different hydrophobicity, the more hydrophobic reagent ion gives a higher retention for an oppositely charged analyte. This is attributed to higher adsorption to the stationary phase surface of the more hydrophobic reagent and a correspondingly higher induced electrostatic surface potential. Since a relative change in retention factor is primarily caused by a change in electrostatic surface potential, it is the surface concentration of the ion pair reagent, and not its detailed molecular structure, which is of importance for retention changes. This important fact is illustrated in **Figure 5** where the retention factor of adrenaline is solely a function of the surface concentration of the three different alkylsulfonates and is independent of the type of ion pair reagent.

Concentration of Organic Modifier in the Mobile Phase

In reversed-phase liquid chromatography, the effect of organic modifier concentration on the retention factor for non-charged analytes is usually described according to eqn [7]

$$\ln k_B(\phi) = \ln k_{wB} - S_B \phi \quad [7]$$

where k_{wB} is the retention factor for analyte B in a water-buffer mobile phase, S_B is a constant for a given analyte-solvent combination, and ϕ is the organic modifier concentration in the mobile phase. The thermodynamic interpretation of eqn [7] is that the free energy of adsorption of the analyte B to the

reversed phase surface is linearly dependent on the organic modifier concentration. In an ion pair system the retention depends on the adsorption of two components, the ion pair reagent and the analyte, respectively. There are therefore two different adsorption energies, and correspondingly, two equilibrium constants for adsorption involved. The logarithm of both these equilibrium constants approximately obey equation [7]. That is, besides the effect on the analyte ion a linear relation with coefficient, S_A , describes the change in $\ln K_A$ with changing organic modifier concentration. The final result is that $\ln k$ for an analyte ion depends on both the value of S_B and S_A . For a mono-charged analyte and ion pair reagent of opposite charge, eqn [6] gives that the slope of the $\ln k_{cB}$ vs ϕ relation becomes $S_B + \frac{1}{2}S_A$, while if they are of similar charge the slope becomes $S_B - \frac{1}{2}S_A$.

In **Figure 6** the logarithm of the retention factor for a positively charged (phenylalanine) and a negatively charged (naphthalene-2-sulfonic acid) analyte is plotted as a function of the volume concentration of methanol in the absence and presence of sodium octylsulfonate, respectively. The dashed line in both figures corresponds to the slope S_B for the corresponding analyte ion, whereas in **Figure 6A** the solid line corresponds to the slope $S_B + \frac{1}{2}S_A$ and in **Figure 6B** it corresponds to the slope $S_B - \frac{1}{2}S_A$.

Effect of pH of the Mobile Phase

For weak acid and basic analytes the mobile phase pH value influences the degree of ionization and con-

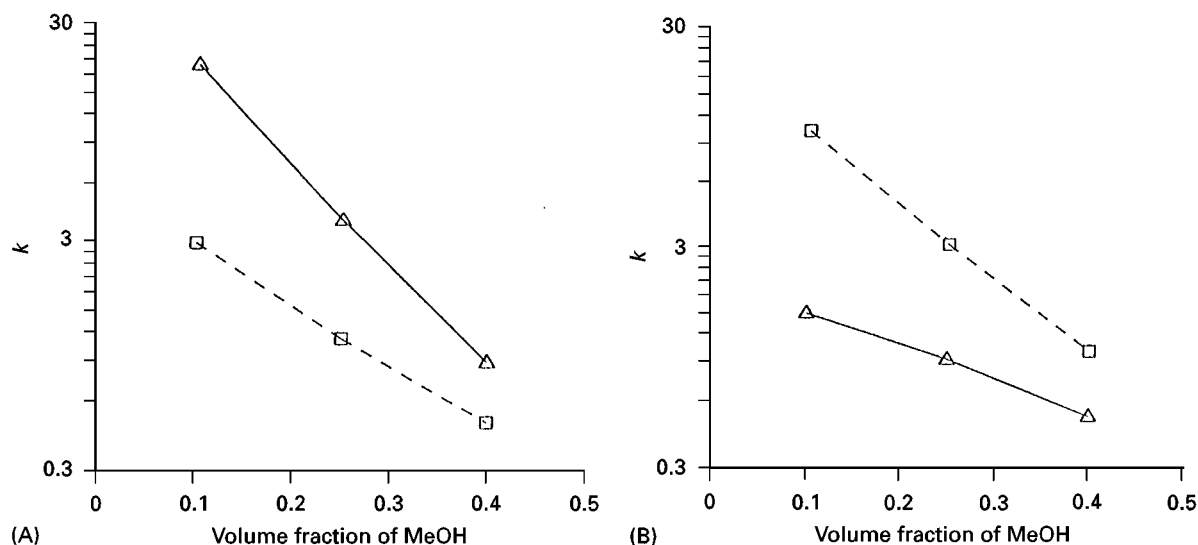


Figure 6 Retention factor for (A) phenylalanine and (B) naphthalene-2-sulfonic acid as a function of the methanol concentration (ϕ) in the phosphate buffer (pH 2.1 and constant ionic strength 175 mM Na^+) in the mobile phase in the absence (□) and presence (△) of 5 mM sodium octylsulfonate pairing ion. (Reproduced with permission from Bartha Á and Ståhlberg J (1994) *Journal of Chromatography A* 668: 255.)

sequently its retention. In a reversed-phase system, with no ion pair reagent added, the retention factor k_B is the weighted sum of the retention factor for the charged, k_{iB} , and the uncharged, k_{uB} , species, respectively:

$$k_B = (1 - f) \cdot k_{uB} + f \cdot k_{iB} \quad [8]$$

where f is the fraction of charged analyte in the mobile phase at the given pH value. Addition of an ion pair reagent to the mobile phase mainly influences the retention of the ionized fraction of the analyte. Furthermore, the influence can be treated with the same formalism as for a fully ionized analyte, i.e. eqn [8] takes the following form:

$$k_B = (1 - f) \cdot k_{uB} + f \cdot k_{oiB} \cdot \exp\left(-\frac{z_{iB} F \Psi_0}{RT}\right) \quad [9]$$

where k_{oiB} is the retention factor of the fully ionized form of the analyte in the absence of the ion pair reagent. Figure 7 shows the retention of a weak base, adenine ($\text{p}K_a = 4.12$), as function of pH in the absence and in the presence of an oppositely charged ion pair reagent (5 mM sodium octylsulfonate).

Choice of Experimental Parameters in IPC

Large changes in retention of ionic analytes may occur when the pH, the concentration of organic

modifier and the concentration of ion pair reagent is varied. The purpose of IPC is to take advantage of these variations in order to achieve a separation.

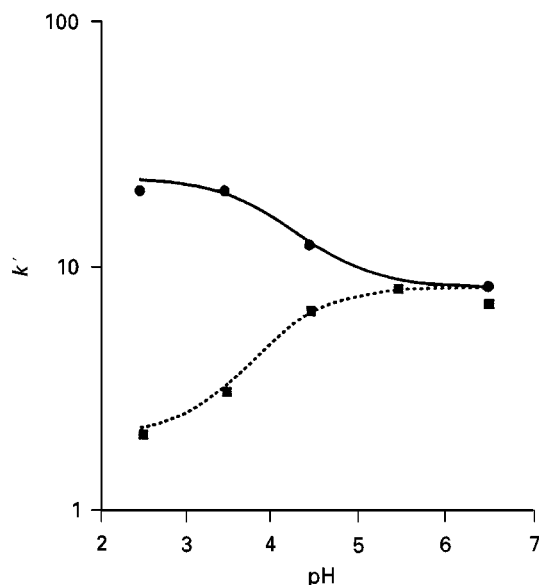


Figure 7 Retention factor for the weak base adenine ($z_{iB} = +1$) as a function of pH in the mobile phase in the absence (■) and presence (●) of the pairing ion sodium octylsulfonate. The theoretical retention plots in the absence of the pairing ion (dashed line, $\Psi_0 = 0$) and in its presence (solid line) are calculated from eqn [9] with the following parameters; $\text{p}K_a = 4.12$, $k_{uB} = 8.2$, $k_{iB} = 2.07$, $z_{iB} F \Psi_0 / RT = -2.398$. (Reproduced with permission from Bartha Á, Ståhlberg J and Szokoli F (1991) *Journal of Chromatography* 552: 13.)

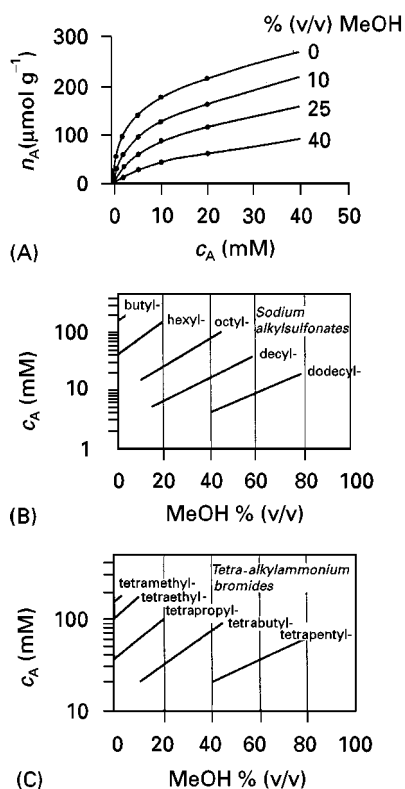


Figure 8 (A) Adsorption isotherm of octylsulfonate to a C_{18} -RP-column with the concentration of MeOH in the mobile phase as parameter. (B) Recommended alkylsulfonate type and concentration for different MeOH concentrations in the mobile phase, and (C) recommended tetraalkylammonium ion type and concentration for different MeOH concentrations in the mobile phase. (Reproduced with permission from Bartha Á, Vigh Gy and Varga-Puchony Z (1990) *Journal of Chromatography* 499: 423.)

This means that method development in this area usually is successful but requires a basic understanding of the physical processes that determine the retention.

In the development of an IPC method, the first point to consider is the relationship between the pK_a value of the analyte ions and the pH value of the mobile phase. To obtain a robust system the mobile phase pH should deviate from the pK_a value with more than two units. The pH is controlled by using a 10–50 mM salt buffer in the mobile phase. The buffer salt not only adjusts the pH but also controls the strength of electrostatic interaction between the ionic analytes and the ion pair reagent.

For changing the retention of an ionic analyte there are mainly three parameters to be varied: the type and mobile phase concentration of the ion pair reagent and the concentration of the organic modifier. The physically important parameter that is changed when these three parameters vary is the surface concentra-

tion of the ion pair reagent, and the corresponding electrostatic surface potential. A guideline for choosing type and concentration of positively and negatively charged ion pair reagents, respectively, as a function of the concentration of MeOH in the mobile phase is shown in Figure 8. The general rules for converting from MeOH to other common types of organic modifiers also apply in this case, e.g. 20% MeOH in the mobile phase corresponds to approximately 8% acetonitrile.

See also: II/Chromatography: Liquid: Mechanisms: Ion Chromatography; Mechanisms: Reversed Phases. Chromatography: Thin-Layer (Planar): Ion Pair Thin-Layer (Planar) Chromatography. III/Chiral Separations: Ion-Pair Chromatography. Peptides and Proteins: Liquid Chromatography.

Further Reading

- Bartha Á and Ståhlberg J (1994) Electrostatic retention model for ion-pair chromatography. *Journal of Chromatography* 668: 255. (The discussion concerning the effect of the different experimental parameters on retention is based on this paper.)
- Bidlingmeyer BA (1980) Separation of ionic compounds by reversed-phase liquid chromatography: an update of ion-pairing techniques. *Journal of Chromatographic Science* 18: 525.
- Chen JG, Weber SG, Glavina LL and Cantwell FF (1993) Electrical double-layer models of ion-modified (ion-pair) reversed-phase liquid chromatography. *Journal of Chromatography* 656: 549.
- Gennaro MC (1995) In: Grushka E and Brown PR (eds) *Advances in Chromatography*, vol. 35. New York: Marcel Dekker.
- Haddad PR and Jackson PE (1990) *Ion Chromatography: Principles and Applications*. Amsterdam: Elsevier.
- Hearn MTW (ed.) (1985) *Ion-pair Chromatography: Theory and Biological and Pharmaceutical Applications*. New York: Marcel Dekker.
- Schill G (1974) In: Marinsky JA and Marcus Y (eds) *Ion Exchange and Solvent Extraction*, vol. 6. New York: Marcel Dekker.
- Snyder LR, Kirkland JJ and Glajch JL (1997) *Practical HPLC Method Development*, 2nd edn. New York: John Wiley.
- Sorel RHA and Hulshoff A (1983) In: Giddings JC, Grushka E and Brown PR (ed.) *Advances in Chromatography*, vol. 21. New York: Marcel Dekker.
- Tomlinson E (1978) Ion-pair high performance liquid chromatography. *Journal of Chromatography* 159: 315.
- Tomlinson E (1983) Ion-pair extraction and high-performance liquid chromatography in pharmaceutical and biomedical analysis. *Journal of Pharmaceutical and Biomedical Analysis* 1: 11.

Large-Scale Liquid Chromatography

H. Colin and G. B. Cox, Prochrom R&D,
Champigneulle, France

Copyright © 2000 Academic Press

Introduction

The 1990s have seen the birth of high performance preparative liquid chromatography (HPPLC) and its recognition by the pharmaceutical and fine chemical industries as a very powerful and versatile purification technique. In contrast to traditional low performance/low pressure preparative chromatography, HPPLC is based on the use of columns of medium to high efficiency, operated at high mobile phase velocities, and consequently at moderate to high pressure – conditions quite similar to those met in analytical chromatography.

The very early work carried out in liquid chromatography at the beginning of the twentieth century (at a time when liquid chromatography was used for preparative purposes only) made use of particles 1–15 μm in diameter. For several reasons, preparative liquid chromatography (PLC) was later carried out with large particles ($>100 \mu\text{m}$) packed in columns of very low efficiencies operated at pressures close to atmospheric. Under such conditions, the kinetic properties of the columns are obviously very poor; the preparative separations require large quantities of mobile phase, long separation times and are expensive. For this reason, for a long time PLC was considered to be inappropriate for industrial purifications and was the choice of last resort. There were three reasons for this poor image: first, the misunderstanding of the effect of the column efficiency and the lack of a theoretical framework to describe the behaviour of columns under highly overloaded conditions; second, the use of low-quality packing materials (large particle size and large size distribution); and third, the lack of proper equipment in general, and adequate column technology in particular. Now that these problems have been addressed, PLC has many advantages.

Particular Effects Related to Column Overloading

For the sake of simplicity, the following discussion is limited to a binary mixture, but the phenomena described are the same for more complex mixtures. It is also assumed that the adsorption isotherms are Langmuirian. This is the case for most practical situations

in chromatography. The total band broadening occurring in the column is the combination of two contributions: that of the intrinsic column efficiency (kinetic term – the column efficiency under an infinitely small injected quantity) and that of the finite mass of product injected (thermodynamic term – related to the amount injected). The equipment itself, besides the column, can also contribute to band broadening, but this is not considered in the present discussion.

When a sufficiently large quantity of product is injected, the thermodynamic term (which is proportional to the injected quantity, to a first approximation) becomes larger than the kinetic term and the total band broadening is primarily controlled by the quantity injected. It has been concluded from this observation that, under high mass overload, there is no reason to use efficient columns in PLC since the contribution of the intrinsic column efficiency is masked by the thermodynamic contribution. This is true as long as pure products are injected, which is obviously not the case when PLC is used.

When a mixture of two products is injected, the elution bands occupy the same section of the column during a certain fraction of their migration through the bed. When this happens, the molecules of each component compete for the same retention sites. When the injected quantity becomes sufficiently large, the molecules that have more affinity for the stationary phase prevent the other ones from interacting with the adsorbent. As a result, the weakly retained product is eluted faster than expected. This is known as a displacement effect. This effect is particularly strong when the weakly retained product is present at a smaller concentration than the strongly retained one. Under such conditions, the peak for the weakly retained component is not only eluted more quickly than if it were injected alone, but it is also narrower and has the typical shape shown in Figure 1A. Better separation is achieved than would be found if the displacement effect were not effective. When the more strongly retained compound is at lower concentration than the weakly retained one, the peak for the second compound is broader than it would be if injected alone. It also starts to be eluted earlier, an effect known as the tag-along effect (see Figure 1B).

It is clearly preferable to optimize the choice of the chromatographic conditions so that the first product is the one at the smaller concentration (typically, the impurity to be removed). Under these conditions, the region where the two products interfere is strongly

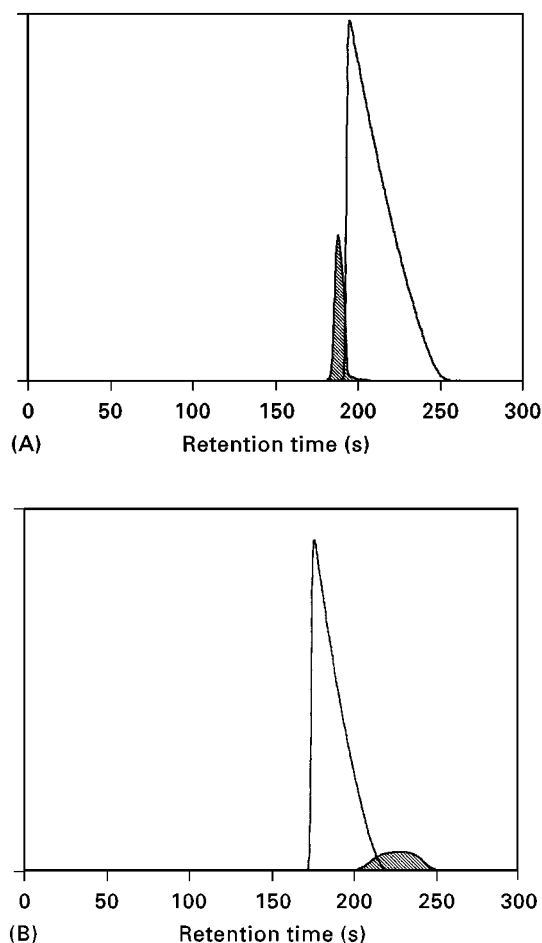


Figure 1

controlled by the column efficiency (see Figure 2) and increasing the column efficiency results in the possibility of injecting (much) more product or recovering more product for a given injected quantity. The possibility of using displacement effects and injecting large quantities is thus associated with columns of sufficient efficiency. Such columns enable higher

production rates, reduce solvent consumption and purification times, and thus decrease purification costs.

The displacement and tag-along effects, as well as the role of the various operating parameters, have been modelled by several groups. Unfortunately, it is not yet possible (and it is questionable if it will be in a near future) to make accurate predictions of the properties of a given chromatographic system under moderate and severe overloading conditions, and thus optimize the operating conditions to minimize the purification cost, for instance. The rigorous treatment of Guiochon and co-workers, based on the simultaneous resolution of the mass balance equations for the various species involved in the chromatographic process, involves numerical integration of a set of differential equations. This treatment is based on the model of competitive Langmuir isotherms and the approach is not simple since it requires knowledge of the composite adsorption isotherms. Major difficulties lie in experiments to measure these composite isotherms and the lack of suitable models to describe them with sufficient accuracy.

Column Technology

In order to get efficient columns of large diameter (i.e. > 5 cm) for preparative purposes, it is necessary to have a packing material of adequate quality and also the appropriate column technology. Column technology is a very critical issue, since it is known that above a certain diameter columns tend to be unstable because of bed settling and the resulting formation of voids in the packing. These voids are very detrimental to the column efficiency and are responsible for band distortion. In addition, large columns are potentially more difficult to pack than small ones, particularly when small particles ($< 50 \mu\text{m}$) are used. Indeed, the high pressure slurry-packing technique used to pack

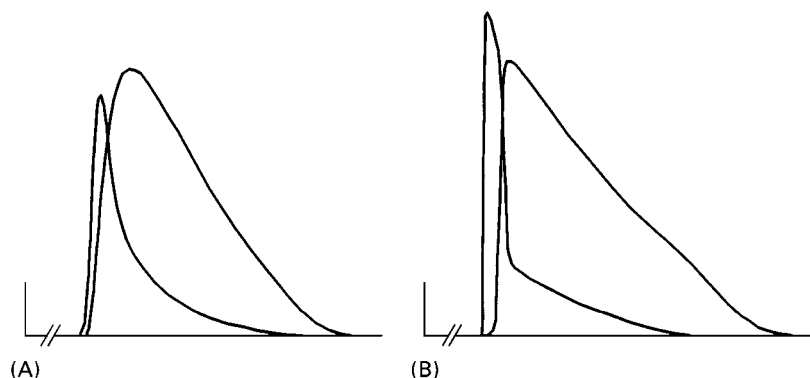


Figure 2

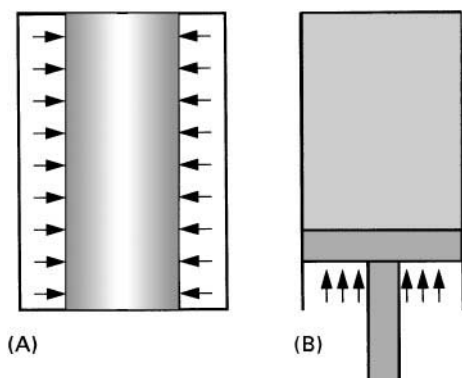


Figure 3 Methods of dynamic compression. (A) Radial compression; (B) axial compression.

analytical columns cannot be used for large diameter columns for both practical and technical reasons.

Various solutions have been proposed to solve the problem of bed stability. It seems that the best approach is to compress the bed of particles, either radially (using columns with flexible walls immersed in a pressurized fluid) or, preferably, axially using a piston (see **Figure 3**). This bed compression must be dynamic so that voids are eliminated as soon as they form. Using dynamic axial compression, it is possible to pack columns of large diameter with small particles offering the same efficiency as analytical columns (see **Figure 4**). This technology is particularly versatile because it gives the operator the possibility of packing the column very easily and quickly with

any type of material. This is clearly important for equipment used in production where downtime has to be minimized. In addition, the length of the bed can be easily adjusted to optimize the column efficiency. Finally, whatever the compression technique used, it is very important to design the column ends properly. Indeed, in order to generate piston flow and avoid band distortion due to unequal flow distribution, it is necessary to spread the flow of liquid evenly across the cross-section of the column.

Packing Materials

The best column technology is useless without the proper packing material. There are two main aspects to consider when selecting the packing material: chemical and physical. The chemical aspect is related to the chemistry of the purification problem and is not discussed here since it is very much product dependent. A material well suited for a given application may be inadequate for another. The physical aspects, however, can be discussed in general terms. The various models of HPPLC have shown that there is an optimum value of the ratio d_p^2/L for any separation problem (d_p is the particle size and L the column length). In typical conditions, for columns operated at a pressure of 30 to 60 bar, an 'optimum' particle size is about 10–20 μm with a column length between 20 and 50 cm. Accordingly, rather small particles have to be used for PLC.

It is also very important to keep the particle size distribution as narrow as possible, since small particles in the distribution have a very strong effect on the column permeability and large particles strongly influence the column efficiency. In other words, a material with a large size distribution tends to produce low-efficiency columns with low permeability. It is usually considered that the ratio d_{p10}/d_{p90} should be less than 1.5 for a good material (d_{p10} and d_{p90} being the particle sizes corresponding to 10% and 90% of the cumulated volume-based size distribution).

Besides the average particle size and the size distribution, other physical properties of the packing material are important, particularly the specific surface area and the pore size. It is desirable to maximize the surface area of the material in order to increase its adsorption capacity. Increasing the surface area, however, usually means decreasing the pore size and thus the access of the molecules to the internal pores of the particles. There exists an optimum pore size and specific surface for each compound to be purified.

Among the other important physical parameters, one should also mention the mechanical strength of the particles, since they must resist the stress of the compression technique used.

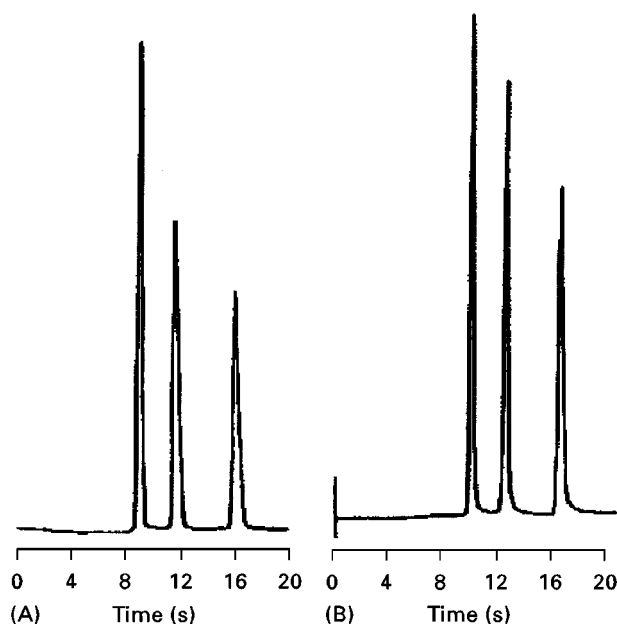


Figure 4 Comparison of chromatograms from columns. (A) 25 cm \times 4.6 mm and (B) 25 cm \times 150 mm.

Optimization of Separation Conditions

The optimization of PLC is not a simple task since many parameters have to be taken into account: kinetics (column efficiency and column design in terms of d_p and L), thermodynamics (choice of the chromatographic system, temperature, degree of column overloading, etc.) and economics. The necessity to take into account economic aspects is important since the most favourable conditions in terms of purification cost do not necessarily correspond to the best chromatographic conditions in terms of quality of separation. Indeed, a better chromatographic mobile phase providing more selectivity may turn out to be more expensive to buy or to recycle (mobile phase recycling is often essential to keep purification costs low). This means that such parameters as the heat of vaporization of the mobile phase and its cost have to be considered. The mobile phase viscosity is also very important since it controls not only the velocity of the eluent at a given operating pressure (and thus the time required for the separation), but also the values of the diffusion coefficients of the products in the mobile phase, and accordingly the column efficiency. Very viscous eluents (such as propanol–water mixtures, for example) should be avoided in preparative chromatography.

A general economic analysis of a purification process by PLC indicates that there are typically two situations to be considered. When the quantity to be purified is low, the optimization should be aimed at maximizing the production rate because time (labour) is the largest contribution to the purification cost. When large quantities have to be processed, the optimization should be aimed at reducing the solvent cost (solvent consumption and regeneration). Many strategies can be envisaged to reduce the cost of PLC, depending on the conditions of the purification in terms of expected production, required purity and recovery ratio, etc. For instance, a purification can be made in several steps. This is often advisable when the concentration of the product of interest in the crude feedstock is low (i.e. less than 50%). In this respect, it is important to clean up the mixture to be purified as much as possible before injecting it (using a preliminary treatment such as flash chromatography, for example).

Various techniques can be used to reduce time and solvent consumption, and thus purification cost. Among them are shave-recycling and flip-flop. Shave-recycling consists of injecting (very) large quantities of feedstock – too large to provide satisfactory recovery of the product of interest at the expected purity. The fraction of the product peak where the purity is acceptable is collected and returned to the column

inlet (typically by using the solvent pump – adequate valving is required). During the second passage through the column, the separation between the product of interest and the impurities is further improved. The pure fraction of the product peak is then collected and, if necessary, the contaminated fraction of the peak is returned to the column for a third cycle. Typically, three or four cycles are made before a new large injection is performed. This shave-recycling approach saves on solvent (no fresh solvent is consumed when the column effluent is returned to the column inlet), reduces product dilution and decreases purification costs.

The flip-flop technique is an optimized back flush operation. It is very common for several impurities to be eluted after the product of interest. If these impurities are not removed from the column before the next injection is made, they can contaminate the product of interest in subsequent purification runs. Backflushing the column is often done to remove the strongly retained impurities. Flip-flop consists of performing the next injection a certain time after the backflush process has been initiated. During this time the weakly retained impurities of the next injection are eluted. Accordingly, during each elution run the flow direction in the column is reversed (hence the name flip-flop). This technique requires very good column stability because of these changes of flow direction.

Another powerful approach employed to reduce purification costs and solvent consumption is the recently ‘rediscovered’ technique of simulated moving bed (SMB), which is of particular interest for binary separation.

Simulated Moving Bed

When working on a large production scale, there are many arguments in favour of continuous processes. The majority of chromatographic processes are, however, batch processes that are incompatible with continuous production. Some years ago, continuous chromatographic processes were developed for large-scale separations in the food and petroleum industries. These processes solved some of the problems of implementation of large-scale chromatography. They are based upon the technique that is now known as simulated moving bed chromatography. The original application areas for this process were in the purification of *p*-xylene (a precursor of polyester plastics) and the separation of glucose from fructose to make high-fructose corn syrups, which are used in the soft drinks industry as a sucrose replacement. A few other applications also based upon this technology exist. There are perhaps 150 of these large-scale, low

pressure SMB systems in the world, responsible for the production of many thousands of tonnes of product each year. More recently, the combination of the new regulatory atmosphere in the pharmaceuticals industry, where pure enantiomers, of racemic drugs are becoming more and more in demand, together with the development of new media for the chromatographic resolution of enantiomers, has resulted in new areas of opportunity for SMB applications. These applications, by virtue of the high value of the products and the requirements for high purity in the industry, are for the most part operated using small particles in high pressure SMB equipment; this parallels the extensive use of HPLC purification methods in production for the pharmaceutical industry.

The basic principle of a true moving bed (TMB) unit is shown in Figure 5. The basis of TMB lies in the idea that in a chromatographic system the 'stationary' phase may be moved as well as the mobile phase. In a binary separation, the two components move at different velocities through the column. If one were to move the packing material in a direction opposite to that of the mobile phase in the column, one could choose a velocity of the packing material relative to that of the mobile phase such that one of the components moved in the original direction, carried by the mobile phase, while the other component, which spends a greater proportion of its time in the stationary phase, would be transported by the packing material in the opposite direction. By injecting in the middle of such a column, one product would emerge from each end of the column (the more retained product is often called the extract and the less retained product the raffinate, see Figure 5). Thus one could inject and collect product in a continuous fashion.

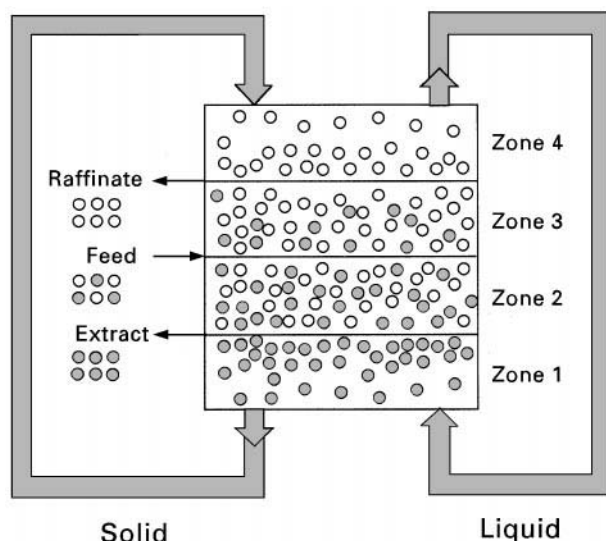


Figure 5 TMB unit.

In practice, many attempts have been made to realize such a countercurrent flow of packing material and mobile phase. None has been really successful, due mainly to the incompatibility of the needs of chromatography (tightly packed beds) and those of the transport of the solid particles (loose, fluid beds). The solution to the problem is to move the entire column, but in this case a column cut into short sections. In this way, rather than moving the bed in a continuous fashion, the individual sections of the column are moved periodically, such that the average bed speed remains that required for continuous separation. The feed inlet and the product outlets are arranged at the interfaces between the sections of the column, facilitating the entry and removal of materials. This principle operation simulates a true moving bed system and is thus called a simulated moving bed, SMB. It has been shown that when the number of columns exceeds about eight (this number depends on the separation problem considered), the performance of SMB is very close to that of TMB.

The removal of the products requires some special arrangements of flow rates in the system. The slower moving product (extract) moves during the separation phase in the direction of the packing material. If, in the section between the solvent inlet and the product outlet, the solvent flow is increased, a velocity will eventually be attained at which the product slows and becomes stationary. At a higher velocity, the product will reverse direction in the system and move with the solvent. This extra flow is removed from the product port; downstream of this port the velocities in the system remain the same as before. This means that in the first part of the column the product is moving toward the exit port in the same direction as the solvent. In the second section, the product is still moving with the packing material, also in the direction of the exit port. The only possible route for this product to take is out of the port, along with the extra solvent used to increase the flow rate beyond that critical for the change in direction of the product. In certain cases, this extra flow is not very large, and can be close in value to that of the feed.

At the other end of the system, the raffinate is removed by bleeding off some of the flow rate at the exit port. This reduces the solvent velocity in the final section of the column set such that the product moves with the packing material rather than the solvent. This means that, in this final section, the product is moved toward the exit port. In the penultimate section, the flow continues as before and the product again is moved in the direction of the outlet port. Thus, this product, too, is eluted from the system at the appropriate product port.

This arrangement for the removal of the products allows the solvent to be recycled. The solvent that elutes from the end of the column set does not (if the flow rates, etc., are controlled correctly) contain any product. It can then be redirected back to the solvent pump with the addition of a make-up flow to compensate for the excess flow removed in the raffinate and extract streams in comparison with that added by the feed. By the same token, the columns that pass the solvent inlet contain no product and so these can be added back at the other end of the column set for reuse. In this way a limited number of columns – usually between 8 and 16 – are used for the separations and the solvent use is also reduced in comparison with the batch operation. It should be noted that, in the majority of SMB system, the columns themselves remain stationary. Their movement is simulated by the use of switching valves, which are used to move the entry and exit ports around the column set.

In comparison with batch chromatography, SMB separations can be performed using smaller columns and less solvent than the equivalent batch separation. This is the result of the reduction in solvent required, the increased efficiency of use of the column and also the reduced need for column efficiency in terms of the number of theoretical plates in the system. Thus, although one requires a greater number of columns, the column set does not have to be as long as for a batch separation using the same column packing. This can lead to some bizarre solutions, in that batch HPLC separations are usually optimized for column lengths of 25 to 50 cm, using particle sizes of around 10 to 25 μm . The equivalent SMB separation, using the same particle size, would require column lengths of only 1 or 2 cm. This is not difficult to realize for a small-scale system, but becomes difficult if large diameter columns – of 50 to 100 cm internal diameter, for example – are envisaged. In this case, larger particle sizes are required in order that the columns can have reasonable product distribution to eliminate band deformation. The optimum size of the particles, columns, etc., for the separation then becomes a question of economics rather than of science.

Conclusions

HPPLC is certainly one of the most powerful purification techniques available today, and as such must be

considered by process and production engineers with the same attention as distillation, crystallization and other more traditional techniques. Provided it is properly used, HPPLC can be cheaper than traditional techniques, provide higher yields, higher degrees of purity and save on purification times, a particularly critical aspect in the highly competitive world of the modern pharmaceutical industry. Properly using HPPLC means understanding the behaviour of columns under highly overloaded conditions and using such beneficial effects as displacement effects. It also means using the right packing material, the right column efficiency and the appropriate column technology, as well as considering alternative strategies such as shave-recycling, backflush, SMB, etc. SMB is of particular interest for binary separations (but not only) and in the near future is expected to become the technique of choice for such separations at large and very large scales.

See Colour Plate 23.

See also: II/Chromatography: Liquid: Column Technology. III/Chiral Separations: Liquid Chromatography. Flash Chromatography. Medium-pressure Liquid Chromatography.

Further Reading

- Bidlingmeyer BA (ed.) (1987) *Preparative Liquid Chromatography* Elsevier: Amsterdam.
- Golshan-Shirazi S and Guiochon G (1988) *Analytical Chemistry* 60: 2364.
- Gvionchon G, Shirazi SG and Katti AM (1994) *Fundamentals of Preparative and Nonlinear Chromatography* Boston: Academic Press.
- Knox JH and Pyper HM (1986) *Journal of Chromatography* 363: 1.
- Miller L, Orihuela C, Fronck R, Honda D and Dapremont O (1999) Chromatographic resolution of the enantiomers of a pharmaceutical intermediate from the milligram to the kilogram scale. *Journal of Chromatography A* 849: 309–317.
- Nicoud RM (1992) *LC-GC INTL*, 5: 43.
- Pynnönen B (1998) Simulated moving bed processing: escape from the high-cost box. *Journal of Chromatography A* 827: 143–160.
- Snyder LR, Dolan JW, Antle DE and Cox GB (1987) *Chromatographia* 24: 82.
- Zhang GM and Guiochon G (1998) Fundamentals of simulated moving bed chromatography under linear conditions. *Advances in Chromatography* 39: 351–400.

Mass Spectrometry Detection in Liquid Chromatography

See II/CHROMATOGRAPHY: LIQUID/Detectors: Mass Spectrometry

Mechanisms: Chiral

I. W. Wainer, Georgetown University Medical Center, Washington DC, USA

Copyright © 2000 Academic Press

The separation of racemic compounds into their constituent enantiomers is now routinely performed by high performance liquid chromatography (HPLC) on chiral stationary phases (HPLC-CSPs). HPLC-CSPs are based on molecules of known stereochemical composition immobilized on liquid chromatographic supports. Single enantiomorphs, diastereomers, diastereomeric mixtures and chiral polymers (such as proteins) have been used as the chiral selector.

The first chromatographic separation of an enantiomeric compound on a CSP was reported in 1939 by Henderson and Rule. In this study, racemic camphor was enantioselectively separated on a column containing lactose as the adsorbent. Some of the other significant advances in this field are presented in Table 1.

The first commercial HPLC-CSP was developed by Pirkle and introduced by the Regis Chemical Company in 1981. By 1996, the number of commercially available HPLC-CSPs had grown to 110. The rapid increase in the availability of this technology was primarily due to its importance in the discovery, development and regulation of pharmaceutical products.

The Basis of Chiral Recognition

In order to utilize the wide range of available HPLC-CSPs effectively, it is important to identify the chiral recognition mechanisms operating on these phases. The enantioselective resolutions obtained on CSPs are the result of the formation of temporary diastereomeric complexes between the enantiomeric solute molecules and immobilized chiral selector (solute/CSP). The difference in energy between the resulting diastereomeric *R*-solute/CSP and *S*-solute/CSP complexes determines the magnitude of the observed stereoselectivity, whereas the sum total of the interactions between the solute and CSP, chiral and achiral, determines the observed retention and efficiency.

In order for two enantiomers to be separated chromatographically, there must be a difference in the free energies of binding (ΔG) between the two transient diastereomeric complexes. The energy difference arising from one such interaction would normally be insufficient to permit resolution. However, chromatography is a weighted time-averaged

view of many dynamic adsorption-desorption processes. These processes occur throughout the entire length of a column and their sum total can be sufficient to allow an observable difference in the retention times of two enantiomers.

The difference in free energy, $\Delta\Delta G$, needed for adequate chromatographic separation is influenced by the efficiency of the system employed. If the chromatographic system is of high efficiency, so that narrow peaks are observed, relatively small $\Delta\Delta G$ values will afford acceptable analytical-scale enantiomer separations.

For a chiral separation where t_{r1} is the retention time of the first eluting enantiomer, t_{r2} is the retention time of the second eluting enantiomer and t_0 is the retention time of an unretained solute (Figure 1). The partitioning of two enantiomerically related analytes between the stationary phase and the mobile phase is defined by the retention factors k_1 and k_2 .

$$k_1 = \frac{(t_{r1} - t_0)}{t_0} \quad [1]$$

Table 1 Some key dates in direct enantioselective separations

1939	Resolution of camphor by column chromatography with lactose as the adsorbent (Henderson and Rule)
1944	Resolution of Troegers base on a lactose column (Prelog and Wieland)
1951	Resolution of amino acid enantiomers by cellulose paper chromatography (Senoh <i>et al.</i>)
1966	Resolution of metallocenes on acetylcellulose columns (Falk and Schlogel)
1966	Initial gas chromatographic resolution on a derivatized dipeptide CSP (Gil-Av <i>et al.</i>)
1968	Resolution of amino acids on a chiral ion exchange resin (Latt and Rieman)
1971	Resolution of DL-proline by chiral ligand exchange chromatography (Davankov and Rogozhin)
1973	Introduction of microcrystalline triacetylcellulose as a liquid chromatography CSP (Hess and Hegll)
1973	Use of agarose-bonded bovine serum albumin for chiral resolution (Stewart and Doherty)
1976	Resolution of helicines by liquid chromatography on 2-(2,4,5,7-tetranitro-a-fluorenylidone)aminopropionic acid (TAPA the first π -acceptance chiral selector: Gil-Av <i>et al.</i>)
1978	Resolution of amino acids on an immobilized chiral crown ether stationary phase (Crom <i>et al.</i>)
1979	<i>N</i> -formyl-L-valine CSP for HPLC (Hara <i>et al.</i>)
1981	(<i>R</i>)- <i>N</i> -(3,5-dinitrobenzoyl) phenylglycine CSP by Regis Chemical Company first commercially available HPLC-CSP (Pirkle)
1982	Bovine serum albumin-based CSP (Allenmark <i>et al.</i>)
1983	α -Acid glycoprotein-based CSP (Hermansson)
1984	Cyclodextrin-based CSP (Armstrong and DeMond)

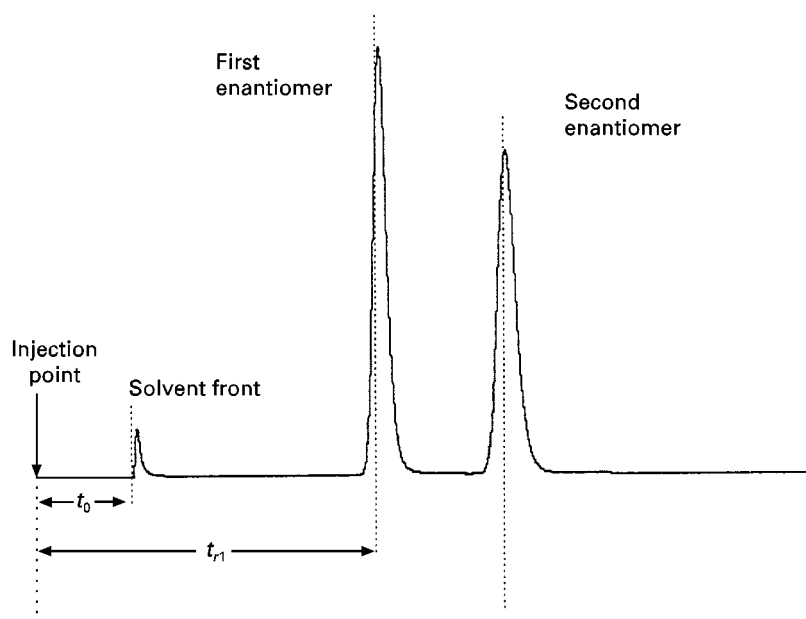


Figure 1 The enantioselective separation of two enantiomers and the measurements required to calculate k_1 , k_2 and α .

$$k_2 = \frac{(t_{r2} - t_0)}{t_0} \quad [2]$$

$$\alpha = \frac{k_2}{k_1} \quad [3]$$

$$\Delta G = -RT \ln K \quad [4]$$

where K is the equilibrium constant for the distribution of a solute between the stationary phase and the mobile phase.

$$\Delta\Delta G = \Delta G_2 - \Delta G_1 \quad [5]$$

where ΔG_1 and ΔG_2 are the free energies of binding for the first and second eluting enantiomers, respectively.

$$\Delta\Delta G = -RT(\ln K_2 - \ln K_1) \quad [6]$$

$$\Delta\Delta G = -RT \ln \frac{K_2}{K_1} \quad [7]$$

$$\Delta\Delta G = -RT \ln \frac{k_2}{k_1} \quad [8]$$

$$\Delta\Delta G = -RT \ln \alpha \quad [9]$$

Chiral Recognition Mechanisms

Chiral recognition is a specific aspect of the much broader area of molecular recognition. In chromatographic terms it usually implies the preferential interaction of one solute enantiomer with another enantiomer immobilized on an inert support. The

three-dimensional spatial arrangement of the solute requires a complementary three-dimensional structure with which to form a sufficient and necessary number of bonded and nonbonded interactions.

To specify the origin of enantioselective adsorption, one must specify the nature of the various interactions between the species involved. It is also necessary to define a model with which to characterize the requirements of enantioselective recognition. The first model was proposed by Easson and Stedman in 1933. In their mechanism, enantioselective receptor binding was the result of the differential binding of two enantiomers to a common site produced by a three-point contact model between ligand and receptor (Figure 2).

In this model, enantiomer 1 was more active than its enantiomorph 2 because 1 was more tightly bound to the receptor (3). The differential binding is a result of the sequence of the substituents, BCD , around the chirally substituted carbon atom which forms a triangular face of the tetrahedral bond array. For enantiomer 1, the sequence matches the complementary triad of binding sites on the receptor 3, $(B'C'D')$, leading to a three-point interaction. The enantiomorph 2 has a mirror image sequence, DCB , and its interaction with 3 occurs at only two of the three sites on the receptor surface, producing a relatively weaker ligand-receptor interaction.

The three-point interaction model was ignored for 15 years until Ogston resurrected it in order to explain the enzymatic decarboxylation of L-serine to L-glycine. The pivotal step in this conversion was the

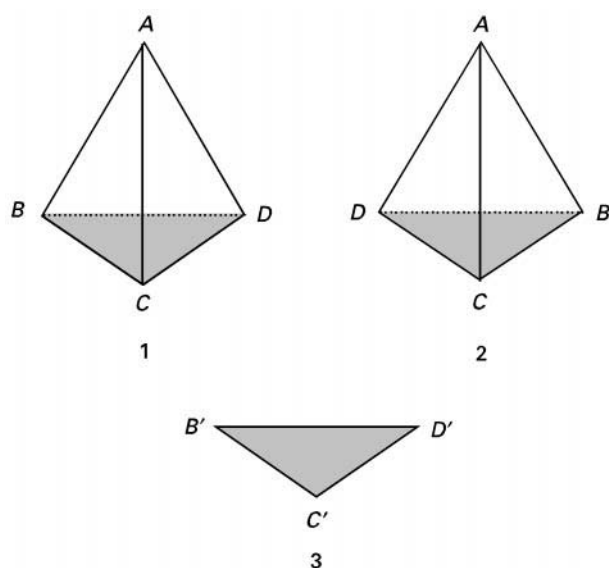


Figure 2 Easson and Stedman's three-point interaction model of chiral discrimination.

stereoselective decarboxylation of the prochiral intermediate metabolite aminomalonic acid. In Ogston's model, the carboxylic moieties on the aminomalonic acid become nonequivalent due to the existence of three nonequivalent binding sites on the enzyme, one of which is responsible for the decarboxylation. Ogston's mechanism was a slight variation of the Easson and Stedman three-point model in that it did not require all three interactions to be attractive.

The first application of the three-point chiral recognition model in chromatography was published by Dalglish in 1952. In this work, amino acid enantiomers were resolved by paper chromatography and a three-point mechanism postulated for the interaction between the chiral cellulose stationary phase and the solute enantiomers. Since its introduction into enantioselective chromatography, the three-point interaction model has been the basis for the rational design of a large number of CSPs as well as the basic explanation for the enantioselective separations achieved on them.

Pirkle was the first to exploit this model in the design of synthetic, small molecule CSPs based upon derivatized amino acids. His initial HPLC-CSP was a 3,5-dinitrobenzoyl derivative of phenylglycine (Figure 3).

As in the Easson and Stedman model, interactions between the enantiomeric solutes and the CSP take place in the plane defined by $B'C'D'$. However, unlike the enzyme model, all of the attractive interactions are contained along the C' axis, including sites for hydrogen bond donation and acceptance, an amide

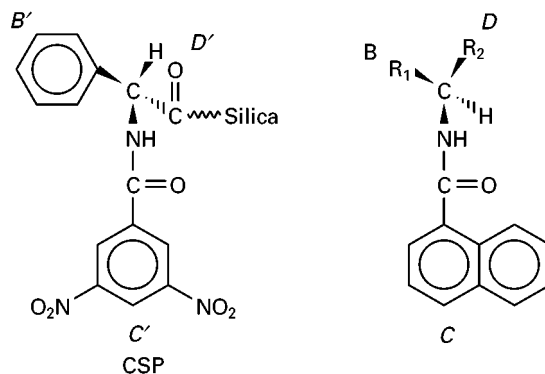


Figure 3 The three-point chiral recognition mechanism, as illustrated by a Pirkle-type CSP.

dipole which can participate in dipole–dipole interactions and the 3,5-dinitrobenzoyl moiety which can act as a site for π acid– π base interactions. The phenyl moiety and hydrogen atom on the B' and C' axes are sites of steric interaction.

In the chiral recognition process involving two enantiomers (BCD , DCB) attractive interactions between the amide moieties on the respective C (solute) and C' (CSP) axes create the solute–CSP complexes. The energetic difference between the R -solute–CSP and S -solute–CSP complexes arises from the steric fit of the BD and DB sequences on the enantiomeric solutes into the $B'D'$ sites on the CSP.

It is clear that the three-point interaction model works in a number of situations, especially with small synthetic CSPs. However, when large chiral biopolymers are used as the CSP, this model does not give an accurate description of how the dissymmetry of one molecule is perceived by a second or of how stereochemically equivalent moieties are distinguished from each other. The problem lies in the perception between point asymmetry and molecular asymmetry. In the former approach, a molecule is broken down into its parts, while in the latter it is viewed as the sum of its parts.

In principle, the three-point model is a static picture of a bimolecular process, essentially the lock-and-key model of enzymatic activity. In enzymology, the lock-and-key model has been superseded by the understanding that the pivotal step in enzymatic conversions involves mutually induced conformational adjustments of the substrate and enzyme – an induced molecular fit. When enantiomeric substrates are involved, the differences in enzymatic activity can be related to the energetic differences involved in the formation of the optimum substrate–enzyme complexes and the related transition state energies.

In analogy with the induced conformational fit utilized in enzyme kinetics, a conformationally driven chiral recognition mechanism has been described for the separation of α -alkyl arylacetic acids on an amylose *tris*(3,5-dimethylphenylcarbamate) CSP (AD-CSP). The chromatographic retentions and enantioselective resolutions of 28 chiral α -alkyl arylacetic acids were related to their respective structures through the construction of quantitative structure–enantioselective retention relationships (QSERR). The QSERR data were combined with molecular modelling studies and the results indicate that the enantioselective discrimination on the AD-CSP proceeds via a three-step process. These steps are:

- Step 1: Distribution of the solute to the stationary phase through hydrogen-bonding interactions between the acid moiety on the solute and amine moieties on the CSP.
- Step 2: Conformational adjustments of the solutes and insertion of the aromatic portion of the solute into a ravine on the CSP.
- Step 3: Stabilization of the solute–CSP complex through electrostatic and hydrogen-bonding interactions within the ravine.

This process can be illustrated using the enantioselective separation of *R*- and *S*-benoxaprofen on the AD-CSP. The optimal interaction between *S*-benoxaprofen and the CSP is illustrated in Figure 4.

Both *R*- and *S*-benoxaprofen form identical hydrogen-bonding interactions – and presumably the same

hydrophobic interactions as well – with the AD-CSP. The energetic differences between the diastereomeric *R*-benoxaprofen–CSP and *S*-benoxaprofen–CSP complexes arise from the internal energies of the two enantiomer conformations which are required to achieve the optimum interactions. The bonding conformation of *R*-benoxaprofen has been calculated to be approximately 250 cal mol^{-1} higher in energy than that of *S*-benoxaprofen. The theoretical enantioselectivity arising from this energy difference was estimated using eqn [9] $\{\Delta\Delta G = -RT \ln \alpha\}$, and the calculated α (1.52) was consistent with the observed α (1.82).

The determining factor in these processes is the molecular chirality of the biopolymer. Enzymes and amylose are large chiral biopolymers with distinct three-dimensional structures. While it is possible to assign specific electrostatic or hydrogen-bonding sites within these molecules, most interactions take place within cavities or ravines. Thus, a more accurate description of the chiral recognition process would be to replace the three-point interaction model with one based on molecular chiralities.

A general chiral recognition process based on this strategy is presented in Figure 5. This process involves the initial formation of the complex, followed by conformational adjustment of the two elements, activation of the complex through additional binding interactions and expression of the molecular chiralities of the two elements in the complex. This process describes enantioselective discrimination by all

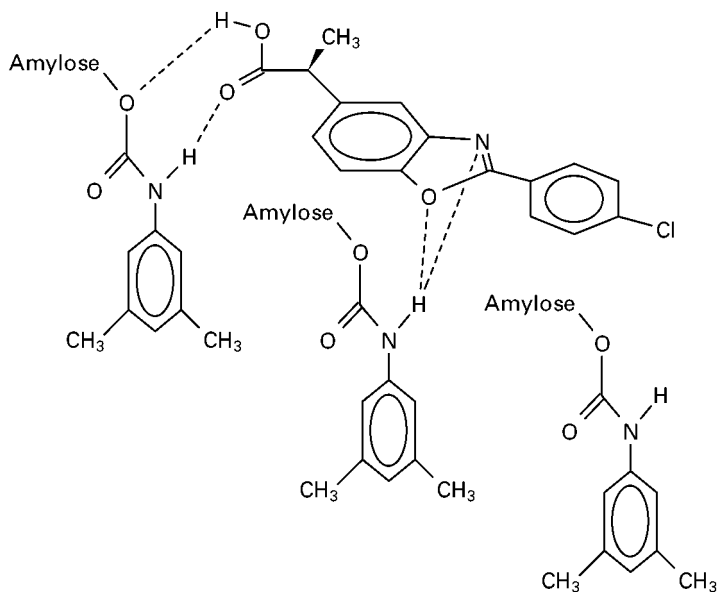


Figure 4 Representative interactions between *S*-benoxaprofen and the AD-CSP, representing a conformationally driven chiral recognition mechanism.

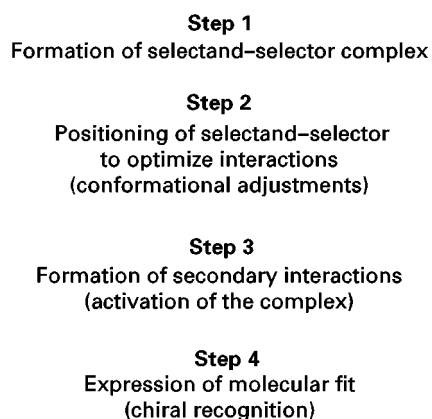


Figure 5 A molecular chiral recognition process.

classes of chiral selectors from biopolymers to derivatized amino acids.

Using Molecular Chiral Recognition to Select a HPLC-CSP

The chiral recognition mechanism presented in Figure 5 can be broken down into its separate parts if one remembers that these parts are interdependent and cannot exist apart from one another. The advantage of considering the steps independently is that it allows for the development of a system for the classification of HPLC-CSPs. If one considers that the key chromatographic step in the chiral recognition process is the formation of the diastereomeric solute-CSP complex, the current HPLC-CSPs can be broken down into five basic types on the basis of the solute-CSP bonding interactions. Using these classes and the molecular structure of the solute, one or more HPLC-CSPs can be selected for the required enantioselective separations. The resulting classes of CSPs are:

- Type I: when the solute-CSP complexes are formed by attractive interactions, such as hydrogen bonding, π - π , dipole stacking, etc., between the solute and CSP. The Pirkle type of CSPs are included in this category
- Type II: when the primary mechanism for the formation of the solute-CSP complex is through attractive interactions, but inclusion complexes also play an important role. The cellulosic and amylosic CSPs are included in this category
- Type III: when the primary mechanism for the formation of the solute-CSP complex is through the formation of inclusion complexes, wherein the sample enters a chiral cavity within the

CSP. The cyclodextrin CSPs are included in this category

- Type IV: when the solute is part of diastereomeric metal complex-chiral ligand-exchange chromatography
- Type V: when the CSP is a protein and the solute-CSP complexes are based on combinations of hydrophobic and polar interactions. CSPs based on immobilized α -acid glycoprotein, bovine and human serum albumin and enzymes such as chymotrypsin are included in this category

Conclusion

Research into chiral recognition on CSPs has expanded the original three-point interaction model into a model of molecular chiral recognition.

See Colour Plates 24, 25.

See also: III/Chiral Separations: Cellulose and Cellulose Derived Phases; Cyclodextrins and Other Inclusion Complexation Approaches; Ligand Exchange; Liquid Chromatography; Protein Stationary Phases; Synthetic Multiple Interaction ('Pirkle') Stationary Phases.

Further Reading

- Booth TD and Wainer IW (1996) Investigation of the enantioselective separations of α -alkyl arylcarboxylic acids on an amylose *tris*(3,5-dimethylphenylcarbamate) chiral stationary phase using quantitative structure-enantioselective retention relationships (QSERR): identification of a conformationally driven chiral recognition mechanism. *Journal of Chromatography A* 737: 157-169.
- Francotte E (1994) Contribution of preparative chromatographic resolution to the investigation of chiral phenomena. *Journal of Chromatography A* 666: 565-601.
- Hara S, Nakagawa T and Terabe S (eds) (1994) International symposium on molecular chirality, Kyoto, Japan, 24-27 May 1994. *Journal of Chromatography A* 694.
- Jinno K (ed.) (1997) *Chromatographic Separations based on Molecular Recognition*. New York: Wiley-VCH.
- Pirkle WH, Pochapsky TC, Burke JA III and Deming KC (1988) Systematic studies of chiral recognition mechanisms. In: Stevenson D and Wilson ID (eds) *Chiral Separations*, pp. 23-36. London: Plenum Press.
- Schreier P, Bernreuther A and Huffer M (1995) *Analysis of Chiral Organic Molecules*. Berlin: Walter de Gruyter.
- Wainer IW (ed.) (1993) *Drug Stereochemistry*. New York: Marcel Dekker.

Mechanisms: Ion Chromatography

P. R. Haddad, University of Tasmania, Hobart, Tasmania, Australia

Copyright © 2000 Academic Press

Introduction

The term ion chromatography (IC) does not refer to a single, specific chromatographic technique, but rather to the specialized application of a collection of established techniques. When introduced in 1975 IC referred only to the separation of inorganic anions and cations using a specific combination of ion exchange columns coupled to a conductimetric detector. Since that time, the definition of IC has expanded greatly and it can be best categorized in terms of the type of analytes separated rather than the manner in which the separation is achieved. We can therefore define IC to be:

the use of liquid chromatographic methods for the separation of inorganic anions and cations and low molecular weight water-soluble organic acids and bases.

While a range of chromatographic methods (e.g. reversed-phase ion interaction chromatography) can be used to separate these types of analytes, it is true to say that the majority of IC separations are performed by ion exchange using specialized stationary phases. In the interests of brevity, the discussion of IC will therefore be confined to ion exchange methods only. The interested reader seeking a broader coverage of the technique is referred to any of the standard texts listed in the Further Reading section.

IC methods employing ion exchange can be divided somewhat arbitrarily into two main groups, largely on the basis of historical development and commercial marketing influences. These groups of methods are referred to as 'nonsuppressed ion chromatography' and 'suppressed ion chromatography'.

Nonsuppressed IC comprises all those methods in which an ion exchange column is used to separate a mixture of ions, with the separated analytes being passed *directly to the detector*. The hardware configuration employed is shown schematically in Figure 1A, from which it can be seen that this configuration parallels the hardware used in traditional high performance liquid chromatography (HPLC). Some of the alternative names proposed for this technique are:

1. single-column ion chromatography
2. electronically suppressed ion chromatography.

The first of these names indicates that only a single chromatographic column is employed and that the eluent is not *chemically* modified prior to entering the detector, whereas the second name pertains to the fact that the background conductance of the eluent can be cancelled *electronically* by certain types of conductivity detectors. 'Nonsuppressed IC' is the most frequently used term and is recommended.

The second group of ion exchange methods consists of those in which an additional device, called the *suppressor*, is inserted between the ion exchange separator column and the detector, as shown in Figure 1B. The function of the suppressor is to modify both the eluent and the analyte in order to improve the detectability of the analytes with a conductivity detector. The suppressor often requires a regenerant solution to enable it to operate for extended periods. Methods using this hardware configuration are referred to as:

1. suppressed ion chromatography
2. chemically suppressed ion chromatography
3. eluent-suppressed ion chromatography
4. dual-column ion chromatography.

The last of these names is misleading because modern suppressors are not columns, but rather flow-through membrane devices. The term 'suppressed IC' is recommended.

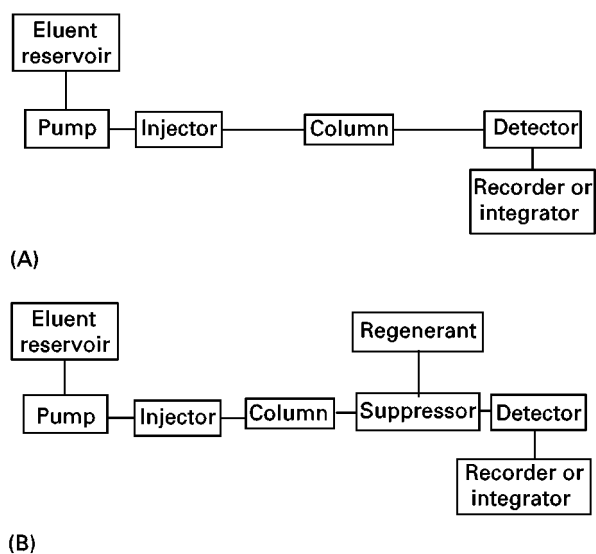


Figure 1 Block diagram showing the instrumental components used in (A) nonsuppressed and (B) suppressed IC.

Stationary Phases for IC

The ion exchange stationary phases used for IC are usually formed by chemical bonding of appropriate functional groups to a suitable substrate such as a polymer or silica. The functional groups used most commonly are sulfonates (for cation exchangers) and quaternary ammonium groups (for anion exchangers). In this respect, IC stationary phases are similar to the conventional ion exchange materials used widely throughout analytical chemistry. However, there are two important factors that differentiate the ion exchangers used in IC. The first is their ion exchange capacity. IC requires ion exchangers with low ion-exchange capacity, typically in the range 10–100 $\mu\text{equiv g}^{-1}$. This requirement can be attributed chiefly to the fact that IC was developed originally for use with conductivity detection, which introduces a preference for eluents of low background conductance in order to enhance the detectability of eluted analyte ions. The diversity of detection methods now available makes it possible to use columns of much higher ion exchange capacity, but because conductivity is still the most commonly employed detection mode, the majority of separations continue to be performed on low capacity materials. The second characteristic of ion exchangers for IC is their greatly enhanced chromatographic efficiency when compared to traditional ion exchangers.

In practice, both of the above-mentioned differentiating characteristics can be achieved by using ion exchangers in which the functional groups are confined to a thin shell around the surface of the stationary phase particle. This both reduces the number of functional groups (and hence the ion exchange capacity) and also limits the diffusion path of analyte ions, thereby improving mass-transfer characteristics and hence chromatographic efficiency. Two main approaches to synthesizing such ion exchangers can be identified. The first involves the use of only a very short reaction time during which the substrate material, i.e. either silica or a polymer such as poly(styrene-divinylbenzene) or poly(methyl methacrylate) is derivatized in order to introduce the ion exchange functional group. For example, a macroporous poly(styrene-divinylbenzene) bead immersed in concentrated sulfuric acid for less than 30 s will give a material in which sulfonic acid functional groups are confined to a very shallow depth (of the order of 20 nm) around the outside of the particle. This produces a 'surface-functionalized cation exchanger', represented schematically in **Figure 2**, in which the confinement of functional groups to the outer layer has been achieved by chemical means. Surface-functionalized anion exchangers can be produced in a similar

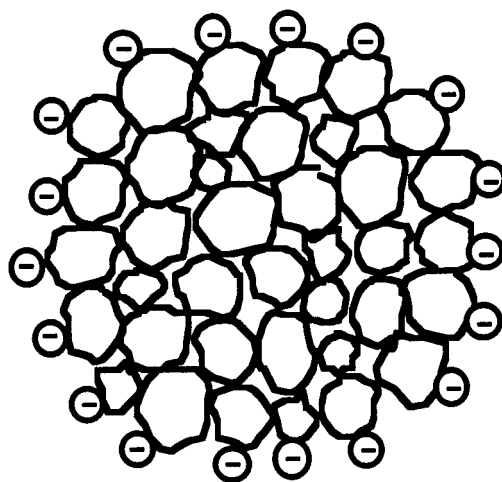


Figure 2 Schematic representation of the cross-section of a surface-sulfonated cation exchange resin. The negative charges represent sulfonic acid groups that are located on the surface of the resin bead. Note that the interior of the bead is not sulfonated.

manner. Historically, surface-functionalized ion exchangers have found most use in nonsuppressed IC.

The second approach to synthesis of ion exchangers for IC involves a physical process for confining the functional groups to the outer layer. These ion exchangers, known as 'agglomerated materials', consist of a central core particle, to which is attached a monolayer of small-diameter particles which carry the functional groups of the ion exchanger. Provided the outer layer of functionalized particles is very thin, the agglomerated particle exhibits excellent chromatographic performance due to the very short diffusion paths available to analyte ions during the ion exchange process. Schematic illustrations of agglomerated anion and cation exchangers are given in **Figure 3**. The central core (or support) particle is

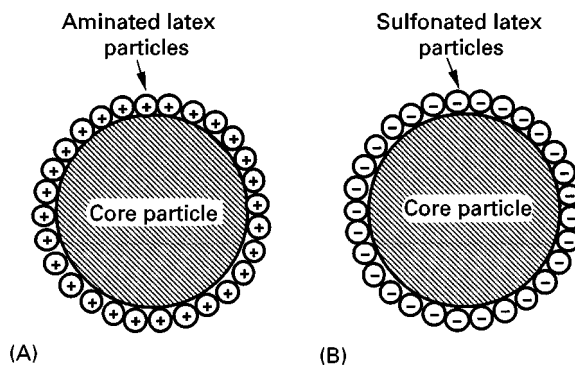


Figure 3 Schematic representation of agglomerated (A) anion and (B) cation exchangers.

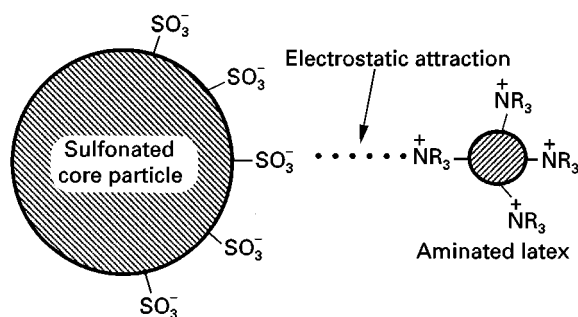


Figure 4 Formation of an agglomerated anion exchange resin using electrostatic binding. Note that the core and the latex particles are not drawn to scale.

generally poly(styrene-divinylbenzene) of moderate cross-linking, with a particle size in the range 7–30 μm , which has been functionalized to carry a charge opposite to that of the outer particles. The outer microparticles consist of finely ground resin or monodisperse latex (with diameters in the approximate range 20–100 nm) that has been functionalized to contain the desired ion exchange functional group. It is this functional group which determines the ion exchange properties of the composite particle, so that aminated (positively charged) latexes produce agglomerated anion exchangers (as illustrated in Figure 3A), while sulfonated (negatively charged) latexes produce agglomerated cation exchangers (Figure 3B). Electrostatic attraction between the oppositely charged core particles and outer microparticles holds the agglomerate together, even over long periods. **Figure 4** shows details of this electrostatic attraction for an agglomerated anion exchanger. Agglomerated ion exchangers are used most frequently in suppressed IC.

Mobile Phases for IC

Mobile phases (or eluents) for IC are similar to those used for regular ion exchange separations in that the eluent must contain a competing ion (of the same charge sign as the analytes to be separated) which serves to displace the analyte ions from the stationary phase and ultimately to elute the analytes from the column. However, eluents in IC must also satisfy the stringent requirement that they should be compatible with conductivity detection. In the case of nonsuppressed IC (in which the eluent is not involved in further reaction before reaching the detector) this means that eluent-competing ions of low limiting equivalent ionic conductance (see discussion of conductivity detection below) are required if direct conductivity detection is to be used. Aromatic car-

boxylates (such as benzoate and phthalate), aromatic sulfonates (such as toluenesulfonate) and complex ions (such as the anionic complex formed between gluconate and borate) are ideal for anion separations, whereas aromatic bases are useful for cation separations. All of these species are bulky ions having low ionic mobility (and hence low conductance) so that direct detection of more mobile analyte ions (such as chloride, sulfate, etc.) is possible using conductivity. Alternatively, indirect conductivity detection is possible using eluent-competing ions having very high values of limiting ionic conductance, such as hydronium ions for cation separations and hydroxide ions for anion separations.

Suppressed IC offers the opportunity for further reaction of the eluent before detection. The purpose of this reaction is to reduce the conductance of the eluent; in most cases acid–base reactions are used. The mechanism of eluent suppression will be discussed further below, but for the present it can be assumed that the process works best when applied to eluents comprising competing ions that can be easily neutralized in an acid–base reaction. For example, carbonate and bicarbonate (or mixtures of the two) can be used for anion separations, while dilute solutions of mineral acids can be used for cation separations.

Many cation separations cannot be achieved simply through correct choice of a suitable eluent-competing cation. Polyvalent cations show such strong electrostatic attraction to sulfonic acid cation exchangers that they can only be displaced by using concentrated eluents. This, in turn, renders conductivity detection difficult. Practical alternatives are created by the use of a complexing agent as the eluent, or by the addition of a complexing agent to an eluent that already contains a competing cation. This serves the dual purpose of reducing the effective charge on the analyte cation (and hence its affinity for the cation exchange sites) and also introduces a further dimension of selectivity between analytes that does not exist when ion exchange is the only retention mechanism in operation. The above approaches are illustrated schematically in **Figure 5**, which shows the equilibria existing between a divalent metal analyte ion M^{2+} , a complexing agent (H_2L), and an ethylenediamine (en) eluent, at the surface of a cation exchange resin. In **Figure 5A**, the eluent contains only the ligand species. Retention of the analyte ion on a cation exchange resin is moderated by the complexation effect of the deprotonated ligand, which can be said to exert a *pulling* effect on the analyte. The eluent pH determines the degree to which the ligand is deprotonated, which in turn governs the retention of the analyte. Retention is also regulated by the type and concentration of the ligand. Tartrate, oxalate, citrate

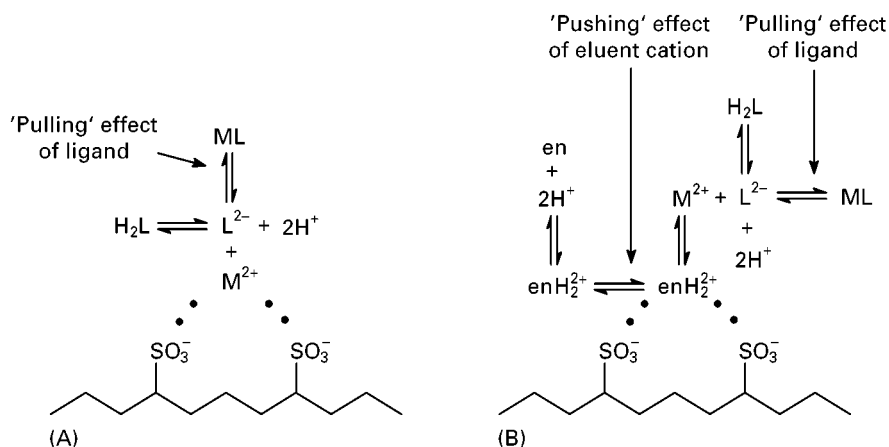


Figure 5 Schematic illustration of the equilibria existing between an analyte cation (M^{2+}), ethylenediamine (en) and an added ligand (H_2L) at the surface of a cation exchanger. In (A) the eluent contains only the ligand, while in (B) the eluent contains both ligand and ethylenediamine.

and α -hydroxyisobutyric acid are examples of typical ligands used as eluent additives.

Figure 5B shows the case where the eluent contains both a ligand and a competing cation (enH_2^+). The retention of the analyte ion, M^{2+} , is influenced by the competitive effect for the sulfonic acid groups exerted by enH_2^+ , and also by the complexation of M^{2+} by the deprotonated ligand L^{2-} . Once again, complexation reduces the effective concentration of M^{2+} and the analyte is therefore less successful in competing for the cation exchange sites. This shows that elution of the analyte results from a combination of the *pushing*, or displacement, effect of the competing cation in the eluent and the complexation, or *pulling*, effect of the complexing agent. The eluent pH influences both the protonation of ethylenediamine and the deprotonation of the added ligand, which in turn controls the degree of complex formation and hence the retention of the analyte. The type and concentration of the added ligand again play a major role in determining analyte retention. For analyte ions of similar ion exchange selectivities, the retention order closely follows the reverse sequence of the conditional formation constants for the analyte–ligand complexes.

Detection in IC

As discussed earlier, the majority of IC separations are performed in conjunction with conductivity detection. However, two further modes of detection, namely indirect UV spectrophotometry and post-column reaction with visible spectrophotometry, also find widespread use. Each of these detection modes will be described briefly.

The normal mode of operation of a detector in IC is the monitoring of a signal (due to the analyte), which appears as an *increase* above the background signal arising from the eluent alone. This is called *direct detection*, and is a useful detection mode whenever the background detector signal due to the eluent alone is small enough to be offset by the zeroing control on the detector. An alternative, namely *indirect detection*, is also possible and involves the measurement of a *decrease* in detector signal when the analyte is eluted and is generally used with eluents that give a high background signal. To function correctly, indirect detection requires that the background composition of the mobile phase must alter in the presence of the eluted analyte and it is this change, rather than a specific characteristic of the analyte itself, that is monitored. Ion exchange chromatography is the most important example of a separation mode that is suited to indirect detection.

Conductivity Detection

Conductivity detection is an important example of bulk property detection and is used commonly when the eluted analytes are ionic, for example acids and bases. However, the major use of this form of detection is for inorganic anions and cations after their separation by ion exchange chromatography. Conductivity detection is universal in response for such analytes, and the detectors themselves are relatively simple to construct and operate.

A solution of an electrolyte will conduct an electrical current if two electrodes are inserted into the solution and a potential is applied across the electrodes. It is relatively straightforward to show that the conductance of a solution, G (having the units of

microsiemens, represented by the symbol μS) is given by:

$$G = \frac{1000\Lambda C}{K} = \frac{\Lambda C}{10^{-3}K} \quad [1]$$

where Λ is the limiting equivalent conductance of the electrolyte (with units $\text{S cm}^2 \text{equiv}^{-1}$), C is the concentration of the electrolyte, expressed as equivalents per litre of solution (equiv L^{-1}), and K is the cell constant (with units of cm^{-1}) determined by the geometry of the electrodes. The conductance can be seen to be proportional to the equivalent conductance of the electrolyte and its concentration. In addition, the lower the cell constant, the higher the conductance. This occurs for cells with large surface area electrodes which are close together.

Since the conductance of the solution results from both the anions and cations of the electrolyte, we must therefore calculate conductance using values for the limiting equivalent ionic conductances (λ) of the individual anions and cations in solution. Equation [1] can now be rewritten as:

$$G = \frac{(\lambda_+ + \lambda_-)C}{10^{-3}K} \quad [2]$$

where λ_+ and λ_- are the limiting equivalent ionic conductances of the cationic and anionic components

of the electrolyte, respectively. Limiting equivalent ionic conductances for some common ionic species are listed in Table 1.

The operating principles of conductivity detection can be illustrated by considering the conductance of a typical eluent prior to and during the elution of an analyte ion. The conductance change, ΔG , produced when an anionic analyte S^- is eluted by an anionic eluent E^- , is given by:

$$\Delta G = \frac{(\lambda_{\text{S}^-} - \lambda_{\text{E}^-})C_{\text{S}}I_{\text{S}}}{10^{-3}K} \quad [3]$$

where C_{S} is the concentration of the analyte and I_{S} is the fraction of the analyte present in the ionic form. Equation [3] shows that the detector response depends on analyte concentration, the difference in the limiting equivalent ionic conductances of the eluent and analyte anions, and the degree of ionization of analyte. The last of these parameters is generally governed by the eluent pH.

Sensitive conductivity detection can result as long as there is a considerable difference in the limiting equivalent ionic conductances of the analyte and eluent ions. This difference can be positive or negative, depending on whether the eluent ion is strongly or weakly conducting. If the limiting equivalent ionic conductance of the eluent ion is low, then an increase in conductance occurs when the analyte enters the

Table 1 Limiting equivalent ionic conductances of some ions in aqueous solution at 25°C

Anion	$\lambda_- (\text{S cm}^2 \text{equiv}^{-1})$	Cation	$\lambda_+ (\text{S cm}^2 \text{equiv}^{-1})$
OH^-	198	H_3O^+	350
$\text{Fe}(\text{CN})_6^{4-}$	111	Rb^+	78
$\text{Fe}(\text{CN})_6^{3-}$	101	Cs^+	77
CrO_4^{2-}	85	K^+	74
CN^-	82	NH_4^+	73
SO_4^{2-}	80	Pb^{2+}	71
Br^-	78	Fe^{3+}	68
I^-	77	Ba^{2+}	64
Cl^-	76	Al^{3+}	61
$\text{C}_2\text{O}_4^{2-}$	74	Ca^{2+}	60
CO_3^{2-}	72	Sr^{2+}	59
NO_3^-	71	CH_3NH_3^+	58
PO_4^{3-}	69	Cu^{2+}	55
ClO_4^-	67	Cd^{2+}	54
SCN^-	66	Fe^{2+}	54
ClO_3^-	65	Mg^{2+}	53
Citrate $^{3-}$	56	Co^{2+}	53
HCOO^-	55	Zn^{2+}	53
F^-	54	Na^+	50
HCO_3^-	45	Phenylethylammonium $^+$	40
CH_3COO^-	41	Li^+	39
Phthalate $^{2-}$	38	$\text{N}(\text{C}_2\text{H}_5)_4^+$	33
$\text{C}_2\text{H}_5\text{COO}^-$	36	Benzylammonium $^+$	32
Benzoate $^-$	32	Methylpyridinium $^+$	30

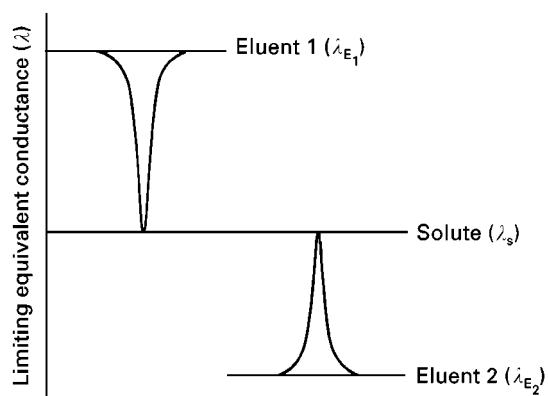


Figure 6 Schematic illustration of the principles of direct and indirect conductivity detection.

detection cell. This detection mode is *direct*, since the analyte has a *higher* value of the measured property than does the eluent ion. Alternatively, an eluent ion with a high limiting equivalent ionic conductance can be employed and a decrease in conductance would occur when the analyte enters the detection cell. This type of detection is *indirect*, where the analyte has a *lower* value of the measured property than does the eluent ion. These detection modes are shown schematically in **Figure 6** and practical examples of direct and indirect conductivity detection are illustrated in

Figures 7 and 8. In **Figure 7A**, the weakly conducting borate–gluconate complex is used as eluent, whilst in **Figure 7B** a suppressed carbonate–bicarbonate eluent is used (see below). In contrast, highly conducting eluent ions are used in **Figure 8**, namely hydroxide (**Figure 8A**) and hydronium (**Figure 8B**) ions. Examination of **Table 1** shows that these are the most strongly conducting ions and should therefore lead to sensitive indirect conductivity detection.

Use of Suppressors with Conductivity Detection

When the conductivity detector is mounted in the usual position for a chromatographic detector, that is immediately after the column, the choice of eluent composition must also take into account the requirements for sensitive conductimetric detection. In many cases, the requirements of conductivity detection also impose constraints on the characteristics of the column used. One way to diminish this interdependence between column, eluent and detector is to insert a device between the column and detector that can chemically or physically modify the eluent. A commonly used device of this type is a suppressor, which achieves signal enhancement in conductivity detection by reducing the conductance of the eluent and simultaneously increasing the conductance of the sample band.

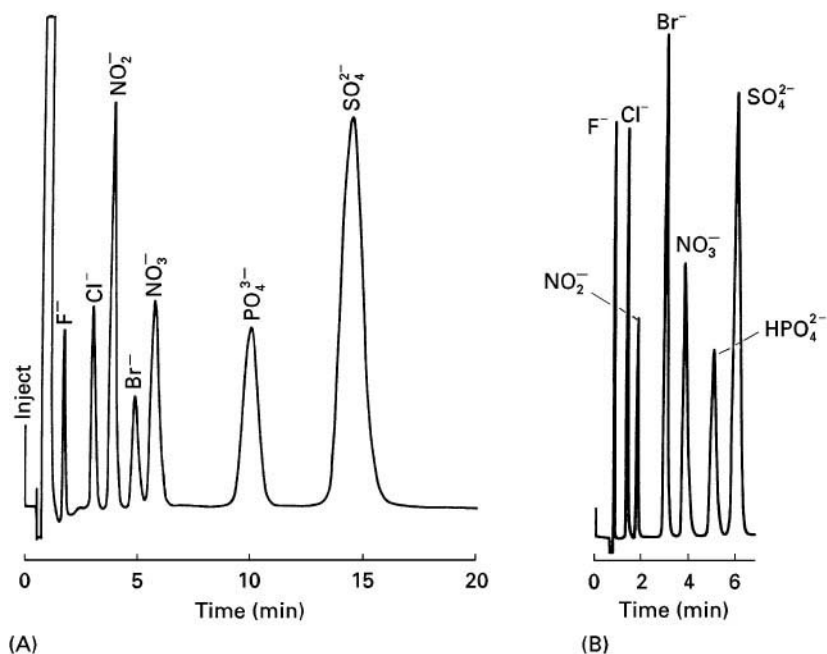


Figure 7 Direct conductivity detection employed in the separation of anions using (A) nonsuppressed and (B) suppressed ion chromatography. (A) A Waters IC Pak A surface-functionalized anion exchange column was used with gluconate–borate as eluent. (B) A Dionex HPIC-AS4A agglomerated anion exchange column was used with a carbonate–bicarbonate eluent. (Chromatograms courtesy of Waters and Dionex.)

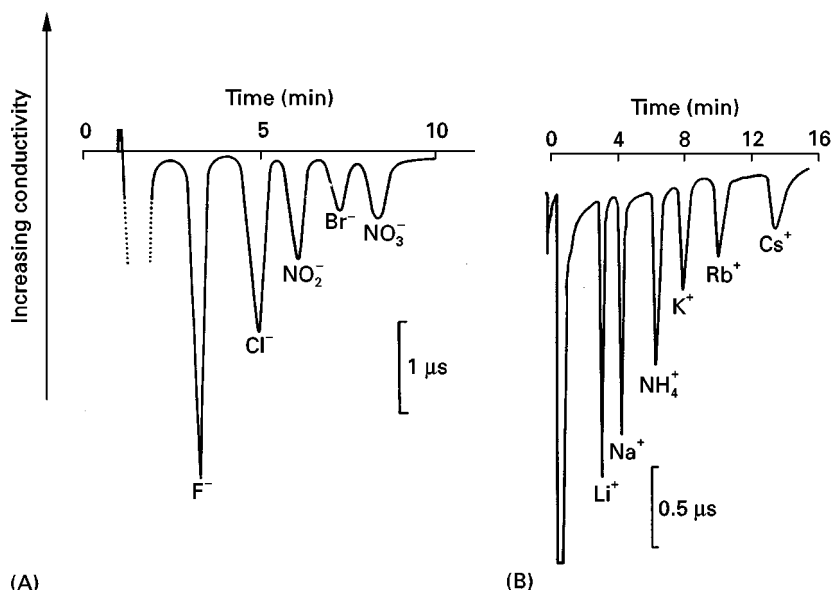
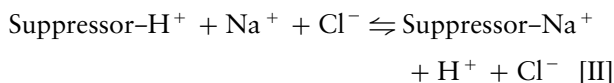
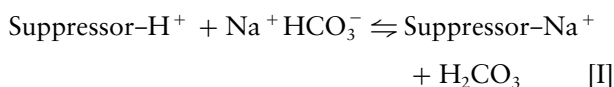


Figure 8 Indirect conductivity detection of (A) anions and (B) cations. (A) A TSK-GEL 620 SA surface-functionalized polymethylmethacrylate anion-exchange column was used with 2 mmol L⁻¹ KOH as eluent. (Reprinted with permission from Okada and Kuwamoto, 1983.) (B) A Waters IC Pak C surface-functionalized poly(styrene-divinylbenzene) cation exchange column was used with 2 mmol L⁻¹ HNO₃ as eluent. (Chromatogram courtesy of Waters.)

The operation of a suppressor can be illustrated by considering the elution of chloride ion with an eluent of NaHCO₃. If the suppressor is capable of exchanging sodium ions in the eluent with hydrogen ions from the suppressor, the first of the reactions below occurs (reaction [I]). The HCO₃⁻ ions are converted into weakly conducting H₂CO₃, and the background conductance of the eluent is said to be suppressed. At the same time, the eluted analyte (in this case, chloride) will also undergo the second of the reactions below in the suppressor (reaction [II]).



The combined result of these processes is that the eluent conductance is decreased greatly, while the conductance of the sample is increased by virtue of the replacement of sodium ions ($\lambda_+ = 50 \text{ S cm}^2 \text{ equiv}^{-1}$) with hydrogen ions ($\lambda_+ = 350 \text{ S cm}^2 \text{ equiv}^{-1}$). The detectability of the analyte is therefore enhanced considerably.

It is important to note that suppression reactions are not limited to acid-base reactions, such as those shown in the above examples, nor are they limited to the detection of anions. Indeed, any post-column reaction that results in a reduction of the background conductance of the eluent can be classified as a sup-

pression reaction. However, the ensuing discussion of suppressor design and performance will be restricted to those which employ acid-base reactions, since these are the most widely used.

Modern suppressors are based on dialysis reactions occurring through ion exchange membranes, with the membrane being generally used as a flat sheet. **Figure 9** gives a schematic representation of the design of a typical flat-sheet (or 'micromembrane') suppressor. The eluent contacts one side of the membrane while a regenerant solution flows in a countercurrent direction on the opposite side of the membrane. In the case of the bicarbonate eluent considered earlier, the membrane would be a cation exchanger and the regenerant would be a solution containing H⁺ ions. The eluent passes through a central chamber that has ion exchange membrane sheets as the upper and lower surfaces. Regenerant flows in a countercurrent direction over the outer surfaces of both of these membranes. Mesh screens constructed from a polymeric ion exchange material are inserted into the eluent cavity and also into the cavities that house the flowing regenerant solution. The entire device is constructed in a sandwich layer configuration with gaskets being used to define the desired flow-paths. The volume of the eluent chamber is very small (< 50 μL), so band-broadening is minimal.

The mode of operation of the suppressor with a NaHCO₃/Na₂CO₃ eluent is illustrated schematically in **Figure 10A**. Sodium ions from the eluent diffuse through the cation exchange membrane and

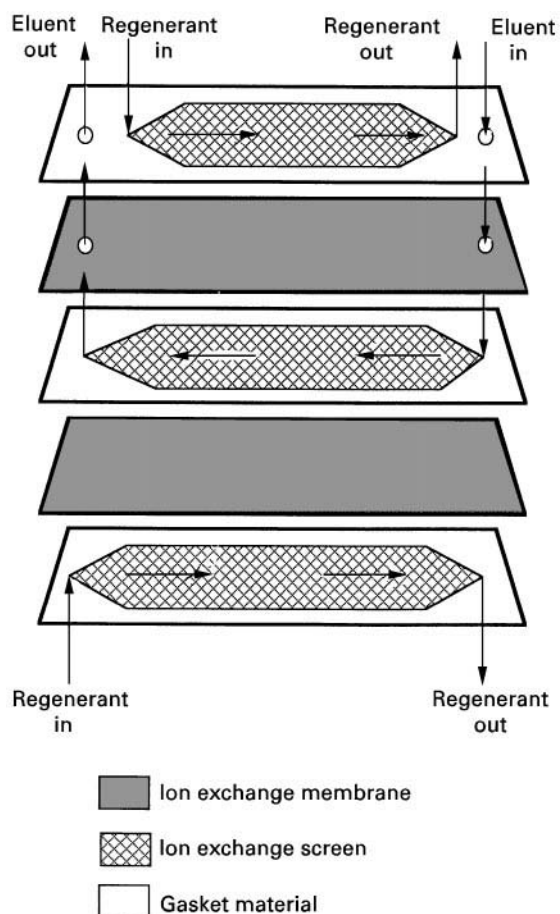


Figure 9 Design of a micromembrane suppressor.

are replaced by H^+ ions from the regenerant, producing the desired suppression reaction. Analyte anions (e.g. chloride) are prevented from penetrating the membrane by the repulsion effect of the anionic functional groups of the membrane and therefore remain in the eluent stream. A schematic representation of the operation of this type of suppressor in the separation of cations using a hydrochloric acid eluent and a barium hydroxide regenerant solution is shown in Figure 10B.

The micromembrane suppressor combines the advantages of other suppression devices, while at the same time eliminating their drawbacks. These advantages can be summarized as:

1. small internal volume, leading to minimal band-broadening effects and hence low detection limits;
2. continuous regeneration;
3. high dynamic suppression capacity, which can be varied readily by changing the nature, concentration and flow-rate of the regenerant;
4. suitable for gradient elution with appropriate eluents;
5. resistant to many organic solvents and ion interaction reagents; and
6. a wider choice of eluent types is possible because of the high dynamic suppression capacities that can be achieved.

A recent adaptation of the micromembrane suppressor replaces the flowing regenerant solution with

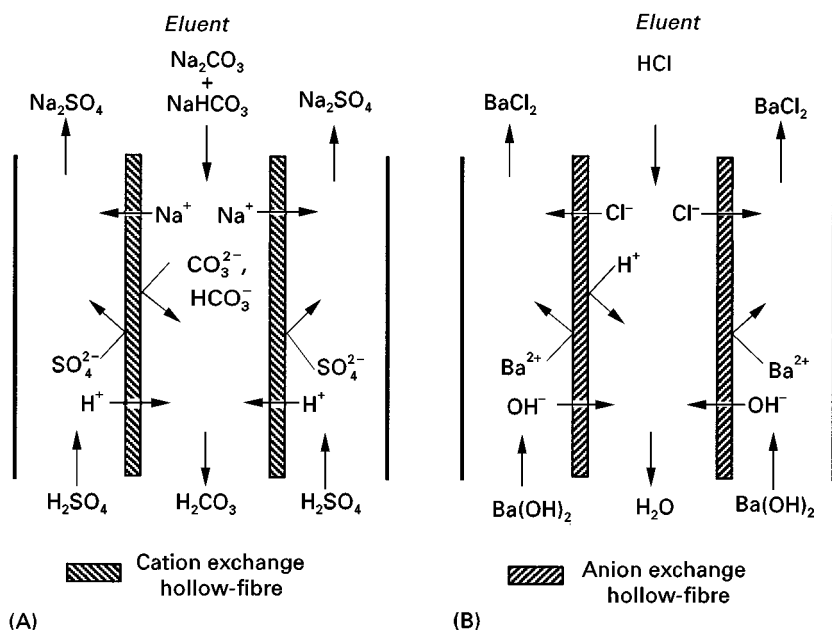


Figure 10 Schematic operation of a micromembrane suppressor for eluents used with (A) anion exchange and (B) cation exchange chromatography.

water and inserts electrodes into the two regenerant compartments. This water is then electrolysed in the regenerant compartments to produce the hydronium and hydroxide ions necessary for the suppression reactions. In addition, the electric field applied to achieve the electrolysis also provides enhanced movement of ions across the membranes and thus more efficient suppression is achieved.

Indirect Spectrophotometric Detection of Anions

Indirect spectrophotometric detection is applied most frequently to the detection of anions and will therefore be discussed in this context only. When an anionic analyte S^{x-} is eluted from an ion exchanger by an eluent containing a competing anion E^{y-} , the absorbance change ΔA is given by:

$$\Delta A = \left(\varepsilon_{S^{x-}} - \frac{x}{y} \varepsilon_{E^{y-}} \right) C_S m \quad [4]$$

where $\varepsilon_{S^{x-}}$ and $\varepsilon_{E^{y-}}$ are the molar absorptivities at the detection wavelength of the analyte and eluent anions, respectively, C_S is the molar concentration of the analyte and m is the detector pathlength in cm. We see that the absorbance change measured by the detector on elution of an analyte is proportional to the analyte concentration, the cell pathlength and to the difference in molar absorptivities between the analyte and eluent anions. Equation [4] shows that indirect detection will result when the molar absorptivity of the analyte anion is less than that of the eluent anion, leading to a negative value for ΔA .

Indirect spectrophotometric detection, also called indirect photometric chromatography and vacancy detection, is a very widely used detection method in IC. Decreased absorbance accompanies the elution of analytes, but the polarity of the detector output is often reversed in order to give positive peaks on the recorder. Provided that Beer's law is followed, then linear calibration plots will result, thereby permitting sample quantification. Eluents such as phthalate, nitrate, sulfobenzoate and benzenetricarboxylate are commonly used for the separation of anions. A typical chromatogram obtained with phthalate as the eluent is shown in Figure 11.

Post-column Reaction Detection of Cations

While alkali metal and alkaline earth cations are detected routinely using conductivity detection, transition metals and lanthanoids are most commonly detected using a post-column reaction (PCR). In most cases, this involves a post-column addition of a colour-forming ligand, generally a metallochromic

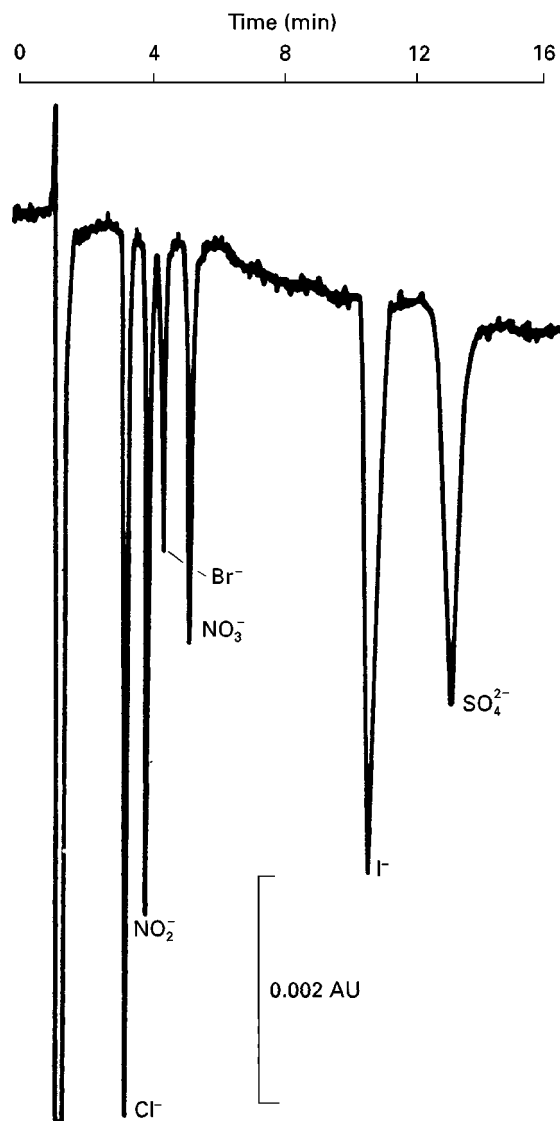


Figure 11 Detection of anions using indirect spectrophotometry. A Vydac 302 4.6 IC surface-functionalized silica anion exchange column was used with 5 mmol L⁻¹ potassium hydrogen phthalate at pH 4.0 as eluent. Detection was at 285 nm. (Reprinted with permission from Heckenberg and Haddad, 1984.)

dye. Typical examples of such dyes are 4-(2-pyridylazo)resorcinol (PAR), which is used for the detection of transition metals, and 2,7-bis(2-arsonophenylazo)-1,8-dihydroxynaphthalene-3,6-disulfonic acid (Arsenazo III), which is used for the detection of lanthanoids. Both dyes react rapidly with a wide range of metal ions to form strongly absorbing complexes that facilitate sensitive detection without the need for complicated reactors or mixing devices. Figure 12 shows a typical chromatogram obtained using Arsenazo I as the PCR reagent.

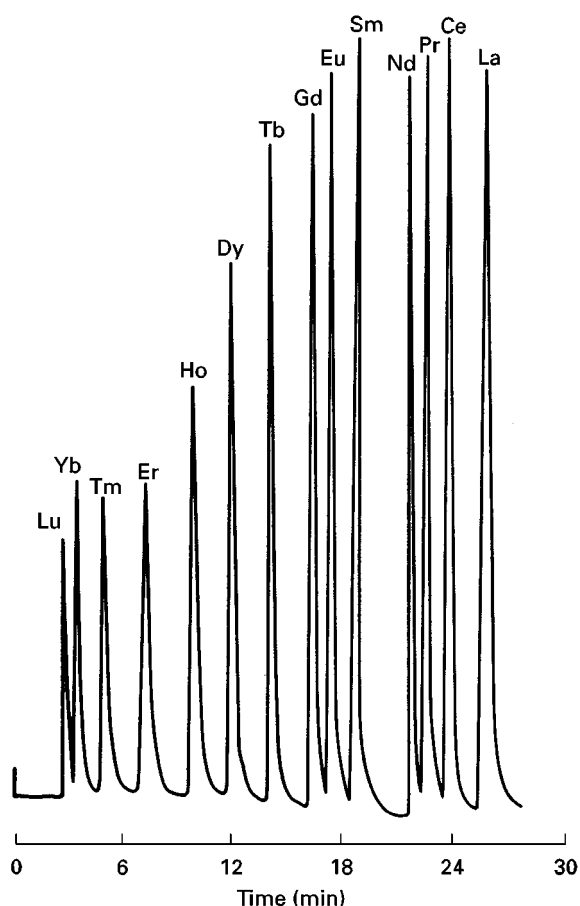


Figure 12 Use of post-column reaction for the detection of lanthanoids. Separation was achieved on a Nucleosil 10SA silica-based cation exchange column using 2-methylactic acid as eluent, with post-column reaction detection with Arsenazo I. (Reprinted with permission from Wang *et al.*, 1984.)

Analytical Performance of IC

IC is now a relatively mature analytical technique and has found application across a wide range of analytes and sample types. Almost all inorganic anions can be determined using IC, as can the alkali metal cations, alkaline earth cations, the first row transition metals and the lanthanoids. However, the availability of sensitive, multielement spectroscopic analytical techniques for the measurement of cations has meant that the major focus of IC has been in the area of anion analysis. About 80% of publications on IC fall into this area.

Variation of the nature of the functional group on the stationary phase can be used as a means to manipulate separation selectivity in IC. For this reason there exists a wide range of stationary phases, and more than 150 different types of IC column are available commercially. It is therefore usually possible to identify a stationary phase suitable for most practical separations. Chromatographic efficiencies of these

columns are typically of the order of 1500 theoretical plates for a 5 cm column packed with a surface functionalized material, and 4500 theoretical plates for a 25 cm column packed with an agglomerated material.

Detection limits are dependent on the particular analyte ion and on the detection mode used. However, if one considers only conductivity detection, then detection limits of 10 ppb (for a 50 μ L injection) and 100 ppb (for a 100 μ L injection) are achievable for suppressed and nonsuppressed IC, respectively. When lower detection limits are required, on-line sample enrichment using a small ion exchange preconcentrator column can be employed, leading to detection limits which are in the ppt range.

IC has found application to a very wide range of samples, but a survey of the literature reveals that the most common application areas are environmental analysis (especially of air and aerosol samples and various natural waters), industrial analysis (such as wastewaters and process samples from pulp and paper manufacture), food and plant analysis, and clinical and pharmaceutical analysis.

See also: I/Ion Exchange. II/Chromatography: Liquid: Detectors: Ultraviolet and Visible Detection. Ion Analysis: Liquid Chromatography. Ion-Exclusion Chromatography: Liquid Chromatography. Metal Complexes: Ion Chromatography.

Further Reading

- Gjerde DT and Fritz JS (1987) *Ion Chromatography*, 2nd edn. Heidelberg: Hüthig.
- Haddad PR and Jackson PE (1990) *Ion Chromatography: Principles and Applications*. Amsterdam: Elsevier.
- Heckenberg AL and Haddad PR (1984) Determination of inorganic anions at parts per billion levels using single-column ion chromatography without sample preconcentration. *Journal of Chromatography* 299: 301–305.
- Okada T and Kuwamoto T (1983) Nonsuppressor ion chromatography of inorganic and organic anions with potassium hydroxide as eluent. *Analytical Chemistry* 55: 1001–1004.
- Shpigun OA and Zolotov YuA (1988) *Ion Chromatography in Water Analysis*. Chichester: Ellis Horwood.
- Small H (1989) *Ion Chromatography*. New York: Plenum Press.
- Small H, Stevens TS and Bauman WC (1975) Novel ion exchange chromatographic method using conductometric detection. *Analytical Chemistry* 47: 1801–1809.
- Tarter JG (ed.) (1987) *Ion Chromatography*. New York: Marcel Dekker.
- Wang W, Chen Y and Wu M (1984) Complementary analytical methods for cyanide, sulfide, certain transition metals and lanthanides in ion chromatography. *Analyst* 109: 281–286.
- Weiss J (1995) *Ion Chromatography*. Weinheim: VCH.

Mechanisms: Normal Phase

R. P. W. Scott, Avon, CT, USA

Copyright © 2000 Academic Press

Introduction

In normal phase chromatography the dominant interactions between the solute and the stationary phase that cause retention and selectivity are polar in nature. If dispersive interactions dominate, then the separation system is called 'reversed phase' chromatography. To comprehend the retention mechanisms involved in normal phase chromatography, it is necessary to understand the nature of the different interactive forces that are involved between the solutes and the two phases and how they occur. The retention of a solute is directly proportional to the magnitude of its distribution coefficient (K) between the mobile phase and the stationary phase which, in turn, will depend on the relative affinity of the solute for the two phases, i.e. the interactive forces between the solute molecules and the two phases. Consequently, the stronger the forces between the solute molecule and the molecules of the stationary phase, the larger the distribution coefficient and the more the solute is retained. There are only three basic types of molecular force, all of which are electrical in nature. These three forces are called 'dispersion forces', 'polar forces' and 'ionic forces'. Despite there being many different terms used to describe molecular interactions (e.g. hydrophobic forces, π - π interactions, hydrogen bonding, etc.) all interactions between molecules are the result of composites of these three basic molecular forces. Dispersion forces arise from charge fluctuations throughout a molecule resulting from random electron/nuclei vibrations. They are typical of those that occur between hydrocarbons and other substances that have either no permanent dipoles or can have no dipoles induced in them. In biotechnology and biochemistry, dispersive interactions are often referred to as 'hydrophobic' or 'lyophobic' interactions, apparently because dispersive substance such as the aliphatic hydrocarbons do not dissolve readily in water. Polar interactions arise from electrical forces between localized charges such as permanent or induced dipoles. Polar forces are always accompanied by dispersive interactions and may also be combined with ionic interactions. Polar interactions can be very strong and produce molecular associations that approach, in energy, to that of a weak chemical bond (e.g. 'hydrogen bonding'). Ionic interactions arise from permanent

negative or positive charges on the molecule and thus usually occur between ions. Ionic interactions are exploited in ion exchange chromatography where the counter-ions to the ions being separated are suited in the stationary phase. To achieve the necessary retention and selectivity between the solutes for complete resolution, it is necessary to select a phase system that will provide the optimum balance between dispersive, polar and ionic interactions between the solute molecules and the two phases.

To achieve retention, the forces between the solute molecules and the stationary phase must dominate. If the molecules are largely dispersive in character then dispersive interactions must dominate in the stationary phase and, by suitable choice of mobile phase, polar interactions are made to dominate in the mobile phase. Conversely, if the substances to be separated are largely polar or polarizable then polar interactions must dominate in the stationary phase and, by suitable choice of mobile phase, dispersive interactions must be made to dominate in the mobile phase. When polar interactions dominate in the stationary phase, historically, the separation system has been termed 'normal' chromatography. When dispersive interactions dominate in the stationary phase, historically, the separation system is said to be 'reversed phase' chromatography. Thus in normal chromatography polar interactions dominate in the stationary phase and dispersive interactions are made to dominate in the mobile phase.

The polar forces that retain solutes in normal chromatography vary in strength and somewhat in mechanism. The strongest polar forces arise from dipole-dipole interactions, where charge centres on the solute molecule interact with the opposite charge centres on the stationary phase. Compounds, such as those containing the aromatic nucleus and thus (π) electrons, are said to be 'polarizable'. When such molecules are in close proximity to a molecule with a permanent dipole, the electric field from the dipole induces a counter dipole in the polarizable molecule. This induced dipole acts in the same manner as a permanent dipole and thus polar interactions occur between the molecules. Induced dipole interactions are, as with polar interactions, always accompanied by dispersive interactions. Aromatic hydrocarbons can be retained and separated purely by dispersive interactions when using a dispersive stationary phase (reversed phase chromatography) or they can be retained and separated by combined induced-polar and dispersive interactions by using a polar stationary phase such as silica gel (normal phase

chromatography). The strongly polar hydroxyl groups inducing dipoles in the easily polarizable aromatic nucleus. A single molecule can possess different types of polarity; phenylethanol, for example, will possess both a permanent dipole as a result of the hydroxyl group and also be polarizable due to the aromatic ring. More complex molecules can have many different interactive groups.

The most common, and in fact traditional, normal phase system used in liquid chromatography consists of silica gel as the stationary phase and a mobile phase that is predominantly an alkane or a mixture containing a high proportion of an alkane. This system will be used to examine the type of interactive mechanisms that can take place in normal phase chromatography. The second solvent(s) can be more dispersive such as methylene chloride or a more polar such as ethyl acetate, *n*-propanol or even ethanol. To reduce retention, either the interactive character of the stationary phase must be reduced or the interactive character of the mobile phase increased or both. Both effects can be achieved by modifying the mobile phase. However, in normal phase chromatography, when employing mixed mobile phases, the interactions on the silica surface can become quite complex and the mechanism of retention needs some discussion. The mechanisms involved in mobile phase interactions with the solute are quite different to those involved with the stationary phase and thus, they will be considered separately.

The Nature of the Surface of Silica Gel

When the silica surface is in contact with a solvent, the surface is covered with a layer of the solvent

molecules. If the mobile phase consists of a mixture of solvents, the solvents compete for the surface which is partly covered by one solvent and partly by the other. Thus, any solute interacting with the stationary phase may well be presented with two, quite different types of surface with which to interact. The probability that a solute molecule will interact with one particular type of surface will be statistically controlled by the proportion of the total surface area that is covered by that particular solvent.

Mono-Layer Adsorption

A solvent can be adsorbed from a solvent mixture on the surface of silica gel according to the Langmuir equation for monolayer adsorption. Examples of mono-layer adsorption isotherms obtained for benzene, chloroform and butyl chloride are shown in **Figure 1**. It is seen that the surface becomes completely covered, and its interactive characteristics severely modified at relatively low concentrations of the second solvent in the mobile phase ($> 10\%$ v/v). If the second solvent is more polar, a quite different type of adsorption isotherm applies. In this case, bi-layer adsorption can take place as shown by the isotherms in **Figure 2**. Bi-layer adsorption is not uncommon and the bi-layer adsorption isotherm equation can be derived by a simple extension of the procedure used to derive the Langmuir adsorption isotherm. It should be noted that, due to the strong polarity of the hydroxyl groups on the silica, the initial adsorption of the ethyl acetate on the silica surface is extremely rapid.

The individual isotherms for the two adsorbed layers of ethyl acetate are included in **Figure 2**. The

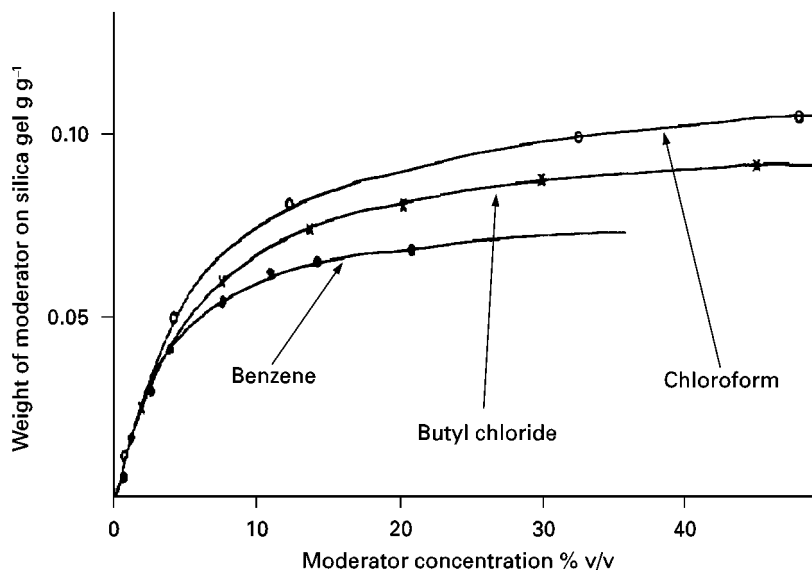


Figure 1 Langmuir adsorption isotherms for benzene, butyl chloride and chloroform.

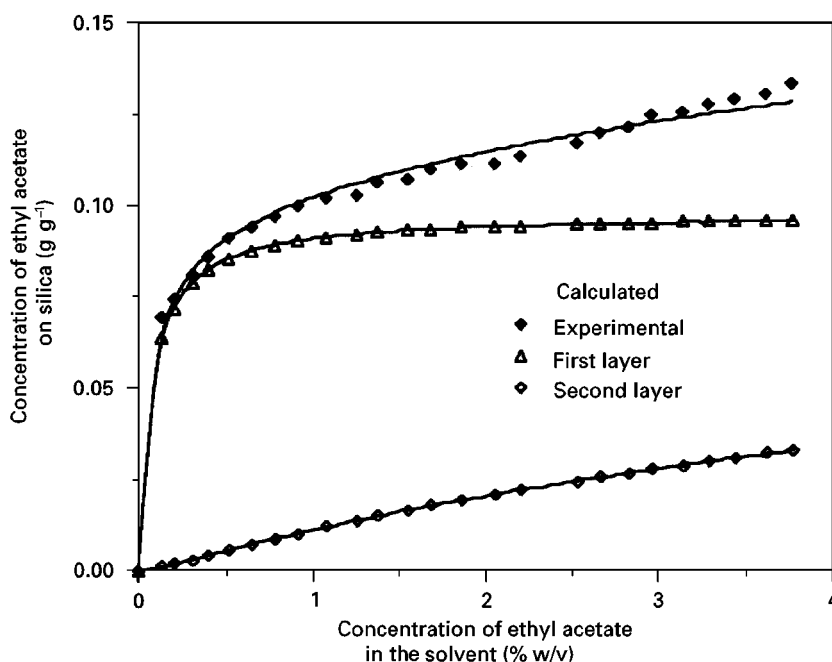


Figure 2 The individual and combined adsorption isotherms for ethyl acetate on silica gel.

two curves, although similar in form, are quite different in magnitude. The first layer which is very strongly held is complete when the concentration of ethyl acetate is only about 1% w/v. At concentrations in excess of 1% w/v the second layer has only just begun to be formed. The formation of the second layer is much slower and the interactions between the solvent molecules with those already adsorbed on the surface are much weaker. Assuming that the total area covered by the first layer will be the same as the area covered by the second layer, then only about one third of the layer is complete at a concentration of about 4% w/v. This is in striking contrast to the formation of the first layer which is virtually complete at an ethyl acetate concentration of 1% w/v.

From the point of view of solute interaction with the surface, it is seen that it can now be very complex indeed. In contrast to the less polar or dispersive solvents, the character of the interactive surface will be modified dramatically as the concentration of the polar solvent ranges from 0 to 1% w/v. However, above 1% w/v, the surface will be modified more subtly, allowing a more controlled adjustment of the interactive nature of the surface.

Multi-layer adsorption is also feasible, for example the second layer of ethyl acetate might have an adsorbed layer of the dispersive solvent *n*-heptane on it. However, any subsequent solvent layers that may be generated will be situated further, and further, from the silica surface and are likely to be very weakly held and sparse in nature. Under such circumstances their presence, if, in fact, real, may have little impact on solute retention.

Interactive Mechanisms on the Surface of Silica Gel in Normal-Phase Liquid Chromatography

It is clear that the interaction of the solute molecules with the stationary phase surface can be quite complex and also change with the composition of the mobile phase. There are two ways a solute can interact with a stationary phase surface. The solute molecule can interact with the adsorbed solvent layer and rest on the top of it. This is called 'sorption interaction' and occurs when the molecular forces between the solute and the stationary phase are relatively weak compared with the forces between the solvent molecules and the stationary phase. The second type is where the solute molecules displace the solvent molecules from the surface and interact directly with the stationary phase itself. This is called 'displacement interaction' and occurs when the interactive forces between the solute molecules and the stationary phase surface are much stronger than those between the solvent molecules and the stationary phase surface. An example of sorption interaction is shown in Figure 3(A). Its linear relationship is clearly demonstrated and it is seen that the distribution coefficient (which controls retention) can be adjusted to any selected value by choosing the appropriate mixture of the two solvents.

Reiterating the equation proposed by Purnell, for two solvents (A) and (B) in GC (see Figure 4):

$$V'_{AB} = \alpha(V'_A - V'_B) + V'_B \quad [1]$$

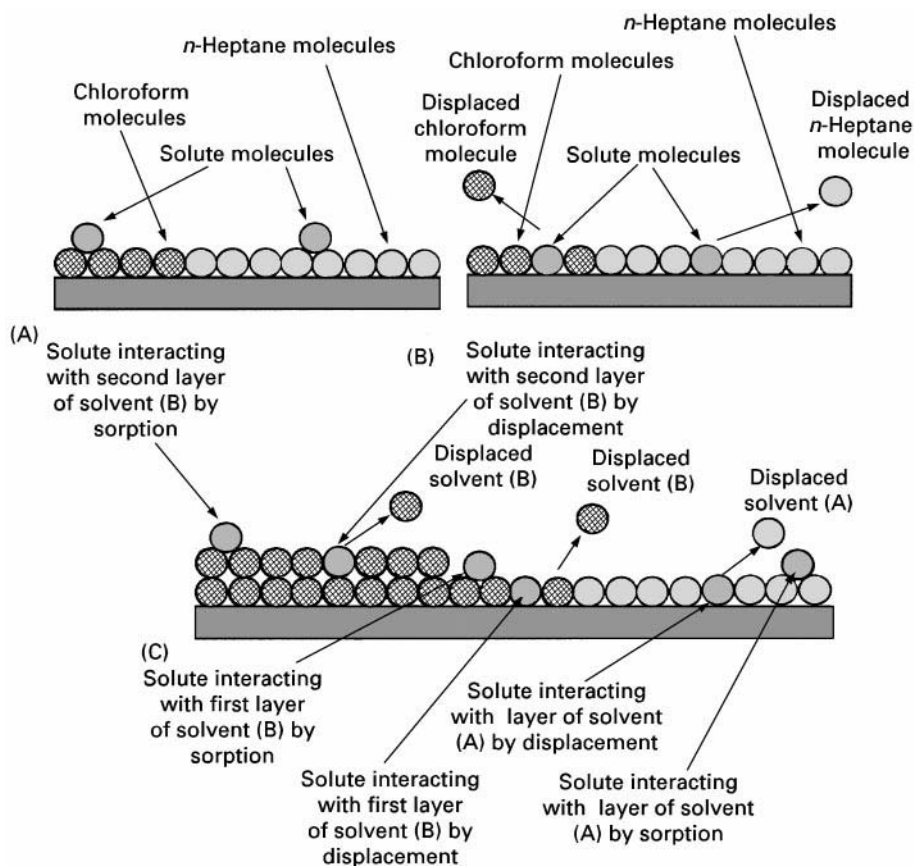


Figure 3 Different forms of molecular interaction with the silica gel surface.

The results of Katz *et al.* can be algebraically expressed in a similar form for LC:

$$K_{AB} = \alpha(K_A - K_B) + K_B \quad [2]$$

For chromatography purposes the product of the distribution coefficient and the volume of stationary

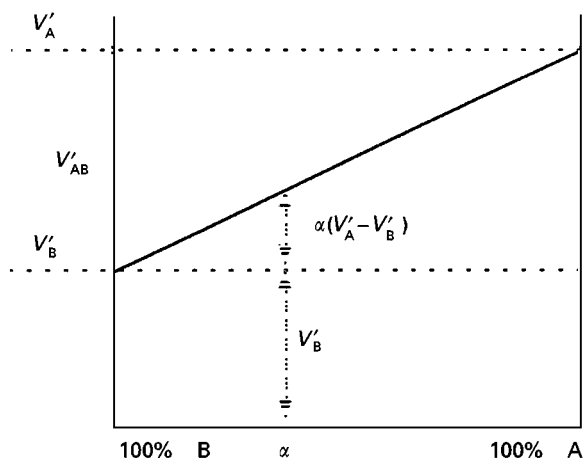


Figure 4 Graph of corrected retention volume against volume fraction of stationary phase.

phase, or stationary phase surface area, gives the corrected retention volume, i.e.:

$$V'_{AB} = K_{AB}\phi, \quad V'_A = K_A\phi \quad \text{and} \quad V'_B = K_B\phi$$

In the experiments of Katz *et al.* (see Figure 5), that validated the relationship given in eqn [4], the distribution coefficients (K) were referred to the solvent phase (mobile phase) whereas in LC it is the mobile phase composition that is changed and the distribution coefficients (K'') are referred to the stationary phase. Thus:

$$K''_{AB} = \frac{1}{K_{AB}}, \quad K''_A = \frac{1}{K_A} \quad \text{and} \quad K''_B = \frac{1}{K_B}$$

or:

$$V''_{AB} = \frac{1}{V'_{AB}}, \quad V''_A = \frac{1}{V'_A} \quad \text{and} \quad V''_B = \frac{1}{V'_B} \quad [3]$$

Substituting for the corrected retention volumes in eqn [3] for inverse phase system:

$$V''_{AB} = \frac{1}{\alpha\left(\frac{1}{V''_A} - \frac{1}{V''_B}\right) + \frac{1}{V''_B}} \quad [4]$$

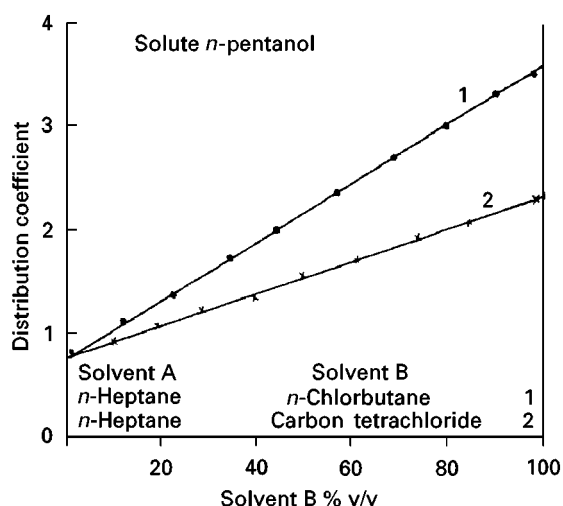


Figure 5 Graphs relating distribution coefficient to solute retention for *n*-pentanol.

Simplifying:

$$V''_{AB} = \frac{V''_A V''_B}{\alpha(V''_B - V''_A) + V''_A} \quad [5]$$

Thus, when $\alpha = 0$, $V''_{AB} = V''_B$ and when $\alpha = 1$, $V''_{AB} = V''_A$.

In practice a more convenient way of expressing solute retention in terms of solvent concentration for a binary solvent mixture as the mobile phase is to use the inverse of eqn [5], i.e.:

$$\frac{1}{V''_{AB}} = \alpha \left(\frac{1}{V''_A} - \frac{1}{V''_B} \right) + \frac{1}{V''_B} \quad [6]$$

If the corrected retention volume in the pure strongly eluting solute is very small compared with the retention volume of the solute in the other pure solvent, i.e. $V''_A \ll V''_B$ which is very often the case in practical LC then eqn [6] simplifies to the simple reciprocal relationship:

$$V''_{AB} = \frac{V''_A}{\alpha} \quad [7]$$

Under these conditions the reciprocal relationship fits experimental data extremely well, particularly at volume fractions below 0.5 of the strongly eluting solute.

In addition, under these conditions the inverse will also apply, i.e.

$$\frac{1}{V''_{AB}} = \frac{\alpha}{V''_A} \quad [8]$$

Equation [8] has been validated by the results from a number of workers in the field and an example of the expected correlation is given by the curves in

Figure 6 for the two enantiomers, (S) and (R) 4-benzyl-2-oxazolidinone. The column chosen was 25 cm long 4.6 mm i.d. packed with 5 μ m silica particles bonded with the stationary phase Vancomycin (Chirobiotic V).

This stationary phase is a macrocyclic glycopeptide Vancomycin that has a molecular weight of 1449.22, and an elemental composition of 54.69% carbon, 5.22% hydrogen, 4.89% chlorine, 8.70% nitrogen and 26.50% oxygen. Vancomycin is a strongly polar stationary phase which contains 18 chiral centres surrounding three 'pockets' or 'cavities' which are bridged by five aromatic rings and thus can readily offer unique enantiomeric selectivity to a wide range of chiral substances. The column was operated in the normal phase mode using mixtures of *n*-hexane and ethanol as the mobile phase. Equation [7] is unambiguously validated by the curves relating the corrected retention volume to the reciprocal of the volume fraction of ethanol shown in Figure 6. It is also seen that an excellent linear relationship is obtained with an index of determination very close to unity.

Although silica gel was taken as an extreme example of a normal phase system, any stationary phase that is polar in nature (bonded silica or polymer based), when used with a predominantly dispersive solvent as the mobile phase, will constitute normal phase chromatography. Expressed in a slightly different way, although the interactive mechanism can be extremely complex and difficult to quantitatively predict, if the prevailing forces in the stationary phase are polar and the eluting forces in the mobile phase

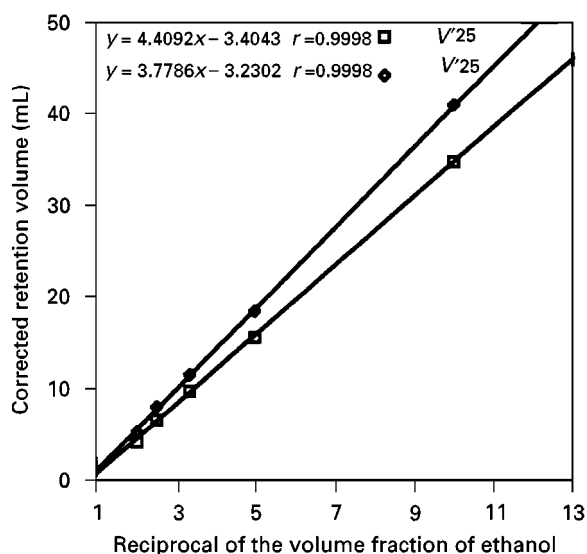


Figure 6 Graph of corrected retention volume of the enantiomers of 4-benzyl-2-oxazolidinone against the reciprocal of the volume fraction of ethanol.

are predominantly dispersive then it is a normal phase system. In practice, normal phase systems are used to separate mixtures of polar substances; they are largely ineffective in separating substances that are largely or exclusively dispersive. For reversed phase chromatography, the converse applies.

See also: II/Chromatography: Liquid: Column Technology; Theory of Liquid Chromatography.

Further Reading

- Hurtubise RJ, Hussain A and Silver HF (1981) *Analytical Chemistry* 53: 1993.
Katz ED, Ogan K and Scott RPW (1986) The distribution of a solute between two phases. *Journal of Chromatography* 352: 67.

- Laub RJ (1983) *Physical Methods in Modern Chromatographic Analysis*, Chapter 4. New York: Academic Press.
Laub RJ and Purnell JH (1975) *Journal of Chromatography* 112: 71.
McCann M, Purnell JH and Wellington CA (1980) *Proceedings of the Faraday Symposium, Chemical Society*, 83.
McCann M, Madden S, Purnell JH and Wellington CA (1984) *Journal of Chromatography* 294: 349.
Robbins WK and McElroy SC (1984) *Liquid Fuel Technology* 2: 113.
Scott RPW and Kucera P (1978) Solute-solvent interactions on the surface of silica gel. *Journal of Chromatography* 149: 93.
Scott RPW and Kucera P (1978) Solute-solvent interactions on the surface of silica gel II. *Journal of Chromatography* 149: 93.

Mechanisms: Reversed Phases

R. P. W. Scott, Avon, CT, USA

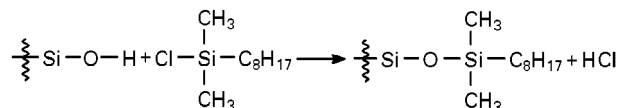
Copyright © 2000 Academic Press

Introduction

In the early days of liquid chromatography (LC), the most commonly used stationary phase was silica gel, which was usually loaded with water and employed with a hydrocarbon mixture such as petroleum ether as the mobile phase. To change the selectivity of the distribution system, the hydrocarbon was sometimes adsorbed on the silica, and water or an aqueous alcohol mixture was used as the mobile phase. For obvious reasons, the latter was termed a reversed-phase system. Since that time, the reversed phase has been defined in a number of different ways: in this article, it is regarded as consisting of hydrocarbon moieties chemically bonded to a silica matrix. Reversed phases are considered to exhibit predominantly dispersive interactions with any solute or solvent with which they are in contact.

The first reversed phase was synthesized by Hálasz and Sebastian in 1969 by refluxing silica with a suitable alcohol (e.g. *n*-octanol) to form the silyl ester, the hydrocarbon chain being linked to the silica by carbon-oxygen-silicon bonds. This bonding proved to be labile, as the hydrocarbon moiety was easily removed by hydrolysis, but was sufficiently stable to allow the potential of such phases to be established. The next year Kirkland and DeStefano used chlorosilane reagents to attach the hydrocarbon chain to the

silica by a silicon-oxygen-silicon bond which proved to be far more stable, at least between pH 4 and pH 8.



Subsequently, other silyl reagents, such as the silyl esters, were also shown to react with silica. Some of these reagents are now commonly used in the production of reversed phases.

Brush Phases

There are three basic types of bonded phases which are produced by the use of the mono-, di- and tri-substituted silanes: brush phases, oligomeric phases and bulk phases. For example, the monochlorosilanes (e.g. octyldimethylchlorosilane) react with the hydroxyl groups on the silica surface to produce dimethyloctylsilyl chains attached to the silica. The alkyl chains are thought to stand out from the surface like the bristles of a brush, hence the term brush phase. After reaction, the material is usually treated with trimethylchlorosilane or hexamethyldisilazane to eliminate any remaining unreacted hydroxyl groups. This procedure is called capping the bonded phase.

The extent to which the silyl groups are reacted is still a subject of some debate. It is thought that the two methyl groups next to the silicon atom of the silyl reagent hinder reaction with adjacent hydroxyl groups on the silica gel surface. Consequently, a considerable amount of unreacted hydroxyl groups will

remain between the bonded moieties even after capping. It has also been suggested that one hydroxyl group may remain situated between each bonded chain. There is certainly evidence of some polar interactions with reversed phases which, if completely covered with hydrocarbon chains, should only exhibit dispersive interactions. However, all reversed phases are predominantly dispersive in character, and it would appear that if there are any hydroxyl groups still present on the surface, their influence on retention is relatively small compared with that of the bonded moieties. However, the residual hydroxyl groups, being strongly polar, can cause separation problems under certain circumstances and thus methods that reduce their effect have been developed and will be discussed later.

Oligomeric Phases

The di-substituted silanes such as methyloctyldichlorosilanes produce oligomeric bonded phases but this involves a more complicated procedure. The silica is first reacted with methyloctyldichlorosilane to link methyloctylchlorosilyl groups to the surface. The product is then treated with water, which hydrolyses the methyloctylchlorosilyl groups to methyloctylhydroxysilyl groups with the elimination of hydrochloric acid. The hydroxy product so produced is then reacted with more methyloctyldichlorosilane, attaching another methyloctylchlorosilyl group to the previous groups. This process of alternately treating the product with the silane reagent and then water can be repeated until eight, 10 or more oligomers are linked to each other and attached to each sterically available hydroxyl group on the surface. It should be noted, however, that hydroxylation of the bonded moiety is not the only possible reaction that can take place with the water. There will be situations where it will be sterically possible for a water molecule to react with two adjacent chains and thus produce some cross-linking. However, a small amount of cross-linking would indeed strengthen the bonded system and could be advantageous.

The product is finally treated with trimethylchlorosilane, or some other capping reagent, to eliminate the last hydroxyl groups formed at the end of the oligomer. The oligomers are layered over the surface and this helps to exclude solutes from interaction with any residual surface hydroxyl groups, making the product extremely stable with almost no polar characteristics. However, due to the complexity of the synthesis (which, ideally, needs to be carried out in a fluidized bed for efficient reaction), oligomeric phases are expensive to manufacture and, consequently, are not generally available.

Bulk Phases

The trichlorosilanes (e.g. octyltrichlorosilane) bond dichlorosilyl moieties to the surface and, in the presence of water, or if water is added, cross-linking occurs and a polymeric hydrocarbon stationary phase is produced. The same procedure can be used as that in the synthesis of oligomeric phases. The silica can be alternately treated with water and the trichlorosilane reagent. Layers of bonded phase are built up on the surface with extensive cross-linking, which produces a multilayer polymeric phase that has been termed a bulk phase. The bulk phases are almost as popular as the brush phases as they tend to have a higher carbon content (more organic material bonded to the surface) and thus provide a greater retention and selectivity. Bulk phases have about the same stability to aqueous solvents and pH as the brush phases.

The residual polarity of the bonded phase arising from the unreacted hydroxyl groups can cause peak tailing under certain circumstances. Consequently, it would be highly desirable to remove them or, at least reduce their effect on solute retention, particularly when present in brush phases. This was partly achieved by Kirkland who used reagents with larger base side chains (e.g. dipropyloctylchlorosilane as opposed to dimethyloctylchlorosilane) which linked a dipropyloctylsilyl group to the surface silicon atom. The larger propyl groups close to the silica surface tended to screen the adjacent hydroxyl groups sterically and thus significantly reduced their interactive availability. This, in turn, reduced their effect on retention. All three types of reversed phase are fairly stable, at least between pH 4 and pH 8 and at ambient temperature. The phase stability decreases as the temperature is raised: to some extent this can be overcome by introducing a phenyl group in the hydrocarbon chain.

Both brush and bulk reversed phases are commonly used in liquid chromatography, but the brush phase, although providing less retention for a given stationary phase loading, appears to be easier to manufacture in a reproducible form. Reversed phases are produced commercially with a range of chain lengths. Commonly available brush reversed-phase chain lengths range from a single carbon (using trimethylchlorosilane or ester as the reagent) to C₃₀.

In general, the retention of a solute increases linearly with the carbon content of the reversed phase, as shown in **Figure 1**. It is seen, however, that the brush phases and the bulk phases fall on different lines. The bulk phases both contain C₁₈ chains but with different degrees of reaction; the ODS has a significant number of the hydroxyl groups unreacted. It appears that the hydrocarbon chains in the bulk

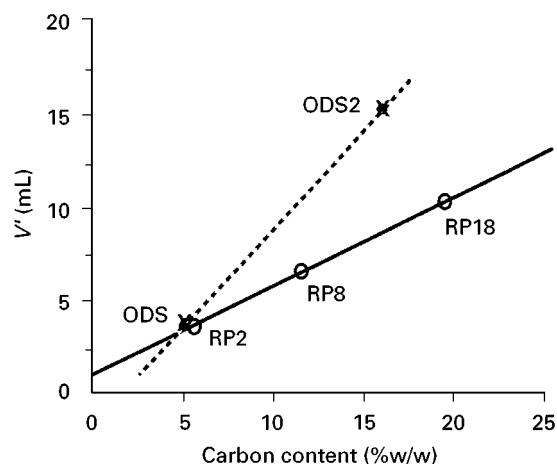


Figure 1 Graph of retention volume (V') against carbon content (%w/w). ODS and ODS2, C_{18} bulk-reversed phases. RP2, RP8 and RP18, C_2 , C_8 and C_{18} brush-reversed phases.

material are more available to the solute than in the brush material, indicating that in the bulk phases, the polymeric material might have a fairly open structure. The brush phases were fully reacted (although, as already discussed, some hydroxyl groups will still be present) and it is seen that retention increases linearly with the chain length.

Reversed phases with long chains and high retention properties, although apparently desirable due to their high selectivity, are not always appropriate. For example, the strong dispersive interactions exhibited by these phases can cause irreversible retention of proteins and other biopolymers, usually accompanied by denaturation. As a result, the C_2 and C_4 phases are very popular in the biotechnology field. In con-

trast, the separation of complex mixtures of stable compounds such as essential oils, fatty acids, pesticides, herbicides and the host of other mixtures produced and used in industry today are best achieved using the longer chain materials.

Particle Shape and Size

Originally, reversed phases were produced from irregularly shaped particles of silica which, after air jet grinding was introduced, were well rounded but not perfectly spherical in shape. The silica was cleaned by various washing procedures to remove heavy metals that were thought to cause peak tailing. This material, when converted to a reversed phase, packed well and provided columns of the expected efficiency (*c.* $L/1.6dp$, where L is the column length and dp the particle diameter). The introduction of spherical silica, which was claimed to pack more easily and was manufactured from silica of greater purity, has now largely replaced the irregular silica. In fact, the retentive properties and efficiencies derived from the spherical silica do not seem to be strikingly different from those produced from irregular silica, if packed properly.

Reversed phases are mostly produced in four particle sizes: 3, 5, 10 and 20 μm . The 3 μm material is usually provided in columns 3 or 5 cm long, giving about 5000 and 8000 theoretical plates respectively. These columns can be operated at 1–2 mL min^{-1} and thus provide fairly fast separations. The 5 μm packings are usually supplied in columns 5 and 10 cm long and the 10 μm particles in columns 10 and 20 cm long. A column 20 cm long packed with 10 μm particles can be expected to provide efficiencies of about 12 000 theoretical plates at a flow rate of 1 mL min^{-1}

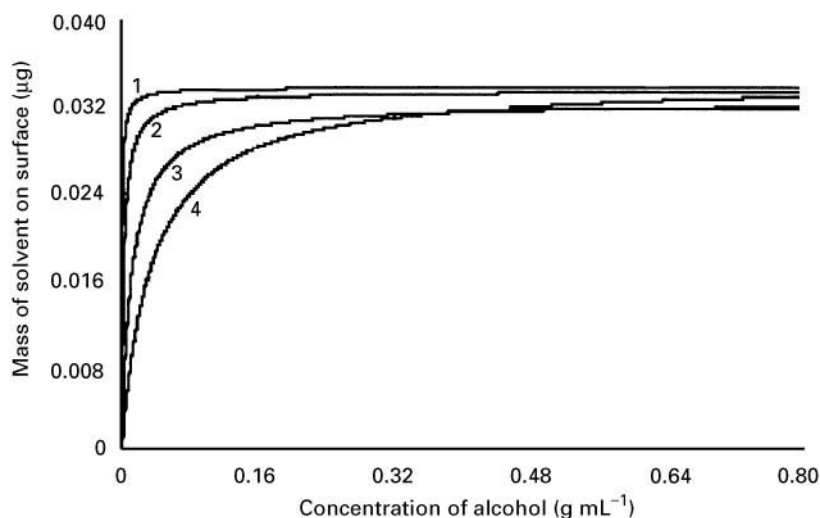


Figure 2 The adsorption isotherms for some aliphatic alcohols on a reversed phase. 1, Butanol; 2, propanol; 3, ethanol; 4, methanol. (Reproduced with permission from Scott, 1993.)

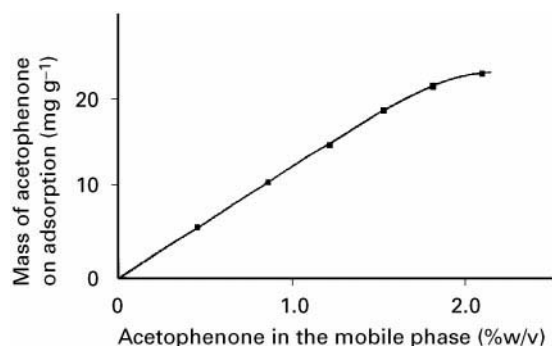


Figure 3 The adsorption isotherm of acetophenone between a reversed phase and an aqueous solvent mixture containing 40.4%w/v acetonitrile. (Reproduced with permission from Scott and Kucera, 1977.)

and is thus very useful in the separation of complex mixtures. The 20 μm packing is almost exclusively used for preparative columns.

Reversed-phase columns are slurry packed, usually employing a methanol–water mixture or ethanol as the packing solvent. There are many proprietary solvent mixtures used in packing reversed-phase columns and the technique has assumed an artificial cloak of mystery. The important aspect of packing is to use a wetting agent (there are many that can be

used successfully) to ensure the particles do not clump together in the packing solvent but are completely dispersed. This can be checked under a low powered microscope. The packing, dispersed in the solvent and wetting agent (often by sonic vibration), is packed by suddenly applying about 8000 psi pressure to the particle dispersion contained in a high pressure reservoir, forcing the slurry through the column; the packing is retained by an appropriate terminal frit.

Interactions on the Surface of Bonded Phases

Solute interactions with the stationary phase in LC, differ from those in gas chromatography (GC) due to the preponderance of solvent that is concurrently interacting with the surface. In fact, in LC, the solute and the solvent interact in exactly the same manner with the stationary phase, but the concentration of the solvent is many orders of magnitude greater than that of the solute. Consequently, an equilibrium arises between the solvent and the stationary phase which is perturbed by the passing presence of the solute. It has been well established that solvents are adsorbed on the surface of a bonded phase as mono- or binary layers according to the Langmuir adsorption isotherm. The equation for the Langmuir adsorp-

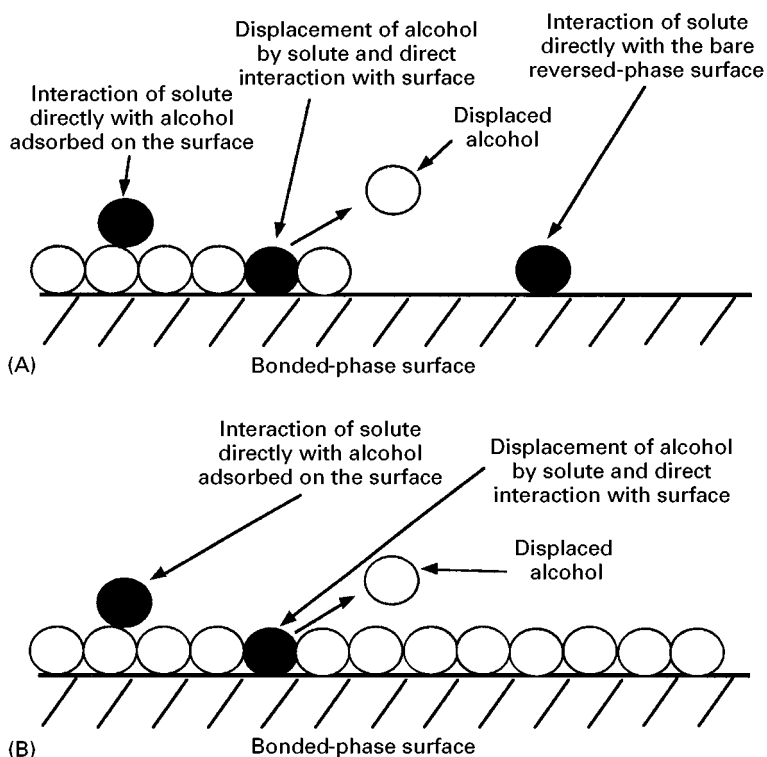


Figure 4 Alternative forms of solute interaction with the surface of a reversed phase. (A) Surface incompletely and (B) surface completely covered with solvent molecules. Open circles, alcohol; filled circles, solute.

tion isotherm of a monolayer is as follows:

$$\alpha = \frac{ac}{b + ac}$$

where α is the fraction of the surface covered by the solute, c is the concentration of the solute in the mobile phase, and a and b are constants.

At high concentrations α becomes unity and the surface is completely covered with the more strongly adsorbed solvent. An example of the monolayer adsorption isotherms of some aliphatic alcohols from their aqueous solutions is shown in Figure 2.

It is seen that the most polar alcohol, methanol, does not saturate the surface until the methanol concentration of the mobile phase is in excess of 30%. In contrast, the surface is completely covered with the more dispersive alcohol, butanol, when its concentration is less than 5%.

In reversed-phase chromatography, aqueous solutions of organic solvents such as methanol and acetonitrile are usually employed as the mobile phase. Consequently the solute molecules will also exhibit Langmuir-type adsorption isotherms when interacting with the surface of a phase. An example of the adsorption isotherm of acetophenone between a mobile phase containing 40.4% v/v acetonitrile (the concentration at which the reversed phase is completely wetted by the solvent) and the phase surface covered with adsorbed solvent is shown in Figure 3.

Only the initial approximately linear part of the isotherm is shown, indicating that the adsorption process is similar to that exhibited by the mobile-phase solvent. It is clear that the solute can interact with the reversed phase in a number of ways depending on the equilibrium conditions that exist between the solvent in the mobile phase and the surface. The alternative forms of interaction are depicted in Figure 4.

In the first case, where the concentration of the solvent is insufficient to cover the entire surface, the solute can interact directly with the uncovered surface, interact with the solvent molecules covering the surface or displace a solvent molecule and interact directly with the surface. All these alternatives will occur during the passage of the solute through the column. In the second case, where the concentration of the solvent is sufficient to ensure that the surface is covered with the solvent molecules, the solute can only interact with the solvent molecules covering the surface, or displace a solvent molecule and interact directly with the surface. The latter can only occur if the interaction energy between the solute and bonded moiety is greater than that between the solute and the adsorbed solvent.

It is seen that the interaction of the solute with the reversed phase can be quite complex and will depend not only on the nature of the solute itself, but on both the nature and concentration of the solvent in the mobile phase. It is clear that a ternary solvent system would be even more complex, and if the solvent composition is changed during development (as in gradient elution) the distribution system at any particular concentration, although possible to calculate from adsorption isotherm data, can be a very complicated procedure indeed.

Applications

Reversed phases are the most commonly used stationary phases in contemporary LC and are employed in over 65% of all analytical applications. They are largely used with water as a component of the mobile

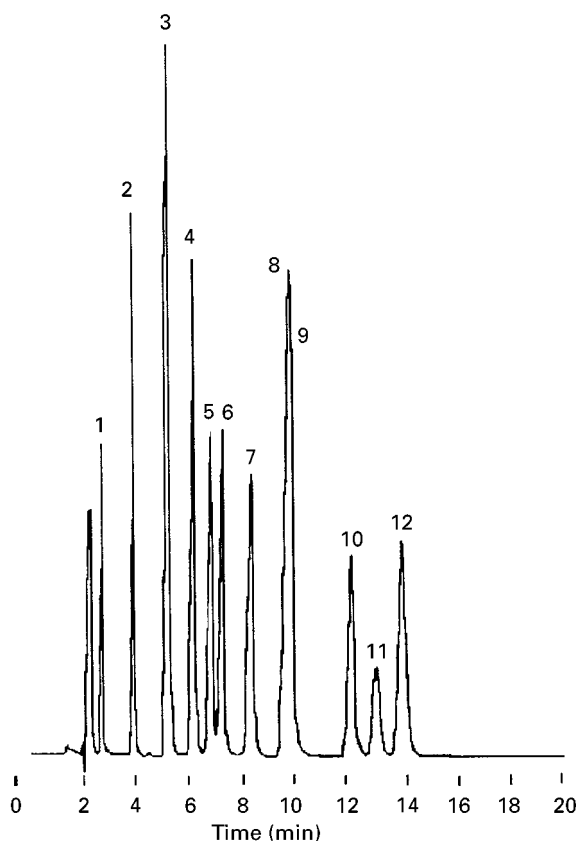


Figure 5 Separation of a sample of explosives. Column: 25 × 4.6 mm i.d. packed with C₁₈ reversed phase. Particle diameter 5 μm. Solvent methanol–water, 50/50 at a flow rate of 1.5 mL min⁻¹. Sample volume 100 μL. 1, HMX (1 μg mL⁻¹); 2, RDX (1 μg mL⁻¹); 3, 1,3,5-trinitrobenzene (2 μg mL⁻¹); 4, 1,3-dinitrobenzene (10 μg mL⁻¹); 5, 2,4,6-trinitrotoluene (1 μg mL⁻¹); 6, tetral (1 μg mL⁻¹); 7, nitrobenzene (1 μg mL⁻¹); 8, 2,6-dinitrotoluene (2 μg mL⁻¹); 9, 2,4-dinitrotoluene (1 μg mL⁻¹); 10, 2-nitrotoluene (0.1 μg mL⁻¹); 11, 4-nitrotoluene (0.5 μg mL⁻¹); 12, 3-nitrotoluene (0.1 μg mL⁻¹).

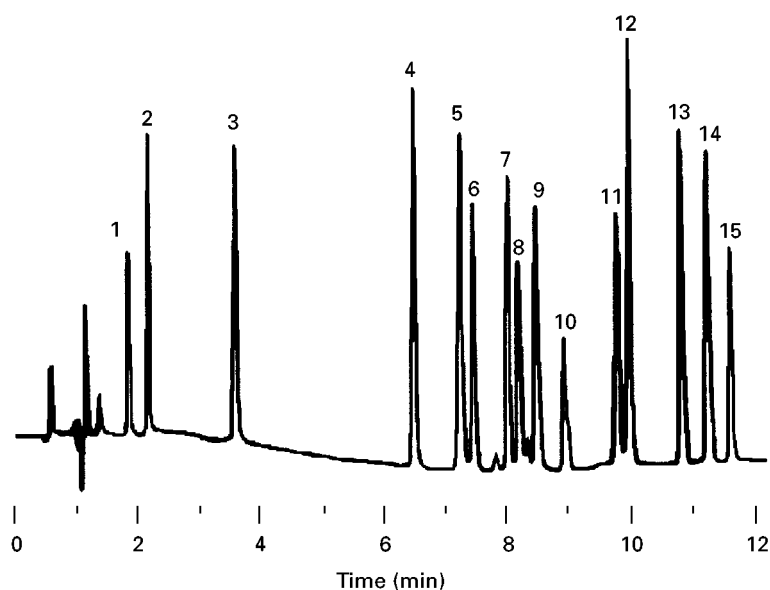


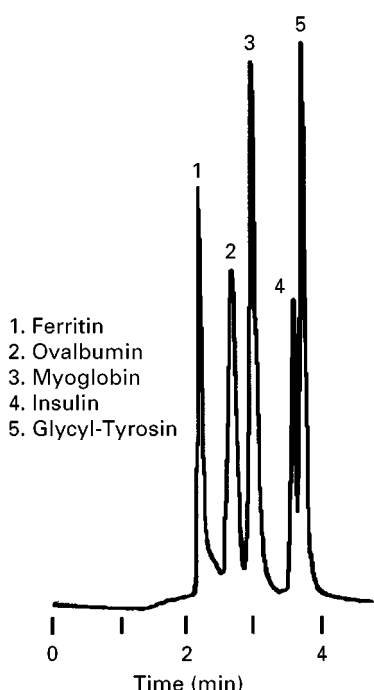
Figure 6 Separation of some urea pesticides on a C_8 reversed-phase column. Column LC 8 reversed phase, 15 cm long, 4.6 mm i.d., 5 μ m particles used with a mobile-phase gradient of 18 : 82 acetonitrile–water to 65 : 35 to acetonitrile–water in 9 min. 1, Methomyl; 2, oxamyl; 3, fenuron; 4, manuron; 5, carbofuran; 6, propoxur; 7, carbaryl; 8, fluometuron; 9, duron; 10, propham; 11, siduron; 12, linuron; 13, chioprophan; 14, barban; 15, neburon.

phase, in binary, ternary and occasionally quaternary mixtures with aliphatic alcohols, nitriles and ethers, e.g. methanol, acetonitrile and tetrahydrofuran. They are also used with ion-pairing reagents in ion chromatography where the reagent is adsorbed as an interactive layer on the surface of the stationary phase. The mechanism of ion-pairing reagents is complex and will be discussed elsewhere.

Reversed phases are used in industrial product quality control, environmental testing, clinical analyses, biotechnological assays, forensic examination and many research programmes. Numerous examples of the use of reversed phases are included elsewhere in this book: some will be given here to illustrate the types of separation possible using predominantly dispersive interactions with the stationary phase. An example of an environmental or forensic type of application is given in **Figure 5**. The separation was carried out on an octadecyl bonded phase using a 50% v/v methanol–water mixture as the mobile phase. The selectivity of the dispersive stationary phase is clearly demonstrated, the more polar materials having strong polar interactions, with the strongly polar mobile phase being eluted first. In contrast, the relatively strong dispersive interactions of the monosubstituted toluenes with the reversed phase cause them to be eluted last. It is also seen that the explosive components are well resolved and detected quantitatively (mostly at the sub-microgram level) with no difficulty. Some samples can be separated by

weaker dispersive interactions using reversed phases with shorter chains. An example of the use of a C_8 reversed phase for the separation of a number of carbamate and urea pesticides is shown in **Figure 6**. The separation is achieved using a gradient that starts with a highly polar binary aqueous mixture containing only 18% v/v acetonitrile to a moderately polar solvent mixture containing 65% v/v acetonitrile. It is seen that excellent separation is obtained in only 12 min.

As discussed earlier, the use of dispersive interactions to separate biologically labile compounds demands the use of short chain length reversed phases to prevent irreversible adsorption and/or solute denaturation. An alternative approach is to use one of the polar bonded phases in a manner where the dispersive interactions dominate but not sufficiently to cause strong adsorption. The amino or diol polar phases have been used in this manner to separate protein and protein-like materials and an example is given in **Figure 7**. It is seen that water containing no solvent is used as the mobile phase, which virtually completely negates the polar interactive capability of the polar stationary phase. The only significant interactions remaining are those with the dispersive moieties of the bonded material. This results in only weak interactions between the solutes and the stationary phase and the separation is attained without significant tailing (a symptom of strong adsorption) or denaturation.



An LC-Diol column, 25 cm long and 6.2 mm I.D. and a Mobile Phase of 0.1 M Potassium Phosphate Buffer at pH 6.8

Figure 7 The separation of some proteins on a polar phase used in the reversed phase mode.

Due to limited pressure available in liquid chromatographs, which is not constrained by pump design but rather by other parts of the chromatograph (in particular the sample valve), the reduction in particle diameter of a column packing is limited in practice. Small particles can only be used with shorter columns, which results in reduced separation times but not an increase in the attainable column efficiency. The shorter columns packed with very small particles also produce extremely small peak volumes that place serious constraints on the sample system and in particular the detector sensor cell. Although in the research laboratory, particles having diameters less than 1 μm may well be developed and their efficacy demonstrated, their general use in analytical laboratories will be very limited for some years to come. Due to the versatility and wide range of operating variables available, difficult separations are more easily achieved by using procedures other than by reducing the particle size to a level where practical difficulties become paramount.

Reversed phases are probably the most effective and popular stationary phases in use today. However, stationary phases employing bonded silica may well

not be the best form of reversed stationary phase to use in the future. The great disadvantage to silica-based stationary phases is their instability in aqueous solvents, particularly at extreme pH. The future stationary phases that will be used in LC are more likely to be some form of macro-reticulated polymeric materials that have been developed and are already quite widely used. These polymeric particles can be prepared with significant surface area and porosity and are extremely inert and stable in aqueous solvent mixtures at the extremes of pH. They can also be prepared with a wide range of polarities linking different chemical groups to their surface and by using different polymer bases.

See also: **II/Chromatography: Liquid:** Column Technology. **III/Pharmaceuticals:** Basic Drugs: Liquid Chromatography. **Porous Polymers:** Liquid Chromatography.

Further Reading

- Buszewski B, Jezierska M, Welniak M and Berek D (1998) Survey of trends in the preparation of chemically bonded silica phases for liquid chromatographic analysis. *Journal of High Resolution Chromatography* 21: 267–281.
- Dorsey JG and Cooper WT (1994) Retention mechanisms of bonded-phase liquid chromatography. *Analytical Chemistry* 66: 857A–867A.
- Kirkland JJ and DeStefano JJ (1970) Controlled surface porosity supports with chemically-bonded organic stationary phases for gas and liquid chromatography. *Journal of Chromatographic Science* 8: 309.
- Kirkland JJ and Henderson JW (1994) Reversed-phase HPLC selectivity and retention characteristics of conformationally different bonded alkyl stationary phases. *Journal of Chromatographic Science* 32: 473.
- Kirkland JJ, Adams JB, van Straten MA and Claessens HA (1998) Bidentate silane stationary phases for reversed phase high-performance liquid chromatography. *Analytical Chemistry* 70: 4344–4352.
- Nawrocki J (1997) The silanol group and its role in liquid chromatography. *Journal of Chromatography A* 779: 29–71.
- Neue UD (1997) *HPLC Columns. Theory, Technology and Practice*. New York: Wiley-VCH.
- Sander LC and Wise SA (1987) Recent advances in bonded phases for liquid chromatography. *CRC Critical Reviews in Analytical Chemistry* 18: 299–415.
- Scott RPW (1993) *Silica Gel and Bonded Phases*. Chichester: Wiley.
- Scott RPW and Kucera P (1977) Examination of five commercially available liquid chromatographic reversed phases (including the nature of the solute-solvent-stationary phase interactions associated with them). *Journal of Chromatography* 142: 213.

Mechanisms: Size Exclusion Chromatography

S. Holding, RAPRA Technology Limited,
Shrewsbury, UK

Copyright © 2000 Academic Press

Introduction

Size exclusion chromatography (SEC), also known as gel permeation chromatography (GPC), is a particularly valuable tool in the measurement of the molecular weights and molecular weight distributions of polymers. There are a number of variations on the basic technique to accommodate the requirements of different polymer types and to elicit additional information. This article seeks to describe the basic technique with particular comment to the often under-appreciated limitations together with detailed comment on the main variations to the basic technique. The relationship between SEC and other techniques for polymer molecular weight techniques will be summarized.

As examples of the technique, Figure 1(A) is an overlay plot of the computed molecular weight distributions for a range of extrusion grades of polystyrene from various producers and Figure 1(B) illustrates the variation in molecular weight for a series of poly(methylmethacrylate) (PMMA) materials polymerized under different conditions. The descriptions in this article will normally relate to the general practice in the use of SEC with polymers soluble in the normal organic solvents. Some comments will also be made on the aqueous-based SEC of processable polymers. Biopolymers, such as polypeptides and proteins are also examined using SEC, but the consideration of appropriate buffers and column packings has not been considered appropriate for separate comment.

SEC – The Basic Technique

SEC is a specific form of liquid chromatography where the only fundamental difference is in the column packing and the separation mechanism. However, the particular requirements of SEC are somewhat different to most other forms of liquid chromatography giving rise to various aspects in the choice of instrumentation, data handling and general practical philosophy.

SEC Columns and the Separation Mechanism

In SEC, the polymer molecules are separated as a function of their size in solution. The column pack-

ings are porous and the separation is achieved according to the degree of access of the polymer molecules to the pores.

The solvent in the column packing pores can be considered as the stationary phase and the interstitial solvent as the mobile phase. A distribution coefficient is established by which the time spent in the pores, or stationary phase, is dependent upon the solvated size of the polymer molecules and on the pore geometry. Since the larger molecules are more restricted in the pore volume available to them, the larger molecules spend less time in the stationary phase and are eluted first; smaller molecules are effectively retarded and elute later.

It is fundamental to SEC that no other separation mechanism (e.g. adsorption) is occurring. As a consequence, the maximum elution volume available to achieve separation is the total pore volume. Molecules which are so large that they are totally excluded from the pores will elute at a volume corresponding to the interstitial or 'void' volume while molecules which can permeate all of the pores will elute at a volume corresponding to the void volume plus the pore volume. Anything eluting at a greater volume than this must be retarded by some additional mechanism.

With consideration to the above requirements, the materials used for SEC column packings are mainly selected for their pore geometry and lack of other interaction with the polymer molecules. In many solvent systems, the potential for adsorption limits the applicability of inorganic packings and polymeric packings are the more usual choice. The bulk of all SEC work with synthetic polymers is carried out using column packings produced from polystyrene, cross-linked with divinylbenzene. In the production of these materials, the pore geometry is manipulated to give variation in pore size and hence 'tailored' to suit particular molecular mass ranges.

In addition to pore size and inertness, the normal chromatographic relationships between packing size and efficiency are applicable but, as noted later, there are limitations to using too small a packing size with the higher molecular weight polymers.

SEC column packings are normally produced with a limited polymer molecular weight applicability but it has been normal practice to use a number of different columns (with specific pore sizes) in series to give an acceptably wide molecular weight range. Typically, to cover a molecular weight range of 2000 to 2 000 000, a bank of columns such as 1×10^3 Å, 1×10^4 Å, 1×10^5 Å and 1×10^6 Å would be used.

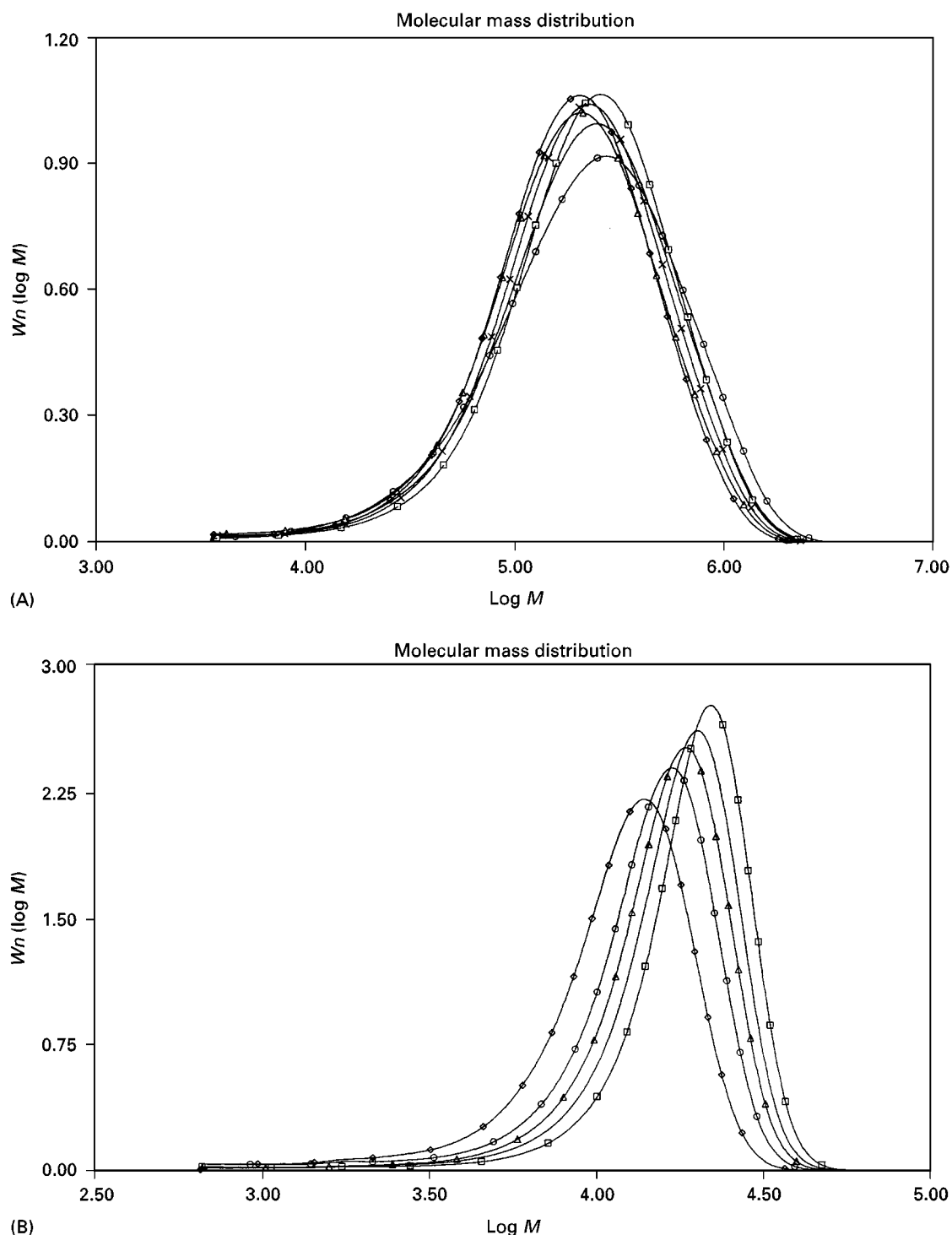


Figure 1 An overlay plot of the computed molecular weight distributions for a range of extrusion grades of polystyrene from various producers.

(The identification of pore size expressed in angstroms is common practice but potentially misleading, since the dimension refers to maximum extended polymer chain length, rather than actual pore size.)

There is potential for using an inappropriate combination of column packings and it is now becoming more common to obtain single columns which the manufacturer has filled with different porosity packings to give a wide molecular weight range. This

'mixed-bed' approach also gives an optimal combination of packing porosities such that a 'linear' calibration is obtained (see later). Even with the mixed-bed approach, a number of columns will normally need to be combined to achieve an acceptable peak capacity.

Efficiency and Resolution

The factors generally affecting column efficiency in other forms of liquid chromatography also apply to SEC, and column efficiency is calculated and expressed in the normal manner. The efficiency as calculated for a specific low molecular weight compound (e.g. an added solvent) will normally be higher than for a truly monodisperse polymer and the efficiency is normally reported for a solvent peak.

The resolution of two given monodisperse components can be sensibly expressed in a similar manner as for other forms of liquid chromatography but in SEC it is also possible to define a 'specific resolution' which relates to the theoretical resolution of two monodisperse polymers having one decade difference in molecular weight. The specific resolution will be dependent upon the gradient of the calibration (as expressed by log molecular weight versus elution volume). If the calibration is linear (on the log molecular weight scale) then the specific resolution will be constant across the molecular weight range.

Column Packing Size and Shear Effects

For some time the normal column packing particle size available has been around 10 μm but, in common with other forms of liquid chromatography, there has been a trend towards increasing the efficiency by producing smaller particle size packings. However, when working with high molecular weight polymers, the higher linear flow velocity associated with the smaller packing sizes can cause shear degradation of the polymer and the particle size must be selected to suit the molecular weight of the sample polymer. The 10 μm material is appropriate for a very wide range of molecular weights but additional efficiency can be obtained by using 5 μm packing for polymers with moderate molecular weights (ca. 10 000 to 100 000) and 3 μm packings can be used for lower molecular weights. For very high molecular weight polymers (ca. > 2 000 000) the use of larger packing size (e.g. 20 μm) should be considered. Where there is potential for shear degradation, lower solution concentrations and lower flow-rates can also reduce this unwanted effect.

SEC Pumps and Flow-Rate

Normal isocratic HPLC pumps are used for SEC work but the requirements for good control of the

flow-rate are probably more severe. Since in SEC, it is an envelope of a multitude of different molecular weight peaks that is being measured, it is not possible to set an identification window and any small variation in flow rate will produce an error in the molecular weight calculation. Variation in flow-rate can be allowed for by the use of an internal marker. For a typical polystyrene, a deliberate correction of the flowrate by 0.2% produces a variation in the calculated weight average molecular weight from 308 000 to 320 000; a variation of approximately 4%.

SEC Concentration Detectors and Sample Concentration

A number of detector types for specific additional information will be considered later but the most basic SEC application requires a concentration detector to monitor the polymer as it emerges from the column.

The most common form of concentration detector encountered in SEC is a differential refractive index (DRI) detector. These detectors are a cost-effective option which are nearly universal in application but they have limited sensitivity and require a very good temperature control. Since SEC is normally used to look at bulk components (rather than trace components), the poor sensitivity is not normally a problem but some difficulties may be encountered where the differential refractive index for the polymer/solvent combination is so small that baseline noise becomes significant.

The other universal detector used in SEC is the ELSD (evaporative light scattering detector, also known as an evaporative mass detector). These units involve atomization of the eluent into a steady flow of inert gas where the solvent is removed and the remaining solute particles are detected by the light scattering they induce. It is important to distinguish between these ELSD and the light scattering from solutions considered later. The ELSD is more expensive than DRI detectors and there are potentially high running costs for the large amount of inert gas consumed. However, they are less affected by any variation in solvent composition or temperature and are more universal in the size of the response regardless of chemical composition of the polymer.

Figure 2 is a schematic diagram of a commercially available evaporative light scattering detector.

Other types of HPLC detector (such as ultra-violet, infrared or radiochemical) are also used for SEC but are more restricted in applicability and are used more as selective detectors to pick out specific components. There are latter comments with regard to the SEC of copolymers.

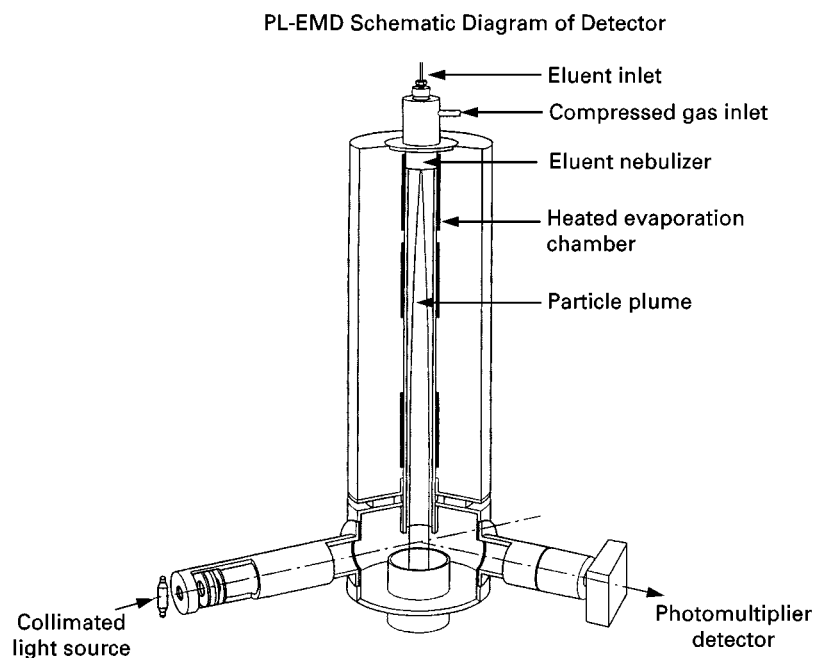


Figure 2 A schematic diagram of a commercially available evaporative light scattering detector. Printed with the permission of Polymer Laboratories Ltd, Church Stretton, Shropshire, UK.

Detector Response to Low Molecular Weight Components

The differential refractive index for a polymer/solvent combination is normally independent of molecular weight at high molecular weight. However, while it is generally known that the refractive index detector response varies with low molecular weight polymers this variation is commonly ignored. As a consequence, SEC results for polymers containing low molecular weight material often do not give an appropriate consideration to the low molecular weight components; this has important implications for many legislative requirements for defining the proportion of low molecular weight material present.

The variation in refractive index response with molecular weight is presumed to be due to the increasing influence of end groups and it seems probable that there are similar effects with most other detector types. For the evaporative light scattering detector, there is similarly the possibility that the more volatile components are lost with the solvent.

SEC Calibration and Data Handling

For SEC a calibration must be obtained by running polymers of known molecular weight. The more usual practice is to run a series of calibrants of very narrow molecular weight distribution (often described as being monodisperse) and known peak molecular weight (M_p) and obtain a calibration of log

M_p versus elution volume. Alternatively, there are procedures for using broad molecular weight distribution calibrants, where the molecular weight distribution is well defined.

In practice, the most commonly used calibrants consist of narrow distribution polystyrenes, and a wide range of these is commercially available. A small range of other polymer types of narrow distribution calibrants is also available but usually with a restricted molecular weight range. The availability of well-defined broad molecular weight distribution calibrants is extremely limited.

The log M_p versus elution volume calibration is usually expressed by an equation which can be a simple linear expression or a polynomial. The software will frequently allow an excellent fit by using a high order polynomial but it is questionable whether an order of three should ever be exceeded. In practice, reasonable good fits are normally obtained using first, second or third order curves but even for third order fits, the potential for variation at low molecular weight, affecting the high molecular weight end of the distribution, is intrinsically present.

The calculation of molecular weight averages and plotting molecular weight distributions from a sample chromatogram and calibration is complex and the use of laboratory computers was introduced early to SEC. However, automatic data handling has often led to inappropriate manipulation of the data and care is always required. The whole chromato-

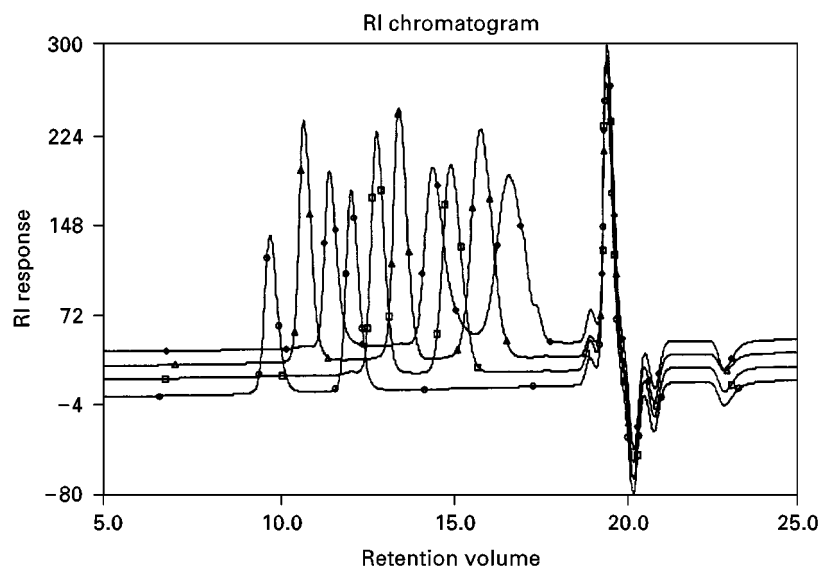


Figure 3 Chromatograms of four solutions containing 10 narrow molecular weight distribution polystyrene calibrants.

gram envelope for the polymer is used in the calculations and any minor variation in baseline placement or integration limits at the extreme ends of the distribution is likely to have significant effects on one of the calculated molecular weight averages.

Measurement of Molecular Weight Averages

All synthetic polymers and many natural polymers have a molecular weight distribution and it is usual to calculate average molecular weights from these distributions. Although there are a considerable number of averages that have previously been used, the most common are the number average, M_n , weight average, M_w , and the z -average, M_z . These are defined as follows:

$$M_n = \sum(N_i \cdot M_i) / \sum N_i$$

$$M_w = \sum(N_i \cdot M_i^2) / \sum(N_i \cdot M_i)$$

$$M_z = \sum(N_i \cdot M_i^3) / \sum(N_i \cdot M_i^2)$$

where N_i is the number of molecules of molecular weight M_i .

The molecular weight is generally calculated from the normalized chromatograms by dividing the chromatogram into slices. The area of each slice (b_i) is measured and the molecular weight (M_i) determined from the calibration curve. The molecular weight averages are then calculated as follows:

$$M_n = \sum b_i / \sum (b_i / M_i)$$

$$M_w = \sum (b_i \cdot M_i) / \sum b_i$$

$$M_z = \sum (b_i \cdot M_i^2) / \sum (b_i \cdot M_i)$$

In practice, the weight average molecular weight generally corresponds to a molecular weight near the maximum of the chromatogram and the repeatability of the measurement from SEC is normally better than for the other averages. The number average molecular weight is sensitive to minor variations at the low molecular weight end of the distribution while the z -average is more influenced by differences at the high end of the distribution.

The term 'polydispersity' is often used as a measure of the width of a molecular weight distribution and is usually the ratio of the weight average to number average molecular weights (M_w/M_n).

Figure 3 shows an overlay of the chromatograms for four solutions containing a total of ten individual, narrow molecular weight distribution polystyrene calibrants and Figure 4 shows the log (molecular weight) versus retention volume calibration derived from these chromatograms.

Figure 5 shows an overlay of one of the chromatograms for one of the above calibrant solutions and a broad molecular weight distribution polymer of unknown molecular weight and Figure 6 shows the calculated molecular weight averages and molecular distribution obtained from applying the calibration to the molecular weight computation with this chromatogram.

In Figure 6, the frequency is expressed as weight fraction per unit of log (molecular weight), $Wn(\log M)$.

The Universal Calibration Procedure

When a polystyrene calibration is applied for the measurement of a polymer other than polystyrene, the results can be expressed as the polystyrene equivalent molecular weights or it might be possible to

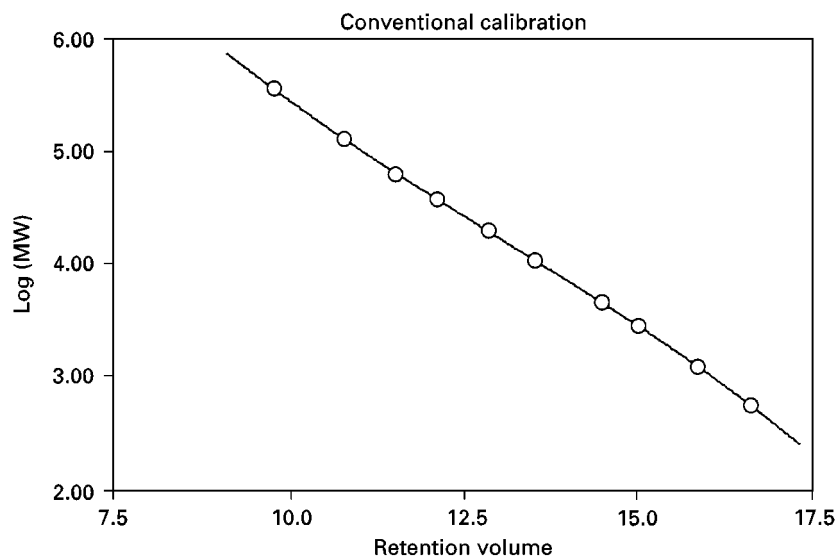


Figure 4 Log (molecular weight) versus retention volume calibration derived from chromatograms shown in Figure 3.

apply a mathematical correction to describe the true molecular weights. The most common mathematical correction, for polymer type, is known as the Universal Calibration Procedure and is based on the early empirical observation that if the calibration is expressed as the log of the product of molecular weight and intrinsic viscosity versus elution volume, then a common calibration is obtained for many polymer types (if the simple log molecular weight vs. elution volume calibrations are plotted, a series of related calibration plots are obtained).

The intrinsic viscosity factor in the universal calibration allows for the variation in solvation between

different polymers. This difference in solvation is closely related to solution viscosity measurements and it is the K and α values from the Mark-Houwink-Sakurada equation which are used in this correction.

The K and α values for both the calibrant and sample polymer types in the solvent used and at the measurement temperature must be known. In practice, the literature contains a lot of data on measured K and α values and if appropriate values are selected with care, the computed molecular weight data can be close to the true values. However, it must be appreciated that the nature of any branching can

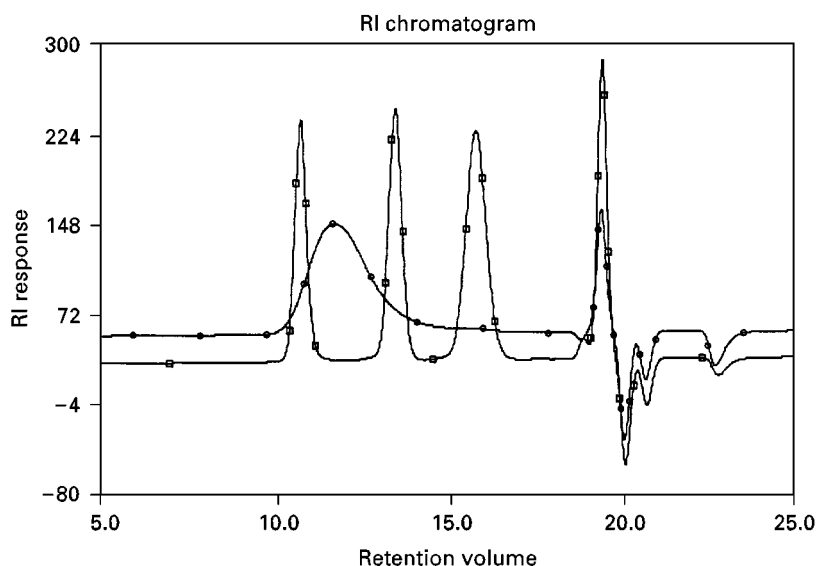


Figure 5 Overlay of one of the chromatograms for one of the above calibrant solutions and a broad molecular weight distribution of unknown molecular weight.

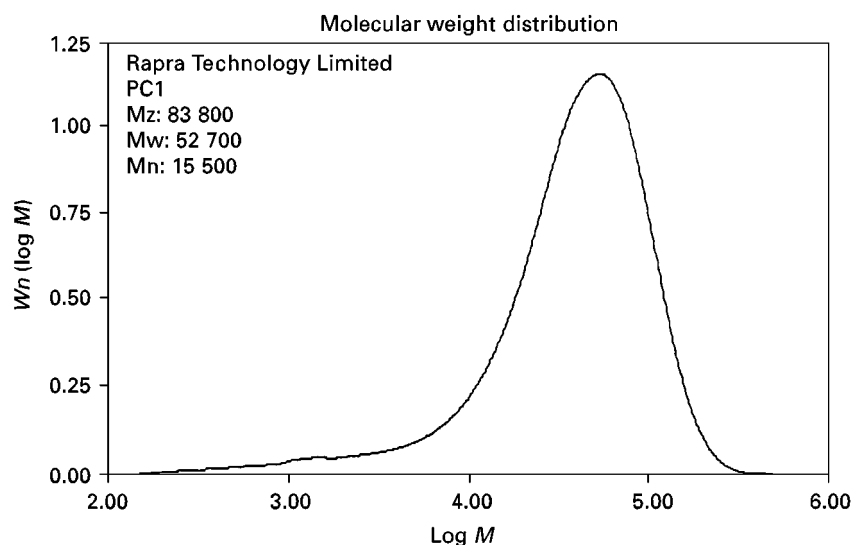


Figure 6 Calculated molecular weight averages and molecular distribution obtained from applying calibration to molecular weight computation with chromatogram in Figure 5. Frequency is expressed as weight fraction per unit of log (molecular weight), $Wn(\log M)$.

have a significant effect on these values and in the literature values were frequently obtained many years ago when the polymer structure might have been somewhat different to common materials today.

The Universal Calibration procedure appears to be appropriate for polymers which have a normal random coil configuration in solution but fails for any polymer type which has any structured conformation in solution. The philosophy behind this approach is also used in combined SEC-viscosity measurements (see later).

High Temperature SEC

In the early days of SEC, it was appreciated that this was a technique that could be used at high temperature and be applied to polymer types for which there was no room temperature solvents, particularly polyethylene and polypropylene, and appropriate commercial instrumentation was soon introduced. Despite this early appreciation of the value of high temperature SEC, it remains a difficult application.

High temperature SEC is carried out either to be able to dissolve the polymers of interest, as with polyolefins, or to reduce the viscosity of the solvents. In practice, SEC of polyolefins requires a minimum temperature of 140°C and is usually carried out with chlorinated aromatic solvents; the SEC of polyesters (such as PET) or polyamides is carried out using phenolic solvents at temperatures of at least 110°C, while SEC with polar solvents, such as dimethylformamide is carried out at temperatures around 80°C. In addition, some SEC is carried out at raised temper-

ature to enhance the efficiency (particularly aqueous SEC).

Polyolefins tend to come out of solution if there is a cool spot in the total instrumentation, which is the main complication with these polymer types but there is potential for other temperature incompatibilities (e.g. temperature cycling on an RI detector). In addition, solvents at high temperature are likely to swell polymer components in the SEC instrumentation (e.g. pump seals) and it is desirable to dedicate the instrumentation to specific applications. With the high temperature SEC using phenolic or polar solvents, the main complications are not necessarily directly related to the high temperature.

SEC with Polar Solvents

Polar polymers normally require the use of polar solvents such as dimethylformamide (DMF), dimethylsulfoxide (DMSO), N-methylpyrrolidine (NMP) or dimethylacetamide (DMAC). Work with these solvents is carried out at raised temperatures (e.g. 80°C), to reduce the viscosity, and it is normal practice to add salts to try and suppress interactions other than SEC. SEC of polyesters and polyamides can be carried out at ambient temperature using fluorinated alcohols but the solvents are excessively expensive and of questionable toxicity.

Although the standard polystyrene-based columns are normally used for SEC with polar solvents, the polystyrene calibrants may not be applicable and the use of alternative calibrant polymers such as polyethyleneglycol/polyethyleneoxide or polymethylmethacrylate is common.

SEC with Phenolic Solvents

As noted above, the SEC of polyesters, such as polyethylene terephthalate and many polyamides is often carried out using phenolic solvents at temperatures of around 110°C or 120°C. Typical solvents are *m*-cresol or *o*-chlorophenol. It is the unpleasant nature of the solvents which is the main problem with these SEC applications but in general the problems of high temperature SEC increase with temperature.

In the author's laboratories, the SEC of polyesters appears to be reasonably straightforward but the weak DRI detector response for polyamides is problematic.

Aqueous SEC

The SEC of polymers in aqueous media has generally been considered more complex due to the frequent need for complex buffer selection and to the requirement for hydrophilic column packings. In the early days of SEC, the hydrophilic column packings available gave significant problems but this appears to have been largely overcome with the advent of high efficiency hydroxymethacrylate packings.

For most water-soluble polymers, it remains necessary to select pH and ion concentration suited to the polymer type of interest and it is not practical to have standard conditions for aqueous SEC work. However, it is usual to raise the temperature to obtain enhanced efficiency.

SEC with Selective Detectors

Fixed wavelength ultra-violet or infra-red detectors are used with a 'universal' detector (such as DRI) and appropriate software to obtain information on how specific chemical groups vary through the molecular weight distribution. However, it should be noted that appropriate spectral windows for the solvent are required to allow this approach to be used and the presence of antioxidants or other additives, in the solution, can be a problem.

Modern diode array detectors can be used to obtain more complex information where applicable.

SEC with FTIR

It should be possible to use the rapid scanning capability of Fourier Transform Infra-Red spectrophotometers to obtain very detailed information on chemical composition but the lack of spectral windows is a severe limitation. Direct combination of SEC and FTIR has been used with tetrachloroethylene as the solvent (which has a very simple infra-red spectrum) to examine ethylenevinyl acetate (EVA) copolymers and a similar direct combination is used for polyolefin samples.

Solvent Removal Approaches

Since the main problem with direct combination of SEC with FTIR is the lack of spectral windows in the solvent, a number of researchers have studied approaches to remove the solvent prior to the FTIR examination.

Laboratory Connections Inc. have developed approaches which use either warm gas or ultra-sonication and vacuum to remove solvent from the atomized eluent and deposit the fractionated material as a thin annulus on a germanium disc. The germanium disc is then transferred to a matching rotating stage located in the infra-red instrument and spectra are recorded as the disc is rotated to mimic the chromatogram. Specialist software allows complex manipulation of the chromatography and spectroscopic data. The quality of spectra that can be obtained without any requirement to overload the chromatographic system is very good and this technique can be used for most SEC approaches and the only real limitation is the potential for losing low molecular weight material with the solvent.

SEC with Light Scattering Detection

Light scattering has long been used as a stand-alone technique for the absolute measurement of the weight average molecular weight of polymers. The classical approach to this technique was to measure the scattered light for a range of different angles and different solution concentrations such as to produce a Zimm plot which would allow determination of both the molecular weight and the shape of the molecule in solution. In the early 1970s, the introduction of laser light scattering instruments allowed the optical cell to be reduced in size to be compatible with a chromatographic detector cell and to work at a low enough angle to avoid the need for extrapolation to zero angle. These Low-Angle Laser-Light Scattering (LALLS) instruments allowed the stand-alone measurement to be carried out far more efficiently but were immediately used for direct combination with SEC such that the 'absolute' measurement of the molecular weight distribution was practical for the first time.

More recently, other instruments have been introduced which measure the scattered light at a range of angles simultaneously; these are known as Multi-Angle Laser-Light Scattering (MALLS) detectors. Instruments have also been introduced which only monitor the light scattered at a right angle (RALLS).

In addition to providing information on the absolute molecular weight distribution, SEC-light scattering is used to obtain information on branching

(basically by comparing the absolute molecular weight with the apparent molecular weight for the linear polymer calibration). The response of the light scattering detector increases dramatically with molecular weight and SEC-light scattering systems are very good at examining any variation at the high molecular weight end of a distribution.

In SEC-light scattering, the solution concentration is an important parameter in the calculation and it is necessary to have accurate information of the differential refractive index for the polymer/solvent (this is a squared term in the calculation). This requirement for information on the differential refractive index is problematic for examination of copolymers.

SEC with Viscosity Measurement

As noted above, it has been empirically demonstrated that for many polymer types, a universal calibration is obtained if the log. product of molecular weight and intrinsic viscosity is used rather than simple log. molecular weight. This is utilized by combining the response of a viscosity detector and a concentration detector to give the universal calibration directly. The viscosity monitor measures the differential pressure as polymer solution travels through a capillary; detectors have been developed which use a single capillary, a pair of capillaries or four capillaries (arranged in a manner analogous to a Wheatstone bridge).

SEC-viscosity is not theoretically an absolute approach but should give the true molecular weight distribution, providing that the polymer of interest conforms to the Universal Calibration approach. As with SEC-light scattering, SEC-viscosity is valuable for obtaining information on branching. Again, the solution concentration is an important parameter in the calculation. The differential refractive index does not appear in the calculation but could produce inaccuracies in the assumed concentration and hence is also problematic for copolymers.

Commercial hardware and software is available for combining SEC-light scattering-viscosity within a single system.

Future Prospects

Although there have been suggestions that other techniques (e.g. matrix-assisted laser-desorption ionization – time-of-flight, MALDI-TOF, mass spectroscopy) might replace SEC, there seems little prospect of this in the near future.

There are new commercial integral SEC systems now available that should simplify some of the more difficult applications and make SEC combined techniques more routine. These developments should ensure that SEC is a main stream technique for the foreseeable future. There will also probably be more utilization of triple-detection (concentration, viscosity and light-scattering) for detailed characterization of specific polymer types.

See also: II/Chromatography: Detectors: Laser Light Scattering. Chromatography: Liquid: Detectors: Refractive Index Detectors; Theory of Liquid Chromatography. III/Gradient Polymer Chromatography: Liquid Chromatography. Synthetic Polymers: Liquid Chromatography.

Further Reading

- Cooper AR (1982) In: Bark LS and Allen NS (eds) *Analysis of Polymer Systems*. London: Applied Science Publishers, London.
- Dawkins JV and Yeadon G (1978) In: Dawkins JV (ed.) *Developments in Polymer Characterisation – 1*. London, Applied Science Publishers.
- Dawkins JV (1984) In: Janca J (ed.) *Steric Exclusion Liquid Chromatography of Polymers*. New York: Marcel Dekker.
- Holding SR and Meehan E (1995) Molecular weight characterisation of synthetic polymers. *Rapra Review Reports*, Volume 7, Number 11.
- Hunt BJ and Holding SR (1989) *Size Exclusion Chromatography*. London: Blackie.

Micellar Liquid Chromatography

M. L. Marina and M. A. García, Universidad de Alcalá, Alcalá de Henares, Madrid, Spain

Copyright © 2000 Academic Press

Introduction

Surfactants are molecules that exist as monomers when they are at low concentrations in solution,

while above their critical micelle concentration (c.m.c.) they associate to form aggregates called micelles. Two zones of different polarity exist in the molecules of surfactants: one is hydrophobic in nature, formed from one or more hydrocarbon chains; the other can be polar or even ionic. According to the nature of this second zone, surfactants are classified into three main categories: ionic (anionic and cationic), nonionic and zwitterionic (amphoteric).

The combination of hydrophobic and hydrophilic properties confers some special characteristics on micellar systems in aqueous solution. This has made these systems applicable in different areas of analytical chemistry, highlighting the increasing interest in their use in separation methods. The ability of micellar systems to solubilize hydrophobic compounds in aqueous solutions, to improve different analytical methodologies, or to develop new analytical methods due to the possibility of increasing sensitivity or selectivity should be emphasized.

In 1980, Armstrong and Henry showed the possibility of employing solutions of surfactants at a concentration above their c.m.c. as mobile phases for high performance liquid chromatography (HPLC), giving rise to micellar liquid chromatography (MLC). This technique, in which nonpolar chemically bonded stationary phases are generally used, constitutes an interesting alternative to aqueous-organic mobile phases in HPLC since micellar mobile phases are low cost and have low toxicity as compared with aqueous-organic mobile phases.

The great variety of interactions that are possible in MLC separations, for example electrostatic, hydrophobic and esteric, and the modification of stationary phase by adsorption of monomeric surfactants, make these systems more complicated than conventional reversed-phase HPLC (RP-HPLC) with aqueous-organic mobile phases. Micelles are not static species, but they exist above the c.m.c. in equilibrium with surfactant monomers. In a chromatographic column, surfactant monomers can be adsorbed on the surface of the stationary phase. For most surfactants and stationary phases, the amount of surfactant adsorbed remains constant after equilibrium between mobile and stationary phase is reached. The adsorption of a surfactant on a silica-bonded stationary phase, such as C_1 , C_8 and C_{18} , can occur in two ways:

1. **Hydrophobic adsorption.** The alkyl hydrophobic chain of the surfactant is adsorbed and the ionic head is in contact with the polar solution, conferring on the stationary phase some ion-exchange properties when charged solutes are separated.
2. **Silanophilic adsorption.** The ionic head of the surfactant is adsorbed by the stationary phase, thus acquiring a more hydrophobic character.

Figure 1 shows the different equilibria existing in MLC. First, a solute can be partitioned between the aqueous mobile phase and the micellar mobile pseudophase, this equilibrium being controlled by a distribution coefficient P_{MW} . Second, this solute can be in equilibrium between the stationary phase and the micellar pseudophase, which is characterized by a distribution coefficient P_{SM} , and finally, a third

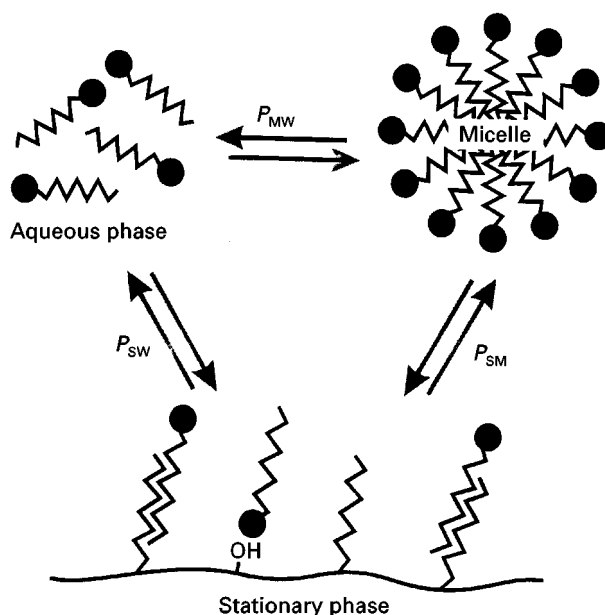


Figure 1 Distribution equilibria of a solute in micellar liquid chromatography. (Reproduced with permission from Marina ML and García MA (1997) *Journal of Chromatography A* 780: 103–116, copyright Elsevier Science Publishers B.V.)

equilibrium can be established for the solute distribution between stationary and aqueous mobile phases (P_{SW}).

Equations Describing Solute Retention in Micellar Liquid Chromatography

Table 1 groups some of the different models developed to describe solute retention in MLC. Some physicochemical models explain the variation of solute retention generally as a function of one or two experimental variables (micellar concentration, organic modifier concentration and pH). Empirical models, without a chemical sense, have also been developed to predict solute retention in MLC under different experimental conditions.

Purely Aqueous Micellar Systems

From equilibria taking place in MLC represented in Figure 1, equations have been developed relating chromatographic retention and concentration of micellized surfactant in solution.

Equation [1] (Table 1) relates the solute elution volume (V_e) in MLC with the micellized surfactant concentration in the mobile phase (C_M) (total surfactant concentration in solution minus c.m.c.). V_s , V_M and v are the stationary phase volume, the void volume of the column and the surfactant molar volume,

Table 1 Retention modelling in MLC

Model	Equations
Physico-chemical	$V_S/(V_e - V_M) = \{V(P_{MW} - 1)/P_{SW}\} C_M + 1/P_{SW}$ [1]
	$1/k = \{K_2/\phi[L_S]K_1\} C_M + 1/\phi[L_S]K_1$ [2]
	$k = (V_S/V_M) \cdot (P_{SW}/V C_M)$ [3]
	$k = \frac{k_0(1 + K_2[C_M]) + k_1(1 + K_4[C_M])K_{am}/[H^+]}{1 + K_2[C_M] + (1 + K_4[C_M])K_{am}/[H^+]}$ [4]
	$k = \frac{\phi K_1[L_S](1 + K_4[A_M])}{1 + (K_3 + K_4)[A_M] + K_2[C_M](1 + K_3[A_M]) + K_3K_4[A_M]^2}$ [5]
Empirical relationships	$\ln k = -S\phi + \ln k_0$ [6]
	$1/k = A\mu + B\phi + C\mu\phi + D$ [7]
	$1/k = A\mu + B\phi^2 + C\phi + D\mu\phi + E$ [8]

respectively. If solute retention is expressed as the retention factor (k), a similar equation is obtained (eqn [2]) relating $1/k$ with C_M through the solute-micelle association constant per monomer, K_2 . Here ϕ is the phase ratio (the ratio of the stationary phase volume to the volume of the mobile phase in the column, V_S/V_M), $[L_S]$ is the stationary phase concentration and K_1 is the binding constant for the solute between the bulk solvent and the stationary phase.

Equations [1] and [2] show that retention of a solute in MLC decreases when micelle concentration in the mobile phase increases. This is in contrast to reversed-phase ion-interaction (or ion-pairing) chromatography, where the surfactant concentration is below the c.m.c. (that is, no micelles exist), and the addition of an ionic surfactant increases retention for compounds that interact electrostatically with it.

For very hydrophobic compounds, a direct transfer retention mechanism from the micellar mobile phase to the modified stationary phase has been proposed. A limit theory has been developed for those compounds where the amount of the solute in the non-micellar aqueous mobile phase can be considered negligible. In this case, k is related to C_M through eqn [3] in Table 1.

For ionized solutes (weak acids, bases and zwitterionic solutes), some equations have also been developed relating k with C_M and pH. As an example, eqn [4] in Table 1 is the derived model for a weak acid. In this equation k_0 and k_1 are the limiting retention factors for the neutral and dissociated forms, respectively, K_4 is the association constant of the

ionized form of the solute with the micellar phase, and K_{am} is the acid dissociation equilibrium constant. The variation of k with pH at a constant micellized surfactant concentration is sigmoidal. Since a shift in the ionization constants can be obtained when the micellized surfactant concentration is modified, optimization of separation conditions must be attained considering both variables simultaneously.

Hybrid Micellar Systems

The addition of an organic modifier to a micellar solution can modify the characteristics of the micellar system (c.m.c. and the aggregation number). This can cause a variation of the solute-micelle interactions that, in turn, can change the chromatographic retention. On the one hand, a high concentration of alcohol can destroy the micellar structure, but on the other hand, the alcohol modifies the structure and composition of the stationary phase because it solvates the bonded hydrocarbon chain. Logically, the separation mechanism with the so-called hybrid mobile phases (micellar phases modified by alcohols) should be more similar to that for conventional aqueous-organic mobile phases than for purely aqueous micellar phases. However, if the integrity of the micelles remains, the addition of an alcohol to micellar mobile phases will not create an aqueous-organic system.

Both physicochemical and empirical models have been developed to describe the retention of solutes with hybrid mobile phases.

Physicochemical models Equation [5] (Table 1), which relates a solute retention factor with the micellized surfactant and alcohol concentrations, can be considered an extension of eqn [2]. This model considers the modification of stationary phase sites and micelle concentration due to the presence of an alcohol, that is, the alcohol can compete with the solute for interaction with the stationary phase and micelles. $[A_M]$ is the alcohol concentration in the mobile phase, and K_3 and K_4 are the association constants of the alcohol with the modified stationary phase and the micellar mobile phase, respectively. Based on the value of these constants and alcohol concentration, some simplified equations can be obtained. This model can predict a nonlinear, linear or quadratic variation of the retention factor with the alcohol concentration in the mobile phase (when micellized surfactant concentration is constant) and a linear variation of the inverse of retention factor with the micellized surfactant concentration (when alcohol concentration remains constant).

Empirical equations These models have no chemical background but are very valuable tools for predicting solute retention as a function of different variables. Among the different empirical equations reported in literature, models can be found relating solute retention to: (1) the organic modifier concentration, and (2) organic modifier and surfactant concentrations.

Empirical equations relating solute retention in MLC to organic modifier concentration Equation [6] (Table 1) is the simplest model relating the retention factor to the organic modifier concentration when surfactant concentration is constant. ϕ is the volume fraction of the organic modifier, S the eluent-strength parameter, and k_0 the retention factor in the absence of the organic modifier. Although this model can explain the decrease in solute retention observed in the presence of organic modifiers, deviations from linearity can be seen and some significant differences are obtained between the intercept and the experimental retention factor in the absence of an organic modifier. From an experimental viewpoint, its applicability is limited because the variation of the surfactant concentration is not considered.

Empirical equations relating solute retention in MLC to organic modifier and surfactant concentrations Equations have been obtained relating the logarithm of the retention factor to the volume fraction of the organic modifier (ϕ) and to the total surfactant concentration in the mobile phase (μ), but their applicability is limited. Other models have been proposed

relating the inverse of the retention factor with these two variables and these, from which eqns [7] and [8] (Table 1) are examples, have shown a more general application range.

An extension of the iterative regression optimization strategy to multiparameter optimizations for the separation of ionic compounds in MLC has also been reported. The parameters examined are surfactant concentration, alcohol concentration and pH. Fairly regular (linear, weakly curved) retention behaviour of compounds as a function of the parameters results in an efficient optimization using a relatively small number of initial experiments.

All the models presented above require a mathematical equation, derived from chemical considerations, or are empirical in nature, but there are other methods that, although also empirical, do not have such requirements; these are artificial neural networks (ANNs). Although ANNs have been known for years, they have been applied only recently to model retention in MLC with hybrid eluents. ANNs are a very promising alternative to classical statistical methods for retention modelling studies in MLC.

Efficiency

One of the main drawbacks of MLC techniques is the loss observed in the chromatographic efficiency as compared with that obtained in RPLC with aqueous-organic mobile phases. This efficiency loss is attributed to the increase in the resistance of solute mass transfer from the mobile phase to the stationary phase. However, the addition of small quantities of an organic modifier to the mobile phase and an increase in the working temperature have shown that efficiencies similar to those obtained in RPLC with aqueous-organic mobile phases may be attained. Other suggestions include working with low flow rates and low surfactant concentrations. Indeed, it has been shown that the use of a high surfactant concentration in the mobile phase may cause efficiency loss.

Surfactant adsorption on the stationary phase seems to have a great influence on the efficiency. The addition of a short or medium chain alcohol causes surfactant desorption out of the stationary phase and improves efficiency. This effect increases with increase in the modifier's concentration and hydrophobicity.

Elution Strength of Micellar Mobile Phases

A disadvantage of MLC techniques is that the eluent strength of micellar mobile phases is quite small.

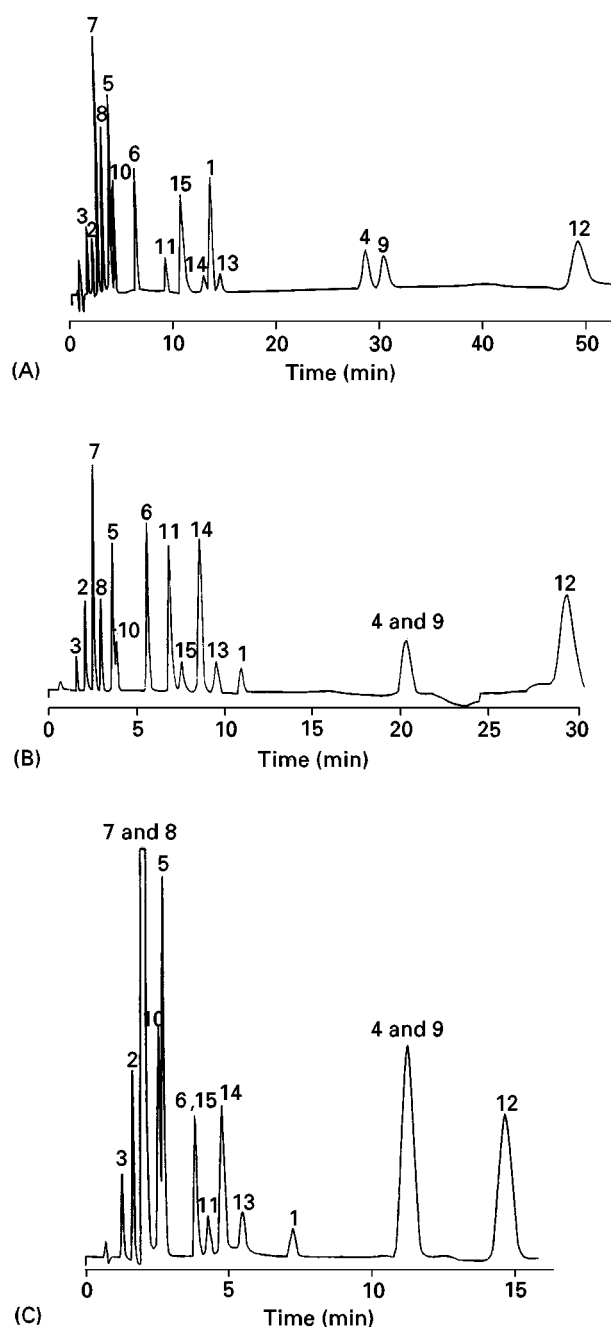


Figure 2 Chromatograms corresponding to the separation of a mixture of 15 benzene and naphthalene derivatives. (A) 0.02 mol L⁻¹ SDS modified with 5% *n*-butanol. (B) 0.035 mol L⁻¹ SDS modified with 5% *n*-butanol. (C) 0.035 mol L⁻¹ SDS modified with 10% *n*-butanol. Key: 1, benzene; 2, benzylic alcohol; 3, benzamide; 4, toluene; 5, benzonitrile; 6, nitrobenzene; 7, phenol; 8, 2-phenylethanol; 9, chlorobenzene; 10, phenylacetone; 11, 3,5-dimethylphenol; 12, naphthalene. Column: Hypersil C₁₈ (10 cm × 4.0 mm i.d.). (Reproduced with permission from García MA, Vera S, Bombin M and Marina ML (1993) Optimization of the separation selectivity of a group of benzene and naphthalene derivatives in micellar high-performance liquid chromatography using a C₁₈ column and alcohols as modifiers in mobile phase. *Journal of Chromatography* 646: 297–305, copyright Elsevier Science Publishers B.V.)

Although the eluent strength of purely micellar eluents increases when the micelle concentration in the mobile phase increases, an increase of the micelle concentration in the mobile phase generally causes an efficiency loss. For these reasons, the addition of organic modifiers to micellar mobile phases is of great interest since it is possible to increase both eluent strength and efficiency. As an example, **Figure 2** shows the chromatograms corresponding to the separation of a mixture of 15 benzene and naphthalene derivatives when the following sodium dodecyl sulfate (SDS) mobile phases are used: 0.02 mol L⁻¹ SDS modified with 5% *n*-butanol (chromatogram A), 0.035 mol L⁻¹ SDS modified with 5% *n*-butanol (chromatogram B) and 0.035 mol L⁻¹ SDS modified with 10% *n*-butanol (chromatogram C). It can be observed that for the same alcohol percentage in the mobile phase, the elution strength increases with the surfactant concentration (Figures 2A and 2B), while for the same surfactant concentration in the mobile phase, elution strength increases with the alcohol percentage (Figures 2B and 2C).

The eluent strength of a micellar mobile phase modified by a short or medium chain alcohol such as methanol, propanol or butanol increases with the length of the alcohol chain as in conventional aqueous-organic systems.

Separation Selectivity

The rate of change in retention of different solutes varies with charge and hydrophobicity of the solute as well as with the length of alkyl chain, charge and concentration of micelles. This causes inversions of elution order that are the result of two competing equilibria: the solute-micelle association, characterized by K_2 , and the solute-stationary phase interaction, characterized by P_{sw} . The parameters K_2 and P_{sw} have a different effect on retention. When P_{sw} increases, retention also increases, but when K_2 increases, retention decreases. When the surfactant concentration in the mobile phase increases, the effect that K_2 has on retention also increases and reversals in elution order can be obtained if the difference in K_2 values for two solutes is large. Therefore, separation selectivity in MLC can be controlled by modifying surfactant nature and concentration. Furthermore, when organic modifiers are added to the mobile phase, the solvent strength parameter for a group of compounds does not have the same ranking for different alcohols owing to the different interaction of these modifiers with the micelles. For these reasons, MLC techniques are very interesting for chromatographic separation.

Although the conditions that optimize separation selectivity in MLC can vary with the nature of the solutes, several workers have shown an increase in separation selectivity for aromatic compounds in MLC with hybrid eluents when the micelle concentration in the mobile phase decreases. However, for a group of amino acids and peptides, an increase in micelle concentration can cause an increase or decrease in selectivity, or even an inversion of the peaks.

The effect of the organic modifier content in the mobile phase seems to be clearer. Generally, separation selectivity in MLC is improved in the presence of an organic modifier and increases with the volume fraction of the modifier in the mobile phase. This result is opposed to that observed in conventional RPLC with aqueous-organic mobile phases in which an increase of the organic modifier content causes a decrease of solute retention and selectivity. The selectivity enhancement observed in MLC when the solvent strength increases has been attributed to the competing partitioning equilibria in micellar systems and/or to the unique abilities of micelles to compartmentalize solutes and organic solvents. For some compounds, however, selectivity can decrease with the content of the alcohol in a micellar (SDS) mobile phase. In this case, for pairs of peaks where the selectivities are reduced by increasing alcohol concentration, a selectivity enhancement is observed with increasing micelle concentration and vice versa. Micelles and alcohols compete to interact with solutes affecting the role of one another in controlling retention and selectivity. The mutual effects of micelles and organic modifiers on each other also require a simultaneous optimization of these two parameters.

The retention mechanism of a solute in MLC can have implications for selectivity. If the retention of a solute in the chromatographic system takes place through a direct transfer mechanism, then the retention factor can be expressed by eqn [3] (Table 1). In this case, and if the surfactant concentration in the mobile phase is high, the selectivity coefficient (α) for a pair of solutes can be calculated from the ratio of their distribution coefficients between the stationary and micellar phases (P_{SM}):

$$\alpha = P_{SM1}/P_{SM2} \quad [9]$$

This equation is useful for two reasons. First, because knowledge about the retention mechanism of compounds in the chromatographic system can be enhanced. In fact, if the experimental selectivity coefficient for a pair of solutes is constant and coincides with the ratio of their respective distribution coeffi-

cients, P_{SM} , it can then be assumed that retention occurs through a direct transfer from the micellar phase to the stationary phase. Second, calculation of the selectivity coefficient from eqn [9] enables prediction of the separation selectivity of two compounds in the chromatographic system, provided the distribution coefficients (P_{SM}) of the solutes are known.

As an example, Figure 3 shows the variation of theoretical and experimental selectivity coefficients as a function of the micellized surfactant concentration in two mobile phases, SDS/5% *n*-propanol (Figures 3A, 3B and 3C) and hexadecyltrimethylammonium bromide (CTAB) modified by 5% *n*-butanol (Figures 3D, 3E and 3F) for three pairs of aromatic solutes. For pyrene/acenaphthene, both of which are highly hydrophobic, a direct transfer mechanism can be assumed for any surfactant concentration in these mobile phases. For pyrene/toluene a direct transfer mechanism can only be assumed for pyrene in all surfactant concentrations. For pyrene/benzamide, benzamide does not experience a direct transfer mechanism except at very high surfactant concentrations. Figure 3 shows that, when both solutes experience a direct transfer mechanism, the experimental and theoretical selectivity coefficients are very similar for all surfactant concentrations in solution, and it is therefore possible to predict the selectivity coefficient from the partition coefficients P_{SM} for the two solutes. When one of the two solutes does not experience a direct transfer mechanism, the theoretical and experimental selectivities are different. This difference decreases under conditions in which the direct transfer mechanism is favoured, i.e. by increasing the solute hydrophobicity, solute-micelle association constants, surfactant concentration in mobile phase and, for mobile phases modified by alcohols, by increasing the polarity of the alcohol. Consequently, the separation selectivity for a pair of solutes shows a tendency to match a limit value close to the ratio of stationary-micellar partition coefficients of two solutes. In this case, the separation selectivity cannot be experimentally modified through a change in the surfactant concentration in the mobile phase.

Applications

Determination of Solute-Micelle Association Constants and Distribution Coefficients

From eqn [1] in Table 1 it can be seen that a plot of the term $V_s/(V_e - V_m)$ versus C_M is linear and the term ' $\nu(P_{MW} - 1)$ ' can be obtained from the slope: intercept ratio. According to Berezin's treatment the term ' $\nu(P_{MW} - 1)$ ' is equal to the solute-micelle

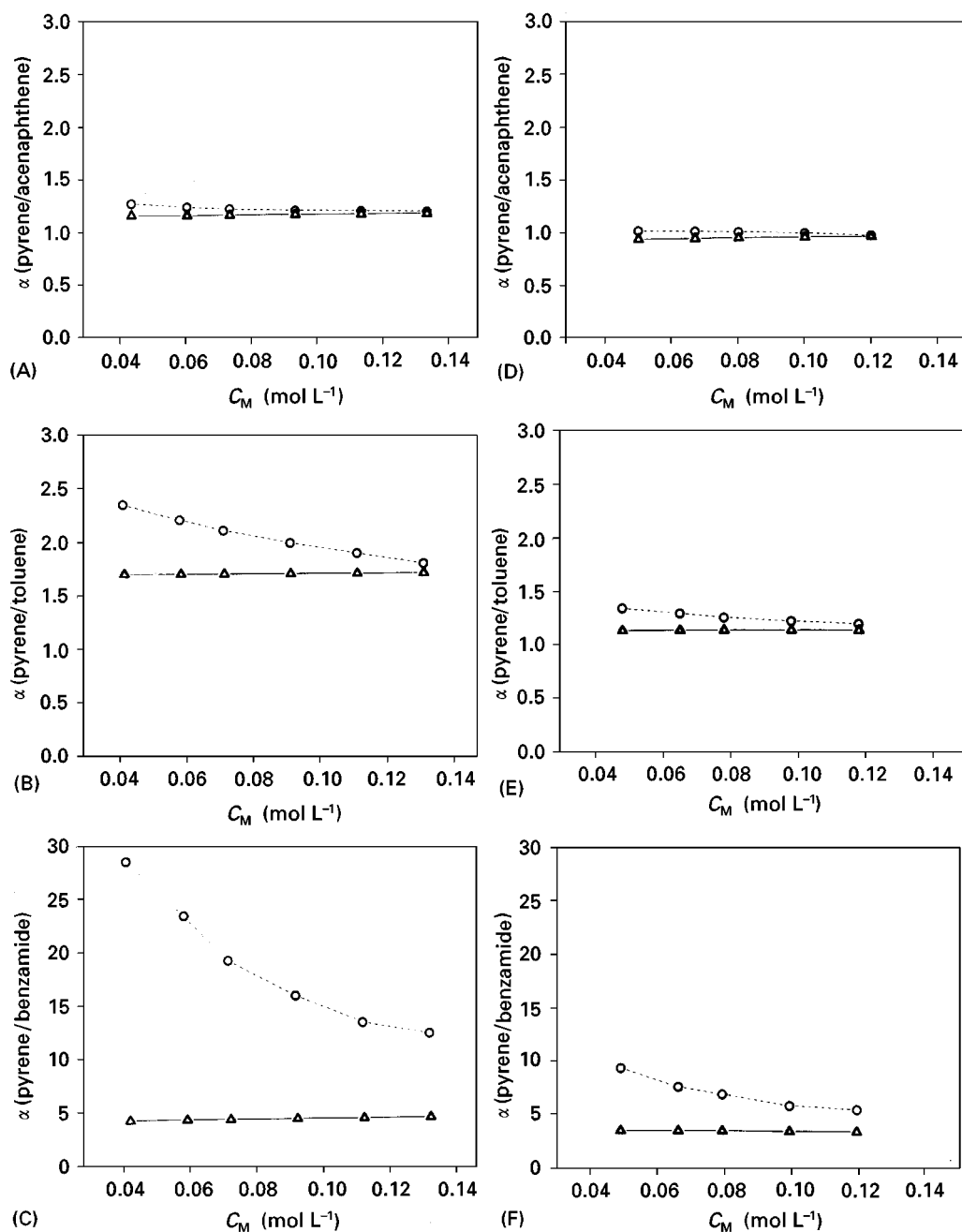


Figure 3 Variation of the experimental (—○—) and theoretical (—△—) selectivity coefficients (α) as a function of the micellized surfactant concentration for three pairs of solutes: pyrene/acenaphthene (A and D), pyrene/toluene (B and E) and pyrene/benzamide (C and F). Mobile phases: A–C, SDS/5% *n*-propanol; D–F, CTAB/5% *n*-butanol. Column: Spherisorb C_8 (15 cm \times 4.0 mm i.d.). (Reproduced with permission from García MA and Marina ML (1996) Influence of alcohol organic modifiers upon the association constants and retention mechanism for aromatic compounds in micellar liquid chromatography. *Journal of Liquid Chromatography and Related Technologies* 19: 1757–1776, copyright Marcel Dekker, Inc.)

association constant per monomer, K_2 , which is the parameter most used to evaluate solute–micelle interactions. Also, the partition coefficient of the solute between bulk water and micelle, P_{MW} , can be obtained if the surfactant molar volume, v , is known. The distribution coefficient, P_{SW} , is obtained directly

from the intercept and the distribution coefficient P_{SM} can be obtained from the ratio P_{SW}/P_{MW} .

In a similar way, the solute–micelle association constant per monomer, K_2 , can be obtained directly from eqn [2] in Table 1 as the slope/intercept ratio of a straight line obtained from a plot of $1/k$ versus C_M .

If the solute-micelle association constant per monomer obtained from eqns [1] or [2] is multiplied by the aggregation number of the micelle, the association constant per micelle is obtained. On the other hand, P_{MW} and K_2 values only depend on the solute and the micellar system employed but not on the stationary phase.

Equations [1] and [2] have frequently been employed with the aim of determining solute-micelle association constants in pure and modified micellar media. Furthermore, good agreement has been found between the values of the association constants obtained by MLC and other techniques.

Figure 4 provides an example of the good linearity obtained for the variation of the term $V_s/(V_e - V_m)$ as a function of C_M for a group of 12 polycyclic aromatic hydrocarbons when an SDS micellar mobile phase modified by 5% *n*-butanol is used.

For highly hydrophobic solutes, the retention of which is described by eqn [3] in Table 1, the variation of $1/k$ as a function of C_M should give a straight

line with an intercept equal to zero; the slope of the line should allow calculation of the distribution coefficient P_{SM} . In these cases, calculation of solute-micelle association constants is not possible and has no chemical meaning.

One of the main drawbacks that this method has is the intrinsic error derived from the determination of a magnitude from a quotient. Error obtained during the determination of K_2 increases with solute hydrophobicity since P_{SW} values for these compounds are elevated (intercept very small, see eqn [1]). With hybrid eluents, the value of P_{SW} decreases and the error in the determination of the solute-micelle association constants for very hydrophobic compounds also decreases (the intercept in eqn [1] increases).

Rapid Elution Gradients

Gradient elution techniques are the most versatile and popular techniques for solving the general elution problem in liquid chromatography. The advantages of gradient elution are enhanced peak resolution, faster analysis times, and better detectability. The major disadvantage is that the compositions of the stationary and mobile phases change during the course of the separation and column regeneration is needed before the next analysis. In order to perform gradient elution in MLC, the concentration of micelles and/or organic modifier may be increased during the course of the separation. In a micellar concentration gradient, re-equilibration time at the end of a gradient run is not necessary, and in an organic modifier gradient the re-equilibration time is very short.

Micellar gradients Rapid micellar elution gradients can be performed in MLC because re-equilibration time for the column is not necessary. This is because the amount of surfactant adsorbed on the stationary phase remains practically constant after reaching equilibrium when the concentration of surfactant in the mobile phase is above the c.m.c. Accordingly, micellar elution gradients are compatible with electrochemical detection. Figure 5 shows the separation of eight organic compounds using a micellar gradient and electrochemical detection.

Organic modifier gradients Organic solvent gradients in MLC require short re-equilibration times at the end of the gradient mainly due to the small range of organic modifier concentration used in MLC in order to maintain micelle integrity. In this case, the change in the concentration of organic modifier is not sufficient to change the concentration of adsorbed surfactant monomer in the stationary phase. In MLC,

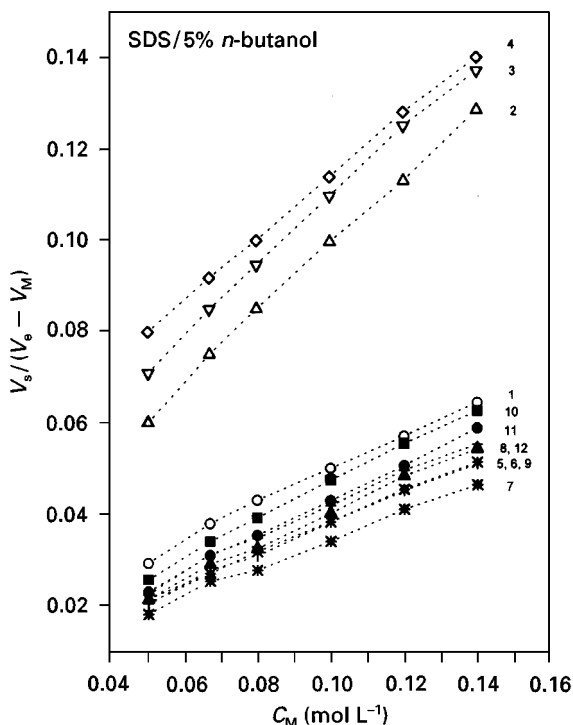


Figure 4 Variation of the term $V_s/(V_e - V_m)$ as a function of C_M for a group of 12 polycyclic aromatic hydrocarbons in an SDS micellar system modified by 5% *n*-butanol. Key: 1, naphthalene; 2, 1-naphthol; 3, 2-naphthol; 4, 1-naphthylamine; 5, pyrene; 6, phenanthrene; 7, 2,3-benzofluorene; 8, fluorene; 9, fluoranthene; 10, acenaphthylene; 11, acenaphthene; and 12, anthracene. Column: Spherisorb C_8 (15 cm \times 4.0 mm i.d.). (Reproduced with permission from Marina ML and Garcia MA (1997) *Journal of Chromatography A* 780: 103-116, copyright Elsevier Science Publishers B.V.)

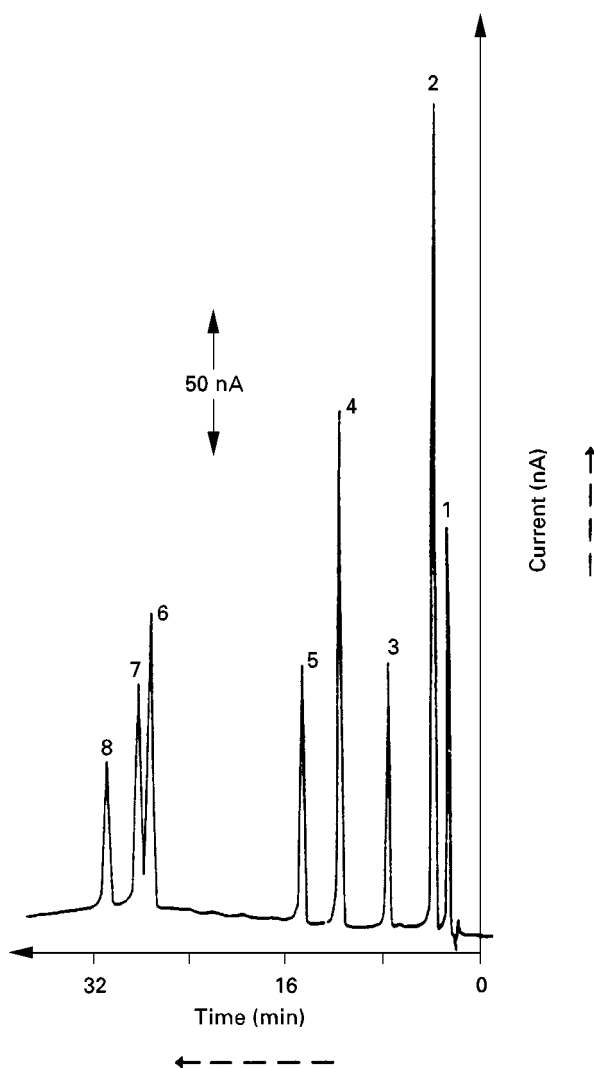


Figure 5 Micellar gradient elution separation with electrochemical detection at +1.2 V. Flow rate: 1.0 mL min^{-1} . Mobile phase A: 0.05 mol L^{-1} SDS/3% 1-propanol, pH 2.5 with phosphate buffer, sodium perchlorate added to balance conductivity with solvent B. Mobile phase B: 0.112 mol L^{-1} SDS/3% 1-propanol, pH 2.5 with phosphate buffer. Gradient program A to B in 12 min. Key: 1, hydroquinone; 2, resorcinol; 3, catechol; 4, phenol; 5, *p*-nitrophenol; 6, *o*-nitrophenol; 7, *p*-chlorophenol; 8, *p*-bromophenol. Column: Altex Ultrasphere C_{18} ($15 \text{ cm} \times 4.6 \text{ mm i.d.}$). (Reproduced with permission from Dorsey JG, Khaledi MG, Landy JS and Lin JL (1984) Gradient elution micellar liquid chromatography. *Journal of Chromatography* 316: 183–191, copyright Elsevier Science Publishers B.V.)

organic modifier gradients are useful since although a limited range of organic modifier may be used, the solvent strength can be compensated with a concurrent micelle concentration gradient. **Figure 6** shows the separation of a mixture of amino acids and peptides in MLC under isocratic and gradient conditions.

Enhancement of Detection Sensitivity

Luminescence detection can be improved in MLC because many solutes show enhanced fluorescence and in some cases room temperature liquid phosphorescence when associated with micelles. The fluorescence intensity of certain compounds in micellar media can be drastically increased as a result of solubilization in the micelle. The location of a solute in the anisotropic medium of micelles, which have a large microenvironment viscosity and different polarity from the aqueous bulk solvent, would result in a decrease in the freedom of movement, shielding of the compounds from nonradiation deactivation, and/or an increase in quantum efficiency. This leads to intensified fluorescence signals and thus to better sensitivity and lower detection limits. Room temperature phosphorescence in solution is possible in the presence of ionic micelles and heavy atom counterions, which increase the population of the triplet excited state molecules and protect them from radiationless deactivation.

Furthermore, many metal–dye complexes show increased absorbance in the presence of micelles. This is

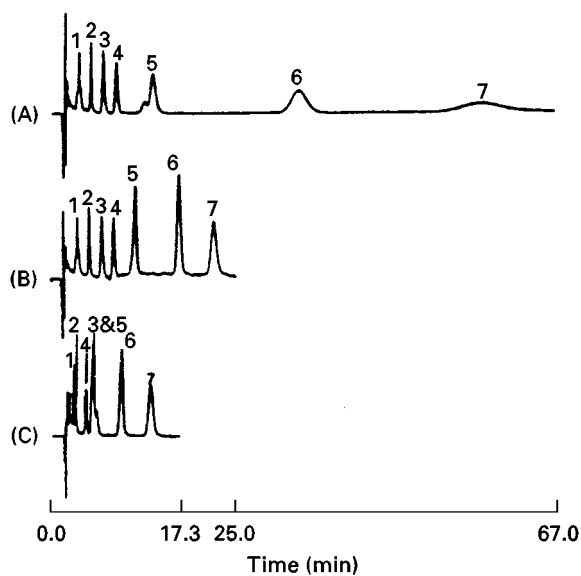


Figure 6 Separation of a seven-component test mixture. Mobile phase: 0.30 mol L^{-1} SDS, 0.02 mol L^{-1} phosphate buffer, pH 2.5 with propanol added. (A) Isocratic separation with 3% 2-propanol, (B) gradient separation with 3 to 15% 2-propanol, and (C) isocratic separation with 15% 2-propanol. Key: 1, aspartic acid–phenylalanine; 2, phenylalanine; 3, lysine–phenylalanine; 4, phenylalanine–phenylalanine; 5, triphenylalanine; 6, tetraphenylalanine; and 7, pentaphenylalanine. Column: Nucleosil C_{18} ($15 \text{ cm} \times 4.6 \text{ mm i.d.}$). (Reproduced with permission from Madamba-Tan LS, Strasters JK and Khaledi MG (1994) Gradient elution in micellar liquid chromatography II. Organic modifier gradients. *Journal of Chromatography A* 683: 335–345, copyright Elsevier Science Publishers B.V.)

due to the capacity of the micelles to produce hyperchromic and bathochromic displacements. Generally, these displacements result in greater sensitivity. In UV/Vis spectrophotometry, the upward displacement of the λ_{\max} of the complex, together with the effect that micellar solutions also have on the λ_{\max} of the ligand, normally enable a more sensitive metal ion determination than that possible in nonmicellar media.

Figure 7 shows a comparison of the detected fluorescent peaks of identical concentrations of three aromatic solutes separated by HPLC. The enhanced fluorescence obtained with an SDS mobile phase with respect to that obtained with a methanol/water mobile phase is observed.

Direct Injection of Biological Fluids

From a bioanalytical viewpoint, a very useful application of MLC is the ability to inject biological fluids (serum, plasma and urine) directly into a chromatographic system with no protein precipitation, analyte extraction steps or pressure build-up problems. These advantages are extremely beneficial in areas such as therapeutic drug monitoring because the analyte extraction steps, traditionally necessary in chromatographic methods, are eliminated. In this way, analysis time is reduced and accuracy and precision are increased because the possible analyte co-precipitation with the protein is avoided.

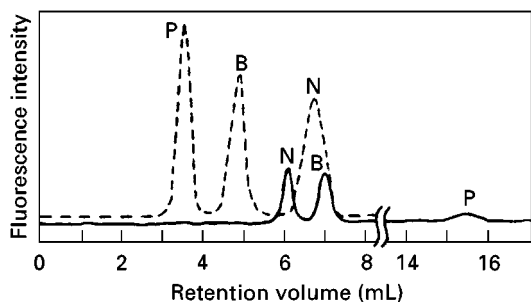


Figure 7 Comparison of the detected fluorescent peaks of identical concentrations of pyrene (P), biphenyl (B) and naphthalene (N) separated by HPLC on a 30 cm \times 4.0 mm i.d. alkyl nitrile column. The broken line (---) shows the separation and enhanced fluorescence obtained with the 0.024 mol L⁻¹ SDS mobile phase. The solid line (—) shows an analogous separation done with a traditional 40 : 60 methanol/water mobile phase. In both separations 10 μ L of solution containing 1.3 \times 10⁻⁷ g (N), 7.0 \times 10⁻⁸ g (B) and 1.1 \times 10⁻⁸ g (P) were injected. (Reproduced with permission from Armstrong DW, Hinze WL, Bui KH and Singh HN (1981) Enhanced fluorescence and room temperature liquid phosphorescence detection in pseudophase liquid chromatography (PLC). *Analytical Letters* 14: 1659–1667, copyright Marcel Dekker, Inc.)

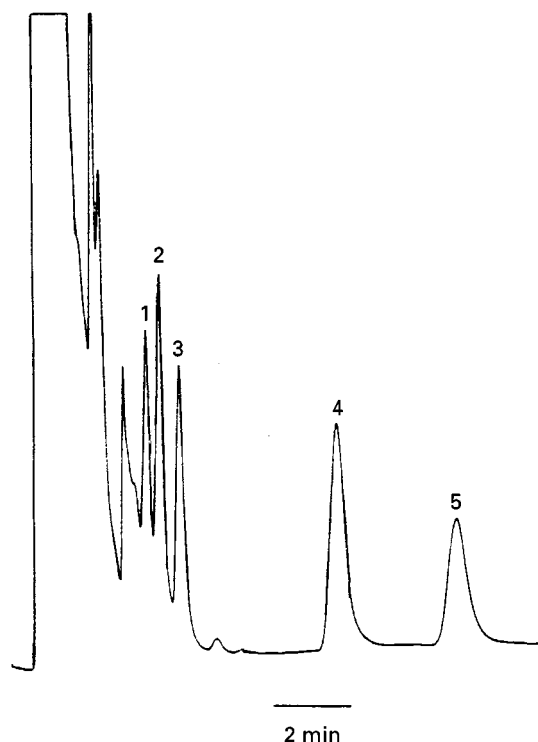


Figure 8 Chromatogram of a urine sample spiked with: 1, amiloride (30 μ g mL⁻¹, 3.67 min); 2, spiro lactone (5 μ g mL⁻¹, 4.02 min); 3, metandienone (1.2 μ g mL⁻¹, 4.57 min); 4, phenylpropanolamine (56 μ g mL⁻¹, 8.63 min); and 5, clostebol (30 μ g mL⁻¹, 11.67 min). Mobile phase: 0.1 mol L⁻¹ SDS/3% 1-pentanol. Flow rate: 1 mL min⁻¹. Column temperature: 60°C. UV detection at 260 nm. Column: Spheri-5 C₁₈ (10 cm \times 4.6 mm i.d.). (Reproduced with permission from Carretero I, Maldonado M, Laserna JJ, Bonet E and Ramis-Ramos G (1992) Detection of banned drugs in sport by micellar liquid chromatography. *Analytica Chimica Acta* 259: 203–210, copyright Elsevier Science Publishers, B.V.)

Micellar systems such as SDS or polyoxyethylene lauryl ether (Brij-35) solubilize the serum proteins and cause their elution with the void volume. Furthermore, surfactant monomers compete with the analyte for protein-binding sites, thereby releasing it for complete quantitation.

Figure 8 shows the separation by MLC of a mixture containing diuretics (amiloride and spiro lactone), anabolic steroids (metandienone and clostebol) and a stimulant (phenylpropanolamine) added to a urine sample at concentrations of μ g mL⁻¹.

Hydrophobicity Estimation for Organic Compounds

Another interesting possibility of MLC techniques is their application to the quantitation of physico-chemical properties of biologically active compounds in QSAR (quantitative structure–activity

relationships) studies, especially for the prediction of hydrophobicity.

Hydrophobicity is commonly understood as a measure of the relative tendency of a solute to prefer a nonaqueous rather than an aqueous environment. Biological activity of many compounds, bioaccumulation of organic pollutants, and soil sorption of contaminants have all been correlated to the lipophilic character of the molecules concerned.

The quantitation of hydrophobicity has both diagnostic and predictive value in various disciplines such as drug design, toxicology and environmental monitoring.

Traditionally, the logarithm of the octanol–water partition coefficient ($\log P_{OW}$) of the nonionized form of a solute has been the most common parameter used to measure the hydrophobicity. The standard ‘shake-flask’ method for determining partition coefficients in liquid–liquid systems has several serious disadvantages. This fact, together with the use of a bulk solvent such as octanol as a model for complex systems such as biomembranes, has been occasionally criticized and has instigated the search for other indirect methods for evaluating hydrophobicity. Among these methods, chromatographic techniques such as reversed-phase TLC and HPLC can be highlighted. From 1977 several QSRR (quantitative structure–retention relationships) studies have appeared in the literature relating the biological activity of a solute and its retention in a chromatographic system. Good linear relationships between the logarithm of the retention factor ($\log k$) for series of organic compounds determined by RPLC and their $\log P_{OW}$ have been obtained.

The linear relationships obtained between $\log k$ determined by chromatographic techniques and $\log P_{OW}$ are based on the relationship existing between the logarithms of the distribution coefficients of a solute in two different systems, provided the interactions that the solute experiences in these systems are similar and the relationship can be expressed by an equation of the Collander type ($\log P_1 = a_1 \log P_2 + a_2$, where P_1 and P_2 are the distribution coefficients of the solute in the two different phases and a_1 and a_2 are constants).

The good linear correlations obtained between $\log k$ and $\log P_{OW}$ in RP-HPLC suggest that the Collander relationship is satisfied, that is, that the interactions of a solute in an aqueous–stationary phase system are similar to the interactions that the solute experiences in an aqueous–octanol one.

As micelles are considered to be simple chemical models for biomembranes, MLC has been investigated as an interesting possibility for evaluating the hydrophobicity of organic compounds. *n*-Octanol is

an isotropic solvent in which the molecular size and shape of the molecules are not important factors; however, micellar systems, like biomembranes, have amphiphilic properties and are anisotropic media so that the size and shape of molecules influence their penetration through them. The solubilization (or partitioning of solute into micelles) closely resembles that of lipid bilayers and both of these are different from the two-phase octanol–water system.

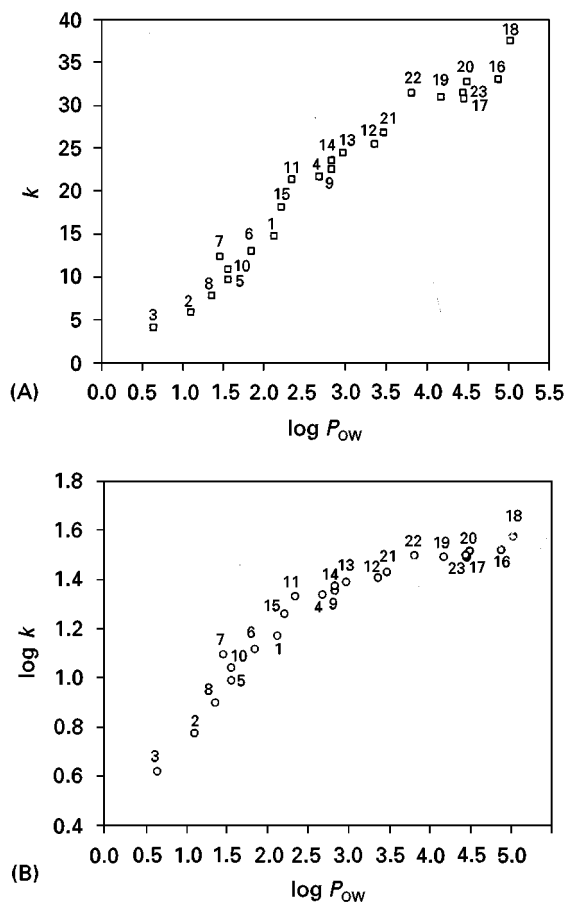


Figure 9 Variation of k (A) and $\log k$ (B) with $\log P_{OW}$ for a group of 23 benzene derivatives and polycyclic aromatic hydrocarbons in a 0.05 mol L⁻¹ CTAB/3% *n*-propanol mobile phase. Key: 1, benzene; 2, benzylic alcohol; 3, benzamide; 4, toluene; 5, benzonitrile; 6, nitrobenzene; 7, phenol; 8, 2-phenylethanol; 9, chlorobenzene; 10, phenylacetonitrile; 11, 3,5-dimethylphenol; 12, naphthalene; 13, 1-naphthol; 14, 2-naphthol; 15, 1-naphthylamine; 16, pyrene; 17, phenanthrene; 18, 2,3-benzofluorene; 19, fluorene; 20, fluoranthene; 21, acenaphthylene; 22, acenaphthene; and 23, anthracene. Column: Spherisorb C₈ (15 cm × 4.0 mm i.d.). (Reproduced with permission from Garcia MA and Marina ML (1994) Study of the k' or $\log k' - \log P_{OW}$ correlation for a group of benzene derivatives and polycyclic aromatic hydrocarbons in micellar liquid chromatography with a C₈ column. *Journal of Chromatography A* 687: 233–239, copyright Elsevier Science Publishers B.V.)

Contradictory results have been obtained concerning which of the two parameters (k or $\log k$) best correlates with $\log P_{OW}$ in MLC. Figure 9 shows the variation of k (Figure 9A) and $\log k$ (Figure 9B) with $\log P_{OW}$ for a micellar mobile phase, 0.05 mol L⁻¹ CTAB modified by 3% *n*-propanol, for a group of 23 benzene derivatives and polycyclic aromatic hydrocarbons. This figure shows that a good linear correlation between $\log k$ and $\log P_{OW}$ can be obtained for solutes with a low hydrophobicity, while, when high $\log P_{OW}$ values are attained, there exists a $\log P_{OW}$ value from which no further change for $\log k$ with $\log P_{OW}$ is obtained. This is due to the change in the retention mechanism of compounds from a three-equilibria mechanism to a direct-transfer mechanism from the micellar mobile phase to the stationary phase with increasing $\log P_{OW}$ for solutes. In fact, for highly hydrophobic compounds, which can become insoluble in water, the predominant equilibrium is the distribution between the micellar and stationary phases. Since these two phases are chemically similar, the distribution coefficient is close to unity and may become independent of solute hydrophobicity. In this way the variation of $\log k$ with $\log P_{OW}$ is represented by a curve.

Conclusion

MLC is a mode of HPLC in which solutions of surfactants at a concentration above their critical micellar concentration are employed as mobile phases. Three different equilibria exist for a solute in MLC. It can distribute between the aqueous mobile phase and the micellar mobile pseudophase, between the stationary phase and the micellar pseudophase, and between stationary and aqueous mobile phases. However, for highly hydrophobic compounds, a direct-transfer mechanism from the micellar to the stationary phase has been proposed. Solute retention is related to the concentration of micellized surfactant in the mobile phase through solute-micelle association constants or distribution coefficients that can be calculated as a direct application of MLC techniques.

The great number of interactions that are possible in MLC separations, such as electrostatic, hydrophobic and esteric, and the modification of the stationary phase by adsorption of monomeric surfactants, make these systems more complicated than conventional RP-HPLC. However, the fact that the amount of the surfactant adsorbed remains constant after equilibrium between mobile and stationary phases allows MLC techniques to achieve rapid micellar and organic modifier gradients.

The control of separation selectivity in MLC can be performed through a great number of parameters;

these include the nature and concentration of the surfactant in the mobile phase, the presence of additives as organic modifiers and salts, and the pH. The fact that the addition of an organic modifier to micellar mobile phases can increase selectivity and reduce analysis time has increased the use of hybrid micellar mobile phases, which also preclude the efficiency loss inherent to MLC as compared to conventional RP-HPLC.

Other applications that can be cited in MLC techniques are directly derived from the special characteristics of micellar solutions. The sensitivity of the detection can be enhanced and biological fluids can be directly injected into the chromatographic systems because of the solubilization of the protein by some surfactants. Finally, the fact that micelles can be considered as chemical models for biomembranes has enabled the application of MLC to hydrophobicity estimation of organic compounds.

See also: II/Chromatography: Liquid: Mechanisms: Reversed Phases. Electrophoresis: Micellar Electrokinetic Chromatography. III/Surfactants: Liquid Chromatography.

Further Reading

- Dorsey JG (1987) Micellar liquid chromatography. *Advances in Chromatography* 27: 167–214.
- Fernández-Lucena F, Marina ML and Rodríguez AR (1991) Determination of metal ions as complexes in micellar media by UV-Vis spectrophotometry and fluorimetry. In: Durig R (ed.) *Vibrational Spectra and Structure*. Amsterdam: Elsevier.
- Hansch C and Leo A (1979) *Substituent Constants for Correlation Analysis in Chemistry and Biology*. New York: Wiley.
- Hinze WL and Armstrong DW (eds) (1987) *Ordered Media in Chemical Separations*, ACS Symposium Series, vol. 342. Washington: American Chemical Society.
- Jiménez O and Marina ML (1997) Retention modeling in micellar liquid chromatography. *Journal of Chromatography A* 780: 149–163.
- Kaliszan R (1987) *Quantitative Structure-Chromatographic Retention Relationships*. New York: Wiley.
- Marina ML and García MA (1994) Micellar liquid chromatography with hybrid eluents. *Journal of Liquid Chromatography* 17: 957–980.
- Marina ML and García MA (1997) Evaluation of distribution coefficients in micellar liquid chromatography. *Journal of Chromatography A* 780: 103–116.
- Medina-Hernández MJ and García-Alvarez-Coque MC (1992) Solute-mobile phase and solute-stationary phase interactions in micellar liquid chromatography. *Analyst* 117: 831–837.
- Mittal KL and Lindman B (eds) (1984) *Surfactants in Solution*, vol. 2. New York: Plenum Press.

Multidimensional Chromatography

P. Campíns-Falcó and R. Herráez-Hernández,
Universidad de Valencia, Valencia, Spain

Copyright © 2000 Academic Press

Trace organic separations are often made difficult by the large number of substances present in various kind of samples, by the similarities among the analytes, and by the need to remove major components in the sample. The advantages of using hyphenated systems to tackle such problems have been demonstrated and sequential separation techniques are also well suited. A characteristic feature of these methods is the use of two or more columns for the separation.

Separation in two dimensions has a substantial history. While methods such as two-dimensional (2-D) electrophoresis and thin-layer chromatography are 2-D in space, coupled column techniques are 2-D in time. In *offline* techniques, the fractions of the first column are collected in vials and reinjected onto the second column later. Interest in these techniques has been revived by increased automation. In 1973 Huber *et al.* proposed a two-channel multicolumn system which allowed an imitation of 2-D chromatography with columns as they existed at that time. In *online* techniques, manual or automatic switching by a valve directs fractions between columns. Electrically controlled valves greatly facilitate the full automation of the chromatographic process, thus increasing the speed and the work capacity of the *high performance liquid chromatography* (HPLC) system. The terms column switching, coupled column chromatography and multidimensional chromatography are used interchangeably.

Column switching includes, in the widest sense, all techniques in which the flow path of the mobile phase is changed by valves, so the effluent from a primary column is passed to a secondary column for a defined period of time. An unlimited number of columns can theoretically be incorporated in a chromatographic network. However, in each successive step, the transferred fraction must be reconcentrated to reduce the dispersion of the analyte in the chromatographic system, and the dead volumes in the connections between columns and in any switching valves must be minimized to achieve maximum separation efficiency. The band spread problem can be approached by making a judicious choice of the order in which the dimensions are sequenced.

Multidimensional separations have been defined by Giddings as having only two criteria. The first is that

sample components must be displaced by two or more separation techniques based on different separating mechanisms. The second is that components separated by any single separation dimension must not be recombined in any further separation dimension. Most coupled-column approaches proposed only subject a portion of the sample to full 2-D or *n*-D analysis and are useful for the resolution of a single fused peak from the first dimension. They do not permit a comprehensive 2-D or *n*-D separation of the entire sample. The term linear heart-cut approach, used by Deans, describes the use of on-off valves in order to isolate an effluent segment which is then injected into a subsequent column. Comprehensive automated systems are useful for the greater resolution of multiple fused peaks from the first dimension column and resolved in the second-dimension orthogonal separation system.

Basic Theory and Configurations

Giddings' treatment of the peak capacity for a single mode leads to the expression:

$$\phi = 1 + \frac{N^{1/2}}{m} \ln(1 + k_n) \quad [1]$$

where $m = 4$ implies unit resolution (4σ separation), N is the plate number, and k_n is the retention factor for the last member of a series of peaks numbered from zero (nonretained) through to n (last peak out). A sequence of independent modes, each having a peak capacity ϕ_i , should exhibit a multiplicative separation effect with an overall result given by:

$$\phi = \phi_1 \times \phi_2 \times \dots \phi_n \quad [2]$$

With a conventional single-column approach the peak capacity increases with dwindling returns. To increase the peak capacity by a factor of 10, a 100-fold increase in column length would be necessary. In coupled chromatography however the effect is, theoretically, multiplicative and leads to an exponential increase with the number of columns within the configuration with different retention mechanisms.

Not all column types are compatible: typical examples of compatible systems with sufficiently different retention mechanisms are size exclusion and normal-phase chromatography, reversed-phase and ion

exchange chromatography, ion exchange and reversed-phase chromatography and polar bonded phase and normal-phase chromatography. The columns employed can have the same or different lengths: even a very short column, like a guard column, is used as the first column for some applications.

When one discrete zone is collected from the first-dimension column and reinjected into the second dimension, the resulting data are two individual one-dimension data sets. In linear coupled-column systems, the peak capacities of the individual columns can be summed, not multiplied. In so-called comprehensive automated system, the resulting data are a matrix, usually represented as a contour plot with each chromatographic separation along an axis.

The multidimensional resolution (R_s) for comprehensive multidimensional chromatography was suggested to be equal to the Euclidean norm of the resolution in each dimension. Schure *et al.* showed that this definition, under a certain set of assumptions, could be utilized to produce an experimentally simple method for 2-D resolution estimation:

$$R_s = \left[-\frac{1}{2} \ln \frac{1-P}{2} \right]^{1/2} \quad [3]$$

where P is the ratio of the difference between the amplitude at the valley and average peak maximum (f) and the average maximum peak (g) of the resulting one-dimensional chromatogram at the peak maxima in the contour plot, as shown in Figure 1 ($t_{1,x}$ and $t_{2,x}$ are the retention times of the peak maxima for peaks 1 and 2 in the x separation axis. The peak maxima in the y dimension are similarly denoted as $t_{1,y}$ and $t_{2,y}$).

A host of methods exist for coupling the various separation systems. In order to set up a switching network, the separation problem must be analysed and a valve configuration selected according to the solution. A review of commonly used switching networks is given by Ramsteiner (see Further Reading). These techniques only require minor modifications to existing equipment and, of equal importance, enable the sample preparation procedures to be completely automated.

For multidimensional chromatography a standard high pressure liquid chromatograph is used with the addition of one or more switching valves. These valves may be simple, manually operated six-, eight- or 10-port valves or may be automatically controlled. An eight-port valve with matching sample loops is typically used when the comprehensive mode of operation is utilized. When coupling two or more separation techniques online, not only has an interface to

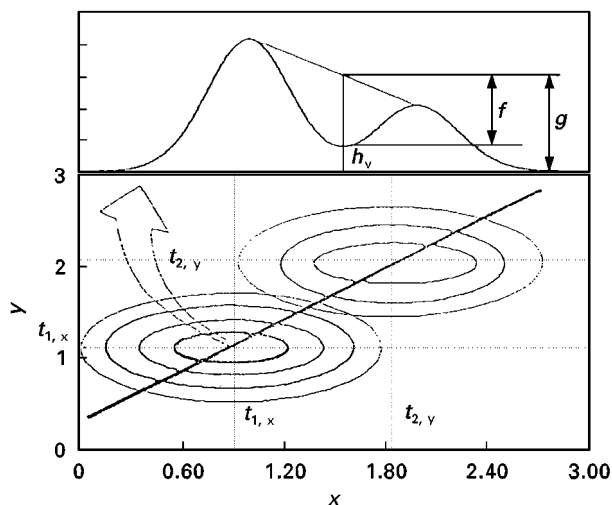


Figure 1 Schematic diagram of the two-dimensional resolution measurement using a 2-D contour (bottom) and the corresponding slice for resolution determination. (Reproduced with permission from Murphy RE, Schure MR and Foley JP (1998) *Analytical Chemistry* 70: 1585–1594. Copyright 1998 American Chemical Society.)

be constructed but attention must be given to the effects of the injection volume and flow rates on the performance of the coupled system.

Scope of Multidimensional Liquid Chromatography

Multidimensional liquid chromatography (LC) is a powerful approach for demands such as improved analyte detectability and separating power, or the generally recognized need to increase sample throughput. In this sense, the main applications of multidimensional systems are analyte purification and enrichment, and improvement of the separation process (for instance, by increasing column length or by reducing the time of analysis), as will be illustrated in some detail below. In addition, because of their inherent flexibility, systems can be designed to achieve various objectives within a chromatographic network.

Sample clean-up

The main drawback of LC for the analysis of complex samples is the time-consuming and laborious nature of the sample pretreatment. Classic methods of clean-up often involve one or more liquid-liquid extractions, which have disadvantages such as the use of large volumes of organic solvents, the risk of contamination or the loss of analytes during evaporation and the final introduction of an aliquot of the (concentrated) extract into the LC column. Whereas

a chromatographic run often requires a few minutes, sample preparation time can be 1–2 h, and typically accounts for at least one-third of the error generated during the performance of the analytical method. Solid-phase extraction, although most commonly used as an offline technique, enables more rapid sample processing. Moreover, since a variety of stationary phases are available, better selectivity is generally achieved. However, the risk of contamination or loss of analytes, and the final introduction of an aliquot of the extract are ever-present drawbacks. In this respect, the employment of coupled columns is very well suited for the purification of complex samples before chromatography and today, coupling LC-LC is a well-established technique for sample clean-up, especially in the analysis of environmental, biomedical, pharmaceutical and food(stuff) samples.

The principle of multidimensional chromatography for sample clean-up is to transfer an effluent cut containing the analytes from a primary to a secondary column, whereas the remaining effluent containing unwanted compounds is vented to waste. In particular, the online coupling of a primary column, for the pre-separation of the analytes, with the analytical column via a switching valve greatly facilitates the analysis, as shown in Table 1. This table compares sample preparation steps typically involved in liquid–liquid extraction, and solid-phase extraction on to disposable cartridges, with those required by the multidimensional approach. As can be deduced from this table, a multidimensional approach drastically reduces, or even eliminates, manual sample preparation steps, and the entire analysis can be fully automated. In addition, the total time required for analysis is greatly shortened and the selectivity that can be reached is comparable to (and

sometimes better than) that obtained with traditional liquid–liquid or solid-phase extraction. Additional advantages over classical procedures are avoidance of an internal standard (and thus of sample dilution) and protection of the analytes during analysis (for example, light-sensitive or oxidation-sensitive compounds, as they can be kept away from light and air).

The success of the clean-up process mainly depends on the type of sample, the working conditions used in the first chromatographic dimension and the configuration of the system.

Type of sample In principle, any liquid sample can be processed by multidimensional LC (solid samples require prior dissolution and homogenization). However, the stability of the chromatographic system is often limited when processing complex matrices. For example, up to several hundred samples can be analysed with satisfactory stability when analysing water samples or biofluids with a low protein content (such as urine). However, regeneration or replacement of the primary column after a few injections may be required for fluids with a large amount of proteins (for instance, plasma or blood) due to the irreversible adsorption of the proteins to the stationary phase, or to the clogging of the pre-column. In most instances, this problem can be overcome simply by centrifugation or filtration of the sample. A prior treatment such as acidification, or the addition of an organic solvent or a selective displacer, aimed to increase the free concentration of analytes tightly bound to matrix constituents may also be required.

Primary column The effectiveness of clean-up mainly depends on the ability of the primary column to

Table 1 Procedures for sample clean-up by liquid–liquid and solid-phase extraction on to a disposable cartridge and multidimensional approach

<i>Liquid–liquid extraction</i>	<i>Solid-phase extraction</i>	<i>Multidimensional LC</i>
Pipetting out the sample	Pipetting out the sample	Primary column conditioning and sample injection
Addition of an internal standard	Addition of an internal standard	
Addition of an organic solvent	Cartridge conditioning	
Agitation		
Centrifugation		Switching-valve rotation Elution of the analytes and insertion into the secondary column
Separation	Elution of the sample	
Possibly re-extraction	Matrix elimination by washing the cartridge	
Agitation		
Centrifugation		
Separation	Elution of the analytes	
Solvent evaporation	Solvent evaporation	
Redissolution	Redissolution	
Filtration	Filtration	
Injection	Injection	

retain selectively the compounds of interest. In general, small columns (often called pre-columns), typically $2\text{--}10 \times 1\text{--}4.6\text{ mm i.d.}$, are preferred. Small size reduces cost, allows fast sampling and prevents band broadening during the analyte transfer to the analytical column. Longer columns provide higher resolution, which might be required for some applications. On the other hand, particle sizes in the $10\text{--}40\text{ }\mu\text{m}$ range are used to prevent pre-column clogging.

The stationary phase must be chosen according to the type of sample and the characteristics of the compounds to be analysed. For example, common reversed-phase materials, which are used in most published procedures, allow the retention of a wide variety of compounds of low to medium polarity. This makes the multidimensional approach very useful in the biomedical field, since proteins, salts and other highly polar matrix constituents are flushed to waste in the first fraction of eluent, while retaining the compounds of interest. Next, the analytes are desorbed and transferred to the analytical column for complete resolution. Obviously, pre-columns with a stationary phase similar to that of the analytical column provide little extra selectivity, but flushing of the pre-column with the correct solvent gives the required selectivity for most applications. This is illustrated in **Figure 2**, which shows the elution time profile obtained for untreated urine ($50\text{ }\mu\text{L}$) in a $20 \times 2.1\text{ mm i.d.}$ pre-column packed with a C_{18} stationary phase. When using water as the mobile phase (washing solvent), the vast majority of matrix components are eliminated from the pre-column

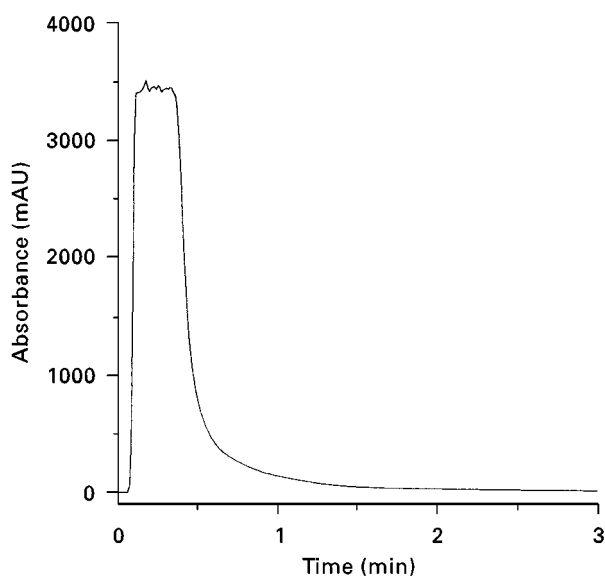


Figure 2 Elution time profile obtained for untreated urine in a pre-column packed with C_{18} stationary phase.

within the first $1\text{--}1.5\text{ mL}$ of eluent. Therefore, satisfactory preseparation can be achieved by incorporating a flushing step, provided that the analytes are not eluted from the first column during the washing stage. As an example, **Figure 3** shows the chromatograms obtained for a urine sample on a C_{18} analytical column, after flushing the pre-column with 1 mL of water. This figure also shows the chromatogram obtained for the same sample when a C_{18} solid-phase extraction cartridge was used offline for sample clean-up. As can be seen from this figure,

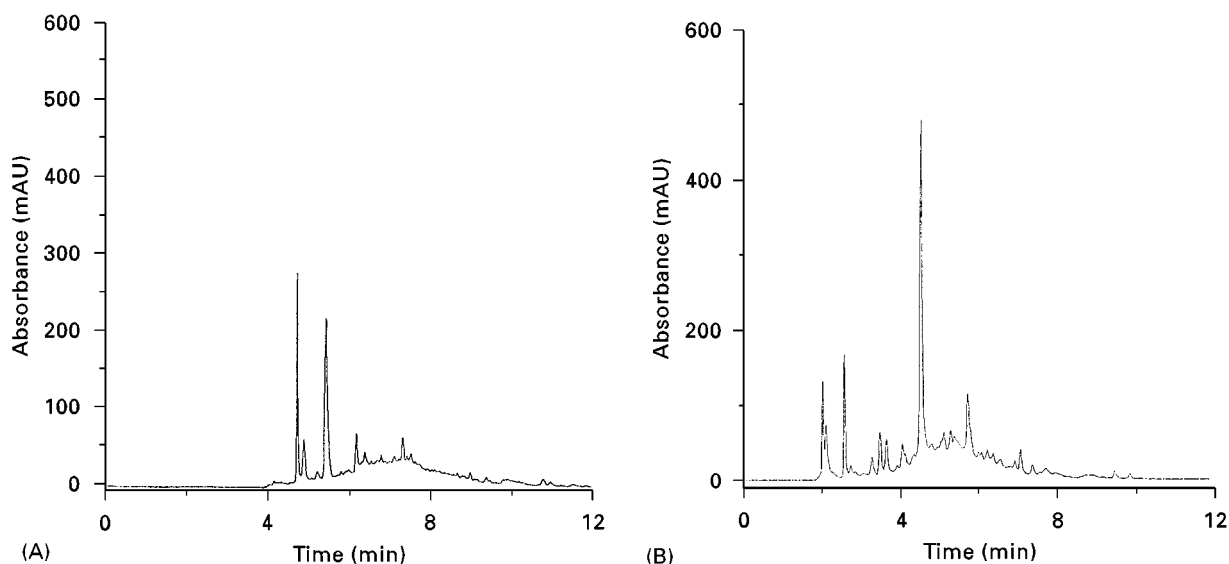


Figure 3 Typical chromatograms obtained from a urine sample by (A) online and (B) offline sample clean-up. Conditions: detection wavelength 230 nm ; analytical column, Hypersil ODS C_{18} ($5\text{ }\mu\text{m}$, $250 \times 4\text{ mm i.d.}$); mobile phase, acetonitrile- 0.05 mol L^{-1} phosphate buffer ($\text{pH } 3$).

the selectivity that can be reached is comparable to or even better than that obtained with solid-phase extraction cartridges. In some instances, selectivity can be improved simply by using a buffer or a specific modifier (an organic solvent or a surfactant) in the washing eluent.

Alternatively, a different chromatographic mode can be used to prepare the analytes. For example, gel permeation materials are effective for the elimination of high molecular mass matrix components before reversed-phase chromatography, which is particularly useful in the analysis of biofluids. A packing material specially designed for this field is the internal surface reversed-phase silica support (ISPR). ISPR materials confine the partitioning phase exclusively to the internal regions of the particles. Therefore, only interaction with small molecules is possible while the macromolecules are unretained since the external surface is nonadsorptive to them. The analysis of polar compounds requires different stationary phases. For example, ion exchangers or metal-loaded phases can be used for the selective retention of polar pesticides from environmental samples. Applications with pro-

tein-coated phases, immobilized antibodies or different copolymers have also been described for the analysis of different kinds of samples. The combination of two or more pre-columns with complementary separation properties can also be used for handling the clean-up of complex matrices.

Configuration The system design also determines the reliability of the system. In the simplest configuration, only a switching valve is required in addition to a basic chromatograph, as shown in **Figure 4**. It should be noted that, during the sampling and clean-up steps, the eluent in the analytical column is stagnant. Therefore, this configuration may lead to considerable baseline fluctuations depending on the elution conditions, which limits its applicability. However, excellent results are achieved when no buffers are used in the mobile phase. This is illustrated in **Figure 4**, which shows the chromatogram obtained for a urine sample spiked with the diuretic triamterene processed with the system shown in the figure. More powerful systems can be achieved at a reasonable cost by using an additional pumping system

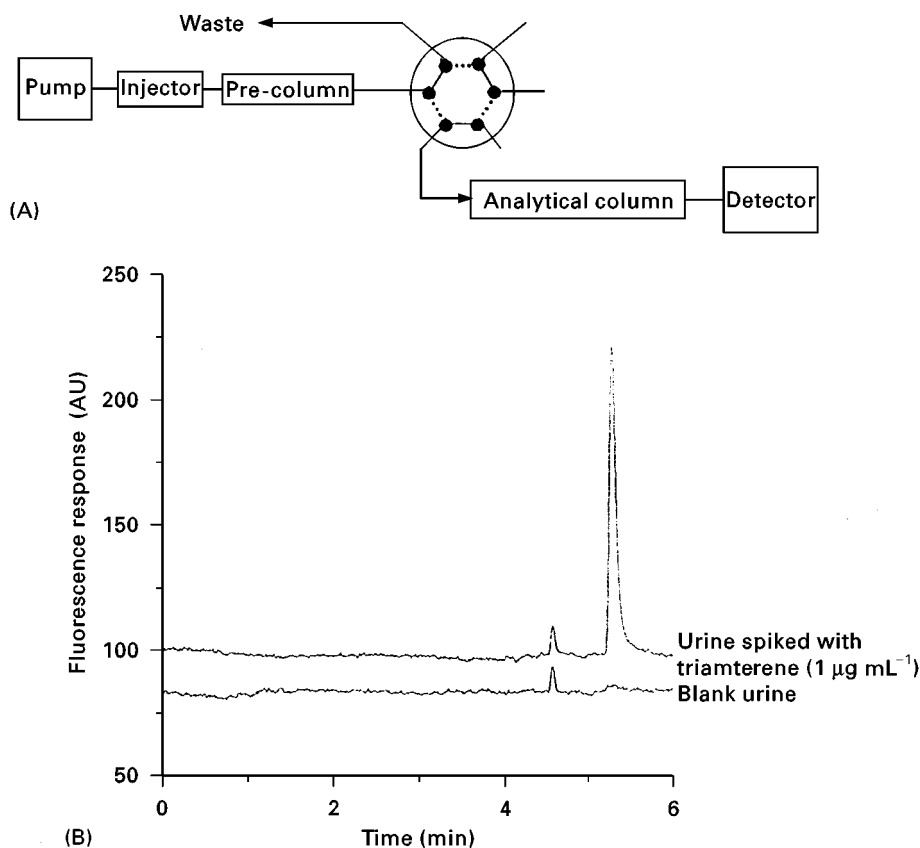


Figure 4 (A) Chromatographic system used for sample clean-up in straight-flush mode and (B) chromatogram obtained for clear and spiked urine sample with triamterene. Conditions: detection, excitation wavelength of 230 nm and emission wavelength of 430 nm; analytical column, LiChrospher 100 RP 18 (5 µm, 125 × 4 mm i.d.); mobile phase, acetonitrile–0.05 mol L⁻¹ phosphate buffer (pH 3). (A) Continuous lines, clean-up; dotted lines, transfer and separation.

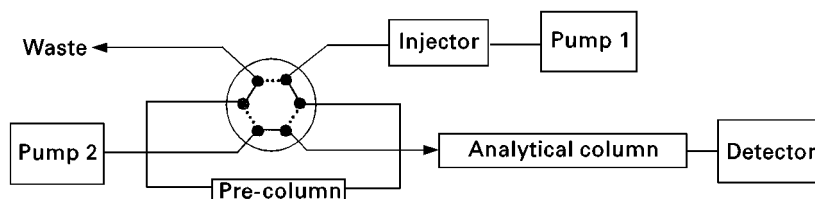


Figure 5 Schematic representation of a conventional chromatographic system with back-flush configuration. Continuous lines, clean-up; dotted lines, transfer and separation.

(Figure 5). In such a way, the analytical column is equilibrated during the clean-up stage, and only the fraction of the eluent containing the compounds of interest is transferred to the analytical column.

Different transfer modes can be used. In forward-flush (also called straight-flush) configurations the flow direction in the pre-column is not changed during the transfer stage, which prevents solid particles retained at the head of the pre-column being sent to the second column. However, for samples containing compounds which are strongly retained in the pre-column, backflush configurations (in which the flow direction of the mobile phase through the pre-column is reversed for the transfer on to the second column) are preferable, because the desorption of the most retained components after every injection is easier.

Sample Enrichment

Sample enrichment is based on analyte retention in a pre-column when a large volume of sample is flushed through it. This column is then connected to the main column for separation of the analytes. An essential condition for this set-up is that the sampling solvent is a weak solvent with respect to the retention mechanism of the analytes in the first enrichment column. For example, since water is a noneluting solvent in reversed-phase LC, large volumes of aqueous samples can be passed through columns packed with hydrophobic chemically bonded phases for enrichment of rather apolar analytes. As for the sample clean-up, greater accuracy and precision can be expected in analyte enrichment by multidimensional LC compared with classical enrichment procedures, which are more time-consuming and prone to errors.

According to the basic principles indicated in the above section, the optimization of the chromatographic conditions should include careful selection of the pre-column (packing and dimensions) and system design, in order to achieve maximum analyte enrichment and minimum peak-broadening. The ultimate enrichment factor is determined by the breakthrough volume of the solute in the pre-column. For most applications, rather small columns, similar to those used in sample clean-up, provide successful results.

The enrichment of apolar compounds can be performed on C_{18} -bonded silica phases, while carbon-based materials or styrene-divinylbenzene provides sufficient resolution for the enrichment of relatively polar compounds (in environmental analysis, for instance). Maximum analyte detectability is reached by using a backflush configuration, which minimizes band broadening. Under optimized conditions, enrichment factors up to several thousand can be achieved.

Unfortunately, sample enrichment also concentrates components other than the analytes, thus limiting the degree of concentration possible. In this sense, the incorporation of washing stage after sample loading may improve the selectivity of the analysis. In such a case, an additional pump is required to deliver the washing solvent. In fact, many systems are designed to effect analyte enrichment and purification simultaneously.

Apart from the good compatibility of the sample with mobile phases used in reversed-phase LC, multidimensional chromatography is especially successful in the biomedical field, because sufficient sensitivity (high to low ng mL^{-1} level) can usually be reached with the direct injection of 0.1–0.5 mL of sample. However, trace analysis in water samples requires much higher sample volumes (50–100 mL). The employment of an LC pump for sampling allows such volumes to be loaded on to the pre-column. Published results demonstrate that detection limits of a few ng L^{-1} can be reached.

Enrichment via a pre-column can also be used to circumvent analyte dilution introduced by a different purification technique, for example, dialysis. Dilution, which is a serious problem when using online dialysis to remove macroconstituents from the sample matrix, can be overcome by refocusing the analytes in a pre-column before the chromatographic separation.

Improvement of the Separation Process

Multidimensional systems can be used to solve many problems encountered in the analysis of complex samples. Of particular interest are those systems designed to enhance the selectivity and to reduce the time of analysis.

The improvement in resolution is probably the most important application of multidimensional LC systems in the present context. The coupling of two or more chromatographic modes with complementary retention mechanisms considerably increases the resolution, provided that the separation modes are compatible. The great differences which are attainable due to the wide variety of separation modes available make multidimensional LC a very powerful tool for the resolution of complex mixtures and much more information can be obtained from a single run, especially if a comprehensive approach is used. A typical example is the analysis of proteins for peptide mapping. Reversed-phase LC coupled to mass spectrometry is generally used for peptide mapping, but the analysis of large proteins is often difficult due to the large number of fragments obtained from the enzymatic digestion of the protein. While mass spectrometry detection is useful to identify the presence of overlapping peaks, data interpretation becomes difficult if a large number of peptides co-elute. Difficulties also arise if the masses of the co-eluting peaks are similar and if the ^{13}C , ^{15}N or ^{18}O peaks overlap. A heart-cutting system combining size exclusion chromatography (SEC) and reversed-phase chromatography greatly facilitates the analysis. Two or more peptides co-eluting in the first SEC column could be transferred and separated in the reversed-phase column, because of the unlikely possibility that they would have the same molecular weight as well as the same hydrophobicity. In this approach, only the fractions containing co-eluting peaks are sampled into the reversed-phase column. A comprehensive configuration, however, offers substantially higher resolution, as fractions of the entire effluent from the SEC column are continuously sampled into the reversed-phase column. As a result, the peak capacity of the system is significantly increased, and exhaustive information from each sample can be obtained (three-dimensional data set). The addition of mass spectrometry allows the molecular weight information to identify accurately the chromatographic peaks. This kind of system has been successfully used for the characterization of proteins such as ovoalbumin and serum albumin in a reasonable time. As an example, Figure 6 shows a typical 2-D chromatogram of a protein sample.

Other interesting applications of two-dimensional systems with part or all of the sample passing into the second dimension deal with the separation of polymers, polymer blends, copolymers or large molecules. The combination of two columns operating under size exclusion and (partition) reversed-phase modes provides complementary information on molecular weight distribution, chemical structure and architec-

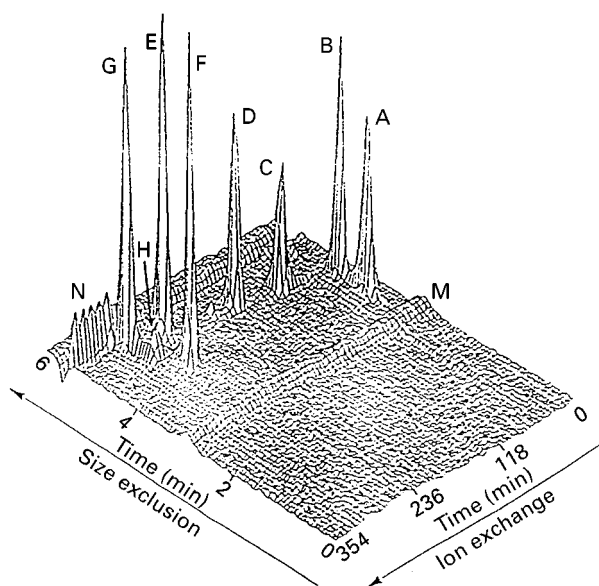


Figure 6 2-D chromatogram of protein sample. Peak A, glucose oxidase; B, ovalbumin; C, β -lactoglobulin A; D, trypsinogen; E, α -chymotrypsinogen A; F, conalbumin; G, ribonuclease A; H, haemoglobin; M, exclusion volume pressure ridge; N, inclusion volume salt ridge. Ovalbumin and α -chymotrypsinogen A at 2%, other proteins at 0.3% (w/v). C1 conditions: $5\ \mu\text{L min}^{-1}$, 0–100% buffer B from 20 to 260 min; buffer A, $0.2\ \text{mol L}^{-1}\ \text{NaH}_2\text{PO}_4$, pH 5; buffer B, $0.2\ \text{mol L}^{-1}\ \text{NaH}_2\text{PO}_4/0.25\ \text{mol L}^{-1}\ \text{Na}_2\text{SO}_4$, pH 5. Valve activated 4 every 6 min; detection at 215 nm, data collection rate 0.5 points per s; plot shows every other point collected for injections 1–60. Each line perpendicular to the ion exchange chromatography time axis represents one injection on the SEC column. (Reproduced with permission from Bushey MM and Jorgenson JW (1990). Automated instrumentation for comprehensive two-dimensional high-performance liquid chromatography of proteins. *Analytical Chemistry* 62: 161–167. Copyright 1990 American Chemical Society.)

ture, thus making possible the complete characterization of complex polymers with a single run. Another example is the separation of groups of compounds in oil samples. The coupling of size exclusion and normal-phase modes enables the separation of oil fractions, and the subsequent resolution of the analytes according to their polarity (if required, the system can be interfaced to a gas chromatograph, for further resolution according to volatility).

An area of special interest is the resolution of enantiomers. Although different combinations have been described, in the most commonly used configuration the first column (achiral) effects a separation of the compounds of interest, whereas only the fraction of the eluent containing the optical isomers is transferred to the second chiral column for enantio-resolution. This simplifies analysis, particularly in the biomedical field, because several matrix compounds can lead to pairs of peaks, thus making the resolution of the compounds of interest difficult. In addition, the

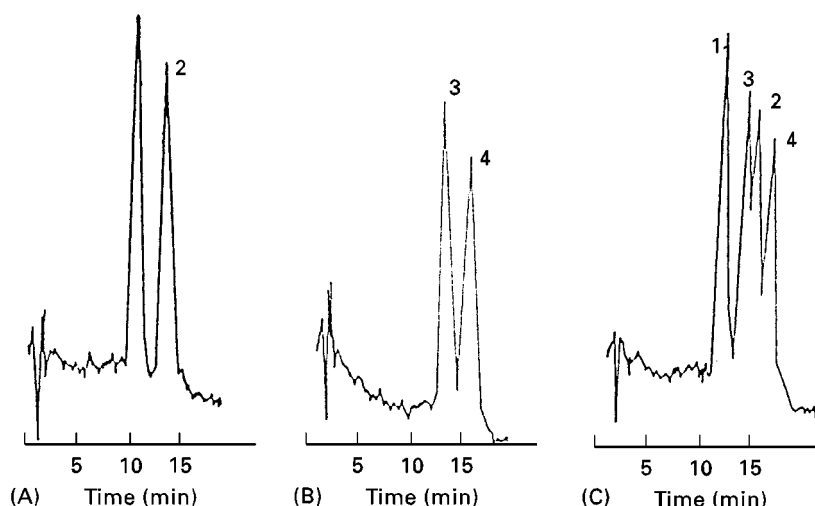


Figure 7 Representative chromatograms for the separation of separation of racemic verapamil (*R,S*-VER) and racemic norverapamil (*R,S*-NOR) on the AGP-CSP. (A) *R,S*-VER; (B) *R,S*-NOR; (C) *R,S*-VER and *R,S*-NOR. 1, *R*-VER; 2, *S*-VER; 3, *R*-NOR; 4, *S*-NOR. (Reprinted from Fried F and Wainer IW (1997) Column-switching techniques on the biomedical analysis of stereoisomeric drugs: why, how and when. *Journal of Chromatography B* 689: 91–104. Copyright 1997, with permission from Elsevier Science.)

chiral column is better protected. An example of the kind of problems encountered in chiral analysis is the inability of many chiral stationary phases to separate parent drugs from metabolites. This is illustrated in **Figure 7**, which shows the chromatograms obtained for the calcium channel-blocking agent verapamil and its major metabolite norverapamil on an AGP chiral column. This column allows the enantioresolution of both compounds but overlap between *S*-verapamil and *R*-norverapamil is observed. The problem can be overcome by using an achiral–chiral system, where verapamil and norverapamil are initially separated from each other on the achiral (reversed-phase) column. The eluent fractions containing verapamil and norverapamil are then selectively transferred to the chiral AGP column for further separation of the enantiomers. A multidimensional approach can also be used to enhance the selectivity by effecting peak compression on an achiral column, after enantioresolution in a primary chiral column. This approach appears as an elegant alternative in

chiral analysis of drugs in biofluids or in multiresidue pesticide analysis.

Another area of application is the analysis of derivatized analytes. In this case, pre-separation or trapping in the first column allows a large amount of unreacted reagent or secondary products to be excluded for the second (analytical) column (**Figure 8**). Solid-phase reagents prepared by immobilizing detection-sensitive reagents on solid supports such as organic polymers can be used as column packings and integrated into the liquid chromatography system in order to form derivatives online. This methodology has been successfully applied to the derivatization of a variety of drugs. During the last 5 years, our research group has been studying the possibility of carrying out derivatizations with conventional octadecylsilica stationary phases. A possible online set-up for this purpose is shown in **Figure 4** or **5**. The system uses a 20×4.6 mm i.d. pre-column packed with an unmodified octadecylsilica stationary phase. This column is used to purify the sample and

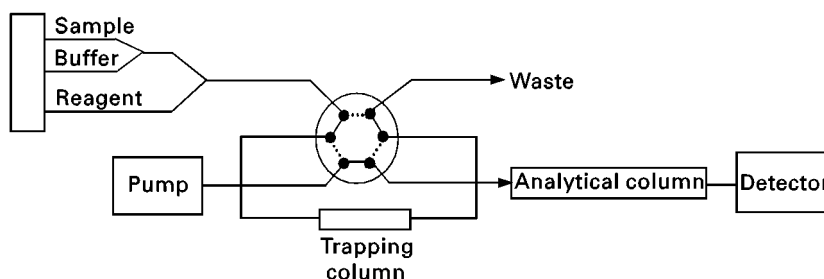


Figure 8 Configuration used for online sample clean-up and derivatization. Continuous lines, derivatization; dotted lines, transfer and separation.

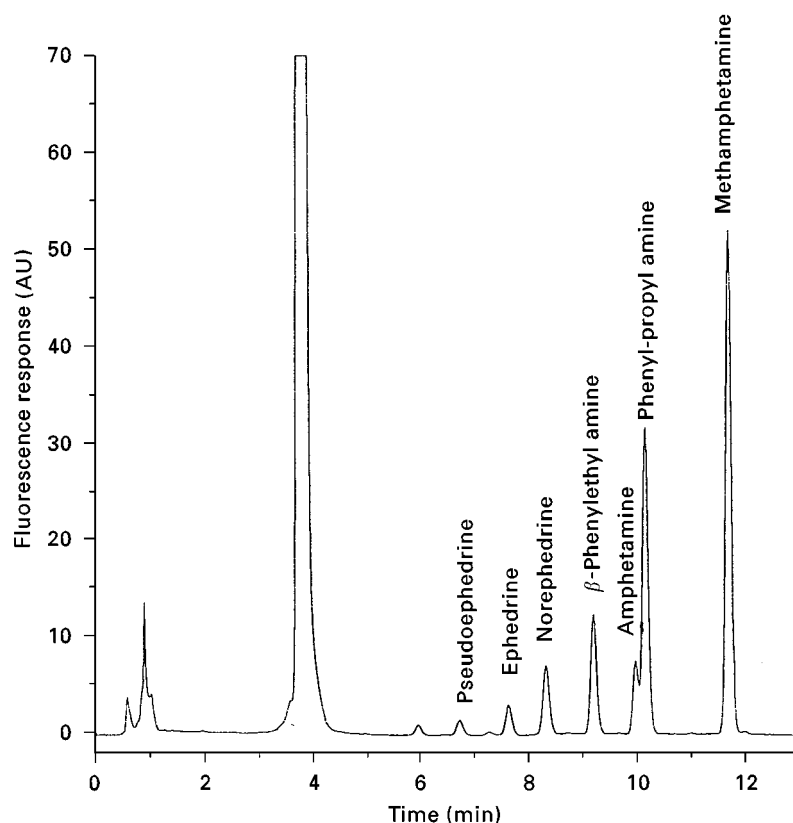


Figure 9 Chromatogram of an aqueous mixture of the amphetamines ($5 \mu\text{g mL}^{-1}$) derivatized online by using the configuration shown in Figure 5. Conditions: derivatization reagent, 9-fluorenylmethyl chloroformate; detection, excitation wavelength 264 nm and emission wavelength 313 nm; analytical column, LiChrospher 100 RP 18 ($5 \mu\text{m}$, $125 \times 4 \text{ mm i.d.}$); mobile phase, acetonitrile–water.

concentrate the analytes; the trapped analytes are derivatized by injection of the derivatization reagent into the pre-column. Finally, the derivatives are transferred to the analytical column by means of a switching arrangement. Some applications based on this methodology have been described for the determination of amphetamine and related compounds in urine, by using reagents such as 1,2-naphthoquinone 4-sulfonate, 9-fluorenylmethyl chloroformate and *o*-phthaldialdehyde. **Figure 9** is an example of the chromatograms obtained by this methodology.

Multidimensional systems can also be used to minimize the separation time of mixtures containing compounds of considerably different retention factors. In a column of high selectivity and under optimized conditions, compounds eluting at the start of the chromatogram can be generally well resolved, but later eluting compounds with long retention times may be difficult to detect. Conversely, if the column has low selectivity, the separation time will be shorter, but early eluting components will be poorly resolved. The coupling of two columns is well suited for such kinds of problems. The first column (short or low selectivity) is used to resolve the late eluting

components in a short time. These compounds are sent directly to the detector, whereas the poorly retained components are transferred to the second column (longer or more selective) for complete resolution. The overall effect is a considerable reduction of the time of analysis. This approach is a good alternative to gradient elution in those cases where a large number of plates is required, where a large number of samples will be analysed (as full automation is possible), or where detectors not compatible with gradient elution will be used.

An interesting form of this alternative is the so-called box car chromatography. The box car configuration involves partial separation of the compounds of interest in the first column, and subsequent transfer to a second column, where they are injected with the maximum frequency permitted by the resolution of the column. In this way, the separation power of the second column is fully utilized, and this considerably increases sample throughput. An example of the box car technique is the analysis of primidone and phenobarbitone in plasma. When utilizing a box car configuration, up to 40 samples per hour can be analysed, and this illustrates the potential of this technique.

Future Developments

Looking to the future, evolutionary development can be expected because the separating power of multi-dimension liquid chromatography is greatly increased over single-dimension liquid chromatography. The simultaneous improvements on both the software and the chromatographic apparatus will lead to a system capable of automatically developing analytical methods for a wide range of analytes in many different matrices. Other desirable aspects are a reasonably short analysis time and flexible operating conditions.

The thrust of multidimensional research will most probably be to improve the combination of separation methods, including coupling to alternative separation techniques.

See also: **II/Chromatography: Thin-layer (Planar):** Modes of Development: Conventional. **Electrophoresis:** Two-Dimensional Electrophoresis. **III/Chiral Separations:** Liquid Chromatography. **Pharmaceuticals:** Chiral Separations: Liquid Chromatography.

Further Reading

- Brinkman UATh (1996) Multidimensionality: a hot topic. *Analysis* 24: M12.
- Campíns-Falcó P, Herráez-Hernández R and Sevilano-Cabeza A (1993) Column-switching techniques for high-performance liquid chromatography of drugs in biological samples. *Journal of Chromatography* 619: 177.
- Cortes HJ (ed.) (1990) *Multidimensional Chromatography*. New York: Marcel Dekker.
- Deans DR (1968) *Chromatographia* 1: 18.

- Freeman DH (1981) Review: Ultrasensitivity through column switching and mode sequencing in liquid chromatography. *Analytical Chemistry* 53: 2.
- Fried K and Wainer IW (1997) Column-switching techniques in the biomedical analysis of stereoisomeric drugs: why, how and when. *Journal of Chromatography* 689: 91.
- Giddings JC (1967) Maximum number of components resolvable by gel filtration and other elution chromatographic methods. *Analytical Chemistry* 39: 1967.
- Herráez Hernández R, Campíns Falcó P and Sevilano Cabeza A (1996) On-line derivatization into precolumns for the determination of drugs by liquid chromatography and column switching: determination of amphetamines in urine. *Analytical Chemistry* 68: 734.
- Holland IA and Jorgenson JW (1995) Separation of nanoliter samples of biological amines by a comprehensive two-dimensional microcolumn liquid chromatography system. *Analytical Chemistry* 67: 3275.
- Huber JFK, Van der Linden R, Ecker E and Oreans M (1973) Column switching in high pressure liquid chromatography. *Journal of Chromatography* 83: 267.
- Krull IS, Deyl Z and Lingeman H (1994) General strategies and selection of derivatization reactions for liquid chromatography and capillary electrophoresis. *Journal of Chromatography B* 659: 1.
- Murphy RE, Schure MR and Foley JP (1998) Effect of sampling rate on resolution in comprehensive two-dimensional liquid chromatography. *Analytical Chemistry* 70: 1585.
- Opiteck GJ, Lewis KC, Jorgenson JW and Anderegg RJ (1997) Comprehensive on-line LC/LC/MS of proteins. *Analytical Chemistry* 69: 1518.
- Ramsteiner KA (1988) Systematic approach to column switching. *Journal of Chromatography* 456: 3.

Normal Phase Chromatography: Mechanisms

See **II/CHROMATOGRAPHY: LIQUID/Mechanisms: Normal Phase**

Nuclear Magnetic Resonance Detectors

M. Dachtler, T. Glaser, H. Händel, T. Lacker, L.-H. Tseng and K. Albert, University of Tübingen, Institute of Organic Chemistry, Tübingen, Germany

Copyright © 2000 Academic Press

Introduction

In many fields of chemistry, biology, pharmacy and medicine, progress is often limited by the ability to resolve complex analytical problems. To this end

analytical techniques have been developed in recent decades dealing with an integrated approach to the separation of mixtures together with structural elucidation of unknown compounds. High performance liquid chromatography (HPLC), gel permeation chromatography (GPC) and supercritical fluid chromatography (SFC), as well as the capillary separation techniques capillary HPLC (CHPLC), capillary electrophoresis (CE) and capillary electrochromatography (CEC) are the most powerful techniques

within the group of chromatographic separation methods. Nuclear magnetic resonance (NMR) spectroscopy, in particular, is useful because of its powerful stereochemical information content but it has the disadvantage of lower sensitivity in comparison to other methods, e.g. mass spectrometry (MS).

The combination of chromatographic separation techniques with NMR spectroscopy is one of the most powerful and time-saving methods for the separation and structural elucidation of unknown compounds and mixtures. Especially for the structure elucidation of light- and oxygen-sensitive substances, for example, hop bitter acids and carotenoid stereoisomers, online liquid chromatography (LC)-NMR has important advantages. Here, structure elucidation with LC-MS is not possible, because the carotenoid isomers exhibit the same fragmentation pattern. Using a classical method with offline separation, enrichment and transfer to a NMR sample tube, the isolated substances would be isomerized. A closed-loop LC-NMR flow-through system solves this problem. Online LC-NMR also allows the continuous registration of time changes as they appear in the chromatographic run. Unequivocal structural assignment of unknown chromatographic peaks is possible by two-dimensional stopped-flow LC-NMR experiments.

NMR Flow Cell Design

Figure 1 shows the design of NMR cells employed for various coupling techniques. For online HPLC-NMR and GPC-NMR coupling, a vertically oriented flow cell with a directly fixed double-saddle Helmholtz coil

is used (Figure 1A). The whole arrangement is centred in the glass dewar of a conventional probe body in which a thermocouple is inserted, allowing temperature-dependent measurements to be made. The internal diameter of the glass tube is 2, 3 or 4 mm, resulting in detection volumes of 60, 120 and 180 μL . The glass walls of the flow cell are parallel within the length of the proton detection coil, and taper at both ends to fit polytetrafluoroethylene (PTFE) tubing (i.d. 0.25 mm). PTFE and glass tubing are connected by shrink-fit tubing. Inverse continuous-flow probes contain an additional coaxial coil (tuned to the ^{13}C resonance frequency) surrounding the ^1H detection coil for heteronuclear $^1\text{H}/^{13}\text{C}$ shift-correlated experiments. This design leads to optimal NMR resolution values with a typical line width of chloroform at the height of the ^{13}C satellites of 9–12 Hz, allowing the determination of coupling constants of 1 Hz in continuous-flow NMR spectra. The disadvantage of this design is the high detection volume, leading to a degraded chromatographic resolution. For analytical HPLC columns (250 \times 4.6 mm i.d.) the plate height is increased for solutes with capacity factors less than 2.5 at detection volumes higher than 48 μL .

The probe design employed for SFC-NMR coupling is shown in Figure 1B. The inner glass tube of the original LC-NMR probe is substituted with a sapphire tube (o.d. 5 mm, i.d. 3 mm, detection volume 120 μL) and the polyetheretherketone (PEEK) capillaries used in the LC-NMR probe are replaced by Titan tubings. A double-tuned proton deuterium coil is directly fixed to the sapphire flow cell. The whole arrangement is centred in the glass dewar of

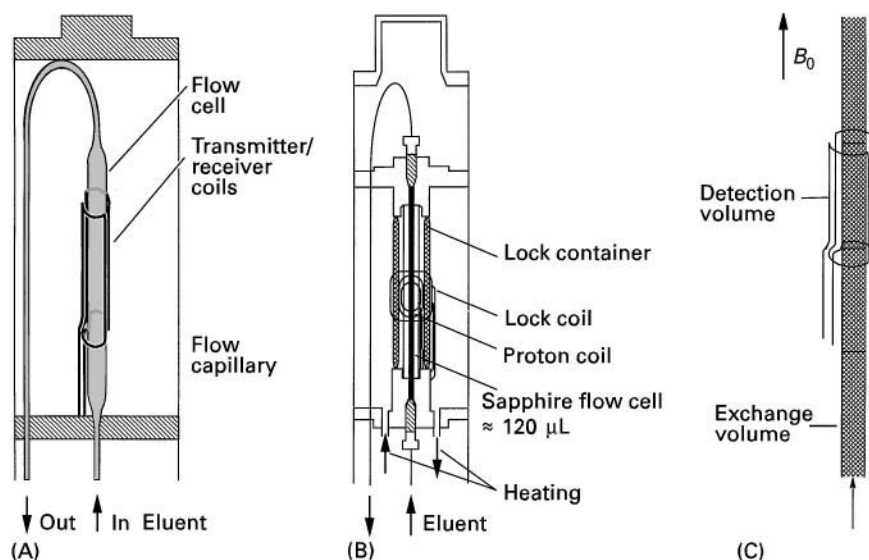


Figure 1 Design of NMR flow cell for: (A) HPLC-NMR and GPC-NMR experiments; (B) SFC-NMR experiments; (C) capillary NMR experiments.

a conventional probe body, in which a thermocouple is inserted, allowing temperature-controlled experiments.

Figure 1C shows the schematic diagram of the capillary NMR detection probe. Here a fused silica capillary is directly inserted within the NMR radio-frequency coil of a 2.0 mm microprobe. Within the area of the NMR detection coil the polyimide coating of the capillary is removed; either capillaries with an i.d. of 180 μm or bubble cell types with an increased i.d. of 220 μm are used.

Experimental Set-up

For online LC-NMR, GPC-NMR and SFC-NMR experiments, the chromatographic separation system consists of either HPLC or SFC pumps together with an injection valve, a separation column (250 \times 4.6 mm i.d.) and an ultraviolet (UV) or refractive index (RI) detector. The system is located at a distance of 2.0 m from an unshielded cryomagnet (Figure 2). With shielded cryomagnets, the chromatographic separation system can be located at a distance of about 30 cm. The outlet of the UV (RI) detector is connected by stainless steel capillary tubing (0.25 mm i.d.) to a switching valve. The valve is used to trap the desired peak in the NMR flow cell for stopped-flow experiments. For online experiments with continuous registration of NMR spectra in distinct time intervals (1–8 s), the switching valve is

open for a continuous flow through the probe to waste. Instead of the switching valve, a Bruker peak sample unit (BPSU) can be used. This technique is advisable when long NMR times are expected. Desired peaks from a separation can be stored in small capillary loops with the help of the peak sample unit. After complete separation, every single peak can be transferred into the probe and the desired stopped-flow experiment can be conducted.

In SFC-NMR experiments the outlet of the high pressure SFC probe is connected to a back-pressure regulator to guarantee supercritical conditions in the detection cell.

A feasible experimental set-up for online capillary LC-NMR coupling is outlined in Figure 3. The separation device for either pressure or electroosmotic flow-driven separations is located at a distance of 2 m from the cryomagnet. Separation is performed on a packed fused silica capillary which is directly fixed in a microprobe. For capillary HPLC separations a T-piece in conjunction with a restriction column is used for flow rate adjustment of the eluent. The HPLC pump, the injection device and the packed separation capillary are connected by fused silica capillaries.

LC-NMR Coupling

The coupling of LC-NMR requires the adjustment of both analytical systems. The flow of the mobile

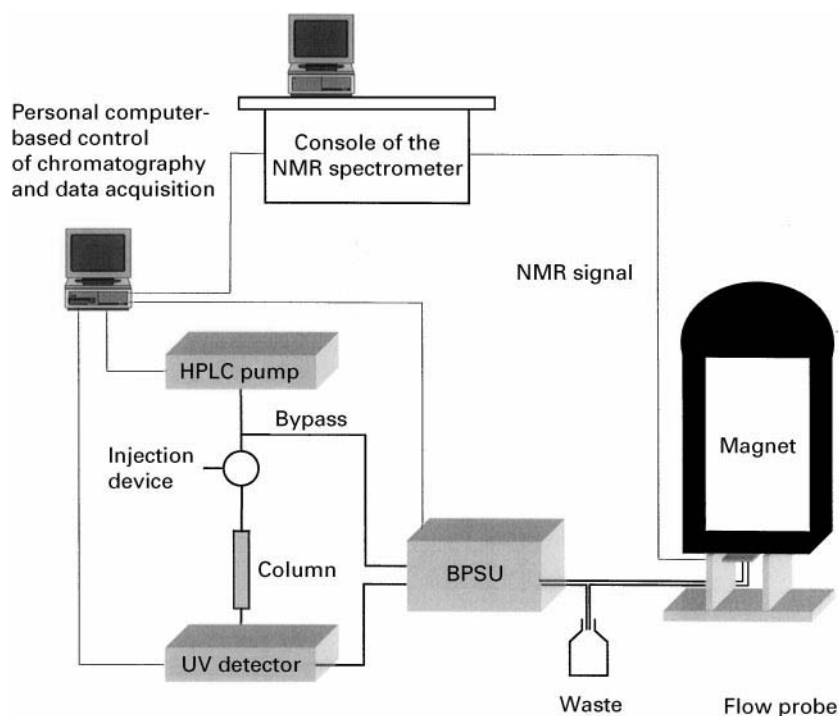


Figure 2 Experimental arrangement for HPLC-NMR, solid-phase extraction (SPE)-HPLC-NMR, GPC-NMR and SFC-NMR experiments. BPSU, Bruker peak sampling unit; fine lines, electronic junction; bold lines, capillary junctions.

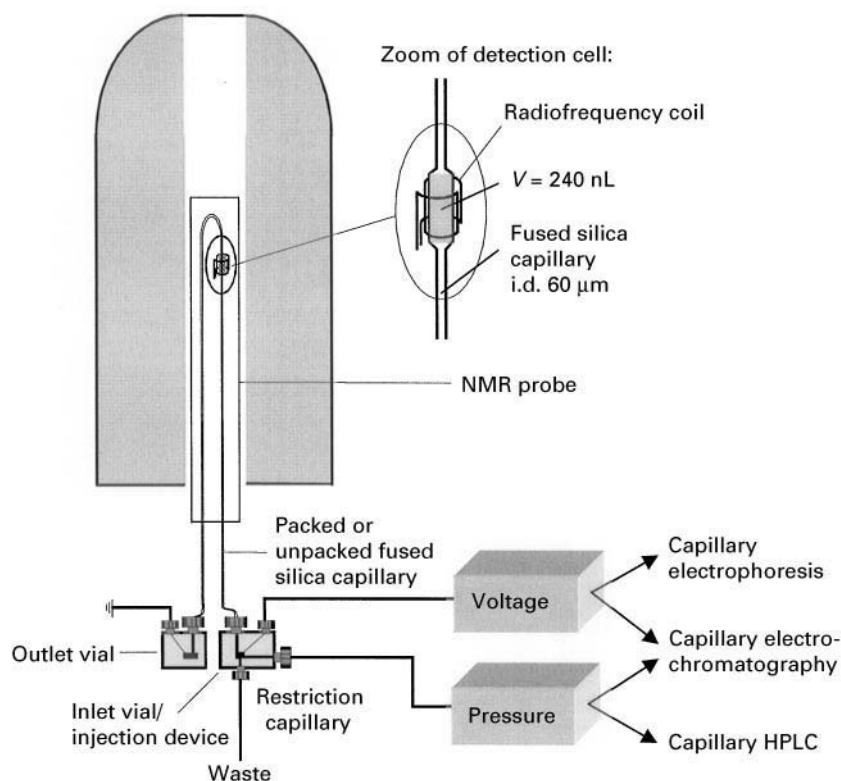


Figure 3 Experimental arrangement for coupling a capillary separation technique with NMR spectroscopy.

phase leads to a restricted exposure period τ for the nuclei in the flow cell. The time τ is defined as the proportion of the detection volume to the flow rate. This is the reason for a shorter transverse relaxation time T_2 , which includes larger NMR signals. On the other hand the equilibrium state will be reached in a shorter time due to the permanent-flow nonexcited nuclei than only through the longitudinal relaxation time T_1 . This allows a quicker repeat time rate for exposure of a spectrum and therefore greater sensitivity.

LC-NMR spectroscopy is a relatively insensitive method requiring sufficient sample concentration in the NMR flow cell. However, the separation column should not be overloaded, because then separation may be impossible. Most HPLC separations are performed with reversed-phase materials using binary solvent mixtures such as acetonitrile–water, acetone–water or methanol–water as mobile phases. The choice of the mobile phase should be suited to the NMR spectroscopy. An obvious advantage is to obtain a small number of solvent signals in the NMR spectrum, because the solvent signals may obscure the sample spectra. Generally, the chromatographic conditions in HPLC-NMR experiments are the same as in conventional chromatography, but water is replaced by deuterated water. The use of deuterated

organic solvents is generally too expensive. For proper adjustment of the receiver gain of the NMR instrument, the solvent signals should be reduced to the height of the sample by applying a solvent suppression technique. Efficient solvent suppression can be performed, for example, by applying a NOESY-type presaturation scheme. With residence times in the order of 5 s and acquisition times of about 1 s, sufficient presaturation time is left even in the continuous-flow mode. Modern techniques like WET or WATERGATE sequences are based on a selective dephasing of the solvent signals using a magnetic field gradient.

Another problem is solvent purity. Most HPLC solvents have small amounts of impurities, often stabilizer additives. These additives have no UV activity and do not affect the chromatographic results, but will be detected in the NMR spectrum.

There exist in principle two general methods for carrying out LC-NMR: continuous-flow and stopped-flow experiments.

Continuous-flow Experiments

With this mode of operation the output of the chromatographic separation is recorded at the same time as the ^1H NMR spectra. In most cases the flow

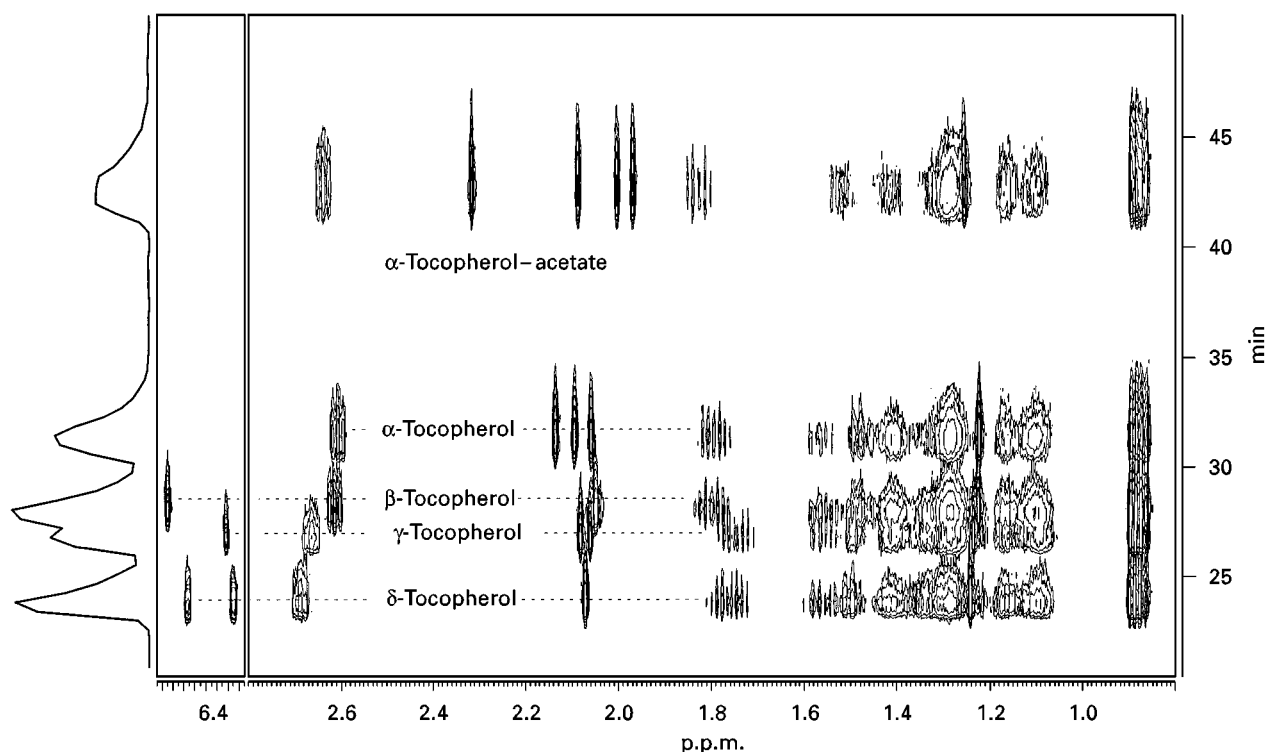


Figure 4 Contour plot (600 MHz) of the separation of tocopherol isomers.

rate of the mobile phase is decreased to yield an NMR scan accumulation of one chromatographic peak. The acquisition of online continuous-flow NMR spectra results in a two-dimensional contour plot of ^1H NMR signals of the separated compounds (x axis = ^1H chemical shift) versus retention time (y axis). **Figure 4** shows the contour plot of the separation of tocopherol isomers on a C_{30} stationary phase in methanol together with 2% CD_3OD . A time interval of 1 s was applied to presaturate the methyl group signal of the solvent. A total of 128 experiments with a time resolution of 27.3 were recorded at a flow rate of 0.3 mL min^{-1} . The chromatogram along the y axis was reconstructed by co-addition of all proton resonances between 0.8 and 1.9 p.p.m. The resolution of this ^1H NMR chromatogram suffers from the small number of 128 data points, but the separation of all five tocopherol isomers is readily apparent.

The structure of the separated compounds can easily be assigned by the methyl group ^1H NMR signals between 2.0 and 2.2 p.p.m. and by the aromatic resonances between 6.4 and 6.5 p.p.m. (**Figure 5**). For instance, the continuous-flow ^1H NMR spectrum of δ -tocopherol shows one signal for the methyl group at C_8 and two aromatic resonances with a small splitting due to the meta coupling between H_5 and H_7 . Thus, unequivocal structural assignment of all different isomers is possible by considering chemical shifts, coupling constants and integration ratios.

Stopped-flow Experiments

In continuous-flow experiments only a short time is available for accumulation of the ^1H NMR spectrum. Thus, this spectroscopic technique can only be used for high concentrations of the sample, since otherwise the signal to noise ratio is too low. The sample is transferred through the flow cell analogous to the continuous-flow experiment, but in the stopped-flow mode the valves of the sample unit switch and the chromatographic run is stopped as soon as the maximum of the peak reaches the flow cell (indicated by UV detector). At this point conventional NMR experiments can be performed and, therefore, the NMR experimental time can be adjusted to the sample concentration. Another advantage of the stopped-flow experiment is the possibility of multidimensional NMR spectra.

In **Figure 6** a correlation spectroscopy (COSY) stopped-flow spectrum of the olefinic protons of the carotenoid all-*trans* zeaxanthin is shown, recorded on a Bruker AMX 400 spectrometer. The number of experiments in F1 dimension was 216, the number of accumulated transients was 256.

Due to the centrosymmetric molecule, the corresponding protons are identical. By means of the cross-peaks in the coupling system, the structure can be elucidated. Proton H_{11} couples with two other protons, H_{10} and H_{12} , while proton H_{15} couples with

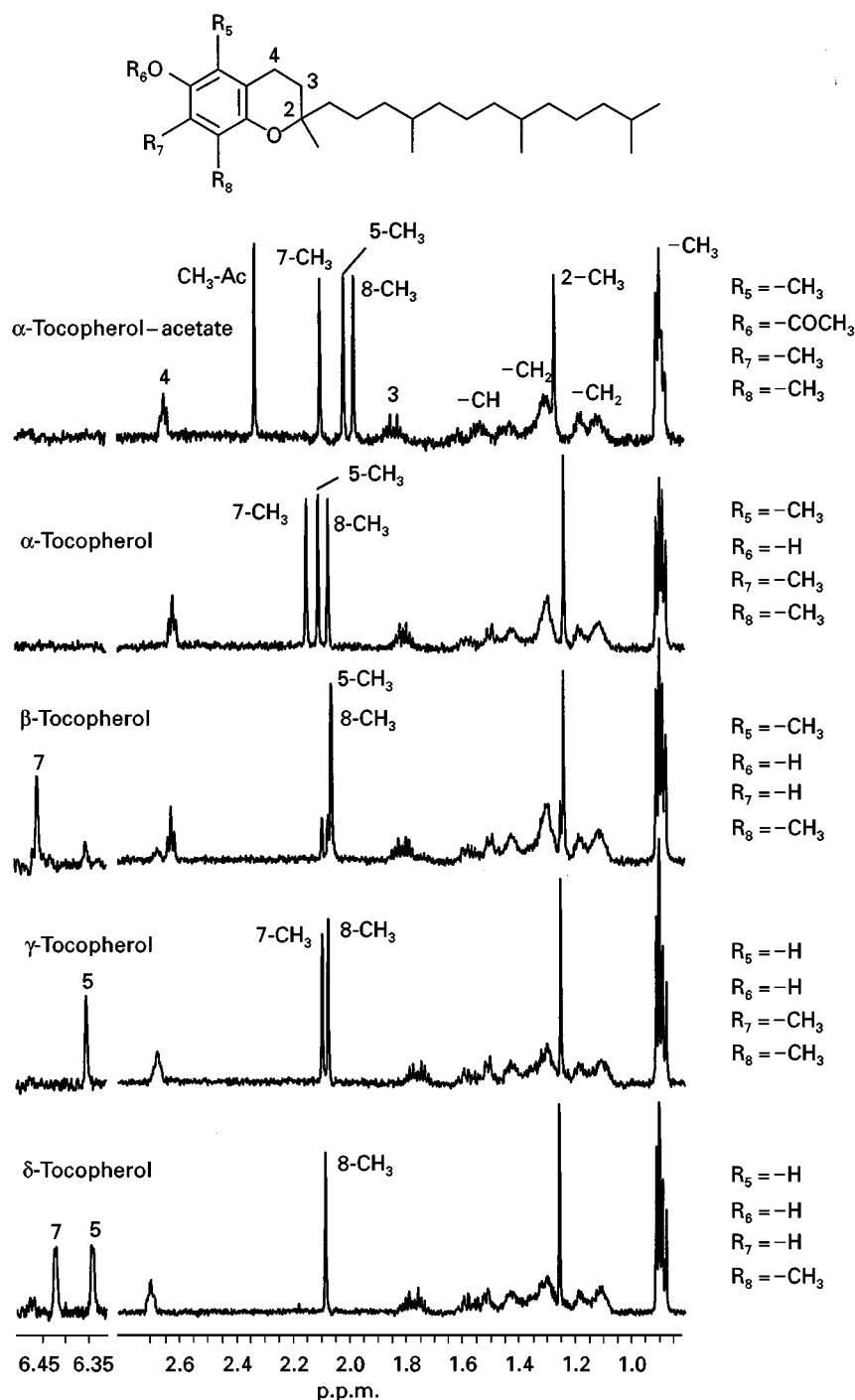


Figure 5 Continuous-flow 1H NMR spectra (600 MHz) of tocopherol isomers.

proton H_{14} . The cross-peak at 6.1 p.p.m. can be assigned to the proton H_7 and H_8 .

Figure 7 shows a stack plot of various zeaxanthin stereoisomers. Due to the *cis*-arrangements, the centrosymmetry of the molecule is repeated. Therefore, different resonance frequencies result for the shielded and unshielded protons. In Figure 7 the 1H NMR

spectra of all-*trans*, 13-*cis* and 9-*cis* zeaxanthin are depicted.

The assignment of *cis/trans* is adapted from the Karplus equation in general, with the difference that the coupling constants are available. In most cases the difference in the chemical shift values in systems with conjugated olefinic protons is more informative. They

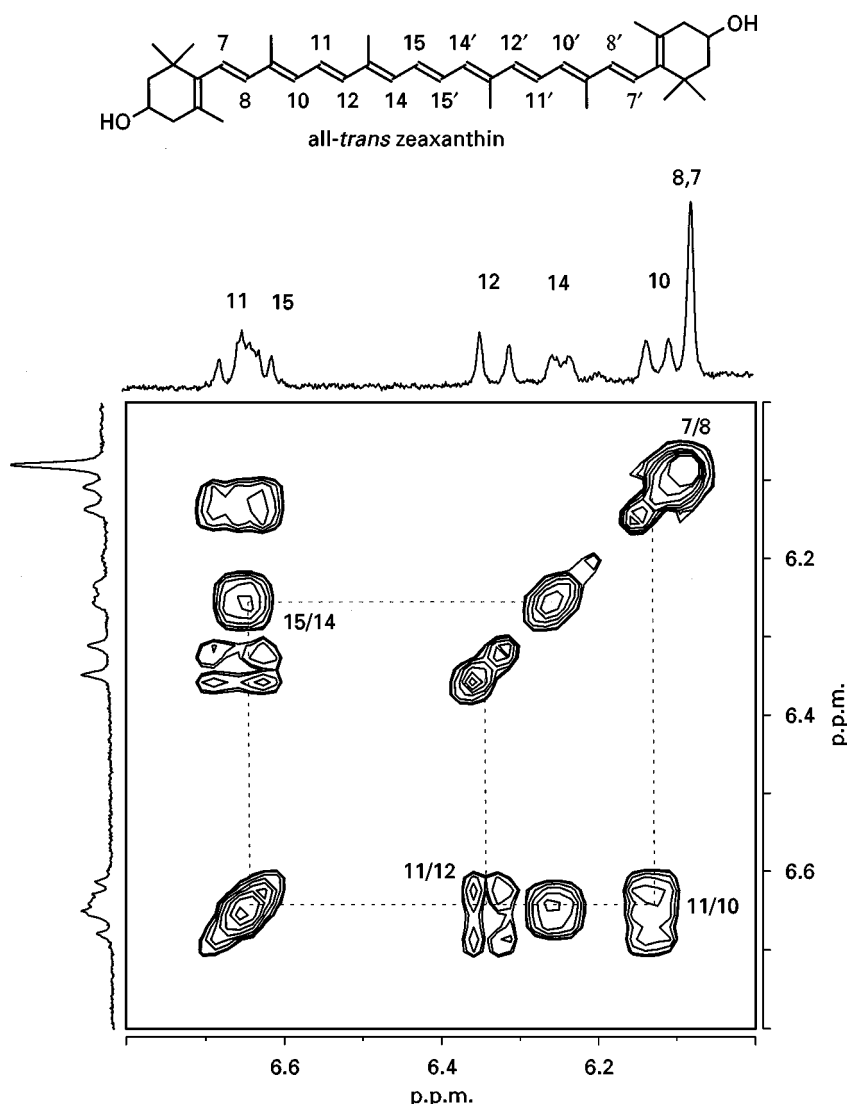


Figure 6 COSY stopped-flow spectrum (400 MHz) of all-*trans* zeaxanthin.

can amount up to 0.6 p.p.m. Looking at the protons of the *cis*-bonding, the outer protons experience a shift to higher field, while the inner protons shift to lower field. As shown in Figure 7, the protons H_{12} and H'_{15} in 13-*cis* zeaxanthin shift to lower field and proton H_{14} to higher field. The protons H_{10} and H'_{15} also show a small influence. The other protons have the same chemical shift values as the all-*trans* zeaxanthin and the *cis*-bonding has no further influence. Analogous effects could be explained for the 9-*cis* zeaxanthin. Here the *cis*-bonding has no effect on the shielded protons and only the unshielded ones are affected.

SPE-LC-NMR Coupling

In order to enhance the sample concentration injected onto the column for HPLC separation, solid-phase

extraction (SPE) can be used. In online SPE, the sample is injected onto a cartridge that replaces the loop of the injection device of the chromatographic system. By switching the valve, the enriched sample is transferred directly onto the separation column. The advantage of online SPE-LC coupling is the direct enrichment of analytes on a cartridge in the HPLC system excluding light and oxygen.

A new online SPE-LC technique in which both the trace enrichment and the separation are performed on one single short HPLC column (10–20 mm in length) is called the SSC (single short column) approach. By performing online sample enrichment before LC-NMR analysis, analyte detectability may be significantly improved. The hyphenation of this approach with NMR spectroscopy can reduce the effective analysis time necessary for separation and structure elucidation. As in conventional LC-NMR coupling,

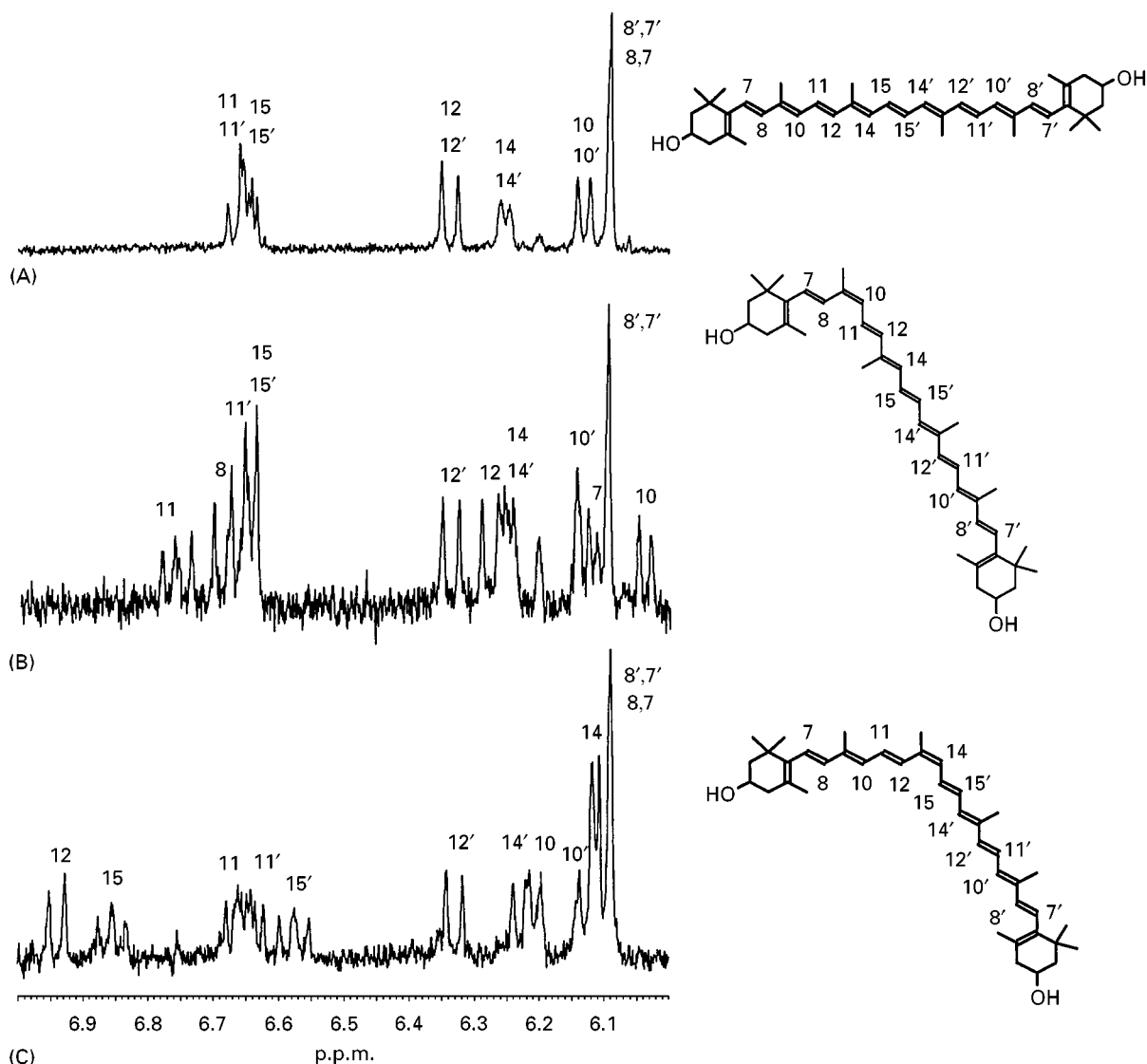


Figure 7 ^1H NMR spectra (600 MHz) of (A) all-*trans*, (B) 9-*cis* and (C) 13-*cis* zeaxanthin.

stopped-flow as well as continuous-flow experiments are possible. The higher concentration of sample is advantageous for continuous-flow LC-NMR experiments. For online SSC-NMR, 10 mL of a $5\ \mu\text{g mL}^{-1}$ mixture was loaded on to a $12.5 \times 4.6\ \text{mm}$ i.d. C_{18} short column and separated on-column with the eluents (A) acetonitrile–0.05% phosphoric acid and (B) water–0.05% phosphoric acid 30 : 70 (v/v) at a reduced flow rate of $0.3\ \text{mL min}^{-1}$ and transferred to the NMR spectrometer. Figure 8 shows the contour plot of the separation of ibuprofen, fenoprofen and naproxen.

In the case of these drugs, the differences between the structures can be determined by the signals in the aromatic region, so the structure of the separated compounds can easily be assigned by the aromatic

resonances. Whereas naproxen is a substituted naphthalene derivative, fenoprofen and ibuprofen both contain a phenyl ring which is meta-substituted in the case of fenoprofen and para-substituted in ibuprofen. For unambiguous structural elucidation, different rows could be extracted from the contour plot to obtain conventional ^1H NMR spectra, as shown in Figure 9 for ibuprofen.

GPC-NMR Coupling

One of the most impressive advantages of continuous-flow ^1H NMR spectroscopy is the direct monitoring of the change in the microstructure of polymers and in the chemical composition of copolymers during GPC. In the case of synthetic polymers, the amount of

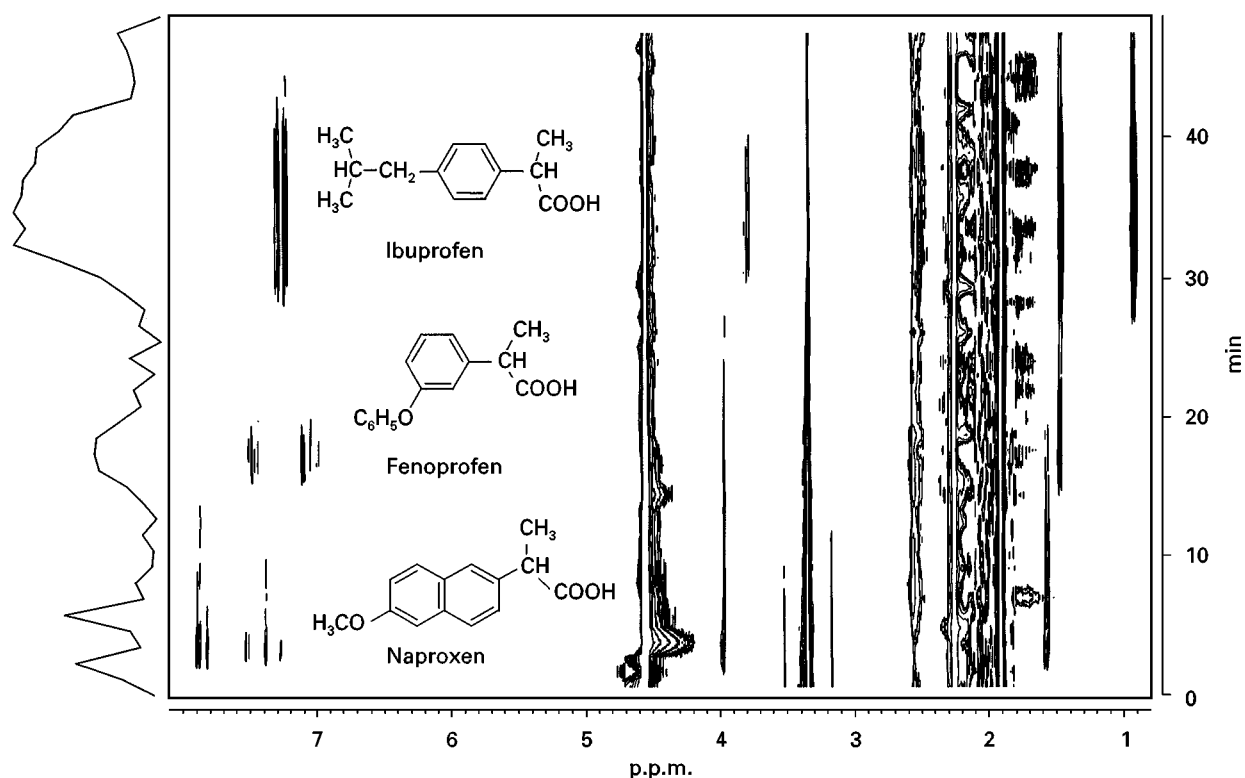


Figure 8 ^1H NMR chromatogram (contour plot, 400 MHz) of an SPE-HPLC separation of ibuprofen, fenopropfen and naproxen.

available sample is not limited and GPC is not sensitive to peak dispersion effects. A NMR flow cell with a detection volume of 120 μL with a 400 MHz spectrometer yields adequate signal-to-noise values within a reasonable resolution time of 8 s.

One example shows the possibilities of GPC-NMR coupling and is typical of a multitude of similar prob-

lems in the chemical industry. Two styrene-butylacrylate copolymers were synthesized under similar conditions, but the physical properties of the copolymers differed. Conventional polymer analysis failed to distinguish between the samples. In both cases the chemical composition and microstructure were identical.

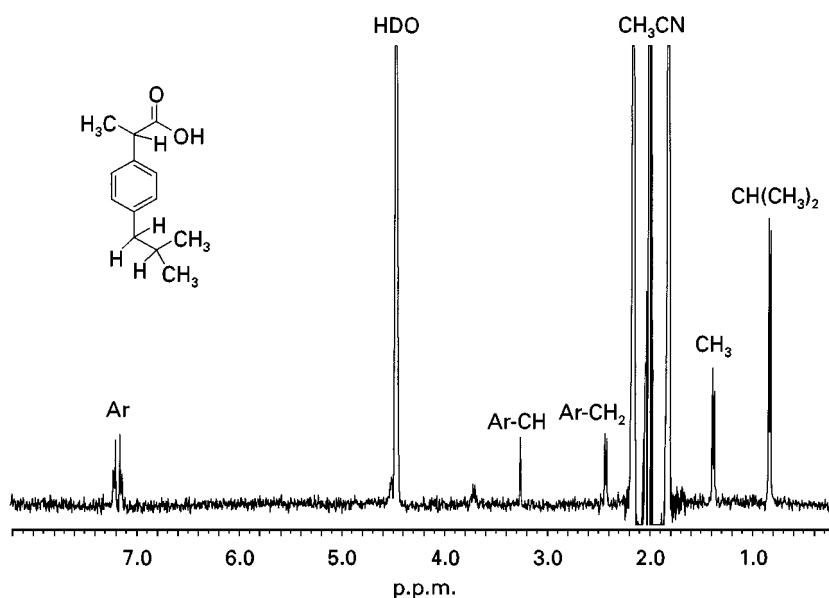


Figure 9 ^1H NMR spectrum of ibuprofen extracted from the SPE-HPLC-NMR run depicted in Figure 8.

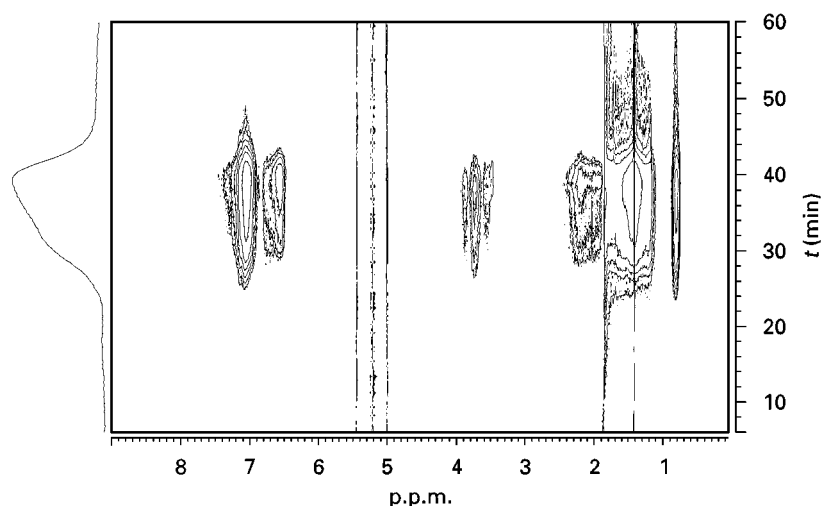


Figure 10 Stacked plot (400 MHz) of the GPC-NMR separation of a styrene-butylacrylate copolymer.

A GPC separation of 100 μL of a 7.5% copolymer solution was performed with a 250×40 mm GPC column using dichloromethane as eluent at a flow rate of 0.4 mL min^{-1} . Sixteen transients were co-

added, defining a time resolution of 8.4 s. The Fourier-transformed spectrum results in a row in the two-dimensional plot of ^1H chemical shifts versus retention times (Figure 10).

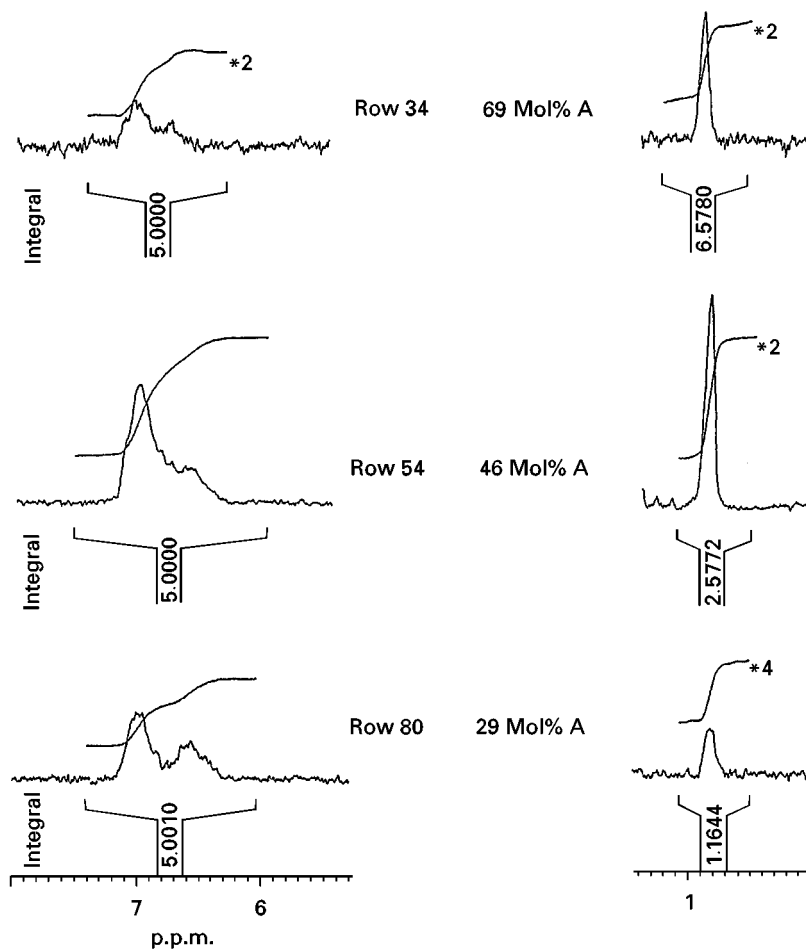


Figure 11 Selected rows of the GPC-NMR separation of a styrene-butylacrylate copolymer (Figure 10) showing signals from the aliphatic and aromatic spectral region.

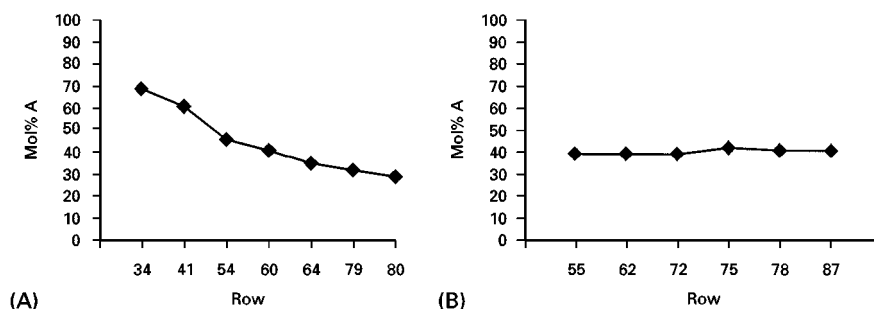


Figure 12 Styrene-butylacrylate copolymer composition versus GPC elution time. (A) Latex A; (B) Latex B.

The methyl group and oxymethylene signals of the acrylate (A) and the aromatic resonances of the styrene (S) units can be used in an online GPC-NMR run to derive information about the molecular weight dependence of the chemical composition.

Within one separation run, up to 128 rows were accumulated, resulting in an overall acquisition time of 42 min. Three selected rows are depicted in **Figure 11**, showing the varying intensities of the CH_3 signals of butylacrylate at 0.85 p.p.m. versus the aromatic signal of styrene at 7 p.p.m. for one copolymer sample.

Thus, the copolymer composition can be directly determined from the elution curves of both signals at any row of the chromatogram. The results from the GPC-NMR coupling for both samples are shown in **Figure 12**. The copolymers show a completely different behaviour in their dependence of the chemical composition on molecular weight.

This example demonstrates the great time-saving nature of the hyphenation of chromatography with NMR spectroscopy. To yield the same information as in the online GPC-NMR run, 128 fractions of the GPC separation would have to be collected and 128

routine ^1H NMR spectra recorded. Whereas the GPC-NMR data were obtained within less than 1 h, offline separation and NMR examination would take at least 3 h.

SFC-NMR and SFE-NMR Coupling

A separation technique employing nonprotonated solvents is SFC, using CO_2 . For SFC-NMR experiments a pressure-stable flow cell has been developed using a sapphire tube instead of glass (**Figure 1B**). At a temperature of 323 K and a pressure of 161 bar, high resolution continuous-flow NMR spectra in supercritical CO_2 can be obtained.

This is demonstrated in **Figure 13**, showing the ^1H NMR spectrum of ethylbenzene in supercritical CO_2 . Often, SFC-NMR separations can be performed with a pressure gradient. Thus, different isomers of vitamin A acetate are easily separated (**Figure 14**).

Supercritical CO_2 can also be used for supercritical fluid extraction (SFE) purposes. As an example, **Figure 15** shows the ^1H NMR spectrum of piperin extracted from black pepper at a temperature of 370 K.

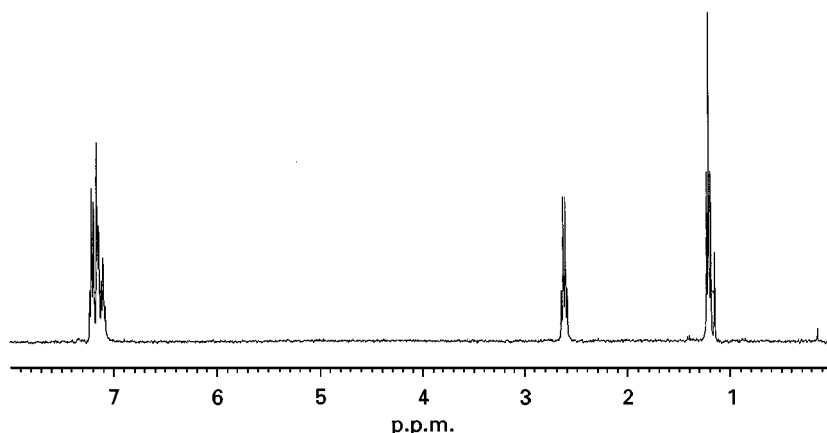


Figure 13 ^1H NMR spectrum (400 MHz) of ethylbenzene in supercritical CO_2 .

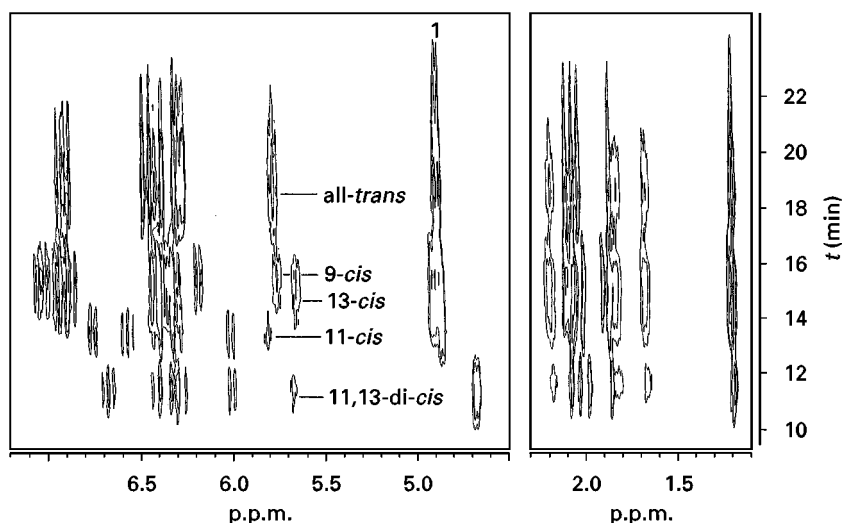


Figure 14 Contour plot (400 MHz) of the separation of vitamin A acetate stereoisomers in supercritical fluid CO_2 . Reprinted from *Journal of Chromatography A*, 761, with permission from Elsevier Science.

Capillary Separations

The above examples clearly show the great advantage of combining efficient separation techniques with NMR detection for the solution of complex analytical problems. In all the applications described, analytical columns (250×4.6 mm) together with sample quantities in the μg range and HPLC analysis times of up to 30 min were employed.

However, there is an increasing need for high-throughput screening and analysis of mixtures containing unknown compounds in the growing field of biotechnology and genetic engineering. Here, only a few nanograms of biologically active mixtures of compounds may be available, and these must be fully characterized. This task can only be performed by miniaturizing the closed-loop separation identifica-

tion system, combining capillary separation technique with nanolitre-scale NMR spectroscopy.

Whereas capillary techniques are already well developed in the field of separations, nanolitre NMR spectroscopy is still in its infancy. Various hardware approaches exist to record NMR spectra on the nanolitre scale. One is the use of a solenoid coil directly attached to the fused silica capillary. The other employed by our group is the application of a microprobe with a double-saddle Helmholtz microcoil. The capillary is fixed within the microcoil in the z -direction of the cryomagnet. This approach has advantages and disadvantages. Because the capillary is inserted within the coil, it can be easily exchanged to meet other separation problems but this design has the inherent disadvantages that the filling factor (the ratio of the coil versus the sample volume) is lower in

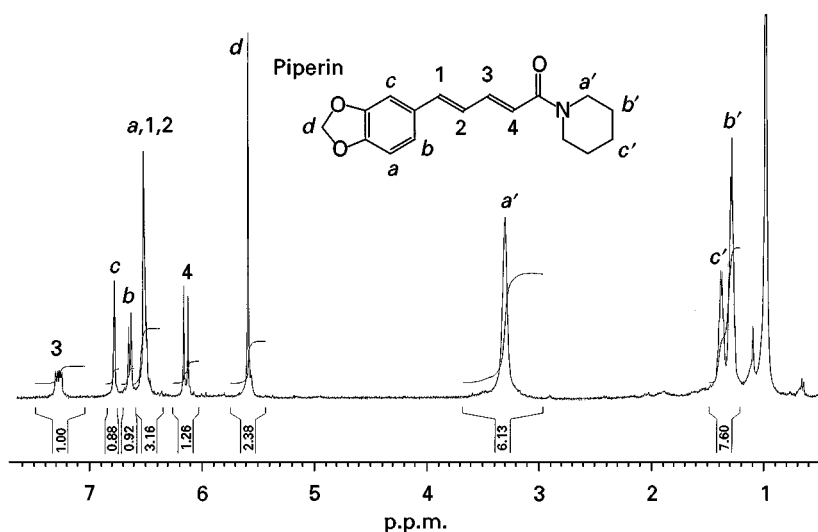


Figure 15 ^1H NMR spectrum (400 MHz) of piperin extracted from black pepper.

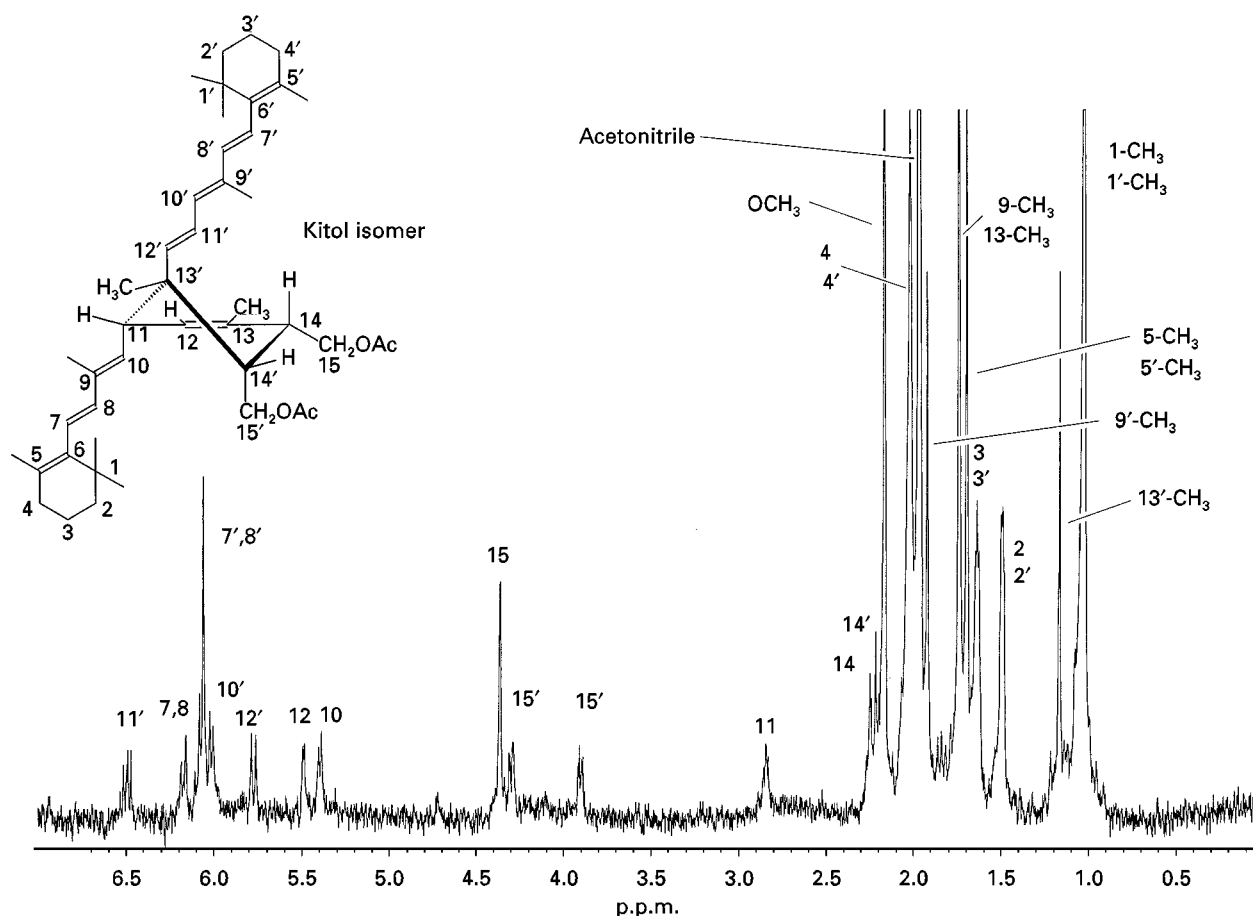


Figure 16 Stopped-flow capillary ^1H NMR spectrum of a vitamin A dimerization product recorded within a capillary (detection volume 200 nL).

comparison to a design where the coil is directly fixed to the capillary. Solenoid coils with a perpendicular orientation to the B_0 direction of the cryomagnet result in a threefold increase in sensitivity in comparison with the Helmholtz microcoil design; however, the currently developed approaches suffer from susceptibility-induced line broadening due to the solenoidal coil fixing to the fused silica capillary. This design has already been improved by the application of a susceptibility-matching fluid and shows potential for further optimization. On the other hand, the orientation of the capillary within the z -direction of the B_0 field has the tremendous advantage that the NMR signal half-width is not affected when electroosmotic flow-driven separation techniques (CE, CEC) are performed. Here, the induced magnetic field of the current within the capillary has no component in the z -direction of the cryomagnet. Thus, a vertically oriented Helmholtz microcoil is a feasible design, at least for capillary separations.

Coupling of capillary HPLC rather than conventional separation techniques with NMR has several distinct advantages. The reduced solvent consump-

tion allows the use of the deuterated solvents, thus rendering elaborate solvent suppression unnecessary. If only a small amount of sample is available, higher concentrations of analyte in the detection cell are obtained when the column dimensions are small. Currently obtained sensitivity levels of this design are in the 500 ng range with acquisition times of some seconds.

One of the first practical results obtained by online capillary HPLC-NMR coupling was the structure elucidation of a vitamin A derivative. The structure of the dimers of vitamin A acetate, so-called kitols, was unknown for a long time because these compounds are sensitive to UV irradiation and to air. The classical procedure of isolation, removal of the extraction solvent and resolution in a deuterated solvent resulted in many isomerization products. By combining a capillary separation together with NMR microcoil detection, structure elucidation of a previously unknown kitol was possible. **Figure 16** shows the capillary ^1H NMR spectrum of the unknown kitol, indicating that the resolution is sufficient to obtain all necessary coupling constants, whereas the hump

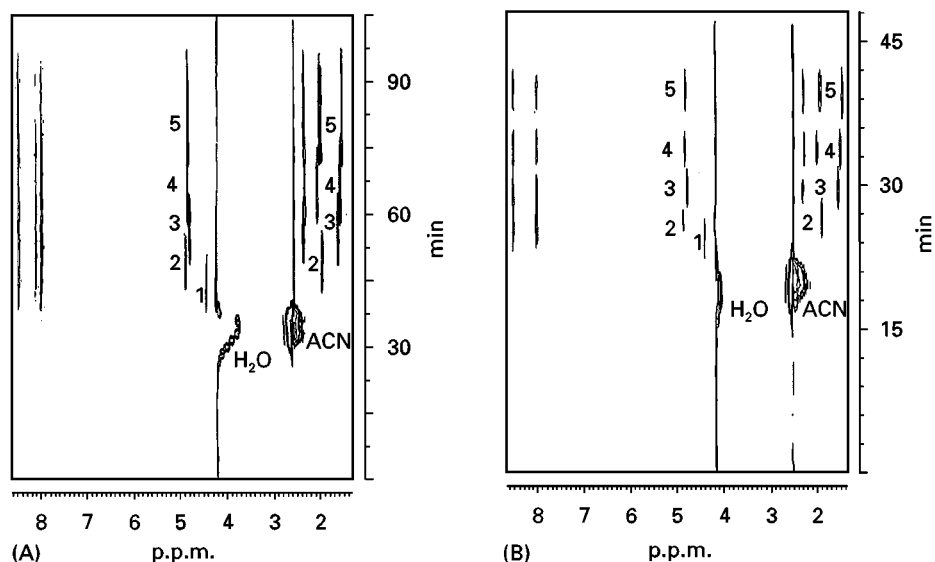


Figure 17 Contour plots of (A) CHPLC and (B) CEC separation of alkylbenzoates: 1, methyl; 2 ethyl; 3, propyl; 4, butyl; 5, pentyl benzoate; ACN, acetonitrile.

(signal line width) at the height of the ^{13}C signals must be further optimized.

A further example is the online CE-NMR and online CEC-NMR separation of alkylbenzoates. Figure 17 shows the contour plot of the separation performed in the CHPLC and the CEC mode. It is evident from the CEC-NMR contour plot that all compounds are baseline-separated, resulting in distinct NMR rows in the two-dimensional display.

This example shows the great power of CHPLC, CE and CEC-NMR to derive unambiguous information of substances in complex organic molecules. The first steps towards a high-throughput separation system have already been made. For the successful performance of real-life applications, NMR sensitivity must be improved. If NMR probes with 1 ng sensitivity become available, an increasing number of capillary separations coupled with nanoscale NMR will be performed in many applications.

See also: II/Chromatography: Supercritical Fluid: Instrumentation. Electrophoresis: Detectors for Capillary Electrophoresis. III/Carotenoid Pigments: Supercritical Fluid Chromatography. Gradient Polymer Chromato-

graphy: Liquid Chromatography. Natural Products: Liquid Chromatography-Nuclear Magnetic Resonance. Pigments: Liquid Chromatography. Polyethers: Liquid Chromatography.

Further Reading

- Albert K (1995) *Journal of Chromatography A* 703: 123–147.
- Albert K (1997) *Journal of Chromatography A* 785: 65–83.
- Braumann U, Händel H, Albert K et al. (1995) *Analytical Chemistry* 67: 930–935.
- De Koenig JA, Hogenboom AC, Lacker T et al. (1998) *Journal of Chromatography A* 813: 55–61.
- Hatada K, Ute K, Kitayama T et al. (1989) *Polymer Bulletin* 21: 489–495.
- Lindon JC, Nicholson JK and Wilson ID (1996) *Progress in NMR Spectroscopy* 29: 1–49.
- Pusecker K, Schewitz J, Gförer P et al. (1998) *Analytical Chemistry* 70: 3280–3285.
- Schlotterbeck G, Tseng L-H, Händel H et al. (1997) 69: 1421–1425.
- Strohschein S, Schlotterbeck G, Richter J et al. (1997) *Journal of Chromatography A* 765: 207–214.
- Wu N, Peck TL, Webb AG et al. (1994) *Analytical Chemistry* 66: 3849–3857.

Partition Chromatography (Liquid-Liquid)

C. Wingren and U.-B. Hansson,
Lund University, Lund, Sweden

Introduction

Partition or liquid-liquid chromatography (LLC) is a powerful separation technique which has been successfully used for the separation and analysis of

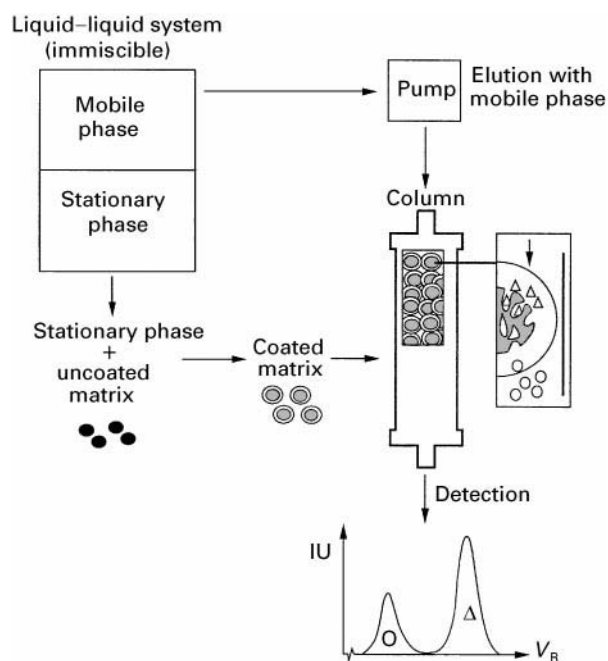


Figure 1 Schematic illustration of LLC. IU, international units; V_R , retention volume.

a wide variety of sample types, including water-soluble and oil-soluble compounds, ionic and nonionic compounds, as well as biopolymers such as nucleic

acids and proteins. The basis of LLC is the distribution of sample molecules between two immiscible liquid phases, a stationary phase and a mobile phase (Figure 1). In conventional LLC, the stationary phase is mechanically held to a support by adsorption. In liquid chromatography (LC), the most widely used supports are those with chemically bonded organic stationary phases. This may be described as a separate LC method: bonded-phase chromatography (BPC).

LLC offers unique selectivity for various samples since a wide range of liquid phases can be used (Table 1). In normal-phase LLC, the support is coated with a polar stationary phase, whereas a relatively nonpolar solvent is used as mobile phase. In reversed-phase LLC, the two LLC phases are interchanged so that the less polar liquid is now the stationary phase and the polar liquid is the mobile phase. LLC systems composed of aqueous/aqueous, aqueous/organic or organic/organic solvents can be used, depending on the particular separation problem. A variety of supports have been used (Table 2), but silica-based matrices appear to be best suited for LLC.

The sample molecules are distributed between the stationary and mobile phases depending on their physicochemical properties and the properties of the

Table 1 Liquid-liquid chromatographic systems commonly used for LLC and LLPC of compounds, nucleic acids and proteins

Sample	Chromatographic system	Stationary phase ^a	Mobile phase
Compounds	Normal-phase LLC	β, β' -Oxydipropionitrile	Pentane, cyclopentane, hexane, heptane or isooctane. Same, but with 10–20% of chloroform, dichloromethane tetrahydrofuran, acetonitrile, dioxane, etc.
		1,2,3-Tris(2-cyanoethoxy)propane	See above
		Triethylene glycol	See above
		Trimethylene glycol	See above
		Ethylene glycol	Di- <i>n</i> -butyl ether or nitromethane
		Dimethylsulfoxide	Isooctane
		Water/ethylene glycol	Hexane/ CCl_4
		Water	<i>n</i> -Butanol
		Nitromethane	CCl_4 /hexane
		Reversed-phase LLC	Methanol/water
Nucleic acids	LLPC	Cyanoethylsilicone	Acetonitrile/water
		Dimethylpolysiloxane	Methanol/water
		Hydrocarbon polymer	
		4.4% PEG 8000/6.2% dextran 500 ^a	
		4.4% PEG 8000/5.2% dextran 500 ^a	
		4.4% PEG 8000/6.2% dextran 500 ^a	
		5.2% PEG 8000/10.0% dextran 40 ^a	
		2.7% PEG 20000/4.5% dextran 500 ^a	
		10% PVP 30/10% dextran 40 ^a	
		PVA 10/dextran 40 ^a	
Proteins	LLPC	11.25% PEG 1500/12.75% potassium phosphate ^a	
		16.75% PEG 1500/16.0% sodium citrate ^a	

^aOr complete system.

LLC, liquid-liquid chromatography; LLPC, liquid-liquid partition chromatography; PEG, polyethylene glycol; PVP, polyvinylpyrrolidone; PVA, polyvinyl alcohol.

Table 2 Supports commonly used for LLC of compounds, nucleic acids and proteins

Sample	Support type	Name	Particle size (μm)	Pore size (nm)
Compounds	LLC	Diatomaceous earth	Chromosorb LC-1	37–44
		Silica, spherical	Spherosil XOA 600	5–8
	Porous		Zorbax	6
		Silica, irregular	Porasil	10
	Pellicular		LiChrosorb Si-60	5, 10
		'Inactive' silica, spherical	Zipax	25–37
			Liqua-Chrom	44–53
			Corasil I	37–50
		'Active' silica, spherical	Perisorb A	30–40
			Vydac	30–44
	BPC			
		Corasil modified with octadecylsilane	Bondapak C ₁₈ /Corasil	37–50
		Perisorb A modified with dimethylsilane	Perisorb-RP-2	30–40
		Zipax modified with octadecylsilane	Permaphase-ODS	25–37
		Vydac modified with ethylnitrile	Vydac SC-polar	30–44
Nucleic acids/proteins	Polyvinyl modified with polyacrylamide		LiParGel 650	25–40
			LiParGel 750	25–40
	Silica modified with polyacrylamide		LiChrospher-Diol 100	10
			LiChrospher-Diol 1000	10
			LiChrospher-Diol 4000	10
			Superdex 200 prep. grade	24–44
	Agarose modified with dextran			

^a Data not available. Exclusion limit for globular proteins of 5×10^6 Da and for dextrans of 10^6 Da.

^b Data not available. Exclusion limit for globular proteins of 5×10^7 Da and for dextrans of 10^7 Da.

^c Data not available. Exclusion limit for globular proteins of 10^6 Da and for dextran of 10^5 Da.

LLC, liquid-liquid chromatography; BPC, bonded-phase chromatography.

phases (and support). In the case of compounds, the separation is generally based on the type and number of substituent groups and by differences in molecular weight (up to about 2000 Da). Hence, LLC is very useful for the separation of homologues and mixtures of compounds of different functionality. Biopolymers (nucleic acid fragments) can be separated mainly owing to differences in molecular weight (up to about 4000 base pairs). In the case of proteins, conditions can be designed in such a way that differences in their overall exposed surface properties are detected. In fact, LLC has proved to be a unique tool for protein analysis, that is for purification and fractionation, detection and separation of conformational isomeric forms, examination of surface properties related to biological specificities and for providing information about the events upon binding of ligand and about possible ligand-induced conformational changes. In this article, we describe the use of LLC for the separation and analysis of compounds, nucleic acids and proteins, focusing on the latter group.

Separation of Compounds

A variety of compounds including detergents, drugs, insecticides, metal chelates, pesticides, phenols, sac-

charides, steroids and vitamins, some of which are shown in Table 3, have been successfully separated using LLC. LLC provides a wide range of separation selectivity since several different liquid-liquid systems can be used. In the case of normal-phase LLC, a number of separations have been performed using either β, β' -oxydipropionitrile (BOP), or one of the various polyethylene glycols (PEGs) as stationary phase. Both liquids are useful for the same type of compounds, although the PEGs may be more selective for alcohols, and BOP is preferred for basic compounds such as amines. Normal-phase LLC is used for more polar, water-soluble compounds, and the solute elution order is similar to that observed in adsorption chromatography. In reversed-phase LLC, cyanoethyl-silicone, hydrocarbon polymers and squalene, among others, have been used as stationary phases. Reversed-phase LLC is generally used to separate compounds with poor water solubility, i.e. non-polar and organic-soluble compounds.

Besides the binary liquid systems normally used in LLC, ternary liquid-liquid systems have also been found useful (Table 1). Such systems are obtained from binary liquid systems by adding a third component (cosolvent) that is miscible with both phases. Either of the two resulting phases can be used as

Table 3 Applications of LLC for separation of compounds

<i>Approach</i>	<i>Application</i>	<i>Examples</i>
Normal-phase LLC	Separation of compounds containing metals	Radioactive metals Isomers of cobalt complexes involved in synthesis of vitamin B ₁₂ Metal- β -diketonates Platinum-metal complexes
	Determination of compounds in biological samples	Vitamins K ₁ and E in serum Phosphatidylcholine in serum 2,4,6-Triiodophenol and other iodinated derivatives in serum Flumequine and 7-flumequine in serum
	Analysis of drugs in food products	Flumethasone pivalate in serum Methyl prednisolone in milk N-Nitrosamines in extract of pork
	Determination of compounds in environmental samples	Pesticides, e.g. mosquito larvacide in salt ponds Insecticides, e.g. imidacloprid in water and soil
	General separations and determinations	Penicillin derivatives Steroids, e.g. derivatized urinary 17-ketosteroids Coumarins Phenols Dinitrophenylhydrazine derivatives Ethylene oxide oligomers
Reversed-phase LLC	Determination of compounds in biological samples	Ritonavis Enoxacin and 4-oxyenoxacin in plasma and tissue Tacrine and its metabolites in plasma and urine Nucleotides in different tissues and body fluids
	Separation of important organic chemical	Antioxidants Plasticizers Nonionic organic dyes
	General separations and determinations	Fat-soluble vitamins, e.g. vitamins A, D, E and K Aromatics Paraffins Olefins and diolefins

LLC, liquid-liquid chromatography.

stationary phase, with the other as mobile phase. As an example, the ternary system formed by water/ethanol/2,2,4-trimethylpentane has been found to be very useful for the separation of many compounds including metal chelates, pesticides and steroids.

Several different supports can be used, but silicas and diatomaceous matrices appears to be best suited. These supports are inert, and have relatively large pores so as to allow ready access of the sample molecules to the stationary phase contained within the porous structure. It may be more convenient to use bonded-phase packings, the main advantage being that they are quite stable, since the stationary phase is chemically bound to the support and subsequently cannot be easily removed in use.

The separation of compounds by LLC is generally based on the type and number of substituent groups and by differences in molecular weight. This is exemplified by the fact that ethylene oxide oligomers (7-14 ethylene oxide units) can be separated by differences in number of functional groups, naphthalene

derivatives by differences in compound type, and 2,4-dinitrophenylhydrazine derivatives (C₂ to C₆) by differences in molecular weight (Table 3).

Modern LLC have been used to separate several biologically important natural and synthetic compounds, including cortisol, derivatized urinary 17-ketosteroids and free underivatized steroids. Many compounds containing metal atoms have been separated using LLC, such as radioactive metals, isomers of cobalt complexes involved in the synthesis of vitamin B₁₂, metal- β -diketonates and platinum metals complexes. Moreover, LLC has also been frequently used for determination of specific compounds in biological samples, as for example vitamins K₁ and E in serum, phosphatidylcholine in serum, 2,4,6-triiodophenol and other iodinated derivatives in serum, and flumequine and 7-flumequine in plasma.

In addition, LLC has been used to analyse drugs in various food products, e.g. flumethasone pivalate in cream, methyl prednisolone in milk and N-nitrosamines in extract of pork. Various derivatives of

penicillin have also been separated using LLC. Moreover, LLC has been used to separate and determine a number of pesticides and insecticides, such as imidacloprid in water and soil.

Reversed-phase chromatography has been used to separate mixtures of fat-soluble vitamins (vitamins A, D, E and K); mixtures of aromatics, paraffins, olefins and diolefins; chlorinated benzenes; and fused-ring aromatics. A wide variety of important organic chemicals such as antioxidants, plasticizers and nonionic dyes has been separated using LLC. Reversed-phase chromatography has also been used to determine compounds in biological samples, including ritonavir, an HIV protease inhibitor, enoxacin and 4-oxyenoxacin in plasma and tissue, and tacrine and its metabolites in plasma and urine. Another important area of application is the separation of nucleotides, nucleosides and bases that are used to examine a variety of biomedical problems.

Separation of Biopolymers

The classical version of LLC uses combinations of an organic and an aqueous or two organic liquid phases, which limits its application to small molecules without defined secondary or tertiary structure. However, the use of LLC for separation of large active biomolecules such as nucleic acids and proteins became possible (at least in theory) when P.-Å. Albertsson succeeded in developing aqueous-aqueous two-phase systems made up of two 'incompatible' water-soluble polymers such as PEG and dextran. Finding suitable supports for these systems was for a long time a major problem, however. Several attempts were made to adsorb the bottom phase onto supports made of agarose beads, polyethers immobilized on Sepharose, silicates and cellulose. The problem was solved by W. Müller in 1986 by combining the affinity of polyacrylamide for the dextran-rich bottom phase of the PEG/dextran system with the mechanical strength of hydrophilic vinyl (LiParGel) or silica (LiChrospher Diol) particles (Table 2). LLC, or LLPC (liquid-liquid partition chromatography), was then intro-

duced as a method for the separation of biopolymers. This technique was later developed further with respect to sensitivity, selectivity and reproducibility by U.-B. Hansson and co-workers, turning it into a powerful tool for protein analysis in particular. It has recently also been shown that dextran-grafted agarose beads (Superdex) can be used as a support for LLPC. LiParGel 650 has been used for the analysis of small as well as of large proteins while LiParGel 750 has mostly been used for the analysis of nucleic acids. LiChrospher-Diol 100 has been used for the analysis of small proteins ($< 100\,000$ Da) while proteins of a wide range of sizes have been analysed on LiChrospher-Diol 1000 or 4000 columns. Superdex is suitable for the analysis of small proteins ($< 100\,000$ Da).

Buffered phase systems formed by polyvinyl pyrrolidone (PVP)/dextran, polyvinyl alcohol (PVA)/dextran and PEG/salt solutions have been used for LLPC, but the PEG/dextran systems are by far the most frequently used (Table 1). A serious drawback of the PEG/dextran systems is, however, the incompatibility between PEG and some proteins such as immunoglobulins. Concentrations of PEG greater than 3% can be used to precipitate antibodies. However, this incompatibility can be partly overcome by adding appropriate salts. IgG can, for example, be solubilized in PEG/dextran systems at pH 7.0, i.e. near its isoelectric point, in the presence of 100 mmol L^{-1} betaine ($\leq 0.8\text{ mg mL}^{-1}$) or 0.1 mol L^{-1} glycine and 0.1 mol L^{-1} sodium chloride ($\leq 2\text{ mg mL}^{-1}$). Hence, the PEG/dextran systems are, for the moment, the obvious choice of two-phase system for LLPC of biopolymers, whereas the usefulness of other phase systems remains to be elucidated.

Nucleic Acids

LLPC in aqueous two-phase systems has been successfully used for DNA fractionation by size, topology and by base sequence, as well as for the fractionation of 'soluble' and ribosomal RNAs (Table 4). Hence, LLPC may provide resolutions unattainable by any other method.

Table 4 Separation of nucleic acids by LLPC

Separation according to:	Examples
Size	DNA fragments, linear relationship for fragments up to about 4000 base pairs Various RNAs from natural sources, e.g. soluble RNAs from tomato plants Ribosomal RNA up to about 30S
Base composition	<i>Eco</i> RI generated fragments from λ DNA Calf thymus DNA
Topology	Fractionation of circular DNAs

LLPC, liquid-liquid partition chromatography.

Fractionation of DNA restriction fragments by size can be performed with DNA fragments up to at least 4000 base pairs (Table 4). Mainly two-phase systems formed by PEG 8000/dextran 500 have so far been applied (Table 1). The separation can be greatly improved by applying a salt-exchange gradient. Side effects, possibly caused by slightly hydrophobic properties of the supports, may strongly influence the fractionation of DNA. Although the influence of the supports on DNA may be obvious, as in the case of proteins (see below), the general applicability of the matrices is not invalidated as the interactions may be exploited as an additional parameter for separation.

DNA may be fractionated according to base composition or sequence using PEG-bound AT- or GC-specific DNA ligands consisting of basic dyes (Table 4). In this way, these ligands will prefer the PEG-rich mobile phase and are subsequently able to shift the partitioning of matching DNA towards this phase. As in the case of DNA, RNA may also be fractionated by LLPC in aqueous two-phase systems due to differences in size. Also large (ribosomal) RNA ranging up to 30 S can be fractionated by LLPC. The high solubility of RNAs in the PEG/dextran systems is also advantageous.

Proteins

The way in which a protein molecule is distributed between the two phases in a given PEG/dextran system depends on its three-dimensional structure and general surface properties and is described by its partition coefficient, K_c (the ratio of the concentration of the molecule in the top phase to that in the bottom phase). Thus, partitioning in aqueous PEG/dextran

two-phase systems offers a unique means of separating proteins in solution with respect to their overall exposed surface properties. In addition, the method is mild so that the conformation of a partitioned protein is not likely to be disturbed.

As in the case of DNA separation, the supports may (strongly) influence the fractionation of proteins. This is illustrated in Figure 2, where LLPC on these supports resulted in different elution profiles for polyclonal IgG, i.e. the supports influenced the partitioning of immunoglobulins in different ways. The exact nature of the observed interactions is still not clear, but they may be determined by the conformation of the molecules together with the properties of the support with respect to pore size and polyacrylamide/dextran coating. Although ideal partitioning is desirable, the general applicability of the matrices is not invalidated as the interactions can be exploited as previously mentioned.

Separation

LLPC can be used to separate a wide variety of proteins including enzymes, hormones, immunoglobulins, serum proteins and transport proteins, some of which are shown in Table 5. LLPC has been successfully used for separations that have previously been difficult, for instance the separation of molecules with similar molecular weight and pI values such as α -1-antitrypsin and albumin, and corticosteroid-binding globulin and a sex hormone-binding globulin. Moreover, LLPC may replace the need of other conventional separation techniques, since LLPC, in contrast to most of these methods, is able to separate proteins owing to differences in several physicochemical properties. As for example, proteins in human sera, which can be separated in a multistep procedure by using a combination of several other techniques such as precipitation, ion exchange chromatography, gel filtration and electrophoresis, can be separated in a single step by LLPC. Furthermore, proteins that can be separated by differences in pI values, as for example isoforms of lactate dehydrogenase and malate dehydrogenase, can be separated by LLPC. In addition, monomeric and dimeric forms of HSA that can be separated by gel filtration and proteins that may be separated by hydrophobic chromatography can also be separated by LLPC. Thus, LLPC in aqueous polymer two-phase systems offers new possibilities to separate proteins in a single step and/or to obtain fractionation that is not readily achieved by other techniques.

Fractionation

LLPC can be used to fractionate proteins and may provide a selectivity and sensitivity unattainable by any other chromatographic method. Some

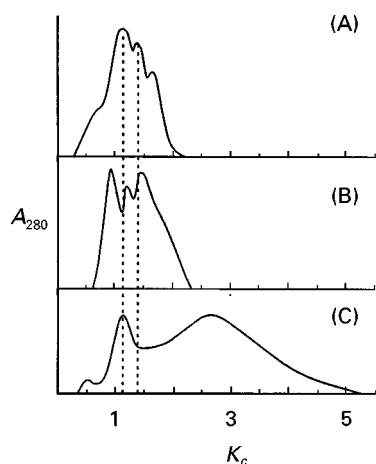


Figure 2 Influence of the support on LLPC of polyclonal IgG: (A) LiParGel, (B) LiChrospher, (C) Superdex. Data adapted from Wingren *et al.*, *Journal of Chromatography* 603, 73 (1992); *Journal of Chromatography* 668, 65 (1994), with permission from Elsevier Science.

Table 5 Separation of proteins by LLPC

<i>Separation problem</i>	<i>Example</i>	<i>LLPC results/comments</i>
Complex system	Proteins in human serum Proteins in goat, sheep, dog and horse serum Proteins in mouse ascites	A single step separation achieved; previously separated in a multistep procedure using a combination of several other methods
Proteins with similar M_r and pI	α -1 antitrypsin and HSA CBG and SHBG from human serum	
Proteins with different pI	Isoforms of LDH Isoforms of MDH	LLPC is able to separate proteins due to differences in 'several' physicochemical properties and may thus replace the need of many conventional separation techniques
Proteins with different M_r Proteins with different hydrophobicity	Monomers and dimers of HSA Human IgG with different relative hydrophobicity	
General separations	Myoglobin, peroxidase, BSA and OVA Cyt c, HSA, β -lactoglobulin, lysozyme, MB, ovotransferrin, OVA and peroxidase ADH, GDH and ferritin ADH, FDH and LDH Transferrin, IgG and HSA	

ADH, alcohol dehydrogenase; BSA, bovine serum albumin; CBG, corticosteroid-binding globulin; Cyt c, cytochrome c; FDH, formate dehydrogenase; GHD, glucose 6-phosphate dehydrogenase; HSA, human serum albumin; LDH, lactate dehydrogenase; LLPC, liquid-liquid partition chromatography; MB, myoglobin; MDH, malate dehydrogenase; OVA, ovalbumin; SHBG, sex hormone-binding globulin.

representative examples, including enzymes and antibodies, are given in **Table 6**. The usefulness of LLPC for this purpose was highlighted in recent studies where several enzymes known to exist in equilibrium between two allosteric forms were analysed. Yeast alcohol dehydrogenase, liver alcohol dehydrogenase, the heart and muscle isoforms of lactate dehydrogenase and two types of hexokinase (fraction I and II of Kaji), are all eluted as two components by LLPC, in spite of the fact that the enzyme preparations appear

to be homogeneous when analysed by other conventional methods such as isoelectric focusing, sodium dodecyl sulfate-polyacrylamide gel electrophoresis (SDS-PAGE) and high performance liquid chromatography-size exclusion (HPLC-SE). Remarkably, an equilibrium between the two components with different surface properties for each of these enzymes can be demonstrated by LLPC. These results show that LLPC can be used to detect and even separate different conformational isometric forms of unliganded enzymes. It

Table 6 Fractionation of proteins by LLPC

<i>Proteins</i>	<i>LLPC results/comments</i>
LADH YADH LDH-H ₄ LDH-M ₄ Hexokinase ^a	An equilibrium between two components with different surface properties detected (i.e. conformational isomeric forms)
sMDH mMDH	Two components with different surface properties detected
Polyclonal IgG Polyclonal IgA Polyclonal IgM	Several components detected
Monoclonal IgG	An equilibrium between at least two components with different surface properties detected (for six of 57 antibodies; conformational isomeric forms?)

^aSimilar results were obtained for two types of hexokinase, fraction I and II of Kaji. LADH, liver alcohol dehydrogenase; mMDH, mitochondrial malate dehydrogenase; sMDH, cytoplasmic malate dehydrogenase; LDH-H₄, heart lactate dehydrogenase; LDH-M₄, muscle lactate dehydrogenase; LLPC, liquid-liquid partition chromatography; YADH, yeast alcohol dehydrogenase.

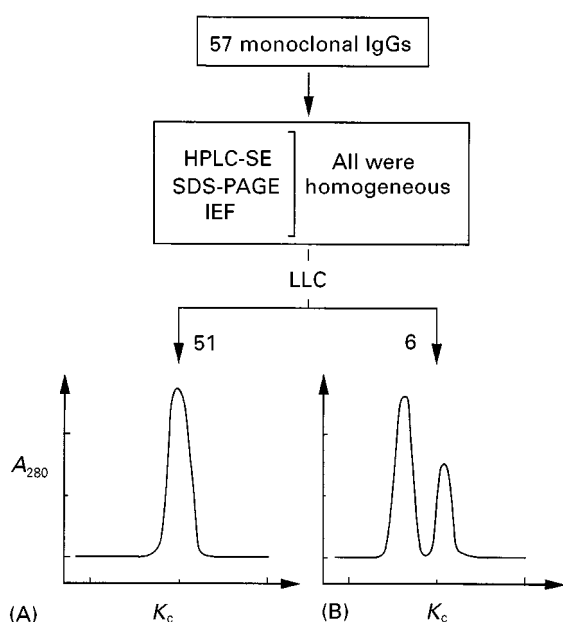


Figure 3 LLPC of 57 monoclonal IgG antibodies containing 95% IgG and homogeneous with respect to their physicochemical properties as determined by HPLC-SE, SDS-PAGE and IEF. The LLPC chromatograms are schematically illustrated in (A), which represents 51 of the IgGs, and (B), which represents six of the IgGs.

may be of interest to note that the LLPC fractionations of the mitochondrial and cytoplasmic isoforms of malate dehydrogenase, the allosteric mechanisms of which are still unclear, also result in two components with different surface properties.

Immunoglobulins are another group of proteins that have been successfully fractionated using LLPC (Table 6 and see below). Purified polyclonal immunoglobulins of IgG, IgM or IgA class can be fractionated into several components using LLPC. In the case of IgG and IgA, it is of a special interest to note that the fractionation is not subclass-related since the

elution profile of each of the subclasses is similar to that of the applied polyclonal antibody population. Surprisingly, some monoclonal antibodies have been found to be fractionated into at least two components by LLPC, in spite of the fact that they are homogeneous with respect to their immunochemical and physicochemical properties (Figure 3). This phenomenon was observed not only for IgG antibodies but also for IgA and IgM myeloma proteins. Recent LLPC experiments have demonstrated that six of 57 monoclonal IgG antibodies seem to exist in an equilibrium between at least two components with different surface properties. Thus, LLPC seems to be able to detect and separate conformational isomeric forms of unliganded antibodies. It has been suggested (using different kinetic techniques) that a tenth of all antibodies may indeed display conformational isomerism.

Specificity

LLPC can be used to examine differences in surface properties of proteins (mainly immunoglobulins) related to their biological specificities; some illustrative examples are given in Table 7.

In early LLPC experiments, polyclonal rabbit IgG antibodies with different specificities were found to exhibit different partition properties (expressed as a partition coefficient, K_c). Since no IgG subclasses have been reported for rabbit IgG, i.e. their Fc parts are likely to be the same, these results indicated that LLC had detected differences in surface properties between IgGs located on structures in their Fab parts. This exciting finding was followed up by more extensive studies in which large sets of well-characterized monoclonal IgG antibodies were analysed by LLPC. These studies clearly showed that there was no correlation between K_c and a single immunochemical and physicochemical property such as light-chain and

Table 7 Examination of surface properties of proteins related to biological specificities using LLPC

Proteins	Example		LLPC results
pAbs with different specificities	anti-IgG, anti-HSA and anti-transferrin		Different K_c values
mAbs with different affinities for the same Ag	Protein Ag	5 mAbs against cytomegalovirus	Different K_c values
		5 mAbs against albumin	Different K_c values
	Hapten Ag	3 mAbs against DNP	Different K_c values
		2 mAbs against T ₃	Different K_c values
		3 mAbs against T ₄	Different K_c values
mAbs with identical affinity for one	Hapten	2 mAbs against T ₃	Identical K_c values
		2 mAbs against T ₄	Identical K_c values
	Epitope	2 mAbs against IgG Fc	Identical K_c values
		3 chimaeric mAbs against NIP	Identical K_c values

pAbs, polyclonal antibodies; mAbs, monoclonal antibodies; Ag, antigen; HSA, human serum albumin; DNP, 2,4-dinitrophenol; T₃, triiodothyronine; T₄, thyroxine; NIP, 5-iodo-4-hydroxy-3-nitrophenyl; K_c , the ratio of the concentration of the molecule in the top phase to that in the bottom phase; LLPC, liquid-liquid partition chromatography.

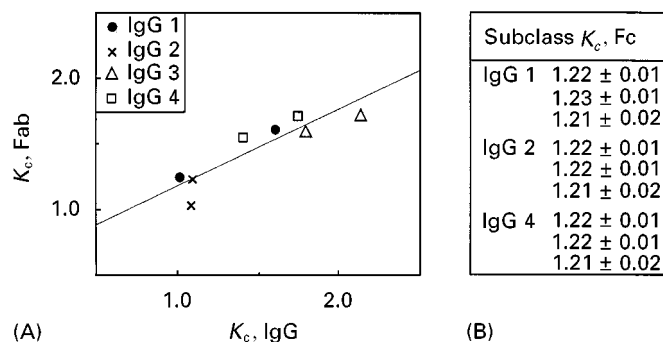


Figure 4 Comparison of the partition properties of (A) intact IgG with those of the corresponding Fab fragments and (B) Fc fragments from one IgG subclass with those of the other subclasses. The partition properties are expressed as a partition coefficient, K_c . The correlation coefficient was (A) 0.80 ($P < 0.05$). (B) The 95% confidence limits of the K_c values are given.

heavy-chain isotypes, charge, size and shape. However, a significant linear correlation between the partition properties of intact IgG1, 2, 3 and 4 and their corresponding Fab fragments was detected (Figure 4). In contrast to the Fabs, Fc fragments from IgG1, 2 and 4 displayed almost identical surface properties (Figure 4). Taken together, the results showed that the differences detected by LLPC between intact IgGs were indeed located on their Fabs.

Further studies have revealed a remarkable relationship between the partition properties of an IgG molecule and the structure of its combining site (specificity; see Table 7). In particular, monoclonal IgG antibodies with different affinities for the same antigen or directed against different antigens are eluted with different K_c values, while monoclonal IgGs with identical affinity constants for the same hapten or the same epitope on a protein are found to have identical K_c values. Moreover, chimaeric anti-NIP antibodies with identical variable regions, corresponding to the human IgG1, 2 and 4 subclasses, display identical surface properties, i.e. differences in the constant part of the heavy chains did not affect the partitioning. Thus, the surface properties of IgGs are, as detected by LLPC, dominated by those of their antigen-binding sites. Recent LLPC experiments have indicated that the antigen-binding site dominance observed for IgG is valid for all the other Ig classes and subclasses provided that antibodies only within a given class or subclass are compared with respect to exposed surfaces. Indications of a dominance of ligand-binding sites for other specific proteins, such as enzymes, have been reported. Taken together, LLPC may offer a unique possibility to screen the antigen-binding sites for differences/similarities in exposed surfaces, even in those cases when we do not know the specificity of the antibodies.

This unique property of LLPC was made use of in a recent study that showed that the LLPC profile for

polyclonal IgG antibodies isolated from the sera of patients with an autoimmune disease (primary Sjögren's syndrome) differed significantly from those of polyclonal IgG isolated from the sera of healthy individuals. These antibodies with 'unique and deviating' specificities could also be isolated by LLPC. Thus, LLPC may provide us with the means to fractionate and isolate specific antibodies 'of unknown specificities'.

Ligand Binding

Finally, LLPC can also be used to study the events upon binding of a ligand by specific proteins in solution. Some typical example, including transport proteins, enzymes and polyclonal as well as monoclonal antibodies, are given in Table 8. In many cases, LLPC can simply be used to separate the ligand-protein complex from either of the free components. This is, for example, the case for most of the enzyme-ligand and antibody-ligand complexes analysed so far.

In recent studies, the capacity of LLPC for analysis of protein-ligand complexes was demonstrated using well-characterized ligand-protein complexes where ligand-induced conformational changes are known to occur. In addition, the ligands in these model complexes are small and almost completely buried upon binding, i.e. the bound ligands themselves would not be responsible for any changes in surface properties observed upon complexation. Small changes in surface properties were detected when rabbit transferrin bound ferric ions, while no changes were observed when human transferrin (which is known to be less flexible) bound the ions. The ligand-induced transition between two conformational isomeric forms could be detected by LLPC for a large number of enzymes, including alcohol dehydrogenase, citrate synthase, glutamate-oxaloacetate transaminase, hexokinase, lactate dehydrogenase, malate dehydro-

Table 8 Examination of the events upon binding of ligand by specific proteins in solution using LLPC

Protein	Ligand	LLPC results/comments
Rabbit transferrin	Fe ³⁺	Small changes in K_c detected
Human transferrin	Fe ³⁺	No changes in K_c detected
CS	Oxaloacetate	Ligand-induced transition between two conformational isomeric forms detected
Hexokinase	Glucose	
GAPDH	NADH or NAD ⁺	
GOT	α -Methyl-aspartate	
LADH	NADH or NAD ⁺	
LDH-M ₄	NADH or NADH + oxamate	
LDH-H ₄	NAD ⁺	
mMDH	Citrate + NAD ⁺	
sMDH	Citrate + NAD ⁺	
PGK	GDP + 3-PGA	
YADH	NADH or NAD ⁺	
pAbs	IgG, HSA or transferrin	Differences in K_c detected, may be interpreted in terms of conformational characteristics
mAb	T ₃	
9 chimaeric mAbs	NIP	Differences in K_c detected; different mAbs formed AgAb with identical K_c
5 mAbs	HSA	
18 mAbs	5 haptens	
		Linear relationship between K_c of unliganded mAbs and their corresponding hapten-mAb complex

CS, citrate synthase; GAPDH, glyceraldehyde-3-phosphate dehydrogenase; GOT, glutamate-oxaloacetate transaminase; HSA, human serum albumin; LADH, liver alcohol dehydrogenase; LDH-H₄, heart lactate dehydrogenase; LDH-M₄, muscle lactate dehydrogenase; mAbs, monoclonal antibodies; LLPC, liquid-liquid partition chromatography; mMDH, mitochondrial malate dehydrogenase; sMDH, cytoplasmic malate dehydrogenase; NIP, 5-iodo-4-hydroxy-3-nitrophenacetyl; pAbs, polyclonal antibodies; PGA, 3-phosphoglycerate; PGK, 3-phosphoglycerate kinase; T₃, triiodothyronine; YADH, yeast alcohol dehydrogenase.

genase and 3-phosphoglycerate kinase. In the case of antibodies, conformational changes may occur upon binding of either hapten (T₃ and NIP) or protein antigens (HSA, IgG and transferrin) that are detectable by LLPC. The surface properties of chimaeric anti-NIP antibodies with identical variable regions, corresponding to the human IgA1, IgA2, IgE, IgG1, IgG2, IgG3, IgG4 and IgM isotypes, have been compared before and after binding of hapten. The hapten-antibody complexes were found to be eluted in a considerably narrower range of K_c values than were the free antibodies. It was concluded that conformational changes, detectable by LLPC, occurred in either IgA1, IgA2, IgE and/or IgM, but not in the IgGs, making the surfaces of the constant regions of the heavy chains of the Ig classes and subclasses more similar. Hence, LLPC may provide us with the means to examine whether ligand binding induces conformational changes in the antibody when in solution.

Almost all the antigen-antibody pair analysed by LLPC so far have formed complexes that are eluted as single homogeneous peaks by LLPC (Figure 5). Moreover, the complexes are eluted with the same value of K_c irrespective of the molar ratio of antigen to antibody at which they are formed (ranging from antigen to antibody excess). Thus, the results imply

that each antigen-antibody pair forms one type of complex with respect to exposed dominant surfaces. This is thought to be the first study reporting such a feature for antigen-antibody complexes.

Remarkably, a linear relationship between the surface properties of unliganded IgGs and their corresponding hapten-IgG complexes has been reported, and it was concluded that the surface properties of

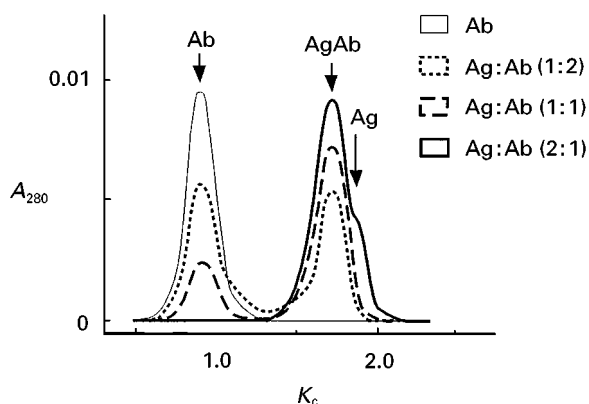


Figure 5 LLPC of antigen-antibody complexes (AgAb) formed at different molar ratios of antigen (Ag) to antibody (Ab) (Ag : Ab = 2 : 1–0.5 : 1). Representative results obtained for one monoclonal IgG antialbumin antibody are shown.

IgG are dominated by those of its antigen-binding sites even after the specific binding of hapten or hapten-carrier at the combining sites. By contrast, the surface properties of protein-antibody complexes are not related to those of the unliganded antibodies. Instead, the surface properties of protein-IgG complexes are related mainly to those of the antigens. Depending on the type of antigen (hapten or protein), LLPC may thus be used to separate antigen-IgG complexes through differences in exposed surfaces of either the antibody combining sites or the antigen. LLPC may thus provide us with new, interesting information concerning the events upon complex formation in solution and possible ligand-induced conformational changes.

See also: III/Nucleic Acids: Liquid Chromatography. Proteins: Ion Exchange. Appendix 1/Essential Guides for Isolation/Purification of Enzymes and Proteins. Essential Guides for Isolation/Purification of Immunoglobulins. Essential Guides for Isolation/Purification of Nucleic Acids.

Further Reading

- Albertsson P-Å (1986) *Partition of Cell Particles and Macromolecules*. New York: Wiley.
- Careri M, Mangia A and Musci M (1996) Applications of liquid chromatography-mass spectrometry interfacing systems in food analysis: pesticide, drug and toxic substance residues. *Journal of Chromatography* 727: 153-184.
- Grune T and Siems WG (1993) Reversed-phase high-performance liquid chromatography of purine compounds for investigation of biomedical problems: application to different tissues and body fluids. *Journal of Chromatography* 618: 15-40.
- Hansson U-B and Wingren C (1998) Separation of antibodies by liquid-liquid aqueous partition and by liquid-liquid partition chromatography. *Separation and Purification Methods*.
- Hansson U-B and Wingren C (1999) Liquid-liquid partition chromatography. In: *Methods in Biotechnology*. Totowa: Humana Press.
- Hansson U-B and Wingren C (1999) Liquid-liquid partition chromatography of proteins. In: Kastner M (ed.) *Protein Liquid Chromatography*. Oxford: Elsevier.
- Müller W (1986) New phase supports for liquid-liquid partition chromatography of biopolymers in aqueous poly(ethyleneglycol)-dextran systems. Synthesis and application for the fractionation of DNA restriction fragments. *European Journal of Biochemistry* 155: 213-222.
- Müller W (1988) *Liquid-Liquid Partition Chromatography of Biopolymers*. Darmstadt: Git-verlag.
- Rizzolo A and Polesello S (1992) Chromatographic determination of vitamins in foods. *Journal of Chromatography* 624: 103-152.
- Walter H and Johansson G (eds) (1994) Aqueous two-phase systems. *Methods in Enzymology* 228.
- Walter H, Brooks DE and Fisher D (eds) (1985) *Partitioning in Aqueous Two-Phase Systems: Theory, Methods, Uses and Application to Biotechnology*. London: Academic Press.
- Wang P and Lee HK (1997) Recent applications of high-performance liquid chromatography to the analysis of metal complexes. *Journal of Chromatography* 789: 437-451.
- Wingren C, Hansson U-B, Magnusson CG and Ohlin M (1995) Antigen-binding sites dominate the surface properties of IgG antibodies. *Molecular Immunology* 32: 819-827.

Physico-Chemical Measurements

R. P. W. Scott, Avon, CT, USA

Copyright © 2000 Academic Press

Chromatography theory establishes that the retention volume of a solute is a function of its distribution coefficient and the variance of the eluted peak is a function of solute diffusivity. Consequently, retention volume measurements can provide distribution coefficient data which, if determined over a range of temperatures, will disclose the necessary thermodynamic information that will help reveal the physical nature of the distribution process. In addition, peak dispersion measurements can furnish accurate diffu-

sion coefficients for almost any solute, in any liquid, at any chosen temperature, assuming appropriate solute solubility and temperature stability. Hence, the use of liquid chromatography to measure physico-chemical properties of a distribution system hinges on the accurate measurement of retention volumes and peak widths.

Gas chromatography retention volume measurements have been used to provide a significant amount of thermodynamic data, including standard free energies, enthalpies and entropies of distribution, together with activity coefficients. These types of physico-chemical measurements were pioneered in the late 1950s. In contrast, the use of liquid chromatography

for the same purposes has not been nearly so prevalent, although in many ways it can be a simpler and a more accurate experimental procedure.

Basic Thermodynamic Theory of Solute Distribution in Liquid Chromatography

The expression that relates the change in *standard free energy* of a solute when transferring from one phase to the other, as a function of the equilibrium constant (the distribution coefficient, K) is as follows:

$$RT \ln K = -\Delta G^0 \quad [1]$$

where R is the gas constant, T is the absolute temperature and ΔG^0 is the standard free energy change.

Now:

$$\Delta G^0 = \Delta H^0 - T\Delta S^0 \quad [2]$$

where ΔH^0 is the standard enthalpy change and ΔS^0 is the standard entropy change.

The enthalpy term represents the energy involved when the solute molecule interacts by electrical forces with a molecule of the stationary phase. However, when interaction takes place, the freedom of movement of the solute molecule is also reduced and it can no longer move in the same random manner that it did in the mobile phase. This new motion restriction is measured as an entropy change. Thus, the free energy change is made up of an actual energy change which results from the work done during the interaction of the solute molecules with those of the stationary phase, and an entropy change that accounts for the resulting restricted movement or loss of randomness, when the solute is associating with the stationary phase.

Continuing:

$$\ln K = -\left(\frac{\Delta H^0}{RT} - \frac{\Delta S^0}{R}\right) \quad [3]$$

It is seen that if the standard entropy change and standard enthalpy change for the distribution of any given solute between two phases could be calculated, then the distribution coefficient (K) and, consequently, its retention volume could also be predicted. Unfortunately, these properties of a distribution system are bulk properties that include, in a single measurement, the effect of all the different types of molecular interactions that are taking place between the solute and the two phases. As a result, it is often difficult to isolate the individual interactive contributions in order to estimate the magnitude of the overall distribution coefficient, or identify how it can be

controlled. Nevertheless, there are a number of ways in which this can be done and, in any event, the thermodynamic approach can provide valuable information with regard to the nature of the distribution.

Rearranging eqn [3]

$$\ln K = -\frac{\Delta H^0}{RT} + \frac{\Delta S^0}{R} \quad [4]$$

Bearing in mind:

$$V_r' = KV_s \quad \text{and} \quad k = \frac{KV_s}{V_m} = \frac{K}{a} \quad [5]$$

where V_r' is the corrected retention volume of the solute, V_s is the volume of stationary phase in the column, V_m is the volume of mobile phase in the column, a is the phase ratio V_m/V_s , and k is the retention factor of the solute. Thus:

$$\ln(V_r') = -\frac{\Delta H^0}{RT} + \frac{\Delta S^0}{R} + \ln(V_s) \quad [6]$$

or:

$$\ln(k) = -\frac{\Delta H^0}{RT} + \frac{\Delta S^0}{R} - \ln(a) \quad [7]$$

It is seen that a curve relating $\ln(V_r')$ or $\ln(k)$ to $1/T$ should give a straight line, the slope of which will be proportional to the standard enthalpy change during solute transfer and the intercept will be related to the standard entropy change (but will include the logarithm of the phase ratio). Thus, the dominant thermodynamic contribution to any specific distribution system can be identified from such curves.

Such curves are called van't Hoff curves and an example of two exaggerated theoretical van't Hoff curves relating $\log(V_r')$ against $1/T$ for two different types of distribution system is shown in **Figure 1**. It is seen that distribution system (A) has a large enthalpy value $[\Delta H^0/RT]_A$ and a low entropy contribution $[-(\Delta S^0/R) + V_s]_A$. The large value of $[\Delta H^0/RT]_A$ means that the distribution is predominantly controlled by molecular forces. The solute is preferentially distributed in the stationary phase as a result of the interactions of the solute molecules with those of the stationary phase being much greater than the interactive forces between the solute molecules and those of the mobile phase. Because the change in enthalpy is the major contribution to the change in free energy, the distribution, in thermodynamic terms, is said to be energy driven.

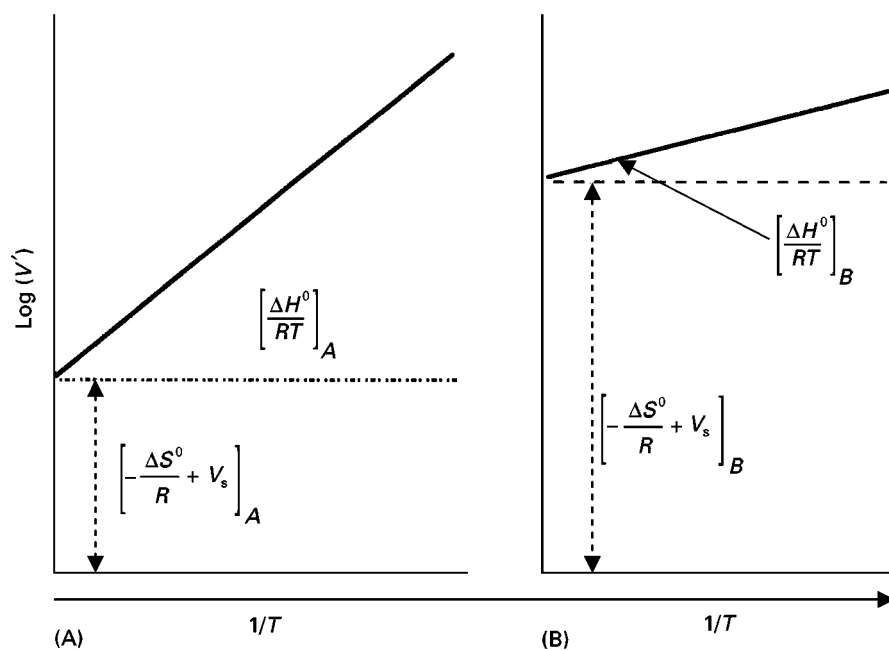


Figure 1 Van't Hoff curves for two different distribution systems. (A) Energy-driven distribution; (B) entropically driven distribution.

In contrast, it is seen that for distribution system *B* there is only a small enthalpy change $[\Delta H^0/RT]_A$, but in this case a high entropy contribution $[-(\Delta S^0/R) + V_s]_B$. This means that the distribution is not predominantly controlled by molecular forces. The entropy change reflects the loss of randomness or freedom that a solute molecule possessed when transferring from one phase to the other. The more random and more free the solute molecule is to move in a particular phase, the greater is its entropy in that phase. In system *B*, the large entropy change indicates that the solute molecules are much more restricted or their movements less random in the stationary phase than they were in the mobile phase. Because the change in entropy in system *B* is the major contribution to the change in free energy, the distribution, in thermodynamic terms, is said to be entropically driven.

Chiral separations and separations dominated by size exclusion are examples where retention and/or selectivity would be entropically controlled. However, chromatographic separations cannot be exclusively energetically driven or entropically driven, but must contain both constituents. In some cases, by careful adjustment of both energetic and entropic components, very difficult and subtle separations can be accomplished.

In most distribution systems met in chromatography, the slope of the van't Hoff curves are positive and the intercept negative. The negative value of the intercept means that the standard entropy change of

the solute has resulted from the production of a less random and more orderly system during the process of distribution into the stationary phase. More importantly, this entropy change reduces the magnitude of the distribution coefficient and attenuates solute retention. Conversely, the greater the forces between the molecules, the greater the energy (enthalpy) contribution, which increases the distribution coefficient and extends the retention. Thus, in liquid chromatography, the enthalpy and entropy changes tend to oppose one another in their effect on solute retention. In fact, there is considerable parallelism shown between the standard entropy and standard enthalpy of a series of solutes for a given distribution system.

This relationship between entropy and enthalpy has been reported many times in the literature. An example of a graph relating ΔH to ΔS is shown in Figure 2. Any increase in enthalpy indicates that more energy is used up in the association of the solute molecule with the molecules of the stationary phase. This means that the intermolecular forces are stronger and thus the stationary-phase molecules hold the solute molecules more tightly. In turn, this implies that the freedom of movement, and the random nature of the solute molecule, are also more restricted, which results in a larger change in standard entropy. It follows that, unless other significant retentive factors are present, any increase in standard enthalpy is usually accompanied by a corresponding increase in standard entropy. If the molecules of one of a pair of closely eluting isomers suffer a greater reduction in

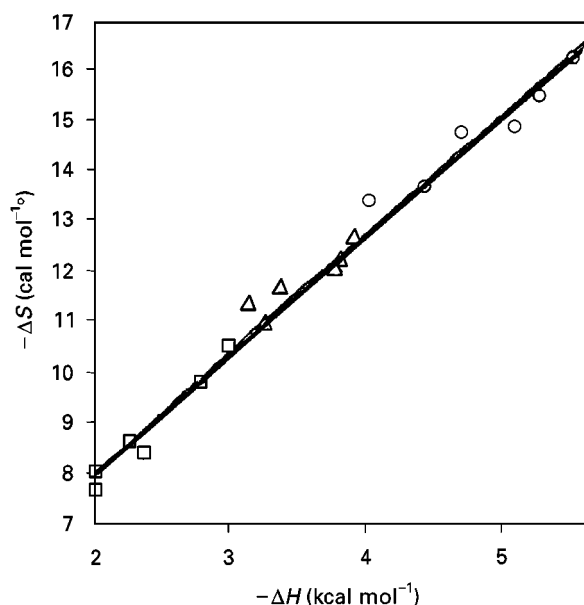


Figure 2 Graph plotting standard free entropy against standard free enthalpy for ether (triangles), thioether (squares) and amine (circles).

freedom or randomness relative to those of the other then, providing the energy changes are similar for the molecules of both isomers, those that experience the greater entropy change will be eluted first.

The van't Hoff curves can help provide even more information on the elution process. If the slope of the $\ln(k)$ versus $1/T$ curves (i.e. the standard free enthalpies) differ for two closely eluting isomers, then the lines must eventually intercept and there must be a temperature of co-elution and a subsequent elution order reversal. This elution order reversal is often not apparent in practice, as the co-elution temperature may occur outside the temperature range over which the distribution system will function satisfactorily for chromatographic purposes. However, in such distribution systems, which will include those used in most chiral separations, the operating temperature is of paramount importance in selecting the optimum operating conditions.

The Distribution of Standard Free Energy

The standard free energy can be used to explain chromatographic retention in two different ways. Firstly, portions of the standard free energy can be allotted to specific types of molecular interactions between the solute molecules and the two phases. Secondly, the molecule can be divided into different parts and each part allotted a portion of the standard free energy. This approach allows the contributions

made by different parts of the molecule to retention to be explained. This concept was suggested by Martin in his early papers, and can be used to relate molecular structure to solute retention. An example of the second approach is as follows.

Thermodynamic Analysis of a Homologous Series

Consider the distribution of the standard free energy throughout an n -alkane molecule, allotting a portion to each methylene group and to the two methyl end-groups. Then, algebraically, this concept can be put in the following form:

$$RT \ln(V'_{r(T)}) = -n\Delta G_{(\text{methylene group})} - m\Delta G_{(\text{methyl group})} \quad [8]$$

where $\Delta G_{(\text{methylene group})}$ is the standard free energy of each methylene group, $\Delta G_{(\text{methyl group})}$ is the standard free energy of each methyl group, n is the number of methylene groups and m is the number of methyl groups ($m = 2$ for an n -alkane).

The concept will now be applied to a simple n -alkane series, the data for which was obtained on the stationary-phase n -heptadecane by Martire and his co-workers. This procedure will show how it is possible to identify the difference between the contribution of a methylene group and a methyl group to solute retention and how the difference can be explained. The curves for $\log(V'_{r(T)})$ against the number of methylene groups in each of the three n -alkanes for seven different temperatures are shown in Figure 3.

The expected straight lines are produced at each temperature and the indices of determination are very close to unity. The slope represents the portion of the standard free energy from each methylene group and each intercept represents the portion from the two methyl groups. It should be noted that the contribution of a single methyl group is seen to be significantly less than that from one methylene group. The slopes (the free energy contribution from a single methylene group, $\Delta G_{(\text{methylene group})}/RT$) and half the intercept (the contribution from one terminal methyl group $\Delta G_{(\text{methyl group})}/RT$) plotted against the reciprocal of the absolute temperature are shown in Figure 4.

These curves provide relative values for the standard enthalpy ($\Delta H_{(\text{methylene group})}/R$ and $\Delta H_{(\text{methyl group})}/R$) and standard entropy ($\Delta S_{(\text{methylene group})}/R$ and $\Delta S_{(\text{methyl group})}/R$) of the distribution for each group, the magnitude of which indicates the manner in which they interact with the stationary phase.

Despite the contribution of a methyl group to the free energy being much less than that of the methylene group, the energies of interaction (the enthalpies)

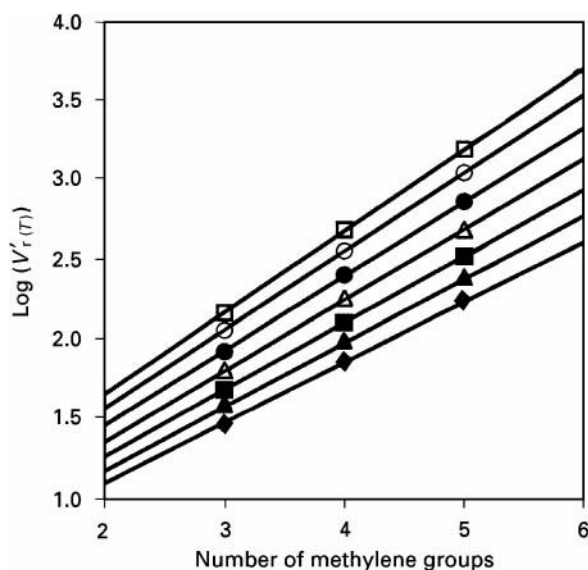


Figure 3 Graph showing $\log(V'_{(T)})$ against number of methylene groups for a series of *n*-alkanes. \square , 22.5°C; $y=0.5150x + 0.6211$, $r=1.0000$. \circ , 30°C; $y=0.4949x + 0.5737$, $r=1.0000$. \bullet , 40°C; $y=0.4706x + 0.5126$, $r=1.0000$. \triangle , 50°C; $y=0.4448x + 0.4631$, $r=1.0000$. \blacksquare , 60°C; $y=0.4216x + 0.4196$, $r=1.0000$. \blacktriangle , 70°C; $y=0.4008x + 0.3751$, $r=1.0000$. \diamond , 80°C; $y=0.3792x + 0.3399$, $r=1.0000$.

of the two groups are very similar. However, the entropy term for the methyl group is nearly 50% greater than that of the methylene group and, as this acts in opposition to the standard enthalpy contribution, it reduces the free energy associated with the methyl group by about 30% relative to that of the methylene group. This entropy difference between the two groups is due to the methylene group being situated in a chain (more rigidly held) and has,

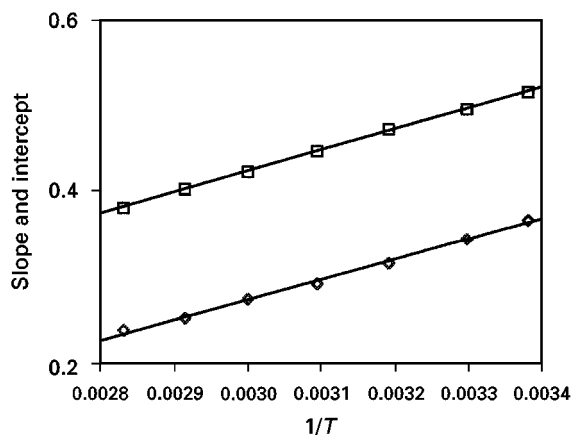


Figure 4 Graph showing intercept and slope from $[\log(V'_{(T)})/\text{number of CH}_2 \text{ group curves}]$ for a series of *n*-alkanes against the reciprocal of the absolute temperature. Squares, CH_2 : $y=246.7281x - 0.3186$; $r=0.9999$. Diamonds, CH_3 groups: $y=235.2839x - 0.4333$; $r=0.9985$.

initially, a much lower entropy before solution in the stationary phase. In contrast, the methyl group, situated at the end of the chain, is much less restricted and thus, on interaction with the stationary phase molecules, the entropy change is much greater. It follows that the introduction of a methylene group into a solute molecule will increase its retention more than the introduction of a methyl group due to the greater change in entropy associated with the methyl group.

Thus, if different portions of the standard free energy of distribution are allotted to different parts of a molecule, then their contribution to solute retention can be revealed. Furthermore, from the relative values of the standard enthalpy and standard entropy of each portion or group, the manner in which the different groups interact with the stationary phase may also be revealed.

The Distribution of Standard Free Energy Between Different Types of Molecular Interactions

In contrast to apportioning the standard free energy between different groups in the solute molecule, it can also be divided between the different types of forces involved in the solute/phase-phase distribution. This approach has been elegantly developed by Martire in his unified theory of retention. In a simplified form, the standard free energy can be divided into portions that result from the different types of interaction, e.g.:

$$\Delta G = \Delta_{\text{dispersive}} + \Delta_{\text{polar}} + \Delta_{\text{ionic}} \quad [9]$$

The polar interactions are often divided into weak, moderate and strong interactions that have, somewhat arbitrarily, been given terms such as π - π interactions, dipole-dipole interactions and hydrogen bonding:

$$\Delta G = \Delta_D + \Delta_{\pi-\pi \text{ interactions}} + \Delta_{\text{dipole-dipole interactions}} + \Delta_{\text{hydrogen bonding}} \quad [10]$$

Nevertheless, it is important to realize that they are not different types of interaction, but are all polar interactions, electrical in nature but of different strengths. In fact, many more terms have been introduced to describe subtly different enthalpic and entropic contributions to retention. In some cases, these extra terms are often introduced to take into account many second-order effects. It must be emphasized, however, that standard free energy is a bulk property, and where a portion is allotted to a particular type of interaction, e.g. dispersive, it will include all

dispersive interactions throughout the whole molecule and not one specific interaction that arises from a particular chemical group.

This approach has been used to determine the so-called binding constants between solute and stationary phase and also to investigate complexation constants. Binding constants and complexation constants have been introduced to distribution system theory largely to account for the wide range of strengths associated with polar interactions between molecules. It follows that some discussion of the physical nature of solute distribution between phases on the molecular level is necessary. Molecules can interact with one another by dispersive forces, polar forces and ionic forces, all of which are electrical in nature. Dispersive forces occur between randomly formed transient dipoles that are continuously generated throughout the molecule. For nonpolar substances, dispersive forces are proportional to their molar volume and polarizability. Polar forces result from charge concentrations dispersed at different parts of a molecule (overall electrically neutral) and can vary widely in strength. At the extreme, the energies involved can approach that of a chemical bond, as in hydrogen bonding. Polar forces may or may not be related to the dipole moment of the substance as internal electrical compensation can take place. Consequently, as dipole moments are calculated from bulk measurements made by external electrical fields, the results are frequently not related directly to the polarity of the substance. For example, the magnitude of the apparent dipole moment of dioxane, as calculated from bulk measurements, is 0.45 Debyes. This compares with 1.15 Debyes for diethyl ether, which theoretically should be about half that of dioxane. Yet dioxane is a very polar substance, soluble in water, whereas ether is weakly polar and relatively insoluble in water. Ionic forces result from the net charges on the molecule and are not germane to this discussion.

Polar interactions can result between molecules with permanent dipoles (which are often very strong) and also between a molecule with a permanent dipole and one which is polarizable (which at the extreme can be very weak). When a polarizable molecule comes into close proximity with a molecule having a permanent dipole, the electric field from the dipole induces a counter dipole in the polarizable molecule. This induced dipole acts in the same manner as a permanent dipole and the polar forces between the two dipoles result in a polar interaction between the molecules. The part of the molecule that is negatively charged due to an asymmetric accumulation of electrons has been given the term an electron donor site, whereas the area of electron depletion in the molecules

(that balances the site of electron accumulation) has been given the term electron acceptor site. More simply, these are basically negatively and positively charged sites on the molecule. Because polar interactions have such a range of strengths, certain ranges of polarity have been assumed to be due to certain types of electrical interaction that have been given the terms nonbonding lone pair, bonding π orbital, vacant orbital, antibonding π orbital, antibonding σ orbital, all of which are based on the accepted electron configuration of the molecule. In practice, however, whatever the cause, the strength of the interaction, and thus its effect on solute retention, is directly related to the intensity of the interacting charges. From the standing of separation technology, whether the introduction of these alternative terms helps to explain the separation process is a moot point, as, even in theory, in most cases the individual effects are extremely difficult to isolate completely from one another.

Martire *et al.* developed a theory assuming that polar interactions constituted the formation of a complex between the solute and the stationary phase with its own equilibrium constant. The complex is assumed to have no vapour pressure and thus remains stationary in the column until, as a result of the equilibrium kinetics, it dissociates again into the individual components. The uncomplexed solute molecule then continues to migrate along the column until complexing again takes place. Experimental data obtained to test the theory led to the conclusion that those solutes that are retained without complexing are retained solely by dispersive forces, whereas retention by polar interactions is the result of complexing. This is one approach to the explanation of retention by polar interactions, but the subject, at this time, remains controversial. Doubtless, complexation can take place, and probably does so in cases like olefin retention on silver nitrate-doped stationary phases. However, if dispersive interactions (electrical interactions between randomly generated dipoles) can cause solute retention without the need to invoke the concept of complexation, it is not clear why polar interactions (electrical interaction between permanent or induced dipoles) need to be considered differently.

Experimental Procedures

The basic apparatus that is recommended for measuring retention volumes in liquid chromatography is shown in Figure 5.

The equipment is standard, but the column oven should be capable of controlling the column temperature within $\pm 0.1^\circ\text{C}$. In addition, some provision should be made for pre-heating the mobile phase to

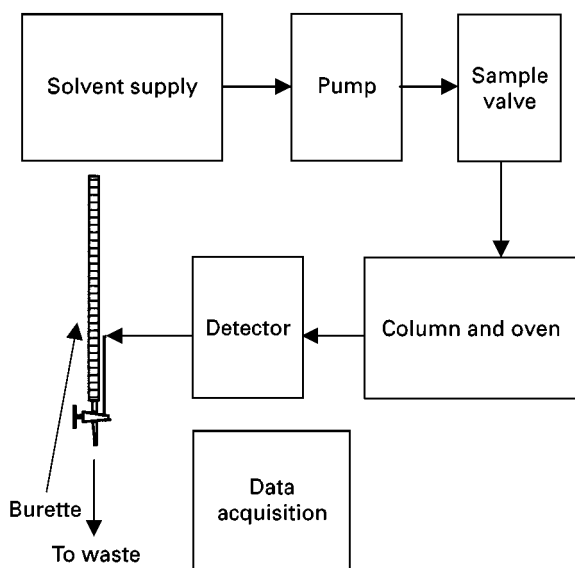


Figure 5 Apparatus for measuring retention volumes.

the correct temperature before it enters the column. The pressure drop across the column is expended as heat in the column, which can result in a significant rise in column temperature. To reduce this thermal effect, the pressure drop across the column must be made minimal and thus, very low flow rates should be employed. There are two basic methods used for measuring retention volumes. The first is to use a pump having a very constant flow rate and obtain values for the retention volume by multiplying the pump flow rate by the accurately measured retention time. The second, a better method, is to make absolute measurements of retention volume, using an accurately calibrated burette connected to the detector outlet.

This arrangement renders the use of an accurate and expensive pump unnecessary and eliminates any residual variation in pump flow rate that may still exist. The experimental procedure is as follows. The burette is read, the sample injected and the pump started. The detector output is observed and when a peak emerges, the pump is shut off at the peak maximum. The system is allowed a minute to reach equilibrium and the burette is read again. The difference between the two readings is taken as the retention volume being measured. Each retention volume should be measured in duplicate (preferably in triplicate) and any two measurements should not differ by more than 2%. After each retention volume measurement, the burette is drained to waste, until just above the lowest calibration, a few minutes allowed for drainage to be complete, and the next retention volume can then be measured. The retention volume is taken as the average of the replicates. The dead vol-

ume can be measured in a number of different ways and the numerous problems associated with dead volume measurement have been discussed in detail by Alhedai *et al.*

There are two column dead volumes that are used in liquid chromatography, the dynamic dead volume and the thermodynamic dead volume. The dynamic dead volume is the volume of the mobile phase that is actually moving, and is usually taken as the retention volume of an ionic salt such as sodium nitroprusside which, due to ionic exclusion, cannot enter the pores of the stationary phase or support. This value is used in peak dispersion theory calculations. The thermodynamic dead volume is taken as the total volume of mobile phase in the column. It is best obtained by weighing the column full of mobile phase, passing a gas through the column, and drying to constant weight. The difference between the full and empty column is taken as the thermodynamic dead volume. The retention volume of the solvent (or one component of a solvent mixture) carrying an isotopic atom can also be employed but a refractive index detector will probably be needed as the detector.

If the mobile phase consists of a mixture of solvents, then an approximate value for the thermodynamic dead volume can be taken as the retention volume of one pure component of the mixture. To minimize errors in dead volume measurement by this method, the retention factor (k) of any solute being examined should be in excess of 5. The corrected retention volume can be taken as the difference between the average retention volume of the solute and the dead volume. An example of a set of results relating corrected retention volume to the reciprocal of the absolute temperature is shown in **Figure 6**.

The information given in **Figure 6** can be used in a number of ways. It is clear that enantiomer B has the higher standard free entropy and is thus the enantiomer that interacts more closely with the chiral stationary phase. The closer association of the B enantiomer with the stationary phase also results in a greater standard free enthalpy and the curves, V_r against $1/T$, will thus have different slopes. Consequently, the two curves will intercept and, despite having different standard free entropies and enthalpies, there will be a temperature of co-elution above which the order of elution will be reversed. In this case, the elution order reversal was not observable as the co-elution temperature was above the maximum permissible for the particular stationary phase.

The linear equations resulting from a curve fit to the data will allow the retention factors (k) and the separation factor (α) of the two enantiomers to be calculated for any temperature. The analysis time, column length and minimum efficiency are a function

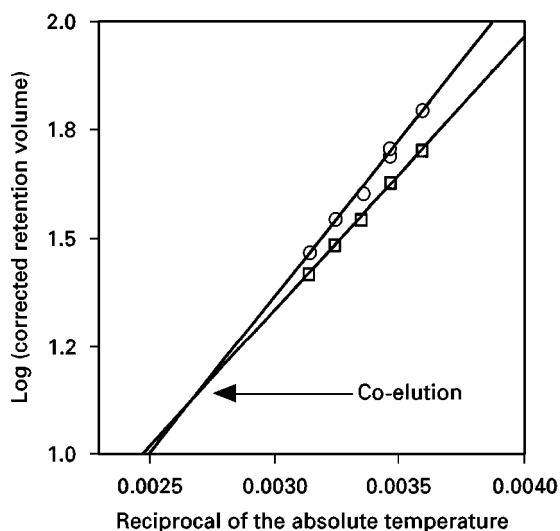


Figure 6 Graph plotting log (corrected retention volume) against the reciprocal of the absolute temperature for a pair of enantiomers separated on vancomycin. Squares, enantiomer A: $y = 631.1694x - 0.5614$; $r = 0.9992$. Circles, enantiomer B: $y = 725.8641x - 0.8116$; $r = 0.9993$.

of the retention factors and separation factor (α) of the two enantiomers. Thus, with an appropriate computer program, the optimum temperature, necessary efficiency and the optimum column length that will provide the minimum analysis time can be calculated from the data given in Figure 6. Finally, values for the standard free enthalpy and entropy for different solutes on different distribution systems can provide an insight into the nature and strength of the molecular interactions involved, which can then be related to molecular structure.

Chromatographic Methods for Measuring Diffusion Coefficients and Molecular Weights

The use of chromatography techniques to measure diffusion coefficients and molecular weights can be used very effectively where other techniques are difficult, cumbersome or time-consuming to employ. Diffusion coefficients are readily obtained by measuring the dispersion of a solute band in the liquid of interest as it passes through an open tube, but certain precautions must be taken. This technique follows directly from the theory of dispersion in open tubes developed by Golay. The van Deemter equation that describes dispersion occurring in a packed column can be used in a similar way to obtain an approximate estimation of the molecular weight of an eluted solute from a packed column.

Diffusion coefficients from dispersion measurements in open tubes Chromatographic techniques employ-

ing open tubes can be used very effectively to determine diffusion coefficients in liquids which, in turn, have been shown to be simply related to molecular weights. This work was pioneered in 1976 by Grushka and Kikta, who showed that the diffusion coefficient of a substance in a specific liquid (the diffusivity) could be determined by measuring its dispersion after passing through a cylindrical tube. According to the theory of band dispersion in an open cylindrical tube, as developed by Golay, the variance per unit length H of the solute band eluted from an open tube carrying no stationary phase is given by:

$$H = \frac{2D_m}{u} + \frac{r^2u}{24D_m} \quad [11]$$

where u is the linear velocity of the liquid through the tube, D_m is the diffusivity of the solute in the liquid and r is the radius of the tube.

Now, if $u \gg D_m/r$, then:

$$H = \frac{r^2u}{24D_m} \quad [12]$$

or:

$$D_m = \frac{r^2u}{24H} \quad [13]$$

As the value of D_m is generally less than 2.5×10^{-5} and the tube diameter is usually about 0.010 in i.d. then, $D_m/r < 10^{-3} \text{ cm s}^{-1}$, thus the condition $u \gg D_m/r$ is easily met in practice.

The apparatus is simple and consists of a solvent reservoir, a pump, a sample valve, the open tube and a suitable detector. The open tube should be jacketed by a larger tube containing circulating water from a thermostat. Temperature control should be $\pm 0.2^\circ\text{C}$. In order to ensure all measurements are accurate, however, some important conditions must be met. The sample valve must be an internal loop valve and have a capacity less than $0.2 \mu\text{L}$; the detector cell must have a small volume certainly not greater than $5 \mu\text{L}$ and preferably less; the open tube must be connected directly to the detector cell with no intervening connecting tube (all commercial detectors have significant lengths of connecting tube between the column and the detector cell, and this connecting tube must be removed or bypassed so that the open tube is connected directly to the cell). These requirements are necessary to ensure that any extra tube dispersion is insignificant compared with that occurring in the open tube. In addition, solute diffusivity is pressure-dependent and thus low flow rates must be used to ensure a minimum pressure drop across the tube. Finally, there must be no radial flow introduced

in the open tube, as this aids diffusion and gives false high values. Consequently, the tube must be perfectly straight between the sample valve and the detector cell. Even a slight curve will produce radial flow and significantly increase the diffusivity as measured, and give false high values.

The band width is measured at the points of inflection at 0.6065 of the peak height. If manual measurements are used, the chart speed should be adjusted so that the peak width is at least 1 cm. The width should be measured with a comparator, reading to an accuracy of ± 0.1 mm. At least three replicate runs should be made and the three replicate values of efficiency should not differ by more than 2%. If the data acquisition system has software that will directly measure column efficiency, then this can be used providing its accuracy is carefully checked manually. Noise on the detector can often introduce inaccuracies that are less likely to occur with manual measurement.

Katz and Scott employed the technique to determine the diffusivities of 70 different solutes in an ethyl acetate-*n*-hexane solvent mixture. Using the data they also demonstrated a relatively simple relationship between the diffusivity and the molecular weight of the solute:

$$\begin{aligned}\frac{1}{D_m} &= A + BV^{1/3}M^{1/2} \\ &= A + BM^{0.833}d^{-0.333}\end{aligned}\quad [14]$$

where V is the molar volume of the solute, M is the molecular weight of the solute, A and B are constants for the solvent system employed, and d is the density of the solute.

Employing the values they obtained for the diffusivities of the different solutes, the relationship between diffusivity and molecular weight as given in eqn [14] is demonstrated by the curves relating $(1/D_m)$ against $(V^{1/3}M^{1/2})$, shown in Figure 7. It is clear that an approximate value of the molecular weight of an eluted solute can be obtained from the diffusivity of the solute which in turn will be related to the band width or the dispersion of the peak.

This procedure has been extended further by Katz to the measurement of high molecular weight materials such as polypeptides and proteins using a packed column. In the first instance, Katz found it necessary to identify the function of k which was included in the resistance to mass transfer term of the van Deemter equation. This was achieved by relating the difference between measured H values (the variance per unit length of the column) and the multipath term, to the reciprocal of the solute diffusivity, using solutes of

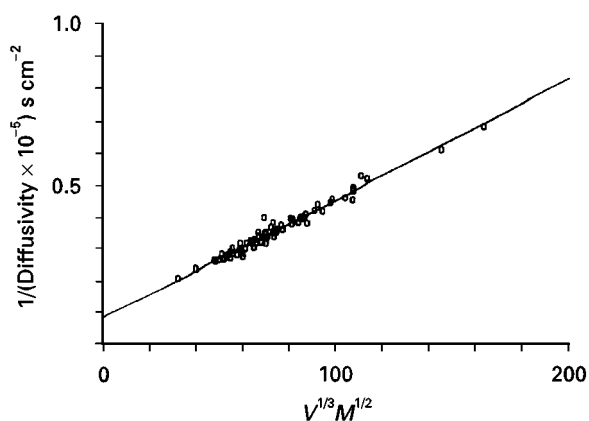


Figure 7 Graph relating the reciprocal of the diffusivity to the product of the cube root of the molar volume and the square root of the molecular weight. Courtesy of Elsevier Science.

known diffusivities. The system was then used to determine the molecular weight of a number of high molecular weight materials. The values obtained were not exceptionally accurate but were practically useful.

In summary, the distribution coefficient and the thermodynamic properties of a distribution system can be easily measured by liquid chromatographic procedures. In addition, information can be gained about the nature of the distribution system and the molecular interactions involved. It is also possible to determine diffusion coefficients and approximate values for the molecular weights of eluted solutes by peak width measurements. Such data, however, may require some rather complex calibration procedures and the results, particularly with respect to the solute molecular weight, may have a precision of only $\pm 20\%$.

See also: II/Chromatography: Liquid: Theory of Liquid Chromatography. III/Physico-Chemical Measurements: Gas Chromatography. Reverse-Flow Gas Chromatography.

Further Reading

- Alhedai A, Martire DE and Scott RPW (1989) Column 'dead volume' in liquid chromatography. *Analyst* 114: 869–875.
- Golay MJE (1958) In: Desty DH (ed.) *Gas Chromatography* 1958, p. 36. London: Butterworths.
- Grushka E and Kikta EJ (1976) Diffusion in liquids. II. The dependence of the diffusion coefficients on molecular weight and temperature. *Journal of the American Chemistry Society* 98: 643–648.
- Laub RJ and Pecsok RL (1978) *Physicochemical Applications of Gas Chromatography*, p. 153. Chichester: John Wiley.

- Liao H-L, Martire DE and Sheridan JP (1973) Thermodynamics of molecular association by gas-liquid chromatography. A comparison of two experimental approaches. *Analytical Chemistry* 215: 2087–2092.
- Martire DE (1989) Generalized treatment of spatial and temporal column parameters applicable to gas, liquid and supercritical fluid chromatography. I. Theory. *Journal of Chromatography* 461: 165–176.
- Martire DE and Reidl P (1968) A thermodynamic study of hydrogen bonding by means of gas-liquid chromatography. *Journal of Physical Chemistry* 72: 3478–3488.
- Scott RPW (1995) *Techniques and Practice of Chromatography*, p. 34. New York: Marcel Dekker.
- Tewari YB, Sheridan JP and Martire DE (1970) Gas-liquid chromatography determination and lattice treatment of activity coefficients for some haloalkane solutes in alkane solvents. *Journal of Physical Chemistry* 74: 3263–3268.
- Van Deemter JJ, Zuiderweg FJ and Klinkenberg A (1956) Longitudinal diffusion and resistance to mass transfer as causes of nonideality in chromatography. *Chemical Engineering Science* 5: 271–280.

Proteins

See II/CHROMATOGRAPHY/Protein Separation

Refractive Index Detectors in Liquid Chromatography

See II/CHROMATOGRAPHY: LIQUID/Detectors: Refractive Index Detectors

Size Exclusion Chromatography: Mechanisms

See II/CHROMATOGRAPHY: LIQUID/Mechanisms: Size Exclusion Chromatography

Theory of Liquid Chromatography

P. A. Sewell, Lathom, Ormskirk, Lancs, UK

Copyright © 2000 Academic Press

Liquid chromatography (LC) involves the separation of the components of a mixture by virtue of differences in the equilibrium distribution of the components between two phases: one which is a liquid (the mobile phase) and moves in a definite direction, the other which is stationary (the stationary phase). Modern LC using very small particles and a relatively high inlet pressure is referred to as high performance liquid chromatography (HPLC).

Stationary Phase

An advantage of LC over gas chromatography is in the variety of types of stationary and mobile phases which may be used, allowing the separation of such diverse molecular species as pharmaceuticals, agrochemicals, proteins, inorganic and organic ions and biopolymers. The use of a stationary phase with a liquid coated physically onto an inert solid support (partition chromatography) has been superseded by the use of a liquid chemically bonded on to the solid support (bonded-phase chromatography). Ideally, the support does not contribute to the separation process, but its particle size and surface properties have a profound effect on the efficiency of the process.

The term liquid–solid chromatography (LSC) covers a range of techniques:

- adsorption chromatography, when the stationary phase is an active solid (e.g. silica, alumina or a polymer) and separation is based on adsorption affinities between the sample molecules and the surface of the active solid
- ion chromatography, which uses an ion exchange medium
- exclusion chromatography using a stationary phase (e.g. a polymer or porous silica) which separates according to molecular size and shape
- affinity chromatography, which utilizes the unique biological specificity of the analyte and ligand interaction with the stationary phase

Liquid chromatography can be carried out within a tube (column chromatography) or on a flat sheet of material (planar chromatography) such as a sheet of paper (paper chromatography) or a layer of stationary phase coated on to a support, e.g. a glass or plastic sheet (thin-layer chromatography, TLC). In column chromatography, the stationary phase (liquid plus support) can fill the whole inside volume of the tube (packed column) or be concentrated along the inside wall of the tube, leaving an unrestricted path for the mobile phase in the middle of the tube (open tubular or capillary column). The term column will be used in a general sense to apply to both column and planar chromatography.

A significant difference between GC and HPLC is the permeability of columns used. The permeability (κ) is a measure of flow resistance:

$$\kappa = \eta L \bar{u} / \Delta P = \eta L^2 / \Delta P t_M \quad [1]$$

where η = viscosity, L = column length, \bar{u} = average mobile phase velocity, ΔP = pressure drop across the column and t_M = residence time for an unretained substance.

Introducing the particle diameter (d_p), the flow resistance parameter (ϕ) is given by:

$$\phi = d_p^2 / \kappa \quad [2]$$

Permeable columns are the most desirable and typically ϕ values are ~ 500 for spherical microparticles.

Mobile Phase

In LC the mobile phase is often called the solvent, but since solid samples have to be made into a solution by dissolution in a sample solvent, the use of the term solvent for the mobile phase may cause confusion. However, in order to avoid solubility prob-

lems when the sample is injected on to the column, it is safest, whenever possible, to make the sample solution using the same liquid as is to be used as the mobile phase, in which case no confusion should arise.

The time taken by a sample to pass through the column (the total elution/retention time: t_R) is a function of the mobile-phase velocity and the volume of mobile phase required to elute the component from the column, the total retention volume (V_R), is given by:

$$V_R = F \times t_R \quad [3]$$

where F is the volume flow rate of mobile phase measured at the column outlet at ambient temperature (T_a) and ambient pressure (P_a). Since column temperatures are usually close to ambient, temperature corrections on flow rate are rarely applied. Volume flow rates are measured from the time required to collect a given volume of mobile phase or with an electronic flow meter. Unlike gas chromatography, liquid mobile phases can be considered as incompressible and the flow rate is uniform throughout the column.

Linear flow rates (\bar{u}) are measured from the retention time, called the hold-up time, of an unretained substance (t_M), i.e. one which moves at the same velocity as the mobile phase:

$$\bar{u} = L / t_M \quad [4]$$

where L is the column length.

However, whereas in gas chromatography it is reasonable to assume that a substance like nitrogen or helium will have negligible solubility in the stationary phases used, in LC finding a species which is soluble in the mobile phase and will not have at least some retention on the stationary phase – therefore giving too high a hold-up time – often proves difficult. Furthermore, with a porous stationary phase, excluded components (not uncommon with mobile phases with a high water content) do not access the total mobile-phase volume and may actually run ahead of the mobile phase, giving too low a hold-up time.

Porosity can be used to verify the hold-up time. The total porosity (ε) of a column is the volume fraction occupied by the mobile phase:

$$\begin{aligned} \varepsilon &= \frac{V(\text{column}) - V(\text{packing material})}{V(\text{column})} \\ &= \frac{4F(\text{mL min}^{-1})t_M(\text{s})}{d_c^2(\text{mm})L(\text{mm})} \end{aligned} \quad [5]$$

where F = volume flow rate, d_c = column diameter and L = column length. For a totally porous material $\varepsilon \sim 0.75$ and ~ 0.4 for porous layer beads.

Thus, values of the hold up time obtained for a given component should give these values according to the type of packing material used. Values < 0.75 indicate the molecule is excluded from the pores of the stationary phase, and values > 0.75 indicate that retention on the stationary phase has occurred.

Choice of mobile phase is fundamental to the separation in LC. Mixtures of solvent, with up to four components are commonly used, so that as well as the chemical nature of the components, miscibility considerations are important. Physical properties, such as viscosity, volatility, refractive index and UV absorption can also limit the choice of mobile phases.

Modes of Liquid Chromatography

Analytical LC is always carried out by elution chromatography where the mobile phase is passed continuously through the column and the sample is fed (or injected) into the system as a finite plug. If the conditions for the analysis are optimized, the sample components can be completely separated from each other. Placing a detector at the end of the column, which responds to some property of the sample, produces a trace (the chromatogram) which is a plot of detector response against time.

If the stationary phase is more polar than the mobile phase, the term normal-phase chromatography is used, and if the stationary phase is less polar than the mobile phase the term reversed-phase chromatography is used.

The General Elution Problem

A typical chromatogram for the separation of a mixture of components which illustrates the character-

istics of chromatography, and is often referred to as the general elution problem, is shown in **Figure 1**.

The properties which the chromatogram illustrates and which must be explained by any theory of chromatography are:

- The components of the mixture elute from the column at different times (retention).
- Peak widths increase with retention time (peak shape and broadening).
- The separation of pairs of peaks is not constant (column resolution).

Chromatographic Retention

Retention parameters are measured in terms of times, mobile-phase volumes or retention factors (k) (previously called capacity factors: k'). If the flow rate is constant, the volumes are proportional to times, e.g. t_R (time) is analogous to V_R (volume).

If a mixture is chromatographed, the time taken for a component to be eluted from the column, the (total) retention time (t_R), is measured from the moment of injection to the appearance of the peak maximum. This, together with the width of the peak measured at the baseline (w) or at half peak height (w_h), and the elution of an unretained peak, are important parameters in chromatography and are illustrated in **Figure 2**, which shows the separation of a two-component mixture eluting with retention times $(t_R)_1$ and $(t_R)_2$, with an unretained component (retention time, t_M).

The retention volume (V_M) of an unretained peak (where $V_M = F \times t_M$) is also called the mobile-phase volume and equals the volume (both inter- and intra-particle) available to the mobile phase in the column.

The adjusted retention time/volume (t'_R/V'_R) is the total elution time/volume minus the retention

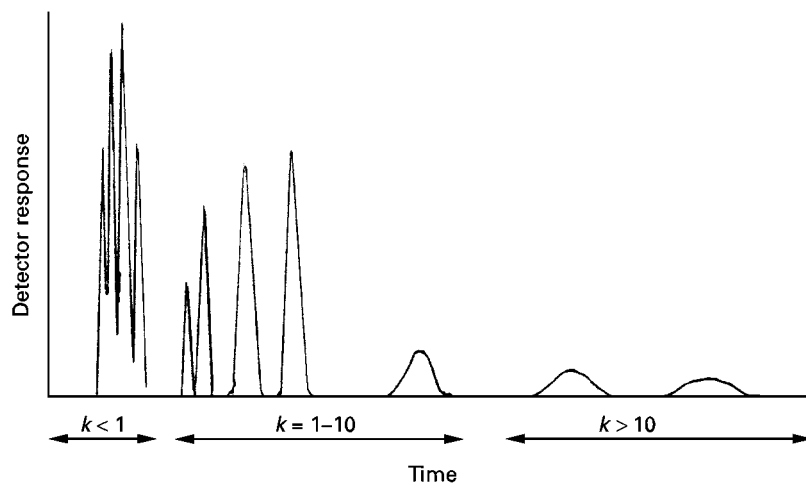


Figure 1 The general elution problem.

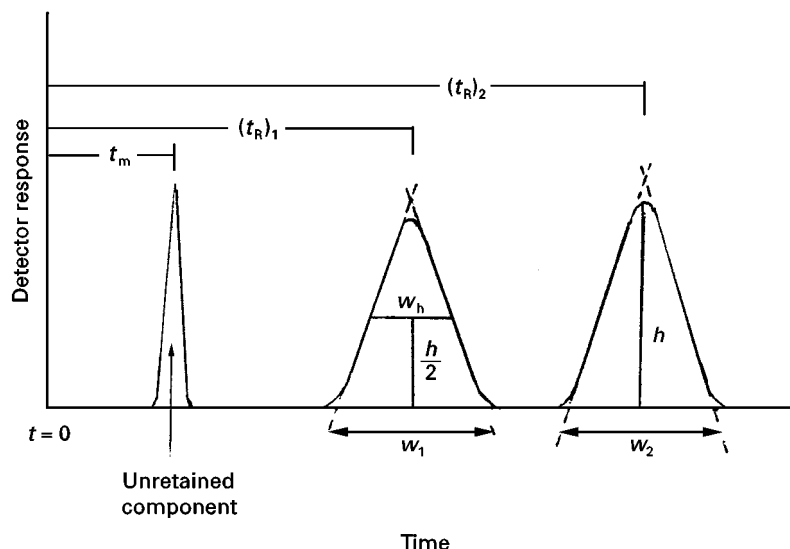


Figure 2 Separation of a two-component mixture showing retention parameters. See text for details.

time/volume of the mobile phase:

$$t'_R = t_R - t_M; \quad V'_R = V_R - V_M \quad [6]$$

The unretained peak, which has no affinity for the stationary phase and does not exhibit exclusion, passes through the column at the same speed as the mobile phase. A substance which shows affinity for the stationary phase moves through the column more slowly than the mobile phase and is said to be retained. The ratio of the two velocities is known as the retardation factor (R):

$$R = \frac{\text{rate of movement of retained peak}}{\text{rate of movement of mobile phase}} \quad [7]$$

A retained component spends time in both the mobile phase (t_M) and the stationary phase (t_S) and retention time t_R is given by:

$$t_R = t_M + t_S \quad [8]$$

The time spent in the stationary phase is dependent on the distribution coefficient (K_c) such that $t_S = K_c V_S$. If C_S and C_M are the concentrations of a component in the stationary phase and mobile phase respectively, the distribution constant is given by:

$$K_c = C_S/C_M \quad [9]$$

The rate of movement of a component through the column is inversely proportional to the distribution constant, i.e. a substance with a high concentration in

the stationary phase (a high distribution coefficient) moves slowly through the column. Components of a mixture are, therefore, separated only if their distribution coefficients differ. Using volumes rather than times we can write:

$$V_R = V_M + K_c V_S \quad \text{or} \quad V'_R = K_c V_S \quad [10]$$

which is the fundamental equation for chromatography, neglecting the effects of nonlinearity of the sorption isotherm and band broadening.

In adsorption chromatography the stationary-phase volume is replaced by the surface area (A_S) of the stationary phase, and the distribution coefficient is changed to the adsorption coefficient (K_A).

An alternative expression (the retention factor: k) for the distribution of a sample component is in terms of the relative number of moles (n) of a component in the stationary and mobile phases, such that:

$$k = n_S/n_M = K_c \cdot (V_S/V_M) \quad [11]$$

$$R = \frac{\text{amount of solute in the mobile phase}}{\text{amount of solute in mobile + stationary phases}} \quad [12]$$

$$\begin{aligned} \text{or } R &= n_M/(n_M + n_S) \\ &= 1/(1 + k) \end{aligned} \quad [13]$$

Substituting the retention factor into the equation:

$$V_R = V_M + K_c V_S \quad \text{gives} \quad V_R = V_M(1 + k) \quad [14]$$

or using retention times:

$$t_R = t_M(1 + k) \quad [15]$$

and on rearrangement:

$$k = (t_R - t_M)/t_M \quad [16]$$

This last expression is widely used as a simple way of expressing retention from values easily measured from the chromatogram, and without the need to measure flow rates.

Since:

$$t_M = L/\bar{u} \quad [17]$$

we can write:

$$t_R = \frac{L}{\bar{u}} (1 + k) \quad [18]$$

Hence the retention time is directly proportional to the column length and inversely proportional to the linear flow rate of the mobile phase.

Peak Shape and Broadening

The variation of solute concentration in the stationary phase with solute concentration in the mobile phase, at constant temperature, is known as the sorption isotherm. Simple chromatographic theory assumes a linear isotherm relationship, i.e. the distribution coefficient is constant. Under these conditions the

retention time is independent of sample concentration and the peak moves with a constant speed. Given a peak profile with plug-shape distribution on injection, this shape should be maintained as the peak passes through the column to emerge at the exit. However, because of longitudinal diffusion in the direction of flow, the peak takes on a Gaussian distribution. If the isotherm relationship is nonlinear (e.g. Langmuir or anti-Langmuir), the distribution coefficient is not constant but varies with solute concentration and there is a distribution of solute velocities across the peak, which is described as tailing or fronting. This relationship between isotherm shape and peak shape is illustrated in Figure 3.

The width of a chromatographic peak is a function of the column efficiency, expressed as the plate number (N), calculated from the following equations depending on the value used for the peak width (Figure 2):

$$N = (V_R/\sigma)^2 = (t_R/\sigma)^2 = 16(t_R/w_b)^2 = 5.545 (t_R/w_h)^2 \quad [19]$$

where σ is the standard deviation of the Gaussian peak.

The column length divided by the plate number gives the plate height or height equivalent to a theoretical plate (H) and normalizes the plate number for column length: $H = L/N$. The concept of plates in chromatographic theory (the plate theory) is by analogy with the distillation process and represents a notional length of the column in which the solute molecules reach a distribution equilibrium. Thus,

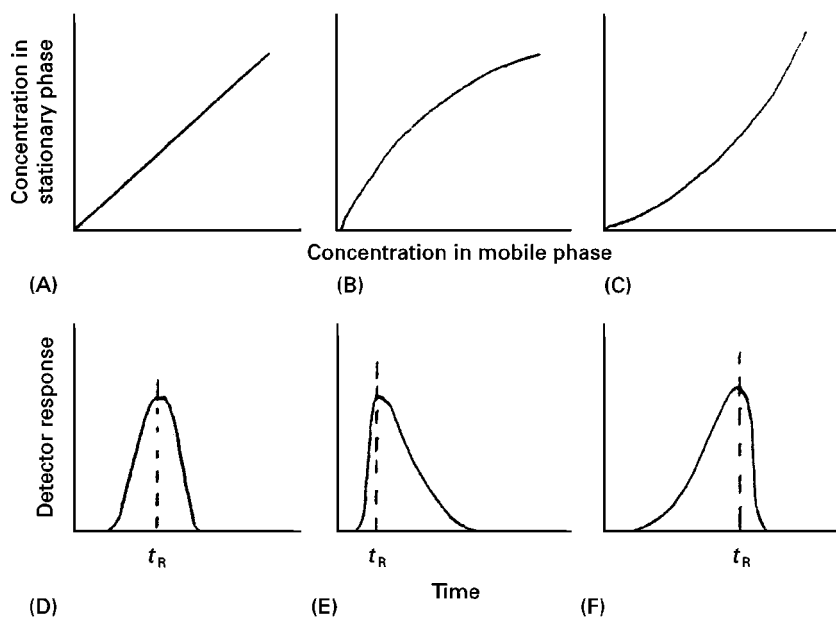


Figure 3 Isotherm shape and their effect on peak shape and retention times. (A) Linear; (B) Langmuir; (C) anti-Langmuir; (D) Gaussian; (E) tailing; (F) fronting.

a large number of theoretical plates corresponds to an efficient column.

Consideration of the chromatographic process as controlled by equilibrium gives a satisfactory explanation of chromatographic retention in term of the distribution coefficients, but in considering band broadening a different approach is required – the rate theory of chromatography. This was first applied by van Deemter, Klinkenberg and Zuiderweg to gas chromatography, but has been extended to include LC. As the solute band passes through the column the band width increases and the solute is diluted by the mobile phase. Although the process of fluid flow is complex, three main contributions to band broadening (i.e. to the variance (σ^2) of the Gaussian peak) may be recognized: the multipath effect (formally called eddy diffusion), molecular diffusion and mass transfer.

The Multipath Effect (the *A* term)

Molecules flowing through a packed bed of stationary phase will take paths of different lengths resulting in a small difference in retention times. This has the effect of broadening the band by an amount dependent on the particle diameter (d_p), such that:

$$A = 2\lambda d_p \quad [20]$$

The packing constant (λ) is an empirical term depending on the shape (spherical or irregular) of the packing material and the packing efficiency, and reaches a minimum value $\cong 0.5$. For open tubular columns there is no *A* term.

Longitudinal Molecular Diffusion (the *B* term)

Solute molecules diffuse in a longitudinal direction (i.e. along the column axis) according to Fick's law of diffusion. The amount of band spreading is directly proportional to the coefficient of diffusion (D_M) of the solute molecules in the mobile phase, and inversely proportional to the mobile-phase flow rate. An obstruction factor (ψ) is introduced to account for the restricted diffusion in a packed bed.

Hence:

$$B = 2\psi D_M/\bar{u} \quad [21]$$

Longitudinal molecular diffusion is only significant in LC if small ($< 10 \mu\text{m}$) stationary-phase particles are used at low mobile phase velocities and with a relatively high solute diffusion coefficient.

Mass Transfer (the *C* terms)

In LC, band broadening due to mass transfer is a complex process involving both the stationary and mobile phases. Two processes are responsible for

band broadening in the stationary phase (stationary phase mass transfer: C_s). The first of these processes involves the finite rate of mass transfer across the mobile-phase/stationary-phase interface. At the head of the column the solute is distributed between the stationary and mobile phases according to the value of the distribution coefficient. As the band moves down the column, solute at the leading edge of the band is continually meeting new stationary phase, into which it dissolves. To maintain the equilibrium, solute will dissolve from the trailing edge of the band out of the stationary phase back into the mobile phase. Because this process is not instantaneous the band is broadened. The second process involves the statistical distribution of the rates of diffusion of individual molecules in the stationary phase, resulting in small differences in the time that individual molecules spend in the stationary phase. A fast-moving mobile mass sweeps the zone more rapidly through the column and accentuates the band broadening as does a greater film thickness (d_f) of stationary phase. A higher rate of solute diffusion in the stationary phase (D_s) will decrease the band broadening so that:

$$C_s = q \cdot \frac{k}{(1+k)^2} \frac{d_f^2 \bar{u}}{D_s} \quad [22]$$

where q is a configuration factor depending on the nature of the stationary phase.

In adsorption chromatography, the C_s term is expressed in terms of the adsorption/desorption kinetics of the solute molecules on the stationary phase.

Band broadening in the mobile phase also results from two different processes. Moving mobile phase mass transfer (C_M) results from frictional forces which modify the laminar flow profile across a channel between two particles, resulting in a higher flow velocity in the centre of the channel. Stagnant mobile-phase mass transfer (C_M^*) is the result of slow diffusion of solute molecules in and out of the pores of a porous stationary phase. The overall mobile-phase mass transfer can be represented by the expression:

$$C_M = f(d_p^2, d_c^2) \cdot \bar{u}/D_M \quad [23]$$

where d_p is the particle diameter and d_c is the column diameter, D_M the solute diffusion coefficient in the mobile phase and \bar{u} is the linear velocity.

Giddings, recognizing that molecules are free to diffuse from one flow path into another, introduced the idea of 'coupling' the multipath term (*A*) and the mobile-phase mass transfer (C_M) so that the variation of the plate height (*H*) with \bar{u} is then given by:

$$H = B/\bar{u} + C_s \bar{u} + C_M^* \bar{u} + \{1/A + 1/C_M \cdot \bar{u}\}^{-1} \quad [24]$$

The contribution of the various terms to the total plate height is illustrated in Figure 4.

Extra-Column Band Broadening

So far, we have only considered band-broadening processes within the chromatographic column itself but, in assessing the overall performance of the system, the instrument as a whole is important. Thus, the injection system, detector and connecting tubing all contribute to the overall peak shape. The objective for injection is to get the sample on to the column in as narrow a plug as possible. Slow transfer of the sample from the injector to the column causes peak broadening and peak tailing. Large dead volumes in the detector can lead to remixing of components and deterioration of the separation as well as dilution of the sample peaks, reducing detection limits. The peak broadening in an open tube (radius r and length L), volume flow rate F , and for a solute with diffusion coefficient D_M is given by:

$$\pi r^4 FL / 24 D_M \quad [25]$$

In particular, short lengths (< 30 cm) of narrow-bore (~ 0.01 in) connecting tubing should be used.

Column Resolution

Chromatographic separation is only achieved when there is a difference in the distribution coefficients of two components, i.e. the molecular interactions (dispersion forces, dipole interactions and hydrogen-

bonding forces) between the sample molecules and the stationary phase are sufficiently different. More fundamentally it is the free energies of distribution $\Delta(\Delta G^\theta)$ of the components of a mixture which must differ. It can be shown that:

$$\Delta(\Delta G^\theta) = -RT \ln \alpha = -RT \ln [(K_c)_2 / (K_c)_1] \quad [26]$$

A stationary phase which produces a large degree of separation is said to have high selectivity. The separation of two components (1 and 2) is expressed by the relative retention (α):

$$\alpha = t'_{R(2)} / t'_{R(1)} = V'_{R(2)} / V'_{R(1)} = k_{(2)} / k_{(1)} = K_{C(2)} / K_{C(1)} \quad [27]$$

If one of the pair is a standard substance, the symbol used for relative retention is r . Having achieved a separation, it is necessary to prevent remixing of the components and the ability to achieve this is a function of the column efficiency, as measured by the plate number. The combined effects of stationary-phase selectivity and column efficiency are expressed in the peak resolution (R_s) of the column:

$$R_s = \frac{(t_R)_2 - (t_R)_1}{(w_1 + w_2)/2} \quad [28]$$

A value of $R_s = 1.5$ is normally considered to represent baseline separation for Gaussian-shaped peaks. To achieve the maximum peak resolution, both high selectivity and column efficiency (giving narrow bands) are required.

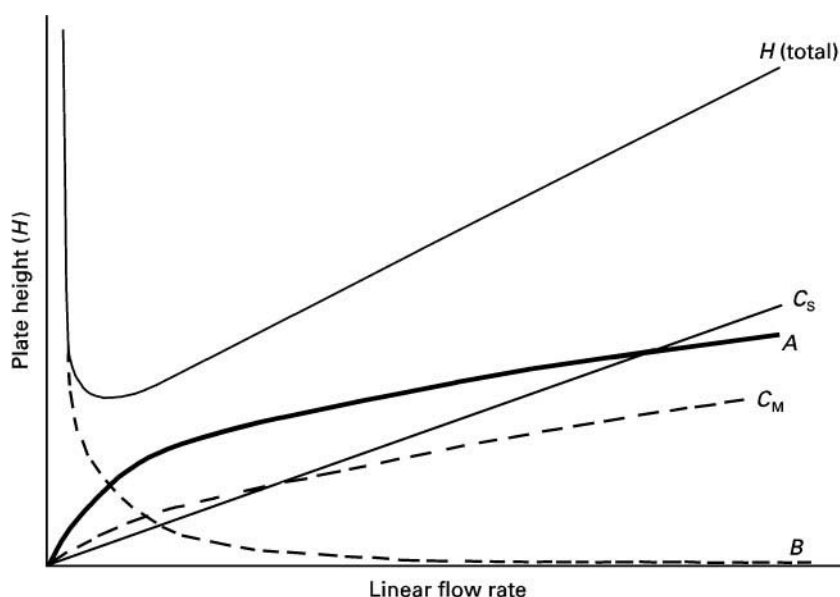


Figure 4 The van Deemter plot for LC and the variation of the terms A , B , C_s and C_M with flow rate. See text for details.

Increased resolution can always be achieved by an increase in column length since the peak separation (Δt_R) is proportional to the distance of migration down the column, but peak width is only proportional to the square root of the migration distance. The penalty for this, however, is longer retention times and an increased inlet pressure of mobile phase.

The Purnell equation shows how peak resolution is related to the retention factor (k), the plate number (N) and the relative retention (α):

$$R_s = \frac{\sqrt{N_2}}{4} \cdot \frac{(\alpha - 1)}{\alpha} \cdot \frac{k_2}{1 + k_2} \quad [29]$$

where the subscript 2 refers to the second peak.

Conditions for obtaining maximum values of the plate number have already been discussed. In LC the relative retention is governed by the nature of the mobile phase as well as the stationary phase. In order to obtain a satisfactory separation, a balance must be achieved between the interactions (dispersion forces, dipole-dipole interactions, dipole-induced-dipole interactions, H-bonded forces), represented in Figure 5 by an interaction triangle.

If the interactions between the sample and stationary phase are too strong, the retention times will be excessively long, whereas if the interactions between sample and mobile phase are too strong, retention times will be too short. Modifications to the mobile phase (e.g. the addition of ion-pairing agents, chiral molecules) may also be used to change stationary-phase-mobile-phase interactions.

The interactions are maximized in the concept of 'like has an affinity for like'. Thus, for a sample which contains predominantly nonpolar species, a nonpolar stationary/mobile phase will optimize the dispersion forces, and polar interactions will be absent. For polar samples a polar stationary/mobile phase will maximize both dipole-dipole interactions and dipole-induced-dipole interactions and the effect of dispersion forces will be reduced. At least a partial separation can be achieved with α values as low as 1.01,

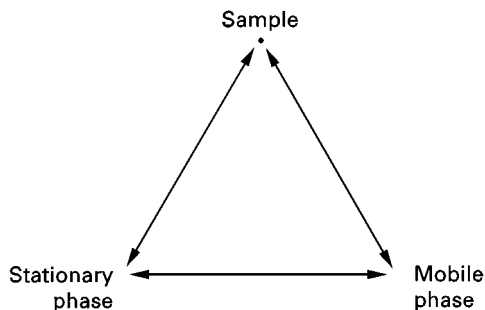


Figure 5 The interaction triangle in LC.

but values in the range 1.5–3.0 are preferable but above values of about 5.0 little additional resolution is achieved.

Peak resolution increases rapidly with increasing k values, but at values > 10 the term $k_2/(1 + k_2) \rightarrow 1$ and the term plays no further part in the resolution. The use of k values < 1 gives very short retention times and poor resolution, so that the optimum for k is between 1 and 10. The retention equation $t_R = L/\bar{u}(1 + k)$ shows that retention times are a function of both the mobile-phase velocity (\bar{u}) and the retention factor.

In LC, temperature has little effect on retention, because of the relatively small values of the enthalpies of solution involved. The van't Hoff equation describes the change in equilibrium constant with temperature and if the phase ratio (V_s/V_M) is independent of temperature we can also write for the retention factor:

$$\frac{d \ln k}{dT} = \frac{\Delta H}{RT^2} \quad [30]$$

where ΔH is the enthalpy of solution (or adsorption) from the mobile phase to the stationary phase.

The main use of temperature control is to increase the reproducibility of retention times, and to increase column efficiency through the effect of temperature on viscosity and diffusion. The first choice to be made is, therefore, the choice of chromatographic mode (normal phase or reversed phase) and the stationary phase. In practice, the reversed-phase mode can be used for samples with a wide range of polarities and is usually the mode of choice. Bonded stationary phases with a hydrocarbon chain attached to the silica surface (e.g. Si-C₁₈) are widely used; the polarity of the phase may be modified by introducing functional groups (e.g. -CN, -NH₂) into the chain.

To select the mobile phase, the concept of solvent strength and polarity is utilized. A strong solvent is one which causes a sample to elute rapidly from the column. Various measures of solvent strength are used:

- solvent strength parameter (E°), based on the adsorption energies of the solvent on alumina
- solvent polarity parameter (P'), based on experimental solubility data which reflects the proton acceptor, proton donor and dipole interactions of the solvent molecule
- the Hildebrand solubility parameter (δ), which measures dispersion and dipole interactions, and hydrogen acceptor and donor properties.

Figure 1 for the general elution problem also shows values of k for different zones of the chromatogram. With low k values ($k < 1$) the peaks are eluted too rapidly and there is no time for separation. With high k values ($k > 10$) elution times are long, the peaks are

broad and the peaks are over-resolved. This problem can be corrected using the technique of gradient elution which is analogous to temperature programming in gas chromatography. Assuming that the chromatogram in Figure 1 was obtained isocratically using a binary mixture of 50% methanol–water, it would be possible to choose a lower solvent strength mixture (e.g. 25% methanol–water) and then increase the methanol content (say to 75%) over a given period of time. This would have the effect of increasing the k values for the early peaks and decreasing the k values for the later peaks, the object being to get all peaks in the optimum region, where k is between 1 and 10. Modern computer-controlled liquid chromatographs have the facility to use isocratic periods and linear and nonlinear gradient programs with multiple ramps to give better control over k values.

The retention equation also indicates that a similar effect could be achieved using the analogous technique of flow programming and changing the mobile-phase flow rate. Having optimized the retention factors by gradient elution, it may still be necessary to alter the selectivity of the system in order to achieve a complete separation. Using the solvent strength parameters, solvents can be classified into eight groups according to their proton acceptor, proton donor and dipole properties and a triangular graph constructed. Solvents are selected from the different classes in order to maximize differences in their properties (bearing in mind the need for solvent compatibility, e.g. miscibility).

For the solvent polarity parameter the value of P' for a binary mixture (AB) is given by:

$$P'_{AB} = \phi_A P'_A + \phi_B P'_B \quad [31]$$

where ϕ_A and ϕ_B are volume fractions of A and B.

From this relationship it is possible to calculate mixtures of solvents having the same solvent strengths, e.g. 45% methanol–water, 52% acetonitrile–water, 37% tetrahydrofuran–water all have the same solvent strength and would give the same retention factors (k), but because of their different proton acceptor/donor and dipole properties they would give different selectivities (α values).

A satisfactory separation is achieved when all three terms in the Purnell equation are optimized.

Future Developments

The theory of LC is well established but a greater understanding of the complexities of fluid flow may lead to improved column performance. Developments in the understanding of the interactions between solute molecules and stationary/mobile phases and the preparation of new stationary phases (e.g. chiral phases) will lead to new applications. Developments in the field of capillary electrophoresis may erode some of the traditional fields of application of LC, e.g. in the analysis of ionic compounds. Developments in instrumentation with new coupled techniques are also a possibility. The most likely area for further development is in the area of data handling and instrument control using the newer breed of computers.

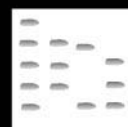
Further Reading

- de Galan L and Billiet HAH (1986) Mobile phase optimization in RPLC by an iterative regression design. *Advances in Chromatography* 25: 63–104.
- Giddings JC (1965) *Dynamics of Chromatography*. New York: Marcel Dekker.
- Hamilton RJ and Sewell PA (1982) *Introduction to High Performance Liquid Chromatography*, 2nd edn. London: Chapman & Hall.
- Hawkes SJ (1983) Modernization of the van Deemter equation for chromatographic zone dispersion. *Journal of Chemical Education* 60: 393–398.
- Kato Y (1987) High performance hydrophobic interaction chromatography. *Advances in Chromatography* 26: 97–111.
- Meyer VR (1998) *Practical High Performance Liquid Chromatography*, 3rd edn. Chichester: Wiley.
- Petryka ZJ (1983) High performance liquid chromatography of porphyrins. *Advances in Chromatography* 22: 215–246.
- Robards K, Hadad PR and Jackson PE (eds) (1994) *Principles and Practice of Modern Chromatographic Methods*. London: Academic Press.
- Sewell PA and Clarke B (1987) *Chromatographic Separations*. London: ACO.
- Snyder LR, Kirkland JJ and Glajch JL (1997) *Practical HPLC Method Development*, 2nd edn. New York: Wiley.
- van Deemter JJ, Zuiderweg FJ and Klinkenberg A (1995) Longitudinal diffusion and resistance to mass transfer as causes of nonideality in chromatography. *Chemical Engineering Science* 50: 3868–3882.

Ultraviolet and Visible Detection in Liquid Chromatography

See II/CHROMATOGRAPHY: LIQUID/Detectors: Ultraviolet and Visible Detection

CHROMATOGRAPHY: SUPERCRITICAL FLUID



Fourier Transform Infrared Spectrometry Detection

M. W. Raynor, Matheson Gas Products, Advanced Technology Center, Longmont, CO, USA

K. D. Bartle, University of Leeds, Leeds, UK

Copyright © 2000 Academic Press

The analytical potential of any separation method is greatly increased when it is combined with a detector that gives qualitative and quantitative information about the separated components. Fourier transform infrared spectrometry (FTIR) has therefore been increasingly used as a detector for supercritical fluid chromatography (SFC), ever since Shafer and Griffiths published the first paper on combined SFC/FTIR in 1983. These researchers recognized that SFC's main application area was the analysis of thermally labile compounds and those too involatile or polar to be analysed by gas chromatography (GC). Furthermore, they realized the potential compatibility of SFC with FTIR detection due to the use of a mobile phase such as carbon dioxide, which has extensive regions of transparency in the infrared (IR) region. Once demonstrated, various SFC/FTIR interfaces were rapidly developed, due to extensive interest from both academia and industry.

The development of FTIR spectrometry itself has also been key to the success of combined SFC/FTIR. In FTIR spectrometry, IR radiation which has been modulated is passed through the sampling area and is detected by a highly sensitive mercury cadmium telluride (MCT) detector. The interferograms, which are plots of IR intensity versus time, are signal-averaged at intervals of less than 1 s and stored on the hard disk of the spectrometer's computer system. The data system then executes a Fourier transform of the interferograms, which are compared against a background to produce an IR spectrum of absorbance (or percentage transmittance) versus wave number. In comparison to a dispersive IR spectrophotometer, which only allows one frequency of radiation to be detected at any one monochromator setting, a FTIR allows all frequencies to be detected simultaneously. Thus, not only can IR absorbance spectra be measured rapidly, a large number of spectra can also be co-added to

increase the sensitivity of the technique (Fellgett's advantage). FTIR is therefore fast enough to measure a number of complete IR spectra in real time during the elution of a chromatographic peak. The FTIR has several other advantages over dispersive instruments. The interferometer in an FTIR instrument uses a gas laser to reference the position of the moving mirror. As a result, these instruments are characterized by high resolution and highly accurate and reproducible frequency determinations, which is particularly useful when spectra have to be co-added or subtracted for background correction (Connes' advantage). FTIR optics also provide much large energy throughput (Jacquinot's advantage) and have minimal light scattering (stray light advantage) in comparison to dispersive instruments that incorporate gratings and narrow slits. In summary, FTIR spectrometry can be used as a highly informative, nondestructive and universal detector for SFC. Since absorption bands can be assigned to individual functional groups in organic molecules, the technique is especially useful for selective detection and the identification of unknown analytes.

When used as a detector for SFC, FTIR is however constrained by two major problems: mid IR absorption by most chromatographically compatible mobile phases and relatively low FTIR sensitivity compared to many of the other commonly used chromatographic detectors. To minimize these problems, various ingenious interfaces have been explored. These designs appear to vary greatly, but they can be classified by essentially two approaches: flow cell interfaces, where the column effluent and analytes are monitored, in real time, by the IR beam as it passes through a high pressure flow cell, and mobile-phase elimination interfaces where the analytes are collected on an IR transparent window (for subsequent IR analysis) as the mobile phase depressurizes at the column outlet. **Table 1** documents the main advances in the development of SFC/FTIR, and the following discussion considers both interface types in more detail.

Flow Cell SFC/FTIR

The flow cell approach involves connecting a high pressure flow-through cell at the end of the separation column and positioning the flow cell in the FTIR beam so that the analytes can be monitored in real time as they elute from the column and flow through

Table 1 Key advances in the development and application of flow cell and mobile elimination interfaces for SFC/FTIR

Year	Development
<i>Flow cell approach</i>	
1983	First demonstration of flow cell SFC/FTIR using carbon dioxide as the mobile-phase (Shafer and Griffiths)
1985, 1986	Demonstration of packed column SFC/FTIR with 10 μL flow cell Evaluation of carbon dioxide and Freon-23
1986	First use of xenon as a mobile phase for capillary SFC/FTIR
1987	Development of Gram-Schmidt orthogonalization for removing baseline drift from reconstructed chromatograms as a result of pressure programming the mobile phase
1988	Introduction of commercial thermostated 1.4 μL flow cell for capillary SFC/FTIR Application to thermally labile compounds such as pesticides and vitamins demonstrated Detection limit for caffeine determined to be ~ 2 ng
1989	Development of 800 nL flow cell for use with 50 μm i.d. capillary columns Use of make-up gas to minimize band broadening in flow cell studies
1990	Stopped flow SFC/FTIR used to improve signal-to-noise ratio of flow cell measurements
1991–94	Comparison of xenon and carbon dioxide as mobile phases for SFC/FTIR
1994	Investigation of 500 nL flow cell for use with 50 μm i.d. capillary columns Practicability of multihyphenated SFC-UV-FTIR system demonstrated
<i>Mobile phase elimination approach</i>	
1986	First demonstration of packed column SFC with deposition on moving KCl plate. Offline diffuse reflectance IR spectra measured from analytes (Shafer and Griffiths; Pentoney)
1986	Use of FTIR microscope to measure IR spectra from 150 μm diameter spot deposited from capillary SFC and restrictor on to a ZnSe plate (Pentoney <i>et al.</i>)
1988	Demonstration of offline mobile phase elimination approach to polymer additives, phenolic carboxylic acids, steroids, polycyclic aromatic hydrocarbons
1989	Comparison of IR sampling techniques evaluated for SFC/FTIR Conventional transmission sampling confirmed to give best sensitivity, reproducibility and adherence to Beer's law
1992	Adaption of first commercial online direct deposit GC/FTIR interface for SFC/FTIR
1995	Performance of real-time direct deposition SFC/FTIR interface characterized Identifiable spectra from 600 pg caffeine demonstrated (Norton and Griffiths) Application to sulfanilamides, silicone oligomers, polyethylene glycol and nonyl phenol oligomers, herbicides

the cell. The IR absorbance is directly proportional to the concentration of the sample in the chromatographic peak that is flowing through the cell at any given time, according to the Beer-Lambert law. A flow restrictor is usually placed after the cell to maintain high pressure in the flow cell, but since FTIR is nondestructive, additional detectors such as a flame ionization detector may be connected in series after the flow cell. A schematic diagram of a SFC/FTIR with a flow cell interface is shown in **Figure 1**. One of the main advantages of online FTIR detection is that chromatograms based on total or selected IR absorbance of the organic molecules can be reconstructed using the Gram-Schmidt algorithm. The retention time data obtained from the Gram-Schmidt reconstructed (GSR) chromatogram is complemented by structural information provided by interpreting IR spectra of the separated components, or by compar-

ing them with a spectral library. The major disadvantage of this interface is the low detection sensitivity obtained, due to the fact that in a dynamic system only a limited number of spectra can be measured as an analyte peak passes through the flow cell.

Flow Cell Compatible Supercritical Mobile Phases

Traditionally, analytes that are incompatible with GC have been separated by liquid chromatography (LC). However, most LC solvents absorb so strongly in the IR region of the spectrum that flow cells with very short pathlengths (typically 100–500 μm) must be used to prevent the solvent bands from completely obstructing wide regions of the spectrum. Detection limits are therefore very high (>20 times higher than in GC/FTIR). One of the advantages of supercritical carbon dioxide, the most commonly used SFC mobile phase, is that it has extensive regions of transparency

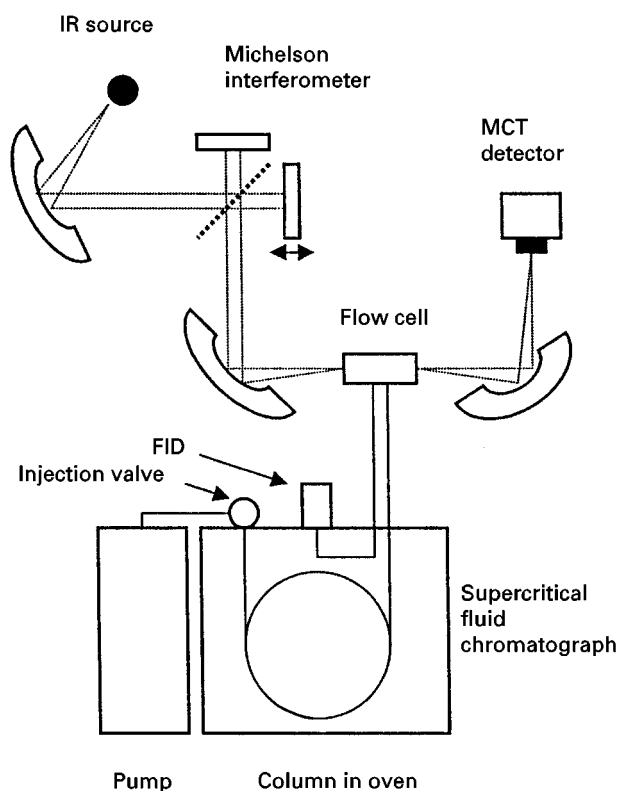


Figure 1 Schematic diagram of SFC/FTIR system with a flow cell interface.

in the IR region of the spectrum, making it more compatible for flow cell SFC/FTIR. However, not all functional groups can be detected and in these cases xenon or other fluids have been used.

CO₂ has two strong infrared-active fundamental vibrational modes, the antisymmetric stretching band that is centred at approximately 2350 cm⁻¹ (ν_3) and the bending mode near 668 cm⁻¹ (ν_2). The symmetry-forbidden symmetric stretch (ν_1) is centred at about 1390 cm⁻¹. These bands obscure the IR spectrum from 2137 to 2551 cm⁻¹ and below 800 cm⁻¹, as shown in Figure 2A. The intensity of ν_1 is enhanced by Fermi resonance with $2\nu_2$, so that two bands at 1390 and 1285 cm⁻¹ are observed in the spectrum. In SFC, the mobile phase is typically programmed from a low density to a higher density to increase the solvent power of the fluid and elute progressively more involatile analytes. As the density of the CO₂ is programmed upwards, these Fermi resonance bands also increase in intensity, as shown in Figure 2B, but are generally not a problem to deal with, as they may be subtracted from the spectra of eluting components if short cell pathlengths (<10 mm) are used. These two Fermi modes also interact with ν_3 to generate a very intense doublet, ($\nu_1 + \nu_3$) and ($\nu_3 + 2\nu_2$), that

obscures the 3504–3822 cm⁻¹ region. Consequently, vibrational modes of functional groups such as the O–H stretch (3500–3800 cm⁻¹), C≡N stretch (2100–2200 cm⁻¹), C–Cl stretch (600–800 cm⁻¹) and aromatic C–H out-of-plane bending modes that absorb below 750 cm⁻¹ cannot be detected in CO₂. It should also be pointed out that the position of absorption bands in the spectra of compounds measured in carbon dioxide vary with the pressure and temperature of the mobile phase. For example, variations up to 10 cm⁻¹ have been observed in spectra measured in liquid versus supercritical CO₂. Modifications of intensity distribution and band width variations were also reported. As a result, the SFC/FTIR spectra obtained using a flow cell are very similar but may not be identical to vapour-phase spectra. However, SFC is generally applied to involatile materials for which

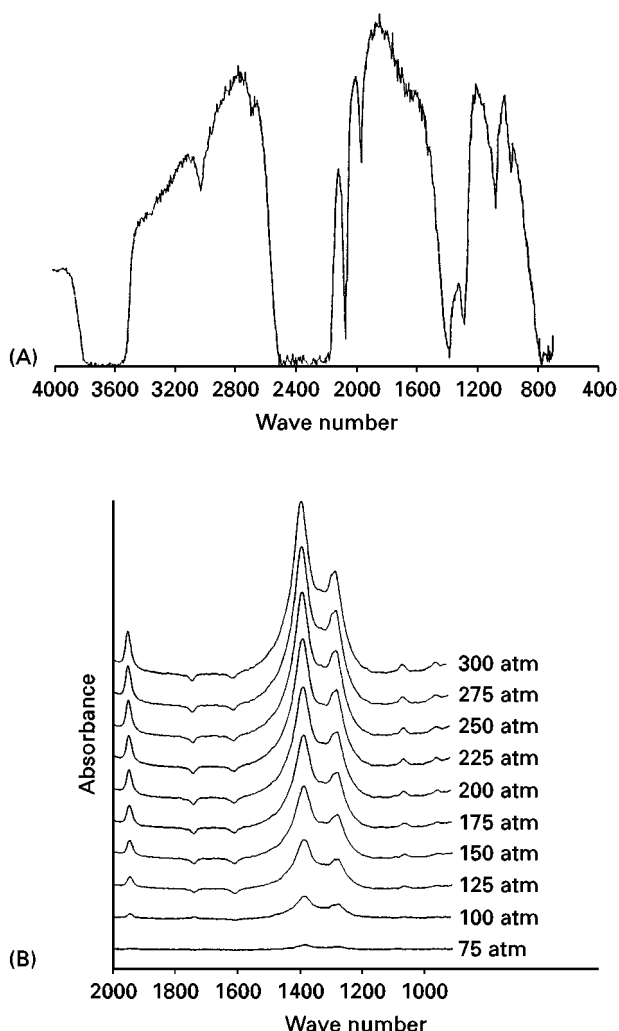


Figure 2 (A) IR spectrum of carbon dioxide at 300 atm and 25°C using an optical pathlength of 10 mm. (B) Increase of absorption of the Fermi resonance bands at 1390 and 1285 cm⁻¹ with increasing CO₂ pressure.

vapour-phase spectra do not currently exist and hence, in the future, libraries of spectra recorded in CO₂ will probably need to be generated.

In cases where detection of the above functional groups is necessary, xenon may be used as an alternative mobile phase. Although xenon is much more expensive than carbon dioxide, it has the advantage of being completely transparent in the IR and background subtraction is less of a problem. However, significant purging with xenon is required to remove the carbon dioxide from the pump and chromatograph completely when changing mobile phases. Spectra measured in xenon also more closely match available vapour-phase library spectra than spectra obtained in carbon dioxide. Xenon is nontoxic, has critical parameters ($T_c = 16.6^\circ\text{C}$, $P_c = 57.6\text{ atm}$) that are similar to carbon dioxide and is compatible with other chromatographic detectors such as the flame ionization detector. Even though only a limited amount of research has been undertaken with xenon as a mobile phase, most reports indicate that it has similar chromatographic properties to carbon dioxide for nonpolar analytes, but is inferior to carbon dioxide for polar analytes.

As far as other fluids are concerned, supercritical nitrous oxide has been shown to be unsuitable for flow cell SFC/FTIR, whereas supercritical sulfur hexafluoride affords transparency solely in the 3000 cm⁻¹ region (i.e. for detection of C-H stretching bands). It has been shown that several chlorofluorocarbons that have moderate critical temperatures and pressures, such as Freon-23 (trifluorochloromethane), have significant regions of transparency and complement carbon dioxide. For example, the O-H stretching region at 3600 cm⁻¹ cannot be monitored in carbon dioxide, but can be monitored in Freon-23. Finally, the addition of polar modifiers is often required to increase the solvent strength of carbon dioxide or to deactivate active sites on stationary phases, especially in packed column SFC. Unfortunately, the addition of a polar modifier such as an alcohol to carbon dioxide reduces the applicability of the online method. Addition of 1% hexanol to CO₂, for example, blocks large regions of the mid-IR spectrum, while addition of 0.2% methanol has been shown to reduce the IR-accessible windows to 3400–2900 cm⁻¹, 2800–2600 cm⁻¹, 2100–1500 cm⁻¹ and 1200–1100 cm⁻¹.

Flow Cell Design Criteria

A number of factors must be considered when using a flow cell interface: choice of chromatographic column (i.e. packed or open tubular), flow cell dimensions, materials of construction of the cell body, windows and seals, the mobile phase and the detection

conditions. A schematic diagram of a high pressure flow cell is shown in **Figure 3**. The major chromatographic requirements of the cell are that it must withstand the high pressures used in SFC (up to 500 atm) and that it has a small volume in relation to the volume of a typical peak eluting from the column to prevent band broadening. To withstand high pressure, most flow cells have been constructed from stainless steel, and ZnS, CaF₂ or ZnSe window materials, have been used with polytetrafluoroethylene (PTFE) or Kel-F seals. To prevent band broadening, the cells must be designed to minimize dead volume in the connections and flow path and the cell volume should not exceed 0.3 SD or about 25% of the volume of a Gaussian peak. However, the peak volume is dependent on the column type. For example, peak volumes in typical 4.6 mm i.d. packed columns are in excess of 40 µL and cell volumes of 10 µL are therefore optimal. For capillary SFC, open tubular columns are typically 50 µm in internal diameter and a typical peak has a width at half height of about 15 s at 150 atm when operated at a flow rate of 1.5 µL min⁻¹. This corresponds to a peak volume of 400 nL and hence the optimal detector volume is in the region of 100 nL. Unfortunately, cells with such small volumes are very difficult to make and are also in conflict with the requirements of the FTIR. Inevitably, a compromise between chromatographic and spectroscopic requirements must be reached.

For maximum IR sensitivity, the dimensions of the flow cell must also be taken into account. According to the Beer–Lambert law, the IR absorbance (A) is dependent on the sample molar extinction coefficient (ϵ), the sample concentration (c) and the cell pathlength (l). Thus, increasing l should improve the signal-to-noise ratio of the spectra obtained. However, l can only be increased so much before absorption by the mobile phase (except with xenon) becomes too intense to allow an adequately low noise level after spectral subtraction. Furthermore, in order to maintain a constant cell volume, the light pipe diameter must decrease as l increases, and this leads to a drop in optical throughput. As the minimum attainable beam diameter is approximately 1 mm using state-of-the-art beam-condensing optics, a cell light pipe diameter less than this must reduce the available energy transmitted through the cell. Consequently, the minimum practical cell diameter is 0.5 mm. Pathlengths of flow cells used in packed column SFC/FTIR have ranged from 5 to 10 mm, while those used with open tubular columns have typically been 1–5 mm to reduce the cell volume as much as possible. Construction details of some flow cells reported in the literature and the experimental conditions under which they were used are summarized in **Table 2**.

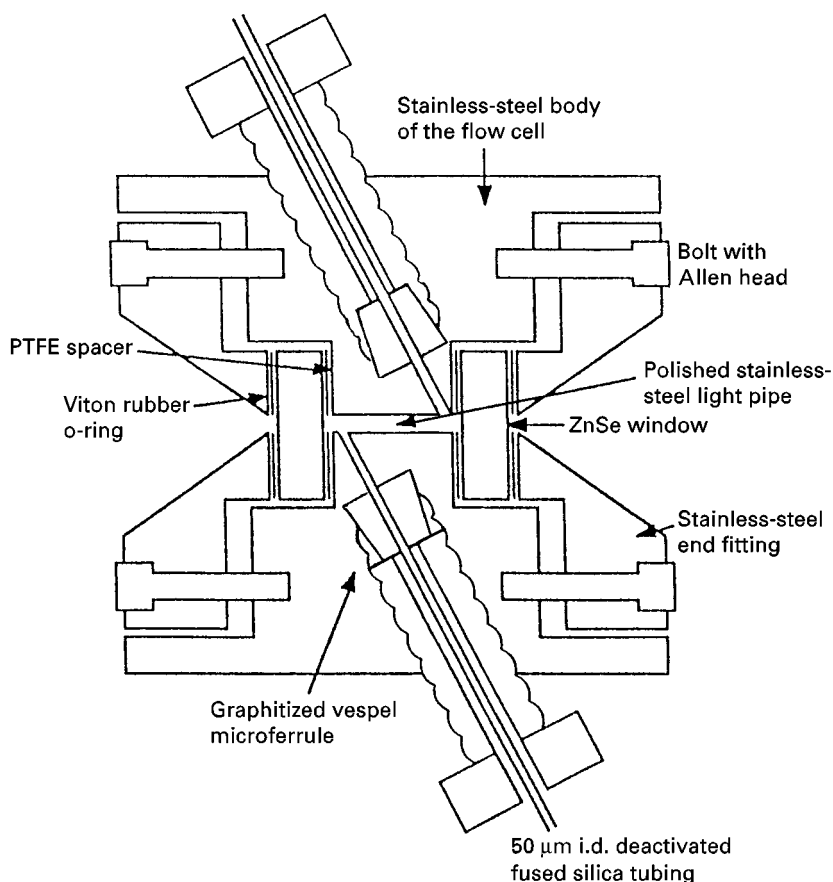


Figure 3 Schematic diagram showing the important design aspects of a high pressure flow cell used for SFC/FTIR.

A number of flow cell SFC/FTIR studies have been performed to determine the minimum identification limit (MIL), defined as the quantity of compound required for identification by spectral interpretation, and the minimum detectable quantity (MDQ), defined as the quantity of material which must be injected to yield an IR response three times the noise level. Although these limits are dependent on the strength of the IR absorption of the compound, an MIL of 10 ng methyl palmitate and an MDQ of 2 ng caffeine have been reported using capillary columns and a flow cell with a 5 mm pathlength.

Application

One of the advantages of the flow cell approach is that chromatograms based on total or selected IR absorbance of the organic molecules can be reconstructed using the Gram-Schmidt algorithm. Further FTIR can also be used as a chemically specific detector, by reconstructing absorbance data in a specific wavenumber region. The IR spectra of the peaks contained in the associated data files can be retrieved and manipulated to remove the spectral features of

the mobile phase. Most packed column studies have been performed with CO₂ at constant pressure and temperature. In this condition, the IR spectrum of the mobile phase does not change during the course of the chromatographic run, facilitating subtraction of the background mobile-phase spectrum from the spectrum of each of the analytes and generation of a GSR chromatogram. In capillary SFC, however, the mobile phase is typically programmed from a low to a high pressure and Gram-Schmidt orthogonalization must be used to prevent this baseline rise. This procedure has been developed: vectors containing the information from the rising baseline are added to the basic set and the chromatogram is then recalculated to remove the baseline drift and to enhance the signal intensity. A flow cell SFC-FTIR analysis of a UV-curing coating in **Figure 4** exemplifies these features.

Many other thermally labile and nonvolatile samples have been analysed by flow cell SFC/FTIR, including free fatty acids, sesquiterpene hydrocarbons, carbamate pesticides, double-base propellants, steroids, triglycerides, aromatic plasticizers and aromatic isocyanates.

Table 2 Experimental details of some packed and capillary column SFC-FTIR studies employing flow cells

Flow cell parameter/study	Jordan and Taylor (1986) ^a	Morin et al. (1986) ^b	Wieboldt et al. (1988) ^c	Raynor et al. (1989) ^d
Mobile-phase	CO ₂ , CClF ₃	Xe, CO ₂	CO ₂	CO ₂
Column dimensions	25 cm × 4.6 mm i.d. (5 µm packing material)	15 cm × 4.6 mm i.d. (5 µm packing material)	10 m × 100 µm i.d. capillary column	10 m × 50 µm i.d. capillary column
Cell volume	8 µL	8 µL	1.4 µL	800 nL
Pathlength	10 mm	10 mm	5 mm	4 mm
Window material	CaF ₂	ZnSe	Not documented	ZnSe
Pressure	200 atm	282 atm	400 atm	400 atm
Temperature	Ambient	Ambient	Ambient to 50°C	Ambient
Beam condenser	Yes, 3 ×	Yes, 4 ×	Yes	Yes
Scans	2 s ⁻¹	3 s ⁻¹	4 s ⁻¹	3 s ⁻¹
Resolution	4 cm ⁻¹	8 cm ⁻¹	4 cm ⁻¹	4 cm ⁻¹

^aJordan and Taylor (1986) *Journal of Chromatographic Science* 24: 82.^bMorin et al. (1986) *Chromatographia* 21: 523.^cWieboldt et al. (1988) *Analytical Chemistry* 60: 2422.^dRaynor et al. (1989) *Journal of Microcolumn Separations* 1: 101.

Mobile-phase Elimination SFC/FTIR

All of the commonly used supercritical fluid mobile phases are gaseous at STP. Thus, analytes can be trapped in some way at the restrictor outlet (connected to the column outlet) as depressurization and evaporation of the mobile phase occur. This is the basis of the mobile-phase elimination approach. Griffith's research group was the first to demonstrate the potential of this methodology in 1986. They realized that this approach had a number of advantages over using a flow cell. Firstly, as most SFC applications were aimed at involatile materials, most of the analytes could be trapped on an IR transparent material at ambient temperature for FTIR analysis. Secondly, as the mobile phase could be easily removed, the complete condensed-phase IR spectrum could be measured without interference from mobile-phase absorbance bands. Thirdly, a large number of scans of the trapped analyte could also be added together to improve the signal-to-noise ratio significantly. Lastly, they recognized that the technique was potentially amenable to mobile phases (and modified mobile phases) that could not be used with flow cells.

Offline Studies

Initial work involved depositing each separated component on a moving glass plate on which a layer of powdered KCl had been laid down from a methanol slurry. A 1 mm i.d. silica packed column and 2% methanol in carbon dioxide was used to separate a mixture of quinones and diffuse reflectance spectra of the separated quinones were measured by moving the substrate into the focused beam from an FTIR spectrometer. Later work by the same group and others showed that it was not necessary to use a pow-

dered substrate and that superior results could be obtained using capillary SFC simply by depositing the eluted compounds on to a zinc selenide or potassium bromide window. The window could then be mounted on the sampling stage of an FTIR microscope and each spot located visually under the microscope. Once located, the transmittance IR spectrum of each spot could be measured by directing the focused FTIR beam through the sample within the microscope.

Important aspects of mobile-phase elimination SFC/FTIR are illustrated in Figure 5. With this approach, the mobile-phase flow from the end of the column is usually split to permit simultaneous detection by another means (for example, using flame ionization or UV absorbance detection) and thus permit identification of the deposition period. When an FID is used, the flow rates of each of the restrictors must be adjusted so that the FID detects the component first. The zinc selenide window can then be moved so that deposition takes place on a fresh area of the window.

Most early depositions were performed offline with the substrate stationary beneath the restrictor. These experiments allowed the shape and dimension of the deposit to be characterized and demonstrated that it was possible to deposit compounds emerging from a capillary SFC column as spots approximately 100 µm in diameter. From a spectroscopic standpoint, minimizing the spot diameter is the key to obtain the maximum FTIR sensitivity since, for a given sample quantity, the average thickness varies inversely with the cross-sectional area. Keeping the spot diameter as small as possible enables the analyte to be deposited as thickly as possible and results in greater IR absorbance according to the Beer-Lambert law.

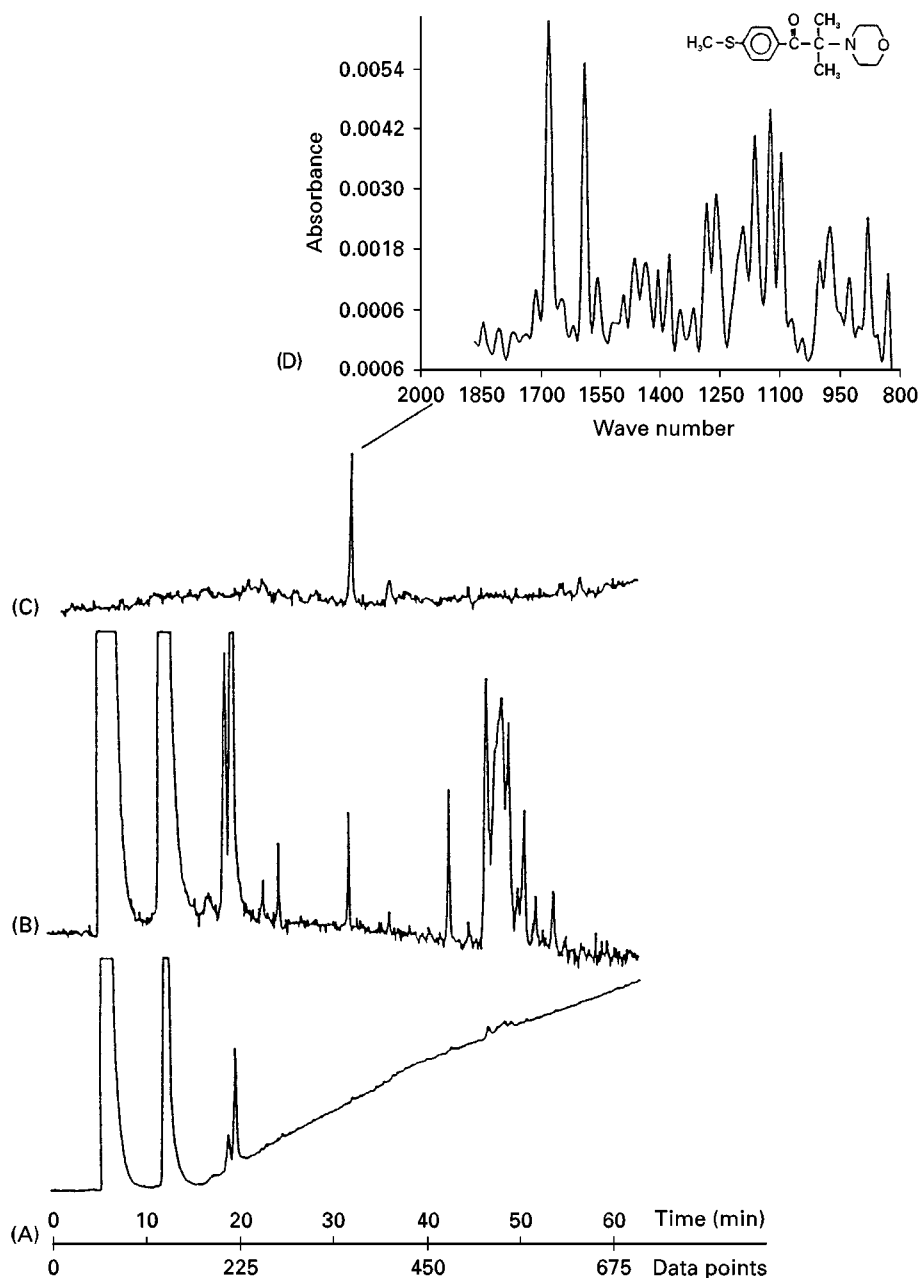


Figure 4 Flow cell SFC/FTIR analysis of an UV-curing coating. (A) Gram-Schmidt reconstructed chromatogram. (B) Gram-Schmidt reconstructed chromatogram with added basis vector 346 to remove the baseline drift from the increased CO₂ absorbance due to the mobile-phase pressure programming. (C) Selective FTIR detection of carbonyl stretching region of an aromatic ketone (1670–1690 cm⁻¹). (D) IR spectrum of photoinitiator detected in the 1670–1690 cm⁻¹ reconstructed chromatogram. Conditions; 10 m × 50 μm i.d. open tubular column; poly(biphenylmethyl)siloxane stationary phase; 65°C; CO₂; pressure programme from 100 to 250 atm at 2.5 atm min⁻¹ followed by 15 min isobaric hold. (Reproduced with permission from Bartle *et al.*, 1989.)

In practice, deposition characteristics depend on the physical properties of the analyte, the temperature of the SFC restrictor (and the window) and the flow rate of the mobile phase leaving the restrictor. Most analytes that are solids can be successfully trapped on a window at room temperature, even though they may exit the restrictor in liquid form. In SFC, the

restrictor must be heated to 100–250°C to prevent it becoming plugged with analytes as they come out of solution from the depressurizing mobile phase. Analytes that are liquid are often too volatile and do not solidify rapidly enough on a surface at ambient temperature; they may be blown off or spread out over the window surface by the expanding mobile

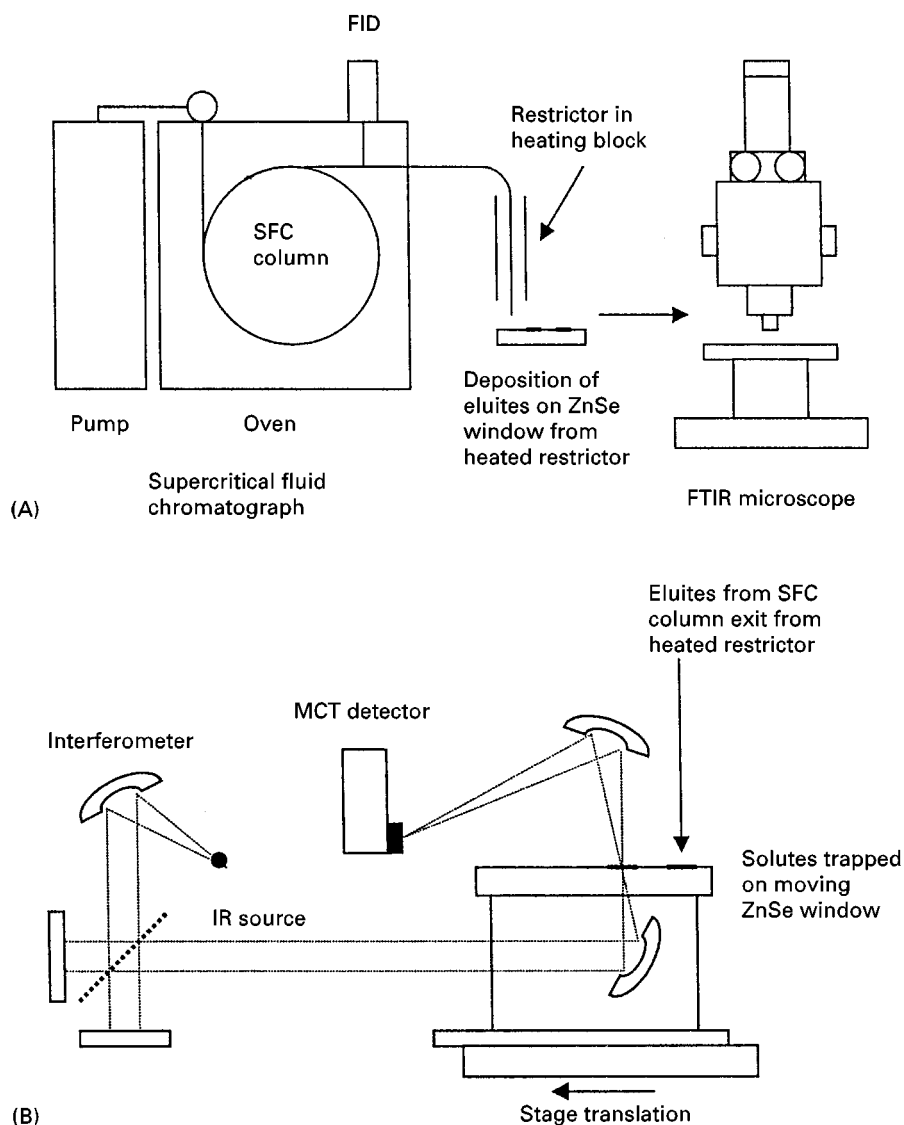


Figure 5 Mobile-phase elimination SFC/FTIR. (A) Offline approach: after deposition on a ZnSe window, the substrate is placed in the focused beam of an FTIR microscope and the spectrum of the eluite is measured with the window stationary. (B) Online approach: after deposition on the moving window, the eluite passes through the focused IR beam.

phase. This was demonstrated by one group who analysed 21 common polymer additives varying in molecular mass from 225 to 1178. Only Topanol OC was unretained on the window, due to its high vapour pressure. The other additives were either deposited as liquids or solids, with spot sizes that ranged from 200 to 300 μm in diameter. By cooling the window, it is possible to capture volatile compounds, but this significantly complicates an otherwise simple interface. High quality IR spectra were typically measured from a 100 ng deposit by adding 1000 scans using a quality IR microscope with an MCT detector. However, it is important to take a suitable background IR spectrum from an area of window where a blank deposit, made during a time when no analytes have eluted, has been

collected. This is because the mobile phase can contain hydrocarbon or other contaminants from the pumping system or column that may be deposited along with the analytes. The IR spectrum of the pure analyte is obtained by subtracting the background IR spectrum from that of the crude analyte.

To date, the interface has been demonstrated by a number of groups, with samples containing phenolic carboxylic acids, steroids, polycyclic aromatic hydrocarbons, indoles, quinones and barbiturates. Most measurements have employed capillary columns for the separation. This is because the commonly used 50–100 μm i.d. open tubular columns operate at very low linear velocities and the gaseous flow rates produced by the expanding mobile phase

are only in the region of $2\text{--}5\text{ mL min}^{-1}$. Because of this, application of the methodology to packed column separations using carbon dioxide and modified carbon dioxide has been questioned. It is indeed difficult to deposit analytes using conventional 4.6 mm i.d. packed columns, because the gaseous flow rates are simply too high ($\sim 500\text{--}1000\text{ mL min}^{-1}$). However, reducing the diameter of the packed column to 1 mm i.d. reduces the volume flow rate by a factor of $(4.6)^2$, or 20 times, and allows successful analyte deposition. This was demonstrated for the analysis of sulfanilamides using a 1 mm i.d. Deltabond-CN packed column with 0.1% water in carbon dioxide as the mobile phase. It was possible to obtain high quality IR spectra from $\sim 120\text{ ng}$ sulfisoxazole.

Online Studies

The logical development of the offline work discussed above has been the commercialization of on-line mobile-phase elimination interfaces, in which deposition occurs on a moving window that then passes through the infrared beam. The Bio-Rad Tracer interface (originally designed for GC/FTIR) was adapted for use with SFC: a $50\text{ }\mu\text{m i.d.}$ fused silica transfer line was used with an integral restrictor

fabricated at the end of the tube. The end of the restrictor was placed $75\text{ }\mu\text{m}$ from the ZnSe window ($60 \times 30\text{ mm}$) and heated to 100°C by a cartridge heater. The ZnSe window was cooled to -10°C with a methanol-dry ice mixture to trap compounds efficiently without condensing the mobile-phase. The speed of translating the deposition window was selected to maintain an appropriate compromise between chromatographic resolution and spectroscopic sensitivity. The best compromise was obtained when the distance moved by the window during the time equal to the full width at half height of the narrowest peak in the chromatogram was equal to the diameter of the spot deposited on the stationary window. For most of the SFC work, the window was moved at a rate of $100\text{ }\mu\text{m min}^{-1}$. In order to remove the expanded mobile phase, 0.1 mTorr pressure was maintained in the interface using a 170 L s^{-1} turbomolecular pump. This pumping speed was fast enough that virtually no absorption due to CO_2 was observed at gaseous mobile-phase flow rates less than 5 mL min^{-1} at STP.

The lowest MIL reported to date for caffeine, using online direct deposition SFC/FTIR, is 600 pg . This is significantly lower than can be achieved using a flow

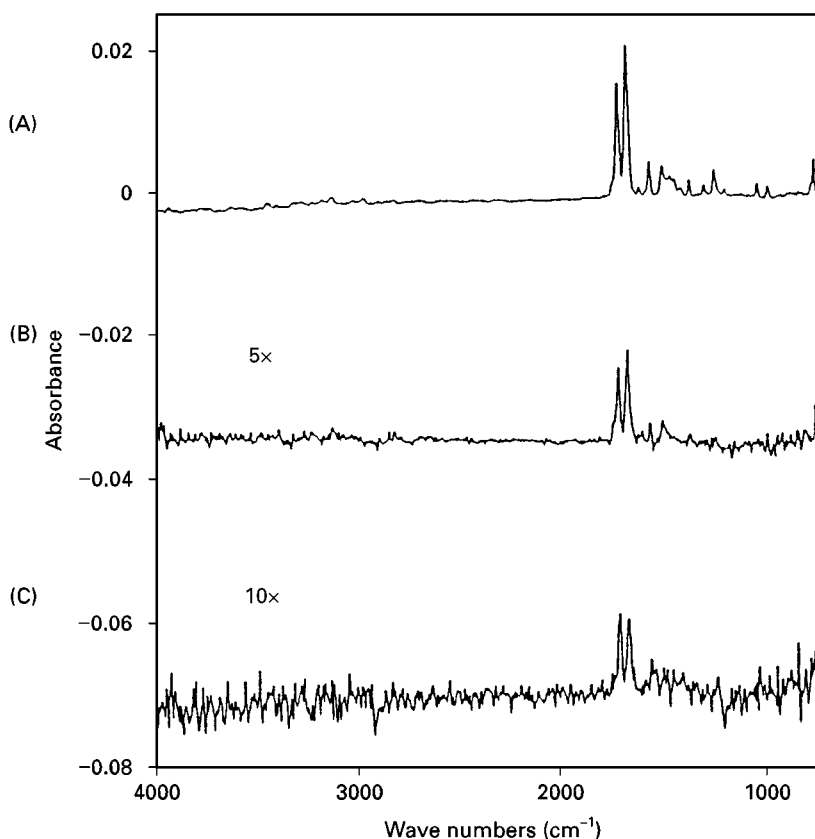


Figure 6 IR spectra measured from (A) 3 ng , (B) 600 pg and (C) 300 pg caffeine during online mobile-phase elimination SFC/FTIR. (Reproduced with permission from Norton and Griffiths, 1995.)

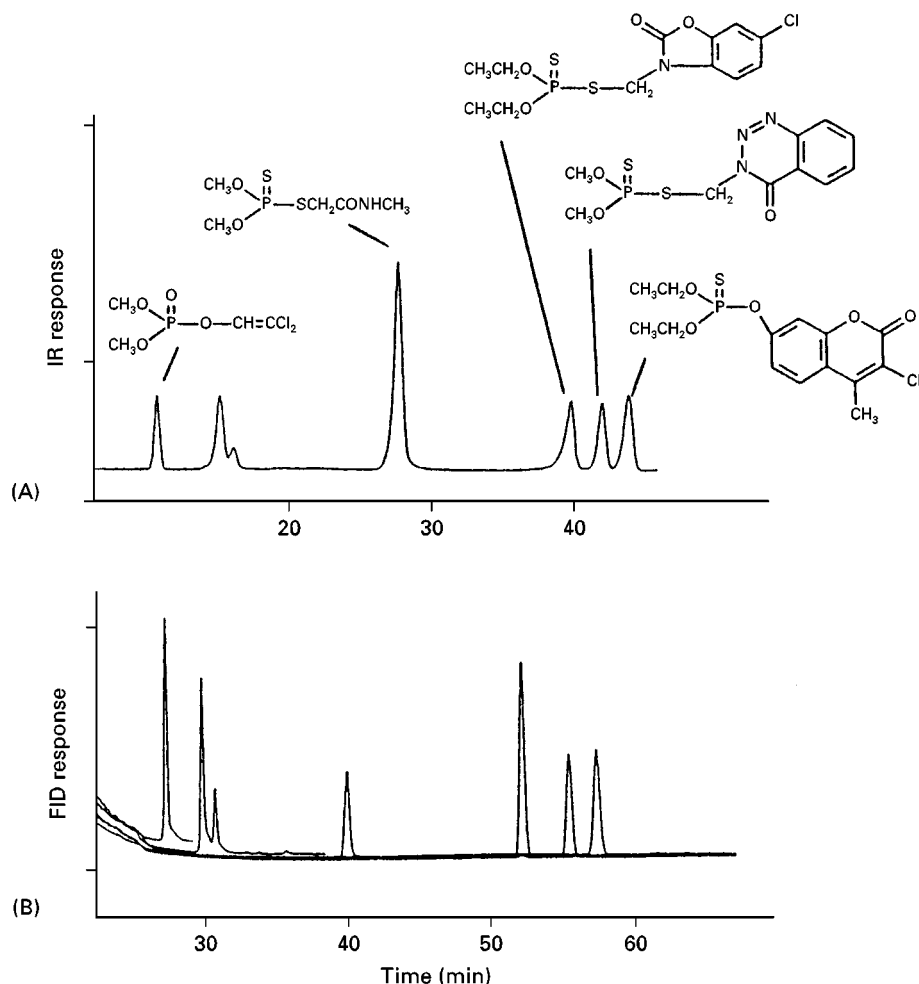


Figure 7 Chromatograms of six cholinesterase inhibitor pesticides. (A) SFC/FTIR Gram-Schmidt reconstructed chromatogram; (B) FID traces for the six pesticides injected individually. (Reproduced with permission from Norton and Griffiths, 1995.)

cell interface. The IR spectra measured from 3 ng, 600 pg and 300 pg caffeine are shown in **Figure 6**. The interface has been further demonstrated for on-line measurement of Gram-Schmidt and functional group reconstructed chromatograms of cholinesterase inhibitor pesticides (**Figure 7**) and polycyclic aromatic hydrocarbons using carbon dioxide and for triazine herbicides using carbon dioxide modified with 2% methanol. Clearly, the possibility of using modified mobile phases is one of the great advantages of the mobile-phase elimination approach.

Future Developments

Since the introduction of the first commercially available SFC system in the early 1980s, hyphenated flow cell and mobile-phase elimination interfaces for SFC/FTIR have attained a high level of sophistication. Although the flow cell approach has a number of advantages, including mechanical simplicity and interfacing with other detectors, mobile-phase elimina-

tion interfaces offer greater sensitivity, the potential of using strongly IR-absorbing mobile phases (including modified mobile phases) and enables library-searchable condensed-phase spectra to be measured. Therefore it is reasonable to expect continued evolutionary development of the latter approach. It is also likely that improvements to the instrumentation will be application-oriented. As solutions to difficult analytical problems are sought, it can be expected that SFC/FTIR will be investigated with new columns such as micro-packed columns (250–300 μm i.d capillaries packed with 2–5 μm HPLC packing materials) and new mobile phases such as the fluorocarbons.

Further Reading

Bartle KD, Raynor MW and Clifford AA *et al.* (1989) Capillary supercritical fluid chromatography with Fourier transform infrared detection. *Journal of Chromatographic Science* 27: 283.

Charpentier BA and Severants (eds) (1988) *Supercritical Fluid Extraction and Chromatography, Techniques and Applications*. Washington, DC: American Chemical Society.

Griffiths PR and de Haseth (1986) *Fourier Transform Infrared Spectrometry*. New York: Wiley.

Jinno K (ed.) *Hyphenated Techniques in Supercritical Fluid Chromatography and Extraction*. Amsterdam: Elsevier.

Lee ML and Markides KE (1990) *Analytical Supercritical Fluid Chromatography and Extraction*. Provo, Utah: Chromatography Conferences.

Messerschmidt RG and Harthcock MA (1988) *Infrared Microspectrometry: Theory and Applications*. New York: Marcel Dekker.

Norton KL and Griffiths PR (1995) Performance characteristics of a real-time direct deposition supercritical fluid

chromatograph-Fourier transform infrared spectrophotometry system. *Journal of Chromatography A* 703: 503.

Pentoney SL Jr, Shafer KH and Griffiths PR (1986) A solvent elimination interface for capillary supercritical fluid chromatography/Fourier transform infrared spectrometry using an infrared microscope. *Journal of Chromatographic Science* 24: 230.

Raynor MW, Davies IL and Bartle KD *et al.* (1988) *Analytical Chemistry* 60: 427.

Shafer K and Griffiths PR (1983) On-line supercritical fluid chromatography/Fourier transform infrared spectrometry. *Analytical Chemistry* 55:1939.

White R (1990) *Chromatography/Fourier Transform Infrared Spectroscopy and Applications*. New York: Marcel Dekker.

Historical Development

K. D. Bartle, University of Leeds, UK

Copyright © 2000 Academic Press

Definition

Above the critical temperature, the vapour and liquid of a substance have the same density and the fluid cannot be liquefied by increasing the pressure; the supercritical fluid has density and solvating power approaching that of a liquid, viscosity similar to that of a gas, and diffusivity intermediate between those of a gas and a liquid. A typical phase diagram is shown in **Figure 1**. It follows that supercritical fluids have

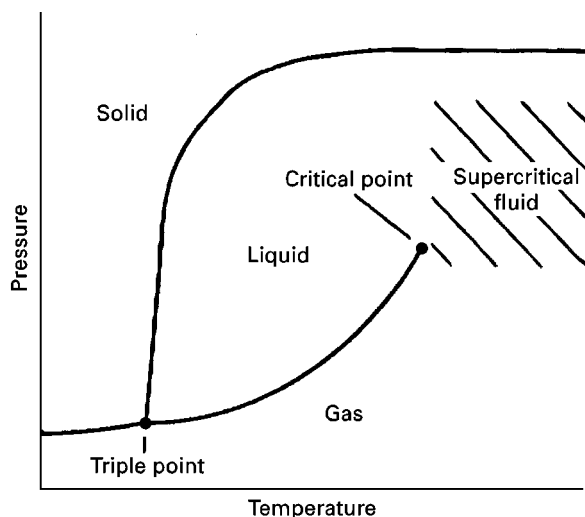


Figure 1 Typical phase diagram of a single substance. (Reproduced with permission from Clifford T(1998) *Fundamentals of Supercritical Fluids*. Oxford: OUP.)

properties which make their use as chromatographic mobile phases very favourable. Thus, gas chromatography (GC) produces narrow peaks and high resolution, but cannot be used for involatile or thermally labile compounds since analytes must be in the vapour phase. High performance liquid chromatography (HPLC) is extensively applied to involatile compounds, but has limited resolution because the high viscosity of the mobile phase limits column length, and the low diffusivity slows the exchange of analyte molecules between liquid streams of different velocity. Supercritical fluid chromatography (SFC) addresses these limitations because of increased solubility (which varies with density and hence applied pressure) for involatile compounds in comparison with GC, and lower viscosity and higher diffusivity in comparison with HPLC.

Both capillary and packed columns are used in SFC, and many of the detectors of both GC and HPLC may be employed. Coupling to spectroscopic detectors has proved fruitful. SFC has established a number of niche areas: it extends the range of GC, it can replace many normal phase HPLC methods and it has many advantages over size-exclusion chromatography.

History

Supercritical fluids have been known (**Table 1**) since Baron Cagniard de la Tour observed in 1822 that, above a certain temperature, a liquid can be converted to a gas without the appearance of a meniscus. In 1869, Andrews fully characterized the critical point in terms of critical temperature T_c and critical

Table 1 Advances in supercritical fluid chromatography

Cagniard de la Tour	Discovery of supercritical state	1822
Andrews	Characterization of critical point	1869
Hannay and Hogarth	Increased solubility in supercritical fluids reported	1879
Lovelock	SFC suggested	1958
Klesper	Demonstration of SFC	1962
Giddings, Sie and Rijnders	Development of dense gas GC and SFC	1966–69
Sie, van Beersum and Rijnders	FID used in SFC	1966
Sie and Rijnders	First use of term 'SFC'	1967
	UV/visible detector used in SFC	1967
Jentoft and Gouw	Pressure programming demonstrated	1978
Randall and Wahrhaftig	SFC coupled to mass spectrometry	1978
Novotny and Lee	Capillary column SFC demonstrated	1981
	Commercial packed column SFC	1982
	Commercial capillary column SFC	1986

pressure P_c . Hannay and Hogarth observed in 1879 that metal halides are soluble in ethanol above the critical point, and as early as 1897 Vuillard reviewed solubility in supercritical fluids. Isolated examples of the use of near-critical solvents for separation appeared between 1930 and 1960; more extensive applications, especially to natural products with the pharmacologically acceptable carbon dioxide have since appeared, based on extensive studies of solubility in supercritical solvents and on the properties of solutions. In parallel with SFC, analytical supercritical fluid extraction (SFE) has been extensively developed as a sample preparation technique.

The original idea for SFC was suggested by Lovelock at an international meeting in 1958, before Klesper, Corwin and Turner separated involatile porphyrins in 1962 using supercritical chlorofluorocarbons at pressures up to 136 bar as mobile phase. In 1966, Sie and Rijnders developed both adsorption and partition chromatography using carbon dioxide, *n*-pentane and isopropanol at temperatures up to 245°C and pressures up to 80 bar.

The advantages of carbon dioxide as a mobile phase were quickly realised: it is an inexpensive material with good solvent properties, convenient T_c and P_c , non-combustible, easily delivered by pumping the liquid, and available in high purity. Although other compounds have since been employed as mobile phases (e.g. N_2O , SF_6 , NH_3 , *n*-butane and *n*-pentane,

xenon, and various fluorocarbons and chlorofluorocarbons), CO_2 has remained the most popular and widely used. Because of the variation of solubility with density and hence pressure, Rijnders suggested in 1967 that pressure programming in SFC should have a similar effect to temperature programming in GC.

In 1970, Jentoft and Gouw constructed a versatile high-resolution SFC chromatograph with a pressure-programming facility for packed columns up to 4-m long and *n*-pentane-methanol mobile phase for temperatures up to 215°C and pressures up to 650 bar; detection was by UV absorption. Styrene oligomers up to $n = 32$ could be analysed with this system. The affinities between GC with a dense gas as mobile phase and SFC were discussed and developed by Giddings between 1966 and 1969.

Novotny pointed out in 1971 the serious limitations in SFC of the pressure gradient generated by the column packing, and realized that SFC should be possible on capillary columns with a much smaller pressure drop. In 1981, Novotny and Lee demonstrated capillary column SFC equipment. Commercial equipment for packed column SFC became available in 1982, and for capillary SFC in 1986.

The 1980–90 period was one of rapid growth in the theory, instrumentation and applications of SFC. A multi-authored text edited by Lee and Markides appeared in 1990 summarizing the state of the art, and remains authoritative. Two series of international conferences on SFC and SFE, one based in USA and the other in Europe began in 1988 and continue.

Instrumentation

Figure 2 illustrates the instrumentation for SFC. The mobile phase is pumped as a liquid and the pressurized fluid passes, via an injection valve, into the column maintained in an oven at a temperature above T_c , and then to a detector. A pressure restrictor to maintain supercritical conditions is located either after the detector or at the end of the column.

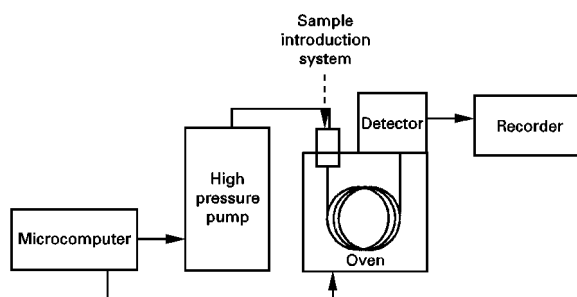
**Figure 2** Schematic diagram of an SFC instrument.

Table 2 Columns in SFC

<i>Column</i>	<i>Internal diameter (mm)</i>	<i>Advantages</i>	<i>Disadvantages</i>
Conventional	2.0–4.6	High capacity	Low overall efficiency
Microbore	1–2	Rapid analysis	Highly activity
Packed capillary	0.2–0.8	Highly selective	
Open tubular	0.05–0.1	Low capacity, high resolution inactive	Long analysis times Selectivity only conferred by stationary phase

Conventional HPLC pumps with cooled heads were used from the start for SFC in packed columns. Syringe pumps were initially used in capillary SFC because of their pulseless operation. Small column diameters necessary in capillary SFC make the method of sample introduction important; small volumes and rapid injection are achieved by a pneumatically operated loop valve with electronic timing.

Columns

Although a full range of columns can be used in SFC, the technique is most usually divided into two categories based on column type, with advantages and disadvantages outlined in **Table 2**. Packed columns for SFC have reflected developments in HPLC: (a) 'conventional' packed columns (up to 4.6 mm i.d.); (b) microbore columns; and (c) packed capillaries with smaller i.d. Most of the work has been carried out on 4.6-mm columns, with 3–10 μm particle size packing materials – usually bonded-silica particles (**Table 3**). It was realized early that the unreacted silanol groups on silica particles which have little activity in reversed-phase HPLC led to peak tailing because of the low polarity of the mobile phase. Such effects led to the almost exclusive addition of organic modifiers (alcohols, ethers, etc.) to the carbon dioxide mobile phase in packed column SFC. These modifiers can influence selectivity and increase the solubility of analytes. A number of specially end-capped silica packings were developed, along with polymer-based

packings, but most of these have had limited use. The low-pressure drop across packed columns has led to the coupling together of columns, with consequent improvement in selectivity and efficiency.

Capillary SFC was only made possible by the development from 1979 onwards of fused silica capillary columns for GC. Because of the slower diffusion of analyte in supercritical fluids, open tubular columns for SFC must have internal diameters less than 100 μm to achieve resolution comparable to that on 200 μm i.d. columns for GC. Lee's group undertook an extensive series of developments of columns for both GC and SFC between 1980 and 1990, basing stationary phase structures on a polysiloxane polymer backbone with pendant groups 'designed' for particular applications. As well as the more usual methyl- and phenyl-containing phases (**Table 3**), polymers with biphenyl, cyanopropyl and ethylene glycol, etc., groups were synthesized; more exotic phases had bonded liquid crystal or chiral groupings. Capillary columns for SFC are highly inert and are usually operated with CO_2 alone as mobile phase.

Detectors

SFC can be carried out with the widest range of detectors of any chromatographic technique: detectors from gas and liquid chromatography are employed, and SFC can be coupled to a number of information-rich spectroscopic detectors (**Table 4**). SFC detection can be carried out in the gas phase after decompression, or in both supercritical and liquid phases. The flame ionization detector (FID) is the most commonly used if unmodified CO_2 is the mobile phase, as is the case for capillary columns, whereas the UV/visible detector is most often used if a mobile phase contains a modifier, e.g. in packed column work. Some limited use has been made of the FID with CO_2 modified by water, formic acid or formamide which give no, or a very small, FID signal.

From 1981 the range of detectors for SFC showed a rapid expansion. The thermionic, electron-capture, photoionization and chemiluminescence detectors from GC, and the fluorimetric and light-scattering

Table 3 Bonded stationary phases in SFC

<i>Packed SFC</i>	<i>Capillary SFC</i>
Octadecyl	Methyl
Octyl	Octyl
Phenyl	Phenyl
Hydroxyl	Biphenyl
Diol	Cyanopropyl
Cyano	Liquid crystal
Amino	Polyether
Chiral	Chiral

Table 4 Detectors in SFC

Type	Established	Developmental
GC type	Flame ionization	Chemiluminescence
	Thermionic	Photoionization
	Flame photometric	Ion mobility
	Electron capture	Element-specific plasma
LC type	UV absorption	Fluorescence
		Light scattering
		Electrochemical
Coupled	Diode array UV	Nuclear magnetic resonance
	Fourier transform IR	Inductively coupled plasma
	Mass spectrometric	spectrometry

detectors from HPLC were all demonstrated in SFC. Element-specific plasma emission detectors were demonstrated in SFC from 1987, and since 1990 electrochemical detection has been explored; if the electrodes are sufficiently small, oxidative and reductive detection is possible in CO₂ containing only small concentrations of water or organic modifier.

The detector providing the most structural information in chromatography is the mass spectrometer (MS); a packed-column SFC–MS interface was first reported in 1978, and a practical SFC interface was developed in 1982 for capillary SFC–MS where the low flow rates permit direct introduction into the ion source. A practical packed-column SFC–MS interface was developed in 1987 to cope with the higher flow rates. SFC with both electron impact and chemical ionization has been demonstrated. The interfacing of capillary SFC to Fourier-transform infrared spectroscopy (FTIR) was achieved as early as 1983. Both solvent-elimination (evaporation of CO₂ to deposit separated compounds on a solid substrate or IR transparent plate) and online direct recording of FTIR spectra in a flow cell with IR transparent optics were developed between 1983 and 1990. A major problem with the latter approach is strong IR absorption by CO₂; alternative supercritical mobile phases, especially xenon, have therefore been employed but xenon is vastly more expensive than CO₂. Recently, NMR detection has been explored in SFC.

Applications

After early exponential growth up to 1990, SFC has consolidated to maintain applications complementing GC and HPLC, mainly in the analysis of lipophilic compounds. **Figure 3** illustrates the perceived application areas. Particularly noteworthy have been applications to: fossil fuels and hydro-

Non-volatile analytes
Thermally unstable analytes } → Extends GC range towards higher molecular weight

Non-detectable analytes
(i.e. lacking UV chromophore) } → Extends normal phase HPLC and SFC (e.g. for oligomers)

Complex analytes

Chiral analytes

Figure 3 Application areas of SFC.

carbons (where simulated distillation at low-temperature and group-type separations have been particularly important); agrochemicals; explosives; drugs and pharmaceuticals (especially those normally analysed by normal-phase HPLC); lipids and other nonpolar biomolecules; industrial chemicals (especially surfactants and polymer additives); and metal chelates and organometallic compounds. A current growth area is in chiral separation, where the rapid speed of analysis in SFC also permits preparative separations. Current developments are aimed at eliminating the distinction between gaseous and supercritical fluid mobile phases.

See also: II/Chromatography: Supercritical Fluid: Instrumentation; Large-Scale Supercritical Fluid Chromatography.

Further Reading

- Berger TA (1995) *Packed Column SFC*. London: Royal Society of Chemistry.
- Clifford T (1998) *Fundamentals of Supercritical Fluids*. Oxford: OUP.
- Gere DR (1983) Supercritical fluid chromatography. *Science* 222: 253.
- Hill HH and McMinin DG (1992) *Detectors for Capillary Chromatography*. New York: John Wiley.
- Klesper E (1978) Chromatography with supercritical fluids. *Angewandte Chemie International Edition English* 17: 738.
- Lee ML and Markides KE (1990) *Analytical Supercritical Fluid Chromatography and Extraction*. Provo UT: Chromatography Conferences Inc.
- McHugh M and Krukonis V (1994) *Supercritical Fluid Extraction*, 2nd edn. Stoneham, MA: Butterworth-Heinemann.
- Novotny M, Springston SR, Peadar PA, Fjeldsted JC and Lee ML (1981) Capillary supercritical fluid chromatography. *Analytical Chemistry* 53: 407A.
- Smith RM (ed.) (1988) *Supercritical Fluid Chromatography*. London: Royal Society of Chemistry.
- White CM (ed.) (1988) *Modern Supercritical Fluid Chromatography*. Heidelberg: Hüthig.

Instrumentation

T. A. Berger, Berger Instruments, Newark, DE, USA

Copyright © 2000 Academic Press

Introduction

Supercritical fluid chromatography (SFC) is an instrumental technique in which a small volume of a sample is entrained in a solvating mobile phase, held near its critical point, and is swept through a stationary bed of particles, or a tube coated with a liquid film. The components of the mixture are separated from each other through differential solvation by the mobile phase, and retention by the stationary phase. SFC can be viewed as a transition technique between GC and HPLC.

A fluid is 'supercritical' when it is raised above its characteristic 'critical point' (a critical temperature, T_c , and a critical pressure, P_c). Most fluids used as SFC mobile phases are gases at room temperature and pressure but all are easily liquefied by raising the pressure. In a supercritical fluid, the molecules are forced close together by an externally applied pressure. Some but not all supercritical fluids act as a solvent. Changing the density of such fluids changes their solvent strength.

Packed vs. capillary columns There are two SFC techniques, using either open tubular (capillary), or packed columns, each of which exploits a different aspect of the technology. Although in 1958 Lovelock originally proposed SFC as a capillary technique, for its first 20+ years SFC was exclusively performed with packed columns. The first commercial instrumentation for packed-column SFC was introduced in 1982 as a modification kit for a HPLC. Capillary SFC was not viable until the late 1970s when stationary phases were first bonded to the surface of the column. Earlier stationary phases were washed out of the column by the SFC mobile phase. In 1981, the groups of Lee at Brigham Young University and Novotny at Indiana University, combined bonded stationary phases with SFC and published the first realistic capillary (open tubular column) SFC chromatograms.

Subsequently, a rather unfortunate controversy raged for some years as to whether capillary or packed columns were 'better'. However, the two techniques are sufficiently different that almost any attempt to compare them will show one or the other unfavourably.

Open tubular or capillary SFC (CSFC) is almost always performed using pressure programming of

pure carbon dioxide as the mobile phase. CSFC can be thought of as an extension of gas chromatography (GC) to higher molecular masses, since the solvation energy of the fluids can replace thermal energy. Elution temperatures can be 200°C or more lower than in GC (i.e. carbon dioxide at 150°C vs. GC with hydrogen at 400°C). The column temperature is almost always maintained at >50°C above the critical temperature.

The fluid solvent strength can be changed in a predictable manner by programming the fluid density (usually pressure, sometimes temperature, rarely both). Carbon dioxide is compatible with the flame ionization detector (FID). The most common uses of CSFC are for the separation of light polymers, surfactants and other homologous series.

Carbon dioxide has a solvent strength similar to hexane or a fluorocarbon. Relatively nonpolar solutes such as hydrocarbons are miscible with carbon dioxide. Polar solutes such as sugars or amino acids are virtually insoluble in carbon dioxide.

Packed columns are, inherently, 10 to 100 times more retentive than capillary columns, due to their higher surface area to void volume ratio. This makes it more difficult to elute molecules from packed columns using pure carbon dioxide. On the other hand, the low polarity of carbon dioxide is incompatible with the solvation of polar molecules.

The most widely used approach to extending SFC to more polar solutes has involved the use of packed columns with binary or ternary mobile phases. Binary fluids consist of a normal liquid such as acetonitrile or methanol mixed with carbon dioxide. Ternary mobile phases consist of a fraction of a percent to several percent of a third, even more polar component, such as trifluoroacetic acid or isobutylamine, added to the liquid modifier. The use of modifiers was pioneered by Jentoff and Gouw in 1969. The use of additives was pioneered by Berger *et al.* starting in 1988.

Once a modifier is added to the mobile phase, the composition of the fluid tends to dominate over its density in determining solvent strength. Pressure programming becomes a secondary control variable. The enhanced solvent strength of modified fluids tends to be less compatible with the inherent low retentivity of capillary columns.

Packed-column SFC can be thought of as an extension of HPLC, using modifier concentration gradients of binary or ternary mixtures near (within 50°C above or below!) their critical temperature. Packed-column SFC is a form of normal-phase chromatography, complementing reversed-phase HPLC, but with

superior speed, and efficiency. The low temperatures used make packed-column SFC ideal for separation of moderately polar, thermally labile molecules. The primary detection scheme with packed columns is UV absorption.

Packed-column and capillary SFC are two different techniques sharing part of a name. As with GC and HPLC there is clearly an overlap between the two. Packed columns are sometimes used with pure carbon dioxide, pressure programming and FID detection, to perform some of the applications more commonly performed by capillary SFC. Some relatively polar solutes are soluble enough in carbon dioxide to allow elution with capillaries and pure carbon dioxide.

Unified chromatography A further problem in defining these techniques is the fact that there are no real borders between GC, SFC and HPLC. One can start an experiment, above the mobile phase critical temperature (T_c) (i.e. as GC), then raise the pressure above the critical pressure (P_c) (to SFC), then drop the temperature below T_c (to LC). In the process the name of the technique changes from GC, to SFC, to HPLC, but there is never more than one phase present, and there is never a phase transition. Changes in solute retention, viscosity, diffusion coefficients, etc., are smooth and continuous, even when the definition of the fluid changes. In packed-column SFC, modifier concentration can be programmed from 0 to 100%. At some intermediate (but not obvious) concentration, the definition of the technique changes from SFC to HPLC. The characteristics of interest in SFC are summarized in Table 1. SFC has additional special advantages when scaled up for preparative use.

There has been some effort to promote SFC as a form of unified chromatography. SFC instrumentation can typically also perform HPLC, and at least

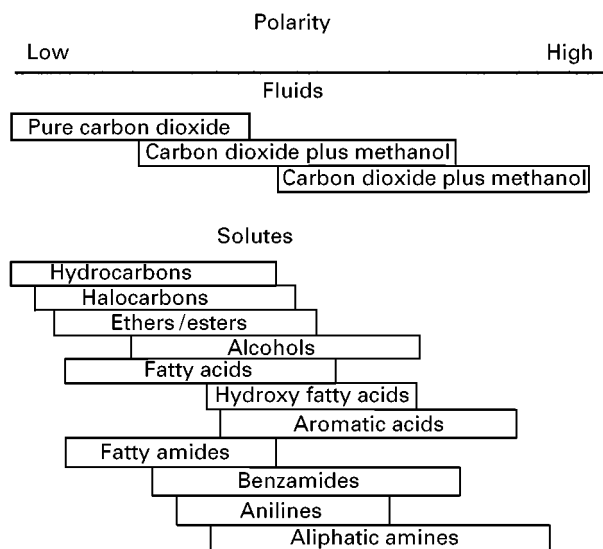


Figure 1 A summary of solute families which have been separated by SFC.

some GC, whereas instrumentation for the other techniques cannot perform much SFC.

Solutes Typical samples separated by packed column SFC consist of low to moderate polarity organic solutes with relative molecular masses $\leq 10\,000$ Da. As a 'rule of thumb', solutes that can be dissolved in methanol or a less polar solvent are good candidates for SFC. On the other hand, solutes requiring water or buffered or pH adjusted water environments are a poor choice. Solute families which have been separated by SFC are summarized in Figure 1. Low polarity solutes are to the left, higher polarity solutes to the right. At the bottom of the figure, there is an attempt to relate the nature of the mobile phase needed to elute the various solute families.

Fluid Characteristics

Other pure fluids used A few common fluids are listed in Table 2. However, carbon dioxide remains the fluid of choice for SFC in spite of its inherently low polarity. It has a modest critical pressure and temperature, is inexpensive, readily available, safe, and compatible with the FID.

Some early work used supercritical pentane mixed with alcohols at $>235^\circ\text{C}$. The flammability of such mixtures means that today they are rarely used. Nitrous oxide has characteristics similar to carbon dioxide but is also an extreme oxidizer. It should not be mixed with fuels such as organic modifiers. Fluids like ammonia are also obviously potentially dangerous and corrosive.

Table 1 Characteristics of interest in SFC

A compressible fluid that acts as a solvent
Solvent strength changes with a physical parameter (pressure)
Very wide range of solvent strength using one binary pair of solvents
Low viscosity
long, high efficiency columns (i.e. $>2\text{ m}$ with $5\text{ }\mu\text{m}$ particles)
low pressure drop at high flow with smaller particles
Higher speed than HPLC – higher diffusion coefficients
3–10 \times higher throughput
much faster re-equilibration
rapid method development
Compatibility with GC detectors, like the FID, ECD, NPD
Transparent in the UV
Complementary selectivity to reversed-phase HPLC
Low cost, environmentally friendly solvents, easily removed

Table 2 Critical parameters of some of the pure fluids used for SFC

	<i>Critical temp. (°C)</i>	<i>Critical pressure (atm)</i>
Carbon dioxide	31.1	72.8
Nitrous oxide	36.4	71.5
Sulfur hexafluoride	45.5	37.0
Trifluoromethane	25.9	47.7
Ammonia	132.3	111.3
<i>n</i> -Pentane	196.6	41.7
Methanol	239.4	79.9
Water	374.1	217.6

Some chlorofluorocarbons have interesting properties but have been banned due to their ozone depletion potential in the environment. Several replacement fluorocarbons, especially F-134a, have recently shown potential for extending the polarity range available with a pure fluid. Sulfur hexafluoride has been used as a mobile phase, particularly in the study of hydrocarbons, but is also an ozone depleter. Its main utility is its compatibility with the FID, although a combustion product is hydrofluoric acid. Fluorocarbons exhibit the same problem.

Density At constant temperature, the log of retention in SFC is a nearly linear function of density. Changing the density of the mobile phase can result in a change in retention of 3 or 4 orders of magnitude. Using carbon dioxide as the mobile phase, the usable density range is from gas-like densities (i.e. 0.002 g cm^{-3}) to a density similar to water ($>0.95 \text{ g cm}^{-3}$). The typical pressure range is 60 to 400 or 600 bar. The typical temperature range is from 40 to 250°C , but temperatures above 150°C are seldom used.

Modifiers None of the pure fluids used in SFC are polar, and polar solutes are typically insoluble in them. Solvent polarity can be increased by adding polar modifiers, such as alcohols to the nonpolar main fluid. The increase in solvent strength is nonlinear. The addition of 2% methanol to carbon dioxide yields a fluid with the polarity one might expect from 10% methanol. This enhanced solvent strength is due to a phenomenon, sometimes called clustering, where the polar modifier molecules tend to cluster together, creating small pockets of greater than expected polarity. Polar solutes tend to be solvated within, and by, these clusters. The clusters are too small to be considered micelles or a different phase. Individual modifier molecules freely exchange in and out of the clusters.

Once a polar organic modifier is added, the composition of the mobile phase dominates over its density in determining the chromatographic retention of a solute. Gradient elution through composition programming becomes the primary means of retention control. Pressure control becomes a secondary variable. The densities of most binary fluids are unknown, and equations of state of binary pairs are inaccurate, making density programming problematic.

In SFC the composition of the mobile phase can be programmed from 0 to 100% modifier. Methanol is among the most polar liquids that is completely miscible with carbon dioxide. On Snyder's solvent strength scale widely used in HPLC, hexane has a strength of 0, water has a strength of 10.4, and methanol has a strength of 5.1. Thus, the solvent strength can be programmed over approximately half the solvent strength scale available in chromatography, using a single binary pair of common solvents. Changing the identity of the modifier can change selectivity.

Additives The polarity range amenable to SFC has been extended significantly by the use of ternary mobile phases consisting of carbon dioxide, methanol, and a low concentration of a much more polar substance called an additive. Without an additive most primary aliphatic amines and most polyfunctional acids will not elute or elute with severe tailing. The inclusion of additives often results in elution of symmetrical peaks with high efficiency. Additives appear to function through multiple mechanisms, although much more work is still required to understand their role better. The most effective additives usually contain stronger members of the same functional group. For example, trifluoroacetic acid is usually effective in improving the elution of other acids, while isopropylamine is effective in eluting amines. Ion pairing, where an acid is added to a base or a base to an acid is seldom effective.

Viscosity One of the more interesting aspects of the fluids used as mobile phases in SFC is their low viscosity, which is more gas-like than liquid-like, even at high densities. For example, the viscosity of carbon dioxide is typically an order of magnitude lower than water. At 20°C and 200 bar the density of liquid carbon dioxide is over 0.9 g cm^{-3} , yet its viscosity is 10.3×10^{-4} poise. At 20°C and atmospheric pressure, the viscosity of water is 100.2×10^{-4} poise. Low viscosity clearly produces the practical advantage of minimizing pressure drops across columns. Very long, high efficiency columns can be used. Compared to HPLC, an SFC column can be run at 2.5 times the flow with 0.25 times the pressure drop. As

the modifier concentration in binary fluids increases, the viscosity of the fluid approaches that of normal liquids.

Diffusion coefficients and speed of analysis Any one column can theoretically be used for GC, SFC or HPLC. Columns can be characterized by the number of 'plates' they exhibit. A column generating many plates can resolve more complex mixtures and is said to have higher efficiency than one generating only a few plates. Another way of describing column efficiency is plate height, H , which is the distance along the column equivalent to one plate. The total number of plates, N , a column exhibits corresponds to the total length, L , divided by the plate height, H ($N = L/H$).

The van Deemter equation, which can be written as: $H = A + 2[D/u] + k[u/D]$, relates the plate height, H , to the solute binary diffusion coefficient in the mobile phase, D , and the linear velocity of the mobile phase through the column, u . Plots of H vs. u show that the minimum value of H (yielding maximum resolving power for a given column) is the same, regardless of the technique, but the optimum speed for pushing the mobile phase through the column depends on the diffusion coefficient of the solute in the mobile phase.

In GC, values for D are of the order of 0.1 to $1 \text{ cm}^2 \text{ s}^{-1}$. In HPLC, a typical D is of the order of $10^{-5} \text{ cm}^2 \text{ s}^{-1}$. Diffusion coefficients in SFC range from 0.01 down to $10^{-4} \text{ cm}^2 \text{ s}^{-1}$. As usually practised, SFC is at least 100 times slower than GC but up to 10 times faster than HPLC. As the modifier concentration is increased in binary fluids, diffusion coefficients approach those in HPLC.

Instrumentation

By the early 1970s, it was generally recognized that HPLC was simpler, easier and more generally applicable than SFC. As an indication of how widespread that conclusion was, no commercial equipment for SFC existed until around 1982. By 1985, commercial SFCs for use with capillary columns appeared. More recently, several companies have introduced instrumentation specifically designed for packed-column SFC or for both packed- and capillary-column SFC.

Instrumentation for Capillary SFC

A schematic representation of the instrumentation required for capillary SFC is shown in Figure 2. In capillary SFC, the main method for changing retention is to change the mobile phase density. Pressure is the primary control variable, temperature is a secondary control variable. The pump is used as a pressure

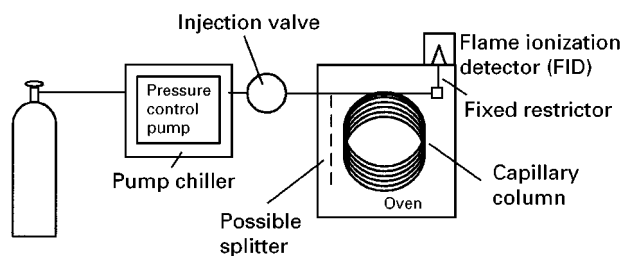


Figure 2 Schematic representation of instrumentation required for capillary SFC.

source. Pressure or density programming is used much like temperature programming is used in GC. Both negative and positive temperature programmes have been used.

Columns The most commonly used capillary columns are 50 or $100 \mu\text{m}$ i.d. and 10 m long, they are made of fused silica tubing. A wide range of stationary phases are available, including many that are more polar than those used in GC. The optimum mobile phase flow rate is inversely related to the density of the fluid and is of the order of 0.1 to 1 cm s^{-1} .

Pumps The most common pumping systems for CSFC are built around 100 to 250 cm^3 syringe pumps, capable of generating pressures of 400 to 600 atmospheres. Syringe pumps are ideal for controlling pressure. When combined with a computer, the pressure of the pump and the temperature of a column oven can be used to calculate the pressure profile required to generate density ramps.

Syringe pumps can be difficult to fill with a single phase. Any gas present must be re-liquefied before the pump can deliver high pressures. Liquefying the gas can require most of the piston displacement. It has become a common practice to purchase carbon dioxide in cylinders with a helium headspace, raising the pressure to a point where the carbon dioxide is always a liquid. In addition, the syringe is chilled using a recirculating bath, further helping to liquefy the fluid.

Capillary columns are seldom used with mixed mobile phases, due partly to the inherent low retentivity of the columns and partly to instrumental difficulties using syringe pumps to generate composition gradients. Syringe pumps cannot control both pressure and (relative) flow simultaneously. When modified fluids are used with syringe pumps they are usually either premixed in a cylinder or made by adding a known volume of a liquid modifier to the syringe then filling with the main fluid (no composition gradients).

Neither binary fluids premixed in a cylinder nor helium headspace should be used. As such cylinders are used up, the concentration of modifier and/or helium in the carbon dioxide changes, changing the fluid solvent strength. Retention can change by a factor of 2 between a nearly full and a nearly empty cylinder.

Flow control reciprocating pumps can be used as a pressure source, when used with a back-pressure regulator (BPR), as shown in **Figure 3**. The pump(s) deliver a large (i.e. 2 mL min^{-1}) flow of mobile phase to a vessel located upstream of the BPR. A tee allows some of the flow to be drawn off to the injection valve and column. The BPR can be programmed to change the pressure in the vessel. The fluid leaving the BPR can be vented or recycled to the inlet of the pump.

Injection High pressure injection valves similar to those for HPLC are used to introduce liquid samples into the chromatograph. Unfortunately, an ideal injection volume for a $50 \mu\text{m}$ i.d. column should be $<4 \text{ nL}$ (a plug 2 mm , 40 column diameters long, in the column). Since there are no fixed loop injectors with such small volumes, split injection schemes are most often used. Timed split injectors move the rotor of a 0.060 to $0.2 \mu\text{L}$ internal loop valve back and forth fast enough so that only part of the loop volume is pushed on to the column.

Traditional flow splitters use a 'tee' mounted just downstream of the valve. A piece of larger inner diameter (i.e. 0.5 mm) stainless steel (s.s.) tubing connects the valve to the tee. The column is usually

pushed through the tee and up inside the s.s. tube until it touches the valve rotor, then it is pulled back $1\text{--}2 \text{ mm}$. A larger volume (i.e. $0.1\text{--}0.5 \mu\text{L}$) sample loop is switched in-line and swept with 10 to 100 times the column flow. Most of this flow and sample is vented through a restrictor mounted in the side arm of the tee.

Split injections tend to give poor reproducibility, due mostly to the difficulty in mixing a liquid sample with a much lower density supercritical fluid a very short time before the split. Many alternate injection schemes have been developed to allow larger injections and/or better reproducibility.

Retention gaps (an empty length of deactivated capillary tubing) allow much larger injections with better reproducibility. By carefully controlling the initial temperature and pressure, the sample can be distributed as an annular film along a retention gap, with the mobile phase passing through the film, along the axis of the tube. Since the fluid rapidly becomes saturated with the sample solvent, only the solvent at the head of the gap is vaporized or dissolved. The film of solvent progressively becomes shorter, while the sample becomes concentrated in the remaining film. When all the solvent is removed, the sample components are concentrated in a narrow band on the retention gap, and are then differentially eluted with a density programme.

Ovens The temperature of the fluid is important in determining its density and thus the retention of solutes. However, temperature has an effect on retention independent of density. To programme an increase in density using only the temperature, the user would start at a high temperature and decrease temperature over time.

In CSFC, the temperature is almost always held at least 50°C higher than the critical temperature. With carbon dioxide as the mobile phase ($T_c \approx 31^\circ\text{C}$) the most common temperatures used are between 100 and 150°C . Since CSFC most often uses GC detectors, along with these higher temperatures, large GC-like ovens are used.

Restrictors With CSFC, the flow of the mobile phase through the column is only indirectly controlled using fixed restrictors mounted on the outlet of the column. Increasing the column head pressure causes large changes in flow (and efficiency) in the column. There are no devices with small enough inner dimensions to allow the pump to act as a flow source (controlling linear velocity), while independently controlling the outlet pressure, without destroying the separation. There have been numerous schemes to minimize changes in flow through restrictors caused by pressure

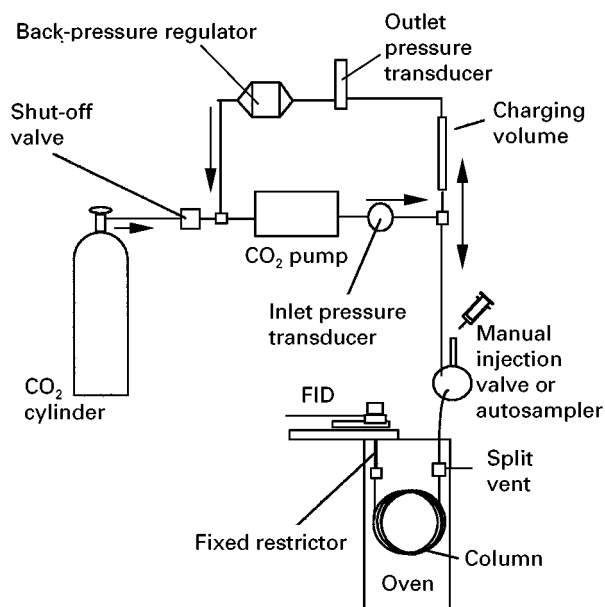


Figure 3 Flow control reciprocating pump used as a pressure source when used with a back-pressure regulator.

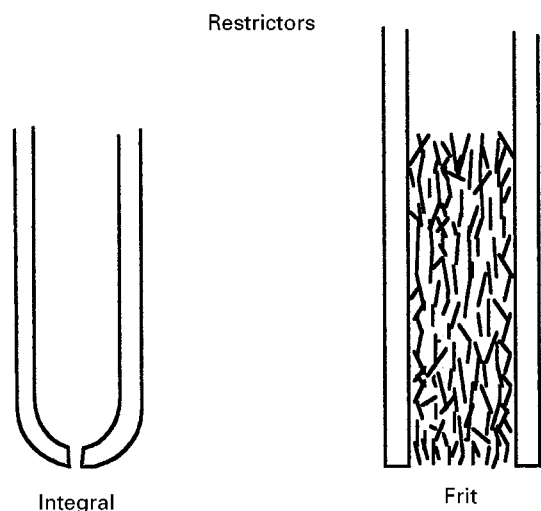


Figure 4 Two types of restrictors in common use.

changes, but they are all relatively complicated or expensive and have not been widely adopted.

There are two types of restrictor in common use: integral and frit, as shown in **Figure 4**. Integral restrictors are 1–2 μm diameter, <25 μm long pinholes formed at the end of a piece of fused silica tubing. They were originally formed on the end of the column and were integral to it. Today, they are usually made of a separate piece of tubing and attached to the column using a butt connector.

Frit restrictors consist of a porous plug of material formed inside a piece of 50 μm i.d. fused silica tubing. The plug is usually 1–2 cm long. Frits have many small tortuous paths.

Integral restrictors have better flow vs. pressure characteristics but are much easier to plug than frit restrictors. However, since the pressure drops along the full length of the frit, the density at its outlet can

be low so that heavier solutes may drop out of solution and are lost inside the frit. For high molecular mass materials, the only choice is an integral restrictor. All restrictors plug over time, changing flow characteristics through the column. Restrictor performance is the weakest link in SFC instrumentation.

Detection One of the greatest advantages of CSFC with carbon dioxide is its compatibility with the flame ionization detector (FID). The FID is universal and exhibits uniform response factors for hydrocarbons, while allowing a change in solvent strength through pressure or density programming. The restrictor at the end of the column is mounted directly in the base of the detector. The fluid expands to a gas in the flame.

Although both UV and fluorescence detectors have been used in CSFC, the light pathlength is typically the column diameter (i.e. 50 μm). Standard HPLC flow cells have pathlengths 200 times longer. Both detection limits and dynamic range are, thus, compromised.

Instrumentation for Packed-column SFC

The instrumentation used for packed-column SFC can be somewhat more complex than capillary SFC as shown in **Figure 5**. Most of the hardware, including injection valves, columns and some detectors, are the same or similar to that used for HPLC. Binary and ternary fluids are the norm, although low polarity solutes can often be eluted with pure carbon dioxide. Changing the mobile phase composition is the most effective way to change solute retention. Composition gradient elution is most common, although pressure, temperature and even flow can also be programmed. Selectivity is often most easily changed by changing the temperature. Pressure is a secondary control variable.

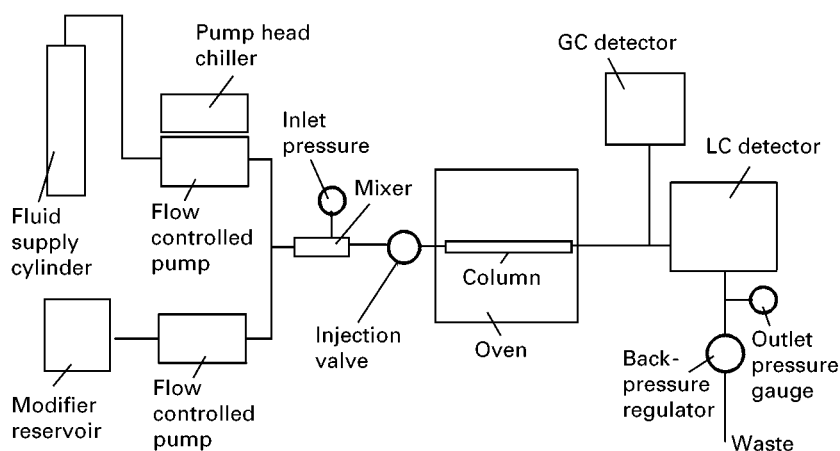


Figure 5 Instrumentation for packed-column SFC.

Columns Standard HPLC columns are used for packed-column SFC. The most common have inner diameters of 2 to 4.6 mm, and are 15 to 25 cm long. Both 1 mm and micropacked fused silica are also sometimes used. The most common packings are 3 to 5 μm diameter totally porous silica, although many other materials have been used. SFC is a 'normal-phase' technique, making the use of more polar bonded phases commoner. The biggest change from HPLC is the growing use of longer packed columns, as much as 2.2 m in length.

Pumps The most common pumping systems in packed-column SFC use multiple high pressure reciprocating pumps operated as flow control devices. Since the main fluid is supplied in a high pressure gas cylinder, gradient switching valves cannot be used to mix modifier with the fluid in SFC. One high pressure pump is used to deliver the main fluid (SF pump) and another is used to pump modifier(s). Used in conjunction with a back-pressure regulator, properly designed pumps allow independent control of flow, composition and pressure.

The head of the SF pump is chilled to ensure the fluid is pumped as a liquid. However, even as a liquid, the fluids used still have a compressibility much higher than normal liquids. To accurately pump these fluids, the pumps need both an extended compressibility compensation range, and the ability to dynamically change compressibility compensation when the pressure and temperature (and composition) are changed. Slightly modified HPLC pumps usually have an inadequate range of compressibility compensation, and never dynamically compensate for the changes in compressibility which accompany pressure and/or composition changes. Using HPLC pumps for SFC results in highly inaccurate and non-reproducible flows and compositions.

Injection Injection is accomplished using standard HPLC injection valves operated in either fixed or partial loop modes. Care must be exercised in choosing the volume and polarity of the sample solvent. SFC is usually a normal-phase technique. Common sample solvents, like methanol, are stronger solvents than the mobile phase. If too much of such a polar solvent is injected, peaks can be distorted and broadened. Injection volumes up to 10 μL can usually, but not always, be tolerated. Smaller amounts of water can be directly injected but only under carefully chosen conditions. Decreasing the polarity of the sample solvent or injecting smaller amounts reduces or eliminates the problem.

Oven The most common temperature range for packed column SFC with binary or ternary fluids is 30

to 50°C, although both higher and lower temperatures are used. With pure carbon dioxide, the temperature is usually held at >60°C.

Since temperature adjustment often has dramatic impact on selectivity, control of the column temperature is more critical than in HPLC. For the separation of enantiomers, subambient temperatures are often desirable. Ovens similar to GC ovens with cryogenic cooling, Peltier heated/cooled ovens, and recirculating baths are all used.

Pressure control Pressure is controlled using a back-pressure regulator mounted at the downstream end of the system. The BPR is used in conjunction with a pressure transducer and feedback loop. Early regulators were mechanical but today are electromechanical, allowing complex programming of the system outlet pressure. Several commercially available back-pressure regulators have small internal volumes which allow peak collection after the device.

Detection Pure carbon dioxide and the FID and often the UV detector can be used to study fats, waxes, silicones, hydrocarbons and other low polarity solutes, where modified fluids are unusual.

Many other GC detectors are compatible with both pure and modified fluids and have been used with either packed or capillary columns. These include: the electron capture detector (ECD) for the study of explosives, flame retardants, pesticides, derivatives of fatty acids, etc.; the thermionic or nitrogen-phosphorus detector (TID or NPD) for the study of pesticides, caffeine in beverages, and many small drug molecules; the sulfur (petroleum, pesticides) and nitrogen chemiluminescence (similar applications to the NPD) detectors; the flame photometric detector (FPD)(petroleum), as well as others. These detectors are often used with packed columns by splitting off a small fraction of the total column effluent through a fixed restrictor.

There are many hundreds of applications of both pure and modified mobile phases using the UV/VIS detector in the speciality chemical, petroleum, pharmaceutical and agricultural chemical sectors. Standard HPLC UV detectors, including photodiode array detectors, need only a high pressure flow cell to become compatible with SFC (fluid density in the cell approaches 0.9–1 g cm^{-3}). Carbon dioxide is completely transparent to below 190 nm. Mixed with acetonitrile or methanol, short wavelengths can be used to maximize detection limits.

Fluorescence detectors also require a high pressure flow cell, complicated by the need for light paths at 90° to each other. Several high pressure 'chiral' detectors are available for differentiating D and

l isomers. Other detectors that have been successfully used with SFC include: mass spectrometry (MS), Fourier transform infrared (FTIR), and the evaporative light-scattering detectors (ELSD). Most atmospheric pressure ionization HPLC-MS interfaces work equally well, or better, as SFC-MS interfaces.

Future Directions

SFC instrumentation is maturing. The unique requirements for pumping these fluids is slowly becoming widely understood. There are unlikely to be further dramatic improvements in the core technologies. However, a wide range of accessories will appear. As more instruments are sold, the cost of production will tend to drop, making SFC more competitive with HPLC. Development of SFC detector interfaces will continue. Recent results with both mass spectrometry and evaporative light scattering detectors, finally indicate equal or better results than in HPLC-MS, or HPLC-ELSD, but with higher throughput.

User training has been another block to the spread of SFC in industry. One of the chief advantages of packed column SFC in industrial environments, particularly in the pharmaceutical industry, is its similarity with HPLC. Technicians familiar with HPLC have little trouble developing expertise in SFC.

Until recently, SFC has been viewed as a research tool, due largely to the relatively high cost of equipment and the need for an expert operator. As equipment is becoming less expensive, and easier to use, it is beginning to be used in routine analysis. Since the number of analysts involved in research is small compared to the number performing routine analysis, the

incorporation of a technique into routine analysis represents a major expansion. This trend should continue, since the surprisingly low cost of operation and environmental friendliness are becoming more widely understood and appreciated.

See also: II/Chromatography: Supercritical Fluid: Historical Development; Theory of Supercritical Fluid Chromatography.

Further Reading

- Ashraf-Korassani M, Fessahaie MG, Taylor LT, Berger TA and Deye JF (1988) Rapid and efficient separation of PTH amino acids employing supercritical CO₂ and an ion pairing agent. *Journal of High Resolution Chromatography* 11: 352.
- Berger TA (1995) *Packed Column SFC*. Cambridge: Royal Society of Chemistry.
- Berger TA and Wilson WH (1993) Packed column supercritical fluid chromatography with 222,000 plates. *Analytical Chemistry* 65: 1451.
- Gere GR (1983) Supercritical fluid chromatography. *Science* 222: 253.
- Giddings JC, Myers MN, McLaren LM and Keller RA (1968) Dense gas chromatography. *Science* 162: 67.
- Lee ML and Markides KE (eds) (1990). *Analytical Supercritical Fluid Chromatography and Extraction*. Provo, Utah: Chromatography Conferences Inc.
- Mourier PA, Eliot E, Caude MH and Rosset RH (1985) *Analytical Chemistry* 57: 2819.
- Novotny M, Springston SR, Peaden PA, Fjeldstead JC and Lee ML (1981) Capillary supercritical fluid chromatography. *Analytical Chemistry* 53: 407A.
- Roberts I (1995) In: Adlard ER (ed.). *Chromatography in the Petroleum Industry*, ch. 11. Amsterdam: Elsevier.

Large-Scale Supercritical Fluid Chromatography

P. Jusforgues and M. Shaimi,
PROCHROM SA, Champigneulle, France

Copyright © 2000 Academic Press

Introduction

Preparative supercritical fluid chromatography (Prep-SFC) came about at the same time as analytical supercritical fluid chromatography (SFC). During the 1960s and 1970s at the time of the early development of SFC, several authors included fraction collectors at the outlet of their analytical supercritical fluid (SF) chromatographs. However, the technological difficulties encountered kept these attempts somewhat marginal. The real interest in Prep-SFC appeared in

1982 when Perrut patented large-scale Prep-SFC with eluent recycling. Since then Prep-SFC has been studied and developed by several teams and on various scales. During the past decade commercial equipment has appeared and applications are reaching industry.

Principle

Prep-SFC is the result of the collaboration of three techniques:

- the principle of the separation is the same as in analytical SFC;
- the scale, the application and the industrial interest is the same as preparative high-performance liquid chromatography (Prep-HPLC);

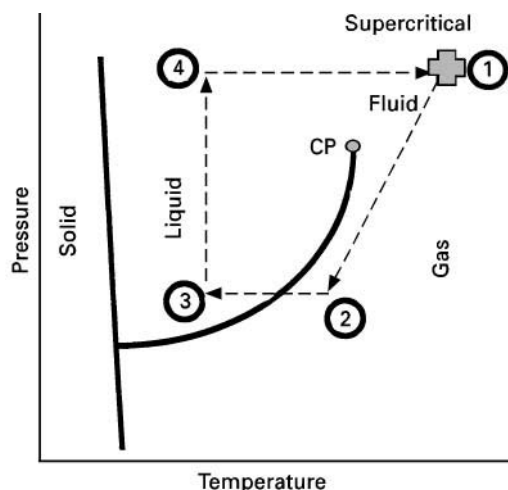


Figure 1 Phase diagram of a pure compound. See the description in the text.

- the economical and practical interest of simple solvent recycling is the same as in industrial supercritical fluid extraction (SFE).

The extensive study of the properties and characteristics of supercritical fluids is not the subject of this article. The main properties relevant to their use in Prep-SFC are good solvent power (comparable to liquids), low viscosity and high diffusion coefficients (intermediate between gases and liquids) and straightforward modulation of solvent properties by pressure adjustment (it is possible to transform a supercritical fluid to a gas by isothermal depressurization).

The principle and characteristics of Prep-SFC can be described with a phase diagram. **Figure 1** shows the eluent cycle in a Prep-SFC process.

At point 1, the eluent is supercritical and the chromatographic separation takes place in the column. At the column outlet, the eluent is depressurized (and heated) to the gas phase at point 2. While in a gas phase the eluent is cleaned and pure fractions collected. The cleaned gaseous eluent is then recycled, through condensation (point 3), recompression (point 4) and heating to the operating temperature (point 1).

This is a description of the simplest Prep-SFC process that uses a pure compound as a supercritical eluent. However, it is often necessary to use a mixture as the supercritical eluent. The secondary component of the eluent is most often a liquid solvent ('the modifier'). A Prep-SFC process that includes a modifier differs from the simple scheme without a modifier and both processes will be described here.

Prep-SFC processes can be classified according to scale. Micro-Prep-SFC is basically the adaptation of an analytical chromatograph to collect small frac-

tions (microgram or milligram size) and is not described here. Laboratory-Prep-SFC is concerned with the purification of larger amounts (hundreds of milligrams or grams). It requires a specific technology, but cannot be considered to be large-scale SFC. It is described briefly later. Pilot-Prep-SFC is intended for the purifications of kilograms per day on columns having an internal diameter of between 5 and 15 cm. It can be used for scale-up studies or even for some small industrial productions. Production-Prep-SFC is for the purification of hundreds of kilograms to tens of metric tons per year. This scale of production takes full advantage of the economics of Prep-SFC.

Important Characteristics

The technique of Prep-SFC is best described by comparing it with Prep-HPLC and the emerging simulated moving bed (SMB) technique, an implementation of countercurrent continuous chromatography.

Prep-HPLC is a very useful tool in the field of high-performance separations. The technique's high flexibility and efficiency means that most separation problems can be solved technically (but not necessarily economically). The main drawback of Prep-HPLC is the huge quantity of expensive solvent that needs to be used. Several strategies have been proposed to eliminate the solvent problem. One of them is SMB which cuts solvent use by up to 10-fold, but needs a higher level of economic investment and is limited to binary separations. Another is Prep-SFC, which reduces the solvent required by a factor of five to 20 (if a modifier is used), or uses no solvent at all (if no modifier is used) but also involves a high level of economic investment and has a limited range of applications.

Selectivity

The range of selectivities accessible by SFC is the same as for HPLC. This is not surprising since selectivity depends on the physical and chemical nature of the stationary and mobile phases. The stationary phases used in Prep-SFC are exactly the same as the ones used in Prep-HPLC. Theoretically, some stationary phases specific to SFC could be used (e.g. cross-linked polymers deposited on a silica support), but phases developed for HPLC are the only ones available in large quantities and, thus, they are the only ones used. Supercritical eluents are fewer in number than the mobile phases used in HPLC and, indeed, carbon dioxide is almost the only supercritical eluent used for Prep-SFC. But the possible use of modifiers, which can be almost any liquid solvent or any mixture, is a powerful parameter for variation of selectivity. Moreover, by changing the operating pressure it

is possible to adjust the solvent strength of the supercritical eluent, since it is compressible, without changing its composition.

The foregoing does not mean that there is no selectivity difference between the two techniques: for a given application, selectivity obtained by SFC can be much higher than by HPLC and vice versa.

Efficiency and Speed

Prep-SFC can attain efficiencies as good as those for Prep-HPLC. A reduction in plate heights of a factor of between two and four are easily obtained leading to efficiencies of between 10 000 and 70 000 plates per metre depending on particle size. Moreover, Prep-SFC has, just like analytical SFC, the advantage of being able to combine high efficiencies with high speed. Indeed, as can be seen in **Figure 2**, in any type of chromatography, a plate height increase (corresponding to a loss of efficiency) is observed when the eluent speed is increased beyond the minimum point. The slope of the curve is correlated to the diffusion coefficient of the sample in the eluent (the higher the diffusivity the smaller the slope). Since diffusion coefficients of supercritical fluids are much smaller than in liquids, the curve is flatter and it is possible to increase the eluent speed (and the productivity) without losing much efficiency. Moreover, in HPLC eluent speed is limited by the pressure drop in the column while in SFC the viscosity of the eluent is much less and such a limitation does not apply. To obtain high efficiencies in large diameter columns, the same difficulties are encountered in Prep-SFC as in Prep-HPLC. For diameters over 5 cm preppacked columns are not

stable enough and lose more than half of their efficiency after a few hours use. This is due to rearrangement of the particles in the column induced by the friction of the flowing solvent. As for Prep-HPLC the solution to this problem is dynamic axial compression columns in which a piston continuously compresses the chromatographic bed, thus preventing the occurrence of voids and the loss of efficiency.

Thermal Degradation

There is no theoretical limit to the operating temperature range of supercritical fluids and some applications use temperatures as high as 200°C. However, the practical temperature range applied to Prep-SFC is from 0 to 100°C and most of the applications are made between 25 and 50°C. These moderate temperatures allow the processing of thermolabile molecules.

Flexibility

The flexibility of use of Prep-SFC is comparable to that of Prep-HPLC. Adjustment of operating parameters to a new feedstock and the start up of a system are simply and quickly performed in a few hours. Prep-SFC is thus well adapted to the type of batch purification often encountered in the pharmaceutical industry. Moreover, separations are not limited to binary separations and it is possible to remove a minor impurity or to isolate one or several compounds from a complex mixture.

Absence or Reduced Use of Solvent

When no modifier is used Prep-SFC can be considered as a 'no-solvent' process because carbon dioxide is used in most cases. The gas is recycled on-line thus there is no solvent consumption, no large storage necessity, no evaporation devices required for downstream processing and no problems with undesirable solvent traces left in the final product. Absence of solvent is also an advantage when it comes to the economics of large-scale separations (see below).

When a modifier has to be mixed with the supercritical main eluent (carbon dioxide), some, but not all, of these advantages are lost. The modifier is added to the eluent concentrations ranging from 0.1 to 25% (more often 1–5%). Thus, only a fraction of the eluent is not recycled on-line which means there is reduced solvent storage and a smaller evaporation plant than for Prep-HPLC. Moreover, the modifier used will very often be a single solvent (not a mixture) which simplifies its evaporation and recycling. The nature of modifiers most often used (methanol, ethanol, isopropanol) means that the toxicity problem of solvent traces left in the final product is

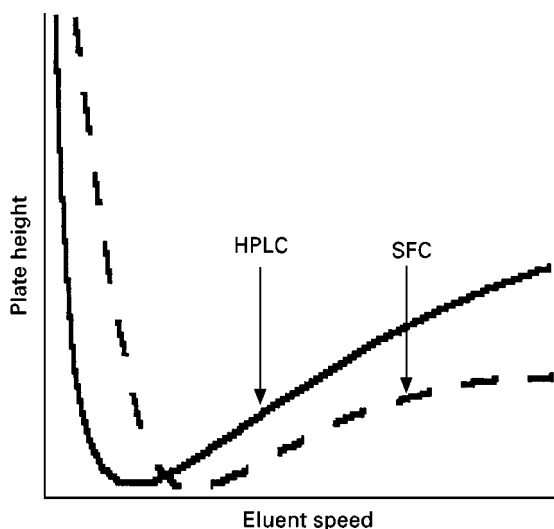


Figure 2 Influence of eluent speed on efficiency. Comparison between high-performance liquid chromatography (HPLC) and supercritical fluid chromatography (SFC).

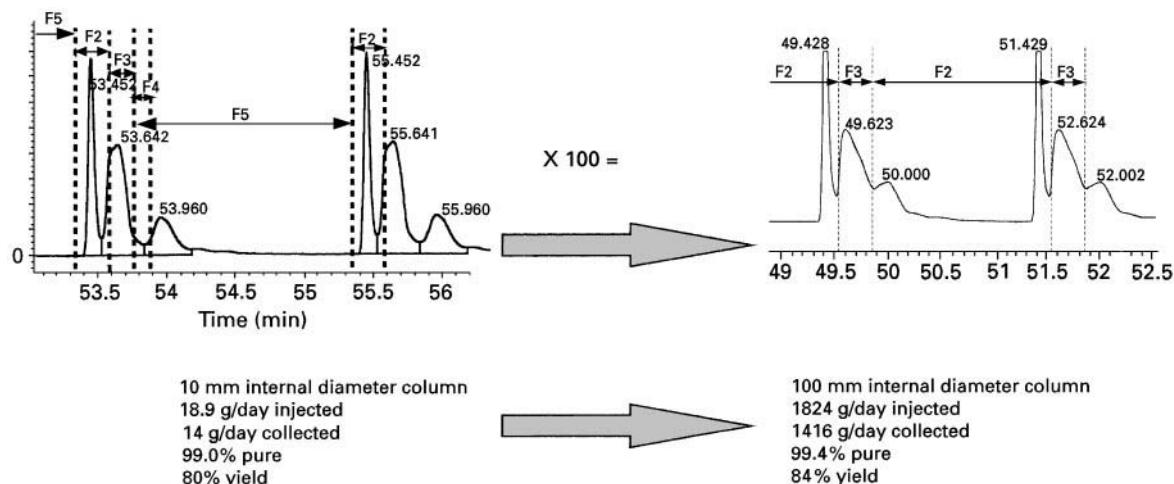


Figure 3 Scale-up example. Purification of an insecticide.

reduced. Finally, the economic advantage over Prep-HPLC is not completely lost because of the reduced quantity of solvent and its ease of recycling.

Scale-up

Scaling up a method developed in the laboratory can be made easily by multiplying the size of the system (flow rates, injected quantity, section of the column, and so on) by the scale factor. This is possible only if the packing material used is the same and the efficiency of the column is the same (this is possible even on very large columns by dynamic axial compression). Figure 3 gives an example of the scaling up possibility.

Limitations

Large and/or polar compounds have a limited solubility in pure carbon dioxide. As has been already mentioned, in this case it is then necessary to add a modifier to the supercritical eluent to enhance the solubilities. The number of applications amenable to Prep-SFC is greatly increased by the use of modifiers. However, some classes of compounds are still insoluble in carbon dioxide and modifier. An example is that some peptides can be dissolved and processed by SFC, but proteins are outside of the range of Prep-SFC.

Another limitation of Prep-SFC is economic. Investment costs for Prep-SFC are much higher than for Prep-HPLC. Savings on solvent consumption will counterbalance the difference in investment cost only for large- or very large-scale applications. For small- or medium-size applications, where both techniques are applicable, HPLC will often be more economical than SFC.

Implementation

Figure 4 shows a schematic flow diagram of a Prep-SFC. Typical pressures and fluid physical states are also indicated.

Eluent tank

The eluent tank (1) contains carbon dioxide under gas-liquid equilibrium at 4.5 MPa and 10°C. It is a buffer volume in the carbon dioxide loop and its volume is about twice the volume of the column. A molecule of carbon dioxide will pass around the system about 15 times per hour. The external carbon dioxide storage tank needs to be only 50 times the volume of the column for one week of operation (compared with the required storage of solvent in HPLC which is 600–1000 times the volume of the column).

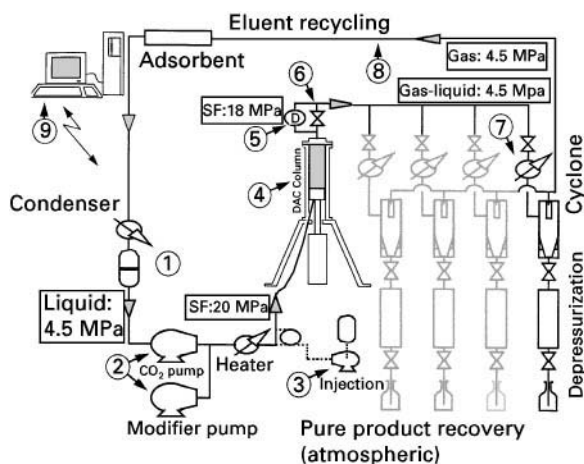


Figure 4 Schematic flow diagram of Prep-SF chromatograph. Legend in text.

Pumps

The carbon dioxide pump (2) is a reciprocating plunger- or membrane-type metering pump. It is a high-pressure pump equipped with one or multiple heads. Pumping is only efficient if the carbon dioxide is kept liquid on the suction side and in the pump head. In order to avoid cavitation it is necessary to cool the eluent tank (1), the suction line and the pump head. Since carbon dioxide is somewhat compressible, reliable pumping is difficult to achieve (the real flow rate differs from the nominal flow rate of the pump) and the efficiency of the pump depends on both inlet and outlet pressures and inlet temperature. Thus, it is better not to rely on the pump to provide a constant flow rate. In the example given the pump is used as a pressure source only, the column inlet pressure is regulated by a pressure regulator and the flow rate is regulated through the depressurization valve (6) at the column outlet. The modifier pump is an ordinary high-pressure liquid metering pump.

Injection Device

For production purposes injections must be made periodically and automatically. The main component of the injection device (3) is a high-pressure metering pump that introduces the sample either directly into the flow of supercritical eluent or into an intermediate injection loop.

Chromatographic Column

The column (4) is similar to Prep-HPLC columns equipped with a dynamic axial compression (DAC) system. A greater thickness of stainless steel is required to withstand the high pressures and a water jacket maintains the operating temperature of the column. Note that, unlike in Prep-HPLC, column outlet pressure is not atmospheric but very close to column inlet pressure (e.g. inlet pressure = 20 MPa and outlet pressure = 18 MPa).

Detector

As in analytical SFC, almost any type of detector (5) can be used (except refractive index detectors): ultraviolet (UV) absorption and so on. UV absorption detectors equipped with a high-pressure cell are used most commonly. Due to the high flow rates, detectors at column outlet must be placed in a split line.

Depressurization Valve

The depressurization valve (6) is a critical piece of equipment. Its function is to reduce the eluent pressure from the operating pressure (e.g. 18 MPa) down

to the recycling line pressure (e.g. 4.5 MPa) and to control the flow rate of the eluent. Depressurization through the valve is almost adiabatic so that it is accompanied by an intense cooling and the fluid at the outlet of the valve is not gaseous but is a gas-liquid mixture (e.g. for carbon dioxide, at 4.5 MPa and 10°C). If the outlet pressure were atmospheric, the physical state of the carbon dioxide would not be a gas-liquid equilibrium but a gas-solid equilibrium (triple point pressure is 0.5 MPa) and the solid would cause random plugging of the tubes. Since the valve is placed at the column outlet, special attention must be given to its design so that it does not include dead volumes that would cause the remixing of the purified fractions.

Traps Lines

A trap line (7) isolates a purified fraction, separates it from the eluent and collects it at atmospheric pressure. There are several ways to achieve this. One configuration is presented in the example which includes a stop valve to select which line is opened when a fraction elutes from the column, a heat exchanger to completely vaporize the carbon dioxide and a cyclone to separate the gaseous carbon dioxide from the liquid sample (or sample dissolved in the modifier). Indeed, the separation cannot be done by a simple decantation, since, after the depressurization, the liquid fraction is highly divided and behaves like a fog that is carried away with the gas. The cyclonic separator is a device that uses the fluid speed to centrifuge it. It has no mechanical moving parts so it is cheap and simple; when properly designed, it can trap 97–100% of the liquid fraction. Also included is a depressurization stage to reduce smoothly the sample pressure from 4.5 MPa to atmospheric pressure.

The number of trap lines required depends on the application. For most industrial processes three to four lines are sufficient. These are a waste line, one or two pure products lines and a mixture line for a fraction requiring recycling (its composition is similar to that of the crude feedstock).

Eluent Recycling

The gas phase is recycled (8). Optionally it can be cleaned with a bed of adsorbents to stop the traces of sample that have not been removed by the cyclones. It is then condensed before being sent back to the eluent tank.

Automation

Although it is possible to imagine a manual version of a Prep-SFC in practice it is almost essential to

Table 1 Examples of production scales

Column diameter (mm)	Column length (cm)	Typical loading capacity		Carbon dioxide flow rate (kg h ⁻¹)
		(g h ⁻¹)	(t year ⁻¹)	
100	10–30	60	0.5	100–200
200	10–30	240	2	400–800
300	10–30	540	4.5	900–1800
500	10–30	1500	12.5	2500–5000

automate. Two pressures, two temperatures and one flow-rate must be controlled. In addition, high-pressure safety and periodic chromatographic functions (injection and collects) must be managed. Finally, data must be acquired and logged.

High-pressure Safety

Supercritical fluids are high-pressure compressible fluids which contain a high level of stored energy that can cause damage if it is abruptly released to atmosphere (unlike high pressure liquids which store little energy because they are not compressible). To prevent any problems associated with pressure release all components are built to withstand pressures much higher than the operating pressure and are certified by regulatory authorities. Safety valves are placed at all critical points in the system and a pressure switch (electromechanical) stops the pressure source (the pump) in case of overpressure. The pump may also incorporate a device to prevent it reaching pressures higher than the maximum operating pressure. Finally, sensors placed all around the system are automatically monitored to prevent any safety problems.

Prep-SFC: What Scale?

Table 1 gives examples of the production scales obtained with different column diameters. These are only typical figures and, depending on the application, actual figures can be bigger or smaller. Pilot or production Prep-SFC can be used for purification of hundreds of grams in a week or for tens of tons in a year as is shown in Tables 2 and 3.

Table 2

3 g (per injection on a 100 mm internal diameter column)
 × 6 (injections per hour)
 × 24 (hours per day)
 × 4 (days per week)
 = 1.7 kg per week

Variants

Working Modes

Various working modes can be implemented in Prep-SFC. They include pressure and/or composition gradients and simulated moving bed SFC (SMB-SFC). Although these techniques may be useful in theory, they are rarely justified by practice and economics. Pressure or composition gradients can be used for selectivity enhancement and/or elution time reduction when the feedstock components have a large range of retention factors. However, with gradients, one of the advantages of Prep-SFC, the speed, is lost since time is required between the two injections to restore the initial pressure or composition, whereas in isocratic Prep-SFC, one can inject the next sample before the previous one is completely eluted.

SMB-SFC offers some of the theoretical advantages of its related technique SMB-HPLC. In SMB-SFC, the feed introduction and the product removal are continuous. The stationary phase is used more efficiently due to the countercurrent process. In SMB-HPLC the high complexity of the system is counterbalanced by savings on the mobile phase consumption, but this is not the case in SMB-SFC because the eluent is already recycled. However, in SMB-HPLC, the elution is necessarily isocratic while in SMB-SFC it is possible to create a pressure gradient in the system and, in some cases, this advantage can bring a decisive productivity increase.

Operating Options

The system described earlier is not the only possible way to implement Prep-SFC. For instance, one can

Table 3

250 g (per injection on a 500 mm internal diameter column)
 × 6 (injections per hour)
 × 24 (hours per day)
 × 300 (days per year)
 = 10.8 t year⁻¹

choose to regulate the flow rate by controlling the pump speed and to control the column outlet pressure by the depressurization valve. The carbon dioxide pressure in the traps can be reduced to atmospheric pressure and the condenser can be replaced by a compressor. It is also possible to add the modifier on the suction side of the main eluent pump.

Applications

Although the principle of Prep-SFC is well established, its commercial availability is relatively new so that there are only a limited number of published applications. One of the first and most studied applications with an industrial opening is the purification of ω -3 unsaturated fatty acids from fish-oil extracts. More precisely, the ethyl esters of eico-sapentaenoic acid ($C_{22:5}$) and docosahexaenoic acid ($C_{20:6}$) are required at a relatively high purity. Pure carbon dioxide is used as an eluent. There is no difficulty in solubilizing the ethyl esters. Large-scale production is envisaged (tens of tons per year). The costing of the process shows that separation by Prep-SFC is two to five times cheaper than Prep-HPLC and the quality of the final product is better.

More recently, other applications have been patented among which one important example is the purification of cyclosporine (a cyclic undecapeptide) with carbon dioxide and an alcohol as modifier. Among the emerging applications under study many chiral separations are candidates to be performed by Prep-SFC. One separation example described below in more detail has been developed in the authors' facilities.

Cis-trans Isomer Separation of Phytol

The separation of the *cis*- and *trans*-isomers of phytol has been chosen as an application of Prep-SFC using carbon dioxide and a modifier (isopropanol) as eluent (see Figure 5).

Phytol is a fatty alcohol and its *trans*-isomer is used in perfumery. The separation has been done on laboratory-scale equipment and has been extrapolated to industrial production. The main steps of the optimization procedure are given below.

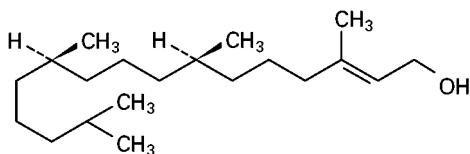


Figure 5 Molecular structure of phytol.

Stationary phase Apolar bonded phases and polymeric phases have been rapidly eliminated because of a lack of selectivity. A classical silica stationary phase was found to give the best separation.

Mobile phase Pure carbon dioxide will not elute the sample so it is necessary to add a modifier. Three alcohols have been tested: methanol (MeOH), ethanol (EtOH) and isopropanol (IPA); IPA gives the best selectivity (see Figure 6).

Overloading The first overloading trials have shown that the thermodynamics of the separation is governed by a concave upward adsorption isotherm (low concentrations migrate faster through the column than high concentrations) even for rather small loadings (10 μ L on a 10 mm internal diameter column). This phenomenon can be clearly seen in Figure 7.

Temperature A rapid screening of operating temperatures in the range of 10–80°C shows the influence of this parameter (see Figure 8). The intermediate temperature (50°C) was chosen to maintain good resolution and short cycle time.

Pressure and modifier content A rapid screening of these two parameters led us to choose 25 MPa and 5.5% (w/w) of IPA in carbon dioxide.

Preliminary trial After establishing the optimum conditions above a preliminary injection was carried out to give the chromatogram shown in Figure 9.

The 4-min cycle time refers to the time elapsed between two successive injections. The total chromatogram duration is 6 min but it is not necessary to wait for the previous injection to be completely eluted before the next injection. With this overlapping injection procedure, the late eluted impurities of the first injection will elute together with the early eluted impurities of the second injection and a 50% increase in productivity is obtained in this particular case. This short cycle time is an advantageous characteristic of Prep-SFC compared to Prep-HPLC where cycle times are closer to 30 min.

Small-scale production On the basis of these results production has been carried out. Figure 10 shows the chromatogram of the repeated injections and Table 4 gives the results of this production step.

Extrapolation of these results to large-scale production can be made directly with a 300 mm internal diameter column and gives 2.3 t year⁻¹ production of the *trans*-isomer from 4 t of feedstock with a product purity of 97.8% and a recovery of greater than 80%.

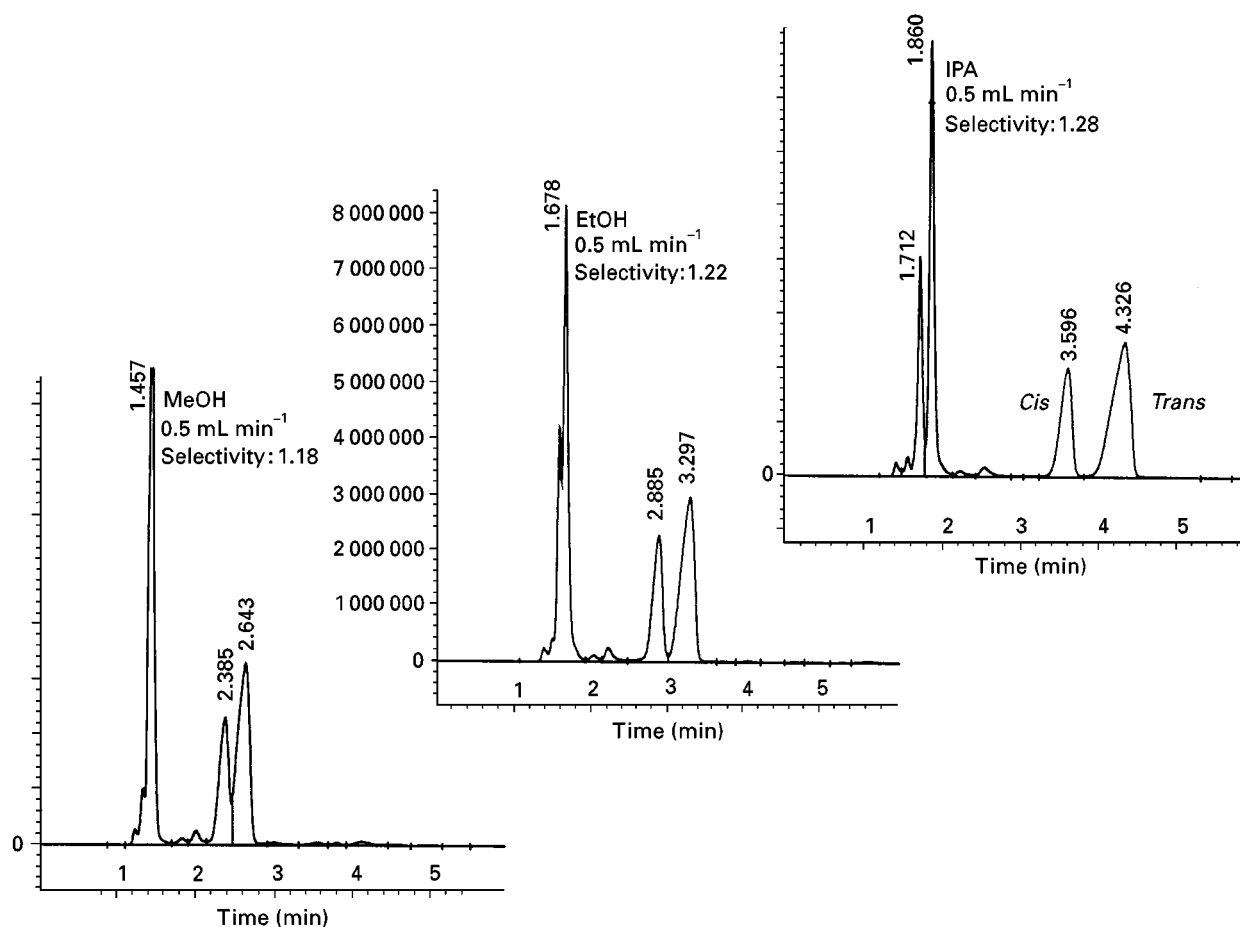


Figure 6 Phytol purification; modifier selection. Stationary phase: silica 15 μm , 100 \AA , AMICON; column: 10 mm \times 250 mm; temperature 50°C; pressure 25 MPa; carbon dioxide flow rate 13.5 g min⁻¹; modifier: MeOH, EtOH or IPA at 0.5 mL min⁻¹ (2.9% w/w); sample: phytol mixture 10 μL .

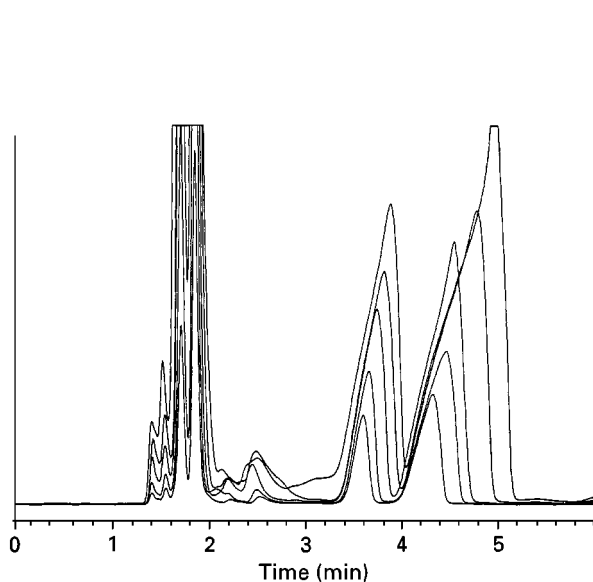


Figure 7 Phytol purification. Peaks distortion due to overload. Modifier: IPA; sample: crude phytol 10, 20, 40, 60, and 100 μL ; other conditions as in Figure 6.

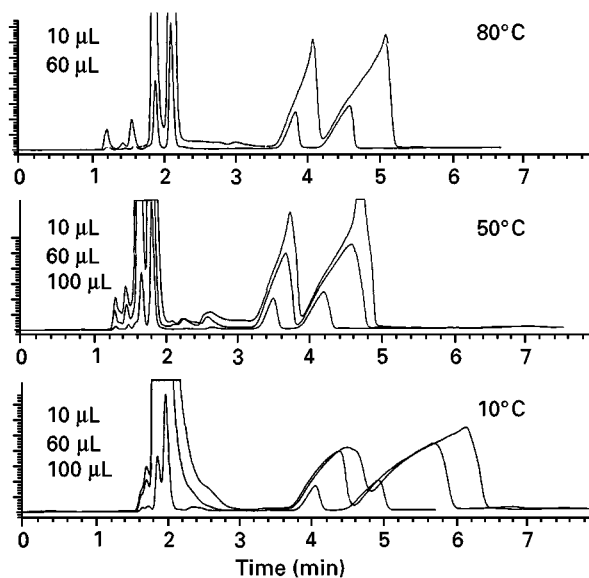


Figure 8 Phytol separation. Influence of temperature. Temperature: 10, 50 and 80°C. Phytol crude: 10, 60, and 100 μL ; other conditions as in Figure 7.

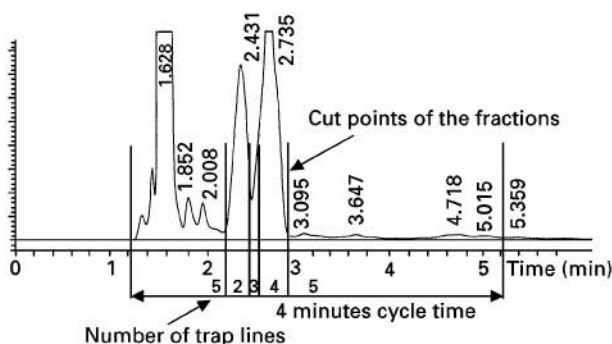


Figure 9 Chromatogram preliminary to production test. Stationary phase: silica 15 μm , 100 Å, AMICON; column: 10 mm \times 250 mm; temperature 50°C; pressure 25 MPa; carbon dioxide flow rate: 13.5 g min⁻¹; modifier: IPA at 1 mL min⁻¹ (5.5% w/w); sample: crude phytol 60 μL = 50.5 mg undiluted; detection: UV absorption at 220 nm.

Economics of Prep SFC

The economics of a separation process depend greatly on the specific application. Indeed, the same Prep-SFC equipment can purify 1 kg per day or 50 kg per day depending on the cycle time, the loadability of the column, the solubility of the sample, the selectivity between the compounds in the sample, and the required purity and recovery. However, it is possible to give the main features of the cost of a separation by Prep-SFC and a reasonable range of costs.

Figure 11 shows a cost breakdown of a typical industrial separation using pure carbon dioxide and no modifier. The total purification cost for this example is about US\$100 per kilogram injected. The range for such a case is US\$20–200 per kilogram. One can see that the capital outlay is half of the total cost while the eluent cost (carbon dioxide) is negligible (2%). The high capital cost is a consequence of working at high pressure and the low cost of the eluent is a consequence of the total on-line recycling of a cheap solvent.

Figure 12 shows the cost breakdown of a typical industrial separation using carbon dioxide and modifier. The total purification cost for this example is

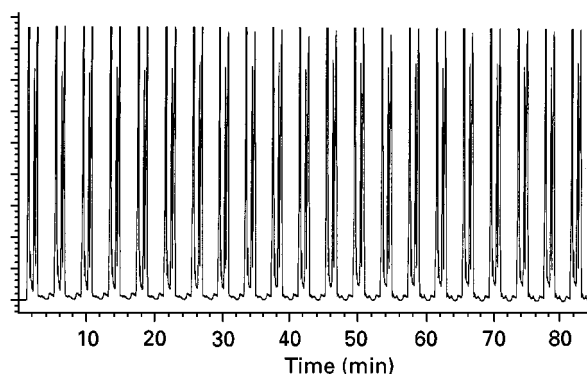


Figure 10 Phytol separation. Preparative chromatogram. Conditions as in Figure 9. One injection every 4 min.

about US\$280 per kilogram injected. The range for such a case is US\$40–400 per kilogram. By comparison with the previous example, the capital cost is slightly higher (an additional pump and bigger traps) and the recycling of the modifier represents 15–30% of the total purification cost. The other costs are similar.

The structure of these cost breakdowns can be compared with Prep-HPLC where the cost of the solvent losses and solvent recycling can represent 60% of the total purification costs. Since an increase in production scale is accompanied by a large decrease of the relative costs (per kilogram of product) except for the consumables (solvent and stationary phase), the purification costs by Prep-SFC and Prep-HPLC will have the tendencies shown in Figure 13 and the choice between Prep-SFC and Prep-HPLC depends on the scale of the purification envisaged. Large scales of production are highly favourable to Prep-SFC.

Lab-Prep-SFC

Lab-Prep-SFC is the purification of hundreds of milligrams or gram quantities. The column internal diameter is typically 10 or 20 mm and the carbon dioxide flow rate is between 10 and 60 g min⁻¹. It is

Table 4 Phytol separation—preparative step results

	Impurities	cis-Isomer	trans-Isomer	Mass of fractions (g)
Crude	7.6%	34.2%	58.2%	1.06
Fraction 2	0.2%	99.3%	0.5%	0.28
Fraction 3	0%	77.2%	22.8%	0.04
Fraction 4	0.2%	2%	97.8%	0.5
Fraction 5	60.6%	5%	34.4%	0.19

One gram of crude has been injected in 1.5 hours on a 10 mm ID column. 95% of the injected material has been collected in four fractions. The *cis*- and *trans*-isomers have been collected with high purities. Only 68 g of IPA were used for the production.

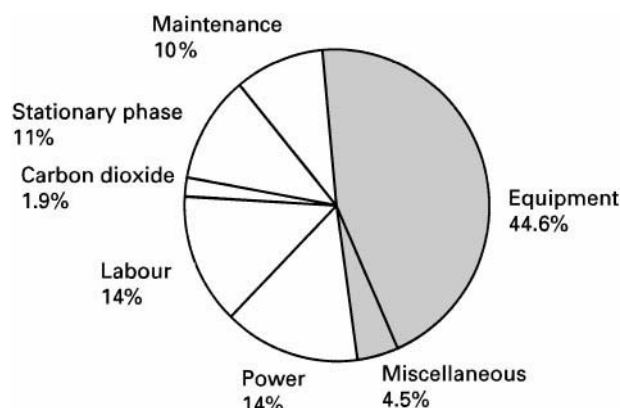


Figure 11 Typical cost of separation by Prep-SFC for a production of 3 t year⁻¹ injected on a 200 mm internal diameter column using pure carbon dioxide as an eluent.

used for two different purposes: application studies preliminary to scale up (see the earlier example) and sample purification for research purpose.

The principle of Lab-Prep-SFC is the same as large-scale Prep-SFC but its technology is slightly different. It is possible, but not necessary, to recycle the carbon dioxide and the columns do not require dynamic axial compression and are slurry prepacked. A UV absorption detector can be installed on-line, and an automated injection device is required for repeated injections, but individual injection facilities by way of a manual injection loop are also necessary for evaluation study purposes.

The interest of Prep-SFC at this scale is not in terms of cost as we have seen that the effect of the savings on solvent is only sensible for large-scale applications. Users of Lab-Prep-SFC are mainly pharmaceutical

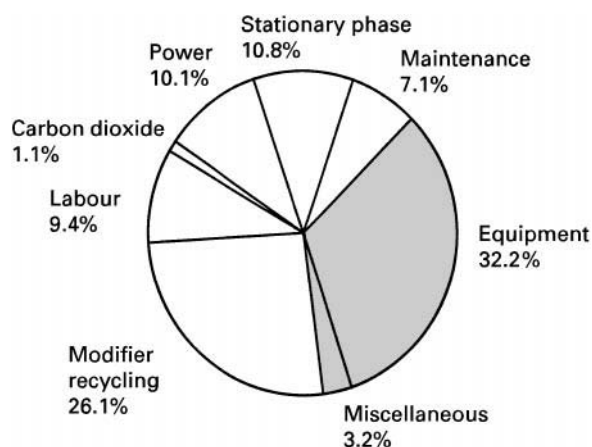


Figure 12 Typical cost of separation by Prep-SFC for a production of 1.6 t year⁻¹ injected on a 200 mm internal diameter column using carbon dioxide and modifier as an eluent.

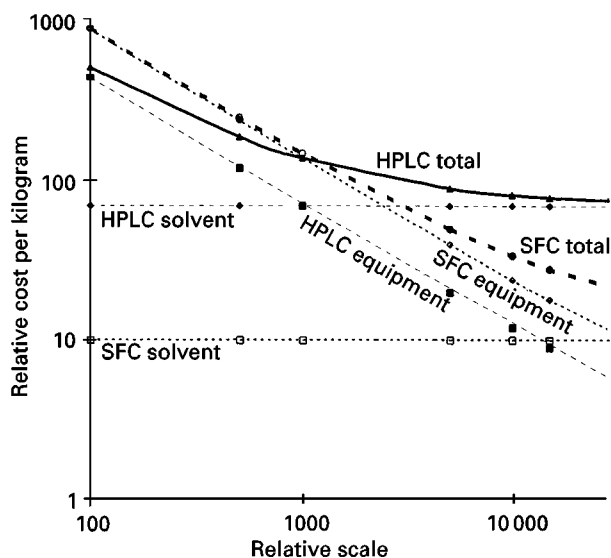


Figure 13 Dependence of the purification costs of Prep-SFC and Prep-HPLC on the scale of purification. Packing, labour and miscellaneous costs have not been included because they are similar for the two processes.

laboratory researchers who find in SFC a way to reduce the quantity of solvents stored in their laboratory and who appreciate the speed of both method development and purification. Then, the interest of Prep-SFC is not measured in dollars per kilogram, but in the number of samples processed per week.

Conclusions

Prep-SFC is a powerful separation technique that gives high purities for difficult separations. The main advantages of this technique can be summed up by comparison with Prep-HPLC: it solves (or considerably reduces) the problems associated with solvents, it is economical at a large scale and fast at a small scale. Its limitations are the relatively high level of investment required and the restricted range of applications due to the low solubility of many biological macromolecules. Given this fact, one can conclude that the principal technical and economic domains of application of Prep-SFC are in the pharmaceutical industry and the high value compounds of the food and fine chemical industries. One can predict that Prep-SFC will not replace Prep-HPLC but should take 15–25% of its market share.

Further Reading

- Berger C and Perrut M (1990) *Journal of Chromatography* 505(1): 37–43.
 Erickson B (1997) *Analytical Chemistry* 71: 683A–686A.

Jusforgues P (1995) In: Subramanian G (eds) *Process Scale Liquid Chromatography*, pp. 153–162. Weinheim: VCH.

Klesper E, Corwin AH and Turner DA (1962) *Journal of Organic Chemistry* 27: 700–701.

Yamauchi Y and Saito M (1994) In: Saito M, Yamauchi Y and Okuyama T (eds) *Fractionation Packed-Column SFC and SFE: Principles and Applications*, pp. 169–178. New York: VCH.

Theory of Supercritical Fluid Chromatography

K. D. Bartle, University of Leeds, Leeds, UK

Copyright © 2000 Academic Press

Introduction

The practising analyst requires of any separation technique that it should provide rapid and efficient resolution of mixtures. The relevant theory, therefore, is concerned with factors which influence chromatographic retention and resolution, and with variables influencing injection and detection.

The special properties of supercritical fluids make them unique chromatographic mobile phases, and the development of supercritical fluid chromatography (SFC) to make use of these properties has been discussed elsewhere. Here, the theory underlying SFC chromatographic parameters is described.

Retention in SFC

SFC is unique among chromatographic techniques in having four variables to change retention: temperature, density or pressure, and mobile-phase composition.

Effect of Column Temperature

The temperature, T , at which an analysis is carried out has an important influence on retention. At constant pressure the retention factor, k , may be either increased or decreased (Figure 1) by increasing the temperature, because of the combined influences of solubility in the stationary and mobile phases, and on vapour pressure, so that resolution may be tuned by adjusting T . A rigorous expression which accounts for the variation of SFC retention with temperature at constant pressure is:

$$\ln k - \ln \phi_m + \ln \left(\frac{\rho}{c^\theta} \right) = C + \frac{\Delta S_s^\theta}{R} - \frac{PV + \Delta H_s^\theta}{RT}$$

[1]

where ϕ_m is the fugacity coefficient of the solute in the mobile phase, ρ is the density of the supercritical fluid, c^θ is the standard concentration and C is a constant. ΔH_s^θ and ΔS_s^θ are respectively the partial molar enthalpy and entropy of solution of the solute in the stationary phase.

The left-hand side of eqn [1] is obtained as follows: experimental values of k ; values of ρ/c^θ from the

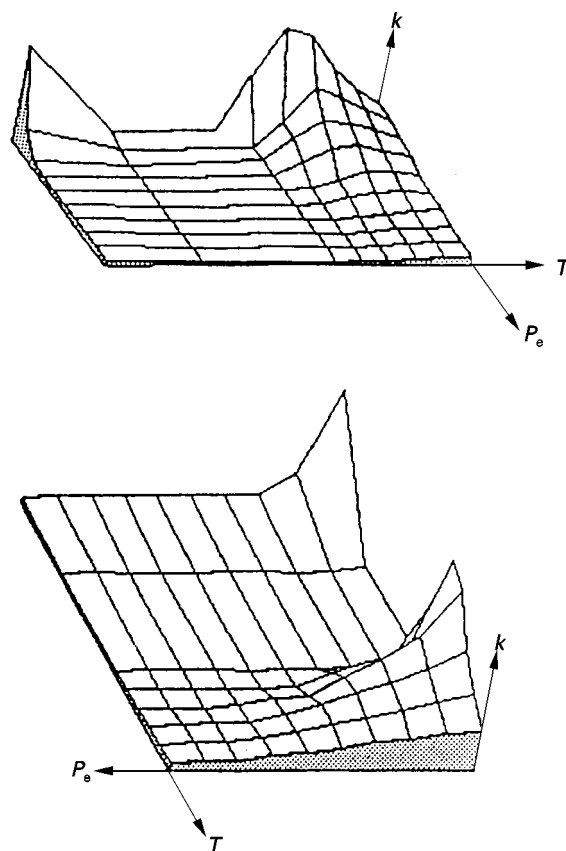


Figure 1 Capacity ratios of pyrene as a function of column end pressure (P_e) and temperature (T). Three-dimensional network shown in two perspectives. Conditions: 25 cm \times 4.6 mm i.d. packed column, 10 μ m silica particles; n -pentane. (Reprinted with permission from Lee ML and Markides KE (eds) (1990) *Analytical Supercritical Fluid and Extraction*. Provo, UT, USA: Chromatography Conferences, Inc.)

IUPAC (International Union of Pure and Applied Chemistry) equation of state for CO₂; and values for ϕ_m are calculated from the Peng–Robinson equation of state. This relationship has been tested for a number of hydrocarbon solutes. Figure 2 shows the individual contributions and total of the left-hand side of eqn [1] for fluorene. It can be seen how the addition of the steepening curves for both $(\ln \rho/c^\theta)$ and $\ln \phi_m$ to the curve of $\ln k$, with its maximum, gives a total which is approximately a straight line when plotted against $1/T$.

The dependence of retention on temperature at constant density is simpler and is predicted via the van't Hoff equation:

$$\frac{d \ln k}{d(1/T)} = -\frac{\Delta H_T^\theta}{R} \quad [2]$$

where ΔH_T^θ is the enthalpy of transfer of solute between phases. It follows that $\ln k$ is a linear function of $1/T$ and that increasing the analysis temperature at constant density always results in a decrease in k .

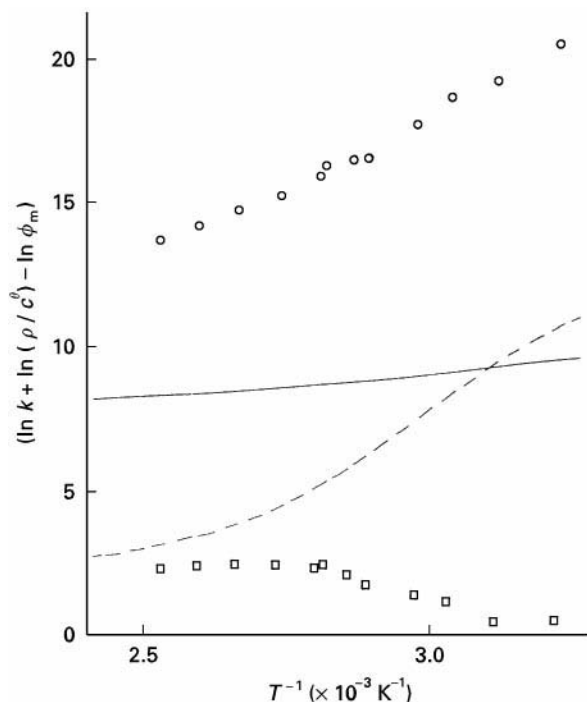


Figure 2 Contributions to $(\ln k + \ln (\rho/c^\theta) - \ln \phi_m)$ for fluorene as a function of reciprocal temperature. Squares, $\ln k$; continuous line, $\ln (\rho/c^\theta)$; dashed line, $\ln \phi_m$; circles, $(\ln k + \ln (\rho/c^\theta) - \ln \phi_m)$. (Redrawn from Bartle KD, Clifford AA, Kithinji JP and Shilstone GF (1988) *Journal of the Chemical Society, Faraday Transactions* 84: 4487, reprinted with permission.)

Effect of Mobile-Phase Density

SFC retention is related to the solubility in the mobile phase and hence to its density, which is varied by changing the pressure. SFC chromatographs usually have software to calculate the pressure necessary to achieve a given density at a given temperature from polynomials fitted to the pressure/density isotherm. Programmed elution is achieved by changing the pressure during the run – the analogue of temperature programming in gas chromatography (GC) and gradient elution in high performance liquid chromatography (HPLC).

The rate of density programming of a homologous series is determined from the relation:

$$\ln k = A_0 + B_0 n - mn\rho \quad [3]$$

where A_0 , B_0 and m are constants, ρ is the density and n is the carbon number of the member of the series. From eqn [3], it can be shown that:

$$\rho = \frac{B_0}{m} - \frac{1}{mn} \quad [4]$$

where $B_0/m = \rho_A$ is the density at which all members of the series co-elute. Thus, as ρ approaches ρ_A , resolution decreases as linear density programming elutes successive members of the series. To elute members of the series at regular time intervals:

$$n = j(t + t') \quad [5]$$

where j is a constant and t' is the reference elution time.

Hence:

$$\rho = \rho_A - \frac{K}{t + t'} \quad [6]$$

where K is another constant. It follows that, if ρ_A is known, homologues can be eluted regularly by asymptotic density programming. ρ_A may be determined from a graph of elution density versus $1/n$ in a linear density run by extrapolation to $1/n = 0$.

It is noteworthy that, as ρ increases, the diffusion coefficient of the solute decreases with concomitant increase of the plate height and loss of resolution. To offset this, the column temperature may be increased during density programming. However, since increasing temperature increases solute vapour pressure and hence solubility (see above), the above approach does not hold when density and temperature programming are combined. In fact, the combined influence of

column pressure, P , and temperature, T , on retention and resolution may be demonstrated by three-dimensional diagrams in which k or mean resolution is plotted versus P or T (Figure 1). Once the general shape of such diagrams is known for a given class of substrate, only a few chromatograms are required to determine how P and T must be changed to improve resolution.

Mobile-Phase Composition

Even high densities of CO_2 may be insufficient to permit migration of certain solutes, and the addition of polar modifiers may be necessary. Chromatographic retention may then be empirically expressed by:

$$k = ax^2 + bx + c \quad [7]$$

where a , b and c are constants and x is the mole fraction of organic modifier. The constant a is often small, so that retention decreases linearly as the mole fraction of organic modifier is increased.

A second approach models SFC retention in terms of solute solubility in the mobile phase via the Hildebrand solubility parameter: δ_s for the stationary phase, δ_m for the mobile phase and δ_i for the solute. The retention variation is represented here by:

$$\ln k = \frac{V_i}{RT}(\delta_m + \delta_s - 2\delta_i)(\delta_m - \delta_s) + \ln\left(\frac{n_s}{n_m}\right) \quad [8]$$

where V_i is the molar volume of the solute, n_s the total number of moles of the stationary phase and n_m the total number of moles of mobile phase. This approach predicts a decrease in retention with increasing modifier content if $\delta_m < \delta_i$, a retention minimum when $\delta_m = \delta_i$, and a retention increase when $\delta_m > \delta_i$. Such correlations are not always observed, and the dielectric constant has also been invoked as a predictor of retention.

Role of the Stationary Phase

The stationary phase influences retention in SFC, as in all chromatography, through interactions with the solute: dispersive, dipole-dipole, dipole-induced and hydrogen-bonding acidic and basic interactions are all possible and retention can be modelled by means of solubility parameters, respectively δ_d , δ_o , δ_{in} , δ_a and δ_b . Retention is then described by:

$$\ln k = V_i(a\delta_d + b\delta_o + c\delta_{in} + d\delta_a + e\delta_b + f) \quad [9]$$

where V_i is the solute molar volume and a - f are weighting factors for given stationary and mobile phases at a given temperature.

The coefficients a - f for each combination can be deduced by means of values of k for probe solutes for which solubility parameters and molar volumes are known. These coefficients then allow retention to be predicted for other solutes, solubility parameters of which have been calculated. In fact, the five individual solubility parameters can be calculated from refractive indices, dipole moments and energies of hydrogen bonding, with calibration using compounds for which relevant data are available. With values for the coefficients a - f and the solubility parameters for a given compound, k for a given mobile and stationary phase is then obtained from eqn [9].

Retention factors and solubility parameters for each probe molecule, stationary phase and mobile phase are combined into an expression of the form of eqn [9]. The series of simultaneous equations is then solved, using a matrix, to give values of the coefficients a - f for each stationary/mobile-phase combination. The coefficients vary greatly on moving from pure CO_2 to 1% modifier, thereafter showing a more gradual variation with increasing modifier content in the mobile phase; this observation is consistent with the formation of a thin layer of modifier on the stationary phase. The coefficients a - f are a measure of the ability of the stationary phase to take part in the five different types of molecular interaction.

Use of the coefficients a - f , solubility parameter and molar volume substituted into eqn [9] yield predicted k values in fair agreement with experimental data. Correspondingly, solubility parameters for compounds for which they are not otherwise available may be obtained. The model has also been extended to difunctional compounds.

Resolution in SFC

Separation in all chromatography and chromatographic theory is defined by the resolution, R_s , between two component peaks:

$$R_s = \frac{\Delta t}{w} \quad [10]$$

where Δt is the separation between peak maxima, and w is the mean baseline peak width. Baseline (99.9%) resolution corresponds to $R_s = 1.5$. The resolution is determined by the number of theoretical plates, N , the capacity factor, k , and the selectivity, $\alpha (= k_1/k_2)$, by:

$$R_s = \frac{N^{1/2}}{4} \left(\frac{\alpha - 1}{\alpha} \right) \left(\frac{k}{1 + k} \right) \quad [11]$$

For a compound with retention time t_R , N is given by:

$$N = 16 \left(\frac{t_R}{w} \right)^2 \quad [12]$$

The column length or height equivalent to a theoretical plate (HETP) is related to average linear mobile phase velocity, \bar{u} , by:

$$H = A + \frac{B}{\bar{u}} + C_m \bar{u} + C_s \bar{u} \quad [13]$$

The A , or multiple-path term, is zero for a capillary column, but, for a packed column:

$$A = 2\lambda d_p \quad [14]$$

where d_p is column packing particle diameter and λ is a constant related to the eddy diffusion coefficient.

The B term defines that portion of H caused by longitudinal diffusion during passage down the column and is given by:

$$B = 2D_M \quad [15]$$

where D_M is the diffusion coefficient of the solute in the mobile phase.

C_m arises from the resistance to mass transfer in the mobile phase, and is proportional to d_c^2/D_M , where d_c is the column diameter for a capillary and the

particle diameter, d_p , for a packed column. C_s , the contribution from solute diffusion in the stationary phase, is proportional to d_F^2/D_s where d_F is film thickness and D_s , the diffusion coefficient in the stationary phase, is generally negligible for a thin coating.

Differentiation of eqn [13] allows the optimum mobile-phase velocity (i.e. for minimum HETP, H_{\min}) to be written as:

$$\bar{u}_{\text{opt}} = \left(\frac{B}{C_m} \right)^{1/2} \quad [16]$$

$$H_{\min} = A + 2(BC)^{1/2} \quad [17]$$

It follows that H_{\min} depends only on k and d so that SFC and HPLC on the same column can only be carried out with the same maximum plate number. Similar considerations hold for SFC and GC (Figure 3). However, \bar{u}_{opt} depends on D_M and is much greater in SFC than in HPLC because of the greater diffusivity of solutes in supercritical fluids; it follows that SFC on a packed column is much more rapid than HPLC on the same column (see Figure 3 and below). Because D_M is less for a supercritical fluid than a gas, however, speed of analysis in capillary SFC is much reduced in comparison with GC. To offset this effect, capillary column diameters of 50 μm

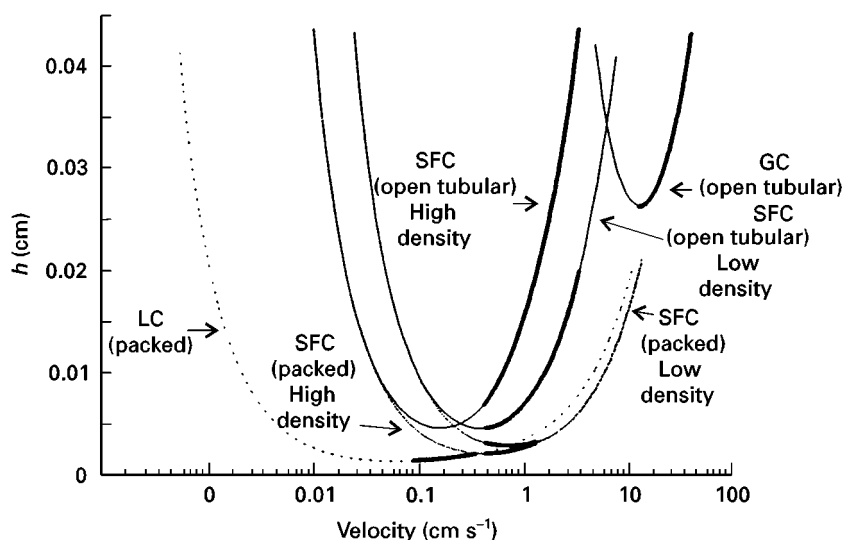


Figure 3 Efficiency as a function of mobile-phase velocity. Commonly used efficiency velocity ranges are highlighted. Packed column conditions: 5 μm particles, values calculated from the Knox equation with $A = 1$, $B = 2$, $C = 0.05$ (for LC), and $C = 0.5$ (for SFC). Open tubular column conditions: 50 μm i.d. (SFC), 300 μm i.d. (GC), values calculated from the Golay equation with $k = 5$. Values for D_m were $10^{-5} \text{ cm}^2 \text{ s}^{-1}$ for liquid, $2 \times 10^{-4} \text{ cm}^2 \text{ s}^{-1}$ for high density supercritical fluid (100°C), $5 \times 10^{-4} \text{ cm}^2 \text{ s}^{-1}$ for low density supercritical fluid (100°C), and $10^{-1} \text{ cm}^2 \text{ s}^{-1}$ for gas.

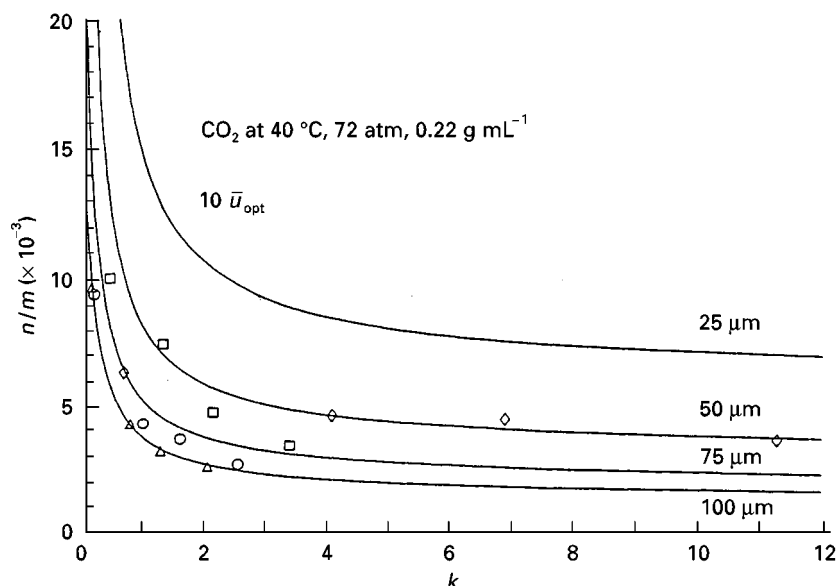


Figure 4 Efficiencies for different column diameters.

are the norm in SFC; in fact, capillary SFC is still often comparatively slow and a column diameter of 25 μm would be desirable. The dependence of C_m on d_c^2 also leads to small preferred column diameters for capillary SFC. Figure 4 illustrates the effect of column diameter on column efficiency.

Speed of Analysis

The analysis time in chromatography for a given solute is calculated from:

$$t_R = \frac{L}{\bar{u}}(1 + k) \quad [18]$$

The relative speed of analysis of packed and capillary column SFC may be compared by means of the parameter H_{\min}/u_{opt} . For values of k between 1 and 5:

$$\begin{aligned} \frac{H_{\min}}{u_{\text{opt}}} &= \frac{2d_p^2}{3D_M} \\ \frac{H_{\min}}{u_{\text{opt}}} &= 0.1 \frac{d_c^2}{D_M} \end{aligned} \quad [19]$$

For equal speeds of analysis, therefore, $d_c = 2.6d_p$. For a given separation, it follows that analysis on currently available capillary columns with i.d. 50 μm is much slower than on columns packed with 3 or 5 μm particles.

On the other hand, speed of analysis is of no value if resolution, i.e. plate number, is insufficient. For equal pressure drops across capillary (maximum plate number N_c) and packed (maximum plate number N_p) columns:

$$\frac{N_c}{N_p} = 4.6 \left(\frac{d_c}{d_p} \right)^2 \quad [20]$$

Hence, from this analysis, a 50 μm capillary generates 450 times as many plates as a column packed with 5 μm particles. However, if N is set at 5000 plates for both columns, a typical ratio of analysis times would be 2.5 in favour of the packed column.

Injector and Detector Requirements

In packed column SFC, injection is normally carried out by switching the contents of a sample loop into the mobile phase. Flow and column diameter here do not generally affect separation efficiency. For capillary SFC, much smaller injected volumes are required, and these are introduced by splitting the injected sample, or more usually by time-split injection, in which the injection valve is opened and closed very rapidly by pneumatic operation. A retention gap, located before the column, may permit focusing of larger amounts of sample. Injection volumes are determined from a general equation which relates τ_i and τ_c , the standard deviations in the peak widths due to the injector (or detector) and the column. N and N_i are respectively the number of theoretical plates provided by the column and the number of those

filled by injector or detector or detector volume:

$$\frac{\tau_i}{\tau_c} = \frac{N_i \left(\frac{n}{k} \right)^{1/2}}{N \left(\frac{n}{k} \right)^{1/2}} \quad [21]$$

From eqn [21], an expression has been derived linking fractional loss of resolution, ΔR_s , due to the injector or detector volume to column and retention characteristics:

$$v_i = 0.866\pi d_c^2 (LH)^{1/2} \left[\frac{1}{(1 - \Delta R_s)^2} - 1 \right]^{1/2} (1 + k) \quad [22]$$

where v_i is the injection volume and L is column length. Since H is a function of d_c , v_i is proportional to $d_c^{5/2}$ and for a $10 \text{ m} \times 50 \text{ }\mu\text{m}$ column operated under practical conditions, a 1% loss of resolution requires an injection volume of only 50 nL.

For equal distribution coefficients, K_D , an equation relating the maximum loadabilities, L_p and L_c , for packed and open tubular columns has been derived:

$$\frac{L_p}{L_c} = 1.24 \left(\frac{d_{pc}}{d_c} \right)^2 \left[\frac{1 + \frac{K_D \varepsilon_i (1 - \varepsilon_e)}{\varepsilon_T}}{1 + \frac{4K_D d_F}{d_c}} \right] \left(\frac{L_p}{L_c} \right)^{1/2} \left(\frac{d_p}{d_c} \right)^{1/2} \quad [23]$$

where d_{pc} is the diameter of the packed column; ε_i , ε_e and ε_T are intraparticle, interstitial and total porosities, respectively; and L_p and L_c are the lengths of the packed and open tubular columns, respectively.

Table 1 lists the maximum sample loadability ratios for different K_D values for typical packed and open tubular columns; as might be expected, sample loadabilities are much greater on packed columns.

Table 1 Sample loadability ratios for different distribution coefficients

K_D	$\frac{L_p}{L_c}$
1	31
10	101
100	373

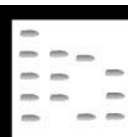
Packed column: $L_t = 20 \text{ cm}$; $d_o = 5 \text{ }\mu\text{m}$; $d_{oc} = 1 \text{ mm}$; $\varepsilon_i = 0.5$; $\varepsilon_e = 0.4$; $\varepsilon_T = 0.7$. Open tubular column: $L_c = 10 \text{ m}$; $d_c = 50 \text{ }\mu\text{m}$; $d_F = 0.2 \text{ }\mu\text{m}$.

Increasing the column diameter is the simplest approach to increasing the sample capacity of packed columns, since the surface area of stationary-phase support particles is generally maximized. However, for capillary columns, sample capacity can be increased by increasing the stationary phase film thickness, d_F . This should also lead, in theory, to a reduction in column efficiency but in practice such a reduction is only small, with film thickness up to $1 \text{ }\mu\text{m}$.

Further Reading

- Anton K and Berger C (eds) (1998) *Supercritical Fluid Chromatography with Packed Columns*. New York: Marcel Dekker.
- Berger TA (1995) *Packed Column SFC*. Cambridge: Royal Society of Chemistry.
- Heaton DM, Bartle KD, Clifford AA, Klee MS and Berger TA (1994) Retention prediction based on molecular interactions in packed-column supercritical fluid chromatography. *Analytical Chemistry* 66: 4253.
- Lee ML and Markides KE (1990) *Analytical Supercritical Fluid Chromatography*. Provo, Utah: Chromatography Conferences.
- Smith RM (ed.) (1988) *Supercritical Fluid Chromatography*. London: Royal Society of Chemistry.

CHROMATOGRAPHY: THIN-LAYER (PLANAR)



Densitometry and Image Analysis

P. E. Wall, Merck Limited, Poole, Dorset, UK

Copyright © 2000 Academic Press

Introduction

Densitometry is a means of measuring the concentration of chromatographic zones on the developed thin-layer chromatography high performance thin-layer chromatography (TLC in HPTLC) layer. The instrument does this without disturbing the substance in the chromatogram. The method and computer-controlled instrumentation produces results that are not only

reproducible, but also highly accurate ($\sim 1\%$ standard deviation). Scanning is a fast process (up to a scan speed of 100 mm s^{-1}) with a spatial resolution in steps from 25 to $200 \mu\text{m}$. Full UV/visible spectra (190–800 nm wavelength) of separated analytes can be recorded at high speed and peaks can be checked for purity by obtaining and comparing spectra from the start, middle and end of the peaks. With the use of highly sensitive charged coupled device (CCD) cameras, the photographic image of the developed TLC/HPTLC plate can be stored as a video image. This can be video-scanned to determine the concentration of separated components or can be printed when required as part of a document for a permanent record of the results. Many images can be stored on the computer hard drive and archived whenever required.

The Development of Modern Scanning Densitometry

The results of a developed TLC/HPTLC plate or sheet can be quantified in a number of ways. Visually, an estimate of concentration can be made. Many related substance tests in the pharmacopoeias rely on the concentration of the sample impurities being less than the standard concentration as seen visually. These are limit tests which depend on the eye of the observer determining that the concentration of the unknown is less than that of the standard. It has been estimated that the human eye can detect down to about $1 \mu\text{g}$ of a coloured spot on a TLC plate with a reproducibility of about 10–30%.

Better quantification can be obtained by eluting the relevant chromatographic zone from the adsorbent followed by spectrophotometry. The position of the zone can be marked out with a sharp bradawl and a microspatula used to scrape away the zone. These scrapings are then transferred to a container where a suitable solvent can be used to dissolve the compounds of interest from the particles of the adsorbent. The mixture is filtered and the concentration of the analyte in solution determined by transmittance/absorption spectrophotometry. There is little to recommend in this procedure as it is both tedious and time-consuming. It also requires meticulous care as errors can easily creep into the procedure. It is difficult to ensure that all the sample is completely removed from the TLC layer and is transferred from the chromatographic zone for further work-up if it is not easily seen in the visible or UV parts of the spectrum.

The technique of scanning densitometry determines the concentration *in situ*. It scans at set spectral wavelengths and does not rely on removal of any of the chromatographic zones from the TLC/HPTLC plate. Hence the previous problems and errors are

eliminated. Scanning densitometry dates back to the 1950s when it was used to scan thin strips of paper chromatograms containing separated amino acids. Since then these primitive instruments have undergone considerable change, to the extent that they are now advanced analytical tools of similar capabilities to modern HPLC instrumentation.

Today's scanning densitometer measures reflectance, quenched fluorescence or fluorescence induced by electromagnetic radiation. For this reason, the instrument is now described as a spectrodensitometer. Although all three detection modes are commonly used, fluorescence is limited by the fact that fewer substances can be induced to fluoresce. Many spectrodensitometers also have an attachment for scanning electrophoresis gels by transmission.

The principle of operation is based on light of a predetermined beam size and wavelength striking the thin-layer surface perpendicularly whilst the TLC plate moves at a set speed under the stationary beam, or alternatively the beam traverses the stationary plate. Some of the electromagnetic radiation passes into and through the layer (transmitted light) whilst the remainder, due to the opaqueness of the layer, is reflected back from the surface. When the light beam passes over an absorbing chromatographic zone, there is a difference in optical response and less of the light is reflected (or transmitted). A photoelectric cell is used to measure the reflected light. When this receives a reduced amount of reflected light due to the presence of an absorbing chromatographic zone, a means is provided of detecting and quantifying the analyte.

Fluorescence quenching mode is really a variation on absorption methods. An inorganic phosphorescent indicator or organic fluorescent indicator is incorporated into the adsorbent layer. The inorganic phosphors give either a bright green or pale blue phosphorescence depending on the compound used. The phosphorescence is very short-lived. Hence it is best observed by continual exposure to UV light at 254 nm. Most HPTLC plates contain the indicator which exhibits the pale blue phosphorescence. This indicator is acid-resistant and allows higher sensitivity of detection of separated analytes due to less intense and less 'noisy' backgrounds. TLC plates containing organic fluorescers which give a bright blue fluorescence when excited by UV light of 366 nm are not as popular. Following chromatographic development, the plates incorporating the fluorophore are scanned at 254 or 366 nm in the absorbance mode. As the sample components absorb the excited radiation, the intensity of the phosphorescence or fluorescence is diminished. Consequently a variation occurs in the reflected light detected by the photomultiplier (or photoelectric cell).

When separated analytes naturally fluoresce under UV light, the spectrodensitometer can be used to scan in the fluorescence mode. The UV light provides the energy in these instances to excite electrons in molecules of the analytes from a ground state to an excited singlet state. As the excited electrons return to the ground state, energy is emitted as radiation at a longer wavelength, usually in the visible range. For best results in using this technique, it is important to use TLC/HPTLC plates which do not contain a phosphorescent or fluorescent indicator to minimize background interference.

Theory of Spectrodensitometry

In spectrophotometric measurements where the absorbance is measured as a result of a beam of light of set wavelength passing through a fixed pathlength of solution, a direct relationship exists between the observed absorbance and the concentration of the solution. This is known as Beer's law. However, it should be pointed out that this relationship is not linear over the whole range of concentration, and it depends on the sample solution being transparent.

As TLC/HPTLC plates are opaque, a somewhat different approach is required. In the 1930s Kubelka and Munk investigated the relationship between absorbance, transmission and reflectance, deriving mathematical expressions to explain the effects of absorbance and reflectance. When a ray of incident light comes into contact with the surface of the opaque TLC layer, some light is transmitted, some is reflected in all directions at the surface and some rays are propagated in all directions inside the adsorbent. The theory which explains to a large degree what is happening in this process is known as the Kubelka-Munk theory. Certain assumptions can be made which simplify the mathematical equations derived. The theory assumes that both the transmitted and reflected components of incident light are made up only of rays propagated inside the sorbent in a direction perpendicular to the plane of the surface. All other directions will lead to longer pathways and hence stronger absorption. These rays therefore contribute little to either the transmitted or reflected light and their contribution can be treated as negligible. When light exits from the sorbent at the layer-air boundary, light scattering occurs, and it is distributed over all possible angles with the surface.

The coefficient of light scatter (S), can therefore be proposed; this depends on the layer thickness. If we assume that this is unchanged in the presence of a chromatographic zone, the following equation can be derived for an infinitely thick opaque layer:

$$\frac{(1 - R_{\infty})^2}{2R_{\infty}} = \frac{2.303}{S} \cdot a_m \cdot C \quad [1]$$

where R_{∞} is the reflectance for an infinitely thick opaque layer, a_m is the molar absorptivity of the sample, c is the molar concentration of the sample and S is the coefficient of scatter per unit thickness.

This equation is clearly less than ideal as the layer has a finite thickness. More meaningful expressions for the intensity of the reflected light, I_R , and the transmitted light, I_T , for a layer of thickness (l) are given by the following hyperbolic solutions:

$$I_R = \frac{\sinh(b \cdot S \cdot l)}{a \cdot \sinh(b \cdot S \cdot l) + b \cdot \cosh(b \cdot S \cdot l)} \quad [2]$$

$$I_T = \frac{b}{a \cdot \sinh(b \cdot S \cdot l) + b \cdot \cosh(b \cdot S \cdot l)} \quad [3]$$

where

$$a = \frac{S \cdot l + K_A \cdot l}{S \cdot l}$$

and

$$b = (a^2 - 1)^{1/2}$$

K_A is the coefficient of absorption per unit thickness.

The application of the equations to quantitative analysis in TLC is quite complex, but it can be greatly simplified by making a number of reasonable assumptions that would hold true for TLC. One thing that eqn [2] immediately reveals is that the relationship between the reflected light and the concentration of the chromatographic zone is nonlinear. This is what is found in practice over the full range of concentrations. The data when graphically displayed fit a polynomial curve (eqn [4]).

$$y = a_0 + a_1 \cdot x + a_2 \cdot x^2 \quad [4]$$

However, over a narrow concentration range the relationship is seen to be linear. This means that if it is necessary to have a calibration curve over the whole range of concentrations, at least four but no more than six standards will be required for the determination of one separated analyte. Of course, only two standards may be needed if the concentrations are close to that of the analyte, because it can be assumed that the curve is linear over a small range.

Although it may seem that errors could easily creep into the determination procedure, this is not the case. The assumptions made have only a negligible effect on the final result. Hence, even including any errors which may originate from the scanning spectrodensitometer, the percentage relative standard

deviation is normally below 2% and quite often well below 1%.

For a wide concentration range, the Michaelis-Menten regression curve can be used. The calibration is calculated as a saturation curve:

$$y = \left(\frac{a_1 \cdot x}{a_2 + x} \right) \quad [5]$$

and is theoretically only permitted within the calibration range (between the largest and the smallest standard amounts applied). This regression always passes through the origin.

In some cases there is a better curve fit to the data if the Michaelis-Menten regression does not pass through the origin. Better resolution is therefore obtained if the data produce a function that does not tend towards zero:

$$y = a_0 + \left(\frac{a_1 \cdot x}{a_2 + x} \right) \quad [6]$$

As before, this is theoretically admissible only within the calibration range.

It is also possible to linearize the data graphically. The simplest transformation procedures involve converting the data on reflectance and concentration into reciprocals, logarithms or squared terms. The following equations can thus be proposed:

$$\log R_e = a_0 + a_1 \cdot \log c \quad [7]$$

$$\frac{1}{R_e} = a_0 + a_1 \left(\frac{1}{c} \right) \quad [8]$$

$$R_e^2 = a_0 + a_1 \cdot c \quad [9]$$

where R_e is the reflectance signal and c is the sample concentration.

Eqns [7] and [9] result in linearization over the middle of the concentration range, whereas eqn [8] showed better linearization, but even this fails at very low concentration. None of these methods is able to linearize the data over the whole concentration range.

A solution to the above is to use nonlinear regression analysis based on second-order polynomials. These can be described by the following equations:

$$\ln R_e = a_0 + a_1 \cdot \ln c + a_2 \cdot (\ln c)^2 \quad [10]$$

$$R_e = a_0 + a_1 \cdot c + a_2 \cdot c^2 \quad [11]$$

Over the whole concentration range, eqn [10] gives the best results. In fact, it has been shown that the

data fit is not compromised when as few as three standards are used over the whole concentration range.

The mathematical treatment of the data for fluorescence intensity can be expressed according to the well-known Beer-Lambert law. The fluorescence emission (F) is given by the equation:

$$F = \theta \cdot I_0 (1 - e^{-a_m \cdot l \cdot c}) \quad [12]$$

where F is the fluorescence emission and θ is the quantum yield.

For low sample concentrations the following assumption can be made:

$$e^{-a_m \cdot l \cdot c} = 1 - a_m \cdot l \cdot c \quad [13]$$

Therefore:

$$F = \theta \cdot I_0 \cdot a_m \cdot l \cdot c \quad [14]$$

It follows that, for low concentrations, the fluorescence emission is linearly dependent on the sample concentration. In practice this proves to be the case even though this equation was derived without taking into consideration the influence of absorption or scatter.

Pre-Scanning Considerations

For quantification by reflectance scanning, there is no limitation on the backing used for the chromatographic layer, whether it be glass, aluminium or plastic. However, it must be said that quality of the scanned results, reproducibility and quantitative accuracy mainly depend on the quality of the spot or band application of the sample and the choice of developing solvents. The use of automated spot and band application equipment results in a noticeable improvement in relative standard deviation. In practical terms, band application gives even greater accuracy than spot application. This is to be expected since a scanning slit length on the spectrodensitometer has to be chosen for a spot such that it covers the whole length, as the concentration of the analyte will vary across the spot, with the highest concentration being in the centre. The slit length also has to allow for any variation caused by migration of spots not occurring in a precisely vertical direction (usually due to solvent vapour not being saturated in the developing chamber). For band development, the concentration of the analyte is the same across the length of the band. Hence, there is more latitude on the choice of slit length. Small slit lengths can be chosen which tend to higher sensitivity. Under these conditions with many separations, coefficient of variation (CV) below 1% can be achieved.

Instrumentation

A number of different types of scanning spectrodensitometers are available. Most are now either partially or fully computer-controlled. The parameters such as track length, number of tracks, distance between tracks, slit length and width, scanning wavelength and speed can all be programmed into the computer. Some spectrodensitometers can perform a pre-scanning run to determine the position of maximum absorption for the separated components on the track: this is particularly useful where spot application has been used. After scanning, the spectrodensitometer generates massive amounts of data from all the tracks, including peak height and area and position of zones (start, middle and end), for every component. Usually a chromatogram can be displayed for all tracks. This can be baseline-adjusted and excess noise from the background of the layer can be subtracted. All peaks can be integrated, ready for possible quantification. Although a number of scanning modes are available, such as linear, radial (scanning from the centre for circular chromatograms) and circular scanning around a ring (circular development), by far the most popular is the linear mode, as shown in **Figure 1**.

Normally, three light sources are used in scanning densitometry: a deuterium lamp (190–400 nm), a tungsten halogen lamp (350–800 nm), and a high pressure mercury vapour or xenon lamp for intense line spectra (254–578 nm), usually required for fluorescence determinations.

Three optical methods (**Figure 2**) have been used in the construction of scanning densitometers:

1. single wavelength, single beam
2. single wavelength, double beam
3. dual wavelength, single beam

Construction 1 requires little explanation and is the type manufactured by most commercial TLC companies. Construction 2 divides the single beam into two by means of a beam splitter, so that one half scans over the chromatographic zone whilst the other scans over the background. Both beams are detected by matched photomultipliers and the difference in the signal measured. In construction 3, two wavelengths as close together as possible are chosen, such that fluctuations caused by light scattering at the light-absorbing wavelength are compensated for by subtracting the fluctuations at the different wavelength at which there is no absorption by the chromatographic zone.

In fixed-beam spectrodensitometers, the stage holding the TLC plate under the light beam moves at a constant rate, propelled by stepping motors. Where the light beam moves, it does so in a zigzag fashion over the surface of the stationary plate. Usually the zigzag scanners incorporate a curve linearization technique for absorption measurements. This uses the hyperbolic solution in eqn [2].

Applications

As the chromatogram is permanently or semipermanently held in the layer after development is complete, a number of useful techniques can be used with a scanning spectrodensitometer both to improve the evaluation of the chromatogram and to collect more important data on the separated analytes.

1. The TLC plate can be scanned at a range of different wavelengths. The optimum wavelength can therefore be chosen for maximum absorption of individual sample components. Of course, if two analytes are not completely resolved, but absorb at different wavelengths, then it is possible to quantify the results without further resolution.
2. UV/visible absorption spectra can be obtained for each separated component. Some commercial software then allows the comparison of such spectra with a library of spectra in order to identify unknowns.
3. Spectra can also be obtained for different parts of the chromatographic zone. Hence, spectra can be obtained for the upslope, apex and downslope of the peak to assist the analyst in looking for any peak impurities. Any changes in the spectrum as the light beam traverses the zone would indicate nonhomogeneity.

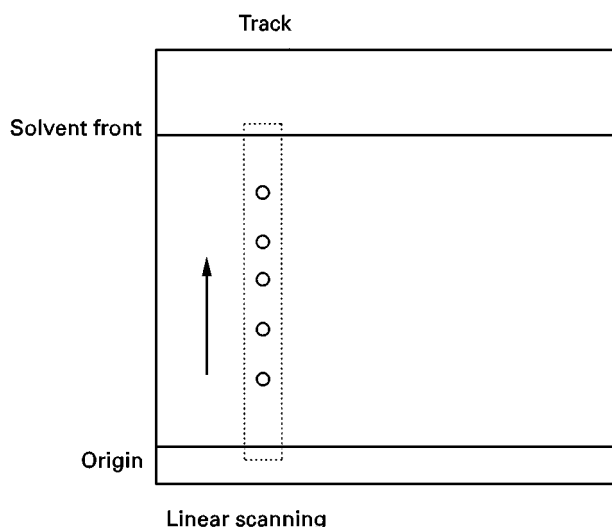


Figure 1 Linear scan of individual tracks using a scanning densitometer. Slit length and width, track length and speed of scan are all pre-selected.

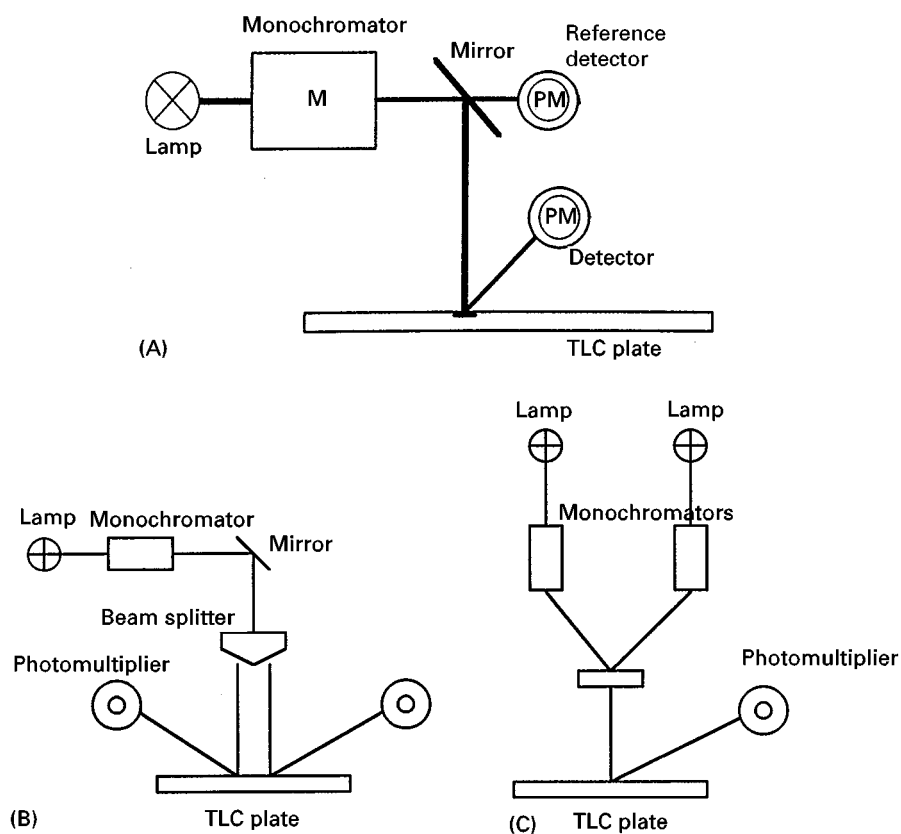


Figure 2 Scanning modes: (A) single beam; (B) single wavelength, double beam in space; (C) dual wavelength, single beam in time. PM, photomultiplier.

- Background subtraction is another useful feature of most spectrodensitometers. Some background noise will always be present, hence the scanner software can subtract a background scan of the TLC plate before quantification.
- Some instruments can scan and image an entire plate, enabling two-dimensional chromatograms to be evaluated (scan time less than 5 min).
- Forensic: drugs of abuse, poisons, alkaloids, inks
- Clinical: therapeutic drug monitoring, identification of metabolic drug disorders
- Environmental: pesticide residues in crops, crop protection agents in drinking water, industrial hygiene
- Industrial: product uniformity, impurity profile, surfactants, synthetic dyes

The widespread use of planar chromatography means that the applications of spectrodensitometry are almost limitless. Hence, there are extensive publications on the use of scanning densitometry in all types of industry and research. Many of the instrument and plate manufacturers also provide application methods and extensive bibliographies. For example, in all of the following areas scanning densitometry has been used for quantification.

- Biomedical: organic acids, lipids, steroids, carbohydrates, amino acids
- Pharmaceutical: stability and impurities of synthetic drugs, antibiotics, drug monitoring, alkaloids
- Food science: mycotoxins (including aflatoxins), drug residues, antioxidants, preservatives, natural pigments, food colours, spices, flavonoids

To give a flavour of the capability of the technique, the following examples can be considered. **Figure 3** shows the scan obtained from the separation of a number of sulfonamides and antibiotics from a complex animal feed matrix on an HPTLC silica gel plate. Scanning at five different wavelengths allows each of the components to be quantified by measurement at its absorption maximum. The three-dimensional presentation also allows the minor impurities to be more clearly identified. Multi-wavelength scanning is also illustrated in **Figure 4** with an automated multiple development (AMD) separation of pesticides in tap water on HPTLC silica gel plates. **Figure 5** illustrates the fluorescence scan of a range of saturated fatty acids from C₆ to C₂₄, an important food application in fats and vegetable oils. The fatty

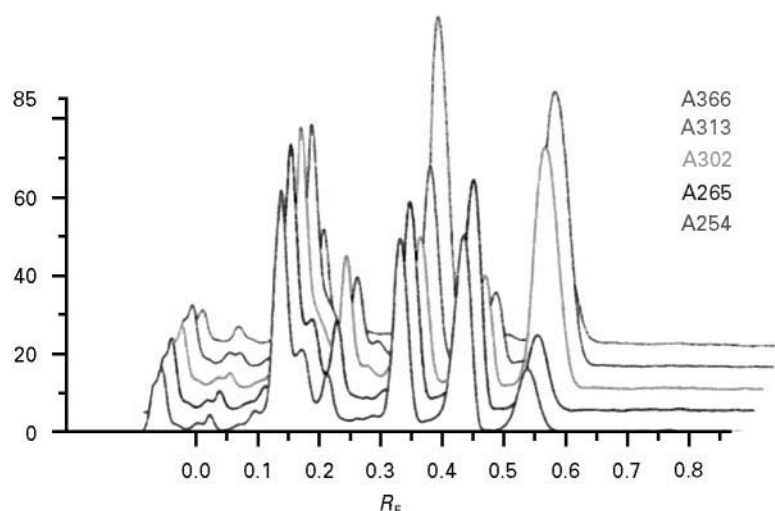


Figure 3 (See Colour Plate 26). Separation of sulfonamides in a complex animal feed matrix on an HPTLC silica gel plate. The plate has been scanned at five different wavelengths and the chromatogram overlaid in a three-dimensional presentation. Reprinted from Camag literature, CAMAG, Muttenz, Switzerland.

acids were derivatized before separation by a unique on-layer technique. The acids are resolved as their dansylcadaverine derivatives on an HPTLC RP18 layer.

The use of spectral identification of an unknown is demonstrated in **Figure 6**. The unknown was eventually identified as morphine, but because ethylmorphine and codeine have such similar spectra (as shown in the overlay), it was necessary to search the spectrum library for the best-fit recorded spectra, and also to check the correlation with the R_F value. This enabled a correlation with morphine of 98.4% to be

obtained for the unknown. This example illustrates the need for the analyst not only to search for the best fit, but also to check the correlation with the R_F value. Had the search been limited to the spectrum library, ethylmorphine could well have been chosen as the unknown.

Video Densitometry

Video densitometry has been developed in the last few years and is now being deployed throughout industry and research. Such instruments use an imag-

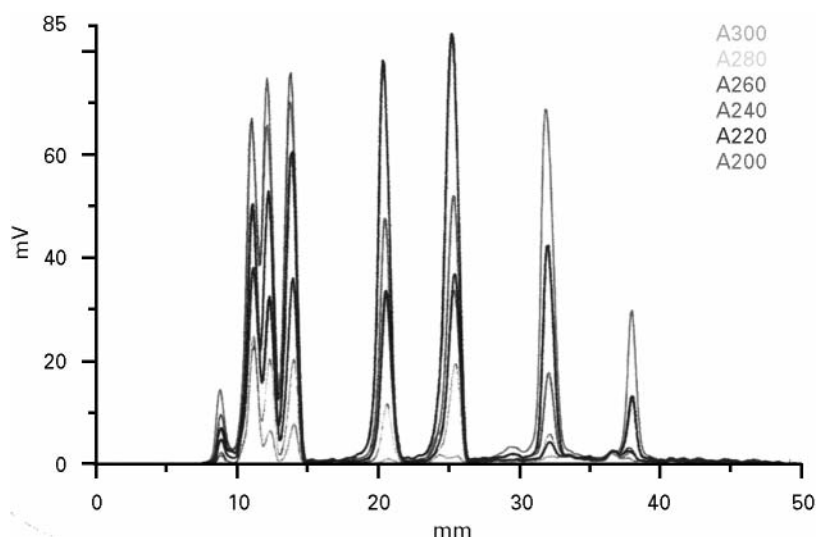


Figure 4 (See Colour Plate 27). Separation of pesticides in tap water on an HPTLC silica gel plate by AMD. Multi-wavelength (six wavelengths) evaluation permits resolution by optical means of fractions insufficiently separated. Reprinted from Camag literature, CAMAG, Muttenz, Switzerland.

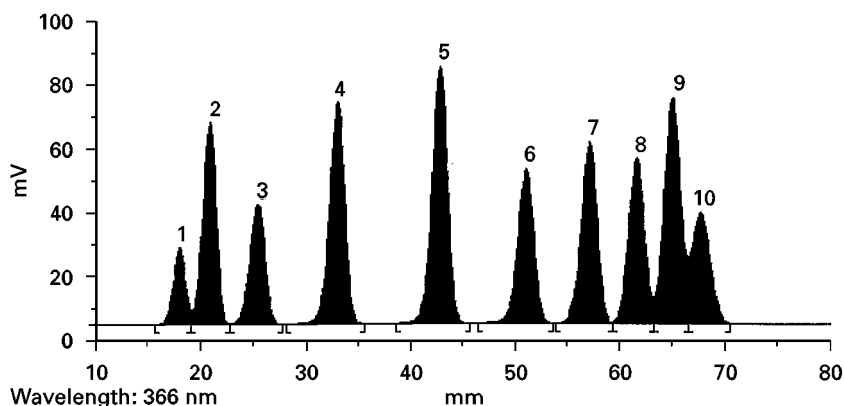
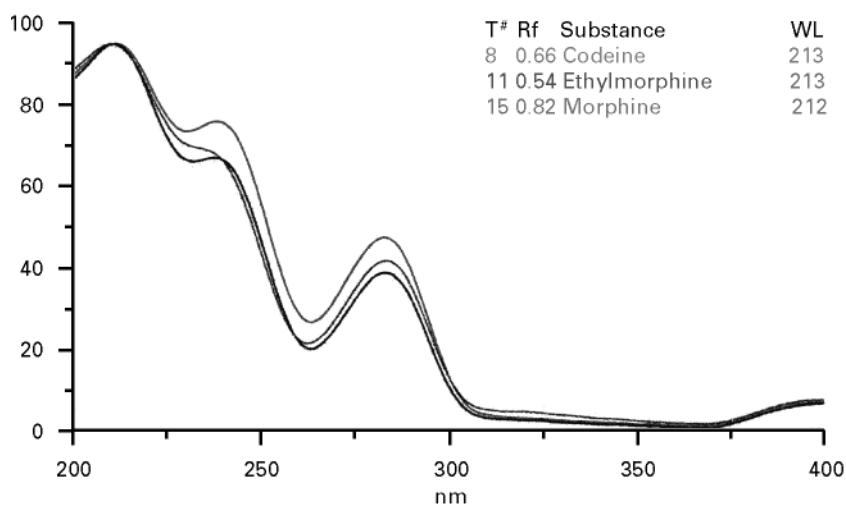


Figure 5 Fluorescence scan of dansylcadaverine derivatized fatty acids separated on an HPTLC silica RP18 plate.

ing system consisting of a high resolution CCD camera with a zoom attachment to focus and enlarge the chromatogram, if required and a suitable illumination system. The camera is linked to a computer (usually a PC) and a video printer. The software controls the camera, as well as all parameters such as brightness, contrast, colour balance and intensity. These can be saved for future use or kept as a record of the results. The chromatogram can be presented as an image on the video printer and can be quantified to

obtain the concentration of analytes using the mathematical procedures used in scanning densitometry. As in spectrodensitometric scanning, the software does all the necessary calculations to determine the concentration of analytes. For weakly fluorescing analytes, a small camera aperture (F:22) can be used with long time integration. This enables the imaging of fluorescing compounds which are often invisible to the human eye. The images can be annotated and that annotation stored separately for



Correlation of spectra without R_F value		Correlation of spectra with R_F value	
Substance	Correlation	Substance	Correlation
Ethylmorphine	0.9924	Morphine	0.9839
Codeine	0.9905	Atenolol	0.9223
Nalorphine	0.9848	Salbutamol	0.9174
Morphine	0.9839	Sotalol	0.8939

Figure 6 (See Colour Plate 28). UV spectra of codeine, ethylmorphine and unknown (morphine) overlaid. Spectra of codeine and ethylmorphine taken from spectral library. Spectrum of morphine taken from chromatogram. Reprinted from Camag literature, CAMAG, Muttens, Switzerland.



Figure 7 Video scan of separation of corticosteroids on an HPTLC silica gel plate. Detection reagent: blue tetrazolium solution. Spot application with automatic equipment.

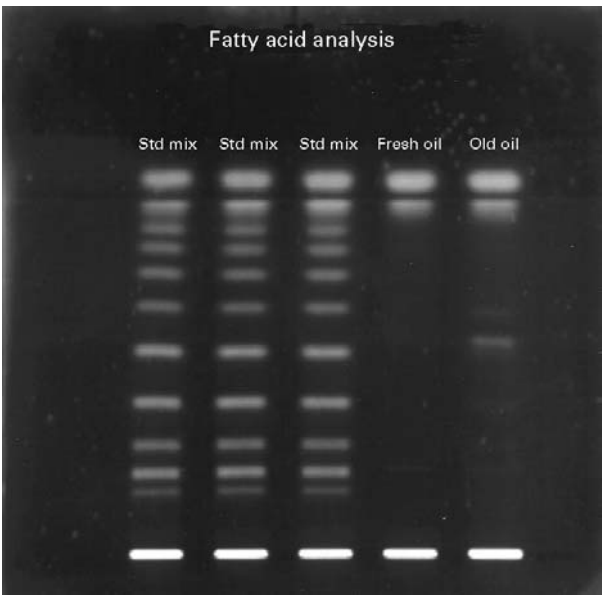
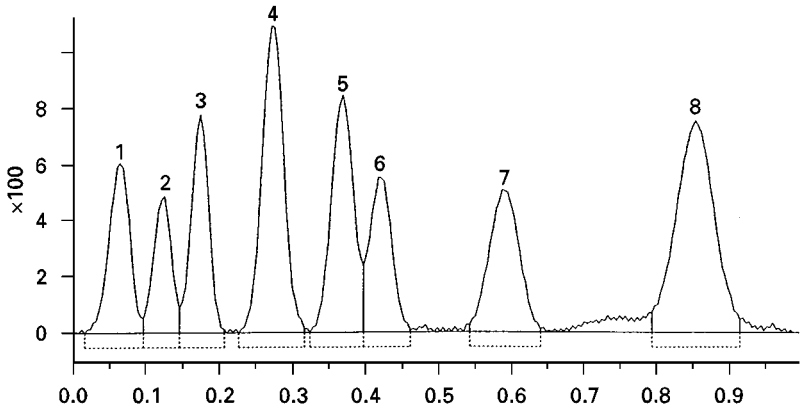


Figure 9 Video scan of separation of pre-derivatized saturated fatty acids on an HPTLC RP18 plate. The plate was scanned at 366 nm to produce fluorescent zones. Band application with automated equipment.



Track 3 Sample a

Peak no	Start		Maximum			End		Area		Subst name
	R _F	H	R _F	H	[%]	R _F	H	A	[%]	
1	0.016	0.0	0.065	606.4	10.76	0.097	50.9	5076.4	9.53	8
2	0.097	50.9	0.126	488.3	8.67	0.146	87.9	3432.6	6.44	7
3	0.146	87.9	0.174	780.2	13.85	0.206	12.1	5353.3	10.05	6
4	0.227	0.0	0.271	1094.6	19.42	0.316	13.8	9440.8	17.72	5
5	0.324	0.0	0.368	844.7	14.99	0.397	240.7	7487.0	14.05	4
6	0.397	240.7	0.417	555.2	9.85	0.462	6.1	4914.6	9.22	3
7	0.543	26.1	0.587	509.7	9.05	0.640	10.6	6065.0	11.38	2
8	0.794	70.3	0.854	755.8	13.41	0.915	46.6	11519.2	21.62	1

Total height, 5634.96; total area, 53288.8.

Figure 8 Video scan of separation of corticosteroids on an HPTLC silica gel plate.

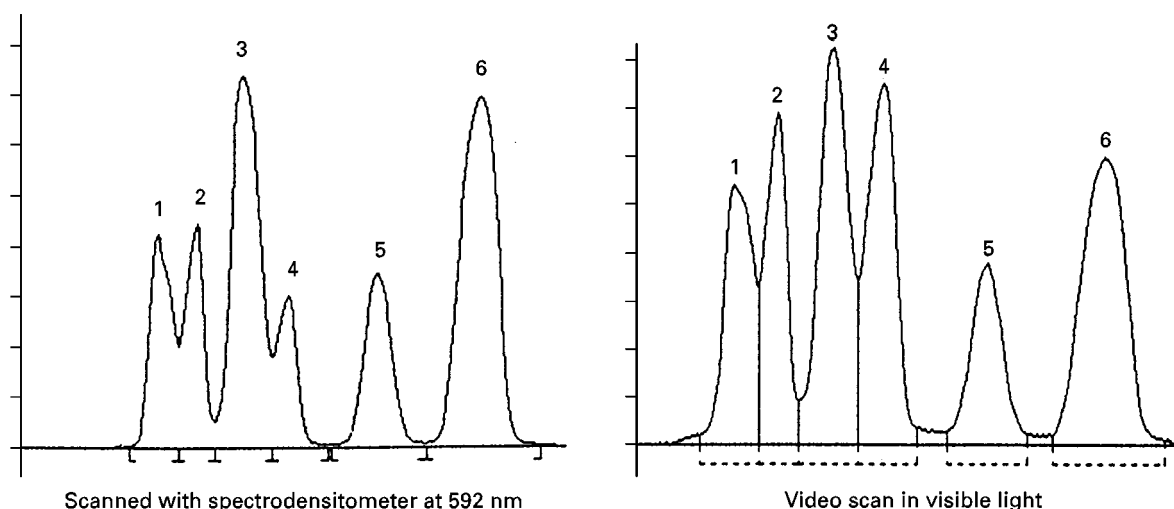


Figure 10 Separation of dye mixture developed on an HPTLC silica gel plate with toluene as mobile phase. Comparison of spectrodensitometric scan with video scanning.

readiness in annotating further images. Such images can be stored in a variety of files which can then be used in a number of well-known office programs, such as Word, and PowerPoint.

The illumination system needs a number of features in order to get the best results from the CCD camera unit. Illumination from above is necessary, both visible light and UV light at 254 and 366 nm (depending on the chromatogram). However, it is essential that the light fittings do not interfere with the camera's field of view. Lighting from below the plate can in some cases also prove advantageous in giving a bright image.

Figure 7 illustrates a video print of a separation of corticosteroids developed on an HPTLC silica gel plate. The steroids were detected with blue tetrazolium reagent. Figure 8 shows the scan taken using the software option available. R_F data is recorded in the table below. Figure 9 illustrates a further video print, this time of fluorescent chromatographic zones, photographed under UV light (366 nm). This is a

separation of derivatized saturated fatty acids from C_6 to C_{24} (conditions as in Figure 5).

Although it is possible to quantify results from the video scan, they are not as accurate as those obtained from a spectrodensitometer. Figure 10 and Table 1 show a comparison of the CV for a six-component dye test mixture separated on an HPTLC layer. Whereas the CVs for spectrodensitometric scan are below 2%, those for the video imaging system are typically from 2 to 4%. As most USP (United States Pharmacopoeia) and EP (European Pharmacopoeia) monographs accept CVs of $\pm 6\%$ in most, if not all, cases, the use of video densitometry is acceptable. However, it should be remembered that for fluorescence quenching and absorption measurements below 254 nm, video densitometry will not show any detection. This is one of the present limitations of the technique. Some substances do require shorter wavelength UV light for their detection. In these instances spectrodensitometry is presently the only solution.

Table 1 Comparison of coefficient of variance (CV) with video scanning and spectrodensitometric scanning. Separation of dyes on an HPTLC silica gel plate using toluene as mobile phase

Dye	R_F	Video scan with white light		Spectrodensitometric scan at 592 nm	
		Mean value (%)	CV (%)	Mean value (%)	CV (%)
Black	0.04				
Grey	0.10	99.4	3.50	101.5	0.83
Red	0.17	102.8	3.10	97.8	0.31
Blue	0.23	103.0	3.52	101.2	1.90
Pink	0.36	99.7	3.46	98.3	0.96
Yellow	0.51	98.6	1.30	98.8	0.56

Future Trends

It seems unlikely that video densitometry will ever replace spectrodensitometry as both techniques have unique advantages. On the one hand spectrodensitometry allows the scanning of TLC/HPTLC plates at selectable wavelengths, the acquisition of UV/visible spectra, the determination of peak purity and high accuracy of results. On the other hand, video scanning provides a computer or printed image that can serve as a permanent record of the results obtained which can be documented at any time in a report. Also, for some requirements the accuracy of scanning is sufficient for quantitative evaluation.

With improved software, both densitometric and video scanners are likely to become still more user-friendly. However, more dramatic improvement in the accuracy and reliability of results is more likely to come from the continual improvements taking place in the quality of adsorbents making up the layer. With the introduction of smaller (4 μm) spherical particle sizes, the quality of separation will improve, hence this will be reflected in the scans and quantitative results obtained with both spectrodensitometry and video scanning.

See also: III/In-Depth Distribution in Quantitative Thin-layer Chromatography.

Further Reading

- Frei MP and Zeiloff K (1992) *Qualitativ und Quantitativ Dünnschicht-Chromatographie*. Weinheim: VCH.
- Geiss F (1987) *Fundamentals of Thin Layer Chromatography*. Heidelberg: Alfred Hüthig Verlag.
- Jork H, Funk W, Fischer W and Wimmer H (1989, 1994) *Thin-layer Chromatography, Reagents and Detection Methods*, vols 1a and 1b. Weinheim: VCH.
- Poole CF and Poole SK (1992) *Chromatography Today*. Amsterdam: Elsevier.
- Sherma J and Fried B (1994) *Thin-layer Chromatography, Techniques and Applications*, 3rd edn. Chromatographic Science Series, vol. 66. New York: Marcel Dekker.
- Touchstone JC (1992) *Practice in Layer Chromatography*, 3rd edn. New York: Wiley-Interscience.
- Touchstone JC and Sherma J (1979) *Densitometry in Thin Layer Chromatography Practice and Applications*. New York: Wiley-Interscience.
- Wall PE and Wilson ID (1995) Thin-layer chromatography-techniques. In: *Encyclopedia of Analytical Science*. London: Academic Press.
- Zlatkis A and Kaiser RE (1977) *HPTLC High Performance Thin-layer Chromatography*. New York: Elsevier.

Historical Development

E. Reich, CAMAG, Muttenz, Switzerland

Copyright © 2000 Academic Press

History

Today the term planar chromatography is commonly used as a synonym for high performance thin-layer chromatography (HPLTC) and conventional thin-layer chromatography (TLC). Originally it referred more generally to a family of techniques including TLC, some types of electrophoresis and paper chromatography, which all have in common a stationary phase in the form of a flat thin layer rather than packed into a column. Modern planar chromatography is a form of liquid chromatography and its history is closely linked to the development of chromatography as an analytical tool.

Early roots go back to Beyrinck who in 1889 separated hydrochloric and sulfuric acid by diffusion through a thin layer of gelatine on a glass plate. With the same technique, Wijsman in 1898 was able to demonstrate the presence of two enzymes in malt diastase. When at the end of the 1930s Tswett's column chromatography became successful, research

focused on a faster microchromatographic method, which allowed the exact identification of adsorbed substances. This situation encouraged the transition from a regular column to an open column, a thin layer of adsorbent.

Izmailov and Shraiber are regarded as the inventors of TLC (Table 1). In 1938 they described a method in which microscopic slides were coated with 2 mm layers of a slurry made of chalk, talc, magnesium oxide, lime aluminium oxide or other adsorbents and water. On drying, a thin adsorbent layer was formed. The authors investigated belladonna and other plant extracts by placing a drop of the extract on to the layer. This resulted in the so-called ultra chromatogram that was visualized under ultraviolet light. The chromatogram was then developed with several drops of solvent. The most important advantage of the new method in comparison to column chromatography was the short time of analysis and the low consumption of adsorbents, solvents and samples.

Crowe reported in 1941 the use of a microchromatographic method to select suitable solvents for column chromatography. The procedure was

Table 1 Key publications that greatly influenced the development of planar chromatography

Author	Reference
Runge	<i>Der Bildungstrieb der Stoffe</i> , Oranienburg, 1855
Goppelsroeder	<i>Kapillaranalyse</i> , Dresden, 1910
Izmailov and Shraiber	<i>Farmatsiya</i> 1938; 3: 1
Crowe	<i>Industrial and Engineering Chemistry Analytical Edition</i> 1941; 13: 845
Consden, Gordon and Martin	<i>Biochemistry Journal</i> 1944; 38: 226
Kirchner, Miller and Keller	<i>Analytical Chemistry</i> 1951; 23: 420
Bate-Smith and Westall	<i>Biochimica Biophysica Acta</i> 1950; 4: 427
Stahl	<i>Pharmazie</i> 1956; 11: 633
Soczewinski	<i>Analytical Chemistry</i> 1969; 41: 179
Snyder	<i>Journal of Chromatography</i> 1971; 63: 15

See also publications listed in the Further Reading section.

based on a thin layer of adsorbent poured loosely into a Petri dish.

Meinhard and Hall achieved the first major improvement in layer quality in 1949 with a method called surface chromatography. They used an aqueous slurry of aluminium oxide, Celite and starch coated on microscope slides to produce chromatographic layers free of cracks.

Several years before that, Martin and Synge had taken a different approach while trying to separate amino acids and their derivatives. They developed partition chromatography, in which the stationary phase was coated on to a support such as silica gel and then filled into a column. Solvents such as chloroform were used for elution. In their search for a complementary micromethod, Consden, Gordon and Martin in 1944 used filter paper as an open column, a technique that has its roots in the capillary pictures of Runge (1855) and in the capillary analysis of Schoenbein and Goppelsroeder (1910). Within about 10 years paper chromatography became a universal chromatographic technique.

For the separation of terpenes, Kirchner, Miller and Keller in 1951 improved the surface chromatography technique by incorporating a mixture of zinc silicate and zinc cadmium sulfide as fluorescence indicator into the layer and leaving the Celite out. From various adsorbents to be used on 0.5×5.25 in glass plates called chromatostrips they chose silica gel as the most suitable for their application.

Although employed successfully by many researchers, the thin-layer method was not used widely for several years.

The situation changed with Egon Stahl, who introduced the term thin-layer chromatography in 1956. He realized that the availability of standardized adsorbents of a narrow range of particle size, suitable equipment for preparing thin layers and suitable examples stimulating the use of the method could lead to a breakthrough in acceptance. In 1958 Merck introduced standardized aluminium oxide, kieselguhr and silica gel according to specifications developed by Stahl. Also based on Stahl's ideas, Desaga brought out a basic TLC kit. The wide publicity given to the technique by Merck and Desaga as well as its recognition as a separate chromatographic method by Chemical Abstracts made TLC more and more popular.

In his fundamental book, *Thin Layer Chromatography – A Laboratory Handbook*, published in 1962, Stahl together with several co-authors, made available the results of systematic research on silica gel and other adsorbents, instrumentation and different techniques as well as on the wide applicability of the technique.

The increasing interest in TLC became apparent in a huge number of published papers and several important books, including those by Randerath (1962), Bobbitt (1963) and Kirchner (1967). Due to its much better performance, higher sample capacity and greater flexibility as regards derivatizing reagents, TLC soon replaced paper chromatography in many applications and found entrance to pharmacopoeias as an official method of analysis.

Further developments of planar chromatography were mainly driven by progress in three areas: plate material, instrumentation and theoretical understanding. In 1996 one of the most comprehensive treatises in the field of planar chromatography was published. The *Handbook of Thin Layer Chromatography*, edited by Sherma and Fried, illustrates the current state of the technique.

Plate Material

Experiments with binders were the first step in the improvement of adsorbents that could be made available as pre-coated layers. For reproducible performance, such layers were required to be homogeneous, reliably attached to the support, not affected by solvents and derivatizing agents and universally applicable. Gypsum, which was initially utilized as a binder, failed to yield layers that met the required criteria. Nevertheless, it was still widely used as binder of adsorbents for custom-made TLC plates. In 1965 organic binders based on polyacrylates/methacrylates were introduced which allowed the layer durability and quality to be significantly improved.

Pre-coated plates featuring a wide range of adsorbents, including aluminium oxide, cellulose, polyamide and silica gel as well as a variety of supports such as glass, aluminium or polyester, were introduced to the market. This was a necessary prerequisite for the evolution of planar chromatography into a reliable quantitative technique.

Due to its unsurpassed flexibility and wide applicability, silica gel 60 (average pore size of 60 Å or 6 nm) became the most widely used of all adsorbents.

Paralleling the development in high performance liquid chromatography, an increase in the separation power of TLC plates was expected to result from the utilization of smaller adsorbent particles. In 1975 Merck developed the high performance TLC plate. The main differences of such plates as compared with conventional layers are based on the use of smaller particles with a narrower size distribution. The HPTLC layer is thinner but much more homogeneous and durable than a traditional layer. Separation power and sensitivity are improved and the plates can be used for trace analysis. When introduced to the market these plates became the foundation for instrumental TLC.

A major drawback in the development of layers made with even finer particles to achieve the goal of further improved performance is the restricted capillary flow in such systems. Without suitable forced flow techniques, 3–5 µm seems to be the lower size limit for HPTLC particles.

Partition chromatography on paper was traditionally used to separate hydrophilic substances such as carbohydrates and amino acids. Because these substances are strongly adsorbed on silica gel, reversed-phase techniques had to be employed in order to use TLC. Impregnation known from paper chromatography was used in the 1960s to accomplish this goal. TLC plates were commonly immersed in solutions of alkanes, mineral, silicone or vegetable oils in petroleum ether and then dried. The reversed phase was used with hydrophilic solvents.

When chemically modified silica gel became available, it was attempted to produce true reversed-phase layers for planar chromatography. However, unlike HPLC, which uses a forced solvent flow, TLC has to rely on capillary forces to transport the solvent through the stationary phase. Therefore, reversed-phase materials were developed that retain some of the hydrophilic character of silica gel. Today, a variety of pre-coated reversed-phase plates is available, including RP2, RP8, RP18 and phenyl-modified silica gel. Some of these phases can be used with up to 100% water in the mobile phase. Hydrophilic-modified silica gels originally developed for HPLC also found applications in planar chromatography.

They offer additional selectivity and are less affected by humidity and the gas phase in the developing chamber than silica gel.

Theoretical Foundation

Martin and Synge have chiefly influenced the basic understanding of the fundamentals of chromatography. The significance of their work was acknowledged when both researchers were awarded the Nobel prize in chemistry in 1952. One term defined by Martin and Synge in their theory of chromatography in 1941 was R as the relative rate of movement. LeRosen used a similar term for adsorption chromatography. In 1944 Consden, Martin and Synge named it R_F as the ratio of rate of movement of the adsorbate zone and rate of movement of the developing solvent. Bate-Smith and Westhall defined another important term, R_M , in 1950.

These terms, R_F and R_M , are of fundamental importance for TLC and today many publications deal with the significance of these values. Very early in the development of TLC, Brenner, Niederwieser, Pataki and Weber offered an in-depth presentation of the theory relevant to the principles of TLC as a chapter in Stahl's book. One of the recent and most detailed discussions of all theoretical aspects is found in *Fundamentals of Thin Layer Chromatography* by Geiss, published in 1987. Currently, research into further theoretical understanding of planar chromatography is published in the *Journal of Planar Chromatography*.

An important difference of planar chromatography from column chromatography is the presence of the gas phase. Stahl summarized the effects of chamber saturation on chromatographic separation in 1962. Attempts to control the effects of the gas phase have resulted in a number of special chambers, such as twin trough chamber (CAMAG), BN chamber (Desaga) and horizontal developing chamber (CAMAG). The underlying theories of these devices have been reviewed and compared in detail by Geiss.

In 1940 Trappe introduced the eluotropic series as an arrangement of solvents according to increasing elution strength. Stahl incorporated the concept into one of the first practical approaches to a systematic method development. He linked the three main components of the TLC system – activity of the stationary phase, polarity of the mobile phase and polarity of the sample mixture – in a scheme in which the corners of a triangle point to appropriate combinations that promise successful separations. For example, a lipophilic sample mixture requires a nonpolar mobile phase and a highly active stationary phase, whereas a hydrophilic sample can be separated with

a polar mobile phase on a deactivated stationary phase. Soczewinski mathematically described the effects of the solvent composition on the R_M value in 1969.

In 1971 Snyder published a systematic approach to adsorption chromatography. He related the resolution of the chromatographic system R_s to the selectivity α , the layer quality characterized by the number of theoretical plates N , and the position of the sample in the chromatogram. Because of the fact that for a given separation the TLC plate and its performance are usually constant, resolution can chiefly be improved by changes in the mobile phase. The solvent strength influences the position of the sample in the chromatogram and the solvent properties can change the selectivity of the system. Solvent strength was discussed extensively by Rohrschneider in 1973, while Snyder in 1974 published the so-called selectivity triangle describing proton donor, proton acceptor and dipolar properties of solvents commonly used in chromatography. For HPLC Snyder, Glajch and Kirkland developed a detailed model for solvent optimization in the early 1980s. This model was adapted for use with TLC by Geiss. Nyiredy, Erdelmeyer and Sticher proposed a similar but more empirical approach to solvent optimization in planar chromatography, the so-called Prisma model, in 1985. Because of its simplicity, usefulness and wide applicability the model was readily accepted for method development in TLC.

Recently, models for computer-aided optimization that are more theoretically based have been applied to TLC. They include window diagrams (Wang, 1990), simplex optimizations (Sabate and Thomas, 1984), overlapping resolution maps (Glajch *et al.*, 1980) and cluster analysis (Windhorst *et al.*, 1990).

A useful parameter to characterize the performance of a planar chromatographic system is the separation number, SN, introduced by Kaiser in 1976. In the following years Guichon and Siouffi investigated the relation of SN to height equivalent to one theoretical plate (HETP).

The separation power of planar chromatography is limited due to the capillary flow of the solvent and the resulting limitations in available separation distance. Several attempts have been made to improve performance; One of these is continuous development. The technique, first proposed by Brenner and Niderwieser in 1961, and later by Soczewinski in 1986, is based on the assumption that resolution of planar chromatography can be improved if the solvent is evaporated at the upper edge of the plate, causing continuous development of the chromatogram.

Another approach, multiple development, involves three techniques:

1. Repetitive development with the same solvent in one direction was first theoretically evaluated by Thoma in 1963.
2. Development with one solvent in one direction followed by a second development perpendicular to it with another solvent (two-dimensional TLC) goes back to the work of Consden, Gordon and Martin (1944), who used the technique on paper to separate amino acids. The concept was re-evaluated by Guiochon *et al.* in 1983.
3. Repetitive development with the same solvents in the same direction over increasing distances was introduced by Perry *et al.* in 1975 as a technique called programmed multiple development (PMD). In 1984 Burger modified the technique, in that he developed the plate with solvents of decreasing strength over increasing distances. The term AMD (automated multiple development) distinguishes it from Perry's technique.

The creation of a forced flow through the layer was the third way of improving the performance of planar chromatography. The first experiments to use forced flow in planar chromatography go back to Hopf, who in 1947 invented the Chromatofuge, a device using centrifugal force to accelerate the flow of the mobile phase. Tyihak, Mincsovcics and collaborators introduced another concept, overpressured layer chromatography (OPLC), in 1977. OPLC is of special importance in the development of planar chromatography because it can be regarded as a hybrid between planar and column chromatography, combining the advantages of both techniques.

Instrumentation

The first instruments or tools specifically for TLC that appeared on the market were plate-coating devices, developing chambers derived from paper chromatography tanks and sample application tools.

In the early days of planar chromatography, plate-coating devices played an important role. They allowed the preparation of more or less uniform TLC layers of variable thickness. Besides primitive tools such as glass rods for spreading suspensions of adsorbents, there were two kinds of instruments. In one kind (Desaga, Shandon) a dispensing unit was moved over a series of glass plates. In the other kind (CAMAG), glass plates were moved beneath the dispenser. There have been motorized versions of both types of instruments. Even though some are still on the market today, such devices have lost their importance with the arrival of pre-coated plates in the late 1960s.

In the following paragraphs other instruments are discussed according to their designation: sample

application, chromatogram development and chromatogram evaluation. For a review of today's state-of-the-art instrumentation, refer to the chapter on planar chromatography – instrumentation.

Sample Application

Hand-held micropipettes and microsyringes in connection with application guides were the first devices used for sample application. Some of them can still be found in TLC laboratories. However, it was soon recognized that sample application was the bottleneck with respect to staffing levels in planar chromatography. Until the introduction of HPTLC material with its need for miniaturization, all attempts to rationalize sample application were based on the arrangement of dosage devices in parallel and their simultaneous actuation. The Morgan applicator (1962) used a series of capillaries, which were simultaneously filled and discharged by manual action. A number of automated devices (CAMAG, 1973; Shandon, 1974; Desaga, 1976) used a series of syringes or peristaltic pumps, which delivered the sample solutions controlled by an electric motor. The degree of automation of the various steps, syringe filling, positioning and rinsing varied from device to device.

With the advent of HPTLC, automatic sample application had to be performed sequentially by one dispensing device. The CAMAG Automatic TLC Sampler I (ATS1) was the first instrument of this kind. It was succeeded by the ATS II and finally by the redesigned ATS3, a fully automated device for sample application in the form of spots or bands. Desaga developed a similar instrument the AS30 which works in conjunction with a commercial HPLC autosampler.

Chromatogram Development

Vertical development of one or more plates in rectangular tanks, sometimes covering the stationary phase with a counterplate to form a so-called sandwich, is commonly regarded as the classical technique of planar chromatography. Exclusively, capillary forces drive the mobile phase. However, beginning in the early 1960s, attempts have been made to design chambers for horizontal development (Brenner; Niederwieser-Chamber, Desaga). The Vario-KS chamber (CAMAG) was designed to optimize development conditions. The short bed continuous development (SBCE) chamber was introduced by Perry in 1979 (Regis).

When HPTLC plates, which can only utilize short developing distances, became available, Kaiser developed the U-chamber for circular development (CAMAG, 1976; **Figure 1**). There was considerable interest in the device. Even densitometers that could



Figure 1 (See Colour Plate 29) CAMAG U-chamber (1976) developed by Kaiser.

evaluate circular chromatograms appeared on the market. Kaiser also postulated another developing mode, anticircular, which had other advantages and merits to the circular mode. It is possible that this caused some confusion among potential users of both the new techniques and within a few years the devices disappeared off the market.

Today interest is focused on chambers that allow automated development with reproducible results. One example is CAMAG's automated developing chamber (ADC). Several, mostly experimental instruments have been constructed for OPLC. Today there is still considerable interest in the technique, especially since a modern instrument is on the market (OPLC-NIT, Engineering Company). Another interesting forced flow technique, high pressure planar chromatography, using the circular developing mode and much higher pressure, was proposed by Kaiser. Unfortunately it was never able to grow beyond the experimental stage.

Modern devices using centrifugal forces to generate a forced flow of the mobile phase through the planar bed are the Rotachrom (Petazon) and Chromatotron (Analtech). Both instruments are primarily used for preparative separations.

Densitometric Evaluation

In the 1960s planar chromatograms were evaluated quantitatively with the help of electrophoresis photometers, some of which had to be modified. The major disadvantage of these instruments was the fact that they used visible light and therefore only coloured substances could be measured. This required some sort of visualization technique to be used.

The first densitometers specifically designed for TLC were those by Zeiss (1965), Shoefel (1967), CAMAG (1978) and Shimadzu (1979). These devices

were fitted with a monochromator, utilized ultra-violet light and measured in the reflection mode, which has advantages over the transmission mode.

In 1976 the first experimental set-up for evaluation of planar chromatograms by video technology was described by Devenyi. In the following years instruments originally designed for the evaluation of electrophoresis gels were adapted for use in TLC. TLC-specific video systems have been available since 1988 (Uniscan, Analtech).

Modern scanning densitometers as well as state-of-the-art video densitometry are discussed in the section on Thin-layer (planar) chromatography – instrumentation.

See Colour Plate 29.

See also: II/Chromatography: Thin-Layer (Planar): Densitometry and Image Analysis; Instrumentation; Layers; Modes of Development: Conventional; Modes of Development: Forced Flow, Overpressured Layer Chromatography and Centrifugal; Spray Reagents; Theory of Thin-Layer (Planar) Chromatography.

Further Reading

- Geiss F (1987) *Fundamentals of Thin Layer Chromatography*. Heidelberg: Huethig.
- Glajch JG, Kirkland JJ, Squire KM and Minor JM (1980) *Journal of Chromatography* 199: 57–79.
- Kirchner JG (1978) *Thin Layer Chromatography*, 2nd edn. New York: Wiley.
- Sabate C and Thomas X (1984) *Journal of High Resolution Chromatography & Chromatography Communications* 7: 104–106.
- Sherma J and Fried B (eds) (1996) *Handbook of Thin Layer Chromatography*. New York: Dekker.
- Stahl E (1967) *Thin Layer Chromatography – A Laboratory Handbook*, 2nd edn. Berlin: Springer.
- Wang Q-S and Wang N-Y (1990) *Journal of Planar Chromatography* 3: 15–19.
- Windhorst G, Kelder J and De Kleijn JP (1990) *Journal of Planar Chromatography* 3: 300–306.
- Wintermayer U (1986) *The Roots of Chromatography: Historical Outline of the Beginning to Thin-layer Chromatography*. Darmstadt: GIT.

Instrumentation

D. E. Jaenchen and E. Reich, Camag,
Muttens, Switzerland

Copyright © 2000 Academic Press

Introduction

At the end of the 1950s thin-layer chromatography was introduced as a rapid, simple technique for qualitative investigations, and it is still widely used in this capacity. With the introduction of high performance plate material (HPTLC) and the availability of dedicated densitometers, thin-layer chromatography has gained increasing acceptance as a quantitative analytical tool. However, to unlock its full potential as an accurate and reliable technique, HPTLC demands the use of instrumentation for the entire process including sample application, chromatogram development and chromatogram evaluation. Since analytical procedures are only as good as their weakest step, additional operations such as *in situ* pre- or post-chromatographic derivatization, as well as sample preparation, require instrumentation for increased reproducibility.

Although several attempts have been made to automate fully the complete TLC process, it seems questionable whether such automation would increase the overall performance of the method. It has proved very difficult to design a device, at a reasonable cost, that

is essentially an automated online system, but at the same time retains the extreme flexibility of the traditional offline design of TLC. One of the many distinct advantages of TLC – the fact that each step can be separated in time and location from all other steps – is very likely to be lost in a fully automated design. Automation of each individual step, perhaps linked by suitable software, appears to be the better choice.

Sample Application

As the first step of planar chromatography, sample application largely determines the overall quality of the separation. All analytes and standards are chromatographed and compared with each other on the same plate, generally by means of migration distance or R_F value. Therefore, exact positioning of the sample during application is crucial for both qualitative and quantitative TLC. Quantitative work also requires exact reproducibility of applied volumes. Furthermore, in order to utilize fully the separation power of the layer, it is important to restrict the dimension of the sample origin in the direction of chromatography. The advantage of instrumentation is mainly derived from a much higher reproducibility of all these parameters.

Generally, two principal sample application techniques are distinguished: application of spots and application of bands. The selection of a sample

application technique depends on factors such as the nature of the analytical task, the type of sample matrix, workload and time constraints, the type of separation layer, and the sample volumes to be applied.

Sample volumes that can be applied as spots delivered in one stroke are 0.5–5 μL on conventional layers and 0.1–1 μL on HPTLC layers. Larger volumes may be applied either as spots by using a device with controllable delivery speed, or by spraying them on in the form of narrow bands.

Sample Application as Spots

The simplest technique to apply samples as spots is to use a fixed volume pipette that fills by capillary action and delivers its content when it touches the layer. Variable volumes can be applied with a syringe, preferably one with micrometer control. Instruments for sample application should ensure two things: first, that the spots are precisely positioned and second, that the layer is not damaged during application. The Camag Nanomat is a mechanized spotting device using fixed volume glass capillaries, which are lowered onto the layer with reproducible contact pressure (Figure 1). The exact position of the spot is mechanically controlled. An instrument designed for the use of microlitre syringes is the Desaga PS 01 Sample Applicator.

Sample Application as Bands

Sample application in the form of narrow bands provides the highest resolution attainable with a given chromatographic separation method. The sample is typically contained in a syringe, which is emptied by a motor. Delivery speed and volume are electronically controlled. A stream of an inert gas such as nitrogen

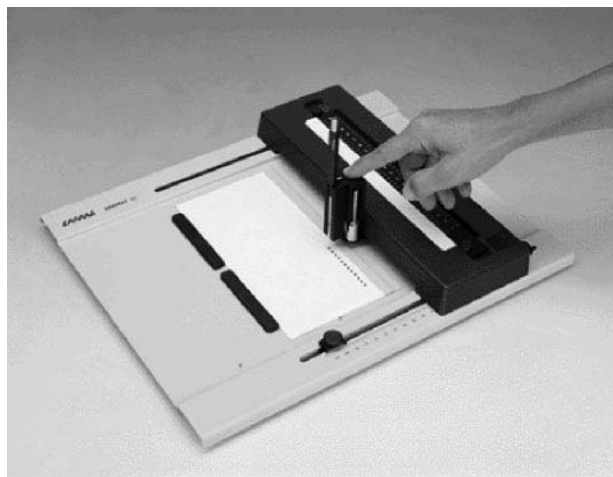


Figure 1 Camag Nanomat.



Figure 2 Camag Linomat IV.

around the tip of the syringe atomizes the sample and creates a band on the TLC plate if either the syringe or the plate is moving linearly. Because large sample volumes can be applied, this technique is able to lower dramatically the determination limits with respect to analyte concentration in the sample solution, e.g. in trace analysis. Another benefit of the spray-on technique for quantitative analysis is the possibility of applying different volumes of the same calibration standard instead of equal volumes of different standard concentrations. The spray-on technique also allows unknowns to be simply over-sprayed with 'spiking' solutions for the standard-addition method.

The Linomat (Figure 2) allows sample application in narrow bands of variable length by a multipassage spray-on technique. The instrument can be used to apply sample volumes of 2–100 μL onto HPTLC plates or conventional layers. By employing the Linomat spray-on technique, the gain in precision of quantitative TLC analysis can be expected to be in the range of 30%, i.e. from 1.5% relative standard deviation to 1.0%, provided that chromatographic resolution is not a problem. If samples are complex, 'dirty', tend to tailing, or are otherwise 'difficult', the choice between band application and spot application may determine whether or not a meaningful quantitative result will be obtained at all.

Automated Sample Application

Sample application in quantitative TLC analysis can take up as much as one third of the time needed for the entire analysis. When carried out manually, this is pure labour time. Therefore, attempts to automate or otherwise rationalize this step have been made since the early days of TLC.

Devices using a series of capillaries or syringes were employed with partial success in conventional TLC.

However, none of the multicapillary or multisyringe devices were truly suitable for the smaller dimensions of HPTLC. Applying samples sequentially proved to be a more appropriate approach to solving the problem of automated sample application without sacrificing precision.

The Camag Automatic TLC Sampler III is a flexible computer-controlled device that can apply samples automatically from a rack of sample vials. The samples are transferred from the vials onto the plate with a steel capillary either as spots by contact or as bands using a multipassage spray-on technique. The sample-dispensing speed, sample volumes and application pattern are freely selectable. Each application step is followed by a programmable rinsing cycle to avoid cross-contamination of samples. Because the software of the instrument is compatible with the software for densitometric chromatogram evaluation, all calibration data need to be entered only once. Another advantage of this automated system is its Good Laboratory Practice/Good Manufacturing Practice (GLP/GMP) compliance.

The Desaga TLC Applicator AS 30 also applies samples to a planar chromatography surface in the form of spots or bands. The differences between the two applicators are that spots are applied by spraying and that a one-passage spray-on process produces bands. The AS 30 Applicator can be coupled with a typical HPLC autosampler. The functionality of such a combination is comparable to that of the ATS III.

Chromatogram Development

Although chromatogram development is the most decisive step in the TLC procedure, important parameters are often not given the attention they deserve. Even as part of quantitative analytical procedures, most planar chromatograms are still developed with rather primitive equipment.

The classical way to develop a planar chromatogram is to place the plate with its lower edge immersed in the developing solvent contained in a tank. While the solvent ascends the plate, the layer interacts with the vapour phase in the tank. Since developing tanks of different manufacturers vary considerably in size, chromatograms developed in one device cannot generally be duplicated in another. It is customary to line the inside of the tank with filter paper soaked with the developing solvent. Although this can be often advantageous, it is not always the case.

A counter plate arranged at a small distance opposite to the layer can largely suppress interaction between the dry or wetted layer and the gas phase. This is called a 'sandwich configuration'. Although sandwich chambers tend to improve the reproducibility of

the separation, secondary fronts, caused by partial solvent de-mixing of complex mobile phases, are often produced and may interfere with resolution of samples.

A limited degree of influence over the gas phase parameters during chromatographic development is offered by the twin-trough chamber. A special advantage of this chamber is the possibility of affecting the separation through preconditioning.

The horizontal developing chamber (HDC; Figure 3) allows a planar chromatogram to be developed in both the sandwich and tank configuration with or without solvent vapour saturation. For development in the HDC, samples can be applied parallel to both opposing edges of the plate, which is then developed from both sides towards the middle. In this way the number of samples per plate can be doubled. However, when used for one-directional development, the HDC also offers advantages in that chromatographic conditions can be standardized. This type of chamber uses very small amounts of developing solvent (2×5 mL for a $20 \text{ cm} \times 10 \text{ cm}$ plate) and offers, therefore, an economical alternative to the conventional developing tank.

Automatic Chromatogram Development

The automatic developing chamber (ADC) provides instrumental control of the classical one-step isocratic chromatogram development. Preconditioning, tank or sandwich configuration, solvent migration distance, and the drying conditions can be preselected and are automatically maintained to ensure high reproducibility of the chromatographic result.

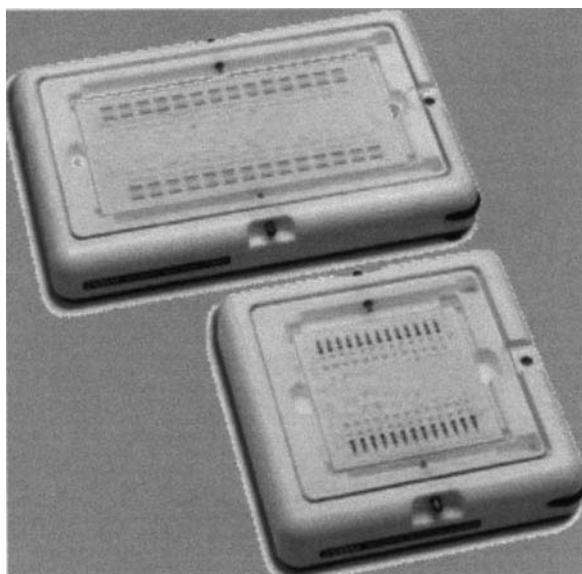


Figure 3 Camag horizontal development chambers.

Computer-Controlled Multiple Development of Planar Chromatograms

Automated multiple development, more particularly when performed as a gradient technique, achieves the maximum resolution feasible within the limited separation distance available on a HPTLC plate. In terms of peak capacity it compares with HPLC while retaining the inherent benefits of planar chromatography. The automated multiple developing system (AMD; Figure 4) serves for this type of chromatogram development. A step gradient of decreasing eluotropic strength and changing selectivity is created and each development proceeds to a higher migration distance than the one before. A typical standard gradient changes the developing solvent from methanol to dichloromethane to hexane in 25 steps over a final migration distance of 65 mm. Between each step the plate is dried under vacuum. The software allows the composition of developing solvent to be specified as well as the developing distance for each step. Solvent volumes are measured with syringes and migration distance of the solvent front is measured with sensors. Preconditioning through the gas phase prior to development is possible.

Forced Flow Layer Chromatography

Several attempts have been made to accelerate the solvent flow in planar chromatography. Applying pressure in the linear or radial direction or using

centrifugal forces have been described. The only technique that has survived is the so-called 'over-pressure layer chromatography' (OPLC), which is described in detail elsewhere in this volume.

Densitometric Chromatogram Evaluation

Principle

During densitometric evaluation of a planar chromatogram, its separation tracks are scanned with a light beam in the form of a slit adjustable in length and width. The photosensor of the densitometer measures diffusely reflected light. The difference between the optical signal from the sample-free background and that from a sample zone (fraction) is correlated with the amount of the respective fractions of calibration standards chromatographed on the same plate. Densitometric measurements of planar chromatograms can be made by absorbance or by fluorescence.

As an alternative to classical densitometry, a planar chromatogram can be evaluated by video technology.

Comparison of Video Technology with Classical Densitometry

Classical densitometry uses the spectral range from 190 to 800 nm with high spectral selectivity. Absorption spectra for substance identification can be recorded within this whole span. In contrast, video technology functions only in the visible range. The UV region – exceptionally productive for planar chromatography – is only indirectly accessible through the use of an UV indicator embedded in the layer and in cases where samples fluoresce. In this respect video technology parallels the human eye.

Spectral selectivity, a strong point of the classical densitometer, is not accessible with a video system. The greater the absorbance of the analyte at or near the excitation maximum of the UV indicator (254 nm), the higher are the sensitivity and accuracy of video quantification. In certain cases they may even become comparable to those of classical densitometry.

In fluorescence mode video and classical densitometry are comparable in respect to detection of emissions in the visible region, caused by long-wave UV light (366 nm). However, video technology lacks the variable-excitation-based selectivity of classical densitometry.

The limitation of image processing to visible light is not caused by the video camera, but by the fact that no solution has yet been found for uniformly illuminating a plate with monochromatic light of a selected

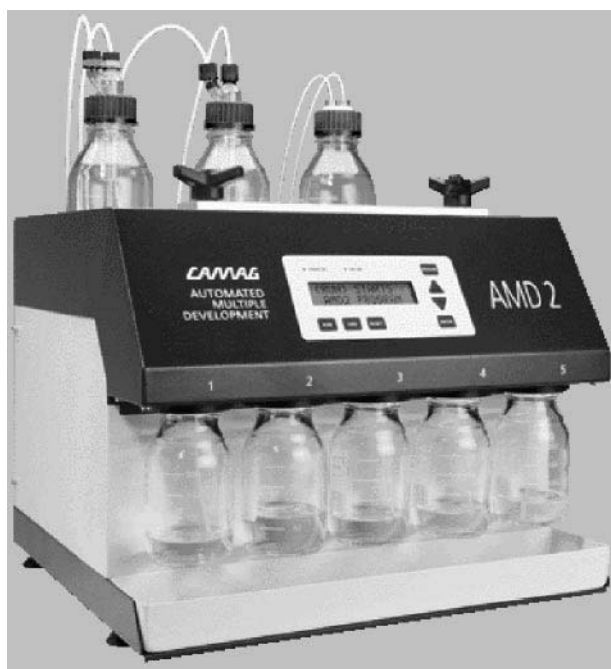


Figure 4 (See Colour Plate 30) Camag automated multiple development chamber AMD 2.

wavelength. *In situ* spectroscopy is only possible with the classical densitometer.

Features of a Modern Chromatography Densitometer

The Camag TLC Scanner 3 may be used to illustrate typical features of a modern densitometer (see Figure 5). Some particulars of other densitometers are also discussed. Technical data for a number of densitometers are given in Table 1.

Two continuum lamps, a deuterium and a tungsten-halogen lamp, in combination with a monochromator generate light of 5–20 nm bandwidths in the spectral range from 190–800 nm. A third, high pressure mercury vapour lamp provides high energy for scanning by fluorescence. The lamps are selected and positioned automatically. Plates up to 20 cm × 20 cm are placed on a stage that is mechanically operated in the *x*- and *y*-directions. The scanning speed is variable to a max of 100 mm s⁻¹. Several cutoff filters can be selected for fluorescence scanning.

All functions of the scanner as well as generation and processing of data are controlled by a personal computer using dedicated software. A typical sequence of quantitative evaluation of a chromatogram includes raw data acquisition, data integration, calibration and calculation of results, and generation of the analysis report.

Raw data are sampled by scanning the chromatogram plate in the direction of chromatography, track by track. Integration is performed from the raw data after all the tracks on a plate have been measured. The system automatically defines and corrects the baseline and sets fraction limits. The operator can accept these or can override the automatic process by manual integration.

In the calibration routine, peak data of the unknowns are related to those of the calibration standards. From several calibration functions, including single- or multi-level with linear or polynomial regression, the most suitable for the task is chosen.

The software automatically stores and retrieves all data files and generates a report containing the date

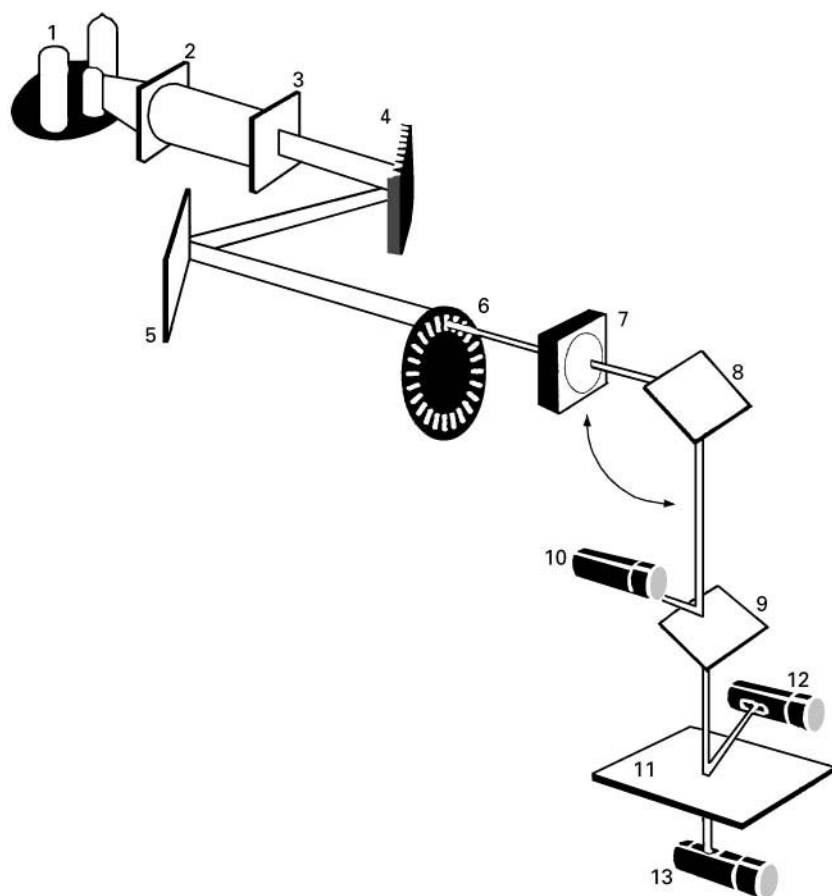


Figure 5 Light path diagram of the TLC scanner. Key: 1, lamp selector; 2, entrance lens system; 3, monochromator entry slit; 4, monochromator grating; 5, mirror; 6, slit aperture disc; 7, lens system; 8, mirror; 9, beam splitter; 10, reference photomultiplier; 11, scanning object; 12, measuring photomultiplier; 13, photodiode (transmission).

Table 1 Technical data for some planar chromatography densitometers

Densitometer	TLC Scanner 3 (CAMAG)	CD-60 (Desaga)	CS-9300 series (Shimadzu)
Scanning mode	Absorbance Fluorescence	Absorbance Fluorescence	Absorbance Fluorescence ^a
Light sources	D ₂ W-halogen Hg	D ₂ W-halogen Hg	D ₂ W Hg ^a Xenon ^a
Spectral range	190–800 nm	210–700 nm	210–650 nm
Slit dimensions			
x-direction	0.05–12 mm	0.4–16 mm	0.4–16 mm ^b
y-direction	0.025–1.2 mm	0.1–0.4 mm	0.4 mm
Size of spot for meander scan	Not available	0.4 × 0.4 mm	0.4 × 0.4 mm
Max. scanning speed	100 mm s ⁻¹	20 mm s ⁻¹	Meander scan <1 mm s ⁻¹ Linear scan <2 mm s ⁻¹
in y-direction			
Spectra recording	No limitation, fully automatic	Max. 29 spectra at manually entered positions	Limited to one track only
Range of spectra recording	190–800 nm ^c	210–700 nm ^d	210–650 nm ^d
Spectrum Library	Yes	No	No

^aOptional.^bSlit scanning simulated by spot scanning at high speed with selectable swing.^cSpectra recording across lamp boundary with lamps stabilized.^dSpectra recording across lamp boundary, lamps not stabilized.

and time of the last change, plus a unique system-generated identification number for GMP/GLP recognition.

Modern scanners are usually able to do more than just quantify the substances on a plate. The following is a selection of other capabilities.

Multiwavelength scanning This expression is often misinterpreted as scanning at selectable wavelengths, a very basic feature of any densitometer fitted with a monochromator. Multiwavelength scanning means that initially acquired raw data of up to ten different wavelengths can be separately processed post-run in the integration and calibration routine. Therefore, each substance can be quantified at the wavelength of its maximum absorbance (see **Figure 6**). Dual-wavelength scanning, which may be used for example to eliminate matrix effects, is a simple variation of multiwavelength scanning.

Recording *in situ* spectra Absorption spectra across the entire range of the monochromator can be measured and, within certain restrictions, so can fluorescence excitation spectra. In the Camag scanner both deuterium and halogen–tungsten lamps remain powered the whole time and are therefore well stabilized. The spectral data can be processed post-run for various purposes:

- to determine the optimum wavelength(s) for quantitative scanning;
- to identify individual fractions by comparison with spectra of authentic standards co-chromatographed on the same plate or stored in a spectrum library;
- to check identity by superimposing the spectra of all fractions within the same R_F window;
- to check the purity of fractions by superimposing the spectra from different positions within a spot.

Scanner validation Automatic instrument validation is available as an option of the software. In the scanner validation procedure the following checks are performed: wavelength adjustment of the monochromator, correct stage positioning; condition and alignment of lamps, condition and alignment of the optical system; and functioning of the electronics. The results, together with the target values, are printed as a validation report.

Features offered by TLC densitometers Instead of scanning a chromatogram track with a fixed slit, it is possible to move a light spot in a zigzag or meander form over the sample zones, whereby the swing corresponds to the length of the slit. This feature, offered by the Desaga CD 60 densitometer and also by the Shimadzu CS 9000 series scanner, is claimed to correct chromatogram distortions. Disadvantages are the lower spatial resolution, particularly in the case of

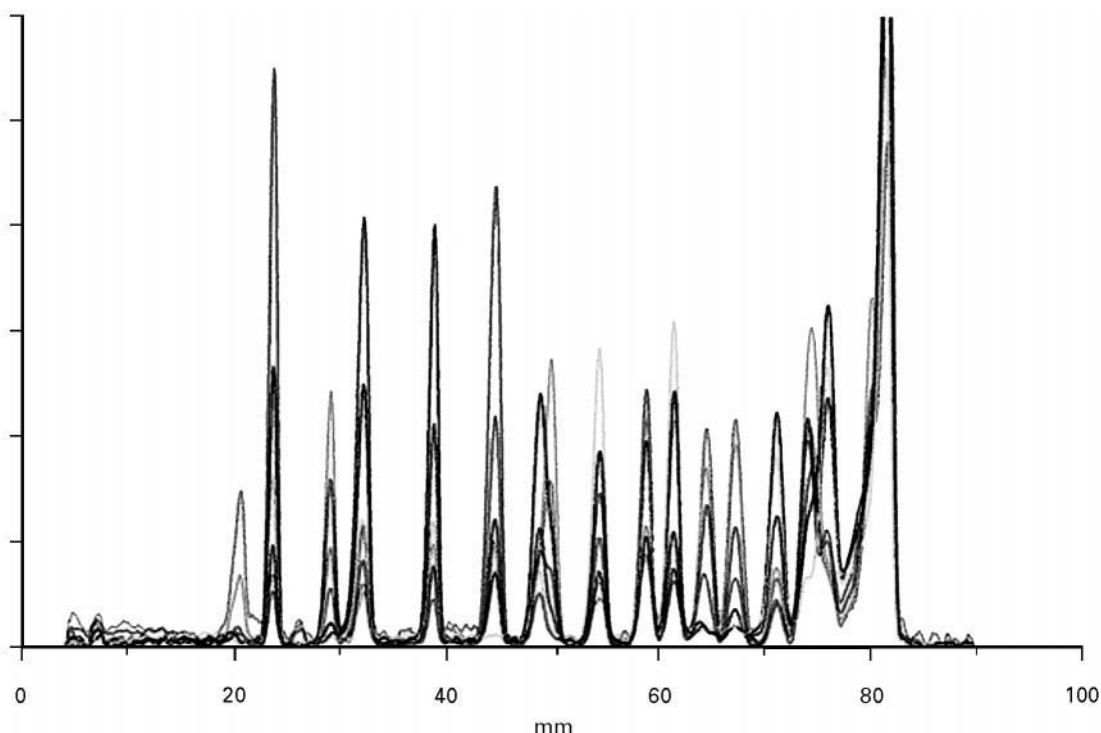


Figure 6 (See Colour Plate 31) Multiwavelength scan of a pesticide mixture after AMD separation.

HPTLC separation material, and unfavourable error propagation, when data of sampling points from different positions are averaged.

Chromatogram Evaluation with Video Technology

A video imaging system typically consists of a lighting module such as Reprostar 3 featuring short-wave UV, long-wave UV and visible light, a charge-coupled device (CCD) camera with zoom objective, computer with frame grabber, and imaging and evaluation software such as VideoStore/VideoScan). Most software allows the user to annotate and manipulate the images. VideoStore image data are archived under observation of GMP/GLP. They can be retrieved any time for quantification with the VideoScan software. Multiple images can be opened and their analogue curves can be compared.

The benefits of chromatogram evaluation by video technology are speed, easy and intuitive operation, and the fact that saved chromatograms can be evaluated at any time if required.

Post-Chromatographic Derivatization

It is an inherent advantage of planar chromatography that fractions are stored on the plate and can readily be derivatized after chromatography in order to render them detectable, to improve detection limit, or to change selectively properties of sample components.

Liquid derivatizing agents can be transferred onto the plate by spraying or dipping. Provided the reagent is suitable, dipping is the preferred technique.

The Chromatogram Immersion device by Camag is an example of an instrument that allows proper execution of the dipping technique. The chromatographic plate must be immersed and withdrawn at a uniform speed to avoid tide marks, which could interfere with densitometric evaluation. By maintaining a defined immersion time, derivatization conditions can be standardized.

Spraying has to be used when two reagent solutions have to be applied in sequence without intermediate drying. Diazotization followed by coupling is an example. There are several sprayers on the market, from simple laboratory atomizer to electropneumatic TLC sprayers.

Whenever reagents are sprayed onto a plate, an efficient dust and mist-removing device should be used to protect laboratory personnel against poisonous or irritating sprays and solvent vapours. Commercial equipment ensures the complete removal of excess spray from the atomizer and spray particles rebounding from the TLC plate. There is no deflection of the spray jet before it reaches the chromatogram, an effect often occurring in a normal laboratory fume hood.

In most cases, the derivatization reaction needs to be completed by heat treatment. Heating the

chromatogram plate uniformly and reproducibly at the desired temperature can be accomplished with a heater specifically designed for this purpose.

Combination of Planar Chromatography with Other Techniques

Combination of planar chromatography and various chromatographic or non-chromatographic methods has been reported frequently. Such combinations include HPLC-TLC, TLC-FTIR, TLC-Raman, TLC-SERS and TLC-MS. Most devices to effect these combinations have been custom-built and only a few are commercially available.

Coupling HPLC with Planar Chromatography

Combining separation techniques that utilize different mechanisms to a multidimensional approach increases the potential of the individual techniques by an order of magnitude. HPLC in reversed-phase mode is one of the most powerful separation techniques available for nonvolatile substances. Online coupling of HPLC with a multiple development system using normal-phase chromatography results in peak capacities of around 500.

A device for mass transfer from HPLC to planar chromatography consists of a sample spray-on device that is connected to the column outlet. Since the maximum quantity of liquid that can be sprayed on a silica layer without washing it away is limited to $10\text{--}60\ \mu\text{L min}^{-1}$, depending on the mobile phase, a microbore HPLC unit is the most appropriate for this technique.

FTIR Evaluation of Planar Chromatograms

The combination of planar chromatography with Fourier transform infrared *in situ* evaluation is a useful method for the identification of complex mixtures and their constituents. Although determination limits ($1\text{--}10\ \mu\text{g}$ per fraction) are higher than those for *in situ* UV spectroscopy, the method can be used for the quantification of substances that exhibit no suitable UV response and are not amenable to derivatization. A major drawback of *in situ* FTIR is the strong absorption of silica gel between $3700\text{--}3100$ and $1650\text{--}800\ \text{cm}^{-1}$. Spectral correction can be achieved by background subtraction of data recorded from an empty track.

Combination of Planar Chromatography with Raman Spectroscopy

Regular Raman spectroscopy as well as the SERS technique (surface enhanced Raman scattering) is

suitable for the identification of substances on a TLC plate. *In situ* Raman generates spectra that are more or less identical with published Raman spectra measured on solids. Detection limits are comparatively poor, i.e. in the range of $0.5\text{--}5\ \mu\text{g}$ per fraction. SERS is suitable for detection and identification of compounds in the picogram range, if the layer is treated with a colloidal silver solution. The user must record a custom library of SERS spectra from a similar layer in order to perform an identification of a totally unknown material.

A multidimensional combination of outstanding separation power is that of HPLC coupled with automated multiple development planar chromatography featuring evaluation by a special SERS technique employing silver deposition via the gas phase.

Combination of Planar Chromatography with Mass Spectrometry (MS)

For the *in situ* identification of compounds separated on a TLC plate, molecules must be desorbed from the layer and then introduced into the ion source of the mass spectrometer. Such desorption can be accomplished by laser ablation or particle beam sputtering techniques. Ionization methods include conventional chemical ionization (CI), fast atom bombardment (FAB), liquid secondary-ion mass spectrometry (liquid-SIMS), and matrix-assisted laser desorption/ionization (MALDI). Mass analysers are either sector field, quadrupole or time of flight (TOF) instruments. The principal limitation of the interesting TLC-MS hyphenation is that there is no MS instrument available that takes $10\ \text{cm} \times 10\ \text{cm}$ or larger plates.

Future Trends

Future developments of instrumentation are likely to focus on improvement of the speed and flexibility of all automated individual steps. The future will see systems that combine the automated steps – sample application, chromatogram development and evaluation by video technology – and have the option to interrupt the process where desired and to interpose additional or alternative steps. Software for control and documentation of all steps of the TLC procedure will be in full GLP/GMP compliance. Other expected developments will be in the area of commercially available interfaces for hyphenated techniques and improved separation media, e.g. spherical material. All this will improve the recognition and acceptance of planar chromatography as a reliable, cost-effective and environmentally friendly method of analysis complementing other chromatographic techniques.

See Colour Plates 30, 31.

See also: II/Chromatography: Thin-Layer (Planar): Densitometry and Image Analysis; Mass Spectrometry; Modes of Development: Conventional; Modes of Development: Forced Flow, Overpressured Layer Chromatography and Centrifugal; Spray Reagents. III/Flame Ionization Detection: Thin-Layer (Planar) Chromatography. Thin-Layer Chromatography-Vibration Spectroscopy. Appendix 2/ Essential Guides to Method Development in Thin-Layer (Planar) Chromatography.

Further Reading

Bertsch W, Hara S, Kaiser RE and Zlatkis A (eds) (1980) *Instrumental HPTLC*. Heidelberg: Hüthig.

Frey H-P and Zieloff K (1993) *Qualitative and Quantitative Thin Layer Chromatography* (in German). Weinheim: VCH Publishers.

Geiss F (1987) *Fundamentals of Thin Layer Chromatography*. Heidelberg: Hüthig.

Grinberg N (ed.) (1990) *Modern Thin Layer Chromatography*. New York: Marcel Dekker.

Jork H, Funk W, Fischer W and Wimmer H (1990) *Thin Layer Chromatography. Reagents and Detection Methods*, vols 1a and 1b. Weinheim: VCH Publishers.

Sherma J and Fried B (eds) (1998) *Handbook of Thin Layer Chromatography*. New York: Marcel Dekker.

Ion Pair Thin-Layer (Planar) Chromatography

I. D. Wilson, AstraZeneca Pharmaceuticals, Macclesfield, Cheshire, UK

Copyright © 2000 Academic Press

Introduction

The separation of polar, ionizable substances can cause problems for simple partition- or adsorption-based chromatographic systems and this is as true in thin-layer, or planar, chromatography (TLC) as for any of the other liquid chromatographic techniques. Often the problem can be dealt with by the simple expedient of controlling the pH of the solvent used for chromatography, in order to suppress the ionization of the solute and thereby reduce its polarity. However, with very polar compounds this is not always a successful strategy and in such circumstances it may be more practical to employ an ion pair (IP) reagent (often referred to as soap chromatography in the early literature). A further benefit of using such an approach is that a hydrophobic IP reagent may, in addition to masking the ionizable group, usefully modify the overall polarity of the complex and thus cause a dramatic change in chromatographic properties. Whilst IP-TLC has not been as widely employed as IP-high performance liquid chromatography (IP-HPLC: described elsewhere in this encyclopedia), there have been sufficient examples of the technique to demonstrate its utility for both acids and bases.

In addition to simply using IP reagents in order to obtain suitable chromatographic separations for substances that are too polar to chromatograph in any other way, this type of TLC has other uses. For example, faced with a mixture of neutral and ionizable compounds, an IP reagent may enable the ana-

lyst to introduce additional selectivity into the system. This can enable the R_F of more acidic or basic compounds to be altered whilst leaving those of neutral solutes unchanged and thereby effecting a separation. The addition of an IP reagent to a system can also provide a rapid indication of which compounds in a mixture are ionizable. There have also been several examples of the use of chiral IP reagents for the separation of enantiomers.

The scope and practice of IP-TLC are described below.

Practical Aspects of IP-TLC

Suitable Ion Pair Reagents for IP-TLC

A range of IP reagents have been used for TLC and high performance TLC (HPTLC). These include both the conventional IP reagents used in other forms of liquid chromatography, such as heptanesulfonic acid, triethanolamine dodecylbenzene sulfonate and sodium dodecyl sulfate for bases and quaternary ammonium salts including tetramethyl, tetrabutylammonium and cetrimide for acids. Some limited work has been performed using 'bolaform' bisquaternary ammonium compounds where two such groups are separated by an alkyl chain of varying length which acts as a spacer.

In addition to these IP reagents, it is arguable that in cases where strong organic acids such as trifluoroacetic acid have been used to enable good chromatography of bases to be obtained, a form of IP chromatography is being performed.

Chiral IP reagents have been employed in a limited number of cases (see below) in order to effect the resolution of certain basic drugs.

Methods for the Use of IP Reagents

When attempting to perform IP-TLC it is worth noting that there are several methods of using the reagents. The best results depend to no small degree on the nature of the reagent and the stationary phases employed. Thus the reagents can be included as additives to the solvent system, can be applied to the plates via impregnation with a suitable concentration of the reagent in a volatile solvent prior to chromatography, or a combination of inclusion in the mobile phase and impregnation. Thus, in the case of small, polar IP reagents such as the quaternary tetramethylammonium salts, inclusion in the mobile phase is essential if chromatography is being attempted on a bonded-silica stationary phase. This is because the reagent is so polar that it is not retained on the stationary phase but migrates with the solvent front. The reagent is thus rapidly removed from the analytes with which the ion pairing is desired, with the result that there is little effect on chromatography. In contrast, any attempt to use the combination of a long chain IP reagent such as sodium dodecyl sulfate or cetrinide as a mobile-phase additive in combination with a bonded phase will invariably be met with disappointing results. This is a direct result of the strong interaction of the nonhydrophilic side chain with the stationary phase, which results in the slow migration of the reagent (if it migrates at all) compared to the solvent. Thus, by the time the advancing solvent front reaches the spots corresponding to the analytes, the concentrations of IP reagent are negligible and no real effect on the subsequent chromatography is seen. For such reagents the prechromatographic impregnation of the stationary phase is essential.

Some of these effects, which illustrate the importance of the correct use of the reagent, are shown in **Figure 1** for a number of dihydroxybenzoic acids with C_2 -bonded HPTLC plates when the quaternary ammonium IP reagent tetrabutylammonium bromide was used. Using the reagent in the mobile phase alone gave unsatisfactory results: there was either little effect or the production of double spots (for ion-paired and nonpaired solute; **Figure 1A**). When the C_2 phase was impregnated with the reagent prior to chromatography, much better results were obtained (**Figure 1B**); maximum effects were seen when the reagent was impregnated into the stationary phase and included in the solvent (**Figure 1C**). Postchromatography, the zones of the plate where the reagent was present were located, due to the lack of a suitable chromophore, using iodine vapour. This provides a simple, rapid and effective method for determining the location of these reagents. This can be important in troubleshooting a separation where the effects obtained are not those anticipated.

The impregnation procedure used can affect the final result and detailed studies have been undertaken to optimize this step. For example, if a paraffin-impregnated silica gel TLC plate is to be used with an IP reagent, there would be an obvious benefit to performing paraffin and IP impregnation with a single solution. However, it has been shown that dipping the plate in paraffin followed by the IP reagent solution results in a much higher quantity of IP reagent being adsorbed than the simultaneous application of paraffin and reagent.

Concentration Effects

In our experience, one of the most important factors in making IP-TLC effective is the concentration of the

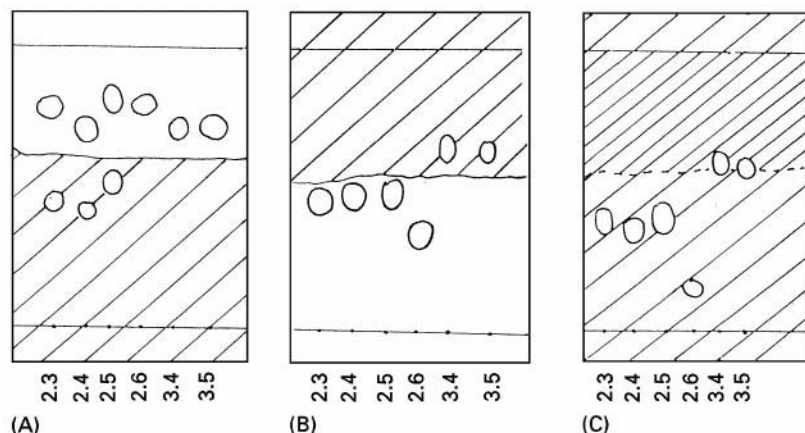


Figure 1 The distribution of IP reagent (tetrabutylammonium bromide) following chromatography as detected using iodine vapour. Shaded areas show the highest concentrations of iodine and thus ion-pair reagent. 2.3, 2.4, 2.5, 2.6, 3.4 and 3.5 are the dihydroxybenzoic acids used as model compounds.

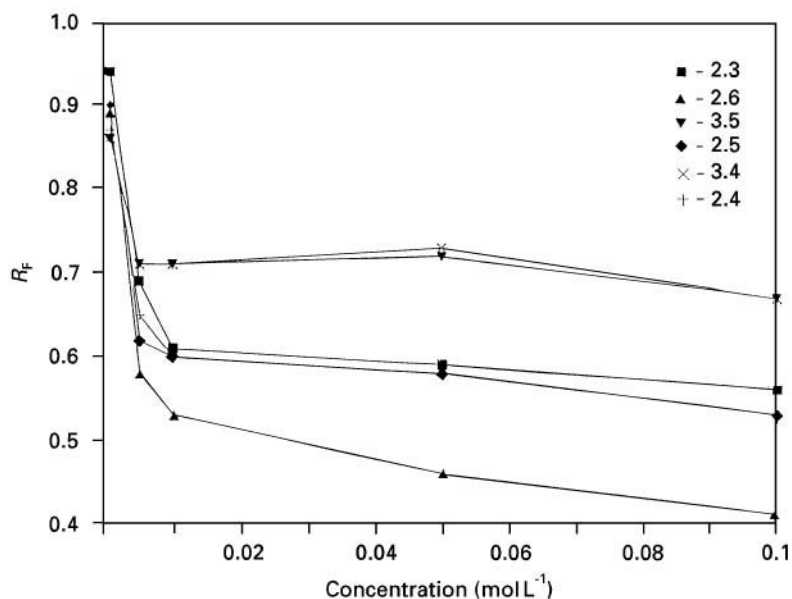


Figure 2 Effect of the concentration of tetrabutylammonium bromide used to impregnate C₂-bonded reversed-phase TLC plates on the R_F values of a range of dihydroxybenzoic acids.

reagent employed. This is shown in Figure 2 for the reagent tetrabutyl ammonium bromide used for a range of dihydroxybenzoic acids on C₂-bonded reversed-phase (RP)-TLC plates. As this figure shows, with methanol–water (1 : 1 v/v) as mobile phase when no reagent is present the test compounds all have R_F values in the range 0.8–0.9. Prechromatographic impregnation of the phase with a solution of the reagent in dichloromethane–ethanol (85 : 15 v/v) at 0.001 mol L⁻¹ was virtually without effect. However, increasing the concentration of the impregnating solution to 0.05, 0.01, 0.5 and 0.1 mol L⁻¹ produced significant reductions in R_F that increased with increasing reagent concentration. Above 0.01 mol L⁻¹ the reduction in R_F observed does not dramatically increase with increasing concentration.

The Role of pH

In IP chromatography in HPLC, the careful control of pH is probably the single most important factor in obtaining retention and ensuring reproducible results. Surprisingly, this is not always the case in IP-TLC and pH effects are often of only marginal significance. In general, with IP reagents such as tetrabutylammonium salts, effects of pH are not observed at all over the range 2–10 (Figure 3). For effects over the range 2–4, there is a gradual decline on silica gel and paraffin-coated silica gel plates and a general decline in R_F is observed with increasing pH on C₁₈-bonded phases (Figure 4). Some of these differences in behaviour between IP reagents may be explained in terms of the way in which the reagents interact with the sta-

tionary phases. A working hypothesis that has been advanced is that on silica gel a reagent such as cetrimide is likely to bond ionically to the acidic surface silanols to form a hydrophobic layer in which the hydrophobic alkyl chains of further cetrimide molecules can sit. As long as the silanols on the silica surface remain ionized this would effectively make a relatively stable ion exchange phase (Figure 5). However, as the pH is lowered, such interactions become less favoured and the layer breaks down with a consequent rapid increase in the R_F of polar solutes. IP reagents such as the tetramethyl- or tetrabutylammonium compounds, which have very different physicochemical properties to cetrimide, would seem at first glance to be much less likely to form this type of ordered layer structure, and so the effect of solvent pH on the surface silanols of the stationary phase would be likely to be less important. Whatever the cause, the susceptibility of IP-TLC to pH effects seems to require the presence of a long aliphatic chain as they are only observed with quaternary ammonium trimethyl-*N*-alkyl IP reagents of C₈ or longer.

It may be advantageous under some circumstances to be able to choose between IP systems that are to all intents and purposes insensitive to solvent pH and those with which pH may be used as another parameter with which to manipulate the separation.

Stationary Phases for IP-TLC

A range of stationary phases have been used for IP-TLC including silica gel, paraffin-coated silica gel

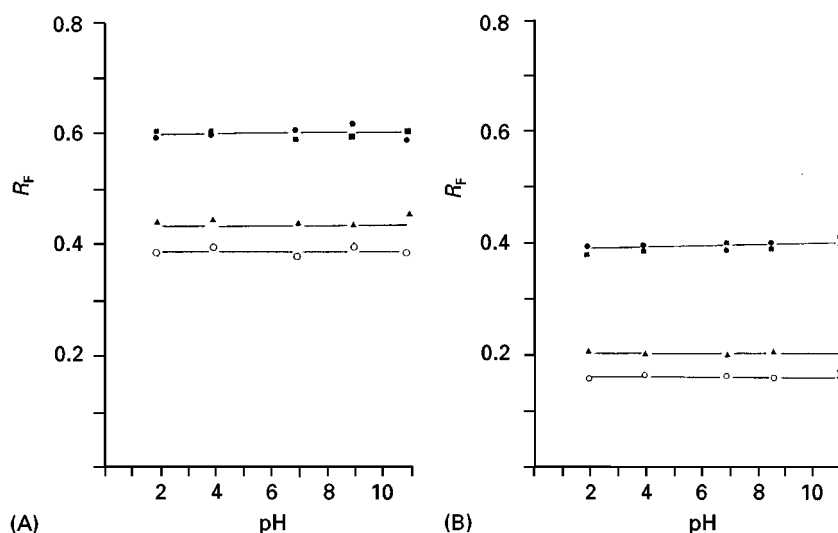


Figure 3 Lack of effect of pH on the R_f values of some dihydroxybenzoic acids on IP-TLC using tetrabutylammonium reagents on (A) paraffin-coated silica gel TLC plates and (B) C_{18} -bonded TLC plates. ■, gentisic acid; ●, 2,5-dihydroxybenzoic acid; ○, 2,6-dihydroxybenzoic acid; ▲, salicylic acid.

and a range from C_2 , C_8 , cyanopropyl, aminopropyl, diphenyl to C_{18} -bonded layers. Chromatography of polar ionic analytes can be obtained with a range of IP reagents on silica gel, paraffin-coated silica gel, alkyl-bonded (C_2 to C_{18}) and diphenyl-bonded layers. However, it is our experience that aminopropyl layers give poor results with IP reagents, and that spot shapes on cyanopropyl layers are poor. It should be noted that these comments are based on limited studies and relatively little work has been done to investigate the use of some of these layers (e.g. cyanopropyl, aminopropyl and diphenyl). It should also be noted that not all reagents can be used with all phases. For example, tetrabutylammonium bromide can be employed with alkyl-bonded stationary phases or paraffin-coated silica gel, but is ineffective on bare silica. In

contrast, cetrимide works well on both bonded stationary phases and silica gel.

Quaternary Ammonium IP Reagents for the TLC of Acids

Reverse-phase IP-TLC In general, the TLC of weakly acidic compounds (e.g. nonsteroidal anti-inflammatory drugs such as ibuprofen or naproxen) can be performed on C_{18} -bonded layers without the need for ion pairing, or indeed for the need for an acidic mobile phase to control the ionization of the analytes. This contrasts with the experience of obtaining satisfactory retention in HPLC for such compounds, but this merely serves to reinforce the fact that the important factors governing retention in RP-TLC and RP-HPLC are not necessarily the same. This may perhaps

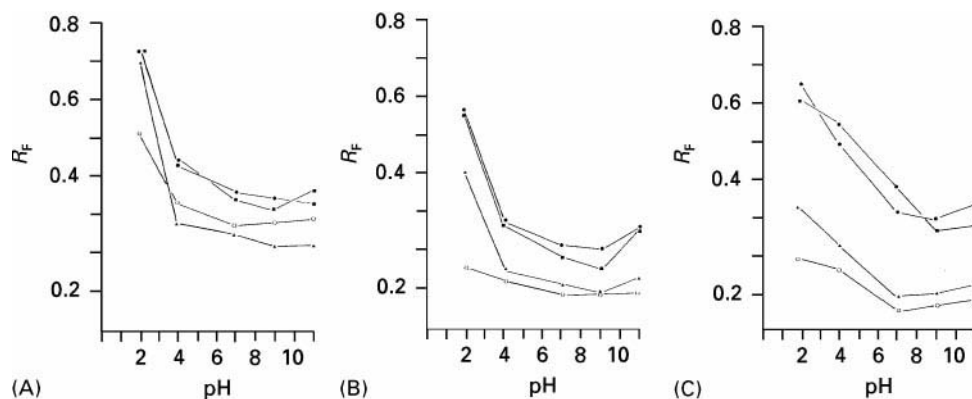


Figure 4 Effect of pH on the R_f values of some dihydroxybenzoic acids on (A) silica gel coated with cetrимide, (B) paraffin-coated silica gel and cetrимide and (C) C_{18} -bonded silica gel and cetrимide.

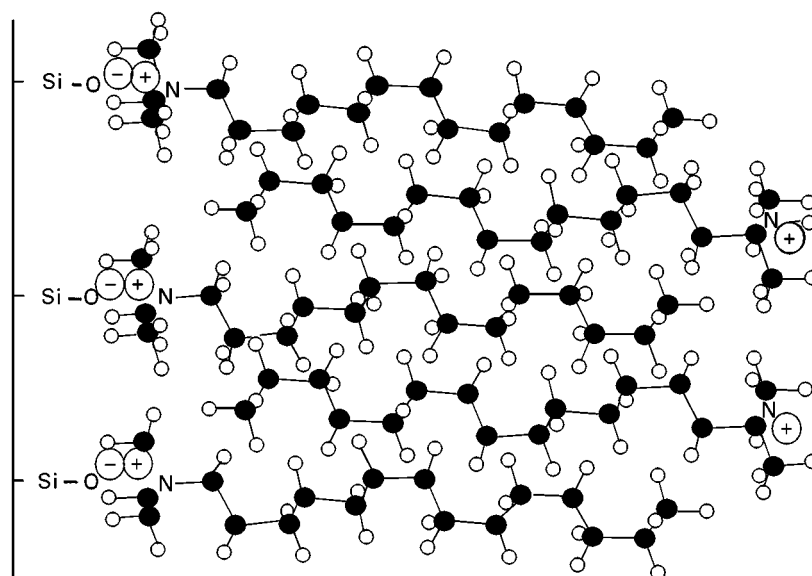


Figure 5 A schematic representation of the possible interaction of long chain IP-reagents with silica gel.

be a result of the acidic nature of the silica surface remaining after the bonding process: this may suppress the ionization of these weak organic acids. This is not to say that IP reagents have no effect on the TLC of such compounds – far from it – and IP reagents can be used to modify R_F for these analytes if required. However, in the case of the RP-TLC of strongly acidic compounds, there is no doubt that the chromatography of such analytes greatly benefits from the use of an IP reagent (and may not be possible without them). Examples of the type of compound where significantly better results are obtained with the employment of an IP reagent (either in terms of ability to modulate R_F or improvements in spot shape) include substances such as mono- and dihydroxylated benzoic acids (e.g. salicylic acid, gentisic acid, etc.). Suitable reagents for the IP-TLC of acidic compounds include tetramethylammonium and tetrabutylammonium salts, cetrimide and the bola-form IP reagents alluded to above.

Acidic IP Reagents for the TLC of Bases

A number of applications of the use of IP-TLC for the chromatography of bases have also been described. That said, it is our experience that the TLC (both normal-phase (NP) and RP) basic compounds can often be performed without recourse to IP systems. Thus, the inclusion of ammonia in NP-TLC systems is often enough to suppress the ionization of weak bases and obtain good chromatography. In RP systems the main problem is usually spot tailing, as the basic analyte interacts with the residual silanols present on

the silica surface. This effect can usually be controlled by using a competing base such as ammonia or triethylamine in the eluent. Alternatively a strong organic acid, such as trifluoroacetic acid (TFA), can be used as a mobile-phase additive (0.1% v/v). It is arguable that this is in fact an ion pairing effect and that the TFA is forming an IP with the basic group on the analyte, thus preventing silanophilic interactions. In HPLC the IP chromatography of bases is usually effected using sulfonic acids such as heptanesulfonic acid and the longer chain dodecylsulfate. Studies have been performed with these reagents on silica gel, silanized silica gel, paraffin-coated silica gel and a range of C_{18} -bonded phases, with the best results usually obtained by coating the reagents on to the plate rather than including them in the mobile phase.

In an early study silanized silica gel was used and the reagents (sodium lauryl ethersulfate or triethanolamine dodecylbenzenesulfonate) were mixed with the stationary phase prior to the preparation of the plates. The amount of reagent employed varied from 0.025% up to 4%, with the maximum effect on the R_F of the test amines seen between 2 and 3%. Later studies showed that a range of reagents, from methyl up to dodecyl sulfonic acids, could be employed with C_{18} -bonded plates and acetone–water (0.1 mol L⁻¹ IP reagent) solvent system for the IP-TLC of analytes such as atropine, codeine, eupaverin and papaverine. Not surprisingly, the authors found that the trend for decreasing R_F of the test solutes was correlated with increasing alkyl chain length for the reagent.

In our own studies the IP-TLC of β -blockers was investigated using silica gel, paraffin-coated silica gel

or C_{18} plates impregnated with sodium dodecyl sulfate. In fact it was possible to obtain good results for these analytes only on the C_{18} -bonded materials. The largest effects on chromatographic behaviour were seen for the dodecyl sulfate reagent.

Overpressure IP-TLC Overpressure TLC (described in detail elsewhere in this Encyclopedia) is a forced flow planar chromatography system whereby the TLC plate is held under pressure beneath an inert and impermeable membrane and the mobile phase is pumped through the layer. This mode of TLC has been used successfully with quaternary ammonium IP reagents using both silica gel and bonded stationary phases and with 10-camphor sulfonic acid on silica gel. When using a reagent such as cetrimide the results were shown to be only really acceptable if the plates were precoated with the reagent, at a concentration of 0.05 mol dm^{-3} . However, if in addition to coating the plates, cetrimide (optimally 0.1 mol dm^{-3}) was also included in the developing solvent, a noticeable improvement in spot shape was seen. Interestingly, and unlike the situation observed for normal IP-TLC, a noticeable dependence of R_F on pH was noted: best results depended upon the stationary phase. So, with bare silica pH 5 gave the best separations whilst on a C_{18} -bonded silica pH 8 was optimal. Later work extended the use of IP-overpressured liquid chromatography (IP-OPLC) to basic compounds with 10-camphor sulfonic acid as the IP reagent, with silica gel as the stationary phase. Interestingly, the investigators noted that this reagent was ineffective when used alone (impregnated into the silica gel by immersion, with or without the reagent also present in the solvent). However, when the plates had previously been impregnated with cetrimide, good results were obtained. This was interpreted as the formation of a double layer of some description. Presumably the cetrimide interacts with the silanols on the surface of the silica gel to form a lipophilic layer on to which the camphor sulfonic acid can be adsorbed. Optimum results are obtained if the plates are pretreated with 0.05 mol L^{-1} solutions of the reagents and both cetrimide and 10-camphor sulfonic acid are present in the eluent at the same concentration. pH effects were also noted in this work, with the best results seen at pH 5.5.

Chiral IP-TLC IP reagents have been used in a limited number of cases in HPLC for the resolution of enantiomers and similar work has also been performed in TLC. Here the aim is to form diastereoisomeric complexes with different chromatographic mobilities rather than mask polar ionizable groups in order to moderate polarity. A number

of IP methods for β -blockers such as propranolol and alprenolol have been reported, based on the use of *N*-benoxycarbonyl-glycyl-L-proline (ZGP) and a diol-bonded HPTLC phase. These plates are firstly pre-washed with dichloromethane and then dipped in the mobile phase to impregnate them with the reagent. The mobile phase consists of a 5 mmol L^{-1} solution of ZGP and 0.4 mmol L^{-1} ethanolamine in dichloromethane. In one method the samples were applied to the plate followed by continuous developments to *c.* 4 cm for 10–20 min. The plates were then dried and the process repeated. Solvent composition for this type of IP-TLC can be critical, and in our hands the inclusion of 2% v/v ethanol to the dichloromethane is essential in order to obtain separation of the enantiomers. With less than this amount of ethanol, no resolution is obtained whilst higher proportions result in increased R_F values for the analytes and a loss of resolution. Sample loading is also an important factor: the best results are obtained with loadings of propranolol of *ca.* $5 \mu\text{g}$ applied as a 1 cm band.

Conclusions

IP-TLC can be used to advantage for the modulation of the chromatography of acidic and basic analytes on a range of stationary phases. The way in which the reagents are used (i.e. in the mobile phase or impregnated on to the plate) depends on the structure of the reagent itself and the nature of the stationary phase. Probably the most important factors controlling the magnitude of the effect obtained when using an IP reagent in planar chromatography are the structure of the reagent (with long chain reagents giving the biggest effects) and the concentration of reagent employed. In contrast to HPLC, pH has relatively little effect in many IP-TLC systems.

See also: II/Chromatography: Liquid: Ion Pair Liquid Chromatography. **Chromatography: Thin-Layer (Planar):** Modes of Development: Forced Flow, Overpressured Layer Chromatography and Centrifugal. **III/Acids:** Thin-Layer (Planar) Chromatography. **Bases: Thin-Layer (Planar) Chromatography. Chiral Separations:** Ion-Pair Chromatography; Thin-Layer (Planar) Chromatography. **Impregnation Techniques: Thin-Layer (Planar) Chromatography.**

Further Reading

Gazdag M, Szepesi G, Hernyes M and Vegh Z (1984) Optimisation of reversed-phase ion-pair chromatography by overpressurized thin-layer chromatography 1. Overpressure thin-layer chromatography. *Journal of Chromatography* 290: 127–134.

- Jost W and Hauk HE (1983) Reversed-phase thin-layer chromatography of nitrogen bases using alkyl sulphonates as ion-pair reagents. *Journal of Chromatography* 264: 91–98.
- Kovacs-Hadady K (1996) A systematic study of the adsorption of different ion-pairing reagents on reversed-phase layers. *Journal of Planar Chromatography* 9: 174–177.
- Lepri L, Desideri PG and Heimler D (1978) Soap thin-layer chromatography of some primary aliphatic amines. *Journal of Chromatography* 153: 77–82.
- Ruane RJ, Wilson ID and Troke JA (1986) Normal- and reversed-phase ion-pair thin-layer chromatography with bifunctional (bolaform) bis(trimethylammonium) ion-pair reagents. *Journal of Chromatography* 368: 168–173.
- Szepesi G, Gazdag M, Pap-Sziklay ZS and Vegh Z (1984) Optimisation of reversed-phase ion-pair chromatography by over-pressurized thin-layer chromatography. III. Over-pressurized thin-layer chromatography using 10-camphor sulphonic acid as ion-pair reagent. *Chromatographia* 19: 422–430.
- Tivert A-M and Backman A (1989) *Journal of Planar Chromatography* 2: 472–473.
- Tomkinson G, Wilson ID and Ruane RJ (1989) Reverse-phase ion-pair high performance thin-layer chromatography of acids on a C-2 bonded silica gel. *Journal of Planar Chromatography* 2: 224–227.
- Wilson ID (1986) Ion-pair reversed-phase thin-layer chromatography of organic acids. Re-investigation of the effects of solvent pH on R_F values. *Journal of Chromatography* 354: 99–106.

Layers

F. Rabel, EM Science, Gibbstown, NJ, USA

Copyright © 2000 Academic Press

Although many new tools, such as high performance liquid chromatography (HPLC) and capillary zone electrophoresis, have been developed for the analytical laboratory, none can be used as quickly or inexpensively as planar or thin-layer chromatography (TLC). This tool can be used as a complete analytical system (from initial separation to final quantitation) or as a stepping stone or aid for other analytical methods. It is one of the few analytical tools that requires no sample clean-up, saving time and money. Many samples can be applied and analysed at the same time on a single TLC plate. With the combinatorial chemistries now being used to develop new drugs, renewed interest in this high throughput tool has become apparent.

One distinct advantage, often overlooked, is that when using TLC for any screening or method development, it shows components at the origin that do not move and will over time contaminate other analytical systems, such as an HPLC column. This potential problem would not be apparent if optimizing solely on the HPLC system. Likewise, samples applied after sample preparation would show whether or not sufficient clean-up was actually accomplished with the sample preparation technique used. This can save countless hours of frustration that would develop long after the initial method was thought to be sufficient for the analytical results needed.

Planar chromatography is also useful when optimizing a solid-phase extraction (SPE) method, when

many SPE tubes and extracting solvents will be tried. Up to 20 samples can be spotted on each side of a 20 × 20 cm TLC plate (Figure 1). Each side can be developed in 10–20 min to just 6–8 cm. A quick look under UV light or spray visualization can show the presence or absence of a compound of interest. This is certainly many times faster than doing the 40 samples on an HPLC system, one at time.

Samples from any fast TLC screening which are found to be positive for the component of interest can be confirmed or further quantified with TLC by applying standards and using densitometry or can be transferred to another analytical technique.

This is a brief review of the layers most often used and referenced in planar chromatography. For details on less used layers or more information on those discussed, the reader is referred to the Stahl book listed in the Further Reading section. A few recommended methods or tips are included within each section, where their use will improve performance or the property of a plate or separation.

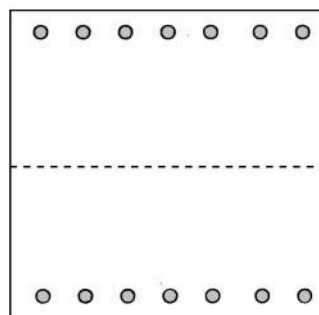


Figure 1 Multi-spotted 20 × 20 cm TLC plate.

Silica Gel

Classical TLC began with silica gel layers and these continue to be the most used today. Silica gel can be used with any solvent system for a separation – from nonpolar to polar, thus accounting for its versatility. **Table 1** shows a list of compounds and classes which can be separated on a silica gel layer.

The separation mode on a silica (or other oxide layer), when a mostly nonpolar mobile phase is used, is the adsorption mode. This mode separates the compounds according to general polarity classes, which is often a necessary initial step if dealing with a multi-component/multipolarity mixture.

The solvents for this mode also contain some polar modifier to balance the selectivity of the silanol sites,

Table 1 Compounds and classes separated by silica gel TLC

Amino acids, derivatized	Flavonoids
Abused drugs	Flavours
Aflatoxins	Fungicides
Alkaloids	Ginsenosides
Allergans	Glycerols
Amines	Glycols
Anaesthetics	Herbal medicines
Analgesics	Herbicides
Anthraquinones	Histamine
Antiarrhythmics	Immunosuppressants
Antiasthmatics	Inorganic ions
Antibacterials	Insecticides
Antibiotics	Lipids
Anticholesterolaemics	Esters
Anticoagulants	Fatty acids
Anticonvulsants	Gangliosides
Antidepressants	Glycolipids
Antifungals	Phospholipids
Antihypertensives	Triglycerides
Anti-inflammatories	Medicinals
Antimalarials	Mycotoxins
Antimicrobials	Nucleotides
Antioxidants	Polyaromatic hydrocarbons
Antiparasitics	Peptides
Antipsoriasis	Pesticides
Antipsychotics	Phenols
Antiseptics	Phenolics
Antituberculars	Pigments
Antitumours	Polyamines
Antiulcers	Polymer additives
Antivirals	Porphyryns
Artificial sweeteners	Prostaglandins
Barbiturates	Proteins
Bile acids	Quats
Bilirubin	Quinine
Carbohydrates	Quinoline
Carboxylic acids	Saccharides
Colchicine	Saponins
Cosmetic components	Steroids
Diuretics	Surfactants
Dyes	Toxins
Essential oils	Vitamins
Explosives	

Table 2 Relationship of silica gel pore size and surface area

Pore size (nm)	Surface area ($\text{m}^2 \text{g}^{-1}$)
6	300
12	170
30	100
50	60

so selective elution is possible. The details for some of these solvent systems are found in other parts of this article in classical texts and in current literature.

The silica gel used for TLC was derived from the silica gel used for column chromatography, placed into a mortar and pestle and reground to a finer particle size. Since the standard pore size for silica gel for column use was 6 nm, this became the *de facto* standard for TLC. Other pore size silica gels are available (4, 8 and 10 nm), but these are not as widely used and so definite conclusions about their possible selectivity differences compared to the 6 nm material cannot be drawn. One difference that could be important is the difference in the surface area of these silicas, as can be seen in **Table 2**. As the pore size increases, the surface area decreases. With less surface area and wider pores, larger molecules, such as biopolymers, separate better.

Also very important in the use of silica gel is the type of silica generated in the manufacturing process. There can be different types of silanols present, as shown in **Figure 2**. The best synthetic method should produce the most homogeneous surface, so that there are no (or minimal) numbers of surface areas of increased binding (with geminal or vicinal silanols), but mostly free silanol sites. Such a silica gel would produce the most symmetrical bands on the plate, with little tailing evident.

There are two particle sizes of silica gels used to make TLC plates. The classical size range is 15–40 μm , which is currently used for most 20 \times 20 cm plates. The newer size range is 3–8 μm and this is used for high performance TLC (HPTLC) plates. As with any chromatographic technique, a smaller particle can give higher efficiency to a separation, is faster since shorter development distances

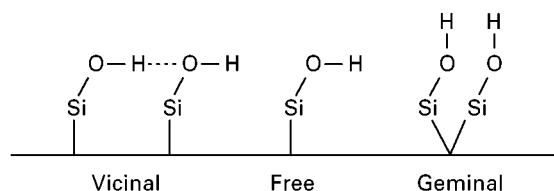


Figure 2 Possible silanol types on silica gel.

are used, and gives more compact spots so the limits of detection are improved. The performance of the HPTLC plates can be further improved if the semi-automatic or automatic devices (Camag, Desaga) are used for spotting and development. For the most part, however, the standard manual spotting techniques and the large volume developing chamber are used for both TLC and HPTLC for routine screening work.

The selectivity and activity of silica gel are determined to a large degree by the amount of water held on to its surface. Generally, a plate is activated to drive off excess water by placing it in an oven at 100°C for 20–30 min. After cooling to room temperature, however, it begins to re-adsorb the atmospheric humidity and rapidly hydrates again. This is not bad, since a completely dry silica would retain compounds too strongly and would need much stronger solvents to move the components.

Chemically Bonded Layers

An ever-expanding line of special phases, many developed first for use in HPLC, are now available as a thin layer. Although their use is not widespread, there are many reasons for using them since they can be excellent scouting tools for HPLC or the reverse – taking a HPLC method and using the solvent systems on the equivalent bonded layer can give a rapid screening tool. Thus, little method development is required, with the exception of some re-ratioing of the mobile-phase components on the thin-layer plate.

The most commonly used HPLC phases are made of silica bonded with various-length alkyl chains, C₁₈, C₈, C₄, CN (cyanopropyl) or aromatic rings, e.g. phenyl. All of these bonded phases are available on a TLC plate for reversed-phase chromatography. They are used as any TLC plate, but often need some organic component in the spotting solvent, since an entirely aqueous solution will not penetrate the bonded hydrophobic surface of some of these layers. The usual methanol–water, acetonitrile–water, tetrahydrofuran–water mobile phases or other combinations of organic solvent–water with acids, bases or buffers can be used. Some highly bonded layers from certain manufacturers need a higher percentage of organic solvent to work well, and to ensure that the layers will not lift away from the support. If a higher percentage of water needs to be used with such layers, the water portion can be made up of 0.5–1 mol L⁻¹ NaCl to help the layer remain intact through the development. Some manufacturers have produced reversed-phase layers that are compatible with solvents containing up to 100% water in the mobile phase.

Other polar bonded layers, like NH₂ (aminopropyl), CN and Diol (propanediol) are often used as a substitute for silica gel with the same type of – mostly nonpolar – mobile phases, but they can also be used with polar mobile phases to accomplish different separations and selectivities.

Aluminium Oxide (Alumina)

Although many metal oxides have been used for TLC, only aluminium oxide has found much use and is available from manufacturers as prepared plates. It can have a vastly different selectivity compared to silica gel since its surface is composed of positive and negative charge sites, with no equivalent to a silanol. Its activity is also very much tied, to the water content on its surface and it is also used with activation. Another difference in this sorbent compared to silica gel is the possibility of making it with a wide range of different pore sizes (6, 9 and 15 nm). Alumina can also be made with acidic, neutral or basic surface character, which provides a range of possibilities for use depending on the compounds being separated. Thus, with a basic layer, acidic components would not move at all, so selective separation (in this case, capture) can begin at the origin where the spotting is done. Thus, a completely different arsenal of analytical tools can be found with these layers and in method development the different layers can be tried side by side to determine the effect of the different surface pHs.

The various-pH alumina layers have been used for separations of alkaloids, amines, antibiotics, lipid, nucleosides, pigments, polyaromatic hydrocarbons, steroids and surfactants. Many researchers seem to fear possible decomposition of components on alumina layers, but this is probably an unfounded myth, and would be just as possible on any high surface area exposed to an oxygen-containing atmosphere and a laboratory with fluorescent lighting.

Cellulose

Another classical column packing made smaller and applied to planar chromatography is cellulose. It has less polarity than an oxide and is hence a much milder sorbent for separation. It is mostly used as a partition chromatographic medium, for separating amino acids, analgesics, antiarrhythmics, antibiotics, carbohydrates, flavonoids, herbicides, inorganic ions, polyaromatic hydrocarbons, phenols, phenolics, pigments and proteins. Its largest use today is for determining amino acid composition using a two-dimensional method (spot in one corner, develop in one direction with one solvent, dry, turn 90° and develop in the

second direction with another solvent). Two-dimensional development gives a much better separation of the > 20 amino acids which can be determined with this method. Some chiral separations have also been performed on cellulose layers, since it possesses a crystallinity that attracts one enantiomeric form more than the other. This chiral recognition can be enhanced and improved by using derivatized celluloses as layers, e.g., acetylcellulose and benzylcellulose.

Polyamide

Polyamide is a sorbent made from the polymer nylon. As the name implies, it has amide linkages throughout the structure, allowing excellent hydrogen bonding to occur on the surface. It has found use in the separation of alkaloids, amino acid derivatives, anilines, antioxidants, catecholamines, dyes, indoles, lactones, nucleotides, -sides, -bases, pesticides, phenols, steroids, sugars, sulfonamides, thiamines or any organic structures with OH or COOH or CHO groups. The mobile phases used on such a layer are as varied as they are for silica gel. For instance, hexane–diethyl ether–acetic acid (1 : 1 : 0.1) has been used for barbiturate separations, benzene–ethyl acetate–formic acid (5 : 10 : 2) has been used for artificial sweetener separations, and water–95% ethanol (6 : 4) has been used for sulfonamide separations. There are a few references to its use (see Further Reading).

Kieselguhr (Diatomaceous Earth)

Kieselguhr or diatomaceous earth is an amorphous silica of fossil origin. Once mined and carefully cleaned, it can be used as a support for TLC. It has a very wide pore size, and very low surface activity compared to silica gel and other TLC sorbents. Because of its inactivity, it is often impregnated with paraffin oil, silicone oil, or similar and used for reversed-phase partition chromatography. Some manufacturers have a prepared TLC layer of a 1 : 1 mixture of silica gel and kieselguhr. It performs like a less active silica gel, with faster mobility of the solutes compared to a pure silica gel layer.

Ion Exchangers

A few ion exchangers derived from cellulose or resinous backbones are available for traditional ion exchange separations. Obviously, these layers are used for separations of ionic compounds, from pharmaceuticals to inorganic salts. These can be found with both weak and strong exchange sites. Ion exchange cellulose layers include diethylaminoethyl (DEAE,

a strongly basic anion exchanger), ECTEOLA (treating alkali cellulose with epichlorohydrin and triethanolamine, a weakly basic anion exchanger), PEI (impregnating cellulose with polyethyleneimine, a strongly basic anion exchanger). The PEI cellulose is widely used to separate nucleic acid derivatives. The resinous layers include the SA (strongly acidic cation exchanger) or the SB (strongly basic anion exchanger). Researchers with an interest in reading more about these and their possible separations should consult the texts in Further Reading.

Impregnated Layers

TLC layers with special properties can be made by adding reagents to the silica gel slurry when the plates are made, or after, by dipping the prepared TLC plate into reagent solutions, or predeveloping them with the reagent solution. Since the prepared layers of this type are limited, and might age if not used, they are prepared mostly by the latter two methods. After drying and activation, they are used in the normal manner.

The most often used impregnated layer is that made with a 1–5% solution of silver nitrate in methanol. This impregnation allows geometric *cis/trans* or C=C bonded isomers to be separated, usually with various lipid mixtures. If made by impregnation, they must be dried and stored in the dark, and wrapped in aluminium foil so that oxidation caused by light does not occur.

Other useful impregnated layers found in the literature include 1% potassium oxalate aiding in the discrimination of polyphosphoinositides, 5–10% magnesium acetate aiding in the separation of phospholipids, and 5% ammonium sulfate, which allows a TLC plate to be charred without spraying with sulfuric acid or other reagents. Whether this dry reagent charring does as good a job for a particular class of compounds as other charring reagents should be investigated.

Pre-scored, Channelled, Preconcentration Zone and Preparative Plates

Other physical devices are also available on thin layers to increase the versatility of the technique. One is the pre-scoring of the glass plate on the back to allow a 20 × 20 plate to be broken into 5 × 20 or 10 × 20 plates. Likewise, a pre-scored 10 × 10 cm HPTLC plate can be broken into 5 × 10 and 5 × 5 sizes (Figure 3). This allows the user to break the plate according to the number of samples needing to be run, to save on plates.

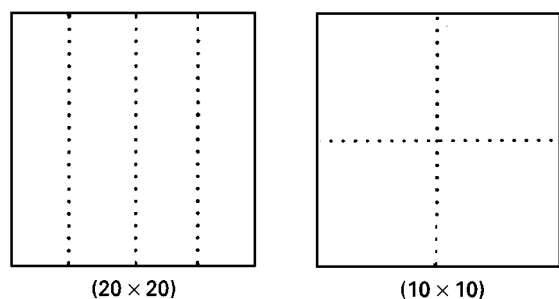


Figure 3 Pre-scored TLC plates.

Other plates have channels placed on the layer about 1 cm apart, 1–2 mm wide, to separate one lane of silica gel from another (Figure 4). Originally it was used to give a blank lane for densitometry background correction, but became widely used to keep samples separated when drugs of abuse testing was done in the 1960s. Now most initial drugs of abuse testing is done with EMIT (enzyme multiplied immunoassay technique) and radioimmunoassay techniques, with confirmation by gas chromatography–mass spectrometry.

Preconcentration Zone

One of the most useful tools designed into a thin layer plate is the preconcentration or pre-spotting zone (Figure 5). This is a 2.5–4 cm area at the bottom of a plate, composed of diatomaceous earth or wide-pore silica gel, to allow heavy loading or vertical (horizontal if doing preparative work) streaking of the sample. As the mobile phase passes through this special material, the sample does two things. If a circular spot, it changes to a band (an oblong circle). If a dilute sample, it also concentrates itself in this band. In this portion of the plate, no separation occurs. The separation begins only after the band transfers from the preconcentration zone into the silica (or, in some cases, the RP18 or other bonded-phase) layer. This

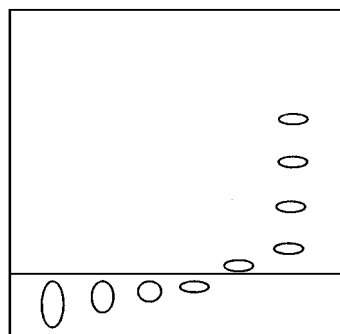


Figure 5 Progressive separation on a preconcentration zone plate.

reforming of the sample (from a spot to a band) gives a more efficient separation, since the band is narrower along the direction of development.

Preparative Layers

These are thicker layers of any of the above sorbents to allow larger quantities of sample solutions to be applied. These layers are 0.5, 1 or 2 mm thick (compared to the usual analytical thickness of 0.25 mm). Usually the sample is applied to the plates as a streak by some automatic device. The thicker the layer, the more sample solution that can be applied (Figure 6). Such a plate is used in the traditional manner, but will generate greater heat of solvation if using a silica plate with a developing solvent with a polar modifier. This will make spots or bands travel faster, and a readjustment of the solvent ratios may be necessary to reduce the band travel.

Binders

Many sorbents made into thin layers do not form a layer that adheres sufficiently strongly. Good binding ability is required so the plate can be handled during activation, spotting, developing and visualiz-

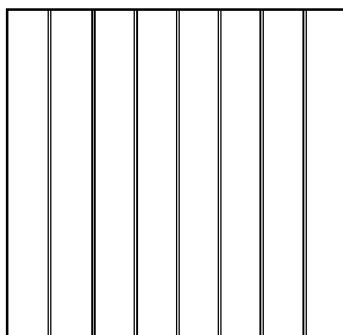


Figure 4 Channelled TLC plate.

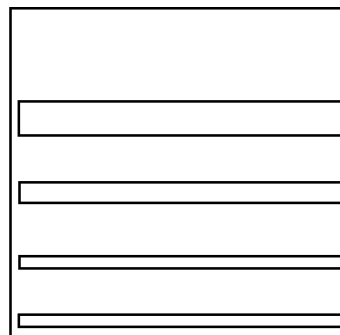


Figure 6 Streaked and developed preparative TLC plate.

ation. If any layer is lost or weakened, then the separation accomplished is lost. A binder of some kind is added to the sorbent formulation when making up the thin-layer plates.

Classically, the binder used for silica gel layers was calcium sulfate hemihydrate (plaster of Paris) added between 10 and 15% by weight. After slurring with water and being applied to the plate, it begins to form the dihydrate within a few minutes. This is called setting and the layer becomes semi-rigid as the water is chemically removed. After further drying, the binder effectively holds the slurry to the glass support. This binder forms what is considered a soft layer, with only a slight resistance to abrasion. As a result, a silica gel G layer needs care in use so that the fragile layer is not damaged when spotting or being moved to and from the developing chamber. This plate is made commercially by only one manufacturer in the USA, or by special order. Most often it is a binder formulation used by researchers making their own plates. Its main advantage is that any spots on such a layer are easily removed for subsequent work.

An alternative binder is a hydrated or fused silica gel, often designated H. A few per cent of this binder also gives a suitable soft-layer plate. This binder is most often used when interference by the calcium sulfate of a G-type of plate has to be eliminated.

Because of the fragile nature of the G and H binders, most planar chromatographic plate manufacturers use polymeric binders. Such polymer binders give a moderate to hard layer that withstands all handling done throughout the TLC process so the integrity of the layer is not harmed. Any damage to the surface done during activation, spotting or visualization can create artefacts and/or affect the results of the chromatography. These plates easily accommodate all stacking, shipping and user steps, and have the selectivity of the classical G-type plate.

The binders used are proprietary but are generally based on a water-soluble polymer such as polyvinyl alcohol (PVA) or polyvinyl pyrrolidone (PVP). These are added to the slurry in a few per cent by weight. They cross-link during drying and heating. They can be made stronger, generally, by reheating before use. This reheating or activation helps not only to dry the silica gel plates, but also to give better reproducibility. Just as important, too, is that the heating makes the binder work better under the conditions of development, even for a reversed-phase plate which is most often going into an organic/water-developing solvent.

Such harder layers are more convenient to use, allowing marking or writing on the top of the plate for identification purposes. Some are more difficult to

spot since the binder imparts some water resistance to the layer. By adding from 5 to 10% ethanol to any aqueous sample (or spray reagent for visualization) the viscosity of the aqueous solutions is dramatically decreased so that penetration into the layer is not a problem.

Often different binders are used on bonded silica gel layers since getting the nonpolar C_{18} silica to stick to a polar glass surface is more difficult. Frequently, too, the bonded phase on a TLC plate is lighter (a smaller percentage by weight) than on the HPLC version to allow a greater solvent range (high or low water content) to be used.

These polymeric binders allowed alternative supports such as aluminium and plastic (usually a polyterphthlate) to be used as supports in addition to glass. With the correct percentage of binder, a certain amount of flexing can be done without cracking or lifting of the layer from these supports. The advantage of these backing materials is that they can easily be cut for resizing or removal of the separated spot. Such plates also allow easy storage, whether stored in the original box or punched and inserted in a file.

If trouble with a binder, such as lifting or bubbling, is observed, the binder may only need re-curing, i.e. reheating, to ensure greater cross-linking and strength. As mentioned above, it is recommended that all TLC plates – silica gel and bonded layers – be heated not only to remove absorbed water but also to make the binder stronger for subsequent steps.

If extraction is to be done from a plate to recover the analyte, the plate should be predeveloped overnight in the solvent (or solvent combination) to be used for the extraction. This will remove unpolymerized binder so it will not wash out into the extract and possibly interfere with further work or characterization. To remove any portion of silica gel from a polymer-bound plate, first wet the area by spraying with methanol-water (1 : 1) to soften the binder. It can then be removed with little flaking or dusting.

Other types of layers that have been around for a number of years are the impregnated and incorporated layers. With the impregnated layer, a fibrous support such as cellulose filter paper or fibreglass paper is impregnated with a silicate solution, treated and dried to form a type of silica gel or hydrated silica. It is very fast, but low resolution separation medium.

With the incorporated layers, the silica gel or bonded silica gel is mixed with fibres of a polyfluoro (or other solvent resistant formulation) polymer and a mat of the combination is cast (like a cellulose paper would be made) and processed to form a sheet. No binders need be added to either of these two types of

layers, but a percentage of the matrix plays no part in the separation.

Often cellulose, alumina and polyamide layers need no additional binders, since their physical properties allow them to form a strong surface bond with the different supports. This can be a combination of hydrogen-bonding ability and fibrous nature of the cellulose, the hydrogen-bonding ability of polyamide, and the particle size range of the alumina.

Supports

Most of the classical layers were prepared on glass since it was generally available and easily handled. It could be cut to any size and Camag and Desaga made special devices for holding the glass plates and dispensing the slurries. The glass had to have an especially smooth surface and often the edges were smoothed to prevent cuts to the operator's fingers while the plates were handled. Any glass used to prepare the TLC plates must be carefully cleaned to remove any grease or oils that might prevent an even layer from being applied.

Pre-scored plates are discussed above, but any glass-supported plate can be cut by placing it face down on a sheet or two of paper towelling and scoring the glass with a carbide scribe (using a steady, hard motion). The plate is then lifted, held along the two edges with a paper towel, and broken, using a combination of bending (away from the score) and a pulling apart to break the plate. A final step is to remove any loose silica (or other sorbent) from the newly cut edges with a paper towel. This prevents edge effects – faster movement of the solvent at any rough, sorbent edges.

With special automated equipment, some manufacturers began to use both aluminium and polyterphthalate plastic supports. Generally, thinner layers were found to be optimal on these flexible layers, but the separations are no different from that found on a glass plate since the other items such as the binder and silica gel are the same. Although most TLC plates sold today are still on glass, some researchers feel that the ability to cut to size or the removal of components after the separation is a distinct advantage. After cutting these plates with scissors or a sharp-bladed instrument, 'edging', discussed above, should be done.

The flexible layers can sag and should be stood in a chamber at a sharper angle (Figure 7) than a rigid glass plate. This is especially true if a chlorinated developing solvent is used. If one of the impregnated or incorporated layers discussed above is used, they require a special holding device or clamps to hang them in the developing chambers, as was used for paper chromatographic separations.

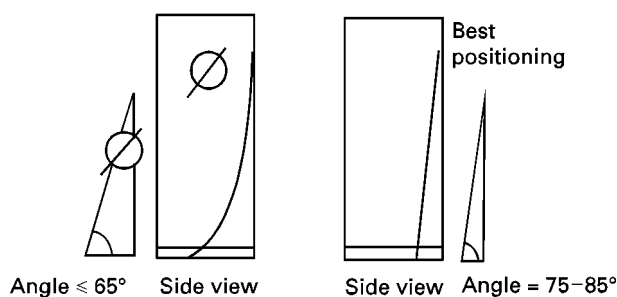


Figure 7 Positioning of flexible-backed TLC plates in a developing chamber.

Fluorescent Indicators

Detection is a special problem which must be considered when beginning a separation. Since most compounds are colourless, this might require considerable time to find the best reagents to spray on to a plate to visualize the components found in the sample. Such spray visualization might need a series of reagents to reveal the different species found in a complex mixture, such as with drugs of abuse.

One method used since the early days of TLC has been incorporation of a fluorescent indicator in the layer. A few per cent by weight of an inorganic salt such as manganese-activated zinc silicate, zinc cadmium sulfide, and others can be used. When visualizing a compound that can absorb the particular wavelength of light used to activate the fluorescent indicator, it will appear as a dark spot against the background fluorescence of the plate. This fluorescent indicator is often activated with either 254 or 366 nm wavelength light. It then fluoresces green, light blue or off-white. Other colours may be seen, too, but these are usually found when an organic fluorescent indicator is used. These latter indicators are often sprayed on after the plate is developed and dried, since they can move with many mobile phases that might be used for developing the plate.

The wavelength of the activation is usually stated after the F designation used by many manufacturers. One other item that might be important regarding fluorescent indicators is the fact that some might not be stable if exposed to strong acids like hydrochloric or sulfuric (i.e. mineral acids). Such strong acids can change the crystal structure of the inorganic salts and make them nonfluorescent. Usually this does not present problems since the fluorescent detection is tried as soon as the plate is dried, and before any other reagents are sprayed on to it for further detection of other types of compounds – ones that would not fluoresce or quench.

Conclusions

Although a simple analytical tool, TLC continues to be an important screening and scouting method for almost all industries. The various TLC layers and supports discussed above are available worldwide and the large amount of literature available continues to show the versatility of this tool. These products allow the chromatographer a wide range of possibilities for attacking an analytical problem with some knowledge and the confidence that success will be attained with a few plates and a few solvent systems.

See also: **II/Chromatography: Thin-Layer (Planar):** Preparative Thin-Layer (Planar) Chromatography. **III/Impregnation Techniques: Thin-Layer (Planar) Chromatography.** **Silver Ion:** Thin-Layer (Planar) Chromatography.

Further Reading

- Fried B and Sherma J (1999) *Thin Layer Chromatography, Techniques and Applications*, 4th edn. New York, NY: Dekker.
- Fried B and Sherma J (1996) *Practical Thin Layer Chromatography – A Multidisciplinary Approach*. Boca Raton, FL: CRC Press.
- Rabel F (1974) *Polyamide Chromatography*. In: Grushka E (ed.) *Bonded Stationary Phases in Chromatography*, pp. 113–137. Ann Arbor, MI: Ann Arbor Science Publishers.
- Stahl E (ed.) (1969) *Thin Layer Chromatography*, 2nd edn. New York, NY: Springer-Verlag.
- Touchstone JC (1992) *Practice of Thin Layer Chromatography*, 3rd edn. New York, NY: Wiley-Interscience.

Mass Spectrometry

W. E. Morden, LGC, Runcorn Research Centre, Cheshire, UK

Copyright © 2000 Academic Press

Introduction

Thin-layer chromatography (TLC) and high performance thin-layer chromatography (HPTLC), collectively often referred to as planar chromatography, in combination with *in situ* mass spectrometry (MS), provides a reliable means for the unequivocal identification of substances separated by this type of chromatography. More specifically, the ability to obtain mass spectrometric information from the separated analytes directly from the TLC/HPTLC sorbent obviates the need to recover the analytes of interest prior to analysis. Although TLC-MS is a useful method of separation and detection, it does have its limitations where complex matrices are encountered. However, tandem mass spectrometric (MS-MS) techniques can be used to enhance the mass spectral data by reducing the interference caused by coeluting analytes or general background noise generated by excipients on the plate.

Practical Considerations

Where the resolution of the separation is high, such as in capillary column chromatography, identification of components based on retention time is a well-established practice. Planar chromatography as normally practised does not achieve a separation efficiency equivalent to that obtained by column chromatography.

Consequently, the identification of components separated by planar methods based solely on R_F values and UV or fluorescence properties will always leave a higher degree of uncertainty about the true identity of the compounds present. Positive identification of unknowns has to be made by subjecting the analyte to a spectroscopic technique such as mass spectrometry.

As with other methods of chromatography, the use of MS as a TLC/HPTLC detector involves the detection and identification of the analyte in the presence of interfering materials from the chromatographic mobile and stationary phases. An analyte separated by planar techniques will be presented to a mass spectrometer along with the stationary phase, any organic phase modifier present, binding agents and fluorescent indicators. It is possible that residual solvents from the mobile phase, some of which may have high boiling points may be present. At best, the mass spectra obtained from a single spot taken from, for example, a silica gel HPTLC plate, will contain ions from the analyte with contributions from all these other compounds. When ionization is by fast atom bombardment (FAB) the situation is exacerbated by the formation of matrix and salt ions. Although useful information can be obtained from TLC/HPTLC-MS experiments, the information so obtained can be improved by using tandem mass spectrometric methods.

Mass Spectrometric Benefits of Planar Separations

The advantages of HPTLC to the mass spectrometrists are equally important. The contribution made by the

chosen detector in evaluating a separation method is often ignored. It is often assumed that the detector of choice is equally sensitive to all analytes presented to it and that the separation method and the detector do not influence each other. As a result, universal detectors that couple high sensitivity, specificity and selectivity are in great demand. A mass spectrometer is such a device. However, the operating limits of the mass spectrometer place some restraints on the chromatographic method of choice. Although the ionization of analytes may be considered as instantaneous, mass analysis is not. However, planar separations do not impose the same constraints on the mass spectrometer since the chromatography is completed prior to the analytes being presented to the mass spectrometer.

Planar Separations as a Sample Clean-up Process

A further use of HPTLC is where the chromatography is simply a clean-up process, or a purification step. The planar separation can be used to remove impurities such as plasticizers or high boiling hydrocarbons. A solvent system can be used that will allow the migration of the contaminants up the plate but will leave the sample of interest at, or close to, the origin. The purified analyte can then be introduced into the mass spectrometer by one of the methods described below.

Instrumentation

The approach to analysis by TLC/HPTLC-MS may be divided into two basic methods: instrumental and manual. The instrumental method involves the use of an automated probe onto which the whole chromatogram is attached. With this method, the integrity of the chromatogram is retained, but is restricted to ionization in the liquid phase by methods such as FAB and the related technique of liquid secondary ion mass spectrometry (LSIMS).

The manual technique involves the removal of the zone of interest from the plate. After removal, the analyte may be extracted from the sorbent prior to analysis, or analysed directly from the sorbent. The manual method is readily implemented and requires no further equipment or interfaces. Also, the classical vapour-phase electron and chemical methods of ionization (EI/CI) can be used.

Sample Application

The most common method of application, and that most suited to MS applications when MS analysis is to be straight from the adsorbent, is by a glass capillary as a spot ('spotting'). For single MS

experiments a single spot is usually sufficient. Where multi-MS experiments are to be performed, such as when tandem mass spectrometry is to be used, the application of a row of replicate spots is the preferred method, the separated analytes from a fresh spot being used as those from a previous one become exhausted. If the analytes are to be removed from the adsorbent before analysis by MS the application of a short line ('streaking') has been found to be the best method. Whether the *spotting* or *streaking* method is used, care is needed during application to keep the analyte origin as compact as possible. A sample that is too large causes poor-quality separations due to the analyte diffusing and causing the spot to broaden. Quantities of sample spotted are in the range of 1–50 $\mu\text{g } \mu\text{L}^{-1}$, 1–10 μL being applied to the plate by multiloading a 1–5 μL capillary.

Care has to be taken not to damage the surface of the adsorbent as this causes the mobile phase to elute unevenly, resulting in distorted spots and so leading to a loss of chromatographic resolution. The type of matrices being studied and the detection limit of the mass spectrometer are then the critical factors in determining to what extent analysis is possible. However, when sample loading needs to be high, the deconvolution-by-mass capabilities of the mass spectrometer often compensate for the reduction in resolution.

Sample Introduction after Planar Separation

Although analysis by planar chromatographic techniques and mass spectrometry has been practised for many years, there remain three principal methods of sample introduction.

The first method involves the analyte of interest being recovered from the adsorbent by elution with an appropriate solvent and introduced into the mass spectrometer's ion source as a discrete sample. After the area of interest of the chromatogram has been identified, usually by visual means, the perimeter of the area of interest, the 'spot', is marked with a soft-leaded pencil. The adsorbent is loosened from the backing with a flat-bladed tool such as a spindle screwdriver or microspatula. The loosened material is removed from the plate and mixed with a small quantity of solvent. Ultrasonication can assist in the extraction process. A small plug of quartz wool packed into a drawn-out Pasteur pipette (Figure 1) acts as a filter medium. The filtered adsorbent is washed with one aliquot of solvent.

Depending upon the method of ionization to be used, the extracted material may be introduced into the ion source by using the direct insertion probe for the ionization of volatile analytes by EI/CI; or by a desorption probe or cassette, such as for analysis by

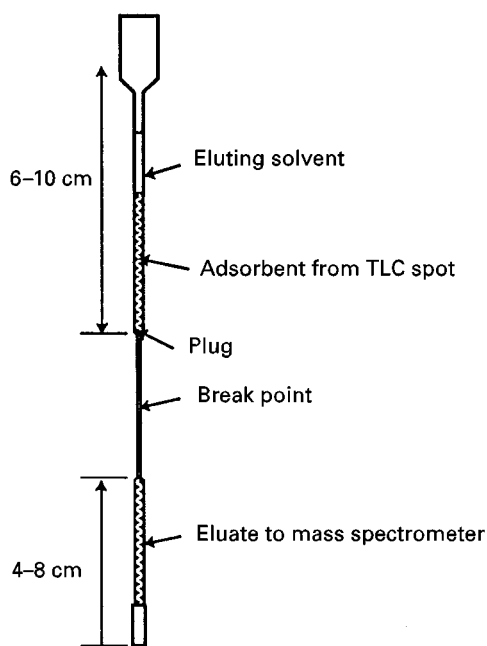


Figure 1 Analyte recovery by solvent elution.

FAB, LSIMS or MALDI (matrix-assisted laser desorption ionization), for the ionization of polar, non-volatile and/or thermally labile analytes. This method of sample introduction is particularly useful when the sample application methods of multispotting or streaking methods are used to obtain sufficient analyte for multi-MS-MS experiments.

In the second method the analyte and adsorbent are not separated. Both are introduced into the ion source simultaneously. After visual location, the spot is scraped off the plate and introduced into the ion source by one of the methods described above.

Both of the above methods destroy the integrity of the chromatogram. A third method of introduction uses a dedicated probe that enables the whole chromatogram to be introduced into the FAB/LSIMS ion source, so that a spatially resolved total ion current chromatogram of the organic material on the adsorbent may be obtained. With this type of probe it is necessary to use aluminium-backed plates. A strip approximately 10 mm × 65 mm, which is essentially one track of a developed plate, is cut out and mounted on the end of the probe. An appropriate matrix is painted down the length of the strip and the chromatogram is driven at a constant rate, with a maximum of 50 mm min⁻¹, by a stepping motor. The pulses to the stepping motor are controlled in conjunction with the scan control of the mass spectrometer, with the result that the whole chromatogram is scanned by the FAB/LSIMS beam. Mass spectral information is acquired for the whole chrom-

atogram. The analysis is analogous to the column chromatography experiment in that the analytes are ionized sequentially throughout the chromatogram.

Sample Concentration

As the HPTLC plate develops, spot diffusion occurs with the result that what was 0.5–1 mm spot at the origin may well be 5 or 6 mm in diameter after complete development. Thus the analyte may well be distributed over 10 times more adsorbent than when at the origin, with the result that when the analytes are introduced into the ion source along with the adsorbent and other extraneous compounds from the plate there is considerably more adsorbent than analyte presented for ionization. Because there is a finite amount of material that can be introduced into the ion source, occasions may arise where there is insufficient analyte available from which good quality mass spectral data may be obtained. Several methods of sample concentration have been devised to overcome this natural spot diffusion phenomenon. For example, an analyte spot can be encircled with a ring of solvent. As the solvent diffuses through the adsorbent the analyte will slowly migrate to, and concentrate at, the centre of the spot. The concentrated spot can then be removed and analysed.

An alternative is where, after chromatographic development on aluminium- and plastic-backed plates, the edge of the plate may be trimmed off using dress-maker's pinking shears. This leaves the plate with a regular saw-toothed edge. The plate is rotated by 180° followed by the application of solvent. The analytes are thus concentrated into the tips of the triangular-shaped segments of the plate. Once concentrated, the zone may be removed from the plate and introduced into the ion source as previously described.

A general method not confined to aluminium- and plastic-backed plates involves scribing a trapezoidal line around the sample spot (Figure 2). A strip, 1–2 mm wide, of the adsorbent on the outside of the

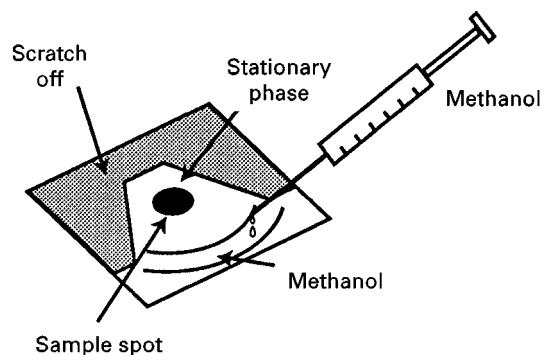


Figure 2 Zone concentration.

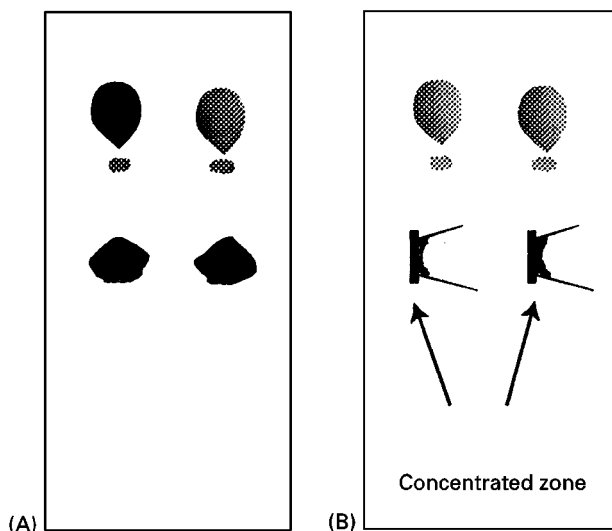


Figure 3 Zones (A) before and (B) after concentration.

line is removed. Then, from a 100 μL syringe, a quantity of an eluting solvent is slowly deposited on the base of the spot. After several tens of seconds the analyte condenses at the top of the trapezoid (Figure 3). The concentrated analyte and adsorbent are removed from the plate and are introduced into the ion source as described previously.

This method of spot concentration completely overcomes the need to overload the plate, with associated loss of chromatographic resolution, to enable sufficient sample to be introduced into the mass spectrometer for ionization. It is highly satisfactory prior to both vapour-phase and liquid-phase ionization.

Obtaining Mass Spectral Data

Vapour-Phase Ionization of the Analytes Directly from the Adsorbent

Where the analytes are volatile and thermally stable and are to be ionized by EI/CI, the zone of interest is concentrated as described earlier and a portion of the adsorbent is placed in a standard quartz sample tube. A small plug of quartz wool is placed on top of the sample to prevent the fine silica being sucked out of the tube during evacuation. The sample tube is then fitted to the direct insertion probe. The volatile analyte is desorbed by heat from the involatile adsorbent.

Where ionization is by MALDI, various methods have been described that enable mass spectra to be obtained directly from the TLC plate. TLC-MALDI takes advantage of the ability of MALDI to ionize fragile, low and high molecular weight compounds with a high degree of sensitivity and without significant fragmentation.

Liquid-Phase Ionization of the Analytes Directly from the Adsorbent

For polar, nonvolatile analytes, the spot is concentrated as described above. The adsorbent is then removed from the plate and slurried directly on the desorption probe with the chosen matrix.

Reducing Surface Effects during FAB/LSIMS Ionization

When compounds with high surface activity properties are present in a mixture, even as minor components, they have been shown to suppress the ionization of the major components during analysis by FAB/LSIMS-MS. Compounds such as surfactants possess these properties to such an extent that analysis by liquid phase ionization is unpredictable. Often the major component (of interest) is suppressed so much that it may not appear to be the major component at all. Planar chromatography has been shown to be an effective way of separating such suppressants from the analyte of interest.

Solo Mass Spectrometer versus Tandem Mass Spectrometry

As described previously, the use of MS as a TLC/HPTLC detector involves the detection and identification of the analyte in the presence of interfering compounds from the chromatographic process. At best, the mass spectra obtained from a single spot after planar separation will contain ions from the analyte and from these other compounds. When ionization is by FAB/LSIMS the situation may be exacerbated by the formation of matrix and salt ions (Figure 4). Although useful information can be obtained from TLC/HPTLC-MS

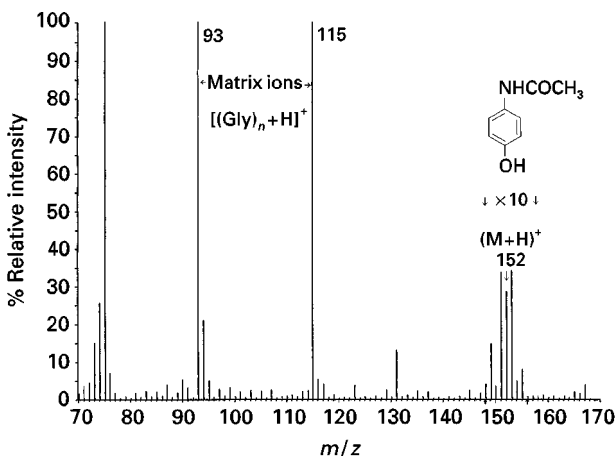


Figure 4 FAB-MS spectrum of paracetamol obtained from urine following ascending chromatography on diol bonded phase.

experiments, the information so obtained can be improved by using tandem mass spectrometric methods.

Tandem mass spectrometry is now a well-established analytical technique. Tandem mass spectrometry offers advantages in three major areas: structure elucidation of organic and biological molecules; the identification of components in complex matrices with or without chromatographic separation; and in trace analysis.

Several types of instrument capable of performing MS-MS analyses are available, the two most common types being the triple-quadrupole and the sector/quadrupole hybrid. In both types of instrument the ions selected in the first analyser are transmitted into the reaction region, normally a gas cell, where frag-

mentation occurs by collisions with a target gas, to yield characteristic product ions to be analysed and detected by the second analyser (Figure 5).

Ionization in Tandem Mass Spectrometry

Although all of the currently available methods of ionization are applicable to tandem mass spectrometry, where planar separations are involved the choice is limited to EI/CI and FAB/LSIMS. Although electron ionization (EI) is still the most commonly encountered method of ionization, and is used extensively in MS-MS studies, ionization methods such as FAB/LSIMS and CI, which normally produce intense ions providing molecular weight information, are preferable. It is desirable to produce as few ions of different m/z values as possible when using MS-MS following planar separations.

The benefits of FAB/LSIMS and CI are two-fold. First, they usually produce a spectrum with fewer interferences, enabling easier selection of precursor ion. Second, an increase in sensitivity is often achieved if all the ions current obtained from an analyte is concentrated in one ion.

Ion Dissociation in Tandem Mass Spectrometry

Although the MS-MS instrumentation is extensive, there is only one basic principle: the measurement of the mass-to-charge ratios of ions before and after dissociation in the reaction region. The change in mass of an ion carrying a single charge is the most commonly measured process and can be represented by the following equation:



where M_p^+ represents the precursor ion, M_d^+ represents the product ion and M_n represents the neutral fragment. The precursor ion may be the ion representing the relative mass of the species but need not necessarily be so; the precursor ion could be any ion formed within the mass spectrometer. However, molecular ions, and ions generated within the ion source, are the major subjects of MS-MS experiments. The product ion, M_d^+ , represented in the above equation may be one of many fragment ions formed by simultaneous dissociation within the reaction region, and as such indicates a direct relationship between it and the precursor ion. The neutral fragment M_n , being uncharged, is not normally detected. However, since M_p^+ and M_d^+ are measured the mass of the neutral fragment may be calculated by difference. These three variables form the basis of most MS-MS experiments and it is this basis that makes tandem mass spectrometry such a powerful analytical tool.

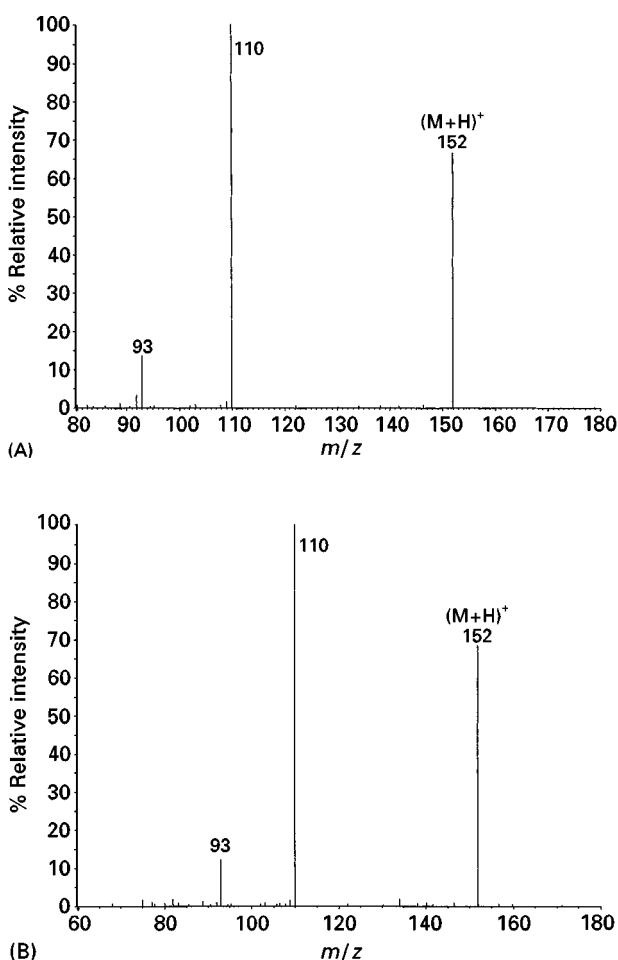


Figure 5 (A) FAB-MS-MS collision induced dissociation product ion spectrum of the $(M+H)^+$ ion from a standard sample of paracetamol following ascending chromatography on diol bonded phase. Collision energy, 60–40 eV; collision gas, argon at an indicated pressure of 3.0×10^{-6} mbar. (B) FAB-MS-MS collision induced dissociation spectrum of the $(M+H)^+$ ion from paracetamol extracted from urine and following ascending chromatography on diol bonded phase. Collision energy, 60–40 eV; collision gas, argon at an indicated pressure of 3.0×10^{-6} mbar.

Scan Functions in Tandem Mass Spectrometry

Although there are several scan functions that can be performed by tandem instruments, the most commonly used function in TLC/HPTLC applications is the product ion scan. The analytical characteristics of TLC/HPTLC-MS-MS product ion analysis contrast it with analysis by chromatography–chromatography–mass spectrometer.

Even so, just as with conventional MS, tandem mass spectrometry has its limitations. MS-MS cannot easily differentiate between isomeric and isobaric species. Isomers tend to produce similar product ion spectra and, since they cannot be separated by mass, two isomers transmitted into the gas cell simultaneously will give a product ion spectrum that is representative of the sum of the individual compounds.

Similarly, if isobaric components of the same elemental composition but of different structure are focused by the first analyser, transmitted into the gas cell and dissociated by collisions, the product ion spectrum obtained from the second analyser will be a compilation of product ions from the two components. It can be seen, therefore, that some form of chromatographic separation such as TLC/HPTLC prior to ionization can enhance the separative and characterization powers of the tandem mass spectrometer. Conversely, the use of MS-MS can greatly enhance the identification and characterization of isomeric and isobaric species separated by planar chromatography.

Conclusions

The use of MS and MS-MS as methods of detection in TLC and HPTLC separations is now well established and has been shown to be a powerful tool in the analyst's armoury. In practice, HPTLC-MS-MS has been shown to be no more technically demanding than traditional TLC-MS, yet the information provided is more detailed. Structurally important diagnostic ions are more easily observed by the elimination of matrix ions and general background clutter. Planar separation should be considered as a complementary technique alongside column methods of chromatographic separation where detection is by mass spectrometric methods. It can be applied to a wide range of polar and nonpolar analytes and is amenable to vapour-phase and liquid-phase methods of ionization. Moreover, where ionization is by laser desorption, separation by planar techniques may be the only choice.

See also: I/Mass Spectrometry.

Further Reading

- Aschcroft AE (1997) *Ionisation Methods in Organic Mass Spectrometry*. London: RSC.
- Barber M, Clench MR, Garner V and Gordon DB (1985) Surface effects in FAB mapping of proteins and peptides. *Biomedical Mass Spectrometry* 12: 355–357.
- Busch KL (1987) Direct analysis of thin-layer chromatograms and electrophoretograms by secondary ion mass spectrometry. *Trends in Analytical Chemistry* 6: 95–100.
- Busch KL (1992) Mass spectrometric detection for thin-layer chromatographic separations. *Trends in Analytical Chemistry* 11: 314–324.
- Busch KL (1996) In: Sherma J and Fried B (eds) *Handbook of Thin Layer Chromatography*, 2nd edition. New York: Marcel Dekker.
- Busch KL, Glish GL and McLuckey SA (1988) *MS/MS Techniques and Applications of Tandem Mass Spectrometry*. New York: VCH.
- Busch KL, Mullis J and Carlsen R (1993) Planar chromatography coupled to mass spectrometry. *Journal of Liquid Chromatography* 16: 1695–1713.
- Hamilton R and Hamilton S (1987) *Thin Layer Chromatography*. Chichester: J Wiley & Sons.
- Johnson T, Martin P, Monaghan JJ, Morden WE and Wilson ID (1992) Thin layer chromatography/mass spectrometry: the advantages of tandem mass spectrometry. *Rapid Communications in Mass Spectrometry* 6: 608–615.
- Masuda K, Harada KL, Suzuki M, Oka H, Kawamura N and Masuo Y (1989) Identification of food dyes by TLC/SIMS with a condensation technique. *Organic Mass Spectrometry* 24: 74–75.
- Mehl JT, Gusev AI and Hercules DM (1997) Coupling protocol for thin layer chromatography/matrix-assisted laser desorption ionisation. *Chromatographia* 46: 358–364.
- Morden WE (1995) *Tandem Mass Spectrometry*. *Encyclopedia of Analytical Chemistry*, pp. 2932–2938. London: Academic Press.
- Morden WE and Wilson ID (1992) TLC combined with tandem mass spectrometry: application to the analysis of antipyrine and its metabolites in extracts of human urine. *Journal of Planar Chromatography* 5: 255–258.
- Morden WE, Somsen GW and Wilson ID (1995) Planar chromatography coupled with spectroscopic techniques. *Journal of Chromatography* 703: 613–665.
- Oka H, Ikai Y, Kondo F, Kawamura N, Hayakawa J, Masuda K, Harada K and Suzuki M (1992) Development of a condensation technique for thin-layer chromatography/fast-atom bombardment mass spectrometry of non-visible compounds. *Rapid Communications in Mass Spectrometry* 6: 89–94.
- Poole CF and Poole SK (1991) *Chromatography Today*. Amsterdam: Elsevier.
- Somogyi G, Dinya Z, Lacziko A and Prokai L (1991) Mass spectrometric identification of thin layer chromatographic spots: implementation of a modified wick-stick technique. *Journal of Planar Chromatography* 3: 191–193.

Modes of Development: Conventional

T. H. Dzido, Medical Academy, Lublin, Poland

Copyright © 2000 Academic Press

In the conventional mode of development in planar chromatography the mobile phase is supplied to the chromatographic plate by direct contact with the adsorbent layer and the flow rate of the eluent is controlled by capillary forces.

The main modes of chromatogram development are linear, circular and anticircular. The most popular mode is linear development owing to its simplicity; no sophisticated equipment is used to apply the eluent to the chromatographic plate, as it is in circular and anticircular modes. In practice, linear development provides the resolution and reproducibility required for most qualitative and quantitative determinations. All three modes can be extended by applying continuous or multiple development.

Linear Development

Linear development is usually performed in a rectangular vessel with ascending migration of the eluent

through the adsorbent layer, from the bottom to the top of the chromatographic plate. The plate is usually positioned vertically in the developing chamber in a few millilitres of solvent. The separation of a standard lipid mixture by this mode of development is presented in **Figure 1A** and **B** by way of example. The separations were performed on a 10×10 cm pre-coated silica gel plate for high performance thin-layer chromatography (TLC), and on a conventional 20×20 cm plate (E. Merck) with eluent composed of methyl acetate-*n*-propanol-chloroform-methanol-0.25% aqueous potassium chloride (25 : 25 : 25 : 10 : 9). A conventional developing chamber (rectangular vessel) was lined with filter paper in order to ensure saturation of the vapour phase with the solvent. Samples were applied on the start line of the chromatographic plate in the form of streaks containing $0.5\text{--}3.0 \mu\text{g mL}^{-1}$ phosphorous lipid. The chromatographic process was performed at room temperature and was stopped when the eluent reached the upper edge of the plate (50 min for high performance TLC and 150 min for conventional plates). Natural lipids, cerebroside, sulfatides, phosphatidylethanolamine, phosphatidylinositol,

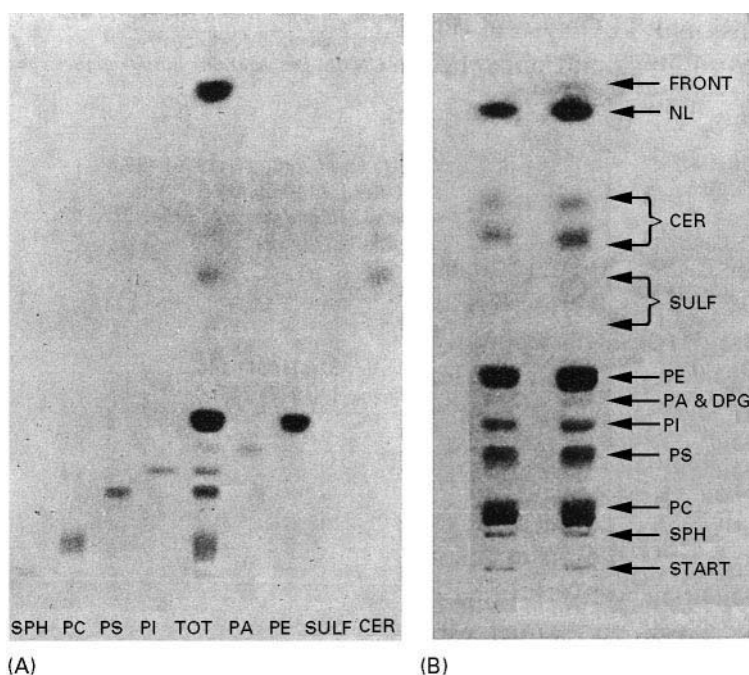


Figure 1 Chromatograms of standard lipids in the solvent methyl acetate-*n*-propanol-chloroform-methanol-0.25% aqueous KCl (25 : 25 : 25 : 10 : 9). (A) Separation on 10×10 cm HPTLC plate; (B) separation on classical pre-coated silica gel plate, 10×20 cm. NL, Neutral lipids; CER, cerebroside; SULF, sulfatides; PE, phosphatidylethanolamine; PA, phosphatidic acid; DPG, cardiolipin; PI, phosphatidylinositol; PS, phosphatidylserine; PC, phosphatidylcholine; SPH, sphingomyelin. Staining: molybdate reagent. (Reproduced with permission from Vitiello F and Zanetta J-P (1973) Thin-layer chromatography of phospholipids. *Journal of Chromatography* 166: 637.)

phosphatidylserine, phosphatidylcholine and sphingomyelin are well separated. In addition, cerebrosides with nonhydroxylated fatty acid chains are separated from those with hydroxylated chains. Similar resolution is observed for sulfatides. The minor brain phospholipids, phosphatic acid and diphosphatidylglycerol show the same migration distance but are well separated from phosphatidylethanolamine and phosphatidylinositol.

Slightly better efficiency can be obtained in horizontal chambers. Solvent migration is not dependent on gravity and equilibration between vapour and liquid is more rapid and uniform (inner chamber volume is small). A cross-section of the horizontal DS (Dzido, Soczewiński) chamber (Chromdes, Lublin, Poland) is shown in Figure 2. Eluent can be supplied to the chromatographic plate simultaneously from its opposite edges so that the number of separated samples can be doubled in comparison to development in a vertical chamber. An example of this type of linear development is illustrated in Figure 3. The samples of a test dye-stuff mixture were spotted along two opposite edges of the 10 × 20 cm high performance TLC plate coated with silica gel. The plate was developed with toluene from opposite directions simulta-

neously. The development stops when both eluent fronts meet each other in the middle of the plate.

Another variation of linear development can be performed by changing the eluent composition during the development process (stepwise or continuous gradient elution). Samples containing components of a wide range of polarity cannot be readily separated in a single isocratic development, but the application of a gradient mobile phase can improve the separation. Figure 4 demonstrates the application of a simple stepwise gradient to increase the separation efficiency of aromatic amines. The separation was performed in an equilibrium sandwich horizontal chamber which allows delivery of very small volumes of eluent to the plate. The glass plates (5 × 20 cm) were covered with a 0.25 mm layer of silica gel, dried in air and activated for 1 h at 80°C and 2 h at 130°C. The solutes were spotted 4 cm behind the solvent front as 0.5% benzene solutions to avoid solvent demixing. A marker (azobenzene, $R_F = 1$) was spotted together with the samples to show the position of the solvent front. Two chromatograms were obtained isocratically; development with constant concentration of the mobile phase with (A) 5% methyl ethyl ketone in cyclohexane, (C) 50% methyl ethyl ketone in cyclohexane

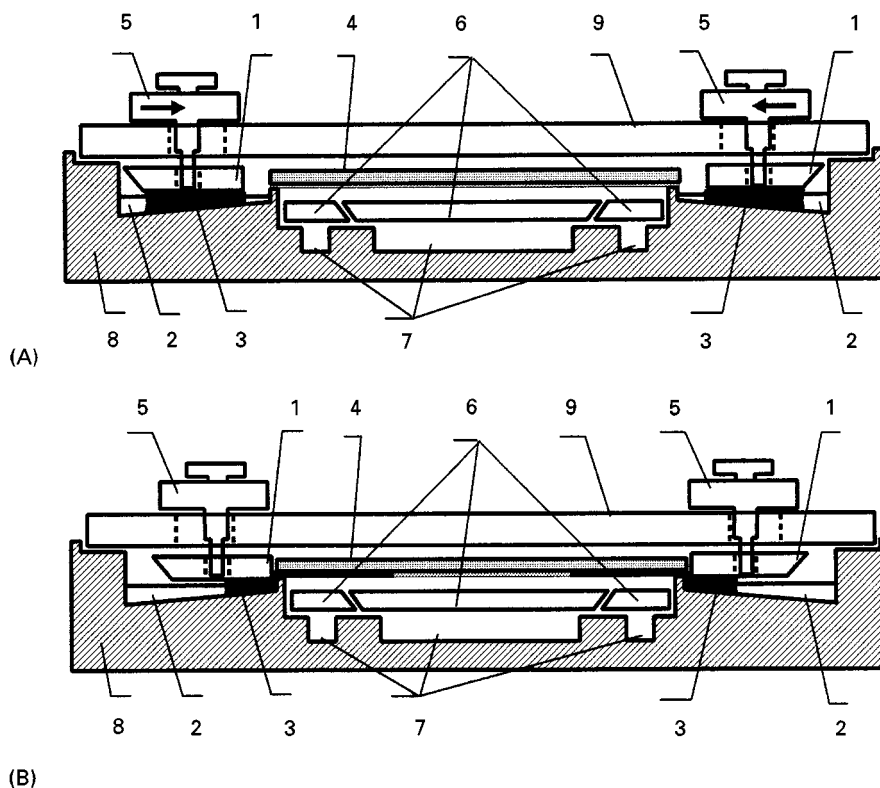


Figure 2 Cross-section of the horizontal DS chamber (Chromdes) (A) before and (B) during development from two opposite edges of the plate. 1, Reservoir cover plates; 2, eluent reservoirs; 3, eluent (black area); 4, chromatographic plate; 5, eluent distributor; 6, trough cover plates; 7, troughs; 8, body of the chamber; 9, glass cover plate.

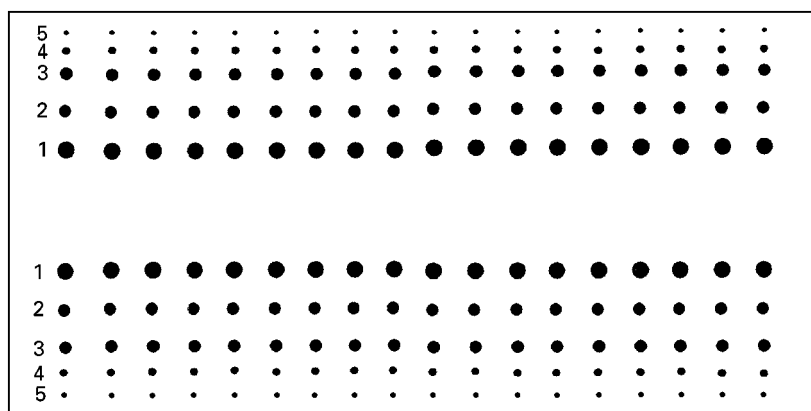


Figure 3 Separation of dyestuff mixture from opposite directions on silica gel high performance TLC plate with toluene. 1, 4-chloro-4'-dimethylaminoazobenzene; 2, fast yellow; 3, 2-nitroaniline; 4, 4-nitroaniline; 5, phenol red.

in cyclohexane and chromatogram (B) with a two-step gradient was performed in the following manner. The plate was first developed with 5% methyl ethyl ketone. When the azobenzene spot has reached the middle of the plate the development was continued with 50% methyl ethyl ketone until the eluent front (with the azobenzene spot) has migrated to the end of the plate which protruded from the chamber. The plate

was dried and the spots were detected by spraying with aqueous sodium hydrogen carbonate and then with bis-diazotized benzidine. All the spots are well separated using the two-step gradient development as opposed to separation by isocratic development.

Figure 5 shows the densitogram of a mixture of glycosides obtained by stepwise gradient development with seven eluent fractions which were applied consecutively to the plate (pre-coated silica gel glass plate for HPTLC, 10 × 10 cm, E. Merck) using a horizontal DS chamber. The volumes and compositions of eluent fractions as solutions of methanol in ethyl acetate were as follows: (1) 0.22 ml 0.0%; (2) 0.11 ml 20%; (3) 0.11 ml 30%; (4) 0.11 ml 2%; (5) 0.11 ml 10%; (6) 0.11 ml 35%; (7) 0.11 ml 100%. Each fraction was introduced into the mobile phase reservoir of the chamber with a micropipette after the previous one had been completely absorbed by the adsorbent layer. The plate was developed for a distance of 8 cm and the glycosides were detected by spraying with a solution of chloramine in trichloroacetic acid, heating for 5–10 min at 100–110°C and scanned with a Shimadzu CS-930 densitometer at 360 nm. The densitogram shows relatively good resolution of the glycosides.

This kind of simple stepwise gradient elution can help solve difficult separation problems, especially for mixtures consisting of solutes with a wide range of polarity, e.g. plant extracts. However, for more complicated stepwise gradients, poorer retention reproducibility is obtained.

Continuous Linear Development

In conventional continuous development the end of the chromatographic plate is immersed in the eluent and the opposite end is extended out of the chromatographic chamber, allowing the solvent to evaporate

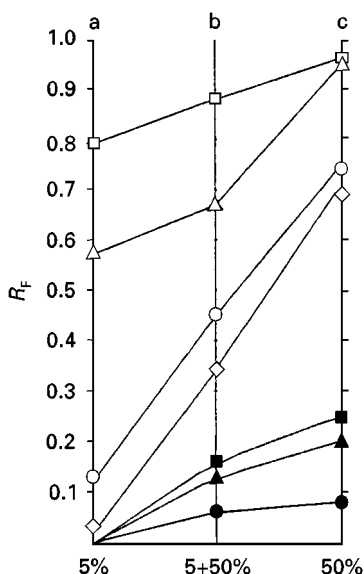


Figure 4 R_f values of aromatic amines obtained on silica gel plate. (a,c) Isocratic development with 5 and 50% solutions of methyl ethyl ketone in cyclohexane, respectively; (b) stepwise development with both solvents. Open squares, *N,N*-dimethylaniline; open triangles, *N*-ethylaniline; open circles, aniline; diamonds, 2-phenylenediamine; filled squares, 3-phenylenediamine; filled triangles, 4-phenylenediamine; filled circles, 3-aminopyridine. (Reproduced with permission from Soczewiński E and Czapińska K (1979) Stepwise gradient development in sandwich tanks for quasi-column thin-layer chromatography. *Journal of Chromatography* 168: 230.)

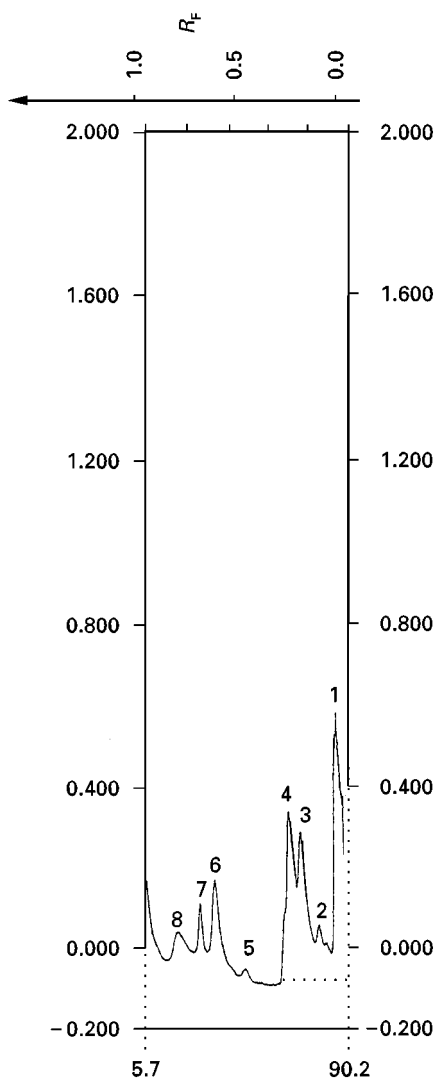


Figure 5 Densitogram of standard mixture of glycosides separated on silica gel high performance TLC plate with stepwise gradient elution (gradient programme given in the text). 1, Acetyl-digitoxine; 2, strophantine; 3, digitaline; 4, desacetylanatoside; 5, lanatoside; 6, convallatoxine; 7, digoxin; 8, digitoxine. (Reproduced with permission from Matysik G, Markowski W, Soczewiński E and Polak B (1992) Computer aided optimization of stepwise gradient profiles in thin-layer chromatography. *Chromatographia* 34: 303.)

and ensuring that solvent migration is continuous and constant; development is performed over the entire length of the plate. Continuous development can also be performed using a very short distance (short bed/continuous development, SB/CD) in comparison to the normal plate length and the eluent strength should then be much weaker than in the conventional development, because several dead volumes of eluent migrate through the layer. Examples of chromatograms with continuous development are shown in Figure 6. Pure chloroform (eluent strength 0.40) and

its mixture with carbon tetrachloride (eluent strength 0.18) were applied as eluents to develop chromatograms on the silica gel G plates, 10 × 10 cm (Camag,

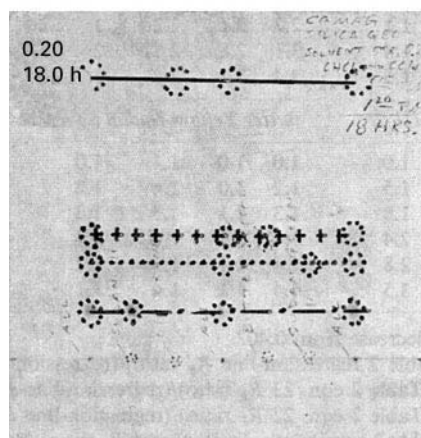
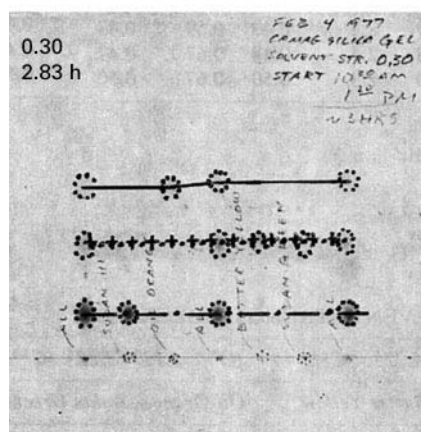
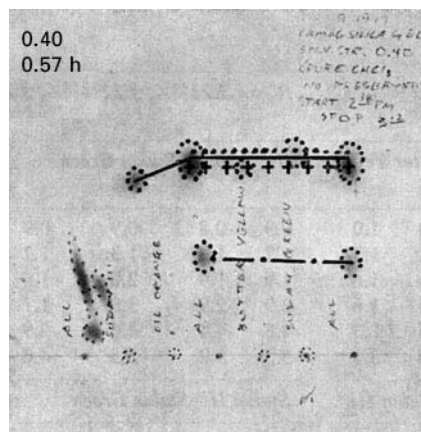


Figure 6 Separation of dye-stuff mixture applying continuous development on 10 × 10 cm silica gel plate with pure chloroform (eluent strength = 0.40) and with solvent mixtures consisting of chloroform and carbon tetrachloride (eluent strength = 0.30 and 0.20), solvent strength (ϵ) marked in the left top corner of the plate. Continuous line, Oil orange; crosses, Butter yellow; dotted lines, Sudan green; dots and dashes, Sudan III. (Reproduced with permission from Perry JA (1979) Solvent strength, selectivity, and continuous development. *Journal of Chromatography* 165: 117.)

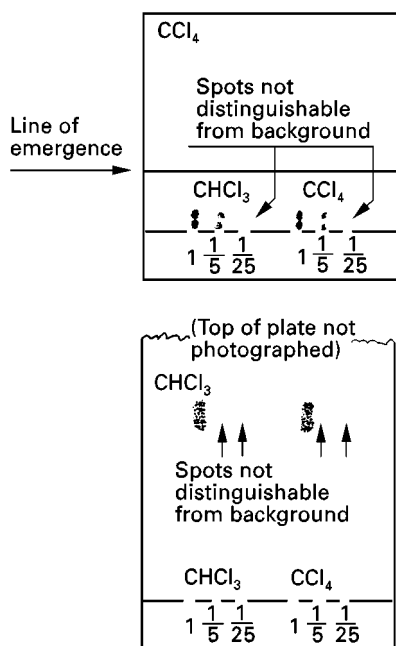


Figure 7 Bottom: chromatogram of a conventional development on 20 cm long silica gel plate with R_F values normally considered about optimal. Top: chromatogram of continuous development on 2.5 cm distance from the solvent level and 1.1 cm from the origin on silica gel plate with solvent of lower solvent strength, with R_F values less than 0.05. (Reproduced with permission from Perry JA (1979) Solvent strength, selectivity, and continuous development. *Journal of Chromatography* 165: 117.)

New Berlin, WI, USA). Eluent strength of the mobile phase applied for the chromatograms shown in Figure 6 was 0.40, 0.30 and 0.20 (marked at the top left corner of each plate). The samples (Oil orange, Butter yellow, Sudan green and Sudan III) were spotted on the plate as benzene solutions. The emergence position (atmospheric boundary) of the plate from the chamber was 7.3 cm from the start line (position of the sample spotting) and 7.8 cm from the eluent level (immersion position of the plate in the solvent). An extraordinary increase in selectivity is observed with solvent of the lowest eluent strength (0.20). However, it is necessary to perform the development for a very long time (18 h) to maintain the same relative retentions as when using pure chloroform (0.57 h). A more efficient separation can be obtained by applying continuous development over a very short distance. The two components of the sample (Oil orange and Sudan green) were separated using SB/CD on a silica gel G plate (10 × 10 cm, Camag, New Berlin, WI, USA) for 35 min with pure carbon tetrachloride. The R_F values obtained were less than 0.05 (Figure 7 (top)). Evaporation of eluent from the plate was carried out at a position 2.5 cm from eluent level and 1.1 cm from the spotting position. For com-

parison, Figure 7 (bottom) demonstrates the results of a conventional development on a 20 cm long bed of the same adsorbent with chloroform as the developing solvent, showing R_F values of about 0.38 and a development time of 90 min. The resolution obtained by the SB/CD mode is better than continuous mode and the development time is also shorter. Additionally, the spot diameter is very small, which leads to better detection levels.

Multiple Development

This mode of development is seldom applied in practice, in comparison to conventional development, but its significance is increasing owing to its greatly increased separation efficiency. A characteristic feature of this mode is repetitive development of the chromatogram on the same plate. Each development is followed by evaporation of eluent from the plate to prepare it for the next chromatographic process. The resolution provided is greater than conventional or continuous development, and mixtures of wide polarity can easily be separated. The spots to be separated are compact, which leads to better detectability. There are three types of multiple development:

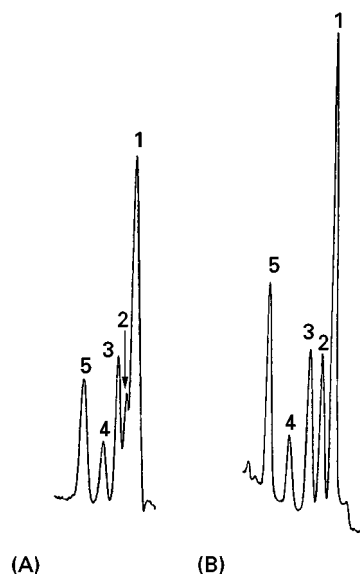


Figure 8 Comparison of (A) conventional and (B) multiple development (4 × 5) + (3 × 7) min for the separation of a mixture of PAH standards. The mobile phase was methanol-water (4 : 1) and the stationary phase octadecylsilanized silica gel. 1, Coronene; 2, benzo[g,h,i]perylene; 3, benzo[a]pyrene; 4, benzo[a]anthracene; 5, fluoranthene. (Reproduced with permission from Butler HT, Coddens ME, Khatib S and Poole CF (1985) Determination of polycyclic aromatic hydrocarbons in environmental samples by high performance thin-layer chromatography and fluorescence scanning densitometry. *Journal of Chromatographic Science* 23: 200.)

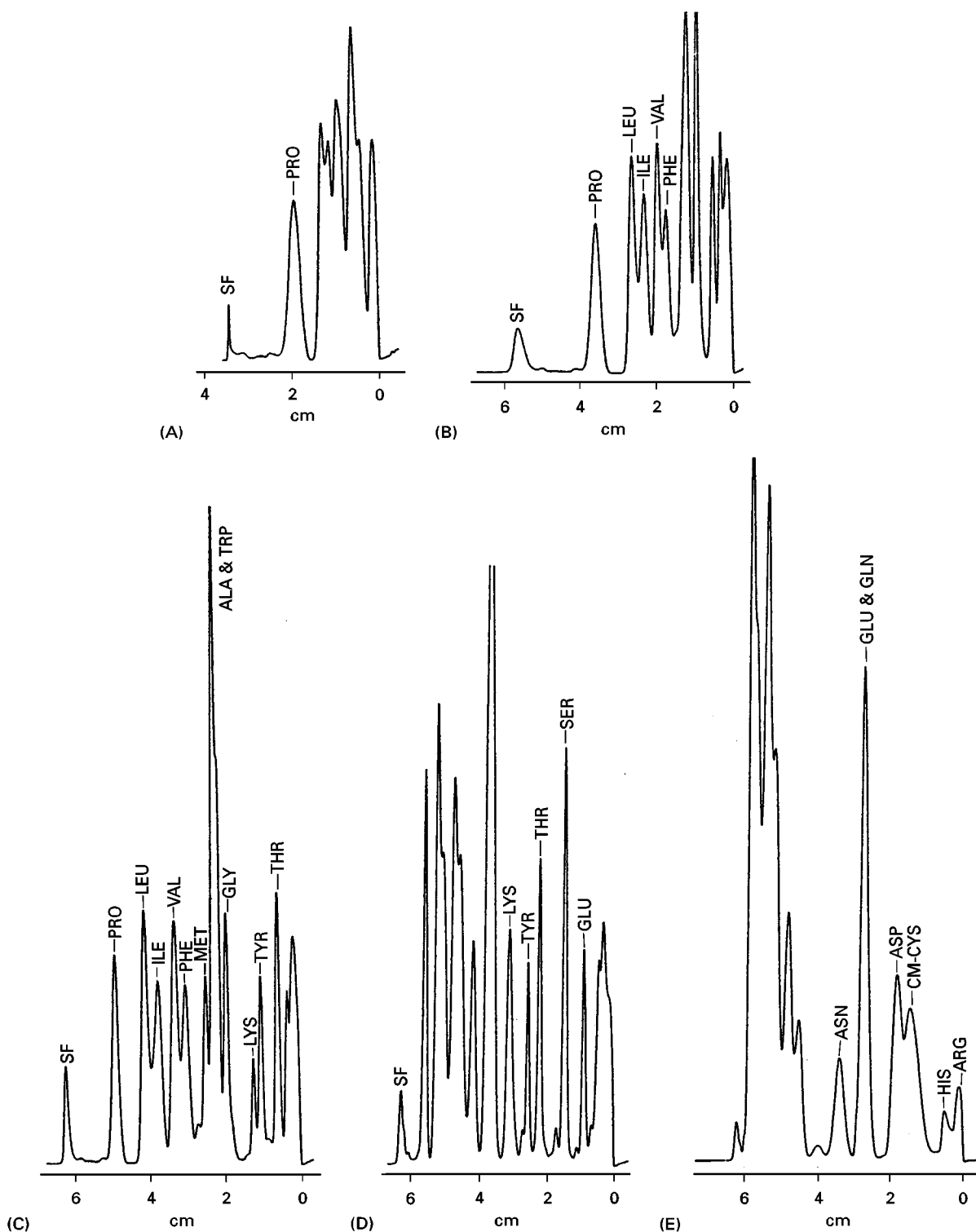


Figure 9 Chromatograms of PTH-amino acids after multiple development on silica gel plate. (A) First development with methylene chloride; (B) Second development with methylene chloride-isopropanol (99:1); (C) third development with methylene chloride-isopropanol (99:1); (D) fourth development with methylene chloride-isopropanol (97:3); (E) fifth development with ethyl acetate-acetonitrile-glacial acetic acid (74.3:25:0.7). (Reproduced with permission from Schuette SA and Poole CF (1982) Unidimensional, sequential separation of PTH-amino acids by high-performance thin-layer chromatography. *Journal of Chromatography* 239: 251.)

1. repetitive development with the same solvent in the same direction
2. repetitive development with the different solvents in the same direction
3. single or repetitive development in one direction with a given solvent, followed by single or repetitive development in the second direction perpendicular to it with another solvent (two-dimensional development)

The first mode is especially applied to the separation of poorly resolved spots, the second to mixtures of a wide range of polarity, and the third mode to separation of complex mixtures with components of similar polarity and/or different polarity.

The example of separation of polyaromatic hydrocarbons (PAH) by repetitive development with the same eluent is demonstrated in **Figure 8B**. The chromatogram was obtained with octadecyl silica layer and methanol–water (4 : 1) as eluent. Chromatogram developments were performed in an SB/CD chamber, position 4 (Regis Chemical Co.). The first four developments were performed for 5 min each and the next three for 7 min each. Between developments the plate was dried using a stream of purified nitrogen. The same PAH mixture was also separated applying conventional single development with the same plate and eluent. **Figure 8B** clearly shows the advantage of multiple development, in comparison to conventional development (**Figure 8A**).

Multiple development using change in eluent strength (stepwise gradient development) of each development stage is suitable for the separation of samples with a wide range of polarities. An example of this approach is shown in **Figure 9** for the separation of PTH-amino acid derivatives. Chromatography was performed on a 10 × 10 cm HPTLC plate coated with silica gel. The spots were applied 0.5 cm from the lower edge of the plate. The plate was developed in a short-bed continuous development chamber. The first development was made with methylene chloride for 5 min with a 3.5 cm development distance (**Figure 9A**). At this stage, only PTH-proline is well separated from the other derivatives. After evaporation of the methylene chloride, the second development was performed with methylene chloride–isopropanol (99 : 1 for 10 min with a 7.5 cm development distance). **Figure 9B** illustrates that five amino acid derivatives can be identified. The third consecutive development was made in the same way as the second (**Figure 9C**). The fourth step was obtained by development with methylene chloride–isopropanol (97 : 3) for 10 min (**Figure 9D**). The most polar PTH-amino acid derivatives are not resolved. Their resolution was achieved in the fifth step with ethyl acetate–

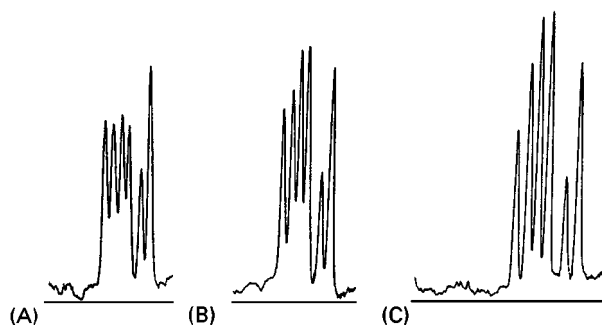


Figure 10 Separation of a mixture of oestrogens by multiple chromatography with fixed solvent entry position (A) and by multiple development with fixed (B) and variable (C) solvent entry position. Conditions are given in the text. The oestrogens, in order of migration, are 17 β -dihydroequilenin, 17 α -dihydroequilenin, 17 β -oestradiol, 17 α -oestradiol, equilenin and oestrone. (Reproduced with permission from Poole SK and Poole CF (1992) Insights into mechanism and applications of unidimensional multiple development in thin layer chromatography. *Journal of Planar Chromatography* 5: 221.)

acetonitrile–glacial acetic acid (74.3 : 25 : 0.7); only two derivatives (GLU, GLN) are not separated (**Figure 9E**).

The separation efficiency of conventional multiple development can be further improved by moving the solvent entry to a higher position on the chromatographic plate for each successive development. **Figure 10** shows the separation of a mixture of six

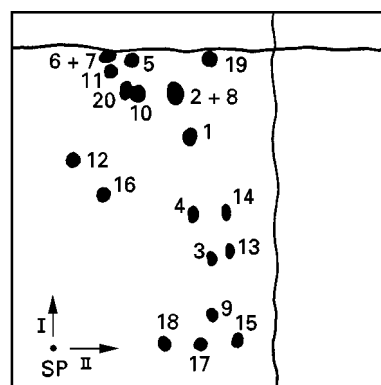


Figure 11 Two-dimensional chromatogram on RP-18 plate. Eluents: in the first direction, hexane–ethyl acetate–acetic acid (80 : 18 : 2); in the second direction, 1 mol L⁻¹ ammonia + 3% potassium chloride in 60% methanol. SP = Starting point. 1, DNP-Gly; 2, DNP-Ala; 3, DNP-Ser; 4, DNP-Thr; 5, DNP-Val; 6, DNP-Leu; 7, DNP-Ile; 8, DNP-Pro; 9, DNP-Met-O₂; 10, DNP-Trp; 11, DNP-Phe; 12, Di-DNP-Tyr; 13, DNP-Asp; 14, DNP-Glu; 15, DNP-CySO₃Na; 16, Di-DNP-Lys; 17, α -N-DNP-Arg; 18, Di-DNP-His; 19, DNP-OH; 20, DNP-NH₂. (Reproduced with permission from Lepri L, Desideri PG and Heimler D (1982) High-performance thin-layer chromatography of 2,4-dinitrophenyl-amino acids on layers of RP-8, RP-18 and ammonium tungstophosphate. *Journal of Chromatography* 235: 411.)

oestrogens on silica gel plates, 5 × 10 cm with a mobile phase of cyclohexane–ethyl acetate (3 : 1, v/v). The chromatograms were scanned at 280 nm. The poorest separation was obtained with simple multiple chromatography (Figure 10A); seven 7 cm developments with fixed solvent entry position at the origin of the plate were used. Separation was improved using multiple development with incrementing times (or distances) of development.

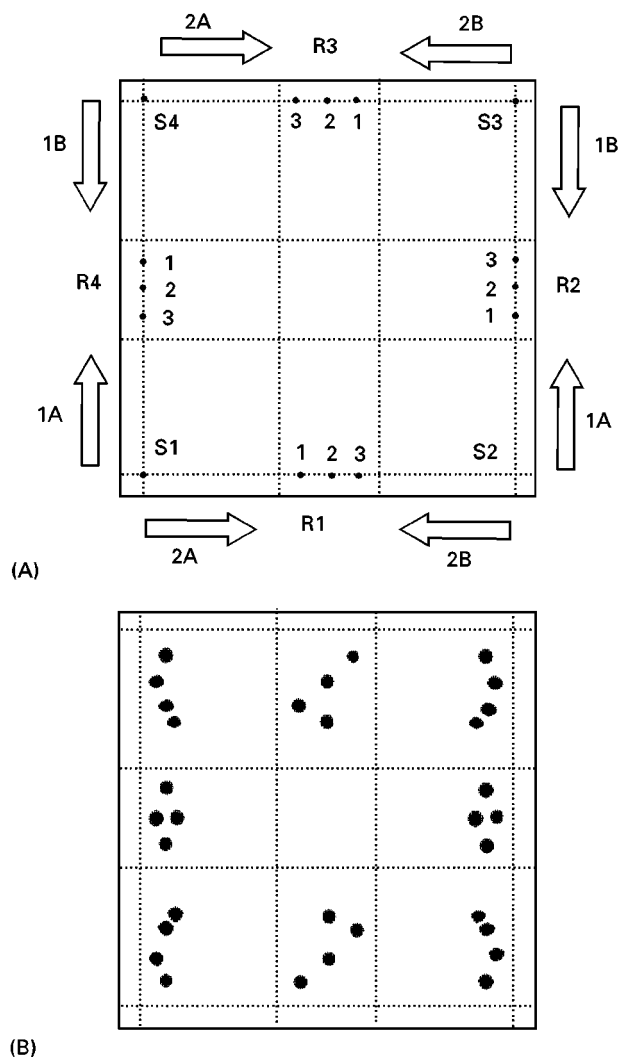


Figure 12 (A) Chromatographic plate prepared for separation of four samples by two-dimensional mode of development. (B) Four two-dimensional chromatograms of hormones on silica gel HPTLC plate, 10 × 10 cm. Eluents: the first direction (two developments simultaneously), heptane–diethyl ether–dichloromethane (4 : 3 : 2); the second direction (two developments simultaneously), chloroform–ethanol–benzene (36 : 1 : 4). 1, Zeranol; 2, *trans*-diethylstilbestrol and *cis*-diethylstilboestrol; 3 dienolestrol. (Part A reproduced from De Brabander HF, Smets F and Pottier G (1998) Faster and cheaper two-dimensional HPTLC using the '4 × 4' mode. *Journal of Planar Chromatography* 1: 369.)

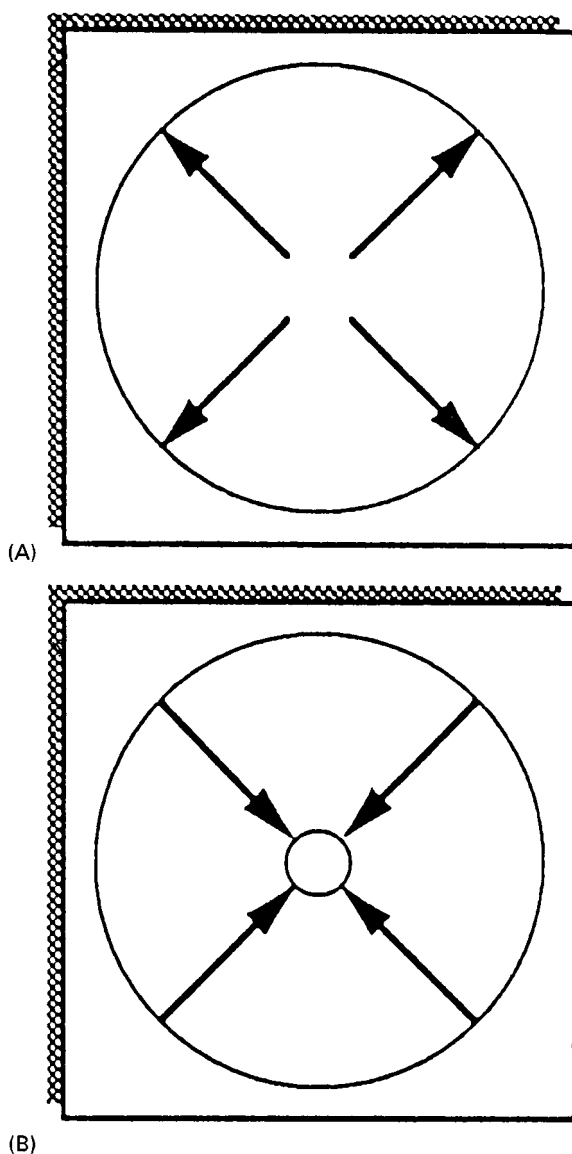


Figure 13 (A) Circular and (B) anticircular development. (Reproduced with permission from Bauer K, Gros L and Saur W (1991) *Thin Layer Chromatography – An introduction*, p. 36. Heidelberg: Hüthig Buch).

Figure 10B shows the chromatogram using nine developments with an incremental increase of the time of each successive development according to the sequence 5, 6, 7, 8, 9, 10, 12, 13, 14 min. However, the best separation was achieved with an incremental increase in the development time, as above, and a variable solvent entry position (0.5 cm below the slowest zone in each development; Figure 10C).

In two-dimensional development the sample is spotted at the corner of the chromatographic plate and developed with the first eluent (in the first direc-

tion). After this development, the eluent is evaporated from the plate; the spots are positioned along the edge of the chromatographic plate. The plate is then rotated through 90° and the next development is performed with the second eluent from the edge with the separated spots of the first development towards the opposite edge. The mixture can be redistributed on the entire plate surface if both eluents (or chromatographic systems) show a dramatic change in selectivity. An example of this mode of separation is shown in Figure 11. Twenty DNP-amino acids were separated using a reversed-phase layer. The sample volume was $0.2\text{--}0.3\ \mu\text{L}$. The spots were visualized in UV light (360 nm with a dried plate or 254 nm when wet). The migration distance was 6 cm. The separations were carried out at 25°C using a Desaga thermostating chamber. The elution in the first direction was performed with hexane–ethyl acetate–acetic acid (80 : 18 : 2) and in the second direction with 1 mol L^{-1} ammonia + 30% potassium chloride in 60% methanol.

Another variant of two-dimensional development is the separation of four samples on one plate instead of one sample on one plate. Figure 12 shows the application of this method to the separation of hormones. The silica gel plate, $10 \times 10\text{ cm}$, is divided into four sample zones and four reference zones, as shown in Figure 12A. The four samples (S1, S2, S3, S4) are spotted at each corner of the plate and the reference solutes on the four reference zones (R1, R2, R3, R4). The plate is introduced into a horizontal DS-chamber (Chromdes) or a linear developing chamber (Camag), which allows the development of the plate from two opposite directions simultaneously with eluent

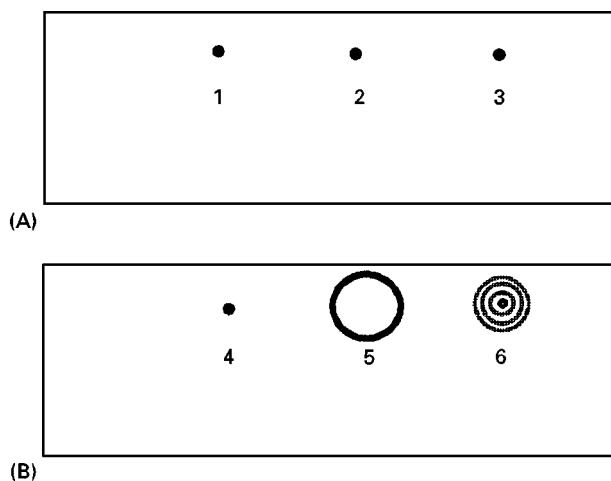


Figure 14 Ring chromatograms of spot test. (A) samples are spotted on the chromatographic plate; (B) circular chromatograms are developed with too weak a solvent (4), too strong a solvent (5) and a suitable one (6).

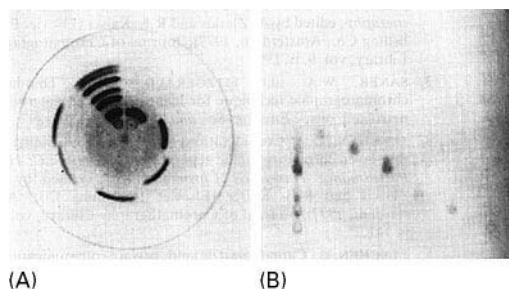


Figure 15 Sugar separation: (A) high performance radial chromatography in the U-chamber, and (B) linear separation performed on high performance TLC plate. (Reproduced with permission from Vitek RK and Kent DM (1978) High performance radial chromatography. *International Laboratory* 73.

1 (heptane–diethyl ether–dichloromethane, 4 : 3 : 2) in two opposite directions: 1A, 1B. When both eluent fronts reach the zone R2–R4 the plate is removed from the chamber and dried. Afterwards the plate is turned through 90° and developed with eluent 2 (chloroform–ethanol–benzene, 36 : 1 : 4) in two opposite directions: 2A and 2B. Before each development the chamber is saturated for 3 min with eluent vapour. After development the plate is sprayed with 5% sulfuric acid in ethanol, dried and heated for

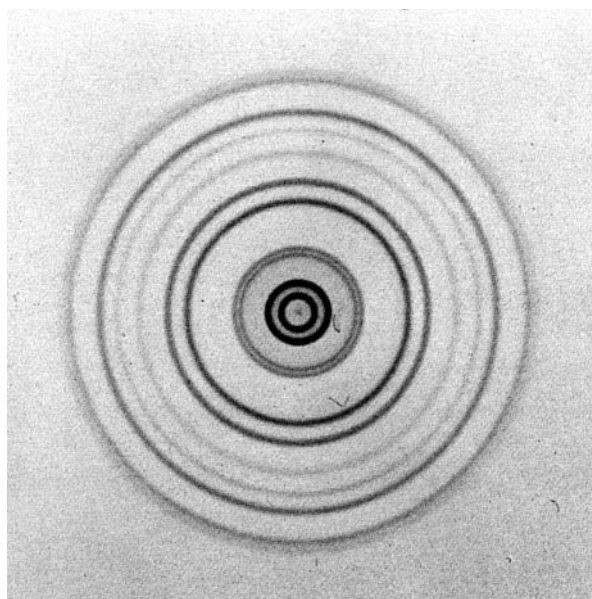


Figure 16 Circular chromatography on pre-coated silica gel high performance TLC plate. Lipophilic dyes, mobile phase; hexane–chloroform– NH_3 70 : 30. (Reproduced with permission from Rippahhn J and Halpaap H (1977) Application of a new high-performance layer in quantitative thin-layer chromatography. In: Zlatkis A and Kaiser RE (eds) *HPTLC High Performance Thin Layer Chromatography*, p. 204. Amsterdam: Elsevier Science.

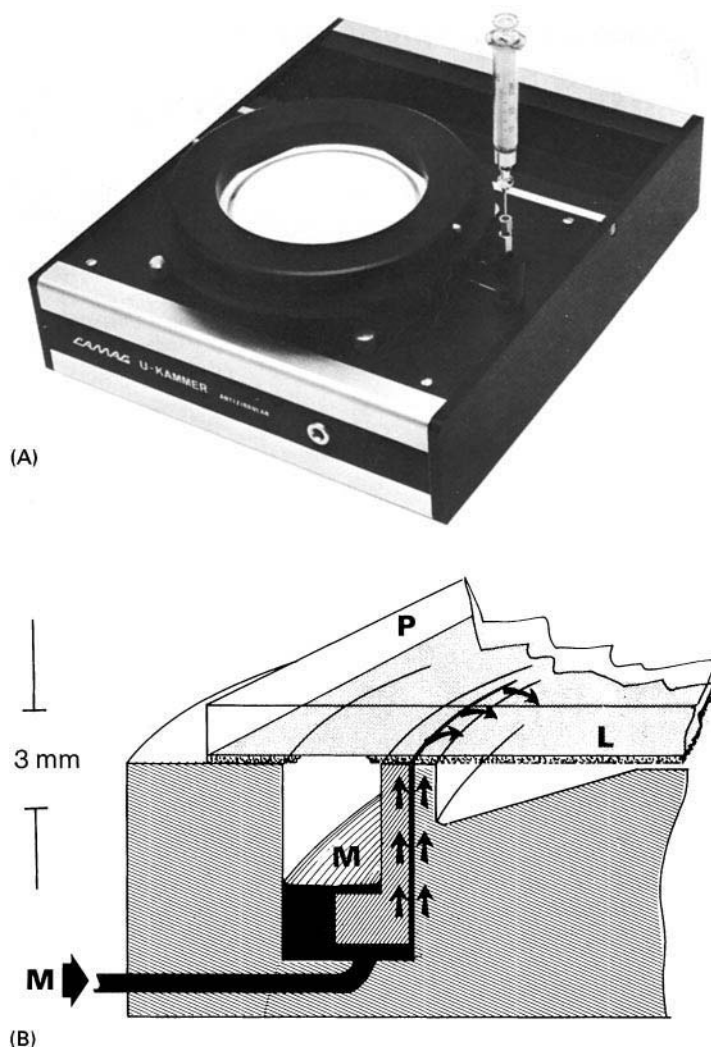


Figure 17 Anticircular U-chamber (Camag). M, mobile phase; P, high performance TLC plate; L, layer. (Reproduced with permission from Bauer K, Gros L and Sauer W (1991) *Thin Layer Chromatography – An Introduction*, p. 41. Heidelberg: Hüthig Buch Verlag.)

5 min at 100°C. The chromatogram shown in Figure 12B was observed in visible or UV light (366 nm).

Radial Development

There are two principal modes of radial development: circular and anticircular. In circular development the mobile phase is supplied at the centre of the chromatographic plate and eluent traverses towards the periphery (Figure 13A). The samples are spotted around the entry position of the mobile phase or are introduced (injected) into the stream of eluent just before its entry on the plate.

A very simple and probably the oldest application of circular development is the spot test, which is used for finding a suitable mobile-phase composition for TLC and HPTLC systems. The sample mixture is spotted on the adsorbent layer in several places and into the centre of each spot different solvents (pure or

occasionally mixtures chosen from the eluotropic series) are applied by a capillary or microsyringe. Then circular development provides ring chromatograms. Different solvents result in various shapes of chromatograms (Figure 14). If a solvent of too low an eluent strength is used, the sample does not move. On the other hand, the sample forms a compressed ring on the outer circle of wetted adsorbent when too strong a solvent is applied. Concentric rings on the entire wetted surface appear when solvents of suitable eluent strength and selectivity are used.

Circular development is also applied to analytical separations. Figure 15a shows an example of sugar separation obtained by circular development. A high performance TLC plate was developed in a U-chamber (Camag) with a solution of *n*-butanol–acetic acid–water (5 : 4 : 0.25). The samples were spotted around the central point of the plate at the entry position of the solvent. Visualization was performed

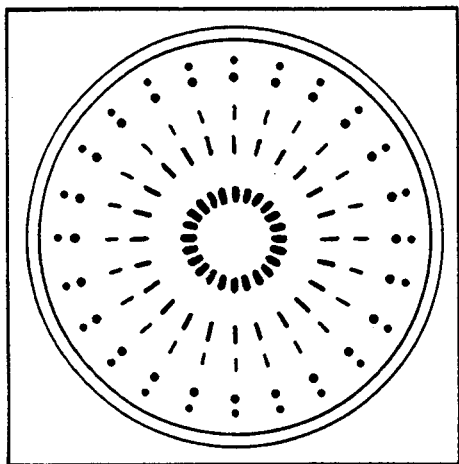


Figure 18 Anticircular chromatogram. (Reproduced with permission from Fenimore DC and Davis CM (1981) High performance thin-layer chromatography. *Analytical Chemistry* 53: 252A.)

with sulfuric acid containing naphthoresorcinol by spraying or dipping with this reagent and heating at 100°C for 5 min. The spots near the origin are symmetrical and compact but those further away are more compressed and elongated at right angles to the direction of development. The sample was also separated in the same chromatographic system, but using linear development on a 10 × 10 cm plate (Figure 15B).

If the sample is introduced in the mobile-phase stream, then separated bands form concentric rings on the chromatographic plate, as shown in Figure 16. This circular chromatogram demonstrates the separation of lipophilic dyes on a silica gel 60 F₂₅₄ high performance TLC pre-coated plate, 10 × 10 cm (E. Merck) with a mobile phase of hexane–chloroform–NH₃, 70 : 30; the distance of development (from entry position of solvent to eluent front) = 30 mm in a Camag U-chamber.

In the anticircular mode of development the mobile phase enters around the entire periphery of the adsorbent layer which is usually formed as a circle by scraping unwanted adsorbent from a square plate.

The samples are applied on an outer circular starting line and development proceeds from the periphery of this circle layer to its centre (Figure 13B). This mode of development can be performed with a Camag anticircular U-chamber, shown in Figure 17.

Anticircular chromatography is seldom applied in practice. An example of a chromatogram obtained by this mode of development is given in Figure 18. The spots are compact near the origin and elongated in the direction of the mobile-phase migration.

Conclusions

Conventional modes of chromatogram development are often applied in analytical practice for both qualitative and quantitative purposes. The most popular among the modes described is linear development. There are several reasons which contribute to this situation, including a simple operation procedure and low cost and time of analysis per sample. These features will still determine a future use of the modes in the analytical practice of planar chromatography in spite of increasing interest in the application of automated and forced-flow development.

See also: II/Chromatography: Thin-Layer (Planar): Instrumentation; Modes of Development: Forced Flow, Over-pressured Layer Chromatography and Centrifugal. **Appendix 2/Essential Guides to Method Development in Thin-Layer (Planar) Chromatography.**

Further Reading

- Geiss F (1987) *Fundamentals of Thin-layer Chromatography (Planar Chromatography)*. Heidelberg: Hüthig.
- Grinberg N (ed.) (1990) *Modern Thin-layer Chromatography*. New York: Marcel Dekker.
- Poole CF and Poole SK (1991) *Chromatography Today*. Amsterdam: Elsevier.
- Sherma J and Fried B (1996) *Handbook of Thin-layer Chromatography*, 2nd edn. New York: Marcel Dekker.
- Zlatkis A and Kaiser RE (1977) *HPTLC High Performance Thin Layer Chromatography*. Amsterdam: Elsevier Science.

Modes of Development: Forced Flow, Overpressured Layer Chromatography and Centrifugal

S. Nyiredy, Research Institute for Medicinal Plants, Budakalász, Hungary

Copyright © 2000 Academic Press

Introduction

Forced-flow planar chromatographic separation can be achieved by application of external pressure (over-

pressured layer chromatography – OPLC), an electric field, or centrifugal force (rotation planar chromatography – RPC). Figure 1 shows schematically the superior efficiency of forced-flow techniques by comparing their analytical performance with those of classical thin-layer chromatography (TLC) and high performance thin-layer chromatography (HPTLC). Forced-flow planar chromatography (FFPC) tech-

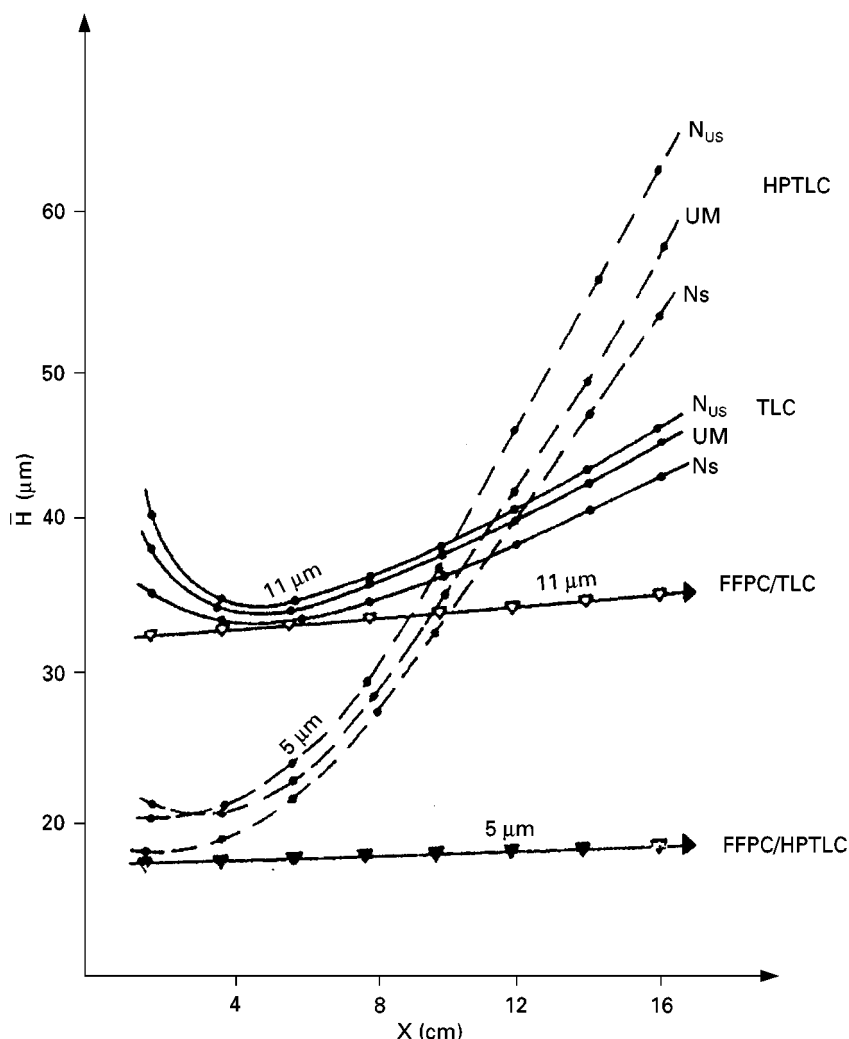


Figure 1 Comparison of the efficiency of analytical TLC and HPTLC chromatographic plates when used with capillary action and forced-flow planar chromatography (FFPC). N_{US} , normal unsaturated chamber; UM, ultramicrochamber; N_S , normal saturated chamber.

niques enable the advantage of optimum mobile phase velocity to be exploited over almost the whole separation distance without loss of resolution. This effect is independent of the type of forced flow.

Although FFPC can be started with a dry layer, as in classical TLC, the forced-flow technique also enables fully online separation in which the separation can be started on a stationary phase equilibrated with the mobile phase, as in high performance liquid chromatography (HPLC). The following FFPC combinations of the various offline and online operating steps are feasible:

- Fully offline process: the principal steps, such as sample application, separation, and detection are performed as separate operations
- Offline sample application and online separation and detection

- Online sample application and separation and off-line detection
- Fully online process: the principal steps are performed as nonseparate operations.

Overpressured Layer Chromatography

In addition to capillary action, the force driving solvent migration in OPLC is the external pressure. Depending on the desired mobile-phase velocity, operating pressures up to 50 bar can currently be used. In OPLC (Figure 2) the vapour phase is completely eliminated; the chromatographic plate is covered with an elastic membrane under external pressure, thus the separation can be performed under controlled conditions. The absence of any vapour space must

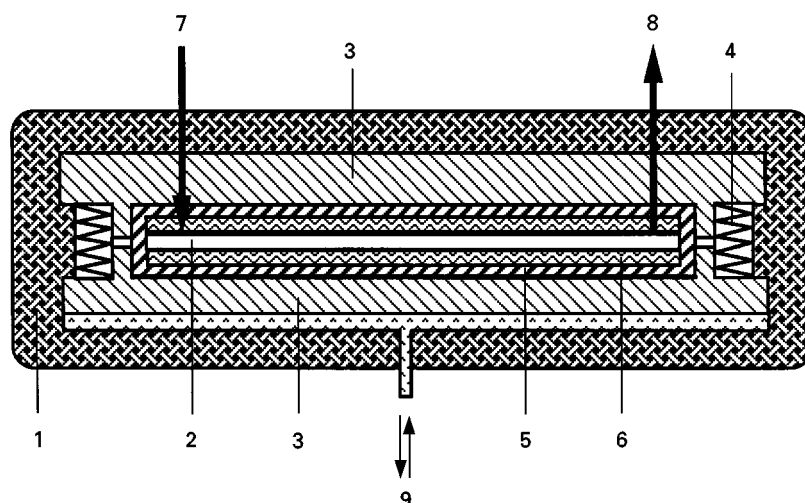


Figure 2 Schematic diagram of online OPLC. 1, Support block; 2, chromatoplate; 3, support plate; 4, spring; 5, cassette system for fixing the chromatoplate between two Teflon layers; 6, Teflon layer; 7, Mobile phase inlet; 8, mobile phase outlet; 9, hydraulic system.

be considered in the optimization of the solvent system, especially in connection with the disturbing zone and multifront effect, which are specific features of the absence of a vapour phase (see section entitled 'Elimination of Typical Problems With Use of OPLC').

Principle of Multi-Layer OPLC (ML-OPLC)

OPLC is suitable for the development of several chromatographic plates simultaneously if the plates are specially prepared. With this multi-layer technique, many samples can be separated during a single chromatographic run. By connecting chromatographic plates in parallel (Figure 3) more HPTLC plates can be developed simultaneously. By circular OPLC, 360 samples of plant extracts can be separated in 150 s. The rapidity and/or efficiency of the OPLC separation of complex samples can be increased by use of ML-OPLC, in which the same or different types of stationary phase can be used for the development of more chromatographic plates.

Principle of Long-Distance OPLC (LD-OPLC)

Long-distance OPLC is a multi-layer development technique with specially prepared plates. Similar to the preparation of layers for linear OPLC development, all four edges of the chromatographic plates must be impregnated with a polymer suspension. The movement of the eluent with a linear solvent front can be ensured by placing a narrow plastic sheet on the layer or scraping a narrow channel in the sorbent for the solvent inlet. Several plates are placed on top of each other to ensure the long running distance. A slit is cut at the end of the first (upper) chromato-

graphic plate to enable the mobile phase to travel to a second layer. Here the migration continues until the opposite end of the second layer, where solvent flow can be continued to the next adjacent chromatographic plate, or the eluent is led away (Figure 4A) if migration is complete. Clearly, on this basis a very long separation distance can be achieved by connecting one plate to another.

Figure 4B shows a typical combination of the same type of chromatographic plate (homoplates). In the arrangement presented, the upper plate has an eluent inlet channel on one side and a slit on the other side for conducting the mobile phase to the next plate. The slit (width approximately 0.1 mm) can be produced by cutting the layer; this enables ready passage of the mobile phase and individual samples without mixing. The cushion of the OPLC instrument is applied to the uppermost layer only, and each plate presses the sorbent layer below. As a consequence of this, glass-backed plates can be used in the lowest position only. The illustrated fully off-line separation is complete when the ' α ' front (the front of the first solvent in an eluent solvent mixture) of the mobile phase reaches the end of the lowest plate.

The potential of the connected layers can be increased by use of different (hetero) stationary phases during a single development; this is shown in Figure 4C, in which the different sorbents are marked with various shades of gray. The eluate can, furthermore, be led from the lower plate, similarly to the way in which it was led in. This gives the possibility of online detection. For this fully online operating mode all layers placed between the highest and lowest plates must have 1 cm cut from the

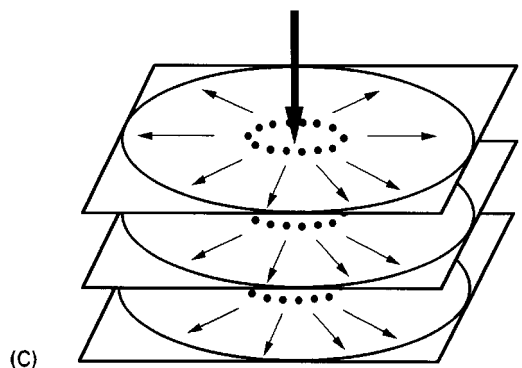
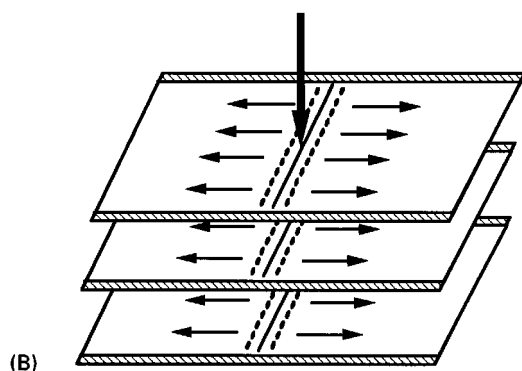
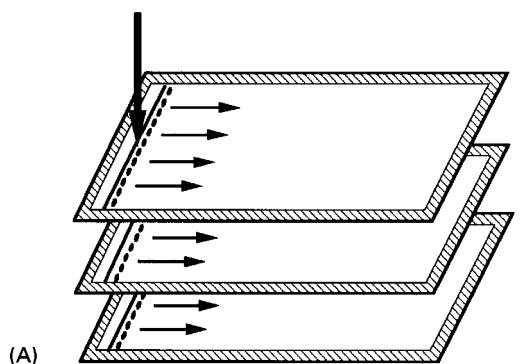


Figure 3 Schematic diagram of multi-layer OPLC (ML-OPLC). (A) Linear one-directional development; (B) linear two-directional development; (C) circular development.

length of the plate, to leave a space for mobile phase outlet.

Analytical OPLC Separations

In OPLC, the most frequent modes of development are linear one- and two-directional (Figure 5A,B). Linear OPLC, however, requires a special chromatographic plate sealed along the edge, by impregnation, to prevent the solvent from flowing off the layer.

The advantage of circular development, in which the mobile phase migrates radially from the centre of the plate to the periphery, is well known for the separation of compounds in the lower R_F range,

where circular development gives 4–5 times greater resolution. The separating power of circular development is better exploited if the samples are spotted near the centre. As the distance between the mobile-phase inlet and sample application increases, the resolution begins to approach that of linear development. No preparation of the plate is necessary for offline circular OPLC (Figure 5C); for online circular OPLC (Figure 5D) a segment-shaped region must be isolated by removing the surrounding adsorbent and impregnating its edges.

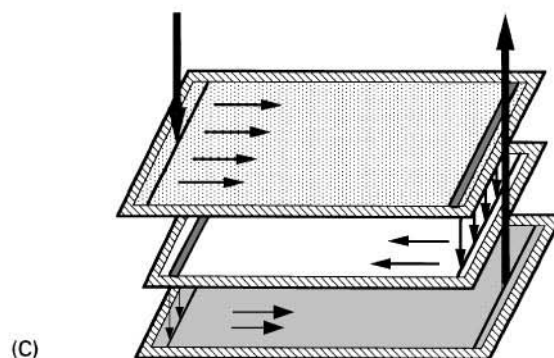
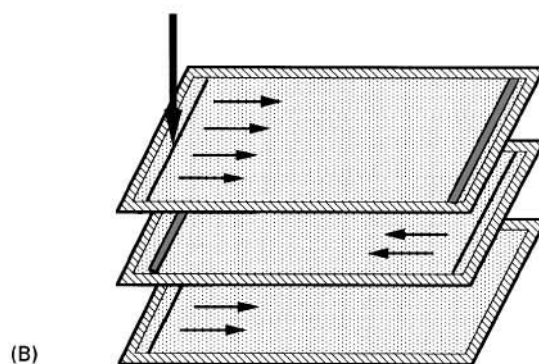
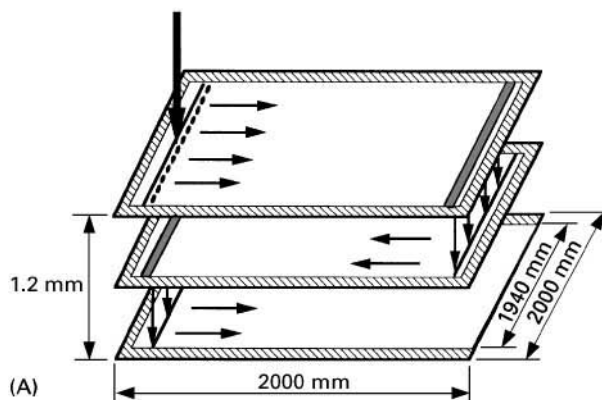


Figure 4 Schematic diagram of long-distance OPLC (LD-OPLC). (A) Principle of the method; (B) fully offline LD-OPLC using homolayers; (C) fully online LD-OPLC using heterolayers.

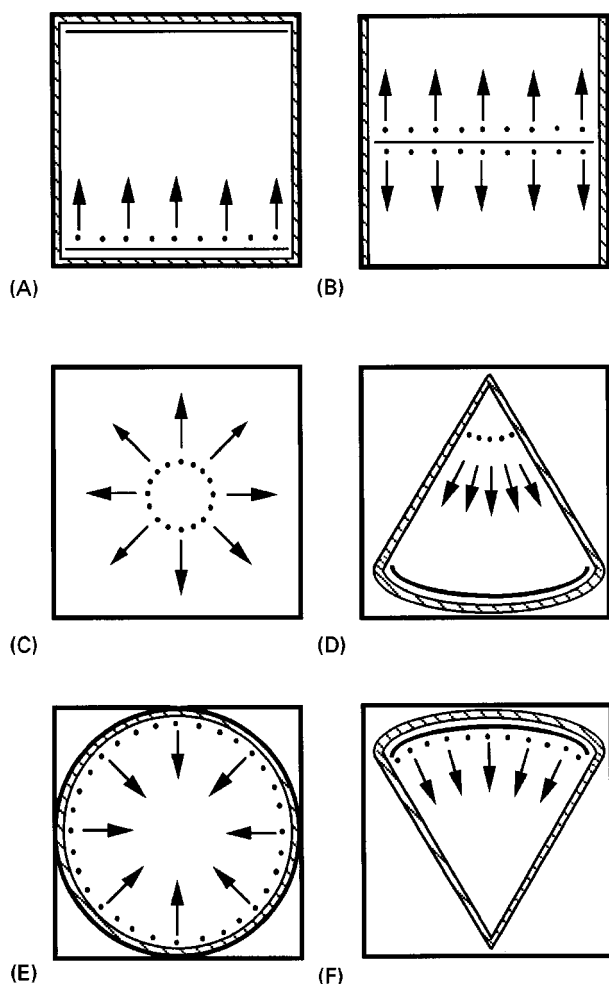


Figure 5 Development modes in analytical OPLC using 20 cm \times 20 cm HPTLC chromatographic plates. (A) Linear unidirectional; (B) linear two-directional; (C) circular with 8 cm development distance; (D) circular with 18 cm development distance, or online circular; (E) anticircular; (F) anticircular with 18 cm development distance, or online anticircular.

Conventional offline anticircular separation (Figure 5E) is rather difficult to perform because of the large perimeter of the mobile-phase inlet (ca. 60 cm for a 20 cm \times 20 cm plate). Fully offline and online anticircular separations can, however, be performed over a separation distance of 18 cm, after suitable preparation of the plate by isolating a segment of the layer (by scraping) and sealing the isolated segment with polymer suspension (Figure 5F).

In linear OPLC the maximum separation distance is 18 cm for 20 cm \times 20 cm chromatographic plates. In offline circular OPLC the maximum separation distance is 10 cm, and only one sample can be analysed. If the distance between the mobile phase inlet and the point of sample application is 2 cm, a separation distance of 8 cm can be achieved; this enables application of more samples.

Micropreparative OPLC Separations

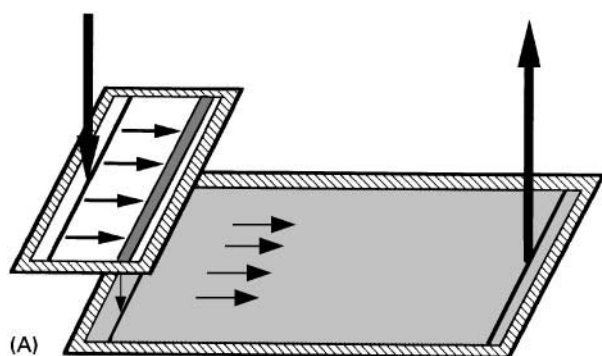
Instrumental methods such as OPLC increase preparation time and costs but also significantly improve efficiency. As a rule of thumb, if the sample contains more than five substances, up to 10 mg of sample can be separated by micropreparative OPLC with linear development on an HPTLC plate. This can be increased five-fold by use of five HPTLC plates and a multi-layer technique; thus preparative amounts can be separated by means of a micropreparative technique. If the sample contains fewer than five substances, the amounts can be increased to 50 mg on a single chromatographic plate. Linear online OPLC is preferable if the structures of compounds to be separated are similar. The circular offline technique can be used if the separation problem is in the lower R_F range.

Probably the most important application of layer switching is in sample clean-up based on a new connection between the layers. A special clean-up effect, sample application and reconcentration, can be achieved simultaneously as shown in Figure 6A, in which the upper plate serves for clean-up. Needless to say, these steps can both be performed in fully offline or fully online operating modes, or in freely chosen combinations of different offline and online steps.

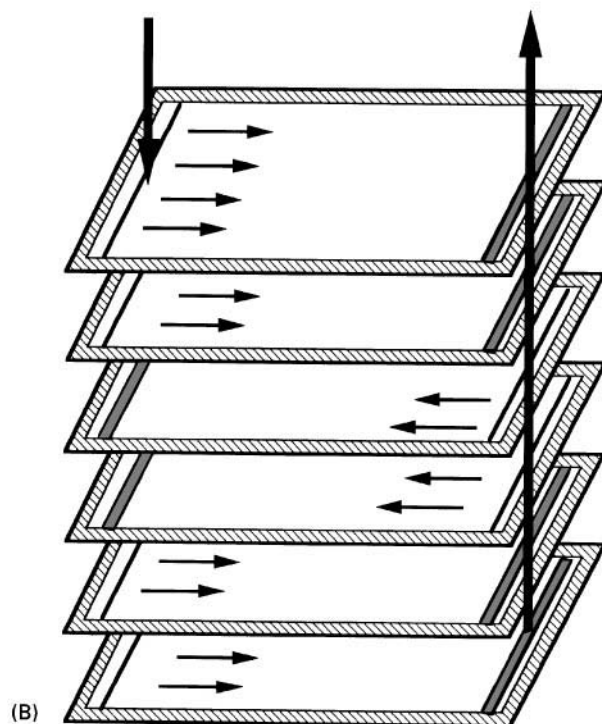
The connection illustrated in Figure 6B is an arrangement suitable for a larger amount of complex sample. In this example micropreparative development can be performed on pre-coated fine particle-size analytical plates. The mobile-phase inlet system with the slits is analogous to that for multi-layer development. In the example illustrated, the direction of mobile-phase migration is the same for each pair of plates. The scraped channels are located at the beginning of the upper two layers and the slits are located at the ends of the adsorbent layers. On reaching the end of the first pair of plates the mobile phase passes through to the adjacent pair of layers. Suitable location of channels and slits ensures mobile phase transport through the whole system. The collector channel at the end of the lowest plate leads the eluate to the outlet.

Preparative OPLC Separations

Whether or not the use of OPLC for preparative separation is necessary depends on the kind of sample to be separated. The potential of linear online OPLC on 20 cm \times 20 cm plates with a separation distance of 18 cm as a preparative method is considerable. Because the average particle size of pre-coated preparative plates is too large, not all the advantages of this method can yet be realized. Generally, preparative online OPLC can be used for separation of 6–8 compounds in amounts up to 300 mg.



(A)



(B)

Figure 6 Micropreparative ML-OPLC separations on analytical HPTLC plates. (A) Schematic diagram of cleanup procedure using fully online LD-OPLC; (B) schematic diagram of fully online LD-OPLC for a large amount of a complex mixture.

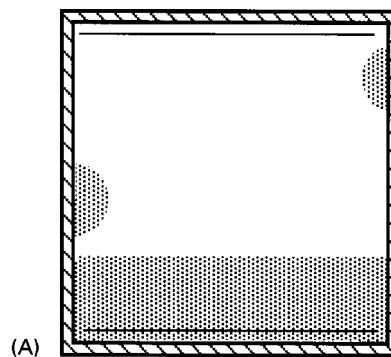
Elimination of Typical Problems with Use of OPLC

It is of practical importance to summarize the most important distorting effects which arise in OPLC and to describe means of eliminating these problems.

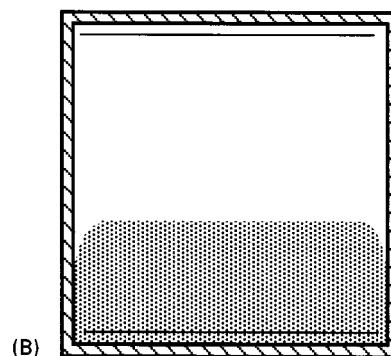
Linear separations require specially prepared chromatographic plates with chamfered edges that are impregnated with a suitable polymer suspension, to prevent solvent leakage at overpressure. For proper preparation of the chromatographic plate, the surface from which the stationary phase has been scratched must be fully cleaned from particles. If this is not achieved, a narrow channel may be formed under the

polymer suspension, resulting in faster migration of part of the mobile phase, because of lack of layer resistance; the mobile phase then re-enters further along the plate ('break-in effect' as shown in Figure 7A). This reduces the value of the separation, at least at the edge(s) of the layer.

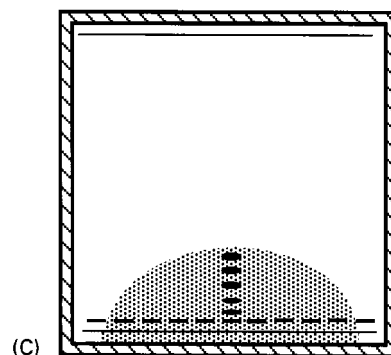
If the area impregnated is too wide, i.e. the edges of the stationary phase covered by the polymer suspension are wider than approximately 1 mm, the 'meniscus effect' can occur (see Figure 7B). As a



(A)



(B)



(C)

Figure 7 Elimination of typical problems in OPLC. (A) 'Break-in effect' – a consequence of improper impregnation of the chromatographic plate; (B) 'meniscus effect' – a consequence of improper impregnation of the chromatographic plate; (C) lack of the appropriate inlet pressure for linear separation.

consequence of this effect – which occurs either in the concave or convex form, depending on the physical properties of the solvents used – the eluent flows more slowly or more quickly on both edges of the chromatographic plate, again distorting quantitative results.

Before starting the separation with the optimized mobile phase, the mobile phase inlet valve is closed and the eluent pump is started to establish an appropriate solvent pressure. The separation is then started by opening the inlet valve; this ensures the rapid distribution of the mobile phase in the inlet channel necessary for linear migration of the mobile phase. If the inlet pressure is too low and the mobile phase does not fill the inlet channel totally, the start of the separation is similar to that for circular development; the distorted linear separation obtained is shown in Figure 7C. No preparation of the plate is needed for offline circular separations.

If multi-component mobile phases are used in unsaturated TLC, the fronts arising from the components can have a decisive influence on the separation. This effect can be substantial in OPLC; the secondary fronts appear as sharp lines because no vapour phase is present. Compounds of the mixture migrating with one of the fronts form sharp, compact

zones whereas tailing or fronting can be observed for compounds migrating directly in front of or behind the α front. With multi-component mobile phases the 'multi-front effect' can appear in two forms. In the first (Figure 8A), one or more fronts can occur between compounds to be separated. In the second, all the compounds to be separated migrate behind the lowest front (Figure 8B), and the fronts do not influence the separation. As the position of the fronts is constant, if the chromatographic conditions are constant, possibly undesirable effects of the multi-front effect can be monitored and taken into account by applying the spots or bands stepwise. Thus for linear separations the sample is applied at different distances ($s = 1, 2, \dots, n$) from the mobile phase inlet channel (Figure 8C). In circular OPLC the samples are applied at points on concentric circles (or rings) with their centres at the mobile phase inlet (Figure 8D). Quantitative evaluation is usually made more difficult, but not impossible, by the multi-front effect, because the phantom peaks formed at the fronts can be measured densitometrically in the substance-free zones at the sides of the chromatographic plates, and thus the values are taken into account. It must be mentioned that the multi-front effect also has a

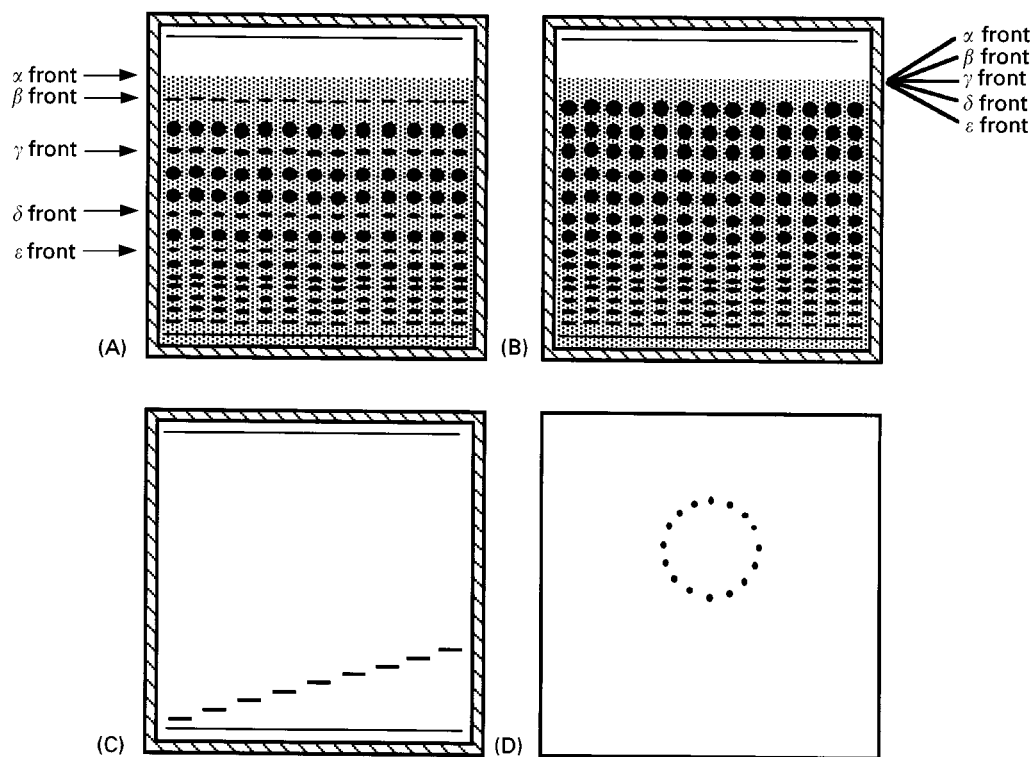


Figure 8 'Multi-front effect' – a consequence of the use of multicomponent mobile phases. (A) The fronts occur between the compounds to be separated; substances migrating with one of the fronts form sharp, compact zones; (B) the compounds to be separated all migrate behind the lowest front, so the fronts do not influence the separation; (C) diagonal application of the samples (as bands) for linear separations to check the place of the different fronts; (D) eccentric application of the samples (as spots) for circular separations to check the place of the different fronts.

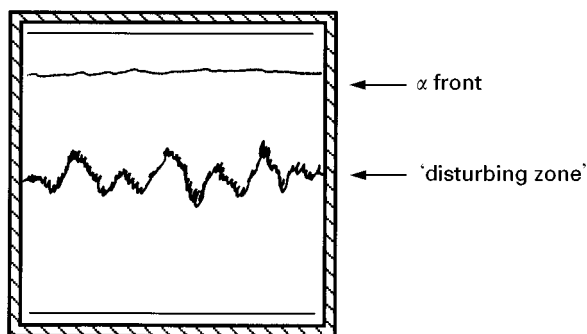


Figure 9 The 'disturbing zone' as a consequence of different air/gas volume ratios adsorbed by the surface of the stationary phase and dissolved in the eluent.

positive effect in preparative separations, because compounds that migrate with α front can be eluted in a very small amount of mobile phase.

If OPLC separation is started with a dry layer, distorted substance zones can sometimes be observed in different R_F ranges, depending on the mobile phase used and the velocity of the mobile phase. This effect appears during the chromatographic process as a zig-zag zone across the width of the plate, perpendicular to the direction of development as a result of the different refractive indices of the solvents in front of and behind this zone. This phenomenon, termed the 'disturbing zone', is depicted in **Figure 9**. The extent of this phenomenon depends on the interrelationship between gas physically bound to the surface of the sorbent and gas molecules dissolved in the mobile phase. Because modification of the location of the 'disturbing zone' is possible within a very narrow range, the only solution to this problem is to conduct a prerun. For separation of nonpolar compounds this can be performed with hexane; for separation of polar substances the prerun can also be performed with hexane or with any component of the mobile phase in which the components are unable to migrate. The selection of this solvent might be considered during optimization of the mobile phase.

Advantages of OPLC

The advantages of the different OPLC methods are summarized as follows:

1. All commercially available chromatographic plates can be used, irrespective of their size and quality; stationary phases prepared from smaller particles can be used without loss of resolution as a result of the overpressure.
2. Mobile phases optimized in unsaturated analytical TLC can be transferred after a suitable prerun.
3. Circular development can be performed without special preparation of the plates; for linear and anticircular development specially prepared plates are necessary.
4. Many samples (up to 72) can be separated rapidly on a single analytical plate and evaluation can be performed densitometrically.
5. Multilayer OPLC is applicable for offline separation of many (up to 360) samples, again with densitometric evaluation.
6. The separation time is relatively short and scale-up for preparative work is simple.
7. All linear separation methods (analytical, micro-preparative, preparative) are online; removal of the separated compounds by scraping off the layer is unnecessary.
8. Online determination of a single analytical sample on fine particle-size analytical plates, and online micro-preparative and preparative separations can be recorded with a flow through detector.
9. Online preparative separation of 10–500 mg samples can generally be performed in a single chromatographic run.
10. The development distance can be easily increased by use of long-distance OPLC.
11. Combination of different adsorbents can be used in long-distance OPLC so that each part of a complex mixture can be separated on a suitable stationary phase.

Rotation Planar Chromatography

The term 'rotation planar chromatography' (RPC) – irrespective of the type and quality of the stationary phase – embraces analytical, offline micro-preparative and online preparative forced-flow planar chromatographic techniques in which the mobile phase migrates mainly with the aid of centrifugal force, but also by capillary action. The centrifugal force drives the mobile phase through the sorbent from the centre to the periphery of the plate. The mobile phase velocity may be varied by adjustment of the speed of rotation.

The different RPC techniques can be classified as normal chamber RPC (N-RPC), micro chamber RPC (M-RPC), ultramicro chamber RPC (U-RPC) and column RPC (C-RPC); the difference lies in the size of the vapour space, an essential criterion in RPC. For analytical separations many samples can be applied. For micro-preparative and preparative purposes only one sample is applied as a circle near the centre of the rotating stationary phase. The separations can be performed either in the offline or online mode. In the latter, the separated compounds are eluted from

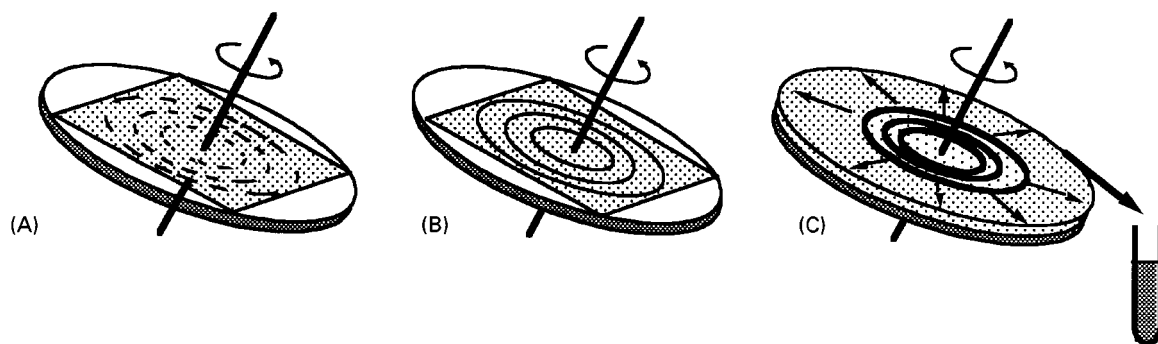


Figure 10 Principles of RPC. (A) Fully offline analytical separation; (B) fully offline micropreparative separation; (C) fully online preparative separation.

the stationary phase by the centrifugal force and collected in a fraction collector (**Figure 10**). All methods can be used for online preparative separations; M-RPC and U-RPC can also be used for analytical and offline micropreparative separations.

Principles of N-RPC, M-RPC and U-RPC

In N-RPC the layer rotates in a stationary chromatographic chamber; in M-RPC – which uses a co-rotating chromatographic chamber – the vapour space is reduced and variable; in U-RPC the layer is placed in the co-rotating chamber from which the vapour space has been almost eliminated. A schematic drawing of preparative M-RPC is shown in **Figure 11**; the layer thickness is approximately 2 mm. When the ultra-microchamber is used, the chromatographic layer is thicker (4 mm); the quartz cover plate is placed directly on the layer so there is almost no vapour space. In N-RPC the quartz plate is removed; this results in a large vapour space.

In all three methods circular development is always used for preparative separations. The sample is applied near the centre of the circular layer, and the

mobile phase is forced through the stationary phase from the centre to the outside of the plate (rotor). The separated compounds are eluted from the layer by centrifugal force and collected in a fraction collector. A detector and recorder can be incorporated before the collector.

M-RPC and U-RPC can be used not only for online preparative separations, but also for analytical and offline micropreparative purposes. Excellent resolution is obtained on HPTLC plates.

Principles of S-RPC

For difficult separation problems a special combination of circular and anticircular development can be performed with the sequential rotation planar chromatography (S-RPC). The mobile phase can be introduced onto the plate at any desired place and, time. In S-RPC the solvent application system – a sequential solvent delivery device – works by centrifugal force (circular mode) and with the aid of capillary action against the reduced centrifugal force (anticircular mode). Generally the circular mode is used for the separation, the anticircular mode for pushing the

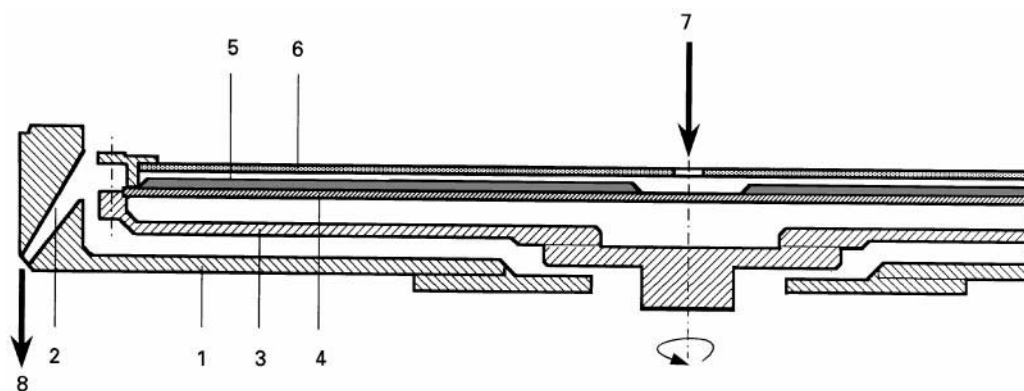


Figure 11 Schematic diagram of preparative M-RPC. 1 = lower part of the stationary chamber, 2 = collector, 3 = motor shaft with the rotating disc, 4 = glass rotor, 5 = stationary phase, 6 = quartz glass cover plate, 7 = mobile phase inlet, 8 = eluent outlet.

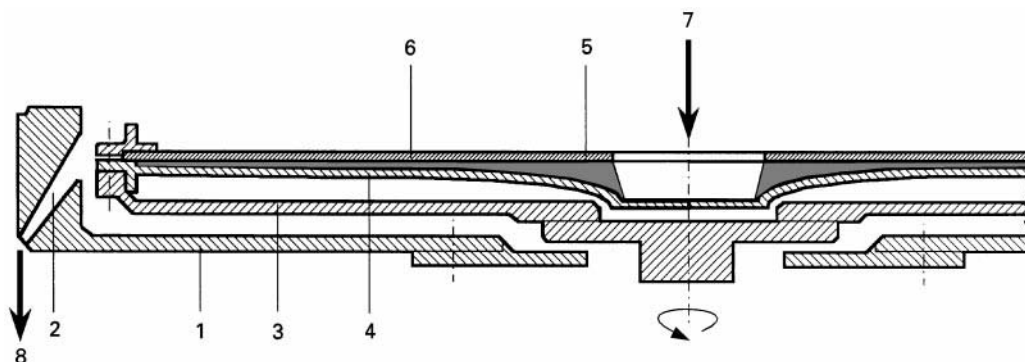


Figure 12 Schematic diagram of preparative C-RPC. 1 = lower part of the stationary chamber, 2 = collector, 3 = motor shaft with the rotating disc, 4 = rotating planar column, 5 = stationary phase, 6 = quartz glass cover plate, 7 = mobile phase inlet, 8 = eluent outlet.

substance zones back to the centre with a strong solvent (e.g. ethanol). After drying the plate with nitrogen at a high rotation speed, the next development with another suitable mobile phase can be started. By combination of the two modes of operation the separation pathway in S-RPC becomes theoretically unlimited.

Principles of C-RPC

In column RPC (see Figure 12) there is no vapour space – the stationary phase is placed in a closed circular chamber (column). The volume of stationary phase stays constant along the separation distance and the flow is accelerated linearly by centrifugal force, hence the name ‘column’ RPC. Because a closed system is used, there is no vapour space and any stationary phase can be used – fine particle size, with or without binder. The rotating planar column has a special geometric design described by eqn [1]

$$h = \frac{K}{(a + br + cr^2)} \quad [1]$$

where r = radius of the planar column, h = actual height of the planar column at radius r , a , b , c , and K = constants.

This design eliminates the extreme band-broadening which occurs normally in all circular development techniques, and so combines the advantages of both planar and column chromatography.

Analytical RPC Separations

In analytical M-RPC there is a vapour space (1 or 2 mm) between the chromatographic plate and the quartz glass cover plate. In analytical U-RPC a soft crepe rubber sheet is placed underneath the analytical plate so that vapour space between the layer and the quartz cover plate is almost eliminated.

In analytical RPC (M-RPC and U-RPC) three development modes are available and the separation distance and number of samples depend on which mode is used. 20 cm × 20 cm plates can be introduced directly into the instrument. In circular mode (Figure 13A) the most commonly used, up to 72 samples can be applied to an HPTLC plate as spots; the separation distance is usually 8 cm. Despite the centrifugal force, the mobile phase direction of flow can be linearized (linear development mode) by scraping channels in the layer (Figure 13B); this reduces the number of samples. The anticircular mode can also be employed with special preparation of the analytical plate (Figure 13C). Although the solvent is delivered

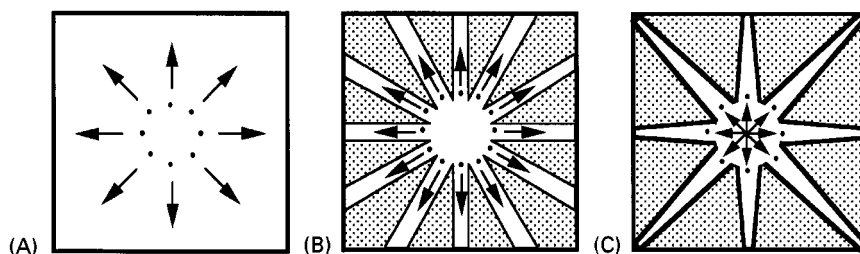


Figure 13 Development modes in analytical RPC on 20 cm × 20 cm HPTLC plates. (A) Circular; (B) linear; (C) anticircular.

at the centre of the plate, in anticircular mode the amount of stationary phase available during development is reduced according to a quadratic relationship by preparation of the layer.

Micropreparative RPC Separations

A mixture of components (5–15 mg) can be applied in the form of a ring near the centre of a single analytical HPTLC plate for isolation of relatively pure compounds by use of U-RPC or M-RPC. The operating process is similar to that used for analytical separations, with the difference that only one sample is applied. Continuous development is possible if a ring of radius 9.8 cm is scraped from the stationary phase, to ensure the regular migration of the mobile phase after it has reached the outskirts of the plate. When the first compounds of interest reach this ring, the separation must be stopped, and either with a stationary rotor or at a rotation speed of 100 rpm the separated components can be scraped out and then the remaining substances can be eluted by the usual procedures, similar to preparative TLC. The separation of ultraviolet (UV)-active compounds can be monitored with a UV lamp during the separation.

Preparative RPC Separations

Because all preparative RPC separations are performed online and no removal of the zones by scratching is necessary, the separation efficiency for the last eluting compounds even increases during the run.

Because M-RPC and U-RPC can be used not only for online preparative separations, but also for analytical purposes, direct scale-up is possible for both analytical methods. From TLC separations using unsaturated or saturated chromatographic tanks, the mobile phase can be transferred via analytical U-RPC and M-RPC to preparative U-RPC and M-RPC, respectively, if the solvent strength and selectivity are kept constant. For scale-up the sample may be applied as a circle to a 20 cm × 20 cm analytical TLC plate and the amount of sample can be increased stepwise in subsequent separations. The adverse effects of different particle sizes and separation distances in the analytical and preparative methods almost cancel each other, so only layer thickness has to be considered in the scale up procedure. The mobile phase flow rate must be adapted to preparative separation, so that the migration of the α front is as fast as in the analytical separation.

Elimination of Typical Problems in RPC

In RPC extra evaporation of the mobile phase occurs owing to the rotation of the chromatographic plate;

this can have undesirable effects. In analytical RPC these are the 'surface effect' and the 'effect of the standing front'. The optimum velocity of rotation depends on the particular separation problem. The flow rate is limited by the amount of solvent that can be kept in the layer (layer capacity) without floating over the surface. The greater the amount of solvent applied, the higher the rotation speed must be to keep the mobile phase within the layer. The parameters, rotation speed, perimeter of solvent application and development mode must be considered when setting the pumping speed, otherwise the mobile phase flows over the top of the applied sample and the layer ('surface effect') distorting the separation. A standing front can occur if after a certain time, the well-separated compounds mix back again because the α front becomes stationary owing to the amount of mobile phase evaporating becoming equal to the amount being delivered. When N-RPC is used for preparative purposes, the 'effect of the change of mobile phase composition' is a typical negative effect, which has to be considered during the optimization of the mobile phase.

Advantages of RPC

The advantages of the different RPC methods, can be summarized as follows:

1. Depending on the properties of the compounds to be separated, the effect of the vapour space, and thus the extent of saturation of the chromatographic system, can be selected freely.
2. All commercially available stationary phases can be used, irrespective of their size and quality; smaller particle size stationary phases can be used without loss of resolution because of the centrifugal force.
3. Mobile phases optimized in saturated or unsaturated analytical TLC, or in HPLC, can be transferred to the various RPC methods.
4. All three basic modes of development (circular, linear, and anticircular) and their combinations can be used for analytical separations.
5. For analytical purposes up to 72 samples can be applied to a single analytical plate, and densitometric quantification can be performed *in situ* on the plate.
6. The separation time is relatively short and scaling up to preparative methods is simple.
7. All preparative methods are online, no scratching out of the separated compounds is necessary, and the preparative separation can be recorded with a flow-through detector.
8. Because of the theoretically unlimited separation distance, the separation power can be increased

Table 1 Comparison of the different analytical and preparative FFPC (OPLC and RPC) methods

Method		OPLC		N-RPC		M-RPC		U-RPC		S-RPC		C-RPC	
Viewpoint		Analytical	Preparative	Preparative	Analytical	Preparative	Analytical	Preparative	Analytical	Preparative	Preparative	Preparative	Preparative
Chamber type		Ultra-micro	Ultra-micro	Normal	Micro	Micro	Ultra-micro	Ultra-micro	Ultra-micro	Normal	Planar column		
Plate (column)		TLC/HPTLC pre-coated	Pre-coated	Self-prepared	TLC/HPTLC pre-coated	Self-prepared	TLC/HPTLC pre-coated	Self-prepared	TLC/HPTLC pre-coated	Self-prepared	Self-filled		
Stationary phase		All available	Silica	Silica	All available	Silica	All available	Silica	All available	Silica	All available		
Layer thickness		0.1, 0.2 mm	0.5–2 mm	1–4 mm	0.1, 0.2 mm	1–3 mm	0.1, 0.2 mm	1–3 mm	0.1, 0.2 mm	1–4 mm	$\bar{x} = 2.24$ mm		
Volume of stationary phase		Constant (increasing)	Constant (increasing)	Increasing	Constant (increasing)	Increasing	Constant (increasing)	Increasing	Constant (increasing)	Increasing and decreasing	Constant		
Particle size of stationary phase		5, 11 μm	$5\text{ }\mu\text{m} < x < 25\text{ }\mu\text{m}$	15 μm	5, 11 μm	15 μm	5–11 μm	15 μm	5–11 μm	15 μm	5 μm		
Separation distance		18 (90) cm	18 cm	10 cm	8(11) cm	10 cm	8(11) cm	10 cm	8(11) cm	Unlimited	9 cm		
Separation mode		Circular, linear, (anticircular)	Linear (circular)	Circular	Circular, linear, (anticircular)	Circular	Circular, linear, (anticircular)	Circular	Circular, linear, (anticircular)	Circular and anticircular	Linear		
Observation		Not possible	Not possible		Coloured and UV active substances can be observed during the chromatographic process								
Detection		Offline, online	Online	Online	Offline	Online	Offline	Online	Offline	Online	Online		
Sample number		Max. 360	1	1	max. 72	max. 72	max. 72	max. 72	max. 72	1	1		
Amount of sample		ng– μg	50–500 mg	50–500 mg	ng– μg	50–500 mg	ng– μg	50–500 mg	ng– μg	50–500 mg	50–500 mg	50–500 mg	50–500 mg

significantly by employing the sequential technique.

9. On line preparative separation of 50–500 mg samples can generally be applied in a single chromatographic run.

Comparison and Outlook of FFPC Methods

The various OPLC and RPC techniques are compared in Table 1. Study of the data shows that OPLC is an excellent technique for analytical separations and that RPC is more ideally suited as a preparative method for isolation of compounds from biological matrices.

The advantage of combining online and offline separations and two-dimensional development can also be exploited in OPLC. The advantage of multiple development methods is the possibility of analytical RPC separations. A realistic means of increasing the efficiency of the planar chromatography of complex samples is the use of long-distance OPLC for analytical separations and sequential RPC for preparative purposes. Working with multi-layer OPLC, the rapidity of the separation can increase significantly, providing new vistas in screening and genetic work.

FFPC techniques will open up a new field of planar chromatography, particularly in the separation of complex samples. It is expected that future research will concentrate on the positive effects (applied pressure in OPLC and higher centrifugal force in RPC) of forced flow. As a consequence, smaller particle size, narrower distribution range, and spherical stationary phases will be needed to achieve maximum resolution.

See also: II/Chromatography: Thin-Layer (Planar): Instrumentation; Modes of Development: Conventional; Preparative Thin-Layer (Planar) Chromatography; Theory

of Thin-Layer (Planar) Chromatography. **Appendix 2/ Essential Guides to Method Development in Thin-Layer (Planar) Chromatography.**

Further Reading

- Botz L, Nyiredy Sz and Sticher O (1990) The principles of long distance OPLC, a new multi-layer development technique. *Journal of Planar Chromatography* 3: 352–354.
- Geiss F (1987) *Fundamentals of Thin Layer Chromatography (Planar Chromatography)*. Heidelberg: Hüthig.
- Nurok D, Frost MC, Pritchard CL and Chenoweth DM (1998) The performance of planar chromatography using electroosmotic flow. *Journal of Planar Chromatography* 11: 244–246.
- Nyiredy Sz (1992) Planar chromatography. In: Heftmann E (ed.) *Chromatography*, 5th edn, pp. A109–150. Amsterdam: Elsevier.
- Nyiredy Sz and Fatér Zs (1994) The elimination of typical problems associated overpressured layer chromatography. *Journal of Planar Chromatography* 7: 329–333.
- Nyiredy Sz, Botz L and Sticher O (1989) ROTACHROM®: A new instrument for rotation planar chromatography (RPC). *Journal of Planar Chromatography* 2: 53–61.
- Nyiredy Sz, Botz L and Sticher O (1990) Analysis and isolation of natural products using the ROTACHROM® rotation planar chromatograph. *American Biotechnology Laboratory* 8: 9.
- Sherma J and Fried B (1995) *Handbook of Thin-Layer Chromatography*. New York: Dekker.
- Tyihák E and Mincsovcics E (1988) Forced-flow planar liquid chromatographic techniques. *Journal of Planar Chromatography* 1: 6–9.
- Tyihák E, Mincsovcics E and Kalász H (1979) New planar liquid chromatographic technique: overpressured thin-layer chromatography. *Journal of Chromatography* 174: 75–81.
- Tyihák E, Mincsovcics E and Székely TJ (1989) Overpressured multi-layer chromatography. *Journal of Chromatography* 471: 375–387.

Preparative Thin-Layer (Planar) Chromatography

S. Nyiredy, Research Institute for Medicinal Plants, Budakalász, Hungary

Copyright © 2000 Academic Press

Introduction

Preparative planar (thin-layer) chromatography (PPC) is a liquid chromatographic technique performed with the aim of isolating compounds, in amounts of 10–1000 mg, for structure elucidation

(mass spectrometry (MS), nuclear magnetic resonance (NMR), Infrared (IR), ultraviolet (UV) etc.), for various other analytical purposes, or for determination of biological activity. PPC is a valuable method of sample purification for preparative purposes and isolation. The scope for modifying operating parameters such as the vapour space, development mode and for offline sample application is enormous in planar chromatography.

In classical PPC the mobile phase migrates by capillary action, whereas if forced-flow PPC (FFPPC) is

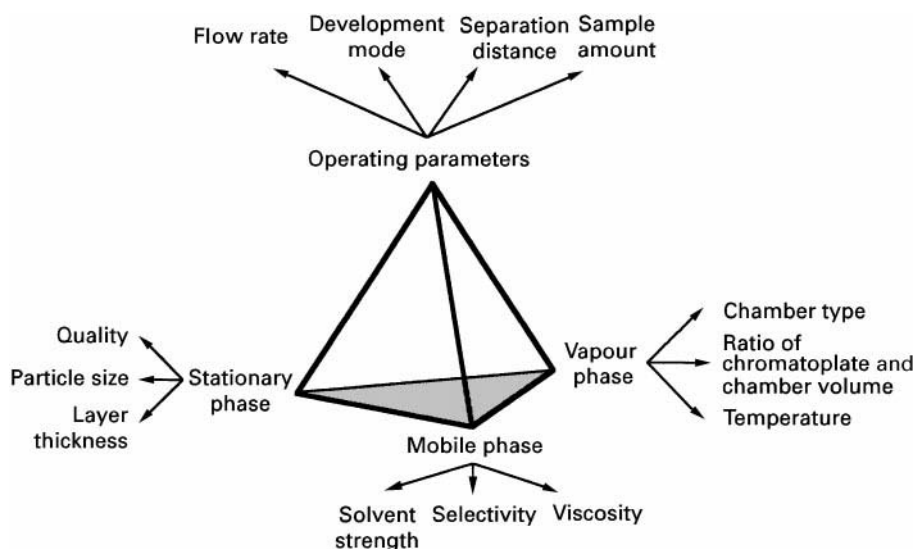


Figure 1 The principal factors affecting preparative layer chromatography.

used, migration of the mobile phase is also promoted either by application of external pressure (overpressured layer chromatography (OPLC)) or by use of centrifugal force (rotation planar chromatography (RPC)). (For more information see the previous entry Modes of development: Forced flow, OPLC and centrifugal.) The enhanced efficiency obtained by use of the optimum mobile phase velocity is independent of layer thickness and of the type of forced flow applied.

Parameters of PPC Separation

One of the most important experimental variables in PPC is the vapour space, because the separation pro-

cess occurs in a three-phase system of stationary, mobile, and vapour phases, all of which interact until equilibrium is reached. The most important factors which might influence a PPC separation are shown in Figure 1.

Stationary Phase

Although alumina, cellulose, and C_2 and C_{18} reversed-phase pre-coated preparative plates are available, silica has been most widely used by far. The silica materials commonly used for PPC have coarse particle sizes (average $\sim 25 \mu\text{m}$) and their distribution range (between 5 and $40 \mu\text{m}$) is also wide; Figure 2

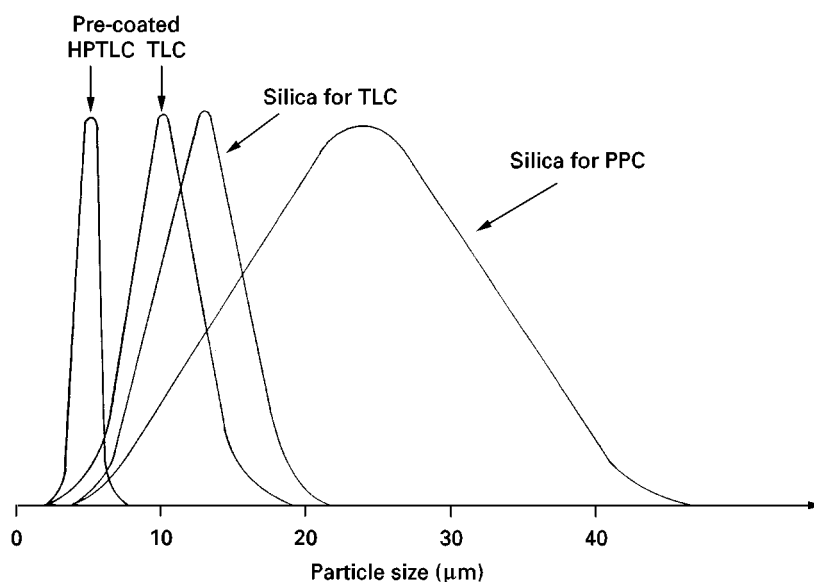


Figure 2 Particle sizes and particle-size distributions of silica stationary phases.

compares the quality of pre-coated analytical (TLC and HPTLC) and preparative plates, and that of silica for TLC. The advantage of making one's own preparative plates is that any desired thickness (< 10 mm) or layer composition (incorporation of salts, buffers, etc.) becomes feasible. Pre-coated $20\text{ cm} \times 20\text{ cm}$ or $20\text{ cm} \times 40\text{ cm}$ preparative plates with layer thicknesses 0.5, 1.0, 1.5, and 2 mm have the advantage of much higher reproducibility. It is generally accepted that higher resolution can be achieved on a thinner preparative layer (0.5–1.0 mm) and the resolution is much more limited on a higher capacity (1.5–2 mm) layer. The loading capacity of a preparative layer increases with the square root of the thickness, practically without loss of separating power so that as a rule of thumb, the loading capacity of a 0.5 mm layer is approximately half that of a 2 mm layer.

Preparative plates are commercially available with or without preadsorbent zones. The preadsorbent zone (generally 4 cm width) serves as a holding zone for the sample until development begins. Soluble compounds migrate with the mobile phase front through the preadsorbent zone and are concentrated in a narrow band as they enter the chromatographic layer, thus improving the resolution. The materials used to manufacture these concentrating zones are kieselguhr or inert silica. Resolution can also be significantly increased by using a layer-thickness gradient that contains a wedge-shaped silica layer ranging in thickness from 0.3 mm at the bottom to 1.7 mm at the top, with an adjacent 700 μm preadsorbent layer for sample application. The cross-sectional area traversed by the mobile phase front increases during migration through the tapered layer, so the cross-sectional flow per unit area is highest at the bottom of the layer and decreases towards the solvent front. As

a result the lower portion of a zone moves faster than the upper portion, keeping each component focused in a narrow band. Theoretical separations on a preparative plate, without and with preadsorbent, and compared with a tapered plate, are depicted in Figure 3A–C. The improved resolution as a result of the greater local mobile phase velocity clearly suggests the wider use of a preadsorbent layer or a layer-thickness gradient if at all possible.

Mobile Phase

The separations can be started in saturated or unsaturated chromatographic tanks. However, on starting the separation in an unsaturated chamber the chromatographic tank becomes saturated during the development because of the long separation time (1–2 h). If saturated chromatographic chambers are used, the optimized analytical mobile phase may be transferred unchanged to PPC. Because the particle sizes and size distribution of sorbents for preparative purposes are larger, and the plates are overloaded with the compounds to be separated, inferior separation is invariably achieved on preparative plates. This means that a successful preparative separation will need an optimized mobile phase.

The 'PRISMA' mobile phase optimization system enables not only optimization of solvent strength and mobile phase selectivity, but also transfer of the optimized mobile phase between the different planar chromatographic techniques. The system is based on the solvent classification by Snyder, who classified more than 80 solvents into eight groups for normal phase (NP) chromatography according to their properties as proton acceptors (X_a), proton donors (X_d), and their dipole interactions (X_n). Because

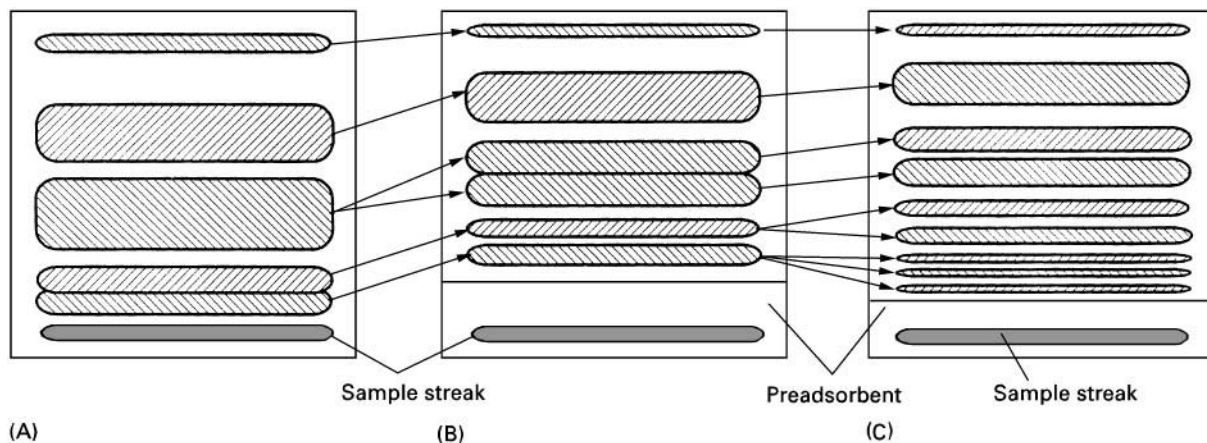


Figure 3 Comparison of separations on different preparative plates. (A) Pre-coated chromatographic plate without concentrating zone, (B) pre-coated chromatographic plate with concentrating zone, (C) pre-coated chromatographic plate with layer-thickness gradient.

$X_a + X_d + X_n = 1$, the solvents can be characterized by two of them (e.g. X_a and X_d), and so a new definition was introduced – the individual selectivity value (S_v), which is the ratio of X_a to X_d . The individual solvent strengths (S_i), selectivity values, and viscosities of the solvents most often used for normal phase PPC, are listed in Table 1.

For characterization of multi-component mobile phases the total solvent strength (S_T) can be defined as the sum of the S_i of the components, weighted by multiplication by their volume fraction. The total selectivity factor (S_V) can be also calculated similarly to the S_T value.

The volatility of the individual solvents must be also considered during the optimization process, otherwise several problems can arise in subsequent steps (elution of the compound from the stationary phase, evaporation of the solvent). It also precludes the use of, e.g. acetic acid as a component of the preparative mobile phase, because of the possibility of chemical degradation during concentration of the isolated compounds. Multicomponent mobile phases should not be used repeatedly, whereas single-solvent mobile phases can be used repeatedly until they become contaminated.

Figure 4 shows the transfer possibilities of the mobile phase, where thick lines indicate direct transfers. The thin lines indicate transfers which are also possible, but the solvent strength and selectivity must generally be changed. The dashed lines indicate direct transfer possibilities for fully online separation processes.

Table 1 Selected solvents for normal phase PPC separation

Selectivity group	Solvents	S_i	$S_v = \frac{X_e}{X_d}$	Viscosity (cP)
—	n-Hexane	0	0.01	0.31
I	Methyl-t-butyl ether	2.7	3.50	0.27
	Diethyl ether*	2.8	4.08	0.23
II	n-Butanol	3.9	3.11	2.98
	Ethanol*	4.3	2.74	1.20
	Methanol	5.1	2.18	0.52
III	Tetrahydrofuran*	4.0	1.90	0.47
	Methoxyethanol	5.5	1.59	0.95
V	Dichloromethane*	3.1	1.61	0.44
	1,1-Dichloromethane	3.5	1.43	0.79
VI	Ethyl acetate*	4.4	1.48	0.45
	Methyl ethyl ketone	4.7	1.59	0.42
	Dioxane*	4.8	1.50	1.20
	Acetone	5.1	1.52	0.32
	Acetonitrile	5.8	1.15	0.39
VII	Toluene*	2.4	0.89	0.59
	Benzene	2.7	0.72	0.69
VIII	Chloroform*	4.1	0.61	0.57
	Water	10.2	1.00	0.95

* Preferred solvent.

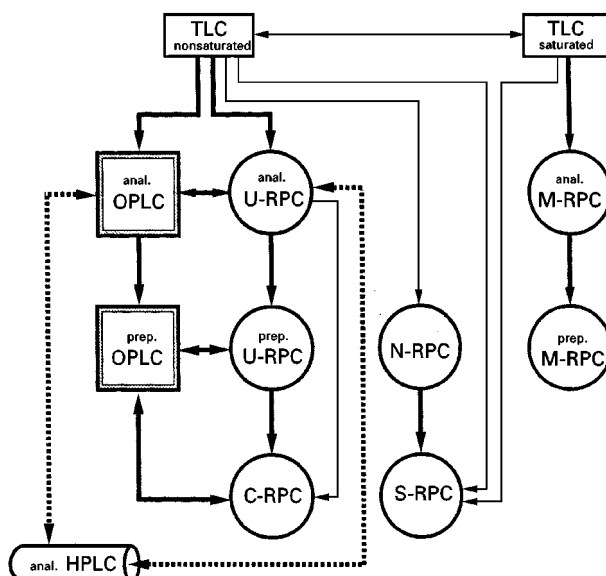


Figure 4 Mobile phase transfer possibilities between different planar chromatographic methods and HPLC, and fully online FFPC techniques.

The optimized TLC mobile phase can be transferred from unsaturated chromatographic tanks to analytical OPLC and U-RPC without modification of the selectivity. If the tank is saturated, the optimized mobile phase can be transferred to M-RPC. Transfer of the corresponding preparative methods (OPLC, U-RPC, M-RPC) from analytical normal-phase FFPC can be performed directly with the same mobile phase. Modification of the mobile phase used in the unsaturated TLC tank is necessary for transfer of preparative N-RPC or S-RPC separations. Direct mobile-phase transfer is also valid from OPLC and U-RPC to C-RPC. With the characterization of the different saturation grade of chromatographic chambers, excellent mobile phase transfer between analytical and preparative planar chromatographic methods and analytical HPLC can be achieved.

Vapour Phase

The selection of the vapour space is a variable offered only by planar chromatography. Three important factors have the greatest influence on this parameter – the chamber type, the ratio of the surface of chromatographic plate to the chamber volume, and the temperature.

Basically, one can distinguish between normal (N) and sandwich (S) chambers. In the conventional N-chamber there is a distance of more than 3 mm between the layer and the wall/lid of the chromatographic chamber. If this distance is smaller, the cham-

ber is said to have the S-configuration. Both types of chromatographic chamber can be used for unsaturated or saturated systems, and the chambers used for FFPPC separation can be also assigned to the earlier mentioned two categories.

Rectangular glass N-chambers are most frequently used for classical PPC (CPPC). Starting the separation with unsaturated chromatographic tanks generally gives higher R_F values for NP systems because of the evaporation of the solvents from the surface of the layer. Disadvantages of using unsaturated tanks are that it can result in a concave solvent front, leading to higher R_F values for solutes near the edges; the reproducibility of this effect and of the R_F values can be poor. If the layer is placed in the chamber immediately after introduction of the mobile phase, separation starts in an unsaturated system which will become progressively more saturated during the course of the separation (Figure 5A). A chamber is saturated when all components of the solvent are in equilibrium with the entire vapour space before and during the separation. A rectangular glass tank (N-chamber) with inner dimensions of 21 cm \times 21 cm \times 9 cm is most frequently used. These tanks can be used for development of two 20 cm \times 20 cm preparative plates with 50–100 mL mobile phase. The chamber must be lined on all four sides with thick filter paper (Figure 5B) thoroughly soaked with the mobile phase (by shaking) and must stand for 60–120 minutes to become saturated with the vapour phase. Each plate must lean against a side wall, so the plates do not touch each other. The advantages of saturated tanks are that the ' α ' front is much more regular and that the separation efficiency is higher for a development distance of 18 cm.

Of the different FFPPC techniques, normal chamber RPC (N-RPC), in which the layer rotates in a stationary N-chamber, belongs to this category. Because of extensive evaporation in the extremely large vapour space, this chamber is practically unsaturated.

S-chambers are very narrow unsaturated tanks, the plate with the layer is usually sandwiched with a glass cover plate (Figure 5C). Saturation can be established with a facing chromatographic plate that has been soaked with the mobile phase (Figure 5D). Part of the stationary phase of the plate to be developed is removed by scraping, so that initially the mobile phase can only reach the level of the facing plate. After sorptive and capillary saturation of this plate, the depth of the mobile phase is increased to start the separation. The U-chamber is a special variety of S-chamber in which the vapour space is reduced (Figure 5E). All basic development modes enable both equilibration before development and a choice of flow rates for separation.

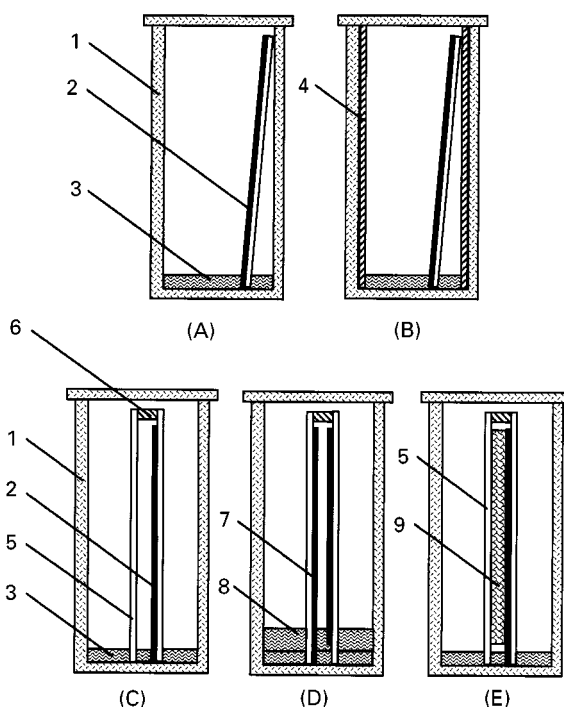


Figure 5 Chamber types used for conventional PPC. (A) Unsaturated N-chamber (1, rectangular chamber; 2, chromatographic plate; 3, mobile phase). (B) Saturated N-chamber (4, filter paper soaked with the mobile phase). (C) Unsaturated S-chamber (5, glass cover plate; 6, spacer). (D) Saturated S-chamber (7, facing chromatographic plate, soaked with the mobile phase; 8, second part of the mobile phase). (E) Ultra-micro chamber, a special variety of S-chamber (5, glass cover plate; 9, elastic inert material).

The chambers used for preparative OPLC separations are unsaturated S-chambers, theoretically and practically devoid of any vapour space. This must be considered in the optimization of the solvent system. M- and U-chambers in RPC also belong to the S-chamber type. The difference between these two chambers is that the former is rapidly saturated, whereas in U-RPC the lid of the rotating chamber is placed directly on the chromatographic plate so that there is practically no vapour space and the chamber must be regarded as unsaturated.

The ratio of the surface area of the chromatographic plate to the chamber volume plays a role only if the separation is started in unsaturated tanks. The higher this ratio, the more unsaturated is the chromatographic chamber.

In saturated chromatography chambers the temperature does not exert a great influence on preparative separations. With unsaturated tanks the composition of the mobile phase plays a more pronounced role and it is important to note that temperature control is now important if separations are to be reproducible.

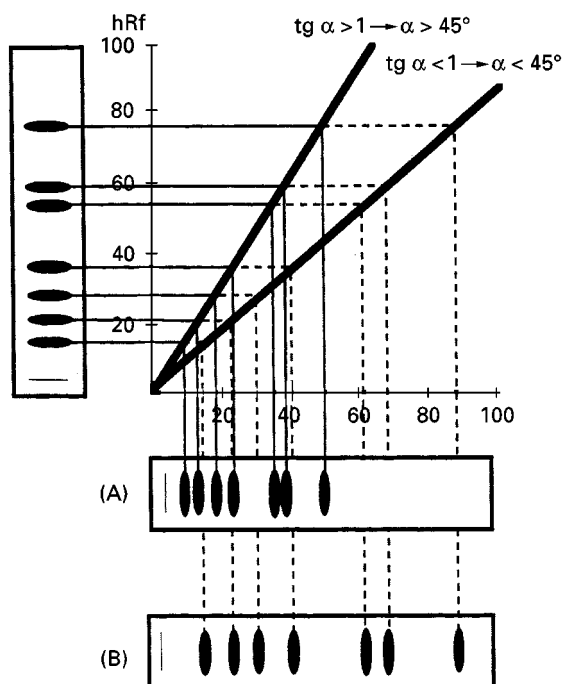


Figure 6 Calculation of the effect of chamber saturation on the separation.

For characterization of chamber saturation, a test-dye mixture can be developed with dichloromethane. If the hR_F values of the dye mixture are the same in different chambers on a given stationary phase, the extent of chamber saturation is identical. For comparison, the hR_F values obtained from different chambers can be depicted in a coordinate system. The hR_F values of any given system are plotted along the y axis and those from the system being compared along the x axis. If the chamber saturation is identical, a linear relationship is obtained, and $\text{tg } \alpha$ for the line is 1. If the hR_F values obtained in the second system were

smaller, the vapour phase was more saturated and $\text{tg } \alpha > 1$, or $\alpha > 45^\circ$. Conversely if $\text{tg } \alpha < 1$, or $\alpha < 45^\circ$, the vapour phase in the second system was less saturated. These possibilities are illustrated by results A and B in Figure 6. With this approach the chamber type can be characterized for a certain separation without specification of the vapour phase. The technique also provides guidelines for the transfer of mobile phases between the different planar chromatographic methods.

Development Mode

The ascending mode, in which the mobile phase moves up the plate, is most frequently used with a maximum separation distance of 18 cm. The angle at which the plate is supported during development affects the rate of development and the shape of the bands. As the angle of the plate decreases towards the horizontal development mode, the flow of the mobile phase increases, but so also does spot distortion. An angle of 75° is recommended as optimum for development. Because descending development has no significant advantages in terms of resolution, it is rarely used.

The advantages of circular development of compounds in the lower R_F range are well known, but it has not been accepted for preparative separations, because the mobile phase velocity would be too slow. However, it is possible to start development not directly from the centre, but from a circle of 2 cm radius, i.e. the mobile phase inlet is not a point, but a circle. Because the size of the mobile phase inlet and the velocity of the mobile phase are related linearly, a relatively high mobile phase velocity can be achieved over a separation distance of 8 cm. Recently a new device has been described which enables a suitable mobile phase velocity to be used in the circular development mode (Figure 7). A solvent reservoir

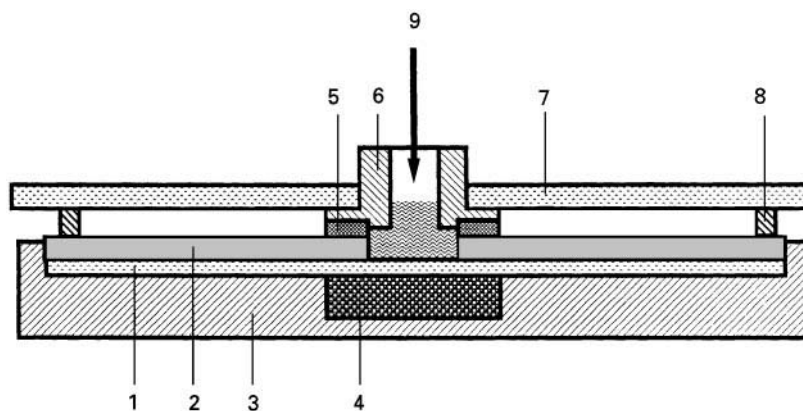


Figure 7 Schematic diagram of a circular preparative chromatography chamber. 1, glass plate; 2, chromatoplate; 3, support block; 4, magnet; 5, Teflon ring; 6, solvent reservoir; 7, quartz glass cover plate; 8, Teflon ring; 9, solvent.

made of steel and a silicone sealing ring are placed on the layer and fixed by a magnet located below the chromatographic plate. To start the separation, adsorbent is scratched from the centre of the plate and the recess produced filled with mobile phase. The device can be used for different types of chamber (N, UM). The entry of sample and mobile phase is regular over the whole cross-section of the preparative layer, irrespective of whether the sample is applied as a liquid or a solid. The device ensures rapid, efficient separation with all the advantages of circular development. The resolution is significantly higher than that obtained from linear development. With the UM chamber the glass cover plate is placed directly on the surface of the chromatographic plate. In the N chamber, the cover plate is placed on a 19 cm diameter metal ring, the height of which can be varied between 0.5 and 2 cm, depending on the type of chamber applied. To start development the solvent reservoir is filled with the appropriate mobile phase and the level of this is kept constant by applying a constant hydrostatic pressure by means of a second reservoir. To stop development the inlet from the second reservoir is turned off.

Anticircular development is accepted in analytical TLC for increasing resolution in the higher R_F range. Because a special device is necessary for such separations, this development mode is rarely used.

Although the different types of multiple development (MD) are rarely used for preparative purposes, the advantage of the method should be understood. In MD the first development length is the shortest and subsequent developments are performed over longer development distances. The last migration distance is the longest and corresponds to the useful development length of the chromatographic plate; it also depends on the nature of the mobile phase. The removal of the mobile phase between development steps is performed by careful drying of the plate. The dried layer is returned to the development chamber for repeated development under the same chromatographic conditions as for earlier development steps.

The most important aspect of MD techniques is the spot-reconcentration mechanism. In each development step the solvent front first contacts the lower part of the chromatographic zone formed in the previous chromatographic step. The molecules at this part of the zone start moving with the mobile phase toward the molecules in the upper part of the chromatographic zone – those still ahead of the solvent front. As the mobile phase front reaches the upper part of the zone, the narrow band developed as a result of the zone reconcentration mechanism migrates and broadens by diffusion in the mobile phase, as in conventional planar chromatography.

In terms of development distance and mobile phase composition, MD techniques can be classified into four basic categories – UMD, IMD, GMD, and BMD (Figure 8). Unidimensional multiple development (UMD) is the repeated development of the chromatographic layer over the same development distance (D) with the same mobile phase (same values of S_{T1} and S_{V1}). In the modification of UMD known as incremental multiple development (IMD) re-chromatography is performed over increasing development distances ($D_1 \rightarrow D_5$) with the same mobile phase (same values of S_{T1} and S_{V1}). In gradient multiple development (GMD), successive chromatographic development steps are performed with a change in solvent strength and selectivity ($S_{T1}, S_{V1}; S_{T4}, S_{V4}$) over the same development distance (D is constant). GMD is required for analysis of multicomponent mixtures spanning a wide polarity range. The most complex multiple development technique is bivariate multiple development (BMD), in which development distance and mobile phase composition are varying simultaneously ($D_1, S_{T1}, S_{V1}; D_4, S_{T4}, S_{V4}$) during successive chromatographic developments. Needless to say, the solvent strength and selectivity of the mobile phase can be changed independently of each other. For the analysis of less complex mixtures of wide polarity range, the preferred technique is BMD with a mobile phase gradient of decreasing solvent strength, when the final chromatographic separation can be detected as a single chromatogram. In BMD the shortest development is performed first with the mobile phase of strongest solvent strength; the chromatographic distance is increased and the solvent strength reduced during successive steps of the chromatography, until finally the last development step is performed over the longest development distance with the weakest mobile phase.

Separation Distance

The separation distance depends on the dimensions of the plate, the mode of development, the particle size, and the size distribution. The last property cannot be influenced by the user of pre-coated chromatoplates. Because in classical PPC capillary action is effective only for plates up to 20 cm in length, the maximum separation distance is 18 cm. For circular development the separation distance is 8–9 cm; in anticircular mode this distance is 8 cm maximum. Despite the short separation distance, correct selection of mobile phase and development mode can give high resolution.

The separation pathway in CPPC can be increased by use of a sequential technique in which the mobile phase supply to the plate is fully variable in time and

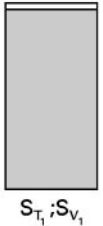




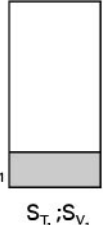
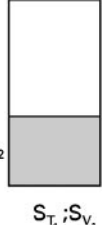
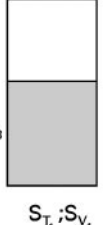





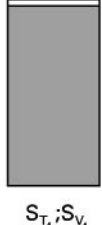
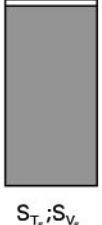

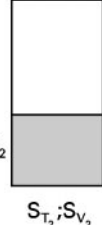




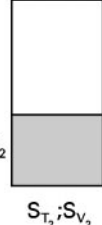



Method	Number of development				
	1	2	3	4	5
U M D					
					
					
					
					

Figure 8 Multiple development possibilities for PPC separations.

location. The principle of this technique is that the mobile phase velocity is much higher at the beginning of separation than later. After an initial separation, the layer is carefully dried, and the mobile phase applicator is placed between two separated zones, irrespective of whether the same or a different mobile phase is used. The supply of mobile phase can be stopped at any time to transfer it directly to the area of the compound zones to be separated. This always gives the highest initial velocity of the mobile phase, which substantially shortens the analysis time. The sequential technique for preparative separations can be performed with a special device—the Mobil- R_F chamber.

The separation pathway in S-RPC becomes theoretically unlimited as a result of a special combination of the circular and anticircular development modes. With this technique the mobile phase can be introduced onto the plate at any desired place and time. The solvent application system works in circular mode and with the aid of capillary action against the reduced centrifugal force (anticircular mode). Generally the circular mode is used for the separation and the anticircular mode for pushing the substance zones back to centre with a strong solvent. After drying the plate at a high rotation speed, the next development with another suitable mobile phase can be started. S-RPC is selected when the separation problem

cannot be solved with a single mobile phase, but optimized mobile phases are available for the separation of the individual compounds. Also the sequence technique can be employed for fast elution of previously separated compounds with a solvent of high strength.

Sample Application

Sample application is one of the most critical steps in PPC. The sample can be applied either offline or online. In offline mode the mobile phase comes into contact with the stationary phase only when sample application is complete; the separation is always started with a dry layer. This mode of application can be used for all PPC methods, irrespective of the driving force (capillary action or forced flow). In online application the sample is dissolved and the stationary phase is always wetted with a solvent – generally it is equilibrated with the starting composition of the mobile phase. This application mode is only possible when forced-flow techniques are used.

Offline Liquid-Phase Sample Application

The preferred method of placing a sample on a preparative layer is to apply it as a narrow streak across the plate. It is highly desirable to have the streak as straight and narrow as possible. With practice it is possible to streak a plate correctly by hand, using a syringe; the use of a Teflon tip on the end of the syringe has the advantage that no mechanical disturbance of the layer occurs. On applying a large amount of sample, the streak can be focused simultaneously and concentrated to a relatively thin line by the sequential technique, especially with nonpolar samples.

Application of a continuous streak can be automated. Most available applications can give a sample zone < 3–4 mm wide and up to 200 mm long for preparative separations. When the layer is not overloaded with sample it is generally accepted that the streak should be applied across the plate 2 cm from both edges. These areas are left free, partly because of the edge effect, which can cause migration of the mobile phase to be faster or slower at the edge than on the centre of the plate. For separations of extremely large amounts, the sample can be applied over the whole width of the plate. Otherwise migration of the mobile phase would be faster in the sample-free areas, resulting in poorer resolution.

When using pre-coated preparative plates with concentrating zones, the quality of streaking is not very important because the sample is applied to a practically inert zone. Pre-coated preparative layers with concentrating zone can be successfully used for PPC and for linear OPLC.

For preparative rotational planar chromatography (RPC), a concentrating zone can be self-prepared. The layer is removed by scraping to furnish a larger inner circle; a slurry with inert material is then cast in this circle. After final drying and scraping, the layer has a preadsorbent zone of approximately 2 cm. For C-RPC separations, after filling the planar column with the selected stationary phase, the last 1 cm can be filled with a deactivated sorbent.

Offline liquid-phase sample application can be used for practically all micropreparative and preparative PPC methods. The only exception is C-RPC, where the solvent for dissolution of the sample is not identical with the mobile phase. The planar column prevents elimination of the sample solvent. The separation may consequently be distorted, especially if the solvent has a higher solvent strength than the mobile phase.

Offline Solid-Phase Sample Application

Preparative solid-phase sample application is especially useful whenever a large amount of sample must be applied and/or the sample is soluble in nonvolatile solvent only. The sample must be dissolved in a suitable solvent and mixed with approximately 5–10 times its weight of deactivated sorbent. The sorbent with the adsorbed sample is dried and then introduced into a layer which has to be prepared to accept it. A 180 mm × 5 mm channel with a U-shaped profile can be scratched from the stationary phase. After removal of the sorbent from the channel, the prepared sorbent with the adsorbed sample is placed in the channel and pressure is applied to ensure optimum contact between the stationary phase of the chromatographic plate and the applied sample. Offline solid phase sample application is useful not only for conventional PPC but also for linear OPLC and C-RPC separations. In OPLC the prepared plate is placed horizontally in the OPLC chamber and the separation can be started with a relatively high inlet pressure. Because of the forced flow, any possible lack of suitable contact has no effect on the efficiency of the separation. With C-RPC the column must first be filled with stationary phase, then with the solid sample. Because of the centrifugal force no lack of suitable contact can occur.

Online Sample Application

In FFPPC the sample can also be applied to a wetted stationary phase, preferably to a plate equilibrated with mobile phase. This mode of application can be used not only for the various methods of preparative OPLC and RPC but also for semipreparative purposes. For plates without a concentrating zone and

online sample application, the separation time is increased because of the longer separation distance. When using the plates with concentrating zone, the effect of the reduced separation distance (2.5–4 cm) is compensated for by the efficiency of the concentrating zone. Because of these results, preparative separations with online sample application and plates with concentrating zones gave practically the same resolution in a shorter time than with the use of offline sample application on plates without concentrating zones. The mode of sample application has no significant influence on the resolution and is independent of the type of plate (analytical, preparative, with or without concentrating zone).

Location and Removal of Separated Compounds

After the preparative chromatographic plate has been developed and the mobile phase evaporated, the separated bands must be located and the desired compounds removed from the plate. If the compounds of interest are coloured, their position on the layer can be located under white light. If they are fluorescent, or become so after post-chromatographic derivatization, their position on the layer can be determined under UV light. Conversely, a PPC plate containing a fluorescent material will indicate the separated compounds as dark zones on a bright background when examined under UV light. Pre-coated plates containing 254 nm or 365 nm fluorescent indicators should be used if possible because they provide a mode of detection which is generally nondestructive.

If the compounds themselves are not visible or fluorescent, detection can be performed by use of iodine vapour or by use of destructive reagents (e.g. vanillin–sulfuric acid). If such a reagent is used for detection of the separated compounds, a vertical channel must be scraped in the layer about half a centimetre from the edge of the streak. After covering the major portion of the layer with a suitable glass plate, the part of the layer which is not covered is sprayed, and thus serves as a guide area. If heating is necessary for detection, the sprayed portion of the plate must be detached from the rest, by use of a glass cutter, because heating the developed preparative plates may lead to decomposition of the compounds of interest.

After location of the desired compound, the subsequent steps are: (1) mechanical removal of the adsorbent zone, (2) extraction of the compound from the stationary phase with a suitable solvent, (3) separation from the residual adsorbent, and (4) concentration of the solvent. The areas of the layer containing the compounds of interest are then scraped off cleanly down to the glass with a suitable scraper. One of the

best methods is to put the adsorbent with the compound to be extracted in an empty receptacle containing a sintered glass filter to retain the adsorbent and to extract the compound with a solvent and the aid of vacuum.

The substance should be highly soluble in the solvent or solvent mixtures used for extraction; the solvent should also be as polar as possible. Chloroform is widely used for nonpolar substances, and ethanol or acetone for polar compounds. If water is the chosen solvent, it should be removed by lyophilization. Because silica is significantly soluble in methanol, this solvent should be avoided. The mobile phase used for the separation is highly recommended also for extraction. As a rule of thumb the volume of solvent (V_{solvent}) required when the chromatographic mobile phase is chosen for extraction is as in equation [1]:

$$V_{\text{solvent}} = 10 \times (1.0 - R_F) \times V_{\text{scraped}} \quad [1]$$

It should be noted that the longer the substance is in contact with the adsorbent, the more likely decomposition is to occur. Once the solution of the compound to be isolated is obtained (free from adsorbent) the extract must be evaporated to dryness. The evaporation temperature should be as low as possible, to avoid decomposition.

Selection of Appropriate PPC Method

All types of PPC can be used for purification and isolation in the micropreparative and preparative range. As a rule of thumb, if the sample contains more than five substances, up to 10 mg of sample can be separated by a micropreparative method and up to 500 mg by a preparative method. If the sample contains fewer than five substances, these values can be increased to 50 and 1000 mg.

Conventional PPC can be used successfully, if: (1) no more than five compounds must be separated, (2) the compounds to be isolated are distributed over the whole R_F range and are present in more or less the same amounts, and (3) the total amount of sample does exceed 150 mg. This is the simplest and therefore the most widely used method.

Online OPLC can be used for the separation of five to seven compounds in amounts up to 300 mg. The use of centrifugal force for online purification and isolation is the oldest forced flow method. Generally, a 15 μm particle size stationary phase is used with all the advantages of the free selection of the size of the vapour space and the development mode. Up to ten compounds in amounts up to 500 mg can be isolated using the appropriate RPC method.

Table 2 Comparison of PPC methods at their present state of development

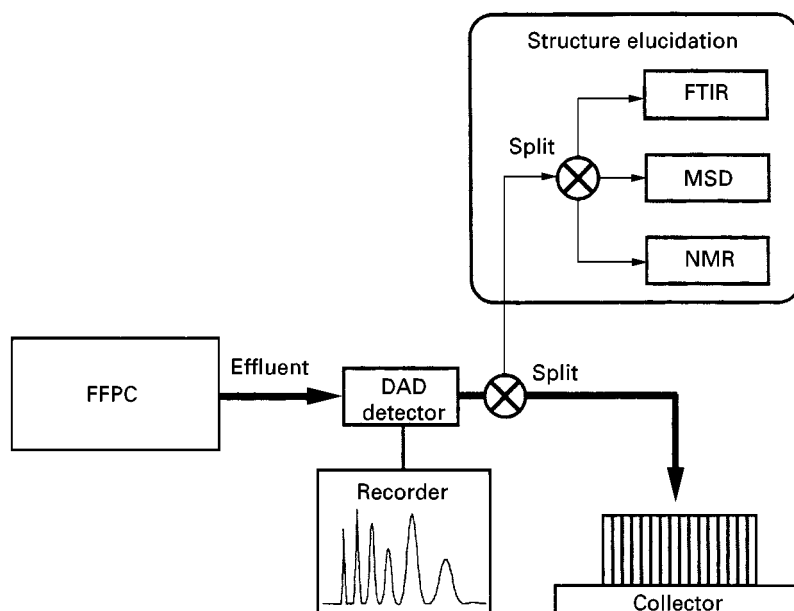
Viewpoint	CPPC	OPLC	RPC (N-, M-, U-, S-, C-RPC)
Migration of mobile phase	Capillary action	Pressure	Centrifugal force/capillary action
Layer/column	Pre-coated	Pre-coated	Self-prepared/filled
Stationary phase	Silica, RP-2, RP-18	Silica	All available
Particle size of stationary phase	$5\text{ }\mu\text{m} < x < 40\text{ }\mu\text{m}$	$5\text{ }\mu\text{m} < x < 40\text{ }\mu\text{m}$	$5\text{ }\mu\text{m} \leq x \leq 15\text{ }\mu\text{m}$
Layer thickness	0.5, 1, 2 mm	0.5, 1, 2 mm	1–4 mm
Volume of stationary phase	Constant	Constant	Increasing (constant)
Vapour space	Normal tank	None	Variable (N, M, UM, none)
Separation distance	18 cm	18 cm	12 cm (unlimited)
Separation mode	Linear (circular)	Linear (circular)	Circular (circular–anticircular)
Isolation	Offline	Online (offline)	Online
Typical amount of sample	50–150 mg	50–300 mg	50–500 mg
Number of compounds	2–5	2–7	2–12

Comparison and Outlook of PPC Methods

The principal differences between classical PPC, OPLC, and RPC are summarized in Table 2 which lists the generally accepted characteristics of the methods. As is apparent, the major difference between the methods is the nature of mobile phase migration. Better resolution can always be achieved by use of forced-flow techniques (OPLC, RPC) because the mobile phase velocity is nearer to the optimum; the use of online separation eliminates the need to scrape the separated compounds from the plate and means that all the compounds migrate over the whole separation distance. This enables connec-

tion of a flow detector, recorder, and fraction collector. These techniques require more sophisticated instrumentation. Unfortunately, the particle size and size distribution of pre-coated plates for OPLC are at present inadequate for this preparative technique.

Modern online forced flow methods enable not only micropreparative (OPLC) and preparative (RPC) separations, but – using appropriate split systems – also the hyphenation of these methods with different spectroscopic techniques like diode-array detection (DAD), FTIR, MS, and NMR, as is apparent from Figure 9. In this way not only isolation but also structure elucidation can be carried out in a single operation process.

**Figure 9** Combination of preparative FFPC and modern spectroscopic methods.

The greatest flexibility with regard to choice of stationary phase, particle size, layer thickness, and chamber type is provided by RPC. Because of the availability of suitable vapour phases and combination of development modes, RPC offers the greatest separating power both in terms of the amount of sample and number of compounds to be separated.

It can be stated that PPC covers a special range of preparative separations. PPC does not compete with column liquid chromatography for purification and isolation of compounds from a complex matrix. Instead, the two approaches are complementary and together they enable successful and rapid separation. It is expected that as a result of development of modern forced-flow and multiple-development techniques, PPC will further expand its importance in the isolation and purification of natural and synthetic products.

See also: II/Chromatography: Liquid: Large-Scale Liquid Chromatography. Chromatography: Thin-Layer (Planar): Densitometry and Image Analysis; Instrumentation; Modes of Development: Conventional; Modes of Development: Forced Flow, Overpressured Layer Chromatography and Centrifugal; Spray Reagents.

Further Reading

Geiss F (1987) *Fundamentals of Thin Layer Chromatography (Planar Chromatography)*. Heidelberg: Hüthig.

Hostettmann K, Hostettmann M and Marston A (1996) *Preparative Chromatography Techniques, Applications in Natural Product Isolation*. Berlin: Springer.

Nyiredy Sz (1995) Preparative layer chromatography. In: Sherma J and Fried B (eds) *Handbook of Thin-Layer Chromatography*. New York: Dekker, pp. 307–340.

Nyiredy Sz (1992) Planar chromatography. In: Heftmann E (ed.) *Chromatography*. 5th edn. Amsterdam: Elsevier, pp. A109–A150.

Nyiredy Sz, Erdelmeier CAJ and Sticher O (1986) Instrumental preparative planar chromatography. In: Kaiser RE (ed.) *Planar Chromatography*. Heidelberg: Hüthig, pp. 119–164.

Nyiredy Sz, Erdelmeier CAJ, Dallenbach-Toelke K, Nyiredy-Mikita K and Sticher O (1986) Preparative on-line overpressured layer chromatography (OPLC): A new separation technique for natural products. *Journal of Natural Products* 49: 885.

Nyiredy Sz, Botz L and Sticher O (1989) ROTACHROM®: A new instrument for rotation planar chromatography (RPC). *Journal of Planar Chromatography* 2: 53–61.

Nyiredy Sz, Dallenbach-Tölke K and Sticher O (1988) The 'PRISMA' optimization system in planar chromatography. *Journal of Planar Chromatography* 1: 336–342.

Poole CF (1992) *Chromatography Today*. Amsterdam: Elsevier.

Szabady B and Nyiredy Sz (1995) The versatility of multiple development in planar chromatography. In: Kaiser RE (ed.) *Modern TLC*. Düsseldorf: Verlag Chemie. pp. 345–367.

Sherma J and Fried B (1995) *Handbook of Thin-Layer Chromatography*. New York: Dekker.

Radioactivity Detection

T. Clark, Zeneca Agrochemicals, Jealott's Hill Research Station, Bracknell, Berkshire, UK

Copyright © 2000 Academic Press

Introduction

Thin-layer chromatography (TLC) is a technique which has been applied to a wide range of chemicals since its introduction in the early 1950s. The only limitation to its use is that a suitable method of detection must be available; however, this limitation is removed when the compounds of interest are radiolabelled. Nevertheless, since the introduction of thin-layer radiochromatography (TLRC), one major drawback in gaining widespread acceptance has been the lack of an easy method to quantify the distribution of radioactivity whilst still maintaining good resolution. The available detection methods have either been very time-consuming (e.g. autoradiogra-

phy) or labour-intensive (e.g. zonal analysis) or could not match the resolution of the TLC separation itself. Over the years TLRC detectors have evolved and significantly improved, starting with scanners in the 1960s, followed by linear analysers in the 1980s and now the new 1990s generation of bioimaging analysers and InstantImager. The limitation of the scanners and linear analysers is that their resolution is lower than can be achieved by TLC itself. New detector technology such as phosphor imaging will lead to a renaissance in the use of TLRC due to the excellent resolution.

Detection and Measurement

The principal methods for detecting and quantifying radioactivity on TLC plates are autoradiography, zonal analysis (plate scraping followed by liquid scintillation counting) and direct measurement using radiation detectors. The method employed for

analysis depends on the available equipment, which generally depends on the amount of money available, and the type of experiment and information required. The various detection methods are discussed below and the technical descriptions in the present review provide information relating to the state-of-the-art modern-day detectors.

Autoradiography

Autoradiography is a detection method in which X-ray or photographic film is exposed to emissions from radioisotopes on TLC plates to produce an image on the film. After exposure (exposure time depends on the amount of radioactivity per zone), the film is developed to reveal the location of the areas of radioactivity as darkened spots or zones of varying optical density. The density is related to the amount of radioactivity in the spot/zone. Quantification can be done either by densitometry using a calibration curve produced by exposure to radioactive standards or by removing the areas of radioactivity (scraping/cutting) and counting them by liquid scintillation. The three principal exposure methods are direct exposure (autoradiography), direct exposure with an intensifying screen and fluorographic exposure (fluorography). The approximate minimum amounts of radioactivity that are required to give a suitable image with a 24 h exposure are shown in Table 1 for the three different exposure methods.

Detection by direct exposure autoradiography involves intimate contact of the TLC plate with a photographic or X-ray film. Direct exposure is useful for all of the β -emitters, with the possible exception of low-level tritium-labelled samples. To improve the detection efficiency for γ -emitting e.g. ^{125}I and high energy β -emitting isotopes (e.g. ^{32}P), the plates are exposed with intensifying screens placed behind the film. Commercially available intensifying screens consist of plates coated with inorganic phosphors. The fraction of radiation that passes completely through the film is absorbed by the phosphor,

which in turn emits light that produces additional exposure of the film. The enhancement in sensitivity using an intensifying screen with preexposed film (see preflashing below) is of the order of 7–10-fold for ^{32}P and 16-fold for ^{125}I when compared to direct exposure without the screen.

Weak β -emitting isotopes (e.g. ^3H), adsorbed on TLC adsorbents, are inefficiently detected by direct exposure to X-ray films. The principal reasons for this inefficiency are the low energy and short range of the β -emissions and the barrier imposed by the protective coating of the X-ray film. To increase the sensitivity for these isotopes, a technique termed fluorography is employed. Fluorography involves the overcoating or impregnation of a scintillator into the TLC plate followed by direct exposure of the treated plate to the X-ray film. The scintillant, being in direct contact with the isotope, emits light when activated by the β -emission and exposes the film photographically. For efficient detection, the spectral sensitivity of the film should be matched to the wavelengths of light emitted by the scintillator. The scintillants can be incorporated by mixing with the adsorbent during preparation of the TLC plate or applied after development. Fluorographic reagents, such as 2,5-diphenyloxazole (PPO), can be added by spraying or dipping the plates.

The sensitivity of the technique can be further improved by lowering the exposure temperature and pretreating the film by partially exposing the film to a controlled flash of light (preflashing) before exposure to the radioactive sample. Preexposure to a flash of light greatly increases sensitivity and corrects the nonlinear response at low exposure levels. For maximum enhancement in sensitivity, both preflashing and cooling to temperatures between -70 and -80°C are utilized.

Zonal Analysis

The basic procedure involves removing areas of chromatographic adsorbent from a TLC plate

Table 1 Approximate lower detection limits on TLC plates for various exposure methods (dpm cm^{-2} with a 24-h exposure)

Exposure method	^3H	^{14}C	^{32}P	^{125}I
Direct exposure (autoradiography)	$2.6\text{--}13 \times 10^5$ ^a	$220\text{--}650$ ^a	500 ^d	1600 ^d
Direct exposure with intensifying screen			50 ^{d,e}	100 ^{d,e}
Fluorographic exposure (fluorography)	$2.0\text{--}6.6 \times 10^3$ ^{b,c}	$50\text{--}450$ ^{b,c}		

^a Average range for direct exposure of film at temperatures between -78.5 and 25°C .

^b Treated with a 7% solution of 2,5-diphenyloxazole (PPO) in diethyl ether and exposed at a temperature of -78°C .

^c Treated with a mixture of 0.5% 2,5-diphenyloxazole (PPO) in methyl anthranilate at -80°C with Kodak X-OMAT AR film.

^d Exposed at a temperature of -78°C .

^e Preexposed Kodak X-OMAT R film with a calcium tungstate X-ray intensifying film. (Reproduced with permission from Clark and Klein, 1996.)

followed by measuring the associated radioactivity with each spot or zone. The zones are removed either by scraping the adsorbent from the plate (plate scraping) or by cutting pieces from flexible-backed plates and transferring the segments into counting vials. In an alternative procedure, which allows isolation of the radiolabelled sample, the plates are segmented and the radioactive components are eluted from the adsorbent with solvents and counted. To ensure maximum recovery of radioactivity by elution with solvent, the adsorbent should first be crushed to a fine powder. Measurement of radioactivity is generally accomplished using a liquid scintillation counter for the weak β -emitters. For the γ -emitters, the sectioned zones are counted without further sample preparation in an appropriate γ -counter.

This technique is relatively sensitive and provides quantitative detection for samples containing low levels of radioactivity. Single peaks containing 100 d.p.m. can be readily detected. Zonal analysis has been reported to be both as sensitive and specific as gas chromatographic-mass spectrometric analysis in the assay of [^{14}C]-labelled clinical samples. When the radiochromatograms are cut into sections and quantified using a γ -counter for the analysis of γ -emitting isotopes, the method is as precise as TLC scanning.

Radiation Detectors

Over the last 30 years or so the detection of radioactivity on TLC plates has taken dramatic leaps forward. Prior to the introduction of radiation detectors, the classical method used for the detection and quantification of radioactivity on a plate involved firstly exposure to X-ray film. This could take from a few hours up to 1–2 months and this technique only located the radioactivity. The second step after location was quantification which was achieved by removing the zone of interest, either by scraping off the silica gel or by cutting away if the plates were aluminium or plastic, followed by liquid scintillation counting. Such a procedure is extremely labour-intensive and is limited in terms of accuracy and resolution (see above).

The first radiation detectors were called radioscaners and these were developed and introduced in the early 1960s. This was a major step forward in the automatic detection and subsequent quantification of radioactive components on TLC plates. The sensitivity and resolution of the instruments were not very high but peaks could be detected and their relative amounts subsequently quantified. At around the same time, spark chambers were also developed for use with TLC plates. Although, these detectors could locate individual components on TLC plates, quantification was not possible.

Another major step forward for radio-TLC came in the early 1980s when the so-called linear analyser was introduced. This instrument was easier to use and more sensitive than the old scanners and was automated to the extent that up to four plates could be run overnight. As a consequence, improved quantitative results were obtained and analysis time was shortened. However, resolution was still not as good as that obtained by using autoradiography and two-dimensional plates could not easily be evaluated.

Currently there are a number of instruments available which have equal resolution to that obtained with autoradiography or are at least approaching it. These instruments include those using the new phosphor imaging technology, the multi-wire system, or the multi-detector system (micro-channel array detector).

The basic functioning of all these detectors is outlined below and a comparison of the advantages and disadvantages of each detector is given later.

Spark chambers The spark chamber is an easy-to-use, low cost technique for photographically locating areas of radioactivity on TLC plates. Exposure times are relatively short and the images obtained on Polaroid film can be quickly transferred back to the original chromatogram using an inbuilt episcopes print projector. This means that the areas of radioactivity can then be removed for efficient counting using a liquid scintillation counter. The spark chamber can also be used for the rapid qualitative screening of plant and tissue sections to assess the degree of uptake.

Reviews of spark chambers and their uses have been published previously. Essentially, the spark chamber consists of electrodes contained in a chamber filled with a mixture of argon containing 10% methane, and this gives a high sensitivity to β -radiation. The gas is ionized by radioactive emissions and these emissions are recorded on film with a camera. The Polaroid film integrates the individual flashes produced over a suitable exposure period. Due to the intensity of the sparks the film is rapidly saturated, leading to blackening of the film, and hence direct quantification is not possible.

Radioscanners These instruments were developed and first sold commercially in the early 1960s and utilize a mechanically driven windowless gas-flow Geiger counter. These counters have an interchangeable aperture plate (collimator slit) which controls the size of the area being measured. The TLC plate is scanned by the moving detector head and the signal obtained from the radioactivity source is amplified and recorded. The resultant chromatogram can then

be printed on a suitable recorder or integrator-plotter. When the speed of the scanner and recorder are synchronized the exact location of the radioactivity on the TLC plate can be obtained by aligning the chromatogram with the TLC plate. Some manufacturers continue to produce radioscanners but, due to the increasing number of new detection systems (described below) which have better sensitivity and resolution, the number of radioscanners available for quantitative TLC has decreased.

Linear analysers The introduction of the linear analyser provided a great boost for the users of radio-TLC since these detectors brought with them not only improved sensitivity and resolution but also much-improved automation. For example, up to four plates, each with several tracks, can be measured overnight and the chromatograms and accompanying quantitative tables automatically printed out. For the first time in this field the resultant data can be stored and reprocessed at a later date. With the development of new desktop publishing software, the chromatograms and quantitative results can be directly transferred into reports or publications.

The linear analysers currently used are based on imaging counters developed for high energy physics and medical imaging in the late 1960s and early 1970s. Essentially, the detector head moves automatically to any track on the TLC plate. Once in position the head is gently lowered on to the surface of this track of the TLC plate and the instrument is then ready to begin measurement. At this point the detector has formed a counting chamber since the TLC plate itself has closed the opening of the detector, making the counting chamber gastight. Immediately the detector is resting on the plate the flow of counting gas (argon/methane) is automatically activated and within a few seconds the counting chamber is purged of air and filled with the counting gas.

There are two kinds of systems available today which function in a similar way: each utilizes a different design to locate the exact position of the radioactivity on the plate. One system uses the resistive anode technique and a schematic diagram of this detector is shown in Figure 1. High voltage is applied to a 25 cm anode wire fixed along the length of a windowless detector (1 cm wide) and positioned directly above the TLC plate. This wire is constructed of carbon-coated quartz and has a high electrical resistance. When a radioactive emission enters the detector, the gas is ionized and electrons are produced along the particle track. The free electrons are accelerated towards the anode wire by the electric field produced by the high voltage. The electrons continue to ionize more gas as they approach the wire, and the

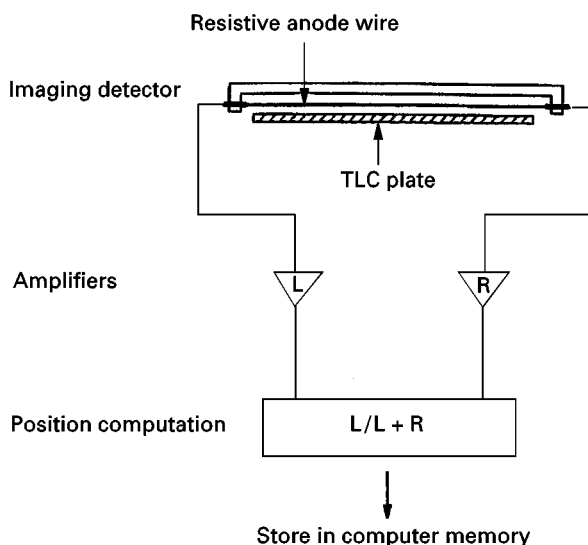


Figure 1 Schematic diagram of a linear analyser detector with a resistive anode wire. (Reproduced with permission from Clark and Klein, 1996.)

resulting number of electrons becomes large enough to be detected electronically. The pulse of electrons is collected on the anode wire near the position of the initial ionization. The charge divides in the wire, and pulses appear in the amplifiers located at both ends of the wire. The amplitude of the pulse measured by each amplifier is proportional to the resistance between that end of the wire and the position where the electrons were collected. The ratio of these two pulses is linearly related to the original position of the event on the wire. The position of each event is calculated and stored in a computer memory to provide a digital image of the distribution of radioactivity on the plate.

The second type of detection system uses the delay wire technique; a schematic diagram of this detector is shown in Figure 2.

The β -radiation (fast electrons) emitted from the radioactive source on the plate ionizes the counting gas which has been specifically chosen so that this process can freely take place. This is the primary mode of ionization and the resultant charged particles, free electrons and positive ions, are then accelerated towards the anode wire and cathode, respectively. In this primary mode of ionization the free electrons are accelerated to such an extent that they themselves cause ionization of the counting gas, producing further free electrons and ions and this is the secondary ionization mode. This continues, causing an avalanche of ions from the primary point of ionization towards the anode wire.

Concurrently, the positive ions produced move relatively slowly towards the cathode. These positive

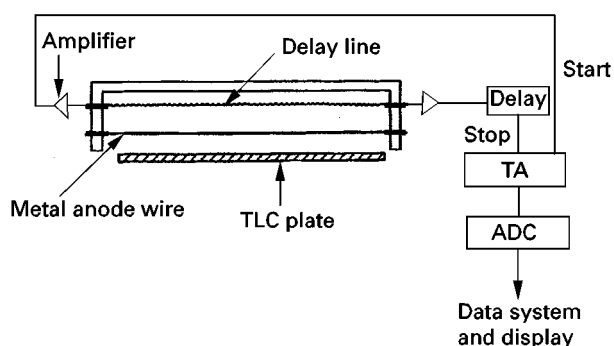


Figure 2 Schematic diagram of a linear analyser detector utilizing a delay wire technique. TA, Time-to-amplitude; ADC, analog-to-digital converter. (Reproduced with permission from Clark and Klein, 1996.)

ions sometimes combine with electrons, producing ultraviolet radiation of sufficient energy to cause further ionizations in a process known as the photoelectric effect. Once sufficient ionization has taken place, a spark is produced, which gives rise to a pulse in both the anode and cathode. The amplitude of the pulse is proportional to the number of ions produced and hence this type of detector is generally called a proportional counter.

The above is a description of the principle of detection. The location of the source of the ionizations is obtained by making use of a delay wire. The delay wire is a very thin wire which is wound over the cathode and pulses pass along this wire in both directions. The pulses are detected by amplifiers at each end of the wire. The arrival of a pulse at one end starts the time-to-amplitude (TA) circuit, while the other pulse is delayed and provides a stop signal in the circuit. The difference between the time of arrival at the two ends of the wire can thus be measured and is proportional to the position of the initial ionization. An analog-to-digital converter (ADC) converts the TA signal to a digital position value that is processed by the data system.

Using this method of detection, the whole of the delay line remains active and thereby the entire length of the chromatogram can be measured at the same time. Once one track of a TLC plate has been measured according to the pre-set time, it automatically moves to the next and the measuring process is repeated.

Radioanalytic imaging system (Ambis) When this instrument was introduced in about 1988, a description of its functioning was reported. The Ambis 4000 directly detects β -particles from a wide variety of isotopes and is suitable for gels, blots, TLC plates and any sample type of the dimensions 20×20 cm. It is

reported in the company literature that this instrument can be 100 times faster than X-ray film.

The detector consists of 3696 individual detector elements (each giving a data point) configured in a hexagonal array. Image quality is improved by increasing the number of data points and this is achieved by moving the sample through 72, 144 or 288 discrete positions. Therefore, counts are recorded in 266 112, 532 224 or 1 064 448 data points (i.e. $3696 \times$ number of discrete positions) from which an image is obtained. This image can then be displayed on a monitor and the areas of radioactivity quantified. A background detector which operates concurrently and in a similar way is located above the main detector, and compensates for background radiation.

Different resolution plates, which have different size and shape apertures, can be inserted into the instrument and these plates control the resolution and efficiency (i.e. sensitivity) of the instrument. In general, this means that, using the correct aperture, the detector can be tuned to obtain maximum resolution (at the expense of sensitivity). Conversely, when the instrument is tuned for maximum sensitivity, this is at the expense of resolution. Therefore, aperture choice is governed by sample size and the number and resolution of components required within the sample.

Multiwire Proportional Counters (MWPC)

Digital Autoradiograph (Berthold) This two-dimensional detector is reported to be 100 times more sensitive than the linear analyser and measures all areas of radiation from a 20×20 cm surface simultaneously.

The radio-TLC plate is placed on the measuring table and is then automatically loaded into the detector, which also controls the flow of the P-10 counting gas (90% argon + 10% methane). The detector is principally a two-dimensional position-sensitive MWPC. Essentially, it consists of three parallel wire planes, X, Y and Z, each with 100 wires. The spacing between the planes and the wires is only a few millimetres. The central plane (Z) is maintained at a positive potential of 1800 V and the counting chamber is filled with P-10 gas. Charged pulses are generated on the Z plane wires by ionizing particles (β -particles). The orthogonally crossed wire planes X and Y, below and above Z, pick up the charge signals from the Z plane at their position of origin, hence the position of the radioactivity on the TLC plate can be located.

The signals from the wire planes are transmitted via preamplifiers, pulse shapers, discriminators and logic circuits to ADC which are finally coupled to a data acquisition system.

InstantImager (Canberra Packard) This microchannel array detector provides direct electronic detection and real-time imaging of radioactivity on flat surfaces such as gels, blots, tissue slices and, of course, TLC plates. The detector consists of an array of 210 420 so-called microchannels (diameter 400 μm) in a 20 \times 24 cm multilayer plate. The microchannel array plate is a laminated surface about 3 mm thick with alternating conductive and nonconductive materials. A voltage step gradient is applied to the successive conductive layers to create a high electric field (approximately 600 volts mm^{-1}) in the microchannels. The β -particle emitted from the radioactive source ionizes a gas (argon with small amounts of carbon dioxide and iso-butane) in one of the microchannels. The electrons produced are accelerated by the high electric field in the microchannel, further ionizing the gas, resulting in a cloud of electrons. In this way the microchannels serve as both collimators and preamplifiers.

The cloud of electrons migrates up an electric field gradient into a multiwire chamber located on top of the multilayer. This chamber consists of an anode plane of thin anode wires and two cathode planes (X and Y), as described above for the Digital Autoradiograph. Further avalanche amplification occurs, resulting in electric pulses in the X and Y cathode tracks. The resultant signals are digitized and then decoded to identify the microchannel in which the primary ionization took place, hence locating the position of the radioactive emission. A schematic representation of the microchannel detector is shown in Figure 3.

BioImaging/phosphor imaging analysers The phosphor imagers make use of an imaging plate which is a two-dimensional sensor formed by a layer of fine crystals of photostimulable phosphor (BaFBr : Eu^{2+}). The emitted β -energy is stored upon exposure. In the reading unit the imaging plate is scanned with a laser beam. The energy of the laser stimulates the stored

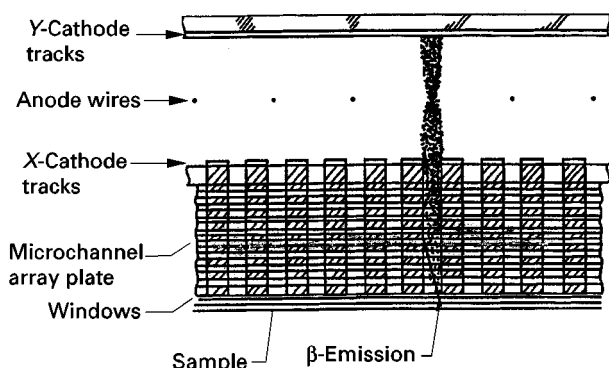


Figure 3 Schematic diagram of the microchannels of the InstantImager. (Courtesy of David Englert, Canberra Packard, Meriden, CT, USA.)

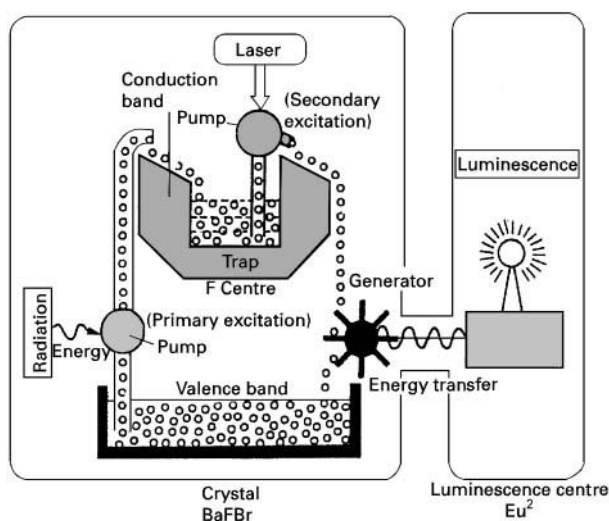


Figure 4 Schematic diagram of the principle of detection of the PhosphorImaging analyser. (Courtesy of Fuji Photo Film Co. Ltd, Tokyo, Japan.)

electrons to return to the ground state and to emit luminescence in proportion to the recorded radiation intensity. This luminescence is collected in a photomultiplier tube and converted into an electrical signal. A schematic diagram of the principle of detection is shown in Figure 4.

Data recording and analysis are carried out at a workstation. After reading, the image data on the imaging plate can be erased by exposure to incandescent light and thus the plate can be reused. Imaging plates for the normal weak β -emitters are available and a specially designed plate for tritium is available. An illustration of the whole imaging process is given in Figure 5.

A prerequisite for good results is to expose the plates in a lead shielding box, particularly those that require longer than 1–2 h exposure time. In this way the contribution of natural background radiation is reduced.

Over the last few years there has been a significant expansion in the variety of instruments available and in the type of imaging plates on offer. Instrumentation has been improved and targeted as far as applications are concerned. For instance, Fuji now has six Phosphor Imaging plate scanners (BAS 1000, 1500, 2000, 2500, 5000 and the new 1800) and Canberra Packard has brought out the Cyclone. Fuji also now offers the FLA 2000 which combines fluorescent and radioisotope detection. The major improvement in the BAS range of instruments has been in resolution, whereby the BAS 5000 can now operate with a resolution of 25 μm , although when used at this high resolution the storage memory required for each scan is extremely high.

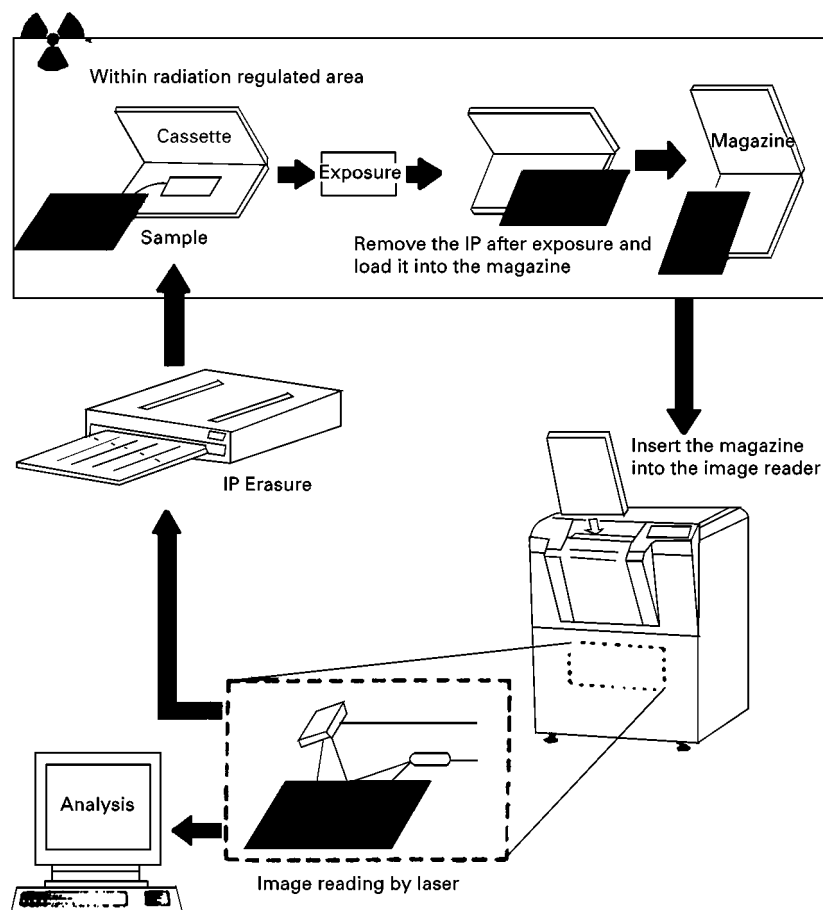


Figure 5 Illustration of the phosphoimaging process. IP, Imaging plate. (Courtesy of Fuji Photo Film Co. Ltd, Tokyo, Japan.)

A further instrument using similar technology, recently introduced by Packard, is the Cyclone™. In this instrument, a solid-state diode laser and confocal optical system moves down the storage phosphor screen as the screen rotates on a carousel. In this process the laser excitation and light collection optics remain in a fixed position relative to the screen surface, so that laser bleed associated with other detectors is eliminated. Furthermore, light collection is increased compared to that obtained with fiberoptic bundles.

A range of imaging plates is now available and these should be chosen according to instrument and requirement. Currently, Fuji is the leading supplier and offers the BAS III, MP, SR, TR and ND imaging plates: care must be taken when selecting a plate because not all plates can be used with all instruments. A range of cassette sizes is also available from Fuji according to plate size.

Comparison of TLRC Detection Methods

As described at the beginning of this article, there are three principal techniques for the analysis of radio-

active components on TLC plates, autoradiography, zonal analysis and mechanical detectors (e.g. linear analysers, phosphor imagers, MWPC detectors). The technique of choice depends on a number of parameters but of primary consideration are sensitivity and resolution. Other parameters to be considered are quantification, linear dynamic range, speed, sample throughput and preservation of sample. A comparative summary of the detection methods with respect to these parameters is shown in Table 2.

Both autoradiography and zonal analysis have a number of drawbacks, including sensitivity and resolution, but primarily both techniques are extremely time-consuming. Linear analysers offer a good compromise between speed, resolution and quantitative accuracy. However, the performance of the linear analysers falls well below that of the currently available MWPC detectors and phosphor imagers in all respects. Sensitivity, quantification and, particularly, resolution are significantly superior, resulting generally in much better quality chromatograms. The phosphor imagers have slightly better resolution than the MWPC detectors but the disadvantage of phosphor imagers is that the chromato-

Table 2 Comparison of thin-layer radiochromatographic analysis techniques

Parameters	Autoradiography	Zonal analysis	Linear analyser	MWPC detector	Phosphor imager
Sensitivity	+	+++++	++	+++++	+++++
Resolution	+++++	+	++	++++	+++++
Quantification	+	+++++	+++++	+++++	+++++
Dynamic range	+++	+++	+++	+++++	+++++
Speed	+	++	+++++	+++++	++++
Sample throughput	+	+	+++	++++	+++++
Preserves sample	Yes	No	Yes	Yes	Yes

+++++, Excellent; +++++, very good; +++, good; ++, satisfactory; +, poor. (Reproduced with permission from Clark and Klein, 1996.)

gram development cannot be seen in real time. Also, for a single plate the analysis time with the MWPC detectors is quicker but when more sample throughput is required, then the phosphor imagers have the advantage since many plates can be exposed simultaneously.

In general, as the newer range of detectors were brought on to the market they were very expensive in comparison to the linear analysers. However, with increasing competition and technological developments, prices are slowly coming down.

Future Developments in TLRC

The new range of detectors have significantly improved sensitivity and resolution; most have a resolution of under 1 mm and the phosphor imagers are able to obtain a resolution of as low as 0.025 mm. Also, current detectors are now able to detect spots of radioactivity on a plate containing less than 10 d.p.m. in a relatively short period of time. As sensitivity and resolution are continually improving, the future major development of TLRC probably lies in the realm of full automation using robots, from the application of multiple samples to the TLC plate, to development and drying, transport to the detector, measurement and finally printing of the chromatogram and quantitative results.

Further Reading

- Clark T and Klein O (1996) Thin-layer radiochromatography. In: Sherma J and Fried B (eds) *Handbook of Thin Layer Chromatography*, 2nd edn. New York: Marcel Dekker.
- Filthuth H (1982) Radioscanning of TLC. In: Touchstone JC (ed.) *Advances in Thin Layer Chromatography*, pp. 89–123. New York: John Wiley.
- Filthuth H (1989a) New detector for radiochromatography and radio-labelled multisample distributions. The digital autoradiograph. *Journal of Planar Chromatography* 2: 198.
- Filthuth H (1989b) Detection of radioactivity distribution with position-sensitive detectors, linear analyzer, and digital autoradiograph. In: Touchstone JC (ed.) *Planar Chromatography in the Life Sciences*, p. 167. New York: John Wiley.
- Hamaoka T (1990) Autoradiography of new era replacing traditional X-ray film bio-imaging analyzer BAS2000. *Cell Technology* 9: 456.
- Johnston RF, Pickett SC and Barker DL (1990) Autoradiography using storage phosphor technology. *Electrophoresis* 11: 355.
- Klein O and Clark T (1993) The advantages of a new bio-imaging analyzer for investigation of the metabolism of ^{14}C -radiolabelled pesticides. *Journal of Planar Chromatography* 6: 369.
- Miyahara J (1989) Visualising things never seen before. The imaging plate: a new radiation image sensor. *Chemistry Today* 223: 29.
- Nakajima E (1993) Radioluminography, a new method for quantitative autoradiography in drug metabolism studies. *Radioisotopes* 42: 228.
- Prydz S (1973) Summary of the state of the art in radio-chromatography. *Analytical Chemistry* 45: 2317.
- Roberts TR (1978) *Radiochromatography, The Chromatography and Electrophoresis of Radiolabelled Compounds*, pp. 45–83. Amsterdam: Elsevier.
- Shulman SD (1982) Quantitative analysis by imaging radiation detection. In: Touchstone JC (ed.) *Advances in Thin Layer Chromatography*, pp. 125–137. New York: John Wiley.

Spray Reagents

P. E. Wall, Merck Ltd, Poole, Dorset, UK

Copyright © 2000 Academic Press

Introduction

The detection of chromatographic zones on a developed thin-layer plate usually relies on the absorption or emission of electromagnetic radiation in the visible or ultraviolet range. Some compounds are visibly coloured, others absorb UV light or exhibit fluorescence when excited by UV or visible light, but most require visualization using an appropriate spraying or dipping reagent. Due to the inert nature of the adsorbents commonly used in thin-layer chromatography (TLC) layers, chemical reactions can be carried out *in situ* without destroying the adsorbent or binder characteristics. Many such detection reagents exist for TLC, and lists of formulations have been collated in a number of publications. Like a number of other features of the TLC procedure, this highlights the versatility and uniqueness of thin-layer chromatography compared with other chromatographic techniques. Often, quite aggressive reagents such as hydrochloric acid or sulfuric acid can be used to detect separated analytes *in situ*. Such reagents are included along with iodine vapour or nitric acid vapour as universal reagents that can be used to visualize a wide range of compounds of different types. Some of these can be termed destructive reagents, particularly those involving charring. Some reagents are much more specific for groups of compounds such as alcohols, aldehydes, ketones, esters or acids. These are termed group-specific reagents. With regard to specificity, this is about the limit of what is possible as no genuine substance-specific reagents exist. When no irreversible chemical reaction is used for detection on the chromatographic layer, the form of visualization is termed non-destructive. Included in non-destructive techniques are visible and UV light, and sometimes the use of iodine or ammonia vapour. The latter two reagents are included as in many cases the 'reaction' is reversible.

Often, separated compounds can be detected and visualized by a combination of the above techniques. A non-destructive technique may be used initially, followed by a universal reagent, and then finally a group-specific reagent to enhance selectivity and sensitivity. Often, for a particular analyte there may be several visualization reagents available, but usually there is a noticeable difference in sensitivity of detection between them. Also stability may play an

important part in the selection of a suitable detection reagent. Some reagents have good stability over a number of weeks, however, there are those that must be made up fresh and used almost immediately. The visualized chromatographic zones may also differ in stability. Some may fade quite quickly, whilst others, although remaining stable, become more difficult to visualize as the background darkens or is affected in some other way by the reagent. Fortunately, the majority of reagents do give acceptably stable results. Sometimes dark or coloured backgrounds can be lightened by exposure of the chromatographic layer to acidic or alkaline vapours. However, all these effects will need to be taken into consideration so that the most effective visualization procedure is used.

After visualization, further analysis can be performed by *in situ* spectrodensitometric scanning in the absorbance, fluorescence quenching, or fluorescence modes, in addition to removing some or all of the separated chromatographic zone for further analysis by infrared (IR), Raman, nuclear magnetic resonance (NMR), mass spectrometry (MS) or radiography. Using these hyphenated techniques, more useful analytical data can be obtained. In fact, the stability of the layers and the detected chromophores often allow useful data to be collected even if the TLC plate had been developed some days or weeks previously.

Non-destructive Methods

Visible Spectrum

Some compounds are sufficiently coloured, for example natural and synthetic dyes, and nitrophenols, to give an absorption in the visible part of the electromagnetic spectrum. However, it is the remaining part of the visible radiation that is reflected and is seen by either the naked eye or light-detecting equipment. Prechromatographic derivatization can often be used to improve resolution of the analytes of interest, but also make them visible to the naked eye. One example of this is the formation of yellow dinitrophenylhydrazones of ascorbic acid and its homologues.

Ultraviolet Spectrum

Colourless separated components on the TLC/high performance (HP) TLC layer may absorb electromagnetic radiation at shorter wavelengths than the visible spectrum. These are detected in the UV range, normally at 400–200 nm. Such compounds are detected using

UV-sensitive detectors, e.g. photomultipliers. Often exposure to UV light at short-wave radiation (254 nm) or long-wave radiation (366 nm) is all that is necessary for absorbing or fluorescing substances to be observed. Most manufacturers' UV lamps and cabinets function at either or both of these wavelengths.

To aid absorbance, many commercial pre-coated TLC layers contain an inorganic phosphorescent indicator or an organic fluorescent indicator. Inorganic indicators used include uranyl acetate (yellow-green), manganese zinc silicate, zinc cadmium sulfide, zinc silicate (green) and tin strontium phosphate (blue). Nearly all silica gel pre-coated plates and sheets contain this type of indicator. Most indicators exhibit a bright green, yellow or blue phosphorescence when excited by UV light at 254 or 366 nm.

Detection by absorbance in these cases relies on the phosphorescence being quenched by the sample components. This process is known as fluorescence quenching because the phosphorescence is very short lived. Hence, the effect is best observed by continual exposure to UV light. In most cases, pink or violet spots/bands are observed for quenching on the green phosphorescent background, whereas grey-black spots/bands are usually seen on the blue background. In most applications, the inorganic indicators are quite stable with little or no elution from developing solvents, and remain unaffected by most dyeing reagents and the temperatures used to effect reactions.

Organic fluorescent indicators can also be used. Most of these fluoresce in long-wavelength UV light (366 nm) and are coded F₃₆₆ or UV₃₆₆ by the manufacturer. Most cellulose pre-coated layers contain this type of indicator. Substances used include optical brighteners, hydroxypyrene sulfonates, fluorescein and rhodamine dyes. Some pre-coated plates are manufactured with both types of indicator present to give possible quenching by sample components at both wavelengths.

The process of fluorescence quenching is caused by the electromagnetic radiation providing the energy to bring about an electronic transition from the ground state to an excited singlet state. As the excited electrons return to the ground state, they emit the energy at a longer wavelength, usually in the visible range. Phosphorescence quenching is slightly different. Rather than returning directly to the ground state, the electrons enter an excited triplet state and then return from there to the ground state. As before, the energy is emitted at a longer wavelength. However, as the decay is longer the process is better described as phosphorescence rather than fluorescence.

Many analytes, however, either absorb insufficiently or not at all by these techniques. In these instances suitable detection reagents are used to give coloured

spots/bands *in situ*. If these are reversible reactions, then they can still be termed non-destructive techniques.

Reversible Reactions

Iodine Vapour

Iodine is a very useful universal reagent, but it should never be overlooked that some reactions with iodine are non-reversible (discussed later in Non-reversible Reactions). The use of iodine as vapour enables the detection of separated substances rapidly and economically before final characterization with a group-specific reagent. Where lipophilic zones are present on a silica gel layer, the iodine molecules will concentrate in the substance zones giving brown chromatographic zones on a yellow background.

Preparation of the reagent simply involves putting a few iodine crystals in a dry chromatography chamber, replacing the lid and allowing the iodine vapour to fill the tank for a few hours. The developed chromatogram is then introduced into the chamber and as soon as the chromatographic zones are recognized, the layer is removed and the results documented. The adsorbed iodine can then be allowed to evaporate from the surface of the layer in a fume cupboard. The chromatogram can then be subjected to further reactions. If more permanent results of the iodine impregnation are required, then the chromatographic zones can be sprayed or dipped in a starch solution (0.5–1%) to give blue starch-iodine inclusion compounds.

Iodine detection works well on silica gel 60 and aluminium oxide layers. However, results are usually poor on reversed-phase layers as the lipophilicity of the layer does not differ appreciably from the substance zones.

Iodine vapour reversible reactions occur with a wide range of organic lipophilic molecules, e.g. hydrocarbons, fats, waxes, some fatty acids and esters, steroids, antioxidants, detergents, emulsifiers, antibiotics and many miscellaneous pharmaceuticals.

Ammonia Vapour

Ammonia vapour is often employed in improving the sensitivity of visualization of organic acids where pH indicators like bromocresol green or bromophenol blue have been used initially. The presence of ammonia has the effect of giving a sharper contrast between the chromatographic zones and the plate background. The process of exposure to ammonia vapour can be carried out simply by holding the chromatographic plate face down over a beaker of strong ammonia solution. However, it can be done more

elegantly by pouring ammonia solution into one compartment of a twin trough developing tank and placing the TLC plate in the dry compartment. With the lid in place the TLC plate is exposed to an almost even concentration of vapour. The process is reversible with time as the ammonia soon evaporates from the adsorbent surface.

Non-reversible Reactions

Destructive Techniques

Most post-chromatographic chemical reactions on the layer could be described as 'destructive' in that a chemical reaction has taken place and visualized compounds are no longer those that were applied as the sample. However, in order that a clear distinction can be seen between a truly destructive technique and a chemical derivatization or other chemical reaction, the destructive techniques described here will be limited to charring and thermal activation.

Charring techniques Charring usually involves treatment of the developed chromatogram with sulfuric acid and then heating at temperatures of 100–180°C for 5–20 min. The reaction is fairly non-specific, detecting most substances that are organic in nature as carbon deposits. Hence, sulfuric acid can also be termed a 'universal reagent'. Sometimes fluorescent chromatographic zones are produced at temperatures below 120°C, but their intensities are very dependent on the time of heating. Most charring occurs at higher temperatures, typically 150–180°C.

Although sulfuric acid charring is a relatively easy technique, there are limitations. Overheating of manufactured pre-coated layers results in the whole layer turning grey or even black. The problem is that commercial binders in pre-coated layers will also char under extreme heat in the presence of sulfuric acid. Most sulfuric acid reagents for dipping and spraying commercial TLC plates consist of a 10–20% v/v solution in water/methanol. Charring reactions will also occur sometimes with other acids, e.g. phosphoric acid. In conjunction with copper acetate, lipids can be detected by charring at 180°C.

A further point to bear in mind is the care that needs to be taken if charring techniques are used in conjunction with reversed-phase silica gel layers. Due to the carbon loading, excessive heating will cause a dark or even black background to appear.

Thermal activation techniques It has been observed that heating some substances to high temperatures on certain chromatographic adsorbents results in

chromatographic zones that are fluorescent under exposure to UV light. This process is known as thermochemical activation. The moderately polar stationary phase, a NH₂-bonded silica gel layer, gives the best results for this type of detection.

It has been postulated that under the catalytic influence of the surface of the silica gel bonded layer, functional groups are eliminated and aromatic ring systems develop, which are excited by long wavelength UV light at 366 nm. In general, compounds with heteroatoms (nitrogen, oxygen, sulfur and phosphorus) more readily undergo this reaction than pure hydrocarbons. Under the influence of the catalytic adsorbent surface, substances rich in π -electrons are formed that conjugate to produce products that are fluorescent when appropriately excited. Changes in pH can alter the excitation and fluorescing wavelengths.

The derivatives formed remain stable for weeks, and the fluorescence can frequently be intensified and stabilized by dipping the chromatogram in organic solvent solutions of Triton X100, liquid paraffin and polyethylene glycol. If the NH₂-bonded layer contains a fluorescent indicator (F₂₅₄), then often appreciable fluorescence quenching can occur under UV light at 254 nm. Sometimes compounds that only weakly fluoresce can exhibit strong fluorescent absorption (e.g. vanillic acid and homovanillic acid). Thermal activation works well for the detection of catecholamines, fruit acids and some carbohydrates.

Chemical Reactions on the Layer

Most chemical reactions on the planar chromatographic layer are carried out after development of the chromatogram. This is described as post-chromatographic visualization and is particularly useful when the presence of 'unknowns' in the sample need to be detected. However, it is also possible, as will be shown later, to carry out a pre-chromatographic derivatization before chromatographic development and this can have significant advantages. As post-chromatographic visualization is the major method of detection, it is this technique that will be given consideration first.

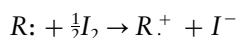
Post-chromatographic visualization Post-chromatographic identification of chromatographic zones can be achieved by spraying or dipping the TLC/HPTLC layer with a universal or group-specific reagent. Sometimes 'destaining' techniques can improve sensitivity where such reagents are employed. Where complex mixtures of large numbers of analytes of differing functionality are involved, sequencing reactions can be used to locate groups of compounds progressively.

The most used and dependable reagents are discussed in detail below, however, this represents only a small fraction of the detection reagents available, and the literature should be consulted for a more comprehensive review. In choosing the best detection reagent, the following points should be borne in mind:

1. Sensitivity of detection.
2. Selectivity of the reagent for the analytes of interest.
3. Background effects, particularly where plates are to be scanned spectrophotometrically.
4. Stability of detection reagent.
5. Stability of the chromatogram after chemical or thermal treatment.
6. Ease of preparation of the spraying or dipping reagent.
7. Hazards associated with the use of particular detection reagent.

Universal chemical reagents

Iodine vapour/solution Iodine reacts chemically with unsaturated compounds, which is rarely reversible on silica gel layers. Also irreversible oxidations, electrophilic substitutions, addition reactions, and the formation of charged transfer complexes have been observed. The so-called 'iodine reaction' is possibly an oxidation with the initial formation of a radical cation as shown in the following reaction equation:



A number of possible reaction pathways can then occur. **Table 1** lists some of the common reactions

that take place on the chromatographic layer with iodine. Iodine also possesses fluorescence quenching properties, hence, chromatographic zones that contain iodine will appear as dark zones on a silica gel layer containing a fluorescent indicator when viewed under UV light at 254 nm.

In the case of both reversible and non-reversible reactions with iodine vapour, the chromatographic zones can be 'fixed' by further treatment with a 0.5–1.0% aqueous starch solution. The well-known deep blue iodine–starch complex is formed, which has good stability. As the reaction is very sensitive it is important to make sure that little iodine remains in the background, otherwise the whole background will be coloured blue!

The detection limits are usually a few micrograms of substance per chromatographic zone, but there are some cases where the detection is lower still (e.g. 200 ng glucose). Iodine may also be applied as a solution and is usually prepared in an organic solvent, such as petroleum spirit, acetone, methanol, chloroform or diethyl ether. A suitable dipping solution would be 250 mg iodine in 100 mL petroleum spirit. Such solutions have the advantage that, in some cases, the iodine is enriched to a greater extent in the chromatographic zones when dissolved in a lipophilic environment than a hydrophobic one. Hence, the sensitivity can be improved.

Ammonia vapour Ammonia vapour has a number of uses in chromatographic zone detection:

1. When pH indicator solutions are used to detect aliphatic and aromatic carboxylic acids and fatty acids, ammonia vapour can help to intensify the colours against a contrasting background (often a reversible reaction).

Table 1 Examples of iodine reactions on the TLC layer with a common range of organic substances

Substance	Reaction
Polycyclic aromatic hydrocarbons, indole and quinoline derivatives	Formation of oxidation products
Quinine alkaloids, barbiturates and calciferol	Addition of iodine to the double bonds
Opiates, brucine, ketazone and trimethazone	Iodine addition to the tertiary nitrogen for the opiates Addition reaction with the $-OCH_3$ group of the brucine Ring-opening reaction in the case of the ketazone and the trimethazone
Thiols and thioethers	Oxidation of sulfur and addition across the double bond in the thiazole ring
Alkaloids, phenthiazines and sulfonamides	Complex formation

2. There are a number of instances where residual chemical detection reagent gives a background colour. Often exposure to ammonia vapour has the apparent effect of bleaching it from the layer. (An example of this is in the use of molybdophosphoric acid reagent, where the background yellow colour is removed.) This effect increases sensitivity of detection.
3. Stabilization of some reactions on the layer is also possible with ammonia vapour. An instance of this is the blue colour of tryptamine after reaction with Gibb's reagent.

Nitric acid vapour Most aromatic compounds can be nitrated with the fumes from fuming nitric acid. The reaction works best if the developed chromatogram is heated to about 160°C for 10 min and introduced whilst still hot into a chamber containing the nitric acid vapour. Generally the chromatographic zones are rendered yellow or brown in colour. They also absorb in UV light at 270 nm. Some substances such as sugars, xanthine derivatives, testosterone and ephedrine fluoresce yellow or blue when excited by long wavelength UV light after such treatment.

Group specific reagents Many reagents give specific reactions with certain organic chemical groups and are called group-specific reagents. In most cases, the reaction mechanism is clearly understood. As a general rule these reagents are very sensitive. It is these reagents that make up the major part of the detection reagent lists that are readily available in a large number of TLC publications. The relative merits of a few of the major group-specific reagents are discussed below.

Oxidation/reduction reactions Often the most frequently used visualization techniques, oxidation/reduction reactions are group-specific depending on the particular reagent used. Some examples of oxidation reactions used in TLC are as follows: Emerson reagent (4-aminoantipyrine–potassium hexacyanoferrate [III]) for detection of arylamines and phenols; phosphomolybdic acid reagent for lipids and some steroids; chlorine–*o*-toluidine reagent for vitamin B₁, B₂, B₆ and triazines; chloramine T reagent for steroids and purine derivatives; and chlorine–potassium iodide–starch reagent for amino, imino and amido groups, and triazine herbicides. Examples of reduction reactions include: tin(II) chloride–4-dimethylaminobenzaldehyde reagent for the detection of aromatic nitrophenols; blue tetrazolium reagent for corticosteroids, Tillman's reagent (2,6-dichlorophenolindophenol) for organic acids including vit-

amin C; and silver nitrate–sodium hydroxide reagent for reducing sugars and sugar alcohols.

Hydrazone formation The reagent mainly employed for hydrazone formation is 2,4-dinitrophenylhydrazine in acidic solution, which provides a specific reagent for carbonyl compounds (aldehydes, ketones and carbohydrates). Yellow or orange-yellow hydrazones, or osazones in the case of carbohydrates, are formed on the chromatogram. Ascorbic acid and dehydroascorbic acid also respond to this reagent. The sensitivity limit is of the order of 10 ng per chromatographic zone.

Dansylation Dansyl chloride and other derivatives are used to produce fluorescent dansyl derivatives of amino acids, primary and secondary amines, fatty acids and phenols. The dansylation of fatty acids is indirect as the acid amides must be formed first. This conversion is readily achieved with the reagent dicyclohexylcarbodiimide. In the next step, dansyl cadaverine or dansyl piperidine is used to form fluorescent derivatives of the amides. The detection limit is 1–2 ng fatty acids.

Diazotization Azo dyes are strongly coloured and can be produced on the TLC layer by reduction to primary aryl amines, diazotization and coupling with phenols. Conversely, phenols can be detected by reaction with sulfanilic acid in the presence of sodium nitrite (Pauly's reagent). The coloured zones formed by such reactions are often stable for a period of months.

A few named reagents exist that rely upon a diazotization reaction to detect specific groups of compounds. Two well-known ones are the Bratton–Marshall reagent and Pauly's reagent. The Bratton–Marshall reagent consists of two spray solutions: the first, is sodium nitrite in acid to effect the diazotization; and the second is a mainly ethanolic solution of *N*-(1-naphthyl)ethylenediamine dihydrochloride. This reagent is used specifically to visualize primary aromatic amines, sulfonamides and urea, and carbamate herbicides. Pauly's reagent is used to visualize phenols, amines, some carboxylic acids and imidazole derivatives.

Metal complexes The cations of a variety of transition metals are electron acceptors and are therefore capable of forming complexes with colourless organic compounds that are electron donors. Coloured complexes are the result caused by electron movement within the orbitals of the central metal ion. The most important of these metal ions that form chelates are Cu²⁺, Fe³⁺ and Co²⁺, which have particular affinity

for compounds that contain oxygen and nitrogen. Examples of this type of chemistry are the biuret reaction with proteins (resulting in the formation of a reddish-violet complex) and the reaction of the Cu^{2+} ion with aromatic ethanolamines (to form blue-coloured chelates). In addition there is the formation of reddish-violet colours of phenolic compounds with the Fe^{3+} ion.

Schiff's base reaction The Schiff's base reaction is a group-specific reaction for aldehydes. The reaction usually occurs under basic conditions with aromatic amines to form a Schiff's base. Aniline is normally used to form a coloured anil or Schiff's base with an aldehyde. Carbohydrates can be visualized with 4-aminobenzoic acid with the formation of coloured and fluorescent Schiff's bases. A similar reaction mechanism occurs with 2-aminobiphenyl for aldehyde detection. One of the most sensitive reagents for reducing sugar visualization, the aniline phthalate reagent, is also a Schiff's base reaction. The limit of sensitivity is 10 µg per chromatographic zone.

Other reactions There are a number of less well-used reactions such as halogenation with bromine or chlorine vapour, esterification of alcohols, hydrolysis reactions, and the formation of charge transfer complexes. Many other popular reagents do not fit into the above categories, yet they do constitute a major part of visualization reagent lists. For some of these, the reaction mechanism has not been fully elucidated. Table 2 lists a selection of visualization reagents together with the classes of compounds visualized.

Sequencing reactions If it is known that particular functional groups may be present in the separated chromatographic zones, then reactions can be ex-

ploited more specifically, not necessarily to give direct identification, but to increase the evidence of the presence or absence of particular analytes. Here, specific reagent sequences can be used to give a wealth of evidence visually. Sequencing reactions are particularly useful where a number of differing functional group compounds are present on a chromatogram. An example illustrating the use of four well-known detection reagents is shown in Figure 1.

Where excess of one reagent has been used that may then interfere with the next reagent in the sequence, washing or 'destaining' steps will be necessary. Rinsing troughs in the form of dipping chambers can be used. Such sequential reactions are always carried out either to prepare a substance for a colour reaction that will follow later or to increase the amount of information that is obtained by exploiting a combination of different independent reactions. Therefore, information is provided that could not be obtained using a single reagent step.

Pre-chromatographic derivatization to enhance detection Group-specific reagents can prove very useful not only in detection but also in determining to some extent the choice of mobile phase for the development of the separation. If we are looking to determine the concentration of a particular compound, or similar compounds with the same functional group in a complex mixture, then prechromatographic derivatization with a group-specific reagent is an effective way of accomplishing this. The derivatization reaction is normally carried out before application of the sample to the chromatographic layer. Lengthy extraction procedures on sample preparation columns to clean up the sample before chromatography are not necessary. Such derivatizations are simple 'test tube' reactions, which usually are not time consuming.

Table 2 Popular visualization reagents for TLC

Visualization reagent	Compound groups visualized
Anisaldehyde-sulfuric acid	Terpenes, steroids, glycosides
Berberine	Fatty acids, triglycerides
Copper(II) acetate-phosphoric acid	Lipids, prostaglandins
Diphenylboric acid-2-aminoethyl ester	Flavonoids, carbohydrates
Dragendorff reagent	Alkaloids and other nitrogen-containing compounds
Ehrlich's reagent	Amines, indoles
Folin and Ciocalteu reagent	Phenols
Gibb's reagent	Phenols, indoles, thiols, barbiturates
Ninhydrin	Amino acids, peptides, amines, amino-sugars
Pinacriptol yellow	Alkyl and aryl sulfonic acids
Potassium hexaiodoplatinate	Alkaloids, nitrogen compounds, thiols
Thymol-sulfuric acid	Sugars, sugar alcohols
Vanillin-sulfuric acid	Essential oils, steroids

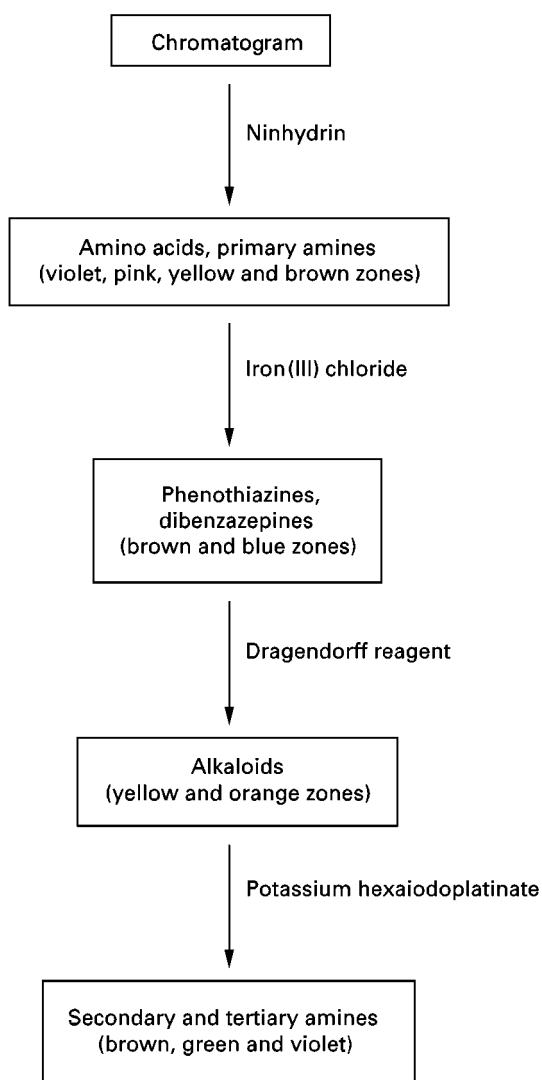


Figure 1 A typical visualization sequence for a TLC chromatogram. The sequence enables the identification of a number of different groups of nitrogen function organic compounds.

An example of such an analytical procedure is the determination of vitamin C in fruit juices. Although it is possible to apply the fruit juices directly to the TLC/HPTLC layer, develop the plate in a suitable solvent mixture, and then use a detection reagent to locate the vitamin C, a more precise and better resolution of the vitamin C can be achieved by derivatizing the sample first with 2,4-dinitrophenylhydrazine to form hydrazones with the keto groups ($>C=O$) present. The sample applied to the plate is then observable by its yellow colour. Using an appropriate solvent mixture for development, the yellow chromatographic zones can be visually observed as they separate and become resolved from each other.

An even more elegant and simple way to achieve prechromatographic derivatization is to carry out the reaction on the layer. At the point where the sample is

to be applied on the chromatographic layer, the derivatization reagents can also be applied. Either the sample can be applied to the layer first, followed by the derivatization reagent shortly afterwards, or it can be done in the reverse order. The advantage of applying the derivatization reagent first is that a complete track across the width of the adsorbent layer can be applied, resulting in complete reaction with the sample when it is dosed, usually as bands, on top of the derivatization reagent. After appropriate drying and reaction time, development of the chromatogram can proceed using a solvent mixture that takes into consideration the polarity of the newly formed compounds.

It is also possible to carry out such 'functional chromatography' within the framework of 2-dimensional separations. The first ascending development is carried out in the usual way with underivatized sample. Before the second development, the separation track is subjected to treatment with a detection reagent specific to the functional group present in the substances (e.g. acids can be esterified, alcohols can be oxidized to ketones or aldehydes, carbonyls can be reduced to alcohols, carbonyls can form hydrazones or semicarbazones). The second development then follows in the usual way at 90° to the first.

Spraying Versus Dipping

Reagents can be applied to TLC/HPTLC plates either by dipping or spraying. The advantages and disadvantages of these approaches are considered below.

Spray Devices

A number of spray devices have been in use for many years. Perhaps the oldest is the atomizer spray, an all-glass unit that uses a rubber bulb to hand pump air into the main unit, which disturbs the detection reagent sufficiently to provide a fine spray out of the exit nozzle. More sophisticated versions have used propellant canisters to provide the means of atomizing the reagent solution into tiny droplets, which can then be evenly sprayed on to the chromatographic layer. As spray guns are relatively inexpensive, they tend to be the most popular spraying devices. However, it is important that the plastic components of the spray gun that come into contact with the detection reagents are solvent resistant. Spray canisters used to contain low-boiling CFCs as propellants, but now contain low-boiling, low-flash point hydrocarbons. More recently, rechargeable electro-pneumatically operated spray systems have become commercially available (an example is shown in **Figure 2**). The basic equipment consists of two spray heads with two different diameter capillaries, together with a charger and spray holder. The smaller diameter



Figure 2 (See Colour Plate 33) An electropneumatically operated spray system for TLC. (Reproduced with the permission of Merck Ltd., UK.)

capillary (0.8 mm) is designed for spraying alcoholic or other low-viscosity solutions, whereas the larger diameter capillary (1.25 mm) is used for more viscous reagents like sulfuric acid. It can, of course, also be used to spray low viscosity reagents at higher rates.

Immersion Devices

In the last few years, dipping or immersion devices for TLC and HPTLC plates have been gaining in popularity. There are obviously benefits with regards to the handling of harmful, irritant or toxic chemicals, but also the uptake of reagent on to the chromatographic layer can be better controlled by immersion.

Chambers for immersion devices need to be as narrow as possible to limit the amount of reagent required, but not so narrow that the chromatographic layer is damaged by contact with the vessel. Manual dipping can be employed, but it is important that the chromatogram is fully dipped and the motion of dipping is done in one constant motion, otherwise 'tide' or 'contour'-like marks will appear on the layer. These will usually interfere with any further spectrophotometric evaluation.

For good reproducibility and reliable constant uptake of reagent into the chromatographic layer, automated immersion devices are essential (an example is shown in Figure 3). These allow precise control of the time of immersion and the rate of dipping, which is essential for good reproducible results.

Future Prospects

The last decade has seen a move away from the use of spray reagents to immersion devices. This trend will inevitably continue as the hazards associated with the spraying of chemical reagents, many of which contain harmful substances, can be avoided by dipping. The greater control over the visualization process that dipping affords is also something that will be encouraged as the whole TLC technique becomes more standardized. Although many chemical reagents are already available, it is likely that new group-specific reagents will be discovered, often replacing those that contain toxic chemicals.

It is in the area of sequencing reactions where probably the greatest growth will occur as only a

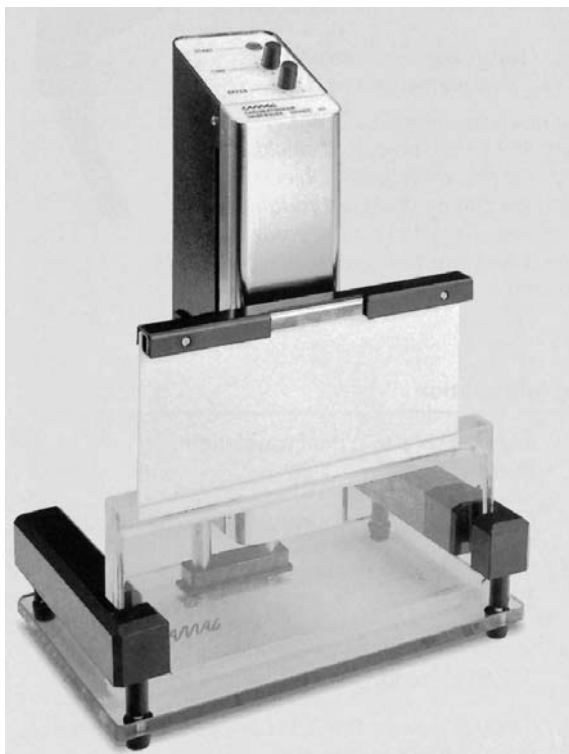


Figure 3 A commercial immersion device for automatic dipping of TLC chromatograms in visualization reagents. (Reproduced with the permission of CAMAG, Switzerland.)

limited number of protocols are presently available. The visualization of the many different types of compounds present in herbal products may well drive the research required.

Pre-derivatization of sample on the TLC plate is proving to be a technique that often results in excellent resolution of analytes of interest. It is to be expected that further protocols will be developed in this area on the basis of reaction sequences that may already be available.

Tables showing the detection of compounds on TLC plates following chromatographic development can be found in appendix 17 on page 4801.

See Colour Plate 33.

See also: II/Chromatography: Liquid: Derivatization. Chromatography: Thin-Layer (Planar): Densitometry and Image Analysis; Instrumentation; Mass Spectrometry. III/Thin-Layer Chromatography-Vibration Spectroscopy. Appendix 2/Thin-Layer (Planar) Chromatography: Detection.

Further Reading

- Jork H, Funk W, Fischer W and Wimmer H (1989, 1994) *Thin-layer Chromatography, Reagents and Detection Methods*, vols 1a and 1b. Weinheim: VCH.
- Stahl E (ed.) (1969) *Thin-layer Chromatography: A Laboratory Handbook*, 2nd edn. Berlin: Springer-Verlag.
- Stahl E (ed.) (1973) *Drug Analysis by Chromatography and Microscopy*. Michigan: Ann Arbor Science.
- Touchstone JC (1992) *Practice in Thin Layer Chromatography*, 3rd edn. New York: Wiley-Interscience.
- Wager H and Bladt S (1996) *Plant Drug Analysis: A Thin Layer Chromatography Atlas*, 2nd edn. Berlin: Springer-Verlag.

Theory of Thin-Layer (Planar) Chromatography

A. Siouffi, Faculté des Sciences de St-Jérôme, Marseille, France

G. Guiochon, University of Tennessee, Knoxville, TN, USA

Copyright © 2000 Academic Press

Introduction

Thin-layer chromatography (TLC) is a simple technique, many runs can be performed at the same time on a single plate, no detection problems occur provided a suitable reagent is used and moreover all solutes are detected. The main drawback is that a good detecting device designed for quantitative work is as expensive as a complete HPLC apparatus.

The observed decline of TLC is mainly due to the belief that efficiency is poor. To perpetuate that idea,

qualitative data are obtained when no care is taken to carry out experiments! The advent of nanoplates coated with fine particles has given a renewed interest in the technique as excellent separations have been reported. By analogy to HPLC (high performance liquid chromatography) the acronym HPTLC (high performance thin-layer chromatography) appeared in the literature. Unfortunately different claims of performance have been published and some misunderstanding between pro and anti HPTLC camps have arisen, leading to fruitless discussions.

In their first paper, Rippahhn and Halpaap reported height equivalent to one theoretical plate (HETP) as low as 15 μm with these nanoplates; on the other hand Delley and Szekely cut a 'normal TLC' plate in four parts to yield the size of nanoplates and obtained identical results. The data of Rippahhn and

Halpaap are effectively comparable to those obtained by HPLC. To compare geometrically different systems, reduced or dimensionless parameters must be used: $h = H/d_p$, the reduced HETP in which H is the observed HETP and d_p the particle diameter. As often no improvement in separation efficiency is observed with HPTLC plates, it is worth reconsidering all the parameters involved in efficiency. Extensive work has been carried out on liquid column chromatography and a proper use of the technique has been defined. The purpose of this article is to consider what is possible or not, which plates are to be used and how to shorten analysis time.

Basic Equations

The aim of the analyst is the complete separation of two (or more) solutes. The resolution of two consecutive Gaussian chromatographic bands is given by:

$$R_s = \frac{2(x_1 - x_2)}{\omega_1 + \omega_2} \quad [1]$$

where x_1 and x_2 are the migration distances of solutes 1 and 2, respectively and ω_1 and ω_2 are base widths of the spots.

If we call L the migration distance of the solvent front, then:

$$R_F = \frac{x}{L} \quad [2]$$

The plate number is given by:

$$N = 16\left(\frac{x}{\omega}\right)^2 = 16\left(\frac{R_F L}{\omega}\right)^2 = \frac{R_F L}{H} \quad [3]$$

Neglecting the variable density of the liquid phase along the plate due to the wide distribution of pore size in the TLC bed, the retardation factor is related to the bed capacity factor through

$$R_F = \frac{1}{1 + k} \quad [4]$$

where k is the retention factor (see HPLC).

The actual relationship is more complex because R_F is somewhat dependent on the experimental conditions, an effect which is neglected as a first approximation. Chromatographers use either R_F or k , depending upon whether they are interested in column or thin-layer chromatography. The parameter α , the relative retention of the two consecutive solutes of interest is given by:

$$\alpha = \frac{k_2}{k_1} = \frac{K_2}{K_1} \quad [5]$$

where K is the well-defined equilibrium constant

$$\frac{\alpha - 1}{\alpha} = \frac{\Delta K}{K} = \frac{R_{F2} - R_{F1}}{R_{F2}(1 - R_{F1})} \quad [6]$$

and

$$\frac{\Delta K}{K} = \frac{\Delta R_F}{R_{F2}(1 - R_{F1})} \quad [7]$$

in which R_{F1} is the smaller retention factor.

When the two spots are close together, $R_{F1} \cong R_{F2}$, and

$$\frac{\Delta K}{K} = \frac{\Delta R_F}{R_F(1 - R_F)} \quad [7a]$$

The resolution is then given by:

$$R_s = \frac{\sqrt{N}}{4} \times \frac{\Delta K}{K} (1 - R_F) \quad [8]$$

According to Snyder, the number of theoretical plates, N , observed in TLC is related to R_F as follows:

$$N = N' \times R_F \quad [9]$$

N' is called the bed efficiency, or the number of hypothetical theoretical plates observed with an inert solute. The Snyder equation is thus written:

$$R_s = \left(\frac{\sqrt{N'}}{4}\right) \left(\frac{\Delta K}{K}\right) (1 - R_F) \sqrt{R_F} \quad [10]$$

From this equation it is impossible to achieve any resolution when R_F is 1 or 0. **Figure 1** shows a plot of the variation of resolution, R_s , with R_F . A maximum is observed when $R_F = 0.33$. However, within the range 0.20–0.50 no dramatic loss of resolution occur as 92% of the maximum efficiency is reached. It is essential to select a solvent that gives an R_F value somewhat larger than 0.33 for the two solutes to be separated, in order to achieve the analysis within a reasonable time.

Rewriting eqn [10] in a more convenient form yields:

$$R = \frac{\sqrt{N}}{4} \times \frac{\Delta R_F}{R_F} \quad [11]$$

R_F is a function of both the ratio of the equilibrium constants K_1 and K_2 of the two solutes and of the plate characteristics. ΔR_F is not a simple measurement of the difficulty of a separation.

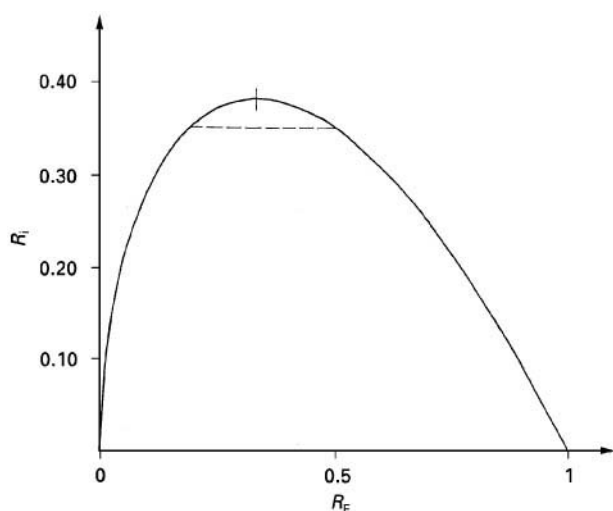


Figure 1 Variation of the resolution between two compounds with the retention of the second compound of the pair. ($R_{F1} \cong R_{F2}$). The figure is drawn assuming that

$$\frac{\sqrt{N'}}{4} \left(\frac{\alpha - 1}{\alpha} \right) = 1$$

thus $R_i = (1 - R_F) \sqrt{R_F}$. (Reproduced with permission from Guiochon G and Siouffi A (1979) *Journal of Chromatographic Science* 16: 368–386.)

The necessary plate number to achieve a given separation is well known in column chromatography:

$$N_{ne} = 16 R_S^2 \left(\frac{\alpha}{\alpha - 1} \right)^2 \times \left(\frac{1 + k}{k} \right)^2 \quad [12]$$

and is written here as:

$$N_{ne} = 16 R_S^2 \left(\frac{\alpha}{\alpha - 1} \right)^2 \times \frac{1}{(1 - R_F)^2} \quad [13]$$

The problem is to achieve N_{ne} with minimum effort and maximum convenience. It is more complicated than in column chromatography as nothing can be done about the speed of the eluent. This flow rate is obviously not constant and we shall consider the laws governing flow rate in TLC in the next section.

Flow Velocity of the Mobile Phase

In normal practice a thin-layer plate is immersed in a tank filled to a height z_0 with the developing solvent. It has been shown that the migration of the mobile phase in a thin-layer plate may be compared to penetration of a liquid by diffusion in interconnected capillaries. A liquid enters a capillary because in doing so it decreases its free energy and more molecules

diffuse from the liquid to the wall of the capillary tube.

The height of ascent, z_M , is governed by two forces acting on the liquid: capillary rise and hydrostatic pressure.

$$z_M = \frac{2\gamma \cos \theta'}{\rho g r} \quad [14]$$

where γ is the surface tension, r is the radius of the capillary, ρ is the density of the solvent, and θ' is the wetting angle.

The smaller the radius, the higher the ascent, and thus smaller particles will govern the rise of eluent. An order of magnitude of r is the radius of the largest sphere that can fall through the hole between three tangent spheres of diameter d_p , i.e. $d_p/15$. Equation [14] does not say anything, however, about the kinetics of the phenomenon.

According to Poiseuille's law, the flow rate in a capillary is given by:

$$Q = \frac{-\pi r^4}{8\eta} \times \frac{\delta P}{\delta x}$$

where η is the viscosity of the liquid and $\delta P/\delta x$ is the pressure gradient along the tube.

As particles are of different sizes and r is not constant, there will obviously be a higher resistance to flow through the smaller tubes. The bulk of the flow will be through the larger capillaries, which fill more slowly behind the solvent front. Thus the volume of liquid is not evenly distributed along the plate; the wet area near the solvent front contains less liquid. A simple glance at a developing plate reveals this fact. In selected experiments the capillary rise can be monitored by UV recording of suitable solvents or, much better, by X-ray absorption. In this latter case the saturation of the porous layer is measured as a function of time and the relationship between the logarithm of the transmitted intensity I and the liquid content is linear. In all cases a plot similar to that of Figure 2 is obtained.

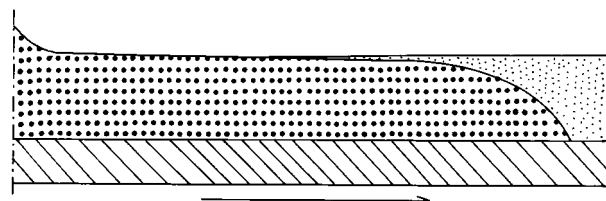


Figure 2 Filling of the layer by the solvent during the course of development.

In consequence we shall not consider further solutes that move at the same speed as the solvent front, as the profile of such a spot would be irregular.

Experimentally the analyst looks at the sharp line separating wet and dry layers. Initially we shall assume that there is no loss of solvent by vaporization and no uptake of vapours by adsorption. It is usually accepted that the distance between the solvent front and the solvent source z_f is related to elapsed time by a quadratic equation:

$$z_f^2 = k_v t \quad [15]$$

k_v is called the velocity constant and depends on the chromatographic system. Thus:

$$k_v = -2b \frac{P_e}{\eta} \Delta P_c \quad [16]$$

where b is the proportionality constant between the rate of advance of the front dz_f/dt and the local flux of mobile phase different from unity.

The term P_e is the permeability of the porous bed given through the Kozeny equation by:

$$P_e = \frac{\varepsilon^3 d_p^2}{180(1-\varepsilon)^2} = P_0 d_p^2 \quad [17]$$

in which ε , the external bed porosity, is the ratio of the volume of interparticle space to the volume of the layer bed.

ΔP_c is the capillary pressure change from the adsorbent saturated with liquid to the dry bed. ΔP_c is proportional to γ , the surface tension of the mobile phase, and inversely proportional to d_p .

$$\Delta P_c = \frac{\gamma}{d_p} \cos \theta' \quad [18]$$

and from eqn [16]

$$k_v = -\frac{2bP_0\gamma}{\eta} d_p \cos \theta' \quad [19]$$

The geometrical factor b has been found to be around 0.8. An expression for k_v in the migration of a liquid in a granular layer has been proposed:

$$k_v = \frac{2bP_0 d_p}{\eta} \left[\gamma \cos \theta' - z_f \frac{d_p \rho g}{12} \right] \quad [20]$$

This assumes that $r = d_p/6$, which is rather large (but the pores of different particles do not connect directly) and it is found that $b = 1$.

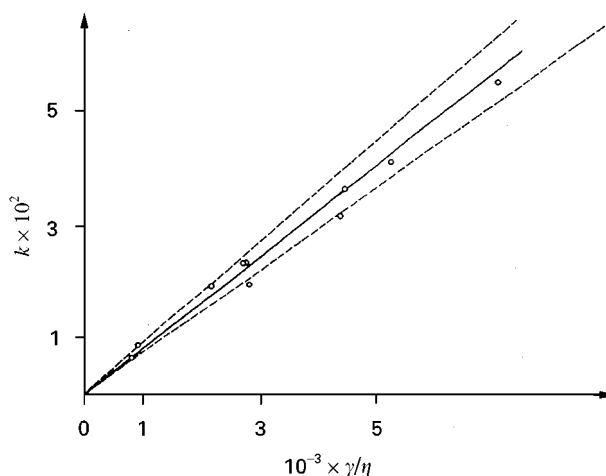


Figure 3 Variation of the velocity constant with the ratio γ'/η for a series of solvents on HPTLC plates; LiChrosorb 5 μm (Merck E, Darmstadt, Germany). (Reprinted with permission from Guiochon G and Siouffi A (1978) *Journal of Chromatographic Science* 16: 598–609.)

Incorporating b into P_0 gives:

$$z_f^2 = \frac{2P_0 d_p \gamma \cos \theta'}{\eta} t = \text{constant} \times t = k_v t \quad [21]$$

The validity of this equation is now well established. As early as 1968, Stahl plotted z_f^2 versus t and obtained a straight line. Stewart had already demonstrated the proportionality between k_v and γ/η . These early experiments were carried out either on paper or on thin layers made with a rather large particle size distribution. More precise data can be gathered from measurements carried out with layers of a narrow particle size distribution (Figure 3).

From the slope of the line the value of P_0 may be derived. Table 1 lists some values obtained with plain silica assuming perfect wettability by solvent so that $\cos \theta' = 1$.

These data from either commercial or homemade plates are in excellent agreement. The coating procedure does not play a significant role and the binding agent has apparently no influence on the hydrodynamics of the plate. In the same way intraparticle

Table 1 Experimental values of P_0

Origin of data	Values of P_0
Stahl	6.7×10^{-3}
Guiochon and Siouffi	8.15×10^{-3}
Ripphahn and Halpaap	6.7×10^{-3}

pore dimensions have no effect as there is no marked difference between Si 60 and Si 100 silica of the same particle size. An experiment was performed on very wide pore silica (Si 50 000) and the velocity constant was the same as the speed was very rapid. The average P_0 value (8×10^{-3}) is rather large when compared to column chromatography (1×10^{-3}).

The proportionality of the velocity constant to the particle diameter has been checked with carefully sorted silica particles and excellent agreement is obtained.

It is convenient to introduce a coefficient of velocity θ , is given by:

$$\theta = \frac{k_v}{d_p} \quad [22]$$

This gives a parameter independent of d_p , which is easier to take into account when calculating the velocity of the eluent in beds made with particles of different diameter. The utility of θ will become apparent in the following sections.

The main drawback of TLC is the presence of a gas phase in contact with the eluent, which yields deviations from the ideal flow velocity. How to get reproducible retention data has given rise to a huge volume of literature. Many practical methods of operations are possible: some workers use saturated tanks in which blotter pads are placed and a certain amount of developing solution is poured over the pads; some workers use nonequilibrated tanks where the plate is placed inside the tank and developed immediately, in contrast to equilibrated tanks where plates are placed in the tank an hour prior to development. Whatever method is used, the presence of the gas phase will influence the solvent front rise through adsorption or vaporization.

Effect of Solvent Vaporization

The observation of most TLC spots shows that solute distribution is not uniform. Precise data have been collected by Hezel and Belenkii, who used a microtome to cut layers 0.05 mm thick. There is a radial flow of liquid phase, which explains why the material in spots is on the surface of the plate, the band being thinner than the layer itself. When a plate is wetted by the mobile phase, vaporization occurs, the flux of which ϕ_v , is given by:

$$\phi_v = \nu l z_f \quad [23]$$

where l is the width of the plate and ν is the rate of vaporization per unit surface area.

ν is the function of $P^0 - P$, the difference between the vapour pressure P^0 of the solvent and its partial

pressure P (if the gas phase is homogeneous, otherwise calculations would be nearly impossible).

The flow of solvent leaving the solvent source, ϕ_s , is proportional to both the cross-sectional area of the layer, el (where e is the thickness of the layer bed), and the aspiration speed, u .

$$\phi_s = elu = \frac{k_v el}{2z_f} \quad [24]$$

The actual flow rate is therefore:

$$el \frac{dz_f}{dt} = \phi_s - \phi_v \quad [25]$$

By combination of the above equations and rearrangement:

$$2z \frac{dz_f}{dt} + \frac{2\nu}{e} z_f^2 - k_v = 0 \quad [26]$$

Integration of this second-order equation and two terms expansion gives:

$$z_f^2 \cong k_v t - \frac{k_v \nu}{e} t^2 = k_v t \left[1 - \frac{\nu}{e} t \right] \quad [27]$$

Equation [27] is valid if the rate of vaporization is small compared to the flow rate inside the layer bed. This is true since from Van Brakel's data the evaporation expressed in terms of the velocity of the rising front is about 0.5 mm day^{-1} with toluene or water. A loss of $1\% \text{ min}^{-1}$ is reasonable.

Effect of Adsorption

Adsorption acts in the opposite direction to vaporization. The building of a monomolecular layer of solvent vapour on the surface of the adsorbent, followed by the appearance of a multilayer adsorption film and possible capillary condensation in the smallest pores when the partial pressure is large, reduces progressively the layer porosity (for example from 0.75 to 0.50 within 15 min).

Let $\varepsilon_{T,0}$ be the bed porosity of the dry adsorbent and $\varepsilon_{T,t}$ the porosity at time t when adsorption has begun:

$$\varepsilon_{T,t} = \frac{V_t}{Se} = \varepsilon_{T,0} - \frac{\nu' t}{e} \quad [28]$$

Here V_t is the total free volume at time t , given by

$$V_t = V_0 - S\nu' t \quad [29]$$

where S is the layer surface area and ν' is the adsorption rate defined in the same way as ν .

To move by dz_f during dt , the solvent front must be supplied by a volume

$$dV = \varepsilon_{T,t} e l dz_f \quad [30]$$

coming from the solvent source and so:

$$dV = \varepsilon_{T,0} e l u \quad [31]$$

Equating expressions for dV gives

$$\varepsilon_{T,t} dz_f = \varepsilon_{T,0} u = \varepsilon_{T,0} \frac{k_v}{2z_f} \quad [32]$$

Combination of the above equations using the same procedure as above gives:

$$\begin{aligned} z_f^2 &= -\frac{k_v \varepsilon e}{v'} \log \left[1 - \frac{v't}{e} \right] \\ &\cong k_v t \left[1 + \frac{v'}{\varepsilon e} t \right] \end{aligned} \quad [33]$$

General Equation

In the classical situation both adsorption and vaporization occur and thus:

$$\frac{2z_f dz_f}{dt} + \frac{2v}{e\varepsilon_t} z_f^2 - \frac{\varepsilon}{\varepsilon_t} k_v = 0 \quad [34]$$

$$z_f^2 = \frac{\varepsilon k_v e}{2v} \left[1 - \left(1 - \frac{v't}{e\varepsilon} \right)^{2v/v'} \right] \quad [35]$$

When $v' = 0$ eqn [27] is valid as $\varepsilon_{T,0}/\varepsilon_{T,t} = 1$. When $v = 0$, eqn [33] is obtained. Integration yields

$$z_f^2 = k_v t \left[1 + \frac{v' - 2v}{2e\varepsilon} t \right] \quad [36]$$

Figure 4 displays the general case when both adsorption and (or) vaporization can occur.

In every case when the development is kept short there is no marked deviation from the quadratic law. A very curious situation arises when $v' = 2v$ as then exact compensation of adsorption is made by vaporization.

Practical Aspects

Plots such as in Figure 4 are quite difficult to obtain and calculations from these curves may be tedious. An easier way is to plot z^2/t versus t , which yields a straight line as shown in Figure 5.

Curve 4 has a negative slope, which means that vaporization predominates. From the slope $k_v v/e$ (k_v

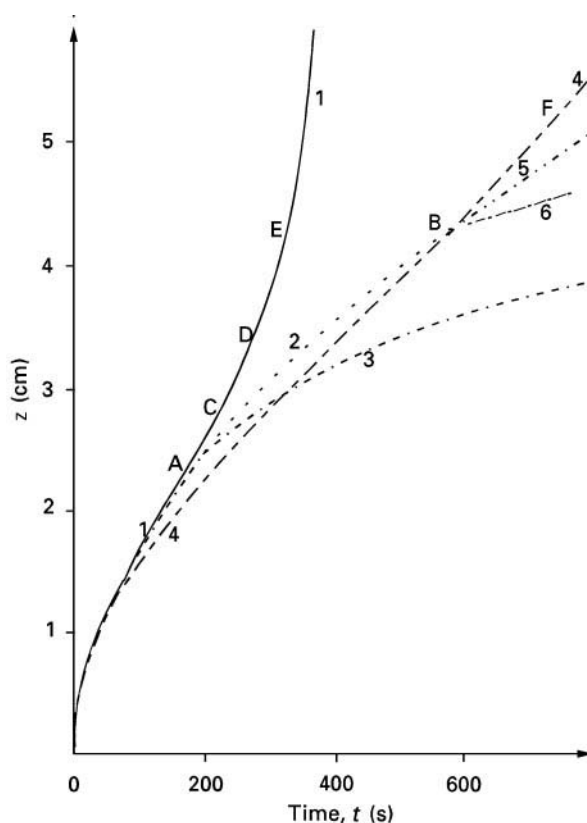


Figure 4 Combination of adsorption and vaporization. Layer thickness, 0.01 cm; velocity constant $k_v = 0.0235 \text{ cm}^2 \text{ s}^{-1}$; porosity of the dry layer, 0.75.

Curve 1 Adsorption speed $v' = 2 \times 10^{-5} \text{ cm s}^{-1}$, vaporization speed $v = 0$. The particles are filled at A ($\varepsilon_t = 0.40$). The total porosity is 0.30 at C, 0.20 at D and 0.10 at E.

Curve 2 $v' = 0$, $\varepsilon_t = 0.4$, $v = 0$, eqn [21] is applied.

Curve 3 $v' = 0$, $v = 1 \times 10^{-5} \text{ cm s}^{-1}$.

Curve 4 $v' = 6 \times 10^{-6} \text{ cm s}^{-1}$, $v = 0$. The particles are filled at B ($\varepsilon_t = 0.40$). The porosity is 0.30 at F.

Curve 5 $v' = 0$, $v = 0$, curves 2 and 5 coincide.

Curve 6 $v' = 0$, $v = 1 \times 10^{-5} \text{ cm s}^{-1}$. (Reprinted with permission from Guiochon G and Siouffi A (1978) *Journal of Chromatographic Science* 16: 598-609.)

is known from the ordinate of the plot, e by plate fabrication) the determination of v is possible (see Table 2). With benzene and toluene (curves 1 and 2) a slight positive slope is observed, which means adsorption. The 'best' curve is curve 3, corresponding to carbon tetrachloride. It should be pointed out that measurements are very imprecise on short development (1 cm or less) as it is difficult to check accurately the solvent front. Table 2 displays the data gathered from Figure 5.

A developing solvent must be carefully chosen. Besides the retention requirements it is necessary to discard solvents that may give high adsorption or vaporization rates. Some properties of common TLC solvents compiled from Rippahhn and Halpaap and

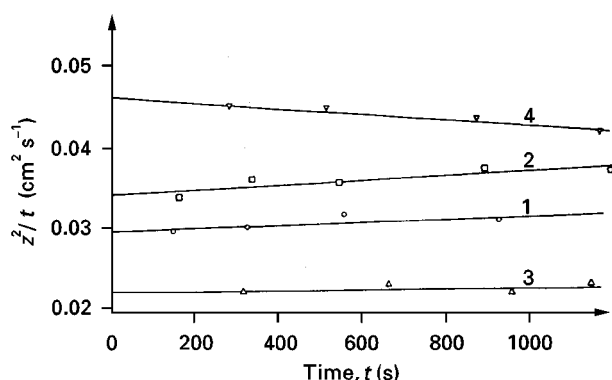


Figure 5 Plots of z^2/t versus t with different solvents on plain silica, $d_p = 5 \mu\text{m}$. Layer thickness 0.2 mm, porosity ε 0.80. Solvents: 1, benzene; 2, xylene; 3, carbon tetrachloride; 4, dichloromethane. (Reprinted with permission from Guiochon G and Siouffi A (1978) *Journal of Chromatographic Science* 16: 598–609.)

our own data are reported in Table 3. θ has been normalized to 5 cm development distance. It is worth checking the time necessary to fill the particles with solvent when adsorption predominates. This time

Table 2 Deviations from the quadratic law (plates 0.2 mm thick of silica Si 60)

Solvent	Curve in Figure 5	$v' - 2v$ (m s^{-1})
Benzene	1	3×10^{-8}
Toluene	2	3×10^{-8}
Carbon tetrachloride	3	0.8×10^{-8}
Dichloromethane	4	-1.3×10^{-8}

may be calculated from:

$$t_s = \frac{\varepsilon - 0.4}{v'} \times e \quad [37]$$

and may be compared with the time needed for the solvent to move by 10 cm (t_3).

With diethyl ether, for example, $t_s > t_3$ (see Table 3); with *n*-pentane, chloroform, dichloromethane and ethyl acetate t_3 is between the time necessary to fill an internal porosity of 0.35 and one of 0.40. A correlation should be possible between v' and P^0 , but this relation is not linear. It is unfortunate that most TLC

Table 3 Velocity constants of various solvents

Solvent	Viscosity η (cP) 20°C	Surface tension γ (N m^{-1})	$\gamma/\eta \times 10^{-5}$ (m s^{-1})	$10^4 \times v'$ (m s^{-1})	$10^2 k_v$	$10^2 \theta$ (m s^{-1})
<i>n</i> -Pentane	0.24	16.0	6.7	10.9 ^a	9.2	115
<i>n</i> -Hexane	0.33	18.4	5.6	5.3	11.8	95
<i>n</i> -Heptane	0.41	20.4	5.0	6.4	8.4	80
Cyclohexane	0.97	25.5	2.6	3.7	5.0	43
Benzene	0.65	28.9	4.4	4.9	8.0	72
Toluene	0.59	28.5	4.8	9.3 ^b	7.1	77
Xylene (P)	0.65	28.4	4.2	4.3	6.1	70
Carbon disulfide	0.36	32.3	8.7	14.9 ^b	11.4	140
Carbon tetrachloride	0.97	27.0	2.8	2.2	5.8	46
Chloroform	0.58	27.1	4.7	8.3 ^a	7.9	75
Dichloromethane	0.43	26.5	6.2	10.4 ^a	8.7	99
Trichloroethylene	0.58	29.3	5.1	8.6 ^a	6.9	82
Diethyl ether	0.23	17.0	7.1	17.0 ^b	8.8	114
Diisopropyl ether	0.35	32.0	9.1	5.9	10.2	145
Dioxane	1.26	35.4	2.8	3.9	4.7	45
Tetrahydrofuran	0.47	26.4	5.6	4.3	10.3	88
Methanol	0.60	22.6	3.8	4.6	5.0	65
Ethanol	1.20	22.7	1.9	2.3	3.1	32
1-Propanol	2.26	23.8	1.05	1.9	2.03	18
2-Propanol	2.50	21.7	0.87	1.1	1.94	15
1-Butanol	2.95	24.6	0.83	—	—	13
<i>i</i> -Butanol	3.95	23.0	0.58	0.85	1.20	10
<i>t</i> -Butanol	2.82	20.7	0.73	0.21	1.0	11.5
Acetone	0.32	23.7	7.4	11.0	11.2	118
2-Butanone	0.43	24.6	5.7	8.3	10.0	91
Ethyl acetate	0.46	23.9	5.2	9.8 ^a	8.0	85
Butyl butyrate	1.03	24.0	2.3	—	—	37
Acetonitrile	0.36	29.3	7.5	8.1	11.4	125
Pyridine	0.97	38.0	3.9	5.3	5.6	64

^aTime t_3 ($z = 10$ cm) is larger than the time necessary to fill the inside of particles in a bed of inner porosity 0.35 (see text).

^bFor these solvents $t_s > t_3$.

data only quote R_F and no information is given on the velocity constant as is usual in HPLC.

Effect on R_F

When adsorption is predominant, the liquid moves inside a layer with constant porosity while the solvent front moves through a layer of decreasing porosity. The front velocity u is different from the bulk velocity u_b . The apparent retention factor $R_{F,a}$ is by definition:

$$R_{F,a} = \frac{x}{z_f} = \frac{z(\text{spot})}{z(\text{solvent})}$$

$$z_f = ut$$

$$x = u_b R_{F,t} t \quad (R_{F,t} \text{ is the true retention factor})$$

$$R_{F,a} = \frac{u_b}{u} \times R_{F,t}$$

$$\frac{u_b}{u} = \frac{\varepsilon_t}{\varepsilon} = \frac{\varepsilon - v't/e}{\varepsilon} = \frac{1 - v't}{\varepsilon e} \quad [38]$$

and thus

$$R_{F,a} = R_{F,t} \left(\frac{1 - v't}{\varepsilon e} \right) \quad [39]$$

R_F can also be modified, and to a much larger extent by modification of the surface activity as a consequence of adsorption of solvent vapour or more active vapours such as water, which it is almost impossible to eliminate from the tank atmosphere.

$R_{F,a}$ may thus be different from one run to another; this is the plague of TLC! Experiments carried out in either equilibrated or saturated tanks decrease $R_{F,a}$. Evidently, time of development is shorter, for example 63 min are necessary for a 10 cm development in an unsaturated tank and only 48 min in a saturated one. Dhont has studied the influence of vapour preadsorption on stability of R_F and showed that equilibrium may require several hours. Adsorption of methyl isobutyl ketone prior to development decreases $R_{F,a}$ from 0.35 to 0.22. Adsorption or vaporization may be decreased to a considerable extent by use of sandwich quasicolumn systems as advocated by Soczewinski or Tyihak.

Reversed-Phase Plates

The number of available stationary phases in TLC is not very large. Silica is still widely used and some separations are better carried out on alumina, cellulose or polyamide. In the above discussion, data were compiled from experiments made with silica on

Table 4 Velocity constants, rate of adsorption, and wetting angles from TLC data with pure organic solvents

Solvent	$k_v \times 10^4 \text{ (m s}^{-1}\text{)}$	$v' \times 10^8 \text{ (m s}^{-1}\text{)}$	$\cos \theta'$
<i>n</i> -Pentane	6.5	4.8	0.87
<i>n</i> -Heptane	4.9	6.0	0.94
<i>n</i> -Dodecane	1.7		0.82
Toluene	4.8	6.4	0.96
Chlorobenzene	3.6	5.3	0.83
Bromobenzene	2.4	5.4	0.71
Acetonitrile	6.1	4.3	0.75

which the contact angle θ' is very large and thus $\cos \theta' = -1$. Alkyl-bonded silica plates are readily available and the number of published separations on these supports is rapidly increasing. These bonded silicas are hydrophobic and some velocity constants with pure organic solvents are given in Table 4.

These data were gathered from plates with average particle size $6.5 \mu\text{m}$ and an assumed P_0 of 7.9×10^{-3} . Apolar solvents completely wet the layer but polar solvents exhibit values of $\cos \theta'$ much lower than 1. These TLC data are consistent with those published by Riedo *et al.* from capillary rise in Pyrex tubes treated with octadecyltrimethyl silane. There is no evident correlation between $\cos \theta'$ and a physical property such as dielectric constant or ability to form hydrogen bonds.

With such plates water-organic solvent mixtures are used and a plot of the cosine of the contact angle versus the water concentration in a water/ethanol eluent is shown in Figure 6.

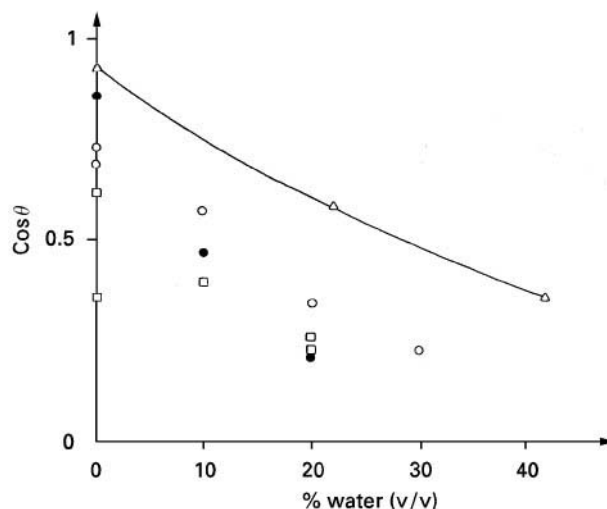


Figure 6 Plot of the cosine of the contact angle versus the water concentration of a water/ethanol mixture. ●, home made plates; ○, Merck plates (no spacer); □, Merck plates (with 1.5 mm spacer). (Reprinted from Guiochon G, Korosi G and Siouffi A (1979) *Journal of Chromatographic Science* 18: 324–329.)

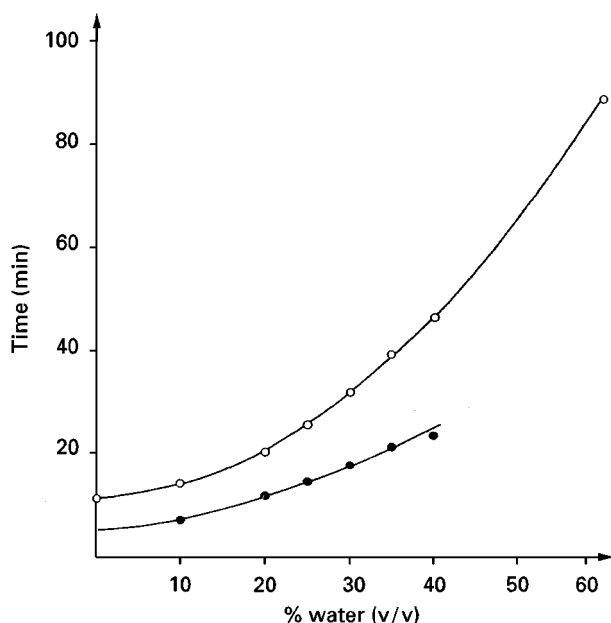


Figure 7 Plot of time necessary to ascend 4 cm versus percentage of water in mixtures of methanol/water and acetonitrile/water. ●, acetonitrile; ○, methanol. Plate LiChrosorb RP-18 (7 μm).

The value of $\cos \theta'$ decreases rapidly as the percentage of water increases. When θ' is close to 90° the solvent is unable to ascend the plate. Even when using a relatively nonviscous organic solvent such as acetonitrile, 30% of water is the upper limit.

In Figure 7, the variation of 4 cm development time with percentage of water is reported, showing the very steep rise of the curve. Analysis may last more than 1 h, which is undesirable. The differences that occur with chain length are rather small but the sequence $\text{RP } 2 < \text{RP } 8 < \text{RP } 18$ is observed. A compromise between the extended hydrophobicity of a totally modified RP phase and the strong hydrophilic character of unmodified silica has been found with layers prepared with a lower degree of silanization. These layers are completely water wetttable (WF plates) and permit the ascent of mobile phases with high water content.

Band Broadening and Plate Height Equation

The Different Parameters

As has been shown above, the speed of the eluent is a complex function of time and space and will not give the desired constant flow rate as in HPLC. Accordingly the plate efficiency is also a complex function of experimental conditions.

According to Giddings, we can use the definition of the local plate height H_l as the proportionality constant between the differential increase in the variance of a Gaussian profile spot and the differential length of migration:

$$H_l = \frac{d\sigma^2}{dx} \quad [40]$$

The average plate height may be defined as:

$$\bar{H} = \frac{\int_0^x H_l dx}{\int_0^x R_F dx} = \frac{\sigma^2}{(z - z_0)R_F} \quad [41]$$

z and z_0 have been previously defined and $(z - z_0)R_F$ is the migration distance of the solute; σ^2 is the variance of the spot to which the contribution due to the starting spot width should be added.

We shall here treat the TLC plate as being equivalent to a normal chromatographic column bed: it is homogeneous, there is one dimensional flow (no vaporization or adsorption). This may seem oversimplified, but most conclusions apply in practice, giving some validity to the model.

We use the conventional Knox reduced plate height equation:

$$h = \frac{B}{v} + Av^{1/3} + Cv \quad [42]$$

where v is the reduced velocity (ud_p/D_m). Here A , B and C are dimensionless coefficients with reference to packing density (A), mass transfer (C) and diffusion (B).

In liquid column chromatography A characterizes the quality of the packing and is usually between 1 and 5; $A = 1$ corresponds to a very good packing. Much work has been done to prepare excellent columns and even now manufacturers each have their own procedure. To our knowledge nothing has been seriously done to improve the packing in TLC, probably because it is easier to achieve a good two-dimensional bed than a three-dimensional one. No precise data on packing in TLC are available but we may suppose a small value of A . The C term characterizes the mass transfer inside the particle. It comes from diffusion in the stagnant mobile phase, kinetics of adsorption-desorption, etc. C varies with R_F (or k) for a given chromatographic system. An average value of 0.01 will be used in most calculations. The B term is mainly a diffusion term. In GC the diffusion in the stationary phase is considered as negligible since the diffusion in the gas phase is several orders of magnitude higher (10^5). In liquid chromatography, the situation is different and the contribution to axial

diffusion resulting from molecular diffusion in the stationary phase may become of the same order of magnitude as the contribution of molecular diffusion in the mobile phase. A rigorous treatment has been published by Giddings and we thus write:

$$B = 2 \left[\gamma_m D_m + \left(\frac{1 - R_F}{R_F} \right) \gamma_s D_s \right] \quad [43]$$

D_m and D_s are diffusion coefficients in the mobile and stationary phases, respectively; γ_m and γ_s are the tortuosity coefficients of the packing and the porous particle, respectively. We shall assume that $\gamma_s \cong \gamma_m$ and assume the same value as in classical column chromatography of 0.7.

Going to a dimensional equation, the local plate height is:

$$H_l = \frac{B D_m}{u} + \frac{A d_p^{4/3}}{D_m^{1/3}} u^{1/3} + \frac{C d_p^2}{D_m} u \quad [44]$$

As

$$u = \frac{\theta d_p}{2z} \quad [45]$$

we can write:

$$H_l = \frac{B D_m}{\theta d_p} z + \frac{A \theta^{1/3} d_p^{5/3}}{(2 D_m)^{1/3}} z^{-1/3} + \frac{C \theta d_p^3}{2 D_m z} \quad [46]$$

We can use eqn [46] to integrate eqn [41].

As we are interested in the chromatographic process we shall consider that the initial spot has a negligible width. This is obviously not true but we can always correct for it using variance addition. In eqn [46], z is the distance of front migration and the integration variable is given by:

$$x = R_F z \quad \text{so that} \quad dx = R_F dz$$

$$H = \int_{z_0}^L \frac{H_l R_F dz}{(L - z_0)} \quad [47]$$

Integration yields:

$$\begin{aligned} \bar{H} = & \frac{B}{\theta d_p} [L + z_0] + \frac{3 A d_p^{5/3} \theta^{1/3}}{2 (2 D_m)^{1/3}} \frac{L^{2/3} - z_0^{2/3}}{L - z_0} \\ & + \frac{C \theta d_p^3}{2 D_m (L - z_0)} \log \frac{L}{z_0} \end{aligned} \quad [48]$$

This equation is difficult to handle and may be rewritten for the sake of simplicity as:

$$\bar{H} = B'(L + z_0) + \frac{A'}{L - z_0} (L^{2/3} - z_0^{2/3}) + \frac{C'}{L - z_0} \log \frac{L}{z_0} \quad [49]$$

where

$$B' = \frac{2 \gamma D_m}{\theta d_p} \quad [50]$$

$$A' = \frac{3}{2} A \frac{d_p^{5/3} \theta^{1/3}}{(2 D_m)^{1/3}} \quad [51]$$

$$C' = \frac{C \theta d_p^3}{2 D_m} \quad [52]$$

It may appear surprising that in such a form eqn [46] does not depend on R_F , but it must be remembered that B depends on R_F and when $\gamma_s D_s$ is close to $\gamma_m D_m$, $B' = 2 \gamma D / \theta d_p R_F$.

A , C and γ are coefficients that depend on the plate itself and are constants. The terms A' , B' and C' do not contribute to \bar{H} in equal ways but they all depend on D_m , d_p and θ .

Influence of D_m Diffusion coefficients depends on the solute. D_m is usually calculated through the Wilke Chang equation:

$$D_m = 7.4 \times 10^{-10} \times \sqrt{\psi_s M_s} \frac{T}{\eta V_i^{0.6}} \quad [53]$$

where M_s is the molecular weight of the solvent, ψ_s an association constant depending on the nature of the solvent (1 for nonassociating solvents, 2 for strong hydrogen-bonding solvents), and V_i is the molar volume of the solute.

High molecular weight solutes will exhibit a low diffusion coefficient. Some values of D_m have been selected to cover the whole range of classical solutes (we have excepted polymers or very low molecular weight compounds that are analysed by SEC or GC, respectively) and values of A' , B' and C' have been computed for a given chromatographic system (d_p , θ , R_F). These values are reported in Table 5.

It is clear from the above data that the B' term is the most important one when the diffusion coefficient is large; its influence decreases slowly as D_m decreases. The plate height increases rapidly with diffusion coefficient (Figure 8). With small particles, H is linearly dependent on L and thus B' is the only term that governs efficiency. This efficiency decreases sharply as L increases. In other words, solutes of high D_m will be poorly separated on small particles with a rather long migration length.

When $d_p = 20 \mu\text{m}$, the situation is completely different. Provided the development length is long enough, all solutes will be separated in the same way,

Table 5 Effect of changing diffusion coefficient on the coefficients of the HETP equation

D_m ($\text{m}^2 \text{s}^{-1}$)	$A' (\times 10^4)$	$B' (\times 10^4)^a$	$C' (\times 10^6)$
3×10^{-9}	4.36	25.4	0.983
2×10^{-9}	4.99	17.0	1.47
1×10^{-9}	6.29	8.48	2.95
7×10^{-10}	7.08	5.93	4.21
5×10^{-10}	7.93	4.24	5.90
3×10^{-10}	9.40	2.54	9.83

Chromatographic conditions: $A = 1$; $C = 0.01$; $10^{-2} \theta = 47.2 \text{ m s}^{-1}$; $z_0 = 0.5 \text{ cm}$; $R_F = 0.7$; $\gamma = 0.7$; $d_p = 5 \mu\text{m}$.

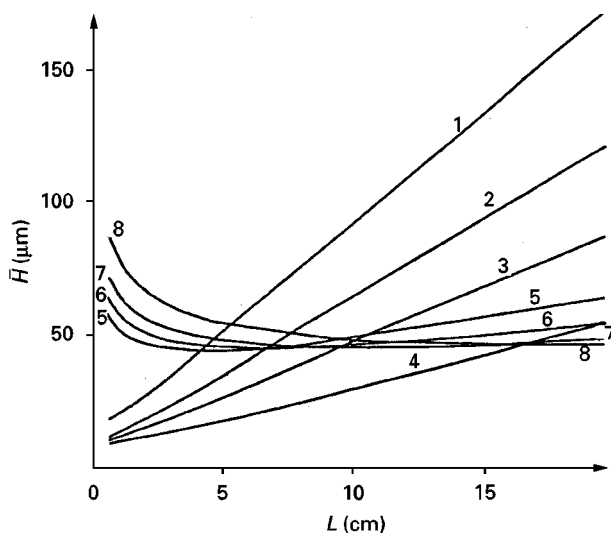
^aAssuming $B' = 2\gamma D_m / \theta d_p R_F$.

a situation that does not occur with small particles. The most interesting feature is that H may be smaller with $20 \mu\text{m}$ particles than with $5 \mu\text{m}$ ones. A dotted round on the curves indicates the length of development when coarse particles become more efficient than fine particles.

Influence of retention From eqn [49], R_F is only involved in the B' term. If R_F is the only variable and the other parameters are kept constant, then we can write:

$$H = \beta \left[D_m + \frac{1 - R_F}{R_F} D_s \right] + \mu + \Gamma \quad [54]$$

As μ, β, Γ are kept constant, a plot of H versus $(1 - R_F)/R_F$ or retention factor would be linear. Such

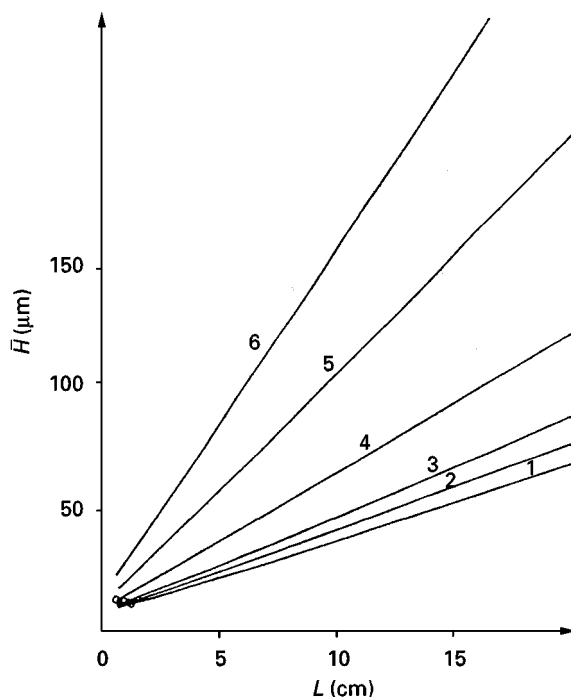
**Figure 8** Plot of HETP versus development distance showing the effect of diffusion coefficient. Curves 1–4 $d_p = 5 \mu\text{m}$. Curves 5–8 $d_p = 20 \mu\text{m}$.

Curves 1 and 5 $D_m = 1 \times 10^{-5} \text{ cm}^2 \text{s}^{-1}$.

Curves 2 and 6 $D_m = 5 \times 10^{-6} \text{ cm}^2 \text{s}^{-1}$.

Curves 3 and 7 $D_m = 5 \times 10^{-6} \text{ cm}^2 \text{s}^{-1}$.

Curves 4 and 8 $D_m = 3 \times 10^{-6} \text{ cm}^2 \text{s}^{-1}$.

**Figure 9** Variation of the apparent HETP with development length. Effect of retention. Particle size $5 \mu\text{m}$. 1, $R_F = 0.9$; 2, $R_F = 0.8$; 3, $R_F = 0.7$; 4, $R_F = 0.5$; 5, $R_F = 0.3$; 6, $R_F = 0.2$. (Reprinted with permission from Guiochon G and Siouffi A (1978) *Journal of Chromatographic Science* 16: 470–481.)

plots can be drawn from data already published and are shown in Figure 9. The fit of a straight line is excellent as long as solutes are not strongly retained, i.e. when $(1 - R_F)/R_F$ is not too large.

Influence of particle size Examination of D_m has shown that different performances may be attained depending on whether fine or coarse particles are considered. Tables 6 and 7 together with Figure 10 allow the comparison of the different terms A' , B' and C' with d_p .

Best efficiencies are obtained with small particles if D_m is small and development length is short. H will increase very rapidly with increasing length of plate if very fine particles are used. If migration is long the coarser particles are more efficient, which is particularly evident from the plots. We have an explanation for the different claims of efficiencies: most demonstrations of HPTLC are made using mixtures of dyes that have rather large molecular weights and low D_m s. Although the nanoplate size prevents long development, some early chromatographers performed development for too long a distance so that efficiency was less than with the older TLC plates. Moreover, the optimal velocity of solvent ($v \cong 3.8$) is kept constant for quite a long time with coarse particles but only for a short time with fine particles. As was

Table 6 Effect of change in particle size on the coefficients of the HETP equation

d_p (μm)	$A' \times 10^4$	$B' \times 10^{4a}$	$C' \times 10^6$
3	3.38	7.06	1.27
4	5.46	5.30	3.02
5	7.93	4.24	5.90
6	10.74	3.53	10.19
7	13.9	3.03	16.2
8	17.3	2.65	24.2
10	25.2	2.12	47.2
12	34.1	1.77	81.6
15	49.5	1.41	153.3
20	79.9	1.06	378.0
25	115.9	0.848	737.0
30	157.0	0.706	1.27×10^3
40	254.0	0.530	3.02×10^3
50	368.0	0.424	5.90×10^3

Chromatographic conditions: $A = 1$; $C = 0.01$; $\theta = 47.2 \text{ cm s}^{-1}$; $z_0 = 0.5 \text{ cm}$.

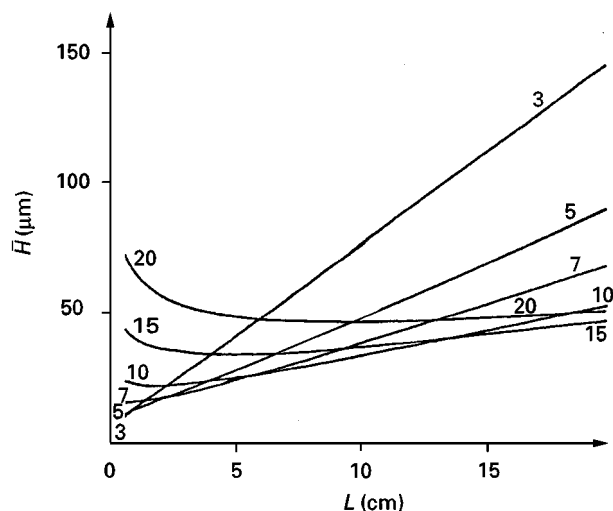
$a\gamma = 0.7$; $R_F = 0.7$; $D_m = 5 \times 10^{-10} \text{ m}^2 \text{ s}^{-1}$. B' is assumed to be $2\gamma D_m/\theta d_p R_F$.

demonstrated in HPLC, the race towards finer and finer particles looks meaningless in TLC for the development ought to be so short that the variance of sample deposition would be too large by far. On the other hand 15 μm particles appear to be a good compromise between efficiency and development length. From these results it is also obvious that one requirement of high performance TLC is the use of particles with a narrow size distribution. The mobile phase velocity is determined by the fine particles and efficiency by the coarse ones, so that one loses on both counts.

Table 7 Effect of change in particle size on coefficients of the HETP equation

d_p (μm)	$A' \times 10^4$	$B' \times 10^4$	$C' \times 10^5$
3	2.69	14.12	0.0635
4	4.34	10.6	0.151
5	6.29	8.48	0.295
6	8.53	7.06	0.510
7	11.03	6.06	0.811
8	13.8	5.30	1.21
10	20.0	4.24	2.36
12	27.1	3.54	4.08
15	39.3	2.82	7.66
20	63.5	2.12	18.9
25	92.1	1.696	36.8
30	125.0	1.412	63.5
40	202.0	1.06	151.0
50	292.0	0.848	295.0

Chromatographic conditions as for Table 6, except $D_m = 1 \times 10^{-9} \text{ m}^2 \text{ s}^{-1}$.

**Figure 10** Plot of HETP versus development distance showing the effect of particle diameter. Diffusion coefficient, $5 \times 10^{-6} \text{ cm}^2 \text{ s}^{-1}$. Numbers on curves represent particle size (μm).

Influence of velocity coefficient θ It is difficult to select a convenient liquid that keeps the critical solute within the R_F range of 0.30–0.60. From the previous conclusions θ must be as large as possible, but θ is imposed by the choice of the chromatographic system and little can be done to change it.

Relative role of the different contributions to band broadening From the above calculations it is clear that the mass transfer C' only plays a minor role unless the plate is poorly prepared or made with very coarse particles, which are not used in current practice. It thus may be neglected in almost all cases, as shown in Figure 11, which gives variation of A' , B' and C' when $d_p = 5 \mu\text{m}$ or— $d_p = 20 \mu\text{m}$ for a given D_m .

As expected from previous discussions, the B' term is often the only one which must be taken into account. For $d_p = 5 \mu\text{m}$ the packing term is only 0.25 H at $L = 1 \text{ cm}$ and 0.03 H at $L = 10 \text{ cm}$. In contrast, it accounts for 0.9 H when $L = 1 \text{ cm}$ and $d_p = 20 \mu\text{m}$. When development distance increases the contribution of molecular diffusion increases as the contribution of packing decreases. Molecular diffusion and packing irregularities are equal when the following condition is satisfied:

$$\frac{L^{2/3} - z_0^{2/3}}{L^2 - z_0^2} = \frac{4\sqrt[3]{2}}{3R_F} \frac{\gamma}{A} \left(\frac{D_m^4}{\theta^4 d_p^8} \right)^{1/3} \quad [55]$$

The balance between these two major contributions may be achieved for particles in the 7–15 μm range with a reasonable development length (3–15 cm).

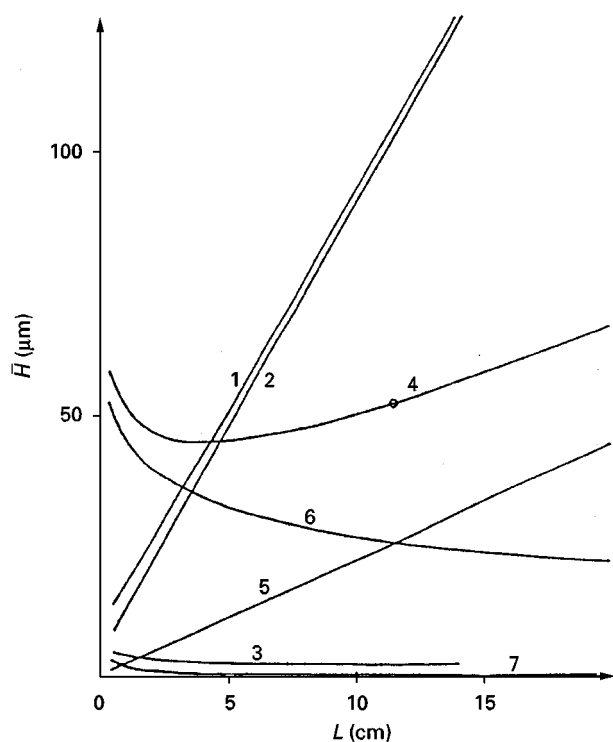


Figure 11 Different contributions to the apparent HETP versus development length. Curves 1, 2 and 3 correspond to particle size 5 μm . Curves 4–7 correspond to particle size 20 μm . Curves 1 and 4, total plate height. Curves 2 and 5 show the contribution of molecular diffusion. Curves 3 and 6 show the packing contribution, while curve 7 shows the mass transfer contribution (this last contribution is too small to be represented when $d_p = 5 \mu\text{m}$). $D_m = 1 \times 10^{-5} \text{ cm}^2 \text{ s}^{-1}$. (Reprinted with permission from Guiochon G and Siouffi A (1978) *Journal of Chromatographic Science* 16: 470–481.)

The H versus L Curve

Collection of experimental data in TLC is much more difficult than in HPLC where a single column can supply much information whereas, the development of many TLC plates is needed for the same purpose.

The relationship between H and L has been checked with small particles carefully sorted; the results are shown in **Figure 12**. The scattering of experimental points on both sides of the theoretical straight line is the consequence of the lack of reproducibility from one plate to another and mainly from the spot shape. The original spot is too large for its contribution to the final spot width to be neglected. It may be corrected but it must be remembered that a Gaussian profile of the injection spot is almost impossible to achieve. Be that as it may, the H versus L line is well predicted by theory.

We used data from Halpaap and Krebs to check our own results. No information was provided on solutes and particle size but the knowledge that ordinary TLC plates are made from 11–15 μm particles

and HPTLC plates from 5–7 μm particles, and that lipophilic dyestuffs are high molecular weight molecules of $D_m \cong 6 \times 10^{-6} \text{ cm}^2 \text{ s}^{-1}$, was used to plot H versus L as shown in **Figure 13**. The fit is not perfect but the main feature is well predicted by theory.

Brinkman has carried out an experimental verification of our conclusions. He performed TLC of solutes of very different D_m such as chloroanilines and dyestuffs. With chloroanilines, he observed a very steep increase in H with development length. To quote Brinkman: ‘a similar steep increase is absent in conventional TLC’. With the dyestuffs the difference between the curves is not so large.

As predicted, the efficiency is better with HPTLC plates over a small development length.

In the same way Tyihak found a striking agreement between observed and theoretical curves and checked experimentally that TLC plates are more efficient than HPTLC plates for a 10 cm development distance.

A careless comparison between experimental and theoretical curves could lead to some fallacies. Experimental plots exhibit a minimum plate height,

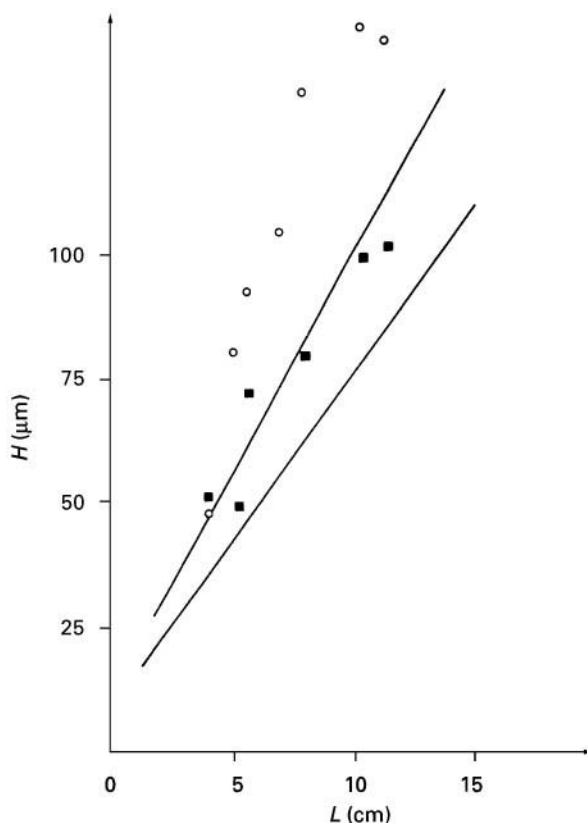


Figure 12 Variation of plate height with development length. Mixture of bis chlorophenyl triazine isomers; solvent CCl_4 . Silica 7 μm particle diameter. ■, $R_F = 0.28$; ○, $R_F = 0.58$. (Reprinted with permission from Guiochon G and Siouffi A (1978) *Journal of Chromatographic Science* 16: 470–481.)

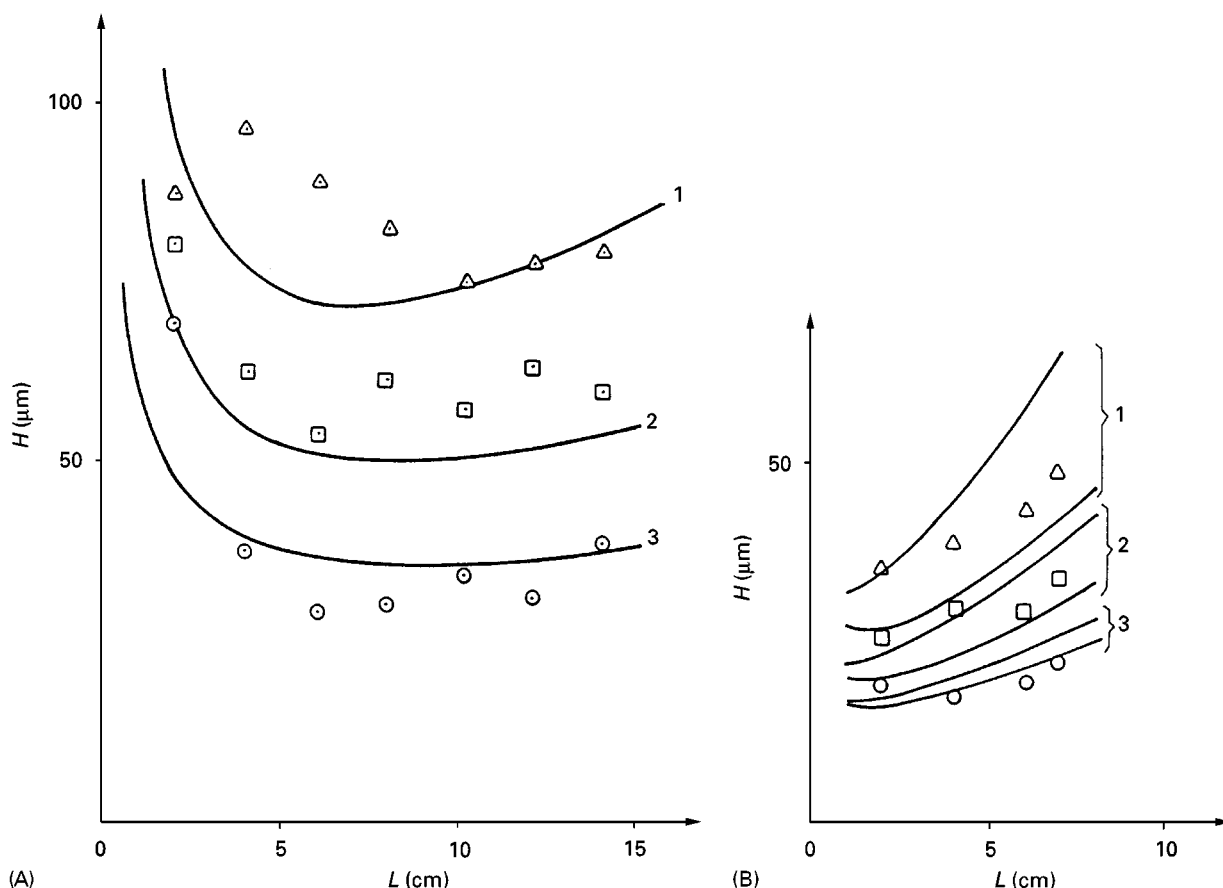


Figure 13 Plots of H versus L from data of Halpaaf H and Krebs KF (1981) *Journal Chromatography* 209: 129–147. Dyestuffs: \circ , violet ($D_m = 6 \times 10^{-6} \text{ cm}^2 \text{ s}^{-1}$; $R_F = 0.75$; $C = 0.10$); \square , green ($D_m = 6 \times 10^{-6} \text{ cm}^2 \text{ s}^{-1}$; $R_F = 0.45$; $C = 0.20$); \triangle , blue ($D_m = 4 \times 10^{-6} \text{ cm}^2 \text{ s}^{-1}$; $R_F = 0.17$; $C = 0.20$).

Experimental points and curves were calculated with $\theta = 70 \text{ cm s}^{-1}$, $\gamma = 0.75$, $A = 0.80$ and $d_p = 15 \mu\text{m}$ for TLC plates. (A) $A = 1.0$ and $d_p = 7 \mu\text{m}$ for HPTLC plates. (B) Curves: 1, blue; 2, green; 3, violet. The lower curves in (B) correspond to the assumption that $\gamma_s D_s = 0.5 \gamma_m D_m$ and all others correspond to $\gamma_s D_s = \gamma_m D_m$. (Reprinted with permission from *Journal of Chromatography*.)

which is not predicted by theory, and measured H are higher than calculated. Currently available spectrophotodensitometers are inadequate to detect carefully a spot of very short migration because their response time is too large, the light spot is too large, and the scanning speed too quick. Halpaap and Ripphahn have corrected the data they published. In Figure 14 we assumed an independent contribution to the spot width. Evidence suggests that experimental data cannot fit theoretical calculations with very short development length because of the lack of a special instrument. This misadaptation of detecting device is a further explanation for the poor efficiency often observed.

Conclusion

In HPLC the analyst carefully selects optimum mobile phase velocity to obtain the lowest HETP and the highest plate count. In TLC the situation is more

difficult to handle. Most often, mobile phase velocity is not considered with much attention and this may lead to erroneous conclusions based solely on observed R_F values. Adsorption or vaporization can dramatically affect retention and it is of the greatest importance to standardize experimental conditions to get reproducible results. A glance at a TLC figure caption is often deceptive since it is rare that information is gathered on the time taken by the solvent front to ascend the plate, the position of the spot above the solvent level (z_0), etc.

Since the mobile phase velocity is not constant the classical HETP equations (van Deemter equation in GC or Knox's equation in HPLC) do not apply. In TLC the HETP equation is of the H versus development length type.

With TLC, low HETP may be generated but the final performances do not compare with HPLC. Nanoplates coated with small particles can provide good performances with short development

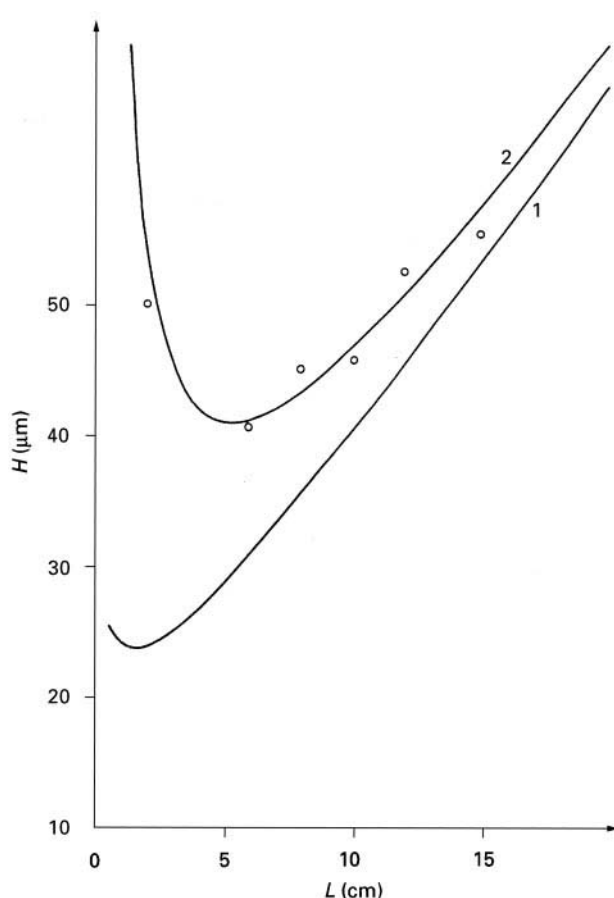


Figure 14 Variation of plate height with development length. Solute: Desaga yellow ($M = 225$); $D_m = 1.37 \times 10^{-9} \text{ m}^2 \text{ s}^{-1}$; $R_F = 0.80$. Solvent: toluene; $\theta = 77$. Packing: silica ($d_p = 11 \text{ }\mu\text{m}$).

Curve 1 Theoretical curve calculated with $\gamma = 0.7$, $A' = 2.48 \times 10^{-3}$, $A = 1$, $B = 2.8 \times 10^{-6}$, $C' = 0.11 \times 10^{-4}$, $C = 0.03$.

Curve 2 curve calculated by adding a constant equipment contribution to the spot variance ($\sigma_{eq} = 4.3 \times 10^{-3} \text{ cm}^2$). (Reprinted with permission from Guiochon G and Siouffi A (1978) *Journal of Chromatographic Science* 16: 470–481.)

distances. The analyst's task is to consider the characteristics of solutes to separate (particularly the diffusion coefficient) and the particle size of the available plates. Then he or she can select the correct plate and the correct development distance to achieve the separation if the plate count is reached under those conditions. It must be remembered that in this article we have only considered the chromatographic experiment. We have not considered extra band broadening from injection (which is important in TLC) or detection devices.

Appendix: Symbols used

b proportionality constant of eqn [16]
 d_p mean particle diameter

e thickness of the layer bed
 h reduced HETP
 k retention factor
 k_v velocity constant
 l width of the plate
 r radius of the capillary
 t time
 t_3 time needed for the solvent to move 10 cm
 u velocity of the solvent front
 u_b velocity of the bulk of the solvent
 v rate of vaporization per unit surface area
 v' adsorption rate
 x_i migration distance of solute i
 z_f distance between the solvent front and the solvent source
 z_M height of capillary ascent
 z_0 height of liquid in the tank

A, B, C constants in the Knox equation
 A', B', C' coefficients in the Guiochon equation
 D diffusion coefficient of the solute
 D_m diffusion coefficient of the solute in mobile phase
 D_s diffusion coefficient of the solute in the stationary phase
 H plate height
 H_1 local plate height
 K equilibrium constant
 L migration distance of the solvent or effective plate length
 M_s molecular weight of the solvent
 N plate number
 N' bed efficiency
 N_{ne} plate number to achieve a given separation
 P_e permeability
 P_0 specific permeability (does not depend on particle size)
 P partial pressure of the solvent
 P^0 vapour pressure of the solvent
 Q flow rate in the capillary
 R_F retention factor in TLC
 $R_{F,a}$ apparent retention factor
 $R_{F,t}$ true retention factor
 R_S Resolution between two consecutive peaks (or spots)
 S layer surface area
 V_i molar volume of the solute
 V_t total free volume at time t

α selectivity or relative retention
 γ surface tension of the mobile phase
 γ_m, γ_s tortuosity coefficients in the mobile (m) and stationary (s) phases
 ε bed porosity

$\varepsilon_{T,0}$	bed porosity of the dry adsorbent
$\varepsilon_{T,t}$	external porosity at time t
ΔP_c	capillary pressure change
η	viscosity of the solvent
θ	specific velocity constant of the solvent
θ'	wetting angle
v	reduced velocity
ϕ_v	flow of solvent vaporized from the wet part of the bed
ϕ_s	flow of solvent across the bed cross-section immediately above the solvent level in the tank
ψ_s	association constant of a solvent
ρ	solvent density
ω_i	base width of spot i

See also: II/Chromatography: Thin-Layer (Planar): Densitometry and Image Analysis; Historical Development; Instrumentation; Layers; Spray Reagents.

Further Reading

- Belenkii BG, Kolegov VI and Nesterov VV (1975) *Journal of Chromatography* 107: 265–283.
 Brinkman UATh, De Vries G and Cuperus R (1980) *Journal of Chromatography* 198: 421–428.
 Delley R and Szekely G (1978) *Chimia* 32: 261–265.
 Dhont JH (1974) *Journal of Chromatography* 90: 203–207.

- Giddings JC (1975) In: Heftmann E (ed.) *Theory of Chromatography In Chromatography*, 3rd edn. p. 27. New York: van Nostrand.
 Halpaap H and Krebs KF (1977) *Journal of Chromatography* 142: 823–853.
 Halpaap H and Rippahhn J (1977) *Chromatographia* 10: 613.
 Hezel U (1976) In: Zlatkis A and Kaiser RE (eds) *High Performance Thin Layer Chromatography*, p. 147. Amsterdam: Elsevier.
 Knox JH (1976) In: Simpson CF (ed.) *Practical High Performance Liquid Chromatography*, p. 19. London: Heyden.
 Riedo F, Czencz M, Liardon O and Kováts ESz. (1978) *Helvetica Chimica Acta* 61: 1912–1941.
 Rippahhn J and Halpaap H (1975) *Journal of Chromatography* 112: 81–95.
 Snyder LR (1968) *Principles of Adsorption Chromatography*, p. 17. New York: Marcel Dekker.
 Soczewinski E (1977) *Journal of Chromatography* 138: 443–445.
 Stahl E (1968) *Zeitschrift für analytische Chemie* 216: 294–305.
 Stewart GH (1966) *Separation Science* 1: 747–756.
 Tyihak E, Mincsovcics E and Kalasz H (1979) *Journal of Chromatography* 174: 75–81.
 Tyihak E, Mincsovcics E and Kalasz H (1980) *Journal of Chromatography* 191: 293–300.
 Van Brakel J and Heertjes PM (1977) *Powder Technology* 16: 75–81.

CRYSTALLIZATION



Additives: Molecular Design

J. H. ter Horst and R. M. van Rosmalen,
Delft University of Technology, The Netherlands
R. M. Geertman, Akzo Nobel Chemicals Research,
Arnhem, The Netherlands

Copyright © 2000 Academic Press

Introduction

Crystallization is the nucleation and growth of a solid phase in a mother liquor. It can be used as a separation technique, because the process results in the separation of the mother liquor and the solid phase. If the mother liquor and the solid phase have different compositions it can also be used as a purification technique. In such cases the mother liquor must contain impurities. The deliberate addition of impurities during the crystallization process, has been widely used to improve both the product quality and the process performance. However, most impurities present during crystallization processes are not added on purpose, but are by-products from previous reactions, dissolved salts and solvents that can have the same kinds of effects.

In industrial crystallization additives are generally used to improve the handling characteristics of the crystalline product or to prevent scaling. By employing correctly selected additives it is possible to reduce caking, improve the free flowing behaviour of a powder, increase the bulk density of a crystalline product, change the crystal size distribution, induce certain polymorphs and improve filtration behaviour.

Varied though this list may seem, all these effects can be achieved by using additives that have very specific interactions with the crystal surface. This fundamental physical effect causes a change in the system parameters when additives are introduced. Detailed knowledge of the molecular structure of the solid-liquid interface is very important for design of additives. Once this interface is understood, it is possible to design molecules that have specific interactions with one or more of the faces of a crystal. Often the same additive can be used in different application. For instance a growth retarder used to prevent scaling of a given compound can, when added after crystallization, also act as an anticaking

agent. Blocking a single crystal face with a certain additive can induce morphology changes, but the same additive can also be used to act as a template for the nucleation of that same crystal face.

In many cases additives are not wanted in the product application. Ferrocyanide is a very effective anticaking agent for salt (NaCl), but the ferrocyanide complex must be destroyed and the iron precipitated prior to electrolysis of the salt for the production of chlorine (Cl_2). Nitrosyltriacetamide is also an effective anticaking agent for salt, but during electrolysis nitrogen trichloride (an explosive) is formed.

Apart from having a very specific influence on a crystal face, additives must also be effective at very low concentrations. Because one of the main uses of additives is in cheap bulk products (costing less than US \$1 kg^{-1}) the price of the additive also acts as an incentive to keep the additive concentrations as low as possible. Expensive additives, even if used in very low amounts, will adversely affect the cost of these cheap bulk products. High additive concentrations always give rise to significant additive incorporation in the crystal and thus decrease the product purity.

Additives that effectively control crystallization processes are also found in nature: the shells of crustaceans are formed as a result of bio-templated growth of calcium carbonate; the growth of the mineral components of our bones and teeth is carefully regulated; and studies of fish in polar regions have revealed some proteins that very effectively block the growth of ice crystals.

After describing the fundamental effects of the additive in the crystallization system, a general procedure for the molecular design of additives will be given. The review ends with some case studies.

Interaction of Impurities and Crystal Surfaces

The effect of an impurity that is present in small quantities (parts per million (ppm) level) cannot be explained solely by its effect on solution bulk parameters such as solubility. The phenomenon that is at the root of all the effects of impurities on process performance and product quality is the interaction of the impurity with the crystal surfaces.

Adsorption of the impurity can take place on flat surfaces, at stepped surfaces and at kink sites (Figure 1). The adsorbed compound can impede the movement of steps on the surface. This is a kinetic effect and causes a reduction in the growth rate of the corresponding crystal surface. For instance the induction time, i.e. the time that elapses until the outgrown nuclei are detectable, can increase because the outgrowth of nuclei takes longer.

Origin and Type of Impurities

In solution crystallization the solvent is an inevitable impurity. Additives play a role in the improvement of product quality (e.g. shape of the crystals, crystal size distribution) or process performance (e.g. filterability). One source of impurities in the crystallization process is the synthesis of the crystal compound, as synthesis by-products greatly affect crystallization.

Impurities can also be classified based on their character. Apart from organic and inorganic compounds, a special group of impurities is the polyelectrolytes, long carbon chain molecules with many functional groups. Because of the large number of functional groups the interaction between polyelectrolytes and crystal surfaces is strong. The large number of functional groups also makes the molecule kinetically very hard to remove, as all the bonded functional groups have to be detached from the surface. One of the detached functional groups remaining bonded to the polyelectrolyte and is thus positioned very near the crystal surface. The attachment of that one functional group onto the surface is faster than the detachment from the surface of the other functional groups of the polyelectrolyte molecule. The strong interaction and the large number of interaction points make polyelectrolytes highly effective additives at very low concentrations. Another special group of impurities is the crystallizing compounds themselves. Long chain hydrocarbons such as fats may cause self-poisoning on certain surfaces if the fat molecules in the melt near the surface have a different conformation from the fat molecules in the surface.

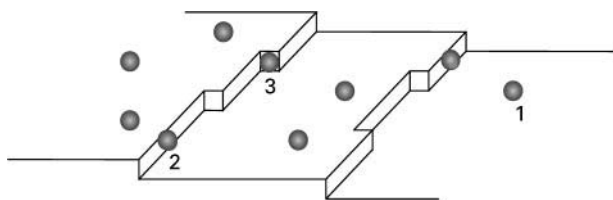


Figure 1 Additive adsorption at various positions on a crystal surface: 1, flat surface; 2, step; 3, kink site.

Predicting the Effects of Impurities

The deliberate addition of an impurity is intended to cause a particular effect, such as a reduction in mineral scale formation or a change in morphology. This effect comes from changes in the kinetic process involved, e.g. for a change in morphology the relative growth rates of the different crystal faces have to change. The function of the additive is thus very specific: the morphology changes if the growth of a specific face is blocked. This is illustrated in Table 1 for a number of desired additive effects. The first column gives the desired effect, the second the kinetic process involved and the third the action acquired by the additive. Table 2 shows whether an interaction with a specific face or all faces is required, at what particular moment the additive should be added and whether it blocks a face or acts as a template. This table shows the close relationship between additives used for different purposes. An anticaking agent is simply an antiscaling agent added after crystallization, and an additive used to block a specific crystal face can in some cases also act as a template for that same face.

Identification of an unintentional impurity and understanding of its effect on the crystallization process requires a kind of reverse engineering. Many impurities are formed as by-products during the synthesis of the compound to be crystallized. By observing how the crystallization process changes in the presence of impurities, the kinetic process involved can be identified. The effect on the process then can be matched with the expected (predicted) effect of one of the impurities present. This is a rather complicated procedure because not all the impurities present that can act on the kinetic processes involved will be known.

The desired effects of additives are changes in the crystal quality or the process parameters. The crystal quality is an overall term for a variety of crystal parameters (morphology, purity, etc.). Changes in the process conditions due to additives, such as better filterability, make the process more efficient. Figure 2 shows the effects of the impurities on the crystal quality and the process conditions. The working directions for both the rational design and the reverse engineering are shown. Key to this figure is knowledge of the interaction of a given compound with the crystalline interface. This interaction determines whether an impurity can, e.g. block growth or induce nucleation of a given face. After evaluating the influence of a given impurity on the morphologically most important faces, the overall effect on the crystal growth and the outgrowth of

Table 1 Additive effects on the crystal growth process

<i>Desired effect</i>	<i>Kinetic process involved</i>	<i>Action required</i>
Anticaking	Dissolution and regrowth of crystalline material	Complete blocking of growth
Antiscaling	Complete blocking of nucleation and/or growth	Complete blocking of growth
Changing morphology (filtration, flowability)	Ratio of growth rates of different faces	Block specific faces
Control of polymorphism	Nucleation of a given polymorph	Mimicing a face of the desired polymorph
Changing crystal size distribution	Changing nucleation/growth ratio	Block specific faces, or block all faces

nuclei can be deduced. From these effects the influence on the crystal quality and the product handling characteristics and ultimately the product properties can be determined. The starting point for designing and studying additives is therefore a study of the molecular structure of the crystalline interface.

Molecular Structure of the Crystal Surface

Both the impurity and the crystal surface determine the strength of the interaction. A crystal has several crystal surfaces, which might have totally different molecular structures. Crystal faces are identified by Miller indices, which indicate how the faces are cut from the crystal unit cell. **Figure 3** shows a unit cell and two crystal surface structures for the compound RDX (cyclotrimethylene trinitramine) with different Miller indices. Since the molecular structures are very different, the interactions of the impurity with the surfaces might also be very different. The growth of one face might be blocked because of strong interactions, while the other face can grow freely because the interactions are only minor. This can cause face-specific growth retardation.

Prediction of the Molecular Structure of the Crystalline Interface

A morphology can be geometrically constructed by drawing planes with an orientation (*hkl*) having a dis-

tance from the origin proportional to the growth rate. The central volume enclosed by the set of planes is the growth form. A face with a large growth rate is positioned far from the origin, and thus its surface area will be small. In contrast, a face with a small growth rate will be close to the origin and have a large surface area (**Figure 4**). This means that the morphology is determined by the slowest growing (*hkl*) faces and that a morphology prediction can be made if the relative growth rates of all the different (*hkl*) faces are known.

Figure 4 also shows the effect of a growth-retarding impurity. Before a crystal face can grow the adsorbed impurity has to be removed from the surface. This takes energy, and thus the growth rate decreases. When face-specific adsorption occurs, surface concentrations of the impurity vary from face to face. The growth retarding effect will then also vary from face-to-face. When face-specific adsorption occurs, the relative growth rates may change, as shown in **Figure 4**.

Nowadays there are several general prediction methods for vacuum morphologies. Here vacuum means that the influence of the solvent or the melt is not taken into account. Donnay and Harker's law states that the importance of a crystal face decreases with interplanar distance d_{hkl} . A morphology can be predicted if the interplanar distance is assumed to be inversely proportional to the relative growth rate of the corresponding crystal face. A prediction method that takes into account the anisotropic energies in the

Table 2 Details of additive effects on product properties

<i>Effect on product property</i>	<i>Interaction with</i>		<i>Addition</i>			<i>Effect on face</i>	
	<i>Specific face</i>	<i>All faces</i>	<i>Before crystallization</i>	<i>During crystallization</i>	<i>After crystallization</i>	<i>Blocking growth</i>	<i>Template induced growth</i>
Anticaking		×			×	×	
Antiscaling		×	×	×		×	
Morphology	×		(×)	×		×	
Polymorphism	×		×				×
Crystal size distribution	(×)	×		×		×	

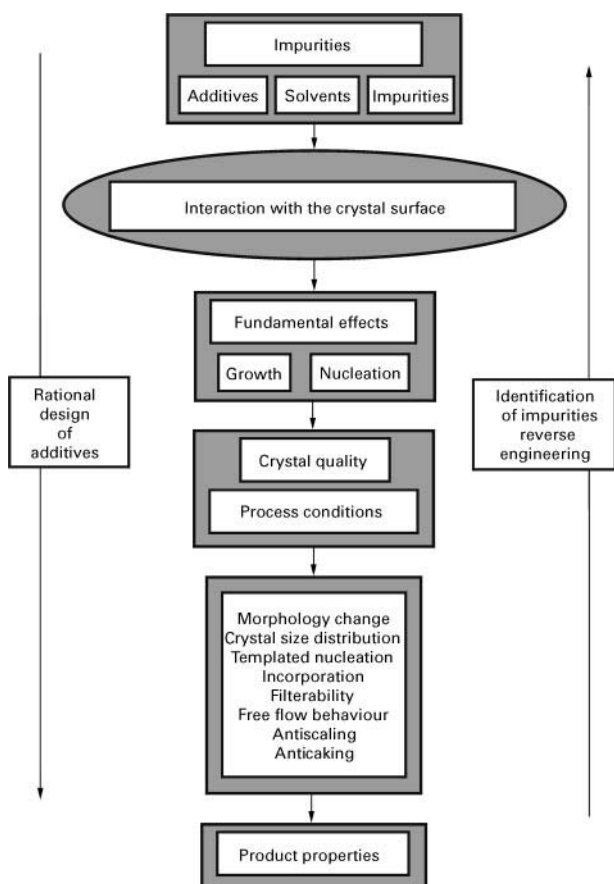


Figure 2 The interaction between the surface and the impurity is the key to the effect of the additive in the crystallization process. This effect translates to changes in the growth and nucleation behaviour of the crystal compound, which in turn affect the crystal quality and process parameters and thus the product properties change.

crystal unit cell is the attachment energy method. The attachment energy is defined as the energy release per growth unit upon adding a growth slice of thickness d_{hkl} onto the corresponding crystal surface. The assumption that the attachment energy is linearly proportional to the relative growth rate of the corresponding crystal surface gives the morphology prediction.

The Design Method

These vacuum morphology prediction methods do not take into account the actual growth processes taking place on a molecular scale at the crystal surfaces. Our goal is to predict the effect of an impurity that affects these growth processes. Such a method should include calculations of the interaction energy between the impurity and the surface. This interaction energy affects the molecular growth processes taking place at the surface.

To make such a prediction, knowledge must first be obtained about the crystal surface structures present. Simple energy calculations determine the morphologically important surface structures. Then more sophisticated calculation methods such as molecular mechanics, molecular dynamics, Monte Carlo techniques or even quantum mechanical calculation methods are needed to calculate the interaction energies of the morphologically important crystal surface structures with the impurity. These interaction energies can be translated into growth rates of the surface structures by assuming a model which interrelates growth rate and interaction energy. The general method for the design of additives is shown in Figure 5.

A good way of determining surface structures and their morphological importance is by performing a periodic bond chain (PBC) analysis. A PBC is an uninterrupted chain of strong bonds between growth units in which periodicity is based on the unit cell parameters and symmetry and which is stoichiometric with regard to the unit cell content. Two sets of intersecting PBCs make a connected net. The connected net can be considered a (hkl) growth slice or growth layer. If a surface does not contain a connected net, the surface cannot grow with a layer growth mechanism and is rough. This means that the relative growth rates of (hkl) surfaces that do not contain connected nets, are very large. These surfaces are not present on the crystal morphology, as a surface needs to contain a connected net to be present. If a surface contains more than one connected net (slices at different heights) more surface structures are possible for one crystal surface. Energy calculations should determine which of the surface structures actually occurs on the surface. However, it is important to remember that the morphologically important surface structure for a particular (hkl) surface may change because of interactions with impurities.

The morphologically important surface structures can be determined by calculating the attachment energy E_a of a surface slice containing a connected net from the bond energies in the slice (the slice energy E_{sl}) and the lattice energy E_{cr} . The attachment energies of all the possible surface structures can be used to determine the relative growth rates of these surface structures:

$$R \propto E_a = E_{cr} - E_{sl}$$

This results in morphologically important crystal surface structures for crystals grown from systems without boundary layer influences such as solvent interactions with the surface structures.

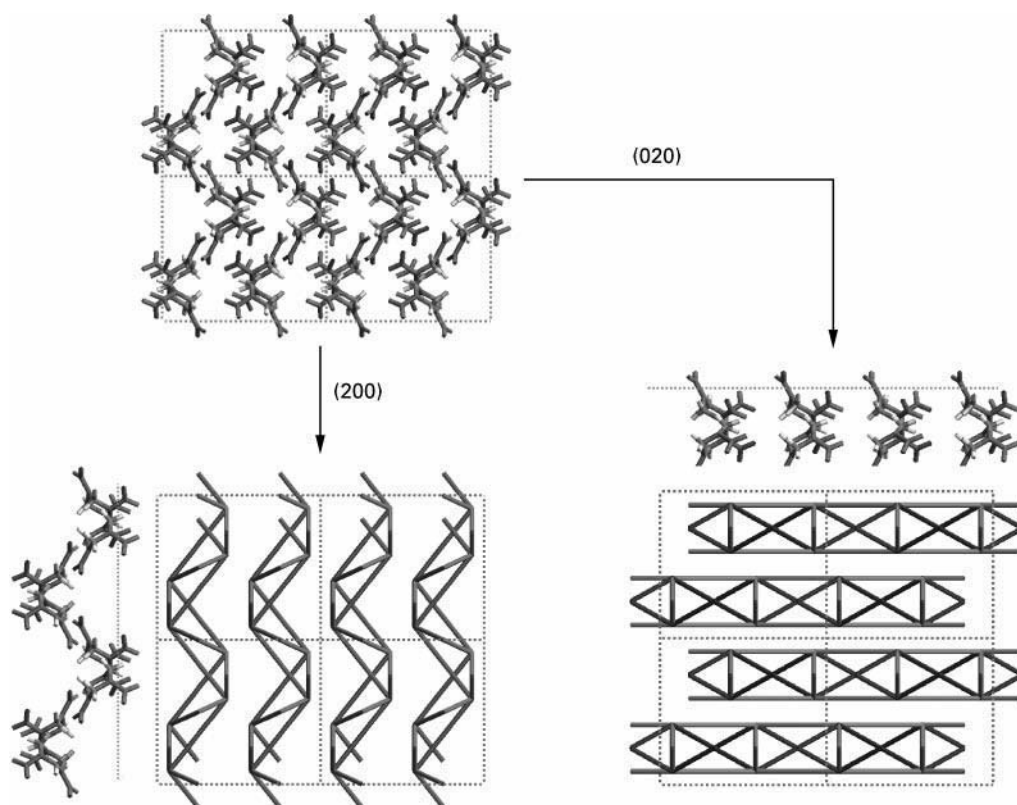


Figure 3 The RDX (cyclotrimethylene trinitramine) unit cell (top left), and the (2 0 0) and (0 2 0) slices, indicating their surface structure. For the (2 0 0) slice the connected net is given on the right of the molecular view of the slice while for the (0 2 0) slice the connected net is given below the molecular view of the slice, as they occur in the unit cell. The surfaces are given perpendicular to the paper. The dotted line in the molecular view of the surfaces indicates the surface.

Commercial software packages nowadays have several tools to calculate interaction energies of one or more impurity molecules on these surface structures.

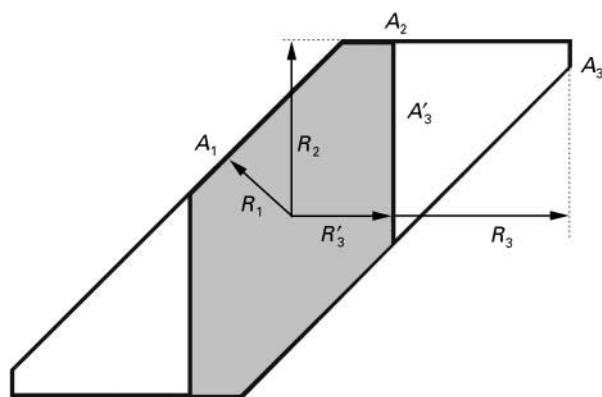


Figure 4 The faces with the smallest growth rates determine the morphology. A growth rate decrease ($R_3 \rightarrow R'_3$) because of a face-specific interaction of the foreign compound causes a morphologically more important surface and thus a change in the morphology.

Once the interaction energies have been calculated, they should be related to the growth rates of the crystal surface structures. The models used for this relation are generally based on the assumption that interaction reduces the growth rate. First the impurity has to be removed from the surface before the face can grow. This takes energy and thus the growth rate decreases. An energy correction term E_s for the vacuum attachment energy can be introduced, which is a function of the interaction of the impurity and the flat crystal surface structure:

$$R \propto E'_a = E_a - E_s$$

In most cases only the interaction of a single ion, complex or molecule with the different crystal surfaces has to be considered. By determining the strongest interactions the corrected attachment energies can be calculated and changes in the morphology can be predicted.

By dynamically simulating a solvent layer on a surface structure (with either a molecular dynamics or a Monte Carlo procedure), the energy changes induced in the solvent layer by the presence of the

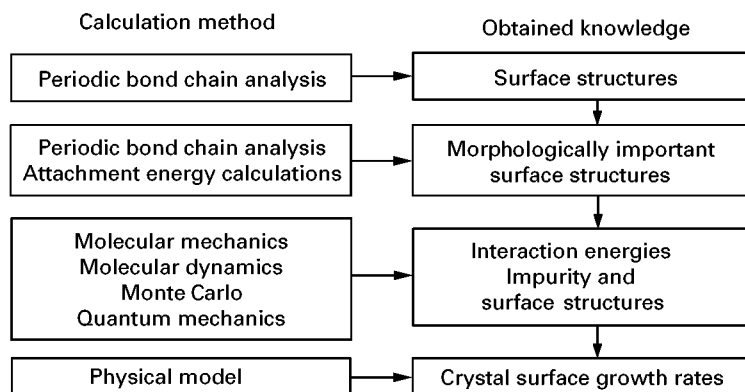


Figure 5 Method of calculating the effect of an impurity on the growth rates of the different crystal faces.

crystalline interface can be estimated, and thus the interaction energy E_s can be calculated. The procedure has to be repeated for all important faces. Though this procedure is somewhat tedious, it yields important insights as to how a solvent can influence the morphology.

Tailor-Made Additives

Tailor-made additives are usually organic additives that are especially designed to aid in the crystallization of a particular organic crystal compound. The additive can be designed to work only on a very specific crystal surface. Again, the additive works by blocking the growth of this crystal surface, making the surface morphologically more important. A characteristic tailor-made additive is very similar to a building unit. The interaction energies needed for adsorption of the building unit and the additive to the surface are similar. Therefore if the additive is adsorbed, it will be relatively hard to remove it from the surface. To retard the growth of the crystal surface, the additive molecule needs a functional group that differs from the growth unit. The functional group may be chosen so that the additive molecule still resembles the building unit, but is smaller. The tailor-made additive is then of the disruptive type. If, because of its functional group, the additive molecule is much larger than the building unit, the additive is of the blocking type (Figure 6).

The attachment energy of a growth unit that belongs to a certain crystal surface can be assumed to be linearly proportional to the growth rate of that crystal face. If the slice to be attached contains an additive, the slice energy changes. However, this change will be small if the additive strongly resembles the building unit (as is the case in both Figure 6B and Figure 6C: $E_{sl} \approx E_{sl}^d \approx E_{sl}^b$). Slices with tailor-made additives will also have a similar attachment energy:

$E_a \approx E_a^{d1} \approx E_a^{b1}$. The difference between crystallization with and without a tailor-made additive is the attachment energy of a subsequent normal slice onto the slice with the additive in it. This attachment energy (E_a^{d2} , E_a^{b2}) is decreased because of the functional group of the additive.

A disruptive type of additive will cause a decrease in the attachment energy E_a^{d2} compared with the normal attachment energy E_a because some bonds between the attaching slice and the surface cannot be made. Because the attachment energy decreases, the growth rate of the crystal surface decreases. During crystallization the disruptive additive can be incorporated in the lattice.

A blocking type of additive will cause a very large decrease in the attachment energy E_a^{b2} compared with the normal attachment energy E_a because the functional group of the additive interferes with the attaching slice. Either the additive has to be removed from the surface or vacancies have to be introduced in the attaching slice to allow the face to grow. This takes large amounts of energy, a large decrease in attachment energy, and thus leads to growth blocking. Instead of having a larger functional group,

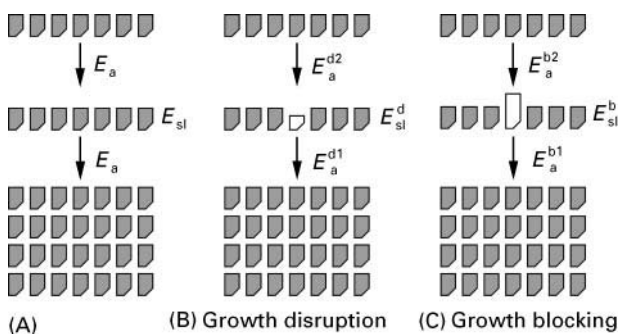


Figure 6 Tailor-made additives can act as growth disrupters or growth blockers.

a blocking additive can also have a functional group that is differently charged from the growth unit, and therefore rejects an incoming growth layer.

This approach can also be used for reverse engineering to find an impurity in the system that causes problems such as incorporation in the lattice or inclusion formation, especially when synthesis by-products that strongly resemble the building units are known to be present as impurities. Disruptive impurities, which have a tendency to incorporate into the lattice, can be distinguished from blocking impurities, which can cause macrosteps and thus inclusion formation. Inclusion formation is the incorporation of pockets of mother liquor into the crystal. A crystal grown from a solution containing a blocking impurity is shown in **Figure 7**. Very large macrosteps are visible on the crystal, and small inclusions also appear in the interior of the crystal.

Incorporation of Impurities

Impurities obviously reduce the purity of the crystalline product and are seldom beneficial to the crystallization processes or the product characteristics. As with the design of additives, it is important to understand how the impurities are incorporated in the crystalline product to reduce their uptake.

In general an impurity is included in the crystalline product through either direct incorporation in the lattice (solid solubility), the formation of inclusions, surface adsorption or poor washing of agglomerates. These incorporation mechanisms will be discussed in more detail.

Solid solutions can only be formed when the impurities mimic the main compound in form and charge.

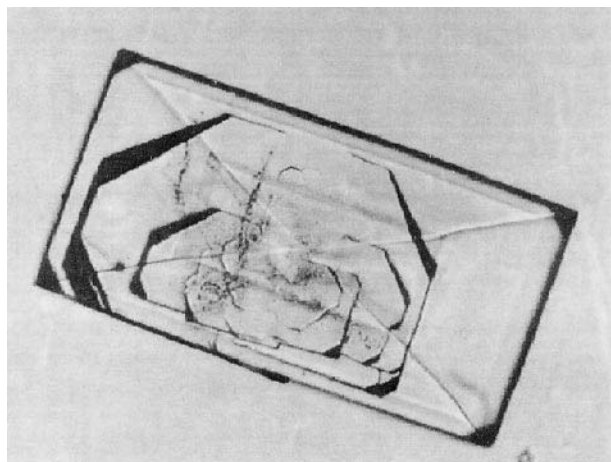


Figure 7 An RDX (cyclotrimethylene trinitramine) crystal grown from the solvent cyclohexanone. A blocking type impurity in the system causes very large macrosteps on a particular surface and inclusions in the interior of the crystal.

They are especially likely to occur with organic crystals where closely related by-products are formed during synthesis of the product. Examples are 2,6-dimethylnaphthalene in naphthalene, cyclohexanone in caprolactam and bromide in sodium chloride. This phenomenon can only occur when the crystallization enthalpy of the impurity is very close to that of the main compound. If that is the case, not only will the impurity be easy to include in the crystal lattice, but the growth will not be retarded. In other words, compounds that form high concentration solid solutions have a very limited influence on the growth of the main compound. If the impurity resembles the main compound to a lesser extent the solid solubility will decrease and growth will be hindered. The free enthalpy involved in the incorporation of polymers or polyelectrolytes, which are the most effective additives in mineral scale prevention, is so large that they are not incorporated in the lattice by direct substitution for molecules or ions of the main component.

A second incorporation mechanism is inclusion formation. Inclusions can be formed in several ways. The most common mechanism in industrial crystallization involves imperfect regrowth of corners damaged by attrition. Pockets of mother liquor are then trapped. The concentration of impurity in the inclusion is then directly related to the concentration in the mother liquor. The overgrowth of poisoned areas is another type of inclusion formation, and occurs at higher driving forces for crystallization. This is essentially the only way to overcome the blocking effects of polymers and polyelectrolytes. As discussed previously, the concentration of polymers or polyelectrolytes in solution is low because these additives are effective at low concentrations and most of the additive is adsorbed on the crystal surface. The amount of additive in the product will therefore not increase much, but of course the amount of other impurities present in the mother liquor, such as solvent, will increase.

A third incorporation mechanism is adherence to the surface. 'Normal' impurities, which cannot be incorporated in the lattice, can be washed off fairly easily. Tailor-made additives, however, are designed to adhere to the surface and are difficult to remove. Partial dissolution of the crystals is not an effective solution as these additives may also hamper the dissolution process. Washing is therefore very useful for the removal of 'normal' impurities, but less so for tailor-made additives.

The formation of voids in agglomerates on impurity uptake is a fourth mechanism of impurity uptake.

In conclusion, impurities that do not hinder crystal growth can be effectively removed from the

product through a combination of careful crystallization and after treatments (washing, etc.). Compounds such as tailor-made additives are much harder to remove.

Case Studies

To illustrate the general principles four cases will be discussed. These cases show the variety of possible applications of additives and the problems sometimes associated with the presence of impurities in the mother liquor. Scaling inhibition is demonstrated using barium sulfate as an example, diesel fuel additives illustrate how the crystal size distribution can be changed, crystallization of α -lactose is a good example of self-poisoning, and the template directed crystallization of calcium carbonate is also discussed.

Scaling problems are often encountered in oil production. The two major scaling problems involve gas hydrates and mineral scaling. Gas hydrates occur when methane and water crystallize under high pressure to form clathrate structures; this can happen in gas pipes on the bottom of the sea. These crystals can scale and block the pipes. Nowadays much research effort is put into the design of additives to prevent these clathrate crystals from blocking the pipes.

Mineral scaling occurs in secondary oil recovery. When the immediate vicinity of a borehole becomes depleted in oil, water is injected in the surrounding rock strata to push the remaining oil from the pores towards the borehole. The pores also contain water that at these deep levels contains a high concentration of barium. When seawater (which contains large amounts of sulfate) is injected, barium sulfate precipitates and the pores silt up. In the worst case the pores are plugged and a new hole must be drilled, which is a very costly operation. Scale formation is inhibited by the addition of low amounts (ppm levels) of polyelectrolytes, for instance polycarboxylates and polysulfonates. Experiments have shown that the molecular structure of the polyelectrolyte determines the effectiveness of the additive. Polyelectrolytes containing sulfonate or phosphonate groups, which closely resemble the sulfate groups in the crystal lattice, are more effective than polyelectrolytes containing only carboxylate groups. Also the way the sulfonate groups are attached to the backbone is important: molecules with the sulfonate group directly attached are more effective than molecules with the sulfonate indirectly attached. The length of the backbone allows each sulfonate group to replace a sulfate in the lattice, thus binding the additive very strongly to the crystal surface, in a zipper-like manner, and inhibiting growth. For instance, 0.1 ppm of a polymaleic acid (polyvinyl sulfonic acid

at a pH of 3.8) decreases the growth rate of barium sulfate by nearly two orders of magnitude (depending on the supersaturation).

Waxes in diesel oil can crystallize at low temperatures. The crystals clog up the fuel filters in cars and prevent the motor from starting. To prevent this problem either wax crystallization should be prevented or only very small crystals should be allowed to form, which can pass through the fuel filter without any problem. As the former option is not very practical (it requires either removal of the waxes or storage of the fuel at higher temperatures) the only option is to add additives that block crystal growth. The design of an additive for such a purpose has been carried out using xylene containing n -C₃₂H₆₆ as a model fuel. A copolymer of fumarate vinyl acetate with different alkyl side chain lengths was used as an additive. The effective concentration at which the additive started to influence the growth of n -C₃₂H₆₆ was determined at a fixed supersaturation as a function of the alkyl side chain length. A clear relationship between the side chain length and the growth inhibition was shown, with a maximum effectiveness when the chain length was very close to the chain length of the solute. This shows that the structural match between the additive and the solute is critical for the effectiveness of the additive.

α -Lactose, a milk sugar, is a disaccharide containing a galactose and a glucose ring. Under influence of an acid, the α -glucose ring can be opened and closed again either in the α or the β form. In the latter form it is a tailor-made additive. The galactose moiety resembles lactose, but the different position of the hydroxyl group (β instead of α) hinders subsequent growth. The ' α -side' of the crystal can therefore be poisoned so the β -lactose molecules cannot attach to the crystal, and only one side is blocked. This results in the typical tomahawk shape of the crystals (Figure 8).

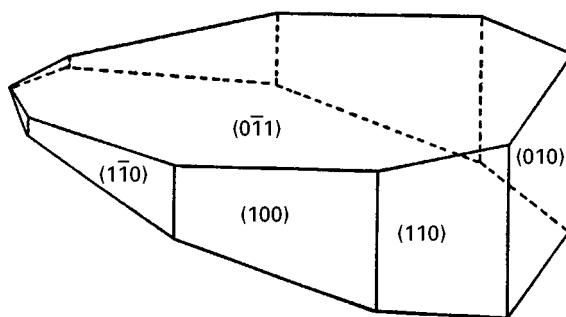


Figure 8 The α -lactose hydrate crystal grown in the presence of β -lactose. The (0 1 0) surface on the right is blocked because β -lactose can adsorb on the surface, causing a blocking impurity as shown in Figure 6C, while on the left the (0 $\bar{1}$ 0) surface is not blocked because the β -lactose can not adsorb on the surface.

A substance that is capable of crystallizing into structurally different but chemically identical crystalline forms exhibits polymorphism. A very common compound that can form polymorphs is water. Under atmospheric pressure and slightly below 0°C ice is formed with a density lower than that of water, so the ice floats on the water. Under higher pressure the ice can crystallize into polymorphs with higher densities that sink. Different polymorphs crystallize under different conditions. However, these conditions may be almost equal for rather complex organic compounds such as pharmaceuticals. In the pharmaceutical industry a strong desire exists to control the crystallization of polymorphs for a number of reasons. The polymorphic form of a pharmaceutical influences its effect and its lethal dosage. The crystallization processes of particular polymorphs are therefore protected by patents.

One way of controlling the crystallization of the correct polymorph is by means of template-directed nucleation of the polymorph. The template mimics a crystal face of the desired polymorph and nuclei of that polymorph can form onto the template. Up to now attention has mainly focused on templates consisting of Langmuir–Blodgett (LB) layers.

Calcite and vaterite are polymorphs of the compound calcium carbonate (calcite is the polymorph that forms under ambient conditions). Stearic acid spreads at the air–water interface, which when compressed as a LB monolayer is highly structured. When the acid group is ionized at higher pH the monolayer surface facing the solution consists of carboxylates that can bind calcium ions from the solution. At higher calcium concentrations calcite grows from the (1 $\bar{1}$ 0) face under the monolayer, while at lower calcium concentrations vaterite grows from the (0 0 1) face under the monolayer. It is suggested that the surface concentration of calcium under the monolayer is important: at high concentrations the calcium ions bonded to the monolayer mimic the (1 $\bar{1}$ 0) face of calcite while at lower concentrations they mimic the (0 0 1) face of vaterite, which is less densely packed with calcium ions. Many examples of template-induced growth are found in nature, as mentioned before and only recently has this technique for controlling polymorphs been exploited.

Concluding Remarks

Additives can be used to improve the handling and quality of crystal products from an industrial crystallization process. The large number of effects that an additive can have on the handling and the quality

all come down to the interaction between the additive and the different crystal surfaces. A general method was given for the design of additives, which involves gaining knowledge of the morphologically important crystal surfaces and on the interaction between these surfaces and the additive.

Further Reading

- Allen MD and Tildesley DJ (1987) *Computer Simulation of Liquids*. Oxford: Clarendon Press.
- Beiny DHM, Mullin JW and Lewtas K (1990) Crystallization of *n*-dotriacontane from hydrocarbon solution with polymeric additives *Journal of Crystal Growth* 102: 801–806.
- Clydesdale G, Roberts KJ and Docherty R (1994) Modelling the morphology of molecular crystals in the presence of disruptive tailor-made additives. *Journal of Crystal Growth* 135: 331–340.
- Clydesdale G, Roberts KJ, Lewtas K and Docherty R (1994) Modelling the morphology of molecular crystals in the presence of blocking tailor-made additives. *Journal of Crystal Growth* 141: 443–450.
- de Goede R (1992) Improvement of melt crystallizations efficiency for industrial applications. In: Pilavachi PA (ed.) *Energy Efficiency in Process Technology*. Elsevier Applied Science.
- Donnay JHD and Harker D (1937) *American Mineralogist* 22: 446.
- Frenkel D and Smit B (1996) *Understanding Molecular Simulation*. New York: Academic Press.
- Hartmann P and Bennema P (1980) The attachment energy as a habit controlling factor. I. Theoretical considerations. *Journal of Crystal Growth* 49: 145–156.
- Hurle DTJ (ed.) (1993) *Handbook of Crystal Growth*, vols 1A–3B. Amsterdam: Elsevier Science.
- Jacquemain D, Wolf SG, Leveiller F, Deutsch M, Kjaer K, Als-Nielsen J, Lahav M and Leiserowitz L (1992) *Angewandte Chemie International Edition English* 31: 130–152.
- Lin CH, Gabas N, Canselier JP and Pèpe G (1998) Prediction of the growth morphology of aminoacid crystals in solution. I. α -Glycine. *Journal of Crystal Growth* 191: 791–802.
- Mann S and Heywood BR (1988) Antifreeze polypeptides come out of the cold. *Nature* 335 (6190): 502–503.
- Mann S, Heywood BR, Rajam S and Birchall JD (1988) *Nature* 334: 692–695.
- Mann S, Heywood BR, Rajam S and Birchall JD (1989) Interfacial control of nucleation of calcium carbonate under organized stearic acid monolayers. *Proceeding of the Royal Society of London, A* 423: 457.
- Mann S, Heywood BR, Rajam S, et al., (1990) *Advanced Materials* 2: 257.
- Mersmann A (ed.) (1995) *Crystallization Technology Handbook*. New York: Marcel Dekker, Inc.

Mullin JW (1993) *Crystallization*, 3rd edn. Oxford: Butterworth-Heinemann Ltd.

Myerson AS, ed. (1999) *Molecular Modeling Applications in Crystallization*. Cambridge: Cambridge University Press.

Sherwood J (1969) Defects in organic crystals. *Molecular Crystals and Liquids* 9: 37.

Sloan ED Jr (1990) *Clathrate Hydrates of Natural Gases*. New York: Marcel Dekker Inc.

Biomineralization

D. Volkmer, University of Bielefeld, Bielefeld, Germany

Copyright © 2000 Academic Press

Many organisms have developed sophisticated strategies to direct the growth of the inorganic constituents of their mineralized tissues. Active control mechanisms are effective at almost all levels of structural hierarchy, ranging from the nanoscopic regime – the nucleation of a crystallite at a specific site – up to the macroscopic regime, where the biophysical properties of the mineralized tissue have to be matched to a certain function.

Among the many open questions, one of the most challenging scientific problems is to gain insights into the molecular interactions that occur at the interface between the inorganic mineral and the macromolecular organic matrix. Biogenic crystals often express exceptional habits that are seemingly unrelated to the morphology of the same type of crystals when grown under equilibrium conditions. For the most widespread calcified tissues it is frequently assumed that a structurally rigid composite matrix consisting of fibrous proteins and thereon adsorbed acidic macromolecules acts as a supramolecular blueprint that templates nucleation of the inorganic phase. Subsequent crystal growth proceeds within a specialized compartment which encloses a suitable aqueous microenvironment. The particular composition of solutes, which often comprises a complex mixture of dissolved electrolytes and macromolecules, has a strong influence on the morphology of the crystals. In the course of mineral deposition, growth modifiers may interact with the maturing crystal in different ways: dissolved macromolecules may be adsorbed onto specific crystal faces, thus slowing down or inhibiting deposition rates along certain crystallographic directions. Adsorbed macromolecules may be completely overgrown by the mineral to produce lattice defects or to introduce discontinuities in the crystal texture.

Efforts in trying to separate and mimic aspects of these complex interactions with simple model systems will help to improve our understanding of crystallization processes that are under biological control.

A profitable knowledge transfer in the direction of biologically inspired design strategies for building new and improved composite materials can be predicted for the near future.

The following account of biomineralization focuses on two special topics of this wide research field, namely ferritin and mollusc shell mineralization, which are considered here as illustrative examples. For a more comprehensive survey which includes further important types of biominerals (e.g. bone or biogenic structures made of amorphous silica) the reader should consider one of the many excellent monographs and review articles on the subject.

Ferritin: From Iron Storage to Nanoparticle Synthesis

Mineral deposition in the iron storage protein (ferritin) may be regarded as an archetypal biological model for the formation of a nanocrystalline mineral phase within a confined space. The structure and function of ferritin have been reviewed in great detail. Ferritin consists of an oligomeric protein shell (apoferritin) and a core of poorly crystalline Fe(III) oxyhydroxide (presumably ferrihydrite, $5 \text{ Fe}_2\text{O}_3 \cdot 9 \text{ H}_2\text{O}$). Iron is temporarily stored within and released from the central cavity of the encapsulating protein shell. The availability of several high resolution three-dimensional structures of apoferritins originating from different organisms provides a reliable basis to discuss possible pathways of iron biomineralization. Current biomimetic strategies to achieve similar properties include mineralization in oil-water microemulsions, block copolymer micelles, or biotechnologically produced capsule-forming proteins.

Apoferritin Structure and Biological Function

Apoferritins with different amino acid compositions have been isolated from eukaryotes as well as

Table 1 Characteristics of ferritins

<i>Iron storage protein</i>	<i>Source</i>	<i>Composition</i>	<i>Physiological functions</i>
Ferritins	Vertebrates Invertebrates	24-mer, predominantly heteropolymeric composed of H-, L- and M-chains Core of crystalline ferrihydrite (polydisperse) Fe/P ratio $\geq 10 : 1$, 1000–3000 Fe(III)/core	Mobile iron storage Iron detoxification Prevention from hydroxyl radical formation
Bacterioferritins	Eubacteria Fungi	24-mer, predominantly homopolymeric Up to 12 haem (cytochrome b_{557}) groups Core of amorphous hydrous ferric phosphate Fe/P ratio 1.1 : 1–1.9 : 1, 600–2300 Fe(III)/core	Precursor to magnetite in magnetotactic bacteria

Adapted with permission from Le Brun N, Thomson AJ and Moore GR (1997) Metal centres of bacterioferritins or non haem-iron-containing cytochromes b_{557} . *Structure and Bonding* 88: 103–138

prokaryotes (Table 1). Sequence similarities of haem-free ferritins and haem-containing bacterioferritins may fall below 20%. However, their quaternary protein structures are almost identical, suggesting that a convergent molecular evolution within different groups of organisms has independently led to an optimal solution for the availability of a mobile temporary iron storage.

While the general physiological effect of ferritin originating from different organisms may differ, it clearly functions as an iron deposit on the molecular scale, owing to several remarkable features:

- the apoferritin creates a confined space which ultimately restricts the maximum size of the inwardly growing mineral phase;
- several anionic residues induce a net negative charge on the inner protein surface which compensates for the positive surface charges of initially formed polycationic Fe(III) oxyhydroxy species;
- the H-chain ferritin subunit contains a ferroxidase centre that catalyses the oxidation of Fe(II) by molecular oxygen to yield Fe(III);
- the L-chain ferritin subunit bears glutamic acid residues in close proximity which point towards the central cavity, thus possibly acting as an active site for crystal nucleation;
- the apoferritin supports long range electron transfer across the protein coat, enabling fast reductive release of Fe(II) ions from the highly insoluble Fe(III) oxyhydroxide mineral.

Apoferritin is built up by 24 structurally complementary subunits that self-assemble to form a hollow shell of an approximate outer diameter of 11 nm. An individual subunit consists of a long 4- α -helix bundle with an additional short α -helix lying at an angle of about 60° to the bundle axis at the C-terminal side of the amino acid chain (Figure 1A). At the beginning of apoferritin self-assembly dimers form mainly through a multitude of hydrophobic

contacts along the juxtaposed 4- α -helix bundles. The complete apoferritin shell is composed of 12 dimers that form the faces of an imaginary rhombic dodecahedron (Figure 1B). The protein shell encloses

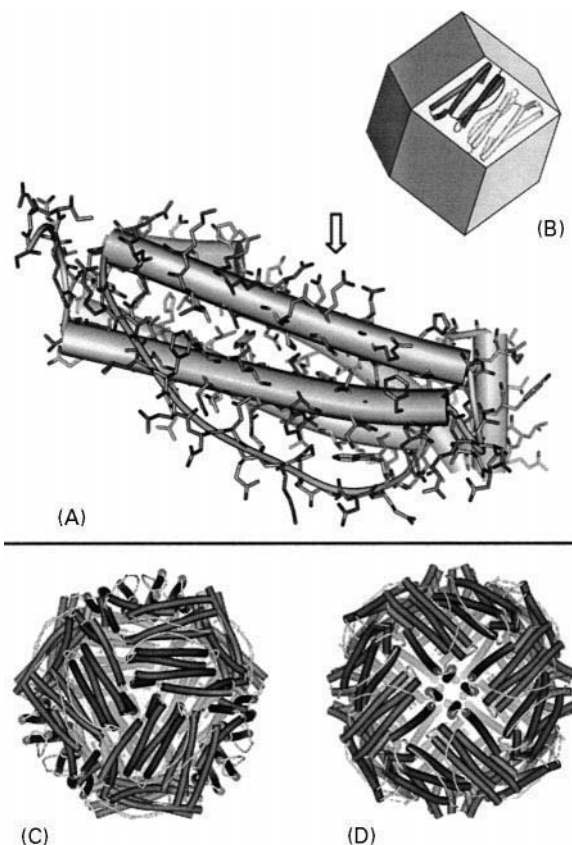


Figure 1 (A) Single apoferritin subunit; α -helix regions of the secondary protein structure are represented as cylinders. The arrow marks a putative mineral nucleation site (here: Glu 57, 60, 61 and 64 of L-chain horse apoferritin, PDB code: 1AEW). (B) Supramolecular architecture of the apoferritin protein shell: 12 subunit dimers form the faces of an imaginary rhombic dodecahedron. (C, D) View along the three-fold channels (the four-fold channels, respectively) of the apoferritin structure. Adapted from Harrison and Arosio (1996).

a nearly spherical cavity of an approximate diameter of 8 nm. The central cavity is accessible through channels of three-fold and four-fold symmetry which are situated at the vertices of the rhombic dodecahedron (Figure 1C, D). While the three-fold channels possess a hydrophilic surface, the four-fold channels are more hydrophobic in nature. The transport characteristics of the ferritin channels are still a matter of controversy. The three-fold channels are likely to be involved in the uptake and release of iron ions as well as in the regulation of the ferritin water content. For the four-fold channels an active role in the uptake of dioxygen has been proposed.

Ferritin Biomineralization

Since ferritin subunits spontaneously self-assemble *in vivo* as well as *in vitro* to yield the complete apoferritin shell, it has been possible to study mineral deposition within the ferritin cavity under various experimental conditions.

Mineral formation within the ferritin cavity proceeds via two different pathways (Figure 2): At low iron content, hydrated Fe(II) ions are taken up from the external medium by the H-chain ferroxidase centre where rapid oxidation takes place. Hydrated Fe(III) ions are released from the ferroxidase centre to

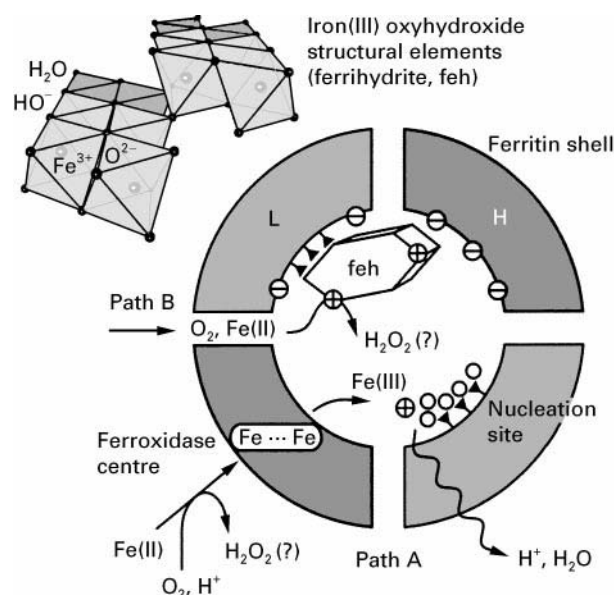


Figure 2 Iron mineral formation in ferritin. A self-assembled heteropolymeric shell forms a spatially confined mineralization compartment composed of H- and L-chain subunits that possess different roles in mineralization. The H-chain contains a pre-organized arrangement of coordinating amino acid residues (ferroxidase centre) which is able to take up two Fe(II) ions and to catalyse their oxidation to Fe(III) ions. The L-chain possesses four highly conserved glutamic acid residues, that are assumed to play a decisive role in Fe(III) mineral nucleation.

enter the ferritin cavity (path A). The inner apoferritin surface bears a multitude of primarily hydrophilic and anionic amino acid residues which point towards the central cavity. In particular, each L-chain subunit contains a distinct array of four potentially coordinating glutamate residues (Figure 1A) that could accumulate a small number of hydrated Fe(III) ions. The immobilized Fe(III) ions start to polymerize, leading to an OH⁻-bridged multinuclear Fe(III) oxyhydroxide cluster. Further cluster growth proceeds via addition of Fe(III) hexaqua cations to the cluster surface with concomitant loss of an H₂O ligand for each established coordinative bond.

On reaching a critical crystallite size, autocatalytic Fe(II) oxidation at the surface of the mineral nucleus outweighs ferroxidase-induced oxidation, and mineral growth continues until most of the cavity is filled by one (or several) Fe(III) oxyhydroxide nanocrystal(s) (path B). The pathways of iron transport into the cavity, as well as the primary product(s) of iron(II) oxidation, are not yet fully established.

Since hydrated Fe(III) ions form polycationic oligomers at the initial stages of polymerization, the general consensus is that L-chain glutamate residues contribute to a negative surface potential on the inside of the apoferritin shell in order to create a thermodynamic sink for Fe(III) oxyhydroxide deposition. In addition to this general effect, a more specific template effect on iron mineral formation has been proposed which takes into account the special arrangement of glutamate residues and the fact that the sequence motif is highly conserved among ferritins from different classes of organisms. The poor crystallinity of the ferritin mineral on the other hand, as well as the fact that nanosized Fe(III) oxyhydroxide particles spontaneously grow from Fe(III)-containing aqueous solutions, challenges this interpretation.

Ferritin Core Structure

The mineral phase of ferritin displays properties similar to the iron oxyhydroxide ferrhydrite which is widespread in nature. This mineral has been traditionally described as amorphous or colloidal ferric hydroxide – Fe(OH₃) – due to its poor X-ray diffracting properties. The actual composition however, is Fe₃HO₈ · 4 H₂O and recent X-ray absorption studies (Fe K-edge XANES and EXAFS spectroscopy) have shown that most of the Fe(III) ions are situated in identical, structurally well-defined coordination environments. A highly hydrated ferrhydrite slowly precipitates from Fe(III)-containing solutions at pH ≥ 2 at room temperature. The Fe(III) hexaqua cations

first oligomerize to yield chains of water-soluble poly-cations in which octahedrally coordinated Fe(III) ions are bridged by hydroxide anions. Further deprotonation and polymerization yield ferrihydrite, which, at close to its zero point of charge at pH 7–8, slowly and irreversibly dehydrates and rearranges to the thermodynamically more stable iron oxide hematite (α -Fe₂O₃). Although the details of the crystal structure and surface properties of ferrihydrite are still controversial, the current data support a structural model in which double chains of edge-sharing iron(III) octahedra are cross-linked via corners (Figure 2, top), similar to the essential structural elements of the mineral goethite (α -FeOOH). The dimensions of coherent X-ray scattering domains for synthetic ferrihydrite are within the range of 1–6 nm, which accounts for the characteristic broadening of X-ray diffraction lines. Temperature-dependent ⁵⁷Fe Mössbauer spectra of synthetic ferrihydrite and ferritin cores display identical features, indicating a superparamagnetic behaviour of the crystalline phase at room temperature and below. Therefore synthetic ferrihydrite precipitates, as well as ferritin cores, may be better described as nanocrystals rather than nanocolloids.

Biologically Inspired Nanoparticle Synthesis

The intriguing supramolecular architecture of ferritin, as well as its unique functional properties, might be taken as a model for the construction of artificial nanocompartments where crystal growth takes place within a spatially confined microenvironment under controlled conditions. Classical approaches that make use of the entrapped water content of oil–water microemulsions are likewise simple to carry out, but as a rule suffer from relatively broad size distributions of the precipitated nanoparticulate materials. For advanced applications, novel synthetic routes will therefore be required to control the dimensions of the desired inorganic nanoparticles. Examples of technologically important compounds which exhibit strongly size-dependent physical and chemical properties range from catalytically active, highly dispersed metal nanocolloids (e.g. Pt, Pd, Rh), quantum-confined semiconductor nanoparticles (CdS, CdSe) to nanoscale ferrimagnetic particles (e.g. γ -Fe₂O₃) and nanocomposite magnetic alloys. Recent examples of biologically inspired synthetic approaches to synthesize nanoscale inorganic materials include the use of biotechnologically engineered apoferritin shells and virus protein cages (capsids), or the use of monodisperse block copolymer micelles as nanoscale reaction compartments (see Further Reading).

From Calcified Tissues to Engineered Crystals

While ferritin represents an example of a nanosized crystalline biomineral, the architecture for example of a vertebrate bone or a mollusc shell spans several length scales. The morphology of the calcified tissue is ultimately encoded in the genome that governs the biosynthesis of required materials at the cellular level of structural hierarchy. Biomineralization therefore, as a highly complex phenomenon of living organisms, cannot be reduced to a single mechanistic aspect. The following representation of CaCO₃ mineralization in molluscs is admittedly a crude simplification which mainly concentrates on structural aspects, while at the same time ignoring the dynamic character of the entire process. Special emphasis here is put on induced CaCO₃ crystal nucleation, i.e. the early stages of crystal growth where the system properties can be described by supramolecular recognition events occurring at the mineral–matrix interface. At this level, common features of ferritin, mollusc shell or bone mineralization do exist: the interaction of highly specialized acidic macromolecules with different surfaces of the growing single crystal. Current research efforts focus on the isolation and characterization of macromolecules from calcified tissues. Functional properties of isolated macromolecules or fractions of macromolecules are systematically investigated for their ability to influence CaCO₃ nucleation, growth and polymorphism. Biologically inspired synthetic strategies try to assemble artificial matrices in order to mimic structural and functional properties of mineralizing tissues.

Crystallochemical Aspects of CaCO₃ Biomineralization

CaCO₃, together with amorphous silica, is the most abundant biomineral. There exist three CaCO₃ polymorphs – calcite, aragonite and vaterite – all of which occur in calcified tissues. A monohydrate (monohydrocalcite) and a hexahydrate form (ikaite) of CaCO₃ have been characterized as metastable precursor phases during the incipient stages of crystal formation (Table 2).

At ambient conditions, calcite is the thermodynamically most stable CaCO₃ polymorph. However, from oversaturated aqueous solutions containing Mg²⁺ at a molar ratio Mg/Ca > 4 (comparable to the composition of seawater), the only observed crystalline phase is aragonite, while at high supersaturation the metastable polymorph vaterite precipitates from solution.

Table 2 Characteristics of the most important CaCO_3 mineral phases

Mineral	Crystal system (space group)	Specific density (g cm^{-3})	Solubility ($-\log K_{sp}$)	Biological occurrence
Calcite (CaCO_3)	Trigonal ($R\bar{3}c$)	2.71	8.48	Very common
Aragonite (CaCO_3)	Orthorhombic ($Pmcn$)	2.93	8.34	Very common
Vaterite (CaCO_3)	Orthorhombic ($P6nm$)	2.54	7.91	Rare
Monohydrocalcite ($\text{CaCO}_3 \cdot \text{H}_2\text{O}$)	Trigonal ($P3_121$)	2.43	7.60	Very rare
Ikaite ($\text{CaCO}_3 \cdot 6\text{H}_2\text{O}$)	Monoclinic ($C2/c$)	1.77	7.12	Unknown

Adapted with permission from Morse JW and Mackenzie FD (1990) *Geochemistry of Sedimentary Carbonate*, p. 41. Amsterdam: Elsevier.

The arrangement of the ions in crystalline CaCO_3 may be described in terms of separate layers of cations and anions. Coordination environments for Ca^{2+} ions (CO_3^{2-} , respectively) in the polymorphs differ from each other, as a result of different successions of layers, as well as different crystallographic orientations of the planar carboxylate groups in the crystal lattices (Figure 3). In calcite, each single densely packed Ca^{2+} layer parallel to the ab plane is situated between single layers of CO_3^{2-} with each layer containing anions oriented in opposite directions. Each Ca^{2+} ion is situated in a distorted octahedral coordination environment of six different CO_3^{2-} anions. In aragonite, the positions of Ca^{2+} ions in the ab plane are nearly identical to those of the calcite structure. In contrast, the CO_3^{2-} anions below and above the Ca^{2+} layer are separated into two layers, which are lifted by 0.98 \AA along the c direction, leading altogether to a ninefold coordination of Ca^{2+} ions.

Shell Formation in Molluscs

It has long been recognized that calcifying organisms have developed active mechanisms to select the poly-

morph, and to control the distribution, shapes and orientations of crystals in their mineralized tissues. Molluscs are among the most thoroughly investigated organisms in this regard; they build concrete shells from CaCO_3 . The mollusc shell may be regarded as a microlaminate composite consisting of layers of highly oriented CaCO_3 crystals which are interspersed with thin sheets of an organic matrix. Crystals within separate shell layers usually consist of either pure aragonite or pure calcite. Vaterite, when present, is usually associated with shell repair. The succession of shell layers, as well as their pronounced ultrastructural features (see Table 3) are important characters in mollusc taxonomy. The main protective functions of the shell are to prevent desiccation, predation and abrasion. The shell also provides support for the body and a site for muscle attachment.

Shell formation occurs in two principal phases. The first involves the cellular processes of ion transport and organic matrix synthesis which occurs in different compartments of the molluscan mineralizing system (Figure 4A). The second phase comprises a series of crystal nucleation and growth processes taking place in a specialized mineralization compartment,

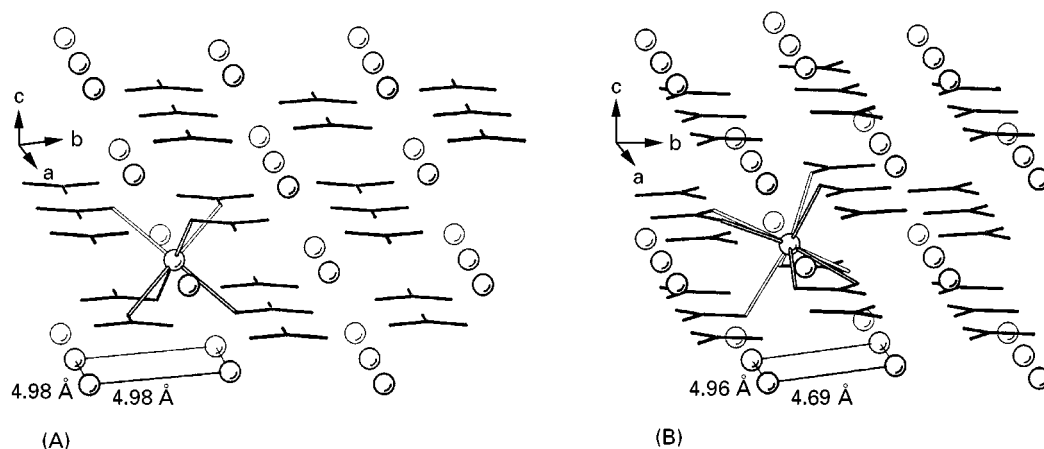


Figure 3 Ion-packing arrangement in the crystal structures of (A) calcite and (B) aragonite. The coordinative bonds between CO_3^{2-} anions (black sticks) and one of the Ca^{2+} ions (open circles) are emphasized with open lines. The minimum distances of Ca^{2+} ions in the ab planes for both crystal lattices are indicated at the bottom.

Table 3 Classification of mollusc shell layers

Shell layer	Composition	Ultrastructural characteristics	Function
Periostracum	Thin layer of hydrophobic sclerotized proteins (periostracin) 3,4-Dihydroxyphenylalanine (DOPA) Asp-rich proteins, chitin (occasionally)	Outer shell surface Little or no ultrastructural order	Space delineation Protection from corrosion Initial substrate for mineralization Camouflage/protective colouring
Prismatic layer	Calcite or aragonite Water-soluble Asp-rich glycoproteins	Outer shell layer extending inward from the periostracum Aggregates of uniformly oriented crystal prisms	$\text{Ca}^{2+}/\text{HCO}_3^-$ storage Multi-layered architecture
Nacreous layer	Aragonite β -Chitin fibrils, silk fibroin-like (Gly-, Ala-rich) framework proteins Water-soluble Asp-rich glycoproteins	Middle or inner shell layer Polygonal, laminar tablets arranged in broad, regularly formed, parallel sheets nearly parallel to the inner shell surface	creates more isotropic structural properties that strengthen the shell against mechanical loading (torsion, fracture)
Foliated layer	Calcite Water-soluble Asp-rich glycoproteins Water-soluble phosphoproteins	Lamellae of parallel and elongate blades of crystals dipping uniformly over large portions of the depositional surface	

Adapted with permission from Wilbur KM and Saleuddin ASM (eds) (1983) Shell formation. In: *The Mollusca*, vol. 4, pp. 236–287. San Diego: Academic Press.

the so-called extrapallial space (Figure 4B). Crystals grow in intimate association with a secreted, highly specialized organic matrix. In order for crystals to form, the extrapallial fluid must become supersaturated with CaCO_3 , which imposes active accumulation strategies upon molluscs that inhabit a freshwater environment, where the external medium is depleted of Ca^{2+} ions. The concentration of Ca^{2+} ions is actively regulated by a Ca membrane transport system that is located in the body and the mantle epithelium. Active carbonate transport has also been postulated for the regulation of HCO_3^- ion concen-

tration. However, as an additional source of hydrogen carbonate, the mollusc may utilize metabolic carbon dioxide from its respiratory system. Any supply of HCO_3^- ions is tightly associated with carbonic anhydrase (CA) activity, an enzyme that catalyses the interconversion of carbon dioxide (CO_2) and carbonic acid (H_2CO_3). High carbonic anhydrase activity is detectable in the extrapallial fluid of molluscs, where the protein seems to be involved in removal of protons from the extrapallial fluid in order to maintain the pH within the appropriate range (7.4–8.3) for mineral formation.

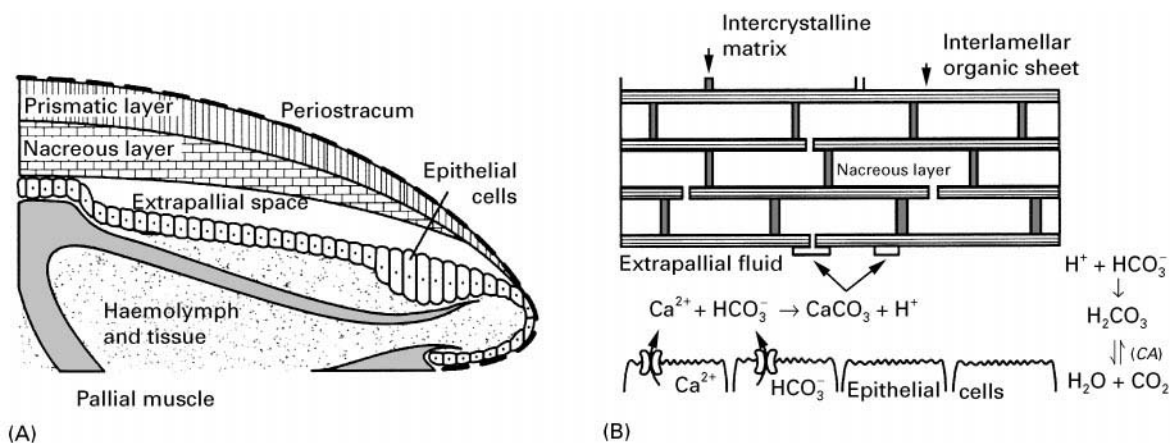


Figure 4 (A) Transverse section of the mantle edge of a bivalve showing the system of compartments. (B) Scheme of ion fluxes at the interface between the outer epithelial cells of the mollusc tissues and the incipient layer of nacre. (Simplified representations, not to scale.)

The extrapallial fluid also contains a complex mixture of inorganic and organic substances. Analysis of several species of marine and freshwater species showed that the major cations present are Na^+ , K^+ , Ca^{2+} and Mg^{2+} while the major anions are HCO_3^- , Cl^- and SO_4^{2-} . The organic components of the extrapallial fluid include amino acids, proteins, mucopolysaccharides and low molecular organic acids (e.g. succinic acid). The organic compounds are secreted by mantle epithelial cells, but their metabolic origins in mollusc tissue have not yet been located.

The Structure of Nacre

Biogenic crystals may use the inner surface of the periostracum, the surface of other, already formed crystals, or the organic matrix as a substrate. Special attention has been drawn to the microstructure of nacre which exhibits an exceptionally regular arrangement of tabular aragonite crystals. Thin interdigitated aragonite plates develop in close association with thin horizontally aligned organic layers (interlamellar sheets) upon which aragonite crystals are nucleated (Figure 4B, Figure 5). In order to grow crystals into a highly regular brickwork-like pattern, numerous nucleation events would have to be synchronized with each other at distant locations. An alternative growth mechanism was proposed to explain the precision by which aragonite platelets are uniformly co-aligned within the same and consecutive layers. According to this model, nacre may be constituted of extended, continuous single crystalline domains of aragonite platelets that are interconnecting by mineral bridges through the perforated interlamellar sheets.

Biologically Induced Crystal Nucleation

Putative Structure of Acidic Nucleation Sites in Calcified Tissues

One of the critical problems in understanding the mechanisms of matrix-associated mineralization is the lack of information on the three-dimensional structures of biological macromolecules that interface with the mineral. A literature search up to the middle of 1999 yielded very few examples where complete or partial information about the primary structure of macromolecules directly involved in mineralization have been determined (Table 4). Macromolecules isolated from mollusc tissues have traditionally been distinguished into two different classes, based on solubility properties. Chemical analysis showed that the insoluble fraction consists

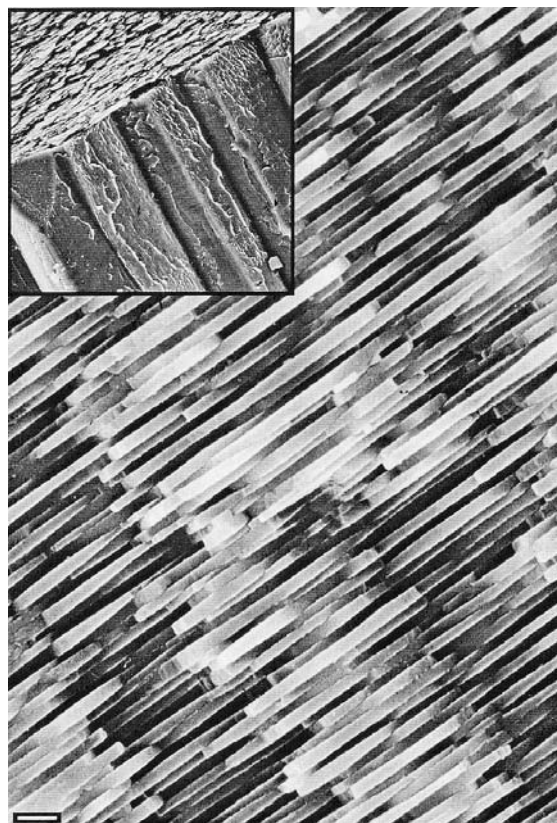
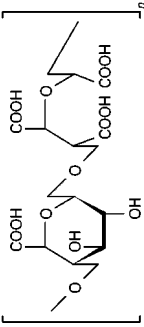


Figure 5 Fractured surface of the nacreous layer of the bivalve mollusc *Atrina rigida*. The inset shows the inner nacreous layer of tabular aragonite crystals (top) and the outer prismatic layer of columnar calcite crystals (bottom). SEM micrographs, scale bar denotes 1 μm . Courtesy of Y. Levi, Department of Structural Biology, Weizmann Institute of Science, Israel.

mainly of fibrous proteins (collagen, chitin) and/or polysaccharides. These macromolecules together build a rigid framework upon which specific macromolecules from the soluble fraction may become adsorbed. The primary function of the insoluble organic matrix is to subdivide the mineralization compartment into an organized network of microcompartments and thus to delimit the available space for crystal growth and/or to constrain the crystal packing arrangement to a certain extent. The surface of this macromolecular assembly may serve as a supramolecular template for oriented nucleation of single crystals, although this structure–function relation is difficult to prove for biological systems *in vivo*.

The macromolecules contained in the soluble fraction have sequence motifs in common which consist of repeating oligomeric units of acidic residues. Table 4 contains further representative examples of functional macromolecules from calcified tissues. However, the heterogeneity of sources/organisms for isolating these macromolecules, their different

Table 4 Representative structural motifs of macromolecules found in calcified tissues

Name	Source	Repeating oligomeric units	Associated mineral	Proposed function	Reference
MS160	Pearl oyster: insoluble protein from the nacreous layer	[Ala ₉₋₁₃] and [Gly ₃₋₁₅]	Aragonite	Framework protein Binding of Asp-rich soluble glycoproteins	Sudo <i>et al.</i> (1997)
MS131	Pearl oyster: insoluble protein from the prismatic layer	[Gly ₃₋₈] and [Glu-Ser-Glu-Glu-Asp-X], (X = Thr or Met)	Calcite	Framework protein Binding of Asp-rich soluble glycoproteins	Sudo <i>et al.</i> (1997)
MSP-1	Scallop shell: soluble glycoprotein from the foliated shell layer	[Asp-Gly-Ser-Asp] and [Asp-Ser-Asp]	Calcite	Induction of oriented nucleation Control of CaCO ₃ polymorphism	Sarashina and Endo (1998)
Nacrein	Pearl oyster: soluble protein from the nacreous layer	[Gly-X-Asn], (X = Glu, Asn, or Asp)	Aragonite	Carbonic anhydrase Ca-binding	Miyamoto <i>et al.</i> (1996)
Type I collagen	Insoluble fibrous scleroprotein from bone	[Gly-X-Y] triple-helices (X, Y frequently Gly, Hyp)	Hydroxyapatite	Framework protein Binding of acidic regulatory proteins	Prockop and Fertala (1998)
Osteonectin	Acidic glycoprotein from bone	[Glu-Glu-Thr-Glu-Glu-Glu]	Hydroxyapatite	High affinity Ca-binding Collagen binding	Fujisawa <i>et al.</i> (1996)
Phosphophoryn	Soluble highly phosphorylated protein from mineralized dentin	[Ser*-Asp] and [Asp-Ser*-Ser*] (Ser* = phosphorylated serine)	Hydroxyapatite	Induction of crystal nucleation Regulation of crystal growth Collagen binding	George <i>et al.</i> (1996)
PS-2	Acidic polysaccharide from <i>P. carterae</i> coccoliths		Calcite	Growth modifier Ca-binding	Marsh (1994)

Sudo S, Fujikawa T, Nagakura T *et al.* (1997) Structures of mollusc shell framework proteins. *Nature* 387: 563-564.

Sarashina I and Endo K (1998) Primary structure of a soluble matrix protein of scallop shell: implications for calcium carbonate biomineralization. *American Mineralogist* 83: 1510-1515.
Miyamoto H, Miyashita T, Okushima M *et al.* (1996) A carbonic anhydrase from the nacreous layer in oyster pearls. *Proceedings of the National Academy of Sciences of the USA* 93: 9657-9660.

Prockop DJ and Fertala A (1998) The collagen fibril: the almost crystalline structure. *Journal of Structural Biology* 122: 111-118.

Fujisawa R, Wada Y, Nodasaka Y and Kuboki Y (1996) Acidic amino acid-rich sequences as binding sites of osteonectin to hydroxyapatite crystals. *Biochimica et Biophysica Acta - Protein Structure and Molecular Enzymology* 1292: 53-60.

George A, Bannon L, Sabsay B *et al.* (1996) The carboxyl-terminal domain of phosphophoryn contains unique extended triplet amino acid repeat sequences forming ordered carboxyl-phosphate interaction ridges that may be essential in the biomineralization process. *Journal of Biological Chemistry* 271: 32869-32873.

Marsh ME (1994) Poly-anion-mediated mineralization - assembly and reorganization of acidic polysaccharides in the Golgi system of a coccolithophorid alga during mineral deposition. *Protoplasma* 177: 108-122.

chemical nature, and their association with different mineral phases clearly rule out a uniform function. They may roughly be divided into five different functional classes:

- concentration regulators: macromolecules that are linked to Ca^{2+} and/or CO_3^{2-} transport and metabolism (e.g. carbonic anhydrase)
- growth inhibitors: acidic macromolecules that strongly bind Ca^{2+} ions and become nonselectively adsorbed on to any arbitrary crystal face which is exposed to the mother liquor
- growth modifiers: acidic macromolecules that interact stereoselectivity with distinct faces of a nascent crystal
- texture modifiers: acidic macromolecules that become occluded and modify texture and mechanic properties of crystals
- nucleators: immobilized acidic macromolecules that form a highly regular template for induced crystal nucleation

Due to the complex nature of interactions in biological matrices, the same acidic macromolecule may belong to more than one of the above mentioned categories and its functional properties may change within different organisms and microenvironments.

To demonstrate a possible mode of molecular interaction between acidic macromolecules and crystal surfaces, this survey of mollusc mineralization will conclude with a brief section about induced CaCO_3 nucleation in biological systems. The body fluids of mineralizing organisms contain crystallization inhibitors that prevent spontaneously formed crystal nuclei from growing into larger crystals. To direct mineral deposition to the appropriate location, active nucleation sites have to exist in mineralizing compartments. The opening section about iron storage has already indicated how the molecular architecture of ferritins may be associated with nucleation of iron minerals. For induced calcite and aragonite nucleation, systematic investigations on biological and suitably assembled artificial systems have shed some light on the structural requirements of a putative nucleation site, especially in mollusc shells. The model of Addadi and Weiner proposes structurally pre-organized domains of acidic residues, that could serve as a supramolecular template for oriented crystal nucleation. Such highly ordered domains could result from acidic macromolecules being adsorbed on a rigid scaffold of insoluble matrix proteins (Figure 6). As an example, the interlamellar organic sheets of mollusc shell nacre consist of thin sheets of β -chitin (a water-insoluble (1 \rightarrow 4)-linked 2-acetamido-2-deoxy β -D-glucan) sandwiched between thicker sheets of silk fibroin-like proteins. Silk fibroin itself possesses microcrystalline

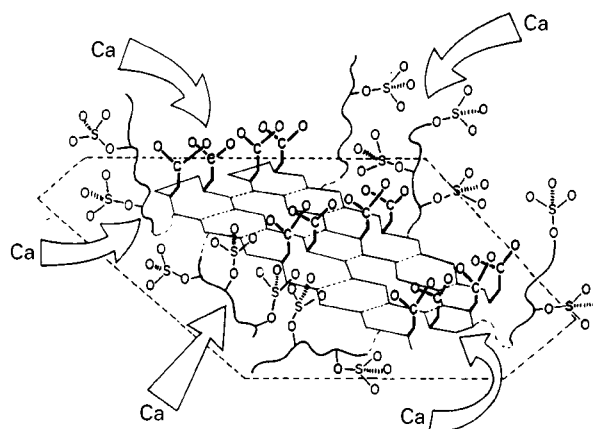


Figure 6 Schematic representation of a putative nucleation site in molluscan tissues. An acidic glycoprotein is anchored to a rigid substrate (as schematized by the broken lines) through hydrophobic or electrostatic interactions. The sulfate groups, linked to flexible oligosaccharide side chains, concentrate Ca^{2+} ions on an Asp-rich oligopeptide domain that is assumed to adapt a highly regular β -sheet conformation. A first layer of Ca ions may thus be fixed and oriented in space, upon which further mineral growth ensues. Reproduced with permission from Addadi and Weiner (1989).

domains of repeating $[\text{Gly-Ala-Gly-Ala-Gly-Ser}]_n$ units that adopt an antiparallel β -pleated sheet conformation. These domains have a highly regular and hydrophobic surface upon which acidic macromolecules are adsorbed from solution. In the course of adsorption, the acidic macromolecules has to fold into the appropriate conformation, in order to maximize its hydrophobic interactions with the silk fibroin surface. Possible candidates for acidic macromolecules interacting with silk fibroin in the described way are oligopeptides that include sequence motifs of $[\text{Asp-X}]_n$, ($\text{X} = \text{Gly}, \text{Ser}$), which have a strong tendency to fold into a β -sheet conformation in the presence of Ca^{2+} ions. As a consequence, the aspartic acid residues of $[\text{Asp-X}]_n$ sequences would be positioned at only one side of the β -pleated sheet, resulting in an organized two-dimensional array of carboxylate ligands.

It is tempting to assume that the carboxylate residues coordinate a first layer of Ca^{2+} ions which would in turn become the first layer of an epitaxially growing CaCO_3 crystal. However, a more profound analysis has so far failed to provide evidence for an epitaxial growth mechanism or a close stereochemical complementarity between the nucleating macromolecules and the incipient CaCO_3 crystal surface. Some properties of the mollusc shell ultrastructure rather point to less sophisticated nucleation strategies; examination of the common crystal orientations in a variety of calcifying organisms reveal that aragonite and calcite single crystals most frequently

nucleate from the *ab* planes. The arrangement of Ca^{2+} ions in this plane (the shortest distance between Ca^{2+} ions is 4.99 Å in calcite, and 4.69 Å in aragonite, respectively; Figure 3) is geometrically not commensurate with the period of amino acid residues in a protein β -strand (approx. 6.9 Å). Moreover, on pointing more or less perpendicular towards the Ca^{2+} ions in the crystal (0 0 1) face, the carboxylate residues of the β -pleated sheet cannot continue the parallel arrangement of planar carbonate anions in the underlying layer(s). The current nucleation model thus does not support the picture of a calcite or aragonite single crystal being nucleated from (0 0 1) crystal faces by virtue of stereochemical selection principles.

Despite the similar positioning of Ca^{2+} ions in the *ab* plane of calcite and aragonite, mollusc shells discriminate between the two polymorphs by secreting them separately in different layers (e.g. prismatic layer and nacre). This suggests that additional factors participate in nucleation. One possibility is that different Mg^{2+} concentrations in the fluids of aragonitic and calcitic layers may be present that could help to shift the balance between the two polymorphs. Another possibility is the presence of polymorph-specific macromolecules that interact with more than one face of the nascent crystal. For a valid explanation of selective nucleation of either polymorph, the current, essentially geometric model will have to be refined. A lot is expected from the first three-dimensional structure of a nucleating macromolecule, although its active conformation may depend on the accompanying insoluble organic matrix in the biological tissues. Finally, novel theoretical approaches are currently being investigated to explore realistic surface properties of the CaCO_3 polymorphs which consider surface relaxation as well as hydration of the outermost ionic layers.

Biologically Inspired Engineering of CaCO_3 Crystals

Several studies have been directed to the phenomenon of heteroepitaxy in CaCO_3 biomineralization. Seminal contributions have come from the group of Mann and co-workers who studied the influence of negatively charged surfactants on crystal nucleation. The group made use of a Langmuir film balance that allows for spreading surfactant molecules as a monolayer at the air–water interface with the charged head groups pointing toward the aqueous subphase. Nucleation of calcite single crystals was observed from monolayers of aliphatic monocarboxylic acids, sulfates or phosphonates. The crystals that grew

underneath the monolayers in general showed a significantly narrower size distribution and reduced nucleation time, as compared to calcite crystals precipitated spontaneously from supersaturated solutions. Moreover, the crystals grew crystallographically oriented relative to the monolayer. Calcite single crystals nucleated preferentially from the {10.0} face underneath compressed monolayers of amphiphilic carboxylic acids, while monolayers of alkylsulfates and -phosphonates led to calcite single crystals that nucleated from the (0 0 1) face. Detailed schemes were proposed to rationalize the different modes of interaction between the different head groups of amphiphiles in the monolayers and the corresponding faces from which the crystals were nucleated.

To gain more precise controls over the relative positions of coordinating residues, patterned self-assembled monolayers of bifunctional ω -terminated alkanethiols ($\text{HS}(\text{CH}_2)_n\text{X}$, $\text{X} = \text{CO}_2^-$, SO_3^- , PO_3^{2-} and OH) have been produced very recently on different supporting metals (Au, Ag) by means of microcontact printing. Depending on the appropriate combination of functional groups, length of alkyl chains, metal substrate and nucleating area, the selective nucleation of calcite single crystals has been achieved for a huge variety of crystallographic orientations. As a unique feature, the self-assembled monolayers allow one to grow isolated and oriented single crystals with a defined separation which is encoded in the tiling of the nucleating areas. The technique has been further employed to grow crystalline CaCO_3 layers that consist of alternating domains of differently oriented calcite single crystals.

The few cited examples demonstrate how model studies may focus on aspects of induced nucleation at organized organic surfaces. Single structural parameters of the organic matrix can be varied systematically and analysed for their influence on crystal nucleation and growth. Results gleaned from these experiments provide important informations that could help to interpret the observed, often highly complex, structures of biominerals. The models studied, furthermore, indicate as to how biologically inspired design and novel technical approaches combine into innovative synthetic strategies for engineering artificial crystalline architectures.

Acknowledgements

The author would like to thank Cia Addadi and Stephen Weiner for valuable discussions. Generous financial support by the MINERVA foundation is gratefully acknowledged.

See also: II/Crystallization: Polymorphism. III/Biological Systems: Ion Exchange Biologically Active Compounds and Xenobiotics: Magnetic Affinity; Supercritical Fluid Crystallization.

Further Reading

- Addadi L and Weiner S (1989) Stereochemical and structural relations between macromolecules and crystals. In: Mann S, Webb J and Williams RJP (eds) *Biom mineralization*, pp. 133–156. Weinheim: VCH.
- Aizenberg J, Black AJ and Whitesides GM (1999) Oriented growth of calcite controlled by self-assembled monolayers of functionalized alkanethiols supported on gold and silver. *Journal of the American Chemistry Society* 121: 4500–4509.
- Briat J-F and Lobréaux S (1998) Iron storage and ferritin in plants. In: Sigel A and Sigel H (eds) *Metal Ions in Biological Systems*, vol. 35, pp. 563–584.
- Chasteen ND (1998) Ferritin. Uptake, storage, and release of iron. In: Sigel A and Sigel H (eds) *Metal Ions in Biological Systems*, vol. 35, pp. 479–514.
- de Leeuw NH and Parker CS (1998) Surface structure and morphology of calcium carbonate polymorphs calcite, aragonite, and vaterite: an atomistic approach. *Journal of Physical Chemistry B* 102: 2914–2922.
- Douglas T and Young M (1998) Host-guest encapsulation of materials by assembled virus protein cages. *Nature* 393: 152–155.
- Fendler JH (ed.) (1998) *Nanoparticles and Nanostructured Films: Preparation, Characterization and Applications*. Weinheim: VCH.
- Gider S, Awschalom DD, Douglas T *et al.* (1995) Classical and quantum magnetic phenomena in natural and artificial ferritin proteins. *Science* 268: 77–80.
- Harrison PM and Arosio P (1996) The ferritins: molecular properties, iron storage function and cellular regulation. *Biochimica et Biophysica Acta – Bioenergetics* 1275: 161–203.
- Harrison PM, Hempstead PC, Artymiuk PJ and Andrews SC (1998) Structure–function relationship in the ferritins. In: Sigel A and Sigel H (eds) *Metal Ions in Biological Systems*, vol. 35, pp. 435–477.
- Heywood B (1996) Template-directed nucleation and growth of inorganic materials. In: Mann S (ed.) *Biomimetic Materials Chemistry*, pp. 143–173. Weinheim: VCH.
- Jambor JL and Dutrizac JE (1998) Occurrence and constitution of natural and synthetic ferrihydrite, a widespread iron oxyhydroxide. *Chemical Reviews* 98: 2549–2585.
- Lippmann F (1973) *Sedimentary Carbonate Minerals. Minerals, Rocks and Inorganic Materials*, vol. 6. Berlin: Springer-Verlag.
- Lowenstam HA and Weiner S (1989) *On Biom mineralization* (Eds Mann, Webb and R.J.P. Williams) New York: Oxford University Press, 7–49.
- Möller M and Spatz JP (1997) Mineralization of nanoparticles in block copolymer micelles. *Current Opinion in Colloid and Interface Science* 2: 177–187.
- Powell AK (1998) Ferritin. Its mineralization. In: Sigel A and Sigel H (eds) *Metal Ions in Biological Systems*, vol. 35, pp. 515–561.
- Schäffer TE, Ionescu-Zanetti C, Proksch R *et al.* (1997) Does abalone nacre form by heteroepitaxial nucleation or by growth through mineral bridges? *Chemistry of Materials* 9: 1731–1740.
- Simkiss K and Wilbur KM (1989) Molluscs – Epithelial control of matrix and minerals. In: *Biom mineralization. Cell Biology and Mineral Deposition*, pp. 230–260. San Diego: Academic Press.
- Weiner S and Addadi L (1997) Design strategies in mineralized biological materials. *Journal of Materials Chemistry* 7: 689–702.

Control of Crystallizers and Dynamic Behaviour

H. J. M. Kramer, Delft University of Technology,
Delft, The Netherlands

Copyright © 2000 Academic Press

Introduction

Ideally industrial crystallizers are operated in such a way that the product specifications are met under conditions that permit profitable, trouble-free production of the desired crystalline material. In industrial practice, however, many operational problems can be encountered that reduce the performance of the crystallizer. The most commonly encountered problems are listed here.

- Deposition of crystal solids on the crystallizer internals, often called scaling or fouling. This results in a reduction of the heat transfer in the heat exchanger or leads to plugging of the process lines and can even hamper the flow pattern and thus the mixing in the crystallizer.
- Alternate feed composition. The resulting changes in the level of supersaturation in the crystallizer can lead to nucleation bursts or depletion of secondary nuclei, having a severe effect on the dynamics of the process.
- Disturbances in the heat exchanger in the crystallizer. This leads to variation in the production yield and the crystal concentration, which in turn

affects the attrition and nucleation kinetics of the process.

- Inappropriate seeding procedures. In batch crystallization processes problems often occur when the amount or size distribution of the seeds crystals or the time of seeding is not optimal. This will result in a final crystal size distribution that is off specification.
- Temperature changes in the crystallizer. This can result in dissolution of the fine crystals in certain zones in the crystallizer, which can have a large impact on the crystallizer dynamics.
- Water injection due to rinse procedures after blockage in product, recycle or circulation lines. This can also result in a temporary decrease in the supersaturation, causing internal dissolution of the fine crystals.

In addition slow, low-order oscillations of the crystal size distribution (CSD) are often observed, which are caused by internal feedback mechanisms in the crystallization process and periodically give rise to an excessive number of fine particles in the product.

To avoid these operational problems, all relevant process variables affecting the crystallization process must be kept within the acceptable limits defined during the design of the process. Not all of the process variables need to be controlled dynamically. Some of them are controlled directly by the equipment design, and others are directly coupled to other variables. Some must be actively controlled to enforce the right process conditions, for instance the temperature profile during a batch cooling process. Others must be manipulated to compensate for the effect of process disturbances. Table 1 shows a list of the major pro-

cess variables for continuous and batch processes. There has been extensive discussion in the literature about the role of each of the process variables and how they are controlled in a variety of crystallizer configurations.

The major process variables in a crystallization process are the level of supersaturation of the solvent, the energy dissipation, the CSD and the distribution of these variables over the crystallizer. These process variables determine to a large extent the kinetic processes (such as nucleation growth and agglomeration) that dominate the crystallization process. They interact with other process variables in a complex way. The presence of interactions and internal feedback mechanisms in the crystallization process limits the success of simple feedback control schemes and favours the use of model-based multivariable controllers, which are able to anticipate these interactions. Unfortunately multivariable control studies for industrial crystallizer are rare and almost completely lack experimental verification.

Depending on the type and scale of the crystallizers, the contents will not be uniformly distributed. Profiles are normally present in the temperature, concentration and particle concentrations, especially around heat exchangers and in baffle and boiling zones. It has recently been shown that the presence of such profiles can have a strong impact on the crystallizer performance. In general these inhomogenities are acceptable as long as the process variables within these zones stay within the acceptable limits and are time-invariant. The main problem in this respect, however, is that the process models normally used for control design do not take account of the presence of these profiles. Compartmental modelling, which has been used to improve the design of industrial crystallizers, should also be applied to control design.

This article gives an overview of the new developments in the control of the CSD for both continuous and batch crystallizers. Attention is focused on the direct control of the CSD either by simple, single-input/single-output feedback control or by multivariable control, using techniques that have been experimentally verified. The reason for this limitation is that process models normally used in crystallization research have a bad reputation with respect to their prediction of the process behaviour. Different crystallizer configurations are analysed with respect to available process actuators. In addition the process models, which form the basis for the controller design and the choice of the measurement technique, are discussed. Some excellent review articles on this topic are used as the starting point of this overview.

Table 1 Process variables to be controlled in industrial crystallizers (after Rawlings *et al.*, 1995)

<i>Continuous operation</i>	<i>Batch operation</i>
Process temperature	(Rate of change in) process temperature
Heat flux to/from process	(Rate of change in) heat flux to/from process
Residence time of crystals	Batch time
Level (volume)	Level (FED batch)(volume)
Feed properties	
Concentration	
Temperature	
Flow rate	
Impurity level	
Slurry concentration	Slurry concentration
Purge flow	
Agitator and pump speed	Agitator and pump speed
CSD	CSD

Modelling of Industrial Crystallizers

The development of an advanced control strategy requires a dynamic model that accurately describes the behaviour of the process. The derivation of such a model implies identification of the model structure and estimation of the model parameters using experimental data, and verification of the model. Parameter estimation falls beyond the scope of this article and will not be covered here.

The modelling of industrial crystallizers is dominated by the presence of the so-called population balance, which describes the evolution in time of the CSD in the crystallizer. The population balance provides a generally accepted approach to the modelling of dispersed phase systems and allows specification of the product quality in terms of the CSD. The general form of the population balance equation (PBE) is as shown in eqn [1]:

$$\begin{aligned} \frac{\partial(n(L)V)}{\partial t} = & -V \frac{\partial(G_L(L)n(L))}{\partial L} + B(L)V - D(L)V \\ & + \sum_{j=1}^m \phi_{v,in,j} n_{in,j}(L) \\ & - \sum_{k=1}^n \phi_{v,out,k} h_{out,k}(L)n(L) \end{aligned} \quad [1]$$

where the amount and the size of the crystals (or particles) are expressed in terms of number density $n(L)$ and crystal length L . V is the suspension volume in the crystallizer, with m streams entering and n streams leaving the crystallizer at volumetric flow rates of ϕ_v . $G_L(L)$ is the linear size-dependent growth rate, and $B(L)$ and $D(L)$ are birth and death rates respectively. Birth and death events can be caused by agglomeration and by the birth of small crystals, called nuclei. The classification function $h(L)$ describes the relation between the CSD in the crystallizer and that in an outlet stream.

As the PBE is a partial differential equation with respect to time t and crystal length L , two boundary conditions are needed to solve it analytically:

$$n(0, t) = \frac{B_0}{G_L(0)} \quad [2]$$

$$n(L, 0) = \text{initial distribution} \quad [3]$$

As primary and secondary nucleation typically involves the birth of small crystals, nucleation is often presented as the birth of nuclei at zero size. Instead of a birth term in the PBE for the nucleation event $B(L)$ that happens over a size range $0 \leq L \leq \gamma$, the birth rate B_0 given by boundary eqn [2] is used. These two

are related as shown in eqn [4]:

$$B_0 = \int_0^\gamma B(L) dL \quad [4]$$

For the second boundary condition a seed population or a population formed by the outgrowth of primary nuclei can be substituted.

The mass balance is given by eqn [5]:

$$\begin{aligned} \frac{dM_{\text{total}}}{dt} = & \phi_{v,feed}(\varepsilon_{\text{feed}}\rho_{\text{feed,liquid}} + (1 - \varepsilon_{\text{feed}})\rho_{\text{crystal}}) \\ & - \phi_{v,product}(\varepsilon\rho_{\text{liquid}} + (1 - \varepsilon)\rho_{\text{crystal}}) \\ & - \phi_{v,vapour}\rho_{\text{vapour}} \end{aligned} \quad [5]$$

The component balances are given by:

$$\begin{aligned} \frac{dM_i}{dt} = & \phi_{v,feed}(\varepsilon_{\text{feed}}\rho_{\text{feed,liquid}}w_{\text{feed,liquid},i} \\ & + (1 - \varepsilon_{\text{feed}})\rho_{\text{crystal}}w_{\text{feed,crystal},i}) \\ & - \phi_{v,product}(\varepsilon\rho_{\text{liquid}}w_{\text{liquid},i} \\ & + (1 - \varepsilon)\rho_{\text{crystal}}w_{\text{crystal},i}) \end{aligned} \quad [6]$$

where $i = 1, \dots, N_{\text{comp}}$, and:

$$M_i = V(\varepsilon\rho_{\text{liquid}}w_{\text{liquid},i} + (1 - \varepsilon)\rho_{\text{crystal}}w_{\text{crystal},i}) \quad [7]$$

where component $i = 1$ is the main compound to be crystallized, and components $i = 2, 3, \dots, N_{\text{comp}}$ are the impurities present.

The distribution coefficients relate the impurity uptake by the solid and the concentration of the impurity in the liquid phase, as shown in eqn [8]

$$k_{\text{distr},i} = \frac{w_{\text{crystal},i}}{w_{\text{liquid},i}} \quad [8]$$

where $i = 2, \dots, N_{\text{comp}}$.

The enthalpy balance with the production rate or solids production P is given by eqn [9]:

$$\frac{dH}{dt} = \phi_{H,feed} - \phi_{H,product} - \phi_{H,vapour} + Q_{\text{heat}} + P\Delta H_{\text{cr}} \quad [9]$$

in which H denotes the enthalpy of the crystallizer content and ϕ_H the enthalpy of the particular stream. Q_{heat} is the effective heat input to the system including heat losses.

In order to complete the model, relations are needed for nucleation and growth. In many cases a size-independent growth rate is determined with a power law relation, as shown in eqn [10]:

$$G_L = k_g \sigma^g \quad [10]$$

where σ is the relative supersaturation. For the secondary nucleation a comparable function is used (eqn [11])

$$B_0 = k_N \sigma^b N^b M_T^j \quad [11]$$

in which N is the stirrer frequency and M_T is the total crystal mass in the crystallizer. Note that B_0 and not B is calculated with this relation. Although these functions are still used, especially in controller design studies, it has been shown that in reality the growth rate function is more complicated and size dependent. In addition, the power law for the nucleation given in eqn [11] is not suitable for describing the dynamics in secondary nucleation dominated crystallization systems and improved relations have proven to give a much better description of these kinetic processes. Here the relations are used because they have been applied in controller design studies. The growth rate is given by eqn [12]:

$$G_L(L) = p_6(C - C_s)^{p_7} \left(1 - \frac{L^{p_8}(L_e^{p_8} + L^{p_8})}{L_e^{p_8}(L^{p_8} + L_a^{p_8})} \right) \quad [12]$$

in which L is the crystal size. In this relation the growth rate decreases beyond a certain crystal size L_a due to attrition, while L_e is the maximum crystal size of the crystals. p_6 , p_7 and p_8 are model parameters, which have to be estimated. The relation for the secondary nucleation is shown in eqn [13]:

$$B_0 = p_3 \left[\int_{p_4}^{\infty} n(L, t) L^{p_5} dL \right]^{p_1} (C - C_s)^{p_3} \quad [13]$$

Here B_0 is calculated assuming that the nuclei have a negligible size. Note that only crystals beyond a certain size p_4 contribute to the secondary nucleation.

State Space Models

The design of model-based controllers requires a state space representation of the process model. As the population balance is a first-order nonlinear partial differential equation, a transformation must be used to get such a form.

Using the definitions of the moments of the distribution, the population balance can be transformed into a set of moment equations (eqn [14]):

$$m_j = \int_0^{\infty} n(L) L^j dL \quad [14]$$

For a continuously operated system with no impurities, a constant V , a size-independent growth rate, no agglomeration, nucleation at zero size, one crystal-free inlet stream, and a nonclassified product stream,

the population balance (eqn [1]) simplifies into eqn [15]:

$$\frac{\partial n(L)}{\partial t} = -G_L \frac{\partial n(L)}{\partial L} - \frac{n(L)}{\tau} \quad [15]$$

with similar boundary conditions. This equation can be reduced to a set of ordinary differential equations using the moment transformation (eqn [16]):

$$\frac{dm_j}{dt} = jG_L m_{j-1} - \frac{m_j}{\tau} + B_0 L_0^j \quad [16]$$

The first four moment equations, together with the kinetic relation (eqns [10] and [11]) and the mass, energy and component balances, form a closed set which describes the crystallization process. Unfortunately, the description will not be very realistic because of the large simplifications which form the basis of this description.

Other methods have been used to obtain a state space model. First of all the method of lines is applied to solve the population balance yielding a state space representation. For controller design this high order nonlinear model was first linearized and then further reduced. As an alternative a black box model was derived using system identification techniques.

Crystallizer Configurations

For continuous crystallization processes several types of crystallizer have been developed, which are used for different applications. The most common types of crystallizers are listed here.

- Forced circulation crystallizer (see Figure 1A). The most widely used crystallizer. It is often treated as a well mixed crystallizer, although several studies have shown that large variations in supersaturation exist within the crystallizer volume. Therefore crystal growth is limited to a small part of the crystallizer (in the vicinity of the boiling zone), and depending on the temperature rise in the external heat exchanger, even dissolution of the fine crystals will take place in that part of the crystallizer. Actuators to control the crystal size distribution are limited although configurations exist with an elutriation leg in which selective removal takes place. The level of supersaturation can be affected by control of the evaporation rate, while the profile can be influenced by adapting the circulation flow rate through the external heat exchanger. The main operational problems encountered with this type of crystallizer are scaling in the boiling zone or in the heat exchanger.

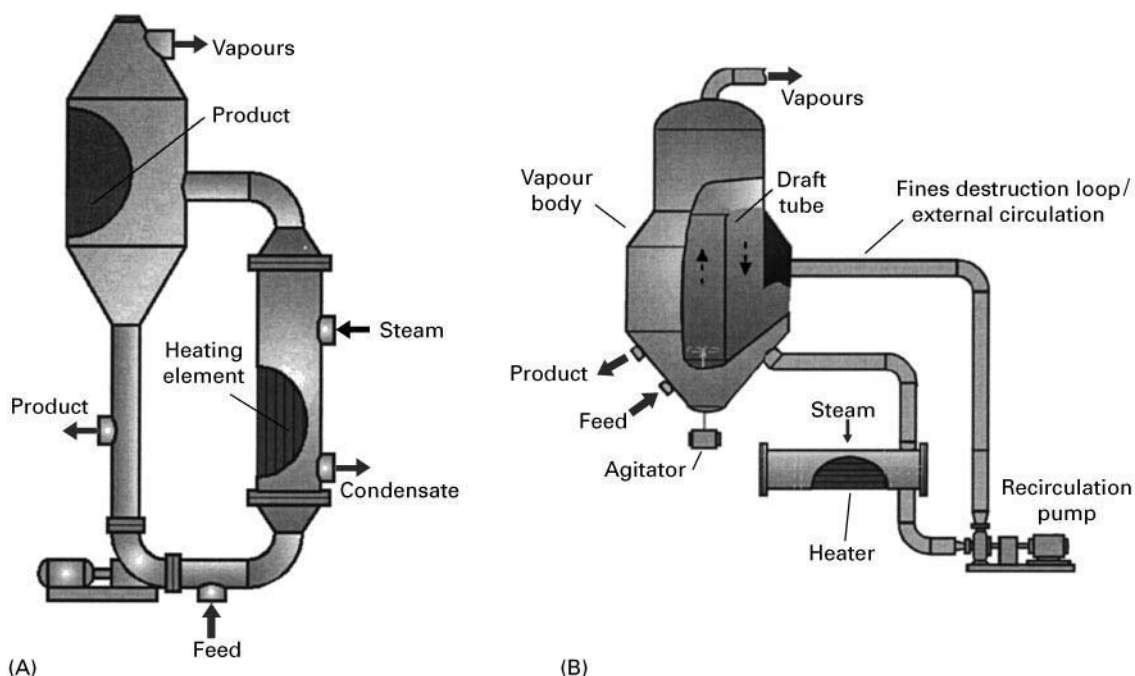


Figure 1 (A) Forced circulation and (B) stirred draft tube baffle (DTB) crystallizer with an external heat exchanger and fines destruction. Both crystallizers are produced by USFilter's HPD.

- Draft tube baffled (DTB) crystallizer (see Figure 1B). This crystallizer enables the generation of larger crystals using fines removal, which is done by installing a skirt baffle to create a settling or annular zone. The flow in the draft tube thus has to be upwards, which is effected by the impeller that also creates most of the attrition fragments. The fines flow can be diluted or heated to partly or totally dissolve the fines. An increase in the fines removal flow increases the number of fines that are removed from the crystallizer, but also increases the cut size of the fines. The fines loop in this way serves as an actuator that can be applied for control of the mean crystal size, although the variation in mean crystal size that can be achieved is limited. The elutriation leg, when present, serves more as a washing device to remove the impurities from the crystal than as a product classifier. The DTB crystallizer is among the best-studied crystallizers, because of the low order oscillations which are often observed. Other operational problems are scaling in the boiling and baffle zones.
- Fluidized-bed crystallizer (see Figure 2A). This crystallizer is especially designed to produce large and uniformly sized crystals. At the top of the bed the crystals are settled, and only the fines leave the crystallizer with the exhausted mother liquor to be circulated through the heat exchanger after mixing with the feed stream. The hot circulated flow enters the vaporizer head, where the solvent is flashed off.

The supersaturated solution leaves the vaporizer through the downcomer, and enters the densely packed fluidized bed at the bottom of the crystallizer. The supersaturation is consumed on its way up, and a coarse product leaves the crystallizer at the bottom. The main control problems are stabilizing the fluidized bed and keeping the supersaturation in the circulation loop, and specifically in the boiling zone and the downcomer, within certain limits to prevent spontaneous (primary) nucleation. Also low-order cycling occurs in this type of crystallizer, which is however much less well studied than the DTB crystallizer. Although fines dissolution already takes place in the circulation loop, a separate fines removal loop can be installed to control the CSD in the crystallizer. In addition a clear liquor overflow stream is sometimes used to control the slurry density in the fluidizer (double draw off).

- Cooling crystallizer (see Figure 2B). In this crystallizer the slurry is circulated through a heat exchanger. For crystallization from solution the slurry is pumped through a tube and shell heat exchanger, with a ΔT range between the tube and the wall of 5–10°C. The temperature decrease in the heat exchanger must be controlled precisely.

As can be seen from these descriptions, the number of available process inputs to manipulate the CSD in the crystallizer is rather limited. The actuator most used

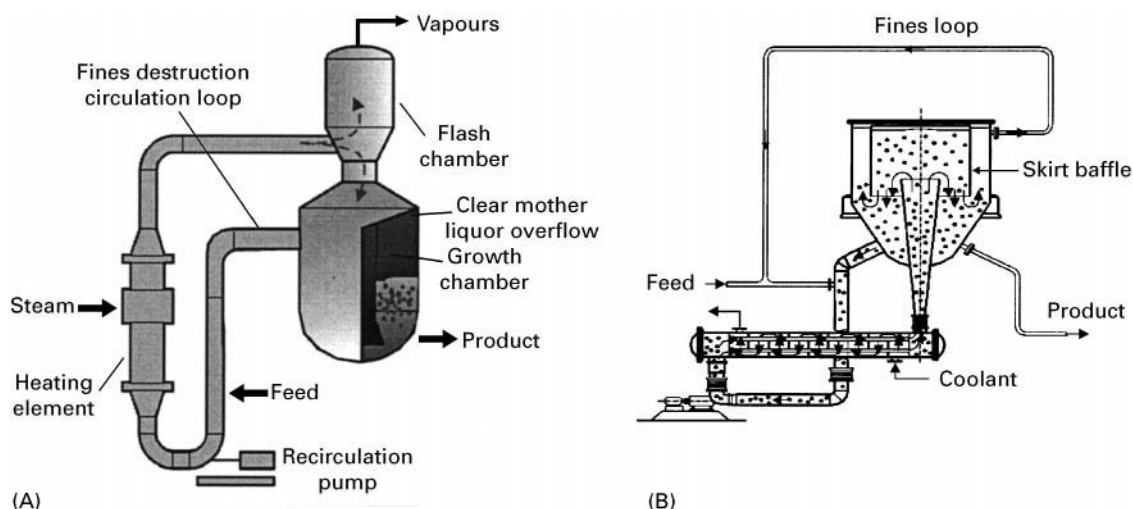


Figure 2 (A) Fluidized bed crystallizer from USFilter's HPD and (B) cooling crystallizers from Swenson.

in control studies is the fines dissolution flow rate, although in industrial crystallizers this flow cannot be manipulated freely. It is constrained on the lower side by the heat input of the system and by the maximum temperature increase of the fines flow. Selective product removal using an external product classifier such as a wet screen or a hydrocyclone seems to be an attractive additional process actuator method, which can be implemented irrespective of the crystallizer used.

Measurements

The on-line measurement of the relevant process variables forms an essential and often difficult part of the control strategy. For the CSD control the most relevant process variables are the supersaturation and one of the characteristics of the CSD. The main measurement techniques are summarized next.

- **Supersaturation.** Except for some crystallization systems (sugars) the direct measurement of supersaturation is either impossible or not accurate enough for control purposes. Recently however several studies have shown that it is possible to measure the supersaturation on-line in a crystallizer using attenuated total reflection (ATR) probes in combination with Fourier transform infrared (FTIR) devices. Successful applications of density measurements have also been reported.
- **On-line CSD measurement.** A number of commercial instruments are available nowadays to determine CSD of crystal slurries. Of these the laser diffraction instruments have been shown to give a reliable measurement in diluted suspensions (at particle concentrations below 1 vol%). A major

drawback to the use of these instruments in a process is the need for an on-line dilution system to dilute the crystal suspension. A more recently developed instrument, measuring the attenuation of planar ultrasonic waves, forms an interesting alternative, because suspensions up to a concentration of 30% (by volume) can be measured without dilution.

- **In-line CSD measurement.** In-line sensors measuring the reflection of laser light and analysing the back-scatter peaks or images enable the analysis of some properties of the CSD inside the crystallizer, which can be of value for control of crystallizers. The main difficulty with the use of these probes is in identification of the relation between the information from the sensor and a process variable which is relevant for the control of the process.
- **Obscuration measurement.** The obscuration is defined as the fraction of light that is obscured by the crystals present in a flow cell and is a measure of the second moment of the distribution. As with laser diffraction this relation is only valid when multiple scattering can be avoided, i.e. at low particle concentrations. Obscuration measurements have been used to measure the number of fines crystals present in the fines removal loop.
- **Particle counter.** An optical particle counter measures the number of particles in a predefined size window in the crystallizer simply by counting the number of pulses from a light detector that are caused by the passage of the particles through a laser beam. The size window is defined as a result of the classification function of the funnel used to withdraw the process liquid from the crystallizer and the detection threshold of the detector, which can be adapted. This counter, which has been

successfully used to control a DTB crystallizer on a pilot-plant scale, forms an attractive alternative to the expensive CSD measurement devices.

The choice of the signal used by the controller, as well as the choice of the instrument, can be decisive for the performance of the controller. Using a CSD measurement, different characteristics of the CSD can be chosen. Analysis of different possibilities suggests that a reduced signal based on a principle component analysis of the raw diffraction data of a Malvern laser diffraction instrument, y_r , gave the best controller behaviour. The median crystal size, however, does not appear to be a suitable signal for control of the CSD, because of large delays in the response and its low sensitivity for changes in the small crystal area.

Control of Continuous Crystallizers

Crystallization Dynamics

As indicated in the introduction, problems in the operation of continuous crystallization processes can lead to large disturbances in the dynamics of an industrial crystallizer. In addition, slow oscillations in the CSD may occur, which do not seem to be caused by process disturbances, but are an intrinsic property for certain process configurations and are related to the internal feedback mechanisms which are present

in the crystallization process. This so-called slow cyclic behaviour is only seen in DTB and fluidized bed types of crystallizer configurations in the presence of fines dissolution and/or classified product removal. Figure 3 shows an example of this behaviour for a 1000 L evaporative DTB crystallizer. For higher values of the fines removal flow rate a limit cycle was reached in the median crystal size, during which the median crystal size varied between 240 and 1040 μm in cycles of about 5–6 h. Oscillatory behaviour has also been reported after selective product removal.

The stability of an open loop continuous crystallizer has been the subject of many studies. The techniques used involve the Laplace transformation of the linearized version of the population balance or conversion to a set of ordinary differential equations using the moment transformation. These solution methods, however, pose severe limitations on the models.

Based on a stability analysis, two types of unstable behaviour, have been identified, namely low order and high order cycling. High order cycling can be caused by very high orders in the power law equation for the nucleation kinetics, which seems unlikely for most crystallization systems. Low order cycling on the other hand can be caused by nonrepresentative product removal.

In more recent work it has been established that simple power law kinetics are unable to explain the

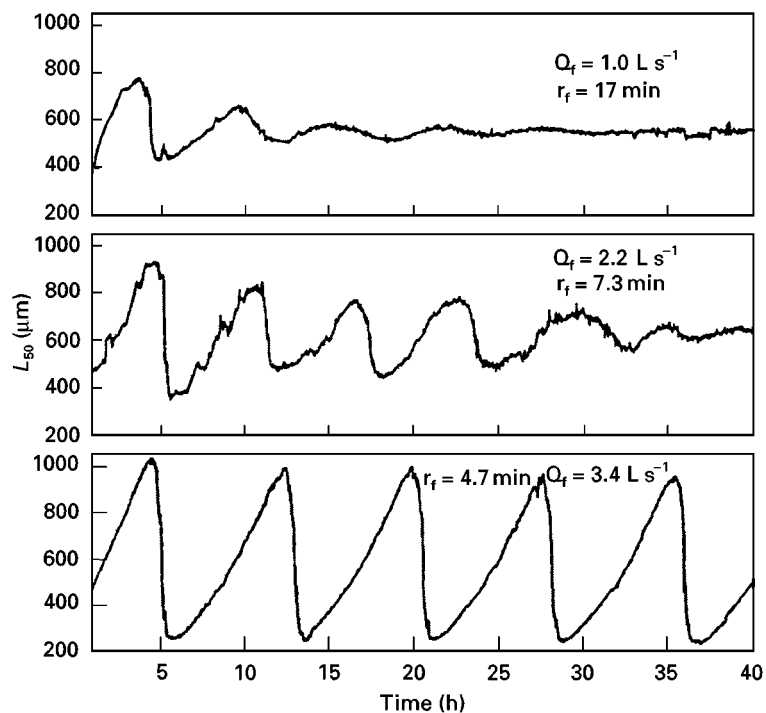


Figure 3 Experimental time response in a DTB crystallizer at start-up of the median crystal size for different fines removal flows (θ_f) and thus different residence times for the fines (r_f). Eek *et al.*, 1995b.

dynamic behaviour in industrial DTB crystallizers. Nucleation models that only take into account crystals beyond a certain minimum crystal size have been shown to give a much better description of the crystallization kinetics.

Some of these limitations in the stability analysis have been removed by using modern analytical techniques, which are based on the reduction of the system of balance and kinetic equations into one single integro-differential implicit equation. The steady state solution of this equation and that of the linearized equation around that point enables an analysis of more complex crystallization models.

Feedback Control

Experimental studies of feedback control schemes for laboratory and bench scale crystallizers have been based on the measurement of the suspension density in the fines removal line by manipulating the fines removal flow. The major drawback of this method is that the manipulation of the fines stream influences not only the number of crystals in the fines flow but also the cut-size of the baffle zone. Therefore the controller will in essence control the fines density removed from the system and not the fines density in the crystallizer.

An in-line Lasentec probe has been used to control a 1000 L DTB crystallizer producing potassium chloride using the fines removal flow as a process actuator. Problems identifying the optimal signal from the sensor and process disturbances affecting the CSD measurements decreased the efficiency of the controller.

The most complete study was one in which the fines removal rate was used as the process actuator to control the process. Figure 4 shows the general control scheme in which u is the process input on which the controller acts, in this case the fines removal rate t and y the process output. d and m are possible process disturbances and the measurement noise respectively.

An on-line particle counter, measuring the number of crystals in a predefined size range (60–100 μm), was used. The control equation is then shown in eqn [17]:

$$Q_f = k_p \left(\varepsilon_n + \frac{T}{T_i} \sum_{n=0}^k \varepsilon_k \right) \quad [17]$$

$$\varepsilon_n = N_f - N_{f,\text{setpoint}}$$

The error ε_k is the difference between the counter output and the set-point value. T is the sample time and T_i the integral or reset time. The following functions of the controller were tested.

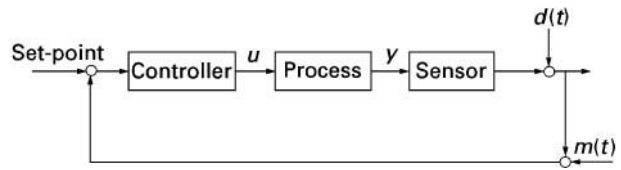


Figure 4 Feedback single-input/single-output control scheme.

1. Stabilization of the process. A considerable reduction in the oscillations after start-up was obtained in closed loop compared with the open loop behaviour (see Figure 5). The severe oscillations resulting from the onset of a product classifier (wet screen) could also be suppressed by the controller (see Figure 6).
2. Set-point tracking. The set-point in the number of fines could be followed by the controller. The changes in the set-point for the number of fines also resulted in changes in the median crystal size of the crystal produced.
3. Disturbance suppression. A process disturbance introduced in the process by closing the product flow for 1 h was analysed. It was shown that open loop response on the disturbance was almost completely suppressed in closed loop operation of the process (see Figure 7).

The choice of the size range for the particle counter, which could be affected by the detector threshold and the settling velocity in the funnel used to discharge the particles from the crystallizer, is essential for the performance of the controller. It has been shown that when the detection size range is moved to particles below 40 μm the controller becomes unstable.

As an alternative to the particle counter, the reduced signal of the laser diffraction instrument was used. Similar results were obtained (see Figure 6).

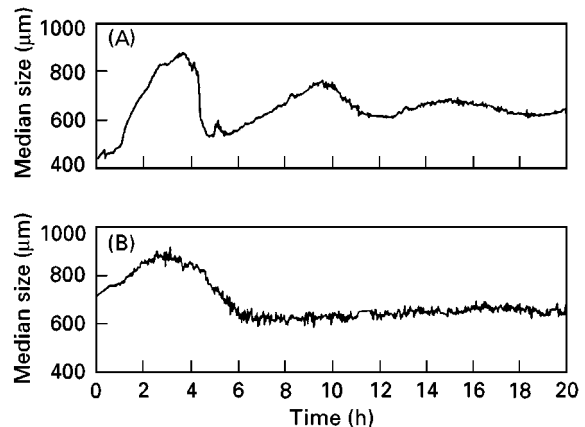


Figure 5 (A) Open and (B) closed loop start up trend of the median crystal size. (Eek, 1995)

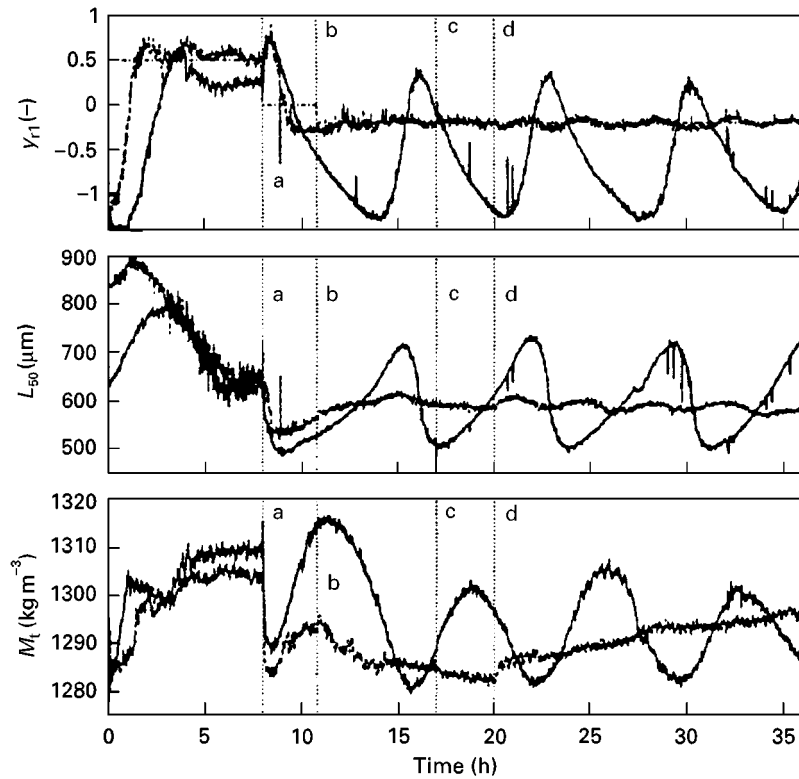


Figure 6 Open and closed loop trends in the y_1 , the x_{50} and the total crystal mass after the onset of a product classifier at a. Points b, c and d represent changes in controller set point and product flow rate respectively. (Eek, 1995.)

Multivariable Control

Only a limited number of multivariable control studies is available and only one of them has been tested experimentally. A state space model must be the basis

for a multivariable control design:

$$\begin{aligned}\dot{x} &= A(t)x(t) + B(t)u(t) \\ y &= C(t)x(t) + D(t)u(t)\end{aligned}\quad [18]$$

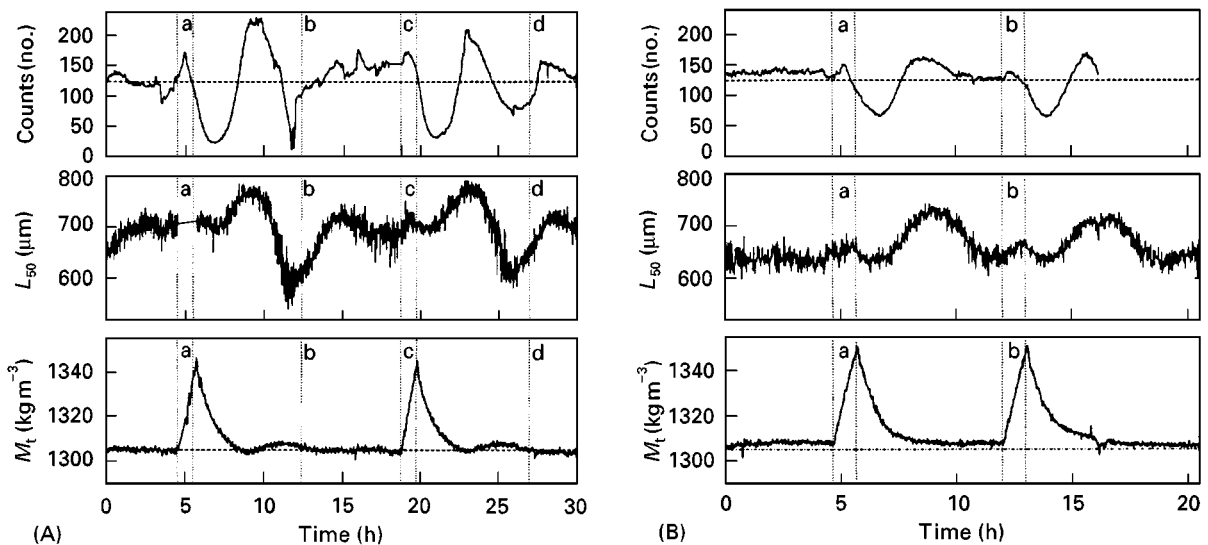


Figure 7 Measured (A) open and (B) closed loop responses of the counter signal, the median crystal size and the product magna density due to a disturbance in the product flow at a and c for the open loop experiment and at a and b for the closed loop experiment (Eek, 1995).

x is the vector of state variables. The crystallizer model must therefore be transformed into a state space representation. This can be achieved by the moment transformation, which is however only valid for a mixed suspension mixed product removal (MSMPR) type of crystallizer with simple crystallization kinetics. Application of the method of lines also yields a state space representation of the model.

An important topic in the design of a multivariable controller is the choice of the input–output pairs. On the basis of a relative gain array analysis with experiments done on a 1 m³ KCl crystallizer, a control structure with the fines, the product and the feed flow rate as process inputs, and the mean crystal size, the weight percentage of solids and the supersaturation as process outputs has been proposed.

On the basis of a controllability analysis the median crystal size has been rejected as an output variable because of the long delays. The control structure shown in Figure 8 was proposed as an alternative. This control structure was experimentally analysed on the 1000 L evaporative DTB crystallizer using a model predictive controller in combination with a state estimator. The controller was based on a linearized first principle model using the method of lines to transform the model into a state space representation. The controller showed good performance with respect to stabilization, disturbance rejection and set-point tracking, which was slightly better than that of a multiloop PI controller. This improvement is related to the interaction, which is taken into account in a multivariable model predictive control (MPC) controller, and the better constraint handling of this controller.

Control of Batch Crystallizers

Batch crystallizers are used extensively for crystallization procedures that are of small capacity and have a high added value, and often when multipurpose reactors are used for the crystallization process. Therefore the control of a batch process differs considerably from that of a continuous process. In addition, although a batch crystallizer can be described by a similar model to the continuously operated crystallizer, because of the inherently nonstationary process conditions and the strong dominant role of the start-

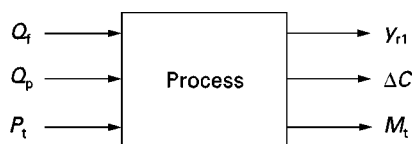


Figure 8 Input–output structure for a multivariable controller (Eek, 1995).

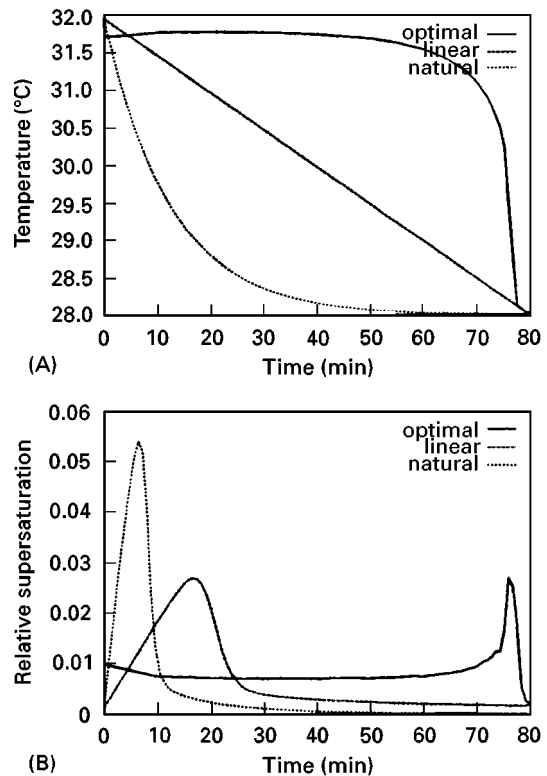


Figure 9 (A) Temperature profiles for a batch cooling KNO₃–H₂O crystallizer and (B) the resulting supersaturation in the crystallizer for different cooling policies (Miller and Rawlings, 1994).

up phase on the product quality process conditions, a completely different control strategy must be followed.

Literature references to the control of batch crystallization processes are mainly directed towards finding cooling or supersaturation profiles (a supersaturation versus time trajectory) that optimizes the product quality of the crystals profile.

Cooling profiles have been determined directly from MSMPR crystallization models with some additional simplifications. Other studies use simulation to calculate a cooling profile that maintains a constant supersaturation or an optimal control theory in combination with an objective function for the final product. The problem with these studies is that they all are limited to strict crystallizer configuration (MSMPR, no fines removal), and simple kinetic models. In addition they are unable to incorporate constraints in the process variables.

An alternative approach is to solve the general multivariable optimal control problem as a nonlinear programming problem.

Using this approach an optimal cooling programme can be calculated. An example is shown in Figure 9, in which a natural, a linear and an optimal

cooling profile are given together with the resulting supersaturation profile for a $\text{KNO}_3\text{-H}_2\text{O}$ system crystallized in a 3 L cooling crystallizer. The curves were determined using a first principle model in which four parameters were estimated using experimental data, maximizing the terminal seed size. Constraints were imposed on the crystallizer temperature and on the production yield. Experimental verification of the optimal cooling profile gave a 9% increase in the terminal seed size over that with linear cooling, and an 18% increase over that with natural cooling.

The determination of optimal cooling profiles is, however, not sufficient for an optimal operation of a batch crystallizer. Uncertainties in the start-up phase and in the crystallization model make the need for on-line measurements and a feedback control relevant. Depending on the reproducibility of the start-up phase, on line optimization procedures might be desirable for optimization of the process.

Conclusions

The control of both continuous and batch crystallizers has been shown to be feasible and can result in a considerable improvement of the process performance. Impressive results have been obtained even with a simple feedback controller, especially in the suppression of the process disturbances and in the stabilization of the process. This makes the application of this CSD control likely in industry in the near future. This progress is based on an extensive analysis of the crystallization process (including the derivation of a reliable process model), the available measurement techniques and the process actuators. On the other hand, because of limitations in the process actuators and the internal feedback loops in the crystallization process, variations in the product specifications (such as the median crystal size) were very limited, especially in continuous crystallization. The situation can only be improved by better crystallizer designs.

It has been shown that there are process models available, that can give a reasonable description of process behaviour. These models are however very empirical in nature and are in principle input-output models. They lack a fundamental description of the underlying (local) phenomena, which is needed to predict the influence of scale, geometry and the physical/chemical properties of the crystallization system. Only then we will be able to design crystallizers and control systems without the need for an extensive research programme.

A better understanding and description of the local crystallization phenomena may also be the key for the

improvement of the multivariable controllers by a better description of the interactions. Results have shown that there is no incentive for a multivariable controller, because the simple feedback controller gives comparable results with much less effort.

Symbols Used

b, g, h, j	Kinetic parameters
B_0	Birth rate ($\text{no. m}^{-3} \text{s}^{-1}$)
$B(L)$	Birth rate (size based) ($\text{no. m}^{-3} \text{m}^{-1} \text{s}^{-1}$)
C	Concentration (kg m^{-3})
C_p	Specific heat ($\text{J kg}^{-1} \text{K}^{-1}$)
C_s	saturation concentration (kg m^{-3})
$D(L, t)$	Death rate ($\text{no. m}^{-3} \text{m}^{-1} \text{s}^{-1}$)
G_L or G	Linear growth rate (m s^{-1})
H	Enthalpy
H_{cr}	crystallization enthalpy (J kg^{-1})
$h(L)$	Classification function (-)
K_N	Nucleation rate constant (-)
k_{distr}	Distribution constant impurity uptake (-)
k_g	Growth rate constant (m s^{-1})
L	Particle length [m]
m_j	j th moment of a distribution (-)
M_T	Total crystal mass per unit crystallizer volume (kg m^{-3})
N_{comp}	No of components (-)
$n(L)$	Number density ($\text{no. m}^{-3} \text{m}^{-1}$)
P	Production rate (kg s^{-1})
$p_1 \dots p_9$	kinetic parameters
t	time (s)
u	process input
V	Crystallizer volume (m^3)
y	process output
y_r	control signal derived from measured light diffraction pattern of the product crystals
w	Mass fraction (-)
ϕ_v	Volumetric flow rates ($\text{m}^3 \text{s}^{-1}$)
ε	Fraction free liquor (-)
ρ	Material density (kg m^{-3})
σ	Relative supersaturation (-)
τ	Residence time (s)

Further Reading

- Beckman JR and Randolph AD (1977) Crystal size distribution dynamics in a classified crystalliser: part II, simulated control of crystal size distribution. *American Institute of Chemical Engineers Journal* 23: 510-520.
- Eek RA, Pouw HAA and Bosgra OH (1995) Design and experimental evaluation of stabilising feedback controllers for continuous crystallisers. *Powder Technology* 82(1): 21-35.

- Eek RA, Dijkstra SJ and van Rosmalen GM (1995b) Dynamic modelling of suspension crystallizers, using experimental data. *American Institute of Chemical Engineers Journal* 41(3): 571–584.
- Kramer HJM, Bermingham SK and van Rosmalen GM (1999) Design of industrial crystallisers for a required product quality. *Journal of Crystal Growth* 198/199: 729–737.
- Miller SM and Rawlings JB (1994) Model identification and control strategies for catch cooling crystallisers. *American Institute of Chemical Engineers Journal* 40: 1312–1327.
- Ó Meadhra RS, Kramer HJM and van Rosmalen GM (1995) A model for secondary nucleation in a suspension crystallizer. *American Institute of Chemical Engineers Journal* 42(4): 973–982.
- Randolph AD and Larson MA (1988) *Theory of Particulate Processes*, 2nd edn. New York, Academic Press.
- Randolph AD, Chen L and Tavana A (1987) A feedback control of CSD in a KCl crystallisation with fines dissolver. *American Institute of Chemical Engineers Journal* 33: 582–591.
- Randolph AD, Beckman JR and Kralievich ZI (1977) Crystal size distribution dynamics in a classified crystalliser: part 1, experimental and theoretical study of cycling in a potassium chloride crystallisation. *American Institute of Chemical Engineers Journal* 23: 500–510.
- Rawlings JB, Miller SM and Witkowski WR (1993) Model identification and control of solution crystallisation processes. *Industrial and Engineering Chemistry Research* 32: 1275–1296.
- Rawlings JB, Sink CW and Miller SM (1995) Control of crystallisation processes. In: Meyerson A (ed.) *Handbook of Industrial Crystallisation*, pp. 103–130. Boston: Butterworth Heinemann.
- Redman T, Rohani S and Strathdee G (1997) Control of the crystal mean size in a pilot plant potash crystalliser. *Transactions of the Institute of Chemical Engineers* 75A: 183–192.
- Rohani S (1995) Control of crystallisers. In: Mersmann A (ed.), *Crystallisation Technology Handbook*. New York: Marcel Dekker, Inc.

Dynamic Behaviour

See II/CRYSTALLIZATION/Control of Crystallizers and Dynamic Behaviour

Geocrystallization

J. A. Gamble, School of Earth Sciences,
Victoria University of Wellington, New Zealand

Copyright © 2000 Academic Press

Magmas are hot (eruption temperatures range between 600°C and 1400°C), multicomponent, but generally silicate-dominated melt systems formed by processes of partial melting in the interior of the earth. Silicon and oxygen are the major constituents of most magmatic systems, apart from those of the carbonatite association, where NaCO₃ and CaCO₃ are significant components. This article considers crystallization in silicate-dominated melt systems. In addition to Si and O, Ti, Al, Fe³⁺, Fe²⁺, Mn, Mg, Ca, Na, K and P comprise the constituents commonly referred to as the ‘major elements’. It has become conventional to refer to these in terms of their oxides, expressed in weight percent (Table 1). Furthermore, magmas typically contain dissolved volatile species, dominated by H₂O, but including SO₂, H₂S, Cl₂, F₂, CO₂, CO and traces of noble gases such as He, Ar and

Xe. Elements such as Rb, Sr, Ba, Zr, Nb, the rare earth elements, Pb, Th and U are present in trace amounts (typically µg g⁻¹ or ppm) and are called ‘trace elements’.

After magmas form, they may move away and separate from their source regions, due principally to

Table 1 Major oxide chemical analyses (wt%) of typical volcanic igneous rocks. All data are from the author's database of chemical analyses

Element oxide	Basalt	Andesite	Dacite	Rhyolite
SiO ₂	49.86	60.35	66.68	73.89
TiO ₂	1.38	0.78	0.58	0.33
Al ₂ O ₃	15.96	17.53	16.5	13.69
Fe ₂ O ₃	5.47	3.37	2.42	1.47
FeO	6.47	3.17	1.93	0.89
MnO	0.32	0.18	0.06	0.08
MgO	6.27	2.79	1.43	0.39
CaO	9.1	5.87	3.51	1.22
Na ₂ O	3.16	3.63	4.03	3.43
K ₂ O	1.55	2.07	2.71	4.53
P ₂ O ₅	0.46	0.26	0.15	0.08

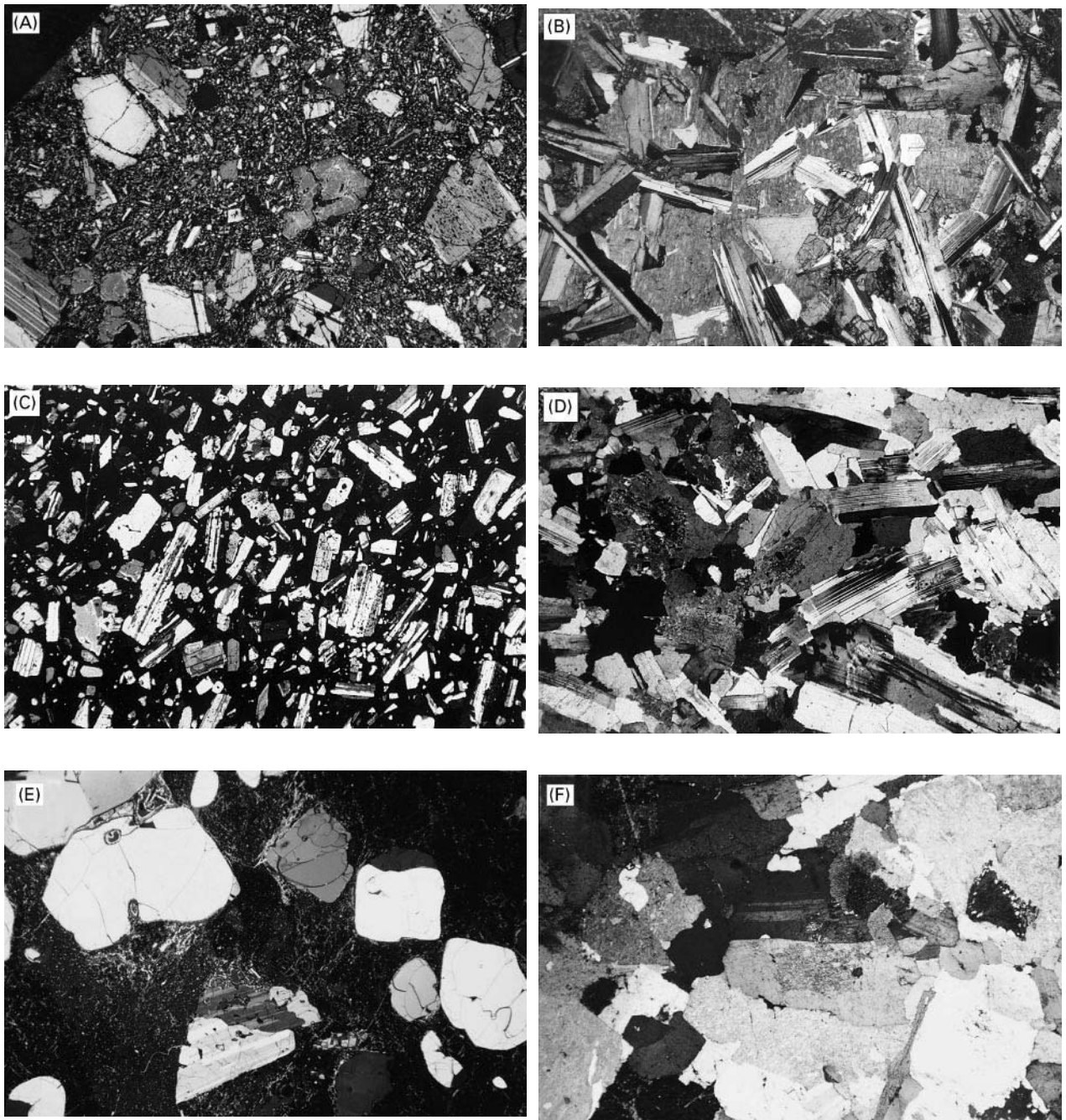


Figure 1 (See Colour Plate 33). Crossed polarizer photomicrographs of (a) a glassy basalt, (b) a gabbro, (c) an andesite, (d) a diorite, (e) a rhyolite and (f) a granite. Each of these photographs was taken at the same magnification (horizontal field is 10 mm across). The bulk composition of the magma forming the basalt and gabbro are broadly similar, as is the bulk composition for the andesite and diorite and the rhyolite and granite. The minerals crystallizing from the basalt and gabbro are similar, as are those in the andesite and diorite and the rhyolite and granite. The clearly observable differences in texture result from differences in crystal growth and nucleation rates. (a) Basalt showing large crystals (phenocrysts) of plagioclase feldspar (grey), Ca-rich pyroxene (purple, at centre) and olivine (yellow, top left) in a finer grained groundmass of these minerals. (b) Gabbro showing crystals of Ca-rich pyroxene (red-orange) enclosing plagioclase (grey-white with multiple twinning) and olivine (blue, green and red grains right of centre). (c) Andesite showing phenocrysts of plagioclase (grey-white with multiple twinning) and pyroxene (yellow, orange-red) set in a fine grained glassy groundmass. (d) Diorite showing a rock comprised of plagioclase feldspar (grey-white multiply twinned crystals), pyroxene, amphibole (green) and interstitial quartz (yellow-grey). Note how the amphibole crystals form a jacket or coating on the pyroxene (centre). (e) Rhyolite showing perlitic cracking in glassy groundmass and phenocrysts of quartz and plagioclase (twinned). Note the corroded and resorbed grain boundaries of the phenocrysts. (f) Granite showing interlocking crystals of plagioclase (twinned), alkali feldspar (turbid, dusty appearance), quartz (clear) and biotite (speckly orange).

the fact that they are less dense and less viscous than their surroundings. Ultimately, they may be emplaced at shallower levels in the Earth, forming igneous intrusions such as batholiths, plutons and sills or erupted at the surface as lava flows or pyroclastic rocks.

Because they are multicomponent melt systems, on cooling, magmas will crystallize a variety of silicate minerals, whose composition is controlled by the bulk composition of the magma and whose grain size is determined by the rates of cooling and crystal nucleation (Figure 1). Thus basaltic magmas will

crystallize Ca-rich pyroxene, Ca-rich plagioclase, Fe-Ti oxides and perhaps olivine, whereas granitic magma will crystallize Na-rich plagioclase, K-rich alkali feldspar, quartz and mica. The ultimate example of undercooling is a natural glass, called obsidian in the case of rhyolite and tachylite in the case of basalt. In nature, volcanic rocks are frequently a mixture of crystals (which grew at depth in the earth) and glass (which quenched on eruption). Intrusive rocks are more likely to be crystalline, with the interlocking minerals displaying a variety of textures

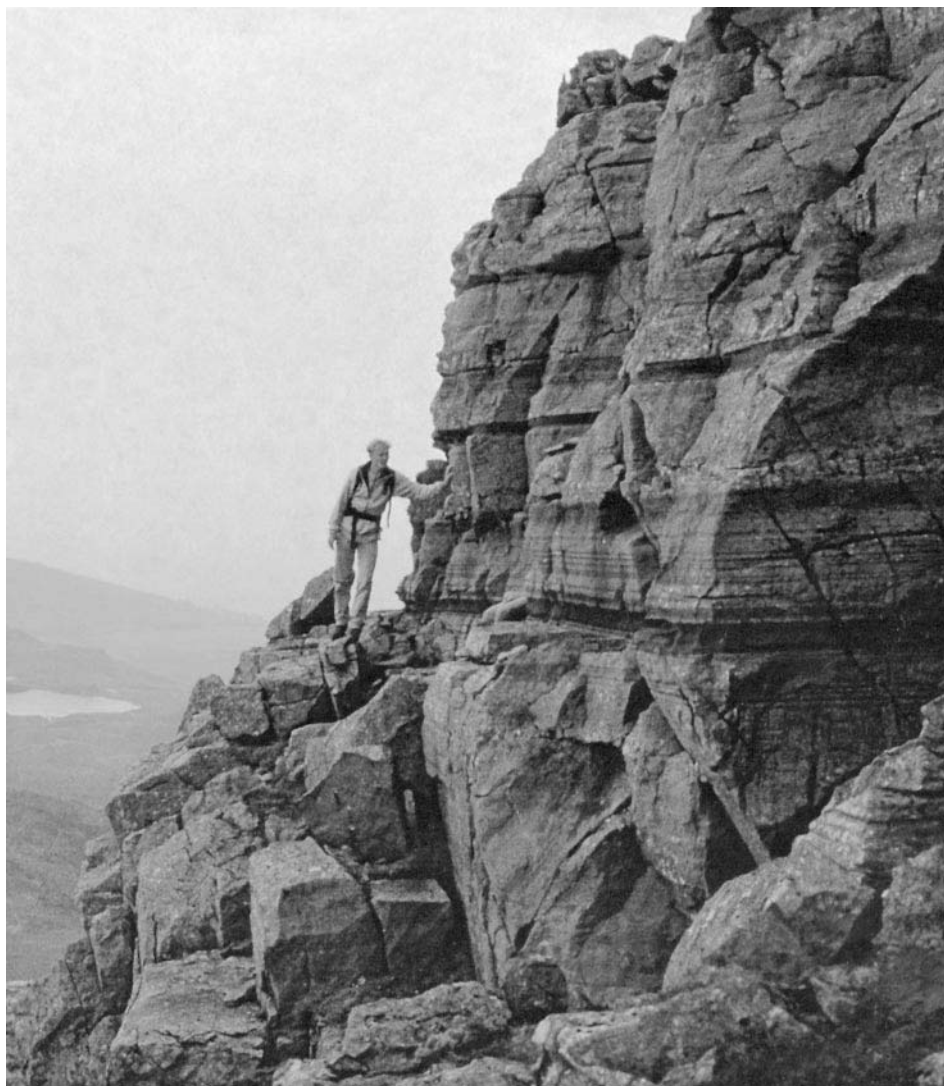


Figure 2 (See Colour Plate 35). Mineral layering in the Rum Igneous Intrusion, NW Scotland. This photograph shows spectacular centimeter-scale mineral layering in Unit 14 of the Eastern Layered Series of the Rum Layered Igneous Intrusion. The Rum Intrusion forms one of a number of layered intrusions, including Skaergaard in East Greenland and The Cullins, on Skye, NW Scotland, which are part of the North Atlantic Tertiary Igneous Province. Now exhumed by the combined effects of erosion and uplift, these intrusions mark the site of crystallizing magma chambers ~ 60 million years ago, during the early rifting stages of the North Atlantic Ocean. The near horizontal layers were formed by sequential precipitation of crystals of different composition (principally plagioclase, pyroxene, olivine and spinel) on the floor of a magma chamber. The darker layers are rich in the minerals olivine and pyroxene, the lighter layers richer in plagioclase. Mimicking sedimentary rocks where the principal hydraulic agent of sorting is a water column, in layered intrusions magma was the hydraulic agent and dense minerals, like spinel and olivine, settled more rapidly than plagioclase, leading to units which are graded from spinel and olivine-rich bases to plagioclase-rich tops.

reflecting the crystallization history of the magma (Figure 1). The minerals crystallizing from the basalt magma are higher temperature solid solutions than those of the granite magmas, deriving from their bulk composition and the higher temperatures of basaltic magmas.

The pioneering high-temperature experimental studies on the effects of magmatic crystallization was undertaken by N.L. Bowen and coworkers during the first half of twentieth century and laid the foundations for understanding how magmas evolve by crystallization. Bowen's textbook, *The Evolution of the Igneous Rocks*, first published in 1928, remains the definitive exposition on the application of phase equilibria to the study of magmatic crystallization. In this book, Bowen championed the role of fractional crystallization as the process most responsible for producing diversity in magmatic rocks. This work received a considerable boost by the discovery of the Skaergaard Intrusion in East Greenland by L.R. Wager in 1931 and subsequent mapping of the intru-

sion by Wager and W.A. Deer. Here, graphic demonstration of the effects of crystal settling layering and the results of fractional crystallization were to spawn an array of terminology and another benchmark text, *Layered Igneous Rocks*. Layered igneous intrusions (Figure 2) are now known to be important examples of subvolcanic magmatic systems where the processes of magmatic differentiation have been preserved.

Phase diagrams remain the most elegant way of appreciating how magmatic crystallization proceeds. Figure 3 is the phase system diopside ($\text{MgCaSi}_2\text{O}_6$)–anorthite ($\text{CaAl}_2\text{Si}_2\text{O}_8$)–albite ($\text{NaAlSi}_3\text{O}_8$) at 1 atm. This system makes a simple proxy for a basaltic magma because it consists of the two major minerals in basalt, plagioclase feldspar (anorthite–albite solid solution) and Ca-rich pyroxene (diopside). The diagram is divided into two primary stability fields by the curved, arrowed line from 1275°C at e to $\sim 1100^\circ\text{C}$ at e' . The upper field is that of diopside, the lower field that of plagioclase (solid solution). The curved line delineates a cotectic of falling temperature

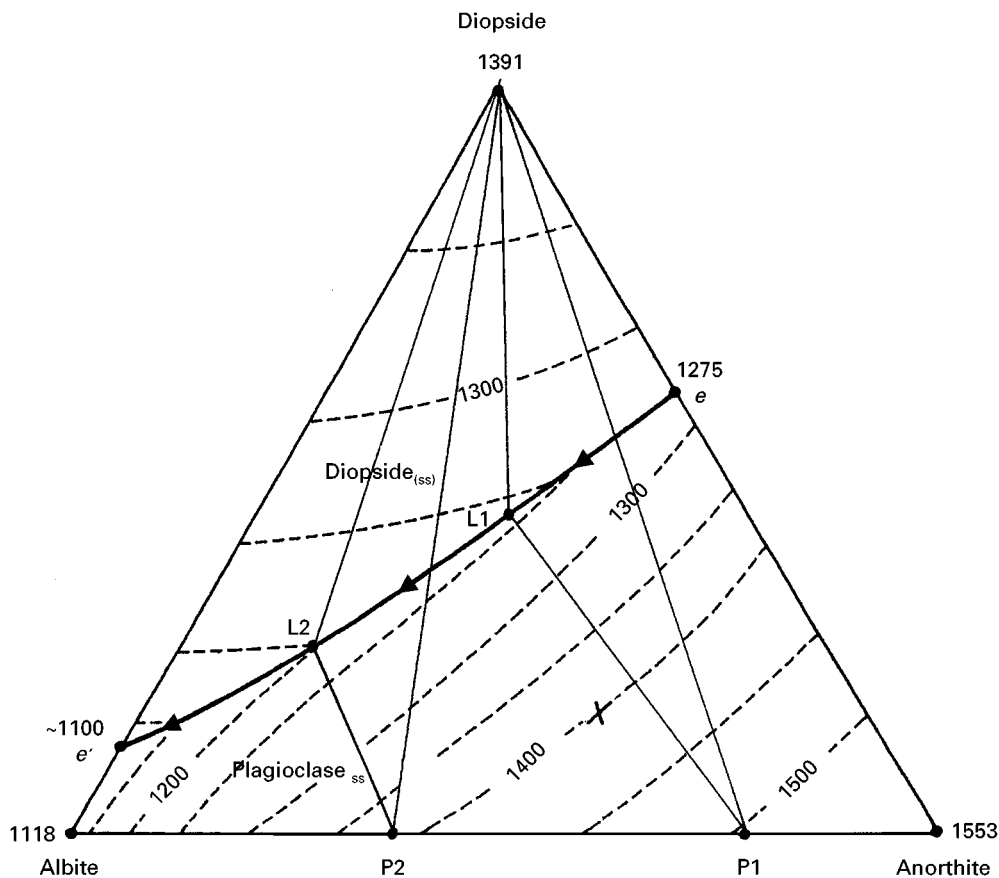


Figure 3 The phase system diopside–anorthite–albite at 1 atm. This system is a particularly useful analogue for the basaltic magma system as it comprises the two major minerals which crystallize from basalt magma, Ca-rich pyroxene (diopside, $\text{MgCaSi}_2\text{O}_6$) and plagioclase feldspar (solid solution, ss, between anorthite ($\text{CaAl}_2\text{Si}_2\text{O}_8$) and albite ($\text{NaAlSi}_3\text{O}_8$)). In this system cooling melts will evolve along the diopside–plagioclase cotectic from right (high temperature) to left (low temperature). Note that in a cooling, crystallizing magmatic system, a liquid (L1) will be in equilibrium with crystals of diopside and plagioclase of composition P1. With cooling, L1 will migrate to L2 and here L2 will be in equilibrium with crystals of diopside and lower temperature plagioclase, P2.

(in direction of arrows) and along which changing liquid compositions will be in equilibrium with diopside and progressively different (lower temperature) compositions of plagioclase. Liquids (L1 and L2) lying along the curve ($e-e'$) will be in equilibrium with diopside and two plagioclase compositions (P1 and P2) such that the lower temperature liquid L2 is in equilibrium with a lower temperature, more sodic, plagioclase (P2).

The process of magmatic fractional crystallization can also be demonstrated effectively through the use of geochemistry. For example, in Figure 4, two bivariate plots of SiO_2 and CaO versus MgO (all in weight percent) are shown for a hypothetical parent magma which is cooling and fractionating olivine [$(\text{Mg}_2\text{SiO}_4)_{90}(\text{Fe}_2\text{SiO}_4)_{10}$]. Note that removal and addition of olivine to the 'parent' magma results in changes to the compositions of the resultant melts. Addition of olivine produces MgO enrichment, removal (extraction) of olivine produces MgO -depleted melts. A further application of this approach is illustrated in Figure 5, which uses the total alkali ($\text{Na}_2\text{O} + \text{K}_2\text{O}$) versus SiO_2 diagram, often referred to

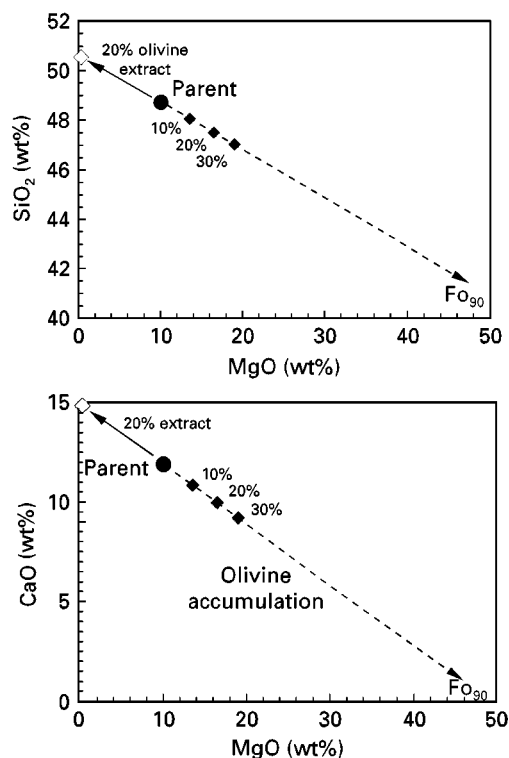


Figure 4 Chemical variation diagrams showing effects of olivine removal and addition to a hypothetical basalt parent magma. Olivine is a relatively simple orthorhombic silicate mineral and crystallizes as a solid solution of Mg_2SiO_4 (forsterite, Fo) and Fe_2SiO_4 (fayalite, Fa) end-members. In basaltic magmas, crystallizing olivine is typically Mg-rich, usually around Fo_{90} , consistent with the high temperatures of these magmas. Removal of Mg-rich olivine will rapidly deplete the residual liquid in MgO . Conversely, addition or accumulation of olivine in the melt will increase MgO .

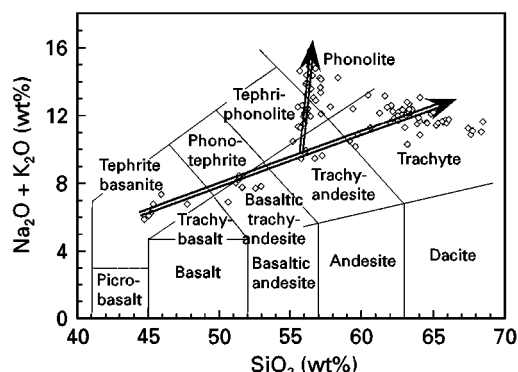


Figure 5 Total alkalis ($\text{Na}_2\text{O} + \text{K}_2\text{O}$, wt%) versus SiO_2 (wt%) for a suite of chemically analysed volcanic rocks (\diamond) which have evolved from a parent (tephrite basanite) composition by fractional crystallization. The bifurcation in the trend derives from a change in the mineral proportions in the fractionating mineral assemblage, around 55–56% SiO_2 , one leading to phonolite the other leading to trachyte.

as the TAS diagram, and the internationally recommended means for classifying volcanic igneous rocks. Data points for a suite of analysed volcanic rocks have been added to this diagram and depict a trend of increasing total alkalis with increasing SiO_2 . Between 55 and 56% SiO_2 the trend splits, with one set of data showing relative enrichment in alkalis. These trends are readily explained by changes in the bulk composition of the fractionating mineral assemblages.

The importance of the process of crystallization in the evolution of magmas and igneous rocks is clear. Through fractional crystallization, which is the natural consequence of a cooling, crystallizing multicomponent magmatic system, a wide spectrum of compositions of igneous rocks can be produced. This, together with the depth at which partial melting takes place, is the major process responsible for producing diversity amongst terrestrial igneous rocks.

See Colour Plates 33, 34, 35.

Further Reading

- Bowen NL (1928) *The Evolution of the Igneous Rocks*. New York: Princeton University Press.
- Cox KG, Bell JD and Pankhurst RJ (1979) *The Interpretation of Igneous Rocks*. London: George Allen and Unwin.
- Ehlers EG (1972) *The Interpretation of Geological Phase Diagrams*. San Francisco: WH Freeman.
- Le Maitre RW, Bateman P, Dudek A, Keller J *et al.* (eds) (1989) *A Classification of Igneous Rocks and Glossary of Terms: Recommendations of the International Union of Geological Sciences Subcommittee on the Systematics of Igneous Rocks*. Oxford: Blackwell Scientific Publications.
- McBirney AR (1993) *Igneous Petrology* (2nd edn). Boston and London: Jones and Bartlett Publishers.
- Wager LR and Brown MG (1968) *Layered Igneous Rocks*. Edinburgh: Oliver and Boyd.

Melt Crystallization

P. J. Jansens, Delft University of Technology,
The Netherlands

M. Matsuoka, Tokyo University of Agriculture and
Technology, Japan

Copyright © 2000 Academic Press

Introduction

Melt crystallization, sometimes referred to as ‘fractional crystallization,’ is a collective term for physical separation processes aimed at purification of organic compounds from a multi-component mixture by crystallization without addition of a solvent. The driving force for crystallization is created by cooling, evaporating or pressuring the melt.

The main advantage of this separation technique is the superior selectivity of the crystallization process caused by restricted mobility in the crystal lattice and strong molecular bonds. The energy consumption can be low because the heat of fusion of most organic compounds is two to four times smaller than their heat of evaporation and the operating conditions are generally mild. Finally, the absence of hazardous solvents is important from an environmental point of view. Disadvantages are the inherent slowness of crystal growth leading to voluminous equipment and the need for intensive slurry handling in certain process designs.

Balancing the merits and drawbacks, melt crystallization is usually applied for ultrapurification (> 99.99%), separation of isomers and purification of thermally unstable components. Some examples of industrial applications are acrylic acid, bisphenol A, caprolactam, cresol, dichlorobenzene, fatty acids, naphthalene, paraffin and xylene.

In this chapter, the designs of conventional and emerging melt crystallization processes are described and evaluated. Also the related field of freeze-concentration of aqueous solutions is briefly touched upon. Extensive coverage of all types of equipment on different scales is beyond the scope of this article. There is a focus on large-scale applications with a bias on state-of-the-art equipment provided by equipment manufacturers rather than the proprietary processes of end-users. More elaborate overviews of the principles and applications of melt crystallization are given in the Further Reading.

Theory

The technical feasibility and economic viability of separation and purification of an organic mixture by

melt crystallization entirely depend on its solid–liquid phase equilibrium (SLE). A survey of SLE data in 1986 demonstrated that more than 70% of organic substances have melting points between 0°C and 200°C, indicating that no special thermal media are needed to achieve separation (Figure 1).

The classification of about 1500 binary systems in the International Critical Tables (Figure 2) has revealed that more than 50% form simple eutectic mixtures and 25% form an intermolecular solid compound which forms simple eutectics with the two constituent components. This type also includes the formation of more than two solid compounds. The formation of a pure solid phase in one crystallization step is feasible for roughly 85% of the systems. The formation of solid-solutions is limited to only 10%, for which complete separation in a single crystallization step is fundamentally impossible.

Even for eutectic systems, however, the product from industrial crystallizers is not 100% pure. This is caused by the adherence of mother liquor to the crystal surface and by the inclusion/entrapment of mother liquor inside the crystals. Further purification is required and this can be achieved by washing and by sweating.

- Washing is done by contacting the crystals with a fresh solvent or, preferably, with pure melted product. This operation removes adhering impurities and is widely used in commercial plants.
- Sweating can be induced by exposing the impure solid phase to slightly elevated temperatures. This operation removes locally dispersed included impurities. Upon a temperature increase, the fraction of liquid inside the crystals increases according to the lever-rule whereby the more impure sections

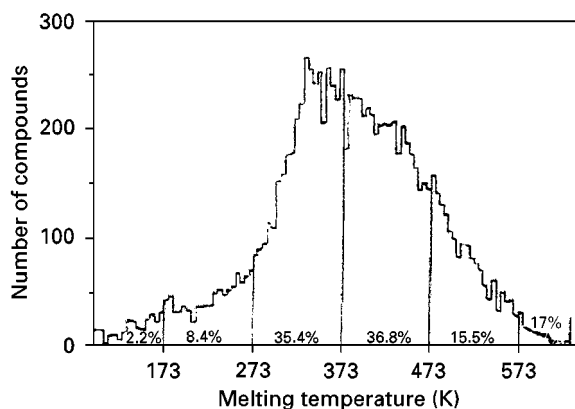


Figure 1 Distribution of atmospheric melting points of organic components (after Matsuoka and Fukushima, 1986).

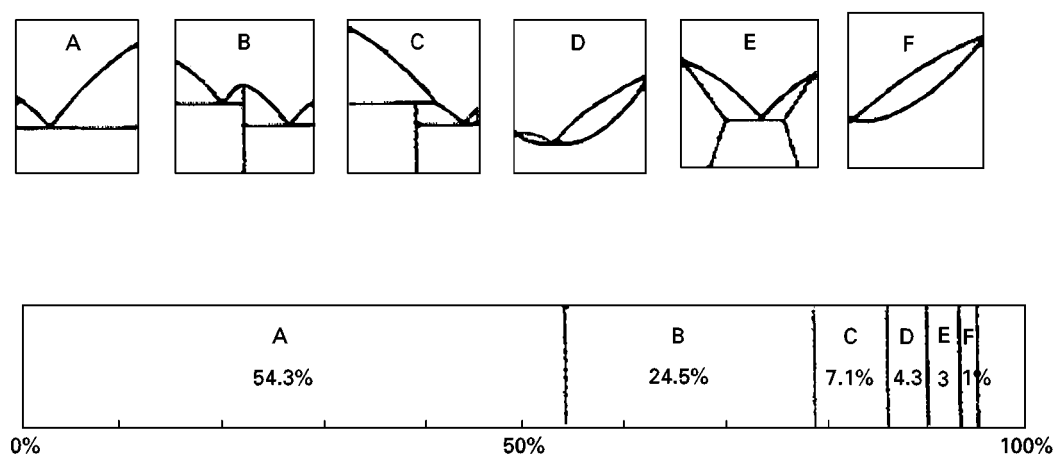


Figure 2 Distribution of binary phase diagrams of organic mixtures (after Matsuoka and Fukushima, 1986).

melt preferentially due to a lower melting point. The impure liquor comes out of the crystalline body through cracks and pores. Sweating can also be applied to solid solution systems and plays an important role as a purification mechanism in layer and suspension growth processes.

Process and Equipment Design

Indirect cooling is the most widely applied technique to produce crystals from a melt. In this context the term 'indirect' refers to the mechanism of heat transfer from the melt to the cooling medium, which takes place via the wall of a heat exchanger. Crystal growth may either take place as a layer on a cooled surface or freely suspended in the mother liquor. The principles of both techniques and their large-scale applications are discussed below. See Table 1 for an overview and an evaluation of both techniques.

Layer Growth

In this technique the crystals grow as a layer fixed and perpendicular to a cooled wall. The heat of crystallization is removed through the crystal layer and the wall. At low growth rates (typically $< 10^{-7} \text{ m s}^{-1}$) and proper mixing of the mother liquor, a stable crystal morphology can be maintained, which results in a good selectivity of the crystallization step. In industrial practice, however, very high growth rates (10^{-6} – 10^{-5} m s^{-1}) must be applied leading to roughening of the crystal surface (cellular and dendritic growth) and consequently to entrapment of impure liquor in the layer. High growth rates are required to achieve a reasonable productivity since the growth area is limited to the heat-exchange area ($\leq 100 \text{ m}^2 \text{ m}^{-3}$).

Industrial layer growth equipment is normally operated batch-wise, whereby static and dynamic processes can be distinguished. In *static equipment*, crystal growth occurs from a stagnant melt. Commercial equipment is manufactured by BEFS Technologies (France) and Sulzer Chemtech (Switzerland). Their similar designs feature a closed rectangular vessel equipped with a high heat-exchange area in the form of finned tubes or structured plates (Figure 3). One full operating cycle takes about one day and comprises five steps: (1) filling of the vessel, (2) crystallization by programmed cooling, (3) sweating by gradual heating, (4) draining of residual mother liquor and (5) melting and draining of the product layer. Equipment sizes range from 0.1 to 35 m^3 . Typical growth rates are in the order of 10^{-6} m s^{-1} but the overall separation efficiency of a full operating cycle is relatively good (up to 99.9 wt% product purity).

In *dynamic processes*, there is forced mixing of the mother liquor during the crystallization step. The mixing is usually achieved by circulating the liquor as a falling film or as a fully developed flow over vertical heat-exchanger tubes. Other designs whereby mixing was achieved by stirring, pulsation or bubbling-through an inert gas, were not successfully commercialized. Sulzer Chemtech provides the dynamic falling film system whereby both the melt as well as the coolant are circulated as falling films over the tube wall (Figure 4).

The turbulent flow regime of the mother liquor enhances heat and mass transfer, which enables higher growth rates of typically 10^{-6} – 10^{-5} m s^{-1} . Similar to the static process, one full operating cycle comprises five stages but is completed in 1.5 h. Tubes are about 0.1 m in diameter and 12-m long while up to 1250 tubes are fitted in one shell.

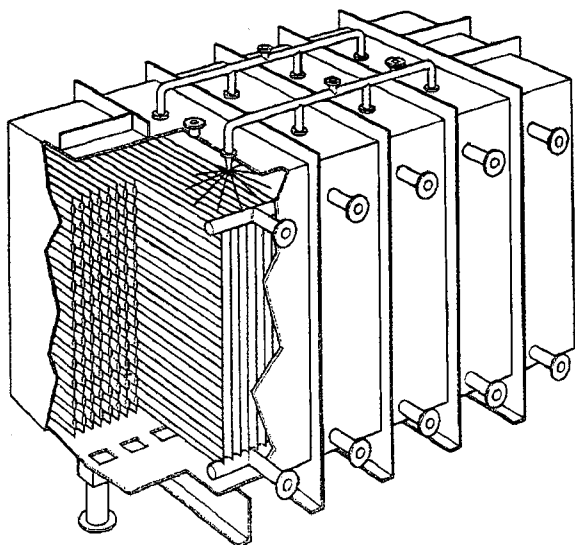
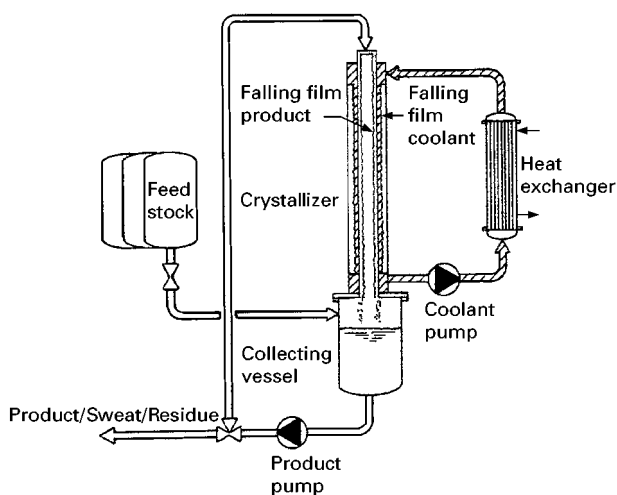
Table 1 Comparison of layer and suspension growth processes (values represent order of magnitude; operation/maintenance relative to distillation)

Parameter	Layer growth	Suspension growth
Crystal surface area	Up to $100 \text{ m}^2 \text{ m}^{-3}$	Up to $10\,000 \text{ m}^2 \text{ m}^{-3}$
Growth rate	10^{-6} – 10^{-5} m s^{-1}	10^{-8} – 10^{-7} m s^{-1}
Mixing intensity	Poor (static)/good (dynamic)	Good
Separation efficiency	Good (static)/moderate (dynamic)	Excellent
Product purity in one stage	$\leq 99.9\%$	$\geq 99.95\%$
Mode of operation	Repetitive batch	Once through, continuous
Heat transfer coefficient	$\sim 200 \text{ W m}^{-2} \text{ K}^{-1}$	$\sim 1250 \text{ W m}^{-2} \text{ K}^{-1}$
Energy efficiency	Good (static)/moderate (dynamic)	Good
Slurry handling	No	Yes
Solid-liquid separation	No	Yes
Design	Simple	Complex
Operational attention	Normal	Above average
Maintenance intensity	Normal	Above average
Scale-up	Multiplication of units	Engineering
Economy of scale	Not good	Good
World-scale plant capacity	$\sim 150 \text{ kT year}^{-1}$	$\sim 350 \text{ kT year}^{-1}$
Feed concentration	Preferably $> 90\%$	Preferably $< 99\%$
Viscosity	$< 10 \text{ cP}$	$< 50 \text{ cP}$
Purification of solid solutions	Suitable	Less suitable
Freeze concentration	Less suitable	Suitable

The overall separation efficiency of one dynamic operating cycle is moderate relative to a static process but the short cycle time makes the dynamic process well suited to sequential countercurrent staging. Staging requires intermediate storage tanks but makes it possible to produce ultrapure products at good recov-

ery. The stages are actually operating cycles which can be executed in the same crystallizer (Figure 5).

One of the drawbacks of the dynamic process until now has been its poor energy efficiency resulting from the need to repeatedly crystallize and melt a product to attain the desired purity. This problem was

**Figure 3** Static crystallizer. (Courtesy of Sulzer Chemtech.)**Figure 4** Dynamic falling film crystallizer. (Courtesy of Sulzer Chemtech.)

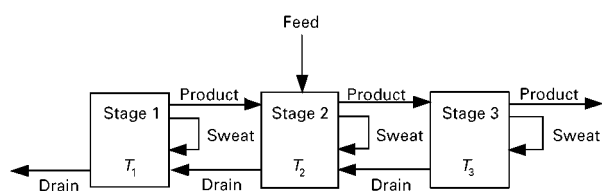


Figure 5 Multistage operation of layer growth processes (temperatures $T_1 < T_2 < T_3$).

addressed by the introduction of heat integration in 1996. The principle is based on a heat pump where a crystallizer alternatively acts as a condenser or as an evaporator for the cooling agent (Figure 6).

Continuous processes, whereby the layer growth occurs on a rotary drum or an endless belt, have been designed but are not applied commercially for purification of organics for various reasons (low selectivity, mechanical complexity, economy of scale).

Static and dynamic layer growth equipment are applied commercially to a wide range of products (e.g. acrylic acid, *p*-xylene, naphthalene, bisphenol A and paraffin). A relatively high feed purity is required, particularly for the dynamic processes, since this promotes the adhesion of the crystal layer to the cooled surface.

Suspension Growth

In this technique, the crystals form and grow freely suspended in the mother liquor. The heat of crystallization is absorbed by the supercooled liquor. High

specific productivity can be achieved at low growth rates because the crystal surface area is very large (up to $10\,000\text{ m}^2\text{ m}^{-3}$). Typical growth rates in industrial units are only 10^{-8} – 10^{-7} m s^{-1} which contributes to an excellent selectivity of the crystallization process.

Suspension growth processes generally comprise separate sections for crystallization and solid–liquid separation. The effectiveness of the final solid–liquid separation has a major impact on the overall separation efficiency. The design of the crystallization section should be focused therefore on producing crystals with a good filterability which means essentially growing large crystals with a narrow size distribution. The fundamentals of modelling particulate processes are also applicable to suspension growth from the melt.

Crystallization section Single-stage crystallization is often unfavourable because the nucleation and growth of all crystals occurs at the lowest operating temperature, which is determined by the yield, from an impurity-rich mother liquor. The simplicity of this design often does not outweigh the potential disadvantages:

- poor filterability of crystals due to high nucleation : growth ratio;
- reduced selectivity due to inclusion or incorporation of impurities;
- moderate energy efficiency;
- difficult solid–liquid separation.

Cascades of crystallizers, operated either cocurrent or countercurrent, are found in most processes. In *cocurrent cascades* crystals and mother liquor are transported in parallel from stage to stage at decreasing temperature. The GMF-CDC (Figure 7) is an example of a cocurrent cascade, where the crystal slurry flows freely from one compartment to the next via openings in the cooling elements. Along the flow direction, the impurities are concentrated in the mother liquor but the nucleation rate and the crystal growth rate decrease. As a result, the filterability of the crystals improves throughout the cascade while a good selectivity is maintained. The product crystals suspended in the impure mother liquor are withdrawn from the cold end of the cascade, which is a major drawback for solid–liquid separation.

In *countercurrent cascades* crystals and mother liquor are transported in opposite directions. TSK (Japan) and Niro-PT (Netherlands) provide similar countercurrent cascades, although the design of the individual stages differs considerably (Figure 8; see also Figure 17). The feed is usually supplied to the hot end of the cascade making sure that here too a large

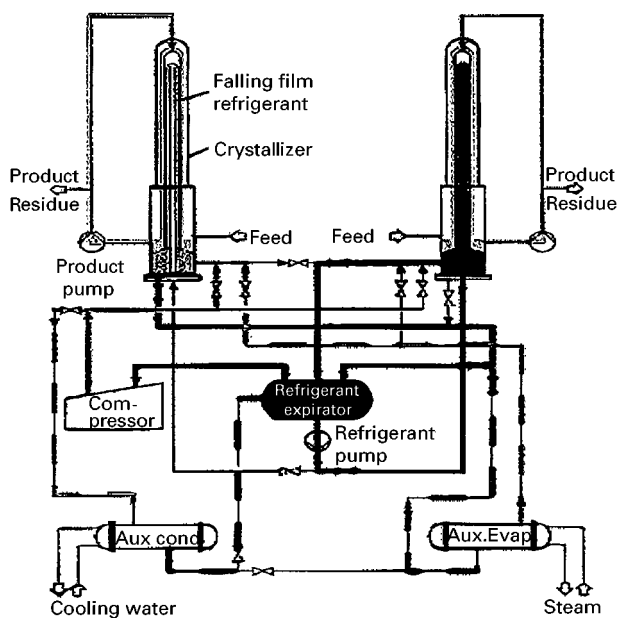


Figure 6 Heat integration of dynamic falling film crystallizers. (Courtesy of Sulzer Chemtech.)

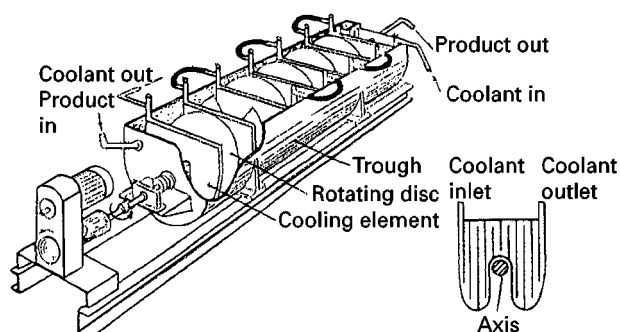


Figure 7 Cocurrent cascade of crystallizers. (Courtesy of GMF-Gouda.)

part of the crystal production occurs at high temperature from a relatively pure mother liquor. Purification of the crystals by Ostwald ripening (growth of large crystals by dissolution of fines driven by a reduction of surface energy) can play a role but it is doubtful whether there is a contribution from sweating. Product withdrawal occurs from the hot end, which simplifies solid-liquid separation.

A comparison of cocurrent and countercurrent crystallizers is shown in Table 2.

Solid-liquid separation section Product recovery is more and more executed in wash columns, which combine an effective solid-liquid separation with a pure melt wash and a single recrystallization step. The principle of wash columns is illustrated by Figure 9. A crystal slurry is pumped into the column, where the mother liquor escapes via a filter leaving behind the crystals as a packed bed. This bed is transported upwards by means of a rotating screw. At the top, the crystals are scraped off, suspended in wash liquid (recycled pure melt) and melted in an external melter. The wash-liquid circuit is kept pressurized, which causes the wash liquid to flow downward (reflux). The wash liquid does not leave the column but recrystallizes on the cold crystal bed, thereby producing the so-called 'wash front'. This front marks steep gradients in concentration, temperature and porosity.

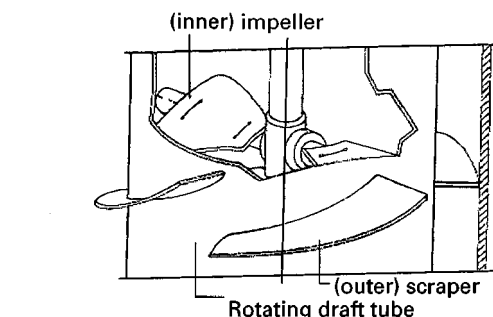
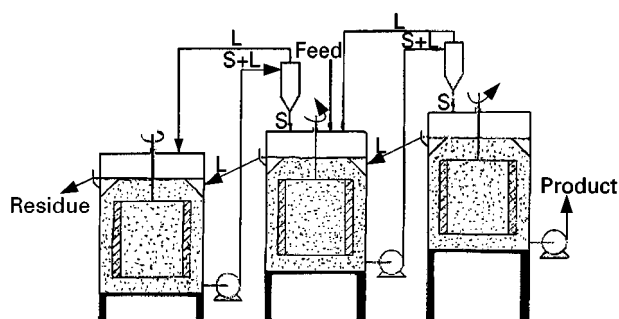


Figure 8 Countercurrent cascade of crystallizers. (Courtesy of Tsukishima Kikai Co. (TSK).)

The crystal bed can be transported under gravity, by hydraulic pressure or via a mechanical aid (screw/piston). The direction of transport is normally downwards for organic crystals and upwards for ice.

If the temperature of the feed slurry is low (single-stage or cocurrent cascade crystallization), more wash liquid will recrystallize causing a large drop in porosity over the wash front. At a given transport force exerted on the crystal bed, the throughput reduces with decreasing porosity due to an increased back-pressure from the wash liquid. Alternatively at constant throughput, the compressive stresses exerted on the crystals increase considerably which may result in deformation of some organic crystals, which are mechanically weak. Ideally, the temperature increase over a wash column should be 2–5°C.

Mass and heat transfer in the wash columns are governed by axial dispersion of the liquid phase while

Table 2 Comparison of crystallization sections consisting of a single-stage, a cocurrent cascade or a countercurrent cascade

Parameter	Single	Cocurrent	Countercurrent
Operating temperature	Constant low	Decreasing	Increasing
Product withdrawal	Cold	Cold end	Hot end
Product crystal filterability	Moderate	Good	Good
Product liquor	Impure	Impure	Relatively pure
Internal slurry handling	None	Limited	Intensive
Equipment and process design	Simple	More complex	Complex

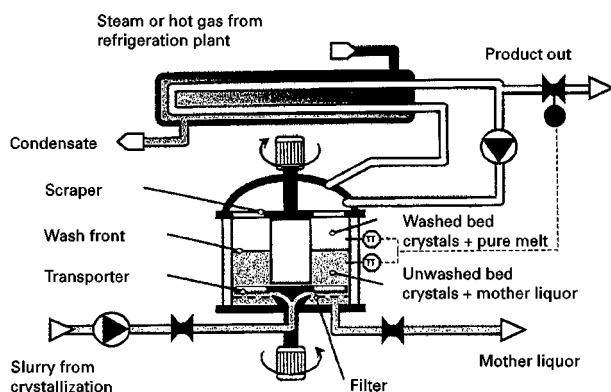


Figure 9 Principle of wash column. (Courtesy of Niro-PT.)

heat-transfer limitation in the solid phase may be neglected. In the more densely packed hydraulic and mechanical wash columns, purification occurs almost exclusively by displacement washing. In the loosely packed gravity wash columns, further purification by sweating occurs because of the longer residence time.

Gravity and mechanical wash columns have been commercialized by TSK and Niro-PT, respectively. TNO (Netherlands) has developed a hydraulic wash column equipped with separate filter tubes. See **Figure 10** and **Table 3** for a more detailed comparison.

Suspension growth equipment is applied commercially to purify various organic products (e.g. *p*-xylene, naphthalene and *p*-dichlorobenzene) but also for concentration of aqueous solutions (freeze concentration, see below). There are virtually no restrictions on feed purity, while a product purity $\geq 99.99\%$ is feasible.

Column crystallizers Column crystallizers are designs where a single-stage crystallizer and a gravity-wash column have been integrated in one shell (similar to distillation columns). The back-mixing column, for example, has been successfully commercialized by Nippon Steel Chemical Co. (Japan) for the purification of naphthalene. The pro-

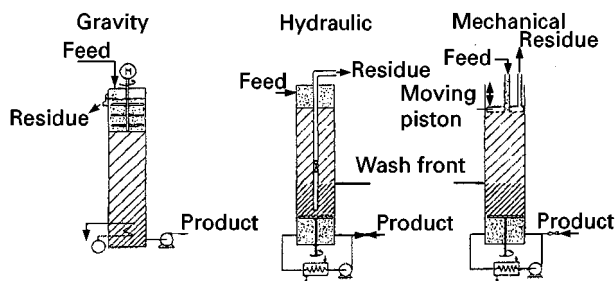


Figure 10 Classification of wash columns based on the crystal transport mechanism (after Jansens and Van Rosmalen, 1994).

duction rate is limited by the capacity of the wash columns ($\leq 1500 \text{ kg m}^{-2} \text{ h}^{-1}$). A new development by Matsuoka is the inclined column crystallizer. The inclination promotes settling and reduced axial dispersion (**Figure 11**).

Alternative Process Designs

Evaporative Melt Crystallization

Direct cooling is the driving force for evaporative crystallization. The heat of crystallization is withdrawn by evaporation of a portion of the mother liquor, which is induced by a reduction of the operating pressure. The vapour phase is condensed in an overhead condensor and refluxed to the crystallizer. Crystal formation and growth take place freely suspended in the bulk of the mother liquor. The main advantage of direct over indirect cooling is that the heat of crystallization is transferred to the cooling medium via a clean condensing duty rather than via a (scrapped) heat exchanger. Hence the heat transfer is more effective while the design and scale-up of equipment can be simplified.

In conventional evaporative crystallization processes, low boiling solvents (propane and carbon dioxide) are used to crystallize heavier organic components but the addition of solvents is not desirable for various reasons (equipment size, safety and the

Table 3 Comparison of wash columns

Parameter	Gravity	Hydraulic	Mechanical
Height : diameter ratio	4–6	1	1
Minimum crystal size	500 μm	150 μm	150 μm
Residence time: whole column	1 h	10–15 min	10–15 min
Residence time: wash section	30 min	3–5 min	3–5 min
Purification mechanism	Washing and sweating	Washing	Washing
Maximum temperature rise	10–15°C	5–10°C	5–10°C
Compressive stress	Negligible	Considerable	Considerable
Capacity	500–1500 $\text{kg m}^{-2} \text{ h}^{-1}$	5000–10 000 $\text{kg m}^{-2} \text{ h}^{-1}$	5000–10 000 $\text{kg m}^{-2} \text{ h}^{-1}$
Scale-up	Proven to 2 m	Under study	Proven to 1.2 m
Equipment design	Simple	More complex	Complex

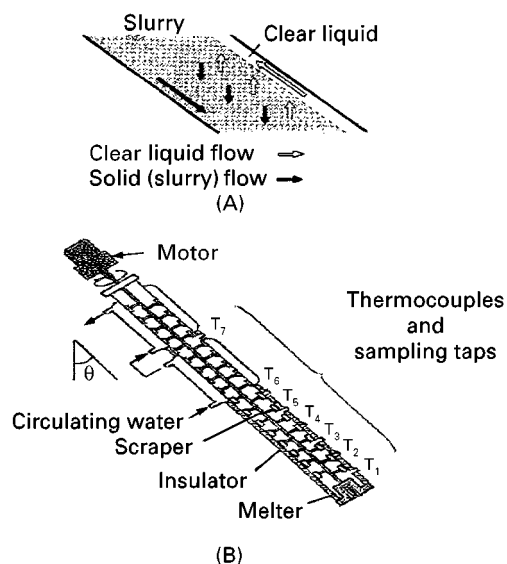


Figure 11 Inclined column crystallizer. (A) Schematic presentation of flows. (B) Experimental facility. (Reproduced with permission from Matsuoka M, Takiyama H and Soutome O (1997) Separation characteristics of an inclined column crystallizer. *Transactions of the Institution of Chemical Engineers* 75(A): 206–212.)

environment, product purity). The potential of applying direct cooling to melt crystallization, however, was not recognized until recently.

In 1993 TSK proposed a purification processes based on evaporative melt crystallization for caprolactam, acrylic acid and bisphenol A. Figure 12 illustrates the set-up of a continuous process featuring a single-crystallization stage and a wash column (purifier).

In recent years, a batch-wise evaporative melt-crystallization process with caprolactam–water as a model system has been developed and optimized. Figure 13

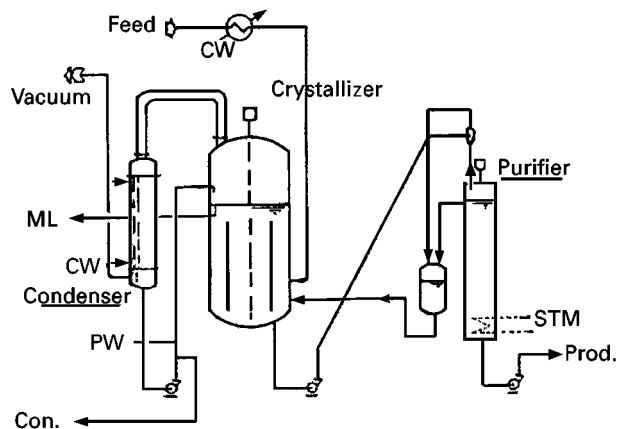


Figure 12 Continuous evaporative crystallization. ML, mother liquor; Con., condensate; Prod., product; STM, steam; CW, cooling water. (Courtesy of Tsukishima Kikai Co. (TSK).)

shows the pressure temperature–fraction temperature (PT–XT) phase diagrams where the three-phase equilibrium curve (S_{CLV}) stretches from the triple point of caprolactam (T_c) to the quadruple point of the binary system (T_q). Lowest operating cost can obviously be achieved near 5 wt% water, where the operating pressure is maximum and the temperature fairly high. Deep vacuum would be required for water concentrations below 1 wt% and above 20 wt%. Operating at a high temperature generates cost savings for the condenser (low area, no chilled cooling water).

Figure 14 shows the PT-trajectory for the batch-wise crystallization of caprolactam from a melt containing 4 wt% of water. Starting from point A, the pressure in the crystallizer is reduced until the vapour–liquid equilibrium is reached at point B and the melt starts to boil. Upon a further reduction of pressure, the evaporation of mainly water causes the melt to cool down but the composition of the melt does not change since the vapour is condensed and refluxed. At point C the solid–liquid–vapour equilibrium is reached and caprolactam starts to solidify. From C to D the crystal content steadily increases to 20 wt%, while the water concentration in mother liquor increases to 5 wt%.

Scale-up to 50–100 m³ crystallizers appears to be feasible, which is world scale for suspension crystallization equipment. Until now, there are few commercial installations with limited capacity. TSK has installed two units for caprolactam with a capacity of 2500 tons per year.

Pressure Crystallization

In this technique, crystallization is induced by compression rather than by cooling. The solid phase of most (organic) materials has a higher density than the liquid phase and consequently the melting point rises with increasing pressure. Benzene, for example, has an atmospheric melting point of 5.5°C but solidifies at room temperature when the pressure is about 2 MPa. Not only the melting points but also solid–liquid phase equilibria shift upward upon a pressure increase, which is illustrated for a mixture of cresols in Figure 15.

An additional advantage of pressure crystallization is found in the transmission of pressure being much faster than the transfer of heat in both liquid and solid phases. This means that a uniform pressure can be established quickly throughout the system. Therefore local variations in supercooling of the mother liquor can easily be avoided.

The separation of cresol isomers by conventional (atmospheric) cooling crystallization is rather difficult due to a high viscosity of the melt. Kobe Steel

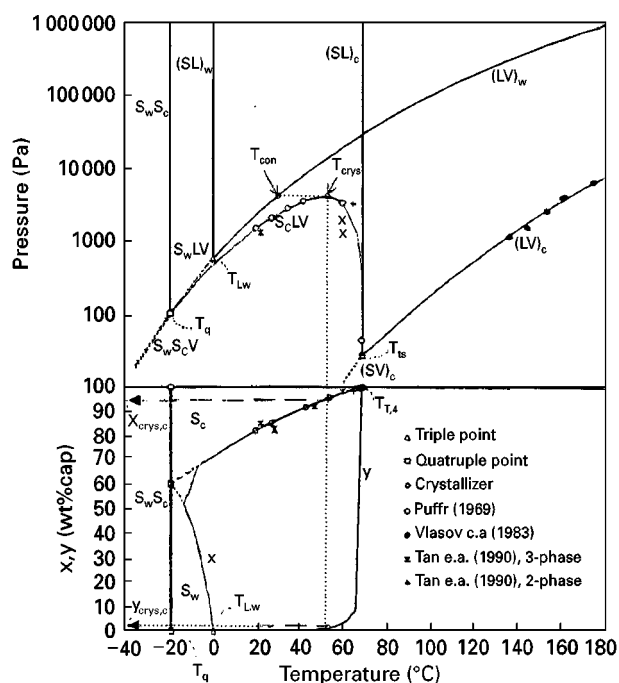


Figure 13 Pressure-temperature-composition diagram of ϵ -caprolactam-water. T_{ti} = triple point component i ; T_q = quatuple point; T_{cryst} = crystallizer temperature; T_{con} = condenser temperature; S_i , L_i , V_i = solid, liquid, vapour phase component i ; $(LV)_i$, $(SL)_i$, $(SV)_i$ liquid-vapour, solid-liquid, solid-vapour equilibrium curves pure component i ; x , y = liquid, vapour concentration (wt%) at three-phase equilibrium; SLV = three-phase equilibrium line with solid phase of component i . (Reproduced with permission from Diepen PJ (1998) *Cooling Crystallization of Organic Compounds*. PhD thesis, Technical University Delft.)

(Japan) developed in the 1970s a pressure-crystallization process, which was applied for the separation of p -cresol from its isomers on a commercial scale. A given amount of slurry from a chiller is fed to a cylindrical pressure vessel, compressed to crystallize and drained to remove residual impure melt (Figure 16). During the subsequent depressuring, purification by sweating can occur. Finally, a cylindrical block of purified crystals is taken out as the product. The operating temperature is 62.5°C at 200 MPa (versus 12.5°C at atmospheric pressure) which effectively reduces the viscosity of the mother liquor. Under these conditions, the selectivity and the rate of crystal growth rate are enhanced while solid-liquid separation is facilitated. Purification by sweating during depressuring is analogous to (thermal) sweating at elevated temperatures.

The features of pressure crystallization can be summarized as follows:

- batch-wise operation;
- product purity up to 99.5%, feasible in one operating cycle from 70 to 80% in feed;

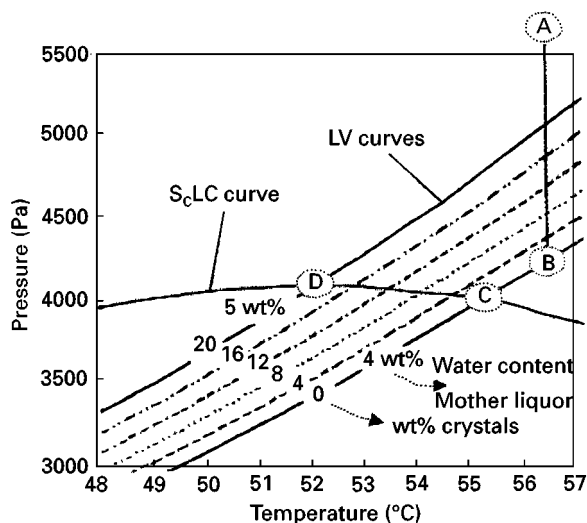


Figure 14 Part of pressure-temperature diagram of ϵ -caprolactam-water. (Reproduced with permission from: Diepen PJ (1998) *Cooling Crystallization of Organic Compounds*. PhD thesis, Technical University Delft.)

- high yield, limited only by the solid-liquid equilibrium of a given system;
- short cycle times, only a few minutes per cycle, due to rapid penetration of pressure;
- low energy consumption – only mechanical energy used for compression;

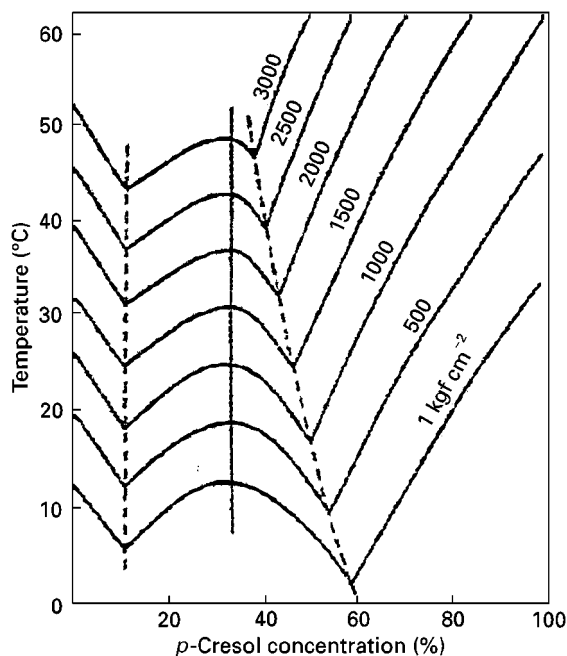


Figure 15 Phase diagram of mixture of p -cresol and m -cresol. (Reproduced with permission from Yasuda M, Sato Y and Suematsu H (1991) p -Cresol with high pressure crystallization. *Kagaku Kogaku* 55(4): 290-291.)

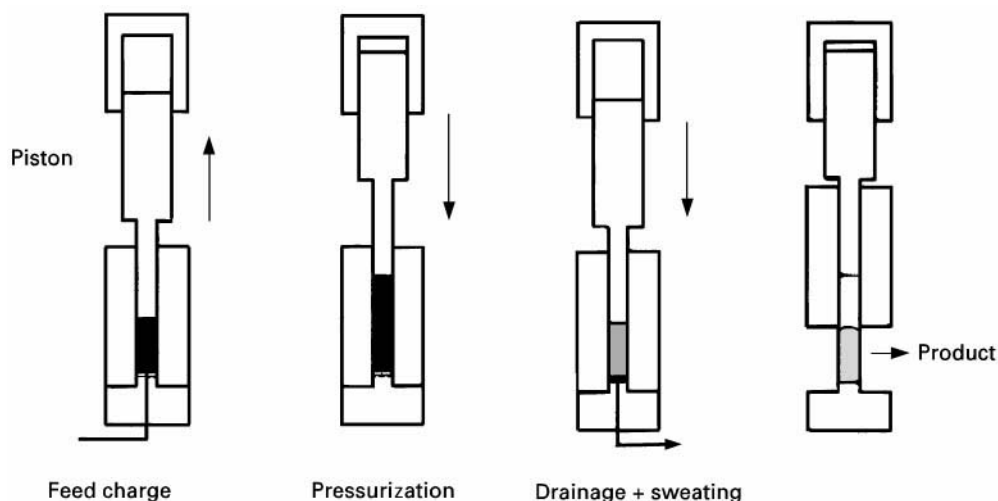


Figure 16 Operating cycle of pressure crystallization process. (Reproduced with permission from Yasuda M, Sato Y and Suematsu H (1991) *p*-Cresol with high pressure crystallization. *Kagaku Kogaku* 55(4): 290–291.)

- simple process design – crystallization, separation and sweating are carried out in a single vessel;
- complex mechanical design – materials selection and construction of mechanical parts are critical factors for success.

The scale-up of pressure-crystallization equipment is not easy due to mechanical complexity, and it becomes increasingly difficult at larger vessel diameters to remove residual melt from the centre of the cake by compression. The production capacity of a single plant is in the order of 500 tons per year.

Freeze Crystallization

Freeze concentration is a separation technology aimed at concentration of aqueous solutions by means of cooling crystallization. This technology is closely related to melt crystallization based on sus-

pension growth in terms of process synthesis and equipment design.

Commercial processes feature a countercurrent cascade of crystallizers while the final solid–liquid separation takes place in mechanical wash columns (**Figure 17**). Indirect cooling is usually preferred over direct cooling to prevent contamination of the concentrate and to contain the volatile components. Large spherical ice crystals can be grown relatively easily through Ostwald ripening. The individual stages of the cascade therefore feature separate sections for nucleation and growth. Crystallization (nucleation) takes place on the surface of the external scraped surface heat exchangers. Ripening (growth) occurs in large stirred vessels.

Nearly identical process flow schemes and equipment designs can also be found in some melt-crystallization processes, e.g. to separate *p*-xylene from its isomers.

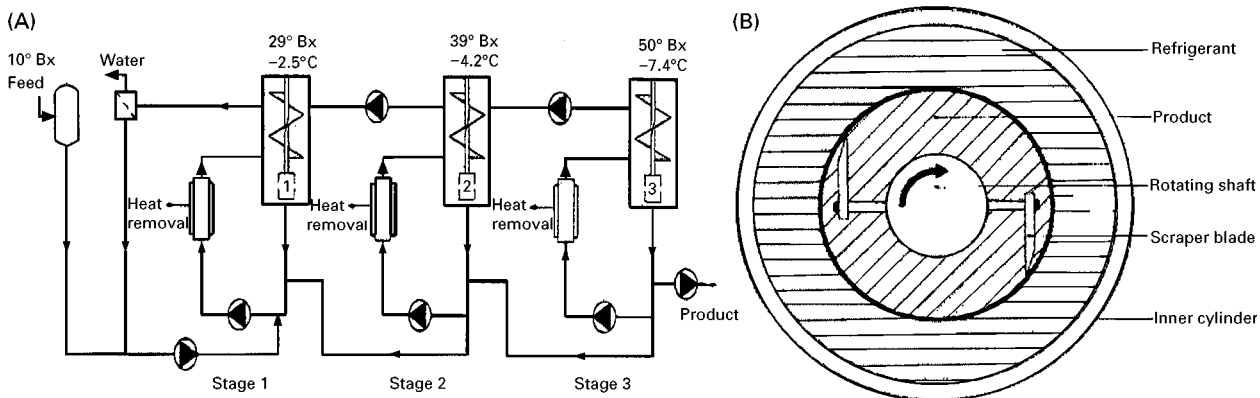


Figure 17 A three-stage countercurrent freeze concentration process. (Courtesy of Niro-PT.) (A) Simplified process flow scheme. (B) Cross-section of a scraped surface heat exchanger. °Bx is a measure for concentration of water phase (based on the breaking index).

Traditionally, most applications are found in the food industry for the concentration of fruit juice, wine, beer and coffee extract. In this field, the advantages of freeze concentration over competing technologies (membranes and evaporation) are the superb preservation of aromas and colour while decay reactions are slowed down by the low operating temperature.

Recently, world-scale installations have come on-stream where wastewater from chemical plants is concentrated. The produced melt water can be re-used as process water while the residual concentrate is incinerated. Here the advantages of freeze concentration are the low energy costs and the capability to concentrate beyond the eutectic point, where salts start to precipitate.

Drawbacks of freeze crystallization are the relatively high investment cost and the above-average maintenance intensity (there are many pieces of rotating equipment).

Conclusion and Future Outlook

Melt crystallization is the third most applied physical separation technology after distillation and extraction. Conventional processes are based on layer or suspension growth by indirect cooling.

- *Layer growth* may be considered as proven and mature technology, whereby the absence of slurry handling is a major advantage. Fully automated semi-continuous units can be delivered as turnkey projects. The need for repeated recrystallization steps to achieve a high product purity, however, increases both investment and operating cost. The desire to develop economically attractive continuously operated equipment seems to be in conflict with the basic characteristic of layer growth on a cooled surface.
- *Suspension growth* is also proven but not yet mature technology. The superior selectivity and high

specific productivity of crystal growth in a suspension create a huge potential, which can be further exploited by simplification of equipment design and minimization of slurry handling.

- *Evaporative melt crystallization* is a relatively young technology which combines the merits of suspension growth with a minimum of slurry handling. For certain applications, such as caprolactam, this technique is expected to take off in coming years.
- *Pressure crystallization* is an alternative technology, which is well suited to purify components with a very low melting point at ambient temperature but elevated pressure. Outside this niche use, pressure crystallization probably cannot compete with indirect/direct cooling crystallization due to high equipment cost.

See Colour Plate 36.

Further Reading

- Arkenbout GF (1995) *Melt Crystallization Technology*. Basel: Technomic Publishing AG.
- Jansens PJ and Van Rosmalen GM (1994) Fractional crystallisation. In: Hurle DJT (ed.) *Handbook of Crystal Growth*, Vol. 2A, ch. 6. Amsterdam: Elsevier Science.
- Matsuoka M and Fukushima H (1986) Determination of solid-liquid equilibrium. *Bunri Gijutsu (Separation Process Engineering)* 16: 4–10.
- Matsuoka M, Takiyama H and Soutome O (1997) Separation characteristics of an inclined column crystallizer. *Transactions of the Institution of Chemical Engineers* 75(A): 206–212.
- Moritoki M (1984) Crystallisation and sweating of *p*-cresol by application of high pressure. *Industrial Crystallization* 84: 369–380.
- Randolph AD and Larson MA (1988) *Theory of Particulate Processes*, 2nd edn. San Diego: Academic Press.
- Sloan GJ and McGhie AR (1988) *Techniques of Melt Crystallization*. New York: John Wiley.
- Yasuda M, Sato Y and Suematsu H (1991) *p*-Cresol with high pressure crystallization. *Kagaku Kogaku* 55(4): 290–291.
- Zief M and Wilcox WR (1967) *Fractional Solidification*. New York: Marcel Dekker.

Polymorphism

M. R. Caira, University of Cape Town, Rondebosch, South Africa

Copyright © 2000 Academic Press

Introduction

When the molecules of a chemical substance are able to crystallize in more than one three-dimensional

structure arrangement, the substance is said to display polymorphism. This phenomenon was discovered in the early nineteenth century but only since the middle of the twentieth century have its wider implications been appreciated by scientists investigating the crystallization, properties and interconversion of solid phases. These implications stem from the fact that different polymorphs of a given substance may

display very significant differences in physical properties such as melting point, colour, hardness, density, electrical conductivity, heat of fusion, solubility and dissolution rate, as well as differences in chemical reactivities. Polymorphism is a common phenomenon which has vital ramifications in the crystallization and processing of pharmaceuticals, in food chemistry, explosives manufacture and in crystal engineering. The profusion of polymorphic forms that might be encountered for a single compound (e.g. up to ten in some instances) has often been viewed as an unwelcome source of confusion, threatening to undermine reproducible isolation of a specific crystalline form. However, those engaged in the study of polymorphism see the benefits this diversity of forms may offer. At the same time, it is recognized that in order to control the polymorphic outcome of the crystallization process, systematic research aimed at a full understanding of the interplay of thermodynamic, kinetic and structural factors involved is paramount. This is a daunting task, however, since the phenomenon of polymorphism is acknowledged to be a complex one with many questions as yet unanswered. Further progress depends critically on a multidisciplinary approach.

Terminology/Nomenclature

Figure 1(A)–(C) are schematic illustrations of different polymorphs of a compound. In (A) and (B), the molecular conformation is retained but the crystal structures are different. The occurrence of a form such as (C), in which the molecule crystallizes with a significantly different conformation gives rise to the term ‘conformational polymorphism’. In addition to

the possibility of forming different (but chemically identical) polymorphs, the molecules of a given substance may upon crystallization from solution incorporate solvent molecules (stoichiometrically or non-stoichiometrically) in the resulting crystal structure. These solvated crystalline forms (examples shown schematically in Figure 1(D) and (E)) are often referred to as ‘pseudopolymorphs’ and are no less important in practice than polymorphs of the parent substance. Thus, for a single organic compound, it is frequently possible to crystallize from solution a series of polymorphs as well as a series of pseudopolymorphs (in the latter case species containing different solvent molecules, either individually or as mixtures). Furthermore, it is possible for a compound to yield pseudopolymorphs which are chemically identical, but structurally distinct (e.g. a monoclinic dihydrate and an orthorhombic dihydrate). Such species may be considered as polymorphic pseudopolymorphs. Since physical properties are ultimately dependent on crystal structure, each of these species will therefore have unique properties. It is also noteworthy that the desolvation (e.g. by controlled heating) of pseudopolymorphs such as those in Figures 1(D) and (E) would yield polymorphs of the parent compound. Hence, this represents another route to isolation of polymorphs in addition to crystallization from solution, melt or vapour.

In the above descriptions of polymorphism and pseudopolymorphism, the simplest connotations of these terms have been used and a digression into semantics has deliberately been avoided. However, it is important to note that difficulties with terminology do arise due to inconsistent use and the multiplicity and overlap of synonymous terms (e.g. ‘crystal form’

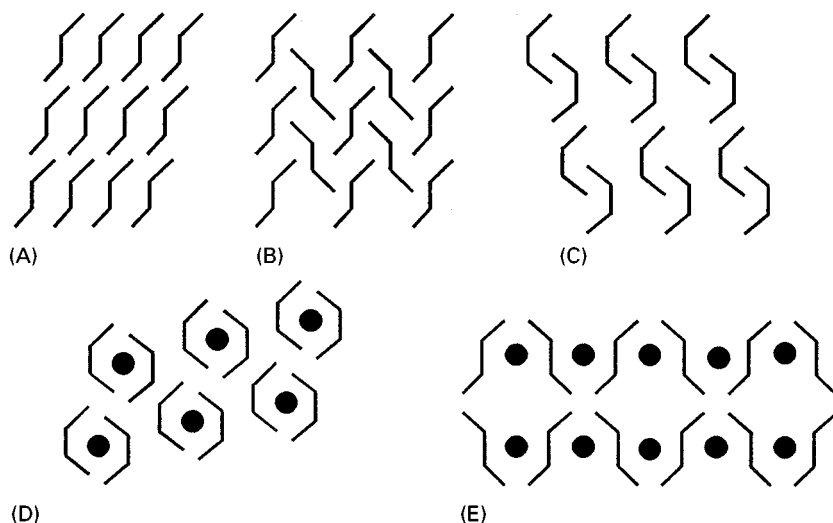


Figure 1 Schematic diagram illustrating polymorphism (A)–(C) and pseudopolymorphism (D), (E); Filled circles represent included solvent molecules.

and 'crystal modification' as synonyms for polymorph; 'solvate', 'inclusion compound', 'clathrate' for pseudopolymorph). Pharmaceutical chemists tend to use 'polymorph' to describe a one-component system and 'pseudopolymorph' for a multi-component system. Finally, it should be noted that amorphous (non-crystalline or 'glassy') states of matter are also relevant in the context of polymorphism, since such phases may arise during transformation of one polymorph into another or during trituration of a crystalline polymorph. Amorphous phases are thermodynamically unstable and will tend to undergo spontaneous crystallization to yield a stable polymorph.

Polymorphic Crystallization and Polymorphic Transformations

Thermodynamic Aspects of Polymorphism

Thermodynamic treatment of a system displaying polymorphism is based on considerations of the Gibbs free energy, G_i , of each polymorph as well as the variation of G_i with the thermodynamic variables temperature (T) and pressure (p). Furthermore, since each polymorph is distinct, each has a characteristic value for its entropy, S_i (≥ 0), under any given conditions of T and p . Considering constant pressure, the thermodynamic relationship $(\partial G_i / \partial T)_p = -S_i$ therefore indicates that the slope of the G - T curve for each polymorph of a compound at any given value of T is (a) negative and (b) different. The stable phase at any given temperature is that polymorph with the lowest value of G , and since the G - T curves for the various polymorphs will generally intersect one another at various temperatures owing to their different slopes, it follows that at a given T , one polymorph will be stable and all others metastable with respect to it. When two G - T curves intersect, the polymorphs they represent are in thermodynamic equilibrium at their transition temperature (T_t) and these phases then have identical values for their Gibbs free energy. Each polymorph thus has a temperature range within which it is stable. (From a thermodynamic viewpoint, the co-existence of several polymorphs of a given substance at e.g. 1 atm, 25°C is a paradox; the reason that this situation arises frequently in practice is that the activation energies for solid-solid transformations to the stable phase are generally very high and such transitions are therefore under kinetic control).

The general principles outlined above can be applied to a dimorphic system, for which the thermodynamic behaviours are classified as being either enantiotropic or monotropic, each of which has practical implications as far as interconversion of the two

polymorphs is concerned. Figure 2 illustrates these cases. Here A, B, and L denote the lower and higher melting polymorphs and their common liquid phase respectively. Intersections of the Gibbs free energy curves of A and B with that of L coincide with the respective melting points $T_{m,A}$ and $T_{m,B}$. In the case of enantiotropy, the curves for A and B intersect at the transition temperature T_t which lies below either of the melting points; furthermore, on either side of T_t , the stability order of A and B is reversed. Each polymorph therefore has a temperature range in which it is stable and the transition between the two is reversible. In practice, processing conditions which involve temperatures near T_t could therefore induce a polymorphic transformation from one stable form to the other (which may or may not be desirable). In the monotropic system, the higher melting polymorph (B) is always the more stable one and the other (A) is metastable with respect to it. If a metastable polymorph is prepared, it may spontaneously convert to the more stable polymorph under conditions conducive to phase transformation.

Using experimental data from differential scanning calorimetry (DSC) together with the thermodynamic relationship $G = H - TS$, the simple curves of Figure 2 can be resolved into their constituent curves depicting the variation of the individual terms H and TS with temperature. An example of such a diagram is shown in Figure 3. Such a composite 'energy/temperature' diagram for a dimorphic system, which includes the curves for both polymorphs, was recommended by Burger and Ramberger in 1979 as a valuable aid in the interpretation of thermal data and for determining polymorphic stability relationships. A set of rules supported by arguments based on statistical mechanics was subsequently formalized from consideration of such diagrams. These rules were intended to be applied in practical situations to determine whether a polymorphic system is enantiotropic or monotropic. For example, according to the 'Heat-of-Transition' Rule, observation of an endothermic effect in a dimorphic system implies the existence of a transition point below it, which in turn requires the dimorphs to have an enantiotropic relationship. In practical cases, where the heat of transition is not measurable due to the slow rate of transformation, the melting points and heats of fusion of the low- and high-temperature polymorphs are determined separately by DSC. The difference between the heats of fusion may then be used instead as an estimate of the heat of transition, leading to a special case of the above rule called the 'Heat-of-Fusion' Rule. A 'Density Rule' relating polymorphic density to thermodynamic stability, and the 'Infrared Rule' which allows entropy rankings from observations of specific

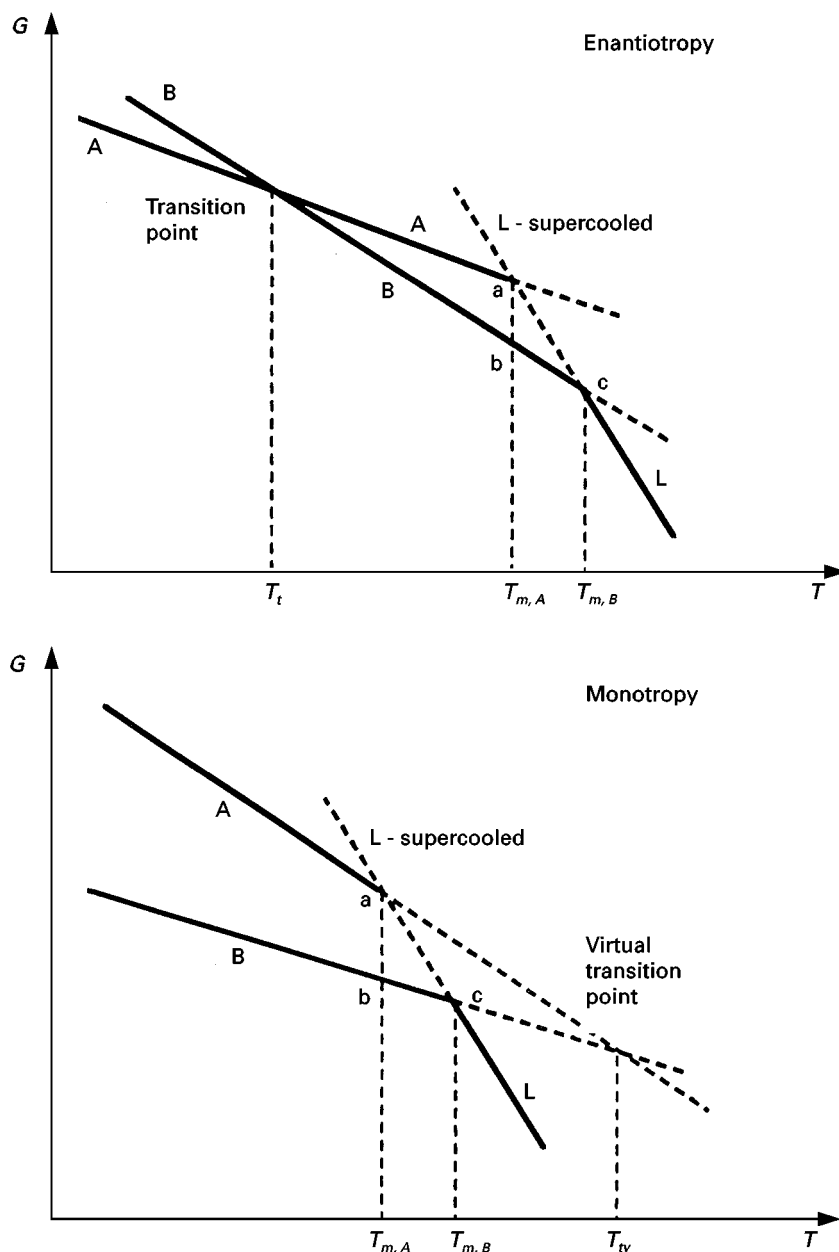


Figure 2 Gibbs free energy-temperature relationships in dimorphic systems. Symbols are defined in the text. (Reproduced with permission from Yu L (1995) *Journal of Pharmaceutical Science* 84: 966, Copyright American Chemical Society and American Pharmaceutical Association.)

infrared frequencies for hydrogen bonded molecular crystals, were also formalized. In more detailed studies of polymorphism, these rules are often applied in an attempt to deduce relative thermodynamic stabilities in a dimorphic pair (especially to determine which is the more stable species at room temperature). Exceptions to the rules are known (conformational polymorphism being acknowledged as a complication) and this may account for the fact that they are not applied universally when the necessary ther-

mal data are available. In 1995, Yu addressed the issue of inferring thermodynamic stability relationships for polymorphs from thermal data using a purely thermodynamic approach. This led to formulae for calculating the Gibbs free energy difference between the polymorphs, ΔG , as well as its temperature derivative. The relative stability of polymorphs can thus be estimated by extrapolation of the value of ΔG to any desired temperature. This work also provided a critical comparison of the derived 'thermodynamic' rules

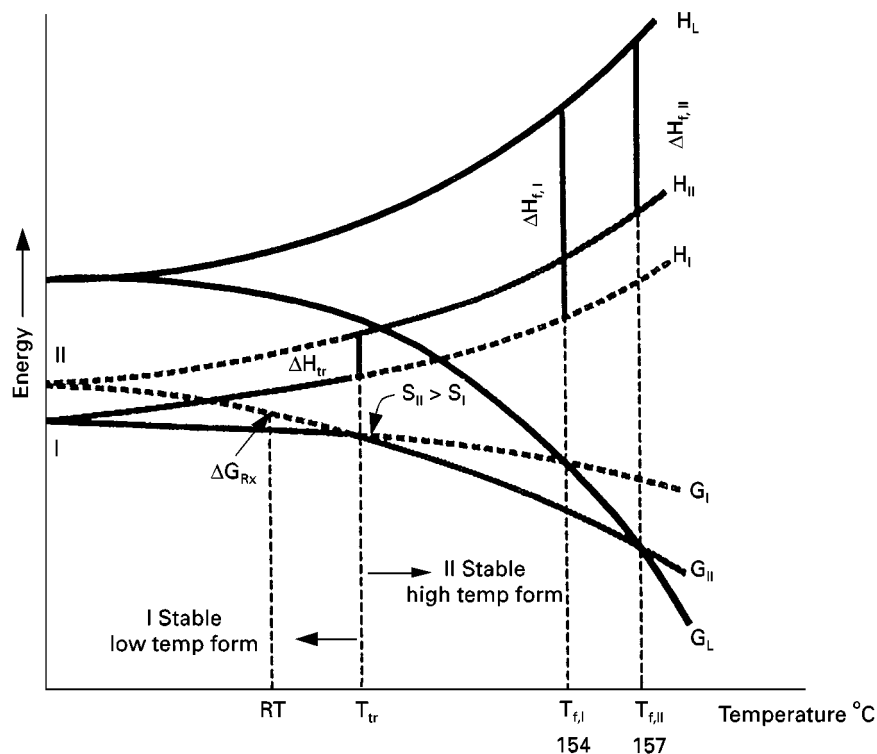


Figure 3 Schematic energy diagram for RG 12525 polymorphs I and II which are enantiotropically related. (Reproduced with permission from Carlton RA, Difeo TJ, Powner TH, Santos I and Thompson MD (1996) *Journal of Pharmaceutical Science* 85: 966. Copyright American Chemical Society and American Pharmaceutical Association.)

with those of Burger and Ramberger showing that, with little exception, they are effectively equivalent, despite the different routes for their derivation. It is likely that this recent endorsement of the Burger and Ramberger rules will lead to more frequent attempts to classify polymorphic systems in terms of enantiotropy or monotropy. A further important outcome of the more recent treatment is that the transition temperature, T_v , is easily estimated by extrapolating the value of the temperature-dependent quantity $\Delta G(T)$ to zero. Knowledge of the value of T_t for a pair of polymorphic forms is of practical importance in the case of enantiotropy and of theoretical interest in the case of monotropy, since for the latter, it is a virtual temperature.

Solubility data provide an alternative means of determining polymorphic transition temperatures. Over a small temperature range, a plot of \ln (solubility) against $1/T$ (a van't Hoff plot) for a polymorph is linear, with a slope related to the enthalpy of dissolution. If the solubility data for two polymorphs of the compound in a common solvent are treated in this way, the point of intersection of the plots will yield the polymorphic transition temperature T_t . An example is illustrated in Figure 4. Furthermore, the heat of transition (ΔH_t) may be calculated as the

difference between the enthalpies of dissolution, since dissolution of either of two polymorphs A and B (distinguishable only in the solid phase) leads to the same species in solution. The above description neglects a common practical problem, namely the possibility

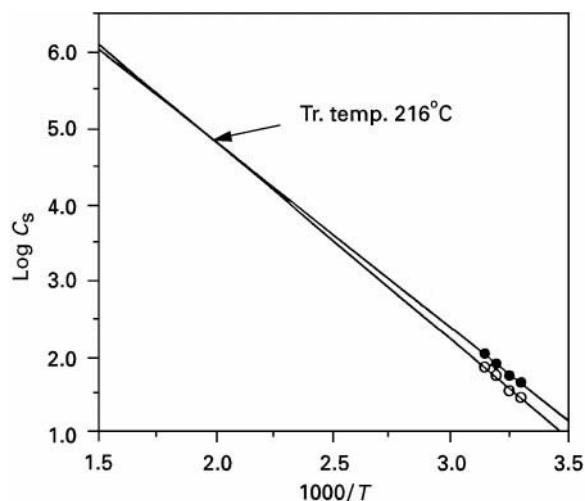


Figure 4 van't Hoff plots for Piretanide Forms A and B at pH 5: ○, Form A; ●, Form B. (Reproduced with permission from Chikaraishi Y, Otsuka M, and Matsuda Y (1995) *Chem. Pharm. Bull.* 43: 1966, Copyright Pharmaceutical Society of Japan.)

of solvent-mediated polymorphic phase transformation during solubility measurement. This type of transformation is but one of several which polymorphs may undergo.

Kinetics of Nucleation and Polymorphism/Pseudopolymorphism

A prerequisite for crystallization of a specific polymorphic phase is the formation of viable nuclei of that phase, nuclei being defined as the smallest molecular aggregates with a configuration resembling that of the final crystal. The probability of nucleation occurring increases with increasing supersaturation of the solution; in such a solution, where incipient nuclei of all possible polymorphs may exist, kinetic factors determine which of these will become viable, i.e. lead to crystallization of a specific polymorph. The critical parameter associated with the formation of a nucleus is the Gibbs free energy of activation, ΔG^* . Nucleation, which proceeds with a rate dependent on ΔG^* , may occur heterogeneously or homogeneously depending on whether random impurities or substrates promoting nucleation are present or not. In the former case, the mechanism of nucleation is associated with a reduction in ΔG^* , relative to the uncatalysed process.

A detailed treatment of homogeneous nucleation shows that the value of ΔG^* is determined by several factors including a geometrical factor specific to the shape of the nucleating cluster, the molecular volume, the interfacial energy (between the nucleating cluster and the crystallization medium), and the chemical potential difference between the crystal and the medium. The crucial point that emerges as regards crystallization of different polymorphs of a given compound from a given medium is, that for each polymorph the values of the various individual factors affecting ΔG^* generally differ. This emphasizes the competitive nature of polymorphic crystallization. In this context, Ostwald's law of stages predicts that nucleation of metastable forms will successively precede that of the stable form, but this has been shown to be valid only in limited regions of chemical potential difference. Since much has still to be learnt regarding evaluation of the individual parameters affecting ΔG^* for individual polymorphs, the problem of predicting polymorphic outcome on the basis of nucleation kinetics remains a complex issue which is receiving continued attention. Molecular dynamics methods have also been applied to the nucleation process with some success. Simultaneous precipitation of different polymorphs occurs frequently in industrial crystallizations. Recent theoretical modelling of this type of process for a dimorphic system has

indicated that polymorphic composition depends on the ratio of the nucleation rates, the ratio of the growth rates and the aggregation tendencies of the two polymorphs.

Crystallization of the solute alone from the medium has been considered thus far. Solvation plays a major role in the crystallization of pseudopolymorphs from solution. Here, the enthalpic advantage associated with particularly strong solute-solvent interactions (e.g. intermolecular hydrogen bonds) outweighs the entropic one associated with liberation of solvent molecules, and the resultant crystals contain entrapped solvent molecules. Theoretical aspects of pseudopolymorphism have not been addressed to any great extent despite the practical importance of these species. A recent survey of documented crystal structures of organic compounds indicates that 15 percent of them contain included solvent molecules.

Types of Polymorphic Transformation

Phase transformations are driven by the tendency for minimization of the Gibbs free energy of the system. In the absence of a liquid phase, the transformation of one polymorph to another of lower Gibbs free energy is possible in principle, but such a process is generally very slow due to the high activation energy associated with nucleation and growth of a new polymorph within the solid matrix of the old one.

The presence of a liquid phase can significantly reduce the activation energy for transformation. Melt-mediated and solution-mediated phase transformations are thus common. In the former, following the melting of a metastable polymorph, the stable polymorph crystallizes (Figure 2, monotropic case, applies here). Solution-mediated polymorphic transformations have received much attention because of their practical importance. Here, a stable solid phase crystallizes from a solution which originally contained a metastable phase, mass transfer being effected through the solution medium. The rate of such a transformation depends on several factors, the most important of which are the difference in solubility of the two polymorphs, the nature of the solvent, temperature and the rate of agitation of the solution. Kinetically, this process has been satisfactorily modelled in terms of dissolution of the more soluble metastable phase (characterized by k_D , the rate constant for dissolution), and crystallization and growth of the stable, less soluble polymorph (rate constant k_G). Experimentally, k_D and k_G are determined from the time-dependence of the supersaturation with respect to the stable phase. Hence, the kinetics of transformation can be either growth-limited or

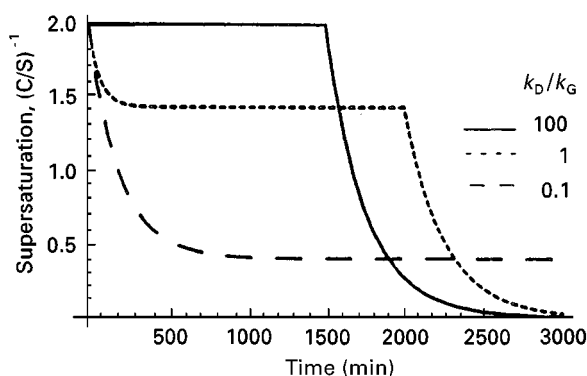


Figure 5 Numerical simulation of the supersaturation-time profiles as a function of the relative rates of dissolution and crystallization during a solution-mediated transformation. Generated from a kinetic model developed by Cardew PT and Davey RJ, (1985) *Proceedings of the Royal Society of London*, A398: 415. (Reproduced with permission from Rodríguez-Hornedo N and Murphy D (1999) *J. Pharm. Sci.* 88: 651. Copyright American Chemical Society and American Pharmaceutical Association.)

dissolution-limited depending on whether the ratio k_D/k_G is large or small. In **Figure 5**, theoretical supersaturation profiles for these extreme cases are compared with the case where the rate constants are equal.

Structural Aspects

The various polymorphs of an organic compound (e.g. those shown schematically in **Figure 1(A)–(C)**), are characterized by different sets of intermolecular interactions (e.g. van der Waals forces, hydrogen bonding, $X-H \cdots \pi$ interactions, where $X = C, N, O$ typically). For molecules containing hydrogen bond donor and acceptor groups, the incidence of polymorphism generally increases owing to the variety of ways in which such molecules can self-

assemble to form supramolecular arrays. **Figure 6** shows portions of the crystal structures of two polymorphs of the drug paracetamol. Despite similar molecular conformations, the intermolecular relationships differ very significantly as a result of the different hydrogen bonding arrangements adopted. Ultimately, it is these features which determine all the observed differences in the physical properties of these polymorphic forms.

Prediction of the crystal structure (or rather, of the family of possible polymorphic structures) of an organic compound from a knowledge of the molecular structure alone is considered a highly desirable goal, but the current state of knowledge of the nature of intermolecular interactions generally prevents its achievement. As to prediction of the outcome of polymorphic crystallization, it would be necessary to invoke additional considerations of thermodynamic, kinetic and solvent effects. These problems are currently being addressed by computational methods with moderate success.

Practical Detection and Analysis of Polymorphs and Pseudopolymorphs

For industrial crystallization, analytical techniques are required for identification of individual polymorphs, quantification of polymorphic mixtures and detection and analysis of pseudopolymorphs. As shown in **Table 1** (which is not exhaustive), many techniques may be used to distinguish polymorphs and to analyse pseudopolymorphs. The primary method is X-ray diffraction, since each crystal structure yields a unique X-ray pattern. As an example, **Figure 7** shows the distinctive powder X-ray diffraction (PXRD) patterns obtained for the monoclinic and orthorhombic polymorphs of a drug substance.

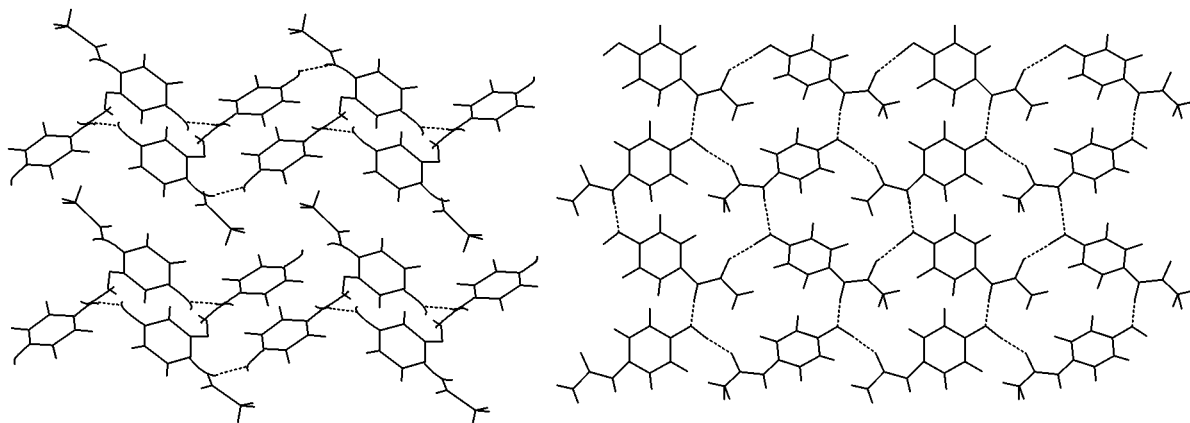


Figure 6 Representative portions of the crystal structures of the monoclinic (left) and orthorhombic (right) polymorphs of paracetamol.

Table 1 Analytical methods suitable for the study of polymorphism and pseudopolymorphism

Analytical method	Principal application for polymorphs and pseudopolymorphs
Elemental analysis	Polymorphs and pseudopolymorphs readily distinguishable due to different chemical compositions
Microscopy	Observation of extinction directions; measurement of refractive indices; determination of optical character (uniaxiality/biaxiality); determination of crystal system
Thermomicroscopy	Visual identification and temperature measurement of desolvation (pseudopolymorphs), polymorphic phase changes, fusion, sublimation, chemical decomposition
Thermogravimetric analysis (TGA)	Measurement of desolvation weight loss (pseudopolymorphs) permitting stoichiometry determination
Differential scanning calorimetry (DSC)	Identification of endothermic events (desolvation, some phase transitions, fusion) and exothermic events (some phase transitions, chemical decomposition)
Infrared spectroscopy	Polymorph identification; detection of included solvents in pseudopolymorphs
Raman spectroscopy	Polymorph identification (complementary to IR)
Powder X-ray diffraction	Primary method for identification of polymorphs and pseudopolymorphs
Single crystal X-ray or neutron diffraction	Complete structural elucidation of polymorphs and pseudopolymorphs
NMR (solution)	Detection of pseudopolymorphs from appearance of peaks due to both parent compound and solvent
NMR (solid state)	Identification of polymorphs and pseudopolymorphs
Solubility measurements	Determination of enthalpies of solution and polymorphic transition temperatures

Detection of more than one polymorph in an industrial crystallization batch may be achieved using this technique since the PXRD patterns are additive. Levels of an adulterating polymorph down to a few percent are detectable. (Near-IR spectroscopy can be equally sensitive in this regard).

When suitable single crystals of the individual polymorphs of a compound can be isolated, complete structural elucidation of each species by X-ray methods is usually possible and highly desirable (cf. Figure 6). The information derived contains all intramolecular parameters (bond lengths, bond angles, conformational parameters) as well as those asso-

ciated with the crystal packing (intermolecular van der Waals contacts and hydrogen bonding) characteristic of each polymorph. These structural parameters can be used to interpret data obtained from other methods. A typical example would be the observation of unequal C=O bond lengths in the molecules of a dimorphic pair, which would account for differences observed in $\nu_{\text{C=O}}$ IR data. For pseudopolymorphs, the observed topology of solvent inclusion (e.g. location within channels, isolated cavities, or layers) and the nature of 'host-guest' hydrogen bonding may be used to explain differences in crystal solvent volatility observed by thermal methods such as DSC. Thus, a knowledge of the crystal structure of each polymorph and pseudopolymorph of a given compound represents a robust foundation for interpretation of many other physicochemical data.

Another major advantage of complete structural elucidation of a polymorph or pseudopolymorph is that the refined parameters may be used to compute an idealized powder XRD pattern for that phase. Such a pattern is invaluable as a primary reference for future identification of that species and for monitoring the purity of the material experimentally during industrial processing.

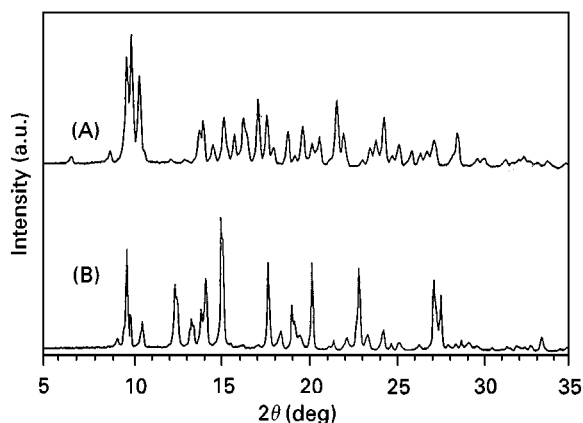


Figure 7 Powder XRD patterns for piroxicam pivalate (A) polymorph 1 (B) polymorph 2. (Reproduced with permission from Cairn MR, Zanol M, Peveri T, Gazzaniga A and Giordano F (1998) *Journal of Pharmaceutical Science* 87: 1608. Copyright American Chemical Society and American Pharmaceutical Association.)

Implications of Polymorphism and Control of Polymorphic Crystallization

Since the Gibbs free energy differences between polymorphs of the same substance are small (typically 2–3 kJ mol⁻¹), even minor changes in crystallization conditions (intentional or otherwise) can lead to the

precipitation of an undesired polymorph or to mixtures of polymorphs. Hence practical difficulties associated with polymorphism manifest themselves prominently in areas where the same compounds undergo repeated crystallization. One notable example is the pharmaceutical industry, where polymorphism and pseudopolymorphism of active agents used in solid dosage forms may have a very significant effect on the efficacy and quality of the formulation. In particular, since different polymorphs of a drug may have different solubilities and different dissolution rates, use of the inappropriate polymorph in a formulation will compromise the bioavailability of the drug. Other problems which could arise include: (a) use of a thermodynamically unstable polymorph which subsequently undergoes spontaneous transformation into a more stable polymorph, with consequent reduction in bioavailability; (b) solvent-mediated conversion of a drug in a suspension resulting in the slow precipitation of an insoluble drug pseudopolymorph (e.g. a hydrate), again leading to reduction in the concentration of therapeutically active material; (c) transformation of the original polymorph to an undesired one induced by processing conditions, e.g. heating, compression, grinding; (d) precipitation of the drug hydrate instead of the desired anhydrous species due to traces of water in the organic crystallizing solvent. Since reproducible behaviour of the dosage form is of paramount importance, pharmaceutical scientists recognize the necessity for a thorough investigation of the polymorphic and pseudopolymorphic behaviour of a drug during its development in order to avert problems of the type described above. Analogous problems, seriously compromising product performance, occur in other industries. Very detailed documentation of crystallization procedures listing all possible parameters is therefore essential in attempting to ensure reproducible outcomes.

Polymorphism can affect other important technological properties such as tablet compaction. In the case of paracetamol (**Figure 6**), the crystal structure of the monoclinic polymorph has a complex three-dimensional hydrogen bonding network which is not conducive to plastic deformation during pressurization. The crystals consequently resist direct compression during tableting. The facile direct compressibility of the orthorhombic polymorph is attributed to the presence of slip planes in the crystal structure which separate the planes of hydrogen bonded molecules (**Figure 6**), rendering this the industrially desired form of the drug.

In the development of solid-state devices, target species displaying second-harmonic generation are crystallographically non-centrosymmetric polymorphs; their selective crystallization, in preference

to inactive centrosymmetric polymorphs of the same compound, is therefore a goal of crystal engineering. Amino acid crystallization is another area affected by polymorphism. For example, precipitation of the α - rather than the β -polymorph of L-glutamic acid is preferred in industry since the former yields a higher solid-liquid separation efficiency.

The above examples highlight the necessity for controlling crystallization mechanisms to ensure precipitation of the desired polymorph. In addition to the computational studies referred to earlier, there are several experimental approaches to this problem (other than solvent-selective polymorphic crystallization), all of which depend on detailed structural knowledge of the stable and metastable polymorphs of the material in question as a basis for understanding the relationship between molecular interactions in the crystallization medium and the supramolecular structures of the polymorphs that might ensue.

Selective crystallization of metastable polymorphs has been achieved by adding inhibitors which retard the growth of the stable polymorph. Inhibitor design is based on identification of the fastest growing crystal faces of the stable polymorph and tailor-making a substrate which will be incorporated along the direction of fastest growth, thereby blocking crystal development. Polymeric inhibitors have been used to control polymorphism in induced enantiomeric resolution of racemates. Essential to these approaches is detailed knowledge of the relationship between crystal morphology and internal structure and this information can usually be obtained only by X-ray diffraction methods.

Another approach to controlling crystallization is based on the knowledge that the molecular topology of a substrate can affect polymorph selectivity and that such heterogeneous nucleation is energetically more favourable than homogeneous nucleation. The mechanism of ledge-directed epitaxy (LDE), illustrated in **Figure 8**, utilizes these principles. Here, a selected substrate, with surface ledges characterized by θ_{sub} , directs the preferred crystallization of that polymorph exclusively whose prenucleation aggregate has a matching dihedral angle θ_{agg} between close-packed crystal planes. A metastable polymorph with θ_{agg} matching θ_{sub} can thus be induced to crystallize in preference to a stable polymorph for which this geometrical condition is not met.

Future Developments

The renewed vigour with which polymorphism as a phenomenon is currently being investigated is motivated by the demand for reliable methods of reproducible crystallization of specific polymorphs of

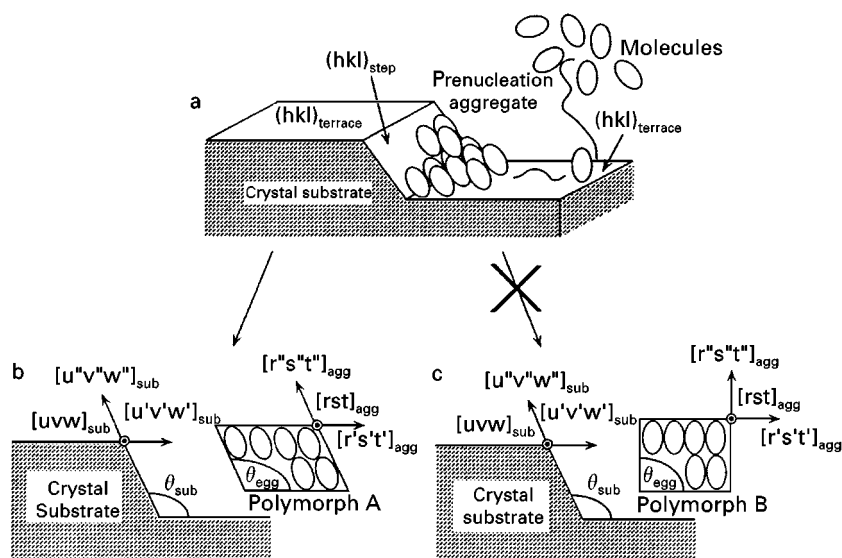


Figure 8 Schematic representation of LDE on a single-crystal substrate and the role of LDE in selective nucleation of polymorphs. Symbols are defined in the original reference. (Reproduced with permission from Bonafede SJ and Ward MD (1995) *Journal of the American Chemical Society* 117: 7853, Copyright American Chemical Society.)

industrially important compounds. In the case of pharmaceuticals, further motivation comes from drug-regulatory bodies (e.g. the FDA) which require details of crystallization procedures for specific drug polymorphs and pseudopolymorphs. It is vital that theoretical development of the subject of polymorphism continues to keep pace with these demands. Computational and experimental techniques, which have during the last decade led to substantial advances in the understanding of the primary event in the crystallization process, namely nucleation, are expected to improve in terms of the complexity of the models employed and in the systems investigated. The strategy of 'rational crystal seeding' epitomized by the LDE technique is likely to be applied more widely to the control of polymorphic crystallization. A consequent growth is expected in the number of reports documenting successful isolation of specific polymorphs utilizing approaches based on deliberate intervention at the nucleation stage. Detailed structural elucidation of metastable polymorphs and microcrystalline polymorphs will be facilitated by the combined use of methods such as computational crystal structure prediction, solid state NMR, high-resolution X-ray and neutron powder diffraction, and single crystal X-ray methods employing synchrotron radiation sources. Accompanying the demand for isolation of particular polymorphs, methods for more rapid analysis and quantification will be needed to satisfy both production and legal requirements. An increase in the number and types of on-line systems for continuous monitoring of polymorphic purity in the industrial environment is also envisaged.

See also: [I/Crystallization](#).

Further Reading

- Bernstein J (1991) Polymorphism and the investigation of structure-property relations in organic solids. In: Garbaczuk JB, James DW (eds) *Organic Crystal Chemistry*. Oxford: Oxford University Press.
- Burger A and Ramberger R (1979) *On the Polymorphism of Pharmaceuticals and Other Molecular Crystals. I. Theory of Thermodynamic Rules*, Vienna: Mikrochimica Acta, 259–271.
- Byrn S R (1982) *Solid State Chemistry of Drugs*. New York: Academic Press.
- Byrn S, Pfeiffer R, Ganey M, Hoiberg C and Poochikian G (1995) Review: pharmaceutical solids: a strategic approach to regulatory considerations. *Pharmaceutical Research* 12: 945–954.
- Caira MR (1998) Crystalline polymorphism of organic compounds. In: Weber E (ed.) *Design of Organic Solids, Topics in Current Chemistry*, Vol. 198, pp. 163–208. Berlin: Springer-Verlag.
- Desiraju GR (1989) *Crystal Engineering*. Amsterdam: Elsevier.
- Dunitz JD and Bernstein J (1995) Disappearing polymorphs. *Acc. Chem. Res.* 28: 193–200.
- Gavezzotti A and Filippini G (1997) In: Gavezzotti A (ed.) *Theoretical Aspects and Computer Modeling of the Molecular Solid State*. Vol. 1, Ch. 3. New York: Wiley.
- Guillory JK (1999) Generation of polymorphs, hydrates, solvates, and amorphous solids. In: Brittain HG (ed.) *Polymorphism in Pharmaceutical Solids*. New York: Marcel Dekker, Inc.

- Klug HP and Alexander LE (1974) *X-Ray Diffraction Procedures for Polycrystalline and Amorphous Materials*. New York: Wiley.
- Rodriguez-Hornedo N and Murphy D (1999) Minireview: significance of controlling crystallization mechanisms and kinetics in pharmaceutical systems. *Journal of Pharmaceutical Sciences* 88: 651–660.
- Sato K (1993) Polymorphic transformations in crystal growth. *Journal of Physics, D: Applied Physics* 26: B77–B84.

- Threlfall TL (1995) Analysis of organic polymorphs, a review. *Analyst* 120: 2435–2460.
- Weissbuch I, Popovitz-Biro R, Lahav M and Leiserowitz L (1995) Understanding and control of nucleation, growth, habit, dissolution and structure of 2-dimensional and 3-dimensional crystals using tailor-made auxiliaries. *Acta Crystallographica, Sect. B: Structural Science B* 51: 115–148.
- Wendlandt WW (1986) *Thermal Analysis*. 3rd edn, New York: John Wiley & Sons.

Zone Refining

C.-D. Ho and H.-M. Yeh, Tamkang University, Taipei, Taiwan, ROC

Copyright © 2000 Academic Press

Introduction

Zone refining is a powerful tool for applying coupled melting and freezing operations for manipulating impurities in crystals, as well as for separating liquid or solid mixtures. It was first used to purify germanium in 1952. Zone refining combines the well-known fact that a freezing crystal differs in composition from its corresponding liquid phase, so that passing a short heater along a solid ingot leads to a purification of the ingot. For improving the separation efficiency and reducing time, a series of narrow heaters moving slowly over a solid ingot can be used in multi-pass zone refining.

Several mathematical models have been presented for modelling multi-pass zone refining processes when zone length affects the separation efficiency. Furthermore, variable cross-sectional area ingots with specified volumes have been introduced to improve the separation efficiency. Analogue simulators were used to simulate zone refining by means of a single mathematical equation that expresses solute concentration as a function of distance for any initial distribution of solute and any number of passes through an ingot of a specified length. These simulators include liquid mechanical and electrical analogue simulators. Thousands of significant papers devoted entirely or largely to some aspect of application of zone refining have appeared in the last two decades. For instance, silicon-on-insulator (SOI) films, and semiconducting and superconducting materials were prepared by zone refining operations.

Separation Theory in Multi-pass Operation

Eqn (1) can be derived by taking the mass balance within the moving zone ABCD or A'B'C'D' as

shown in **Figure 1**. It is based on the following assumptions: (a) constant distribution coefficient; (b) uniform composition and no diffusion in the molten zone; (c) no change in density during melting and freezing; (d) a constant cross-sectional area for the ingot.

$$\frac{d\bar{C}_n(Z)}{dZ} + \frac{\left(\frac{dY_n(Z)}{dZ} + k\right)}{Y_n(Z)} \bar{C}_n(Z) = \frac{k\bar{C}_{n-1}[Z + Y_n(Z)]}{Y_n(Z)} \left(1 + \frac{dY_n(Z)}{dZ}\right), \quad 0 \leq Z \leq 1 - Y_n(Z) \quad [1]$$

$$\frac{d\bar{C}_n(Z)}{dZ} + \frac{\left(\frac{dY_n(Z)}{dZ} + k\right)}{Y_n(Z)} \bar{C}_n(Z) = 0, \quad 1 - Y_n(Z) \leq Z \leq 1 \quad [2]$$

and the boundary conditions of eqns (1) and (2) become:

$$\text{at } Z = 0, \quad \bar{C}_n = \frac{k}{Y_n(0)} \int_0^{Y_n(0)} \bar{C}_{n-1}(Z) dZ \quad [3]$$

$$\text{at } Z = 1 - Y_n(Z),$$

$$\bar{C}_n = \frac{k}{Y_n(Z)} \left[1 - \int_0^{1-Y_n(Z)} \bar{C}_n(Z) dZ \right] \quad [4]$$

in which:

$$\bar{C}_n(Z) = C_n(x)/C_0 \quad [5]$$

$$Y_n(Z) = l_n(x)/L \quad [6]$$

$$Z = x/L \quad [7]$$

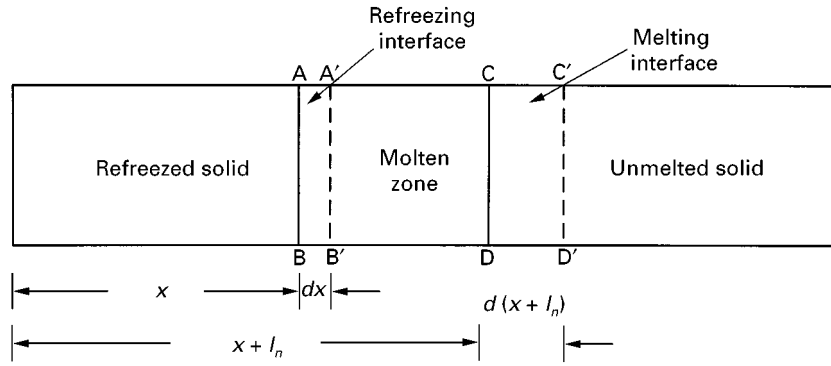


Figure 1 Schematic diagram of zone-refining operation.

The initial solute concentration of the ingot, C_0 , is uniform, the amount of solute, $W_{n,i}$, either transporting away from ($k < 1$), or into ($k > 1$) the i th section after the n th pass, can be calculated by:

$$W_{n,i} = \int_{x_i}^{x_{i+1}} \|C_0 - C_n(x)\| A dx \quad [8]$$

Since the original amount of solute in the ingot is $W_0 = ALC_0$, where A is the cross-sectional area of the ingot, the fraction of solute removed, $f_{n,i}(Y_{n,i}(Z))$, in each section after n passes, is expressed as:

$$f_{n,i}(Y_{n,i}(Z)) = \frac{W_{n,i}}{W_0} = \frac{\int_{Z_i}^{Z_{i+1}} \|1 - \bar{C}_n(Z)\| dZ}{\int_{Z_i}^{Z_{i+1}} \|1 - \bar{C}_n(Z)\| dZ} \quad [9]$$

Once the values of $f_{n,i}(Y_{n,i}(Z))$, $i = 1, 2, \dots, I$ for each section are known, the overall amount of solute removed $F_n(Y_n(Z))$ can be obtained by summing up these values as:

$$F_n(Y_n(Z)) = \sum_{i=1}^I f_{n,i} = \sum_{i=1}^M f_{n,i} = \frac{1}{2} \sum_{i=1}^M f_{n,i} \quad [10]$$

where x_I is the place where $C_n(x) = C_0$ or $\bar{C}_n(Z) = 1$.

Normal Freezing

The optimal zone length Y_1^* for maximum $F_q(Y_1)$ is obtained by solving the equation, $dF_1(Y_1)/dY_1 = 0$, with the use of eqns (9) and (10), since $dF_1(Y_1)/dY_1$ is less than zero for $k < 1$ and $dF_1(Y_1)/dY_1$ is larger than zero for $k > 1$. In order to meet both requirements, therefore, Y_1 must be as large as possible, i.e. normal freezing for all values of the distribution coefficient. Accordingly, the optimal zone length for the first pass is:

$$l_1 = L \quad \text{or} \quad Y_1^* = 1 \quad [11]$$

Varying Optimal Zone Length in Each Pass

The optimal variable zone length $Y_{n,i}^*(Z)$, the corresponding concentration distribution $\bar{C}_n^*(Z)$ and the fractions of solute removal for each section, $f_{n,i}(Y_{n,i}(Z))$, were determined numerically for different values of k with M sections. After the optimal zone length $Y_{n,i}^*(Z)$ for a maximum solute removal $f_{n,i}(Y_{n,i}(Z))$ in each section were achieved, the maximum $F_n(Y_{n,i}^*(Z))$ as well as the corresponding best function of the optimal variable zone length, $Y_n^*(Z)$, were calculated from eqn (10). The optimal functions of variable zone length for up to ten passes are presented graphically in Figure 2.

Constant Optimal Zone Length in All Passes

For constant zone length $Y_{1 \rightarrow n}$ in all passes, $dY_{1 \rightarrow n}/dZ = 0$ and $Y_1 = Y_2 = \dots = Y_n$. In this case, eqns (1)–(7) still apply with $Y_n(Z)$ substituted by $Y_{1 \rightarrow n}$. The optimal zone lengths $Y_{1 \rightarrow n}^*$ for maximum solute removal $F_n(Y_{1 \rightarrow n}^*)$ in n -passes were obtained as follows. First, $\bar{C}_n(Z, Y_{1 \rightarrow n})$ was obtained from eqns (1) and (2) numerically with M sections and with the use of eqns (3) and (4) as well as the given value of $Y_{1 \rightarrow n}$. $F_n(Y_{1 \rightarrow n})$ was then calculated from eqns (9) and (10) and finally, $Y_{1 \rightarrow n}^*$ was obtained from the requirement, $dF_n(Y_{1 \rightarrow n})/dY_{1 \rightarrow n} = 0$.

The optimal values of $Y_{1 \rightarrow n}^*$ are shown in Figure 3 as a function of k with pass number n .

Constant Optimum Zone Length in Each Pass

For this case, we have $dY_n/dZ = 0$ but $Y_{n-1} \neq Y_n$. Eqns (1)–(7) are applicable if $Y_n(Z)$ is substituted by Y_n . The optimal zone lengths Y_n^* for each pass in n -passes were obtained by following the same calculation procedure described in previous sections. The results are shown in Figure 4.

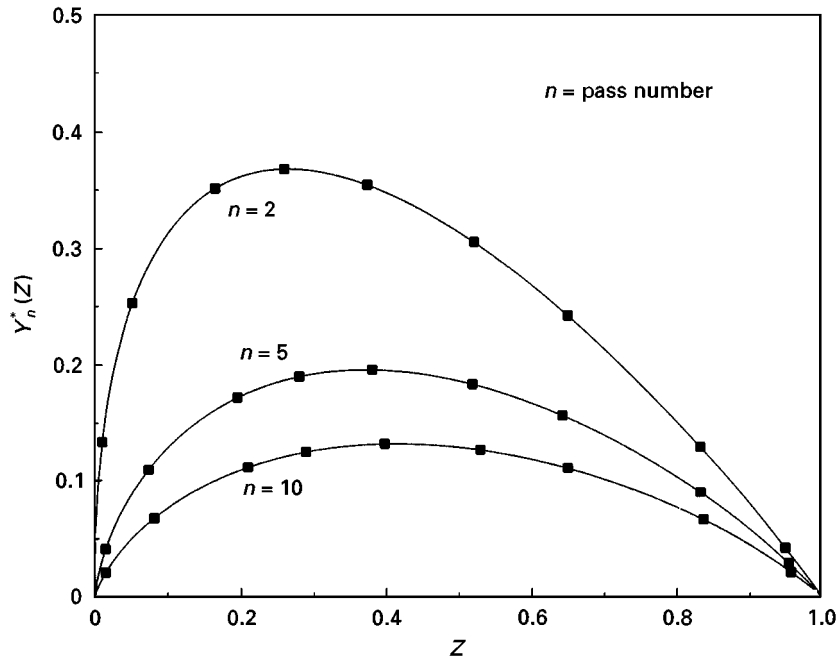


Figure 2 Numerical values of the optimal variable zone length for each pass.

Separation Theory in Analogue Simulators

Zone Refining Simulator for $k < 1$

Zone refining region, $0 \leq x \leq (L - l)$ Figure 5 shows a zone refining simulator for $k < 1$. The ingot is operated by an array of vertical tubes, such as

burettes, of equal internal area a , each with a stopcock, connected in parallel to a common horizontal tube leading to the zone tube. The solute concentration at any point is represented by the height of the liquid level in the tube. Initially, the zone tube is emptied and ingot tubes are filled to height h_0 . The number of open tubes, m , corresponds to the zone length.

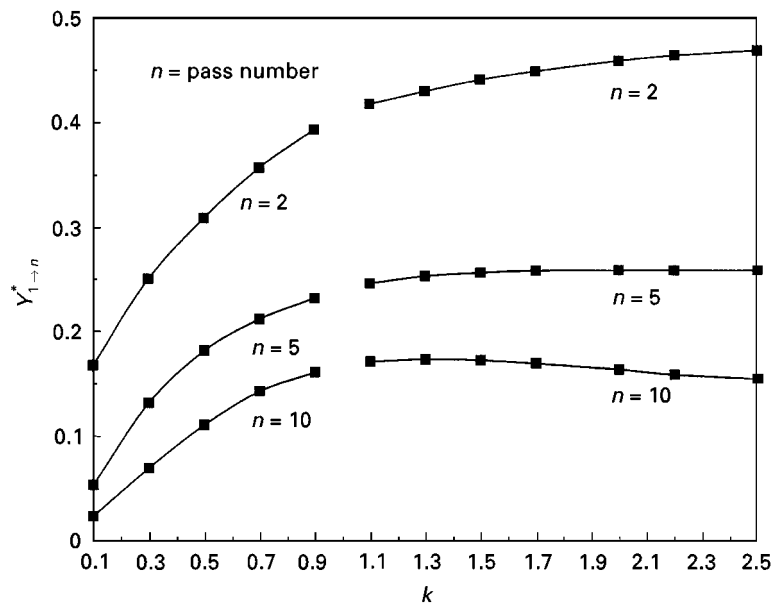


Figure 3 Numerical values of the constant optimum zone length for all passes.

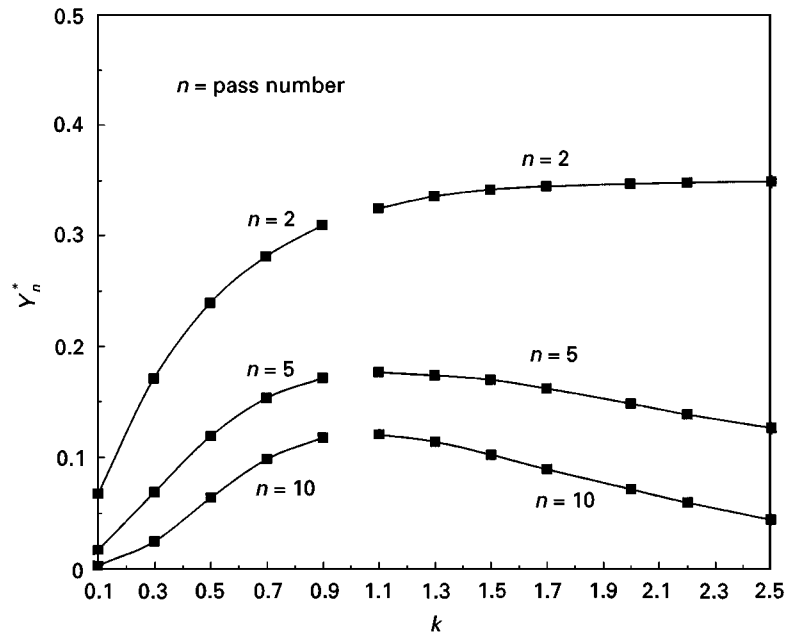


Figure 4 Numerical values of the constant optimal zone length for each pass.

The area a_z of the zone tube determines the value of k that is operated, in accordance with:

$$a_z = \frac{ma(1-k)}{K} \quad [12]$$

The liquid level in tube i after the n th pass is:

$$h_i^n = \frac{(m-1)ah_{i-1}^n + ah_{m+i-1}^{n-1} + a_z h_{i-1}^n}{ma + a_z}, \quad i = 1, \dots, N-m \quad [13]$$

It can be seen that the horizontal tube in conjunction with the zone tube performs the essential operations of a travelling molten zone: namely, taking in solute at the leading end; remixing it with the solute in the zone; and freezing out. At the trailing end, a solute concentration is k times that in the zone. In the analogue simulator, as the molten zone advances, it opens the next tube in line, produces the same liquid height in the zone tube and the empty tube connected to it, and then leaves this height in the closed off tube.

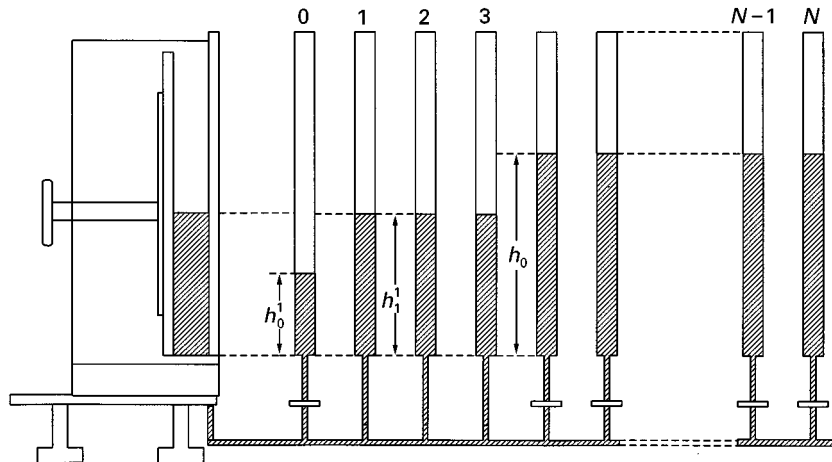
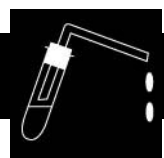


Figure 5 Hand-operated liquid-level zone refining simulator for $k < 1$.

Further Reading

- Bertein F (1958) Simple analogue apparatus for study of treatment of an ingot by zone melting. *Journal of Physics in Radium* 19: 121A.
- Bertein F (1958) Electrical analogue for study of treatment of an ingot by zone melting. *Journal of Physics in Radium* 19: 182A.
- Davies LW (1959) The efficiency of zone refining processes. *Transactions of the American Institute of Mechanical Engineers* 215: 672.
- Ho CD, Yeh HM and Yeh TL (1997) Multipass zone refining with specified ingot volume of frustum with sine-function profile. *Separation and Purification Technology* 11: 57–63.
- Ho CD, Yeh HM, Yeh TL and Sheu HW (1997) Simulation of multipass zone refining processes within whole ingot. *Journal of the Chinese Institute of Chemical Engineers* 28: 271–279.
- Ho CD, Yeh HM and Yeh TL (1998) Numerical analysis on optimal zone lengths for each pass in multipass zone refining processes. *Canadian Journal of Chemical Engineers* 76: 113–119.
- Ho CD, Yeh HM and Yeh TL (1999) The optimal variation of zone lengths in multipass zone refining processes. *Separation and Purification Technology* 76: 113–119.
- Lawson WD, and Nielsen S (1962) In: Schoen HM (ed.) *New Chemical Engineering Separation Techniques*. New York: John Wiley and Sons Inc.
- Lord NW (1953) Analysis of molten-zone refining. *Transactions of the American Institute of Mechanical Engineers* 197: 1531.
- Pfann WG (1964) *Zone Melting*, 2nd edn. New York: John Wiley and Sons Inc.

DISTILLATION



Azeotropic Distillation

F. M. Lee and R. W. Wytcherley,
GTC Technology Corporation, Houston, Texas, USA
Copyright © 2000 Academic Press

Introduction

An azeotrope occurs when the composition of a vapour in equilibrium with a liquid mixture has the same composition as the liquid. Azeotropic distillation takes advantage of azeotropes that form naturally between many components. Azeotropic distillation involves the formation of an azeotrope, or the use of an existing azeotrope, to effect a desired separation.

For almost 100 years the existence of naturally occurring azeotropes has been used to purify chemicals. In 1902, Young reported using benzene as an azeotropic agent to dehydrate ethanol. This first industrial application was in a batch mode and therefore not conducive to widespread commercial use. Twenty years elapsed before a continuous commercial process was developed. In 1923, Backus, Keyes and Stevens of the United States, and Guinot of France developed continuous azeotropic distillation processes for the dehydration of ethanol. As with Young's batch process, the continuous processes relied upon the ethanol–benzene–water ternary azeotropic mixture for dehydrating ethanol. From that time, azeotropic distillation processes have grown to become an indispensable tool in today's industries.

Desirable properties for an azeotropic entrainer are:

1. Heterogeneous azeotrope for ease of entrainer recovery
2. Commercially available and inexpensive
3. Nontoxic
4. Chemically stable
5. Noncorrosive
6. Low latent heat of vaporization
7. Low viscosity to provide high tray efficiencies
8. Low freezing point to allow ease of handling and storage

Azeotropic distillation is an essential unit operation in today's processes. Applications using azeotropic distillation are readily apparent in the chemical process industry (CPI), speciality chemicals and food industries. Applications from various industries are listed in **Table 1**.

The main advantages of azeotropic distillation are in allowing the separation of chemicals that cannot feasibly be separated by conventional distillation, such as systems containing azeotropes or pinch points, and improving the economics of the separation by saving energy and increasing recovery. The main disadvantages of azeotropic distillation are the larger diameter column required to allow for increased vapour volume due to the azeotropic agent, and an increase in control complications compared with simple distillation.

A minimum-boiling azeotrope can be formed by the introduction of an azeotrope-forming compound (entrainer) to an existing azeotropic mixture or close-boiling mixture for which separation by

Table 1 Industrial applications of azeotropic distillation

Industry	Application	Separation involved	Typical entrainers
CPI	Acetic acid recovery or purification	Acetic acid/water	Ethyl acetate, butyl acetate
CPI	Terephthalate acid solvent recovery	Acetic acid/water	Ethyl acetate, butyl acetate
CPI	Preparation of high purity esters	Water/esters to change equilibrium	Alcohol
CPI	THF purification	THF/water azeotrope	<i>n</i> -Pentane
Speciality chemicals	Purification of 1,1,1,2-tetrafluoroethane (refrigerant)	1,1,1,2-tetrafluoroethane/hydrogen fluoride and/or 1-chloro-2,2-difluoroethylene	Components present in system
Speciality chemicals	Recovery of perchloroethylene (dry cleaning solvent)	Perchloroethylene and residue	Water
Speciality chemicals	Solvent recovery from tyre manufacturing	Contaminated solvents	Water
Food	Alcohol dehydration	Alcohol/water azeotrope	Benzene, cyclohexane
Food	Production of L-aspartyl-L-phenylalanine methyl ester (sweetener)	Acetic acid/toluene azeotrope	Water

CPI, chemical process industry.

conventional distillation is not feasible. One example is alcohol dehydration. Ethanol and water form a minimum-boiling azeotrope with ethanol as the major component and therefore ethanol cannot be completely dehydrated by conventional distillation. Benzene forms a ternary azeotrope with ethanol and water, which boils at a lower temperature and will therefore remove the water (with some ethanol) overhead, leaving dry ethanol as a bottoms product.

In some cases, an azeotrope that exists within the system can be used advantageously to purify a compound, as in the production of esters. The esterification of alcohols involves a reversible reaction. Being equilibrium limited, the reaction will not go to completion in the presence of the product. If one of the products is removed (in this case water) utilizing the water/alcohol azeotrope (almost all alcohols from C₂ to C₂₀ form azeotropes with water) the reaction is driven in favour of the ester product. A comprehensive list of many azeotrope-forming compounds can be found in the publication *Azeotropic Data III*, by Horsely (see Further Reading section).

Relative volatility is a comparison of the volatilities of the components in the mixture. When the compositions of the vapour and liquid phases are the same, the volatilities of the components are the same and the relative volatility is equal to 1. The further the relative volatility is away from 1, the easier it is to separate the components of the mixture. Figure 1 illustrates the number of theoretical stages required to separate two components to 99% purity compared with the relative volatility of the mixture. As can be

seen, the number of trays required asymptotically approaches infinity and the separation becomes impossible as the relative volatility approaches unity. A relative volatility close to unity could indicate the presence of a pinch point. It is technically feasible to separate components that form a pinch point, but often not economic due to the large number of stages required to effect the separation.

Homogeneous azeotropes exist when the vapour is in equilibrium with a single liquid phase. In a homogeneous azeotropic system, the entrainer must be recovered by additional fractionation or extraction. Figure 2 illustrates the homogeneous azeotropic

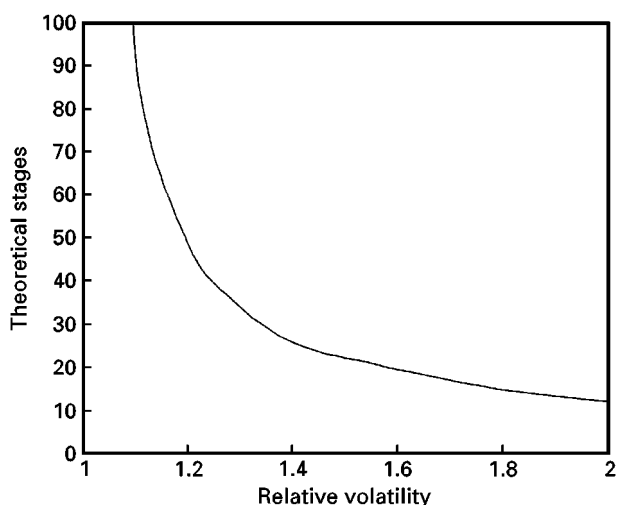


Figure 1 Relative volatility versus theoretical stages required to separate two components to 99% purity.

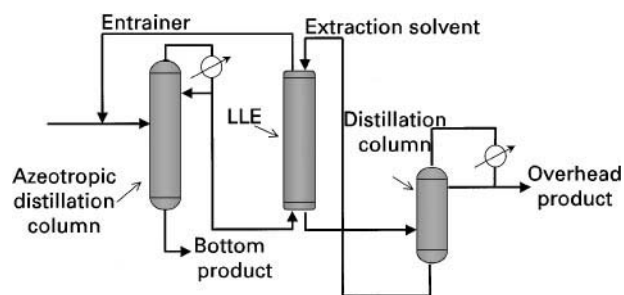


Figure 2 Typical homogeneous azeotropic distillation system utilizing a liquid-liquid extraction (LLE) column to separate the overhead product from the entrainer.

distillation system. Heterogeneous azeotropes exist when the vapour is in equilibrium with two liquid phases. Heterogeneous azeotropic distillation is widely used for the separation of azeotropic or close-boiling mixtures by forming a minimum-boiling azeotrope and taking advantage of the liquid-liquid immiscibility to recover the entrainer. **Figure 3** illustrates a typical azeotropic distillation system of a heterogeneous azeotrope.

Acetic Acid Recovery

There are many industrial processes where acetic acid and water coexist and must be separated. One such process is the production of terephthalic acid. Terephthalic acid (TA) is a polyester raw material used to produce fibres, films and bottles. Terephthalic acid production is important because of the phenomenal growth of this product in the market. The worldwide purified terephthalic acid (PTA) production is currently 15 million tonnes per year, with a growth rate of 12% per annum expected well into

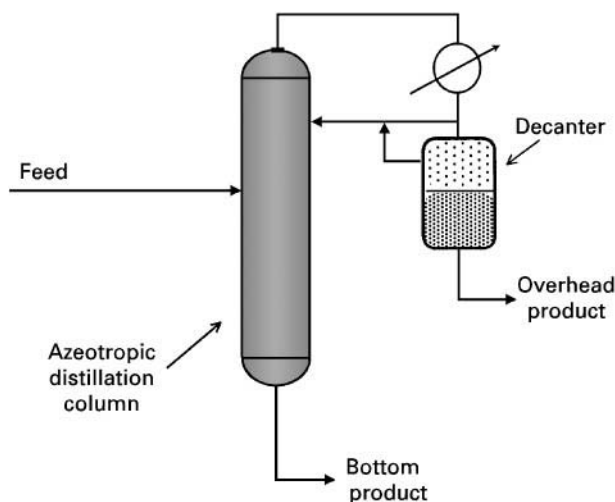


Figure 3 Typical heterogeneous azeotropic distillation system.

the twenty-first century. Let us examine the operational advantage of using azeotropic distillation in the production of purified terephthalic acid.

The production of PTA includes two main sections, oxidation and purification. Within the oxidation unit, *p*-xylene is catalytically oxidized to produce crude TA. **Figure 4** shows a PTA oxidation section block diagram. Acetic acid is present in the oxidation reactor as a solvent and has also been found to be beneficial in the oxidation reaction itself.

Critical to the efficient and economical operation of a PTA plant is the recovery and recycling of the acetic acid solvent. The acetic acid must be separated from the water that is produced as a product of oxidation. Water and acetic acid exhibit a pinch point at high water concentrations making it very difficult to recover the pure acid. **Figure 5** illustrates the water/acetic acid pinch point on a graph of the fraction of water in liquid phase versus the fraction of water in the vapour phase.

In this process, a clean separation of acetic acid from water is vital. If the acetic acid recycled to the reactor contains too much water, the oxidation reaction will be inhibited, resulting in a decrease in overall yield. If the water being disposed as waste contains acetic acid, the acid must be treated within a wastewater treatment facility. Therefore, any acid losses count against the process economics both as increased make-up solvent required and increased wastewater treatment costs.

The acetic acid recovery unit separates the acetic acid to be recycled to the reactor, from water that can be polished for disposal. A conventional acetic acid recovery unit in a PTA process consists of the low and high pressure absorbers and the acid dehydration column. The low pressure absorber uses water to absorb acetic acid and methyl acetate (reaction by-product) from the TA drier gas. The high pressure absorber uses water to absorb acetic acid and methyl acetate from the reactor off-gas. These streams generally make up 25% of the feed to the dehydrator and contain less than 30% concentration of acetic acid. The remaining feed to the dehydrator column comes

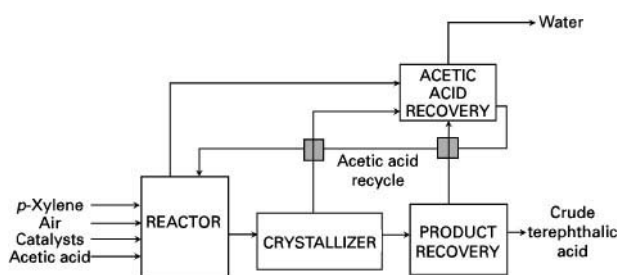


Figure 4 PTA oxidation section block diagram.

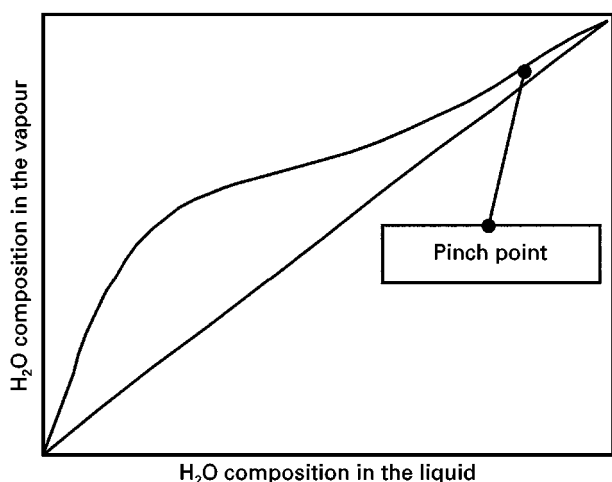


Figure 5 Diagram illustrating acetic acid/water pinch point on a graph of the fraction of water in the liquid phase versus the fraction in the vapour phase.

from the crystallizers. **Figure 6** shows a conventional acetic acid recovery unit using azeotropic distillation in a PTA process.

Typically the acetic acid/water separation of the acid recovery unit is accomplished by either conventional distillation or azeotropic distillation. Separation of acetic acid and water by conventional distillation requires a very tall column, containing 70 to 80 trays.

Preferably, the acid dehydration column in the solvent recovery unit can be operated as an azeotropic distillation column. As an example, let us assume the azeotropic agent used is *n*-butyl acetate. *n*-Butyl acetate and water exhibit limited miscibility and therefore form a heterogeneous azeotrope which boils at 90.2°C. *n*-Butyl acetate is added in sufficient quantities to form an azeotrope with all the water being fed

to the dehydration column. The *n*-butyl acetate/water azeotrope can then be distilled as an overhead stream, leaving the pure acetic acid as the bottoms product. The heterogeneous azeotrope forms two phases upon condensation, with the top layer containing almost pure *n*-butyl acetate saturated with water. The bottom phase contains almost pure water saturated with *n*-butyl acetate. The top (entrainer) phase is recycled back to the dehydration column. The bottom phase (aqueous) is fed to a stripping column where the relatively small amount of entrainer is removed as an azeotrope with the overhead back to the dehydration column and water is removed as the bottom product.

The use of azeotropic distillation in the PTA process has economic and environmental advantages over conventional distillation for acetic acid recovery. Due to the lowered heat of vaporization of the azeotrope compared with that of water alone, azeotropic distillation can save one-third the energy of conventional distillation. Since azeotropic distillation results in a cleaner separation, the amount of acetic acid lost in the aqueous discharge can be reduced by almost 40%. **Table 2** shows the substantial advantages of using azeotropic distillation in this commercial application.

Production of PTA is just one illustration of azeotropic distillation being used in the commercial separation of acetic acid and water. Azeotropic distillation is also used in the production of acetic acid. The most popular methods for producing acetic acid are methanol carbonylation, butane or naphtha catalytic liquid-phase oxidation (LPO) and acetaldehyde oxidation. Methanol carbonylation is used for more than 90% of all new acetic acid capacity worldwide. In methanol carbonylation methanol and carbon monoxide are reacted over a rhodium catalyst under gentle operating conditions to produce acetic acid. The reaction produces low boiling by-products which are flash distilled to recover the rhodium catalyst. The remaining acid is dehydrated by azeotropic distillation much the same way as described in the PTA acetic acid recovery unit.

Butane/naphtha catalytic liquid-phase oxidation was once the most favoured method for the production of acetic acid. Along with acetic acid, a host of other components are produced such as

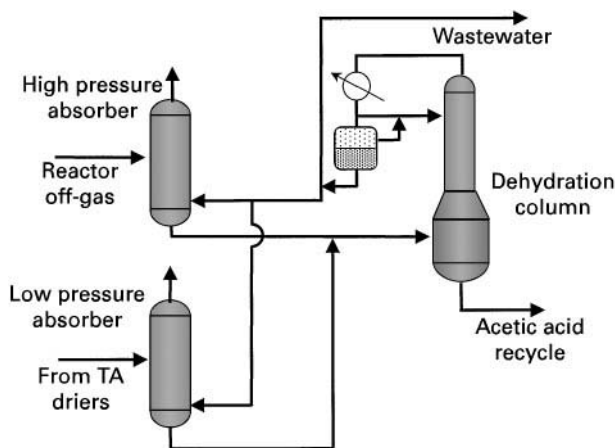


Figure 6 Conventional acetic acid recovery unit using azeotropic distillation in a PTA process.

Table 2 Comparison of distillation methods for PTA production

Parameter	Conventional distillation	Azeotropic distillation
Energy, J h ⁻¹	139	92
Acetic acid in WW, t yr ⁻¹	400	250

WW = wastewater.

formic, propionic and butyric acids. Azeotropic distillation is used to separate the formic acid and water from the aqueous reactor product.

In acetaldehyde oxidation, ethanol is dehydrogenated oxidatively to acetaldehyde using a silver, brass or bronze catalyst. Acetaldehyde is oxidized in the liquid phase over cobalt and manganese catalysts to produce acetic acid. The final purification process uses ethyl acetate to azeotropically remove formic acid and water. The acetic acid product is removed as a side stream from the azeotropic column.

Alcohol Dehydration

Azeotropic distillation for alcohol dehydration has the longest history of use within the industry. Beginning with the work of Young, who demonstrated the first industrial application, azeotropic distillation is still used today in the production and dehydration of alcohol. Alcohol production is present in the CPI, speciality chemicals and food industries, and although the end use and perhaps the alcohol purity requirements vary, the method of production using azeotropic distillation is similar.

Prior to Young's work, absolute alcohol was prepared by distilling the alcohol with a dehydrating agent such as freshly ignited lime. This method required the major component (alcohol) to be boiled overhead leaving the minor component (water) at the bottom. Young's objective was to find a method of removing the minor component as the overhead product. When two different chemicals are distilled together, often a minimum boiling point occurs where a mixture of the two chemicals will distil off first, with the last portion being the compound in excess. Since ethanol is a hydroxyl compound like water and yet an organic compound, it should exhibit analogies to both water and hydrocarbons. Therefore, ethanol should form azeotropes with water and organic compounds. If an azeotroping agent such as benzene is used (in Young's time benzene and heptane were preferred due to their availability), the fractions would come off as follows: ternary water/benzene/alcohol azeotrope; alcohol and benzene azeotrope; and water and benzene azeotrope. At this point, all the water should be removed, leaving anhydrous alcohol. Young performed his azeotropic dehydration of alcohol by a batch method. While popular for distilling strong spirits, this batch method did not catch on commercially. It was not until Backus *et al.* and Guinot developed continuous azeotropic distillation processes that it became a commercial success.

As an example of an alcohol dehydration process, let us examine ethanol dehydration. Dilute water/

ethanol solutions can be rectified to produce an ethanol-rich stream containing a maximum of about 89.4 mol% ethanol at atmospheric pressure. The introduction of benzene as a heterogeneous azeotropic entrainer to the top of the column, which is fed with an 89.4 mol% aqueous ethanol feed, produces the ternary ethanol/benzene/water azeotrope. This ternary azeotrope boils at 64.9°C and is easily separated from ethanol (b.p. = 78.4°C), which is removed as the bottom product. The ternary ethanol/benzene/water azeotrope forms two liquid phases with the benzene-rich phase fed back to the column. The aqueous phase contains nearly equimolar proportions of ethanol and water which is rectified to produce water as the bottom product and the binary ethanol/water azeotrope as the overhead product. The concentrated ethanol/water azeotropic stream is recycled back to the feed for the dehydration column. **Figure 7** illustrates a typical ethanol dehydration process.

Production of Esters

Esters are produced by reacting alcohols with organic acids. The reaction is reversible and therefore unless one of the products is removed, the ester yield is limited. Assuming the reaction is equilibrium-limited and not rate-limited, higher conversions can be obtained by removing one of the products. For instance, if during the reaction the water is removed, the reaction will be driven by equilibrium to produce more ester product. High purity esters can be produced with azeotropic distillation to simultaneously remove water and alcohol from the esters using aromatic and aliphatic hydrocarbons as entrainers.

Mato Vazquez *et al.* found isobutyl acetate, *n*-butyl acetate and *iso*amyl acetate could be purified using an entrainer such as *n*-heptane, methyl cyclopentane or various other hydrocarbons to simultaneously remove the water and alcohol. The reaction products are fed to an azeotropic column where the entrainer is used to remove the alcohol and water as overhead

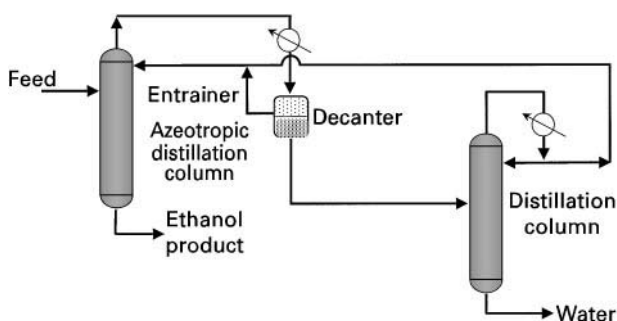


Figure 7 Typical ethanol dehydration process using azeotropic distillation.

products. Final purification of the ester product is carried out in a rectification column with only a few stages. The entrainer is recovered using a one-step liquid–liquid extraction (LLE) column with water as the extractant.

Wuest *et al.* found they could prepare ethyl chloroacetate by addition of ethanol to a melt of chloroacetic acid and *p*-toluene sulfonic acid and purify the ester product using azeotropic distillation. The ester and water form a minimum boiling binary azeotrope and therefore affect the ester/alcohol separation. Water and ethyl chloroacetate are removed overhead and the product is decanted. In this manner the ester is practically alcohol-free. This process avoids formation of the ternary ester/alcohol/water azeotropes which are difficult to separate.

Hills *et al.* found that azeotropic distillation is useful in the purification of esters produced using an enzymatic route. For example, isopropyl myristate can be prepared with lipase or immobilized lipase from myristic acid and propane-2-ol. The water produced in the reaction is removed by azeotropic distillation.

Conclusion

For almost 100 years azeotropic distillation has been an essential tool in the separation and purification of many industrial chemicals. There are distinct advantages to using azeotropic distillation, including energy savings, increased recovery and ability to separate components contained in close boiling, pinch point and azeotropic mixtures. Azeotropic distillation will undoubtedly remain a viable alternative for simplifying difficult separations found in industry.

See also: I/Distillation. II/Distillation: Energy Management; High and Low Pressure Distillation; Historical Development; Instrumentation and Control Systems; Modelling

and Simulation; Multicomponent Distillation; Theory of Distillation; Vapour–Liquid Equilibrium: Correlation and Prediction; Vapour–Liquid Equilibrium: Theory.

Further Reading

- Catalogue of Successful Hazardous Waste Reduction/Recycling Projects.* Energy Pathways Inc. and Pollution Probe Foundation (1987) Prepared for Industrial Programs Branch, Conservation & Protection Environment Canada, March, p. 84.
- Guinot H and Clark FW (1938) Azeotropic distillation in industry. *Transactions of the Institute of Chemical Engineers* 16: 189–199.
- Hills GA, Macrae AR and Poulina RR (1989) Eur. Pat. Appl. EP383,405, 16 Feb.
- Horsely LH (1973) *Azeotropic Data III*. Washington DC: American Chemical Society.
- Mato Vazques F, Bonilla Alonso D and Gonzalez Benito G (1990) Purification of commercial acetic acid esters by azeotropic distillation. Part I. Selection of azeotropic agents. *Quim. Ind. (Madrid)* 36(5): 444–449.
- Mato Vazques F, Bonilla Alonso D and Gonzalez Benito G (1990) Preparation of high-purity esters and recovery of azeotropic agents. Part II. Purification of commercial acetic acid esters by azeotropic distillation. *Quim. Ind. (Madrid)* 36(6): 543–547.
- Ohura H, Uchida Y, Yasaki A and Kishimoto S (1993) EP 0 529 413 A2. 13 Mar.
- Taylor AM and Wheelhouse RW (1992) EP 0 467 531 A1. 22 Jan.
- Te C and Shih TT (1989) Development of an azeotropic distillation scheme for purification of tetrahydrofuran. *Fluid Phase Equilibria. 5th International Conference on Fluid Properties and Phase Equilibria for Chemical Process Design*, 30 Apr–5 May, Vol. 52, pp. 161–168. Banff, Alberta, Canada.
- Wuest W, Leischner H and Esser H (1989) Eur. Pat. Appl. EP 315,096, 10 May.
- Young S (1902) The preparation of absolute alcohol from strong spirit. *Journal of the Chemical Society* 81: 707–717.

Batch Distillation

M. Barolo, Università di Padova, Padova, Italy

Copyright © 2000 Academic Press

Introduction

The interest in batch distillation has been steadily increasing in the last few years. This is a natural reflection of a change in industrial trends. In fact, the

shift towards the production of high value-added and low volume speciality chemicals and biochemicals has been much more marked in the last decade than in the past. Within firms producing specialized chemicals and biochemicals, batch distillation is a ubiquitous method for separating products from process inventories, for recovering components that are used in one of the process steps (like solvents, for example), and for removing undesired components

from an effluent stream. Examples of industrial applications of batch distillation include: the recovery of chloroform, butanol, water, organic and inorganic acids from process broths in the pharmaceutical industry; the concentration of acetone from dilute aqueous mixtures and the removal of water from butyl alcohol in the fine chemistry industry and the manufacture of alcoholic beverages from fermented mixtures in the food and beverages industry.

The success of batch distillation as a method of separation is undoubtedly due to its flexibility. In fact, a single batch column can separate a multicomponent mixture into several product cuts within a single batch but if the separation were carried out continuously, either a train of columns or a multi-pass operation would be required. Also, whenever completely different mixtures must be processed from day to day, the versatility of a batch column is still unexceeded. These attributes are crucial for responding quickly to a market demand characterized by short product lifetimes and severe specification requirements.

Equipment Arrangements and Process Modelling

Simple Distillation

The simplest batch distillation apparatus is shown in Figure 1. The operation is known as simple distillation or differential distillation. This is the oldest manifestation of distillation itself; it was used by many ancient cultures as a way of producing alcoholic beverages, essential oils and perfumes.

With regard to the separation of a binary mixture, the batch apparatus is run as follows. The pot is continuously heated, so that a vapour rich in the more volatile component is produced, condensed and collected in the external receiver. Indicating with x_B and y the instantaneous mole fractions of the more volatile component in the liquid and vapour phases in equilibrium, and with H_B the molar amount of boiling liquid remaining in the pot, the following material balances hold during any small time interval:

$$dH_V = -dH_B \quad [1]$$

$$y dH_V = -d(H_B x_B) \quad [2]$$

where dH_V is the molar amount of vapour produced during the same time interval. Combining [1] and [2], and integrating from the original feed conditions (H_F moles of boiling liquid of mole fraction z) to the present conditions, leads to the so-called Rayleigh equation:

$$\ln \frac{H_B}{H_F} = \int_z^{x_B} \frac{dx'_B}{y - x'_B} \quad [3]$$

Eqn [3] can be integrated numerically or graphically. It relates the amount of liquid remaining in the pot to the composition of this liquid. The molar amount H_D and average composition \bar{x}_D of the liquid accumulated in the receiver can be determined from the following material balances:

$$H_F = H_B + H_D \quad [4]$$

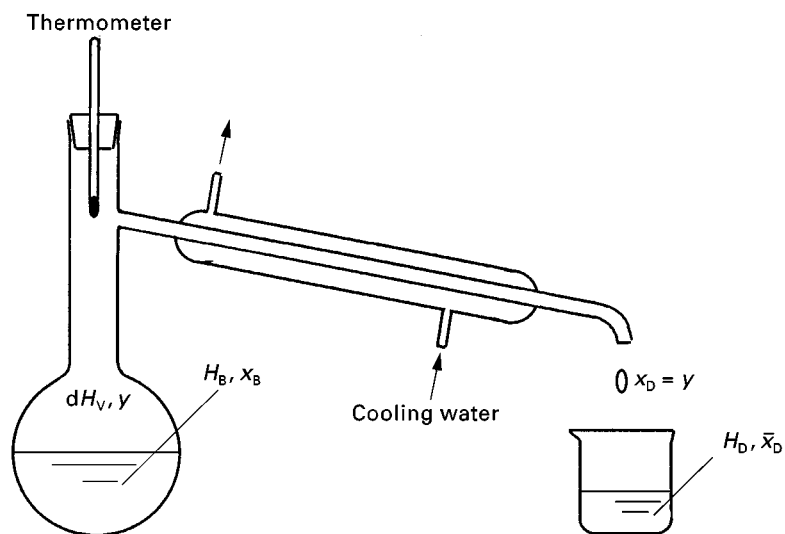


Figure 1 Apparatus for simple distillation.

and:

$$H_F z = H_B x_B + H_D \bar{x}_D \quad [5]$$

If the system displays a constant relative volatility (α), the integration of eqn [3] can be performed analytically, leading to:

$$\ln \frac{H_B}{H_F} = \ln \frac{1-z}{1-x_B} + \frac{1}{\alpha-1} \ln \frac{x_B(1-z)}{z(1-x_B)} \quad [6]$$

A graphical representation eqn [6] is presented in **Figure 2**. It is shown that, for a given fractional purification x_B/z of the feed, a larger amount of liquid can be recovered at the end of the batch when the feed is leaner in the more volatile component. It is also clear that it is not possible to obtain a finite amount of the pure heavy component, whatever the feed composition.

For a mixture of N_c components, N_c Rayleigh equations of the form [3] can be derived, and an iterative procedure is usually employed in order to determine the composition profile of each component as a function of the amount of liquid remaining in the still. In the case of constant relative volatility mixtures, direct calculation of the composition profiles can be accomplished by defining the amount b_i of the i th component remaining in the pot ($b_i = H_B x_{B,i}$). It can be shown that:

$$\frac{b_i}{f_i} = \left(\frac{b_j}{f_j} \right)^{\alpha_{i,j}} \quad [7]$$

where j is an arbitrarily chosen reference component, $f_i = H_F z_i$, and $\alpha_{i,j}$ is the relative volatility of the i th component with respect to the reference one. From

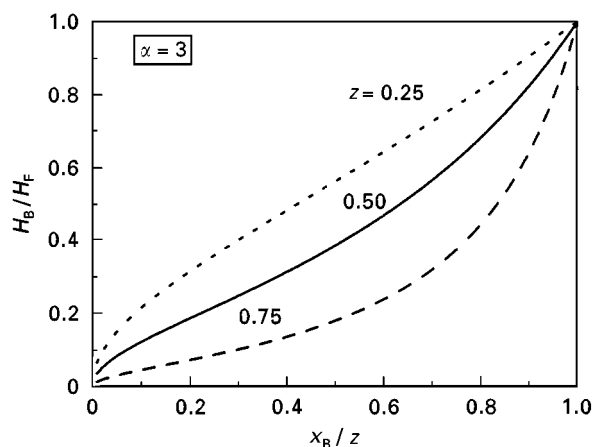


Figure 2 Simple distillation: fraction of the initial charge recovered after the purification of three different binary feeds from a light impurity.

the definition of b_i , it follows that:

$$x_{B,i} = \frac{b_i}{\sum_{i=1}^{N_c} b_i} \quad [8]$$

Differential distillation is a very simple way of separating a mixture of several components into cuts of different purities, for example for laboratory applications. However, it permits only rough separations, even with large energy consumption (it is a one-theoretical-stage operation). This is the reason why multistaged columns with reflux are employed whenever a sharper separation is needed.

Batch Rectification

A typical batch distillation column (a batch rectifier) is shown in **Figure 3**. The feed mixture is charged to a large reboiler, to which a heating medium (e.g. steam) is also fed. The vapour reaching the top of the column is condensed, and partially returned as reflux. A distillate stream is withdrawn, which sequentially feeds a series of tank receivers. The column may be a staged or a packed one.

Since in practice it is much more frequently requested to operate an existing column rather than to design a new one, only the issues of modelling and operating an existing rectifier will be addressed in the following sections.

Regardless of the operating mode, the column-modelling approaches can be grouped into three main classes: short-cut modelling, approximate modelling and rigorous modelling.

Short-cut models Short-cut models usually assume that the column dynamic behaviour can be approximated as a sequence of steady states (pseudo-steady-state approximation), which in turn is true when the column and reflux drum hold-ups can be neglected compared to that of the reboiler. This assumption allows the short-cut models that have been devised for the design of continuous columns to be employed at every time step in the simulation of batch columns. When binary mixtures are considered, a graphical representation of the process can be obtained by means of classical McCabe–Thiele diagrams. For multicomponent mixtures, a modification of the Fenske–Underwood–Gilliland design approach is often employed for simulating the batch column operation.

The main advantage of these models is their speed of computation; the main limits are their poor accuracy, and the fact that most of them are limited to constant relative volatility mixtures. They are mostly employed in preliminary process design and

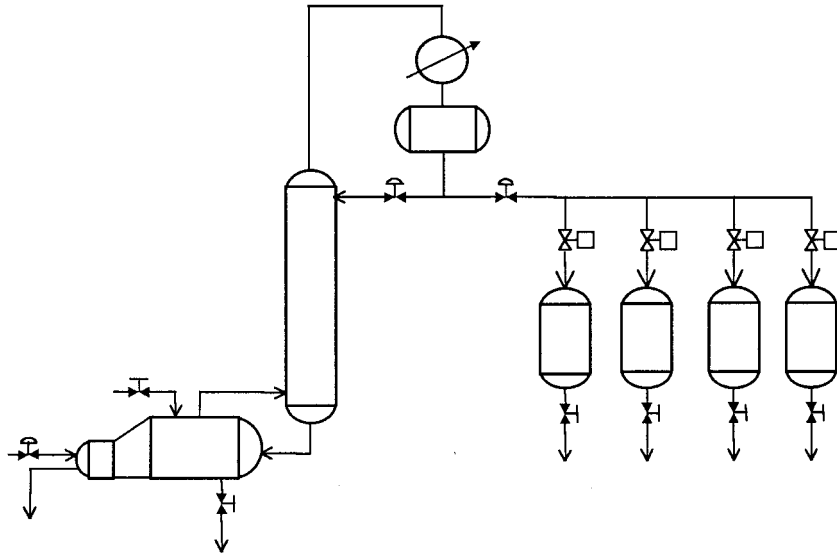


Figure 3 Sketch of a batch rectifier.

optimization studies, when a large number of cases need to be evaluated quickly, and a result of limited accuracy is acceptable. Rigorous results can be obtained by the subsequent use of more accurate models.

Approximate models Approximate models are used whenever a more realistic representation of the column dynamics is required. In this case, the tray and reflux drum liquid hold-ups are explicitly taken into account, even though they are usually assumed to be constant throughout the whole operation. Other usual assumptions are: boiling feed, total condensation without subcooling, perfect mixing in all parts, negligible vapour hold-ups, constant boil-up rate, constant molar overflows, ideal tray behaviour and negligible pressure drops and heat losses.

The set of equations usually employed to model a column with a separating capacity of N ideal trays is as follows:

Reboiler

$$\frac{dH_B}{dt} = L - V \quad [9]$$

$$\frac{d(H_B x_{B,j})}{dt} = Lx_{1,j} - Vy_{B,j} \quad j = 1, 2, \dots, Nc - 1 \quad [10]$$

Bottom tray (tray 1)

$$H_1 \frac{dx_{1,j}}{dt} = L(x_{2,j} - x_{1,j}) - V(y_{1,j} - y_{B,j}) \quad j = 1, 2, \dots, Nc - 1 \quad [11]$$

Tray i

$$H_i \frac{dx_{i,j}}{dt} = L(x_{i+1,j} - x_{i,j}) - V(y_{i,j} - y_{i-1,j}) \quad j = 1, 2, \dots, Nc - 1 \quad [12]$$

Top tray (tray N)

$$H_N \frac{dx_{N,j}}{dt} = L(x_{D,j} - x_{N,j}) - V(y_{N,j} - y_{N-1,j}) \quad j = 1, 2, \dots, Nc - 1 \quad [13]$$

Reflux drum

$$\frac{dH_D}{dt} = 0 \quad (V = L + D) \quad [14]$$

$$H_D \frac{dx_{D,j}}{dt} = V(y_{N,j} - x_{D,j}) \quad j = 1, 2, \dots, Nc - 1 \quad [15]$$

Thermodynamic equilibrium in stage i

$$y_{i,j} = K_{i,j} x_{i,j} \quad j = 1, 2, \dots, Nc - 1 \quad [16]$$

Summation constraints

$$x_{i,Nc} = 1 - \sum_{k=1}^{Nc-1} x_{i,k} \quad [17]$$

$$y_{i,Nc} = 1 - \sum_{k=1}^{Nc-1} y_{i,k} \quad [18]$$

In the above equations, H_i , H_D and H_B are the tray, reflux drum and reboiler hold-ups respectively; $x_{i,j}$ is the mole fraction of component j in stage i ; L , V and D are the liquid, vapour and distillate molar flow rates (respectively); $K_{i,j}$ is the vapour/liquid equilibrium ratio of component j in stage i ; and t is the time. Any suitable thermodynamic model can be used for the representation of the equilibrium ratio; deviations from the ideal tray behaviour can be taken into account using the Murphree tray efficiency concept. Due to possible wide ranges in the relative volatilities and/or large differences in tray and reboiler hold-ups, the system of differential equations is frequently stiff. As a starting point for the integration, it is often assumed that the reboiler, reflux drum and all trays are filled with the boiling liquid feed at the beginning of the operation.

Approximate models provide a fairly accurate description of the column dynamics, and are frequently used in process design and process optimization applications.

Rigorous models When a still more accurate description of the process dynamics is needed (for example, when it is required to model accurately the operation of an existing column), a rigorous model should be employed. In this case, almost all of the previous assumptions are relaxed, which considerably increases the computational load. The deter-

mination of the system and equipment parameters (like the Murphree tray efficiency, for example) is done by fitting some of the modelled profiles to actual plant data.

Other Column Arrangements

In the attempt to improve the flexibility of batch distillation operation as a whole, a closer look at alternative column configurations has been undertaken in the last few years. These different kinds of columns have been known since the 1950s, but a thorough understanding of their dynamic behaviour and features has only recently been achieved.

In the batch stripper represented in Figure 4A, the feed is charged to the reflux drum, while multiple cuts are withdrawn from the bottom of the column sequentially. In the middle-vessel batch column (Figure 4B), the feed is charged to an intermediate vessel, and the product/impurity removal is accomplished simultaneously from both the top and the bottom ends. The reboilers of both columns may be considerably smaller than the reboiler of a batch rectifier.

Potential improvements in column productivity, with respect to conventional batch rectifiers, may be very large when using these alternative configurations. However, to date it is not possible to provide general guidelines for determining *a priori* the best column configuration for a certain separation.

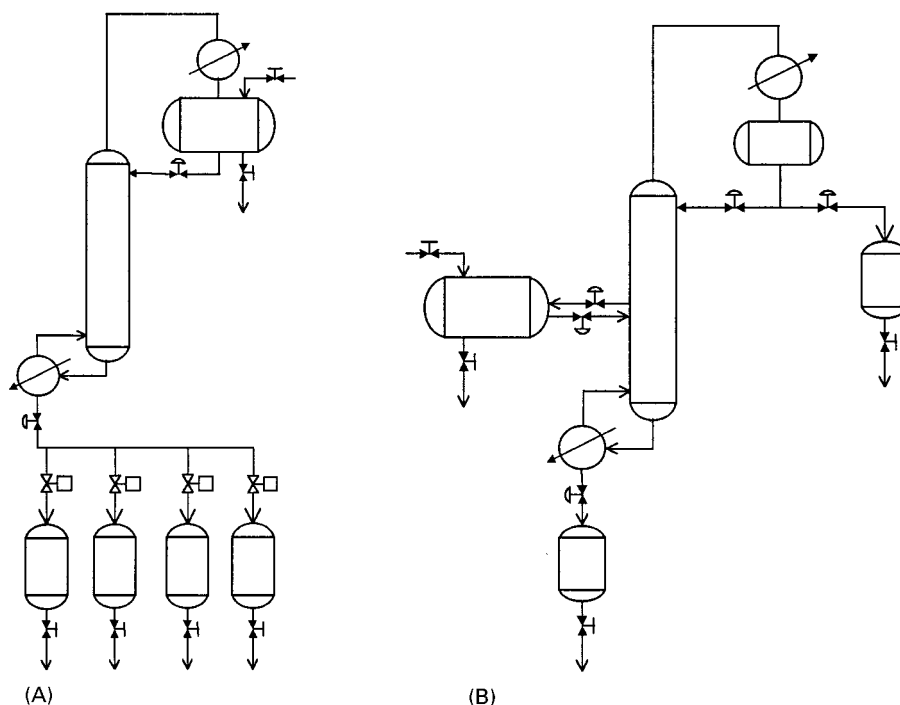


Figure 4 Sketch of (A) a batch stripper and (B) a middle-vessel batch column.

A preliminary simulation with a simplified model (or even with a short-cut one) should be used to assess the most profitable configuration for separating a given feed (amount and composition), subject to the given purity constraints.

Column Operation

The operation of a batch rectifier only will be considered in here. The most popular operating modes are: constant reflux ratio (with variable distillate composition), constant distillate composition (with variable reflux ratio) and total reflux (no product take-off). The former two operations are in fact semi-batch operations; the latter one is truly a batch operation. Operation at optimal reflux ratio should be mentioned too, but – since it is often accomplished through a series of constant reflux ratio sequences – this operating mode will not be considered here. In the following, the components are numbered in order of decreasing ease of separation (i.e. component 1 is the most volatile one, component 2 is the second most volatile, and component N_c is the least volatile).

From a practical point of view, regardless of the operating policy, the operation of a multicomponent column is carried out in three steps: (i) a start-up phase; (ii) a main cut production phase; and (iii) a slop cut removal phase. The last two steps are repeated sequentially. The following actions take place during the start-up phase: the column and receivers are possibly cleaned from the materials processed in the previous batch; cooling of the condenser is started; steam is fed to the reboiler, so that the material to be processed is heated up to its bubble point and starts to vaporize; as soon as the overhead vapour has been condensed and has filled the reflux drum, liquid is returned to the top of the column, and the column is run at total reflux; consequently, the column trays are sequentially filled with liquid.

The start-up procedure is very general, and goes on until either the steady state is approached, or the lighter product purity specification is reached in the reflux drum. The other two phases vary according to the operating policy employed.

Constant Reflux Ratio Operation

In the case of the separation of a binary mixture, a short-cut modelling approach is useful in order to have a graphical representation of the process. In a McCabe–Thiele diagram, at a given value $r = L/D$ of the reflux ratio, the slope of the operating line is fixed during the operation (Figure 5).

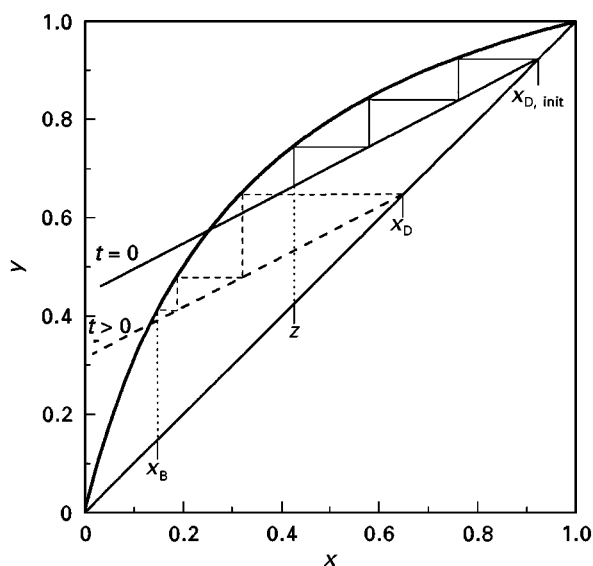


Figure 5 Binary batch distillation at constant reflux ratio (three-ideal-stage column).

While the distillation is proceeding, the operating line shifts down along the diagonal line. The mole fraction of the more volatile component in the distillate is continuously decreasing, and, at any instant of time, the reboiler composition is determined by stepping off N stages along the operating/equilibrium lines.

If both the top and the bottom purity specifications (x_D^{spec} and x_B^{spec} , respectively) are assigned, the reflux ratio should be chosen such that the final amount H_B^{final} of bottom product, as calculated through eqns [4] and [5] with $x_B = x_B^{\text{spec}}$ and $\bar{x}_D = x_D^{\text{spec}}$, is the same as the amount calculated by means of the Rayleigh equation:

$$\ln \frac{H_B^{\text{final}}}{H_F} = \int_{x_B^{\text{spec}}}^{x_D^{\text{spec}}} \frac{dx_B}{x_D - x_B} \quad [19]$$

The integral of eqn [19] can be evaluated numerically or graphically. The total amount Q_r of energy to be supplied at the reboiler is given by:

$$Q_r = \lambda(r + 1)H_D^{\text{final}} \quad [20]$$

where λ is the molar latent heat of vaporization of the mixture, and H_D^{final} is the final amount of distillate product collected.

For a multicomponent mixture, after starting up the column, the product removal is started at a constant and finite reflux ratio, and it continues until the average composition of the accumulated product (product 1) falls below the specification. At this point (called the cut-off point), the distillate composition is

neither sufficiently rich in component 1 to allow further accumulation of product 1, nor is it sufficiently rich in component 2 to allow beginning the withdrawal of product 2. Therefore, the distillate stream is diverted to another tank, and the collection of slop cut 1 is started. When the concentration of component 2 in the reflux drum meets the second product's specification, the distillate stream is diverted to a third receiver, and the accumulation of product 2 is initiated. The operation proceeds this way until all the products but the heaviest have been collected in the receivers. The heaviest product (product N_c) is recovered in the reboiler at the end of the operation. Therefore, at the end of the operation N_c main cuts (products) and at most $N_c - 1$ slop cuts are obtained. The slop cuts need to be reprocessed in subsequent batches.

It should be noted that, unless this issue has been addressed at the column design stage, the whole tray

hold-up drains to the reboiler when the steam supply is stopped. This must be taken into account when estimating online the final reboiler composition in order to detect the time when the distillation should be interrupted.

The plot of a typical evolution of the profiles of the average product composition, product amount and instantaneous distillate composition for the separation of a nonazeotropic ternary mixture at constant reflux ratio is shown in Figure 6. The profiles were determined with the approximate model described previously, and a constant relative volatility mixture was considered.

The dynamic behaviour of the column is characterized by a 'front' of each component sequentially moving from the bottom to the top of the column. If the column has enough stages, the top trays virtually separate a binary mixture made of the current most volatile component and its adjacent

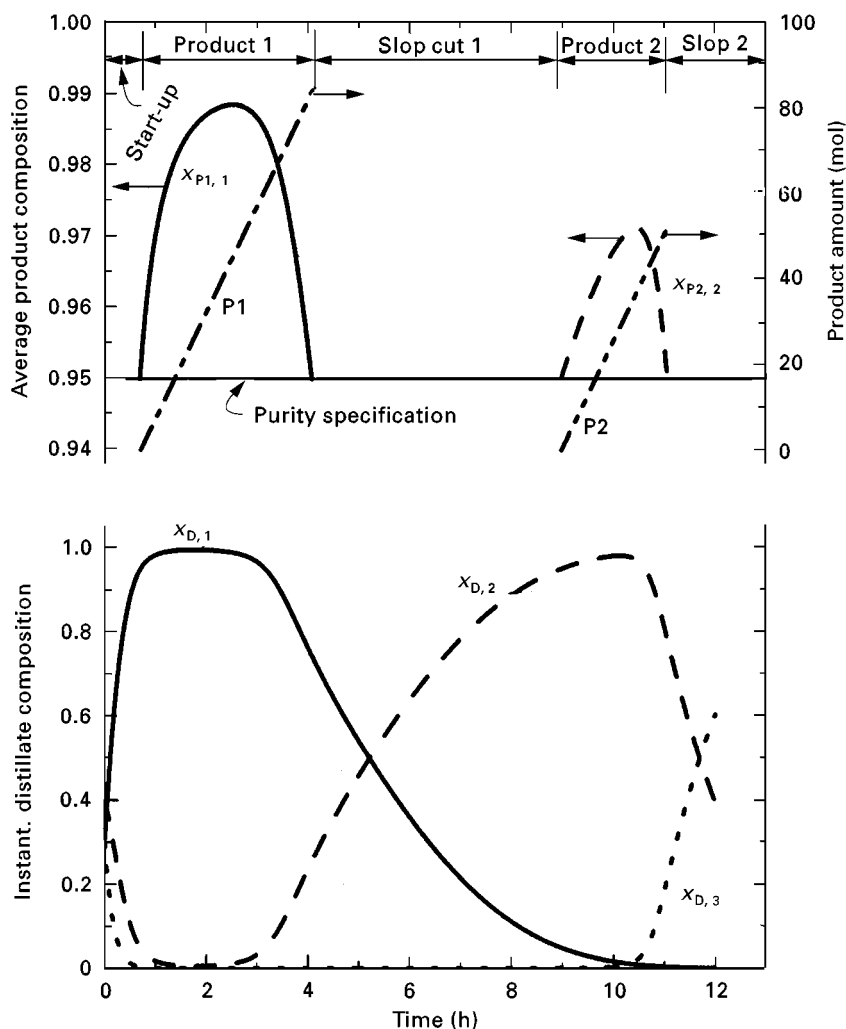


Figure 6 Typical evolution of the profiles of the average product composition, product amount and instantaneous distillate composition for an ideal ternary mixture under constant reflux ratio operation.

component in the scale of relative volatilities. This may prove advantageous for the control of the operation.

Operation at constant reflux ratio is the most popular in industry, because it is very easy to accomplish. However, some considerations deserve attention at this point. In order to implement this operating policy practically, a measure of the distillate and reboiler compositions should be available online, which is not usually the case. Therefore, the product composition needs to be inferred from secondary measurements, which should be available online quickly and at a low cost (like temperature and flow rates, for example). Also, operating the column at a constant reboiler duty is often easier than operating it at constant vapour boil-up, as was done in the previous numerical example. Finally, it should be noted that the column pressure may be decreased during the batch in order to improve the ease of separation of the less volatile components.

Constant Distillate Composition Operation

For the separation of a binary mixture under the quasi-steady-state assumption, a quick glance at the process can be obtained again by using a McCabe–Thiele representation, as shown in Figure 7.

In order to get the desired specification x_D^{spec} from the very beginning of the operation, the initial value of the reflux ratio must be such that the feed composition z is exactly obtained in the still when stepping off N stages from x_D^{spec} . Then, the reflux ratio (hence, the

slope of the operating line) is continuously increased during the batch in order to keep the distillate composition on specification. The operation is interrupted when either the reboiler composition has reached the desired composition, or the reflux ratio is so high that continuing the operation would be uneconomical (or even impossible, in an actual column).

The determination of the total amount of energy that needs to be supplied to the still is obtained by the following equation:

$$Q_r = \lambda \int_0^{H_D^{\text{final}}} (r + 1) dH_D \quad [21]$$

whose integration requires knowing r as a function of H_D . By combining eqns [4] and [5], with $\bar{x}_D = x_D^{\text{spec}}$, it is found that:

$$H_D = H_F \frac{z - x_B}{x_D^{\text{spec}} - x_B} \quad [22]$$

which enables relating the instantaneous reboiler composition (x_B) to the amount of product (H_D) collected up to the same instant. Therefore, since the reflux ratio can be related to x_B at any instant of time, eqn [21] can be easily integrated.

In a multicomponent separation, product 1 is collected until the reflux ratio reaches the prespecified maximum value. Then, the reflux rate is decreased in order to allow a quick removal of the remaining traces of the most volatile component (these traces are accumulated in slop cut 1). At the same time, this enables the front of the second lightest component to build up in the column so that, when the reflux drum composition meets the specification for product 2, the accumulation of this product is started. The production phase and the slop removal phase are then repeated sequentially; product Nc is eventually recovered from the reboiler.

Since operation at constant distillate composition is inherently a feedback operation, some kind of feedback from the plant is needed in order to be able to determine the correct value of the reflux ratio at any instant. When the distillate composition measurement is not available online, the most convenient feedback signal that can be used is a pilot tray temperature measurement. This strategy is similar to the one applied for one-point composition control in continuous columns. In principle, temperature control should be applied to binary mixtures only, but it can be extended to multicomponent mixtures, provided that the column has enough trays. Note that, similarly to continuous distillation, the measuring element must be placed somewhat down from the top of the column in order to ensure sensitivity of the temperature

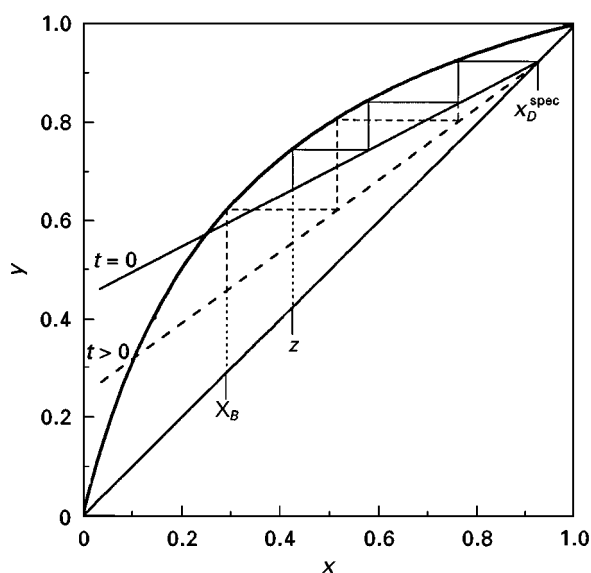


Figure 7 Binary batch distillation at constant distillate composition (three-ideal-stage column).

response to changes in the distillate composition. Therefore, if good control at a constant set point is provided, the product purity usually increases while this product is being removed from the column. This is because the separating capacity of the column increases during the batch, due to the increase of the reflux rate.

From a practical point of view, this kind of operation is harder to implement than constant reflux ratio, even if a measure or an estimate of the distillate composition is available online. Because the dynamics of the process may change significantly as the batch proceeds, conventional proportional plus integral controllers often prove to be inadequate for tight composition control. Care should be taken when the reflux rate increases widely, because the liquid loading to the column might increase to a point that flooding conditions are reached.

Total Reflux Operation

This operation is the best suited for binary mixtures, whose components should be recovered at a relatively high degree of purity. The feed charge H_F is split between the reflux drum (H_D kmol) and the reboiler (H_B kmol), and the column is operated at total reflux for the whole duration of the batch. Under the assumptions of quasi-steady-state operation and constant relative volatility, the operation can be analysed easily. For a given pair of product specifications, the minimum number N_{\min} of theoretical stages necessary in order to achieve the desired separation can be determined from the Fenske

equation:

$$N_{\min} = \frac{1}{\ln \alpha} \ln \frac{x_D^{\text{spec}}(1 - x_B^{\text{spec}})}{x_B^{\text{spec}}(1 - x_D^{\text{spec}})} \quad [23]$$

If the operation is feasible in the available column, the requested top and bottom hold-ups are calculated immediately by eqns [4] and [5], with $x_B = x_B^{\text{spec}}$ and $\bar{x}_D = x_D^{\text{spec}}$.

At any time t , the operating line is parallel to the diagonal line in a McCabe–Thiele diagram (Figure 8), and moves towards the diagonal as time progresses according to the following dynamics:

$$V(y - x) = H_D \frac{dx_D}{dt} \quad [24]$$

or:

$$V(y - x) = -H_B \frac{dx_B}{dt} \quad [25]$$

Since, at time t , the following material balance holds true:

$$\frac{x_D - z}{z - x_B} = \frac{H_B}{H_D} \quad [26]$$

the reflux drum and reboiler compositions at the same time instant can be determined by using the auxiliary line \overline{FQ} , where the abscissa a_Q of the auxiliary point Q on the x -axis is such that:

$$\frac{a_Q - z}{z} = \frac{H_B}{H_D} \quad [27]$$

The segment \overline{BD} is drawn, where B is on the diagonal line with $a_B = x_B$, and D is on the auxiliary line \overline{FQ} with $a_D = x_D$. The product compositions at time t are correct if the segment \overline{BD} is parallel to the x -axis.

The total amount of heat to be supplied to the reboiler is given by:

$$Q_r = \lambda H_D \int_z^{x_D^{\text{spec}}} \frac{dx_D}{y - x} = -\lambda H_B \int_z^{x_B^{\text{spec}}} \frac{dx_B}{y - x} \quad [28]$$

From a practical standpoint, the advantages of this operating mode are:

- the column always operates at its maximum fractionating capacity;
- column operation is very easy: only a level controller is necessary, which keeps the reflux drum hold-up at the specified value; no product switchovers are required;
- neither the yield nor the quality of the products is influenced by variations in the heating rate or interruption of the distillation.

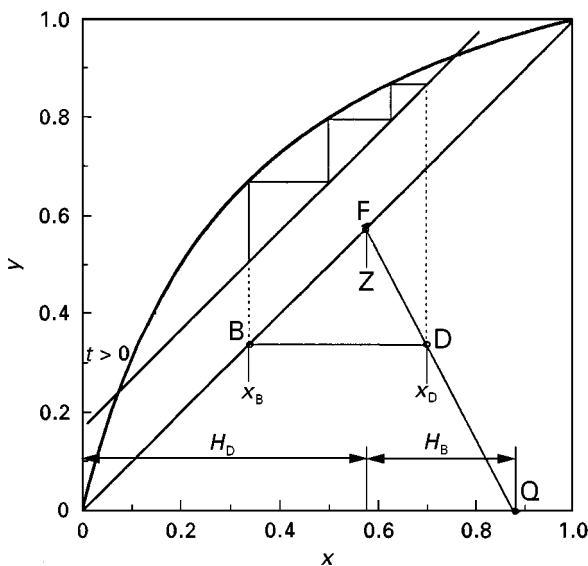


Figure 8 Binary batch distillation at total reflux (three-ideal-stage column).

However, it should also be observed that unavoidable uncertainties in the feed amount, feed composition and column hold-up would act in such a way as to prevent reaching the desired purity specifications for both products. In order to ensure that the more valuable product is recovered on specification, the hold-up of the vessel containing this product should be set somewhat smaller than requested theoretically; a conventional temperature controller may be cascaded to the reflux drum level controller in order to adjust the level setpoint online, according to the desired purity requirements. Another way to reduce (and even eliminate) the effect of the uncertainties is using a middle-vessel batch column.

For multicomponent separations, a cycling operation may be employed: the column is operated at total reflux until a steady state is approached; distillate is then taken as total draw-off for a short period of time; then, the operation is switched back to total reflux, and the operating cycle is repeated.

Conclusion

As was noted in the Introduction, batch distillation as a way of separating a given mixture in multiple fractions is becoming more and more frequent, especially in the fine chemicals, pharmaceutical, biochemicals, food and beverages industries. While it is true that batch distillation usually consumes more energy than continuous distillation, it nevertheless provides more flexibility and requires less capital investment. This is an economic incentive, particularly when small volume or high added-value products are to be recovered. Still, there is a certain reluctance among operators to use this process. In fact, its unsteady nature, together with the need for monitoring, switching and discharging a series of cuts, may unavoidably confuse plant personnel.

From an engineering perspective, modelling and simulation of the operation is no longer as hard a task as it was in the past. The understanding of the process is fairly comprehensive (at least for conventional columns), so that all the operating steps characterizing a batch distillation process can be modelled in some detail. The availability of computer hardware at low cost makes it possible to solve all the model equations in a reasonably short time. It should be stressed that the availability of a reliable process model is a crucial issue for profitably utilizing an

existing batch column. If a good model is available, then it can be used to find out the optimal operating policy for the batch, i.e. to determine which are the sequence of reflux ratios during the batch and the strategy for reprocessing slop cuts between batches that would maximize a prescribed profit function. A process model can also prove useful for the closed-loop control of the operation. Advanced control strategies employ process models to get online estimations of the product compositions, thus eliminating the need to resort to expensive hardware analysers; more efficient control laws than the classical proportional plus integral algorithm can also be developed if a process model is available. Finally, process models can be employed within a training programme to instruct the plant personnel on how to interpret the column dynamics, and its response to process uploads: this may prove useful in improving the operator's confidence about this unsteady unit operation.

See also: II/Distillation: Historical Development; Instrumentation and Control Systems; Multicomponent Distillation; Pilot Plant Batch Distillation; Theory of Distillation.

Further Reading

- Diwekar UM (1995) *Batch Distillation: Simulation, Optimal Design, and Control*. Bristol: Taylor-and-Francis.
- Hart DR (1992) Batch distillation. In: Kister HZ (ed.) *Distillation Design*. New York: McGraw-Hill.
- Holland CD (1966) *Unsteady State Processes with Applications in Multicomponent Distillation*. Englewood Cliffs: Prentice-Hall.
- Luyben WL (1990) *Process Modeling, Simulation, and Control for Chemical Engineers*. New York: McGraw-Hill.
- Macchietto S and Mujtaba IM (1996) Design of operation policies for batch distillation. In: Reklaitis GV, Sunol AK, Rippin DWT and Hortaçsu Ö (eds) *Batch Processing Systems Engineering – Fundamentals and Applications for Chemical Engineering*. Berlin: Springer.
- Muhrer CA and Luyben WL (1992) Batch distillation. In: Luyben WL (ed.) *Practical Distillation Control*. New York: Van Nostrand Reinhold.
- Robinson CS and Gilliland ER (1950) *Elements of Fractional Distillation*. New York: McGraw-Hill.
- Rose LM (1985) *Distillation Design in Practice*. Amsterdam: Elsevier.
- Seader JD and Henley EJ (1998) *Separation Process Principles*. New York: John Wiley.
- Stichlmair JG and Fair JR (1998) *Distillation: Principles and Practice*. New York: Wiley-VCH.

Control Systems

See II/DISTILLATION/Instrumentation and Control Systems

Energy Management

T. P. Ognisty, The M. W. Kellogg Company,
Houston, TX, USA

Copyright © 2000 Academic Press

Introduction

Distillation dominates separation processes in the petrochemical industry and consumes nearly 95% of the total energy used in commercial separations. The energy used in distillation is approximately 3% of the total energy consumed in US industry. Distillation columns provide reliable, cost-effective separation for large throughputs and high purity product requirements. Distillation is an energy-intensive process and economics drive the need to optimize energy consumption in all aspects of its design.

In the pioneer years of distillation development, energy was comparatively cheap compared to capital costs. Reflux ratios of 1.2–1.5 times the minimum were commonly used to obtain an economical balance between operating and fixed costs. Columns were designed with large design margins to allow for feed changes and the lack of accuracy in physical properties, tray hydraulics and tray efficiency. By providing excess exchanger and tray capacity, product purity could be maintained by adjusting the tower operation to compensate for design uncertainty.

With the advent of the oil crises of the 1970s and 1980s, the energy costs became the major factor in column costs and created an urgency to find ways to reduce the energy requirements of distillation. Several techniques for analysing columns and plants were extensively developed and published in this era. Among the notable advances is 'exergy' analysis, developed primarily in Europe, and 'pinch' technology. This trend has subsided somewhat as more efficient methods of design and experience have eventually replaced the older technologies. The more exciting opportunities are in revamping older plants and designing new products. The introduction of high speed computers has also played a significant role in producing more accurate and more extensively evaluated designs. Physical and transport properties continue to be obtained more accurately. As the regulatory requirements for pollutant emissions and wastewater reduction became more stringent, many new studies has been directed towards reducing emissions from fired heaters and steam boilers used to supply heating requirements in columns. Wastewater

reductions of steam condensate blowdowns and cooling water make-up have become subject to tighter restrictions. Distillation column design will become more extensive and complex as the stringency of requirements continues to increase.

The primary objective of distillation column design is to produce the desired products with the minimum amount of energy expenditure and capital cost. The energy consumption in distillation columns is affected by the physical properties of the system, the utilities available for heating and cooling, the internals for contacting the liquid and vapour and the arrangement of the column separation sequence.

Measurement of Energy Performance

In order to determine the energy performance of a distillation column, two thermodynamic principles are applied to give a measurement method for determining the value of design improvements.

Availability or Exergy Analysis

The concept of availability or available useful work is a convenient way to determine the thermodynamic minimum amount of energy required for doing work in a steady flow process. The availability is referred to as exergy in Europe. The availability function is defined as:

$$A \equiv H - T_a S$$

where H is the enthalpy, S is the entropy and T_a is the reference temperature (298 K). A higher value of availability indicates that more work can be extracted as compared to a lower value. For example, high pressure steam is more valuable than steam at atmospheric pressure, although the latent heat values are about equal.

The change in availability represents the amount of shaft work that can be extracted from a system as it flows from an initial to final state. It also defines the minimum work required to achieve a change in a flowing system. This available shaft work, W_s , is defined in terms of the availability change, or:

$$-W_s \equiv \Delta A = \Delta H - T_a \Delta S$$

These properties are readily available from data references or process simulators and can be applied to all types of plant equipment in a process.

Heat Engines

A Carnot heat engine is useful in determining the theoretical maximum heat efficiency of an ideal, reversible distillation. The heat engine analogy consists of the simple column arrangement depicted in **Figure 1**. Heat is added at the bottom of the tower at a high level of temperature and then removed at the top of the tower at a lower temperature. This degradation in heat provides the work to separate the feed into the products. If we consider a distillation column as a heat engine, then the theoretical minimum work required for the heat engine is:

$$W_{\text{heat}} = Q_{\text{reboiler}}(1 - (T_a/T_{\text{reboiler}})) - Q_{\text{condenser}}(1 - (T_a/T_{\text{condenser}}))$$

The availability change of the streams in and out of the column is equal to this heat work minus a lost work term to account for thermodynamic inefficiency, or:

$$A_{\text{products}} - A_{\text{feeds}} = W_{\text{heat}} - W_{\text{lost}}$$

To account for real processes, a lost work term is included to account for irreversible changes within the column. This extra work is required to overcome pressure, temperature and composition driving forces. There are a number of commercial algorithms for determining each driving force contribution to lost

work. These lost work contributions are generally classified as:

1. Momentum loss due to pressure drop.
2. Heat transfer loss from temperature difference.
3. Mixing losses due to composition differences.

As the lost work term increases, the reboiler and condenser loads must increase in order to supply the same amount of useful work. As the driving forces approach zero, the lost work approaches zero and less energy is wasted.

For a particular column design, the availability of the feed and products and the theoretical minimum work are fixed. The lost work energy is solved by difference. The actual heat duty required for the distillation column will be the sum of the theoretical minimum plus the lost work, or $(W_{\text{heat}} + W_{\text{lost}})$. By comparing values of this sum, the designer has a yardstick in which to rate different column designs. For existing columns, a simple calculation of the total lost work will quickly focus as approach towards the most potentially beneficial areas. For example, if the lost work is less than 5% of the total heat duty, then this is probably within the design margin of the equipment and not worth pursuing.

Distillation Design Guidelines

A thermodynamic analysis provides information about the theoretical limits and does not address the issues of expense and implementation. Exergy studies should include capital costs with a payback period for a proper economic assessment.

The following list is a collection of design guidelines and practical constraints to be considered in searching for better energy schemes:

1. In order to distil vapour and liquids, the pressure must be below the critical pressure.
2. Accurate physical properties are required; proper models for nonideal solutions and azeotropes should be checked.
3. Thermally unstable components may limit the reboiler temperatures.
4. Air and/or water-cooling are preferred to the more expensive refrigeration.
5. Operational flexibility is usually required for feed changes and plant turndown.
6. Distillation columns do not work well at less than the minimum reflux ratio and at pinch points.
7. Heat integration may not be practical; transporting fluid over large distances may not be econ-

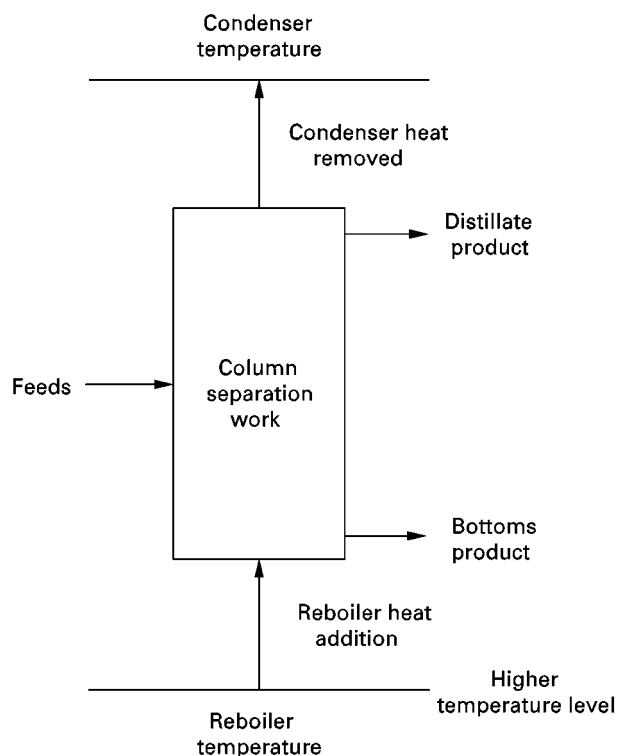


Figure 1 Distillation heat engine analogy.

omical; excessive temperatures result in film boiling; interaction between columns should be controlled.

8. Shipping weight and total height restrictions tend to limit the maximum number of trays or packing in one tower shell.
9. Lowering the operation pressure is a simple way to reduce energy consumption. Increasing pressure is the simpler way to increase capacity.
10. Lower energy consumption usually requires higher capital costs.

McCabe–Thiele Diagrams

One of the best visual aids for distillation is the ubiquitous McCabe–Thiele diagram. Despite its many limitations, the diagrams show the basic relationship between the equilibrium curve and the composition profiles throughout the column. A typical McCabe–Thiele diagram is illustrated in **Figure 2**. Heating or cooling changes the internal vapour and liquid flows and this effect can be seen as a shift in the slope of the operating lines in the diagram. For energy management, we are interested in seeking ways to minimize the difference (the composition driving forces) between the operating and equilibrium curves.

The absolute minimum energy expenditure will occur if external heating or cooling is applied to each stage to adjust the operating line so that it coincides with the equilibrium curve. This condition is impractical, since an infinite number of stages would be

required. The goal is to design a column with an approach as close as possible to equilibrium, but with an acceptable number of stages. A few successful designs exist that provide internal continuous cryogenic cooling in a small tray section. These types of columns that have continuous, internal heat exchangers are called dephlegmators.

There are numerous practical applications in the industry where adding *just a few select* external heating or cooling locations will provide a cost-effective reduction in energy.

Intermediate Heating and Cooling

Pumparounds

One of the earliest methods for saving significant amounts of energy was developed for crude units. Pumparounds are used extensively in atmospheric and vacuum towers to remove heat at selected stages. Liquid is withdrawn from an intermediate product stage, externally cooled and then pumped back to the column at a higher elevation. This arrangement is shown in **Figure 3**. The hot liquid from the tower is used to supply heat to several sources. The remaining cooled liquid is returned to the column and used to cool the column vapour. Pumparounds have the effect of shifting the operating lines *at select intervals* closer to the equilibrium curve to improve energy consumption. The sub-cooled liquid provided in the pumparound reduces the cold utility requirements and size of the overhead system. The cooling tower and condensers are less expensive and thermal and wastewater pollution is reduced. The hot pumparound liquid has the additional role of recovering heat supplied in the feed furnaces by transferring it to feed pre-heat, steam generation and heating for downstream units.

Intercondensers and Interreboilers

Another useful technique for reducing the utility loads is to add intermediate exchangers. **Figure 4** shows the effect of adding an inter-reboiler on a McCabe–Thiele diagram. The benefit of this modification is that the *reboiler* heat duty is reduced by the amount of duty used in the inter-reboiler. Since the temperature level will be less than the reboiler temperature, it may be possible to use a process stream for the heating. If this heat integration is feasible, then significant savings of the reboiler utility, such as high pressure steam, can be achieved. The internal column flows below the interreboiler stage will be reduced, but the stage requirement will increase since the operating line will be closer to the equilibrium curve. For this reason, the addition of intermediate exchangers is

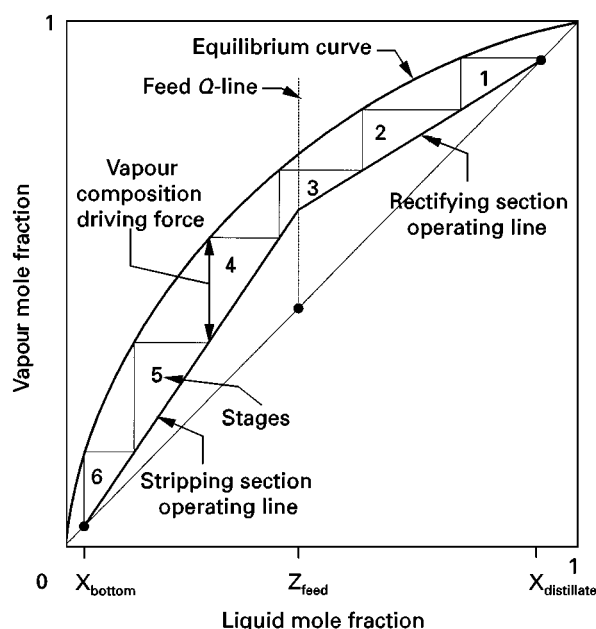


Figure 2 Typical McCabe–Thiele diagram.

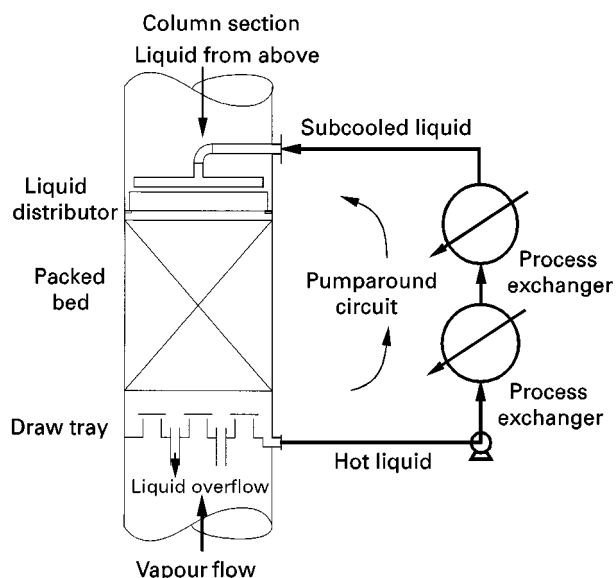


Figure 3 Pumparound section.

usually economical only when a few extra stages will be required. An analogous result will be obtained with an inter-condenser. The condenser utility load will be reduced, the internal flows in the stages above the condenser will be reduced, but more stages will be required. The benefits of intermediate cooling or condensing are particularly economical when an expensive refrigerant is used as the condenser cooling medium.

There are semi-rigorous calculation methods for determining how much heat can be added or removed

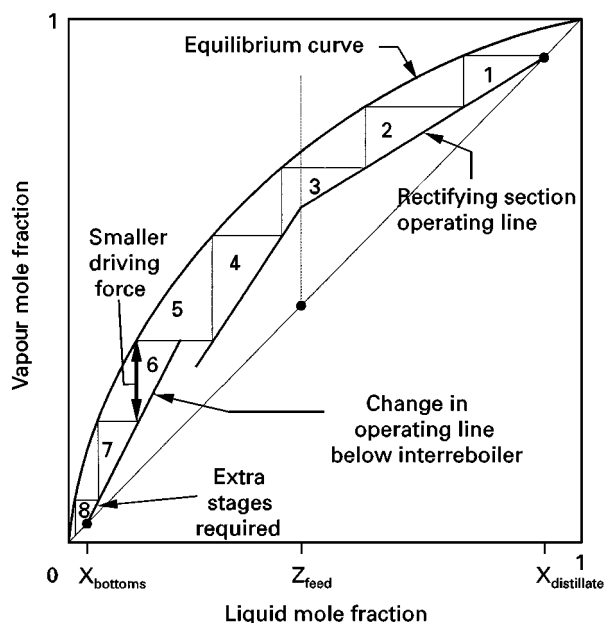


Figure 4 McCabe-Thiele diagram with interreboiler.

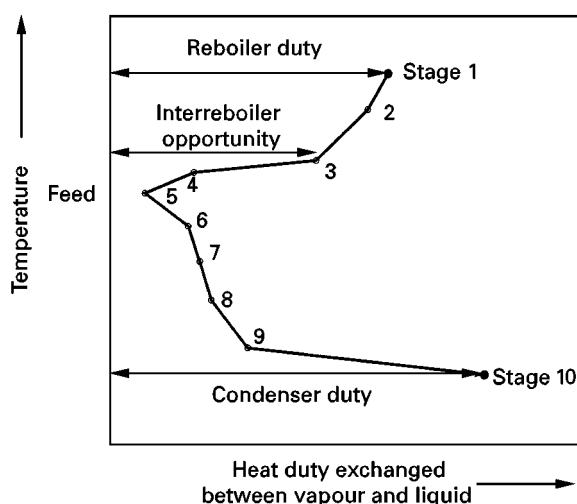


Figure 5 Column grand composite curve.

at a particular temperature level. One technique, which is an extension of 'pinch' technology, is to generate a column grand composite curve (CGCC). These curves plot the heat transferred between the vapour and liquid versus stage temperature. A typical example is shown in Figure 5. The best opportunities for using intermediate heat exchangers exist in the regions where large amounts of heat are exchanged at temperatures significantly different to that of the reboiler or condenser. When deciding upon how much heat will be added or removed, one should consider the extra stages that will be required and allow for a suitable design margin for flexibility. If this type of region exists near the feed locations, then feed conditioning may be an option. Adding a feed exchanger will generally be less expensive than adding an intermediate exchanger on the column.

Feed Conditioning

The feed is introduced into the column where the temperature and composition roughly match the column profile. The feed is at higher pressure in order to flow into the column. The location of the feed stream can be optimized with a few judicious choices with a process simulator. The feed quality and location can also be adjusted within limits to lower the reboiler or the condenser duty, but not both. The best opportunities for utilizing feed exchangers are during revamps when there is excess vapour- and liquid-handling capacity in one section of a column. For example, if the trays above the feed can handle more fluid traffic without modification, but the bottom section trays are capacity-limited, then installing a feed pre-heater can be used to unload the bottom traffic. The

energy penalty will be increased condenser duty, but internal modifications or tower replacement may be avoided.

Prefractionation

In a multi-component column separation, the presence of lighter nonkey components will limit the purity of the light key. At the top of the tower, the light key will actually be the heavier component and its composition will reach a maximum value and then decrease as it is fractionated from the lightest components. By removing these lighter non-key components from the feed in a pre-absorber, the column can now produce a higher purity product. Removing the light components from the feed reduces the flow to the column, so that pre-absorbers can be used to unload the rectifying section of an existing column. In analogous fashion, the addition of a pre-stripper will unload heavy components from the stripping section of a column. **Figure 6** shows an illustration of a pre-stripper column arrangement. The additional feed to the last column will usually provide a modest energy saving for that column.

Heat Pumping

A significant saving in condenser duty can be achieved by compressing the overhead vapour to a temperature that can be used to reboil the bottoms liquid. A typical heat-pumped column is shown in **Figure 7**. The compressor is a significant addition to the total capital costs. This scheme is feasible if the distillation involves a close boiling mixture where the top and bottom temperatures are not significantly different. The most common industrial application is propane/propylene splitters, which require large

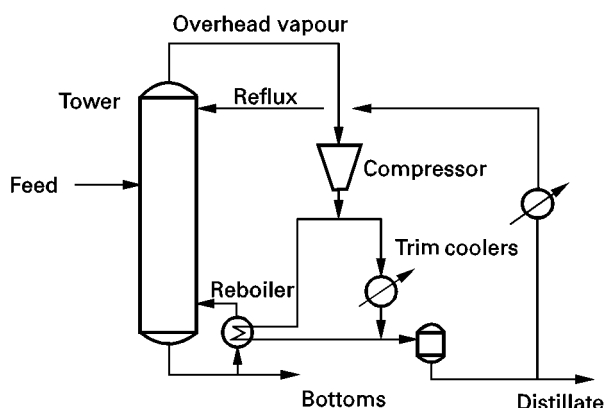


Figure 7 Heat-pumped column.

amounts of heating and cooling energy. A large reduction in cooling water and wastewater products provides a large incentive to heat pump these types of columns.

Extractive and Azeotropic Distillation

Instead of modifying the heat exchange in columns, a reduction in energy is possible by altering the physical properties of the mixtures. For mixtures that are difficult to distil, a solvent may be added to increase the relative volatility of the mixture. If a suitable solvent can be found with a relatively low volatility, then the separation process is known as extractive distillation. A typical extraction distillation column arrangement is illustrated in **Figure 8**. This process is economical to use when a small amount of inert solvent can permit an easier (less expensive) separation of the original products. An additional tower is required to remove the solvent from the heavier product.

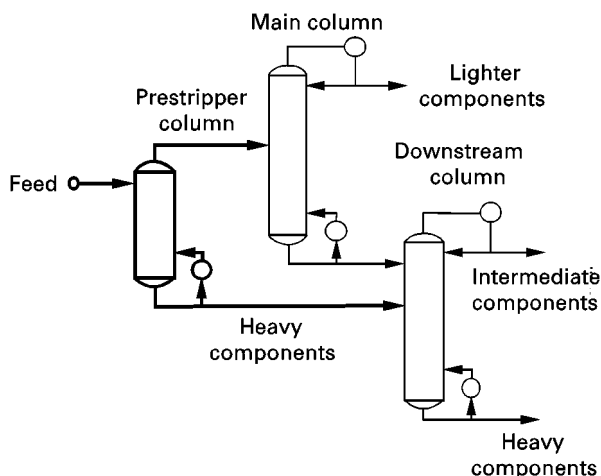


Figure 6 Prestripper column sequence.

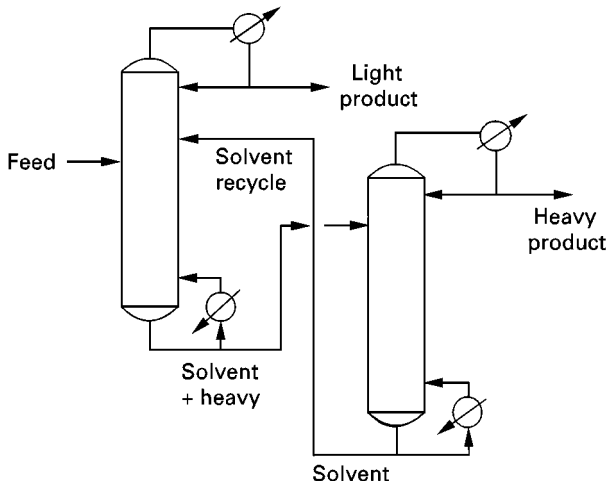


Figure 8 Extractive distillation configuration.

If the addition of a light component can alter an azeotrope, then the process is termed azeotropic distillation. The entrainer often forms a new low boiling azeotrope that is relatively easy to separate from the heavier product. The entrainer is separated from the lighter product with an additional column and/or condensed to two liquid phases that are separated in a settling drum. Azeotropes are common in the specialty chemicals industry and most configurations are proprietary.

Extractive or azeotropic distillation should be considered a last resort option. Finding a suitable solvent or entrainer that is inexpensive and relatively inert is the key to a practical design.

Column Internals Selection

The choice of internals can have impact on energy efficiency, control response and downstream equipment. The function of trays or packing is to promote efficient heat and mass transfer by intimate contacting of the vapour and liquid. For trays, a portion of the vapour energy is expended in the form of pressure drop to produce liquid droplets and to overcome the liquid head on the tray. In contrast, the contact area in packing is mainly created by the spreading of liquid over the metal surfaces and by rivulet flow. For these reasons, the pressure drop in packing is significantly less than in trays.

This becomes an important characteristic in high vacuum distillation, where the pressure and temperature changes dramatically from top to bottom as pressure drop increases. A tower pressure change from 50 mm Hg to 25 mm Hg will double the volumetric flow of vapour and will have a major impact on the tower size. The normal design pressure drop for *one* tray is 3–5 mm Hg, which will limit the number of trays that can be used. Low pressures and temperatures in the top of the tower have an impact on the cost and performance of the condenser and vacuum system. Using lower pressure drop internals reduces the exergy losses associated with momentum and temperature difference. For these reasons, packed ns are favoured for vacuum distillations.

There also is an advantage to lowering pressure drop in a column when the overhead vapour is fed to a compressor. Changing from trays to packing during a capacity increase revamp is a convenient way to avoid compressor changes. If the pressure drop through the tower is reduced, the increase in compressor suction pressure may just compensate for the new capacity increase.

By virtue of lower pressure drop and liquid hold-up, packed columns have relatively faster response to changes in flow and composition changes. The faster

acting control of the column reduces the energy waste of recycling off-spec product.

Column Sequencing

The sequencing and arrangement of columns to obtain multiple products has a major impact on energy and capital costs. In order to separate X amount of products, a minimum of $X - 1$ simple, conventional columns are required. If the products are removed as distillates, the arrangement is called a direct sequence. The direct sequence is favoured when the distillations are at high pressure and require refrigeration, such as olefin production. An indirect sequence is used if the products are withdrawn as bottoms. Indirect sequencing favours lower heat consumption. In many petrochemical plant configurations, both sequences are used or mixed as dictated by the many product requirements. An illustration of the direct and indirect sequence arrangement is given in Figures 9 and 10.

A number of heuristics have evolved from experience of sequencing columns. A few of the more common guidelines are listed below:

1. Leave the most difficult separations to the end. The binary separation of high purity products requires larger towers and higher energy consumption when non-key components are present.
2. Direct sequences are favoured when heating costs are less than cooling costs.
3. Less energy is expended when the top and bottom product flows are about equal.

The column sequencing depends upon numerous factors that make each case different. Refining, ethylene, aromatic and specialty chemical plants all have unique properties and idiosyncrasies that make generalizations difficult. The column arrangements

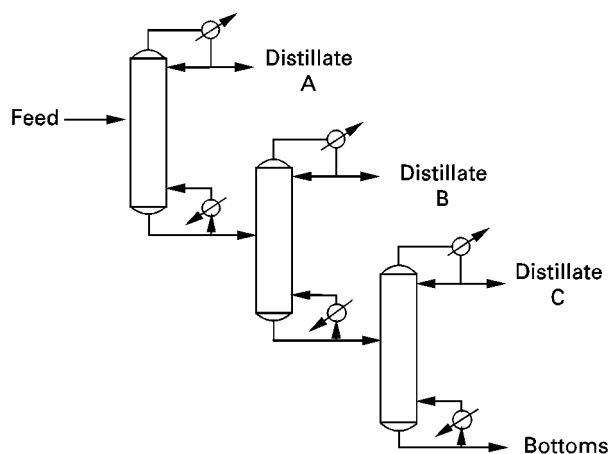


Figure 9 Direct column sequence.

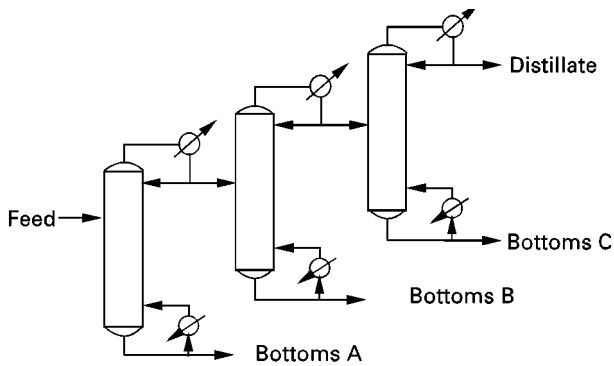


Figure 10 Indirect column sequence.

are commonly integrated with the total plant optimization to minimize overall capital costs, energy consumption and pollution reduction. Techniques such as pinch technology and exergy analysis are used to evaluate the global effect of equipment changes to arrive at the best plant design, which may not coincide with the best column design.

Distributed Distillation

Distributed distillation is a separation technique that minimizes the lost work due to mixing and recycling of fluids within a column. The energy consumption can be reduced by making a separation between the most volatile and least volatile components with the rest of the components distributed between the top and bottom. An easy separation between components

with the highest relative volatility will yield the minimum boil-up and reflux for any column. This concept is illustrated in Figure 11. A distributed column sequence will theoretically consume less energy, but will require more columns. The energy savings have been reported to be upwards of 30%.

To lower the capital costs, the column can be thermally coupled as described in the Petlyuk configuration shown in Figure 12. Thermal coupling is used to describe the situation when liquid from a column is used to supply reflux and vapour is used to supply boil-up to another column. Several variations of this arrangement are used to eliminate heat exchangers in column designs. Combining the two columns together and providing a partition to form a *divided wall column* reduces the capital cost. Three products can be produced from one column, one reboiler and one condenser, as compared to a conventional sequence that requires two columns and four exchangers. The commercial use of divided wall columns tends to be limited to separations with significant amounts of intermediate components.

The Future of Energy and Distillation

Distillation is a mature separation technology and will remain dominant in the near future. Despite the high energy requirements, distillation is a cost-effective method for separating large quantities of material into high purity products. Other separation methods are specific in application and lack the

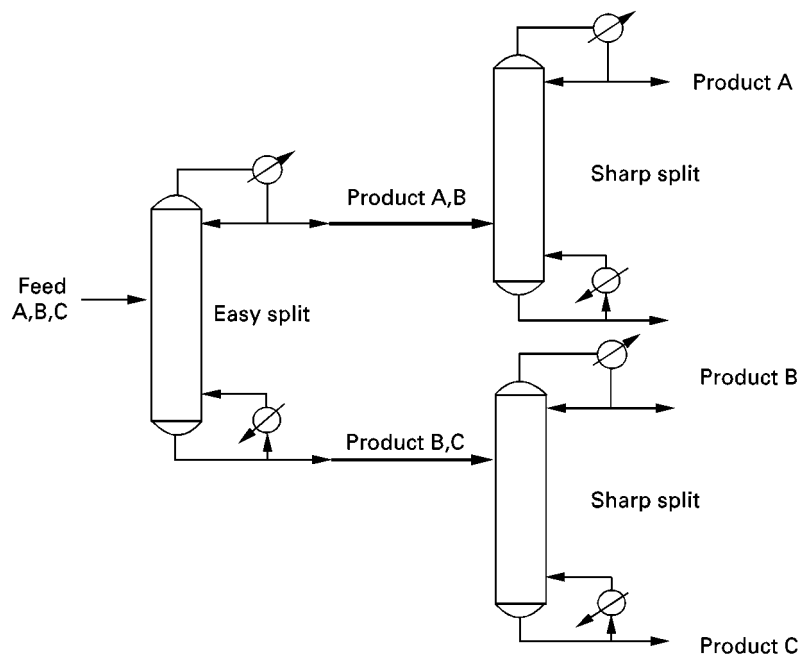


Figure 11 Distributed column sequence.

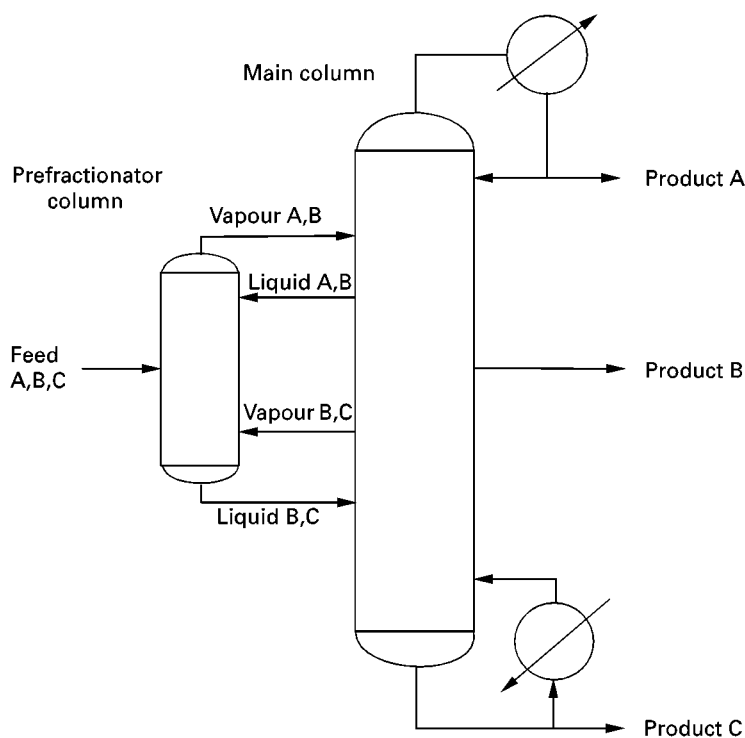


Figure 12 Petlyuk configuration.

versatility of distillation. Current research efforts have been evolutionary and the majority of the industry is reluctant to test any technology that has not been commercially proven. Therefore, even promising new technology changes are slow and cautious. Many research efforts have started to combine the best features of different separation methods to save energy and capital costs. The future of distillation will always depend upon energy costs and change will occur when these costs become unacceptable.

See also: II/Distillation: High and Low Pressure Distillation; Historical Development; Modelling and Simulation; Multicomponent Distillation; Packed Columns: Design and Performance; Pilot Plant Batch Distillation; Theory of Distillation; Tray Columns: Design; Vapour-Liquid Equilibrium: Theory.

Further Reading

- Dhole VR and Linhoff B (1993) Distillation column targets. *Computers in Chemical Engineering* 17 (56): 549–560.
- Dodge BF (1994) *Chemical Engineering Thermodynamics*. New York: McGraw-Hill.
- Fonyo Z (1974) Thermodynamic analysis of rectification—I. Reversible model of rectification. *International Chemical Engineer* 14(1): 18–27.
- Kaibel G Blass E and Kohler J (1990) Thermodynamics—guidelines for the development of distillation column arrangements. *Gas Separation and Purification* 4: 109–114.
- Kaibel G (1992) Energy integration in thermal process-engineering. *International Chemical Engineer* 32 (4): 631–641.
- King CJ (1971) *Separation Processes*. New York: McGraw-Hill.
- Liebert T (1993) Distillation feed preheat – is it energy efficient? *Hydrocarbon Processing* 3: 37–42.
- Linhoff B, Dunford H and Smith R (1983) Heat integration of distillation columns into overall process. *Chemical Engineering Science* 38: 1175–1188.
- Petterson WC and Wells TA (1977) Energy-saving schemes in distillation. *Chemical Engineer* (September): 78–86.
- Sussman MV (1980) *Availability (Exergy) Analysis*. Lexington, MA: Mulliken House.
- Terranova BE and Westerberg AW (1989) Temperature–heat diagrams for complex columns. I. Intercooled/interheated distillation columns. *Ind. Eng. Chem. Res.* 28: 1374–1379.
- Treybal RE (1968) *Mass-Transfer Operations*, 2nd edn. New York: McGraw-Hill.
- US Department of Energy (1994) *Assessment of Potential Energy Savings in Fluid Separation Technologies*. Document DOE/ID/124763-1, December. Washington, DC: US Department of Energy.
- Vogler TC (1988) Thermodynamic availability analysis for maximizing a systems efficiency. *C.E.P.* 25–42.

Extractive Distillation

F.-M. Lee, GTC Technology Corporation,
Houston, TX, USA

Copyright © 2000 Academic Press

Introduction

In the first half of the twentieth century, extractive distillation (ED) became an important industrial process when World War II demanded high purity toluene for explosive production and butadiene for synthetic rubber production. Over the years, substantial developments in ED have been carried out in terms of novel solvent discovery for a particular separation, as well as the development of more sophisticated ED tower internal designs. In the petroleum and petrochemical industries, ED has been found effective in separating mixtures of aromatics/nonaromatics, diolefins/olefins, olefins/paraffins and naphthenes/paraffins.

This article will briefly review the basic concept of ED, and summarize the development of ED technologies for the applications in the following areas:

1. Aromatic purification from refining and petrochemical streams.
2. Cycloparaffin (cyclohexane or cyclopentane) recovery from naphtha or natural gas liquid.
3. Light olefins from light hydrocarbon mixtures.

The basis of ED is the increase of relative volatility between the close-boiling components caused by introducing a selective solvent, which has stronger affinity with one type of the components in the mixture. If there is a single liquid phase (no phase separation), the solvent selectivity can be measured from the experimentally observed relative volatility (α) between the key components in the presence of solvent as:

$$\alpha = (Y_1/X_1)/(Y_2/X_2)$$

where X_1 and X_2 are the mole fractions of components 1 and 2, respectively, in the liquid phase, and Y_1 and Y_2 are those in the vapour. All compositions are measured on a solvent-free basis.

In some cases, liquid-phase separation may occur in the ED tower, especially in the upper portion of the tower where less polar components are concentrated. Under this condition, the solvent phase can reject a second liquid phase, which can be defined as the raffinate liquid phase. The liquid in the solvent-rich phase is defined as the extract liquid phase. The solvent selectivity is determined by the relative vola-

tilities of the key components in the two interrelated liquid phases and the common vapour phase, according to the following formulae:

$$\alpha_r = (\gamma_{1r}p_{1r})/(\gamma_{2r}p_{2r})$$

$$\alpha_e = (\gamma_{1e}p_{1e})/(\gamma_{2e}p_{2e})$$

where α_r and α_e are the relative volatilities of components 1 and 2, respectively, in the raffinate phase and extract phase; γ_{1r} and γ_{2r} are the activity coefficients in the raffinate phase, and γ_{1e} and γ_{2e} are the activity coefficients in the extract phase; and p_{1r} , p_{2r} , p_{1e} , and p_{2e} are the vapour pressures of the pure components (which can be estimated from an Antoine equation).

A schematic diagram of a typical ED process is presented in **Figure 1**. During a normal run, a polar, high-boiling (low volatility) solvent is introduced to near the top of the ED tower. As the nonvolatile solvent flows down the column, it preferentially associates the more polar components in the ascending vapour mixture, thus increasing the relative volatility between the polar and less polar components. The process feed stream is introduced to the middle portion of the ED tower. The more polar components are concentrated in the rich solvent, exiting the bottom of the ED tower, while the less polar components are concentrated in the overhead raffinate stream. The tower reflux stream is provided to knock down the entrained solvent from the overhead raffinate stream.

The solution, rich in polar compounds from the bottom of the ED tower, is fed to the solvent stripper, where the polar components are stripped from the solvent by heat alone or by heat and a stripping gas, such as steam. The lean solvent is then recycled to the ED tower from the bottom of the stripper.

Aromatic Purification from Refining and Petrochemical Streams

Advantages and Principle of ED Technology

Although liquid-liquid extraction (LLE) technologies have dominated the industrial processes for purifying benzene, toluene, xylene (BTX) aromatics from refining and petrochemical streams, ED technologies have gained ground quickly since the 1980s for more recent grassroots plant installations. In comparison to LLE, ED has the following advantages:

1. *Lower capital costs.* ED requires two major process units (ED tower and solvent stripper), while

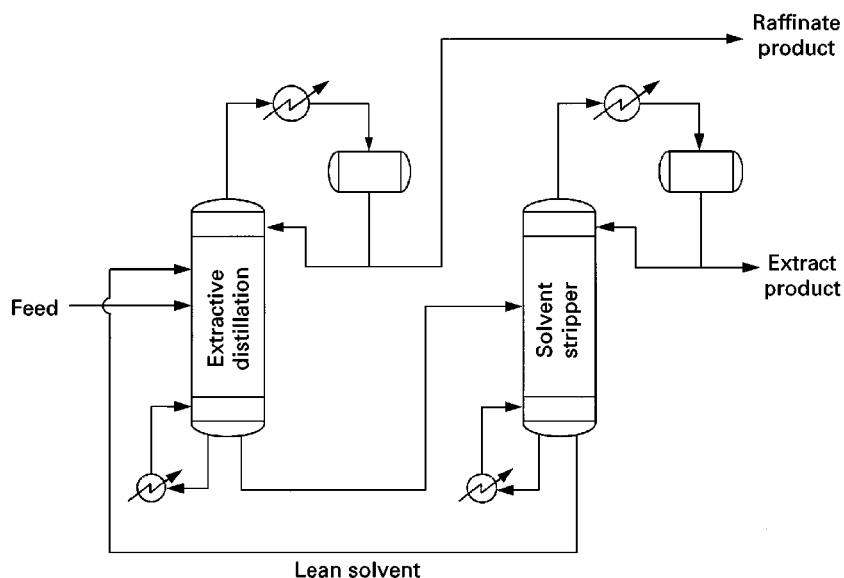


Figure 1 Configuration of an ED process.

the popular LLE, using sulfolane as the solvent, requires four major process units, including LLE tower, extractive stripper, solvent recovery column, and raffinate wash tower (see Figure 2).

2. *Higher operational flexibility.* LLE uses only solvent selectivity (polarity) for separation, while ED uses both solvent selectivity and boiling point for separation, so it has one extra dimension for operational flexibility.

3. *Less physical property restrictions.* Interfacial tension and density difference between the liquid phases are important concerns for LLE, but not for ED.

The principle of ED for aromatic purification was studied as early as 1944. One example was the recovery of toluene from paraffins using phenol as the selective solvent. The effect of phenol on a paraffin-toluene mixture is plotted in liquid-vapour

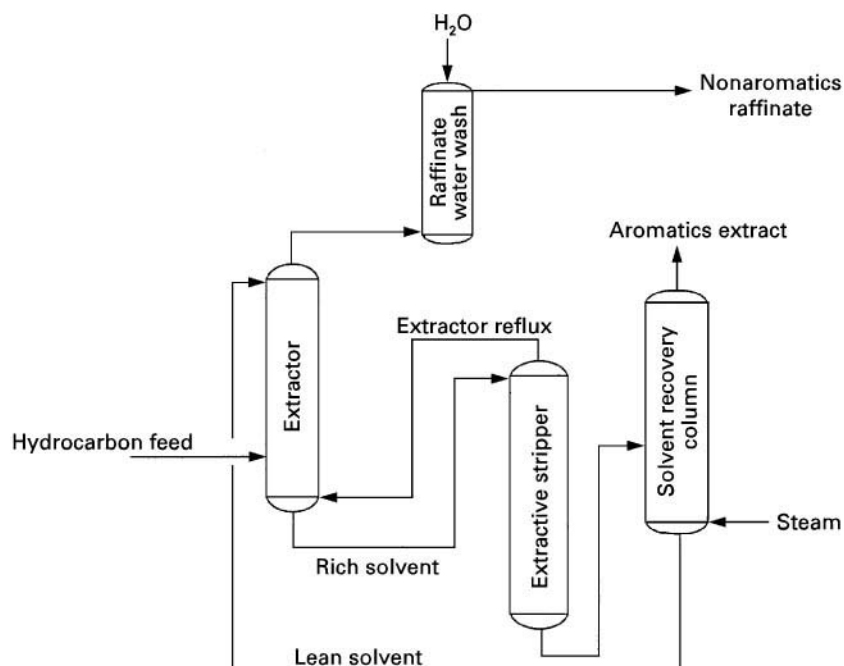


Figure 2 Configuration of liquid-liquid extraction using sulfolane for aromatic recovery.

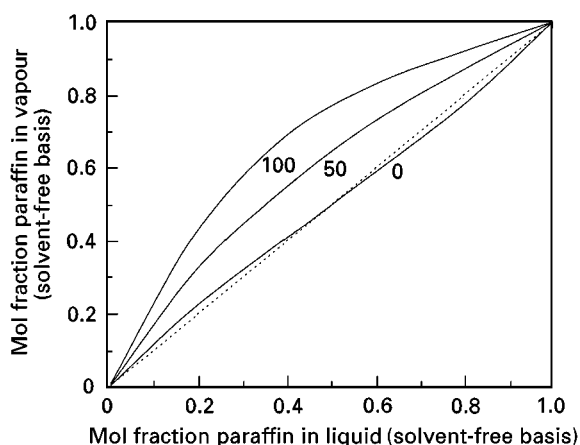


Figure 3 Effect of phenol on the vapour-liquid equilibrium of paraffin and toluene. Numbers on curves refer to mol% solvent in liquid.

diagrams as shown in Figure 3, in which the paraffin is considered as a hypothetical octane having the same boiling point as toluene. In the absence of phenol, there exists an azeotrope of paraffin and toluene. However, at 50 mol% phenol, the azeotrope is destroyed and the mixture is easily separated; at 100 mol% phenol, the separation between paraffin and toluene becomes very easy. Figure 4 illustrates the effect of phenol on the change in relative volatility between paraffin and toluene. Phenol causes an increase of activity coefficient for both paraffin and toluene, but the activity coefficient of the paraffin increases to a greater extent than that of toluene. Therefore, the relative volatility of paraffin over toluene can be increased from 1.0 (no separation) to 3.7 (easy separation) at near zero hydrocarbon concentration in phenol (infinite dilution).

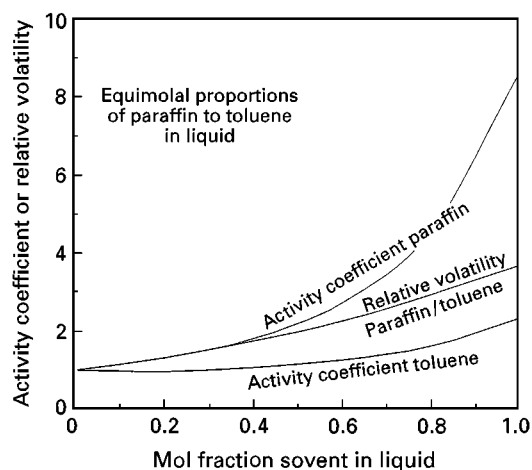


Figure 4 Effect of phenol on the activity coefficient of paraffin and toluene.

The vapour-liquid equilibria of the paraffin-toluene-phenol system were applied to test a commercial ED tower for toluene purification. As shown in Figure 5, the McCabe-Thiele diagram, drawn on a phenol-free basis, was used to carry out the theoretical calculations from tray to tray in the ED tower.

The calculated results were then compared with the actual results generated from a commercial ED tower with 2.1 m diameter and 65 trays. The hydrocarbon feed tray and the solvent feed tray are located at trays 19 and 39 (counted from the bottom of the tower), respectively. The tower was operated at a solvent-to-feed ratio (S/F) of 2.5, a reflux-to-overhead ratio (R/D) of 2.75, and reboiler temperature at 170°C under 1.3 atm bottom pressure. On the basis of the charge, overhead and bottoms analyses, tray-to-tray calculations were made.

Figure 6 shows the calculated concentration profiles for each component plotted against theoretical tray number. It also shows the plot of the tray analyses against actual tray number. The overall efficiencies calculated over small sections of the tower are given in Table 1. The average of the overall tray efficiencies throughout the tower is about 50%.

Based on the above principle, much more rigorous algorithms for tray-to-tray calculation of ED towers for multicomponent systems have been developed in

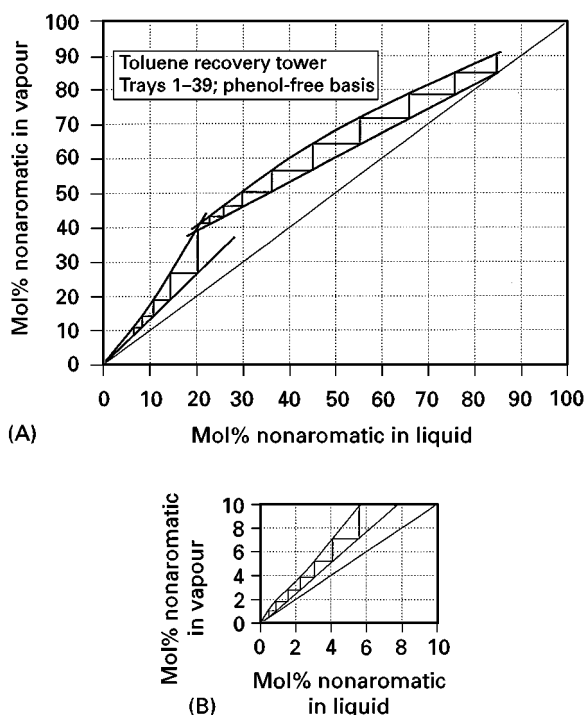


Figure 5 McCabe-Thiele diagram for paraffin and toluene separation in the presence of phenol. Part (B) is an enlargement of part of the diagram in (A).

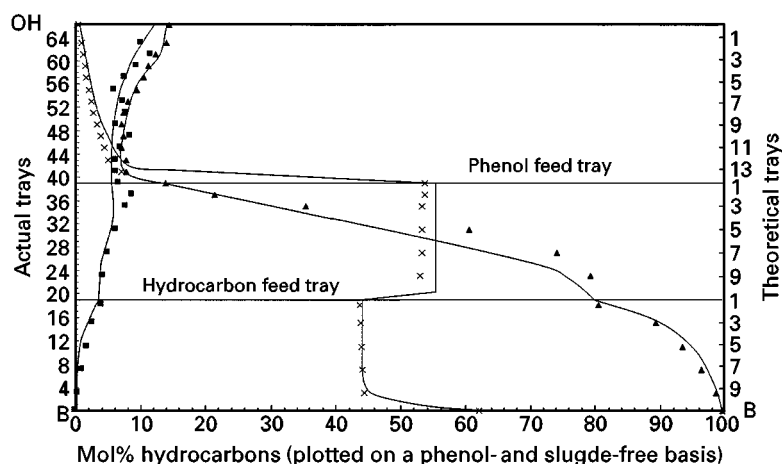


Figure 6 Calculated versus actual concentration profile of the components in an ED tower. Key: ■, methylcyclohexane; ▲, toluene; × phenol; —, calculated values.

recent years, with the help of advanced vapour-liquid equilibrium theories and high-speed computers.

Handling Two Liquid Phases in ED Towers

One of the challenges of ED technology for aromatics purification is the handling of the possible formation of two liquid phases in the upper portion of the ED tower where nonaromatics are concentrated. The occurrence of a second liquid phase is due to the fact that the nonaromatics, such as paraffins, naphthenes and olefins, have significantly lower solubility in the polar solvent than aromatics.

One way to solve the problem of two liquid phases in the ED tower is to select a polar solvent that has

enough solvency to dissolve both aromatics and nonaromatics in the mixture under process condition. In general, however, solvents with a high selectivity for compounds to be separated will have a reduced solvency (capacity), and vice versa. The selectivity versus solvency of the common commercial solvents for aromatic extraction is shown in Figure 7. Therefore, in order to eliminate two liquid phases, one may have to compromise the solvent selectivity, sometimes to a great extent.

A better way is to cope with two liquid phases in the ED tower, without sacrificing the solvent selectivity, for the following reasons:

1. Two liquid phases normally reduce the solvent selectivity in the three-phase equilibrium (vapour-liquid-liquid) condition in the ED tower. However, this can be compensated by intrinsic selectivity of a highly selective solvent. For example, the performance of sulfolane was

Table 1 Tray efficiency of ED tower for toluene purification

Section of tower trays	Theoretical trays	Actual trays	Overall efficiency (%)
<i>Below phenol feed tray</i>			
1-3	1.8	3	60.0
4-7	2.7	4	67.5
8-11	2.1	4	52.5
12-15	1.5	4	37.5
15-18	1.8	3	60.0
23-27	2.1	4	52.5
27-30	2.5	4	62.5
31-34	2.65	4	66.0
35-39	2.35	5	47.0
<i>Above phenol feed tray</i>			
43-65	10.8	23	47.0
49-65	8.6	17	50.7
57-65	4.5	9	50.0
61-65	2.8	5	56.0

All trays numbered from bottom of tower.

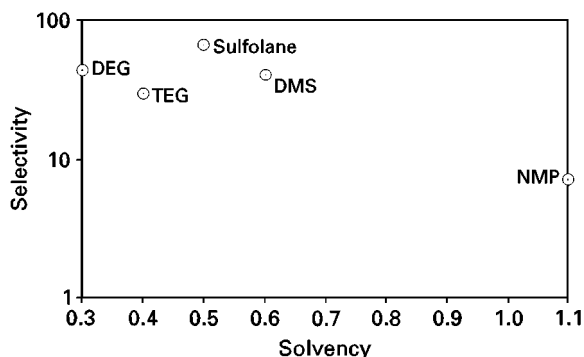


Figure 7 Selectivity versus solvency (solubility) of the common commercial solvents. DEG, diethylene glycol; TEG, triethylene glycol; DMS, dimethyl sulfoxide; NMP, *N*-methyl pyrrolidone.

compared with those of *N*-formyl morpholine (NFM) and *N*-methyl pyrrolidone (NMP). The ability of these solvents to enhance the relative volatility of *n*-heptane over benzene (an aromatic and nonaromatic separation) in a one-stage equilibrium cell was determined. Table 2 shows that, although two liquid phases were observed using sulfolane as the solvent, sulfolane still gave a better performance than the other solvents where a single liquid phase existed in the mixture.

- Two liquid phases have no ill effects on the efficiency of small tray or packed towers with diameter from 0.08 m to 0.46 m. However, in larger towers, the heavy liquid phase tends to accumulate on the tray if the liquid phases are not well mixed. This problem can be eliminated by tray designs promoting gas agitation, forcing the two liquid phases to behave as a homogeneous liquid. For larger packed columns, liquid-liquid redistributors are specially designed to allow separate distribution of the two liquid phases.

Computer simulations have been developed which are capable of accurately predicting the development of two liquid phases in the ED tower. In one approach, the simulation algorithm starts from linearized pressure, temperature and concentration profiles and feed conditions given by the program operator. New estimates of composition are solved, using the material balance and equilibrium relationship for each tray. Then the equilibrium constants are re-estimated and a new temperature gradient is established to calculate a tray-by-tray energy balance. Accumulated errors are calculated for the energy, material and equilibrium balances. Appropriate column operation restraints are factored in at this point. A correction factor is found for the temperature, rate profiles, and liquid composition profile by inverting the accumulated error matrix. These correction factors are used to form new iterative estimates of composition to start the process again until the correction factors are small enough to call the components converged.

Table 2 ED solvent screening for aromatics recovery

Solvent	Relative volatility (<i>n</i> -heptane/benzene)	Number of liquid phases
Sulfolane	3.9	2
DMSO	3.6	1
NFM	3.1	1
NMP	2.6	1

Feed: 20% *n*-heptane and 80% benzene; pressure 1 atm; DMSO, dimethyl sulfoxide; NFM, *N*-formyl morpholine; NMP, *N*-methyl pyrrolidone.

Multicomponent vapour-liquid and liquid-liquid equilibria solutions are required for the algorithm. Two activity coefficient models, NRTL (nonrandom two liquids) and UNIQUAC (universal quasichemical), are readily extendable to multicomponent systems and capable of such solutions. Experimental activity coefficients, γ , at infinite dilution are used for calculating binary parameters for the NRTL equation. These parameters are then tested using experimental liquid-liquid ternary data, experimental vapour-liquid equilibrium data, and data from pilot plant or commercial plant. The NRTL equation is used in the algorithm to calculate activity coefficients and is given in the following equations:

$$\ln \gamma_1 = x_2^2 [\tau_{21}(G_{21}/(x_1 + x_2 G_{21}))^2 + \tau_{12}(G_{12}/(x_2 + x_1 G_{12}))^2]$$

$$\ln \gamma_2 = x_1^2 [\tau_{12}(G_{12}/(x_2 + x_1 G_{12}))^2 + \tau_{21}(G_{21}/(x_1 + x_2 G_{21}))^2]$$

where

$$\ln G_{12} = -\beta_{12}\tau_{12}$$

$$\ln G_{21} = -\beta_{21}\tau_{21}$$

$$\tau_{12} = (\eta_{12} + S_{12}T)/RT$$

$$\tau_{21} = (\eta_{21} + S_{21}T)/RT$$

and where G_{ij} , η_{ij} , S_{ij} and β_{ij} are empirical constants, γ_i is activity coefficient, R is the gas universal constant, T is absolute temperature, and x_i is liquid phase mole fraction of component i .

The simulation uses a Newton-Raphson-based flash algorithm that checks for two liquid phases by checking Gibbs free energies for components the program operator lists as possible second liquid phase formers. If two liquid phases are indeed present, regular solution theory provides a method of combining the liquid-phase activity coefficients.

State-of-the-art ED Technologies

The modern state-of-the-art ED technologies for BTX aromatic purification are based on several solvent systems: sulfolane, NFM and NMP. Proprietary cosolvents may be blended into the base solvent to enhance the performance in specific applications.

Table 3 summarizes the key performance parameters of LLE and ED for aromatics recovery. ED process can provide up to 25% savings in capital investment as compared with the commercially available LLE processes. This saving is attributable to the

Table 3 Comparison of aromatic recovery technologies

System	UDEX TM	Arosolvan TM	Sulfolane TM	Morphylane [®]	GT-Aromex TM
Solvent	Tetra-EG	NMP	Sulfolane	N-formyl morpholine	Proprietary
ISBL capital cost (million US\$)	9.5	11.0	10.7	11.0	8.1
<i>Utilities</i>					
Power (kWh per t of feed)	—	6.6	2.4	4.6	4.8
Steam (kcal per kg of feed)	211	225	177	250	194
Cooling H ₂ O (gal per lb of feed)	19	—	—	16	21
<i>Aromatics recovery</i>					
Benzene	99.9%	99.9%	99.9%	99.9%	95.0%
Toluene	99.5%	99.5%	99.0%	99.5%	99.5%
Xylene	95%	95%	95%	97%	100%
Solvent-to-feed ratio (v/v)	4 : 1	0.4 : 1	2 : 1	3 : 1	3 : 1

Data are for 1994 construction, extraction section only; all processes are pro rata for 1600 metric tons day⁻¹ reformate feed; sources include SRI International, Handbook of Solvent Extraction, Petroleum Refining Technologies & Economics, and licensor literature.

smaller number of operating units, as mentioned above. The ED process recovers more xylenes but less benzene than LLE processes.

The Morphylane[®] process offered by Krupp Koppers uses NFM as the selective solvent. A schematic diagram of the Morphylane[®] process is given in Figure 8. The diagram is very similar to the general ED process scheme as shown in Figure 1, except the nonaromatic vapour exiting the top of the ED tower contains a small amount of NFM solvent (0.9 wt%), which must be recovered. Two methods are used for this solvent recovery, both of which require additional equipment and expense: (1) a separate solvent recovery column; and (2) additional trays or packings fitted to the top of the ED tower (above the solvent tray), using nonaromatics as the reflux to flush NFM back into the ED tower. To use the second method,

the feedstocks to the ED tower must contain only very small amounts of critical components, such as methylcyclohexane and dimethylcyclopentane in pyrolysis gasoline feedstock, or C₇ olefins in reformate feedstock.

The Morphylane[®] process is available in commercial applications for recovering high purity benzene from C₆ fraction, or pure benzene and toluene from the C₆–C₇ fraction of reformate or pyrolysis gasoline. For example, the process has been commercially tested with a feedstock from a mixture of C₆ reformate fraction and a C₆ fraction of a pyrolysis gasoline. The plant had a top-fitted solvent recovery system. The results are summarized in Table 4. Approximately 98% benzene recovery with 99.9% benzene purity was achieved with this process. This process, however, has not been applied to the recovery of higher

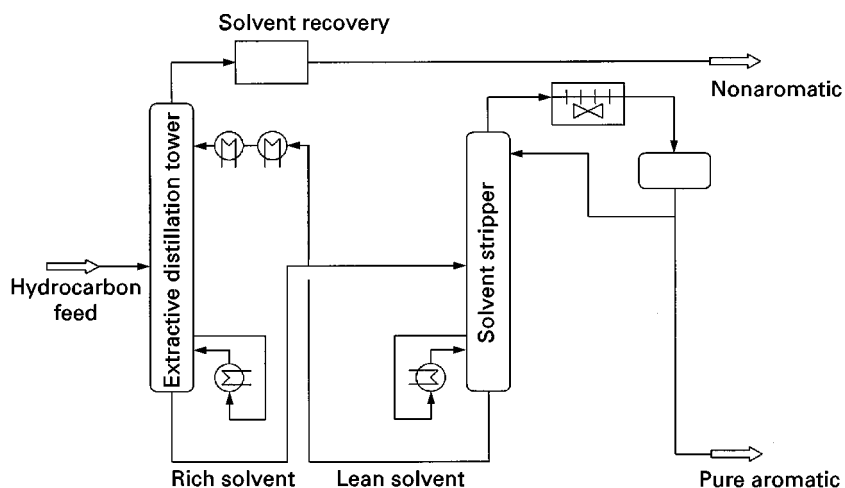
**Figure 8** Schematic diagram of the Morphylane[®] process for aromatic purification.

Table 4 ED performance for benzene recovery from the C₆ fraction

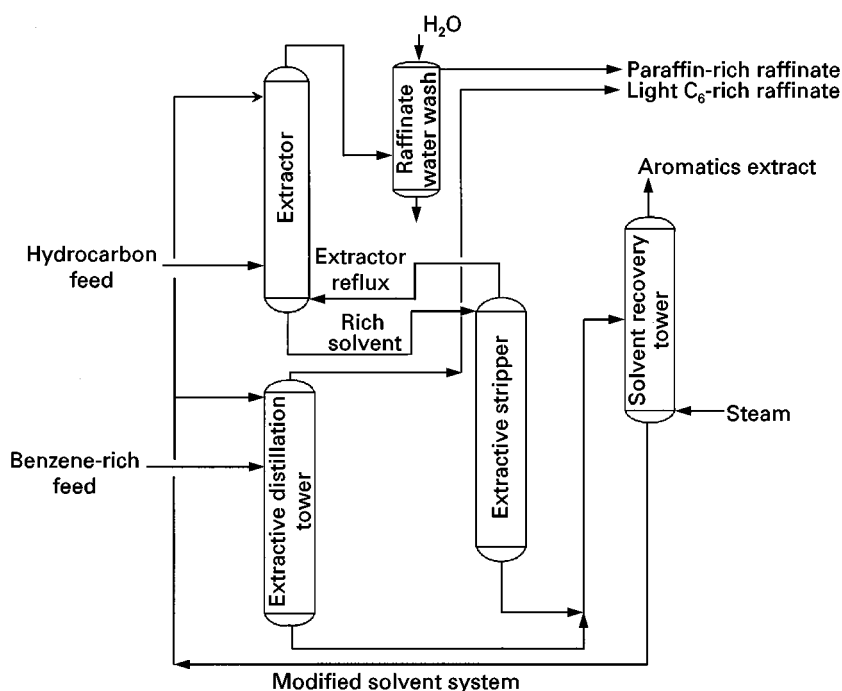
Parameter	Units	Value
Throughput	t h ⁻¹	23.0 (approx. 116%)
Benzene production	t h ⁻¹	12.89
Benzene purity	wt %	99.98
Benzene yield	wt %	98.11
Solvent consumption	g t ⁻¹ aromatics	6.0
Solvent in benzene product	ppm	Not ascertainable
Steam consumption (16 × 10 ⁵ Pa) (including benzene column)	kg t ⁻¹ feed	564
Energy consumption for extractive distillation only	kg t ⁻¹ feed	349
16 × 10 ⁵ Pa steam	Gcal t ⁻¹ feed	0.161

boiling aromatics, such as mixed xylenes or C₉⁺ and higher aromatics, probably because of the relatively low boiling point of NFM.

The GT-BTXSM process offered by GTC Technology Corporation is available for recovering not only benzene and benzene/toluene, but also a full range of aromatics (benzene, toluene and xylenes) with high purity and recovery. The process uses a proprietary sulfolane-based solvent blend. Due to the high boiling point of the solvent, the process is very effective in recovering higher boiling aromatics, such as xylenes

and C₉⁺ and higher aromatics. Unlike the Morphylane[®] process, the overhead nonaromatics stream from the ED tower in the GT-BTXSM process contains essentially no solvent, and does not require a separate solvent recovery tower.

A hybrid concept of the GT-BTXSM process can be used to increase substantially the capacity of the liquid-liquid extraction unit and improve the quality of the benzene product, through retrofitting of the existing unit. The retrofitting can be carried out using this hybrid concept without requiring extensive modifications, investment or lengthly shutdown time. Figure 9 shows a new process using a hybrid of the sulfolane liquid-liquid extraction process with the GT-BTXSM process that bypasses part of the feed around the original extraction section. In the hybrid scheme, the ED tower is better suited to purifying the benzene-rich feed than the liquid-liquid extraction unit, and it is not subject to the maximum aromatics limit in the hydrocarbon charge. The ED tower nonaromatic stream (rich in cyclohexane) may be recycled to the reformer unit for producing more benzene, while the raffinate stream from the liquid-liquid extractor (rich in paraffins) could be routed to gasoline blending or used as a feedstock for naphtha cracking to produce ethylene and pyrolysis gasoline. The major changes are modifications of the solvent system to be compatible with both extraction operations and to make the appropriate tie-ins to the ED tower.

**Figure 9** Hybrid scheme for aromatic recovery process expansion.

Cyclohexane Recovery from Naphtha or Natural Gas Liquid

In recent years, ED technology has also been applied to the separation of paraffins and cycloparaffins, a much more difficult separation than aromatics and nonaromatics. One of the major developments was cyclohexane recovery from naphtha or natural gas liquid (NGL) streams. Cyclohexane, an important raw material for the nylon industry, exists naturally in naphtha and NGL streams. However, recovery of high purity cyclohexane from naphtha or NGL through conventional distillation is virtually impossible, owing to the close-boiling C_7 isomers in the streams. Since the polarity difference between cyclohexane and C_7 isomers is substantially smaller than that for aromatic and nonaromatic compounds, no extractive solvent has been found that can effect the separation. However, through the use of a cosolvent (to enhance the solvency of the mixed solvent), an ED process has been commercialized to recover high purity cyclohexane directly from an NGL fraction containing 85% cyclohexane.

Many solvent blends show synergistic improvement over what would be expected by pure component mixing. To test the concept, experiments were conducted in a one-stage vapour-liquid equilibrium (VLE) cell to compare the selectivity of five solvents. To a hydrocarbon mixture of 85 wt% cyclohexane (C_6) and 15 wt% 2,3 dimethylpentane (2,3-DMP), a selective solvent or a mixed solvent was added, at a solvent-to-feed ratio (S/F) of 7.0. The relative volatility of 2,3-DMP over C_6 was measured in the equilibrium cell with various solvents. Table 5 presents a comparison of relative volatilities obtained for five solvents tested, including a proprietary mixed solvent (MIST) from Phillips Petroleum Company. MIST solvent, discovered by investigating the combinations of many other solvents, has a significantly higher relative volatility than the other single solvents.

Computer simulations were carried out to confirm the results on solvent screening from the one-stage

Table 6 Computer simulation for solvent comparison

<i>Solvent</i>	<i>2,4-DMP recovery (%)</i>	<i>C_6 purity (wt%)</i>	<i>Separation factor^a</i>
MIST	85.5	97.5	586
TEG	53.7	92.4	115
Sulfolane	51.7	92.1	106
NMP	45.9	91.2	84
EG ^b	0.0	85.0	0

^aSeparation factor

$$= \frac{\text{mole fraction 2,4-DMP raffinate/mole fraction } C_6 \text{ raffinate}}{\text{mole fraction 2,4-DMP extract/mole fraction } C_6 \text{ extract}}$$

^bSimulation failed to converge.

Premises: 99% C_6 recovery, overhead product allowed to vary; S/F weight ratio = 16; 25 equilibrium stages (solvent fed on stage 24, hydrocarbon fed on stage 12); reflux fixed at 0.48 (hydrocarbon feed).

VLE cell for the mixed and single solvents shown in Table 5. These simulations were based on experimental physical property data, such as the infinite dilution activity coefficients of binary solvent-hydrocarbon mixtures. Again, NRTL thermodynamic correlations were used to predict the occurrence of two liquid phases and a Newton-Raphson convergence method was used to carry out the simulations.

Simulations of a ED process separating an 85/15 wt% C_6 /2,4-DMP mixture were made to compare the MIST solvent with four common extraction solvents, ethylene (EG), triethylene glycol (TEG), sulfolane and N-methyl pyrrolidone (NMP). The simulations were for a 25 theoretical stage ED tower at a S/F ratio of 16. The C_6 recovery in the extract stream was specified at 99.0% and the overhead raffinate product was allowed to vary. Table 6 shows that the MIST solvent has a separation factor 5 times greater than TEG, which has the highest separation factor of the single solvents.

The MIST solvent was first tested in a 150 mm diameter ED pilot plant using as the feedstock a refinery stream that had an average composition as shown in Table 7. Based on the successful pilot plant study, a commercial plant purifying 100 metric tonnes per day cyclohexane was designed, constructed and commissioned in 1991.

Table 5 Equilibrium cell study for C_6 and 2,3-DMP separation

<i>Solvent</i>	<i>No. of liquid phases</i>	<i>Relative volatility (2,3-DMP/C_6)</i>
(No solvent)	1	0.84
EG	2	1.02
TEG	2	1.06
Sulfolane	2	1.07
NMP	1	1.07
MIST	1	1.22

Light Olefin and Paraffin Separations

The synthetic rubber process, brought to a successful culmination during World War II, required large quantities of butadiene; consequently normal

Table 7 Average ED pilot plant feedstock

Components	wt%
Cyclohexane	89.1
2,2-Dimethylpentane	1.3
2,4-Dimethylpentane	4.0
3,3-Dimethylpentane	0.1
2,3-Dimethylpentane	0.9
2-Methylhexane	1.6
3-Methylhexane	1.1
2,2,3-Trimethylbutane	0.8
Dimethylcyclopentanes	1.0
<i>n</i> -Heptane	0.1

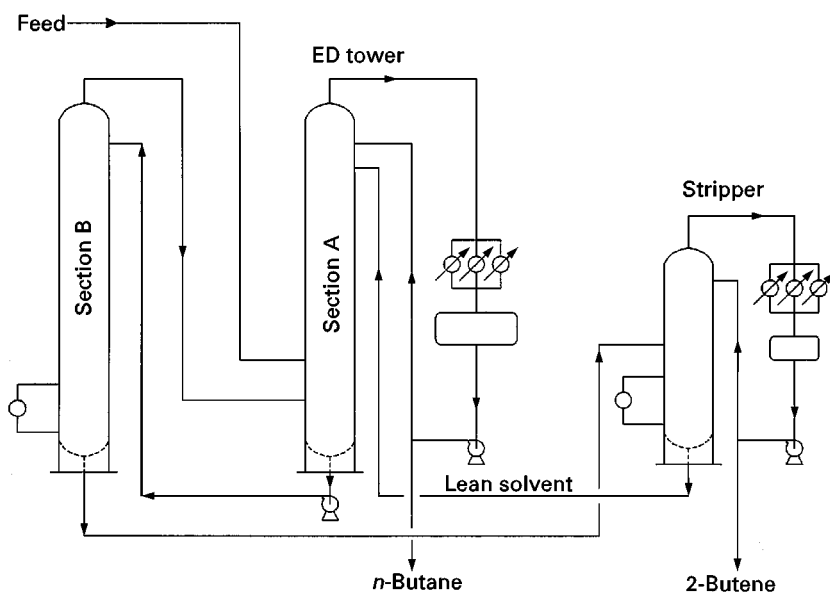
butenes, the feedstock to butadiene units, were also in great demand. ED process technology was developed to recover high purity *n*-butenes suitable for producing butadiene to feed the synthetic rubber process. In this case, the selective solvent, developed by Shell Development Company in Houston, Texas, USA, was a mixture of 85% acetone and 15% water.

Later, furfural was used as an ED solvent for separating isobutane from butene-1, *n*-butane from butene-2, and butene-1 from butadiene. As shown in Figure 10, furfural was tested in an ED tower consisting of two 50-tray sections in series for separating butene-2 from *n*-butane. Solvent was charged to a tray, which was several trays from the top of the first section (A), and flowed to the bottom of this section. It was pumped together with dissolved hydrocarbons to the top of the second section (B), and

withdrawn from the bottom of this section together with hydrocarbon bottoms. The solvent and bottoms are separated in a smaller 20-tray stripper tower, the solvent-free bottoms being removed as overhead and stripped solvent circulated back to the ED tower. Hydrocarbon feed is charged at some point below the solvent feed, near the bottom of the first section or top of the second section of the ED tower.

For *n*-butane and 2-butene separation, the purity of 2-butene was 94.6 vol% with only 39.4 vol% recovery. For mixed butanes and mixed butenes separation, the purity of mixed butenes was 88.7 vol% with 96.7 vol% recovery, and for butadiene and butenes separation, the purity of butadiene was 96.9 vol% with 89.7 vol% recovery. Obviously, these results did not meet the industrial requirements for producing high purity product with high recovery.

Further studies were carried out to screen solvents for olefin and paraffin separations. For example, a comprehensive solvent screening study was conducted for *n*-butane and butene-2 separations. Eighty solvents were evaluated, including ester-type solvents containing hydroxyl groups, aldehyde groups, amine groups, nitrile groups, nitro groups, ketone groups, nitrogen; ether-type solvents; and miscellaneous solvents. It was found that aniline and furfural were the most selective solvents. The VLE data for *n*-butane and 2-butenes in furfural and aniline solvents are given in Figures 11 and 12. Although *N*-formyl morpholine was also tested among the nitrogen-containing solvents for *n*-butane and 2-butenes separation,

**Figure 10** Schematic ED process diagram for separating 2-butene and *n*-butane.

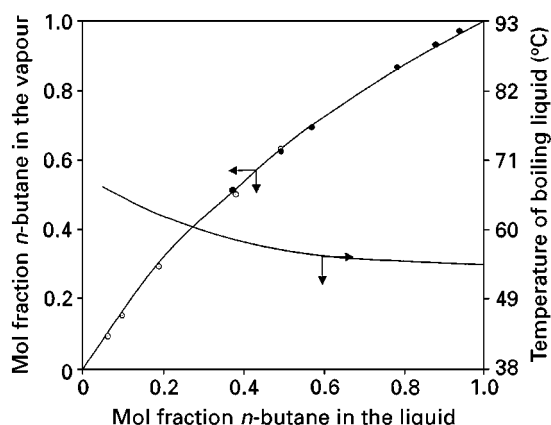


Figure 11 Vapour-liquid equilibrium of *n*-butane and 2-butene in Furfural. Solvent dosage: ●, 3.7; ○, 4.5. Pressure, 3862 mmHg.

for unknown reasons the solvent was not considered for commercialization until recently.

Krupp Koppers has offered the BUTUNEX process, an ED process using *N*-formyl morpholine as the selective solvent, for recovering 1-butene and 2-butene from C_4 hydrocarbon streams. On the basis of such a feedstock with the composition of 25.6% isobutane, 32.7% *n*-butane, 26.6% 1-butene and 15.1% 2-butene, the following yields can be

achieved:

1-Butene	95.6%
2-Butene	99.1%
Butanes	98.9%

The purity of 1-butene and 2-butene products can be 99.6% and 95.9%, respectively.

Conclusions

Since the 1940s, ED technology has gone through extensive development for solving many difficult separation problems in the petroleum and petrochemical industries. The development in cosolvent selection tailored for a specific separation and the advancement in tower internal design have made ED a competitive process. In many cases, ED processes can be more efficient and economical than conventional LLE in terms of capital investment, energy consumption and ease of operation. It is anticipated that the ED technology will be selected more frequently in the future for the petroleum and petrochemical industries.

See also: II/Distillation: Theory of Distillation. III/Reactive Distillation.

Further Reading

- Benedict M and Rubin LC (1945) Extractive and azeotropic distillation: I. Theoretical aspect. *Transactions of the American Institution of Chemical Engineers* 41: 353–370.
- Brown RE and Lee FM (1991) Way to purity cyclohexane. *Hydrocarbon Processing* May: 83–86.
- Doherty MF and Knapp JP (1993) Distillation, azotropic and extractive. In: *Kirk-Othmer Encyclopedia of Chemical Technology*, 4th edn, vol. 8, pp. 358–398. New York: John Wiley and Sons.
- Drickamer HG and Hummel HH (1945) Application of experimental vapor-liquid equilibria to an analysis of the operation of a commercial unit for the purification of toluene from petroleum. *Transactions of the American Institute of Chemical Engineers* 41: 607–629.
- Gentry JC and Kumar CS (1998) Improve BTX Processing Economics. *Hydrocarbon Processing* (March): 69–74.
- Lee FM and Gentry JC (1997) Don't overlook extractive distillation. *Chemical Engineering Progress* 93 (10): 56–64.

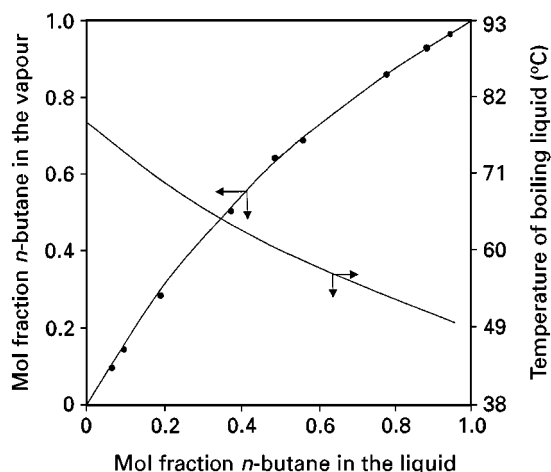


Figure 12 Vapour-liquid equilibrium of *n*-butane and 2-butene in aniline. Solvent dosage, 5.0; pressure, 3862 mmHg.

Freeze-Drying

G.-W. Oetjen, Chemical Engineering,
Lübeck, Germany

Copyright © 2000 Academic Press

Introduction

Freeze-drying is a process, in which a product is first frozen and then dried by sublimation of the ice. The total process involves four steps: freezing; sublimation of the ice, called main drying (MD); desorption of the water bound to the solid, called secondary drying (SD); and packing in containers to exclude absorption of water and/or oxygen from the atmosphere. By freeze-drying a product unstable in water is transformed into a dry, stable product. The process has to be developed to satisfy four demands on the finished product: its volume remains that of the frozen substance; the structure and the biological activity of the dried solid correspond as far as possible to those of the original substance; the dried product remains stable during storage, if possible at temperatures up to $+40^{\circ}\text{C}$ and for up to 2 years; and with the addition of water the original product is quickly reconstituted. This article summarizes the problems and solutions to achieve these aims.

Theoretically, sublimation of ice can be done at atmospheric pressure; however, the vapour pressure of ice between -10°C and -40°C is approximately 2.6–0.13 mbar and 1 kg of ice has a volume of approximately 470 m^3 at -10°C and 8400 m^3 at -40°C . To transport these volumes at atmospheric pressure the gas volume has to be approximately 400–8000 times larger than that of the vapour. Therefore all freeze-drying plants today are vacuum plants, in which the air is reduced to some 10% of the vapour pressure, to allow the free flow of vapour at velocities up to 100 m s^{-1} .

The first organ tissues were freeze-dried in 1890 and in 1932 a vacuum freeze-drying plant was built, but only after 1940 did it become an industrial process with the freeze-drying of blood plasma and penicillin.

Freezing

Structure of Water and Ice

In a water molecule the two H atoms form an almost tetrahedral angle with a strong dipole moment. A shell of about four water molecules exists at a distance of 28 nm, followed by a second at approximately

45 nm, and beyond 80 nm no shell can be identified. In addition to this short range order, a network of hydrogen bonds exists with a very short lifetime of 10^{-12} to 10^{-13} s .

In sub-cooled, very pure water the nucleation of ice crystals (homogeneous nucleation) starts around -41°C . Normally water contains about 10^6 particles which act as nuclei for crystallization (heterogeneous crystallization). They become more effective as their structure approaches that of ice. Ice crystals exist in nine forms, of which the cubic and hexagonal at under atmospheric pressure. The growth rate of crystals depends on the diffusion of molecules to the nuclei, on finding a suitable place, and on the transportation of the freed energy to the heat sink. With extreme cooling rates (of the order of $10^5^{\circ}\text{C min}^{-1}$), crystallization can be avoided and water solidifies into an amorphous, glass-like phase. **Figure 1** shows that the amorphous phase of ice is only stable below -160°C ; in the range -160°C to -130°C amorphous and cubic phases can exist, and between -130°C and -65°C all the forms can be present, depending on the speed of warming. It is technically impossible to cool pure water quickly enough, to produce glassy ice; even small droplets (1 mm) injected into liquid nitrogen may freeze at a rate less than $10^3^{\circ}\text{C min}^{-1}$. The freezing behaviour of water changes completely if other substances are present in the water, e.g. cryoprotective agents (CPAs). The most widely used CPAs are:

- protein: human serum albumin, gelatin
- amino acids: glycine, arginine, alanine
- alcohols: mannitol, polyethylene glycol (PEG)
- carbohydrates
 - monosaccharides: glucose, fructose
 - disaccharides: lactose, maltose, sucrose, trehalose
 - polysaccharides: dextran, cyclodextrins
- others
 - metals
 - surfactants
 - polymers
 - buffer salts

They all protect in one way or another, alone or in combination, the original quality of the product to be freeze-dried.

As an example of a CPA the influence of glycerol concentration is shown on the right-hand side of **Figure 1**. The temperature of homogenous nucleation

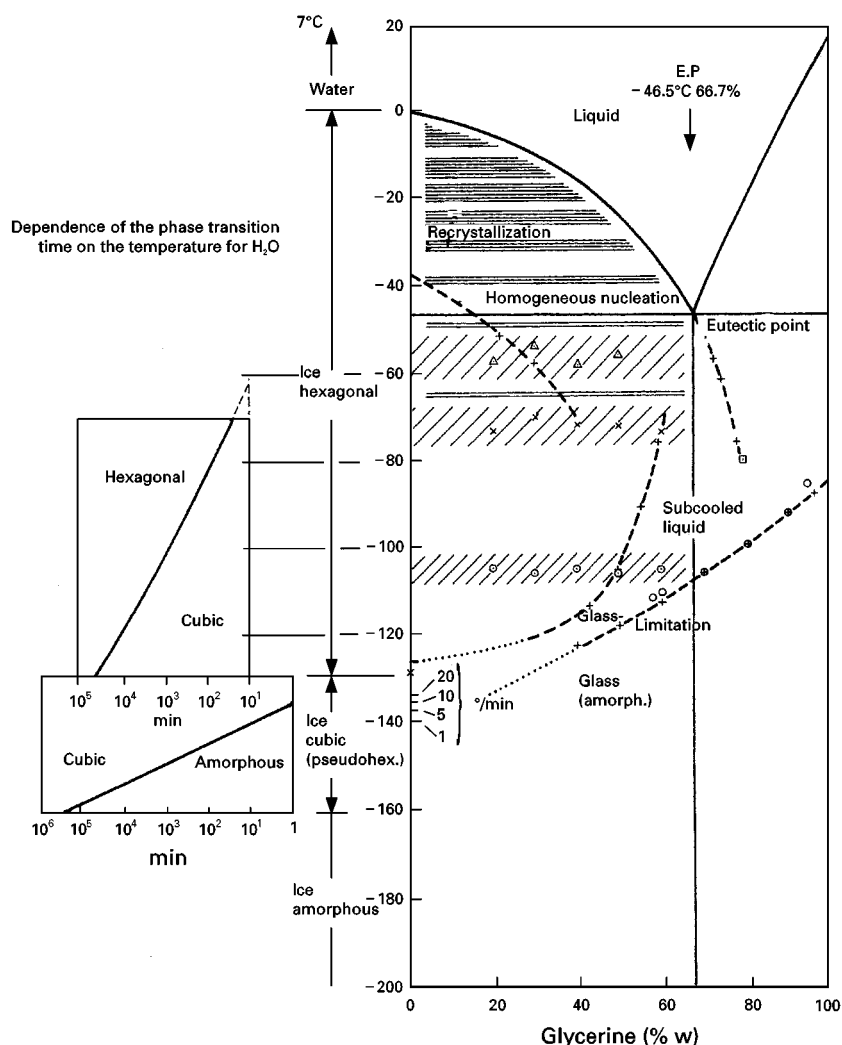


Figure 1 Phase diagram, water-glycerine. On the left-hand side the dependence of the phase transformation time from the ice temperature is shown: at -140°C amorphous ice transforms into cubic ice in approximately 10 min. (From Umrath, W. Kurzbeitrag für die Tagung Raster-Elektronenmikroskopie in Medizin und Biologie, unpublished, Brühl.)

(T_{hn}) can be reduced by about 20°C , the devitrification temperature (T_{g}) can rise by almost 35°C and sub-cooled liquids can exist down to very low temperatures. Polyvinyl pyrrolidone reduces T_{hn} only a few degrees, while T_{g} can be changed by more than 70°C . The freezing of a product is mostly done so quickly that no equilibrium state is reached during the process. The structure of the frozen product depends therefore not only on its components but also very much on the freezing rate and the temperature at the end of the freezing process. Generally speaking, during slow freezing the nuclei have time to grow and the solution in between the ice crystals becomes increasingly concentrated. During quick freezing only small crystals can grow and the remaining solution can become so viscous that the water

molecules cannot diffuse to the crystals and they become part of the solidified liquid (glass) between the ice crystals.

The freeze concentration may, among other effects, change the pH, the water structure around proteins and extract water from cells. The unfrozen water will crystallize during warming when the mobility of the molecules is sufficiently increased. The crystallization can be very abrupt, warm the surroundings, melt it at least partially and destroy the structure. The freezing of a product is as critical as the drying – in some respects even more so. The structure achieved during freezing and solidification determines the main and secondary drying process, the reconstitution of the dried product and its storage capability. Therefore it is mandatory to analyse the

formation of the structure and the factors which influence it.

Methods of Structure Analysis

A number of methods have been described to supply information during freezing. Electrical resistance during cooling and warming (ER) is measured in a test vial at different freezing and warming rates. For a more accurate interpretation of the function $\log(ER) = f(T)$ the first derivative of the plot is calculated as shown in Figure 2. The advantages of the method are: sample size is of the order of a product in

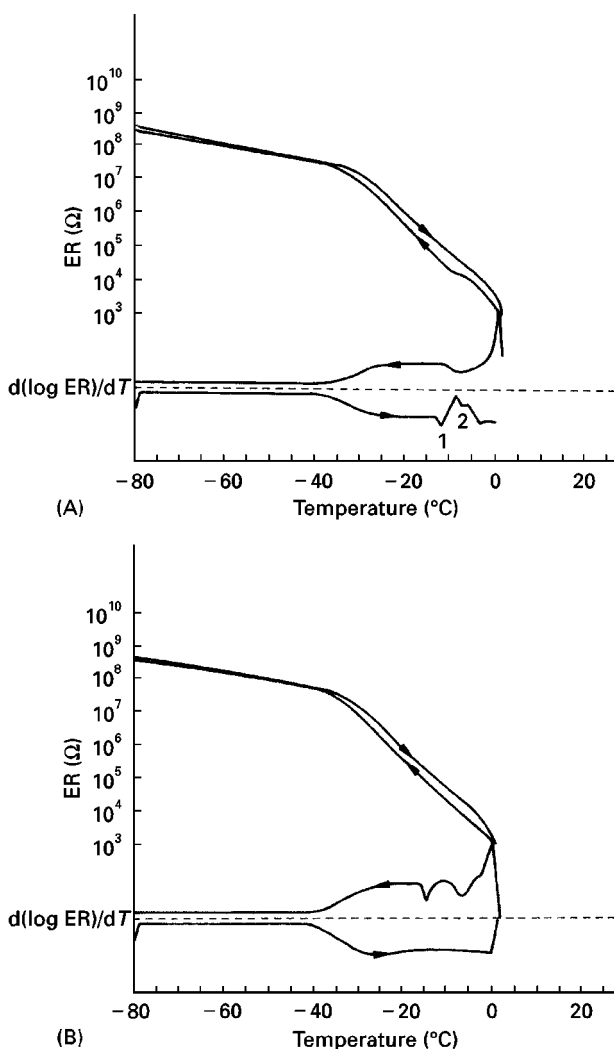


Figure 2 (A) Electrical resistance (ER) of a pharmaceutical product as a function of temperature during cooling at $1^{\circ}\text{C min}^{-1}$ and warming at $3^{\circ}\text{C min}^{-1}$. Heat transfer medium and product are approximately uniformly heated. (B) Measurement of the electrical resistance as in A, but with the wall of the vial insulated by a plastic tape up to the filling height of the product. Heat is therefore mostly removed through the bottom of the vial. (A and B from Willemer, H., Köln, unpublished measurements.)

a vial; it simulates heat transfer from the shelf to the vial/product; and the equipment is relatively inexpensive and easy to operate. The disadvantages are that interpretation needs some experience, the measured data reflect the mobility of ions and the amount of energy used or freed during an event cannot be calculated. In Figure 2A, the heat transfer medium and product are at a similar temperature; in Figure 2B, the wall of the test vial is isolated from the heat transfer medium to simulate the freezing of a product in a vial on the shelf. In Figure 2A, the effect of subcooling during freezing can be seen at about -10°C , but the derivative shows it more clearly between -3°C and -10°C . During warming at event 1 (-12°C) the structure softens, allowing unfrozen water to crystallize, represented by the increase in resistance. In Figure 2B the crystallization energy cannot be quickly removed: freezing occurs in two steps. During warming, events 1 and 2 are not found, all freezable water is crystallized during cooling.

Differential scanning calorimetry (DSC) compares heat flows, one to and from the sample and the other to and from a substance with no transitions in the measuring range. Roos and Karel showed by DSC (Figure 3) the influence of unfrozen water on T_g of fructose (1) and glucose solutions (2). After rapid freezing ($30^{\circ}\text{C min}^{-1}$) to -100°C T_g of fructose and glucose is at -88°C and -84°C respectively; at -48°C and -44°C respectively the unfrozen water crystallizes, followed by the melting of ice. If the products are thermally treated or annealed (after freezing the product is warmed to -48°C for 15 min and then cooled again to -100°C), T_g , called T_g' if all freezable water is frozen, is raised to -58°C and -57°C and no crystallization event is measurable. Time and temperature of annealing must be carefully determined to achieve a certain mobility of the molecules without collapse of the structure (see Figure 9B). The advantages of DSC are the quantitative measurement of the changes in the heat capacity of the sample and the energy freed or used in an event. The disadvantage is the small sample (milligrams), which can behave differently from a product in vials (grams) and the cost of the equipment.

In a cryomicroscope the sample can be optically observed during cooling and warming at different rates. Some models also permit freeze-drying of the sample. Willemer has shown (Figure 4) the structure of a Factor VIII solution during warming after quick freezing. This product must be freeze-dried at a temperature of the sublimation front of the ice (T_{ice}) below -44°C and if annealing is necessary it may be possible at -43°C to -42°C for several minutes but a longer time at -45°C is recommended. The advantage is the visual confirmation of data gained by

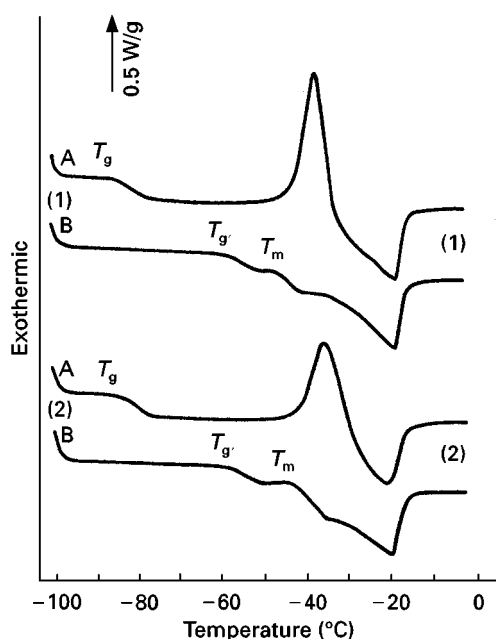


Figure 3 Results of annealing (thermal treatment) on the formation of ice in a 60% fructose solution (1) and in a 60% glucose solution (2). Curve A: after cooling at $30^{\circ}\text{C min}^{-1}$ down to -100°C , the DSC plots have been recorded during warming at $5^{\circ}\text{C min}^{-1}$. T_g approximately -85°C and -88°C , respectively, for fructose and glucose. At approximately -48°C and -44°C respectively, ice crystallization starts clearly, followed by the beginning of the melting of ice. (During freezing only a part of the water has been crystallized.) Curve B: after cooling down to -100°C , the product has been warmed at $10^{\circ}\text{C min}^{-1}$ to -48°C , kept for 15 min at this temperature (thermal treatment), cooled down again at $10^{\circ}\text{C min}^{-1}$ to -100°C , and the DSC plot (B) measured during rewarming. During thermal treatment all freezable water is crystallized, and T_g is increased to -58°C and -57°C , respectively. During warming, no crystallization can be detected. (Reproduced with permission from Roos and Karel, 1991.)

other methods, e.g. ER or DSC, and the possibility to analyse the image quantitatively by computer. The disadvantages are high cost and the relatively small region of the sample that can be observed.

Nuclear magnetic resonance (NMR) provides information, among other things about free or bound water (e.g. to protein molecules), the influence of unfrozen water on the collapse temperature and the crystallization of amorphous dry products. Hanafusa has shown by NMR (Figure 5) how the amount of unfrozen (bound) water in a 0.57% ovalbumin solution is reduced by the addition of a 0.01 M solution of sucrose or glycerol. Similar information can be gained for a coffee extract with 25% solids: during freezing and rewarming at -70°C 0.01 g water per gram solid are unfrozen, at -40°C 0.1 g per gram and at -20°C approximately 30%; thereafter the amount increases rapidly. This extract has to be freeze-dried

at a $T_{\text{ico}} < -20^{\circ}\text{C}$, otherwise the structure would collapse. The unique advantage of NMR is the ability to discriminate between free, crystallized and bound water.

More details concerning these methods and additional procedures have been reported by Oetjen.

Freezing Rates

The freezing time can be estimated by an equation developed by Steinbach:

$$t_f = \Delta J / \Delta T \rho_g (\sigma^2 / 2\lambda_g + d / K_{su})$$

where t_f = freezing time; ΔJ = enthalpy difference between the initial freezing point and the final temperature; ΔT = difference of temperature between the freezing point and the cooling medium; d = thickness of the product parallel to the direction of prevailing heat transfer; ρ_g = density of the frozen product; λ_g = thermal conductivity of the frozen product; and K_{su} = surface heat transfer coefficient between cooling medium and the freezing zone.

In this equation K_{su} has to be measured for each type of vial or tray used. The flatness of the bottoms

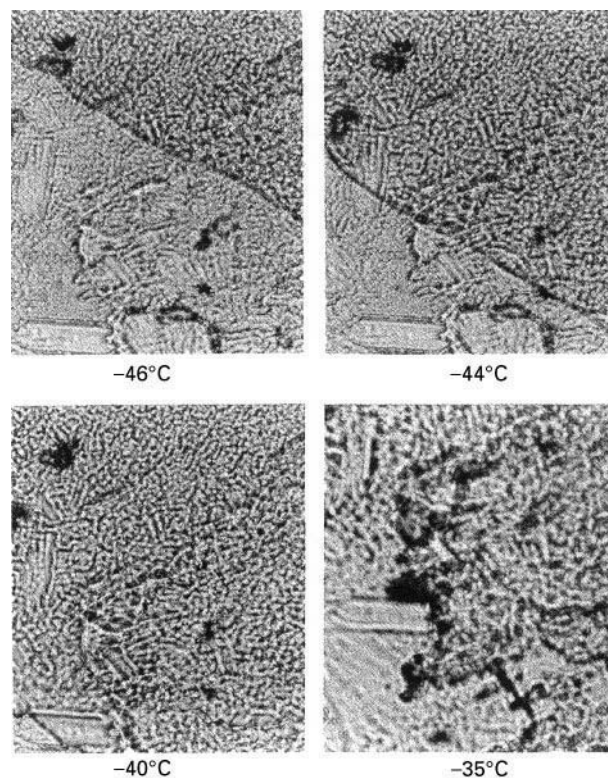


Figure 4 Photographs taken with a cryomicroscope of Factor VIII solutions at four temperatures. At -40°C the structure is still visible, but is more coarse compared with the appearance at -44°C . At -35°C the structure is collapsed. (Reproduced with permission from Willemer, 1996.)

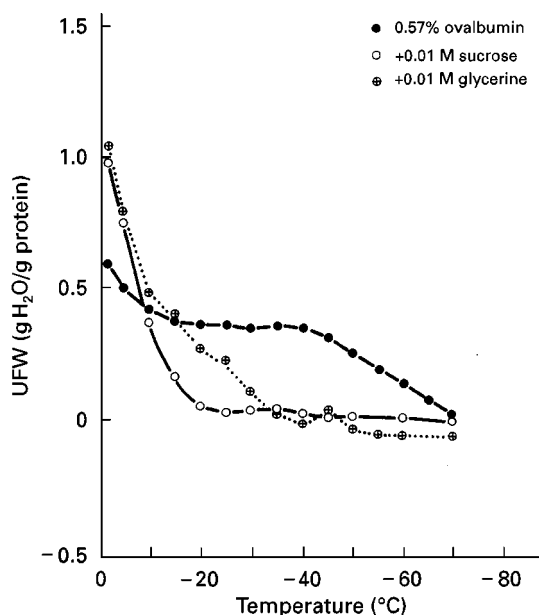


Figure 5 Unfreezable water (UFW) in a 0.57% ovalbumin solution as a function of the freezing temperature with different CPAs. (Reproduced with permission from Hanafusa, 1992.)

can change K_{su} by a factor of two – if the vials are in trays without machined bottom surfaces by a factor four and more. With K_{su} measured, t_f can be estimated with an error of 10–15%.

Main or Sublimation Drying

The main drying process (MD) has been photographed in a cryomicroscope by Kochs *et al.* as shown in **Figure 6**. The ice crystals grow extremely uniformly using a special freezing method. The ice sublimates and the remaining solids show their original structure after freezing. During sublimation the temperature of the ice at the sublimation front (T_{ice}) has to be kept well below the collapse temperature T_c .

As can be seen in **Figure 6** T_{ice} cannot be measured by a sensor because the ice front travels. If the valve between chamber and condenser (8 in **Figure 11**) is closed for a short time (< 3 s) the water vapour pressure in the chamber rises until the saturation pressure (ρ_g) of the ice front is reached. The rising pressure is measured 100 times per second and the change in the slope (after 2.14 s), if saturation is reached, is determined as 0.286 mbar, corresponding to -32.7°C as shown by Haseley and Oetjen in **Figure 7**. This procedure is called barometric temperature measurement (BTM). It permits checking T_{ice} during MD (e.g. every 10 min). To estimate the main drying time (t_{MD}) the following equation

developed by Steinbach is used:

$$t_{MD} = (\rho_g \zeta_w LS \Delta m d) / T_{tot} \{ (1/K_{tot}) + (d/2 \cdot \lambda_g) + (d/2 LS b/u) \}$$

where ρ_g = density of the frozen product (kg m^{-3}); ζ_w = amount of water (kg kg^{-1}); LS = sublimation energy (2.805 kJ kg^{-1}); T_{tot} = temperature difference ($T_{sh} - T_{ice}$); K_{tot} = total heat transmission coefficient from the shelf to the sublimation front of the ice; λ_g = thermal conductivity of the frozen product; d = thickness of the layer (m); Δm = content of frozen water; and b/μ = permeability ($\text{kg m}^{-1} \text{ h}^{-1} \text{ mbar}^{-1}$) for water vapour through the dried product.

T_{tot} is known, if T_{ice} is measured and K_{tot} has to be measured once for each type of container; one can

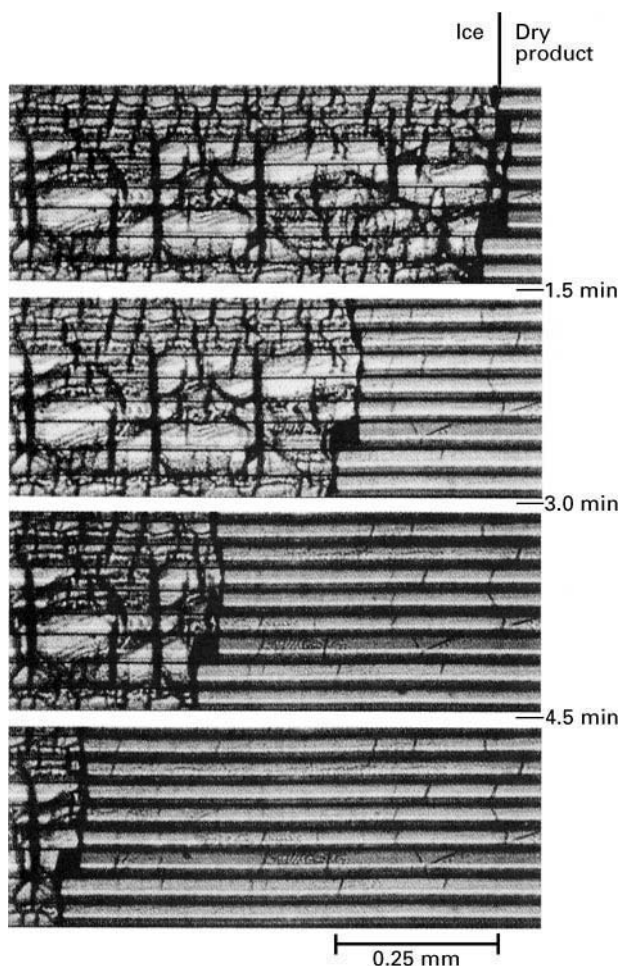


Figure 6 Course of main drying observed using a cryomicroscope, in which freeze-drying is carried out. The hydroxyethyl starch solution is optimally frozen. The dark lines show the form of the sublimated ice crystals. (Reproduced with permission from Kochs *et al.*, 1991.)

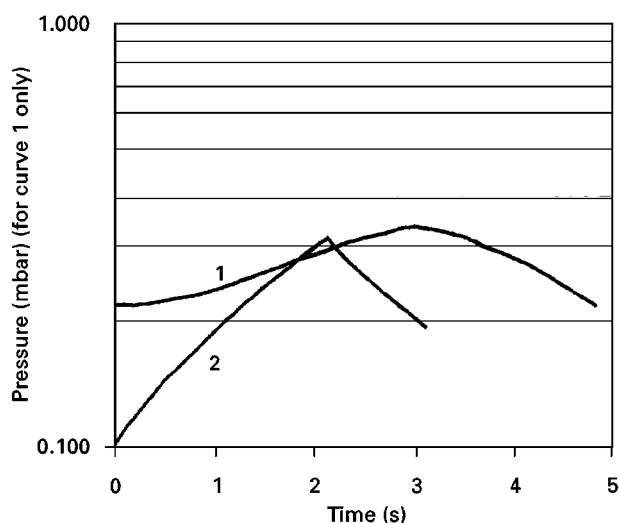


Figure 7 Pressure rise as a function of time. 1, Pressure rise in the chamber after the valve is closed; 2, first derivative of 1. The maximum of 2 is reached at 2.14 s; the related equilibrium vapour pressure $p_g = 0.286$ mbar, corresponding to $T_{ice} = -32.7^\circ\text{C}$. (Reproduced with permission from Haseley and Oetjen, 1998.)

expect values between 60 and $120 \text{ kJ m}^{-2} \text{ h}^{-1} \text{ }^\circ\text{C}^{-1}$. K_{tot} is only slightly dependent on the operation pressure up to 0.1 mbar; then it increases up to 1 mbar by a factor of two. λ_g is, in most cases, the figure for pure ice. Δm has to be determined for each product by methods described above. $b/\mu = 1.3 \times 10^{-2} \text{ (kg m}^{-1} \text{ h}^{-1} \text{ mbar}^{-1})$ is an average which is often found in practice, it can vary by a factor of two, but

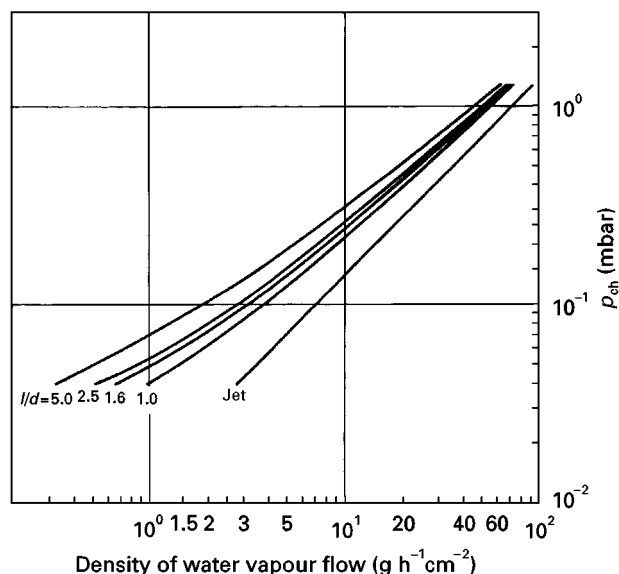


Figure 8 Density of water vapour flow ($\text{g cm}^{-2} \text{ h}^{-1}$) as function of p_{ch} with jet flow and different l/d as parameter. (Reproduced with permission from Oetjen, 1999.)

the term with b/μ in most freeze-drying processes only has an influence of a few per cent on t_{MD} . The standard deviation of T_{ice} , measurements during MD in the range of -15 to -45°C should be $< 0.5^\circ\text{C}$, if measured automatically. t_{MD} is in most cases governed by the value of T_{tot} and the term $(1/K_{tot})$. The term $(d/2 \cdot \lambda_g)$ is, for d values below 10 mm, of the order of 10% or less of $1/K_{tot}$ growing to approximately 50% at $d = 35$ mm. T_{ice} is the result of a thermodynamic equilibrium between heat transfer to the sublimation front and energy consumption for sublimation. Both depend on several factors, but the heat supply and vapour transport to the condenser are most important during MD. Therefore the operation pressure is a very effective tool to control T_{ice} , if the shelf temperature is kept constant and the condenser temperature is always below a maximum, which depends on the water vapour pressure in the chamber and the design of the plant. By changing the operation pressure, e.g. from 0.1 mbar to 0.8 mbar, T_{ice} can be controlled between -30°C and -20°C . For another product, a different product thickness or a different plant, the pressure range and its controlled range are different, but the dependence is reproducible. Since T_{ice} depends also on the structure of the frozen product it can be used to prove that the structure of products in different runs is homogeneous and sufficiently identical. If the structure contains unfrozen water, T_{ice} data will from time to time jump by 1°C or more (when the water evaporates) and the data will be different for a product frozen at different freezing rates.

At the end of MD the ice is mostly sublimed and the measured T_{ice} decreases below the standard deviation of T_{ice} during MD. This effect can be used to change automatically from main to secondary drying (SD), e.g. if the measured T_{ice} becomes 2 – 3°C smaller than the average during MD. Other criteria are often suggested, such as an increase of product temperature, a decrease in operating pressure or a decrease in partial pressure of water vapour, but it is more difficult to use these other methods quantitatively.

Besides heat transfer, the water vapour transport from the chamber to the condenser is often critical in a freeze-drying process. The length (l) and diameter (d) of the connection between chamber and condenser in a freeze-drying plant as shown in Figure 11 determine the vapour flow, assuming that the other flow resistances in the chamber are relatively small by comparison. The vapour flow can be estimated using the Günther-Jaekel-Oetjen equation. Figure 8 shows that: the vapour flow density decreases in a nonlinear manner with the chamber pressure; the relation of l/d is of increasing importance with decreasing pressure; for example, at 4×10^{-2} mbar the vapour

flow density at $l/d = 5$ is only 30% that at $l/d = 1$. Right-angle bends contribute to the length not only by their physical dimensions but, depending on the design, by a factor of four or more of the measured length. For operation pressures below about 10^{-1} mbar, $l/d > 2.5$ should be avoided.

Secondary or Desorption Drying

Desorption Rates

During secondary drying (SD), water that is removed is more less bound to solid molecules. The amount of water removed is small (e.g. 10% of solids), compared to 10 times the weight of solids during MD. The behaviour of water molecules close to a protein surface has been described by Bellissent-Funel and Teixeira. The water molecules are in a monolayer around the protein with a reduced mobility compared with bulk water.

The desorption of bound water can be measured during SD by measuring the pressure rise in the chamber after closing the valve to the condenser for 60–120 s. The length of time is not critical since the temperature does not change quickly in this phase. The pressure rise ($dp \text{ s}^{-1}$) can be converted into the desorption rate (DR) using:

$$\text{DR} = 2.89 \times 10^2 (V_{\text{ch}}/m_{\text{so}}) (dp/dt)$$

where DR = desorption of water vapour in per cent of solids per hour; V_{ch} = chamber volume (L); dp = pressure rise (mbar); dt = time of dp (s); and m_{so} = mass of solids (g).

The course of DR describes not only the progress of the secondary drying quantitatively, but also reflects the structure of the frozen product as shown by Haseley and Oetjen in Figure 9. In Figure 9A DR data are shown for a 10% mannitol solution frozen in vials on the shelves of the freeze-drying plant at a rate of $0.5\text{--}0.8^\circ\text{C min}^{-1}$. In Figure 9B the same solution in the same vials is frozen in liquid nitrogen and in Figure 9C the solution is frozen in liquid nitrogen but annealed before freeze-drying. From these figures the following conclusions can be drawn. (1) Slow freezing of 10% mannitol solutions results in structures in which the water is bound in several forms. The DR plots as a function of time are not single-valued. (2) Freezing at rates of more than $30^\circ\text{C min}^{-1}$ produces structures with a more uniform desorption behaviour. DR plots show the influence of the operating conditions during MD: (1) run 6 in Figure 9B is collapsed, and the water has dissolved part of the solids, forming a sticky cake. The water

vapour of 378 vials resulted in an unstable T_{ice} , which is $5\text{--}7^\circ\text{C}$ higher than in all other runs. (2) The systematic influence of T_{sh} is shown in Figure 9B and C. (3) The influence of p_c is shown in Figure 9C, and the influence of annealing or low T_{ice} is demonstrated by comparing Figure 9B and C: without annealing, DR plots bend between 3% and 5% per hour; with annealing this effect practically disappears. The exceptions prove the sensitivity of the measurements: run 1 (Figure 9B) is freeze-dried at $T_{\text{ice}} = -36.9^\circ\text{C}$, others at approximately -34.9°C ; run 5 (Figure 9B) is annealed at -40°C but for 8 h; runs 2 and 3 (Figure 9C) are annealed at a temperature 1°C too high and 1.5°C too low for 18 min. Annealing reduces the amount of unfrozen water.

Residual Moisture Content

The integration of DR over time results in the amount of water which can still be desorbed; this is called desorbable water, dW or residual moisture content. In Figure 10 Haseley and Oetjen show the calculated plots from the DR data of Figure 9B and C. From the lower part of Figure 10, it follows that the heat conductivity of the annealed product during SD is almost 100% higher and more uniform than that of the unannealed product. The upper part shows that the correctly treated products and the one dried at a low T_{ice} during MD will dry more quickly than the others.

Storage

The storage capability of a dried product depends generally on its chemical and structural qualities. The complexity of the problem is highlighted, for example, by the storage stability of therapeutic proteins. The degradation of a protein, the irreversible change in primary structure, conformation or state of aggregation in a glassy surrounding depends on the thermodynamic behaviour of the glass as well as on the qualities of the protein produced during freezing and freeze-drying, as shown by Pikal. The storage temperature of such products has to be well below T_g of the dried formulation; nevertheless unfolding or aggregation of unfolded molecules can occur because of poor interaction between the stable glass structure and movements in protein configurations. From this example some simplified guidelines can be proposed. There are no general rules to estimate the maximum storage time at a maximum tolerable temperature – both depend even on small changes in the formulation of a drug or the variations between two types of fruits or the processing methods of extracts (e.g. coffee). In many cases the maximum storage time is

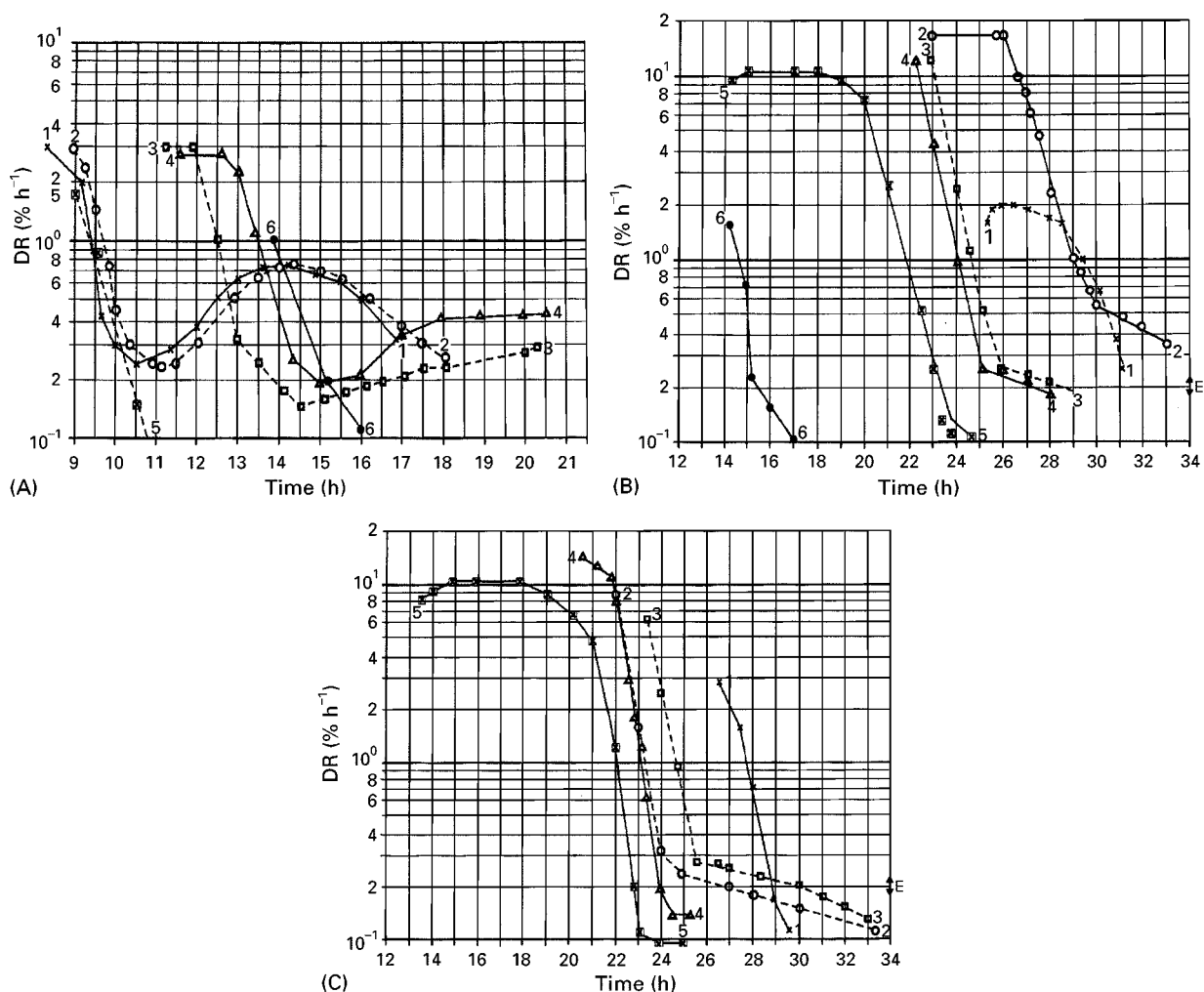


Figure 9 (A) Desorption rate (DR) as a function of time of a 10% mannitol solution frozen on the shelves of the freeze-drying plant at a rate of $0.5\text{--}0.8^{\circ}\text{C min}^{-1}$. In all runs: 300 vials at an operation pressure (p_c) = 0.3 mbar during MD. Runs 1 and 2 at a shelf temperature (T_{sh}) = 20°C ; runs 3 and 4, $T_{sh} = 5^{\circ}\text{C}$. Plot 5 egg albumin and plot 6 saccharose for comparison. (B) DR as in A, but the solution is frozen in liquid nitrogen at a rate between 35°C and $66^{\circ}\text{C min}^{-1}$. During MD all runs at $p_c = 0.15$ mbar, except run 1 = 0.08 mbar and T_{sh} in run 1 = -5°C ; in run 2 = 0°C ; in runs 3–6 = 0°C for the first 11 h, thereafter until end of MD 10°C . In runs 1–5, 126 vials; in run 6, 378 vials. Run 5 intentionally changed from MD to SD 7 h earlier than in runs 3 and 4. (C) DR as in B, but the frozen mannitol was annealed at slightly different temperatures and times:

Run	Annealing temperature ($^{\circ}\text{C}$)	Annealing time (min)
1	– 24	18
2	– 23.5	18
3	– 26	18
4	– 24.5	18
5	– 24	20

All runs at $p_c = 0.15$ mbar, T_{sh} in the first 11 h = 0°C , thereafter 10°C , during SD = 30°C except run 1 $p_c = 0.08$ mbar and $T_{sh} = -5^{\circ}\text{C}$ in the first 11 h. (Reproduced with permission from Haseley and Oetjen, 1999.)

inversely related to the maximum temperature and depends strongly on the residual moisture content ($\pm 1\%$ or less can be decisive). For crystallized products (e.g. antibiotics) the crystal structure must not

change during storage and for glassy products the maximum storage temperature has to be well below T_g (see above). The main difference between the stresses during drying and storage is the length of the

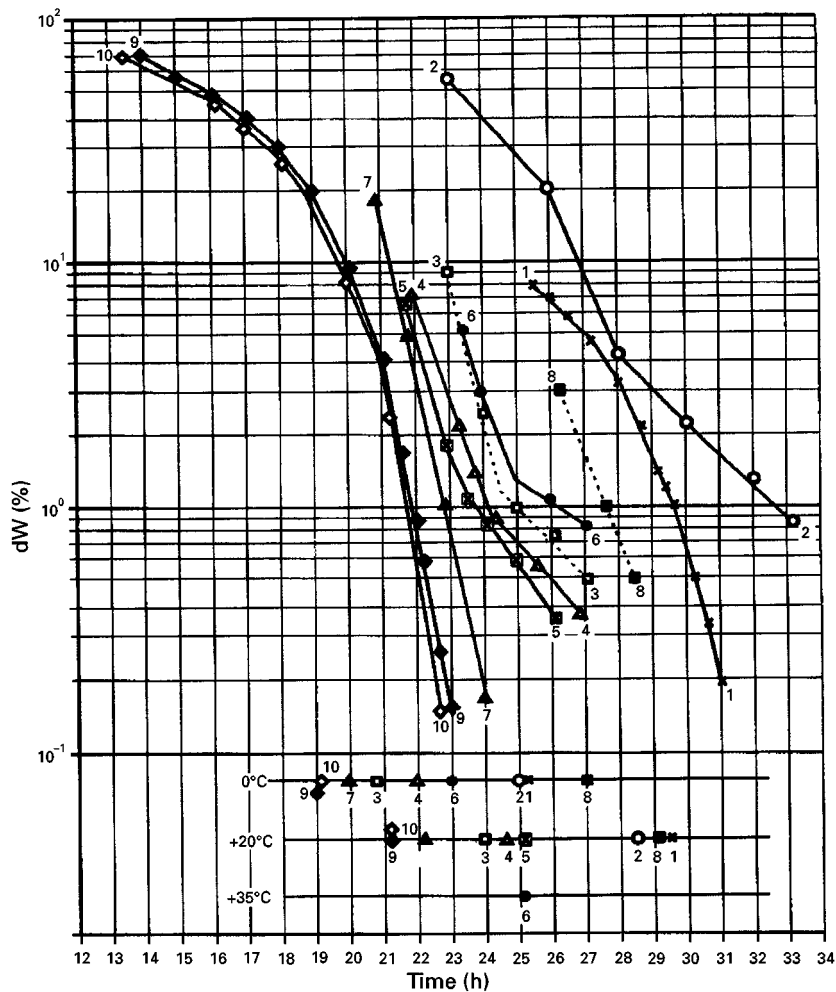


Figure 10 Residual moisture content shown as desorbable water (dW) during secondary drying. Plot 1 = plot 1 in Figure 9B; 2 = 2 (9B); 3 = 3 (9B); 4 = 4 (9B); 9 = 5 (9B); 5 = 2 (9C); 6 = 3 (9C); 7 = 4 (9C); 8 = 1 (9C); 10 = 5 (9C); except run 1, $p_e = 0.08$ mbar and $T_{sh} = -5^\circ\text{C}$ in the first 11 h. (Reproduced with permission from Haseley and Oetjen, 1999.)

effective time: a few hours as opposed to many months up to years.

Relaxation time in molecular configurations may be large compared with the drying cycle, but this may be totally different for the long-term storage time. Besides temperature-induced changes, the residual moisture content (RM) can increase the mobility of molecules and promote chemical reactions. The RM at the end of drying can be as specified; nevertheless moisture can diffuse from the stoppers closing the vials into the product, raising the RM by several per cent during storage. Stoppers and the gas in the container of the product have to be dried carefully. On the other hand, 'the drier the better' is unjustified for many products. The Maillard reaction increases with decreasing water activity ($a_w = p/p_s$, where p = vapour pressure of the product and p_s = saturation vapour pressure) as well as the oxidation of fats. Influenza virus in a freeze-dried formulation shows the

largest decrease in infectivity at 0.4% and 3.2% RM, while at 1.7% it is about 30 times less. Tissue plasminogen activator and human growth factor in certain formulations are optimally stabilized if they are surrounded by a monolayer of water molecules (which may not be distributed evenly).

Freeze-Drying Equipment

Figure 11 shows a freeze-drying plant, designed for maximum current demands. The condenser is cooled by liquid nitrogen controllable between -70°C and -100°C (T_{co}); the brine for the shelves is temperature-controlled (T_{sh}) between $+60^\circ\text{C}$ and -80°C (cooling by liquid nitrogen); the four-stage pump set can reach about 5×10^{-5} mbar (p_e); the vials can be closed shelf by shelf by a hydraulically operated

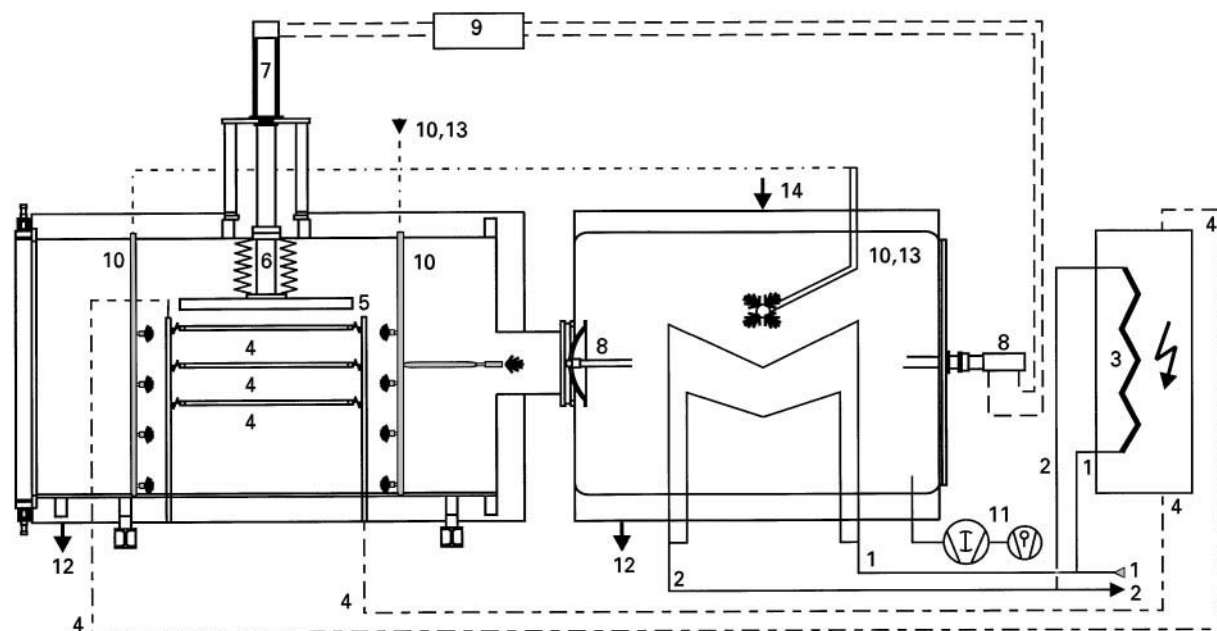


Figure 11 Freeze-drying plant condenser and shelves cooled with liquid nitrogen. Clean In Place system in chamber and condenser. 1, liquid nitrogen inlet to condenser and heat exchanger; 2 nitrogen outlet from the condenser and heat exchanger; 3, heat exchanger for the brine in the shelves; 4, brine to and from the shelves; 5, pressure plate for closing vials; 6, piston rod with bellows; 7, hydraulic piston for 5 and 6; 8, hydraulically operated valve; 9, hydraulic system; 10 and 13, water and steam inlets; 11, pumping system; 12, water outlet. (Courtesy of Steris GmbH, Hürth, Germany.)

pressure plate; the connection between chamber and condenser is as short as technically possible; the valve between chamber and condenser is operated by a fast hydraulic piston; chamber and condenser can be cleaned by a pressure spray and cleaning system (clean-in-place); chamber, condenser and all components within them can be sterilized by the pressureless Vaporized Hydrogen Peroxide (VHP)[®] process; loading and unloading of the plant is fully automatic; the documentation and control of the total process from loading to freezing, to drying, to closing of the valves, to venting and unloading can be automatic with no thermocouples in the product; this includes the change from MD to SD, the calculation of the moisture content during SD and the termination of the secondary drying at a specified moisture content.

If no extreme temperatures are required, refrigerant compressors can be used for the condenser down to $T_{co} \approx -80^{\circ}\text{C}$ and for the brine down to $T_{sh} \approx -60^{\circ}\text{C}$, and a three-stage pump set is sufficient. If steam sterilization is mandatory, the equipment has to be built for pressures up to 2.5 bar and temperatures up to 125°C .

At the other end of the line of freeze-drying equipment laboratory installations are found, of which a typical example is shown in Figure 12. Usually the product is frozen in vials or trays in a separate freezer

or in the condenser of the plant and the shelves are only heated. The chamber is often a bell jar, $T_{co} \approx -45^{\circ}\text{C}$, $p_e \approx 0.05$ mbar. It is not advisable to use this type of plant as a pilot plant for process development, because the product temperature is not sufficiently uniform and cannot be controlled accurately, especially in the low temperature area.

Regulatory Issues

In the *Validation Documentation Inspection Guide*, US Department of Health and Human Services, Food and Drug Administration, 1993, process validation is defined as follows:

- Establishing documented evidence, which provides a high degree of assurance that a specific process will consistently produce a product meeting its predetermined specifications and quality attributes.
- The *Guide to Inspections of Lyophilization of Parenterals*, published by the US Food and Drug Administration, July 1993, contains among others the chapters 'Lyophilization Cycle and Controls', 'Cycle Validation' and 'Lyophilizer Sterilization/Design'.

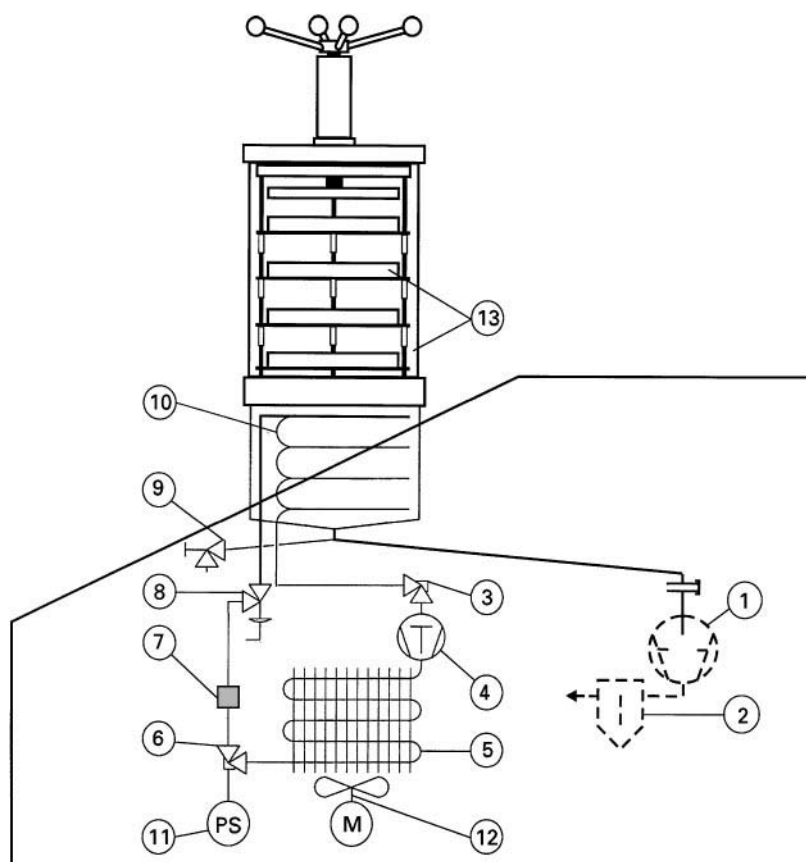


Figure 12 Schema of a laboratory freeze-drying plant: 1, two-stage vacuum pump; 2, exhaust filter; 3, valve; 4, refrigeration compressor; 5, liquefaction of refrigerant; 6, valve; 7, filter; 8, injection valve; 9, drain valve; 10, ice condenser; 11, pressure switch; 12, ventilator; 13, drying chamber with heated shelves and closing system for stopper of vials. (Lyovac® GT 2, Courtesy of Steris GmbH, Hürth, Germany.)

In the European Union, the directive 91/356 EEC provides the principles and guidelines of Good Manufacturing Practice (GMP). In a series of annexes, supplementary guidelines are covered, but up until 1996 only 'Annex 1: Manufacture of Sterile Medical Products' has been revised. In spite of all these guidelines and annexes, Monger summarized the situation for the user of freeze-drying processes and installations as follows: 'It might be expected that some substantial guidance would be provided. Regrettably, this is not so'.

Powell-Evans provided a range of advice on how to 'streamline validation', which he calls 'one of the most time-consuming and costly exercises faced by pharmaceutical manufacturers'. The qualification and validation of freeze-drying installations and processes for the production of pharmaceuticals cannot be summed up in this section. For cosmetic and food products regulatory issues, depending on the country of manufacturing and use, have also to be followed.

Conclusion

Freeze-drying is the most complex and costly conservation process of all drying methods. However, it is the only way for many pharmaceutical products to maintain their original qualities for an acceptable time at readily available temperatures or even at room temperature and above. For food and cosmetic products it provides an opportunity to supply the customers with stable high quality products which can be easily used. For many products, e.g. some antibiotics and some food ingredients, simpler methods of preservation have been developed but in pharmaceuticals there is an increase in the number of products which have to be frozen and freeze-dried at low temperatures using tightly controlled processes. The tendency to automate the whole procedure is promoted by three goals: (1) to have little or no personnel in the sterile areas; (2) to restrict the volume of sterile areas as much as possible, for example by enclosing the whole production line from vial filling to



Figure 13 (See Colour Plate 37). Isolator, Class 100, for filling, transportation and loading of vials into the freeze-drying plant. Decontamination of the isolator and the equipment therein is accomplished by vaporized hydrogen peroxide (VHP). The VHP 100® generator can be seen in the centre in front of the isolator. (Courtesy of Steris GmbH, Hürth, Germany.)

unloading from the chamber in isolators as shown in **Figure 13**; (3) to exclude human error as much as possible and to have each step documented by computer.

To automate an existing process can be more difficult than to develop a new automated process. This is based on several factors. The formulation of the drug has to reflect the automation, e.g. filling and loading can require hours, during which the solution has to be stable, possibly at room temperature. Freezing of the product on the shelves and drying in the chamber have to be executed without temperature sensors in the product; other methods of temperature control have to be used, tested and installed. Criteria have to be defined for the automatic change from main to secondary drying. Automatic termination of the secondary drying has to be effected when certain measurable events are accomplished. Besides these main points several others have to be evaluated. More accurate and independent sensor systems will influence freezing and drying procedures. The required data processing and the actuators to fulfil the commands are available today.

See Colour Plate 37.

Further Reading

Bellissent-Funel MC and Teixeira J (1999) Structural and dynamic properties of bulk and confined water. In: Rey

L and May JC (eds) *Freeze-Drying/Lyophilization of Pharmaceutical and Biological Products*, pp. 53–77. New York: Marcel Dekker.

Hanafusa N (1992) The behavior of hydration water of protein with the protectant in the view of HNMR. In: May JC and Brown F (eds) *Developments in Biological Standardization*, vol. 74, pp. 241–253. Basel: Karger.

Kochs M, Körber Ch, Nunner B and Heschel I (1991). The influence of the freezing process on vapor transport during sublimation in vacuum-freeze-drying. *International Journal of Heat and Mass Transfer* 34: 2395–2408.

Monger P (1997) Freeze dryer validation. In: Cameron P (ed.) *Good Pharmaceutical Freeze-Drying Practice*, p. 157. Buffalo Grove, IL: Interpharm Press.

Oetjen GW (1999) *Freeze Drying*, ch. 1.1.5. Weinheim: Wiley-VCH.

Oetjen GW (1999) *Freeze Drying*, ch. 1.2.4. Weinheim: Wiley-VCH.

Pikal MJ (1999) Mechanisms of protein stabilization during freeze-drying and storage: the relative importance of thermodynamic stabilization and glassy state relaxation dynamics. In: Rey L and May JC (eds) *Freeze-Drying/Lyophilization of Pharmaceutical and Biological Products*, pp. 161–198. New York: Marcel Dekker.

Steinbach G (1971) *Equations for the Heat and Mass Transfer in Freeze-Drying of Porous and Non-Porous Layers and Bodies*, pp. 674–683. Washington, DC: International Institute of Refrigeration.

High and Low Pressure Distillation

A. R. Jose and J. Lopez-Toledo,

Instituto Tecnológico de Celaya,

Celaya, Gto. Mexico

Copyright © 2000 Academic Press

Introduction

Engineers and scientists frequently have the problem of separating a mixture into its components or need to purify a specific product. To solve the problem they usually apply a heuristic procedure, such as the following McMaster five-stage method:

1. Identify and define the problem.
2. Propose and develop several alternatives to solve the problem.
3. Based on available resources, choose one or two of the best alternatives.
4. Work on the chosen alternatives in greater detail and compare them before selecting the most appropriate solution.
5. Evaluate and decide if the problem has been solved.

Let us assume that, for step 1, the problem is identified as the recovery of one or more organic compounds from a mixture, or the purification of a specific chemical.

In order to apply the second step, the differences in physical properties are taken into account. Sometimes the physical properties of the components are very different, so that, if two phases already exist in the mixture, mechanical separations such as filtration or decanting may then be used. But more often the components of the mixture form a single phase and other differences in physical properties need to be found.

When a homogeneous mixture is formed with components of different vapour pressure or different boiling points, then distillation may be one of the several alternatives proposed in step 2. As will be seen later, the relative volatility (α) of a mixture is:

$$\alpha_{i,j} = \frac{K_i}{K_j} = \frac{y_i/x_i}{y_j/x_j} \approx \frac{p_i^0 \gamma_i \phi_j}{p_j^0 \gamma_j \phi_i} \quad [1]$$

where K_i and K_j are the equilibrium constant for components i and j respectively. These K values provide for each component a linear relationship for the

mole fraction in the gas phase and the mole fraction of the same component in the liquid phase. Eqn [1] shows that the equilibrium constant and relative volatility depend on the ratios of vapour pressure, liquid-phase activity coefficients (γ) and vapour-phase fugacities (ϕ).

The relative volatility α is a measure of the ease of the separation.

- If $\alpha = 1.0$ the separation is not possible by distillation.
- If $\alpha \geq 1.2$, distillation will probably be a good alternative, and should be chosen as the next step.

In step 4, the distillation system should be designed. The design and analysis of these columns operating at high and low pressure form the core of this manuscript and are presented in the next sections.

Finally, in step 5, the scientist or engineer debates whether the problem have been solved satisfactorily. If this is the case, the problem is finished; if not, it is necessary to go back and start again.

Distillation

Distillation is based on diffusion of one or more components through a mixture operating at a temperature, pressure and composition that assures the presence of liquid and vapour phases. In distillation, the mass transfer is due to a concentration difference moving from a place of high concentration to one of low concentration; it is not bulk movement as a result of a pressure gradient, like pumping liquid through a pipe.

Relative Volatility

The key separation factor in distillation is the relative volatility, defined by eqn [1]. As the value of relative volatility increases, the easier it is for components to be separated by distillation.

The number or theoretical stages required to separate two species to a desired degree is strongly dependent on the value of α .

The variation of this parameter with pressure is shown in **Figure 1** for the system ethane–propane. As seen, α is greater at low pressure than at high pressure. Therefore, at low pressure (e.g. 1 atm), for

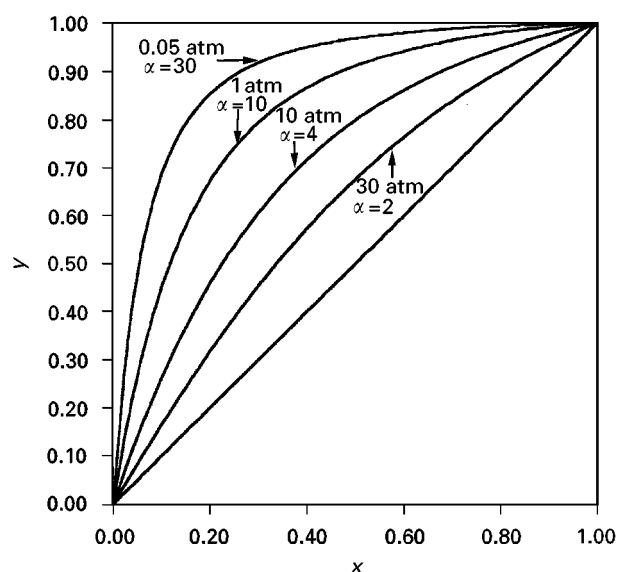


Figure 1 Variation of relative volatility with pressure.

a specified separation, the number of theoretical stages is less than at high pressure (e.g. 10 atm). In this case, why not use low pressure for this separation? As will be seen later, the temperature at the top and bottom of the column plays an important role in this decision. At low pressure (0.05 atm) top temperature -130°C , while at high pressure (30 atm) top temperature is 10°C . Therefore, distillation at high pressure is used since it is much easier and more economical to reach 10°C than -130°C .

Classification, Equipment and Design of Distillation Columns

Distillation is the separation process most used in the chemical and petrochemical industry; as shown in Table 1, its operation is classified into several forms.

Most of the time, distillation is carried out in vertical columns or towers (like the packed column shown in Figure 2) where the liquid descends while the vapour ascends to the top of the column. The vapour left at the top of the tower is condensed and at least a fraction is returned back to the top of the tower as liquid reflux. Part of the liquid leaving the bottom of the column is vaporized in a reboiler and returned to the column as boil-up.

How the distillation equipment operates and how it is calculated has been modified over the years. Figure 3 shows some developments related to distillation.

The design or sizing of distillation equipment requires the calculation of diameter and height of the column. Diameter depends on volumetric flow rates of liquid and vapour inside the column, and these are functions of the total amount of the mixture feed to the column and the reflux or boil-up ratios. The desired purity of the components at the top and bottom of the tower dictates the height of the column. First, the theoretical or ideal plates are calculated, then efficiency is estimated to convert from ideal to real stages. By specifying the distance between plates (30–60 cm), and providing space for about four plates at the top of the column and six for the bottom for disengagement of the phases, the total height of the shell is determined. Figure 4 shows a block diagram for a typical design of a distillation column.

Distillation at high and low pressures involves special characteristics, summarized in Table 2.

With Internal Devices of Distillation Columns

There are three types of internal devices which provide the intimate contact between phases in a distillation column. These are tray, random packing and structured packing.

Table 1 Different classifications of distillation equipment or operation

Amount of compound to be separated	Solute recovery Fractionation
Mode of operation	Steady-state Unsteady-state Batch Semibatch Start and shut-down Stagewise contact Continuous contact
Mixing between phases	None Plates Bubble cups Sieve Valve
Internal device used	Packing Random Structured
System characteristics	Flash Fractionation Azeotropic Extractive
Operating pressure	Low High vacuum Medium vacuum Low vacuum Medium High

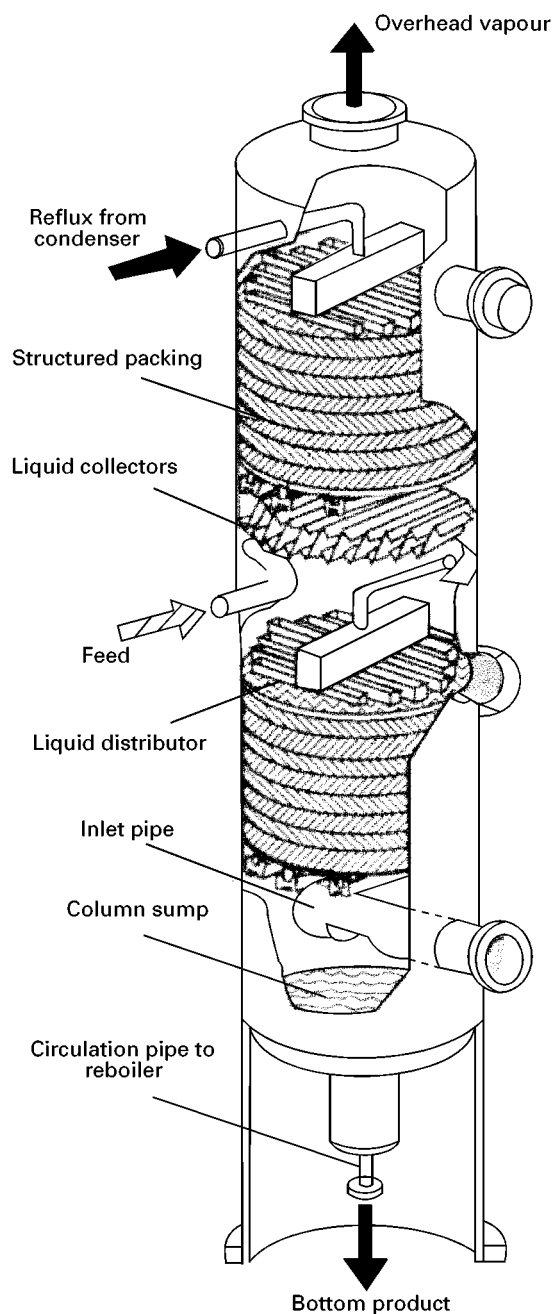


Figure 2 Distillation column equipped with structured packing.

Each has advantages and disadvantages. Trays have been used for many years. Random packings have also been used over three generations of design. Structured packings have replaced trays, especially in applications at low and atmospheric pressures. At high pressure, trays perform better than packings.

For any application one must determine whether tray or packing is the most appropriate. The following factors are an indication of when trays or packings are favoured.

Factors favouring trays

- High liquid rate (this occurs when high column pressures are involved);
- large diameter (packing prone to maldistribution);
- complex columns with multiple feed/take-offs;
- feed composition variation;
- scale-up less risky;
- columns equipped with tray weigh less than those equipped with some packings.

Factors favouring packings

- vacuum conditions;
- low pressure drop required;
- in smaller diameter columns (where trays are more difficult to install, diameters 0.6–0.9 m or less);
- corrosive system (more construction materials available);
- foaming;
- low liquid hold-up.

High Pressure Distillation

As seen from Table 3, distillation at high pressure cover a wide range of applications that have some of the following characteristics:

1. The compounds have low molecular weight (like C_2 , C_3 , C_4 hydrocarbons).
2. Cooling water can be used in the condenser.
3. A change in pressure could change the azeotropic point by more than 10% (in mole fraction).
4. Energy is integrated between condensers and reboilers of different columns.

Sometimes the increase in pressure is limited by the heat sensitivity of the bottom product (it could polymerize or degrade) or by its critical temperature or pressure. As is known, at the critical conditions only one phase exists. If the mixture reaches this point two phases cannot exist anymore and therefore separation is not possible. It is necessary, therefore, to be careful when one is thinking of the operating column pressure.

The upper pressure could be limited by economical conditions. If water is used as cooling medium at the top, the pressure required may be too high and therefore it would be necessary to use a refrigerant. Some authors recommend a upper pressure value of 1.48 MPa using a total condensation with water, 2.52 MPa using partial condensation with water, and if the pressure required is higher than this value it is recommended to fix the top pressure at 2.86 MPa using partial condensation with a refrigerant.

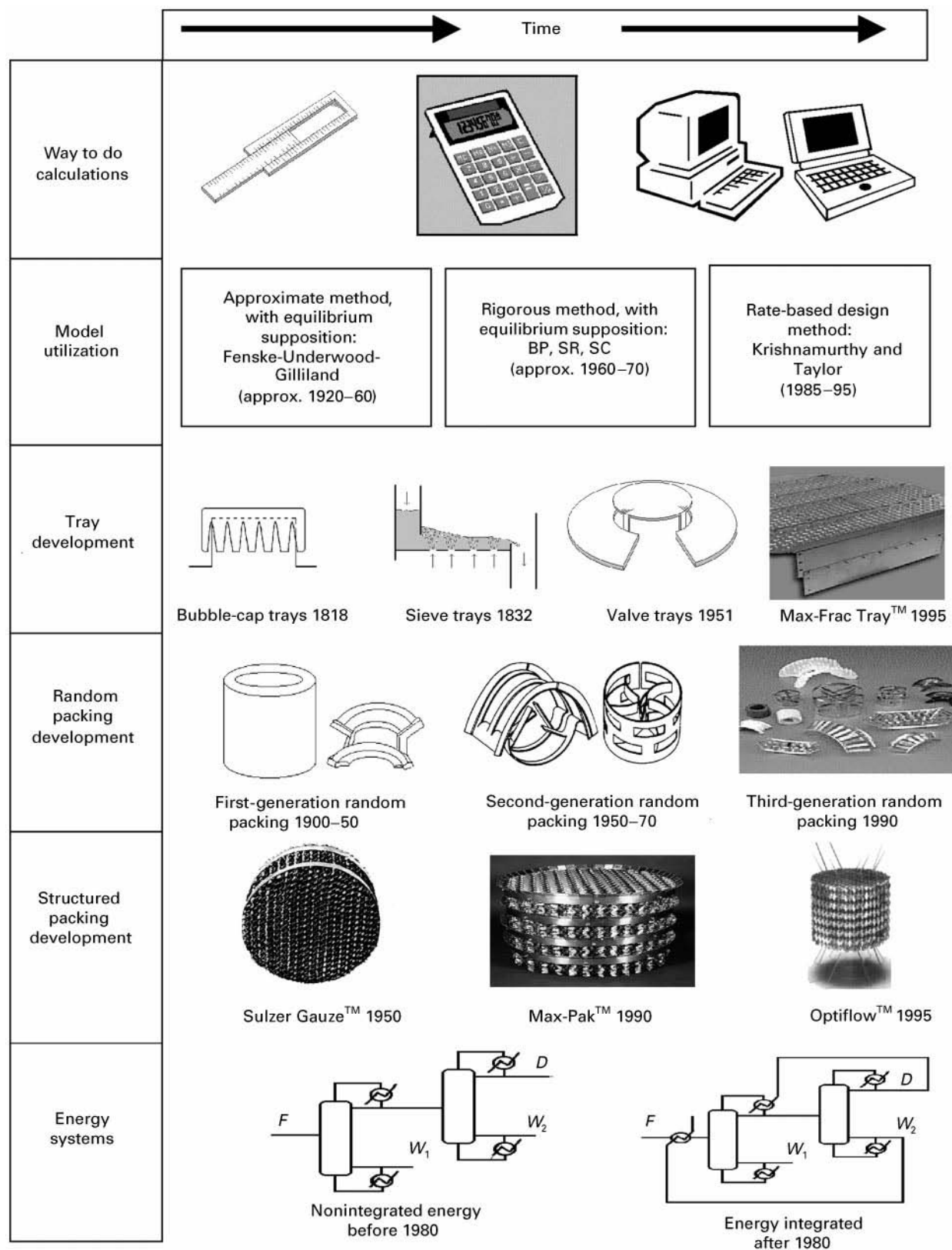


Figure 3 Paradigm shifts related to distillation. (With permission from Chemical Engineering Process (1972) 68 (8): 16).

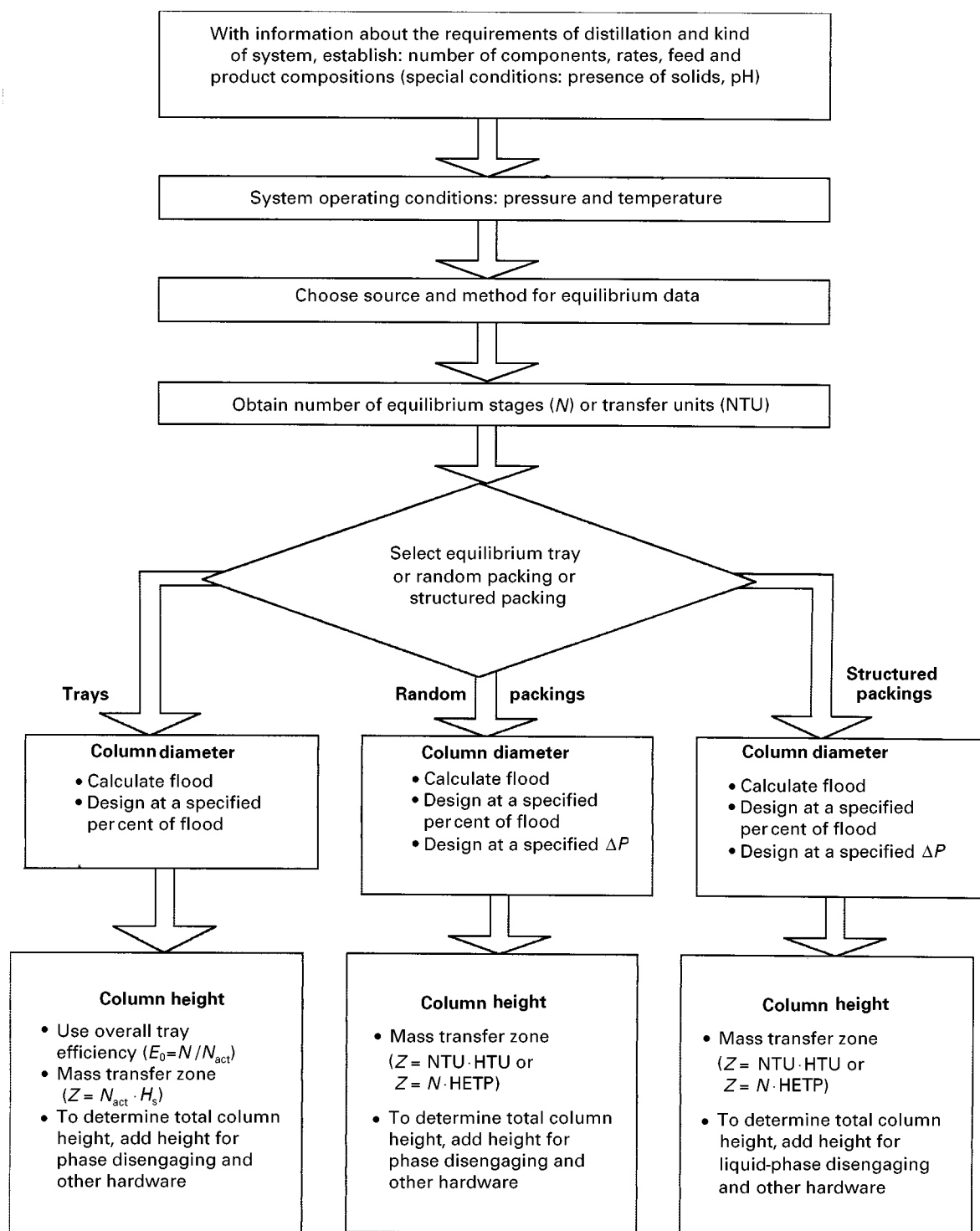


Figure 4 Procedure for designing a distillation column.

The upper pressure also could be limited by cost. If pressure is increased above 1 MPa, all equipment costs begin to go up. For instance, a stainless steel column with sieve trays could double in cost when the pressure is raised from 0.1 to 3 MPa. A similar rela-

tionship exists for other equipment and materials of construction.

Some specific applications of high pressure distillation are given in Table 3. Most applications are in the petrochemical industry, but another very important

Table 2 Characteristics of high and low distillation operation

Feature	Low pressure	High pressure
When is it used?	Products sensitive to temperature (thermal degradation) Avoid using high pressure steam Break azeotropes and allow separation of the system; also when a significant change occurs at the azeotropic composition (about 5%) with change in pressure When trains of distillations columns with energy integration are desired allow energy of overhead vapour partially to vaporize the bottom of the other column)	Gas feeds (C ₂ /C ₃ /C ₄ separation, air separation and ammonia recovery) Allow water to be used in the condenser
Liquid density	High molecular weight of components No significant change	Low molecular weight of components Decreases slowly when pressure increases
Vapour density	Low; decreases if pressure decreases	Increases quickly if pressure increases
Liquid diffusivity	Low; increases slowly if pressure increases	Increases quickly if pressure increases
Vapour diffusivity	High; decreases if pressure increases	Low; decreases quickly if pressure increases
Liquid viscosity	High; decreases quickly if pressure increases	Low; decreases quickly if pressure increases
Vapour viscosity	High; no significant change at low or high pressure	High; no significant change at low or high pressure
Relative volatility	Increases if pressure decreases	Decreases if pressure increases
Flow parameter $F_p = \frac{L}{G} \sqrt{\frac{\rho_G}{\rho_L}}$	< 0.1	> 0.3

application is cryogenic air separation. This is based on a low and high pressure distillation column. The reboiler of the low pressure upper column (0.13 MPa) cools the condenser of the high pressure lower column (0.60 MPa). As can be seen, the high pressure column does not have a high pressure value but neither is it at atmospheric pressure.

The Further Reading section cites a good report on high pressure distillation by Brierley which gives some tips on improving an existing column and de-

signing a new one. High pressure distillation begins about 1 MPa, where liquid density, liquid viscosity and surface tension are unusually low, while vapour density is high. Trays are recommended as internal devices, especially above 2 MPa; below this value, trays and packings must be evaluated. Many problems in high pressure distillation could be avoided with an appropriate design. Available design methods for low pressure can be applied to high pressure but with some corrections, specifically in downcomer design because this is where liquid flooding usually starts in high pressure distillation, while in low pressure, the bottleneck is the vapour flow through the active area. Downcomer design should consider both downcomer back-up and downcomer velocity.

Three flow regimes may exist in industrial columns: spray, froth and emulsion (see Further Reading). In high pressure distillation, tray operation is usually in the emulsion regime, where liquid loads are high and vapour velocities comparatively low. However, in small diameter column (less than 1.5 m) at low liquid loads or at the low end of the high pressure range (about 1 MPa), froth and spray regimes can be found. In the spray regime, flooding is caused by excessive entrainment of liquid from the active area to the tray above. It increases the tray pressure drop and the entrained liquid recirculates to the tray below. The larger liquid load in the downcomer and the increased tray pressure drop together cause the downcomer to overfill, so that the tray floods. In the emulsion

Table 3 Specific applications of high pressure distillation

Application	Pressure Range
Ethylene plant	
Demethanizer	32 MPa
Deethanizer	27 MPa
C-2 splitter	16 MPa
Depropanizer	19 MPa
Debutanizer	5 MPa
Dimethyl ether (DME) production (via the dehydration of methanol)	
DME column	1.60 MPa
Water column	0.75 MPa
Production of heptenes from propylene and butenes:	
C ₃ + C ₃ = /mixture separation	0.60 MPa
Miscellaneous hydrocarbons	
Propylene/propane separation	2.1 MPa
Cryogenic air separation	
Lower column	0.6 MPa

regime, there is little entrainment of liquid by the vapour; instead, the high liquid load causes the downcomer to overflow and the tray to flood. In the froth regime, which is between the spray and the emulsion ones, flooding may be by either mechanism, depending on tray spacing and the particular combination of vapour and liquid loads.

A new model for the design or analysis of sieve tray columns has been developed at the University of Texas at Austin, in its Separation Research Program. This model applies to both low and high pressure columns. The model was adjusted with a wide experimental database from the open literature and also from the Separation Research Program facilities.

The equipment used to perform distillation at high pressure is basically the same as that used for close to atmospheric pressure, but the following special considerations should be taken into account.

1. The physical properties move in the direction indicated in Table 2 (liquid density, liquid viscosity and surface tension are low and vapour density is high).
2. The thickness of the shell and column peripheral equipment must be greater.
3. The advantage in capacity and/or efficiency of structured packing over random packing and plates decreases as the pressure increases.
4. At very high pressure the efficiency of distillation decreases, due to back-mixing.
5. At very high pressure the use of plates (standard and high capacity) is more reliable than packing.

The design equations for packed columns are basically the same, with one possible correction to the height of a transfer unit (HTU) value, to take into account the deviation from plug flow:

$$HTU_{\text{total}} = HTU_{\text{plug flow}} + HTU_{\text{back-mixing}} \quad [2]$$

Remember that at high pressure the density of gases increases by several orders of magnitude; the opposite is true for the diffusivity of the gas phase, and the surface tension decreases to very low values.

Low Pressure Distillation

Modern society is becoming ever more demanding in the quality of the products it uses and for health and environmental reasons a better removal of some components is required. This better purification of many products sometimes requires operating at very low pressure. Fortunately, the development of industrial

equipment to obtain better and lower vacuum has been maintained. The cost of carrying out these operations is of course more expensive than at around atmospheric pressure. The increase in cost is inversely proportional to the absolute operating pressure.

Distillation at low pressure is used for special cases with one or more of the following characteristics:

1. heat sensitive products;
2. liquid feeds or liquid residue with high viscosity;
3. liquids with fouling and/or foaming tendencies;
4. low operating pressure (medium and high vacuum);
5. low residence time.

The applications may be classified into four groups:

- distillation or evaporation of sensitive organic chemicals;
- concentration of foods, chemicals, polymers and biological compounds;
- recovery of organic solvents;
- desolventing, devolatilization and finishing of polymer solutions.

Table 4 shows the levels of vacuum used and also lists representative equipment. Some advantages of vacuum and molecular distillation are:

- low residence time;
- high selectivity due to the higher values for relative volatility;
- cheaper heating requirements.

Some of these special kinds of distillation are discussed below.

Agitated Thin-film or Wiped-film Evaporators (WFE) and Short Path Distillation Equipment

For medium vacuum distillation, thin-film evaporators are used with or without agitation, but evaporators with scraping blades provide better performance and flexibility. Where there are heat-sensitive substances, thermal decomposition may occur during evaporation. Decomposition increases exponentially with temperature and linearly with duration of thermal load. A gentle distillation method therefore reduces the evaporation temperature and the residence times at high temperature.

Since the evaporation temperature depends on pressure, evaporation is performed under vacuum at considerably lower temperatures. If, in addition to applying vacuum, the thickness of the material on the

Table 4 Classification of low pressure distillation

	Approximate pressure	Typical equipment
Low vacuum	760 to 1 Torr (1000 to 1.315789 mbar)	Vacuum column internals Plates Random packing Structured packings
Medium vacuum	1 to 10^{-3} Torr (1.315789 to 0.013157 mbar)	Thin-film evaporators Agitated thin-film evaporators
High vacuum	10^{-3} to 10^{-7} Torr (0.013157 to 0.0000013 mbar)	Short path distillation Molecular distillation Rotary stills Falling-film stills Wiped-film stills Centrifugal stills

Adapted with permission from Eckles AJ (1997) Difficult to process? Vacuum it! *Chemical Engineering* 94–100.

evaporator wall is reduced, lower evaporation temperature and shorter residence times can be achieved.

Most WFE are vertical cylinders where the feed material is distributed to the inner surface; as the liquid flows downward, axially arranged blades or roller wipers distribute the liquid as a thin film which is constantly mixed. In Figures 5 and 6, two types of WFE are shown. Figure 5 illustrates a WFE with rotating blades, while Figure 6 shows a unit with roller wipers and condenser. The last feature is a distinct characteristic of short path evaporators and molecular distillation stills. These types of equipment

operate at the lowest pressure and provide the lowest pressure drop.

The double-walled evaporator jacket is heated continuously with a heating medium. A vacuum system (often a combination of several individual pumps) reduces the pressure in the distillation chamber.

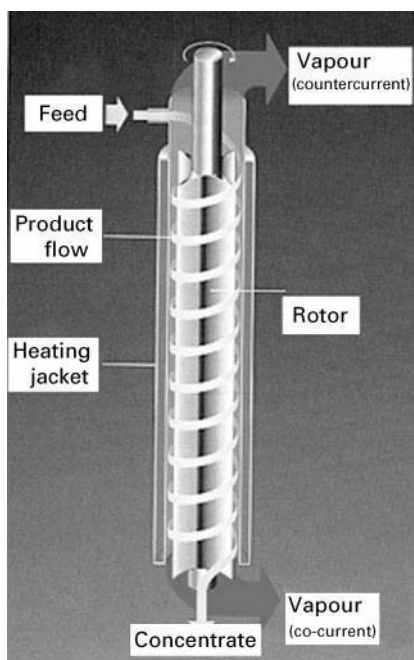


Figure 5 Agitated thin- or wiped-film evaporator (WFE) with rigid blade rotor.

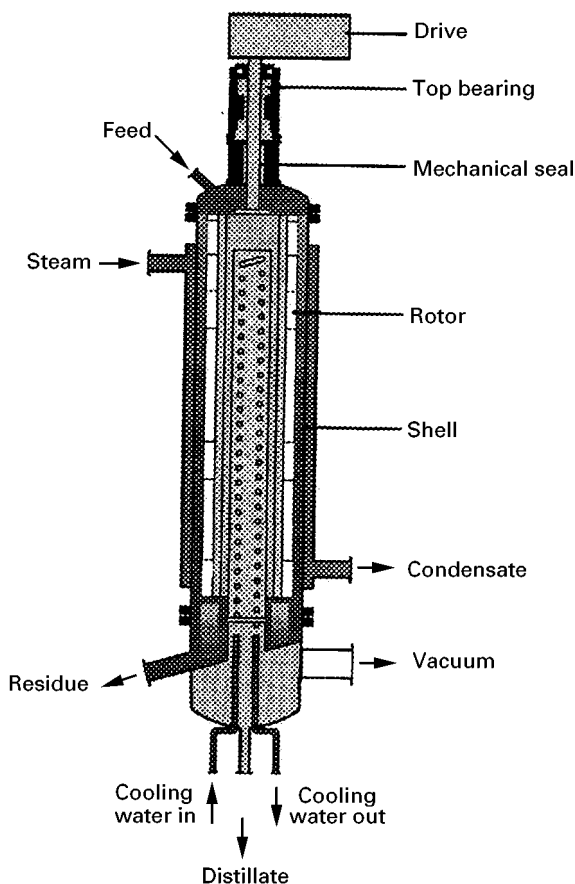


Figure 6 Wiped-film evaporator or short-path distillation equipment, with roller wiper system.

Depending on the temperature and the pressure in the distillation chamber, vapours leave through the vapour discharge and travel to an external condenser. Involatile substances are discharged at the lower end of the evaporator.

The cylindrical evaporation chamber is externally heated with hot pressurized water, steam or heat transfer oils.

Essential parts of a WFE are the rotating blades or roller wiper system, which are axially arranged in the evaporator. The blades (or roller wiper system) influence the following aspects:

- Film thickness: the components to be evaporated are more easily separated from a thin film.
- Uniformity of distribution: uniform distribution of the feed material on the evaporator surface promotes excellent heat transfer and avoids overheating.
- Mixing of the film: optimal mixing within the liquid film increases the complete separation of the components, thus enhancing evaporation.
- Residence time: if gentle distillation is required, heat-sensitive materials can be heated in the evaporator for only a short period of time. With a well-constructed blade or wiper system, the residence time can be considerably reduced.

Thin-film evaporators can be totally vacuum-sealed, thus avoiding any oxidation of product caused by penetration of air.

Discharge of the distillate vapours takes place above the feed nozzle. This is why undistilled liquid droplets, which may occur during flash evaporation, are trapped in the head of the evaporator and then flow back to the evaporator surface.

McKenna (see Further Reading) provides equations to design or analyse operation of a WFE. Some of the important equations to calculate the final concentration C_F of the residual liquid are:

$$C_F = \frac{C_0 - C^*}{(1 + \alpha)^{n_{\text{total}}}} + C^* \quad [3]$$

$$\alpha_n = 2\pi^{1.5} \text{Dif}^{0.5} \frac{w^{0.5} d_e^2 \tan \phi}{QN_b^{0.5}} \times \left[1 + \frac{2N_b Q^{0.5}}{\pi^{2.5} d_e^2 w^{0.5} \tan \phi} \left(\frac{\pi d_e}{N_b} - l_b \sin \phi \right)^{0.5} \right] \quad [4]$$

$$n_{\text{tot}} = \frac{H_e d_e}{d_e H_s} = \frac{H_e N_b}{d_e \pi \tan \phi} \quad [5]$$

Advantages of the process of WFE and short path distillation Thin-film evaporators offer a number of advantages. If higher operating pressure and temperature are required for economic reasons, thermally sensitive materials can still be processed because of the short residence times utilized in WFE equipment.

The thin liquid film and turbulent mixing of the film result in very quick attainment of equilibrium. This is especially important if a complete separation of a low boiling, volatile component out of the residue is required. This is why thin-film evaporators are successfully used as reboilers for rectification columns.

Thin-film evaporators are excellent degassers. If, for example, small quantities of a volatile component have to be removed down to only a few p.p.m., the evaporation capacity is not very important. The main goal in this case is to transfer the portions to be separated as completely as possible to the surface of the film. The transport is achieved by the roller wiper or blade system.

Molecular Distillation

Molecular distillation may be considered as a special version of evaporative distillation in which the liquid is evaporated without boiling, but in such circumstances that the evaporating molecules reach the condenser surface without obstruction. Three conditions for molecular distillation are:

1. Pressure must be lower than 0.001 mmHg. This low pressure is required to ensure that the molecules do not collide with each other.
2. The distance between evaporation and condensation surfaces is of the same order of magnitude as the mean free path of the molecules and the free motion of the molecule is not mechanically hindered.
3. The temperature of the condenser surface should be between 50 and 100°C lower than that of the evaporation surface to prevent re-evaporation of molecules.

The mean free path λ is given by:

$$\lambda = \frac{1}{\sqrt{2}\pi\sigma^2 N} \quad [6]$$

where σ is the diameter of the molecule in centimetres and N is the number of molecules in 1 cm³. By reducing the pressure to very low values, N decreases, giving values for λ of 1–3 cm, in the range of the distance between evaporator and condenser surface.

In molecular distillation the maximum or theoretical rate of evaporation was proposed by Langmuir in 1916:

$$W_e = 0.0583 P_{\text{mm}} \sqrt{\frac{M}{T}} \quad [7]$$

where M is the molecular mass and T is the absolute temperature.

The relative volatility is given by:

$$\alpha_{1,2} = \frac{p_1^0 \gamma_1 \sqrt{M_2}}{p_2^0 \gamma_2 \sqrt{M_1}} \quad [8]$$

From these two equations it may be seen that molecular weight of the compounds involved is an important consideration.

Equipment for molecular distillation and medium vacuum is expensive, but it is economically justified for the separation of high value products such as vitamins, fats, essential oils and hormone concentration.

Typical unit operations and applications for medium and high vacuum using WFE, short path

Table 5 Specific applications of low pressure distillation

<i>Unit operations where wiped-film evaporators (WFE) are used</i>	
Evaporation	Drying
Concentration	Degassing
Distillation	Reactions
Stripping	Deodorizing
Heating	

<i>Distillation</i>	<i>Concentration</i>
<i>Application of WFE for distillation and concentration at pressure of 1–1000 mbar</i>	
Acrylonitrile	Extract solutions
Essential oils	Insulin
Amines caprolactam	Peroxides
Quinoline derivatives	Phospholipids
Diocetyl phthalate	Pyrethrum
<i>WFE for distillation and concentration of viscous products</i>	
Fatty alcohols	Resins
Waxes	Honey
	Glue
	Polymers
	Lubricant oils
	Silicone fluids
<i>WFE for distillation and concentration of products liable to encrust the heated surface</i>	
Used oils	Contaminated effluents
Solvents containing impurities	Residue products from rectification and evaporation plants

equipment or molecular distillation are shown in Table 5.

Technologies to Improve Distillation Processes

There are several ways of improving the separation of mixtures into the desired products. Some of these combine distillation with other processes (like adsorption, stripping, pervaporation, reverse osmosis, membranes, etc.). Others are improvements to the internal devices (such as high efficiency trays or high efficiency packings). There are also the so-called enhanced distillation methods (like extractive distillation, homogeneous and heterogeneous azeotropic distillation, reactive distillation, heat integration, high gravity distillation, spinning cone distillation, mechanical vapour recompression, and pressure swing distillation). Further information about these technologies can be found in the texts cited in the Further Reading section.

Conclusion

In the 21st century, distillation at high, medium and low pressure, will continue to be a much used method for the separation of components from homogeneous mixtures.

See also: **I/Distillation. II/Distillation:** Historical Development; Theory of Distillation. **Membrane Separations:** Filtration.

Further Reading

- Billet R (1979) *Distillation Engineering*. New York: Chemical.
- Brierley RJP (1994) High-pressure distillation is different! *Chemical Engineering Progress* 90 (7): 68–77.
- Dean JA (1995) *Analytical Chemistry Handbook*. New York: McGraw-Hill.
- Hewitt GF, Shires GL and Polezhaev YV (eds) (1997) *Encyclopedia of Heat and Mass Transfer*. Boca Raton, FL: CRC Press.
- Holló J, Kurucz E and Boródi (1971) *The Applications of Molecular Distillation*. Budapest: Akademiai Kiadó.
- Humphrey JL and Keller GE II (1997) *Separation Process Technology*. New York: McGraw-Hill.
- Kister HZ (1990) *Distillation Operation*. New York: McGraw-Hill.
- Kister HZ (1992) *Distillation Design*. New York: McGraw-Hill.
- Lockett MJ (1986) *Distillation Tray Fundamentals*. Cambridge: Cambridge University Press.

McKenna TF (1995) Design model of a wiped film evaporator. Application to the devolatilization of polymer melts. *Chemical Engineering Science* 50 (3): 453–467.

Seader JD and Henley EJ (1998) *Separation Process Principles*. New York: Wiley.

Treybal RE (1980) *Mass-Transfer Operations*, 3rd edn. New York: McGraw-Hill.

Historical Development

M. S. Ray, Curtin University of Technology,
Perth, Western Australia

Copyright © 2000 Academic Press

Introduction

Distillation is one of the oldest and most widely studied unit operations in chemical engineering. It is familiar as a separation technique to chemical, process and petroleum engineers and to chemists. The common techniques, design methods and numerous applications have been extensively documented in monographs and in the journal literature (and conference proceedings) over many decades. Specialist texts and more general handbooks should be familiar to those working in related fields, therefore these standard sources are not documented here. The importance of distillation and its future directions have been discussed by Kunesh *et al.* (1995) and by Porter (1995) (see Further Reading). This article presents a state-of-the-art overview of distillation by concentrating on recent advances and possible future developments.

Sources of Information and Data

For a subject as old as distillation, and with such a wide range of applications, there is an extensive collection of published information. With the advent of electronic databases and online web-based resources it has become much easier to perform literature searches on particular topics and to keep abreast of the current literature and recent developments. For this reason an extensive reference list to journal articles is not provided in the Further Reading at the end of this article. Selected papers are included that can be used to locate related references. Author or subject searches of the journal literature (from 1956 to the present, with six-monthly updates) can easily be performed by using the **CHERUB™** *Chemical Engineering Database* (compiled by M. S. Ray) which is included on the *Engineering & Applied Science CD-Rom Database*. The ability to easily search the chemical engineering literature is a recent development, and is an important advantage for distillation re-

searchers. Another useful reference source is a series of annual update bibliographic papers on 'Equilibrium-staged Separations' (e.g. *Separation Science and Technology* 32(18): 3067–3083, 1997). Patent searches can also be performed on the web, e.g. www.ibm.com/patents, and www.uspto.gov (the website of the US Patent & Trademark Office). Several handbooks and monographs (and CD-ROMs) containing property data useful for distillation systems have also been compiled, e.g. C. L. Yaws (transport properties data and thermodynamic diagrams); J. Gmehling and co-workers (including VLE data, heats of mixing, azeotropic data); and the *American Institute of Chemical Engineers' Design Institute for Physical Property Data (DIPPR)* publications.

Prediction of Vapour–Liquid Equilibria (VLE) Data

Significant advances in the interpretation and prediction of vapour–liquid equilibria (VLE) data have been made since the 1970s. These advances developed from the publication of a range of equations of state (EOS) based upon the application of traditional thermodynamic principles and relationships. The EOSs provide interpretation or evaluation of available experimental VLE data. The Wilson model (1964) is probably the most popular for dealing with liquid-phase activity coefficients because it has only two adjustable parameters, and it works well for both binary and multicomponent systems. The prediction of nonidealities in binary mixtures using the UNIQUAC model (1975) is rather more complex. Subsequent and related studies led to the development and use of the Group Contribution Methods such as ASOG and UNIFAC for the prediction of VLE data. The latter is widely used when actual system data are not available, provided that an approximate nonideality correction is acceptable. New methods are being developed and probably the one showing most promise and of general applicability is known as: A Generalized Approach to Phase Equilibria (AGAPE, 1995).

There are many EOS models described in the literature but only a few have wide use for engineering

applications. The Redlich–Kwong equation (1949) and its modification by Soave (1972), and the Peng–Robinson equations (1976) have broad general application for nonpolar components and are the most widely used, especially in the refining and gas processing industries. For highly nonideal components, use of the EOS requires an appropriate mixing rule. The alternative approach is direct application of liquid activity model parameters in the EOS. A collection of papers relating to the development of the Peng–Robinson EOS over 20 years was published in 1998 (*Industrial and Engineering Chemistry Research* 37(5): 1579–1706).

The availability of commercial software packages, e.g. flowsheeting design packages such as HYSYSTM and PRO/IITM (see below), have made the prediction and evaluation of equilibrium data quicker and easier. These packages were generally developed for use by the oil and gas industry and refining companies, and they include extensive VLE prediction equations integrated within the design methods. Some of these prediction methods have been developed specifically for use with common petroleum systems (e.g. Chao-Seader; Grayson-Streed).

Applications of the Design Methods

Distillation design methods are well established and described in detail in the traditional reference texts (see Kister, 1992). The original methods were formulated in the 1920s and 1930s such as the McCabe–Thiele (1925) and Ponchon–Savarit (1921, 1922) methods for binary mixtures, and the rigorous multicomponent analogues of the Lewis–Matheson (1932) and Thiele–Geddes (1933) procedures. Use of the latter trial-and-error methods emphasized the need for the incorporation of suitable numerical techniques to ensure that the solution (of number of stages) would actually converge, and also to reduce the time spent performing the calculations. Designers later came to rely on short-cut design methods, e.g. Fenske (1932), Underwood (1945, 1946, 1948), Smith–Brinkley (1960), etc., to provide ‘ballpark’ results before embarking upon the detailed rigorous calculations. Easier access to mainframe computers in the 1960s, and desktop machines in the late 1970s meant that the time required to perform the numerical calculations was reduced, and developments then centred on design methods which simplified the problem formulation, e.g. matrix manipulation techniques.

The arrival in the 1980s of general flowsheeting design packages such as HYSIMTM and PRO/IITM (replaced by HYSYSTM and PRO/IITM in the 1990s) shifted the design emphasis away from the develop-

ment of specific design methods to the use of commercially available packages which could provide quick and easy short-cut designs. These developments meant that the designer was liberated from tedious calculation but still required a sound knowledge of distillation principles and the ability to analyse the simulation results in order to avoid serious errors. Many papers have been published in the mid-1990s concerning the limitations of the simulation methods (e.g. *Chemical Engineering Progress* 91(6): 63–75, 1995; *Chemical Engineering Education* 31(1): 46–51, 1997), and the problems that can occur if too great an emphasis is placed upon their use with too little feedback from experienced designers (e.g. *Chemical Engineering Progress* 94(6): 63–77, 1998).

Other design packages are available, the most recent developments being the *Computational Fluid Dynamics* (CFD) modelling software. Such packages may be useful for modelling effects within distillation equipment rather than straightforward applications of the equilibrium stage calculations. CFD is discussed later in this article in relation to possible future developments.

Advances in Column Design

The basic equipment used to achieve a separation has not changed significantly within the last half century. A tray (or packed) column is still used to provide contact area between the liquid and vapour phases in order to achieve mass transfer and hence the desired separation. Tray columns are generally preferred (packed columns are used for particular types of separations, or specific situations) and the equipment consists of tall vertical towers with a large percentage of internal free space. Distillation is also characterized by its thermal design requirements and is an energy-intensive process. Advances in column design have tended to focus on improvements in energy usage and/or improved separation efficiencies. Two examples from the literature are the Hige distillation unit and the integral dual column. The Hige high-performance distillation or extraction unit described by Ramshaw (*The Chemical Engineer* (IChemE) June: 17–21, 1987) attempted to utilize centrifugal fields to improve the separation efficiency and to reduce the column size. The dual distillation columns (see US Patent no. 4 681 661 (1987) and *The Chemical Engineer* (IChemE) December: 21, 1987) consists of two concentric columns (the stripping and rectifying sections) arranged one within the other, the reason being an attempt to better utilize heat effects and also to reduce the column height. Neither of these developments (or numerous others described in the literature) has been widely adopted by industry,

possibly because they do not offer significant cost advantages (or because of the conservative nature of the chemical processing industry).

Column Developments

These have centred mainly on a better understanding of the fluid dynamics within the column and specifically across the trays (the first book on this topic was by Lockett in 1986), and also on improved prediction methods for determining plate and overall column efficiencies. A better knowledge of the interrelation of these two aspects is beginning to emerge from several research groups, e.g. Biddulph and co-workers, and their studies of the relationship between Marangoni surface tension effects and plate efficiencies (*American Institute of Chemical Engineers Journal* 37(8): 1261–1264, 1991). A development since the 1970s is the preference for sieve trays, rather than bubble or valve trays which were prevalent up to that time. The *AIChE Bubble Tray Design Manual* (1958) is still used (with modifications) and quoted, even for the calculation of sieve tray efficiencies for which it was not intended and for which it provides rather poor results. However, this older method has provided a starting point for recent studies which examine the significance of fluid-related variables (such as surface tension) and how this knowledge can be used to design more efficient tray columns.

Many papers have been published in the more industry-orientated journals (e.g. *Chemical Engineering* (NY), *Chemical Engineering Progress* and *Hydrocarbon Processing*) concerning column operation and performance problems. These papers also discuss particular aspects of internal column design and use of the newer structured packings, now available as alternatives to tray systems, in relation to column performance and operation. The use of high efficiency packings requires a better understanding of the hydrodynamic conditions and the mass transfer processes that occur in the packing. Fouling and plugging within distillation equipment can become serious problems and they are areas in need of better understanding. High surface area packings are popular because they promote efficiency, however they are also more prone to fouling problems.

If solids are present in a stream then design solutions generally act to keep the solids moving. Therefore any liquid maldistribution within the column or tray channelling (due to initial vapour maldistribution) must be corrected to avoid plugging problems. Plugging and fouling have varying effects depending upon the actual in-service conditions, and hence it is difficult to devise generic strategies or solutions. General advice tends to focus upon the need for good

distributor design, good wetting (and wettability) of the mass transfer surface, and good distribution of the flow streams within the equipment.

Papers describing column operational problems, such as product draw limitations especially for column revamps (*Chemical Engineering Progress* 94(6), 63–77, 1998), are particularly useful for designers and process operators.

Energy-intensive Nature of Column Design

The energy-intensive nature of column design and operation is unlikely to change significantly, mainly because the requirements for the reboiler to provide vapour flow and the condenser to provide liquid product are essential aspects of the separation. An additional constraint is that the heat removed by the condenser is typically low grade and of little use elsewhere in the plant. Traditional solutions have been to use vacuum operation in the column to lower the boiling point of the mixture (especially for heat-sensitive materials), and to utilize low-grade heat from other plant operations to provide the reboiler duty. Attention has been directed towards lowering the energy requirements of a column, e.g. by reducing the reflux ratio. Energy-saving revamps have replaced trays with packings in order to create more theoretical stages within a column, and hence reduce the reflux rate and boil-up rate. The integration of columns within a sequence and the use of overhead vapours in another column's reboiler (e.g. by use of a Rankine cycle) have also been considered. Energy saving and integration techniques have become standard design procedures since the 1970s (including the use of pinch technology and heat exchanger network design). However, it is difficult to achieve (or to envisage) large scale reductions in the thermal requirements of distillation due to the inherent basis of the separation itself, i.e. latent heat of vaporization is required for the essential partial vaporization at each stage. The most likely developments in this area are the use of hybrid systems, e.g. membranes + distillation, which effect a part of the separation in a less energy-intensive operation (see the section below on developments and applications).

Particular Techniques and Situations

This section considers only two specific aspects of distillation operations, namely process control and difficult separations (e.g. azeotropes).

Chemical Process Control

This was mainly in the hands of electrical/instrument engineers until the mid-1960s, and most of the

published literature reflected their particular expertise. Since that time process control has developed as a significant area of chemical engineering expertise and publication. Many academics have adopted and published in this field (see Luyben, 1992) and there are also several handbooks and practical texts dealing with plant operations (e.g. Shinskey, 1984). Distillation was one of the primary chemical engineering unit operations to be researched and developed in depth for process control applications. This was because of the scope offered by distillation as a control problem and the range of options and alternatives available. The focus of distillation control is usually the product specification, but the critical operations of reboiler and condenser performance, the uncertainty of feed-point location, the reflux rate, and the need for correct internal functioning (e.g. fluid flow on and between the trays) means that several complex relationships and problems need to be considered together. The number of publications dealing specifically with distillation control attests to the complex nature of the problem and the number of approaches and applications that are possible within any single situation. An additional consideration for the designer is the possible number of column arrangements, utilizing several columns, and their possible alternative specifications (hence the advantages offered by simulation packages), and therefore the integration of individual column control within the overall control of a set of distillation operations.

Developments in distillation control have focused on several areas, generally searching for optimal solutions to the following:

1. Individual column control (including reflux streams, and reboiler and condenser operation and performance).
2. Control of a column required to perform a specific separation (e.g. heat-sensitive mixtures) or a particular type of application (e.g. separation of azeotropes or close-boiling mixtures; reactive distillation).
3. Control of sequences and arrangements of several columns.

Distillation control has developed into a multifaceted problem incorporating mass transfer and separations, process modelling and optimization techniques, instrumentation and control functions, and the application of simulation packages in order to evaluate a range of possible problem solutions. Control theory has now developed to include a range of advanced techniques such as adaptive control, model-based control, and the use of neural networks which supplement the basic approaches offered by combina-

tions of proportional, integral and derivative (P-I-D) control functions.

Difficult Separations

Difficult separations using distillation techniques depend primarily upon the nature and properties of the components in the mixture, rather than the physical arrangement of the equipment such as bubble caps versus sieve trays, tray versus packed columns, etc. Reactive distillation is an exception to this generalization (see next section). Distillation contrasts with other separation techniques such as membranes and adsorbents where the characteristics of the actual separation media have a significant effect upon the ability to separate the components. This is why generic distillation methods have been developed and used effectively whereas there is no single theory or method available for the design of either membrane or adsorption systems. However, distillation was developed in order to separate mixtures of components exhibiting significant differences in relative volatilities and boiling points and problems arise where this is not the case. In particular, azeotropes exhibit no difference in volatility (at certain conditions) and hence no change in the composition of the mixture obtained. Traditional approaches have been either to avoid the conditions where an azeotrope forms, or (more likely) the addition of a solvent or entrainer which 'breaks' the azeotrope but which also requires an additional column(s) to remove and recycle the solvent. The common azeotropes are well known and documented, e.g. ethanol/water, acetone/chloroform, etc. Recent developments have centred on the ability to predict the occurrence of an azeotropic mixture (or a mixture with very little difference in component volatilities), and also on the application of the traditional design methods to the design of a range of column configurations. These configurations aim to produce an optimum separation in terms of product specification, minimum use and recycle of solvent, effective and feasible control schemes, minimum capital and operating costs. Computer-based property packages have been developed specifically to predict azeotrope formation, and the vapour-liquid equilibria data can then be used in an appropriate column simulation package to evaluate the alternative equipment arrangements. Researchers have developed prediction and property packages by the application of basic thermodynamic principles, and also utilizing specific equations of state (see section on VLE data above). The property packages have also included data on available solvents. The aim is generally to combine azeotrope prediction with solvent selection, and full specification of the combined mixture properties for use in column design simulations.

Developments and Applications

Reactive or Catalytic Distillation

Reactive or catalytic distillation has emerged as a significant development in recent years, the original patents were obtained by L.A. Smith in the early 1980s. Several research groups have considered a range of specific systems and applications and a substantial body of literature has been published. The main system that has been investigated and reported is the production of methyl *tert*-butyl ether (MTBE) mainly due to the high efficiency of the process, and also the related systems of ethyl *tert*-butyl ether (ETBE) and *tert*-amyl methyl ether (TAME). The technique includes reactive (homogeneous catalyst) or catalytic effects (heterogeneous catalyst acts as the packing) within the traditional distillation equipment. The design requires a combination of the well-known mass and energy balance equations with the individual reaction mechanisms, and consideration of heats of reactions. The design of such systems requires modelling of the mass transfer, reaction and separation, thermal effects, and the inherent control systems. An additional requirement is the knowledge of any possible side reactions and by-product formation, and their effect on the final separation of the mixture produced.

If a catalyst is required then the physical installation of this material, its removal and replacement, and its effect upon the fluid dynamics within the column become important additional operational and design considerations. The distillation column now becomes a countercurrent two-phase flow, fixed-bed reactor. Packed beds typically have a void fraction of 0.7 (even up to 0.95), whereas small catalyst particles result in a voidage of 0.3–0.4 which makes countercurrent operation impractical. Therefore catalyst support structures must be designed and incorporated to provide a voidage of at least 0.5, and in addition allow for expansion and contraction of the bed, and provide a uniform catalyst spatial distribution. An alternative is to manufacture the catalyst in the shape of a distillation packing. For certain systems there are distinct advantages from employing reactive distillation, but their dynamics are complex and careful consideration of the operation and control are required in order to avoid potential difficulties.

Hybrid Separation Systems

Hybrid separation systems combining two or more unit operations have become popular in the 1990s, and there are numerous examples in the journal literature. Many of the examples have combined distillation with a membrane-type technique, thus aiming to

utilize the well-known data and methods (and separation efficiency) of distillation with the low temperature advantages offered by membrane systems. Osmotic distillation (or isothermal membrane distillation) has been developed specifically for applications requiring the retention of flavours and fragrances (*Chemical Engineering Progress* 94(7): 49–61, 1998). This hybrid process can concentrate solutes to very high levels at low temperatures and pressures, and it is particularly suitable for sensitive solute materials. It can also effect the selective removal of a single volatile solute from an aqueous solution. The process involves the transfer of volatile components between two inherently miscible liquid streams, separated by a semipermeable membrane, the driving force being provided by differences in component activity between the streams. The strip solution becomes diluted during separation/transfer and must be reconcentrated by distillation (or evaporation). Many other examples of membrane–distillation systems can be found in the literature. Alternative hybrid systems include crystallization–distillation, solvent extraction–distillation, pervaporation–distillation, and fluidized reaction–distillation. These systems have been described in some detail including patents, although generally the work is directed towards a particular application or problem.

The Future: Developments and Applications

Future developments would seem to be most closely linked to the areas already outlined in this chapter rather than sudden and unexpected applications. Distillation is a mature separation technology and developments are likely to be in incremental advances in our knowledge and understanding of the process itself, and in the underlying principles that determine its ultimate effectiveness for separating components.

The most likely areas for significant advances and developments are:

1. Further combinations of mass transfer effects within distillation equipment (tray or packed columns), developing the current trends of reaction with distillation (reactive and/or catalytic distillation), and hybrid systems of membranes (or other techniques) with distillation.
2. Improvements in separation effectiveness (and costs) including attempts to reduce the size of the equipment, increased efficiencies, and reductions in energy requirements.
3. More reliable prediction and modelling techniques directed towards VLE predictions, efficiency models and predictions, and improvements in the CAD

modelling packages in order to identify practical limitations of the simulations at an early stage.

4. Development of separation systems incorporating distillation in order to address specific environmental problems and applications.

Significant applications are expected in the use of *computational fluid dynamics (CFD) packages* for prediction of effects occurring within distillation equipment. This is a different area of research from the use of the flowsheeting packages and the calculation of equilibrium stages. The CFD approach (generally using commercial packages such as PHOENIXTM and FLUENTTM) has been used to predict single-phase flow patterns (of a vapour phase) from numerical solutions of the Navier–Stokes equation, turbulence equations, and the continuity equation. If the equations of momentum and mass transfer are inserted into the CFD methodology then it may be possible to predict the flow patterns and their effects upon tray performance. However, the major challenge is the consideration and modelling of the three-dimensional froth height and its shape.

Reviews of the state-of-the-art in distillation and the need for and possible directions of future research have been discussed by Fair (1988), Kunesh *et al.* (1995) and Porter (1995). Assessments of advances and developments in distillation equipment regularly appear in the journal literature, e.g. *Chemical Engineering* (NY), December 1992; *Hydrocarbon Processing*, February 1989; *The Chemical Engineer* (IChemE), September 1987. Fouling and plugging in equipment and a better understanding of the internal flow mechanisms and regimes are areas receiving and requiring further attention, as discussed earlier. Most new ideas tend eventually to become either an academic curiosity, or niche applications, and approximately every 10 years a new technique gains attention and prominence, e.g. reactive distillation, membrane-distillation.

See Colour Plate 38.

See also: II/Distillation: Energy Management; Instrumentation and Control Systems; Modelling and Simulation; Theory of Distillation.

Further Reading

- CHERUBTM – CHEMical Engineering Reference User Bibliography on the *Engineering & Applied Science* CD-ROM from INFORMIT, Melbourne, Victoria, Australia (published semi-annually by subscription; details available from this author).
- CAD Design Packages: HYSIMTM (1987) and HYSYSTM (1996), Hyprotech Ltd, Alberta, Canada; PRO/IITM (1984) and PROTESSTM (1996). California, USA: Simulation Sciences Inc.
- Fair JR (1988) Distillation: whither, not whether. *Chemical Engineering Research and Design* 66: 363–370.
- Kister HZ (1990) *Distillation Operation*. New York: McGraw-Hill.
- Kister HZ (1992) *Distillation Design*. New York: McGraw-Hill.
- Kunesh JG, Kister HZ, Lockett MJ and Fair JR (1995) Distillation: Still towering over other options. *Chemical Engineering Progress* 91(10): 43–54.
- Luyben WL (1992) *Practical Distillation Control*. New York: Van Nostrand Reinhold.
- Porter KE (1995) Why research is needed in distillation. *Chemical Engineering Research and Design* 73(4): 357–362.
- Shinskey FG (1984) *Distillation Control*, 2nd edn. New York: McGraw-Hill.
- Sneesby MG, Tadé MO, Datta R and Smith TN (1998) Detrimental influence of excessive fractionation on reactive distillation. *American Institute of Chemical Engineers Journal* 44(2): 388–393.
- Tadé MO, Sneesby MG, Datta R and Smith TN (1997) ETBE synthesis via reactive distillation. Part 1: Steady-state simulation and design aspects; Part 2: Dynamic simulation and control aspects. *Industrial and Engineering Chemistry Research* 36(5): 1855–1869 and 1870–1881.

Instrumentation and Control Systems

B. Roffel, University of Twente, Faculty of Chemical Engineering, Enschede, The Netherlands

Copyright © 2000 Academic Press

Introduction

Distillation columns have been widely used in the past to separate mixtures of liquids into individual components. And even though new separation techniques are being developed, distillation remains the

most important separation method applied in the process industries today.

The layout of a simple distillation column is shown in **Figure 1**. A single feed enters the column at the side and two products are produced: the light or most volatile components are withdrawn from the top and heavy components are removed from the bottom. Heat (in the case shown, steam) for evaporation of the liquid is supplied to the reboiler, and heat is removed (in this case, through cooling water) at the top in the condenser. The nomenclature used in this

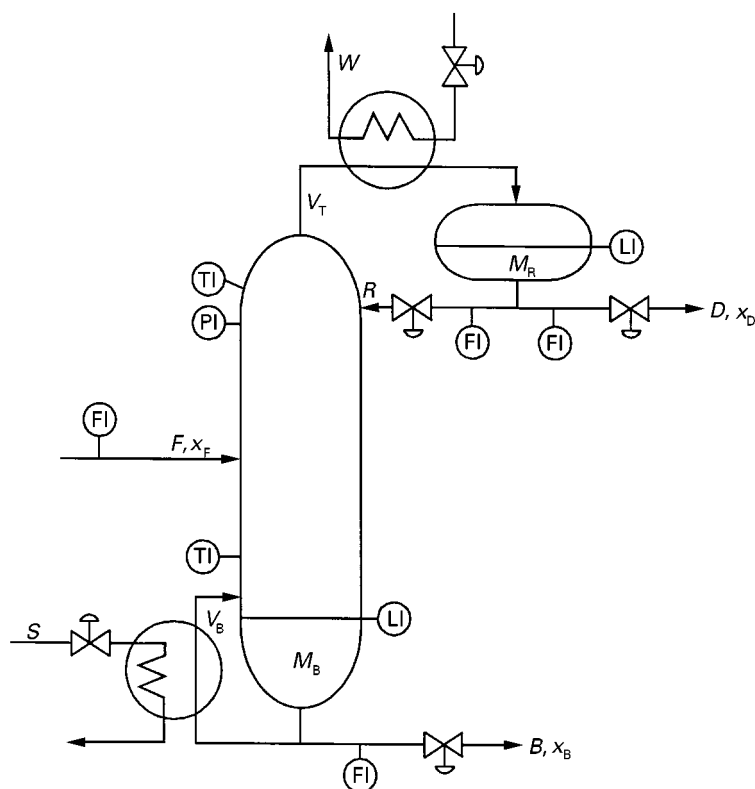


Figure 1 Distillation column layout.

chapter is shown in **Figure 1**, where V = vapour flow, F = feed flow, R = reflux flow, D = distillate flow, B = bottom flow, x = composition, M = mass hold-up and W and S are cooling water and steam flow respectively. In order to maintain constant separation in the distillation column, it should be well instrumented and controlled. The treatment of instrumentation and control techniques will focus primarily on packed columns or columns with trays.

A number of excellent books and review articles have been written about distillation control. Shinskey's book (1984) is a very practical one and provides a good introduction to the subject of distillation control, although a detailed explanation of different approaches to control alternatives is always clear to the novice. The book by Buckley *et al.* (1985) provides a comprehensive treatment of pressure, level and protective controls; control of composition is restricted to a short treatment of composition dynamics in binary columns. The book edited by Luyben (1992) is probably the best starting point: It has been written by several experts in the field of distillation dynamics, instrumentation and control. It provides a comprehensive treatment of distillation models, distillation simulation, identification of distillation processes and selection and comparison of control structures. In addition, several chapters are devoted to

particular case studies. The *Process Control Instrument Engineers' Handbook* (Liptak, 1995) also provides three interesting sections on distillation control: one section discusses basic controls, another section discusses advanced controls and in a subsequent section the subject of relative gain calculations is reviewed. The handbook also provides a wealth of information on instrumentation.

A book which gives a good introduction to batch distillation control is the one by Fisher (1990) and Luyben (1992) gives a good overview. Three review articles should be mentioned as a starting point for further reading; the first one is by Tolliver and Waggoner (1980: 195 references), another is written by McAvoy and Yang (1986: 270 references), and the one by Skogestad (1992) also provides easy-to-understand material: it has 206 references.

Because vapour and liquid with a certain energy content are present in the column, basic instrumentation includes measurements of the vapour hold-up (column pressure), liquid hold-ups (column bottom level and reflux drum level) and generally a number of temperatures along the column. In addition, the in- and outgoing flows are usually measured, as shown in **Figure 1**.

Since the feed to the distillation column is often fixed by a preceding process, no control valve is

shown in this flow, although sometimes the feed pre-heater control valve is used to control the amount of feed that vaporizes. This means that five manipulable flows remain and there are essentially five degrees of freedom for control. However, the vapour and liquid hold-ups have to be controlled, which means that $5 - 3 = 2$ degrees of freedom remain, which are generally used for composition control.

Distillation columns pose some interesting control problems. First of all, the process is often highly nonlinear. Secondly, there are five variables to be controlled (pressure, P , level, h_B , level, h_R , composition, x_D , composition, x_B) and five variables which can be manipulated (flows R , D , B , S and W). How the coupling between these controlled and manipulated variables should be established has been an interesting field of study for many years. In our approach a matrix (Figure 2) is constructed where all variables are listed; for each combination of controlled output and manipulated input the control quality is determined. The control quality can be established on the basis of speed of control, power of control and the requirement of minimal interaction between control loops. The speed of control is related to the period of oscillation of the control loop at the limit of stability. The shorter this period, the higher the speed of control. The power of control relates to the range over which control is effective. For an acceptable combination, the speed of control should be large, as

should the power of control – in other words, the controlled output should respond quickly to changes in the manipulated process input. However, there are not always five variables to be controlled. It could be that there is no strict requirement for the column pressure, in which case it is often optimal to minimize the pressure and open the cooling water valve of the condenser completely. It could also be that there is a strict requirement for the top product composition but no requirement for the bottom composition, in which case there would be an extra degree of freedom.

The issue of column operation, column instrumentation and selection of the right pairing between controlled process outputs and manipulated inputs will be considered in more detail in the following sections.

Objectives for the Separation Process

The main objective of the distillation process is usually the recovery of a valuable component from the feed. In that case there is also often a quality requirement for this valuable component. If the purity of the valuable component is low, then the product has little value. If the concentration meets the specification, then the product value is high.

There may be no distinct quality requirement, in which case the economic value of the product could be a continuous function of the product properties.

Let us assume that both top and bottom product represent an economic value. Then an economic objective for the operation of the process could be defined as:

$$J = c_D D + c_B B - c_F F - c_S S \quad [1]$$

where c_D is the top product value (\$ kg⁻¹), c_B the bottom product value (\$ kg⁻¹), c_F the cost of the feed (\$ kg⁻¹) and c_S the cost of the steam (\$ kg⁻¹). The use of cooling water usually involves little cost and fixed costs do not play a role in the optimization of the operation.

If F is fixed and the overall material balance $F = B + D$ is substituted in eqn [1], then the variable part J_d of eqn [1] can be written as:

$$J_d = D - \frac{c_S}{c_D - c_S} S \quad [2]$$

Figure 3 shows both terms as a function of the steam flow to the column reboiler. When S increases, the yield of the valuable product approaches asymptotically a value which is equal to the amount of top product which is present in the feed: $D_{\lim} = F X_{F,lk} / X_{D,lk}$, where the subscript lk refers to the light key component.

	Basic control				
	P	h_B	h_R	x_D	x_B
W					
B					
D					
R					
S					

Figure 2 Control matrix, showing controlled and manipulated variables.

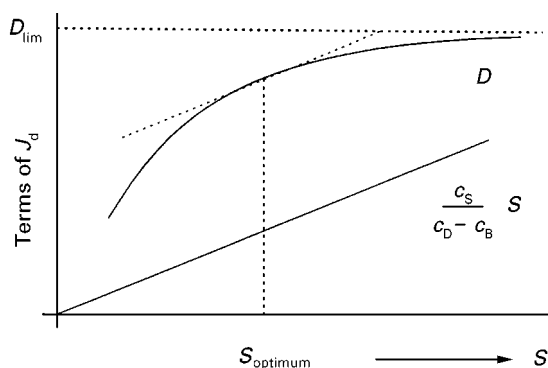


Figure 3 Optimal steam usage in distillation process.

The maximum value of J_d is found when the tangent to the curve for D parallels the straight line for $c_s S / (c_D - c_B)$, as shown in **Figure 3**. The optimum point may be located within the operation area. But at different values of the feed, however, some constraint may make the optimum point unreachable, in which case the optimum lies on the constraint.

Control of Vapour Inventory

There are a number of ways to control the vapour inventory or column pressure. Even though one of the five flows indicated in **Figure 2** could be used for pressure control, only the use of W and S gives sufficient power of control. If S were used for pressure control, a step increase in S would result (via higher pressure and top temperature) in an increase in the vapour flow in the top. Consequently, the concentration of the less volatile components in the top would increase, resulting a higher top temperature and consequently a higher vapour flow in the top. This positive feedback can sometimes be so strong that the pressure finally attains a lower value (inverse response). Therefore, the most common method of pressure control is through manipulation of the coolant flow, W .

If a water-cooled condenser is used, the water flow rate is manipulated to control pressure: if an air-cooled condenser is used, the fan speed is generally changed. The attractiveness of this pressure control option is that the condensed liquid is at its bubble point and is not subcooled, as may be the case with other pressure control options.

If there are incondensable gases in the system, pressure could also be controlled through manipulation of a bleed valve, through which the gases are bled from the column. The bleed valve is often installed on top of the reflux drum.

It should be emphasized that the pressure has a large degree of self-regulation. If the pressure in a column increases, the temperature will also increase

and because of this the heat transfer in the condenser will increase; consequently the pressure will decrease again to a certain extent.

The general recommendation for pressure control is:

1. if the condenser performs partial condensation, control the column pressure by manipulating the vapour flow leaving the column;
2. if there is no net vapour flow from the column, the next preferred option is to control pressure by manipulating condenser duty, e.g. by changing the coolant flow.

Control of Liquid Inventory

Liquid inventory of the distillation process can be controlled by controlling the liquid levels: the base level in the column, h_B , and the level in the reflux drum, h_R . Often the levels serve the purpose of smoothing disturbances, hence for control of the reflux drum level the combination (h_R, D) or (h_R, R) is suitable, since W is already used for pressure control and B and S provide insufficient power of control.

For bottom-level control, D is unsuitable since the power of control is nil. Hence both (h_B, S) and (h_B, B) are suitable combinations, since they both have a large power of control.

Under normal circumstances the most logical combinations are to use the distillate flow for controlling the reflux drum level and the bottom flow for controlling the column base level.

In columns with a small distillate flow, D , and a large reflux flow, R , this scheme does not work so well. This problem can be partly eliminated by establishing a ratio controller between distillate and reflux flow. When the distillate is then increased, the ratio controller will increase the reflux flow accordingly. However, in many cases with a small distillate flow, the reflux is used for reflux drum-level control. A similar situation holds for the bottom of the column. If the bottom draw-off B is very small, level control using the liquid draw-off might not work well. In that case one could use the steam flow for base-level control. However, increasing the steam flow to the reboiler (and accompanying larger vapour flow in the column) might temporarily increase the bottom level in the column. In the long term, however, increased heat input will result in increased evaporation and consequently a lower bottom level (**Figure 4**). This response is called inverse response or nonminimum phase response and is not desirable for control purposes.

For tray columns this effect can easily be quantified using detailed column models. Assuming that any increase in vapour flow will propagate through the

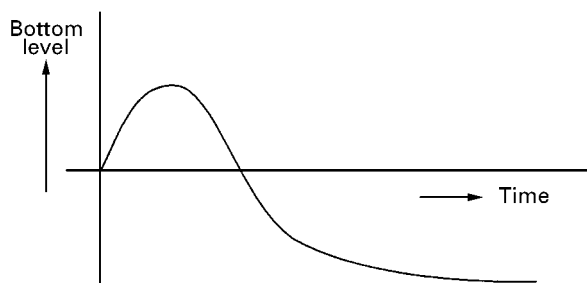


Figure 4 Bottom-level response to a positive change in steam flow.

column relatively rapidly, linearizing liquid dynamics and using deviation variables, the liquid flow from tray 1 can be written as (Figure 5):

$$\delta L_i = \lambda \delta V + \frac{1}{\tau_L} \delta M_i \quad [3]$$

in which:

$$\lambda = \left(\frac{\partial L}{\partial V} \right)_{M_i}, \quad \tau_L = \left(\frac{\partial M}{\partial L} \right)_V \quad [4]$$

where τ_L is the tray hydraulic time constant. Neighbouring trays will have similar parameter values, hence the term $\lambda \delta V$ is the same everywhere, and therefore initially all changes in liquid flows will remain the same. The mass balance on each tray will

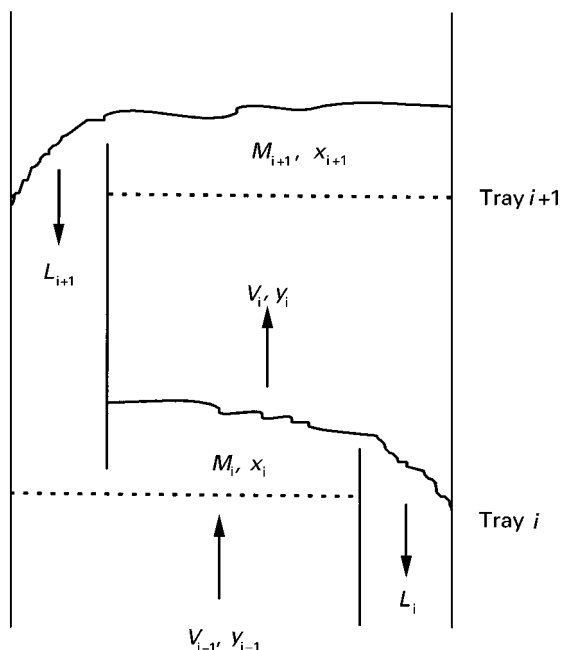


Figure 5 Schematic of a stage of a distillation column.

therefore initially remain at equilibrium, resulting in no change of liquid content on the trays. However, for the top tray, N , where the same flow of liquid (reflux) is still entering, a mass balance combined with eqn [4] gives:

$$\delta M_N = \frac{\tau_L \lambda \delta V}{1 + s \tau_L} \quad [5]$$

Substituting eqn [5] into eqn [3] and writing the result for the entire column yields for the liquid flow change for the bottom tray:

$$\delta L_1 = \lambda [1 - G_d(s)] \delta V \quad [6]$$

with:

$$G_d(s) = \frac{1}{(1 + \tau_L s)^N} \quad [7]$$

For the column bottom level it can then be written that:

$$\delta h_B = \frac{K_B}{s} \{ \lambda [1 - G_d(s)] - 1 \} \delta V \quad [8]$$

where K_B is the gain of the bottom level in response to vapour flow changes.

From eqn [8] it can be seen that an inverse response can exist, as long as λ is not equal to zero. The magnitude of the inverse response depends on the magnitude of λ . For some columns negative values of λ have been found; for others λ is positive. It can be shown that bottom-level control on the steam (vapour flow) is strongly delayed by the effect of λ when $\lambda > 0.5$. The physical interpretation of the so-called λ -effect is that with large tray loads, an increase in vapour flow will lead to stagnation of the liquid flow and consequently λ will be larger than 1. With small tray loads an increase in vapour flow will push more liquid off the tray, thus a larger liquid flow to the lower bottom will result. Figure 6 summarizes all options for control.

Quality Control

The response of the key components to variations in liquid and vapour flow can be approximated by the algebraic sum of the relative flow variations followed by a first-order response with a large time constant:

$$\delta x_i = \left(\frac{\delta L_{i+1}}{L_{i+1}} - \frac{\delta V_{i-1}}{V_{i-1}} \right) \frac{K_x}{1 + \tau_x s} \quad [9]$$

	Basic control				
	P	h_B	h_R	x_D	x_B
W	++		+	+	+ unless $\hat{\lambda} > 0.5$
B		++ unless $V_B/B \gg 1$			
D			++ unless $R/D \gg 1$	+	
R			+	++	
S	+	+ unless $\hat{\lambda} > 0.5$		+	++ unless $\hat{\lambda} > 0.5$

Figure 6 Possibilities for the control scheme.

where L and V are the liquid and vapour flow respectively (see Figure 5), K_x is the gain for concentration responses and τ_x is a large time constant for concentration responses, usually in the order of hours. This time constant is approximately proportional to the square of the number of trays.

For control of the bottom quality, the reflux R or distillate flow D are unsuitable candidates, since there is a large dead time in the dynamic response between the flow and the composition. The steam flow S and coolant flow W are acceptable candidates for bottom quality control, unless, for the same reason as holds for bottom-level control, the parameter:

$$\hat{\lambda} = \frac{V_i}{L_i} \left(\frac{\partial L}{\partial V} \right)_{M_i} \quad [10]$$

is larger than 0.5. The bottom flow B does not have a direct impact on the bottom quality; it could have some impact via a level controller.

For top quality, R , W and S are all suitable candidates for control. If, however, pressure is controlled by manipulating coolant W , the only viable option for bottom composition control is the steam flow S , after which the only remaining option for control of the top quality is the reflux R . Not in all cases, however, is there a dual composition requirement, which leaves more options for composition control.

Location of Sensors

It is important to provide the column with adequate sensors: flow measurements and pressure measurements at various locations, for example above the top tray, at the feed tray and below the bottom tray in order to be able to calculate pressure differentials for the purpose of detecting flooding. Temperature sensors should also be positioned at various locations along the column. In many cases temperatures can be used to infer composition. When the temperature difference between top and bottom of the column is small, inferring composition from temperature measurements is generally not feasible, even though in some cases temperature differences may still provide a reasonable composition estimate. An advantage of using temperature differences is that it is insensitive to pressure changes; unfortunately, the correlation between temperature difference and product composition is often highly nonlinear. In multicomponent mixtures, the relation of tray temperature to key component composition is not unique. Furthermore, the tray temperature to key product composition may also be nonlinear. Therefore, care must be taken in using temperatures for controlling composition. For high purity distillation columns sometimes the logarithm of the temperature (or composition) is used to linearize the response of the distillation column.

When the temperature difference between column top and bottom is large, several temperatures should be measured at trays above and below the feed tray, where under normal circumstances the temperature break is located. These temperatures should then be averaged and could be used in manipulating, for example, the steam flow.

An excellent treatment of sensor and valve issues in distillation control is given by Luyben (see Further Reading); the location of temperature sensors receives an especially comprehensive treatment.

For a distillation column first the base control scheme should be established, i.e. pressure, reflux drum level and column bottoms level should be controlled. Then two variables remain available for control of composition, say the reflux R and steam flow S .

If temperature is used for control of composition, the problem of proper temperature sensor location becomes prime importance.

If only one composition is controlled, a simple procedure could be followed. By giving a small change in the reflux R , the sensitivity $\delta T_i / \delta R$ can be determined for each tray. A similar procedure can be followed for the steam flow S . A typical plot for a toluene-*o*-xylene column with 30 trays is shown in Figure 7. It can be seen that a 1% change in steam

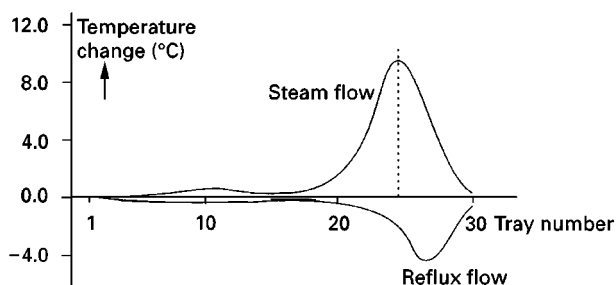


Figure 7 Gain matrix graph for the toluene-*o*-xylene column.

flow causes a temperature change of about 10° at tray 24. A 1% change in the reflux flow causes a maximum temperature change on tray 26 of about -4° . Therefore the sensitivity of the temperature to changes in steam flow is larger than the sensitivity for changes in reflux flow. Where there is dual composition control, sensor sensitivity should be balanced against sensor interaction. One tool that has been used to accomplish this is singular value decomposition. The sensitivity matrix X , which contains the sensitivity of the temperature on each tray for changes in reflux and steam and thus contains two columns and 30 rows, is now decomposed into three individual matrices:

$$[U, S, V] = \text{SVD}(X) = USV^T \quad [11]$$

Luyben gives a comprehensive treatment of the use of the individual matrices and their physical meaning and suggests computing a new function (combination of the principal components) for each tray:

$$Z_i = |U_{1,i}| - |U_{2,i}| \quad [12]$$

The maximum of Z_i is an indication for the best location of the first sensor, while the minimum of Z_i gives the best location for placement of the second sensor. For the toluene-*o*-xylene column this was calculated and the results are shown in Figure 8. The

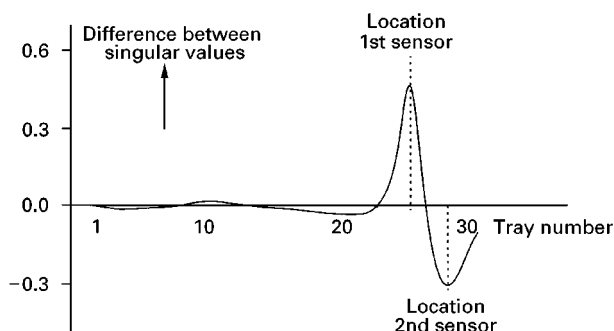


Figure 8 Sensor placement based on U-vectors.

best location for the first temperature sensor is tray 25, and the best location for the second sensor is tray 28. Note that the location has changed somewhat compared to the best locations for the single composition control problem (trays 24 and 26). This is a result of the process of reducing the interaction between the vector components at the other trays.

In many columns temperature has been used to control the separation process. For binary systems at constant pressure there is a unique relationship between temperature and composition. For multicomponent mixtures, often a simple relationship may be found between temperature and composition. If the column pressure is not controlled tightly, temperature measurement should compensate for pressure variations:

$$T_{\text{compensated}} = T_{\text{measured}} + S(P_{\text{reference}} - P_{\text{measured}}) \quad [13]$$

where S is the inverse of the slope of the vapour pressure-temperature curve at normal operating conditions.

No matter how attractive it is to control temperature rather than composition, the ultimate objective of the separation process is to control composition(s). This means that an analyser should be used to indicate the true compositions. There are, however, a number of disadvantages using analysers in control. First of all, analysers are highly sophisticated instruments and are therefore expensive and require extensive maintenance. In addition, the sampling system of analysers is prone to malfunctioning and as analysers are often used for multiple streams the response can exhibit a large dead time. This means that simple feedback control using analysers often results in poor control performance and dead time compensation techniques often have to be used to improve performance.

Analysers are well suited for use in a cascade control set-up, where the temperature (or combination of temperatures) controls one of the flows and the analyser controller resets the temperature controller setpoint. Figure 9 shows one possibility, using the reflux as manipulated variable.

Control Configurations

From Figure 6 it is clear that controlling the top composition by the reflux (R) and the bottom composition by the vapour flow V (or steam flow S) is just one possible option. This control option is called the RV configuration or energy balance structure and it is probably one of the more frequently used options for dual composition control in many distillation columns. In the literature other options for controlling

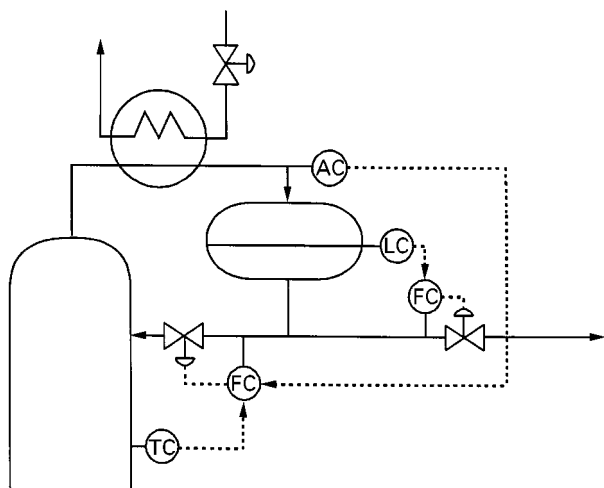


Figure 9 Composition control in a cascade structure.

both top and bottom composition are discussed and compared, such as the *DV* configuration and *RB* configuration, which are called the material balance structures.

Use of Feedforward and Decouplers

In many cases the top and bottom composition control loops will show interaction and it is advisable to

design and implement decouplers. Depending on the required purity of the products and on the selected control configuration, decoupling is sometimes difficult to achieve. However, for many industrial distillation columns, decoupling considerably improves the performance of the composition control loops Figure 10.

The main source of disturbances usually enters the column with the feed. Whereas the feed composition may vary somewhat, the feed flow varies considerably in many cases. In those situations it might be worthwhile applying feedforward control. If the reflux is controlling the top composition and the steam flow the bottom composition, then feedforward affects both these flows on a column feed change. The principle for the reflux controller is shown in Figure 11, which shows a feedforward controller for feed flow changes. In a similar manner, a feedforward controller for feed composition changes could be implemented. Reflux affects the tray temperature, say via a model G_R . If the feed affects the tray temperature via a model G_F , then the feedforward controller has the structure G_F/G_R . One word of caution is necessary: care should be taken to identify properly both models, since a poorly designed feedforward controller may cause poorer control performance than no feedforward controller at all.

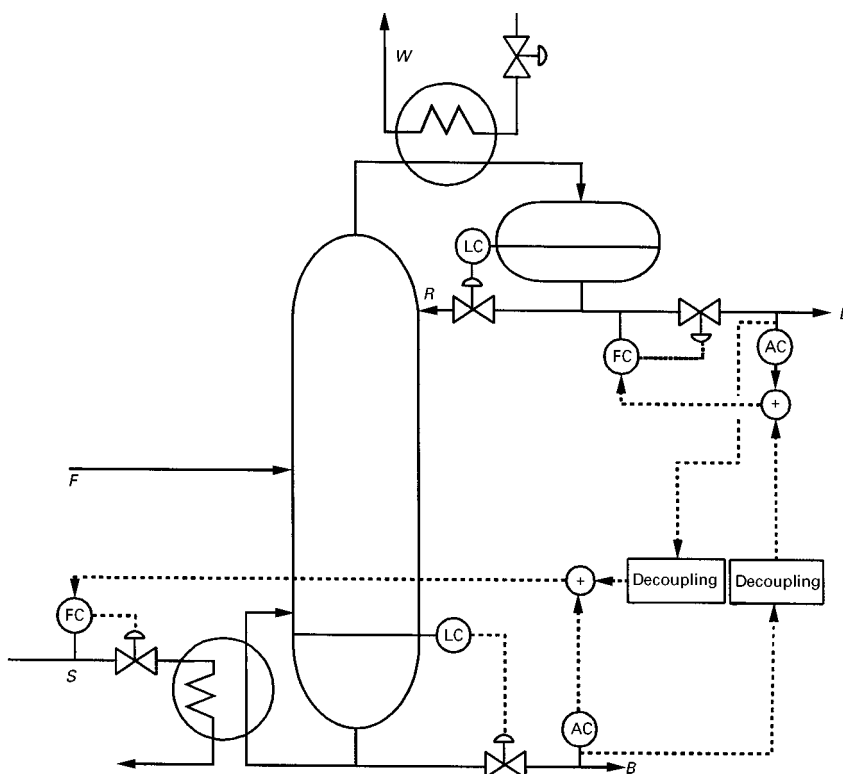


Figure 10 Example of dual analyser control using *DV* configuration with decoupling.

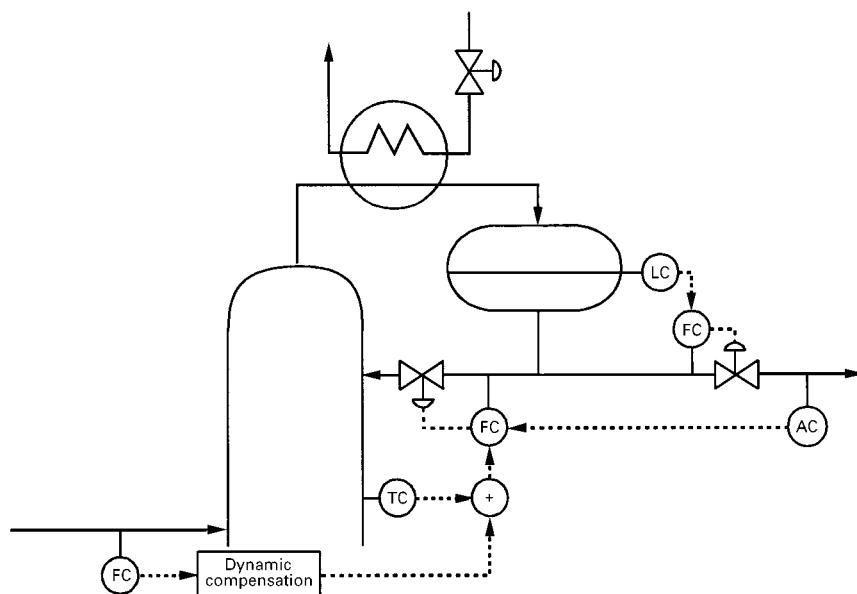


Figure 11 Principle of feedforward control.

Ratio Control

From eqn [9] it follows that keeping L/V constant will reduce variations in the concentration. Figure 12 shows this ratio control implemented. Usually one cannot directly measure the vapour flow V , but a reasonable estimate can be made in many ways, for example from a static heat balance over the condenser:

$$V_{\text{top}} = F_{\text{water}} c_{\text{water}} (T_{\text{water,in}} - T_{\text{water,out}}) / \Delta H_c \quad [14]$$

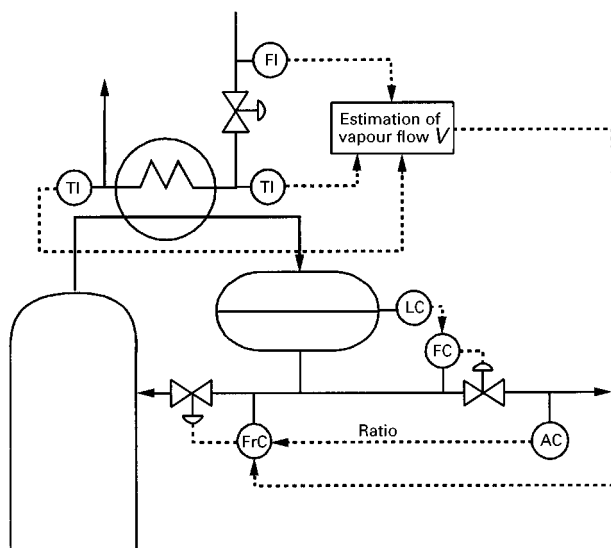


Figure 12 Ratio control between vapour flow and reflux flow.

in which ΔH_c is the heat of condensation and c_{water} is the specific heat of water.

Although this estimate of the vapour flow is not dynamically correct, the quality controller can be tuned such that the control scheme works well.

Multivariable Control

It is possible to consider the 5×5 control problem as an integrated problem for which an integrated controller should be designed. One technique which tries to accomplish this is multivariable predictive control. In this design all the input–output relationships of the process are identified by means of proper plant testing. Based on the models, a controller is designed, which adjusts all five process inputs simultaneously utilizing all measured process outputs. In its unconstrained version the controller is:

$$\Delta u = (A\Gamma A^T + \Gamma_m)^{-1} A^T \Gamma e \quad [15]$$

in which Δu is a vector with the changes in process inputs, A is a matrix with step weight coefficients which represent the model dynamics, Γ is a diagonal matrix with weights representing the relative importance of the process outputs, Γ_m is a diagonal matrix with penalties for the process input changes and e is a vector of process output error predictions into the future.

Model predictive control works well for distillation columns; it becomes more attractive for larger systems, such as heat-integrated distillation columns.

One of the major benefits of model predictive control is its capability in handling constraints. In that case the control problem is usually solved using quadratic programming or some other optimization technique. Commercial software packages are available for model identification and controller implementation.

Conclusion

Instrumentation and sensor location has been discussed for a distillation column. In addition, a comprehensive treatment is given of the various options for control. It is shown that some understanding of column dynamics is necessary in order to select the proper control schemes.

See also: I/Distillation. II/Distillation: Historical Development; Theory of Distillation.

Further Reading

Buckley PS, Luyben WL and Shunta JP (1985) *Design of Distillation Control Systems*. Research Triangle Park: Instrument Society of America.

Fisher TG (1990) *Batch Control Systems, Design Application and Implementation*. Triangle Research Park: Instrument Society of America.

Liptak BG (ed.) (1995) *Process Control Instrument Engineers' Handbook*, 3rd edn, sections 8.12–8.14. Oxford: Butterworth-Heinemann.

Luyben WL (1990) *Process Modelling, Simulation and Control for Chemical Engineers*, 2nd edn. McGraw-Hill.

Luyben WL (1992) *Practical Distillation Control*. Van Nostrand Reinhold.

McAvoy TJ and Yang YH (1986) Survey of recent distillation control results. *ISA Transactions*, 25(1): 5–21.

Roffel B and Chin PA (1981) *Computer Control in the Process Industries*. Ann Arbor, Michigan: Ann Arbor Science.

Roffel B and Rijnsdorp JE (1987) *Introduction to Process Dynamics, Control and Protection*. Ann Arbor, Michigan: Ann Arbor Science.

Shinsky FG (1984) *Distillation Control for Productivity and Energy Conservation*, 2nd edn. New York: McGraw-Hill.

Tolliver TL and Waggoner RC (1980) Distillation column control: a review and perspective from the CPI. *Instrument Society of America*, 35: 83–106.

Laboratory Scale Distillation

R. C. Gillman, Riverside Organics Inc., Lincoln Park, MI, USA

Copyright © 2000 Academic Press

Distillation on a scale ranging from research quantities as small as ten milligrams to multikilogram lots is commonly encountered in the laboratory. Based upon the physical and chemical properties of the substance to be isolated, in addition to those of the attendant impurities and the quantity of impure product to be distilled, a technique can often be chosen which will result in a product of adequate purity in one operation. It may be said that planning a synthesis should include consideration of the difficulty one may encounter in separation of the mixture of products resulting therefrom; on the bench several alternate routes to the desired product may be available, and the resultant mixtures will differ in ease of separation. Since the quantities are not large, more expensive reagents may be chosen, if desirable, than would be acceptable in a manufacturing process. A major saving in time and effort can often be thus effected.

Resort is commonly had to three broad classes of distillation, steam distillation, flash or simple distillation, and fractional distillation. The first, finding use in separation of substances volatile with steam from those which are not steam-volatile, often uses the basic equipment of simple distillation described below, with steam being sparged into the distilland; either the product is collected as part of the condensate of the residual distilland is enriched in the desired product by removal of steam-volatile impurities. This technique, when applicable can be a powerful and convenient method requiring less skill and attention than fractional distillation.

Simple, or flash, distillation is in general used to separate individual compounds from mixtures consisting of substances whose boiling points differ by at least 40°C, and mixtures of volatile and nonvolatile components. The method consists of simply boiling the mixture in a vessel equipped with a device, commonly referred to as a 'head' which conducts the vapour to a condenser wherefrom the resultant liquid is collected. The head is usually equipped with a means by which the vapour temperature may be

observed. No forced reflux is used in this method of rectification; all the vapour reaching the head is condensed as efflux. In order to minimize entrainment of droplets, some form of dephlegmator can be interposed between the pot and the head. This technique can be conducted at pressures ranging from atmospheric to the lowest pressure available; pressures as low as 0.01 torr are not unusual. Very small quantities of product can be distilled using a device known as a 'kugelrohr (ball-tube) apparatus'; it is constructed of two or more spherical globes connected linearly by glass tubing to each other and to a vacuum source. The globe most remote from the vacuum source is charged with the distilland and vacuum is applied; the unit is rotated by hand in a horizontal position while the globe containing the distilland is heated by flame or oil bath. The vapour condenses in the globe nearer the vacuum source.

It must be stated that the development of preparative gas chromatography, a powerful and convenient method, has in most cases obviated the necessity of distillation of quantities less than 25 g. Separations hardly realizable with the most sophisticated and cumbersome techniques can be accomplished in minutes using this method; the fractions taken are usually of a high degree of purity as isolated.

The remaining method, fractional distillation, is normally used to purify quantities of crude product larger than approximately 100 g, although apparatus such as the Podbielniak column, constructed of a metal helix fitted snugly into a small-diameter glass column, have been utilized successfully to fractionate amounts less than a tenth as large. The separation efficiency of such a column can be very high but throughput is very low. As stated, preparative gas chromatography is currently the method of choice for small quantities. For rectification of larger quantities a variety of apparatus is available, and the choice of equipment rests upon the predicted difficulty of the separation to be accomplished. As mentioned, on the bench one may be able to choose a synthetic scheme which results in an easily purified crude product; when this is not feasible recourse is had to a more efficient system capable of separating components whose boiling points lie close together.

As a rule of thumb, if the components of a mixture differ in boiling point by at least 30°, satisfactory partition can be achieved by use of Vigreux column, which is constructed of a glass tube 16–25 mm in diameter 20 cm to 1 m in length having tiers of indentations spaced 1.5–2 cm apart. The fractionating efficiency of the Vigreux column is quite good considering the ease and economy of construction of the unit.

Due to its relative openness the throughput of such a column is quite high, and as a result this type of

column has become the workhorse in many preparative laboratories; its efficiency may be further enhanced by operating it under forced reflux. Throughput of 0.1–1.5 L h⁻¹ are common when using this column. An additional advantage to use of this column is the ease of repair; most repairs can be made in the laboratory.

In cases where the boiling point differentials between component is less than 30°C, use of a more efficient column to effect partition will usually be found advantageous. These units are of three basic types; the first in which contact between liquid and vapour in the column is forced by mechanical construction of the column, the second in which the structured packing is used to present a large surface area to promote vapour-liquid interaction in the column (such as a bubble-cap column), and the third, a column filled with glass or metal objects of various geometries such as metal saddles, glass beads, and glass helices. The last type is often referred to as 'dumped packing'.

Units of the first type, whereby the vapour and liquid are forced into contact by the construction of the column are fairly efficient and can be designed for a reasonably high throughput. They are, however, very expensive and quite fragile when constructed of glass; thus, while they have found major application in industrial processes, where the construction is only of metal, in the laboratory they have not found use to the extent to which packed columns are used. Repairs to glass columns of this type are difficult and expensive.

The second type, structured column packings, are usually made up of a fairly closely woven metal mesh, which is then crimped and rolled into cylindrical sections which are pushed into a glass or metal column; the packed length of such a column typically will be 0.6–3.0 m for laboratory use, with diameters of 25–100 mm. The packing itself can be fabricated from many different metals, for instance stainless steels, monel, or tantalum depending on the chemical nature of the product to be purified. The advantages of this type of column are relatively high throughput, low pressure drop and moderate to high fractionation efficiency. They can be designed to operate at pressures as low as 0.1 mmHg and even greater than atmospheric pressure. In practice, however, the high vapour velocities and low vapour densities encountered at pressures less than 1 mmHg result in significant degradation of column efficiency, especially if a moderate throughput is required. As to size, a column of this type whose internal diameter is about 25 mm would be suitable for use with a distillation pot of 5 L capacity, while for use on a 50 L pot a column of 75–100 mm internal diameter would

suffice. In addition, this type of column is quite easily constructed, easily repaired if broken, and can be used to predict the performance of an industrial unit of similar construction. In the laboratory, throughput of $0.1\text{--}2.0\text{ L h}^{-1}$, depending on pressure, can be expected.

The last group of columns, the so-called 'dump packed' type, are as a group the most efficient at fractionation and can be the most tedious to use. They can be filled with a variety of packings, from Raschig rings (short sections of glass tubing) to columns packed with single turn glass helices dropped individually into the column. The latter is one of the most efficient fractionating columns ever devised, but as will be seen, is more suitable for distillation of smaller batches. In practice, columns of this design intended for laboratory use are $0.6\text{--}2.5\text{ m}$ in length, with internal diameters of $15\text{--}60\text{ mm}$. Packing fabricated of perforated metal should be purchased after consultation with the manufacturer; a nominal size of $0.4\text{--}1.0\text{ cm}$ is usually chosen for bench use. Of the various packing components, a column filled with glass helices of $4.5\text{--}8.0\text{ mm}$ diameter has proven to have the greatest efficiency per unit column length but this advantage is offset to some extent by the low throughput and high pressure drops attendant with use of these units. Raschig rings are cut to a length approximating their external diameter from glass tubing $6\text{--}12\text{ mm}$ in size. Columns filled with dumped packing have one advantage other than efficiency in that they can easily be emptied and refilled with some other type of packing should such be desirable; conversely, structured packing, once installed can be difficult if not impossible to remove from the column without out ruining it. The disadvantages of dumped packings are a tendency to form channels through which vapour can pass without contacting liquid, low throughput, and, in most cases, high pressure drop, in addition to being prone to flooding. As a result these columns are seldom used at pressures below 10 mmHg ; fractionation efficiency and throughput suffer markedly at lower pressures. In spite of these disadvantages columns of this construction have found use in many laboratories because of their ability to successfully perform separations not possible with columns of other design. Throughputs of $0.025\text{--}0.5\text{ L h}^{-1}$ can be expected from these columns.

General Comments

The efficiency of any distillation column is dependent to some extent upon its being operated under adiabatic conditions. Thus, distillation columns are usually insulated, enclosed within a silvered vacuum jacket, or enclosed within a heated jacket the temper-

ature of which can be measured and controlled to within about 3°C of the vapour in the column. Too much heat will result in superheating of the vapour, causing insufficient condensation and reboiling as the vapours proceed up the column; too little heat can result in excessive condensation and flooding in the column.

Since maximum efficiency also depends upon operation at or near thermal equilibrium it is important to be able to change from one fraction to another without interrupting the distillation. A number of designs are available from scientific laboratory glass supply houses to accomplish this. In this connection, it will be found convenient to install some form of manostatic device in the vacuum line to prevent pressure fluctuations during the course of the distillation.

The source of heat input to the pot must be provided with various zones such that the heat input to the flask may be restricted to the area of the flask immersed in the distilland as the distillation proceeds. Failure to control the heat input in this way will result in serious superheating of the vapour as the distillation nears its end; driving superheated vapour into the column will result in significant loss of efficiency.

Finally, allusion was made to use of forced reflux during fractionation; it is exceedingly important to the maintenance of column equilibrium and thus fractionation efficiency. Even with a simple column such as the Vigreux, use of a partial takeoff head will result in increased ability of the system to furnish fractions of relatively high purity. In the case of packed columns control of reflux is absolutely essential to proper column performance; in its absence vapour-liquid equilibrium is never established resulting in loss of up to 90% of the fractionating efficiency of the column. Typically, reflux ratios (reflux ratio is defined as the ratio of the amount of condensate returned to the column to the amount of condensate collected as efflux) as high as 50:1 are not uncommon during difficult separations; ratios approaching 1:3 are sometimes used during centre cuts or end fractions. Various means to effect reflux control are available from laboratory glass suppliers, from simple devices utilizing manual control by means of a stop-cock to elaborate units in which a magnetically controlled valve is used to divert the condensate stream either to the column or to the receiver.

Caution

Since a difficult fractionation may consume days, during which the pot is at constant reflux, heed must be paid to considerations of thermal stability in the distilland, especially since small quantities of acids or bases can, and do accelerate thermal degradation of

some organic chemicals. In fact, some thermal decompositions have been shown to be autocatalytic. It therefore may be well to consider flash distillation of the crude product prior to subjecting it to fractional distillation to remove trace non-volatiles and/or non-volatiles which would accelerate decomposition or lead to excessively high pot temperatures. In some cases one might consider the addition of a stabilizing agent to the pot to retard decomposition.

Closing Remarks

With all of the above having been stated, fractional distillation, particularly at reduced pressure, can be viewed as an opportunity to see physical chemistry at work. When selecting a system one hopes will result in satisfactory partition of components it will be

helpful to consider properties other than the boiling point. For example, if a mixture of intermolecularly bound substances is to be separated by distillation, their partition is likely to be more difficult than the differentials between their boiling points would indicate. On the other hand, a mixture of alkanes may well be more easily separable than comparison of their boiling points would otherwise indicate. In any case practice is necessary, both conducting distillations and selecting systems for distillation. Once experience has been gained it is satisfying to be able to rationalize the results of a fractionation in terms of physico-chemical principles. One positive note: since distillation does not result in loss of product, in the worst case one can recombine all the fractions and redistill using different conditions and, if necessary, a different system.

Modelling and Simulation

J. R. Haas, UOP LLC, Des Plaines, Illinois, USA

Copyright © 2000 Academic Press

Introduction

Rigorous computer modelling of all types of fractionation columns has become a necessary part of the development and design process. There are numerous software products available to do these calculations. An understanding of the basic mathematics used in these programmes is helpful to select, use and troubleshoot a column model. Explained here are the basic equations, numerical and solution methods commonly used.

Stage and Column Models

A rigorous method describes a column as a group of equations and is the mathematical engine to solve and satisfy these equations to calculate the operating conditions of the column.

Column design and performance calculations present the column at steady state, that is, what enters the column matches what leaves it (material and energy balances), i.e.:

$$\begin{aligned} \sum (\text{molar feed flow rates}) \\ = \sum (\text{molar product flow rates}) \end{aligned}$$

$$\begin{aligned} \sum (\text{mass feed flow rates}) \\ = \sum (\text{mass product flow rates}) \end{aligned}$$

$$\begin{aligned} \sum (\text{moles of any component in the feeds}) \\ = \sum (\text{moles of the component in the products}) \end{aligned}$$

$$\text{Feed enthalpy} + \text{Heat added}$$

$$= \text{Product enthalpy} + \text{Heat removed}$$

Figure 1 shows a complex column with one feed and one side product. The top stage of the column is a partial condenser, with a vapour product, D , and a liquid product, d . The reflux is the liquid, L_0 , and the reflux ratio is $L_0/(D + d)$. The bottoms product, B , leaves stage $N + 1$, the reboiler. The stages are numbered from the top, with the condenser as stage 0, the top tray in the column, stage 1, the bottom tray, stage N , and the reboiler, as stage $N + 1$.

An ideal or equilibrium stage is where vapour and liquid entering and leaving the stage are perfectly mixed and there are no inhibitions to material transfer between the phases. The material and energy flows in and out of a simple stage, with no feeds or side products, is stage j depicted in Figure 2, and i represents the component number. Components are numbered from 1 to the last, C .

The enthalpy terms, H_i and h_i , are molar enthalpies of the vapour and liquid leaving the stage, respectively. These molar enthalpies are multiplied by the total flow rates, V_i and L_i , leaving the stage to give the total energy leaving the stage in each phase.

The feed stage model (stage f in Figure 2) for an equilibrium stage assumes that the feed liquid mixes

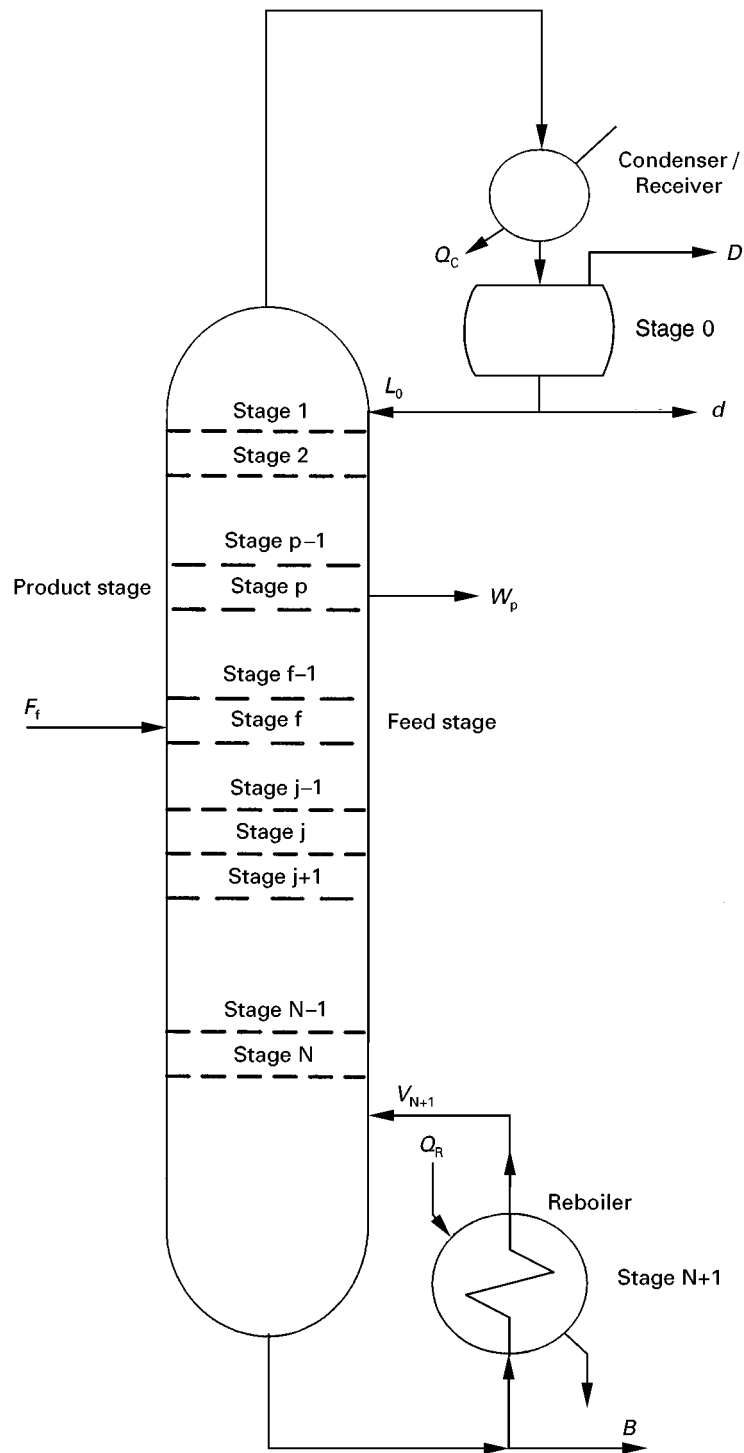


Figure 1 Overall column model with external variables.

with the liquid entering the feed stage while feed vapour mixes with vapour leaving the stage (though special consideration is made for the vapour feed at the bottom of absorber/stripper columns). The distribution is found by an adiabatic flash of the feed at the

feed stage pressure before the feed enters the column. Regardless of whether the feed is subcooled liquid or superheated vapour, or if true mixing occurs, the assumption of an equilibrium stage is maintained in most rigorous methods.

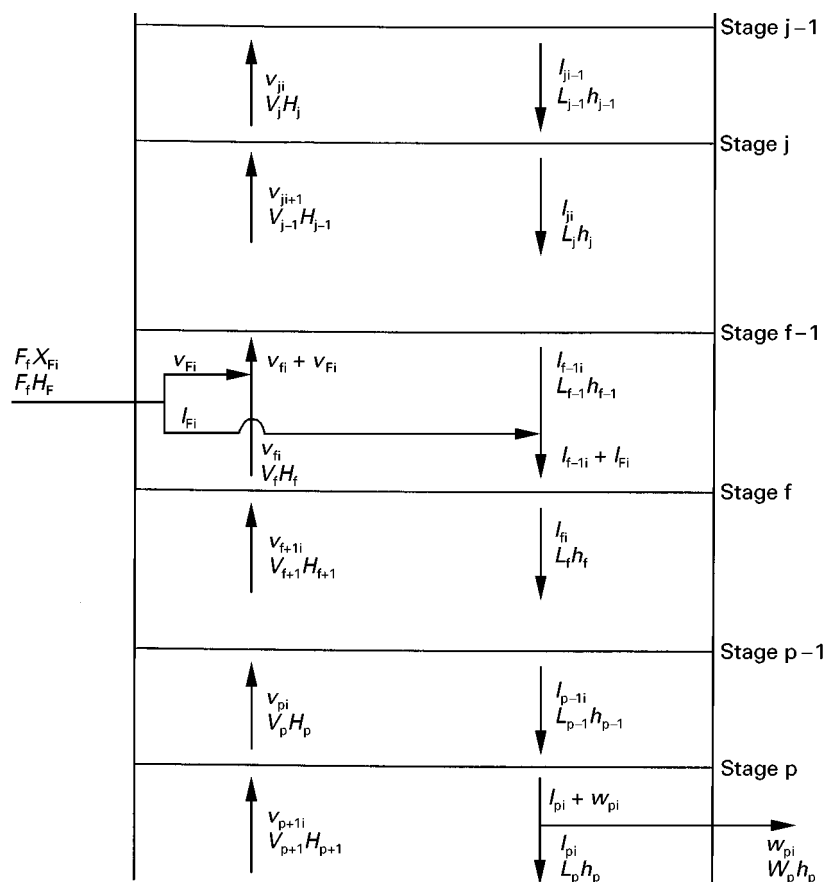


Figure 2 Model of stage variables.

Similar models are drawn for the bottom and top stages of any column, plus other equipment such as product withdrawal stages (stage p of Figure 2), pump-around returns and draws, and inter-reboilers and inter-condensers. Since a reflux, reboiler vapour, feeds, or returns are often subcooled, superheated, or very different in composition from the material on the stage, the assumption of an equilibrium stage rapidly becomes invalid.

Equations of Distillation Modelling

The basic equations below fully describe a distillation column. These equations define the overall column total material balances, energy balances, and product compositions. Internal to the column, they describe equilibrium conditions, internal (stage-to-stage) component and total material balances, and internal energy balances. The independent variables of a column are the product rates and compositions, internal vapour and liquid rates and compositions, and stage temperatures. Equilibrium constants, also called K values, and mixture enthalpies are dependent vari-

ables. Each stage is assumed to be at equilibrium (a theoretical stage), though an efficiency can be applied in the equations.

The equations were first referred to as the MESH equations by Wang and Henke (1966). The MESH acronym stands for:

- Material or flow rate balance equations, both component and total.
- Equilibrium equations including the bubble and dew point equations.
- Summation or Stoichiometric equations or composition constraints.
- Heat or enthalpy or energy balance equations.

The MESH variables are referred to as state variables. These are:

- Stage temperatures, T_j
- Internal total vapour and liquid rates, V_j and L_j
- Stage compositions, y_{ji} and x_{ji} , or instead, component vapour and liquid rates, v_{ji} and l_{ji}

The equilibrium equation is:

$$y_{ji} = K_{ji}x_{ji} \quad \text{or} \quad v_{ji}/V_j = K_{ji}l_{ji}/L_j$$

The equilibrium constant or K -value, K_{ji} , can be a complex function itself, dependent on the compositions, x_{ji} and y_{ji}

$$K_{ji} = K_{ji}(T_j, P_j, x_{ji}, y_{ji})$$

The dependence of K_{ji} on x_{ji} and y_{ji} often appears in the MESH equations. The component rates can also be expressed in the terms of each other, giving:

$$v_{ji} = l_{ji}(K_{ji}V_j/L_j) = l_{ji}S_{ji}$$

and

$$l_{ji} = v_{ji}(L_j/K_{ji}V_j) = v_{ji}A_{ji}$$

$K_{ji}V_j/L_j$ is termed the stripping factor, S_{ji} , while $L_j/K_{ji}V_j$ is termed the absorption factor, A_{ji} .

The summation equation or composition constraints simply states that the sum of the mole fractions on each stage is equal to unity. For the liquid phase:

$$\sum_{i=1}^C x_{ji} - 1 = 0 \quad \text{or} \quad \sum_{i=1}^C l_{ji}/L_j - 1 = 0 \quad \text{or} \quad \sum_{i=1}^C y_{ji}/K_{ji} - 1 = 0$$

and for the vapour phase:

$$\sum_{i=1}^C y_{ji} - 1 = 0 \quad \text{or} \quad \sum_{i=1}^C v_{ji}/V_j - 1 = 0 \quad \text{or} \quad \sum_{i=1}^C K_{ji}x_{ji} - 1 = 0$$

For a simple column (single feed, no side products), the overall component balance equation is:

$$f_i - d_i - b_i = 0$$

The component balance for the simple stage (no feed or side product), j , of Figure 2, is:

$$v_{j+1} + l_{j-1} - v_{ji} - l_{ji} = 0$$

The component balance for feed stage, f , of Figure 2 will add the liquid portion of the feed, l_{Fi} , while the vapour portion, v_{Fi} , is added to the component balance for stage $f-1$. For the product stage, p , the

material withdrawn, w_{pi} , is subtracted from the component material balance. By convention, material leaving a tray has a negative value and material entering a tray has a positive value.

The total material balances are organized in the same manner as the component balances. The total material balance for the simple stage of Figure 2 is:

$$V_{j+1} + L_{j-1} - V_j - L_j = 0$$

The same convention applies to feed and product trays where the total flow rate of a feed, F_j , is positive and the product, W_{ps} , is negative.

The equilibrium equation and the composition constraint are combined to get the bubble point equation:

$$\frac{1}{\sum_{i=1}^C l_{ji}} * \sum_{i=1}^C K_{ji}l_{ji} - 1 = 0$$

and the dew point equation:

$$\frac{1}{\sum_{i=1}^C v_{ji}} * \sum_{i=1}^C \frac{v_{ji}}{K_{ji}} - 1 = 0$$

These, or some variation, are important in some methods to find the stage temperature, especially for more narrow boiling mixtures.

The energy balance equations are required in any rigorous method. In narrow-boiling mixtures, they influence the internal total flow rates. In wide-boiling mixtures and in columns where there are great heat effects (e.g. oil refinery fractionators) they also strongly influence stage temperatures. The overall energy balance for a column with one feed and side product is:

$$FH_F - DH_D - Bh_B - WH_W + Q_R - Q_C = 0$$

The enthalpy terms, H and h , are per mole of mixture. Note that the enthalpies of the top and side products are written so that a vapour or liquid enthalpy can be substituted, depending on the phase of the product. The energy balance for the simple stage, j , of Figure 2 is:

$$v_{j+1}H_{j+1} + L_{j-1}h_{j-1} - V_jH_j - L_jh_j = 0$$

The enthalpies (energy per mole) for each phase are functions of temperature, pressure and composition:

$$H_j = H_j(T_j, P_j, y_{ji})$$

$$h_j = h_j(T_j, P_j, x_{ji})$$

For feed stages, side product stages, and stages with inter-condensers or inter-reboilers, additional terms are included in the energy balance equations. The energy balance for the reboiler is:

$$L_N h_N - V_{N+1} H_{N+1} - B h_{N+1} + Q_R = 0$$

and for a partial condenser with both vapour and liquid products:

$$V_1 H_1 - L_0 h_0 - d h_0 - D H_0 - Q_C = 0$$

Subcooling is accounted for in h_0 (the enthalpy of the reflux, L_0 , and the liquid distillate, d).

Most computer simulations work with ideal stages but to characterize a stage for the deviation from ideality or equilibrium, stage efficiencies are often used in some software. Commonly, a Murphree vapour efficiency is used for each component, given as:

$$E_{MVji} = \frac{y_{ji} - y_{ji-1}}{y_{ji}^* - y_{ji-1}}$$

where y_{ji}^* is what the vapour composition would be if the vapour were in equilibrium with the actual liquid on the stage and y_{ji} and y_{ji-1} are actual vapour compositions. If the absorption factor is used, the vapour efficiency can be expressed in terms of variables already presented:

$$E_{MVji} = \frac{v_{ji} - v_{ji+1}(V_j/V_{j+1})}{(K_{ji} V_j/L_j)l_{ji} - v_{ji+1}(V_j/V_{j+1})}$$

A vaporization efficiency, E_{ji} , based on the Murphree efficiency is defined as:

$$E_{ji} = E_{MVji} + (1 - E_{MVji}) \frac{y_{ji+1}}{K_{ji} x_{ji}}$$

This can be used in the MESH equations to account for stage nonideality. This vaporization efficiency is applied to the equilibrium constant, K_{ji} , and appears as the product $E_{ji} K_{ji}$. The vaporization efficiency does solve a computational problem in placing an efficiency in the MESH equations. A major disadvantage of the vaporization efficiency is that it does vary with composition. Near the top of a high purity column, as y_{ji+1} and x_{ji} approach unity, E_{ji} also approaches unity, and so a vaporization efficiency does not truly reflect stage nonidealities.

Another efficiency method is the bypass method where some of the vapour flow of a component entering the stage is sent to the next stage to account for its

inefficiency in separation. The bypass method cannot be used on trays that have material leaving or entering from outside the column such as a feed tray, product draw tray, pump-around return or draw tray, or side-stripper return or draw tray. The bypass method will cause one of these trays to be out of mass balance. Some of the trays adjacent to these trays are also affected by these actions. In some columns, this eliminates a large number of trays and makes results difficult to apply.

Caution then should be used in any choice of efficiency. More often, it is usually best to perform the rigorous calculation using ideal stages and then apply an overall column efficiency based on sound engineering judgement and experience to account for stage nonideality, and calculate the number of actual trays or packing height.

Rigorous Computational Methods

Classification of the Methods

The rigorous methods can be divided into four basic classes. These are:

- The bubble point methods (BP)
- The sum-rates methods (SR)
- The 2N Newton methods
- The global Newton or simultaneous correction (SC) methods.

The BP methods get their name because the stage temperatures are found by directly solving the bubble point equation. The BP methods generally work best for narrow-boiling, ideal or nearly ideal systems; where composition has a greater effect on temperature than the latent heat of vaporization.

The sum-rates (SR) method is suitable for modelling absorbers and strippers with extremely wide-boiling systems, especially those with non-condensables. In these columns, temperatures are the dominant variables and are found by a solution of the stage energy balances. Compositions do not have as great an influence in calculating the temperatures as do heat effects or latent heats of vaporization.

The 2N Newton methods calculate temperatures and total flow rates together but compositions are still calculated in a separate, dependent step. The name 2N Newton means that there are two equations per stage for a total of $2 \times N$ functions and variables per column solved simultaneously by a Newton-Raphson method. The 2N Newton methods have been shown to work well for wide-boiling mixtures including refinery fractionators, absorber-stripper columns and reboiled absorbers.

The first three classes are referred to as equation tearing or decoupling methods because the MESH equations are divided and grouped or partitioned and paired with MESH variables to be solved in a series of steps. The SC methods attempt to solve all of the MESH equations and variables together. Additional classes are:

- Inside-out methods
- Relaxation methods
- Homotopy–continuation methods
- Nonequilibrium models.

The relaxation, inside-out and homotopy–continuation methods are extensions of whole or part of the first four methods in order to expand the range of columns, and to solve difficult systems or columns. The nonequilibrium models are rate-based or transport phenomena-based methods that do away altogether with the ideal stage concept and eliminate any use of efficiencies. They are best suited for columns where a theoretical stage is difficult to define and efficiencies are difficult to predict or apply by any means.

Numerical Methods – The Newton–Raphson Technique

The MESH equations form a large system of inter-related, nonlinear, algebraic equations. The mathematical method used to solve all or part of these equations as a group is the Newton–Raphson method. An understanding of the numerical method is needed to understand the performance of all column methods. Detailed discussion of the Newton–Raphson method and its variations can be found in Holland's (1981) text.

The Newton–Raphson is an approximation technique. It assumes in the derivatives that the MESH equations are linear over short distances and the slopes will point towards the answers. The MESH equations can be far from linear and the predictions can take the next trial well off the curves, and move away from the solution. In some rigorous methods based on Newton–Raphson, a poor set of starting values can cause the calculation never to approach a solution. Also, the calculation can oscillate, with values swinging to either side of the solution. The independent variables calculated in a trial need to move the column to a solution. The software should include means to prevent or detect these problems and improve stability, e.g. by damping or limiting the change to the next set of variables. A Newton–Raphson method will normally take even steps toward the solution.

Global Newton Methods

One group of methods that is very popular is the global Newton methods, also called the simultaneous correction (SC) methods. A common one is that of Naphtali and Sandholm (1971), but there are numerous applications in the literature and global Newton methods have been extended to include additional equations and variables for solving three-phase and reactive distillation columns.

In the global Newton methods, all of the equations are solved together in a Newton–Raphson technique. The methods vary in their choice of variables and MESH equations for the Newton–Raphson calculation but none of the MESH equations are solved in any separate step. In the BP, SR and 2N Newton methods, the component balances and compositions lag the other MESH calculations (since K values and enthalpies are generated using the compositions from the previous trial) and compositions of each component are calculated independently of the others MESH variables. These are major disadvantages with highly nonideal systems, where K values (especially activity coefficients γ_{ji}) and enthalpies are highly composition dependent and where the composition of one component cannot be readily decoupled from those of others. The global Newton method includes the component balances among the Newton–Raphson independent functions and compositions join other MESH variables as independent variables.

The global Newton methods are the most sensitive of the rigorous methods to the quality of the initial values and often require initial values near the answer. This, and applying the methods to a full range of column equipment and specifications, is their greatest problem. Variations on global Newton methods are used in the inside-out, relaxation, homotopy and nonequilibrium methods, where their power and reliability is extended.

Inside-out Methods

The inside-out algorithm has become one of the most popular methods because of its robustness and its ability to be applied to the solution of a wide variety of columns. The inside-out concept was developed by Boston (1980). Russell (1983) presented an inside-out method that works well for many refinery fractionators. The inside-out methods are now the methods of choice for mainstream column simulation and have displaced other methods.

In older methods, the MESH variables of temperatures, total flow rates and component flow rates are the primary solution variables and are used to generate the K values and enthalpies from complex correlations. These methods update the MESH variables in

an outer loop with the K values and enthalpies updated whenever the MESH variables change. The inside-out concept reverses this by using the complex K value and enthalpy correlations to generate parameters for simple K value and enthalpy models. These parameters are unique for each stage and become the variables for the outside loop. The inside loop consists of the MESH equations and is a variation on other methods. In every step through the outside loop, the simple models are updated using MESH variables from the inside loop. This sets up the next pass through the inside loop. Since the K values and enthalpies are simple, the inside loop works well for a wide range of mixtures and is little affected by the nonideality of mixtures or the quality of the initial values.

The outer loop K value model is based on a simple composition-independent K method:

$$\ln K_{bj} = A_j + B_j(1/T_j - 1/T^*)$$

where T^* is a reference temperature for the K value correlation. Outer loop variables, A_j and B_j , are generated for each stage from a reference $K_{bj\text{Ref}}$ of a composite component:

$$\ln K_{bj\text{Ref}} = \sum_{i=1}^C w_i \ln K_{ji(\text{actual})}$$

where the w_i are weight factors. The temperatures and compositions used to get the $K_{ji(\text{actual})}$ are the latest from the inside loop. Simple relative volatilities are among the outside loop variables, and are used in the K_b method to calculate the temperatures and whenever K values are needed in the inside loop:

$$\alpha_{ji} = K_{ji(\text{actual})}/K_{bj\text{Ref}}$$

These simple relative volatilities change little over the range of temperatures that is seen on a given stage and greatly simplify temperature and composition calculations in the inside loop. For nonideal mixtures, an activity coefficient for each component accounts for composition effects in the inside loop. This activity coefficient has a simple model, similar to the K_b model:

$$\ln \gamma_{ji}^* = a_{ji} + b_{ji}x_{ji}$$

where the new outer loop variables, a_{ji} and b_{ji} , for each component are determined from the actual activity coefficient model at the current stage temperature and stage composition.

The simple K values used in the inside loop are easily determined from:

$$K_{ji(\text{simple})} = K_{bj}\alpha_{ji}\gamma_{ji}^*$$

Simple models for the enthalpy of a phase are also used to reduce effects such as that caused by components moving past their critical conditions. Thus, the outside loop calculation consists of updating the terms of the simple K value, activity and enthalpy models which are updated after each inside loop solution using the latest temperatures and compositions from the inside loop.

The inside loop consists of the actual calculation of the MESH variables using the simple K value and enthalpy models. Boston initially used an inside loop solution method similar to a bubble point method and from that it may appear that the Boston method is most appropriate for narrow-boiling mixtures. However, the forcing style of the method also allows it to work well for wide-boiling mixtures. The Boston method works well for tall, high purity (superfractionator) type columns, but has been extended to absorbers, to three-phase distillation, and to reactive distillation by using other arrangements of the MESH equations.

The Boston method includes a middle loop to allow for column specifications and constraints. The arrangement of equations in the inner loop, where the solution of the MESH variables occur, may allow for only a few control or specified variables, such as fixed reflux ratio and product rates. The middle loop adjusts the control variables to meet the specifications. The middle loop can be built as an optimization method with process specification equations and economic objectives and constraints.

Russell's (1983) method differs from Boston's in the inside loop by a solution method of the MESH equations that includes specifications for product quality, stage temperatures, internal flow rates, etc., without the use of a middle loop to solve these. Here, for each heat exchanger in the column, plus each additional side product, an additional specification and operating variable is added to the problem. Russell's method has been found to work well for refinery fractionators with side strippers and other similar columns.

Relaxation Methods

A relaxation method finds a steady-state solution of a column as if it were an operating column changing with time. The column is initialized using some realistic condition and then makes steps to the steady-state conditions by successive approximations of the

unsteady-state distillation equations. These unsteady-state equations are modifications to the MESH equations to include changes in the MESH variables with respect to time. This mimics the physical start-up of the column, but the objective is not to follow the dynamic operation but to seek the steady-state solution.

Homotopy–Continuation Methods

Homotopy or continuation methods are applied to difficult-to-solve columns, and are a simple means of forcing a solution. The MESH equations can be difficult to solve, due either to the nature of the column (many feeds or side products, side strippers, near minimum reflux, etc.) or to the nonidealities of the K values or enthalpies. For three-phase systems, azeotropic systems or systems of columns with two or more feed/recycle stream combinations, there may be more than one calculated solution. The method must be forced to reach the desired solution. Homotopy methods begin with a known solution of the column and from there follow a path to the desired solution. The known solution can be at different conditions or with much simpler K value and enthalpy methods and stepped changes are made from there, solving the column equations at each step, until the final solution is reached.

Nonequilibrium or Rate-based Methods

Stage efficiency prediction and scale-up from ideal or equilibrium stages to the actual design can be difficult and unreliable for many columns. For highly nonideal, polar and reactive systems, such as amine absorbers and strippers, prediction and use of efficiencies is particularly difficult. In such mixtures, mass transfer and not equilibrium often limits the separation.

Nonequilibrium methods attempt to get around the difficulty of predicting efficiencies by replacing the equilibrium stage concept. Instead, they apply a transport phenomena approach for predicting mass transfer rates. Here, the bulk vapour and liquid phases are not at equilibrium with each other, but there is equilibrium at the interface between phases with a movement from the bulk phase through the interface (Figure 3). The net loss or gain of material and energy at the interface is expressed as transfer rates. The mass and energy transfer rates are dependent on the mass and energy transfer coefficients for each phase which are in turn dependent on composition and conditions of each bulk phase and at the interface.

The correlations for the mass and heat transfer coefficients and interface also take into account packing or tray geometries for the actual column. The total mass and energy rates are calculated from integrating the mass and energy fluxes across the total interface surface.

Krishnamurthy and Taylor (1986) present and test a nonequilibrium model which includes rate equations among the traditional MESH equations. These include individual mass and energy balances in the vapour and the liquid and across the interface. An equilibrium equation exists for the interface only. The solution methods for these equations are the same as the global Newton methods.

The total mass transfer rates are added to an expanded set of the MESH equations called the MERQ equations. The new MERQ acronym stands for:

Material balances for each component – one for the bulk vapour, one for the bulk liquid and one across the interface.

Energy balance equations – one for the bulk vapour, one for the bulk liquid and one across the interface.

Rate equations for mass transfer for all but one component – one from the interface to the bulk vapour and one from the bulk liquid to the interface, plus one energy transfer rate equation from the liquid to the vapour.

Equilibrium equation at the interface only.

Outlook

New rigorous methods for fractionation modelling may no longer be forthcoming and most enhancements will be driven by greater acceptance of nonequilibrium methods, and to other methods by their application to more complex fractionators and difficult systems of components. Teaching concepts of equations and solution may be limited to what is necessary to understand a programme's options, diagnostics and why a programme acts in a certain manner. There should be greater emphasis on knowledge of the physical reality of a column and where the actual process is sensitive, to help set up a problem. Software improvements are needed more in analysis and troubleshooting thought processes, tools and reports. Some of these tools may be a return to use of pre-computer tools such as x - y , McCabe–Thiele, and Hengstebeck diagrams and shortcut methods. While computers continue to become more common, faster and easier to use, they should never be a substitute for sound engineering experience and judgement.

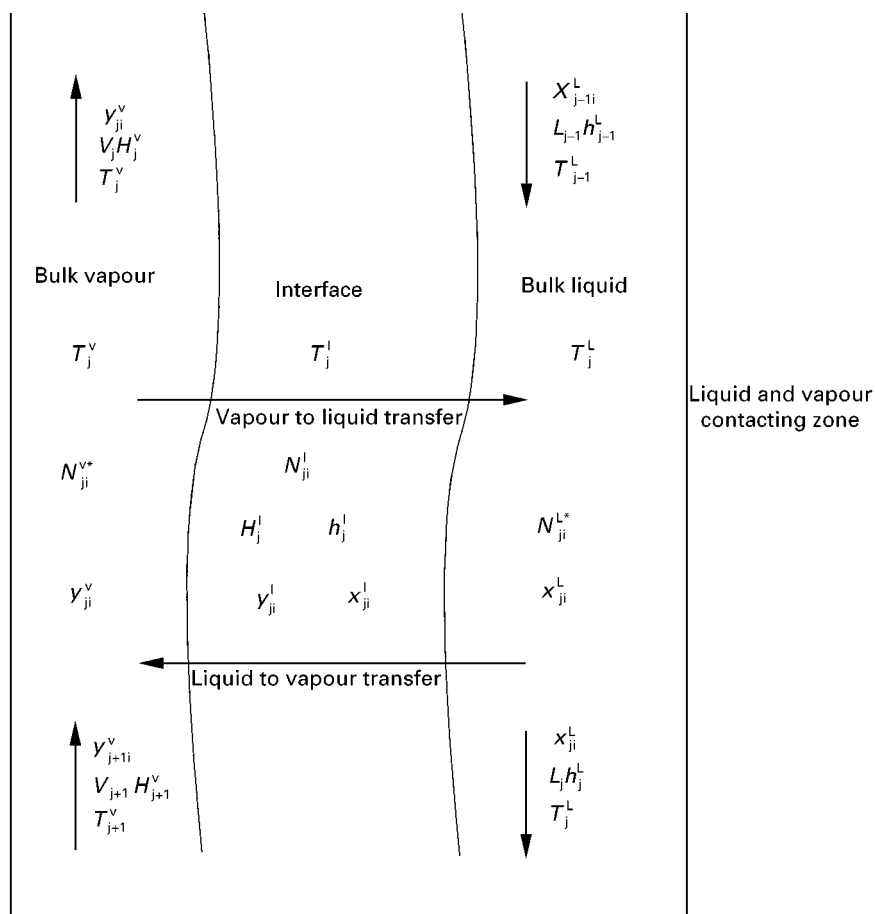


Figure 3 Model of a nonequilibrium separation and mass transfer.

See also: II/Distillation: Historical Development; Theory of Distillation; Vapour-Liquid Equilibrium: Correlation and Prediction; Vapour-Liquid Equilibrium: Theory.

Further Reading

- Boston JF (1980) Inside-out algorithms for multicomponent separation process calculations. American Chemical Society Symposium Series No. 124: 135.
- Brierley RJP and Smith RI (1979) DISTPACK – Using a combination of algorithms to solve difficult distillation and absorption problems. Chemical Engineering Symposium Series No. 56: 89.
- Friday JR and Smith BD (1964) An analysis of the equilibrium stage separations problem—formulation and convergence. *American Institute of Chemical Engineers Journal* 10: 689.
- Holland CD (1981) *Fundamentals of Multicomponent Distillation*. New York: McGraw-Hill.
- Ketchum RG (1979) A combined relaxation–Newton method as a new global approach to the computation of thermal separation processes. *Chemical Engineering Science* 34: 387.
- Kister HZ (1992) *Distillation Design*. New York: McGraw-Hill.
- Kister HZ (1995) Troubleshooting distillation simulation. *Chemical Engineering Progress* 16(6): 63.
- Krishnamurthy R and Taylor R (1986) Multicomponent mass transfer theory and applications. In Cheremisinoff NP (ed.) *Handbook of Heat and Mass Transfer*. Gulf Publishing Company.
- Lockett MJ (1986) *Distillation Tray Fundamentals*. Cambridge, UK: Cambridge University Press.
- Naphtali L and Sandholm DS (1971) Multicomponent separations calculations by linearization. *American Institute of Chemical Engineers Journal* 17: 148.
- Russell RA (1983) A flexible and reliable method solves single-tower and crude-distillation-column problems. *Chemical Engineering* 90(20): 53.
- Taylor R, Wayburn TL and Vickery DJ (1987) The Development of Homotopy methods for the solution of separation process problems. International Chemical Engineering Symposium Series No. 104: B305.
- Wang JC and Henke GE (1996) Tridiagonal matrix for distillation. *Hydrocarbon Processing* 45(8): 155.

Multicomponent Distillation

V. Rico-Ramirez and U. Diwekar,
Carnegie Mellon University, Pittsburgh, PA, USA

Copyright © 2000 Academic Press

Introduction

Distillation is the oldest separation process and the most widely used unit operation in industry. It involves the separation of a mixture based on the difference in the boiling point (or volatility) of its components. The reason for the wide acceptance of distillation is that, from both kinetic and thermodynamic points of view, distillation offers advantages over other existing processes for the separation of fluid mixtures:

1. Distillation has the potential for high mass transfer rates because, in general, in distillation there are no inert materials or solids present.
2. The thermodynamic efficiency for distillation is higher than the efficiency of most other available processes in the chemical industry.

Designing a distillation column involves: (1) selecting the type of column, mostly based on heuristics; (2) obtaining the vapour–liquid equilibrium data using thermodynamics; and (3) finding the design variables such as number of equilibrium stages and operating conditions required to obtain the desired separation based on mass and energy balances.

When the mixture to be separated contains two components, the design of a column can be accomplished by using *graphical methods*. However, for multicomponent systems the design methods are more difficult and are the focus of this article.

Fundamentals

Simple Distillation

Distillation began as a simple still. In such an operation, a liquid mixture is heated (see Figure 1). As a result, a vapour stream richer in the more volatile components comes off, while the liquid, richer in the less volatile components, remains in the still. The vapour stream is condensed and collected in the condenser.

The analysis of simple distillation for a binary mixture presented in 1902 by Lord Rayleigh marks the earliest theoretical work on distillation. Consider Figure 1. Let F (moles) be the initial feed to the

still and x_F (mole fraction) be the composition of component A of the mixture. Let B be the number of moles of material remaining in the still, x_B the mole fraction of component A in the still, x_D the mole fraction of component A in the vapour dB produced during an infinitesimal time interval dt . The differential material balance for component A can be written as:

$$\ln \left(\frac{B}{F} \right) = \int_{x_F}^{x_B} \frac{dx_B}{x_D - x_B} \quad [1]$$

Complex mass and heat transfer processes occur in distillation processes and it is generally assumed that the vapour formed is in thermodynamic equilibrium with the liquid. Hence, the vapour composition (x_D) is related to the liquid composition (x_B) by an equilibrium relation of the functional form $x_D = f(x_B)$. Note that, because of the unsteady nature of simple distillation, the equilibrium relationship between x_D and x_B holds only for each infinitesimal time interval dt .

The exact equilibrium relationship for a particular mixture may be obtained from a thermodynamic analysis and is also dependent upon temperature and pressure.

Thermodynamics and Equilibrium Data

Accurate and reliable thermodynamic data for vapour–liquid equilibrium is essential to distillation

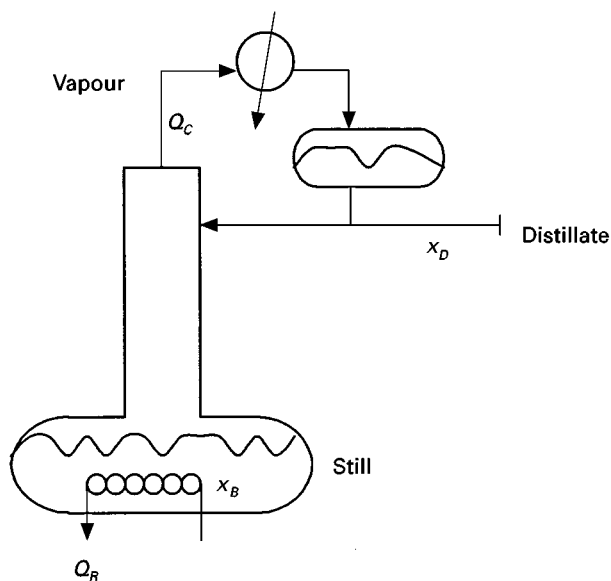


Figure 1 Simple distillation – a still.

design. For binary mixtures, these data are generally presented in the form of tables containing the liquid and vapour equilibrium compositions over a range of temperatures for a fixed pressure. The same information can also be plotted in what is called an x - y diagram. For multicomponent mixtures, however, vapour liquid equilibrium data are difficult to represent in graphical or tabular form. In such case, K values are used instead.

K value and relative volatility The K value of a component i is a measure of the tendency of such component to vaporize. A K value is defined by:

$$K_i = \frac{y_i}{x_i} \quad [2]$$

where y_i is the equilibrium composition of the vapour phase for a composition x_i of the liquid phase. K values are a function of temperature, pressure and composition, and they are widely reported for binary and multicomponent mixtures. An associated concept is the relative volatility, $\alpha_{i,j}$, which is a measure of the ease of separation of components i and j by distillation:

$$\alpha_{i,j} = \frac{K_i}{K_j} \quad [3]$$

Ideal and nonideal systems An ideal system is one in which the liquid phase obeys Raoult's Law and the vapour phase obeys the ideal gas law. For such systems, the K value is given by:

$$K_i = \frac{y_i}{x_i} = \frac{p_i^0}{P} \quad [4]$$

where p_i^0 is the vapour pressure of pure component i and P is the pressure of the system. Note that p_i^0 is a function of temperature.

For a nonideal system, the K values can also depend upon the composition of the mixture and are expressed in terms of fugacity coefficients, where ϕ_i^V is the vapour phase fugacity coefficient and γ_i^L is the liquid phase activity coefficient, as given below:

$$K_i = \frac{\gamma_i^L}{\phi_i^V} \cdot \frac{p_i^0}{P} \quad [5]$$

Azeotropic systems represent examples of nonideal mixtures for which eqn [5] has to be used.

Classification of Distillation Processes

There are many criteria under which one can classify distillation: type of accessories, operating mode,

design calculation assumptions, etc. Distillation can either be binary or multicomponent. According to the type of accessories used to increase the mass transfer in the separation process, a distillation column can be packed (use of packing) or staged (use of plates). It can be batch or continuous. Also, according to the assumptions made and accuracy expected in a distillation design calculation, a calculation technique can either be a shortcut method or a rigorous method.

Packed columns and staged columns Although simple distillation in a still historically represents the start of the distillation process, a complete separation of the components of the mixture using this process is not possible. Therefore, the application of these stills is restricted to laboratory-scale distillation, where high purities are not required or when the mixture is easily separable.

One can look at simple distillation as consisting of one equilibrium stage where a liquid and a vapour are in contact with one another and mass and heat transfers take place between the two phases. If N such stages are stacked one above the other, and are allowed to have successive vaporization and condensation, that results in a substantially richer vapour and weaker liquid (in terms of the more volatile component) in the condenser and the reboiler, respectively. This multistage arrangement is representative of a distillation column, where the vapour from the reboiler rises to the top and the liquid from the condenser is refluxed downwards (see Figure 2). The contact between the liquid and the vapour phase is established through accessories such as packing or plates. When the accessory is a stack of plates, then the result is a column of trays. Similarly, if the accessory is packing, the result is a packed column.

Continuous distillation and batch distillation The basic difference between a batch column and a continuous column is that in continuous distillation the feed is continuously entering the column, while in batch distillation the reboiler is normally fed at the beginning of the operation. Also, while the top products are removed continuously in both batch and continuous operations, there is no bottom product in a conventional batch distillation. Since in a continuous operation the total product flow equals that of incoming feed or feeds, the process reaches a steady state. In batch distillation, on the other hand, the reboiler becomes depleted over time, so the process is unsteady. Such differences are illustrated in Figure 3.

Batch distillation is a direct extension of the simple distillation still, where the Rayleigh equation

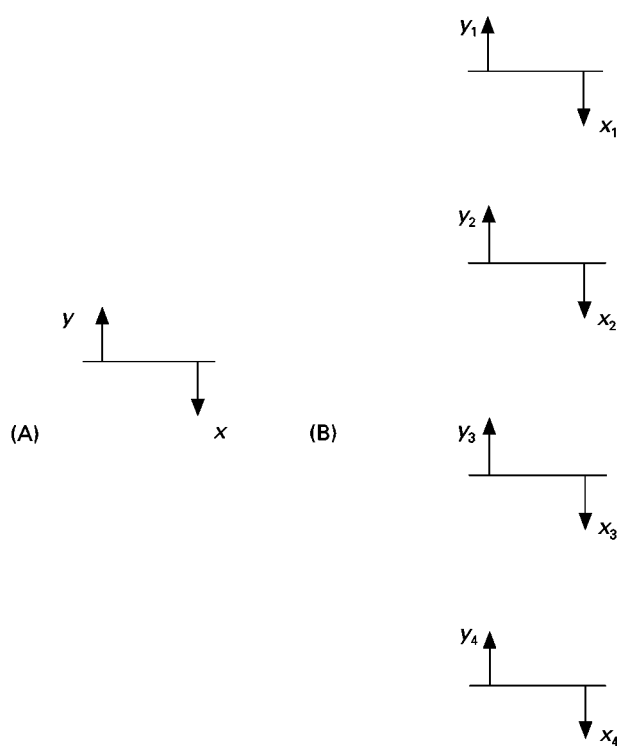


Figure 2 Equilibrium processes. (A) Single stage; (B) multi-stage.

(eqn [1]) is applicable. However, in both batch and continuous distillation, multistage mass transfer and thermodynamic equilibrium stage calculations are used for obtaining the steady-state relationship be-

tween the product composition (instantaneous in case of batch) and feed composition.

Multicomponent Multistage Equilibrium Calculations

This section is divided in two parts. In the first we discuss approximate methods (or shortcut methods); the second part corresponds to rigorous methods. The approaches are different depending upon the operation mode of the column, that is, a continuous operation or a batch operation.

In this section, our attention is focused on the approaches to the design of continuous columns. The reader can refer to the book by Diwekar (1995) for batch distillation calculations.

Shortcut Methods

Approximate methods constitute a useful for the synthesis, analysis and design of distillation separations. The main advantage of shortcut methods is that they can provide the feasible region of operation. They also provide large saving in computer time, and sometimes, they are sufficiently accurate that more expensive rigorous methods are not justified.

Concept of N_{\min} and R_{\min} Minimum number of plates, N_{\min} , and minimum reflux, R_{\min} , are very important concepts in the design of distillation processes, as they are considered to be the limiting conditions in the operation of a distillation column.

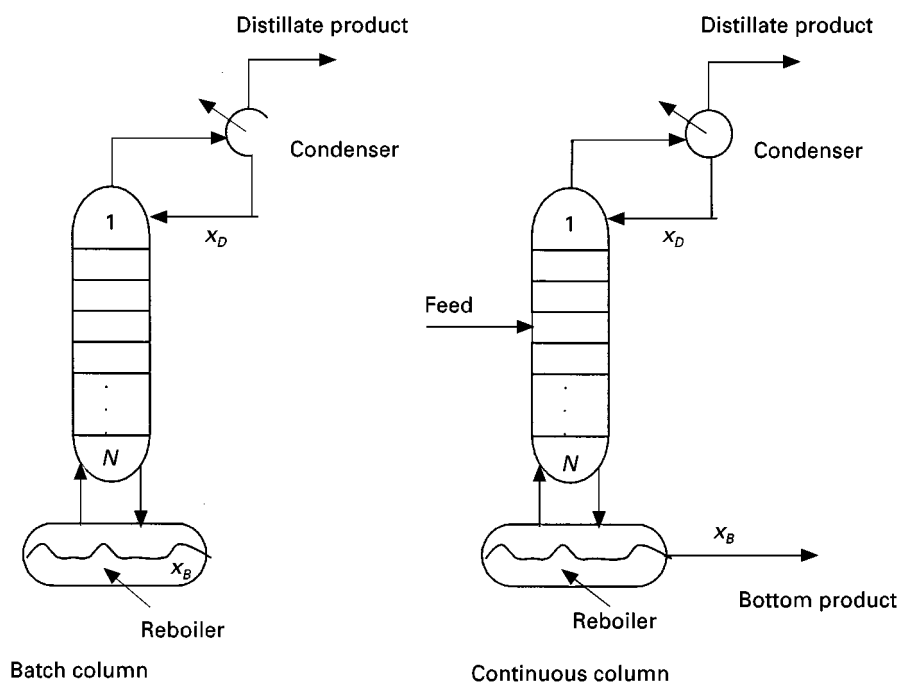


Figure 3 Batch distillation versus continuous distillation.

N_{\min} corresponds to the number of trays required for separation in a situation in which the external reflux ratio R (ratio of the liquid refluxed to the distillate rate) of the column is infinite. This corresponds to total reflux operation.

R_{\min} corresponds to the minimum value of the external reflux ratio required to achieve the specified separation in a situation in which the number of trays of the column is infinite.

Fenske–Underwood–Gilliland method The most popular of these shortcut methods is the Fenske–Underwood–Gilliland method (FUG). The basic assumptions of such a method are:

1. The system is ideal.
2. Constant molar overflow (as in the McCabe Thiele method for binary mixtures).
3. The separation is essentially taking place between the light key component and the heavy key component. The light key (lk) is the lightest component appearing in the bottom and the heavy key (hk) is the heaviest component appearing in the top.

In the FUG method:

1. Fenske's equation is used to calculate the minimum number of trays, N_{\min} .
2. Underwood's equation is used to estimate the minimum reflux, R_{\min} .
3. Gilliland's correlation is used to calculate the actual number of trays, N (for any R given), or the reflux ratio, R , (for any N given) in terms of previous limiting values N_{\min} and R_{\min} .

The Fenske equation is:

$$N_{\min} = \frac{\log \left[\left(\frac{x_{Dlk}}{x_{Blk}} \right) \cdot \left(\frac{x_{Bhk}}{x_{Dhk}} \right) \right]}{\log(\alpha_{lk,hk})} \quad [6]$$

where $\alpha_{lk,hk}$ is the relative volatility between the light key component and the heavy key component. Since it can be expected that the value of α changes for each tray of the column, the geometric average of this value is generally used:

$$\alpha^N = \alpha^N \cdot \alpha_{N-1} \dots \alpha_1 \quad [7]$$

The Underwood equation can be written as:

$$\sum_i \frac{\alpha_i \cdot x_{i,D}}{\alpha_i - \theta} = R_{\min} + 1 \quad [8]$$

where θ is a root of the equation:

$$\sum_i \frac{\alpha_i \cdot x_{i,F}}{\alpha_i - \theta} = 1 - q \quad [9]$$

such that $\alpha_{hk} \leq \theta \leq \alpha_{lk}$. α_{hk} and α_{lk} are the relative volatilities of the key components (light and heavy) in the calculation. As stated earlier, such components are the ones that the designer uses as the basis for the separation.

Finally, the Gilliland correlation is given by:

$$\frac{N - N_{\min}}{N + 1} = 1 - \exp \left[\left(\frac{1 + 54.4G}{11 + 117.2G} \right) \cdot \left(\frac{G - 1}{G^{0.5}} \right) \right] \quad [10]$$

where

$$G = \frac{R - R_{\min}}{R + 1} \quad [11]$$

The main assumptions of the Underwood equation are the assumption of constant molar flow rates and an ideal system. Such assumptions constitute the main limitation of the algorithm.

Rigorous Methods

Recent developments in computer hardware and software have made it possible to use rigorous methods for the design of distillation processes. In these methods, the assumption of constant molar flow rates is no longer considered. The implication of removing such an assumption is that rigorous methods not only consider mass balances, but also enthalpy balances for each of the trays of the column. Thus, rigorous methods require simultaneous convergence of mass and energy equations. Depending on the calculation sequence, there are several rigorous methods reported in the literature. The most important of these methods are: (1) Thiele–Geddes; (2) tridiagonal methods; (3) Naphtali–Sandholm; (4) inside-out algorithms; (5) Θ convergence methods; and (6) $2N$ Newton methods. The method of Naphtali–Sandholm and the inside-out algorithm, which are commonly used nowadays, are discussed in this work to give an idea of the scope and applications of rigorous methods.

MESH equations Most rigorous methods involve the solution of the so-called MESH equations. For each stage n in a distillation column (and for each component i in a mixture of C components), the equations representing mass balance (M), equilibrium relationships (E), summation of compositions (S) and energy balance (H), constitute the MESH equations. In addition, both K values and enthalpies

are generally given as functions of temperatures, pressures and compositions. The generalized form of the MESH equations for the equilibrium stage shown in Figure 4 and the expressions for K values and enthalpies are present in Table 1.

Naphtali-Sandholm method In the Naphtali-Sandholm method, the number of variables of the MESH equations is reduced by the introduction of component flow rates and side streams. Furthermore, the summation of compositions are eliminated. Those modifications result in the equations presented in Table 2.

To solve the system of MESH equations given in Table 2, the vectors of variables and equations are ordered as follows. Variables:

$$\bar{X} = [\bar{X}_1, \bar{X}_2, \dots, \bar{X}_n, \dots, \bar{X}_N] \quad [12]$$

where N is the number of stages and

$$\bar{X}_n = [v_{n,1}, v_{n,2}, \dots, v_{n,C}, T_n, l_{n,1}, l_{n,2}, \dots, l_{n,C}]^T \quad [13]$$

Equations:

$$\bar{F} = [\bar{F}_1, \bar{F}_2, \dots, \bar{F}_n, \dots, \bar{F}_N] \quad [14]$$

where

$$\bar{F}_n = [\hat{H}_n, M_{n,1}, M_{n,2}, \dots, M_{n,C}, E_{n,1}, E_{n,2}, \dots, E_{n,C}]^T \quad [15]$$

The solution process is iterative, using one of the several variations of the Newton method. Thus, corrections at each iteration k are obtained from

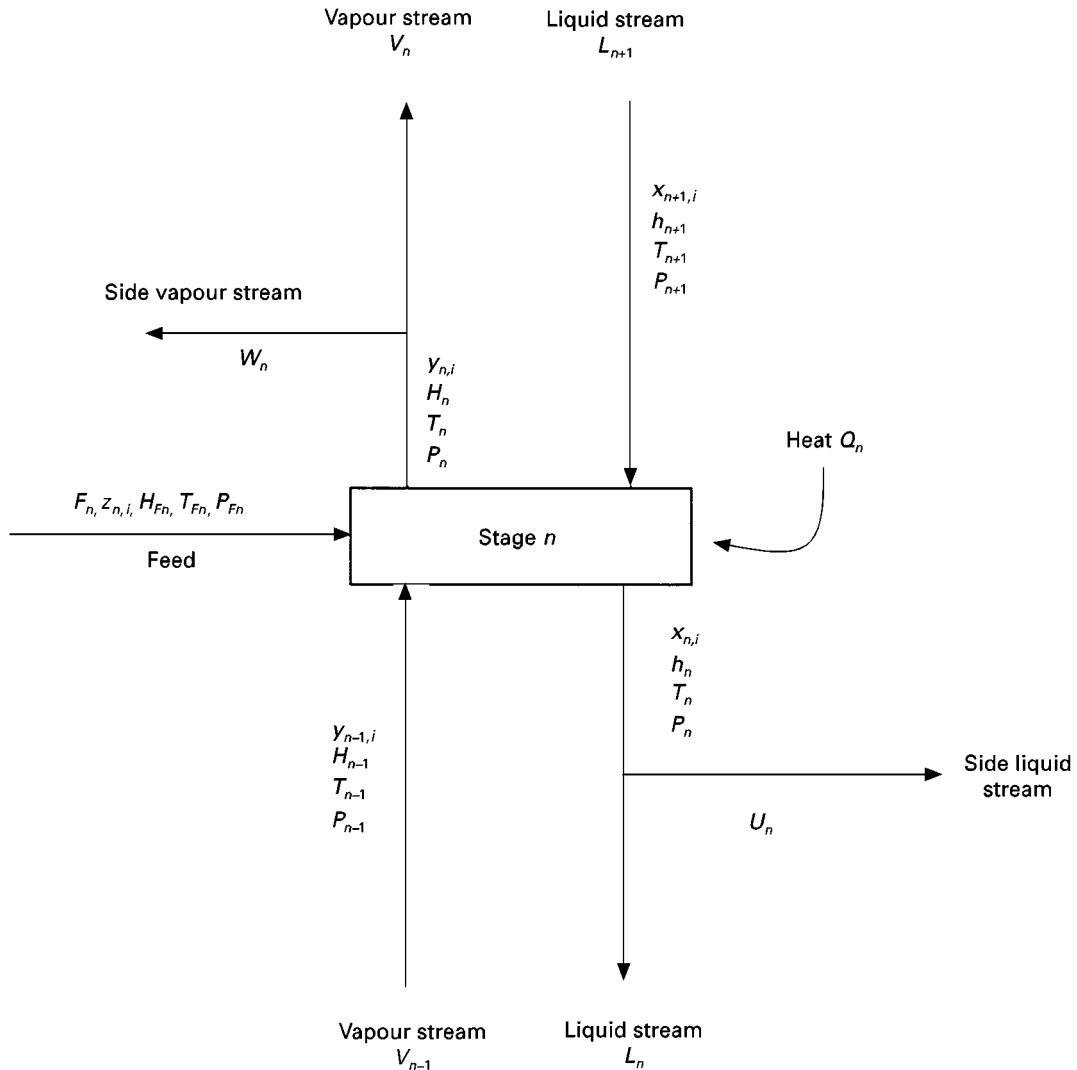


Figure 4 Equilibrium stage. Derivation of MESH equations.

Table 1 MESH equations

Relationship	Equation
Mass balance	$L_{n+1} \cdot x_{n+1,i} + V_{n-1} \cdot y_{n-1,i} + F_n \cdot z_{n,i} - (L_n + U_n) \cdot x_{n,i} - (V_n + W_n) \cdot y_{n,i} = 0$
Equilibrium	$y_{n,i} = K_{n,i} \cdot x_{n,i}$
Summation of compositions	$\sum_i y_{n,i} - 1 = 0$
H energy balance	$L_{n+1} \cdot h_{n+1} + V_{n-1} \cdot H_{n-1} + F_n \cdot H_{F_n} - (L_n + U_n) \cdot h_n - (V_n + W_n) \cdot H_n - Q_n = 0$
K values and enthalpies	$K_{n,i} = K_{n,i}(T_n, P_n, x_n, y_n)$
	$H_{n,i} = H_{n,i}(T_n, P_n, y_n)$
	$h_{n,i} = h_{n,i}(T_n, P_n, x_n)$

(classical Newton–Raphson equations):

$$\Delta \bar{F}^{(k)} = - \left[\left(\frac{\partial \bar{F}}{\partial \bar{X}} \right)^{-1} \right]^{(k)} \cdot \bar{F}^{(k)} \quad [16]$$

$$\bar{X}^{(k+1)} = \bar{X}^{(k)} + t \cdot \Delta \bar{X}^{(k)} \quad [17]$$

where t is such that $0 \leq t \leq 1$. t is the factor that ensures progress toward the solution of the system at equations of each iteration.

Inside-out algorithm In the Naphtali–Sandholm method, the temperatures and component flowrates are the primary solution variables (see eqn [13]) and

are used to generate the K values and enthalpies from complex correlations. Hence, such a method updates the primary variables in an outer loop, with the K values and enthalpies updated in an inner loop whenever the primary variables change.

In inside-out algorithms, the previous situation is reversed. These methods use complex K values and enthalpy correlations to generate parameters for simple K values and enthalpy models. Hence, these parameters become the variables for the outside loop. The inside loop then consists of the MESH equations. In every step through the outside loop, the simple K values and enthalpy models are updated by using the MESH variables from the inside loop. This sets up the next pass through the inside loop. The book by Kister (1992) provides detailed guidelines for the use of the various inside-out methods.

Table 2 MEH equations for method of Naphtali and Sandholm

Relationship	Equation
Component flow rates and side streams	$v_{n,i} = y_{n,i} \cdot V_n$
	$l_{n,i} = x_{n,i} \cdot L_n$
	$f_{n,i} = z_{n,i} \cdot F_n$
	$s_n = U_n/L_n$
	$S_n = W_n/V_n$
M	$M_{n,i} = l_{n,i} \cdot (1 + s_n) + v_{n,i} \cdot (1 + S_n) - l_{n+1,i} - v_{n-1,i} - f_{n,i}$
E	$E_{n,i} = K_{n,i} \cdot l_{n,i} \cdot \left(\sum_k v_{n,k} / \sum_k l_{n,k} \right) - v_{n,i} = 0$
H	$\hat{H}_n = h_n \cdot (1 + s_n) \cdot \sum_i l_{n,i} + H_n \cdot (1 + S_n) \cdot \sum_i v_{n,i} - h_{n+1} \cdot \sum_i l_{n+1,i} - H_{n-1} \cdot \sum_i v_{n-1,i} - H_{F_n} \cdot \sum_i f_{n,i} - Q_n = 0$

Special Separations

When the components of a mixture have low relative volatilities, or when the mixture contains a large number of components, separation by distillation becomes difficult and expensive because a large number of trays or a large number of columns are required for the separation. Furthermore, some systems may show nonideal behaviour such as the formation of azeotropes or a reversal of the relative volatility with the change in pressure from top to bottom in a column. Complex systems which have these characteristics are common in the pharmaceutical and synthetic chemical industry.

This section presents a brief review of separations in which the traditional distillation process is altered, but the general principles of multicomponent distillation still apply. Three broad categories of such special separations exist: azeotropic distillation, extractive distillation and reactive distillation. Petroleum distillation will also be discussed since it represents a case

in which the complexity of the mixture (petroleum) requires special considerations for the separation.

Azeotropic Distillation

Highly nonideal systems, with components having close boiling points among them, often produce azeotropes. Azeotropes can be identified by using an x - y diagram. When an azeotrope is present, the equilibrium curve crosses the line $x = y$ (45° line), as shown in Figure 5.

Azeotropes limit the separation that can be achieved by conventional distillation. Sometimes it is possible to shift the equilibrium by changing the pressure of the system sufficiently to move the azeotrope away from the region where the separation must be made. Other cases, however, require the addition of a new material in order to achieve separation.

In azeotropic distillation, the equilibrium behaviour of the mixture is modified by adding a new material (called the solvent or entrainer). The added entrainer forms a minimum boiling point azeotrope with one or more components and distils overhead. The distillate is generally heterogeneous, that is, it is composed of two immiscible liquids when condensed. Such a heterogeneous nature facilitates the separation of the product from the entrainer.

Extractive Distillation

Extractive distillation also involves the addition of the third component to the mixture (solvent or entrainer). However, in the case of extractive distillation, the solvent is a relatively high boiling point material, which is present at high concentration on each stage and exits at the bottom. To improve the efficiency of the process, the entrainer has to be added

at the top of the column, so that its concentration on each stage will be enough to produce the desired effect in the equilibrium of the original mixture. Finally, the entrainer is separated from the bottoms product in another distillation column.

Reactive Distillation

The idea of combining reaction and separation in a single apparatus has been extensively investigated. Doherty and Buzad (1992) present a survey of the available design techniques for reactive distillation. Reactive distillation is particularly attractive whenever a chemical reaction provides the favourable effect of reacting away azeotropic mixtures so that the behaviour of the liquid phase is simplified. In addition, it has been shown that reactive distillation has the potential of eliminating recycle costs when a liquid reaction involves a large excess of one reactant.

In general, the current trend in reactive distillation design is using experimental results from bench-scale problems in the initial stages of the design, and then using computer-aided simulation tools for scale-up and operability issues.

Possible profitable applications of reactive distillation processes are numerous. However, an incomplete understanding of the interactions of the many nonlinear phenomena such as chemical reaction, phase equilibrium, mass transfer and countercurrent flow has prevented the widespread use of such processes. Considerable research effort in the area is currently being conducted.

Petroleum Distillation

Petroleum distillation is particularly difficult because of the large number of components of the mixture and large scale of the processes. This type of distillation involves products that are not easily identifiable components. Instead, separation is achieved in terms of pseudo-components, which are generally characterized in terms of their true boiling point ranges (TBP), an average relative molecular mass and an API gravity. TBP data are widely available and are generally presented in form of curves.

There are two main approaches to the design of petroleum distillation columns. The first consists of the solution of mass and energy balances based on empirical correlations, and is basically a calculation by hand. This approach was developed by Packie.

In the second approach, each pseudo-component is characterized for properties (such as vapour pressure and enthalpy) by using homologous-series approaches. Thus, rigorous mass and energy balances can then be applied to determine the separation in

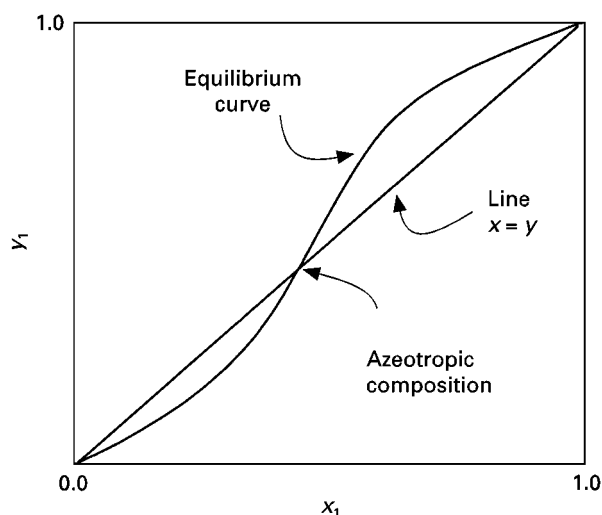


Figure 5 Azeotropic behaviour.

terms of the reflux ratio. Several efficient computer programs following this approach have been developed.

Packed Columns

Several approaches exist for the design of packed columns. These are based on the concepts of number of transfer units (NTU), height of transfer units (HTU) and height equivalent to a theoretical plate (HETP). The last of these concepts is the most widely used.

Since methods for the design of staged distillation columns are well developed, a common approach is to calculate the number of trays N using such approaches and then to find the height of the packed column, h , by the relation:

$$h = N \cdot \text{HETP} \quad [18]$$

There exist various correlations for predicting the value of the HETP. One of most commonly used is the Sherwood correlation. It can be expected that HETP will change with respect to the operating conditions, physical properties of the liquid, etc., so, it is calculated in terms of correlations containing many factors.

Nonequilibrium Distillation

All the mathematical methods (binary, rigorous, shortcut) presented earlier assume that each stage in the column is an equilibrium stage. In reality, however, this assumption is rarely satisfied.

Stage Efficiency

An approach to nonequilibrium calculations is the use of the concept of stage efficiency. The most common approach is to modify the rigorous methods with the introduction of the so-called Murphree efficiency in the calculations. The Murphree efficiency in a stage calculation can be defined as:

$$E_{M_i}^L = \frac{x_{out,i} - x_{in,i}}{x'_i - x_{in,i}} \quad [19]$$

for the liquid and

$$E_{M_i}^V = \frac{y_{out,i} - y_{in,i}}{y'_i - y_{in,i}} \quad [20]$$

for the vapour. x'_i are the compositions of the liquid that would be in equilibrium with the outlet composition of the vapour. y'_i are the compositions of the

liquid that would be in equilibrium with the outlet composition of the liquid.

Mass Transfer Rates

It has been shown that stage efficiency prediction and scale-up are difficult and unreliable. For highly nonideal, polar and reactive systems, a transport phenomena approach for predicting mass transfer rates is preferred. Such mass transfer rates are calculated continuously along the column similarly to the HETP calculation for packed columns.

Nonequilibrium models for the calculation of mass transfer rates assume that, while the bulk vapour and liquid phase are not in equilibrium with each other, there is an equilibrium at the interface. Hence, the net loss or gain for a component at the interface is expressed in a rate form. For instance, the net gain by the vapour because of the transfer at the interface is:

$$N_{ij}^{V0} = N_{ij}^V \cdot da_i \quad [21]$$

where N_{ij}^V is the vapour flux of the component at some point through the interface and da_i is the interface area through which the flux passes. The mass transfer rates for liquid and vapour, N_{ij}^V and N_{ij}^L , are dependent on the mass transfer coefficients for each phase. There exist several correlations for the heat and mass transfer coefficients and these are dependent on the compositions in the bulk phase, the temperatures in the bulk phase and interface, and on the packing or tray geometries.

Industrial Applications

Distillation is by far the most widely used separation technique in the petroleum, natural gas and chemical industries so, applications of multicomponent distillation are numerous. A couple of industrial applications are described in this section.

Primary Distillation of Crude Oil

A typical configuration for the distillation of a crude oil unit includes two main columns, an atmospheric tower and a vacuum tower (see Figure 6). In the atmospheric tower, crude oil is rectified (at a pressure no greater than 275.8 kPa (40 psi); to yield a distillate product containing light hydrocarbon gas, light and heavy naphtha, kerosene, diesel oil, and a bottom product of heavier components (TBP greater than 420°C). Each of the side streams of the atmospheric tower are sent to side strippers that have a partial reboiler or steam stripper. The side stream strippers serve to remove the light components. Stripping by

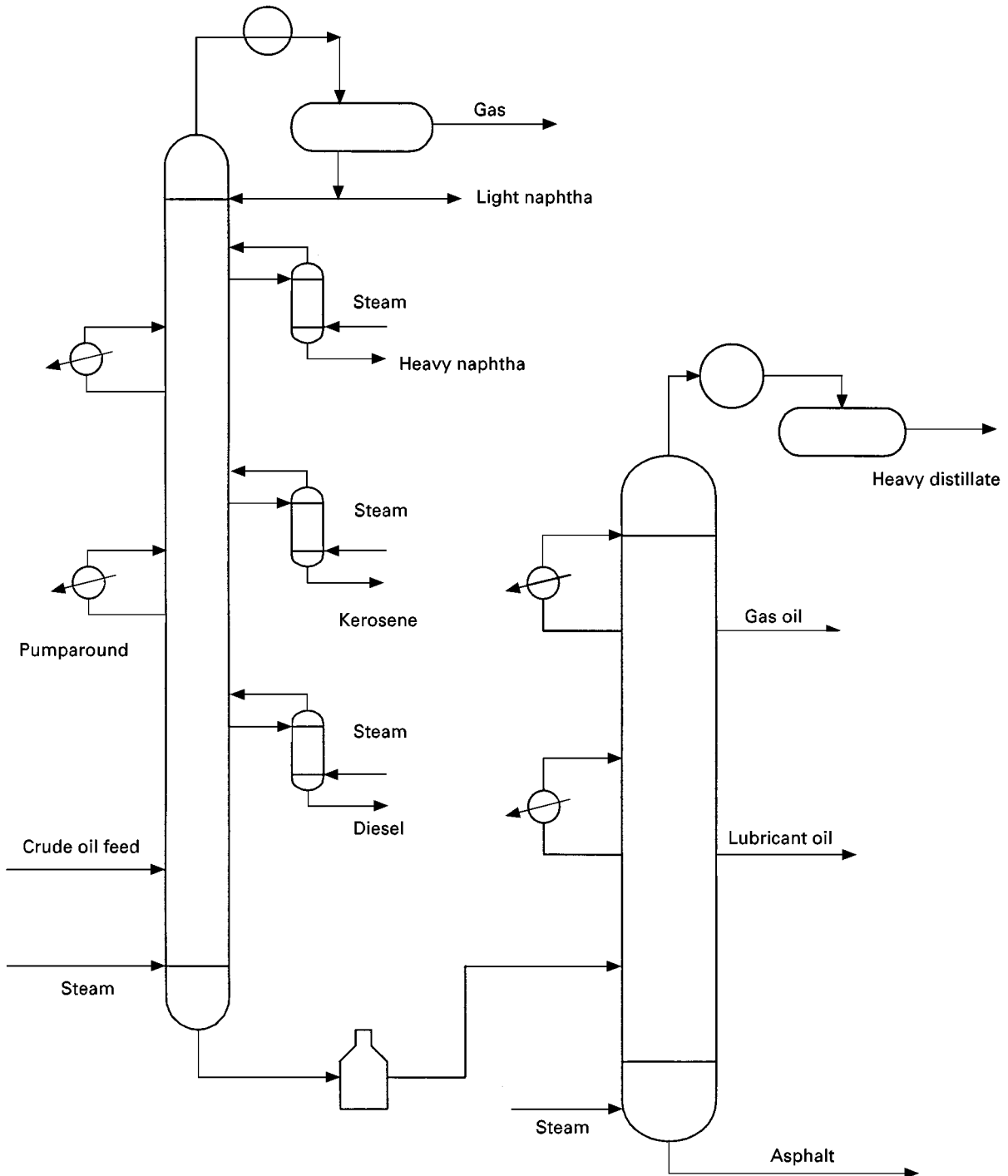


Figure 6 Crude oil distillation unit.

steam is also frequently used in the bottom of the tower.

The bottom product of the atmospheric tower is further separated by rectification in the vacuum tower. The feed-tray pressure of a vacuum tower is usually 6 kPa (45 Torr). Vacuum towers are mainly designed to obtain heavy distillates such as gas oil,

lubricating oils and bunker fuels with asphalt as the bottom product.

The pump-around systems shown in both of the towers serve to make much larger liquid flows on the intermediate stages and produce a net increase in liquid flow. This serves as a point of control to keep the plates from running dry.

Highly developed procedures for the preliminary design of fractionators that process petroleum are commercially available through computer programs. The program 'REFINE' of the ChemShare Corporation and the 'PROCESS' (now PRO-II) program of Simulation Sciences Inc. are two examples.

Ethylene and Propylene Production

The manufacture of ethylene and propylene is one of the most important operations of the petrochemical industry. In that process, ethylene and propylene are formed from the thermal cracking of other hydrocarbons, such as ethane, propane and naphtha. The mixture resulting from the thermal cracking is very complex. Hence, the mixture has to be separated into relatively pure ethylene and propylene, ethane and propane to be used as a recycle, methane and hydrogen to be used as fuel, and heavier products to be used for gasoline. A typical refinery gas feed to the separation system of this process contains hydrogen, ethylene, methane, ethane, propane, propylene and lower compositions of other heavy hydrocarbons. The distillation sequence most commonly used for the separation of the mixture is shown in Figure 7.

In a high pressure plant (no refrigeration is needed for condensation of products), the distillation sequence consists of five distillation columns:

1. Demethanizer
2. Deethanizer
3. Ethylene/ethane separator
4. Depropanizer
5. Propylene/propane separator.

Both the propylene/propane and the ethylene/ethane separator require high towers with large diameters because such mixtures contain components with very close relative volatilities. A plant that uses the configuration described here was built by Pullman Kellogg Inc., Houston, Texas.

In the case of a lower pressure plant, the deethanizer precedes the demethanizer because refrigeration is required for the feed of the demethanizer. So, by placing the deethanizer first, important utility savings are obtained.

Future Work

Enormous progress has been made on the application and design of distillation technology. However, challenges still exist in some areas, which lead to the following ongoing research:

1. Improvement of mass transfer coefficients in packed distillation columns. Great effort is being made on the design of efficient packings and accurate correlation of their performance.

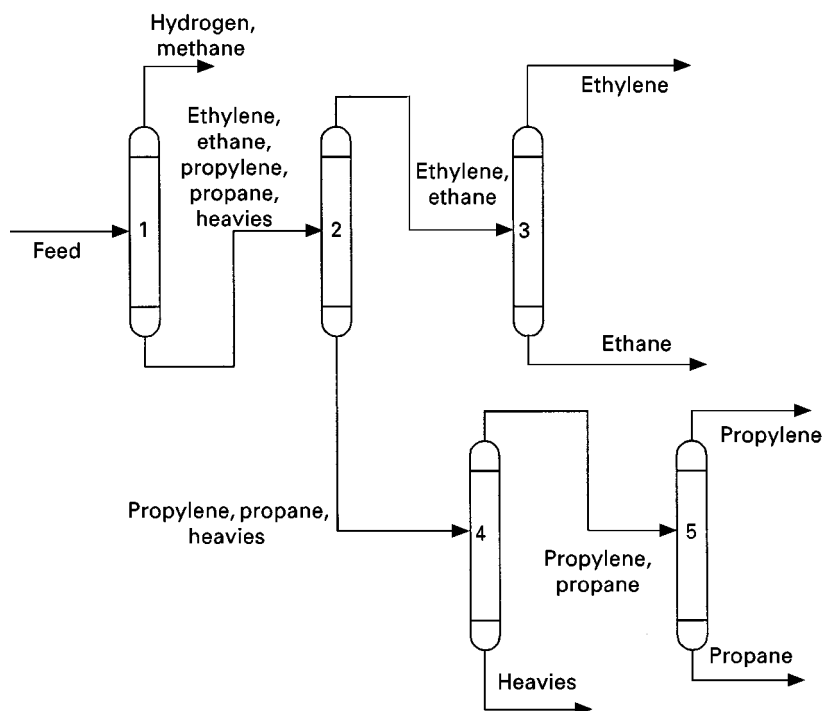


Figure 7 Separation of products of the manufacture of ethylene and propylene.

2. The simulation, synthesis and design of reactive and azeotropic distillation. Such topics still constitute a gap in the knowledge of distillation technology.
3. Investigation of complex configurations for batch distillation processes.
4. Use of optimization methods for obtaining optimal configuration and design of batch and continuous distillation processes.
5. Online optimization and control of columns.

See also: II/Distillation: Batch Distillation; Theory of Distillation; Vapour-Liquid Equilibrium: Correlation and Prediction; Vapour-Liquid Equilibrium: Theory.

Further Reading

Diwekar UM (1995) *Batch Distillation: Simulation, Optimal Design and Control*. Series in Chemical and Mechanical Engineering. Washington, DC: Taylor & Francis.

Doherty MF and Buzad G (1992) Reactive distillation by design. *Transactions of the Institution of Chemical Engineers* 70: part A.

Gmehling J and Onken U (1977) *Vapor-Liquid Equilibrium Data Collections*, DECHEMA Chemistry Data series, vol. 1. Frankfurt:

Henley EJ and Seader JD (1981) *Equilibrium-Stage Separation Operations in Chemical Engineering*. New York: Wiley.

Holland CD (1981) *Fundamentals of Multicomponent Distillation*. New York: McGraw-Hill.

King CJ (1980) *Separation Processes*, 2nd edn. New York: McGraw-Hill.

Kister HZ (1992) *Distillation Design*. New York: McGraw-Hill.

Perry RH, Green DW and Maloney JO (1984) *Perry's Chemical Engineers' Handbook*, 6th edn. New York: McGraw-Hill.

Schweitzer PA (1979) *Handbook of Separation Techniques for Chemical Engineers*. New York: McGraw-Hill, The Kingsport Press.

Treybal RE (1980) *Mass Transfer Operations*, 3rd edn. New York: McGraw-Hill.

Packed Columns: Design and Performance

L. Klemas, Bogota, Colombia

J. A. Bonilla, Ellicott City, MD, USA

Copyright © 2000 Academic Press

Use of Packing in Distillation

Use of packing in mass transfer has its origins in the early 1800s for simple applications such as alcohol distillation, and in sulfuric acid plant absorbers. Glass balls, coke or even stones were used as packing materials. Nevertheless packings for distillation were not established until the 1930s with the use of regular shape materials such as ceramic Raschig rings and Berl saddles, as well as the availability of distillation calculations such as the McCabe–Thiele and Ponchon–Savarit methods. Early in the second half of the century, the use of packing for distillation went through a transformation, producing the second-generation packings (see Table 1). Regular and improved shape of packings, such as pall rings, became available with larger open areas that permitted a substantial increase both in capacity and column efficiency. In the 1960s Sulzer introduced the wire-mesh packings with very high efficiency (low height equivalent to a theoretical plate, HETP), resulting in a new transformation in the use of packings. In the 1970s

and 1980s all major mass-transfer equipment manufacturers developed structured packings. Compared to the traditional tray columns spectacular improvements in plant capacity were achieved, but also some projects were pitfalls, when the expected benefits did not materialize. Manufacturers started realizing that liquid distributors had to be improved, but there was no coherent understanding, nor correlations, that could lead to a safe distributor-column system design. Many manufacturers returned to trays, producing new improved designs, using the area under the downcomer for vapour flow: these trays are offered with new names that indicate their increased vapour flow capacity (Maxyflow, Superfrack, etc.). The need for good distribution and its effect on the column efficiency are now well understood, allowing safe design and efficient applications for random and structured packings in large industrial columns.

General Concepts

Distillation separation is based in relative volatility that makes it possible to concentrate the more volatile components in the vapour phase while the less volatile ones remain in the liquid phase. Distillation columns are countercurrent vapour-liquid mass-transfer devices, where the required separation and purification of components is achieved.

Table 1 Evolution of packing

	<i>First generation, before 1950</i>	<i>Second generation, 1950–1970</i>	<i>Third generation, after 1970</i>
Random packings	Rashing rings Lessing rings Saddles	Intalox® (Norton) Pall Rings ^a	IMTP® (Norton) CMR® (Koch Glitsch) Chempak® ^b Fleximax® (Koch Glitsch) Nutter Ring® (Nutter)
Grids		C-Grid (Koch Glitsch) ^c EF-25 (Koch Glitsch) ^c	
Structured packing		Wire-mesh type ^d	Sulzer BX and CY Mellapak® (Sulzer) Flexipack® (Koch Glitsch) Gempack® (Koch Glitsch) Intalox® (Norton) Montz packing (Montz)

^aDeveloped by BASF, still marketed (or variations of it) by most packing manufacturers.

^bDeveloped by Leva, marketed by Nutter.

^cVariations of these grids are now offered by most packing manufacturers.

^dDeveloped by Sulzer, they are now offered by other manufacturers.

The main variable influencing the column design requirements is the relative volatility, α . **Figure 1** illustrates the effect of α on the column performance:

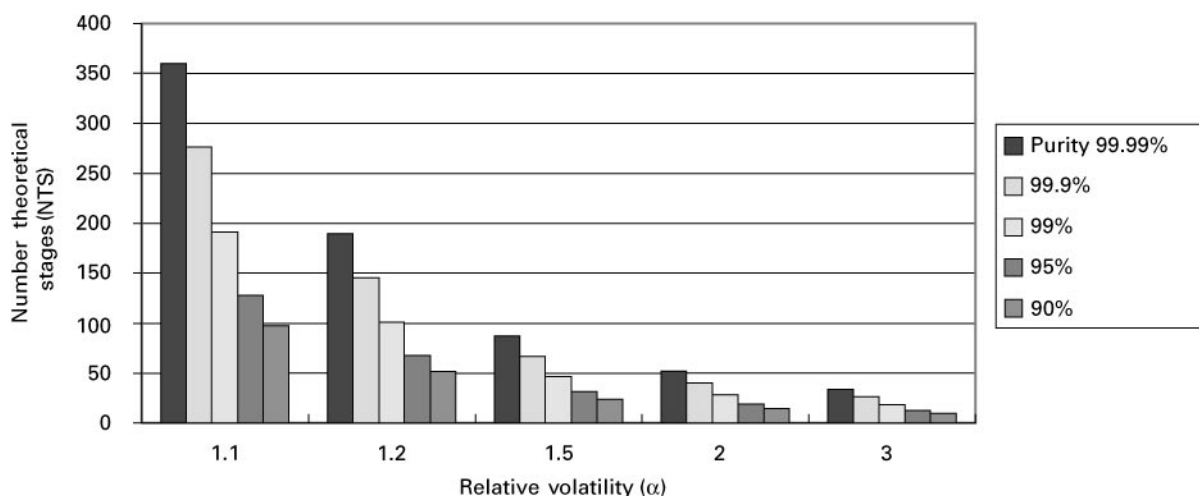
- As α increases, the number of theoretical stages (NTS) required to achieve a fixed product quality decreases, since NTS is proportional to $1/\ln(\alpha)$. As α decreases and approaches 1, the number of stages required increases approaching infinity. At any given α , the minimum number of stages required to achieve a given separation corresponds to a total reflux operation. At total reflux all overhead vapours are condensed and returned to the column as

reflux, so that there is no net product. The minimum reflux sets the limiting slope of the operating line, required to achieve a given separation.

- At constant α , the NTS increases as the product purity increases. The increase is proportional to the logarithm of the key components purity ratio.

It can be also demonstrated that:

- At constant product purity, the minimum reflux decreases as α increases.
- At constant product purity, the minimum number of stages decrease as α increases.
- At constant α , the minimum reflux decreases as the product purity decreases.

**Figure 1** Number of stages required vs. relative volatility at several product purities.

- At constant α , the minimum number of stages increases as the product purity increases.

All these statements say that α defines the separation difficulty. For values around 1.1 and lower, separation by distillation becomes very difficult, requiring very large and expensive columns. For $\alpha = 1$ the mixture is azeotropic and would require the addition of selective entrainers if azeotropic or extractive distillation is to be applied.

Packed Column Description

Figure 2 illustrates a tower with structured packing. In addition to the packing itself, packed columns require other internals to assure the performance of the packing. These internals are:

- Liquid feed pipes to deliver the fluid to the liquid distributors, as seen at the top of the tower and at the intermediate distributor.
- Liquid collection and mixing as shown below the top bed.
- Liquid draw-off sump and pipe as shown below the top bed.
- Liquid redistributors, as presented between the two beds.
- Vapour feed pipes as shown at the vapour inlet nozzle, at the bottom of the tower.
- Packing support plates resting on beams and levelled rings welded to the vessel.
- Hold-down plates.

Incorrect design or incorrect installation of any of these elements can lead to tower failure. One of the most critical elements, and often the culprit of tower failures, is the liquid distributor.

Packing Selection

Figures 3 and 4 illustrate random and structured packings. There are many parameters to be considered in the selection of packings; in some cases, there are one or two considerations that dictate the selection, such as capacity for a revamp, which could favour structured packing. There are also some considerations or applications, such as high-pressure distillation, that could make structured packing a questionable choice. Table 2 gives some general guidelines on packing selection.

Pressure Drop in Packed Beds

The dry-bed pressure gradient is given by the following equation:

$$\Delta P_d = C_1 \rho_g u_g^2 \quad [1]$$

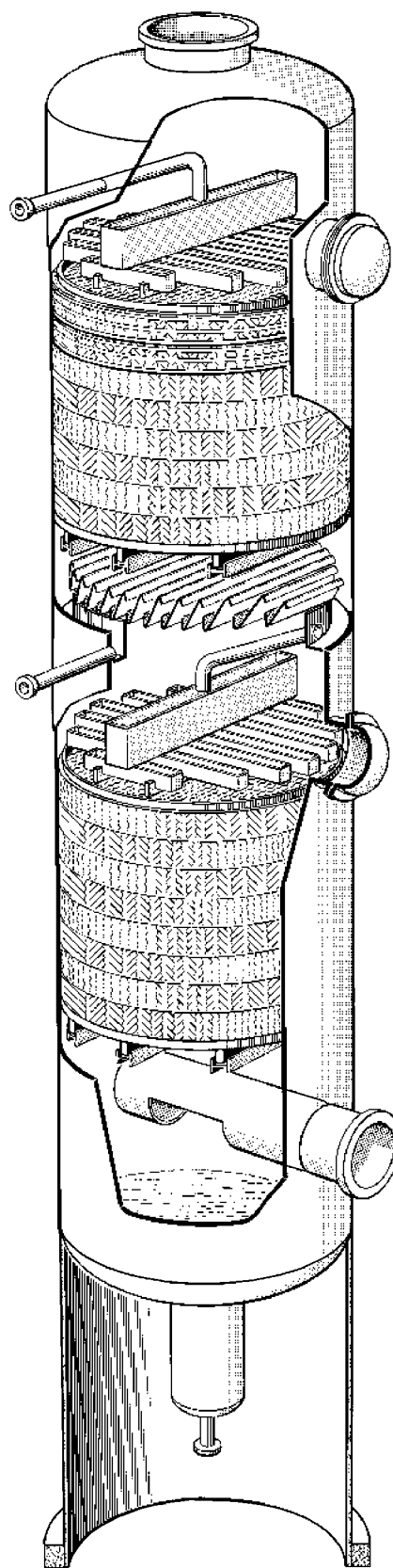


Figure 2 Packed tower illustration. (Photo courtesy of Sulzer Chemtech.)



Figure 3 Random packings: (A) IMTP®. (Photo courtesy of Norton Chemical Process Products Corporation.) (B) Nutter Ring®. (Photo courtesy of Sulzer Chemtech.) (C) Cascade Mini-Rings® (CMR™) and Fleximax®. (Courtesy of Koch-Glitsch Inc.) (D) Pall Rings metal and plastic. (Courtesy of Koch-Glitsch Inc.)

Leva extended the correlation to irrigated beds:

$$\Delta P_i = C_1 10^{\beta u_1} \rho_g u_g^2.$$

Robbins developed the following set of general pressure-drop correlations:

$$\Delta P = C_2 G_f^2 10^{C_3 L_f} + 0.4(L_f/20\,000)^{0.1} (C_2 G_f^2 10^{C_3 L_f})^4 \quad [2]$$

where:

$$G_f = G(0.075/\rho_g)^{0.5} (F_p/20)^{0.5} 10^{0.024 \rho_g} \quad (\text{for pressures over 1 atm})^*$$

*Note: in this correlation the original term $10^{0.3 \rho_g}$ was replaced by $10^{0.024 \rho_g}$ since the original correlation predicts too high a pressure drop.

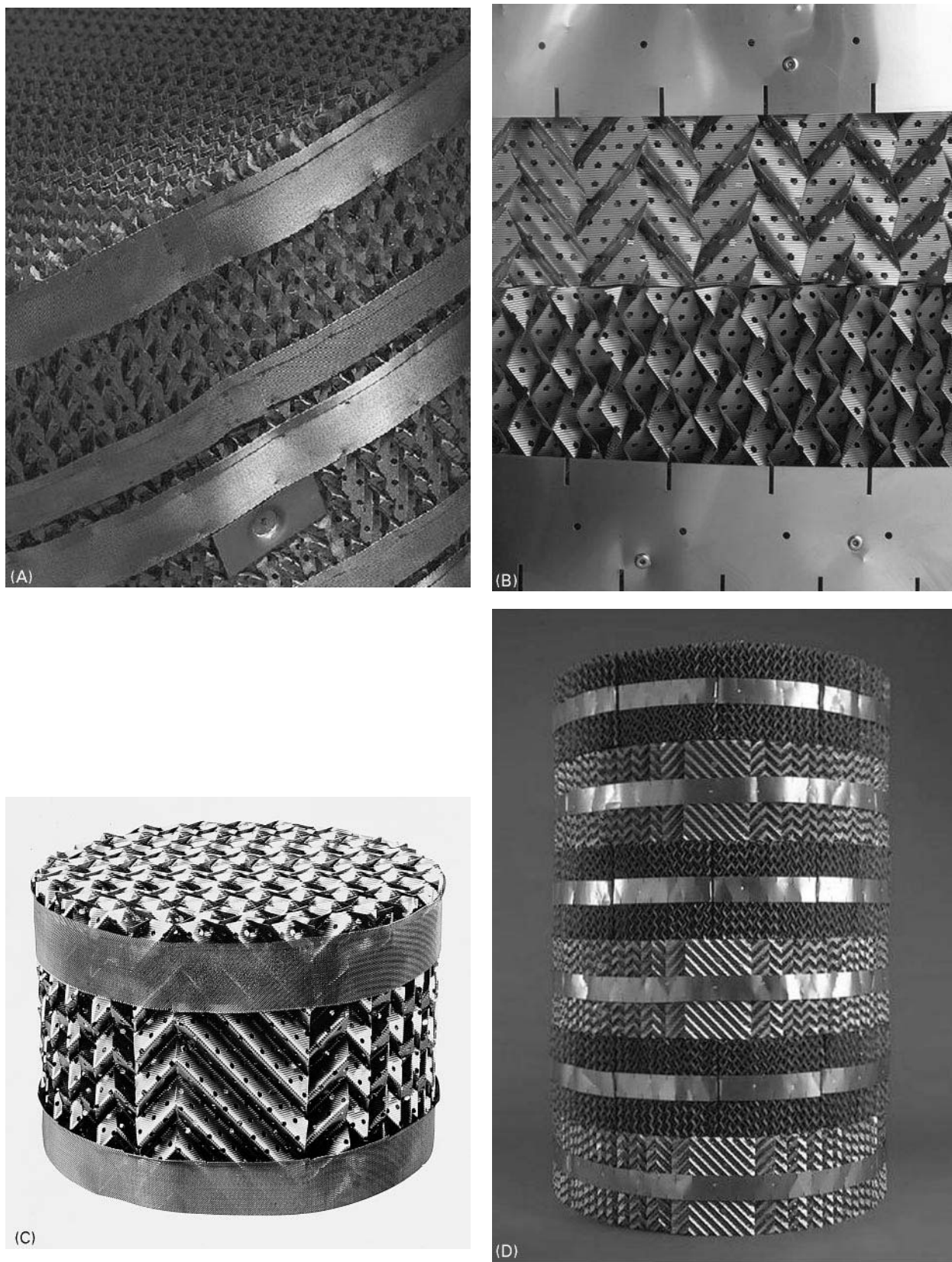


Figure 4 Structured packings: (A) Wire gauze structured packing. Close view, packing and wiper bands. (Photo courtesy of Koch-Glitsch Inc.) (B) Two structured packing layers rotated 90°. (Photo courtesy of Koch-Glitsch Inc.) (C) One structured packing element for small towers. (Photo courtesy of Sulzer Chemtech.) (D) Structured packed bed for a small tower. (Photo courtesy of Koch-Glitsch Inc.) (E) Packed bed for a large tower built in sections. (Photo courtesy of Norton Chemical Process Products Corp.)

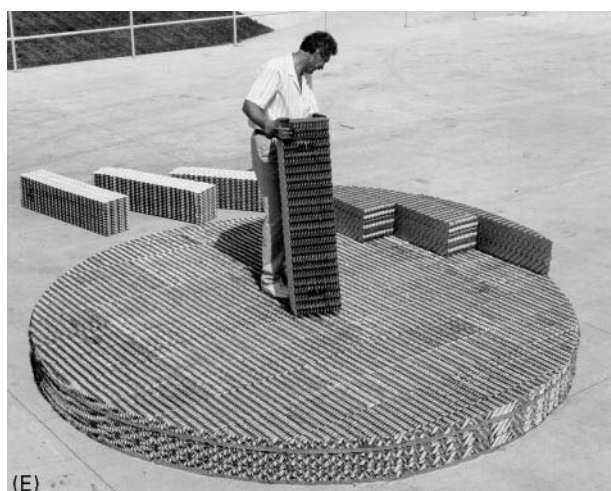


Figure 4 Continued

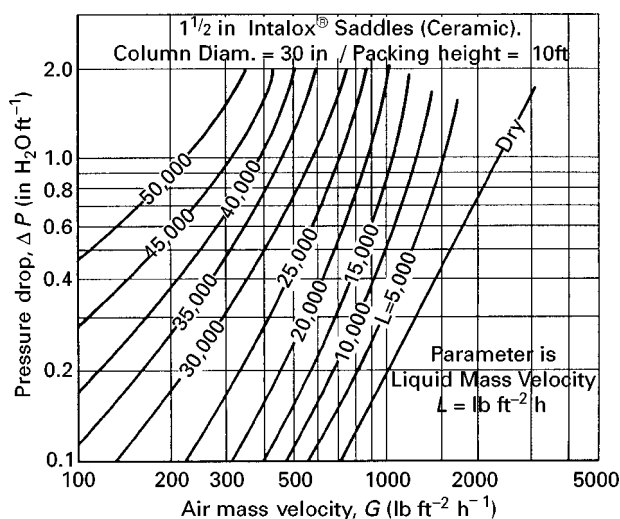
$$L_f = L(62.4/\rho_1)(F_p/20)^{0.5}\mu_1^{0.1} \text{ (for } F_p \text{ over 15)}$$

$$C_2 = 7.4 \times 10^{-8} \text{ and } C_3 = 2.7 \times 10^{-5}$$

For the case of dry packing $L_f = 0$, the pressure-drop equation reduces to:

$$\Delta P = C_2 G_f^2 = C_2 (0.075/20) F_p G^2 / \rho_g. \quad [3]$$

Figure 5 presents a family of pressure drop-lines at constant liquid flow as a function of the vapour flow. The constant liquid rate lines start parallel to the

Figure 5 Bed ΔP vs. rates. (Permission from Gulf Publishing Company.)

dry-column line (which is a function of the drag only). Equation [3] allows calculation of the packing factor, F_p , by measuring the slope of the dry-packing pressure-drop data. As the vapour rate increases, the slope of the constant liquid rate lines increase; this increase is also proportional to the liquid rate. The initial departure from the dry-line slope indicates interaction between the vapour and liquid, and represents a loading point. Efficient mass-transfer operations can be achieved only above the loading

Table 2 Packing selection guidelines (trays included as a reference)

Application in distillation	Random packing	Structured packing	Traditional trays	High-capacity trays
Pressure drop/theoretical stage	2	1	3	3
Maximum capacity ^a	2	1	3	2
Efficiency at high pressure	2	4	2	1
Efficiency at low pressure	2	1	2	3
Efficiency at low liquid rate ^c	2	1	3	4
Efficiency at high liquid rate ^d	3	4	2	1
Low residence time	2	1	4	4
High residence time	3	4	1	1
Heat transfer	2	1	2	2
Foaming systems	2	2	3	3
Non-metallic services ^b	1	2	4	4
Fouling systems	4 ^f	2 ^f	1 ^e	1 ^e
Efficiency in high δ systems	2	4	1	1
Inspection and maintenance	3	4	1	1
Low cost	2	4	1	3

Application rating: 1, best; 2, good; 3, fair; 4, poor.

^aEfficiency may be reduced at high capacities.

^bAs may be required based on corrosion protection considerations, such as ceramic.

^cSystems below 5 gallons min⁻¹ ft⁻².

^dSystems over 15 gallons min⁻¹ ft⁻².

^eApplies to sieve trays, specially dual-flow, not to valve trays.

^fIt would require a fouling-resistant distributor, which may result in reduced efficiency.

point. For any given liquid rate, as the vapour rate further increases, the pressure-drop line slope increases rapidly until the line becomes near vertical. At this point the flow and ΔP are unstable, and the bed is flooded; the vapour flow does not allow the liquid to flow down the bed and there is massive entrainment of liquid in the vapour phase and mass transfer is no longer viable.

For most packings, bed flooding occurs between 1 and 2 inches of water-pressure drop per foot of packing. Pressure drop at flooding seems to be a function of the packing size. Kister cited Zenz and later Strigle and Rukovena observations indicating that flooding (ΔP_f) is higher for smaller size packings, and proposed a correlation to determine the pressure drop at flooding as a function of the packing factor.

$$\Delta P_f = 0.115(F_p)^{0.7} \quad [4A]$$

We also obtained by regression from data published by Strigle:

$$\Delta P_f = 0.146F_p^{0.75} \text{ inch liquid ft}^{-1} \text{ or} \quad [4B]$$

$$\Delta P = 0.146S_g F_p^{0.75} \text{ inch H}_2\text{O ft}^{-1} \quad [5]$$

Pressure drop at incipient loading may be estimated:

$$\Delta P_l = 0.072S_g F_p^{0.75} \quad [6]$$

and pressure drop at maximum efficiency loading may be estimated by:

$$\Delta P_e = 0.082S_g F_p^{0.75} \quad [7]$$

All the above correlations have been regressed for metallic random packings (Pall Rings and IMPT®).

For column design, it is well-accepted practice to assume flooding at 1 inch of water per foot of packing pressure drop and design the packing for an operation at 80% flood. However, when reliable packing-factor information is available, the use of the calculated ΔP_f , using one of the eqns [4A], [4B] and [5], is a more accurate approach.

Caution: Presence of foam, even incipient foam, has a great impact on a packing column pressure drop and performance and should be avoided. Amines, insoluble fine solids (such as corrosion products), high-viscosity organic liquid (0.5–1 cP or higher) and immiscible liquids are known to foam. For these systems, or other systems known to be prone to foam, continuous or intermittent dosing of antifoam agents may be required to maintain an efficient packed-column operation. Nevertheless, uncontrol-

led antifoam injection is known to aggravate foaming problems. Filtration of liquids and adsorption of contaminants on activated carbon has proven valuable to control foaming in some systems such as amines.

Flooding Correlations

Several generalized flooding and pressure-drop correlations have been proposed for commercial packings. Sherwood, Shipley and Holloway presented the first correlation between a 'flow parameter' X defined as:

$$X = (L/G) (\rho_g/\rho_l)^{0.5} \quad [8]$$

and a 'flooding parameter' Y defined as:

$$Y_f = (u_g^2/g_c)(a/\varepsilon^3)(\rho_g/\rho_l)\mu^{0.2} = (G_f^2/g_c)(a/\varepsilon^3)\mu^{0.2}/(\rho_g\rho_l). \quad [9]$$

Sherwood and co-workers correlated dumped and stacked random packing data and found that Y_f is around five times higher for stacked than for dumped packing, which means that mass velocity at flood is over two times higher for stacked packing. This was the precursor idea for the later development of 'structured' packings.

Lobo and Friend presented a similar correlation of Y and X with indication of pressure-drop lines and flooding line.

Leva proposed a similar correlation with the same flow parameter given by eqn [8] and modified the flooding parameter $Y_f = (G_f^2/g_c)(a/\varepsilon^3)\mu^{0.2}(\rho_w/\rho_l)^2/\rho_l$. According to this correlation, minimum loading Y_m occurs at about one-third of Y_f which means that loading starts at 50% of the mass flow rates corresponding to the flooding point.

Eckert observed that the packing geometrical properties factor (a/ε^3) did not represent correctly the packing in the flooding correlations. He introduced a packing factor, F_p . The value of F_p is determined experimentally from pressure-drop data. The new flooding parameter became:

$$Y_f = (G_f^2/g_c)F_p\mu^{0.2}(\rho_w/\rho_l)^2/(\rho_g\rho_l) \quad [10]$$

and is correlated to the same flow parameter $X = (L/G) (\rho_g/\rho_l)^{0.5}$.

The most recent proposed correlation was presented by Strigle (see Figure 6):

$$Y = C_s F_p^{0.5} (\mu/S_g)^{0.05} = C_s F_p^{0.5} v^{0.05} \quad [11A]$$

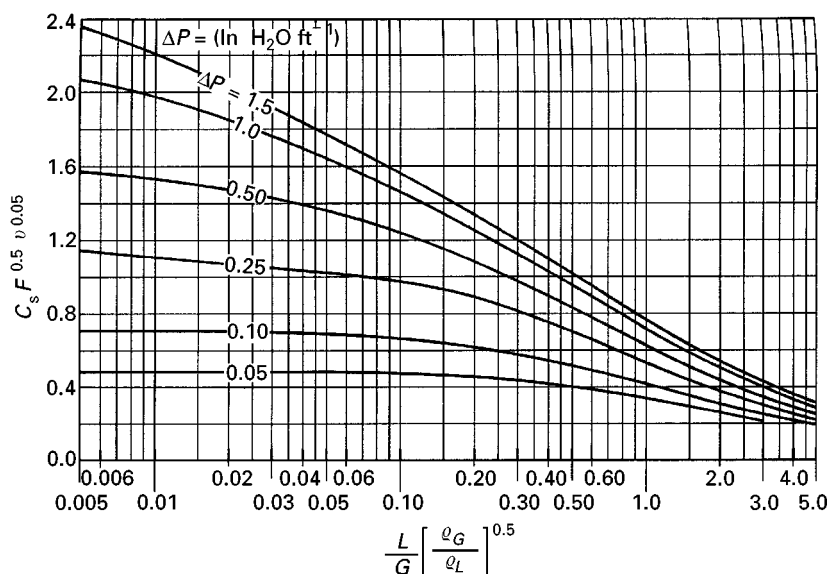


Figure 6 Strigle pressure drop chart. (Permission from Gulf Publishing Company.)

Y is the vapour flow parameter and is a function of vapour capacity factor $C_s = u_g(\rho_g/(\rho_l - \rho_g))^{0.5}$, the packing factor and the kinematic viscosity $v = \mu/S_g$. Note that at flooding $Y = Y_f$. Y is plotted in a linear ordinate as a function of the flow parameter X in a logarithmic abscissa and a family of constant ΔP lines. No flooding line is shown. The advantage of the linear ordinate is that it is easier to interpolate than the older log-log charts.

Figure 7 presents the flooding lines of packings as a function of the packing factor F_p and the flow parameter X . The ordinate is the modified flooding parameter Y_f^* , defined as follows:

$$Y_f^* = Y_f/F_p^{0.5} = C_s v^{0.05} \quad [11B]$$

Y_f^* is plotted as a function of the flow parameter X , eqn [8], at constant packing factors.

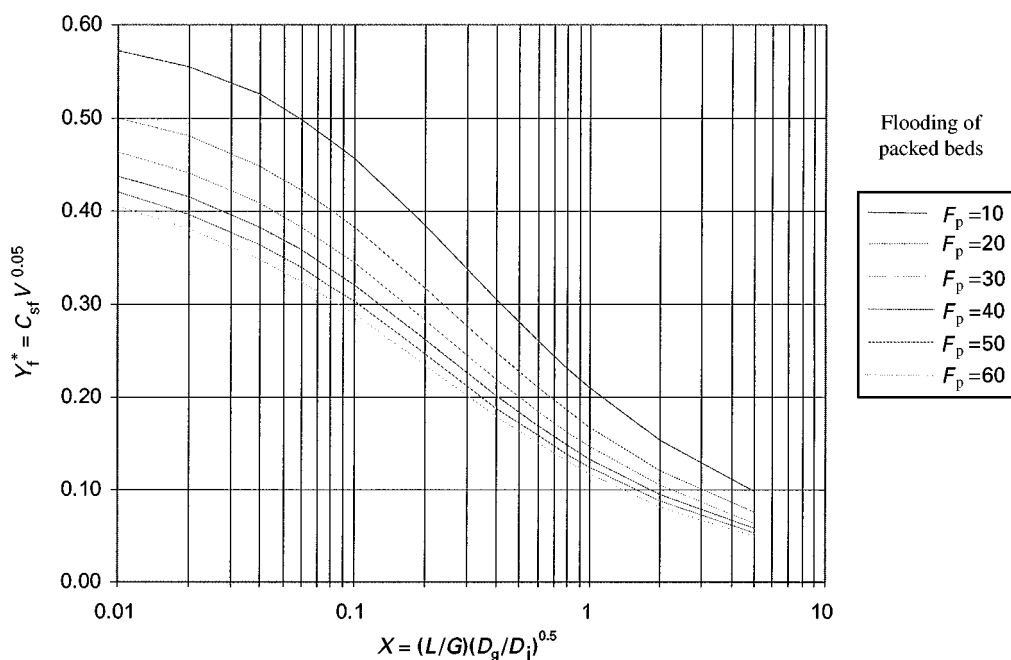


Figure 7 Modified flooding parameter as a function of the flow parameter.

Comparing Packed Column vs. Tray Tower Capacity

Table 5 presents packing capacities, calculated from the above relations, compared to tray flooding capacities at several tray spacings.

Packed Tower Diameter

Figures 6 or 7 can be used to determine the column diameter. Using Figure 7 the procedure is as follows:

1. Determine the value of the abscissa $X = L/G(\rho_g/\rho_l)^{0.5}$.
2. Obtain from the manufacturer the selected packing F_p value, or from Tables 3 or 4.
3. Determine the ordinate $Y_f^* = C_s v^{0.05}$ from Figure 7.
4. Calculate the capacity factor at flood C_s from the Y_f^* value, the gas velocity at flood $u_g = C_s(\rho_l - \rho_g)^{0.5}/\rho_g$ and the flooding gas mass velocity $G_{fl} = u_g \rho_g$.
5. Determine the column cross-sectional area $A_c = V/(0.8G_{fl})$, based on 80% of the G flooding rate. This is standard design practice for new column sizing, and allows for normal flow fluctu-

ations that occur in actual operations and for process control requirements.

6. Determine the column diameter $D_c = 12(4A_c/\pi)^{0.5}$.

Turndown and Minimum Wetting Flow

In general, the turndown of a packed tower is limited to the turndown of the liquid distributor, which is its ability to reduce liquid load and still maintain a homogeneous distribution. Most standard liquid distributors can operate efficiently at 50% of its design liquid load; turndown as low as 25% can be achieved.

To operate efficiently as mass-transfer devices, packing should be homogeneously wetted to assure use of the total surface. Minimum recommended values of liquid irrigation depend on the packing material and surface wettability, as follows:

Random packing

Ceramic	0.2 gallons min ⁻¹ ft ⁻²
Surface-treated or rusted metals	0.5 gallons min ⁻¹ ft ⁻²
Glass, glassed ceramic and stainless steel	1.0 gallons min ⁻¹ ft ⁻²
Plastics	1.5–2.9 gallons min ⁻¹ ft ⁻²

Table 3 Random packing design parameters

Packing metal	Nominal size	Packing factor (F_p)	Specific surface ft ² ft ⁻³ (a)	Void ft ³ ft ⁻³ (e)	Bulk density (lb ft ⁻³)
Pall Rings	0.625	81	103	0.918	39.9
	1	56	61	0.953	23.1
	1.5	40	39	0.971	14.3
	2	27	30	0.969	14.1
	3.5	18	18	0.972	13.9
CMR®	0	60	103	0.957	20.96
	1	38	76	0.968	15.51
	1.5	33	57	0.961	18.66
	2	26	44	0.970	14.29
	2.5	21	38	0.974	12.54
	3	14	32	0.979	10.22
	4	12	23	0.985	7.36
IMTP®	5	8	15	0.989	5.46
	No 15	51	88.7	0.961	17.9
	No 25	41	69.8	0.970	14.1
	No 40	24	46.9	0.969	14.6
	No 50	18	31.2	0.981	9.3
	No 60	16	25.3	0.982	8.7
Nutter Rings®	No 70	12	17.5	0.984	8.1
	0.7	N/A	69	0.978	11.0
	1.0	30	51	0.978	11.1
	1.5	24	38	0.978	11.3
	2.0	18	29	0.979	10.8
	2.5	16	25	0.982	9.0
	3.5	13	20	0.984	8.3

Table 4 Structured packing design parameters

Packing 45° Crimp angle	Size	Packing factor	Specific surface ft ² ft ⁻³ (a)	Void fraction (ε)	Bulk density (lb ft ⁻³)
Mellapak® (Sulzer)	125Y	10	35	0.989	5.09
	250Y	20	78	0.987	5.61
	350Y	23	107	0.983	7.8
	500Y	34	155	0.975	10.92
Sulzer BX (Gauze)	BX	21	150		
Gempack® (Koch Glitsch)	4A	55	138.1	0.942	17
	3A	23	91.4	0.962	9.9
	2A	15	67	0.972	6.3
	1A	9	35	0.977	4.7
Intalox® (Norton)	1T	28.0	95.2	0.980	10.14
	2T	20.0	65.3	0.984	8.23
	3T	15.0	51.9	0.987	6.55
	4T	13.5	40.6	0.986	6.75
	5T	12.0	27.0	0.991	4.5
Montz	B1-100		30		
	B1-200	20	61	0.94	
	B1-250		76		
	B1-300	33	91		

Structure packings

Surface-treated metals	0.2 gallons min ⁻¹ ft ⁻²
Plain surface metals	0.5 gallons min ⁻¹ ft ⁻²

especially for high-purity separations, only gravity distributions are used. **Table 6** illustrates the main type of distributors and the main factors to be considered for selection:

Type of Liquid Distributors

Liquid distributors can be gravity or pressure fed depending on how the liquid is introduced to the distributor. Pressure distributors are limited to heat transfer and some simple mass-transfer operations, mainly in stripping or absorption. For distillation,

Table 5 Relative capacity of packing and trays^a

Tray spacing	Ratio of packing to tray capacity according to packing factor (F _p)					
	10	20	30	40	50	60
36 inches	1.15	0.96	0.87	0.81	0.76	0.73
24 inches	1.45	1.22	1.10	1.03	0.97	0.93
18 inches	1.90	1.60	1.44	1.35	1.27	1.22
12 inches	2.41	2.03	1.84	1.71	1.62	1.55

^aTray capacity based on the column full cross-sectional area, without discounting any area for downcomers (which implies high-capacity trays). For conventional trays the ratio of packing capacity/tray capacity will be higher. Tray capacity taken from the generalized correlation of tray flooding proposed by Fair JR and Matthews RL (*Petroleum Refiner* 37(4): 153). The packing capacity taken from the generalized correlations presented by RF Striegler Jr and Figure 6).

- *Pipe orifice headers (POH)* (**Figure 8**) consist of a pipe ladder arrangement with calibrated orifices drilled in the pipe laterals in a uniform layout. POH can be pressure or gravity fed.
- *Pan distributors (PAN)* (**Figure 9**) consist of a flat horizontal plate (tray) with uniformly spaced calibrated orifices that allow the passage of liquid to the packing below. Round or rectangular risers (chimneys), located within the orifice pattern, distribute the vapour to the packing above. The riser layout should be uniform and should not interfere with the uniformity of the orifice layout. PAN distributors are always gravity fed.
- *Narrow trough distributors (NTD)* (**Figure 10A and 10B**). This distributor is composed of a series of narrow (3–4 inches) parallel troughs fed by one or more larger troughs (parting boxes) oriented at 90° from the narrow troughs. The narrow troughs distribute the liquid to the packing below, through calibrated orifices drilled at the bottom or at the wall. NTD are always fed by gravity.
- *Spray nozzle header (SNH)* (**Figure 11**). They are similar to POH but spray nozzles are used instead of orifices. The density of nozzles in the SNH is lower than the density of orifices in the POH. The SNH relies on the liquid cone leaving the nozzle for

Table 6 Guidelines for distributor selection

	Gravity-fed distributors			Pressure-fed distributors	
	POH	PAN	NTD	POH	SNH
Uniformity	1	1	1	2	3
High-purity fractionation	1	1	1	3	3
Maximum drip points per area	2	1	1	2	2
For large diameter towers (over 10 ft)	1	3	1	1	1
Leakage potential	C	H ^a	C	C	C
For high liquid rates	2	1	2	2	1
For high vapour rates	1	3	1	1	1
Residence time	C	A	B	C	C
Solids handling	3	3	2 ^b	2	1
Turndown	1	1	1	1	3
Easy installation and levelling	1	3	2	1	1
Cost	B	A	A	C	C

1, Good; 2, fair; 3, poor; A, high; B, medium; C, low.

^a Unless it is seal-welded.

^b Very good if a V-notch is provided at the top of the trough wall for liquid flow. Nevertheless, the quality and turndown of the distributor are affected.

further spreading. This results in either an overlap or a gap of the cone projection over the packed bed, and deteriorates the uniformity of the distribution. SNHs can handle very large liquid rates and are very efficient for heat transfer.

Liquid Mixing, Redistribution and Maximum Bed Height

Initial liquid distribution is essential to achieve good packed tower efficiency. Hoek suggested that at a given flow rate, each packing has its natural distribution determined by its radial spreading coefficient. Although this effect does spread the initial liquid distribution, this effect is not sufficient to correct poor initial distribution. Radial concentration gradients already established at the top of the bed cannot be compensated by additional packing. The result is permanent efficiency loss.

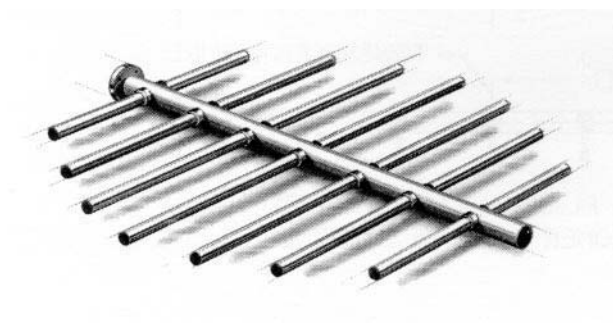


Figure 8 POH distributor. (Courtesy of Norton Chemical Process Products Corp.)

In general, if a good distribution is established at the top of the bed, the packing will develop its natural distribution and maintain it for bed depths of 10 NTS or more. Columns requiring more than 10 NTS per section should be subdivided into several packing beds to maintain coefficient HETP values. Liquid redistribution, and often mixing, are required between these bed sections.

Distributor Design Parameters

Distributor Liquid Level and Hole Diameter

The basic distributor design equation relates the total orifice open area, the liquid head and the volumetric flow:

$$Q = C_o n a_0 (h - h_d)^{0.5} \quad [12]$$

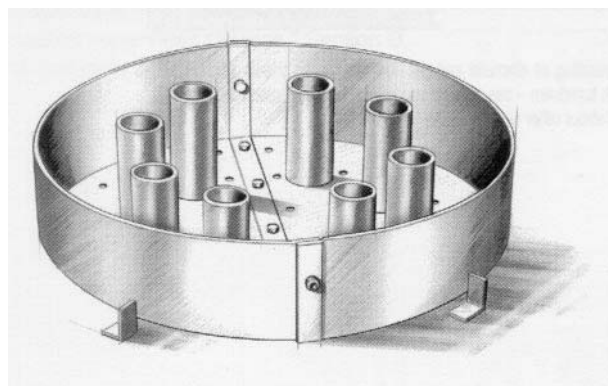


Figure 9 PAN distributor.

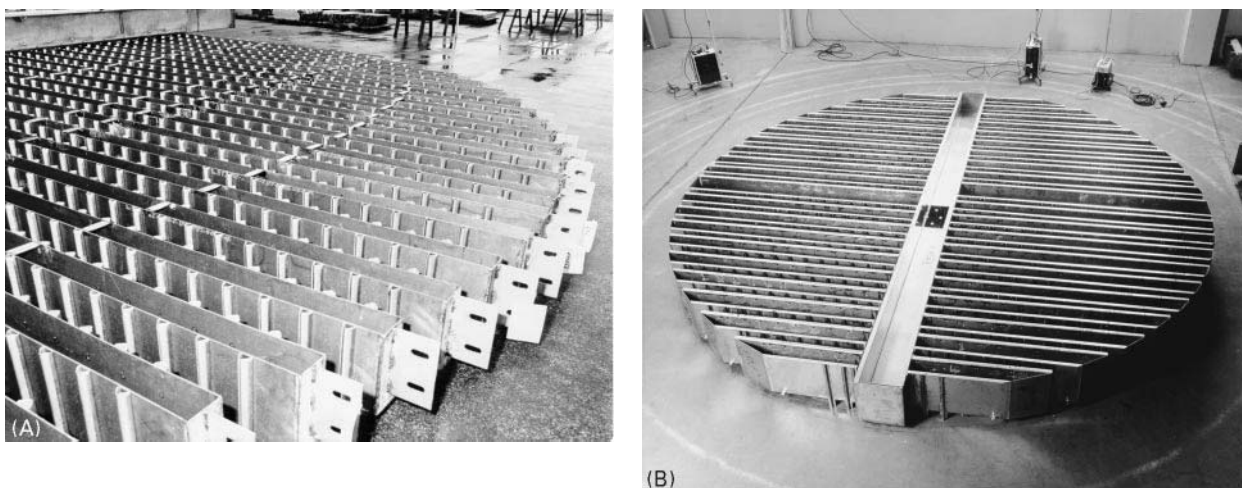


Figure 10 NTD distributor: (A) Photo courtesy of Norton Chemical Process Products Corp. (B) Photo courtesy of Koch–Glitsch Inc.

where Q is the volumetric flow rate, C_o the orifice flow coefficient, n the number of orifices, a_o the open area of one orifice, h the liquid head over the orifice, and h_d the vapour-pressure drop across the distributor given in head of liquid. The value of C_o varies between 0.5 to 0.8 and is near 0.6 for most commercial distributors. Using this value, eqn [12] becomes:

$$Q = 4.0nd^2(h - h_d)^{0.5}$$

and:

$$n = 0.25Q/d^2(h - h_d)^{0.5} \quad [13]$$

The minimum recommended orifice diameter, to prevent plugging, is 3/8 inch for carbon steel and 1/8 inch for stainless steel. The minimum recommended liquid level at minimum flow is 2 inches. If a 50% turndown is specified, the required liquid level at normal liquid load becomes 8 inches.

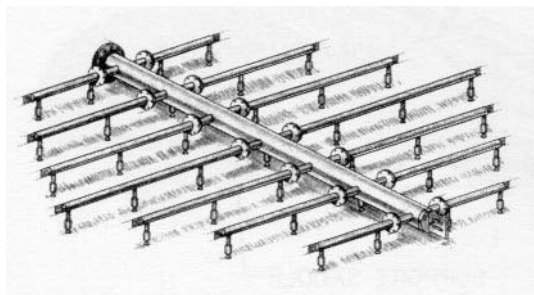


Figure 11 SNH distributor. (Courtesy of Norton Chemical Process Products Corp.)

Uniformity of the Drip Point Layout

Density of liquid drip points is not enough to assure a good distributor quality. The distribution must be homogeneous; the same amount of liquid should irrigate the packing at any fraction of the tower cross-sectional area. Areas near the tower wall should receive the same amount of liquid as areas near the centre.

Other Considerations

A number of factors need to be considered when selecting and designing packing and distributors.

Ratio Tower to Packing Size

The minimum recommended ratio of the tower diameter to the packing size is 8. In the case of structured packings, this ratio applies to the ratio of the tower diameter to the crimp size.

Fouling

Some solids are usually present even in 'clean systems' because of corrosion products, especially after maintenance shutdowns, when rust and debris can remain in the tower. The tower shell metallurgy should be adequate to prevent formation of scale or corrosion products that can plug distributors. Distributors with small orifices should be protected with filters in all liquid lines entering the tower. In other cases, solids are expected to be present because of the process itself. In these cases the distributor should be designed to handle the solids. A NTD distributor with V-notches for liquid overflow is adequate to handle

some slurries. SNHs can also handle slurries but their application is limited to heat transfer.

Vapour Distribution Requirements

Vapours entering the tower have a kinetic energy proportional to their velocity, which is converted into pressure as the vapour turns to start flowing upward in the tower. The resulting radial pressure profile is not uniform; areas of higher pressure would allow higher vapour up-flow. This is especially critical for low-pressure drop packings such as structured packings. Vapour radial velocity profiles are corrected by pressure drop and by diffusion devices. The following is the recommended practice for vapour distribution:

- Low vapour inlet velocity (velocity head below 0.5 inches of water): no inlet distributor required, provide as minimum $1\frac{1}{2}$ column diameters, or 36 inches between the top of the vapour inlet nozzle and the bottom of the bed.
- Intermediate vapour inlet velocity (velocity head between 0.5 and 1.5 inches of water): provide an inlet vapour diffuser directing vapour flow down the tower. This type of device can be a horizontal pipe with the bottom half cut as shown at the bottom of the column in **Figure 2**. Vertical baffles can be provided for better vapour distribution. The purpose of these baffles is to stop the horizontal velocity component of the vapour.
- High vapour velocity (velocity heads above 1.5 inches of water): provide an inlet vapour diffuser, as described above, plus a small riser chimney tray with a pressure drop of a minimum of 2 inches of water. The pressure drop can be created by orifices at the bottom of the risers. A vapour distributor, as shown in **Figure 12** is a good alternative to the vapour diffuser in critical systems.

Distributor Testing

Water test of assembled distributors at the manufacturer's workshop is always a good practice for all high-efficiency distributors. The test should determine liquid rate gradients under the distributor, liquid level in the distributor itself at design and

turndown liquid rate, liquid level gradient in the trough and uniformity of the drip point layout. These parameters should be compared to the distributor design parameters and adjustments made to the distributor if necessary. **Figure 13** shows a distributor testing facility.

Packing Performance in Distillation

Factors to Consider in Determining the Column Design HETP

The height equivalent to a theoretical plate (HETP) is determined by the following main three factors:

Intrinsic geometric shape and size of the packing

This factor determines the surface per unit of volume, and the packing capacity of establishing effective vapour liquid interfacial surface. It is a well-known fact that, for any packing, the smaller its particle size, the larger its surface : volume ratio, and the lower the HETP value. All the other factors being equal, numerous available data tend to indicate that the expected reference packing $HETP_o$ may be correlated as follows:

$$HETP_o = K_p / F_p^f \quad [14]$$

where F_p is the packing factor. The constants K_p and f for different types of commercial packing are correlated as in **Table 7** for a reference system.

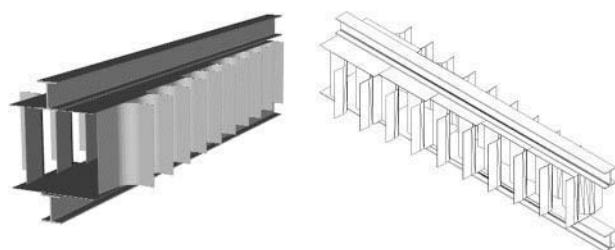


Figure 12 Vapour distributor. (Courtesy of Sulzer Chemtech.)



Figure 13 Distributor testing facilities. (Photo courtesy of Koch-Glitsch Inc.)

Table 7 HETP correlation factors for a reference system, regressed by the authors for eqn [14]

Packing	Constant K_p	Exponent f
<i>Structured packings</i>		
Sulzer Mellapak®	126	0.73
Koch Flexipac®	100	0.69
Koch-Glitsch Gempak®	120	0.76
Average of above structured packings	106	0.70
<i>Random metallic packings</i>		
Koch-Glitsch CMR®	73	0.43
Norton IMPT®	198	0.69
Pall Rings	250	0.69
Average above random packings	110	0.50

properties:

$$\text{HETP} = \text{HETP}_o (\mu\alpha/S_g\delta)^n / (\mu\alpha/S_g\delta)_o^n \quad [15]$$

when the n exponent best fit is between 0.15 and 0.21. Replacing HETP_o from eqn [14] into eqn [15], and using the reference system we obtain:

$$\text{HETP} = (2.0K_p/F_p^f) (\mu\alpha/S_g\delta)^{0.2} \quad [16]$$

In addition, theoretical considerations suggest that the HETP is related to $\lambda = m/(L/V)$, the ratio of the slopes of the equilibrium line and operating line, by the correlation:

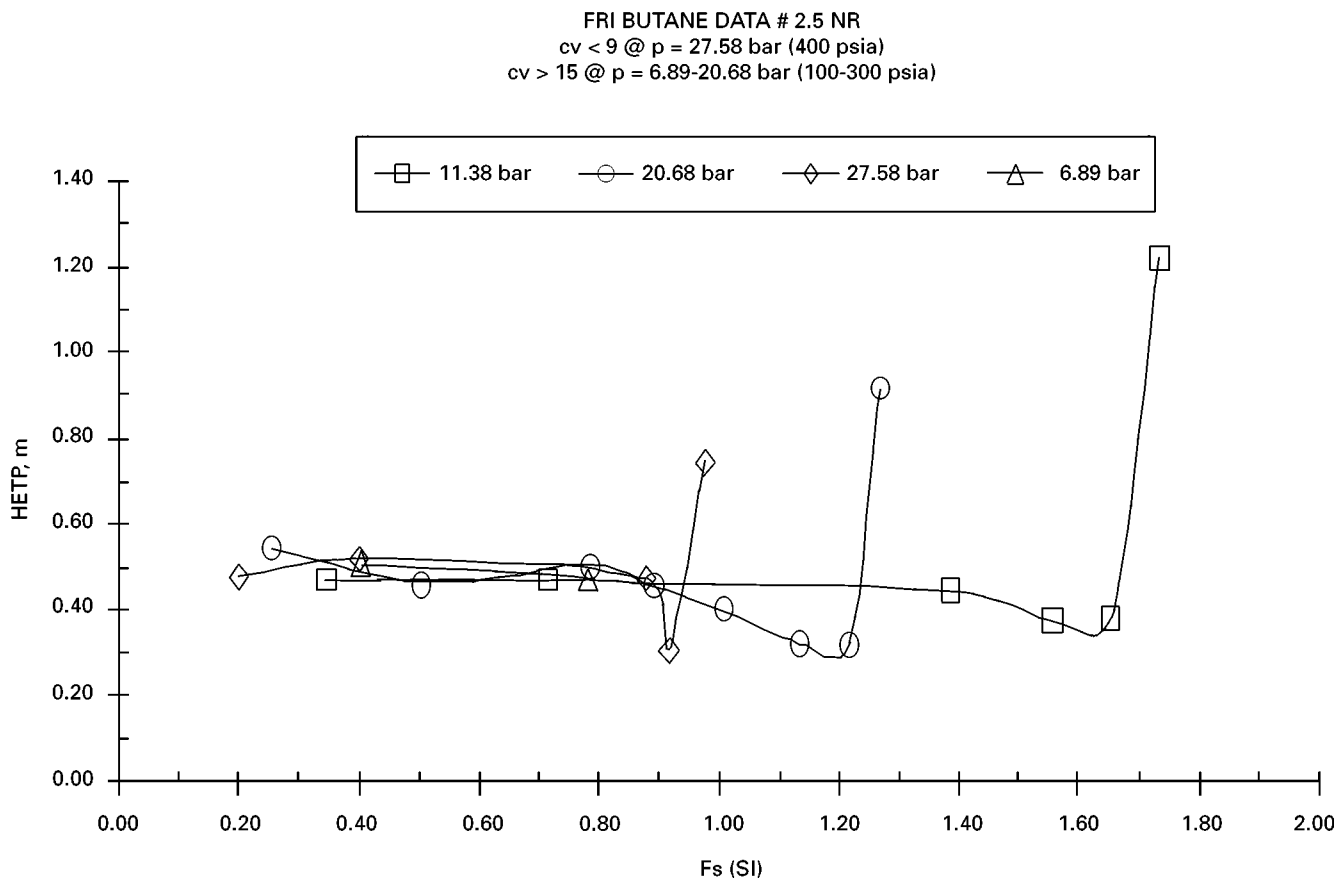
$$\text{HETP} = \lambda \ln(\lambda)/(\lambda - 1) \text{HTU}$$

System properties Numerous investigations have tried to correlate experimental HETP data with the distillation system fluid physical properties. The best and most consistent correlations tend to confirm that the HETP is proportional to reference HETP_o and a factor proportional to the system physical

where HTU is the height of a transfer unit. Then:

$$\text{HETP} = (2.0K_p/F_p^f) (\mu\alpha/S_g\delta)^{0.2} f(\lambda) \quad [17]$$

Packing loading Figure 14 shows the pilot plant performance of Sulzer/Nutter ring No. 2.5 in

**Figure 14** HETP vs. loads. (Courtesy of Sulzer Chemtech.)

isobutane-n-butane separation. Note that although only the vapour rate appears in the abscissa, actually both the vapour and the liquid rates increase in the same proportion since the chart was developed at total reflux. All packings present similar curves in small size experimental columns. The initial HETP is high (low efficiency) owing to the low loads that result in liquid maldistribution, poor packing wetting and little interaction between the vapour and the liquid (this left section of the curve is not shown in Figure 14). Nevertheless, the HETP continuously decreases as the loads increase. At a point, corresponding to the loading point of the packing, the HETP becomes constant over a range of loads. This range represents the operating range of the packing. As the loads continue to increase, the HETP shows a dip corresponding to high interaction between the fluids, followed by a rapid increase in the HETP caused by recirculation of liquid within the bed. This corresponds to the initial flooding of the bed.

Maldistribution

Liquid maldistribution has a very large effect on column distillation performance. Liquid maldistribution is originated by uneven liquid flow from the distributor to the top section of the packing. Some degree of maldistribution cannot be avoided and it is related to the following factors.

Drip points density (total drip points/column cross-section area) In principle, a smaller number of drip points equates to a higher initial maldistribution. This could be solved by constructing distributors with a high number of drip points. However, there are physical and mechanical limits that make it difficult to build distributors with more than 20 drip points ft^{-2} . It has also been demonstrated that if the distributor deck is not levelled, the resulting maldistribution effect may increase as the number of drip points is increased above an optimal number. The optimal number of drip points is related to the liquid irrigation flow as follows (Figure 15):

Liquid irrigation $\text{g} \cdot \text{m}^{-1} \cdot \text{ft}^{-2}$	0.25	0.5	1.0	2.0	4.0
Optimum number drip points per square foot	5	8	13	21	32

Furthermore, the drip points themselves may create additional maldistribution if they are not evenly distributed across the entire column cross-sectional area. Poor construction making holes of variable diameters or unlevelled installation of the distributor will also

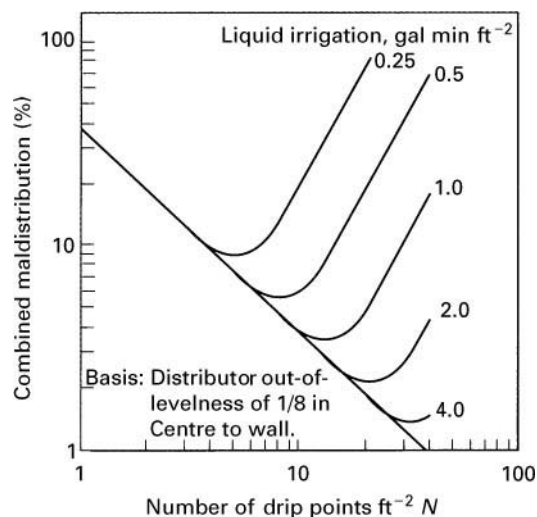


Figure 15 Effect of number of drip points and liquid irrigation rate on maldistribution. (Permission from Chemical Engineering Progress.)

induce additional maldistribution. Operational problems such as plugging of the distributor deck areas will cause large sectors to be dry, thus producing a macroscopic or sectorial maldistribution.

Maldistribution and spreading factor Initial maldistribution produces a condition of uneven liquid/vapour flow ratio across the column cross-sectional area. Some areas or spots are underirrigated and some are overirrigated. The column packing does spread the liquid resulting in some correction or attenuation of the initial maldistribution. The overall weighted maldistribution is attenuated better in small diameter columns than in larger columns. This is determined by the nondimensional number (Z_b/CD_c^2) , where Z_b is the bed height in feet, D_c the column diameter in inches, and C is the spreading factor in $\text{ft} \cdot \text{in}^{-2}$ units (see Figure 16). The spreading factor is related to the packing particle size and the liquid irrigation.

The lost column efficiency is proportional to the liquid maldistribution, and this effect is amplified by the number of theoretical stages required to achieve the separation. Figure 17 presents a useful correlation for the calculation of the column efficiency in packed distillation columns.

Liquid distributor quality The liquid distributor intrinsic maldistribution, M_d (related to its design and manufacture) should be measured at the factory by a water test measuring the liquid flow under each subsection of the column cross-section. The smaller and more numerous the test area subdivisions, the more precise will be the maldistribution

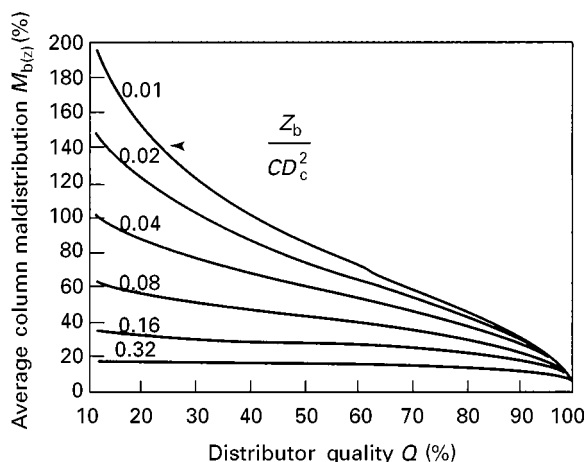


Figure 16 M vs. Z_b/CD_c^2 . (Permission from Chemical Engineering Progress.)

measurement. The mathematical expression of the maldistribution is:

$$M_d = 100[\Sigma((L_i/L_{av} - 1)^2)/n]^{0.5} \quad [18]$$

for each point area subdivision from $i = 1$ to $i = n$. The following is the correlation between distributor quality and its maldistribution:

$$Q_d (\%) = 100/[1 + (M_d/100)^2] \quad [19]$$

If the distributor quality is 90%, the actual measured maldistribution should not exceed 33%. A 95% quality implied a maximum measured maldistribution of 23%.

Total maldistribution Additional maldistribution can originate from operational factors related to levelness and obstructions. The total initial maldistribution, M_o , can be calculated by:

$$M_o = (\Sigma M^2)^{0.5} \quad [20]$$

Assuming a maximum operational maldistribution $M_{op} = 15\%$, and using a 90% distributor quality ($M_d = 33\%$), the total effective operating maldistribution at the top of the packing is $M_o = (33^2 + 15^2)^{0.5} = 36.2$.

The effective bed attenuated maldistribution is calculated by the following equation:

$$M_{bz} = M_o/[1 + 0.16M_o(Z/CD_c^2)] \quad [21]$$

With this M_{bz} value, the bed efficiency E_z may be obtained from Figure 17. The calculated bed efficiency should be used to correct the packing HETP and obtain the bed operating HETP_{op}:

$$\text{HETP}_{op} = \text{HETP } E_z/100 \quad [22]$$

$$\text{HETP}_{op} = [(2.0 K_p/F_p^f)(\mu\alpha/S_g\delta)^{0.2} f(\lambda)]E_z/100. \quad [23]$$

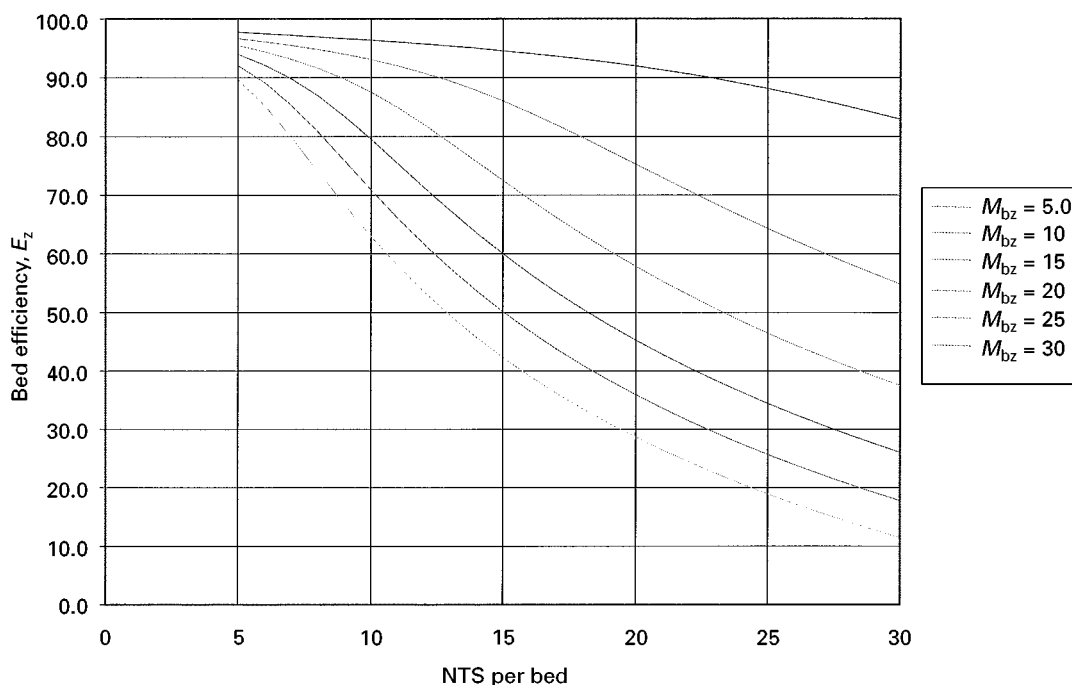


Figure 17 Efficiency vs. NTS.

The bed effective number of theoretical stages can be calculated by:

$$\text{NTS} = Z/\text{HETP}_{\text{op}}. \quad [24]$$

For a column requiring more than 10 NTS, it is in general advantageous to subdivide the packing in two or more beds and limit the NTS per bed to around 10. The lower the NTS per bed, the higher the resulting bed efficiency. The limiting factor of subdividing the column into a large number of redistributed beds, is the extra column height (or the effective packed height loss for column revamps) necessary to accommodate each redistributor, and the resulting increased cost. For new columns, the optimal number of beds is the one that results in the required performance at minimum cost, for revamps, it is often the one that results in the maximum available overall NTS. The best choice in each case is determined by an optimization.

Future Developments

With the ability to accurately design and predict the performance of packings in distillation, it is expected that the use of packings in distillation will become better accepted, not only for plant revamps but also for grass roots applications. The design and evaluation of liquid distributors needs to be better understood by users and equipment manufacturers; standard methods for distributor quality rating should be implemented based on the basic concepts presented in this contribution. Readers interested in further exploring the column design methods outlined in this article may download a free demo of BDSIM at url <http://www.geocities.com/~combusem/BDSIM.HTM>

Nomenclature

A_c	Column cross-sectional area	ft ²
ΔP	Packing pressure drop	in ft ⁻¹
C	Packing spreading factor	ft in ⁻²
C_o	Orifice flow coefficient	
C_1, C_2, C_3	Constants in pressure drop correlations	
d	Orifice diameter	in
D_c	Column diameter	in
E_z	Bed efficiency	%
C_s	Vapour capacity factor, defined by $C_s = u_g(\rho_g/(\rho_l - \rho_g))^{0.5}$	ft s ⁻¹
ρ_g	Gas density	lb f ⁻³
ρ_l	Liquid density	lb f ⁻³
u_g	Vapour velocity	ft s ⁻¹

h	Liquid head over distributor orifice	inches of liquid
h_d	Vapour pressure drop across liquid distributor	inches of liquid
G	Vapour flow mass velocity	lb ft ⁻² h ⁻¹
G_f	Vapour flow mass velocity (in Robbins equation)	lb ft ⁻²
V	Vapour flow	lb h ⁻¹
L	Liquid mass flow	lb ft ⁻² h ⁻¹
L_f	Liquid mass flow	lb ft ⁻² h ⁻¹
L_i	Liquid mass flow at point i	gallons min ⁻¹ ft ⁻²
L_{av}	Liquid average mass flow	gallons min ⁻¹ ft ⁻²
F_p	Packing factor	
K_p	HETP correlation factor	
n	Number of measured points (in distributor testing)	
HETP	Height equivalent of a theoretical plate	in
HTU	High of a transfer unit	in
μ_l	Liquid viscosity	cP
S_g	Liquid specific gravity	
X	Flow factor = $(L/G)(\rho_g/\rho_l)^{0.5}$	
Y	Vapour flow parameter. At flooding $Y = Y_f$	
Y_f, Y_f^*	Flooding parameters, defined by eqns [10] and [11]	
a	Packing surface area	ft ² ft ⁻³
a_0	Open area of one drip point	
α	Relative volatility	
ε	Void fraction	
δ	Surface tension	dynes cm ⁻¹
g_c	Gravitational constant	32.2 ft s ⁻²
NTS	Number of theoretical stages	
R	Reflux ratio	
R_m	Minimum reflux ratio	
M_d	Maldistribution originated by the distributor design	%
M_o	Total initial maldistribution	%
M_{bz}	Effective bed maldistribution	%
Q	Liquid flow	gallons min ⁻¹
Q_d	Distributor quality	%
Z_b	Bed height	ft
ν	Kinematic viscosity constant = μ_l/S_g	
λ	Ratio of the equilibrium curve slope to the operating line slope	

See also: **I/Distillation:** Historical Development; Modeling and Simulation; Theory of Distillation; Tray Columns: Performance; Tray Columns: Performance; Vapour-Liquid Equilibrium; Correlation and Prediction; Vapour-Liquid Equilibrium: Theory.

Further Reading

- Bonilla J (1993) Don't neglect liquid distributors. *Chemical Engineering Progress* 83(3): 47.
- Eckert JS (1961) *Chemical Engineering Progress* 57(9): 54.
- Fair JR and Matthews RL (1958) *Petroleum Refiner* 37(4): 153.
- Klemas L and Bonilla J (1995) Accurately assess packed-column efficiency. *Chemical Engineering Progress* 91(7): 27.

- Kister HZ (1992) *Distillation Design*. New York: McGraw-Hill.
- Leva M (1954) *Chemical Engineering Progress* 50(10): 51.
- Lobo WE *et al.* (1945) *Transaction of the American Institute of Chemical Engineers* 41: 693.
- Robbins LA (1991) *Chemical Engineering Progress*, May, p. 87.
- Sherwood TK, Shipley GH and Holloway FA (1938) *Industrial and Engineering Chemistry* 30.
- Strigle RF Jr (1994) *Packed Tower Design and Applications*. Houston: Gulf Publishing.
- Strigle RF Jr and Rukovena F (1979) *Chemical Engineering Progress* 75(3): 86.
- Zenz FA (1953) *Chemical Engineering*, August, p. 176.

Pilot Plant Batch Distillation

**M. A. P. de Carvalho and
W. R. Curtis**, The Pennsylvania State University,
PA, USA

Introduction

Laboratory distillation encompasses an operating range from millilitres in bench-top devices to pilot units with the capacity for producing several hundred kilograms of product per day. While the design of bench-top assemblies is generally geared towards the achievement of a specified purity grade of the desired product, quantitative predictions are not usually feasible for such equipment and their construction relies a great deal on ingenuity and craftsmanship. For dedicated applications, glassware companies offer off-the-shelf equipment. This article will therefore focus on the pilot-scale units, where the analytical principles of mass and heat transfer can be applied to the operation, design and optimization of the equipment.

The section on theory presents analytical descriptions of batch distillation for three different approaches in order of decreasing complexity. It starts with a comprehensive model for a nonadiabatic, non-zero hold-up, nonconstant molar overflow, nonideal multicomponent column. The second model presented neglects stage hold-ups and assumes adiabatic stages and constant molar overflows to arrive at a set of equations describing the transient behaviour of the equipment, which can be solved for a binary system using a simple spreadsheet. If constant relative volatility and operation at minimum reflux are further

assumed, the derivation of a third model is possible, where the transient states within the equipment are given by direct analytical expressions.

The design of a batch column can be a challenging task because batch distillation presents unique considerations that are not addressed in most of the available literature, which is concerned with continuous operation. The section on design is a collection of advice and criteria for the design of batch columns. Specific information is given about equipment for batch distillation and accompanying instrumentation and safety circuitry. Details are drawn from a pilot-scale column that is installed in Penn State University's Department of Chemical Engineering. The section on column operation extends the scope of the two preceding sections by providing information on establishing operating strategies and operating protocols for batch runs. Much of this information is based on hands-on experience acquired with the column described in the subsection on equipment.

The last section is a synopsis of numerical techniques that have been developed in recent years to facilitate the optimization of the operation and design of batch columns. Inherent difficulties associated with the implementation of these numerical techniques into computer codes prevents their widespread use in equipment operation and design. However, it is likely that these techniques will be integrated into commercial simulators in the near future and be readily available to users with little knowledge of programming. The aim here is to introduce the reader to the topic, rather than to offer extensive coverage,

providing references for those interested in further reading.

Theory

The theory of batch distillation permits design, operation and optimization calculations by integrating the concepts of thermodynamic equilibrium, mass and heat transfer, energy and material balances to solve the problem of predicting the compositions and flow rates of process streams. The traditional approach to the development of governing equations is to model the equipment as a stack of equilibrium stages. Departures from ideality are taken into account by introducing the concept of stage efficiencies. Modelling in terms of equilibrium stages is convenient because of the availability of extensive equilibrium data for multicomponent systems and the associated predictive thermodynamic models. Packed columns, which do not possess physical mass transfer stages, can be translated into this technical framework by the use of the transfer unit concept (see, for example, McCabe *et al.*, 1993).

Relinquishing or including levels of complexity and interdependence in the fundamental equation and process variables will result in more or less rigorous treatments, with gains in accuracy usually being accompanied by substantial drawbacks in complexity and computational difficulty. Hereunder, three different sets of model equations are presented in decreasing levels of complexity. A rigorous approach to the problem involves the solution of a set of time-dependent differential and algebraic equations for the material and heat balances and for the equilibrium relations. Batch columns are usually constructed so that there is only one section, either above or below the feed stage. The typical column design depicted in **Figure 1** represents the rectifying section. From this simplification it is possible to write the following equations to define the problem completely in each stage except the top stage and the feed drum (reboiler).

Total material balance

$$\frac{dh_{\text{tot},i}^L}{dt} = L_{i-1} + V_{i+1} - L_i - V_i \quad [1]$$

Component material balances

$$h_{\text{tot},i}^L \frac{dx_{i,j}}{dt} = L_{i-1}x_{i-1,j} + V_{i+1}y_{i+1,j} - L_ix_{i,j} - V_iy_{i,j} \quad [2]$$

$i = 1, N_{\text{stage}}, j = 1, NC$

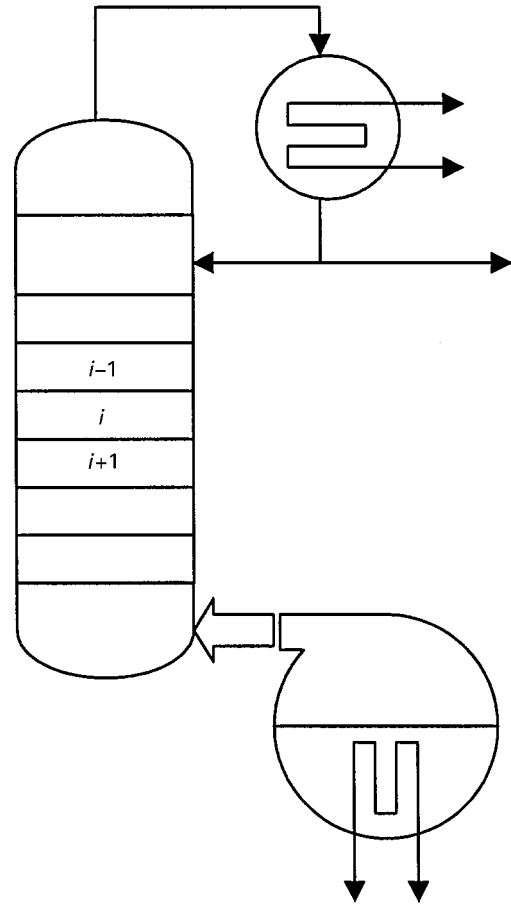


Figure 1 Batch distillation column schematic for a rectifying configuration.

Energy balance

$$\left(h_{\text{tot},i}^L \sum_{x=1}^{NC} x_{i,j} \frac{dH_{i,j}^L}{dT} \right) \frac{dT}{dt} = L_{i-1}x_{i-1,j}H_{i-1,j}^L + V_{i+1}y_{i+1,j}H_{i+1,j}^V - L_ix_{i,j}H_{i,j}^L - V_iy_{i,j}H_{i,j}^V + Q_i \quad [3]$$

$i = 1, N_{\text{stage}}, j = 1, NC$

Vapour liquid equilibrium relation

$$y_{i,j} = f(x_{i,j}) \quad [4]$$

Summation of liquid mole fractions

$$\sum_{j=1}^{NC} x_{i,j} = 1 \quad [5]$$

Summation of vapour mole fractions

$$\sum_{j=1}^{NC} y_{i,j} = 1 \quad [6]$$

Liquid total hold-up constraint

$$h_{\text{tot},i}^L \left(\sum_{j=1}^{\text{NC}} x_{i,j} v_j \right) = \text{Vol} \quad [7]$$

Eqns [1]–[7] ignore the tray hydraulic behaviour and assume identical compositions for the liquid hold-up within a stage and the liquid outflow out of the stage. Other major features and assumptions of the model are nonadiabatic stages, negligible vapour hold-up and constant volumetric liquid hold-up. The assumptions concerning the hold-up are very reasonable and the equations can be readily translated to real stages by the introduction of Murphree tray efficiencies as correction factors for either the liquid or the vapour compositions.

For the top stage, the liquid inflow is related to the distillate outflow by the reflux ratio, and for the feed drum, the depletion of material should be taken into account. There is also no liquid outflow for the reboiler, thereby decreasing the number of necessary equations by one (eqn [7]). The following equations are the modified set for the situation in the top stage and reboiler.

Top stage: total material balance

$$\frac{dh_{\text{tot},1}^L}{dt} = DR_D + V_2 - L_1 - V_1 \quad [8]$$

Component material balances

$$h_{\text{tot},1}^L \frac{dx_{1,j}}{dt} = DR_D x_{D,j} + V_2 y_{2,j} - L_1 x_{1,j} - V_1 y_{1,j} \quad [9]$$

Energy balance

$$\begin{aligned} & \left(h_{\text{tot},1}^L \sum_{x=1}^{\text{NC}} x_{1,j} H_{1,j}^L \frac{dH_{1,j}^L}{dT} \right) \frac{dT}{dt} \\ &= DR_D x_{D,j} H_{D,j}^L + V_2 y_{2,j} H_{2,j}^V - L_1 x_{1,j} H_{1,j}^L \\ & \quad - V_1 y_{1,j} H_{1,j}^V + Q_1 \end{aligned} \quad [10]$$

For the feed drum (reboiler) the following equations are modified.

Total material balance

$$\frac{dh_{\text{tot},R}^L}{dt} = L_{N \text{ stage}} - V_R \quad [11]$$

Component material balances

$$h_{\text{tot},R}^L \frac{dx_{R,j}}{dt} = L_{N \text{ stage}} x_{N \text{ stage},j} - V_R y_{R,j} \quad [12]$$

Energy balance

$$\begin{aligned} & \left(h_{\text{tot},R}^L \sum_{x=1}^{\text{NC}} x_{R,j} H_{R,j}^L \frac{dH_{R,j}^L}{dT} \right) \frac{dT}{dt} \\ &= L_{N \text{ stage}} x_{N \text{ stage},j} H_{N \text{ stage},j}^L - V_R y_{R,j} H_{R,j}^V + Q_R \end{aligned} \quad [13]$$

The set of equations written for all the stages forms a system of nonlinear differential algebraic equations, with initial conditions given by the original charge in the feed drum, tray hold-ups and tray composition profiles and internal flow rates. The vector of initial conditions represents a pseudo steady-state solution for an initial feed whose composition is equal to the vapour in equilibrium with the liquid charge of the feed vessel. The transient behaviour is obtained by the simultaneous solution of eqns [1]–[13], which requires linearization and a combination of matrix inversion and integration techniques.

Despite the large range of computational complexity, simulations of batch distillation show that, in most cases, short-cut and rigorous models agree very well. A distinct advantage of the simplified models is they can be implemented in a spreadsheet. In these models the stage hold-up is considered negligible, except for the feed drum (reboiler) where the following equations hold for the total and volatile component material balances in a column operating at constant distillate composition and variable reflux.

Total cumulative material balance

$$\bar{D} = \bar{V} - \bar{L} \quad [14]$$

$$\begin{aligned} dW &= -d\bar{D} = \left(1 - \frac{\bar{L}}{\bar{V}} \right) d\bar{V} = \left(1 - \frac{R}{R+1} \right) d\bar{V} \\ &= (1-S) d\bar{V} \end{aligned} \quad [15]$$

Cumulative component balance

$$W_i x_{wi} = W x_w + (W_i - W) x_D \quad [16]$$

By differentiating and rearranging one gets:

$$W = \frac{W_i (x_{wi} - x_D)}{(x_w - x_D)} \quad [17]$$

$$-dW = \frac{W_i (x_D - x_{wi}) dx_w}{(x_D - x_w)^2} = d\bar{D} \quad [18]$$

If eqn [18] is substituted in [15] one gets:

$$(1 - S) d\bar{V} = \frac{W_i(x_D - x_{wi}) dx_w}{(x_D - x_w)^2} \quad [19]$$

The total amount of vapour produced will then be:

$$\bar{V} = \int_{x_{wi}}^{x_{wf}} \left[\frac{W_i(x_D - x_{wi})}{(1 - S)} \right] \frac{dx_w}{(x_D - x_w)^2} \quad [20]$$

Since the cumulative vapour produced is $\bar{V} = \theta V$, the time θ necessary for a run is calculated from the above equation as:

$$\theta = \int_{x_{wi}}^{x_{wf}} \left[\frac{W_i(x_D - x_{wi})}{V} \right] \frac{dx_w}{(1 - S)(x_D - x_w)^2} \quad [21]$$

The total amount of distillate produced can be found by integration of eqn [18]:

$$\int_0^{\bar{D}_f} d\bar{D} = \int_{x_{wi}}^{x_{wf}} \frac{W_i(x_D - x_{wi}) dx_w}{(x_D - x_w)^2} \quad [22]$$

Finally, rearrangement of eqn [16] yields:

$$W_i x_{wi} - (W_i - W)x_D = W x_w \quad [23]$$

$$W_i x_{wi} - \bar{D} x_D = W x_w \quad [24]$$

The above can be differentiated to give the following result:

$$d(W_i x_{wi} - \bar{D} x_D) = d(W x_w) \quad [25]$$

$$- d(\bar{D} x_D) = d(W x_w) \quad [26]$$

$$- x_D d\bar{D} = x_w dW + W dx_w \quad [27]$$

The remaining amount of charge in the still is then calculated by combining the above equation with the total differential balance $dW = -d\bar{D}$ and subsequently integrating the resultant expression:

$$\frac{dW}{W} = \frac{dx_w}{x_D - x_w} \quad [28]$$

$$\ln \frac{W_f}{W_i} = \int_{x_{wi}}^{x_{wf}} \frac{dx_w}{x_D - x_w} \quad [29]$$

Eqns [20]–[22] provide an efficient way of calculating the total amounts of vapour and distillate produced and the time necessary for the separation without having to solve the system of equations comprised by eqns [1]–[13]. This calculation provides an economic benchmark since it defines the optimum time for a run, based on the recovered product value and the operating costs. As the run time increases, the cumulative revenues given by the total amount of recovered product multiplied by its value will first increase but then approach an asymptotic value. The decreased economic benefit results either because the amount of distillate decreases (as in the case of constant composition distillate) or because the product stream becomes progressively less pure (as in the case of constant reflux ratio operation). The operating costs on the other hand increase steadily with time and the profit function, which combines these two costs, undergoes a maximum, after which the profit will decrease, as illustrated by **Figure 2**.

An analytical solution can be found for a limiting case which assumes an infinite number of stages (corresponding to minimum reflux) and constant relative volatility. At minimum reflux the operating line ends at a pinch zone and x_w is located in the equilibrium

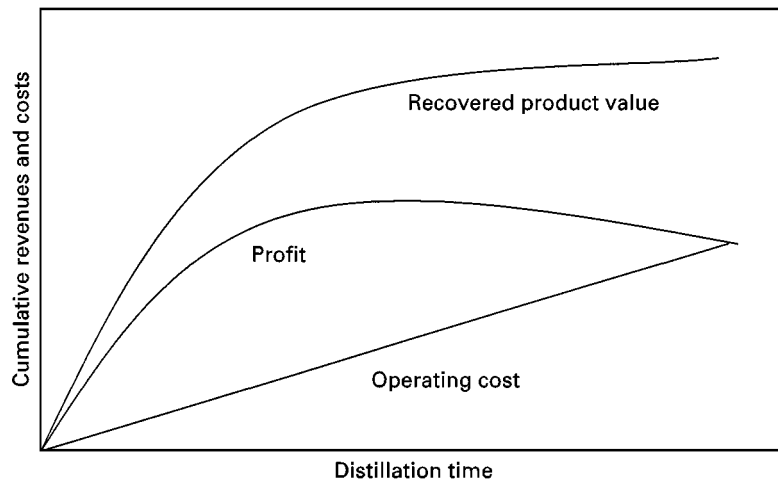


Figure 2 Optimum profit profile: operating costs versus length of time. Recovered product increases rapidly at first but then levels off.

line. The slope of the operating line is then given by:

$$S = \frac{d\bar{L}}{d\bar{V}} = \frac{x_D - y_w}{x_D - x_w} = \frac{R}{R + 1} \quad [30]$$

Under the constraint of constant relative volatility the equilibrium relation becomes:

$$y_w = \frac{\alpha x_w}{1 - x_w(\alpha + 1)} \quad [31]$$

If one takes advantage of eqns [30] and [31], analytical forms for the cumulative distillate production and remaining charge left in the feed still can be derived for the cases of either constant reflux ratio or constant distillate composition operation.

For constant reflux ratio, eqn [15] can be integrated to the expression for the total vapour requirement:

$$\bar{V} = (R + 1)\bar{D} = (R + 1)(W_i - W_f) \quad [32]$$

Combination of eqns [15], [30] and [31] yields the functional dependence of distillate composition, x_D on recycle ratio, R , composition of the remaining feed, x_w in the reboiler and relative volatility, α :

$$x_D = \frac{(R + 1)\alpha x_w - R x_w - R x_w^2(\alpha - 1)}{1 + x_w(\alpha - 1)} \quad [33]$$

Substitution of eqn [33] into the general mass balance expression, eqn [29] and subsequent integration produces an analytical form for the mass balance given by:

$$\ln \frac{W_f}{W_i} = \frac{1}{(R + 1)(\alpha - 1)} \ln \left[\left(\frac{1 - x_{wi}}{1 - x_{wf}} \right) \left(\frac{x_{wf}}{x_{wi}} \right) \right] + \left(\frac{1}{R + 1} \right) \ln \left(\frac{1 - x_{wf}}{1 - x_{wi}} \right) \quad [34]$$

If the column is operated at constant distillate composition, direct integration of eqn [29] produces the expression for the mass balance:

$$\frac{W_f}{W_i} = \left(\frac{x_D - x_{wi}}{x_D - x_{wf}} \right) \quad [35]$$

The integration of eqn [20], however, requires the development of an expression for the time-dependent operating line, which is accomplished by substitution

of eqn [31] into [30] to yield:

$$\frac{d\bar{L}}{d\bar{V}} = \frac{x_D + x_D x_w (\alpha - 1) - \alpha x_w}{(x_D - x_w) [1 + x_w(\alpha - 1)]} \quad [36]$$

Substitution of [36] into the general expression for the vapour requirement (eqn [20]) and integration leads to the vapour requirement equation when the column is operated at constant distillate composition and variable reflux:

$$\bar{V} = \frac{W_i(x_D - x_{wi})}{(1 - x_D)(x_D)(\alpha - 1)} \times \left\{ (1 - x_D) \ln \left[\left(\frac{x_D - x_{wf}}{x_D - x_{wi}} \right) + \left(\frac{x_{wi}}{x_{wf}} \right) \right] + x_D \alpha \ln \left[\left(\frac{x_D - x_{wf}}{x_D - x_{wi}} \right) \left(\frac{1 - x_{wi}}{1 - x_{wf}} \right) \right] \right\} \quad [37]$$

Eqns [34] and [37] were developed by Bauerle and Sandall, assuming the ideal pinched columns operating at minimum reflux. None the less, their application to real columns yields good approximated results if the equipment operates in a near-pinched zone at the bottom. This is often the case for columns with five or more theoretical stages.

Design

The operation of a batch distillation column, even pilot-scale equipment, is often as technically involved as operation of an industrial-scale column, and the same amount of care in start-up and safety procedures should be taken. Whether designing a new column or revamping an existing one, the necessary safety and physical properties data such as flash and ignition points, flammability and toxicity must be compiled for each component in the mixture. Predictive equations or experimental values for the vapour pressures of all components and binary equilibrium data should be compiled together with parameters of equations of state or activity coefficient models whenever available. Other physical properties to be included are liquid and vapour heat capacities, heats of vaporization and viscosities.

Once the physical property data bank has been put together, preliminary design calculations can be performed. For a multicomponent distillation column a light-key and a heavy-key component should be chosen in order to reduce the preliminary design to a pseudo-binary system. At this point it is possible to use graphical methods like McCabe-Thiele or even something more involved like Ponchon-Savarit to

carry out a case study to find out the system response in terms of required number of theoretical stages for a specified purity at different reflux ratios. To accomplish this, the optimization techniques described later can be useful, but since they are also hard to implement. The alternative approach of using a simplified calculation method such as presented in the section on column operation might be more desirable. This initial set (reflux ratio — number of theoretical stages) will permit the preliminary design.

Depending on the intended purpose of the laboratory-scale column, these initial calculations are likely to be sufficient for specifying the details of column design. Reboiler and condenser heat loads permit sizing of steam and condensation coils. Environmental concerns have introduced complexities in design which were not previously an issue for pilot-scale distillation. Current regulations at our site require condensate return to steam generation facilities to recover waste heat. Even a moderate condenser heat load can require prohibitively large quantities of cold tap water and the condenser heat load for even a small distillation column will typically be substantially larger than can be handled by laboratory-scale recirculated chillers. Much of the final decisions on absolute sizing will be dependent upon available facilities and the anticipated intensity of column use. It is important to get to a reasonably accurate preliminary design early in the design process, so that such practical constraints can be considered.

In many situations, a laboratory-scale distillation column will be used for multiple separations, or as a testing ground for additional full-scale design data. Under these circumstances, design for flexibility is a primary concern. Instead of focusing on detailed physical property information, the data collection should focus on obtaining ranges of anticipated physical properties as well as ranges in batch size. The actual design should then reflect the appropriate bounds of properties and separations that may be encountered. It should be kept in mind that there is a practical minimum volume that can be handled, due to tray hold-up, while larger volumes can be handled with multiple batches. Undersizing either reboiler or condenser heat transfer capacity may render the column useless for a specific separation.

In most batch distillation operations, the lighter component is the desired product and the actual column is the rectifying section of a continuous tower. The preceding discussion in this section as well as in the next section implicitly assume this situation. Nevertheless, there might arise design situations where the economical interest lies in the heavier compounds. In more complex operations the designer might even be faced with the task of devising a separ-

ation sequence involving two or more columns. For the case where it is desired to recover the heavy component, the calculations for the number of stages should be performed as a stripping column instead.

Since the principles and computational basis of distillation are quite advanced, additional assumptions allow the derivation of simple expressions for the distillate composition and flow rate and the amount of material left in the feed drum. These assumptions render the evaluation of columns with recycle amenable to straightforward solutions.

The remainder of this section includes a description of a versatile laboratory distillation column and its instrumentation and safety systems.

Equipment

Batch distillation equipment can be custom-made to meet particular design specifications or be directly purchased by catalogue selection if no stringent construction features or materials are required. Ordering can be greatly facilitated by a previous search of the manufacturers or suppliers in the worldwide web. Equipment intended to be used for research or educational purposes should be made of glass whenever possible, given the easy observation of the internal flow regimes and their change with the internal flow rates. An existing batch glass column is described here as an example.

Figure 3 shows a distillation column which has a simple conceptual design but is versatile enough to be used for research or teaching applications. The column is atmospheric and functions as the rectifying section of a regular distillation column. The feed drum doubles as a kettle vessel where the feed is vaporized by a coil heater having steam as the heating medium. Instrumentation is reduced to the essentials: the distillate and reflux flow rates are controlled by varying the rotation speed of the distillate and reflux pumps, and the feed flow rate can be controlled by varying the steam pressure in the coil. The safety system consists of a relay actuated by the occurrence of any of the failure conditions in the column, which are pressurization within the equipment, zero flow of condenser cooling water or loss of power to the ventilation system. When any of these conditions occurs, steam admission to the feed drum is switched off.

The pumps are actuated in the remote mode by a driver board that receives signals in the range between 4 and 20 mA from an analog output board installed in a PC. The connection between the pump driver board and the analog output board consists of a screw terminal connector. The variation of the output signal to the pumps is accomplished via

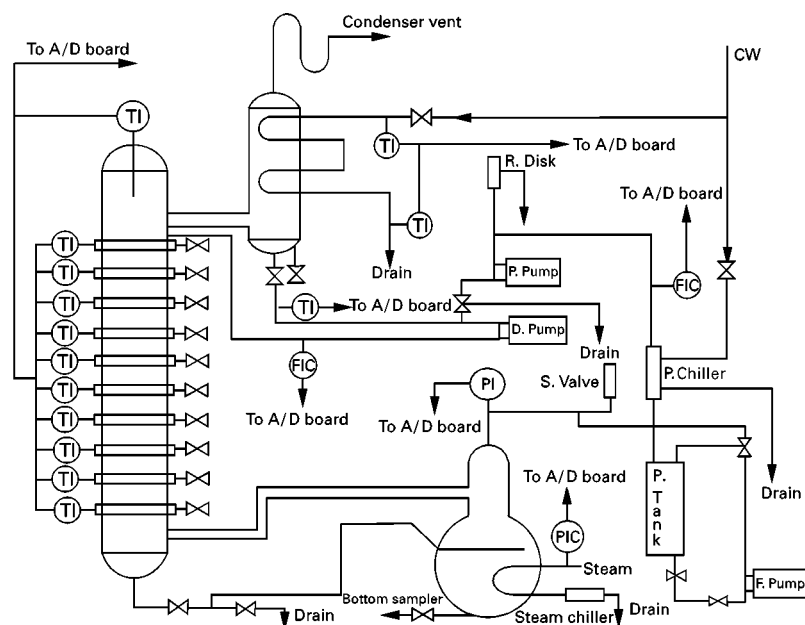


Figure 3 Rectifying batch distillation column. The abbreviations are as follows: A/D board = analog to digital interface board, CW = cooling water, D. Pump = distillate pump, F. Pump = feed pump, FIC = flow indicator control, P. chiller = product chiller, P. Tank = product tank, PI = pressure indicator, PIC = pressure indicator control, R. Disk = rupture disk, S. Valve = safety valve and TI = temperature indicator.

a software utility provided with the board that emulates a control panel, where each of the instruments hooked to the board is assigned a channel number displayed in the panel screen. The user varies the pump flow rate by changing the output current at the computer screen. Manual local control of each pump is also provided in case of failure of the computer-interfaced control. The stepper motor of the steam valve for the feed drum steam coil is also interfaced in a comparable manner.

The column is also provided with thermocouples for each stage, including condenser and reboiler. The thermocouples are wired to a screw terminal connector, that provides the interface to an analog/digital I/O board installed in the PC. When there is a significant difference between the boiling points of the two components of a binary system, the stage temperature is an efficient and straightforward way of evaluating compositions. Under these circumstances, the real-time composition profile within the column can be updated to the computer screen. Sample ports for the liquid phase are installed in every stage, including the condenser and reboiler to corroborate thermal measurements under circumstances where thermal gradients are not sufficiently steep to provide accurate composition correlation. The composition analysis can be performed by a variety of methods. If there is a significant density difference between components being separated, composition can be deduced from a density-concentration curve. Density can be deter-

mined gravimetrically, or equipment is available for online density measurement. A particularly versatile online implementation of density measurement is in the condensate stream of an off-set condenser as described in more detail below. If one of the components is an organic acid, sample analysis can be carried out either by titration or by the measurement of any other property related to the dissociation state (such as pH), provided the metering apparatus is sufficiently accurate to discriminate stage-to-stage differences. For organic mixtures, other properties such as refractive index may also be used as analytical method.

The feed drum in the described pilot-scale column is a large glass bulb equipped with a steam heating coil to vaporize the feed. A pressure relief rupture disk provides a mechanical fail-safe against reboiler pressurization. Another pressure gauge is installed at the steam inlet to the coil. The steam outlet is provided with a trap to ensure the total condensation of the steam, and therefore the use of its latent heat. A useful energy balance is achieved by cooling the condensate as it is discharged to the drain. The heat load to the column can be crudely calculated by measuring the discharge flow rate and multiplying this value by the heat of vaporization of the steam at the inlet pressure.

The distillate is collected in a separate vessel whose volume equals approximately half that of the feed drum. The product collection vessel is fitted to permit

charging of material to the feed drum. The remaining material in the drum after a batch processing can be discharged by a valve in the bottom. The subsequent batch charge can also be combined with the remaining heavy ends of the previous operation.

The off-set condenser depicted in Figure 3 provides for direct measurement of condensate flow rate. This eliminates the need to calculate condensate from the condenser energy balance. This is particularly important for pilot-scale units where complete condensation may not be achieved at high boil-up rates. The condensed top vapours drip down and accumulate in the bottom part of the vessel, from which they are removed either to the distillate tank or back to the column as reflux. A match between the condensation rate and sum of product and liquid flow rate returned to the column can be assured by visual monitoring of the condenser liquid level or computer monitoring of the liquid head in the bottom of the condenser with a pressure transducer. The gas entrance to the condenser doubles as a liquid overflow in the event of excessive condensate accumulation.

Instrumentation and Safety Circuits

Although a batch distillation column can be run manually by an attentive and experienced technician, the dynamic nature of operation requires extensive instrumentation for all but the simplest mode of operation. To gain the flexibility necessary for the operation at constant distillate composition, flow rates of the reflux and distillate must be independently controlled. In small units devoted to research, flow control can be easily accomplished by varying the speed of a gear pump through a control panel displayed on a computer screen. The connection of the pump to the computer consists of a driver board wired to a screw terminal connector. The latter is attached to an analog output board. The output signal to the driver board can be varied based on the results of calculations performed by external application programs. If the top composition is to be kept constant, the update on the reflux rate can be calculated by a user routine with the aid of operating charts such as those described later. The value of the reflux rate translated to flow rates (typically current values) controls the distillate and reflux pumps. The product and reflux flow rates must be constrained to balance the rate of condensation. This is conveniently accomplished by monitoring the condenser level as an indicator of the difference between boil-up and distillate and product flow rates. The direct use of the heat load output to control the condenser level is not recommended due to the large dead-time between a change in the reboiler conditions and the resulting effect in the liquid

level. The result of the reflux calculation is stored in a data buffer from which it can be retrieved by another application and used to update the corresponding analog output channel.

Analog and digital I/O boards can also be installed to retrieve information such as cooling water temperature and flow rate, steam pressure, flow rate to the reboiler and the temperature profile of the column. The stage temperature is a direct indicator of stage composition; however, it is only useful as a control variable when the temperature variation between successive stages is significant. The greatest variation in temperature during the batch run will take place in the reboiler which is an excellent means of monitoring overall progress of the separation.

Variation of the heat load to the column can be actuated remotely by fitting the steam valve with a stepper motor. A variable heat load adds operation flexibility and can be used in conjunction with other strategies to maximize recovery and purity of a desired component at a lower energy cost. For example, the feed drum contains the highest fraction of the volatile component at the beginning of the process. Therefore, the column can be started up at a lower boil-up rate, which will be gradually increased to match the enrichment of the charge in the heavier component. Figure 3 shows typical column instrumentation, and data acquisition and control.

Three operating conditions are monitored constantly and may independently activate the safety system, stopping steam delivery to the reboiler by closing a steam safety valve that precedes the steam controller valve. These monitored conditions are the column pressure, cooling water flow and ventilation fans. The pressure transducers, flow transmitter and power to the fans are set up as a logic relay where loss of any one of the direct current voltages is sufficient to actuate the steam safety valve. It is important to choose the logic of these circuits such that electrical and mechanical failures will default to termination of the batch run. The safety system circuitry is depicted in Figure 4.

Column Operation

While dedicated laboratory-scale distillation can be used for solvent recovery, experimental laboratory-scale columns are used for collection of design data. The operational objective is usually to maximize the recovery of a component under the constraint of a desired purity level. The feature of the batch process which distinguishes it from the more familiar continuous counterpart is its inherently transient nature. The continuously changing feed composition must be

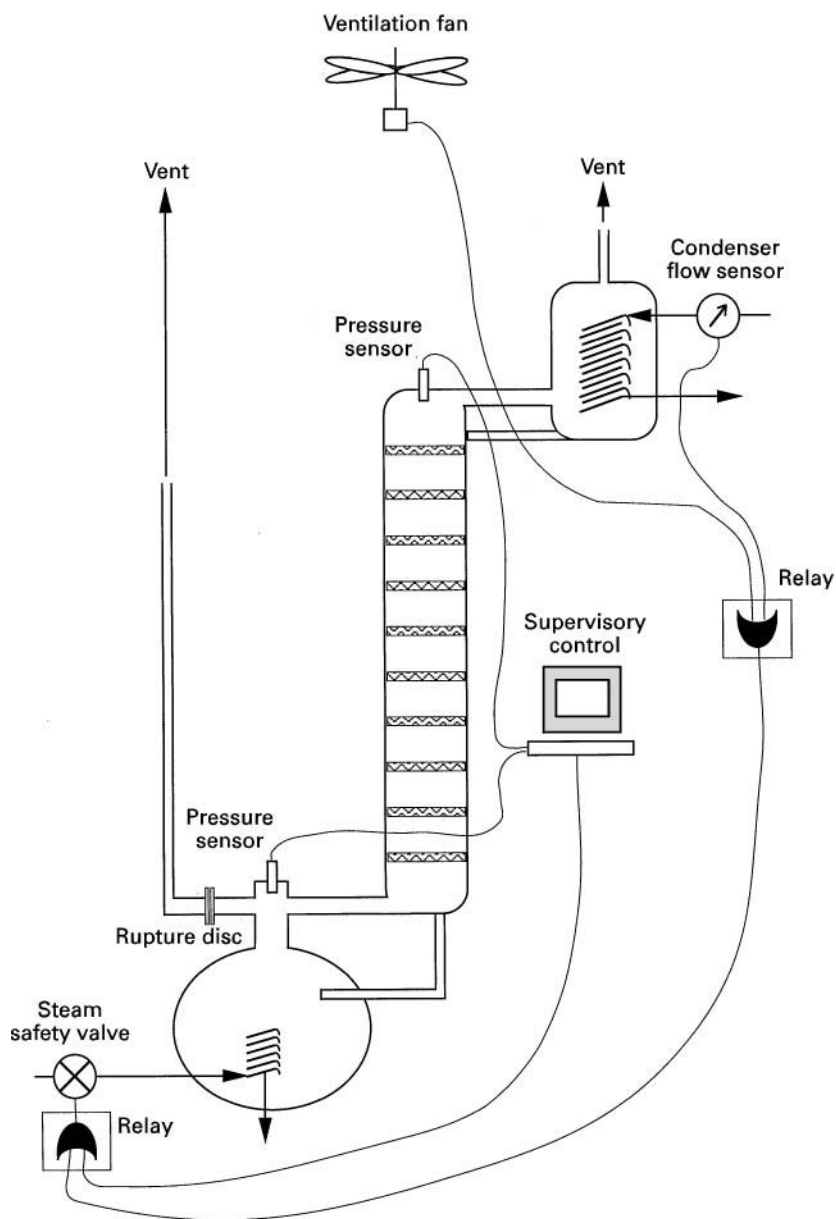


Figure 4 Safety system circuitry.

accounted for in the calculation theory. A variety of operation and completion criteria may be used depending on the process economics, equipment characteristics and product value. Several different basic operational modes are possible:

1. total reflux, with periodic dumping of the accumulated material from the condenser to the distillate tank;
2. constant reflux, with continuous variation of the instantaneous distillate composition, starting above and finishing below the desired product specification;
3. constant composition, with variable reflux ratio in order to keep the instantaneous distillate composition constant.

Operation strategies can take advantage of all three of these operational modes.

Initially the column is operated at total reflux with subsequent product collection at a purity higher than the final product specification. After this initial cut is withdrawn to the product tank, operation is switched to the constant composition mode and the equipment is run until the reflux ratio becomes so high that product collection is minimal. At this point the

operation is switched to the constant reflux mode and continued until the average composition of the distillate drops to the desired level, when the equipment is shut down. Variations on this approach are often required due to equipment limitations. If the column is to be operated manually, then it might be difficult to maintain constant distillate composition. Also, if the column consists of less than five ideal stages, it is more advantageous to operate at constant reflux.

Prior to the initiation of any operational procedure, it is necessary to elaborate an operation schedule that can be used as a guide throughout the run. Although the procedures discussed here can be implemented for columns with a very low level of automation, they can also be used in application programs that run as a part of an automated control loop. One can use simplified calculation methods (e.g. McCabe–Thiele) or resort to more extensive numerical computations if the effect of some variables such as the hold-up is to be taken into account. Independent of the calculational basis, better predictions of the composition profiles can be obtained if the stage efficiencies or at least the overall efficiency is known. Efficiencies depend on the physical properties of the system, particularly the viscosity and the relative volatility, but also on the geometric characteristics of the equipment. Determination of the overall and stage efficiencies can be easily accomplished by running the column at total reflux. When the column has reached

steady state, the composition profiles within the column must be determined. The overall efficiency is easily calculated by stepping off theoretical stages in the McCabe–Thiele diagram between the equilibrium and the operating line, which at total reflux coincides with $y = x$. The number of theoretical stages is determined when the bottom composition is crossed. The Murphree efficiency for stage n receiving liquid from stage $n - 1$ and vapour from stage $n + 1$ is defined as:

$$\eta_M = \frac{y_n - y_{n-1}}{y_n^{\text{eq}} - y_{n-1}} \quad [38]$$

Eqn [38] is a measure of the degree of separation achieved in the vapour going from stage $n + 1$ to stage n and can be visualized in the McCabe–Thiele diagram as a segment ratio, as shown in **Figure 5**. The maximum degree of separation is represented by the difference in the denominator, where the vapour leaving the stage is in equilibrium with the liquid phase of the same stage.

Determination of the vapour-phase composition is often more difficult than liquid and sample ports are generally only provided for the liquid phase. It is therefore useful to define Murphree efficiency of the liquid compositions as:

$$\eta_M = \frac{x_{n+1} - x_n}{x_{n+1} - x_n^{\text{eq}}} \quad [39]$$

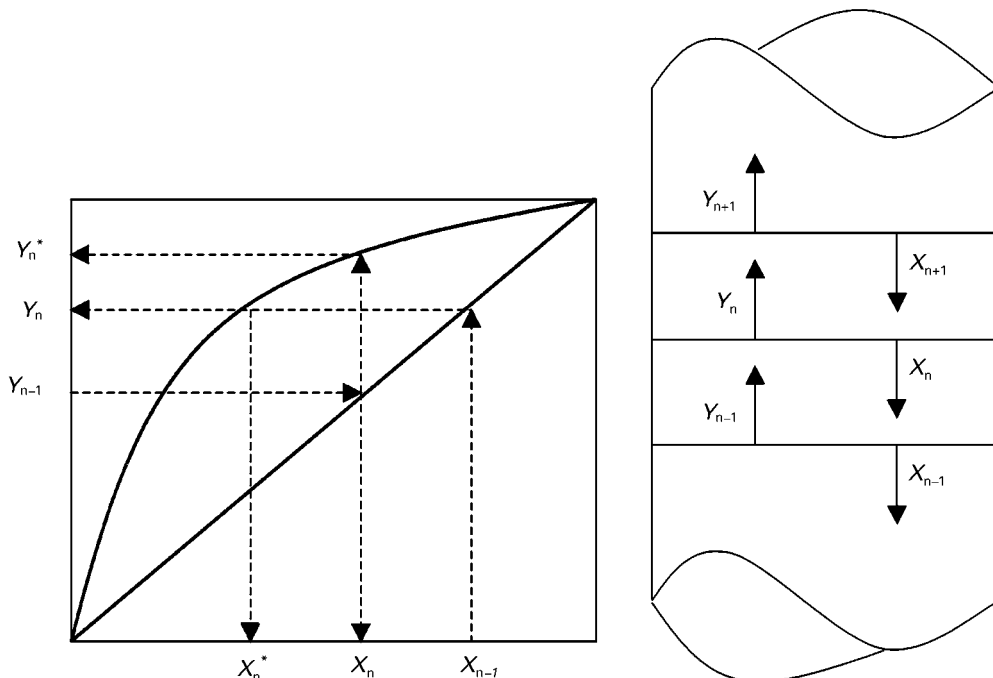


Figure 5 Representation of stage efficiencies.

Once the efficiencies are determined, an operation schedule at constant reflux should be prepared. The operation schedule consists of a family of curves where the reflux ratio is plotted as a function of reboiler composition, holding the distillate composition constant as depicted in Figure 6. The curves can easily be generated in a spreadsheet if the equilibrium curve for the system can be regressed as an analytical form, $x = f(y)$. A distillate composition (x_D) is fixed as the fulcrum, around which all the operating lines pivot, as defined for different reflux ratios (R_D), as shown in Figure 7. Since the number of ideal stages is known, the bottoms composition (x_B) is found for each operating line by stepping off these stages between the equilibrium curve and the operating lines. Once x_B is found for a particular operating line, the reflux ratio is changed, thereby defining another operating line, and the procedure is repeated to find the corresponding x_B . In this way, a set of data points (R_D , x_B) corresponding to a fixed distillate composition x_D is determined. The next set is determined by the same procedure, changing the value of x_D . These plots of R_D versus x_B represent the reflux ratio required to achieve a specified distillate composition at a given composition within the reboiler.

The R_D versus x_B curves can either be used in manual operation or integrated into an automated control strategy, where information about the feed drum composition is used to calculate the new required reflux ratio to keep x_D constant. The choice of x_D will depend on the minimum acceptable purity for the product. Sometimes, even when a higher purity is desired, the operating x_D may be imposed by equipment restrictions. The flow rate range of the pumps, for example, might restrict operation to a certain range of the reflux ratio. In this case, switching to

a lower distillate composition will allow longer runs, thus increasing the total amount of product.

Stopping criteria for an industrial distillation is generally dictated by economics. Operating costs accumulate continuously with time, because of energy and labour costs, as discussed above.

Optimization Techniques

Optimization of batch distillation operations is not addressed with the same frequency as the continuous-case counterpart. The likely reason for the scarcity of publications in this area lies in the transient nature of the problem, which introduces a system of differential equations to describe the dynamics. The optimization problem therefore consists of a target functional (see below) to be minimized and a set of constraints embodied by the differential equations for the time-dependent behaviour of material and energy balances and algebraic equations for phase equilibrium and column hydraulics plus additional constraints such as bounds on certain variables. Optimization problems with nonlinear algebraic model equations and constraints can be solved in a straightforward way by nonlinear programming strategies. On the other hand, unconstrained problems with differential equation models can be handled through the calculus of variations. Models that combine both of these features are currently optimized by imposing some level of approximation to the problem. The problems usually reported in the literature for batch distillation can be classified as:

1. Maximum distillate problem: to maximize the amount of distillate of a specified purity for a specified time.

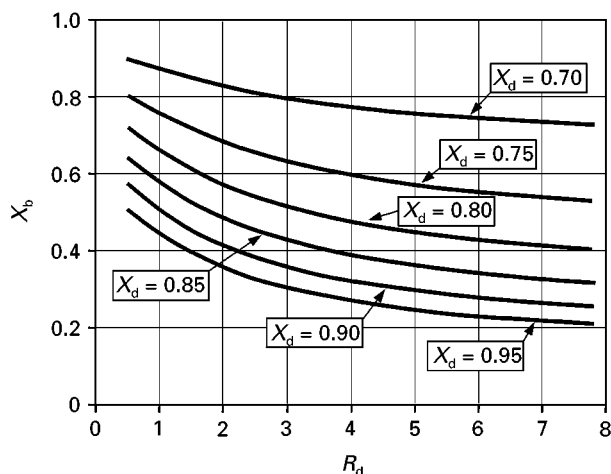


Figure 6 Operation schedule at constant composition. Reflux schedule (based on 45% η overall). X_B is the reboiler composition, X_d is the distillate composition and R_d is the reflux ratio.

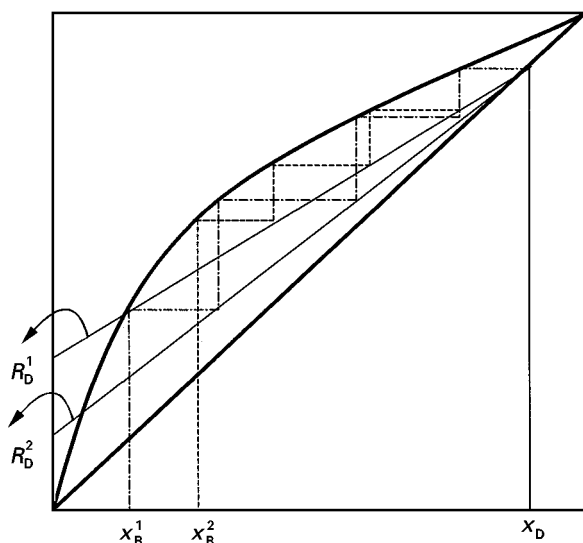


Figure 7 Construction of the operation schedule.

2. Minimum time problem: to minimize the batch time needed to produce a prescribed amount of distillate of a specified purity.
3. Maximum profit problem: to maximize a profit function for a specified purity of distillate.

The maximum profit problem for a column operated at constant distillate composition involves the evaluation of the net profit of the column along its batch run time. The net profit function behaviour has already been discussed. The profit curve displays an extrema and the profit optimization problem therefore seeks the value of the batch run time (a number) that will maximize the net profit function. It is amenable to a simple graphic solution that can be obtained from a spreadsheet as long as a simple zero hold-up model is employed to describe the column operation. On the other hand, the solution of the maximum distillate problem is given by a time-dependent function (the distillate flow rate) that will maximize the cumulative distillate production, a function of the distillate flow rate. This latter function of another function is called a functional.

In this section some of the recently developed techniques to extremize functionals are briefly reviewed. The objective is to offer the reader an introduction to the theme, and provide useful references for further information. The optimization problem belonging to one of the above categories can be posed in terms of an objective function subjected to constraints such as:

$$\text{Min}_{u(t), z(t), p} \Phi = \Psi(z(b), p) + \int_a^b G(z(t), u(t), p) dt \quad [40]$$

subject to:

$$\dot{z}(t) = F(z(t), u(t), p) \quad [41]$$

$$g(u(t), z(t)) \leq 0 \quad [42]$$

$$g_f(z(b)) \leq 0 \quad [43]$$

$$z(a) = z_0 \quad [44]$$

$$z(t)^L \leq z(t) \leq z(t)^U \quad [45]$$

$$u(t)^L \leq u(t) \leq u(t)^U \quad [46]$$

In the above set of equations the integral part of the objective function to be minimized can be viewed as the total amount of distillate, withdrawn as top product, whereas the function $\psi(z(b), p)$ may account for the final hold-up within the equipment, which can be incorporated into the product at the end of a batch run. The vector $z(t)$ represents the state variables of the system, such as composition, internal flow rates and temperatures, and the vector p represents constant parameters. The vector $u(t)$ carries the control profiles, i.e. the variables used to manipulate eqn [40] and achieve the minimization goal. Distillate of a specified purity can be maximized for instance by changing the reflux ratio. The time-dependent reflux ratio would be then the control variable $u(t)$ for such an optimization problem. The constraints represented by eqn [41] embody the material and energy balances, which are written in their transient form for the batch problem. Algebraic constraints included in eqn [42] may represent the equilibrium relations and the summation of the liquid mole fractions. Inequality constraints with lower and upper bounds (eqns [45] and [46]) may represent either purity requirements in the product or physical constraints in the maximum and minimum attainable values of the control variables. Initial and final states of the system are also written as constraints, as represented by eqns [44] and [43] respectively.

The optimal control problem posed above seeks the time-dependent control profile (control function) that minimizes the objective functional (i.e. a function of functions represented by eqn [40]). It can be solved in a variety of ways, depending on how one chooses to handle the differential equation constraints. Methods based on the calculus of variations use Lagrange multipliers and slack variables to restate the constrained problem of eqns [40]–[46] as an unconstrained one. Since the minimum of the constrained problem is equivalent to the minimum of the unconstrained one, the augmented problem is

represented by:

$$\begin{aligned} \text{Min}_{u(t), z(t), p} \Phi^1 = & \psi(z(b), p) + v^T g_f(z(b)) \\ & + \int_a^b [G(z(t), u(t), p) \\ & + \lambda^T(t)(F(z(t), u(t), p) - \dot{z}(t)) \\ & + M^T(t)(g(u(t), z(t)) + s^2)] dt \end{aligned} \quad [47]$$

By analogy to Hamilton's equation of motion, one can define a Hamiltonian as:

$$\begin{aligned} H(z(t), u(t), p) = & G(z(t), u(t), p) + \lambda^T F(z(t), u(t), p) \\ & + M^T(g(u(t), z(t)) + s^2) \end{aligned} \quad [48]$$

And therefore the problem in [47] becomes:

$$\begin{aligned} \text{Min}_{u(t), z(t), p} \Phi^1 = & \psi(z(b), p) + v^T g_f(z(b)) \\ & + \int_a^b [H(z(t), u(t), p) - \lambda(t)\dot{z}(t)] dt \end{aligned} \quad [49]$$

The minimum of the latter is found in the usual way by taking the derivatives of the augmented problem with respect to all the independent variables (z , v , λ , s , u , t). Setting those to zero and taking into account the conditions for a fixed initial condition problem ($dt|_{t_0} = 0$, $dz|_{t_0} = 0$), one obtains the following variational formulation.

State equations

$$\dot{z} = \frac{\partial H}{\partial \lambda} \quad [50]$$

Co-state equations

$$-\dot{\lambda} = \frac{\partial H}{\partial z} \quad [51]$$

Stationary condition

$$\frac{\partial H}{\partial u} = 0 \quad [52]$$

$$\frac{\partial H}{\partial M} = 0 \quad [53]$$

$$\frac{\partial H}{\partial s} = 0 \quad [54]$$

Pontryagin's maximum principle

$$H(x^*, u^*, \lambda^*, t) \leq H(x^*, u^* + \delta u, \lambda^*, t) \quad [55]$$

Boundary condition

$$(\phi_z + \psi_z^T v - \lambda)^T|_b dz(b) + (\phi_t + \psi_t^T v + H)|_b dt(b) = 0 \quad [56]$$

For problems with constraints in the control variables like those given by eqn [46], the stationary condition must be modified to include Pontryagin's maximum principle which establishes that the solution values for the constrained control variables must lie along an optimal path. That is, any variation in the optimal control profile $u^*(t)$ at time t , while keeping the state and co-state variables $z(t)$, $\lambda(t)$ and $M(t)$ at their optimal values, will force an increase in the value of the Hamiltonian. This replaces the unconstrained minimum condition of eqn [52] and is stated mathematically in eqn [55]. Also, the second term of the boundary condition in eqn [56] vanishes for fixed-time problems.

Solution of the optimization problem of eqns [40]–[46] in its variational formulation requires integration of two sets of differential equations given by [50] and [51] to get the state variables z and adjoint variables λ for the ordinary differential equation (ODE). Since these equations are also a function of the control profile $u(t)$, their integration is first performed with guessed values of this vector. Eqns [53] and [54] are used to find the second set of adjoint variables (M) and the slack variables (s^2) associated with the constraint on $g(u(t), z(t))$. Finally, eqn [52] or [55] provides the updated values for $u(t)$, the control profile, whereas the adjoint variables for the boundary conditions are calculated from eqn [56]. The whole procedure involves successive iterations of the control vector and can be computationally intensive, especially for problems with many constraints.

An alternative solution can be formulated to overcome the difficulty posed by the differential constraints. Eqns [40]–[46] are discretized using finite elements. Within each element, function approximation is expressed in terms of orthogonal polynomials and the resulting problem is amenable to a mathematical treatment intended to minimization problems involving only algebraic equations.

Discretization of the optimal control problem leads to the nonlinear problem model given below. This formulation consists of the discretized objective function of the original problem, the continuity equations for state variables and inequality constraints in the

original formulation.

$$\text{Min}_{u_{ij}, z_{ij}, p, \Delta \zeta_i} \Phi = \psi(z_f, p) + \sum_{i=1}^{NE} \sum_{j=1}^K w_{ij} G(z_{ij}, u_{ij}, p, \Delta \zeta_i) \quad [57]$$

subject to:

$$\Delta \zeta_i r_{ij} = \dot{z}_{K+1} \tau_{ij} - \Delta \zeta_i F(z_{ij}, u_{ij}, p) = 0 \quad [58]$$

$$g(u_{ij}, z_{ij}, \Delta \zeta_i) \leq 0 \quad [59]$$

$$g_f(z_f) \leq 0 \quad [60]$$

$$z_{10} - z_0 = 0 \quad [61]$$

$$z_{i0} - z_{K+1}^{i-1}(\zeta_i) = 0 \quad i = 2, \dots, NE \quad [62]$$

$$z_f - z_{K+1}^{NE}(\zeta_{NE+1}) = 0 \quad [63]$$

$$z_{ij}^L \leq z_{ij} \leq z_{ij}^U \quad [64]$$

$$u_{ij}^L \leq u_{ij} \leq u_{ij}^U \quad [65]$$

$$\sum_{i=1}^{NE} \Delta \zeta_i = \zeta_{\text{Total}} \quad [66]$$

Problem discretization introduces the time element lengths ($\Delta \zeta_i$) as additional variables. Thus, variables in [57]–[66] include: $\Delta \zeta_i$, the finite element lengths for $i = 1, \dots, NE$; z_f , the value of the state at the final time; z_{ij} and u_{ij} , the collocation coefficients for the state and control profiles where i refers to the element and j to the collocation point within each element; and p , any additional design parameters (such as boil-up rate and final time). In addition, w_{ij} are quadrature weights from the integral in [40]. Lagrange polynomials are applied for the orthogonal collocation within the finite elements. The order of the collocation method should be equal to the index of the system of the state variable differential constraints and algebraic equations. The index is equal to the number of times the algebraic equations must be derived in order to recover the standard form of a first-order ODE.

The solution of eqns [57]–[66] looks for the values of the coefficients z_{ij} and u_{ij} of the polynomial approximation for the state variables and control profiles respectively. In addition, the discretized problem also includes the length of the discretization interval $\Delta \zeta_i$. The problem variables are partitioned into a set of state variables (z_{ij}) and optimization variables (u_{ij} and $\Delta \zeta_i$), which provides a solution strategy where the state variables are calculated separately using the state equations, whereas the control profile and element lengths are obtained via the solution of a quad-

ratic programming problem as follows (see Logsdon and Biegler, in the Further Reading section):

Equation [58] is solved in each element for the values of z_{ij} in the interior collocation points, starting with the first element, from the initial values of the state variables and guessed element lengths ($\Delta \zeta_i$) and control profiles (u_{ij}). The rightmost (exterior) collocation point for the state and control profiles in eqn [58] is calculated from the values at the interior collocation points by:

$$z_{i,k+1} = \sum_{j=0}^k z_{ij} \phi_j \quad [67]$$

$$u_{i,k+1} = \sum_{j=1}^k z_{ij} \theta_j \quad [68]$$

where ϕ_j and θ_j in the above equation are Legendre's orthogonal polynomials.

Continuity for the state variables is ensured by eqn [62] which establishes the equality between the state variables of the rightmost collocation point of element $i - 1$ and their initial value in element i . The initial value problem presented in eqn [58] is thus integrated element-by-element using a marching technique with collocation within each element.

After a new set of state variables is generated by the technique described above, the control profiles (u_{ij}) and element lengths ($\Delta \zeta_i$) are updated using a successive quadratic programming algorithm that solves the following:

$$\text{Min}_{\Delta \zeta} \nabla \Phi^T \mathbf{Z} \Delta \zeta + \frac{1}{2} \Delta \zeta^T (\mathbf{Z}^T \mathbf{B} \mathbf{Z}) \Delta \zeta \quad [69]$$

subject to:

$$\mathbf{g} + \nabla \mathbf{g}^T \mathbf{Z} \Delta \zeta \leq 0 \quad [70]$$

In the above problem, the variables u and $\Delta \zeta$ were included in the vector $\Delta \zeta$ and the inequality constraint is the same as that of the original problem formulation. ($\mathbf{Z}^T \mathbf{B} \mathbf{Z}$ is the Hessian matrix of the objective function Φ and it is also updated during the quadratic programming step using the BFGS (Broyden–Fletcher–Goldfarb–Shanno) formula). The reduced gradients for the objective and constraint functions appearing in eqns [69] and [70] above are calculated in the iteration t during the integration step according to the formula:

$$\{\mathbf{Z}^T \nabla \Phi\}_j = \frac{\partial z_{t,k+1}}{\partial \zeta_j} \frac{\partial \Phi}{\partial z_t} \quad \{\mathbf{Z}^T \nabla \mathbf{g}_n\}_j = \frac{\partial z_{c,k+1}}{\partial \zeta_j} \frac{\partial \mathbf{g}_n}{\partial z_c} \quad [71]$$

In the equation above, the partial derivatives of the state variables at the rightmost exterior collocation point (z_{k+1}), in relation to the optimized vector ξ , is calculated, via chainruling, by the formula:

$$\frac{\partial z_{i,k+1}}{\partial \xi_j} = \frac{\partial z_{i,k+1}}{\partial z_{i-1,k+1}} \frac{\partial z_{i-1,k+1}}{\partial z_{i-2,k+1}} \dots \frac{\partial z_{i,k+1}}{\partial \xi_j} \quad [72]$$

The new set of control variables and element lengths calculated in the optimization step replaces the old one and the integration step is performed once again. The Kuhn-Tucker conditions, which determine the attainment of constrained minimum, are then checked and the calculations are stopped if these conditions have been reached. Otherwise, the optimization step is performed again and the whole procedure is repeated.

The preceding development typifies the complexity involved in rigorous optimization of batch distillation. The gains of reduced costs or shorter process times that can be achieved by such an optimization would not probably be worth the effort for routine operation. None the less, it is possible to utilize sophisticated laboratory-scale distillation units to test alternative control strategies indicated by computational approaches.

List of Variables

Section 2 – Theory

Variables

b	=	tray hold-up
H	=	molar enthalpy
\bar{D}	=	cumulative distillate production, moles
L	=	liquid molar internal flow rate
\bar{L}	=	cumulative amount of reflux, moles
MW	=	molecular weight
Q	=	heat load
R	=	reflux ratio
S	=	$R/(R + 1)$
T	=	temperature
t	=	time
V	=	vapour molar internal flow rate
v	=	liquid molar volume
Vol	=	volume of the stage
\bar{V}	=	cumulative vapour production, moles
W	=	moles of material left in the still
x	=	liquid molar fraction
y	=	vapour molar fraction

Superscripts

L, V = liquid and vapour phases

Subscripts

i, j	=	tray number, component
i	=	initial
f	=	final
R	=	reboiler
w	=	material in the still
tot	=	total

Section 5 – Optimization Techniques

Variables

a	=	initial condition for the optimization problem
b	=	final condition for the optimization problem
G	=	component of the objective function due to the integral state
H	=	Hamiltonian function
M	=	Lagrange multipliers for the algebraic inequality constraints
p	=	vector of design parameters
t	=	time
s^2	=	vector of slack variables for the inequality constraints
u	=	vector of control variables
z	=	vector of state variables

Superscripts

U, L	=	upper and lower limits of the constrained variables
--------	---	---

Subscripts

z	=	derivative with respect to z
b	=	evaluate at point b

Greek alphabet

$\Delta \xi$	=	vector of time-finite element lengths
θ	=	Lagrange polynomial approximation for the control variables
λ	=	Lagrange multipliers for the differential equality constraints
ν	=	Lagrange multipliers for the inequality constraints at final conditions
ϕ	=	Lagrange polynomial approximation for the state variables
Φ	=	objective function
Ψ	=	term of the objective function evaluated at final conditions

See also: II/Distillation: Historical Development; Instrumentation and Control Systems; Theory of Distillation.

Further Reading

Al-Tuwaim MS and Luyben WL (1991) Multicomponent batch distillation. 3. Shortcut design of batch distillation columns. *Industrial and Engineering Chemistry Research* 30: 507.

- Bauerle GI and Sandall OC (1987) Batch distillation of binary mixtures at minimum reflux. *AIChE Journal* 33: 1034.
- Block B (1961) Batch distillation of binary mixtures provides versatile process operations. *Chemical Engineering* 68: 87.
- Chiotti OJ and Iribarren OA (1991) Simplified models for binary batch distillation. *Computers and Chemical Engineering* 15: 1.
- Diwekar UM and Madhavan KP (1991) Batch-Dist: a comprehensive package for simulation, design, optimization and optimal control of multicomponent, multifraction batch distillation columns. *Computers and Chemical Engineering* 15: 833.
- Diwekar UM (1992) Unified approach to solving optimal design-control problems in batch distillation. *AIChE Journal* 38: 1551.
- Kumana JD (1990) Run batch distillation processes with spreadsheet software. *Chemical Engineering Progress* 6: 53.
- Lewis F (1986) *Optimal Control*. New York: John Wiley.
- Logsdon JS and Biegler LT (1990) On the simultaneous optimal design and operation of batch distillation columns. *Transactions of the Institution of Chemical Engineers, Part A* 68: 434.
- Logsdon JS and Biegler LT (1992) Decomposition strategies for large-scale dynamic optimization problems. *Industrial and Engineering Chemistry Research* 32: 692.
- Logsdon JS and Biegler LT (1993) Accurate determination of optimal reflux policies for the maximum distillate problem in batch distillation. *Chemical Engineering Science* 47: 851.
- McCabe WL, Smith JC and Harriott P (1993) *Unit Operations of Chemical Engineering*, 5th edn. New York: McGraw-Hill.
- McCausland I (1985) *Introduction to Optimal Control*. Malabar, FL: Robert Krieger.
- Rao S (1996) *Engineering Optimization*. New York: John Wiley.
- Van Dongen DB and Doherty MF (1985) On the dynamics of distillation processes – VI. Batch distillation. *Chemical Engineering Science* 40: 2087.

Sublimation

J. D. Green, BP Amoco Chemicals, Hull, UK

This article is reproduced from *Encyclopedia of Analytical Science* Copyright © 1995 Academic Press

Introduction

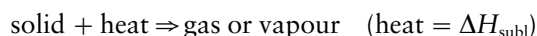
Sublimation is not a procedure that is generally regarded as an analytical technique. It is a process, however, by which compounds can be purified or mixtures separated and as such can be of value as a single step or as an integral part of a more complex analytical method. It is applicable to a range of solids of inorganic or organic origin in a variety of different matrices and can be particularly useful when heat-labile materials are involved.

As a method of sample purification sublimation has been used to produce high-purity materials as analytical standards. A specific and common example of sublimation used as a means of purification is the removal of water from heat-labile materials in the process known as freeze-drying. The technique is described more fully below.

As a separation technique fractional sublimation has been used either to purify samples for analysis by removing undesirable components of the matrix or to remove the analyte from the matrix for subsequent analysis.

Principles

Sublimation is the direct conversion of a solid to a gas or vapour:



The heat supplied in this endothermic process is termed the heat of sublimation (ΔH_{subl}). The conditions under which sublimation occurs may be predicted for a given substance from its phase diagram, but in practice it is more common to use typical experimental parameters to determine the optimized procedure.

The heat of sublimation is a crucial parameter in deciding upon the applicability of sublimation to a particular substance, or indeed on the possibility of separating two components in a mixture.

An empirical approach to determining the appropriate temperature and pressure for sublimation can be used based upon previously determined data. The temperature (T , °K) and pressure (P) of sublimation can be related by an expression of the form:

$$\log_{10} P \text{ (mmHg)} = A - (B/T)$$

in which the constants A and B for compounds of interest are available from published tables. The

result of the sublimation process can be seen in a freezer where ice sublimates and resolidifies as crystals. Iodine is a common substance that sublimates at room temperature and pressure; the result of this can be observed in a reagent bottle of the element.

The theory and mechanism of sublimation is of less practical importance to analytical procedures than it is in some other specialized areas of chemical science. Knowledge of sublimation characteristics can aid improvements in the stability of materials used at high temperatures or low pressures. For analytical purposes it should be sufficient to recognize that rates of sublimation depend upon the topology of the vaporizing surface (dislocations, atomic steps and ledge concentrations) and upon any atomic rearrangement that occurs during the sublimation process.

Experimentally, to effect sublimation, a number of criteria need to be satisfied. Firstly, the sample in question must be maintained at a temperature that ensures a sufficiently high vapour pressure for sublimation to occur, whilst remaining below that point at which the material either decomposes or melts. Secondly, a secondary surface must be available on which the sublimated vapour can condense or solidify. A number of experimental arrangements have been used that allow these criteria to be established; these are described in a later section of this article. It is also possible to enhance the sublimation process by changing the physical parameters under which the process is carried out:

- The sample may be heated in order to increase its vapour pressure.
- The application of a vacuum to the apparatus encourages vaporization and enhances the sublimation.
- Selectively cooling part of the apparatus increases the efficiency of the condensation process.
- Using an entraining gas can improve the mass transport in the system and thereby increase the overall efficiency of the sublimation process.

Apparatus

The simplest form of sublimation apparatus consists of a beaker or porcelain dish on top of which is placed an upturned watch-glass. The beaker contains the solid to be sublimed and the underside of the watch-glass provides the surface upon which the sublimed components condense (Figure 1). A perforated filter paper is commonly placed between the beaker and the watch-glass to prevent sublimate falling back into the sample.

A variant upon the above system uses an upturned funnel instead of a watch-glass as the condensing

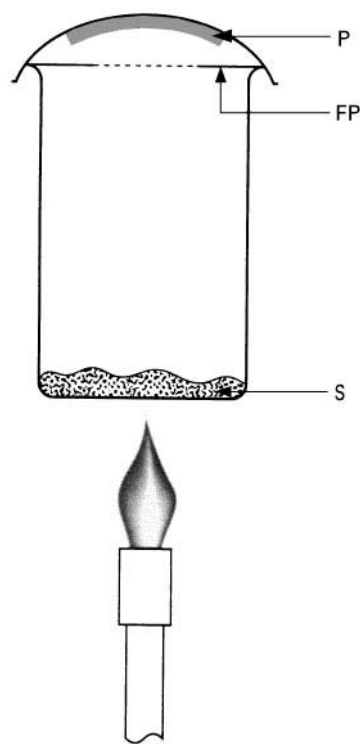


Figure 1 Simple apparatus for demonstrating the principles of sublimation. S, sample; P, sublimate (product); FP, perforated filter paper.

surface and an appropriately placed sealing ring improves the performance (Figure 2). Coils through which coolant is circulated can promote the sublimation process.

An early form of sublimation apparatus of which the above arrangements are derivatives (Figure 3)

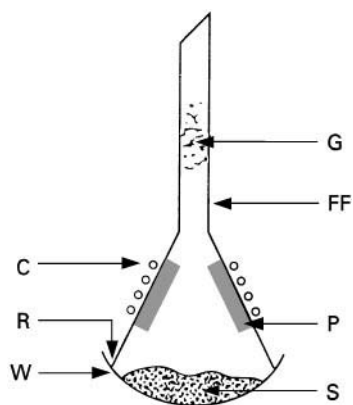


Figure 2 Apparatus for simple sublimation at atmospheric pressures. Watch-glass, W, with sample, S, surmounted by filter funnel, FF, with cooling coils, C, glass wool, G, and collected sublimed product, P. A sealing ring, R, is included between the watch-glass and filter funnel.

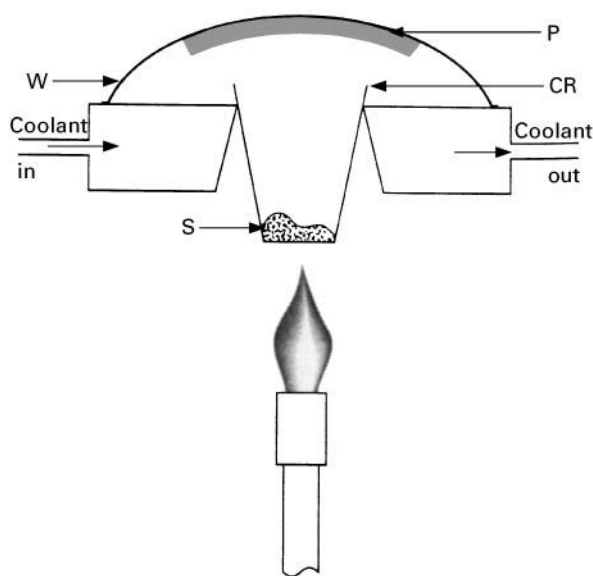


Figure 3 Early form of sublimation apparatus. The heated crucible, CR, rests in the cooling device. The sublimate product, P, collects on the underside of the watch-glass, W. S, sample.

included a means of cooling the surface on which the sublimate condenses. Cooling can be achieved in a number of ways, for example, using filter papers moistened with cool water, or in the case of the upturned funnel, a suitably shaped coil of circulating coolant liquid can be placed around the surface.

Sublimation under reduced pressure uses a modified form of apparatus in which a sealed enclosure allows a vacuum to be applied. The cooled surface is orientated with respect to the sample so as to maximize the condensation once sublimation has occurred (Figure 4). Reducing the distance that the sublimed substance(s) must travel is beneficial provided the necessary temperature gradient between sample and condensing surface can be maintained. An alternative arrangement for sublimation applications is shown in Figure 5.

Freeze-drying, a special application of the sublimation principle, uses apparatus of a different kind (Figure 6). The sample is dispersed around the walls of a round-bottomed flask whilst it is frozen by immersion in a suitable freezing mixture, for example dry ice-acetone. The flask is then attached to the evacuating system which usually comprises an oil vacuum pump protected from the ice sublimate by a train of condenser traps. Over a period of typically several hours the ice sublimates from the sample and condenses in the traps. Air is then admitted to the apparatus and the dried sample can be removed whilst the sublimed ice is drained off as water through the drain tap. Frequently this system is used to dry heat-sensitive

materials such as enzymes and the process has been termed lyophilization.

Sublimation of metallic elements from rock or ore samples requires high temperatures. The equipment used is based upon silica furnace tubes in order to withstand the necessary conditions. The silica tube is heated in a furnace and the sublimate condenses either on a cool part of the tube or on a cooled surface immediately after leaving the tube.

The conditions of sublimation must be chosen according to the requirements of the application. For simple purification the sample temperature is raised slowly, under reduced pressure if necessary, until sublimate is observed on the condensing surface. These established conditions should then be maintained until no further sublimation appears to be occurring, at which point the sample temperature can be raised again if other components of the sample can be further removed. At any point in this cycle the apparatus can be dismantled and the sublimate removed. This process allows selective separation or fractional sublimation to be carried out.

Applications

Sublimation is applicable to a wide range of organic and inorganic compounds in an equally wide range

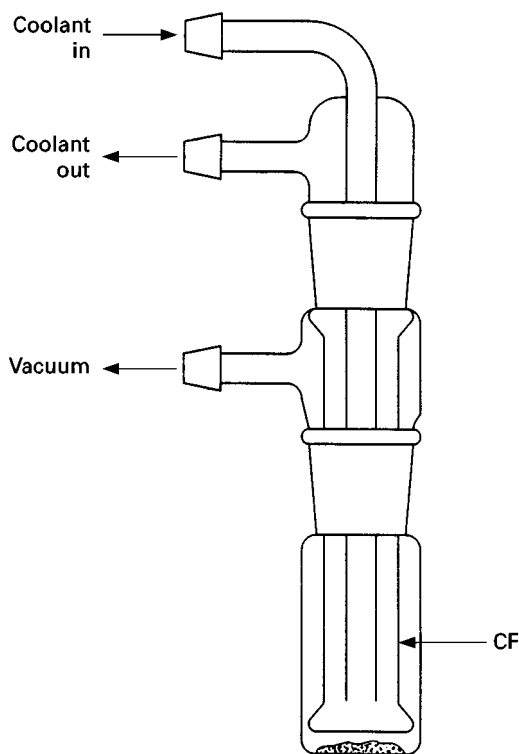


Figure 4 Apparatus for sublimation at reduced pressure. Coolant is circulated through the cold finger, CF, whilst a vacuum is applied to the sample chamber.

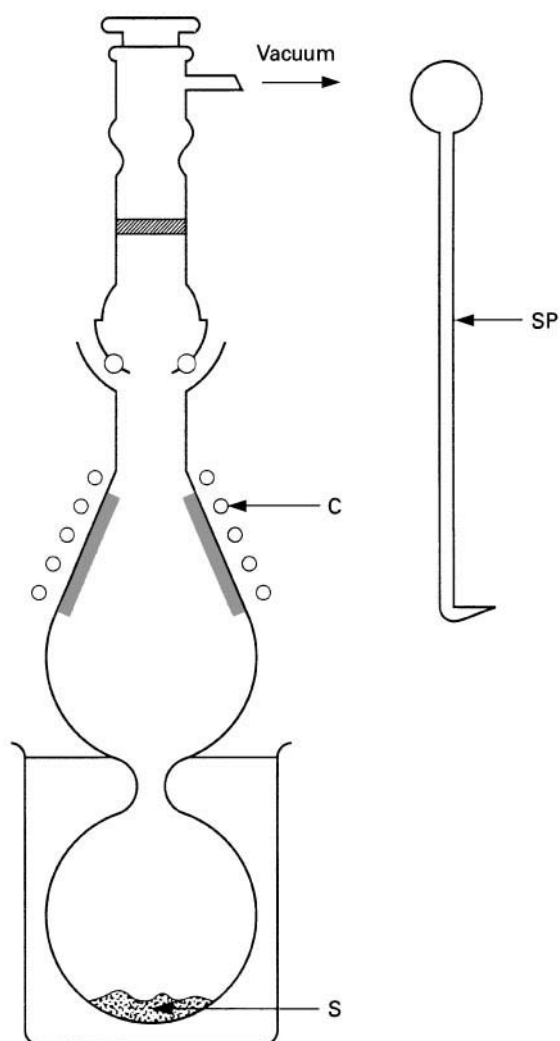


Figure 5 Improved sublimation apparatus proposed by Eisenbraun *et al.* (1978). Sample, S, sublimates from the lower to the upper chamber where condensation takes place on the cooled surface. A vacuum is applied to the apparatus and cooling coils, C, improve the condensation process. A specially formed spatula, SP, can be used to help remove the sublimate after the upper part of the apparatus is removed.

of different matrices. Sublimable substances include ice, iodine, arsenic(III) oxide, cadmium sulfide, ammonium chloride and a large number of organic compounds. Common matrices from which substances are sublimed include biological fluids, plant materials, carbonaceous materials, samples of crude organic solids and samples of rocks and ores.

Sublimation as a method of applying substances to thin-layer chromatography (TLC) plates involves the sample being sublimed and the vapour produced being directed by means of a drawn capillary onto the surface of a TLC plate which is slowly moved in one dimension. This results in the sublimed materials being deposited upon the TLC plate in a differential

mode – the most easily sublimed compounds are deposited first whilst those requiring a higher temperature are deposited later. The TLC plate is then developed in the normal way to give what has been termed a ‘thermofractogram’ in which the substances are separated as a function of their heats of sublimation along one axis and as a function of their chromatographic characteristics along the other axis. This approach has been applied to a wide range of substances including pharmaceutical preparations, plant components and foodstuffs.

Only a very limited number of standard methods have been reported in which sublimation is an important aspect. These comprise an ASTM standard for measurement of sublimation from thermionic emitters, and two standards from Germany and Japan testing the stability of dyes and printing inks to sublimation. The first covers the determination of the quantity, rate, and identity of sublimed, evaporated, or sputtered materials, whilst the latter two are concerned with textile materials and semi-manufactured products.

Sublimation is often the mechanism by which pre-concentration of an analyte is effected, although this fact is frequently not appreciated. Dynamic headspace concentration from solid samples such as plant materials, foodstuffs or polymeric materials occurs by sublimation of the volatile components. Indeed, given appropriate apparatus that can be operated at different temperatures for dynamic

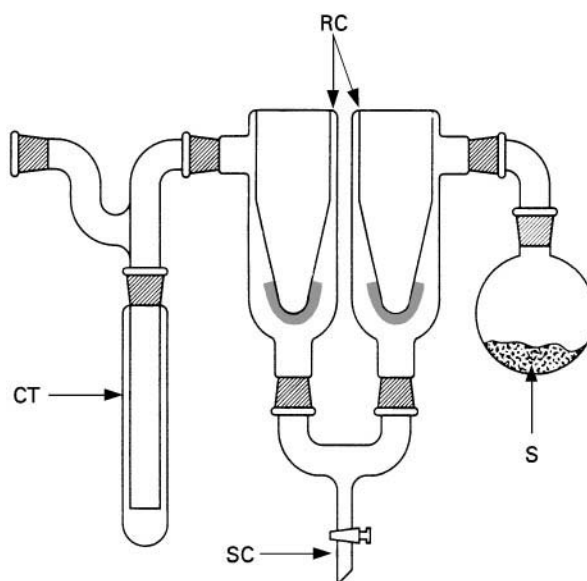


Figure 6 Typical freeze-drying apparatus. The frozen sample, S, is attached to the condenser assembly and a vacuum is applied. A cold trap, CT, protects the pump as ice sublimates from the sample and subsequently condenses in the refrigerant condensers, RC. On completion of the drying the sample is removed and the collected ice melts and drains from the system through the stopcock, SC.

headspace concentration, the heat of sublimation can be determined for various compounds.

Derivatization procedures carried out on crude samples can produce materials with improved sublimation characteristics. This technique has been used to produce volatile compounds of lanthanides and actinides which have then been sublimed prior to analytical determinations. Derivatives have been made using β -diketones (hexafluoroacetylacetone or acetylacetone), benzoyltrifluoroacetone and thenoyltrifluoroacetones.

Low-temperature sublimation, which in some circumstances is termed freeze-drying, has been used to separate water, as ice, from biological fluids such as serum, urine or saliva. The technique has been particularly useful in paediatric cases where sample volumes are extremely low. Determinations have then been accomplished using IR spectroscopy or mass spectrometry. Preparation of physiological samples for determination of deuterium oxide has included sublimation techniques prior to spectrophotometric determinations.

Low-temperature sublimation has been used to prepare samples for cryo-scanning electron microscopy (SEM) analysis in order to examine herbicide particles in a water suspension. The sublimation of herbicide-containing frozen water droplets provides a suitable etching of the surface for the SEM technique.

High-temperature sublimations are often the methods of choice in sample preparations from mineral ores, particularly in the case of trace enrichment of noble metals and the actinides and lanthanides prior to activation methods. Temperatures of 800–1200°C are typical. The procedure is carried out in silica tubes with entrainment gases, for example air or argon, being used to increase the sublimation process.

Polycyclic aromatic compounds have been separated using sublimation techniques from a variety of samples including coal, solids derived from oil, coal and petroleum processing, and residues (soots) resulting from the use of such fossil fuels.

A variety of miscellaneous applications have been developed for separation from difficult matrices and purification of specific materials. These include:

- Mercury separated from impurities by conversion to its iodide followed by sublimation.
- Isolation of proazulene and chamomile from the flower heads of plants.
- Isolation of aroma compounds from wheat and rye samples prior to determination using isotope dilution methods.
- Determination of tin in cassiterite.
- Selective sublimation of molybdenum and tungsten.

Sublimation is used in some procedures for the preparation of samples for SEM in which gold is sublimed in vacuum from a heated tungsten filament to the sample being examined.

See also: II/Distillation: Freeze-Drying.

Further Reading

- Chickos JS (1987) Heats of sublimation. In: Liebman JF and Greenberg A (eds) *Molecular Structure and Energetics*, vol. 2. Weinheim, Germany: VCH Publishers.
- Davies M (compiler) (1991–1992) Sublimation pressure for organic compounds. In: Lide DR (ed.) *CRC Handbook of Physics and Chemistry*, 72nd edn, pp. 5–91. Boca Raton: CRC Press.
- Eisenbraun EJ, Moyer CJ and Vuppapalaty P (1978) Sublimation apparatus: design improvement. *Chemistry and Industry* 229–230.
- Holden CA and Bryant HS (1969) Purification by sublimation. *Separation Science* 4(1): 1–13.
- Somorjai GA (1968) Mechanism of sublimation. *Science* 162: 755–760.
- Stahl E (1976) Advances in the field of thermal procedures in direct combination with thin-layer chromatography. *Accounts of Chemical Research* 9: 75–80.

Theory of Distillation

I. J. Halvorsen and S. Skogestad, Norwegian University of Science and Technology (NTNU), Trondheim, Norway

Copyright © 2000 Academic Press

Introduction

Distillation is a very old separation technology for separating liquid mixtures that can be traced back to

the chemists in Alexandria in the first century AD. Today distillation is the most important industrial separation technology. It is particularly well suited for high purity separations since any degree of separation can be obtained with a fixed energy consumption by increasing the number of equilibrium stages.

To describe the degree of separation between two components in a column or in a column section, we

introduce the separation factor:

$$S = \frac{(x_L/x_H)_T}{(x_L/x_H)_B} \quad [1]$$

where x denotes mole fraction of a component, subscript L denotes light component, H heavy component, T denotes the top of the section, and B the bottom.

It is relatively straightforward to derive models of distillation columns based on almost any degree of detail, and also to use such models to simulate the behaviour on a computer. However, such simulations may be time-consuming and often provide limited insight. The objective of this article is to provide analytical expressions that are useful for understanding the fundamentals of distillation and which may be used to guide and check more detailed simulations:

1. minimum energy requirement and corresponding internal flow requirements
2. minimum number of stages
3. simple expressions for the separation factor

The derivation of analytical expressions requires the assumptions of:

1. equilibrium stages
2. constant relative volatility
3. constant molar flows

These assumptions may seem restrictive, but they are actually satisfied for many real systems, and in any case the resulting expressions yield invaluable insights, also for systems where the approximations do not hold.

Fundamentals

The Equilibrium-Stage Concept

The equilibrium (theoretical)-stage concept (Figure 1) is central in distillation. Here we assume vapour-liquid equilibrium (VLE) on each stage and that the liquid is sent to the stage below and the vapour to the stage above. For some trayed columns this may be a reasonable description of the actual physics, but it is certainly not for a packed column. Nevertheless, it is established that calculations based on the equilibrium-stage concept (with the number of stages adjusted appropriately) fits data from most real columns very well, even packed columns.

One may refine the equilibrium stage concept, e.g. by introducing back-mixing or a Murphree efficiency factor for the equilibrium, but these 'fixes' often have relatively little theoretical justification, and are not used in this article.

For practical calculations, the critical step is usually not the modelling of the stages, but to obtain a good description of the VLE. In this area there has been significant advances in the last 25 years, especially after the introduction of equations of state for VLE prediction. However, here we will use simpler VLE models (constant relative volatility) which apply to relatively ideal mixtures.

Vapour-Liquid Equilibrium

In a two-phase system ($PH = 2$) with N_c nonreacting components, the state is completely determined by N_c degrees of freedom (f), according to Gibb's phase rule:

$$f = N_c + 2 - PH \quad [2]$$

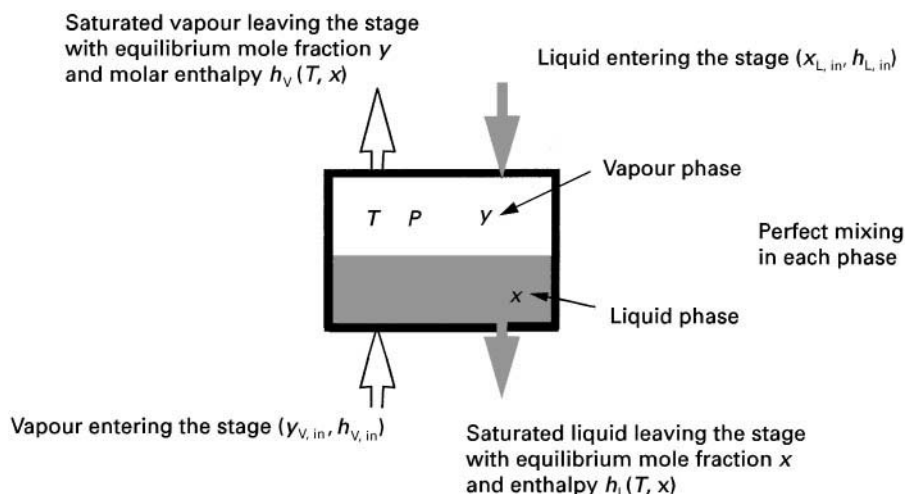


Figure 1 Equilibrium-stage concept.

If the pressure (P) and $N_c - 1$ liquid compositions or mole fractions (x) are used as degree of freedom, then the mole fractions (y) in the vapour phase and the temperature (T) are determined, provided that two phases are present. The general VLE relation can then be written:

$$\begin{aligned} [y_1, y_2 \dots y_{N_c-1}, T] &= f(P, x_1, x_2 \dots x_{N_c-1}) \\ [y, T] &= f(P, x) \end{aligned} \quad [3]$$

Here we have introduced the mole fractions x and y in the liquid and vapour phases respectively, and we trivially have $\sum_{i=1}^n x_i = 1$ and $\sum_{i=1}^n y_i = 1$.

In ideal mixtures, the VLE can be derived from Raoult's law which states that the partial pressure p_i of a component (i) in the vapour phase is proportional to the vapour pressure (p_i^o) of the pure component (which is a function of temperature only: $p_i^o = p_i^o(T)$) and the liquid mole fraction (x_i):

$$p_i = x_i p_i^o(T) \quad [4]$$

For an ideal gas, according to Dalton's law, the partial pressure of a component is proportional to the mole fraction $p_i = y_i P$ and since the total pressure $P = p_1 + p_2 + \dots + p_{N_c} = \sum_i p_i = \sum_i x_i p_i^o(T)$ we derive:

$$y_i = x_i \frac{p_i^o}{P} = \frac{x_i p_i^o(T)}{\sum_i x_i p_i^o(T)} \quad [5]$$

The following empirical formula is frequently used to compute the pure component vapour pressure:

$$\ln p^o(T) \approx a + \frac{b}{c + T} + d \ln(T) + eT^f \quad [6]$$

The coefficients are listed in component property databases. The case with $d = e = 0$ is called the Antoine equation.

K-values and Relative Volatility

The K -value for a component i is defined as: $K_i = y_i/x_i$. The K -value is sometimes called the equilibrium constant, but this is misleading as it depends strongly on temperature and pressure (or composition).

The relative volatility between components i and j is defined as:

$$\alpha_{ij} = \frac{(y_i/x_i)}{(y_j/x_j)} = \frac{K_i}{K_j} \quad [7]$$

For ideal mixtures that satisfy Raoult's law we have:

$$\alpha_{ij} = \frac{(y_i/x_i)}{(y_j/x_j)} = \frac{K_i}{K_j} = \frac{p_i^o(T)}{p_j^o(T)} \quad [8]$$

Here $p_i^o(T)$ depends on temperature so the K -values will actually be constant only close to the column ends where the temperature is relatively constant. On the other hand, the ratio $p_i^o(T)/p_j^o(T)$ is much less dependent on temperature, which makes the relative volatility very attractive for computations. For ideal mixtures, a geometric average of the relative volatilities for the highest and lowest temperature in the column usually gives sufficient accuracy in the computations: $\alpha_{ij} = \sqrt{\alpha_{ij, \text{top}} \cdot \alpha_{ij, \text{bottom}}}$.

We usually select a common reference component r (usually the least volatile or heavy component), and define:

$$\alpha_i = \alpha_{ir} = p_i^o(T)/p_r^o(T) \quad [9]$$

The VLE relationship (eqn [5]) then becomes:

$$y_i = \frac{\alpha_i x_i}{\sum_i \alpha_i x_i} \quad [10]$$

For a binary mixture we usually omit the component index for the light component, i.e. we write $x = x_1$ (light component) and $x_2 = 1 - x$ (heavy component). Then the VLE relationship becomes:

$$y = \frac{\alpha x}{1 + (\alpha - 1)x} \quad [11]$$

This equilibrium curve is illustrated in Figure 2.

The difference $y - x$ determines the amount of separation that can be achieved on a stage. Large relative volatilities imply large differences in boiling points and easy separation. Close boiling points imply relative volatility closer to unity, as shown below quantitatively.

Estimating the Relative Volatility from Boiling Point Data

The Clapeyron equation relates the vapour pressure temperature dependency to the specific heat of vaporization (ΔH^{vap}) and volume change between liquid and vapour phase (ΔV^{vap}):

$$\frac{dp^o(T)}{dT} = \frac{\Delta H^{\text{vap}}(T)}{T \Delta V^{\text{vap}}(T)} \quad [12]$$

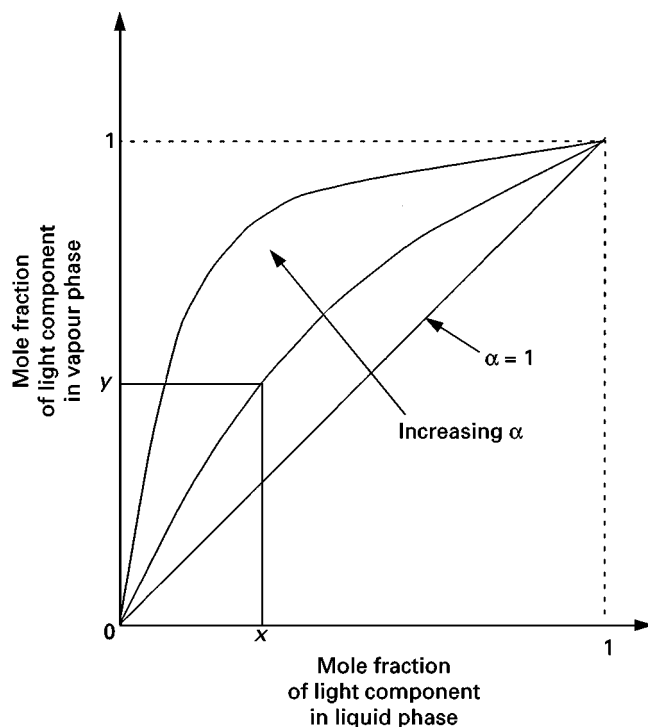


Figure 2 VLE for ideal binary mixture: $y = \alpha x/1 + (\alpha - 1)x$.

If we assume an ideal gas phase, and that the gas volume is much larger than the liquid volume, then $\Delta V^{\text{vap}} \approx RT/P$, and integration of Clapeyron's equation from temperature T_{bi} (boiling point at pressure P_{ref}) to temperature T (at pressure p_i°) gives, when ΔH_i^{vap} is assumed constant:

$$\ln p_i^{\circ} \approx \left(\frac{\Delta H_i^{\text{vap}}}{R} \left(\frac{1}{T_{\text{bi}}} \right) + \ln P_{\text{ref}} \right) + \frac{\left(-\frac{\Delta H_i^{\text{vap}}}{R} \right)}{T} \quad [13]$$

This gives us the Antoine coefficients: $a_i = (\Delta H_i^{\text{vap}}/R) (1/T_{\text{bi}}) + \ln P_{\text{ref}}$, $b_i = -\Delta H_i^{\text{vap}}/R$, $c_i = 0$. In most cases $P_{\text{ref}} = 1$ atm. For an ideal mixture that satisfies Raoult's law we have $\alpha_{ij} = p_i^{\circ}(T)/p_j^{\circ}(T)$ and we derive:

$$\ln \alpha_{ij} = \frac{\Delta H_i^{\text{vap}}}{R} \frac{1}{T_{\text{bi}}} - \frac{\Delta H_j^{\text{vap}}}{R} \frac{1}{T_{\text{bj}}} + \frac{\Delta H_j^{\text{vap}} - \Delta H_i^{\text{vap}}}{RT} \quad [14]$$

We see that the temperature dependency of the relative volatility arises from different specific heats of vaporization. For similar values ($\Delta H_i^{\text{vap}} \approx \Delta H_j^{\text{vap}}$), the expression simplifies to:

$$\ln \alpha_{ij} \approx \underbrace{\frac{\Delta \bar{H}^{\text{vap}}}{R \bar{T}_b}}_{\beta} \frac{T_{\text{bj}} - T_{\text{bi}}}{\bar{T}_b} \quad \text{where } \bar{T}_b = \sqrt{T_{\text{bi}} T_{\text{bj}}} \quad [15]$$

Here we may use the geometric average also for the heat of vaporization:

$$\Delta \bar{H}^{\text{vap}} = \sqrt{\Delta H_i^{\text{vap}}(T_{\text{bi}}) \cdot \Delta H_j^{\text{vap}}(T_{\text{bj}})}$$

This results in a rough estimate of the relative volatility α_{ij} , based on the boiling points only:

$$\alpha_{ij} \approx e^{\beta(T_{\text{bj}} - T_{\text{bi}})/\bar{T}_b} \quad \text{where } \beta = \frac{\Delta \bar{H}^{\text{vap}}}{R \bar{T}_b} \quad [16]$$

If we do not know $\Delta \bar{H}^{\text{vap}}$, a typical value $\beta \approx 13$ can be used for many cases.

Example For methanol (*L*) and *n*-propanol (*H*), we have $T_{\text{BL}} = 337.8$ K and $T_{\text{BH}} = 370.4$ K and the heats of vaporization at their boiling points are 35.3 and 41.8 kJ mol⁻¹ respectively. Thus $\bar{T}_b = \sqrt{337.8 \cdot 370.4} = 354$ K and $\Delta \bar{H}^{\text{vap}} = \sqrt{35.3 \cdot 41.8} = 38.4$. This gives $\beta = \Delta \bar{H}^{\text{vap}}/R \bar{T}_b = 38.4/(8.83 \cdot 354) = 13.1$ and $\alpha \approx e^{13.1 \cdot 32.6/354} \approx 3.34$ which is a bit lower than the experimental value.

Material Balance on a Distillation Stage

Based on the equilibrium-stage concept, a distillation column section is modelled as shown in Figure 3.

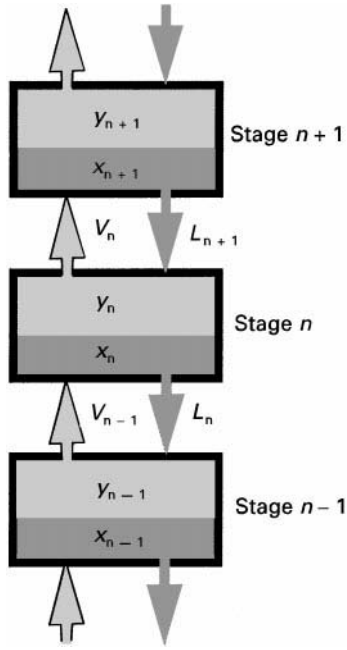


Figure 3 Distillation column section modelled as a set of connected equilibrium stages.

Note that we choose to number the stages starting from the bottom of the column. We denote L_n and V_n as the total liquid and vapour molar flow rates leaving stage n (and entering stages $n-1$ and $n+1$, respectively). We assume perfect mixing in both phases inside a stage. The mole fraction of species i in the vapour leaving the stage with V_n is $y_{i,n}$, and the mole fraction in L_n is $x_{i,n}$.

The material balance for component i at stage n then becomes (in mol s^{-1}):

$$\frac{dN_{i,n}}{dt} = (L_{n+1}x_{i,n+1} - V_n y_{i,n}) - (L_n x_{i,n} - V_{n-1} y_{i,n-1}) \quad [17]$$

where $N_{i,n}$ is the number of moles of component i on stage n . In the following we will consider steady-state operation, i.e.: $dN_{i,n}/dt = 0$.

It is convenient to define the net material flow (w_i) of component i upwards from stage n to $n+1$ (mol s^{-1}):

$$w_{i,n} = V_n y_{i,n} - L_{n+1} x_{i,n+1} \quad [18]$$

At steady state, this net flow has to be the same through all stages in a column section, i.e. $w_{i,n} = w_{i,n+1} = w_i$.

The material flow equation is usually rewritten to relate the vapour composition (y_n) on one stage to the

liquid composition on the stage above (x_{n+1}):

$$y_{i,n} = \frac{L_{n+1}}{V_n} x_{i,n+1} + \frac{1}{V_n} w_i \quad [19]$$

The resulting curve is known as the operating line. Combined with the VLE relationship (equilibrium line), this enables us to compute all the stage compositions when we know the flows in the system. This is illustrated in **Figure 4**, and forms the basis of McCabe–Thiele approach.

Assumption about Constant Molar Flows

In a column section, we may very often use the assumption about constant molar flows. That is, we assume $L_n = L_{n+1} = L$ (mol s^{-1}) and $V_{n-1} = V_n = V$ (mol s^{-1}). This assumption is reasonable for ideal mixtures when the components have similar molar heats of vaporization. An important implication is that the operating line is then a straight line for a given section, i.e. $y_{i,n} = (L/V)x_{i,n+1} + w_i/V$. This makes computations much simpler since the internal flows (L and V) do not depend on compositions.

The Continuous Distillation Column

We study here the simple two-product continuous distillation column in **Figure 5**. We will first limit ourselves to a binary feed mixture, and the component index is omitted, so the mole fractions (x, y, z) refer to the light component. The column has N equilibrium stages, with the reboiler as stage number 1. The feed with total molar flow rate F (mol s^{-1}) and mole fraction z enters at stage N_F .

The section above the feed stage is denoted the rectifying section, or just the top section, and the most volatile component is enriched upwards towards the distillate product outlet (D). The stripping section, or the bottom section, is below the feed, in which the least volatile component is enriched towards the bottoms product outlet (B). (The least volatile component is stripped out.) Heat is supplied in the reboiler and removed in the condenser, and we do not consider any heat loss along the column.

The feed liquid fraction q describes the changes in liquid and vapour flow rates at the feed stage:

$$\Delta L_F = qF \quad [20]$$

$$\Delta V_F = (1 - q) F$$

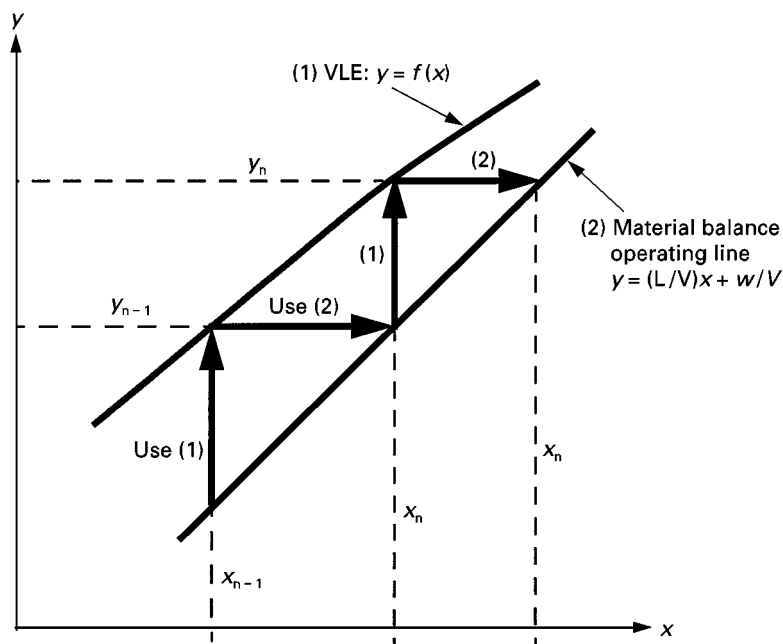


Figure 4 Combining the VLE and the operating line to compute mole fractions in a section of equilibrium stages.

The liquid fraction is related to the feed enthalpy (h_F) as follows:

$$q = \frac{h_{V,\text{sat}} - h_F}{\Delta H^{\text{vap}}} = \begin{cases} > 1 & \text{Subcooled liquid} \\ = 1 & \text{Saturated liquid} \\ 0 < q < 1 & \text{Liquid and vapour} \\ = 0 & \text{Saturated vapour} \\ < 0 & \text{Superheated vapour} \end{cases} \quad [21]$$

When we assume constant molar flows in each section, we get the following relationships for the flows:

$$\begin{aligned} V_T &= V_B + (1 - q)F \\ L_B &= L_T + qF \\ D &= V_T - L_T \\ B &= L_B - V_B \end{aligned} \quad [22]$$

Degrees of Freedom in Operation of a Distillation Column

With a given feed (F , z and q), and column pressure (P), we have only 2 degrees of freedom in operation of the two-product column in Figure 5, independent of the number of components in the feed. This may be a bit confusing if we think about degrees of freedom as in Gibb's phase rule, but in this context Gibb's rule

does not apply since it relates the thermodynamic degree of freedom inside a single equilibrium stage.

This implies that if we know, for example, the reflux (L_T) and vapour (V_B) flow rate into the column, all states on all stages and in both products are completely determined.

External and Internal Flows

The overall mass balance and component mass balance is given by:

$$F = D + B \quad [23]$$

$$Fz = Dx_D + Bx_B$$

Here z is the mole fraction of light component in the feed, and x_D and x_B are the product compositions. For sharp splits with $x_D \approx 1$ and $x_B \approx 0$ we then have that $D = zF$. In words, we must adjust the product split D/F such that the distillate flow equals the amount of light component in the feed. Any deviation from this value will result in large changes in product composition. This is a very important insight for practical operation.

Example Consider a column with $z = 0.5$, $x_D = 0.99$, $x_B = 0.01$ (all these refer to the mole fraction of light component) and $D/F = B/F = 0.5$. To simplify the discussion set $F = 1$ (mol s⁻¹). Now consider a 20% increase in the distillate D from 0.51 to

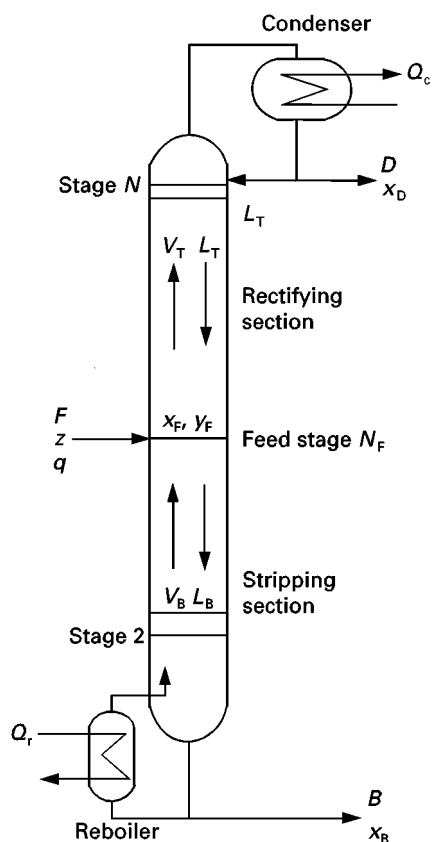


Figure 5 An ordinary continuous two-product distillation column.

$0.6 \text{ (mol s}^{-1}\text{)}$. This will have a drastic effect on composition. Since the total amount of light component available in the feed is $z = 0.5 \text{ (mol s}^{-1}\text{)}$, at least $0.1 \text{ (mol s}^{-1}\text{)}$ of the distillate must now be heavy component, so the amount mole fraction of light component is now at its best $0.5/0.6 = 0.833$. In other words, the amount of heavy component in the distillate will increase at least by a factor of 16.7 (from 1% to 16.7%).

Thus, we generally have that a change in external flows (D/F and B/F) has a large effect on composition, at least for sharp splits, because any significant deviation in D/F from z implies large changes in composition. On the other hand, the effects of changes in the internal flows (L and V) are much smaller.

McCabe–Thiele Diagram (Constant Molar Flows, but any VLE)

The McCabe–Thiele diagram where y is plotted as a function x along the column provides an insightful graphical solution to the combined mass balance (operation line) and VLE (equilibrium line) equations. It is mainly used for binary mixtures. It is often used to

find the number of theoretical stages for mixtures with constant molar flows. The equilibrium relationship $y_n = f(x_n)$ (y as a function of x at the stages) may be nonideal. With constant molar flow, L and V are constant within each section and the operating lines (y as a function of x between the stages) are straight. In the top section the net transport of light component $w = x_D D$. Inserted into the material balance eqn [19] we obtain the operating line for the top section, and we have a similar expression for the bottom section:

$$\text{Top: } y_n = \left(\frac{L}{V}\right)_T (x_{n+1} - x_D) + x_D \quad [24]$$

$$\text{Bottom: } y_n = \left(\frac{L}{V}\right)_B (x_{n+1} - x_B) + x_B$$

A typical McCabe–Thiele diagram is shown in Figure 6.

The optimal feed stage is at the intersection of the two operating lines and the feed-stage composition (x_F, y_F) is then equal to the composition of the flashed feed mixture. We have that $z = qx_F + (1 - q)y_F$. For $q = 1$ (liquid feed) we find $x_F = z$ and for $q = 0$ (vapour feed) we find $y_F = z$ (in the other cases we must solve the equation together with the VLE). The pinch, which occurs at one side of the feed stage if the feed is not optimally located, is easily understood from the McCabe–Thiele diagram, as shown in Figure 8 (see below).

Typical Column Profiles – Pinch

An example of a column composition profile is shown in Figure 7 for a column with $z = 0.5$, $\alpha = 1.5$, $N = 40$, $N_F = 21$ (counted from the bottom, including the reboiler), $y_D = 0.90$, $x_B = 0.002$. This is a case where the feed stage is not optimally located, as seen from the presence of a pinch zone (a zone of constant composition) above the stage. The corresponding McCabe–Thiele diagram is shown in Figure 8. We see that the feed stage is not located at the intersection of the two operating lines, and that there is a pinch zone above the feed, but not below.

Simple Design Equations

Minimum Number of Stages – Infinite Energy

The minimum number of stages for a given separation (or equivalently, the maximum separation for a given number of stages) is obtained with infinite internal flows (infinite energy) per unit feed. (This always holds for single-feed columns and ideal

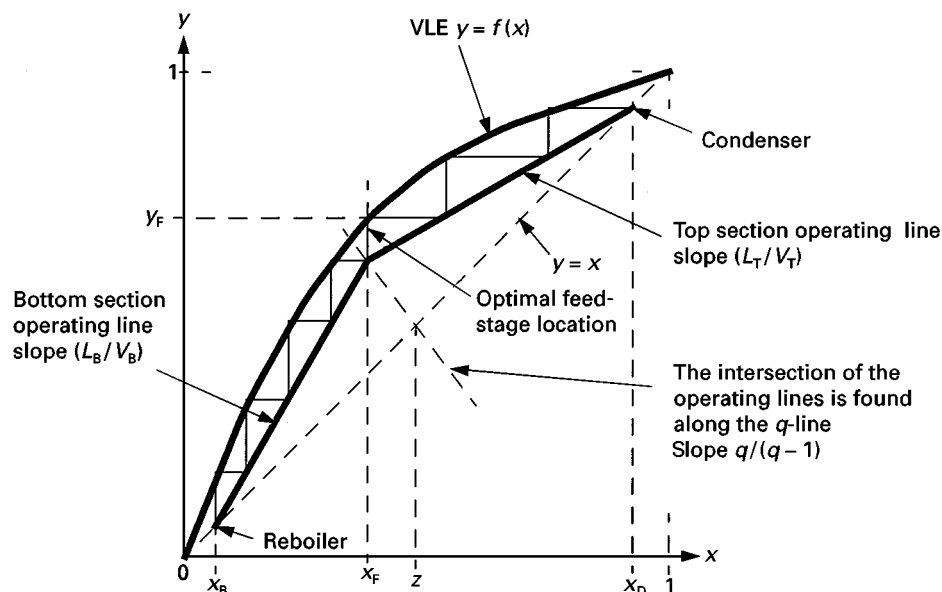


Figure 6 McCabe–Thiele diagram with an optimally located feed.

mixtures, but may not hold, for example, for extractive distillation with two feed streams.)

With infinite internal flows (total reflux) $L_n/F = \infty$ and $V_n/F = \infty$, a material balance across any part of the column gives $V_n = L_{n+1}$, and similarly a material balance for any component gives $V_n y_n = L_{n+1} x_{n+1}$. Thus, $y_n = x_{n+1}$, and with constant relative volatility

we have:

$$\alpha = \frac{y_{L,n}/x_{L,n}}{y_{H,n}/x_{H,n}} = \frac{x_{L,n+1}/x_{L,n}}{x_{H,n+1}/x_{H,n}} \quad [25]$$

For a column or column section with N stages, repeated use of this relation gives directly Fenske's

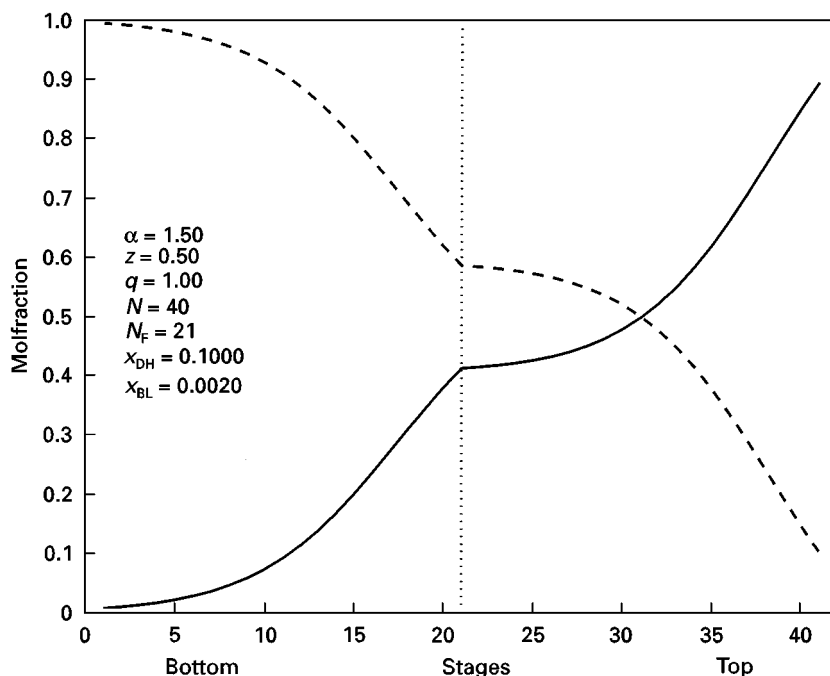


Figure 7 Composition profile (x_L , x_H) for case with nonoptimal feed location. Continuous line, light key; dashed line, heavy key.

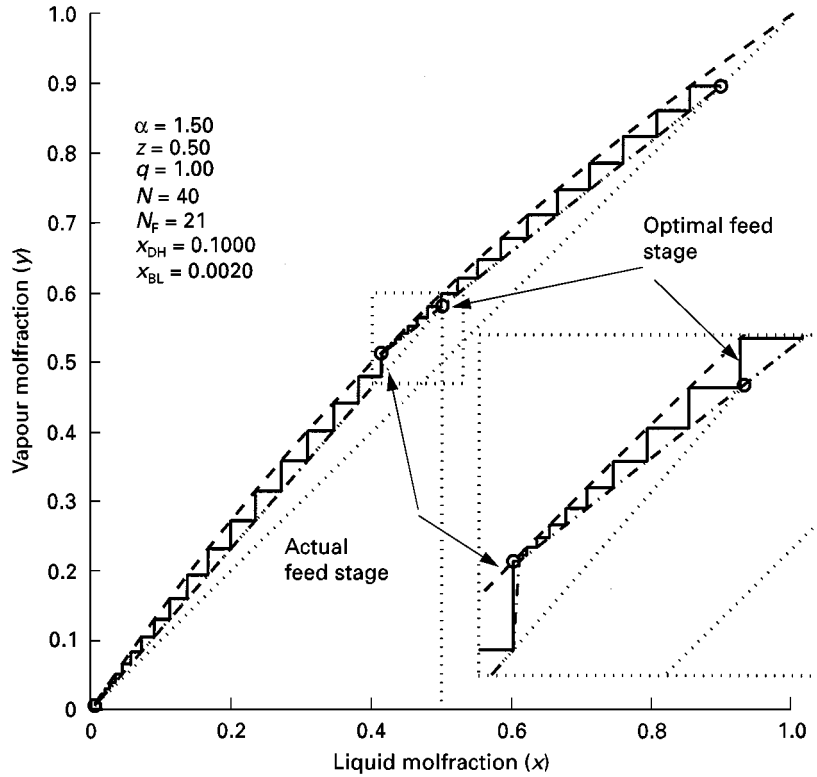


Figure 8 McCabe-Thiele diagram for the same example as shown in Figure 7. Observe that the feed stage location is not optimal.

formula for the overall separation factor:

$$S = \left(\frac{x_L}{x_H} \right)_T / \left(\frac{x_L}{x_H} \right)_B = \alpha^N \quad [26]$$

For a column with a given separation, this yields Fenske's formula for the minimum number of stages:

$$N_{\min} = \frac{\ln S}{\ln \alpha} \quad [27]$$

These Fenske expressions do not assume constant molar flows and apply to the separation between any two components with constant relative volatility. Note that although a high purity separation (large S) requires a larger number of stages, the increase is only proportional to the logarithm of the separation factor. For example, increasing the purity level in a product by a factor of 10 (e.g. by reducing $x_{H,D}$ from 0.01 to 0.001) increases N_{\min} by about a factor of $\ln 10 = 2.3$.

A common rule of thumb is to select the actual number of stages $N = 2N_{\min}$ (or even larger).

Minimum Energy Usage – Infinite Number of Stages

For a given separation, an increase in the number of stages will yield a reduction in the reflux (or equiva-

lently in the boil-up). However, as the number of stages approaches infinity, a pinch zone develops somewhere in the column, and the reflux cannot be reduced further. For a binary separation the pinch usually occurs at the feed stage (where the material balance line and the equilibrium line will meet), and we can easily derive an expression for the minimum reflux with $N = \infty$. For a saturated liquid feed ($q = 1$) (King's formula):

$$L_{T\min} = \frac{r_{L,D} - \alpha r_{H,D}}{\alpha - 1} F \quad [28]$$

where $r_{L,D} = x_{L,D}/zF$ is the recovery fraction of light component, and $r_{H,D}$ of heavy component, both in the distillate. The value depends relatively weakly on the product purity, and for sharp separations (where $r_{L,D} = 1$ and $r_{H,D} = 0$), we have $L_{T\min} = F/(\alpha - 1)$. Actually, eqn [28] applies without stipulating constant molar flows or constant α , but then $L_{T\min}$ is the liquid flow entering the feed stage from above, and α is the relative volatility at feed conditions. A similar expression, but in terms of $V_{B\min}$ entering the feed stage from below, applies for a saturated vapour feed ($q = 0$) (King's formula):

$$V_{B\min} = \frac{r_{H,B} - \alpha r_{L,B}}{\alpha - 1} F \quad [29]$$

For sharp separations we get $V_{Bmin} = F/(\alpha - 1)$. In summary, for a binary mixture with constant molar flows and constant relative volatility, the minimum boil-up for sharp separations is:

$$\begin{aligned} \text{Feed liquid, } q = 1: \quad V_{Bmin} &= \frac{1}{\alpha - 1}F + D \\ \text{Feed vapour, } q = 0: \quad V_{Bmin} &= \frac{1}{\alpha - 1}F \end{aligned} \quad [30]$$

Note that minimum boil-up is independent of the product purity for sharp separations. From this we establish one of the key properties of distillation: we can achieve any product purity (even infinite separation factor) with a constant finite energy (as long as it is higher than the minimum) by increasing the number of stages.

Obviously, this statement does not apply to azeotropic mixtures, for which $\alpha = 1$ for some compositions but we can get arbitrarily close to the azeotropic composition, and useful results may be obtained in some cases by treating the azeotrope as a pseudo-component and using α for this pseudo-separation.

Finite Number of Stages and Finite Reflux

Fenske's formula $S = \alpha^N$ applies to infinite reflux (infinite energy). To extend this expression to real columns with finite reflux we will assume constant molar flows and consider three approaches:

1. Assume constant K -values and derive the Kremser formulas (exact close to the column end for a high purity separation.)
2. Assume constant relative volatility and derive the following extended Fenske formula (approximate formula for case with optimal feed-stage location):

$$S \approx \alpha^N \frac{(L_T/V_T)^{N_T}}{(L_B/V_B)^{N_B}}$$

Here N_T is the number of stages in the top section and N_B in the bottom section.

3. Assume constant relative volatility and derive exact expressions. The most used are the Underwood formulas which are particularly useful for computing the minimum reflux (with infinite stages).

Constant K -Values – Kremser Formulas

For high purity separations most of the stages are located in the corner parts of the McCabe–Thiele diagram where, according to Henry's law, we may approximate the VLE relationship, even for nonideal mixtures, by straight lines:

Bottom of column:

$$y_L = H_L x_L \text{ light component; } x_L \rightarrow 0$$

Top of column:

$$y_H = H_H x_H \text{ heavy component; } x_H \rightarrow 0$$

where H is Henry's constant. (For the case of constant relative volatility, Henry's constant in the bottom is $H_L = \alpha$ and in the top is $H_H = 1/\alpha$.) Thus, with constant molar flows, both the equilibrium and mass-balance relationships are linear, and the resulting difference equations are easily solved analytically. For example, at the bottom of the column we derive for the light component:

$$\begin{aligned} x_{L,n+1} &= (V_B/L_B)H_L x_{L,n} + (B/L_B)x_{L,B} \\ &= s x_{L,n} + (1 - V_B/L_B)x_{L,B} \end{aligned} \quad [31]$$

where $s = (V_B/L_B)H_L > 1$ is the stripping factor. Repeated use of this equation gives the Kremser formula for stage N_B from the bottom (the reboiler would here be stage zero):

$$x_{L,N_B} = s^{N_B} x_{L,B} [1 + (1 - V_B/L_B)(1 - s^{-N_B})/(s - 1)] \quad [32]$$

(assuming we are in the region where s is constant, i.e. $x_L \approx 0$). At the top of the column we have for the heavy component:

$$\begin{aligned} y_{H,n-1} &= (L_T/V_T)(1/H_H)y_{H,n} + (D/V_T)x_{H,D} \\ &= a y_{H,n} + (1 - L_T/V_T)x_{H,D} \end{aligned} \quad [33]$$

where $a = (L_T/V_T)/H_H > 1$ is the absorption factor. The corresponding Kremser formula for the heavy component in the vapour phase at stage N_T counted from the top of the column (the accumulator in stage zero) is then:

$$y_{H,N_T} = a^{N_T} x_{H,D} [1 + (1 - L_T/V_T)(1 - a^{-N_T})/(a - 1)] \quad [34]$$

(assuming we are in the region where a is constant, i.e. $x_H \approx 0$).

For hand calculations one may use the McCabe–Thiele diagram for the intermediate composition region, and the Kremser formulas at the column ends where the use of the McCabe–Thiele diagram is inaccurate.

Example We consider a column with $N = 40$, $N_F = 21$, $\alpha = 1.5$, $z_L = 0.5$, $F = 1$, $D = 0.5$, $V_B = 3.206$. The feed is saturated liquid and exact

calculations give the product compositions $x_{H,D} = x_{L,B} = 0.01$. We now want to have a bottom product with only 1 p.p.m. heavy product, i.e. $x_{L,B} = 1.e - 6$. We can use the Kremser formulas to estimate easily the additional stages needed when we have the same energy usage, $V_B = 3.206$. (Note that with the increased purity in the bottom we actually get $D = 0.505$.) At the bottom of the column $H_L = \alpha = 1.5$ and the stripping factor is $s = (V_B/L_B)H_L = (3.206/3.711)1.5 = 1.296$.

With $x_{L,B} = 1.e - 6$ (new purity) and $x_{L,N_B} = 0.01$ (old purity) we find by solving the Kremser equation [31] for the top with respect to N_B that $N_B = 34.1$, and we conclude that we need about 34 additional stages in the bottom (this is not quite enough since the operating line is slightly moved and thus affects the rest of the column; using 36 rather than 34 additional stages compensates for this).

The above Kremser formulas are valid at the column ends, but the linear approximation resulting from the Henry's law approximation lies above the real VLE curve (it is optimistic), and thus gives too few stages in the middle of the column. However, if there is no pinch at the feed stage (i.e. the feed is optimally located), then most of the states in the column will be located at the column ends where the above Kremser formulas apply.

Approximate Formula with Constant Relative Volatility

We will now use the Kremser formulas to derive an approximation for the separation factor S . First note that for cases with high purity products we have $S \approx 1/(x_{L,B}x_{H,D})$. That is, the separation factor is the inverse of the product of the key component product impurities.

We now assume that the feed stage is optimally located such that the composition at the feed stage is the same as that in the feed, i.e. $y_{H,N_T} = y_{H,F}$ and $x_{L,N_B} = x_{L,F}$. Assuming constant relative volatility and using $H_L = \alpha$, $H_B = 1/\alpha$, $\alpha = (y_{L,F}/x_{L,F})/(y_{H,F}/x_{H,F})$ and $N = N_T + N_B + 1$ (including total reboiler) then gives:

$$S \approx \alpha^N \frac{(L_T/V_T)^{N_T}}{(L_B/V_B)^{N_B}} \frac{c}{(x_{H,F}y_{L,F})}$$

where:

$$c = \left[1 + \left(1 - \frac{V_B}{L_B} \right) \frac{(1 - s^{-N_B})}{(s - 1)} \right] \times \left[1 + \left(1 - \frac{L_T}{V_T} \right) \frac{(1 - a^{-N_T})}{(a - 1)} \right]$$

We know that S predicted by this expression is somewhat too large because of the linearized VLE. However, we may correct it such that it satisfies the exact relationship $S = \alpha^N$ at infinite reflux (where $L_B/V_B = V_T/L_T = 1$ and $c = 1$) by dropping the factor $1/(x_{H,F}y_{L,F})$ (which as expected is always larger than 1). At finite reflux, there are even more stages in the feed region and the formula will further overestimate the value of S . However, since $c > 1$ at finite reflux, we may partly counteract this by setting $c = 1$. Thus, we delete the term c and arrive at the final extended Fenske formula, where the main assumptions are that we have constant relative volatility, constant molar flows and that there is no pinch zone around the feed (i.e. the feed is optimally located):

$$S \approx \alpha^N \frac{(L_T/V_T)^{N_T}}{(L_B/V_B)^{N_B}} \quad [35]$$

where $N = N_T + N_B + 1$. Together with the material balance, $Fz_F = Dx_D + Bx_B$, this approximate formula can be used to estimate the number of stages for column design (instead of e.g. the Gilliland plots), and also to estimate the effect of changes of internal flows during column operation. However, its main value is the insight it provides:

1. We see that the best way to increase the separation S is to increase the number of stages.
2. During operation where N is fixed, the formula provides us with the important insight that the separation factor S is increased by increasing the internal flows L and V , thereby making L/V closer to 1. However, the effect of increasing the internal flows (energy) is limited since the maximum separation with infinite flows is $S = \alpha^N$.
3. We see that the separation factor S depends mainly on the internal flows (energy usage) and only weakly on the split D/F . This means that if we change D/F then S will remain approximately constant (Shinskey's rule), that is, we will get a shift in impurity from one product to the other such that the product of the impurities remains constant. This insight is very useful.

Example Consider a column with $x_{D,H} = 0.01$ (1% heavy in top) and $x_{B,L} = 0.01$ (1% light in bottom). The separation factor is then approximately $S = 0.99 \times 0.99 / (0.01 \times 0.01) = 9801$. Assume we slightly increase D from 0.50 to 0.51. If we assume constant separation factor (Shinskey's rule), then we find that $x_{D,H}$ changes from 0.01 to 0.0236 (heavy impurity in the top product increases by a factor 2.4), whereas $x_{B,L}$ changes from 0.01 to 0.0042 (light

impurity in the bottom product decreases by a factor 2.4). Exact calculations with column data: $N = 40$, $N_F = 21$, $\alpha = 1.5$, $z_L = 0.5$, $F = 1$, $D = 0.5$, $L_T/F = 3.206$, given that $x_{D,H}$ changes from 0.01 to 0.0241 and $x_{B,L}$ changes from 0.01 to 0.0046 (separation factor changes from $S = 9801$ to 8706). Thus, Shinsky's rule gives very accurate predictions.

However, the simple extended Fenske formula also has shortcomings. First, it is somewhat misleading since it suggests that the separation may always be improved by transferring stages from the bottom to the top section if $(L_T/V_T) > (V_B/L_B)$. This is not generally true (and is not really 'allowed' as it violates the assumption of optimal feed location). Second, although the formula gives the correct limiting value $S = \alpha^N$ for infinite reflux, it overestimates the value of S at lower reflux rates. This is not surprising since at low reflux rates a pinch zone develops around the feed.

Example Consider again the column with $N = 40$, $N_F = 21$, $\alpha = 1.5$, $z_L = 0.5$, $F = 1$, $D = 0.5$; $L_T = 2.706$. Exact calculations based on these data give $x_{HD} = x_{LB} = 0.01$ and $S = 9801$. On the other hand, the extended Fenske formula with $N_T = 20$ and $N_B = 20$ yields:

$$S = 1.5^{41} \times \frac{(2.706/3.206)^{20}}{(3.706/3.206)^{20}} = 16\,586\,000 \times \frac{0.34}{18.48} = 30\,774$$

corresponding to $x_{HD} = x_{LB} = 0.0057$. The error may seem large, but it is actually quite good for such a simple formula.

Optimal Feed Location

The optimal feed-stage location is at the intersection of the two operating lines in the McCabe-Thiele diagram. The corresponding optimal feed-stage composition (x_F, y_F) can be obtained by solving the following two equations: $z = qx_F + (1 - q)y_F$ and $y_F = \alpha x_F / (1 + (\alpha - 1)x_F)$. For $q = 1$ (liquid feed) we find $x_F = z$ and for $q = 0$ (vapour feed) we find $y_F = z$ (in the other cases we must solve a second-order equation).

There exists several simple short-cut formulas to estimate the feed point location. One may be derived from the Kremser equations given above. Divide the Kremser equation for the top by the one for the bottom and assume that the feed is optimally located to derive:

$$\frac{y_{H,F}}{x_{L,F}} = \frac{x_{H,D}}{x_{L,B}} \alpha^{(N_T - N_B)}$$

$$\times \frac{\left(\frac{L_T}{V_T}\right)^{N_T} \left[1 + \left(1 - \frac{L_T}{V_T}\right) \frac{(1 - a^{-N_T})}{(a - 1)}\right]}{\left(\frac{V_B}{L_B}\right)^{N_B} \left[1 + \left(1 - \frac{V_B}{L_B}\right) \frac{(1 - s^{-N_B})}{(s - 1)}\right]}$$

The last big term is close to 1 in most cases and can be neglected. Rewriting the expression in terms of the light component then gives Skogestad's short-cut formula for the feed stage location:

$$N_T - N_B = \frac{\ln \left(\left[\frac{(1 - y_F)}{x_F} \right] \left[\frac{x_B}{(1 - x_D)} \right] \right)}{\ln \alpha} \quad [36]$$

where y_F and x_F at the feed stage are obtained as explained above. The optimal feed-stage location counted from the bottom is then:

$$N_F = N_B + 1 = \frac{[N + 1 - (N_T - N_B)]}{2} \quad [37]$$

where N is the total number of stages in the column.

Summary for Continuous Binary Columns

With the help of a few of the above formulas it is possible to perform a column design in a matter of minutes by hand calculations. We will illustrate this with a simple example.

We want to design a column for separating a saturated vapour mixture of 80% nitrogen (L) and 20% oxygen (H) into a distillate product with 99% nitrogen and a bottoms product with 99.998% oxygen (mole fractions).

Component data Normal boiling points (at 1 atm): $T_{bL} = 77.4$ K, $T_{bH} = 90.2$ K, heat of vaporization at normal boiling points: 5.57 kJ mol⁻¹ (L) and 6.82 kJ mol⁻¹ (H).

The calculation procedure when applying the simple methods presented in this article can be done as shown in the following steps:

1. Relative volatility: The mixture is relatively ideal and we will assume constant relative volatility. The estimated relative volatility at 1 atm based on the boiling points is $\ln \alpha \approx (\Delta \bar{H}^{\text{vap}}/R\bar{T}_b) [(T_{bH} - T_{bL})/\bar{T}_b]$ where $\Delta \bar{H}^{\text{vap}} = \sqrt{5.57 \cdot 6.82} = 6.16$ kJ mol⁻¹, $\bar{T}_b = \sqrt{T_{bH} T_{bL}} = 83.6$ K and $T_H - T_L = 90.2 - 77.7 = 18.8$. This gives $(\Delta \bar{H}^{\text{vap}})/(R\bar{T}_b) = 8.87$ and we find $\alpha \approx 3.89$ (however, it is generally recommended to obtain α from experimental VLE data).
2. Product split: From the overall material balance we get $D/F = (z - x_B)/(x_D - x_B) = (0.8 - 0.00002)/(0.99 - 0.00002) = 0.808$.

3. Number of stages: The separation factor is $S = (0.99 \times 0.99998)/(0.01 \times 0.00002) = 4950000$, i.e. $\ln S = 15.4$. The minimum number of stages required for the separation is $N_{\min} = \ln S / \ln \alpha = 11.35$ and we select the actual number of stages as $N = 23$ ($\approx 2N_{\min}$).
4. Feed-stage location: With an optimal feed location we have at the feed stage ($q = 0$) that $y_F = z_F = 0.8$ and $x_F = y_F/(\alpha - (\alpha - 1)y_F) = 0.507$. Skogestad's approximate formula for the feed-stage location gives:

$$\begin{aligned} N_T - N_B &= \ln \left(\left[\frac{(1 - y_F)}{x_F} \right] \left[\frac{x_B}{(1 - x_D)} \right] \right) / (\ln \alpha) \\ &= \ln \left(\left[\frac{0.2}{0.507} \right] \times \left[\frac{0.00002}{0.01} \right] \right) / 1.358 \\ &= -5.27 \end{aligned}$$

corresponding to the feed stage $N_F = [N + 1 - (N_T - N_B)]/2 = (23 + 1 + 5.27)/2 = 14.6$.

5. Energy usage: The minimum energy usage for a vapour feed (assuming sharp separation) is $V_{\min}/F = 1/(\alpha - 1) = 1/2.89 = 0.346$. With the choice $N = 2N_{\min}$, the actual energy usage (V) is then typically about 10% above the minimum (V_{\min}), i.e. V/F is about 0.38.

This concludes the simple hand calculations. Note again that the number of stages depends directly on the product purity (although only logarithmically), whereas for well-designed columns (with a sufficient number of stages) the energy usage is only weakly dependent on the product purity.

Remark 1 The actual minimum energy usage is slightly lower since we do not have sharp separations. The recovery of the two components in the bottom product is $r_L = (x_{L,B}B)/(z_{FL}F) = 0.9596$ and $r_H = (x_{H,B}B)/(z_{FH}F) \approx 0$, so from the formulas given earlier the exact value for nonsharp separations is $V_{\min}/F = (0.9596 - 0.0 \times 3.89)/(3.89 - 1) = 0.332$.

Remark 2 For a liquid feed we would have to use more energy, and for a sharp separation:

$$V_{\min}/F = 1/(\alpha - 1) + D/F = 0.346 + 0.808 = 1.154$$

Remark 3 We can check the results with exact stage-by-stage calculations. With $N = 23$, $N_F = 15$ and $\alpha = 3.89$ (constant), we find $V/F = 0.374$, which is about 13% higher than $V_{\min} = 0.332$.

Remark 4 A simulation with more rigorous VLE computations, using the Soave-Redlich-Kwong (SRK) equation of state, has been carried out using the HYSYS (Hypnotech Ltd.) simulation package.

The result is a slightly lower vapour flow due to a higher relative volatility (α in the range 3.99–4.26 with an average of 4.14). More precisely, a simulation with $N = 23$, $N_F = 15$ gave $V/F = 0.291$, which is about 11% higher than the minimum value $V'_{\min} = 0.263$ found with a very large number of stages (increasing $N > 60$ did not give any significant energy reduction below V'_{\min}). The optimal feed stage (with $N = 23$) was indeed found to be $N_F = 15$.

Thus, the results from HYSYS confirm that a column design based on the very simple short-cut methods is very close to results from much more rigorous computations.

Multicomponent Distillation – Underwood's Methods

We present here the Underwood equations for multicomponent distillation with constant relative volatility and constant molar flows. The analysis is based on considering a two-product column with a single feed, but the usage can be extended to all kinds of column section interconnections.

It is important to note that adding more components does not give any additional degrees of freedom in operation. This implies that for an ordinary two-product distillation column we still have only two degrees of freedom, and thus we will only be able to specify two variables, e.g. one property for each product. Typically, we specify the purity (or recovery) of the light key in the top and of the heavy key in the bottom (the key components are defined as the components between which we are performing the split). The recoveries for all other components and the internal flows (L and V) will then be completely determined.

For a binary mixture with given products, as we increase the number of stages, there develops a pinch zone on both sides of the feed stage. For a multicomponent mixture, a feed region pinch zone only develops when all components distribute to both products, and the minimum energy operation is found for a particular set of product recoveries, sometimes denoted as the preferred split. If all components do not distribute, the pinch zones will develop away from the feed stage. Underwood's methods can be used in all these cases, and are especially useful for the case of infinite number of stages.

The Basic Underwood Equations

The net material transport (w_i) of component i upwards through a stage n is:

$$w_i = V_n y_{i,n} - L_{n+1} x_{i,n+1} \quad [38]$$

Note that w_i is always constant in each column section. We will assume constant molar flows ($L = L_n = L_{n-1}$ and $V = V_n = V_{n+1}$) and, assuming constant relative volatility, the VLE relationship is:

$$y_i = \frac{\alpha_i x_i}{\sum_i \alpha_i x_i} \quad \text{where } \alpha_i = \frac{(y_i/x_i)}{(y_r/x_r)} \quad [39]$$

We divide eqn [38] by V , multiply with the factor $\alpha_i/(\alpha_i - \phi)$, and take the sum over all components:

$$\frac{1}{V} \sum_i \frac{\alpha_i w_i}{(\alpha_i - \phi)} = \frac{\sum_i \frac{\alpha_i^2 x_{i,n}}{(\alpha_i - \phi)}}{\sum_i \alpha_i x_{i,n}} - \frac{L}{V} \sum_i \frac{\alpha_i x_{i,n+1}}{(\alpha_i - \phi)} \quad [40]$$

The parameter ϕ is free to choose, and the Underwood roots are defined as the values of ϕ which make the left-hand side of eqn [40] unity, i.e.:

$$V = \sum_i \frac{\alpha_i w_i}{(\alpha_i - \phi)} \quad [41]$$

The number of values ϕ satisfying this equation is equal to the number of components.

Most authors usually use a product composition or component recovery (r) in this definition, e.g. for the top (subscript T) section or the distillate product (subscript D):

$$w_i = w_{i,T} = w_{i,D} = D x_{i,D} = r_{i,D} z_i F \quad [42]$$

but we prefer to use w since it is more general. Note that use of the recovery is equivalent to using net component flow, but use of the product composition is only applicable when a single product stream is leaving the column. If we apply the product recovery, or the product composition, the defining equation for the top section becomes:

$$V_T = \sum_i \frac{\alpha_i r_{i,D} z_i F}{(\alpha_i - \phi)} = \sum_i \frac{\alpha_i x_{i,D}}{(\alpha_i - \phi)} D \quad [43]$$

Stage-to-Stage Calculations

With the definition of ϕ from eqn [41], eqn [40] can be simplified to:

$$\frac{L}{V} \sum_i \frac{\alpha_i x_{i,n+1}}{(\alpha_i - \phi)} = \frac{\phi \sum_i \frac{\alpha_i x_{i,n}}{(\alpha_i - \phi)}}{\sum_i \alpha_i x_{i,n}} \quad [44]$$

This equation will be valid for any of the Underwood roots, and if we assume constant molar flows and

divide an equation for ϕ_k with the one for ϕ_j , the following expression appears:

$$\left(\frac{\sum_i \frac{\alpha_i x_{i,n+m}}{(\alpha_i - \phi_j)}}{\sum_i \frac{\alpha_i x_{i,n}}{(\alpha_i - \phi_j)}} \right) = \left(\frac{\phi_k}{\phi_j} \right)^m \left(\frac{\sum_i \frac{\alpha_i x_{i,n}}{(\alpha_i - \phi_k)}}{\sum_i \frac{\alpha_i x_{i,n}}{(\alpha_i - \phi_j)}} \right) \quad [45]$$

and we note the similarities with the Fenske and Kremser equations derived earlier. This relates the composition on a stage (n) to a composition on another stage ($n+m$). The number of independent equations of this kind equals the number of Underwood roots minus 1 (since the number of equations of the type as in eqn [44] equals the number of Underwood roots), but in addition we also have $\sum x_i = 1$. Together, this is a linear equation system for computing $x_{i,n+m}$ when $x_{i,n}$ is known and the Underwood roots are computed from eqn [41].

Note that so far we have not discussed minimum reflux (or vapour flow rate), thus these equations hold for any vapour and reflux flow rates, provided that the roots are computed from the definition in eqn [41].

Some Properties of the Underwood Roots

Underwood showed a series of important properties of these roots for a two-product column with a reboiler and condenser. In this case all components flows upwards in the top section ($w_{i,T} \geq 0$), and downwards in the bottom section ($w_{i,B} \leq 0$). The mass balance yields: $w_{i,B} = w_{i,T} - w_{i,F}$ where $w_{i,F} = F z_i$. Underwood showed that in the top section (with N_c components) the roots (ϕ) obey:

$$\alpha_1 > \phi_1 > \alpha_2 > \phi_3 > \alpha_3 > \dots > \alpha_{N_c} > \phi_{N_c}.$$

And in the bottom section (where $w_{i,n} = w_{i,B} \leq 0$) in general we have a different set of roots denoted (ψ) computed from $V_B = \sum_i [\alpha_i w_{i,B}/(\alpha_i - \psi)] = \sum_i [\alpha_i (-r_{i,B} z_i)/(\alpha_i - \psi)] = \sum_i [\alpha_i (-(1-r_{i,D})) z_i/(\alpha_i - \psi)]$ which obey:

$$\psi_1 > \alpha_1 > \psi_2 > \alpha_2 > \psi_3 > \alpha_3 > \dots > \psi_{N_c} > \alpha_{N_c}.$$

Note that the smallest root in the top section is smaller than the smallest relative volatility, and the largest root in the bottom section is larger than the largest volatility. It is easy to see from the defining equations that $V_T \rightarrow \infty \Rightarrow \phi_i \rightarrow \alpha_i$ and similarly $V_B \rightarrow \infty \Rightarrow \psi_i \rightarrow \alpha_i$.

When the vapour flow is reduced, the roots in the top section will decrease, while the roots in the bottom section will increase, but interestingly Underwood showed that $\phi_i \geq \psi_{i+1}$. A very important result

by Underwood is that for an infinite number of stages $V \rightarrow V_{\min} \Rightarrow \phi_i \rightarrow \psi_{i+1}$.

Then, at minimum reflux, the Underwood roots for the top (ϕ) and bottom (ψ) sections coincide. Thus, if we denote the common roots (θ), and recall that $V_T - V_B = (1 - q)F$, we obtain the following equation for the common roots (θ) by subtracting the defining equations for the top and bottom sections:

$$(1 - q) = \sum_i \frac{\alpha_i z_i}{(\alpha_i - \theta)} \quad [46]$$

We call this expression the feed equation since only the feed properties (q and z) appear. Note that this is not the equation which defines the Underwood roots and the solutions (θ) apply as roots of the defining equations only for minimum reflux conditions ($N = \infty$). The feed equation has N_c roots (but one of these is not a common root) and the $N_c - 1$ common roots obey: $\alpha_1 > \theta_1 > \alpha_2 > \theta_2 > \dots > \theta_{N_c-1} > \alpha_{N_c}$. Solution of the feed equation gives us the possible common roots, but all pairs of roots (ϕ_i and ψ_{i+1}) for the top and bottom section do not necessarily coincide for an arbitrary operating condition. We illustrate this with the following example.

Example Assume we start with a given product split (D/F) and a large vapour flow (V/F). Then only one component i (with relative volatility α_i) can be distributed to both products. No roots are common. Then we gradually reduce V/F until a second component j (this has to be a component $j = i + 1$ or $j = i - 1$) becomes distributed, e.g. for $j = i + 1$ one set of roots will coincide: $\phi_i = \psi_{i+1} = \theta_i$, while the others do not. As we reduce V/F further, more components become distributed and the corresponding roots will coincide, until all components are distributed to both products, and then all the $N_c - 1$ roots from the feed equation are also roots for the top and bottom sections.

An important property of the Underwood roots is that the value of a pair of roots which coincide (e.g. when $\phi_i = \psi_{i+1} = \theta_i$) will not change, even if only one, two or all pairs coincide. Thus all the possible common roots are found by solving the feed equation once.

Minimum Energy – Infinite Number of Stages

When we go to the limiting case of infinite number of stages, Underwood's equations become very useful. The equations can be used to compute the minimum energy requirement for any feasible multicomponent separation.

Let us consider two cases: first we want to compute the minimum energy for a sharp split between two adjacent key components j and $j + 1$ ($r_{j,D} = 1$ and

$r_{j+1,D} = 0$). The procedure is then simply:

1. Compute the common root (θ_j) for which $\alpha_j > \theta_j > \alpha_{j+1}$ from the feed equation: $(1 - q) = \sum_i [a_i z_i / (a_i - \theta)]$
2. Compute the minimum energy by applying θ_j to the definition equation:

$$V_{T,\min}/F = \sum_{i=1}^j a_i z_i / (a_i - \theta_j).$$

Note that the recoveries

$$r_{i,D} = \begin{cases} 1 & \text{for } i \leq j \\ 0 & \text{for } i > j \end{cases}$$

For example we can derive King's expressions for minimum reflux for a binary feed ($z_L = z$, $z_H = (1 - z)$, $\alpha_L = \alpha$, $\alpha_H = 1$, and liquid feed ($q = 1$)). Consider the case with liquid feed ($q = 1$). We find the single common root from the feed equation: $\theta = \alpha / (1 + (\alpha - 1)z)$, (observe $\alpha \geq \theta \geq 1$, as expected). The minimum reflux expression appears as we use the defining equation with the common root:

$$\frac{L_{T,\min}}{F} = \frac{V_{T,\min}}{F} - \frac{D}{F} = \sum_i \frac{\theta r_{i,D} z_i}{(\alpha_i - \theta)} = \frac{\theta r_{L,D} z}{\alpha - \theta} + \frac{\theta r_{H,D} (1 - z)}{1 - \theta}$$

and when we substitute for θ and simplify, we obtain King's expression: $L_{T,\min}/F = (r_{L,D} - \alpha r_{H,D}) / (\alpha - 1)$. Another interesting case is minimum energy operation when we consider sharp split only between the most heavy and most light components, while all the intermediates are distributed to both products. This case is also denoted the preferred split, and in this case there will be a pinch region on both sides of the feed stage. The procedure is:

1. Compute all the $N_c - 1$ common roots (θ) from the feed equation.
2. Set $r_{1,D} = 1$ and $r_{N_c,D} = 0$ and solve the following linear equation set ($N_c - 1$ equations) with respect to $[V^T, r_{2,D}, r_{3,D}, \dots, r_{N_c-1,D}]$ ($N_c - 1$ variables):

$$V^T = \sum_{i=1}^{N_c} \frac{a_i r_{i,D} z_i}{(a_i - \theta_i)} : \quad V^T = \sum_{i=1}^{N_c} \frac{a_i r_{i,D} z_i}{(a_i - \theta_{N_c-1})} \quad [47]$$

Note that, in this case, when we regard the most heavy and light components as the keys, and all the intermediates are distributed to both products, King's very simple expression will also give the correct

minimum reflux for a multicomponent mixture (for $q = 1$ or $q = 0$). The reason is that the pinch then occurs at the feed stage. In general, the values computed by King's expression give a (conservative) upper bound when applied directly to multicomponent mixtures. An interesting result which can be seen from King's formula is that the minimum reflux at the preferred split (for $q = 1$) is independent of the feed composition and also independent of the relative volatilities of the intermediates.

However, with the Underwood method, we also obtain the distribution of the intermediates, and it is easy to handle any liquid fraction (q) in the feed.

The procedure for an arbitrary feasible product recovery specification is similar to the preferred split case, but then we must only apply the Underwood roots (and corresponding equations) with values between the relative volatilities of the distributing components at the limit of being distributed. In cases where not all components distribute, King's minimum reflux expression cannot be trusted directly, but it gives a (conservative) upper bound.

Figure 9 shows an example of how the components are distributed to the products for a ternary (ABC) mixture. We chose the overhead vapour flow ($V = V_T$) and the distillate product flow ($D = V - L$) as the two degrees of freedom. The straight lines,

which are at the boundaries when a component is at the limit of appearing/disappearing (distribute/not distribute) in one of the products, can be computed directly by Underwood's method. Note that the two peaks (P_{AB} and P_{BC}) give us the minimum vapour flow for a sharp split between A/B and B/C. The point P_{AC} , however, is at the minimum vapour flow for a sharp A/C split and this occurs for a specific distribution of the intermediate B, known as the preferred split.

King's minimum reflux expression is only valid in the triangle below the preferred split, while the Underwood equations can reveal all component recoveries for all possible operating points. (The shaded area is not feasible since reflux and vapour flow rates have to be positive ($V > D$, $V > (1 - q)F$).

Further Discussion of Specific Issues

The Energy Balance and the Assumption of Constant Molar Flows

All the calculations in this article are based on the assumption of constant molar flows in a section, i.e. $V_n = V_{n-1} = V$ and $L_n = L_{n+1} = L$. This is a very common simplification in distillation computations, and we shall use the energy balance to see when we can justify it. The energy balance is similar to the

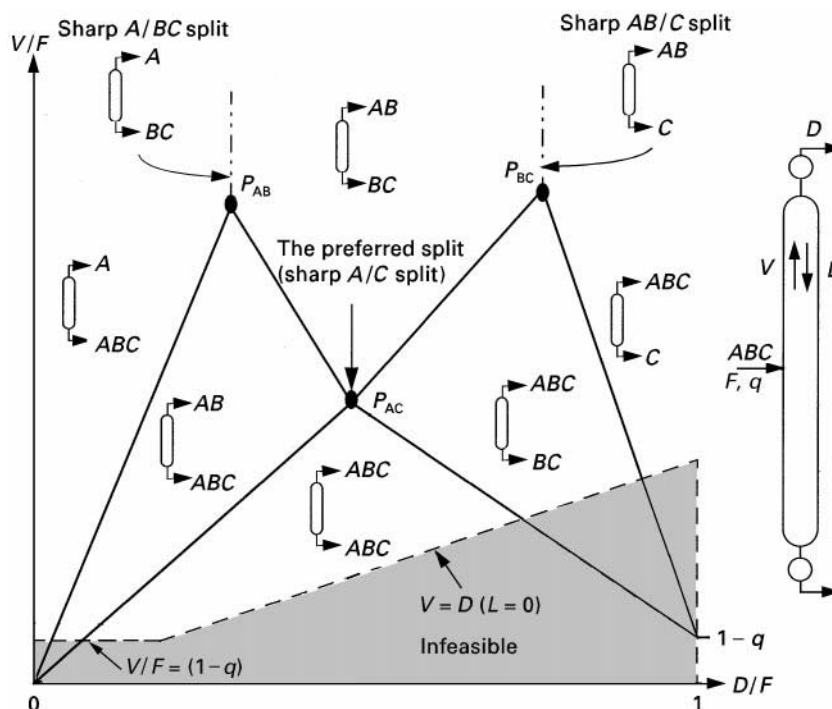


Figure 9 Regions of distributing feed components as a function of V and D for a feed mixture with three components: ABC. P_{ij} represents minimum energy for sharp split between components i and j . For large vapour flow (above the top sawtooth), only one component distributes. In the triangle below P_{AC} , all components distribute.

mass balance, but now we use the molar enthalpy (h) of the streams instead of composition. The enthalpy is computed for the actual mixture and will be a function of composition in addition to temperature (or pressure). At steady state the energy balance around stage n becomes:

$$L_n h_{L,n} - V_{n-1} h_{V,n-1} = L_{n+1} h_{L,n+1} - V_n h_{V,n} \quad [48]$$

Combining this energy balance with the overall material balance on a stage ($V_{n-1} - L_n = V_n - L_{n+1} = W$ where W is the net total molar flow through a section, i.e. $W = D$ in the top section and $W = B$ in the bottom section) yields:

$$V_n = V_{n-1} \frac{h_{V,n-1} - h_{L,n}}{h_{V,n} - h_{L,n+1}} + W \frac{h_{L,n} - h_{L,n+1}}{h_{V,n} - h_{L,n+1}} \quad [49]$$

From this expression we observe how the vapour flow will vary though a section due to variations in heat of vaporization and molar enthalpy from stage to stage.

We will now show one way of deriving the constant molar flow assumption:

1. Choose the reference state (where $h = 0$) for each pure component as saturated liquid at a reference pressure. (This means that each component has a different reference temperature, namely its boiling point (T_{bpi}) at the reference pressure.)
2. Assume that the column pressure is constant and equal to the reference pressure.
3. Neglect any heat of mixing such that

$$h_{L,n} = \sum_i x_{i,n} c_{PLi} (T_n - T_{bpi}).$$

4. Assume that all components have the same molar heat capacity, c_{PL} .
5. Assume that the stage temperature can be approximated by $T_n = \sum_i x_{i,n} T_{bpi}$. These assumptions give $h_{L,n} = 0$ on all stages and eqn [49] for change in boil-up is reduced to:

$$V_n = V_{n-1} \frac{h_{V,n-1}}{h_{V,n}}$$

6. The molar enthalpy in the vapour phase is given as: $h_{V,n} = \sum_i x_{i,n} \Delta H_{bpi}^{vap} + \sum_i x_{i,n} c_{PV,i} (T_n - T_{bpi})$ where ΔH_{bpi}^{vap} is the heat of vaporization for the pure component at its reference boiling temperature (T_{bpi}).
7. We assume that c_{PV} is equal for all components, and then the second summation term above will become zero, and we have: $h_{V,n} = \sum_i x_{i,n} \Delta H_{bpi}^{vap}$.
8. Then if $\Delta H_{bpi}^{vap} = \Delta H^{vap}$ is equal for all components we get $h_{V,n} = h_{V,n-1} = \Delta H^{vap}$, and thereby constant molar flows: $V_n = V_{n-1}$ and also $L_n = L_{n+1}$.

At first glance, these assumptions may seem restrictive, but the assumption of constant molar flows actually holds well for many industrial mixtures.

In a binary column where the last assumption about equal ΔH_{bpi}^{vap} is not fulfilled, a good estimate of the change in molar flows from the bottom (stage 1) to the top (stage N), due to this effect for a case with saturated liquid feed ($q = 1$) and close to pure products, is given by: $V_N/V_1 \approx \Delta H_H^{vap}/\Delta H_L^{vap}$, where the molar heat of vaporization is taken at the boiling point temperatures for the heavy (H) and light (L) components respectively.

Recall that the temperature dependency of the relative volatility is related to different heat of vaporization also, thus the assumptions of constant molar flows and constant relative volatility are closely related.

Calculation of Temperature when Using Relative Volatilities

It may seem that we have lost the pressure and temperature in the equilibrium equation when we introduced the relative volatility. However, this is not the case since the vapour pressure for every pure component is a direct function of temperature, thus it is also the relative volatility. From the relationship $P = \sum p_i = \sum x_i p_i^o(T)$ we derive:

$$P = p_r^o(T) \sum_i x_i \alpha_i \quad [50]$$

Remember that only one of P or T can be specified when the mole fractions are specified. If composition and pressure are known, a rigorous solution of the temperature is found by solving the nonlinear equation:

$$P = \sum x_i p_i^o(T) \quad [51]$$

However, if we use the pure component boiling points (T_{bi}), a crude and simple estimate can be computed as:

$$T \approx \sum x_i T_{bi} \quad [52]$$

For ideal mixtures, this usually gives an estimate which is a bit higher than the real temperature; however, a similar approximation may be done by using the vapour composition (y), which will usually give a lower temperature estimate. This leads to a good estimate when we use the average of x and y , i.e.:

$$T \approx \sum \left(\frac{x_i + y_i}{2} \right) T_{bi} \quad [53]$$

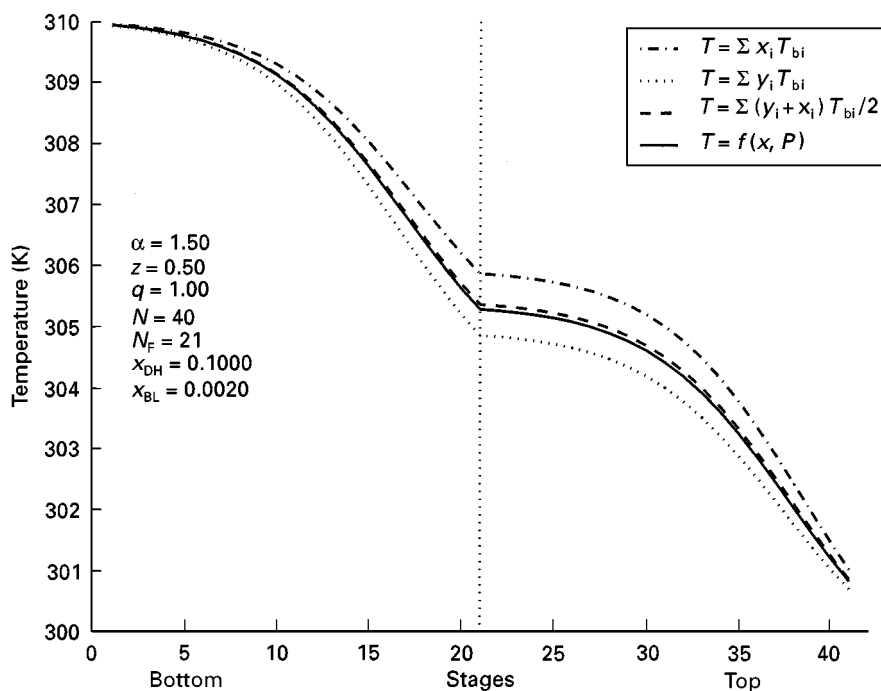


Figure 10 Temperature profile for the example shown in Figure 7 (continuous line) compared with various linear boiling point approximations.

Alternatively, if we are using relative volatilities we may find the temperature via the vapour pressure of the reference component. If we use the Antoine equation, then we have an explicit equation:

$$T \approx \frac{B_r}{\log p_r^\circ - A_r} + C_r \quad \text{where } p_r^\circ = P / \sum_i x_i \alpha_i \quad [54]$$

This last expression is a very good approximation to a solution of the nonlinear eqn [51]. An illustration of how the different approximations behave is shown in Figure 10. For that particular case (a fairly ideal mixture), eqns [53] and [54] almost coincide.

In a rigorous simulation of a distillation column, the mass and energy balances and the VLE have to be solved simultaneously for all stages. The temperature is then often used as an iteration parameter in order to compute the vapour pressures in VLE computations and in the enthalpy computations of the energy balance.

Discussion and Caution

Most of the methods presented in this article are based on ideal mixtures and simplifying assumptions about constant molar flows and constant relative volatility. Thus there are many separation cases for nonideal systems where these methods cannot be applied directly.

However, if we are aware of the most important shortcomings, we may still use these simple methods for short-cut calculations, for example, to gain insight or check more detailed calculations.

See also: II/Distillation: Historical Development; Instrumentation and Control Systems; Modelling and Simulation; Vapour-Liquid Equilibrium: Theory.

Further Reading

- Franklin NL and Forsyth JS (1953) The interpretation of minimum reflux conditions in multicomponent distillation. *Chemical Engineering Research and Design* 31. Reprinted in volume 75, December 1997, pp. 56–81.
- King CJ (1980) *Separation Processes*, 2nd edn. New York: McGraw-Hill.
- Kister HZ (1992) *Distillation Design*. New York: McGraw-Hill.
- McCabe WL, Smith JC and Harriot P (1993) *Unit Operations of Chemical Engineering*. New York: McGraw-Hill.
- Shinskey FG (1984) *Distillation Control – for Productivity and Energy Conservation*. New York: McGraw-Hill.
- Skogestad S (1997) Dynamics and control of distillation columns – a tutorial introduction. *Chemical Engineering Research and Design* 75: 539–562.
- Stichlmair J and James RF (1998) *Distillation: Principles and Practice*. New York: Wiley.
- Underwood AJV (1948) Fractional distillation of multicomponent mixtures. *Chemical Engineering Progress* 44: 603–614.

Tray Columns: Design

K. T. Chuang and K. Nandakumar,
University of Alberta, Edmonton, Alberta, Canada

Copyright © 2000 Academic Press

Distillation has remained an important separation technology for the chemical process industries. In 1997 it was reported in the journal *Chemical Engineering* that about 95% of all worldwide separation processes use this technology. In the USA alone, some 40 000 distillation columns represent a capital investment of about US \$8 billion. They consume the energy equivalent of approximately 1 billion barrels of crude oil per day. Such columns are used in refineries, petrochemical plants, gas processing plants and organic chemical plants to purify natural gas, improve gasoline, produce petrochemicals and organic products, recover pollutant species, etc.

Distillation can be carried out in a tray or a packed column. The major considerations involved in the choice of the column type are operating pressure and design reliability. As pressure increases, tray columns become more efficient for mass transfer and can often tolerate the pressure drop across the trays. The design procedure for the large diameter tray column is also more reliable than that for the packed column. Thus, trays are usually selected for large pressurized column applications.

Distillation trays can be classified as:

1. cross-flow trays with downcomers (see **Figure 1A**);
2. countercurrent trays without downcomers (also known as dual-flow trays) (see **Figure 1B**).

The dual-flow tray allows the gas and liquid to pass through the same tray openings. This results in a limited operating range because the dispersion height is very sensitive to the gas/liquid flow rates. In general, dual-flow trays are employed only in cases where high capacity or high resistance to fouling are required. However, because of its narrow operating range, the market share is small and such trays will not be discussed further.

The cross-flow tray utilizes a weir on the downcomer to control the spray height on the tray, and thus provides a stable gas-liquid dispersion over a wide range of gas/liquid flows. A tray is the combination of a tray deck, where froth is generated to provide vapour-liquid contact, and a downcomer, where the vapour-liquid mixture is separated. The bulk of the vapour rises from the aerated liquid through the vapour disengagement space to the tray above. However, the passage of the liquid from the

top to the bottom of the column occurs mainly via downcomers.

There are three types of cross-flow trays: (1) sieve, (2) valve and (3) bubble cap. Among them, sieve trays offer high capacity and efficiency, low pressure drop, ease of cleaning, and low capital cost, but smaller turndown ratio. Although the design procedure is similar for all three types of trays, only sieve tray performance data are readily available in the public domain. The valve and bubble cap designs are often protected by patents, and thus the performance data are supplied by the vendors. This article describes the procedure for designing an optimum sieve tray. A similar procedure can be applied in principle to the valve and bubble cap trays, provided critical performance data are available.

The cost of a tray column is determined by two factors:

1. column diameter, which determines the throughput;

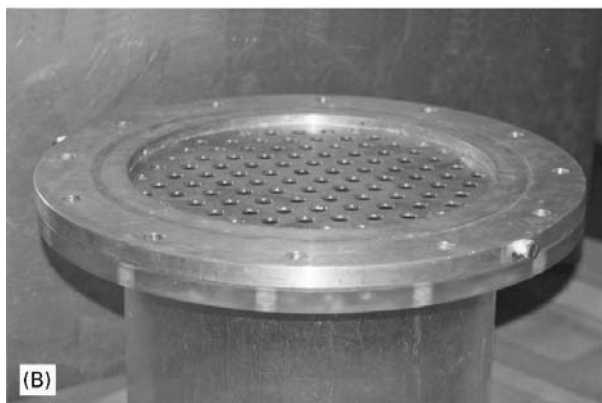
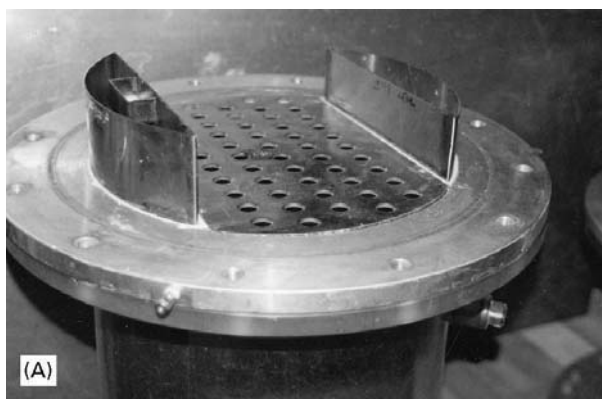


Figure 1 (A) Sieve tray with downcomer in a 30 cm diameter column. (B) Dual-flow tray in a 30 cm diameter column.

2. column height, which delivers the number of equilibrium stages required for the separation.

The minimum cost is generally achieved when the column volume is minimized. The final selection of the tray design is based on the combined cost of the column shell, internals and installation.

It should be noted that the fraction of the cross-sectional area available for vapour-liquid disengagement decreases when the downcomer area is increased. Thus, optimum design of the tray involves a balance between the tray area and the downcomer area (i.e. the capacity for the tray deck should match the capacity of the downcomer). The correlations for sizing trays are implicit in column diameter, tray spacing and tray geometry, thus requiring trial-and-error calculations to arrive at the final selection.

Characteristics of Tray Operation

Typical tray layout is shown in Figure 2, and tray operation is shown in Figure 3. High speed photography of a large operating tray indicates that the vapour erupts through the liquid sporadically. The holes that are not erupting do not weep appreciably at a vapour rate above the weep point, although the supporting of the liquid by the vapour is not absolutely complete. The interaction of vapour and liquid on a properly designed tray results in a highly turbulent two-phase mixture of a high specific interfacial area with net

liquid movement in a crossflow direction to the rising vapour stream. The aerated liquid may be either liquid-continuous (froth) at relatively low vapour velocities or vapour-continuous (spray) at high vapour velocities.

The maximum capacity of a sieve tray is reached when the tray is flooded. This may be due to excessive spraying (entrainment) taking place in the intertray space or the froth in the downcomer backing-up to reach the top of the outlet weir. The onset of flooding is accompanied by a sharp increase in tray pressure and a sharp decrease in tray efficiency.

As vapour rates decrease to the point that the vapour flow cannot totally support the liquid on the tray, some liquid will weep through the holes. If the weepage is so severe that no liquid flows over the outlet weir, the tray cannot operate stably under these dumping conditions. The minimum capacity of the tray is normally reached when moderate weepage is encountered. Ideally, a sieve tray should operate in the shaded area shown in Figure 4 to ensure proper operation.

Tray efficiency can be divided into two components:

1. point efficiency as determined by the vertical flow of vapour through the froth;
2. tray efficiency enhancement by the crossflow of liquid.

The physical properties of the vapour-liquid mixture determine the point efficiency, although froth height, which influences the gas residence time, also has a significant effect, especially for low efficiency systems. Liquid flow pathlength determines the liquid residence time and the extent of crossflow tray efficiency enhancement. Entrainment and weeping depress tray efficiency by disrupting the concentration profile in the column. The froth height and the liquid flow path are two parameters that are optimized to give maximum tray efficiency. Other geometric variables, such as open hole area, hole diameter and downcomer arrangement, also affect tray hydraulics and efficiency. The goal for a tray design is to reach maximum tray efficiency without compromising hydraulic stability.

The steps required for tray column design are shown in Figure 5; a detailed discussion of each step is given below.

Input Data

Once sieve trays are selected for a given application, the input data that are required in the design calculations include density, viscosity, surface tension, diffusivity and flow rate of the liquid stream, as

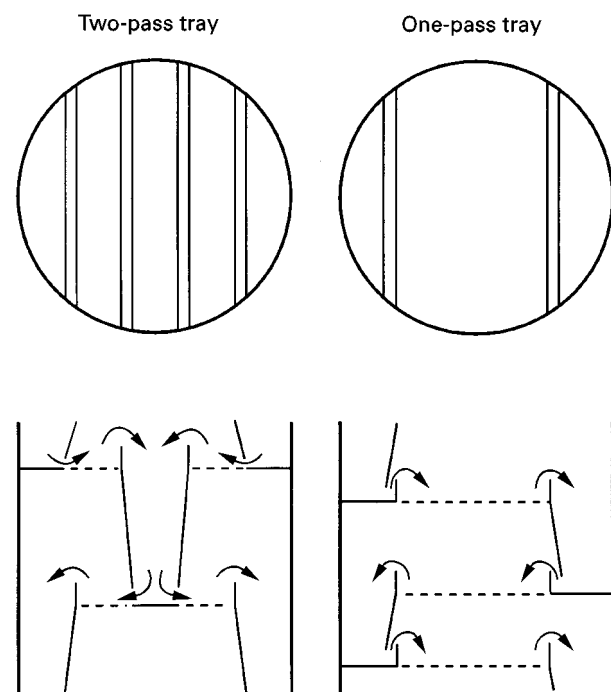


Figure 2 Tray layouts.

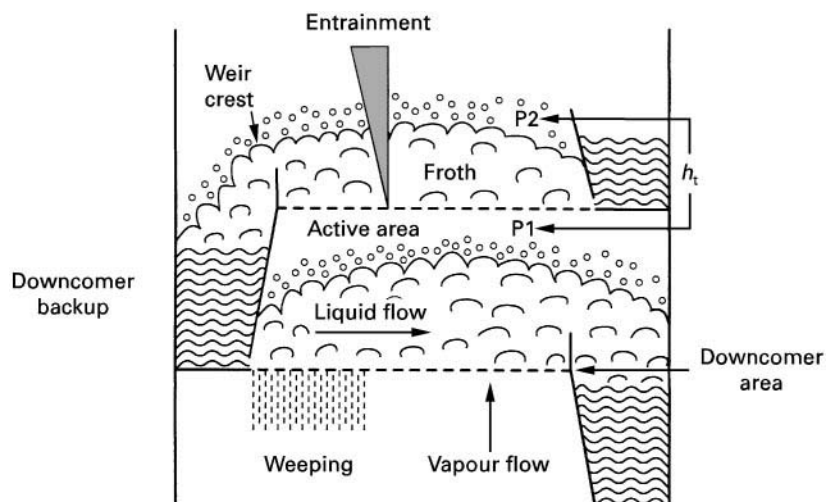


Figure 3 Tray operation schematic diagram.

well as density, diffusivity and flow rate of the vapour stream. This information can be obtained by performing tray-to-tray distillation calculations; several commercial computer packages are available for this purpose (e.g. PRO II, ASPEN PLUS, HYSIM).

As the physical properties and the vapour and liquid flow rates vary throughout a given column, it is difficult to provide a single design for the entire column. Instead, the column is divided into a number of sections. Within each section, trays are designed with the same layout. Normally the section is a set of trays bounded by two column penetrations (feed and/or drawoff). Tray design calculations should be performed to ensure that trays at the top and bottom of the section meet the design requirements.

Preliminary Specifications

Tray Spacing

Tray spacing is set by maintenance requirements, and also by support structure design in large-diameter columns. Sufficient crawl space must be provided for tray cleaning and repair. From these considerations, the minimum tray spacing is about 12 in (30 cm) for column diameter less than 5 ft, and (150 cm) and 18 in (45 cm) for a column diameter greater than 10 ft (300 cm). In general, it is best to keep tray spacing to a minimum, which is often the most economical.

Downcomer Area

The downcomer area at the top is sized such that the velocity of the ascending vapour bubbles exceeds the downflow velocity of the liquid. The size is related to

the stability of the froth in the downcomer and determined by the residence time required for achieving the separation of the two-phase mixture. For non-foaming systems, such as lower alcohols, a residence time of 3 s is sufficient, whereas for extremely high foaming systems such as caustic regenerators, 9 s is required.

To prevent the liquid coming off the bubbling area from splashing against the column wall, the minimum downcomer width is 5 in (12.7 cm). Also, the minimum side chord length should be 60% of the column diameter. This is required to maintain good liquid distribution on the tray.

Since the separation of the vapour-liquid mixture is complete at the bottom of the downcomer, a sloped downcomer can be used to maximize the active tray area. In this case, the downcomer area at the bottom should be about 60% of that at the top.

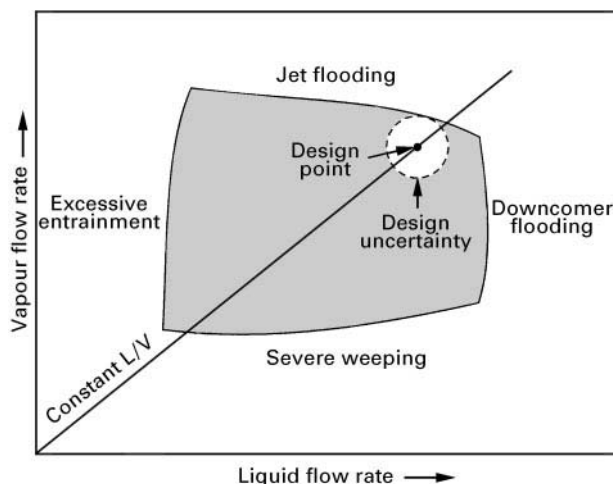


Figure 4 Sieve tray performance diagram.

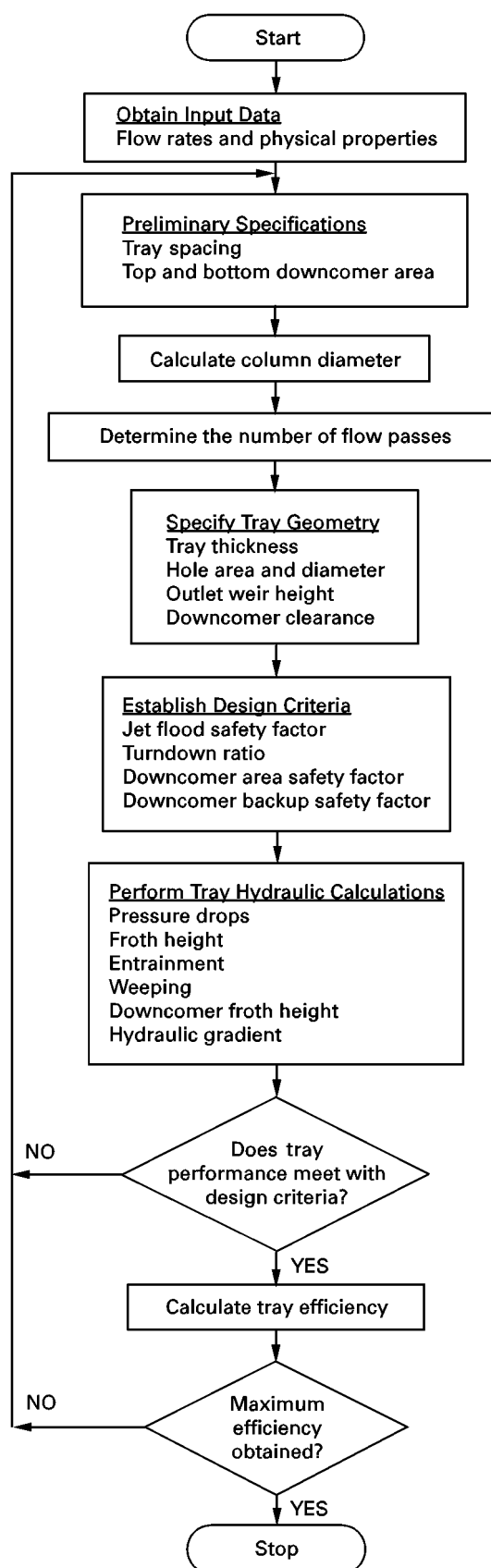


Figure 5 Sieve tray design procedure.

It should be noted that the downcomer area occupies only a small fraction of the cross-sectional area. Thus, a small overdesign does not result in a significant economic penalty.

Column Diameter

The column diameter can be calculated once the tray spacing and downcomer area have been specified. The Fair correlation, based on the Souders and Brown criterion, is recommended by most designers. The vapour flooding velocity can be calculated from eqn [1].

$$U_{N,f} = C_{SB} \left(\frac{\rho_L - \rho_V}{\rho_V} \right)^{0.5} \left(\frac{\sigma_L}{20} \right)^{0.2} \quad [1]$$

In eqn [1] C_{SB} is the Souders–Brown coefficient, ρ_L and σ_L (dyne cm^{-1}) are liquid density and surface tension, respectively, and ρ_V is the vapour density in the same units as ρ_L . $U_{N,f}$ is based on the net area, $A_N(\text{ft}^2)$, which is the active area plus one downcomer area. The unit for $U_{N,f}$ is ft s^{-1} . The most popular empirical formula for calculating C_{SB} is given in eqn [2].

$$\begin{aligned} C_{SB}(\text{ft s}^{-1}) = & 0.04232 + 0.1674 T_s \\ & + (0.0063 - 0.2686 T_s) F_{IV} \\ & + (0.1448 T_s - 0.008) F_{IV}^2 \end{aligned} \quad [2]$$

In this equation $F_{IV} = (L/V)(\rho_V/\rho_L)^{0.5}$, T_s is tray spacing in feet, and L and V are mass flow rates of the liquid and vapour. The C_{SB} is valid for trays with a fractional hole area greater than 10%. For areas of 8% and 6%, C_{SB} should be multiplied by 0.9 and 0.8, respectively.

Knowing $U_{N,f}$ and the total vapour flow rate, the column diameter can be calculated by assuming that the column will be operated at a lower vapour velocity, say 80% of the flood point.

Number of Flow Passes

The number of flow passes is set to allow the tray to operate at a weir loading that does not result in excessive weir crest. The weir loading can be calculated once the column diameter and the downcomer area are determined. The optimum weir loading is 4–6 US gallons per minute and the maximum loading is about 20. Downcomer choking, which causes liquid build-up on the tray, may occur if the maximum value is exceeded. Increasing the number of flow passes provides a solution to this problem (see Figure 2). However, shorter liquid flow path and possible maldistribution of liquid and vapour streams in multipass trays may result in lower tray efficiency.

As a rule of thumb, the liquid and vapour handling capacity are a direct function of weir loading and column area, respectively. Since weir length and column area are proportional to column diameter and diameter squared, respectively, the use of multipass trays is often necessary for large-diameter columns.

Tray Geometry

Tray geometry should be chosen so that hydraulic and efficiency calculations can be performed to arrive at the optimum design. The following parameters must be specified for tray design calculations.

Tray Thickness

The choice of material for the fabrication of trays is dependent mainly on the corrosion properties of the process fluids. In general, tray thickness is about gauge 10 (0.134 in; 3.40 mm) for carbon steel and gauge 12 (0.109 in; 2.77 mm) for stainless steel. For economic reasons the holes are punched, which dictates that the thickness must be less than the hole diameter.

Hole Diameter

Small holes with a diameter in the range of $\frac{3}{16}$ to $\frac{1}{4}$ in (4.76–6.35 mm) give better hydraulic and mass transfer performance than the large ones in the range of $\frac{1}{2}$ to $\frac{3}{4}$ in (12.7–19.0 mm). However, large-hole trays are cheaper and show more resistance to fouling. Choose the hole size according to design requirements.

Hole Area

The hole area is normally in the range of 5–16% of the bubbling area. Lower hole area allows the tray to operate at higher efficiency and turndown ratio, but at the expense of higher pressure drop. Since the operating pressure of the column dictates the maximum allowable pressure drop, the hole area is selected according to the type of service. Recommended values are 5–10% for pressure and 10–16% for vacuum operations.

Hole areas below 5% are not used because the distance between holes becomes excessive and liquid channelling may occur. However, the distance can also be adjusted by changing the hole diameter. In general, the hole pitch should not be larger than 2.5 in (6.35 cm). On the other hand, if the hole areas are greater than 16%, significant weeping and entrainment may coexist and the design equations may not apply under these conditions.

Weir Design

Outlet weirs are used to control the froth height on the tray. For most trays, the outlet weir height is about 1–4 in (2.5–10 cm) and the downcomer clearance, where the liquid is discharged from the bottom of the downcomer onto the tray below, should be 0.5 in (1.25 cm) smaller than the outlet weir height to ensure a positive downcomer seal.

From the above discussion, it may be concluded that the object of tray design is to obtain the optimum combination of the following parameters:

1. column diameter
2. tray spacing
3. top and bottom downcomer area
4. hole diameter and hole area
5. outlet weir height and downcomer clearance.

Design Criteria

The trays should be designed for maximum throughput. However, owing to inaccuracies in the design equations and fluctuation of process conditions (e.g. flow rates, temperature and pressure), safety factors are needed to ensure stable column operation at all times (see Figure 4).

Jet Flood Safety Factor

The jet flood safety factor (JFSF) is defined as the ratio of vapour velocity required to entrain the entire liquid flow (U_{\max}) to the operating velocity (U_{op}). It is a useful measure of entrainment and hydraulic stability. The typical JFSF value is 1.2.

Turndown Ratio

For various reasons, the column may be operated at a reduced throughput. Weeping is encountered if the vapour velocity can no longer support the liquid on the tray. Although flow dynamics permit stable operation as long as dumping is avoided, tray efficiency suffers because weeping reduces the vapour–liquid contact. The turndown ratio is the ratio of the design vapour flow rate to the flow rate that permits some weeping without seriously affecting the tray efficiency. Recommended weepages at turndown conditions for vacuum and pressure operations are 3% and 7%, respectively.

Downcomer Area Safety Factor (DCASF) and Downcomer Backup Safety Factor (DCBUSF)

The liquid handling capacity of a tray is determined by downcomer design and tray spacing. The DCASF determines the approach of the top downcomer area

to the minimum area to the minimum area required for vapour–liquid disengagement. The DCBUSF determines the approach of the downcomer froth height to the downcomer depth (= tray spacing + outlet weir height). Safety factors in the range of 1.5–2.0 are recommended.

Pressure Drop

The pressure drop across an operating tray should be specified if it affects the number of equilibrium stage requirements for the separation. This is often the case for vacuum applications. Stable operation can be obtained at a pressure drop of 1–3 in (2.5–7.6 cm) of liquid per tray for vacuum and 2–5 in (5.1–12.7 cm) for pressure operations.

Design Calculations

Tray Hydraulics

The hydraulic performance of a sieve tray for a given layout may be calculated using the methods presented in 'Distillation/Tray Columns: Performance'.

Tray Efficiency

Tray efficiency is a strong function of the physical properties of the vapour and liquid streams. It is also affected, to a lesser extent, by the flow rates and tray layout. In the latter case, only hole diameter, hole area and weir height have a small influence on the tray efficiency. The optimum design, which gives the maximum number of equilibrium stages in a column, is often obtained at minimum tray spacing and minimum number of flow paths that satisfy the hydraulic design criteria.

Conclusions

A well-designed tray should be economical while meeting all process design requirements. Economic

considerations suggest that it is best to use the smallest column diameter and height that satisfy the process requirements within reasonable safety allowances. Process requirements include accommodation of the expected liquid and vapour flow ranges and the optimization of tray efficiency.

See also: II/Distillation: Packed Columns: Design and Performance; Theory of Distillation; Tray Columns: Performance.

Further Reading

- Billet R (1979) *Distillation Engineering*. New York: Chemical Publishing Co.
- Fair JR (1963) In: Smith BD (ed.) *Design of Equilibrium Stage Processes*. New York: McGraw-Hill.
- Fair JR (1987) In: Rousseau RW (ed.) *Handbook of Separation Process Technology*, ch. 5. New York: John Wiley.
- Fair JR, Steinmeyer DE, Peuney WR and Crocker BB (1997). In: Perry RH and Green D (eds) *Perry's Chemical Engineers' Handbook*, 7th edn, sect. 14. New York: McGraw-Hill.
- Humphrey JL and Keller GE II (1997) *Separation Process Technology*. New York: McGraw-Hill.
- Kister HZ, (1992) *Distillation Design*. New York: McGraw-Hill.
- Lockett MJ (1986) *Distillation Tray Fundamentals*. Cambridge: Cambridge University Press.
- Lygeros AI and Magoulas KG (1986) Column flooding and entrainment. *Hydrocarbon Processing* 65: 43–44.
- McCabe WL, Smith JC and Harriott P (1993) *Unit Operations of Chemical Engineering*, 5th edn. New York: McGraw-Hill.
- Ogboja O and Kuye A (1991) A procedure for the design and optimization of sieve trays. *Transactions of the Institution of Chemical Engineers* 445.
- Rose LM (1985) *Distillation Design in Practice*. Amsterdam: Elsevier.

Tray Columns: Performance

K. Nandakumar and K. T. Chuang, University of Alberta, Edmonton, Alberta, Canada

Copyright © 2000 Academic Press

Introduction

As pointed out in the article entitled distillation tray columns: design, a sieve tray is designed with a num-

ber of objectives in mind. They include: (i) achieving high efficiency of contact between the liquid and the vapour so that the phases leaving a tray are as close to equilibrium conditions as possible; (ii) balancing the tray deck area provided for vapour/liquid contact with the downcomer area provided for disengagement of the two phases so that neither limits the capacity of the column to process large amounts of feed; and (iii) avoiding detrimental operating

conditions in the column such as *weeping*, *flooding* or high vapour *entrainment*.

Numerous geometrical factors have to be selected by the designer such as: (i) column diameter; (ii) tray spacing; (iii) top and bottom downcomer area; (iv) number of flow passes; (v) hole diameter and density; (vi) tray thickness; and (vii) weir design. This is a highly empirical process which depends on empirical design equations that describe the tray hydraulics and rule-of-thumb guidelines that have evolved over several decades of operating experience. Thus, the design of sieve tray columns has remained an art, although commercial process simulation software packages such as ASPEN, PRO II, HYSIM, etc., are trying to codify these procedures into their design packages. The conceptual steps in the design procedure together with the rule-of-thumb guidelines have been presented in the Tray Columns: Design article. Since frequent reference will be made to that article, we will henceforth refer to it simply as Part I.

In contrast, the performance analysis problem is relatively more scientific, in the sense that a series of well-defined steps leads to the estimation of the Murphree tray efficiency, the *column efficiency* and the *actual number of trays*. The overall column efficiency, E_o , is defined as:

$$E_o = \frac{N_{\text{equilibrium}}}{N_{\text{actual}}} \quad [1]$$

where $N_{\text{equilibrium}}$ is obtained from stagewise equilibrium design calculations. Performance evaluation boils down to estimating E_o so that the actual number of trays, N_{actual} , can be determined. The overall column efficiency, E_o , is related to the Murphree tray efficiency, E_{MV} , through the Lewis relationship (assuming constant slopes of equilibrium and operating lines), given by:

$$E_o = \frac{\ln [1 + E_{MV}(\lambda - 1)]}{\ln \lambda}$$

where $\lambda = mG/L$ is the separation factor, m is the slope of the equilibrium line, and (G, L) are the vapour and liquid flow rates in kmol s^{-1} . Thus the Murphree tray efficiency, E_{MV} , must be estimated in order to determine the column efficiency. The Murphree tray efficiency is defined to provide a measure of departure from the assumption of *ideal equilibrium tray* that is used to determine the number of *ideal stages* required to achieve a given separation. It is defined as:

$$E_{MV} = \frac{y_n - y_{n-1}}{y_n^* - y_{n-1}} \quad [2]$$

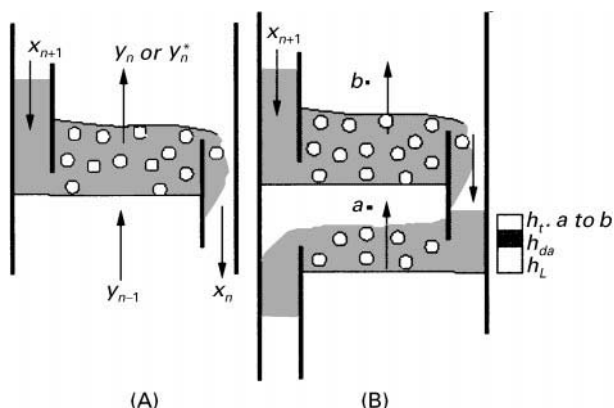


Figure 1 (A) Murphree tray efficiency. (B) Head in the downcomer.

Figure 1A illustrates various compositions. y_n is the actual composition of the vapour stream leaving tray n , while y_n^* is the composition that is in equilibrium with the exit liquid stream.

These two compositions would be the same, if and only if the condition of *ideal equilibrium tray* is satisfied. Since it is never satisfied in practice, it is important to be able to predict the tray efficiency. In fact, the compositions are not even uniform across the tray deck. Hence the above definition is applied at a local point on the tray and the point efficiency is integrated with the *variations in flow conditions* to predict a tray efficiency. The relationship between the inputs and the sequence of calculations is shown in Figure 2.

In Figure 2 the *point efficiency* is a function of local flow conditions such as local mass transfer coefficients in the liquid and vapour phases. The *dry Murphree* tray efficiency incorporates the effects of liquid and vapour distribution on the *point efficiency*, while the *wet Murphree* tray efficiency incorporates the additional effects of entrainment and weeping.

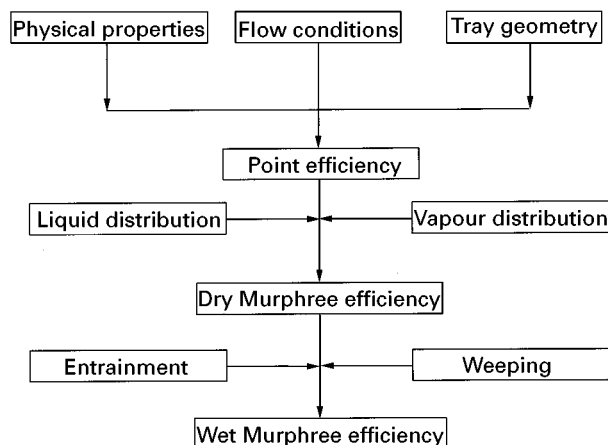


Figure 2 Steps in performance evaluation.

The tray efficiency, E_{MV} , clearly depends on: (i) the geometrical design parameters chosen as outlined in Part I; (ii) the physical properties of the system such as density, viscosity, surface tension, etc.; and (iii) the operating conditions like the vapour/liquid flow rates.

Having selected the design parameters identified in Part I, the objective of the performance analysis step is to predict: (i) the tray hydraulics (including the pressure drop, the flow regime, the froth density, the entrainment and weeping factors); (ii) the point efficiency; (iii) the Murphree tray efficiency; and (iv) the column efficiency. In the initial stages of designing a *new tray column*, there is feedback between the design and performance analysis steps to arrive at a set of optimal design parameters, as outlined in the flow chart (Figure 5 of part I). But the performance analysis steps to be outlined in this part, are also useful in analysing the performance of an *existing tray column*, although the opportunity to pick optimal design conditions is not present as one is forced to deal with an existing tray.

An excellent summary of the equations used to study the performance of a sieve tray column can be found in Zuiderweg (1982), Lockett (1986) and Kister (1992) (see Further Reading). The detailed steps involved in the performance analysis include: (i) the pressure drop prediction; (ii) froth height and density calculations; (iii) point efficiency prediction; and (iv) tray efficiency prediction. The inputs required are: (i) tray geometry; (ii) physical properties; and (iii) flow conditions.

Steps in Performance Analysis

Pressure Drop Calculation in Vapour Phase

The pressure drop in the vapour phase across a sieve tray is modelled as (Zuiderweg, 1982):

$$\Delta P = \Delta P_{\text{dry}} + \rho_l g h_l \quad [3]$$

where the dry pressure drop is given by:

$$\Delta P_{\text{dry}} = \frac{1}{2} \rho_G \left(\frac{u_{g,h}}{C_D} \right)^2 \quad [4]$$

Here, g is the acceleration due to gravity, h_l is the liquid height or hold-up in metres, $u_{g,h}$ is the vapour velocity in the hole in metres per second, C_D is the drag coefficient, and (ρ_G, ρ_l) are the densities of the vapour and liquid, respectively. The second term in eqn [3] represents the static head due to the liquid hold-up on the tray. Hence the liquid height, h_l must be predicted from correlations that depend on the

weir geometry. One such equation that predicts the liquid height is given by:

$$h_l = 0.6 H_w^{0.5} p^{0.25} (FP/b)^{0.25} \quad 25 \text{ mm} < H_w < 100 \text{ mm} \quad [5]$$

Here, H_w is the weir height in metres, p is the pitch of the holes in the sieve plate in metres, $FP = (u_l/u_g) \sqrt{(\rho_l/\rho_g)}$ is the flow parameter, b is the weir length per unit bubbling area in metres⁻¹.

The discharge coefficient, C_D in eqn [4] is a function of the flow conditions near a hole. It is in fact dependent on the liquid present on the tray. It is correlated by:

$$C_D = 0.7 \left[1 - 0.14 \left(\frac{g h_l \rho_l}{u_{g,h}^2 \rho_g} \right)^{2/3} \right] \quad [6]$$

All of the quantities appearing on the right-hand side have been defined previously.

Pressure Drop Calculation in the Liquid Phase

The liquid is transported down through the *downcomer*. The capacity of the downcomer should be sufficient to handle the liquid load without becoming the rate limiting factor, i.e. without the liquid backing up the downcomer to a significant extent. Figure 1B shows the pressure differential components making up the total head differential on the liquid side as the liquid backs up the downcomer to a height of h_{dc} . The extent of liquid back-up can be estimated from:

$$h_{dc} = h_t + h_{da} + h_L \quad [7]$$

where h_t is the pressure difference between points a and b in the vapour phase that is necessary to keep the vapour flowing upwards, h_L refers to the effective clear liquid height on the tray deck that must be overcome by the liquid in the downcomer, and h_{da} refers to the pressure loss due to the liquid flow under the downcomer apron. Note that h_t is necessary to keep the upward flow of vapour, but acts as a pressure differential that works against the natural liquid flow in the downcomer. If this pressure differential is large, the liquid will back up more in the downcomer. This points out the coupling between the pressure loss in the vapour phase through the tray deck area and the liquid flow in the downcomer. An optimal design must balance these two factors carefully. h_L and h_t can be estimated from the correlations provided in the previous section. h_{da} can be estimated from:

$$h_{da} = 165.2 U_{da}^2$$

where h_{da} is in millimetres of liquid and U_{da} is the velocity under the downcomer apron in metres per second.

Froth Height and Density Calculation

The froth density (or the two-phase density) has been measured using gamma ray techniques. The average liquid volume fraction on a sieve tray, defined as $\bar{e}_l = h_l/h_b$, is correlated by:

$$\frac{1}{\bar{e}_l} - 1 = c_1 \left[\frac{u_g}{(g h_l)^{0.5}} \left(\frac{\rho_G}{\rho_L} \right)^{0.5} \right]^n \quad [8]$$

Here, h_b is the froth or bed height in metres and u_g is the vapour velocity on bubbling area in metres per second. The constants c_1 and n depend on the type of flow regimes. In the *spray regime*, they take on the values of $c_1 = 265$ and $n = 1.7$, while in the *mixed/emulsion regime*, they are 40 and 0.8. This requires one to estimate the flow regime to be expected under a given set of operating conditions. In Figure 3 of Part I, we identified the limits of operation to lie between the weeping and flooding conditions as the vapour rate is increased. Even within this permissible range of operation, the flow condition has been observed to change from *spray* to *froth* to *emulsion* to *bubble flow* regimes. The transition into the spray regime is given by the capacity factor defined as:

$$CF = u_g \left(\frac{\rho_g}{\rho_l} \right)^{0.5} = 0.85 \frac{g^{0.5} h_l^{1.5} \cdot F}{d_h}$$

Here, CF is the capacity factor defined as $u_g \sqrt{(\rho_G/\rho_L)}$ in metres per second, u_g is the vapour velocity in the bubbling area in metres per second, F is the fractional hole area per unit bubbling area and d_h is the hole diameter in metres. The transition from the spray/froth to emulsion/bubble flow regime is controlled by the ratio of horizontal liquid momentum to vertical vapour momentum and is given by:

$$\frac{u_l}{u_g} \left(\frac{\rho_l}{\rho_G} \right)^{0.5} = \frac{FP}{b \cdot h_l} > 3.0$$

where u_l is the horizontal liquid velocity, u_g is the vapour velocity on bubbling area in metres per second, and FP is the flow parameter defined in eqn [5], b is the weir length per unit bubbling area in metres⁻¹, h_l is the liquid height or hold-up in metres.

Point Efficiency Calculation

There are many empirical correlations for predicting the mass transfer efficiencies on sieve trays. The most recent one is that proposed by Chen and Chuang (1993). It is based on data from industrial sized columns of Fractionation Research Inc. The point effi-

ciency is related to the overall number of transfer units by:

$$E_{OG} = 1 - e^{-N_{OG}} \quad [9]$$

Chen and Chuang present the following correlation for N_{OG} using data free of weeping and entrainment. But the data set spans both the froth and spray regimes:

$$N_{OG} = \frac{11 \frac{1}{\mu^{0.1} \phi^{0.14}} \left[\frac{\rho_L F_s^2}{\sigma^2} \right]^{1/3} (D_G t_G)^{0.5}}{\lambda \frac{11}{14} \left(\frac{D_G \rho_G}{D_L \rho_L} \right)^{0.5} \left(\frac{M_G L}{M_L G} \right) + 1} \quad [10]$$

Here $\lambda = mG/L$ is the separation factor, $F_s = u_s \sqrt{\rho_G}$ is the superficial F-factor in kg^{0.5}/m^{0.5}s, $t_G = h_f/u_s$ is the vapour-phase contact time in seconds, and h_f is the froth height in metres. Note that this correlation combines the *geometrical parameters* such as ϕ , the fractional perforated area, A_b , the bubbling area, the *system properties* such as densities (ρ_L , ρ_G), diffusivities (D_L , D_G) viscosity (μ), the interfacial tension (σ) in newtons per metre, the molecular weights (M_L , M_G), and *operating conditions* such as (L , G), flow rates. This correlation appears to predict the point efficiencies to within 5% of experimental data over a wide range of pressures.

Murphree Tray Efficiency Calculation

The point efficiency model presented above is based on a detailed examination of mass transfer at the vapour/liquid interface. The *ideal equilibrium tray assumption* used in the McCabe-Thiele method asserts that the flow condition on a tray is homogeneous everywhere. If that were true, the point efficiency would be the same everywhere on the tray. But there is strong evidence that the flow is not homogeneous, the degree of inhomogeneity being larger in large diameter columns. Several researchers have tried to measure the velocity profiles across a sieve tray and increasingly computational fluid dynamics is being used as a tool to predict such flow fields. (See for example Solari and Bell (1986) and Mehta *et al.* (1998)). This information on flow profile must be integrated with the point efficiency calculations in order to predict a Murphree tray efficiency. One such method is given below as an illustration. This model considers only the effect of *longitudinal mixing*. A measure of the effective diffusivity, D_E is needed in this model. Models of other flow configuration are discussed in Lockett (1986):

$$\frac{E_{MV}}{E_{OG}} = \frac{1 - e^{-(\eta + Pe)}}{(\eta + Pe) \{ 1 + [(\eta + Pe)/\eta] \}} + \frac{e^{-\eta} - 1}{\eta \{ 1 + [\eta/(\eta + Pe)] \}} \quad [11]$$

where:

$$\eta = \frac{Pe}{2} \left[\left(1 + \frac{4\lambda E_{OG}}{Pe} \right)^{1/2} - 1 \right]$$

and Pe is the Peclet number, defined as $Pe = Z_l^2/D_E t_l$. Here Z_l is the length of liquid travel, or the distance between the two weirs and t_l is the liquid residence time. The effective diffusivity is given by:

$$\sqrt{D_E} = 0.0124 + 0.017u_G + 0.0025L + 0.0150W \quad [12]$$

where D_E is in square feet per second, u_G is superficial gas velocity, expressed as cubic feet per second divided by the active bubbling area in square feet. As the Peclet number becomes large, this model predicts efficiency enhancement much large than unity. In large diameter columns (large Z_l) the *Peclet* number can tend to take a large value which would suggest significant efficiency enhancements. But it should be remembered that the above model considers only the *longitudinal mixing* process. In large diameter columns, the liquid flow structure can be much more complicated as documented by Solari and Bell (1986). Hence, predicted values of E_{MV}/E_{OG} greater than 1.2 by the *longitudinal mixing* model should be viewed with caution, as they may not be realized in the field.

Effect of Entrainment on Murphree Tray Efficiency

The effect of entrainment on the Murphree tray efficiency is estimated from:

$$E_{MV,entrain} = E_{MV} \left[\frac{1}{1 + E_{MV}\psi/(1 - \psi)} \right] \quad [13]$$

where:

$$\psi = \frac{e}{L + e} = \frac{\text{absolute entrainment}}{\text{total liquid flow rate}}$$

where e is the entrained liquid in moles per hour. Zuiderweg presents the following empirical equation to predict the liquid entrainment in the spray regime:

$$\psi = 1.0 \times 10^{-8} \left(\frac{h_b}{H_s} \right)^3 \left(\frac{u_{g,h}}{u_l} \right) \quad \text{for } 0.3 < \frac{h_b}{H_s} < 0.9$$

Here H_s is the tray spacing in metres, h_b is the bed height as defined in eqn [8], $u_{g,h}$ is the vapour velocity in the hole in metres per second and u_l is the horizontal liquid velocity.

Weeping Point Determination

When the vapour velocity is too small, the liquid on a tray deck can flow down through the holes on the

sieve plate, instead of the downcomer, which is the preferred path for the liquid. If weeping is significant, then it results in mixing of liquid streams between two neighbouring trays, thus degrading the performance of the column. The need to avoid weeping places a limit on the minimum vapour velocity. Zuiderweg presents the following correlations to predict the minimum operating limit.

Mixed/free bubbling regime

$$CF_w = F\sqrt{gh_l} \left[1 - 0.15 \frac{FP}{bh_l} \right]$$

Emulsion flow regime

$$CF_w = 0.45F\sqrt{gh_l}$$

where $CF_w = u_g \sqrt{\rho_G/(\rho_L - \rho_G)}$ is the capacity factor at the weep point in metres per second, and F is the fractional hole area per unit bubbling area. Correlations to estimate the type of flow regime are given by Zuiderweg. Note that weeping will seldom occur in the spray regime as vapour velocities are sufficiently large under design conditions. The effect of weeping on the tray efficiency calculation has been studied by Kageyama (1969).

Extensions to Multicomponent Systems

The methods outlined above have been developed largely using experimental data for binary, two-phase systems. The question of whether they can be applied to multicomponent systems can be examined as follows. Tray hydraulics factors such as pressure drops, flow regimes, froth densities, etc., depend only on the fluid mechanics of the two-phase mixture on sieve trays; hence one can expect the correlations to be useful for multicomponent mixtures as long as mixture properties for densities, viscosities, interfacial tensions, etc., are used. On the other hand, the point efficiency (and hence the Murphree tray efficiency) depends on the mass transfer resistance of each component species in each phase. Since the diffusivities and the equilibrium ratios (or the slope of the equilibrium curve, m) could vary for each species, the point efficiency will be different for each species. The correlation given in eqn [10] is based on binary mass transfer data.

In the pseudo binary method of calculation (see Kister, 1992) two components are identified as the *light key* and *heavy key* components and the

Murphree tray efficiency is determined for such a binary pair. One then has the option of either using the efficiency so calculated for all of the remaining components or repeating the procedure for all possible binary pairs. Such detailed estimates of component efficiencies are then used as inputs to advanced process simulators such as ASPEN.

Issues Relating to Scale-up of Efficiency Data

Since the point efficiency data and correlations (like eqn [10] are (or should be) based on local conditions, they should, in principle, remain valid on all scales. They are then integrated with flow conditions to predict the overall tray efficiency. Correlations such as eqn [11], which provide this function of integrating the point efficiency to provide tray efficiency, do not remain valid at all scales. It has been well documented that the liquid flow patterns change quite dramatically depending on the diameter of the column and the location of the weirs near the downcomer. In future one can expect *computational fluid dynamics* to provide detailed flow information using models that remain scale invariant over a wide range of diameters.

Concluding Remarks

A series of correlations taken from the literature are presented. They permit the evaluation of the performance of a sieve tray, once a set of design parameters has been chosen as outlined in Part I. At the design stage of a new sieve tray column, one can embed this design and performance analysis steps into an optimization procedure, in such a way that the design parameters may be altered until a specified objective function is satisfied. The objective function could be

a cost function that includes the capital cost of the equipment (which determines the column diameter, tray spacing, etc.) and operating costs (which determine the reflux and reboil rates and the number of ideal stages).

See also: II/Distillation: Historical Development; Instrumentation and Control Systems; Theory of Distillation; Tray Columns: Design; Packed Columns: Design and Performance; Vapour-Liquid Equilibrium: Correlation and Prediction; Vapour-Liquid Equilibrium: Theory.

Further Reading

- Chen GX and Chuang KT (1993) *Prediction of Point Efficiency for Sieve Trays in Distillation*. I & EC Research, vol. 32, p. 701.
- Fair JR *et al.* (1997) In: Perry RH and Green D (eds.), *Perry's Chemical Engineers' Handbook – Section 14*, 7th edn. New York: McGraw-Hill.
- Kageyama, O. Plate efficiency in distillation towers with weeping and entrainment, I. Chem. E. Symposium Series No. 32.
- Kister HZ (1992) *Distillation Design*. New York: McGraw-Hill.
- Lockett MJ (1986) *Distillation Tray Fundamentals*. Cambridge University Press.
- Mehta B, Chuang KT and Nandakumar K (1998) Model for liquid phase flow on sieve trays. *Transactions of the Institute of Chemical Engineers*, part A (in press).
- Rose LM (1985) *Distillation Design in Practice*. Amsterdam: Elsevier.
- Rousseau RW (1987) *Handbook of Separation Process Technology*, New York: John Wiley & Sons.
- Solari RB and Bell RL (1986) Fluid flow patterns and velocity distributions on commercial scale sieve trays. *American Institute of Chemical Engineers Journal* 32: 640.
- Zuiderweg FJ (1982) Sieve trays: A view of the state of the art. *Chemical Engineering Science* 37: 1441.

Vapour-Liquid Equilibrium: Correlation and Prediction

B. C.-Y. Lu, University of Ottawa, Ottawa, Ontario, Canada,

D.-Y. Peng, University of Saskatchewan, Saskatoon, Saskatchewan, Canada

Copyright © 2000 Academic Press

Introduction

Distillation is a process used to separate liquid mixtures into two or more streams, each of which has a composition that is different from that of the

original mixture. The process involves both the vaporization of the original liquid in order to generate the vapours and the subsequent condensation of the vapours to form the desired liquid products. It is evident that vapour-liquid equilibria (VLE) are essential to this separation process. Typical temperature-composition (T - x - y) diagrams, pressure-composition (P - x - y) diagrams, and vapour-liquid composition (x - y) diagrams for completely miscible binary systems are depicted in Figure 1.

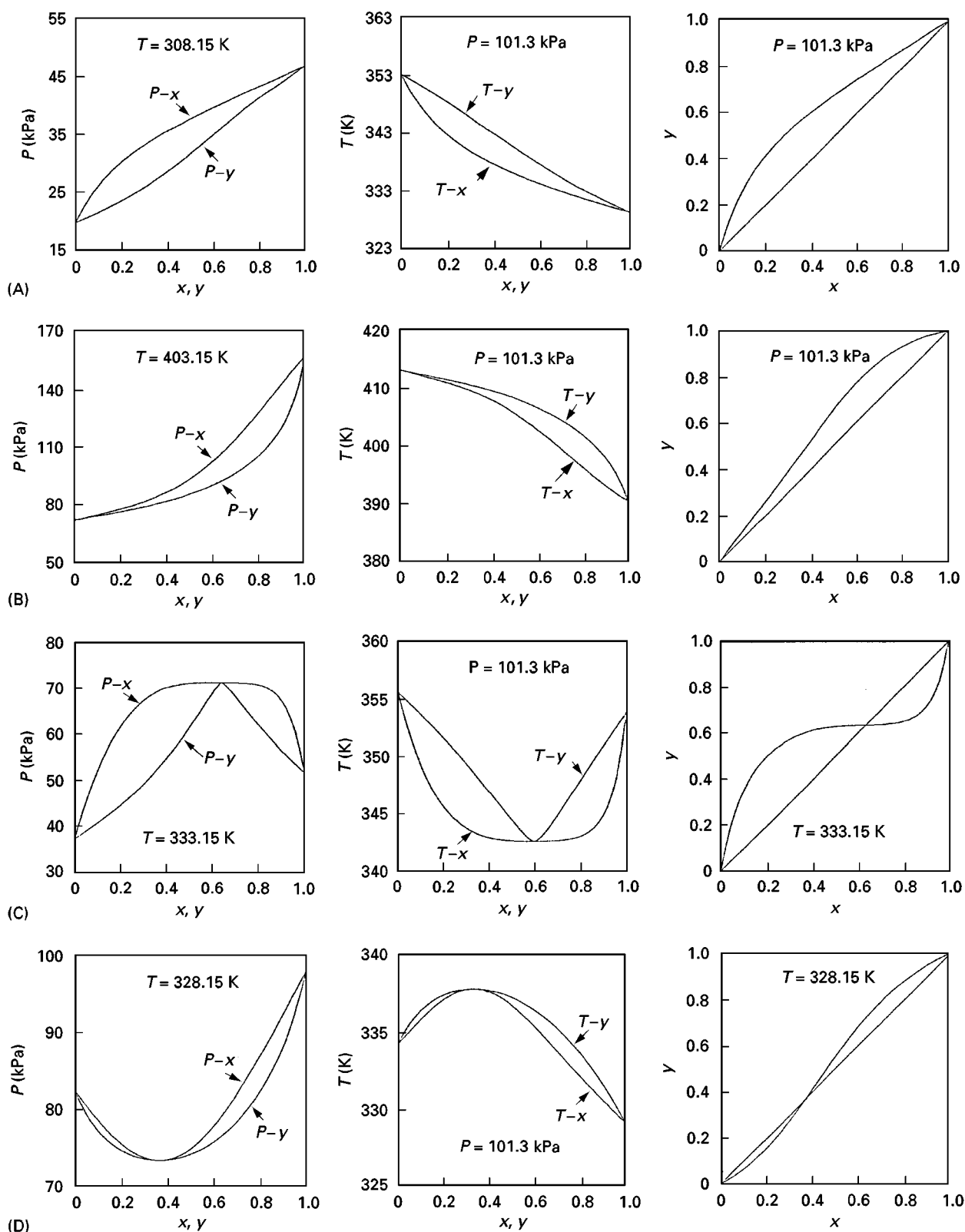


Figure 1 Four types of binary P - x - y , T - x - y and x - y equilibrium phase diagrams. Correlation curves are for: (A) System acetone + benzene. (B) System 1-butanol + acrylic acid. (C) System cyclohexane + 2-propanol. (D) System acetone + chloroform.

Consider an N -component closed system in which a liquid mixture at temperature T and pressure P is in equilibrium with a vapour mixture at the same temperature and pressure. The condition of thermodynamic equilibrium is that the chemical potentials of the components in both phases must satisfy the equality relation:

$$\mu_{iV} = \mu_{iL} \quad (i = 1, 2, \dots, N) \quad (\text{constant } T) \quad [1]$$

The introduction of the quantity called fugacity by G.N. Lewis has facilitated the application of this condition. The fugacity of a system, f , at constant temperature is defined in the following two equations:

$$dG = RT d \ln f \quad [2]$$

and:

$$\lim (f/P) = 1 \quad \text{as } P \text{ approaches zero} \quad [3]$$

where, in eqn [2], G is the molar Gibbs energy.

The fugacity of a component i in a solution is related to the chemical potential of the same component by the equation:

$$d\mu_i = RT d \ln \hat{f}_i \quad [4]$$

A practical expression for vapour-liquid equilibrium consideration thus takes the form:

$$\hat{f}_{iV} = \hat{f}_{iL} \quad [5]$$

where the subscripts V and L indicate fugacity in the vapour phase and liquid phase, respectively. Correlation and prediction of vapour-liquid equilibria must satisfy the equal fugacity condition. The main concern is to relate these fugacities to T , P , and the compositions of the liquid and vapour phases.

Design of distillation operations requires reliable experimental vapour-liquid equilibrium values for conditions corresponding to the desired operation. Available data may frequently be either fragmentary or for conditions different from the desired operating conditions. On many occasions, the needed experimental values are not available at all. In order to make suitable interpolation and extrapolation of the available data, and to make acceptable estimates of unavailable data, it is necessary to take advantage of the limited data available and apply prediction methods developed on the basis of reasonable assumptions. In this article, discussion is limited to correlation and prediction of the vapour-liquid equilibrium values for organic and nonelectrolyte mixtures at conditions such that Raoult's law cannot be

used to represent the behaviour of all components over the complete concentration range. The emphasis is placed on the equilibrium T - P - x - y .

Correlation of Vapour-Liquid Equilibria (VLE)

The quality of the available experimental data is the first concern of any VLE correlation. It is known that a considerable proportion of experimental values are not of good quality owing to the impurity of the chemicals and poor equilibrium stills used, equipment set-ups, and operator errors. In many instances there are quantitative discrepancies among the experimental results for the same system investigated under the same thermodynamic conditions by different authors. Therefore, it is desirable to determine whether the available experimental values are thermodynamically consistent prior to correlation. Consistency tests can be applied whenever the measured properties are more than those that are needed, on the basis of the phase rule, to define the intensive properties of the system under consideration. Although the thermodynamic consistency of experimental data does not guarantee their correctness, inconsistent data are definitely not acceptable.

There are two frequently used methods in correlating vapour-liquid equilibria. One is through the gamma-phi approach, and the other is by means of an equation of state. A comparison of the two methods is presented in Table 1.

Thermodynamic Consistency Test of Data

The Gibbs-Duhem equation is a differential equation that represents the interrelationship among the changes of T , P and composition (in terms of chemical potentials) of an equilibrium system. The equation has the form:

$$-ns dT + nv dP - \sum n_i d\mu_i = 0 \quad [6]$$

When the Gibbs-Duhem equation is applied to the experimental results for systems under isothermal conditions and at low to moderate pressures, eqn [6] is reduced to $\sum n_i d\mu_i = 0$. In terms of liquid activity coefficient, which is defined by:

$$\gamma_i = \hat{f}_{iL}/x_i f_i^{\text{sat}} \quad [7]$$

the simplest expression for testing thermodynamic consistency has the form:

$$\sum x_i d \ln \gamma_i = 0 \quad [8]$$

Table 1 Comparison of vapour-liquid equilibrium calculation methods

Method	Gamma-phi approach	Equation-of-state approach
Advantage	Applicable to a wide variety of mixtures, including polar systems, electrolytes, and polymers. Simple solution models suffice for the correlation of vapour-liquid equilibrium data.	Applicable to a given system over wide ranges of temperature and pressure, including the supercritical region Thermodynamic properties, such as the enthalpy and entropy, can be consistently calculated from the same equation of state.
Disadvantage	Difficult to apply to systems involving supercritical components. Additional correlations must be used to represent the volumetric behaviour and thermal properties.	A single equation cannot represent the properties of all components precisely at the same time. Conventional mixing and combining rules are not applicable to systems containing polar components, polymer molecules, or electrolytes.

In eqn [7], the standard-state fugacity, f_i^{sat} , is the fugacity of component i at the system temperature. The standard state is usually taken to be the pure liquid at the T and P of the system. As data for binary systems are the basis for further correlation, it is desirable to have their consistency tested first. The simplest method is the 'visual test', which is independent of the models of equations used for expressing the excess Gibbs energy. A brief description of the visual test method is presented in **Table 2** with examples depicted in **Figure 2**. More precise testing methods, such as the point-by-point test and the area test, which take into consideration the effect of temperature change on the data for systems at isobaric conditions or the effect of pressure change on the data for systems at isothermal conditions, are available. However, excess enthalpies or volume changes owing to the mixing of components may be required. Whenever the liquid activity coefficients obtained from experimental data can be represented by an integrated Gibbs-Duhem equation (an appropriate modelling equation for γ), the data are considered thermodynamically consistent. For high pressure VLE, testing methods such as those developed by Won and Prausnitz in 1973 and Christiansen and Fredenslund in 1975 may be applied.

Gamma-Phi approach

In the gamma-phi approach, the dimensionless fugacity coefficients ϕ and the activity coefficients γ are used to describe the vapour phase and the liquid phase:

$$\hat{f}_V = \hat{\phi}_i y_i P \quad [9]$$

$$\hat{f}_L = \gamma_i x_i f_i^{\text{sat}} \quad [10]$$

The fugacity coefficients can be calculated from the vapour phase PTv composition data by means of an equation of state, such as the virial equation. When the system pressure is low, either of the volume-explicit virial equation and the pressure-explicit virial equation may be truncated after the second term and used for the calculation. The resulting expressions are respectively:

$$\ln \hat{\phi}_i = (P/RT) \left(2 \sum y_i B_{ij} - B \right) \quad [11]$$

and:

$$\ln \hat{\phi}_i = (2/v) \sum y_i B_{ij} - \ln Z \quad [12]$$

In these two equations, the expression:

$$B = \sum \sum y_i y_j B_{ij} \quad [13]$$

Table 2 Visual test of consistency of activity coefficients for binary systems

1. $\log \gamma_1$ evaluated at $x_1 = 0.25$ should be approximately equal to $\log \gamma_2$ evaluated at $x_1 = 0.75$.
2. Let α be the value of $\log \gamma_1$ evaluated at $x_1 = 0$ and β be the value of $\log \gamma_2$ evaluated at $x_1 = 1$.
 $\log \gamma_1$ evaluated at $x_1 = 0.5$ should be approximately equal to 0.25β .
 $\log \gamma_2$ evaluated at $x_1 = 0.5$ should be approximately equal to 0.25α .
3. If α is greater than or equal to β , then the value of $\log \gamma_1$ evaluated at $x_1 = 0.5$ should be less than or equal to the value of $\log \gamma_2$ evaluated at $x_1 = 0.5$.
4. If α is less than β , then the value of $\log \gamma_1$ evaluated at $x_1 = 0.5$ should be greater than the value of $\log \gamma_2$ evaluated at $x_1 = 0.5$.
5. Both $\log \gamma_i$ versus x_i curves show horizontal tangency as x_i approaches unity and $\log \gamma_i$ approaches zero.
6. If there is a maximum (or minimum) on one of the $\log \gamma_i$ versus x_i curves, there is a corresponding minimum (or maximum) on the other curve at the same x_i .
7. If there is neither a maximum nor a minimum on the curves, both curves should be on the same side of the horizontal line that is representing $\log \gamma_i = 0$.

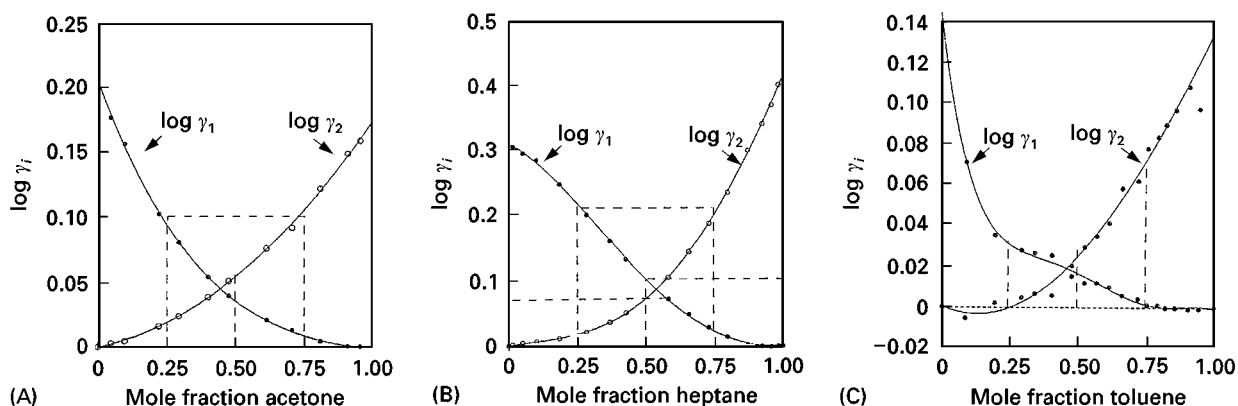


Figure 2 Visual consistency test of binary vapour-liquid equilibrium of (A) the acetone + benzene system at 318.15 K (Brown I and Smith F (1957) Liquid-vapor equilibrium VIII. The system acetone + benzene and acetone + carbon tetrachloride at 45°C. *Australian Journal of Chemistry* 10: 423–428), (B) the heptane + 3-pentanone system at 368.15 K (Geiseler G and Koehler H (1968) Thermodynamic behavior of the binary systems methyl ethyl ketoxime/n-heptane, diethyl ketone/n-heptane, and methyl ethyl ketoxime/diethyl ketone. *Berichte, Bunsengesellschaft fuer Physikalische Chemie*. 72: 697–706), (C) the toluene + n-octane system at 101.3 kPa. (Bromiley EC and Quiggle, D (1933) Vapor-liquid equilibria of hydrocarbon mixtures. *Industrial and Engineering Chemistry* 25: 1136–1138).

is used for the second virial coefficient of the mixture under consideration. When $i \neq j$, the cross second virial coefficient B_{ij} represents the interaction between molecule i and molecule j . Z is the compressibility factor of the mixture. The ϕ_i values obtained from eqns [11] and [12] are practically identical. A generalized method proposed by Hayden and O'Connell in 1975 may be used for predicting the second virial coefficients for pure components and the cross second virial coefficients. For an ideal gas mixture, $\hat{\phi}_i$ is unity.

Expressions are available for representing the dependence of γ_i on the composition of the solution. The activity coefficients are related to the excess Gibbs energy function by the equation

$$G_i^E = RT \ln \gamma_i \quad [14]$$

where $G_i^E = (\partial n G^E / \partial n_i)_{T,P,n_j}$. Some of these expressions, such as the two-parameter equations of van Laar, those of Margules, and the multiparameter equations of Redlich and Kister, are listed in Table 3. Additional expressions involving higher-order terms, such as those based on the local composition concept proposed by Wilson in 1964, the nonrandom two-liquid (NRTL) model by Renon and Prausnitz in 1968, and the universal quasi-chemical theory (UNIQUAC) equation by Abrams and Prausnitz in 1975, are frequently applied to activity coefficient calculations for binary and multicomponent systems.

According to eqn [8], the relation between $\ln \gamma_1$ and $\ln \gamma_2$ for a binary system at constant temperature and at low to moderate pressure, is given by:

$$x_1(d \ln \gamma_1 / dx_1) + x_2(d \ln \gamma_2 / dx_1) = 0 \quad [15]$$

which indicates that the two activity coefficients are not independent of each other. These activity coefficients may be evaluated by means of the equations listed in Table 4. If the vapour phase can be considered ideal at low pressures, the calculation of γ is much simplified. Pure-component fugacities may be substituted directly by the pure-component vapour pressures:

$$p_i \equiv y_i P = \gamma_i x_i p_i^{\text{sat}} \quad [16]$$

where p_i is the partial pressure of component i , P the system pressure, and p_i^{sat} the vapour pressure of pure component i .

The effect of temperature on $\ln \gamma_i$ is a concern in data correlation; a suitable representation of the temperature effect permits the determination of data for isobaric conditions from data for isothermal conditions, and vice versa. However, a consistency test for isothermal data is much easier than that for isobaric data because the pressure effect is generally much smaller than the temperature effect. The effect of temperature on $\ln \gamma_i$ is related to the partial molar enthalpy. Lu in 1959 considered the variation of excess enthalpies with temperature for binary systems and suggested that the variation of $\ln \gamma_i$ at constant liquid composition be represented by an expression involving three terms for data interpolation and extrapolation:

$$\ln \gamma_i = a + (b/T) + c \ln T \quad (\text{constant composition}) \quad [17]$$

In the absence of excess enthalpy data, isothermal data determined at three conditions suffice for the

Table 3 Selected activity coefficient models

Name	$G^E/(RT)$	$\ln \gamma_i$
Margules	$G^E/(RT) = x_1 x_2 (Ax_1 + Bx_2)$	$\ln \gamma_1 = x_2^2 [B + 2(A - B)x_1]$ $\ln \gamma_2 = x_1^2 [A + 2(B - A)x_2]$
van Laar	$G^E/(RT) = ABx_1 x_2 / (Ax_1 + Bx_2)$	$\ln \gamma_1 = A[1 + Ax_1/(Bx_2)]^{-2}$ $\ln \gamma_2 = B[1 + Bx_2/(Ax_1)]^{-2}$
Redlich–Kister	$G^E/(RT) = x_1 x_2 [A + B(x_1 - x_2) + C(x_1 - x_2)^2 + D(x_1 - x_2)^3 + \dots]$	$\ln \gamma_1 = a_1 x_2^2 + b_1 x_2^3 + c_1 x_2^4 + d_1 x_2^5 + \dots$ $\ln \gamma_2 = a_2 x_1^2 + b_2 x_1^3 + c_2 x_1^4 + d_2 x_1^5 + \dots$ where: $a_1 = A + 3B + 5C + 7D + \dots$ $b_1 = -4(B + 4C + 9D) + \dots$ $c_1 = 12(C + 5D) + \dots$ $d_1 = -32D + \dots$ $a_2 = A - 3B + 5C - 7D + \dots$ $b_2 = 4(B - 4C + 9D) + \dots$ $c_2 = 12(C - 5D) + \dots$ $d_2 = 32D + \dots$
Wilson	$G^E/(RT) = -\sum_i x_i \ln (\sum_j x_j \Lambda_{ij})$	$\ln \gamma_i = 1 - \ln (\sum_j x_j \Lambda_{ij}) - \sum_k [x_k \Lambda_{ki} / (\sum_j x_j \Lambda_{kj})]$
NRTL	$\frac{G^E}{RT} = x_1 x_2 \left(\frac{\tau_{21} G_{21}}{x_1 + x_2 G_{21}} + \frac{\tau_{12} G_{12}}{x_2 + x_1 G_{12}} \right)$ where: $\tau_{12} = \frac{\Delta g_{12}}{RT}$, $\tau_{21} = \frac{\Delta g_{21}}{RT}$ $\ln G_{12} = -a_{12} \tau_{12}$, $\ln G_{21} = -a_{12} \tau_{21}$	$\ln \gamma_1 = x_2^2 \left[\tau_{21} \left(\frac{G_{21}}{x_1 + x_2 G_{21}} \right)^2 + \frac{\tau_{12} G_{12}}{(x_2 + x_1 G_{12})^2} \right]$ $\ln \gamma_2 = x_1^2 \left[\tau_{12} \left(\frac{G_{12}}{x_2 + x_1 G_{12}} \right)^2 + \frac{\tau_{21} G_{21}}{(x_1 + x_2 G_{21})^2} \right]$
UNIQUAC	$G^E = G^E(\text{combinatorial}) + G^E(\text{residual})$ $\frac{G^E(\text{combinatorial})}{RT} = x_1 \ln \frac{\Phi_1}{x_1} + x_2 \ln \frac{\Phi_2}{x_2} + 5 \left(q_1 x_1 \ln \frac{\theta_1}{\Phi_1} + q_2 x_2 \ln \frac{\theta_2}{\Phi_2} \right)$ $\frac{G^E(\text{residual})}{RT} = -q_1 x_1 \ln (\theta_1 + \theta_2 \tau_{21}) - q_2 x_2 \ln (\theta_2 + \theta_1 \tau_{12})$ $\Phi_1 = \frac{x_1 r_1}{x_1 r_1 + x_2 r_2}$, $\theta_1 = \frac{x_1 q_1}{x_1 q_1 + x_2 q_2}$ $\ln \tau_{21} = -\frac{\Delta u_{21}}{RT}$, $\ln \tau_{12} = -\frac{\Delta u_{12}}{RT}$	$\ln \gamma_i = \ln \frac{\Phi_i}{x_i} + 5q_i \ln \frac{\theta_i}{\Phi_i} + \Phi_i \left(l_i - \frac{r_i}{r_j} \right) - q_i \ln (\theta_i + \theta_j \tau_{ji}) + \theta_j q_j \left(\frac{\tau_{ji}}{\theta_i + \theta_j \tau_{ji}} - \frac{\tau_{ij}}{\theta_j + \theta_i \tau_{ij}} \right)$ where: $i = 1, j = 2$ or $i = 2, j = 1$ $l_i = \frac{z}{2}(r_i - q_i) - (r_i - 1)$ $l_j = \frac{z}{2}(r_j - q_j) - (r_j - 1)$

determination of isobaric data within a reasonable range of temperatures. Similarly, if isobaric vapour–liquid equilibrium data are available at three conditions, isothermal data can be obtained by the same approach and then tested for consistency. The number of sets of vapour–liquid equilibrium data required can be reduced when excess enthalpies are available, but generally one set of experimental values should be used in the correlation. In the absence of the required data for the determination of parameters in eqn [17], $RT \ln \gamma_i$ at a given composition may be assumed to be constant as an approximation. The correlated results can also be used for the prediction purposes.

Equation-of-State Approach

Fugacities of both phases are represented in this approach by the same equation of state, which provides a relationship between the intensive thermodynamic variables T , P , v and composition. Such an equation may be explicit in P or v . The pressure-explicit equations in the form of:

$$P = P(T, v, x_1, x_2, \dots, x_{n-1}) \quad [18]$$

are more useful for solving phase-equilibrium problems. In terms of the fugacity coefficients, $\hat{\phi}_{iV}(=\hat{f}_{iV}/y_i P)$ and $\hat{\phi}_{iL}(=\hat{f}_{iL}/x_i P)$, formulation of vapour–liquid equilibria is based on the equilibrium

Table 4 Barker's method for the determination of activity coefficients from experimental data

At equilibrium:

$$\begin{aligned} f_i^l &= f_i^v \\ \hat{\phi}_i^v &\equiv \frac{f_i^v}{y_i P} \quad (\text{by definition}) \\ y_i P \hat{\phi}_i^v &= x_i \gamma_i f_i^l \\ \hat{\phi}_i^l &= \frac{f_i^l}{P}, \quad \hat{\phi}_i^{\text{sat}} = \frac{f_i^{\text{sat}}}{p_i^{\text{sat}}} \end{aligned}$$

Therefore:

$$\begin{aligned} y_i P \hat{\phi}_i^v &= x_i \gamma_i \hat{\phi}_i^l P \\ \ln(y_i P \hat{\phi}_i^v) &= \ln(x_i \gamma_i) + \ln \hat{\phi}_i^l + \ln P \\ &= \ln(x_i \gamma_i) + \ln \hat{\phi}_i^{\text{sat}} + \frac{v_i^l}{RT}(P - p_i^{\text{sat}}) + \ln p_i^{\text{sat}} \end{aligned}$$

Hence:

$$\ln \gamma_i = \ln \frac{y_i P}{x_i p_i^{\text{sat}}} + \ln \hat{\phi}_i^v - \ln \hat{\phi}_i^{\text{sat}} - \frac{v_i^l(P - p_i^{\text{sat}})}{RT}$$

For a binary system:

$$B = y_1^2 B_{11} + 2y_1 y_2 B_{12} + y_2^2 B_{22}$$

Let:

$$\delta_{12} = 2B_{12} - B_{11} - B_{22}$$

Then:

$$B = y_1 B_{11} + y_2 B_{22} + y_1 y_2 \delta_{12}$$

At low pressure:

$$\begin{aligned} Z &= \frac{P\tilde{V}}{RT} = 1 + \frac{BP}{RT} \\ \ln \hat{\phi}_1^v &= \left(\frac{B_{11} + y_2^2 \delta_{12}}{RT} \right) P \end{aligned}$$

 For pure component i :

$$\begin{aligned} \ln \phi_i &= \int_0^P (Z_i - 1) \frac{dP}{P}, \quad \left(Z_i = 1 + \frac{B_i P}{RT} \right) \\ \ln \phi_i^{\text{sat}} &= \int_0^{p_i^{\text{sat}}} (Z_i - 1) \frac{dP}{P} = \frac{B_{ii}}{RT} p_i^{\text{sat}} \\ \ln \gamma_1 &= \ln \frac{y_1 P}{x_1 p_1^{\text{sat}}} + \left(\frac{B_{11} + y_2^2 \delta_{12}}{RT} \right) P - \frac{B_{11}}{RT} p_1^{\text{sat}} - \frac{v_1^l(P - p_1^{\text{sat}})}{RT} \\ &= \ln \frac{y_1 P}{x_1 p_1^{\text{sat}}} + \frac{(B_{11} - v_1^l)(P - p_1^{\text{sat}})}{RT} + \frac{y_2^2 \delta_{12} P}{RT} \end{aligned}$$

Similarly:

$$\ln \gamma_2 = \ln \frac{y_2 P}{x_2 p_2^{\text{sat}}} + \frac{(B_{22} - v_2^l)(P - p_2^{\text{sat}})}{RT} + \frac{y_1^2 \delta_{12} P}{RT}$$

 Barker JA (1953) Determination of activity coefficients from total-pressure measurements. *Australian Journal of Chemistry* (1953) 6: 207–210.

equations:

$$y_i \hat{\phi}_{iV} = x_i \hat{\phi}_{iL} \quad (i = 1, 2, \dots, N) \quad [19]$$

$$RT \ln \hat{\phi}_i = \int_V^\infty [(\partial P / \partial n_i)_{T,V,n_j} - RT/V] dV - RT \ln Z \quad [20]$$

 with both the $\hat{\phi}_{iV}$ and $\hat{\phi}_{iL}$ calculated from the equations:

The advantage of this approach is that it is applicable to calculations of VLE at high pressures and it

can also be used to obtain other configurational properties such as enthalpy, entropy and volume changes of mixing, which are useful in the design of distillation columns.

The first equation of state with a theoretical foundation was proposed by van der Waals in 1873, several decades after the ideal gas equation of state had been formulated. This equation not only yields qualitatively correct representation of the phase behaviour of a real fluid, but also provides the basis of the principle of corresponding states. Hundreds of equations of state have been developed since the publication of the van der Waals equation. They may be theoretical, semi-theoretical or empirical. However, most of the modifications are generally limited to a specific purpose.

In order to apply an equation of state to vapour-liquid equilibrium calculations for pure components, a suitable equation should satisfy the three conditions at a given saturation temperature:

$$\nu_{V,\text{calc.}} = \nu_V, \quad \nu_{L,\text{calc.}} = \nu_L, \quad f_{V,\text{calc.}} = f_{L,\text{calc.}} \quad [21]$$

Mixing and combining rules for the equation parameters are required for extending its application to mixtures. However, most of the practical equations available at present have their inherent advantages and disadvantages and may not satisfy both of the volumetric conditions.

The equations of state expressed in terms of polynomials in volume are of practical importance. For VLE calculations, especially when the properties under consideration are limited to T , P and compositions, the simplest and frequently used form is that which is cubic in ν . In spite of their shortcomings, these cubic equations are the most frequently used in practice at present. Currently, the most popular two-parameter cubic equations of state include the Soave-Redlich-Kwong equation (1972):

$$P = RT/(\nu - b) - a/[\nu(\nu + b)] \quad [22]$$

and the Peng-Robinson equation (1976):

$$P = RT/(\nu - b) - a/[\nu(\nu + b) + b(\nu - b)] \quad [23]$$

Both equations can be obtained from a general form of a four-constant cubic equation of the van der Waals type:

$$P = RT/(\nu - b) - a/[(\nu + c_1b)(\nu + c_2b)] \quad [24]$$

Additional multiparameter cubic equations, which are of the form represented by eqn [24] but developed for improving the representations of pure-component

vapour pressures, saturated liquid volumes, the critical compressibility factors, and phase behaviour of polar-nonpolar mixtures, appear continuously in the literature. The maximum number of parameters in a cubic equation is five. A list of some selected cubic equations of state is presented in Table 5. In some of the cubic equations, different repulsion terms (the first term on the right-hand side of the equations listed in the table) have been adopted. The forms of these equations are frequently influenced by the desire to improve the theoretical basis of the equation, and that of fitting the volumetric properties. It should also be mentioned that one of the inherent limitations of a two-parameter equation is that the critical compressibility factor is a constant for all components. The ability of a cubic equation in VLE representation is controlled by the selection of an adequate temperature function for the parameter ' a ' for vapour pressures of pure components, and a set of suitable mixing and combining rules for all the parameters of the equation for mixtures.

Temperature function for ' a ' The importance of using a proper temperature function to represent the parameter ' a ' cannot be overemphasized. In the 1960s, Wilson began the consideration of the temperature effect on the parameter ' a ' of the Redlich-Kwong equation. The expression which has gained wider acceptance was developed by Soave for the same equation in 1972. The parameter ' a ' was expressed by:

$$a = a_c \alpha \quad [25]$$

with α expressed by a function involving the reduced temperature $T_r (= T/T_c)$ in the form:

$$\alpha = [1 + m(1 - T_r^{1/2})]^2 \quad [26]$$

where the subscript c refers to the critical-point condition, and m represents a quadratic function of the acentric factor of Pitzer. This form and its variations have been adopted subsequently in many cubic equations. A selected set of temperature functions for the parameter ' a ' is listed in Table 6.

Mixing and combining rules To extend the application of his equation of state to representing the behaviour of mixtures, van der Waals proposed that the constants ' a ' and ' b ' be expressed by:

$$a = \sum \sum x_i x_j a_{ij} \quad [27]$$

$$b = \sum \sum x_i x_j b_{ij} \quad [28]$$

Table 5 Selected cubic equations of state and the corresponding fugacity coefficient expressions

Equation of state	Fugacity coefficient for pure component i	Fugacity coefficient for component i in mixture ^a
Soave–Redlich–Kwong (1972) $P = \frac{RT}{v-b} - \frac{a(T)}{v(v+b)}$	$\ln \phi = Z - 1 - \ln(Z - B) - \frac{A}{B} \ln \left(1 + \frac{B}{Z} \right)$ <p>where: $A = \frac{aP}{R^2 T^2}$, $B = \frac{bP}{RT}$, $Z = \frac{Pv}{RT}$</p>	$\ln \phi_i = \frac{B_i}{B} (Z - 1) - \ln(Z - B) - \frac{A}{B} \left(\frac{2 \sum_j y_j a_{ji}}{a} - \frac{B_i}{B} \right) \ln \left[1 + \frac{B}{Z} \right]$
Peng–Robinson (1976) $P = \frac{RT}{v-b} - \frac{a(T)}{v(v+b) + b(v-b)}$	$\ln \phi = Z - 1 - \ln(Z - B) - \frac{A}{2\sqrt{2}B} \ln \left[\frac{Z + (1 + \sqrt{2})B}{Z + (1 - \sqrt{2})B} \right]$ <p>where: $A = \frac{aP}{R^2 T^2}$, $B = \frac{bP}{RT}$, $Z = \frac{Pv}{RT}$</p>	$\ln \phi_i = \frac{B_i}{B} (Z - 1) - \ln(Z - B) - \frac{A}{2\sqrt{2}B} \left(\frac{2 \sum_j y_j a_{ji}}{a} - \frac{B_i}{B} \right) \ln \left[\frac{Z + (1 + \sqrt{2})B}{Z + (1 - \sqrt{2})B} \right]$
Patel–Teja (1982) $P = \frac{RT}{v-b} - \frac{a(T)}{v(v+b) + c(v-b)}$	$\ln \phi = Z - 1 - \ln(Z - B) + \frac{a}{2RTN} \ln \left[\frac{Z + M}{Z + Q} \right]$ <p>where: $B = \frac{bP}{RT}$, $Z = \frac{Pv}{RT}$</p> $M = \left(\frac{b+c}{2} - N \right) \frac{P}{RT}$ $N = \left[bc + \frac{(b+c)^2}{2} \right]^{-1/2}$ $Q = \left(\frac{b+c}{2} + N \right) \frac{P}{RT}$	$RT \ln \phi_i = -RT \ln(Z - B) + RT \left(\frac{b_i}{v-b} \right) - \frac{\sum_j x_j a_{ji}}{d} \ln \left(\frac{Q+d}{Q-d} \right) + \frac{a(b_i + c_i)}{2(Q^2 - d^2)} + \frac{a}{8d^3} \{ c_i(3b + c) + b_i(3c + b) \} \times \left\{ \ln \left(\frac{Q+d}{Q-d} \right) + \frac{2Qd}{Q^2 - d^2} \right\}$ <p>where:</p> $Q = v + \frac{b+c}{2}, \quad d = \sqrt{bc + \frac{(b+c)^2}{4}}$
Adachi–Lu–Sugie (1983) $P = \frac{RT}{v-b_1} - \frac{a(T)}{(v-b_2) + (v+b_3)}$	$\ln \phi = Z - 1 - \ln(Z - B_1) + \frac{a}{RT(b_2 + b_3)} \ln \left(\frac{v-b_2}{v+b_3} \right)$	$\ln \phi_i = \frac{b_{1i}}{v-b_1} - \frac{a}{RT(b_2 + b_3)} \left[\frac{b_{2i}}{v-b_2} + \frac{b_{3i}}{v+b_3} \right] + \frac{a}{RT(b_2 + b_3)} \left(\frac{2 \sum_j y_j a_{ji}}{a} - \frac{b_{2i} + b_{3i}}{b_2 + b_3} \right) \times \ln \left[\frac{v-b_2}{v+b_3} \right] - \ln(Z - B_1)$ $\left[b_j = \sum_i x_i b_{ji} \right]$
Iwai–Margerum–Lu (1988) $P = \frac{RT}{v-b} - \frac{a(T)}{v^2 + ub(v-b)}$	$\ln \phi = Z - 1 - \ln Z + \ln \left(\frac{v}{v-b} \right) - \frac{1}{RT} \left[\frac{a}{(c^2 - 4bc)^{0.5}} \right] \times \ln \left[\frac{2v-c + (c^2 - 4bc)^{0.5}}{2v-c - (c^2 - 4bc)^{0.5}} \right]$ <p>where:</p> $Z = \frac{Pv}{RT}, \quad c = -bu$	$\ln \phi_i = \frac{b_i}{v-b} + \ln \frac{v}{v-b} - \ln Z + \left[\frac{a}{RTA} (v^2 - cv + cb) \right] \times [(b_i c + c_i b)(2v - c) + c_i(2bc - cv)] + \left[2 \sum_j x_j a_{ji} + \frac{a}{A} (2(b_i c + c_i b) - cc_i) \right] \times \frac{1}{RT\sqrt{A}} \ln \frac{2v-c-\sqrt{A}}{2v-c+\sqrt{A}}$ <p>where:</p> $A = c^2 - 4bc$

^aThe mixing rule: $a = \sum_i \sum_j x_i x_j a_{ij}$, $b = \sum_i x_i b_i$, $c = \sum_i x_i c_i$, $a_{ij} = (a_i a_j)^{1/2} (1 - k_{ij})$. References: Adachi YB, Lu BC-Y and Sugie H (1983) A four-parameter equation of state. *Fluid Phase Equilibria* 11: 29–48. Iwai Y, Margerum R and Lu BC-Y (1988) A new three-parameter cubic equation of state for polar fluids and fluid mixtures. *Fluid Phase Equilibria* 42: 21–41. Patel NC and Teja AS (1982) A new cubic equation of state for fluids and fluid mixtures. *Chemical Engineering Science* 37: 463–473. Peng D-Y and Robinson DB (1976) A new two-constant equation of state. *Industrial and Engineering Chemistry Fundamentals* 15: 59–64. Soave G (1972) Equilibrium constants from a modified Redlich–Kwong equation of state. *Chemical Engineering Science* 27: 1197–1203.

Table 6 Some different forms of the α function

Form	Reference
$\alpha = 1 + m(1 - T_r)$	1
$\alpha = [1 + m(1 - \sqrt{T_r})]^2$	2
$\alpha = [1 + m_1(1 - \sqrt{T_r}) + m_2(1/T_r - 1)]^2$	3
$\alpha = [1 + m_1(1 - \sqrt{T_r}) + m_2(1 - T_r)(0.7 - T_r)]^2$	4
$\alpha = 1 + m_1(1 - T_r) + m_2(1/T_r - 1)$	5
$\alpha = 10^{[m(1 - T_r)]}$	6
$\alpha = \{1 + [m_1 + m_2(1 + \sqrt{T_r})(0.7 - T_r)](1 - \sqrt{T_r})\}^2$	7
$\alpha = 10^{f(T_r)}$, $f(T_r) = m_3(m_0 + m_1 T_r + m_2 T_r^2)(1 - T_r)$	8
$\alpha = \exp[m_1(1 - T_r) + m_2(1 - \sqrt{T_r})^2]$	9
$\alpha = T_r^{(m_2-1)m_3} \exp[m_1(1 - T_r^{m_2+m_3})]$	10

References: 1. Wilson GM (1964) Vapor-liquid equilibria, correlation by means of a modified Redlich-Kwong equation of state. *Advances in Cryogenic Engineering* 9: 168-176. 2. Soave G (1972) Equilibrium constants from a modified Redlich-Kwong equation of state. *Chemical Engineering Science* 27: 1197-1203. 3. Harmens A and Knapp H (1980) Three-parameter cubic equation of state for normal substances. *Industrial and Engineering Chemistry Fundamentals* 19: 291-294. 4. Mathias PM (1983) A versatile phase equilibrium equation of state. *Industrial and Engineering Chemistry, Process Design and Development* 22: 385-391. 5. Soave G (1984) Improvement of the van der Waals equation of state. *Chemical Engineering Science* 39: 357-369. 6. Adachi Y and Lu BC-Y (1984) Simplest equation of state for vapor-liquid equilibrium calculations: a modification of the van der Waals equation. *American Institute of Chemical Engineers Journal* 30: 991-993. 7. Stryjek R and Vera JH (1986) PRSV: An improved Peng-Robinson equation of state for pure compounds and mixtures. *Canadian Journal of Chemical Engineering* 64: 323-333. 8. Yu JM and Lu BC-Y (1987) A three-parameter cubic equation of state for asymmetric mixture density calculations. *Fluid Phase Equilibria* 34: 1-19. 9. Melhem GA, Saini R and Goodwin BM (1989) A modified Peng-Robinson equation of state. *Fluid Phase Equilibria* 47: 189-237. 10. Twu CH, Bluck D, Cunningham JR and Coon JE (1991) A cubic equation of state with a new alpha function and a new mixing rule. *Fluid Phase Equilibria* 69: 33-50.

The simplest combining rules for ' a_{ij} ' and ' b_{ij} ' are obtained by using the geometric mean for a_{ij} and the arithmetic mean for b_{ij} , i.e:

$$a_{ij} = (a_i a_j)^{1/2} \quad [29]$$

$$b_{ij} = (b_i + b_j)/2 \quad [30]$$

A binary interaction parameter k_{ij} is frequently introduced in eqn [29] to correct the discrepancy generated by the geometric mean:

$$a_{ij} = (a_i a_j)^{1/2} (1 - k_{ij}) \quad [31]$$

Occasionally, a binary interaction parameter l_{ij} is introduced in eqn [30] to yield improved b_{ij} values:

$$b_{ij} = (b_i + b_j)(1 - l_{ij})/2 \quad [32]$$

More recently, new mixing rules, such as the one proposed by Wong and Sandler in 1992, with im-

proved theoretical considerations have appeared in the literature. A list of some mixing and combining rules is presented in Table 7.

In general, vapour-liquid equilibrium of a great variety of mixtures, including polar-nonpolar mixtures, can be well represented. For a given mixture, the equation-of-state mixing rules with one set of parameters can frequently represent the data over wide ranges of temperature and pressure.

Examples of binary data representation by means of the two approaches are depicted in Figure 3.

Prediction of Vapour-Liquid Equilibria

Although vapour-liquid equilibria have been investigated for more than 10 000 systems, values resulting from various combinations are still unknown. It would be impractical to determine experimentally all the systems needed individually.

In principle, experimental values of some thermodynamic properties can be used to estimate other properties. For examples, binary vapour-liquid equilibrium can be estimated from the liquid activity coefficients calculated from mutual solubility data for the same mixture, and the infinite-dilution activity coefficients measured from gas-liquid chromatography can be used to predict the vapour-liquid equilibria over the complete concentration range. Some prediction methods are briefly described below with emphasis placed on binary mixtures. Extending the

Table 7 Some mixing and combining rules for cubic equations of state

van der Waals/Berthelot

$$a_{ij} = (a_i a_j)^{1/2}$$

$$a = \sum_i \sum_j y_i y_j a_{ij}, \quad b = \sum_i y_i b_i$$

Modified van der Waals/Berthelot

$$a = \sum_i \sum_j y_i y_j a_{ij} \quad b = \sum_i \sum_j y_i y_j b_{ij}$$

$$a_{ij} = (a_i a_j)^{1/2} (1 - k_{ij})$$

$$b_{ij} = \frac{1}{2}(b_i + b_j)(1 - c_{ij})$$

Wong-Sandler

$$b - \frac{a}{RT} = \sum_i \sum_j \left(b_{ij} - \frac{a_{ij}}{RT} \right)$$

$$b_{ij} = \frac{b_i + b_j}{2} (1 - k_{ij})$$

$$a_{ij} = \frac{a_i + a_j}{2} (1 - k_{ij})$$

$$\frac{a}{b} = \sum_i \frac{x_i a_i}{b_i} - \frac{G^E}{CRT}$$

where: G^E is a selected excess Gibbs energy model
 C is characteristic of the equation of state

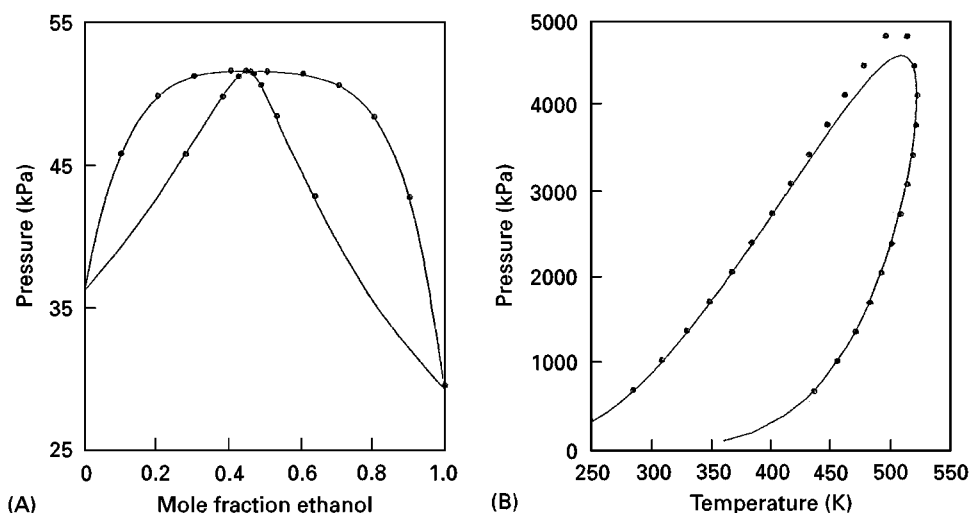


Figure 3 (A) Correlating the phase behaviour of the (ethanol + benzene) system at 323.15 K by means of the gamma-phi approach. The lines represent the values calculated by using the Margules equations and the points represent the experimental values reported by ND. Litvinov (1952) Isothermal equilibrium of vapor and liquid in systems of three fully miscible liquids. *Zhurnal Fizicheskoi Khimii* 26: 1405–1412. (B) Predicting the phase behaviour of the (0.2654 mole fraction ethane + 0.7346 mole fraction *n*-heptane) mixture by means of the equation-of-state approach. The smooth curve represents the values calculated by using the Peng–Robinson equation, and the points represent the experimental values reported by WB Kay (1938) Liquid–vapor phase equilibrium relations in the ethane-*n*-heptane system. *Industrial and Engineering Chemistry* 30: 459–464.

application to multicomponent mixtures is feasible once good correlation of the vapour–liquid equilibria of its constituent binary systems becomes available.

Prediction from Pure Component Properties

Application of the regular solution theory For mixtures containing nonpolar components that are not much different in size and shape, the regular solution theory of Hildebrand leads to a semi-quantitative prediction of γ_k values of all components in a mixture. In terms of the solubility parameter, the activity coefficients of the components in a regular solution can be calculated from the equation:

$$RT \ln \gamma_k = v_k (\delta_k - \delta)^2 \quad [33]$$

where the volume average solubility parameter is given by:

$$\delta = \sum \Phi_i \delta_i \quad [34]$$

and the volume fraction Φ_i is defined by:

$$\Phi_i = x_i v_i / \sum x_j v_j \quad [35]$$

The solubility parameter for substance k , δ_k , is defined by:

$$\delta_k = (\Delta U_k^V / v_k^V)^{1/2} = [(\Delta H_k^V - RT) / v_k^V]^{1/2} \quad [36]$$

where ΔU_k^V and ΔH_k^V are, respectively, the molar energy and enthalpy of vaporization of pure liquid k at temperature T . The assumption involved here is that T is well below the critical temperature in order to make the approximation valid. The calculated liquid activity coefficients can then be used to obtain the desired vapour–liquid equilibrium values. For a binary mixture:

$$RT \ln \gamma_1 = v_1 \Phi_2^2 (\delta_1 - \delta_2)^2 \quad [37]$$

$$RT \ln \gamma_2 = v_2 \Phi_1^2 (\delta_1 - \delta_2)^2 \quad [38]$$

Should a binary interaction parameter be required to improve the data representation, an extension of the approach to the prediction of multicomponent vapour–liquid equilibrium may not be practical; attempts made to correlate the binary parameters have not been successful.

Liquid activity coefficients at infinite dilution γ^∞ Values of γ^∞ are particularly useful for obtaining the parameters of any of the two-constant equations for the excess Gibbs energy; the γ^∞ values for a binary system are the parameter values. For example, $\gamma_1^\infty = A$ and $\gamma_2^\infty = B$ for the van Laar and Margules equations presented in Table 3. If a three-parameter equation is used, the third parameter must be determined by an independent approach.

The modified separation of cohesive energy density (MOSCED) method proposed by Thomas and Eckert

in 1984 may be used to predict γ^∞ values from pure component parameters. This method is based on a modified regular solution theory and the assumption that the forces contributing to the cohesive energy are additive. It has been reported that the average error of 3357 γ^∞ values predicted by this method was 9.1%.

In general, calculated equilibrium vapour compositions are relatively insensitive to moderate errors in the γ^∞ used in the calculation.

Prediction of Binary γ Values Using Azeotropic or Mutual Solubility Data

Prediction from azeotropic data Many binary systems exhibit azeotropic behaviour. At an azeotropic condition, the compositions of the liquid and vapour phases are identical. At low pressures, the liquid activity coefficients can be simply calculated by:

$$\gamma_1 = P/p_1^{\text{sat}} \quad \text{and} \quad \gamma_2 = P/p_2^{\text{sat}} \quad [39]$$

The parameters of any two-parameter expression of the excess Gibbs energy can then be obtained and used for extrapolating vapour-liquid equilibrium over the complete concentration range.

Prediction of γ values from mutual solubility data

The thermodynamic consideration applicable to a binary system at vapour-liquid equilibrium is also applicable to a partially miscible binary liquid mixture at equilibrium. Hence, the activity coefficients of the two liquids at the temperature at which the solubilities were experimentally determined can be expressed by:

$$\gamma'_1 x'_1 = \gamma''_1 x''_1 \quad \text{and} \quad \gamma'_2 x'_2 = \gamma''_2 x''_2 \quad [40]$$

where the two superscripts refer to the two liquid phases. Applying these relationships to any two-parameter expression of the excess Gibbs energy leads to the determination of the parameter values, which permit vapour-liquid equilibrium estimation of the mixture.

Prediction of γ from Group Contribution Methods

In group contribution methods, the calculation of thermodynamic properties of pure fluids is based on the assumption that each molecule is an aggregate of functional groups. Langmuir in 1925 extended the concept to mixtures. Redlich, Derr, Pierotti and Papadopoulos developed a group interaction model for heats of solution in 1959. Adopting the concepts presented by these authors, Wilson and Deal suggested in 1962 a solution of the groups approach by

which liquid activity coefficients can be estimated on the basis of group contributions. In this approach, the logarithm of the activity coefficient of a component is assumed to be the sum of two contributions: the configurational contribution, which accounts for the differences in molecular size, and the group interaction contribution, which accounts for the intermolecular forces originating from the different functional groups.

The group contribution approach to calculating γ is attractive because through this approach it is possible to estimate vapour-liquid equilibria of nonideal mixtures without experimentation. Although a large number of mixtures can result from pure compounds, the functional groups, such as CH_2 , OH, CO, COO and COOH, that constitute these compounds are limited. If the activity coefficients of the mixture components could be obtained from a knowledge of the interactions of these groups, and with the assumption that the contribution to γ by one group within a molecule is independent of that made by any other group in that molecule, a relatively small number of parameters would suffice for the prediction of the activity coefficients for mixtures containing the same groups. This assumption implies that the contribution of the group interaction is independent of the nature of the molecule.

Two of these approaches are mentioned here.

Analytical solutions of groups (ASOG) method

Following the concept of the solutions of groups of Wilson and Deal, the analytical solutions of groups (ASOG) method was first presented by Derr and Deal in 1969. Basically, the practical application of the solutions of groups concept involves the reduction of liquid activity coefficients obtained from experimental data for vapour-liquid equilibria into a number of binary group interaction parameters. The working equations of the ASOG method are presented in Table 8.

Kojima and Tochigi in 1979 calculated the group interaction parameters for 31 groups and used the method to predict the vapour-liquid equilibria for 936 binary systems, 103 ternary systems, five quaternary systems, and two quinary systems at low pressures. They reported that the average absolute deviation of the predicted vapour compositions was 1.2%.

Universal functional group activity coefficient (UNIFAC) method

The universal functional group activity coefficient (UNIFAC) method proposed by Fredenslund, Gmehling and Rasmussen and the ASOG method are based on the same principle of group contributions. The main difference between these two methods is in the equations used for

Table 8 The analytical solution of groups (ASOG) method

1. $\ln \gamma_i = \ln \gamma_i^S + \ln \gamma_i^G$
2. $\ln \gamma_i^S = 1 - r_i - \ln r_i$
 where: $r_i = \frac{v_i}{\sum_j x_j v_j}$
 x_j = mole fraction of molecule j
 v_j = number of atoms other than hydrogen in molecule j
3. $\ln \gamma_i^G = \sum_k v_{ki} (\ln \Gamma_k - \ln \Gamma_k^{(i)})$
 where: v_{ki} = number of atoms other than hydrogen in group k in molecule i
 $\ln \Gamma_k = 1 - C_k - \ln D_k$
 $\ln \Gamma_k^{(i)} = 1 - C_k^{(i)} - \ln D_k^{(i)}$
 $C_k = \sum_j \frac{X_j A_{jk}}{D_j}, \quad C_k^{(i)} = \sum_j \frac{X_j^{(i)} A_{jk}}{D_j}$
 $D_k = \sum_j X_j A_{kj}, \quad D_k^{(i)} = \sum_j X_j^{(i)} A_{kj}$
 $X_L = \frac{1}{S} \sum_i x_i v_{Li}, \quad X_L^{(i)} = \frac{v_{Li}}{\sum_k v_{ki}}$
 $A_{kL} = \exp\left(m_{kL} + \frac{n_{kL}}{T}\right)$
 $S = \sum_i x_i \sum_k v_{ki}$

representing the excess Gibbs energy. The Wilson equation is used in the ASOG method, whereas the two-parameter universal quasi-chemical (UNIQUAC) equation of Abrams and Prausnitz is used in the UNIFAC method. The working equations of the UNIFAC method are presented in Table 9. There are 50 main groups together with their subgroups for the determination of the parameters involved in the calculation. For γ calculations for multicomponent systems, the adjustable binary parameters are evaluated from binary vapour–liquid equilibrium data.

Prediction using Equations of State

The equations of state successfully used for correlation of binary vapour–liquid equilibria can be used for the purposes of predicting multicomponent vapour–liquid equilibria, provided that the binary interaction parameters of all the constituent binary systems are available. All the parameters should be obtained by regression of the binary data using the same mixing and combining rules. Interpolated and estimated values of these parameters are available for some systems, but their values are subject to frequent revision.

Additional Comments on Applications

There is no simple equation of state that can represent satisfactorily the three conditions of eqn [21] over

a wide range of temperature. Experience indicates that equations that could meet the equal fugacity condition as well as v_v or v_L would be suitable for the intended vapour–liquid equilibrium calculations. Should a situation arise such that the saturated liquid molar volume is required in the estimation, cubic equations containing more parameters may be selected for the representation. Adachi and Lu in 1990 suggested that it is possible to assign different two-parameter or three-parameter cubic equations to different components of the binary mixture under consideration, and then use a four-parameter cubic equation to combine the equations in the vapour–liquid equilibrium calculations for mixtures.

Special case should be applied when equations of state are used to represent the experimental data measured at or near theoretical points of the fluids.

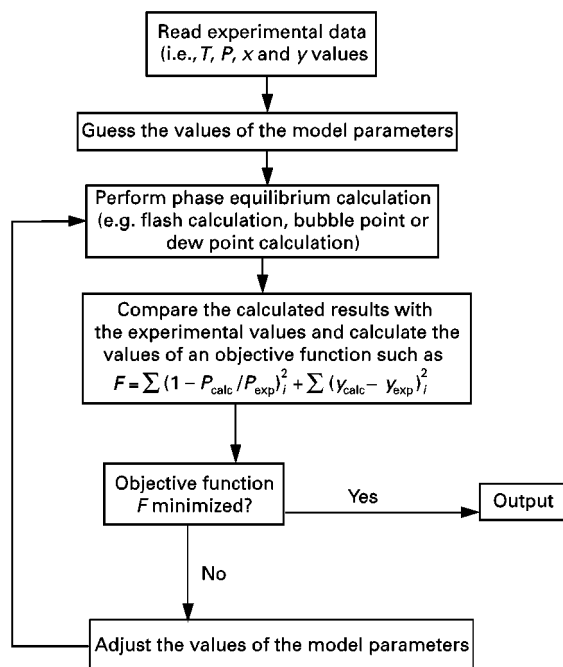
The selection of mixing and combining rules plays a crucial role in the application of equations of state to the correlation and prediction of vapour–liquid equilibria. The importance of selecting an appropriate expression for the excess Gibbs energy cannot be overemphasized.

The prediction of binary vapour–liquid equilibria from pure-component properties by means of the MOSCED method is attractive. However, poor results are obtained for systems where steric considerations are significant. The general applicability of this model is limited due to the difficulties involved in

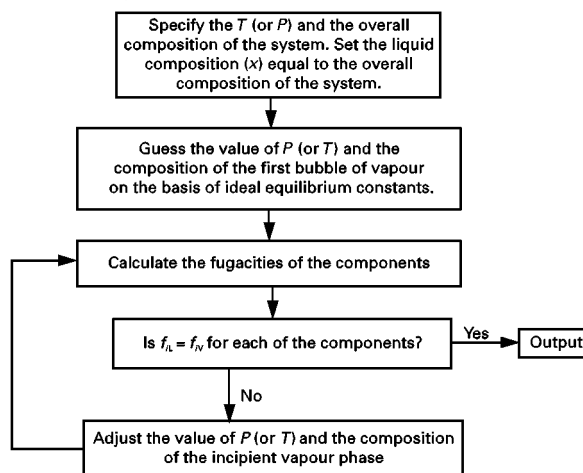
Table 9 The UNIFAC method

1. $\ln \gamma_i = \ln \gamma_i^G + \ln \gamma_i^R$
2. $\ln \gamma_i^G = 1 - J_i + \ln J_i - 5q_i \left(1 - \frac{J_i}{L_i} + \ln \frac{J_i}{L_i}\right)$
 where: $J_i = \frac{r_i}{\sum_j x_j r_j}, \quad L_i = \frac{q_i}{\sum_j x_j q_j}$
 $r_i = \sum_k v_k^{(i)} R_k, \quad q_i = \sum_k v_k^{(i)} Q_k$
 R_k = volume parameter for group k
 Q_k = surface area parameter for group k
 $v_k^{(i)}$ = number of subgroups of type k in molecule of species i
3. $\ln \gamma_i^R = q_i \left[1 - \sum_k \left(\frac{\theta_k \beta_{ik}}{S_k} - \rho_{ki} \ln \frac{\beta_{ik}}{S_k}\right)\right]$
 where: $\rho_{ki} = \frac{v_k^{(i)} Q_k}{q_i}$
 $\beta_{ik} = \sum_m \rho_{mi} \tau_{mk}$
 $\theta_k = \frac{\sum_i x_i q_i \rho_{ki}}{\sum_i x_i q_i}$
 $S_k = \sum_m \theta_m \tau_{mk}$
 $\tau_{mk} = \exp\left(-\frac{\alpha_{mk}}{T}\right)$
 α_{mk} = group interaction parameter

(A) Correlation



(B) Bubble point calculation



(C) Dew point calculation

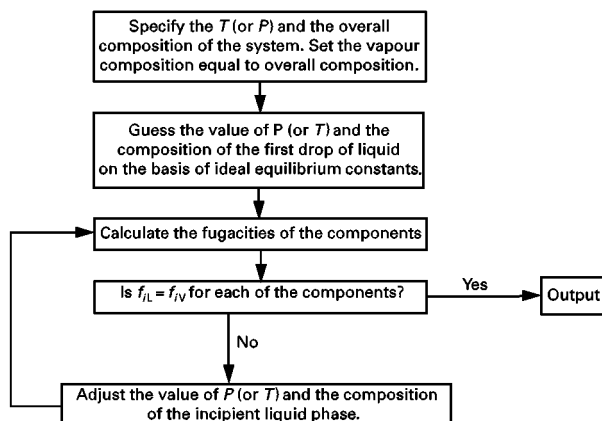


Figure 4 Algorithms for correlating and predicting vapour–liquid equilibrium values.

the determination of pure component parameters. Furthermore, the approach cannot be used for aqueous mixtures, nor for systems with very large γ^∞ values.

In general, the accuracy of prediction depends on the availability of some reliable binary data for either the system of interest or another one that is closely related to it.

All the group-contribution methods are approximate. The fundamental assumption involved in the group solution approach is additivity, and the estimated γ values are necessarily approximate.

Finally, computer software packages for vapour–liquid equilibrium calculations are available commercially from a number of process engineering software

development companies. Typical algorithms for data correlation and prediction are depicted in Figure 4.

See also: II/Distillation: Modelling and Simulation; Multicomponent Distillation; Theory of Distillation; Vapour–Liquid Equilibrium: Theory. III/Physico-Chemical Measurements: Gas Chromatography.

Further Reading

Abrams DS and Prausnitz JM (1975) Statistical thermodynamics of liquid mixtures. New equation for the excess Gibbs energy of partly or completely miscible systems. *American Institute of Chemical Engineering Journal* 21: 116–128.

- Adachi Y and Lu BC-Y (1990) Taking advantage of available cubic equations of state. *Canadian Journal of Chemical Engineering* 68: 639–644.
- Christiansen LJ and Fredenslund A (1975) Thermodynamic consistency using orthogonal collocation or composition of equilibrium vapor compositions at high pressures. *American Institute of Chemical Engineers Journal* 21: 49–57.
- Derr EL and Deal CH Jr (1969) Analytical solutions of groups. Correlation of activity coefficients through structural group parameters. *Proceedings of International Symposium of Distillation* 3: 40–51.
- Denbigh K (1981) *The Principles of Chemical Equilibrium*, 4th edn. Cambridge: Cambridge University Press.
- Fredenslund A, Gmehling J and Rasmussen P (1977) *Vapour-Liquid Equilibria Using UNIFAC*. Amsterdam: Elsevier.
- Gmehling J, Onken U and Arlt W (1974–1990) *Vapour-Liquid Equilibrium Data Collection*; Dechema Chemistry Data Series, vol. I, parts 1–8. Frankfurt: Dechema.
- Hala E, Pick J, Fried V and Vilim O (1967) *Vapour-Liquid Equilibrium*, 2nd edn. Oxford: Pergamon Press.
- Hayden JG and O'Connell JP (1975) Generalized method for predicting second virial coefficients. *Industrial and Engineering Chemistry. Process Design and Development* 14: 209–216.
- Knapp H, Doring R, Oelrich L, Plocker U and Prausnitz JM (1982) In: Behrens D and Eckerman R (eds) *Chemistry Data Series, Vol. VI: VLE for Mixtures of Low Boiling Substances*. Frankfurt: Dechema.
- Kojima K and Tochigi T (1979) *Prediction of Vapour-Liquid Equilibria by the ASOG Method*. New York: Elsevier.
- Lewis, GN and Randall M (1923) *Thermodynamics and the Free Energy of Chemical Substances*. New York: McGraw-Hill.
- Lu BC-Y (1959) Heats of mixing and vapor-liquid equilibrium calculations. *Canadian Journal of Chemical Engineering* 37: 193–199.
- Lu BC-Y (1962) Binary vapor-liquid equilibrium data: Thermodynamic consistency tests. *Canadian Journal of Chemical Engineering* 40: 16–24.
- Malanowski S and Anderko A (1992) *Modelling Phase Equilibria, Thermodynamic Background and Practical Tools*. New York: John Wiley.
- Papadopoulos MN and Derr EL (1959) Group interaction. II. A test of the group model on binary solutions of hydrocarbons. *Journal of American Chemical Society* 81: 2285–2289.
- Prausnitz JM, Lichtenthaler RN and de Azevedo EG (1999) *Molecular Thermodynamics of Fluid-Phase Equilibria*, 3rd edn. Englewood Cliffs, NJ: Prentice-Hall.
- Raal JD and Muhlbauer AL (1998) *Phase Equilibria, Measurement and Computation*. Washington, DC: Taylor & Francis.
- Redlich O, Derr EL and Pierotti GJ (1959) Group interaction. I. A model for interaction in solutions. *Journal of American Chemical Society* 81: 2283–2285.
- Reid RC, Prausnitz JM and Poling BE (1987) *The Properties of Gases and Liquids*, 4th edn. New York: McGraw-Hill.
- Renon H and Prausnitz JM (1968) Local compositions in thermodynamic excess functions for liquid mixtures. *American Institute of Chemical Engineers Journal* 14: 135–144.
- Starling KE (1977) *Fluid Properties for Light Petroleum Systems*. Houston, TX: Gulf Publishing Co.
- Thomas ER and Eckert CA (1984) Prediction of limiting activity of coefficients by a modified separation of cohesive energy density model and UNIFAC. *Industrial and Engineering Chemistry. Process Design and Development* 23: 194–209.
- Walas SM (1985) *Phase Equilibria in Chemical Engineering*. Boston: Butterworth.
- Wilson GM (1964) Vapor-liquid equilibrium. XI. A new expression for the excess Gibbs energy of mixing. *Journal of American Chemical Society* 86: 127–130.
- Wilson GM and Deal CH (1962) Activity coefficients and molecular structure – activity coefficients in changing environments – solutions of groups. *Industrial and Engineering Chemistry Fundamentals* 1: 20–23.
- Won KW and Prausnitz JM (1973) High-pressure vapor-liquid equilibria. Calculation of partial pressures from total pressure data. Thermodynamic consistency. *Industrial and Engineering Chemistry Fundamentals* 12: 459–463.
- Wong DSH and Sandler SI (1972) A theoretically correct mixing rule for cubic equations of state. *American Institute of Chemical Engineers Journal* 38: 671–680.

Vapour-Liquid Equilibrium: Theory

A. S. Teja and L. J. Holm, Georgia Institute of Technology, Atlanta, GA, USA

Copyright © 2000 Academic Press

Introduction

The concept of an equilibrium stage in distillation is based on the assumption that the vapour leaving the

stage is in equilibrium with the liquid leaving the same stage. The use of this concept in the design of distillation columns requires a description of how the components of a multicomponent mixture distribute between the two phases in equilibrium. This description is provided by phase equilibrium thermodynamics.

The equilibrium relationship for any component i in an equilibrium stage is defined in terms of the

distribution coefficient or K value:

$$K_i = \frac{y_i}{x_i} \quad [1]$$

where y_i is the mole fraction of component i in the vapour phase and x_i is the mole fraction of i in the liquid phase. The more volatile components of a mixture will have higher K values, and vice versa. In distillation, the efficiency of separation of two components is often compared via a quantity called the relative volatility α_{ij} :

$$\alpha_{ij} = \frac{K_i}{K_j} = \frac{y_i/x_i}{y_j/x_j} \quad [2]$$

A relative volatility close to unity means that the separation of the two components is likely to be difficult, whereas a relative volatility much greater or much less than unity means that few equilibrium stages are likely to be needed for separation. For binary system, eqn [2] can be rearranged to give:

$$y_i = \frac{\alpha_{ij}x_i}{1 + (\alpha_{ij} - 1)x_i} \quad [3]$$

Eqn [3] is plotted in **Figure 1** for various (constant) values of the relative volatility. Note that an increase in the relative volatility leads to an increase in the concentration of the more volatile component in the vapour phase. When the relative volatility has a value of 1, $y_i = x_i$ and separation is no longer feasible. A relative volatility of 1 also signifies the existence of an azeotrope or a critical point. A framework for the correlation and prediction of K values (and hence

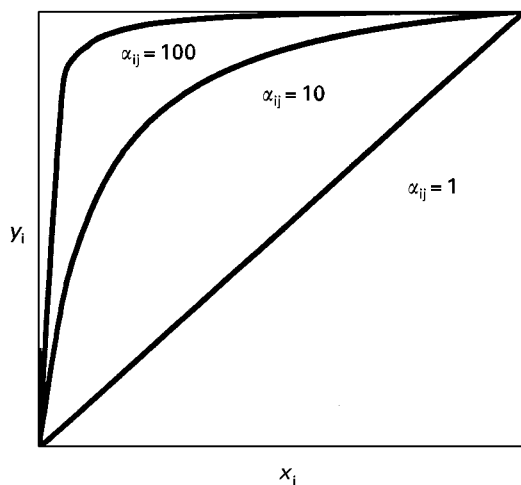


Figure 1 The y - x behaviour of a binary mixture at constant temperature for various values of the relative volatility α_{ij} .

relative volatilities) is provided by thermodynamics and is discussed below. A more detailed discussion may be found in textbooks of thermodynamics (see Further Reading).

Thermodynamic Framework

Vapour–liquid equilibria (VLE) can be modelled using the thermodynamic relationship for the equality of fugacities of a component i in the vapour and liquid phases. Thus:

$$\hat{f}_i^L = \hat{f}_i^V \quad (i = 1 \text{ to } m) \quad [4]$$

where m is the total number of components in the system, and L and V represent the liquid phase and the vapour phase, respectively. In order to use this relationship, the fugacities must first be related to the compositions in the two phases in equilibrium. This is done using the following thermodynamic relationship in terms of the variables T , P and n_i :

$$RT \ln \left(\frac{\hat{f}_i}{z_i P} \right) = \int_0^P \left[\left(\frac{\partial V}{\partial n_i} \right)_{T,P,n_j} - \frac{RT}{P} \right] dP \quad [5]$$

or the equivalent relationship in terms of T , V and n_i :

$$RT \ln \left(\frac{\hat{f}_i}{z_i P} \right) = \int_V^\infty \left[\left(\frac{\partial P}{\partial n_i} \right)_{T,V,n_j} - \frac{RT}{V} \right] dP - RT \ln \left(\frac{PV}{RT} \right) \quad [6]$$

In the above equations, z_i is either x_i or y_i depending on the phase being considered, and n_i is the number of moles of component i in that phase. The quantity $(\hat{f}_i/z_i P)$ is called the fugacity coefficient $\hat{\phi}_i$ of component i in the mixture.

Ideal Systems

In the case of an ideal gas mixture, substitution of the ideal gas equation $PV = nRT$ into eqn [5] leads to:

$$\hat{f}_i^V = y_i P \quad [7]$$

Similarly, substitution of the volume additivity relation for ideal liquid mixtures $V = \sum n_i v_i^L$ (where v_i^L is the molar volume of component i at the temperature and pressure of the solution) leads to:

$$\hat{f}_i^L = x_i f_i^L \quad [8]$$

where f_i^L is the fugacity of pure liquid i at the pressure and temperature of the solution. At constant temperature, the effect of pressure on the pure liquid

fugacity can be obtained from:

$$d \ln f_i^L = \frac{v_i^L}{RT} dP \quad [9]$$

Integration of eqn [9] from the saturation pressure to the system pressure leads to:

$$f_i^L = f_i^{\text{sat}} \exp \int_{P_i^{\text{sat}}}^P \frac{v_i^L}{RT} dP \quad [10]$$

where $f_i^{\text{sat}} (= \phi_i^{\text{sat}} P_i^{\text{sat}})$ is the fugacity of pure i at saturation, ϕ_i^{sat} is the fugacity coefficient of pure i at saturation, and P_i^{sat} is the vapour pressure of pure i . The liquid molar volume v_i^L can often be assumed to be constant with respect to pressure (since liquids are incompressible), thus simplifying the exponential terms of eqn [10], called the Poynting factor, to:

$$\exp \left(- \int_{P_i^{\text{sat}}}^P \frac{v_i^L}{RT} dP \right) \approx \exp \left(\frac{v_i^L (P_i^{\text{sat}} - P)}{RT} \right) \quad [11]$$

At low pressures ($P < 1$ MPa), the Poynting terms and ϕ_i^{sat} both approach unity and eqn [10] reduces to:

$$f_i^L = P_i^{\text{sat}} \quad [12]$$

Thus, for the simplest case of an ideal gas mixture in equilibrium with an ideal liquid solution at low pressures, eqns [4]–[12] lead to Raoult's law:

$$x_i P_i^{\text{sat}} = y_i P \quad [13]$$

and, therefore:

$$K_i = \frac{y_i}{x_i} = \frac{P_i^{\text{sat}}}{P} \quad [14]$$

and:

$$\alpha_{ij} = \frac{P_i^{\text{sat}}}{P_j^{\text{sat}}} \quad [15]$$

The relative volatility of a system that obeys Raoult's law is thus a ratio of two vapour pressures and is a function only of the temperature. The y_i versus x_i behaviour at constant temperature is therefore as shown in Figure 1, and the P - x - y behaviour of such a system is shown in Figure 2. A feature of this system is that the P - x behaviour (or the bubble curve) is linear and given by:

$$P = P_i^{\text{sat}} + x_1 (P_1^{\text{sat}} - P_2^{\text{sat}}) \quad [16]$$

Only a small number of systems containing chemically similar components obey Raoult's law, and then

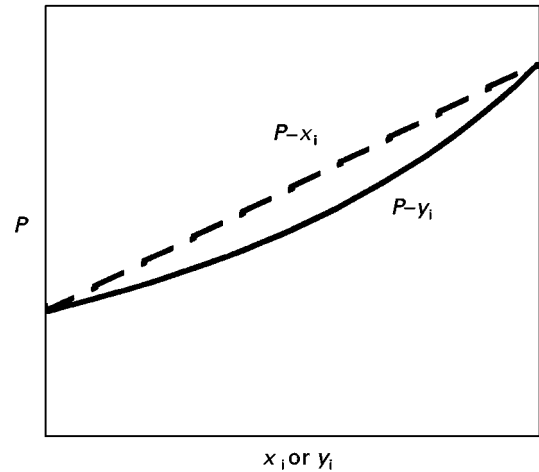


Figure 2 The P - x - y behaviour at constant temperature of a binary mixture that obeys Raoult's law. The dashed line shows the P - x behaviour or the bubble curve. The solid line represents the P - y behaviour or the dew point curve.

only at low pressures (< 1 MPa). As a consequence, K values can be predicted from pure component data only for such mixtures. The majority of real systems are nonideal and their thermodynamic description is discussed below.

Nonideal Systems

Figure 3A, B shows the P - x - y behaviour of systems that exhibit small negative and positive deviations from Raoult's law, whereas Figure 3C and D show systems that exhibit large negative and positive deviations from Raoult's law, respectively. Large deviations from Raoult's law often lead to the formation of minimum pressure (maximum boiling) or maximum pressure (minimum boiling) azeotropes, as shown in Figure 3C and D. The relative volatility has a value of unity at the azeotropic composition. Nonideal behaviour depicted in these figures can be described using two approaches – the activity coefficient approach and the equation of state approach.

Activity coefficient approach In this approach, vapour-phase fugacities are written in terms of the vapour-phase composition as follows:

$$\hat{f}_i^V = \hat{\phi}_i^V y_i P \quad [17]$$

where $\hat{\phi}_i^V$ is the vapour-phase fugacity coefficient of component i , y_i is the mole fraction of i in the vapour phase and P is the total system pressure. In addition, liquid-phase fugacities are written in terms of the liquid-phase composition as follows:

$$\hat{f}_i^L = \gamma_i x_i f_i^0 \quad [18]$$

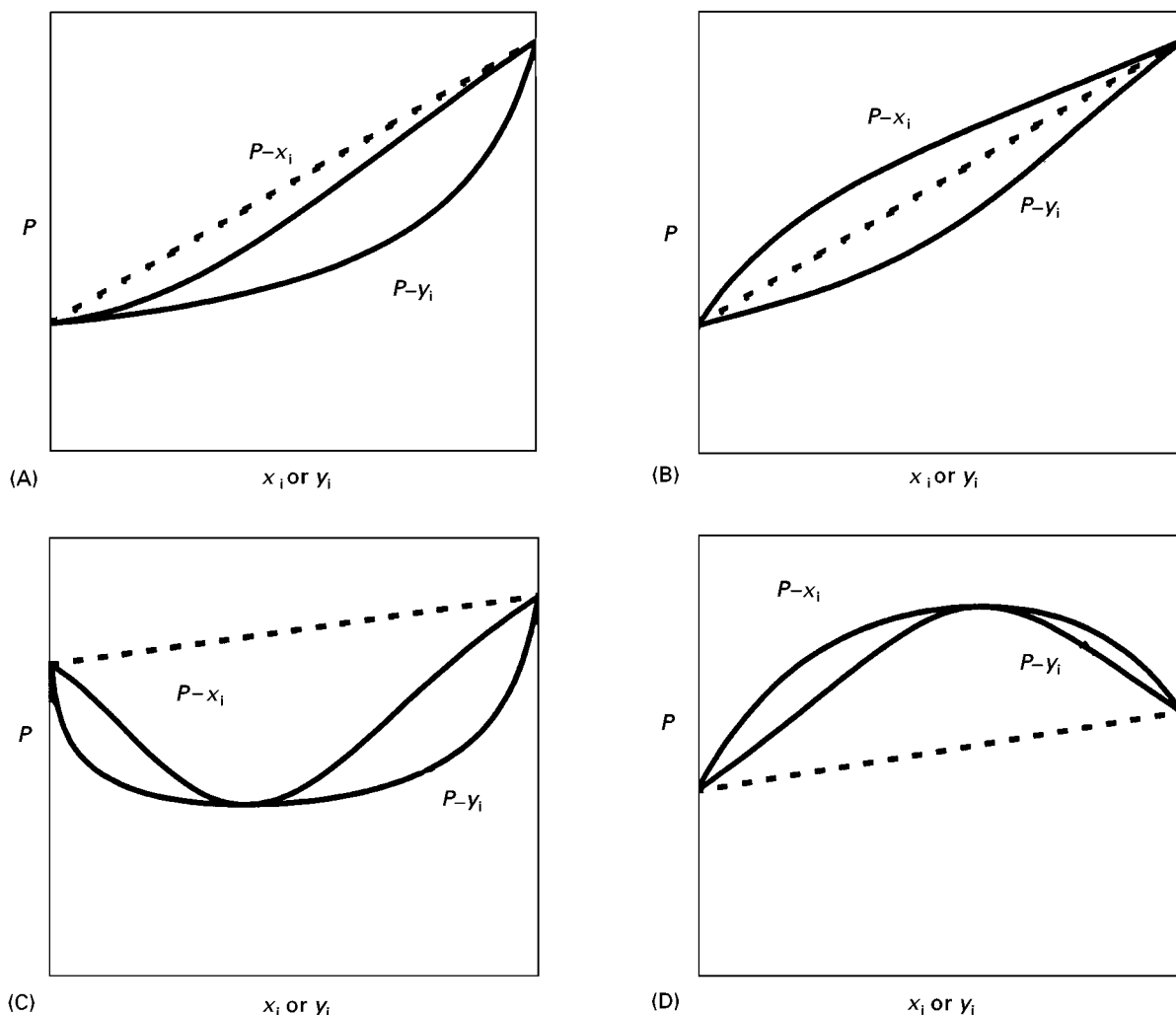


Figure 3 (A) The P - x - y behaviour of a system that exhibits small negative deviations from Raoult's law. The P - x behaviour of a system that follows Raoult's law is shown by the broken line. (B) The P - x - y behaviour of a system that exhibits small positive deviations from Raoult's law. Raoult's law behaviour is shown by the broken line. (C) The P - x - y behaviour of a system that exhibits significant negative deviations from Raoult's law leading to the formation of a minimum pressure (maximum boiling) azeotrope. (D) The P - x - y behaviour of a system that exhibits significant positive deviations from Raoult's law leading to the formation of a maximum pressure (minimum boiling) azeotrope.

where γ_i is the activity coefficient of component i in the liquid phase, x_i is the mole fraction of i in the liquid phase and f_i^0 is the fugacity of pure liquid i at the pressure and temperature of the system. Combining eqns [17] and [18], we obtain:

$$\gamma_i x_i f_i^0 = \hat{\phi}_i^V y_i P \quad [19]$$

At low pressures (< 1 MPa), eqn [19] can be simplified further to yield:

$$\gamma_i x_i P_i^{\text{sat}} = \hat{\phi}_i^V y_i P \quad [20]$$

as discussed in the previous section. Often $\hat{\phi}_i^V \sim 1.0$ for vapour phases at moderate pressures.

Hence:

$$\gamma_i x_i P_i^{\text{sat}} = y_i P \quad [21]$$

and:

$$K_i = \gamma_i P_i^{\text{sat}} / P \quad [22]$$

Vapour pressures at subcritical temperatures may be obtained from experimental data using equations such as the Antoine equation. Activity coefficients may be obtained from excess Gibbs energy g^E models, as described below.

Equation of state approach The equation of state approach uses eqn [17] for the vapour phase and an

analogous expression for the liquid phase. Thus, for the liquid phase:

$$\hat{f}_i^L = \hat{\phi}_i^L x_i P \quad [23]$$

Substituting these relationships into eqn [4] results in:

$$\hat{\phi}_i^V y_i = \hat{\phi}_i^L x_i \quad [24]$$

and:

$$K_i = \hat{\phi}_i^L / \hat{\phi}_i^V \quad [25]$$

The calculation of K values is therefore reduced to the calculation of fugacity coefficients in the equation of state approach and, at moderate pressures, to the calculation of activity coefficients in the activity coefficient approach.

Calculation of Fugacity Coefficients

Calculation of the fugacity coefficient using eqn [5] or eqn [6] requires knowledge of the P - V - T - x behaviour of the system. This information is obtained from an equation of state. Two representative types of equation of state will be discussed below – a volume-explicit virial equation and a pressure-explicit cubic equation. A more detailed discussion of types of equation of state is available elsewhere (see Further Reading).

Volume-explicit Virial Equation

Virial equations of state are infinite-series expansions of the compressibility Z as a function either of the density or pressure. The pressure series may be written as:

$$\begin{aligned} Z = \frac{PV}{RT} &= 1 + B'P + C'P^2 + \dots \\ &= 1 + \frac{BP}{RT} + \frac{(C - B^2)}{(RT^2)}P^2 + \dots \end{aligned} \quad [26]$$

where B is the second virial coefficient, C the third virial coefficient, and so on. Typically, the two-terms truncated form of the virial equation is used for gases at low pressures:

$$Z = 1 + B'P = 1 + \frac{BP}{RT} \quad [27]$$

which can be rearranged in the volume-explicit form:

$$V = \frac{RT}{P} + B \quad [28]$$

The truncated virial eqn [28] is only applicable to gases at densities that are less than about half the critical density. One of the advantages of the virial equation, however, is that virial coefficients can be calculated from intermolecular potential functions. Also, statistical mechanics provides rigorous expressions for the composition dependence of the virial coefficients. Thus, the mixture second virial coefficient is given by:

$$B = \sum_i \sum_j y_i y_j B_{ij} \quad [29]$$

where B_{ii} is the second virial coefficient of component i and B_{ij} is a cross second virial coefficient. Substitution of eqns [28] and [29] into eqn [5] leads to:

$$\ln \hat{\phi}_i^V = \frac{P}{RT} [B_{ii} + \frac{1}{2} \sum_k \sum_l y_k y_l (2\delta_{ki} - \delta_{kl})] \quad [30]$$

where $\delta_{kl} = 2B_{kl} - B_{kk} - B_{ll}$. The fugacity coefficient of any component in the vapour phase can thus be calculated if the second virial coefficients of the pure components and the cross second virial coefficients are available. Since the truncated virial equation is only applicable to gases at low to moderate pressures, fugacity coefficients calculated using eqn [30] are generally only employed when eqn [20] is used to calculate VLE.

Pressure-explicit Cubic Equation of State

Cubic equations of state express the pressure as a cubic function of the molar volume, and their origin stems from the van der Waals equation, which was the first cubic equation of state to represent qualitatively both vapour and liquid phases. Several hundred modification of the van der Waals equation have been reported in the literature. An example of a recent modification that is better able to represent P - V - T - x data for both vapour and liquid mixtures is the equation of state proposed by Patel and Teja in 1982. This equation may be written as:

$$P = \frac{RT}{v - b} - \frac{a\alpha}{v^2 + bv + cv - bc} \quad [31]$$

where:

$$a = \alpha \Omega_a \frac{R^2 T_c^2}{P_c} \quad [32]$$

$$b = \Omega_b \frac{RT_c}{P_c} \quad [33]$$

$$c = \Omega_c \frac{RT_c}{P_c} \quad [34]$$

$$\alpha = [1 + m(1 - \sqrt{T/T_c})]^2 \quad [35]$$

$$\Omega_a = 3\zeta_c^2 + 3(1 - 2\zeta_c)\Omega_b + \Omega_b^2 + 1 - 3\zeta_c \quad [36]$$

$$\Omega_c = 1 - 3\zeta_c \quad [37]$$

$$\zeta_c = P_c v_c / RT_c \quad [38]$$

and Ω_b is the smallest positive root of:

$$\Omega_b^3 + (2 - 3\zeta_c)\Omega_b^2 + 3\zeta_c^2\Omega_b - \zeta_c^3 = 0 \quad [39]$$

In the above equations, the subscript c denotes a value at the critical point. Note that by setting the parameter $c = 0$ in eqn [31], the Patel-Teja equation reduces to the Redlich-Kwong-Soave equation of state; and by setting $c = b$, it reduces to the Peng-Robinson equation of state. Both the Redlich-Kwong-Soave and the Peng-Robinson equations are widely used in process design calculations. For non-polar fluids, ζ_c and m are calculated from the following relationships in terms of the acentric factor ω :

$$\zeta_c = 0.329032 - 0.076799\omega + 0.0211947\omega^2 \quad [40]$$

$$m = 0.452413 + 1.30982\omega - 0.295937\omega^2 \quad [41]$$

A knowledge of P_c , T_c and ω is therefore sufficient to calculate the parameters of the equation of state. Alternatively, ζ_c and m may be calculated from experimental values of the vapour pressure and liquid density of the substance. Several other forms of eqn [35] suitable for complex molecules have been proposed.

The parameters a , b and c for a mixture can be calculated using the following mixing rules:

$$a\alpha = \sum_i \sum_j z_i z_j (a\alpha)_{ij} \quad [42]$$

$$b = \sum_i z_i b_i \quad [43]$$

$$c = \sum_i z_i c_i \quad [44]$$

where z_i can be x_i or y_i and $(a\alpha)_{ij} = (1 - k_{ij})\sqrt{(a\alpha)_i(a\alpha)_j}$, k_{ij} is a binary interaction parameter that is usually obtained by fitting experimental VLE data.

The fugacity coefficient can be obtained by substituting eqns [31]–[44] into eqn [6] leading to:

$$\ln \hat{\phi}_i = \ln \left(\frac{\hat{f}_i}{z_i P} \right) = \frac{b_i}{v - b} - \ln \left[\frac{P}{RT} (v - b) \right] - \frac{2 \sum_j x_j \alpha_{ij} a_{ij}}{RT[4bc + (b + c)^2]^{1/2}}$$

$$\begin{aligned} & \times \ln \left(\frac{(2v + b + c) + [4bc + (b + c)^2]^{1/2}}{(2v + b + c) - [4bc + (b + c)^2]^{1/2}} \right) \\ & + \frac{2a\alpha(b_i + c_i)}{RT((2v + b + c)^2 - [4bc + (b + c)^2])} \\ & + \frac{a\alpha}{RT[4bc + (b + c)^2]^{3/2}} \\ & \times [c_i(3b + c) + b_i(3c + b)] \\ & \times \left[\ln \left(\frac{(2v + b + c) + [4bc + (b + c)^2]^{1/2}}{(2v + b + c) - [4bc + (b + c)^2]^{1/2}} \right) \right. \\ & \left. - \frac{2(2v + b + c)[4bc + (b + c)^2]^{1/2}}{(2v + b + c)^2 - [4bc + (b + c)^2]} \right] \quad [45] \end{aligned}$$

Eqn [45] can be used to calculate both the vapour- and liquid-phase fugacity coefficients. In the case of vapour phase, $z_i = y_i$ and v is the vapour molar volume, whereas for the liquid phase, $z_i = x_i$ and v is the liquid molar volume. The ratio of the two fugacity coefficients yields the K value under the conditions of interest.

Calculation of Activity Coefficients

Activity coefficients, γ_i are generally calculated by differentiation of the excess Gibbs energy g^E :

$$RT \ln \gamma_i = \left(\frac{\partial n g^E}{\partial n_i} \right)_{T, P, n_j} \quad [46]$$

A number of expressions have been proposed for g^E as a function of composition. Some of the more popular of these are outlined below.

Margules Equation

The Margules equation is one of the simplest expressions for the molar excess Gibbs energy. For a binary solution:

$$\frac{g^E}{RT} = x_1 x_2 (A_{21} x_1 + A_{12} x_2) \quad [47]$$

where A_{12} and A_{21} are binary parameters dependent on temperature, but not on the composition. The Margules activity coefficients in a binary mixture are obtained by differentiation of eqn [47] and are given by:

$$\ln \gamma_1 = [A_{12} + 2(A_{21} - A_{12})x_1]x_2^2 \quad [48]$$

$$\ln \gamma_2 = [A_{21} + 2(A_{12} - A_{21})x_2]x_1^2 \quad [49]$$

A_{12} and A_{21} are generally obtained by fitting VLE data. Note that the value of the activity coefficient of each component tends to unity as the mole fraction of that component goes to unity. This behaviour is inherent in all g^E models. The Margules equation works well for binary systems in which the two components are very similar in size, shape and chemical nature. Margules parameters for a large number of systems are tabulated in DECHEMA books on VLE data.

Van Laar Equation

The van Laar equation for the excess Gibbs energy may be written as:

$$\frac{g^E}{RT} = \frac{2a_{12}x_1x_2q_1q_2}{x_1q_1 + x_2q_2} \quad [50]$$

where q_1 and q_2 are the effective volumes of the two molecules and a_{12} is an interaction parameter. Differentiation according to eqn [46] leads to the following expressions for the activity coefficients:

$$\ln \gamma_1 = \frac{A_{12}}{\left[1 + \frac{A_{12}x_1}{A_{21}x_2}\right]^2} \quad [51]$$

$$\ln \gamma_2 = \frac{A_{21}}{\left[1 + \frac{A_{21}x_2}{A_{12}x_1}\right]^2} \quad [52]$$

where $A_{12} = 2q_1a_{12}$ and $A_{21} = q_2a_{12}$. As in the case of the Margules equation, the two parameters A_{12} and A_{21} are obtained by fitting VLE data. The van Laar equations have been shown to work well for a number of binary systems where the size, shape and chemical nature of the components are dissimilar, and parameters for many binary systems have been tabulated in the DECHEMA data books.

Wilson Equation

The Margules equation is based on the assumption that the ratio of species 1 to species 2 molecules surrounding any molecule is the same as the ratio of the mole fractions of species 1 and 2. A different class of g^E models has been proposed based on the assumption that, around each molecule, there is a local composition that is different from the bulk composition. The Wilson equation is such a local composition model and the Wilson excess Gibbs energy has the following form for a binary system:

$$\frac{g^E}{RT} = x_1 \ln(x_1 + \Lambda_{12}x_2) - x_2 \ln(x_2 + \Lambda_{21}x_1) \quad [53]$$

where Λ_{12} and Λ_{21} are parameters specific to the binary pair. These parameters are defined in terms of

the molar liquid volume v_i of the pure component i , and the energies of interaction λ_{ij} between the molecules i and j as follows:

$$\Lambda_{ij} = \frac{v_j}{v_i} \exp\left[-\frac{\lambda_{ij} - \lambda_{ii}}{RT}\right] \quad [54]$$

The expression for the liquid activity coefficients are:

$$\ln \gamma_1 = -\ln(x_1 + \Lambda_{12}x_2) + x_2 \left(\frac{\Lambda_{12}}{x_1 + \Lambda_{12}x_2} - \frac{\Lambda_{21}}{x_2 + \Lambda_{21}x_1} \right) \quad [55]$$

$$\ln \gamma_2 = -\ln(x_2 + \Lambda_{21}x_1) + x_1 \left(\frac{\Lambda_{21}}{x_2 + \Lambda_{21}x_1} - \frac{\Lambda_{12}}{x_1 + \Lambda_{12}x_2} \right) \quad [56]$$

The Wilson equation has two parameters Λ_{12} and Λ_{21} (or equivalently, $\lambda_{12} - \lambda_{11}$ and $\lambda_{21} - \lambda_{22}$) and is able to correlate VLE data for a wide variety of miscible systems, including those containing polar or associating components in nonpolar solvents. However, the equation is incapable of predicting liquid–liquid immiscibility in a system.

For multicomponent mixtures, the Wilson equation is written as follows:

$$\ln \gamma_k = -\ln \left[\sum_{j=1}^m x_j \Lambda_{kj} \right] + 1 - \sum_{i=1}^m \frac{x_i \Lambda_{ik}}{\sum_{j=1}^m x_j \Lambda_{ij}} \quad [57]$$

Note that only binary parameters Λ_{ij} are required to evaluate activity coefficients in multicomponent systems. These parameters are obtained by fitting VLE data for the binary pairs, and many of these parameters have been tabulated in the DECHEMA data books. Moreover, because a temperature dependence is included in eqn [54], the same binary parameters may be used over a range of temperatures (although no more than about 50 K).

NRTL Equation

The NRTL (non-random two-liquid theory) equation is also based on a local composition model for the excess Gibbs energy. However, it is applicable to miscible as well as partially miscible systems due to the inclusion of a third binary parameter in the model. The expression for the molar excess Gibbs energy is:

$$\frac{g^E}{RT} = x_1x_2 \left[\frac{\tau_{21}G_{21}}{x_1 + x_2G_{21}} + \frac{\tau_{12}G_{12}}{x_2 + x_1G_{12}} \right] \quad [58]$$

where τ_{ij} and G_{ij} are defined as:

$$G_{ij} = \exp(-\zeta_{ij}\tau_{ij}) \quad [59]$$

$$\tau_{ij} = \frac{g_{ij} - g_{ji}}{RT} \quad [60]$$

g_{ij} describes the energy of interaction between component i and j and ζ_{ij} ($=\zeta_{ji}$) is a nonrandomness parameter which is often set equal to 0.3. Thus, only two parameters τ_{ij} and τ_{ji} (or, equivalently, $g_{ij} - g_{ji}$ and $g_{ji} - g_{ii}$) are required per binary pair.

The activity coefficients expressions are as follows:

$$\ln \gamma_1 = x_2^2 \left[\tau_{21} \left(\frac{G_{21}}{x_1 + G_{21}x_2} \right)^2 + \frac{\tau_{12}G_{12}}{(x_2 + G_{12}x_1)^2} \right] \quad [61]$$

$$\ln \gamma_2 = x_1^2 \left[\tau_{12} \left(\frac{G_{12}}{x_2 + G_{12}x_1} \right)^2 + \frac{\tau_{21}G_{21}}{(x_1 + G_{21}x_2)^2} \right] \quad [62]$$

A major advantage of the NRTL equation lies in its ability to represent highly nonideal systems, particularly partially miscible systems.

For multicomponent mixtures, the liquid-phase activity coefficients are expressed as:

$$\ln \gamma_i = \frac{\sum_{j=1}^m \tau_{ji} G_{ji} x_j}{\sum_{l=1}^m G_{li} x_l} + \sum_{j=1}^m \frac{x_j G_{ij}}{\sum_{l=1}^m G_{lj} x_l} \left(\tau_{ij} - \frac{\sum_{r=1}^m x_r \tau_{rj} G_{rj}}{\sum_{l=1}^m G_{lj} x_l} \right) \quad [63]$$

As with the Wilson equation, only binary data are needed to calculate activity coefficients in multicomponent systems, and these parameters have been tabulated in the DECHEMA data books for many systems. Furthermore, because of the inclusion of the temperature in eqn [60] the parameters obtained by fitting VLE data at one temperature may be used to calculate VLE at other temperatures (within a range of about 50 K).

UNIQUAC Equation

The UNIQUAC (universal quasi-chemical theory) equation expresses the molar excess Gibbs energy as a sum of a combinatorial part and residual part.

$$g^E = g^E(\text{combinatorial}) + g^E(\text{residual}) \quad [64]$$

The combinatorial part accounts for differences in the size and shape of the molecules, whereas the residual contribution accounts for energetic interactions.

$$\frac{g^E(\text{combinatorial})}{RT} = x_1 \ln \frac{\Phi_1}{x_1} + x_2 \ln \frac{\Phi_2}{x_2} + \frac{z}{2} \left(q_1 x_1 \ln \frac{\theta_1}{\Phi_1} + q_2 x_2 \ln \frac{\theta_2}{\Phi_2} \right) \quad [65]$$

$$\frac{g^E(\text{residual})}{RT} = -q_1 x_1 \ln(\theta_1 + \theta_2 \tau_{21}) - q_2 x_2 \ln(\theta_2 + \theta_1 \tau_{12}) \quad [66]$$

where:

$$\Phi_i = \frac{x_i r_i}{\sum_j x_j r_j} \quad [67]$$

$$\theta_i = \frac{x_i q_i}{\sum_j x_j q_j} \quad [68]$$

$$\tau_{ji} = \exp \left(-\frac{a_{ji}}{RT} \right) \quad [69]$$

In eqn [65] z is a coordination number ($=10$ usually), Φ_i are volume fractions, and θ_i are surface area fractions for component i . The volume and surface area parameters r_i and q_i can be evaluated from pure component molecular structure information and are tabulated in the DECHEMA data books. Thus, there are two binary parameters a_{ij} and a_{ji} in the UNIQUAC model and these are found by fitting binary VLE data. The activity coefficient expressions become:

$$\ln \gamma_1 = \ln \frac{\Phi_1}{x_1} + \left(\frac{z}{2} \right) q_1 \ln \frac{\theta_1}{\Phi_1} + \Phi_2 \left(l_1 - \frac{r_1}{r_2} l_2 \right) - q_1 \ln(\theta_1 + \theta_2 \tau_{21}) + \theta_2 q_1 \left(\frac{\tau_{21}}{\theta_1 + \theta_2 \tau_{21}} - \frac{\tau_{12}}{\theta_2 + \theta_1 \tau_{12}} \right) \quad [70]$$

$$\ln \gamma_2 = \ln \frac{\Phi_2}{x_2} + \left(\frac{z}{2} \right) q_2 \ln \frac{\theta_2}{\Phi_2} + \Phi_1 \left(l_2 - \frac{r_2}{r_1} l_1 \right) - q_2 \ln(\theta_2 + \theta_1 \tau_{12}) + \theta_1 q_2 \left(\frac{\tau_{12}}{\theta_2 + \theta_1 \tau_{12}} - \frac{\tau_{21}}{\theta_1 + \theta_2 \tau_{21}} \right) \quad [71]$$

where:

$$l_i = \left(\frac{z}{2} \right) (r_i - q_i) - (r_i - 1) \quad [72]$$

The UNIQUAC equation is applicable to a wide range of systems, including partially miscible systems.

For multicomponent systems, the UNIQUAC equation becomes:

$$\ln \gamma_i = \ln \frac{\Phi_i}{x_i} + \frac{z}{2} q_i \ln \frac{\theta_i}{\Phi_i} + l_i - \frac{\Phi_i}{x_i} \sum_{j=1}^m x_j l_j - q_i \ln \left(\sum_{j=1}^m \theta_j \tau_{ji} \right) + q_i - q_i \sum_{j=1}^m \frac{\theta_j \tau_{ij}}{\sum_{k=1}^m \theta_k \tau_{kj}} \quad [73]$$

Once again, only pure component and binary data are needed to calculate the parameters. UNIQUAC parameters for over 6000 binary systems have been tabulated in the DECHEMA data series on VLE.

UNIFAC Group Contribution Method

When values of Margules, van Laar, Wilson, NRTL or UNIQUAC parameters are not available in the literature, or when no VLE data for the system of interest have been measured, the UNIFAC (UNIQUAC functional group activity coefficients) method may be used to estimate activity coefficients. The UNIFAC method is a group contribution technique for the estimation of the parameters a_{mn} of the excess Gibbs energy model. The method expresses the molar excess Gibbs energy as a sum of a combinatorial part and a residual part and uses the same combinatorial part as the UNIQUAC equation. In terms of the activity coefficient:

$$\ln \gamma_i = \ln \gamma_i^C + \ln \gamma_i^R \quad [74]$$

$$\ln \gamma_i^C = \ln \frac{\Phi_i}{x_i} + \left(\frac{z}{2} \right) q_i \ln \frac{\theta_i}{\Phi_i} + \Phi_i \left(l_i - \frac{r_i}{r_j} l_j \right) \quad [75]$$

$$r_i = \sum_k v_{ki} R_k \quad [76]$$

$$q_i = \sum_k v_{ki} Q_k \quad [77]$$

The group R_k , and the group area Q_k have been tabulated for a large number of groups. v_{ki} is the number of groups of k kind in molecule i .

The residual contribution is expressed as follows:

$$\ln \gamma_i^R = \sum_k Q_k (\ln \Gamma_k - \ln \Gamma_k^{(i)}) \quad [78]$$

$$\ln \Gamma_k = Q_k (1 - \ln E_k - F_k) \quad [79]$$

$$\ln \Gamma_k^{(i)} = Q_k^{(i)} (1 - \ln E_k^{(i)} - F_k^{(i)}) \quad [80]$$

$$E_k = \theta_1 \psi_{1k} + \theta_2 \psi_{2k} + \theta_3 \psi_{3k} + \dots \quad [81]$$

$$F_k = \frac{\theta_1 \psi_{k1}}{E_1} + \frac{\theta_2 \psi_{k2}}{E_2} + \frac{\theta_3 \psi_{k3}}{E_3} + \dots \quad [82]$$

$$\theta_m = \frac{X_m Q_m}{\sum_n X_n Q_n} \quad [83]$$

$$\psi_{mn} = \exp \left(- \frac{a_{mn}}{T} \right) \quad [84]$$

$$X_m = \frac{\sum_i x_i v_{mi}}{\sum_i \left(x_i \sum_k v_{ki} \right)} \quad [85]$$

Since the group volume parameters R_k and the group area parameters Q_k are known, the only unknowns in the UNIFAC equations are the group interaction parameters a_{mn} and a_{nm} . These have been tabulated for a large number of groups. Moreover, updated parameters are published regularly in the literature. The UNIFAC method has been successfully applied to a wide variety of binary and multicomponent systems.

Examples of Use

Subcritical Vapour–Liquid Equilibria

Figure 4 shows the P - x - y behaviour of the methanol–water system at 313 K calculated using the activity coefficient approach. Activity coefficients were obtained from the Wilson equation using parameters $\Lambda_{12} = -449.3$ and $\Lambda_{21} = -835.9$ reported in DECHEMA data books. Fugacity coefficients in the vapour phase were assumed to be equal to 1.0. Note that the Wilson parameters were obtained by fitting the data, and therefore reproduce the experimental

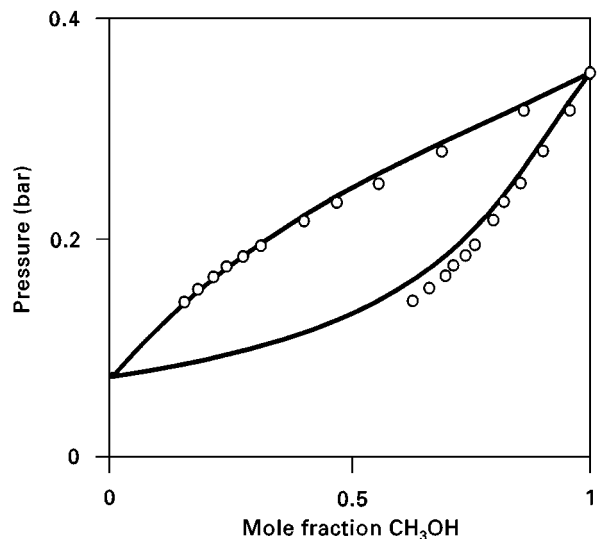


Figure 4 The P - x - y behaviour of methanol–water at 313 K correlated with the Wilson equation.

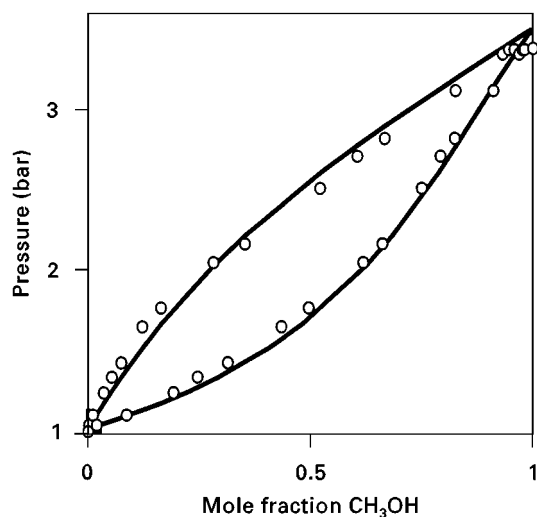


Figure 5 The P - x - y behaviour of methanol-water at 373 K predicted using Wilson equation constants obtained at 313 K.

data (open circles) reasonably well in this system. Figure 5 shows that when the same parameters are used to calculate VLE data for methanol-water at 373 K, good agreement is obtained with experimental data.

Figure 6 shows the P - x - y behaviour at 313 K of the same system correlated using the Patel-Teja equation of state. Two k_{ij} values were required to correlate the data ($k_{12} = -0.0923$ and $k_{21} = 0.0748$) and, in general, excellent agreement was obtained between calculated and experimental values. Moreover, the equation of state was successful in predicting data at

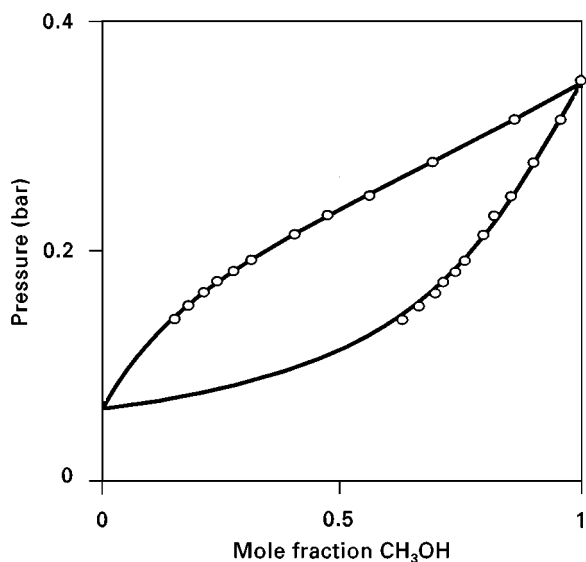


Figure 6 The P - x - y behaviour of methanol-water at 313 K correlated with the Patel-Teja equation.

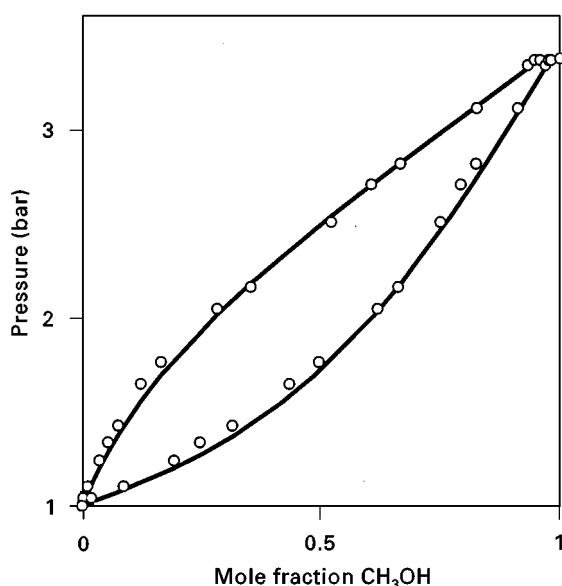


Figure 7 The P - x - y behaviour of methanol-water at 373 K predicted with Patel-Teja equation using binary parameters obtained at 313 K.

373 K using the same values of the k_{ij} parameters, as shown in Figure 7.

Supercritical Vapour-Liquid Equilibria

Figure 8 shows the P - x - y behaviour of the carbon dioxide-propane system at 328 K predicted using the equation of state approach with the Patel-Teja equation of state. The two binary interaction

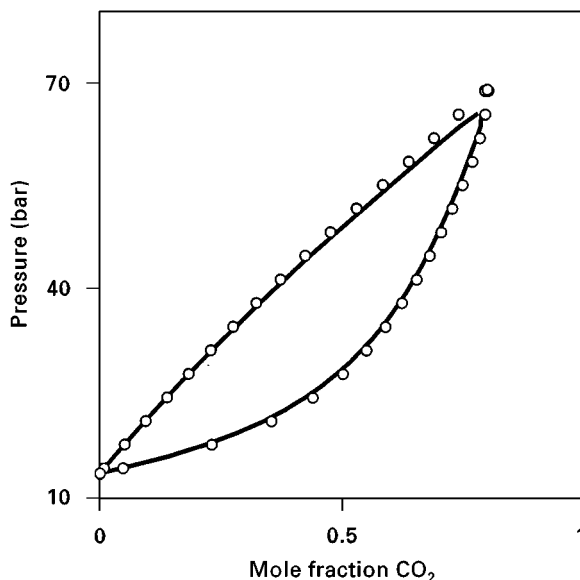


Figure 8 The P - x - y behaviour of CO_2 -propane mixtures at 328 K predicted using the Patel-Teja equation of state with binary parameters obtained from data at 244 K.

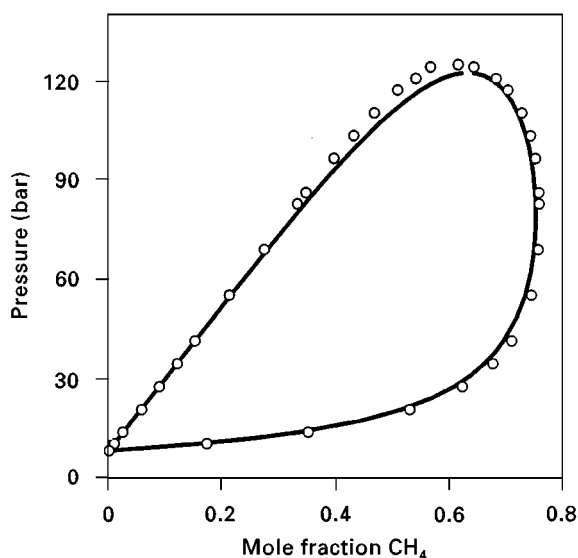


Figure 9 The P - x - y behaviour of methane- n -butane mixtures at 344 K predicted using the Patel-Teja equation of state with binary parameters obtained from data at 186 K.

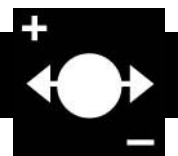
parameters ($k_{12} = 0.143$ and $k_{21} = 0.121$) were obtained by fitting data at a much lower temperature of 244 K. The predictions are in excellent agreement with experiment, even though the extrapolation is to a temperature that is above the critical temperature of carbon dioxide (304 K). A similar extrapolation using the Patel-Teja equation of state is shown in Figure 9 where VLE in the methane- n -butane system at 344 K have been predicted using binary parameters ($k_{12} = 0.021$ and $k_{21} = 0.002$) obtained at 186 K. Note that the extrapolation is carried out to a temperature that is well above the critical temperature of methane (190 K). Finally, it should be added that the activity coefficient approach described above cannot be used to correlate or predict supercritical VLE behaviour.

See also: II/Distillation: Historical Development; Modeling and Simulation; Multicomponent Distillation; Theory of Distillation; Vapour-Liquid Equilibrium: Correlation and Prediction.

Further Reading

- Dymond JH and Smith EB (1980). *The Virial Coefficients of Pure Gases and Mixtures: A Critical Compilation*. New York: Oxford University Press.
- Fredenslund A, Gmehling J and Rasmussen P (1977) *Vapour-liquid Equilibria Using UNIFAC - A Group Contribution Method*. New York: Elsevier Science.
- Ghemling J, Onken U and Arlt W (eds) (1978) *Vapour-liquid Equilibrium Data Collection*. Frankfurt: DE-CHEMA.
- Hansen HK, Rasmussen P and Fredenslund A *et al.* (1991) Vapour-liquid equilibrium by UNIFAC group contribution. 5. Revision and extension. *Industrial & Engineering Chemistry Research* 30: 2352-2355.
- Knapp H, Reichl A and Sandler SI (1998) Analysis of thermodynamic model equations: mixing rules in cubic equations of state. *Industrial & Engineering Chemistry Research* 37: 2908-2916.
- Patel NC (1996) Improvements of the Patel-Teja equation of state. *International Journal of Thermophysics* 17: 673-682.
- Patel NC and Teja AS (1982) A new cubic equation of state for fluids and fluids mixtures. *Chemical Engineering Science* 37: 463-473.
- Prausnitz JM, Lichtenthaler RN and Gomes de Azevedo E (1999) *Molecular Thermodynamics of Fluid-phase Equilibria*, 3rd edn. Englewood Cliffs: Prentice Hall.
- Reid RC, Prausnitz JM and Poling B (1987) *The Properties of Gases and Liquids*, 4th edn. New York: McGraw-Hill.
- Smith JM, Abbott MM and Van Ness HC (1996) *Introduction to Chemical Engineering Thermodynamics*, 5th edn. New York: McGraw-Hill.

ELECTROPHORESIS



Agarose Gels

J. R. Shainoff, Cleveland State University,
Cleveland, Ohio, USA

Copyright © 2000 Academic Press

Development

Agarose is a uniquely nonadhesive hydrocolloid that has found many uses in the separation sciences

following Araki's preparation of it in 1937 as an apparently sulfate-free component distinct from the sulfate-rich agaropeptin in agar. Agar and many of the other hydrocolloids derived from certain species of seaweed had been used mainly in food preparation dating back to the seventeenth century in Japan. Agar was introduced as a medium for immunoelectrophoresis by Grabar and Williams in 1953, and the original technique is occasionally used today. Citrated agar electrophoresis is the current principal method for identification of haemoglobin variants. Agar was

applied by Polson in 1961 for chromatographic separations based on molecular sieving, following which its use gradually gave way to agarose beginning with Hjertén. A word-search of the Medline abstracts indicates that the number of papers per year employing agarose electrophoresis did not surpass agar electrophoresis until 1976.

The sulfate content of grades of agarose supplied for laboratory use is generally below 0.12% compared to 4% in agarpectin (see Armisen, 1997). The ease with which agarose can be cast into gels without additives or cross-linking agents and its inertness towards interacting with proteins and nucleic acids are the principal reasons for its popularity as a separation medium. All that is needed to prepare gels is to dissolve the agarose powder by careful heating to boiling or near boiling temperatures, and let the clear solution cool. Gelation proceeds spontaneously and completely as the solution cools. In addition to the simplicity of gel casting with agarose and its inertness towards interacting with proteins and nucleic acids, it offers many other advantages as a separation medium, such as easy sample recovery, nontoxicity, and amenability to cast and use it in an open faced format. The latter option underlies its unique applicability to numerous immunoelectrophoretic procedures. Agarose is very porous compared to polyacrylamide, and that limits its suitability in unmodified form for sieving-based separations of proteins with molecular masses below 60 kDa. On the other hand, its high permeability makes it, again, superior to polyacrylamide for immunochemical studies.

Properties of Agarose Gels

Chemically, agarose is a polysaccharide composed of alternating D- and L-galactose biose (agarobiose) units in chains that are on the order of 400 agarobiose units in length, ~120 kDa. Rees and Arnott each characterized the gelation as proceeding initially through pairing of the 120 kDa chains into 0.8–1.4 nm thickness double helical coils, followed by lateral coalescence of the helical dimers into thick protofibrils with average thickness of the order of 24 nm, although the number of helical dimers can range from 5 to 5000. By contrast, conventional polyacrylamide gels have fibre thickness of only 0.4 nm. Gelation occurs as the thick protofibrils interlink at their loosely coiled ends into a net-like matrix (Figure 1). The gels are translucent because of light scattering by the thick fibrils, but become transparent on drying. The ability to form thick, strong fibres enables agarose to form gels at concentrations down to 0.2% as utilized in studies by Serwer. The incorporation of

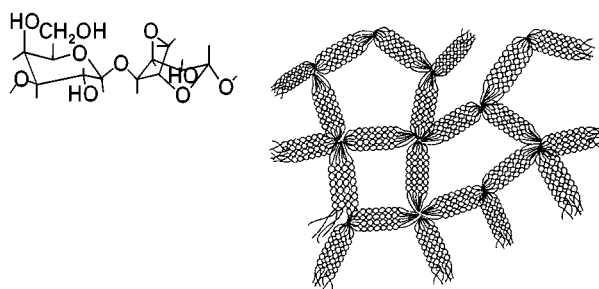


Figure 1 Depiction of structure of the agarose biose unit and the structure of interlocking aggregates of coiled coil dimers of agarose chains based on electron microscopy and X-ray diffraction. (Reproduced with permission from Westermeier, 1997.)

the agarose into thick rather than thin fibres makes the gels highly porous at concentrations up to 6%, the limit to which agarose can be dissolved without resorting to autoclave temperatures. Concentrations up to 16% can be reached by autoclaving.

The high porosity makes agarose superior to polyacrylamide for separation of large proteins, polypeptides, complexes with size ranging from 100 kDa to several megadaltons, and for DNA fragments ranging from 1000 to 23 000 bp. In the interest of retaining the gel casting simplicity of agarose while enhancing its sieving capacity, nonsupercoiling hydroxyalkylated agarose derivatives have been developed which, according to Chrambach, have fibre thicknesses of the order of 0.8 nm, approaching polyacrylamide, but have gel strengths that are low compared to unmodified agarose. Recently, blends of agarose derivatives have been formulated which have improved strength.

The sulfate present in most commercial agarose induces a slight electroendosmosis (EEO) during electrophoresis. Electroendosmosis is the flow of buffer through the gel. In effect it arises because the negatively charged sulfate groups in the matrix cannot move towards the anode which results in a compensatory pumping of buffer to the cathode. The slight effect on mobility of proteins is usually of little consequence; however, it can have pronounced effects on mobilities of buffer boundaries in discontinuous buffer systems used for sharpening bands in the applied samples. It can also induce syneresis and collapse of gels with discontinuous buffer systems due to unequal electroendosmosis across the buffer boundaries. Thus, some of the numerous buffer systems that have been described in the computer output by Jovin for polyacrylamide gels do not work well with agarose gels. Many do, nevertheless. The zero-EEO agarose which is used for isoelectric focusing has its electroendosmotic tendency neutralized by charge-balancing with electropositive groups. The additives in some

zero-EEO agaroses contribute to background staining.

The gelation of agarose depends entirely on hydrogen bonding, and is inhibited by chaotropic agents such as concentrated (~20%) glycerine or urea. Although the high concentrations of these substances usually used in biochemical procedures can block the gelation, they do not appreciably affect gels once solidified. As with all electrophoresis, concentrated ionic chaotropes such as guanidine-HCl and KSCN which are used as protein solubilizing and denaturing agents should be removed and replaced with either urea or SDS prior to electrophoresis. Since the aggregation of agarose is fully reversible, gels can melt under high current. Also, agarose gels are compressible, and tend to drop out of vertical electrophoresis cells unless supported. The ability using weights to mechanically compress agarose gels to within a few per cent of original thickness can be used to advantage. Gels containing more than 2.5% agarose will rehydrate to the original thickness within a fraction of an hour, but gels with 1% or less agarose have a greatly reduced tendency to rehydrate.

Agarose Derivatives

Numerous agarose derivatives have been described for affinity chromatography where addition of charged groups is not critical. All derivatives prepared for electrophoresis involve modifications not imparting electrical charges. As indicated earlier, hydroxyethylated (FMC BioProducts) and hydroxymethylated agarose (Hispanagar, SA) are low melting derivatives which form gels with thin fibres for enhanced sieving. These low melting agaroses have been used to impart sieving during capillary electrophoresis. Allylglycidyl agarose, a very low melting derivative, is frequently used in place of bis-acrylamide for cross-linking acrylamide into stronger gels. All of the commercially available derivatives yield gels with low melting points. That is because the agarose is derivatized in a molten state. As we learned in studies on alkylation of agarose with either glycidol or allylglycidyl ether from preparing glyoxyl agarose and its analogues, the hydroxyl groups involved in the hydrogen bonding functioning in gelation are protected during derivatization of the agarose in the gel state, and the derivatized agarose gel retains much of its original melting and gelling characteristics.

Glyoxyl agarose (oxidized glyceryl agarose) has acetaldehyde substituent groups which can be utilized to form Schiff's base linkages with protein amino groups. At pH < 8.5, these Schiff's base linkages are too dissociated to retard electrophoresis of the pro-

teins. Once separated on the glyoxyl agarose gel, the proteins can be driven to bind to it, either reversibly by immersion in pH 10 buffer to suppress dissociation of the Schiff's base linkages or by immersion in buffer containing sodium cyanoborohydride which rapidly and specifically drives alkylation of amino groups of the protein with the aldehyde groups in the gel matrix. This functionality enables the gel to be used sequentially and repetitively as a protein-separating and immobilizing medium. It can also fix small peptides containing at least a single amino group, but does not fix nucleotides. By compositing it with a removable polyacrylamide filler, it can be used for separations over any molecular weight range.

Agarose/Polyacrylamide Composites

These media were constructed initially to provide a supporting agarose matrix for polyacrylamide at concentrations below 3–4% which do not form firm gels. The combinations can yield exceedingly strong gels (Figure 2) and provide facility to achieve a wide range of sieving characteristics. As described by Peacock and Dingman in 1968, strong gels are obtained only when formulated to allow the agarose to gel before the acrylamide polymerizes. By using either non-cross-linked polyacrylamide or cross-linkers such as alkali or periodate degradable 1,2-dihydroxyethylene-bis-acrylamide instead of the usual bis-acrylamide, the poorly-permeable acrylamide filler can be removed leaving a highly permeable agarose matrix to allow direct immunochemical characterization of the fixed components of the electropherogram.

Electrophoresis

Initial applications of agarose electrophoresis focused heavily on diagnostic separations of plasma proteins, particularly lipoproteins, with great improvement over results obtained with paper or with starch which had been used earlier. Straight analytical separations were followed by more definitive immunoelectrophoretic protein identifications. These separations were usually applied to native, undenatured proteins. Following introduction in 1967 of sodium dodecyl sulfate (SDS) by Shapiro, Viñuela and Miazal as a carrier enabling polyacrylamide-based separation of proteins according to molecular weight by imposing overwhelming negative charge over the original and by denaturing conformational differences between proteins, the practice was widely adopted as a rapid means for separating large-sized proteins on agarose. The converse approach of separating proteins according to differences in isoelectric points

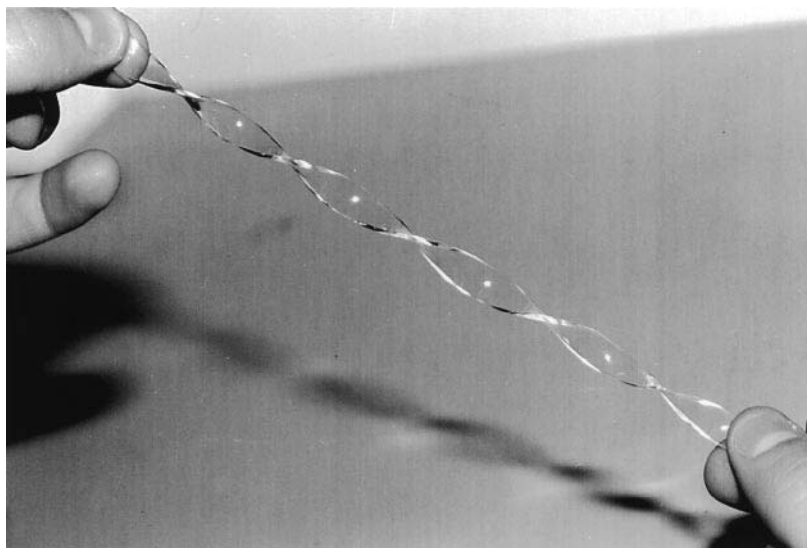


Figure 2 Demonstration of the strength of agarose/polyacrylamide composite gels. (Reproduced with permission from Shainoff, 1993.)

independent of molecular size by establishing a pH gradient across the gel was demonstrated in 1969 by Vesterberg, but a decade passed before the development of zero-EEO agarose enabled this separation method to be used with agarose.

Equipment and Buffer Systems

Agarose gels are usually used for electrophoresis on a horizontal platen on which the gels are placed between anodic and cathodic electrode chambers filled with buffer and connected to the gel with buffer-filled wicks. Except for the usual need to purchase a platen that can be cooled with circulating water, this is a simple arrangement that is easily set up, largely because of the ease with which agarose gels are cast either open faced or in cassettes consisting of two spacer-separated glass plates which can be separated from the gel because the gel is nonadherent. The use of wicks can be troublesome, because voltage is lost across them, and this produces much of the heating and vapour condensation in the chamber. Voltage drop across the gels must be gauged directly from the gel rather than the power supply. Condensation of vapour on the gel is easily prevented by simply laying a vapour barrier, usually GelBond® (FMC Bio-Products), over the gel. For nucleic acid electrophoresis the use of wicks has been obviated by a technique known as 'submarine' electrophoresis in which the gel is laid into a buffer-filled platform connecting the electrode chambers. The submarine mode is usually not applicable to protein electrophoresis because proteins tend to diffuse into the surrounding buffer, while nucleic acids which have very low diffusion

constants migrate almost entirely due to the applied voltage with little diffusion. Running agarose gels in vertical format with electrode chambers directly above and below the gel-containing cassette, as generally used with polyacrylamide gels, is seldom recommended because of the tendency of agarose to synerese and slip out of the cassette, a problem that can be prevented by use of etched rather than clear glass for the cassette. Slipping can also be prevented by partially immersing the cassette into dilute 0.5% agarose, and letting the agarose drain and dry before pouring the running gel.

Sample applications into agarose gels were initially made by either cutting or punching a slot or hole to receive the solution. This approach continues to be used with nucleic acids which form sharp bands as they migrate out of the nonrestrictive sample solution into the migration-restrictive gel, but comparatively little band sharpening occurs with proteins which easily permeate the gels. Further, the wells induce band distortions of proteins due: (i) to partial permeation into the sides of the wells prior to electrophoresis; and (ii) to uneven voltage drops across the wells. Because of the ease with which solutions can be imbibed into agarose following a temporary compression with blotting paper, samples can be drawn into the gels in nicely demarcated bands through a 'sample application foil', thin plastic overlays with slots through which the samples are drawn into the gels. Large samples need band-sharpening which can be achieved either mechanically by temporarily overlaying a dialysis membrane and thick gel to produce a sharp voltage drop near the origin, or by use of discontinuous buffer systems.

A method for sharpening bands at the beginning of runs at the outset of electrophoresis was devised by Ornstein and Davis using a discontinuous buffer system, 'disc electrophoresis', in which proteins and all but common electrolytes stack in hypersharp bands at the boundary between initial buffer ions producing low conductivity and secondary buffer ions producing high conductivity with a common counter ion. The discontinuous buffer systems worked predictably with over 7000 computer generated buffer systems based on the pK_a values of the leading and trailing buffering ions, as far as known, with polyacrylamide gels which produce no EEO, but only a few have been tested and found to yield operable systems with agarose, as already noted.

The ability to run agarose gels horizontally in a virtual open-faced format is its real advantage. That enables the gels to be cut and manipulated post-electrophoresis to conduct secondary electrophoretic operations with it. This facility has made it the usual medium for immunoelectrophoretic analyses.

Staining

With the exception of silver staining, all commonly used staining methods (Coomassie-based, fluorescent, chemiluminescent, and colloidal-type) work well with agarose, colloidal Coomassie being one of the fastest. An important consideration is to minimize exposure to acid which hydrolytically weakens the gel. Unlike polyacrylamide, agarose gels can be directly immunostained as illustrated (Figure 3), but the antibodies should be free of large entrapable aggregates.

Immunoelectrophoresis

These methods are based on immune-precipitate (precipitin) formation at antigen/antibody equivalence, analogous to Ouchterlony immunodiffusional analyses in which antibody and antigen placed in separate wells in agar(ose) form precipitin arcs in the gel at position(s) depending on levels of antigen and antibody in the wells. In the method of Grabar and Williams the proteins under analysis are separated on agar gels, then lateral slots are cut approximately 8 mm to each side of the gel to accommodate antibody. After a day lateral diffusion of the protein bands towards the counter-diffusing antibody one or more precipitin arcs will form in the gel depending on the antibody and antigen heterogeneity. Quantitation of antigen/antibody by this method requires considerable effort and multiple runs. A simpler approach to quantitation was devised by Laurell, using a method known as 'rocket immunoelectrophoresis'.

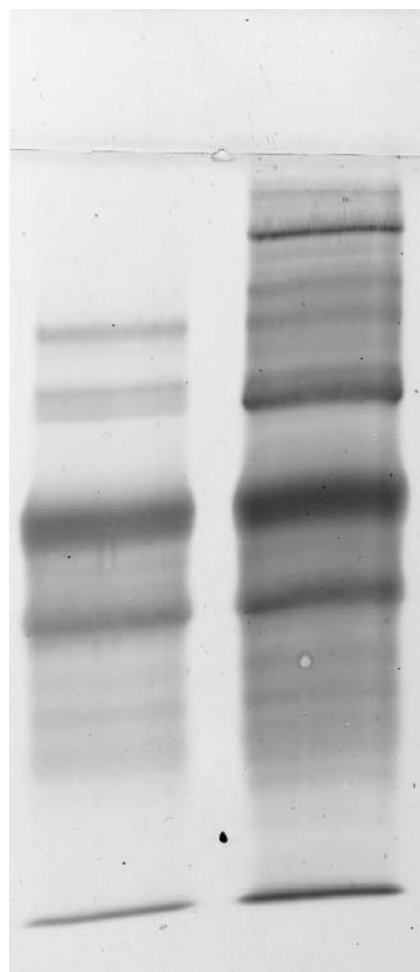


Figure 3 (See Colour Plate 39). Direct dual immunostaining of a polyacrylamide/glyoxyl-agarose composite gel to profile fibrinogen γ -chain (grey), α -chain (amber) cross-linking and hybrid α/γ -chain (umber) cross-linking by plasma transglutaminase (right lane), and the chain composition of plasma fibrinogen. The illustration depicts sieving equivalent to a regular polyacrylamide gel, and subsequent rendering of the gel for antibody permeation by removing the polyacrylamide. (Reproduced with permission from Shainoff *et al.*, 1991, *Journal of Biological Chemistry* 266: 6429.)

In the method of Laurell, the gel is poured with antibody added to it at 56°C, and wells are punched in the solidified gel to accommodate the antigen solution. As the antigen moves by electrophoresis out of the well it sweeps soluble immune complexes along with it in a comet-shaped profile until the antigen/antibody levels become equivalent, whereupon the comet-shaped precipitin arc comes to a virtual stop because the antibodies themselves do not migrate at around pH 8.6. The area contained within the arc is usually directly proportional to the antigen level. Because of the ease with which agarose gels can be cut and filled with interposed gels open-faced, this technique is amenable to a myriad of variations, as described by Axelsen and associates.

In one variation of the Laurell method, called crossed immunoelectrophoresis, the proteins are subjected to pre-electrophoresis, and antibody-containing agarose is cast around a strip of the gel. Then, in a crossed electrophoresis the antigens are transferred out of the primary gel into the antibody where they form rocket(s) in line with their initial position. The technique is 'found' useful for quantifying multiple antigens and variant forms of an antigen. If the initial gel contains SDS, it should be quenched by adding nonionic detergent such as Lubrol® to the antibody-containing gel. In the event that the protein becomes insoluble when stripped of SDS, initially it can be fixed, then probed with charge-enhanced carbamylated primary antibody. Retained antibody is measured by electrophoresis into secondary antibody, as illustrated in **Figure 4**. Use of secondary antibodies is also essential when using monoclonal IgG antibodies as primary probes, because these monoclonal antibodies do not form immunoprecipitates on their own unless the epitope is multiply expressed in the antigen.

Direct Immunoprobing

Because of the permeability of agarose gels to antibody it is possible to probe electropherograms directly. Direct immunoprecipitation within the gel is seldom used because of uncertainties of levels or antibody required for substantial precipitation of un-

known levels of antigen. The proteins are usually fixed or immobilized, and probed by imbibing labelled antibody into and out of the gel. If secondary antibodies are to be used to report retention of the primary antibody, the primary antibody should in turn be fixed before the secondary probing to avoid dissociative losses of the primary during the secondary probing which takes periods of the order of an hour. Glyoxyl agarose was developed to enable these fixations by chemical immobilization.

Blotting

This widely used procedure involves transfer of components out of the gel on to a blotting membrane to immobilize them for immunostaining or compositional analysis on an open-faced surface. It is an essential means for probing reactivities of components separated on polyacrylamide because of the low permeability of the gel. Much uncertainty attends this 'blotting', because the transfers are incomplete, and frequently nil with high molecular mass proteins. These proteins not only transfer slowly, but often precipitate within the gel as SDS transfers away from them. Also, very low molecular mass peptides fail to be retained by the blotting membrane.

While blotting from polyacrylamide gels is usually effected by crossed electrophoresis, the transfers out of agarose gels are more simply effected by either compressing them against the membrane supported on filter paper stacks (a method that yields only partial transfer), or by light vacuum suctioning of buffer through the gel on to the membrane supported on a 'gel drier'. However, when SDS is present it must either be quenched by a prior 15 min immersion in buffer containing 1–2% nonionic detergent, or precipitated by immersing the gel in 0.1 M KCl.

Affinity Electrophoresis

These methods use specific ligands, either added to the buffer or immobilized on the gel matrix, to induce shifts in mobilities or apparent concentrations of target proteins. Again, ability to work with open-faced gels to interpose ligand-rich zones makes it an ideal medium for these procedures, as devised with numerous examples from crossed immunoelectrophoresis. With glyoxyl agarose a ligand containing at least a single amino group can be imbibed into the gel through a mask and fixed in place.

Conclusion

Equipment and supplies for general electrophoresis on agarose have undergone little change over the last

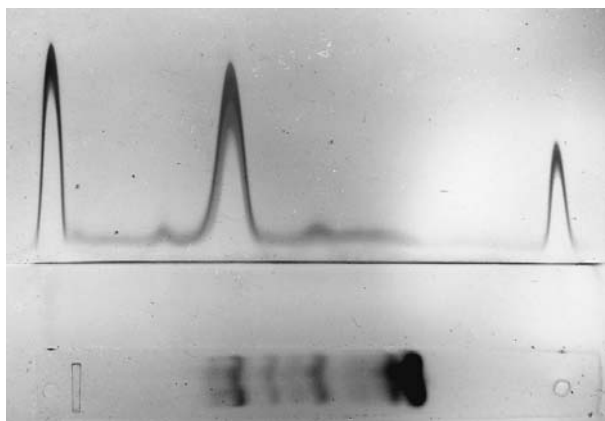


Figure 4 Crossed immunoelectrophoresis to profile plasma fibrinogen derivatives in plasma by: (i) probing the electropherogram with primary antifibrinogen antibodies; and (ii) measuring the retained antibody by displacing to form rockets in secondary gel containing anti-IgG antibodies, with standards for the IgG forming the left- and right-most peaks. This approach was made necessary because insolubility of fibrinogen and its high molecular mass derivatives, once denatured by SDS, cannot be transferred out of the primary electropherogram to form rockets directly. (Reproduced from Dardik *et al.*, 1989, *Cleveland Clinical Journal of Medicine* 56: 451.)

two decades. Improved imaging systems and labelling agents for high sensitivity detection and linear quantitation by fluorescence and chemiluminescence offer attractive alternatives to immunostaining and the use of radioisotopes, and have made rapid automated nucleic acid sequencing possible. Except for those involved in nucleic acid work, few laboratories perform electrophoresis on agarose on a day-to-day basis; thus, accessories for many techniques such as immunoelectrophoresis have been dropped by suppliers. There may be a revival because of growing interest in several proteins which are not separable in polyacrylamide matrices, von Willebrand factor multimers for diagnosis of certain types of von Willebrand's disease, and high molecular mass derivatives of fibrinogen as markers of vascular disease.

More efficient cooling and thermal control would allow the application of much higher voltages for high performance agarose electrophoresis above the present limitations imposed by gel meltdown. By using an apparatus in which the gel is enveloped with a membranous bladder for cooling, von Willebrand factor multimers can be separated in 20 min runs producing resolution superior to that obtained with the usual overnight runs widely used through the 1990s.

Precast polyacrylamide gels have become popular, and precast agarose gels are available for submarine electrophoresis. Compressibility of agarose is the principal detriment to precasts for other modes of electrophoresis. Agarose/polyacrylamide composites would not be subject to that drawback, and would probably be marketable in precast form because they offer advantages and are not as easily constructed as gels of agarose itself.

Summarily, agarose gels are simple to construct. They are highly porous and ideal for separating high

molecular mass proteins and nucleic acids, and can be modified or composited to extend their utility.

See Colour Plate 39.

Further Reading

- Andrews AT (1989) In Peacock AR and Harrington WF (eds) *Electrophoresis. Theory, Techniques, and Biochemical and Clinical Applications*, 2nd edn. New York: Oxford University Press.
- Armisen R (1997) In Imeson A (ed.) *Thickening and Gelling Agents for Food*, 2nd edn, pp. 1–21. London: Blackie.
- Axelsen NH (1975) *Quantitative Immunoelectrophoresis. New Developments and Applications*, Oslo: Universitetsforlaget.
- Axelsen NH, Kroll J and Weeke B (1973) *A Manual of Quantitative Immunoelectrophoresis. Scandinavian Journal of Immunology*, Vol. 2, Supplement no. 1, Oslo: Universitetsforlaget.
- Buzás Z and Chrambach A (1982) Un-supercoiled agarose with a degree of molecular sieving similar to that of crosslinked polyacrylamide. *Electrophoresis* 3: 130–134.
- Chrambach A (1985) *The Practice of Quantitative Gel Electrophoresis*. Weinheim: VCH.
- Hames BD and Rickwood D (1981) *Gel Electrophoresis of Proteins*. Oxford: IRL Press.
- Orban L, Hahn E and Chrambach A (1988) Discontinuous buffer systems optimized for the agarose gel electrophoresis of subcellular particles. *Electrophoresis* 9: 167.
- Pharmacia Fine Chemicals (1982) *Isoelectric Focusing, Principles and Methods*. Uppsala: Pharmacia.
- Serwer P (1980) A technique for electrophoresis in multiple-concentration agarose gels. *Analytical Biochemistry* 101: 154–159.
- Shainoff JR (1993) Electrophoresis and direct immunoprob- ing on glyoxyl agarose and polyacrylamide composites. *Advances in Electrophoresis* 6: 61–177.
- Westermeyer R (1997) *Electrophoresis in Practice*. Wein- heim: VCH.

Autoradiography Electrophoresis

See II/ELECTROPHORESIS/Detection Techniques: Staining, Autoradiography and Blotting

Blotting

See II/ELECTROPHORESIS/Detection Techniques: Staining, Autoradiography and Blotting

Capillary Electrophoresis

S. F. Y. Li and Y. S. Wu, National University of Singapore, Singapore

Copyright © 2000 Academic Press

Introduction

The migration of charged particles under the influence of an electric field was discovered and characterized theoretically more than 100 years ago by Kolrausch *et al.* Foreseeing the possibility of separation of charged species through the application of a voltage, the term 'electrophoresis' was coined soon after. However, early attempts to use electrophoresis as an analytical tool were persistently frustrated by the existence of Joule heating, which acts to discount the electrophoretic effect. Thus a way of combatting the thermal effect during the electrophoretic process was needed. By 1950s, Tiselius *et al.* found that a variety of substances such as agarose and polymeric gels could serve as stabilizing agents in electrophoretic analysis owing to their anticonvective properties. This eventually led to the creation of slab gel electrophoresis, which has become a fundamental technique for the study of proteins, DNA fragments and other biomacromolecules in life sciences and biotechnology. Notwithstanding its great success, slab gel electrophoresis has its drawbacks with respect to speed and automation when compared with contemporary chromatographic techniques such as high performance liquid chromatography (HPLC).

A straightforward way to speed up an electrophoretic separation process is to apply higher electric fields, and this necessitates systems able to release the heat generated more efficiently. Electrophoresis with a tube as a separation channel is hence an attractive choice since the desired surface-to-volume ratio can be achieved by simply reducing the tube radius. Performing electrophoresis based on the tube format has an added advantage in that simultaneous detection may be implemented in a way analogous to HPLC, thus rendering the entire procedure fast and automatic. Running electrophoresis with a tube configuration was initiated by Hjerten as early as the 1960s, and further attempted by Virtanen *et al.* and Mikkers *et al.* in 1970s. During this period, the adopted inner diameters of tubes were in the range of 0.2–3 mm, and thermal effects confined the applied voltage to around 1000–2000 V, which was of the same order as in typical slab gel electrophoresis. As a consequence, despite these pioneering efforts to perform

free solution electrophoresis with in-line monitoring, the full potential with respect to column performance was not yet attained. Also, complexity in instrumental design deterred follow-up by ordinary electrophoresis practitioners.

A milestone for column-based electrophoresis was set in the early 1980s, when Jorgenson *et al.* introduced capillary zone electrophoresis (CZE) with on-column optical detection. They found that with the inner diameter of the capillaries scaled down to 80 μm , voltages as high as 30 kV could be applied without incurring overheating problems. Thus the separation time for most charged species, from small molecules to macromolecules, was shortened to less than 30 min, which is comparable to modern chromatographic methods. For the first time outstanding column efficiencies of several hundred thousand plates was routinely obtained. The unprecedented performance, relatively simple instrumentation, concurrent with the widespread availability of fused silica capillary columns by the mid-1980s quickly aroused the interests of both electrophoresis practitioners and chromatographers, thus making capillary electrophoresis (CE) one of the most exciting research areas. Today, it has become an indispensable branch of modern separation science. The powerful separation ability of CE was exemplified in an early electropherogram concerning the resolution of derivatized peptides originated from egg white lysozyme (Figure 1).

This article serves as an introduction to CE. It covers the basic principles, various aspects of instrumentation, separation modes and major applications. Some future trends of CE are discussed in the final section.

Fundamentals

Electrophoretic Migration of Ions

The uniform motion of an ion under an electric field can be recognized as a result of balancing electromotive and frictional forces of the ion in solution:

$$qE = 6\pi r\eta u \quad [1]$$

where q is the effective charge of the ion concerned, E is electric field, while r is the ion's Stokes radius, η is the dynamic viscosity of the solution, and u is the linear velocity of the ion. The important parameter, electrophoretic mobility (μ), is defined as the ion's

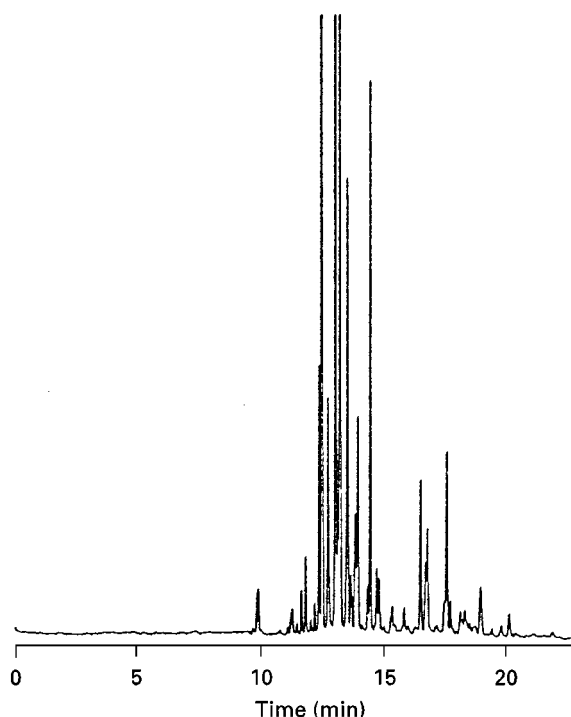


Figure 1 Capillary zone electrophoresis separation of fluor-escamine-labelled peptides obtained from a tryptic digest of reduced and carboxymethylated egg white lysozyme. (Adapted with permission from Jorgenson JW and Lukacs KD (1981) Zone electrophoresis in open-tubular glass capillaries: preliminary data on performance. *Journal of High Resolution Chromatography and Chromatographic Communications* 4: 230–231.)

linear velocity per unit of electric field:

$$\mu = \frac{u}{E} = \frac{q}{6\pi r\eta} \quad [2]$$

From eqn [2], it can be seen that the ion's effective charge, its size and the viscosity of the solution decide ionic mobility. Thus in a given system ionic mobility is an intrinsic property of an ion. Usually ionic mobility cannot be directly derived from eqn [2], as the parameters are not easily accessible quantities. Instead it can be measured based on relevant experimental data, i.e. how long an ion takes to travel through a certain distance under a definite electric field, as follows:

$$\mu = \frac{u}{E} = \frac{L_{\text{eff}}}{t_m} \times \frac{1}{E} = \frac{L_{\text{eff}}}{t_m} \times \frac{1}{V/L_{\text{tot}}} = \frac{L_{\text{eff}} \times L_{\text{tot}}}{V \times t_m} \quad [3]$$

where L_{eff} and L_{tot} are the effective migration length (from inlet to detection window) and total migration length, respectively, V is the applied voltage, and t_m is the migration time of the ion. For a CE system operated under a constant voltage, L_{eff} , L_{tot} and V are all

fixed. Hence electrophoretic mobility, the inherent attribute of an ion is directly reflected by its migration time. This provides the theoretical basis of using migration time as a means of identifying an ion in CE.

Electroosmotic Flow (EOF)

Electroosmosis is a fundamental electrokinetic effect involving movement of the bulk solution against a charged solid surface under the influence of an electric field. In the case of CE, the capillary inner wall usually carries negative charges due to the deprotonation of silanol groups. For the part of the liquid adjacent to the capillary wall, build-up of cations takes place to counterbalance the negative charges on the capillary surface. According to Stern's double layer model the solution containing net cations can be divided into two regions, namely a rigid layer and a diffuse double layer. The rigid layer is immediately adjacent to the capillary wall, so the cations within it are largely immobilized owing to the strong electrostatic interaction with the wall. The diffuse layer is slightly away from the wall, hence the cations inside are mobile. Upon the application of a voltage, these cations together with their surrounding hydrating water will migrate towards the cathode. The cohesive nature of water causes the whole solution inside the capillary to be dragged forward, generating a net flow across the capillary. This is named the electroosmotic flow (EOF). The magnitude of the EOF can be described via the Helmholtz equation:

$$\mu_{\text{eo}} = \frac{\epsilon \zeta}{4\pi\eta} \quad [4]$$

where ϵ is the dielectric constant of the buffer solution, ζ is the zeta-potential across the diffuse layer, and η is the viscosity of the electrolyte. Unlike conventional electrophoresis where EOF is regarded as unfavourable and thus usually suppressed, in CE it has several important positive implications.

First, the existence of an EOF offers a simple and highly efficient way of driving a separation system. The zeta-potential is uniformly distributed within an extremely narrow cylindrical region along the whole capillary so the bulk electrolyte solution is pumped out of the capillary with virtually no pressure drop (Figure 2). A 'plug-like' flow is obtained, which subsequently contributes to high column performance. This is advantageous over the conventional pumping methods such as in HPLC, where the pressure-based flow always introduces a parabolic profile thus adding to the loss of column efficiency.

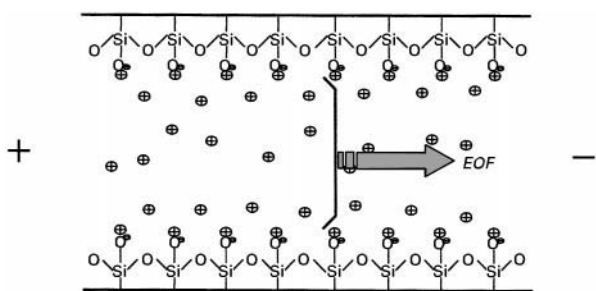


Figure 2 The generation of electroosmotic flow (EOF) in a silica capillary.

Second, the presence of EOF affects the apparent mobilities of ions (**Figure 3**). In any electrophoretic separation system where EOF is not fully suppressed, the observed mobility of a charged species will be the resultant of its effective electrophoretic mobility and EOF:

$$\mu_{\text{obs}} = \mu_{\text{ep}} + \mu_{\text{eo}} \quad [5]$$

Under normal conditions, with EOF directed towards the cathode, obviously cations will be accelerated, while anions will be decelerated. If the magnitude of the EOF exceeds the mobilities of the anions, the anions will be swept towards the detection side, thus allowing the simultaneous analysis of cationic and anionic species. As the magnitude and direction of EOF will affect how long the analytes stay inside the separation capillary, manipulation of EOF often becomes a core issue for effecting a satisfactory resolution. Since the formation of EOF involves two phases (capillary wall and running buffer), any modification to their chemistries will bring about a change in EOF.

Causes of Band Broadening

As in a chromatographic process, in electrophoresis it is necessary to contain the ionic species within narrow bands while creating sufficient mobility differences. How narrow a band is depends not only on the various dispersive factors inherent to the electrophoretic process, but also on how well the whole process is performed. The common causes of band

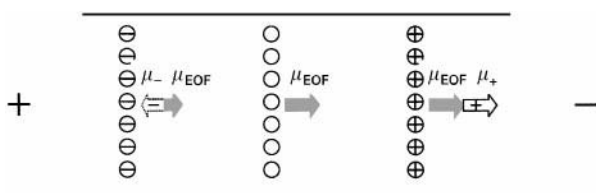


Figure 3 Effect of EOF on the apparent mobilities of anions and cations.

broadening in CE include longitudinal diffusion, injection-related volume overloading, thermal effects, electrodispersion, wall adsorption, etc. These band broadening mechanisms are deemed to be random and independent events, so that the concept of summation of variances can be used to evaluate the contributions of individual factors to the overall band broadening effect, that is:

$$\sigma_{\text{tot}}^2 = \sigma_{\text{diff}}^2 + \sigma_{\text{inj}}^2 + \sigma_{\text{therm}}^2 + \sigma_{\text{wall}}^2 + \sigma_{\text{electr}}^2 + \sigma_{\text{other}}^2 \quad [6]$$

A brief description of these band broadening factors is given below.

Longitudinal diffusion In the course of electrophoretic transportation of an analyte band along the capillary, the sample molecules will inevitably have a tendency to enter the surrounding buffer solution because of the apparent concentration difference, leading to a wider and more dilute sample band. According to Einstein's diffusion equation, band dispersion due to longitudinal diffusion is a function of diffusion coefficient and time:

$$\sigma_{\text{diff}}^2 = 2D_m t \quad [7]$$

Under an ideal situation, longitudinal diffusion becomes the only unavoidable band broadening process. Therefore it defines the maximum attainable column efficiency in CE. Based on chromatographic theory, the maximum obtainable theoretical plates (N) can be derived as follows:

$$\begin{aligned} N &= \frac{L^2}{\sigma^2} = \frac{L^2}{2D_m t} = \frac{L^2}{2D_m \times (L/v)} \\ &= \frac{L^2}{2D_m \times [(L_{\text{eff}} \times L_{\text{tot}})/\mu V]} = \frac{\mu V}{2D_m} \end{aligned} \quad [8]$$

Thus the maximum column efficiency in CE is proportional to the mobility and voltage, while inversely proportional to the diffusion coefficient. Considering that mobilities of ions range between 10^{-4} and $10^{-3} \text{ cm}^2 \text{ V}^{-1} \text{ s}^{-1}$, diffusion coefficients from 10^{-7} to $10^{-5} \text{ cm}^2 \text{ s}^{-1}$, and an applied voltage up to 10^4 V , the attainable theoretical plate number would be in the order of 10^5 – 10^6 , which is much higher than any conventional HPLC approach. Eqn [8] also suggests that in principle CE should be well suited for the separation of high-mass charged particles such as biopolymers, since their diffusion coefficients are extremely low. This has been demonstrated in the most successful resolution of DNA fragments and proteins where plate numbers of 10^6 have been reached. It should be emphasized

that eqn [8] is only valid under the precondition that longitudinal diffusion plays a predominant role among the various band broadening mechanisms. In other words, to achieve the maximum column efficiency, the electrophoretic separation should be carried out in such a way that all the other potential band dispersions are curbed well below the magnitude of the longitudinal diffusion effect.

Injection related volume overload During sample injection, a finite volume of sample is placed onto the capillary. The length of this starting plug will contribute directly to the final band width. Treating the original band as rectangular in shape, the variance of this plug can be expressed by:

$$\sigma_{inj}^2 = \left(\frac{l_{inj}}{12}\right)^2 \quad [9]$$

where l_{inj} is the initial plug length. As a rule of thumb, loss of efficiency due to any extraneous dispersion factor should be kept within 10% of the maximum theoretical column efficiency. Assuming a moderate plate number in the order of 10^5 as defined by longitudinal diffusion, it can be easily estimated that the acceptable injection length should be a few millimetres. For the commonly employed capillaries with inner diameter between 50 and 75 μm , the above length is equivalent to only a few nanolitres. So it is obvious that CE's high column efficiency will pose very stringent restriction on the sample size. Any attempt to increase the injection volume in an aim to enhance detection sensitivity may result in a significant loss of column efficiency.

Thermal gradient effect An electrophoretic process is always accompanied by certain amount of thermal effects due to the passage of a current through the resistive medium (Joule heating). For a CE system, the electrical power (P) responsible for the generation of heat can be estimated through the following equation:

$$P = V \times I = \frac{V^2}{R} = \frac{V^2 \pi r^2 \lambda c}{L} \quad [10]$$

where V is the applied voltage, r and L are capillary inner radius and length, respectively, while λ and c are respectively the molar conductivity and the concentration of the electrolyte solution. While heat generation is uniform for the whole electrolyte solution, heat dissipation is apparently not: the nearer the electrolyte is to the capillary wall, the faster is the heat transferred out to the surroundings. Consequently, a temperature gradient is generally present in the radial direction of the capillary, which is

equivalent to the superimposition of a parabolic profile to the otherwise plug-like ion boundaries and bulk flow, as any temperature gradient will be translated into viscosity and mobility gradients in the solution. To minimize the influence of thermal effects on the overall column efficiency, it is imperative to limit the heat generation while maximizing the heat dissipation. In this regard, the use of narrow bore capillaries is particularly recommended because it favours the above two aspects simultaneously. According to eqn [10], for a certain CE system, heat generation may also be controlled through balancing the buffer composition and separation potential.

Wall adsorption effect The capillary surface, like most solid surfaces, never behaves in a completely inert manner to foreign compounds. In HPLC, it has been well known that peak anomalies are often the result of some specific interaction (e.g. hydrogen bonding) between the residual silanol groups and analytes. While similar adverse effects cannot be ruled out, in CE the problem is exacerbated by the fact that under a typical operation condition, the silanol groups along the wall are mostly deprotonated to give a negatively charged capillary surface. When an analyte with a positive charge travels along the capillary, the electrostatic force will tend to attract the analytes onto the wall, causing additional band broadening. This is a feature of the analysis of proteins owing to their low diffusion coefficients and multiple charge sites. Significant efforts have been made to tackle this problem, mostly through the suppression of EOF or complete reversal of the charge status of the capillary wall.

Electrodispersion Electrodispersion is the result of Ohm's law during the electrophoretic separation. It may appear in two instances. First, if the conductivity of the injection plug is larger than that of the buffer solution, an isotachopheresis effect will occur to dilute the original band till the conductivity is equal to the surrounding buffer. Second, during the separation, an analyte zone is 'submerged' into the buffer solution. Any mismatch of its mobility with its co-ions in the buffer will render the local electric field different from that in the normal running buffer. If the mobility of the sample ion is larger than that of its co-ions, then there will be a lower electrical field for the analyte zone. Thus any sample ions diffusing out of the zone will experience a higher electric field, and these ions will speed up along the migration direction. This causes the ions at the rear to re-enter the zone, whereas the ions at the front will drift away from the zone. The accumulative effect of such phenomenon is the formation of a tailing band showing a sharp

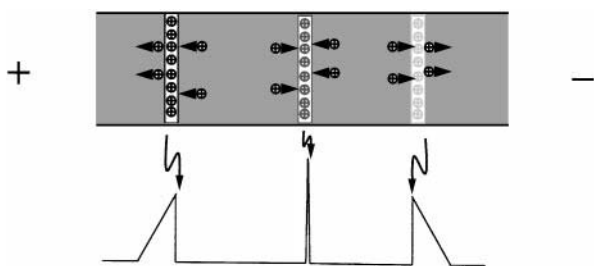


Figure 4 Mobility mismatch-induced band broadening.

trailing boundary but a broadened leading boundary. By a similar argument, if the analyte ion is of lower mobility than the co-ion, a fronting band is expected (Figure 4). The higher the sample concentration compared to the buffer concentration, the more pronounced are the nonuniformities with respect to conductivity and field strength, and eventually more severe is the band asymmetry.

From the above discussion it is obvious that, to prevent possible loss of column efficiency due to electrodispersion, the conductivity of the injection plug and the actual sample concentration should be sufficiently low. Theoretical study had shown that, to confine the electrodispersion-related band broadening at a level comparable to longitudinal diffusion, the sample concentration should be two orders below the buffer concentration. To some extent, it is the electrodispersion that limits the mass loadability of a CE system.

Instrumentation

CE can be performed with relatively simple instrumentation as depicted in Figure 5. A capillary containing an appropriate separation medium spans two buffer reservoirs, to which the high voltage power

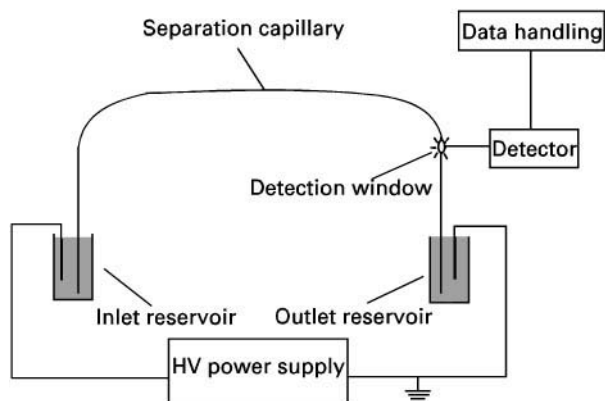


Figure 5 Instrumental setup of a capillary electrophoresis system.

supply is connected via the platinum electrodes. Following the introduction of sample at the capillary inlet, a high voltage is applied, thus driving the analytes to travel inside the capillary with different velocities. Somewhere close to the capillary outlet, an on-line detector is installed to monitor the separation process. The resulting signals are fed to the data acquisition device, and finally the result is presented in the form of an electropherogram.

Apart from these fundamental components, commercial CE instruments are commonly equipped with some dedicated facilities, such as an autosampler, pressure regulating unit, capillary thermostating, and comprehensive supporting software. These added functions allow a sequential analysis of different samples under prespecified conditions, thus ensuring better reproducibility, accuracy and higher throughput. Two modern commercial systems are shown in Figure 6.

High Voltage Power Supply

A high voltage power source delivering stable DC potential of ± 30 kV will satisfy the requirement of most CE applications. Many power supplies offer additional features such as polarity switching, constant potential/current setting, and an interlocked

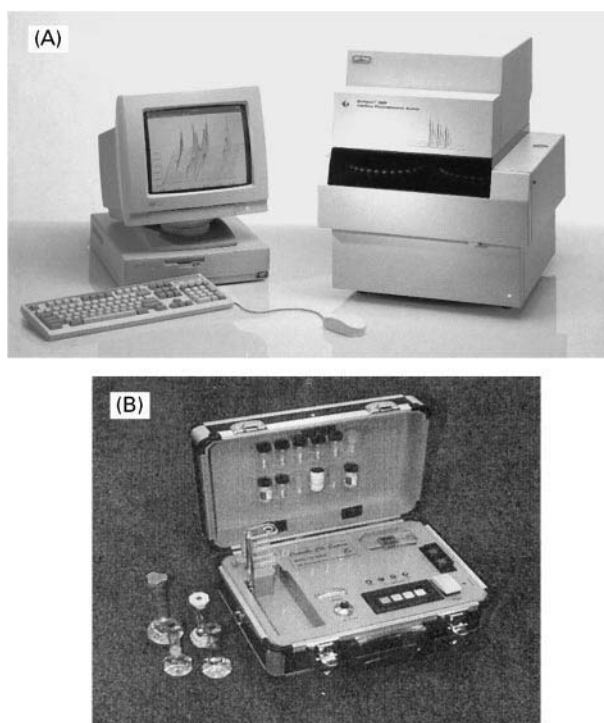


Figure 6 Commercial CE systems. (A) Bench top CE system. Photograph courtesy of Bio-Rad Laboratories. (B) Portable CE system. Photograph courtesy of CE Resources Pte. Ltd.

antieletrical shock loop. In the commercial CE instruments, the power supply is designed with digital communication capability, so that more information such as a current curve can be tracked and retrieved, and the applied voltage can be programmed.

Separation Capillary

Although capillaries made of glass or polymer (e.g. Teflon or Nylon) have found occasional application, fused silica capillaries are used predominantly in CE, largely due to their strength, flexibility and most importantly their excellent UV transparency. Usually the fused silica capillary is coated with a layer of polyimide to enhance its durability. For on-column optical detection a small segment of this coating needs to be removed to provide the detection window. The most commonly used CE capillaries have inner diameter between 20 and 75 μm , outer diameter 100–400 μm and are about 30–100 cm in length.

Sample Injection

To achieve high column efficiency and good quantitative results, sample injection must be performed in a reproducible manner. Since the injection volume in CE is in the nanolitre range, which precludes the use of conventional injection methods, alternative approaches have to be pursued. Hydrodynamic injection and electrokinetic injection have turned out to be the most widely employed sampling techniques.

Hydrodynamic injection introduces a sample based on a pressure difference in the two sides of the capillary. For a laboratory-built instrument, this is realized by simply lifting up the sample vial together with the capillary inlet for a certain period of time (typically a few seconds). The hydrodynamic force will siphon a band of sample solution into the capillary. For commercial instruments, the pressure drop is created by either applying pressure at the inlet side, or imposing a vacuum at the outlet vial. The injection volume can be calculated based on Poiseuille's law:

$$V_{\text{inj}} = \frac{\Delta P \pi r^4 t}{8 \eta L} = \frac{\rho g \pi r^4 \Delta h t}{8 \eta L} \quad [11]$$

where ΔP and Δh are the pressure and height differences, respectively, while r , t , η and L represent capillary inner radius, injection time, solution viscosity and capillary total length, respectively.

Electrokinetic injection is based on the transportation of sample ions by electrophoretic movement and EOF. Normally a lower voltage than that for separation purpose is applied for a certain amount of time to allow analytes to migrate into the capillary. The

injection volumes of individual components can be calculated through the following equation:

$$V_{\text{inj}} = \frac{(\mu_i + \mu_{\text{eo}}) \pi r^2 V t}{L} \quad [12]$$

where μ_i , μ_{eo} are the mobilities of the analyte and EOF, respectively, and V is the injection voltage. For electrokinetic injection the injected amounts of different analytes are dictated by the mobilities of the respective analytes. Thus it is different from hydrodynamic injection, where the sample plug is of entirely the same composition as the original sample solution. To avoid sample injection bias, hydrodynamic injection is preferred. However, in some circumstances hydrodynamic injection may be impracticable (e.g. owing to the high viscosity or low permeability of the separation medium). Electrokinetic injection is then the only viable option, such as in capillary gel electrophoresis. On the other hand, sometimes electrokinetic injection may be exploited in favour of CE operation. For example, it can be employed to diminish the interference of the sample matrix if the components concerned are of low mobilities. Moreover, if the sample is of low conductivity, then sample enrichment during electrokinetic injection is possible by taking advantage of the sample-stacking effect.

Detection

In CE, sample separation is accomplished in an electrolyte solution, so detection strategies analogous to HPLC are adopted. Compared with HPLC, CE column efficiencies are at least one order of magnitude higher, which suggests that solute bands will be narrow and the average concentration of the analyte zone is several times higher than for HPLC. As far as a concentration-sensitive detector concerned, this implies a larger detection signal output. However, so far for CE the concentration sensitivity is usually lower than its HPLC counterparts. This apparent contradiction stems mainly from the small sample size, which poses great difficulties for detection. The fundamental detection schemes in CE fall into three categories: optical (UV absorptive and fluorescent) detection, electrochemical detection, and various hyphenating techniques (typically mass spectrometric detection). The sensitivities of the different detection methods are compared in Figure 7.

UV adsorbance This is the most commonly used detection method for CE, mainly because of its simplicity. It is frequently implemented by modifying a HPLC-type UV detector. The normal flow cell is

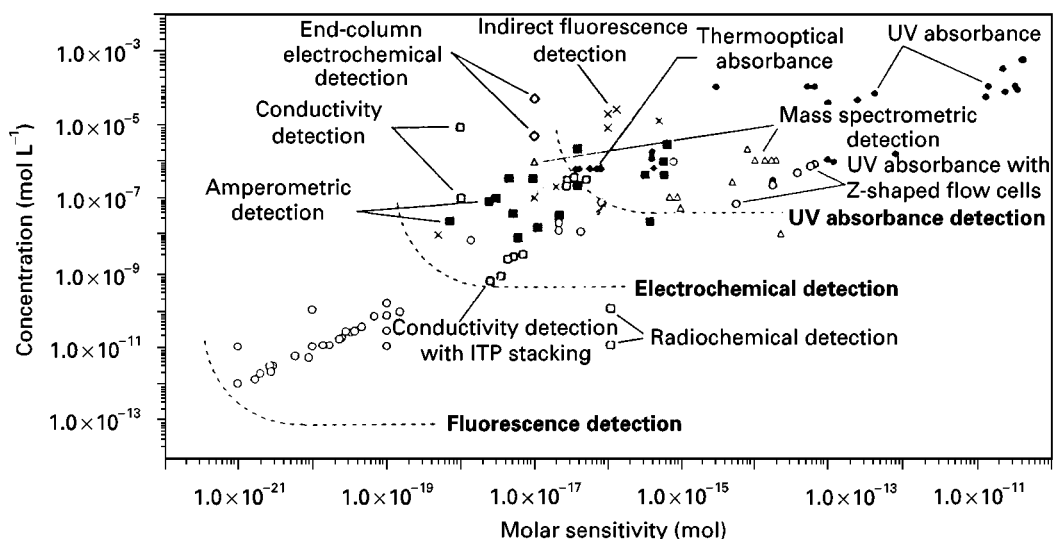


Figure 7 Comparison of sensitivities of various CE detection methods. (Adapted with permission from Landers JP (ed.) *Handbook of Capillary Electrophoresis*, 2nd edn, chap. 10, pp. 425–448. Boca Raton, FL: CRC Press.)

removed and the capillary is mounted directly between the incident lens and photocell, in conjunction with a corresponding aperture. Such on-column detection configuration, though easy to execute, provides only a moderate detection sensitivity with the lower detection limits around 10^{-5} to 10^{-6} mol L $^{-1}$, as it is associated with two major problems. First, since the capillary is illuminated radially, the maximum optical path is equivalent to the inner diameter of the capillary. This severely reduces the achievable absorbance according to Lambert–Beer’s law. Second, due to its unique cylindrical geometry, the capillary tends to act like a lens to defocus the incoming light, thus posing difficulties in light orientation and collection. As a consequence, signal noise and nonlinearity are further aggravated. By bending the capillary into Z-shape or creating a bubble feature on the capillary body, the optical pathlength can be considerably increased. These efforts, coupled with improved detection optics, enhance the detection limits to 10^{-7} mol L $^{-1}$. The capillary can also be connected to an HPLC-type flow cell (pathlength ~ 1 mm) as in the HP system.

Fluorescence detection Fluorescence detection is so far the most sensitive detection mode available to CE due to the fact that the measurement is performed against a ‘dark’ background, and fluorescence intensity is less pathlength dependent but directly proportional to excitation power. On-column fluorescent detection can also be realized through adaptation of an HPLC-type detector. Once again, due to the presence of the lens effect of the capillary, improvement of the detection optics is necessary to ensure better

focusing of excitation light and more effective collection of emission light. An important development in CE fluorescence detection is the introduction of laser-based excitation sources. Owing to its outstanding coherence, a powerful laser source can be focused into an extremely sharp beam to illuminate the core part of the capillary, thus producing emission light of high intensity. As a result, detection limits of 10^{-9} – 10^{-11} mol L $^{-1}$ can be obtained routinely, which is at least two orders of magnitude more sensitive than the conventional approach. Single molecule detection has been demonstrated by fine-tuning the CE system and utilizing laser-induced fluorescence (LIF) detection. A major drawback of fluorescence detection is that the number of analytes with native fluorescence is far less than that with UV absorbance. Therefore, to make use of this highly sensitive detection scheme, derivatization of analytes by tagging with a fluorescent group is often needed.

Indirect photometric detection For compounds without any chromophore, indirect detection offers a simple, effective way to take advantage of the convenience of on-column optical detection. Here a UV-absorbing or fluorescent compound with the same sign as the sample ions is added to the running buffer to provide a stable background. During the electrophoretic separation, the sample ions will displace a certain amount of background ions due to electroneutrality requirements. Thus the passage of a sample zone through the detection window will appear as a negative peak. In principle, the quantification of a sample in such a way involves differentiating a signal from two large responses, hence the detection

sensitivity is lower than that for direct photometric detection. To achieve an acceptable detection limit, the background concentration should be kept low. Under such circumstance, any mismatch of mobilities between the sample ions and background co-ions will give rise to a considerable electrodispersion, hence leading to severely distorted peaks. Therefore, selecting a suitable CE background is of special significance for the implementation of indirect optical detection.

Electrochemical detection In electrochemical detection, sample bands are monitored in terms of an electrical signal. Depending on the application, the measured quantity can be conductivity, voltage or current. Accordingly it is referred to as conductimetry, potentiometry or amperometry, respectively. Unlike optical detection in which the measurement output depends strongly upon the available volume, in electrochemical detection the signal relates only to the part of solution that is directly contacting the electrode surfaces. Thus, wherever volume insufficiency precludes the employment of photometric detection, e.g. in case where ultra-narrow bore capillary is used to facilitate fast separation, electrochemical detection may still be a viable choice. Moreover, as long as the analyte is electrochemically active, the detection can be performed directly without involving derivatization, as it may be for photometric detection. Due to these advantages, electrochemical detection gradually gains its popularity in CE practice.

There are two major difficulties involved with implementing electrochemical detection for CE. The first comes from the fact that, it is not easy to make an electrochemical detector function well in the presence of a high voltage, because the separation voltage will produce noise that swamps the minute response of the analytes. Thus, decoupling of the separation electric field from the detection system has to be done to facilitate the measurement. The insulation of the separation voltage can be realized by introducing a fracture or a gap structure in the capillary through which the electrical grounding is made, such that the segment behind the fracture or the gap can be used for the accommodation of the electrochemical electrodes. Alternatively, to shield off the high voltage, the detecting elements may be mounted immediately outside the outlet of the separation capillary. A more elegant way is to etch the capillary end to generate an enlarged conical cuvette from where the detecting electrodes are installed. In this way the interference of high voltage can be eliminated because the electric field decays very rapidly before the enlarged conical part. The second difficulty stems from the need to

fabricate microelectrodes and mount them into an extremely small space, usually defined by the separation capillary. While the current state-of-the-art allows the preparation of microelectrodes with dimensions down to several μm , the installation of the microsensing elements to the detection region is a task requiring complicated microfabrication techniques and great patience. All three types of electrochemical detection have shown their feasibility in CE with typical detection limits in the range of 10^{-7} – 10^{-9} mol L $^{-1}$.

Hyphenation with mass spectrometry Following the great success in interfacing HPLC with mass spectrometry, it is a logical move to explore the potential of CE-MS. For a successful implementation of CE-MS, keeping a proper electrical contact at the MS side is essential. This has been achieved through a variety of means, such as contacting via coaxial sheath flow, or through a liquid junction. Sheathless contact has been realized by attaching the metal-coated separation capillary tip directly to the ion source emitter. For sample ionization and transportation, the electrospray ionization interface (ESI) is predominantly adopted, mainly because ESI is operated under almost atmospheric pressure, thus not conflicting with CE separation. Moreover, ESI ionization works with electrostatically induced nebulization, in which compounds are ionized with different charge status depending on their relative molecular masses and shapes. In principle, this allows determination of relative molecular mass for a large range of compounds, from small molecules to large biopolymers (such as proteins and polysaccharides). Thus it is applicable to all types of CE analytes. As for the mass analyser, the high efficiency of CE separation demands a mass analyser with a fast scan rate. The time-of-flight (TOF) mass spectrometer is probably the most promising candidate, but the quadrupole mass spectrometer is currently the workhorse for CE-MS owing to its commercial availability and relatively low cost. Its insufficient scan speed may be compensated partially through the manipulation of the electric field, i.e. when a certain analyte is migrating out of the capillary, the applied voltage can be reduced temporarily, such that the analyte of interest will remain in the ionization chamber for a longer time. With careful optimization of parameters, CE-MS has shown detection limits in the attomole range (10^{-18} mol mass).

Separation Formats of CE

One of the advantages of CE is that many types of separation can be performed with the instrument

described in Figure 2. This is made possible by simply altering the separation medium inside the capillary and utilizing an appropriate buffer system. The commonly employed separation formats in CE can be divided into the following.

Capillary Zone Electrophoresis (CZE)

Among the various CE formats CZE is the simplest and most popular. Here a homogenous free solution is employed to maintain a constant electric field along the capillary. Ionic species are separated inside this supporting solution according to their different charge-mass ratios, thus forming segregate zones. The desired separation selectivity can be achieved by simply optimizing the parameters of the carrier electrolyte particularly pH, as well as ionic strength and the type and concentration of various EOF modifiers. A number of secondary equilibria are available to strengthen the separation selectivity further.

Although CZE is commonly performed with an aqueous buffer, it can also be implemented in a non-aqueous medium by using organic solvents and compatible conductive salts. The effect of replacing water with an organic solvent in CE can be understood from the fact that organic solvents possess significantly different viscosities and dielectric constants compared with water. Thus, changes in the magnitude of EOF and migration behaviours of charged analytes are expected in non-aqueous CE, which can be seen from eqns [2] and [4]. Furthermore, organic solvents differ in their capacity to stabilize equilibria. Thus, in organic media, the charge status of organic analytes can be dramatically different from that in an aqueous medium, hence leading to quite different separation selectivity. Additionally, it is evidenced that organic media are capable of promoting certain mechanisms such as inclusion interaction and ion-pair formation, which enhance possibilities of achieving the desired separation. Moreover, with a water dominated buffer, it is very difficult to conduct CE separations of hydrophobic analytes. Under such circumstances, switching to a non-aqueous buffer system would provide an efficient solution. Finally, it is noted that, when an organic medium is utilized for CZE separations, the electrophoretic current is reduced considerably. As a result, even though capillaries of relatively wide inner diameter are employed, Joule heating is at a manageable level, thus enabling the enhancement of detection sensitivity through the usage of wide bore capillaries. In short, non-aqueous CZE is an attractive means for extending the applicability of CE.

Capillary Gel Electrophoresis (CGE)

For this format, polymeric networks are present along the electrophoretic pathway of analytes, which causes charged species to be resolved on the basis of their physical sizes rather than charge-to-mass ratios. Accordingly this separation process is also commonly known as 'molecular sieving'. It is particularly suitable for the separation of biomacromolecules consisting of numerous repeat charge units, such as DNA fragments, SDS-denatured proteins and polysaccharides (Figure 8). CGE may be considered as an adaptation of traditional gel electrophoresis into its capillary format. However, traditional gel electrophoresis use only cross-linked polyacrylamide (so called 'chemical gel'), while for CGE both cross-linked polymer gels and various polymer solutions can be employed to create the sieving pores. The use of polymer solutions instead of chemical gels facilitates renewing of the sieving medium by simply flushing out the original solution, and refilling with another. It also alleviates some technical problems associated with chemical gel such as gel shrinkage, bubble formation and matrix collapse, hence improving the separation reproducibility.

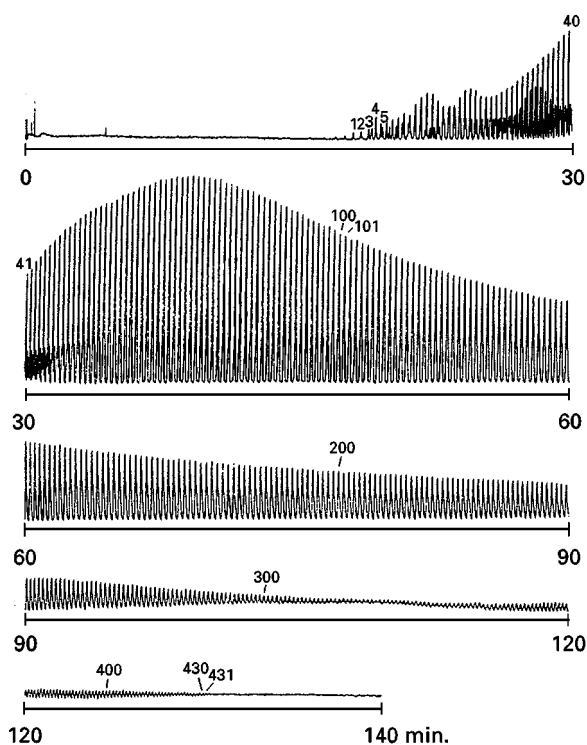


Figure 8 CGE separation of poly(uridine 5'-phosphate). (Adapted with permission from Yin HF, Lux JA and Schomburg G (1990) Production of polyacrylamide gel filled capillaries for capillary gel electrophoresis (CGE): influence of capillary surface pretreatment on performance and stability. *Journal of High Resolution Chromatography* 15: 624–627.)

Capillary Isotachopheresis (CITP)

In CITP, a leading electrolyte of higher mobility than any of the sample components is filled into the separation capillary and outlet reservoir, while a terminating electrolyte of lower mobility than any of the sample components is placed in the inlet reservoir. The sample is applied from the capillary inlet. This arrangement ensures that there will be no mixing of sample with the two electrolytes during the whole electrophoretic process. As a consequence, upon application of an electric field, the main change happens inside the sample band itself, i.e. the sample components tend to 'queue up' according to their effective mobility orders. These components are relocated with corresponding changes in their concentrations and band lengths. Ultimately a series of consecutive 'pure zones' containing only the individual substances are formed. This is the steady state as there will be no more changes for the sample except that all the zones will continue to migrate out of the capillary with an identical velocity (hence the term 'isotachopheresis'). Unlike the other types of CE separation, in CITP the concentration of a specific zone is predetermined by the concentration of the leading electrolyte and the relative mobility of the ion of interest with respect to the leading electrolyte, while the sample amount is reflected by the zone length. Due to the unique stepwise increase in electric field starting from the leading electrolyte side, which prevents a component from drifting off its own band, sharp boundaries can be maintained more readily. Therefore CITP can be implemented using tubes of relatively large i.d. (e.g. 0.2–0.8 mm). Nevertheless, CITP as an analytical tool has largely lost its popularity since the advent of CZE, probably due to the fact that a thorough knowledge of the sample is required before the separation. Furthermore, the isotachopherogram is usually step-shaped, and the steps are not time related, thus rendering automatic identification and quantification difficult. CITP is often applied as a sample pre-concentration step before CZE separations to enhance detection sensitivity.

Capillary Isoelectric Focusing (CIEF)

This is another example of an adaptation of a conventional electrophoresis principle to a capillary format. CIEF exploits differences in isoelectric points (pI s), a unique characteristic of amphoteric compounds under which its acidic and basic groups dissociate to an equal extent, so that the whole molecule exhibits no net charge. It is only suitable for the separation of compounds like amino acids, peptides and proteins. The operation of CIEF relies on a mixture of carrier

ampholytes with isoelectric points in a certain range and in close proximity to each other. Such a mixture is commonly formed by a series of synthetic poly-amino polycarboxylic acids. The capillary is filled with the carrier ampholyte solution and a small amount of sample, and dipped into the buffer reservoirs that contain acid and base, respectively. Under the electric field, different ampholytes will migrate along the capillary until they reach positions corresponding to their pI values, where they stand still. Collectively a stable pH gradient is formed across the capillary. The sample components, too, will migrate until they find positions equivalent to their pI values. When such a steady state is obtained, an immobilization step (by utilizing electrophoretic movement or pressure) is performed, and the separated analyte bands will be forced out and passed through the detector. If the carrier ampholyte mixture is well prepared and a sufficient time is allowed for the electric focusing process, a very high column efficiency can be realized.

Micellar Electrokinetic Chromatography (MEKC)

Neutral species can never be resolved with traditional electrophoretic techniques since they have no electrophoretic mobility. After the birth of CE, this problem was solved by Terabe *et al.* through the addition of a charged surfactant to the running buffer. Typically a negatively charged surfactant is added at a concentration above its critical micelle concentration (CMC). Under such circumstances, micelles are formed, which allow neutral compounds to be retained based on their hydrophobicities. Under an electrical field, the negatively charged micelles move toward the anode side, while a strong EOF moves toward the cathode side (Figure 9). As EOF usually exceeds the electrophoretic mobility of micelles, the micelles will eventually be swept out in the same

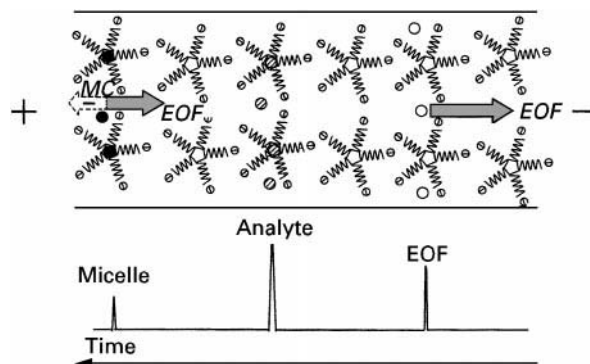


Figure 9 Separation mechanism of MEKC.

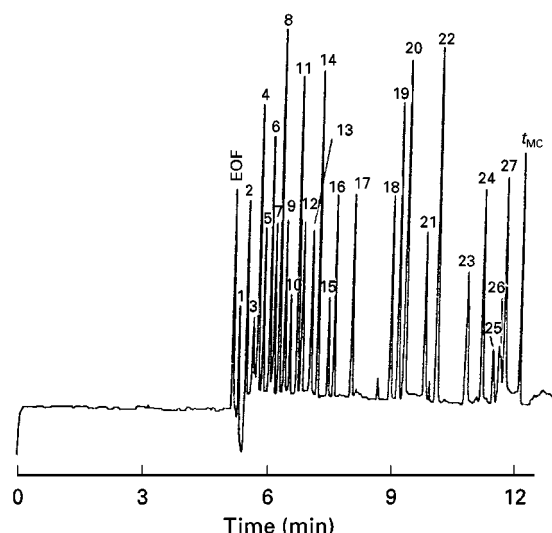


Figure 10 Separation of small neutral aromatic compounds by bile salt-based MEKC. (Unpublished results.)

direction. Thus a migration time window is defined within which the neutral compounds can be separated according to their affinities for the micelle micro-environment. If a positively charged surfactant is used, then similar resolution of neutral analytes can again be obtained, the only difference being that the EOF will be reversed owing to the adsorption of cationic surfactant molecules onto the capillary. The polarity of the separation voltage, therefore, needs to be reversed. The micelle-forming reagents for MEKC are not limited to synthetic detergents – any chemical with similar surface activity can be employed. These include biogenic surfactants such as bile salts (**Figure 10**), and as some synthetic high mass-to-charge polymers.

Affinity Capillary Electrophoresis (ACE)

Compared with other types of CE techniques, ACE represents a relatively recent development. Introduced in the early 1990s, ACE is performed on the basis of specific or non-specific affinity interactions between receptor and ligand molecules, typically biomolecules. Theoretically, if either receptor or ligand is a charge species, their binding complex would show a different electrophoretic mobility from that of the parent molecule due to the changes in charge-mass ratio. Thus, measuring the changes in electrophoretic mobility of the receptor via CZE mode provides an excellent way to study aspects of the receptor–ligand binding.

Depending on the binding strength of the receptor–ligand pair and the operational procedure, ACE

can be divided into three different categories, namely, non-equilibrium mode, dynamic equilibrium mode and immobilizing mode. Equilibrium ACE is well suited to studying strong binding systems, in which the sample is injected as an equilibrated mixture of receptor and ligand, whereas the electrophoresis medium contains only the supporting buffer. In such cases, CE serves merely as a tool to separate and determine the free and bound receptor molecules. Dynamic equilibrium ACE is typically employed for weak to moderate binding system, in which the receptor is injected as the sample, while ligand of varied concentration is incorporated in the running buffer. In this case, free and bound molecules are not separated due to the fast on-and-off kinetics, but rather, they are detected as single peaks. The immobilizing mode is self-explanatory, for which ligand is attached to the capillary wall, or more commonly, onto a supporting material via an appropriate bonding chemistry, while sample (receptor) is driven over the active surface by application of an electric field. Again, the migration behaviour of the receptor is a good indication of receptor–ligand interaction strength.

ACE has become a powerful tool in diverse fields, including the measurement of binding constants, the study of binding kinetics, the determination of interaction stoichiometry, the characterization of biomolecules and the separation of enantiomers, etc. ACE has been applied to the investigation of a number of biologically important systems, such as the interaction of polypeptides with immunoglobulins, polypeptides, carbohydrates, nucleic acids, drugs, etc.

ACE bears some resemblance to classical gel affinity electrophoresis and conventional affinity chromatography, in that they all utilize specific interactions to effect separations. However, ACE inherently has an unsurpassed advantages, that is, the buffer conditions (ionic strength and pH) can be finely tuned to give a perfect mimic of the real physiological environment, so that more precise characterisation of many binding processes is possible, provided the wall adsorption problem can be addressed properly.

Applications

The introduction of CE has resulted in a dramatic expansion of the applicability of electrophoresis as a separation tool. While conventional slab gel electrophoresis is mainly limited to the separation of biosubstances such as proteins and DNA fragments, CE has been utilized to resolve a much broader spectrum of substances, ranging from simple ions

through small molecules to macromolecules. High mass biomolecules such as proteins, DNA and polysaccharides can be separated by CZE as well as CGE. Smaller charged molecules such as amino acids, peptides, organic acids and amines can be resolved via CZE. Simple ions, both cations and anions, can be easily separated via CZE with conductivity detection. CZE separations of ions with indirect UV detection, dubbed as capillary ion analysis (CIA) has been accepted rapidly as an alternative to ion chromatography owing to its simplicity, speed and low cost. The separation of various neutral compounds has been made possible through MEKC or CEC. Chiral separations, an area hardly touched by conventional electrophoresis, is increasingly carried out by CE. Many chiral selectors (cyclodextrin derivatives, amino acids, proteins, optical micelles, etc.) may be added to the buffer solution to induce enantiodiscrimination based on one of several mechanisms (host-guest complexation, ligand exchange and solubilization by micelles, etc.). The unequal stability of dynamically formed diastereoisomers cause the optical isomers to be moved out of the capillary with different velocities, and enantioseparation is achieved. Because of its far-reaching capabilities, CE is becoming ubiquitous in almost all analytical fields.

Future Prospects

The introduction of CE in the early 1980s has had a huge impact on numerous scientific fields. It can be anticipated that in the future CE will continue to evolve into a fully fledged analytical technique that will benefit many research disciplines. Based on the characteristics of CE and its current status, several directions deserving special attention can be envisaged.

CE is hailed for its high column efficiency and outstanding mass sensitivity. The concentration sensitivity of CE remains relatively low compared to HPLC, thus limiting its applications in areas such as trace impurity determination and environmental analysis. Therefore, improving the detection sensitivity will continue to be a topic for development. Creative detection configurations, interplay from micro-mechanic and microelectronics, together with advancement of light sources, may remarkably enhance the sensitivity of optical detection. To facilitate the use of electrochemical detection, efforts must be made to provide better microelectrodes with reasonable ruggedness. With the enhanced performance and reduced cost, a more common use of sophisticated hyphenation techniques such as CE-MS is expected.

On the other hand, the ability of CE to handle extremely small sample quantities is attractive for the direct probing of micro-entities. The recently emerged single cell analysis is a good example of this. With further improvements in sampling techniques and detection schemes, it is believed that in the near future, CE-based methodologies will allow us to investigate the chemistries of a wider spectrum of cells, thus enriching our knowledge about many biological processes essential to life.

Finally, due to its instrumental simplicity, CE is amenable to further miniaturization. CE on a glass chip has been successfully demonstrated by borrowing microfabrication concepts from the microelectronics industry. These devices feature the integration of injection, separation and detection, as well as sophisticated designs with intricate patterns and multi-channel arrays, thus producing an unprecedented analytical platform which is fully manipulated by applying voltages. As the plate format possesses an excellent ability for heat dissipation, electric fields up to 2000 V cm^{-1} may be applied across the separation channels, hence shortening the analytical time scale to minutes or even seconds. With continuous maturity of relevant technologies, such an ultra-high speed separation method may provide a solution to some formidable tasks including DNA sequencing.

See also: **II/Electrophoresis:** Electrochromatography Thin Layer.

Further Reading

- Baker DR (1995) *Capillary Electrophoresis*. New York: Wiley.
- Engelhardt H, Beck W and Schmitt T (1996) *Capillary Electrophoresis: Methods and Potentials*. Braunschweig/Wiesbaden: Vieweg.
- Guzman NA (ed.) (1993) *Capillary Electrophoresis Technology*. New York: Marcel Dekker.
- Jorgenson JW and Phillips M (eds) (1987) *New Directions in Electrophoretic Method*. Washington, DC: American Chemical Society.
- Kevin DA (ed.) (1996) *Capillary Electrophoresis Guidebook: Principles, Operation and Applications*. Totowa, NJ: Humana Press.
- Kuhn R and Hoffstetter-Kuhn S (1993) *Capillary Electrophoresis: Principles and Practice*. Berlin/New York: Springer-Verlag.
- Landers JP (ed.) (1997) *Handbook of Capillary Electrophoresis*, 2nd edn. Boca Raton, FL: CRC Press.
- Li SFY (1992) *Capillary Electrophoresis: Principles, Practice and Applications*. Amsterdam: Elsevier.
- Vindeogel J and Sandra P (1992) *Introduction to Micellar Electrokinetic Chromatography*. Heidelberg: Huthig.
- Weinberger R (1993) *Practical Capillary Electrophoresis*. Boston: Academic Press.

Capillary Electrophoresis Detection

See II/ELECTROPHORESIS/Detectors for Capillary Electrophoresis

Capillary Electrophoresis–Mass Spectrometry

M. Hamdan, GlaxoWellcome Medicines Research Centre, Verona, Italy

P. G. Righetti, University of Verona, Verona, Italy

Copyright © 2000 Academic Press

Introduction

Capillary zone electrophoresis (CZE) is widely recognized as a powerful analytical technique in its own right, known for its high separation efficiency, short analysis times and low-volume sample requirements. These characteristics made CZE a popular method for the analysis of peptide mixtures, protein digests, drug substances and biotechnological products. The coupling of CZE with electrospray ionization mass spectrometry (ESI–MS), first reported by Olivares *et al.* in 1987, has added further capabilities, in particular for obtaining molecular mass information and structural details when tandem mass spectrometry (MS–MS) is used. However, it can be said that the major advantage of such coupling is that the migration time is not the only parameter used for identifying the eluted components. These times are subjected to variations between runs, yet such variations become irrelevant when, in the same run, highly diagnostic mass spectra are obtained.

Depending on the ionization method, CZE can be coupled to a mass spectrometer either directly (online) or indirectly (offline). In the latter mode of operation, ^{252}Cf plasma desorption and matrix assisted laser desorption can be used. The online coupling of CZE is more common and usually performed by electrospray ionization (ESI) or fast atom (ion) bombardment (FAB). Although online CZE/MS is the more common form of application, offline analysis has the advantage of allowing separation in non-volatile buffers, which are highly undesired in ESI.

It goes without saying that every analytical technique has its limitations and CZE/MS is no exception. One of the main limitations of this experimental arrangement is its relatively poor sample concentration/ion sensitivity. Approaches to reduce such limitations included online preconcentration, sample

stacking, and the increasing use of time-of-flight (TOF) analysers which use ESI and TOF analysers with and without a quadrupole in between. The innovative feature of this class of instruments is their fast scanning, which allows the acquisition of a number of full spectra per second. Additionally, as all ions in each spectrum are sampled at the same moment in time, spectra are free of mass discrimination or peak skew typical of slow scanning systems that must scan over a narrow chromatographic/electrophoretic peaks.

Capillary electrochromatography (CEC) is another technique which is currently undergoing a rapid phase of advancement and development. This technique was revived by Jorgenson and Lukacs in 1981; these authors used 0.005 mol L^{-1} phosphate buffer, $170 \mu\text{m}$ packed column and 30 kV separation voltage to separate 9-methylanthracene and perylene. This technique has recently become more diffuse because of a number of advances in both CE instruments and detection techniques including electrospray mass spectrometry. However, on-column UV detection and in-column laser-induced fluorescence detection remain the most commonly used methods. Despite its high sensitivity, the latter method is subjected to interferences by buffer fluorescence. In MS detection, the column is commonly packed right up to the point where the sample is injected into the mass spectrometer. The combination of CEC with mass spectrometry provides reliable molecular weights and in many cases structural information, which makes it highly attractive for a wide range of applications. For more details on this topic, the reader is referred to recent extensive reviews, covering the methodology of CEC and its coupling to MS, by Colòn *et al.* (1997) and Rentel *et al.* (1999). Interestingly, packed-CEC offers the possibility of higher sample capacity and the utilization of simpler mobile phases, which are more compatible with MS.

Experimental Aspects

One of the main advantages of CZE is that it requires simple instrumentation, which generally consists of

a high-voltage power supply, two buffer reservoirs, a capillary and a detector. Coupling of such instrumentation to a mass spectrometer requires the replacement of one of the buffer reservoirs with a suitable interface and some simple electronic circuit to accommodate the presence of an additional 3–5 kV required for the operation of the ion source.

Interfacing CZE to a mass spectrometer has been effected in a number of ways, yet all of them can be traced to two general configurations: liquid junction interface and coaxial sheath flow. The liquid junction interface, first described by Minard *et al.* in 1988, was used to couple a CZE to a continuous-flow FAB source. In such a configuration the CE capillary terminates in a 20 μm block that contains either the matrix solution for FAB ionization or the sheath solution for ES ionization. The inlet of the transfer capillary is aligned in close proximity to the cathode end of the CE capillary, an alignment considered critical, since the gap must be sufficiently wide to allow enough matrix or sheath fluid to maintain a stable ion beam. On the other hand, the same gap should be small enough to prevent analyte diffusion, upon exiting the CE capillary, which would otherwise result in peak broadening. The main disadvantage of this configuration is associated with the dead volume caused by a long transfer line which together with the mixing effects in the interface and the presence of the FAB matrix renders the separation efficiency of this interface poorer than that of the coaxial sheath flow. Liquid-junction interface has been redesigned to allow easier mounting and alignment of the CE and continuous-flow FAB capillaries. The same interface was further modified by Caprioli *et al.* in 1989, who

used it for the analysis of synthetic mixtures of peptides and protein digests.

The first successful coupling of CE with MS was effected by Olivares *et al.* in 1887, wherein the cathode end of the CE capillary terminated within a stainless-steel capillary which completed the electrical circuit and established contact with the CE side. An improved version of this interface was developed by the same research group, where the metal contact at the CE terminus was replaced by a thin sheath of liquid flow. In comparison with the liquid-junction interface, the coaxial sheath-flow interface provided both better sensitivity and better resolution, yet this did not mean that the interface was trouble free. A number of difficulties can derive from the use of sheath liquid: ionic and neutral species within this liquid compete for protonation in the ESI process, thus lowering the overall sensitivity. The composition of the sheath liquid commonly includes a volatile organic acid (1% formic or acetic acid) in a mixed water–organic solvent, a composition which is different from that of the electrophoretic buffer. During the CE, sample ions and other species present in the buffer exit the capillary at the MS end, and, simultaneously, counterions from the liquid sheath enter the column and migrate toward the injection end. These moving ion boundaries can influence migration order, times and resolution. The same phenomenon has the advantage of allowing some analysis in the presence of difficult-to-spray electrolytes (such as phosphate- or borate-containing buffers).

Figure 1 gives the up-to-date version of a commercial coaxial sheath-flow interface constructed and marketed by Micromass (Manchester, UK).

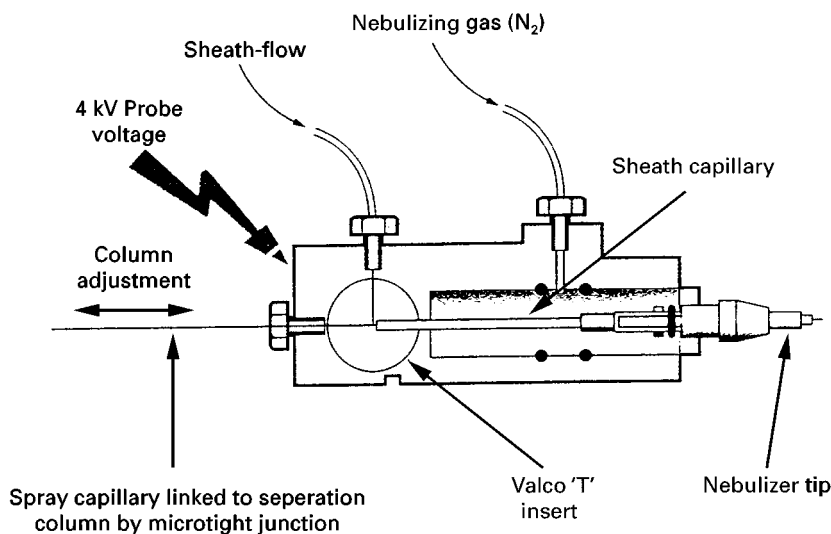


Figure 1 The main components of a sheath-flow probe which can be used to couple CZE to a Q-TOF or to a single/triple quadrupole instruments. (Courtesy of Micromass, Manchester, UK.)

Representative Examples

CZE/MS in Peptide Analysis

One of the advantages of coupling CZE to ES mass spectrometry is the formation of multiply charged ions which allows simple analysers such as quadrupoles to measure the mass to charge ratios (m/z) of relatively large biomolecules. Indeed, the majority of CZE/MS applications have been in the field of biological and biochemical research. A number of reports have appeared on the characterization of synthetic mixtures of peptides and proteins, where the unusually high resolution of CZE permits the separation of sequences which may differ by a single amino acid residue. This advantage has been exploited in the use of CZE/ES–MS to examine a number of reaction mixtures of peptides obtained by solid-phase synthesis; two representative examples are considered here. A reaction mixture obtained by solid-phase synthesis of neuropeptide Y (NPY) analogue, [Leu³¹, Pro³⁴]-NPY. This peptide has 36 amino acid residues, a relative molecular mass of 4222 and is known to play a major role in the central and peripheral nervous system. Online CZE/ES–MS analysis of this mixture resulted in a fairly complex UV and total ion current (TIC) electropherograms which, in addition to the target peptide, contained a number of side products. The use of mass spectrometry allowed reliable identification of all the components of the mixture, although some of the side products differed by a single amino acid residue in sequences containing over 30 residues. These measurements allowed unambiguous identification of the various components of the mixture which are summarized in **Table 1**.

A second and less complex reaction mixture associated with the same synthesis was also examined by the same technique which yielded the total ion current electropherogram in **Figure 2(A)**. Deconvolution of the mass spectra in **Figure 2** (panels 1–4) yielded the relative molecular masses 4222 (1), 2441

(2), 3577 (3) and 3789 (4). The first molecular mass coincides with the desired peptide, while the other three masses are associated with a number of incomplete sequences which are summarized in **Table 2** which clearly shows an excellent agreement between the calculated and measured masses, fully based on CZE/MS measurements. Given the complex procedure associated with solid-phase synthesis of peptides, it is evident that the use of online CZE/MS is an indispensable analytical tool for the initial characterization of the product and for providing a reasonable indication on the yield of synthesis.

CZE/MS can also give reliable information on unexpected processes in the course of solid-phase synthesis of peptides. To underline this statement, two cases are considered. A series of newly synthesized peptides investigated, corresponding to portions of the extracellular domain of human granulocyte-macrophage colony-stimulating factor receptor α -subunit. A solution containing 3 mg mL⁻¹ of the peptide [PRAKHSVKIRAADVRLN], $M_r = 2084$, was examined by full-scan CZE/MS, which yielded UV and TIC electropherograms, each of which contained three peaks of almost equal relative heights. The associated ES mass spectra revealed the presence of the desired peptide together with its acetylated version in one of the three TIC peaks. It is fair to say that without the use of online MS detection, the identification of the latter component would have been very unlikely. A second case refers to online CZE/MS of an NPY analogue which exhibited a TIC electropherogram containing seven peaks, two of which yielded $M_r = 4222$ which implied the presence of two different configurations of the same sequence within the same crude of synthesis. This deduction was found in accord with existing literature describing undesirable side products observed in solid-phase synthesis of peptides and small proteins. One such side product can be invoked by the formation of succinimide of the Asp residue (β -aspartyl peptide) which, in the present case, has the same M_r as the

Table 1 Proposed peptide sequences, corresponding to relative molecular masses (M_r) obtained from the ES mass spectra associated with various peaks in a TIC electropherogram obtained by online CZE/MS of NPY analogue reaction mixture

Peptide chain	M_r calculated	M_r measured	Proposed sequence
Ac [Leu ³¹ ,Pro ³⁴]-NPY	4222	4222 \pm 1	Ac-YPSKPDNPGEDAPAEDLARYYSALRHYINLLTRPRY-NH ₂
H-12-36-NH ₂	3022	3022 \pm 1	H-APAEDLARYYSALRHYINLLTRPRY-NH ₂
Ac[Leu ³¹ ,Pro ³⁴]-NPY	4222	4222 \pm 1	Ac-YPSKPDNPGEDAPAEDLARYYSALRHYINLLTRPRY-NH ₂
Ac(5-36)	3789	3789 \pm 1	Ac-PDNPGEDAPAEDLARYYSALRHYINLLTRPRY-NH ₂
Ac(4-36)	3917	3917 \pm 1	Ac-KPDNPGEDAPAEDLARYYSALRHYINLLTRPRY-NH ₂
Ac(3-36)	4004	4004 \pm 1	Ac-SKPDNPGEDAPAEDLARYYSALRHYINLLTRPRY-NH ₂
Ac(20-36)	2440	2441 \pm 1	Ac-YYSLRHYINLLTRPRY-NH ₂
Ac(7-36)	3577	3577 \pm 1	Ac-NPGEDAPAEDLARYYSALRHYINLLTRPRY-NH ₂
Ac(5-36)	3789	3789 \pm 1	Ac-PDNPGEDAPAEDLARYYSALRHYINLLTRPRY-NH ₂

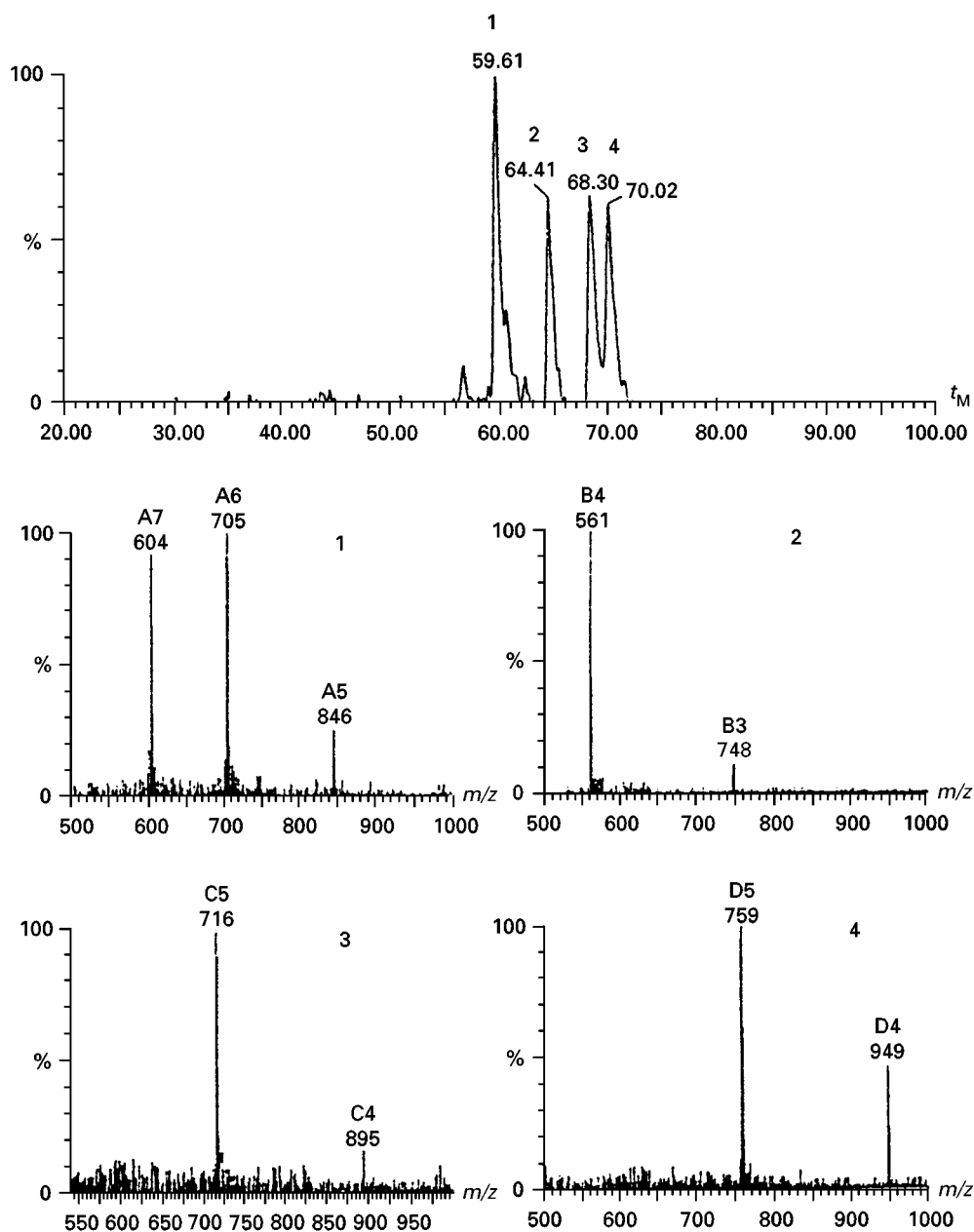


Figure 2 Upper frame: total ion current (TIC) electropherogram of a crude of synthesis associated with [Leu³¹,Pro³⁴]-NPY. Lower frames: associated positive ES mass spectra of the TIC peaks: (1) t_M = 59.61 min; (2) t_M = 64.41 min; (3) t_M = 68.30 min; and (4) t_M = 70.02 min.

NPY analogue. The mechanism responsible for such reaction is depicted in Figure 3.

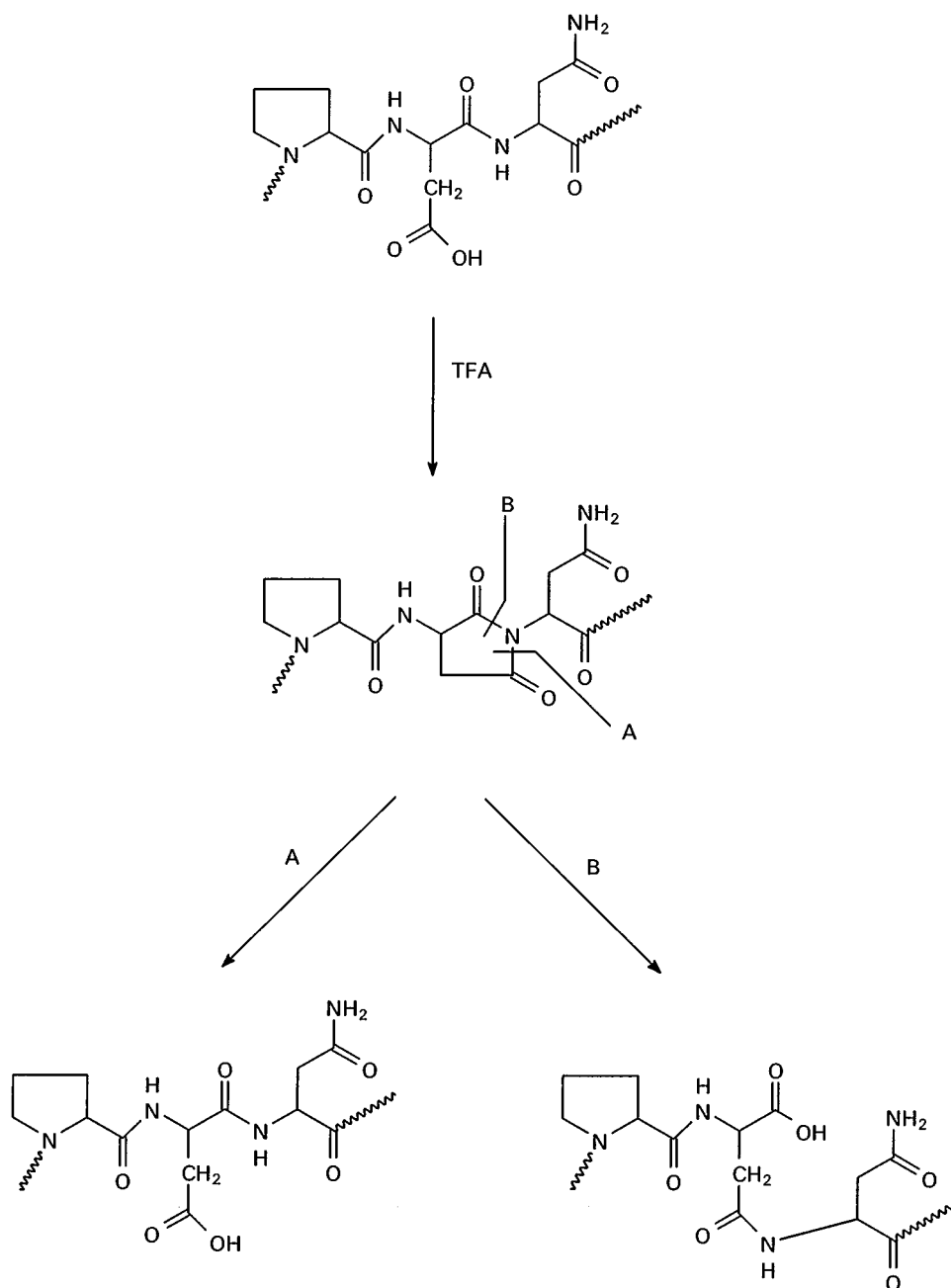
Forensic Application of CZE/MS

Most drugs of forensic interest are commonly analysed by GC/MS or extraction followed by IR analysis. Separation of benzodiazepines and ergot alkaloids by GC is difficult and differences in the IR

spectra are small. On the other hand, the analysis of these compounds by CE/MS is characterized by short analysis times and specific MS information. Forensic drug chemists, investigating drugs of abuse, also find the analysis of drugs such as LSD challenging because of microgram quantity dosage and the fact that GC/MS analysis is rather demanding owing to column adsorption and thermal lability. This is also true for psilocybin, the psychoactive agent in certain

Table 2 Proposed peptide sequences, corresponding to relative molecular masses (M_r) obtained from the ES mass spectra associated with the components arising from the synthesis of [Leu³¹,Pro³⁴]-NPY

Peptide chain	M_r calculated	M_r measured	Proposed sequence
Ac[Leu ³¹ ,Pro ³⁴]-NPY	4222	4222 \pm 1	Ac-YPSKPDNPGEDAPAEDLARYYSALRHYNLLTRPRY-NH ₂
Ac(20–36)	2440	2441 \pm 1	Ac-YYALSALRHYNLLTRPRY-NH ₂
Ac(7–36)	3577	3577 \pm 1	Ac-NPGEDAPAEDLARYYSALRHYNLLTRPRY-NH ₂
Ac(5–36)	3789	3789 \pm 1	Ac-PDNPGEDAPAEDLARYYSALRHYNLLTRPRY-NH ₂

**Figure 3** Representation of succinimide formation using partial sequence containing Asp⁶ and two adjacent amino acids, Asn⁷ and Pro⁵ taken from the sequence of [Leu³¹,Pro³⁴]-NPY. (Reproduced with permission of John Wiley & Sons Ltd.)

mushrooms, owing to the presence of the highly labile phosphate moiety. The absence of complex preparative extractions for CE analysis of both drugs allows their separation without causing undesired decomposition.

The fact that many forensic drugs have closely related isomeric structures renders CE/MS a powerful tool for their separation and identification. For instance, phenethylamines are historically a difficult group to analyse due to the large number of isomers including both D- and L-optical isomers. Twelve optical isomers of ephedrine, pseudoephedrine, norephedrine, norpseudoephedrine, amphetamine and methamphetamine have been separated in under 30 min using CE. It is worth noting that this class of compounds tends to give strong $[M + H]^+$ signals in ES ionization which makes them ideal for CZE/MS analysis.

A separation of 18 common drugs of abuse was accomplished in less than 40 min using CE buffered with phosphate/borate, with sodium dodecyl sulfate (SDS) as a micellar phase and acetonitrile as an organic modifier. The main advantage of this method over other screening techniques is that acidic, basic and neutral drugs can be screened through a single analytical method, where extraction procedures are unnecessary.

Clandestine manufacturers of illegal drugs pose additional challenges to the forensic scientist, since samples submitted for analysis tend to contain complex mixtures of chemicals, including thermally reactive and labile components. CZE with and without MS detection can be a powerful tool for such type of analysis. For example, the frequently encountered methamphetamine can be analysed by CE allowing the identification of its isomeric composition which can be eventually used to construct evidence concerning its synthetic pathway and the source of the sample.

An additional problem with samples from clandestine laboratories is the presence of unreacted precursors and adulterants that may interfere with the analysis of the target compound(s). For instance, under typical GC/MS conditions, certain mixtures of chemicals associated with methamphetamine will derivatize the illegal drug to a compound that is not controlled, resulting in an inconclusive analysis. Using a number of CE methods, such interference can be easily avoided.

CZE/MS is also highly suitable for the analysis of biological samples which may contain traces of illegal drugs or poisons in a complex matrix. Extensive reviews cite over sixty references on the use of CE for the analysis of drugs in biological samples including drugs of abuse in urine, cocaine and morphine in hair

and barbiturates in serum. Other examples include the chiral separation of racemethorphan and racemorphan in urine using a cyclodextrin/SDS/propanol buffer and the micellar CE separation of nitrazepam and its metabolites in urine. An extensive review is available on the use of CZE coupled to tandem mass spectrometry to identify a variety of drugs and metabolites. All these reviews are listed in the **Further Reading**.

Forensic Analysis of Inorganic Explosives

Capillary electrophoresis is also widely used in the analysis of inorganic ions in criminal cases, material such as black powder, flash powder, ammonium nitrate and home-made explosive mixtures. The inorganic anions resulting from an explosive reaction of such materials are among the most important evidence used to determine the nature of an inorganic explosive. For many years, the most powerful tool in these investigations was ion chromatography (IC). The introduction of CE for anion analysis provided a simpler, faster and slightly more sensitive technique for performing such analysis. It is interesting to note that CE separations are based on differences in charge-to-mass ratios of the solvated ions, while IC separations are the result of complex interactions between the ions and the stationary phase. As a result, the migration order is quite different in the two methods and a nearly orthogonal relationship exists between the relative retention times.

The reliable analysis of certain alkyl-substituted organophosphorus acids, which are the primary hydrolysis products of neurotoxic agents, has become very important in the last few years owing to the likelihood of an international agreement that will forbid the development, production and stockpiling of chemical warfare agents and weapons. CZE coupled to ion spray mass spectrometry was applied in the negative ion mode to investigate five organophosphonic acids, which are the primary hydrolysis products of neurotoxic agents. The MS spectra exhibited a very abundant $[M - H]^-$ signal with minimal fragmentation. The authors reported sensitivity in the range 10–30 pg using the single-ion recording (SIR) mode.

Conclusions

The examples cited in this work have to be considered as only a part of the capabilities of CE with and without MS coupling. The literature cites varied areas of application of such powerful methodology. As new applications of CE continue to appear, the

advantages and importance of CE in conjunction with mass spectrometry have also become appreciated. Analytical chemists are faced with the challenge of increasing sample complexity and decreasing sample quantities. Because of the complexity observed with most biological mixtures, there continues to be a need for the development of a highly efficient separation technique in conjunction with a sensitive and specific detector. The low quantities of analytes often available require nanoseparation techniques. The mass spectrometer is a selective and broadly applicable detector for analytical separations. It can provide information regarding the structure of unknown components present in a sample mixture with high specificity and sensitivity. The coupling of CE with MS combines the extremely high-resolving power and structural information in one system. Like any other separation technique such as GC–MS and LC–MS, the principal advantage of CE–MS is that analytes are identified by both their differential separation and their molecular masses and/or fragmentation patterns. An analytical separation that precedes MS analysis is often necessary to assure correct interpretation of the mass spectral data.

Fast, high-efficiency separation techniques are becoming ever more important in the race to discover new drugs. The potential complexity of libraries produced by automated parallel synthesis, combinatorial and genetically manipulated natural product chemistries are driving many developments in separation sciences.

CE, CEC and nano-LC are all potential candidates for such analyses and each has a requirement for a fast, sensitive detection system.

Further Reading

Aumatell A and Wells RJ (1993) *Journal of Chromatographic Science* 31: 502–508.

- Cai J and Henion J (1995) *Journal of Chromatography A* 703: 667–692.
- Caprioli RM (1990) *Continuous-Flow Fast-Atom Bombardment*. New York: John Wiley.
- Caprioli RM, Moore WT, Martin M, DaGue BB, Wilson K and Moring S (1989) *Journal of Chromatography* 480: 247–257.
- Casazza A, Curcuruto O, Hamdan M, Bisello A and Peggion E (1995) *Journal of Chromatography A* 715: 227–240.
- Colòn LA, Reynolds KJ, Alicea-Maldonado R and Fermier AM (1997) *Electrophoresis* 18: 2162–2174.
- Foret F, Thompson TJ, Vouros P, Karger BL, Gebauer P and Bocek P (1994) *Analytical Chemistry* 66: 4450–4458.
- Karas M, Bahr U and Giessmann U (1991) *Mass Spectrometry Review* 10: 335–358.
- Kostiainen R, Bruins AP and Hakkinen VMA (1993) *Journal of Chromatography* 634: 113–118.
- Lurie IS (1992) *Journal of Chromatography* 605: 269–275.
- McCord BR, Hargadon KA, Hall KE and Burmeister SG (1994) *Analytica Chimica Acta* 288: 43–56.
- Northrop DM, McCord BR and Butler JM (1994) *Journal of Capillary Electrophoresis* 1: 58–168.
- Olivares JA, Nguyen NT, Yonker CR and Smith RD (1987) *Analytical Chemistry* 59: 1230–1232.
- Rentel C, Gfroerer P and Bayer E (1999) *Electrophoresis* 20: 2329–2336.
- Rovatti L, Curcuruto O, Hamdan M, Cassano E, Galoppini C and Rovero P (1996) *Rapid Communications in Mass Spectrometry* 10: 1504–1508.
- Sundqvist B and MacFarlane RD (1985) *Mass Spectrometry Review* 4: 421–460.
- Tagliaro F, Aiello C, Dorizzi R, Ghielmi S and Marigo M (1993) *Journal of Chromatography* 638: 303–309.
- Thormann W, Maier P, Marcolli C and Binder F (1991) *Journal of Chromatography* 545: 445–460.
- Thormann W, Molteni S, Caslavská J and Schutz A (1994) *Electrophoresis* 15: 5–12.
- Wernly P and Thormann W (1991) *Analytical Chemistry* 63: 2878–2882.

Capillary Electrophoresis–Nuclear Magnetic Resonance

K. Pusecker and J. Schewitz, University of Tübingen, Tübingen, Germany

Copyright © 2000 Academic Press

Miniaturization is an important current trend in separation science and the development of capillary elec-

trophoresis (CE), capillary HPLC (cHPLC) and capillary electrochromatography (CEC) are milestones in this respect. The electrophoretic techniques especially can achieve rapid and efficient separations using only very small volumes and they have become research tools with widespread applications. The advantages of this miniaturization are obvious: less sample is

required, less solvent is consumed, and the separation times are shorter.

The second trend in separation science is toward information-rich detection modes. Although UV-VIS fluorescence, and electrochemical detectors provide sensitive and simple detection, the information is generally not sufficient for unequivocal characterization or structural elucidation of compounds. For this purpose the coupling of capillary separation methods with electrospray mass spectrometry (ESI-MS) has proven to be highly successful. ESI-MS is an extremely sensitive detector and in many cases information about mass and fragmentation gives detailed structural information.

The enormous sensitivity gain in nuclear magnetic resonance (NMR) spectroscopy in recent years also enables the wider application of directly-coupled HPLC–NMR. NMR spectroscopy is considered one of the most powerful methods for determining chemical, dynamic, and spatial structural properties of organic compounds. Its capability to distinguish between most structural, conformational, and, in special cases, optical isomers is highly complementary to the information gained from MS experiments. NMR spectroscopy is nondestructive and spectra are recorded in solution. A combination with additional detectors is possible, e.g. HPLC–UV–NMR, HPLC–MS–NMR.

The miniaturization of liquid chromatography (LC)–NMR has additional advantages. The small volumes of eluent consumed in capillary separation techniques make the use of fully deuterated solvents economically feasible. Therefore, problems associated with protonated solvents are prevented. NMR solvent suppression techniques which can lead to distortion of parts of the spectra are no longer necessary. Thus, the entire range of the ^1H -NMR scale can be used in one- and two-dimensional experiments. The supplementary benefit of conserving material is particularly interesting for valuable samples, such as natural products or labelled proteins.

However, the NMR spectrometer is one of the least sensitive of all possible LC detectors. The miniaturization of the LC–NMR coupling for the application of capillary separation techniques requires a reduction of the detection volume by a factor of approximately 1000 in comparison to conventional LC–NMR systems. On these conditions, the techniques seemed to be incompatible. Despite these problems, because of the great potential of the technique, efforts have been made in the past few years to enable coupling of capillary techniques to NMR spectroscopy. To date, two different experimental approaches have been developed and evaluated. They differ mainly in the type of radiofrequency (rf) coil that is used for the

NMR detection. This variation leads to different strengths and weaknesses of the two systems, which allow or hinder their use for particular applications.

Set-up for CE–NMR Coupling

The design of an interface for the coupling of capillary separation techniques with NMR spectroscopy is simple in principle. Since phase transfer is not necessary, detection can be carried out in the fused-silica capillary, which is used for CE separation. The detection takes place on-column similar to a common UV detection. The capillary is built into an NMR probe head. Even the inlet and outlet vials of the CE can be incorporated inside this probe, but for practical reasons to allow easy sample loading, it is more useful to retain the inlet outside the NMR spectrometer. In any case both vials are maintained at the same height to avoid siphon flow. The separation equipment, e.g. power supply or HPLC pump, have to be placed outside the magnetic field. High voltage is applied to one end of the capillary and the other vial is grounded. With vials outside the magnet (inlet vial or both vials) a capillary length of approximately 150–200 cm is required. This means the capillary is three to four times longer than a common CE capillary.

The limiting factor of the whole system is the low sensitivity of the NMR spectroscopy. The parameters that affect the detection limit are the type and size of the radiofrequency coil, the detection volume, and the so-called filling factor, the ratio of coil and sample volume. A optimal detection cell fills the purpose-built microcoil completely. Furthermore, the inner diameter of the used fused-silica capillaries have to fulfill the chromatographic requirements. Especially for electrophoretic techniques, the inner diameter of the capillaries is therefore limited ($\leq 100\ \mu\text{m}$) and the size of the coil has to be adapted to these requirements.

Two different microcoil NMR configurations have been used for online coupling of capillary separation techniques with NMR spectroscopy. One approach is based on a solenoid rf coil wound directly on the CE capillary (Figure 1). The detection volume for the system is thereby determined by the inner diameter of the capillary and the length of the coil. With $75\ \mu\text{m}$ capillaries and a typical coil length of approximately 1 mm, detection volumes of 5–8 nL are obtained. Solenoid coils are positioned in a horizontal direction in the NMR spectrometer, perpendicular to the main magnetic field. The other approach uses saddle-type rf coils (Figure 2). The detection unit consists of a coil fixed onto a glass tube, into which the capillary is inserted. Due to technical problems, the reduction of

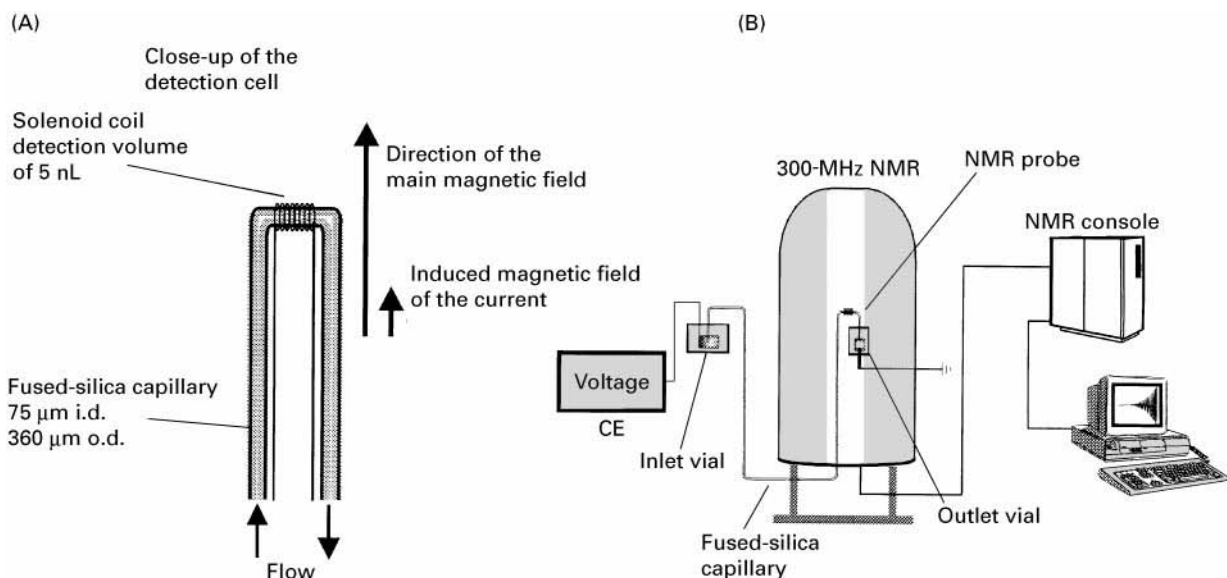


Figure 1 (A) Solenoid NMR interface. (B) Instrumentation of the solenoid NMR probe system. Adapted with permission from Gfrörer *et al.* (1999) *Analytical Chemistry News and Features* 71: 315A–321A, and Olsen *et al.* (1999) *Analytical Chemistry*, 71: 3070–3076.

the coil diameter is restricted. The smallest available coils have diameters of 1.5–2.0 mm and a length of 5–9 mm. To optimize the filling factor, special NMR capillary cells have been fabricated to a predetermined size by etching a standard fused-silica capillary with a HF solution only in the detection region. While the inner diameter in this part was widened, the rest

of the capillary remained nearly the original diameter of 75 μm allowing the application of electrophoretic separation techniques. By varying the duration of etching, detection volumes between 180 and 440 nL were obtained. In contrast to the solenoid coil, the saddle coil is situated vertically in the NMR spectrometer, parallel to the main magnetic field.

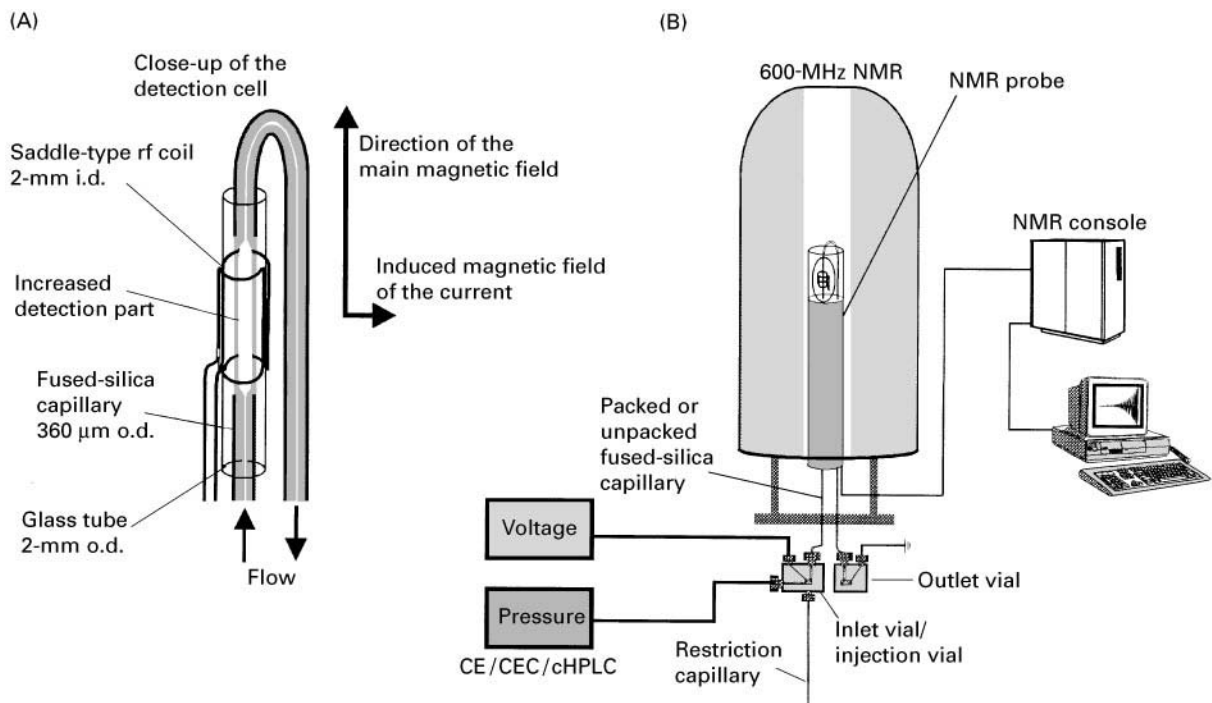


Figure 2 (A) Saddle-type NMR interface. (B) Instrumentation of the saddle-type NMR probe system. Adapted with permission from Gfrörer *et al.* (1999) *Analytical Chemistry News and Features* 71: 315A–321A.

Development of the Solenoid NMR Probe System

In 1994 Wu *et al.* described the first capillary electrophoresis NMR system with a solenoid rf microcoil. The coils were produced by winding copper wire around fused-silica capillaries with inner diameters of 75–530 μm . The resulting NMR detection cells had volumes of 5–200 nL. The possibility of an online NMR detection was shown for CE separation of amino acids. The set-up was not suitable for routine operation, e.g. each sample had to be loaded externally, after which the probe was inserted. The structural information of the NMR spectra was limited due to large line widths (7–200 Hz). The electrophoretic current had a clear effect to the NMR line width.

Further developments of this solenoid system focused on the NMR detection of mass limited samples. In 1995, Olson *et al.* presented a new microcoil design. Several modifications were devised to obtain higher resolution. The fabrication of the coil was slightly changed and the outer diameter of the capillary was increased (357 μm o.d., 75 μm i.d.). The main improvement was the reduction of the effect of magnetic susceptibility caused by the proximity of the rf coil to the sample. A perfluorinated organic liquid was used to match the susceptibility of the surrounding medium to that of the coil material. This lowered the static magnetic field inhomogeneities in the sample and thus improved resolution and line shape (line width < 1 Hz). As a consequence of the improved resolution, the sensitivity of the system increased. Limits of detection in the range of 100 pmol were reported for arginine, sucrose and a seven amino acid peptide using a 5-nL detection cell.

In 1998 Subramanian *et al.* presented solenoid microcoil probes for direct or inverse ^{13}C -NMR detection. Heteronuclear NMR techniques are an important component in determining full-structure information on unknown compounds. Due to the low relative sensitivity of ^{13}C -NMR, the detection volume was increased in comparison to the previous design. Capillaries with inner diameters of 700 μL were used for the fabrication of the probe. The resulting detection cells had volumes of 550–1200 μL . The natural-abundance ^{13}C -NMR limit of detection was below 100 nmol. One-dimensional ^{13}C -NMR spectra and two-dimensional ^1H - ^{13}C inverse-correlation NMR spectra were acquired using samples in the tens of micrograms range.

In 1999, Olson *et al.* applied the optimized NMR interface for CE–NMR coupling. Arginine, glycine and triethanolamine were used as model compounds

to investigate in more detail the influence of the electrical current on the NMR signals. It was confirmed that for geometries, in which capillary and static field are not parallel, the electrophoretic current induces a magnetic field, which degrades the spectroscopic information obtainable from the CE–NMR spectra. To circumvent this effect, the electrophoretic voltage was periodically interrupted to obtain high resolution spectra. In addition, different sample-loading techniques including field-amplified stacking for sample preconcentration, were evaluated. Flow profiles were observed by the detection of the water signal of the loaded samples.

Development of the Saddle-type NMR Probe System

First results of this approach were reported by Behnke *et al.* in 1996. The LC capillary was mounted inside a modified NMR microprobe equipped with a 2.5-mm double-saddle Helmholtz coil. In static NMR experiments, a line width of 3 Hz could be achieved in 75- μm i.d. capillaries. However, this arrangement adversely affected the filling factor of the system and thus the sensitivity using this configuration was reduced significantly. First, coupling experiments with this system were performed with cHPLC. In comparison with CE, cHPLC provides a higher sample capacity and offers the possibility of peak preconcentration by the application of gradient elution. Online and stopped-flow NMR experiments of dansyl amino acids were carried out in 315- μm i.d. capillaries.

The sensitivity of the saddle-type system was improved by Schlotterbeck *et al.* in 1997. Decreasing the inner diameter of the rf coil from 2.5 to 2 mm improved the filling factor and thus the sensitivity and the line shape of the system. For online cHPLC–NMR experiments, the inner diameter of the capillary was increased to 180- μm i.d. in the detection region and this led to a limit of detection of 150 pmol. The feasibility of the interface was proved by its application to vitamin derivatives. The structure of a so-far unknown kitol, a retinyl acetate dimer, was determined from one- and two-dimensional ^1H -NMR spectra in both continuous and stopped-flow measurements.

In 1998 the configuration was modified for the application of electrophoretic techniques by Pusecker *et al.* The most important alteration was a purpose-built CE–NMR capillary. This capillary had a detection cell with an inner diameter of 190 μm corresponding to a detection volume of 240 nL, whilst the rest of the capillary still had the usual CE diameter of approximately 75 μm . CE–NMR measurements proved that for the saddle geometry, in which capillary and static magnetic field are parallel, the

spectroscopic information is not degraded by a magnetic field gradient induced by the electrophoretic current. The suitability of the configuration for electrophoretic methods was investigated by the application of CE and CEC–NMR spectroscopy to model systems. The favourable capabilities of the CEC–NMR coupling in view of the increased sample capacity and separation efficiency were demonstrated for the separation of five alkyl benzoates.

The optimization of the filling factor by a further increase of the detection volume to 440 nL improved sensitivity and line shape. A line width < 0.8 Hz was reported by Schewitz *et al.* The system was applied to the analysis of mixtures of pharmaceuticals and drug metabolites, nucleotides, peptides, natural products and ingredients of soft beverages. The possibility of CE stopped-flow NMR experiments was shown for an adenosine dinucleotide. The flow was halted by switching off the voltage at a retention time corresponding to the first NMR signals of the dinucleotide. By means of this stopped-flow mode, it is possible to accumulate spectra for a longer period of time. This enables the acquisition of two-dimensional NMR experiments. These techniques are substantial in determining full-structure information on unknown compounds. As an example, the two-dimensional TOCSY

NMR spectrum of the adenosine dinucleotide is shown in Figure 3. In this spectrum cross-peaks indicate those protons which are coupled to each along an unbroken chain of couplings. Hence the coupling of each desoxyribose is clearly observable in two separate spin-coupling connectivities.

In 1999, a final improvement was made by Gfrörer *et al.* who coupled a gradient-elution CEC–NMR system to the interface. As an example, Figure 4 shows the CEC–NMR separation of paracetamol metabolites extracted from human urine. The result is viewed as a contour plot with the CEC separation time on the vertical axis and the chemical shift on the horizontal axis. The peaks that spread throughout the figure arise from the residual water and acetonitrile in the deuterated solvents of the buffer. In addition, sets of peaks related to paracetamol and endogenous material are observed. Those marked (1) can be assigned to the paracetamol glucuronide. Clear identification is possible via the diagnostic shifts of the glucuronic acid at $\delta = 3.8$ and 4.2. The component marked (2) is the paracetamol sulfate. The NMR spectrum of the third compound is consistent with the endogenous material hippurate (3). The appropriate individual rows taken from the contour plot are shown on the right-hand side of Figure 4.

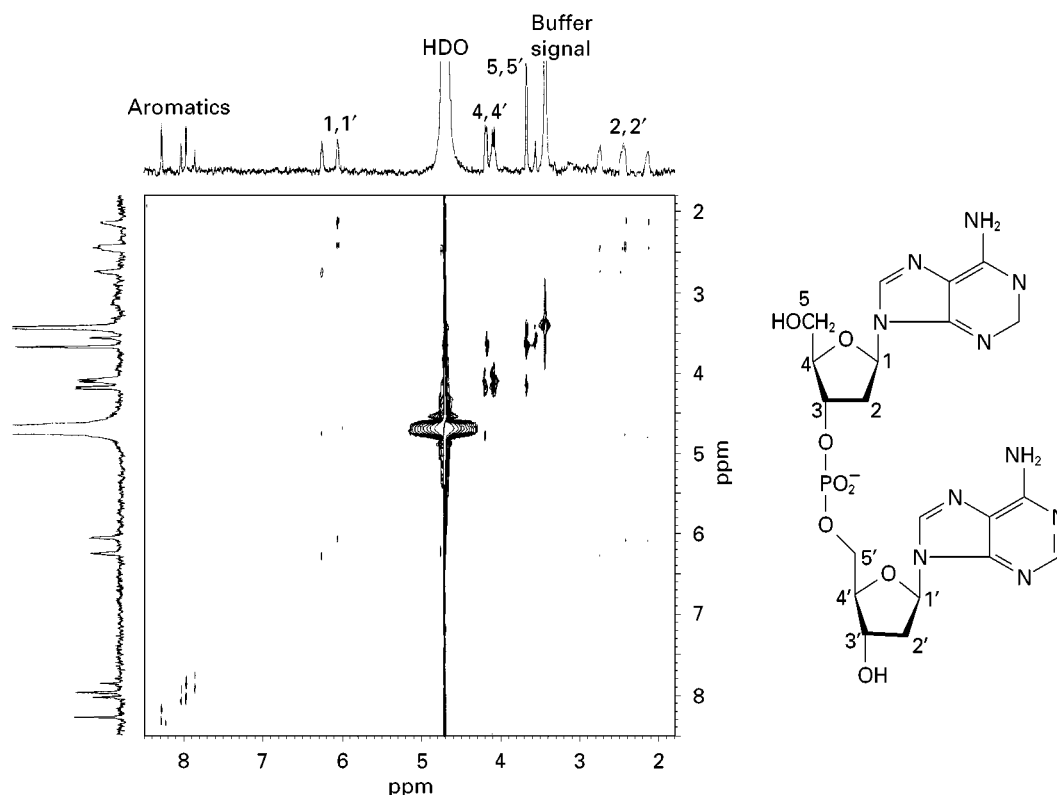


Figure 3 Two-dimensional CE ^1H – ^1H -TOCSY NMR spectrum of adenosine dinucleotide. Adapted with permission of Schewitz *et al.* (1999) *Chromatographia* 50: 333–337.

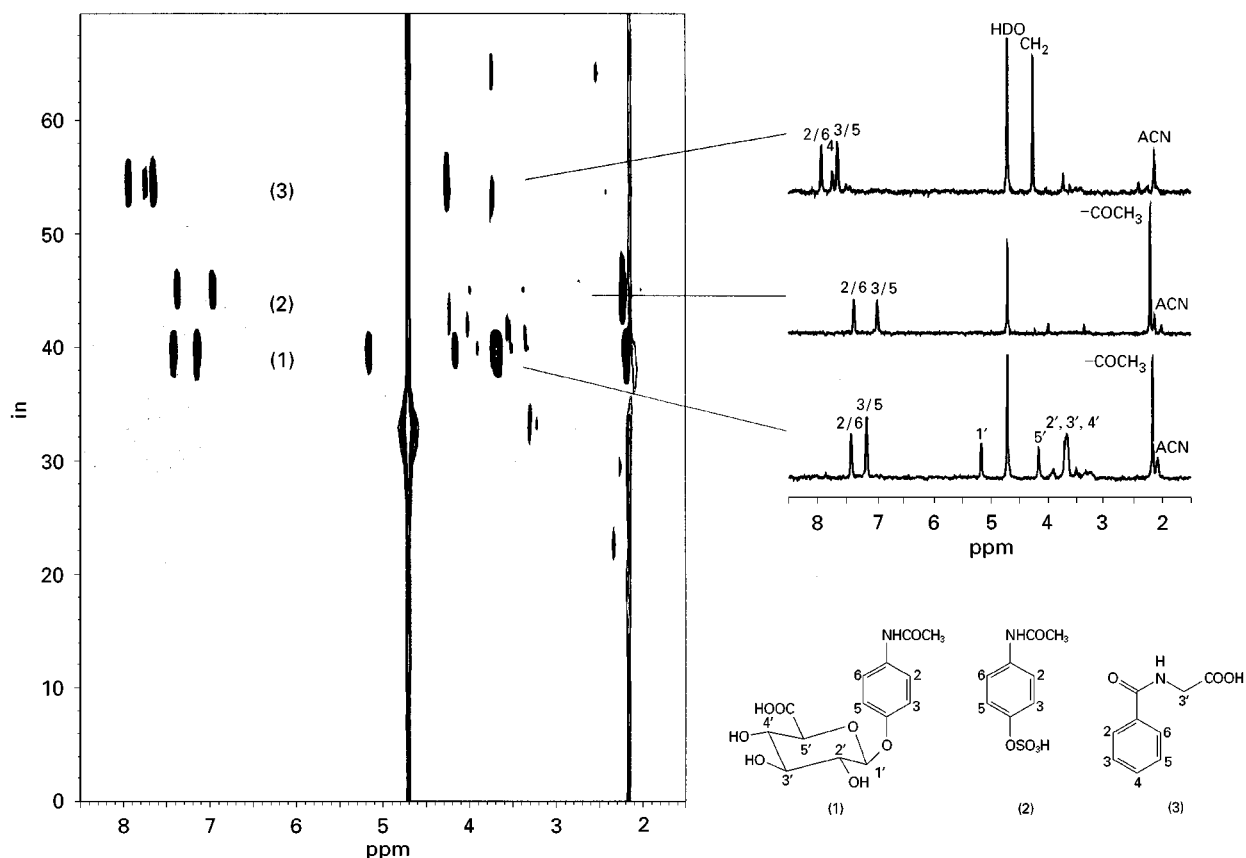


Figure 4 On-flow contour plot of the ^1H -NMR detected CEC separation of human urine. ^1H -NMR spectra on the right side are extracted from the contour plot. (1) Paracetamol glucuronide; (2) paracetamol sulfate; (3) hippurate. Adapted with permission from Pusecker *et al.* (1998) *Analytical Communications* 35: 213–215.

Comparison of the Systems

Both types of NMR detection system have strengths and weaknesses. The substantial advantage of the solenoid system is its better sensitivity. The low detection limit resulting from the perfect filling factor of the system allows extremely small detection volumes. This is important for electrophoretic separations, where the peaks often have volumes in the order of a few nanolitres and larger detection cells thus limit separation efficiency. It is obvious that the arrangement is well suited for mass limited samples, but unfortunately the small detection volume is offset by the need for high sample concentrations. Typically, these have been $>30\text{ mM}$ but in some examples concentrations of $>50\text{ mM}$ were necessary, and this then leads to a limitation in the number of possible applications. The approach may need special sample injection techniques like the field-amplified stacking.

Another problem of the solenoid CE–NMR set-up is the complex interdependence on flow rate, electric field and current. The current, which passes through the capillary, produces a magnetic field gradient

that perturbs the uniformity of the main magnetic field of the NMR spectrometer. Large NMR line widths and reduced structural information are the consequences. High-resolution NMR spectra are only obtainable by periodic stopped flow capillary electrophoresis when the interruption of the current enables the acquisition of NMR spectra. However, this technique makes the already long separation times even longer.

The most important advantage of the saddle system is its easier handling capability. Already there is a large number and a wide range of reported applications to support this assertion. There are several reasons. Firstly, as described above, the capillary is arranged vertically in the saddle-type probe. Because the shim systems used for the field homogeneity adjustment in cryomagnets are optimized in the vertical z -direction parallel to the magnetic field, the shimming procedure is facilitated in comparison to the solenoid system. Furthermore, the coil is not permanently attached to the separation capillary, thus allowing the capillary to be easily exchanged for different applications without the risk of damaging

the rf coil. Finally the distance between coil and sample is relatively large and so problems with susceptibility do not occur.

On the other hand, the size of the saddle coil is problematic. Due to technical problems, it is not possible to reduce the coil diameter beyond a certain limit. To obtain a suitable filling factor, the detection cell has to be enlarged and the resulting detection volumes of 180–440 nL are much larger than in conventional CE and might be thought to lead to lowered separation efficiency of electrophoretic techniques. However, the fabrication method of these NMR cells produces cell profiles that avoid mixing and turbulent flows and thus the separation efficiency is not seriously compromised. Assuming a sufficient separation of the components large detection cells can even have advantages. Longer residence times of the components allow an improvement in the signal-to-noise ratio of the NMR spectra through the accumulation of an increased number of scans and the higher level of solvent reduces the necessary sample concentration to < 10 mM.

The two systems are complementary in approach and both have made contributions to a better understanding of the challenges involved in coupling CE and NMR. A decision on which type will find more widespread application will be determined by future improvements of the systems and possibly by the type of applications to which this technology will be applied.

Future Developments

Numerous obstacles to coupling capillary separation techniques with NMR spectroscopy have already been overcome. In the short term, the development is likely to be focused on the improvement of the NMR interface and a goal must be implementation of the advantages of solenoid and saddle systems. An interface that combines sensitivity and small detection volumes of the solenoid arrangement with the easy handling of the saddle-type configuration and thus allow routine and automated operations will find extensive use in the future.

One way to reach this goal might be the application of the new cryo-probe technology to capillary NMR spectroscopy. Such probes already exist for conventional NMR spectroscopy and provide, in favourable circumstances, an improvement in signal-to-noise ratio of approximately 400%. This is achieved by cooling the rf coil to reduce the level of thermal noise. This might increase the sensitivity of a saddle coil by a substantial factor without the need of a size reduction.

Another improvement would be integration of UV detection directly into the NMR probe. This would allow the performance of real stopped-flow measurements and this would, for example, circumvent the

problem of NMR line broadening by the electrical current for the solenoid interface.

Usually, capillary separation science techniques are optimized to handle minimal amounts of sample. However, because of the desirability of direct combination with NMR spectroscopy, new technologies have to be developed that allow an effective separation of relatively large sample amounts in small volumes without a reduction of the efficiency. There are many possible improvements, which are necessary in order to increase the capabilities of this new hyphenated technique. With forthcoming advances in the sensitivity of NMR spectroscopy, CE–NMR and CEC–NMR will become practical and useful methods in situations which require separation and structural determination of components of mixtures in severely mass-limited situations.

See also: II/Chromatography: Liquid: Electrochromatography; Nuclear Magnetic Resonance Detectors. **Electrophoresis:** Capillary Electrophoresis; Capillary Electrophoresis–Mass Spectrometry. **III/Clinical Applications:** Capillary Electrophoresis.

Further Reading

- Behnke B, Schlotterbeck G, Tallarek U, Strohschein S, Tseng L-H, Keller T, Albert K and Bayer E (1996) *Analytical Chemistry* 68: 1110–1115.
- Gfrörer P, Schewitz J, Pusecker K, Tseng L-H, Albert K and Bayer E (1999) *Electrophoresis* 20: 3–8.
- Gfrörer P, Schewitz J, Pusecker K and Bayer E (1999) *Analytical Chemistry* 71: 315A–321A.
- Lacey ME, Subramanian R, Webb GA, Olson DL and Sweedler JV (2000) *Chemical Reviews*, in press.
- Olson DL, Peck TL, Webb AG, Magin RL and Sweedler JV (1995) *Science* 270: 1967–1970.
- Olson DL, Lacey ME and Sweedler JV (1998) *Analytical Chemistry* 70: 257A–264A.
- Olson DL, Lacey ME, Webb AG and Sweedler JV (1999) *Analytical Chemistry* 71: 3070–3076.
- Pusecker K, Schewitz J, Gfrörer P, Tseng L-H, Albert K and Bayer E (1998) *Analytical Chemistry* 70: 3280–3285.
- Schewitz J, Gfrörer P, Pusecker K, Tseng L-H, Albert K, Bayer E, Wilson ID, Bailey NJ, Scarfe GB, Nicholson JK and Lindon JC (1998) *Analyst* 123: 2835–2837.
- Schewitz J, Pusecker K, Gfrörer P, Tseng L-H, Albert K and Bayer E (1999) *Chromatographia* 50: 333–337.
- Schlotterbeck G, Tseng L-H, Händel H, Braumann U and Albert K (1997) *Analytical Chemistry* 69: 1421–1425.
- Subramanian R and Webb GA (1998) *Analytical Chemistry* 70: 2454–2458.
- Subramanian R, Sweedler JV and Webb GA (1999) *Journal of the American Chemical Society* 121: 2333–2334.
- Webb AG (1997) *Progress in Nuclear Magnetic Resonance Spectroscopy* 31: 1–42.
- Wu N, Peck TL, Webb AG, Magin RL and Sweedler JV (1994) *Analytical Chemistry* 66: 3849–3857.

Capillary Gel Electrophoresis

R. Freitag, Swiss Federal Institute of Technology, Lausanne, Switzerland

Copyright © 2000 Academic Press

Introduction

Electrophoresis covers a number of bioseparation techniques where charged substances are separated due to differences in migration speed in an electrical field. Since the 1950s, electrophoresis has been routinely used by biochemists to separate, quantify and identify large biopolymers, such as proteins, DNA and complex carbohydrates. In the early days electrophoresis was typically performed in slab or rod-shaped gels, which were necessary to hold the electrophoresis buffer and to minimize the dispersion of the analyte bands by suppressing convection caused by Joule heating and electroosmosis. At that time, electrophoresis was therefore commonly gel electrophoresis.

Electrophoretic separation is based on differences in the charge density (the mass-to-charge ratio) of the analytes. Small, highly charged molecules move faster than large, low charged ones, while uncharged molecules do not move at all. This is a powerful principle, for example for the separation of native proteins and peptides. Other biomolecules such as DNA restriction fragments and carbohydrates are very similar in chemical structure and therefore almost identical in charge densities. For these molecules gel electrophoresis represents a unique opportunity. Gels can be prepared to provide a sieving effect in the relevant mass range and thereby allow separation of charged molecules not according to their charge density but according to their size.

In 1981 Jörgenson and Lukacs published a series of landmark papers, in which they demonstrated both theoretically and practically how electrophoresis could be carried out in free solution as long as capillaries of small inner diameter were used and how the previously unwelcome electroosmotic effect could be used to advantage. The era of (free zone) capillary electrophoresis (CZE) began. Gels were no longer necessary, since the 'wall effect' in capillaries of less than 100 μm i.d. is sufficient to stabilize the flow. Capillary electrophoresis (CE) was seen as a complementary analytical technique to both liquid chromatography and 'conventional' slab/rod gel electrophoresis. In the following decade, research and application of free zone capillary electrophoresis ex-

ploded and several variants of the basic technique were established. In 1989 the first commercial CE instrument entered the market.

Capillary gel electrophoresis (CGE) was resurrected in 1983 by Hjerten, albeit for protein separations. It would probably have rested there, since protein CGE subsequently encountered severe problems. Instead it was the human genome project that helped to establish CGE as the important analytical technique it is today. The aim of this project is to determine the sequence of the over 3 billion base pairs that form the human genome. DNA sequencing requires the separation and identification of DNA fragments that differ in length by a single base. The progress of the project is largely determined by the speed of the respective analytical techniques.

The efficiency of CGE is extremely high and up to 3 million plates per metre are routinely reached. Heat dissipation is more effective in thin capillaries compared to conventional gels. As a consequence, much stronger fields can be used in CGE without loss in resolution. This results in significantly reduced analysis times. An example, the single base resolution of oligoadenylates containing from 12 to 60 nucleotides, is shown in **Figure 1**.

Current high throughput instruments use ultrathin capillaries and oligonucleotide primers that are covalently attached to different fluorescent dyes. The restriction digests of all four primers can therefore be analysed in the same sample. A comparison between CGE and conventional gel electrophoresis shows that even though more samples can be analysed in parallel in slab gels, CGE resolves a given sequence at least three times faster. **Table 1** summarizes some additional advantages and disadvantages of CGE over conventional gel electrophoresis.

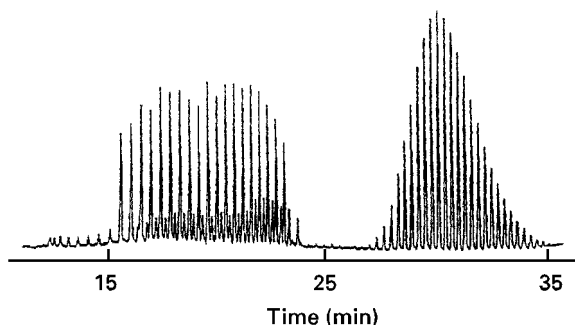


Figure 1 Single base resolution of oligoadenylates containing from 12 to 60 nucleotides by CGE. (Adapted with permission from Baba Y, Matsuura T, Wakamoto K and Tsuchiko M (1991) *Journal of Chromatography* 558: 273–284.)

Table 1 Comparison of capillary and conventional gel electrophoresis*Advantages of CGE*

- Smaller sample volume
- Less buffer, gel and reagent consumption. The latter is especially important, since DNA gel electrophoresis requires toxic and/or mutagenic substances (e.g. ethidium bromide)
- Shorter analysis time
- Higher resolution
- Higher efficiency (over several million plates per metre)
- Reliable quantification of the analyte concentration by on column or off column flow through detector (UV absorbency, fluorescence, mass spectrometer, etc.) instead of staining and semiquantitative evaluation in the gel by densitometry
- Other than conventional slab gel electrophoresis, CGE can be fully automated from sample injection to separation, detection and data processing steps
- Semipreparative applications become much easier, since the molecules pass through and exit the capillary. In conventional gels, the zones are stained within the gel, from which they can only be removed by manual cutting of blotting

Disadvantages of CGE

- Restriction in sample size
- CGE gels are more difficult to prepare
- Capillary coating often necessary to reduce electroosmosis

Gel Filled Columns for Capillary Gel Electrophoresis

Cross-linked chemical gels and physical gels such as agarose are just as popular in CGE as in conventional slab gel electrophoresis. However, since the capillary wall effect exerts its stabilizing influence, solutions of entangled polymers are also used.

Naked fused silica capillaries show electroosmosis above a pH of 3. As a consequence the electrophoresis buffer flows towards the cathode. In capillary gel electrophoresis electroosmosis would lead to extrusion of the gel from the capillary. A possible way to avoid this is to coat the inner silica surface with a neutral polymer. Table 2 summarizes the more common types of capillary coating. Ideally, the coating should be effective in suppressing electroosmosis as well as the interaction of the analytes with the capillary wall. The preparation should be reproducible and the coating should be stable for a long time and over a wide pH range. Most coatings are attached to the wall by covalent bonds. However, dynamic coatings consisting of ionic, zwitterionic or nonionic molecules that are simply adsorbed to the wall either as monolayer or as bilayer are also used.

Chemical Gels

A general outline for preparing a cross-linked gel column for CGE is given in Table 3. Cross-linked polyacrylamide (PAA) gels are prepared by radical copolymerization of acrylamide as monomer and – most frequently – *N,N'*-methylenebisacrylamide (BIS) as cross-linker. $(\text{NH}_4)_2\text{S}_2\text{O}_8$ is commonly used as initiator in combination with *N,N,N',N'*-tetramethylethylenediamine (TEMED). Riboflavin (< 5 ppm) has been used as light sensitive initiator but requires the use of UV transparent capillaries. The polymerization of acrylamide can also be started by γ -radiation (^{60}Co source).

The resulting gels have well defined, fairly small average pore sizes of 2 to 8 nm. The %T, %C nomenclature is used for their characterization, with:

$$\%T = \frac{g_{\text{acrylamide}} + g_{\text{crosslinker}}}{100 \text{ mL solvent}}$$

corresponding to the monomer concentration:

$$\%C = \frac{g_{\text{crosslinker}} \times 100}{g_{\text{crosslinker}} + g_{\text{acrylamide}}}$$

corresponding to the crosslinker concentration.

Table 2 Common types of capillary coatings

Coating	Comments
Polyacrylamide with Si–O–C bond	Very common, easy to prepare
Polyacrylamide with Si–C bond	Improved hydrolytic stability, difficult to prepare
Polyethylene glycol	Very common
Nonionic surfactants	TWEEN and BRIJ series
LC type stationary phases	C ₁ , C ₈ , C ₁₈ , i.e. weakly, moderately and highly hydrophobic
GC type stationary phases	e.g. DB-17 (50% phenylmethyl silicone)

Table 3 Outline for the preparation of a cross-linked sieving matrix for CGE

Prepare stock solution of monomer, cross-linker, buffer, etc.
Cut/burn detection window if necessary
Pretreat the inner surface of the silica capillary (coating, activation, etc.)
Introduce mixture of monomer (cross-linker)/initiator/catalyst/stabilizing agent (if necessary)
Initiate polymerization
Pre-electrophoresis (to remove impurities and assure constant run conditions and a stable baseline)

Single strand oligonucleotides are typically separated in 2.5%T/3.3%C or 4%T/3.3%C gels. A higher cross-linker concentration gives a tighter sieve and thus higher size selectivity. An increase in the monomer concentration also results in a gel matrix with smaller pores. Lower %T/%C values result in a reduced selectivity but allow coverage of a wider analyte size range. An increased column length can compensate for the loss in resolution, albeit only at the price of increasing the analysis time. A reduction of the cross-linker concentration for a given monomer concentration results in larger pores. A 3%T/0.5%C gel has, for example, been found to give excellent resolution of double-stranded DNA restriction fragments varying from 5 to 12 000 base pairs.

Polyacrylamide is a popular gel matrix because of its electroneutrality. With time, however, it will be hydrolysed to charged polyacrylate, especially at high temperatures (high field strength) and extreme pH values. When the polyacrylate concentration becomes too high, an electroosmotic flow can be observed, which finally results in expulsion of the gel from the capillary. In order to prevent this, the gel may be covalently anchored to the wall coating. This calls for polymerizable (double bonds) groups in the coating. Alternatively, coating and gel formation can be done simultaneously in activated capillaries.

The preparation of gel-filled capillaries is not simple and only four out of five capillaries produced can actually be used. Problems arise in a number of areas, but a major cause of concern is the formation of bubbles during production, transport and use (injection!) of the gel-filled capillaries. Bubbles lead at best to loss in resolution and changing separation patterns and at worst to the total breakdown of the

electrical field, especially at high field strengths ($> 300 \text{ V cm}^{-1}$).

If the gel and the capillary wall coating are not physically linked, bubble formation is less of a problem, since the wall and the gel can move relative to one another. The reduced stability of the gel under these circumstances is another matter. Whereas capillaries with wall-bound gels can often be used for more than 100 runs, the number of separation that can be performed with the mobile gels tends to be an order of magnitude lower.

Bubble formation during polymerization is largely due to shrinkage of the gel during the process (higher density of the gel than the monomer mixture). **Table 4** summarizes approaches to circumvent this problem. In the case of the laterally aggregated polyacrylamide gels, a hydrophilic polymer such as polyethylene glycol (PEG) is added to the reaction mixture. The more hydrophobic PEG coordinates a large amount of water leaving the growing polyacrylamide strands to form hydrogen bridges mainly among themselves. As a result, thick gel fibres are formed and subsequently stabilized by cross-linking (**Figure 2**). The laterally aggregated gels have larger pores than homogeneous polyacrylamide gels of similar %T/%C. Their sieving behaviour depends also on the concentration and molecular mass of the PEG and should be determined experimentally in each case.

Physical Gels and Entangled Polymers

In physical gels the network structure is formed by noncovalent interactions such as van der Waals forces and hydrogen bonds rather than chemical

Table 4 Suggestions for the polymerization of bubble-free cross-linked PAA gels

Polymerization at high pressure (400 bar) to equalize the density of the monomer mixture and the final gel
Sequential polymerization starting with the gel formation at one end of the capillary and slowly progressing to the other, for instance by:
• irradiation (1 cm min^{-1})
• thermal (slow immersion into a heated water bath or slow removal from a cold one)
• isotactic polymerization (the initiator is placed between the leading and the terminating electrolyte and slowly moves through the capillary by isotachopheresis)

Laterally aggregated polyacrylamide gels (formed in the presence of a hydrophilic polymer such as polyethylene glycol)

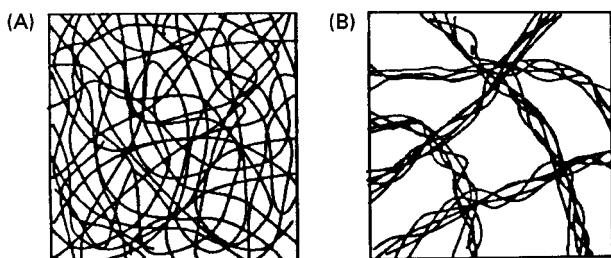


Figure 2 Hypothetical model for 'laterally aggregated' gels. (a) Homogeneous network of cross-linked PAA. (b) Heterogeneous network of PAA in the presence of PEG 2000 (Reproduced with permission from Kuhn R and Hoffstetter-Kuhn S (1993) *Capillary Electrophoresis: Principles and Practice*, Springer Verlag.)

cross-linking. If large analyte molecules try to transverse this dynamic structure they also encounter a size-dependent resistance (sieving effect). The type and number of physical gels used in CGE is much more varied than the chemical gels. Mixed physical gels containing, for example, polyacrylamide and cellulose, are also possible. Both solid and liquid sieving matrices are known. Physical gels are often cheaper than chemical gels. They have a more flexible pore structure and can be operated at higher temperatures (50–70°C) and field strength (up to 1000 V cm⁻¹).

Examples of solid physical gels include agarose gels at room temperature and linear polyacrylamide gels with %T > 8 (the %C would be zero in this case). Such high %T polyacrylamide gels also have to be prepared by *in situ* polymerization. The size selectivity is a function of the polymer concentration and can be similar to that of the cross-linked polyacrylamide gels (Figure 3). Agarose is a natural polysaccharide network of 1,3-linked β -D-galactopyranose and 1,4-linked 3,6-anhydro- α -L-galactose. Purified agarose for electrophoresis can be obtained from a number of chemical suppliers. The matrix exhibits a wide range of pore diameters from several hundred nanometres to several micrometres and has high mechanical strength. Agarose is biologically inert and stable between pH 4 and 9. The gel liquefies around 65°C and solidifies again at 35°C. In the molten state it is easily injected into (or removed from) the capillary. Agarose gels can be used below and above the gelling point. Gel filled capillaries (0.3–5% by weight) are stable for a couple of days. No treatment of the capillary walls is necessary. To improve the stability of the gel a small amount of a polyalcohol such as sorbitol may be added.

Entangled polymer solutions are liquid sieving matrices. They are essentially low viscosity gels and can be replaced after each analysis. Hydrolysis or contamination of the network is thus less problematic. Gel formation in entangled polymer solutions de-

pends on the polymer concentration. In dilute solution the polymer molecules are hydrodynamically isolated. For a certain polymer volume fraction Φ^* (overlap threshold) the chains begin to entangle and interact. As a consequence a highly dynamic network is created. Experimentally, Φ^* can be determined by plotting the logarithm of the specific viscosity versus the polymer volume fraction. For $\Phi < \Phi^*$ the curve has a slope of approximately 1.0; for $\Phi > \Phi^*$ the slope increases.

Linear polyacrylamide has to be used at concentrations of at least 6%T to ensure sufficient size discrimination. The solution is then already very viscous and difficult to handle. Other hydrophilic polymers have much lower threshold values. The corresponding solutions are therefore less viscous and can be easily injected and replaced. Among them are various cellulose derivatives (overlap threshold approximately 0.3%), such as methylcellulose, hydroxymethylcellulose, hydroxyethylcellulose and hydroxypropylmethylcellulose. The sieving efficiency depends also on the molecular mass of the cellulose. Molecules weighing more than 900 000 g mol⁻¹ make good

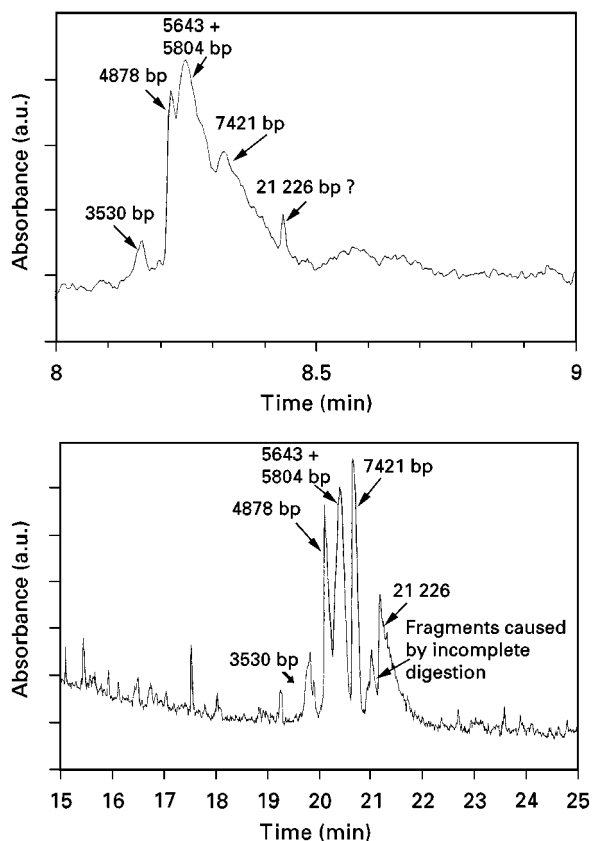


Figure 3 Separation of lambda-DNA restriction fragments (*Eco*RI). Top, 2% polyacrylamide gel; bottom, 4% polyacrylamide gel. (Adapted with permission from Hebenbrock K, Schügerl K and Freitag R (1993) *Electrophoresis* 14: 753–758.)

sieving gels for DNA fragments (polymer concentration 0.5%). For protein separation dextran or polyethylene rather than cellulose derivatives are used to prepare the gels. This has the additional advantage of allowing detection of the proteins at the more sensitive wavelength of 214 nm.

Both physical and chemical gels can be further modified, for example by the incorporation of cyclodextrins or antibodies into the matrix, to allow more specific interactions.

Separation in Capillary Gel Electrophoresis

Two models are used in CGE to describe the separation. The Ogston model considers the gel as a labyrinth of interconnecting pores and channels with an average pore (mesh) size of ζ . The analyte molecules are pictured as rigid spheres with a radius R . Small molecules can pass unhindered through a large fraction of the pores, they therefore move fast but larger molecules are slower. If the pore size of the gel is assumed to be a function of the polymer concentration, the following equations can be used to describe the situation:

$$\mu_g = \mu \exp[-Tb(R + r)^2]$$

and:

$$\mu_g = \mu \exp[-0.25\pi((R + r)\zeta)^2]$$

where μ_g is the analyte mobility in the gel matrix; μ is the analyte mobility in free solution for $E \rightarrow 0$; T is the polymer concentration; b is a constant; R is the radius of gyration of the analyte molecule and r is the average radius of the network pores.

The term $b(R + r)^2$ is also called the retardation coefficient, k . To obtain μ , the mobility of the analytes in free solution is extrapolated to a field strength of zero. A plot of μ_g versus T , the Ferguson plot, results in a straight line with a slope of k and an intercept of μ . This plot is used to determine the size separation range of the gel. If the plot is not linear, the assumption that the analytes are rigid spheres with a radius $R < r$ is no longer true.

Biopolymers are flexible molecules rather than rigid spheres and can therefore in reality pass through pores with radii of less than their own radius of gyration. The reptation model considers the analytes as dynamic and essentially chain-like structures that snake and wriggle headfirst through the network in a reptation (hence the name) type of motion. In this model the length of the flexible macromolecule is considered large in comparison to the distance be-

tween neighbouring knots in the network. The analyte mobility is proportional to the reciprocal of the chain length or, for nucleic acids, to the base number, N , of the molecule:

$$\mu_g \approx 1/N$$

Larger molecules are again more handicapped than smaller ones. For a flexible macromolecule the transition from the Ogston sieving model to the reptation model takes place when R becomes approximately 1.4 times ζ , depending on the nature (globular proteins, rod-shaped DNA molecules) and the flexibility of their structure. For very large molecules neither model holds true, because the electrical field deforms the molecular structure. For DNA fragments the equation is valid up to approximately 1000 base pairs, depending on the applied field strength. The mobility of larger DNA fragments is actually higher than expected. This leads to a co-migration of larger fragments with smaller ones, especially at high field strength and in high %T gels.

Instrumentation and Methodology

CGE requires no special instrumentation and can be carried out on the same type of instrument as standard capillary electrophoresis. All that is required in addition to the gel filled column is a high voltage power supply and a detector. Most commercial systems are automated to a high degree and also include an autosampler/injection module and a data handling station.

CGE uses continuous electrolyte systems. The separation of the analyte molecules is therefore a kinetic process. In general, all buffer systems for capillary electrophoresis can also be used in CGE. By far the most popular are TRIS-borate buffers (50 or 100 mM TRIS, 50, 100, 250 mM borate, pH 7.6–8.5, up to 5 mM EDTA), especially for the separation of DNA fragments and nucleotides.

While the separation of the native molecules is possible, denatured molecules are sometimes easier to analyse. In this case, denaturing agents, such as high concentrations of urea (5–8 M) are added to the separation buffer, in order to destroy the tertiary and quaternary structure of the molecules. A special case is polyacrylamide gel electrophoresis of proteins in the presence of the surfactant sodium dodecyl sulfate (SDS-PAGE). The protein structure is fully denatured under these conditions including cleavage of the disulfide bonds by a reducing agent such as mercaptoethanol. The remaining polypeptide chains bind SDS in a constant weight ratio (1.4 g SDS per gram of protein) to yield detergent-protein complexes of

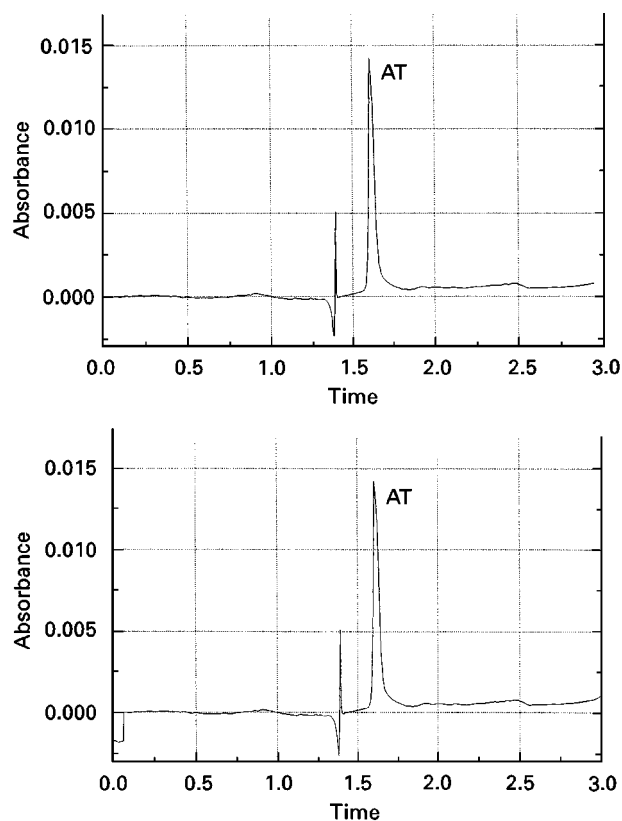


Figure 4 Determination of the molecular mass of recombinant human antithrombin III. Top, calibration using pepsin (34.7 kDa); ovalbumin (45.0 kDa); bovine serum albumin (69.0 kDa); and phosphorylase subunit B (97.4 kDa) as markers. Bottom, recombinant h-AT III. (Reproduced with permission from Reif O-W and Freitag R (1994) *Journal of Chromatography* 680: 383–394.)

constant charge density. SDS-PAGE in slab gels is a standard method for purity control and mass estimation of proteins. SDS-PAGE in capillaries has been used for similar purposes (Figure 4). Ethidium bromide is a selective intercalating agent for double stranded DNA. The positively charged molecule can be used to optimize the separation of large DNA restriction fragments in CGE (Figure 5). It lowers the charge density and thereby the migration speed of the negatively charged DNA molecules.

Sample Introduction

Two basic types of injection principle are used in capillary electrophoresis. One is injection by pressure (vacuum suction or gravity), i.e. hydrodynamic injection, the other is electrokinetic injection. Pressure injection cannot be used with cross-linked gels, although it may be an option for some of the low viscosity entangled polymer solutions. In most cases it would either not succeed in pushing the sample into the capillary or destroy the gel.

For electrokinetic injection the capillary is placed into the sample vial and the electric field is switched on (typically between 1 and 20 s and 100 and 400 V cm⁻¹). The analyte molecules migrate into the capillary due to electrophoresis. Electrokinetic injection is biased towards small, highly charged molecules which are then over-represented in the introduced sample. In capillary gel electrophoresis the problem is less pronounced, since all analyte molecules are assumed to have identical mass to charge ratios, i.e. differ very little in migration speed.

The surface of the capillary inlet is very important (Figure 6). To ensure an even surface, the respective end of the capillary should be cut off with a microtome or snapped off cleanly after scoring with a sapphire cleaver.

Detection

The most common detection principles in CE are optical or column detectors (UV absorbance and (laser induced) fluorescence, LIF). Fluorescence and especially LIF detection allow very low limits of detection (LOD) to be reached. Unfortunately only a few biological molecules show native fluorescence. DNA molecules require pre- or postcapillary derivatization with a fluorescing agent, e.g. a fluorescence-labelled hybridization probe or primer. FITC, JOE, TAMRA, FAM and ROX have been used as labels in DNA sequencing. Proteins have been detected using their native fluorescence at 280 to 340 nm

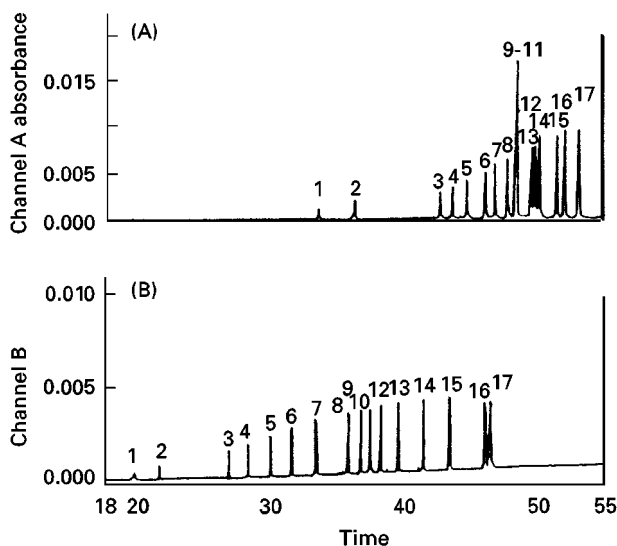


Figure 5 Effect of ethidium bromide addition on the resolution of a restriction fragment digest (pBR 322 by Msp I). Top, no ethidium bromide; bottom, 1 µg mL⁻¹ ethidium bromide. (Reproduced with permission from Guttman A and Cooke N (1991) *Analytical Chemistry* 63: 2038.)

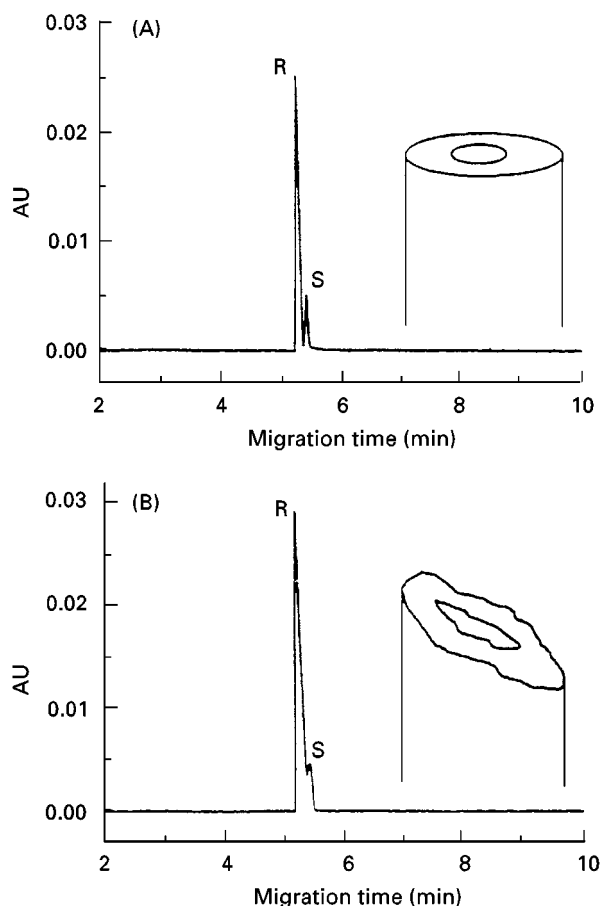


Figure 6 Effect of the physical shape of the inlet of a gel-filled capillary on the resolution of naproxen enantiomers. (Reproduced with permission from Guttman A and Schwartz HE (1995) *Analytical Chemistry* 67: 2279–2283.)

(tryptophan residues). However, since the quantum yield is often low, labels such as fluorescein isothiocyanate (FITC 494 to 525 nm) are also used (Figure 7).

The problem with UV absorbance in CGE is the short optical pathway (inner diameter of the capillary), which leads to low sensitivity. Bubble and z-shaped cells can be used, but the bubble cell makes the capillary fragile, while the z-shaped cell lowers the resolution. In gel-filled capillaries the sensitivity suffers further because of the low UV transparency of most gels. The transparency of a PAA-filled capillary (6%T, 5%C) at 260 nm is 15% lower than that of a water-filled one; even lower if additives like urea or PEG are used. Instead of on-column detection, an off-column detector connected with a sheath flow interface can be used. In addition, several suppliers offer UV-transparent gels either of the cross-linked or the entangled type. The composition of these gels is usually proprietary.

Special Techniques

Varying the magnitude and the direction of the field, so-called pulsed field electrophoresis, can improve the resolution especially for DNA separation, since fragments of up to 10 million base pairs can be analysed. Since the larger molecules are assumed to snake through the gel, they need to orientate themselves in the field before they can advance. If the field is regularly inverted, the advance of the larger molecules is more affected than that of the smaller ones and as a consequence their separation is improved.

Voltage ramping has been shown to improve the separations of mixtures of small and large molecules. First high voltage is used to separate the smaller fragments, afterwards the larger fragments are separated with a gradually or abruptly decreased voltage. Field programming may also aid fraction collection, since the extremely sharp peaks of CGE are difficult to 'catch' unless the analyte migration is reduced by lowering the voltage.

Future Developments

CGE is a rapidly maturing technique and the need for high resolution bioanalytical techniques can be expected to increase rather than decrease in the near future. Up to now application of capillary gel electrophoresis has been dominated by DNA analysis. The potential of the method for protein analysis has not been realized. However, the demands of the modern biopharmaceutical industry for fast and reliable protein characterization techniques may soon change this.

The speed of CGE can be further accelerated by more stable gels (higher field strength) or by using several capillaries in parallel (array). If the sample size could be reduced further, the need for template amplification, e.g. by the polymerase chain reaction (PCR) would be reduced. Detection may be improved by increased use of high molecular weight mass spectrometers (MS). They can be linked to the CE instrument, for example by an electrospray ionization (ESI) interface. As these detectors become more affordable, their use in CGE will increase. Mass spectrometers combine a high sensitivity with being nearly universal detectors. When MS-MS is used more structural information of the analytes become available.

Capillary electrophoresis in many ways is already a microtechnique. However, further miniaturization is possible and the CE on a chip need not be far ahead. Such microchip CE will most likely use gel filled 'capillaries' to realize the maximum number of theoretical plates over the short separation distance.

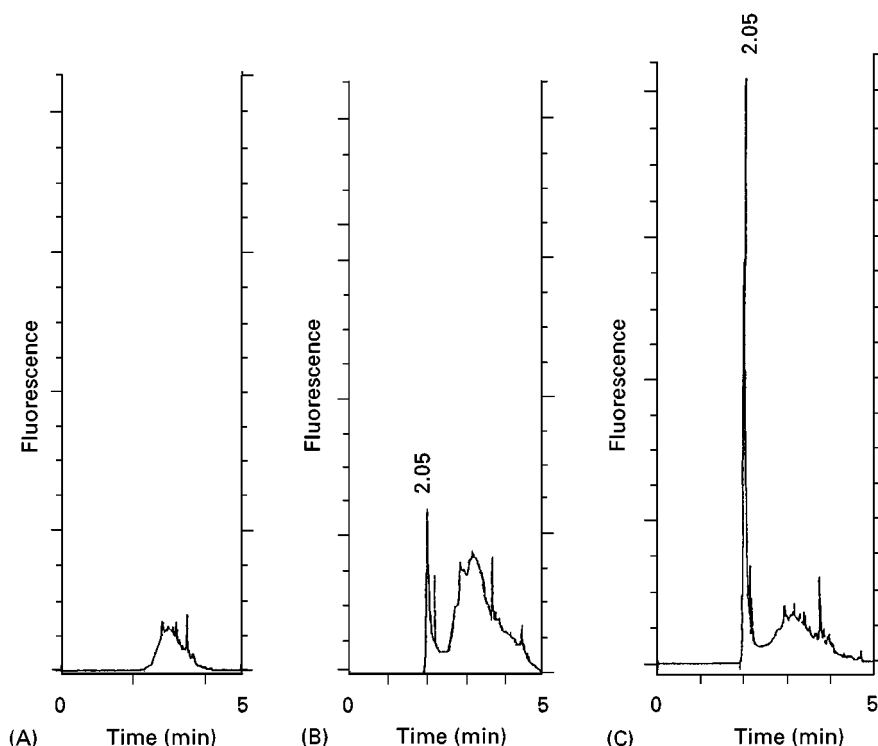


Figure 7 Quantification of human immunoglobulin G (h-IgG) using FITC-labelled Protein G. A, no IgG; B, $250 \mu\text{g mL}^{-1}$; C, 1 mg mL^{-1} . (Adapted with permission from Reif O-W, Lausch R, Scheper Th and Freitag R (1994) *Analytical Chemistry* 66: 4027–4033.)

Further Reading

- Beale SC (1998) Capillary electrophoresis. *Analytical Chemistry* 70: 279. (This journal prints every two years a review on capillary electrophoresis. The article is written by an expert in the field and covers more or less all developments in CE including CGE of the preceding years.)
- Grossmann PD and Colburn JC (eds) (1996) *Capillary Electrophoresis: Theory and Practice*. San Diego: Academic Press.
- Grossmann PD and Soane DS (1991) Capillary electrophoresis of DNA in entangled polymer solutions. *Journal of Chromatography* 559: 257. This paper treats the two models for separation in CGE (Ogston and reptation) in more detail.
- Jörgenson JW and Lukacs KD (1981) High resolution separation based on electrophoresis and electro-osmosis. *Analytical Chemistry* 53: 1298.
- Kuhn R and Hoffstetter-Kuhn S (1993) *Capillary Electrophoresis: Principles and Practice*. New York: Springer Verlag.
- Landers JP (ed.) (1994) *Handbook of Capillary Electrophoresis*. Boca Raton: CRC.
- Li SFY (1992) *Capillary Electrophoresis*. Amsterdam: Elsevier.
- Lunte SM and Radzik DM (1996) *Pharmaceutical and Biomedical Applications of Capillary Electrophoresis*. Oxford: Pergamon Press.
- Schwartz H and Guttman A (1995) *Separation of DNA by Capillary Electrophoresis*. Fullerton, CA: Beckmann Primer 607397.

Capillary Isoelectric Focusing

P. G. Righetti, University of Verona,
Faculty of Sciences, Verona, Italy
C. Gelfi, ITBA, CNR, Segrate, Milan, Italy

Isoelectric focusing (IEF) possibly represents the electrokinetic method with the highest resolving power. In IEF, amphoteric compounds are sorted in order of their isoelectric points (pI) in a steady-state pH gradient. Good resolution is favoured by both a low diffusion coefficient and a high mobility slope at the pI ,

conditions which are well satisfied by most proteins. A high field strength and a shallow pH gradient further enhance resolution. There are two basic variants of IEF: (1) in soluble, amphoteric buffers, called carrier ampholytes (CA) and (2) in insolubilized, non-amphoteric buffers (the latter technique is known as immobilized pH gradients, IPG). In this article we will deal with the former, i.e. CA-driven IEF, since IPGs have not as yet been implemented in capillaries. In fact, in IPGs, the buffers (acrylamido weak acids and bases) have to be grafted onto a support which at present is only a polyacrylamide gel. In addition, the gradient is created 'artificially', outside the electric field (whereas in CA-IEF the pH gradient has to be generated and maintained by the electric field itself), and thus gel casting requires the use of a two-vessel gradient mixer, with the simultaneous pouring of a density and a pH gradient in a flat-gel slab format. In normal use IPGs additionally require that the gel cassette is opened and that the polyacrylamide slab, with the grafted pH gradient, is exhaustively washed, so as to eliminate salts, ungrafted buffers and catalysts. This preparation sequence means that preparing an IPG in a capillary format is not a straightforward process.

The theory of IEF and IPGs, as well as the chemistry of the buffers adopted, has been covered elsewhere. Here we will focus on the techniques used in capillary IEF (CIEF), namely: one- and two-step focusing methods, pH gradient determination, sample preconcentration systems and some application examples.

General Considerations

CIEF combines the high resolving power of conventional IEF with the advantages of automation and speed. The separation of charged analytes takes place in a pH gradient created in a capillary by carrier ampholytes under the influence of an electric field. The concentrating effect that occurs during the focusing step, enables components present in small quantities to be detected. A major difference between IEF and CIEF is the detection method: in CIEF detection is performed in most cases with an ultraviolet (UV) or photodiode array detector placed near one end of the capillary. In order to visualize the stationary zones formed in the capillary, its content must therefore be mobilized in an additional step so that they pass in front of the detector window. To date, most of the reagents used in CIEF (carrier ampholytes, solubilizers and so on) have been adopted from traditional IEF. A number of reviews have already appeared on the topic of CIEF (see the Further Reading section).

A principal difference between IEF in a gel and in a capillary is that, in the latter, mobilization of the focused proteins past the detector has to be carried out if an on-line imaging detection system is not used. Three techniques are mainly used: chemical and hydrodynamic flow mobilization (in coated capillaries) and mobilization utilizing the electrosmotic flow (in uncoated or partially coated capillaries). These techniques are discussed further below.

Focusing in Internally Coated Capillaries

At any pH value above pH 2 the fused silica surface will progressively acquire negative charges due to ionization of weakly acidic silanol groups which are fundamental constituents of any vitreous material. Accordingly, close to the capillary wall (in the diffuse part of the double layer) there will be more positive than negative ions (electroneutrality will thus not prevail in the double layer). In an electric field, the hydrated, positively charged surface layer will move toward the negative pole, thus producing an electrosmotic flow (EOF), which can be observed as a bulk fluid movement. Such an EOF pump is not, in itself, deleterious to the analyte zone, since it has a flat profile (except in the few nanometre thickness of the double-layer); however, in the case of proteins, strong adsorption may ensue, due to multipoint attachment of positively charged species to the negative charges of the wall. In addition, particles migrating in directions opposite to the bulk liquid flow might never reach the detector. The electrosmotic mobility (μ_{eo}) is inversely proportional to the viscosity (in the double layer). Thus, by coating the inner surface of the capillary with a hydrophilic, non-ionic polymer, there will be two beneficial effects: the charges will be masked and, in general, suppressed and, additionally, the viscosity in the double layer will be so high as to virtually eliminate EOF. A typical coating consists in first reacting the wall with a bifunctional agent (γ -methacryloxypropyltrimethoxysilane) and then covalently affixing a monolayer of linear polyacrylamide to the dangling double bonds. Many other coating procedures have been described and have been reviewed by Chiari *et al.* (1996).

Focusing Step

The coated capillary is filled entirely with sample solution mixed into at least 1% carrier ampholytes (the sample should be desalted so as to avoid pH gradient drift). One end of the tube is then pressed into a 1% agarose gel, prepared either in 20 mM NaOH or in 20 mM phosphoric acid (representing

the cathodic and anodic solutions, respectively). The gel plug thus inserted into the tube end prevents zone-deformation by hydrodynamic flow in the tube during the subsequent focusing step. A constant voltage of 4000–6000 V is applied. When the steady-state has been attained, which occurs when the current has dropped to about 10–25% of the starting value, the voltage is switched off and elution started immediately as described below.

Elution and Detection Step

In such a system, due to suppression of EOF, the focused stack of carrier ampholytes and proteins is arrested; thus ways have to be found to transport the stack past the detector. A number of procedures can be adopted: (1) apply a mechanical pump to the capillary and generate a hydrodynamic flow (at the end of the IEF process); (2) replace the base at the cathode with acid or the acid at the anode with base and (3) salt mobilization. This latter technique has attained wide popularity. When a salt (e.g. NaCl) is added at the anolyte, mobilization will be towards the anode; conversely, if added to the catholyte, the train of bands will elute at the cathode. **Figure 1** shows

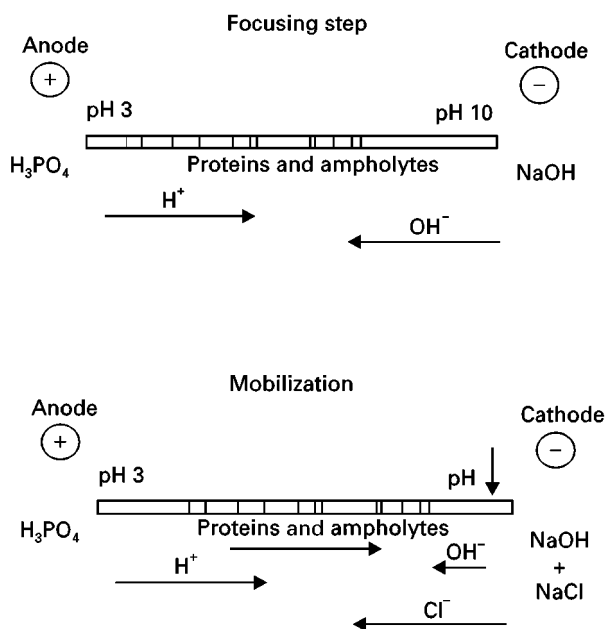


Figure 1 Focusing in internally coated capillaries. The focusing (upper) and mobilization (lower) steps. In the upper drawing the steady-state is shown as an arrested stack of proteins and CA buffers. Only protons and hydroxyl ions move from the respective electrodes carrying most of the current. In the lower drawing, addition of NaCl to the cathode is shown to mobilize the stack of proteins and CA buffers towards and past the detector port (represented as a large vertical arrow close to the cathode). (Reproduced by permission of Bio Rad, Hercules, CA, USA.)

a representation of this process: the upper part depicts the steady-state, characterized by a stationary pattern of focused proteins in an arrested pH gradient. In this stage, current is carried mostly by protons and hydroxyl ions moving from the anodic and cathodic compartments, respectively (and also by the to and fro movement of the CA buffers about the *pI* position!). On addition of the salt (typically 20–80 mM) at the cathodic reservoir, the stack of proteins and CA buffers is mobilized towards the cathodic side (past the detector). The time required for mobilization is about 15 min at 360 V cm^{-1} . During mobilization the current which had reached a minimum at the end of the focusing stage (typically $1 \mu\text{A}$) rises again to as high as $50 \mu\text{A}$. It is during mobilization that the train of zones, titrated away from the *pI* by the cations or anions (other than protons or hydroxyl ions) entering the tube from one of the electrode reservoirs, transits in front of the detector and is registered as a series of bands. Ideally, proteins and peptides should best be monitored at 210 (or even 190) nm where the absorbance of the amido bond is 20–50 times higher than at 280 nm. However, at the low wavelengths the CA buffers also produce a UV signal (rather similar for Ampholine and Biolyte, quite different in the case of Pharmalytes) which could be mistaken as sample zones. Thus, in an IEF experiment, it is best to read the sample at 280 nm.

Elution by Vacuum or Pressure Under Voltage

An alternative elution method consists in applying a vacuum of 5 mmHg while still under high voltage. The vacuum causes the focused proteins to flow past the detector, while the voltage maintains the pH gradient and zone sharpness even in the presence of distorting effects due to laminar flow. First, the entire tube is filled with NaOH (catholyte). Then, by hydrodynamic flow, approximately two-thirds of the capillary length is filled with carrier ampholytes. This is followed by a short sample plug, which is subsequently insulated from strong anolyte (which might, by contact, denature some proteins). At this point liquid pumping is stopped and the focusing process takes place between the phosphoric acid as anolyte and the NaOH as catholyte. Mobilization is again accomplished by a vacuum-driven hydrodynamic flow under voltage. The detection limit for proteins at 280 nm is as low as 1.3 ng, while the signal linearity is in the range of 1.3–10.7 ng (an eight-fold concentration range). Interestingly, this sensitivity is of the same order of magnitude as that reported for silver staining of sodium dodecyl sulfate-denatured protein zones and two to three orders of magnitude higher than conventional Coomassie Brilliant Blue staining.

pI Measurements

In its simplest approach unknown *pI* values can be assessed by plotting the *pI* values of a set of markers, co-focused with the proteins under investigation, versus their relative mobility on elution. This plot is linear and thus a high precision (approximately ± 0.1 pH unit) is obtained (see Figure 2). *pI* values as low as 2.9 and 2.75 can be determined. In another approach monitoring the current in the mobilization step can be adopted for *pI* assessments. If the peaks of the mobilized stack of proteins are monitored simultaneously with the rising current due to the passage of the salt wave in the capillary one can correlate a given *pI* value (which should already be known from the literature) with a given current associated with the transit of a peak at the detector port. The system can thus be standardized and used for constructing a calibration graph to be adopted in further work, without resorting to 'internal standards'. One such graph correlating current with *pI* values is shown in Figure 3: this appears to be a precise method, since the error is only about 0.03 pH units. The use of low M_r substituted aromatic aminophenols, which fulfil all the requirements for *pI* standards for CIEF and assure a 0.06% *pI* reproducibility, have also been proposed. In another method dansylated peptides have been synthesized for use as *pI* markers for evaluating pH gradient formation.

On Isoelectric Precipitation

Proteins have nett negative and nett positive charges at pH values above and below their *pI* values. This decreases the risk of aggregation, which ultimately

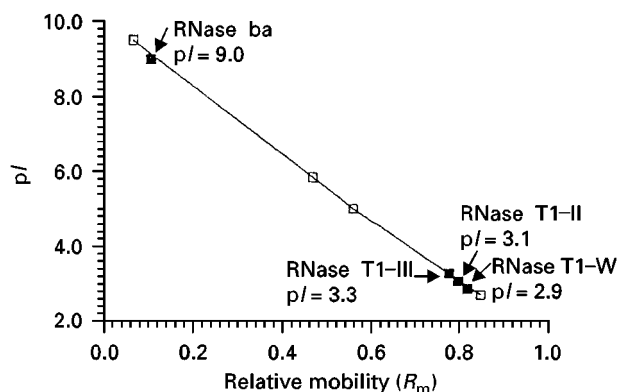


Figure 2 Calibration graph for *pI* determination using a set of marker proteins. The markers (open squares) are ribonuclease A (*pI* 9.45); carbonic anhydrase (*pI* 5.90); β -lactoglobulin (*pI* 5.1) and unsulfated cholecystikinin flanking peptide (*pI* 2.75). The four solid squares represent four unknown proteins whose *pI*s have been determined by linear interpolation in the calibration graph. (Reproduced from Chen SM and Wiktorowicz JE (1992) *Analytical Biochemistry* 20: 84–98 by permission.)

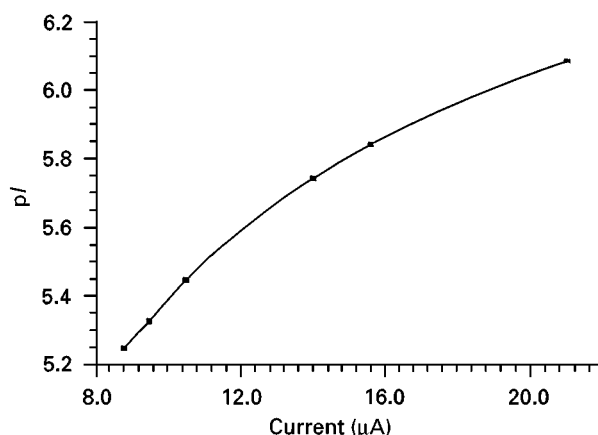


Figure 3 Calibration graphs for *pI* determination using the current during the mobilization step as a parameter in capillary IEF. The six experimental points represent six forms of transferrin, containing different amounts of sialic acid and of iron. (Reproduced from Kilar F (1991) *Journal of Chromatography* 545: 403–406, by permission.)

may lead to precipitation. However, at, or in the proximity, of their *pI* value proteins exhibit a minimum of total charge and thus a solvation minimum. This increases the risk of aggregation, and is further enhanced by the extremely low ionic strength conditions prevailing in IEF. When protein molecules precipitate they probably aggregate by hydrophobic interactions. It seems logical therefore to try to suppress precipitation by supplementing the CA buffers with agents known to decrease hydrophobic interactions, such as ethylene glycol (10–40% v/v) or detergents (1–4% w/v). The detergents should be either non-ionic or zwitterionic, so as to be compatible with the focusing process; in addition, they should preferably be transparent at 280 nm so as to minimize interference with protein detection. There are some simple ways to reduce protein interaction and precipitation: one is to use dilute protein solutions (aggregation is proportional to protein concentration); the other is to increase the CA buffer concentration up to 4%, since this leads to an increase in total ionic strength. Conti *et al.* (1997) have investigated the use of a large number of solubilizers and proposed mixtures of mild agents capable of fully preserving the three-dimensional structure and full activity of biomolecules. Among the solubilizing agents are non-detergent sulfobetaines, taurine, Good's buffers such as bicine and CAPS, polyols, such as sucrose, sorbose, sorbitol and mixtures thereof.

The Detection System

As discussed above, the standard absorption wavelength for detection in IEF is 280 nm, the typical

absorption maximum of proteins. As an alternative method a universal concentration gradient imaging system not requiring a mobilization step can be used. This system is based on the Schlieren shadowgraph methods and uses a He-Ne laser to probe the capillary content and a charge-couple device (CCD) as a detector. The capillary has to be square, not covered by polyimide and rather short (4 cm). Focusing is completed in 2 min, resolution is of the order of 0.02 pH units and the mass detection limit appears to be of the order of the picomole level. As an alternative, a whole column UV absorbance detection consisting in transporting the entire column past the detector (the capillary, of course, has to be UV transparent) can be used. In this set-up the optical configuration consists of a 5 mW argon ion laser (with either a 496.5 or a 514.5 nm lasing line) probing the entire length of a 4 cm long, square glass capillary and using as a detector a 1204-pixel CCD camera. Focusing and imaging are usually completed in 2–4 min. The problem is that only coloured proteins (those that absorb in this wavelength region) can be efficiently detected (e.g. haemoglobin, myoglobin and cytochrome-c). Finally, a mass spectrometer has been proposed as a detector after CIEF: it should be noted that the technique becomes two-dimensional, since proteins are then mapped by both charge and mass.

Focusing in Dynamically Coated Capillaries

Three groups have reported approaches on the possibility of focusing in dynamically coated capillaries. The techniques will be reviewed below.

Dynamic Coating with Methylcellulose

Rather than completely eliminating EOF one might try to reduce it to such an extent as to allow attainment of steady-state conditions; from there on, the bulk flow would keep the 'arrested' stack moving past the detection window. This approach would then obviate the need for performing salt, vacuum or hydrodynamic mobilization; focusing and elution being accomplished in one step. A simple way for modulating EOF is to add viscous polymer solutions. The capillary can be conditioned with 0.1% methyl cellulose, mixed with sample and CA buffers and used to fill the entire column. It has been found that by increasing the anolyte concentration to 25 mM phosphoric acid also allows the detection of acidic proteins. Finally, it has been assessed how deleterious different amounts of salt (NaCl) present in the sample would be to the focusing process. As little as 10 mM

of NaCl in the sample suffices to entirely destroy the separation so salt in the analyte must be kept below this level.

Dynamic Coating with Hydroxypropyl Methylcellulose

In another system, the dynamic agent used for partial coating is hydroxypropyl methylcellulose (HPMC). In this approach, some interesting variants have been adopted. A new capillary is first rinsed for 20 min with 1 M NaOH and then for 10 min with 0.1 M NaOH containing 0.3% HPMC. It is during this final washing that conditioning of the capillary and partial coating with HPMC occurs. This etching procedure (with 1 M NaOH), followed by a short renewal of the dynamic coating (0.3% HPMC in 0.1 M NaOH) is shown to provide data of the highest reproducibility. The sample proteins are dissolved in 2.5% Ampholine solution, without any addition of HPMC. The anolyte is the standard 10 mM phosphoric acid solution, whereas the catholyte consists of 20 mM NaOH in the presence of 0.1% HPMC. The sample is introduced as a plug, occupying only 10–50% of the capillary length at the anodic side, the remaining being filled with catholyte. Since the entire stack of proteins will eventually be displaced towards the cathode by the EOF, this initial sample plug distribution allows more time to reach a good focusing pattern prior to sample passage in front of the detector.

Dynamic Coating with Adsorbed Surfactants or Polymers

In another variant, reduction of EOF via derivatization of capillaries with a hydrophobic coating (octadecylsilane) followed by adsorption of either a surfactant (Brij 35, PF-108) or a hydrophilic polymer (e.g. polyvinyl alcohol, polyvinyl pyrrolidone, methylcellulose) has been proposed. The procedure is as follows: the capillary is first treated with 1 M NaOH for 30 min, followed by several washings with deionized water and methanol (30 min each). The residual methanol is evaporated in an oven at 90°C for 2 h, while flushing the capillary with a stream of nitrogen at 400 kPa. While still in the oven at 90°C, a solution of octadecyltrichlorosilane in 50% toluene is flushed through the capillary for 6 h. After silylation, the capillary is rinsed for 20 min with methanol and then with water for 30 min. Surfactant solutions (in general 0.4%) are pumped continuously through the capillary for an additional 6 h in order to complete the coating process. Coating via adsorption of detergent (or methylcellulose 4000) is shown to reduce the EOF of the native, untreated capillary, to approximately 3–5% of the original value but the

residual EOF still allows adequate flow to obviate the need for a separate mobilization step. Based on the resolution of haemoglobin variants proteins that varied 0.03 pH units in isoelectric point were resolvable.

Sample Preconcentration Systems

Typical preconcentration steps commonly used in biochemical analysis (especially for macromolecules) such as lyophilization, ultrafiltration, partition between two polymer aqueous phases, osmotic removal of water and chromatographic adsorption-desorption, will entail large losses when the sample volume is 1–10 μL or less, as is customary in capillary zone electrophoresis (CZE). A number of electrophoretic methods for concentrating biopolymers (especially peptides and proteins), while partially depleting them of strong electrolytes (often a problem in all IEF procedures), have been described. In practice the whole electrophoresis tube is filled with the sample solution to be concentrated and then the sample is allowed to migrate against the end of the tube where a gradient of conductivity or viscosity exists and is arranged in such a way as to continuously slow down sample electrophoretic migration. The sample will finally collect in a narrow zone of the tube (typically 0.2–0.5 mm in width). A 400–1000-fold concentration is obtained when a 200 mm long tube is filled completely with the sample and still more if an electrode vessel is also loaded with sample. As an alternative, an on-line isotachophoretic (ITP) concentration process of very large injection volumes prior to CZE analysis can be adopted. Sample volumes up to 25 μL can be concentrated by this system. As concentrating large volumes would take a relatively long time, depending on the migration path length, a system of coupling a narrower bore to a larger bore capillary is generally utilized in order to speed up the process. Finally, after the ITP concentration step the sample can be analysed by CZE via a T-junction connected to another electrolyte reservoir (i.e. one has to resort to a three-pole column).

Some Application of Examples

A vast body of applications already exists; a number of them can be found in the reviews listed in the Further Reading section. We will consider some selected examples here. By using umbilical cord blood which contains only three major haemoglobin (Hb) components (Hb F, Hb A and Hb F acetylated, F_{ac}) it is possible to perform thalassaemia screening provided a good separation is obtained between Hb A and Hb F_{ac} , which have minute differences in pI values. In order to improve the separation the pH 6–8

Ampholine is admixed with an equimolar mixture of 'separators', namely 0.2 M β -alanine and 0.2 M 6-aminocaproic acid, which flatten the pH gradient in the focusing region of the three major components. Figure 4 shows this separation obtained by CIEF. The method is simple, can unambiguously detect any

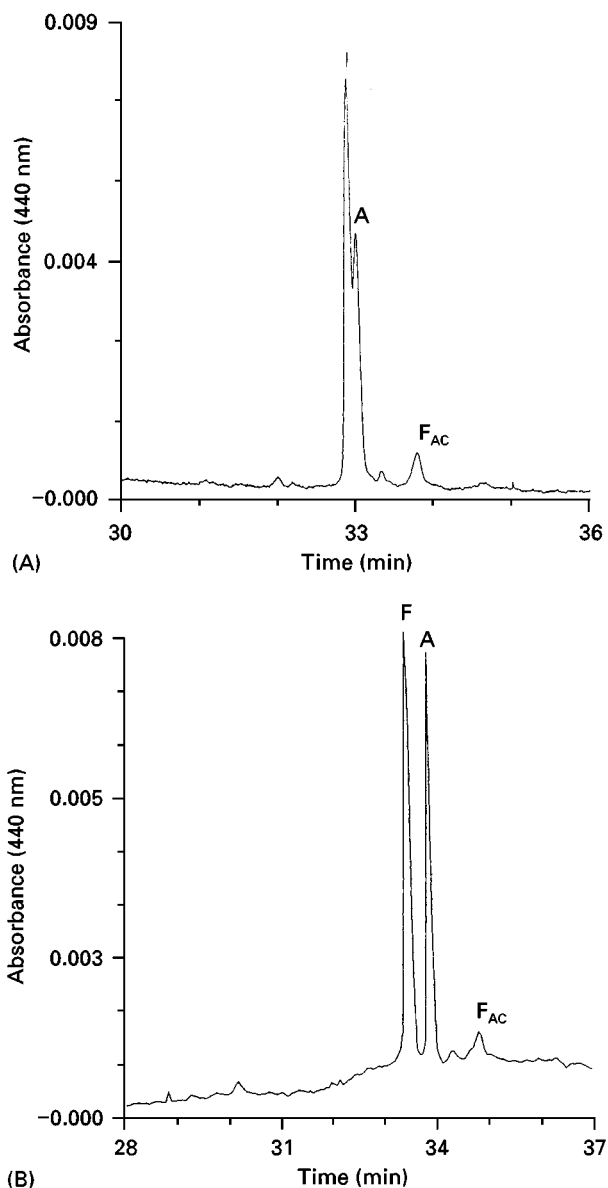


Figure 4 Separation of Hb F, A and F_{ac} by capillary IEF. Background electrolyte: 5% Ampholine, pH 6–8, added with 0.5% TEMED (panel A) and additionally with 3% short-chain polyacrylamide and 50 mM β -Ala (panel B). Anolyte: 20 mM H_3PO_4 ; catholyte: 40 mM NaOH. Sample loading: by pressure, for 60 s. Focusing run: 20 kV constant at 7 μA (initial) to 1 μA (final current), 20°C. Capillary: coated with poly(AAEE), 25 μm internal diameter, 23.6/19.1 total/effective length. Mobilization conditions: with 200 mM NaCl added to anolyte, 22 kV. Detection at 415 nm. (Reproduced from Conti M, Gelfi C and Righetti PG (1995) *Electrophoresis* 16: 1485–1491, by permission.)

thalassaemic condition and can be easily performed on a routine basis in a neonatal unit. Using the same principle Conti *et al.* have also attempted CIEF separation of Hb A from Hb A_{1c} (the glycated form of Hb A), the latter component being of diagnostic value for the long-term control of diabetic patients (glucose

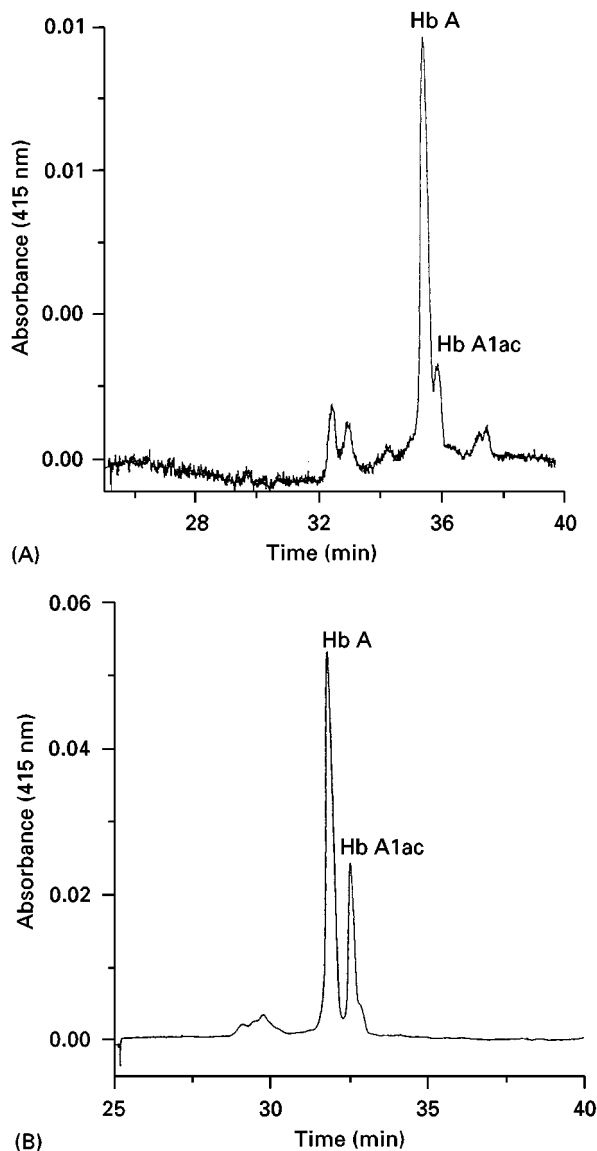


Figure 5 Separation of Hb A from A_{1c} by capillary IEF in the absence (A) and in presence (B) of 3% short-chain polyacrylamide and an equimolar mixture of 'separators', 0.33 M β -Ala and 0.33 M 6-amino caproic acid. Background electrolyte: 5% Ampholine, pH 6–8, added with 0.5% TEMED. Anolyte: 20 mM H_3PO_4 ; catholyte: 40 mM NaOH. Sample loading: by pressure, for 60 s. Focusing run: 20 kV constant at 7 μ A (initial) to 1 μ A (final current), 20°C. Capillary: coated, 25 μ m internal diameter, 23.6/19.1 total/effective length. Mobilization conditions: with 200 mM NaCl added to anolyte, 22 kV. Detection at 415 nm. (Reproduced from Conti M, Gelfi C, Bianchi-Bosisio A and Righetti PG (1996) *Electrophoresis* 17: 1590–1596, by permission.)

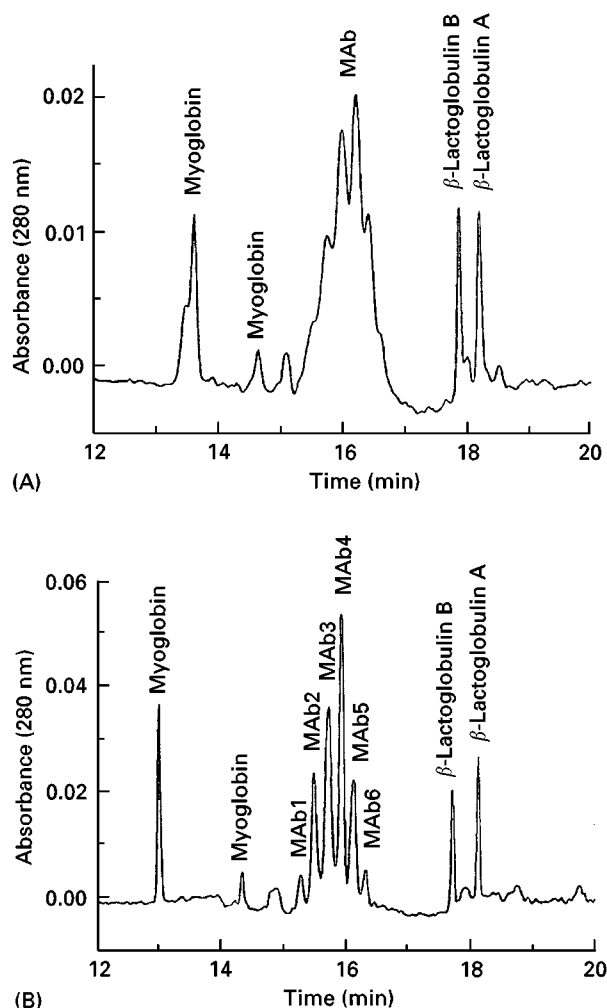


Figure 6 CIEF of a mouse monoclonal antibody using pressure mobilization. Focusing for 2 min at 10 kV, followed by mobilization at low pressure (0.5 psi) at (A) 10 kV and (B) 20 kV. Concentration of the marker proteins: 50 ng μ L⁻¹; concentration of desalted antibody: 0.5 μ g μ L⁻¹. Ampholyte solution: 4% Pharmalyte, pH 3–10, 1% TEMED in 0.8% methyl cellulose. Anolyte: 10 mM H_3PO_4 ; catholyte: 20 mM NaOH. (Reproduced from Schwer C (1995) *Electrophoresis* 16: 2121–2126, by permission.)

binds irreversibly to Hb molecules; the percentage of Hb A_{1c} varies with the blood glucose concentration to which red blood cells have been exposed during their circulating lifetime, see Figure 5). A good separation of monoclonal antibodies is shown in Figure 6: as mobilization was obtained by pressure under voltage it shows the importance of working under high voltage during this step.

Further Reading

Chiari M, Nesi M and Righetti PG (1995) Surface modification of silica walls: a review of different methodologies. In Righetti PG (ed.) *Capillary Electrophoresis in Analytical Biotechnology*. Boca Raton: CRC Press. pp. 1–36.

- Conti M, Galassi M, Bossi A and Righetti PG (1997) Capillary isoelectric focusing: the problem of protein solubility. *Journal of Chromatography A* 757: 237–245.
- Liu X, Susic Z and Krull IS (1996) Capillary isoelectric focusing as a tool in the examination of antibodies, peptides and proteins of pharmaceutical interest. *Journal of Chromatography A* 735: 165–190.
- Pritchett TJ (1996) Capillary isoelectric focusing of proteins. *Electrophoresis* 17: 1195–1201.
- Righetti PG (1983) *Isoelectric Focusing: Theory, Methodology and Applications*, Amsterdam: Elsevier.
- Righetti PG (1990) *Immobilized pH Gradients: Theory and Methodology*. Amsterdam: Elsevier.
- Righetti PG and Bossi A (1998) Isoelectric focusing of proteins and peptides in gel slabs and in capillaries. *Analytica Chimica Acta* 372: 1–19.
- Righetti PG, Gelfi C and Conti M (1997) Current trends in capillary isoelectric focusing of proteins. *Journal of Chromatography B* 699: 91–104.
- Righetti PG, Bossi A and Gelfi C (1997) Capillary isoelectric focusing and isoelectric buffers: an evolving scenario. *Journal of Capillary Electrophoresis* 4: 47–59.
- Rodriguez-Diaz R, Wehr T and Zhu M (1997) Capillary isoelectric focusing. *Electrophoresis* 18: 2134–2144.
- Steinmann L, Mosher RA and Thormann W (1996) Characterization and impact of the temporal behaviour of the electroosmotic flow in capillary isoelectric focusing with electroosmotic zone displacement. *Journal of Chromatography A* 756: 219–232.
- Strege MA and Lagu L (1997) Capillary zone electrophoresis and isoelectric focusing of biotechnology-derived proteins. *Electrophoresis* 18: 2343–2352.
- Taverna M, Tran NT, Merry T, Horvath E and Ferrier D (1998) Electrophoretic methods for process monitoring and the quality assessment of recombinant glycoproteins. *Electrophoresis* 19: 2527–2594.

Capillary Isotachophoresis

J. Sádecká and J. Polonský, Faculty of Chemical Technology, Bratislava, Slovak Republic

Copyright © 2000 Academic Press

Introduction

Isotachophoresis (ITP) is one of the fundamental electrophoretic separation techniques, where charged constituents are separated in an electric field due to their differences in their electrophoretic mobilities.

The moving boundary electrophoretic experiments and theoretical developments were the forerunners of isotachophoresis. Even by 1923, Kendall and Crittenden had described separation of some metals and acids by – as they called it – the ‘ion migration method’, which was in fact isotachophoresis. They concluded that ion concentrations were in accordance with the Kohlrausch regulation function. In 1942, Martin did his first experiments on what he called ‘displacement electrophoresis’ as an analogue of displacement chromatography. In 1963, Everaerts and Martin started their work on isotachophoresis. Up to 1970 several names had been used for what Kendall had called the ion migration method: these included the ‘moving boundary method’, ‘displacement electrophoresis’, ‘steady-state stacking’, and ‘ionophoresis’. In 1970, Haglund introduced a name, based on the characteristic feature of the electrophoretic technique, namely the equal velocity of the sample zones in the steady state: isotachophoresis (ITP). The basic theory and early development in the field of iso-

tachophoresis was described in 1976 by Everaerts in his fundamental book. An outline of the development of isotachophoresis is given in Table 1. Some advances in isotachophoresis are described in detail below.

ITP in Closed Systems

Up to 1990, ITP was carried out in commercial apparatus in 200–500- μm i.d. narrow-bore plastic capillaries and with closed systems, i.e. no electroosmotic flow (EOF) occurred.

Basic Theory

Under the influence of an applied electric field, E , ionic species will move towards the electrode with a migration velocity, v , of:

$$v = m \times E \quad [1]$$

where m is the effective mobility of an ionic species. The effective mobility depends on various factors, for example, the ionic radius, shape and charge of the ion, degree of dissociation, pH, dielectric constant and viscosity of the solvent, and temperature.

Typically, ITP is performed with a constant current and it is not possible to separate cations and anions in the same run (unidirectional isotachophoresis).

It is characteristic of ITP that the sample to be separated is injected between two different electrolyte solutions. The first solution (the leading electrolyte) contains an ion (the leading ion) with the same charge

Table 1 Development of isotachophoresis

Year	Development of:	Attributed to:
1897	Regulation function	Kohlrausch
1930	Moving boundary electrophoresis	Tiselius
1942	Displacement electrophoresis	Martin
1968	Capillary tube apparatus for isotachophoresis	Verheggen, Everaerts
1970–1989	ITP in closed systems, 200–500 μm i.d. narrow-bore plastic capillary with minimized EOF	
	Column-coupling ITP	Everaerts
1970–1980	Thermometric, conductometric, potentiometric and UV detection	Everaerts
1981	Refractometric detection	Bresler
1981	Offline ITP-MS	Kenndler
1983	Radiometric detection	Kaniansky
1984	Fluorimetric detection	Reijenga
1984	Amperometric detection	Kaniansky
1985	Absorption spectra	Hanibalová
1989	ITP in open system, 100 μm i.d. fused-silica capillary with EOF, online ITP-MS	Udseth
1990	ITP in open system, 25–50 μm i.d. fused-silica capillaries	Thormann
1990	Online ITP-CZE (column coupling)	Kaniansky
1991	Offline ITP-PIXE	Hirokawa
1993	Bidirectional ITP	Hirokawa
1995	Raman spectroscopic detection	Walker

sign as that of the sample ions, but with an effective mobility higher than that of the fastest moving sample ion. The second solution (the terminating electrolyte) contains an ion (the terminating ion) with the same charge sign, but with an effective mobility slower than that of the slowest moving sample ion. The polarity of the electric field has to be such that the leading ion migrates to the electrode that is placed on the same side of the sample as the leading electrolyte. After application of an electric field to the system, each ionic species will have a different migration velocity according to eqn [1] and hence the isotachophoretic process starts.

The process of isotachophoresis may be divided into two parts. In the first part, the separation of the ions proceeds and the migration velocity of the individual ions in the mixed zones is different. In the second part (in the steady state) the ions have already separated from one other and all move with the same velocity, v :

$$v = m_L E_L = m_i E_i = m_T E_T \quad [2]$$

where L is the leading ion, i is the i th ion and T is the terminating ion.

A schematic representation of the cationic and anionic modes in ITP experiments without EOF is given in Figure 1(A,B). As the ionic species are arranged in order of decreasing effective mobilities, the electric field strengths increase on the terminating ion side.

The increase in the electric field strength in the consecutive zones induces the zone-sharpening effect. When a zone has attained the steady state, the bound-

ary will not broaden further, which is in contrast to zone electrophoresis, where the peaks are broad owing to adsorption and diffusion. This effect can easily be explained. If an ion diffuses into a preceding zone, where the electric field strength is lower than the value that corresponds to its velocity, its velocity will decrease according to eqn [2], and it will be overtaken by its own zone. If an ion diffuses into a zone with a higher electric field strength, then it will obtain a higher migration velocity according to eqn [2], until it reaches its own zone.

It is characteristic for the steady state that the concentration of each component is adjusted to the value following from the Kohlrausch regulation function in the form:

$$c_i = c_L \frac{m_L + m_R}{m_L} \times \frac{m_i}{m_i + m_R} \times \frac{z_L}{z_i} \quad [3]$$

where R is the common counterion, Z_i is the ionic charge. In the steady state, the concentration C_i of the i th ion is always adjusted to a certain value depending only on the concentration of the leading electrolyte C_L and on the mobility of the ions i , L and R. From the analytical point of view this is a very important feature of ITP. It can be concluded that for a given set of experimental conditions, the zone length is a direct measure of the amount of an ion present in the zone. Another important consequence of these properties is the concentration effect of isotachophoresis. In fact, a species more concentrated in the original sample is diluted during the separation and, a species originally too dilute is concentrated during the separation.

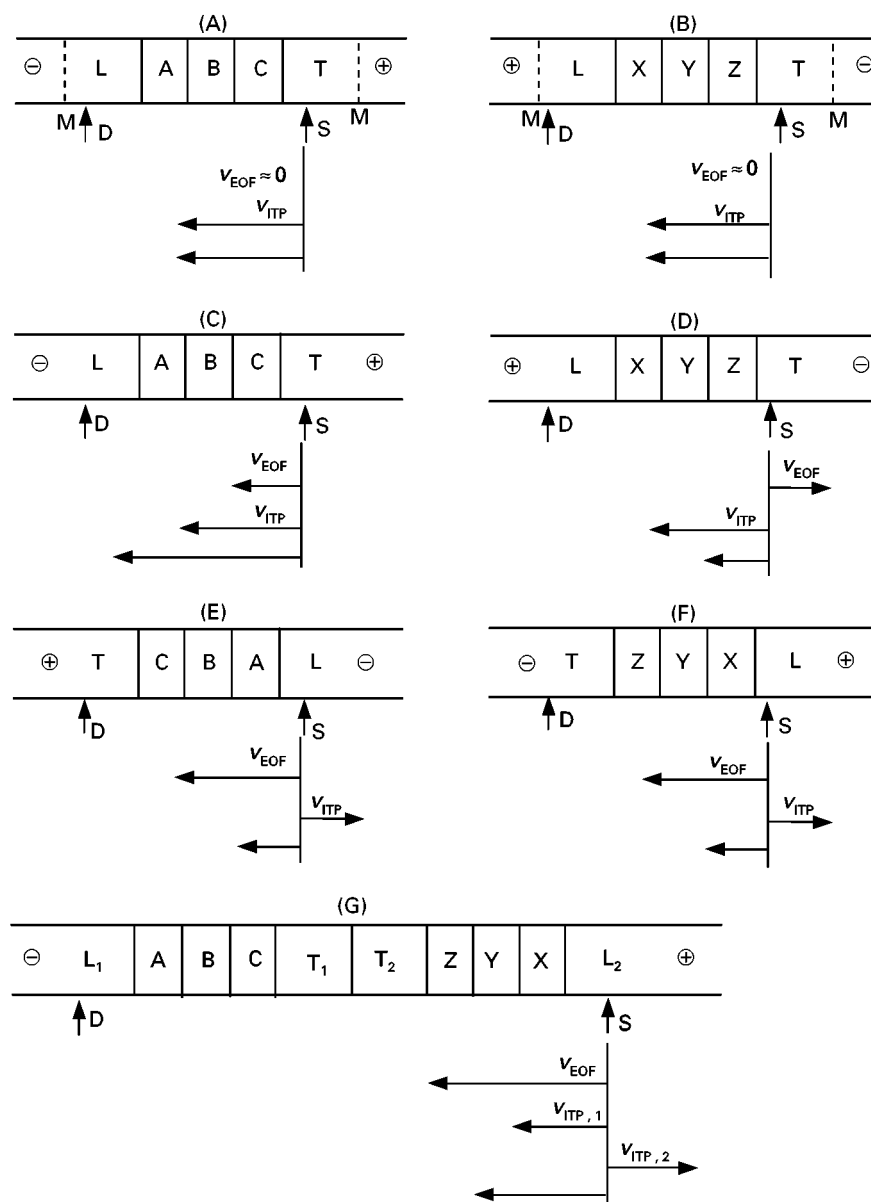


Figure 1 Schematic representation of the two modes in unidirectional ITP experiments without EOF: (A) the cationic separation of a mixture of cations A, B, and C with $m_A > m_B > m_C$; (B) the anionic separation of a mixture of anions X, Y, and Z with $m_X > m_Y > m_Z$. The four modes in unidirectional ITP with EOF: (C) the cationic cations as in (A); (D) the anionic anions as in (B); (E) the reversed cationic; (F) the reversed anionic; (G) Schematic representation of the bidirectional ITP; separation of mixture of cations A, B and C and anions X, Y and Z. L_1 = leading cation; T_1 = terminating cation; L_2 = leading anion; T_2 = terminating anion. Only steady state is presented. S = sample inlet; D = detector position, L = leading ion, T = terminating ion, v_{EOF} = velocity of EOF; v_{ITP} = isotachopheretic velocity; \leftarrow or \rightarrow = net velocity; M = semipermeable membrane. For further explanation, see text.

In ITP, the response is usually recorded against time with a detector placed at the end of capillary (Figure 2).

The identity of a species is characterized by the effective mobility (or a quantity proportional to the effective mobility). This is usually the response of the universal detector. It is called the height (step height) or the relative height (relative step height, rsh) of the

zone, and is given by the relation:

$$rsh_i = \frac{h_i - h_L}{h_T - h_L} \quad [4]$$

where h_i is the step height of the compound, h_L is the step height of the leading ion and h_T is the step height of the reference ion (usually the terminating ion)

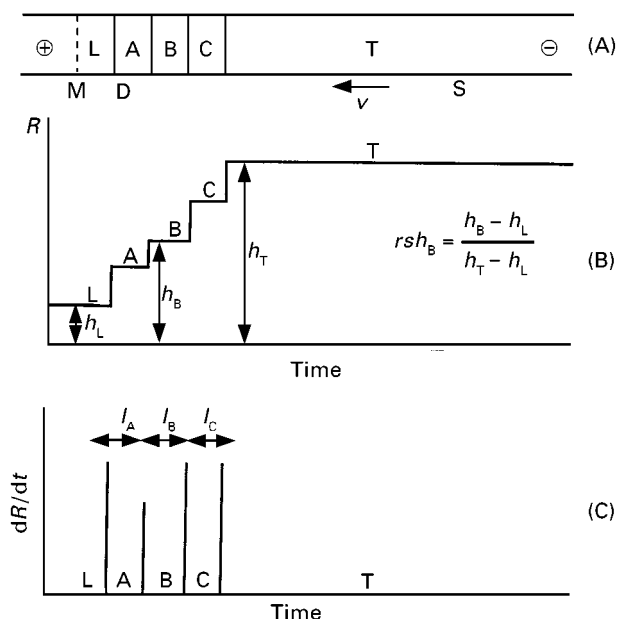


Figure 2 Graphical representation of response R from universal detector [(B) linear; (C) differential] for the different anions A, B, and C, moving in the steady state of an isotachopheric analysis (A). L = leading anion; T = terminating anion; S = sample inlet; D = detector position; M = semipermeable membrane. For further explanation, see text.

(Figure 2B). The values obtained in this way are then compared with those of standard species measured under the same experimental conditions.

The quantification is in general simplified by differentiating the signals and measuring the distance between the inflection point (Figure 2C). The zone lengths l_i are directly proportional to the number of ions (n_i): $l_i = K_i n_i$. The constant K_i depends on the equipment and the current used. A universal calibration constant (the response factor RF, eqn [5], which is independent of the diameter of the capillary, construction of the universal detector and driving current used during detection, has been introduced. For each component, the RF depends only on the concentration of the leading electrolyte:

$$RF = \frac{l \times I}{|z| \times F \times Q} \quad [5]$$

where l is the zone length (seconds), I is the driving current (amps), $|z|$ is the charge of the ion (equiv mol⁻¹), F is Faraday's Number (coulombs equiv⁻¹) and Q the amount injected (mol).

Based on the mathematical models for isotachophoresis described, computer programs have been set up for calculation of the parameters of the different zones. Unfortunately, only a few schemes

can be used for simulating capillary isotachophoresis at realistic current densities without causing either severe oscillations or unexpected program termination.

Online Coupling of ITP with CZE (Column-Coupling Instrumentation)

Column-coupling instrumentation (see below) of the separation unit for ITP as described by Everaerts has been shown to be suitable for online coupling of ITP and CZE. The extensive studies of Kaniánský and Marák give a good impression of the potential of combined ITP-CZE.

The online combination of ITP and CZE is a very effective tool for increasing the separation capability and sensitivity of CZE. It is characterized by isotachophoresis in the first capillary followed by online transfer of the sample cut into the second capillary where zone electrophoresis proceeds.

In principle, there are three ways of performing an ITP-CZE combination technique as far as the electrolyte systems are concerned. The simplest way is to use the terminating electrolyte as the background electrolyte (BGE) for CZE; the second possibility is to use the leading electrolyte as BGE and the third possibility is to use a totally different BGE.

ITP has the advantage of much higher loading volumes, e.g. microlitres instead of nanolitres in CE. In addition, ITP is a concentration technique. The combination of these features makes ITP, in principle, an ideal technique for sample pretreatment. In ITP-CZE, a 10⁴-fold concentration increase can be achieved, and this even for a component present in a 10⁵-fold excess of the matrix.

ITP in Open Systems

Since the early 1990s, commercial instruments for CZE have been available generally with open-tubular fused-silica capillaries with an inner diameter between 20 and 100 μm, together with an on-column detector placed towards one end of the capillary. As this apparatus can be used for ITP it was of interest to study the possibilities for ITP in open systems. If ITP experiments are performed in open-tubular fused-silica capillaries, the negative surface charge of untreated fused-silica causes an EOF towards the cathode. This EOF will influence the ITP system and four different modes can be observed. In Figure 1(C), the cationic ITP mode is shown. The EOF will generally act in the direction from the anode to the cathode and as a result the cationic ITP system will be pushed towards the cathode with a higher velocity compared with cationic experiments in closed systems. In

Figure 1(D), the anionic ITP mode is shown. This mode can be applied if the velocity of the leading ion is greater than that of the EOF during the whole experiment. Only in this case will anions with mobilities slower than that of the EOF also migrate to the anode according to the isotachopheretic condition. The reversed cationic mode (Figure 1E) can be applied if there is a reversed EOF (e.g. using coated capillaries or additives to the electrolyte) with a velocity greater than that of the cationic system. Here the cathode must be placed at the sample inlet end and the anode at the detector end. Although the ITP separation takes place in the direction of the cathode, there will be a net velocity of the ITP system in the direction of the detector end and components will be detected in a reversed order compared with a normal cationic ITP system. In Figure 1(F), the reversed anionic mode is presented. Here the anode is placed at the sample inlet end, the cathode at the detector end and components will be detected in a reversed order compared with a normal anionic ITP system.

As the velocity of the EOF is extremely important in the migration behaviour of ITP systems, much effort must be put into controlling EOF. The velocity of the EOF strongly depends on the choice of the leading and terminating electrolyte and it also varies with the composition of the sample. Moreover, the velocity of the EOF continuously changes during the analysis and is first determined by the composition of the leading electrolyte and finally by that of the terminating electrolyte. Varying EOF velocities cause irreproducible migration times and zone length and the results of quantitation are erroneous. The addition of methylhydroxyethylcellulose to the electrolytes and sample largely suppresses the EOF in order to improve quantitation. In spite of the addition of methylhydroxyethylcellulose, the reproducibility of the zone lengths with time is poor, and an internal standard is, therefore, needed. Hence the reproducibility in ITP quantitative analysis in open systems is a problem similar to that in electrophoresis. Generally, closed systems are to be preferred to open systems for quantitative analysis.

The presence of an EOF, however, facilitates the development of bidirectional ITP for the simultaneous determination of anionic and cationic components. In bidirectional ITP, the leading electrolyte for cations must be simultaneously the terminating electrolyte for anions, and vice versa the leading electrolyte for anions must be the terminating electrolyte for cations. That is, the counterions (cations) coexisting with the leading anions play the role of the terminating cation, and the counterions (anions) coexisting with the leading cations play the role of the termina-

ting anion. In a fused silica capillary in the presence of a cathodic EOF, cationic sample trains can be detected with a detector placed towards the cathodic end of the capillary. However, anionic species can be detected only at pH > 6. At pH > 6, the velocity of the EOF is greater than that of the anionic ITP system and hence the anions migrate slowest since they are attracted to the anode, but are still carried by the EOF towards the cathode (Figure 1G).

Instrumentation for ITP

Separation Capillary

The actual separation takes place in a PTFE (polytetrafluoroethylene) or a silica capillary. The separation capacity can be increased by extending the length of the capillary, but the analysis time and the maximum voltage required also increases. From the instrumental point of view, the column-coupling system (Figure 3) frequently used today has led to significant progress. It consists of a pre-separation unit with a capillary of larger diameter (e.g. 0.8 mm) equipped with the detector and bifurcation block, to which an analytical capillary of small diameter (e.g. 0.3 mm) is connected. At the beginning of the analysis, the driving current passes through the pre-separation capillary only. The detection system in the first capillary is employed to evaluate analysis. In addition, it provides the information necessary to control the transfer of the analytes into the second capillary and the removal of the sample constituents which are led out of the separation compartment after the first stage. At a suitable moment, the driving current is switched so that it passes through the analytical capillary and thus introduces the required sample zones into this capillary where further separation takes place. Column coupling enables use of different leading electrolytes in the pre-separation and analytical capillaries, thereby influencing the subsequent separation, separation of mixtures containing components in ratios up to 1 : 1000 without increasing the voltage and without prolonging the analysis time, and application of ITP in combination with CZE.

Electrode Chamber, Electrodes and Power Supply

The capillary is connected on each side to an electrode chamber provided with a platinum electrode. In closed systems, the chamber, filled with the leading electrolyte, is connected to the capillary via a semipermeable membrane. The terminator chamber is connected via a multiway switching valve, which is open in the course of the analysis. In open systems, the ends of the capillary are placed in electrolyte reservoirs (electrode chamber).

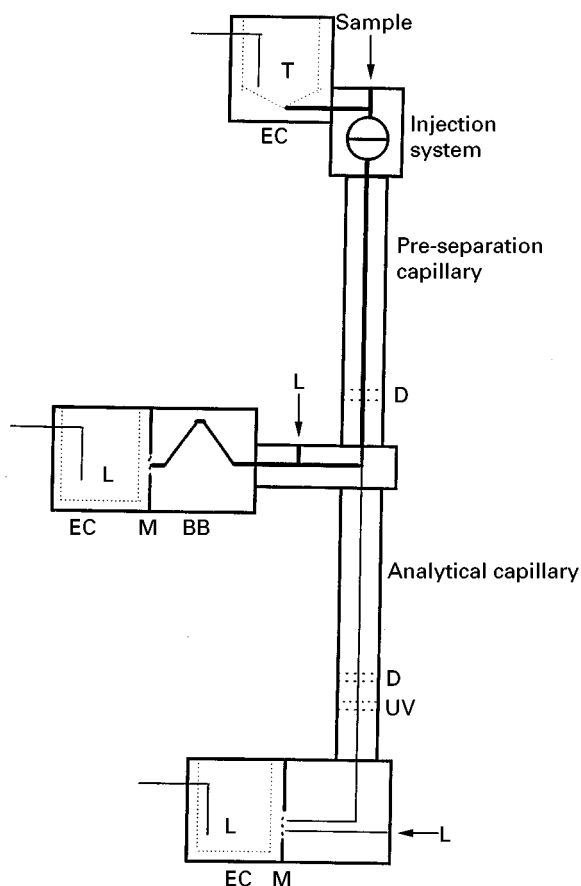


Figure 3 Column-coupling isotachopheretic system. EC = electrode compartment; BB = bifurcation block; D = conductivity detector; UV = UV detector; L = leading electrolyte; T = terminating electrolyte; M = semipermeable membrane.

A high-voltage power supply capable of delivering 500 μ A at up to 20–30 kV d.c. is needed. The constant current regulation of the power supply must be extremely well designed.

Injection System

In closed systems, the sample can be introduced by a microsyringe through a septum or by a multi-port valve system. In open systems, the sample can be vacuum-aspirated or loaded electrokinetically.

Detection

The first universal online detector was the thermocouple detector. Owing to its low sensitivity, the thermocouple detector was replaced with universal contact detectors, which sense the electrical resistance or potential gradient in the zones. The disadvantage of contact detectors is polarization of the sensing electrodes. To solve this problem, a universal contactless high-frequency conductivity detector was pro-

posed in the 1970s. Detection based on differences in the refractive index of various zones was introduced in 1981. The disadvantage of this system was the necessity of working with high electrolyte concentrations, which resulted in slow analysis.

In 1991, McDonnell and Pawliszyn developed a new refractive index detector for ITP consisting of a He–Ne laser or a laser diode and photodiode position sensor. The direction of the beam is deflected when it passes through the refractive index gradient produced by the sample zone. By using this detector, a few nanomoles of sample can be detected. The development of a selective UV-absorption detector for ITP had been an important contribution to the development of ITP in the 1970s. The UV detector is now a common component of commercial apparatus. In most cases only the wavelengths 254 and 280 nm have been utilized for detection. Arlinger had shown in 1974 that a UV detector could be applied as a pseudo-universal detector. UV-absorbing counterions were used, for which the molar absorption was pH-dependent. As each zone has its own defined pH and concentration, the pH and concentration difference gave rise to an absorbance difference sufficiently large to be detectable.

Sometimes it can be advantageous to use a UV-absorbing spacer in order to make the detection of consecutive zones of nonabsorbing ionic species possible. In some instances it is possible to detect boundaries between two consecutive non-UV-absorbing zones because of the trace amounts of UV-absorbing impurities which are present in most electrolytes and which concentrate as markers between the separated non-UV-absorbing zones. Great attention has been paid to development of new selective detectors for ITP, to facilitate the identification of compounds in the detected zones. Sensing of absorption spectra in isotachopheretic zones is one of the possibilities. Fluorimetric detection is a highly sensitive method. In ITP, the equipment designed initially for the dual-wavelength UV detection has been employed for fluorimetric zone detection. Zones of fluorescing compounds or of compounds quenching counterion fluorescence can be detected.

In 1991, Hirokawa introduced a new specific detection method for metal ions. He used an offline combination of ITP and particle-induced X-ray emission (PIXE), which is a multi-elemental method with high sensitivity. As the method is based on the characteristic X-rays emitted by target elements, it has a high specificity for the determination of the elements even if they are not separated. Radiometric detection of compounds labelled with a radioactive isotope is a specific method. Its principle is the detection of the radiation emitted from the labelled

compound zone passing the window of Geiger-Müller tube. Electrochemical detection, owing to its high sensitivity and specificity, is widely used in liquid chromatography. Its direct use in ITP is hindered by the presence of the driving electric field. To minimize disturbances due to the driving current, post-column amperometric detection has been employed. The separated constituents are hydrodynamically transported from the separation compartment into the detection cell. The hydrodynamic transport causes the dispersion to increase, therefore, the resolving power of post-column detection is lower in comparison, with for example, the conductivity detector. However, this disadvantage can be outweighed by its inherent selectivity and/or sensitivity.

The online combination of ITP with mass spectrometry was first demonstrated in 1989. The ITP/MS interface is based on electrospray ionization. Separations were conducted in open-tubular untreated fused-silica capillaries. The interface requirement of strong electroosmotic flow did not significantly degrade separations and both high sensitivity (limit of detection 10^{-9} mol L $^{-1}$) and high resolution can be obtained. Recently, Walker has demonstrated that a fiberoptic Raman probe can be used to obtain real-time intracapillary Raman spectra during ITP. Even at 2×10^{-5} mol L $^{-1}$ initial concentration, Raman spectra were obtained at a good signal-to-noise ratio.

Preparative Procedures in Isotachopheresis

Capillary isotachopheretic analysers can be used for preparative purpose in a discontinuous arrangement only. Once the separation has been performed, the analysis is discontinued and the analysed compound zone is isolated by using a microsyringe, a specially designed fractionating valve placed at the end of the separation capillary or a counterflow of leading electrolyte (Figure 4).

Continuous free-flow isotachopheresis (Figure 5) was developed to fractionate large-scale samples continuously. The separation field of continuous free-flow isotachopheresis is typically a thin film of fluid flowing between two parallel plates. An electric field is applied perpendicular to the flow direction. The leading and terminating electrolytes and the sample solution are continuously supplied with a multifold peristaltic pump into one end of the electrophoretic chamber and are collected with a multifold pump at the other. The leading and terminating electrolytes used for the electrode compartments circulate by pumps during migration. A dialysis membrane iso-

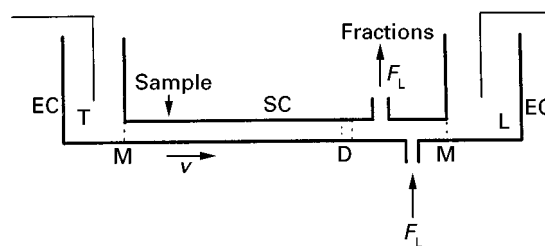


Figure 4 Capillary preparative isotachopheresis with a counter-flow of leading electrolyte. EC = electrode compartment; SC = separation capillary; D = detector; M = semipermeable membrane; L = leading electrolyte; T = terminating electrolyte; F_L = counter flow of leading electrolyte.

lates the separation chamber from the electrode compartments.

In recycling electrophoresis, in order to increase the electric charge applied to the sample, the fraction from each channel are continuously reinjected into the inlet port of the separation chamber. This instrumentation allows a high throughput and complete separation of the injected sample. Typical operation is batchwise, in contrast to continuous free-flow isotachopheresis.

Future Developments

Isotachopheresis underwent major development in the years 1970–1990. Over the last ten years CZE has occupied the major part of both the theory and applications of electrophoresis. Despite this, capillary isotachopheresis has kept its position as a special technique with unique features. Concentrating and

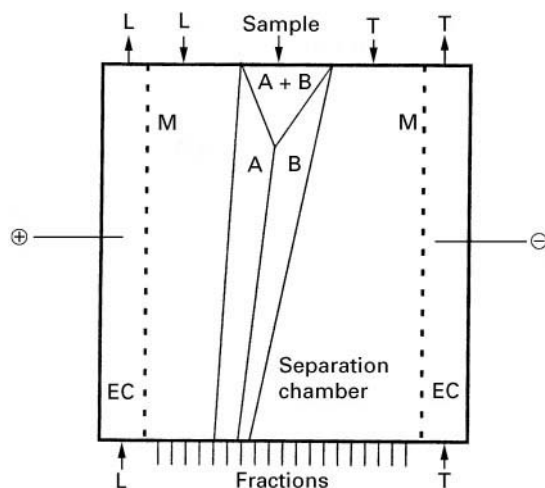


Figure 5 Continuous free-flow isotachopheresis. EC = electrode compartment; M = semipermeable membrane; L = leading electrolyte; T = terminating electrolyte; sample = mixture of A and B.

zone sharpening make it possible to obtain, in particular cases, much better results than when using CZE. Most promising is the combination of ITP with CZE where ITP serves as a preconcentration and pre-separation step for analysis of samples with complex matrices. Unfortunately, there is only one manual ITP–CZE system still commercially available.

Further Reading

- Boček P, Deml M, Gebauer P and Dolník V (1988) *Analytical Isotachophoresis*, pp. 5–237. Weinheim: VCH.
- Boček P, Gebauer P, Dolník V and Foret F (1985) Recent developments in isotachophoresis. *Journal of Chromatography* 334: 157–195.
- Everaerts FM, Beckers JL and Verheggen ThPEM (1976) *Isotachophoresis. Theory, Instrumentation and Applica-*

- tions*, Journal of Chromatography Library, vol. 6, pp. 7–282. Amsterdam: Elsevier.
- Gebauer P and Boček P (1997) Recent application and developments of capillary isotachophoresis. *Electrophoresis* 18: 2154–2161.
- Hirokawa T, Watanabe K, Yokota Y and Kiso Y (1993) Bidirectional isotachophoresis. *Journal of Chromatography* 633: 251–259.
- Hjalmarsson SG and Baldesten A (1981) A critical review of capillary isotachophoresis. *CRC Critical Reviews in Analytical Chemistry* 11: 261–352.
- Kaniansky D and Marák J (1990) On-line coupling of capillary isotachophoresis with capillary zone electrophoresis. *Journal of Chromatography* 498: 191–204.
- Thormann W (1990) Isotachophoresis in open-tubular fused-silica capillaries. Impact of electroosmosis on zone formation and displacement. *Journal of Chromatography* 516: 211–217.

Cellulose Acetate

G. Destro-Bisol, University 'La Sapienza',
Rome, Italy

M. Dobosz and V. Pascali, Catholic University,
Rome, Italy

Copyright © 2000 Academic Press

The introduction of zone electrophoresis, pioneered by König in 1939, played a crucial role in the progress of electrokinetic separations. With this technique, molecules migrate as zones with sharp boundaries in a supporting medium immersed in a buffer solution under the application of an electric field. Zone electrophoresis was quickly found to be superior in performance to Tiselius's original technique of moving boundary electrophoresis and replaced it entirely – to be superseded in turn by displacement electrophoresis and isoelectric focusing (IEF). Interestingly, the term 'zone electrophoresis' was first suggested by Tiselius himself.

Kohn first used cellulose acetate (CA) as a supporting medium for zone electrophoresis in 1957, as a superior substitute for plain filter paper. Since then, CA has been used in many electrophoretic protocols, for both research and clinical investigations (Table 1). Nowadays CA electrophoresis is a widespread technique.

In this article we explain what CA is and why it is used in electrophoresis. This is followed by a brief overview of the uses of CA in various electrophoretic contexts. Finally, some recent and innovative applications of CA in electrophoretic protocols are discussed.

General Concepts

Preparation of CA

CA sheets employed in electrophoresis are made of a molecular matrix, similar in structure to a sponge but a thousand times smaller. This matrix is obtained by letting acetic anhydride react with cellulose and dissolving the product in an organic solvent, that can evaporate quickly. After letting the solvent evaporate in closely-controlled conditions of temperature and humidity, a highly permeable matrix is obtained with a uniformly distributed microporosity. The spatial volume of the pores may account for 80% of the total matrix size, ensuring ideal permeation by any

Table 1 Historical sequence of main applications of CA to electrophoretic protocols in different areas of research and clinical investigations

Year	Application
1957	CA is used as an electrophoretic support (Kohn)
1971	Application to conventional electrophoresis of white cell and red cell enzymes (Meera Khan)
1975	Application to isoelectric focusing of alpha-1-antitrypsin in human serum and 6-phosphogluconate dehydrogenase (Harada)
1984	Application to counterflow affinity isotachophoresis of antigens in biological fluids with low protein contents (Abelev and Karamova)
1992	Introduction of CA for protein transfer from polyacrylamide gels
1993	Introduction of protocols for reusing CA

electrolytic solution. When shaped into gel sheets CA has better resistance to the dehydration involved in the dissipation of heat and is more easily handled. Thus, pre-gelled CA membranes (also referred to as Cellogel™) are the first choice of support for many electrophoretic applications. For better handling, some commercial versions of Cellogel™ come welded to an inert support of polyester plastic (Mylar™). These commercial forms of CA pass practically unchanged through the entire separation–staining–destaining cycle of a classical electrophoretic experiment.

There are several major factors accounting for the versatile electrophoretic properties of CA: (1) the cellulose chain length, which ranges from a few to millions of individual molecules; (2) the degree of acetylation (from 0.1% to 44%); (3) the pore size (between 50 Å and 10 µm), the random pore distribution and the volume of the pores compared with the solid matrix (20% to 80%). The spatial coiling of cellulose molecules, the type and concentration of wetting agents and the presence of residual contaminants may also be important factors.

CA as an Electrophoretic Medium

Migration of molecules through the CA matrix depends mainly on the net charge on the molecule, the buffer pH and ionic strength and the intensity of the electric field. The difference in surface net charge between the molecular species in a sample to be separated is perhaps the most important point to consider. Proteins are amphoteric, like their constituent amino acids, and they may be charged positively or negatively depending on the pH of the solvent medium (the buffer solution, in an electrophoretic experiment).

In gel electrophoresis a sieving effect may affect the separation, depending on the critical relationship between the spatial shape of a protein species and the pore size of the matrix medium. Because of the extremely large cellulose matrix pores, the mobility of proteins in CA electrophoresis is a direct function of their surface net charge, whereas molecular weight and shape are less important. For example, the human heavy α -2 macroglobulin (M_r : 1 000 000; pI 5.9) moves faster than the much lighter haptoglobin (M_r 100,000; pI 6.1) in alkaline buffer solutions.

As in most electrophoretic protocols, to improve a CA separation the ideal buffer pH and ionic strength, strip temperature, voltage, current, electroosmosis and time of separation should be selected. The optimal ionic strength is between 0.01 and 0.1 (mequiv L⁻¹). Although mobility is theoretically enhanced at high temperature, proteins are easily heat

denatured so the separation temperatures should be kept below 50°C. Moreover, since CA electrophoresis is traditionally carried out with no cooling, separation voltages should not exceed 500 V (60 V per linear centimetre in gel strips), and the current should be adjusted to less than 2.5 mA cm⁻². CA contains polar groups – hydroxy (OH⁻) and acetyl (CH₃COO⁻) radicals – that become charged at the pH system and move towards the anode through the cellulose matrix. This produces a counter-reaction, displacing buffer toward the cathode and interfering with the separation of the molecules of interest (endosmosis). Prolonged separation times may thus lead to the creation of artefacts due to the combined effects of heat, buffer turbulence and the counter-diffusion of molecules. Running times should be altered accordingly.

A few fundamental properties make CA electrophoresis notably superior to electrophoresis using filter paper: (1) the CA matrix is homogeneous, microporous and chemically pure, reducing molecular adsorption to a minimum; (2) instant heat dissipation occurs in the matrix, which does not need to be cooled; (3) the amount of protein needed is very small (1 mg or less); (4) the inherent buffering–staining–destaining system is very simple; (5) stained CA strips have no background; (6) the standard electrophoretic apparatus required is simple and inexpensive (Figure 1).

For most purposes – especially for routine clinical investigations – small-scale CA electrophoresis (with membranes < 10 cm long) is widely used (Figures 2 and 3). Larger scale membranes (usually 20 cm long) suit a variety of research analytical purposes and micropreparative applications.

CA in Electrophoretic Protocols

Conventional Electrophoresis

CA was originally introduced as a classical support for analytical zone electrophoresis but found a much broader range of applications. Essentially, it can now be used for both analytical and preparative purposes. Preparative applications exploit the speed of CA separations, the absence of molecular interaction, and the easy recovery of biologically active substances from the matrix.

CA is popular in clinical laboratories in which some well-established routine analyses are performed, e.g. for haemoglobin, serum proteins, lipoproteins and lactate dehydrogenase. Isoforms of many enzymes and proteins from different tissues come out very clear-cut on CA – a fact that is (or has been) of particular interest for anthropogenetic and

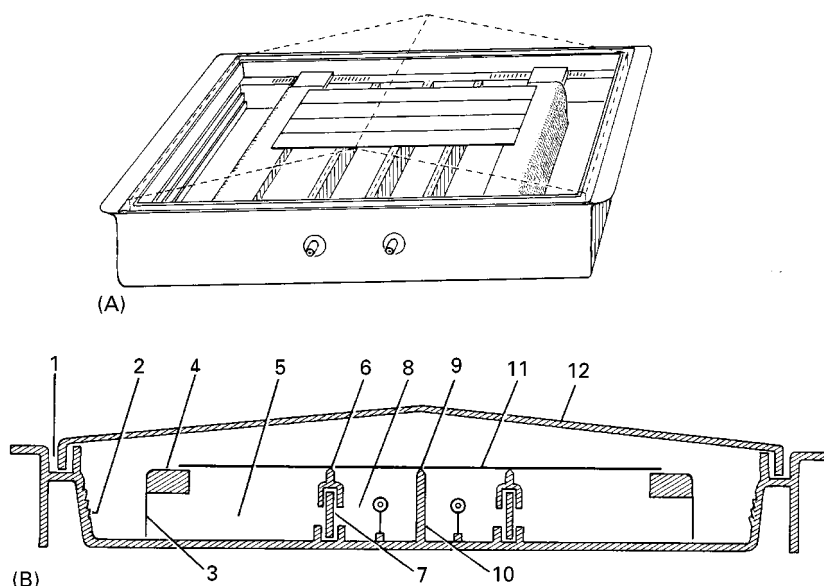


Figure 1 Description of a universal electrophoretic apparatus for CA electrophoresis (redrawn and modified from Kohn, 1957). The CA strips (11) are supported at each end by the shoulder pieces (4) and when taut are just clear of the top edge of the centre partition (10). The top edge of this centre partition is formed as a row of pyramids (9) which support the strip should it tend to sag. When using long strips, strip supports (6) may be fitted to the labyrinth partitions (7) that form the connections between the buffer compartments (5) and electrode compartments (8). Filter paper wicks (3) connect the CA strips to the buffer compartments. The internal sides of the tank are stepped all round (2) as an aid to buffer level checking. The lid (12) fits in a recess (1) moulded all round the tank.

forensic purposes and for the biochemical characterization and classification of various pathogenic microorganisms such as *Leishmania* and *Trypanosoma* species.

In addition to one-dimensional electrophoretic methods, two-dimensional CA electrophoretic protocols are also available. A summary of important applications is given in Table 2.

Detection and Quantitation

Any protein stain can be used with CA, provided that the solution does not contain a cellulose solvent. Aqueous staining solutions are preferred to alcoholic ones, since with the latter strips tend to shrink and curl unless they are passed through an aqueous bath.

Staining solutions for CA are less concentrated than those used in filter paper electrophoresis, and they can be repeatedly used with no appreciable loss of sensitivity.

A wide range of analytical applications can be listed with an impressive variety of fully compatible staining methods, including Coomassie blue brilliant, Ponceau red, Nigrosin, Schiff, gold and silver stain, different types of immuno-staining, and many different types of enzyme specific staining. A 5% (w/w) aqueous solution of acetic acid is a universal washing solution for reducing the background.

The simplest way of evaluating the results is by visual inspection of stained strips, which should be carried out against a strong light source to improve the assessment of the separation pattern.

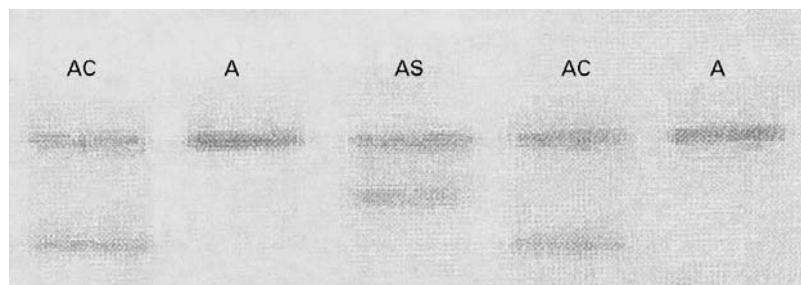


Figure 2 Electrophoretic separation of human haemoglobin variants A, C and S. Ponceau red staining was used to visualize haemoglobin bands, and the anode was on top.

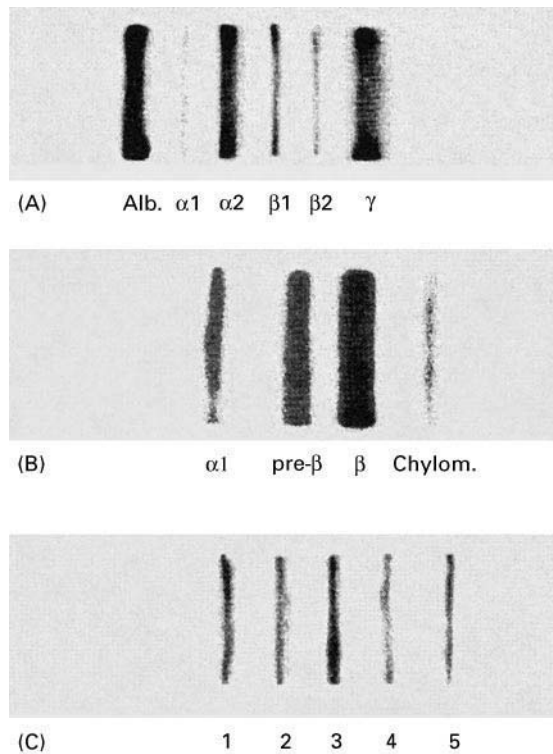


Figure 3 Routine clinical electrophoretic separations on CA: (A) serum proteins; (B) lipoproteins; (C) Lactate dehydrogenase isoenzymes. Samples were obtained from healthy patients.

Quantitative determinations can be carried out by elution or by scanning of the stained strips. Once stained, protein bands can be easily eluted from the membrane by an appropriate buffer system (a classical system is Tris (2-amino-2-hydroxymethylpropane-1,3-diol) or Barbitone elution buffer over Ponceau red stained bands). Alternatively, a solvent (e.g. chloroform-ethanol 9:1 v/v) can be used to dissolve the membrane and recover the protein

of interest. To enhance the recovery efficiency, gelled CA blocks (about 0.5 cm thick, instead of much thinner 0.5 mm supports) can be used.

Scanning is preferred to elution for routine clinical applications. To reduce background and increase sensitivity, CA strips should be cleared prior to scanning. As with filter paper it is important to use oil with the same refractive index as the support. CA strips cleared with oil may be returned to their original dry state by using a solvent such as ether. By contrast, swelling agents such as acetic acid and dioxan used in conjunction with heat treatment, permanently clear CA.

Isoelectric Focusing

CA has ideal features to suit IEF separations. CA is virtually a non-sieving matrix enabling a quasi-free fractionation of macromolecules according to their respective isoelectric points (pI , the pH at which there occurs an equal number of negative and positive surface charges). CA is easily soaked with very small amounts of carrier ampholyte species, allowing them to be eluted in due course with no damage to stained-destained proteins; this in turn allows densitometry measurements and storage.

Unfortunately, the combined effect of CA electroosmotic flow and the low ionic strength of commercial ampholines can seriously impair the resulting separation of proteins at their isoelectric points. To overcome these drawbacks, CA has been variously treated with surface active agents or with methylating agents. Such treatments can partly – if not wholly – reduce the osmotic flow. Also, a high concentration of carrier ampholytes should be used to cover broad pH ranges (8% v/v instead of the customary 2% v/v) and electrolyte additives at low concentration (such as 0.2 M lysine and 0.2 M acetic acid) should help stabilize narrow pH intervals. Untreated CA strips give better results when 5% β -mercaptoethanol and 5 M urea are used as stabilizing agents.

Alternative strategies to circumvent electroosmosis, which differ in effectiveness, involve shortening the inter-electrode distance or using ‘chemical spacers’ to flatten the pH gradients at the appropriate segment of separation. These devices may help to create high field strengths with low voltages. Recently, thermoelectric cooling has been used to stabilize CA IEF gradients.

Counterflow Affinity Isotachopheresis

Isotachopheresis or ‘displacement’ electrophoresis permits simultaneous concentration and effective separation of surface-charged substances, including biological macromolecules. With this analytical method,

Table 2 Some recent applications of CA electrophoresis

Year	Application
1994	Introduction of thermocooling apparatus for CA IEF Sequential electrophoresis, with detection of 21 different alleles in ESD-2 locus in <i>Drosophila buzzatii</i>
1995	Improved separation of apolipoproteins by use of surfactant Tween 20
1996	Rapid screening of biochemical loci of rat Highly sensitive detection of urinary proteins using colloidal silver staining
1997	Detection of superoxide dismutase isozymes to distinguish between <i>tsetse</i> blood meals of human and non-human origin CA electrophoresis used as the method of choice for alpha-thalassaemia screening IEF on CA applied to the analysis of microheterogeneity of immunoglobulins and serum protein fraction

proteins are stacked as closely spaced, narrow bands between the 'leading' and the 'trailing' ions. Iso-tachopheresis on CA gels takes advantage of the absence of sieve effect in this matrix to study sets of interacting biological macromolecules, such as antigen/antibody and glycoprotein/lectin systems. However, electroosmosis once again interferes with this application. Abelev and Karamova were able to overcome this drawback by demonstrating that the cathodic counterflow, combined with the constant flow of liquid through the membrane, stabilizes separations. The counterflow may be also used as a 'conveyer belt' to move immunoreagents through antigens or antibodies immobilized onto the membrane. Abelev and Karamova used a discontinuous buffer system, in which the two buffers have the same cation and differ in the anion species (chloride as the leading ion and β -alanine as the trailing ion). Under these conditions, macromolecules are separated between the two anions.

Abelev and Karamova's method was originally developed to analyse proteins in highly dilute biological fluids such as urine, tears, and cerebrospinal and amniotic fluids, and it turned out to also be useful for detecting low levels of urinary monoclonal immunoglobulin light chains (Bence Jones protein) and alpha-fetoprotein in various pathological conditions.

CA as a Reusable Electrophoretic Support

CA separations are faster than those on other supports, usually with no resolution loss. However, CA sheets cost considerably more than starch, agar, agarose or polyacrylamide gel sheets.

Recently, a wash method has been described that makes it possible to recycle CA strips. The procedure has been shown to work even after using the strips for analysis of a variety of erythrocyte isoenzymes, which notoriously expose the support matrix not only to the strain of the electric field but also to many somewhat elaborate biochemical colorimetric treatment steps. Surprisingly, none of these stages seem to irreversibly affect the mechanical and physicochemical properties of the CA. In fact, after a variety of enzyme activity tests (adenosine deaminase, adenylate kinase, carbonic anhydrase, erythrocyte acid phosphatase, esterase D, glutathione peroxidase, glyoxalase 1, phosphoglucomutase and 6-phosphogluconate dehydrogenase) Cellogel™ returns to its original features if soaked/washed in water and methanol for a short time. In the course of double blind trials, no difference in band sharpness and resolution was noticed between new and used Cellogel™ strips. The procedure can be repeated two or three times if care is taken to avoid

warping strips with absolute methanol soaking or rough handling.

Blotting Proteins from Polyacrylamide Gels to CA Sheets

Different electrophoretic species run in the same gel for the same time with the same electric field settings. The end of a given experiment is currently set depending on the specific requirements of the molecules to be separated, in zone electrophoresis as well as in IEF.

To achieve optimal resolution of different protein constituents of the same sample, various experiments are often carried out, only differing in voltage and duration. To save time, a simple method involves repeatedly blotting a polyacrylamide gel with CA sheets at various stages of separation. The blots obtained in this way can be stained and the protein species made to show the optimal resolution.

The advantages that can be obtained from CA blots of the same acrylamide gel are great, the most outstanding being:

1. various stages of a single protein separation can be tested in one experiment, to improve the protocol;
2. common and rare variants of a single electrophoretic pattern can be detected, each under optimal separation;
3. several proteins can be analysed at optimal conditions in the same experiment;
4. all the allele products may be discriminated by isotachopheretic mechanisms (in non-equilibrium IEF) and isoelectric point (in true equilibrium IEF) within the same run.

Conclusion

Almost uniquely among the various supports for electrokinetic separations, CA electrophoresis is still intensively used for both research and routine applications. The reasons for this long-lasting success are clear: simplicity of use, low cost, versatility and cost effectiveness. These same factors are likely to provide the general basis for the continuing use of CA in the future.

Acknowledgement

The drawing of Figure 1 was provided by Niccolò Falchi of the Department of Animal and Human Biology, University of Rome 'La Sapienza'.

Further Reading

Abelev GI and Karamova ER (1984) Counterflow affinity isotachopheresis on cellulose acetate membranes. *Analytical Biochemistry* 142: 437–444.

- Ambler J (1978) Isoelectric focusing of proteins on cellulose acetate gel membranes. *Clinica Chimica Acta* 85: 183–191.
- Destro-Bisol G and Santini SA (1995) Electrophoresis on cellulose acetate and Cellogel: current status and perspectives. *Journal of Chromatography A* 698: 33–40.
- Golias TL (1971) *Helena Laboratories Electrophoresis Manual*. Beaumont, Texas: Helena Laboratories.
- Grunbaum BJ, ed. (1980) *Handbook for Forensic Individualization of Human Blood and Bloodstains*. Gottingen: Sartorius.
- Harada H (1975) Isoelectrofocusing in cellulose acetate membrane: the method and application. *Clinica Chimica Acta* 63: 275–283.
- Kohn J (1970) Electrophoresis and immunodiffusion techniques on cellulose acetate membrane. *Methods in Medical Research* 12: 243–260.
- Meera Khan P (1971) Enzyme electrophoresis on cellulose acetate gel: zymogram patterns in man–mouse and man–Chinese hamster somatic cell hybrids. *Archives of Biochemistry and Biophysics* 145: 470–483.
- Righetti PG (1976) *Isoelectric Focusing, Theory, Methods and Applications*. Amsterdam: Elsevier.
- Schneider RG (1978) Methods for detection of hemoglobin variants and hemoglobinopathies in the routine clinical laboratory. *CRC Critical Reviews in Clinical Laboratory Sciences* 9: 243–271.

Deoxyribonucleic Acid, Theory of Techniques for Separation

J. Noolandi, Xerox Research Centre of Canada,
Mississauga, Ontario, Canada

Copyright © 2000 Academic Press

Introduction

Separation of biochemical molecules can be carried out in gels or polymer solutions and, in specific cases, in free solution, using constant or variable electric fields. Gels are used primarily in deep-dish containers, submerged in buffer, and polymer solutions are used in glass capillaries, with inner diameters less than 100 μm . Thin gels between two glass plates have been used for separating and sequencing single-stranded DNA molecules. We begin the theoretical discussion by considering the separation of double-stranded DNA molecules (dsDNA) in submarine gels under constant electric field conditions.

Geometrical Sieving Model for Small DNA Molecules in a Constant Electric Field

Ogston was the first to calculate the fractional volume available to a sphere of radius R in a gel of a given concentration. The gel itself was modelled as a random array made up of fibres of radius r . Within this description, a sphere with a radius $R \gg r$ cannot pass through the network if the sphere is not allowed to deform. This geometrical model predicts that the electrophoretic mobility of DNA molecules, as a result of molecular ‘sieving’, varies as:

$$\frac{\mu}{\mu_0} \propto \exp \left[- \left(\frac{R_g}{a} \right)^2 \right] \quad [1]$$

where R_g is the radius of gyration of the DNA molecule, μ_0 is the free solution mobility, a is the average pore size of the gel, and the exponential dependence of the mobility arises from the assumption of Poisson statistics for the distribution of spaces in a random network of straight fibres. This model describes the mobility of small molecules when they first encounter the gel fibres as obstacles to molecular motion. The analysis of experimental data using eqn [1] is highly model dependent, but can provide some guidance for the development of new gel structures for more efficient electrophoretic separations of small molecules.

Entropic Trapping of Small DNA Molecules

For DNA in the entropic size regime, the deformable molecules select the larger pores in order to maximize locally their conformational entropy. However, in order to accomplish this, they must squeeze through the narrow channels connecting the larger pores. The corresponding polyelectrolyte dynamics is dominated by an activation process in this regime, where the electrophoretic mobility is given by an inverse power law (> 1) over a size range that is larger than for the Ogston regime, but smaller than for the beginning of reptation, which is discussed in the next section.

Gel Electrophoresis of Large DNA Molecules in a Constant Electric Field

Figure 1 shows a schematic picture of a gel matrix, in which a DNA molecule is embedded. For a molecule that is much longer than the average spacing between the chemical cross-links of the gel fibres, the molecule cannot move through the gel as a random coil, rather

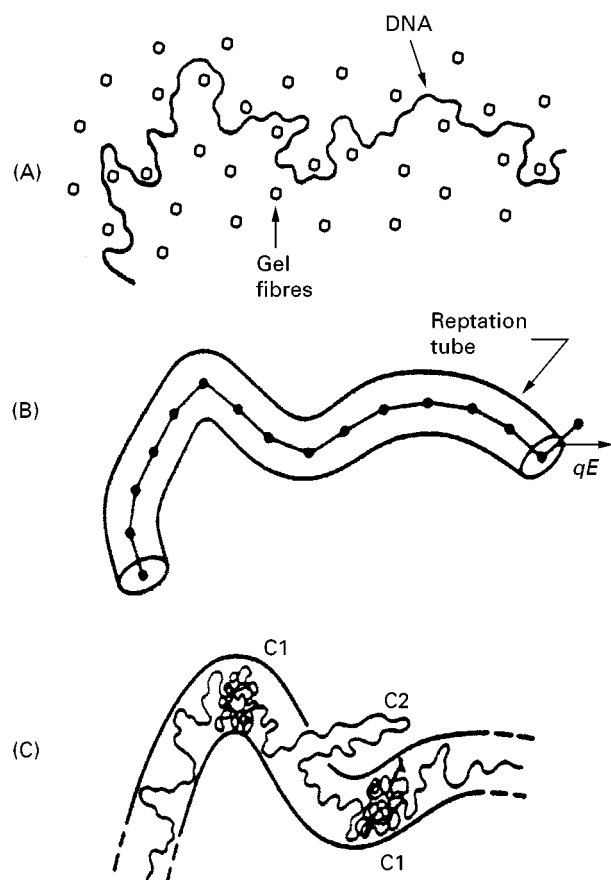


Figure 1 Schematic representation of a DNA molecule in a two-dimensional gel (A), in which the open dots represent obstacles corresponding to the gel fibres. (B) Shows how the obstacles hindering the motion of the molecule are approximated by a tube and the polymer by a chain of beads; the electric field exerts a force qE on the last bead and orients the segment leaving the tube. The tube is defined by the molecular conformation so that an extended conformation (with less DNA per gel pore) has a longer tube. (C) Charge gradients (C1) along the tube axis, and field-driven tube leakages (C2) are neglected in the biased reptation model.

it must reptate (from the Latin *reptare*, to creep) around the obstacles (cross-links), in a way that is analogous to the movement of polymer molecules in a self-entangled polymer melt. In this situation, the natural length scale is the average pore size of the gel, a . In terms of this length scale, we define a number of different quantities that arise in a theoretical description of the problem. One of these is the number of gel pore segments, N , occupied by the molecule:

$$N = \frac{M}{M_a} \quad [2]$$

where M is the relative molecular mass of the molecule and M_a is the average relative molecular mass in a gel

pore. Under the influence of an electric field, M_a can change as a function of time, depending on the stiffness of the molecule, the pore size, the magnitude of the electric field, and other factors. Another important quantity is the scaled effective electric field, E_{eff} :

$$E_{\text{eff}} = \frac{e_1 M_a E a}{2k_B T} = \frac{E}{E_a} \quad [3]$$

which defines the intrinsic electric field parameter E_a . The net charge per nucleotide for DNA is denoted by e_1 . This quantity depends on the native charge on the molecule, as well as on the charge screening properties of the buffer solution used for the electrophoretic separation. A simple way of understanding the limitations for separating large molecules in a gel using constant electric fields is as follows.

For constant a and M_a , the electrical force F_1 on the molecule in the longitudinal direction (also known as the tube axis, if the molecule is considered to fill a 'tube' made up of occupied gel pores) is:

$$F_1 = (qE) \cdot \left(\sum_i \frac{\mathbf{r}_i}{a} \right) \quad [4]$$

where $q = e_1 M_a$ is the average net charge of the molecule in a gel pore, and \mathbf{r}_i/a is the unit vector pointing from pore i to pore $i + 1$ along the molecule, where the dot in eqn [4] indicates the dot product of two vectors. This expression reduces to:

$$F_1 = qE \frac{h_x}{a} \quad [5]$$

where h_x is the end-to-end distance of the molecule in the field direction. The force is time-dependent and fluctuates during electrophoretic migration. Opposing the migration along the tube is a friction coefficient $\xi = \xi_0 N$, where ξ_0 is the friction coefficient per tube segment, as defined by eqn [2]. The instantaneous velocity of the chain along the longitudinal axis is then:

$$v_1 = \frac{F_1}{\xi} = \left(\frac{qE}{\xi} \right) \left(\frac{h_x}{a} \right) \quad [6]$$

and the average mobility of the centre of mass (defined as the velocity per unit electric field in the field direction) is given by:

$$\mu = \frac{\langle v_1(h_x/N) \rangle}{E} = \mu_0 \frac{\langle h_x^2 \rangle}{N^2} \quad [7]$$

where $\mu_0 = q/\xi_0 a$, and the geometrical factor (h_x/N) in eqn [7] takes into account the fact that the vector

h is in general not parallel to the direction of the electric field. For small electric fields and/or small molecules, $\langle h_x^2 \rangle$ proportional to N , giving μ proportional to $1/N$. In this regime the molecules reptate while retaining their random-walk conformations. For large molecules and/or high electric fields, the molecules become stretched in the electric field direction during migration, and $\langle h_x^2 \rangle$ is proportional to N^2 , resulting in a mobility that is independent of the molecular mass, according to eqn [7].

Figure 2 shows a log-log plot of the reduced electrophoretic mobility, μ/μ_0 , from Slater and co-workers as a function of the scaled molecular size, $N = M/M_a$, for different values of the scaled electric field. From top to bottom, $E_{\text{eff}} = 1.0, 0.2, 0.1, 0.01$. For small molecular sizes, the mobility is independent of the field intensity and decreases as $1/N$. For large molecular sizes, the mobility is independent of size and increases as E_{eff}^2 . The small minimum in the mobility is a phenomenon known as band inversion, for which, in a limited size range, large molecules can move faster than smaller molecules. Noolandi and co-workers have shown that this is a statistical effect where linear molecules, which have two free ends, can migrate into slowly moving 'J' or 'U' states for different time intervals, depending on the specific electrophoresis conditions. Since the bands of DNA molecules are not in order of increasing size in this

region, one has to be careful not to mislabel the molecular fragments.

In summary, the basic reason for the constant plateau mobility in Figure 2 is that for stretched molecules the electrical driving force and the opposing friction both scale linearly with length, and the resulting ratio is independent of length. For freely draining molecular coils in free solution, the same effect occurs, with the result that it is not possible to separate freely draining polyelectrolytes according to size in free solution electrophoresis. However, there are ways to overcome this limitation at least partly for free solution electrophoresis, as we discuss later. Next we turn to overcoming the limitations of constant field gel electrophoresis.

Pulsed Field Gel Electrophoresis of Large DNA Molecules

In constant field gel electrophoresis the maximum size of dsDNA that can be separated is about 50 kilobases. In pulsed-field gel electrophoresis separations up to a few megabases can be achieved. In this section we explain why such an increase in separation latitude takes place.

The plateau mobility is reached because of molecular stretching in a constant electric field. Schwartz and Cantor showed that the way to avoid this is to change the electric field constantly, either in magnitude and/or direction. The disadvantage of doing this is that it can take a long time to separate large molecules (separating dsDNA molecules a few megabases in size can take a few days). The advantage, of course, is that it is possible to separate large molecules at all, provided that the variations in the electric field are chosen properly. Changes in the magnitude and/or direction of the electric field force the molecules to adapt to the new electrophoresis conditions. However the adaptation time (also known as the 'relaxation' time) is very specific to the molecular size, average gel pore diameter, and electric field changes. It follows that there are a large number of ways to implement this process. Some pulsed-field gel separations use electric fields of the same magnitude and only change the field direction in two dimensions. Others keep the electric field in one dimension (forwards and backwards) for different time periods and with different amplitudes). We use the one-dimensional case developed by Turmel and co-workers as an example of how separations can be carried out by tuning the pulse times to the relaxation times of the molecules in the gel.

Figure 3 is a schematic illustration of the displacement of two types of molecules, molecular masses

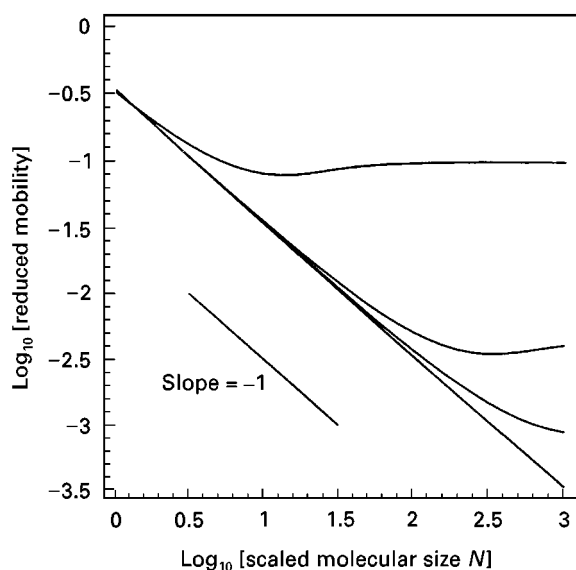


Figure 2 Log-log plot of the reduced electrophoretic mobility μ/μ_0 as a function of the scaled molecular size $N = M/M_a$ for different values of the scaled constant electric field E_{eff} (see text). For small molecular sizes the mobility is independent of the constant field intensity and decreases with size as $1/N$. For large molecular sizes, the mobility is independent of size and increases as E_{eff}^2 . The electrophoretic mobility has a shallow minimum for intermediate molecular sizes.

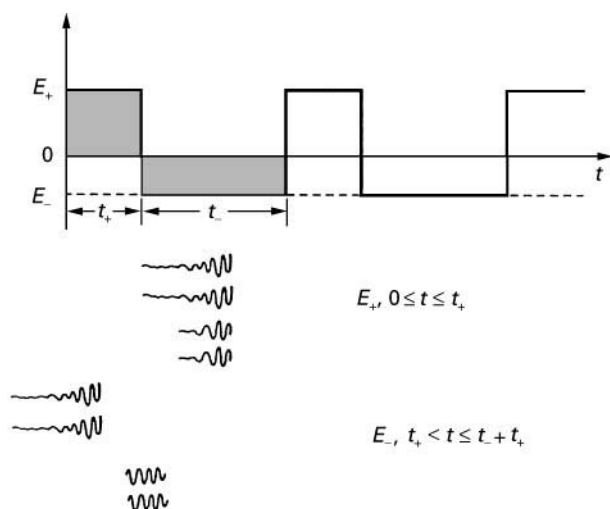


Figure 3 Pulse shape for gel separations of large DNA molecules, using zero-integrated-field electrophoresis (ZIFE). As explained in the text, this pulse shape allows the proper size-migration distance to be maintained at all times, and gives rise to a sharp drop in the electrophoresis mobility as a function of size for fixed pulse parameters. For given electric field amplitudes, the reverse pulse time, t_- , defines the relaxation time of the largest molecule that can adapt to the lower electric field and have a net forward displacement during one complete cycle.

M_1 and M_2 ($M_1 < M_2$), when subjected to a high field forward pulse, followed by a low field backward pulse of longer duration than the forward pulse. During the pulse duration t_+ , with field intensity E_+ , the displacements of molecules M_1 and M_2 are $\mu(E_+, M_1)E_+t_+$ and $\mu(E_+, M_2)E_+t_+$ respectively, where the dependence of the mobilities on the field strength and molecular size has been explicitly indicated. During the reverse pulse of duration t_- , with absolute field intensity E_- , the reverse displacement of the shorter molecule is $-\mu(E_-, M_1)E_-t_-$, if t_- is long enough to allow the shorter molecule to relax to the new electric field in the backward direction. The net displacement of the shorter molecules over the time period $t_+ + t_-$ is then $\mu(E_+, M_1)E_+t_+ - \mu(E_-, M_1)E_-t_-$. However, for the longer molecule M_2 , the reverse displacement is $-\mu(E_+, M_2)E_-t_-$, if the time interval t_- is too short to allow the longer molecule relax to the lower electric field intensity E_- in the reverse direction. The net displacement of the longer molecule is then $\mu(E_+, M_2)E_+t_+ - \mu(E_+, M_2)E_-t_-$, and vanishes when $E_+t_+ = E_-t_-$. This is known as the zero-integrated field condition. With this condition the displacement of the shorter molecule becomes $[\mu(E_+, M_1) - \mu(E_-, M_1)]E_+t_+$, which is in the forward direction since $\mu(E_-, M_1) < \mu(E_+, M_1)$ if $E_- < E_+$. The zero-integrated pulse form allows the proper molecular size versus displacement in the gel to be maintained at all

times, avoiding the problem of band inversion. Although the tight DNA bands achieved by this process is an advantage, the running time for experiments is longer than for some other pulse schemes. Its usefulness depends on the specific requirements of the practitioner. The pulse times are determined experimentally using known molecular size markers, which show a sharp drop in mobility when the relaxation times are reached for a given size range. Using this information, a general electric field pulse scheme can be programmed for separating unknown DNA size distributions.

Capillary Zone Electrophoresis (CZE)

Capillary electrophoresis of DNA is a specific example of a technique used to separate molecules known as capillary zone electrophoresis (CZE), in which fused silica capillaries have their ends inserted in electrolyte reservoirs which also contain electrodes. This powerful analytical technique, as discussed by Gordon and co-workers, has been developed over the past decade in a number of different academic and industrial laboratories. Here the walls of the fused silica capillaries have a negative charge resulting from the ionization of the surface silanol groups in aqueous solution. When a potential difference is established between the electrodes, a bulk flow of fluid towards the cathode takes place. This is called electroosmotic flow, and results from the electrical double layer formed at the wall-electrolyte interface. The electroosmotic velocity is given by:

$$V_{eo} = \mu_{eo}E = \frac{\varepsilon\varepsilon_0\zeta E}{\eta} \quad [8]$$

where $\zeta = \delta\sigma/\varepsilon_0$, and μ_{eo} is the electroosmotic mobility, E is the electrical field, ε_0 the permittivity of the vacuum, ε the relative permittivity, ζ the zeta potential, η the viscosity, δ the double layer thickness and σ the surface excess charge density. The double layer thickness is inversely proportional to the square root of the molar concentration of the buffer solution. The electroosmotic flow enables the separation of charged molecules according to their different electrophoretic mobilities. In this method, positively charged molecules are eluted first because their electrophoretic motion and the electroosmotic motion are in the same direction. Negatively charged molecules try to move in the opposite direction, but if their electrophoretic mobility is less than the electroosmotic mobility, the net result is that they are eluted later than the positive molecules. Thus electroosmotic flow can be considered as a built-in pump which is useful for carrying out electrokinetic separations.

Clearly this process cannot separate neutral molecules if only an electrolyte is used. Sometimes micelles are dissolved in the separation electrolyte, resulting in some separation of uncharged species because of their partitioning between the micelles and the electrolyte. More commonly, one packs the capillary with a stationary phase, which can be bonded to the walls of the capillary, or formed by close packed small particles. The flow profile in the capillary has a nearly flat (plug-like) profile instead of the usual parabolic profile for Poiseuille flow when a viscous, incompressible fluid is pushed through a cylindrical tube by a pressure difference. The nearly flat flow profile makes the separation and detection of small amounts of analyte easier. This technique is known as capillary electrochromatography (CEC). The packing of the capillaries can be carried out electrokinetically, using commercially available small (a few μm) porous silica particles.

A number of different theoretical strategies have been used to increase the sensitivity of analyte detection. Programming of the electric field to achieve uniform sensitivity for on-line detection has been used, and theories for maximizing the signal-to-noise ratio for the case of laser-induced fluorescence and UV absorbance detection in capillary electrophoresis have been developed. In particular, for rather general conditions, the ratio of the number of fluorescent molecules in two analyte bands can be shown to be proportional to the ratio of the heights of the band peaks. This is useful for fluorescent analytes, and for cases where nonfluorescent analytes are labelled with fluorescent probes prior to detection.

Capillary Electrophoresis of DNA Molecules in Free Solution

In free solution the electrophoretic mobility of a free draining polyelectrolyte coil is equal to the ratio of its electric charge to its friction coefficient. Since both quantities scale linearly with molecular mass, the mobility is independent of molecular size. Hence the only way to separate molecules of different size in this case is to break the scaling symmetry of the charge and/or friction with size. As shown by Voelkel and Noolandi, adding a molecular unit with a different charge and friction to one of the ends of a linear polyelectrolyte, such as DNA, will change the free solution mobility to:

$$\mu(M) = \mu_0 \frac{M + q_{\text{eff}}}{M + \xi_{\text{eff}}} \quad [9]$$

where μ_0 is the free solution mobility of the unlabelled free draining polyelectrolyte, q_{eff} is the ratio of the

effective charge carried by the label expressed in terms of the charge per monomer unit of the polyelectrolyte, and ξ_{eff} is the friction of the label expressed in terms of the friction per monomer unit of the polyelectrolyte. In this approximation the hydrodynamic interaction of the label and the polyelectrolyte is neglected. The free solution mobility is now a function of the molecular mass. However the effectiveness of this strategy depends on the size of the label, compared with the rest of the molecule, and the amount of the band broadening caused by Brownian motion and other effects. In practice this approach seems viable for separating single-stranded DNA molecules up to several hundred bases long for DNA sequencing applications. While gel separations of single-stranded DNA molecules can routinely be carried out for sizes well over 500 bases, free solution separations, which are only effective for shorter fragments, can be carried out only an order of magnitude faster.

Capillary Electrophoresis of DNA Molecules Using Dilute Polymer Solutions

A separation mechanism that combines aspects of both free solution and gel electrophoresis is separation in capillaries using ultrathin polymer solutions. Here the DNA molecules drag along the polymer molecules that they encounter during migration. The capture and release of the unentangled polymer molecules results in the separation of DNA molecules. This new type of separation mechanism, developed by Barron and co-workers, is based on hydrodynamics, drag forces and molecular collisions, and is best suited for high throughput applications. The theoretical basis for the separation is still under development.

Capillary Electrophoresis of DNA Molecules Using Entangled Polymer Solutions

As pointed out by Slater, entangled solutions, as opposed to a gel, involve physical, instead of chemical, cross-links. For polymer solutions, we consider concentrations $c > c^*$, where c^* is called the critical concentration for entanglements:

$$c^* = \frac{M}{\left(\frac{4\pi}{3}R_g^3\right)} \quad [10]$$

M is the relative molecular mass, and R_g is the radius of gyration of the polymer molecule. For $c > c^*$ the polymer coils overlap and a loosely associated polymer network is formed. From the theory of polymer networks in solution we can characterize the mean pore size by a 'blob' dimension:

$$\xi = 1.4R_g \left(\frac{c^*}{c} \right)^{3/4} \quad [11]$$

However we must bear in mind that we are dealing with loosely associated networks, and that the physical cross-links are temporary, as opposed to chemically cross-linked networks. As discussed by Viovy and Heller, for low electrophoretic mobilities the dissociation and reassociation times of the network become important, because they occur on the same timescale as the transit time of the DNA molecules through the network. As a consequence, it is not possible to achieve better separations of DNA molecules through a concentrated polymer solution than through a gel, however polymer solutions are more easily processed (injected or removed) through capillary channels than cross-linked gels because of their low viscosities. Some polymer solutions have strongly temperature-dependent properties, which allows more latitude in the processing conditions.

Future Developments

Separations of biomolecules are being carried out on smaller and smaller devices, using miniaturized fluid-handling devices and detection systems. Making use of recent rapid developments in the area of microelectromechanical systems (MEMS), which exploits advances in microlithography for the semiconductor industry, new biochips and biosensors have been designed that enable faster analytical and diagnostic techniques to be carried out than was possible with macroscopic devices. As shown by Chee and co-workers, hundreds of thousands of DNA oligonucleotide probes can be assembled on a glass microchip, and combined with micromachined capillary electrophoresis injectors and separators. Complete hybridization patterns can be revealed in a matter of minutes, using laser-induced fluorescence. The implications for the entire biotechnology industry are revolutionary. Coupled with the knowledge obtained from the Human Genome Program, in which the estimated 100 000 human genes are in the process of being discovered and sequenced, thousands of genetic variations can be analysed in a single experiment, making possible the rapid localization of disease-causing genes.

From the theoretical point of view, there are several areas where advances are necessary to keep up with the rapid developments in instrumentation. First, new software codes are required to enable the rapid deciphering and processing of the massive amounts of bioinformation that are being generated. Second, detection systems with higher resolution than is currently available must be designed to interpret the spectral data that are available with the use of laser-induced fluorescence. Finally, theoretical modelling of the behaviour of electrolytes and biomolecules in microchannels in the presence of electric fields will be useful in understanding the ultimate capability of microdevices for the applications that we have mentioned.

See Colour Plate 40.

Further Reading

- Barron AE, Blanch HW and Soane DS (1994) A transient entanglement coupling mechanism for DNA separation by capillary electrophoresis in ultradilute polymer solutions. *Electrophoresis* 15: 597–615.
- Chee M, Yang R, Hubbell E *et al.* (1996) Accessing genetic information with high-density DNA arrays. *Science* 274: 610–614.
- Gordon MJ, Huang X, Pentoney SL Jr and Zare RN (1988) Capillary electrophoresis. *Science* 242: 224–228.
- Noolandi J, Rousseau J, Slater GW, Turmel C and Lalande M (1987) Self-trapping and anomalous dispersion of DNA in electrophoresis. *Physics Review Letters* 58: 2428–2431.
- Ogston AG (1958) The spaces in a uniform random suspension of fibres. *Transactions of the Faraday Society* 54: 1754–1757.
- Schwartz DC and Cantor CR (1984) Separation of yeast chromosome-sized DNAs by pulsed field gradient gel electrophoresis. *Cell* 37: 67–75.
- Slater GW, Mayer P, Hubert SJ and Drouin G (1994) The biased reptation model of DNA gel electrophoresis: a user guide for constant field mobilities. *Applied and Theoretical Electrophoresis* 4: 71–79.
- Slater GW (1996) Electrophoresis theories. In: Heller C (ed.) *Analysis of Nucleic Acids by Capillary Electrophoresis*, ch. 2. Berlin: Vieweg Press.
- Turmel C, Brassard E, Forsyth R, *et al.* (1990) High resolution zero integrated field electrophoresis (ZIFE) of DNA. In: Birren B and Lai E (eds). *Current Communication in Molecular Biology. Electrophoresis of Large DNA Molecules*, p. 101. Cold Spring Harbor, NY: Cold Spring Harbor Laboratory.
- Viovy JL and Heller C (1996) Principles of size-based separations in polymer solutions. In: Righetti PG (ed) *Capillary Electrophoresis in Analytical Biotechnology*, ch. 11. Boca Raton, FL: CRC Press.
- Voelkel A and Noolandi J (1995) Mobilities of labeled and unlabeled single stranded DNA in free solution electrophoresis. *Macromolecules* 28: 8182–8189.

Detection of Proteins in Electrophoresis

See II/ELECTROPHORESIS/Proteins, Detection of

Detection Techniques: Staining, Autoradiography and Blotting

P. J. Wirth, National Cancer Institute, Bethesda, MD, USA

Copyright © 2000 Academic Press

Introduction

Polyacrylamide gel electrophoresis (PAGE) is a highly reliable and widely used technique for the separation, identification and characterization of proteins and protein mixtures. Although two-dimensional (2D)-PAGE, which combines protein isoelectric focusing (IEF) in the first dimension with sodium dodecyl sulfate (SDS)-PAGE molecular sieving in the second dimension, provides the highest resolution allowing one to separate 1000–2000 individual polypeptide spots on a single gel, 2D-PAGE is technically very demanding. However, in the vast majority of applications, one-dimensional (1D)-PAGE, specifically SDS-PAGE, provides sufficient resolution and is especially well suited for the simultaneous analysis of multiple protein samples on a single gel. Since its introduction in 1951, very few modifications to the basic protocols for preparing and running 1D-PAGE gels have been made, although considerable advances have been introduced for the detection and analysis of PAGE separated proteins.

Post-electrophoretic gel staining is the most frequently used method for the detection of individual protein bands or spots on 1D- and 2D-PAGE gels, respectively, although procedures for prestaining proteins prior to PAGE have been described. Detection is usually performed either *in situ* within the polyacrylamide gel matrix itself or following Western electroblot transfer of proteins from PAGE gels on to polymeric membrane support matrixes. Detection systems include organic dye and metal salt-based staining protocols, fluorescent group tagging, specific protein–ligand/receptor interactions, enzymic activity detection, as well as group-specific (e.g. glyco-, phospho-, lipoproteins, etc.) staining and immunological detection of antibody–antigen complexes. Alternatively, proteins which have been labelled with radioactive molecules, either prior to or post-electrophoretically, can be visualized using autoradio-

graphic and fluorographic detection on X-ray film. Although a plethora of protein staining and visualization protocols have been described, none is totally ideal and often the use of multiple protein staining and/or protein labelling procedures is necessary.

Protein Staining

Organic Dyes

Many of the organic dyes and stains that have been adopted for the detection of proteins in polyacrylamide gels and on membranes have been derived from dyes originally developed for the textile industry. Currently the most commonly used dyes include Amido Black, Procion Blue RS, Ponceau S, Alcian Blue, Fast Green FCF, Coomassie^{1,2} Brilliant Blue R-250 (R = reddish hue) (CBB-R) and Xylene Cyanine Brilliant G (confusingly referred to as Coomassie Brilliant Blue G-250) (G = greenish hue) (CBB-G). Recently, inorganic metal ion-based staining procedures have been developed that provide highly sensitive methods of protein visualization.

CBB-R and CBB-G are the most sensitive, convenient and economical to use of the commonly available dyes, and have become the reagents of choice for protein staining. CBB-R is a nonpolar, sulfated aromatic dye that is generally used in methanolic acetic acid solutions where excess CBB is removed from the gel matrix by destaining. An acidic environment is required for optimal CBB staining to enhance ionic interactions between the dye molecules and basic amino groups of the protein as well as to augment dye–protein interactions due to hydrogen bonding, van der Waals attraction and hydrophobic bonding.

¹ Any reference to a trademark or proprietary product does not constitute endorsement of that product by the US government and does not imply its approval to the exclusion of other products.

² CoomassieTM is a registered trademark held by the Imperial Chemical Industries (ICI). Equivalent CBB dyes under their own trademarks include Serva Blau (Blue) R or G, PAGE blue 83 (R) or 90 (G), Kenacid blue R, Supranocyanin 6B or G, Brilliant Blue R and Microme no. 1137.

Typically, CBB staining is performed using a 0.1–0.2% CBB-R (w/v) in aqueous (v/v) 45% methanol and 10% acetic acid. The duration of staining is dependent on gel thickness and polyacrylamide composition and destaining is performed using either passive diffusion or electrophoretic destaining. After destaining, gels can be stored in 7.5% acetic acid in which the dye–protein complex is fixed and the colour is relatively stable.

An alternative CBB-based procedure exhibiting very low background staining has been described using CBB-G. Incubation of gels in a colloidal suspension of CBB-G in aqueous trichloroacetic acid (TCA) results in the formation of dye–protein complexes, in which CBB-G interacts with proteins only at the surface of the gels and does not penetrate into the gel matrix, thus minimizing background staining. Major protein bands are visible within 5–10 min and for optimal staining of less abundant proteins gels should be left in the staining solutions for several hours to overnight followed by destaining in 5% TCA.

Amido Black (Buffalo black NBR, naphthalene black 12B, aniline blue black, naphthol blue black, acid black 1 and amido schwarz) was probably the first dye used to stain proteins in polyacrylamide gels; however, its use today is less frequent because of the availability of more sensitive CBB-based protocols. None the less, Amido Black still enjoys numerous applications because of its rapid staining and destaining properties.

A dye especially well suited for quantitation applications is Fast Green FCF (food green 3). Fast Green exhibits a greater linearity of staining as compared to CBB-R and also has the capacity to form stable coloured complexes with histones, thereby making it a useful group-specific stain. In contrast to CBB, Fast Green does not bind to carrier ampholytes and can be used for staining of proteins in IEF gels.

Recently, protein staining procedures utilizing calconcarboxylic acid *N,N*{1-(2-hydroxy-4-sulfo-1-naphthylazo)-2-hydroxy-3-naphthoic acid}, Eriochrome Black T/rhodamine B, Evans blue/rhodamine B, and CBB/Bismark Brown R have been introduced with reported sensitivity comparable or better than CBB in SDS-PAGE gels. A very useful general protein stain that also displays group-specific staining is Stains-all™, a cationic carbocyanine dye, which stains sialoglycoproteins and phosphoproteins blue and almost all other proteins red. Table 1 summarizes some of the more commonly used organic dyes for protein staining.

Silver Staining

For most applications, visualization of proteins with CBB is sufficiently sensitive. However, if one is inter-

ested in determining the absolute purity or trace amounts of a protein then more sensitive techniques must be utilized. To accomplish this, Merrill developed an ultrasensitive silver staining procedure based on photographic principles. Silver staining is upward to 100-fold more sensitive than CBB-R with sensitivity comparable to, or greater than, autoradiography, for selected polypeptides. It should be noted, however, that many proteins respond differently to silver staining. Some proteins may not stain at all, so sensitivity values for silver staining may vary from protein to protein.

Silver staining or silver shadowing procedures can be divided into three basic categories: diamine or ammoniacal silver stains; chemically developed nondiamine type; and photoreduction silver stains. The diamine or ammoniacal silver stains utilize ammonium hydroxide to form soluble silver–diamine complexes and proteins are visualized by acidification, usually with citric acid in the presence of formaldehyde. Diamine stains are rather time-consuming (overnight fixation and 6 h staining) but are particularly good for the staining of gels thicker than 1 mm. The nondiamine chemical development stains are generally more rapid than the diamine stains but display higher backgrounds and are best suited for gels 1 mm or thinner. Image development of nondiamine stains occurs as a result of selective reduction of silver ions to elemental metallic silver by formaldehyde under alkaline pH. The photoreduction silver stains are the most rapid, allowing the visualization of protein patterns within 10 min after electrophoretic separation; however, they are the least sensitive of the silver-based staining methods.

While most proteins stain monochromatically with silver, yielding brown or black spots and bands, certain silver stains can produce varying shades of black, blue brown, red and yellow and the staining of individual proteins appears to be group-specific. Lipoproteins tend to stain blue while glycoproteins appear yellowish-brown, or red. Colour formation has been shown to be highly dependent on the size and distribution of the silver grains within the gel as well as the refractive index of the gel and standardized colour-based silver staining kits are commercially available.

Reverse Staining

In contrast to the positive-staining procedure described above, alternative but generally less sensitive staining procedures based on the formation of insoluble metal (zinc, copper and potassium) salts have also been described. These methods, commonly

Table 1 Reagents useful for protein visualization on gels and membrane supports

Stain/dye	Sensitivity	Gel	Membranes			Comments
			NC	PVDF	Nylon	
<i>Organic dyes</i>						
Coomassie Brilliant Blue (CBB-R) and (CBB-G)	100–1000 ng	yes	yes	yes	no	Permanent, convenient to use, sensitive, anionic, relatively high background (CBB-R), (> 1 h) ^a
Ponceau S	1–2 µg	yes	yes	yes	no	Reversible, low background, rapid staining/destaining (<2 min)
Amido Black	1–2 µg	yes	yes	yes	no	Permanent, low background, anionic stain, stains histones and orosomucoids (>30 min)
India Ink (colloidal carbon)	80–100 ng	no	yes	yes	yes	Permanent, very sensitive, low background, sensitivity dependent upon source/lot of ink (>2 h), useful for charged nylon membranes
Fast Green FCF	1–2 µg	yes	yes	yes	no	Permanent, linearity of staining>CBB, does not bind IEF ampholytes, stains histones (30 min)
Stains-All™	1–2 µg	yes	yes	yes	no	General protein and nucleic acid stain, stains RNA (bluish purple), DNA (blue), most proteins (red) sialoglycoproteins and phosphoproteins (blue)
Periodic acid–Schiff (PAS)	25–100 ng	yes	yes	yes	no	General protein and glycoprotein stain. Silver enhancement increases sensitivity (~0.4 ng)
Procion Blue RS	1–2 µg	yes	yes	yes	no	Anionic, hydrophobic dye, occasionally used
Alcian Blue	500–700 ng	yes	yes	yes	no	Useful for staining glycosaminoglycan
Eosin Y	10 ng	yes	yes	yes	no	General protein stain, stains sialoglycoproteins
Congo Red	500 ng	yes	yes	yes	no	Low background, rapid (5 min), anionic stain
<i>Fluorescent stains</i>						
Dansyl chloride	100–200 ng	yes	yes	yes	no	Stains all types of proteins, including proteoglycans
SYPRO Red/Orange	100 ng	yes	no	no	no	Exhibits a greater linearity of staining than CBB, SDS-PAGE only, does not require protein fixation, will not stain nucleic acids
Fluorescamine	6–10 ng	yes	yes	yes	no	Neither fluorescamine nor its degradation products are fluorescent, low backgrounds
Fluorescein isothiocyanate	50 ng	yes	yes	yes	no	Rapid, can be used as pre-electrophoretic tag
Metal salt complexes						
Silver	1–3 ng	yes	yes	yes	no	Permanent, very sensitive, stains nucleic acids, hundreds of modifications, time-consuming
Colloidal gold (Aurodye™)	1–3 ng	yes	yes	yes	no	Permanent, very sensitive, silver enhancement increases sensitivity
Potassium chloride	10–100 ng	yes	no	no	no	Reversible, SDS-PAGE only, negative stain, whiter bands on opaque background
Iron (Ferridye™)	1–3 ng	yes	yes	yes	yes	Permanent, useful for nylon membranes
Copper (iodide/chloride)	10–100 ng	yes	no	no	no	Reversible, rapid (5 min), SDS-PAGE only, negative stain, clear bands on opaque background
Copper phthalocyanine	10–100 ng	yes	yes	yes	no	Reversible, rapid (<2 min), sensitive
3,4',4'',4''' tetrasulfonic acid						
Zinc/imidazole SDS	10–100 ng	yes	no	no	no	Reversible, metal chelate stain, SDS-PAGE only, negative stain, clear bands on opaque background, does not require protein fixation, protein eluted from gels with high efficiency (>90%)

^aStaining/destaining time. NC, Nitrocellulose; PVDF, polyvinylidene fluoride.

referred to as negative or reversible staining, are limited to SDS-containing gels and produce a semi-opaque background on the gel surface where proteins are detected as whiter or transparent bands or spots when viewed against a black background or when back-lit. Staining procedures are rapid (within 15 min), display intermediate sensitivity between that of CBB and silver staining, and since minimal protein fixation is required, proteins are readily eluted from gels (>90%) for biochemical characterization including Western immunoblotting, amino acid composition analysis and Edman N-terminal amino acid microsequencing.

Fluorescent Protein Labelling

Fluorescent methods for protein visualization are extremely sensitive but are less frequently used than the CBB/silver staining protocols due to their relative complexity (e.g. they require ultraviolet illumination for protein visualization, and fluorescence signal intensities diminish with time) and increased cost. Proteins can be tagged either pre- or post-electrophoretically with fluorescent sensitive dye(s) via covalent interaction of the dye with terminal $-NH_2$ groups of the proteins. Fluorophores most commonly utilized to label proteins prior to electrophoresis include dansyl chloride (1-dimethylaminonaphthalene-5-sulfonyl chloride), fluorescamine (4-phenylspiro(furan-2[3H]-1'-phthalan-3,3' dione), MDPF (2-methoxy-2,4-diphenyl-3-(2H)-furanone), DACM (N-(7-dimethylamino-4-methylcoumarinyl)maleimide) and OPA (o-phthaldialdehyde). Although dansyl chloride was the first fluorescent dye used for pre-electrophoretic labelling of proteins, fluorescamine has found increasing use since neither fluorescamine nor its hydrolysis products are fluorescent. Fluorescamine is capable of detecting as little as 6 ng of myoglobin while MDPF, which is 2.5 times more sensitive than fluorescamine, is very useful for quantitative applications and displays a linear staining response from 1 to 500 ng.

Proteins can also be detected post-electrophoretically using fluorescent reagents such as ANS (1-anilinonaphthalene-8-sulfonate), Bis-ANS, fluorescamine, *p*-hydrazinoacridine and OPA. Since labelling is usually performed under nondenaturing conditions, these reagents can be used quite advantageously for the rapid detection of proteins during preparative electrophoresis. Generalized procedures for both pre- and post-labelling with fluorescent dyes have appeared in reviews by Hames and Rickwood and Merril. Table 1 briefly summarizes the major metal-based and fluorescent dyes used to stain proteins on polyacrylamide gels.

Autoradiographic Detection

Labelling of proteins either prior to or post-electrophoretically using radioactive isotopes remains the most sensitive method for protein detection. Individual radiolabelled protein bands or spots are usually detected in one of three ways: liquid scintillation counting, autoradiography and fluorography. Modifications to facilitate the detection of proteins expressed at very low concentrations (e.g. transcription factors, cytokines, single copy gene products) or proteins labelled with low energy β -particle-emitting radioisotopes, such as [3H], include indirect autoradiography which utilizes intensifying screens for signal enhancement and fluorography.

Autoradiography

In autoradiography dried polyacrylamide gels containing radiolabelled proteins are placed in direct contact with the appropriate X-ray film (e.g. Kodak X-Omat AR, Kodak SB-5, Kodak BMS2, Kodak BMR2, Fuji RX) where radioactive emissions (β -particles and/or β/γ -radiation) react with the silver halides in the film emulsion, resulting in the formation of elemental silver atoms which are visualized following photographic development of the films. [^{14}C]-, [^{35}S]-, [^{32}P]-, [^{125}I]- and [^{131}I]-labelled proteins are readily detected using direct autoradiography while [3H]-labelled proteins are very weakly detected due to severe quenching of their low energy β -emissions by the polyacrylamide gel matrix.

Fluorography and Indirect Autoradiography

To enhance the detection of low abundance proteins and proteins labelled with low energy β -type emitters, fluorographic and indirect autoradiographic methodologies have been developed. Both procedures provide enhanced autoradiographic imaging of low to medium energy β -particle emitters (3H , ^{14}C or ^{35}S) and involve the conversion of the emitted energy from the respective isotopes to photons of visible light, which become the predominant exposing radiation. This is accomplished either by the incorporation of an organic scintillator, PPO (2,5-diphenoxoxazole), directly into the polyacrylamide gel matrix prior to fixation, drying and exposure to film (fluorography) or by the use of calcium tungstate X-ray intensifying screens (indirect autoradiography), as originally developed by Bonner and Laskey and Mills, respectively. For optimal sensitivity, film exposure utilizing X-ray intensifying screens such as Kodak X-OMATIC and Dupont Cronex Lightning Plus or Cronex Quanta II should be performed at low temperatures ($-70^\circ C$) to stabilize latent image formation. This results in up to a 30–40-fold increase in the

detection of [^{125}I] and 8–10-fold increase in sensitivity to [^{32}P]. Additional rare earths (europium-activated barium fluorochloride or terbium-activated mixtures of lanthanum oxysulfide and gadolinium oxysulfide) are available and these appear to be more efficient than calcium tungstate for [^{32}P] detection but result in higher background film darkening. The sensitivity of fluorography can be further increased by pre-flashing (< 1 ms) or hypersensitizing the film before main exposure. This step has the added benefit of correcting the so-called toeing effect or nonlinear relationship between the radioactivity in a sample to the absorbance of the film image, thus permitting quantitative measurements. If an autoradiogram or fluorogram is too faint then it is possible to intensify the images up to 10-fold by incubation of the X-ray film in [^{35}S]-thiourea which complexes with the silver ions in the film to form silver [^{35}S] sulfide.

Storage Phosphor Imaging

Two of the most serious limitations to the use of X-ray film for the visualization of isotopically labelled proteins are relative insensitivity to low energy β -radiation and a nonlinear, limited dynamic range of film darkening to radiation exposure. An alternative to X-ray film for the detection and quantification of autoradiography is photostimulable storage phosphor imaging. Storage phosphor imaging exhibits a dynamic exposure range of more than five orders of magnitude (100 000 : 1 versus 300 : 1 for X-ray film) and a 10–250-fold greater sensitivity than autoradiography to β -emissions. Dried gels containing radiolabelled proteins are exposed to imaging screens composed of a thin layer of $\text{BaFBr} : \text{Eu}^{+2}$ crystals in an organic binder in the same manner in which X-ray film is exposed. Incident radiation (β -particles, γ -rays, X-rays) from labelled proteins induces excitation of the Eu^{+2} ions in the phosphor complex which stores this energy as a latent image. The latent images are scanned with a helium–neon laser which releases the stored energy as blue photons and the intensity of luminescence is quantitated. [^{14}C], [^{35}S], [^{32}P], [^{33}P], [^{125}I] and [^{131}I] are readily detected and quantitated.

Labelling of Proteins with Radioactive Isotopes

The most commonly used isotopes include [^{14}C], [^{35}S], [^{32}P], [^3H] and [^{125}I], although metal isotopes such as [^{59}Fe], [^{45}Ca], [^{63}Ni] and [^{75}Se] have been used to identify iron, calcium and nickel binding proteins and Se-cysteine-containing proteins, respectively. Whereas [^{32}P]-orthophosphate has been used for the introduction of radioactive phosphate groups into proteins, the substitution of [^{33}P] for [^{32}P] has gained in popularity because of significantly increased res-

olution band sharpness as well as increased safety factors afforded by the lower energy [^{33}P] emitter as compared to [^{32}P].

In vitro metabolic labelling of cells or tissue sections in short term culture by incorporation of isotopically labelled amino acid(s) precursor molecules during the cellular growth phase is usually performed using either [^3H]-leucine or [^{35}S]-methionine/cysteine. The use of [^{35}S]- is favoured because of its higher energy β -emitter potential (0.167 vs. 0.018 MeV), higher specific activity (> 1000 vs. 50 Ci mmol^{-1}) and lower cost than [^3H]-labelled molecules. The extent of incorporation of [^{35}S]-methionine is, however, dependent upon methionine content of the individual proteins and proteins lacking methionine would be undetected using [^{35}S]-methionine labelling. This problem has been circumvented by labelling with [^{14}C] amino acid mixtures, although this method is less favoured due to significantly higher cost and lower specific activity (50 mCi mmol^{-1}) of [^{14}C] versus [^{35}S]. Proteins which are post-translationally modified via glycosylation can be labelled with [^3H]/[^{14}C]-galactose, mannose, N-acetyl-glucose and galactoseamine (carbohydrates), respectively, while lipoproteins and certain membrane-associated polypeptides can be labelled with [^3H]/[^{14}C] palmitate and myrisoylate.

Radioactive Stains

The use of radioactive stains for the *in situ* detection of proteins has found limited applications because of the availability of relatively few radiolabelled reagents. [^{59}Fe]-ferrous bathophenanthroline has been used to label radioactively a series of protein markers in polyacrylamide gels post-electrophoretically using simple staining and destaining procedures.

Protein Blotting

One the major advances in the analysis of proteins has been the development of post-electrophoretic techniques for the transfer and immobilization of proteins from the polyacrylamide gel matrix to thin support membranes. Originally based on DNA Southern and RNA Northern blotting principles, protein-blotting protocols were similarly developed by Towbin and co-workers utilizing the electrophoretic elution of proteins separated by PAGE to nitrocellulose (NC) sheets. The major advantage of protein electroblotting is that separated proteins are transferred from the gel matrix, where their access to detection reagents is severely hindered, to the surface of a membrane where the protein molecules are readily accessible. Although protein blotting has traditionally been associated with the immunodetection of

antigen–antibody complexes (Western immunoblotting), blotted proteins are amenable to analysis and characterization via a multitude of visualization and overlay techniques. These include general protein staining and autoradiography, group-specific ligand binding, receptor–ligand interaction, enzymic activity determination as well as amino acid composition and primary amino acid sequence analysis of individual spots or bands. A single protein blot offers numerous advantages not afforded by polyacrylamide gels. It is easily handled and manipulated, can be stored for up to 1 year and the blot can be used for multiple successive analyses. Once a signal has been obtained and recorded, the blot can be erased by removing the probe or stain while retaining the original protein pattern on the membrane and the blot reprobed. Protein blotting has been said to add a second and third dimension to 1D and 2D-PAGE, respectively.

Various types of membranes have been used for protein blotting and immobilization. Nylon and NC sheets (thin film on cellulose esterified with nitric acid) were first used but recently different types of polyvinylidene fluoride (PVDF) membranes have been introduced. A detailed description of protein-blotting methodology, including the advantages and disadvantages of the various blotting membranes, is beyond the scope of this article (see Further Reading).

Immunological Detection

Immunological or group-specific detection of protein(s) on blotted membranes is far and away the most utilized method for protein detection but is limited by the availability of appropriate antibodies/ligands. Following protein transfer, membranes are incubated with dilute protein solutions (e.g. bovine serum albumin, gelatin or instant nonfat dry milk) to block nonspecific binding sites on the membranes. The membrane-bound proteins are incubated with either monoclonal or polyclonal antibodies directed against specific target antigens or group-specific ligands (e.g. Concanavalin A for the detection of glycoproteins, ^{59}Fe and ^{45}Ca to detect iron- and calcium-binding proteins, and [^{32}P]-labelled DNA to detect DNA binding proteins). NC and PVDF membranes are most frequently used since nylon membranes with their intrinsically higher binding affinity for proteins are more difficult to block. If antibodies are used, then blots are incubated with a second antibody that has been directed toward the primary antibody and has been tagged with a reporter label. Typically, the second anti-species antibody may be radiolabelled (^{125}I) or conjugated with an enzyme (e.g. horseradish peroxidase (HRP), alkaline phosphatase (AP) or β -galactosidase). The resulting (antigen–1 $^{\circ}$ antibody)–2 $^{\circ}$ antibody complex is detected

either autoradiographically or colorimetrically using an appropriate chromogenic substrate. The advantages of enzyme-conjugated antibodies are ease of handling and storage and rapid development of colour (min vs. day). Sensitivity is usually in the range of 0.1–10 ng of antigen/band. While this sensitivity is approximately 10–100-fold less sensitive than autoradiographic or fluorographic detection, it is possible to achieve a similar level of enhanced sensitivity using peroxidase–antiperoxidase (PAP) sandwiching.

Recently, modifications have been developed for the use of light emission (luminescence) as an end point for protein–antibody detection on membranes. Although substrates which produce colour complexes exist for both AP and HRP, the HRP luminescent system, in which blue light is generated by the HRP-mediated oxidation of luminol, is the most sensitive system. This system, commonly known as the ECL (enhanced chemiluminescence) Western blotting system, provides excellent signal-to-noise ratio and is extremely rapid and sensitive.

In the basic (nonenhanced) chemiluminescent reaction, HRP is used to oxidize a peracid, resulting in a raised oxidation state of the haem Fe in HRP. Relaxation of this excited state to initial (ground) state occurs in a two-step process. At each relaxation a luminol radical is formed and, as each radical decays, light is emitted. However, in the ECL reaction, an enhancer molecule is added which reacts with the haem Fe in place of the luminol molecule, resulting in the formation of enhancer radicals which themselves react to produce luminol radicals and light is emitted. The enhancer molecules increase light emission greater than 1000-fold over luminol alone. Light emission on membranes rises rapidly over the first 5 min, remains at maximum for 15 min, and then declines with a $t_{1/2}$ of 60 min. Typical exposures for ECL are of the order of a few seconds to minutes and are capable of detecting 1 pg or less of protein.

Total Protein Staining

Blotted membranes can be stained with many of the general protein stains used for polyacrylamide gels including Amido Black, CBB, Ponceau S, Fast Green and India ink (Table 1). Amido Black and Ponceau S are preferred to CBB-R because stained membranes can be destained quickly to leave very low backgrounds, whereas CBB-R gives higher backgrounds. India ink (colloidal carbon) is the most sensitive of the above dyes and can detect as little as 80 ng of protein but staining sensitivity is highly dependent upon dye source and lot. Silver staining is also possible as well as the use of colloidal gold and iron sol stains. Both silver and gold stains can detect as little as 1–5 ng protein on NC and PVDF membranes and

the sensitivity of gold stain can be further enhanced by incubation with a silver lactate solution such that as little as 400 pg of protein per band can be detected. Although nylon or charged nylon membranes possess the greatest protein-binding capacities (450 vs. 80 $\mu\text{g cm}^{-2}$ (NC/PVDF)), staining of nylon membranes is very problematic. Anionic organic dyes as well as colloidal gold and silver are not useful for staining nylon membranes due to extremely high backgrounds. However, colloidal sols are especially useful for the detection of proteins on nylon membranes. On nylon membranes the positively charged colloidal iron particles bind to negatively charged SDS-denatured proteins and protein staining can be intensified using potassium ferricyanide, which gives deep blue-stained bands with low backgrounds. India ink and a modified silver stain have been reported to have been used to stain charged nylon membranes.

A less frequent, but none the less useful method for the visualization of protein bands on NC and charged nylon membranes involves protein iodination *in situ* with chloramine T/potassium iodide, followed by formation of a purple complex between the bound iodine and starch.

Autoradiographic Detection

Electroblotting of proteins radiolabelled with ^{14}C or ^{35}S permits more efficient autoradiography since the gel matrix is no longer present to quench the β -emissions. The minimum level of ^{14}C or ^{35}S that can be detected in 24 h is about 400 dpm cm^{-2} . While fluorography is necessary to detect ^3H on polyacrylamide gels, ^3H exposure can be detected directly on electroblots using autoradiography, although 2×10^4 dpm cm^{-2} is required for detection in 24 h. The efficiency of detection for all isotopes is enhanced if fluorography is employed (100 dpm and 500 dpm cm^{-2} for $^{14}\text{C}/^{35}\text{S}$ and ^3H , respectively).

Future Developments

PAGE, in particular 2D-PAGE, remains the method of choice for the separation of complex protein mixtures. This has necessitated the development of highly sensitive protein visualization protocols incorporating both nonradioactive and radioisotopic imaging

methodologies. The development of methods for the transfer of polypeptides from gels to membranes where they are readily accessible to react with stains, specific antibodies, group-specific ligands and detailed structural characterization, including amino acid microsequencing and mass spectral analysis, has permitted the identification of previously unidentified proteins. Further developments are likely to take place in low background staining polyacrylamide formulations and modified membrane support matrices in which proteins may be bound either covalently or which form reversible covalent bonds. Such proteins can be easily and selectively eluted for more detailed biochemical studies. Future advances are likely to take place in the development of more sensitive and group-specific dyes/stains and increased speed and sensitivity of detection systems such as the enhanced bioluminescent and chemiluminescent systems, as well as the development of faster and more sensitive photographic detection film.

Further Reading

- Bonner WM (1983) Use of fluorography for sensitive isotope detection in polyacrylamide gel electrophoresis and related techniques. *Methods in Enzymology* 96: 215–222.
- Dunbar BS (ed.) (1994) *Protein Blotting*, p. 242. New York: Academic Press.
- Gershini JM (1988) Protein blotting: a manual. *Methods in Biochemistry Analysis* 33: 1–58.
- Hames BD and Rickwood D (eds) (1990) *Gel Electrophoresis of Proteins*, p. 383. New York: IRL Press.
- Laskey RA and Mills AD (1977) Enhanced autoradiographic detection of ^{32}P and ^{125}I using intensifying screens and hypersensitized film. *FEBS Letters* 82: 314–316.
- Merril CR (1990) Gel staining techniques. *Methods in Enzymology* 182: 477–488.
- Towbin H, Staehelin T and Gordon J (1979) Electrophoretic transfer of proteins from polyacrylamide gels to nitrocellulose sheets. Procedure and some applications. *Procedures of the National Academy of Science (USA)* 76: 4350–4354.
- Wirth PJ and Romano A (1995) Staining methods in gel electrophoresis, including the use of multiple detection methods. *Journal of Chromatography (A)* 698: 123–143.

Detectors for Capillary Electrophoresis

Thomas Kappes and Peter C. Hauser, University of Basel, Switzerland

Detection is a particularly critical issue in capillary electrophoresis (CE) because of the extremely small cell volumes available. Considerable effort has gone into overcoming this limitation and a bewildering

variety of methods has been described, ranging from the straightforward adaptation of existing chromatography detectors to less obvious and highly experimental techniques. The path has not been smooth, but many obstacles have turned out to be less serious than anticipated. Optical methods have proved very useful despite the short pathlengths involved. Electrochemical detection methods, intuitively considered incompatible with the applied high voltage and long neglected in favour of optical means, are now readily implemented. However, the development of detection methods is still in flux and it may take several more years before maturity is reached and different methods have found their established roles for particular applications.

The Detection Challenge

The internal diameters of the capillaries employed in CE range from 100 μm down to about 5 μm and a single analyte zone is approximately 1 mm long. Because the detection volume has to be smaller than the peak volume available, detection volumes range from about 1 pL to 1 nL. In high performance liquid chromatography (HPLC), in contrast, detection volumes of at least 1 μL are available. One would therefore expect sensitivities for CE to be several orders of magnitude lower than those in HPLC and, as a consequence, the detection limits to be much inferior. However, in CE the sample does not experience significant dilution before it reaches the detector, as is the case in HPLC, because of the flat flow profile in CE. Therefore, the sensitivities are not in fact as significantly degraded in comparison with HPLC as might be expected. Nevertheless the issue of detection limits is still critical in CE and detector sensitivity is not always adequate. Preconcentration by electrostacking is sometimes advocated, but this method is only possible for samples with low ionic strength and generally leads to poor precision unless an internal standard is employed.

Because of the small detection volumes, on-column detection schemes are required to avoid band broadening, rather than detector cells attached in an off-column arrangement as is the case in chromatography. A unique property of detection in electrophoresis, which is not shared with chromatography, is the fact that there is a dependence of the peak area (expressed on a time basis) on migration velocity. However in practice this is usually of no concern. Detection methods may be grouped according to whether a bulk property of the solution (such as conductivity, refractive index) or a specific attribute of the analytes (such as optical absorption or fluorescence, redox activity or membrane permeability) is

monitored. Detectors used in the first case tend to be more universal, but generally suffer from the presence of a large background signal against which small changes have to be distinguished. This often leads to poor signal-to-noise (S/N) ratios and hence relatively high detection limits. The exploitation of specific interactions is generally better in this regard, but each method is usually only applicable to a certain class of analytes. Some of the specific detection methods also allow additional information on the analyte to be gathered, which may be desirable as migration times can never be taken as absolute proof of identity. These detectors may be termed 'information rich', and include for example mass spectrometers, photodiode arrays and voltammetric detectors.

Important general characteristics of detectors are their sensitivity, dynamic range, and linearity. The term sensitivity generally denotes the gradient of the calibration curve but the precision of the measurement (S/N ratio) has to be considered as well for a complete evaluation. Often, the term sensitivity is used to indicate the lowest concentration that may be detected (limit of detection, LOD) and these parameters are of course interrelated. In CE detection limits are sometimes quoted in terms of the detectable mass or number of moles, as impressive figures in the pico- or atto-gram or -mole range can be given because of the small sample volumes used. However, the standard concentration limits are much more useful and meaningful. The dynamic range is encompassed by the detection limit and by a maximum where a loss of sensitivity occurs. Wide dynamic ranges are desirable as they simplify sample preparation, but they often go hand-in-hand with relatively poor precision. The upper concentration limit in capillary electrophoresis is generally determined by the ionic strength of the background buffer (typically 1–10 mmol).

The choice of detector is guided by the requirement of the application in terms of detection limit, selectivity and information requirements but to a large degree also by commercial availability, cost, robustness and ease of use. Some features of the major detection methods are summarized in Table 1.

Optical Methods

Optical detection methods are more widely employed than any other detection means. Commercial CE instruments with optical absorption detectors were introduced in 1989 and are available from a variety of instrument manufacturers. The detectors employed have often been adapted from devices used in HPLC and this may be part of the reason for the prevalence of the ultraviolet (UV) absorption detection method.

Table 1 Main detection methods for capillary electrophoresis

Method	Features	Detection limits ^a (mol L ⁻¹)
UV/Vis absorption	Readily available commercially	10 ⁻⁷
Indirect UV/Vis absorption	Compromise with poorer detection limits for nonabsorbing species such as most inorganic ions	10 ⁻⁵
Fluorescence	Good detection limits but most species require derivatization; available commercially	10 ⁻⁹
Laser fluorescence	Elaborate; excellent detection limits; available commercially	10 ⁻¹¹
Conductometry	Good for small ions; available commercially	10 ⁻⁶
Amperometry	Simple, but only possible for electroactive ions; not available commercially	10 ⁻⁸
Mass spectrometry	Provides information on peak identity; expensive; interfaces available commercially	10 ⁻⁸

^aThe values given should be considered as rough guides only, as these are often very much dependent on species and instrumental set-up. UV/Vis, ultraviolet-visible.

Fluorescence-based detectors are not as widely used but are also on the market.

To carry out on-column detection the usual polyimide protection coating has to be removed from the column by burning, by dissolution with hot sulfuric acid, or by mechanical scraping, to form a window into the capillary. The material is fairly brittle, so that care has to be taken to avoid breakage once the protective cladding has been removed. Fused silica capillaries are transparent even below 200 nm, so that the near-UV range is readily accessible.

The basic cell arrangement for absorbance measurement through a capillary is illustrated in Figure 1. Generally, besides the light source, there is a monochromator or optical filter to define the wavelength employed, a lens and aperture, and a photodetector. Variations of this arrangement are possible. Most commonly wavelengths in the UV range from about 250 nm down to 185 nm are employed, using different types of sources such as deuterium lamps, but instruments that include the visible range are also available. Variable wavelength as well as fixed wavelength arrangements are in use. It is important to get a high light intensity transmitted onto the detector for best S/N ratio. The usual UV light sources, such as deuterium lamps, are larger than the optical cell and it is only possible to focus

a small fraction of the radiation emitted through the cell even with the best available lenses. Ball lenses, mounted directly adjacent to the capillary, are often employed. Apertures are required to minimize the amount of stray light reaching the detector. Optical fibres can be used for transmission of the radiation as this allows efficient electrical shielding of the photodetector and at the same time the distal ends form the optical apertures. Absorbance detectors based on light-emitting diodes (LEDs) and laser diodes have also been demonstrated. These devices give high baseline stability because of the absence of flicker noise present in discharge lamps and allow the construction of battery operated instruments because of their low power consumption. However, these devices are not available for the UV wavelength range.

The circular cross-section of the capillary is far from ideal for absorbance measurements because it is not possible to pass collimated light through the interior of the tube without refraction. This means that changes in the refractive index of the solution are a potential source of interference. In practice, however, the only serious limitation appears to be the short optical pathlength, which leads to low sensitivity according to the Lambert-Beer law. For this reason the largest capillary diameters that allow efficient cooling are usually employed in absorbance detection, typically with an internal diameter of 50–75 μm . Different methods of increasing the sensitivity in absorbance detection have been described. These include the use of rectangular capillaries, capillaries bent in a Z-shape to obtain a longitudinal light path, multipass cells by multiple reflections in silver-coated capillaries, and so-called bubble cells formed on the capillary itself. Only the last approach is reasonably easily implemented, and it appears to be the only one that is commercially available (albeit at a cost much higher than that of ordinary capillaries).

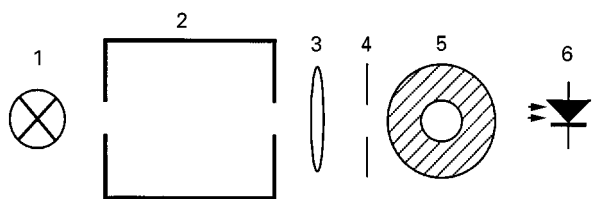


Figure 1 Schematic representation of absorbance detector. 1, Light source; 2, monochromator or optical filter; 3, lens; 4, aperture; 5, capillary; 6, photodiode or photomultiplier tube.

The internal diameter of the capillary is widened in the detector region by a factor of about three, thereby increasing the sensitivity by the same magnitude.

A different approach to increase the sensitivity of absorption measurements is the use of thermo-optic methods. Here the heat evolved following the absorption of light is sensed indirectly. In the thermal lens method the refraction of a laser light beam is measured, using a relatively simple arrangement. Two light beams perpendicular to each other are employed. One of the beams is of a wavelength that is absorbed by the analytes. The heat evolved through absorption of light leads to a refractive index gradient in the capillary which is monitored by the second beam. A variation on this technique has been reported that uses intensity-modulated light. This leads to a vibration of the capillary that may again be detected with a second probe beam. Ordinary refractive index detection has also been described using the deflection of a laser beam but neither of these two techniques has gained much acceptance.

Most organic analytes possess chromophoric groups that show intrinsic absorbance in the near-UV range, so most methods are based on this wavelength region. It has been demonstrated that for these species it is preferable to use wavelengths that are as short as possible (below 200 nm) for the best sensitivity. Photodiode-array detection is also possible. This technique yields additional qualitative information on the identity of the detected species and allows peak inhomogeneity to be detected. However, the S/N ratio and therefore the detection limit, which is always critical in CE, are degraded because of the reduced integration time available, and the method requires considerable computing power, because of the large amount of data acquired. Ions that do not show absorbance in the UV/Vis range, such as inorganic species or completely saturated organics, may be determined by indirect methods. These methods rely on the displacement of dye molecules of equal charge as the analyte species (to maintain electroneutrality) so that a decrease in absorbance is detected. This is more demanding on the stability of the system than the direct absorbance method and the detection limits are generally higher. However it is the only method employing optical absorbance detectors to be available for most inorganic anions. Chromate is often used as the background ion but other species, some for the visible wavelength range, have also been reported. Inorganic cations can also be detected by indirect means, but many of them are best determined via the formation of coloured complexes using non-discriminating ligands.

Fluorescence detection is also possible and is commercially available. However, few species display in-

trinsic fluorescence, so derivatization reactions have to be employed. Derivatization may be classified as pre-column, on-column or post-column according to the scheme employed. Fluorescence has the great advantage of much higher sensitivity than absorbance measurements. Detection limits approaching single molecule detection have been achieved. Lasers appear to be ideal light sources for fluorescence measurements, as the light is produced in a tightly focused beam well matched to capillaries, but inexpensive sources are not available for the UV range and available lasers are often plagued by insufficiently stable output intensities. This limits their use, especially for the more universal indirect detection scheme. Nevertheless, impressive results have been obtained for microbiological applications (e.g. in neuroscience) that include the analysis of single cells. Chemiluminescence detection is usually based on the influence of analytes on the efficiency of one of several available chemiluminescence reactions. The achievable sensitivities are very high, a feature this method has in common with fluorescence. Its implementation is similar to post-column fluorescence detection in that a pumped reagent stream has to be merged with the column effluent in a suitable small-scale mixing device prior to detection in a light-tight enclosure with a photomultiplier tube.

Electrochemical Methods

Electrochemical detection techniques in general are developing rather more slowly than optical techniques, even though some of the earliest examples of open tubular electrophoresis were based on electrochemical detection. It was considered that the electrical field applied for separation was a serious hindrance. Also, the exposure of the detector to the buffer solution (which is not the case for the optical methods) is a potential source of problems as the electrodes may corrode or be affected in other ways. While the common optical detection methods have reached maturity, the same cannot be said for the electrochemical methods. Of the three reported methods, namely conductimetry, amperometry and potentiometry, the former is the only one that is commercially available at this time. Nevertheless, these methods have attracted considerable attention and in general are much simpler than other methods.

In an early approach to conductivity detection, the cell was formed by drilling a hole perpendicularly through the capillary with a laser and then inserting two small wires that faced each other. In this way the two detector electrodes were not exposed to a voltage gradient. Another approach, which is still used by some workers for amperometric detection, is to

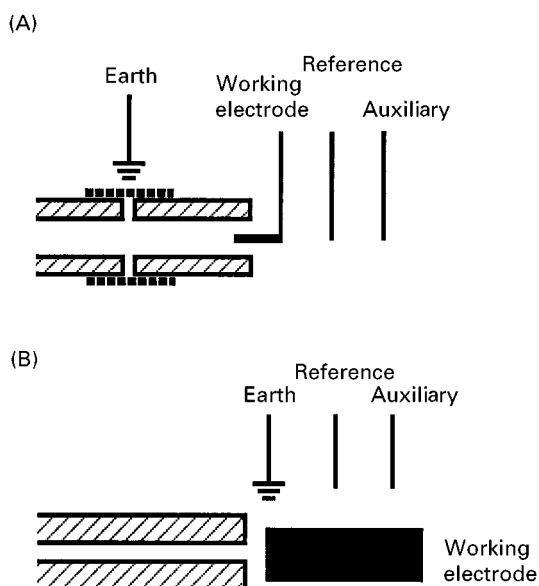


Figure 2 Common arrangements for electrochemical detection. (A) Decoupled configuration with on-column detection using a micro-electrode. (B) Wall-jet arrangement possible with capillaries with internal diameters of 50 μm or less, showing a relatively large electrode at a suitable distance from the capillary end.

decouple the detector from the electrical field. This is achieved by creating a small gap in the capillary and using a sleeve typically made of an ion exchange membrane to provide a contact to the electrical earth. This arrangement is illustrated in Figure 2A. The analytes are pushed forward to the detector electrode(s) by the pressure created by the electroosmotic flow. This arrangement is ideal in an electrical sense but cumbersome to implement. However, it was later realized that if electrodes are positioned immediately outside the end of capillaries that have internal diameters of 50 μm or less, then the electrical bias on the detector is minimal. This arises because the cross-section of the liquid volume outside the capillary is considerably larger than that inside, so that the remaining voltage drop between the end of the capillary and the electrophoretic earth electrode located a few millimetres away is a few hundred millivolts only. Inside the capillary voltage drops of 30 V mm^{-1} are typically encountered. Also, the electrical current through the capillaries is considerably lower for smaller internal diameters. This so-called wall-jet arrangement (Figure 2B) is the one used in commercial instruments for conductivity detection, and this same configuration is also frequently employed for the other two electrochemical detection methods. A further feature of the wall-jet configuration is the use of electrodes with diameters larger than the internal diameter of the capillary, which was found to be possible without significant loss of peak resolution.

This allows the construction of relatively simple cells for the alignment of capillary ends and electrodes.

In conductimetric detection it is essentially the same property which is responsible for the separation, namely the mobility in the electrical field giving rise to a detector signal. This means that in principle any species that can be separated by CE may be detected by conductimetry. However, the need for an electrolyte in the running buffer leads to the presence of a background signal against which the analyte signal has to be measured. As the analyte displaces ions of the same charge (the same feature exploited in indirect absorbance detection), it is the difference in conductivity (caused by a difference in mobility between background and analyte ions) that leads to a detectable signal. To optimize the sensitivity the conductivity of the background buffer should be low, a requirement that conflicts with the need for matching the mobility of the buffer to that of the analytes to prevent peak tailing or fronting. A compromise therefore has to be made. For analytes with low conductivity indirect detection may be employed using a background electrolyte with high conductivity.

Conductivity detection can also be carried out in a contactless configuration with two tubular electrodes placed over the capillary. These then form capacitors (albeit with small capacitance values) with the liquid, whose conductivity can be probed with an applied high frequency alternating current. Electrode degradation is prevented in this mode. The sensitivity of conductivity detection can be improved by the so-called suppressed detection technique, known from ion chromatography, in which the background conductivity is largely removed by using a weak acid or base that is rendered neutral by ion exchange before the detection cell. However, for CE an arrangement similar to that used for electrical decoupling is required for suppression. This is difficult to implement and the method has not found wide use.

Amperometric detection may be employed for ions that are electroactive, i.e. that can be reduced or oxidized at electrodes. Different classes of species show this property, including heavy metal ions, certain inorganic anions, and many different organic molecules that incorporate reactive groups such as phenols, aldehydes, amines, etc. Many applications of amperometric detection have been reported but these have certainly not been fully explored yet. As the detection limits of amperometry tend to be good this approach is useful when low concentrations are to be determined. Please note that the terms 'electrochemical detection' and 'EC detection' are often employed with the sole connotation of amperometric detection, a usage that has evolved in the context of HPLC detection methods. This may lead to confusion as

conductimetry and potentiometry clearly are electrochemical methods as well.

At this stage detector cells for amperometry have to be constructed in-house as (at least to our knowledge) no commercial units are available. However, all the other parts required to set up a CE instrument, including potentiostats to operate the detector, are available commercially in modular form. In the wall-jet arrangement, the voltage applied to the working electrode by the potentiostat circuitry is superimposed by a voltage bias that is not only dependent on the applied separation voltage but also on parameters such as buffer composition, capillary diameter and the exact position of the electrode. For this reason some workers continue to use the decoupled detector. Amperometric detection in CE in principle requires a total of four electrodes at the detector end of the column. Besides the detector electrode (the working electrode of the potentiostat circuitry) and the electrophoretic earth, a reference electrode and a counter (or auxiliary) electrode are required. It is possible to simplify this configuration by employing the electrophoretic earth as a pseudo-reference and as a counter electrode as well.

Different electrode materials may be used in amperometric detection including gold, platinum and glassy carbon to suit different applications. The use of copper wire electrodes has proved to be useful as several oxidation reactions are catalysed on this material. Pulsed amperometric detection (PAD) may be employed when reaction products lead to a fouling of the electrode. Voltammetric detection in which the applied electrode potential is swept rapidly and repeatedly over the range of interest to gain additional information on the peak identity via the redox potential is also possible. Somewhat higher detection limits may have to be accepted, however, for these pulsed methods.

Potentiometric detection with ion selective electrodes is the least reported of the three electrochemical detection methods. The matching of a separation method with a sensor (rather than a detector which by definition is not selective) may appear to be a contradiction, but ion selective electrodes are in fact rarely highly selective and may be tailored to be responsive to a range of ions. So-called Hofmeister electrodes discriminate solely on the basis of the lipophilicity of the anions or cations, and are therefore at least in principle well suited for the determination of singly charged organic species. Early reports on this technique were based on micropipette ion selective electrodes known from physiological studies on single cells. These electrodes consisted of glass capillaries, with tip diameters of a few micrometres, that were filled with a viscous organic solvent incorporating an ionophore and acted as ion selective membranes.

However, these electrodes were not very robust and have now been superseded by more reliable miniature coated-wire ion selective electrodes. These detectors have been used to detect a variety of inorganic and organic species that otherwise could not be detected with CE, or could only be detected with difficulty. It is possible to use a copper wire electrode as a simple potentiometric detector for amino acids in CE.

In summary, the three electrochemical methods may be considered to be complementary. Conductivity detection is a versatile general method that works best for small ions of high mobility. Amperometric detection is useful for electroactive ions and good detection limits can be expected. Potentiometric detection has currently been relatively poorly explored, but may prove to be a useful alternative for large, singly charged ions that cannot be detected amperometrically or by direct optical absorption measurements.

Other Methods

Detection methods other than optical or electrochemical methods have also been reported. One method that is fairly widely used is mass spectrometric detection, including detection by inductively-coupled plasma mass spectrometry, and commercial interfaces are available. Detection by nuclear magnetic resonance is also an established technique. These methods are covered elsewhere in this encyclopedia. Radioisotope detection has been reported and good detection limits have been achieved.

Future Developments

The acceptance of CE depends to a large extent on the availability of suitable robust detection methods with good detection limits. Shortcomings appear to exist for trace analysis of organic species that do not fluoresce, and for inorganic species. Thermooptic and chemiluminescence methods are promising in this regard as are the electrochemical methods of amperometry and conductivity. The last two methods appear to have reached some degree of maturity and it is hoped that these will become more readily available commercially.

See also: II/Chromatography: Liquid: Detectors: Ultra-violet and Visible Detection; Detectors: Mass Spectrometry; Detectors: Fluorescence Detection.

Further Reading

Baker D (1995) *Capillary Electrophoresis*. New York: John Wiley.

- Doble P and Haddad PR (1999) Indirect photometric detection of anions in capillary electrophoresis. *Journal of Chromatography A* 834: 189.
- García Campaña AM, Baeyens WRG and Zhao Y (1997) Chemiluminescence detection in capillary electrophoresis. *Analytical Chemistry* 69: 83A.
- Jandik P and Bonn G (1993) *Capillary Electrophoresis of Small Molecules and Ions*. Weinheim: VCH Publishers.
- Landers JP, ed. (1997) *Handbook of Capillary Electrophoresis*. Baton Rouge: CRC Press.
- Li SFY (1993) *Capillary Electrophoresis, Principles, Practice and Applications*. Amsterdam: Elsevier.
- Liu BF, Liu LB and Cheng JK (1999) Analysis of inorganic cations as their complexes by capillary electrophoresis. *Journal of Chromatography A* 834: 277.
- Lucy CA and Wu Q (1998) Characteristics and calibration of conductivity detection in capillary electrophoresis. *Journal of Chromatographic Science* 36: 33.
- Nouadje G, Siméon N, Nertz M and Couderc F (1996) Électrophorèse capillaire et détection par fluorescence induite par laser. *Analisis* 24: 360.
- Polesello S and Valsecci SM (1999) Electrochemical detection in the capillary electrophoresis analysis of inorganic compounds. *Journal of Chromatography A* 834: 103.
- Saz JM and Díez-Masa JC (1994) Thermo-optical spectroscopy: new and sensitive schemes for detection in capillary techniques. *Journal of Liquid Chromatography* 17: 499.
- Voegel PD and Baldwin RP (1997) Electrochemical detection in capillary electrophoresis. *Electrophoresis* 18: 2267.
- Weinberger R (1993) *Practical Capillary Electrophoresis*. Boston: Academic Press.

Discontinuous Electrophoresis

M. J. Doktycz, Oak Ridge National Laboratory,
Oak Ridge, TN, USA

Copyright © 2000 Academic Press

Introduction

Electrophoresis is one of the most powerful tools in the arsenal of separation scientists. It is commonly employed in the field of biochemistry, where separation of complex mixtures of proteins or nucleic acids is a continuing challenge. Numerous variants of electrophoresis have been described with the goal of optimizing the speed and effectiveness of the separations. One important electrophoretic variable is the separation matrix. It provides the retarding forces, or sieving qualities, that counter the electrophoretic transport. These forces can ultimately effect the separation and can be altered by the matrix type or concentration. Cross-linked or linear forms of polymers such as agarose or acrylamide are common choices. Different formats for the electrophoresis medium can also have dramatic effects on the resolution and separation time. This is exemplified by recent uses of microcapillary formats which greatly speed up separations. Another component that dictates the speed and resolution of electrophoretic separations is the charge-carrying buffer ion. The buffer is a universal component of electrophoresis, independent of gel constitution or format. This component is often overlooked, though attention to this aspect can be beneficial in developing electrophoresis-based separation techniques.

Proper buffer selection offers several practical advantages, including optimum separation times, in-

creased band concentration and reduced effects of diffusion. The resolution of closely migrating species results from the proper choice of the pH, concentration, and type of buffer ion. These physical characteristics define the conductivity of the electrophoretic medium and affect the transport of the molecules to be separated. Inorganic ions, such as chloride anion, have high conductivities in comparison to the ionized form of weak acids and bases. Such high mobility ions offer little advantage when used for the electrophoretic separation of large, less mobile biomolecules but slower-moving ions, such as those of weak acids or weak bases, are more useful choices. These not only buffer the pH but, due to the slower mobility of these ions, lead to better separation of charged macromolecules.

Zonal electrophoresis utilizes a single buffer in the gel and reservoirs. An alternative to the continuous buffer, zonal separations is a discontinuous system where multiple ionic components are used. The presence of multiple ionic components in electrophoresis leads to discontinuities in the voltage gradient, pH and ionic strength due to the different physical mobilities of the ions involved. These different mobilities lead to the formation of discrete zones of ions that, under equilibrium conditions, travel at a constant rate in an applied electric field. Adjustment of these mobilities involves alteration of the ion concentration and potential gradient of the zone. Sharp boundaries can exist between these zones, with the ionic concentration being dictated by the Kohlrausch regulating function. The technique is similar or identical to a number of electrophoresis techniques that are known as discontinuous multiphasic, multizonal,

displacement, isotachopheresis and moving boundary electrophoresis. The primary advantages of discontinuous buffer systems over continuous buffer, zonal separation are their ability to concentrate dilute samples, enhance resolution between closely migrating species and provide defined reference fronts.

Implementation

Most of the electrophoretic techniques that exploit the differential migration of ions in an electric field trace their origins to the work of Kohlrausch. In 1897, Kohlrausch presented the equations that describe ionic migration in an electric field. In later decades, Tiselius furthered electrophoretic techniques and accomplished the separation of serum proteins using moving boundary electrophoresis. In 1958, Poulik published the use of the discontinuous buffer technique for the separation of proteins in a starch gel and, a few years later, Ornstein and Davis described the theory of discontinuous buffer systems for the separation of serum proteins in polyacrylamide gels. The Ornstein and Davis 'disc' electrophoresis system concentrated the sample by placing it between buffers of different mobility and then performed the separation using zone electrophoresis. In 1965, Richards applied the technique for the separation of nucleic acids. Since this period, discontinuous buffer systems, or similar techniques, have seen consistent usage in protein separations. Theoretical treatments that aid in the design of appropriate buffer systems have been extended. This has led to the description of various buffer systems for the separation of both acidic and basic proteins and the development of 'spacer' ions for resolving closely migrating proteins. The application to nucleic acid separations has been sporadic. This is perhaps due to the lower reliance on charge differences for the separation of nucleic acids. In

contrast to proteins, nucleic acids have a near constant mass-to-charge ratio giving them a common free electrophoretic mobility. Typically, zonal gel systems that fractionate solely on size are used. However, discontinuous buffer systems do offer advantages for certain nucleic acid separations.

In practice, a leading ion is chosen such that the mobility of this ion is greater than all others in the system. This ion is incorporated into the separation matrix (or in some applications, an anti-convective matrix). The trailing ion(s), with a mobility slower than the leading ion, is placed in the top buffer reservoir while a counterion, common to all zones, is placed in the bottom buffer reservoir. For open-faced gel systems, the samples are loaded directly on to the separation matrix, while for vertical slab systems the sample can be loaded on top of the gel. As the moving boundary is established, the sample will be concentrated in a very thin moving boundary. The analytes to be separated will stack themselves in the order of their ionic mobility and, in the case of discontinuous electrophoresis, may be further fractionated by the use of a sieving gel. The resultant bands are easily detected with conventional techniques, using stains or fluorescent or radioactive labels. A description of a typical experimental set-up, and the identity of the various ionic species for an anionic separation, is shown in Figure 1.

Only the concentration of the leading ion can be chosen freely. During electrophoresis, the ionic concentration and potential gradient of the trailing zones will be regulated to compensate for the lower mobility. This regulating function is known as the Kohlrausch regulating function. Under equilibrium conditions, the leading and trailing ions migrate at the same rate (isotachopheresis). This causes the ion concentration in a trailing zone to be lower, and the voltage gradient to be higher, than that in a leading

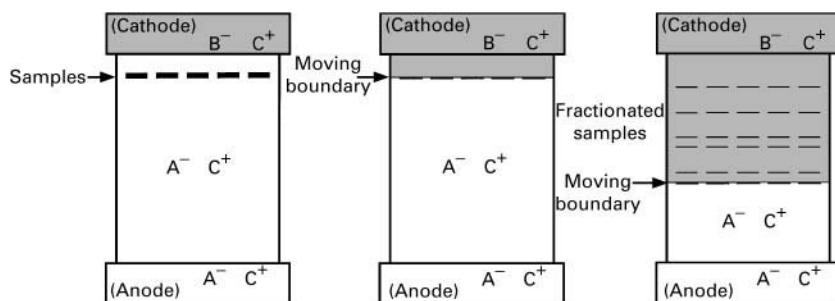


Figure 1 Pictorial description of the progress of an electrophoretic separation using a discontinuous buffer system. The initial set-up is shown on the left. A trailing anion, B^- , is placed in the cathodal buffer reservoir while the leading ion, A^- , is placed in the gel. This leading anion has a mobility that is greater than all other anions in the system. A common counterion, C^+ , is used throughout the reservoirs and gel. The centre panel shows the sample being concentrated by the moving boundary created by the dissimilar anions. As this boundary traverses through the gel, the sample components, with mobilities that are slower than the trailing anion, will be fractionated in the trailing zone. Those ions with an intermediate mobility will be retained in the moving boundary. This is shown on the right.

zone. These differences compensate for the lower free mobility. The migration rate of the ions can be followed by observing the position of the boundary between the zones. This boundary is self-sharpening, as 'trailing ions', if present in the leading zone, will be in a low field region and slow down, while 'leading ions' in the trailing zone will be in a high field region and speed up. This boundary can be conveniently demarcated by incorporation of a low concentration of a dye with a mobility intermediate between the leading and trailing zone. Alternatively, conductivity or thermal changes can be monitored to detect the passing of the boundary. Multiple boundaries can exist with each one defining a distinct zone. Since the concentration of ions in the zone is regulated, the size of the zone will depend on the quantity of material and the concentration of the leading ion. Thus, dilute samples can be concentrated and different ions can be sorted based on their mobilities.

Selection of appropriate buffer systems usually requires some knowledge of the charge and mobility of the analytes to be separated. Many buffer systems, which span the entire range of pH values, have been described. These systems are especially useful for the separation of proteins that are charged under specific pH values. The mobilities of the charged analytes to be separated are also critical. For molecules that are subsequently to be fractionated within the trailing zone, the trailing ion should have a mobility that is similar to or intermediate between the ions to be separated. Tuning the mobility of the trailing ion to that of the analyte can minimize the conductance changes across the sample. This can lead to sharp band profiles and enhance the resolution of closely migrating species. Reference to previously tabulated buffer mobilities will aid in the selection of an appropriate buffer system. The development of new buffer systems can be accomplished empirically or through simple application of the equations describing discontinuous electrophoresis.

Advantages

The primary advantage of discontinuous buffer systems is the ability to concentrate the sample zone. The passage of the moving boundary has the effect of sweeping the sample into an extremely thin starting band. For analytical applications this can lead to reduced band widths and higher resolution separations. This feature has obvious advantages for the characterization of closely migrating species. For preparative applications, the result is the concentration of dilute samples. Another advantage of discontinuous buffer systems is their use as an analytical tool for defining relative mobilities. The mobility of

the ion front is easily defined and can serve as a reference for defining relative mobilities. Furthermore, the mobility of the front is reproducible and independent of the gel matrix. These features can be convenient for analytical and forensic applications. Additionally, the mobility of sample ions can be altered by changing the mobility of ions in the trailing zone. This can lead to the tailoring of separations by defining the size range that can be fractionated. Sample ions that are not of interest can remain trapped in an ion front, allowing examination of particular ions. Finally, discontinuous buffer systems are compatible with virtually any gel format, as its use is independent of the gel matrix or the physical format of the gel. Since it alters only the buffer system, the only complication is selecting an effective buffer. Fortunately, the characteristics of many buffer systems have been described and designing new systems is a straightforward task, as described below.

Figure 2 exemplifies some of the features of discontinuous buffer systems for nucleic acid separations. Shown here is a portion of a DNA sequencing gel using a denaturing formate-glycine discontinuous buffer system. An intermediate zone, with a mobility between the formate leading ion and the glycine trailing ion, was inadvertently created from contaminating ions in the gel or sample loading buffer. For analytical application, care should be taken to ensure that extraneous ions are absent. However, the presence of this ion species demonstrates the effects of stacking limits on the size selection and band concentration of DNA sequencing products. DNA bands smaller than 106 bases are trapped in the first ion front while DNA sizes 115–166 are trapped in the second front. The DNA sizes that are trapped in the ion fronts define the stacking limits and cannot be separated because their mobility is between that of the migrating ion zones. Since the DNA is not freely electrophoresing, these stacking limits could be altered by changes to the gel matrix. The intermediate ion zone demonstrates other features. Its size is directly proportional to the amount of contaminating ion that is present. Larger amounts of contaminating ion would expand this zone. Additionally, the eight DNA bands in this zone are much sharper than the bands migrating behind the second front, even after the 30 cm migration distance. This is due to the concentrating effects of the leading ion front and the closely matched mobility between these DNA bands and the ions in the zone.

Theoretical Description

Calculation of the ion concentrations and basic characteristics of the leading and trailing ion zones are

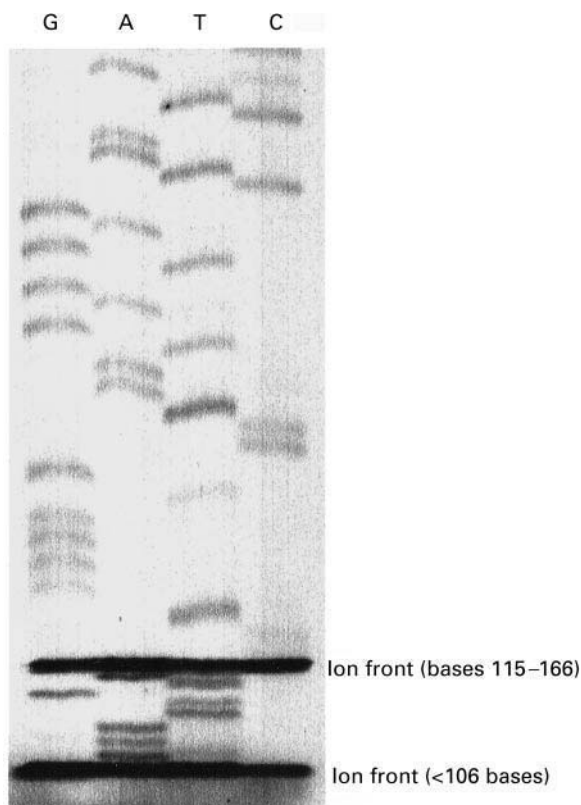


Figure 2 The differential effects of stacking limits on the migration of DNA sequencing products on a 6% polyacrylamide gel (containing 5% bis-acrylamide cross-linker) with a 50 mmol L⁻¹, pH 9.0 formate leading ion, glycine trailing ion. The sequence between the two fronts, AAATTGTT, corresponds to fragment lengths of 107–114 bases; the sequence behind the front, CTGG, corresponds to fragment lengths of 167–170 bases. Fragment lengths between 115 and 166 bases are concentrated in the second front while fragment lengths < 107 bases are concentrated in the first front.

easily accomplished through use of a few simple equations. The starting point is the Kohlrausch regulating function (R) that describes the moving boundary condition:

$$\sum \frac{C}{m} = R_n \quad [1]$$

where C is the concentration of the ion in zone n and m is the mobility of the ion. These values are signed according to the charge of the ion. For the set-up described in Figure 1, the regulating functions characterizing the two zones would be equal under moving boundary conditions and:

$$\frac{C_1^{A-}}{m_{A-}} + \frac{C_1^{C+}}{m_{C+}} = \frac{C_2^{B-}}{m_{B-}} + \frac{C_2^{C+}}{m_{C+}} \quad [2]$$

where the concentration subscripts denote the zone. This relationship, along with the condition for

electroneutrality:

$$C_1^{A-} + C_1^{C+} = 0 = C_2^{B-} + C_2^{C+} \quad [3]$$

allows definition of the basic relationship between the concentration of ions in the different zones and their mobilities:

$$\frac{C_1^{A-}}{C_2^{B-}} = \frac{m_{A-}(m_{B-} - m_{C+})}{m_{B-}(m_{A-} - m_{C+})} \quad [4]$$

This relationship can be defined for every boundary in a discontinuous electrophoresis system. The relationship is valid for strong electrolytes and weak electrolytes. For weak electrolytes, the concentration value represents the total of the ionized and un-ionized forms. The fraction of the trailing species that is ionized, $X(n)$, can be determined after calculation of the amount of counterion that crosses the boundary into the trailing zone. When using a weak electrolyte as the counterion, a final expression for the counterion concentration in the trailing zone is:

$$C_2^{C+} = C_1^{C+} + C_1^{A-} \left(\frac{m_{C+}}{m_{A-}} \left(1 - \frac{(m_{A-} + m_{C+})}{(m_{C+} + m_{B-})} \right) \right) \quad [5]$$

where the counterion concentrations are the total concentration (both ionized and un-ionized forms). The fraction ionized, $X(n)$, can then be calculated from the ion equilibrium constants of the trailing ion and counterion. The net mobility accounts for the actual transport of the trailing acid species and is defined as:

$$\text{net mobility}(n) = m_n X[n] \quad [6]$$

The net mobility should be tuned closely to the sample's mobility. Sample mobilities faster than the trailing ion net mobility will be retained in the ion front. Details regarding these equations and more rigorous definitions can be found in numerous references.

A few characteristics of discontinuous buffer systems are apparent from examining the above equations. First, the equilibrium concentration of the trailing ion is independent of its initial concentration. It is determined by the free mobilities of the ions in the system and the concentration of the leading ion. Therefore, only the leading ion conditions can be chosen freely. Second, since the trailing ion has a slower mobility than that of the leading ion, the concentration of the trailing ion must be lower than that of the leading ion. This bears directly on the conductance and potential gradient of the trailing

zone. The zone conductance, κ , can be calculated from the ion concentrations, free mobilities and Faraday's constant (F). It can also be related to the field strength (volts (V) per unit length (l)) through Ohm's law, as shown (where i is the current and A the cross-sectional area of the gel):

$$\kappa = F [(\text{net mobility}(B^-))(C_2^{B^-}) + (\text{net mobility}(C^+))(C_2^{C^+})] = \frac{i}{A(V/l)} \quad [7]$$

Since the ion concentrations and ion mobilities in the trailing zone are lower than that in the preceding zone, the potential gradient in a trailing zone will be higher than the leading zone. This is what allows the trailing ions to migrate at the same rate as the leading ions, despite their lower physical mobility. Tuning the ionic strength is critical for optimizing separations. It affects the size of the migrating zone, the speed of the separation and the joule heating. The joule heating further influences resolution. Therefore, a high potential gradient for a given current, or heat output, will be preferable.

The above equations can be implemented on simple spreadsheet software to determine the physical characteristics of discontinuous buffer systems. A few example buffer systems are shown in Table 1. These buffer systems have been designed to vary the trailing ion type and the trailing ion net mobility while keeping the ion speed constant. A Tris-formate buffer, at a formate concentration of 50 mmol L⁻¹, has been selected as a common leading ion. Tris is used as a common counterion. The ion speed and voltage gradient would be determined by the applied current. These buffer systems exemplify some of the characteristics of discontinuous buffer systems. As can be seen, the trailing ion concentration is lower than the leading ion concentration and a wide range of net mobilities can be achieved when using a common

leading ion. Also notice that the net mobility, or actual transport of the trailing ion, is lower than the free mobility when using weak electrolytes. Such buffer systems can be used to assess the stacking limits, or mobility, of the analytes to be separated. Sample ions that migrate in the ion front will have a mobility intermediate between the leading and trailing ions. Those sample ions that have a mobility slower than the net mobility of the trailing ion will migrate more slowly than the ion front and will electrophorese within the trailing zone.

Other examples of calculated buffer systems are shown in Table 2. These buffer systems vary the trailing ion type while keeping the ionic strength of the trailing phase constant. This is accomplished by varying the leading ion concentration to allow for a predetermined ion concentration in the trailing zone. All the buffer systems in Table 2 use a formate leading ion of varying concentration and have a common trailing ion concentration of 30 mmol L⁻¹. Even with a common trailing ion concentration, a 50% change in the conductance can be obtained. This allows for increased voltages to be applied without increasing the current. As with the buffer systems described in Table 1, a range of trailing ion net mobilities is obtained. Other buffer systems, that define different ranges of net mobilities, different pH values or different conductivities, could be similarly calculated to address particular separation problems or analytical characterizations.

Outlook

Electrophoretic techniques that exploit the differential migration of ions are over 100 years old. Though the applications and physical formats have evolved, the underlying technique continues to endure. The iteration of discontinuous buffer systems has had intermittent use since its introduction over 30 years ago. This is presumably due to the perceived added

Table 1 Examples of discontinuous buffer system using constant leading ion conditions^a

Trailing ion species	m Mobility ($\times 10^4 \text{ cm}^2 \text{ V}^{-1} \text{ s}^{-1}$)	Leading ion pH	Concentration of trailing ion species (mmol L ⁻¹)	Ion concentration (mmol L ⁻¹)	Net mobility ($\times 10^4 \text{ cm}^2 \text{ V}^{-1} \text{ s}^{-1}$)	κ Trailing zone conductance ($\text{cm}^2 \Omega^{-1} \text{ mol}^{-1}$)
Hepes	1.45	8.0	26.4	25.1	1.38	0.98
Tricine	2.18	8.0	33.6	27.1	1.76	1.25
Asparagine	2.80	8.5	38.2	23.2	1.70	1.20
Glycylglycine	2.85	8.0	38.5	27.8	2.06	1.47
Taurine	3.27	9.0	41.0	27.2	2.17	1.54
Glycine	3.74	8.0	43.4	9.4	0.81	0.58

^aThe leading ion in all cases is 50 mmol L⁻¹ formate (ion mobility of $5.50 \times 10^{-4} \text{ cm}^2 \text{ V}^{-1} \text{ s}^{-1}$) buffered with Tris (ion mobility of $2.60 \times 10^{-4} \text{ cm}^2 \text{ V}^{-1} \text{ s}^{-1}$) to the indicated pH. The counterion in all cases is Tris.

Table 2 Examples of discontinuous buffer systems with constant trailing ion concentration^a

Trailing ion species	Concentration of trailing ion species (mmol L ⁻¹)	Ion concentration (mmol L ⁻¹)	Net mobility ($\times 10^4$ cm ² V ⁻¹ s ⁻¹)	Trailing zone conductance (cm ² Ω ⁻¹ mol ⁻¹)	Leading ion concentration (mmol L ⁻¹)
Hepes	31.6	30	1.38	1.17	60
Tricine	37.2	30	1.76	1.38	55
Asparagine	49.4	30	1.70	1.56	65
Glycylglycine	41.5	30	2.06	1.58	65
Taurine	45.2	30	2.17	1.70	55
Glycine	138.5	30	0.81	1.83	160

^aThe leading ion in all cases is formate (ion mobility of 5.50×10^{-4} cm² V⁻¹ s⁻¹) at the indicated ion concentration. The counterion in all cases is Tris (ion mobility of 2.60×10^{-4} cm² V⁻¹ s⁻¹).

complexity of the technique or ignorance of the technique's advantages. However, the benefits of sample stacking, mobility tailoring and an ionic reference front are unchanged and unique when compared to zonal buffer systems. With new applications and challenges for electrophoretic separations, renewed attention to the technique is certain.

Further Reading

- Allen RC and Budowle B (1994) *Gel Electrophoresis of Proteins and Nucleic Acids*. Berlin: Walter de Gruyter.
- Allen RC and Doktycz MJ (1996) Discontinuous electrophoresis revisited: a review of the process. *Applied and Theoretical Electrophoresis* 6: 1–9.
- Davis BJ (1964) Disc electrophoresis II. Method and application to human serum proteins. *Annals of the New York Academy of Science* 121: 404–427.
- Doktycz MJ (1993) Discontinuous electrophoresis of DNA: adjusting DNA mobility by trailing ion net mobility. *Analytical Biochemistry* 213: 400–406.
- Jovin TM (1973) Multiphasic zone electrophoresis. I. Steady-state moving-boundary systems formed by different electrolyte combinations. *Biochemistry* 12(5): 871–878.
- Jovin TM (1973) Multiphasic zone electrophoresis. IV. Design and analysis of discontinuous buffer systems with a digital computer. *Annals of the New York Academy of Science* 209: 477–495.
- Martin AJP, and Everaerts FM (1970) Displacement electrophoresis. *Proceedings of the Royal Society of London A* 316: 493–514.
- Morris CJOR and Morris P (1976) Theoretical aspects of electrophoresis. In: *Separation Methods in Biochemistry*, pp. 705–760. New York: Halsted Press.
- Ornstein L (1964) Disc electrophoresis – I. Background and theory. *Annals of the New York Academy of Science* 121: 321–349.
- Richards EG and Lecanidou R (1971) Quantitative aspects of the electrophoresis of RNA in polyacrylamide gels. *Analytical Biochemistry* 40: 43–71.
- Vesterberg O (1989) History of electrophoretic methods. *Journal of Chromatography* 480: 3–19.
- Yarmola E and Chrambach A (1995) Band width measurement in automated gel electrophoresis apparatus: DNA dispersion in a discontinuous system and in a single buffer. *Electrophoresis* 16: 345–349.

Electrochromatography

T. Shafik and A. G. Howard, University of Southampton, Southampton SO17 1BJ, UK

Copyright © 2000 Academic Press

Introduction

The application of electric fields to planar chromatographic media in order to drive and/or enhance separations is as old as planar chromatography itself. There is evidence to suggest that paper electrophoresis was first performed several years prior to the first

reports of paper chromatography. Research in the field has been intermittent, with periods of considerable activity separated by long periods of inactivity. This is at least partly due to attention being diverted away from planar methods to modern high-efficiency column techniques. It is quite conceivable that modern chromatography would be very different, with a much stronger focus on planar techniques, had more development work been carried out on thin layer electrochromatography (TLE).

The subject is enjoying something of a revival with significant advances having been made during the

1990s. If this trend continues, planar electrochromatography may take its place as a powerful tool in the modern analytical laboratory offering new modes of separation at speeds that are currently unavailable in conventional thin-layer chromatography (TLC).

Definitions

The term TLE will be used to refer to all techniques carried out within chromatographically active thin layers and with electric fields being employed to influence the separation. This will encompass a number of different modes of separation, including those that are dominated by electrophoretic analyte migration but which, due to the nature of the layer, include some element of chromatographic retention. Conventional gel-based electrophoresis is therefore distinguished from TLE by the electrophoresis in TLE being carried out in a chromatographically active layer of material such as silica, alumina or cellulose. TLE therefore excludes gel electrophoresis carried out in cast gel slabs of materials such as polyacrylamide that are commonly used for the separation of proteins and DNA. Paper electrophoresis is now largely obsolete and is not therefore covered.

Advantages of TLE

Thin-layer chromatography has proved to be one of the most successful chromatographic techniques ever devised. This success owes largely to its simplicity and versatility compared with column techniques. The main drawback of TLC is the low solvent velocity achieved through capillary action. This leads to long separation times and means that the optimum flow velocity (for chromatographic efficiency) is seldom reached. Electric fields can be used to cause the migration of the analyte, either by directly exerting a force on the molecules, or by causing the eluting solvent to flow, carrying with it the analyte. This can result in migration velocities of one to three orders of magnitude greater than those achieved through capillary action and can introduce an electrophoretic component to a separation, facilitating the separation of difficult mixtures.

Electrophoresis

This is the migration of ionized species under the influence of an electric field. Ions in an electric field experience a force proportional to their charge, causing them to accelerate in the direction of the field. Ions in solution, not interacting with a solid support, reach a terminal velocity dependent on the magnitude of the force and their interaction with the solvent. Therefore, different ions will migrate through the

solvent at different rates. This can be used to separate different ions and is known as free solution electrophoresis.

If the solvent is within a bed of chromatographically active media such as silica, the migrating ions can interact with the solid support, adding a chromatographic component to the separation. At this point, it is simpler to refer to the separation as electrochromatography, which encompasses both electrophoretic and chromatographic effects.

The ionic mobility u can be expressed in terms of the ion's velocity v in a given electric field strength E by $u = v/E$. This only applies to free solutions, since migration through the channels of a solid support follows a tortuous path that deviates from a straight line by a quantity dependent upon the properties of the solid support. The important point is that the migration velocity, both in free solution and through a bed of chromatographic media, is proportional to the potential applied. In order to achieve greater migration velocities, it is necessary to apply higher potentials.

Electroosmosis

Electroosmotic flow arises from the formation of an electrical double layer at a solid-liquid interface. This is due to the presence of charged species on the solid surface; either in the form of surface ionized groups (e.g. SiO^- in the case of silica) or because of the preferential adsorption of ions from the solution. In most cases it is a combination of both. The surface charges are counterbalanced by ions in solution, which form an immobile, strongly bound layer near the surface and a mobile, solvated layer extending into the liquid. Under the influence of an applied potential, the solvated layer of counterions moves, causing bulk solvent flow (Figure 1).

This means of inducing solvent flow has been successfully applied to capillary column chromatography, producing capillary electrochromatography (CEC). Using electroosmotic flow (EOF) to pump solvent through a column generates a 'plug' flow profile, which is distinct from the parabolic profile generated by hydraulic pumping. This results in reduced band broadening in CEC. It also allows the use of very fine chromatographic supports, which would be impossible to use in pressure-driven systems owing to back-pressure constraints. These factors combine to give high linear flow rates, of the order of 1 mm s^{-1} , allowing very fast, efficient separations.

As with electrophoretic migration, the EOF velocity increases linearly with applied potential. This makes it generally desirable to apply higher potentials in order to achieve faster migration rates.

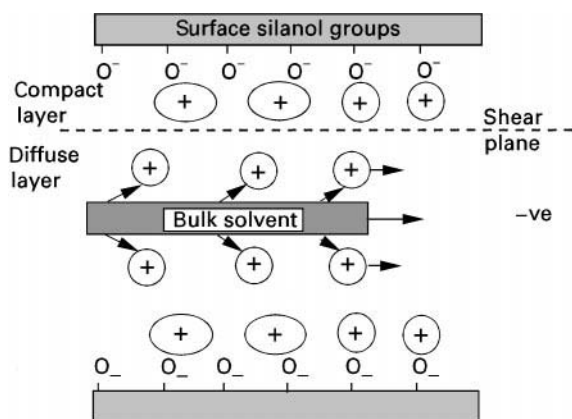


Figure 1 A schematic representation of double layer formation at a silica surface.

Modes of Migration

In standard TLC, the migration of a sample molecule is controlled by its interaction with the bed of chromatographic media and the partition of the solute into the eluting solvent. In electrically driven TLC, the solutes may be made to move in a number of different ways.

If the sample molecules are ionic in the solvent used, the application of an electric field will exert a force on them and they will migrate electrophoretically. As they migrate they are also subject to chromatographic partitioning between the solvent and the stationary phase. The individual components separate from each other by migrating at different velocities, each compound having a characteristic migration velocity that reflects the conflict between electrophoretic migration and chromatographic retention.

If, however, the sample molecules are uncharged in the solvent, they will only migrate if the solvent is made to flow. Whereas in standard TLC this is achieved by capillary action, in electrically driven TLC, with the right solvent and adsorbent, it can be achieved through EOF. The separation that results from an electroosmotically driven TLE experiment is, in the absence of electrophoretic effects, similar to that obtained by conventional TLC, but it is obtained much more rapidly.

There is a third mode by which solvent flow can be induced through a thin layer chromatographic media during an electrochromatography experiment. When a current flows through a wetted layer of chromatographic material the layer heats up. The power which has to be dissipated from the plate depends on the current flow and hence the resistance of the wetted plate. When the solvent is unevenly distributed through the plate this leads to an uneven evaporation

of solvent from the plate causing capillary solvent migration to occur as a direct result of Joule heating. This effect is more extreme with vertically mounted plates, which under gravity drain solvent to the base of the plate. In some experiments, evaporative flow can be considerably larger than that which is generated by electroosmosis. This can be falsely identified as EOF and is particularly evident in experiments carried out with vertically mounted plates. In horizontally mounted plates, with a solvent reservoir at each end of the plate, solvent is replenished least quickly at the center of the plate. If the rate of evaporation is initially assumed to be uniform across the plate, then the middle of the plate will dry out more quickly. This leads to solvent flow from both ends of the plate towards the middle being superimposed upon any EOF.

The current flow through the solvent-wetted chromatographic layer is dependent on the overall electrical resistance of the plate, which is a function of the ionic density in the solvent. These ions may originate from soluble ionic species in the chromatographic material, dissolved ions in the solvent or dissociated solvent molecules. The smaller the ionic density, the higher the overall plate resistance and the smaller the current. Unless adequate cooling is provided, the input of power will cause a temperature rise in the thin layer. This will lead to evaporation of the solvent, the rate of which will depend upon the rate of power influx, the volatility of the solvent and degree of external cooling. This is the main limitation controlling the magnitude of the potential that can be employed in TLE to achieve faster migration rates.

Various methods of cooling the plates have been used in order to reduce solvent evaporation. Immersion of the plate in a solvent that is immiscible with the eluting solvent has been employed in various separations, with CCl_4 being the most popular coolant for aqueous eluent systems. The purpose of the solvent bath is to provide direct cooling to the plate surface. This approach was experimentally clumsy and limited the range of analytes, since analyte solubility in the 'coolant' must be considered. It was later dropped in favour of the use of cooling pads in contact with the TLE plate, achieving cooling rates in excess of 0.1 W cm^{-2} . With high-conductivity aqueous systems this arrangement allowed the applied potential to be raised to 160 V cm^{-1} , generating migration velocities of up to 0.1 mm s^{-1} .

Solvents with limited volatility, such as higher alcohols, propylene carbonate and formamides have been used to reduce evaporation. This approach did not however gain popularity owing to several experimental limitations, the most important of which is the difficulty in removing the eluting solvent from the

chromatographic material following an experimental run. This is usually necessary in order to visualize the separated compounds.

Historical Development

The development of TLE occurred in tandem with that of paper electrophoresis (Table 1). This is not surprising, since both techniques require similar apparatus and reagents, and are generally used to achieve the same types of separation. TLE has always had an advantage over the paper technique in terms of chromatographic performance. The finer and more uniform surface structure achievable on thin layers results in considerably reduced band broadening when compared with fibrous media.

The earliest experiments were carried out in the 1940s using paper and layers of silica gel. A wide range of analytes was separated, largely employing aqueous systems. The high conductivity of the aqueous systems limited the applied potential to 10–50 V cm⁻¹ but the electrophoretic separations achieved at these potentials were still a considerable improvement on those obtained by the equivalent paper chromatography/TLC separations. The run times were typically of the order of 1–3 h, but some experiments, particularly protein separations, were run for as long as 24 h.

The development of gas chromatography (GC) and high-pressure liquid chromatography (HPLC)

enabled high-efficiency separations to be achieved and diverted attention away from planar techniques. This led to thin-layer electrophoresis/electrochromatography being largely abandoned in the late 1960s in favour of the column techniques. Very few publications between 1970 and 1998 cite the use of TLE.

Following a period of active research into planar techniques between 1940 and 1960, interest in TLE has been sporadic at best. Long periods of inactivity have been punctuated by occasional reports of technical advances and/or applications of the technique. Possibly one of the most important of these is a paper by Pretorius *et al.*, which described very high-speed separations both on TLC plates and in columns utilizing EOF to mobilize solvent. This paper set a precedent, by using nonaqueous and low aqueous solvents, potential gradients of around 1000 V cm⁻¹ could be used – potentials at least five times greater than had been previously employed. The experiments carried out in columns were quickly followed up by several other research groups and are considered the direct predecessor of modern capillary electrophoresis (CE) and CEC.

Experimental Techniques

Development Chambers

Historically, the majority of TLE experiments have been carried out in the horizontal mode, with solvent reservoirs at both ends of the plate. This set-up continues to be used today by several groups, and is shown in Figure 2. The plates are supported with the chromatographic surface either up or down.

Solvent is transported to and from the plates by wicks, which also serve as electrical contacts. A range of materials has been used as wicks, including filter paper, sintered glass and felt. The electrodes are usually submerged in the solvent and made of an inert conductive material, such as silver, stainless steel, carbon or platinum.

A less popular approach involves the use of vertical plates, with solvent at the base of the plate (Figure 3). Electrical contact is made via the solvent at the base

Table 1 Developments in thin-layer electrochromatography

1937	Earliest recorded use of paper electrophoresis, separation of snake venom proteins followed by UV detection (Konig)
1946	Earliest recorded use of 'thin-layer' electrophoresis, in a slab of silica jelly. Method used for the separation of amino acids and peptides (Consden <i>et al.</i>)
1954	First use of electroosmotic flow as driving force to effect a separation. Polysaccharides separated on collodion membranes (Mould and Synge)
1961	Separation of amines and amino acids by thin-layer electrophoresis (Honnegar)
1963	Investigation of the characteristics of solution flow in thin-layer electrophoresis on a range of thin-layer chromatography (TLC) media. (Kowalczyk)
1974	High-speed separation of organic compounds on silica TLC plates and in columns in electric fields (Pretorius <i>et al.</i>)
1994	Planar electrochromatography on non-wetted thin layers (Pukl <i>et al.</i>)
1998	TLE separation of non-polar dyes on commercial reversed-phase TLC plates using electroosmotic flow (Nurok <i>et al.</i>)
1999	Quantification of electroosmotic and separation of basic pyrimidines by thin-layer electrochromatography (Howard and Shafik)

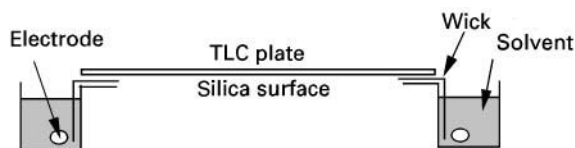


Figure 2 A horizontal tank design for thin-layer electrochromatography.

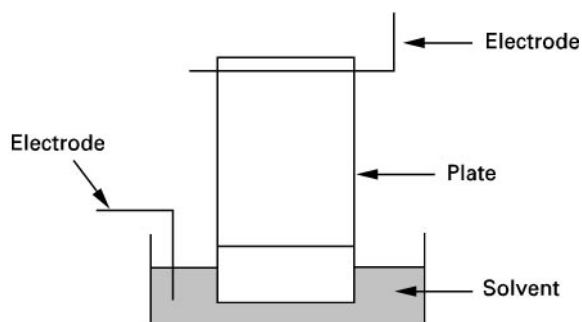


Figure 3 A vertical tank design for thin-layer electrochromatography with bottom solvent feed.

and an electrode fixed at the top of the plate. While in such systems the solvent is sometimes described as migrating up the plate because of electroosmosis, this may not always be strictly true. The main limitation of this arrangement stems from the lack of solvent reservoir at the top of the plate, and uneven solvent evaporation from the plate can impart a capillary-driven component to the solvent migration. This makes it difficult to differentiate between electroosmotic solvent flow and capillary solvent flow. Some workers have placed a second solvent reservoir at the top of the plate, and generated electroosmosis in a downward direction.

Chambers are usually sealed from the atmosphere in order to provide a solvent-saturated atmosphere, thus reducing evaporation. Some arrangements employ a cover plate, usually glass, in direct contact with the chromatographic surface in order to minimize evaporative effects.

Plates

A wide range of stationary phases, mobile phases and operating conditions have been employed in TLE. The layer is frequently 50–200 μm thick on a backing material of glass or organic polymer. Aluminium-backed plates are not suitable for use in TLE because of their electrical conductivity. TLE has been carried out on all thin layer adsorbents used for TLC, with silica, microcrystalline cellulose and alumina attracting the greatest interest.

Plates are generally 10–20 cm long and 5–20 cm wide. Longer plates tend to suffer from evaporative flow more than short ones and are generally avoided. The width of the plate is limited only by the current that the power supply is able to deliver at the required potential.

Solvent Systems

The majority of TLE separations have so far been carried out in aqueous buffer systems similar to those

used in TLC. More recently, the use of nonaqueous systems has been shown to be useful in achieving faster and more efficient separations.

Potentials, Currents and Power Supplies

Potentials used in aqueous TLE are in the range of 10–100 V cm^{-1} , with currents of around 10–100 mA. This generates power levels of around 1–100 W. At the higher power levels, plate cooling is essential in order to prevent drying out. When nonaqueous systems are used, potentials between 200 and 2000 V cm^{-1} are used, with currents of 0.01–2 mA, generating between 0.02 and 20 W. Cooling of plates run at higher potential is seldom employed. Cooling is rarely necessary and very difficult to achieve due to the inherent incompatibility of high thermal conductivity and good electrical insulation characteristics in materials.

Starting Conditions

The layers are usually pre-wetted with the eluting solvent following sample application. This is achieved by spraying or dipping. Some experiments have been carried out using dry plates, but with limited success.

Sample Application and Visualization

The same methods of applying and viewing sample spots and bands used in TLC are employed in TLE.

Applications

Thin layer electrochromatography can be divided into three main forms depending on the major factor governing the separation. While not mutually exclusive, since most separations include some element of the other modes, these broadly arise from electrophoretic solute migration, electroosmotic solvent flow and the natural spin-off from the heating effects arising from the applied potential, electrothermal elution.

The most commonly encountered examples of TLE are based around electrophoretic separations in aqueous solvent. Not surprisingly, given the historical success of paper electrophoresis, several workers have used thin layers of microcrystalline cellulose. In addition, cellulose acetate and silica have been used for the separation of proteins. Other applications have included the separation of starches, amino acids (and various derivatives) (Figure 4), organometallic compounds (Figure 5) and transition metal ions.

Electrophoretic separations are not limited to aqueous solvent systems and the higher resistance of nonaqueous solvents gives the advantage of lower currents and reduced heating effects. The separation

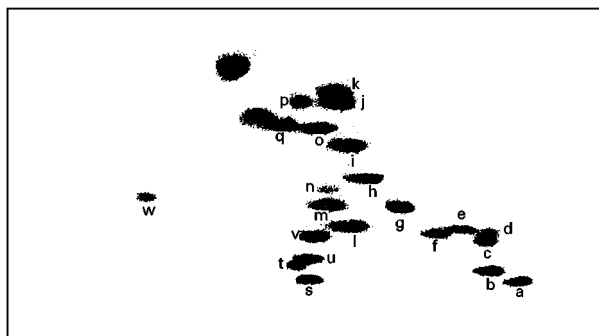


Figure 4 The separation of amino acids by two-dimensional thin layer electrophoresis–thin-layer chromatography with an aqueous electrolyte. The chromatographic media was plastic-backed cellulose layer. Electrophoresis in the first dimension using a 4% (v/v) aqueous formic acid electrolyte was followed by chromatographic elution in the second dimension with butanol–0.4% pyridineacetic acid (22:10:10, v/v/v). Adapted from E. McEvoy-Bowe (1985) *Journal of Chromatography* 347: 199–208, with permission.

of a number of dyes using ethanol as the solvent is shown in **Figure 6**. In this separation electroosmotic flow effects were suppressed to reveal the electrophoretic migration of the charged dyes, resulting in completely different elution orders.

In TLE, solvent migration from EOF is easily confused with capillary-induced flow resulting from localized solvent evaporation. Broadly speaking, EOF is to be expected from wet polar solvents, protic solvents or from those that are capable of autoprotolysis.

With vertical tank systems, and particularly those employing nonpolar solvents, there must remain some uncertainty over whether thermal effects have been responsible for any solvent migration observed. This is the case in the pioneering planar systems studied by Pretorius (**Figure 7**), in which nonpolar solvents such as benzene were allegedly used. Our attempts to reproduce this work with a vertical tank system resulted in an electrically driven solvent

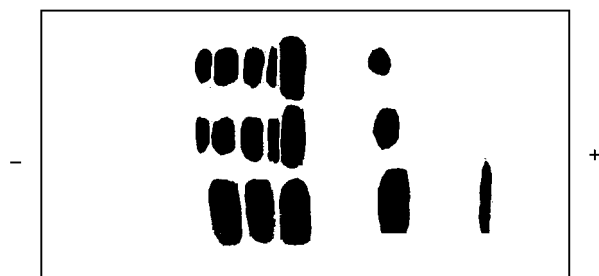


Figure 5 A thin-layer electropherogram of platinum chloroamine complexes. The chromatographic media was microcrystalline cellulose thin layers and electrolyte was 0.1 M NaClO₄, at 500 V for 5 min. Adapted from M Lederer and E Leipzig-Pagani (1998) *Analytica Chimica Acta* 358: 61–68, with permission.

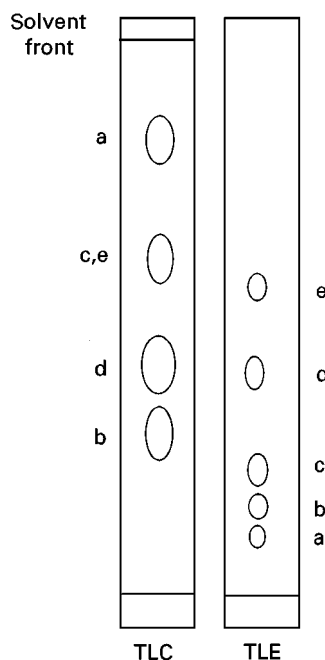


Figure 6 Nonaqueous thin-layer electrochromatography (TLE) and conventional thin-layer chromatography (TLC) of a dye mixture: (a) Oil Blue, (b) Rhodamine B, (c) Neutral Red, (d) Diazine Green, (e) Brilliant Green. The chromatography media was silica (electroosmotic flow suppressed) and the solvent was ethanol.

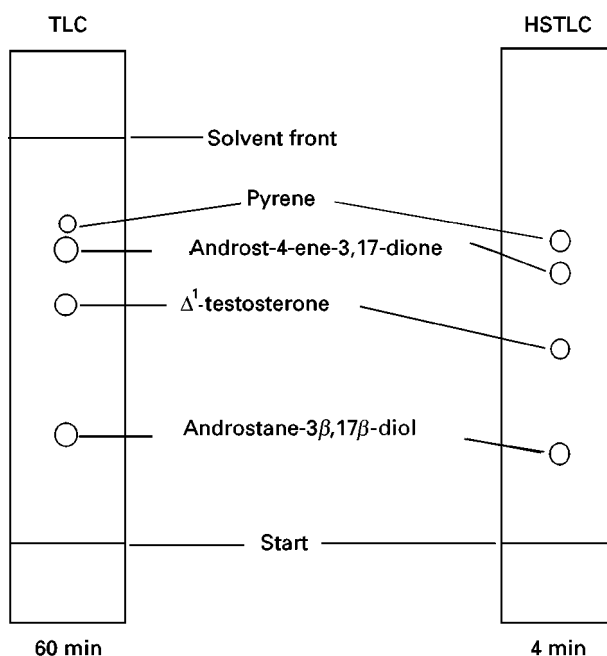


Figure 7 An early thin-layer electrochromatography (TLE) separation of nonionic compounds. The chromatography media was dichlorodimethylsilane-treated silica and the solvent was unspecified. Adapted from V. Pretorius *et al.* (1974) *Journal of Chromatography* 99: 23–30, with permission.

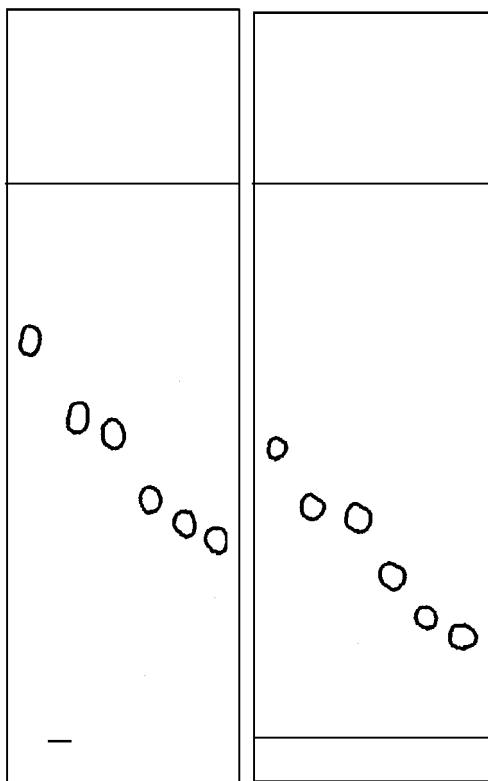


Figure 8 Conventional thin-layer (left) and electroosmotic (right) separation of pyrimidines employing identical silica layer chromatographic media and eluting solvent (ethanol) (TLC *ca.* 15 min; TLE 7 kV, 90 s). Adapted from AG Howard and T Shafik (1999) *Journal of Chromatography* 844A: 333–340, with permission.

migration and chromatographic separation resulting largely from thermal effects and not EOF. By changing to more polar solvents, in a horizontal tank, we have shown that true electroosmotic flow could be achieved. The separation of a number of pyrimidines on silica eluted with ethanol showed elution characteristics similar to those obtained by conventional TLC, but with higher separation efficiency and in one tenth of the time (Figure 8).

More recently, high-voltage nonaqueous TLE employing electroosmosis as the main driving force has been applied to the separation of a wide range of acidic, basic and neutral organic compounds, with considerable success.

Further Reading

- Howard AG, Shafik T, Moffatt F and Wilson ID (1999) *Journal of Chromatography* 844: 333–340.
- Kowalczyk JS (1996) *Chemical Analysis (Warsaw)* 41: 157–171.
- Poole CF and Wilson ID (1997) *Journal of Planar Chromatography* 10: 332–335.
- Pretorius V, Hopkins BJ and Schieke JD (1974) *Journal of Chromatography* 99: 23–30.
- Sargent JR (1975) *Methods in Zone Electrophoresis*, 3rd edn. Poole: BDH Chemicals Ltd.
- Smith IW (1960) *Chromatographic and Electrophoretic Techniques*, vol. 1. London: Heinemann Medical Books Ltd.
- Tsuda T (1995) *Electric Field Applications in Chromatography, Industrial and Chemical Processes*. Weinheim: VCH.

Electrochromatography in Thin-Layer Electrophoresis

See II/ELECTROPHORESIS/Electrochromatography

Electrophoresis Using Cellulose Acetate

See II/ELECTROPHORESIS/Cellulose Acetate

Electrophoresis: Discontinuous

See II/ELECTROPHORESIS/Discontinuous Electrophoresis

Gel Electrophoresis in Capillary Electrophoresis

See II/ELECTROPHORESIS/Capillary Gel Electrophoresis

Immunoelectrophoresis

F. Lampreave, M. Piñeiro, S. Carmona and M. A. Alava,
Facultad de Ciencias, Universidad de
Zaragoza, Zaragoza, Spain

Copyright © 2000 Academic Press

Development

The discovery that antigen–antibody interaction could be produced not only in liquids, but also on gel media, such as agar or agarose gels, with the formation of insoluble immunoprecipitates, opened the door to the development of the gel diffusion techniques for immunoprecipitation analysis. The first of these techniques, known as double diffusion, was introduced by Ouchterlony in 1948. In this technique, the antigens (proteins) and the corresponding antibodies (immunoglobulins, Ig) are located on a thin agar gel, in small and separated wells. The simple diffusion of the antigen and the antibody produce precipitation lines between the two wells where the interaction of these molecules occurs.

Advances in gel immunoprecipitation techniques occurred in 1953, when Grabar and Williams described immunoelectrophoresis (IE), in which the high resolution of electrophoresis and the specificity and sensitivity of the immunological reactants are combined. The immunoelectrophoretic techniques had a very rapid development during the 1960s and early 1970s, because they are adequately suited to the analysis of complex mixtures of proteins. The first attempts to improve the immunoelectrophoretic technique pursued two main objectives: to increase its speed (IE was rather slow, mainly due to the time-consuming immunodiffusion step) and to achieve quantitative methods (IE is basically qualitative).

In a short period of time new techniques based on crossed immunoelectrophoresis (CIE), rocket immunoelectrophoresis (RIE), counter IE, crossed-affinity IE (CAIE) and charge shift IE, were introduced.

This article describes all the techniques in which electrophoresis and immunoprecipitation steps performed in agar or agarose gels are combined. Diffusion-type techniques, such as double immunodiffusion and the quantitative radial immunodiffusion, will not be described. Other immunochemical techniques, such as enzyme-linked immunosorbent assay (ELISA) and Western blotting, in which immunoprecipitation is not produced, will be considered elsewhere.

Conventional Immunoelectrophoresis

The scheme in Figure 1A shows the principles of the techniques, such as it was originally introduced and generally used by many workers. The first step consists of electrophoresis in 1% agar-agar or agarose gels, prepared in different buffers at pH ranging from 8.2 to 8.6 (Veronal 0.025 mol L^{-1} , pH 8.2 is one of the buffers frequently used). The sample to be analysed, usually a complex mixture of proteins, is applied in small wells located in the middle of agar-agar gels, or partially displaced towards the extreme nearest to the cathode when agarose gels are used. Most of the proteins, for example in blood sera or plasma, have a negative net charge in buffers with pH higher than 7.0. Thus, when a continuous electrical field is applied to the gel, the tendency of these proteins is to move towards the anode with a migration rate which mainly depends on charge-to-size ratio. However, the migration rate is in part reduced by the electroendosmotic effect due to the negative charges in polymeric molecules of the gel. This electroendosmotic effect is greater in agar-agar than in agarose gels. The extension of the electrophoretic run can be precisely fixed by controlling the migration of a marker. One of the markers routinely used is the protein stain Amido black. The second step is a double immunodiffusion performed in the same gel plate (Figure 1A). For this, longitudinal channels are cut parallel to the direction of the electrical flow and separated 4 mm from the original wells where the samples were applied. The channels are filled with the

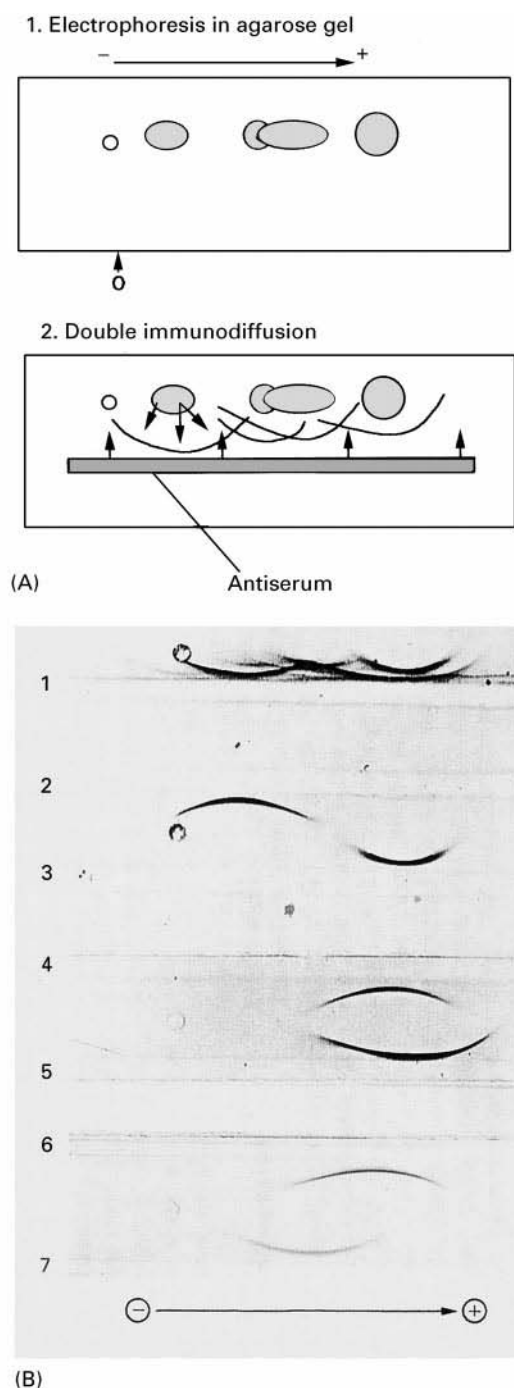


Figure 1 (A) Schematic representation of the principle of conventional immunoelectrophoresis. 1, Electrophoresis of the sample in agar or agarose gels; 2, double immunodiffusion of the separated proteins and the corresponding antiserum. (B) Application of the technique to the study of specificity of various antisera. In all wells, fetal pig serum was applied. In the channels, the following antisera were assayed: 1, anti-fetal pig serum, 2, anti-transferrin; 3, anti-albumin; 4, anti- α -fetoprotein; 5, anti- α_1 -antitrypsin; 6, anti- α_1 -acid glycoprotein; 7, anti-fetuin. (With permission from Lampreave, F, González-Ramón N, Martínez-Ayensa S, Hernández MA, Lorenzo HK, García-Gil A and Piñeiro A (1994) *Electrophoresis* 15: 672-676.)

corresponding antiserum and the plate is maintained in a humid, sealed box, for a period of between 24 and 48 h. Under these conditions, the combination of the radial diffusion of the proteins from the circular or ovoid spots obtained after the electrophoretic run, with the uniform diffusion of the antibodies, occurring in a perpendicular direction to the channel, produces arcs of precipitation in the different electrophoretic zones.

The IE patterns can be directly visualized or photographed, in the wet gel, by dark-field illumination. In this method the oblique light from a circular source placed below the plate is directed through the gel and transmitted at an angle of about 25° . The immunoprecipitates are visible as white lines on the dark background. To preserve the plates and before staining the immunoprecipitates, it is necessary to wash the gel plates extensively so that all the unprecipitated materials are removed. The wash is accomplished by immersing the gel plates in a buffered saline solution (0.01 mol L^{-1} phosphate, NaCl 0.15 mol L^{-1} buffer, pH 7.4) for 1-3 days, and with several changes of liquid. Alternatively, a quick procedure can be carried out by placing several paper towels on the gel plate and applying a moderate pressure for some minutes. In this way, the liquid and all the soluble material are removed from the gel and absorbed by the paper towels. Then, the plate is submerged in the saline solution until the gel almost recovers its original thickness. Repeating this drying/soaking cycle, it is possible to achieve effective and rapid washing of the plates. Finally, the plates are dried and the immunoprecipitates stained, commonly with Coomassie blue or Amido black. The sensitivity of the method, using these conditions, allows the detection of proteins with concentrations ranging from 3 to $20 \mu\text{g mL}^{-1}$. Specific staining methods have been introduced to facilitate the identification of single proteins. For example, Sudan black can be used to detect lipoproteins and periodic acid (Schiff reagent) for polysaccharides and glycoproteins. There are also specific staining procedures for some proteins, such as ceruloplasmin, hemopexin, etc.

IE has been used to analyse complex mixtures of proteins from tissue extracts; to detect impurities during the monitoring of protein purifications; to detect differential expression of protein during growth and differentiation; to study the expression of single proteins during pathological situations and to detect protein polymorphisms. Figure 1B shows an example of the application of the IE technique. In the plate, the specificity of different antisera against six proteins isolated from fetal pig sera (albumin, α -fetoprotein, α_1 -acid glycoprotein, α_1 -antitrypsin, fetuin and transferrin) is analysed by attaching them to

a fetal pig serum by this technique. As reference, the same fetal pig serum is analysed against a polivalent anti-fetal pig antiserum.

Counter Immuno-electrophoresis

This technique is a modification of conventional IE, that is performed in agar-agar gels at pH 8.0. Under these conditions, the antibodies are positively charged whereas the antigens present a negative net charge. Antigen and antibodies are applied in wells of 3 mm diameter, as indicated in **Figure 2**. Antibodies are placed on the well nearest to the anode and the sample in that close to the cathode. By applying a voltage across the gel the antigen and the antibodies move towards each other, forming lines of precipitation between the two wells. For this technique, the utilization of agar-agar gels is convenient since the medium, at the pH commonly used, generates a significant electroendosmotic flow that increases the cathodic movement of the antibodies. This technique can be used to detect both antigen and antibodies; rapidity is the main advantage.

Crossed Immuno-electrophoresis

Crossed IE is another approach in IE which is well suited for qualitative and quantitative analysis. The method, which was originally named two-dimensional electrophoresis or antigen-antibody crossed IE, offers not only higher resolution and simpler interpretation of the results than in conventional IE but it can also be standardized for quantitative analysis.

The principles of this technique are presented in **Figure 3A** and consist of two electrophoretic runs, both in 1% agarose gel plates. Veronal 0.05 mol L^{-1} pH 8.6, 1 mmol L^{-1} calcium lactate is a buffer that is frequently used. Samples are applied in wells of around 3 mm

diameter and a current applied for about 3–4 h at a potential gradient of 10 V cm^{-1} (to achieve a total electrophoretic run of around 6 cm). Afterwards, a longitudinal strip of 1 cm width, which includes the separated protein fractions, is cut off and transferred to a plate with the second agarose gel (prepared in the buffered solution as above) that contains the antiserum corresponding to the material to be tested.

The second run is carried out in a perpendicular direction to the first separation, at a potential gradient of around 5 V cm^{-1} . The time of this electrophoretic step varies depending on the mobility of the antigens. For complex mixtures, and depending on the relative proportions between antigens and antibodies, periods of around 6–10 h may be needed. Under these conditions, precipitation peaks are produced in which the height prevails over the width. Furthermore, the area of each peak is now related to the amount of protein contained in the sample.

Identification of proteins in the crossed immuno-electrophoretic patterns, though simpler than in the patterns obtained by conventional IE, presents difficulties when complex mixtures of proteins are analysed. For that reason, some modifications to crossed IE, such as fused rocket IE, line IE, tandem crossed IE, crossed line IE and crossed IE with intermediate gel, have been introduced.

Crossed IE techniques enable the easy comparison of the content of a determined protein in different samples. **Figure 3B** shows an example of the potential of this technique, applied to the study of the acute-phase proteins in pigs. The comparison of the crossed immuno-electrophoretic patterns of blood serum from the same pig before (left) and 48 h after the induction of acute inflammation by turpentine injection (right, acute-phase serum), permits detection of important differences in the concentration of some plasma proteins. Especially notable is the increase of peak 9, that corresponds to the major acute-phase protein in pigs, called Pig-MAP, which could be detected through this technique.

Crossed IE can also be applied to the study of membrane proteins. For this it is convenient to solubilize them with nonionic detergents, such as Triton X-100, that better preserve the structural and functional properties of these proteins. The detergent does not cancel out the antigenic properties of the membrane proteins, nor does it impede the antigen-antibody reaction. In the characterization of membrane proteins it is important to know whether the proteins studied possess hydrophobic domains that anchor them to the hydrocarbon interior of the bilayer, or whether they are externally bound to the membrane. Charge-shift immuno-electrophoresis permit the user to easily obtain that information even in

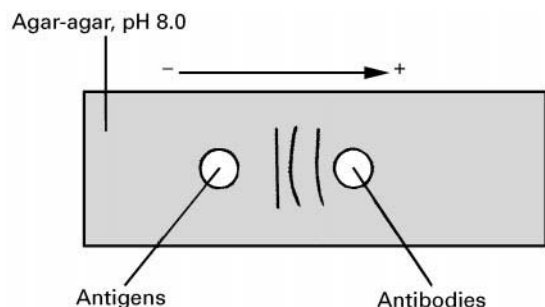


Figure 2 Principle of counter IE. This technique is developed in agar-agar gels, at pH 8.0. Antigens move towards the anode and antibodies to the cathode, due to its charge and to the electroendosmotic effect. (With permission from Lampreave F and Piñeiro A (1992) Concentration of major plasma proteins in serum and whole-tissue extracts of porcine fetuses during development, *Journal of Reproduction and Fertility* 95: 441–449.)

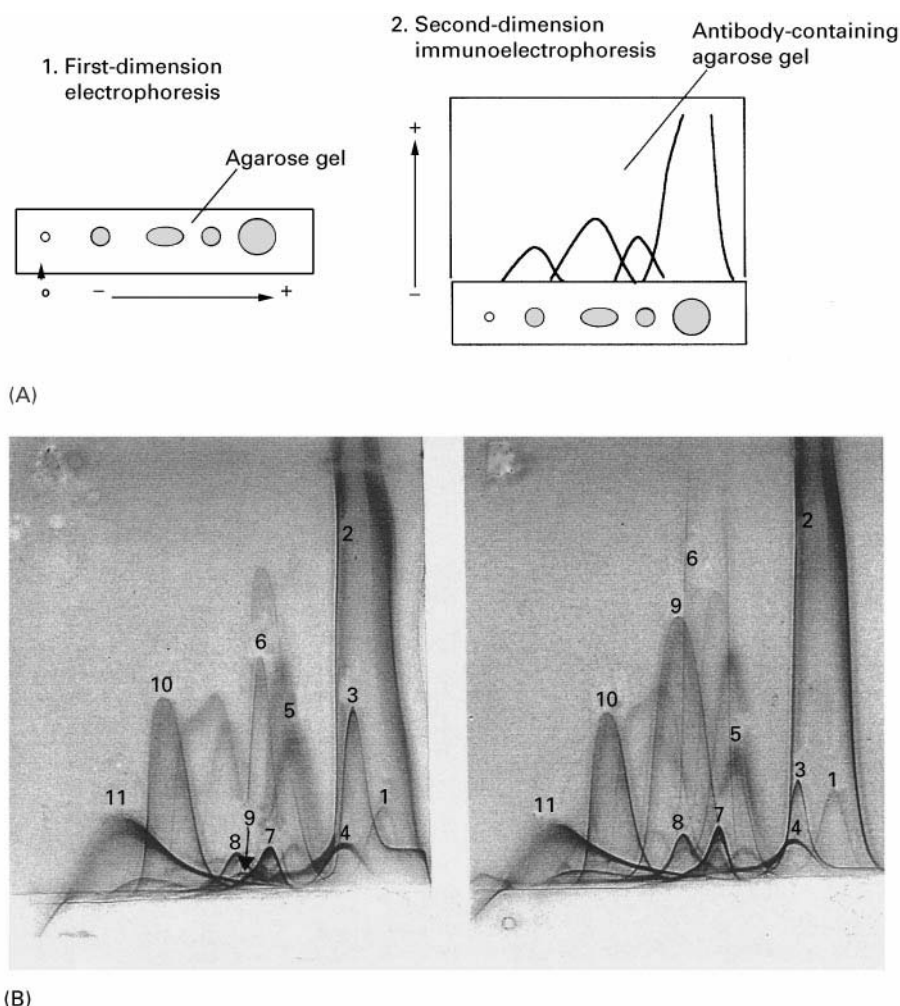


Figure 3 (See Colour Plate 41). (A) Schematic illustration of crossed IE. 1, Agarose electrophoresis of the sample (O = origin, corresponding to the well where the sample is applied); 2, a longitudinal strip of the first-dimension gel is transferred into a second-dimension gel containing a polyvalent antiserum. The second-dimension IE is performed perpendicularly to the first-dimension run. (B) Example of use of the crossed IE technique. The blood serum from the same pig is analysed (left) before and (right) 48 h after turpentine injection. The changes in the protein concentrations, induced by inflammation, can easily be studied by analysing the area (or height) of the different-numbered peaks. (With permission from Lampreave, F, Alava MA and Piñeiro A (1996) *Trends in Analytical Chemistry* 15: 122–129.)

complex mixtures. Membrane proteins are solubilized either with Triton X-100 alone or mixed with other detergents, for example, Triton X-100/sodium deoxycholate (an anionic detergent) and Triton X-100/cetyltrimethylammonium bromide (a cationic detergent). Afterwards, these three membrane extracts are analysed comparatively by crossed IE. The detergent-induced shift in mobility provides a method to distinguish between hydrophilic and amphiphilic proteins.

Rocket Immunoelectrophoresis

This immunochemical method, introduced by Laurell in 1966, is suitable for the quantitative estimation of

proteins. In this case (Figure 4A) there is only one electrophoretic run carried out in 1% agarose gel (plates of uniform thickness of about 1.5 mm) in Veronal buffer, pH 8.6 as described before, but including an appropriate quantity of an adequate antiserum. The samples are applied in separated wells of 3 mm diameter, located near the extreme of the plate in contact with the cathode. To obtain quantitative results, different dilutions from a primary standard (a solution of the purified protein of known concentration) or a secondary standard (a serum previously evaluated using a primary standard) are applied on the gel. The electrophoresis is accomplished over periods ranging from 4 to 6 h depending on the charge of

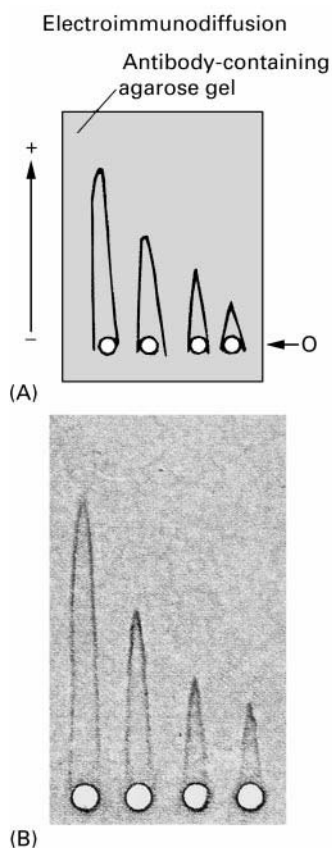


Figure 4 (A) Schematic representation of rocket IE. The electrophoresis is carried out in agarose gel containing specific antiserum against the protein to be determined. The area of the rockets (or its height) is proportional to the content of protein in the sample. (B) Application of this technique to the quantification of human α -fetoprotein. To improve sensitivity, the first immunoprecipitates (developed with rabbit antiserum to human α -fetoprotein) were treated with glucose oxidase-labelled sheep antibodies to rabbit immunoglobulins. From left to right, solutions containing α -fetoprotein concentrations of 720, 360, 180 and 120 ng mL⁻¹ were assayed.

the antigen and on the relationship between the amount of antigen and antibodies included in the gel plate. The immunoprecipitates formed in this case have the shape of a rocket, the area (or height) of which is proportional to the concentration of the antigen applied in the well. The concentration of the protein in unknown samples can be determined by reference to the calibration line obtained by representing the height versus the concentration of each standard.

This technique can be applied to any protein with a net charge that differs from that of the antibodies. Some proteins, such as, for example IgG, hardly move during electrophoresis using a pH 8.6 buffer. In these cases, the mobility of the antigen to be determined can be increased by carbamylation of the sample with KCNO.

Rocket IE is the most sensitive of the conventional immunelectrophoretic methods and allows one to accomplish the quantification of proteins (using stains to visualize the immunoprecipitates) up to concentrations close to 1 μ g mL⁻¹. This sensitivity can be increased by combining immunochemical methods. Figure 4B shows an example of one of these methods applied to determine human α -fetoprotein. During the electroimmunodiffusion, the first antigen-antibody reaction is produced using a rabbit antiserum containing the specific antibodies (Ig). In a second step, the plate is incubated with glucose oxidase-labelled sheep antibodies to rabbit Ig. Finally, the glucose oxidase bound to immunoprecipitates is revealed by incubating the plate with a solution that contains glucose, MTT-tetrazolium and phenazide methasulfate. The immunoprecipitates stain blue-violet over a fainter background of similar colour. This method provides reproducible results and allows the quantification of α -fetoprotein at concentrations as low as 50 ng mL⁻¹.

Crossed-affinity Immunelectrophoresis (CAIE)

Affinity electrophoresis refers to any technique in which two or more components specifically interact during an electrophoretic run. Affinity electrophoresis in agarose gels, combined with subsequent immunochemical detection (CAIE), was introduced by Bog-Hansen in 1975 as a useful tool for the characterization of biospecific macromolecular interactions. This technique permits, among other things, the demonstration of ligand-binding proteins, enumeration of binding sites and estimation of binding constants, with the added advantage of being adequate for determination of very small quantities in impure materials.

An important field of application of CAIE has been the study of the interaction of glycoproteins and lectins. Lectins are animal and mostly plant-derived proteins that specifically interact with the carbohydrate components of glycoconjugates. There is a considerable amount of information in the literature about the biochemical properties of numerous lectins and on the type of glycan structures that they can recognize. Using different lectins in the first electrophoresis run (affinity electrophoresis step), CAIE permits the analysis of the heterogeneity of glycoproteins in complex mixtures. The serum protein glycoforms, after fractionation by lectin affinity electrophoresis, can be revealed with specific antibodies and finally quantified.

Figure 5A shows a schematic illustration of the CAIE technique. First, the serum proteins are subjected to electrophoresis (generally at pH 8.2–8.6)

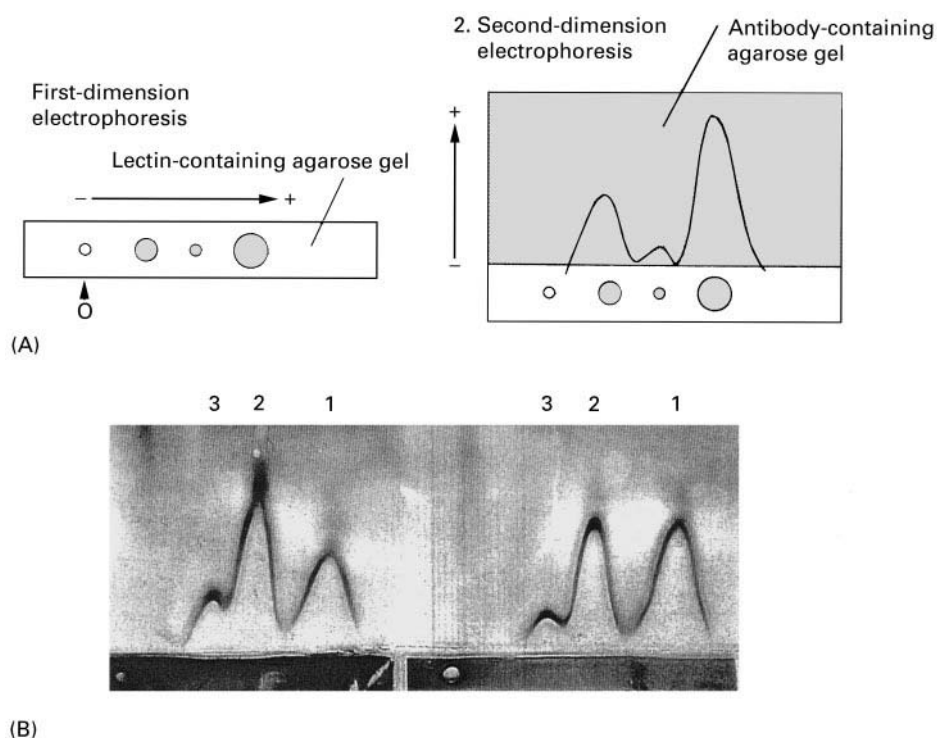


Figure 5 (A) Schematic representation of the CAIE technique. O, origin, corresponding to the well where the sample is applied in the first-dimension electrophoresis. (B) CAIE patterns of human α_1 -acid glycoprotein from (right) healthy individuals and (left) patients with inflammatory processes. The numbered peaks correspond to microforms of α_1 -acid glycoprotein in decreasing order of mobility.

in lectin-containing agarose gels (first-dimension gel). The lectin is added to the melted agarose (at around 55°C) before pouring the gel. Under these conditions most of the lectins used in CAIE do not have sufficient mobility. The proteins are fractionated in their different glycoforms, whose mobility depends on their corresponding affinity for the lectin. The first-dimension gel is then transferred into a second-dimension agarose gel containing specific antibodies against the protein to be analysed. The second-dimension electrophoresis produces for many serum glycoproteins fused precipitating peaks, which corresponds to the different microforms present in the sample. The CAIE patterns can be visualized by the methods described in the previous immunochemical techniques. The amount of each glycoform is related to the corresponding immunoprecipitating area that can be calculated by planimetry or by triangulation.

Figure 5B shows, as an example, the CAIE patterns of α_1 -acid glycoprotein from human serum. In the first dimension gel, 1 mg mL^{-1} of the lectin Concanavalin A was included. The second-dimension gel contained specific rabbit antiserum against human α_1 -acid glycoprotein. The different peaks have been labelled in decreasing order of mobility. Peak 1 corresponds to glycoforms of the human α_1 -acid glycoprotein that did not react with the lectin and contains tri- and tetra-antennary glycans; peak 2 corresponds to weakly

reactive glycoforms of the protein containing one bi-antennary glycan; finally, peak 3 corresponds to strong reactive glycoforms containing at least two bi-antennary glycans.

Equipment and General Methods

Agarose gels (1% w/v) are prepared in the described buffers on glass plates of different size according to need. For example $9 \times 12\text{ cm}$ plates are suited for conventional IE (they permit the analysis of eight samples or seven antisera) and also for RIE (in this case, about 20 samples can be applied). For the CIE and CAIE techniques, $4 \times 9\text{ cm}$ and $7.5 \times 10\text{ cm}$ glass plates can be used for the first and the second electrophoretic run, respectively. In all cases, one of the surfaces of the glass plates is coated with an agarose solution (1% w/v, in distilled water) that, after being dried, serves as an anchor for the agarose gel. To ensure regular thickness throughout the gel plate, which is essential for the reproducibility of quantitative methods, the melted agarose is poured between two glass plates separated by rigid spacers of around 1.5 mm thickness.

When antibodies, purified proteins or lectins are to be added to the gel, the agarose solution must be previously equilibrated around 55°C in a thermostated water bath to avoid protein denaturation. The

growth of microorganisms is avoided by the addition of preservatives to the agarose solutions, for example 0.1% sodium azide or 0.01% sodium merthiolate.

Simple equipment is commercially available, though much can be made in-house. The electrophoresis system only requires two electrophoretic tanks (provided with platinum wire and connected to the electrodes), and an adjustable power supply delivering voltage up to 400 V at 400 mA. The connection between the agarose plates and the buffer in the tanks can be accomplished through filter-paper wicks previously wetted in electrophoretic buffer (the same as that used for preparing the gel). To avoid excessive warming of the gel during electrophoresis, it is convenient to cool the agarose plates using a system connected to tap water. This allows the electrophoresis to be run at room temperature in the laboratory, alternatively, it can be carried out in a cold room at 5°C.

A great number of polyvalent and specific antisera prepared in goat, sheep or rabbits can be obtained from different suppliers or obtained in-house.

Present and Future Developments

Though most immunoelectrophoretic techniques described here were developed at least 25 years ago, they still enjoy great popularity and continue to be excellent tools for biochemists and immunologists. IE and CIE are very useful techniques for the characterization of complex mixtures of proteins and for the study of certain pathological situations that evolve with changes in plasma protein patterns. CAIE is a powerful technique for detecting glycoprotein microforms using different lectin specificities. Advances in the characterization of new lectins with restricted specificity represent a future development in this field. CAIE can also be applied to many affinity systems, including the important contribution of monoclonal antibodies in the affinity electrophoresis step.

Immunoelectrophoretic techniques are time- and antisera-consuming techniques. These limitations

could be improved by including the capillary methods commonly used in capillary electrophoresis systems.

Further Reading

- Bøg-Hansen TC, Bjerrum OJ and Ramlau J (1975) Detection of biospecific interaction during the first dimension electrophoresis in crossed immunoelectrophoresis. *Scandinavian Journal of Immunology* 4 (Suppl. 2): 141.
- Breborowicz J and Mackiewicz A (eds) (1992) *Affinity Electrophoresis: Principles and Application*. Boca Raton: CRC Press.
- Dolnik V (1997) Capillary zone electrophoresis of proteins. *Electrophoresis* 18: 2353.
- Grabar P and Williams CA (1953) Méthode permettant l'étude conjuguée des propriétés électrophorétiques et immunochimiques d'un mélange de protéines. Application au sérum sanguin. *Biochimica Biophysica Acta* 10: 193.
- Helenius A and Simons K (1977) Charge shift electrophoresis: simple method for distinguishing between amphiphilic and hydrophilic proteins in detergent solution. *Proceedings of the National Academy of Science of the USA* 74: 529.
- Laurell CB (1966) Quantitative estimation of proteins by electrophoresis in agarose gel containing antibodies. *Analytical Biochemistry* 15: 45.
- Ouchterlony Ö (1948) In vitro method for testing the toxin-producing capacity of diphtheria bacteria. *Acta Pathologica Microbiologica Scandinavica* 25: 186.
- Ouchterlony Ö and Nilsson LÅ (1986) Immunodiffusion and immunoelectrophoresis. In: Weir M, Herzenberg LA, Blackwell C and Herzenberg LA (eds) *Handbook of Experimental Immunology* 4th edn, vol. 1. *Immunochemistry*, Ch. 32. Oxford: Blackwell Scientific Publications.
- Ressler N (1960) Two-dimensional electrophoresis of proteins antigens with an antibody containing buffer. *Clinica Chimica Acta* 5: 795.
- Uriel J (1971) Color reactions for identification of antigen-antibody precipitates in gels. In: Williams CA and Chase MW (eds) *Methods in Immunology and Immunochemistry*, vol. III, p. 294. New York: Academic Press.
- Williams CA (1971) Immunoelectrophoretic analysis. In: Williams CA and Chase MW (eds) *Methods in Immunology and Immunochemistry*, vol. III, p. 235. New York: Academic Press.

Isoelectric Focusing

P. G. Righetti and A. Bossi, University of Verona, Verona, Italy

C. Gelfi, ITBA, CNR, Segrate, Milan, Italy

Copyright © 2000 Academic Press

Isoelectric focusing represents a unique electrokinetic method in that it is based on steady-state patterns

attained by amphoteric species (mostly proteins and peptides) along a pH gradient under the influence of an electric field. Due to a continuous balancing of diffusion away from the pI (isoelectric point) and pI-driven electric forces, extremely sharp zones are obtained, characterized by a very high resolving power. This article will consider conventional isoelectric focusing (IEF) in soluble, amphoteric buffers; and immobilized pH gradients (IPG) in insolubilized,

non-amphoteric buffers. In the latter case, guidelines will be given on how to optimize linear and nonlinear pH gradients and examples will be shown on the unique resolving power of the technique.

Conventional Isoelectric Focusing

In principle, pH gradients could be obtained by diffusion of non-amphoteric buffers but such 'artificial' gradients would be altered by changes in electric migration and diffusion of the buffer ions. Thus, Svensson in 1961 introduced the concept of 'natural' pH gradients, created and stabilized by the electric current itself. The buffers used in this system required two fundamental properties: first amphoterism, so that they could reach an equilibrium position along the separation column and secondly 'carrier' ability. This last concept is more subtle, but just as fundamental. Any ampholyte cannot simply be used for IEF; only a carrier ampholyte, that is a compound capable of transporting the current (a good conductor) and capable of carrying the pH (a good buffer). With this notion, and with Vesterberg's elegant synthesis of such ampholytes in 1969, present-day conventional IEF was born.

Some Basic Theoretical Concepts

Here some basic equations governing the IEF process will be considered. The most important is the one governing the distribution profile of an ampholyte about its isoelectric point. Under steady-state conditions (obtained by balancing the simultaneous electrophoretic and diffusional mass transports), Svensson derived the following differential equation describing the concentration profile of a focused zone:

$$C\mu i/qk = D\left(\frac{dC}{dx}\right) \quad [1]$$

where C is the concentration of a component in arbitrary mass units per arbitrary volume unit; μ is the electric mobility in $\text{cm}^2 \text{V}^{-1} \text{s}^{-1}$ of ion constituent except H^+ and OH^- , with positive sign for cationic and negative sign for anionic migration; i is the electric current in A; q is the cross-sectional area in cm^2 of electrolytic medium, measured perpendicularly to the direction of current; k is the conductance of the medium, in $\Omega^{-1} \text{cm}^{-1}$; D is the diffusion coefficient in $\text{cm}^2 \text{s}^{-1}$ of a given ionic component with mobility μ ; and x is the coordinate along the direction of current increasing from 0 to the anode towards the cathode.

Each term in eqn [1] expresses the mass flow per second and square centimetre of the cross-section: to the left being the electric and to the right the diffu-

sional mass flows. If eqn [1] is re-written in the form:

$$\left(\frac{i\mu}{q}\right)\left(\frac{dx}{k}\right) = D\left(\frac{dC}{C}\right) \quad [2]$$

it is seen that it is possible to integrate it if μ is known as a function of pH and D as a function of C . Specifically, if the conductance, the diffusion coefficient, and the derivative:

$$p = -\frac{d\mu}{dx} = -\left[\frac{d\mu}{d(\text{pH})}\right]\left[\frac{d(\text{pH})}{dx}\right] \quad [3]$$

(where p is the ratio between the protein titration curve and the slope of the pH gradient over the separation axis) can be regarded as constant within the focused zone, then $\mu = -px$ and one obtains the following analytical solution:

$$C = C_0 \exp\left[-\frac{(pix^2)}{(2qkD)}\right] \quad [4]$$

where x is now defined as being zero at the concentration maximum C_0 . This is a Gaussian concentration distribution with inflection points at:

$$x_i = \pm \sqrt{\left(\frac{qkD}{pi}\right)} \quad [5]$$

where x_i represents the width of the Gaussian distribution of the focused zone measured from the top of the distribution of the focused ampholyte to the inflection point (one standard deviation). The course of the pH gradient is $d(\text{pH})/dx$ and $d\mu/d(\text{pH})$ represents the titration curve of the ampholyte. It should be kept in mind that this Gaussian profile holds only if and as long as the conductivity of the bulk solution within the zone is constant. Constant conductivity along a pH gradient is quite difficult to maintain, especially as one approaches pH extremes (below pH 4 and above pH 10), if for no other reason, because the non-negligible concentration of H^+ and OH^- present in the bulk liquid begins to contribute strongly.

Another important equation regards the resolving power in IEF, expressed in $\Delta(\text{pI})$ units, i.e. in the minimum difference of surface charge between two adjacent proteins that the IEF technique is able to resolve. If two adjacent zones of equal mass have a peak-to-peak distance three times greater than the distance from the peak to inflection point there will be a concentration minimum approximating the two outer inflection points. Taking this criterion for resolved adjacent proteins, Rilbe derived the following equation for minimally but definitely resolved zones:

$$\Delta(\text{pI}) = 3\sqrt{\left(\frac{D[d(\text{pH})/dx]}{E[-d\mu/d(\text{pH})]}\right)} \quad [6]$$

This equation shows that good resolution should be obtained with substances with a low diffusion coefficient (D) and a high mobility slope [$d\mu/d(\text{pH})$] at the isoelectric point – conditions that are satisfied by all proteins. Good resolution is also favoured by a high field strength (E) and a shallow pH gradient [$d(\text{pH})/dx$]. It will be seen that, whereas in conventional IEF the limit to the resolving power is approximately 0.01, in IPGs it is 0.001 pH units.

The Carrier Ampholyte Buffers

Recall that the buffer capacity of an ampholyte in the isoprotonic state decreases with increasing ΔpK across the isoprotonic point, linearly at first, then exponentially. Let us take as an example a hypothetical ampholyte, with $\text{pK}_1 = 4.6$ (a carboxyl group) and $\text{pK}_2 = 6.2$ (an amino group), having thus a $\text{pI} = 5.4$ and $\Delta\text{pK} = 1.6$. If we titrate this ampholyte in the pH 4–7 range, encompassing the two pK s, and if we plot the accompanying buffering power (β), degree of dissociation (α) and slope of the pH gradient, we will have the plot shown in Figure 1(A). It can be seen that there is still a substantial buffering power at the pI of the ampholyte, with a corresponding degree of ionization less than unity, and that the titration curve is smooth throughout the pH gradient explored, with

only a small deviation about the pI of the ampholyte, indicating that this species is indeed a ‘good’ carrier ampholyte. Now take an ampholyte with $\text{pK}_1 = 4.6$ but with $\text{pK}_2 = 9.3$, thus with a $\text{pI} = 6.95$ and $\Delta\text{pK} = 4.7$. If we now titrate it in the pH 4–10 range, again encompassing the two pK values, we will have the graph shown in Figure 1(B). It can be seen now that at the theoretical pI value the ampholyte does not have any appreciable buffering power and that it is fully ionized. In addition, it is not only isoelectric at $\text{pH} = 6.95$, but indeed almost at any pH in the interval 5–9, as seen by the abrupt sigmoidal shape in the pI environment. This species will be a ‘bad’ carrier ampholyte, useless for a well-behaved IEF fractionation.

An important prerequisite for a good carrier ampholyte is that it has a high conductivity at its pI . Regions of low conductivity will absorb much of the applied voltage, thus reducing the field strength and hence the potential resolution in other parts of the gradient. It has been demonstrated that good conductivity is associated with small values of $\text{pI} - \text{pK}$. This is also true for the buffering capacity of an ampholyte. Thus, the parameter $\text{pI} - \text{pK}$ (equivalent to $\frac{1}{2} \Delta\text{pK}$) becomes the most important factor in selecting carrier ampholytes exhibiting both good conductivity and buffering capacity (β).

Methodology

The structure of carrier ampholytes (CA) and their general properties are illustrated in Figure 2. CAs are oligoprotic amino carboxylic acids, each containing at least four weak protolytic groups, at least one being a carboxyl group and at least one a basic nitrogen atom, but no peptide bonds. In a typical synthesis, a mixture of oligoamines (four to six nitrogens in length, linear and branched) reacts with an α - β -unsaturated acid (typically acrylic or itaconic acids), at a nitrogen–carboxyl ratio of 2 : 1.

The mechanism of developing a pH gradient in IEF is illustrated in Figure 3. Before passage of the current, the column is at constant pH (Figure 3A) and the multitude of amphoteric buffers is randomly distributed, resulting in a reciprocal neutralization. However, each individual CA species will have its own titration curve (see Figure 2, lower left side) defining different mobilities in the electric circuit. After starting the experiment the different CAs will migrate at different velocities in the column, the most acidic and most basic compounds being the fastest moving ions. As a result of this sorting process, a pH gradient will form, sigmoidal at first (Figure 3B), with an uneven voltage gradient. After 1 h, the various CA buffers will have separated further, and at this point an almost linear pH gradient has been established

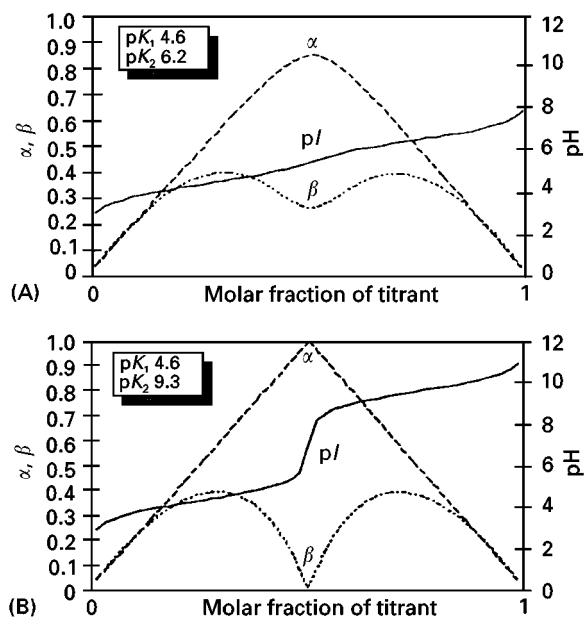


Figure 1 Degree of ionization (α) and buffering power (β) of a good (A) and a poor (B) carrier ampholyte. (A) computer simulations obtained assuming a $\text{pK}_1 = 4.6$ and a $\text{pK}_2 = 6.2$ ($\text{pI} = 5.4$). The ampholyte was titrated in the pH 4–7 interval. (B) Computer simulation obtained by assuming a $\text{pK}_1 = 4.6$ and a $\text{pK}_2 = 9.3$ ($\text{pI} = 6.95$). The ampholyte was titrated in the pH 4–10 interval. Note the sharp sigmoidal transition in the pI region in (B), suggesting total lack of buffering power (Wenger P and Righetti PG, unpublished observations).

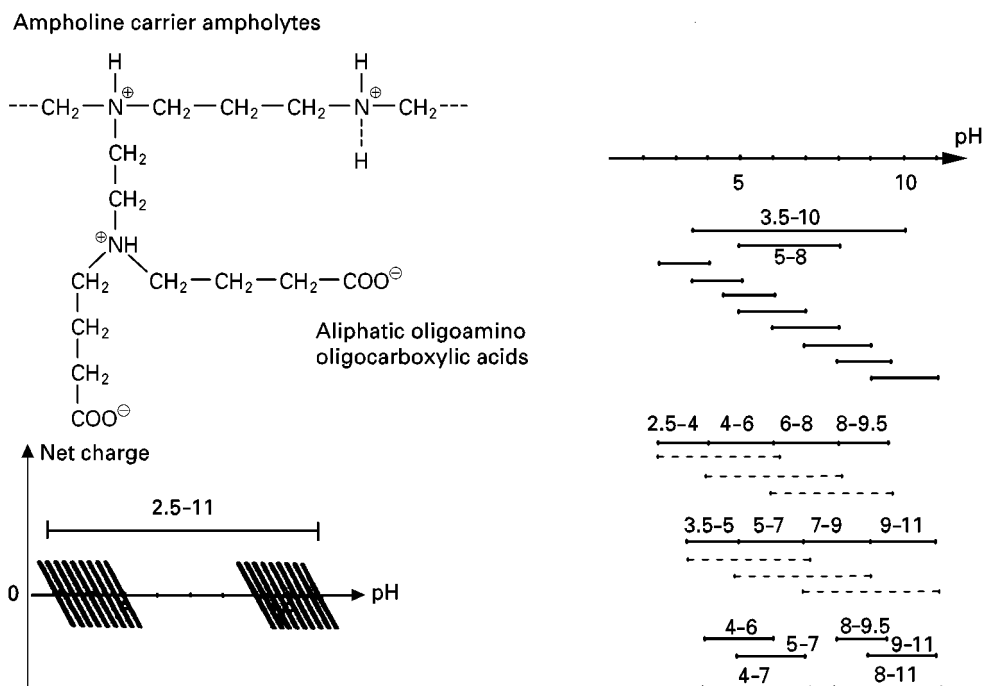


Figure 2 Composition of Ampholine. On the upper left side a representative chemical formula is shown (aliphatic oligoamino oligocarboxylic acids). On the lower left side, portions of hypothetical titration curves of carrier ampholytes are depicted. Right: different pH cuts for wide and narrow range ampholytes (by permission of LKB Produkter AB).

which spans the pH range defined by the pIs of the ampholytes (Figure 3C). After 1.5 h the CAs have separated into symmetrical zones with overlapping

Gaussian profiles. Now the system has achieved a steady-state, i.e. a balance between electrophoretic transport and diffusion away from the pI, and no

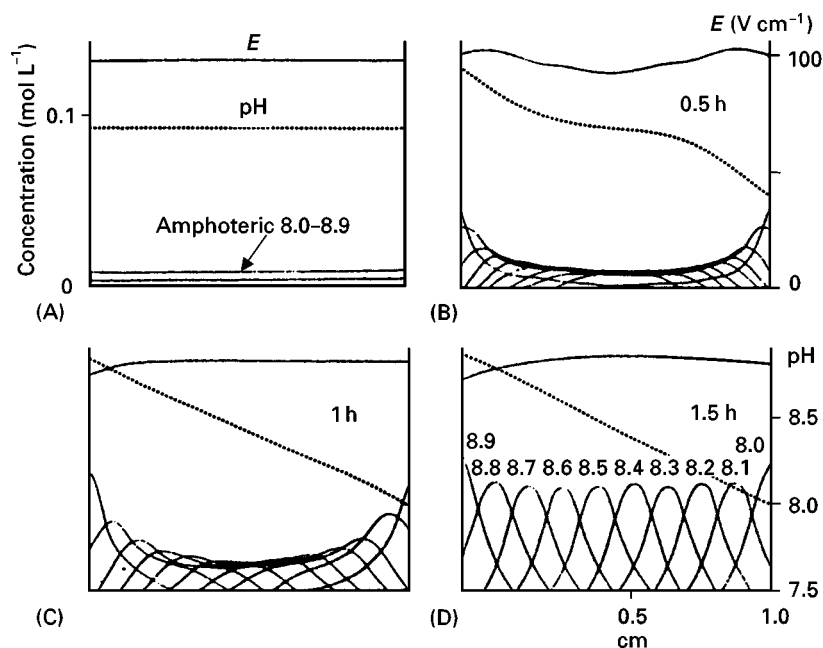


Figure 3 Calculated time development of a focusing process involving 10 ampholytes in a closed vessel. The p/s of the ampholytes are evenly distributed in the pH 8.0-8.9 range. The initial distribution of the amphoteric buffers is indicated in (A). The calculation was performed assuming a constant voltage (100 V cm⁻¹) across the system. The anode is positioned to the right in the diagrams. Each x-axis represents the distance from the cathode on the same scale as in (D). (Reproduced with permission from Schaefer-Nielsen, 1986.)

further mass transport is expected (Figure 3D). As long as the local concentration of the different CA species does not change the slope of the pH gradient will be kept constant with time. Proteins will keep migrating against this CA distribution profile eventually reaching their *pI* position.

By and large, most analytical IEF runs are performed in horizontal chambers: the polyacrylamide gel slab rests on a cooling block [generally made of glass or coated aluminium or even beryllium oxide (used as the heat shield of the space shuttle)]. This horizontal configuration allows one to dispose of electrode reservoirs and of all the hydraulic problems connected with vertical chambers (tight seals, etc.): in fact, anolyte and catholyte are soaked in filter paper strips resting directly on the open gel surface. In addition, most modern chambers contain a cover lid with movable electrodes which can be adjusted to any gel length (generally from 10 to 25 cm electrode distance). Since thick gels (e.g. 2 mm thick) generate thermal gradients through the gel thickness, resulting in skewed zones (essentially all horizontal chambers have cooling only on one gel face) ultrathin gels (0.2–0.5 mm) supported on a reactive polyester foil (Gel Bond PAG) are preferred today.

Immobilized pH Gradients (IPG)

IPGs are based on the principle that the pH gradient, which exists prior to the IEF run itself, is copolymerized, and thus immobilized within the polyacrylamide matrix. This is achieved by using as buffers a set of up to 10 non-amphoteric, weak acids and bases, called Immobilines, having the following general chemical composition: $\text{CH}_2=\text{CH}-\text{CO}-\text{NH}-\text{R}$, where R denotes either three different weak carboxyls, with *pK*s of 3.1, 3.6, and 4.6 (Table 1), or five tertiary amino groups, with *pK*s of 6.2, 7.0, 8.5, 9.3

and 10.3 (Table 2). This set of eight weak buffers is complemented by a strong acid (*pK* of approximately 1, 2-acrylamido-2-methyl propanesulfonic acid) and a strong base (*pK* > 12, quaternary aminoethyl-acrylamide), used only as titrants. During gel polymerization, these buffering species are incorporated into the gel (84–86% conversion efficiency at 50°C for 1 h), by the same free radical reaction used to activate the acrylamide double bond. Figure 4 shows a segment of a hypothetical structure of an Immobiline matrix and the process of focusing two proteins in it. It is seen that only the proteins migrate to their steady-state position, whereas the Immobilines remain fixed at their original grafting position in the gel, where a fixed ratio of buffering/titrant ions defines the pH locally. This means that the pH gradient is stable indefinitely (but it has to pre-exist before the onset of polymerization) and can only be destroyed if and when the polyacrylamide gel is hydrolyzed. Given the sparse distribution of Immobilines in the gel they behave as isolated charges, able to effectively contribute to the ionic strength of the medium. In conventional IEF, on the contrary, at steady-state the ionic strength is exceedingly low (less than 1 mequiv L^{-1}) since the focused carrier ampholytes form an inner salt, and this often results in protein precipitation and smears both at the *pI* and in its proximity. In IPGs the high ionic strength existing in the matrix (typically 10 mequiv L^{-1}) induces protein solubilization at the *pI* value (thus CA-IEF is similar to a 'salting-out' milieu and IPGs to a 'salting-in' environment).

Immobiline-based pH gradients can be cast in the same way as conventional polyacrylamide gradient gels by using a density gradient to stabilize the Immobiline concentration gradient, with the aid of a standard, two-vessel gradient mixer. As shown earlier, these buffers are no longer amphoteric as in

Table 1 Acidic acrylamido buffers

<i>pK</i>	Formula	Name	<i>M_r</i>
1.0	$\begin{array}{c} \text{CH}_3 \\ \\ \text{CH}_2=\text{CH}-\text{CO}-\text{NH}-\text{C}-\text{CH}_3 \\ \\ \text{CH}_2-\text{SO}_3\text{H} \end{array}$	2-Acrylamido-2-methylpropanesulfonic acid	207
3.1	$\begin{array}{c} \text{CH}_2=\text{CH}-\text{CO}-\text{NH}-\text{CH}-\text{COOH} \\ \\ \text{OH} \end{array}$	2-Acrylamidoglycolic acid	145
3.6	$\text{CH}_2=\text{CH}-\text{CO}-\text{NH}-\text{CH}_2-\text{COOH}$	<i>N</i> -Acryloylglycine	129
4.6	$\text{CH}_2=\text{CH}-\text{CO}-\text{NH}-(\text{CH}_2)_3-\text{COOH}$	4-Acrylamidobutyric acid	157

Table 2 Basic acrylamido buffers

<i>pK</i>	Formula	Name	<i>M_r</i>
6.2	$\text{CH}_2=\text{CH}-\text{CO}-\text{NH}-(\text{CH}_2)_2-\text{N} \begin{array}{c} \diagup \diagdown \\ \diagdown \diagup \end{array} \text{O}$	2-Morpholinoethylacrylamide	184
7.0	$\text{CH}_2=\text{CH}-\text{CO}-\text{NH}-(\text{CH}_2)_3-\text{N} \begin{array}{c} \diagup \diagdown \\ \diagdown \diagup \end{array} \text{O}$	3-Morpholinopropylacrylamide	198
8.5	$\text{CH}_2=\text{CH}-\text{CO}-\text{NH}-(\text{CH}_2)_2-\text{N}(\text{CH}_3)_2$	<i>N,N</i> -Dimethylaminoethylacrylamide	142
9.3	$\text{CH}_2=\text{CH}-\text{CO}-\text{NH}-(\text{CH}_2)_3-\text{N}(\text{CH}_3)_2$	<i>N,N</i> -Dimethylaminopropylacrylamide	156
10.3	$\text{CH}_2=\text{CH}-\text{CO}-\text{NH}-(\text{CH}_2)_3-\text{N}(\text{CH}_2\text{H}_5)_2$	<i>N,N</i> -Diethylaminopropylacrylamide	184
> 12	$\text{CH}_2=\text{CH}-\text{CO}-\text{NH}-(\text{CH}_2)_2-\text{N}^+(\text{CH}_2\text{H}_5)_3$	<i>N,N,N</i> -Triethylaminoethylacrylamide	198

conventional IEF, but are bifunctional: the buffering group is located at one end of the molecule and at the other end there is the acrylic double bond which will disappear during the grafting process. The three carboxyl immobilines have rather small temperature coefficients of ionization (dpK/dT) in the 10–25°C range due to their small standard heats of ionization (approximately 1 kcal mol⁻¹) and thus exhibit negligible *pK* variations over this temperature range. On the other hand, the four basic immobilines exhibit rather large ΔpK s in the same temperature range (as much as $\Delta\text{pK} = 0.44$ for the *pK* 8.5 species) due to their larger heats of ionization (6–12 kcal mol⁻¹). Therefore, for reproducible runs and pH gradient calculations, all the experimental parameters have been fixed at 10°C. Temperature is not the only variable that will affect immobiline *pK*s (and therefore the actual pH gradient generated): additives in

the gel that will change the water structure (chaotropic agents such as urea) or lower its dielectric constant, and the ionic strength itself of the solution, will alter *pK* values.

Narrow and Ultranarrow pH Gradients

We define the gradients (in the gel slab) from 0.1 to 1 pH unit as ultranarrow and narrow gradients, respectively. Within these limits one can generally work on a 'tandem' principle, i.e. choosing a 'buffering' Immobiline (e.g. a base or an acid), having its *pK* within the desired pH interval, and a 'non-buffering' Immobiline (e.g. an acid or a base), having its *pK* at least 2 pH units removed from either *pH*_{min} or *pH*_{max} of the pH range. The latter will therefore provide equivalents of acid or base, respectively, to titrate the buffering group, but will not itself buffer in the desired pH interval. For these calculations one

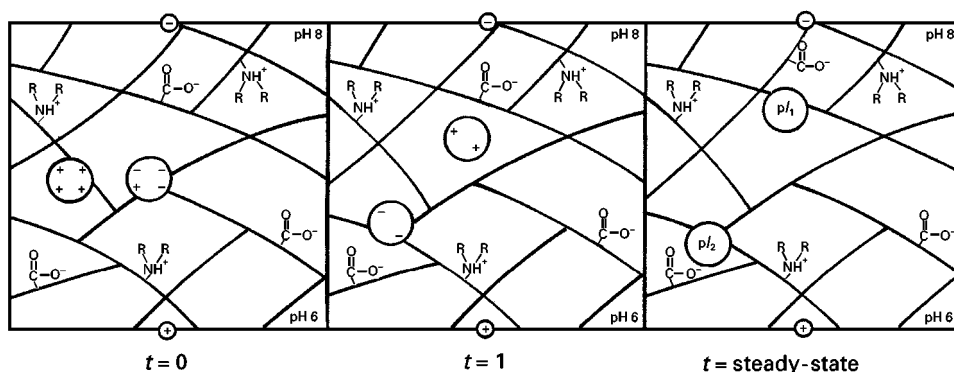


Figure 4 Hypothetical structure of an Immobiline gel and mechanism of the focusing process. The acrylamido acid and basic groups are shown grafted on the polyacrylamide matrix. Two proteins are shown migrating in the gel at the times $t = 0$, at $t = 1$ and finally at the steady-state, where they reach they respective *pI* values (*pI*₁ and *pI*₂) as points of zero net charge (by permission of LKB Produkter AB).

can resort to modified Henderson–Hasselbalch equations and to rather complex nomograms or simply adopt tabulated recipes, 1 pH unit wide, which start with the pH 3.8–4.8 interval and end with the pH 9.5–10.5 span, separated by 0.1 pH unit increments (58 such recipes have been tabulated). If a narrower pH gradient is needed this can be derived from any of the 58 pH intervals tabulated by a simple linear interpolation of intermediate Immobiline molarities.

Extended pH Gradients

For wider pH intervals, several buffering species have to be mixed and the situation becomes considerably more complex. This has been solved with the aid of computer programs designed specifically for this purpose. The basic findings are: first for generating a linear pH gradient the buffering power has to be

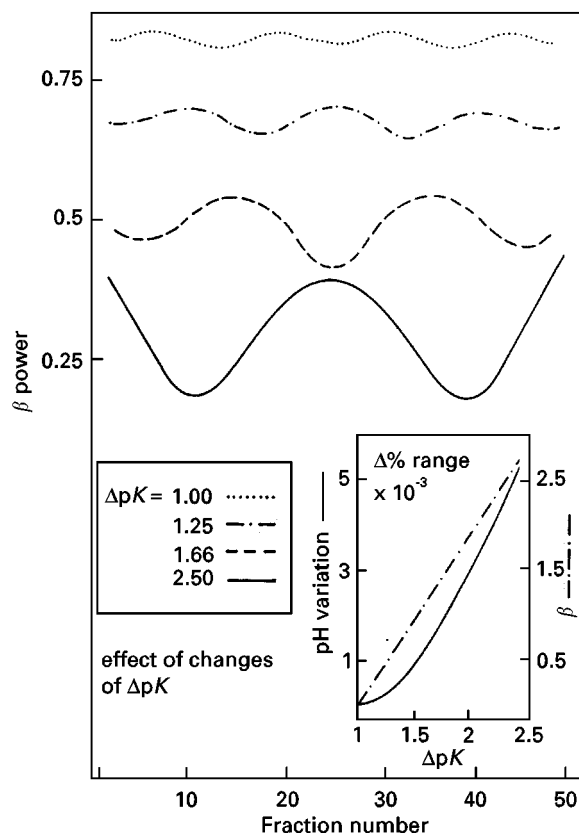


Figure 5 Effect of changes in the number of (evenly spaced) buffering components. The optimal concentrations of fictitious buffers (bases) with pK s differing by 1, 1.25, 1.66 and 2.5 pH units, were calculated so as to cover the pH 4.5–8.5 range. The resulting courses of β power are shown as a function of ΔpK . The insert is a plot of percentage variation, in comparison with the case $\Delta pK = 1$, of the ranges of deviation of pH (left scale) and of β (right scale). Note that the smoothest β power is obtained with $\Delta pK = 1$ (from Gianazza *et al.*, 1983, with permission of Elsevier Science Publishers).

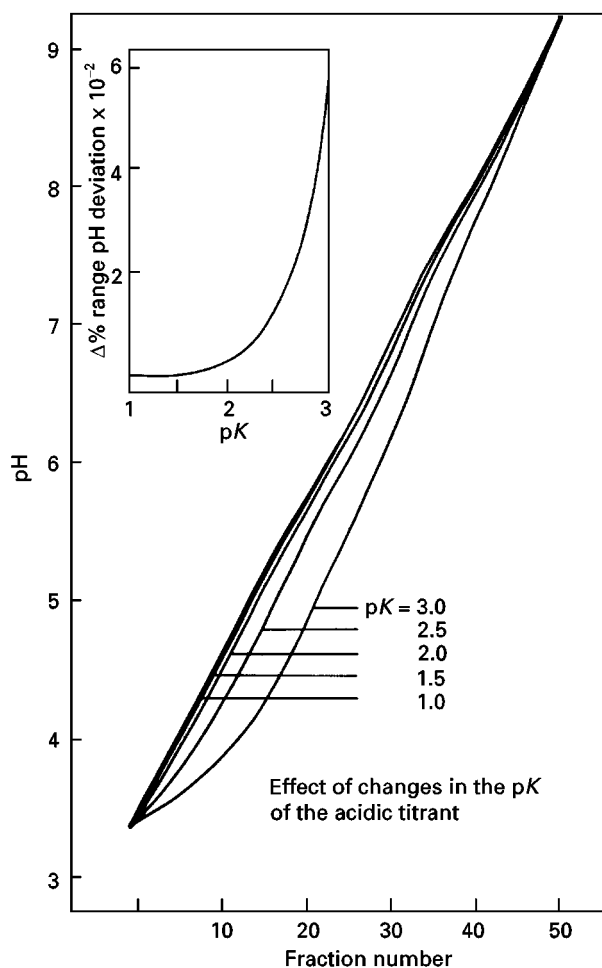


Figure 6 Effect of changes in the pK of the acidic titrant. A reference Immobiline mixture was titrated to the same pH value with fictitious acids whose pK was 0.5, 1.0, 1.5, 2.0 and 2.5 pH unit lower than the gradient's limit (in this case, $pH_{\min} = 3.5$) and the pH course was calculated for the five cases. The insert is a plot of the percentage variation of deviation from linearity as the titrant's pK increases (from Gianazza *et al.*, 1983, with permission of Elsevier Science Publishers).

constant throughout the desired pH interval (this is best achieved when the pK values are spaced at 1 pH unit intervals, see Figure 5). Secondly, to avoid deviations from linearity, the titrants should have pK s well outside pH_{\min} and pH_{\max} of the wanted pH range (in general, at least 2 pH units removed from the limits of the pH interval) (see Figure 6). As a consequence of this, for pH ranges wider than 3 pH units, two additional Immobilines are needed as titrants: one strongly acidic ($pK < 1$) and one strongly basic ($pK > 12$). There are two ways of generating extended pH intervals. In one approach the concentration of each buffer is kept constant throughout the span of the pH gradient and 'holes' of buffering power are filled by increasing the amounts of the buffering species bordering the largest ΔpK s; in the

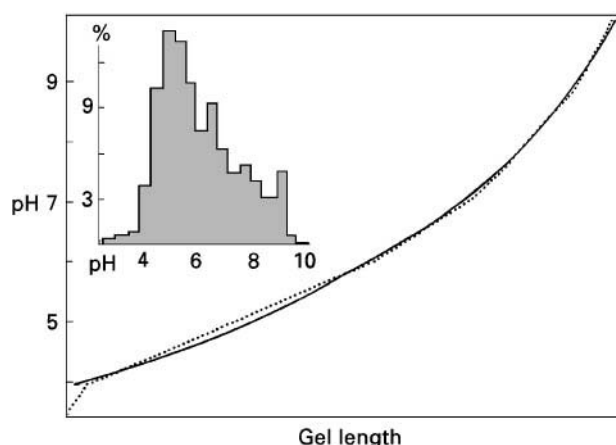


Figure 7 Non-linear pH 4–10 gradient. Ideal (dotted line) and actual (solid line) formulation courses. The shape for the ideal profile was computed from data on the statistical distribution of proteins p/s. The relevant histogram is redrawn in the figure inset (from Gianazza *et al.*, 1985; by permission of VCH).

other approach (varying buffer concentration) the variation in concentration of the various buffers along the width of the desired pH gradient results in a shift of their apparent pKs with a concomitant evening-out of the ΔpK values. With the available recipes, preparation of any Immobiline gel is now

a trouble-free operation, as all the complex computing routines have already been performed and no further calculations of any type are required.

Non-linear, Extended pH Gradients

IPG formulations have been given only in terms of rigorously linear pH gradients. While this has been the only solution adopted so far, it might not be the optimal one in some cases. Altering the pH slope in some portions of the gradient might be required in those pH regions overcrowded with proteins. The reasons for resorting to non-linear pH gradients are given in the histogram of **Figure 7**. With the relative abundance of different species it is clear that an optimally resolving pH gradient should have a gentler slope in the acidic portion, and a steeper course in the alkaline region. Such a general course has been calculated by assigning to each 0.5 pH unit interval in the pH 3.5–10 region a slope inversely proportional to the relative abundance of proteins in that interval. The ideal (dotted) curve in **Figure 7** was obtained by such a procedure. What is also important here is the establishment of a new principle in IPG technology, namely that the pH and density gradients stabilizing it need not be co-linear. The possibility exists of modulating the former by locally flattening of pH

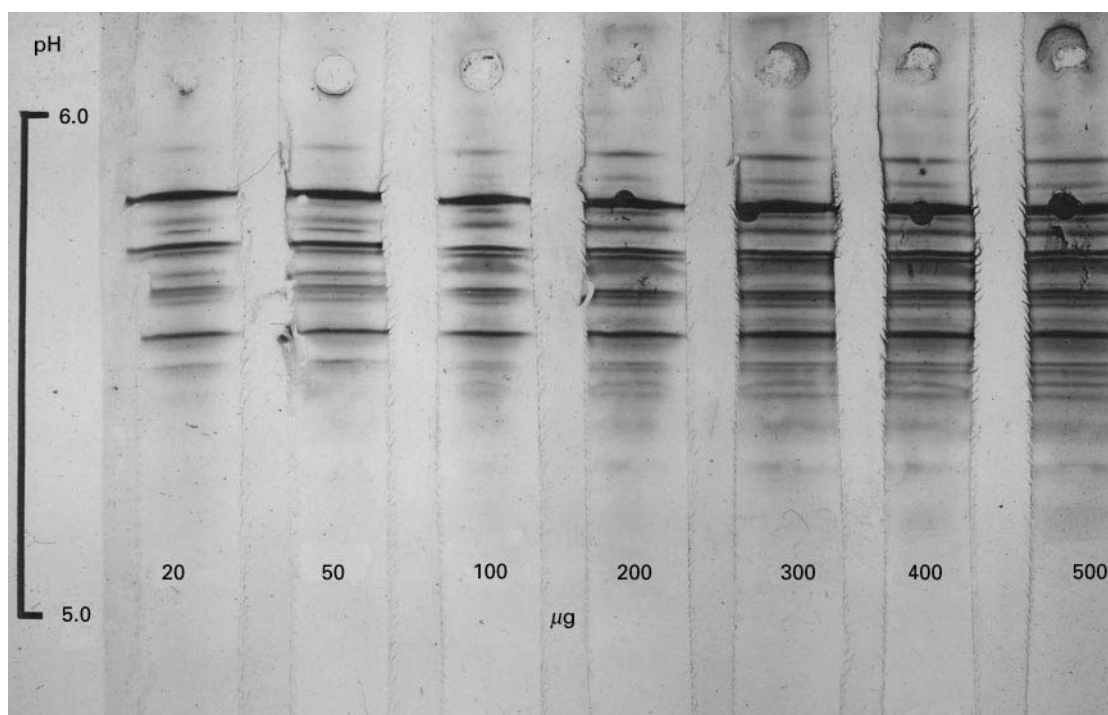


Figure 8 IEF of conalbumin in an IPG pH 4.5–6.5 gradient. Gel: 5%T, 3%C polyacrylamide, equilibrated in 10% glycerol. All samples were applied in round basins punched through the gel thickness at the cathodic side as 20 μ L droplet (20–500 μ g protein). Staining with Coomassie Blue R-250 in ethanol/acetic acid in presence of copper sulfate. Notice that, although the gel thickness is only 0.5 mm, there is no overloading effect in such a wide interval of protein concentration (from Righetti PG and Ek K, unpublished observations).

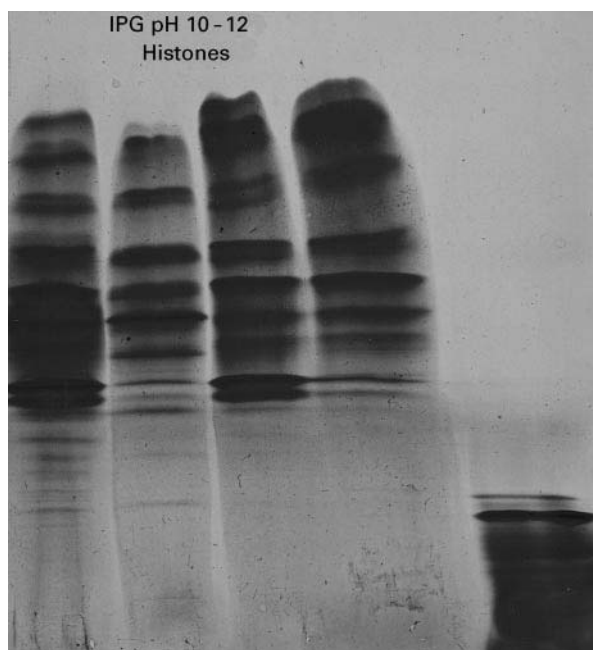


Figure 9 Focusing of histones in an IPG pH 10–12 nonlinear interval. Gel: 6% T, 4% C polyacrylamide matrix, containing an IPG 10–12 gradient, reswollen in 7 M urea, 1.5% Nonidet P-40 and 0.5% Ampholine pH 9–11. The gel was run at 10°C under a layer of light paraffin oil at 500 V for the first hour, followed by increasing voltage gradients, after sample penetration, up to 1300 V for a total of 4 h. The samples (2 mg mL⁻¹, 50 µL seeded) were loaded in plastic well at the anodic gel surface. Staining with Coomassie Brilliant Blue R-250 in Cu²⁺. Histone samples (from left). (1) VII-S (Lys-rich); (2) VI-S; (3) II-AS and (4) VIII-S (Arg-rich, subgroup F), from calf thymus. The pI 10.6 marker (cytochrome C) is in track 5 on the right side (from Bossi *et al.*, 1994, by permission of Elsevier Science Publishers).

gradients for increased resolution, while leaving unaltered the latter.

Although only one example of a nonlinear extended pH gradient is given here, clearly the possibility exists of modulating in the same fashion any narrower pH interval.

Examples on the Resolving Power

What can IPGs achieve in practice? Figure 8 gives an example of a separation carried to the limit of a small-scale preparative load. Even when conalbumin is greatly overloaded, up to 500 µg in a single

track, no smears or precipitations occur, while faint bands become visible. Another interesting example, at the very limit of any focusing technique, is given in Figure 9. Here histones are seen focused at the steady-state in a very alkaline pH 10–12 gradient. It can be appreciated that all histones have a pI in the pH range 11–12, as they should, given their amino acid composition. Previous data obtained by conventional IEF had attributed to them pIs in the pH 9–10 interval, clearly grossly underestimated.

Further Reading

- Bossi A, Gelfi C, Orsi A and Righetti PG (1994) Isoelectric focusing of histones in extremely alkaline immobilized pH gradients: comparison with capillary electrophoresis. *Journal of Chromatography A* 686: 121–128.
- Gianazza E, Dossi G, Celentano F and Righetti PG (1983) Isoelectric focusing in immobilized pH gradients: generation and optimization of wide pH intervals with two-chamber mixers. *Journal of Biochemical Biophysical Methods* 8: 109–133.
- Gianazza E, Giacom P, Sahlin B and Righetti PG (1985) Non-linear pH courses with immobilized pH gradients. *Electrophoresis* 6: 53–56.
- Righetti PG (1983) *Isoelectric Focusing: Theory, Methodology and Applications*. Amsterdam: Elsevier.
- Righetti PG (1990) *Immobilized pH Gradients: Theory and Methodology*. Amsterdam: Elsevier.
- Righetti PG, van Oss CJ and Vanderhoff JW (eds) (1979) *Electrokinetic Separation Methods*. Amsterdam Elsevier.
- Rilbe H (1976) Theory of isoelectric focusing. In: Catsim-poolas N (ed.) *Isoelectric Focusing*, pp. 14–52. New York: Academic Press.
- Rilbe H (1996) *pH and Buffer Theory: a New Approach*. Chichester: John Wiley.
- Schaefer-Nielsen C (1986) Computer simulation of pH gradient formation in isoelectric focusing. In: Dunn MJ (ed.) *Gel Electrophoresis of Proteins*, pp. 1–36. Bristol: Wright.
- Svensson H (1961) Isoelectric fractionation, analysis and characterization of ampholytes in natural pH gradients. Scandinavica I. The differential equation of solute concentration at steady state and its solution for simple cases. *Acta Chemica Scandinavica* 15: 325–341.
- Vesterberg O (1969) Synthesis of carrier ampholytes for isoelectric focusing. *Acta Chemica Scandinavica* 23: 2653–2666.

Isoelectric Focusing in Capillary Electrophoresis

See II/ELECTROPHORESIS/Capillary Isoelectric Focusing

Isotachophoresis

T. Hirokawa, Hiroshima University, Higashi-hiroshima Japan

Copyright © 2000 Academic Press

Introduction

Isotachophoresis (ITP) is one of the electrophoretic techniques useful for the analysis and isolation of ionic substances. The first successful analysis using this method was reported for alkali earth metals and amino acids by Longworth in 1953. The use of glass capillaries was first reported by Martin and Everaerts in 1967 after the successful separation of metal cations using a glass capillary by Konstantinov and Oshurkova in 1963 and of carboxylic acids using a paper strip by Schumacher and Studer in 1964. Although various names had been used for this method, the name ITP was proposed by Haglund in 1970 and has been widely accepted. It is interesting to note that the root of the present capillary electrophoretic methods is ITP.

An ITP separation is due to the different electrophoretic mobilities of the sample components in a similar manner to the other electrophoretic techniques. However, ITP has some characteristic features which distinguish it from the other electrophoretic techniques. This article, summarizes the theoretical background of ITP separations and then describes the analytical and preparative equipment used. Finally, separation strategies are given together with typical examples of ITP.

Electrophoretic Mobility and Velocity

Effective mobility μ of an ionic substance in a solution can be expressed as a function of many factors as follows:

$$\mu = f(m_0, K_a, \text{pH}, T, \eta, \varepsilon, I, K_s, C_{\text{comp}}) \quad [1]$$

where m_0 is the absolute mobility of a solvated ion, K_a the acid dissociation constant, pH the pH of the solution, T the temperature, η the viscosity of the solvent used, ε the dielectric constant of the solvent, I the ionic strength, K_s the stability constants of the complexes or ion pairs formed, and C_{comp} the concentration of the complex-forming agent or the ion pair-forming agent.

Eqn [1] shows that the effective mobility is a complex function of the properties of the sample ion, the solvent used and the coexisting ions. A basic idea of the electrophoretic separation is to vary the mobilities of the ions being separated by varying some of the factors in the above function.

The migration velocity of the ion $(v)_i$ can be expressed as:

$$v_i = \mu E \quad [2]$$

where E is the potential gradient of the electrical field. Consequently the difference of the electrophoretic velocities among separands is the driving force of the electrophoretic separation.

The name of 'isotachophoresis' comes from the Greek for equal (*iso, iso*) velocity (*tacho, tachoz*) sample dragging (*phoresis, foreesqai*). Although this name characterizes its principle as described later, if the sample velocities were the same throughout the migration process, there would be no separation.

Principle of ITP

Operational Electrolyte System and Separation Principle

Two different electrolytes (a leading and a terminating electrolyte) are used in ITP and this is the important point which distinguishes it from other electrophoresis method. A sample solution is injected at the boundary of the two electrolyte solutions as shown in Figure 1(A). The leading electrolyte is usually a pH-buffered electrolyte containing leading ions (L) with the same sign as the sample ions and appropriate counterions with pH-buffering ability. Usually, Cl^- and K^+ or NH_4^+ are used as the leading ions because of their large mobilities. The terminating electrolyte contains terminating ions (T) together with appropriate counterions.

For successful ITP separations, the effective mobilities of A and B in Figure 1 should fulfil the following relationship:

$$\mu_L > \mu_A > \mu_B > \mu_T \quad [3]$$

At the initial stage of migration, a homogeneous mixed zone (A + B) is formed as shown in Figure 1(B), where A and B migrate with different velocities under the same potential gradient. In this case, v_A is greater than v_B in the mixed zone. A forms a pure zone in the leading side of the mixed zone, and

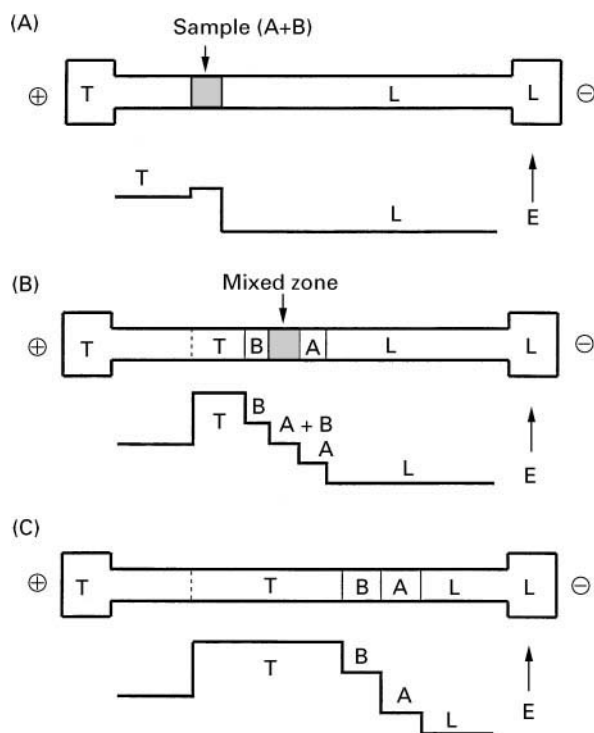


Figure 1 Separation process in isotachophoresis. (A) Before migration. (B) Separation process forming a mixed zone AB. (C) Complete separation (a steady state). L, leading zone; A, B, sample zone; T, terminating zone; E, potential gradient.

B forms a pure zone at the terminating side of the mixed zone. After a while, the mixed zone diminished and the sample components A and B are separated to form independent zones (Figure 1C). It should be noted that the migrating zones differ from those in zone electrophoretic migration. Once they are separated, they never mix again and the zone lengths are kept constant according to the sample amount as long as the migration current is applied. This is the isotachophoretic steady state.

When the migration order is as shown in Figure 1(C), the following relations are valid:

$$\begin{aligned}\mu_{A,A} &> \mu_{A,B} \\ \mu_{B,A} &> \mu_{B,B}\end{aligned}\quad [4]$$

where $\mu_{A,A}$ and $\mu_{B,B}$ denote the effective mobility of A and B ions in the steady state zone and $\mu_{A,B}$ and $\mu_{B,A}$ denote the effective mobility of A ions in the B zone and that of B ions in the A zone. This relation keeps the boundary between A and B zones very sharp (self-sharpening effect).

At the isotachophoretic steady state where the zone lengths of all samples are constant and no mixed zone

remains, the following relations are valid for a constant current:

$$v_L = v_A = v_B = v_T \quad [5]$$

$$E_L\mu_L = E_A\mu_A = E_B\mu_B = E_T\mu_T \quad [6]$$

From eqns [3] and [6] the following relationships between the potential gradient of zones (Figure 1) apply:

$$E_L < E_A < E_B < E_T \quad [7]$$

Therefore the separated zones can be detected by the use of a potential gradient detector and a conductivity detector besides spectroscopic detectors.

It should be noted that the pH of the ITP system is different in the different zones. The pH buffering counterions are continuously supplied from the leading electrolyte, and they regulate the pH of the sample zones. Usually the following relationship is valid for an anion analysis:

$$\text{pH}_L < \text{pH}_A < \text{pH}_B < \text{pH}_T \quad [8]$$

The reversed relationship holds in a cationic analysis. The difference $|\text{pH}_L - \text{pH}_T|$ is usually less than 1 when the pH buffering counterion is selected properly. Since the pH of the zones are thus not constant in contrast to zone electrophoresis, the effective mobility dependence of the samples on the pH of the leading electrolyte cannot be estimated straightforwardly. And this makes the separation optimization of isotachophoresis difficult in comparison with zone electrophoresis.

The pH buffers conventionally used are summarized in Table 1 for anion analysis. To keep good buffering capacity of the leading electrolyte, the pH_L

Table 1 pH buffers used for anionic analyses

Buffer	pK_a	pH_L range
Glycylglycine	3.140	2.6–3.6
β -Alanine	3.552	3.0–4.0
ϵ -Aminocaproic acid	4.373	3.8–4.8
Creatinine	4.828	4.2–5.4
Histidine	6.040	5.4–6.4
Imidazole	7.150	6.4–7.4
TRIS ^a	8.076	7.4–8.4
Ammediol ^b	8.780	8.2–9.2
Ethanolamine	9.498	9.0–10.0

^aTRIS, tris(hydroxymethyl)aminomethane.

^bAmmediol, 2-amino-2-methyl-1,3-propanediol. These buffers are used to adjust the pH of an electrolyte containing a leading ion such as hydrochloric acid.

should satisfy the following relationship:

$$pK_Q - 0.5 < pH_L < pK_Q + 0.5 \quad [9]$$

where pK_Q is the pK_a of the buffers used. The maximum buffering capacity is obtained at $pH_L = pK_Q$.

The isotachophoretic steady state is achieved when the following four conditions are fulfilled:

- The leading and the terminating electrolyte are chosen properly to satisfy eqn [3].
- A constant migration current is applied.
- Mass balance of the counterion is kept: the molar amount of the pH buffer flowing into the sample zone in a unit time should be equal to the amount flowing out the sample zone.
- Electroneutrality is kept in each zone as in normal electrolyte solutions.

ITP is bidirectional in principle, since electrophoretic phenomena are bidirectional. In fact, isotachophoretic stacking zones can be formed simultaneously for anionic and cationic components in a sample when a suitable electrolyte system is chosen. In bidirectional ITP, the anolyte and the catholyte are the leading electrolyte and the terminating electrolyte for anions, and vice versa for cations.

Although the selection of the operational electrolyte system for bidirectional isotachophoresis is not too difficult, the difference between the pH of an anolyte and that of a catholyte is restricted.

Qualitative Analysis

The effective mobility of a sample component is uniquely determined under a given set of experimental conditions and this allows qualitative analysis. In practice, some qualitative indices have been proposed using some different definitions on the basis of the ratio of the potential gradients or the conductivities of the separated zones. We have proposed R_E , which is defined for the component A as follows:

$$R_{E,A} = E_A/E_L = \mu_L/\mu_A \quad [10]$$

Figure 2 shows the experimental definition of R_E values using step heights, where the asymmetric potential of the potential gradient detector (δh) is corrected by the use of an internal standard. By comparing such qualitative values of samples with those of reference standards, tentative qualitative analysis can be done. Additional information by a UV/VIS online detector may be useful. For exact identification, ITP zones are fractionated and the fractions analysed by independent analytical methods.

Quantitative Analysis

In ITP, the concentration of ions in the steady-state zone is determined by their effective mobilities and by the concentration of the leading ion. Therefore, dilute components in a sample are concentrated according

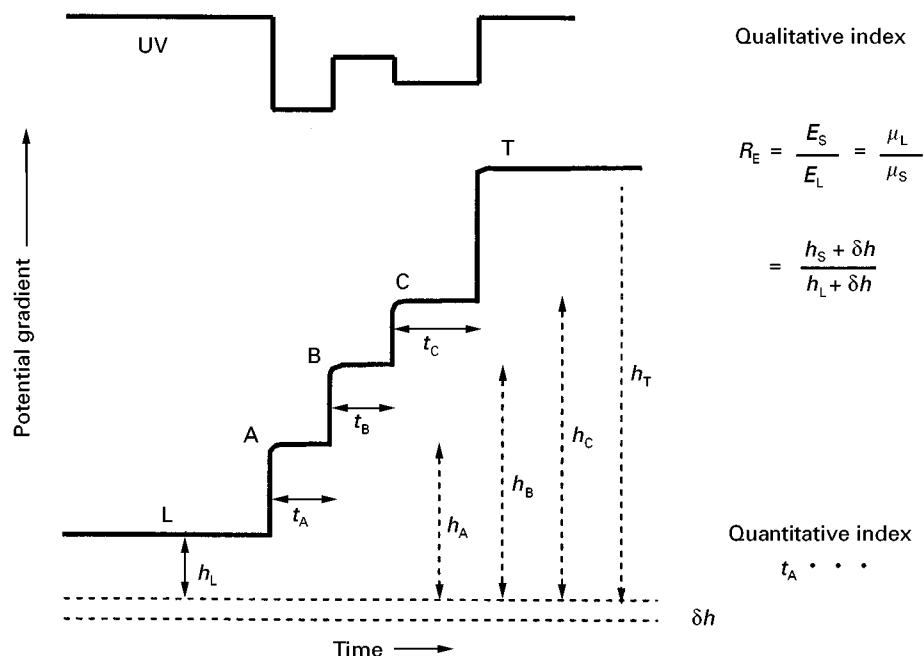


Figure 2 Isotachopherograms and experimental definition of R_E values. L, leading zone; A, B, C, sample zone(s); T, terminating zone; h , step height; δh , step height corresponding to an asymmetric potential of a potential gradient detector, which can be determined using theoretical R_E value of internal standard; R_E , corrected R_E value of sample. The subscript S denotes component A, B or C.

to Kohlrausch's regulating function and conversely the concentrated components are diluted during migration. The following relation is valid among the total equivalent concentrations of the samples (C^t):

$$C_L^t > C_A^t > C_B^t > C_T^t \quad [11]$$

The quantitative index is the time-based zone length as shown in Figure 2. The absolute zone length of the sample A (l_A in cm) can be defined as:

$$l_A = 1000n/(C_A^t \pi r^2) \quad [12]$$

where n is the amount of applied sample (moles) and r the radius (cm) of the separation tube at a detector.

The zone passing time, t (s) is equal to the actual zone length divided by the ITP velocity, v (cm s^{-1}). When both the sample ion and the buffer ion are monovalent, t_A can be expressed as follows:

$$t_A = Fn(1 + \mu_Q/\mu_A)/i \quad [13]$$

where F is the Faraday constant, μ_Q the mobility of the buffer ion, μ_A that of sample A, and i the migration current.

Instrumentation

Separation System for ITP Analyser

A typical diagram of ITP analyser is shown in Figure 3 for unidirectional ITP. A separation tube connecting two electrodes is made of polytetrafluoroethylene (PTFE) or fused silica, whose inner diameter is 0.2–0.5 mm. A PTFE tube as large as 1 mm inner diameter is frequently used before detection as a pre-column to increase column hold up or electric charge for better resolution. An additional leading electrode chamber can be used to apply high current during pre-separation to reduce analysis time. The chamber is connected appropriately to the separation tube before the detector. The leading and the terminating electrode chamber are typically 20 mL in volume.

The separation tube is also filled with a leading electrolyte and a terminating electrolyte. The boundary is formed at a sample injection port and a sample solution is introduced there typically by using a microsyringe. Sample components are separated during migration and their zones are detected using appropriate detectors.

Detectors

The quality of the detector employed determines and limits the qualitative and quantitative analysis of ITP.

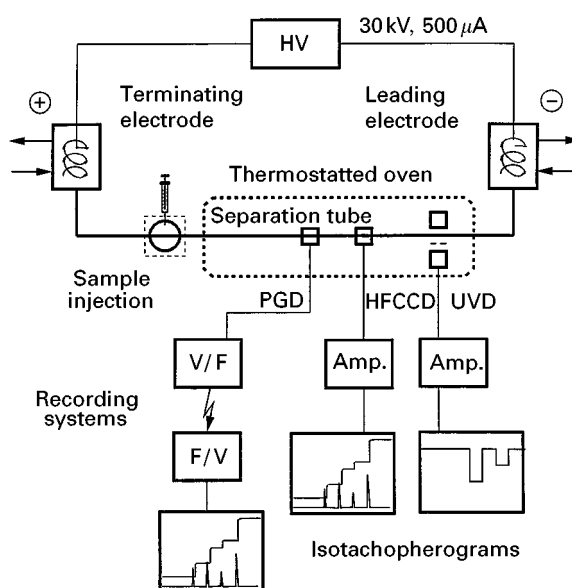


Figure 3 ITP apparatus with potential gradient detection (PGD), high-frequency contactless conductivity detection (HFCCD), and ultraviolet detection (UVD). HV, high-voltage power supply (constant current); V/F, voltage-frequency converter; F/V, frequency-voltage converter.

There are two demands on the detector; firstly to accurately reflect the separation occurring in ITP and secondly to obtain the isotachopherogram from the analysis with high reproducibility.

Detectors for ITP can be divided into universal and specific types. The signal from universal detectors is directly proportional to the effective mobilities of the ionic species, and these detectors detect zones of all components separated in the narrow-bore tube. Thermometric, potential gradient and conductivity detectors belong to this class. The detection limit of potential gradient and conductivity detectors is sub-nanomole but that of thermometric detector is rather high. On the other hand, specific detectors such as UV spectrophotometers allow the identification of some components directly, or at least can give additional information about zones.

In Figure 3, three detection systems using a high-frequency contactless conductivity detector (HFCCD), a potential gradient detector (PGD), and an ultraviolet detector (UVD) are shown. Since the sensing electrodes of PGD directly contact the solution in the capillary, this system needs a device to isolate high voltage. In Figure 3, a photocoupler is used for this purpose (IP-1B, IP-2A, IP-3A, Shimadzu, Kyoto, Japan, production discontinued). A transformer is used in the usual (contact type) conductivity detection (a.c. method). Although the sensitivity of a contactless detector is lower than the direct contact

detector, the merit of HFCCD is obviously that the detection system needs no such isolation device.

Preparative ITP Apparatus

Capillary type ITP is useful not only for analytical purposes but also for preparative purposes. Capillary type (CITP) is useful for batch processing of a small amount of sample.

In addition to direct cutting of the capillary section containing the target of interest, preparative methods in CITP can be classified into three types, as shown in Figure 4. Figure 4(A) shows a preparative ITP system reported by Arlinger for the fractionation of the entire sample zones. This system was used in the LKB Tachofrac (Bromma, Sweden, 1983, production discontinued). The zones were swept gradually by a counterflow of a leading electrolyte (ex. $3 \mu\text{L min}^{-1}$) on applying migration current, and the fractions were fixed on a cellulose acetate strip. The separated zones were successively pushed out through a T-branch by applying a counterflow and the zones were continuously fixed on the strip by an electric spray. The linear

velocity of the counterflow was set only a few percent higher than the isotachophoretic migration velocity so as not to dilute the sample by the leading electrolyte. The fractions on the strip can be analysed by immunological and radioactive methods. The zymogram technique can be used directly on the strip. The fractions have to be eluted, for analysis by other methods.

A dropwise fractionating method was developed utilizing a counterflow technique. The schematic diagram of the apparatus is shown in Figure 4(B). When the sample zone is pushed out from a T-branch, a spray effect is usually observed due to electrostatic forces. This can be a convenient interfacing technique but it disturbs dropwise fractionation. The electric spray and fluctuation of the drop rate due to electrostatic forces are suppressed by a very simple electrostatic device: As shown in Figure 4(B), the exiting fraction is surrounded by a copper coil, which is connected to a nozzle. The fractions are collected directly into small test tubes on the fraction collector through the coil. By using this technique, complete recovery of the mobile components in the injected samples is possible with minimum risk of loss and contamination. It should be noted, however, that mixing of adjacent sample zones cannot be avoided. The average volume of one drop was ca. $5 \mu\text{L}$ and the deviation was estimated as $+10\%$. A few nanomoles of the sample components are contained in a drop. The concentration of samples in the fractionated drops or the amount of the target in a fraction was adjustable by changing the flow rate of the leading solution. A typical counterflow of a leading electrolyte was ca. $12 \mu\text{L min}^{-1}$, which is much higher than the Arlinger-type apparatus.

Figure 4(C) shows another method reported by Kobayashi *et al.*, where the separated sample zones are discontinuously isolated by using a microsyringe. Kobayashi *et al.* used a potential gradient detector (PGD) with a sample-removal port to fractionate the target zone immediately after the tail of the zone was detected by the PGD. Although the method was not intended for the successive fractionation of the entire sample zones, the ease of operation is notable. This technique was employed for IP-1B and IP-2A instruments (Shimadzu, Kyoto, Japan, production discontinued).

Figure 4(D) shows other discontinuous fractionation technique using a specially designed fractionating valve placed at the end of the separation capillary. After trapping the target zone in the valve, the zone is flushed out.

In addition, the separation tube used was a series of four separation tubes (inner diameter of the tubes, 5–0.5 mm) in order to increase the amount of

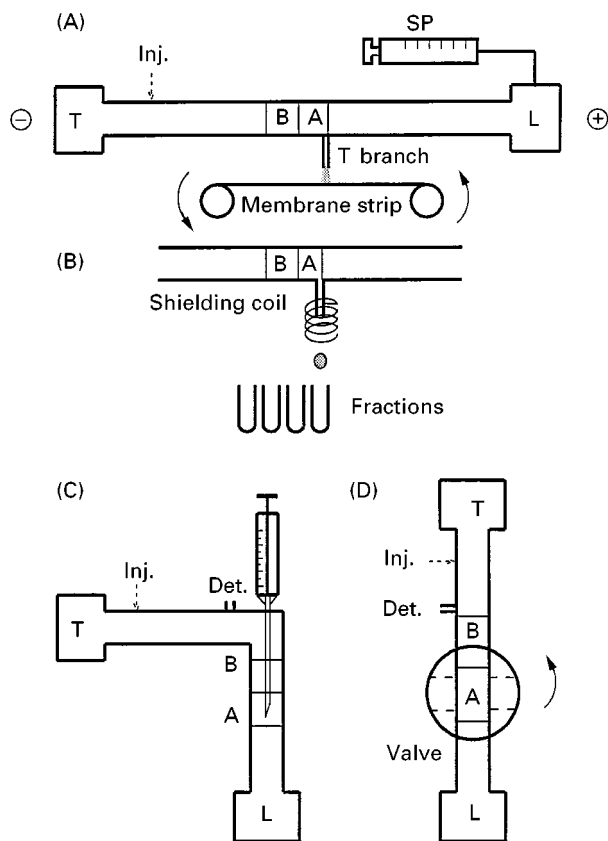


Figure 4 Preparative methods in capillary-type isotachopheresis. (A) Arlinger's counterflow method. (B) Modified Arlinger's method. (C) Microsyringe method. (D) Fractionation valve method. A and B, samples; L, leading electrolyte; T, terminating electrolyte; Inj., sample injection port; SP, a counterflow pump; Det., a detector.

sample separated. The tube of 5 mm inner diameter was made of acrylic resin and the maximum injectable sample volume was 2.5 mL.

Free-flow apparatus Since no solid media are used in free-flow electrophoresis (FFE), the most important point in instrumentation is the stabilization of the separated zones for any electrophoresis mode. Unstable zones may be caused by unstable operational electrolyte, sample flow, heat convection, density-driven flow, electroosmosis, etc. Bier *et al.* and Thormann *et al.* summarized several different methods for stabilizing the zones. A flat-type FFE is treated here, although there are several different approaches using different geometries, such as a thin film between parallel plates, a cylindrical laminar flow between two coaxial cylinders, etc.

Continuous FFE apparatus utilizing a thin flowing fluid was originally designed by Hanig for zone electrophoresis. Prusik and Wagner *et al.* designed and constructed similar apparatus, suggesting that several modes of electrophoresis can be used. At present, the only FFE apparatus available is the Octopus continuous electrophoresis apparatus from Dr. Weber GmbH (Kirchheim-Heimstetten, Germany). By using this apparatus, up to several grams of pure substances can be prepared daily, although the amount depends on the properties of the sample. Figure 5 illustrates the electrolyte circuits of an FFE system (Octopus)

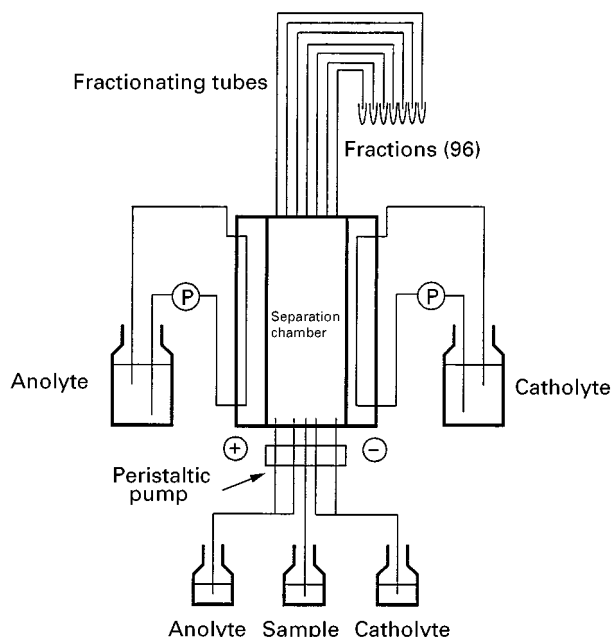


Figure 5 Electrolyte circuits of a free-flow electrophoresis apparatus (Octopus, Dr. Weber GmbH). Outer dimensions of separation chamber are $640 \times 180 \times 80$ mm, Separation area is 500×100 mm (variable thickness 0.4–2.0 mm). P, pumps.

when operated in continuous free-flow isotachophoresis (CFFITP) mode. The effective size of a typical separation chamber is 10-cm wide, 50-cm high and 0.4-mm thick. The sample solution is supplied with a multifold peristaltic pump together with an anolyte and a catholyte. Overflow of the separation chamber is collected as 96 fractions. The flow rate is variable in the range $0.3\text{--}100\text{ mL h}^{-1}$. The sample residence time is variable in the range 1–40 min. High flow rate and small residence time allow stable flow and consequently stable position of zones.

The anolyte and catholyte are circulated by pumps during migration. A dialysis membrane isolates the separation chamber from the electrode compartments. The electrolyte solutions may be denatured (the pH will change) after a few hours operation. The separation chamber can be thermostatted and separation can be monitored with a VIS CCD detection system which can be positioned near the end of the chamber. To obtain pure fractions, the positions of the sample zones at the end of the sample chamber should be stable. The positions are dependent on several factors such as the electric field strength, temperature of the electrolytes, flow rate, and sample and buffer composition. Since these factors are closely correlated with each other, careful control is needed. Sufficient residence time and separation distance are necessary especially when mobility differences are small. For this purpose, a larger separation chamber or a counterflow technique should be used as reported by Prusik (a 50×50 cm square chamber with a thickness of 0.5 mm).

Separation Strategy and Typical Applications

Operational electrolyte conditions should be optimized to obtain the best quality of separation by changing electrolyte parameters so that the difference of the effective mobilities of the target components should be as large as possible. Strictly speaking, the separability depends on the mobility difference in the mixed zone (see Figure 1). However, to a first approximation, the mobility differences at the steady state or the difference of the R_E values may be used for the criterion for optimization of separations.

For separation optimization in electrophoresis, a theoretical approach is sometimes very useful. In isotachophoresis especially, the pH and the ionic strength of the separated zones are different to one other. The optimum electrolyte system can be determined by iterative computer calculations where the effective mobilities of the species being separated at the steady state are calculated using their

physicochemical constants, and the differences of the effective mobilities compared. This method may be called computer-aided separation optimization, which enables the determination of the electrolyte conditions such as the pH without time-consuming 'trial-and-error' experiments. Some examples of simulation are also included in this section.

pH Effect

When the sample contains weak electrolytes, the pH of the leading electrolyte (pH_L) should be carefully chosen to obtain high separability among the components, since the effective mobilities of weak electrolytes change drastically according to the pH of the solution. This pH effect on the effective mobility is the most important and should be examined first.

Figure 6 shows the simulated and the observed isotachopherograms for a test mixture of pyrophosphoric (P_2O_7), triphosphoric (P_3O_{10}), tetraphosphoric (P_4O_{12}) acids, and 15 nucleotides, AMP, ADP, ATP, CMP, CDP, CTP, GMP, GDP, GTP, IMP, IDP, ITP, UMP, UDP and UTP. The pH_L was adjusted to 4.7 with creatinine. The optimum pH_L range was rather limited, because CTP may form a mixed zone with

UDP at low pH_L and with ATP at the high pH_L . Obviously from this example, the pH of the leading electrolyte should be carefully chosen in order to obtain high separability for weak electrolytes. For this purpose, computer simulation of the isotachophoretic steady state is useful, when the mobility and dissociation constants are available. In fact, the optimum pH_L of the above separation has been determined by simulation.

Solvent Effect

Since the mobility is strongly affected by the viscosity of the solvent and the dissociation constants depend on the dielectric constant of the solvent, the use of a nonaqueous solvent or a mixed solvent may improve electrophoretic separations (the solvent effect). The other advantage of the use of a nonaqueous systems is that it enables the analysis of substances with low water solubility. Many solvents have been successfully applied for isotachophoresis, such as methanol, ethanol, dioxane, acetone, propanols, dimethylformamide, etc. The migration behaviour in a nonaqueous solvent is very different from that in an aqueous solvent. The use of a mixed solvent

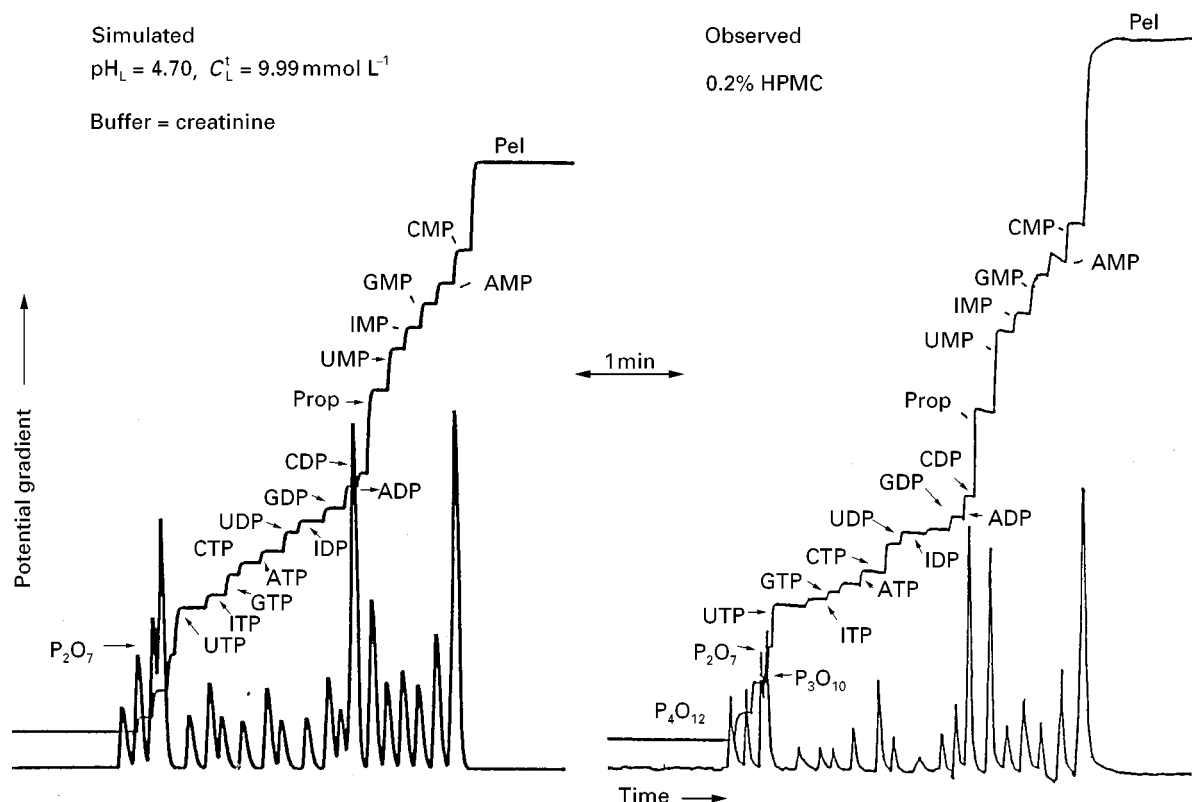


Figure 6 Simulated and observed isotachopherograms of 19 anions, AMP, ADP, ATP, CMP, CDP, CTP, GMP, GDP, GTP, IMP, IDP, ITP, UMP, UDP, UTP, pyrophosphoric acid (P_2O_7), triphosphoric acid (P_3O_{10}), tetraphosphoric acid (P_4O_{12}) and propionic acid (Prop) at $\text{pH}_L = 4.7$ (creatinine buffer). The terminator was pelargonic acid (Pel). Current, $75 \mu\text{A}$. Sample amounts, 1.2–3 nmol. The leading electrolyte contained 0.2% hydroxypropylmethylcellulose (HPMC). Buffer, creatinine. C_L^+ , concentration of leading ion.

(aqueous–nonaqueous) provides further possibilities for mobility control to improve separations.

Figure 7(A) and (B) show the simulated and observed isotachopherograms at pH 8 using triethanolamine buffer when methanol is used as solvent. The leading ion is perchlorate. Obviously, the separation is complete. On the other hand, insufficient separation was predicted for the aqueous system where the leading ion was chloride when $\text{pH}_L = 3.6$ (β -alanine buffer), as shown in Figure 7(C). Apparently the step heights of 2-naphthalenesulfonate, picrate and *o*-chlorobenzoate were similar and they may form a mixed zone in the actual analysis. No satisfactory separation was estimated when pH effects in the aqueous system were used.

Thus it is evident that the separation behaviour in isotachophoresis is strongly affected by the solvent used. As demonstrated above, high separability can be expected by the use of methanol solvent for particular samples but it should be noted that carboxylic acids are esterified gradually on standing in methanol solution, although the production of esterified compounds during analysis is negligible.

Complex-forming Effect

The use of a complex-forming agent is a traditional technique to improve separability especially in the case of metal ions. To achieve complex-forming equilibria, a constant amount of the complex-forming agent should be supplied continuously to the sample

zone. The complexing agent can be supplied as the counterion in the leading electrolyte, as neutral ligand (crown ether and cyclodextrin), or as the terminating ions.

Complex formation is very useful for the separation of metal ions. A typical example of the isotachophoretic separation of metal ions utilizing the complex-forming effect was reported for lanthanides, where α -hydroxyisobutyric acid (HIBA) was used as the complexing agent. The concentration of the complexing agent and the pH of the leading electrolyte should be optimized to obtain a good separation. By adding malonic acid to the main agent HIBA, 15 rare-earth ions (lanthanide and yttrium) were successfully separated as shown in Figure 8.

Conclusion

Isotachophoresis is a useful analytical technique with high reproducibility. However, ITP is not a very familiar technique to many chromatographers. Possible reasons are absolute sensitivity of ITP is in the sub-nanomole range, which is low in comparison with recent capillary electrophoresis (CE) techniques; auto-samples are not available; and stepwise recording is not readily accepted by chromatographers. However, it should be noted that the relative sensitivity of ITP is comparable with CE especially when the detection method is the same (e.g. UV detection), since a relatively large volume of a sample (e.g.

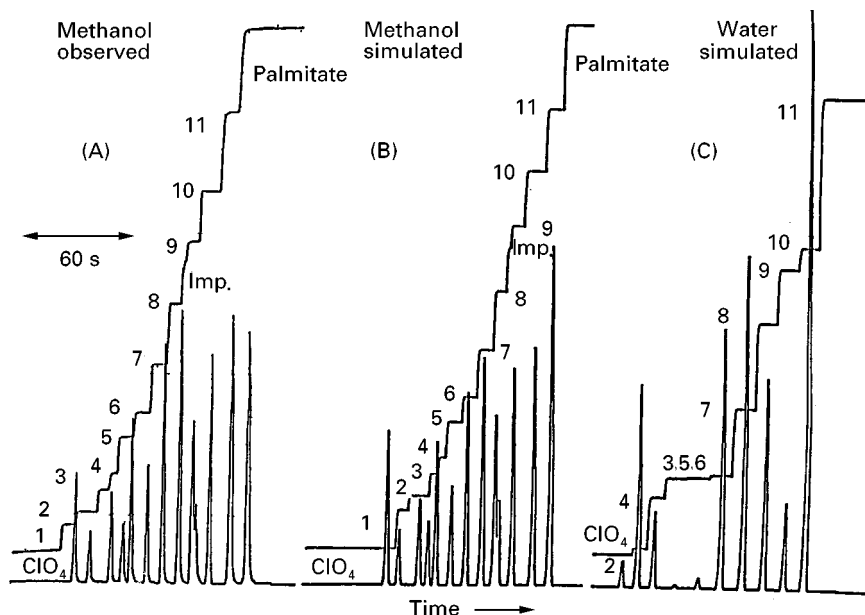


Figure 7 The observed (A) and the simulated isotachopherogram (B) of (1) bromide, (2) chloride, (3) picrate, (4) formate, (5) 2-naphthalenesulfonate, (6) *o*-chlorobenzoate, (7) *p*-chlorobenzoate, (8) 3-hydroxybutyrate, (9) crotonate, (10) propionate and (11) pelargonate ions in methanol as solvent. The leading ion was $10 \text{ mmol L}^{-1} \text{ ClO}_4^-$ and the buffer used was triethanolamine ($\text{pH}_L = 8.06$). (C) The simulated isotachopherogram of the above samples except for bromide. The leading ion was 10 mmol L^{-1} chloride and the buffer used was β -alanine ($\text{pH}_L = 3.6$). The terminator was pelargonate. Imp., impurity of the used electrolyte system.

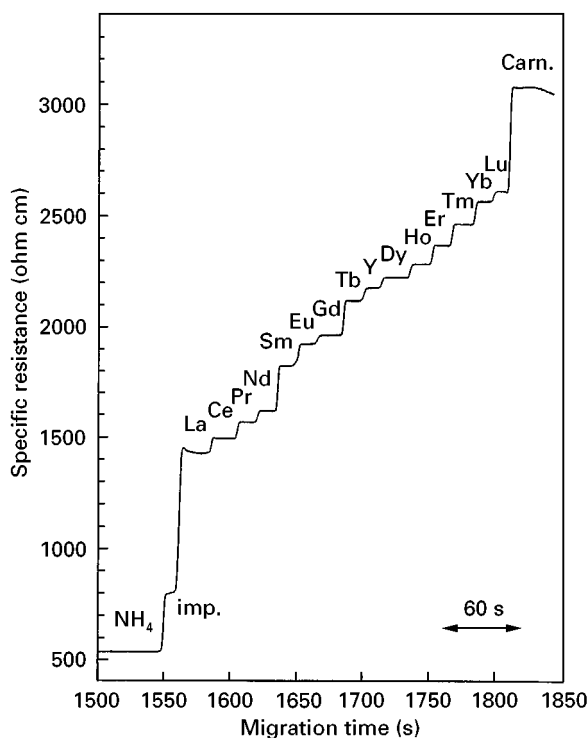


Figure 8 The observed isotachopherogram of 15 rare-earth ions (lanthanide ions and yttrium ion). HIBA, the complex-forming agent α -hydroxybutyric acid. The leading ion, 20 mmol L⁻¹ NH₄⁺; pH buffer = 2-ethyl-*n*-butyric acid (pH_L = 4.8). The sample amount was 0.33 mmol L⁻¹ × 5 μ L. Migration current = 40 μ A. The terminator is carnitine hydrochloride. (Carn.) imp., impurity of the used electrolyte system.

100 μ L) can be injected. For preparative purpose, ITP is sometimes better than CE especially when the sample size is relatively large. In order to utilize the favourable features of ITP, an automated apparatus is needed or a method should be found to use commercial CE apparatus for ITP.

Further Reading

- Babetskii VG, Zhukov MYu and Yudovich VI (1989) *Mathematical Theory of Electrophoresis*. New York: Plenum.
- Bocek P, Deml M, Gebauer P *et al.* (1988) In: Radola BJ (ed.) *Analytical Isotachophoresis*. Basel: VCH.
- Everaerts FM, Beckers JL, Verheggen ThPEM (1976) *Isotachophoresis. Theory, Instrumentation and Application*. Amsterdam: Elsevier.
- Gebauer P, Caslavská J and Thormann W (1991) *Journal of Biochemical and Biophysical Methods* 23: 97.
- Hirokawa T, Nishino M, Aoki N *et al.* (1983) Table of isotachophoretic indices. I. Simulated qualitative and quantitative indices of 287 anionic substances in the range pH 3–10. *Journal of Chromatography* 271: D1–D106.
- Li SFY (1992) *Capillary Electrophoresis, Principles, Practice and Applications*. Amsterdam: Elsevier.
- Moscher RA, Saville AD and Thormann W (1992) *The Dynamics of Electrophoresis*. Weinheim: VCH.
- Pospichal J, Gebauer P and Bocek P (1989) Measurement of mobilities and dissociation constants by capillary isotachophoresis. *Chemical Reviews* 89: 419–430.

Isotachophoresis in Capillary Electrophoresis

See II/ELECTROPHORESIS/Capillary Isotachophoresis

Mass Spectrometry Detection in Capillary Electrophoresis

See II/ELECTROPHORESIS/Capillary Electrophoresis-Mass Spectrometry

Micellar Electrokinetic Chromatography

M.-L. Riekkola, Laboratory of Analytical Chemistry, University of Helsinki, Finland

Introduction

Micellar electrokinetic capillary chromatography (MEKC), first introduced by Shigeru Terabe and co-workers in 1984, has extended the potential of

capillary electromigration techniques to the separation of uncharged analytes. With its impressive separation efficiency and flexibility, MEKC has become a popular technique especially in the pharmaceutical and biomedical fields.

Above their critical micelle concentration (CMC), surfactant monomers added to an electrolyte solution form aggregates called micelles. Individual micelles are not significantly larger than the solutes being separated. On account of their small size and large number, they have a high surface area-to-volume ratio. Their structures are dynamic, with the average residence time of a surfactant monomer in the micelle being in the order of 1 ms or less. Separation in MEKC is based on the partitioning of analytes between the micelles and the aqueous phase, in the presence of electroosmotic flow. The micelles act as a pseudo-stationary phase. The mechanism of the analyte-micelle interaction is mainly determined by hydrophobic and electrostatic interactions. MEKC was originally developed to exploit the advantages of capillary electrophoretic techniques (high efficiencies, the requirement of only minute amounts of sample and reagent, fast analysis time) in the separation of neutral solutes of closely similar structure, but it is also applicable to the separation of charged

compounds. A basic capillary electrophoresis (CE) instrument is used, and the separations are carried out usually in uncoated fused silica capillaries after hydrodynamic injection.

Separation in MEKC

When one or more micelle-forming surfactants are added to the electrolyte solution at concentrations above their CMC, partition of the analytes into the micellar pseudo-stationary phase increases the selectivity of the separation system. The overall separation of compounds is based on their differential solubilization into the micelles and on the migration velocities of the micelles under the electric field, in the presence of electroosmotic flow (EOF). The separation principle for an anionic surfactant is illustrated in Figure 1.

The separation of neutral analytes is based on their partitioning between the aqueous phase and the micellar stationary phase. When solutes interact strongly with the micelles their migration time is comparable to that of the micelles, t_{mc} , allowing the solutes to serve as micelle markers. Neutral analytes migrate with times t_1 and t_2 , which lie inside a window formed by the migration times of the neutral

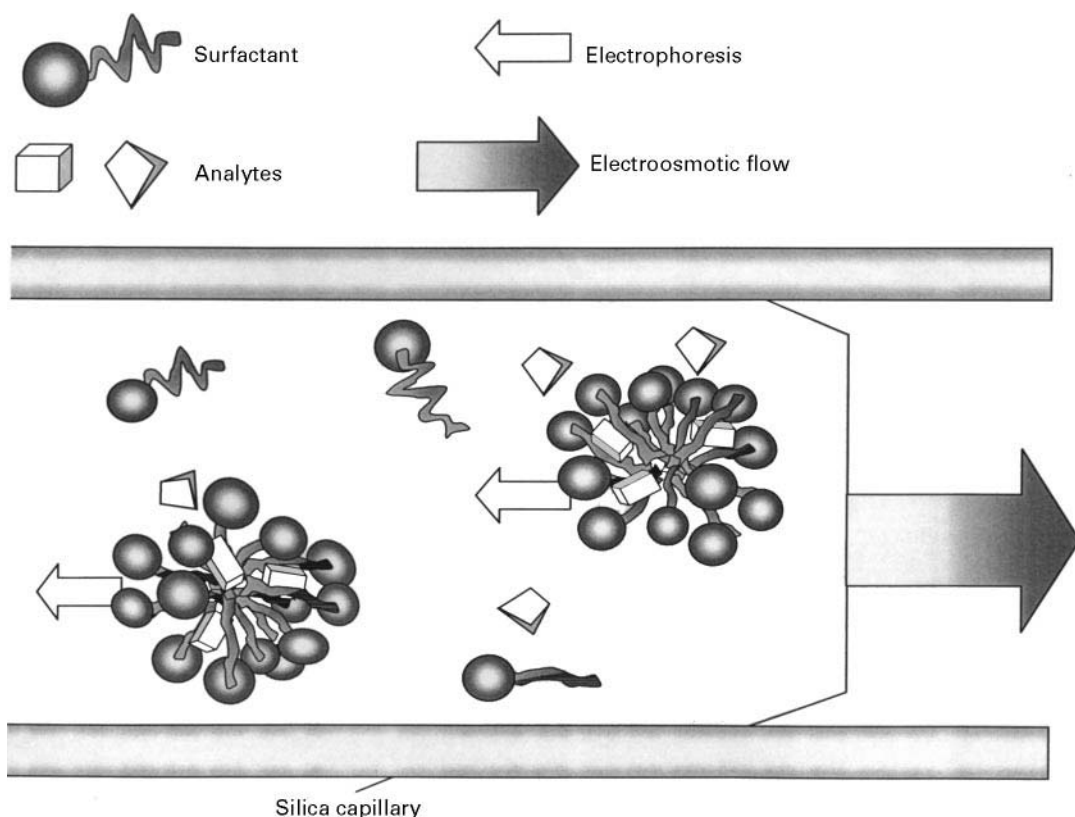


Figure 1 Schematic depiction of separation in micellar electrokinetic capillary chromatography.

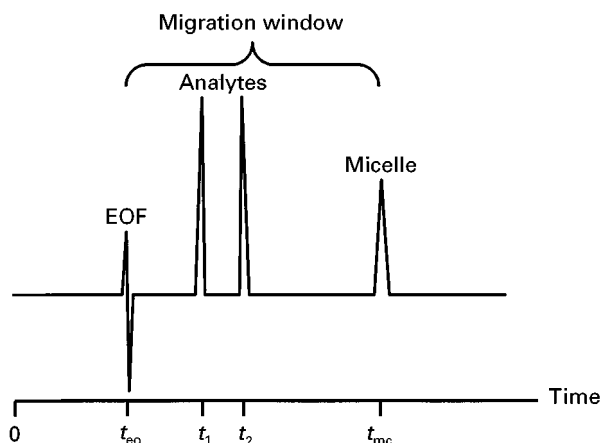


Figure 2 Migration window for neutral solutes in micellar electrokinetic capillary chromatography. EOF, electroosmotic flow.

electroosmotic flow marker, t_{eo} , and the micelle marker, t_{mc} (Figure 2). A relatively polar molecule (e.g., acetone, acetonitrile, formamide, methanol, 1-propanol or tetrahydrofuran) can be used as electroosmotic flow marker, and usually a highly hydrophobic, neutral compound such as Sudan III, Sudan IV, dodecanophenone, Orange OT, or Yellow OB as micelle marker. The migration window is finite because the micelles themselves migrate out of the capillary. Even though the peak capacity is restricted by the migration window, high separation efficiencies can be achieved. A wide migration time window is favourable for high resolution, but then a long analysis time may be required.

The micellar phase is not a true stationary phase because it is moving along the capillary towards the detector. When the analyte is permanently retained, its migration time (t_m) is identical with the migration time of the micelle (t_{mc}). Therefore, the term 'retention factor' used in chromatography should be replaced by the term 'partition factor' in MEKC. The partition factor k_{mekc} is described as:

$$k_{mekc} = \frac{n_{mc}}{n_{aq}}$$

where n_{mc} and n_{aq} are the numbers of the analytes in micellar and aqueous phases, respectively. In the case of a neutral analyte, k_{mekc} can also be calculated directly from the migration times:

$$k_{mekc} = \frac{t_m - t_{eo}}{t_{eo}(1 - t_m/t_{mc})}$$

However, there may be variations in k_{mekc} depending on EOF and the micelle marker; in particular, the

choice of the micelle marker may have a significant effect on the value.

The selectivity α can then easily be determined by the ratio of the partition factors of two compounds:

$$\alpha = \frac{k_{mekc2}}{k_{mekc1}}$$

The most effective way to alter the selectivity of nonpolar analytes in MEKC is to change the micellar phase by changing the type of surfactant. When compounds are neutral, factors such as concentration of electrolyte and micellar solutions, pH, voltage and temperature have a relatively minor effect on the selectivity of the system. When the compounds are charged, on the other hand, variations in pH may induce changes in the dissociation of the compounds, affecting their charge, and thereby the solute-micelle ionic interactions and electrophoretic mobilities.

The resolution in MEKC is determined by the equation given by Terabe *et al.*:

$$R_s = \frac{\sqrt{N}}{4} \left(\frac{\alpha - 1}{\alpha} \right) \left(\frac{k_{mekc2}}{1 + k_{mekc2}} \right) \left(\frac{1 - t_{eo}/t_{mc}}{1 + (t_{eo}/t_{mc})k_{mekc1}} \right)$$

where N is the plate number. The resolution of the system depends on the efficiency, the selectivity, the partition factor and the migration time window.

Surfactants

Unique selectivities are achieved in MEKC through appropriate choice of anionic, cationic, nonionic and zwitterionic surfactants (Table 1). Surfactants are molecules with distinct hydrophobic and hydrophilic parts. The CMC increases dramatically with the alkyl chain length of the surfactant. At Kraft temperature, T_{Kr} , the solubility of the surfactant increases rapidly. T_{Kr} is the point at which surfactant solubility equals the CMC. The Kraft point varies with the surfactant, increasing with the length of the alkyl chain. Surfactant concentrations above the CMC and temperature above the Kraft point are required for the formation of micelles. Changes in temperature, concentration of surfactant, pH, ionic strength, additives in the aqueous phase and structural groups in the surfactant may cause changes in the size, shape and aggregation number of the micelles. In aqueous media, surfactants with bulky or loosely packed hydrophilic groups and long, thin hydrophobic groups tend to form spherical micelles, while those with short, bulky hydrophobic groups and small, close-packed hydrophilic groups tend to form lamellar cylindrical micelles. Factors that decrease the electrostatic repulsion between the head groups of ionic surfactants favour micelle

Table 1 Typical surfactants used in MEKC, with their critical micelle concentration (CMC)

Surfactant	CMC (mM)	Temperature (°C)
<i>Anionic</i>		
Sodium dodecyl sulfate (SDS)	8.2	25
Sodium tetradecyl sulfate (STS)	2.1	25
Sodium decyl sulfate	33	40
Sodium dodecyl sulfonate	11.4	40
Sodium <i>N</i> -lauroylmethyl- <i>N</i> -taurate	8.7	25
Lithium perfluorooctane sulfonate (LiPFOS)	6.3	25
<i>Cationic</i>		
Cetyltrimethylammonium bromide (CTAB)	0.92	25
Cetyltrimethylammonium chloride (CTAC)	1.3	30
Tetradecyltrimethylammonium bromide (TTAB)	3.6	25
Dodecyltrimethylammonium bromide (DTAB)	16	25
Dodecyltrimethylammonium chloride (DTAC)	20	25
Cationic fluorosurfactant (Fluorad FC 134)	na	
<i>Nonionic and zwitterionic</i>		
Octyl glucoside (OGLU)	25	25
Polyoxyethylene (23) dodecanol (Brij-35)	0.1	na
Polyoxyethylene (20) sorbitane monooleate (Tween 80)	0.01	na
Polyoxyethylene (20) sorbitane monolaurate (Tween 20)	0.059	na
3-[3-(Chloroamidopropyl) dimethylammonio]-1-propane-sulfonate (CHAPS)	4.2–6.3	na
<i>Chiral surfactants</i>		
Sodium <i>N</i> -dodecanoyl-L-valinate (SDVal)	2	na
Sodium <i>N</i> -dodecanoyl-L-glutamate (SDGlu)	na	
Digitonin (DIG)	na	
<i>Bile salt surfactants</i>		
Sodium cholate (SC)	12.5	25
Sodium deoxycholate (SDC)	10	25
Sodium taurocholate (STC)	4	25
Sodium taurodeoxycholate (STDC)	6	na
Sodium glycodeoxycholate	na	

na, not available.

formation leading to lower CMC in electrolyte solutions than in pure water.

Many physical properties change dramatically at the CMC. These changes can be exploited by determining the CMC of surfactants in CE electrolyte solutions, for example by measuring surface tension, light scattering, refractive index, electrical conductivity or electrophoretic mobility. The data are plotted against surfactant concentration, and a change in the slope corresponds to the CMC. However, the CMC obtained may differ according to the method used because micellization is a gradual aggregate growth which occurs over a finite concentration range. CMC values for the most commonly used surfactant, sodium dodecyl sulfate, in selected electrolyte solutions are listed in Table 2.

Anionic Surfactants

Anionic surfactant systems are preferred in MEKC because the electrophoretic migration of the micelles is in the opposite direction to the electroosmotic flow,

and the micelles do not interact with the negatively charged walls of the fused silica capillaries. Anionic surfactants with alkyl chain and polar group, such as sodium decyl sulfate, sodium *N*-lauroyl-*N*-methyltaurate, sodium tetradecyl sulfate, and especially sodium dodecyl sulfate (SDS) are the most widely used. Simultaneous separation of neutral and positively charged compounds is not possible at low pH because the EOF is too slow to carry the micelles to the cathode.

Most studies with anionic surfactants have been carried out under neutral or basic conditions. The most frequently used anionic surfactant, SDS, forms relatively spherical micelles with hydrophobic tail groups oriented towards the centre and charged head groups along the outer surface. The surfaces of SDS micelles possess a large net negative charge, giving them a large electrophoretic mobility toward the anode.

Another group of anionic surfactants, which has been widely used in separations of both neutral and ionic analytes, is bile salts. Bile salts have a hydroxyl-substituted steroidal backbone with hydrophilic and

Table 2 CMC values of SDS in selected electrolyte solutions at 25°C

<i>Electrolyte solution</i>	<i>CMC (mM)</i>	<i>Method of determination</i>
50 mM AMPSO ^a (pH 9.0)	3.6	Conductometric titration
50 mM AMPSO ^a (pH 9.0)	3.9	CE
50 mM AMPSO ^a (pH 8.7)	2.7	Surface tension
20 mM PIPES ^b , 20 mM NaOH (pH 7.0)	3.8	Conductometric titration
100 mM BES ^c , 100 mM NaOH (pH 7.0)	3.1	Conductometric titration
100 mM borate, 50 mM phosphate (pH 7.0)	2.9	Conductometric titration
5 M urea, 100 mM borate, 50 mM phosphate (pH 7.0)	4.4	Conductometric titration
20% DMSO (v/v), 25 mM sodium tetraborate, 50 mM sodium dihydrogen phosphate (pH 7.0)	6	Conductometric titration
20% acetone (v/v), 25 mM sodium tetraborate, 50 mM sodium dihydrogen phosphate (pH 7.0)	6.3	Conductometric titration
20 mM sodium tetraborate (pH 9.2)	3.1	CE
20 mM sodium tetraborate (pH 8.0)	5.5–9.6	CE
5 mM sodium tetraborate–acetonitrile (85 : 15, v/v)	7.3	CE
5 mM sodium tetraborate (pH 9.2)	5.3	CE
100 mM sodium tetraborate, 100 mM sodium dihydrogen phosphate (pH 6.0)	2	CE
100 mM sodium tetraborate, 100 mM sodium dihydrogen phosphate (pH 6.5)	2.4	CE
100 mM sodium tetraborate, 100 mM sodium dihydrogen phosphate (pH 7.0)	3.1	CE
100 mM sodium tetraborate, 100 mM sodium dihydrogen phosphate (pH 7.7)	4	CE
50 mM CHES ^d (pH 10.0)	2.9–5.2	CE
50 mM CHES ^d (pH 10.0)	2.7–5.4	CE
80 mM CHES ^d (pH 10.0)	1.6–2.2	CE
100 mM CHES ^d (pH 10.0)	1.2–2.4	CE
50 mM ammonium acetate (pH 9.0)	1.7–2.7	CE

^aAMPSO = 3-[(1,2-dimethyl-2-hydroxyethyl)amino]-2-hydroxypropanesulfonic acid; ^bPIPES = piperazine-*N,N*-bis(2-ethanesulfonic acid) monosodium salt; ^cBES = *N,N*-bis(2-hydroxyethyl)-2-aminoethanesulfonic; ^dCHES = 2-(*N*-cyclohexylamino)ethanesulfonic acid.

hydrophobic faces and they form helical micelles. Bile salts have a lower solubilizing effect on hydrophobic compounds than does SDS.

Cationic Surfactants

Unlike anionic surfactants, positively charged surfactants, monomers and micelles are strongly attracted to the negatively charged surface of the fused-silica capillary wall and thus have a significant effect on EOF. Cationic surfactants such as long-chain alkylammonium salts may even cause a reversal of EOF through electrostatic interactions with the capillary surface, and this may occur at surfactant concentrations below the CMC. The capability for reversed EOF has been successfully exploited in MEKC separations.

Neutral and Zwitterionic Surfactants

Although neutral surfactants with zero electrophoretic mobilities cannot be exploited in the MEKC separation of nonionic solutes, they can be applied to the separation of ionic solutes. Since problems with Joule heat do not arise when nonionic surfactants are used at high concentration, large voltages can be used even when surfactants are added to the buffer in high concentration. Like the neutral surfactants, the zwitterionic surfactants do not

contribute to the net conductivity of the electrolyte solution.

Mixed Micelles

Selectivity in MEKC can often be improved by using mixed surfactants. Clearly different selectivities from those obtained with the corresponding single micelles can be achieved. Some mixed micellar systems are presented in Table 3.

High Molecular Mass Surfactants

The high molecular mass surfactants used in MEKC are either oligomers of monomeric surfactants or block copolymers with surface-active properties. It has been proposed that the micelle is formed of a single molecule, and accordingly it has been termed a 'molecular micelle'. Because their CMC values are close to zero, molecular micelles are considered to be highly stable irrespective of the experimental conditions.

Surfactants and Cyclodextrins

Cyclodextrins (CD) are the most popular chiral selectors for chiral separations by MEKC. The separation mechanism is based on differential partitioning of solutes between the micellar and CD aqueous phase.

Table 3 Selected mixed micellar systems used in MEKC

Mixed micellar system	Surfactants in the mixture ^a
Anionic–nonionic surfactants	SDS and Brij-35 SDS and Tween 60 SDBS and Brij-35 SDS and Tween 20 Bile salts and polyoxyethylene-4-dodecyl ether
Anionic–anionic surfactants	SDS and sodium cholate SDS and sodium octyl sulfate SDS and bile salts Two different bile salts LiPFOS (fluorocarbon) and LiDS (hydrocarbon)
Anionic–cationic surfactants	Fluorosurfactants FC 128 and FC 134
Anionic–zwitterionic surfactants	SDS and SB-12
Nonionic–nonionic surfactants	Tween 20 and Tween 80 Triton X-100 and Brij-35
Cationic–cationic surfactants	TTAC and OTAC TTAB and DTAB

^aSDS = sodium dodecylsulfate; Brij-35 = polyoxyethylene (23) dodecanol; Tween 20 = polyoxyethylene (20) sorbitane monolaurate; Tween 60 = polyoxyethylene (20) sorbitane monostearate; SDBS = sodium dodecyl benzenesulfonate; LiPFOS : lithium perfluorooctane sulfonate; LiDS = lithium dodecyl sulfate; SB-12 = *N*-dodecyl-*N,N'*-dimethyl-3-ammonio-1-propanesulfonate; TTAC = tetradecyltrimethylammonium chloride; OTAC = octyltrimethylammonium chloride; DTAB = dodecyltrimethylammonium bromide.

Most of the surfactants used in separations have been anionic.

Optimization of Separation

Resolution in MEKC is a highly complex and non-linear function of experimental variables and is very difficult to optimize systematically. In a search for the optimal conditions for separation, several mathematical models have accordingly been developed. Often just a few test runs are needed to predict the best overall running conditions, though this naturally depends on the number of parameters included in the optimization strategy. When more than one surfactant is added to the electrolyte solution, the situation is complicated by the possible micelle–micelle interactions. Examples of the statistical optimization schemes used in MEKC are listed in **Table 4**.

Detection

Of the various detection systems employed in MEKC separations, optical systems are the most extensively used, and ultraviolet detectors (UV) used in conjunction with commercial CE instruments are a typical solution.

The sensitivity of mass spectrometry (MS), and the possibility of obtaining molecular information on compounds, make the on-line coupling of MEKC with MS highly attractive. Electrospray ionization (ESI) has been one of the most popular ionization techniques in coupled CE–MS. Although MEKC is a convenient separation technique for neutral analytes, problems are encountered in the on-line MEKC–ESI–MS interface connection because the micelles in the electrolyte solution are nonvolatile and tend to contaminate the MS. A number of approaches have been developed to overcome the problems of separating neutral compounds, while at the same time preventing micelles from entering the mass spectrometer. These include use of the heart-cut technique, high molecular mass surfactants, a semipermeable membrane interface, anodically migrating micelles, and the partial filling technique. An electrospray–chemical ionization interface is a possibility for certain types of online MEKC–MS applications.

Applications

MEKC has been applied to a wide variety of compounds, including phenols and chlorinated phenols, amino acids, several pharmaceuticals and their metabolites, porphyrins, peptides, nucleic acids, nucleosides and oligonucleotides. The capability for direct injection of biological fluids (plasma, serum, urine) is a special feature of electrokinetic capillary analysis. Effective solubilization of the biological matrix components by surfactants, and increased selectivities due to hydrophobic interactions with the micellar pseudo-stationary phase are evidently advantageous in bioanalysis. The use of MEKC for therapeutic and diagnostic drug monitoring has also proven to be of considerable value.

Future Directions

The great advantage of MEKC is the feasibility to manipulate the selectivity simply by changing the composition of the micellar phase. Even though several surfactants have shown their potential to act as micellar pseudo-stationary phase, the versatility of the technique and the range of applications can be further extended by developing new synthetic micelle-forming surfactants like polyelectrolytes or exploiting mixed micelles or biomembranes as pseudo-stationary phases. Understanding the mechanisms involved will greatly facilitate the systematic optimization of the large number of experimental parameters leading to better, faster, easier, and more reliable separations. In addition, studies are still needed to clarify new possibilities to couple MEKC with mass spectrometry.

Table 4 Statistical optimization schemes used in MEKC

Optimized parameter	Parameters varied	Modelling
Selectivity and resolution	pH, [SDS], [borate]	CCD ^c , desirability functions
Selectivity and resolution	pH, [SDS], [sodium cholate], [AMPSO] ^a	CCD, desirability functions
Resolution	[acetonitrile], [urea]	Iterative regression strategy
Resolution	9 for a stepwise screening, followed by 3: pH, [SDS], [acetonitrile]	Fractional factorial design, full factorial design, RSM ^d
Yield for the derivatization of some dipeptides	Reaction time, T, ionic strength, pH, [isopropanol]	Fractional factorial design, CCD, RSM
Selectivity	pH, [SDS]	Iterative regression strategy
Resolution	[SDS], [acetonitrile]	CABRO II ^e
Precision and efficiency	[SDS], V, T	FUMI ^f
Resolution	T, V, ionic strength, [SDS], [HPMC] ^b , [β -cyclodextrin]	PLS ^g
Resolution	[SDS], [urea]	CABRO II
Resolution	pH, [SDS]	CAMOS ^h
Resolution	pH, [buffer], [SDS], [SDS + sodium heptyl sulfate], [acetonitrile]	Plackett–Burman statistical design
Resolution	[SDS], [<i>N,N</i> -dimethylformamide], ionic strength	ORM ⁱ
Resolution	pH, [SDS], [tetrabutylammonium salt]	ORM
Resolution	pH, [SDS]	ORM
Resolution	[SDS], [isopropanol], [β -cyclodextrin]	Full factorial design
Resolution	pH, [SDS]	Full factorial design

^aAMPSO = 3-[(1,2-dimethyl-2-hydroxyethyl)amino]-2-hydroxypropanesulfonic acid; ^bHPMC = hydroxypropyl methylcellulose; ^ccentral composite design; ^dresponse surface modelling; ^ecomputer-assisted bivariate resolution optimization II; ^ffunction of mutual information; ^gpartial least squares; ^hcomputer-assisted multivariate optimization strategies; ⁱoverlapping resolution mapping. V, voltage; T, temperature.

Further Reading

- Camilleri P (1998) *Capillary Electrophoresis, Theory and Practice*, 2nd edn, pp. 135–182. New York: CRC Press.
- Guzman NA (1993) *Capillary Electrophoresis Technology*, pp. 65–87, 693–704. New York: Marcel Dekker.
- Khaledi MG (1998) *High-Performance Capillary Electrophoresis*, pp. 77–140. New York: John Wiley.
- Poole CF and Poole SK (1997) Interphase model for retention and selectivity in micellar electrokinetic chromatography. *Journal of Chromatography A* 792: 89–104.
- Riekkola M-L, Wiedmer SK, Valkó IE and Sirén H (1997) Selectivity in capillary electrophoresis in the presence of micelles, chiral selectors and non-aqueous media. *Journal of Chromatography A* 792: 13–35.
- Rosen MJ (1989) *Surfactants and Interfacial Phenomena*, 2nd edn, pp. 108–206. New York: John Wiley.
- Terabe S, Otsuka K, Ichikawa K, Tsuchiya A and Ando T (1984) Electrokinetic separations with micellar solutions and open-tubular capillaries. *Analytical Chemistry* 56: 111–113.
- Terabe S (1989) Electrokinetic chromatography: an interface between electrophoresis and chromatography. *Trends in Analytical Chemistry* 8: 129–134.
- Vindeogel J and Sandra P (1992) *Introduction to Micellar Electrokinetic Chromatography*, pp. 1–231. Heidelberg: Hüthig Buch Verlag.

Microtechnology

T. McCreedy, University of Hull, Hull, UK

Copyright © 2000 Academic Press

Introduction

Electrophoresis is an established separation technique, frequently used for mixtures ranging from pro-

teins and DNA to small anions and cations. However, perhaps its greatest strength lies in its remarkable ability to separate charged macromolecules. Reports describing electrophoretic separations started to appear in the 1930s, but the most significant developments really took place in the 1940s and 50s when separations with a paper or gel support matrix were used for the separation of macromolecules. The early

methods used relatively large scale apparatus, but during the later 1960s, and early 1970s, reports appeared describing separations being performed in small bore tubes filled with buffer solution. This work was extended in the early 1980s, with capillaries being a key feature of the basic methodology. This was the start of capillary electrophoresis (CE); however, it was not until the mid 1980s that great interest was shown towards a new approach to separation science. From that moment, development and commercialization came very quickly and soon there were a number of commercial instruments available for routine laboratory use.

It is not possible to cover all aspects of electrophoresis in an article such as this; indeed there are several topics that have been omitted. Fluid logic devices and freeze-melt switching are two such examples; another important area not included is the use of parallel bundles of microcapillaries that permit multiple analyses to be performed at a high throughput.

The basic element of any CE system is the separation capillary, typically 10–100 μm internal diameter and 30–100 cm long. Each end of the capillary is located in a small reservoir, which contains buffer solution and a platinum anode or cathode; typically potentials of up to 30 kV can be applied between them. Detection is achieved by a range of in-line detection methods, such as ultraviolet absorbance and other detection methods, such as mass spectrometry, can be interfaced to the capillary.

Separation is achieved due to the differing electrophoretic mobilities of the analytes in the sample, but in addition electroosmotic flow (EOF) takes place. This phenomenon gives rise to bulk flow of the solution in the capillary without the need for an external pump. For a unmodified silica capillary, the direction of flow would be from the anode to the cathode, which enables all uncharged species to be carried to the detector. This technique offers very high separation efficiencies and rapid analysis. This feature, coupled with the simplicity of the instrumentation, makes the technique ideally suited to miniaturization.

Interest in miniaturizing analytical systems is not new; indeed, the idea of a micro total analysis system (often referred to as μTAS) has been mooted for some time within the scientific community (see, for example, the paper by Martin cited in Further Reading). The ideal approach is to include sample manipulation and detection on a chip-sized device; this has given rise to the term 'lab on a chip'. Such systems employ microstructures fabricated on glass or other substrates to form integrated devices rather than attempting to construct miniaturized systems from discrete components. However, there is also consider-

able interest in the development of discrete components, such as micropumps. The conference proceedings from the recent Micro Total Analysis Systems '98 give some indication as to the diversity of the developments. While on-chip injection is feasible, some prior degree of preparation may still be necessary. For example, particulate matter would quickly block the channels, so pre-filtering would be required in such situations. Before examining in more detail electrophoresis on chips, it is important to consider the fabrication of such microchannel devices.

Fabrication of Electrophoresis Devices

There are numerous fabrication methods available, and the complexity of possible designs is virtually limitless. A popular fabrication technique is the use of photolithographic masking in conjunction with wet or chemical etching. The simplest case would be the fabrication of a single channel in a piece of glass. First, the glass would be coated with a layer of deposited metal and subsequently photoresist, e.g. by spin coating, then the pattern mask is placed on top of the photoresist. This masked surface is subsequently exposed to ultraviolet light, which transfers the pattern on to the photoresist. The unprotected area can then be removed, along with the underlying metal surface. An etching solution, such as hydrofluoric acid/nitric acid, is used to etch away the glass, forming the channel in the chip. This surface of the chip protected by the metal and photoresist layer does not etch. This process can be seen in **Figure 1**. There are a few problems with this approach; the first is that only certain materials can be etched. The second is that, as the channel is etched deeper, the width also increases. This becomes more of a problem as the depth increases, resulting in channel with nonvertical sides. This problem can also create difficulties at channel intersections, which do not have true intersecting corners due to the accelerated etching of the exposed corners.

There are many alternatives to the wet etch approach. Dry etch processes include reactive ion and laser etching; these offer a way to cut precise channels of small dimensions. Silicon is gaining in popularity as an alternative substrate to glass for chip fabrication, and by employing more than one etching technique complex devices can be produced.

In order to use polymeric materials, such as silicone rubber, or fluoropolymers for chip fabrication, new approaches are required. This may take the form of stamping, imprinting or injection moulding of the polymeric material. The approach offers a significant alternative to wet etching of channels directly,

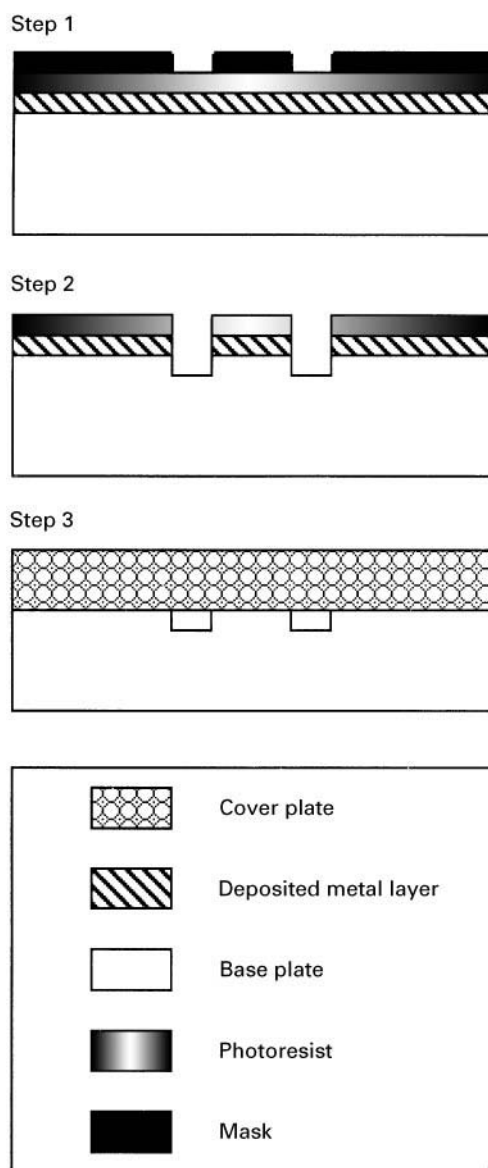


Figure 1 The fabrication process for a separation chip fabricated from silica. The first step is to place the mask on top of the silica base plate covered in deposited metal and photoresist (step 1). After this has been exposed to UV light, the chip is developed to remove the exposed photoresist and metal. It is then etched, e.g. with hydrofluoric/nitric acids (step 2); etching does not occur where the metal and photoresist remains. The final stage (step 3) is the bonding of the cover plate on to the base plate. The two etched channels can clearly be seen.

primarily since it allows the use of a wide range of new materials, and the prospect of mass production. It requires a template to be constructed, often by wet etching or mechanical milling. This template can be considered as the negative image of the channels, and is often finally produced in a more durable material, such as nickel. From this robust template, it is pos-

sible to mass-produce thousands of channel systems with considerable speed.

All of these methods create half the chip; the next step is to attach the cover plate, i.e. the other half of the chip. It is common to locate the holes for the necessary reservoirs in this plate; the reservoirs themselves are frequently constructed by attaching cylinders, e.g. truncated pipette tips, to the top plate. For glass and silica-based systems, it is a simple step to bond the top plate on to the channels by a heating and cooling cycle (the cooling cycle is required to avoid thermally stressing the glass). The fixing of the top plate to polymeric materials can be more complex; however, perhaps the simplest method is to use a thermally activated adhesive to laminate the top plate on to the chip. Typical channel dimensions are 200 μm wide by 60 μm deep, and vary in length from 5 mm to several centimetres. Of course, many other channel dimensions can be created. Some typical patterns can be seen in Figure 2.

Theoretical Considerations

There are two important effects that need to be considered when discussing electrophoresis in microchannels; these are similar to the more conventional capillary electrophoresis. The first is electrophoretic mobility, and the second is electroosmotic flow (EOF). EOF is otherwise referred to as electroendosmotic flow.

Electrophoretic Mobility

This process forms the basis for the separation in the channel, and dictates the migration velocity of a given ion in the channel. The electrophoretic mobility (μ_e) is related to the migration velocity (v) by eqn [1], where E is the electric field strength:

$$v = \mu_e E \quad [1]$$

The units of μ_e , v and E are $\text{cm}^2 \text{V}^{-1} \text{s}^{-1}$, cm s^{-1} , and V cm^{-1} respectively. The electrophoretic mobility is proportional to the ionic charge and frictional forces. Thus, if two mobile species differ in either their charge or the frictional forces, then separation will occur. Since uncharged molecules have an electrophoretic mobility of zero, movement will not occur; this is why electrophoresis cannot separate neutral molecules. For ions of the same size, μ_e will be greater for ions with greater charge while for ions of the same charge, μ_e will be greater for smaller ions.

Electroosmotic Flow

This is a process which gives rise to the flow of buffer through the channel. It can be quite significant,

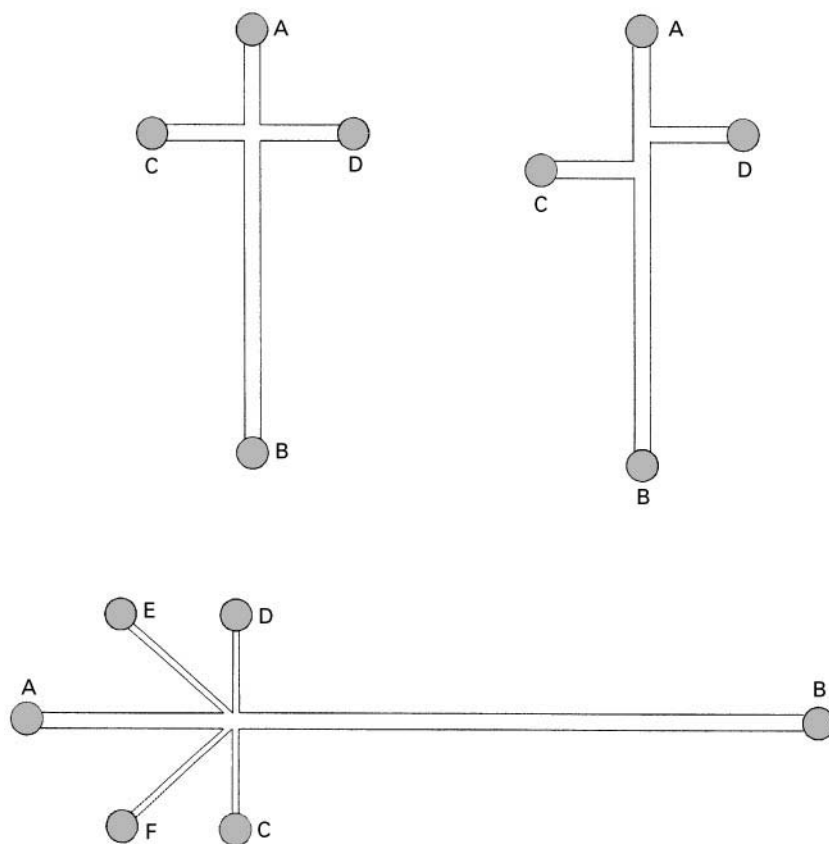


Figure 2 Some typical channel arrangements. Reservoirs A and B start and terminate the separation channel. Reservoirs C and D permit a known amount of sample to be injected into the separation channel. The reservoirs E and F permit the addition of other reagents to the separation channel.

reaching linear velocities of around 5 cm min^{-1} or greater. The rate of movement due to EOF is normally greater than the electrophoretic mobility, thus ensuring that all ionic (and uncharged) species pass the detector. However, unlike electrophoretic mobility, EOF will only occur in the presence of an electrical double layer at the surface of the channel. In **Figure 3**, an axial view of a channel etched in glass can be seen; the surface is covered in silanol groups.

When the pH of the buffer is above $\sim \text{pH } 9$, all the silanol groups are ionized. Cations from the buffer migrate towards the negative wall of the channel, and a double layer is formed. When a voltage is applied across the channel, these cations migrate towards the cathode, thereby inducing bulk flow. Electro-driven flow has a characteristically flat profile compared to the parabolic profile observed for pressure-driven systems. This significantly reduces the dispersion due to flow, and is considered to be a reason for the high efficiency separations possible. Another reason for the low dispersion observed is that the Reynolds numbers for liquids in such a system are very low, which results in limited dispersion. The electroosmotic mo-

bility (μ_{EOF}) is given in eqn [2] where η is the viscosity of the buffer, ϵ is the dielectric constant of the buffer and ζ is the zeta potential (charge on the capillary wall):

$$\mu_{\text{EOF}} = (\epsilon\zeta/\eta) \quad [2]$$

The EOF velocity can be calculated from eqn [3] which has striking similarities to eqn [1]. Here, the EOF velocity (v) is related to the electroosmotic mobility (μ_{EOF}), and the electric field gradient (E):

$$v = \mu_{\text{EOF}}E \quad [3]$$

From this, it is apparent that the overall velocity of the ionic species is the algebraic sum of the migration velocity, and the EOF velocity. By summing the two velocity terms and subsequent rearrangement of the equation, the actual velocity (v_a) of an ionic species is given by eqn [4]:

$$v_a = (\mu_E + \mu_{\text{EOF}})E \quad [4]$$

Situations do arise, such as during the analysis of anions with high electrophoretic mobility, when the

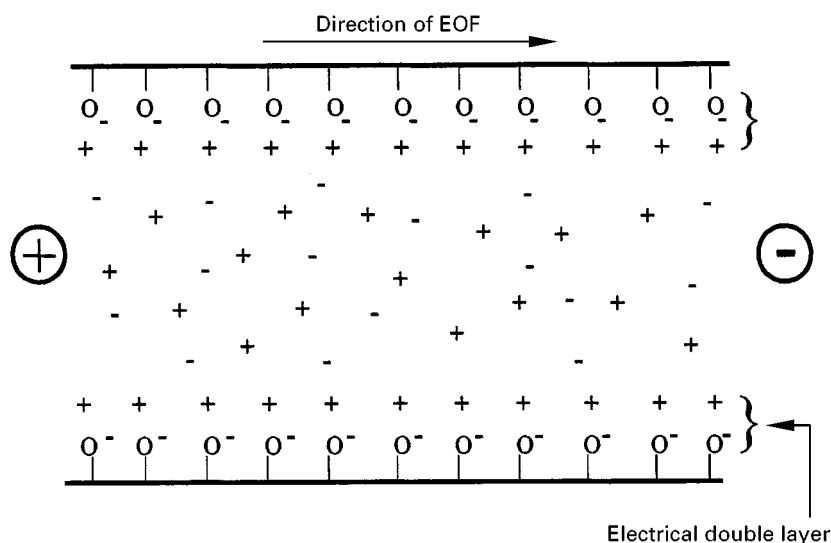


Figure 3 The double layer formed in silica channel. The layers of cations which collect along the walls of the channel will migrate towards the cathode when a voltage is applied. This gives rise to the electroosmotic flow (EOF) with the characteristic flat flow profile.

direction of EOF needs to be reversed. This can be achieved by coating the walls of the channels with a cationic surfactant. This gives an apparently positive charge to the walls, so that anions (not cations) will form the double layer. Then, when the potential is applied, EOF will be in the opposite direction. Since the influence of the double layer is generally considered to extend less than $1\text{ }\mu\text{m}$ into the solution, overlap of the double layer should not be an issue for channels of greater than $5\text{ }\mu\text{m}$ minimum dimension. However, for channels of smaller dimension, the flat flow profile model may no longer be valid, and great care should be exercised in describing the flow.

To prevent EOF completely, the walls of the channel need to be rendered neutral. In silica channels, this ought to be achievable by coating the walls with a compound such as trimethylchlorosilane, to end-cap all terminal silanol groups. However, in practice, it is impossible to eliminate all EOF since residual surface charge remains. Since many microsystems are now being constructed from polymeric substrates, EOF normally does not occur to any appreciable extent. This is due to the absence of ionizable or charged surface groups. In this situation, EOF could be induced by coating the walls of the channel with a charged compound, such as cetyltrimethylammonium bromide.

Practical Considerations

Perhaps the key practical consideration is whether integrated on-chip detection will be employed, or whether the separated compounds will be transferred to another device, such as a mass spectrometer. In

a similar context to conventional capillary electrophoresis separations, on-chip detection is the ideal option, since it minimizes dispersion and the dead volume associated with the transfer of analytes from the chip to a detector. The dead volume will normally be far in excess of the separation volume, thus band broadening will be a serious problem.

The other key issue is sample introduction. The simplest system relies on the EOF to introduce the sample into the separation capillary. Consider the channel arrangement in **Figure 4**. The channels are etched into silica, and no deactivating treatment is applied. Under normal conditions (I), the applied voltage between reservoirs A and B induces EOF. In addition, the potential field gradient will give rise to electrophoretic separations.

Since only buffer is flowing, this does not give rise to any apparent separation effect. When the voltage is manipulated such that it is now between reservoirs C and D (II), EOF is induced between the reservoirs, thus the sample is introduced, and occupies a small section of the main channel. Once the voltage is restored between A and B, the separation step begins (III). Here, the sample is moved by the EOF towards reservoir D, and separation occurs due to electrophoretic mobility.

In situations where EOF is insignificant due to the absence of surface charge, the injection step relies either on the electrophoretic movement of the analytes or an applied pressure. There is, of course, a potential problem with electrophoretic mobility, and that is the discriminatory effects observed between analytes of high and low electrophoretic mobility. Pressure, on the other hand, offers a simple

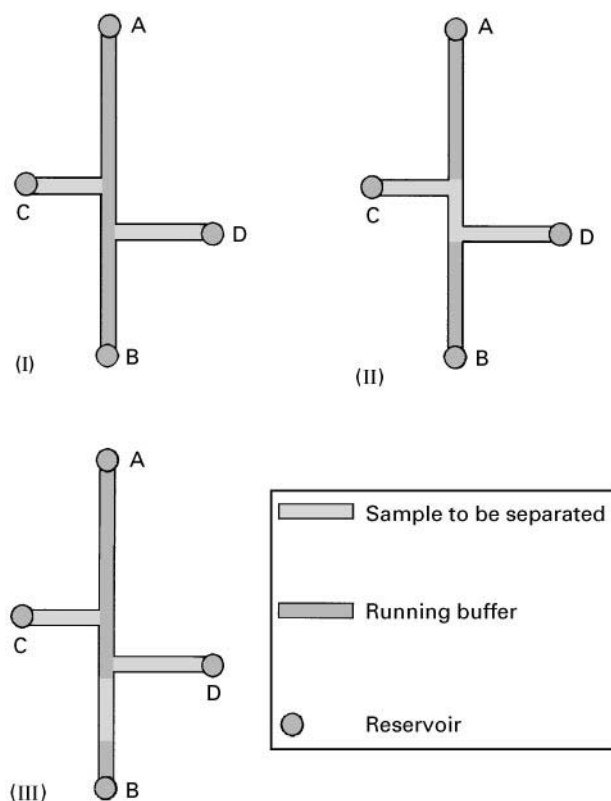


Figure 4 Sample introduction into the separation channel. (I) When the voltage is applied between reservoirs A and B, the separation channel is filled with running buffer. (II) To inject a sample, the voltage is applied between C and D: the sample moves into a short section of the separation channel. (III) With the voltage restored across A and B, the sample moves along the separation capillary, and separation occurs.

and nondiscriminatory route for sample introduction. This can be achieved by either applying pressure to one reservoir in order to force the analyte through the system, or by deformation of the chip (in situations where the polymer is flexible). In either case, a valveless injection method is used; this greatly simplifies the operational aspect of these systems.

Applications

In this section, several types of application will be considered. While much of the discussion will be related to the separation of compounds on chips using electrophoresis, it is impossible to neglect the potential of EOF alone for fluid mobility, which is unaffected by back-pressure.

Electrophoretic Separations

Much of the literature available on chip-based electrophoretic separations features capillary zone elec-

trophoretic (CZE) separations; however, there are many other types of separation possible, such as isotachopheresis and electrokinetic focusing.

Perhaps the simplest applications are based on CZE within silica microchannels. Here EOF and electrophoretic mobility can be utilized, the EOF for injection and bulk flow of solutions through the capillary, and electrophoretic mobility for the actual separation process. A typical separation capillary would be 50 mm long, 45 μm wide and 8 μm in depth, with an applied potential in the range 600–1200 V along the 50 mm length. The types of samples that can be separated by this technique are extensive (not surprising, given the diversity of the applications for conventional CZE) but include small anions and cations, monoclonal antibodies, theophylline and DNA fragments. There are a number of potential detectors, but those based on optical or electrochemical methods are the most frequently used.

Electrochemical detection can easily be incorporated on to a microchip, but requires the detector to be located after the high voltage section of the channel. This is necessary to prevent the high voltage causing interference with the detection. This can be achieved in such a system as described above, by locating the electrochemical detector in the channel just after the ground electrode. The EOF occurring in the channel would pump the fluid along the channel from the ground electrode to the detector electrodes. Over this short region, band broadening should not pose a significant problem. It is similar in principle to the porous junction technique widely used in conventional CE. It is possible to achieve limits of detection of micromolar levels or better with electrochemical detection.

Spectroscopic methods fall into two main classes – absorbance and fluorescence. Absorbance measurements are simple to effect, but commonly suffer from relatively low sensitivity. This is primarily due to the channel dimensions resulting in a very small path length. Measurements across a 50 μm channel would give rise to a very small absorbance, since absorbance is proportional to path length. It is possible to increase the path length (Figure 5), but absorbance measurements do not have the sensitivity of fluorescence measurements, although they are generally applicable to a wider range of analytes. In addition, for practical reasons, dual-channel systems are not easily set up and this can lead to instability in the detector signal.

Fluorescence measurements can provide limits of detection in the picomolar range (varying from around 2 pmol L^{-1} upwards), and have even been reported for counting single chromophore molecules. Generally, the excitation source is directed along the

to an electrophoretic separation chip is one possible answer. However, there is no reason why reactions cannot be carried out on such devices. Since it does not require the investment of a large chemical plant, the reactions can be performed where required, thus reducing the need to transport hazardous chemicals across countries. Since many reactors can be constructed on a single chip, and many chips located in the same area, it is evident that this technology will provide hazardous or chemically unstable chemicals where they are required.

Further Reading

- Altria KD (ed.) (1996) *Capillary Electrophoresis Guidebook, Principles, Operation, and Applications*. New Jersey: Humana Press.
- Harrison DJ and Van den Berg A (eds) (1998) *Micro Total Analysis Systems '98*. Dordrecht: Kluwer Academic Publishers.
- Haswell SJ (1997) Developments and operating characteristics of microflow injection analysis systems based on electroosmotic flow. *Analyst* 122: 1R–1OR.
- Manz A and Becker H (1997) *Microsystem Technology in Chemical and Life Sciences*. Berlin: Springer.
- Madou M (1996) *Fundamentals of Microfabrication*. Boca Raton: CRC.
- Martin AJP (1962) Opening lecture. In: Van Swaay M (ed.) *Fourth International Symposium on Gas Chromatography*. London: Butterworths.
- Oefner PJ, Bonn GK and Chiesa C (1995) *Encyclopaedia of Analytical Chemistry*, pp. 1041–1152. London: Academic Press.
- Pethig R and Markx GH (1997) Applications of dielectrophoresis in biotechnology, *Trends in Biochemistry* 15: 426–432.
- Regnier F (1999) The evolution of analysis in life science research and molecular medicine: the potential role for separations. *Chromatographia* 49: S56–S64.
- Tsuda T (ed.) (1995) *Electric Field Applications*, pp. 47–73. Weinheim: VCH.

Nonaqueous Capillary Electrophoresis

S. H. Hansen, I. Bjørnsdottir and J. Tjørnelund,
Royal Danish School of Pharmacy, Copenhagen,
Denmark

Copyright © 2000 Academic Press

Electrophoresis is a separation technique that is normally performed in an aqueous environment. This is due to the fact that the separation mechanism is based on the difference in migration rate of charged species in an electric field. Species (ions/molecules or particles) with a difference in their charge over size ratio will exhibit a difference in migration rate. Most charged species are fairly soluble in aqueous media and thus water is the most obvious solvent for electrophoresis. However, in a number of nonaqueous solvent systems, it is possible to obtain sufficient conductivity to perform electrophoresis. If such systems are utilized with the technique of capillary electrophoresis, a number of advantages compared to aqueous systems are obtained in the separation of small molecules. Nonaqueous electrophoresis of biopolymers like polysaccharides, nucleic acids and proteins is not of practical use due to lack of solubility of such molecules in organic solvents.

Nonaqueous Capillary Electrophoresis

Only a few attempts to perform nonaqueous paper electrophoresis have been described and these articles

were reviewed in 1978. In 1984 nonaqueous capillary electrophoresis (NACE) was briefly mentioned in a single publication, but not utilized further. However, since 1993 the use of nonaqueous media for capillary electrophoresis has seen renewed interest in the separation of drug substances due to the high separation selectivity obtained in these systems.

The electrophoretic migration of the solutes is influenced by the nature of the solvent or solvent mixture used for the electrophoresis medium in three main ways:

1. The mobility may change due to changes in the size of the solvated ion.
2. The dielectric constant of the organic solvent may influence the equilibrium of the protolytic dissociation. The higher the value of the dielectric constant, the higher the degree of ionization of acids and bases.
3. The acid–base property of the solute, expressed by its pK_a value, may change due to the differentiating effect of many organic solvents.

The latter effect of the three is the most significant, as the dissociation constant, K_a , may change many orders of magnitude for different solvents.

The increased selectivity of separation in organic solvents compared to aqueous systems is due to the fact that the levelling effect of water is eliminated. If

Table 1 Classification of organic solvents according to their Brønsted acid–base behaviour

Solvent designation		Relative acidity	Relative basicity	Examples
Amphiprotic	Neutral	+	+	<i>MeOH</i> , glycerol, phenol, <i>tert</i> , butyl alcohol
	Protogenic	+	—	Sulfonic acid, formic acid, <i>acetic acid</i>
	Protophilic	—	+	Liquid ammonia, <i>FA</i> , <i>NMF</i>
	Dipolar protophilic	—	+	<i>DMSO</i> , <i>DMF</i> , tetrahydrofuran, 1,4-dioxan, pyridine
Aprotic	Dipolar protophobic	—	—	<i>MeCN</i> , acetone, nitrobenzene, sulfolane, <i>PC</i>
	Inert	—	—	Aliphatic hydrocarbons, benzene, 1,2-dichloroethane, tetrachloromethane

— indicates weaker and + indicates stronger acid or base than water. DMF, *N,N*-dimethylformamide; DMSO, dimethyl sulfoxide; FA, formamide; MeCN, acetonitrile; MeOH, methanol; NMF, *N*-methylformamide; PC, propylene carbonate. Solvents *in italic* are the ones that are preferred for NACE. Reproduced with permission from Tjørnelund J and Hansen SH (1999) *Journal of Biochemistry and Biophysical Methods* 38: 139–153.

strong acids or bases are dissolved in water, they all show up with about the same acid or base strength. If the same acids or bases are dissolved in organic solvents they will exhibit very different protolytic behaviour depending on the degree of dissociation, which again depends on the solvent in question.

Important factors influencing the choice of organic solvent or solvent mixture for a given separation are volatility, the dissolving power towards suitable electrolytes, viscosity and dielectric constant, UV transparency and, last but not least, the effect on the separation selectivity of the system. Information on the viscosity and volatility, the auto protolysis constant, the dielectric constant at standard conditions and the UV transparency of the neat solvents may be found in the literature. In contrast, data on solvent mixtures and systematic studies of how to choose solvents and electrolytes in order to control the selectivity of the electrophoretic system are limited

and thus the choice of separation media is still a matter of trial and error. Solvents may be classified according to their Brønsted acid–base behaviour; a simplified version of this classification is shown in Table 1.

Practical Considerations

Choice of Organic Solvent

The physical chemical properties of the organic solvents preferred for NACE are given in Table 2 and, as mentioned above, the physical constants have a major impact on the choice of solvent or solvent mixture for a given electrophoretic separation. Some of the more practical considerations are the chemical resistance of parts in the CE instrument towards the solvent, the volatility of the solvent, the solvating power of the solvent towards electrolytes, the UV transparency and the viscosity of the solvent.

Table 2 Physicochemical parameters of selected solvents

Solvent	Viscosity, η (cP)	Dielectric constant, ϵ	ϵ/η	pK_{auto}	T_{boil} ($^{\circ}\text{C}$)	UV cutoff (nm) (1 cm cuvette)
Water	0.89	78.4	89.9	14	100	<200
FA	3.3	111	33.6	16.8	210	275
NMF	1.65	182	110.3	10.7	182	275
DMF	0.8	36.7	45.9	29.4	153	260
DMSO	1.99	46.7	23.4	33.3	189	260
MeOH	0.544	32.7	60.6	17.2	65	205
PC	2.5	64.4	25.7	Not detected	242	200–230
MeCN	0.34	37.5	110.3	Not detected	82	200–230
Glycerol	945	42.5	0.045	—	290	205
Acetic acid	1.04 ₃₀	6.152	5.91	14.45	118	—

All values are at 25°C unless otherwise stated in subscript. For abbreviations, see Table 1. Reproduced with permission from Tjørnelund J and Hansen SH (1999) *Journal of Biochemistry and Biophysical Methods* 38: 139–153.

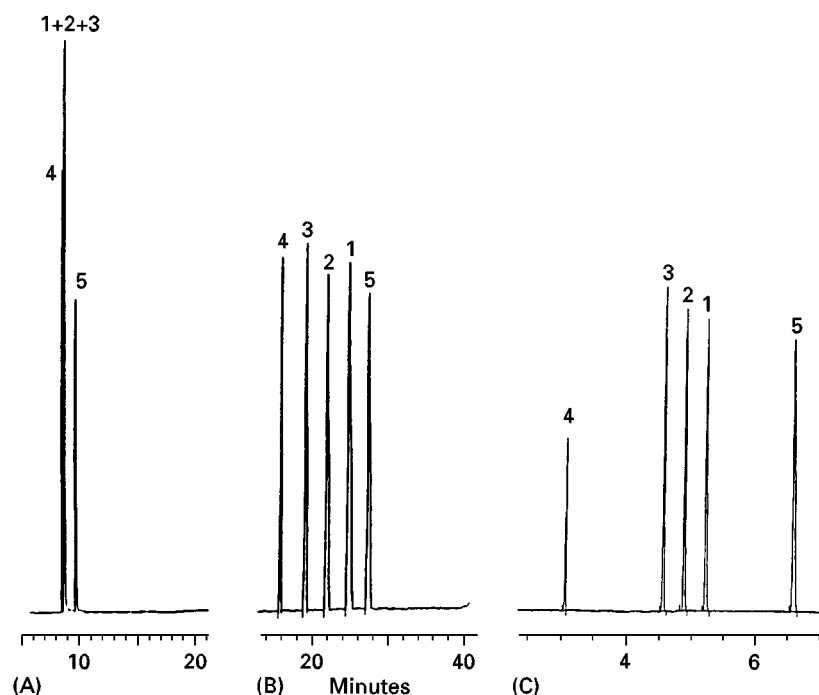
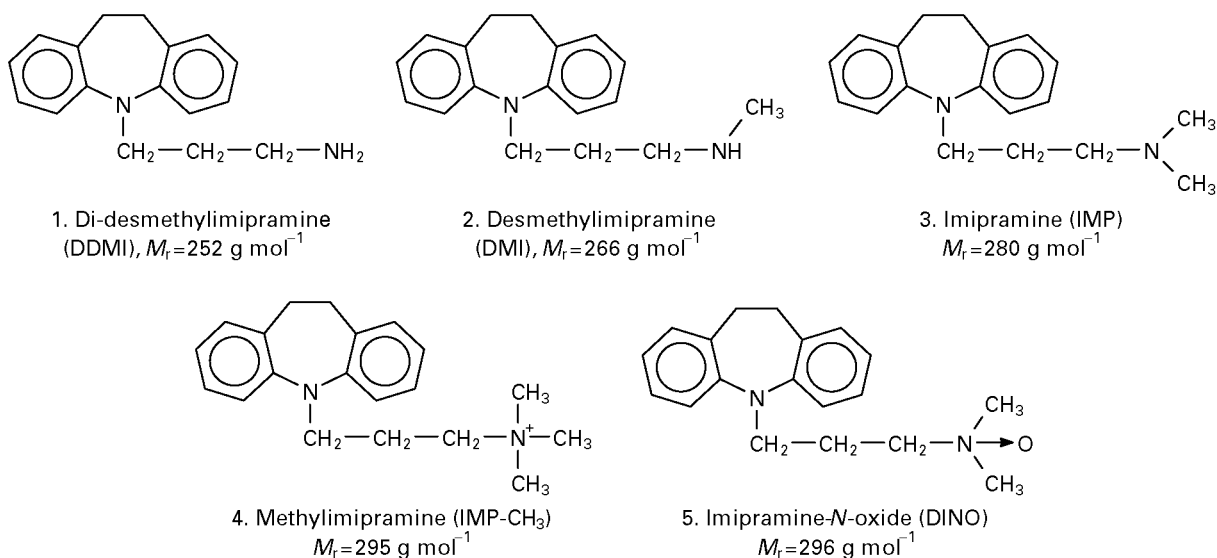


Figure 1 Electropherograms of imipramine and four derivatives. (A) 50 mmol L⁻¹ 6-aminocaproic acid pH 4.0; (B) 50 mmol L⁻¹ 6-amino caproic acid pH 4.0 with 25 mmol L⁻¹ of 3-(*N,N*-dimethylmyristylammonium)propanesulfonate and 15 mmol L⁻¹ of Tween® 20 added. Apparatus: Quanta 4000. Conditions: 64 cm (56 cm to the detector) \times 75 μm i.d. capillary, hydrostatic (10 cm) injection for 15 s, ambient (27–30°C), 20 kV (62 μA) and UV detection at 214 nm. (C) 25 mmol L⁻¹ ammonium acetate and 1 mol L⁻¹ acetic acid in acetonitrile. Apparatus: HP3DCE instrument. Conditions: 64 cm (55.5 cm to the detector) \times 50 μm i.d. capillary, injection of 3 s at 5 kPa (50 mbar), 25°C, 25 kV (7 μA) and UV detection at 214 nm. Adapted with permission from Bjørnsdottir I, Tjørnelund J and Hansen SH (1996) Selectivity enhancement in capillary electrophoresis using nonaqueous media. *Journal of Capillary Electrophoresis* 3: 83–87.

Solvents with a high vapour pressure and thus a high volatility (e.g. methanol (MeOH) and acetonitrile (MeCN)) may be inconvenient for automated analysis in some instruments due to problems with evaporation of the electrophoresis medium from the

run buffer vials as well from the sample vials. In CE the detection is often performed by measuring the UV absorbance of the analyte at a relatively short wavelength (e.g. at 214 nm or below) in order to increase the sensitivity. However, many organic sol-

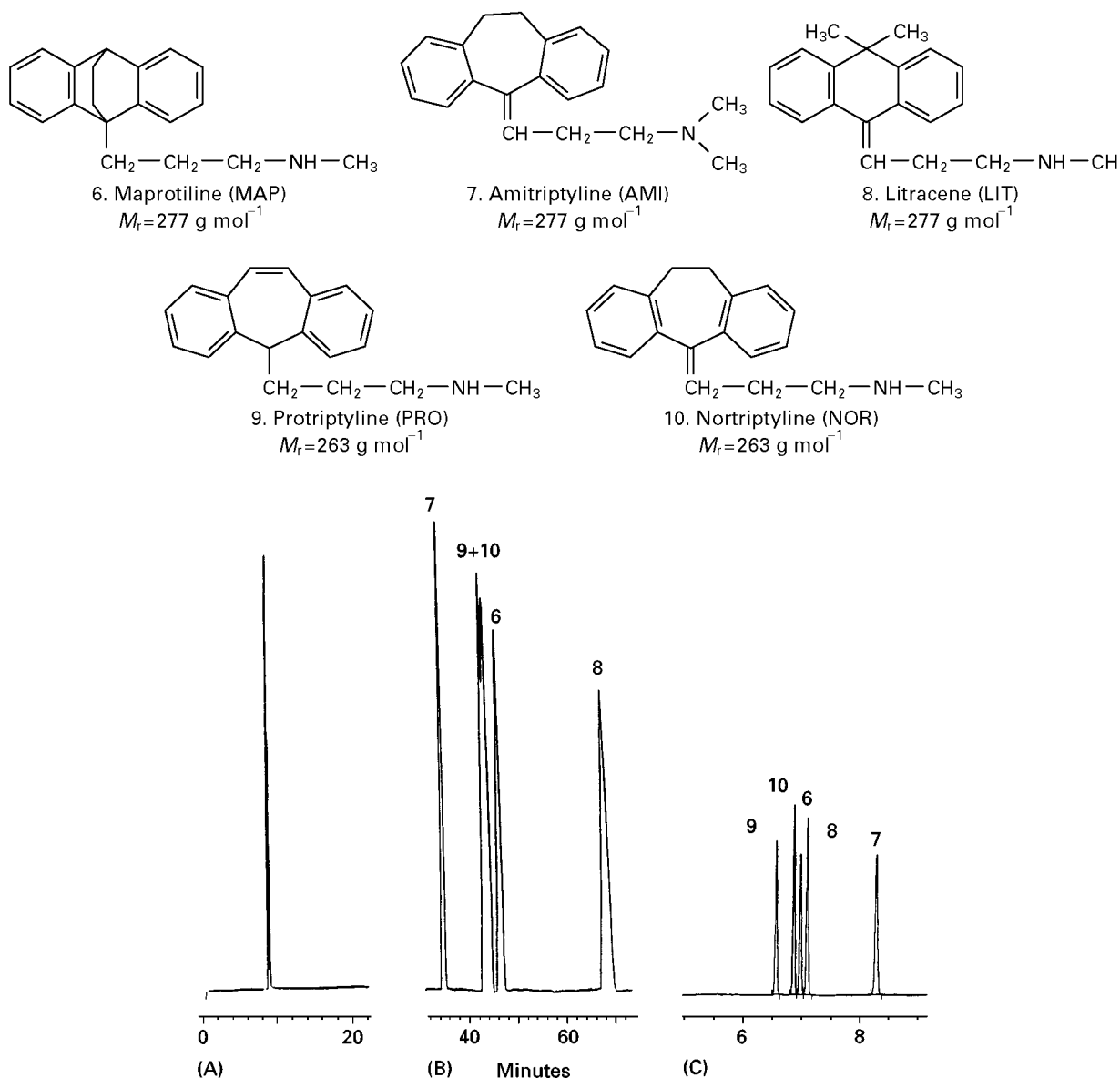


Figure 2 Electropherograms of five basic drugs with equal or very similar mass over charge ratio. (A) 50 mmol L⁻¹ 6-aminocaproic acid pH 4.0; (B) 50 mmol L⁻¹ 6-amino caproic acid pH 4.0 with 25 mmol L⁻¹ of Tween® 20 added. Apparatus and conditions as in Figure 1A. (C) 25 mmol L⁻¹ ammonium acetate and 100 mmol L⁻¹ sodium acetate in methanol + acetonitrile (1 : 1 v/v) and 25 kV (23 μ A). Apparatus and other conditions as in Figure 1C. Adapted with permission from Bjørnsdottir I, Tjørnelund J and Hansen SH (1996) Selectivity enhancement in capillary electrophoresis using nonaqueous media. *Journal of Capillary Electrophoresis* 3: 83–87.

vents have a UV cutoff at 214 nm or above (Table 2). Nevertheless, solvents like MeCN and MeOH may be used for measurements performed at a wavelength as low as 200 nm as the light path through the capillary is very short compared to the 1 cm cuvette used for the determination of the UV cutoff wavelength. The amides and dimethylsulfoxide can only be used when detection at wavelengths above *c.* 245 nm is sufficient of the application.

On the positive side, organic solvents often intensify the fluorescence relative to what is observed for

given solutes in aqueous media. This has been used to decrease detection limits in NACE for analysis of tetracyclines in biological matrices.

Choice of Electrolyte

The choice of electrolyte is important and will influence the separation. However, due to the low solubility of many electrolytes in organic solvents, it can be difficult to find a suitable electrolyte. The more polar solvents, like MeOH, DMSO, formamide, *N*-methylformamide and *N,N*-dimethylformamide, possess

a good solvating power towards the electrolytes commonly used in NACE. So far, ammonium acetate has been the most frequently used electrolyte in NACE systems and acetic acid or sodium acetate have often been used in combination with ammonium acetate in order to adjust the acid–base properties of the electrophoresis medium. Quaternary ammonium salts have also been used a number of times with success, e.g. in the separation of phenols and carboxylic acids. More rarely, Tris, magnesium acetate, citric acid, formic acid, trifluoroacetic acid and methanesulfonic acid have been used.

When coupling CE to mass spectrometry (MS), it is an advantage to choose a volatile electrolyte, e.g. ammonium acetate, in order to limit background noise or cluster ion formation.

Other Additives

A number of polyalcohols and surfactants such as the Tweens® have been used as additives. Their primary function is to decrease the electroosmotic flow (EOF) and thus prolong the time for electrophoretic separation.

Also chiral separations are possible in NACE using either cyclodextrines or chiral counter ions as additives.

Reversal of EOF

The separation of anionic solutes in CE may lead to extended time of analysis due to their migration in the direction opposite to EOF. One method of decreasing the analysis time is to reverse the EOF, thus making the anions migrate in the same direction as the EOF. In aqueous CE, the addition of long alkyl chain trimethylammonium ions is used for this purpose, e.g. in the analysis of inorganic anions and phenols. This principle may also be used in NACE. However, the long alkyl chain trimethylammonium ions are not able to form hemimicelles at the inner capillary surface when using nonaqueous solvents and thus the EOF is not reversed. Addition of the polycation hexadimethrine bromide to the nonaqueous electrophoresis medium may result in suitable and stable systems with reversed EOF, even when used at fairly low concentrations (0.001–0.05%).

Applicability of NACE

In CE the separation of solutes is due to differences in the charge over size ratios and thus very similar substances may be difficult to separate in aqueous CE unless special mechanisms like micellar electrokinetic chromatography (MEKC) are involved. Of course this involves addition of one or more surfactants.

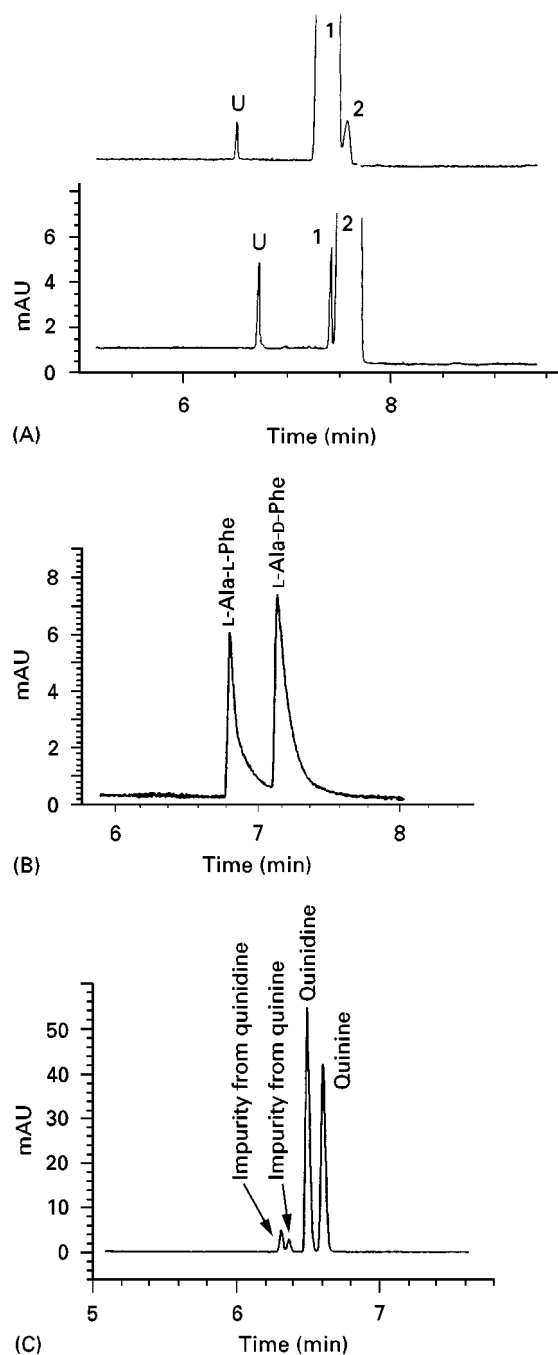


Figure 3 Electropherograms of *cis-trans*- and diastereo-isomers. (A) Separation of *cis*- and *trans*-flupenthixol decanoate using 50 mmol L⁻¹ ammonium acetate and 1 mol L⁻¹ acetic acid in methanol + acetonitrile (1 : 1, v/v), above: *cis*-flupenthixol decanoate with 0.5% *trans*-isomer added; below: *trans*-flupenthixol decanoate. Conditions: 64 cm (55.5 cm to the detector) × 50 μm i.d. capillary, injection for 3 s at 5 kPa (50 mbar), 25°C, 30 kV (9 μA) and UV detection at 230 nm. Test solution: 5.0 mg mL⁻¹ of the sample in methanol + acetonitrile (1 : 1 v/v). Peak identity: 1, *cis*-flupenthixol decanoate; 2, *trans*-flupenthixol decanoate; U, unknown. (B) Separation of dipeptides (diastereomers); (C) separation of quinine and quinidine (diastereomers). Conditions as in (A) with a detection wavelength of 214 nm. Adapted with permission from Hansen SH, Bjørnsdottir I and Tjørnelund J (1997) Separation of cationic *cis-trans* (Z-E) isomers and diastereomers using nonaqueous capillary electrophoresis. *Journal of Chromatography A* 792: 49–55.

Table 3 Applications of NACE in analysis of food, pharmaceuticals and biological fluids

<i>Solvents</i>	<i>Electrolytes</i>	<i>Analytes</i>
<i>Applications within food</i>		
NMF-dioxane (1 : 1 v/v)	40 mmol L ⁻¹ Tris, 2.5 mmol L ⁻¹ anthraquinone-2-carboxylic acid	Free saturated long chain fatty acids (<i>n</i> -C ₁₄ - <i>n</i> -C ₂₆). Separation of dimeric and trimeric acids and hydrogenated fish oil
NMF	500 mmol L ⁻¹ magnesium acetate tetrahydrate	Tetracycline (TC), oxytetracycline (OTC), chlorotetracycline (CTC), demeclocycline, 4-epitetracycline, anhydrotetracycline, 4-epianhydrotetracycline, and desmethyltetracycline
Propylene carbonate	Tetraalkylammonium ions, long chain trimethylammonium ions 20 mmol L ⁻¹ tetradecylammonium bromide (vitamin K ₁ and preservatives)	TC, OTC and CTC in milk and plasma Phenanthrene, β -naphthol, preservatives: methylparaben, ethylparaben and propylparaben, thiourea (EOF marker) and vitamin K ₁
<i>Applications within pharmaceuticals</i>		
10–100% MeOH	Ammonium acetate, acetic acid	Haloperidol and synthetic putative metabolites, pyrazoloacridine and mifentidine
Mixture of MeOH and H ₂ O	Ammonium acetate, acetic acid	Haloperidol, cimetropium and mifentidine
MeOH	5 mmol L ⁻¹ ammonium acetate, 100 mmol L ⁻¹ acetic acid	Haloperidol and its synthetic putative metabolites, pyrazoloacridine and its synthetic putative metabolites, mifentidine and its synthetic putative metabolites
MeOH and mixture of MeOH and MeCN	Ammonium acetate, tetrabutylammonium bromide, tetrabutylammonium hydrogen sulfate and tetrapentylammonium bromide	Tamoxifen and four phase I metabolites
MeOH, MeCN, mixture of MeOH and MeCN, formamide, NMF, DMF, DMA, DMSO	25 mmol L ⁻¹ ammonium acetate, 0–1 mol L ⁻¹ acetic acid or 100 mmol L ⁻¹ sodium acetate Application: 25 mmol L ⁻¹ ammonium acetate, 1 mol L ⁻¹ acetic acid in MeCN	Imipramine, di-desmethylinipramine, desmethylinipramine, methylimipramine and imipramine- <i>N</i> -oxide. Maprotiline, amitriptyline, litracene, protriptyline and nortriptyline. Application: imipramine <i>N</i> -oxide and impurities
MeOH : MeCN : DMF (45 : 49 : 6 v/v/v)	25 mmol L ⁻¹ ammonium acetate, 10 mmol L ⁻¹ citric acid and 118 mmol L ⁻¹ methanesulfonic acid	Tetracycline and three degradation products. Tetracycline, oxytetracycline, doxycycline, desmethyltetracycline and chlortetracycline
MeOH : MeCN (1 : 1 v/v)	20 mmol L ⁻¹ ammonium acetate, 1 mol L ⁻¹ acetic acid	Morphine analogues, antihistamines, antipsychotics and stimulants
Formamide, NMF or DMF	Citric acid or acetic acid mixed with Tris. Chiral selectors: β -CD, γ -CD and derivatized β -CD. Addition of long chain alkyl ammonium salts investigated	Racemic mixtures of chlorphedianol, chlorcyclizine, ethopropazine, mianserin, nefopam, primaquine, propiomezine, trihexyphenidyl, trimeprazine, trimipramine and thioridazine
NMF, formamide and mixtures of both	25–200 mmol L ⁻¹ β -CD, 10 mmol L ⁻¹ NaCl	Dansylated amino acids
NMF	5–100 mmol L ⁻¹ β -CD and 10 mmol L ⁻¹ NaCl	Dansylated amino acids
MeOH	Ammonium acetate, acetic acid, quinine	<i>N</i> -3,5-dinitrobenzylated amino acids, (±)-1,1'-binaphthyl-2,2'-diyl hydrogen phosphate and <i>N</i> -[1-(1-naphthyl)ethyl]phthalomic acid
MeCN	(±)-Camphorsulfonic acid potassium or sodium salt, 1 mol L ⁻¹ acetic acid 0.2 mol L ⁻¹ Tween 20	Atenolol, bisoprolol, bunitrolol, metoprolol, pindolol, propranolol, salbutamol, ephedrine, epinephrine, cisapride and synthetic impurities
Formamide	Tetra- <i>n</i> -butylammonium perchlorate. Chiral selector: (+)-18-crown-6-tetracarboxylic acid	1-Naphthylethylamine, 1-phenylethylamine, phenylalanine, DOPA, tryptophan, norephedrine, noradrenaline and 2-amino-1,2-diphenylethanol

Table 3 *Continued*

<i>Solvents</i>	<i>Electrolytes</i>	<i>Analytes</i>
Formamide, NMF, DMF, DMA, DMSO, MeOH, MeCN and mixtures of MeOH and MeCN	25 mmol L ⁻¹ ammonium acetate, 1 mol L ⁻¹ acetic acid	Morphine, codeine, normorphine, thebaine, noscapine and papaverine. Application: morphine in opium tincture
MeOH : MeCN (75 : 25)	25 mmol L ⁻¹ ammonium acetate, 1 mol L ⁻¹ acetic acid	Morphine
NMF	500 mmol L ⁻¹ magnesium acetate tetrahydrate	Oxytetracycline in an ointment
Mixtures of MeOH and MeCN	Ammonium acetate, ammonium chloride, acetic acid, trifluoroacetic acid, formic acid, methane sulfonic acid	<i>Cis-trans (Z-E)</i> isomers of chlorprothixene, thiothixene, clopenthixol, flupenthixol, flupenthixol decanoate, clomiphene and diastereomers: L-Ala-L-Phe, L-Ala-D-Phe; quinine, quinidine, cinchonine and cinchonidine
Mixtures of MeOH and MeCN	Sodium acetate	A range of penicillins, cephalosporins and nonsteroidal anti-inflammatory drugs
MeOH	20 mmol L ⁻¹ CAPS and 0–40 mmol L ⁻¹ Brij 35	Mesoporphyrin, coporphyrin, pentaporphyrin, hexacarboxylporphyrin, heptacarboxylporphyrin and uroporphyrin
<i>Applications within biological fluids</i>		
10–100% MeOH in H ₂ O	20 mmol L ⁻¹ ammonium acetate, 1% acetic acid	Pyrazoloacridine, two metabolites and a synthetic degradation product in urine
NMF	500 mmol L ⁻¹ magnesium acetate tetrahydrate	Tetracycline (TC), oxytetracycline (OTC), chlortetracycline (CTC), demeclocycline, 4-epitetracycline, anhydrotetracycline, 4-epianhydrotetracycline and desmethyltetracycline. TC, OTC and CTC in cow milk and human plasma
MeOH	5 mmol L ⁻¹ ammonium acetate, 100 mmol L ⁻¹ acetic acid	Mifentidine and three metabolites in rat liver homogenate
MeOH : MeCN (1 : 1 v/v)	50 mmol L ⁻¹ ammonium acetate, 159 mmol L ⁻¹ sodium acetate and 0.002% (w/v) hexadimethrine bromide	Acetylsalicylic acid and three metabolites: salicylic acid, salicyluric acid and gentisic acid in plasma and urine

Reproduced with permission from Bjørnsdottir *et al.* (1998) *Electrophoresis* 19: 2179.

NACE provides high separation power of very similar substances without using additives like surfactants or cyclodextrins. In **Figures 1** and **2** the separation of very similar substances using NACE are compared to separation in an aqueous CE and a MEKC system. As seen in **Figure 2**, even substances expected to have identical mass over charge may be separated in a short time compared to the aqueous systems. **Figure 3** shows the separation of *cis-trans* isomers and diastereoisomers. These isomers are also expected to have the same mass over charge ratio. The use of NACE in the analysis of food, pharmaceuticals and biological fluids has been reviewed by Bjørnsdottir and co-workers and in **Table 3** an overview of applications is given. An important practical consequence of using a NACE separation medium is that the organic phases resulting from either simple extractions or from eluents from solid-phase extractions can be injected directly into the system, thereby saving time.

Furthermore, some NA solvents seem promising for CE-MS experiments due to the volatility of the solvents and the relatively low current generated in the organic solvents. The low current is comparable to the current generated in electrospray MS interfaces and therefore the stability of online CE-MS is optimized.

Two questions are often raised in connection with practical work with NACE. How important is it that the electrophoresis medium is really nonaqueous? This is not crucial. A content of water up to 1% will not influence the separation efficiency and selectivity significantly. Is it possible to perform quantitative analysis using NACE? Yes, if steps against evaporation are taken when volatile solvent are used, the reliability of the methods is comparable to that of aqueous systems (**Table 4**). A number of applications including validated quantitative methods are given in **Table 4**.

Table 4 Validation data from quantitative NACE analysis of food, pharmaceuticals and biological fluids

Analytes	Linearity (r^2)	Repeatability of inj. (%RSD)	LOD	Accuracy
Free saturated long chain fatty acids ($n\text{-C}_{14}\text{-}n\text{-C}_{26}$)	0.994 ($n_{16}\text{-}n_{20}$) 0.985 ($n_{22}\text{-}n_{26}$)	Inter-day: 2.1–39% ($n = 6$) at three concentration levels	0.025 mmol L ⁻¹	nd
Tetracyclines in plasma and milk	0.999	Inter-day repeatability of the method: 3.6–10.2% ($n = 6$) at three concentration levels	25 ng mL ⁻¹ of TC, OTC or CTC	97.2% Oxytetracycline ($n = 6$, %RSD = 4.2%) and 63.3% ($n = 6$, %RSD = 3.6%) at two conc. in milk
Vitamin K ₁ , propylparaben and methylparaben	0.993	~ 3% ($n = 6$) at three concentration levels for all three analytes	nd	98% Vitamin K ₁ ($n = 6$, %RSD = 4.95%) 96% Propylparaben ($n = 6$, %RSD = 4.45%) 82% Methylparaben ($n = 6$, %RSD = 2.26%)
Tetracycline and three degradation products	0.993–0.998	Inter-day: 3.4–13% (five concentration levels)	nd	nd
Oxytetracycline in an ointment	> 0.999	Inter-day: 2.8–4.4% for peak area ($n = 6$) at three conc. levels. For migration time: > 0.8% within day ($n = 8$) and < 3.3% in-between days ($n = 6$)	nd	96.1–97.3% Oxytetracycline at three concentration levels ($n = 6$)
Morphine in pharmaceutical products	> 0.999	Inter-day: 2.0% ($n = 6$)	0.2 µg mL ⁻¹	100.7–101.2% (three concentrations)
Acetylsalicylic acid and three metabolites: salicylic acid, salicyluric acid and gentisic acid in plasma and urine	Good in the range: 5–500 µg mL ⁻¹	Inter-day: plasma: 0.8–5.0% ($n = 6$), urine: 1.0–5.4% ($n = 6$) at three conc. levels	LOQ : 5 µg mL ⁻¹ in plasma and 25 µg mL ⁻¹ in urine	Plasma: 65–99%, urine: 75–97%

nd, not determined; LOQ, limit of quantitation. Reproduced with permission from Bjørnsdottir *et al.* (1998) *Electrophoresis* 19: 2179.

Concluding Remarks

The primary advantages of using nonaqueous media for CE may be outlined in four statements:

1. The separation selectivity is improved by using neat organic solvents and the selectivity can easily be altered by changing the nature of the organic solvent or using mixtures of organic solvents.
2. Analysis of hydrophobic compounds is facilitated as their solubility is higher in organic solvents than in aqueous media.
3. Sample preparation is facilitated as extracts obtained with organic solvents may be injected directly into the nonaqueous system (e.g. the eluate from a solid-phase extraction cartridge, when using MeOH or MeCN as the eluent, may be used for CE without further treatment).
4. The relatively low current generated in organic solvents combined with the volatility of the solvents seems to be promising for CE-MS experiments.

Further Reading

- Altria KD (1998) *Analysis of Pharmaceuticals by Capillary Electrophoresis*, p. 223. Braunschweig/Wiesbaden: F. Vieweg.
- Bjørnsdottir I, Tjørnelund J and Hansen SH (1998) Nonaqueous capillary electrophoresis – its applicability in the analysis of food, pharmaceuticals and biological fluids. *Electrophoresis* 19: 2179.
- Hansen SH, Tjørnelund J and Bjørnsdottir I (1996) Selectivity enhancement in capillary electrophoresis using nonaqueous media. *Trends in Analytical Chemistry* 4: 175.
- Korchennaya EK, Ermakov AN and Bochkova LP (1978) Electrophoresis in nonaqueous and mixed solvents. *Journal of Analytical Chemistry USSR* (Engl. transl.) 33: 635.
- Kenndler E (1993) Organic solvents in capillary electrophoresis. In: Gusman NA (ed.) *Capillary Electrophoresis Technology*, pp. 161–183. New York: Marcel Dekker.
- Sarmini K and Kenndler E (1997) Review, Influence of organic solvents on the separation selectivity in capillary electrophoresis. *Journal of Chromatography A* 792: 3.
- Valko IE, Sirén H and Riekkola M-L (1997) Capillary electrophoresis in nonaqueous media: an overview. *LG-GC International* 10: 190.

Nuclear Magnetic Resonance Detection in Capillary Electrophoresis

See II/ELECTROPHORESIS/Capillary Electrophoresis-Nuclear Magnetic Resonance

One-dimensional Polyacrylamide Gel Electrophoresis

P. G. Righetti, University of Verona, Verona, Italy

Copyright © 2000 Academic Press

Electrophoresis is based on the differential migration of electrically charged particles in an electric field. As such, the method is applicable only to ionic or ionogenic materials, i.e. substances convertible to ionic species (a classic example being neutral sugars, which form negatively charged complexes with borate). In fact, with the advent of capillary zone electrophoresis (CZE) it has been found that a host of neutral substances can be induced to migrate in an electric field by inclusion in charged micelles, e.g. of anionic (sodium dodecyl sulfate, SDS) or cationic (cetyltrimethylammonium bromide, CTAB) surfactants. Even compounds that are not ionic, ionogenic, or complexable can often be analysed by CZE as they are transported past the detector by the strong electroosmotic flow on the capillary walls.

Basically, if one plots the velocity of a zone against the pH in the same zone, electrophoretic techniques can be divided into four main types: zone electrophoresis (ZE) together with moving-boundary electrophoresis (MBE), discontinuous (disc) electrophoresis, isotachopheresis (ITP) and isoelectric focusing (IEF). **Figure 1** represents this classification. It can be seen that IEF and ITP are based on principles that are 'perpendicular' to ZE and MBE. In particular, in IEF, once steady-state conditions have been attained, all proteins reach a zero-velocity ($v = 0$, pH-axis). It is then clear that ITP closes the ring of possibilities: all zones move with the same velocity, but at different pH. Alternatively, electrophoretic techniques may be enumerated in chronological order, as follows: moving boundary electrophoresis (MBE), zone electrophoresis (ZE), disc electrophoresis, isoelectric focusing (IEF), sodium dodecyl sulfate/polyacrylamide gel electrophoresis (SDS-PAGE), two-dimensional (2-D) maps, isotachopheresis (ITP), staining techniques, immobilized pH gradients (IPG), and capillary zone electrophoresis.

ZE became a reality when hydrophilic gels (acting as an anticonvective support) were discovered. Grabar and Williams in 1953 first proposed the use of an agar matrix (currently abandoned in favour of a highly purified agar fraction, agarose). They also combined, for the first time, electrophoresis on a hydrophilic support with biospecific detection (immunoelectrophoresis). Barely two years after that, Smithies (1955) applied another gel, potato starch. The starch blocks were highly concentrated matrices (12–14% solids) and subsequently introduced a new parameter in electrophoretic separations: molecular sieving. Human sera, which in cellulose acetate or paper electrophoresis, were resolved in barely five bands, now produced a spectrum of 15 zones. The most important discovery, however, came with the introduction of polyacrylamide gels and disc electrophoresis; this discovery was thoroughly debated in

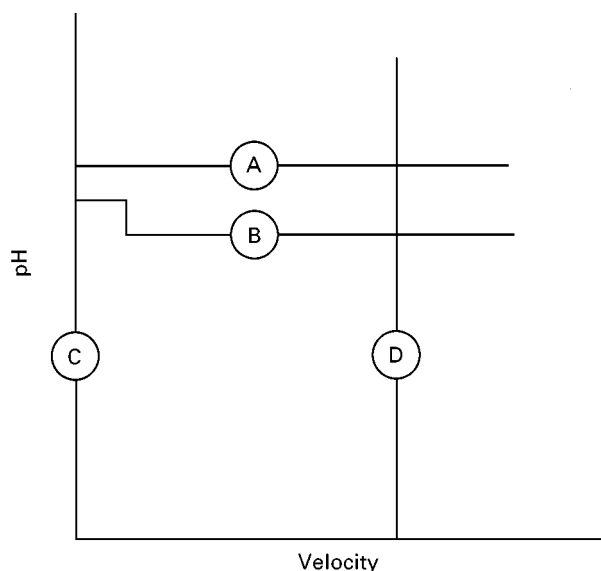


Figure 1 Classification of the four modes of electrokinetic techniques. The velocity of a zone is plotted against the pH in the same zone. (A) zone and moving boundary electrophoresis; (B) discontinuous electrophoresis; (C) isoelectric focusing; (D) isotachopheresis. (Reproduced with permission from Routs RJ (1971) PhD thesis, University of Eindhoven.

a classic electrophoretic volume, which appeared in December, 1964 in the *Annals of the New York Academy of Sciences* (a collectors item!). This was like the explosion of a supernova in the firmament of electrokinetic methodologies. Although most of the above-mentioned techniques belong to the category of one-dimensional PAGE, we will only mention three of them here in detail: disc electrophoresis, SDS electrophoresis and pore-gradient-gel electrophoresis. The other techniques such as IEF and ITP, being steady-state methods, are best performed in non-sieving media. The technique of moving-boundary electrophoresis died out long ago.

Discontinuous Electrophoresis

In 1959 Raymond and Weintraub described the use of polyacrylamide gels (PAG) in ZE, which offered UV and visible transparency (starch gels are opalescent) and the ability to sieve macromolecules over a wide range of sizes. **Figure 2** gives a scheme of reaction for producing polyacrylamide gels from the standard mixture of monomers, acrylamide and the cross-linker Bis. It should be noted that although this matrix should be neutral (except where accidental hydrolysis of acrylamide to acrylic acid occurs), in reality it is not completely devoid of charges; at the

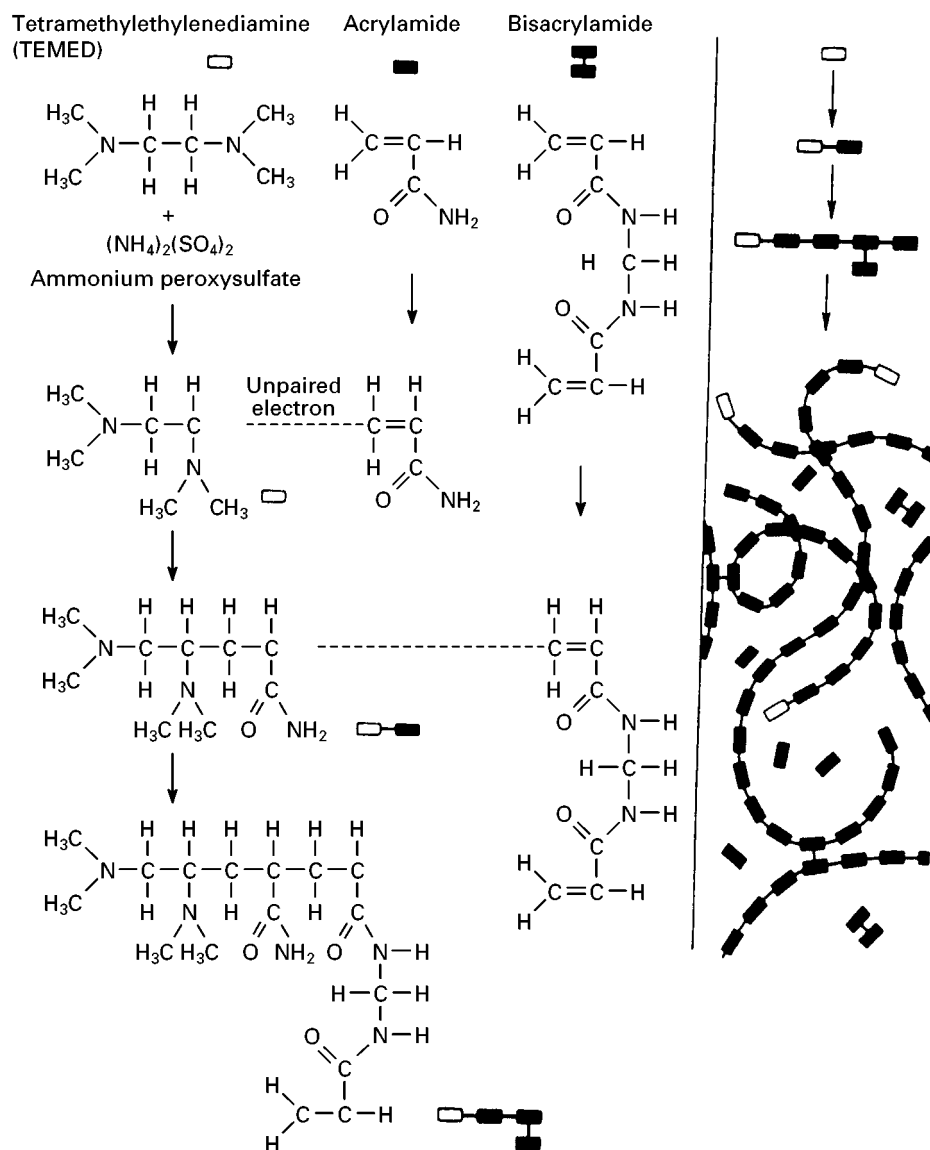


Figure 2 The polymerization reaction of acrylamide. The chemical formula of acrylamide, *N,N'*-methylenebisacrylamide (Bis) and of the initiators (peroxysulfate and *N,N,N',N'*-tetramethylethylenediamine, TEMED) are shown. On the right-hand side, growing polyacrylamide chains, in equilibrium with free monomers, are illustrated. In this particular case, it is assumed that the chain termini are TEMED molecules, although peryoxysulfate could be just as well incorporated.

chain termini either initiator, N,N,N',N' -tetramethylethylenediamine (TEMED), or sulfate, could be incorporated which would impart positive or negative charges, respectively. The fact that polyacrylamides always exhibit a residual electroosmotic flow towards the cathode suggest that an excess of negative charges is incorporated over positive ones (TEMED).

In 1964, Ornstein and Davis created discontinuous (disc) electrophoresis by applying to PAG a series of discontinuities (of leading and terminating ions, pH, conductivity, and porosity), thus further increasing the resolving power of the technique. In discontinuous disc electrophoresis (the principle of which is outlined in Figure 3), the proteins are separated on the basis of two parameters: surface charge and molecular mass. The matrix is divided into three sections (from bottom up): a 'separation', or 'running' gel, a 'spacer' or 'stacking' gel, and a sample gel. A sharp discontinuity exists at the running/stacking interface: the bottom gel is a tightly knit sieve (with small pores), while the second and third layers are minimally sieving, open-pore structures. At the same interface, a second discontinuity exists in pH. In fact, the running gel is titrated at pH 8.9, whereas spacer and sample gels are buffered at pH 6.7. This gel region at

pH 6.7 is also a low conductivity region (third discontinuity), which means that a voltage gradient will be generated in this zone when an electric current is passed through it. Below and above it (in the cathodic chamber) high-conductivity regions are found. A fourth discontinuity exists at the interface between the upper gel end and the liquid in the cathodic compartment: below it only Cl^- (leading, L) ions are present, while above it only glycinate (trailing or terminating, T) ions are found.

Why is there the need for such a complicated system? This intricate set up must satisfy the Kohlrausch regulating function, which is at the heart of ITP (in fact, movement of ions in the first two gel segments will be according to ITP rules). If all the ions in the system are arranged in such a way that $\mu_L > \mu_P > \mu_T$ (where μ is the mobility of leading, protein and terminating ions, respectively), then, upon playing a voltage gradient, they will migrate down the gel cylinder with equal velocities and the boundary between each adjacent species will be maintained. As soon as the electric circuit is closed, Cl^- (fastest moving) ions are swept down the column towards the anode. Just behind this boundary, all protein ions will start arranging themselves in order of their mobilities, with the lowest pI component next to the Cl^- boundary and

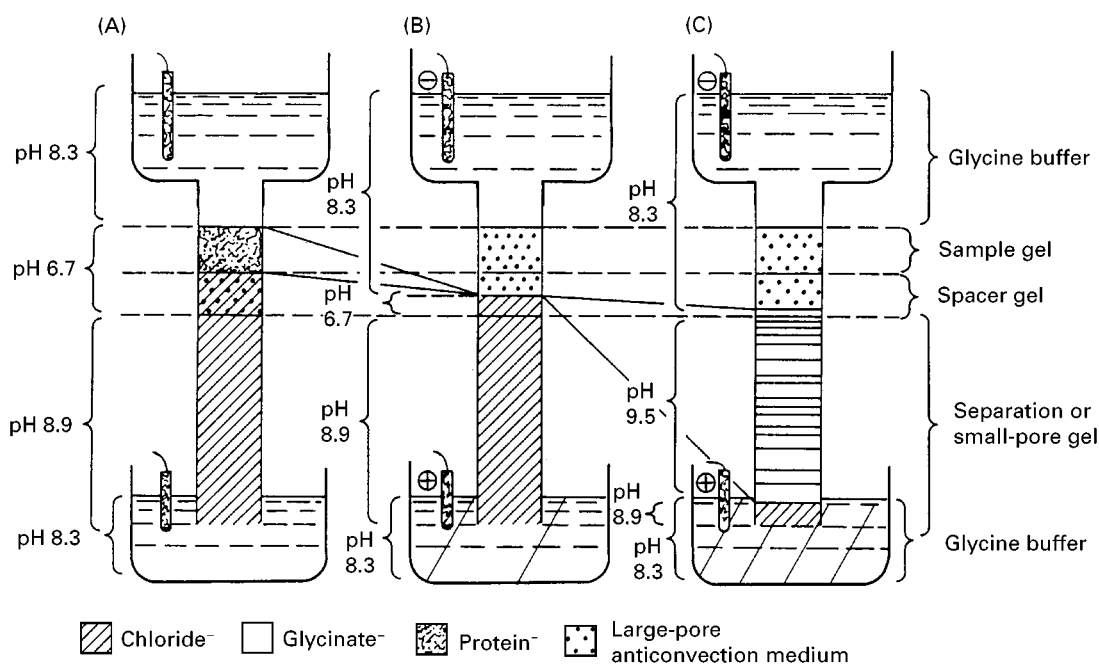


Figure 3 Principle of discontinuous disc electrophoresis. (A) Sample in sample gel; (B) sample concentration in stacking gel; (C) sample separation in running gel. From top to bottom, the following phases are encountered: glycine buffer at pH 8.3 in the cathodic reservoir; sample gel and spacer gel, both titrated to pH 6.7; small-pore running gel, titrated to pH 8.9; and glycinate buffer again in the anodic reservoir at the bottom. In part (C) it is seen that, as the glycinate boundary sweeps down the gel past the protein zones, the pH increases from 8.9 (in A and B) up to 9.5. (Reproduced with permission from Ornstein, 1964.)

the highest pI species closing the procession. The last 'wagon of the train' is the glycinate (terminating) ion; and explains why the sample and spacer gels are titrated at pH 6.7. Gly has a theoretical pI of 6.1 but, as shown by its titration curve, it is almost isoelectric, even at pH 6.7; its anionic mobility, therefore, is extremely small, in any event smaller than the slowest protein ion.

Thus, in the sample and spacer gels, two basic phenomena occur: (1) all protein ions are sorted out and physically separated according to their pI s, and (2) each protein ion is strongly concentrated in extremely thin starting zones (the disc barely a few micrometres thick and a concentration process of up to 1000- to 10 000-fold). This isotachophoretic 'train', however, does not have a long life; as it enters the running gel, the train 'runs off the tracks'. Only the 'locomotive' (Cl^-) of the train is unaffected; the various protein wagons now overrun each other, since they experience a strong frictional force, due to the highly sieving matrix, so that now their velocity is a function of their charge/size ratio. In addition, as the almost isoelectric Gly enters the pH 8.9 zone, its negative charge density strongly increases so that it jumps ahead and closely follows the Cl^- ion. As Gly sweeps down the running gel, the pH increases from pH 8.9 to 9.5 (approaching the pK value of the Gly amino group) so that now the net charge on Gly is -0.5 . As a consequence of this further jump in pH, all proteins experience an additional mobility increment. One might wonder why, after taking on such an experimental burden in forming the ITP train, one should then destroy it and continue the run in the plain zone electrophoretic mode. There are reasons for this. First, the ITP train, while maintaining high resolution due to lack of degradation of zone boundaries, has the main defect that the zones are contiguous and continuous, i.e. they are not separated by blank zones of plain buffer. As a result, when staining the gel, one would only see a single, continuous zone of protein ions, with no visible separation between zones. Second, whereas the sharp protein discs formed during the stacking (ITP) process are separated solely by surface charge, during migration in the running gel, separations continue on the basis of an additional parameter i.e. the mass. The small loss of resolution due to diffusion of the protein discs in the running gel is more than compensated for by the resolution increments due to size (coupled to charge) fractionation in this gel zone. Although disc electrophoresis is no longer in vogue, it was an extremely useful analysis technique for at least 20 years after its inception. Moreover, the general principle has not been abandoned and it is used today as a stacking technique in both SDS and capillary electrophoresis.

Disc electrophoresis could also be used for deriving physico-chemical parameters of the proteins under analysis. In 1964, Ferguson showed that one can derive parameters which are proportional to both the surface charge and the mass of the macromolecule. This can be accomplished by plotting the results of a series of experiments with polyacrylamide gels of varying porosity. For each protein under analysis, the slope of the curve $\log m_T$ (electrophoretic mobility) vs gel density (%T) is proportional to molecular mass, while the y -intercept (Y_0) is a measure of surface charge. Examples of these plots are shown in Figure 4. In Figure 4A the two parallel lines indicate charge isomers; in Figure 4B, the fanning out lines indicate a family of constant charge and different mass; in Figure 4C, the two crossing lines indicate proteins differing in both charge and mass. Recently, non-linear Ferguson plots have been reported (Chrambach, 1988), related to the reptation mode of DNA in sieving media.

Sodium Dodecyl Sulfate (SDS) Electrophoresis

SDS electrophoresis fractionates polypeptide chains essentially on the basis of their size. It is therefore a simple, yet powerful and reliable, method for molecular mass determination. In 1967 Shapiro *et al.* first reported that electrophoretic migration in SDS is proportional to the effective molecular radius and, thus, to the M_r of the polypeptide chain. This means that SDS must bind to proteins and cancel out differences in molecular charge, so that all components will migrate solely according to size. Surprisingly, large amounts of SDS appear to be bound (an average of 1.4 g SDS/g protein). This means that the number of SDS molecules bound is of the order of half the number of amino acid residues in a polypeptide chain. This amount of highly charged surfactant molecules is sufficient to overwhelm effectively the intrinsic charges of the polymer coil, so that their net charge per unit mass becomes approximately constant. If migration in SDS (and disulfide-reducing agents, such as 2-mercaptoethanol, in the denaturing step, for a proper unfolding of the proteins) is proportional only to M_r , then, in addition to cancelling out charge differences, SDS also equalizes molecular shape differences (e.g. globular vs rod-shaped molecules). This seems to be the case for protein-SDS mixed micelles. These complexes can be assumed to behave as ellipsoids of constant minor axis (*c.* 1.8 nm) and a major axis proportional to the length of the amino acid chain (i.e. to molecular mass) of the protein. The rod length for the 1.4 g SDS/g protein

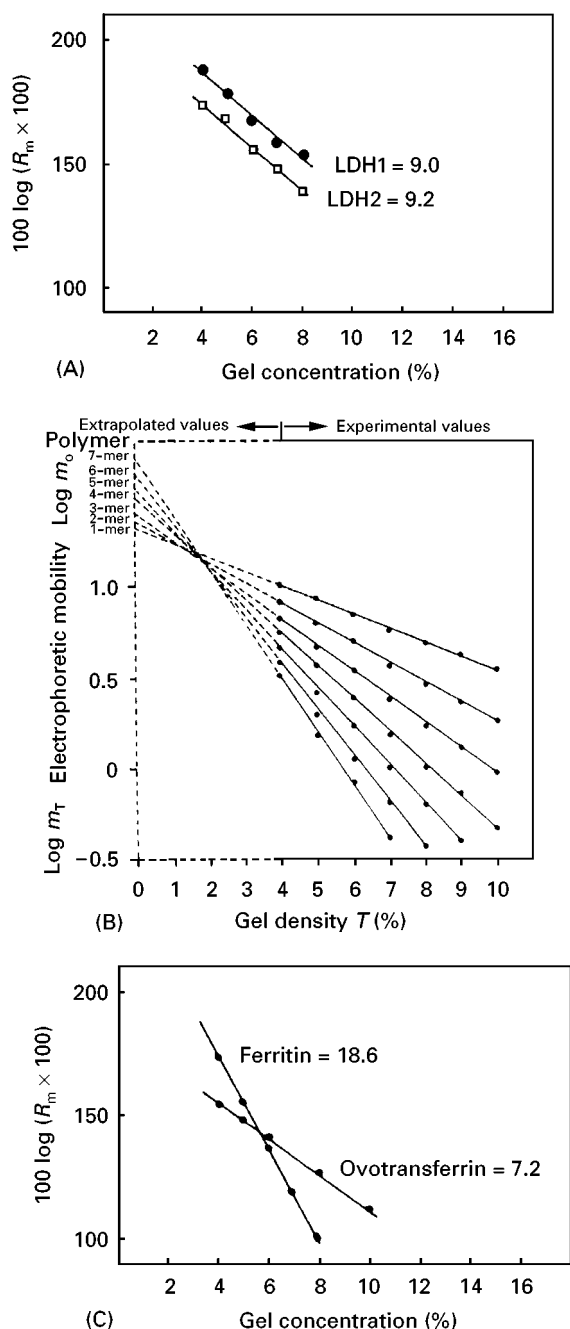


Figure 4 Ferguson plots ($\log R_m$, relative mobility, vs %T, total monomer concentration) in the case of: (A) lactic dehydrogenase (LDH) 1 and 2 (isomers of charge, exhibiting the same mass); (B) serum albumin (polymeric forms, from monomer to heptamer, having constant charge and pure size difference, since all curves meet in gel-free environment, at 2% T where polyacrylamide will liquefy); (C) ferritin and ovalbumin, two totally unrelated proteins differing in both size and charge. (Parts (A) and (C) reproduced with permission from Hedrick and Smith, 1968 and Part (B) from Thorun, 1971.)

complex is of the order of 0.074 nm per amino acid residue. For further information on detergent properties, see Helenius and Simons (1975).

In SDS electrophoresis, the proteins can be prelabelled with dyes that covalently bind to their $-\text{NH}_2$ residues. The dyes can be conventional, like the blue dye Remazol, or fluorescent, such as dansyl chloride, fluorescamine, O-phthalaldehyde, and MDPF (2-methoxy-2,4-diphenyl-3[2H]-furanone). Prelabelling is compatible with SDS electrophoresis, as the size increase is minimal, but would be anathema in disc electrophoresis or IEF, as it would generate a series of bands of slightly altered mobility or pI from an otherwise homogeneous protein. Although at its inception SDS electrophoresis used continuous buffers, today the preferred set up is via discontinuous buffers and matrices, simplified from the original disc electrophoresis assembly (see Figure 5). This ensures much higher resolving power, due to formation of ultrathin protein zones.

For treatment of data, the sample and M_r standards are electrophoresed side-by-side in a gel slab. After detection of the polypeptide zones, the migration distance (or R_F) is plotted against $\log M_r$ to produce a calibration curve (Neff *et al.*, 1981) from which the M_r of the sample can be calculated (see Figure 6). It should be noted that in a gel of constant %T, linearity is obtained only in a certain range of molecular sizes. Outside this limit a new gel matrix of appropriate porosity should be used. Two classes of proteins show anomalous behaviour in SDS electrophoresis: glycoproteins (because their hydrophilic oligosaccharide units prevent hydrophobic binding of SDS micelles) and strongly basic proteins, e.g. histones (because of electrostatic binding of SDS micelles through their sulfate groups). The first anomaly can be partially alleviated by using alkaline Tris/borate buffers, which will increase the net negative charge on the glycoprotein and thus produce migration rates well correlated with molecular size. The migration of histones can be improved by using pore-gradient gels and allowing the polypeptide chains to approach the pore limit.

Porosity Gradient Gels

When macromolecules are electrophoresed in a continuously varying matrix concentration (which results in a porosity gradient) rather than in a gel of uniform concentration, the protein zones are compacted along their track, as the band front is, at any given time, at a gel concentration somewhat higher than that of the rear of the band, so that the former is decelerated continuously. A progressive band sharpening thus results. There are other reasons for resorting to gels of graded porosity. We have seen that disc electrophoresis separates macromolecules on the basis of both size and charge differences. If the influence of molecu-

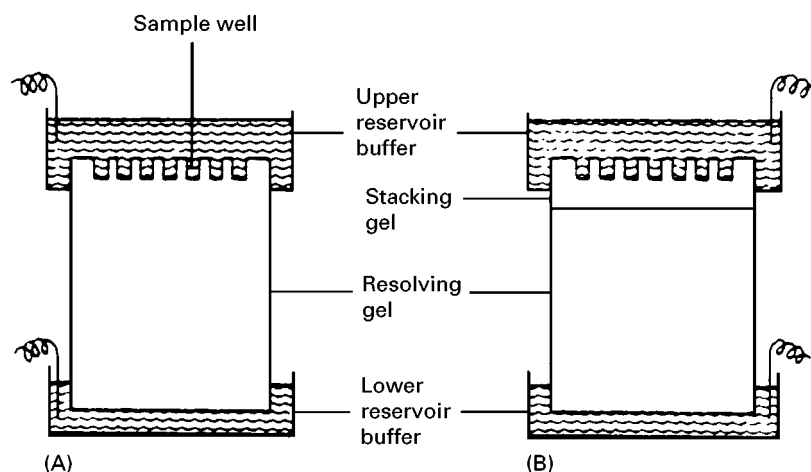


Figure 5 Typical set up of a gel slab for SDS electrophoresis in a continuous (A) or discontinuous (B) gel and buffer system. In both cases, the sample is applied as a dense liquid layer in pockets precast in the gel slab by the teeth of the comb. Note that this mode of sample deposition avoids the use of the third gel phase, the sample gel, as typically adopted in disc electrophoresis.

lar charge could be eliminated, then clearly the method could be used with a suitable calibration for measuring molecular size. This has been

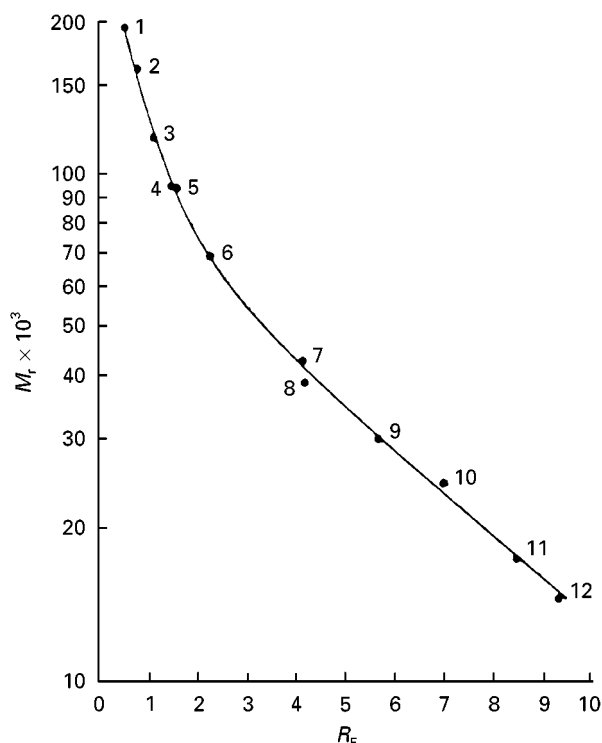


Figure 6 Typical $\log M_r$ vs R_F plot after an SDS-PAGE run. Note that the plot is linear only in the M_r 15 000–60 000 Da range. The M_r markers are: (1) myosin (194 000 Da); (2) RNA polymerase (β - β -subunit, 160 000 Da); (3) β -galactosidase (116 000 Da); (4) phosphorylase B (94 000 Da); (5) RNA polymerase (δ -subunit; 95 000 Da); (6) bovine serum albumin (68 000 Da); (7) ovalbumin (43 000 Da); (8) RNA polymerase (α -subunit; 38 400 Da); (9) carbonic anhydrase (30 000 Da); (10) trypsinogen (24 500 Da); (11) β -lactoglobulin (17 500 Da); and (12) lysozyme (14 500 Da). (Reproduced with permission from Neff *et al.*, 1981.)

accomplished by overcoming charge effects in two main ways. In one such way, a relatively large amount of charged ligand, such as SDS, is bound to the protein, effectively swamping the initial charges present on the protein molecules and giving a quasi-constant charge-to-mass ratio. However, in SDS electrophoresis, proteins are generally dissociated into their constituent polypeptide subunits, and the concomitant loss of functional integrity and antigenic properties cannot be prevented. Therefore, the size of the original, native molecule must be evaluated in the absence of denaturing substances.

In the second method for M_r measurement, this can be done by relying on a mathematical cancelling of charge effects, following measurement of the mobility of native proteins in gels of different concentrations. This is the so-called 'Ferguson plot' discussed above. As a third method for molecular size measurements one can use gels of graded porosity. This method is characterized by high resolving power and relative insensitivity to variability in experimental conditions. See Figure 7 for a typical experimental set up for casting porosity gradients in gel slabs. Under appropriate conditions (at least 10 kV \times hours), the mobility of most proteins becomes constant and eventually ceases as each constituent reaches a gel density region in which the average pore size approaches the diameter of the protein (pore limit) (Margolis and Kenrick, 1968). Thus, the ratio between the migration distance of a protein to that of any other becomes a constant after the proteins have all entered a gel region in which they are subjected to drastic sieving conditions. This causes the electrophoretic pattern to become constant after prolonged migration in a gel gradient. The gel concentration at which the migra-

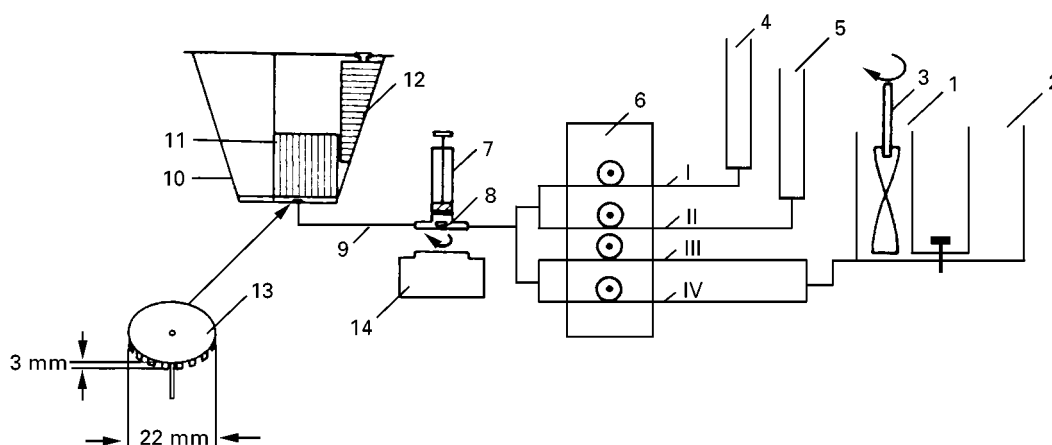


Figure 7 Scheme of the apparatus used for the simultaneous preparation of eight gradient gel slabs. (1) and (2) two-chamber mixer; (3) stirrer; (4) reservoir for peroxosulfate; (5) reservoir for TEMED; (6) proportioning pump; (7) modified disposable syringe, used as small chamber mixer; (8) magnetic bar; (9) tube connecting the stirrer to the gel casting apparatus (10); (11) gel cassettes; (12) wedge; (13) distributor; (14) magnetic stirrer; I and II, 0.5 mm i.d. vinyl tubings; III and IV, 3.16 mm i.d. vinyl tubings. (Reproduced with permission from Rothe and Purkhanbaba, 1982.)

tion rate for a given protein becomes constant is called the 'pore limit'. If this porosity is properly mapped with the aid of a suitable set of marker

proteins, it is possible to correlate the migration distance to the molecular mass of any constituent in the mixture.

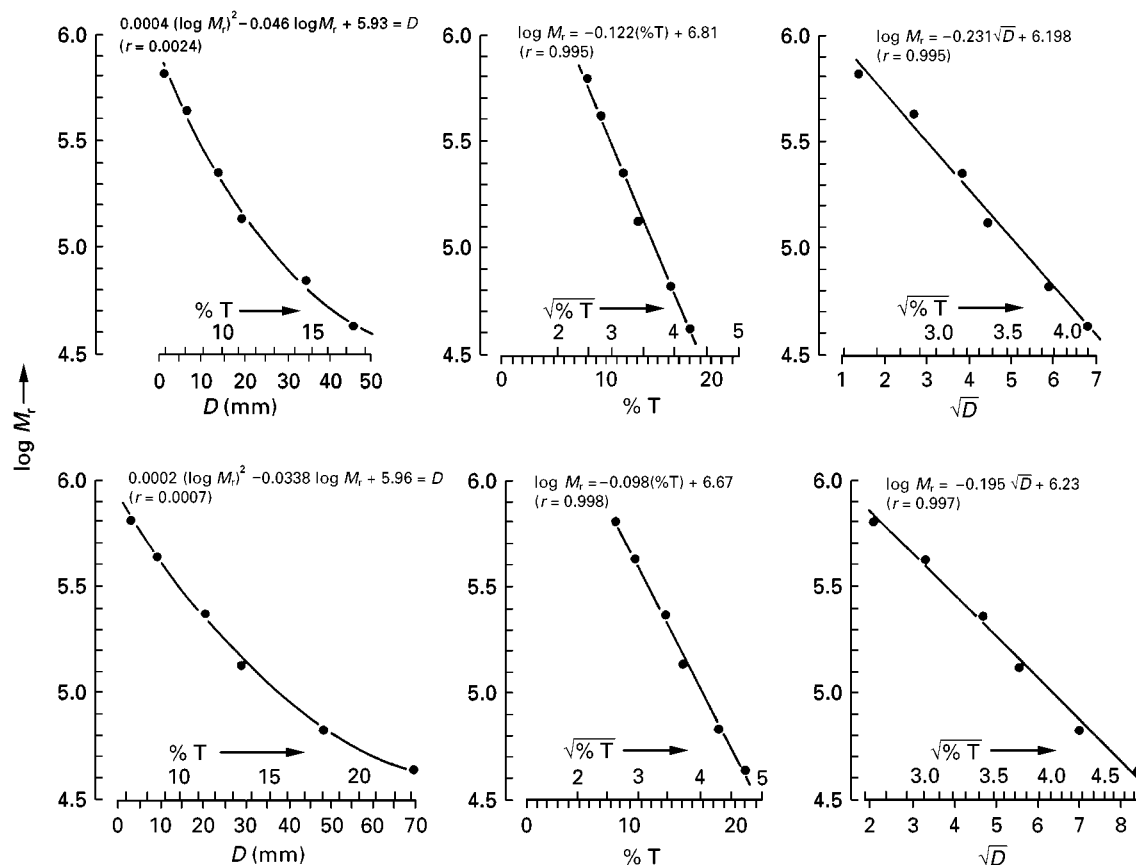


Figure 8 Typical $\log M_r$ vs migration distance (D) or gel composition (%T) plots after pore-gradient electrophoresis. Note that these plots are non-linear, whereas when $\log M_r$ is plotted against \sqrt{D} or $\sqrt{\%T}$ a linear relationship is obtained. (Reproduced with permission from Rothe and Purkhanbaba, 1982.)

After electrophoresis has finished, the experimental data gathered can be handled in two ways: a two-step or a one-step method. The most promising two-step approach appears to be that of Lambin and Fine (1979), who observed that there is a linear relationship between the migration distance of proteins and the square root of electrophoresis time, provided that time is kept between 1 and 8 h. The slopes of the regression lines of each protein in the above graph are an indication of molecular size. When the slopes of the various regression lines thus obtained are plotted against the respective molecular masses, a good linear fit is obtained, which allows M_r measurements of proteins of between 2×10^5 and 10^6 Da. The shape of the proteins (globular or fibrillar), their carbohydrate content (up to 45%) and their free electrophoretic mobilities (between 2.1 and $5.9 \times 10^{-5} \text{ cm}^2 \text{ V}^{-1} \text{ s}^{-1}$) do not seem to be critical for proper M_r measurements by this procedure. One-step methods have been described by Rothe and Purkhanbaba (1982). These authors found that when $\log M_r$ is plotted against either D (distance migrated) or %T (acrylamide + Bis), a nonlinear correlation is always obtained. However, when $\log M_r$ is plotted vs $\sqrt{\%T}$ or \sqrt{D} , a linear regression line is obtained, which allows the accurate determination of M_r values of proteins (standard deviation of $\pm 3.7\%$; see Figure 8. The correlations $\log M_r - \sqrt{\%T}$ or $\log M_r - \sqrt{D}$ are not significantly altered by the duration of electrophoresis. Therefore, a constant M_r value should be obtained for a stable protein, no matter how long electrophoresis takes. More recently, Rothe and Maurer (1986) have demonstrated that the relationship $\log M_r$ vs \sqrt{D} is also applicable to SDS electrophoresis in linear polyacrylamide gel gradients.

Further Reading

- Chrambach A (1988) Particle and gel fiber properties derived from the mobilities in gel electrophoresis: the dilectics of Ferguson plots. In: Schafer-Nielsen (ed.) *Electrophoresis* 88, pp. 28–40. Weinheim: VCH.
- Davis BJ (1964) Disc electrophoresis. II: method and application to human serum proteins. *Ann. N.Y. Acad. Sci.* 121: 404–427.

- Ferguson KA (1964) Derivation of size and charge of proteins from polyacrylamide gel electrophoresis at different %T. *Metabolism* 13: 985–995.
- Frederick JF (1964) Gel electrophoresis. *Ann. N.Y. Acad. Sci.* 121: 307–650.
- Grabar P and Williams CA (1953) Methode permettant l'etude conjugée des proprietes electrophoretiques et immunochimiques d'un melange de proteins; application au serum sanguine. *Biochim. Biophys. Acta* 10: 193–201.
- Hedrick JL and Smith AJ (1968) Size and charge isomer separation and estimation of M_r of proteins by disc gel electrophoresis. *Arch. Biochem. Biophys.* 126: 155–163.
- Helenius A and Simons K (1975) Solubilization of membranes by detergents. *Biochim. Biophys. Acta* 415: 29–79.
- Lambin P and Fine JM (1979) M_r estimation of proteins by electrophoresis in linear polyacrylamide gradient gels in the absence of denaturing agents. *Anal. Biochem.* 98: 160–168.
- Margolis J and Kenrick KG (1968) Polyacrylamide gel electrophoresis in a continuous molecular sieve gradient. *Anal. Biochem.* 25: 347–358.
- Neff JL, Muniz N, Colbourn JL and de Castro AF (1981) Convenient procedures for SDS and conventional disc electrophoresis. In: Allen RC and Arnauds P (eds) *Electrophoresis* 81, pp. 49–63. Berlin: de Gruyter.
- Ornstein L (1964) Disc electrophoresis. I: background and theory. *Ann. N.Y. Acad. Sci.* 121: 321–349.
- Raymond S and Weintraub L (1959) Polyacrylamide gel: a new matrix for zone electrophoresis of proteins. *Science* 130: 711–712.
- Rothe GM and Maurer WD (1986) One dimensional PAA-gel electrophoretic techniques to separate functional and denatured proteins. In: Dunn MJ (ed.) *Gel Electrophoresis of Proteins*, pp. 37–140. Bristol: Wright.
- Rothe GM and Purkhanbaba M (1982) Determination of M_r and Stokes' radii of non-denatured proteins by PAGE. I: an equation relating total polymer concentration, the M_r of proteins in the range 10^4 – 10^6 and duration of electrophoresis. *Electrophoresis* 3: 33–42.
- Shapiro AL, Vinuela E and Maizel JV Jr (1967) M_r estimation of polypeptide chains by electrophoresis in SDS-polyacrylamide gels. *Biochem. Biophys. Res. Commun.* 28: 815–820.
- Smithies O (1955) Zone electrophoresis in starch gels: group variations in the serum proteins of normal adults. *Biochem. J.* 61: 629–636.
- Thorun W (1971) Estimation of the size of albumin oligomers via Ferguson plots. *Z. Klin. Chem. Klin. Biochem.* 9: 3–13.

One-dimensional Sodium Dodecyl Sulfate Polyacrylamide Gel Electrophoresis

G. L. Jones, University of New England, Armidale, Australia

Copyright © 2000 Academic Press

Introduction

Technical and Developmental Details of Basic Technique

Any ion will undergo electrophoresis to migrate in an electric field. Proteins are complex polyions with a net charge at all pH values other than its isoelectric point. Problems associated with convective disturbance in free solution led early researchers to consider various supporting media for electrophoresis such as paper, cellulose acetate and various thin layer materials where the separation depends largely on the charge density at a given pH. The reader should refer to the separate articles on Electrophoresis Theory and Cellulose Acetate Electrophoresis for further details. Other early workers considered the properties of various gels where the pore size approximates the size of the protein molecules themselves leading to a separation based on both charge and molecular size. The extent of molecular sieving depends on the pore size of the gel being used. For example, the pore size of agarose gels is sufficiently large that sieving of most proteins is minimal, whereas larger DNA molecules are sieved very well. Again, for a discussion of this refer to the separate article on Agarose Electrophoresis.

The pore size of polyacrylamide gels may be changed in a systematic and reproducible fashion by varying the percentage of monomer and crosslinker to give a matrix which maximizes the molecular sieving effect for a wide range of proteins and the reader should refer to the separate article on Polyacrylamide Gel Electrophoresis (PAGE) for a discussion on varying porosity in this medium.

Native proteins, however, often occur as multiple supramolecular assemblies of many peptide subunits in different configurations affected by non-covalent bonding, particularly in the case of membrane proteins. Shapiro *et al.* (1967) first demonstrated the potential of the superior protein dissociating qualities of sodium dodecyl sulfate (SDS) in an electrophoretic system designed to separate individual polypeptides on the basis of their molecular weight alone but the definitive publication in this area is undoubtedly that of Laemmli (1970) who first

combined a discontinuous buffer system (see separate article on Discontinuous Electrophoresis) with the use of SDS in sample preparation and gel electrophoresis. Protein complexes are solubilized and dissociated with such high efficiency in 2% SDS and 5% mercaptoethanol that typically over 90% of the protein in a crude lysate will enter the gel matrix and be resolved.

In the discontinuous system, proteins are dissolved by denaturing treatment at 100°C with the dissociating agents SDS and mercaptoethanol in a Tris-HCl buffer at pH 6.8. Gels are constructed in two stages both containing 0.1% SDS. The separating gel in the original Laemmli publication was formed using 30% stock acrylamide monomer with 0.8% bisacrylamide as a cross-linker. A final solution was made to 8 or 10% acrylamide containing 0.375 M Tris-HCl pH 8.8. The resolving (separating) gel is polymerized using tetramethylethylenediamine (TEMED) (catalyst) and ammonium persulfate (free radical initiator). A 'stacking' gel (at 3% acrylamide) is then cast on top of the resolving gel in the same manner but containing 0.125 M Tris-HCl at the same pH as the buffer in which the protein mixtures were dissociated (pH 6.8). The electrode buffer contains 0.025 M Tris/0.192 M glycine to a pH of 8.3 also with 0.1% SDS. Upon electrophoresis, protein anions in the form of rod-shaped SDS complexes are compressed in the stacking gel between the leading chloride ions and the trailing glycinate ions which, because of the pH difference between buffer systems, progressively close the gap as electrophoresis proceeds. (Again, see the separate articles on Discontinuous Electrophoresis and Iso-tachophoresis). The result is a concentration or stacking of the SDS-protein anions as extremely sharp bands ($\approx 5\text{--}10\text{ }\mu\text{m}$) behind the leading chloride ion in strict order of mobility. These complexes then enter the separating gel and since, supposedly, the charge-mass ratio is invariant (see later for a caveat) are separated by molecular sieving according to their molecular size only. Gels of particular acrylamide concentration and therefore pore size may be calibrated using standard proteins of known molecular weight. By extrapolation, reliable molecular weight estimates of large numbers of polypeptides in a complex mixture may be obtained. Proteins are fixed in the gel after electrophoresis using a 50% trichloroacetic acid solution and stained in a Coomassie blue solution. Radiolabelled proteins were also detected by autoradiography. For a more detailed

discussion please refer to the separate article on Detection Techniques, Staining, Autoradiography and Blotting.

In the original Laemmli procedure, gels were electrophoresed in small glass cylinders and since the absolute mobility of SDS-polypeptides varied slightly from gel to gel the relative mobility of standard and unknown bands was calculated as the ratio between the mobility of the protein and the mobility of the tracking dye, bromphenol blue (BPB), which travels with the SDS-micelle front behind the leading buffer front.

A major improvement on the original procedure uses rectangular slab gels of uniform thickness (typi-

cally 0.5–1.5 mm) with sample wells (typically 10–30) set into the stacking gel. Electrophoretic apparatus was originally constructed according to a variety of *ad hoc* patterns, in house, from perspex, using gels polymerized between notched glass plates, although now most laboratories use commercially available equipment. The use of such equipment (see the separate article on Slab Gel Electrophoresis: Equipment) has led to highly standardized reliable separations since standards and unknowns may be run under identical conditions. The apparent molecular weights of unknowns may be obtained by extrapolation from a plot of log MWt vs. mobility of standard proteins. **Figure 1** shows how individual

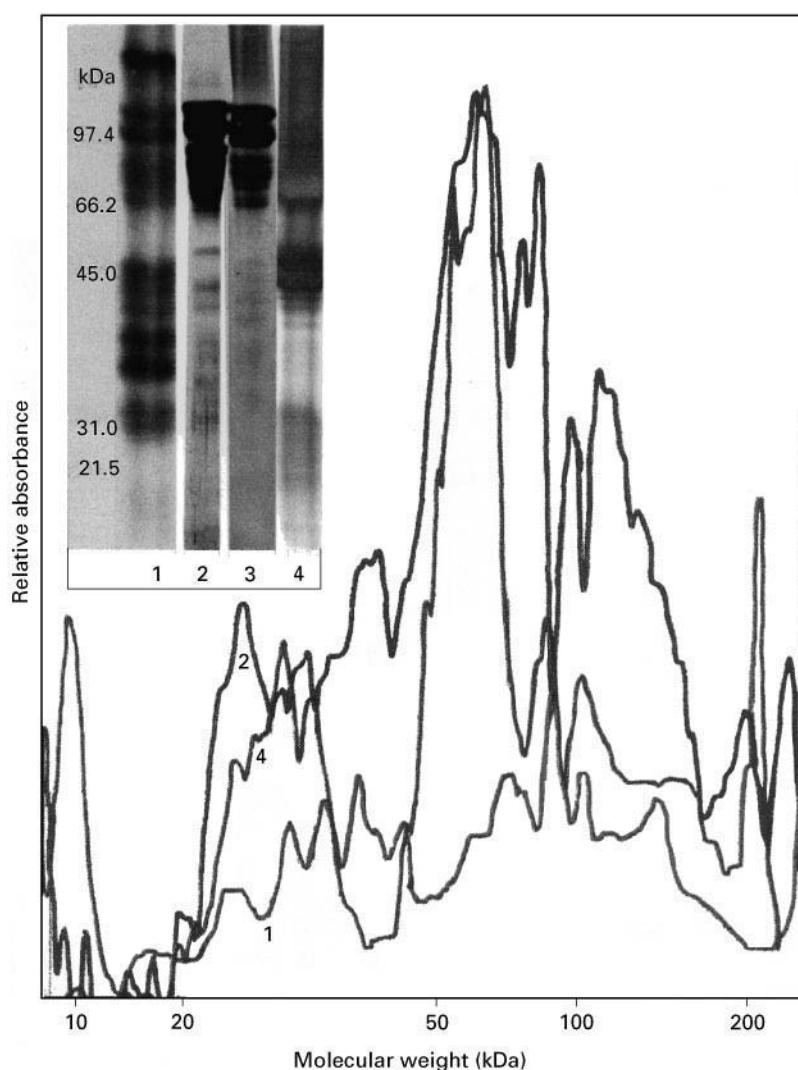


Figure 1 (See Colour Plate 41). The inset shows the separation of human head hair proteins using 12% sodium dodecyl sulfate-polyacrylamide gel electrophoresis with the point of migration of standard proteins to the left under the heading kDa: lanes 1–3 *S*-carboxymethylated proteins; lane 4 reduced non-*S*-carboxymethylated proteins: lane 1 ^{14}C Autoradiograph; lanes 2 and 4, silver stain; lane 3, Coomassie stain. The main body of Figure 1 shows a densitometric profile of the separated lane 1 (autoradiograph ^{14}C -*S*-carboxymethylated, green). Lane 2 (silver stain, *S*-carboxymethylated, red); lane 4 (silver stain, non-*S*-carboxymethylated). Molecular weights were extrapolated from a plot of log MWt vs. relative migration of standard proteins.

zones in a complex mixture of human hair keratins may all be assigned an apparent molecular weight and how the entire molecular weight profile is apparently shifted 20–40 kDa higher after S-carboxymethylation.

Although several alternative sample extraction and buffer systems are available (see later), the use of the basic Laemmli system has proved so robust and reliable that it has revolutionized protein characterization in complex mixtures to the extent that proteins of widely differing function are routinely described according to their apparent molecular mass on Laemmli SDS-PAGE. The explosive increase in the use of this technique across a comprehensive range of the biological sciences is illustrated in Figure 2 showing the number of citations each year of the Laemmli (1970) publication.

I will now discuss subsequent major methodological developments of the basic Laemmli protocol.

Other SDS-PAGE Systems

The SDS-PAGE technique may also be performed with the simpler continuous phosphate buffer system of Weber and Osbourne, although dilute samples are not concentrated by stacking as they are in the discontinuous system of Laemmli. In general, however, very dilute protein samples may be concentrated by precipitation with trichloroacetic acid or acetone prior to loading.

Separations of peptides and protein mixtures ranging in molecular weight from 300 kDa down to about 10–12 kDa may be optimally achieved using resolving gels of different fixed acrylamide concentrations as, for instance, shown in Figure 3A (7.5%) or B (10%) for the separation of phosphoproteins during the invasion of human red blood cells by the malarial parasite. Alternatively, a gradient mixer may be used to produce resolving gels with a linear or concave concentration gradient.

Peptides of less than 10 kDa are not resolved using the normal Laemmli system even at maximal acrylamide concentration so a variety of modified buffer systems have been introduced to allow the separation of, for example, cyanogen bromide and proteolytically cleaved peptides for structural analysis of proteins. The original Swank and Monckres system uses SDS/urea and is capable of resolution down to 2 kDa, although some undesirable modifications of amino acids may take place in the presence of urea. Other buffer systems designed to fractionate low molecular weight peptides such as the tricine and the modified Laemmli system have been more recently introduced to address this problem. For a detailed technical discussion of the preparation of gels using these various

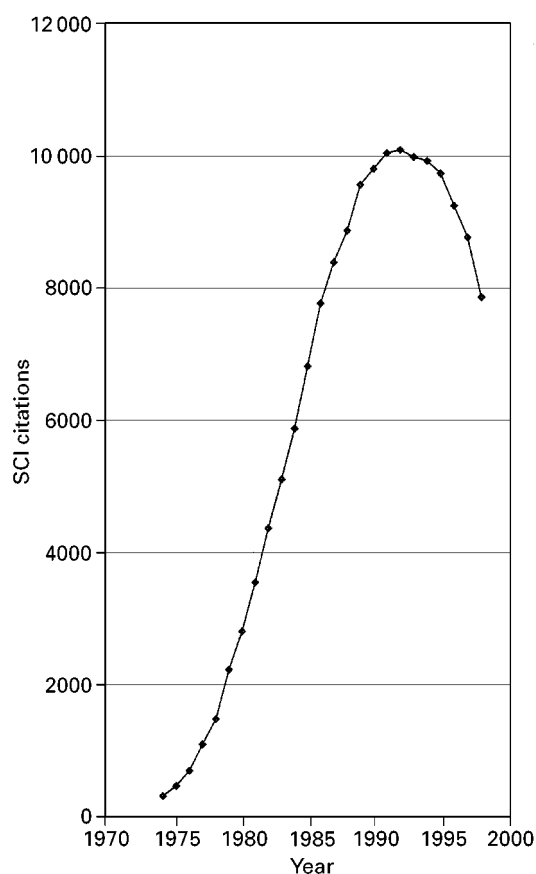


Figure 2 The number of SCI citation of the original Laemmli, U.K. (1970) paper on sodium dodecyl sulfate-polyacrylamide gel electrophoresis for each year from 1974 (when SCI started).

buffer systems one should refer to one or more of the following generally excellent technical guides available (*Current Protocols in Molecular Biology*; *Gel Electrophoresis of Proteins – A Practical Approach*; *Protein Purification, Principles – High Resolution Methods and Techniques*).

Identification of Resolved Protein Zones

Protein bands may be directly visualized by scanning unstained unfixed gels at A_{280} but most workers employ a protein stain after fixation. Coomassie R-250 dye binds noncovalently to proteins giving deep blue bands on a clear background after diffusion (see Figure 5) or electrophoretic destaining. Alternatively, fixed proteins may be revealed by the precipitation of silver granules from an alkaline silver nitrate solution. The procedure is more complicated than the dye-binding protocol but can be up to 100 times more

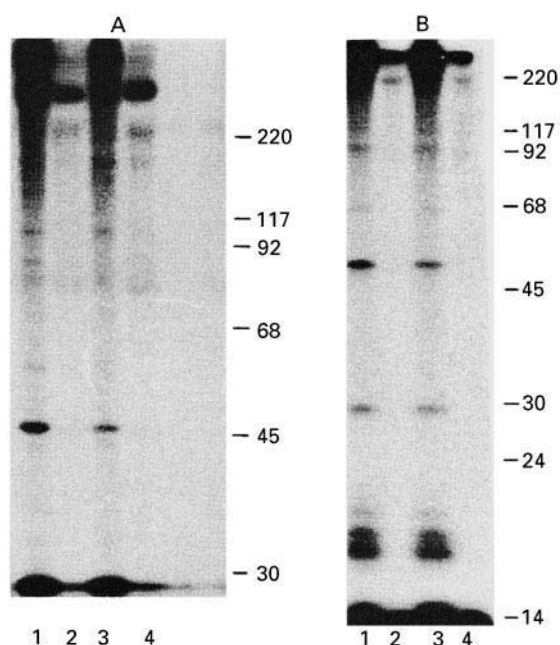


Figure 3 Sodium dodecyl sulfate-polyacrylamide gel electrophoresis showing protein phosphorylation in human blood cells parasitized with the malarial organism *Plasmodium falciparum* using continuous metabolic labelling with ^{32}P phosphate. A, 7.5% Resolving gel; B, 10% Resolving gel. Mobility of molecular weight standards indicated in kiloDaltons to the right of gel A and gel B. Lane 1, parasite pellet (mature shizonts) 36 h post label; lane 2, infected red cell ghost 36 h post label; lane 3, parasite pellet (new rings) 50 h post label. Lane 4, infected red cell ghost 50 h post label.

sensitive. Several commercial kits are now available, ensuring the robust reproducibility of the once notoriously fickle silver staining technique. Because of this and the added sensitivity the silver staining technique has now become standard in most laboratories. Proteins vary markedly in their affinity for either Coomassie dye or silver. The insert to **Figure 1** (lanes 2 and 3) shows a comparison of the proteins separated from human hair after solubilization and carboxymethylation using either silver stain or Coomassie stain respectively. The differing sensitivities are obvious. Lane 1 shows the same proteins labelled with ^{14}C iodoacetic acid and revealed by autoradiography. Note that the lower molecular weight zones are very strongly labelled whereas they stain relatively weakly with silver (lane 2) and very poorly with Coomassie dye (lane 3).

Detection of Radiolabelled Proteins

Proteins may be radiolabelled during synthesis in the presence of labelled amino acids. ^{35}S methionine is commonly used in this regard. **Figure 4**, for instance, shows biosynthetic labelling in human lymphocytes

before and after heat shock. ^3H and ^{14}C labelled amino acids are also used as is ^{32}P phosphate (see **Figure 3**) to label phosphoamino acids. ^{35}S , ^{14}C and ^{32}P may be detected by direct autoradiography by placing fixed dried gel slabs against suitably sensitized X-ray film. The sensitivity of detection depends, on the level of incorporation of the particular

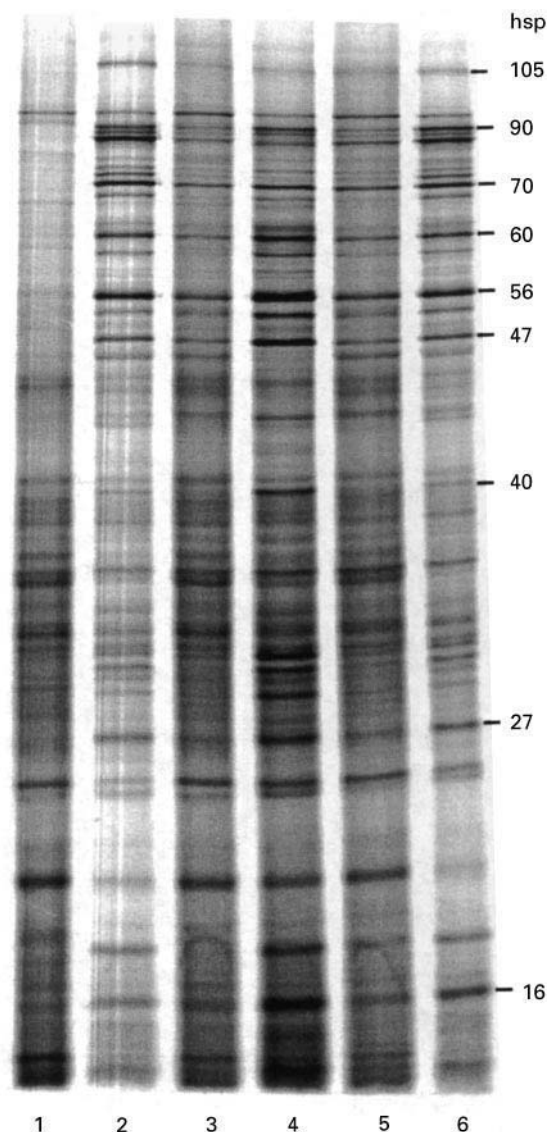


Figure 4 A 10% sodium dodecyl sulfate-polyacrylamide gel electrophoresis separation of ^{35}S methionine-labelled proteins from human lymphocytes after different recovery periods from 1 h heat shock at 42°C . Control cells from the same individual were maintained at 37°C . Lane 1, 2 h control; lane 2, 2 h after heat shock; lane 3, 3-h control; lane 4, 3 h after heat shock; lane 5, 4-h control; lane 6, 4 h after heat shock. Numbers to the right of the gel indicate the position of major heat shock proteins (hsp) induced after heat shock. Hsps are routinely classified according to their apparent molecular weight (105, 90, 70 kDa, etc.) after one-dimensional SDS-PAGE. (Thanks to my PhD student D. Visala Rao for this gel.)

amino acid into the particular protein zone but also on the isotope itself. For example after a 24-h exposure about 300–500 d.p.m.cm² of ³²P will give a visible band whereas about tenfold this level of radioactivity is required to produce a visible band using ³⁵S or ¹⁴C label. ³H label is not detected because the low β -emissions do not penetrate the gel matrix. A fluor may be introduced into the gel matrix prior to gel drying to detect ³H-labelled proteins as well as to improve the sensitivity to ¹⁴C and ³⁵S.

Proteins may also be labelled post synthetically using such reagents as ¹⁴C iodoacetic acid which preferentially labels available sulphydryl groups (see Figure 1, insert lane 1) and ¹²⁵I which preferentially labels available tyrosine groups. Many laboratories use phosphoimaging whereby the radioactive proteins in the gel excite a phosphorescent screen and the number of excitation events is directly digitized. Although this instrumentation is rather expensive it obviates the need for X-ray film and gives results in hours rather than days. Effective concentrations are said to be linear over six orders of magnitude whereas the linear range for X-ray film detection rarely covers one order of magnitude. For further details see the separate article on Detection Techniques: Staining, Autoradiography and Blotting. Radioactivity may also be quantified in gels after slicing and solubilization. In this case, a generally useful labile crosslinker N,N'-diallyltartardiamide (DATD) is often used in place of bisacrylamide.

Identity of Individual Protein Zones

The appearance of single discrete zones on SDS-PAGE, sometimes used as an indicator of homogeneity in protein purification (see Figure 5), does not preclude the possibility of multiple comigrating protein species with differing independent functions. Zones may be identified immunologically after Western blotting onto a suitable matrix and again the reader should refer to the separate article on Detection Techniques: Staining, Autoradiography and Blotting in this series for further details.

Although the process of the SDS-PAGE results in largely inactive proteins, some techniques allow *in situ* renaturation followed by specific enzyme detection (for proteases, for example). A potentially powerful development involves a second dimension SDS-PAGE separation of the entire repertoire of protein zones separated in the first dimension after co-stacking with a protease that retains its activity in the presence of SDS. In this way, a comprehensive peptide map of the proteins may be obtained and homologous proteins identified within or between species. Proteolytic fragments, so separated, may also

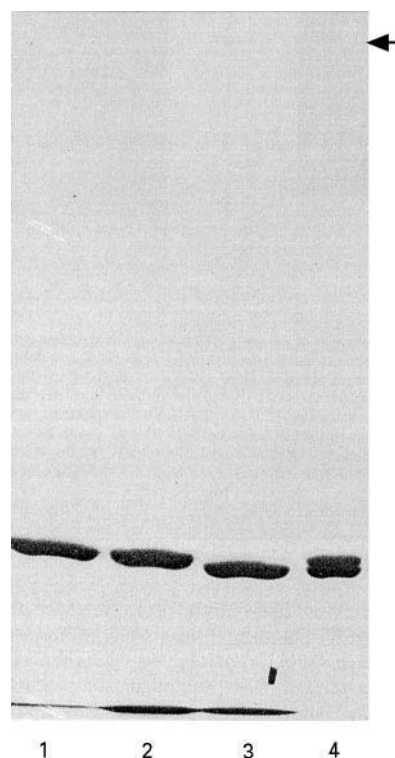


Figure 5 Sodium dodecyl sulfate-polyacrylamide gel electrophoresis of purified human carbonic anhydrase I. The horizontal arrow indicates the interface between the 4% stacking gel and the 10% resolving gel. (1) Purified Caucasian enzyme; (2) purified normal component from isoelectric focusing; (3) purified variant component from isoelectric focusing; (4) purified heterozygote mixture before resolution of normal and variant components. Reproduced with permission from Jones GL and Shaw DC (1982) *Biochemical Genetics* 20: 943.

be transferred onto a PVDF membrane and sequenced.

Glycoproteins may be distinguished using the specific periodic acid-Schiffs (PAS) stain whereas phosphoproteins may be detected by intact cell metabolic labelling with ³²P phosphate (see Figure 3) or with [γ -³²P] ATP in crude lysates.

Scanning and Quantification of Individual Protein Zones

Proteins identified by specific or nonspecific staining techniques or by autoradiography or fluorography may be quantified in a relative sense after densitometric scanning of stained gels, photographs or autoradiographs. The inset to Figure 1 shows the separation of human hair proteins before (lane 4) and after (lanes 1–3) ¹⁴C-S-carboxymethylation. Proteins are detected by ¹⁴C autoradiography (lane 1),

Coomassie (lane 2) or silver stain (lanes 2 and 4). The main body of Figure 1 shows a gel scan of lane 2 (red) and lane 4 (blue) as well as the scan of the autoradiograph (lane 1, green) according to the apparent molecular weight of each component in the complex densitometric scan. Readers should refer to the separate article on Instrumentation for Scanning gels for further details in this field.

Anomalous Migration in SDS-PAGE

The precise structural relationship of SDS to protein during SDS-PAGE is unknown but various studies have indicated that a wide variety of proteins all bind a relatively constant amount of SDS ($\approx 1.4 \text{ g SDS g}^{-1}$ protein) and adopt a similar flexible rod shape regardless of their native configuration. It is this supposedly constant very high and uniform charge-mass ratio which allows for reliable molecular weight determination since migration rate therefore depends on molecular sieving alone. Having said this, even the original paper of Laemmli referred to the anomalously slow migration of a bacteriophage point mutant. The very basic proteins, histones, behave so anomalously that special buffer conditions in the presence of urea must be employed to determine reliably their molecular weights. Glycoproteins also show anomalous migration. In this laboratory we have, over the years, seen direct evidence of discrete changes in apparent migration in SDS-PAGE related to single mutations which change the charge on a protein without significantly affecting its calculated molecular weight. Figure 5, for instance, shows an SDS-PAGE separation of purified carbonic anhydrase 1 (CA1) from a Caucasian blood donor (lane 1) or an Australian Aboriginal donor (lane 4) who is heterozygous for a polymorphic variant CA1-9. The normal and the variant component of the heterozygote were resolved by isoelectric focusing (lanes 2 and 3, respectively). The variant component differed from the normal component at only one position (Asp \rightarrow Gly) although the apparent molecular weight after SDS-PAGE was 27 kDa compared with 28.5 Da. From this and other previous studies with defined point mutations of defined proteins we propose that each extra negative charge on a modified protein results in retardation on SDS-PAGE such that its apparent molecular weight is greater by 1.5 kDa. We have applied this rule of thumb to changes in the apparent molecular weights of the keratins of human hair after *S*-carboxymethylation which substitutes an extra negative charge for each thiol. See Figure 1 for general molecular weight shift of hair proteins after *S*-carboxymethylation – compare the profile from lane 4 (red) with the profile from lane 2 (blue). Given the

published molecular weights of the unmodified keratins we were then able to calculate an apparent thiol content in rough agreement with previous estimations assuming that each thiol group was substituted with an extra negative charge after carboxymethylation (lane 2).

We are therefore convinced that electrophoretic migration of SDS-protein complexes is not totally independent of charge of the native protein and furthermore that if a one-dimensional SDS-PAGE system could be suitably calibrated, the relationship we have described could become useful in studies where the net charge on a given protein is changed genetically or epigenetically in an incremental way.

Conclusions

Over the past 30 years, one-dimensional SDS-PAGE has become a standard technique in most biological and biomedical laboratories. It offers a powerful combination of resolution (up to 200–300 components in crude mixtures), reliability, versatility (pore size, extraction conditions and buffer systems can be tailored precisely to the conditions required for particular proteins) and reproducibility (different laboratories all refer confidently to certain proteins by their apparent molecular weight on SDS-PAGE, e.g. Hsp 70; see Figure 4). In addition, selectivity may be enhanced by using a variety of detection methods ranging from nonspecific staining, metabolic and postmetabolic radiolabelling to highly specific immunological detection after Western blotting. One may confidently expect that one-dimensional SDS-PAGE will continue to play a central role in protein separation in biological laboratories for many years to come, even though Figure 2 suggests that the technology uptake is now stable in that the citation rate peaked in 1990. It may be that improvements in two-dimensional technology (see the article on Two-dimensional SDS-PAGE) and the developing discipline of proteomics involving ever more powerful software to analyse complex two-dimensional protein gels will see a slow erosion of the central position of one-dimensional SDS-PAGE in isolation as method of choice in the resolution of complex protein mixtures.

See Colour Plate 42.

Further Reading

- Gallagher SR (1996) 1D SDS-PAGE. In: Ausubel *et al.* (eds) *Current Protocols in Molecular Biology*, vol. 2, ch. 10. Massachusetts: John Wiley and Son.
- Hames BD and Rickwood D (eds) (1990) *Gel Electrophoresis of Proteins: A Practical Approach*, 2nd edn. New York: Oxford University Press.

- Hunkapiller MW, Lujan E, Ostrander F and Hood LE (1983) Isolation of microgram quantities of proteins from polyacrylamide gels for amino acid sequence analysis. *Methods in Enzymology* 91: 227.
- Laas T (1989) Electrophoresis in gels. In: Janson J-C and Ryden L (eds) *Protein Purification – Principles, High Resolution Methods and Applications*. New York, Weinheim and Cambridge: VCH Publishers.
- Laemmli UK (1970) Cleavage of structural proteins during the assembly of the head of bacteriophage T4. *Nature* 227: 680.
- Matsudaira PT and Burgess DR (1978) SDS microslab linear gradient polyacrylamide gel electrophoresis. *Analytical Biochemistry* 87: 386.
- Schagger H and von Jagow G (1987) Tricine-sodium dodecyl sulfate-polyacrylamide gel electrophoresis for the separation of proteins in the range from 1 to 100 kDa. *Analytical Biochemistry* 166: 368.
- Shapiro AL, Vinuela E and Maizel Jr JV (1967) Molecular weight estimation of polypeptide chains by electrophoresis in SDS-polyacrylamide gels. *Biochem. Biophys. Res. Commun.* 28: 815.
- Takano E, Maki M, Mori H, Hatanaka N, Marti T, Titani K, Kannagi R, Ooi T and Murachi T (1988) Pig heart calpastatin: identification of repetitive domain structures and anomalous behaviour in polyacrylamide gel electrophoresis. *Biochemistry* 27: 1964.
- Weber K, Pringle JR and Osborn M (1972) Measurement of molecular weights by electrophoresis on SDS-acrylamide gel. *Methods in Enzymology* 26: 3.

Polyacrylamide Gel Electrophoresis

See **II/ELECTROPHORESIS/One-dimensional Polyacrylamide Gel Electrophoresis;**
II/ELECTROPHORESIS/One-dimensional Sodium Dodecyl Sulphate Polyacrylamide Gel Electrophoresis;
II/ELECTROPHORESIS/Two-dimensional Polyacrylamide Gel Electrophoresis

Porosity Gradient Gels

G. M. Rothe, Johannes Gutenberg-University, Mainz, Germany

Copyright © 2000 Academic Press

Introduction

The high resolving power of polyacrylamide (PA) gels for proteins, peptides and nucleic acids can be improved by using gradient gels instead of homogeneous (i.e. single concentration) gels. However, a more specific separation of polynucleotides in PA gels affords separation by incorporating a 40–80% denaturant gradient (7 mol L⁻¹ urea, 40% (v/v) formamide) into a homogeneous PA gel (of e.g. 6.5% (w/v) total polymer concentration) or applying a temperature gradient to a homogeneous PA gel.

In PA gradient gels the average pore radius decreases with increasing gel concentrations, i.e. in the direction of the migrating protein (polynucleotide) bands. This results in a sharpening of the bands because the molecules at the front of the moving band are slower than those at the rear. Because of this effect, gradient gels need not be covered by a stacking gel, as in disc gel electrophoresis. In porosity gradient

gels with a steep increase of polymer concentration (e.g. from 4 to 30% T (w/v) where %T = g acrylamide + g Bis = N,N'-methylenebisacrylamide (Bis) per 100 mL) proteins of a large size range (approximately 10⁴–10⁶ Da) can be separated. In shallow gradients (> 4% T to < 30% T), the separable size range of proteins is limited but they still provide an improved band sharpening.

There are two modes to run porosity gradient gels: a fixed-time mode, where electrophoresis is terminated after a certain time, and a time-dependent mode, which means that a number of consecutive electrophoretic mobilities are registered. Fixed-time electrophoresis is performed if protein (polynucleotide) patterns are to be screened, such as in population genetics or when determining the molecular mass of sodium dodecyl sulfate (SDS) denatured proteins. Molecular size properties of non-denatured proteins, however, cannot be elucidated that way, but afford time-dependent investigation of protein mobilities. On the other hand, time-dependent PA gradient gel electrophoresis not only offers the possibility to estimate the molecular mass of native proteins and enzymes but also allows determination of their Stokes radius, frictional coefficient, free electrophoretic

mobility and nett charge. A number of different (iso)enzyme systems have been classified in this way and comparisons between related species used to study the evolution of enzyme systems.

Porosity gradient gels can be easily prepared using one of the different devices on the market. Ready-to-use pore gradient gels are commercially available (Amersham Pharmacia Biotech, Freiburg, Germany; Gradipore, 200 Harris Street, Pyrmont NSW 2009, Sydney, Australia). Porosity gradient gels can be prepared in casting glass cassettes either without any further support or by adhering them to a silanized glass plate or a reactive polyester film. The latter two methods are employed when ultra-thin gels are to be used horizontally. Glass cassette cast PA gradient gels without any further support are used vertically.

Porosity of Polyacrylamide Gradient Gels

In 1962 Ornstein and Davis were the first to suggest a formula to estimate roughly the average pore diameter of homogeneous PA gels:

$$p_{av} \text{ (nm)} = 12.67 \times (\%T)^{-1/2} \quad [1]$$

where p_{av} (nm) is the average pore diameter in nanometres and % T is the total acrylamide concentration (g acrylamide + g Bis in 100 mL).

Based on the Ogston model which describes dextran gels as assembled from arbitrarily arranged gel

rods, Raymond and Nakamichi related the average pore diameter of PA gels to the total polymer concentration (T) as follows:

$$p_{av} \text{ (nm)} = K \times d \times (100 \times p)^{1/2} \times (\%T)^{-1/2} \quad [2]$$

where K is the factor resulting from the angle in which the gel rods are linked together (1.5), d (nm) is the diameter of a PA gel rod (0.5), p (g cm⁻¹) is the density of gel rod (1.2). This results in:

$$p_{av} \text{ (nm)} = 8.216 \times (\%T)^{-1/2} \quad [3]$$

The largest pore diameter in a PA gel of a certain concentration is, however, much larger than the average pore diameter (Figure 1). Moreover, the largest pore diameter deviates increasingly from the average pore diameter with decreasing gel concentration. The pores therefore are statistically distributed, but the standard deviations of the average pore radii and the distribution function (Gaussian or logarithmic distribution) are unknown.

The generally held assumption of a random meshwork of cross-linked individual PA rods could not be confirmed by electron microscope images. They revealed sponge-like structures in the submicron range. Such structures are in accordance with the mode in which gels polymerize. PA molecules first arrange as high molecular aggregates that are in the sol state and not interconnected. Thereafter, cross-linkage to a three-dimensional gel occurs: this is indicated by an abrupt start of gelation.

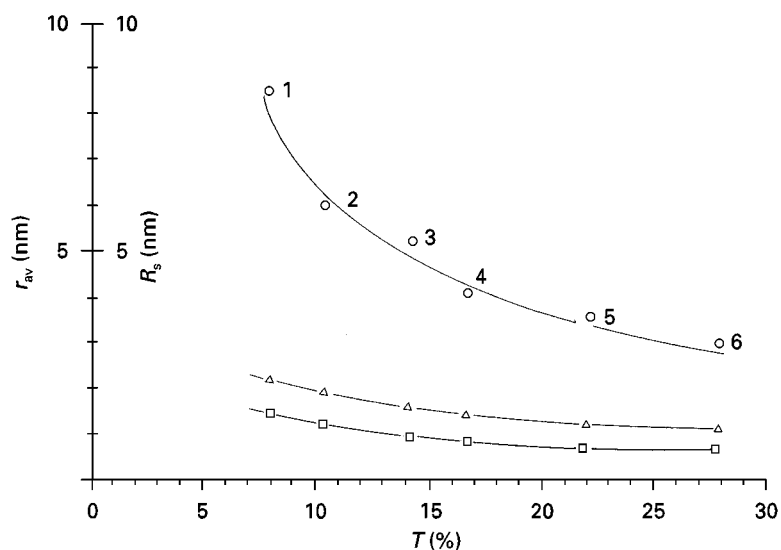


Figure 1 Plot of average pore radius (r_{av} (nm)) against PA gel concentration (T (%)). Triangles, average pore radii calculated as suggested by Ornstein and Davis (1962). Squares, average pore radii calculated as suggested by Raymond and Nakamichi (1962). Circles, maximum pore radii as marked by native proteins of known radius: 1, thyroglobulin; 2, ferritin; 3, catalase; 4, lactate dehydrogenase; 5, bovine serum albumin; 6, ovalbumin. Reproduced with permission from Rothe and Maurer (1986).

Analytical Separation of Native Proteins in a Glass Cassette-Cast Porosity Gradient

Gradient preparation is performed with acrylamide solutions of high and low concentrations, usually by using a two-chamber gradient mixer, although more sophisticated gradient formers have been developed. Linear PA gradients are usually prepared by the technique which was first described by Martin and Ames in 1961 for the preparation of linear sucrose gradients. Glass cassette-cast gels are mostly 82×82 (140) mm or 125×250 mm and a thickness of 3.0, 1.0, 0.8, 0.5 or 0.1 mm.

Preparation of a Batch of Unattached Gradient Gels

Polyacrylamide gradient gels cast in glass cassettes may be prepared individually or simultaneously in batches (Figure 2). The latter method saves time and, although the gradients usually deviate slightly from each other, they are well suited to determine protein patterns, e.g. isozyme patterns as in population genetics. Any form of gradient (linear, concave, convex) may be prepared but linearly increasing gradients of total polymer concentration are most commonly used.

The device shown in Figure 3 can prepare six gradient gels simultaneously. In each gel the PA concentration increases linearly from top to bottom from approximately 5 to 25% T . The gels are encased in glass cassettes of internal dimensions 172×82

$\times 1.0$ mm. Each cassette is fitted with a slot former and inserted in a gel-casting device. The linear PA gradient is prepared by using a two-chamber gradient mixer, a separate reservoir (for the catalyst solution), a proportioning pump, a 1 mL mixing chamber (and a reservoir filled with sucrose and a pump to lift the gradient into the cassettes). The device shown in Figure 3 is used as follows: The inner chamber (1) and the connecting tube (3) to the outer chamber (2) of the gradient mixer are filled with 57 mL of T_{\min} solution. Then the tube (3) to chamber (2) of the mixer is closed. Afterwards 57 mL of the T_{\max} solution is pipetted into chamber (2) of the gradient mixer. Now 22.5 μ L of N,N,N',N' -tetramethylethylenediamine (TEMED) is mixed with the T_{\min} and the T_{\max} solution, respectively. A separate reservoir (4) is filled with 35 mL of gel buffer containing 50 mg ammonium persulfate. The connection between chamber (1) and (2) of the gradient mixer is opened, after which the stirrer (5) of the gradient mixer and the stirrer (6) of the mixing chamber (7) as well as the peristaltic pump (8) are switched on. Immediately after chamber (1) is empty, the pump (8) is switched off and a sufficient amount of sucrose solution (50% (w/v)) is pumped from the corresponding reservoir (9) with the help of a separate pump (10) underneath the gel cassettes (12) to lift the whole gradient into the cassettes, which are in the gel-casting device (14).

The T_{\min} and T_{\max} solution contain acrylamide and Bis at the same ratio (acrylamide-Bis = 24 : 1). The T_{\min} solution contains 4.205 g acrylamide and

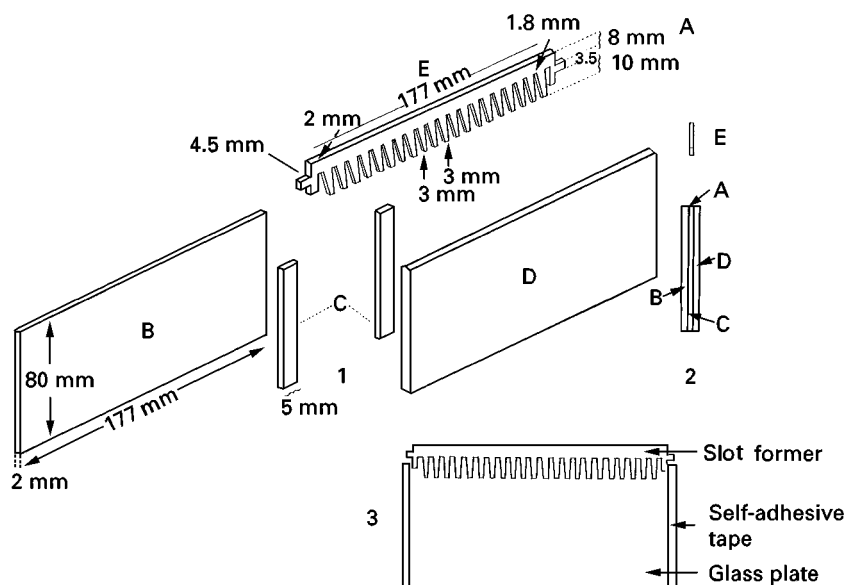


Figure 2 Assembly of a glass cassette to cast a PA (gradient) gel slab. A, Slot former; B, front and D rear glass plate of cassette; C, left and right distance bar. 1, Exploded view of cassette; 2, side view; 3, front view. Procedure according to Pharmacia, Uppsala, Sweden. Reproduced with permission from Rothe (1991).

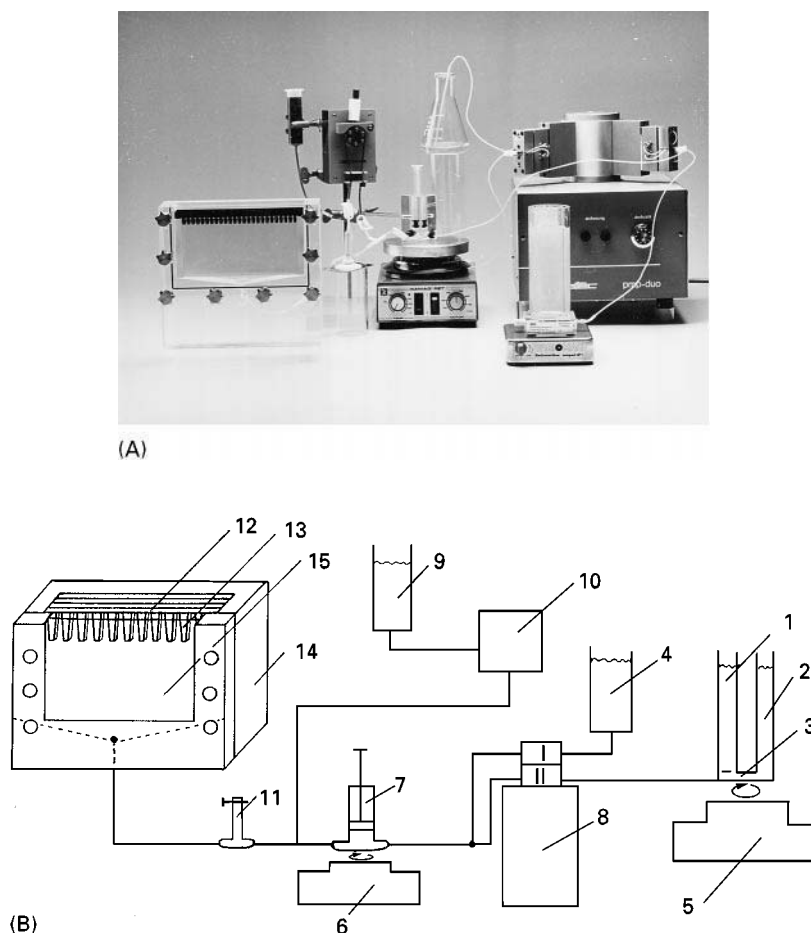


Figure 3 (A) Device for preparing a batch of six PA porosity gradient gels. (B) Scheme for preparing a batch of six porosity gradient gels each encased in a glass cassette without further support. 1 and 2, chambers of the gradient mixer (1 with magnetic bar); 3, connecting tube between both chambers which can be closed by a stopcock (not shown); 4, reservoir to hold the catalyst solution (ammonium persulfate); 5 and 6, stirrers; 7, mixing chamber (modified 1 mL syringe); 8, two-channel pump; 9, reservoir to hold sucrose solution; 10, one-channel pump; 11, air trap; 12, gel cassettes with 13, inserted slot formers; 14, gel-casting apparatus (made of perspex) with 15 removable front plate. Reproduced with permission from Rothe (1994).

0.175 g Bis per 100 mL gel buffer while the T_{\max} solution contains 31.54 g acrylamide and 1.314 g Bis in 100 mL gel buffer. The T_{\min} and T_{\max} solutions are diluted upon gradient formation with catalyst solution by a factor of 1.255 (Figure 3) and the gel solution is pumped to about 5 mm above the slot template. This results in a final concentration range of approximately 5–25% T . (Mixing both catalysts into the T_{\min} and T_{\max} solution is also possible but carries the danger that the gel may solidify before being completely cast in the cassette). Prior to use all solutions are brought to room temperature and degassed. The ammonium persulfate solution should be prepared freshly each time. 90 mmol L⁻¹ Tris, 45 mmol L⁻¹ boric acid and 2.5 mmol L⁻¹ EDTA-Na₂, pH 8.4 is used as gel and electrode buffer. Further buffer systems are given in Table 1.

Vertical Electrophoresis

Glass cassette-cast gradient gels are mounted vertically into an electrophoretic apparatus consisting of an upper and lower electrode vessel (Figure 4). The upper buffer tank has rubber gaskets into which two or four cassettes can be inserted. The lower electrode vessel is filled with cooled buffer; the upper electrode vessel with the inserted gel cassettes is mounted into the electrophoresis apparatus and filled with electrode buffer. Then the samples (enriched with 10% sucrose) are added to the slots (with a Hamilton syringe). Afterwards the voltage is switched on (≤ 40 V cm⁻¹) for 15 min for the proteins to migrate into the gel. Finally the buffer is circulated from buffer tank to buffer tank at the same voltage. The lower buffer tank is cooled to 5°C during electrophoresis by a cooling coil.

Table 1 Buffer systems used in porosity gradient gel electrophoresis to separate native proteins

Gel buffer	Electrode buffer	%T range	Authors
0.35 mol L ⁻¹ Tris HCl, pH 8.9	0.06 mol L ⁻¹ , Tris, 0.40 mol L ⁻¹ glycine, pH 8.3	3–20	Kopperschläger <i>et al.</i> (1969)
0.09 mol L ⁻¹ Tris, 0.08 mol L ⁻¹ boric acid, 0.003 mol L ⁻¹ EDTA–Na ₂ , pH 8.3	Same as gel buffer	4–26	Anderson <i>et al.</i> (1972) Lasky (1978)
0.01 mol L ⁻¹ Tris, 0.08 mol L ⁻¹ glycine, pH 8.3	Same as gel buffer	5–30 5–15	Slater (1969)
0.04 mol L ⁻¹ Veronal–Na, 0.04 mol L ⁻¹ Tris, 0.01 mol L ⁻¹ glycine, 0.04 mol L ⁻¹ ethanolamine, 0.001 mol L ⁻¹ EDTA–Na ₂ pH 9.8	Same as gel buffer	5–30	Lambin and Fine (1979)
0.01 mol L ⁻¹ Na–phosphate, pH 7.2	Same as gel buffer	5–30	Lambin and Fine (1979)

References as given in Rothe and Maurer (1986). Reproduced with permission from Rothe and Maurer (1986).

PA gradient gel electrophoresis under nondenaturing conditions has proved to be advantageous compared to electrophoresis in homogeneous gels, e.g. in plant population genetics. Figure 5 gives an example.

Separation of Native Proteins in an Ultra-Thin Support-Bound Porosity Gradient

To prepare a thin gradient gel of the dimensions 120 × 250 × 0.5 mm fixed to a derivatized clear and flexible polyester foil (e.g. manufactured by Gel

Bond, Marine Colloids, Rockland, MN, USA or Serva, Heidelberg, Germany), the gel-forming devices shown in Figure 6 may be used. (When the cassettes are assembled the slot formers must not touch the opposite glass wall but leave a space of 0.1 mm in between). The following solutions may be used to form a gradient ranging from 3 to 30% T:

1. gel buffer: 90 mmol L⁻¹ Tris, 80 mmol L⁻¹ boric acid, 2.5 mmol L⁻¹ EDTA–Na₂, pH 8.4;
2. electrode buffer: 1 in 2 diluted gel buffer;
3. stock acrylamide solution (30% T: 28.8 g acrylamide plus 1.2 g Bis plus 50 mL gel buffer, made to 100 mL with distilled water);

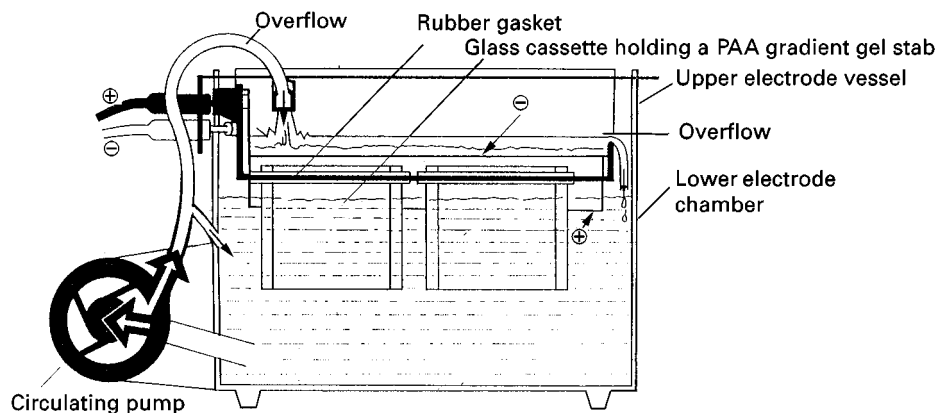


Figure 4 Vertical electrophoretic apparatus in which up to four glass cassette-cast porosity gradient gels can be inserted. Upper electrode vessel with 2 rubber gaskets to hold 2 to 4 glass cassettes, each containing a porosity gradient made of PA; +, –, electrodes. Modified from an instruction leaflet published by Pharmacia, Uppsala, Sweden.

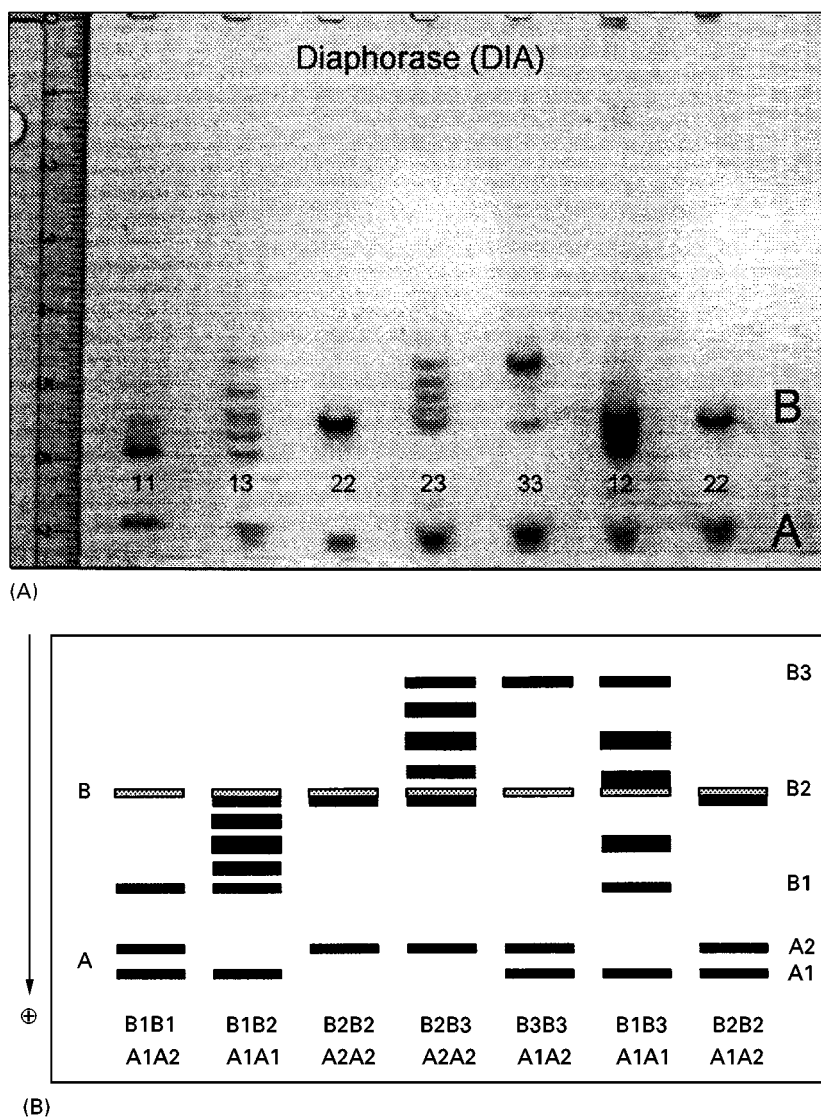


Figure 5 Electrophoresis of plant diaphorase isoenzymes in a 4–20% *T* PA gradient gel of 0.8 mm thickness (length 175 mm, height 75 mm). (A) Zymogram of diaphorase enzymes (numbers indicate genotypes of the tetrameric enzyme at locus B). (B) Schematic representation of genotypes at locus DIA-A and DIA-B. Enzyme source: leaf buds of seven different trees of European beech (*Fagus sylvatica* L.). Conditions of electrophoresis: gel and electrode buffer: 45 mmol L⁻¹ Tris, 40 mmol L⁻¹ boric acid, 1.25 mmol L⁻¹ EDTA-Na₂; pH 8.4; running time 4 h; voltage gradient 40 V cm⁻¹; temperature 5°C.

Enzyme extraction: 1.5 mL Eppendorf tubes containing 150 mg of green bud leaves, 50 mg of quartz sand and 600 µL of extraction medium were cooled from underneath with ice water. A motor-driven grinding cone adapted in the shape of the tube (rotating at 700 rpm) was used to homogenize the material. The extraction medium contained in 100 mL: 1.21 g Tris, 1.43 g Na₂HPO₄, 60 mg L-cysteine, 210 mg ascorbic acid, 14 g sucrose, 40 mg NADP, 15 g polyclar AT (PVPP) and 1 g polyethylene glycol, pH 7.5 (with H₃PO₄). The homogenate was centrifuged for 30 min at 4°C and 10 000 *g* and the clear supernatant used as crude enzyme extract. Samples of 8 µL were applied per lane. Diaphorase isozymes were visualized histochemically (60 mL 25 mmol L⁻¹ Tris-HCl, pH 8.5, containing 24 mg NADH, 1.5 mg 2,5 dichlorophenolindophenol-Na × 2H₂O (DCPIP) and 1.8 mL MTT (500 mg 100 mL⁻¹ aq. bidest. water). Anode at bottom. A, Enzymes of gene locus DIA-A; B, locus DIA-B. In (A) not all genotypes indicated in (B) are shown.

4. dense acrylamide solution (30% *T*: to 6.5 mL stock solution is added, shortly before use, 20 µL TEMED (1 in 10 with H₂O diluted solution) and 5 µL ammonium persulfate solution (40% w/v in distilled water));
5. light acrylamide solution (3% *T*: 1 vol of stock acrylamide solution is diluted with 4.5 vol distilled water and 4.5 vol of gel buffer shortly before use and 40 µL TEMED (1 in 10 with distilled water diluted solution) and 10 µL ammonium persulfate

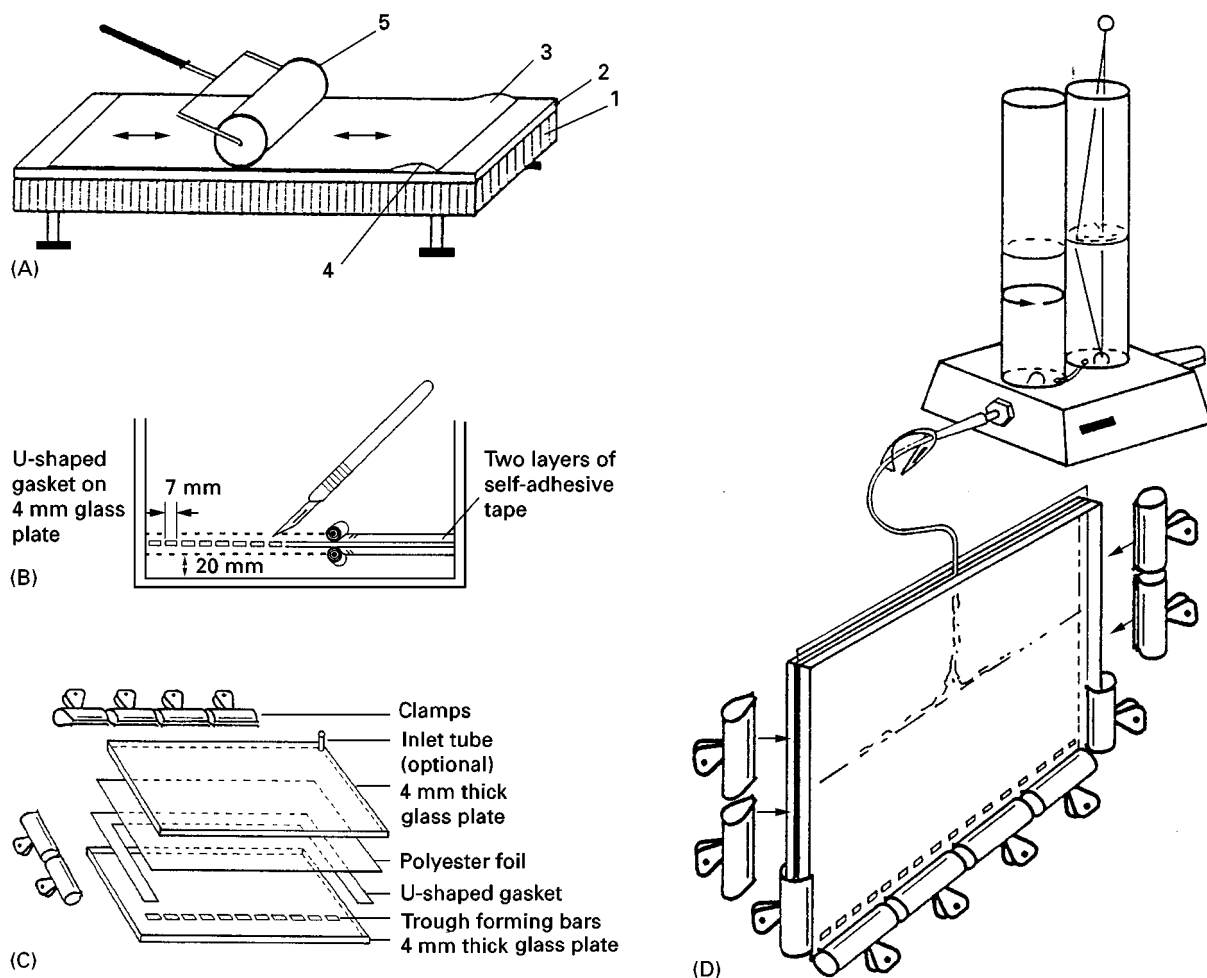


Figure 6 Preparation of an ultra-thin PA gradient gel fixed to a polyester foil. (A) Rolling the polyester foil (reactive side up, e.g. Gel Bond) on to one of the glass plates used to build the casting glass cassette: 1, levelling table; 2, glass plate; 3, hydrophilic side of polyester foil; 4, water layer; 5, rubber roller. (B) Trough template preparation. The bars are prepared from two layers of self-adhesive tape with a scalpel. (C) Assembling the glass cassette to cast the PA gradient. (D) Casting the porosity gradient: two-chamber mixer and glass cassette. Reproduced with permission from Rothe (1991).

solution (40% w/v in distilled water) is added. The gradient is made of 6.5 mL of dense acrylamide solution and 6.5 mL of light acrylamide solution. After gradient formation, 2 mL of light acrylamide solution is overlaid; the slots must be situated in the middle of the 3% T range.

Horizontal Electrophoresis

Before electrophoresis, the gel is taken out of the cassette. A few drops of kerosene are put on the cooling plate of the opened electrophoretic apparatus (Figure 7) and the gel, firmly adhering to the polyester foil, is placed on it, carefully avoiding the inclusion of air bubbles. Both ends of the gel are connected with the buffer vessels by paper wicks or a household sponge-like material. A 15–30 min pre-electrophor-

esis is performed at 1000 V (50 V cm^{-1}). Then the slots are filled with protein solution (or electrode buffer) and the power is turned on again at a voltage of 1000 V for approximately 2 h. Afterwards the gel, fixed on the polyester foil, may be stained for proteins or (iso)enzymes (Figure 8).

Determination of the Course and Concentration of a Porosity Gradient Gel

The course and % T range of laboratory-made PA gradient gels can be controlled by densitometry if a coloured dye such as *p*-nitrophenol is added to the denser acrylamide solution prior to gradient formation. After polymerization, the increase in colour

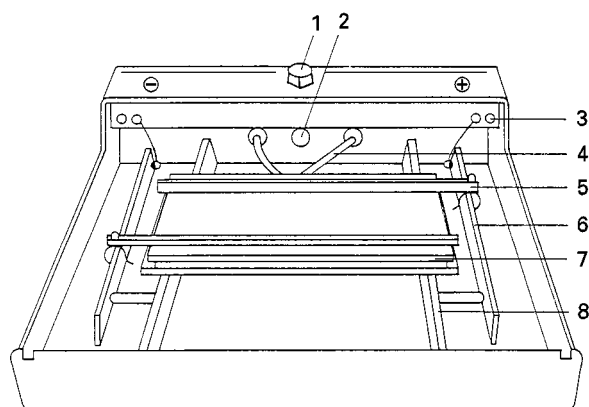


Figure 7 Horizontal electrophoretic apparatus with cooling plate. 1, Cover lock; 2, gassing stud; 3, high voltage connection of the lid; 4, flexible tube to the cooling plate; 7, with a cooling device (not shown); 5, electrode bar (used in isoelectric focusing); 6, electrode ledge; 8, support for cooling plate. For PA gradient gel electrophoresis the electrode bars are replaced by two buffer vessels (not shown) under the cooling plate and connected to the electrode ledge. The gel is connected to the buffer reservoirs by (paper) wicks (not shown). Reproduced with permission from Rothe (1991).

intensity from top to bottom of the gel can be used to measure the course of the gradient and its precise concentration in polyacrylamide. For a 1 mm thick gel 15 mg *p*-nitrophenol may be added to 100 mL of the dense acrylamide solution. After gelation the colour intensity is quantified by densitometry at 405 nm. Whilst the course of the gradient can be seen directly on the densitogram, the %*T* range of the gradient can be calculated with the formula:

$$T(\%) = T_s \times (E_{405} - E_p) \times M_r \times (c \times d \times \epsilon)^{-1} \quad [4]$$

where T_s (%) is PA concentration of stock solution, E_{405} is absorbance of *p*-nitrophenol, E_p is absorbance of empty cassette at 405 nm, c (g L^{-1}) is concentration of *p*-nitrophenol in stock acrylamide solution ($c = 0.150$), M_r (g L^{-1}) is mol mass of *p*-nitrophenol ($M_r = 139.1$), d (mm) is thickness of gel (e.g. 0.5), E [L (mol mm)^{-1}] = molar extinction coefficient of *p*-nitrophenol at 405 nm ($\epsilon = 1728$) and T (%), as in eqn [1].

Cross-Linkers Other than Bis and Mixed Polyacrylamide Gels

PA is normally cross-linked with Bis to obtain an electrophoretic matrix. The use of *N,N'*-(1,2-dihydroxyethylene)bisacrylamide (DHEBA) instead of Bis gives gels that can be solubilized in dilute periodic

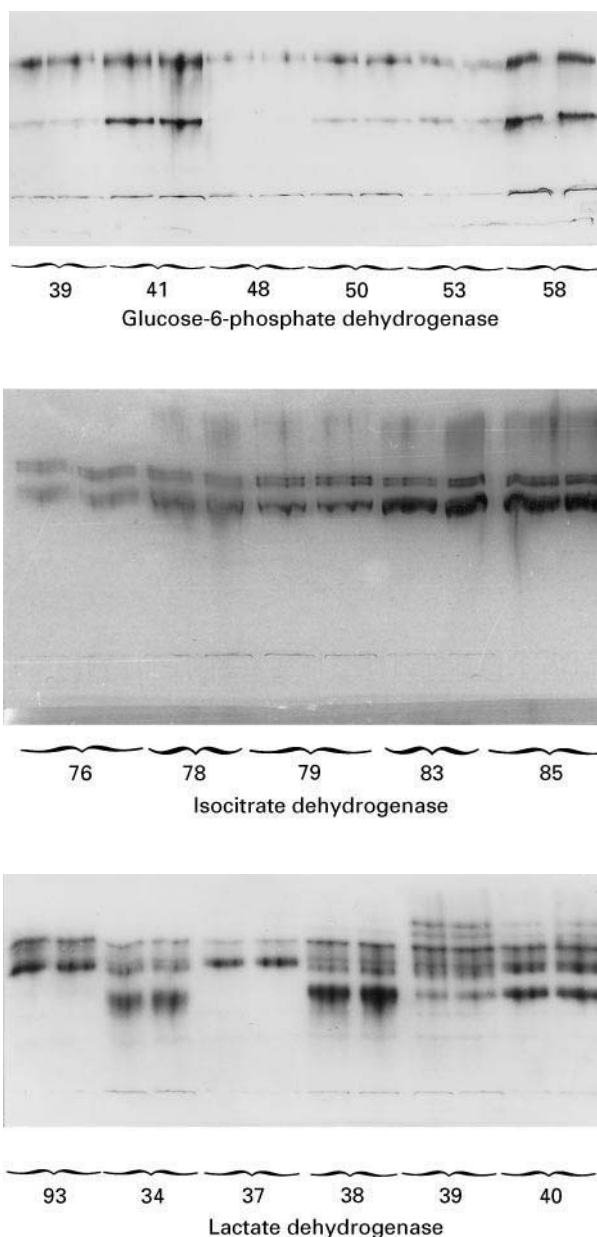


Figure 8 Electrophoresis of plant (iso)enzymes on ultra-thin PA gradient gels fixed on a polyester film. Gel dimensions: $240 \times 120 \times 0.5$ (mm); PA gradient from 4 to 28% *T*. Enzyme source: current-year (1989) needles of Norway spruce (*Picea abies* L., Karst.) sampled from a variety of clones (clone numbers indicated) of the multiple clone variety East Prussian Late Spruce (Hessische Forstliche Versuchsanstalt, Hann. Münden, Germany). Enzyme extraction: 2 g of fresh needles was homogenized in 10 mL of homogenizing medium (0.1 mol L^{-1} Na-phosphate, pH 7.5, containing 5% w/v Polyclar AT and 0.5% w/v Triton X-100). The crude extract was centrifuged for 30 min at 38 000 g and the supernatant concentrated by a factor of 4 using the ultrafiltration system Centrisart I (Sartorius, Göttingen, Germany). Samples of $10 \mu\text{L}$ were applied per lane. Conditions of electrophoresis: 1000 V for 90 min at 4°C ; gel and electrode buffer: 45 mmol L^{-1} Tris, 40 mmol L^{-1} boric acid, 1.25 mmol L^{-1} EDTA- Na_2 , pH 8.4. Enzymes were stained histochemically. Anode at top. Reproduced with permission from Rothe (1991).

acid or dilute aqueous solutions of bases to liberate proteins after the electrophoretic separation. Gradient flat gels ($140 \times 120 \times 3$ mm) with an increasing acrylamide concentration but a constant ratio of DHEBA have been used to separate protein mixtures from fruit with radio-labelled amino acids. Following electrophoresis, gel slices containing protein zones are placed in a glass scintillation counting vial fitted with a Teflon-lined plastic cap, 1 mL of 0.025 mol L^{-1} periodic acid is added and the vials are sealed. After incubation for 48 h at 50°C , 10 mL of Mix I scintillation fluid is added, and the vials cooled overnight before counting. PA gels produced with DHEBA may be used with the common alkaline buffer systems except borate buffers, which form negatively charged complexes with the *cis*-1, 2-diol structure of the cross-linker DHEBA.

To improve the retardation of PA gradient gels for low molecular mass proteins, a mixture of acrylamide, Bis and *N,N',N'*-triallylcitric triamide has been suggested.

The use of *N*-substituted acrylamido derivatives, such as *N*-acryloyltris(hydroxymethyl)aminomethane (NAT) gives PA gels with larger pores, although the pores are still smaller than those of agarose. Gels of similar pore sizes can be made from allyl-activated agarose and acrylamide or *N*-substituted acrylamido derivatives. The mixed-bed gels of agarose-acrylamide have average pore sizes which are about 30% larger than those of a regular 3.3% Bis cross-linked gel with the same %*T*.

Size Estimation of Native Proteins and Enzymes

The size of native proteins can be deduced from their migration behaviour in homogeneous or gradient gels. Both methods have the advantage that crude tissue or cell extracts can be used as the protein source, provided a specific staining method exists with which they can be located in the gel after electrophoresis. The method with homogeneous gels uses a number of gels of different PA concentration in the range of 4–35% *T* and estimates the relative electrophoretic mobility referred to Bromophenol blue (R_F value) of a set of marker proteins and the sample protein(s). From these values the gel concentration is estimated at which the electrophoretic mobility is zero (or would become zero). This is achieved by plotting the logarithm of the %*T* concentration ($\log T$) in which the mobility is measured against the respective R_F value. In the underlying linear function ($\log T = -k \times R_F + \log T_{\text{lim}}$), the value of T_{lim} represents the exclusion limit, the %*T* concentration at which protein mobility stops. The T_{lim} values cal-

culated for a number of marker proteins can be correlated to their corresponding Stokes radii (R_S) to obtain a calibration line. A linear function is obtained when R_S is plotted against the reciprocal of T_{lim} ($R_S = a \times 1/T_{\text{lim}} + b$). Into this equation the exclusion limit of a sample protein is inserted and this then allows calculation of the corresponding Stokes radius.

Polyacrylamide gradient gel electrophoresis can also be used to estimate the molecular size of non-denatured proteins, provided it is performed in a time-dependent way. The following physicochemical properties of native proteins (enzymes) are obtainable:

1. molecular mass (M_r);
2. hydrodynamic radius (Stokes radius (R_S));
3. frictional coefficient (f/f_o) (molecular eccentricity, considering the molecular shape as a rotational ellipsoid and f/f_o as the quotient of the ratio of the two half axes of the rotational ellipsoid, f = half axis of ellipsoid, f_o = half axis of circle);
4. isomeric nature of multiple protein forms (size isomers or charge isomers);
5. free electrophoretic mobility (and nett negative charge (valence Z , charge Q)) at the pH value of the electrophoresis.

The mathematical procedures used to calculate these parameters are bound by several preconditions:

1. The PA gradient increases linearly (at a constant ratio of acrylamide to Bis). The gradient range however, can be chosen freely.
2. The electrophoretic pH value and the voltage gradient are chosen in a way that marker and sample proteins migrate sufficiently.
3. The same buffer system has been used as gel and electrode buffer, if net charges are to be obtained.
4. The sizes of the marker and sample proteins fit the pore range of the PA gradient.
5. Marker and sample proteins have migrated on the same gel slab.
6. Parts of the gel slab which have been cut into two or more parts and stained differently are re-equilibrated to the original gel length before protein migrations are measured.
7. Approximately 10 (or more) time-dependent migration distances of marker and sample proteins are accurately measured.

Estimation of the Maximum Migration Distance and Recognition of Size Isomers

With increasing times of electrophoresis under non-denaturing conditions, the migration of proteins in a PA gradient gel gradually decreases (Figures 9–11).

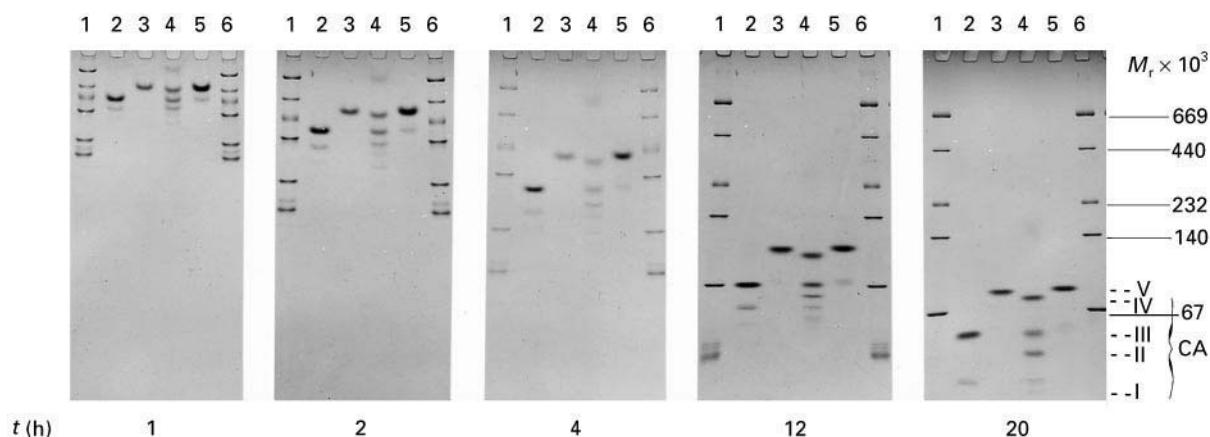


Figure 9 Time-dependent migration patterns of marker proteins and carbonic anhydrase (EC 4.2.1.1) (iso)enzymes from mammalian erythrocytes. Lanes 1 and 6, marker proteins. Lanes 2–5; carbonic anhydrases from (2) bovine, (3) human, (4) rabbit and (5) canine. Mol mass of marker proteins: ovalbumin (45 000), bovine serum albumin (67 000), lactate dehydrogenase (140 000), catalase (232 000), ferritin (440 000) and thyroglobulin (669 000). Linear PA 4–30% T gradient (acrylamide-Bis = 24 : 1), 300 V per 73 mm of gel length, 5°C. Running times: 2, 8 and 16 h. Gel and electrode buffer: 90 mmol L⁻¹ Tris, 80 mmol L⁻¹ boric acid, 1.25 mmol L⁻¹ EDTA-Na₂-H₂O, pH 8.4. Protein staining with Coomassie brilliant blue. Enzyme preparations from Sigma, Munich, Germany. Reproduced with permission from Rothe (1991).

Migration of globular proteins comes to an end when the maximum pore size of a gel region equals their own size. The corresponding migration distance is called the maximum migration distance (D_{\max} (mm)). The maximum migration distance can be obtained from a number of time-dependent protein migrations (D (mm)) (Figures 9 and 10) which are directly measured on the gel after proteins have been visualized following electrophoretic separation (Table 2). To obtain the maximum migration distance of a certain protein, the following mathematical approximation procedure can be applied: the migration distances are double-logarithmized ($\ln(\ln D)$) and plotted versus the reciprocal of the square root of electrophoretic migration time, $1/t^{1/2}$ (t (h)). This results in a straight line (Figure 11) whereby the transformed migration values ($\ln(\ln D)$) and the transformed times of electrophoresis ($t^{-1/2}$) are interrelated by the equation:

$$\ln(\ln D) = -a \times t^{-1/2} + b \quad [5]$$

where a and b are the slope and the intercept of the corresponding straight line. The equation predicts that at very high values of t , $t^{-1/2}$ reaches zero. This means that the maximum migration of a protein (D_{\max} (mm)) can be taken from the intercept of the straight line with the ordinate in a plot of $\ln(\ln D)$ versus $t^{-1/2}$ provided protein migrations were larger than 2 mm and a sufficient number of different migration distances are registered. Letting t approximate to infinity means that eqn [5]

becomes:

$$\ln(\ln D) = \ln(\ln D_{\max}) = b \quad [6]$$

and:

$$D = D_{\max} = \exp(e^b) \quad [7]$$

A plot of $\ln(\ln D)$ versus $t^{-1/2}$ can also be used to distinguish size isomers from charge isomers. Equally sized but differently charged forms of an enzyme or protein system are recognized by the fact that the straight line of each enzyme form intersects at the same point on the $\ln(\ln D)$ axis as is for example the case with mammalian carbonic anhydrase (cf. Figure 11) and mammalian lactate dehydrogenase. On the other hand, migration of charge isomers should result in lines of equal slope. Proteins differing in charge and size, however, give straight lines with both different slopes and intercepts.

Estimation of Stokes Radius and Molecular Mass

The maximum migration distance of globular proteins is related to the maximum gel pore radius at the respective gel concentration (cf. Figure 1). Therefore, the maximum migration distances (D_{\max}) of proteins can be correlated to their Stokes radius (R_s). A linear relationship is obtained if the logarithm of the maximum migration distance ($\ln D_{\max}$) of proteins is plotted versus the logarithm of their Stokes radius ($\ln R_s$):

$$\ln D_{\max} = -m \times \ln R_s + b \quad [8]$$

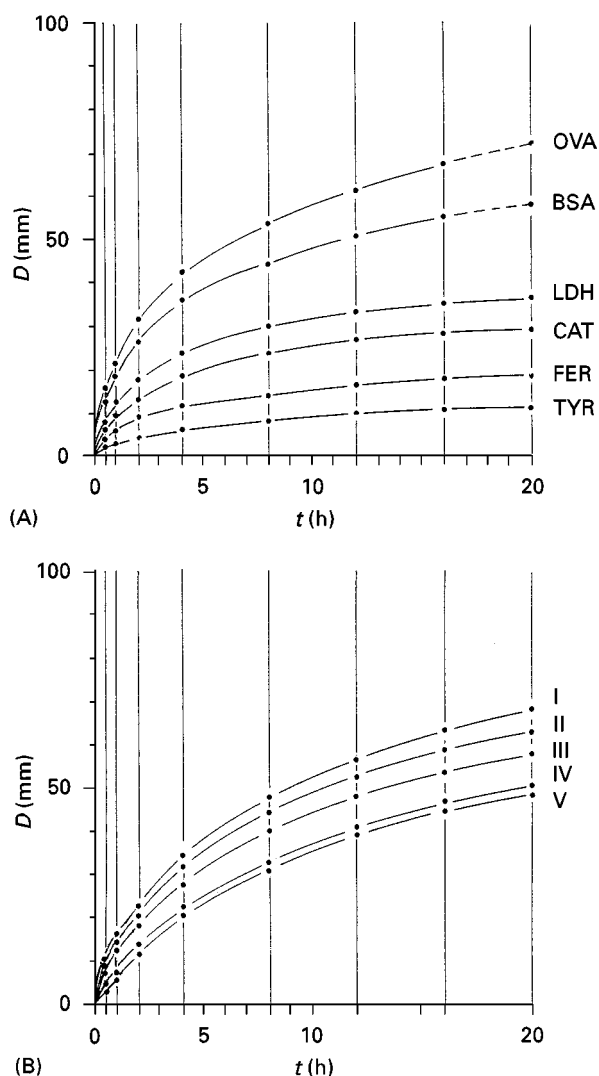


Figure 10 (A) Plot of migration distances (D (mm)) of marker proteins and (B) of five different carbonic anhydrases versus times of electrophoresis (t (h)) in a linear PA gradient gel of 4–30% T . Conditions of electrophoresis are given in Figure 9. Migration distances and times of electrophoresis as listed in Table 2. OVA, Ovalbumin; BSA, bovine serum albumin; LDH, lactate dehydrogenase; CAT, catalase; FER, ferritin; TYR, thyroglobulin. Marker proteins and carbonic anhydrases were migrated on the same gradient gel. Purified enzyme preparations (Sigma, Munich, Germany) comprised carbonic anhydrases from bovine (I–III), rabbit (III, IV), human (V) and canine (V) erythrocytes. (Reproduced with permission from Chrambach *et al. Advances in Electrophoresis* Vol 4: pp 351–358.)

where $\ln D_{\max}$ equals e^b of eqn [7], and m and b represent the slope and intercept of the straight line (Figure 12).

It has been shown that a similar equation correlates the logarithm of the maximum migration distance ($\ln D_{\max}$) to the logarithm of the molecular mass ($\ln M_r$):

$$\ln D_{\max} = -z \times \ln M_r + c \quad [9]$$

where $\ln D_{\max}$ equals e^b of eqn [7], and z and c represent the slope and intercept of the straight line (Figure 12).

Knowing the maximum migration distance of any native globular protein, the calibration line can be used to calculate the molecular mass of the protein by inserting the calculated $\ln D_{\max}$ value and the values of the slope (z) and the intercept (c) of the calibration line into the equation $\ln D_{\max} = -z \times \ln M_r + c$ (Table 3) or inserting the $\ln D_{\max}$ value and the values of the slope (m) and the intercept (b) of the calibration line into the equation $\ln D_{\max} = -m \times \ln R_s + b$ (Table 4).

When using PA gradients of 4–30% T and a buffer of pH 8.4 (45 mmol L⁻¹ Tris, 40 mmol L⁻¹ boric acid, 1.25 mmol L⁻¹ EDTA-Na₂, pH 8.4) a number of markers can be used, ranging from carbonic anhydrase (M_r 30 000, R_s 3.05) to thyroglobulin (M_r 669 000, R_s 8.50; Table 5). β -Galactosidase (M_r 116 000, R_s 4.23) and carbonic anhydrase (Sigma, St Louis, MO, USA) are run in the same lane and the other marker proteins are run in a separate one. The marker proteins bovine serum albumin, lactate dehydrogenase, catalase, ferritin and thyroglobulin can be obtained as a freeze-dried mixture (Amersham Pharmacia Biotech, Freiburg, Germany) and dissolved in a solution of pure ovalbumin (Boehringer, Mannheim, Germany). Separation times depend on the voltage gradient and may range from 0.5 to more than 20 h (Table 2).

Estimation of Frictional Coefficient

The frictional coefficient (f/f_o) relates the hydrodynamic volume of a protein molecule to its molecular mass. According to Siegel and Monty, the Stokes radius (R_s) of a protein is related to its molecular mass (M_r) by the following equation:

$$R_s \text{ (m)} = f/f_o \times (3 \times v \times M_r)^{1/3} \times (4 \times \pi \times N_A)^{-1/3} \quad [10]$$

where R_s (m) is the Stokes radius, f/f_o is the frictional coefficient (equivalent to the quotient of the half axes of a rotational ellipsoid), v (m³ g⁻¹) is the partial specific volume (the reciprocal of the average density of a protein, ($v = 0.75 \times 10^{-6}$), N_A (mol⁻¹) is Avogadro's number ($N_A = 6.022 \times 10^{23}$), and M_r (Da = g mol⁻¹) is the molecular mass of a protein. By substituting the actual values one obtains:

$$R_s \text{ (m)} = f/f_o \times 66.1 \times 10^{-12} \times M_r^{1/3} \quad [11]$$

The geometric mean radius of a molecular mass equivalent sphere is defined as R_m (m). It is obtained

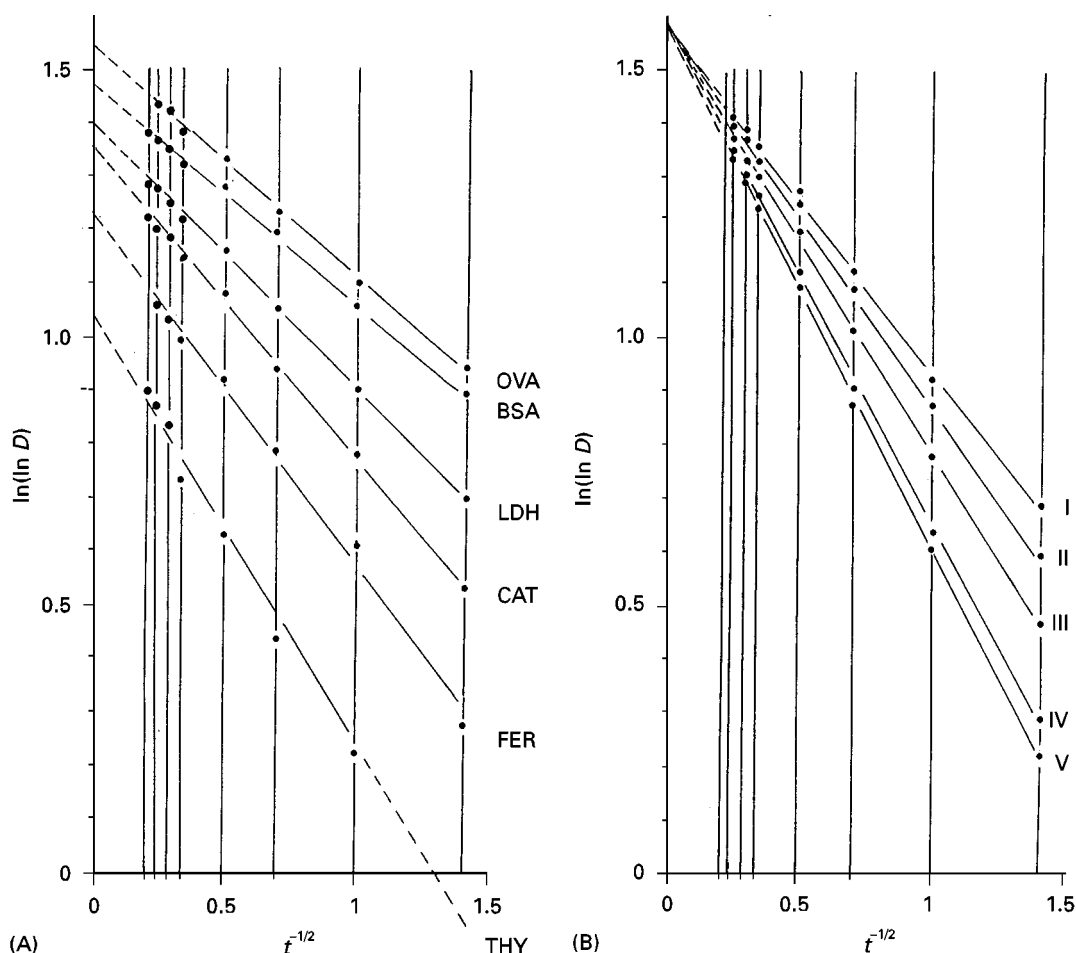


Figure 11 Plot of transformed migration distances ($\ln(\ln D)$) against transformed migration times ($t^{-1/2}$) of (A) marker proteins and (B) five carbonic anhydrase variants. Migration distances and times of electrophoresis as listed in Table 2. Abbreviations as in Figure 10. The common point of intersection of the various straight lines marked I–V on the $\ln(\ln D)$ axis indicates that the investigated enzymes are size isomers. Reproduced with permission from Rothe (1991).

by setting $f/f_o = 1$ in eqn [11] to give eqn [12]:

$$R_s (\text{m}) = 66.1 \times 10^{-12} \times M_r^{1/3} \quad [12]$$

This means that R_s and R_m are interrelated through the frictional coefficient:

$$R_s = f/f_o \times R_m \quad [13]$$

The frictional coefficient can be obtained from the experimentally obtained M_r and R_s values and eqn [13].

Extremely high frictional ratios are to be expected for molecules with rod-like or fibrous structures, which are characterized by a high axial ratio such as fibrinogen or myosin or by bulky and voluminous globular molecules with normal axial ratios. Examples of the latter are the spider-like immunoglobulin M, the shell-like apoferritin or the branched α -macroglobulin. Usually, native proteins and enzymes do not belong to these groups of proteins.

In eqn [11] the frictional coefficient of native proteins is assumed to be constant. However, when analysing the molecular mass (M_r) and Stokes radius (R_s) of more than 60 native proteins it became apparent that the frictional coefficient increases with increasing protein size (see Further Reading). A more precise equation relating R_s and M_r is the following:

$$R_s (\text{m}) = M_r^{0.0225} \times 55.1 \times 10^{-12} \times M_r^{0.0142} \times M_r^{1/3} \quad [14]$$

According to this expression the frictional coefficient of globular proteins equals $f/f_o = M_r^{0.0225}$ and increases with molecular masses of 10^3 to 9×10^6 from $f/f_o = 1.17$ to $f/f_o = 1.43$ while the factor 66×10^{-12} of the expression of Siegel and Monty ($R_s (\text{nm}) = f/f_o \times 66.1 \times 10^{-12} \times M_r^{1/3}$) increases from 61×10^{-12} to 67×10^{-12} .

As an average, the frictional ratio of globular proteins sized 45–100 kDa is $f/f_o = 1.23$, for those in the range of 100–500 kDa $f/f_o = 1.28$ and in the range of

Table 2 Time-dependent migration distances of marker proteins and carbonic anhydrase (iso)enzymes from erythrocytes of four mammalian species in a porosity gradient gel from 4 to 30% *T*

Protein		Time <i>t</i> (h) of electrophoresis ($1/\sqrt{t}$ given in brackets)							
		0.5 (1.41421)	1 (1.00000)	2 (0.70711)	4 (0.50000)	8 (0.35355)	12 (0.28868)	16 (0.25000)	20 (0.22361)
Ovalbumin	<i>D</i> (mm)	13.05	20.25	31.5	44.0	54.0	61.0	67.5	
Bovine serum albumin	<i>D</i> (mm)	11.7	17.8	26.5	36.3	43.5	47.5	50.5	53.2
L-lactate dehydrogenase	<i>D</i> (mm)	7.5	11.9	17.5	24.5	30.2	33.3	35.5	37.5
Catalase	<i>D</i> (mm)	5.5	8.8	13.2	18.8	23.5	26.6	28.5	30.0
Ferritin	<i>D</i> (mm)	3.7	6.5	9.0	12.0	14.3	16.6	17.9	18.9
Thyroglobulin	<i>D</i> (mm)	1.9	3.5	4.7	6.5	8.0	10.0	10.8	11.6
Bovine I	<i>D</i> (mm)	7.3	12.5	21.5	35.5	48.2	56.0	62.5	
Bovine II	<i>D</i> (mm)	6.3	11.0	19.0	32.5	45.0	52.3	58.8	68.0
Bovine, rabbit III	<i>D</i> (mm)	5.0	8.8	15.5	27.5	40.1	47.5	52.0	58.0
Rabbit IV	<i>D</i> (mm)	3.8	6.7	11.8	21.5	33.6	41.0	45.7	50.2
Canine, Human V	<i>D</i> (mm)	3.5	6.3	11.2	20.0	32.5	39.8	44.5	48.5

D (mm), Time-dependent migration distances of marker proteins and carbonic anhydrase (EC 4.2.1.1) variants. Gel length (*D* (mm)) and gel concentration (*T* (%)) are interrelated by the equation $T = \alpha D + \beta$ where $\alpha = 0.3528 \pm 0.0054$ and $\beta = 4.1116 \pm 0.2344$; the correlation coefficient is $r = 0.9985$. Reproduced with permission from Rothe (1991).

500–1000 kDa $f/f_o = 1.43$. From these data and the Stokes radius of a globular protein its molecular mass can be estimated:

$$M_r = (1/(f/f_o))^3 \times 3463 \times R_s^3 \quad [15]$$

with M_r , f/f_o and R_s as in eqn [10].

This can be exemplified by mammalian liver alcohol dehydrogenase (EC 1.1.1.1), which has a molecular mass of 80 kDa and a Stokes radius of 3.5 nm; the

average frictional coefficient of globular proteins in that range is $f/f_o = 1.23$. By inserting these values into eqn [15] one obtains: M_r (Da) = $(1/1.23)^3 \times 3463 \times 3.5^3 = 79\,791$.

Determination of Migration Velocities

The migration velocity of a protein migrating in an electrophoretic support medium can be obtained by computing the quotient of the difference in the distance migrated between two consecutive time

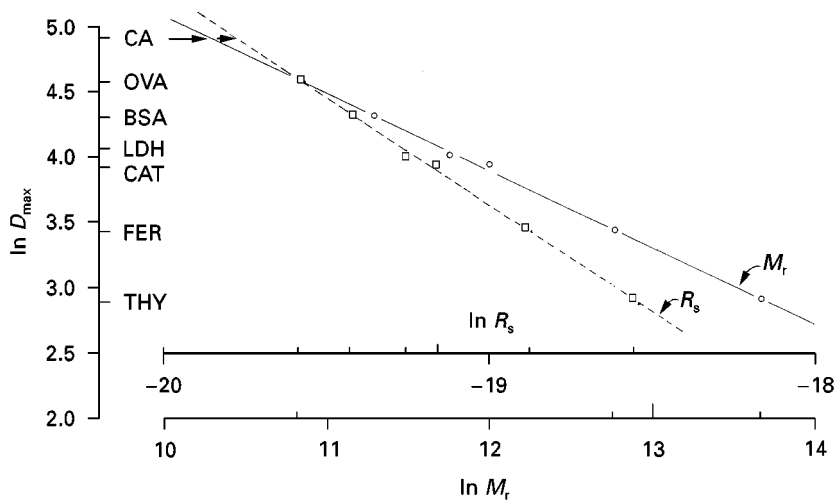


Figure 12 Calibration lines to calculate the molecular mass (M) and Stokes radius (R_s) of five carbonic anhydrase isoenzymes. The logarithm of the maximum migration distance ($\ln D_{\max}$) correlates linearly to the logarithm of the mol mass ($\ln M_r$) and the logarithm of the Stokes radius ($\ln R_s$), respectively. CA, Carbonic anhydrase (average $\ln D_{\max}$ of isozymes I–V); OVA, ovalbumin; BSA, bovine serum albumin; LDH, lactate dehydrogenase; CAT, catalase; FER, ferritin; THY, thyroglobulin. The calculated mol masses and Stokes radii are listed in Tables 3 and 4.

Table 3 Calculated molecular mass of marker proteins and mammalian carbonic anhydrase (iso)enzymes and calculation of percentage of deviation of the calculated values from the literature

Protein	Mol mass (M_r (g mol^{-1})) ^a	$\ln M_r$	Frictional coefficient (f/f_0)	Calculated mol mass (M_r)			
				$\ln M_r$	M_r^b	Deviation ^c (%)	$\ln D_{\max}$
Ovalbumin	43 000	10.6690	1.18	10.8234	50 181	+ 16.7	4.6563
Bovine serum albumin	67 000	11.1125	1.34	11.2981	80 668	+ 20.4	4.3537
L-lactate dehydrogenase	140 000	11.8494		11.7695	129 249	− 7.7	4.0532
Catalase	232 000	12.3545	1.27	12.0356	168 653	− 27.3	3.8836
Ferritin	440 000	12.9945	1.40	12.7717	352 110	− 20	3.4144
Thyroglobulin	669 000	13.4135		13.6949	886 379	+ 32	2.8259
Carbonic anhydrase							
Bovine I				10.5233	37 171		4.8476
Bovine II				10.4904	35 968		4.8686
Bovine/rabbit III	38 000			10.5373	37 695		4.8387
Rabbit IV				10.5775	39 241		4.8131
Canine/human V	29 700			10.5462	38 032		4.8330
Arithmetic mean				10.5346	37 594		4.8404

^aLiterature values.^bThe molecular mass of bovine carbonic anhydrase as estimated by sequence analysis was reported to be 28 980 while that of the enzyme from mouse was found to be 29 068.^cThe molecular sizes calculated are compared with the literature data and the percentage deviation indicated.

Reproduced with permission from Rothe (1991).

intervals during electrophoresis, and the corresponding time difference:

$$v \text{ (mm s}^{-1}\text{)} = (D_1 - D_0) \times (t_1 - t_0)^{-1}$$

$$v \text{ (mm s}^{-1}\text{)} = (D_2 - D_1) \times (t_2 - t_1)^{-1}$$

$$v \text{ (mm s}^{-1}\text{)} = (D_3 - D_2) \times (t_3 - t_2)^{-1}$$

$$\vdots$$

$$v \text{ (mm s}^{-1}\text{)} = (D_Z - D_{Z-1}) \times (t_Z - t_{Z-1})^{-1}$$

Eqn [16] summarizes this procedure:

$$v \text{ (mm s}^{-1}\text{)} = (D_n - D_m) \times (t_n - t_m)^{-1} = dD \times dt^{-1} \quad [16]$$

where D_n (mm) equals the migration distance of a protein at a time t_n (s) and D_m (mm) equals its migration distance at a time t_m (s) where $t_n > t_m$ (Figure 13).

Table 4 Calculated Stokes radius of marker proteins and mammalian carbonic anhydrase (iso)enzymes and calculation of percentage of deviation of calculated values from the literature

Protein	Stokes radius (R_s (nm)) ^a	$\ln R_s$	Calculated Stokes radius (R_s)			$\ln D_{\max}$
			$\ln R_s$	R_s (nm)	Percentage deviation ^b	
Ovalbumin	3.05	− 19.6081	− 19.5992	3.08	+ 0.9	4.6563
Bovine serum albumin	3.55	− 19.4563	− 19.4285	3.65	+ 2.8	4.3537
L-Lactate dehydrogenase	4.20	− 19.2881	− 19.2590	4.32	+ 2.9	4.0532
Catalase	5.25	− 19.0650	− 19.1634	4.76	− 9.3	3.8836
Ferritin	6.10	− 18.9150	− 18.8987	6.20	+ 1.6	3.4144
Thyroglobulin	8.50	− 18.5832	− 18.5668	8.64	+ 1.7	2.8259
Carbonic anhydrase						
Bovine I			− 19.7070	2.76		4.8476
Bovine II			− 19.7189	2.73		4.8686
Bovine/rabbit III			− 19.7020	2.78		4.8387
Rabbit IV			− 19.6876	2.82		4.8131
Canine/human V			− 19.6988	2.78		4.8330
Arithmetic mean			− 19.7030	2.77		4.8404

^aLiterature values.^bThe molecular sizes calculated are compared with the literature data and the percentage deviation indicated.

Reproduced with permission from Rothe (1991).

Table 5 Marker proteins that can be used to estimate the native molecular size of proteins

Marker protein	M_r	R_s
Carbonic anhydrase	30 000	2.43
Ovalbumin	45 000	3.05
Bovine serum albumin	67 000	3.55
β -Galactosidase	116 000	4.23
Lactate dehydrogenase	140 000	4.20
Catalase	232 000	5.25
Ferritin	440 000	6.10
Thyroglobulin	669 000	8.50

M_r (Da), Molecular mass; R_s (nm), Stokes' radius of proteins. These markers can be taken when using PA gradients of 4–30% T and a buffer of pH 8.4 (45 mmol L⁻¹ Tris, 40 mmol L⁻¹ boric acid, 1.25 mmol L⁻¹ EDTA-Na₂, pH 8.4).

Correlating Migration Velocities and Migration Distances

The migration velocities may be plotted against the corresponding migration distances at the end of each time interval to correlate migration velocities and migration distances (Figure 13). The function by which v and D are interrelated is best described by the following exponential equation:

$$v \text{ (mm s}^{-1}\text{)} = \varepsilon(D_{\max} - D)^\delta \quad [17]$$

where ε , D_{\max} and δ are constants, D (mm) is the independent variable and v (mm s⁻¹) the dependent variable. D_{\max} represents the maximum migration distance which a protein can cover, i.e. the migration distance at which the migration velocity becomes zero. If this point is reached then $D_{\max} = D$ and:

$$v \text{ (mm s}^{-1}\text{)} = \varepsilon(D - D)^\delta = 0 \quad [18]$$

Eqn [17] can be used to relate the apparent migration velocity (v) of a protein to the PA concentration (T (%)) that corresponds to the migration distance travelled during a given period of electrophoresis. When using a linear gel gradient, the PA concentration and the gel length are interrelated by eqn [19]:

$$D = \alpha^{-1}(T - \beta) \quad [19]$$

whilst T_{\max} (%), the stacking gel concentration, is related to the maximum distance D_{\max} (mm) by eqn [20]:

$$D_{\max} = \alpha^{-1}(T_{\max} - \beta) \quad [20]$$

Substituting eqns [19] and [20] into eqn [17] yields the formula:

$$v \text{ (mm s}^{-1}\text{)} = \varepsilon[(T_{\max} - \beta) \times \alpha^{-1} - (T - \beta) \times \alpha^{-1}]^\delta \quad [21]$$

which can be arranged to:

$$v \text{ (mm s}^{-1}\text{)} = \varepsilon \times \alpha^{-\delta} \times (T_{\max} - T)^\delta \quad [22]$$

and:

$$v \text{ (mm s}^{-1}\text{)} = h \times (T_{\max} - T)^\delta \quad [23]$$

where $h = \varepsilon \times \alpha^{-\delta}$.

This derivation shows that, indeed, the apparent migration velocity of a protein (v) is related by the same function to the distance (D) as to the PA concentration (T) it has reached in a linear pore gradient, although the constants (ε and D_{\max} , respectively, h and T_{\max}) are different. The exponent δ in both equations, however, is the same.

Eqn [23] predicts that zero protein mobility ($v = 0$) results if the apparent gel concentration (T (%)) is equal to the stacking gel concentration (T_{\max} (%)), i.e. if $T = T_{\max}$. The apparent free electrophoretic mobility of a protein unhindered by the PA matrix (μ (mm s⁻¹)), can be calculated by simply extrapolating its apparent mobility to zero T (%):

$$\mu \text{ (mm s}^{-1}\text{)} = h \times (T_{\max} - 0)^\delta \quad [24]$$

thus:

$$\mu \text{ (mm s}^{-1}\text{)} = h \times T_{\max}^\delta \quad [25]$$

This expression may be used to divide eqn [23] to yield eqns [26] and [27]:

$$v \times \mu^{-1} = (h \times (T_{\max} - T)^\delta) \times (h \times T_{\max}^\delta)^{-1} \quad [26]$$

which can be rewritten as:

$$v = \mu[1 - (T \times T_{\max}^{-1})]^\delta \quad [27]$$

The value of the quotient $(T_{\max} - T) \times T_{\max}^{-1}$ ranges from one ($T = 0$) to zero ($T = T_{\max}$) and thus the value of v extends from the apparent free electrophoretic mobility (μ) to zero.

This means that, in a linear PA gradient, the apparent migration velocity (v) of a protein (migrating under a constant electrical field strength) is equal to its apparent free mobility (μ) times a retardation factor $[1 - (T \times T_{\max}^{-1})]^\delta$ which depends on the PA concentration (T) that the protein has just reached and its exclusion limit (T_{\max}). This factor always takes

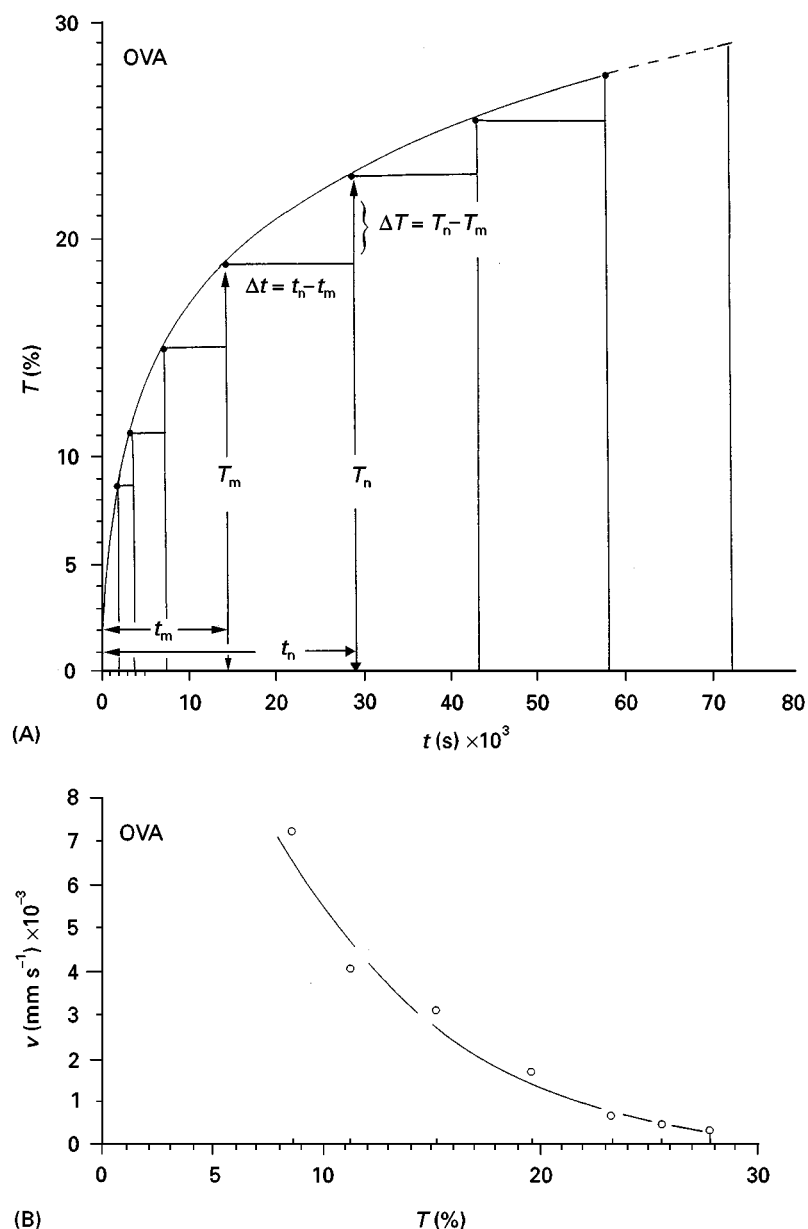


Figure 13 (A) Estimation of the migration velocity of a protein (OVA, ovalbumin) in a linear PA gradient gel. T_n , migration distance at a longer time of electrophoresis (t_n); T_m , migration distance at a shorter time of electrophoresis (t_m). (B) Plot of the resulting migration velocities (v (mm s $^{-1}$) versus the corresponding gel concentrations (T (%)) at the end of each time interval.

values between zero and one and increases exponentially with increasing gel concentrations.

In order to solve eqn [23] (v (mm s $^{-1}$) = $h \times (T_{\max} - T)^\delta$), the following sequence of calculations is recommended:

1. determination of the maximum migration distance of the protein under investigation from a plot of $\ln(\ln D)$ vs. $t^{-1/2}$ (eqn [5])
2. computation of the maximum gel concentration (T_{\max}) by use of eqn [20] ($D_{\max} = \alpha^{-1}(T_{\max} - \beta)$);
3. calculation of the gel concentration equivalent to the migration distances with eqn [19] ($D = \alpha^{-1}(T - \beta)$), (the values of the constants α and β may be obtained from a gel scan at 405 nm if *p*-nitrophenol has been mixed into the more concentrated of the two solutions used to prepare the gradient gel);
4. then the values of $(T_{\max} - T)$ are calculated
5. finally the constants h and δ in eqn [23] are calculated by plotting $\ln v$ vs. $\ln(T_{\max} - T)$ and performing a linear regression analysis with these data,

i.e. taking the logarithmized version of eqn [23]:

$$\ln v = \delta \times \ln(T_{\max} - T) + \ln b \quad [28]$$

Calculation of the Free Electrophoretic Mobility

The free electrophoretic mobility (U ($\text{m}^2 \text{V}^{-1} \text{s}^{-1}$)) of a protein results from its apparent free electrophoretic mobility unhindered by the gel matrix (μ ($\text{m} \text{s}^{-1}$)) and the electric field strength E (V m^{-1}) acting on it:

$$U = \mu \times E^{-1} (\text{m s}^{-1} (\text{V m}^{-1})^{-1} = \text{m}^2 \text{V}^{-1} \text{s}^{-1}) \quad [29]$$

The apparent free electrophoretic mobility can be obtained by applying eqn [25] (μ (mm s^{-1}) = $b \times T_{\max}^{\delta}$). The free electrophoretic mobilities of various marker proteins and five different mammalian carbonic anhydrases calculated by these procedures are listed in Table 6.

Computation of the Nett Charge

Estimation of the number of unit charges (Z) in a nondenatured protein requires prior knowledge of its Stokes radius (R_s) and its apparent free electrophoretic mobility (μ) or its free electrophoretic mobility (U). In addition to this, the ionic strength (I) and viscosity (η) of the buffer system used to estimate Z and R_s must be known. Time-dependent gradient gel electrophoresis can be used to determine the Stokes radius of a protein and its free electrophoretic mobility.

At a first approximation, the free electrophoretic mobility, unhindered by a gel matrix (U ($\text{m}^2 \text{V}^{-1} \text{s}^{-1}$)), can be described by eqn [30]:

$$U = (Z \times \varepsilon) \times (6 \times \pi \times \eta \times R_s)^{-1} \\ (C (\text{Pa s m})^{-1} = \text{m}^2 (\text{V s}^{-1})) \quad [30]$$

where Z is the number of unit charges (1); ε is the unit charge (protonic charge) = 1.602×10^{-19} (C); $\pi = 3.14 \dots$; η is the dynamic viscosity of the medium (Pa s); R_s is the Stokes radius (m) and the following coherences $1 \text{ C} = 1 \text{ A s}$, $1 \text{ Pa} = 1 \text{ N m}^{-2}$, $1 \text{ V A} = 1 \text{ W}$ and $1 \text{ W s} = 1 \text{ N m}$.

Since migration of proteins is studied in buffered solutions, there are also positive and negative buffer ions present, in addition to the protein ions. The small ions of sign opposite to that of the protein, also called counterions, are present in excess and to be found in the vicinity of the protein molecules. The electric field which drives the protein molecules also acts on the counterions, but in the opposite direction and since the migrating counterions drag solvent along with them and the solvent in turn acts on the protein, the nett effect is a secondary force on the protein opposite in direction to the primary force. The migration velocity of the protein molecules towards the electric field may therefore be reduced well below that predicted by eqn [30], an effect known as the electrophoretic effect. This is why eqn [30] must be corrected by a retardation factor (F),

Table 6 Free electrophoretic mobility (U) and net negative charge (valence, Z ; charge, Q) of several marker proteins and carbonic anhydrase (iso)enzymes from mammalia at pH 8.4

Protein	U ($\text{m}^2 (\text{V s})^{-1} \times 10^{-9}$) $I = 0.529 \times 10^{3a}$ (mol m^{-3})	Negative charge		
		$I = 0.1 \times 10^{3b}$ (mol m^{-3})	Z	Q ($C \text{ molecule}^{-1}$) $\times 10^{-19}$
Ovalbumin	3.45	5.99	13.06	20.92
Bovine serum albumin	4.40	7.85	22.42	35.92
Lactate dehydrogenase	3.27	6.00	22.63	35.25
Catalase	2.60	4.94	21.43	34.33
Ferritin	3.28	6.38	43.81	70.18
Thyroglobulin	2.78	5.62	68.46	109.67
CA I	1.58	2.69	4.93	7.90
CA II	1.17	1.99	3.58	5.74
CA III	1.05	1.79	3.32	5.32
CA IV	0.851	1.46	2.75	4.41
CA V	0.734	1.25	2.31	3.70

^a Ionic strength of electrophoretic buffer system.

^b Free electrophoretic mobility at ionic strength 0.1×10^3 ($\text{m}^2 (\text{V s})^{-1}$).

CA, Carbonic anhydrase (iso)enzymes from mammalian erythrocytes: (bovine, I, II), bovine, rabbit (III), rabbit (IV) and canine, human (V). Conditions of electrophoresis: linear polyacrylamide gradient from 4 to 27% T (acrylamide-Bis = 24 : 1); gel length 73 mm; buffer system 90 mmol L^{-1} Tris; 80 mmol L^{-1} boric acid; 1.25 mmol L^{-1} EDTA- Na_2 , pH 8.4 ($I = 529$ (mol m^{-3}); field strength: 41 V cm^{-1} ; 4°C.

Reproduced with permission from Rothe (1991).

the quantity of which depends on the composition and strength of the small ions of the buffer used. Henry proposed a method for computing this factor using the formula:

$$F = (X_1(\kappa \times R_s)) \times (1 + (\kappa \times R_s))^{-1} \quad [31]$$

where X_1 is a function of $\kappa \times R_s$. Introducing this factor into eqn [30] yields eqn [32]:

$$U = (Z \times \varepsilon) \times (6 \times \pi \times \eta \times R_s)^{-1} \times (X_1(\kappa \times R_s)) \times (1 + (\kappa \times R_s))^{-1} \text{ (m}^2 \text{ V s}^{-1}\text{)} \quad [32]$$

The function $X_1(\kappa \times R_s)$ is complicated but always gives values between 1.0 and 1.5, as shown in **Figure 14**. According to Henry, three different equations must be used to compute the values of the function X_1 . If $\kappa \times R_s > 24$ then the first of the three equations indicated in **Figure 14** must be used. When $\kappa \times R_s \leq 5$ the last of the three equations in **Figure 14** is applied. In the range between the two border values 5 and 24, a linear equation is taken, which is also

given in **Figure 14**. It is somewhat difficult to calculate the X_1 values when $\kappa \times R_s \leq 5$. Therefore, **Table 7** provides a number of values in the range of $\kappa \times R_s = 0.01$ –5. Kappa ($\kappa \text{ (m}^{-1}\text{)}$) represents the reciprocal of the radius of the ion cloud, i.e. the radius of the cloud of counterions surrounding the protein. Depending on the ionic composition, ionic strength and temperature of the solution, κ acquires values ranging from zero to infinity, and at increasing ionic strengths the value of κ increases whilst the radius of the ionic cloud decreases and vice versa. In a salt-free solution, $\kappa = 0$ so that the electrophoretic mobility U is not influenced at all, whilst conversely it decreases permanently in solutions with increasing salt concentrations. The value of kappa can be obtained from the equation:

$$\kappa = [(2N_A \times \varepsilon^2) \times (D_0 \times D \times k \times T)^{-1}]^{1/2} \times I^{1/2} \text{ (m}^{-1}\text{)} \quad [33]$$

where $N_A = 6.025 \times 10^{23} \text{ (mol}^{-1}\text{)}$; ε is the unit charge (protonic charge) = $1.602 \times 10^{-19} \text{ (C)}$; D_0 represents

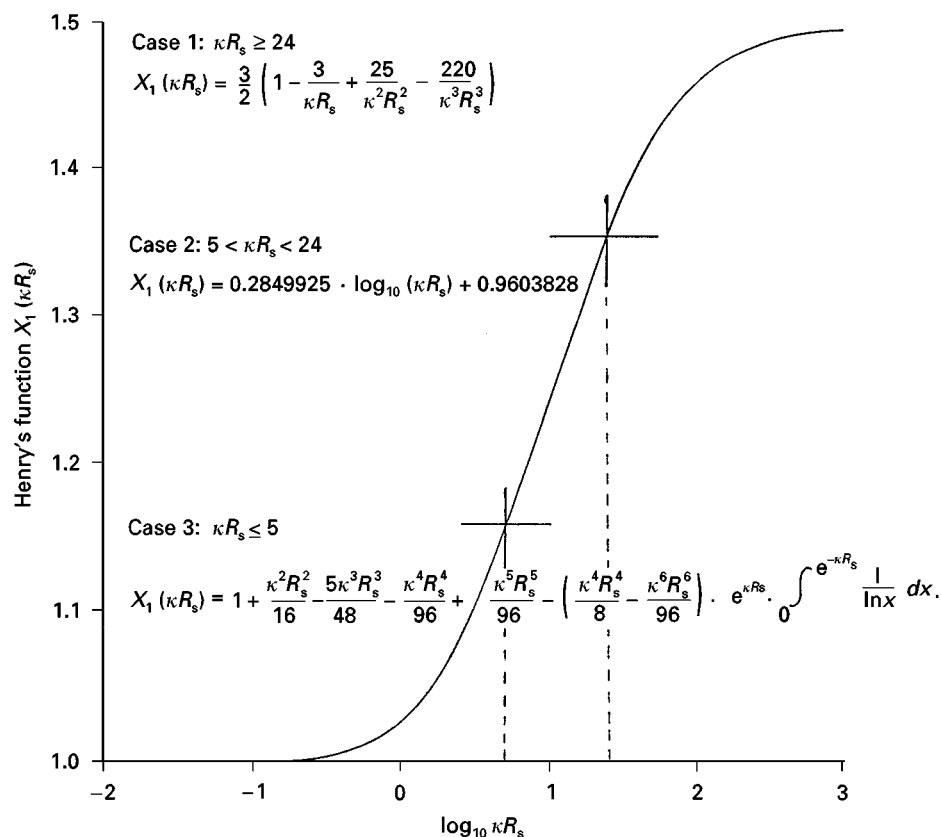


Figure 14 Graphical representation of Henry's function $X_1(\kappa R_s)$. Depending on the value of κR_s three different equations must be used to compute the values of X_1 . If $\kappa R_s > 24$ (case 1), the first of the three equations given is used. The second equation (case 2) comes into use if $5 \leq \kappa R_s \leq 24$ while the third equation (case 3) is applied if $\kappa R_s \leq 5$. In the latter case, Table 6 provides a number of values. Reproduced with permission from Rothe (1991).

Table 7 Values of Henry's function ($X_1(\kappa \times R_s)$) if $\kappa \times R_s < 5$ (cf. Figure 14)^a

$\kappa \times R_s$	$\log_{10}(\kappa \times R_s)$	X_1 according to Overbeek's modification of Henry's equation	$\kappa \times R_s$	$\log_{10}(\kappa \times R_s)$	X_1 according to Overbeek's modification of Henry's equation
0.01	-2	1.0000062	1.95	0.2900346	1.0632127
0.05	-1.30103	1.0001452	2.00	0.30103	1.0651048
0.10	-1	1.0005451	2.05	0.3117539	1.0669887
0.15	-0.8239087	1.0011577	2.10	0.3222193	1.0688642
0.20	-0.69897	1.001951	2.15	0.3324385	1.0707308
0.25	-0.60206	1.0028994	2.20	0.3424227	1.0725882
0.30	-0.5228787	1.003982	2.25	0.3521825	1.0744361
0.35	-0.455932	1.005181	2.30	0.3617278	1.0762744
0.40	-0.39794	1.0064817	2.35	0.3710679	1.0781027
0.45	-0.3467875	1.0078712	2.40	0.3802112	1.0799208
0.50	-0.30103	1.0093387	2.45	0.3891661	1.0817286
0.55	-0.2596373	1.0108744	2.50	0.39794	1.0835259
0.60	-0.2218487	1.0124701	2.55	0.4065402	1.0853126
0.65	-0.1870866	1.0141185	2.60	0.4149733	1.0870886
0.70	-0.154902	1.0158129	2.65	0.4232459	1.0888537
0.75	-0.1249387	1.0175476	2.70	0.4313638	1.0906078
0.80	-0.09691	1.0193175	2.75	0.4393327	1.0923509
0.85	-0.0705811	1.0211181	2.80	0.447158	1.094083
0.90	-0.0457575	1.0229452	2.85	0.4548449	1.0958039
0.95	-0.0222764	1.0247952	2.90	0.462398	1.0975136
1.00	0.0	1.0266648	2.95	0.469822	1.0992121
1.05	0.0211893	1.028551	3.00	0.4771213	1.1008994
1.10	0.0413927	1.0304511	3.05	0.4842998	1.1025754
1.15	0.0606978	1.0323626	3.10	0.4913617	1.1042402
1.20	0.0791812	1.0342836	3.15	0.4983106	1.1058938
1.25	0.09691	1.0362118	3.20	0.50515	1.1075361
1.30	0.1139434	1.0381455	3.25	0.5118834	1.1091672
1.35	0.1303338	1.0400832	3.30	0.5185139	1.1107871
1.40	0.146128	1.0420233	3.35	0.5250448	1.1123958
1.45	0.161368	1.0439644	3.40	0.5314789	1.1139934
1.50	0.1760913	1.0459054	3.45	0.5378191	1.11558
1.55	0.1903317	1.0478451	3.50	0.544068	1.1171554
1.60	0.20412	1.0497825	3.55	0.5502284	1.1187199
1.65	0.2174839	1.0517167	3.60	0.5563025	1.1202734
1.70	0.2304489	1.0536469	3.65	0.5622929	1.1218159
1.75	0.243038	1.0555723	3.70	0.5682017	1.1233477
1.80	0.2552725	1.0574921	3.75	0.5740313	1.1248686
1.85	0.2671717	1.0594059	3.80	0.5797836	1.1263788
1.90	0.2787536	1.0613129	3.85	0.5854607	1.1278783
3.90	0.5910646	1.1293672	4.45	0.64836	1.1450647
3.95	0.5965971	1.1308456	4.50	0.6532125	1.1464318
4.00	0.60206	1.1323134	4.55	0.6580114	1.1477892
4.05	0.607455	1.1337709	4.60	0.6627578	1.1491371
4.10	0.6127839	1.135218	4.65	0.667453	1.1504754
4.15	0.6180481	1.1366549	4.70	0.6720979	1.1518043
4.20	0.6232493	1.1380816	4.75	0.6766936	1.1531238
4.25	0.6283889	1.1394981	4.80	0.6812412	1.1544341
4.30	0.6334685	1.1409047	4.85	0.6857417	1.1557352
4.35	0.6384893	1.1423012	4.90	0.6901961	1.1570272
4.40	0.6434527	1.1436879	4.95	0.6946052	1.1583101
			5.00	0.69897	1.159584

^aValues were calculated using eqn [3] of Figure 14 (cf. Overbeek JTG (1950) *Advances in Colloid Science*, 3: 97-135). Tolerance of values: 10^{-6} , calculation of integral: 7 digits. Data from Rothe (1991).

the dielectric constant of vacuum = 8.8542×10^{-12} ($\text{C V}^{-1} \text{m}^{-1} = \text{C}^2 \text{N}^{-1} \text{m}^{-2}$); D is the temperature-dependent dielectric constant of water (without dimension, cf. Table 8), k is Boltzmann's con-

stant = 1.3805×10^{-23} ($\text{J K}^{-1} = \text{N m K}^{-1}$); T is absolute temperature (K) and I is the ionic strength (mol m^{-3}) of the buffer that was used for electrophoresis.

Table 8 Dielectric constant (D) of water depending on the temperature t ($^{\circ}\text{C}$)

t ($^{\circ}\text{C}$)	D	t ($^{\circ}\text{C}$)	D
0	87.90	18	80.93
5	85.90	20	80.18
10	83.95	25	78.36
15	82.04	30	76.58

Reproduced with permission from West (1976–1977).

By substituting these values into the equation one obtains:

$$\kappa = [(2 \times 6.025 \times 10^{23} \times (1.602 \times 10^{-19})^2) \times (8.8542 \times 10^{-12} \times 1.3805 \times 10^{-23})^{-1}]^{1/2} (\text{K m} (\text{mol})^{-1})^{1/2} \times (I (D T)^{-1})^{1/2} (\text{mol m}^{-3} \text{K}^{-1})^{1/2} \quad [34]$$

thus:

$$\kappa = 1.590608013 \times 10^{10} (\text{K m mol}^{-1})^{1/2} \times (I (D T)^{-1})^{1/2} (\text{mol m}^{-3} \text{K}^{-1})^{1/2} \quad [35]$$

At a temperature of 5°C (278 K), the dielectric constant of water is 85.90 (cf. Table 8). Inserting both values into eqn [35] yields eqn [36]:

$$\kappa = 1.02930525 \times 10^8 (\text{m mol}^{-1})^{1/2} \times \sqrt{I (\text{mol m}^{-3})^{1/2}} \quad [36]$$

The ionic strength I (mol m^{-3}) is calculated using the formula:

$$I = 1/2 \sum c_i Z_i^2 (\text{mol m}^{-3}) \quad [37]$$

where $\sum c_i$ (mol m^{-3}) represents the concentrations of the ionic species of the buffer times their squared charges (Z_i).

Taking, for example, a 90 mmol L^{-1} Tris, 80 mmol L^{-1} boric acid, 1.25 mmol L^{-1} EDTA- Na_2 buffer of pH 8.0, the ionic strength of this buffer is:

$$I = 1/2 \sum c_i Z_i^2 (\text{mol dm}^{-3}) \quad [38]$$

thus:

$$I = 1/2 [(0.09 \times 1^2) + (3 \times 0.08 \times 1^2) + (0.08 \times (-3)^2) + (2 \times 0.00125 \times 1^2) + (0.00125 \times (-2)^2)] \quad [39]$$

which becomes:

$$I = 0.52875 (\text{mol dm}^{-3}) \quad [40]$$

or:

$$I = 0.52875 \times 10^3 (\text{mol m}^{-3}) \quad [41]$$

Substituting this value into eqn [36] gives:

$$\kappa = 1.02930525 \times 10^8 (\text{m mol}^{-1})^{1/2} \times (528.75)^{1/2} (\text{mol m}^{-3})^{1/2} \quad [42]$$

which rearranges to:

$$\kappa = 2.366842604 \times 10^9 (\text{m}^{-1}) \quad [43]$$

Taking ferritin as an example, with a Stokes radius of 6.20×10^{-9} (m), then $\kappa \times R_s = 14.67$. The log of $\kappa \times R_s$ equals 1.167 and using this value one obtains from the equation in case 2 shown in Figure 14, a value of 1.293 for the function X_1 ($\kappa \times R_s$). Thus, inserting these values into eqn [31], it follows that:

$$F = (X_1(\kappa \times R_s)) \times (1 + (\kappa \times R_s))^{-1} = 1.293 \times (1 + 14.67)^{-1} = 0.08251 \quad [44]$$

To calculate the number of nett charges in ferritin, eqn [32] must be solved for Z :

$$Z = ((U \times 6 \times \pi \times \eta \times R_s) \times \epsilon^{-1}) \times ((1 + (\kappa \times R_s)) \times (X_1(\kappa \times R_s))^{-1}) \quad [45]$$

From gradient gel electrophoresis results, the free electrophoretic mobility of ferritin was calculated as $U = 3.28 \times 10^{-9}$ ($\text{m}^2 \text{V}^{-1} \text{s}^{-1}$). Substituting this value, that of factor F and the value for the temperature-dependent dynamic viscosity (η (N s m^{-2})) of water as taken from Table 9 into eqn [45], the number of unit charges that ferritin acquires under the electrophoretic conditions indicated above can be computed as:

$$Z = (3.28 \times 10^{-9} \times 6 \times \pi \times 1.519 \times 10^{-3} \times 6.20 \times 10^{-9}) \times (1.602 \times 10^{-19})^{-1} \times ((1 \times 0.08251)^{-1}) \quad [46]$$

which works out to:

$$Z = 44.05 \quad [47]$$

The actual charge on the molecule is given by $Z \times \epsilon$ [C molecule^{-1}] = $44.05 \times 1.602 \times 10^{-19} = 7.057 \times 10^{-18}$ (Table 6).

Table 9 Dynamic viscosity (η (N s m⁻²)) of water depending on the temperature (t (°C))

t (°C)	$(N s m^{-2}) \cdot 10^{-3}$	t (°C)	$(N s m^{-2}) \cdot 10^{-3}$
0	1.787	16	1.109
1	1.728	17	1.081
2	1.671	18	1.053
3	1.618	19	1.027
4	1.567	20	1.002
5	1.519	21	0.9779
6	1.472	22	0.9548
7	1.428	23	0.9325
8	1.386	24	0.9111
9	1.346	25	0.8904
10	1.307	26	0.8705
11	1.271	27	0.8513
12	1.235	28	0.8327
13	1.202	29	0.8148
14	1.169	30	0.7975
15	1.139		

Reproduced with permission from West (1976–1977).

Evaluation of the Free Electrophoretic Mobility at an Ionic Strength of 0.1 mol L⁻¹

For reasons of comparability, the free electrophoretic mobility obtained for a given set of experimental conditions may be corrected to an effective mobility at an ionic strength of 0.1 mol L⁻¹. This can be achieved by substituting the relevant values into Abramson's equation:

$$U_{0.1} = (U_{>0.1}(\kappa_{>0.1} \times R_S + 2.4)) \times (\kappa_{0.1} \times R_S + 2.4)^{-1} \quad [48]$$

where $U_{0.1}$ and $U_{>0.1}$ (m² V⁻¹ s⁻¹) represent the free electrophoretic mobilities at an ionic strength of 0.1 (mol m⁻³) and > 0.1 (mol m⁻³) respectively; $\kappa_{>0.1}$ and $\kappa_{0.1}$ represent the reciprocal of the effective thickness of the ionic cloud at ionic strength of 0.1 (mol m⁻³) and > 0.1 (mol m⁻³) respectively and R_S (m) is the Stokes radius of the protein.

For the experimental conditions given earlier:

$$\kappa_{0.1} = 1.02930525 \times 10^8 \text{ (m mol}^{-1}\text{)}^{1/2} \times (0.1 \times 10^3)^{1/2} \text{ (mol m}^{-3}\text{)}^{1/2} \quad [49]$$

thus:

$$\kappa = 1.02930525 \times 10^9 \text{ (m}^{-1}\text{)} \quad [50]$$

Taking ferritin as an example, for which U (m² V⁻¹ s⁻¹) = 3.28×10^{-9} (at $I = 0.529 \times 10^3$ (mol m⁻³), if $\kappa_{>0.1} = 2.366842604 \times 10^9$ and $R_S = 6.20 \times 10^{-9}$ (m) are determined and substituted into eqn [48], it follows that:

$$U_{0.1} = ((3.28 \times 10^{-9}) \times (2.366842604 \times 10^9 \times 6.20 \times 10^{-9} + 2.4)) \times (1.02930525 \times 10^9 \times 6.20 \times 10^{-9} + 2.4)^{-1} \quad [51]$$

thus:

$$U_{0.1} = 6.377 \times 10^{-9} \text{ (m}^2 \text{ V}^{-1} \text{ s}^{-1}\text{)} \quad [52]$$

The free electrophoretic mobilities at $I = 0.52875 \times 10^3$ (mol m⁻³) and at $I = 0.1 \times 10^3$ (mol m⁻³) of several marker proteins and some carbonic anhydrase isozymes are listed in Table 10.

Table 10 Free electrophoretic mobility of ferritin in buffered solution

Experimental conditions	Free mobility U (m ² V ⁻¹ s ⁻¹) $\times 10^{-9}$	Reference
Moving boundary method $I = 0.1$ (mol L ⁻¹), 0 (°C), pH 8.6	– 6.1	Mazur <i>et al.</i> (1950)
Agarose gel electrophoresis $I = 0.05$ (mol L ⁻¹), + 20 (°C), pH 6.8	– 10.5	Gosh <i>et al.</i> (1974)
Disc electrophoresis $C = 2\%$; 0 (°C), pH 8.88 $I = 0.0034$ (mol L ⁻¹) $I = 0.10$ (mol L ⁻¹)	– 10.97 – 5.67	Rodbard <i>et al.</i> (1971)
PA gradient gel electrophoresis 5–30 T (%), acrylamide–Bis = 24 : 1; + 4 (°C), pH 8.4 ^a $I = 0.529$ (mol L ⁻¹) $I = 0.10$ (mol L ⁻¹)	– 3.28 – 6.38	Rothe (1991)

^aElectrophoretic conditions; 90 mmol L⁻¹ Tris, 80 mmol L⁻¹ boric acid, 1.25 mmol L⁻¹ EDTA–Na₂, pH 8.4; separation distance 73 mm, voltage gradient 41.1 (V cm⁻¹)

References are given in Rothe (1991).

The result of calculating the net protonic charge of a protein of course remains unaffected whether the ionic strength of the experiment or that of a buffer strength of 0.1 mol L^{-1} is used.

Comprehensive Equation Describing Electrophoretic Mobility of Proteins Migrating in a Linear PA Gradient Gel

As explained above, the velocity with which a protein migrates in a linear PA gradient gel depends on its apparent free electrophoretic mobility times a retardation factor (eqn [27]):

$$v = \mu \times [1 - (T \times T_{\max}^{-1})]^\delta \text{ (m s}^{-1}\text{)} \quad [27]$$

where v is the migration velocity (m s^{-1}), T (%) is the PA concentration which the migrating protein of mobility v has reached and T_{\max} (%) represents the exclusion limit of the migrating protein.

Since $U = \mu \times E^{-1}$ ($\text{m}^2 \text{V}^{-1} \text{s}^{-1}$), it follows that:

$$v \times E^{-1} = U \times [1 - (T \times T_{\max}^{-1})]^\delta \text{ (m V}^{-1} \text{s}^{-1}\text{)} \quad [53]$$

U is defined by eqn [32] as equivalent to:

$$U = (Z \times \varepsilon) \times (6 \times \pi \times \eta \times R_s)^{-1} \times (X_1(\kappa \times R_s)) \times (1 + (\kappa \times R_s))^{-1} \text{ (m}^2 \text{V s}^{-1}\text{)}$$

with the definitions given above.

Using all this information, a complete description of the electrophoretic mobility of proteins migrating in a linear PA gradient gel can then be given by the equation:

$$v \times E^{-1} = (Z \times \varepsilon) \times (6 \times \pi \times \eta \times R_s)^{-1} \times (X_1(\kappa \times R_s)) \times (1 + (\kappa \times R_s))^{-1} \times [1 - (T \times T_{\max}^{-1})]^\delta \text{ (m}^2 \text{V s}^{-1}\text{)} \quad [54]$$

with the definitions as given above.

Sodium Dodecyl sulfate Porosity Gradient Gel Electrophoresis

Polyacrylamide gradient gels also offer greater possibilities for the electrophoretic separation of proteins in the presence of SDS. Porosity gradient gels have a much higher resolving capacity, for example the two chains of haemoglobin of $M_r = 15\,126$ and $15\,866$ Da, respectively, can be clearly separated in a 3–30% T gradient gel. An 8% T continuous PA-SDS gel does not exhibit this resolving capacity. In SDS porosity gradient gel electrophoresis the

use of continuous buffer systems is recommended (Table 11) since partial deloading of SDS-protein complexes has been observed when the gel contained SDS but not the electrode buffer. This results in a confusing multitude of bands.

Estimation of Molecular Mass of Denatured Proteins and Small Peptides

When SDS electrophoresis is performed in a linear PA gradient gel of 3–30% T , a linear relationship can be set up between the logarithm of the mol mass ($\log M_r$) and the log of the PA concentration ($\log T$) reached by proteins after a certain time of electrophoresis. The validity of the corresponding relationship $\log M_r = -a \times \log T + b$ has been confirmed with some 40 proteins between 14 and 950 kDa. In PA gradient gels in the presence of SDS the molar mass of both unreduced and 2-mercaptoethanol-reduced proteins as well as the molar mass of glycoproteins can be determined with the same accuracy ($\pm 5\%$, Table 12). Ribonuclease and lysozyme binding normal amounts of SDS migrate anomalously in homogeneous SDS gels but not in SDS PA gradient gels. Papain and pepsin, which also bind only traces of SDS, migrate regularly in SDS PA gradient gels.

The migration distance of proteins in linear SDS PA gradient gels and their respective mol mass can also be correlated by the equation:

$$\log M_r = -a \times \sqrt{D} + b \quad [55]$$

where D (mm) is the migration distance. This relationship can be applied to SDS-complexed and reduced and to SDS-complexed nonreduced proteins, to glycoproteins and to carbohydrate-free proteins (Figure 15). The relationship is not affected by the buffer system, the concentration of the cross-linker within 1–8% C or the concentration range of the gradient within 3–30% T at the commonly used gel length of 8–15 cm. The value of the constants a and b , on the other hand, are changed when the experimental parameters are altered. If SDS electrophoresis is performed in a linear gradient gel of approximately 6–27% T , the relationship $\log M_r = -a \times \sqrt{D} + b$ is practically independent of the time of electrophoresis. This means that the molecular mass estimation can be made when the best resolution of a set of proteins has been obtained. It is not necessary to wait until the proteins have reached their exclusion pore size. On the contrary, under prolonged electrophoresis protein-SDS complexes can reach a pore size where the complexing SDS is stripped off the protein molecules which leads to erroneous banding patterns. This is particularly

Table 11 Gel and buffer systems used in SDS PA gradient gel electrophoresis to separate denatured proteins

PA range (%T) (acrylamide-Bis)	Gel shape (dimensions (mm))	Buffer systems		Current or voltage per gel	Running time (h)	Correlation (M_r range (kDa))	Notes	Authors
		Gel buffer	Electrode buffer					
3–30 (30 : 0.8)	Column (150 × 6)	0.1 mol L ⁻¹ Na-phosphate, 0.1% SDS, 5–15% (v/v) glycerol, pH 7.0	0.1 mol L ⁻¹ Na-phosphate, 0.1% SDS, pH 7.0	4 mA	24	— (12–125)	<i>a</i>	Exposito and Objeski (1976)
3–30 (9.62 : 0.38)	Slab gel (length: 80)	10.75 g Tris, 5.04 g boric acid 0.93 g EDTA-Na ₂ , pH 7.2	0.01 mol L ⁻¹ Na-phosphate, 1% SDS, 1% 2- mercaptoethanol, pH 7.2	40 V	16	log M_r vs. log T (13–950)	<i>b</i>	Lambin <i>et al.</i> (1976), Lambin (1978)
1.5–40 (12.57 : 1)	Microcolumn i.d. 0.43, length 15	0.1 mol L ⁻¹ Na-phosphate, pH 7.2, 0.1% SDS or 0.35 mol L ⁻¹ Tris-sulfate, 0.1% SDS, pH 8.5, or 0.05 mol L ⁻¹ Tris-glycine, 0.1% SDS, pH 8.4, or 0.065 mol L ⁻¹ Tris-borate, 0.1% SDS, pH 9.3	29 g glycine plus Tris to pH 8.4, 1 g SDS, H ₂ O to 1000 mL	60 V	2	log M_r vs. R_F (13–300)	<i>c</i>	Rüchel <i>et al.</i> (1974)
1.5–40 (12.57 : 1)	Microcolumn (i.d. 0.43, length 15)	4 g Tris and H ₂ SO ₄ to pH 8.4, H ₂ O to 10 mL	29 g glycine plus Tris to pH 8.4, 1 g SDS, H ₂ O to 1000 mL	60 V	0.33	log M_r vs. R_F (13–300)	<i>c</i>	Rüchel <i>et al.</i> (1974)
3–30 (28 : 1)	Slab gel (width 80, length 80, thickness 1)	0.04 mol L ⁻¹ Tris, 0.02 mol L ⁻¹ Na-acetate, 0.02 mol L ⁻¹ Na-EDTA, pH 7.4, 0.2% SDS	Same as gel buffer	150 V	0.5–8	log M_r vs. \sqrt{D} (13–950)	<i>d</i>	Rothe (1982)

^aGels were stored at room temperature before use in a solution which contained 0.1 mol L⁻¹ Na-phosphate, 0.01% SDS, 15% glycerol, 2 mmol L⁻¹ EDTA-Na₂ and 0.01% NaN₃. Samples were dissolved at 100°C for 3 min in 0.01 phosphate buffer, pH 7, containing 2.5% SDS, 5% 2-mercaptoethanol, 10% glycerol and 0.005% Bromophenol blue. On each column 20–100 µg protein was loaded.

^b T (%) g acrylamide plus g Bis per 100 mL solvent. Protein samples (0.5 mg mL⁻¹) were incubated in 0.01 mol L⁻¹ phosphate buffer, containing 1% SDS, pH 7.2 for 3 min in a 100°C bath; for cleavage of disulfide bridges 1% 2-mercaptoethanol was added. The % T concentration reached by each protein after electrophoresis was determined and log T plotted versus log $mol\ mass$.

^cResolution was found to be better in discontinuous than in continuous buffer systems. Samples (1 mg protein mL⁻¹) were treated for 2 min at 100°C with 1% SDS and 1% 2-mercaptoethanol in 0.035 mol L⁻¹ Tris-sulfate, pH 8.6, 0.35 mol L⁻¹ Tris-sulfate, pH 8.6 or 0.1 mol L⁻¹ phosphate. Complete removal of SDS from proteins can be achieved with SDS-free electrode buffers. The activity of β -galactosidase denatured with SDS and separated on an SDS-free PA gradient gel could be restored to 10%.

^d \sqrt{D} , square root of migration distance (D (mm)). Re-evaluation of the data from Lambin (1978), Lasky (1978) and Poduslo and Rodbard (1980) confirmed the validity of the log M_r – \sqrt{D} relationship, found when evaluating time-dependent SDS-porosity gradient gel electrophoresis using marker proteins in the range of 10–330 kDa.

References as given in Rothe and Maurer (1986). Reproduced with permission from Rothe and Maurer (1986).

true when in an alkaline buffer system the upper electrode buffer contains no SDS.

In SDS electrophoresis with linear PA gradients ranging from 3 to 30% T , polypeptides in the range

of 1.4–10 kDa cannot be resolved. Separation is possible, however, in 10–18% T gels in the presence of 0.1% SDS and 7 mol L⁻¹ urea (cf. Tables 13 and 14).

Table 12 Separation characteristics of some proteins in SDS PA gel electrophoresis and deviation of calculated mol masses from those given in the literature

No.	Protein	M_r (Da) (literature value)	3–30% T, C = 8.4% ^a				3–30% T, C = 3.8% ^b			
			D (mm)	M_r^c ± %	T (%)	M_r^d ± %	D (mm)	M_r^c ± %	T (%)	M_r^d ± %
1	Prealbumin	13 745	51.5	− 0.4	20.7	− 4.0	56	− 1.7	22.4	− 6.8
2	Lysozyme	14 314	53.5	− 16.5	21.4	− 20.4	51.5	+ 16.9	20.8	+ 13.6
3	Ribonuclease B	14 700	52	− 10.0	20.9	− 14.0	55.5	− 6.0	22.2	− 10.3
4	Haemoglobin	15 500	51	− 8.6	20.5	− 11.2	55	− 8.7	22	− 12.3
5	Avidin	16 000	49.5	− 1.7	20	− 4.2	51	+ 7.1	20.6	+ 4.8
6	Soybean trypsin inhibitor	20 095	47	− 6.6	19.2	− 9.2	50	+ 10.4	20.3	− 12.7
7	Papain	23 426	44.5	− 4.0	18.3	− 4.8	48	+ 15.1	19.6	− 16.5
8	α-chain of IgG	23 500								
9	Chymotrypsinogen A	25 666	43.5	− 5.6	18	− 7.0	44	+ 4.8	18.2	− 4.8
10	Carbonic anhydrase B	28 739	41	+ 1.8	17.1	+ 2.2	42	+ 5.5	17.5	− 4.7
11	Carboxypeptidase A	34 409	40	− 8.1	16.7	− 6.3	39.5	− 9.5	16.7	− 9.0
12	Pepsin	34 700	37.5	+ 11.0	15.9	+ 12.5	37.5	+ 0.4	16	+ 1.8
13	Glycerol-3-phosphate dehydrogenase	35 700	37.5	+ 7.9	15.9	+ 9.4	36	+ 6.4	15.5	+ 7.9
14	Lactate dehydrogenase	36 180	37.5	+ 6.4	15.9	+ 7.9	37	− 1.0	15.8	+ 1.0
15	Aldolase	38 994	36	+ 11.5	15.4	+ 13.1	35	+ 3.2	15.1	+ 6.0
16	Alcohol dehydrogenase	39 805	35.5	+ 13.8	15.2	+ 16.4	34.5	+ 4.2	14.9	+ 7.7
17	α ₁ -Acid glycoprotein	40 000	35	+ 18.0	15	+ 21.7	32	+ 20.6	14.1	+ 23.9
18	Ovalbumin	43 000	35.5	+ 5.4	15.2	+ 7.8	35.5	− 9.1	15.3	− 7.2
19	Fibrinogen γ chain	47 000								
20	Glutamate oxalacetate transaminase	50 000	32.5	+ 16.7	14.2	+ 19.2	29	+ 16.6	13	+ 21.9
21	Heavy chain IgG	50 000								
22	Fibrinogen β chain	56 000								
23	Catalase	57 500	32	+ 5.9	14	+ 9.1	29	+ 1.4	13	+ 6.0
24	Fibrinogen α chain	63 500								
25	Albumin monomer	66 290	31.5	+ 10.7	13.8	+ 14.9	28	+ 8.2	12.7	− 12.3
26	Heavy chain IgM	72 000								
27	Transferrin	76 000	30.5	− 8.6	13.5	− 6.0	24	+ 7.6	11.3	+ 12.4
28	Plasminogen	81 000	29	− 1.8	13	+ 0.7	23	+ 8.5	11	+ 12.2
29	Phosphorylase b	96 800	25.5	+ 14.2	11.8	+ 17.1	21	+ 5.3	10.3	+ 8.9
30	Ceruloplasmin	124 000	23.5	+ 8.8	11.1	+ 11.6	17	+ 13.2	8.9	+ 16.2
31	Albumin, dimer	132 580	24	− 3.3	11.2	+ 1.4	17.5	+ 1.6	9	+ 6.2
32	Immunoglobulin G	150 000	21.5	+ 10.6	10.4	+ 13.4	15	+ 11.4	8.2	+ 13.4
33	Immunoglobulin A	160 000	22	+ 1.6	10.6	+ 0.1	14	+ 14.5	7.8	+ 17.2
34	Reduced α ₂ -macroglobulin	190 000								
35	Albumin, trimer	198 870	19.75	+ 0.8	9.8	+ 2.6	12	+ 11.8	7.1	+ 12.6
36	Immunoglobulin A	320 000	16	− 3.1	8.5	− 3.5	9	− 4.0	6.1	− 8.4
37	Thyroglobulin	330 000	16.5	− 11.6	8.7	− 12.4	11	− 25.4	6.8	− 26.6
38	Fibrinogen	340 000	15	+ 3.3	8.2	+ 0.4	8.5	− 4.2	5.9	− 8.8
39	α ₂ -Macroglobulin	380 000	15.5	− 13.2	8.3	− 13.1	8	− 9.0	5.8	− 16.0
40	Immunoglobulin A, trimer	480 000	13	− 4.8	7.5	− 9.5	6.5	− 12.4	5.2	− 20.6
41	Immunoglobulin M	950 000	8.75	− 9.1	6	− 20.1				
	Average % deviation			± 7.8		± 9.6		± 8.7		± 11.2
	Lambin (1978)					± 5.9				± 7.4

^a The gel buffer contained no 2-mercaptoethanol (gel length 78.5 mm).^b Gel buffer with 2-mercaptoethanol (gel length 81 mm), gel and electrode buffer as well as conditions of electrophoresis as given in Table 8. M_r (Da), mol mass; D (mm), migration distance; T (%), g acrylamide plus g Bis per 100 mL, as reached by a protein.^c M_r ± %, %-deviation of calculated mol mass from the literature value using the relationship $\log M_r = a \times \sqrt{D} + b$.^d M_r ± %, %-deviation of calculated mol mass from the literature value using the relationship $\log M_r = a \times \sqrt{T} + b$.

Reproduced with permission from Rothe and Maurer (1986).

Separation of Urinary Proteins and Diagnosis of Proteinurias

Diagnosis of pathological urinary profiles and estimation of the molecular size of the corresponding

proteins is possible by SDS PA gradient gel electrophoresis under nonreducing conditions. Protein patterns may be estimated in micro-sized ($43 \times 50 \times 0.45$ mm) SDS gradient gels of 8–25% T fixed to a plastic backing (GelBondTM) as they are

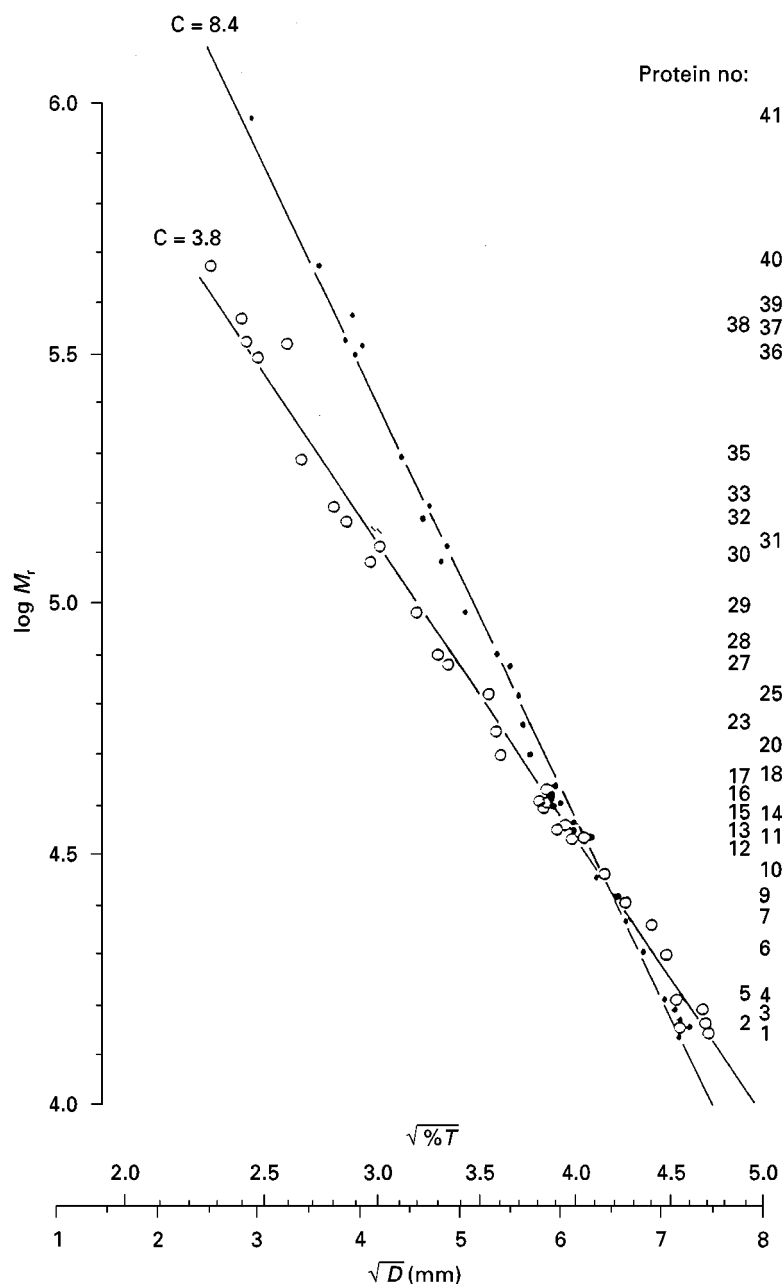


Figure 15 Migration distances of denatured proteins and protein subunits obtained by SDS PA gradient gel electrophoresis. The logarithm of the molecular mass of proteins ($\log M_r$) is linearly correlated to the square root of the PA concentration ($\sqrt{\%T}$) which they reached upon electrophoresis. Also, $\log M_r$ is linearly correlated to the square root of the migration distance (\sqrt{D} (D (mm))) which proteins reached upon electrophoresis. Reproduced with permission from Rothe (1994).

commercially available together with a suitable horizontal electrophoretic apparatus (Phast system) and an automated silver staining device (Amersham Pharmacia Biotech). The method has the advantage that urine samples need not be concentrated or desalted before electrophoresis. Samples may be stored frozen at -20°C after addition of sodium azide and after particulate removal by centrifugation. Samples with

protein concentrations above 0.30 mg mL^{-1} must be diluted. Proteins must not be reduced (e.g. with 2-mercaptoethanol) since under SDS and nonreducing conditions the quaternary structure of all major serum proteins excreted in urine is unaffected, except haemoglobin which is split into its monomers and dimers. **Figure 16** shows some selected protein patterns of renal malfunctions.

Table 13 Gel and buffer system used to separate small peptides in SDS PA gradient gel electrophoresis

Acrylamide (g 100 mL ⁻¹)	Bis (g 100 mL ⁻¹)	Gel buffer (pH)	Electrode buffer (pH)	Correlation (M_r (Da) range)	Authors
10–18	0.5–0.9	Stacking gel: 5% acrylamide, 0.13% Bis, 0.067 mol L ⁻¹ Tris-HCl, pH 6.8, 0.1% SDS, 0.067% ammonium persulfate and 0.067% TEMED; separation gel: 0.45 mol L ⁻¹ Tris-HCl, pH 6.9, 0.1% SDS, 0.05% ammonium persulfate, 0.05% TEMED, 7 mol L ⁻¹ urea	0.05 mol L ⁻¹ Tris, 0.38 mol L ⁻¹ glycine, 0.1% SDS, pH 8.5	log M_r vs. D (1400–17 000)	Hashimoto <i>et al.</i> (1983), Laemmli (1970)

M_r (Da), mol mass; D (mm), migration distance; TEMED, *N,N,N',N'*-tetramethylethylenediamine. The buffer solution containing 10% acrylamide (0.5% Bis) contains no sucrose while the buffer solution containing 18% acrylamide (0.9% Bis) contains 10% (w/v) of sucrose. The PAA concentration and the sucrose concentration increase linearly from top to bottom. The system can also be used to separate lipopolysaccharides and phospholipids. The addition of iodoacetamide to samples prior to electrophoresis eliminated artifacts currently observed in silver staining of protein bands. Log M_r correlates linearly with migration distance (D (mm)) in the mon mass range of 1.4 (kDa) to 17 (kDa). Flat gels of the dimensions 150 × 140 (height) × 1 (mm) were used. Gels were run for at least 15 h at 120 V. Samples were heated for 2 min at 100°C in a sample buffer containing 10% sucrose, 0.0625 M Tris-HCl, pH 6.8, 2% SDS, 10 mM dithiothreitol and 0.0025% Bromophenol blue (if necessary they were treated with iodoacetamide). Reproduced with permission from Rothe and Maurer (1986).

Table 14 Mol masses of polypeptides and peptides employed for urea-SDS gel electrophoresis

Protein	Mol mass (Da)	
	Literature value ^a	Computed ^b
Ovalbumin	46 000	
Carboxypeptidase A	34 500	<i>c</i>
Myoglobin	17 200	
Myoglobin I + II	14 900	
Cytochrome <i>c</i>	12 300	<i>c</i>
Myoglobin I	8270	
Cytochrome <i>c</i> I	7760	
Myoglobin II	6420	
Bovine trypsin inhibitor	6160	<i>c</i>
Adrenocorticotrophic hormone	4550	6500
Insulin	5700	
Insulin B chain	3400	
Insulin A chain	2300	
Glucagon	3460	1800
Cytochrome <i>c</i> II	2780	
Myoglobin III	2550	
Cytochrome <i>c</i> III	1810	
Bacitracin	1400	
Polymyxin B	1225	2200

^aValues as cited by Swank and Munkres (1971).

^bValues calculated by Swank and Munkres (1971) using least-squares regression analysis and assuming a linear correlation between log M_r (M_r , mol mass (Da)) and migration distance D (mm).

^cThe mol masses of these proteins also deviate considerably if a straight line in a log M_r vs. D plot is drawn through the points of carboxypeptidase A and bacitracin.

References as given in Rothe and Maurer (1986). Reproduced with permission from Rothe and Maurer (1986).

Diagnosis of the following proteinurias is possible:

1. Proteinuria in the normal range of total protein
2. Orthostatic (postural) proteinuria
3. Post-renal proteinurias
 - (a) Post-renal haematuria
 - (b) Local excretion of proteins
4. Bence-Jones proteinuria
5. Lower and upper urinary tract infections: cystitis and pyelonephritis
6. Diabetes mellitus

Concluding Remarks

Gradient gel electrophoresis has many advantages over conventional gel electrophoresis. Gradient range and course can be adapted to any individual separation problem, and protein bands are much sharper than in Cellogel or starch gel electrophoresis. So far, for example, more than 20 enzyme bands of an enzyme system such as plant acid phosphatase have been clearly resolved and genetically interpreted, and crude enzyme extracts can be used as the enzyme source, provided a specific detection (staining) system is available. The disadvantages are few compared to conventional gel electrophoresis, such as availability of gradient gel, a load of two to three times more enzyme activity per cm² of gel cross-section as compared to starch gels, and the exclusive migration of proteins towards the cathode (anode), whereas in Cellogel and starch gel electrophoresis both cathodically and anodically migrating proteins can be detected within the matrix.

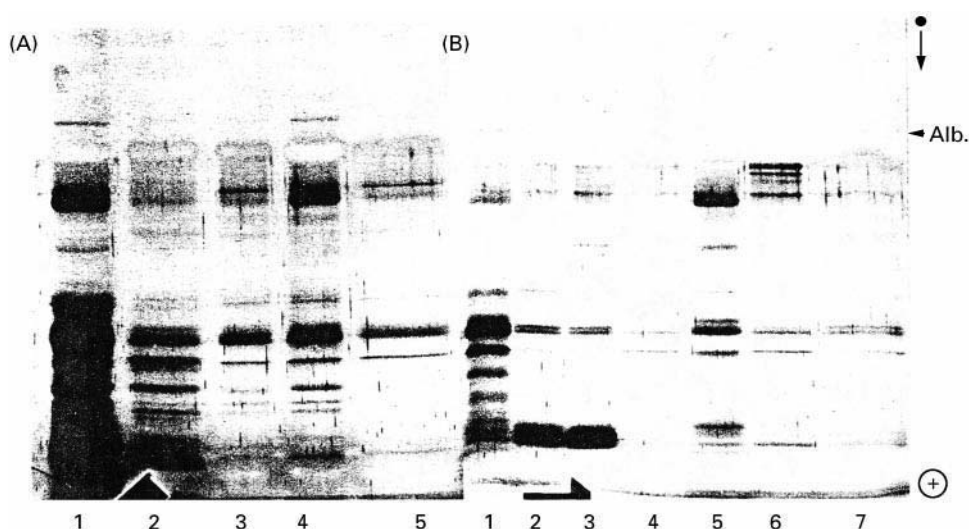


Figure 16 Separation of urinary proteins by macro SDS PA gradient gel electrophoresis. Gel: 4–20% *T*. Running conditions: 3 h at 350 V, 50 mA. Samples: up to 50 μ L urine. (A) and (B) show urine samples from paediatric patients with pyelonephritis at various stages of follow-up. Series A: 1, acute phase; 2, and 3, urine taken at weekly intervals; 4, reinfection (acute phase); 5, 1 week follow-up. Series B: 1, acute phase; 2–4, follow-up at weekly intervals (note blood contamination in 2 and 3, α - and β -globin chains at 16 kDa), 5, reinfection, 6, and 7, weekly follow-up. Black dot and vertical arrow on the right side of the gel represent the application point and migration direction, respectively. + Gel polarity. Alb., albumin. Reproduced with permission from Bianchi-Bosisio *et al.* (1991).

In addition to pure PA gels, matrices of mixed polymers can be used for porosity gradients. However, this possibility has been rarely used, although it could extend the separation possibilities.

PA gradients are widely used to determine the molecular mass of SDS-denatured proteins, because this method offers a larger separation range and a much better resolution of protein bands. However, native, time-dependent PA gradient gel electrophoresis has much more possibilities to offer, such as differentiation between size and charge isomers, determination of the molecular size of native proteins and (iso)enzymes (M_r , R_s), estimation of the molecular excentricity (f/f_o), and calculation of the net negative charge at a given pH value. Using these possibilities the evolution of homologous proteins in related animal and plant species can be studied as well as the net charge of isozymes from different cells compartments.

Further Reading

- Abramson HA (1933) Electrokinetic phenomena. *Journal of General Physiology* 16: 593–603.
- Altland K and Altland A (1984) Forming reproducible density and solute gradients by computer-controlled co-operation of stepmotor-driven burettes. *Electrophoresis* 5: 143–147.
- Bianchi-Bosisio A, D'Agrosa F, Gaboardi F *et al.* (1991) Review, Sodium dodecyl sulphate electrophoresis of urinary proteins. *Journal of Chromatography* 569: 243–260.

- Chiari M, Campoleoni A, Conti P *et al.* (1996) Electrophoretic separation of biopolymers in a matrix of polyacrylamide covalently linked to agarose. *Electrophoresis* 17: 473–478.
- Felgenhauer K (1974) Evaluation of molecular size by gel electrophoretic techniques. *Hoppe-Seyler's Zeitung für Physiologische Chemie* 355: 1281–1290.
- Henry DC (1931) The cataphoresis of suspended particles. Part I. The equation of cataphoresis. *Proceedings of the Royal Society A* 133: 106–140.
- Horvath ZS, Corthals GL, Wrigley CW and Margolis J (1994) Multifunctional apparatus for electrokinetic processing of proteins. *Electrophoresis* 15: 968–971.
- Lasky M (1978) Protein molecular weight determination using polyacrylamide gradient gels in the presence and absence of sodium dodecyl sulfate. In: Catsimopoulos N (ed.) *Electrophoresis*, pp. 195–210, Amsterdam: North Holland.
- Righetti PG and Tudor G (1981) Isoelectric points and molecular weights of proteins – a new table. *Journal of Chromatography* 220: 115–194.
- Rothe GM (1982) Applicability of the log MM/\sqrt{D} relationship to linear polyacrylamide gradient gel electrophoresis under a wide range of experimental conditions. *Electrophoresis* 3: 255–263.
- Rothe GM (1991) Determination of the size, isomeric nature and net charge of enzymes by pore gradient gel electrophoresis. In: Chrambach A, Dunn MJ and Radola BJ (eds) *Advances in Electrophoresis*, vol. 4, pp. 251–358. Weinheim: VCH.
- Rothe GM (1994) *Electrophoresis of Enzymes: Laboratory Methods*, p. 307. Berlin: Springer Verlag.

- Rothe GM (1994) Molecular relationship and possible evolution of 15 enzyme loci in five *Pinaceae* species. In: Zin-Suh K and Hattener H (eds) *Conservation and Manipulation of Genetic Resources in Forestry*, pp. 161–141. Seoul: Kwang Moon Kag.
- Rothe GM and Maurer WD (1986) One dimensional PAA-gel electrophoretic techniques to separate functional and denatured proteins. In: Dunn MJ (ed.)

- Gel Electrophoresis of Proteins*, pp. 37–140. Bristol: Wright.
- Tanford C (1961) *Physical Chemistry of Macromolecules*, p. 417, pp. 425–532. New York: John Wiley.
- Wedler G (1982) *Lehrbuch der physikalischen Chemie*, pp. 172–212. Weinheim: Verlag Chemie.
- West RC (eds) (1976–1977) *Handbook of Chemistry and Physics*, 57th edn. Cleveland, Ohio: CRC Press.

Proteins, Detection of

M. J. Dunn, National Heart and Lung Institute, Imperial College School of Medicine, Heart Science Centre, Harefield Hospital, UK

Copyright © 2000 Academic Press

Introduction

After polyacrylamide gel electrophoresis, it is essential that separated protein zones be detected for subsequent analysis, whether this is to be done by simple visual inspection or by quantitative computerized densitometry. In the early days of electrophoresis, methods for the detection of separated zones (ultra-violet absorption, Schlieren optics) were limited and insensitive. The subsequent development of organic dyes able to react with proteins made stains such as Bromophenol Blue and Amido Black 10B popular. In particular, Coomassie Brilliant Blue was for many years the method of choice for protein detection following gel electrophoresis owing to its relatively high sensitivity. However, the need for increased sensitivity resulted in the development of a group of staining methods based on the use of silver (approximately 0.1 ng of protein per band). Recently, there has been a renewed interest in the use of fluorescent methods of protein detection as they provide high sensitivity equivalent to silver staining combined with excellent linearity and extended dynamic range. Detection methods based on the use of radiolabelling also provide high sensitivity but cannot be applied in all situations. Finally, methods are available for the detection of groups of proteins with specific post-translational modifications, for example glycoproteins, phosphoproteins and lipoproteins.

Fixation

After electrophoresis is complete, the gel is removed from the apparatus for localization of the separated zones. Procedures have been described for the direct visualization of unfixed proteins within gels. How-

ever, for the majority of protein detection methods it is necessary to precipitate and immobilize (i.e. 'fix') the separated proteins within the gel and to remove any nonprotein components which might interfere with subsequent staining. Gels that are to be used for visualization of enzymatic activity of the separated proteins must not be fixed. The best general purpose fixative is 20% w/v trichloroacetic acid (TCA) as it gives effective precipitation of most proteins. Acid methanol (or ethanol), typically a solution containing 10% v/v acetic acid, 45% v/v methanol, and 45% deionized water, is often used for gel fixation, but it should be noted that this can be ineffective for small proteins, basic proteins and glycoproteins. Aqueous solutions of reagents such as 5% w/v formaldehyde or 2% w/v glutaraldehyde can be used to cross-link proteins covalently to the gel matrix, but this is not a commonly used approach.

Coomassie Brilliant Blue

The most popular general protein-staining procedures following gel electrophoresis are based on the use of the non-polar, sulfated triphenylmethane Coomassie stains, developed for the textile industry, Coomassie Brilliant Blue (CBB) R-250 is most often used and requires an acidic medium for electrostatic interaction between the dye molecules and the amino groups of proteins. Staining is usually carried out using 0.1% w/v CBB R-250 in the same acid methanol solution used for fixation (10% acetic acid, 45% methanol). Depending on gel thickness and polyacrylamide concentration, staining can take from 30 min to several hours. In practice, it is often convenient to stain the gel overnight and then destain it by several changes in the same acid methanol solution until intense blue protein zones can be seen against a clear background. This method is able to detect a minimum of around 100 ng protein per band (**Figure 1**), so that for complex mixtures containing several hundred components, it is necessary to load relatively high amounts of total protein (> 50 µg).

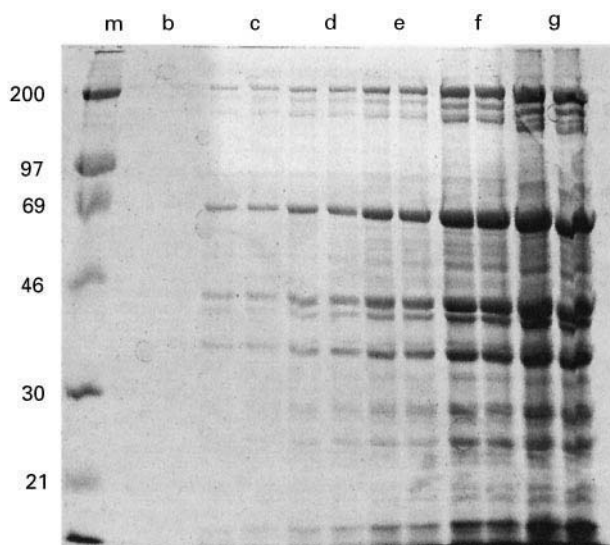


Figure 1 SDS-PAGE separation of human heart proteins (lanes b–g). Lane (a) contains the molecular weight marker proteins and the scale at the left indicates protein size in kDa. The gel has been stained with Coomassie Brilliant Blue R-250. The sample protein loadings were (b) 1 µg, (c) 5 µg, (d) 10 µg, (e) 25 µg, (f) 50 µg, (g) 100 µg.

More sensitive staining (down to 10 ng protein per band) can be achieved using the dimethylated form of the dye, CBB G-250, as a 0.1% w/v colloidal dispersion in 2% w/v phosphoric acid, 10% w/v ammonium sulfate, and 20% v/v methanol. An additional advantage of this method is that the colloidal dye only binds to the separated proteins as it is unable to penetrate the gel matrix. This means that no destaining step is required and the intensity of staining can be controlled by visual inspection during the staining process. Related dyes such as Acid Violet 17, Serva Violet 49 and Fast Green FCF also form colloids in strongly acidic solutions and stain proteins in gels with low background.

Silver Staining

Silver has been known to be able to develop images for over two hundred years, first being usefully exploited in photography and then rapidly adopted for use in histological staining procedures. The ability of silver to detect proteins following their separation by gel electrophoresis was first recognized by Merrill and his colleagues in 1979. Subsequently, more than a hundred silver-staining procedures have been described and this group of methods has become the standard approach for the sensitive detection of gel-separated proteins. However, certain classes of proteins, such as calcium-binding proteins and glycoproteins, stain rather poorly, with an inverse relationship

between the intensity of silver staining and the proportion of the molecule that is composed of carbohydrate. Pre-staining with cationic dyes prior to silver staining can significantly improve the sensitivity of detection of glycoproteins.

Depending on the method, silver staining is between ten and a hundred times more sensitive than staining with CBB R-250, and is able to detect low nanogram amounts of protein. There can be problems in using silver staining as a quantitative procedure as it is known to be non-stoichiometric. However, staining intensity is linear over a 40-fold range, comparing well with the 20-fold linear range of CBB R-250. Above this limit, the stain becomes non-linear, resulting in saturation and even negative staining of bands and spots at very high protein concentrations, making quantitation of such protein zones impossible. In a two-dimensional electrophoresis study of human leukocyte proteins, over 200 spots were observed to have coefficients of variation less than or equal to 15% when data from replicate patterns were analysed. In dilution experiments, the majority (> 80%) of the proteins were found to have a linear relationship between the amount of protein loaded and the spot volume. An additional problem with the quantitation of silver staining is that the relationship between staining intensity and protein concentration may be different for each protein. However, it is often forgotten that this is also the case for staining with CBB R-250.

All silver-staining procedures depend on the reduction of ionic silver to its metallic form, but the precise mechanism involved in the staining of proteins has not been fully established. It has been proposed that silver cations complex with protein amino groups, particularly the ϵ -amino group of lysine, and with sulfur residues of cysteine and methionine. However, staining cannot be attributed exclusively to specific amino groups suggesting that some other component of protein structure is also responsible for differential protein staining.

Procedures for silver staining can be grouped into two main types depending on the chemical state of the silver when used for impregnating the gel. The first group comprises alkaline methods based on the use of ammoniacal silver or diamine solution, prepared by adding silver nitrate to sodium-ammonium hydroxide mixture. Copper can be included in these diamine methods to give increased sensitivity, probably by a mechanism similar to the Biuret reaction. The silver ions complexed to proteins in the gel are then developed by reduction to metallic silver with formaldehyde in an acidified environment, usually using citric acid. In the alternative group of methods, silver nitrate in a weakly acidic (around pH 6.0)

solution is used for gel impregnation. Development is subsequently achieved by the selective reduction of ionic silver to metallic silver by formaldehyde made alkaline with either sodium carbonate or sodium hydroxide. Any free silver is washed out of the gel prior to development to prevent precipitation of silver oxide that would result in high background staining.

The majority of silver staining procedures are monochromatic, resulting in dark brown to black protein zones. However, if the development time is extended with saturation of the zones of highest protein concentration, then colour effects can be produced. In a comparative study of several methods based on both the silver diamine and silver nitrate approaches, the most rapid procedures were found to be generally less sensitive than those which were more time-consuming. The use of glutaraldehyde pre-treatment of the gel and silver diamine as the silvering agent were found to be the most sensitive and example of a gel stained with a method of this type is shown in **Figure 2**.

Increasingly, proteins are being visualized in gels for subsequent identification and characterization by techniques such as mass spectrometry. In this case, glutaraldehyde cannot be used and silver-staining protocols that omit this reagent must be used. However, this modification results in a decrease in sensitivity and uniformity of staining as well as an increase in background.

It is a common experience that silver-staining procedures can give rise to problems when based on the

use of laboratory-prepared reagents. If care is not taken with the use of high-purity water, reagents and glassware, then problems of high background staining, surface 'mirror' effects and poor reproducibility can be experienced. Many of these problems can be alleviated using one of the commercially available silver-staining kits (for example from Amersham-Pharmacia Biotech, Bio-Rad Laboratories, Richmond, CA, USA).

Reverse Stains

One disadvantage of the standard protocols for staining with Coomassie Blue dyes and silver is that it is essential to use a fixation step prior to staining. Unfortunately, this can result in reduced recovery of proteins from the gel for subsequent chemical characterization. Reverse stains have been developed to specifically overcome this problem. The result of these stains is a semi-opaque background on the gel surface, while the proteins are visible as transparent zones using back-lighting. The process of staining is rapid, requiring generally between 5 and 15 min. After staining, the proteins can be eluted after chelation of the metal ions with agents such as EDTA. It should be noted that reverse stains are not suitable for quantitative applications.

A variety of reverse-stain methods suitable for visualizing proteins after SDS-PAGE have been described. The most popular methods have been those using potassium chloride, copper chloride and zinc chloride, with the last being the most sensitive. The zinc imidazole-staining method is quite sensitive, with a limit of detection of around 10 ng protein per band. In the presence of imidazole, free or weakly bound zinc ions are readily precipitated as zinc imidazole, while tightly bound ions associated with proteins do not precipitate. This results in clear protein zones on an opaque background.

Fluorescent Detection Methods

Many of the problems inherent in the quantification of gel-separated proteins visualized by silver staining can be overcome using detection methods based on the use of fluorescent compounds. This group of methods is highly sensitive and generally exhibits excellent linearity and a high dynamic range, making it possible to achieve good quantitative analysis, particularly if a suitable imaging device is used.

Two approaches can be used, the first being to couple the proteins with a fluorescent-labelled compound prior to electrophoresis. Examples of such compounds are: dansyl chloride; fluorescamine (4-phenyl-[furan-2(3H)-1-phthalan]-3,3'-dione);

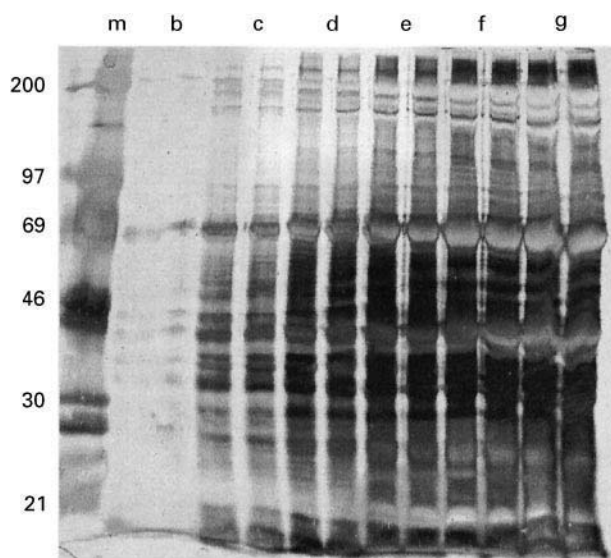


Figure 2 SDS-PAGE separation of human heart proteins (lanes b–g). Lane (a) contains the molecular weight marker proteins and the scale at the left indicates protein size in kDa. The gel has been silver stained. The sample protein loadings were (b) 1 µg, (c) 5 µg, (d) 10 µg, (e) 25 µg, (f) 50 µg, (g) 100 µg.

o-phthaldialdehyde (OPA) + a thiol; and MDPF (2-methoxy-2,4-diphenyl-3(2H)-furanone). The last reagent has a reported sensitivity of 1 ng protein per band and is linear over the range 1–500 ng protein per band.

The main disadvantage of pre-electrophoretic staining procedures is that they can cause protein-charge modifications, for example fluorescamine converts an amino group to a carboxyl group when it reacts with proteins. Such modifications usually do not compromise SDS-PAGE unless a large number of additional charged groups are introduced into the protein. However, they result in altered mobility during other forms of electrophoresis, giving rise to altered separations by native PAGE, IEF and two-dimensional electrophoresis. Recently, compounds that react with cysteine or lysine residues have been described and used successfully for two-dimensional electrophoresis separations. The cysteine-reactive reagent monobromobimane has been used to label proteins prior to analysis by two-dimensional electrophoresis. Using a cooled CCD camera to measure fluorescence, the limit of detection was found to be 1 pg protein per spot.

In an alternative approach, two amine-reactive dyes (propyl Cy3 and methyl Cy5) have been synthesized and used to label *Escherichia coli* proteins prior to electrophoresis. These cyanine dyes have an inherent positive charge, which preserves the overall charge of the proteins after dye coupling. The two dyes have sufficiently different fluorescence spectra that they can be distinguished when they are present together. This allowed two different protein samples, each labelled with one of the dyes, to be mixed together and subjected to two-dimensional electrophoresis on the same gel. This method, which has been termed 'difference gel electrophoresis (DIGE)', has great potential for improving the efficiency of detection of differences in two-dimensional electrophoresis protein profiles between different samples.

For two-dimensional electrophoresis, one approach to overcoming the problems associated with charge modification during the IEF dimension is to label the proteins while present in the first dimension gel after IEF, prior to the second dimension separation by SDS-PAGE. Two fluorescent labels that have been used in this way are MDPF and a fluorescent maleimide derivative.

The alternative approach, which also overcomes the problem of protein-charge modifications, is to label the proteins with fluorescent molecules such as 1-aniline-8-naphthalenesulfonate (ANS) and OPA after the electrophoretic separation has been completed. However, these two methods suffer the disadvantage of relative insensitivity. Recently, two post-

electrophoretic fluorescence staining reagents, SYPRO orange and red (Molecular Probes, Eugene, Oregon, USA), have been described. These stains have a very high sensitivity (1–2 ng protein per band) and excellent linearity with a high dynamic range. Using a fluorescence imaging device, the SYPRO dyes have been shown to be linear over three orders of magnitude in protein quantity. The other advantage of this method is that staining can be achieved in only 30 min, compared with staining with silver and CBB R-250 which can take from 2 h to overnight. Gels can be stained without fixation so that they can be subjected to subsequent Western blotting procedures. However, staining with these reagents requires that the proteins are complexed with SDS, so that if the gels are fixed prior to staining or electrophoresis is carried out in the absence of this detergent, then the gels must be incubated in a solution of SDS prior to staining. An SDS-PAGE gel separation visualized using SYPRO red is shown in Figure 3.

Metal Chelate Stains

This recently developed group of stains have been developed specifically for compatibility with characterization methods such as mass spectrometry as they do not use reagents such as glutaraldehyde or formaldehyde which reduce their efficacy. Although a stain of this type, using the pink bathophenanthroline disulfonate/ferrous complex, was described over twenty

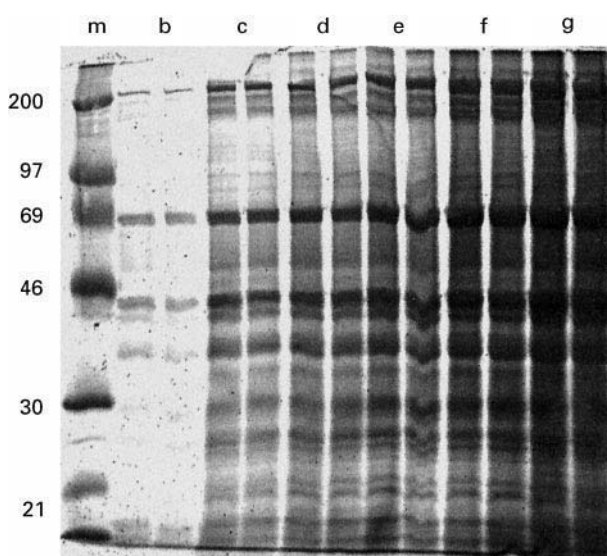


Figure 3 SDS-PAGE separation of human heart proteins (lanes b–g). Lane (a) contains the molecular weight marker proteins and the scale at the left indicates protein size in kDa. The gel has been stained with SYPRO red. The sample protein loadings were (b) 1 µg, (c) 5 µg, (d) 10 µg, (e) 25 µg, (f) 50 µg, (g) 100 µg.

years ago, its insensitivity (600 ng protein) ensured its lack of acceptance. Sensitivity can be increased by introducing ^{59}Fe into the complex, but only to a level equivalent of colloidal Coomassie Blue staining.

The poor performance of these dyes resulted in a recent investigation of luminescent metal chelate stains. Such stains utilizing metal chelates complexed to certain transition metal ions (e.g. europium, terbium, and ruthenium) offer much greater sensitivity compared to the previous colorimetric methods. Of particular interest is SYPRO Ruby, a proprietary ruthenium-based metal chelate stain (Molecular Probes, Eugene, Oregon, USA). This allows one-step, low background staining of proteins in polyacrylamide gels without resorting to lengthy destaining procedures. The linear dynamic range of this dye extends over three orders of magnitude, thus surpassing silver and Coomassie stains in performance. Its sensitivity is claimed to be up to thirty times more sensitive than silver staining. Moreover, staining times (unlike silver protocols) are not critical and staining can be carried out overnight without overdevelopment.

Radioactive Detection Methods

Metabolic labelling of proteins with a radiolabelled amino acid prior to their separation by gel electrophoresis represents a very sensitive method for the detection of proteins and is ideal for the analysis of protein synthetic events occurring in response to an experimental intervention. This approach is most commonly used in combination with *in vitro* cell culture systems, but it is also possible to radiolabel synthetically the proteins of small pieces of fresh tissue in this way. In this method, the cells or tissue are incubated in the presence of the radiolabelled amino acid for a period of time, normally between 3 and 24 h. It is important to use a tissue culture medium that has been depleted of the amino acid used for radiolabelling. The most commonly used amino acids for radiolabelling are [^{35}S]-methionine and [^{14}C]-leucine. [^3H]-amino acids can be used, but these are more difficult to detect due to the weak energy of their beta emissions. Methods are also available for synthetic radiolabelling to detect specific post-translational modifications of proteins.

Proteins can also be radiolabelled post-synthetically, prior to their separation by gel electrophoresis, using a variety of methods such as radioiodination with ^{125}I or reductive methylation with [^3H]-sodium borohydride. However, most of these methods result in significant charge modification of the target proteins, generally precluding their use for electrophoretic techniques other than SDS-PAGE.

Following electrophoresis of radiolabelled proteins, the gel must normally be dried prior to detection of the radioactive zones. Thin gels cast on plastic supports can be dried, after equilibration in 3% w/v glycerol, in air or in an oven at 40–50°C. It is also possible to air-dry gels which have not been cast on supports. These should be equilibrated in 3% w/v glycerol and placed between two cellophane sheets supported in a plastic frame. The gels are then dried in hot air at 40–50°C; the process usually taking 2 or 3 h. The best method for drying gels which are not on supports is by heating them under vacuum. Gels should be soaked in 3% w/v glycerol prior to drying. Gradient polyacrylamide gels are particularly prone to cracking and these can be protected by soaking in a solution containing 1% w/v glycerol and 2% v/v dimethyl sulfoxide (DMSO). Gels can be dried down onto filter paper or onto cellophane. A temperature of 80°C is normally used, but it is better to use a lower temperature (40–60°C) for gels at risk of cracking (i.e. thick, high percentage or gradient gels).

Radiolabelled proteins are most easily detected by direct autoradiography, in which the dried gel is placed in contact with X-ray film and exposed for the appropriate time. This method works satisfactorily for isotopes such as ^{14}C , ^{35}S , ^{32}P and ^{125}I , but is not suitable for ^3H owing to its low-energy beta-emissions which are not able to penetrate the gel matrix. Much sensitive detection can be achieved using fluorography in which the gel is impregnated with a scintillant, such that low-energy beta particles excite the fluor molecules to emit photons which can be detected on a suitable (usually blue-sensitive) X-ray film. In the original procedure, 2,5-diphenyloxazole (PPO) which must be dissolved in DMSO, was used. However, fluorography with commercially available enhancers is simpler and less tedious than the original PO-DMSO method, and produces equivalent results. Pre-exposure of the X-ray film to a brief flash of light (approximately 1 ms) increases the sensitivity of fluorography by two- or threefold. The use of an intensifying screen and exposure at low temperature (–70°C) also result in a significant increase in sensitivity.

Techniques of autoradiography and fluorography are simple and require little specialized equipment, apart from the access to darkroom facilities. However, prolonged exposure times are often required to achieve the desired level of sensitivity of protein detection. Moreover, the nonlinear response of X-ray film and its limited dynamic range present severe problems to accurate quantitation. To overcome these problems several devices for detecting radiolabelled proteins directly in gels have been described. The best and most practical of these

approaches are imaging devices based on the use of photostimulable storage phosphor-imaging screens.

Detection of Specific Biological Compounds

Detection of Glycoproteins

Proteins with limited glycosylation can be detected following gel electrophoresis with the general protein stains such as CBB R-250 and silver. However, such staining gives no direct indication that these proteins are glycosylated and the methods are much less sensitive if the proteins are more highly glycosylated. Proteoglycans are usually stained with cationic dyes, such as Alcian Blue or Toluidine Blue, which bind to the negatively charged glycosaminoglycan side chains. Glycoproteins have generally been detected using variations of the Schiff base reaction, involving oxidation with periodic acid followed by staining with Schiff reagent, Alcian Blue or a hydrazine derivative. A twofold increase in sensitivity can be achieved with methods in which Alcian Blue is used as the primary staining agent followed by subsequent enhancement using a neutral silver-staining protocol.

An alternative approach to the analysis of glycosylated proteins is to radiolabel then *in vitro*, followed by gel electrophoretic separation of the radiolabelled proteins and their detection. N-linked sugar labelling can be achieved using [³H]-mannose and terminal O-linked N-acetylglucosamine can be labelled by galactosyltransferase and UDP-[³H]-galactose.

Probably the most versatile reagents for the characterization of glycosylated proteins following their separation by electrophoresis are radiolabelled, fluorescent or enzyme-conjugated lectins. Although it is possible to use these directly in the gel matrix, much better results are achieved using Western blotting techniques.

Detection of Phosphoproteins

The most commonly used approach to the analysis of protein phosphorylation is to radiolabel cells in culture with either [³²P]-orthophosphate or [γ -³²P]-ATP. An alternative approach, which avoids the use of radioactive materials, is to use antibodies which are specific to phosphotyrosine, phosphothreonine and phosphoserine in combination with Western immunoblotting.

Detection of Lipoproteins

Lipoproteins can be stained following electrophoresis with Sudan black B. Prenylated proteins can be

radiolabelled prior to electrophoresis with [³H]-mevalonolactone, while fatty acylated proteins can be radiolabelled with [³H]-palmitic or [³H]-myristic acid.

Detection of Enzymes

It is generally considered that specific enzyme activities can only be visualized following gel electrophoresis if native conditions have been used. However, there are several reports demonstrating that SDS-denatured proteins can also be visualized provided that it is possible to achieve at least partial renaturation of their spatial configuration. Such renaturation is most effective if disulfide bonds are not essential for enzymic activity and if the native protein is not composed of subunits of different molecular weights. Pre-electrophoresis of gels is usually recommended to remove unreacted acrylamide monomers and catalysts.

Enzyme staining can be achieved by incubating the unfixed gel in a solution of the appropriate reagents using either fluorogenic or chromogenic substrates. This method works well if the final reaction product is insoluble. However, a soluble reaction product will rapidly diffuse resulting in loss of resolution. It is generally preferable to use a print or gel overlay technique. In this approach, the substrates and other reagents are either impregnated into a filter or included in a thin layer of agarose or polyacrylamide gel cast on a glass or plastic support. The overlay is then placed in direct contact with the surface of the separation gel and following a suitable period of incubation, the enzymic activity is visualized on the overlay. Methods are available for the visualization of a large number of enzyme activities following gel electrophoresis.

See also: III/Proteins: Capillary Electrophoresis; Electrophoresis. Electrophoresis: Detection Techniques: Staining; Autoradiography and Blotting

Further Reading

- Fernandez-Patron C, Castellanos-Serra L, Hardy E, Guerra M, Estevez E, Mehl E and Frank R (1998) Understanding the mechanism of the zinc-ion stains of biomacromolecules in electrophoresis gels: Generalization of the reverse-staining technique. *Electrophoresis* 19: 2398–2406.
- Laskey RA (1980) The use of intensifying screens or organic scintillators for visualizing radioactive molecules resolved by gel electrophoresis. *Methods in Enzymology* 65: 363–371.
- Merrill CR (1987) Detection of proteins separated by electrophoresis. In: Chrambach A, Dunn MJ and Radola BJ (eds). *Advances in Electrophoresis*, Vol. 1, p 111–139. Weinheim: VCH.

- Neuhoff V, Arold N, Taube D and Ehrhardt W (1988) Improved staining of proteins in polyacrylamide gels including isoelectric focusing gels with clear background at nanogram sensitivity using Coomassie Brilliant Blue G-250 and R-250. *Electrophoresis* 9: 255–262.
- Rabilloud T (1990) Mechanisms of protein silver staining in polyacrylamide gels: a 10-year synthesis. *Electrophoresis* 11: 785–794.
- Rabilloud T (1992) A comparison between low background silver diamine and silver nitrate protein stains. *Electrophoresis* 13: 429–439.
- Rothe GM (1994) *Electrophoresis of Enzymes: Laboratory Methods*. Berlin: Springer.
- Shevchenko A, Wilm M, Worm O and Mann M (1996) Mass spectrometric sequencing of proteins from silver-stained polyacrylamide gels. *Analytical Chemistry* 68: 850–858.
- Steinberg TH, Jones LJ, Haugland RP and Singer VL (1996) SYPRO orange and SYPRO red protein gel stains: One-step fluorescent staining of denaturing gels for detection of nanogram levels of protein. *Analytical Biochemistry* 239: 223–237.
- Sutherland JC (1993) Electronic imaging of electrophoretic gels and blots. In: Chrambach A, Dunn MJ and Radola BJ (eds). *Advances in Electrophoresis*, Vol. 6, pp. 3–42. Weinheim: VCH.
- Unlu M, Morgan ME and Minden JS (1997). Difference gel electrophoresis: A single gel method for detecting changes in protein extracts. *Electrophoresis* 18: 2071–2077.
- Urwin VE and Jackson P (1993) Two-dimensional polyacrylamide gel electrophoresis of proteins labelled with the fluorophore monobromobimane prior to first-dimensional isoelectric focusing: Imaging of the fluorescent protein spot patterns using a charge-coupled device. *Analytical Biochemistry* 209: 57–62.
- Wirth P and Ramano A (1995) Staining methods in gel electrophoresis, including the use of multiple detection methods. *Journal of Chromatography A* 698: 123–143.

Staining

See II/ELECTROPHORESIS/Detection Techniques: Staining, Autoradiography and Blotting

Theory of Electrophoresis

K.S. Pitre, Dr. Harisingh Gour University, Sagar, India

This article is reproduced from *Encyclopedia of Analytical Science*, Copyright © 1995 Academic Press

Principles

Electrophoresis is a very separation technique which involves the separation of charged species (molecules) on the basis of their movement under the influence of an applied electric field. It is widely used by chemists and biochemists in studies related to medical technology, environmental research, food and water analysis, pollution control and forensic investigations. The development and applications of electrophoretic separation methods are an example of the fruitfulness of using physical methods in tackling biological and biochemical problems.

The migration of charged colloidal particles in an electric field was originally given the name cataphoresis or electrophoresis. Because there has been some diversity of opinion about the definition of a colloid, and thus about the distinction between colloidal and molecular systems, there has also been some differ-

ence of opinion as to how widely the term ‘electrophoresis’ should be used. Some authors prefer the term ionophoresis to describe the movement of relatively small molecules or ions under such conditions.

The 1940s and 1950s witnessed very rapid developments in the applications of methods making use of the migration of particles in an electric field. These applications covered the whole range of particle sizes from the largest protein molecules to small molecules like amino acids, sugars (at high pH) and even simple inorganic ions, using the sample types of procedures and apparatus. Although it is not a form of chromatography, the differences in the rates of migration of the charged particles provide a powerful means of separating biocolloids such as proteins, polysaccharides and nucleic acids, as well as for the characterization of their components. For these reasons, and also for historical reasons, it is now general practice to use the term ‘electrophoresis’ to refer to all these procedures. Electrophoresis pertains to the transport of electrically charged particles – ions, colloids, macromolecular ions or particulate matter – in an electric field.

Electrophoresis experiments are usually carried out to obtain information on the electrical double layers surrounding the mobile particles, to analyse a mixture, or to separate it into components. Interpretation of experimental results requires a theory connecting the electrophoretic mobility with the fundamental quantities relating to the electric double layer – the electrical potential, charge and structure.

The electrical double layer is not restricted to the interface between electrically conducting phases. For example, if a glass rod is immersed in an aqueous electrolyte, then it will carry a double layer of ions wholly within the electrolyte phase. This double layer originates from the specific adsorption of a Helmholtz layer of anions or cations from solution onto the glass surface. The resulting excess of charge is neutralized by a diffuse or Gouy layer dispersed further out in the solution. If we consider the case of two insulating phases, namely glass and oil, the double layer at the interface may be considered to arise either from the specific adsorption of ions generated by very weak electrolytes or from the orientation of dipolar molecules. The behaviour of the diffuse or mobile component of the double layer may be correlated with a class of phenomena which includes electrokinetic effects.

Electrokinetic effects are associated with the relationship between the relative motion of two phases (generally a liquid and a solid) and the electrical properties of the interface between them. Electrokinetic phenomena arise in microheterogeneous systems, i.e. in cases when one phase is dispersed in another. Electrokinetic effects may be classified into four groups: (1) electroosmosis, (2) electrophoresis, (3) streaming potential and (4) sedimentation potential.

1. *Electroosmosis* is the movement of a liquid along a capillary, a system of capillaries or a porous plug under the influence of an externally applied electric field.
2. *Electrophoresis* is the movement of solid particles under the influence of an electric field applied to the medium in which the particles are suspended. In this case the disturbance of the double layers attached to the solid moving particles produces the effect. It may be regarded as the reverse of electroosmosis, in which the solid phase is fixed and it is the movement of the liquid phase that is induced by the applied electric field. In both electrophoresis and electroosmosis the applied potential difference sets up a mechanical force which results in the movement of one phase.
3. *Streaming potential* is the building up of potential difference between the upstream and downstream

ends of liquid flow. This is caused by friction between the moving liquid layer and the wall of the capillary, the system of capillaries or the porous plug.

4. *Sedimentation potential* (Dorn effect) is the converse of electrophoresis and results in the building up of potential difference between the top and the bottom of a vessel in which dispersed solid particles are suspended in a liquid.

The theoretical treatment of the electrical double layer depends on its geometry. The double layer at a flat interface constitutes the most simple case, which we can analyse to explain many of the facts connected with double layers. The boundary between two phases is a layer of finite dimensions. The properties of the two adjacent phases change gradually over a certain distance. These changes depend both on geometrical factors and on the forces between the molecules. The density and orientation of the molecules, even in a one-component system, undergo a gradual change when going from one phase to another, e.g. from the liquid to the gas phase. In multicomponent systems the boundary layer concentrations are different from those in the bulk, leading to what is called adsorption. Though these changes near phase boundaries are limited to only a very few layers of molecules, all the properties of the phases are changed in this transition layer.

When one or both phases contain ions, the transition layer may be much more extended. In such a case, one type of ion is strongly concentrated at the phase boundary by short-range forces. When ions of one sign are adsorbed at the phase boundary, ions of the opposite sign will be attracted by the resulting electric field and will accumulate near the phase boundary. This accumulation is opposed by their Brownian movement. As a result an electrically neutral double layer is formed which may extend to a considerable thickness (a few tens of nanometres).

In order to apply simple mathematical treatment to electrokinetic phenomena it is assumed that the diffused double layer acts as a parallel plate electric capacitor whose plates are d cm apart, each carrying a charge e per cm^2 . The zeta potential, i.e. ζ , the potential difference between the plates, is given by eqn [1]:

$$\zeta = 4\pi ed/D \quad [1]$$

where D is the dielectric constant of the medium between the hypothetical plates. This is the fundamental equation for the quantitative treatment of all types of electrokinetic phenomena.

When a liquid is forced by electroosmosis through the fine capillaries of a porous diaphragm, two opposing factors will determine the flow, namely the force of electroosmosis and the frictional force between the moving liquid layers and the capillary wall. When the two forces become equal, the flow attains a uniform rate. If u is the uniform velocity so obtained and d is the effective thickness of the double layer across which the flow takes place, then the velocity gradient in the double layer may be taken as equal to u/d . Since the velocity at one side, i.e. the wall, is zero, and the average value on the other side, i.e. in the moving liquid, is u , the force due to frictional effects is equal to $\eta u/d$, where η is the coefficient of viscosity of the liquid. If E is the potential gradient across the membrane and e is the charge per cm^2 at the boundary of movement, then the electrical force causing electroosmosis is equal to Ee . Hence at the steady state eqn [2] applies:

$$Ee = \eta u/d \quad [2]$$

Substituting the value for d from eqn [2] in eqn [1] we obtain eqn [3]:

$$\zeta = 4\pi\eta u/DE \quad [3]$$

Following on from this discussion of electrokinetic phenomena, electrophoresis takes place due to the presence of an electrical double layer at the interface between the dispersed phase and the dispersion medium, and the consequent presence of a zeta potential. On applying an external electromotive force, positive and negative portions of the double layer are displaced relative to each other. Since the particles in a solution are free to move, they will migrate under the influence of the applied electric field. As has been noted previously, the double layer surrounding a particle may be treated as a capacitor. We can therefore derive a relationship for the observed velocity u' of the particle from eqn [3], namely eqn [4]:

$$u' = \zeta DE/4\pi\eta \quad [4]$$

Here the quantity $u'/E = U$ represents the particle's mobility, i.e. the velocity for a potential gradient of 1 V cm^{-1} .

Consider the case of a comparatively large spherical particle of radius R carrying a charge q in a medium of dielectric constant D . According to electrokinetic theory the potential of the particle may be given by q/DR . If the charge is identified with that present in the diffused double layer only, then the potential is ζ and since the thickness of the Helm-

holtz double layer is negligible compared with the radius of large particles, R may be taken as equal to the radius of particle plus its Helmholtz layer. This can be written as shown in eqn [5]:

$$\zeta = q/DR \quad [5]$$

From eqns [4] and [5] we get eqns [6] and [7]:

$$u' = qE/4\pi\eta R \quad [6]$$

$$U = q/4\pi\eta R \quad [7]$$

where U is the electrophoretic mobility. If the surrounding medium is an electrolyte, the interaction between the charged and migrating particles will reduce the zeta potential, ζ , of the particle. The magnitude of this effect has been evaluated by Debye and Hückel, who observed that ζ is reduced by a factor of $1/(1 + KR)$, where $1/K$ is ionic length. K is of the order of 10^{-7} – 10^{-8} cm and can be calculated in terms of ionic charges in the electrolyte, the concentration and dielectric constant of the electrolyte and the radius at which the ionic atmosphere would need to be concentrated to obtain the potential of the ion. The electrophoretic mobility for a comparatively large spherical particle in an electrolyte may be given by eqn [8]:

$$U = \left(\frac{q}{4\pi\eta R} \right) \left(\frac{1}{1 + KR} \right) \quad [8]$$

Eqn [8] is not applicable to small spherical particles where the curvature of the double layer is too large for streaming to take place entirely in the direction of the applied field. In such a case the electrical force on the particle is equal to the viscous drag as given by Stokes' law. Considering the effect of the electrolyte on the zeta potential (as in eqn [8]) the result for a small spherical particle is given by eqn [9]:

$$U = \left(\frac{q}{6\pi\eta R} \right) \left(\frac{1}{1 + KR} \right) \quad [9]$$

Debye and Hückel made an exact treatment and found that the factor 4 in eqn [8] is strictly only applicable for cylindrical particles, and it should be replaced by the factor 6 (as in eqn [9]) for spherical particles. Eqns [8] and [9] are thus the special cases of a general expression covering all sizes of particle. A slight modification can be made to eqn [9] to give the electrophoretic mobility according to:

$$U = \left(\frac{q}{4\pi\eta R} \right) \left(\frac{1}{1 + KR} \right) f(KR) \quad [10]$$

where $f(KR)$ is a complicated function of K and R . More elaborate equations for electrophoretic mobility have been derived by taking into account the finite sizes of ions in the double layer attached to the particle. Gorin has also given a treatment for cylindrical particles.

Looking at the consequences of the complications associated with the theoretical deviation of the relationship between the electrophoretic mobility and the shape of the particle, attempts have been made to solve the problem experimentally. However, the experimental results are equally inconclusive. Abramson established that the electrophoretic mobility is independent of the shape of the moving particles by performing experiments on the movement of spherical particles of some oils and of needles of asbestos and *m*-aminobenzoic acid coated with the same protein.

The applicability of eqns [8] and [9] (for spherical particles) can also be tested by the comparison of electroosmotic and electrophoretic mobilities using a microelectrophoresis cell made of the same material as the suspended particle, e.g. glass or quartz. If eqn [8] is correct, then the ratio of the two mobilities should be unity; on the other hand if eqn [9] is correct, the ratio should be 1.5. Experiments with spherical particles and surfaces, all coated with adsorbed protein to ensure that the surfaces were the same, indicated that the mobility ratio was approximately unity, as required by eqn [8]. Objections have been raised to this conclusion on the grounds that the independence of electrophoretic mobility with respect to the shape of particles and the value of unity for the mobility ratio were due to the use of a liquid medium containing a relatively high concentration of the electrolyte. The objectors stated that if the electrolyte concentration is less than 1 mmol L^{-1} then the ratio of electrophoretic to electroosmotic mobility is unity. Other workers also questioned the conclusion, and as such the situation is somewhat uncertain. However, eqn [8] may be regarded as reasonably adequate for particles of any shape.

Factors Affecting Electrophoretic Mobilities

Several factors have a definite influence on the electrophoretic mobilities of charged molecules or ions.

Nature of the Charged Molecule

The nett charge, size, shape and relative mass of particles has a great influence on their electrophoretic mobilities. The charge-to-size ratio of molecules is an important parameter. The higher its charge-to-size

ratio (e/r), the faster a molecule will migrate under given conditions.

Nature of the Electrophoretic System

As well as the characteristics of the substances to be separated, there are several parameters relating to the electrophoretic system itself that have a pronounced effect on the electrophoretic mobilities of the molecules or ions. These parameters are as follows.

1. The ionic composition of the electrophoresis buffer.
2. The temperature.
3. The pH of the electrophoresis buffer.
4. The applied voltage.
5. In the case of zone electrophoresis, the type of support medium chosen, and if the support medium is gel, its pore size.

Ionic composition of the electrophoresis buffer

A charged macromolecule becomes surrounded by an ionic atmosphere of opposite charges because of interactions between ionizable groups on the surface of the charged molecule and ions in the electrophoresis buffer. As a result, both its net charge and its electrophoretic mobility are decreased. This effect is quite pronounced in the electrophoretic separation of proteins, since different proteins have different amino acid side chains which interact to varying degrees with the ions in the solutions used.

In order to minimize these 'counterion' effects it is advisable to use an electrophoresis buffer with as low an ionic strength as possible. However in some cases, such as with polypeptides and polynucleotides, electrophoresis has to be carried out in solutions of high ionic strength, otherwise these macromolecules will not be soluble. It therefore becomes necessary to choose a suitable salt concentration.

Temperature Temperature plays a pronounced effect on electrophoresis. In an electrophoretic run, heat (Joule's heat) is generated and may affect the electrophoresis in a number of ways.

1. *Diffusion*. An increase in temperature causes an increase in the diffusion of migration zones of charged molecules. If the electrophoresis takes a long time (several hours) diffusion effects become more significant.
2. *Evaporation*. It is customary to perform electrophoresis in a closed system to avoid loss of water by evaporation, which increases with temperature. This evaporation results in the drying out of the supporting medium and also leads to an

increase in the ionic strength of the buffer during the analysis.

3. *Viscosity.* In gel electrophoresis an increase in temperature can change the viscosity of the medium. Since this takes place during the electrophoretic run, the interpretation of the results may become complex.
4. *Distortion of zones.* During an electrophoretic run, particularly in column gels if cooling is inadequate, the portions of the migration zones in the warmer parts of the gel move faster than those in the cooler parts. This difference in migration speeds produces curved bands. This may result in the overlap of neighbouring zones and consequently in poor resolution.
5. *Convection currents.* During an electrophoretic run the warmer solution in the centre of the apparatus has a lower density than the cooler solution close to the walls. This density gradient induces convection currents in the solution. Since water has its maximum density at 4°C, and the smallest variations in density of aqueous solutions are observed around this temperature, it is advisable to perform electrophoresis at a temperature as close as possible to 4°C. However, the viscosity of an aqueous solution increases as the temperature is lowered, which may result in an increase in the frictional resistance to the migration of the charged molecules. If the temperature is maintained at 4°C the electrophoretic mobilities of the charged molecules will be relatively low. It is therefore necessary to choose an optimal temperature for a particular electrophoretic run and maintain it throughout the course of analysis.

pH of the electrophoresis buffer pH has a marked effect on the nett charge on a protein molecule. At a definite pH value, i.e. at the isoelectric point, the nett charge on the molecular is zero. Molecules acquire a nett positive charge at pH values below their isoelectric points. At pH values above their isoelectric points, they acquire a nett negative charge. Thus different molecules (e.g. proteins) at any particular pH value will have different nett charges. To optimize the separation of a mixture of (protein) molecules the buffer pH must be chosen on the basis of the nett molecular charges. For example in an electrophoretic run two or more proteins may migrate together to give only one band. If the analysis is done at a different buffer pH value it may result in the appearance of extra protein bands, indicating the presence of other proteins in the sample.

Applied voltage In electrophoresis the applied voltage plays an important role. The migration velocity of

a molecule is proportional to the field strength across the medium. The higher the applied voltage, the larger the field strength across the medium, and the faster a molecule will migrate. Thus, the charged molecules will migrate more quickly with increasing voltage. This saves time and reduces the diffusion of migrating molecules. However, with increasing voltage the current also increases, resulting in greater power generation (the power increases as the square of the current).

Some of this power is dissipated as heat (Joule's heat). The heat generated can have serious effects on an electrophoretic analysis, as discussed previously. It is therefore necessary to select a definite value of applied voltage. The voltage (or current) should be large enough to allow rapid migration of charged molecules, but not so large as to generate excessive heat.

Support medium In zone electrophoresis different types of support media are used. The selection of the most suitable support medium for a particular zone electrophoretic analysis is based on the following considerations.

1. Sample quality.
2. Size of the molecules – whether they are small or large. If a sieving gel has to be used its pore size (concentration) is chosen so as to suit the molecular size under study.
3. The time required for analysis.

Types of Electrophoresis

Electrophoresis analysis can be divided into three main types, as listed here.

1. moving-boundary electrophoresis
2. zone electrophoresis
3. steady-state electrophoresis.

Moving-Boundary Electrophoresis

Moving-boundary or free solution electrophoresis was first proposed by Picton and Linde in 1892 and was fully developed by Tiselius in 1930, finding wide application between 1935 and the 1950s. Its principle use was in protein research, where it provided invaluable results.

The apparatus for moving-boundary electrophoresis, in its simplest form, consists of a U-tube with a rectangular cross-section (**Figure 1**). It is partially filled with the solution to be analysed (protein solution) and a buffer solution is layered over it. Electrodes are immersed in the buffer solution.

When an electromotive force is applied across these electrodes the charged molecules move towards the appropriate electrode. If the solution under study is

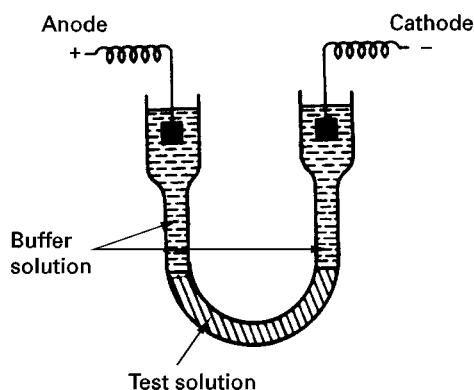


Figure 1 Apparatus for moving-boundary electrophoresis.

coloured and contains several components with different electrophoretic mobilities, then their migration can be observed as multiple moving boundaries in the system. Where the migration boundary is not visible to the naked eye it may be made visible by causing it to fluoresce as a result of exposure to ultraviolet (UV) light. In such a case the apparatus should be made of quartz. In the case of protein solutions which have a refractive index slightly greater than that of the buffer, there will be a change in refractive index at the protein boundary in the apparatus, which can be detected by optical methods.

After completion of the electrophoretic analysis the different fractions containing the components separated from the original sample can be analysed using appropriate methods.

Moving-boundary electrophoresis has proved to be useful in the determination of complex heterogeneous samples. However, it has a drawback in that only the slowest and fastest moving components of a sample can be obtained in pure form.

Zone Electrophoresis

Zone electrophoresis results in the complete separation of the components of a mixture in the form of discrete zones. The separated zones may be stabilized

in a number of ways which include the use of support media, density gradients and free zone techniques.

Use of support media An important development in electrophoresis was the use of support media for stabilizing zones of electrophoretically separated mixtures. A porous medium such as filter paper, cellulose acetate film, a gel, glass beads, granular starch or polyvinyl particles, etc., is used as the support medium. The separatory power of some of the gels exceeds that of other media or free solution.

The most common apparatus for zone electrophoresis using support media is depicted in **Figure 2**.

The sample is placed on the support medium in the form of a spot or narrow band at the sample origin. On subjecting it to electrophoresis the components of the sample separate into bands which are kept distinct by the presence of the support medium.

Zone electrophoresis in density gradients An important method that allows complete separation of complex mixtures involves carrying out electrophoresis in a density gradient column. The density gradients are usually solutions of substances such as ethylene glycol, glycerol, sucrose, etc., which do not ionize or interact with the materials under examination.

Free zone electrophoresis Although it is a complex technique, by using this method it is reasonably simple to recover the separated components at the end of analysis. The electrophoretic analysis may be performed in two ways, by rotation of the electrophoresis vessel during the run or by streaming a continuous film of buffer across the electrophoretic system, in a direction perpendicular to the applied electric field. These techniques are not in common use because they require elaborate equipment and are expensive.

Steady-State Electrophoresis

The fundamental basis of this method is that, after electrophoresis has proceeded for a certain length of

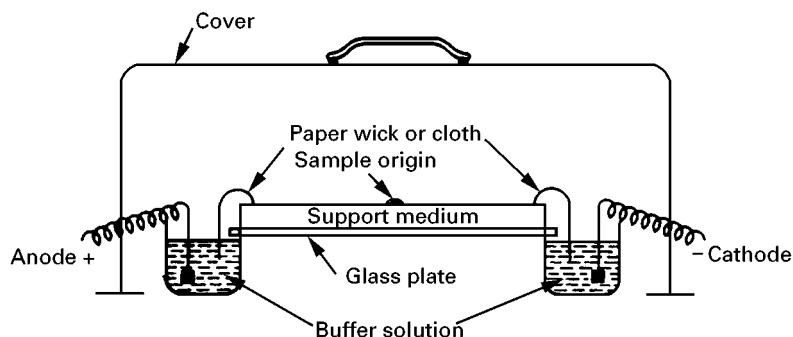


Figure 2 Apparatus for zone electrophoresis.

time, a state known as the steady-state is reached in which no further changes to either the position or the width of the zone of the separated components occur with time. Steady-state electrophoresis involves two types of techniques, isoelectric focusing and isotachophoresis.

Isoelectric focusing In this technique the charged components of the sample move through the medium under the influence of an applied electric field until they ultimately reach a position in the pH gradient where their net charge is zero and hence they do not migrate any more. This pH is their isoelectric point. The individual bands may be collected from the apparatus, and examined chemically or biologically.

This technique has very high resolving power, and may be used preparatively. It is not applicable to some compounds (proteins) that precipitate at their isoelectric point, which makes their recovery difficult.

Isotachophoresis This technique is particularly applicable to the separation of charged components with small relative molecular masses, such as some drugs and polypeptides of medical interest. In this technique all the charged components become stacked one behind the other, depending upon their electrophoretic mobilities.

To achieve a good separation of two charged components from one another by isotachophoresis, their electrophoretic mobilities must differ at least by 10%.

Comparison of Moving-Boundary and Zone Electrophoresis

In moving-boundary electrophoresis a differential movement of the charged particles towards one or the other of the electrodes is observed. Separation takes place as a result of differences in mobilities. The mobility of a particle is approximately proportional to its charge-to-mass ratio. However, this technique suffers from several disadvantages, one of the most serious being the tendency of the separated components to mix by convection as a consequence of thermal and density gradients and mechanical vibrations. Thus, careful thermal regulation and isolation from mechanical vibrations is essential. Also, elaborate optical systems are often required for locating and measuring the fraction, making this method quite expensive.

Many of these experimental difficulties associated with moving-boundary or free solution electrophoresis may be avoided if separations are carried out in a supporting medium (zone electrophoresis), such as

on paper. This prevents convection currents from distorting the electrophoretic pattern. This technique closely resembles the various chromatographic methods, with the additional parameter of a superimposed electric field. The separations mainly depend upon the properties of the medium and may result primarily from the electrophoretic effect or from a combination of electrophoresis and adsorption, ion exchange, or other distribution equilibria.

Practical Problems

The Joule's heat generated in an electrophoretic run causes various problems, including changes in the pH of the buffer medium, diffusion and distortion of the zones, and evaporation and convection currents. It should be remembered that these effects may occur simultaneously, which may complicate the results. It is therefore necessary to optimize the temperature for a particular analysis and keep it constant.

In paper electrophoresis there is liable to be variability in the quality of paper from batch to batch, and also perhaps within one sheet. Some papers have adsorptive properties that may affect the electrophoretic mobility of the molecules under study. Ionizable groups may produce an electroosmotic effect on the paper, which in turn may distort the migration characteristics of the separating components. The physical and chemical inhomogeneity of the support medium also has a pronounced effect on the migration of substances which in turn affects the results.

The method used for the detection of sample components separated by electrophoresis depends on the type of electrophoresis, the nature of the molecules to be detected, and the purpose of analysis. Some detection methods are listed in **Table 1**.

Separations using electrophoretic methods may not be adequate for very complex mixtures. Resolutions may be improved substantially by combining electrophoresis with some other separation technique. The sample subjected to electrophoresis in one direction while the other separation analysis is carried out in a perpendicular direction (so-called two-dimensional techniques).

Applications

Electrophoresis involves the separation of charged species on the basis of their movement under the influence of an applied electric field. It has found wide applications in the characterization of biological molecules (proteins and nucleic acids). The main applications of electrophoresis have been in the separation of biological molecules, which includes molecules with

Table 1 Methods of detection for quantitative analysis of sample components separated by electrophoresis

Optical methods	UV absorption
	Staining
	Fluorescence
Raidiochemical methods	Liquid scintillation counting Autoradiography
Biological assay and immuno-methods	Immunoelectrophoresis Rocket electrophoresis

relatively lower relative molecular masses such as amino acids, and also molecules of higher relative molecular masses such as proteins and polynucleotides (including RNA and DNA molecules). An example of the use of paper electrophoresis follows.

Paper electrophoresis has been extensively used in almost all laboratories where proteins and other similar macromolecular electrolytes are investigated. The apparatus (Figure 2) consists of two electrode chambers placed 15 cm apart. There is also a device which can support up to six (30 cm) filter paper strips between the electrodes. A d.c. supply source (0–250 V) is used to apply the desired voltage across the electrodes. The two electrode chambers are filled to equal heights with the buffer solution. The buffers commonly used for this purpose are (1) Aronsson and Gronwall buffer, i.e. dimethyl barbiturate buffer, which is a mixture of 20.60 g sodium dimethyl barbiturate and 2.80 g barbituric acid with a pH of 8.6, and (2) Consden and Powell buffer, i.e. borate buffer, which is a mixture of 1.77 g sodium hydroxide and 9.60 g orthoboric acid with a pH of 8.6.

Whatman paper (M540) strips (about 30 cm long) are cut and dipped in a container of buffer until they are thoroughly wet. The excess buffer is then removed by laying them out on a large sheet of filter paper. The strips are then immersed into the electrode chambers so that the ends of the strips dip in the buffer solutions. The sample is applied at the centre of the paper. The paper strips are allowed to stand for about 1 h, to equilibrate the bed with the liquid evenly throughout the paper. The power supply is then switched on and the voltage adjusted to about 75 V. Excellent sharply defined separations of serum proteins into five fractions within a span of 2 cm can be obtained within 1 h. If the run is extended to 16 h, a pattern approximately 12 cm long with five fractions may be obtained. On completing the run the fractions are measured by staining. The dye most commonly employed for this purpose is amido black 10B. The paper strip is dried and developed in a dye bath containing a saturated solution of the dye in a mixture of methanol and glacial acetic acid (9 : 1

v/v). Staining is allowed for 10 min with constant shaking.

After the electrophoretogram has been stained, the excess of dye is removed (destaining) by dipping the stained paper in baths of methanol–glacial acetic acid (9 : 1 v/v) several times. This destaining procedure is a slow process and can be made more efficient and faster by opting for electrophoretic destaining. After destaining, the paper strip is dried and scanned in a densitometer, i.e. the strip is illuminated and moved along the light source, the transmittance showing the distribution of the separated compounds. On plotting the reciprocal of transmittance against the wavelength one or more maxima are observed, depending upon the number of components. The amount of each component can be estimated by measuring the area under each peak. The estimation of serum proteins can also be done by an elution method. The destained paper strip is cut transversely into small pieces 5 mm wide, one unstained small strip at the end of the paper providing the blank value. The elution is done in 1.0 mol L⁻¹ NaOH in 50% ethanol + 0.25% (0.25 g per 100 mL) ethylenediaminetetraacetic acid (EDTA). After elution is over, the optical density is measured using a colorimeter.

A more rapid separation of serum proteins can be achieved using polyacrylamide gel electrophoresis. However, paper electrophoresis is still of particular interest where small amounts of protein need to be isolated for further analysis or testing.

Further Reading

- Antropov LI (1975) *Theoretical Electrochemistry*. Moscow: Mir Publishers.
- Bier M, ed. (1956) *Electrophoresis: Theory Methods and Applications*. New York: Academic Press.
- Glasstone S (1956) *An Introduction to Electrochemistry*. New York: D van Nostrand.
- Longworth LG (1943) A differential moving boundary method for transference numbers. *Journal of the American Chemical Society* 65: 1755–1765.
- Longworth LG (1939) A modification of the Schlieren method for use in electrophoretic analysis. *Journal of the American Chemical Society* 61: 529–530.
- Melvin M (1987) Analytical chemistry by open learning. In: Kealey D (ed.) *Electrophoresis*. New York: Wiley.
- Scott ND and Svedberg T (1924) Measurements of the mobility of egg albumin at different acidities. *Journal of the American Chemical Society* 46: 2700–2707.
- Svedberg T and Tiselius A (1926) A new method for the determination of proteins. *Journal of the American Chemical Society* 48: 2272–2278.
- Svedberg T and Jette ER (1923) The cataphoresis of proteins. *Journal of the American Chemical Society* 45: 954–957.

Two-dimensional Electrophoresis

M. Fountoulakis, F. Hoffman-La Roche Ltd.,
Pharmaceutical Research-Gene Technology, Basel,
Switzerland

Copyright © 2000 Academic Press

Introduction

Two-dimensional (2D) polyacrylamide gel electrophoresis is a classical technique for the separation of proteins. It first appeared in the mid-1970s but for a long time it only found limited applications. Recently it has enjoyed an impressive renaissance. The major reasons for this are the introduction of the immobilized pH gradient (IPG) strips and the development of analytical methods capable of identifying proteins present in very low quantities. 2D electrophoresis represents the core methodology of the new, technology-driven science **proteomics**. Proteomics finds a wide application, in both clinical diagnosis and in pharmaceutical research, for the detection of novel drug targets. **Figure 1** demonstrates the application of 2D electrophoresis for the detection of variable protein levels between diseased and healthy brain tissue. In a sample from the parietal lobe of the brain of a patient with Alzheimer's disease, a strong spot representing glial fibrillary acidic protein (GFAP), a marker for neuronal loss, is pres-

ent, whereas in the control sample, the corresponding spot is very weak.

The aim of proteomics is the high throughput analysis of the proteome (protein complement expressed by a genome) of various organisms or tissues. It consists of two steps: (1) the separation of protein mixtures by 2D electrophoresis, and (2) the identification of the separated proteins by analytical techniques, such as mass spectrometry and amino acid composition analysis. The process is facilitated by the use of highly sophisticated software for advanced image analysis and the high reproducibility of images in intra- and inter-laboratory studies. The 2D electrophoresis itself involves: (1) separation of the proteins on the basis of differences in their net charge, called isoelectric focusing (IEF), and (2) separation of the focused proteins on the basis of differences in their molecular masses. **Table 1** gives a summary of the most significant chronological events in the development of 2D electrophoresis. The state-of-the-art technology will be discussed without entering into extensive technical details that can be found in the literature provided.

First-Dimensional Separation (IEF)

Proteins carry positively and negatively charged side groups and are, therefore, amphoteric molecules. The

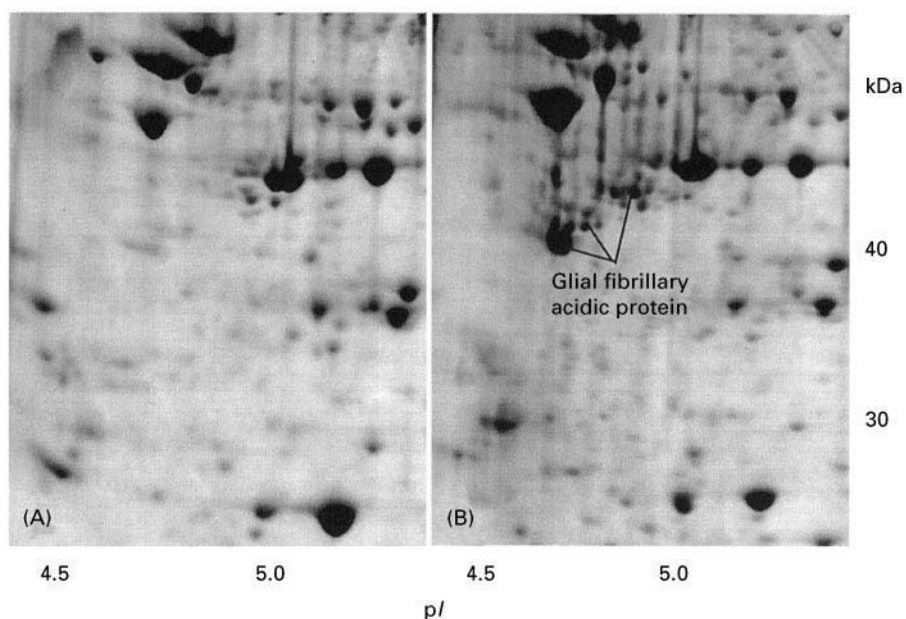


Figure 1 Partial 2D gel images showing human brain proteins from a control (A) and a patient with Alzheimer's disease (B). The proteins were separated on pH 3–10 nonlinear strips, followed by 9–16% SDS gels, stained with colloidal Coomassie blue. The spots representing glial fibrillary acidic protein (GFAP) in (B), a known marker of neuronal loss, are indicated.

Table 1 Important advances in 2D electrophoresis technology

1970	Introduction of sodium dodecyl sulfate in 1D gel electrophoresis to efficiently separate complex protein mixtures (Laemmli UK, <i>Nature</i> 227: 680)
1975	Separation of protein mixtures by 2D gel electrophoresis using tube gels and pH gradients formed with carrier ampholytes (O'Farrell PH, <i>Journal of Biological Chemistry</i> 250: 4007)
1980–1990	Pioneering work to improve pH gradient stability; synthesis of Immobilines and preparation of IPG strips (Bjellqvist B, <i>Journal of Biochemistry Biophysics Methods</i> 6: 317); electrotransfer of proteins from gels to PVDF membranes
1990–today	IPG strips became commercially available; introduction of sigmoidal strips, efficient separation of basic proteins, improvement of gel staining and protein solubilization techniques (Bjellqvist, Dunn, Goerg, Hochstrasser, Rabilloud, Righetti and others); development of high throughput protein analytical techniques (MALDI-MS, amino acid analysis); development of software for protein identification and image comparison; establishment of databases accessible via the WorldWideWeb; sequencing of the complete genome of microorganisms; preparation of 2D protein maps for organs, cell lines, organisms; new terms <i>Proteome</i> , <i>Proteomics</i> were introduced

protein charge depends on the pH value of the solution. IEF is an equilibrium process, during which, under the influence of a high voltage field the proteins move along a pH gradient, according to their net charge, to a position, where they have no net charge and consequently stop moving. This pH value is called the isoelectric point (pI). The resolving power of IEF is defined by the equation of Svensson:

$$\Delta pI = [D[d(pH)/dx] \cdot E - du/d(pH)]^{1/2}$$

where ΔpI = resolution capacity (pI difference required to resolve neighbouring spots), D = diffusion coefficient of the protein, E = field strength ($V\ cm^{-1}$), $d(pH)/dx$ pH gradient, $du/d(pH)$ mobility slope at pI.

According to this equation, the resolution capacity is influenced by the pore size of the gel, which affects the diffusion of the protein, the slope of the pH gradient and the voltage value.

An efficient and reproducible protein separation during IEF requires a stable pH gradient. There are two pH gradient systems in use. In the first one, the pH gradient is created by an excess of carrier ampholytes during the IEF run. Ampholytes are amphoteric compounds of low molecular mass with closely related pI values. Upon application of an electric field, the ampholyte molecules move and align themselves between the electrodes, forming a pH gradient, which increases from anode to cathode. This type of IEF is usually performed in tube acrylamide gels.

In the second pH gradient system, the pH gradient is immobilized and has been formed prior to IEF run. IPGs are formed by acrylamide derivatives, called immobilines, which are weak acids and bases with a buffering capacity. Immobilines are copolymerized in a polyacrylamide gel, such that a pH gradient is formed between basic and acidic molecules. When an electric field is applied, the pH gradient does not move. Only the charged molecules of the protein sample move and are focused according to their pIs into

narrow bands. This type of IEF is usually performed in strips of acrylamide gel fixed on a plastic sheet.

Carrier Ampholytes

The pH gradient formed by the carrier ampholytes during IEF can be affected by the amount of total protein loaded. Proteins when applied in large quantities, having themselves a buffering capacity, can affect the focusing position along the pH gradient and consequently the reproducibility. Therefore, factors such as protein quantity, temperature, voltage and chemicals can strongly affect performance. Only small quantities of protein (of the order of 0.1 mg) should be applied for IEF with the carrier ampholytes approach. The difficulties in controlling the various factors which affect reproducibility together with the difficulties of preparing and transferring the tube gels to the second dimensional separation, contribute to the reasons why carrier ampholyte-based IEF remained a scientific speciality of only a few laboratories. Nevertheless, these laboratories are able to control the conditions affecting reproducibility, so that IEF with carrier ampholytes is still used. This approach allows a very reliable protein quantification of complex mixtures. Because only a small amount of protein can be applied, 2D gels made following the carrier ampholyte approach are more suitable for analytical purposes. IEF based on carrier ampholytes can efficiently separate proteins with pIs within the pH range of 3–8. Proteins with higher pIs separate poorly due to cathodic drift during isofocusing. The cathodic drift is the result of a high electroosmotic flow, caused by the charged groups on the glass walls of the gel tubes.

IPG Strips

The increased application of two-dimensional gel electrophoresis today is to a large extent due to the introduction of IPG strips. The major advantage of using IPG strips is the ability to maintain high

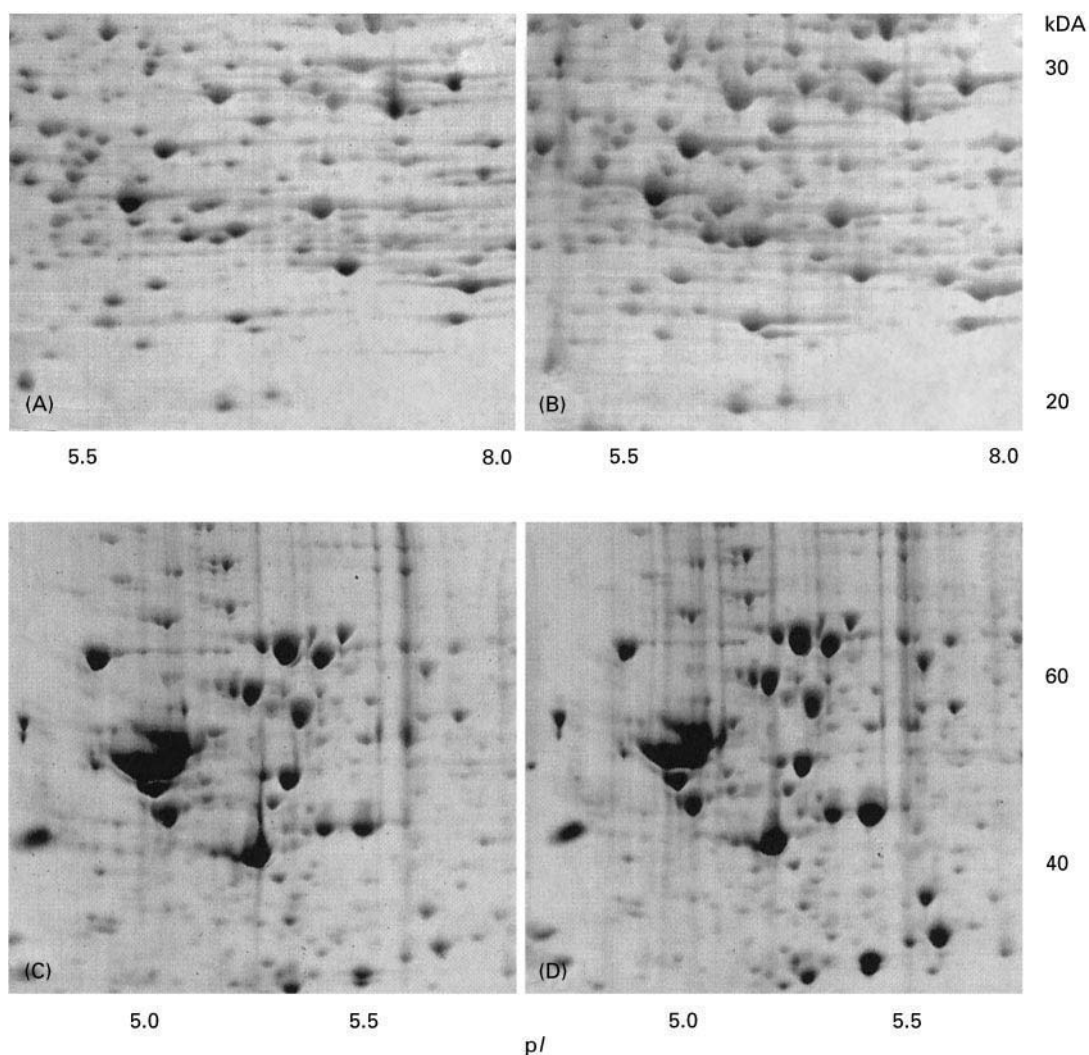


Figure 2 Partial 2D gel images showing the high fidelity in the reproducibility of separation of bacterial (A, B) and mammalian (C, D) proteins. The proteins were separated as stated in the legend to Figure 1. (A, B). Separation of proteins of *Haemophilus influenzae* were 1.5 and 3.0 mg, respectively. (C, D) Separation of rat brain proteins, 1.5 and 2.0 mg, respectively.

reproducibility. The increase in reproducibility has allowed a high throughput analysis of proteomes and the application of larger sample quantities, a requirement for protein spot analysis. **Figure 2** provides examples of the reproducibility of separation of bacterial and mammalian proteins, following IEF on pH 3–10 nonlinear IPG strips. Although minor differences can be detected, the reproducibility concerning both the position and the intensity of the protein spots can be considered as satisfactory.

As mentioned earlier, immobilines are polymerized in a gradient, in a polyacrylamide gel, and the gel is then dried on a plastic sheet. Before the IEF run, the dry strips are rehydrated in a specific rehydration solution, containing a reducing agent, ampholites and high concentrations of urea and a zwitterionic or

nonionic detergent (usually CHAPS). Rehydration can also be performed in a solution containing the protein sample to be analysed (see sample application). Large numbers of strips can be rehydrated at a time and this represents an advantage of the method regarding high throughput analysis and performance. Today, IPG dry strips are commercially available from Amersham Pharmacia Biotechnology in two lengths—11 and 18 cm and in three pH ranges—3–10, 4–7 and 6–11. The pH 3–10 strips are available in a linear and non-linear (sigmoidal) form. The latter allow a more efficient focusing of proteins with pI values between 4.5 and 7. A large percentage of proteins from various organisms have pI values within this range. The dry strips can be kept frozen at -20°C for a long time (the expiration date is indicated on the packaging).

The use of narrow pH range strips (i.e. of 1 pH unit) provides a higher resolution and allows the detection of protein isoforms; this is an additional advantage of IEF using IPG strips. Strips of more narrow pH ranges are not currently commercially available and have to be prepared by the user. IPG strips can be made in any biochemical laboratory using a gradient marker and Immoblines of various pK values which can be purchased. Recipes for the preparation of IPG strips can be found in handbooks, for example in *Electrophoresis in Practice* (see Further Reading). On the narrow pH range the spots appear stretched compared to the wide range strips. **Figure 3** shows an example of a protein which appears as one spot following IEF after focusing on a pH 3–10 strip and as five spots after IEF on a pH 4–7 strip. IEF on strips of an even narrower pH range would result in the detection of additional spots resulting from further isoforms of the protein. Following IEF, the IPG strips can be either immediately used for the second dimensional separation or stored frozen at -20°C for long periods (for example, in petri dishes sealed with parafilm). Strips stored for 4 months have been used at -20°C without any

effect on the spot resolution. Longer storage times of up to 1 year have been reported.

Sample Preparation

Careful sample preparation is a prerequisite of a successful analysis. Most proteins are soluble and are easily recovered in the sample preparation solution, which includes urea, CHAPS, a reductant and, optionally, protease inhibitors. Recovery of the proteins that are insoluble in this solution is often a problem. A centrifugation step is necessary for removal of nondissolved material. The addition of thiourea and of a noncharged reducing agent, such as tributyl phosphine, to the sample buffer increases protein solubility during IEF. It would appear that hydrophobic interactions between proteins and the acrylamide gel of the IPG strips are responsible for protein losses during IEF. Nucleic acids present in the sample can also seriously affect spot resolution. Enzymatic digestion with an endonuclease prior to sample application is usually recommended.

Sample Application

The protein application mode can affect the amount of protein entering the IPG strip during IEF. There are several ways of applying the sample. In the system supplied by Amersham Pharmacia Biotechnology (Multiphor II), the sample is usually loaded into application cups (also supplied by Amersham Pharmacia Biotechnology). Up to 150 μL can be applied in one cup. The cups are fixed in special 'cup accommodating bridges' which are placed near the basic or acidic end of the strip. It seems that sample application at the basic end of the strip is more advantageous compared to the application at the acidic end. We have, however, found that simultaneous sample application at both the basic and the acidic ends of the strip can result in the detection of more and stronger protein spots compared to sample application at only one end. It also allows the simultaneous application of sample volumes larger than 150 μL . From a technical point of view, sample application using the cups is the most difficult operation to perform. The cups should touch the polyacrylamide gel on the strip, otherwise the sample will leak; they should also not damage the gel at the contact point, otherwise the proteins will not enter the strip.

An alternative method of sample application is the rehydration of the strip in a solution containing the protein sample. This approach is convenient to perform and theoretically it should result in the detection of all proteins present in the sample. However, more comparative studies are required to prove that this approach is more efficient than the loading of sample

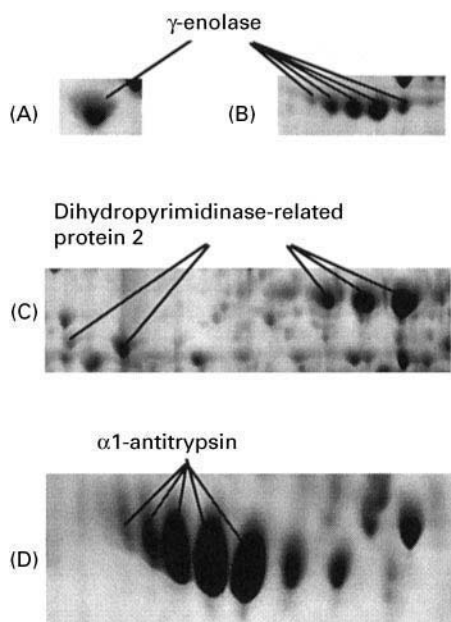


Figure 3 Partial 2D gel images showing examples of proteins represented by multiple spots. (A, B) γ -enolase from human brain. The protein is represented by one spot when IEF was performed on pH 3–10 nonlinear IPG strips (A), and by five spots when IEF was performed on pH 4–7 strips (B). (C) Dihydropyrimidinase-related protein 2 from human brain shows a high heterogeneity, represented by five spots, localized into two regions on the gel. (D) α 1-antitrypsin from human cerebrospinal fluid is represented by many spots, most likely denoting different glycoforms of the protein.

into cups. Amersham Pharmacia Biotechnology has recently introduced a new IEF apparatus (IPGphor) in which sample application and IEF can be performed. The strips are placed in special ceramic strip holders and rehydrated for the desired time in a solution containing the protein sample. Each strip holder holds a single IPG strip throughout rehydration and IEF. IEF starts automatically after rehydration according to the conditions programmed. Whether the performance of IEF will be improved with the use of this instrument is not clear at present.

The quantity of protein to be applied on the strip naturally depends on the goal of the analysis. If the identification of protein spots is intended, the amount loaded should be in the order of 1 mg or higher, depending on the number of proteins in the mixture. A 1D gel analysis of the sample prior to 2D electrophoresis may provide helpful information as to defining the right protein quantity. If large amounts of protein are applied, a percentage of the proteins may not enter the strip. Presently, this constitutes a drawback of the IPG strip approach. Because certain proteins in the sample (mainly major components) only partially enter the strip, this can result in an unreliable quantification of a particular protein in a given mixture. While the application of 15 mg or more of protein sample has been reported, we consider that 2–4 mg is the limit for a productive separation, using the strips that are presently available.

IEF using IPG strips can separate basic proteins efficiently with pIs up to about 12. The introduction of low concentrations of isopropanol in the rehydration buffer improves focusing of basic proteins. Hydrophobic proteins probably precipitate at the point of application and efficient separation has not yet been reported. Hydrophobic proteins can be analysed in a different 2D electrophoresis system, which uses the interaction of the proteins with a cationic detergent in the first dimension rather than pI. The second dimension is, as described below, dependent on the molecular mass. The separated proteins form approximately a diagonal line. Relatively, only a small number of proteins can be successfully separated using this approach.

Second-Dimensional Separation (Sodium Dodecyl Sulfate-Polyacrylamide Gel Electrophoresis, SDS-PAGE)

Following IEF, the proteins are separated according to their molecular masses. During this nonequilibrium

step, the proteins are negatively charged by addition of the anionic detergent SDS. Upon application of an electric field, the charged proteins move along a porous polyacrylamide gel and are separated according to their size. A reducing agent is also included to disrupt disulfide bonds. In comparison with IEF, SDS-PAGE is relatively easy to control. The terms ISO-DALT and IPG-DALT are often used to mean 2D gel electrophoresis employing IEF with carrier ampholytes or IPG strips, respectively.

Horizontal or more usually vertical slab gels, running in a discontinuous buffer system are employed. A high throughput analysis is facilitated by the use of tanks accommodating 6–20 gels running in parallel. An efficient separation of thousands of proteins present in complex mixtures, can only be performed on gels of a large format (18 × 20 or 25 × 25 cm). Either gradient gels or gels of a constant acrylamide concentration can be used. Because of the complexity of the

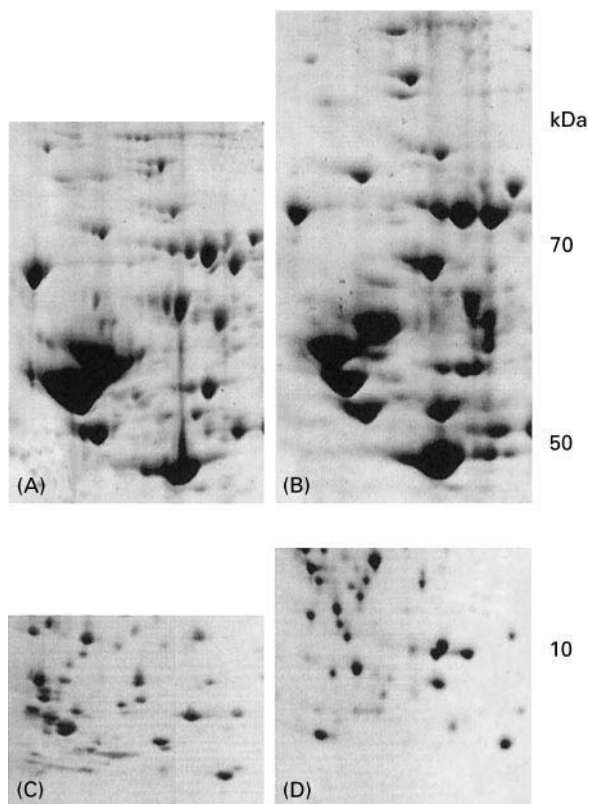


Figure 4 Partial 2D gel images showing an improved spot resolution by using different acrylamide concentrations. Separation of rat brain proteins on a 9–16% SDS gel (A) and on a 7.5–16% SDS gel (B). Separation of low molecular mass soluble proteins from *H. influenzae* on 9–16% SDS gel (C) and on a 10% SDS Tricine gel (D). (B, D) The gel parts comprising the corresponding proteins shown in A and B, respectively, are longer on account of the different acrylamide concentrations.

technology and the large diversity of the samples to be analysed, and in order for the data to be useful to a broad research community, 2D PAGE has been to a large extent standardized. In the second dimension, for example, we usually use 9–16% linear gradient gels. This gel system represents a good compromise, as it separates proteins between 5 and 200 kDa. However, efficient separation is limited to a range of approximately 15–40 kDa. Outside this range, in particular above 50 and below 10 kDa, the separation is often suboptimal. For more efficient separation, gels of a different acrylamide concentration should be tried. **Figure 4** gives examples of the improved separation of high molecular mass brain proteins using gels of lower acrylamide concentration and of low molecular mass proteins from *Haemophilus influenzae*, using gels with Tricine as the trailing ion instead of Tris.

For spot visualization, the gels can be stained with either silver or Coomassie blue (usually colloidal Coomassie blue), depending on the quantity of pro-

tein sample applied and the aim of analysis. Silver stain may be preferentially used for gel comparison studies, whereas staining with Coomassie is preferred when the spots are intended for protein identification. Colloidal Coomassie blue has the advantage that the stain is sensitive enough and the gels can be easily destained with water. The simultaneous staining of many gels in one tank substantially increases the throughput. Apart from silver and Coomassie blue, several other protein detection methods exist, such as staining with various metals, labelling with fluorescent agents or detection of radiolabelled compounds, after gel drying and exposure, for example to a film.

Proteome Analysis

An essential step of proteomics is the identification and mapping of the proteins separated by 2D electrophoresis. From a mammalian organism, comprising approximately 100 000 possible gene products,

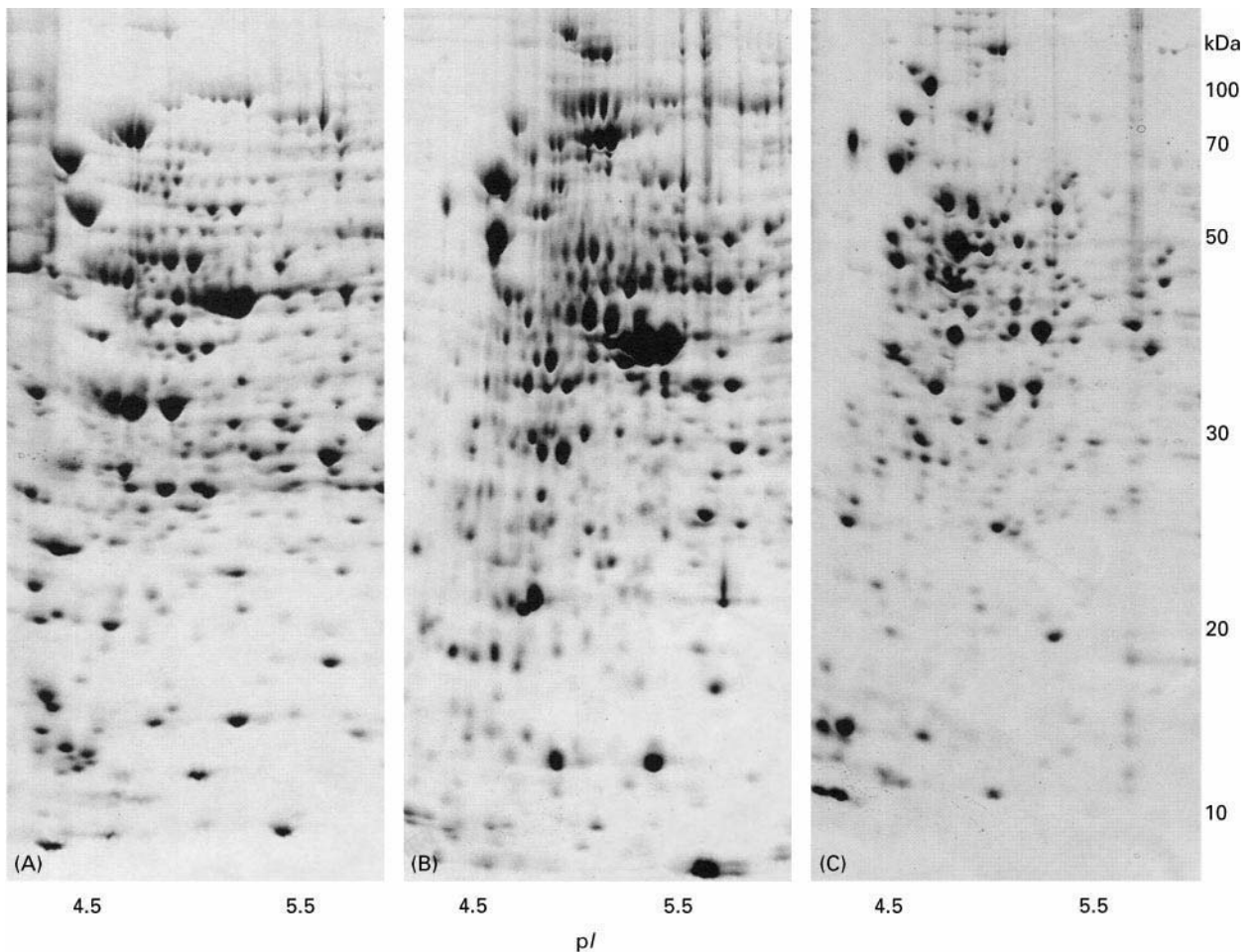


Figure 5 Partial 2D gel images showing soluble proteins of (A) *H. influenzae*, (B) *E. coli* and (C) *B. subtilis*. The proteins were separated as stated in the legend to Figure 1. Note the similarity in the distribution of the major proteins in the three bacterial organisms.

approximately 1000–2000 protein spots can be visualized on one 2D-gel, using Coomassie blue. Higher numbers can be detected, following staining with silver or after radiolabelling. Approximately one-half of the visible spots are available in sufficient quantities to be analysed for identification. **Figure 5** shows the analysis by 2D electrophoresis of the proteomes of three bacteria, *H. influenzae*, *Escherichia coli* and *Bacillus subtilis*. The genomes of the three microorganisms have been completely sequenced, so that theoretically all expressed proteins can be mapped. This has however not yet been accomplished. The largest 2D proteome maps, such as that of *H. influenzae* prepared at F. Hoffmann-La Roche, Basel, include approximately 500 mapped proteins. Many of the unidentified proteins are not expressed in sufficient amounts to be visualized.

For the mapping of proteomes of the various organisms, protein enrichment steps need to be introduced before analysis. We have used several chromatographic steps, such as heparin chromatography, hydrophobic interaction chromatography, chromatofocusing, hydroxyapatite chromatography and several other approaches, to enrich the low-abundance gene products of *H. influenzae* and *E. coli*.

Additional enrichment steps are required for an efficient mapping of proteins present at low abundance, such as cytokines or transcription factors. **Figure 6** shows an example of protein enrichment by hydrophobic interaction chromatography. One protein (enolase), represented by a strong spot in the 2D map of the total protein extract, is highly enriched after chromatography. Another example of protein enrichment, this time using heparin chromatography is shown in **Figure 7**. In two fractions collected from the column, proteins which are not visible in the 2D gel image of the total extract can also be detected.

On a 2D map, proteins are often represented by more than one spot. **Figure 3C** shows an example of a brain protein represented by five spots, in two locations, with different *pI* and *M_r* values. Presently, we do not know the reasons and the biological significance for most of these cases of observed heterogeneity. It may be the consequence of post-translational modifications, such as deamidation, phosphorylation or glycosylation, which result in the alteration of the *pI* of the molecule and its focusing position. Another reason may be the carbamylation of the protein upon contact of the sample with urea. In **Figure 3D** an

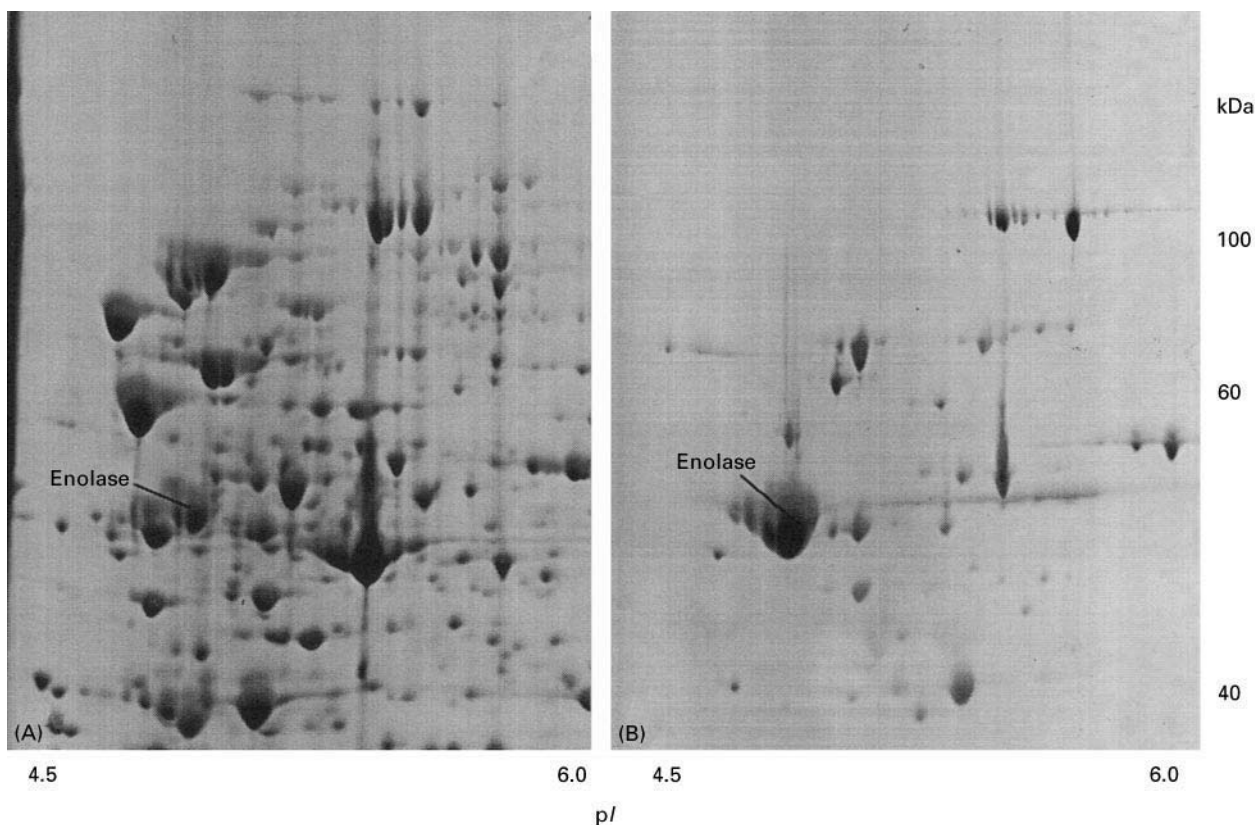


Figure 6 Partial 2D gel images showing the enrichment of enolase by hydrophobic interaction chromatography. (A) Total extract; (B) proteins from a fraction collected from the column.

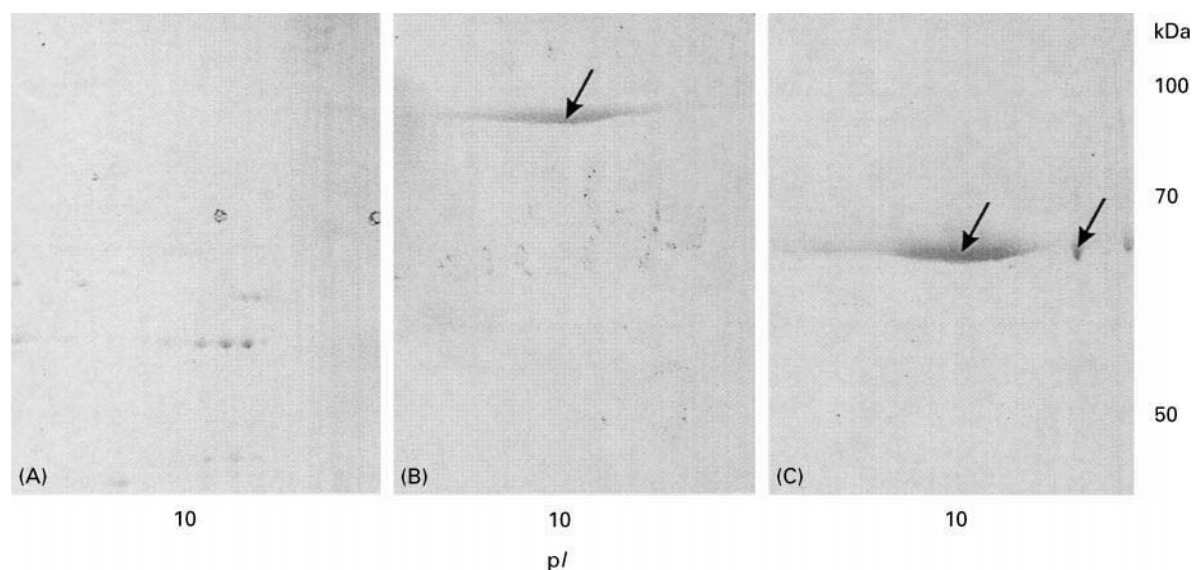


Figure 7 Partial 2D gel images showing the enrichment of low abundance proteins of *H. influenzae* by heparin chromatography. (A) Total extract; (B, C) proteins from fractions collected from the heparin column. The arrowheads indicate spots representing two proteins (B, topoisomerase I; C, ATP-dependent RNA helicase) which are not visible in total extract (A).

example of protein heterogeneity, most likely due to glycosylation, is presented.

Following 2D electrophoresis, proteins can be identified by mass spectrometric analysis of the peptides resulting from the in-gel digestion with a specific

protease, such as trypsin. In another approach, the proteins can be electrotransferred onto membranes and identified by immunoreaction with specific antibodies, by N-terminal sequencing or amino acid composition analysis. For those proteins for which the

Table 2 Steps in the preparation of 2D electrophoresis

IPG strip rehydration and sample preparation

Protein extraction, centrifugation, recovery in sample solution

Sample application

Application in cups at either or at both ends of the strip or strip rehydration in a solution containing the protein sample

First dimensional separation (isoelectric focusing)

Start at 200 V and increase gradually to 5000 V; keep 5000 V for 6–48 h, depending on sample, quantity and strip range; narrow pH range strips require longer focusing times

Reduction and alkylation of proteins on IPG strip

Equilibration of strip with reducing and alkylating agents or freeze until use

Second dimensional separation (SDS-PAGE)

Preparation of gel of the desired acrylamide concentration; gels should carry a label to identify them afterwards; establishment of contact between strip and gel with agarose solution; run at 40 mA/gel

Protein fixing and staining or blotting

Fixation of proteins within the gel and staining with silver or Coomassie blue or drying of the gel and exposure to a film or phosphorimager for detection of radiolabelled proteins or electrotransfer of proteins to membranes for immunoblot, MS or amino acid analysis

Gel scanning

Storage of image in a database

Gel comparison

Gel comparison and protein quantification using specific software; comparison with database master gels via the WorldWideWeb

Identification of proteins

Identification of protein spots from gels by mass spectrometry or from membranes by N-terminal sequencing, amino acid composition analysis, MS or immunoblots

genomic sequence is in a database, the most efficient identification method presently available is matrix-associated laser desorption ionization mass spectrometry (MALDI-MS) with which about 500 spots can be analysed daily by one person. The method tolerates small amounts of salt in the sample, so that no time-consuming desalting steps are required after digestion. Several approaches using a combination of protein digestion on membranes and MS have also been reported. **Table 2** summarizes the essential steps of 2D electrophoresis and protein analysis.

Future Developments

2D electrophoresis is still in a developmental stage. Several technical improvements, mainly concerning further simplification of the technology and possible automation, an increase in reproducibility and sensitivity, and expansion of the pH detection spectrum, have to be achieved in order for the method to become routine in any biochemical laboratory. Gel grinding techniques, together with sophisticated software using the mass spectroscopic data, may be developed to produce a gel image without previous staining of the gel. Such a development could be decisive as to whether the technology will reach its major goal, i.e. the investigation of biological problems by a faithful comparison of protein expression levels. The completion of the sequencing of more genomes together with improvements in the analytical techniques will also

lead to a more widespread application of the technology.

See Colour Plate 43.

Further Reading

- Anderson L (1991) *Two-dimensional Electrophoresis: Operation of the ISO-DALT System*. Rockville: Large Scale Biology Press.
- Fountoulakis M and Lahm H-W (1998) Hydrolysis and amino acid composition analysis of proteins. *Journal of Chromatography* 826: 109.
- Hames BD and Rickwood D (1990) *Electrophoresis of Proteins: A Practical Approach*. Oxford: IRL Press.
- Humphrey-Smith I, Cordwell SJ and Blackstock WP (1997) Proteome research: Complementarity and limitations with respect to the RNA and DNA worlds. *Electrophoresis* 18: 1217.
- Kleinert T (1990) *Elektrophoretische Methoden in der Proteinanalytik*. Stuttgart: Georg Thieme Verlag.
- Righetti PG (1990) *Immobilized pH Gradients: Theory and Methodology*. Amsterdam: Elsevier.
- Smith BJ (1997) *Methods in Molecular Biology: Protein Sequencing Protocols*, vol. 64. Totowa: Humana Press.
- Walsh BJ and Herbert B (1998) Setting up Two-dimensional Gel Electrophoresis for Proteome Projects. http://rbams3115/Pages/2DPAGE/ABRFNews_2dpage.html
- Westermeyer R (1993) *Electrophoresis in Practice*. Weinheim: VCH Verlagsgesellschaft.
- Wilkins MR, Williams KL, Appel RD and Hochstrasser DF (1997) *Proteome Research: New Frontiers in Functional Genomics*. Berlin: Springer.

Two-dimensional Polyacrylamide Gel Electrophoresis

J.-D. Tissot and P. Schneider,

Service Régional Vaudois de Transfusion Sanguine,
Lausanne, Switzerland

M. A. Duchosal, Centre Hospitalier Universitaire Vaudois,
Lausanne, Switzerland

Copyright © 2000 Academic Press

Introduction

The evolution of tools utilized in biology and medicine, together with the exponential progress accomplished recently in the area of bioinformation, enables analysis of whole organism constituents. Such analyses are best exemplified by complete genomic sequences of different microorganisms, and by the recent development in techniques permitting dissection of the whole protein repertoire of an individual, namely its proteome. Furthermore, the dramatic growth in the number of genome projects as

well as the speed with which genome sequences are determined has generated huge amounts of information. This progress has boosted techniques, notably two-dimension polyacrylamide gel electrophoresis (2D-PAGE), enabling the analysis of a proteome consisting of all the proteins expressed by a genome. Such analyses give information on the effector molecule itself, namely the protein, and take into account highly sophisticated mechanisms regulating gene expression. 2D-PAGE is the most powerful tool to separate a multitude of polypeptides that are contained in a single biological sample. Various procedures have been described to separate proteins according to biophysical parameters. In 1975, O'Farrell, Klose and Scheele described optimized 2D procedures in which proteins were denatured and separated by electrophoresis on polyacrylamide gel. The first gel dimension comprised a separation according to the protein charge by isoelectric focusing,

and the second gel dimension separated proteins according to their sizes. Thus, peptides are separated from one another according to two independent biochemical properties. 2D-PAGE was shown to be particularly valuable in the study, as well as in the identification of thousands of cellular or secreted proteins, including many of those present in human plasma/serum (Figure 1).

During the past few years, tremendous progress has been made in the field of 2D-PAGE. The 2D technique has been simplified, and, more importantly, made reproducible. Commercially manufactured im-

mobilized pH gradients (IPGs), with both acidic and basic high resolution power and precast sodium dodecyl sulfate (SDS) PAGE gels are now available. In addition, progress in protein solubilization and in the development of systems allowing high loading capacities has been made.

More than 20 years after its birth, 2D-PAGE is now a major technique in protein sciences. Over the past few years there has been an exponential increase in the creation and expansion of protein databases such as the SWISS-2DPAGE, the HEART-2DPAGE and the HSC-2DPAGE. Furthermore, tools have been developed to

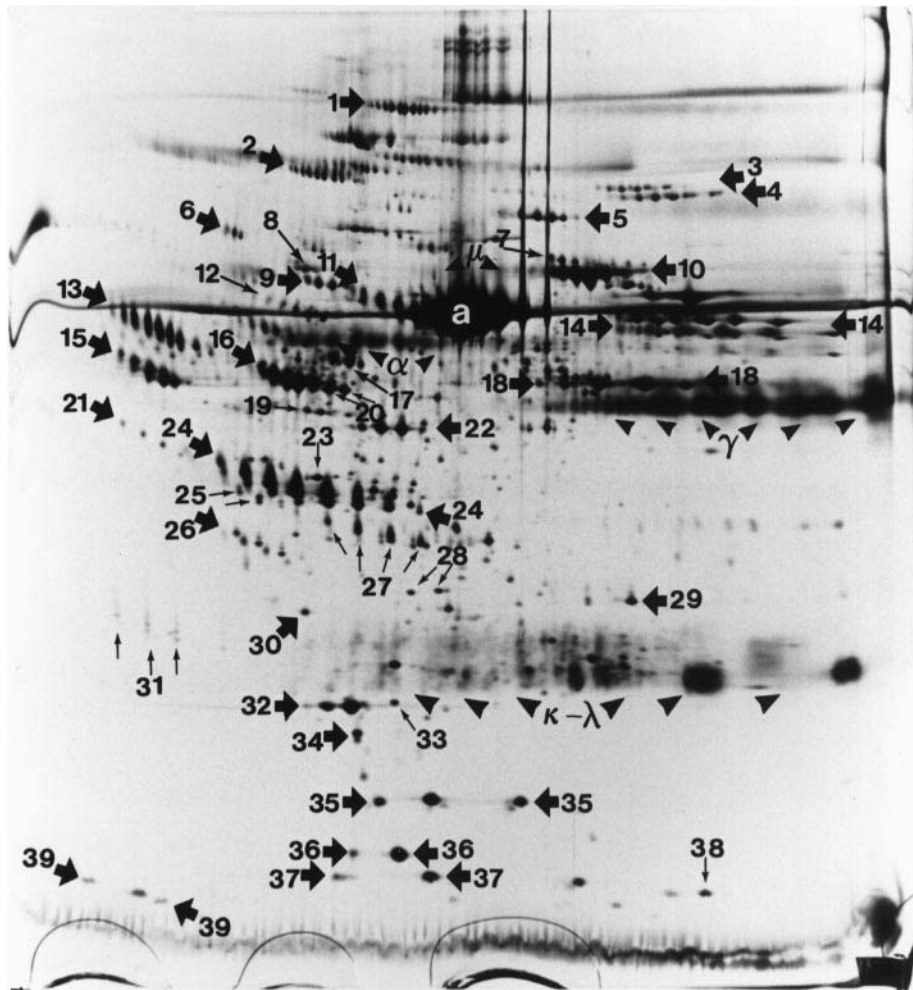


Figure 1 The normal human plasma 2D map. Polypeptides (0.3 μ L of plasma) were separated by pH 3.5–10 carrier ampholyte gradient, followed by gradient 9–16% T polyacrylamide gel electrophoresis in the presence of sodium dodecyl sulfate (SDS). The ammoniacal silver-stained gel was photographed with the higher molecular weight at the top and the acidic side on the left. 1, α_2 -macroglobulin; 2, ceruloplasmin; 3, glu-plasminogen; 4, lys-plasminogen; 5, complement factor B; 6, complement C1s; 7, protransferrin; 8, prothrombin; 9, α_1 -B-glycoprotein; 10, transferrin; 11, hemopexin; 12, α_2 -antiplasmin; 13, α_1 -antichymotrypsin; 14, fibrinogen α chain; 15, α_2 -HS-glycoprotein; 16, α_1 -antitrypsin; 17, antithrombin III; 18, fibrinogen β chain; 19, extended fibrinogen γ chain; 20, Ge-globulin; 21, lysin-rich glycoprotein; 22, fibrinogen γ chain; 23, apolipoprotein A-IV; 24, haptoglobin β chain; 25, Zn- α -glycoprotein; 26, apolipoprotein J; 27, cleaved haptoglobin β chain; 28, apolipoprotein E (phenotype E 3/4); 29, γ chain of complement C₄; 30, α_1 -microglobulin; 31, apolipoprotein D; 32, apo A-I; 33, proapolipoprotein A-I; 34, retinol-binding protein; 35, haptoglobin α_1 chain; 36, transthyretin (prealbumin); 37, haptoglobin α_2 chain; 38, haemoglobin β chain; 39, apolipoproteins C-II and C-III; a, albumin; μ , polyclonal heavy chains of IgM; α , polyclonal heavy chains of IgA; γ , polyclonal heavy chains of IgG; κ - λ , polyclonal Ig light chains. Reproduced with permission from Tissot and Spertini (1995).

compare 2D gels images across the Internet. Most importantly, methods for the analysis of 2D gels are continually improving. The high sensitivity and throughput of these techniques now enable the characterization of hundreds of proteins from a whole cell, tissue or body fluid. Proteins can be identified according to primary parameters such as their isoelectric points, apparent molecular mass, real mass and protein N- or C-terminal sequence tag, but also according to secondary attributes such as peptide mass fingerprint, peptide fragmentation data or amino acid composition. Interfacing and integrating databases from 2D gels such as SWISS-2DPAGE, SWISS-PROT, GenBank, EMBL nucleotide sequence database, dbest, GSBD and the NLM's MEDLINE bibliographical reference database provide researchers with invaluable tools to study both genome and proteome. The continuing progress accomplished in both proteome research and bio-information will contribute to the implement of the *Cyber-Encyclopedia of the Proteome*, as suggested by R.D. Appel. This development increases the need for simple protocols to run reproducible 2D gels and is an important step for investigators involved in proteomics. Several well-written protocols and reviews are accessible in the literature or through the World Wide Web (<http://expasy.hcuge.ch/ch2d/technical-info.html>; <http://www.abdn.ac.uk/~mmb023/2dhome.htm>). We will review here some of the important features that must be evaluated in order to implement a new 2D-gel laboratory.

Sample Preparation and Protein Solubilization

2D-PAGE is an ideal separation tool. Nevertheless, sample preparation and protein solubilization are still a key step that is frequently ignored. In addition, there is no universal and ideal sample buffer for 2D-PAGE. The goal of sample preparation is to maximize solubilization and disaggregation of the tissues while preventing protein degradation. For these reasons, and because samples have various characteristics, protocols have to be adapted according to the origin of the samples. Sample preparation is quite easy with soluble proteins such as those of plasma or cerebrospinal fluid, but presents major difficulties in the presence of membrane or nuclear proteins. Tissue samples are usually mechanically disrupted (ultrasonication, rapid agitation in the presence of glass or zirconium microspheres), washed in a low salt buffer and then chemically (lysis buffer) solubilized. Constituents such as nucleic acids, lipids or salts can interfere with both solubilization and with the electrophoretic properties of the proteins. Before loading, nonsolubilized material must be eliminated by high

speed centrifugation. To break down interpolypeptide disulfide bonds and to maintain reducing conditions, components such as dithiothreitol, dithioerythritol or β -mercaptoethanol are used. The solubility problem can be alleviated to a large extent by the proper use of a combination of chaotropes and detergents in combination. Urea is a common constituent of protein sample preparations, and in its presence care must be taken to avoid heating above 32°C, which causes carbamylation of peptides. Impressive improvements in protein solubilization have been obtained with a denaturing solution containing urea, thiourea and detergents (both nonionic and zwitterionic). The ideal conditions would combine the highest chaotropic power (i.e. 2 mol L⁻¹ thiourea and 7–8 mol L⁻¹ urea) with a detergent cocktail (3-[(3-cholamidopropyl)dimethylammonio]-1-propane sulfonate, Triton X-100).

The main problem encountered with thiourea is the strong inhibition of acrylamide polymerization. Another problem complicating protein separation by 2D-PAGE is that, at high concentrations, many proteins are prone to precipitation, resulting in poor resolution after isoelectric focusing. In order to load large amounts of proteins, investigators have overcome the problem by using 'in gel' application of the samples, avoiding the use of sample cups and eliminating precipitation at the same application site.

Isoelectric Focusing

In 1964, synthetic carrier ampholytes (aliphatic oligoamino and oligocarboxylic acids) were synthesized allowing separation of peptides according to their charges. For 2D-PAGE, carrier ampholyte isoelectric focusing is usually performed in an ampholyte–polyacrylamide matrix that is polymerized in a glass tube. After sample loading, polypeptides are concentrated into narrow bands within a continuous pH gradient in the polyacrylamide gel matrix. Proteins migrate in an electric field until they arrive at a position in which they have no net charge, i.e. their isoelectric point (pI). Isoelectric focusing is useful because: (i) no diffusion of proteins occurs because of the focusing effect; (ii) it offers a resolution allowing the separation of microheterogeneous populations of proteins; and (iii) the pI of the protein can be estimated. In the past, pH gradients were generated by carrier ampholytes or amphoteric buffer moving freely within an acrylamide matrix.

Practically, many factors can affect measurement of the apparent pI of the proteins during isoelectric focusing with carrier ampholytes: (i) since the proteins have their own inherent charges, they can act as ampholytes themselves and affect pH during focus-

ing; (ii) the carrier ampholytes have a higher mobility than the proteins; (iii) some proteins may never reach steady state due to polyacrylamide gel matrix restriction; (iv) ampholyte-protein interactions may alter the observed pI of the proteins. Temperature, time, voltage and salt concentration are other parameters that may dramatically influence the determination of the pI . Finally, the basic proteins are not detected without using nonequilibrium pH gradient electrophoresis. Nowadays, many of these problems have been resolved by the development of isoelectric focusing with an IPG. The pH gradient is created by copolymerization of acrylamide/ N,N' -methylenebisacrylamide with acrylamido derivatives, containing either carboxyl or tertiary amino groups as buffers and sulfate groups (acidic) or quaternary ammonium (basic) as strong titrants (Immobilines). This method is a true equilibrium method, which significantly improves the feasibility of the 2D-PAGE.

Recently, highly reproducible, commercially available, wide-range as well as narrow-range IPGs have been produced. The latter gradients allow a pH scale that enables comparison of several 2D gel maps generated with many IPGs in the first dimension and with various biological samples. IPGs also offer the possibility of determining pI without major differences from the calculated pI values, unless there are significant post-translational protein modifications. Nowadays, with the improvements of IPG production, it is possible to detect proteins with pI s up to pH 12 in a single IPG gel with highly reproducible protein patterns.

Finally, as mentioned in the previous section, entire IPG gels can be used for sample application, with the protein entering the gels during their rehydration. This approach is useful because it eliminates precipitation at the sample application site, it improves the resolution over the entire pH range of the gels, and it allows precise control of protein amounts and sample volumes loaded on to the IPG gels. Up to 5 mg of proteins can be loaded on wide IPG gels and up to 15 mg on narrow pH range gels. Contrarily to isoelectric focusing with carrier ampholytes, electroendosmosis (transport of water towards the cathode at low pH values or towards the anode at high pH values) is generally not a problem with IPGs. Currently, isoelectric focusing using carrier ampholytes still has a place in a 2D laboratory, because the resolution of particular proteins is sometimes better.

From the First to the Second Dimension

Transfer of the first-dimension spaghetti-like gels after isoelectric focusing in the presence of am-

pholytes used to be a manipulation challenge for beginners in the field of 2D-PAGE. Extrusion of the gels from the glass tubes was difficult, and the gels frequently broke into several pieces. With the use of IPG strips, which are deposited on a plastic backing material, the transfer is easy. Practically, after the first dimension run, the strips are equilibrated in buffers containing SDS in order to maintain proteins in solution and to reduce $-S-S-$ bonds. Subsequently, strips are placed over SDS gels that may or may not contain a stacking gel.

SDS-PAGE

In the second dimension, polypeptides are separated according to their size in a gel matrix. Practically, after electric focusing in reducing conditions, proteins are separated into their polypeptide components. The latter are mixed with SDS-containing buffers. SDS binds to polypeptides at a constant mass ratio (1.4 g SDS per gram of protein). As a consequence, polypeptides organize as rod-like molecules, with a diameter of 1.8 nm, and their lengths depend on their molecular weight. The bound SDS molecules contribute to a strong negative charge, which effectively swamps the intrinsic charge of the polypeptides. Thus, in general the SDS-polypeptide complexes have the same mass/charge ratio and, in a sieving polyacrylamide matrix, they will migrate according to their molecular weight. Glycoproteins and lipoproteins can migrate abnormally as they are not easily saturated with SDS.

The gel matrix is most frequently composed of polyacrylamide generated by polymerization of acrylamide monomers into long chains that are cross-linked. Usually, cross-linkers are bifunctional components such as N,N' -methylenebisacrylamide (bis) or diacrylpiperazine. Polymerization of acrylamide is initiated either by the use of ammonium persulfate or riboflavin, and is accelerated by the use of N,N,N',N' -tetramethylethylenediamine (TEMED). Oxygen inhibits polymerization, and thus gel mixtures are usually degassed. The composition of a polyacrylamide gel is defined by two parameters: % T and % C . The % T (w/v) is the total concentration of the monomer (acrylamide plus cross-linker), whereas % C corresponds to the ratio (w/w) of the cross-linker to the acrylamide. The pore size of the polymerized acrylamide will depend on these two parameters, but since pore formation is random, pore sizes will never be totally uniform. The choice of the mean pore size will depend on the molecular weight of the proteins to be studied. The second-dimension SDS-PAGE can be performed with home-made vertical or horizontal systems, using linear or gradient polyacrylamide

(9–16%) gels. Commercially manufactured gels are also available. The advantages of the latter reside in their reproducibility and safety (polymerized acrylamide being clearly less neurotoxic as compared with monomeric acrylamide). The sensitivity as well as the resolution power of the protein detection must be kept in mind before choosing optimal conditions for SDS-PAGE. Gels polymerized with the photoinitiator system, composed of methylene blue, toluene sulfinate and diphenyliodonium chloride, lead to low resolution power after silver staining. Resolution can be restored if methylene blue is replaced by riboflavin. Gels polymerized with the riboflavin/sulfinate/iodonium system yield better results upon *N*-terminal microsequencing after blotting than gels polymerized with the standard TEMED/ammonium persulfate system.

Protein Visualization

Several methods have been described to detect protein spots after 2D-PAGE. These methods use reactants

such as Coomassie Brilliant Blue R-250, Amido Black, Ponceau S, Fast Green, negative staining, silver staining, fluorescein and radioisotopes. The two most popular approaches are Coomassie Brilliant Blue R-250 and silver staining. A good stoichiometric relationship has been documented between protein abundance and integrated optical density of protein spots for Coomassie Brilliant Blue R-250. The silver staining methods are more sensitive than those using Coomassie Blue and can detect as little as 1–4 ng of proteins. Several methods of silver staining of proteins have been described, with the most rapid ones being usually less sensitive and less reproducible than the more time-consuming ones. Among the latter methods, those using silver–diamine complex give the most uniform sensitivity. However, they require special home-made gels and cannot be applied to several electrophoretic systems. For these reasons, protocols based on silver nitrate are of more general use and are favoured. A variety of systems using different metal cations (K^+ , Cu^{2+} , Zn^{2+}) has been

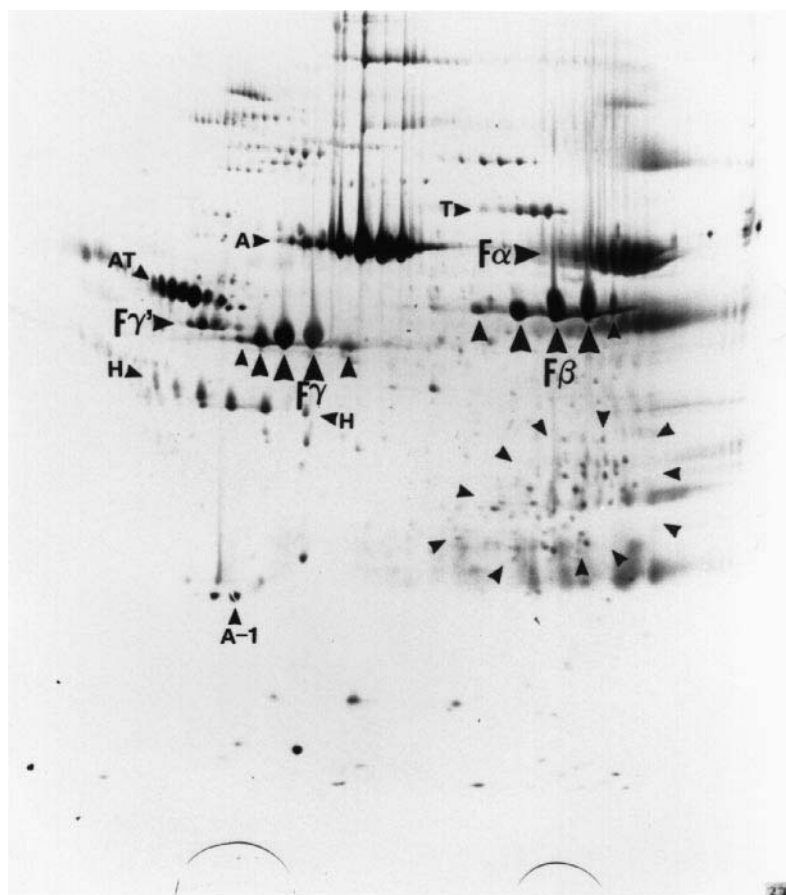


Figure 2 Microheterogeneity of proteins. 2D gel of a cryoprecipitate containing fibrinogen (cryofibrinogen). A, albumin; AT, α_1 -antitrypsin; T, transferrin; H, haptoglobin β chain; A-1, apolipoprotein A-1; $F\alpha$, fibrinogen α chain; $F\beta$, fibrinogen β chain; $F\gamma$, fibrinogen γ chain; $F\gamma'$, extend fibrinogen γ chain. Unknown protein spots are shown by arrowheads. All major identified proteins present charge microheterogeneities. First dimension: immobilized pH gradient.

developed to stain SDS-PAGE separated proteins without the need for fixative, organic dye or chemical modifier. SDS proteins stain negatively upon gel treatment with solutions of heavy metal salts. The zinc imidazolate reverse-staining method offers the advantage of combining good sensitivity, rapidity and reversible interaction. Furthermore, the zinc imidazolate reverse-staining method can be used in situations where Coomassie Brilliant Blue R-250 or silver staining is inappropriate or fail to produce detection of the polypeptides of interest.

Protein Microheterogeneity

Polypeptides separated by 2D-PAGE rarely appear as single spots, and most are resolved as multiple spots characterized by charge and size microheterogeneities (Figure 2).

Microheterogeneity is due to several factors that frequently occur together. The first cause of microheterogeneity is genetic polymorphism where heterozygote individuals express both forms of the gene (Figure 3); the second is related to protein co- and post-translational modifications. These modifications are multiple and have all the potential of modifying a protein's charge, hydrophobicity, conformation and/or stability. Furthermore, the 'one gene one polypeptide' paradigm is challenged by the alternative splicing of many genes responsible for synthesizing several proteins from a single gene. An important feature of 2D gel analysis is that various protein isoforms generated by co- and/or post-translational modifications can be separated by isoelectric focusing and/or by SDS-PAGE. Among the modifications which lead to a charge-dependent change to a protein, acylation, alkylation, carboxymethylation, phosphorylation, sulfation, carboxylation, sialylation and proteolytic processing are involved. Finally, glycosylation of proteins may lead to both charge and size modifications, and microheterogeneity of a protein may reflect the presence of several glycoforms.

Protein Identification

Several approaches have been used to identify proteins after 2D-PAGE. Co-migration with purified known proteins and Western blotting were employed by the pioneers of the 2D field. The use of specific antibodies and the recent developments of antigen-antibody interactions with enhanced chemiluminescence allow detection and identification of traces of proteins. However, monoclonal antibodies may not detect denatured polypeptides. Nowadays, proteins are identified by microsequencing, amino

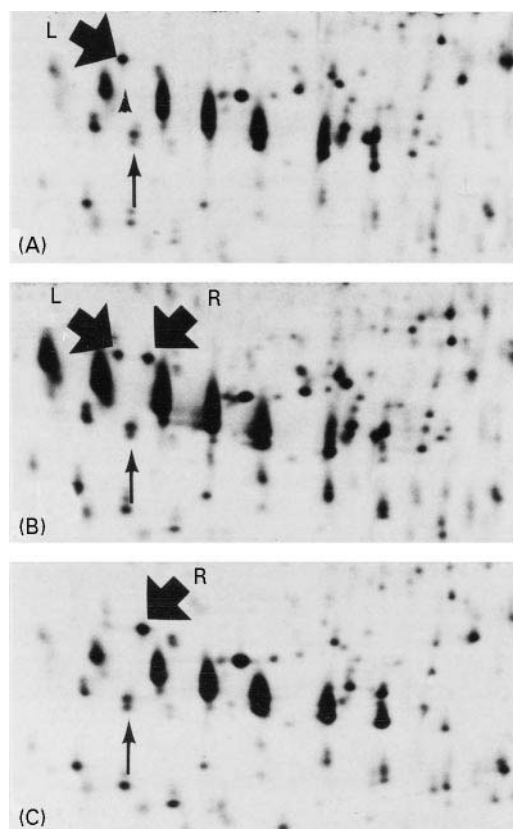


Figure 3 Genetic heterogeneity of plasma proteins. Close-up of the human plasma 2D map corresponding to the haptoglobin β chain (pH 3.5–10 carrier ampholyte gradient). (A) L form (homozygous); (B) L–R forms (heterozygous); (C) R form (homozygous). A reference spot is shown by the arrowhead. This genetic polymorphism is less detectable with immobilized pH gradients. Note the microheterogeneity of haptoglobin β chain spots, which present both charge and size heterogeneities.

acid analysis, peptide mass fingerprinting and/or mass spectrometry. The development of automated, high throughput technologies for the rapid identification of proteins is in progress. Automation already exists in several stages of the protein identification process. This includes automated acquisition of matrix-assisted laser desorption ionization-time-of-flight mass spectra and peptide mass fingerprinting. Bioinformation allows identification of proteins by mixing several databases (a classified index can be found at the following address: <http://expasy.hcuge.ch/alinks.html#Proteins>).

Data Management

Many investigators have analysed their 2D gels by holding two, sometimes three gels together towards a light source, and tried to identify differences between them (Figure 4). However, analysis of a multitude of 2D gels, with its bulk of information is greatly

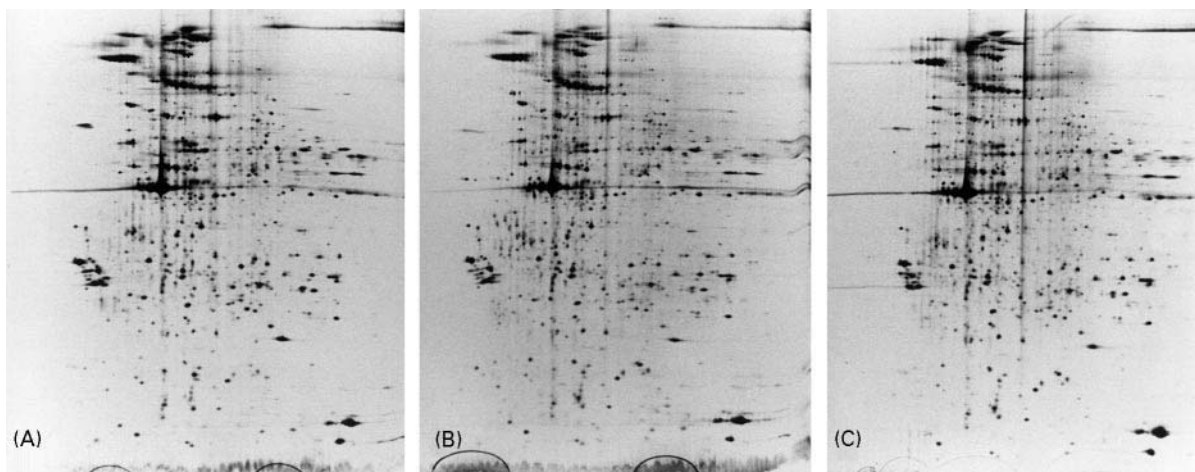


Figure 4 Analysis of 2D gels. 2D gels of human platelets from a single blood donor (pH 3.5–10 carrier ampholyte gradient). (A) Platelets stored with leukocytes, 1 day after collection; (B) platelets stored in the presence of leukocytes, 7 days after collection; (C) platelets stored in the absence of leukocytes, 7 days after collection. Without computerized analysis, it is not possible to draw a definitive conclusion from the comparison of this set of gels. Reproduced with permission from Sarraj-Reguieg A, Tissot JD, Hochstrasser DF, von Fliegener V, Bachmann F and Schneider P (1993) Effect of prestorage leukocyte reduction on proteins of platelets obtained by apheresis. *Vox Sanguinis* 65: 279.

facilitated by the use of computer-based data processing. The improvements in image acquisition and image analysis allow clear spot detection, background subtraction, spot matching and database construction. Furthermore, interpretation of 2D-PAGE images is facilitated by statistical methods, artificial intelligence and machine-learning programs. Ascendant hierarchical classification sorts the image into meaningful groups. The use of correspondence analysis and ascendant hierarchical clustering allows identification of new, potentially important proteins. Many database of 2D gel master images are accessible through the World Wide Web (Internet sites can be found at the following addresses: <http://www.expasy.ch/ch2d/2d-index.html> or <http://www.lmmb.ncifcrf.gov/ABRF97/abrf3.html>). It is also possible to compare 2D gels from various laboratories, or 2D gels with masters, on the World Wide Web by using the flicker created by P.F. Lemkin (accessible at <http://www-lecb.ncifcrf.gov/flicker/>).

Protein Functions

After 2D-PAGE analysis of cells, thousands of spots are observed. Such an observation is frequently impressive, but not very useful. Identification of the polypeptide sequence corresponding to a spot is already undergoing major progress. However, understanding the protein's function(s) remains the final goal of any analysis. It is also relevant to study the expression level, the phosphorylation state, the sub-cellular location, the association with other proteins and the rate of synthesis or degradation of the

proteins of interest. Combination of all this information will make possible the study of a functional proteome.

Concluding Remarks

Amino acids are like letters. Amino acids make proteins; letters make words. Proteins are like words. Some are known, others are unknown. Proteome databases are like dictionaries; they contain a lot of information and are very useful. Organization of the words makes the texts; organization and regulation of protein production make the cells. 2D-PAGE is a major proteomics tool. The technique should be applied to resolve specific biological problems. It should not be used for random investigations.

Further Reading

- Bjellqvist B, Basse B, Olsen E and Celis JE (1994) Reference points for comparisons of two-dimensional maps of proteins from different human cell types defined in a pH scale where isoelectric points correlate with polypeptide compositions. *Electrophoresis* 15: 529.
- Chevallet M, Santoni V, Poinas A *et al.* (1998) New zwitterionic detergents improve the analysis of membrane proteins by two-dimensional electrophoresis. *Electrophoresis* 19: 1901.
- Corbett JM, Dunn MJ, Posch A and Görg A (1994) Positional reproducibility of protein spots in two-dimensional polyacrylamide gel electrophoresis using immobilised pH gradient isoelectric focusing in the first dimension: an interlaboratory comparison. *Electrophoresis* 15: 1205.

- Görg A, Boguth G, Obermaier C, Posch A and Weiss W (1995) Two-dimensional polyacrylamide gel electrophoresis with immobilized pH gradients in the first dimension (IPG-Dalt): the state of the art and the controversy of vertical versus horizontal systems. *Electrophoresis* 16: 1079.
- Görg A, Boguth G, Obermaier C and Weiss W (1998) Two-dimensional electrophoresis of proteins in an immobilized pH 4–12 gradient. *Electrophoresis* 19: 1516.
- Humphrey-Smith I, Cordwell SJ and Blackstock WP (1997) Proteome research: complementarity and limitations with respect to the RNBA and DNA words. *Electrophoresis* 18: 1217.
- Rabilloud T, Vuillard L, Gilly C and Lawrence JJ (1994) Silver-staining of proteins in polyacrylamide gels: a general overview. *Cellular and Molecular Biology* 40: 57.
- Rabilloud T, Adessi C, Giraudel A and Lunardi J (1997) Improvement of the solubilization of proteins in two-dimensional electrophoresis with immobilized pH gradients. *Electrophoresis* 18: 307.
- Rabilloud T (1998) Use of thiourea to increase the solubility of membrane proteins in two-dimensional electrophoresis. *Electrophoresis* 19: 758–760.
- Sanchez JC, Rouge V, Pisteur M *et al.* (1997) Improved and simplified in-gel sample application using reswelling of dry immobilized pH gradients. *Electrophoresis* 18: 324.
- Tissot JD and Spertini F (1995) Analysis of immunoglobulins by two-dimensional gel electrophoresis. *Journal of Chromatography A* 698: 225.
- Traini M, Gooley AA, Ou K *et al.* (1998) Towards an automated approach for protein identification in proteome projects. *Electrophoresis* 19: 1941.
- Wilkins MR, Williams KL, Appel RD and Hochstrasser DF (eds) (1997) *Proteome Research: New Frontiers in Functional Genomics*. Berlin: Springer-Verlag.

EXTRACTION



Analytical Extractions

M. K. L. Bicking, ACCTA Inc., Woodbury, MN, USA

Copyright © 2000 Academic Press

Introduction

The process of generating analytical data involves some combination of planning, sampling, sample preparation, quantification, data review and reporting. Initially, each step in the method required comparable effort. Sample preparation, generally involving some form of extraction followed by analyte enrichment, has in the past been a laborious process, with only a few tools available. Likewise, quantification usually consisted of a 'wet' chemistry process such as titration or precipitation. Before the development of personal computers, the planning, sampling, data review and reporting steps also required considerable effort. Since each step presented formidable challenges to the analytical scientist, the relative importance of each step remained about the same.

Modern techniques, particularly chromatography, have changed the situation. The rapid and successful development of gas and liquid chromatography dramatically reduced quantification steps from hours or days to a matter of minutes, often with better accuracy and precision. The other steps in the method,

especially sample preparation, were regarded as of secondary importance, serving only to support the ultimate (i.e. chromatographic) step in the method. Since most of the creative – and financial – resources flowed into chromatography development, research in the other areas slowed and sample preparation came to be viewed as the 'low tech' part of the method.

Chromatography is now considered a mature science, being an integral part of nearly every analytical laboratory. The slower pace of chromatographic research, coupled with outside pressures to improve the efficiency of the entire analytical method, has finally resulted in an increased interest in sample preparation. These efforts have produced a number of advances that improve efficiency, selectivity and time required. The discussion will provide an overview of some of the many sample preparation principles and techniques available, focusing on the analytical extraction part of the process. The goal is to provide the reader with a more balanced view of this important part of analytical methodology.

Principles of Extraction

Developing a successful extraction as part of an analytical method requires an understanding of the chemical and physical principles involved. Thus, we will begin this discussion of analytical extraction by focusing on the underlying principles that make the techniques work. Only with understanding and

appreciation of these principles can full advantage be taken of them.

Definition of Analytical Extraction

Extraction is the process of moving one or more compounds of interest (analytes) from their original location (usually referred to as the sample or matrix) to a physically separate location where further processing and analysis occur. The sample may be a solid, liquid or gas. The separate location is usually a fluid (an extracting solvent), but extractions into the gas phase and on to solid sorbents are also common. Finally, the word analytical implies that this process involves small amounts of analyte (as opposed to preparative extraction). Most analytical methods aim at complete extraction although situations frequently exist where good analytical results are possible with only partial extraction.

Thermodynamics and Kinetics

These two terms are often interchanged, when in fact they have very different chemical meanings. Thermodynamics is the study of energy, in this case the energy associated with the chemical process of extraction. Through this study of energy, we can determine if the process is favourable or unfavourable. That is, will this extraction give a good result or a bad one? Even if the process is favourable, it may not happen quickly because of kinetic factors. Kinetics is the study of the rate at which these processes occur.

It is important to realize that these two principles are completely independent of each other. Complete extraction is not necessarily a fast process and devel-

opment of a successful extraction method requires that consideration to be given to both aspects.

Like Dissolves Like

A compound will be soluble in, or mix with, another compound that is chemically like it. That is, the two compounds must be from the same, or similar, chemical families. This simple principle is an implied requirement in every analytical extraction. The concept of moving analytes from the matrix to some other location requires them to be transported using some medium in which they are soluble. Therefore, we must carefully consider how the like-dissolves-like concept can help to achieve the desired result: extracting the desired compounds and not extracting the undesired ones.

Figure 1 illustrates how simple changes in molecular structure can have a profound influence on solubility behaviour. This plot shows the solubility of three related amino acids in water. Amino acids are generally considered to be polar, so their solubility in the polar solvent, water, is generally high. As nonpolar functionality is added to the molecule, in the sequence from glycine to phenylalanine, the nonpolar character of the entire molecule increases (i.e. it becomes less like water). The result is a significant reduction in water solubility.

The same situation exists when considering the relative solubility of any compound in a series of solvents. A higher solubility will be observed when the solvent is most like the compound in question. The reader is referred to the Further Reading section for additional examples.

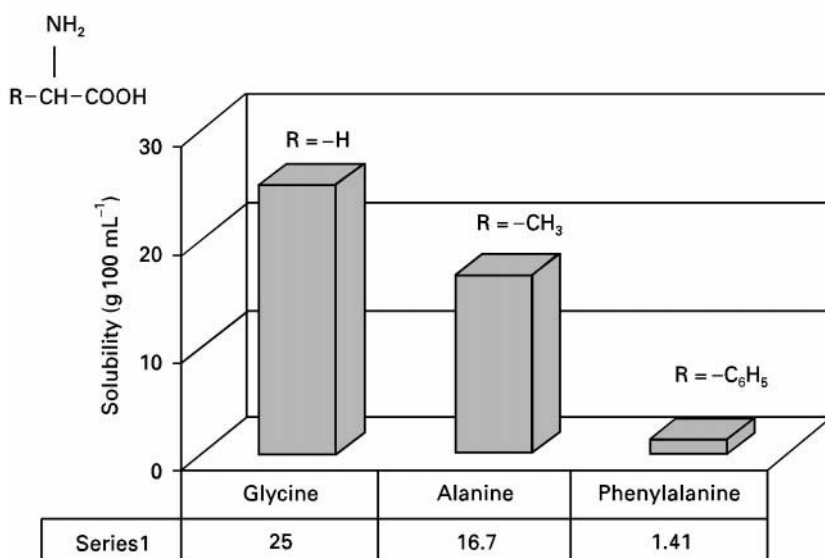


Figure 1 Solubility of amino acids in water as a function of structure.

Temperature Effects

Temperature has an effect on three important phenomena: solubility, vapour pressure and kinetics. While increasing temperature generally increases the magnitude of each effect, there are some aspects of this principle that are particularly relevant to analytical extractions.

Effect of temperature on solubility In most cases involving organic analytes, increasing the temperature of a liquid results in increased analyte solubility. **Figure 2** illustrates that for the same three amino acids as shown in **Figure 1** a temperature increase from 0 to 75°C results in a three- to fourfold increase in solubility. Even marginally soluble compounds show a dramatic improvement from this simple change in conditions. Indeed, as will be seen later, this principle is used in most extraction procedures.

Effect of temperature on vapour pressure Increasing the temperature of a liquid will result in an increase in vapour pressure. Boiling occurs when the vapour pressure above the liquid equals the applied (usually atmospheric) pressure.

Figure 3 shows calculated vapour pressures for several common solvents. Note that the vapour pressure is relatively large at temperatures as much as 20°C below the boiling point of the solvent. Simple evaporation in a stream of nitrogen at room temperature uses this fact to evaporate a solvent rapidly without boiling. If the applied pressure is raised, the boiling point is also raised, so that the solvent can be maintained in its liquid state at higher temperatures. Press-

urized fluid extraction uses this phenomenon to advantage. Similarly, lowering the applied pressure, as in a rotary evaporator, reduces the boiling point, allowing faster evaporation at lower temperatures. Finally, at any given temperature, the relative vapour pressure of each compound above the liquid phase provides an estimate of the relative evaporation rates of the liquids. Such knowledge is essential when performing critical steps such as solvent evaporation or solvent exchange.

Effect of temperature on kinetics All chemical processes are affected by the temperature at which the process is occurring, although the exact change in reaction rate with temperature is unique for any process. However, many reaction rates will approximately double for each 10°C increase in temperature, and this rule of thumb can be a helpful guide in understanding the effects of temperature changes. These changes can be either positive or negative, depending on whether the temperature change is increasing or decreasing. For example, storing samples and solutions at low temperatures slows down evaporation and degradation. These processes are about four times slower if the solution is stored at 4°C compared to room temperature.

Effect of pH

The pH of an aqueous sample will influence the success or failure of an extraction for acidic and basic analytes. Acids and bases involve an equilibrium between two forms, one neutral and one ionic. Each form has significantly different chemical and physical properties, as noted in **Table 1**.

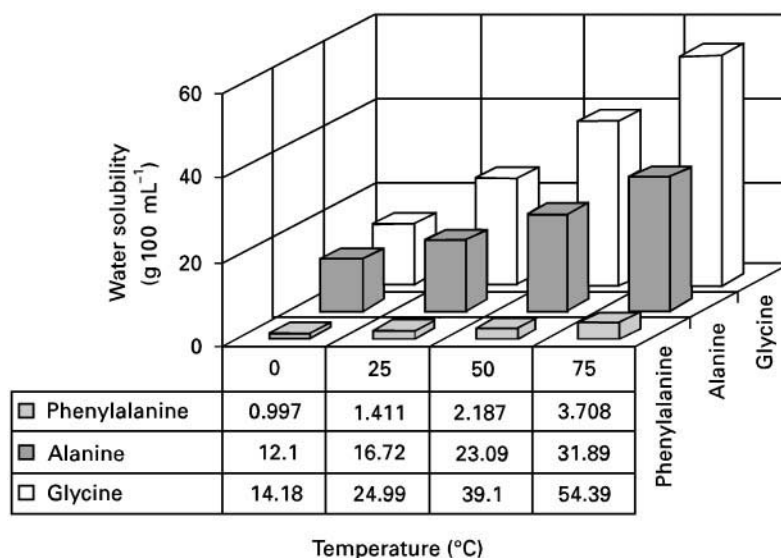


Figure 2 Solubility of amino acids in water as a function of temperature.

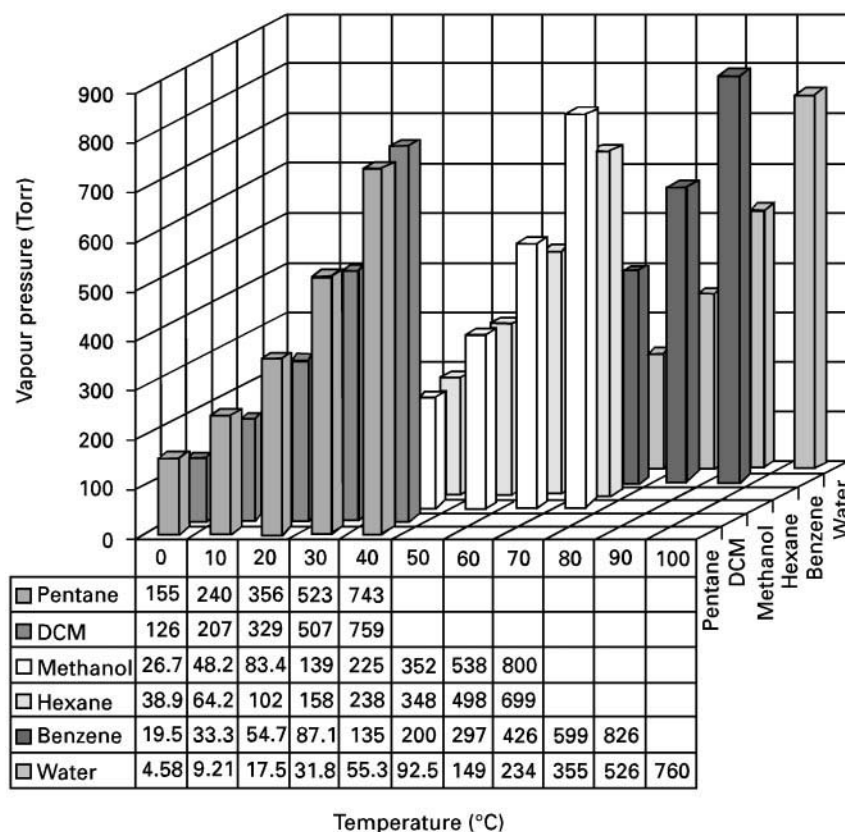


Figure 3 Vapour pressure of common solvents as a function of temperature. (Calculated from data in *Handbook of Chemistry and Physics* (1971).)

Extraction of organic acids from water is only practical at pH values more than two units below the pK_a of the acid. Only at this pH is most of the compound in the neutral form and amenable to extraction with an organic solvent. Similarly, to keep a base, such as an aromatic amine, in the neutral (extractable) form, the pH of the solution must be adjusted to at least two units above the pK_b of the base. Readings with a pH meter are likely to be unstable and/or unreliable in the presence of organic solvents, and the equilibrium constant, K_a , is also

likely to change, often in an unpredictable way. Any required pH adjustments and measurements must, therefore, be made before the organic component is added.

Two-phase Distribution Equilibria

Definitions The process of extraction, by definition, requires that the analyte be transferred from the matrix to a different phase. When the extracting medium first contacts the matrix, the analytes will become distributed between the two phases in a well-defined ratio. Since the matrix is usually a liquid or solid, and the extracting medium can be a solid, liquid or fluid, this usually refers to liquid-liquid and liquid-solid distribution equilibria.

These distribution equilibria can be described by several important equations. First, the distribution ratio, D , for extracting from phase 1 into phase 2 is defined as:

$$D = \frac{C_2}{C_1}$$

where C is the stoichiometric concentration of the analyte in each of the phases. (Actually, D is related

Table 1 Properties of individual forms in acid-base equilibria

Neutral form		Ionic form	
HA + H ₂ O	\rightleftharpoons	A ⁻ + H ₃ O ⁺	
Acid		Conjugate base	
B + H ₂ O	\rightleftharpoons	BH ⁺ + OH ⁻	
Base		Conjugate acid	
More soluble in organic solvents		Less soluble in organic solvents	
Insoluble in water		Soluble in water	
More volatile		Nonvolatile	
Sour/bitter taste, bad odour		Little odour	

to the ratio of activities rather than concentration, but in dilute solution the difference is negligible.)

This ratio is a constant that depends on the analyte, the two phases, the composition of the phases (pH, ionic strength, etc.) and the temperature.

The fraction extracted, θ , in any one equilibration is defined as:

$$\theta = \frac{D\beta}{1 + D\beta}$$

where β is the phase ratio, the ratio of the volumes of the two phases ($= V_2/V_1$). The fraction remaining in the initial phase (V_1) is, of course $1 - \theta$.

The amount extracted depends on the physico-chemical interactions between the two phases and the analyte, and the volume of each phase. A change in these variables will cause a change in the extraction result.

Effect of analyte structure on D Actual values of D in Table 2 show how simple changes in molecular structure have a profound influence on the success of an extraction.

The addition of nonpolar functional groups (methyl- and chloro-) to benzene make the molecule more nonpolar, so that the new molecule favours the hexane phase (larger value for D). Conversely, adding polar groups (amine, hydroxy, carboxylic acid) makes the molecule more like the water phase (smaller D). It is important to keep these general principles in mind when developing an extraction method and understanding the results.

Multiple extractions When multiple extractions are performed on the same sample, the amount extracted into phase 2 and the amount remaining in phase 1 are calculated using the equations shown in Table 3.

In general, several extractions with the same total volume of extracting solvent will always produce better recovery than a single extraction with the same

Table 3 Equations used for multiple extractions

Extraction number	Fraction extracted into phase 2	Fraction remaining in phase 1
1	θ	$1 - \theta$
2	$\theta(1 - \theta)$	$(1 - \theta)^2$
3	$\theta(1 - \theta)^2$	$(1 - \theta)^3$
n	$\theta(1 - \theta)^{n-1}$	$(1 - \theta)^n$

volume of solvent, although it is seldom worth carrying out more than three extractions.

Effect of variations in D and β The effects of variations in D and β on extraction results are shown in Table 4. The total recovery after multiple extractions is calculated for various combinations of D and β . These calculations show the importance of all three variables: phase ratio, distribution ratio and number of extractions.

In summary, two-phase distribution equilibria are an important part of every analytical extraction, and the laboratory scientist must ensure that all critical variables are controlled in order to generate reliable results.

Other Principles

The preceding principles do not represent an exhaustive list. Certainly, there are other chemical principles that contribute to the extraction process, but play a more minor role. Some of these are discussed briefly below.

Time A longer extraction time will usually produce better recoveries, but this effect assumes that the

Table 2 Distribution ratios for extraction from water into hexane

Analyte	Added functional group	Functional group category	D (25°C)
Benzene			275
Toluene	-CH ₃	Nonplar	970
Chlorobenzene	-Cl	Nonpolar	950
Nitrobenzene	-NO ₂	Moderately polar	31.2
Aniline	-NH ₂	Polar	0.90
Phenol	-OH	Polar	0.13
Benzoic acid	-COOH	Very polar	0.051

Reproduced with permission from Sekine and Hasegawa (1977)

Table 4 Total per cent recovery as a function of β , D and number of extractions

Phase ratio $\beta = V_2/V_1$	D	After 1st extraction	After 2nd extraction	After 3rd extraction	After 4th extraction
1/1	1	50	75	88	94
	2	67	89	96	
	10	91	99		
	100	99			
1/4	1	20	36	49	59
	2	33	56	70	80
	10	71	92	98	99
	100	96	99		
1/10	1	9	17	25	32
	2	17	31	42	52
	10	50	75		
	100	91	99		

Reproduced with permission of ACCTA, Inc.

analytes, reagents and solvents are nonvolatile, stable and do not react with each other. If these assumptions are not valid, longer extraction times may actually produce poorer recoveries.

Ionic strength The addition of ionic species to an aqueous solution results in a 'salting-out' effect. This procedure often enhances extraction of neutral organic analytes from water by increasing D .

Surface area Reducing the particle size of a solid matrix, thereby increasing contact areas between phases, can cause a dramatic increase in extraction rates.

Stirring/mixing Adequate stirring enhances the rate of procedures that are otherwise limited by diffusion processes.

Analytical Extraction Techniques

This discussion will focus on the most popular traditional techniques, and provide an introduction to some of the newer extraction technologies. In each case, the principles involved will be considered together with some practical operating tips.

Liquid-Liquid Extraction Techniques

Separatory funnel techniques There are few limitations on what size or type of liquid samples can be extracted, except that the two liquid phases must be immiscible and unreactive with each other. Separatory funnels are available to handle samples from as small as a few millilitres to several litres. Extraction times vary from 1 to 15 min, depending on the specific requirements of the method, but equilibration is usually fast in all but the most viscous liquids. As noted in the section on principles of extraction, multiple extractions with a smaller volume of extracting solvent are preferred over a single extraction with a larger volume. The primary disadvantages of separatory funnels are the labour necessary, the need to evaporate an often large volume of solvent and the formation of emulsions.

The following practical points should be considered:

- **Funnel size:** to allow adequate mixing, the flask size should be chosen so that at least 25% of the funnel volume is free space.
- **Venting:** regular venting is a required safety procedure, especially at the start of the extraction process.
- **Draining layers:** too much time should not be

wasted draining off one layer, except after the final equilibration.

- **Shaking:** the most important variable is the time spent shaking the two layers, not the intensity of the shaking. Because of this, automated shakers provide adequate extraction, even though the intensity of mixing may be quite low.

Continuous liquid-liquid extractors These systems are usually reserved for larger water samples and/or situations where a long extraction time is required. There are two basic design types, depending on whether the extracting solvent is more dense (Figure 4) or less dense (Figure 5) than water. In each design, the solvent in the flask is heated to boiling, causing solvent vapours to collect in the condenser. The condensed solvent then passes through the sample in the main chamber.

The principles are the same as for separatory funnel extractions. However, each drop of solvent represents a separate two-phase distribution system with a small phase ratio but high surface area and fast extraction kinetics. Since each drop represents an equilibration step, the extraction consists of thousands of multiple extractions. The result is generally a high analyte

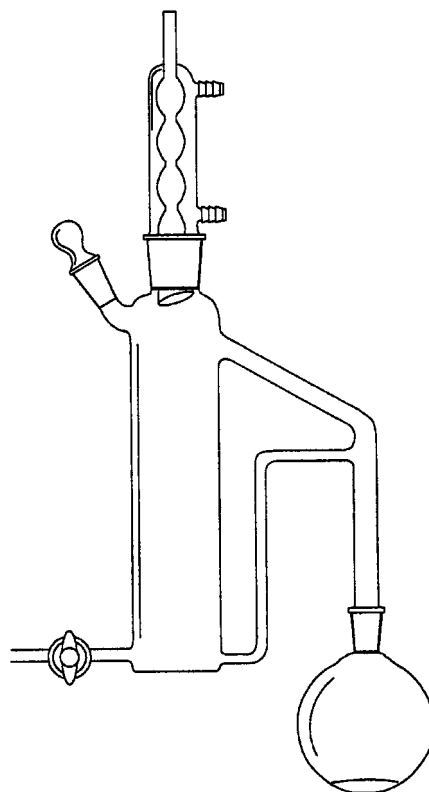


Figure 4 Continuous liquid-liquid extractor for use with extracting solvents that are denser than water. (Reproduced from Burford and Hawthorne (1994) *Journal of Chromatography A* 65: 75-94, with permission of ACCTA, Inc.)

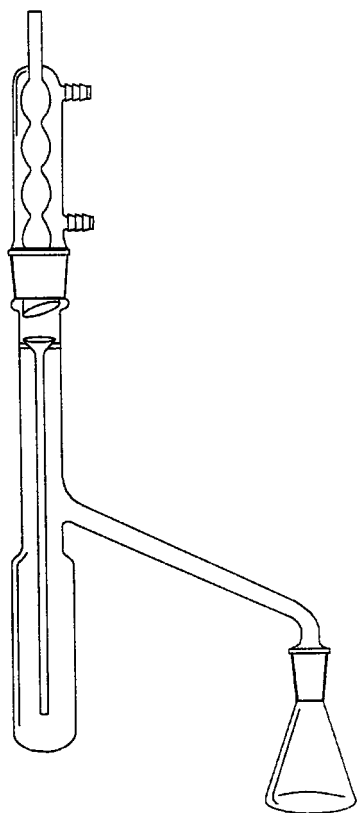


Figure 5 Continuous liquid-liquid extractor for use with extracting solvents that are less dense than water. (Reproduced with permission of ACCTA, Inc.)

recovery. The primary disadvantages are the set-up time, lengthy extraction time (6–24 h), and large quantities of solvent. The latter problem has been solved somewhat by integrated extraction systems that allow extraction, evaporation and concentration of solvent in one apparatus.

For continuous liquid-liquid extractors the following considerations are important:

- The extractor only works properly if the condensed solvent passes through the bulk of the sample, rather than along the sides of the flask.
- The reflux (boiling) rate determines the overall extraction rate, and some minimum rate must be maintained to ensure complete extraction.
- Emulsions can be a problem. See below for ways to deal with them.

Other liquid-liquid extraction devices While the chemistry and mechanics of liquid-liquid extraction have not changed, many practical variations have improved the speed and convenience of the technique. Two examples of these improvements are the Mixxor™ extractor (New Biology Systems Ltd, Haifa,

Israel) and the VectaSep CLE® system (Whatman, Inc., Clifton, NJ, USA).

The Mixxor™ system (Figure 6) consists of a receiver and piston assembly. The aqueous sample is placed in the receiver (B) with a small quantity of immiscible organic solvent (D). The sample is extracted by moving piston (A) up and down a number of times. After extraction, the plunger is moved to the bottom and the separated organic solvent is forced into the axial chamber (C), where it is easily removed. The entire extraction and separation process is completed in less than 5 min and can provide a concentration factor of 30 or more. Extractors are available for samples with volumes ranging from 2 to 50 mL. This system is more convenient than separatory funnels, although at the expense of some flexibility in sample and extraction solvent volumes. Also, the design precludes the use of heavier-than-water solvents.

The VectaSep CLE® system (Figure 7) is particularly useful for smaller samples. The extraction solvent is placed in the larger tube. The sample (1.5 mL) is added to the sample dispenser, which is then placed in the extraction tube and centrifuged, typically for 10 min at 3500 rpm. Centrifugal force pushes the sample through a dispersion membrane in the bottom of the sample dispenser, causing the sample to emerge as small droplets which travel along

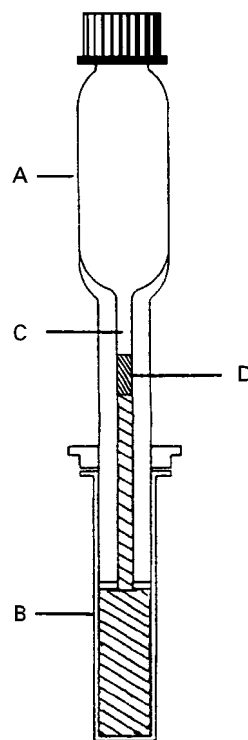


Figure 6 Mixxor™ extraction device. (A) Upper chamber; (B) sample reservoir; (C) axial chamber; (D) organic solvent. (Reproduced with permission of New Biology Systems Ltd.)

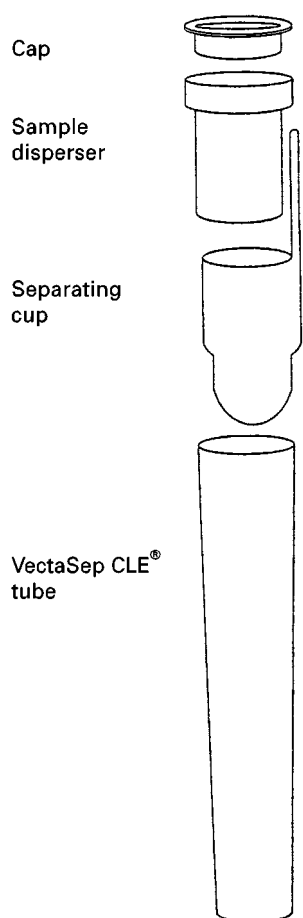


Figure 7 VectaSep CLE extraction system. (Reproduced with permission of Whatman, Inc.)

the inside of the tube to the bottom. After centrifugation, the sample dispenser is removed and the separating cup is added to locate the phase separation boundary. Evaporation of the upper organic layer then deposits extracted analytes in the separating cup, where they can be readily redissolved in an appropriate solvent. Although sample size and extraction solvent choices are somewhat limited, this system makes clever use of the extraction principles discussed earlier. In this case, the sample is passed through the extraction solvent (a reverse of the other methods) in small droplets, increasing surface area (kinetics) and offering a very favourable phase ratio.

These systems offer advantages in terms of sample handling, safety and efficiency considerations. So, despite their limitations, both of these systems, and others like them, merit consideration as a replacement for the more traditional techniques.

Emulsions No discussion of liquid–liquid extraction would be complete without mention of the emulsion problem. Emulsions are a mixture of two nor-

mally immiscible phases that won't separate in practice. This problem is often caused by the presence of surfactants or solids at the phase interface, high viscosity of one of the phases, or a small phase ratio (not enough organic phase). Although each emulsion is unique, one of the following remedies will often result in separation into two distinct layers:

- Wait: many emulsions will disappear with sufficient time.
- Gentle mechanical agitation/stirring with a glass rod or spatula.
- Immersion in an ultrasonic cleaning bath.
- Add 'a salt': this makes the aqueous phase less like the organic phase.
- Increase the phase ratio: add more organic phase.
- Pass through a bed packed with glass wool or diatomaceous earth.
- Centrifuge.
- Freeze the aqueous layer with dry ice/acetone or liquid nitrogen, then simply pour off the organic layer.

Liquid–Solid Extraction Techniques

Soxhlet techniques The Soxhlet extractor (Figure 8) is one of the oldest extraction systems available but is still very common. A solid sample is placed in an extraction thimble inside the middle chamber. Upon boiling, the solvent vapours from the bottom flask travel up to the condenser and then drip through the sample. The sample is soaked in solvent (a two-phase distribution equilibrium), which then returns to the flask when the liquid reaches the top of the siphon. The sample is exposed to fresh solvent after every siphon cycle, usually at a rate of about six cycles per hour. Typical extraction times are 6–24 h. Once assembled and operating, there is little that can go wrong with this system. However, operators must be aware of the following general hints:

- Proper cycling is required: the rate (cycles per hour) is usually specified in the method, and the operator must ensure that the unit siphons in distinct events rather than continuously draining.
- Solvent level in the thimble: if too high, sample may be lost from the thimble, contaminating the extract.
- Moisture content: dry samples work best; add a drying agent to remove free moisture.

The system requires a large volume of organic solvent, and extraction time is long. Despite these limitations, the Soxhlet extractor is still in widespread

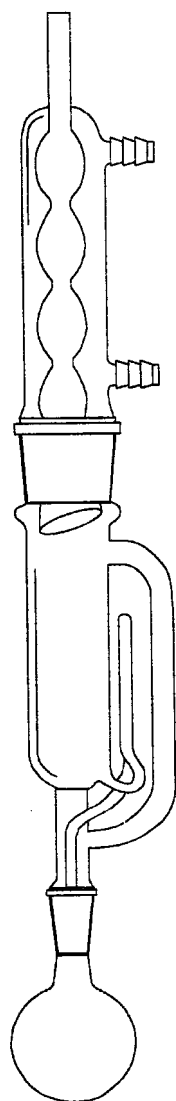


Figure 8 Soxhlet extractor. (Reproduced with permission of ACCTA, Inc.)

use, primarily because of its excellent reputation for providing complete extraction. Indeed, Soxhlet values are often used as the standard against which other extraction methodologies are compared.

Modified Soxhlet extractors The lengthy Soxhlet extraction times have prompted the development of modified extractors, such as the Soxtec[®] system (Foss Tecator AB, Höganäs, Sweden). The sample is placed in an extraction thimble, but the thimble is then directly immersed in boiling solvent, rather than bathed in cooler condensed solvent. The increased temperature means faster extraction kinetics. After about 1 h equilibration, the sample is removed from the solvent and flushed with fresh condensed solvent for an additional hour. The apparatus even allows

the evaporation and collection of solvent, further improving efficiency. These alternatives offer considerable advantages in terms of time and solvent use, and results are generally comparable to the traditional method.

Solid-phase extraction Solid-phase extraction (SPE) is an alternative to liquid-liquid extraction where the extraction solvent is replaced with a solid sorbent. The sorbent is usually packed into a cartridge (Figure 9) that can vary in size from about 1 mL to more than 50 mL. The quantity of sorbent can range from about 500 mg to 10 g. Extraction is accomplished by forcing the aqueous sample past the sorbent (via vacuum or pressure), causing analytes in the sample to be sorbed. This two-phase distribution is similar to the partitioning that occurs in chromatography. After the sample has passed through the sorbent bed, the sorbed analytes are eluted with a strong solvent, such as methanol, acetonitrile or carbon disulfide.

The SPE process involves the following sequential steps:

- Conditioning/cleaning of the sorbent with an organic solvent such as methanol
- Extraction of the sample.
- Air drying or rinsing to remove any remaining sample.
- Elution of analytes using a strong organic solvent.

SPE offers three primary advantages over conventional liquid-liquid extraction: reduced solvent usage, extraction speed and selective chemistry. In an ideal method, only a few millilitres of organic solvent may be necessary for an extraction and it is possible to extract and elute 10 100-mL samples or more in as little as 15–20 min. Finally, by varying the nature of the sorbent, it is possible to achieve selective extraction and/or selective elution. For example, a minor change in bonded phase from a C₁₈ phase to a C₈ phase can actually result in a significant change in selectivity. The shorter chain C₈ phase is less retentive towards more hydrophobic molecules and exposes somewhat more of the polar character from the underlying silica. This trend can be extended using even shorter aliphatic bonded phases or by adding a polar functional group to the chain (e.g. cyano- or phenyl-). There are no analogous series in liquid-liquid systems.

There are a host of sorbents available, including more polar functional groups, polymer-based, ion exchange, affinity and chelating materials. Nearly every liquid-liquid extraction method has an SPE counterpart, and almost all provide equal if not better

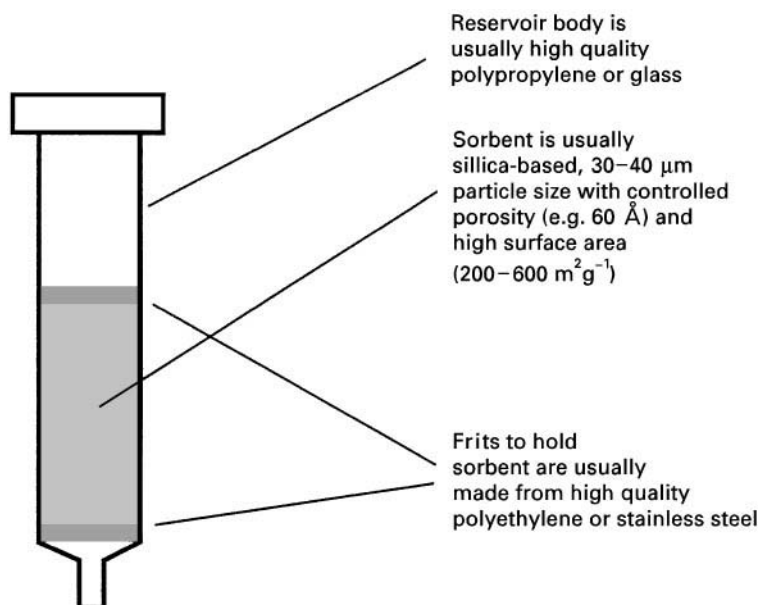


Figure 9 Solid-phase extraction (SPE) cartridge design. (Reproduced with permission of ACCTA, Inc.)

results, with considerably less effort. It should also be noted that SPE can be performed on nonaqueous samples using a polar sorbent, but this application is usually used for sample clean-up rather than extraction.

Finally, it is important to note SPE's limitations:

- High particulate samples will often plug the frits.
- Extracting capacity (total extractable mass) is more limited than with conventional solvent extraction.
- Reproducibility (batch-to-batch) can be a problem, although this is less of a concern now than during early development of the technique.

Membrane disc extraction Membrane extraction discs, first sold under the brand name Empore® (3M, St Paul, MN, USA), are an alternative SPE system. In the membrane discs the sorbent is enclosed in a support network rather than simply being packed into a cartridge. The unique Empore® design consists of 90% (w/w) sorbent particles (8–10 μm diameter), in a network of polytetrafluoroethylene fibrils, in a disc format that resembles a thicker version of conventional synthetic membrane filters. A typical disc is about 0.5 mm thick with diameters ranging from 1 to 90 cm.

A membrane disc extraction method would typically consist of the following steps:

- Pre-washing the disc with the final eluting solvent.
- Pre-wetting the disc with methanol or some other

solvent that is miscible with the sample (which is usually aqueous).

- Extraction, i.e. drawing the sample through the disc.
- Elution of analytes, which involves a soak with the elution solvent for a period of time, followed by elution with the aid of a vacuum. This elution step may be repeated with different solvents if necessary.

Membrane discs have the same advantages over liquid–liquid extraction as SPE but are superior to conventional SPE because the extraction rate is faster; flow rates of 100–200 mL min⁻¹ are typical. The small particles also provide greater capacity and uniformity of packing. Unfortunately, the discs are more sensitive to the presence of particulates, so a pre-filter is often necessary.

Early applications of membrane discs focused on environmental analysis, where large sample sizes made the fast extraction rates attractive. Membrane discs can also be formulated into SPE-like cartridges, allowing the efficient processing of small clinical samples (e.g. serum, urine, etc.). Use of membrane disc applications continues to grow, although the number of reported applications is not as high as SPE, due to the relative age of the two techniques.

Solid-phase microextraction Solid-phase microextraction (SPME) is another version of liquid–solid extraction techniques. In this system, the extraction

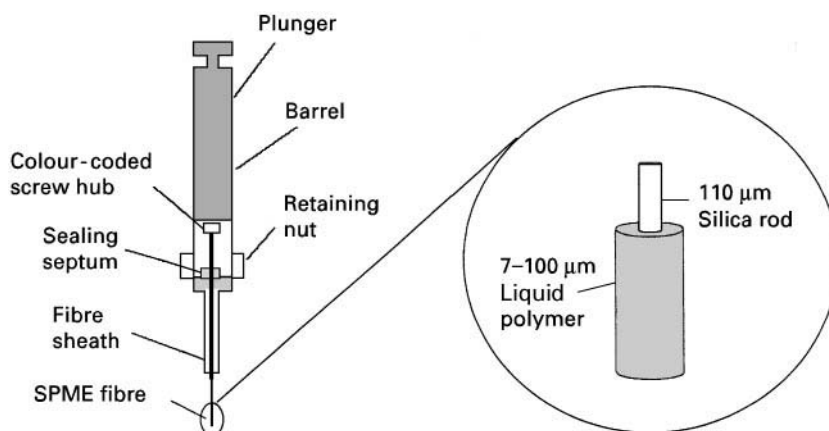


Figure 10 Solid-phase microextraction system. (Reproduced with permission of ACCTA, Inc.)

phase consists of a fused silica fibre coated with a sorbent (e.g. dimethylsilicone or other immobilized polymer) with thicknesses ranging from about 10 to 100 μm (Figure 10). The fibre is placed in contact with the liquid or gas sample and analytes are sorbed on to the phase, from which they are directly desorbed into a chromatograph.

Unlike the other techniques discussed here, SPME is a completely solvent-free extraction method. The extraction step tends to be rapid, usually requiring 10–20 min, and desorption can take only a few seconds. Thus, a fast analysis with a good lower limit of detection is possible, since the entire extract is analysed. Furthermore, the selectivity and extractability can be affected by changes in fibre chemistry as well as solution pH, ionic strength, etc. Sampling by immersion in the sample or extraction from the headspace above the liquid (often a faster extraction) provides additional flexibility. However, SPME, by its nature, is not applicable to as wide a range of samples as other techniques, and there are currently a more limited number of sorbents available compared to SPE. However, SPME offers some unique advantages that make it an attractive alternative for many applications.

Pressurized Fluid Extraction

So far, each extraction medium discussed has been either a conventional liquid or solid, each performing its function at or near room pressure and at or below the boiling point of the liquid phase. Experimentally, these conditions are easiest to attain in the laboratory and require relatively unsophisticated equipment. Unfortunately, in some cases these conditions can also result in slow extraction kinetics and/or incomplete extraction because of the (relatively) mild conditions employed. Such problems can often be solved

simply by maintaining the extraction fluid at a higher pressure so that higher temperatures can be used. This can result in a dramatic improvement in extraction efficiency. In addition to the pressurization of conventional solvents in a closed vessel, supercritical fluids may also be used at high temperature and pressure.

Accelerated liquid extraction As noted earlier, increased temperature improves solubility and extraction kinetics, and increases the vapour pressure. In addition, an increase in applied pressure causes an increase in the boiling point of a liquid. Logically, then, one would expect improvement in extraction results at higher applied pressure, where the increased boiling point would then allow liquid extractions above the normal boiling point of the solvent. This approach has been successfully applied in two different ways.

In the first method, called microwave-assisted solvent extraction (MASE), the sample and extraction solvent are placed in a sealed vessel, usually constructed of polytetrafluoroethylene or other inert polymer. When placed in a microwave field, polar materials (e.g. water) absorb energy and the sample heats up. Since the vessel is closed, the pressure also increases, resulting in a significantly elevated boiling point. For example, hexane–acetone mixtures can be used at 115°C, which is more than 40°C above the boiling point of either solvent. The increased temperature has several beneficial effects on the extraction, such as increased solubility, faster diffusion, reduced viscosity and reduced surface tension (increased wettability).

This approach is also used for sample digestion in inorganic analysis, and succeeds for the same reasons – temperature-related improvements in reaction rates.

The second approach uses conventional electrical conduction heating in a sealed stainless steel vessel (Dionex Corporation, Salt Lake City, UT, USA) to accomplish the same effect. With this equipment, the pressure and temperature can be set independently, whereas in the MASE process the pressure increase results from the temperature increase.

Both methods allow Soxhlet-type extractions to be completed in 30 min or less and require small solvent volumes. This approach has received widespread acceptance because it draws from existing experience with organic extraction solvents. The basic chemistry of the extraction does not change significantly, only the rate. In theory, then, any liquid solvent-based extraction method could be adapted for accelerated liquid extraction.

The primary disadvantages involve the safety aspects associated with the use of organic solvents at high temperatures and pressures. In addition, the same process that enhances analyte extraction may also cause extraction of other unwanted components from the matrix. However, the reductions in solvent use and extraction time make accelerated liquid extraction an attractive alternative to unpressurized techniques.

Supercritical fluid extraction As the temperature and pressure on a compound are raised, a point is reached, called the critical point, where the substance is no longer a gas or liquid, but has properties intermediate between these two states. Supercritical fluids are good solvents with gas-like viscosities and diffusivities and no surface tension.

Carbon dioxide is the most popular choice for a supercritical fluid, because of its relatively low critical point (31°C, 73 atm). Supercritical fluid extraction (SFE) then involves placing the sample in a high pressure vessel and contacting the sample with the supercritical fluid. Extraction temperature can be varied from about 40°C to more than 150°C while pressures may be adjusted between 100 and as high as 680 atm or more. Since carbon dioxide is actually a nonpolar fluid, 10–20% of polar modifiers such as methanol can be added to improve the range of solubilities. A typical extraction will be complete in less than 20 min.

SFE receives much attention because the extractions are fast and, with carbon dioxide as the extraction fluid, evaporation of the extracting medium is spontaneous upon decompression to atmospheric conditions. The ability to control extracting power, through changes in temperature, pressure and modi-

fier, offers more selectivity and flexibility than with liquid solvents. While SFE is not a universal replacement for liquid solvent-based methods, it is clearly the best choice for many specific applications, especially foods, natural products, polymers and environmental samples.

Final Comments

Analytical extraction (and sample preparation in general) has returned to its rightful place as an equally important part of the analytical method. There are many options available to achieve extraction, depending on the type and size of sample as well as other more practical considerations. The laboratory worker can choose from 100-year-old techniques that still provide excellent results, or instrumental-based technologies that offer faster extractions on smaller samples.

The extraction step, as a distinct part of the analytical method, will retain its importance as long as chromatographic procedures are used for quantification. The objective of moving the analytes from the sample to the point of quantification will still be required. Future research is likely to focus on better ways of accomplishing this movement, resulting in reduced solvent usage and sample size, automation and online transfer of extracts to subsequent processing and quantification steps. But throughout these changes, it will be important to remember that, although the names may change, the chemistry will remain the same.

Further Reading

- Freiser H (1973) Solvent extraction. In: Karger BL, Snyder LR and Horvath C (eds). *An Introduction to Separation Science*, Ch. 9. New York: Wiley-Interscience.
- Lopez-Avila V, Young R and Teplitsky N (1996) Microwave-assisted extraction as an alternative to Soxhlet, sonication, and supercritical fluid extraction. *Journal of the Association of Official Analytical Chemists International* 79: 142–156.
- Peleg I and Vromen S (1983) An efficient novel device for solvent extraction. *Chemistry and Industry* 61: 615–616.
- Sekine Y and Hasegawa Y (1977) *Solvent Extraction Chemistry*, p. 105. New York: Marcel Dekker.
- Weast RC (ed.) (1971) *Handbook of Chemistry and Physics*, p. C-743, D-151. Cleveland, OH: Chemical Rubber Co.
- Zhang Z, Yang MJ and Pawliszyn J (1994) Solid phase micro-extraction. *Analytical Chemistry* 66(17): 844A–853A.

Analytical Inorganic Extractions

K. A. Anderson, Oregon State University, Corvallis, OR, USA

Copyright © 2000 Academic Press

Historical Development

Trace elemental analysis is under constant development and the challenging analyses of today become the routine of tomorrow. Despite recent and rapid advances in analytical instrumentation, it is still necessary in many applications to use separation and preconcentration techniques prior to the analytical determination. Typically, the reason for performing a separation and/or preconcentration step is to bring the concentration of the trace element to a detectable level and/or separate it from interfering substances in the sample matrix. Separation and preconcentration are therefore a frequent component of an analytical scheme. Inorganic solvent extractions are also used extensively in industrial applications. Moreover a rapidly developing field, elemental speciation, will depend in part on sophisticated separation techniques such as liquid-liquid inorganic extractions.

Inorganic solvent extractions have been known and performed since the nineteenth century. The extraction of uranyl nitrate into diethyl ether was reported in the 1840s, but it was some time later before quantitative understanding of the inorganic liquid-liquid extraction distribution equilibria was forthcoming. Nernst presented the thermodynamical explanation of the distribution in the 1890s. Chelate extraction was also developing at this time, most notable was the use of 1,5-diphenylcarbohydrazide which chelated with chromium. The work of Fisher in the 1920s with dithizonates is noteworthy; this group studied the distribution of the elements as a function of reagent concentration, metal, complexing agents and pH. During this time, a wide array of solvent extraction methods was developed.

Rapid and distinguished progress in inorganic extractions occurred during World War II, most as part of the 'Manhattan Project' research in atomic energy. One of the most significant applications of liquid-liquid extraction in inorganic chemical technology was the separation of uranium and plutonium from nuclear reaction fission products in the late 1940s. Later, inorganic extractions replaced ion exchange at the beginning of the nuclear fuel cycle for separating uranium from other leach liquors.

Hydrometallurgical applications of liquid-liquid inorganic extractions are numerous and remain the contemporary choice of separation for many processes today. In addition, as environmental regulations develop, increased interest in recovery methods for metals from a variety of waste streams will no doubt renew interest in metal separation techniques.

The prevailing industrial use of inorganic solvent extraction includes the separation of the lanthanide (III) ions. Individual lanthanides are widely used in many of today's 'high-technology' applications for example, lasers (neodymium in yttrium-aluminum garnet), superconducting materials, specialty ceramics, catalyst, the nuclear industry and colour video phosphors.

Inorganic Processes

Solvent extraction, ion exchange, volatilization and precipitation are the most commonly used separation approaches for trace elemental analysis. Inorganic preparation schemes generally follow a flow diagram, as shown in Figure 1.

The processes by which extraction of inorganic compounds occur using organic solvents are varied and may be relatively involved. Consequently, attempts to classify inorganic extraction processes are difficult. Attempts have been made, based on the identity of the extracted compound, or of the extracting agent, or pH of the extraction solution. For the purposes of this chapter, a simple subdivision will be adopted based on the extraction reagent used.

Extraction Considerations

The need for separation and/or preconcentration in trace metal analyses are fundamentally related to available instrumentation and instrumental

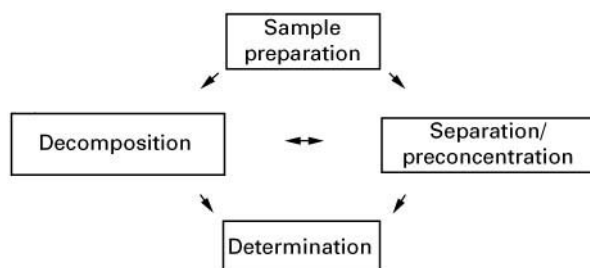


Figure 1 Inorganic preparation flow diagram.

Table 1 Comparison of a select list of analytical techniques^a

Comparison	ASV	Flame AAS	ET-AAS	ICP-AES	NAA	ICP-MS
General detection limits	0.1–0.01 mg L ⁻¹ (ppb)	1–5000 mg L ⁻¹ (ppb)	0.1–0.001 mg L ⁻¹ (ppb)	1–100 mg L ⁻¹ (ppb)	1–1000 mg L ⁻¹ (ppb)	0.01–1 mg L ⁻¹ (ppb)
General sensitivity	Excellent, select elements	Moderate, refractories poor	Excellent, refractories limited	Moderate, refractories excellent	Moderate	Excellent
Instrument maturity	Well established	Well established	Well established	Established and growing	Established	New and growing
Interferences	Some	Few, well understood	Many, controllable	Spectral	Few	Moderate, mass overlap
Instrument availability	Readily	Readily	Readily	Readily	Specialized laboratory	Specialized laboratory
Instrument-specific inorganic extraction	Developed	Numerous, well developed	Well developed	Developed	Well developed	Undeveloped

^aAbbreviations: ASV, anodic stripping voltametry; Flame AAS, flame atomic absorption spectrometry; ET-AAS electrothermal atomic absorption spectrometry; ICP-AES, inductively coupled plasma atomic emission spectrometry; NAA, neutron activation analysis; ICP-MS: inductively coupled plasma mass spectrometry.

capabilities. Basically, separation and/or preconcentration are needed when one of the following situations occurs: concentration of analyte is below the sensitivity of the instrumental method; interferences exist in the sample (relative to the instrument to be used); or physical or chemical states of the sample are not appropriate for the instrument. Sensitivities for elements varies with the instrumental method and are relative to matrix type; however, a general listing of sensitivities of commonly used analytical equipment is given in **Table 1**.

The impetus for doing an extraction will therefore depend on the availability of instruments and the capability of the instrument relative to the matrix type (i.e. interferences). Inorganic extraction schemes are typically instrument specific. Although instrument development has significantly reduced detection limits, availability of some of the more state-of-the-art equipment is still limited to specialized or well-equipped laboratories. The need for separation and preconcentration therefore still exist. Speciation studies will also continue to support development and research into inorganic separations from complex matrices.

Because atomic absorption spectrometry (AAS) is readily available, but the detection limits are high in relation to today's needs, there are numerous solvent extraction methods available for metals in AAS analysis. Several excellent sources are listed in Further Reading; these have lengthy tables of inorganic extraction schemes.

Theory and Equations of Inorganic Solvent Extraction

The solvent extraction process to separate and/or preconcentrate an analyte of interest is performed by using two immiscible solvents. A complex (typically neutral in charge) is formed with the element of interest, typically in an aqueous solution and will partition into a mutually insoluble (organic solvent) phase. The Nernst partition (or distribution law) states that at equilibrium a given solute will be distributed between two essentially immiscible liquids according to the following equation:

$$K_D = \gamma_o[A]_o / \gamma_{aq}[A]_{aq}$$

where K_D is the distribution coefficient (also called the partition coefficient) and $[A]$ is the concentration of the analyte, γ are activity coefficients, subscript 'o' denotes organic phase and the 'aq' subscript denotes aqueous phase. The above equation holds true in only the most rigorously well-defined thermodynamic systems. For simplicity the relationship assumes that no side reactions occur in either the aqueous or organic phase and that no stable intermediates are formed with the analyte (e.g. metal) of interest. From a practitioner's standpoint, the total amount of analyte (e.g. metal) transferred from one phase to the other is of most interest. An empirical distribution ratio, D , is defined by the simplified relationship given below:

$$D = [A_T]_o / [A_T]_{aq}$$

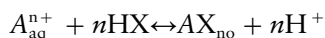
where $[A_T]_o$ includes all (T = total) complexes of the analyte of interest in the organic phase and activity coefficients are assumed unity. The assumption of $\gamma = 1$ for chelating extractions is reasonable. However, for ion-pair extractions where the electrolyte concentration is high, to assume unity for the activity coefficients is a poor assumption. The simplifying relationship is still often employed, however, with the assumption that the (γ_o/γ_{aq}) ratio will remain constant.

The extraction efficiency, $\%E$, which defines the amount of analyte transferred from the aqueous phase to the organic phase, is defined as follows:

$$\% \text{ Extraction} = 100D / \{D + (V_{aq}/V_o)\}$$

where V_{aq} is the volume of the aqueous phase and V_o is the volume of the organic phase. An important property of the above relationship is that the extraction efficiency is independent of the initial analyte concentration. High extraction efficiencies can be achieved when the V_{aq}/V_o ratio is small (that is, small aqueous volumes used with large organic volumes). There is of course a practical limit to this approach. Multiple extractions with reasonable volumes perform better than a single extraction with one large volume. Large values of D , distribution ratio, correspond to high extraction efficiencies (e.g. $D = 100$ then $\%E = 99\%$, $D = 0.1$ then $\%E = 10\%$, for a 1 : 1 volume ratio).

An extraction reaction may be described by the general chemical equation given below:



where A is the analyte of interest (e.g. metal ion) with charge n^+ , HX is the extracting agent (e.g. chelating agent). Note, that extracting agents are often acidic. From the following extraction reaction the equilibrium constant, K_{ex} is:

$$K_{ex} = [AX_n]_o [H^+]^n / [A^n]_{aq} [HX]^n_o$$

By substituting the distribution ratio, D , the equation simplifies to:

$$K_{ex} = D \{ [H^+]^n / [HX]^n_o \}$$

hence:

$$D = K_{ex} [HX]^n_o / [H^+]^n$$

The logarithmic form for the distribution coefficient is then:

$$\log D = \log K_{ex} + npH + n \log [HX]_o$$

From this model, for a given system, the degree of extraction increases as the concentration of the chelate $[HX]_o$ increases. Extraction increases with increasing pH (decreasing hydrogen concentration) in the aqueous phase. A one unit increase in pH results in a factor of 10 increase in the distribution coefficient for $n = 1$; for $n = 2$, the distribution coefficient increases by a factor of 100. Hydrolysis of the metal ion and decreased solubility of the chelate occur at high pH limiting this general approach.

Plots of $\log D$ versus pH (or $\%E$ versus pH or versus $pH_{1/2}$) are often used to define extraction systems. These types of plots produce sigmoidal curves, with the overall position relative to the pH axis dependent on K_{ex} with the slope $= n$. For purposes of comparison, if $D = 1$ (i.e. $E = 50\%$) and $[HX]_o = 1$, the pH is constant and equal to $\log K_{ex}/n$. This term is referred to as $pH_{1/2}$, and is characteristic of the extraction process. Analyte/chelate agent values of $pH_{1/2}$ are often cited and are used as a measure of the feasibility of separating two analytes.

Further theoretical discussion is beyond the scope of this chapter but includes topics on solvent properties, such as the solvent Hildebrand parameter, solvent dielectric constant, and complex properties such as the complex size, polarity and polarizability, as well as pH, temperature and reaction kinetics.

Inorganic Solvent Extractions

The essential prerequisite for an element to be extracted from an aqueous solution is that it be part of a neutral complex. Charge neutrality reduces the electrostatic interactions between the element (analyte of interest) complex and water and therefore lowers the solubility of the complex in water. Consequently, the neutral complex can be extracted into the less polar organic solvent. General attributes and chemical properties that can facilitate separation are: charge neutrality, increase size of complex formed and incorporation of hydrophobic or organophilic properties. These general attributes can be accomplished by several mechanisms including the element associated with naturally occurring complexants, chelate complexes formed with analyte and ion-associated (ion-paired) complexes. All three mechanisms can and will form a neutral complex with the analyte of interest. Depending on the ligands (complex associated with the element) other chemical properties such as complex size and hydrophobic/organophilic properties can be incorporated.

Extraction Schemes

Classification schemes are numerous and no one scheme covers all systems. The most common

schemes are based on the form of the extracted element that transfers into the organic phase. This simplified classification scheme is adequate for the discussion here. However, even with simple schemes the categories are not exclusive, and some extraction agents could be classified into other categories. The experimental process of inorganic extraction of a neutral complex, regardless of the type of complex, is essentially the same. The neutral complex's interaction with the aqueous phase, including but not limited to the solubility, depends on the charge and polarity of the overall complex. The first step is to generate a neutral complex with the analyte of interest through one of the mechanisms listed above. A small volume of organic solvent is added to the sample mixture. For example, a 1 L aqueous sample may be extracted into 40 mL of organic solvent. Extraction can be performed in a separatory funnel or by using a mechanical shaker table. The pH of the mixture may need to be manipulated, depending on the exact extraction scheme used. In addition, masking agents may be used to obtain specificity (see below). After mixing, the two phases are separated and the procedure is generally repeated several times. The organic phase is combined from each extraction. The concentration of the elements in the sample is increased by 1–3 orders of magnitude in the organic phase. The extract can then be further pre-concentrated if needed (back-extraction, evaporation, etc.) or analysed directly, for example by flame AAS.

Naturally occurring complexants Elements that can form neutral complexes can already exist in naturally occurring water systems. These complexes are formed essentially with covalent bonding between the element and naturally occurring ligand(s). Ligands are molecules or ions bonded to a central metal ion and tend to be Lewis bases; also included in this category would be undissociated covalent species. Examples of this category would include I_2 and B_2 , the halides of some metals ($GeCl_4$, $HgCl_2$, $AsCl_3$) and oxides of some metals (OsO_4). The extraction of these types of compounds would proceed in the same manner as for chelates and ion-associated complexes.

Chelates A chelate is a type of ligand. A multidentate (*dentate* is Latin for tooth) ligand that uses more than one atom to bind to a metal in a coordination complex, see Figure 2. The metal is the electron-pair acceptor and the chelating agent the electron-pair donor. When binding to the metal ion, the chelate (ligand) forms a ring of atoms, of which the metal is one member. The chelate complex charge exactly neutralizes the charge on the metal ion. Most rings contain > 4 and < 8 atom members; the most stable

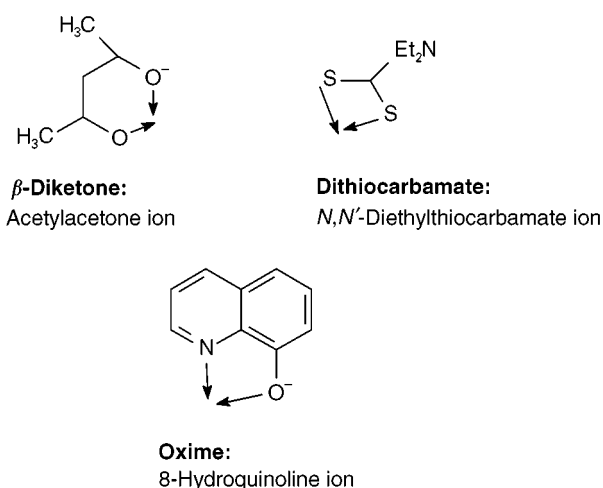


Figure 2 Chemical structures of typical chelate-metal complexes.

typically is a 5-membered ring. Bidendate describes a chelate where two atoms from the chelate complex bond to the metal and tridentate would indicate three coordinating atoms. Many chelating extractants are weak acids, therefore, control of pH is important in many extracting schemes.

An exhaustive treatment of every chelate system is beyond the scope of this chapter. Table 2 lists a selection of chelate types with one or two specific chelate agents listed below these. To describe the selectivity of each is not possible in a brief chapter, a sense of the ability of each chelate reagent is given by listing the wide range of complex-forming metals that are possible. Detailed information about the selectivity, solvent and other experimental conditions can be found in the references listed in Further Reading. The list in Table 2 include inorganic extraction procedures for a wide array of instrumental methods including: flame AAS, electrothermal (ET)-AAS, inductively coupled plasma-atomic emission spectroscopy, (ICP-AES), neutron activation analysis (NAA), spectrophotometric, chromatographic, flame photometry, and polarography. In addition, most of the chelate groups listed in Table 2 are compatible with more than one organic solvent. Solvent flexibility in an analytical scheme allows an extended range of instrumental methods which can be used for the determination.

Inorganic extraction, utilizing chelates, for analytical separation and/or preconcentration has been exploited for many instrumental systems. For flame AAS analysis, often the inorganic solvent extraction is designed to increase the concentration of elements of interest and, most importantly, reduce the concentration of alkali and alkaline earth elements (i.e. leave most of them in the aqueous phase). This separation

Table 2 A select list of inorganic extraction systems

	<i>Metals extracted</i>
<i>Chelating agents</i>	
<i>Oxines</i>	
-8-Hydroxyquinoline -(and derivatives)	> 50 metals
<i>α-Dioximes</i>	
-Dimethylglyoxime	Ni, Pd, Co
<i>Dithizones</i>	
-Diphenyldithiocarbazone	> 30 metals
<i>Dithiocarbamates</i>	
-sodium diethyldithiocarbamate	> 50 metals
-Sodium <i>N,N'</i> -phenylacetyldithiocarbamate	> 50 metals
<i>β-Diketones</i>	
-Acetylacetone	> 50 metals
-Thenoyltrifluoroacetone	> 50 metals
<i>Nitrosoarylhydroxylamines</i>	
-Ammonium <i>N</i> -Nitroso- <i>N</i> -phenylthiohydroxylamine (cupferron)	> 30 metals
<i>Organophosphorus acids</i>	
-di- <i>n</i> -butylphosphoric acid	> 30 metals
-Di(2-ethylhexyl)phosphoric acid	> 30 metals
1-Nitroso-2-naphthol	Co(II)
1-(2-Pyridylzao)-2-naphthol (PAN)	> 50 metals
<i>Ion-pair agents</i>	
<i>Chelated ion-pairs</i>	
-ethylenediaminetetraacetic acid (EDTA)/halide	> 30 metals
-1,10-phenanthroline/perchlorate	Fe (II)
<i>Non-chelated ion-pairs</i>	
-tetraalkylammonium salts	> 50 metals
-tetraphenylarsonium salts	> 50 metals
<i>Halide ion pairs</i>	
-HCl	> 50 metals
-HF	> 50 metals
-HI	> 50 metals

is especially necessary for many natural water samples such as seawater, brines, etc. Trace element analyses of clinical samples such as blood, urine, etc., also benefit from inorganic extraction for flame AAS analysis as well as other determination techniques (ET-AAS, ICP-AES, etc.). Radiochemistry separations for NAA also often use inorganic extraction techniques that utilize chelating schemes.

Extraction schemes have also been developed which leave the analyte of interest in the aqueous phase and remove interferences through the organic phase. This technique has limited applicability owing to the limited solubility of the (starting reagent) chelate in organic solvents.

Ion association (ion pair) Neutral complexes can be formed through ion association (ion-pair) and extracted from an aqueous solution into an organic solvent. Ion association inorganic extracts encompass a wide range of extraction schemes. General sub-groupings include chelated ion pairs, nonchelated ion pairs and halide-cation ion-pairs. The halide-cation pairs are typically extracted into oxygen-containing solvents, such as methyl isobutyl ketone, diethyl ether and alcohols. A select list of ion pair extracting agents is given in Table 2.

Maximizing the coulombic forces of attraction between the ion pairs facilitates extraction of the ion pairs. The dielectric constant of the solvent is a large contributor to the overall extractability of a scheme. Enhancement of the extraction of ion-associated complexes is increased by the addition of electrolytes, called 'salting-out'. The salting-out effect may be attributed to the increase in anion concentration, as well as the decrease of the dielectric constant of the aqueous phase. Complexes can be formed by ligands coordinated to the metal and an appropriate counter anion that neutralizes the total charge. One of the ions (either the complexed ligand or the anion) typically contains a large hydrophobic group(s) which further enhances extraction of the ion pair into the organic phase.

Factors Affecting Inorganic Solvent Extractions

Control of pH is critical to ensure conditions are favourable for the formation of the desired complexes. The extraction specificity needed influences the acceptable range of pH. Many inorganic extraction schemes use buffers. The lack of a buffer in an inorganic extraction should be viewed with suspicion, since the quantity of metal extracted is strongly pH dependent. In addition, chelating agents will alter the pH of the solution. Several buffers have been used for inorganic extractions for AAS determination, including borate, phosphate, citrate, acetate and formate. Acetate should not be used if lead or silver or other stable metal acetates are to be determined. Buffers can be a significant source of contamination, as can any unpurified reagent added to a sample.

The nature of the solvent is of special importance for inorganic extractions. There are several criteria which should be evaluated when choosing a solvent for an inorganic extraction. The solvent should have the following characteristics:

- Extracts the desired metal chelates
- Immiscible with aqueous solution (i.e. low solubility in water); for convenience, density > water if the sample is drawn off
- Does not form emulsions

- Compatible with the analytical determination technique
- Environmentally safe and nontoxic
- Available in an acceptably uncontaminated state.

In the case of flame AAS, ketones or esters are commonly used extraction solvents. The list of organic solvents used in inorganic extractions is extensive.

Masking Agents

When the desired specificity for separation cannot be controlled sufficiently by pH modification, addition of a masking agent will frequently be used. Masking agents are complexing agents that form water-soluble complexes which then compete with the extracting agent. The masking agents prevent the extraction of the metals they react with, by forming water-soluble complexes (strong polar complexes) which remain in the aqueous phase. Some extracting agents are specific and many others can be made specific using pH control and/or a masking agent. The most commonly used masking agents include cyanide, thiocyanate, thiosulfate, tartrate, carbonate, citrate, fluoride, bromide, iodide and ethylenediaminetetraacetic acid (EDTA). The effectiveness of masking agents is pH specific, ranging from acidic to basic conditions. In some schemes, more than one masking agent may be used.

Applications

Inorganic extractions are used in both analytical and industrial fields. Chelates form an important part of inorganic extractions and have extensive application in many areas of science and industry.

As discussed above, analytical applications include the separation and/or preconcentration of an analyte for determination. Another analytical application is the use of inorganic extraction techniques for reagent purification by removing trace metals (e.g. purification of aqueous buffers). Extraction of metals into nonpolar organic phases crosses many scientific disciplines. For example, crown ethers are used extensively as phase transfer catalysts. Crown ethers extract an element (e.g. K^+) from the aqueous phase into an organic phase. The K^+ ion is engulfed (chelated) in the centre of the crown ether. A class of antibiotics, the ionophores (e.g. nonactin, valinomycin, gramicidin, etc.) work much like crown ethers: they alter the permeability (distribution) of bacterial cells to metal ions and thereby disrupt their metabolism.

An example of a large-scale inorganic metallurgical extraction, is the Purex process used to extract ura-

nium isotopes and plutonium. Once the uranium ore (e.g. carnotite) is crushed, it is concentrated by physical means; the uranium is then further concentrated by flotation methods. The ore is then roasted and leached with sulfuric acid (often with an oxidizing agent) and precipitates as sodium diuranate, a bright yellow solid called 'yellowcake'. This solid dissolves in nitric acid producing uranyl nitrate. The inorganic solvent extraction (Purex process) extracts the uranyl nitrate from the aqueous solution into tributyl phosphate in an inert hydrocarbon diluent: the impurities remain in the aqueous phase.

The aim of speciation studies is to identify and quantify all species that together combine to comprise the total element concentration. This is typically achieved by physicochemical techniques. A range of physicochemical separation techniques has been applied to speciation studies, including inorganic solvent extraction.

Inorganic chelate extractions are used extensively in industrial applications. A brief listing includes the following applications:

- Metallurgical extraction
- The chelate: (EDTA)
 - used in water softeners
 - boiler scale removal
 - industrial cleaning
 - soil metal micronutrient transport
 - food preservation
- The chelate: nitrilotriacetic acid (NTA)
 - similar applications to those listed for EDTA
- Ion exchange resins can be chelates
 - water purification processes
- Zeolites are a type of chelating ion exchange resin
 - water purification processes

Future Developments

Although instrument development has had a significant impact on inorganic extractions and the direction of research on separation and preconcentration techniques, there remains an extensive need and interest in inorganic solvent extraction techniques. One area which is currently under intense investigation is speciation. Chemical-physical methods of separation incorporating inorganic extractions remain an important part of this field. Another area of development is the recovery and removal of metals from industrial waste streams.

See also: II/Chromatography: Liquid: Ion Pair Liquid Chromatography. Ion Exchange: Theory of Ion Exchange. III/Ion Analysis: Liquid Chromatography.

Further Reading

- Batley GE (1989) *Trace Element Speciation: Analytical Methods and Problems*. Boca Raton: CRC Press.
- Howard AG and Statham PJ (1993) *Inorganic Trace Analysis Philosophy and Practice*. New York: John Wiley and Sons, Inc.
- Minczewski J, Chwastowska J and Dybczynski R (1982) *Separation and Preconcentration Methods in Inorganic Trace Analysis*. New York: John Wiley and Sons Inc.
- Mizuike A (1983) *Enrichment Techniques for Inorganic Trace Analysis*. New York: Springer-Verlag.
- Ruthven DM (ed) (1997) *Encyclopedia of Separation Technology*. New York: John Wiley and Sons Inc.
- Swaddle TW (1990) *Applied Inorganic Chemistry*. Calgary: University of Calgary Press.
- Tatsuya S and Yuko H (1977) *Solvent Extraction Chemistry: Fundamentals and Applications*. New York: Marcel Dekker, Inc.
- Vandecasteele C and Block CB (1993) *Modern Methods for Trace Element Determination*. New York: John Wiley and Sons Inc.
- VanLoon JC (1985) *Selected Methods of Trace Metal Analysis*. New York: John Wiley and Sons, Inc.
- Zolotov YA (1970) *Extraction of Chelate Compounds*. Ann Arbor: Humphrey Science Publishers.

Extraction With Supercritical Fluid

See II/ EXTRACTION / Supercritical Fluid Extraction

Inorganic Extractions

See II/ EXTRACTION / Analytical Inorganic Extractions

Microwave-Assisted Extraction

V. Lopez-Avila, Midwest Research Institute,
Cupertino, CA, USA

Copyright © 2000 Academic Press

Introduction

Common extraction techniques for solid matrices include Soxhlet extraction, sonication extraction, supercritical fluid extraction (SFE), microwave-assisted extraction (MAE), and accelerated-solvent extraction (ASE).

Soxhlet extraction allows use of large amount of sample (e.g. 10–30 g), no filtration is required after the extraction, the technique is not matrix dependent, and many Soxhlet extractors can be set up to perform in unattended operation. The most significant drawbacks of Soxhlet extraction are: long extraction times (e.g. up to 24–48 h), large amount of solvent usage (300–500 mL per sample), and the need for evaporation after sample extraction.

Sonication extraction is faster than Soxhlet extraction (30–60 min per sample) and allows extraction of

large amount of sample with a relatively low cost, but it still uses about as much solvent as Soxhlet extraction, is labour intensive, and filtration is required after extraction.

The newer extraction techniques such as SFE, MAE, and ASE are very attractive because they are a lot faster, use much smaller amounts of solvents, and are environmentally friendly techniques. For example, SFE uses carbon dioxide or modified carbon dioxide (e.g., carbon dioxide containing a small amount of an organic solvent known as modifier) for extraction. Carbon dioxide is a nontoxic, nonflammable, and environmentally friendly solvent. Furthermore, the extraction selectivity can be controlled by varying the pressure and temperature of the supercritical fluid and by the addition of modifiers.

MAE uses microwaves that can easily penetrate into the sample pores causing the solvent trapped in the pores to heat evenly and rapidly. In contrast to conventional heating where it takes a long time for the vessel to heat and then transfer its energy to the

Further Reading

- Batley GE (1989) *Trace Element Speciation: Analytical Methods and Problems*. Boca Raton: CRC Press.
- Howard AG and Statham PJ (1993) *Inorganic Trace Analysis Philosophy and Practice*. New York: John Wiley and Sons, Inc.
- Minczewski J, Chwastowska J and Dybczynski R (1982) *Separation and Preconcentration Methods in Inorganic Trace Analysis*. New York: John Wiley and Sons Inc.
- Mizuike A (1983) *Enrichment Techniques for Inorganic Trace Analysis*. New York: Springer-Verlag.
- Ruthven DM (ed) (1997) *Encyclopedia of Separation Technology*. New York: John Wiley and Sons Inc.
- Swaddle TW (1990) *Applied Inorganic Chemistry*. Calgary: University of Calgary Press.
- Tatsuya S and Yuko H (1977) *Solvent Extraction Chemistry: Fundamentals and Applications*. New York: Marcel Dekker, Inc.
- Vandecasteele C and Block CB (1993) *Modern Methods for Trace Element Determination*. New York: John Wiley and Sons Inc.
- VanLoon JC (1985) *Selected Methods of Trace Metal Analysis*. New York: John Wiley and Sons, Inc.
- Zolotov YA (1970) *Extraction of Chelate Compounds*. Ann Arbor: Humphrey Science Publishers.

Extraction With Supercritical Fluid

See II/ EXTRACTION / Supercritical Fluid Extraction

Inorganic Extractions

See II/ EXTRACTION / Analytical Inorganic Extractions

Microwave-Assisted Extraction

V. Lopez-Avila, Midwest Research Institute,
Cupertino, CA, USA

Copyright © 2000 Academic Press

Introduction

Common extraction techniques for solid matrices include Soxhlet extraction, sonication extraction, supercritical fluid extraction (SFE), microwave-assisted extraction (MAE), and accelerated-solvent extraction (ASE).

Soxhlet extraction allows use of large amount of sample (e.g. 10–30 g), no filtration is required after the extraction, the technique is not matrix dependent, and many Soxhlet extractors can be set up to perform in unattended operation. The most significant drawbacks of Soxhlet extraction are: long extraction times (e.g. up to 24–48 h), large amount of solvent usage (300–500 mL per sample), and the need for evaporation after sample extraction.

Sonication extraction is faster than Soxhlet extraction (30–60 min per sample) and allows extraction of

large amount of sample with a relatively low cost, but it still uses about as much solvent as Soxhlet extraction, is labour intensive, and filtration is required after extraction.

The newer extraction techniques such as SFE, MAE, and ASE are very attractive because they are a lot faster, use much smaller amounts of solvents, and are environmentally friendly techniques. For example, SFE uses carbon dioxide or modified carbon dioxide (e.g., carbon dioxide containing a small amount of an organic solvent known as modifier) for extraction. Carbon dioxide is a nontoxic, nonflammable, and environmentally friendly solvent. Furthermore, the extraction selectivity can be controlled by varying the pressure and temperature of the supercritical fluid and by the addition of modifiers.

MAE uses microwaves that can easily penetrate into the sample pores causing the solvent trapped in the pores to heat evenly and rapidly. In contrast to conventional heating where it takes a long time for the vessel to heat and then transfer its energy to the

solvent, MAE is very fast since the heat is transferred directly to the solvent (provided that the solvent absorbs microwaves). MAE is promising because: it is fast (e.g. 20–30 min per batch of as many as 12 samples); MAE uses small amounts of solvents as compared to Soxhlet and sonication extraction (30 mL in MAE versus 300–500 mL in Soxhlet extraction); it allows full control of extraction parameters (time, power, temperature); stirring of the sample is possible in MAE; allows high temperature extraction; and no drying agents are needed in MAE since water absorbs microwaves very fast and thus can be used to heat up the matrix. MAE has several drawbacks that contributed to its slow acceptance such as: extracts must be filtered after extraction, which slows down the operation; polar solvents are needed; cleanup of extracts is needed because MAE is very efficient (e.g. ‘everything’ gets extracted); and the equipment is moderately expensive.

Accelerated solvent extraction is a fairly new extraction method that was approved recently by the U.S. Environmental Protection Agency (EPA) as Method 3545. The extraction is done in a closed-vessel at elevated temperatures (50° to 200°C) and pressures (1500–2000 psi). This technique is attractive because it is fast (e.g. extraction time is approximately 15 min per sample), uses minimal solvent (15–40 mL), no filtration is required after the extraction, and the instrumentation allows extraction in unattended operation. At least 24 samples can be processed sequentially and different sample sizes can be accommodated (e.g. 11, 22, and 33-mL vessels are available).

Theoretical Considerations in MAE

Microwaves are high-frequency electromagnetic waves placed between radio frequency and the infrared regions of the electromagnetic spectrum (their frequency range from 0.3 to 300 GHz corresponding to wavelengths of 1 m to 1 mm). In contrast to conventional heating where the heat penetrates slowly from the outside to the inside of an object, in MAE the heating appears right in the core of the body that is being heated, and the heat spreads from the inside to the outside of that body. The microwave energy affects molecules by ionic conduction and dipole rotation. In ionic conduction, the ions in solution will migrate when an electromagnetic field is applied. The resistance of solution to this flow of ions will result in friction and, thus, heating of the solution. Dipole rotation means realignment of the dipoles with the applied field. At 2450 MHz, the dipoles align and randomize 4.9×10^9 times per second; this forced

molecular movement results in molecular ‘friction’ and, thus, heating of the solution.

Selection of proper solvents is the key to a successful extraction. In selecting solvents, consideration should be given to the microwave-absorbing properties of the solvent, the interaction of the solvent with the matrix, and the analyte solubility in the solvent (the principle of ‘like dissolves like’ is still applicable in MAE). The larger the dipole moment of the solvent the faster the solvent will heat under microwave irradiation. For example, hexane (dipole moment is < 0.1 Debye) will not heat, whereas acetone with a dipole moment of 2.69 Debye will heat in a matter of seconds. Thus, a mixture of hexane and acetone is an ideal solvent for compounds of environmental significance, and many applications described here use hexane–acetone (1 : 1).

Other important factors under considerations include: 1. the compatibility between the extraction solvent and the analytical method used in the analysis of the extract (the less polar solvents seem to be preferred for gas chromatographic analysis, whereas the more polar ones for liquid chromatographic analysis and immunoassay techniques) and 2. the selectivity of the solvent. Little has been reported in the literature on the selectivity of MAE because the technique is so efficient that it can not be regarded as a selective extraction technique. ‘Everything gets extracted’ so a cleanup step after the extraction is needed in almost all cases.

When MAE is conducted in closed vessels, the temperature achieved during the extraction will be greater than the boiling points of the solvents. For most of the solvents (e.g. acetone, acetone–hexane, dichloromethane–acetone), the temperature inside the vessel is two to three times the boiling point of the solvent. These elevated temperatures result in improved extraction efficiencies of the analyte from the sample matrix. The reader should refer to **Table 1** for a listing of solvents and their maximum closed-vessel temperatures achieved at 175 psi.

Instrumentation for MAE

The features of commercially available MAE systems are identified in **Table 2**. The equipment (**Figure 1**) used for closed-vessel MAE consists of a magnetron tube, an oven where the individual extraction vessels (closed vessels) are set up on a turntable or rotor, monitoring devices for temperature and pressure, and electronic components. It usually includes specific safety features such as rupture membranes for the extraction vessels, an exhaust fan to evacuate air from the instrument cavity, a solvent vapour detector (monitors the presence of solvent vapour in the

Table 1 Solvent boiling point and closed vessel temperature^a

<i>Solvent</i>	<i>Boiling point (°C)</i>	<i>Closed vessel temperature (°C) at 175 psi</i>
Dichloromethane	39.8	140
Acetone	56.2	164
Methanol	64.7	151
Ethanol	78.3	164
Acetonitrile	81.6	194
2-Propanol	82.4	145
Acetone–hexane (1 : 1)	52 +	156
Acetone–cyclohexane (70 : 30)	52 +	160
Acetone–petroleum ether (1 : 1)	39 +	147
Dichloromethane–acetone (1 : 1)	^b	160 ^c
Toluene–methanol (10 : 1)	^b	110–112 ^c
Toluene–methanol (1 : 10)	^b	146 ^c

^aAdapted from Kingston and Haswell.^bInformation not available.^cTaken from Reference 2.

microwave cavity and shuts off the microwave energy whenever solvent vapour is detected in the instrument cavity), an expansion container (the extraction vessels are connected to this expansion container through vent tubing; in case the membrane ruptures, due to increased pressure in the vessel, then vapour is re-

moved through the rupture vent tube), and an isolator located in the wave guide that diverts reflected microwave energy into a dummy load to reduce the microwave energy within the cavity. One manufacturer of microwave equipment uses resealable vessels. In this case, vessels are placed on a sample rotor and secured with a calibrated torque wrench for uniform pressure. If the pressure exceeds the vessel limits, a spring device (Milestone's patented technology) allows the vessel to open and close quickly, thus releasing the excess pressure. These sample rotors are available with (perfluoroalkoxy)polymer (PFATM) and (tetrafluoroalkoxy)polymer (TFMTM) liners with pressure ratings of 435 psi to 1450 psi. Another safety feature which was added to the microwave system is the 'movable wall'. To prevent the door from being blown away, a door frame on spring-loaded, high-impact steel bars was added such that the door moves out and in to release pressure from the microwave cavity.

Typical pressures reached with most closed-vessel systems (first-generation) were 105 psi, but today's technology can handle pressures as high as 1500–1600 psi. A special rotor, which houses six thick-walled vessels capable of working at 1600 psi, is available commercially on several systems, including the CEM's MARS-5, Milestone's Ethos-1600,

Table 2 Features of commercially available MAE systems^a

<i>Model/ manufacturer</i>	<i>Power (watts)</i>	<i>Sensors</i>	<i>Max. pressure (bar)</i>	<i>Vessel volume (mL)</i>	<i>Vessel material</i>	<i>Number of vessels</i>	<i>Max. temp. (°C)</i>
Multiwave/ Anton Paar GmbH, Austria	1000	Pressure	70	100	TFM/ceramics	12	230
		control in	70	100	TFM/ceramics	6	260
		all vessels	130	50	TFM/ceramics	6	260
		Infrared	130	50	Quartz	6	300
		temperature measurement in all vessels	130	20	Quartz	6	300
MARS-6/CEM, USA	1500	Infrared	36	100	TFM	14	300
		temperature measurement in all vessels	100	100	TFM	12	300
Ethos 900/1600, Milestone, USA	1600	Pressure	30	120	TFM or PFA	10	240
		control in	100	120	TFM	6	280
		all vessels					
		Temperature control in all vessels	30 100	120 120	TFM or PFA TFM	12 10	240 280
Model 7195/ O.I. Corp. USA	950		13	90	TFM	12	200
			40	90	TFM	12	200
Soxwave 100/ 3.6 Prolabo, France	250	Temperature control	Open vessel	250	Quartz	1	
			Open vessel	100 or 250	Quartz	6	

^aLopez-Avila V (1999) *Critical Reviews in Analytical Chemistry* 29: 195, reprinted with permission of CRC Press, Boca Raton, FL.

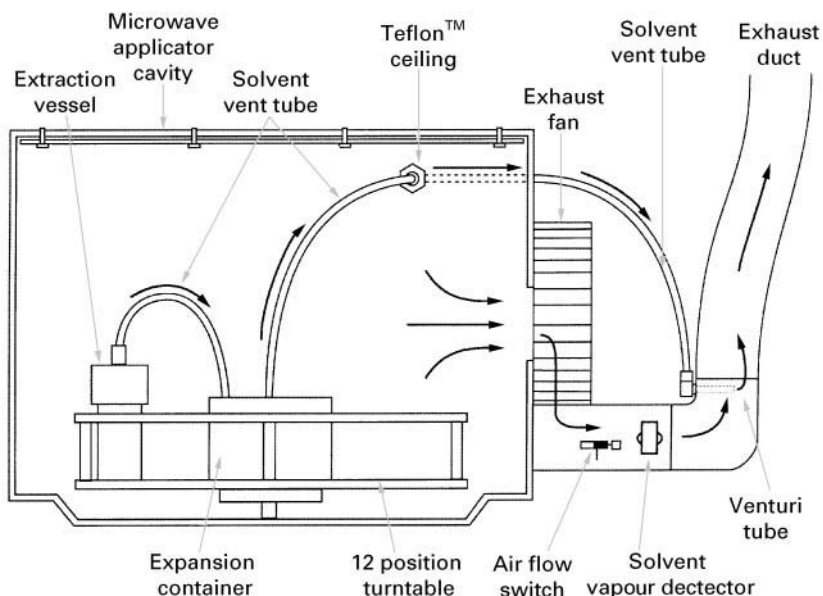


Figure 1 Schematic diagram of a closed vessel MAE system.

and Plazmatronika's UniClever system. In the Milestone system, for example, if the operating pressure inside the vessel exceeds the vessel limits, a special spring device will allow the vessel to open and close, thus reducing the pressure.

The vessels are typically made of microwave transparent materials (e.g. polyetherimide, or TFM) and are lined with perfluoroalkoxy or TeflonTM liners. A new microwave system introduced recently by one

manufacturer uses magnetic stir bars, which allow extraction with polar and nonpolar solvents while agitating the sample and solvent to achieve efficient mixing and improve analyte recoveries.

Figure 2 shows a schematic of CEM's lined digestion vessel with and without temperature and pressure control. Vessel body and cap are made of UltemTM, a polyetherimide. The cap and cover of the control vessel are modified to allow

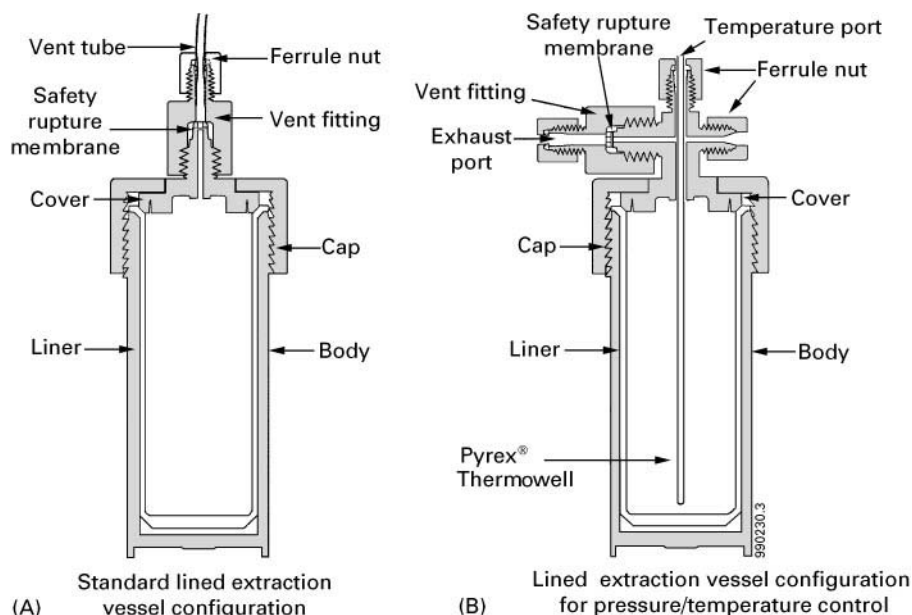


Figure 2 (A) Standard lined extraction vessel and (B) lined extraction vessel with pressure temperature control.

a pressure-sensing tube and a fibre optic temperature probe. The fibre optic probe is microwave transparent and is positioned in the control vessel using a glass thermal well. Infrared temperature sensors are also used to monitor the temperature inside the vessel. As the turntable revolves, the infrared sensor measures the temperature of each vessel. More detail on the pressure and temperature feedback control can be found elsewhere.

Additional features such as magnetic stirring of the extraction solvent inside multiple sample vessels is possible, at least on one commercial system (Ethos 1600 Labstation from Milestone, Inc.). Moreover, nonpolar solvents, such as hexane, can now be heated at elevated temperatures by use of magnetic stir bars made of Milestone's proprietary fluoropolymer Weflon™. (This polymer absorbs the microwave energy and subsequently transfers heat to the surrounding medium.)

All closed vessel systems that are available commercially are multivessel systems which evenly space the vessels on a carousel or rotor and rotate them through a pattern on 360° oscillating turntable.

Specific Applications for MAE

Selected MAE applications are identified in Table 3.

Polycyclic Aromatic Hydrocarbons (PAHs)

Work done by V. Lopez-Avila *et al.* indicated that PAHs, with the exception of more volatile compounds such as naphthalene, can be extracted quantitatively (recovery > 80%) from soil and sediment matrices with hexane–acetone (1 : 1) at temperatures of 115°C. Typical extraction times for batches of up to 12 samples (5 g each) are 10 min at 100% power (1000 watts). The lower recoveries of naphthalene, acenaphthene, and acenaphthylene were attributed to the presence of water in the soil matrix (to prepare a representative aged soil sample, water was added to the soil matrix to bring its water content to 30%).

Other successful microwave-assisted extractions of PAHs from soils, sediments, and fly ash have been reported with hexane–acetone (1 : 1), acetone alone, dichloromethane alone, dichloromethane–toluene (50 : 50), acetone–petroleum ether (1 : 1), methanol–toluene (9 : 1), and toluene–water.

Dean *et al.* reported on a direct comparison between Soxhlet, MAE, and SFE for PAHs and concluded that the major advantage of MAE is the speed of extraction, but they also acknowledged that without additional cooling after extraction it takes approximately 30 min until the vessels can be opened and extracts processed. Barnabas, Dean and

coworkers also investigated the effects of pressure, temperature, extraction time, and percent of methanol modifier added to the extraction solvent in order to optimize the extraction.

Chee *et al.* reported a 5-min heating at 115°C with 30 mL hexane–acetone (1 : 1) as the optimum extraction conditions for a 5 g sample, conditions which are very similar to those reported by V. Lopez-Avila *et al.*

Optimization of MAE of PAHs using open-vessel technology was conducted by Budzinski *et al.*, who reported that the optimum conditions are 30% water, 30 mL dichloromethane, and 10 min heating at 30 W power. When considering that the time needed to reach the boiling point is about 2 min (for dichloromethane), a heating time of 10 min is more than sufficient to extract PAHs quantitatively from the matrix, especially when adding water which is supposed to cause swelling of the matrix.

Organochlorine pesticides (OCPs)

Onuska and Terry extracted aldrin, dieldrin, and DDT from soils and sediments using acetonitrile, isooctane, or a mixture of isooctane–acetonitrile (1 : 1, v/v) and achieved quantitative recoveries using five or seven 30-s irradiations with microwave energy. They also reported that MAE recoveries increase as the moisture content of the soil increases up to 15%. Fish and Revesz used hexane–acetone as extraction solvent and reported that OCP recoveries improved when changing from 1 : 1 hexane–acetone to 2 : 3 hexane–acetone. The latter solvent has a composition similar to the azeotropic vapour in the Soxhlet extractor.

Lopez-Avila *et al.* extracted 45 OCPs from freshly spiked and 24-h aged soil samples with hexane–acetone (1 : 1, v/v). For the freshly spiked soil, 38 compounds had recoveries between 80 and 120%, six compounds had recoveries between 50 and 80%, and the recovery of captafol was above 120%. For the spiked soil samples aged for 24 h, 28 compounds had recoveries between 80 and 120%; 12 compounds had recoveries between 50 and 80%; three compounds including captafol, captan, and dichlone were poorly recovered; and chloroneb and 4,4'-DDT had recoveries above 120%.

When recoveries from freshly spiked soil were compared to those from aged spiked soil, it was found that the recovery of captafol dropped from 122% to 36%, the recovery of captan dropped from 106% to 21%, and the recovery of dichlone dropped from 78% to 10%. Captafol and captan appear to be quite stable upon irradiation of soil/solvent suspensions, but dichlone was found to disappear upon irradiation

Table 3 Selected MAE applications reported in the literature

Analyte	Matrix	Solvent	MAE conditions	Ref.
17 PAHs, 14 phenols, 20 organochlorine, 13 miscellaneous compounds (e.g. chlorinated benzenes, nitroaromatic compounds and phthalate esters)	3 Reference marine sediments 3 Reference soils Topsoil	Hexane–acetone (1 : 1)	Closed-vessel extraction at 80°C, 115°C for 5, 10, 20 min	2, 3, 4, 41
PAHs	Soil	Acetone–dichloromethane	29 min at 120°C in closed vessel	6
PAHs	Marine sediments Mussel tissue Air particles	Dichloromethane Dichloromethane–toluene (50 : 50) Acetone–hexane (50 : 50)	5 to 40 min irradiation at 30 to 90 W in open vessel, 10 min irradiation at 30 W in open vessel	7
PAHs	Reference marine sediments	Hexane–acetone (1 : 1)	5 min at 115°C in closed vessel	8
PAHs	Reference marine sediments	Dichloromethane	5 to 10 min at 35°C in open vessel	9, 10
PAHs	Fly ash	Hexane–acetone (90 : 10)	70°C in closed vessel	11
PAHs	Soil	Acetone	20 min at 120°C, closed vessel	12
PAHs	Marine sediments	Dichloromethane Acetone–hexane (1 : 1)	5 and 15 min at 115° and 135°C, closed vessel	13
PAHs	Reference marine sediment Reference soil Reference river sediment Reference sewage sludge Industrial soil Marine sediment	Dichloromethane Dichloromethane–toluene (50 : 50) Acetone–hexane (50 : 50, 60 : 40) Acetone	10 min, 30 watts, open vessel	14
Organochlorine pesticides	Sediment saturated with distilled water (1 g sample and 2 mL water)	Acetonitrile Isooctane Isooctane–acetonitrile (1 : 1)	30 s irradiation in open vessel; repeat up to five times	15
16 Phenols, 20 organochlorine pesticides	Topsoil Clay soil Sand Reference soil	Hexane–acetone (1 : 1)	Closed-vessel extraction at 115°C for 10 min	16
16 PAHs 10 Organochlorine pesticides 4 Aroclors 6 Phthalate esters 7 Organophosphorus pesticides 5 Fungicides/herbicides	Water samples preconcentrated on C18 membrane discs	Acetone Dichloromethane	1, 3, 5, 10 min at 80°C, 100°C, 120°C, closed vessel	17
PCB 153	Seal Blubber	<i>n</i> -Hexane	Several 30 s extractions at 1000 W	18
PCB 180 PCB 138 <i>p,p'</i> -DDE Hexachlorocyclohexane Hexachlorobenzene	Pork fat Cold liver	Ethyl acetate–cyclohexane (1 : 1)	Several irradiations at 250 to 1000 W in increments of 100 W	19
PCBs	Municipal sewage sludge	Hexane–acetone (1 : 1)	10 min, 30 W, open vessel	20
PCBs	River sediments	Hexane–acetone (1 : 1)	15 min, closed vessel	21

Table 3 *Continued*

Analyte	Matrix	Solvent	MAE conditions	Ref.
C ₁₆ -C ₃₂ hydrocarbons 20 PAHs 4 Organochlorine pesticides PCBs	Marine sediments	Toluene-water (1 : 5 to 1 : 2)	6 min, closed vessel	22
Phenol	Soils	Hexane and hexane-acetone (2 : 8) with pyridine and acetic anhydride for <i>in-situ</i> derivatization	130°C in closed vessel	23, 24
Methyl phenols				
Nonyl phenol	Water samples preconcentrated on C18-packed cartridge, C18-packed disc Sediments	Dichloromethane Acetone-petroleum ether (1 : 1)	5 and 15 min at 100°C to 120°C, closed vessel	25
Phenol 2-Chlorophenol 2-Methylphenol 2-Nitrophenol 2,4-Dichlorophenol	Soil	Acetone-hexane (various ratios)	Closed vessel	26
Imidazolinone herbicides	Soil	0.1 M ammonium acetate/ammonium hydroxide (pH 9-10)	3 to 10 min irradiation at 125°C in closed vessel	27-29
Atrazine and degradation products	Lupin seeds Rat feces	Water followed by 0.35 N HCl	Closed vessel, 95-98°C	30
Atrazine Simazine Prometryne	Sandy loam Clay Bentonite Florisil	Methanol Acetone-hexane (1 : 1) Dichloromethane Water		31
Atrazine Simazine Metazachlor Desisopropyl atrazine Desethyl atrazine	Sand Peat Clay	Dichloromethane with water, methanol, and acetone Acetonitrile-0.5% ammonia in water (70 : 30)	5 to 45 min at 30°C to 130°C, 20 min at 115°C	32, 33
Atrazine	Soil	Water	3, 4 and 5 min closed vessel	34
Organotin compounds (mono-, di- and tributyltin; mono-, di- and triphenyltin)	2 Reference sediments	50% acetic acid Isooctane Methanol Water Artificial sea water	1 to 7 min irradiation in open vessel, up to 160 W	35
Organotin compounds	Sediments	0.5 M ethanoic acid in methanol	3 min, open vessel	36
Butyl and phenyl organotin	Reference marine biological matrix Tuna tissue Mussel tissue	25% tetramethyl-ammonium hydroxide in water	3 min at 90°C, 115°C and 130°C, closed vessel	37
Organotin compounds	Sediments	11 M acetic acid NaBEt ₄	3 min at 50 to 60 W, open vessel	38
Organomercury compounds	Sediments Reference biological materials	2 M nitric acid 2 M hydrochloric acid 25% tetramethyl-ammonium hydroxide	3 min at 60 W, open vessel 2 to 4 min at 40 to 60 W, open vessel	38
Methylmercury	Aquatic sediments Certified reference sediments	Digestion with 6 M HCl (methylmercury is extracted at room temperature by complexation with cysteine acetate and toluene)	10 min at 120°C, closed vessel	39

of the solvent. (The recovery of dichlone from solvent was only 5.5% after heating at 145°C for 5 min and 2.6% after 20 min at the same temperature.) Microbial degradation may be responsible for the low recoveries of captafol and captan, whereas in the case of dichlone, it is quite likely that this compound is not stable under the conditions used. Nonetheless, these recoveries are higher than those obtained by Soxhlet or sonication extraction.

Water samples can also be extracted by MAE; however, they have to be preconcentrated first on a membrane disc or some adsorbent material. Chee *et al.* used C₁₈-membrane discs and then extracted the discs with 20 mL solvent (acetone and dichloromethane) in a closed-vessel MAE system at 80°C, 100°C and 120°C for 1, 3, 5 and 10 min. Acetone was found to give higher recoveries than dichloromethane. This approach would allow extremely low detection limits since several discs generated by processing a large volume of sample can be extracted in one vessel.

Vetter and coworkers extracted OCPs from fatty tissues (e.g. seal blubber) with solvents such as hexane and ethyl acetate (1 : 1). To transfer heat to hexane, which is microwave transparent, discs of Weflon™ (2.5 cm in diameter × 0.3 cm thickness) were used in the extraction vessel. The yield of extractable fat and recoveries of OCPs after seven irradiation cycles were comparable to those obtained by Soxhlet extraction. Since ethyl acetate-cyclohexane (1 : 1, v/v) seems to extract more fat than hexane, a gel permeation chromatography step after extraction is a must.

Polychlorinated Biphenyls (PCBs)

MAE of PCBs was reported by Lopez-Avila *et al.*, Onuska and Terri, Chee *et al.*, Pastor *et al.*, Dupont *et al.* and Kodba and Marsel. Lopez-Avila *et al.* used hexane-acetone (1 : 1, v/v) and reported that the average recoveries from typical soil matrices were greater than 70% for the Aroclors 1016 and 1260 and the method precision was better than 7%. Furthermore, there was no degradation of PCBs upon heating of solvent/soil suspensions with microwave energy. Three reference materials and 24 soils from a Superfund site, most of which contained Aroclors, were extracted by MAE and analysed by both GC/ECD and enzyme-linked immunosorbent assay (ELISA). Because ELISA is very sensitive and its detection range is quite narrow, the hexane-acetone extracts were first diluted with methanol and subsequently with the assay buffer (which contained 50% methanol) to bring the Aroclor concentrations to less than 5 ng mL⁻¹. These data indicate excellent

agreement between the certified Soxhlet/GC/ECD data and the MAE-ELISA data (correlation coefficient 0.9986; slope 1.0168) and the MAE-GC/ECD data and the MAE-ELISA data (correlation coefficient 0.9793; slope 1.0468).

Other solvents used successfully to extract PCBs from environmental samples include isooctane, acetone and dichloromethane, and toluene-water.

Phenols

MAE of phenolic compounds was reported by Lopez-Avila *et al.*, Llompart *et al.*, Chee *et al.* and Egizabal *et al.* Acetone-hexane seems to be the preferred solvent for 16 phenolic compounds and dichloromethane, acetone-petroleum ether (1 : 1) were reported to work well for extraction of nonylphenol. The only compounds found to degrade during MAE are 2,4-dinitrophenol and 4,6-dinitro-2-methylphenol. MAE recoveries for phenolic compounds are usually higher than the classical extraction method recoveries, and the method precision is significantly better for MAE (e.g. coefficient of variation of 3% for MAE as compared to 15% for Soxhlet and 20% for sonication).

Herbicides

Imidazolinones (e.g. imazapyr, imazetapyr, imazethapyr, imazaquin, etc.) are extracted from soil with 0.1 M ammonium acetate/ammonium hydroxide (pH 9–10) in a 10-min extraction. A variety of soil samples fortified at 1 to 50 p.p.b. exhibited an average recovery of 92% (standard deviation 13%).

Triazine herbicides have been successfully extracted from soil by MAE with water, methanol, acetone-hexane (1 : 1), dichloromethane, acetonitrile-0.5% ammonia in water (70 : 30), dichloromethane-water (50 : 50), methanol-dichloromethane (10 : 90). Water seems to be preferred since it is very polar solvent and can interact strongly with polar matter in soils to enhance the desorption of triazines; it is a cheap, safe, and environmentally friendly solvent; and it heats up very quickly when irradiated with microwave energy microwave energy. Xiong *et al.* reported that direct heating of soil with water gave a 73.4% recovery for atrazine from soil and, therefore, stated that 'MAE is not only a simple heating'.

Organotin and Organomercury Compounds

Methods reported in the literature for the determination of organotin compounds in soils use extraction with organic solvents in the presence of complexing agent, or leaching with acetic or hydrochloric acid assisted by sonication or some sort of shaking.

Open-vessel MAE was recommended to accelerate the leaching with 50% acetic acid aqueous solution, and the data showed that a 3-min irradiation at 60 W was sufficient to recover tributyl tin from certified reference sediments. Ethanoic acid (0.5 M in methanol) was also reported. When dealing with biological matrices (e.g., tuna tissue, mussel tissue), solubilization with tetramethylammonium hydroxide (TMAH) for a 3 min at 90°C, 115°C, and 130°C in a closed vessel was demonstrated to be as efficient as the hot-plate procedure. Schmitt *et al.* reported on the integration of the solubilization step with the derivatization/extraction step by using 11 M acetic acid for solubilization and NaBEt₄ for derivatization using an open vessel MAE system.

Organomercury compounds can be extracted from sediments with 6 M hydrochloric acid at 120°C for 10 min in closed vessel or 2 M nitric acid and 2 M hydrochloric acid after 3 min irradiation at 60 W in open vessel. Pure acetic acid and 1 M sulfuric acid could only extract 85% and 55%, respectively. Microwave-assisted digestion of the biological tissue with 25% TMAH for 2–4 min at 40–60 W gave quantitative recovery of both organomercury and inorganic mercury.

Additives in Polymers

Antioxidants such as the Irganox 1010, Irganox 1076, and Irgaphos 168, which are added to polymers to protect them during end-use applications, can be extracted with > 95% efficiency by MAE with *n*-heptane–acetone in a few minutes. Higher temperatures (e.g. 140°C) were used by Jordi *et al.* with cyclohexane–chloroform–triethylamine (45:45:10) to dissolve polyethylene and extract compounds such as Tinuvin 770, Tinuvin 622, Tinuvin 144, and Chimisorb 81.

Natural Products

Extraction of oils from mint leaves and other materials of biological origin is a patented process known as the 'microwave-assisted process'. Other reports on MAE of natural products include that of Young, Bichi *et al.* and Mattina *et al.* Young extracted ergosterol from fungi and spores by MAE with methanol and 2 M sodium hydroxide. Bichi *et al.* extracted pyrrolizidine alkaloids from *Senecio paludosus* and *Senecio cordatus* dried plants by MAE with methanol at 65 to 100°C for 20 to 30 min. Mattina *et al.* reported on the extraction of taxanes from *Taxus* biomass by MAE with ethanol. Using 5 g of freshly harvested needles (moisture content 55 to 65%) soaked in 5 mL of water prior to MAE and 10 mL ethanol at 85°C for 9 min resulted in about 90%

recovery. This procedure would significantly reduce the costs of the extraction of taxanes from biomass with no reduction in the extraction yields.

See also: II/Extraction: Supercritical Fluid Extraction; Ultrasound Extractions. III/Environmental Applications: Soxhlet Extraction. Solid-Phase Extraction with Disks.

Further Reading

1. For a comprehensive text on MAE, see *Microwave-Enhanced Chemistry* edited by H.M. (Skip) Kingston and Stephen J. Haswell, American Chemical Society, 1997.
2. Lopez-Avila V, Young R and Beckert WF (1994) *Analytical Chemistry* 66: 1097–1106.
3. Lopez-Avila V, Young R, Benedicto J, Ho P, Kim R and Beckert WF (1995) *Analytical Chemistry* 67: 2096–2102.
4. Lopez-Avila V, Young R and Teplitsky NL (1995) *Journal of AOAC International* 79: 142–156.
5. Fish JR and Revesz R (1996) *LC-GC* 14: 230–234.
6. Dean JR, Barnabas IJ and Fowles IA (1995) *Analytical Proceedings Including Analytical Communications* 32: 305–308.
7. Budzinski H, Baumard P, Papineau A, Wise S and Garrigues P (1995) Presented at the 15th PAC Symposium, Belyirule, Italy, 1995.
8. Chee KK, Wong MK and Lee HK (1996) *Journal of Chromatography A* 723: 259–271.
9. Budzinski H, Papineau A, Baumard P and Garrigues P (1995) *Analytical Chemistry* 321: 69–76.
10. Letellier M, Budzinski H, Garrigues P and Wise PS (1996/7) *Spectroscopy* 13: 71–80.
11. Hsu TB and Chen YS (1996) *Organohalogen Compounds* 27: 450–454.
12. Barnabas IJ, Dean JR, Fowles IA and Owen SP (1995) *Analyst* 120: 1897–1904.
13. Chee KK, Wong MK and Lee HK (1996) *Journal of Chromatography A* 723: 259–271.
14. Budzinski H, Letellier M, Garrigues P and Le Menach K (1999) *Journal of Chromatography A* 837: 187–200.
15. Onuska FE and Terry KA (1993) *Chromatographia* 36: 191–194.
16. Lopez-Avila V, Young R, Kim R and Beckert WF (1995) *Journal of Chromatographic Science* 33: 481–484.
17. Chee KK, Wong MK and Lee HK (1996) *Analytica Chimica Acta* 330: 217–227.
18. Hummert K, Vetter W and Luckas B (1996) *Chromatographia* 42: 300–304.
19. Vetter W, Weichbrodt M, Hummert K, Glotz D and Luckas B (1998) *Chemosphere* 37: 2439–2449.
20. Dupont G, Delteil C, Camel V and Bermond A (1999) *Analyst* 124: 453–458.
21. Kodba ZC and Marsel J (1999) *Chromatographia* 49: 21–27.

22. Pastor A, Vasquez E, Ciscar R and de la Guardia M (1997) *Analytica Chimica Acta* 344: 241–249.
23. Llompart MP, Lorenzo RA, Cela R, Paré JRJ, Bélanger JMR and Li K (1997) *Journal of Chromatography A* 757: 153–164.
24. Llompart MP, Lorenzo RA, Rosa A, Cela R, Li K, Bélanger JMR and Pare JRJ (1997) *Journal of Chromatography A* 774: 243–251.
25. Chee KK, Wong MK and Lee HK (1996) *Journal of Liquid Chromatography and Related Technology* 19: 259–275.
26. Egizabal A, Zuloaga O, Etxebarria N, Fernandez LA and Madariaga JM (1998) *Analyst* 123: 1679–1684.
27. Stout SJ, da Cunha AR and Allardice DG (1996) *Analytical Chemistry* 68: 653–658.
28. Stout SJ, da Cunha AR, Picard GL and Safarpour MM (1996) *Journal of Agriculture and Food Chemistry* 44: 3548–3553.
29. Stout SJ, da Cunha AR and Safarpour MM (1997) *Journal of AOAC International* 80: 426–432.
30. Steinheimer TR (1993) *Journal of Agriculture and Food Chemistry* 41: 588–595.
31. Xiong G, Tang B, He X, Zhao M, Zhang Z and Zhang Z (1999) *Talanta* 48: 333–339.
32. Hoogerbrugge R, Molins C and Baumann BA (1997) *Analytica Chimica Acta* 348: 247–253.
33. Molins C, Hogendoom EA, Heusinkveld HAG, Van Harten DC, Van Zoonen P and Baumann RA (1996) *Chromatographia* 43: 527–532.
34. Xiong G, Liang J, Zou S and Zhang Z (1998) *Analytica Chimica Acta* 371: 97–103.
35. Donard O, Lalere B, Martin F and Lobinski R (1995) *Analytical Chemistry* 67: 4250–4254.
36. Lalere B, Szpunar J, Budzinski H, Garrigues P and Donard OFX (1995) *Analyst* 120: 2665–2673.
37. Rodriguez I, Santamarina M, Bollain MH, Mejuto MC and Cela R (1997) *Journal of Chromatography A* 774: 379–387.
38. Schmitt VO, de Diego A, Cosnier A, Tseng CM, Moreau J and Donard OFX (1996/7) *Spectroscopy* 13: 99–111.
39. Vazquez MJ, Carro AM, Lorenzo RA and Cela R (1997) *Analytical Chemistry* 69(2): 221–225.
40. Lopez-Avila V, Benedicto J, Charan C, Young R and Beckert WF (1995) *Environmental Science and Technology* 29: 2709–2712.
41. Onuska FI and Terry KA (1995) *Journal of High Resolution Chromatography* 18: 417–421.
42. Freitag W and Angew JO (1990) *Makromolecular Chemistry* 175: 181–185.
43. Jordi HC, Savage W and Bichard F (1995) Paper presented at Pittcon '95, Paper No. 1209.
44. Pare JRJ (1991) US Patent 5,002,784.
45. Young JC (1995) *Journal of Agriculture and Food Chemistry* 43: 2904.
46. Bichi C, Beliarab FF and Rubiolo P (1992) *Lab 2000* 6: 36
47. Mattina MJI, Berger WAI and Denson CL (1997) *Journal of Agriculture and Food Chemistry* 45: 4691.

Multistage Countercurrent Distribution

G. Johansson, Chemical Center, Lund, Sweden

This article is reproduced from *Encyclopedia of Analytical Science*, Copyright © 1995 Academic Press.

Theory

The separation of chemical compounds by partitioning between two liquid phases, so-called liquid–liquid extraction, can be made more effective by using it as a cascade process. One way in which this can be carried out is by multiplicative partitioning, also called countercurrent distribution (CCD). This process, in which complete partition equilibrium is achieved in each step, is presented schematically in Figure 1. The principle is that two sets of liquid phases, the upper and lower phase, come into contact with each other stepwise. The bottom phases are numbered 0, 1, 2 and so on. The sample to be analysed (fractionated) is included in the first system (containing bottom phase number 0). Before each transfer of the upper phases (to the right in Figure 1) the two-phase systems are equilibrated by mixing and

the sample components are distributed between each pair of phases (each full two-phase system). The partitioning of a pure substance between the phases of a two-phase system can be expressed either by a partition coefficient, K , defined as the ratio of the concentrations (C) of the component in the phases:

$$K = \frac{C \text{ (in phase I)}}{C \text{ (in phase II)}} \quad [1]$$

or by a partition ratio, G , defined as the ratio of the masses (m) of the components in the phase:

$$G = \frac{m \text{ (in phase I)}}{m \text{ (in phase II)}} \quad [2]$$

K and G are related by eqn [3]:

$$G = K \frac{\text{Volume (phase I)}}{\text{Volume (phase II)}} \quad [3]$$

In the following the upper phase is chosen as phase I. A convenient way of analysing the CCD process is to calculate the amounts (in fractions) of a pure

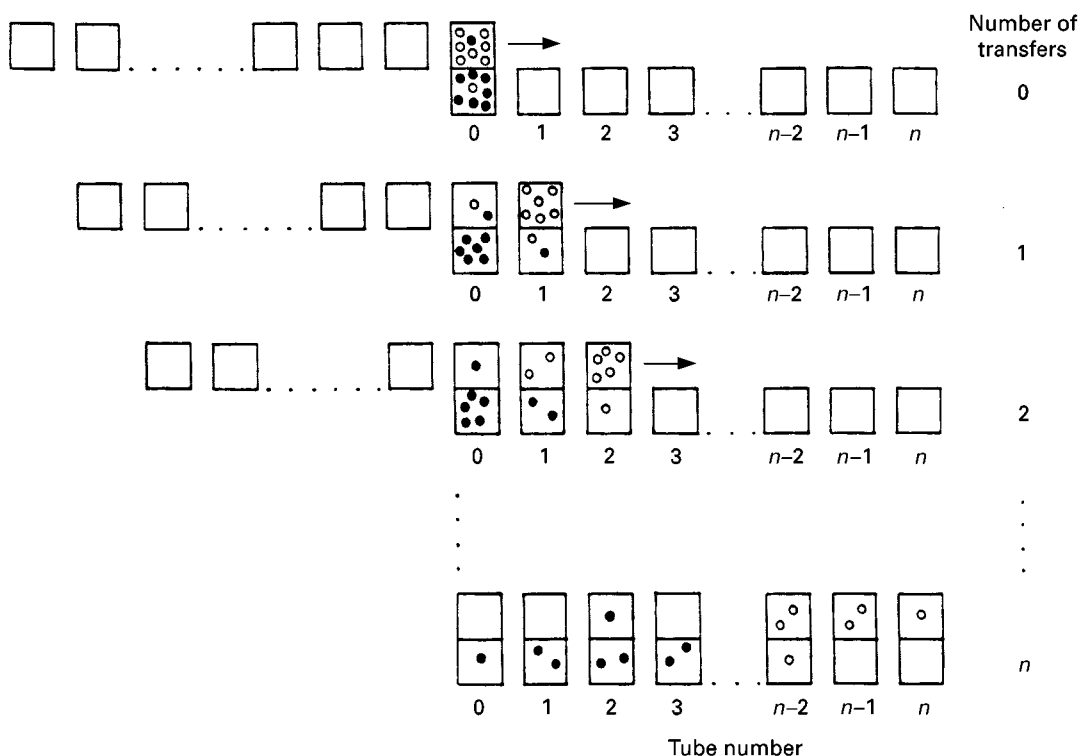


Figure 1 Principle of CCD. The upper phases are transferred stepwise from left to right. Between each transfer the two-phase systems are equilibrated by shaking and the phases are allowed to settle. Filled circle, substance with small G value; open circle, substance with large G value.

component in the various phases based on its G value. In the initial two-phase system (number 0) the component is distributed with the fractions p in the upper phase (phase I) and q in the lower phase (phase II). By definition $p + q = 1$. When the upper phase of system number 0 is combined with the pure lower phase number 1 equilibration of this system will make the transferred fraction p distribute as p/q ($= G$) giving the fraction p^2 in the upper phase and the fraction pq in the lower phase. In the new system number 0, with a new upper phase, the remaining fraction q will partition likewise and the equilibration results in the fraction pq in the upper phase and q^2 in the lower

phase. The resulting distribution after 10 transfers in the 11 tubes 0–10 is shown in **Figure 2**. In the same figure the material in each tube (upper plus lower phase) has been calculated. These values are the same as the terms obtained when $(q + p)^{10}$ is written as a polynomial. More generally, the amount of material $T_{n,i}$ (in fractions), in tube number i after a CCD with n transfers is given by eqn [4]:

$$T_{n,i} = \frac{n!}{i!(n-i)!} p^i q^{n-i} \quad [4]$$

The volume ratio is kept constant during the process. By using the relations $G^i = p^i/q^i$ and $(1 + G)^n =$

pq^{10}	$10p^2q^9$	$45p^3q^8$	$120p^4q^7$	$210p^5q^6$	$252p^6q^5$	$210p^7q^4$	$120p^8q^3$	$45p^9q^2$	$10p^{10}q$	p^{11}	Amount in upper phase
q^{11}	$10pq^{10}$	$45p^2q^9$	$120p^3q^8$	$210p^4q^7$	$252p^5q^6$	$210p^6q^5$	$120p^7q^4$	$45p^8q^3$	$10p^9q^2$	$p^{10}q$	Amount in lower phase
0	1	2	3	4	5	6	7	8	9	10	i
q^{10}	$10pq^9$	$45p^2q^8$	$120p^3q^7$	$210p^4q^6$	$252p^5q^5$	$210p^6q^4$	$120p^7q^3$	$45p^8q^2$	$10p^9q$	p^{10}	Amount in each tube

Figure 2 Distribution of a component which partitions in the ratio p/q between the upper and lower phase—after a CCD with 10 transfers. The amounts are given in fractions, i.e. $p + q = 1$.

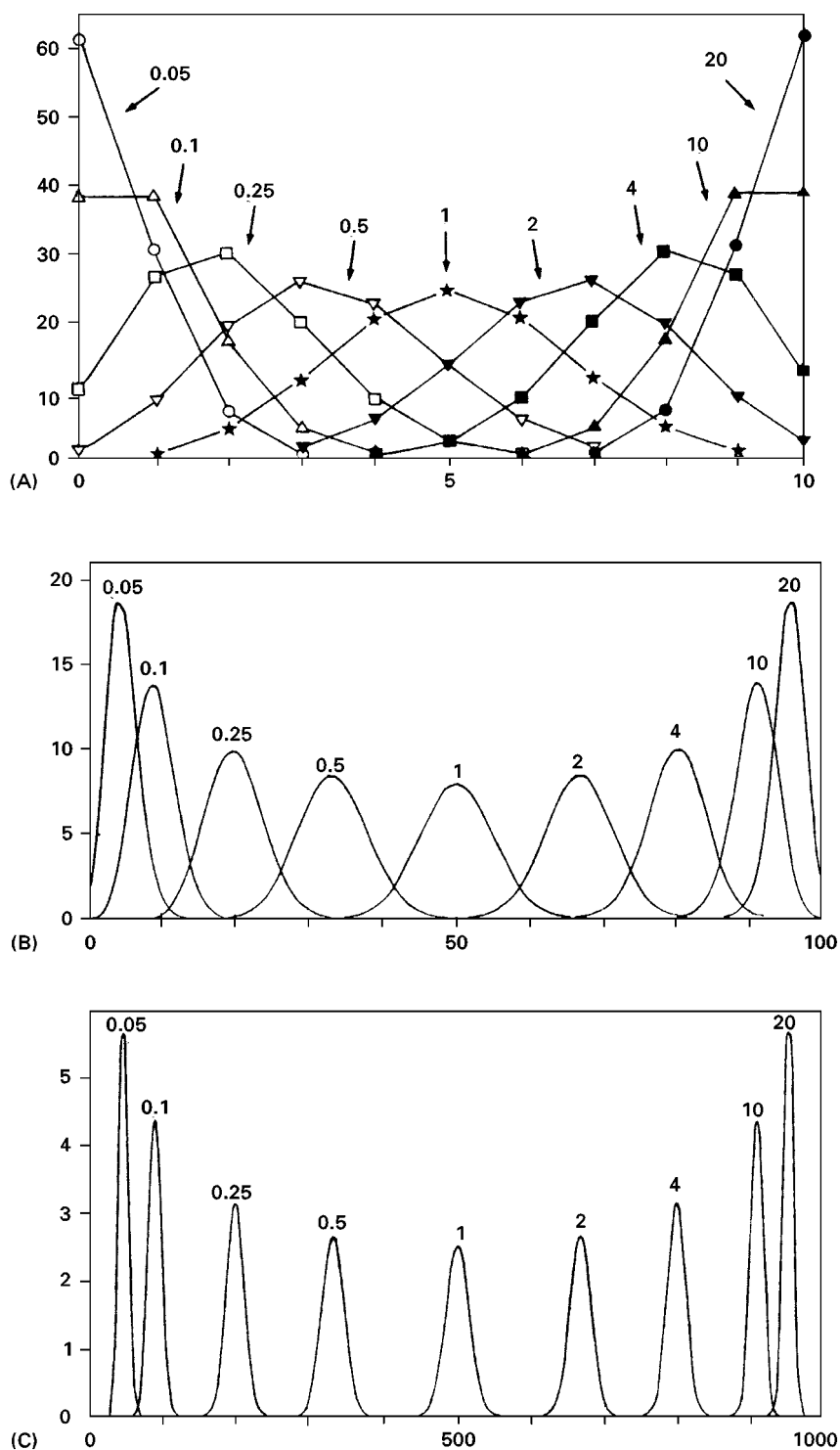


Figure 3 The resulting CCD profiles after (A) 10 transfers, (B) 100 transfers and (C) 1000 transfers for substances with the indicated G values.

$(1/q)^n$, eqn [5] is obtained:

$$T_{n,i} = \frac{n!}{i!(n-i)!} \frac{G^i}{(1+G)^n} \quad [5]$$

This relationship has been used to calculate the distribution profiles in Figure 3 for three cases: i.e. with the number of transfers (n) equal to 10, 100 and 1000. In each case the distributions of components with

G values of 0.05, 0.1, 0.25, 0.5, 1, 2, 4, 10 and 20 are shown. The resolution of components with various G values increases with the increase in the number of transfers. This is due to the fact that the difference in the position (tube number) of the peaks (with given G values) is proportional to the number of transfers, while the peak width only increases with the square root of the number of transfers.

The width of a peak Δr , covering 99.7% of the compound, can be approximately calculated using eqn [6]:

$$\Delta r = \frac{6\sqrt{nG}}{(1 + G)} \quad [6]$$

The relative width of a peak, $\Delta r_{\text{rel}} = \Delta r/n$, is given in Table 1 for $G = 1$ and a number of n values.

The most effective separation of two components, with partition coefficients K_1 and K_2 , is achieved when their distribution peaks are oriented symmetrically around the middle of the tube train, i.e. tube $i = n/2$. This, as can be seen in Figure 3, is equal to the relation $G_1 = 1/G_2$ which can be written as $G_1 \times G_2 = 1$. By combining this relation with eqn [3] the volume ratio, V , to be used for optimal separation can be calculated as shown in eqn [7]:

$$V = \frac{1}{\sqrt{K_1 K_2}} \quad [7]$$

The ratio between the K values of two substances 1 and 2 is called the separation factor, β , and is a measure of the separability of the substances. In Table 2 the number of transfers necessary for virtually complete (more than 99.5%) separation has been calculated for various β values.

The G value of a component which has its maximum peak value in tube number \hat{i} after n transfers is given by the approximate eqn [8]:

$$G = \hat{i}/(n - \hat{i}) \quad [8]$$

Table 1 The absolute, Δr , and relative, Δr_{rel} , peak width (percentage of the total number of tubes) of a substance with $G = 1$ after a CCD with n transfers

n	Δr (no. of tubes)	Δr_{rel} (%)
20	13	67
50	21	42
100	30	30
200	42	21
500	67	13
1000	95	9.5
2000	134	6.7
5000	212	4.2

Table 2 Number of transfers, n , in a CCD necessary to separate two substances, 1 and 2, with a given separation factor $\beta = K_1/K_2$. The volume ratio is chosen in such a way (eqn [7]) that $G_1 \times G_2 = 1$

β	G_1	G_2	n
2	0.709	1.414	264
3	0.577	1.732	110
4	0.500	2.00	70
9	0.333	3.00	30
16	0.250	4.00	20
25	0.200	5.00	16
36	0.167	6.00	14
49	0.143	7.00	12
81	0.111	9.00	10
400	0.050	20.0	6
2500	0.020	50.0	4

The G value can also be obtained by comparing the amount of a substance in two consecutive tubes, numbers i and $i + 1$. By combining the expressions for $T_{n,i}$ and $T_{n,i+1}$ obtained from eqn [5] the G value is obtained as in eqn [9]:

$$G = \frac{T_{n,i+1}}{T_{n,i}} \frac{i+1}{n-i} \quad [9]$$

By following the apparent G values over a distribution peak the presence of several substances differing slightly in their G values can be detected.

Various Modes of Multiplicative Partitioning

The basic process of CCD has been described, but it can be varied in a number of ways.

Single Withdrawal Procedure

In this process the addition of fresh upper phases is not stopped after n transfers, but continues from the left while the overflowing upper phases (to the right) are collected. This process is therefore similar to a chromatographic system with the lower phases corresponding to the stationary phase of the column and the upper phases corresponding to the elution liquid. Substances with high G values are easily eluted in this way while those with low G values need a great number of steps to be carried through the CCD train. The greater the number of transfers the more diluted the substance will be when leaving with the overflowing upper phases. Likewise the upper phases can be chosen as the stationary phase and the lower phases can be used as the eluting phases. In this case substances with low G values rapidly eluted.

O'Keefe Partitioning

The multiplicative partitioning can be carried in such a way that a new portion of the solute mixture to be separated is added after each transfer step. This method of carrying out the partitioning is called O'Keefe partitioning. Several two-phase systems are arranged in a row and a solute sample is included in the centre system. After equilibration and settling all the upper phases are moved one step to the right and the overflowing upper phase is collected. Then all the lower phases are moved one step to the left and the one to the extreme left is collected. The remaining set is completed with one fresh lower phase (to the right) and one fresh upper phase (to the left) to restore the original number of systems. After addition of a new portion of solute to the centre system the next cycle takes place. Substances with $G > 1$ will be recovered in the upper phases collected to the right and substances with $G < 1$ in the lower phases removed to the left. This process is used when large amounts of substances are to be separated. The number of systems is usually small, e.g. 7, 9 or 11.

A similar process, called Watanabe–Morikawa partitioning, differs in that the ongoing addition of solute mixture is done in the first system of the row. This is useful when only components with high or low G values are to be isolated.

Description of Some CCD Apparatus

CCD with only a few transfers (up to 10) can easily be carried out by using a set of separating funnels for mixing, settling and phase separation. For small phase volumes, 0.5–5 mL, the separating funnels can be replaced by test tubes and the upper phases can be transferred with the aid of a pipette. For CCDs with more than 10 transfers it is strongly advised that some kind of automatic apparatus is used. Some examples of such apparatuses are presented next.

All-Glass CCD According to Craig

Several glass units, allowing mixing, settling and phase transfers (Figure 4) are arranged in batteries on a horizontal axis. Movement about this axis can be used to gently mix the phases, to put the glass units in position for settling of the phases and for decanting the upper phases, respectively. The times for each part of the CCD cycle as well as the number of transfers can be programmed. Standard types of such machines allow 50 transfers while more advanced machines may be used for up to 1000 transfers. The glass units can be obtained in various sizes but standard tubes have space for *c.* 2 mL (fixed amount) of lower phase and up to 5 mL of upper phase.

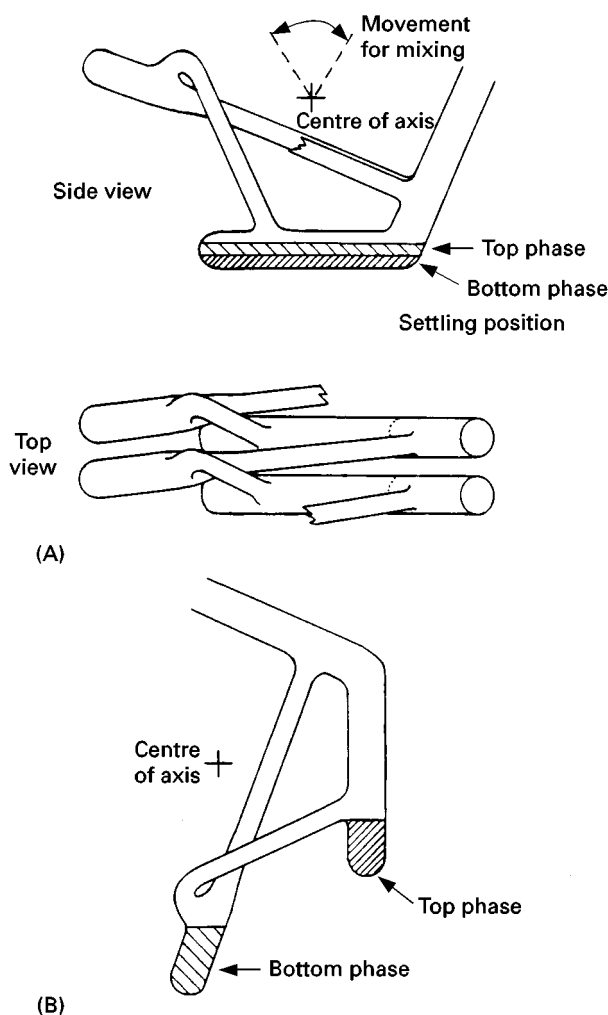


Figure 4 Section of the all-glass apparatus for CCD constructed by Craig. (A) Two segments (or tubes) are shown from side and top views. Normally 50–1000 tubes are connected and placed on a horizontal rack which allows simultaneous mixing of all tubes. (B) By turning the axis the upper phases can be decanted. When returning to the original position the upper phases are transferred to the neighbouring tube.

Thin-Layer CCD According to Albertsson

This CCD apparatus is designed to be used with aqueous two-phase systems which normally need a long time for settling. By using systems with low heights, only a few millimetres, the settling time will be acceptable (5–20 min). The operating unit (Figure 5) consists of two circular plates of polyacrylic plastic, one on top of each other: the lower plate (stator) is fixed while the upper one (rotor) can be rotated stepwise. Both plates have 60 (or 120) radially oriented cavities which pair-wise form containers for the two-phase systems. The cavities of the stator contain the lower phases (normally 0.8 mL) while the upper phases (0.2–2 mL) are situated in the

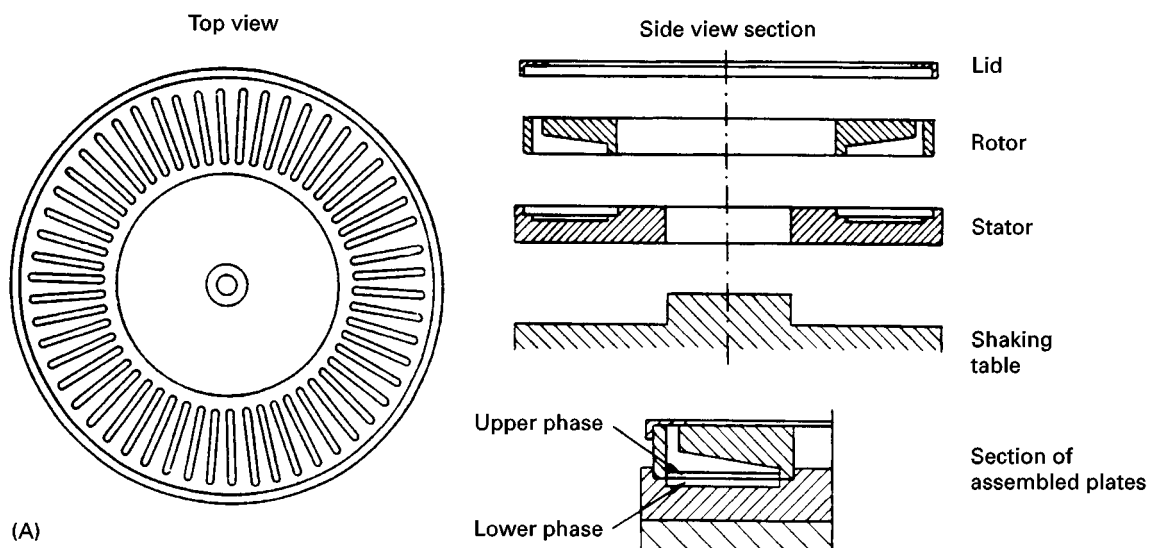


Figure 5 Thin-layer CCD apparatus according to Albertsson. (A) The two discs of polyacrylic plastic contain matching cavities for the upper and lower phases and by rotation the upper plate can move all upper phases relative to the lower ones. See text for further details. (Adapted from Albertsson P-Å (1986) *Partition of Cell Particles and Macromolecules*, 3rd edn, p. 126. New York: Wiley (interscience), by permission.) (B) A thin-layer CCD machine constructed by Albertsson.

cavities of the rotor and therefore can be transferred relative to the lower phases by rotating the upper plate. The two plates are placed on the shaking table of a machine which also contains a drive for the upper plate rotation. The phase systems are added to each container (chamber) via openings in the upper side of the rotor. These openings, during the run, are covered with a ring-formed lid. The shaking and settling periods and number of transfers are controlled by an automatic unit. After the CCD run is completed the two-phase systems can be collected by use of a fraction collector. This is a circular rack with the same number of test tubes (4 mL) as chambers. The rack is placed over the inlet holes and is inverted together with the plates which are then emptied.

Centrifugal CCD According to Åkerlund

This kind of CCD machine uses centrifugation to speed up the settling of the phases. It consists of an outer ring with cavities for the lower phases (attached to a bottom plate) and an inner plate with cavities for the upper phases (Figure 6.) The inner plate can rotate relative to the outer ring. When the chambers have been loaded with systems they are covered with a lid. As in the case of the thin-layer machine the functional unit is placed on a (round) table which can be shaken. In this case, however, the table can also rotate to allow centrifugation of the mixed systems which speeds up the settling of the phases. The upper phases are then transferred to the neighbouring lower

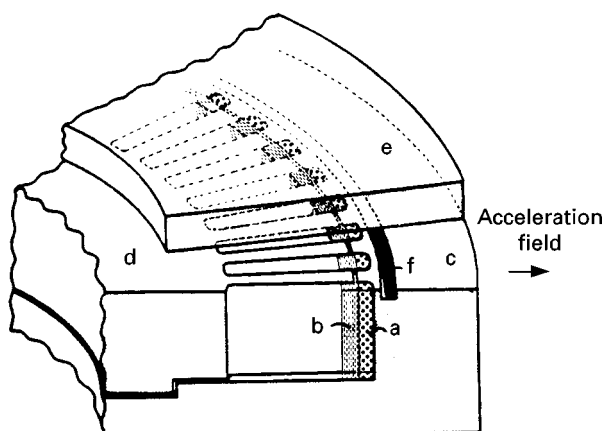


Figure 6 Centrifugal CCD according to Åkerlund. A section of the circular separation unit is shown. It is composed of four units: c, the outer ring with cavities for the lower phase; d, the inner plate with cavities for the upper phase; e, the lid; and f, an O-ring for sealing. The position of the two-phase system during centrifugation is shown, with the upper phase, a, and the lower phase, b. (From Johansson G, Åkerlund H-E and Olde B (1984) *Journal of Chromatography* 311: 277, by permission.)

phases by rotation of the inner plate when the whole system is still spinning and the phases are in a vertical position. After the transfer the centrifugation is stopped and a new cycle begins with the shaking process. After the run the phases are collected by pipette.

Continuous apparatus, such as extraction columns and coil planet centrifuges, also corresponds to a CCD process but differs in that no discrete steps are used and equilibrium is not reached.

Analytical Applications

Many metal ions can be separated by using various kinds of water/organic solvent systems for counter-current distribution. Metal chelators, such as dithizone, 8-quinolinol, cupferron, dimethylglyoxime and acetylacetone, are used specifically to extract metal ions into the organic phase. Likewise certain anions such as halides, thiocyanate or nitrate can be used. For example, uranium and plutonium have been separated by using an aqueous phase containing 8 mol L^{-1} nitric acid.

Biochemical Applications

CCD has been used for fractionation of a number of biochemical substances and cellular particles as well as cells and viruses. Peptides, proteins and nucleic acids have been fractionated by using aqueous two-phase systems composed of water and the two polymers dextran and poly(ethylene glycol) (PEG). The partition coefficients of the solutes can be adjusted by addition of various salts to the two-phase system and

by adjusting the pH value. More selective adjustment of the partitioning has been carried out by linking an affinity ligand to one of the phase-forming polymers which then is concentrated in one of the phases.

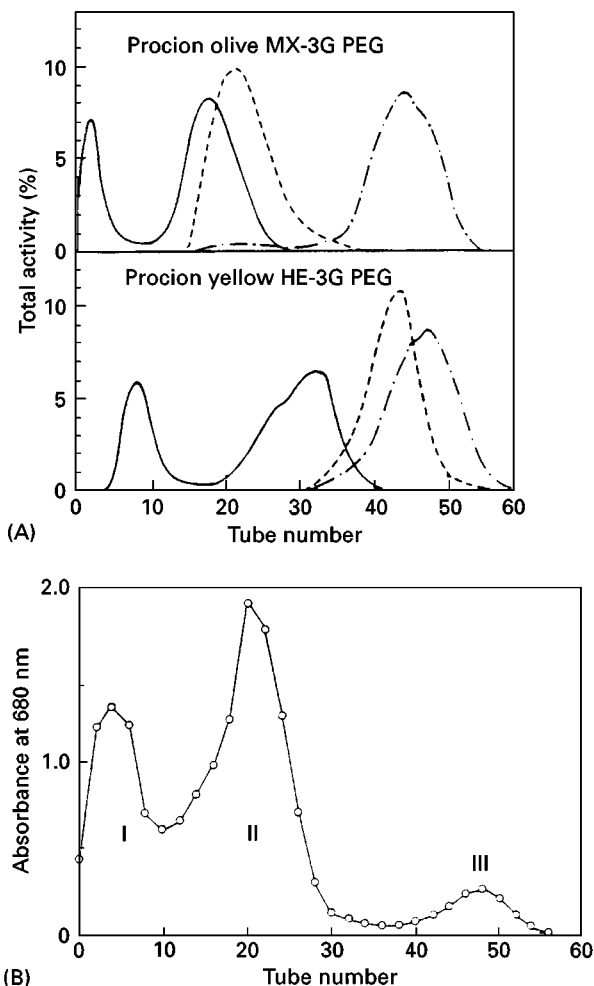


Figure 7 Countercurrent distribution of proteins and cell organelles. (A) Distribution of the enzymes hexokinase (—), 3-phosphoglyceratekinase (---), and phosphofructokinase (·····) when an extract of baker's yeast was applied to a CCD with 55 transfers. The textile dyes Procion olive MX-3G or Procion yellow HE-3G were used as PEG-bound affinity ligands enriched in the mobile upper phase. Composition of two-phase system: 88% (w/w) water, 7% (w/w) dextran 500, 5% PEG with $M_r = 8000$, including dye-PEG, 1% of total PEG 50 mmol L^{-1} sodium phosphate buffer, pH 7.0, 0.2 mmol L^{-1} ethylenediamine-tetraacetic acid and 5 mmol L^{-1} 2-mercaptoethanol. Volume ratio, 1.5. Temperature, 3°C . A centrifugal CCD apparatus was used with 5 min shaking and 3 min settling (centrifugation). (Adapted from Johansson G, Joelsson M and Åkerlund H-E (1984) *Journal of Chromatography* 298: 483, by permission.) (B) Fractionation of photosynthetic particles, chloroplasts, from spinach using a thin-layer CCD apparatus with 56 transfers and a dextran-PEG two-phase system. Peak I, intact chloroplasts surrounded by their envelope; peak II, naked thylakoid membranes (class II chloroplasts); peak III, chloroplasts surrounded by a 'bag' of plasma membrane also containing cytoplasm, mitochondria and peroxisomes. (From Larsson C, Collin C and Albertsson P-Å (1971) *Biochimica Biophysica Acta* 245: 425, by permission.)

Biological membranes, cell organelles, whole cells and viruses can be fractionated by CCD in the same kind of systems. In this case, however, the particles partition between the two liquid phases and the interface between them. The CCD is therefore usually carried out using a stationary interface. This is achieved by using a smaller volume of the lower phase than is needed to fill the lower cavities. Therefore, a portion of the upper phases will also be stationary. The *G* value satisfying eqn [5] is in this case defined as the amount of a pure compound, at equilibrium, in the mobile part of the upper phase divided by the amount of the compound in the rest of the system (stationary upper phase, interface and lower phase). Examples of CCD of proteins and of chloroplasts, the photosynthetic organelle in green plant cells, are given in Figure 7.

See also: II/Chromatography: Countercurrent Chromatography and High-Speed Countercurrent Chromatography: Instrumentation.

Further Reading

- Åkerlund H-E and Albertsson P-Å (1994) Thin-layer countercurrent distribution and centrifugal countercurrent distribution apparatus. *Methods in Enzymology* 228: 87–99.
- Craig LC (1962) Countercurrent distribution. In: Florkin M and Stotz EH (eds) *Comprehensive Biochemistry*, vol. 4, pp. 1–31. Amsterdam: Elsevier.
- Hecker E (1995) *Verteilungsverfahren im Laboratorium*. Weinheim: Verlag Chemie.
- Morris CJOR and Morris P (1976) *Separation Methods in Biochemistry*, 2nd edn, pp. 638–702. London: Pitman.

Solid-Phase Extraction

C. F. Poole, Wayne State University, Detroit, MI, USA

Copyright © 2000 Academic Press

Solid-phase extraction is a method used to isolate analytes from a gas, fluid or liquid by their transfer to and retention on a solid-phase sorbent. After separation of the sorbent from the sample the analytes are recovered by elution using a liquid or fluid, or by thermal desorption into the gas phase. If the analytes are recovered from the sorbent in a final volume that is only a fraction of the sample volume, then concentration as well as isolation is achieved. In addition, if the sorption step, any subsequent rinse steps, and the elution conditions are selective for retention and recovery of the analyte, then matrix simplification is achieved. Isolation, concentration and matrix simplification are the primary goals of solid-phase extraction.

Probably the earliest application of solid-phase extraction was the use of charcoal-filled columns in the 1950s to isolate organic contaminants from surface waters for toxicity evaluation. The large volume of water generally sampled (more than 1000 L over several days) precluded the use of liquid-liquid extraction techniques. The subsequent evolution of solid-phase extraction techniques is summarized in Figure 1.

The introduction of macroporous polymers in the early 1970s was responsible for rekindling interest in solid-phase extraction and extending its scope to air sampling and the isolation of drugs from

biological fluids. These sorbents had reasonable mechanical strength compared with gels, a large surface area and sample capacity, low water retention, and gave high sample recoveries by solvent desorption. Compared with carbon the overall analyte recovery was generally better and irreversible adsorption and catalytic activity greatly diminished. These

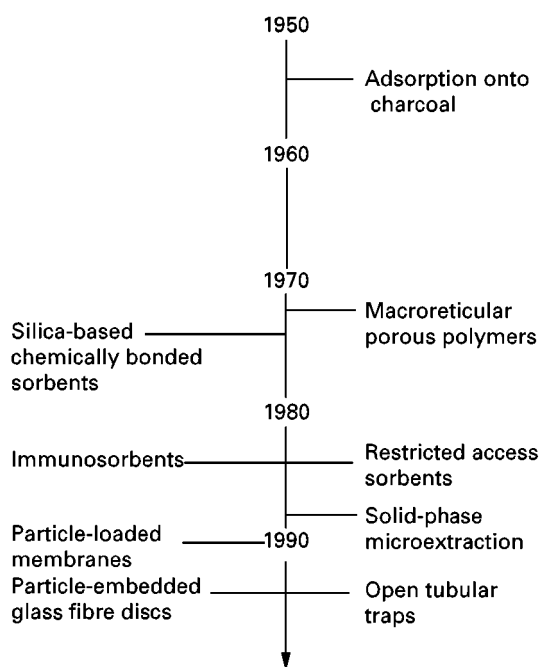


Figure 1 Time line showing the general evolution of solid-phase extraction techniques.

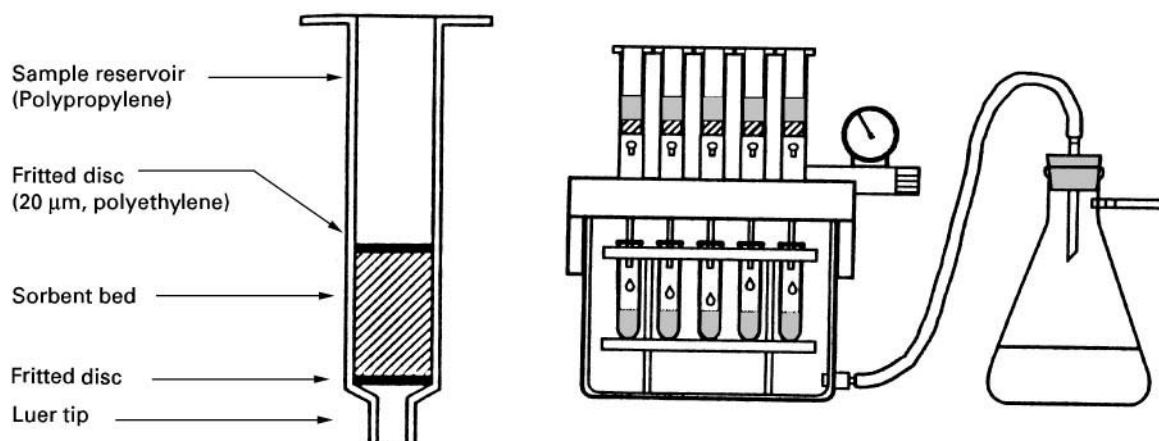


Figure 2 Schematic diagram showing the typical construction of a solid-phase extraction cartridge and a vacuum manifold for parallel sample processing.

properties, together with a reduction in the amount of material needed for identification due to improved instrumentation, resulted in the general use of small columns, similar in size to those in use today. Porous polymers with high thermal stability and low water retention revolutionized the room temperature sorbent extraction of volatile organic compounds from air or purge gas from water samples. Trapped compounds were thermally desorbed directly into a gas chromatograph for analysis. Automated systems based on the above process are used for routine analysis today.

Solid-phase extraction for liquid samples became a widely used laboratory technique with the introduction of disposable sorbent cartridges containing porous, siloxane-bonded silica particles, sized to allow sample processing by gentle suction (Figure 2). A typical solid-phase extraction cartridge consists of a short column (generally an open syringe barrel) containing a sorbent with a nominal particle size of 50–60 µm, packed between porous metal or plastic frits. A large number of sorbents are in use today corresponding to the desire for general purpose, class-specific and even compound-specific extractions.

Slow sample processing rates for large sample volumes, low tolerance to blockage by particles and sorbed matrix components, and problems arising from the low and variable packing density of cartridge devices spawned the development of alternative sampling formats based on disc technology. At least three different designs for solid-phase extraction discs are offered commercially today. The particle-loaded membranes consist of a web of polytetrafluoroethylene (PTFE) microfibrils, suspended in which are sorbent particles of about 8–10 µm diameter. The membranes are flexible with a homogene-

ous structure containing 80% (w/w) or more of sorbent particles formed into circular discs 0.5 mm thick with diameters from 4 to 96 mm. For general use they are supported on a sintered glass disc (or other support) in a standard filtration apparatus using suction to generate the desired flow through the membrane (Figure 3). Particle-embedded glass fibre discs contain 10–30-µm sorbent particles woven into a glass fibre matrix. The small diameter discs are rigid and self-supporting, while the larger diameter discs require a supporting structure. Speediscs® (Figure 4) consist of a sandwich of 10-µm sorbent particles held between two glass-fibre filters, with a screen to hold the filters in place. Disc technology has contributed directly to the automation of solid-phase extraction through the development of the multiwell extraction plate (Figure 5), which is used for the clean-up of samples in high-throughput screening techniques for drug development. Direct coupling of solid-phase extraction and high pressure liquid chromatography for on-line sample processing and analysis is now routine and the direct coupling of solid-phase extraction and gas chromatography for the analysis of liquid samples has moved beyond the research phase. Several research groups have demonstrated the direct coupling of solid-phase extraction and electrophoretic and thin-layer chromatographic separation techniques.

Replacement for Liquid–Liquid Extraction

Solid-phase extraction was introduced as a replacement for liquid–liquid extraction to give a practical and economic solution to the real and perceived problems associated with solvent extraction techniques. Liquid–liquid extractions are labour

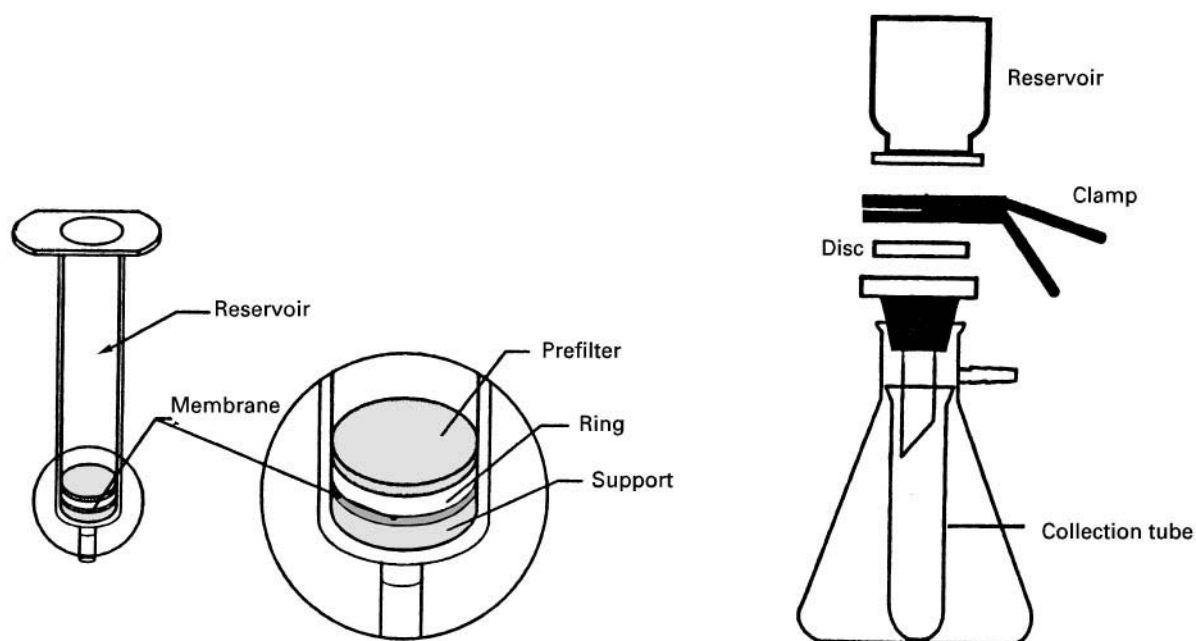


Figure 3 Typical cartridge and vacuum filtration formats for solid-phase extraction using discs.

intensive, difficult to automate, and frequently plagued by practical problems, such as emulsion formation. Liquid-liquid extractions also tend to consume large volumes of high purity solvents, which may have significant health hazards and disposal costs associated with their use. In contrast, solid-phase extraction benefits from lower intrinsic costs, reduced processing times, low solvent consumption and simpler processing procedures. Solid-phase extraction procedures are easily automated using robotics, or special purpose flow processing units that

simultaneously extract samples and prepare them for automatic injection, or by using centrifugal analysers, which can batchwise process multiple samples. Solid-phase extraction is convenient for field sampling since it minimizes the transport and storage problems of bulk samples, which have to be returned to the laboratory for processing.

Solid-phase extraction techniques have their own, although different, problems to those of liquid-liquid

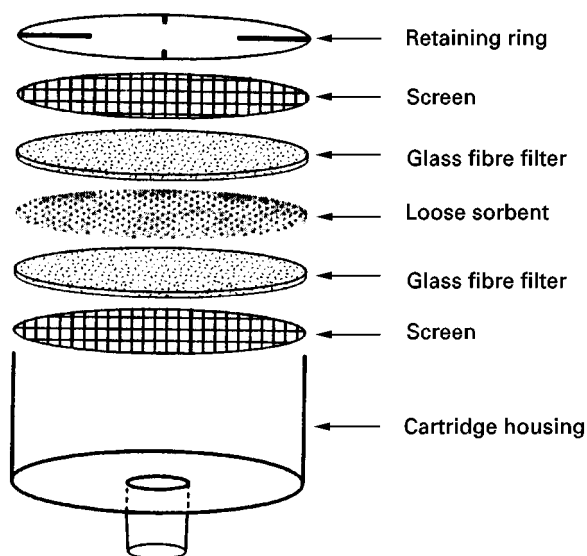


Figure 4 Exploded-view of the Speedisc® used for solid-phase extraction.

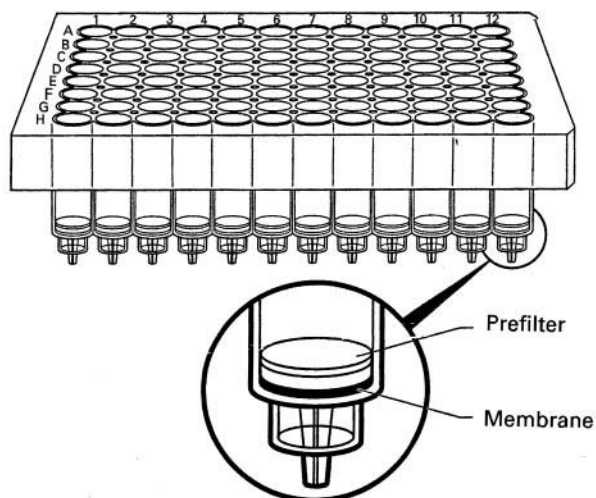


Figure 5 Multiwell plate for automated solid-phase extraction. (Reproduced with permission from Plumb RS, Gray RDM, and Jones CM (1997). Use of reduced sorbent bed and disc membrane solid-phase extraction for the analysis of pharmaceutical compounds in biological fluids, with applications in the 96-well format. *Journal of Chromatography B* 694:123-133.)

extraction. The sorption properties of manufactured sorbents are not as reproducible as solvent properties. Basic drugs, for example, are often retained on silica-based, chemically bonded sorbents by a mixed retention mechanism involving non-specific sorption by the bonded phase and ion exchange interactions with accessible, dissociated silanol groups. The mixed retention mechanism can interfere in the recovery of analytes since solvent elution may be ineffective for removing ionically bound analytes, and the extent of binding through ionic sites can vary for different sorbent lots. Sorbents tend to have a higher level of contamination by manufacturing and packaging materials than do solvents. The chemical background from impurities may interfere in the subsequent analysis of the sample. Solvent rinsing of cartridges and discs and the running of blanks to establish background contamination levels diminishes sample throughput and adds significantly to solvent consumption and processing costs. Sample processing problems, such as column overloading, displacement and blocking of sorbent pores, easily go unnoticed, resulting in changes in analyte recovery. Sample overload and displacement are more important for extraction based on adsorption than for extraction based on absorption.

When choosing between liquid-liquid or solid-phase extraction for a particular problem, economic, as well as technical features, should be taken into consideration. In this sense, liquid-liquid and solid-phase extraction techniques should be considered complementary approaches, and although the general trend is towards the replacement of liquid-liquid extraction methods by solid-phase extraction, this is never likely to be a complete replacement.

Disc Versus Cartridge Format

Cartridges have a small cross-sectional area, a slow sample processing rate, and a low tolerance to blockage by particles and adsorbed matrix components. For large sample volumes containing suspended particles, discs are likely to function better. Discs provide shorter sample processing times due to their larger cross-sectional area and decreased pressure drop, enabling higher sample flow rates to be used. The larger cross-sectional area also reduces problems with plugging. For example with a high particle burden, discs with integral or separate depth filters are available, as well as different materials that can be added to the surface of the disc as filter aids.

Because of the low packing density of typical cartridge devices, longer sorbent beds than are needed for extraction are used to compensate for reduced retention resulting from channelling. Increased bed

mass results in increased non-specific matrix adsorption and dirtier extracts. The use of smaller particles and the greater mechanical stability of discs reduces channelling, and the optimized use of bed mass results in a cleaner background and lower interferences due to reduced matrix adsorption. For small sample sizes it is easier to miniaturize discs than cartridges, and several disc devices (e.g. microdiscs, pipette tips, etc.) that contain only a few milligrams of sorbent for processing small samples are available. Immobilized analytes on microdiscs facilitate integrated sample processing techniques such as in-vial extraction and on-disc derivatization.

Inorganic Oxide Adsorbents and their Applications

The most important adsorbents for extraction and matrix simplification are silica gel, alumina, Florisil and diatomaceous earths. Silica gel, prepared from sodium silicate using the sol-gel procedure, is the most widely used general-purpose adsorbent. Silica gels used for solid-phase extraction have surface areas of about $300\text{--}800\text{ m}^2\text{ g}^{-1}$, pore sizes from 4–10 nm, and an apparent pH of 5.5–7.5. The apparent sorbent pH is characterized as the observed pH of a 5% (w/w) aqueous suspension. Alumina is prepared by the low temperature dehydration ($< 700^\circ\text{C}$) of alumina trihydrate and is a mixture of γ -alumina with small amounts of α -alumina (less active form) and sodium carbonate. Depending on processing conditions, alumina is available as neutral ($\text{pH } 7.5 \pm 0.5$), weakly acidic ($\text{pH } 6.0 \pm 0.5$), acidic ($\text{pH } 4.5 \pm 0.5$) and basic ($\text{pH } 9.5 \pm 0.5$) forms. Adsorbents used for extraction and matrix simplification have a surface area of about $150\text{ m}^2\text{ g}^{-1}$ and a pore size of 6 nm. Florisil is a magnesium silicate prepared by precipitation from a mixture of magnesium sulfate and sodium silicate solutions followed by calcining at about 1200°C . It has a surface area of about $250\text{--}300\text{ m}^2\text{ g}^{-1}$ and an apparent pH of about 8.5. Diatomaceous earths are flux-calcined forms of natural silica with very small surface areas. They are used as a filter aid and as a dispersant for liquid extraction using matrix dispersion techniques (see matrix dispersion).

The general extraction mechanism and applications of the inorganic oxide adsorbents are summarized in Table 1. Adsorbent properties that increase retention are a larger surface area and a high activity. Adsorbent activity is controlled by the intentional addition of water to the dried adsorbent prior to use and by drying extracts with anhydrous sodium sulfate, or a similar drying agent, prior to applying the extract to the adsorbent. A small column of

Table 1 General applications of solid-phase extraction**(1) Inorganic oxide adsorbents**

- Isolation of low and medium polarity analytes from non-aqueous solutions
- Isolation of cations (alumina and silica) and anions (alumina) from buffered aqueous solutions
- Matrix simplification by fractionation into groups containing a similar number and type of functional group

Examples

- ⇒ Isolation of organochlorine pesticides and polychlorinated biphenyls from transformer oil, animal fats and oils, etc. using Florisil.
- ⇒ Isolation of lipids by chromatography over silica gel using chloroform to elute simple lipids, acetone to elute glycolipids and methanol to elute phospholipids.
- ⇒ Group fractionation of polycyclic aromatic compounds (hydrocarbons, *N*-containing and *OH*-containing) in synthetic fuels over alumina using a step solvent gradient.
- ⇒ Isolation of paraquat and diquat from high moisture crops in a pH 9 aqueous extract using silica gel
- ⇒ Mycotoxins in feeds using silica gel
- ⇒ Pesticides in foods, feeds and soil extracts; alkaloids, pigments and flavour compounds from plants; sugars and caffeine in cola beverages, inorganic anions and organic acids in aqueous solution using alumina; steroids and vitamins from creams and oil-based suspensions.

(2) Low specificity sorbents (aqueous solutions)

- Isolation of neutral and ionizable analytes from aqueous solution. Weak acids and bases by ion suppression. Strong acids and bases using ion pair extraction (alternative to ion exchange)
- Retention increases with solute size and is reduced by polar interactions (particularly hydrogen-bonding) and ionization
- Polar bonded phases provide only weak retention and are not particularly useful unless elution of the analyte is a problem from non-polar sorbents

Examples

- ⇒ Isolation of agricultural and industrial chemicals from surface waters using C₁₈, carbon or poly(styrene-divinylbenzene) (PS-DVB)
- ⇒ Isolation of drugs from biofluids using C₁₈, C₈, PS-DVB or cyanopropyl (CN)
- ⇒ Isolation of macromolecules from biofluids and fermentation broth using C₄
- ⇒ Isolation of pigments and colouring materials from beverages and food extracts using C₁₈
- ⇒ Isolation of carbohydrates and nucleosides from biofluids using AMINO
- ⇒ Isolation of proteins, peptides and surfactants using DIOL

(3) Low specificity sorbents (organic solvents)

- Retention depends on the type and number of functional groups. Solute size is not important
- CN Strong dipole-type interactions and weak hydrogen-bond acidity
- AMINO Strong hydrogen-bond base and weak hydrogen-bond acid. Weak dipole interactions
- DIOL Strong hydrogen-bond acid and weak hydrogen-bond base with significant capacity for dipole-type interactions

Examples

- ⇒ Isolation of polar pesticides from fats and oils
- ⇒ Isolation of polycyclic aromatic compounds from fuel oils
- ⇒ Active ingredients from ointments and suppositories

(4) Ion-exchange sorbents

- In general strong ion exchangers are used to isolate weak acid/bases of opposite charge and weak ion exchangers strong acid/bases
- Retention selectivity can be adjusted by manipulating the sample pH and ionic strength
- Choice of competing ion, its concentration and eluent pH controls selectivity for matrix simplification and elution
- Isolation of macromolecules in an active form may require special non-denaturing sorbents based on cellulose, agarose or dextran

Examples

- ⇒ Isolation of carboxylic, sulfonic and phosphoric acids, phenols, amines and inorganic ions from water
- ⇒ Isolation of amino acids, organic acids, nucleosides and nucleotides from biofluids
- ⇒ Isolation of organic acids and bases from coal-derived and synthetic fuels
- ⇒ Isolation of organic acids, phenols and amines from wine, fruit juices and food extracts

sodium sulfate connected in tandem with the adsorbent cartridge can be used as an additional precaution. The Brockmann scale (based on the relative retention of test dyes, see Table 2) provides a widely used standardized scale of adsorbent activity. Adsorbents of defined activity are prepared by adding a known amount of water to the adsorbent, shaking to avoid clumping, and then allowing the adsorbent to equilibrate overnight in a closed container. Analyte properties that increase retention depend on the num-

ber and type of functional groups present. Hydrogen-bonding functional groups are strongly retained, those with a significant dipole-character are retained to a lesser extent, and polarizable functional groups are the least retained. Irreversible adsorption and catalytic degradation of sensitive analytes can occur on all inorganic oxide adsorbents and is a source of low recovery for some analytes. Alumina and silica can function as selective ion exchange sorbents with buffered aqueous samples (see Table 1).

Table 2 Standardization of adsorbent activity

Brockmann activity grade	Percentage of water (w/w)		
	Alumina	Silica gel	Florisil
I ¹	0	0	0
II	3	5	7
III	6	15	15
IV	10	25	25
V	15	38	35

¹Activate sorbents by heating alumina at 400°C for 8–12 h, silica gel at 180°C for 8–12 h, and Florisil at 130°C for 8–12 h.

Coating silica or alumina with chemical reagents, such as sulfuric acid, sodium hydroxide, alkaline potassium permanganate, silver nitrate, etc., is used to improve the selectivity of the isolation of some analytes from their matrix. Silver nitrate, for example, improves the isolation of olefins from hydrocarbons due to formation of charge-transfer complexes. Acids can be used for the selective isolation of bases and vice versa. Silica impregnated with 2,4-dinitrophenylhydrazine is widely used for the selective isolation of volatile ketones and aldehydes from air for analysis by high pressure liquid chromatography.

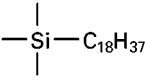
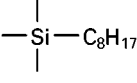
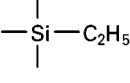
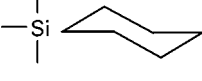
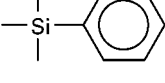
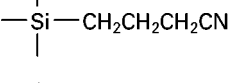
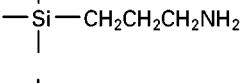
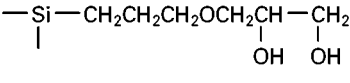
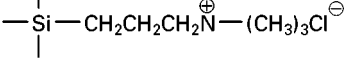
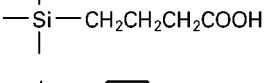
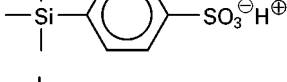
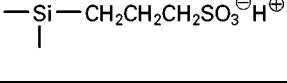
Low Specificity Sorbents and Their Applications

Low specificity sorbents include silica-based, chemically bonded sorbents, macroreticular porous polymers and various forms of carbon. Silica-based, chemically bonded sorbents are derived from materials developed for high pressure liquid chromatography. They are generally prepared by reaction of monofunctional or trifunctional silanes with silica gel followed by end-capping in some cases. Trifunctional reagents result in sorbents with a polymeric-bonded layer of higher carbon loading and greater acid stability and are the more common type of sorbent in general use. Chemically bonded sorbents can be prepared with a wide range of bonding densities, pore sizes and functional group types. Some common examples are given in Table 3. Chemically bonded sorbents with large surface areas, long alkyl chains and high phase loading maximize retention of small analytes from aqueous solution, while wide-pore materials with low phase loading and short alkyl chains are generally used to isolate macromolecules. Chemically bonded sorbents with immobilized polar functional groups are used to isolate analytes from organic solutions, based on their selective interactions with analyte polar functional groups (see Table 1).

The macroreticular porous polymers are copolymers of styrene-divinylbenzene or acrylic esters, prepared by suspension polymerization to yield particles consisting of agglomerates of randomly packed microspheres permeated by a network of holes and channels (Table 4). They are used exclusively for extraction from aqueous solution and are more retentive than most chemically bonded phases. They possess a high sample capacity and are frequently used in large-scale isolation studies and for the purification of industrial products. Tenax[®], a polymer based on 2,6-diphenyl-4-phenylene oxide, revolutionized the sorbent trapping of volatile organic compounds from air and the purge-and-trap analysis of volatile organic compounds in water. It exhibits strong retention of semivolatile organic compounds (>C₇) at room temperature with little adsorption of water vapour and can be rapidly heated to high temperatures, without thermal breakdown, for the recovery of analytes by thermal desorption. Since no single adsorbent is ideal for trapping all analytes it is common practice to use cartridges packed with several adsorbent beds in series, so that a broad range of compounds with different molecular weight and polarity can be trapped on a single cartridge. Besides Tenax, different forms of carbon, silica gel and liquid-coated sorbents are used. In a multiple bed cartridge, each bed protects the next, increasingly active bed, by preventing compounds from being held so strongly that they cannot be desorbed quickly without decomposition. During thermal desorption the carrier gas passes through the trap in the reverse direction to the sample flow and the desorbed compounds are swept onto the separation column in a gas chromatograph. A cryogenic interface may be used to refocus the desorbed sample to improve the chromatographic separation. The complete processes of desorption and separation can be automated for sample cartridges stored in an autosampler.

The common forms of carbon used in solid-phase extraction are granular activated carbon, graphitized carbon blacks and carbon molecular sieves. Granular activated carbons are prepared by the low temperature oxidation of vegetable charcoals. They have large surface areas (300–2000 m² g⁻¹), a wide pore size distribution, and a heterogeneous surface containing active functional groups. Their use in solid-phase extraction is largely confined to the isolation of dissolved organic compounds in surface waters, and as the sorbent material in personal monitors for sampling workplace atmospheres. The most common form of personal monitor makes use of a sorbent cartridge filled with activated charcoal in conjunction with a small pump to maintain a fixed flow of air through the cartridge. Trapped volatile compounds

Table 3 Structures of silica-based chemically bonded sorbents

Type	Functional group	Structure
C ₁₈	Octadecyl	
C ₈	Octyl	
C ₂	Ethyl	
CH	Cyclohexyl	
PH	Phenyl	
CN	Cyanopropyl	
NH ₂	Aminopropyl	
DIOL	2,3-Dihydroxypropoxypropyl	
SAX	Trimethylaminopropyl (quaternary amine)	
CBA	Carboxypropyl	
SCX	Benzenesulfonic acid	
PRS	Propylsulfonic acid	

are then eluted with carbon disulfide or another solvent, or can be thermally desorbed by microwave heating, for separation by gas chromatography. Poor reproducibility of activated carbons and their variable chemical and catalytic activity result in limited laboratory use. Graphitized carbon blacks are more refined and generally nonporous, with surface areas between about 5–100 m² g⁻¹. They are used primarily for the room temperature trapping of volatile organic compounds (>C₄), either separately or in combination with Tenax®. Carbon molecular sieves have small pores and large surface areas (> 500 m² g⁻¹

with some >1200 m² g⁻¹). They are used primarily for the room temperature trapping of volatile organic compounds (C₁ and C₂), usually as a component of a multiple-bed sorbent trap for air sampling and purge-and-trap analysis.

Foamed polyurethanes, composed of agglomerated spherical micrometer-sized particles bonded to one another in a rigid and highly permeable structure, are suitable for sampling semivolatile organic compounds (e.g. airborne pesticides and polychlorinated biphenyls) at high flow rates. They are frequently used in conjunction with high-volume air samplers on

Table 4 Characteristic properties of some macroreticular porous polymer sorbents

<i>Amberlite sorbents</i>	<i>Mean pore diameter (nm)</i>	<i>Specific surface area (m² g⁻¹)</i>	<i>Pore volume (mL g⁻¹)</i>	<i>Sample molecular weight limit</i>
XAD-2 (STY-DVB)	9	300	0.65	20 000
XAD-4 (STY-DVB)	4	725	0.98	
XAD-7 (MMA)	9	450	1.14	60 000
XAD-16 (STY-DVB)	10	800	1.82	40 000
XAD-2010 (STY-DVB)	28	660	1.80	
DAX-8 (MMA)	22.5	160	0.79	150 000

STY-DVB, styrene-divinylbenzene; MMA, methylmethacrylate.

account of their low pressure drop compared with standard sorbent cartridges. They are used less frequently for water analysis where macroreticular porous polymers are considered a better choice.

Compound and Class-specific Sorbents and their Applications

Various forms of selective sorbents for solid-phase extraction based on ion exchange, bioaffinity, molecular recognition, and restricted access are used to supplement the general class of sorbents discussed above. Ion exchange is used to isolate ionizable compounds (usually) in aqueous solution with sorbents containing fixed ionic sites of opposite charge to the analytes of interest. Ion-exchange sorbents are usually classified as weak or strong depending on the identity of the ionic group and whether its charge is independent of the sample pH (strong ion exchanger) or can be manipulated by changing the pH (weak ion exchanger). Some examples of typical silica-based ion-exchange sorbents are indicated in Table 3. Ion-exchange sorbents with a porous polymer backbone are also commonly used and have a higher exchange capacity and a wider pH-operating range than silica-based sorbents. For many applications either silica-based or porous polymer ion-exchange sorbents with the same immobilized ionic groups can be used interchangeably, although, because of non-specific adsorption of matrix components, the chemical background of the extracts might be different. Ion-exchange sorbents are particularly attractive for the isolation of ionizable substances since the neutral molecules, which may interfere in the final chromatographic analysis, are easily rinsed from the sorbent without affecting the recovery of the ionized components. Mixed-mode sorbents containing ion-exchange sites and alkyl groups co-bonded to silica in either cartridge or disc format are popular in clinical and pharmaceutical laboratories, where they are used for the isolation of ionized drugs and their metabolites from biological fluids. Standard protocols using

mixed-mode sorbents have been developed for the isolation of most drugs of abuse (e.g. amphetamines, barbiturates, cocaine, opiates, etc.). The strong retention and the use of efficient rinse solvents results in cleaner extracts compared with single-mode sorbents, suitable for screening by thin-layer chromatography and confirmation by gas chromatography-mass spectrometry.

Resin-bound phenylboronic acids are used for the isolation of compounds with vicinal diol groups such as steroids, catecholamines and nucleotides. Surface-bonded macrocyclic ligands, cryptands, can be used for the selective isolation of metal ions. The cryptands can be synthesized with a variety of cavity sizes suitable for the isolation of different metal ions. The metal ion is sorbed in the cavity of the cryptand until released by elution with a solution of a complexing agent with a high binding constant for the metal.

Immunosorbents have been used for a long time for sample pretreatment in medicine and biology, but more general applications, such as to environmental analysis, are relatively recent. In part, this is due to the difficulty of making antibodies selective to small molecules, as well as a lack of familiarity among analytical chemists of the procedures used to make specific antibodies. Immunosorbents are prepared by covalently bonding a suitable antibody to an appropriate sorbent. A high degree of molecular selectivity is obtained based on the specificity of the antibody-antigen (analyte) interaction. Because specificity is high, immunosorbents are able to isolate target analytes from complex matrices in a single step with minimal co-extraction of matrix interferences. By taking advantage of cross-reactivity, class-specific immunosorbents for the isolation of mycotoxins, phenylurea herbicides and polycyclic aromatic hydrocarbons have been developed. Manufactured immunosorbents have been available for only a short time and the range of products is still narrow. A laboratory familiar with the techniques for raising and isolating antibodies is required.

Molecular imprinting is a technique used for preparing polymers with synthetic recognition sites

having a predetermined selectivity for a specified analyte. The imprint is obtained by arranging polymerizable functional monomers around a template (the analyte). Template–monomer complexes are formed in solution through molecular interactions and subsequently fixed in place by cross-linking. Removal of the template from the resulting polymer matrix creates vacant recognition sites that exhibit affinity for the analyte. For the time being, it is impossible to predetermine the experimental conditions for successful imprinting of target analytes. The template molecule may be difficult to leach from the imprinted polymer, reducing the binding capacity of the polymer, but more seriously, it may lead to contamination of sample extracts. Only a few practical applications using molecularly imprinted polymers for solid-phase extraction have been demonstrated so far, most of which are for the isolation of drugs from biological fluids, but the future for this technology looks very promising. Molecularly imprinted polymers should be easier and cheaper to produce in chemical laboratories than antibodies while, at least in theory, they should be capable of similar specificity.

Restricted access sorbents have been developed for the isolation of low molecular weight compounds, generally drugs, directly from biological fluids with minimum sample pretreatment. They work by preventing access of macromolecules (proteins) to those regions of the sorbent where retention of the analyte occurs. Restricted access to the retentive part of the sorbent is provided by either a physical diffusion barrier, such as a pore diameter, or by a chemical diffusion barrier, such as a polymer network at the outer surface of the particle. In addition, the outer surface of the particles must be non-adsorptive and protein-compatible. Restricted access sorbents are commonly used for automated on-line sample processing in liquid chromatography. In this case, a short precolumn packed with the restricted access material is interfaced to a separation column by a six-port switching valve. The biofluid is injected directly onto the precolumn, which retains the analytes of interest. Potentially interfering sample constituents are then flushed to waste. Macromolecules (proteins) pass through the precolumn unretained and do not interfere in the subsequent separation of the analytes. The analytes retained on the precolumn are eluted on-line to the separation column and detected. Simultaneously the precolumn is reconditioned (or exchanged) before processing the next sample. An important consideration for automated sample processing is the ability of the restricted access sorbent to repeatedly extract the analyte without change in properties or accumulation of sample matrix components.

Sample Processing Considerations

Solid-phase extraction cartridges are available in a range of sizes containing from about 35 mg to 10 g of sorbent, with the 100 mg and 500 mg sorbent cartridges (or discs) being the most widely used for extraction and the larger cartridge sizes for sample clean up. As a rough guide, the sorbed sample capacity of a solid-phase extraction device is about 1–5% of the sorbent mass. The sample volume that can be processed depends primarily on the breakthrough volume of the analyte, the concentration of the analyte matrix, sample flow rate, and the sorbent mass. The sample volume is often selected to conform to the needs of the instrumental detection step, and as instrumental methods of determination have improved in sensitivity, sample volumes have decreased in size. Regulatory authorities often indicate action levels in concentration units, which can also be used to define an adequate sample volume for analysis.

Sorbent selection is based on the considerations summarized in **Figure 6**. The sample solvent (aqueous or organic), the analyte type (non-polar, polar or ionized), and whether it is ionized (strong or weak, acid or base) provides a logical guide for method selection. Organic compounds soluble in polar organic solvents but difficult to dissolve in solvents of intermediate polarity, can be extracted in the reversed-phase mode if they can be reconstituted in aqueous solution.

Sample processing involves four distinct steps. Initially, the sorbent is conditioned with solvent to improve the reproducibility of analyte retention and to reduce the carrythrough of sorbent impurities at the elution stage. The conditioning solvent is then replaced with the same solvent as the sample solvent and the sample passed through the sampling device at a controlled flow rate. Optionally, after the sample has been processed, the sorbent is rinsed with a weak solvent to displace undesired matrix components from the sorbent without displacing the analytes. Finally, the analytes of interest are eluted from the sorbent in a small volume of strong solvent for subsequent determination. Hidden in the above description of events are a number of sub-steps that can dramatically influence analyte recovery if not adequately optimized (**Table 5**). The conditioning step is critically important for processing aqueous samples using particle-loaded membranes. The high surface tension of water combined with the microporosity of the discs results in slow and uneven flow through the discs and low analyte recovery if the discs are not first conditioned with an organic solvent. For large sample volumes, a small amount of the same organic solvent is usually added to the sample to maintain a constant

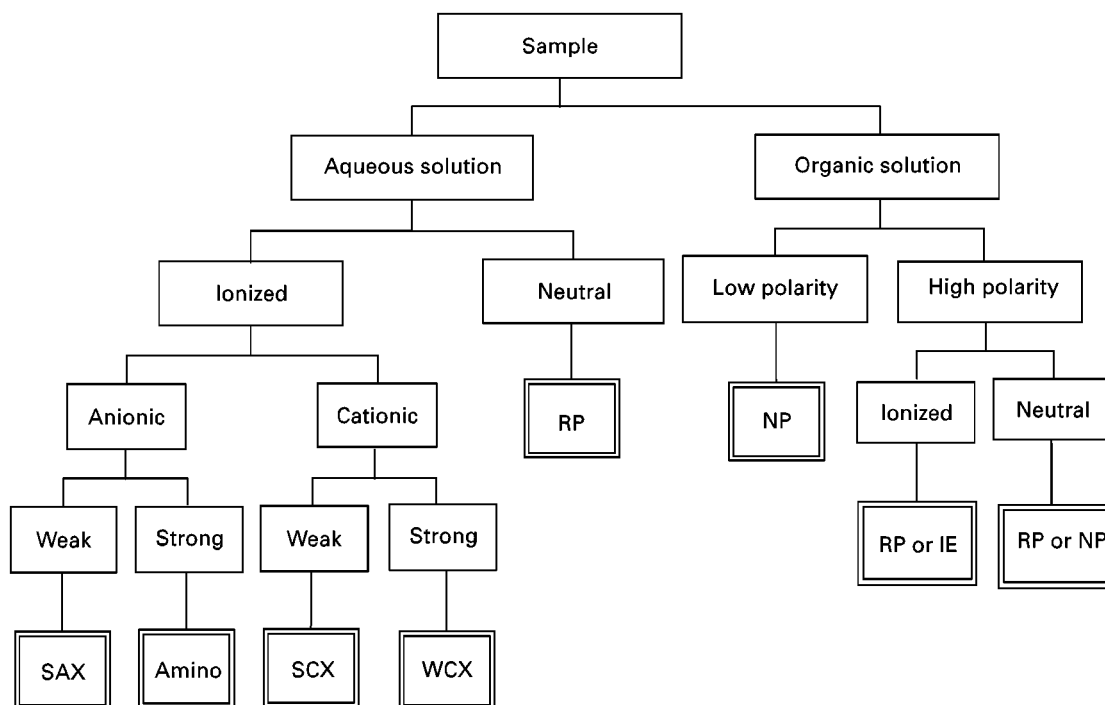


Figure 6 Method development guide for the isolation of organic compounds from liquid samples. SAX, strong anion exchanger; SCX, strong cation exchanger; WCX, weak cation exchanger; RP, reversed-phase sampling mode; NP, normal-phase sampling mode; IE, ion exchange sampling mode.

sample flow rate. The drying step between processing aqueous samples and eluting the retained analytes with a water-miscible organic solvent is also important. The purpose of the drying step is to reduce the volume of water co-eluting from the sampling device permitting further concentration of the eluent by the gas-blow down method. Drying, by suction or storage in a vacuum desiccator, should be sufficient to remove water trapped in the pores, but excessive drying can result in low analyte recovery from evaporation or inefficient elution. A new porous polymer sorbent, prepared by copolymerization of divinylbenzene and *N*-vinylpyrrolidone (Oasis HLB), and solvated by water alone, has been suggested as a solution to this problem. Recently, it was shown that all sample-processing steps are amenable to computer-aided method development, replacing the traditional experimental trial-and-error approach by fast computer simulations.

Automation

Automation provides a better utilization of laboratory resources, unattended and out-of-hours operation and improved precision compared with manual methods. Common approaches to automation differ significantly. Using robotics, samples are processed

(usually) in a similar manner to manual methods. Using flow-processing schemes, samples are extracted in parallel with computer or microprocessor control of solvent management. Sorbent conditioning, sample condition, solvent selection, rinse and elution steps are performed automatically and can be varied for method development. Positive displacement instead of suction is used for solvent control, and advanced units can be programmed to replace sorbent cartridges to increase sample throughput and inject extracts into different chromatographic instruments. On-line analysers with a direct coupling to chromatographic instruments are widely used. Solid-phase extraction using short precolumns and a switching valve interface is a routine method for analysis by liquid chromatography. Advanced systems even allow programmed replacement of the sorbent cartridges and unattended 24-hour operation. The recovery and separation steps of purge-and-trap and sorbent trapping of volatile organic compounds from air are easily automated using thermal desorption with cold trapping, if required, for the direct injection of analytes into a gas chromatograph. Major strides have been made in the on-line solid-phase extraction of water samples with solvent desorption directly into a gas chromatograph. This method is not far from becoming routine today.

Table 5 Experimental variables that influence recovery of analytes by solid-phase extraction

-
- Conditioning solvent (typically 3–5 bed volumes)
 - ⇒ Ensures reproducible retention and flow. Critical step for particle-loaded membranes
 - ⇒ Helps to minimize contamination of extracts by sorbent impurities
 - ⇒ Replace by sample solvent before processing sample
 - Flow rates (typical range 0.2–1.5 mm s⁻¹)
 - ⇒ More critical for cartridges than discs due to their variable and heterogeneous packing density (channelling)
 - ⇒ More critical when the sample volume exceeds the breakthrough volume as typical sampling devices provide too few theoretical plates for flow-independent retention
 - Sample properties
 - ⇒ Dilute viscous samples with a weak low viscosity solvent to reduce sample processing time
 - ⇒ Remove excessive particle matter by filtration or centrifugation to maintain a constant sample-processing rate. Concentrated hydrochloric acid is effective for dissolving inorganic particles in water samples
 - ⇒ Add small volume of organic solvent (1–3% v/v) to large volume water samples to ensure sorbent remains solvated and to maintain a constant (fast) sample-processing rate. Important for particle-loaded membranes
 - ⇒ Adjust pH to reduce ionization of weak acids and bases for reversed-phase sampling
 - ⇒ Maintain ionic strength approximately constant for samples and standards with reversed-phase sampling conditions. Ionic strength is a critical parameter for ion-exchange extraction
 - ⇒ Deproteinization of biofluids may be required for acceptable recovery of low molecular weight analytes for reversed-phase sampling
 - ⇒ Precipitation of inorganic acids (sulfate, phosphate, etc.) by barium hydroxide is sometimes required for acceptable recovery of organic acids from biofluids using ion-exchange extraction
 - Drying time (typically 1–5 min, but sometimes considerably longer)
 - ⇒ Sufficient to remove all sample solvent trapped in the sorbent pores
 - ⇒ Excessive drying may result in low recovery of analytes from evaporation or retention in poorly solvated regions of the sorbent
 - Rinse solvent (optional)
 - ⇒ Small volume of intermediate strength solvent to elute matrix components. Analytes remain immobilized on the sorbent
 - ⇒ Biological fluids, plant extracts and soil extracts often require a rinse step but surface waters may not
 - Eluting solvent (ideally 2–3 bed volumes but often larger)
 - ⇒ Should be a strong solvent able to displace all analyte from the sorbent in a small volume
 - ⇒ Should normally be volatile and miscible with the sample solvent
-

Future developments

Solid-phase extraction is approaching maturity and is a familiar laboratory operation for many analytical chemists. Advances are expected in the area of specific sorbents based on molecular imprinting or bioaffinity designed for the convenient isolation of target compounds in complex matrices. Advances are also expected in the use of computer-aided method development for the prediction of sampling and recovery conditions by simulation to replace tedious experimental trial-and-error approaches. A wider use and further development of automated solid-phase extraction systems can be expected, particularly in those industries where high sample throughput or round-the-clock process monitoring are important.

See also: **II/Affinity Separation:** Immobilised Boronates and Lectins; Imprint Polymers. **Extraction:** Solvent Based Separation. **III/Airborne Samples:** Solid Phase Extraction. **Immunoaffinity Extraction.** **Immobilised Boronic Acids:** Extraction. **Molecular Imprints for Solid-Phase**

Extraction. Restricted-Access Media: Solid-Phase Extraction. Solid-Phase Extraction with Cartridges. Solid-Phase Extraction with Disks. Solid-Phase Matrix Dispersion: Extraction. Sorbent Selection for Solid-Phase Extraction. Appendix 2/Essential Guides to Method Development in Affinity Chromatography.

Further Reading

- Dean JR (1998) *Extraction Methods For Environmental Analysis*. Chichester: John Wiley.
- Hennion M-C and Pichon V (1994) Solid-phase extraction of polar organic pollutants from water. *Environmental Science and Technology* 28: 576A–583A.
- Masque N, Marce RM and Borrull F (1998) New polymeric and other types of sorbents for solid-phase extraction of polar organic micropollutants from environmental water. *Trends in Analytical Chemistry* 17: 384–394.
- Mayer ML and Poole CF (1994) Identification of the procedural steps that affect recovery of semi-volatile compounds by solid-phase extraction using cartridge and particle-loaded membrane (disk) devices. *Analytica Chimica Acta* 294: 113–126.

- Pinchon V, Bouzige M, Miegé C and Hennion M-C (1999) Immunosorbents: natural molecular recognition materials for sample preparation of complex environmental matrices. *Trends in Analytical Chemistry* 18: 219–235.
- Poole CF, Poole SK, Seibert DS and Chapman CM (1997) Determination of kinetic and retention properties of cartridge and disk devices for solid-phase extraction. *Journal of Chromatography B* 689: 245–260.
- Poole CF and Poole SK (1991) *Chromatography Today*. Amsterdam: Elsevier.
- Seibert DS and Poole CF (1998) A general model for the optimization of sample processing conditions by solid-phase extraction applied to the isolation of estrogens from urine. *Journal of High Resolution Chromatography* 21: 481–490.
- Sellergren B (1999) Polymer- and template-related factors influencing the efficiency in molecularly imprinted solid-phase extractions. *Trends Analytical Chemistry* 18: 164–174.
- Simpson NJK (2000) *Solid Phase Extraction: Principles, Strategies, and Applications*. New York: Marcel Dekker.
- Thurman EH and Mills MS (1998) *Solid-Phase Extraction, Principles and Practice*. New York: John Wiley.

Solid-Phase Microextraction

J. Pawliszyn, University of Waterloo, Waterloo, Canada

Copyright © 2000 Academic Press

Introduction

Solid-phase microextraction (SPME) was introduced as a solvent-free sample preparation technique in 1990. The basic principle of this approach is to use a small amount of the extracting phase (usually less than 1 μL) compared to the sample matrix. Sample volume can be very large, when the investigated system, for example air or lake water, is sampled directly. The extracting phase can be either a high molecular weight polymeric liquid, similar in nature to chromatographic stationary phases, or it can be a solid sorbent, typically of a high porosity to increase the surface area available for adsorption.

To date the most practical geometric configuration of SPME utilizes a small fused silica fibre, usually coated with a thin film of polymeric phase. The fibre is mounted for protection in a syringe-like device (Figure 1A). The analytes are absorbed or adsorbed by the fibre coating (depending on the nature of the coating) until an equilibrium is reached in the system. The amount of an analyte extracted by the coating at equilibrium is determined by the magnitude of the partition coefficient (distribution ratio) of the analyte between the sample matrix and the coating material.

In SPME, analytes typically are not exhaustively extracted from the matrix. However, equilibrium methods are more selective because they take full advantage of the differences in extracting phase/matrix distribution constants to separate target analytes from interferences. Exhaustive extraction can be achieved in SPME when the distribution constants are large enough. This can be accomplished for most compounds by cooling the fibre coating. This

concept was tested using a piece of microtubing coated on the outside instead of a solid rod and supplying liquid carbon dioxide into the tube to achieve an internally cooled fibre. In exhaustive extraction, selectivity is sacrificed to obtain quantitative transfer to target analytes into the extracting phase. One advantage of this approach is that, in principle, it does not require calibration, since all the analytes of interest are transferred to the extracting phase. On the other hand, the equilibrium approach usually requires calibration through the use of surrogates or standard addition to quantify the analytes and compensate for matrix-to-matrix variations and their effect on distribution constants.

Since equilibrium rather than exhaustive extraction occurs in microextraction methods, SPME is ideal for field monitoring. It is unnecessary to measure the volume of the extracted sample and therefore the SPME device can be exposed directly to the investigated system for quantitation of target analytes. Thin coatings of extracting phase result in fast separations. In addition, extracted analytes are introduced to the analytical instrument inlet system by simply placing the fibre in the desorption unit (Figure 1B and 1C). This convenient, solvent-free sample introduction process facilitates sharp injection bands and rapid separations. These features of SPME result in the integration of the first steps in the analytical process: sampling, sample preparation and introduction of extracted mixture to the analytical instrument. For example, total analysis time in field applications can be as low as a few minutes when portable instrumentation is used.

The equilibrium nature of the technique also facilitates speciation in natural systems since the presence of a minute fibre, which removes small amounts of target analytes, is not likely to disturb the system. Because of the small size, coated fibres can

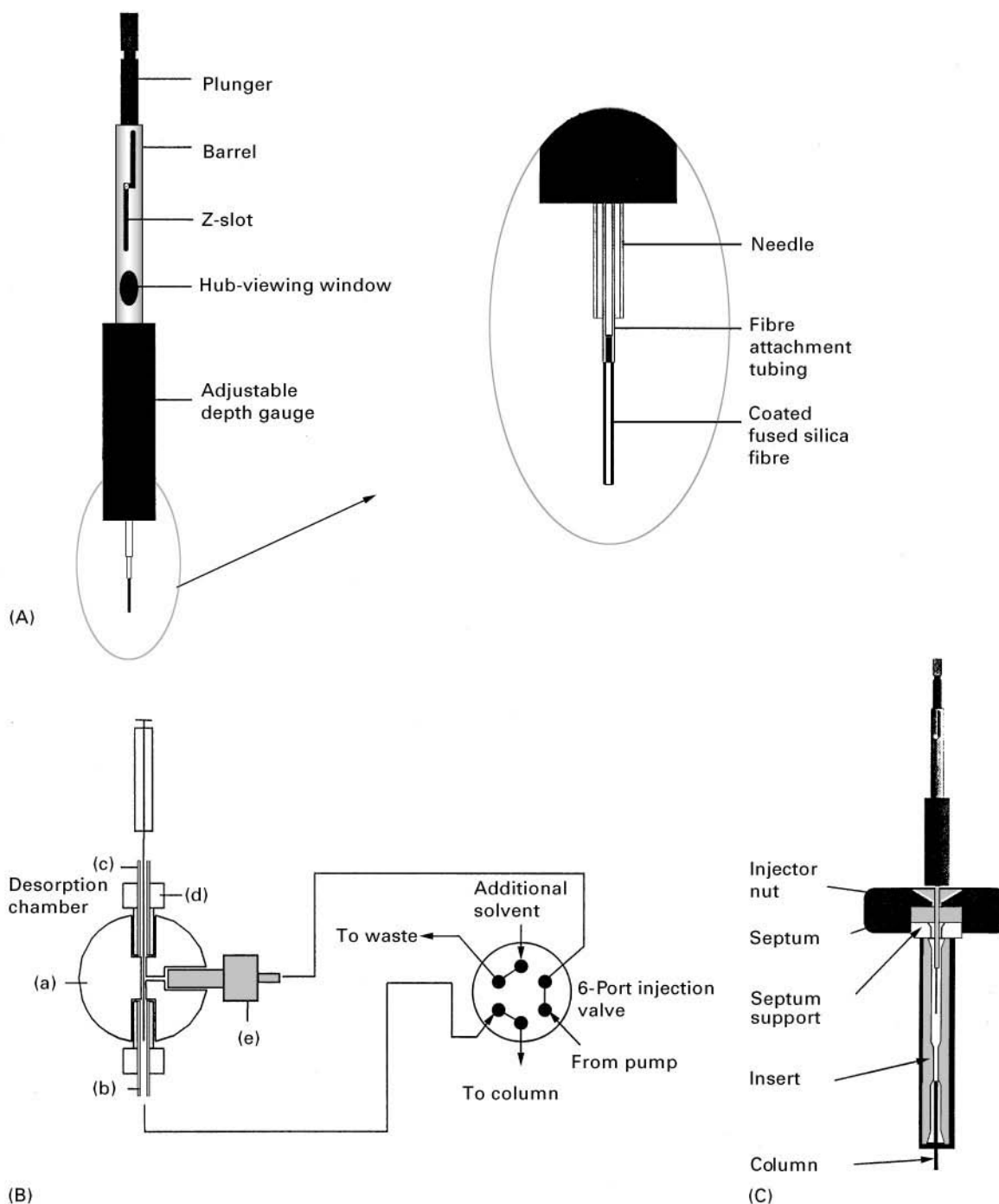


Figure 1 (A) Design of a commercial SPME device. (B) SPME-HPLC interface: (a) stainless steel (SS) 1/16" tee; (b) 1/16" SS tubing; (c) 1/16" polyetheretherketone (PEEK) tubing (0.02" i.d.); (d) two-piece finger-tight PEEK union; (e) PEEK tubing (0.005" i.d.) with a one-piece PEEK union. (C) SPME-GC interface.

be used to extract analytes from very small samples. For example, SPME has been used to probe for substances emitted by a single flower bloom during its lifespan.

Figure 1A illustrates the commercial SPME device manufactured by Supelco, Inc. (Bellefonte, PA, USA).

The fibre, glued into a piece of stainless steel tubing, is mounted in a special holder. The holder is equipped with an adjustable depth gauge, which makes it possible to control repeatably how far the needle of the device is allowed to penetrate the sample container (if any) or the injector. This is important, as the fibre can

be easily broken when it hits an obstacle. The movement of the plunger is limited by a small screw moving in the z-shaped slot of the device. For protection during storage or septum piercing, the fibre is withdrawn into the needle of the device, with the screw in the uppermost position. During extraction or desorption, the fibre is exposed by depressing the plunger, which can be locked in the lowered (middle) position by turning it clockwise (the position depicted in Figure 1A). The plunger is moved to its lowermost position only for replacement of the fibre assembly. Each type of fibre has a hub of a different colour. The hub-viewing window permits a quick check to be made of the type of fibre mounted in the device.

If the sample is placed in a vial, the septum of the vial is first pierced with the needle (with the fibre in the retracted position) and the plunger is lowered, which exposes the fibre to the sample. The analytes are allowed to partition into the coating for a predetermined time, and the fibre is then retracted back into the needle. When gas chromatography (GC) is used for analyte separation and quantitation, the fibre is inserted into a hot injector, where thermal desorption of the trapped analytes takes place (Figure 1C). All extracted compounds are introduced to the analytical instrument facilitating high sensitivity of determinations. The fibre desorption process can be automated by using an appropriately modified, commercially available syringe autosampler. For high performance liquid chromatography (HPLC) applications, a simple interface mounted in place of the injection loop can be used to re-extract analytes into the desorption solvent (Figure 1B). The extraction phase

can also coat the inner wall of the capillary. This approach to microextraction can be automated using a number of commercially available autosamplers, but it is limited to extraction of relatively clean samples, which do not plug capillaries.

The SPME device is suitable for both spot and time-averaged sampling. As described above, for spot sampling, the fibre is exposed to a sample matrix until equilibrium is reached between the sample matrix and the coating material on the fibre. In the time-average approach, on the other hand, the fibre remains in the needle during the exposure of the SPME device to the sample. The coating works as a trap for analytes that diffuse into the needle, resulting in the integration of concentration over given time.

SPME sampling can be performed in three basic modes: direct extraction, headspace extraction and extraction with membrane protection. Figure 2 illustrates the differences between these modes. In direct extraction mode (Figure 2A), the coated fibre is inserted into the sample and the analytes are transported directly from the sample matrix to the extracting phase. To facilitate rapid extraction, some level of agitation is required to transport the analytes from the bulk of the sample to the vicinity of the fibre. For gaseous samples, natural flow (e.g. convection) is frequently sufficient to facilitate rapid equilibration, but for aqueous matrices, more efficient agitation techniques, such as fast sample flow, rapid fibre or vial movement, stirring or sonication are required to reduce the effect of the depletion zone produced close to the fibre as a result of slow diffusional analyte

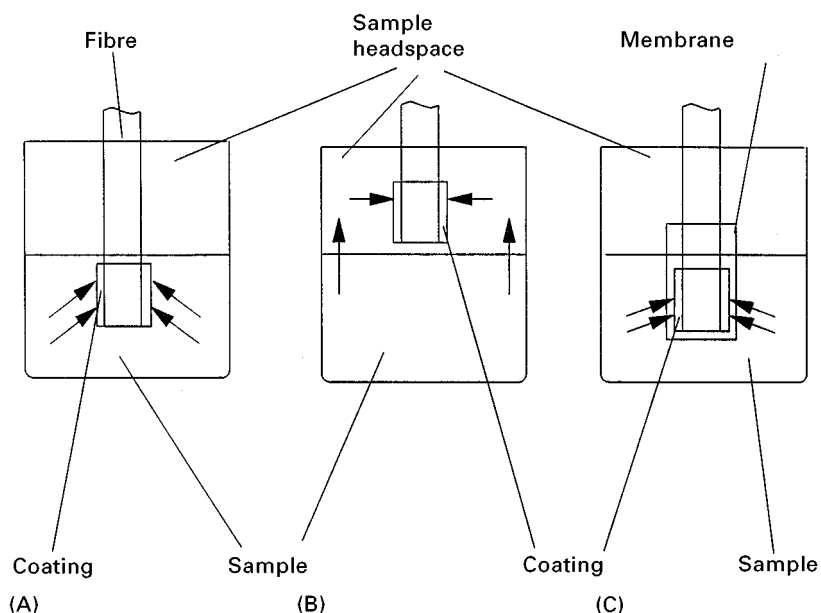


Figure 2 Modes of SPME operation: (A) direct extraction, (B) headspace extraction and (C) membrane-protected SPME.

transport through the otherwise static layer of liquid surrounding the fibre.

In the headspace mode (Figure 2B), the analytes are extracted from the gas phase equilibrated with the sample. The primary reason for this modification is to protect the fibre from adverse effects caused by non-volatile, high molecular weight substances present in the sample matrix (e.g. humic acids or proteins). The headspace mode also allows matrix modifications, including pH adjustment, without affecting the fibre. In a closed system consisting of a liquid sample and its headspace, the amount of an analyte extracted by the fibre coating does not depend on the location of the fibre, therefore the sensitivity of headspace sampling is the same as the sensitivity of direct sampling as long as the volumes of the two phases are the same in both sampling modes. Even when headspace is not used in direct extraction, a significant sensitivity difference between direct and headspace sampling can occur only for very volatile analytes. However, the choice of sampling mode has a significant impact on the extraction kinetics. When the fibre is in the headspace, the analytes are removed from the headspace first, followed by indirect extraction from the matrix. Therefore, volatile analytes are extracted faster than semivolatiles. Temperature has a significant effect on the kinetics of the process, since it determines the vapour pressure of analytes. In general, the equilibration times for volatile compounds are shorter for headspace SPME extraction than for direct extraction under similar agitation conditions, for the following reasons: (i) a substantial portion of the analytes is present in the headspace before the extraction process begins; (ii) there is typically a large interface between sample matrix and headspace; and (iii) the diffusion coefficients in the gas phase are typically higher by four orders of magnitude than in liquids. The concentration of semivolatile compounds in the gaseous phase at room temperature is small, consequently headspace extraction rates for those compounds are substantially lower. These rates can be improved by using efficient agitation or by increasing the extraction temperature.

In the third mode (SPME extraction with membrane protection, Figure 2C), the fibre is separated from the sample by a selective membrane, which lets the analytes through while blocking the interferences. The main purpose for the use of the membrane barrier is to protect the fibre against adverse effects caused by high molecular weight compounds when very dirty samples are analysed. While extraction from headspace serves the same purpose, membrane protection allows the analysis of less volatile compounds. The extraction process is substantially slower than direct extraction because the analytes

have to diffuse through the membrane before they can reach the coating. Use of thin membranes and increase in extraction temperature, applied to analysis of polyaromatic hydrocarbons (PAHs) in matrices containing humic matter, result in shorter extraction times.

Theoretical Aspects of Solid-phase Microextraction Optimization and Calibration

Thermodynamics

SPME is a multiphase equilibration process. Frequently, the extraction system is complex, as in a sample consisting of an aqueous phase with suspended solid particles having various adsorption interactions with analytes, plus a gaseous headspace. In some cases specific factors have to be considered, such as analyte losses by biodegradation or adsorption on the walls of the sampling vessel. In the discussion below we will only consider three phases: the fibre coating, the gas phase or headspace, and a homogeneous matrix such as pure water or air. During extraction, analytes migrate between all three phases until equilibrium is reached. The following discussion is limited to partitioning equilibrium involving liquid polymeric phases such as poly(dimethylsiloxane). The method of analysis for solid sorbent coatings is analogous for low analyte concentration, since the total surface area available for adsorption is proportional to the coating volume if we assume constant porosity of the sorbent.

The mass of an analyte extracted by the polymeric coating is related to the overall equilibrium of the analyte in the three-phase system. Since the total mass of an analyte should remain constant during the extraction, we have:

$$C_0 V_s = C_f^\infty V_f + C_h^\infty V_h + C_s^\infty V_s \quad [1]$$

where C_0 is the initial concentration of the analyte in the matrix; C_f^∞ , C_h^∞ and C_s^∞ are the equilibrium concentrations of the analyte in the coating, the headspace and the matrix, respectively; V_f , V_h and V_s are the volumes of the coating, the headspace and the matrix, respectively. If we define the coating/gas distribution constant as $K_{fh} = C_f^\infty / C_h^\infty$, and the gas/sample matrix distribution constant as $K_{hs} = C_h^\infty / C_s^\infty$, the mass of the analyte absorbed by the coating, $n = C_f^\infty V_f$, can be expressed as:

$$n = \frac{K_{fh} K_{hs} V_f C_0 V_s}{K_{fh} K_{hs} V_f + K_{hs} V_h + V_s} \quad [2]$$

Also:

$$K_{fs} = \frac{K_H}{K_F} = K_{fh}K_{hs} = K_{fg}K_{gs} \quad [3]$$

since the fibre/headspace distribution constant, K_{fh} , can be approximated by the fibre/gas distribution constant K_{fg} , and the headspace/sample distribution constant, K_{hs} , by the gas/sample distribution constant, K_{gs} , if the effect of moisture in the gaseous headspace can be neglected. Thus, eqn [2] can be written as:

$$n = \frac{K_{fs}V_fC_0V_s}{K_{fs}V_f + K_{hs}V_h + V_s} \quad [4]$$

The equation states, as expected from the equilibrium conditions, that the amount of analyte extracted is independent of the location of the fibre in the system. It may be placed in the headspace or directly in the sample as long as the volumes of the fibre coating, headspace and sample are kept constant. There are three terms in the denominator of eqn [4] which give measures of the analyte capacity of each of the three phases: fibre ($K_{fs}V_f$), headspace ($K_{hs}V_h$) and the sample itself (V_s). If we assume that the vial containing the sample is completely filled (no headspace), the term $K_{hs}V_h$ in the denominator, which is related to the capacity ($C_h^\infty V_h$) of the headspace, can be eliminated, resulting in:

$$n = \frac{K_{fs}V_fC_0V_s}{K_{fs}V_f + V_s} \quad [5]$$

Equation [5] describes the mass absorbed by the polymeric coating after equilibrium has been reached in the system. In most determinations, K_{fs} is relatively small compared to the phase ratio of sample matrix to coating volume ($V_f \ll V_s$). In this situation the capacity of the sample is much larger compared to capacity of the fibre, resulting in a very simple relationship:

$$n = K_{fs}V_fC_0 \quad [6]$$

The above equation emphasizes the field-sampling capability of the SPME technique. It is not necessary to sample a well-defined volume of the matrix since the amount of analyte extracted is independent of V_s as long as $K_{fs}V_f \ll V_s$. The SPME device can be placed directly in contact with the investigated system to allow quantitation.

Prediction of distribution constants In many cases, the distribution constants present in eqns [2]–[6] which determine the sensitivity of SPME extraction

can be estimated from physicochemical data and chromatographic parameters. For example, distribution constants between a fibre coating and gaseous matrix (e.g. air) can be estimated from isothermal GC retention times on a column with a stationary phase identical to the fibre-coating material. This is possible because the partitioning process in gas chromatography is similar to the partitioning process in SPME, and there is a well-defined relationship between the distribution constant and the retention time. The nature of the gaseous phase does not affect the distribution constant, unless the components of the gas, such as moisture, swell the polymer, thus changing its properties. A most useful method for determining coating-to-gas distribution constants uses the linear temperature programmed retention index (LTPRI) system, which relates retention times relative to the retention times of *n*-alkanes. The logarithm of the coating-to-air distribution constants of *n*-alkanes can be expressed as a linear function of their LTPRI values. For poly(dimethylsiloxane) (PDMS), this relationship is $\log K_{fg} = 0.00415 \cdot \text{LTPRI} - 0.188$. Thus, the LTPRI system permits interpolation of the K_{fg} values from the plot of $\log K_{fg}$ versus retention index. The LTPRI values for many compounds are available in the literature, hence this method allows estimation of K_{fg} values without experimentation. If the LTPRI value for a compound is not available from published sources, it can be determined from a GC run using a GC column coated with the same material as the fibre.

Estimation of the coating/water distribution constant can be performed using eqn [5]. The appropriate coating/gas distribution constant can be found by applying techniques discussed above, and the gas/water distribution constant (Henry's constant) can be obtained from physicochemical tables or can be estimated by the structural unit contribution method.

Some correlations can be used to anticipate trends in SPME coating/water distribution constants for analytes. For example, a number of investigators have reported correlation between the octanol/water distribution constant, K_{ow} , and K_{fw} . This is to be expected, since K_{ow} is a general measure of the affinity of compounds for the organic phase. It should be remembered, however, that the trends are valid only for compounds within homologous series, such as aliphatic hydrocarbons, aromatic hydrocarbons or phenols; they should not be used to make comparisons between different classes of compounds, because of different analyte activity coefficients in the polymer.

Effect of extraction parameters Thermodynamic theory predicts the effects of modifying certain

extraction conditions on partitioning and indicates parameters to be controlled for reproducibility. The theory can be used to optimize the extraction conditions with a minimum number of experiments and to correct for variations in extraction conditions, without the need to repeat calibration tests under the new conditions. For example, SPME analysis of outdoor air may be done at ambient temperatures that can vary significantly. A relationship that predicts the effect of temperature on the amount of analyte extracted allows calibration without the need for extensive experimentation. Extraction conditions that affect K_{fs} include temperature, inorganic salt concentration, pH and organic solvent content of the water.

Kinetics

The kinetic theory is useful to optimize the extraction conditions by identifying 'bottlenecks' in SPME and indicating strategies to increase extraction speed. In the discussion below we will limit our consideration to direct extraction (Figure 3).

Perfect agitation Let us first consider the case where the liquid or gaseous sample is well agitated. In other words, the sample phase moves rapidly with respect to the fibre, so that all the analytes present in the sample have access to the fibre coating. In this case, the equilibration time, defined as the time required to extract 95% of the equilibrium amount (Figure 4) of an analyte from the sample, corresponds to:

$$t_e = t_{95\%} = \frac{2(b-a)^2}{D_f} \quad [7]$$

Using this equation one can estimate the shortest equilibration time possible for a practical system by substituting appropriate data for the diffusion coefficient of an analyte in the coating (D_f) and the fibre-coating thickness ($b-a$). For example, the equilibration time for the extraction of benzene from a highly agitated aqueous solution with a 100 μm PDMS film is expected to be about 20 s assuming diffusion coefficient of $10^{-5} \text{ cm}^2 \text{ s}^{-1}$ in PDMS. Equilibration times close to those predicted for agitated samples have

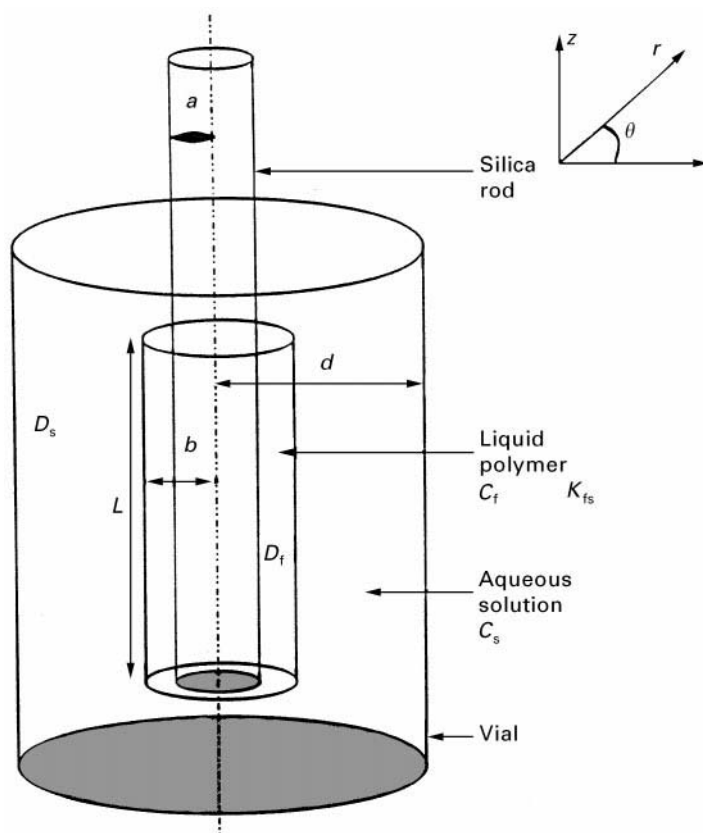


Figure 3 Graphic representation of the SPME/sample system configuration, with dimensions and parameters labelled as follows: a , fibre coating inner radius; b , fibre coating outer radius; L , fibre coating length; d , vial inner radius; C_f , analyte concentration in the fibre coating; D_f , analyte diffusion coefficient in the fibre coating; C_s , analyte concentration in the sample; D_s , analyte diffusion coefficient in the sample; K_{fs} , analyte distribution coefficient between fibre coating and sample; $K_s = C_f/C_s$. (With permission from Louch *et al.* (1992) *Analytical Chemistry* 64: 1187.)

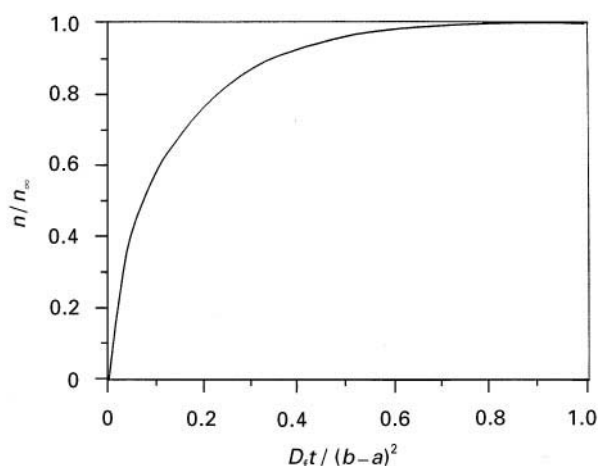


Figure 4 Mass absorbed versus time for a well-agitated solution of infinite volume. (With permission from Louch *et al.* (1992) *Analytical Chemistry* 64: 1187.)

been obtained experimentally for extraction of analytes from air samples (because of high diffusion coefficients in gases) or when high sonication power is used to facilitate mass transfer in aqueous samples. However, in practice there is always a layer of unstirred water around the fibre, although a high stirring rate will reduce its thickness.

Practical agitation Independently of the level of agitation, fluid contacting the fibre surface is always stationary, and as the distance from the surface increases, the fluid movement gradually increases until it corresponds to the bulk flow in the sample. To

model mass transport, the gradation in fluid motion and convection of molecules in the space surrounding the fibre surface can be simplified by a zone of a defined thickness in which no convection occurs, and perfect agitation in the bulk of the fluid everywhere else. This static layer zone is called the Prandtl boundary layer (**Figure 5**). Its thickness is determined by the agitation conditions and the viscosity of the fluid.

The equilibration time can be estimated for practical cases from the equation below:

$$t_e = t_{95\%} = 3 \frac{\delta K_{fs}(b-a)}{D_s} \quad [8]$$

where $(b-a)$ is the coating thickness on the fibre, D_s is the diffusion coefficient of the analyte in the sample fluid, K_{fs} is the distribution constant of the analyte between the fibre and the sample and δ is a boundary layer thickness. This equation can be used to predict equilibration times when the extraction rate is controlled by the diffusion in the boundary layer. The extraction time calculated using eqn [8] must be longer than the corresponding time predicted by eqn [7].

Conclusion

SPME is gaining acceptance principally because of its simplicity, speed and low cost of operation. The detection limits are comparable to a total extraction technique since all extracted analytes are introduced to the analytical instrument in SPME versus only a fraction for a total extraction techniques. Selectivity

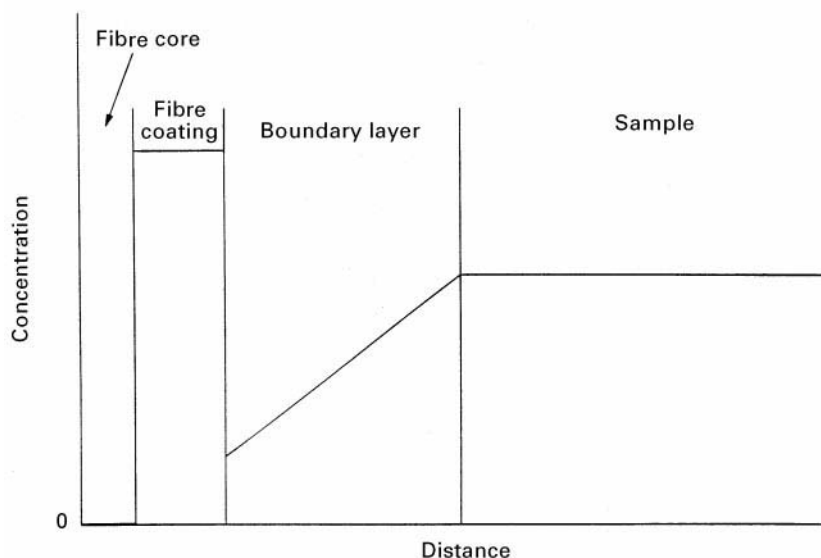


Figure 5 Boundary layer model configuration showing the different regions considered and the assumed concentration versus radius profile for the case when the boundary layer determines the extraction rate.

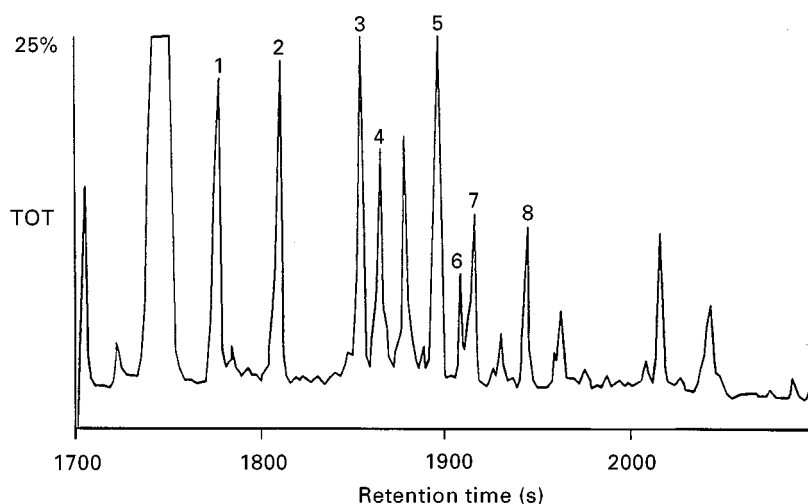


Figure 6 Reconstructed GC-MS chromatogram indicating short chain fatty acids in a sewage sample. Peak assignment: 1, acetic; 2, propionic; 3, isobutyric; 4, butyric; 5, pivalic; 6, isovaleric; 7, valeric; 8, hexanoic acids. The peaks correspond to pyrenylmethyl esters of these acids.

of the technique is controlled by chemical properties of the coating and it is determined by the appropriate distribution constants. Selecting the appropriate fibre allows discrimination against interferences and therefore a separate clean-up step is not necessary. In addition, the coating can contain derivatization reagent, which can specifically bind target analytes, resulting in high specificity and sensitivity of the pro-

cess. **Figure 6** shows a chromatogram obtained after selective headspace SPME extraction of low molecular weight carboxylic acids from a sewage sample by poly(acrylate)-coated fibre containing 1-pyrenyl-diazomethane which selectively reacts with the target analytes. New coatings and reagents will allow expansion of SPME applications to new areas such as inorganic analysis and analysis of biomolecules.

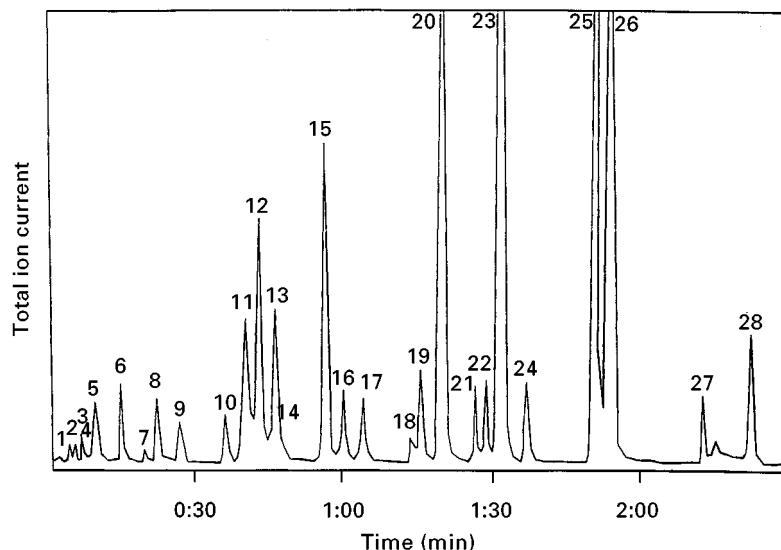


Figure 7 Separation of purgeables A, B and C on a Vocol column. Conditions: 0° – $30^{\circ}\text{C min}^{-1}$ 70° ; 2.1 atm, dedicated injector, capacitor voltage 24 V, MS detector, mass range 45–250. Peak assignment: 1, chloromethane; 2, vinyl chloride; 3, bromomethane; 4, chloroethane; 5, trichlorofluoromethane; 6, 1,1-dichloroethene; 7, dichloromethane; 8, 1,2-dichloroethene; 9, 1,1-dichloroethane; 10, trichloromethane; 11, 1,1,1-trichloroethene; 12, tetrachloromethane; 13, benzene; 14, 1,2-dichloroethane; 15, trichloroethene; 16, 1,2-dichloropropane; 17, bromodichloromethane; 18, 2-chloroethyl vinyl ether; 19, *cis*-1,3-dichloropropene; 20, toluene; 21, *trans*-1,3-dichloropropene; 22, 1,1,2-trichloroethane; 23, tetrachloroethylene; 24, dibromochloromethane; 25, chlorobenzene; 26, ethylbenzene; 27, tribromomethane; 28, 1,1,2,2-tetrachloroethane.

In addition to solvent-free sample extraction, SPME is also a solvent-free sample introduction technique which facilitates design of a simple, low volume injection system. The net result is rapid desorption and good chromatographic separation, especially when flash-heated injectors are used. **Figure 7** illustrates 2.5 min extraction and separation of 28 Environmental Protection Agency volatile priority pollutants, which is over an order of magnitude faster than the standard purge and trap technique. This approach is particularly useful in combination with online SPME extraction. As eqn [6] indicates, it is possible to integrate sampling with a sample preparation step. This not only results in elimination of analyte losses to container walls and degradation during the transport, but also saves time and transport costs. This is particularly true when online SPME extraction is combined with field portable GCs.

Another interesting feature of SPME which is currently being explored includes speciation of analytes in complex matrices. The small amount of extracting phase does not disturb the equilibrium existing in the natural system and therefore allows quantitation of individual species or the determination of distribution

constants in a multiphase system. In addition, the fibre can be made very specific, so separation using chromatographic systems may not be necessary. Therefore development of coupling between SPME with other analytical instrumentation, such as mass spectrometry and inductively coupled plasma-mass spectrometry will facilitate high sensitivity and a large throughput.

See also: **II/Extraction:** Solid-Phase Extraction; Solvent Based Separation. **III/Environmental Applications:** Solid-Phase Microextraction; **Solid-Phase Microextraction:** Overview.

Further Reading

- Kolb B and Ettre LS (1997) *Static Headspace Gas Chromatography. Theory and Practice*. New York: Wiley-VCH.
- Pawliszyn J (1997) *Solid Phase Microextraction. Theory and Practice*. New York, NY: Wiley-VCH.
- Schwarzenbach R, Gschwend P and Imboden D (1993) *Environmental Organic Chemistry*. New York, NY: John Wiley.
- Young AD (1989) *Boundary Layers*. Oxford: BSP Professional Books.

Solvent Based Separation

R. G., P. M. Harper and Martin Hostrup,
CAPEC, Technical University of Denmark, Lyngby,
Denmark

Copyright © 2000 Academic Press

Introduction

Separation involves removal of one or more of the constituent parts from a mixture. A solvent is that constituent of a solution that is liquid in the pure state, is usually present in the larger amount, and has dissolved the other constituent (a solute) of the solution. The solute may be a solid, a liquid or a gas. The solvent may be a single compound or a mixture of compounds. Solvent-based separation techniques become necessary when separation or removal of a solute(s) from a mixture become difficult or infeasible by conventional separation techniques such as distillation. If the addition of a solvent causes a totally miscible liquid to split into two liquid phases and produce the necessary property difference, the solvent-based separation technique is commonly known as liquid-liquid extraction. If the addition of a solvent causes the coexisting vapour and liquid phases to have different properties, the solvent-based

separation technique is called extractive distillation. **Figure 1A** and **1B** highlight the change of the mixture properties as a result of the addition of a solvent. In **Figure 1A**, the difference between the properties of the liquid and vapour for the binary azeotropic mixture of ethanol-water with and without the addition of solvents is highlighted. It is clear from **Figure 1A** that addition of a solvent removes the barrier of the azeotropic condition. **Figure 1B** highlights through a ternary diagram that addition of the solvent causes the totally miscible binary liquid mixture (components 1 and 2) to split into two liquid phases, a solvent-rich phase and a solute-rich (1 or 2) phase.

Examples of industrial processes employing solvent-based separation techniques are numerous. Almost all chemical, petrochemical, biochemical and pharmaceutical processes employ one or more solvent-based separation techniques. In chemical and petrochemical processes, solvents are used mainly to separate components from liquid and/or gaseous mixtures, while in biochemical and pharmaceutical processes, solvents are typically employed for dissolving or removing solids. Use of a solvent to extract aromatic compounds from a petroleum by-product

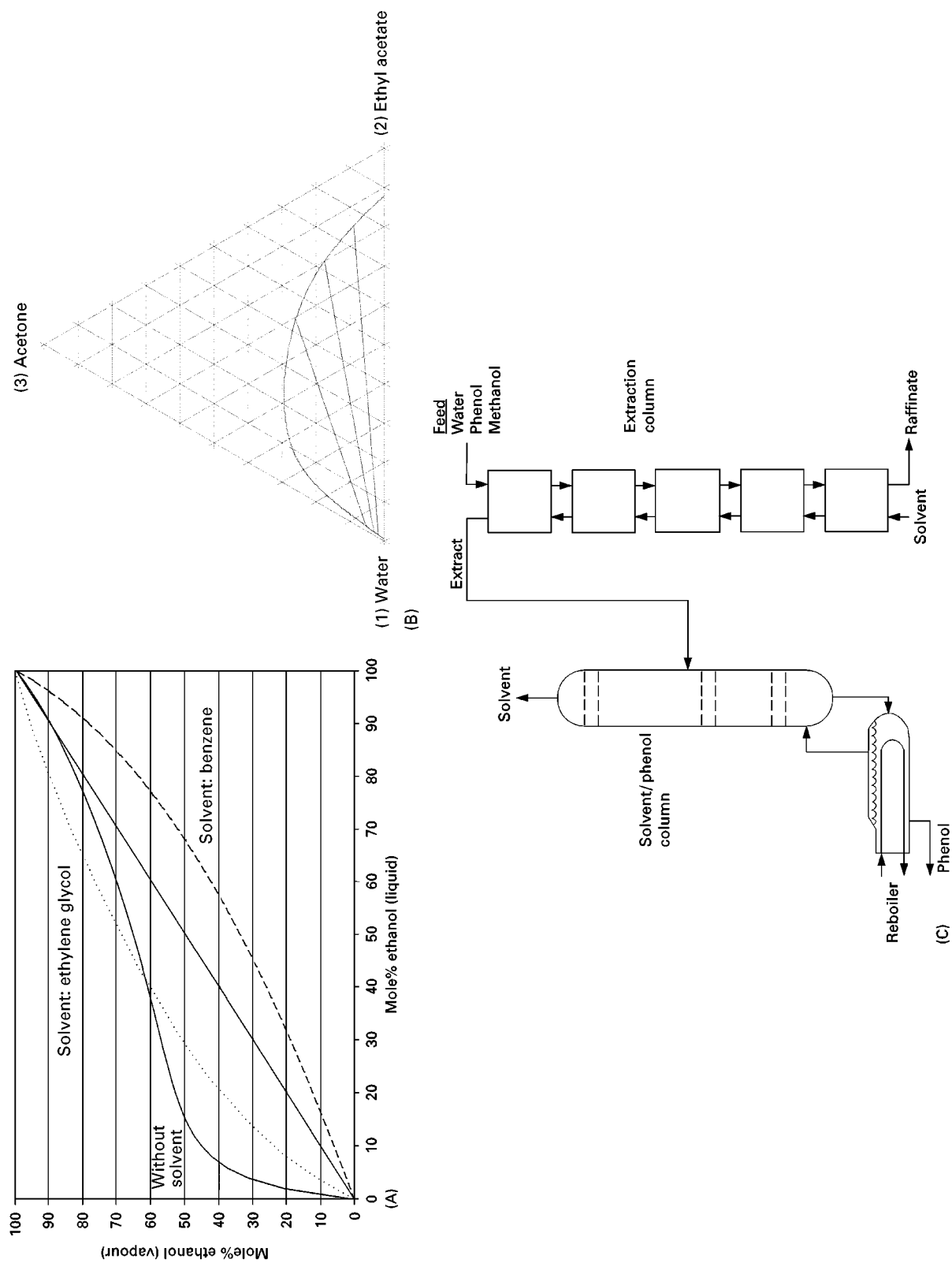


Figure 1 (A) VLE phase diagrams for ethanol-water (pressure 1 atm) with and without solvents (plotted on a solvent-free basis). (B) Ternary LLE diagram for acetone-water-ethyl acetate. (C) Process flowsheet for separation of phenol from wastewater.

Table 1 Classification of important solvent-based separation techniques

<i>Separation technique</i>	<i>Solute property</i>	<i>Number and identity of phase</i>	<i>Separation barrier</i>	<i>Separation phenomena</i>	<i>Solvent function</i>
Liquid-liquid extraction	Totally miscible solutes	Two liquid phases	Total miscibility	Property differences in liquid phases	Addition of solvent causes phase split
Extractive distillation	Solutes from azeotrope or are close boiling	Vapour and liquid phases	Azeotropes or relative volatilities	Property differences in vapour and liquid phases	Addition of solvent breaks the azeotrope but does not cause liquid phase split
Azeotropic distillation	Solutes from azeotrope or are close boiling	Vapour and two liquid phases	Azeotropes or relative volatilities	Property differences in vapour and two liquid phases	Addition of solvent breaks the azeotrope but also causes liquid phase split
Absorption	Absorbed gases in liquid	Vapour and liquid phases	Solubility of gases	Differences in solubility	Solvent must be able to dissolve the solute (gas)
Stripping	Entrained liquids in gases	Vapour and liquid phases	Solubility of liquids	Differences in solubility	Solvent must be able to dissolve the solute (liquid)
Leaching	Solid particles	Solid(s) and liquid phase	Solubility of solids	Differences in solubility	Solvent must be able to dissolve the solute (solid)

or removal of a chemical species (undesirable by-product or raw material) from a wastewater stream through solvent-based separation are typical examples of industrial application. Figure 1C illustrates the removal of phenol from water through solvent based liquid-liquid extraction. An important feature in this and most other vapour-liquid and/or liquid-liquid solvent-based separation techniques is that the solvent is recovered and recycled back to the solvent-based separation unit.

A logical criterion for classification of solvent-based separation techniques is the number and identities of the coexisting phases and the function of the solvent. Table 1 gives a list of some of the well-known solvent-based separation techniques, classified in terms of the number and identities of the coexisting phases and function of the solvent. It can be noted from Table 1 that the selected solvent is directly related to the separation task and the separation technique and indirectly related to factors such as cost of operation, the efficiency of separation and the environmental impact. Therefore, solvent selection plays an important role in solvent-based separation. While solvents and solvent-based separation techniques have been known for a very long time, use of efficient search techniques, such as computer-aided molecular design (CAMD) and computer-aided database search, are fairly new. This article highlights the computer-aided methods and tools related to solvent selection.

Solvent Selection: Problem Formulation

Problem formulation is an important first step in solvent selection as it is necessary first to define the functions of the solvent before attempting to find suitable candidates. Each problem, characterized in terms of solvent and solute properties, needs to address a set of issues related to separation task, performance, environmental impact and problem-specific (special) considerations. The solvent selection problem is formulated in terms of a set of properties (target properties) and their values (target values). A two-step procedure, consisting of a problem identification step (identifies the solvent functions and issues that need to be addressed) and a criteria for evaluation step (selects target properties and their target) is recommended.

Properties

The properties of the selected solvent define, to a large extent, the type of the solvent-based separation technique. Consider the binary azeotropic mixture of ethanol-water and the solvents benzene or ethylene glycol. If benzene is used as the solvent, the resulting solvent-based separation process is called azeotropic distillation because ethanol-water-benzene forms a heterogeneous azeotropic system, as shown in Figure 2A. If, on the other hand, ethylene glycol is used as a solvent, the solvent-based

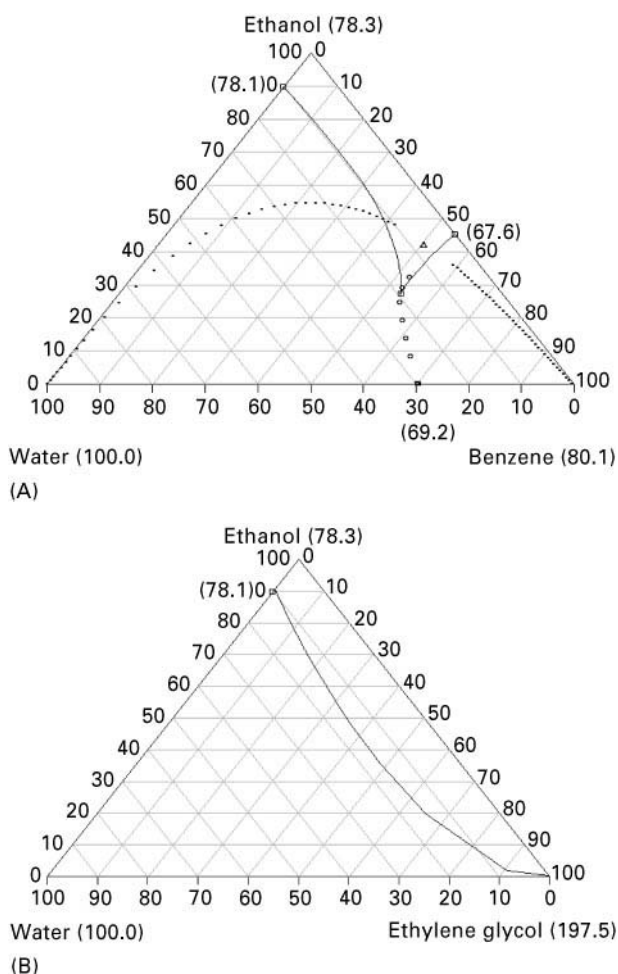


Figure 2 (A) Ternary VLE diagram for ethanol–water–benzene (solvent). (B) Ternary homogeneous VLE diagram for ethanol–water–ethylene glycol (solvent). Key: ..., heterogeneous liquid boiling surface; ○, vapour line; △, critical point; □, azeotropes. All temperatures in °C.

separation technique is called extractive distillation because ethanol–water–ethylene glycol forms a homogeneous azeotropic system, as shown in Figure 2B.

Table 2 gives a list of different types of solvent properties that may be considered in the selection/design of a solvent. These properties are classified in terms of pure component, mixture and environmental. Table 3 expands on the nature of the environmental properties. While the pure component and environmental properties are usually available for a large number of chemical species, the mixture properties usually need to be estimated through suitable property prediction methods.

Problem Identification

Solvents are well known for their different applications and, therefore, functions. They may be employed as cleaning agents, as paint additives, as separ-

ating agents and many more. Each application of the solvent is related to different sets of desirable functions and undesirable effects (or functions). The main question that needs to be asked here is what functions will the selected solvent perform? The answer depends, to a large extent, on the properties of the solute and/or the mixture to be separated. Properties, for pure compounds and mixtures, provide a framework for classifying the different solvent functions and their undesirable effects in a systematic and structured way.

Criteria for Evaluation

Since in solvent selection problems, one is looking for alternatives that match approximately the desirable solvent functions but not the undesirable solvent effects, numerical values of properties can be used to evaluate candidate solvents. Based on the identified separation task, the question of which properties (target properties) should be considered in defining the solvent functions and what should be the property values (target values) is addressed in this step. The exact target values for the target properties are obtained by trial and error. However, if a known solvent is being substituted, then the target values are obtained from the solvent that needs to be substituted. In Table 2, two types of criteria for evaluation are shown – simple and general. As simple, the minimum number of properties that may define the desired solvent properties for each solvent based separation is highlighted, while as general, a comprehensive list of properties is highlighted.

Example

Consider the process from Figure 1C – the effluent water stream from an industrial process contains 7% w/w of phenol, which needs to be removed through liquid–liquid extraction. The desired solvent, when added to the phenol–water system, must cause a phase split such that the solvent-rich phase will contain significantly more phenol than water while the water-rich phase will contain very little phenol or solvent. It should be possible to separate easily the solvent from phenol. That is, the solvent must not form azeotrope, it must have a reasonable difference in boiling point and vapour pressure from phenol, and it must have a density lower than that of water in order to have free convection flow in the extraction column. If the solvent has a high environmental impact, the loss of the solvent through the water-rich phase will have to be reduced. If the solvent is unable to remove enough phenol, more solvent may need to be used. It should pose a low risk of explosion (the flash point temperature should be as high as possible).

Table 2 Solvent selection problem formulation with properties

Property	Solvent design									
	L-L Extraction		Extractive distillation		Azeotropic distillation		Solid separation		Gas absorption	
	Simple	General	Simple	General	Simple	General	Simple	General	Simple	General
<i>Pure</i>										
Solubility parameter	*		*		*		*			
Surface tension		*								*
Viscosity		*								
Boiling point	*	*	*	*	*	*				
Melting point	*	*	*	*	*	*	*	*	*	*
Density		*								
Vapour pressure			*	*	*	*			*	*
Heat of fusion								*		
<i>Mixture</i>										
Selectivity		*		*		*		*		*
Solvent loss.		*								
Solvent power		*		*		*		*		*
Distribution coefficient		*								
Phase split	*	*			*	*				
Azeotropes		*		*		*				
Mixture viscosity		*								
Henry's law constant									*	
Environmental	*	*	*	*	*	*	*	*	*	*

To ensure a minimal loss of the solvent to the water stream, the solvent should have very low miscibility in water and a high octanol–water partition coefficient. It should be possible to separate the solvent easily from phenol (must not form azeotrope, must

have a reasonable difference in boiling point and vapour pressure from phenol, and must have a density lower than that of water in order to have free convection flow in the extraction column). For the process in Figure 1C, the target properties and their target values are given in Table 4.

Table 3 Specific environmental concerns

Environmental property	Health concern	Safety concern	Environmental concern
<i>Implicit</i>			
Toxicity	*		*
Biological persistence			*
Chemical stability		*	
Reactivity	*	*	
<i>Explicit</i>			
Biodegradability			*
Vapour pressure	*	*	*
Henry's law constant in water			*
log <i>P</i>	*		*
Water solubility			*
Flash point		*	
Biological oxygen demand			*
Vapour density	*	*	
Evaporation rate	*	*	
LD ₅₀	*		*
Ozone depletion potential			*

Solvent Selection: Methods and Tools

Methods

Solutions of solvent selection problems formulated above require a multistage approach (see Figure 3).

Table 4 Problem formulation for separation of phenol from wastewater

Target property	Target value
Partition coefficient (log <i>P</i>)	> 1.5
Solvent loss	< 0.0015
Liquid density at 298 K	< 0.95
Normal boiling point	< 450 K
Vapour pressure at 360 K	> 0.03 bar
Flash temperature	> 300 K
Selectivity	> 8
Capacity	> 2
Separation factor	> 80
Other properties	Must not form azeotrope with phenol
	Acceptable environmental properties

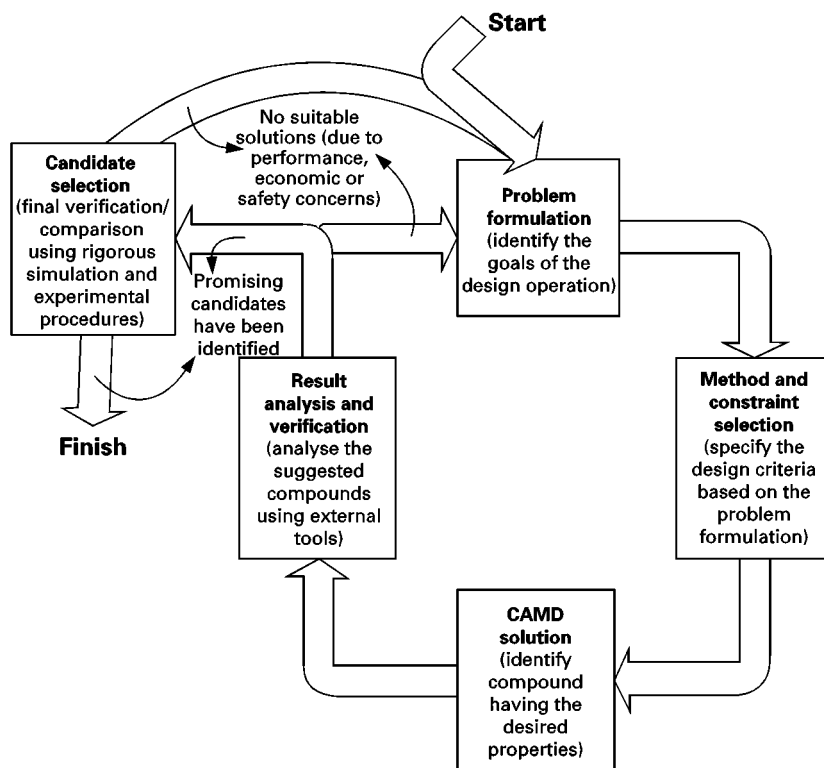


Figure 3 Multilevel approach to solvent selection.

After problem formulation, a list of feasible solvent alternatives is determined and ordered according to a specified criterion. The best feasible candidates are then analysed in terms of separation task, performance, environmental impact and special considerations in order to determine the most appropriate solvent(s). If none are found, it is necessary to go back to the problem formulation stage and relax some target property values or go back to the stage for determination of alternatives and use another search space. Thus, solvent selection is also a design problem requiring a trial-and-error solution approach.

List of solvent alternatives Determination of the list of solvent alternatives is based on the 'generate and test' paradigm. That is, first generate a list of solvent candidates and then analyse (test) the candidates to determine those that match the specified target property values. The methods available can be classified into three types: database search, CAMD and hybrid.

The database search approach involves a search in one or more databases for compounds that match the specified target property values. For this approach, an efficient search engine (or computer-aided technique) is needed. For solvent selection problems involving only pure component target properties, efficient search engines based on so-called pattern matching are available. Difficulties are encountered, however, when mix-

ture properties are also included in the target properties and when the databases do not contain all the target properties for all the compounds. In such cases, an efficient and comprehensive search is almost impossible and reliable property estimation methods are needed.

In the CAMD technique, molecular structures of chemically feasible compounds are generated, the specified target properties for the generated molecules are estimated and those that match the specified target property values are included in the list of alternatives. The CAMD technique is therefore a more efficient search technique that is able to overcome the difficulties related to solvent selection problem formulations involving pure component as well as mixture target properties and incomplete databases. CAMD techniques, however, depend on the accuracy of the property estimation methods used for prediction of target properties for the generated molecules. The search space is not limited by the molecules present in a database but by the number of molecular structures that can be generated and by the application range of the property estimation methods used.

Combining the search based on databases with CAMD, a multilevel hybrid approach is obtained. In this approach, in level 1, a database search is carried out only with respect to the pure component target properties. This gives an idea of the types of molecules that are likely to be selected as solvents. Level 2

uses this information as initial estimate and employs CAMD to solve the solvent selection problem for the pure component and mixture properties that it can estimate with acceptable accuracy. At the end of level 2, a larger list of alternatives than level 1 is obtained. In level 3, those molecules that can be found in the database are identified and their target properties are verified, resulting in an updated list of alternatives. This list is now used for checking the remaining target properties (such as environmental properties and special properties that are found in special databases). Screening out the molecules that do not satisfy the target properties based on these databases produces a further refinement of the list of alternatives. Finally, in level 4, selected molecules from level 3 are investigated in terms of atomic structure, bond length, bond angle, energies, etc., through links to molecular modelling programs.

Final selection Since the list of alternatives contains more than one solvent, all of which match the specified target property values, it is necessary to determine the most appropriate solvent from this list. Therefore, it is necessary to define a selection criterion, for example, an objective function (F) that is either minimized or maximized. This objective function may be an explicit function of the target properties (see eqn [1]) or an implicit function of the target properties (see eqn [2]):

$$F = (S_p, S_s) \quad [1]$$

$$F = f(D_s(S_p, S_s), T(S_p, S_s), P(S_p, S_s)) \quad [2]$$

In the above equations, S_p is solvent power, S_s is selectivity, D_s is a vector of specified products, T is a vector of operating temperatures and P is a vector of operating pressures. Since the target properties of eqn [1] are known for the solvents in a generated and tested list of alternatives, use of eqn [1] simply means ordering the molecules in ascending order and selecting the optimal for further analysis (for example, pilot plant study). In this case, the solvent with the maximum value of F is regarded as the optimal solvent. In eqn [2], the evaluation of F needs other calculations (such as process simulation) in order to determine the values of D_s , T and P corresponding to an optimal F . Two solution approaches are commonly applied – an enumeration approach and a simultaneous solution approach. In the enumeration approach, the optimal value for F in eqn [2] is determined for each solvent through process simulation/optimization, generating a set of values for F , D_s , T and P corresponding to each solvent in the generated list of alternatives. The optimal solvent then corresponds to the minimum (or maximum) F in the

generated set. In the simultaneous solution approach, the solvent identity is an integer variable and adding it as an optimization variable in the process optimization problem gives a mixed integer nonlinear programming (MINLP) problem formulation, which determines the optimal solvent and the optimal F simultaneously.

Tools

From the above section, it is clear that the tools that are needed for solution of the solvent selection problem are databases, search engines, property estimation methods, process simulators and numerical methods (such as a MINLP-solver). It should be noted that all the tools might not be necessary for all solvent selection problems. Also, different sets of tools are needed depending on the chosen method of solution. In this article, only the use of search engines with the hybrid approach, which includes database search, CAMD and property prediction, is highlighted. Table 5 gives a list of various tools that may be used in solving solvent selection problems.

Search engine The hybrid generate-and-test approach (search engine–CAMD algorithm) has four levels. Each level has its own generate-and-test algorithms. Higher levels use additional molecular structural information compared with lower levels. Levels 1–2 are group contribution based (thereby employing macroscopic representation of the molecule), while levels 3–4 are based on atomic (microscopic) representation of the molecule. Switch from level 1–2 to 3–4 needs a conversion of macroscopic representation to microscopic representation.

Level 1 This level generates sets of building blocks (*fragments*) by combining first-order functional groups. These sets are capable of forming at least one feasible molecular structure. Simultaneous calculation of related properties (that are dependent only on first-order groups) and screening of the generated structures is performed to control the problem size and execution time. The algorithm here is based on a modified set of rules. Building blocks are classified according to type. Feasibility rules are based on the number of groups from a specific class a compound may contain. Valency rules are used to determine the number of groups with one, two, three and four connections that are to be used in molecule structure generation. The main steps of the level 1 algorithm are illustrated in Figure 4.

Level 2 This level generates molecular structures by combining elements of the individual fragment sets

Table 5 List of tools for solvent selection problems

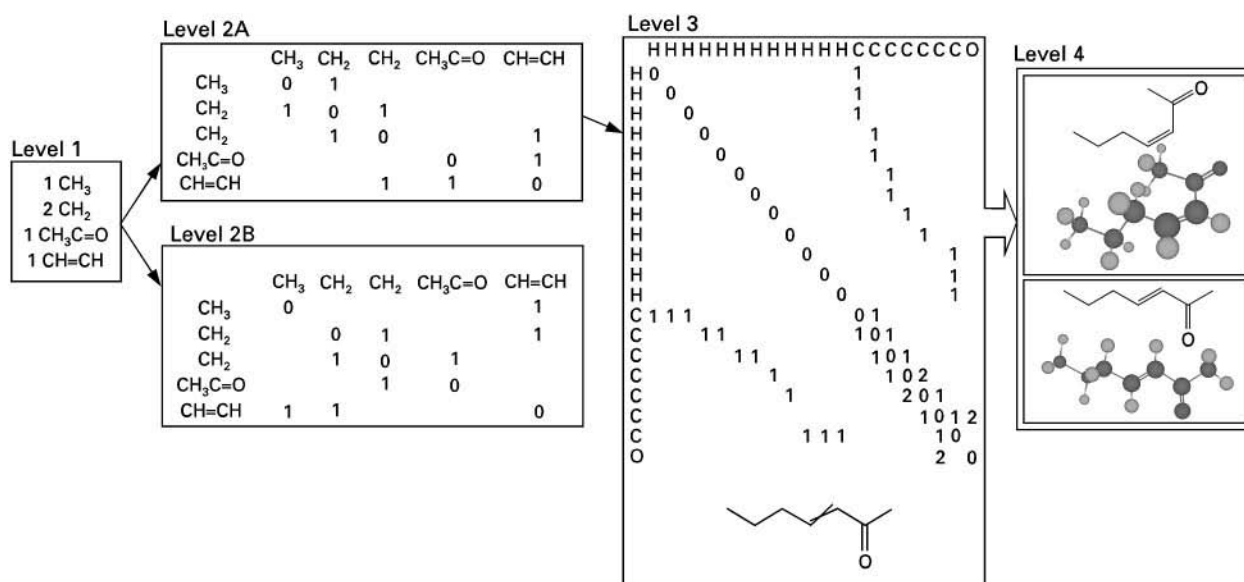
Tool	Type	Contact information
ProCAMD	CAMD	CAPEC
Synapse	CAMD	Molecular Knowledge Systems, Inc.
EFDB	Electronic database (environmental fate)	Syracuse Research Corporation
ChemBank—RTECS	Electronic database (health, safety, physical properties, environmental data)	SilverPlatter Information Inc.
Dortmund Data Bank	Electronic database (mixture and physical properties)	DDBST GmbH
PHYSPROP	Electronic database (physical properties)	Syracuse Research Corporation
SOLVDB	Electronic database (solvents)	Syracuse Research Corporation
NIST WebBook	Online database (physical properties)	NIST
CS Chemfinder	Online database (physical properties, links to other sources)	Cambridge Soft Inc.
SMSWIN	Phase behaviour calculations	AstraZeneca
Process Design Studio	Phase behaviour calculations	CAPEC
ChemDraw 5.0 Ultra	Property prediction	Cambridge Soft Inc.
ACD/Labs Physico-Chemical Laboratory	Property prediction	Advanced Chemistry Development inc.
Cranium	Property prediction	Molecular Knowledge Systems, Inc.
ProPred 2.5	Property prediction	CAPEC

from level 1 to form molecular structures. First- and second-order groups are considered. The main feature of this algorithm is that it is pseudorecursive, all allowed combinations are considered, and efficiency is maintained by continuous removal of duplicate structures. Also, the combination rules satisfy conditions of chemical feasibility. Use of second-order groups allows the estimation method to differentiate between some isomers.

Level 3 In this level, the selected candidates from level 2 are given an atomic representation. Note that

the atomic representation also defines the connectivity of the molecules. Therefore, property prediction methods based on connectivity indices can be employed to predict properties that could not be predicted earlier (due to unavailable group contributions) or to verify previously estimated values.

Level 4 In this level, generation and testing enters an interactive mode. For any selected candidate from level 3, it is possible to use molecular modelling programs such as MOPAC or Chem3D from Cambridge Soft Corp. A three-dimensional graph (or

**Figure 4** Hybrid CAMD search engine.

molecular model) is created by applying a set of standard or default bond lengths and angles for the various types of connections. As a result the true molecular model of a compound, which can be further analysed in terms of conformers, stability, properties, etc., is obtained.

Application Examples

Problems

Solutions of solvent selection problems with the database search approach and the hybrid approach are illustrated. Tools listed in Table 5 have been used for solution of these problems, which involve solvent-based vapour-liquid, liquid-liquid and solid-liquid separations. For the removal of morphine, all the solution steps for solvent selection with the hybrid approach are highlighted. For the other examples, only the problem formulation in terms of target properties and the final results are presented. Also, for solution with the database search approach, only pure component target properties have been considered.

Database Search Approach

For the separation of phenol from water by liquid-liquid extraction, solution of the problem (as defined in Table 4) finds, among others, butyl acetate and toluene as solvents that match the pure component target properties.

For the purification of ethanol from a binary mixture of ethanol-water, solvents for extractive or azeotropic distillation are sought. The pure component target properties are: normal boiling point (T_b) < 473 K; melting point (T_m) > 270 K; flash point (F_T) > 320 K; solubility parameter (δ) between 15 and 20 MPa^{1/2} for azeotropic distillation or 28 and 35 MPa^{1/2} for extractive distillation. Note that δ of ethanol is around 26 MPa^{1/2} and that of water is around 47.8 MPa^{1/2}. A value of δ far from water and closer to ethanol will be selective to ethanol and will likely cause a phase split. Benzene, toluene and cyclohexane satisfy the target property values for azeotropic distillation. Ethylene glycol satisfies the requirements for extractive distillation. Figure 2A and 2B also confirm this result.

For the separation (removal) of phenol present as a solid, a solvent is needed to dissolve it. The solvent target properties may be defined with T_m > 270 K, T_b < 473 K and $23.5 < \delta < 25.5$ MPa^{1/2}. A search of the database gives furfuryl alcohol, aniline, *N,N*-dimethylformamide and furfural. The solvent function of aniline related to dissolving solid phenol is validated through the computed solid-liquid phase diagram for the phenol-aniline mixture (see Figure 5).

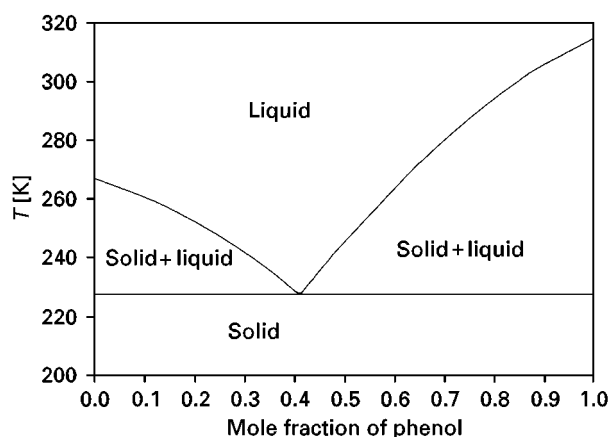


Figure 5 Computed SLE phase diagram for aniline-phenol.

Hybrid Approach

The solvent selection problem for the removal of phenol from wastewater has been solved with the ProCAMD (see Table 5). The summarized results from ProCAMD are shown in Figure 6. Compared with butyl acetate and toluene, this solvent has been found to have a higher F (eqn [1]) and is environmentally acceptable.

Identification of a solvent for morphine

Problem formulation In the production of morphine a solvent is needed for dissolving the solid. Known solvents for morphine include cyclohexane, tetrachloromethane, toluene and benzene. It is desired to find alternative solvents capable of dissolving morphine. Furthermore, in order not to contaminate the product with toxic substances, in case of solvent inclusions after crystallization, the compound should be nonaromatic and have a low toxicity.

Constraint selection Solubility is a mixture property. To be able to predict solubility to some degree of accuracy it is necessary to have access to a method for calculation of activity coefficients. For complex compounds (such as morphine) very few group-contribution-based property estimation methods are able to describe the molecular structure (see Figure 7). Therefore, the search for alternative solvents is carried out using pure component properties as criteria for evaluation. It is well known that two compounds having similar solubility parameters (δ) are highly likely to be miscible. The search for solvents for morphine can therefore be expressed as a search for compounds being liquid at ambient temperatures and having a solubility parameter as close as possible to that of morphine ($\delta = 26.3$ MPa^{1/2}).

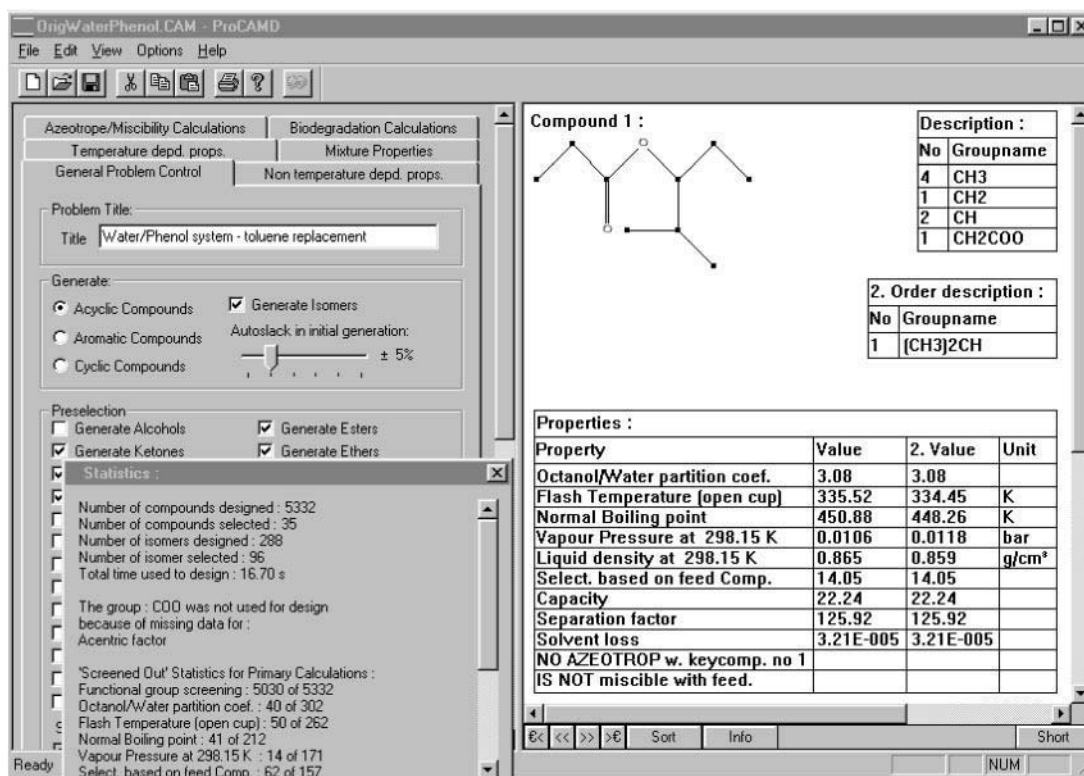


Figure 6 Results for phenol-wastewater separation (screenshot from ProCAMD).

Design specifications

- *Compound type* acyclic alkanes, ethers, esters, aldehydes, ketones, alcohols;
- $T_b > 350$ K; $T_m < 273$ K;
- $22 < \delta < 30$ (exclusion of the lowest ranking candidates);
- *performance measure* $|26.3 - \delta|$ should be as low as possible.

Generation of alternatives The ProCAMD package (see Table 5) was used, generating 348 candidates fulfilling the requirements. After performing a structure search to identify substances with known CAS registry numbers two candidates, 1,5-pentanediol and acetol, were selected based on having a solubility parameter close to that of morphine.

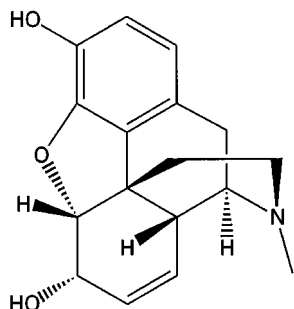


Figure 7 Molecular structure of morphine.

Analysis and verification To verify the predicted values of the properties used as design specifications a search in available databases was carried out and the experimental values compared to the predicted. Furthermore the RTECS database (see Table 5) was consulted in order to investigate the health and environment properties of the selected compounds. The result of the investigations and the predicted properties are shown in Table 6.

Candidate selection From the data listed in Table 6 it is clear to see that among the known and generated solvents 1,5-pentanediol is the most promising candidate and should be selected for further testing in an experimental setting.

Future Developments

As current and future separation problems become more difficult due to complex molecular structure of solutes, changes in environmental regulations and demands for material and energy conservation, the solvent selection problem is also becoming more difficult. It is no longer feasible to attempt to solve the solvent selection problem with a single database. Computer-aided techniques provide the necessary framework to solve the current and future solvent selection problems. The current hybrid approaches,

Table 6 List of solvents for separation of morphine

Solvent	CAS-NO	Predicted			Experimental			Compound class (RTECS)
		T_b (K)	T_m (K)	δ (MPa ^{1/2})	T_b (K)	T_m (K)	δ (MPa ^{1/2})	
Benzene	71-43-2				353.24	278.68	18.73	C,D,M,T,S
Toluene	108-88-3				383.78	178.18	18.32	C,M,T,S
CCl ₄	56-23-5				349.79	250.33	17.55	C,D,M,T,S
Cyclohexane	110-82-7				353.87	279.69	16.76	M,S
1,5-Pentanediol	111-29-5	491	253	27.0	512.15	257.15	26.45	S
Acetol	116-09-6	418	226	27.2	418.65	256.15	25.75	M

D, drug; S, primary irritant; T, reproductive-effector; M, mutagen; C, tumorigen.

however, need to integrate aspects of molecular modelling and computational chemistry before acceptable solutions to problems involving complex solutes and tight environmental regulations can be obtained. Finally, it should be noted that having a good solvent means easier design/operation of the solvent-based separation technique. Therefore, it is important to formulate correctly the solvent selection problem and to find reliable results in the form of optimal solvents.

Further Reading

Barton AFM (1985) *CRC Handbook of Solubility Parameters and Other Cohesion Parameters*. Boca Raton, FL: CRC Press.

Fredenslund AA, Gmehling J and Rasmussen P (1972) *Vapour-Liquid Equilibrium Using UNIFAC*. Amsterdam: Elsevier.

Harper P, Gani R, Kolar P and Ishikawa T (1999) Computer aided molecular design with combined molecular modelling and group contribution. *Fluid Phase Equilibria* 337: 158–160.

Horvath AL (1992) *Molecular Design*. Amsterdam: Elsevier

Lo TC, Baird MHI and Hancon C (1987) *Handbook of Solvent Extraction*. New York: John Wiley.

Marcus Y (1998) *The Properties of Solvents*. New York: John Wiley.

Mavriounioutis M (ed.) (1998) Special issue on design of chemical compounds. *Computers and Chemical Engineering Journal* 22: 713.

Seader JD and Henley E (1998) *Separation Process Principles*. New York: John Wiley.

Steam Distillation

L. Ramos, Free University, Amsterdam, The Netherlands

Copyright © 2000 Academic Press

Sample preparation is nowadays the limiting step in the trace analysis of organic pollutants in environmental and biological samples. Looking forward to the laboratory of the future, versatile and universal sample enrichment techniques are required, which can produce fast and valid data, with low costs in terms of solvent consumption and operator involvement. A selectivity higher than that of the classical exhaustive extraction methods or the simultaneous elimination of the interference material could be an additional requirement, as it would reduce the amount of solvents and adsorbents used by reducing or eliminating the subsequent clean-up step. Possible additional benefits deriving from a low manual manipulation of the samples would be a reduction in the

risk of contamination and loss of the analytes, as well as an easier automation of the process.

Steam distillation extraction-solvent extraction (SDE) has been presented as such a universal sample enrichment technique. SDE allows the simultaneous extraction, clean-up and concentration of the target compounds in a closed system, with short analysis times (1–8 h) and by using small amounts of organic solvents (a few mL). This paper reviews this assumption for the case of the analysis of less volatile organic pollutants in environmental samples. The SDE advantages and shortcomings for such an analysis have been discussed.

Introduction

The monitoring of toxic organic chemicals in environmental and biological samples is a major concern in many different fields. However, the large variety of compounds of interest, the differences existing in

their environmental levels and physico-chemical properties, and the complexity of the matrices typically investigated make the development of universal analytical methods for such an analysis a very difficult goal. This is especially true for the most toxic organic pollutants as their high toxicity makes their reliable detection and accurate quantification at the trace level more relevant.

Most of the procedures described in the literature for the analysis of less volatile organic pollutants are time-consuming, laborious and specific for the determination of an analyte (or family of compounds) in a selected matrix. Examples of selective extraction of the target compounds, allowing their determination without any additional clean-up, can be found in the literature. However, most of these procedures involve sophisticated and expensive analytical techniques, such as supercritical fluid extraction or gel permeation chromatography. On the other hand, the efficiency of these methods have been recognized to be highly matrix-dependent. Because of these unresolved shortcomings, classical exhaustive extraction techniques, i.e. liquid-liquid extraction, LLE, solid-liquid extraction or Soxhlet extraction, are still widely used in official methods and routine applications. Due to the low selectivity of these methods, subsequent elimination of the co-extracted material is recommended. Such a clean-up step is mandatory for reliable trace level determination of lipophilic and bio-accumulative pollutants in biological and complex environmental samples.

Steam distillation-solvent extraction (SDE) has been used mainly for the extraction and concentration of fragrance and flavour compounds. However, a variety of SDE methods reporting sample preparation for the analysis of pollutants in environmental samples can be found in the literature. Most of these methods allow the simultaneous extraction, clean up and concentration of the target compounds. The investigated compounds range from volatile polar and non-polar pollutants to non-ionic surfactants. This article reviews the suitability and the limitations of SDE for the determination of less volatile trace organic pollutants, such as pesticides, polychlorinated biphenyls (PCBs), polychlorinated dibenzo-p-dioxins and furans (PCDD/Fs), or surfactants, in environmental and biological matrices. The most relevant variables affecting the efficiency of the SDE of these compounds are discussed and the results of some selected applications reviewed.

General Considerations

According to the theoretical model developed by Rijks *et al.*, in 1983, the efficiency of the SDE process

increased with the extraction time and with the liquid and vapour flows. The process also depends on analyte-specific parameters related to the activity coefficient (calculated from the water solubility of the analyte at 100°C) and the gas-liquid distribution coefficient of the compound in water at the process temperature (i.e., 100°C for water steam). Not unexpectedly, the recoveries increased with the affinity of the target compounds for the extracting solvent. This theoretical model is applicable only under ideal conditions, which are achieved when all volumes and flow rates remain constant and there is ideal mixing and equilibrium at every stage. In spite of these limitations, the model reflects the effect of several experimental factors on the SDE process. In fact, the different modifications carried out on the SDE devices originally described by Likens and Nickerson in 1964 and by Flath and Forrey in 1977 reveal the influence of several parameters on the recoveries of the target compounds. The modifications were mainly focused on increasing the size of the vapour chamber and/or the condensing surface to allow a more complete mixing of the solvent and steam vapours, as well as on the miniaturization of the system. As a consequence of the changes in design (Figure 1), the efficiency of the extraction was increased, the analysis time reduced and the field of SDE expanded through the analysis of residue levels of less volatile pollutants in environmental samples.

Due to the characteristics of the technique, the feasibility of SDE for the analysis of less volatile compounds depends on their (i) potential for forming azeotropes with water and (ii) relative solubility in water and in the extraction solvent. However, the SDE of the target compounds from complex samples can be expected to occur only after destruction or degradation of the main matrix components, which usually entrap the analytes (see below). Therefore, as stated by Nash in 1984, the applicability of the SDE technique to the analysis of this kind of environmental matrices would be limited by the resistance of the investigated compounds to the selected degradation procedure. Alternatively, in some cases, co-distillation solvents have been used to improve the SDE efficiency by reducing the surface tension of the water and by increasing the extraction power (polarity) of the organic solvent. Finally, rather different results have been published about the suitability of adding anti-foam agents in applications involving fatty samples (see Table 3).

Application of SDE to the Analysis of Aqueous Samples

Water was one of the first environmental samples selected to evaluate the feasibility of the SDE

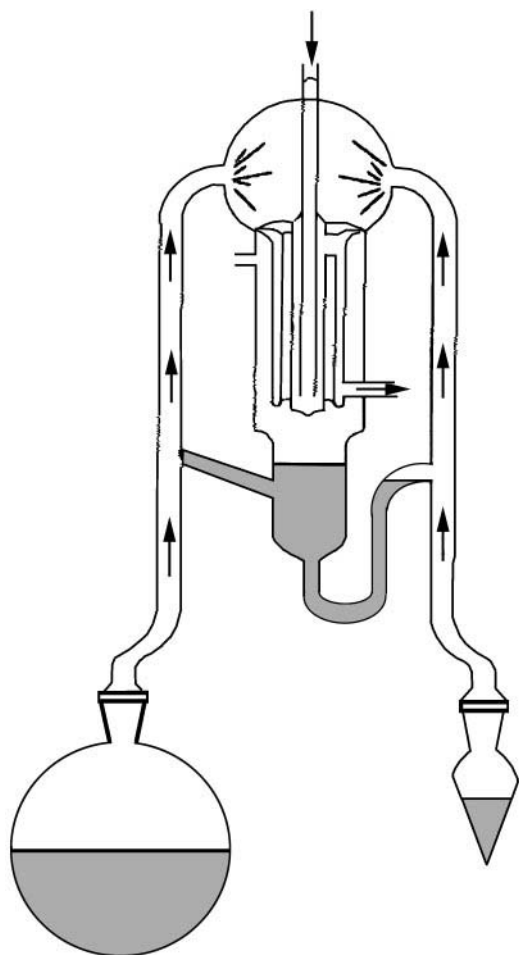


Figure 1 A typical SDE modern design.

technique for the determination of less volatile organic contaminants levels. **Table 1** summarizes relevant data concerning some reported methods for the analysis of this matrix.

Quantitative recoveries of spiked organochlorinated pesticides, OCPs (globally, in the range 90–106 ppb), and PCBs (globally, in the range 70–104 ppb) in aqueous samples have been reported using the SDE technique. The reported methods allowed the simultaneous extraction and concentration of the analytes in 1–1.3 h in a relatively small amount of a non-polar solvent (1–15 mL). Usually, no additional treatment of the sample or the organic extract was required. The SDE technique was favourably compared with other widely used extraction procedures, such as LLE or solid-phase extraction (SPE) by Ramos *et al.* in 1995, e.g. similar recoveries have been published for the analysis of PCBs in water at the ppb (ng mL^{-1}) level by using SDE, LLE or SPE. However, the higher repeatability of the SDE procedure (relative standard deviations, RSD, lower than 10%) and

the small amount of organic solvent involved, as well as the short sample preparation times, makes SDE a valuable alternative technique for such an extraction, especially when a large number of analyses have to be carried out.

Nevertheless, some limitations of SDE have also been reported for less volatile pollutants in water samples. Nash *et al.* in 1984 studied different parameters affecting the efficiency of the steam distillation process. They concluded that this technique is probably limited to compounds with a vapour pressure of about 1 kPa at 100°C. Their results also showed that the performance of SDE depends on the concentration investigated and that recoveries tend to increase with the spiking level.

Similar tendencies have been observed by Ramos *et al.* in 1995 when using the SDE technique for the extraction of water spiked with the 2,3,7,8-substituted-CDD/Fs at different levels of concentration ($0.25\text{--}2\text{ ng mL}^{-1}$, $0.025\text{--}0.2\text{ ng mL}^{-1}$ and $0.0025\text{--}0.02\text{ ng mL}^{-1}$). The recoveries obtained for the lower and higher boiling point congeners (tetra- and octa-CDD/Fs, respectively) are consistently lower than those found for the rest of the investigated congeners: respectively 40–76% and 73–137% at the highest level of concentration investigated, 39–60% and 62–92% at the intermediate, and 37–55% and 25–72% at the lowest spiking level. These results also show that the SDE recoveries for a given compound decrease with the concentration level when using *n*-pentane as the extraction solvent. The simple substitution of *n*-pentane for a solvent more selective for the PCDD/Fs (dichloromethane) increases recoveries from 25–73% to 71–139% for tetra- to hepta-CDD/Fs at the $0.0025\text{--}0.02\text{ ng mL}^{-1}$ level. However, no additional improvement is obtained for the octa-CDD/F recoveries (38–56%). In spite of the low recoveries obtained for OCDD/F, the proposed SDE procedure compares favourably with results previously published by using LLE or SPE in terms of repeatability, analysis time and solvent consumption.

Good recoveries (in the range 84–100%) have been reported by Meissner *et al.* for the analysis of surfactants such as fatty alcohol sulfates and alkyl polyglycosides in water (**Table 1**). SDE of the fatty alcohols yielded by hydrolysis and subsequent LLE of the original compounds is an attractive technique for the effective clean-up and concentration of these complex mixtures of compounds at the trace level. On the other hand, the application of SDE to the extraction of fatty alcohol ethoxylates with more than three ethoxy units in the molecule cannot be accomplished due to their high solubility in water.

Table 1 SDE methods for the analysis of less volatile organic pollutants in aqueous samples

Compound	Spiking level (ng mL ⁻¹)	Solvent (mL)	Extraction time (h)	Cc. factor ^a (water : solvent, v/v)	Post-treatment ^b	Recovery (%)	RSD (%)	Ref.
OCP	0.004–0.016	Isooctane/toluene (15)	1	167 : 1	NR ^c	90–104	?	Hemmerling <i>et al.</i> (1991)
Arochlor 1016, 1242, 1248, 1254	0.016	Isooctane/toluene (15)	1	167 : 1	NR	98–100	?	
OCP	0.4–4.0	n-pentane (1)	1.3	50 : 1	NR	97–106	?	Godefroot <i>et al.</i> (1982)
Arochlor 1260	10	n-pentane (1)	1.3	50 : 1	NR	81–104 ^d	?	
Toxic PCBs	0.01–1.0	n-pentane (2)	1	50 : 1	Concentration	70–115	< 10	Ramos <i>et al.</i> (1995)
PCDD/Fs	0.025–2.0	n-pentane (2)	1	50 : 1	Concentration	49–139	< 10	
PCDD/Fs	0.0025–0.02	Dichloromethane (2)	1	50 : 1	Change of solvent	49–139	< 10	
Fatty alcohol sulfates	500 nM	Ethyl acetate (2)	3 ^e	100 : 1	Derivatization	87–100	5.6–7.0	Meissner <i>et al.</i> (1999)
Alkyl poly- glycosides	2 µM	Ethyl acetate (2)	4 ^e	25 : 2	Derivatization	84	?	

^aConcentration factor.^bPost-SDE treatment required.^cNR, not required.^dRecoveries for some selected peaks.^eThe SDE was conducted after hydrolysis with 4 M H₂SO₄ plus liquid-liquid extraction with diethyl ether of the hydrolysate and concentration.

Application of SDE to the Analysis of Non-Fatty Environmental Samples

Table 2 summarizes relevant data related to some reported SDE methods for the analysis of less volatile organic pollutants in non-fatty environmental samples. Most of the reported SDE applications referred to the analysis of OCPs and toxic aromatic compounds, e.g. PCBs, polychlorinated naphthalenes (PCNs), or polynuclear aromatic hydrocarbons (PNAs), in soils and sediments. Contrary to what might be expected from the high complexity of these samples, most of the methods did not include any further pre-treatment of the matrix but blending with the selected volume of water. Only a few procedures involving drastic treatments (e.g. blending of the sample with H₂SO₄ and K₂Cr₂O₇) during the SDE to guarantee the destruction of the soil or sediment components in which the target compounds could be entrapped, can be found in the literature.

The efficiency (or need) of such a drastic treatment is difficult to evaluate from the data published. In general, high (quantitative) recoveries have been reported for freshly spiked analytes (globally in the range 78–102% for PCBs and OCPs at the 20–90 µg g⁻¹ level) with all the procedures (Table 2).

However, the efficiency of the proposed SDE methods for the extraction of endogenous pollutants from weathered samples has been scarcely evaluated. In these studies, Seidel *et al.* (1993) and Cooke *et al.* (1980) found concentrations very close or below the limit of detection have usually been reported for the endogenous contaminants, but the lack of comparison of the SDE results with those obtained by standard or more exhaustive methods, i.e. Soxhlet extraction, do not allow any discussion about the methods used.

Dunnivant *et al.* in 1988 reported recoveries ranging from 47 to 99% for SDE of certified sediments with PCBs at the 2.34–24.6 µg g⁻¹. However, as quoted above, this SDE method involved a digestion of the sample under drastic conditions.

In a closely related study, Nash *et al.* compared the efficiency of steam distillation with subsequent organic solvent extraction to that of Soxhlet extraction for the analysis of pesticides in soil, plant tissues and air (polyurethane foam filters). Both procedures provided similar recoveries for the spiked samples (in the ranges 80–90%, 80–90% and 90–100%, respectively). However, the SDE levels determined for weathered soils blended with water were 40–50% lower than the concentrations found by the Soxhlet procedure. The study also showed that the efficiency

Table 2 SDE methods for the analysis of less volatile organic pollutants in non-fatty environmental samples (symbols as in Table 1)

Matrix	Compound	Spiking level ($\mu\text{g g}^{-1}$)	Pre-treatment	Solvent	Extraction time (h)	Post-treatment	Recovery (%)	RSD (%)	Ref.
Sediment	Arochlor 1016	50	Blended with 2.5 L water	Isocot/tol ^a (15)	1	Elimination S	78	?	Veith <i>et al.</i> (1977)
Weathered sediment	PCBs, PCNs, PNAs	–	Blended with 0.8–1.1 L water	n-Hexane (10)	2.2	Concentration	–	1.1–23	Cooke <i>et al.</i> (1979)
Sediment	Chlorinated benzenes	100–1000	Blended with 0.25 L water	n-Hexane (10)	3	Elimination S	76–91	0.5–21	Onuska <i>et al.</i> (1985)
Sediment	Chlorinated benzenes	10–100	Blended with 0.25 L water	n-Hexane (10)	3	Elimination S	71–88	1.4–33	
Sediment	Chlorinated benzenes	1–10	Blended with 0.25 L water	n-Hexane (10)	3	Elimination S	66–89	1.4–17	
Certif. Sediment	PCBs	2.34–24.6	200 mL H ₂ SO ₄ + K ₂ Cr ₂ O ₇	n-Hexane (15) ^b	8	Alumina	47–99	0.3–5.4	Dunnivant <i>et al.</i> (1988)
Sediment	PCBs	33.6–90.0	200 mL H ₂ SO ₄ + K ₂ Cr ₂ O ₇	n-Hexane (15) ^b	8	Alumina	102	4.7–9.3	
Soil	HCb	20.0	100 g soil + 20 mL water + 10 mL ethanol + ultrasonic; 1 min	Petrolbenzine (?)	1	NR	100	2.7	Seidel <i>et al.</i> (1993)
Weathered soil	Endogenous OCP	–	100 g soil + 20 mL water + 10 mL ethanol + ultrasonic; 1 min	Petrolbenzine (?)	1	NR	–	–	
Particulate	PCDD (homologues)	0.045–8.56 ^c	150 g (sample + water) + HCl + sonication	n-Hexane (10)	3	Basic alumina	85–116 ^d	?	Townsend <i>et al.</i> (1989)
Fruits, vegetables	OCCs, OCPs	0.01–1.0	5–10 g sample blended with 0.25 L water	n-Hexane (5)	1.5	NR	66–108	?	Hemmerling <i>et al.</i> (1991)
Fruits, vegetables	PCBs	0.1	5–10 g sample blended with 0.25 L water	n-Hexane (5)	1.5	NR	68–89	?	
Sediments	Chiral PCBs	–	5 g sample blended with 4 g Cu + 50 mL water	n-Pentane (2)	1	NR	–	–	Glausch <i>et al.</i> (1996)
Sewage sludge	Nonylphenol polyethoxylates	100 ^e	1 g sample blended with 0.1 L water	Cyclohexane (1–2)	3	NR (HPLC) Alumina (GC)	< 30 ^f	?	Lee <i>et al.</i> (1997)
Toothpaste	Fatty alcohol sulfates	–	30 g sample + 50 mL 4M H ₂ SO ₄ + LLE (diethyl ether, 10 mL) + concentrat.	Ethyl acetate (2)	3	Derivatization	–	–	Meissner <i>et al.</i> (1999)

^aIsocotane/toluene.^bReplace hexane layer after 1, 2, 4 and 8 h intervals.^cRange for different homologues.^dMass balance calculations for the whole SDE system by comparison with the initial amount.^eTotal concentration for all NP_nEO ($n = 1–17$).^fBy comparison with SFE, except for NP1EO.

of the SDE depends on the soil type and, in agreement with that mentioned for aqueous samples, on the volatility of the selected compounds. The less volatile the compound, the lower the recovery: SDE recoveries for DDT were only 21–60% of those found by Soxhlet extraction.

Onuska and Terry observed a similar trend when comparing the SDE and the Soxhlet efficiencies for the extraction of spiked chlorinated benzenes from a sediment. The concentrations found using SDE were 14–36% lower than those using the Soxhlet method, except for pentachlorobenzene and 1,3-dichlorobenzene, which were not determined by the latter procedure. The authors also reported a decrease in the SDE recoveries of the target compounds as the investigated concentration level decreased (Table 2). The recoveries of the studied chlorinated benzenes decreased from 76–91% to 66–89% as the spiking level decreases from 100–1000 $\mu\text{g g}^{-1}$ to 1–10 $\mu\text{g g}^{-1}$.

In a recent study, Meissner *et al.* used SDE for the determination of fatty alcohol sulfates in cosmetics (toothpaste) by combining this technique with a hydrolysis treatment. However, the application of SDE to the analysis of nonylphenol polyethoxylates in sewage sludge by Lee *et al.* failed when compared with the more efficient supercritical fluid extraction technique.

In general, the published SDE methods for the analysis of non-fatty environmental samples involve longer extraction times (1–8 h) than those reported for aqueous samples (1–1.3 h). In addition, and contrary to that proposed by the theoretical model of Rijks *et al.*, the recoveries of less volatile compounds from non-fatty complex samples have been found to be independent of the vapour flow rates. However, it is important to note that in this study by Seidel ethanol was added to the water flask to improve the OCP recoveries, and that the possible effect of a co-distillation solvent was not included in the theoretical model.

Application of the SDE to the Analysis of Fatty Biological Samples and Food

Due to the high lipophilicity of some of the most toxic pollutants, such as OCPs, PCBs and PCDD/Fs, the classical procedures for the analysis of these pollutants in fatty samples were based on an exhaustive extraction of the lipids from the matrix. Subsequent removal of the co-extracted lipids has been widely recognized as the main problem with these kinds of methods, especially when analysing samples with high fat contents such as dairy products. Because of the characteristics of the SDE technique, the disruption of the strongly bound pollutant-matrix in these

samples can be accomplished before SDE by degradation of the matrix components entrapping the target compounds. Treatment with 1–2 M sulfuric acid followed by ultrasonication in a bath and heating of the sample during the SDE process has been found to be one of the most efficient procedures for breaking down the matrix structure allowing steam distillation of the analytes. Furthermore, this acid treatment allowed a simultaneous clean up of the final extract as the matrix components form more polar products, which can then be easily separated from the non-polar analytes. According to the published results, most samples submitted to this kind of treatment did not require any additional clean up. Filek *et al.* report good recoveries for the SDE of OCPs from dairy products when using this type of acid pre-treatment: in the range 83–126% for powdered milk and human milk spiked at the 20.0–51.3 ng g^{-1} level, and in the range of 73–111% for a certified dairy product (OCP levels ranging from 1.5 to 6.6 ng g^{-1}). However, the SDE method failed when it was used for the extraction of the endogenous PCBs from dairy products with different fat contents. According to the reference method, the PCBs detected by Ramos *et al.*, in 1998 ranged from 2 to 0.01 ng g^{-1} in the investigated matrices. Nevertheless, most of the PCB congeners were found to be non-detectable with the SDE procedure and, when found at quantifiable levels, the reported concentrations were less than 26% of those determined by the reference method.

Rather similar results were reported by Seidel and Lindner in 1993 for the analysis of the OCPs in dairy products and human milk as none of the investigated compounds were found to be at a quantifiable level. However, no additional comparison with a reference method was included in this study, in which 10 g of sample was blended with water and ethanol. In this case, the alcohol, added as a co-distillation solvent, would also be able to disrupt the fat globule thereby allowing the SDE of the analytes. An important shortcoming of this kind of approach is the formation of large oil drops during the extraction, which increase the diffusion layer and hinder the SDE process. Filek *et al.* proposed blending of the sample with surfactants has been proposed as a possible solution for the case of fatty matrices without natural emulsifiers.

When no pre-treatment of the fatty sample was carried out, a co-distillation (total, according to Yoon *et al.*, or partial, according to Ramos *et al.*) of the lipids with the less volatile compounds occurred. Then, a post-treatment for isolation of the target compounds from the co-extracted matrix components was required. Following the implication of these results, it is rather surprising that neither pre- nor post-treatment of the sample was included

Table 3 SDE methods for the analysis of less volatile organic pollutants in fatty environmental samples (symbols as in Table 1)

Matrix	Compound	Spiking level (ng g^{-1})	Pre-treatment	Solvent	Extraction time (h)	Post-treatment	Recovery (%)	RSD (%)	Ref.
Fish tissue	PCBs	1700	Blended with 2.5 L water	Isooct/tol.(15)	7–14	NR	82–85	?	Veith <i>et al.</i> (1977)
Muscle, liver, kidney	PCBs, PCNs, ΣDDT^a	5000	Blended with 0.1 L water	n-Heptane (10)	2	Concentration	67–100	1.0–20	Dunnivant <i>et al.</i> (1988)
Muscle, liver, kidney	PCBs, PCNs, ΣDDT^a	1000	Blended with 0.1 L water	n-Heptane (10)	2	Concentration	65–85	?	
Dairy products, Human milk	Endogenous OCPs	–	10 g sample + water + ethanol	Petrobenezine (?)	1	NR	–	?	Seidel <i>et al.</i> (1993)
Pumpkin seed	OCPs	100	10 g sample + water + ethanol + surfactant	Petrobenezine (?)	1	NR	65–89	6–12	
Certif. dairy product	OCPs	1.5–6.6	5 g sample + 80 mL 2 M H_2SO_4 + ultrasonic, 1 min + 1 mL ethanol + surfactant	Petrobenezine (20)	1.5	Concentration	73–111	?	Filek <i>et al.</i> (1995)
Powdered milk, Human milk	OCPs	20.0–51.3	5 g sample + 80 mL 2 M H_2SO_4 + ultrasonic, 1 min + 1 mL ethanol + surfactant	Petrobenezine (20)	1.5	Concentration	83–126	?	
Powdered milk	Endogenous PCBs	–	15 g sample + 60 mL 1 M H_2SO_4 + ultrasonic, 1 min	Dichlorometane (2)	60–90	$\text{SiO}_2\text{-HSO}_4$	< 26	?	Ramos <i>et al.</i> (1998)
Dairy products	PCBs	0.5	15 g sample + 60 mL 1 M H_2SO_4 + ultrasonic, 1 min	Dichlorometane (2)	60	$\text{SiO}_2\text{-HSO}_4$	< 10	?	
Herbal essential oils	OCPs	500–10 000	Blended with 0.05 L water	?	?	LLE (hexane : ethyl ether) + H_2SO_4	83–105	2.4–10	Rajendran <i>et al.</i> (1991)
	OPPs	500–10 000	Blended with 0.05 L water	?	?	LLE (hexane : ethyl ether) + H_2SO_4	72–116	0.5–10	

^aDDT + DDE + TDE.

in some of the first reported applications of SDE for the analysis of toxic aromatic compounds in biological matrices. The investigated samples included fish tissues, muscle, liver and kidney and, although satisfactory recoveries (67–100%) were reported for the spiked PCBs, PCNs and Σ DDT (i.e. DDT + DDE + TDE), it is important to note that the spiking level in these experiments ranged from 1000–5000 ng g⁻¹ (Table 3). Even at such a high level of concentration, the authors reported an evident dependence of SDE recoveries on the analyte concentration. In fact, Cooke *et al.* found that the PCB, PCN and Σ DDT recoveries from animal tissues decreased from 67–100% to 65–85% when the spiking level decreased from 5000 to 1000 ng g⁻¹. According to this trend, it can be concluded that the very low levels of the endogenous pollutants in environmental samples together with the typical complexity of the matrix would be the main reasons for the disappointing results reported for some SDE applications involving non-spiked fatty samples.

See also: **II/Extraction:** Analytical Extractions; Solid-Phase Extraction; Solid-Phase Microextractions; Supercritical Fluid Extraction. **Distillation:** Extractive Distillation.

Further Reading

- Cooke M, Nickless G, Povey A and Roberts DJ (1979) Polychlorinated biphenyls, polychlorinated naphthalenes and polynuclear aromatic hydrocarbons in Severn estuary (UK) sediments. *Science of Total Environment* 13: 17–20.
- Cooke M, Roberts DJ and Tillett ME (1980) Polychlorinated naphthalenes, polychlorinated biphenyls and DDT residues in British birds of Prey. *Science of Total Environment* 15: 237–246.
- Dunnivant FM and Elzerman AW (1988) Determination of polychlorinated biphenyls in sediments, using sonication extraction and capillary column gas chromatography-electron capture detection with internal standard calibration. *Journal of the Association of the Official Analytical Chemistry* 71: 551–556.
- Filek G, Bergamini M and Lindner W (1995) Steam distillation-solvent extraction, a selective sample enrichment technique for the gas chromatographic-electron capture detection of organochlorine compounds in milk powder and other milk products. *Journal of Chromatography A* 712: 355–364.
- Glausch A, Blanch GP and Schurig V (1996) Enantioselective analysis of chiral polychlorinated biphenyls in sediments samples by multidimensional gas chromatography-electron capture detection after steam distillation-solvent extraction and sulfur removal. *Journal of Chromatography* 723: 399–404.
- Godefroot M, Stechele M, Sandra P and Verzele M (1982) A new method for the quantitative analysis of organochlorine pesticides and polychlorinated biphenyls. *Journal of High Resolution Chromatography Communications* 5: 75–79.
- Hemmerling C, Risto C, Augustyniak B and Jenner K (1991) Untersuchungen zur aufbereitung von Lebensmittel- und Umweltpuben für die rückstandsbestimmung von pestiziden und PCB mittels kontinuierlicher wasserdampfdestillation. *Die Nahrung* 35: 711–719.
- Lee HB, Peart TE, Bennie DT and Maguire RJ (1997) Determination of nonylphenol polyethoxylates and their carboxylic acid metabolites in sewage treatment plant sludge by supercritical carbon dioxide extraction. *Journal of Chromatography A* 785: 385–394.
- Meissner C and Engelhardt H (1999) Trace analysis of surfactants derived from fatty alcohols. II. Hydrolysis and enrichment techniques. *Chromatographia* 49: 12–16.
- Nash RG (1984) Extraction of pesticides from environmental samples by steam distillation. *Journal of the Association of the Official Analytical Chemistry* 67: 199–203.
- Onuska FI and Terry KA (1985) Determination of chlorinated benzenes in bottom sediments samples by WCOT column gas chromatography. *Analytical Chemistry* 57: 801–805.
- Rajendran N and Venugopalan VK (1991) Bioconcentration of endosulfan in different body tissues of estuarine organisms under sublethal exposure. *Bulletin of Environmental Contamination and Toxicology* 46: 151–158.
- Ramos L, Blanch GP, Hernández L and González MJ (1995) Recoveries of organochlorine compounds (PCBs, PCDDs and PCDFs) in water using steam distillation-solvent extraction at normal pressure. *Journal of Chromatography A* 690: 243–249.
- Ramos L, Tabera J, Hernández L and González MJ (1998) Selective extraction of polychlorinated biphenyls from dairy products using steam distillation solvent extraction at normal pressure. *Analytica Chimica Acta* 376: 313–323.
- Rijks J, Curvers J, Noy T and Cramers C (1983) Possibilities and limitations of steam distillation-extraction as a preconcentration technique for trace analysis of organics by capillary gas chromatography. *Journal of Chromatography* 279: 395–397.
- Seidel V and Lindner W (1993) Universal sample enrichment technique for organochlorine pesticides in environmental and biological samples using a redesigned simultaneous steam distillation-solvent extraction apparatus. *Analytical Chemistry* 65: 3677–3683.
- Townsend DI, Lamparski LL and Nestrick TJ (1989) Laboratory simulation and potential mechanisms explaining PCDD congener group ratio behaviour on particulates from combustion sources. *Chemosphere* 16: 1753–1757.
- Veith GD and Kiwus LH (1997) An exhaustive steam-distillation and solvent-extraction unit for pesticides and industrial chemicals. *Bulletin of Environmental Contamination and Toxicology* 17: 631–636.

Supercritical Fluid Extraction

A. A. Clifford, University of Leeds, Leeds, UK

Copyright © 2000 Academic Press

Supercritical Fluids

It is now 170 years since Baron Charles Cagniard de la Tour discovered that, above a certain temperature, single substances do not condense or evaporate, but exist only as fluids. In the following decades the 'critical point' was characterized, with its parameters: the critical temperature and pressure. In recent years fluids have been widely exploited at conditions above, but not too far removed from, their critical temperatures and pressures. The term 'supercritical fluids' has been coined to describe these media. Their value lies in the fact that they can have properties intermediate between those we associate with gases and liquids, and also that the properties can be controlled by pressure as well as temperature. Consequently, supercritical fluids can often provide optimum conditions for both experiments and processes. Equally important, especially as regulations become tougher, is that supercritical fluids offer environmental advantages. This is mainly because carbon dioxide and water are available as solvents. The disadvantages of supercritical fluids are that high pressures and sometimes temperatures are involved, and, in the case of water, there are corrosion problems. As the technology to overcome them is available, these disadvantages become cost and convenience factors to weigh against potential advantages. Consequently, supercritical fluids are being exploited in specialized areas. Amongst these is supercritical fluid extraction (SFE), on both an industrial and analytical scale.

Substances used as supercritical fluids include hydrocarbons, such as propane and ethene, water and ammonia, fluorinated hydrocarbons and even xenon. However, one compound, carbon dioxide, has so far been the most widely used in extraction, because of its convenient critical temperature, cheapness, chemical stability, non-flammability, stability in radioactive applications and non-toxicity. Large amounts of carbon dioxide released accidentally could constitute a working hazard, given its tendency to blanket the ground, but hazard detectors are available. It is an environmentally friendly substitute for other organic solvents. The carbon dioxide that is used is obtained in large quantities as a by-product of fermentation, combustion and ammonia synthesis and would be released into the atmosphere sooner rather than later, if it were not used as a supercritical fluid. Its polar

character as a solvent is intermediate between a truly non-polar solvent such as hexane and weakly polar solvents. Because the molecule is non-polar it is often classified as a non-polar solvent, but it has some limited affinity with polar solutes because of its large molecular quadrupole. It has a particular affinity for fluorinated compounds and is useful for working with fluorinated metal complexes and fluoropolymers.

To increase the affinity of carbon dioxide to a variety of solutes, substances are added as 'modifiers' or 'entrainers'. The characteristics they impart include increased or decreased polarity, aromaticity, chirality, and the ability to further complex metal-organic compounds. For example, methanol is added to increase polarity, aliphatic hydrocarbons to decrease it, toluene to impart aromaticity, [R]-2-butanol to add chirality, and tributyl phosphate to enhance the solvation of metal complexes. They are often added in 5% or 10% amounts by volume, but sometimes much more, say 50%. They can have significant effects when added in small quantities and in these cases it may be the effect on surface processes rather than solvent character which is important. For example, the modifier may be effective in extraction by adsorbing onto surface sites, preventing the readsorption of a compound being extracted.

Because supercritical fluids have properties intermediate between those of gases and liquids to an extent controlled by pressure, optimum conditions can be sought for extraction. The medium can be adjusted for compounds to be sufficiently soluble to be removed, while at the same time the viscosity and diffusion coefficients can be high enough to bring about relatively rapid mass transport. **Table 1** shows typical values for the density and viscosity of a gas, supercritical fluid and liquid, taking carbon dioxide as an example. Density is more than half that of the liquid, giving rise to reasonable solubility. Moreover, by controlling the solvent density SFE can, to some extent, be made selective. In contrast, however, the viscosity of a supercritical fluid is much closer to that of a gas than that of a liquid. Thus pressure drop through a supercritical extraction cell is less than for the equivalent liquid process. Diffusion coefficients, also shown in Table 1 for naphthalene in carbon dioxide, are higher in a supercritical fluid than in a liquid. They are approximately inversely related to the fluid density. The advantage shown in the table is seen not to be so great and the main diffusional advantage lies in the fact that typical supercritical solvents have smaller molecules than typical liquid solvents. The diffusion coefficient for naphthalene in

Table 1 The density, ρ , and viscosity, η , of carbon dioxide and the diffusion coefficient for naphthalene in carbon dioxide, D , under gas, supercritical and liquid conditions

	$\rho/\text{kg m}^{-3}$	$\eta/\mu\text{Pa s}$	$D/\text{m}^2 \text{s}^{-1}$
Gas, 313 K, 1 bar	2	16	5.1×10^{-6}
Supercritical, 313 K, 100 bar	632	17	1.4×10^{-8}
Liquid, 300 K, 500 bar	1029	133	8.7×10^{-9}

a typical liquid would be closer to $1 \times 10^{-9} \text{ m}^2 \text{s}^{-1}$. Thus diffusion coefficients in supercritical fluid experiments and processes are typically an order of magnitude higher than in a liquid medium. This has the advantage of faster transport in the narrow passages typical in an extraction.

Application to Extraction

Because of the properties of a supercritical fluid, as described above, SFE can be more rapid than liquid extraction. Furthermore, the solvent is removed more easily, and fractionation of the extract by reducing the pressure in stages is feasible. SFE was first exploited on a process scale and this application continues to develop. On an industrial scale the first and most famous example is the 'natural' decaffeination of green coffee beans by the Hag process initiated in Bremen. Hops are also extracted by SFE on a large scale. Apart from these large-scale processes, more than 30 high-value oils, flavours and essences are extracted commercially in batch processes.

SFE is also used in chemical analysis to replace liquid extraction for sample preparation for a wide range of systems. SFE is now being used for the Total Diet Study programme of the US Food and Drug Administration. Usually, SFE is more rapid, less laborious and involves solvents which are less hazardous. Efforts still have to be made to make it more quantitative, but in fairness to SFE, extraction is often incomplete using a liquid. SFE is sometimes used on-line with an analytical method such as gas chromatography; it is most successful for some polymer and plant extractions. Table 2 summarizes the principle analytical applications of SFE.

Laboratory-Scale SFE

SFE is carried out on a laboratory scale for both sample preparation and for initial studies on possible industrial processes. A range of commercial equipment is available to carry out experimental studies

conveniently. A simple system is shown schematically in Figure 1. It can be assembled in-house and shows the principles involved. The fluid, typically carbon dioxide, is supplied from a cylinder with a dip tube to a pump, which can be a pump designed for liquid chromatography capable of delivering up to 5 mL per minute at a pressure of 400 bar and displaying the pressure and the flow rate. The pump head must be accessible so that it can be cooled by circulating an ethylene glycol and water mixture from a cooler, so that the fluid substance is pumped as a liquid. An alternative method of ensuring this is to use a fluid supply with an overhead pressure of around 100 bar of helium. In this case, cooling the pump head is not necessary, but the fluid will contain a small percentage of helium. The pumped fluid substance then passes into a controlled heater, which can be an oven for gas chromatography. It first passes through a length (typically 0.3 m) of stainless steel tubing into an extraction cell, rated for 400 bar at 100°C, which is fitted with a frit at the exit end (often both ends) to keep the sample matrix to be extracted in place. The exit tube is then connected to a restrictor to maintain the pressure in the system. This can be of stainless steel or, alternatively, a quartz capillary, in which case the connector will have a graphitized ferrule. The effluent then passes through a collecting solvent to trap the extracted compounds. Because of the cooling effect as the fluid expands to atmospheric pressure, it is usually necessary to heat the restrictor and the simplest way of doing this is with a domestic hair dryer. Evaporation of the collecting solvent may occur and it will be necessary to add solvent to the vial during the extraction. This simple device, although often satisfactory, can suffer from blocking of the

Table 2 Examples of the use of SFE in analytical sample preparation

Matrix	Examples of analytes extracted
Soils, sludges, water	Agrochemicals, polychlorobiphenyls, polycyclic aromatic hydrocarbons, fuel hydrocarbons, phenols, surfactants, metals
Food and animal tissue	Veterinary drugs, pesticides, anabolic steroids, mycotoxins, fats
Human milk and serum	Drugs
Polymers, food packaging	Low oligomers, polymer additives
Herbs, cosmetic products	Flavours, fragrances
Plant tissue	Alkaloids, various natural products, triglycerides
Fly ash, engine emissions	Polycyclic aromatic hydrocarbons, dioxins
Sedimentary rocks	Biomarker hydrocarbons
Fermentation broths	Biologically active compounds

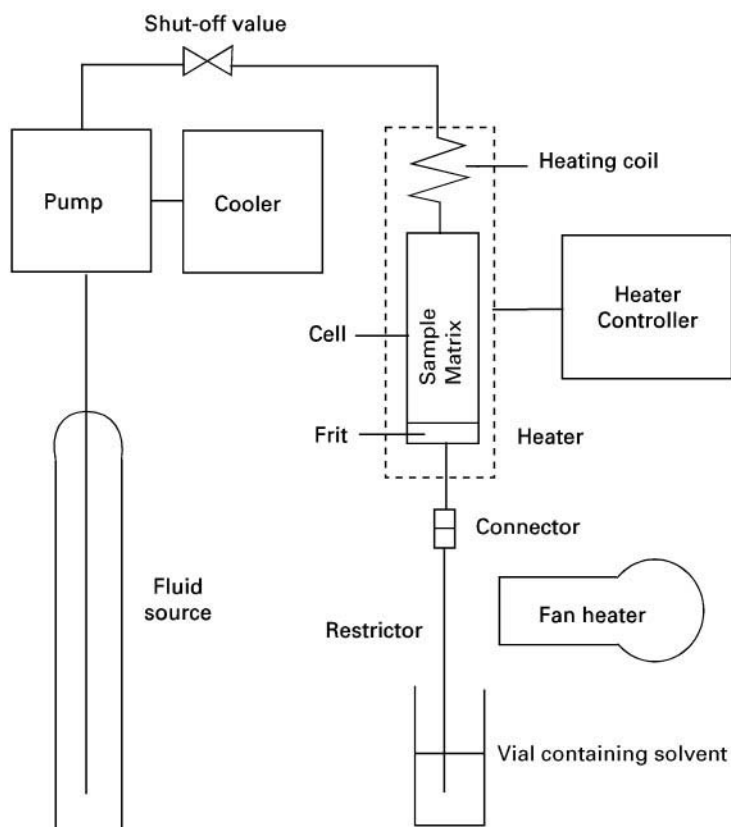


Figure 1 Schematic diagram of a simple system for carrying out SFE on a laboratory scale.

restrictor and loss of extracted compounds because of inefficient trapping. Furthermore, it does not allow independent control of the flow rate and pressure. More sophisticated commercial methods of pressure control and trapping are available.

In a representative experiment, a 1 mL cell is loaded with 0.5 g of the material to be extracted, (previously dried and ground to particles of 0.1 mm diameter). Carbon dioxide is pumped at a rate of 0.5 mL min^{-1} , measured as liquid at the pump. The temperature is 50°C and the pressure of 400 bar is maintained by a restrictor of $25 \mu\text{m}$ internal diameter and 12 cm length. The effluent is trapped in 3 mL of dichloromethane, ready for analysis by gas chromatography after an internal standard had been added. The extraction is carried out for 30 min. However, conditions for SFE vary widely and the details for a particular application can be found in the many reports now in the literature.

If a modifier is required, a second liquid pump must be added to the system and the output liquid fed into a mixing chamber just before the shut-off valve in Figure 1. Modifiers are usually added in relatively small amounts, say 5% or 10% by volume. It is possible to purchase cylinders of carbon dioxide al-

ready containing small amounts of common modifiers, such as methanol or acetone. If a modifier is used, the trapping solvent is conveniently the same as the modifier, as modifier will precipitate in the collection vial. Trapping is usually more efficient if a modifier is used.

The experiment described above is described as dynamic extraction, as the fluid is continuously flowing through the cell. Static extraction can also be carried out in a similar system if a second shut-off valve is inserted after the extraction cell. During an experiment, the cell is pressurized with fluid and the cell isolated so that contact between the matrix and fluid can occur for a period of about 30 minutes. A short dynamic stage is then carried out to remove the fluid, containing the dissolved extract, from the cell. For a static extraction, a modifier may be added as liquid to the cell before closing it.

SFE can readily be coupled to gas chromatography by passing the restrictor through a septum into the injection port of a chromatograph. This procedure can be much more sensitive, as all the extracted material is transferred to the chromatograph, whereas in an off-line experiment, only a small fraction of the collection solvent will be injected. Thus the procedure

is applicable for example to the analysis of pesticides at low levels. To carry out this procedure, the first section of the chromatographic column is cooled and the carrier gas turned off. SFE is then carried out with the carbon dioxide, or other fluid substance, passing out through the column and the extracted materials depositing at the inlet of the column. SFE is then stopped and the carrier gas passed through the column to flush out the carbon dioxide. The column is then raised to the analysis temperature and chromatography carried out.

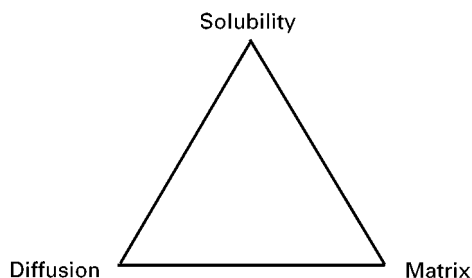
Pilot and Process-Scale SFE

The basic process of extraction on a process scale is analogous to that on a laboratory scale and is shown schematically in **Figure 2**. The fluid substance, such as carbon dioxide, is pumped as a liquid and therefore is initially cooled to, say, 5°C, which must allow for some heating during pumping, and kept in a cooled reservoir. A system for adding a proportion of liquid modifier, not shown, may be incorporated. The fluid is then heated to the extraction temperature and pumped into an extraction cell, which is maintained at this temperature. The matrix to be extracted is packed into the extraction cell in a mesh basket to prevent it being carried out of the cell during extraction. Following extraction, the pressure is reduced to precipitate the extract through a control valve. The flow rate of fluid is controlled by the rate of pumping and the pressure in the extraction cell is controlled by the setting of the control valve for a particular pumping rate. Control systems may be used to control the extraction conditions. Reduction of pressure causes cooling of the fluid and so heat input is required, as shown. The precipitated material is collected at the base of the collection vessel, which has temperature control and also pressure control from the control valve on the fluid exit. A series of collection vessels at successively lower pressures may be employed to trap all the extract and separate it into fractions to some extent. A trapping liquid, such as a vegetable oil, may be used on a process scale to give a particular product. Trapping onto a surface, such as active charcoal, may also be used, particularly for volatile products, followed by thermal desorption. On a process scale the fluid leaving the collection vessel is likely to be cooled for recycling.

Mechanisms and Kinetics of SFE

Although extraction is essentially a complex process in which many factors, including procedural parameters, are involved, in a basic theoretical approach

the process of extraction can be considered to involve the three factors shown in the SFE triangle below.



The solute must, firstly, be sufficiently soluble in the supercritical fluid to be removed by solution in the fluid flow. If this is not the case, it will be revealed by interpretation of the kinetic recovery curve, as shown below. If solubility is insufficient, the situation may be improved by adding a modifier to the fluid, as described earlier.

Secondly, the solute must be transported sufficiently rapidly, by diffusion or otherwise, from the interior of the matrix in which it is contained. The diffusion process may be normal diffusion of the solute, or it may involve diffusion in the fluid thorough pores in the matrix. The time-scale for diffusion will depend on the diffusion coefficient and the shape and dimensions of the matrix or matrix particles. Of these the shortest dimension is of great importance, as the times depend on the square of its value. Values for this quantity of 1 mm or preferably less are usually necessary.

Thirdly, the solute must be released by the matrix. This last process may involve desorption from a matrix site, passage through a cell wall, or escape from a cage formed by polymer chains. It can be slow and in some cases it appears that part of the substance being extracted is locked into the structure of the matrix. An example is the SFE of additives and lower oligomers from polymers, which can give much lower results than obtained by dissolving the polymer in a solvent, or using liquid extraction at higher temperatures, which swells the polymer to a greater extent. Thus SFE will not always give the total amount of a compound in a sample, only the amount extractable under particular SFE conditions. It may be that the latter is of interest, for example for determination of the migration of additives from polymers into food-stuffs, but if the total amounts are required, SFE may not be applicable. Preliminary experiments, and comparisons with other methods, are necessary. It can be strongly temperature-dependent and thus higher temperatures may improve the situation. The addition of modifiers may often reduce the matrix effect; in fact modifiers are often more important in this respect

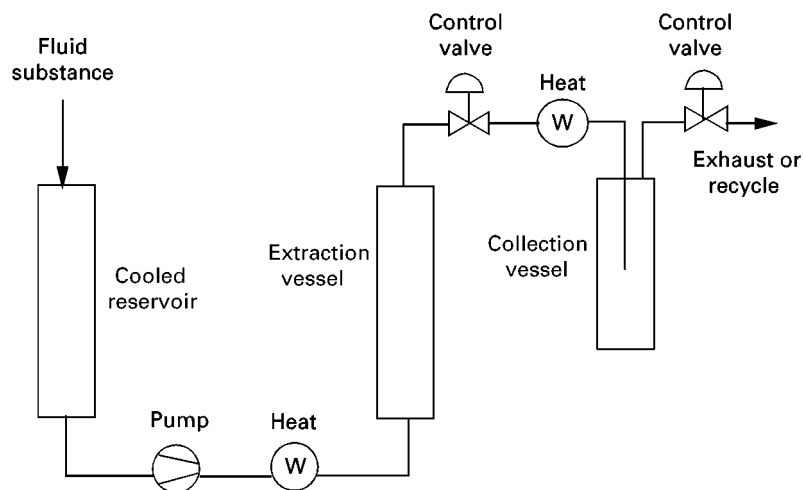


Figure 2 Schematic diagram of SFE on a process scale.

than in enhancing solubility. The mechanism is thought to involve interactions with surfaces. It should be emphasized here that the matrix effect also occurs with liquid solvent extraction. The fact that solvent strength can be varied in a supercritical fluid means that the matrix effect is more obvious in this medium and can be studied in more detail. The advantage is that conditions can often be found in SFE where the matrix effect is minimized.

A related problem is the presence of water. Water is not very soluble in many fluids, such as carbon dioxide, and it can 'mask' the substances to be recovered. The rate of extraction may sometimes be equal to the rate of water removal. It may be necessary to dry the material to be extracted in air or by admixture with

a drying agent, such as diatomaceous earth or anhydrous magnesium sulfate. Reduction of the water content of plant material from, say, 80% (as measured by mass loss at 100°C) down to 10% may be desirable, provided valuable volatiles are not lost in the process. However, water may assist extraction by acting as a modifier, as is believed to be the case for coffee decaffeination.

Modifiers or entrainers added to the fluid, as discussed earlier, may be beneficial to any of the above factors. They may improve the solubility of the compounds to be extracted and this was originally thought to be their most important role. However they often improve diffusion by absorption into a polymer and swelling it, for example. Modifiers

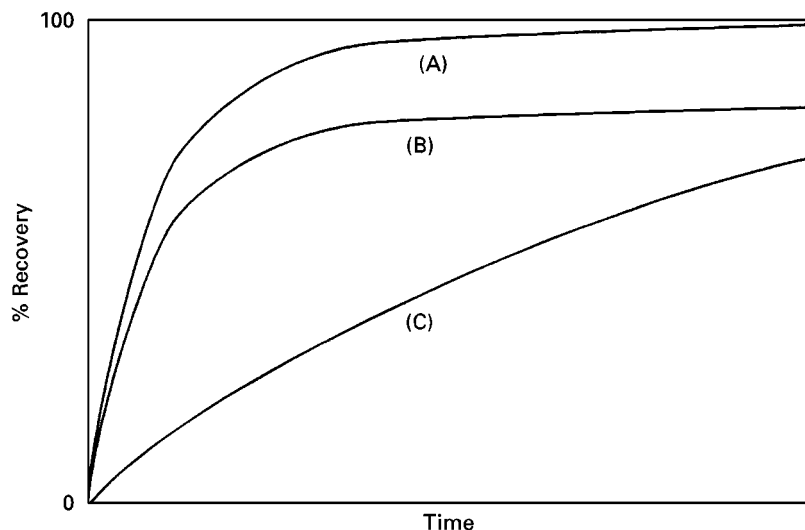


Figure 3 Examples of schematic recovery curves, where recovery is controlled by (A) diffusion; (B) diffusion and matrix effects; and (C) by solubility.

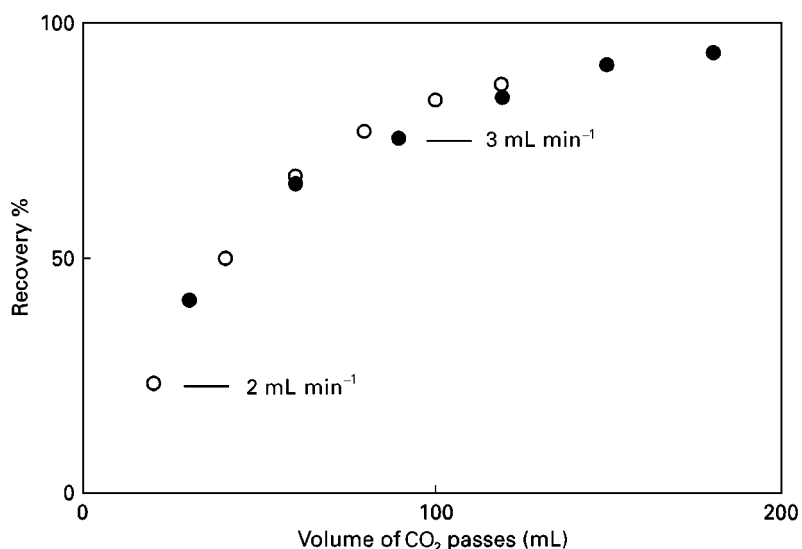


Figure 4 Extraction of lycopene from tomato paste at 100°C and 400 bar at two flow rates plotted against the volume of CO₂ passed.

may improve the matrix factor by adsorbing on surface sites. Modifiers, such as methanol, can reduce the water problem by improving its solubility in the fluid.

Figure 3 shows examples of the types of curves of recovery versus time that can be obtained in SFE. Curve (A) is a typical curve obtained when the process is controlled by diffusion. When matrix effects are significant, the results may have the form of (B). Curve (C) is an example of recovery behaviour when the extracted compound is not very soluble in the extracted fluid. It is thus highly desirable, when developing a procedure for a particular application, to carry out kinetic experiments to obtain curves of recovery versus time. The curves can then be used to investigate the reaction mechanism, as well as determine a suitable extraction time. These developments are detailed in some of the books listed in the bibliography. Kinetic experiments are done by replacing the collection vial periodically. As extraction is faster initially, the time intervals are smaller near the beginning of an extraction. A representative series of times for changing over the collection vial is 2, 5, 10, 20, 30, 40 and 60 min. The total amount extracted can also be compared with liquid extraction.

An example of an experimental recovery curve is now given in Figure 4 for the extraction of lycopene from 0.5 g of tomato paste, dried by mixing with diatomaceous earth, at 100°C and 400 bar. Flow rates of 2 mL min⁻¹ and 3 mL min⁻¹ per minute (measured as liquid at the pump) were used, and the results plotted not against time, but against the volume of CO₂ passed (i.e. the time multiplied by the flow rate). The fact that the two curves approx-

imately coincide, indicates that the extraction is principally by the partition of lycopene between CO₂ and the tomato paste matrix, which in turn is related to the solubility of lycopene in CO₂.

Conclusions

Supercritical fluid extraction can be a clean alternative to liquid solvent extraction both for analytical sample preparation and for production scale, because environmentally friendly solvents such as carbon dioxide can be used instead of organic solvents. Some applications are found to be more successful than others. It requires more expensive equipment and a greater commitment to process development than liquid extraction. Nevertheless, it is being applied in specific areas, such as for polymer additives in analytical chemistry and as a method for obtaining valuable compounds from plants on a process scale.

See Colour Plate 44.

See also: **II/Chromatography: Supercritical Fluid:** Large-Scale Supercritical Fluid Chromatography. **III/Environmental Applications:** Supercritical Fluid Extraction. **One-line Sample Preparation: Supercritical Fluid Extraction.** **Polymers:** Supercritical Fluid Extraction.

Further Reading

Bright FV and McNally MEP (1992) Supercritical Fluid Technology. *ACS Symposium Series 488*. Washington DC: American Chemical Society.
Clifford, T (1998) *Fundamentals of Supercritical Fluids*. Oxford: Oxford University Press.

- King JW and List GR (1996) *Supercritical Fluid Technology in Oil and Lipid Chemistry*. Champaign, Illinois: American Oil Chemists' Society.
- King MB and Bott TR (1993) *Extraction of Natural Products Using Near-Critical Solvents*. Glasgow: Blackie.
- Lee ML and Markides KE (1990) *Analytical Supercritical Fluid Chromatography and Extraction*. Provo, Utah: Chromatographic Conferences, Inc.
- Lynch TP in Adlard ER (1995) Chromatography in the Petroleum Industry. *Journal of Chromatography Library* Vol. 56. Amsterdam: Elsevier.
- McHugh MA and Krukonis VJ (1994) *Supercritical Fluid Extraction*, 2nd edn. Boston: Butterworth-Heinemann.
- Page SH, Sumpter SR and Lee ML (1992) Fluid phase equilibria in supercritical fluid chromatography with CO₂-based mixed mobile phases: a review. *Journal of Microcolumn Separations* 4: 91.
- Westwood SA (1993) *Supercritical Fluid Extraction and its Use in Chromatographic Sample Preparation*. Glasgow: Blackie.

Ultrasound Extractions

C. Bendicho and I. Lavilla,

Universidad de Vigo, Facultad de Ciencias
(Química), Vigo, Spain

Copyright © 2000 Academic Press

Introduction

Sound is transmitted through a medium by inducing vibrational motion of the molecules forming part of it. Human hearing threshold is reached when the frequency of sound is higher than 16–18 kHz. Ultrasound comprises the region of frequencies between 18 kHz and 100 MHz, the upper limit not being sharply defined (Figure 1). This broad region can still be divided into two different regions: power ultrasound between 20 and 100 kHz and diagnostic ultrasound between 1 and 10 MHz. The above classification relies on the capability of energy transmission into the medium at the lower frequencies, which induces the cavitation phenomenon.

Relevant applications of ultrasonic energy include its use in animal communications (e.g. bat navigation and dog whistles), medicine for fetal imaging, underwater range finding (SONAR) and nondestructive testing for metal flaws. Recently, ultrasound has also been considered a potential source for enhancement of chemical reactivity. A large variety of chemical and industrial processes rely on high intensity ultrasonica-

tion, e.g., cleaning, drilling, soldering, acceleration of chemical reactions, emulsification, sterilization, flotation, homogenization, dissolution, deaggregation of powder, disruption of biological cells, extraction, crystallization, oxidation, etc. A further advantage of the above-mentioned ultrasound-assisted processes is the relative simplicity of both method development and instrumentation.

A brief description of ultrasound fundamentals as well as a discussion of its applications for solid-liquid extraction is given below.

Fundamental Features of Ultrasound

Vibrations Induced by Ultrasound

Sound waves are usually represented as a series of vertical lines, with intensity being related to separation between them, or as a sine wave where intensity is related to the amplitude (Figure 2).

Ultrasonic irradiation of a liquid medium gives rise to an acoustic pressure (P_a) which is added to the hydrostatic pressure (P_h) which exists in the medium. The acoustic pressure depends on time according to the following expression:

$$P_a = P_A \sin 2\pi ft$$

where f is the frequency of the wave (> 16 kHz), t is the time and P_A is the maximum pressure amplitude of the wave. At the point where the lines are close to each other, pressure is higher than normal (i.e. compression region), whereas at the point where the lines are furthest apart, pressure is lower than normal (i.e. rarefaction region).

The intensity of the wave can be defined as the energy transmitted per second per cm² of fluid and can be related to P_A as follows:

$$I = P_A^2(2\rho c)^{-1}$$

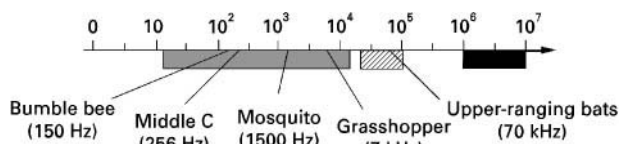


Figure 1 Sound frequencies (Hz, cycles per second). ■, human hearing 16 Hz–16 kHz; ▨, power 20 kHz–100 kHz (clearing plastic welding sonochemistry); ■, high frequency 1 MHz–10 MHz (medical diagnosis, chemical analysis). (From Mason TJ (1991).)

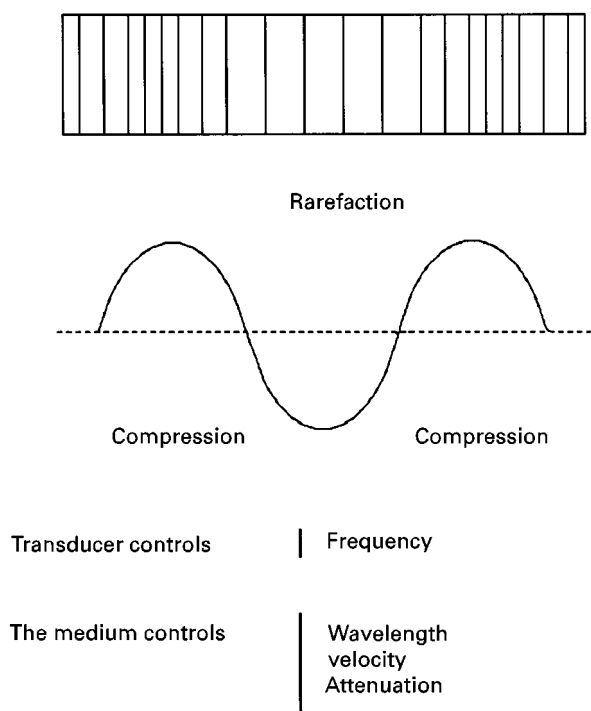


Figure 2 Sound motion in a liquid medium.

where c is the velocity of sound in the medium and ρ is the density of the medium.

Attenuation of Sound in a Liquid Medium

The intensity of the ultrasonic wave decreases with increasing penetration into the medium. Molecular vibration induced by the sound wave results in loss of intensity of the wave, which is transformed into heat. Heating occurs in the sites of compression and cooling at the sites of rarefaction. Since the compressibility of liquids is small, there is little heating caused by ultrasound as waves pass through the medium. The heating effect is caused by the degradation of acoustic energy due to absorption, following the equation:

$$I = I_0 \exp(-2\alpha d)$$

where I is the intensity at distance d from the ultrasound source and α is the absorption coefficient.

The Phenomenon of Cavitation

The pressure wave caused by ultrasound transmitted in a liquid medium will, in turn, cause an oscillation of the molecules around their mean position. When a large negative pressure (P_c) is applied to the liquid, where P_c (rarefaction pressure) = $P_a - P_h$, the distance between molecules can overcome a critical distance R , under which the liquid breaks down so that cavitation bubbles form. The R distance for water is

around 10^{-8} cm and the pressure involved is 10.1×10^5 kPa, where $P_c = 2\sigma/R$, σ is the surface tension. The cavitation process can be observed at much lower negative pressure (e.g. 10.1×10^4 kPa), as a result of the presence of gas nuclei as dissolved gas, suspended gas bubbles, or gas bubbles caused by heat fluctuations within the liquid. The cavitation threshold decreases with degassed liquids or as consequence of the increase in hydrostatic pressure.

Cavitation can be divided into two classes: transient and stable. Stable cavities oscillate around some equilibrium size (R_0) over several rarefaction-compression cycles. In contrast, transient cavities usually exist over one acoustic cycle, increasing their size during the cycle and collapsing into smaller bubbles. The time required for a bubble to collapse is usually shorter than the period of the acoustic wave, and therefore P_m (i.e. pressure in the liquid at the moment of transient collapse, $P_m = P_h + P_a$) can be considered as constant during collapse. This time can be expressed as:

$$t = 0.915 R_m (\rho/P_m)^{1/2}$$

where R_m is the radius of the cavity at the moment of collapse.

Temperatures and pressures reached inside a cavitation bubble containing nitrogen in water at ambient temperature and pressure before collapsing are nearly 4200 K and 975 bar, respectively. The high temperature existing inside cavitation bubbles accounts for radical formation, whereas the shock wave caused by bubble implosion may be responsible for the increased chemical reactivity.

Influence of Different Parameters on the Cavitation Process

The different processes occurring during cavitation (i.e. nucleation, bubble growth and collapse) can be affected by parameters such as liquid medium, intensity and hydrostatic pressure, which are among the most important.

Thus, the formation of cavitation bubbles decreases on increasing ultrasonic frequency. This is due to insufficient time for the rarefaction cycle to allow the growth of the bubble so that disruption of the liquid can be produced.

As expected, cavitation is decreased in viscous media as a result of the increased negative pressure in the rarefaction region needed for disruption of the liquid.

The number of nuclei for cavitation depends on temperature. An increase of temperature from -10 to $+50^\circ\text{C}$ causes an increase in sonochemical effects as a result of the increased cavitation. Nevertheless,

when temperature exceeds 50°C the decrease in surface tension and increase in vapour pressure within the cavity will result in a lower P_{\max} and, consequently, sonochemical effects will diminish.

The increase in gas content within the liquid leads to a lower cavitation threshold and intensity of the shock wave released on the collapse of the bubble. It has been observed that the use of monoatomic gases (He, Ar, Ne) provides more effective cavitation than diatomic gases (N_2 , O_2 , air).

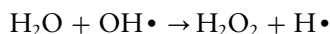
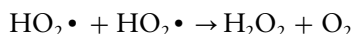
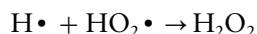
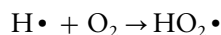
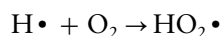
External pressure also influences the cavitation process. Thus, when the external pressure is increased (P_h), a lower cavitation threshold and intensity of cavitation collapse are observed. When $P_h - P_a > 0$, it means that the negative phase of the sound will no longer exist, hence eliminating cavitation.

Finally, another factor that can influence cavitation is intensity, which enhances cavitation.

Effect of Power Ultrasound on Chemical Systems

Homogeneous Medium

Mechanical and chemical effects caused by cavitation fall into three different processes (Figure 3). First, the cavitation bubble contains solvent vapour which is subject to high temperatures and pressures on collapsing. This promotes the formation of reactive species, e.g. radicals. For example, when water is used as solvent the following reactions take place:



Second, surface-active reagents can accumulate at the interface between the bubble and the bulk liquid. Finally, in the surrounding of the bubble, an intense shock wave will be produced causing enormous shear forces.

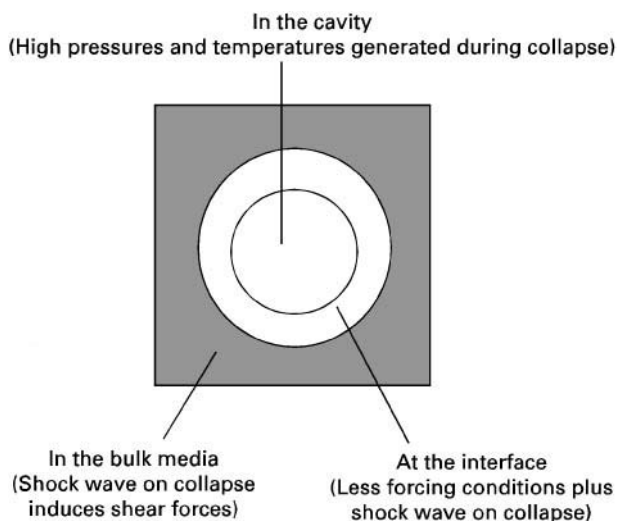


Figure 3 Cavitation effects in a homogeneous liquid.

Heterogeneous Medium

In this case, there are two types of cavitation collapse that can affect the surface of solids (Figure 4): (1) cavitation collapse on the surface of the solid due to the presence of surface defects,

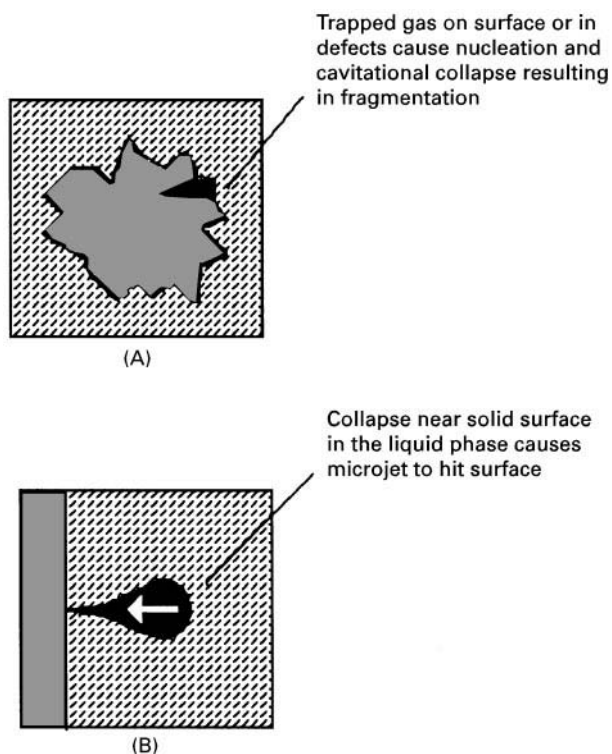


Figure 4 Cavitation effects at a solid-liquid interface: (A) cavitation collapse on the surface of a solid particle; (B) cavitation collapse close to a surface of a solid particle.

entrapped gases or impurities; (2) cavitation collapse close to a surface causing a microstreaming of solvent to impinge on the surface (i.e. cleaning action of ultrasound). It has been observed that ultrasonic irradiation can cause particle rupture (i.e. disruption) which results in a decrease in particle size and an increase in surface area for reaction. Alternatively, cavitation collapse in a medium containing two immiscible liquids can cause the formation of an emulsion.

Instrumentation

Among the several types of sonicator systems currently available, mostly bath and probe-type sonicators are used. Both systems are based on an electromagnetic transducer (i.e. device capable of converting mechanical or electrical energy into high frequency sound) as a source of ultrasound power, commonly operating at a fixed frequency of 20 kHz.

Ultrasonic sources used now rely on the piezoelectric effect discovered by Curie (1880). Ultrasonic processors implement transducers which are based on the changes in dimension of some materials on application of an electrical potential across opposite faces. When the potential is modulated at high frequency, the material converts the electrical energy into mechanical energy (sound). A sufficiently high alternating potential will result in the generation of ultrasound. The first ultrasonic transducer was reported by Galton in 1883, who tried to establish the threshold frequency of human hearing.

Bath Systems

In these systems the transducer is usually placed below a stainless steel tank, the base of which is the source of ultrasound (Figure 5). Some tanks are also provided with a thermostatically controlled heater. Typically, the ultrasound power levels delivered by

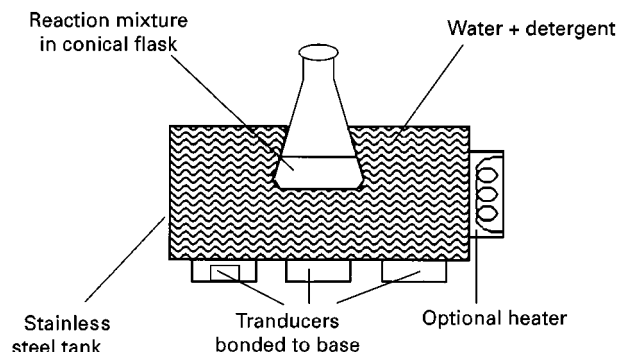


Figure 5 Schematic diagram of an ultrasonic bath.

most commercial ultrasonic baths (e.g., 1–5 W cm⁻²) are sufficient for cleaning, degassing of solvents and extraction of adsorbed metals and organic pollutants from environmental samples, but are less effective for extraction of analytes bound to the matrix. The power should be great enough to cause cavitation within the extraction vessel placed inside the bath; this is not always achieved with commercial ultrasonic baths.

An important factor influencing extraction efficiency is the position of the extraction vessel inside the bath. For a bath with a single transducer on the base, the extraction vessel must be located just above the transducer, since power delivery will be a maximum at this position. In order to obtain reproducible results, the bath must be either thermostatted or preheated at the equilibrium temperature (i.e. maximum temperature measured in the liquid under continuous running conditions) since most cleaning baths warm up slowly during operation. An important drawback of most cleaning baths is the lack of power adjustment control.

Probe Systems

Probe-type sonicators are able to deliver to the extraction medium up to 100-fold greater power than that of an ultrasonic bath, so that a better performance is expected. One main feature for the successful application of ultrasonic probes for many chemical processes is that the ultrasonic energy is not transferred through the liquid medium to the extraction vessel but introduced directly into the system (Figure 6). The ultrasonic probe consists of the following components:

- A generator which is the source of alternating electrical frequency (typically 20 kHz). The generator allows tuning to be carried out for optimum performance.

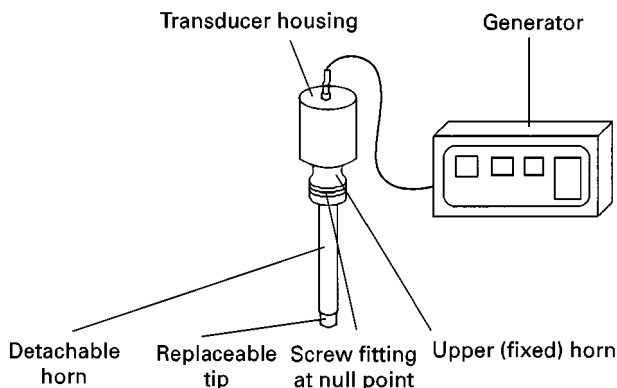


Figure 6 Schematic diagram of a probe-type sonicator.

- Ability of the ultrasonic processor to be used in pulsed mode operation which allows the medium to cool between pulses of sonication.
- The upper horn element – a piece of titanium to which the detachable horn is attached, forming both the emitter or booster.
- A detachable horn, usually made of a titanium alloy, which allows the vibration of the fixed horn to be transmitted to a chemical system. Tip erosion can occur as a result of cavitation. Depending on the volume of sample to be irradiated a range of detachable horns can be used.

Despite the improved performance displayed by probe-type sonicators for solid-liquid extraction compared with cleaning baths, a series of problems can arise with the use of these sonicators. Volatile components can be lost due to the 'degassing' effect of the ultrasound power. Ultrasound irradiation by means of probes is accompanied by a large amount of heat generated during operation, hence some cooling of the sonication vessel is required.

Ultrasound-Assisted Extraction

Extraction techniques are widely accepted as a prerequisite for analytical determination of both organic and inorganic analytes in a large variety of samples.

As a part of an analytical process, sample preparation is considered to be an essential step so that the entire process can be simplified. In this case, the ability of many analytical systems to handle liquid samples has brought about the development of separation methods which fulfil a main objective, i.e. to obtain quantitative analyte leaching from the solid matrix using a suitable solvent, with little or no matrix release, so that matrix effects can be kept to a minimum during the measurement steps. For speciation applications, a last condition of a solid-liquid extraction method must be the maintenance of the species integrity during treatment.

Table 1 shows the most relevant methods for treatment of solid samples based on analyte extraction. An important requirement of most techniques shown is that solvents at high temperature (i.e. at boiling point) or pressure must be used. In contrast, operation with ultrasonic processors can be performed at ambient temperature and normal pressure, and mild chemical conditions can be used in most cases.

Sonication is usually recommended for pretreatment of solid environmental samples for the extraction of nonvolatile and semivolatile organic com-

pounds from solid, such as soils, sludges and wastes. When comparing the different methods available for analyte extraction from solid samples, sonication is considered as an effective method since unsophisticated instrumentation is required and solid-liquid separations can usually be performed in a short time using diluted reagents and low temperatures. To date, most of applications of ultrasonic extraction have been carried out for organic compounds, but the usefulness of ultrasound for element extraction is still to be explored. Some examples of solid-liquid extraction of some elements with the use of ultrasound are shown in Table 2. It should be pointed out that for many applications reported in this table, operation conditions were intended to obtain a homogeneous slurry so that a representative aliquot could be sampled; specific optimization of the variables influencing ultrasound-assisted extraction processes was not performed. Significant variables influencing the solid-liquid extraction process with a probe-type sonicator are sonication time, vibrational amplitude of the probe, acid concentration, particle size and solid concentration in the liquid. In general, the presence of an acidic liquid is an important prerequisite for quantitative extraction to be achieved; nitric acid at low concentration (e.g. 3–5% v/v) is usually chosen for extraction of elements from solid samples.

Quantitative extraction can be achieved for some analytes such as As, Cu, Pb, Cd, etc., from plant and animal tissues. Nevertheless, incomplete extraction has been observed from samples containing a typical inorganic matrix (e.g. sediment). It is believed that this finding is related to the ability of ultrasound to penetrate the solid material. A further variable that influences the solid-liquid extraction is the analyte-matrix interaction. Thus, strongly bound analytes should be more difficult to extract, thereby requiring more stringent extraction conditions. A relationship between extractability and binding characteristics of elements in the sample is yet to be established.

The extraction efficiency obtained with ultrasound could be increased by addition of glass beads which promote particle disruption by focusing the energy released by cavitation, and by physical crushing. Particle disruption could also be enhanced by increasing hydrostatic pressure and viscosity. The use of a bubbling gas during sonication gives rise to an enhanced formation of H_2O_2 and hydroxyl radicals ($\text{OH}\cdot$) thus aiding analyte extraction from oxidizable materials. In general, the use of probe-type sonicators at the appropriate vibrational amplitude and sonication time is required so that extraction efficiency can be improved for strongly-bound elements.

Table 1 Extraction methods from solid samples.

<i>Sample pretreatment method</i>	<i>Principles of the technique</i>
Accelerated solvent	Sample is placed in a sealed container and heated to a temperature higher than its boiling point, causing pressure in the vessel to rise.
Automated Soxhlet	A combination of hot solvent leaching and Soxhlet extraction; sample in thimble is first immersed in boiling solvent and then the thimble is raised for Soxhlet extraction with solvent refluxing.
Forced-flow leaching	Sample is placed in a flow-through tube, and solvent is pumped or pushed through high-pressure nitrogen gas, while the tube is heated near the boiling point of solvent.
Gas phase	After equilibrium, analytes partition themselves between a gas phase and the solid phase at a constant ratio; with static headspace extraction, volatiles are sampled above the solid; with dynamic headspace extraction, volatiles are sampled by continuously purging the headspace above a sample with inert gas, trapping them on a solid medium, and then thermally desorbing them into a gas chromatograph.
Homogenization	Sample is placed in a blender, solvent is added, and sample is homogenized to a finely divided state; solvent is removed for further work-up.
Pervaporation	Volatile substances present in a heated donor phase placed inside a pervaporation module evaporate through a porous membrane and the vapour condenses on the surface of a cool acceptor stream on the other side of the membrane.
Solid-liquid extraction	Sample is shaken together with the appropriate solvent in a container and the liquid separated by filtration
Sonication	Finely divided sample in a container is immersed in ultrasonic bath with solvent and subjected to ultrasonic irradiation; an ultrasonic probe or cell disrupter can also be used.
Soxhlet extraction	Sample is placed in a disposable, porous container (thimble); constantly refluxing solvent flows through the thimble and leaches out analytes that are collected continuously.
Supercritical fluid	Sample is placed in flow-through container and a supercritical fluid (e.g. CO ₂) is passed through sample; after depressurization, extracted analyte is collected in solvent or trapped on adsorbent and desorbed by rinsing with solvent.
Thermal	A form of dynamic headspace analysis, but the sample is heated (controlled) to much higher temperatures (as high as 350°C).

Contents based on Majors RE (1996) *LC-GC International*, 638 and Luque de Castro MD and Papaefstathiou I (1998) *Trends in Analytical Chemistry* 17: 41.

Future Prospects

The use of ultrasound as a sample preparation method for solid-liquid extraction is widespread in many laboratories and can be regarded as fast and effective. Extractions based on sonication have been employed for the isolation of weakly-bound organic compounds from solid samples such as soils, animal tissue, plants, etc., and are comparable to methods involving more intensive treatments (e.g., Soxhlet, accelerated solvent, etc.). However, ultrasound applied to solid-liquid extraction of inorganic analytes has rarely been attempted, perhaps owing to the inefficient sonochemical effects caused by most ultrasonic baths, which are more extended than probe-type sonicators. Ultrasound irradiation from high-inten-

sity ultrasonic processors opens the door to new perspectives, mainly concerning those analytes that are strongly-bound to the matrix. Thus, extraction of elements from solid samples is feasible under optimized sonication conditions, hence avoiding the more intensive treatments commonly employed for matrix decomposition (i.e. dry or wet ashing procedures). New possibilities of ultrasound lie in its use as selective extraction techniques for metal speciation in conjunction with the appropriate leaching reagents. Thus, ultrasound-accelerated sequential extraction schemes for metal partitioning in environmental solid samples (e.g. soil, sediment, sewage sludge) or selective extraction of physicochemical forms of elements constitute new sample preparation strategies which deserve further research.

Table 2 Percentage of metal extracted into the liquid phase of slurries prepared in an acidic diluent and subsequently homogenized by sonication

Sample	Element and percentage of extraction	Sonication system	Reference
Bovine liver	Cd (111%)	Bath	1
Bovine liver	Mn (100%), Fe (72%)	Probe	2
Cabbage leave	Cd (89%), Pb (1%)	Probe	3
Cabbage root	Cd (86%), Pb (1.5%)	Probe	3
Carbon	Cr (14%)	Probe	4
Carbon	Cu (69%), Cr (2%)	Probe	5
Lemon leaves	Cd (67%), Cu (88%), Mn (98%)	Bath	1
Orchard leaves	Cd (100%), Cu (88%), Pb (98%)	Bath	1
Oyster	Cd (99%), Pb (98%)	Bath	6
Prawns	Se (88%)	Bath	6
Rice flour	Cd (100%)	Bath	1
Sediment	Cr (30%)	Probe	4
Sediment	Cu (60%), Cr (10%)	Probe	5
Silica gel	As (60%), Cr (65%), Ni (77%)	Probe	7
Spinach	Cu (98%), Cr (74%)	Probe	5
Spinach	Mn (100%), Zn (74%), Fe (36%), Cu (100%)	Probe	2
Talc	As (59%), Cr (61%), Ni (74%)	Probe	7
Tomato leaves	Mn (70%), Fe (70%), Cr (51%)	Probe	2
Tomato leaves	Mn (92%)	Bath	1
Wheat flour	Mn (97%), Fe (88%)	Probe	2

1, Minami H *et al.* (1996). *Spectrochimica Acta, Part B*, 51: 211. 2, Miller-Ihli NJ (1990) *Fresenius Journal of Analytical Chemistry* 337: 271; 3, Dobrowolski R and Mierzwa J (1993) *Fresenius Journal of Analytical Chemistry* 346: 1058. 4, Miller-Ihli NJ (1994) *Journal of Analytical Atomic Spectrometry* 9: 1129. 5, Miller-Ihli NJ (1993) *Fresenius Journal of Analytical Chemistry* 345: 482.6, Mierzwa J *et al.* (1997) *Analytical Science* 13: 189. 7, Mierzwa J and Dhindsa HS (1988) *Atomic Spectroscopy* 19: 6.

See also: III/Ultrasound-Assisted Metal Extractions.

Further Reading

- Ashley K (1988) Ultrasonic extraction of heavy metals from environmental and industrial hygiene samples for their subsequent determination. *Trends in Analytical Chemistry* 17: 366.
- Barceló D (1993) *Environmental Analysis. Techniques, Applications and Quality Assurance*. Amsterdam: Elsevier.
- Dean JR (1998) *Extraction Methods for Environmental Analysis*. Chichester: Wiley.
- Lorimer JP and Mason TJ (1987) Sonochemistry. Part I – The physical aspects. *Chemical Society Reviews* 16: 239.

Luque de Castro MD and da Silva MP (1997) Strategies for solid sample treatment. *Trends in Analytical Chemistry* 16: 16.

Majors RE (1996) The changing role of extraction in preparation of solid samples. *LC-GC International*, 638.

Mason TJ (1991) *Practical Sonochemistry. User's Guide to Applications in Chemistry and Chemical Engineering*. Chichester: Ellis Horwood.

Mason TJ and Lorimer JP (1988) *Sonochemistry: Theory, Applications and Uses of Ultrasound in Chemistry*. Chichester: Ellis Horwood.

Suslick KS (1988) *Ultrasound: Its Chemical, Physical and Biological Effects*. Weinheim: VCH.

FLOTATION



Bubble–Particle Adherence: Synergistic Effect of Reagents

B. J. Bradshaw and C. T. O'Connor, University of Cape Town, Rondebosch, South Africa

Copyright © 2000 Academic Press

Introduction

It is well known in the practice of flotation that mixtures of various collectors often behave with greater effectiveness than would be expected from their individual known characteristics. This phenomenon is a classical example of synergism in flotation, in which the combined effect exceeds the sum of the linearly weighted partial effects. Such phenomena are not only consciously applied by adding mixtures of reagents, especially collectors, but may also occur inadvertently since many industrial reagents are synthesized from less than absolutely pure chemicals, resulting in the presence of small amounts of different product molecules which are often capable of having a positive synergistic effect on the flotation behaviour. Such synergism can have a significant effect not only on the recovery but also on the selectivity of specific minerals in differential flotation. The manner in which reagents interact in order to achieve a synergistic effect is a complex function of their chemical nature as well as their chemisorptive or physisorptive properties. The former will determine whether the chemical composition of the reagent changes when another compound is present through, for example, a dimerization reaction. The latter will determine how competitive or synergistic adsorption will influence the ultimate flotation behaviour. The analysis of synergism between reagents in flotation is complicated by the fact that the roles and interactions of the different classes of reagents are difficult to isolate due to the complexity of the flotation process, viz. the frother is added to stabilize the froth zone but can also interact with the collector and affect the performance of the collection zone.

This review firstly discusses those properties of pure collectors, frothers, depressants and activators which are pertinent to their potential synergistic

behaviour. The interactions between collectors, frothers and each other are then reviewed. The emphasis here is on sulfide minerals but similar effects have been extensively reported in the case of oxide flotation. Finally, an hypothesis is proposed to explain the synergism observed when mixtures of thiol collectors are used in the flotation of pyrite. This represents a typical sulfide mineral flotation system and will serve to highlight how the various sub-processes of flotation may be influenced in a synergistic manner, thus influencing the ultimate flotation performance.

Functional Roles of Pure Reagents

Collectors

The predominant functional role of collectors is to induce hydrophobicity by adsorption onto the desired mineral and they are therefore concentrated at the mineral–water interface. Collectors are heteropolar molecules containing a nonpolar hydrocarbon chain, which renders the particle hydrophobic, and a polar group that interacts with the mineral surface.

Collector molecules can be divided into three classes: nonionic, which are largely insoluble and used in the flotation of coal and graphite; cationic, which are typically amine salts and used in the flotation of silicates and sulfides at alkaline conditions; and anionic, which are used to float basic minerals such as metal oxides and sulfides. Fatty acids are used for the flotation of nonsulfide minerals such as apatite, calcite, feldspar and hematite. Sulfonates and sulfates are used for apatite as their frothing properties limit their usefulness for other systems. Sulfhydryl or thiol collectors are used for the flotation of sulfide minerals and, of these, xanthates, first patented in 1925, are still the most widely used.

The mechanism of mineral–collector bonding depends on the collector type and the nature and charge of the mineral surface and can occur via physisorption or chemical bonding. There are several modes of chemical interaction of the collector with the mineral surface. In the case of physisorption, the collector does not interact with the mineral surface. The attachment is due primarily to van der Waals forces and the Gibbs free energy of adsorption is relatively low. In the case of chemisorption, when the collector interacts with the mineral surface without movement of the metal ions from their lattice sites, this produces

monolayer coverage. When the surface chemical reactions are associated with movement of metal ions from their lattice sites, multilayers may form. If a reaction occurs in the bulk solution between dissolved ions and the collector, a hydrophobic surface will only be established if there is bulk precipitation on the mineral surface.

Sulfide minerals are semiconductors and react electrochemically with thiol collectors according to the mixed potential model. This involves the cathodic reduction of oxygen and the anodic oxidation of collectors. The electrochemical potential of the system and the thermodynamics of the respective reactions determine the nature of the surface products. Depending on the nature of the surface products formed, the collector may however be physisorbed, such as in the case of the neutral dithiolate, or chemisorbed, as in the case of the metal thiolate. Naturally, when mixtures of collectors are used, a combination of these mechanisms and products may occur, possibly resulting in an enhanced flotation performance.

Frothers

Frothers are added to create a stable dispersion of bubbles in the pulp which will subsequently create a reasonably stable froth and which will allow selective drainage from the froth of entrained gangue and improve the flotation selectivity. The frother also affects the flotation kinetics. They are nonionic heteropolar molecules and, unlike collectors, are not associated with particular categories of minerals. The frothing ability of a compound is associated with hydroxyl ($-OH$), ester ($-COOR$) and carbonyl ($-CO$) chemical groups, and commercial frothers can be divided into three main categories: alcohols, alkoxyparaffins, polyglycols and polyglycol ethers. The polar end of the frother molecule forms hydrogen bonds with the water and no mineral-frother bonds are formed. The nonpolar end is hydrophobic so that the frother concentrates at the air-water interface and is thus described as being surface-active. This affects the surface tension, which indicates the difference between the surface activity of frothers and causes a stable froth to form. In general, increased surface activity results in increased floatability and froth stability.

Depressants

The role of depressants, which are either inorganic salts, such as sodium silicate, sodium sulfite or organic compounds such as polysaccharides, dextrin and starch derivatives, guar gums, carboxymethylcellulose and alginates, is to reduce the collection of

unwanted gangue which consists of typically talcaceous or other oxide minerals. This is done by either enhancing the hydrophilic nature of the gangue surface, by preventing the formation of hydrophobic species which might adsorb on the gangue surface or by preventing the coating of unwanted slimes on the mineral surface. Mechanisms of depression also include the formation of large aggregates and the complexation of the collector in solution.

Activators

Activators are specifically added to enhance flotation performance, usually by modifying the surface of the particle in some way so as to make it more amenable to interaction with the collector. They may however have unexpected effects, for example, by complexing with other ions in solution and rendering particles less floatable. Copper sulfate, for example, is a well-known activator. Under certain circumstances, in sulfide flotation, the copper may ion-exchange with surface ions, creating a readily floatable particle but in different pulp conditions may complex as a hydroxy species and depress the particles. Such effects may be considered synergistic but fall outside the scope of this article. Another commonly used activator is sodium sulfide or bisulfide which is used as a sulfidizing reagent for tarnished or oxidized ores.

Synergistic Interactions Between Reagents

There has been a considerable amount of work done on the effects of mixing reagents in flotation. Table 1 summarizes much of this literature with respect to type of reagents mixed, minerals tested, measurements made and the benefits observed.

Collector-Collector Interactions

The use of mixtures of collectors has long been recognized in plant practice and has been shown to enhance flotation performance. These benefits have been reported for a wide range of collector mixtures (anionic, cationic and nonionic) and include lower dosage requirements, improved selectivity and rates and extents of recovery and an increase in the recovery of coarse particles. In many cases an optimum ratio of constituent collectors was shown to exist. Dithiophosphates are a class of thiol collectors that are so widely used in mixtures that they are known as promoters.

Using measurements obtained from experimental techniques shown in Table 1, a number of mechanisms have been proposed by various authors to

Table 1 The effects of mixing reagents in Flotation

<i>Interactions</i>	<i>Reagents^a (ratios tested)^b</i>	<i>Mineral systems^c</i>	<i>Techniques</i>	<i>Benefit of mixture</i>	<i>Reference</i>
Collector: collector Thiol–thiol	Ethyl X: amyl X (2: 1, 1: 2 mass)	Arsenopyrite (P)	Batch flotation	Higher rates of recovery with mixtures. Optimum mixtures: ethyl X: amyl X (1: 2) for arsenopyrite and (1: 1) for galena	Plaskin <i>et al.</i> (1954)
	Ethyl X: amyl X: diethyl DTP (1: 1 mass)	Arsenopyrite (P)			
	Ethyl X: butyl X: diethyl DTP (1: 1 mass)	Galena (P)	Radiographic adsorption techniques	More even collector coverage on mineral surface with mixture	Plaskin and Zaitseva (1960)
	<i>n</i> -propyl DTC: <i>n</i> -hexyl DTC: cyclohexyl DTC: di propyl DTC (10: 90; 50: 50; 90: 10)	Pyrite ore with quartz gangue (South Africa) (1.27% Sulfur)	Batch flotation	Increased recoveries for all mixtures. Optimum ratio: <i>n</i> -propyl DTC: cyclohexyl DTC (90: 10)	Bradshaw and O'Connor (1994)
	Butyl X: butyl DTP (50: 50)	Galena (P)	Adsorption Bubble pick-up	Preferential DTP adsorption from mixture with no increased mass picked up by bubble	Wakamatsu and Numata (1979)
	Isopropyl DTC: iso propyl X (1: 2 mass)	Chalcopyrite ore (Canada) (1.1% Cu)	Batch flotation	Better results with DTC: X mixture than with pure DTC	Falvey (1969)
	Di-isobutyl DTP: iso butyl X (30: 70; 50: 50; 70: 30 mass)	Platinum group metal (PGM) ore	Batch flotation	Recovery improved from 73.2% for pure X to 80% with 70: 30 mixture	Mingione (1984)
	Di-isobutyl DTP: SMBT (50: 50 mass)	Auriferous pyrite ore (0.38 g/t Au, 1% Sulfur)		Recovery improved from 73.8% for pure SMBT to 79.9% with mixture	
	Di-isobutyl DTP: SMBT (50: 50; mass)	Sphalerite ore (1.5% Zn)		Recovery improved from 90% for pure SMBT to 95% with mixture	
	Isobutyl X: cyano diethyl DTC (12: 44 mass)	Chalcopyrite/pyrite with quartz gangue (China)	Batch flotation	Chalcopyrite recovery increased from 92.4% to 92.8% with 12: 44 mixture	Jiwu <i>et al.</i> (1984)
	DTP: MTP (types unspecified) (75: 25; 50: 50; 25: 75)	Mixed copper sulfide ore	Batch flotation	Optimum recovery at 75: 25 due to combination of collector properties	Mitrofanov <i>et al.</i> (1985)

Table 1 *Continued*

<i>Interactions</i>	<i>Reagents^a (ratios tested)^b</i>	<i>Mineral systems^c</i>	<i>Techniques</i>	<i>Benefit of mixture</i>	<i>Reference</i>
	Ethyl X : di-ethyl DTC (80 : 20; 66 : 33; 50 : 50; 33 : 66; 20 : 80)	Hazelwoodite (SP)	Adsorption Surface tension Microflotation	Optimum ratio: 33 : 66 for lower surface tension, increased microflotation recovery and extent of adsorption	Critchley and Riaz (1991)
	SMBT : amyl X (70 : 25 mass)	Gold and arsenopyrite ore (France)	Batch flotation	Gold and arsenopyrite recovery increased with use of mixture	Van Lierde and Lesoille (1991)
Collector : collector Thiol-thiol	Isopropyl X : dicresyl DTP (95 : 5)	Mixed copper sulfide/ oxide ore (2.9% Cu)	Batch flotation	Enhanced rate and recovery with mixture. Recovery from 80-83% Cu	Adkins and Pearse (1992)
	<i>n</i> -butyl X : cyclohexyl DTC (95 : 5; 90 : 10; 85 : 15; 50 : 50)	Pyrite ore with quartz gangue (South Africa) (0.83% S)	Batch flotation	Recovery increased for all mixtures. Highest recovery for 50 : 50 mixture	Bradshaw and O'Connor (1997)
	<i>n</i> -butyl X : cyclohexyl DTC (90 : 10)	Pyrite (P)	Bubble loading Thermochemical	Increased bubble loading and heat of adsorption with mixture	
Thiol-anionic	Ethyl X : sodium oleate (10 : 90; 20 : 80; 40 : 60; 60 : 40; 80 : 20)	Pyrite (polished section) Gold (polished section)	Surface tension Contact angle	Largest contact angle corresponded to low surface tension with 3 : 1 mixture	Valdiviezo and Oliveira (1993)
Thiol-anionic polymers	Ethyl X : amino acid glycine (1 : 1)	Chalcocite (P), galena (P), pyrite (P)	Microflotation	Higher recoveries obtained for all sulfides with mixture	Hanson <i>et al.</i> (1988)
	Butyl X : hydrolysed polyacrylamide (90 : 10)	Mixed sulfide ore with gold	Batch flotation	90 : 10 mixture increased gold recovery 3% above that obtained with pure X	Orel <i>et al.</i> (1986)
Thiol-cationic	Ethyl X : ammonium bromide (05 : 1; 1 : 1; 2 : 1; 4 : 1)	Pyrite (P), quartz (P)	Surface tension Microflotation	Lowest surface tension for 1 : 1 mixture Increased recovery with all mixtures	Buckenham and Schulman (1963)
Collector : frother	Ethyl X : alkyl alcohols	Chalcocite (P)	Frothability	Enhanced frothability with X added to alcohols	Leja and Schulman (1954)
	Ethyl X : α -terpinol	Chalcocite (P)	Microflotation Frothability	Increased recovery with increasing dosage of frother with xanthate. Only froths in 3 phase	Lekki and Laskowski (1971)

Table 1 *Continued*

<i>Interactions</i>	<i>Reagents^a (ratios tested)^b</i>	<i>Mineral systems^c</i>	<i>Techniques</i>	<i>Benefit of mixture</i>	<i>Reference</i>
	Ethyl X : α -terpinol (1 : 1)	Chalcocite ore	Batch flotation	Increased recovery due to joint frother-collector interactions	Lekki and Laskowski (1975)
	Butyl X : 41G	Galena (polished section)	Contact angle	Contact angle on mineral increased with addition of frother to X	Harris (1982)
	Xanthogen formate : MIBC	Copper sulfide ore (Chile)	Batch flotation Plant practice	Collector dosage reduced 40% to achieve same recovery, which reduced cost and selectivity	Crozier and Klimpel (1989)
Collector : frother	Ethyl X : alkyl alcohols Range of molar concentrations	No mineral	Surface tension Film thickness	Reduced film thickness and surface tension with increasing addition of X	Manev and Pugh (1993)
Frother : frother	MIBC, pine oil, cresylic acid, PPG	Various copper sulfide ores	Plant practice	Survey of 66 plants showed 37% used mixtures of frothers	Crozier and Klimpel (1989)

^aReagents tested as components of the mixture are separated by a colon. Where more than two reagents are in the list, all the reagents listed have been tested at all the ratios specified in brackets.

^bRatios are mole ratios unless otherwise specified as mass ratios (mass).

^cIn cases where the origin or grade of the ore is not included in Table 1, this information was not available in the original reference. X, Xanthate class of reagents; DTC, dithiocarbamate class of reagents; DTP, dithiophosphate class of reagents; MTP, monothiophosphate class of reagents; SMT, sodium mecaptobenzothiazole; PPG, polypropylene glycol; 41G, a proprietary frother containing triethoxybutane manufactured by NCP; MIBC, methyl isobutyl carbinol; (P), pure mineral sample with no gangue component; (SP), synthetically prepared pure mineral sample.

explain the fact that the mixtures give a flotation performance greater than that expected from the contributions of each individual component. These proposals are based on effects related to adsorption of the collectors on the surface of the particle, interactions between the reagents, either in the bulk or at the surface, or changing froth characteristics.

When using mixtures of collectors it has often been observed that there is a greater surface coverage of the adsorbed collectors on the mineral than would have been expected from their weighted averages. This could either enhance the overall hydrophobicity of the mineral surface or result in an adsorbed surface layer of collector molecules more suitable for frother-collector interactions. The increased mineral hydrophobicity could result from the formation of a more evenly distributed surface species. The change in hydrophobicity can be measured by, for example, changes in contact angle, bubble loading and ultimately the recovery in batch flotation tests. It has also been proposed that, for certain systems, when a mixture of collectors is exposed sequentially to a surface

which, by definition, must have a heterogeneous distribution of energetically different sites, the weaker collector will adsorb preferentially on the strong sites and the strongly adsorbing collector, added subsequently, will adsorb on the weaker sites. In this way as many sites as possible are utilized for adsorption, thus enhancing the hydrophobicity. Single collector addition may only result in adsorption on strongly adsorbing sites, forming nonuniform coverage and thus a less than optimal adsorption capacity. It is possible that such an effect will not be observed if the collectors are pre-mixed before addition, thus emphasizing the fact that synergism may depend on the sequence of addition as much as on the presence of a mixture.

The grade of the concentrate is largely a function of the depressant used, which affects the froth zone characteristics. The presence of hydrophobic solids in the froth phase will destabilize the froth, causing bubble coalescence in the froth which results in improved drainage and consequently increased selectivity and grades. The presence of hydrophilic or only

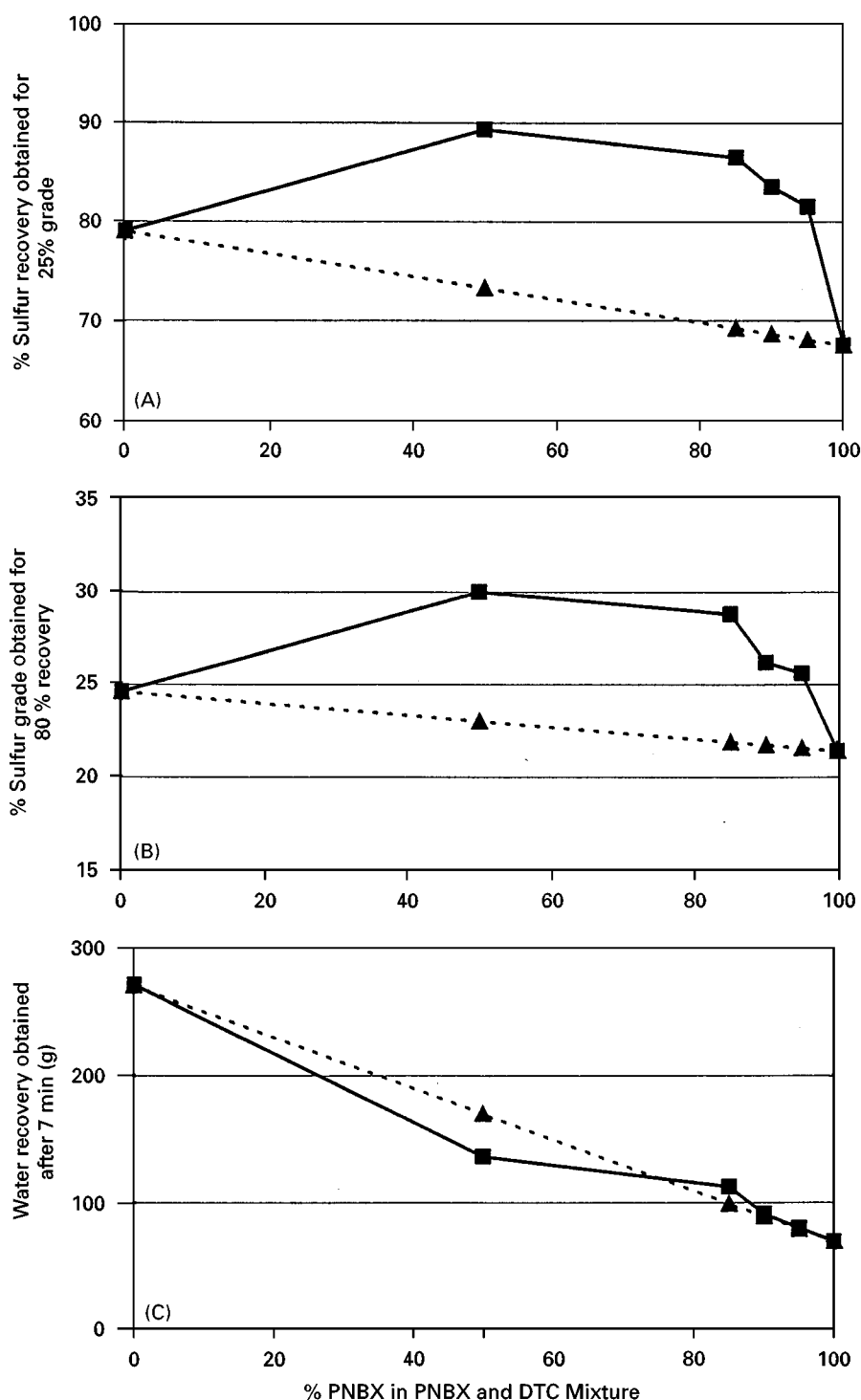


Figure 1 The effect of mixtures of collectors on batch flotation performance of a low-grade pyrite ore at pH 4. Values measured (squares) were compared with those predicted from the linearly additive mole ratio contribution of potassium *n*-butyl xanthate (PNBX) and dithiocarbamate class of reagents (DTC; triangles) for (A) % sulfur recovery obtained for 25% grade; (B) % sulfur grade obtained for 80% recovery; and (C) water recovery obtained after 7 min (g).

slightly hydrophobic minerals can stabilize the froth zone and thereby decrease the grade achieved. The use of a combination of collectors resulting in both

physisorbed and chemisorbed surface products can also affect the froth structure and influence the final grade achieved. It is also often observed that

enhanced performance is achieved when a strong collector with no frothing properties is used with a weaker collector with frothing properties. The former increases coarse particle recovery and the latter increases fine particle recovery. This is however not a true synergistic effect since the combined effect is the sum of the individual effects.

Collector-Frother Interactions

Before the collision of a mineral particle and an air bubble, adsorbed layers of reagents are present at both interfaces. At the time of collision, there are interactions between these layers which are affected by the nature and charge of the respective molecules. Any associated molecules are anchored to the mineral group by the polar groups of the collector. The strength of this film determines the tenacity of attachment of the mineral to the bubble and the ultimate success of the flotation process. When the molecular associations between frother and collector are suitably balanced the appropriate mechanical properties of the film at the interface are created, resulting in good recoveries and grades. If the collector or frother dosages are too high, the molecules would be too densely packed and penetration and successful attachment would not take place. This supports the well-known phenomenon that too high a dosage of reagents can result in reduced recoveries. In this case synergistic interactions between the frother and collector that improved flotation performance at the lower dosages are no longer possible at the higher dosage.

Frother molecules can accumulate at the mineral surface, without enhancing its hydrophobicity and, at

the time of collision with a bubble, re-orientate quickly, facilitating mineral-bubble attachment. This produces a stable three-phase froth and strong tenacity of mineral-bubble attachment. An alternative explanation is that at the mineral-water interface the alkyl chains of frother and collector molecules are held together by van der Waals forces. Frothers are able to hydrogen-bond with the oxygen atom in the collector molecule. These associations are only formed when a mineral is present. The frother's ability to interact with the collector is thus more significant than its surface activity, which is required to produce a stable froth zone. This also explains why detergents are not suitable frothers. It has moreover often been shown that the collector can affect frothing properties and that the frother can affect mineral hydrophobicity.

The surface activity and thus frothability of the frother is very sensitive to the presence of small amounts of other substances, such as impurities or collector molecules. The chemical nature of certain combinations of frothers and collectors may result in interactions occurring at the point of collision of the pure components. The properties of frothers can sometimes be additive, with the mixing of stronger and weaker frothers to form medium-strength frothers.

Synergistic Interactions – A Case Study

Synergistic enhancement of flotation performance has been observed in batch flotation tests with a low

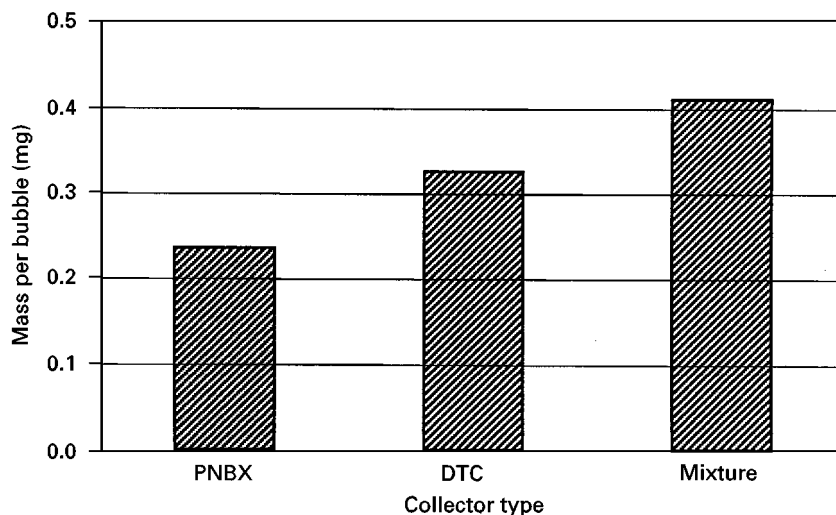


Figure 2 The mass loading per bubble for bubbles of average diameter of 1.2 mm of pyrite with equimolar amounts of potassium *n*-butyl xanthate (PNBX), dithiocarbamate class of reagents (DTC) and the 90 : 10 mixture of collectors added at pH 4.

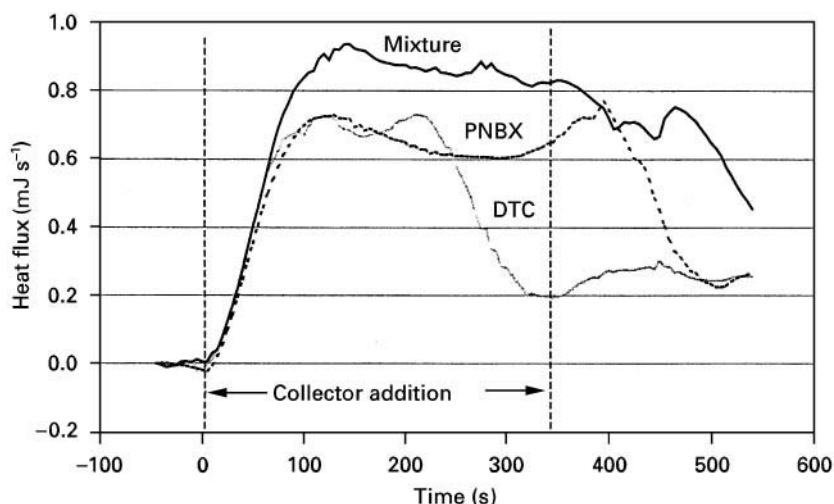


Figure 3 The difference in heat flux measured when equimolar amounts of potassium *n*-butyl xanthate (PNBX), dithiocarbamate class of reagents (DTC) and 90 : 10 mixture of collectors are added to pyrite at pH 4.

grade pyrite ore using thiol collectors at pH 4. The collectors tested were potassium *n*-butyl xanthate (PNBX) and an alkyl dithiocarbamate collector. Performance was analysed using grade-recovery data as well as water and mass recoveries and the rate of sulfur recovery. The froth surface was analysed using digital image analysis. In all experiments the total molar concentration of collector was constant.

Figure 1 shows the batch flotation results as represented by sulfur grade at 80% recovery, the sulfur recovery at 25% grade and the water recovery, all as a function of mole ratio of components. It is clear that the grades and recoveries are greater than would be expected from a merely linearly additive effect and are synergistically enhanced. Obviously pure collectors may not show linearity with respect to dosages but in the present case the dosages were in the range where these differences were minimal. The change in water recovery, however, was linearly proportional to the molar contribution of the components and clearly the synergistic effect was only influencing the behaviour of the solid particles. Digital image analysis of the froth showed that, when the mixture of collectors was used, the froth was more mobile and the froth surface bubble size was larger. This may be due to the frother-collector interactions, decreasing froth stability, increasing drainage of entrained material and increasing the grades obtained.

In order to elucidate the mechanisms of synergism, the extent of bubble loading and the heats of adsorption were measured for the respective collectors and collector mixtures using pure pyrite at pH 4,

(Figure 1). Figure 2 shows that, for bubbles of average diameter of 1.2 mm, increased bubble loading resulted from the use of a mixture of collectors and Figure 3 shows that when a mixture of collectors was used there was a stronger adsorption than in the case of the pure xanthate, where multilayer adsorption of dixanthogen is indicated, and in the case of dithiocarbamate where pseudo-monolayer adsorption is indicated. In this example, the synergistic effect observed is attributed to increased mineral hydrophobicity, which is thought to be due to the weakly adsorbing dixanthogen adsorbing in multilayers around the strongly adsorbing dithiocarbamate, which acts as a sort of anchor on the surface of the mineral particle. The ultimate result is an increase in bubble loading, an improvement in froth characteristics and a greater grade and recovery.

Further Reading

- Bradshaw DJ and O'Connor CT (1997) The synergism of mixtures of thiol collectors in the flotation of low grade pyrite ores. In: Hoberg H and von Blottnitz H (eds) *Proceedings of the XX International Minerals Processing Congress, Aachen*, vol. 3, pp. 343–354. Germany: GMBH Publishers.
- Fuerstenau DW (1995) Where are we in flotation chemistry after 70 years of research? In: *Proceedings of the XIX International Minerals Processing Congress, San Francisco*, SME, vol. 3, pp. 3–18.
- Harris PJ (1982) Frothing phenomena and froths. In: King RP (ed.) *Principles of Flotation*, pp. 237–250. Johannesburg: South African Institute of Min. Metall.

- Klimpel RR and Hansen RD (1988) Frothers. In: Somasundaran P and Moudgil BM (eds) *Reagents in Mineral Technology*, pp. 387–409. New York: Marcel Dekker.
- Laskowski JS (1993) Frothers and flotation froth. *Mineral Processing and Extraction Metall. Review* 12: 61–89.
- Leja J (1989) Interactions of surfactants. *Mineral Processing and Extraction Metall. Review* 5: 1–22.
- Leja J and Schulman JH (1954) Flotation theory: molecular interactions between frothers and collectors at solid-liquid interfaces. *Transactions of the A.I.M.E.* 199: 221–228.
- Lekki J and Laskowski JS (1971) On the dynamic effect of frother-collector joint action in flotation. *Transactions of Institute of Min. Metall.* 80: C174–C180.
- Mingione PA (1984) Use of dialkyl and diaryl dithiophosphate promoters as mineral flotation agents. In: Jones MJ and Oblatt R (eds) *Reagents in the Minerals Industry*, pp. 19–24. London: Inst. Min. Metall.
- List of References from Table 1**
- Adkins SJ and Pearse MJ (1992) The influence of collector chemistry on the kinetics and selectivity in base metal sulfide flotation. *Mineral Engineering* 5: 295–310.
- Bradshaw DJ and O'Connor CT (1994) The flotation of pyrite using mixtures of dithiocarbamates and other collectors. *Mineral Engineering* 7: 681–690.
- Bradshaw DJ and O'Connor CT (1997) The synergism of mixtures of thiol collectors in the flotation of low grade pyrite ores. In: Hoberg H and von Blottnitz H (eds) *Proceedings of the XX International Minerals Processing Congress*, Aachen, vol. 3, pp. 343–354. Germany: GMD Publishers.
- Buckenham MH and Schulman JH (1963) Molecular association in flotation. *Transactions of the Institute of Mineral and Metallurgy* 7: C1–C6.
- Critchley JK and Riaz M (1991) Study of synergism between xanthate and dithiocarbamate collectors in flotation of heazlewoodite. *Transactions of the Institute of Mineral and Metallurgy* 100: C55–C57.
- Crozier RD and Klimpel R (1989) Frothers: plant practice. *Mineral Processing and Extractive Metallurgy Review* 5: 257–279.
- Falvey JJ (1969) *Dialkyl Dithiocarbamate as Froth Flotation Collectors*. US patent no. 3 464 551.
- Hanson JS, Barbaro M, Fuerstenau DW, Marabini A and Barbucci R (1988) Interaction of glycine and a glycine-based polymer with xanthate in relation to the flotation of sulfide minerals. *International Journal of Mineral Processing* 23: 123–135.
- Harris PJ (1982) Frothing phenomena and froths. In: King RP (ed.) *Principles of Flotation*, pp. 237–250. Johannesburg: South African Institute of Mining and Metallurgy.
- Jiwu M, Longling Y and Kuoxiong S (1984) Novel frother collectors for flotation of sulfide minerals–CEED. In: Jones MJ and Oblatt R (eds) *Reagents in the Minerals Industry*, pp. 287–290. London: Institute of Mining and Metallurgy.
- Leja J and Schulman JH (1954) Flotation theory: molecular interactions between frothers and collectors at solid-liquid interfaces. *Transactions of the American Institute of Mining, Metallurgical and Petroleum Engineers* 199: 221–228.
- Leja J (1989) Interactions of surfactants. *Mineral Processing and Extraction Metallurgy Review* 5: 1–22.
- Lekki J and Laskowski JS (1971) On the dynamic effect of frother-collector joint action in flotation. *Transactions of the Institute of Mining and Metallurgy* 80: C174–C180.
- Lekki J and Laskowski JS (1975) A new concept of frothing in flotation systems and general classification of flotation frothers. In: *Proceedings of the XI International Minerals Processing Congress*, Universita de Calgari, Calgari, pp. 427–448.
- Manev E and Pugh RJ (1993) Frother/collector interactions in thin froth films and flotation. *Colloids and Surfaces* 70: 289–295.
- Mingione PA (1984) Use of dialkyl and diaryl dithiophosphate promoters as mineral flotation agents. In: Jones MJ and Oblatt R (eds) *Reagents in the Minerals Industry*, pp. 19–24. London: Institute of Mining and Metallurgy.
- Mitrofanov SI, Kuz'kin AS and Filimonov VN (1985) Theoretical and practical aspects of using combinations of collectors and frothing agents for sulphide flotation. 15e Congres International de Mineralurgie, vol. 2, pp. 65–73. St. Etienne: Societe de l'Industrie Minerale et du Bureau de Recherches Geologiques et Minerres.
- Orel MA, Chibisov VM and Lapatukhin IV (1986) Use of mixtures of butyl xanthate and hydrolyzed polyacrylamide when floating gold-containing ore. *Soviet Journal of Non-ferrous Metals* 27: 97–98.
- Plaskin IN and Zaitseva SP (1960) Effect of the combined action of certain collectors on their distribution between galena particles in a flotation pulp. (Mintek translation no. 1295, June 1988.) Naachnye Soobshcheniya Institut Gonnogo dela Imeni AA Skochinskogo, Akademiya Nauk SSSR, Moskva, Report no. 6, pp. 15–20.
- Plaskin IN, Glembofskii VA and Okolovich AM (1954) Investigations of the possible intensification of the flotation process using combinations of collectors. (Mintek translation Feb. 1989.) Naachnye Soobshcheniya Institut Gonnogo dela Imeni AA Skochinskogo, Akademiya Nauk SSSR, Report no. 1, pp. 213–224.
- Valdiviezo E and Oliveria JF (1993) Synergism in aqueous solutions of surfactant mixtures and its effect on the hydrophobicity of mineral surfaces. *Mineral Engineering* 6: 655–661.

Van Lierde A and Lesoille M (1991) Compared effectiveness of xanthate and mercaptobenzothiazole as gold and arsenopyrite collectors. In: *Proceedings of the XVII International Minerals Processing Congress*, Dresden, vol. IV, pp. 111–119.

Wakamatsu T and Numata Y (1979) Fundamental study on the flotation of minerals using two kinds of collectors. In: Somasundaran P (ed.) *Fine Particle Processing*, American Institute of Mining, Metallurgical and Petroleum Engineers, New York, pp. 787–801.

Bubble-Particle Capture

J. Ralston, University of South Australia,
The Levels, Adelaide, Australia

Copyright © 2000 Academic Press

Introduction

Bubble-particle capture is the heart of froth flotation. For efficient capture to occur between a bubble and a hydrophobic particle, they must *first* undergo a sufficiently close encounter, a process that is controlled by the hydrodynamics governing their approach in the aqueous environment in which they are normally immersed. Should they approach quite closely, within the range of attractive surface forces, the intervening liquid film between the bubble and particle will drain, leading to a critical thickness at which rupture occurs. This is then followed by movement of the three-phase-line contact line (the boundary between the solid particle surface, receding liquid phase and advancing gas phase) until a stable wetting perimeter is established. This sequence of drainage, rupture and contact line movement constitutes the *second* process of attachment. A stable particle-bubble union is thus formed. The particle may only be dislodged from this state if it is supplied with sufficient kinetic energy to equal or exceed the detachment energy, i.e. a *third* process of detachment can occur.

The capture (or collection) efficiency E of a bubble and a particle may be defined as:

$$E = E_C \times E_A \times E_S \quad [1]$$

where E_C is the collision efficiency, E_A is the attachment efficiency and E_S is the stability efficiency of the bubble-particle aggregate. This dissection of capture efficiency into three parts was originally proposed by Derjaguin and Dukhin (1960–61) and focuses attention on the three zones of bubble-particle capture where, in order, hydrodynamic interactions, surface forces and forces controlling bubble-particle aggregate stability are dominant.

This article describes each of the substeps in the bubble-particle capture process. The individual processes and efficiencies are focused upon, since they provide the key to understanding the substeps. Our knowledge of the various efficiencies has been enhanced by six important publications, referred to in **Table 1**, each of which signalled major advances in our understanding and catalysed further research in this interdisciplinary field of colloid and flotation science.

Processes and Substeps

Process 1: Collision Efficiency

For a batchwise flotation process, the flotation recovery (the mass of particles recovered in a given time t) R is given by:

$$R = 1 - \exp - t \left(\frac{3GhE_C E_A E_S}{2d_b V} \right) = 1 - \exp(-tk) \quad [2]$$

where G is the volumetric gas flow rate of a swarm of bubbles of diameter d_b passing through a particle suspension of volume V and depth h , and:

$$k = \frac{3GE_C E_A E_S h}{2d_b V} \quad [3]$$

The flotation rate constant k is directly analogous to that obtained in chemical reaction kinetics. Its value will be partly determined by the substep(s) in bubble-particle collision, attachment and detachment processes, as well as by physical variables such as G . (For a constant G and constant bubble size distribution, d_b will be an appropriate average.)

Equation [2] has been shown to apply, for example, to a system of monodisperse polystyrene latex particles floating under batchwise conditions. A plot of $\ln(1 - R)$ versus t yields the rate constant k . For systems that are polydisperse in particle size and/or in which particles of different hydrophobicities are present, the recovery then becomes the sum of a series of exponential terms and the plot of

Table 1 Key papers in understanding fundamental flotation substeps (details of references are given in Further Reading)

Date	Area of research
1948	A fundamental paper by Sutherland on the kinetics of the flotation process appeared in Australia. This paper invoked induction time, described particle size effects in flotation, and catalysed other similar approaches. While it was preceded by other efforts, this paper was the first comprehensive effort to describe recovery, size and time data in a fundamental manner.
1960–61	In Moscow, Derjaguin and Dukhin produced a key paper on the theory of flotation of small and medium-sized particles. Hydrodynamics, surface forces and diffusiophoresis were all used in this theory. This seminal work resulted in an acceleration of fundamental flotation research worldwide.
1972	Blake and Kitchener, working together in London, published some very careful measurements of the thickness of aqueous films on hydrophobic quartz surfaces. Film thicknesses, measured as a function of salt concentration, were shown to depend on the electrical double layer force. Film instability occurred on hydrophobic surfaces at film thicknesses less than about 60 nm. This value, which was smaller than the range of the electrical double layer force, represented the combined effects of hydrophobic force, surface heterogeneities and external disturbances. Blake and Kitchener's film thickness studies hinted at the length dependence of hydrophobic forces, information which was subsequently obtained by surface force experiments after 1982.
1976	Scheludko and colleagues in Bulgaria considered how particles might become attached to a liquid surface and developed the capillary theory of flotation.
1977	Anfruns and Kitchener published the first measurements of the absolute rate of capture of small particles in flotation. This was the first critical test of collision theory under conditions where the bubble and particle surface chemistry was characterized and controlled.
1983	Schulze published a key textbook on the physicochemical substeps that are important in flotation, drawing on a wide range of hydrodynamic, surface chemical and engineering information. Originally published in German, once translated into English the book captured an international audience.
c. 1980–present	There has been a strong interest in developing reliable collision models (Dai <i>et al.</i> , 1998). The surface force apparatus and, recently, the atomic force microscope colloid probe technique, have provided very useful insight into electrical double layer, van der Waals and hydrophobic forces (Israelachvili, 1985; Fielden <i>et al.</i> , 1996). Thin film drainage has been investigated between a rigid and a deformable interface (Miklavcic <i>et al.</i> , 1995). Attachment efficiencies have been measured (Hewitt <i>et al.</i> , 1995). Reliable methods for measuring contact angles on particles have been developed (Diggins <i>et al.</i> , 1990). Major theoretical and experimental advances in describing dynamic contact angles on well-defined surfaces have been made (Blake, 1993).

$\ln(1 - R)$ versus t will show curvature, reflecting the different contributions to the recovery from the various particles present in the mixture.

In the metallurgical literature, R versus t data are frequently analysed by assuming that the pulp consists of 'fast' and 'slow' floating components, allowing the respective rate constants (k_f and k_s) and fractions (f_f and f_s) to be determined. Although this is a gross simplification of the real multicomponent situation, much valuable information may be gleaned from such an analysis. In fact the latter is frequently used to examine the flotation behaviour of particles of a specific size range in flotation circuits, where the behaviour of an individual flotation cell or bank of cells may be approximated to a batchwise process.

Derjaguin and Dukhin were the first to distinguish three zones of approach of a bubble and a particle

on the basis of the different kinds of force in each zone (Figure 1). This model is a very useful one and helps to identify the various contributions to capture efficiency. However, it should not be taken to mean that there are well-defined boundaries between each zone; rather they grade into one another, the importance of the various contributing effects in each zone being more accurately identified as further information becomes available.

Zone 1 is a region far from the bubble surface where hydrodynamic forces are dominant, controlling E_C in eqn [1]. Hydrodynamic drag forces act to sweep the particle around the bubble, viscous forces tend to retard this relative motion between the two, while particle inertial and gravitational forces move the particle towards the bubble.

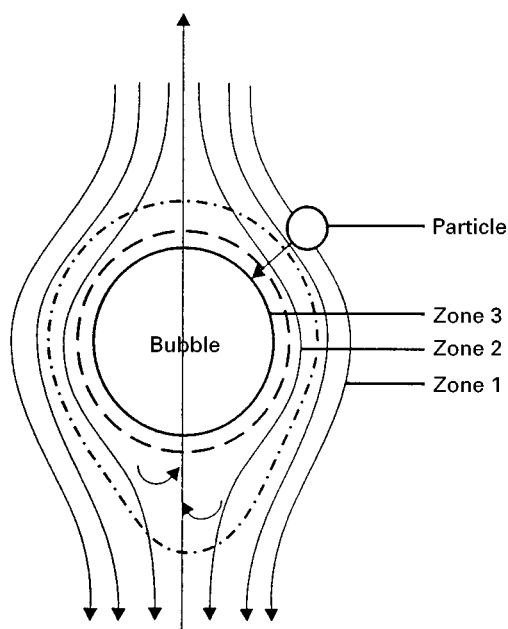


Figure 1 Hydrodynamic (1), diffusiophoretic (2) and surface force (3) zones of interaction between a bubble and a particle. (Reproduced with permission from Derjaguin BV and Dukhin SS (1960–61). *Theory of flotation of small and medium-size particles. Transactions of the Institute of Mining and Metallurgy* 70: 221–246, Figure 1).

Broadly speaking, all models of collision efficiency predict that E_C decreases with particle size at constant bubble size down to a particle diameter of about $0.5 \mu\text{m}$. Then, Brownian diffusion probably takes over as the predominant capture mechanism (although this has not been proven), the collision efficiency increasing with decreasing size as the tiny particles (virtually 'solute molecules') move towards the bubble surface. In 1948 Sutherland made the first significant contribution to the treatment of collision efficiency. His hydrodynamic treatment of the process of particle and bubble approach in zone 1 was carried out without any consideration of particle inertia, bubble deformation or film thinning, deficiencies that were in part recognized by Sutherland and Wark in 1955.

The Sutherland theory, based on potential theory or streamline flow, shows that the concentration, C , of mineral floated at a time t is related to its initial concentration, C_0 , by the recovery, R as:

$$R = \frac{C_0 - C}{C_0} = \left\{ 1 - \exp - t \left[\frac{3\pi\phi R_b R_p V_t N_B}{\cosh^2(3V_t \lambda / 2R_b)} \right] \right\} \quad [4]$$

where R_b and R_p are the bubble and particle radii, V_t is the bubble-particle relative velocity, λ is the

induction time, N_B is the number of bubbles per unit volume, and ϕ is the fraction of particles retained in the froth following bubble-particle attachment. The reader should note the relationship between eqns [2], [3] and [4], which are the basis for a first-order model, largely based on pulp microprocesses. Despite the deficiencies of the Sutherland model, his 'first approximation theory' yields results that are in fair agreement with experimental determinations of particle trajectories, touching angles and collision efficiencies, obtained from model experiments performed in a vertical flow tube with individual particles and a single bubble. For more detailed treatments of the hydrodynamic aspects of bubble-particle collision the reader is referred to the extensive literature available.

The inability of collision theories to describe adequately the collection process between bubbles and smooth and angular particles was vividly demonstrated by Anfruns and Kitchener in 1977. Their experiments, the first measurements of absolute rate of capture, gave results in only fair agreement with collision theory, assuming every collision resulted in capture of their very hydrophobic particles.

Process 2: Attachment Efficiency

Derjaguin and Dukhin identified zone 2 in Figure 1 as that region where diffusion effects are important. A strong electric field exists in this zone, since the liquid flow around the moving bubble gives rise to a tangential stream at its surface that destroys the equilibrium distribution of adsorbed ions there. Where surfactant is present it is continually swept from the upper to the lower surface of the bubble. Transport of ionic surfactant to the moving bubble surface therefore takes place, leading to the establishment of a concentration gradient. A strong electric field of order 3000 V cm^{-1} is established when the cation and anion diffusion coefficients differ, as they generally do. Hence charged particles entering zone 2 will experience an electrophoretic force in precisely the same way as in an electrophoresis cell and will be either attracted towards, or repelled from, the bubble surface. The term 'diffusiophoresis' was coined for this phenomenon, i.e. the 'diffusiophoretic force' therefore acts on the particle as an additional force.

To date, however, evidence confirming the presence or absence of diffusiophoresis in flotation is equivocal and sparse. Apart from noting its possible contribution to capture efficiency, it is not pursued further here.

In zone 3, surface forces predominate once the thin film between the bubble and the particle is reduced

much below a few hundred nanometres. These forces can accelerate, retard or even prevent the thinning of the liquid film between the particle and the bubble. From a thermodynamic point of view, the free energy of a liquid film differs from the bulk phase from which it is formed. This excess free energy was originally called the 'wedging apart' or 'disjoining' pressure by Derjaguin and represents the difference between the pressure within the film, p^f , and that in the bulk liquid adjacent to the solid surface, p^l . Note that for a bubble pushed against a flat solid surface, immersed in water, p^b , the pressure within the bubble, is equal to p^f . Derjaguin and his school, as well as Scheludko, performed experimental measurements of disjoining pressures, providing both the first real verification of the DLVO theory of surface forces (named after Derjaguin, Landau, Verwey and Overbeek), as well as the first accurate experimental estimates of the Hamaker constant. The disjoining pressure (π) depends on the film thickness, h , and:

$$\pi(h) = p^f - p^l \quad [5]$$

For mechanical equilibrium in a stable film $\pi(h) > 0$ and $d\pi/dh < 0$.

If the liquid film is stable at all thicknesses the liquid is said to wet the solid completely and the solid is said to be hydrophilic. This occurs, for example, when an air bubble approaches a clean silica surface immersed in water – in this instance the Hamaker constant is negative and the corresponding van der Waals force is repulsive for the silica–water–air triple layer. For an unstable film the thin film must drain, then rupture, and the resulting three-phase line of contact (tpic, vapour–water–solid) must expand to form a wetting perimeter before the particle can adhere to the bubble. Each of these events will have a characteristic time associated with it, the sum of which must be less than the contact time between the bubble and the particle if bubble–particle capture is to occur. The contact time is generally of the order of 10^{-2} s or less. The induction time, λ (see eqn [4]) is normally taken as the time required for bubble–particle adhesion to occur, once the two are brought into contact, i.e. it is the sum of the thin film drainage and tpic spreading times ($t_{\text{film}} + t_{\text{tpic}}$) and is synonymous with the attachment time. Rupture is a very fast process and is not a significant contributor to λ .

When a bubble is pressed against a solid surface, through water, the intervening film is generally not plane parallel. Rather the edge of the film thins quickly and a small, thicker dimple is trapped in the centre, because the bubble is deformable. This is essentially a kinetic phenomenon, caused by the outflow being greatest at the very edge of the film in the initial stages

of drainage. The existence of this dimple has been detected experimentally. Hydrodynamic theories attempting to describe the profile and evolution of the dimple have been proposed but with very limited success in describing experimental data. Surface deformation of bubble surfaces can also occur under the influence of electrostatic interactions (and possibly other surface forces as well) aside from any kinetic effects.

An unstable film arises when there is a net attractive force between the particle and the bubble. This normally occurs when there is an attractive hydrophobic force involved, since the van der Waals and electrostatic forces are repulsive, except in rare circumstances. The measurement of this hydrophobic force, its length dependence and theoretical origins are subjects of intense research effort. In recent times it has become possible to measure the hydrophobic force, in a configuration relevant to the flotation process, by attaching a small particle to the cantilever in an atomic force microscope (Figure 2). The particle is then pressed against a captive bubble and the force–separation distance profile determined. In this fashion, the various surface forces may be explored.

Experimental evidence relating to film drainage in systems where soluble surfactants are present is rather equivocal. Adsorption and desorption processes coupled with possible molecular reorientation make any theoretical interpretation difficult. Unfortunately these are the very systems that are of primary interest to mineral processing. Furthermore additional complications ensue when one considers a particle approaching a bubble in flotation. The nature of the bubble surface (i.e. whether it is mobile or immobile) will influence the thinning of the thin film between bubble and particle. This makes any solution of the Navier–Stokes equation for film drainage difficult, particularly in the case of the

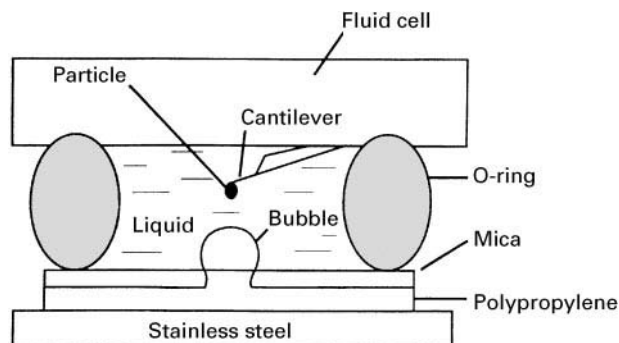


Figure 2 Experimental arrangement for the measurement of forces between a particle and a bubble using the atomic force microscope colloidal probe technique [from Fielden, Hayes and Ralston (1996), *Langmuir*, 12, 3721–3727, with permission].

angular particles that are normally present in flotation. It is worth recalling at this point the observations that smooth spheres float more slowly than angular particles under otherwise identical conditions, presumably because the asperities on the angular particles lead to increased film drainage rates and/or rupture.

The kinetics of movement of the tplc are of central importance in many processes, apart from flotation. During the movement of the tplc a dynamic contact angle is established. Irrespective of whether the 'surface chemical', 'hydrodynamic' or mixed 'surface chemical/hydrodynamic' approaches are used, there is as yet no general theory that adequately describes tplc kinetics on all surfaces. One cannot generally calculate *ab initio* what the spreading velocity of the tplc will be when an air bubble spreads over a mineral surface immersed in water in the presence of a surfactant. Part of the problem at least is due to the fact that poorly characterized experimental systems have been used where any generalization has been obscured by the same time-dependent adsorption/desorption/molecular reorientation processes that complicate thin film drainage rate studies. Physical and chemical surface heterogeneities on the particle surface also strongly influence the tplc kinetics.

At present only the crudest estimates of t_{film} and t_{tpic} can be made. Hence various experimental methods for determining λ are frequently resorted to. A potentially valuable approach to the calculation of induction times, based on bubble deformation and restoration, has been developed.

These experimental methods for determining induction times are generally based on either pressing a bubble against a smooth mineral surface or against a bed of particles. The disadvantages of all current methods for determining λ include: (1) insufficient understanding of the process of bubble deformation and energy dissipation during bubble-particle collision; (2) insufficient information concerning the behaviour of the attractive hydrophobic forces during the bubble-particle interaction (e.g. how the thin film of liquid evolves during the time a particle slides or rolls around a bubble; it may well be incorrect to assume that bubble-particle interaction ceases when the particle passes the bubble equator); (3) the absence of data on t_{film} , e.g. influence of surfactant type and concentration on thin-film drainage mechanisms and rate; and (4) the absence of data on t_{tpic} as a function of hydrophobicity, physical and chemical surface heterogeneities and surfactant type.

The most appropriate method for determining induction times is probably through direct observation of bubble-particle interactions in a flotation cell under well-defined conditions. The necessary theory can

then be developed. For the present the Sutherland and similar approaches (eqn [4]) serve as useful approximations in determining λ from experimental flotation data of the type normally generated.

Kinetic effects certainly have a strong influence on bubble-particle collision and attachment efficiencies. The latter provides the key to selective separations in flotation. Once attachment has occurred, the interplay between particle size and contact angle in the environment of the flotation cell becomes of paramount importance and is the next subject of our discussion.

Process 3: Stability Efficiency and Detachment

Flotation limits for coarse particles The essential problem in understanding bubble-particle aggregate stability is to determine whether or not the adhesive force, acting on the tplc, is large enough to prevent the destruction of the aggregate under the dynamic conditions that exist in flotation. It is important to understand the physics of the problem before moving on to a mathematical description. Let us consider a smooth spherical particle located at the fluid interface. Once the equilibrium wetting perimeter has been established following spreading of the tplc, the static buoyancy of this volume of the particle will act against the gravitational force (Figure 3). The hydrostatic pressure of the liquid column of height Z_0 acts against the capillary pressure. The 'other detaching forces' require further discussion. Since they arise from the particle motion relative to the bubble, velocity-dependent drag forces will oppose the detachment of the particle from the bubble. An analysis of these forces is extremely complex and has not been reported to date. Therefore any force balance will necessarily be quasistatic and approximate.

The net adhesive force, F_{ad} , is equal to the sum of the attachment forces, F_{a} , minus the detachment forces, F_{d} , i.e.:

$$F_{\text{ad}} = F_{\text{a}} - F_{\text{d}} \quad [6]$$

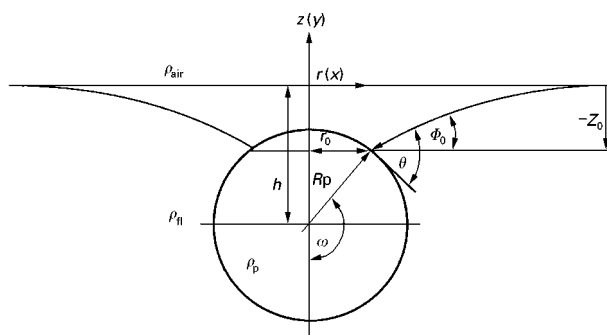


Figure 3 Location of a smooth spherical particle at a fluid interface. (From Schulze (1983) *Physicochemical Elementary Processes in Flotation*. Amsterdam: Elsevier.)

The particle will not remain attached to the bubble if F_{ad} is negative but will be present in the liquid phase.

The mathematical description of the various forces that dictate the equilibrium position of particles at liquid-vapour or liquid-liquid interfaces has followed an evolutionary trail. Analogous processes of interest, for example, include pigment 'flushing', where a solid particle is induced to transfer from one liquid phase to another by appropriate surface modification with surfactants, and the stabilization of emulsion droplets by solid particles.

The actual problem of the balance of forces operating on a particle at a liquid-air interface has been considered by Sutherland and Wark, who considered the case of a gas bubble attached to a plane solid surface of infinite extent and used this as a model for bubble-particle adhesion in flotation. Since this work there have been other very notable contributions. It was Princen who proposed the first extensive and generalized treatment of the forces acting on a particle at fluid interfaces. This theory was developed further by Schulze in 1977 and expanded in 1983.

Consider the case of a spherical particle at a liquid-air interface. We assume that the system is in a quasistatic state and that the contact angle corresponds to that for a static system. The dynamic contact angle can depart significantly from the static value, depending in part on the velocity of the tpic. If the particle oscillates around its equilibrium position, the tpic would be expected to move to some extent. Hence a full analysis would need to account for the velocity-dependent drag forces mentioned above and link these to contact angle dynamics. Since this is an intractable problem at present, a simpler approach is necessary.

Let us suppose that a spherical particle of radius R_p is attached to a bubble of radius R_b where R_b is much greater than R_p , as shown in Figure 3. By understanding the forces that operate on the particle, it is possible to calculate the energy of detachment. The forces acting upon the particle are as follows:

- Capillary force, F_c , acting in the vertical direction along the tpic:

$$F_c = 2\pi r_0 \gamma \sin \phi_0 = -2\pi R_p \gamma \sin \omega [\sin(\omega + \theta)] \quad [7]$$

where γ is the liquid-vapour surface tension.

- Static buoyancy of the fractional volume of the immersed particle, F_b :

$$F_b = \frac{\pi}{3} R_p^3 \rho_l g [(1 - \cos \omega)^2 (2 + \cos \omega)] \quad [8]$$

- Hydrostatic pressure, F_h , of the liquid column of height Z_0 on the contact area:

$$F_h = -\pi r_0^2 \rho_l g Z_0 = -\pi R_p^2 (\sin^2 \omega) \rho_l g Z_0 \quad [9]$$

- Capillary pressure, F_p , in the gas bubble which acts on the contact area πr_0^2 :

$$F_p = P_g \pi r_0^2$$

which for a spherical bubble is given approximately as:

$$F_p \approx \pi R_p^2 \sin^2 \omega \left(\frac{2\gamma}{R_b} - 2R_b \rho_l g \right) \quad [10]$$

- Gravitational force, F_g :

$$F_g = \frac{4}{3} \pi R_p^3 \rho_p g \quad [11]$$

where ρ_p is the particle density.

- Extra detaching forces, F_d , which are denoted approximately and generally as the particle mass multiplied by a generalized acceleration b_m in the flotation cell:

$$F_d \approx \frac{4}{3} \pi R_p^3 \rho_p b_m \quad [12]$$

It is worth remarking that it is bubble-particle aggregates that are actually accelerated in the flotation device, thus ρ_p is in fact an approximation ($\Delta\rho = \rho_p - \rho_l$).

At equilibrium, the sum of these forces, $\sum F$, must equal zero.

The energy of detachment, E_{det} , corresponds to the work done in forcing a particle to move from its equilibrium position, $h_{eq}(\omega)$ at the liquid-vapour interface to some critical point, $h_{crit}(\omega)$, where detachment occurs and the particle moves into the liquid phase. The sum of the various forces, $\sum F$, is related to E_{det} by:

$$E_{det} = \int_{h_{eq}(\omega)}^{h_{crit}(\omega)} \sum F dh(\omega) \quad [13]$$

Equation [13] may be solved by introducing the various forces and carrying out a numerical integration. The detachment process takes place when the kinetic energy of the particle equals E_{det} . The kinetic energy of the particle is given by $\frac{2}{3} \pi R_p^3 \rho_p V_t^2$, where V_t is the relative (turbulent) velocity of the particle, acquired due to stresses on the bubble-particle

aggregate in the turbulent field of the flotation cell, as the aggregate collides with other bubbles or aggregates or due to other modes of excitation. V_t is determined experimentally as the velocity of gas bubbles in the flotation cell and ρ_p is the density of the particle.

The maximum floatable particle diameter based on the kinetic theory, $D_{\max,K}$, is given as:

$$D_{\max,K} = 2 \left[\frac{3}{2\pi\rho_p V_t^2} \int_{h_{eq}(\omega)}^{h_{crit}(\omega)} \left\{ \frac{2}{3} \pi R_p^3 \rho_1 g \right. \right. \\ \times \left[1 - \frac{2\rho_p}{\rho_1} - \cos^3 \omega + \frac{3h}{2R_p} \sin^2 \omega \right. \\ \left. \left. - \frac{3}{a^2 R_p^2} \sin \omega \sin(\omega + \theta) \right] \right. \\ \left. \left. - \pi(R_p \sin \omega)^2 \left(\frac{2\gamma}{R_b} - 2R_b \rho_1 g \right) \right\} dh \right]^{1/3} \quad [14]$$

Equation [14] may be solved by numerical integration or by plotting each of the kinetic and detachment energies as a function of R_p at constant γ and ρ_p and specified V_t . ρ_1 refers to the density of the fluid and γ is the surface tension at the liquid-vapour interface. This equation has been shown to describe adequately both the detachment of a sphere from a liquid-vapour interface and the behaviour of hydrophobic angular quartz particles between approximately 30 and 120 μm in diameter under flotation conditions.

Flotation limits for fine particles The only theoretical study to date dealing with the limit of floatability of fine particles was published by Scheludko and co-workers in 1976. The limit is the critical work of expansion required to initiate a primary hole or three-phase contact line during bubble-particle approach – a requirement that is met by the kinetic energy of the particles. The matching of these two quantities enables a minimum particle diameter, $D_{\min,K}$, for flotation to be obtained:

$$D_{\min,K} = 2 \left[\frac{3\kappa^2}{V_t^2 \Delta\rho \gamma \{1 - \cos \theta\}} \right]^{1/3} \quad [15]$$

where κ is the line tension, opposing expansion of the tpic. Molecules that are present in a line have a free energy that is different from those at a surface – in fact there is an excess linear free energy and a linear tension in an analogous fashion to that of excess surface free energy and surface tension.

In fact,

$$\kappa = \left(\frac{\partial F}{\partial L} \right)_{T,V,W} \quad [16]$$

where F is the Helmholtz free energy, L is the contact line, T is the temperature, V is the volume and W is the thermodynamic work. The Young-Dupré equation becomes:

$$\gamma_{S/V} - \gamma_{S/L} = \gamma_{L/V} \cos \theta \pm \frac{\kappa}{r} \quad [17]$$

The line tension is important for small contact radii and can oppose or reinforce $\gamma_{L/V} \cos \theta$. It counteracts the formation of the tpic in Scheludko's theory which neglects thin film drainage and other hydrodynamic effects. Experimental data for hydrophobic, angular quartz particles between about 10 and 35 μm in average diameter follow a general trend that is predicted by eqn [15], although quantitative agreement is poor. If a pseudo-line tension, embracing surface heterogeneities, replaces κ in eqn [15], then this in turn enables D_{\min} in eqn [15] to be re-expressed in terms of a critical bubble radius below which attachment does not occur. Reconciliation between theory and experiment is then achieved although the concept of pseudo-line tension needs to be placed on a firmer experimental foundation.

The Future

In terms of our fundamental understanding, there is no entirely adequate collision model that can correctly account for particle size and inertial effects in the presence and absence of soluble surfactants. Thin film drainage is poorly understood when one of the interfaces is both physically and chemically heterogeneous, and the other is deformable. The nature of the hydrophobic interaction between a particle and a bubble requires both experimental and theoretical verification. There is no reliable model at present to describe the movement of a three-phase contact line over a physically and chemically heterogeneous surface. Thus major research challenges exist that, if they are to be successfully overcome, must embrace systems where surfactants are both present and absent.

From a separation technology point of view, froth flotation will continue to be one of the principal means by which ores are successfully beneficiated for many years to come. Increasingly the technique is also being used in the deinking of paper, soil remediation, plastics recycling and heavy metal ion decontamination, to name but a few examples. Both research and practice are expected to accelerate strongly over the next decades as new techniques and theoretical approaches are used.

Further Reading

- Anfruns JF and Kitchener JA (1977) Rate of capture of small particles in flotation. *Transactions of the Institution of Mining and Metallurgy, Section C* 86: C9–C15.
- Blake TD and Kitchener JA (1972) Stability of aqueous films on hydrophobic methylated silica. *Journal of the Chemical Society, Faraday Transactions I* 68: 1435–1442.
- Blake TD (1993) Dynamic contact angles and wetting kinetics. In: Berg JC (ed.), ch. 5. *Wettability*. New York: Marcel Dekker.
- Collins GL and Jameson GJ (1976) Experiments on the flotation of fine particles: the influence of particle size and charge. *Chemical Engineering Science* 31: 985–991.
- Crawford R and Ralston J (1988) The influence of particle size and contact angle in mineral flotation. *International Journal of Minerals Processing* 23: 1–24.
- Dai Z, Dukhin SS, Fornasiero D and Ralston J (1998) The inertial hydrodynamic interaction of particles and rising bubbles with mobile surfaces. *Journal of Colloid and Interface Science* 197: 275–292.
- Derjaguin BV and Dukhin SS (1960–61) Theory of flotation of small and medium-size particles. *Transactions of the Institute of Mining and Metallurgy* 70: 221–246.
- Diggins D, Fokkink LGJ and Ralston J (1990) The wetting of angular quartz particles. *Colloids and Surfaces* 44: 299–313.
- Drelich J and Miller JD (1992) The effect of surface heterogeneity on pseudo-line tension and the flotation limit of fine particles. *Colloids and Surfaces* 69: 35–43.
- Fielden ML, Hayes RA and Ralston J (1996) Surface and capillary forces affecting air bubble–particle interactions in aqueous electrolyte. *Langmuir* 12: 3721–3727.
- Hewitt D, Fornasiero D, Ralston J and Fisher LR (1993) Aqueous film drainage at the quartz–water interface. *Journal of the Chemical Society, Faraday Transactions* 89: 817–822.
- Hewitt D, Fornasiero D and Ralston J (1995) Bubble particle attachment. *Journal of the Chemical Society, Faraday Transactions* 91: 1997–2001.
- Israelachvili JH (1991) *Intermolecular and Surface Forces*, 2nd edn. London: Academic Press.
- Laskowski JS and Ralston J (1992) *Developments in Mineral Processing. Colloid Chemistry in Mineral Processing*. Amsterdam: Elsevier.
- Lynch AJ, Johnson NW, Manlapig EV and Thorne CG (1981) *Mineral and Coal Flotation Circuits: Their Simulation and Control*. Amsterdam: Elsevier.
- Miklavcic SJ, Horn RG and Bachmann (1995) Colloidal interaction between a rigid solid and a fluid drop. *Journal of Physical Chemistry* 99: 16357–16364.
- Ralston J (1992) The influence of particle size and contact angle in flotation. In: *Colloid Chemistry in Mineral Processing*, ch. 6. Amsterdam: Elsevier.
- Scheludko A, Toshev BV and Bojadjev DT (1976) Attachment of particle to a liquid surface (capillary theory of flotation). *Journal of the Chemical Society, Faraday Transactions* 72: 2815–2828.
- Schulze HJ (1983) *Physico-chemical Elementary Processes in Flotation: An Analysis from the Point of View of Colloid Science Including Process Engineering Considerations*. Amsterdam: Elsevier.
- Sutherland KL (1948) Kinetics of the flotation process. *Journal of Physical Chemistry* 52: 394–425.
- Sutherland KL and Wark IW (1955) *Principles of Flotation*. Melbourne: Australasian Institute of Mining and Metallurgy.
- Ye Y and Miller JD (1989) The significance of bubble–particle contact time during collision in the analysis of flotation phenomena. *International Journal of Mineral Processing* 25: 199–219.

Column Cells

I. M. Flint, Canadian Process Technologies Inc., Vancouver, BC, Canada

M. A. Burstein, NPACI, Edcenter on Computational Science and Engineering, SDSU, San Diego, CA, USA

Copyright © 2000 Academic Press

Introduction

History

The first pneumatic flotation cell, which used air sparging through a porous bottom and horizontal slurry flow, was patented in 1914 by Callow. The first countercurrent column flotation device was designed and tested by Town and Flynn in 1919. Cross-current

pneumatic flotation machines were widely used in industry in the 1920s and 1930s, but were later replaced by the impeller-type flotation devices in mineral-processing plants. Dissolved-air flotation became the main type of flotation for water treatment applications. These substitutions were the result of the absence of effective and reliable air spargers for fine bubble generation and the lack of automatic control systems on the early columns. During this period, both the poor flotation selectivity and entrainment of slimes characteristic of impeller-type cells were offset by the use of complex flow sheets using large numbers of cleaner stages and recycle lines. Column flotation devices were reintroduced

for mineral processing in Canada by Boutin and Wheeler in 1967, at which time washwater was added to the froth to eliminate entrainment of hydrophilic materials to the float product. By the late 1980s column flotation had become a proven industrial technology in the mineral industry. These separators are routinely used on their own or in conjunction with other types of devices within separation circuits. This technology is currently being applied to liquid-liquid separations (oil-water, organic solvent-liquid), solid-liquid, or solid-solid separations in many industries.

Comparative Strengths and Weaknesses

Column cells are flotation devices that also act as three-phase settlers where particles move downwards in a hindered settling environment. Within the vessel there is a distribution of particle residence times dependent on settling velocity that may impact on the flotation of large particles. Impeller devices do not suffer from this effect to the same degree but do require higher energy input to suspend larger particles.

The low turbulence in columns means particles usually have low momentum, which in turn may reduce the probability of collection by passing bubbles. As a result, fine particle recovery may be hindered when compared to the capabilities of impeller-type designs.

The mechanism of particle-bubble collision in columns is different from intensive mixing devices such as impeller cells. Under the low intensity mixing caused only by a rising bubble swarm, particle drift from the liquid streamlines is caused mainly by gravity and inertial forces and also by interception, while in mechanical cells, according to many researchers, bubble-particle collision occurs at their relative movement within a turbulent vortex or at adjacent vortices. Also, as velocities of both bubble and particle during the attachment are slower under the quiescent conditions in a column, the contact time is generally higher. Therefore, probabilities of both collision and adhesion (components of attachment probability) are different to those in mechanical flotation processes.

The lower velocity gradient and less intensive shear forces in the vicinity of rising bubbles under low turbulent conditions in a column lead to reduced detachment probability. The latter is most important for improvement of recovery for coarse, heavy or weakly hydrophobic particles.

A column can support a deep froth bed and may use washwater to maintain a downward flow of water in all parts of the vessel. This essentially eliminates the entrainment of hydrophilic particles in the

float product when the vessel is used for solid-solid separation. This property, along with the absence of stray flows of feed material to the float product by turbulence, means that column devices are normally superior to impeller-type machines for the selective separation of fine particles.

In immiscible liquid separation duties, columns do not emulsify the material like impeller devices.

The bubbles used in a column are usually generated within the size range that maximizes interfacial surface flux and collection intensity through the vessel. Dissolved air systems nucleate micrometer-sized bubbles on particles which require very low downward liquid velocities in large volume vessels to separate the bubble and water. Also, dissolved air systems cannot provide air hold-up higher than approximately 4–6%, due to limited gas solubility and lower flooding limits caused by the microbubbles. In mechanical cells, bubbles are usually generated by shear action of the impeller; thus, bubble size is dependent on both air flow rate and impeller rotation speed. As such, bubble size cannot be controlled independently of cell turbulence.

The height-to-diameter ratio of a column is significantly higher than the impeller-type machines. As a result, control and consistency of flow are more critical. The column requires much less floor space to operate.

Control Systems

Control systems are designed to maintain separation in a changing environment by maintaining operating variables at their optimum values for process performance. The configuration used depends on the variability of the vessel feed, the ability of the operating and instrumentation staff, the availability of detectors and other parts, capital costs and the goals of the project. The most basic system only controls the interface level, between the aqueous suspension and froth phases, while complex systems can integrate expert systems or other forms of artificial intelligence into a full-grade/recovery adjustment strategy.

All columns perform best when flows are constant, therefore operation should be as close to steady-state conditions as possible. Good control systems limit damage due to variations by maintaining constant flows in earlier stages, establishing a recycle within the column system, or compensating by changing conditions within the vessel.

Level

The goal of a level control system is to maintain a constant aqueous suspension depth despite changes

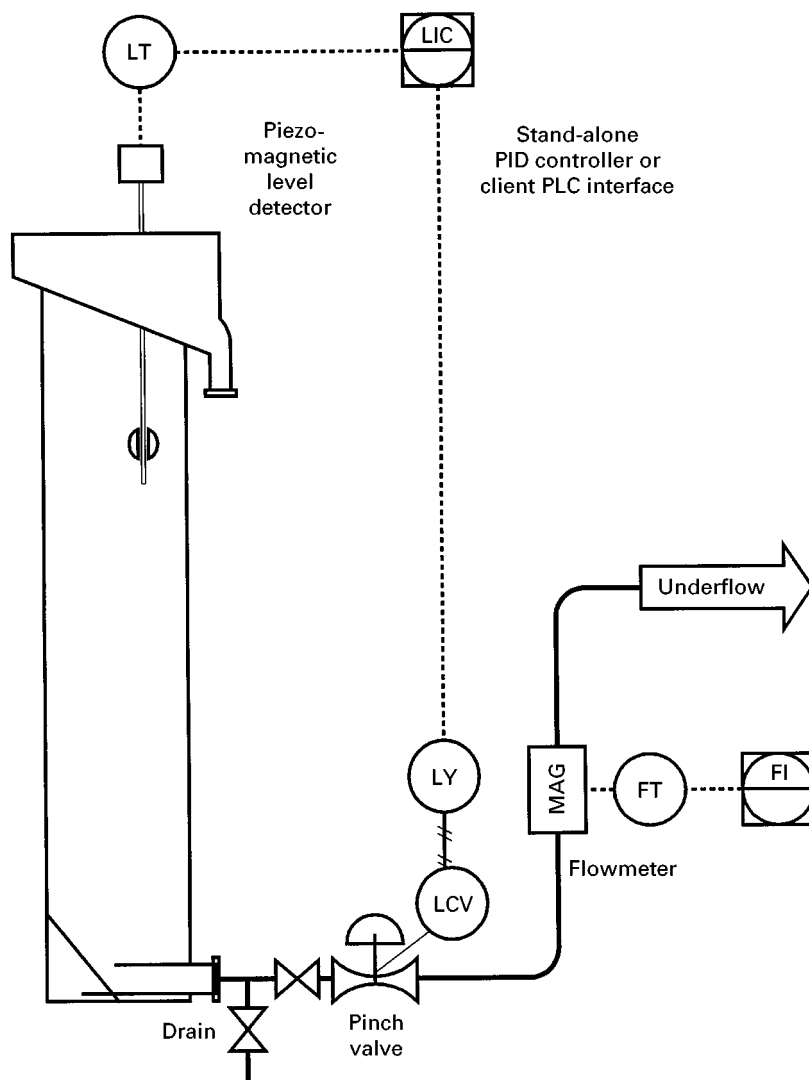


Figure 1 Example of level control loop. LT, level transmitter; LIC, level indicator and control; LY, level D/A signal conversion; LCV, level control device; MAG, magnetic flow detector; FT, flow transmitter; FI, flow indicator; PID, proportional-integral-derivative; PLC, programmable logic controller.

in feed flow, floatable material concentration or air rates. An example of this control is found in **Figure 1**. In water-oil separation, a periodic level rise may be organized to dump an accumulated organic pad. The simplest method of controlling level is to adjust the discharge height of the underflow using a 'gooseneck' or alternative form of gravity control. If this is not possible, then the level must be detected and that signal used to control either a variable-speed pump or control valve through a controller device. Detection devices include floats; pressure, capacitance, conductance, and ultrasonic transducers, or combinations of these devices. The set point for the level is determined from the desired froth depth. Generally, the higher the level, the greater is the recovery of the floating component and the lower its content in the overflow

(froth product). In more complicated systems, the level control may be used with froth or oil pad depth data to control overflow grade, with flow-monitoring devices for predictive control based on incoming feed, or multiple monitors to compensate for variations in air rate or feed composition.

Air

The purpose of the air loop is to control a volumetric flow of air through the column or to maintain a three-phase density within the vessel. In basic control systems air rate is controlled manually based on a monitored air flow rate. In slightly more advanced systems, the flow is controlled through an automatic valve to compensate for pressure changes (**Figure 2**).

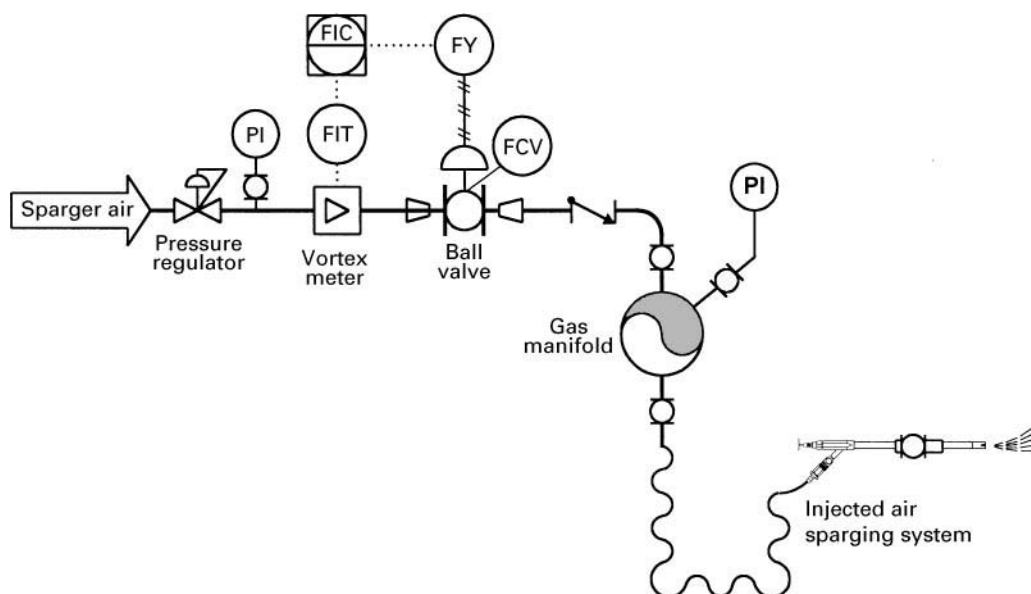


Figure 2 Example of air control loop. PI, pressure indicator; FIT, flow indicator and transmitter; FIC, flow indicator and controller; FY, flow D/A signal conversion; FCV, flow control device.

Air rate may be linked to predictive- or recovery-based systems.

Bias

Bias is defined as a downward flow of liquid through the froth zone. Positive or downward bias is usually used when two suspended substances must be separated from each other. If multiple separation stages are in operation, it is usually used on the last stage. The downward flow of water through the froth is controlled by varying the water rate added to the froth zone. This flow may be monitored by temperature, conductance or by flow differences (water added to froth minus overflow water, or amount of liquid in underflow minus its amount in feed). The actual bias needed depends on the distribution of the water through the froth and the hydrophilic particle sizes.

Bias may be estimated using the difference in slurry flows (**Figure 3**) or, more accurately, by first calculating the liquid volumetric flows using flow and density meters.

Advanced Controls

It is possible – although not common – to control a column to separate according to a grade-recovery response curve. As grade increases or decreases in the feed, level, air rate and bias may be adjusted to achieve the most economical performance. This type of control requires a good predictive model based on theoretical knowledge, past experience and test work that uses information from upstream processes to

adjust column parameters in anticipation of changes (feed-forward control). Predictive systems provide feed-forward control and can incorporate either knowledge base or models (statistical or deterministic) into the control loop. Excessive complexity of models or control strategy does not improve the results as the uncertainty in parameters grows. Such a system also requires extensive online detection equipment such as density, flow and pressure meters. When these controls are implemented they are either model-based systems or some form of artificial intelligence (knowledge base, neural network systems based on fuzzy logic principles).

Operating Parameters

Process-operating variables are those inputs to the separator that may change with time and can be used to control the production quantity and quality. These include column control variables such as gas rate, washwater rate and froth or oil pad levels. There are also variables that may be controlled but are usually not even monitored, like bubble size distribution, and variables that depend on other parts of the operation such as volumetric feed rate, and feed solids characteristics: concentration, liberation and particle size distribution.

Gas (Air)

Gas (air) rate is an effective parameter to control separation since the probability of particle collision

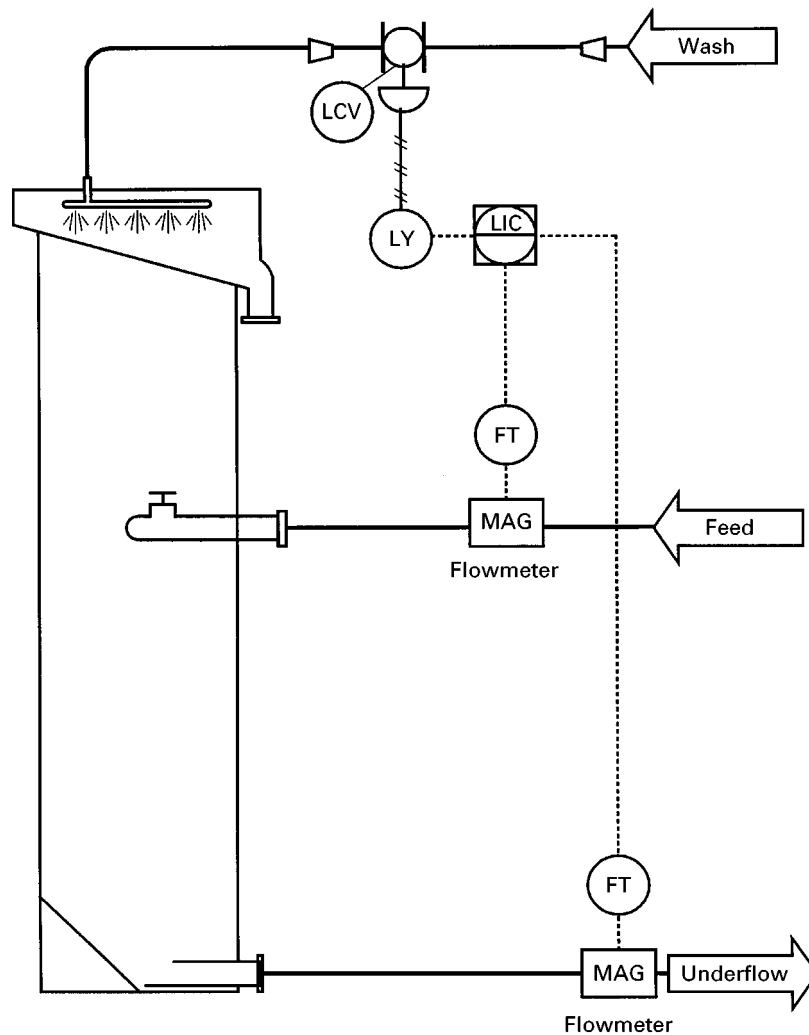


Figure 3 Example of differential feed-underflow bias control loop. LCV, level control device; LY, level D/A signal conversion; LIC, level indicator and control; FT, flow transmitter; MAG, magnetic flow detector.

with bubbles is dependent on the number of bubbles and their size distribution. The maximum particle surface flux removed depends on bubble surface area flux. As surface area flux increases, so does the probability of material-bubble aggregation (collection) within a specific range. This range is bounded by the increased mixing intensity as flooding limits are approached and the increase in bubble size that is usually associated with an increase in gas flow. The total removal capacity, known as carrying capacity, can also be controlled by the gas rate since it is proportional to the specific bubble surface area. The carrying capacity is determined as the maximum amount of material which can be transported into froth in unit time from a unit cross-sectional area of a column. It varies depending on particle size (for solid separation) and density of the floating substance. The carrying capacity can be estimated from the balance

of the available bubble surface area and particle surface flux. The normal range of superficial air velocity is $1.0\text{--}2.5\text{ cm s}^{-1}$. In buoyant material separations, high gas rates may reduce the three-phase density of the aqueous suspension within the column to a density lower than that of the product. This will cause an unstable pad that will sink if not quickly removed from the system.

Volumetric Feed Rate

The volumetric feed rate determines the vessel retention time and strongly influences vessel mixing. An increase in superficial suspension velocity results in lower gas limits as flooding will occur at lower gas rates and increases the size of microbubbles which become entrained by downward flow to the underflow. However, higher slurry velocities also decrease

the negative influence of mixing on grade and recovery (higher Peclet number) and lessen the retention time difference between fine and coarse particles due to the settling. Typically, superficial feed velocity is $0.5\text{--}1.3\text{ cm s}^{-1}$.

Feed Solids

An increase in the percentage of solids contained in the feed increases the residence time of those solids in the case of constant-column throughput of solids. The maximum solids load is determined by the viscosity of the system and may be only 0.25–2% (weight/weight) for paper de-inking applications to almost 70% for calcite/silica separation.

Washwater

Mineral separation columns can provide a positive bias which causes displacement of the feed liquid phase with washwater in the overflow. This substitution virtually eliminates entrained fines from the overflow product. Washwater distribution on to or into froth and its flow rate should be individually tuned for each application depending on feed and concentrate size distributions, froth stability, height and mobility, and on process objectives. Excessive washwater supply causes froth disruptions, loss of recovery and dilution of products. Typically, superficial washwater flow rate does not exceed 0.15 cm s^{-1} , although optimal rates depend on washwater distribution design and froth rheology. Washwater is not normally used in mineral roughing or scavenging operations, oil–water separations, or systems where entrainment is not a factor.

Froth Depth (Solid Separation)

The froth level maintained within the column is highly variable depending on the application. Some vessels may be operated with no froth, such as oil–water separators, or mineral columns operating on very large particles. In other cases, like molybdenite flotation, a froth as deep as 1.5 m may be run to ensure minimal entrainment and high selectivity. In general, a deep froth gives more opportunities for grade/recovery control and compensates for poor washwater distribution. Froth depth in mineral (solid–solid separation) column flotation typically varies from 15 to 300 cm. The gas hold-up in froth gradually increases upwards due to froth sineresis and drainage along plateau canals. The entrained fine particles return back to the lower (collection) section of the column by net downward liquid flow in the froth (in the case of positive bias). Experimental data confirm that, in some cases, upgrading of the product

occurs mainly in the froth zone, and not at the collection stage.

It is important to note that an increase in froth depth decreases the volume of the remainder of the column which may be detrimental to overall performance.

Organic Pad (Liquid Separation)

In an oil separation vessel a hydrocarbon pad may be maintained at the top of the column. A deep pad minimizes water entrainment into the overflow but may increase the stripping of light hydrocarbons. When high air rates are used and the organics pad is not removed, droplets of organic phase may form and drop through the aerated zone of the column. Air rates must be lowered or the organics pad continuously removed as a froth to prevent sinking of the floated organics.

Bubble Size

Some types of spargers allow the change of bubble size distribution at nearly constant overall air rate. Both break-up and coalescence of bubbles occur after formation by the sparging devices which results in an equilibrium size distribution above a certain distance from the spargers. The average and deviation of this distribution depend on the surface tension at the air–water interface and turbulence in the cell. Generally, smaller bubbles provide higher collection intensity and carrying capacity, but loaded microbubbles may sink or be entrained in the downward slurry. Also, maximum gas rate (at column flooding point or transition to a churn-turbulent regime) is reduced with decreasing bubble size, meaning that there is a specific bubble size that gives the maximum upward rising surface area flux. The point of column flooding can be estimated (in the assumption of cross-section flow uniformity and narrow bubble size distribution) from the drift flux model. In many cases a combination of smaller bubbles that provide the separation and coarser transport bubbles that coalesce with the smaller bubbles results in optimal flotation rates.

Column Circuits

Column cells can be used to perform many functions. These include separation within a grinding circuit (unit cell), as an initial (primary or rougher) or scavenging separator whose purpose is maximum recovery of material, or as a final separator (cleaner or recleaner) used to produce a pure product. They can also be used to process bleed streams from other processes. There are many examples of column usage, including base metal and industrial mineral

separation, iron ore purification, coal cleaning, solvent extraction and oil–water separation, paint recovery and newspaper de-inking. In addition, columns can be used to remove hydrophobic substances, or materials dissolvable in hydrophobic liquids, from water or soils. Examples are DDT, polycyclic aromatic hydrocarbons (PAHs) or other dangerous chemicals, oil production from tar sands, or the purification or removal of algae or bacteria from cultures. All of these separations fall into three categories: solid–solid, solid–liquid and liquid–liquid separations.

Solid–Solid Separations

In order to get a good separation, the solids present must be liberated: that is, not physically or chemically attached, be suspended in a liquid medium and the flotation kinetics of the materials must be different. One or more stages of separation may be needed, depending on the kinetics and chemistry of the separation. To achieve sharper separation when difference in flotation rate of components is not high and/or material is not completely liberated, complicated flowsheets including multiple recycle lines and regrinding are used. Regrinding operations for middlings are used to avoid over-grinding of the bulk of material as it would cause reduction in flotation rate and selectivity for fine particles. For finely disseminated ores, entrainment is a substantial factor

reducing sharpness of separation. Entrainment is a process of particle transfer to froth without their attachment on to bubble surfaces. This phenomenon can be explained by movement of small particles in the wake behind the rising bubble or within the static layer of liquid surrounding it. In machines with intensive mixing (impeller cells) the entrainment can also be caused by local upward slurry flows. These flows are not present in columns therefore reducing overall entrainment intensity and improving separation efficiency. A classical flotation flowsheet includes several cleaning stages generally linked by recycle of the cleaner tailings to previous stages. When more than one material is floatable and separation depends only on degrees of hydrophobicity (molybdenite–chalcopyrite), four to six stages may be required. If insufficient recovery is achieved in the primary vessel (rougher flotation), scavenger cells may be used. In general, all stages do have a common separation goal. For example, silica (impurity) is floated away from hematite in a four stage iron ore circuit in **Figure 4**. This circuit, or variations of it, is common when the valuable product is hydrophilic or an under-flow product of the column. The example gives four stages of separation; however, in many cases fewer stages are required.

The circuit for a hydrophobic product is shown in **Figure 5**. The second cleaner stage of this circuit is generally not needed unless the separation is between

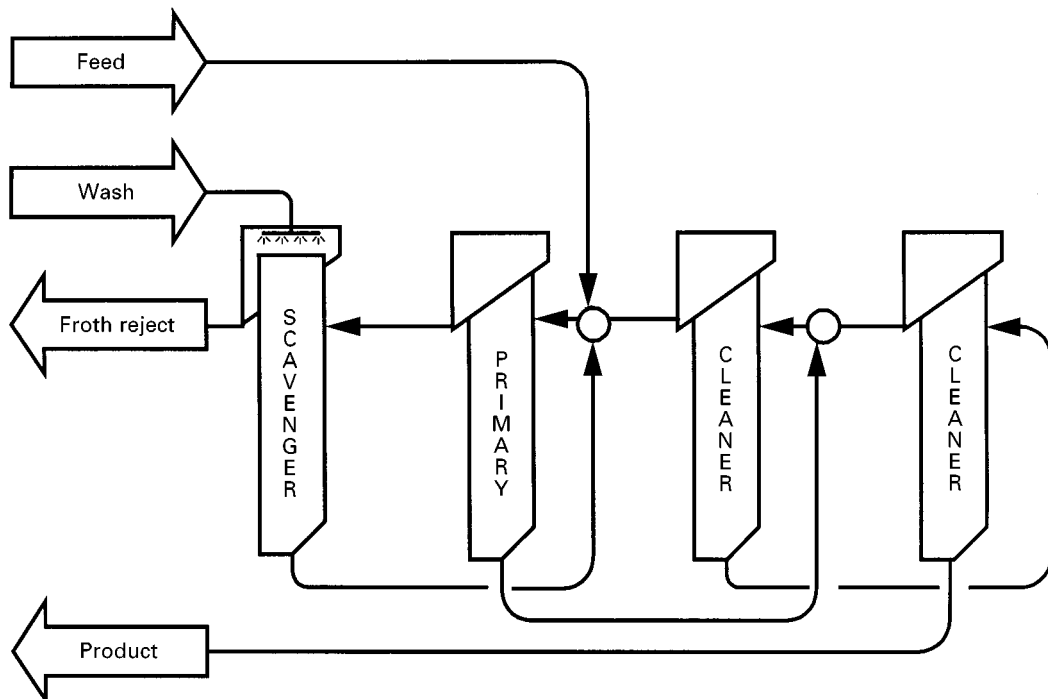


Figure 4 Hydrophilic product, solid–solid four-stage separation circuit. Example of iron ore.

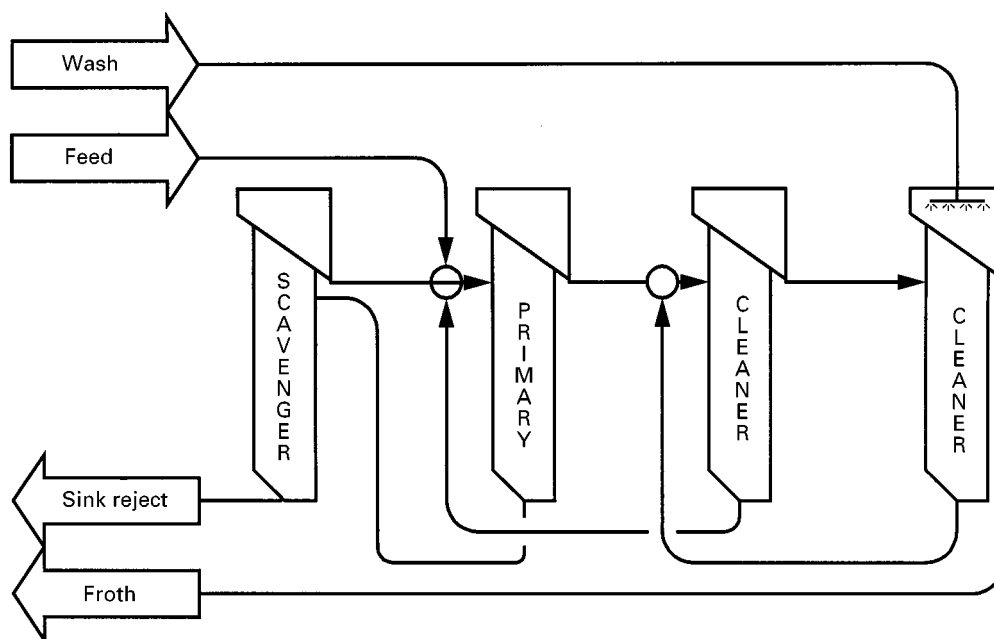


Figure 5 Hydrophobic product, solid–solid four-stage separation circuit. Example of copper or plastics float.

hydrophobic materials with similar flotation rates. As an example, this configuration or variations of it can be used in phosphate, copper, zinc and plastics separations, or for soil remediation.

Solid-Liquid Separations

In many circumstances a solid is present in a liquid stream that must be removed. Flotation is often a viable precursor stage, used to increase the percentage of solids, prior to filtration. This type of system can be used to float coal and associated PAHs from run-off water and upgrade the percentage of solids from p.p.m. levels up to 10–25%. **Figure 6** gives an example of such a circuit where PAHs from coking coal are floated from a contaminated site run-off

water without removing the naturally occurring sand and silt.

Flotation can also be considered as an alternative to settling of naturally hydrophobic materials in wastewater treatment. This type of separation may also be used to remove bacteria or algae from water, or many solid substances from reaction vessels.

Liquid-Liquid Separations

Immiscible liquids of any kind can be separated from water by flotation. The bubbles act to increase the kinetics of the naturally floating droplets such as diesel, crude oil, kerosene or the organics used in solvent-liquid extraction processes. Some examples are hydrocarbon separation from water on oil

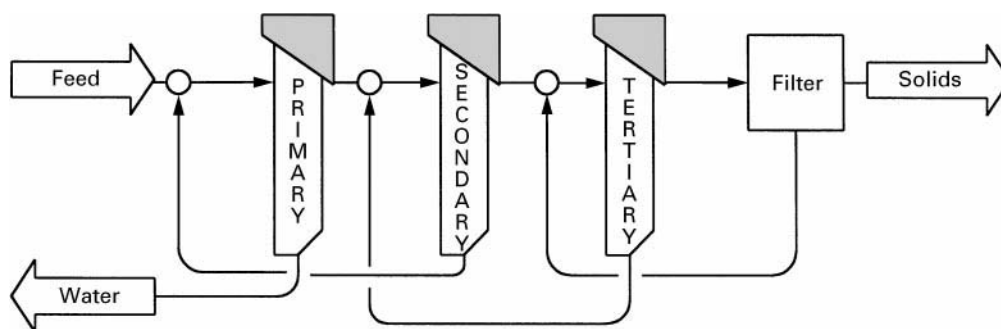


Figure 6 Example of solid-solid separation: PAH from run-off water. Input of approximately 500 p.p.m. solids; filter feed of approximately 24% solids.

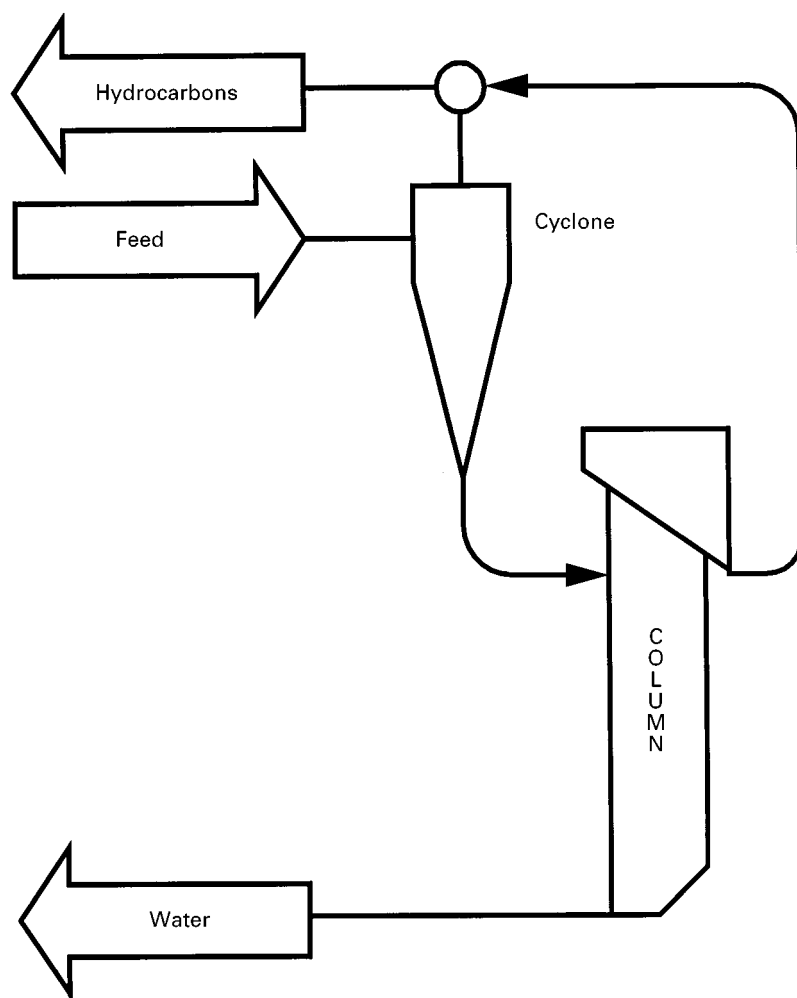


Figure 7 Treatment of oil platform process water; generalized circuit.

production platforms prior to final release of water, site run-off remediation and organics separation in hydrometallurgy. Columns are capable of removing freely floating hydrocarbons but usually not emulsified or dissolved hydrocarbons. In order to remove emulsified forms of hydrocarbons, a pre-aeration unit must be installed.

Oil production application Large amounts of water are involved in the extraction and production of oil. Column cells are used in the water treatment stage of production prior to release of the water back into the environment. In a typical circuit, as shown in **Figure 7**, water from the process is first passed through a cyclone or corrugated plate separator then to a column. The hydrocarbon concentrate from both of these vessels is returned for processing.

Site run-off remediation Sites that contain hydrocarbon contamination such as refineries and distribu-

tion depots often have run-off waters that contain entrained hydrocarbons. These can be treated effectively with flotation technology using a circuit containing a column either working on its own or in conjunction with a settling tank. If emulsified hydrocarbons are present, a pre-aeration unit may be required on the column in order to achieve contamination level under 15 p.p.m.

Organic-aqueous separation in solvent-liquid extraction circuits The solvent liquid extraction circuits employed in most hydrometallurgical processes require the removal of essentially all of an organic solvent from an aqueous medium in more than one stream. Initial separation is usually done in settlers. Columns with or without a pre-aeration unit can be used as secondary separation devices prior to filtering. The advantage of columns over many other devices is their ability to compensate for wide fluctuations in both aqueous and organic flows.

Conclusion

Column flotation has become the standard proven industrial flotation technique rather than an experimental method during the last decade. Nevertheless, its use in mineral-processing plants is mainly restricted at present to cleaning operations. The future of flotation equipment development lies in the combination of the advantages of impeller and column flotation and in the use of pneumatic machines in roughers.

As a greater share of flotation operations are used for unconventional areas such as environmental applications (water treatment, soil remediation, etc.) and ultrafine and colloid particle separation, special machines will be developed combining flotation attachment at intensive aeration and mixing conditions and three-phase separation in a quiescent environment. This leads to the concept of pre-aeration in a reactor (a unit for attachment of recovering phase on to gas bubbles) and de-aeration in a separator (a unit for separation of loaded bubbles from the bulk of three-phase suspension). Additional coarser bubbles can be added in a separator as a carrier to enhance the removal of loaded microbubbles by coalescence.

This concept and other types of new combined flotation machines will provide for more effective

and efficient separation for a wide range of applications.

See also: I/Flotation. II/Flotation: Froth Processes and the Design of Column Flotation Cells.

Further Reading

- Agar GE, Huls BJ and Hyma DB (eds) (1991) *Column '91. Proceedings of an International Conference on Column Flotation*, June 2–6, 1991. Sudbury, Ontario, Canada: Canadian Institute of Mining and Metallurgy and Petroleum.
- Boutin P and Wheeler DA (1967) Column flotation development. *Canadian Mining Journal* 88: 94.
- Finch JA and Dobby GS (1990) *Column Flotation*. New York: Pergamon.
- Gomez CO and Finch JA (eds) (1996) *Column '96. Proceedings of the International Symposium on Column Flotation*, August 26–28, 1996. Montreal, Quebec, Canada: Canadian Institute of Mining and Metallurgy and Petroleum.
- Pal R and Masliyah J (1991) Process dynamics and control of a pilot flotation column. *Canadian Metallurgical Quarterly* 30: 87–94.
- Rubinstein JB (1995) *Column Flotation, Processes, Designs and Practices*. Basel, Switzerland: Gordon and Breach.
- Yingling JC (1993) Parameter and configuration optimization of flotation circuits, part I: a review of prior work. *International Journal of Mineral Processing* 38: 21–40.

Column Flotation Cells

See II/FLOTATION/Froth Processes and the Design of Column Flotation Cells

Cyclones for Oil/Water Separations

M. T. Thew, University of Bradford,
Bradford, UK

Copyright © 2000 Academic Press

Synopsis

Though the solid–liquid hydrocyclone has been established for most of the 20th century, satisfactory liquid–liquid separation performance did not arrive until the 1980s. The offshore oil industry had a need for compact, robust and reliable equipment for removing finely divided contaminant oil from water. This need was satisfied by a significantly different

type of hydrocyclone, which of course had no moving parts.

After explaining this need more fully and comparing it with solid–liquid cyclonic separation in mineral processing, the advantages that the hydrocyclone conferred over types of equipment installed earlier to meet the duty are given.

Separation performance assessment criteria are listed prior to discussing performance in terms of feed constitution, operator control and the energy required, i.e. the product of pressure drop and flowrate.

The environment for petroleum production sets some constraints for materials and this includes the problem of particulate erosion. Typical materials

used are mentioned. Relative cost data for types of oil separation plant, both capital and recurrent, is outlined, though sources are sparse. Finally, some pointers to further development are described, as the oil industry looks to equipment installed on the sea bed or even at the bottom of the wellbore.

Introduction to Liquid-Liquid Hydrocyclones

This article covers the application of hydrocyclones to remove or concentrate dispersed oil from water. Two main classes of operation relating to their use with water-continuous liquid exist. Firstly as removers of oil contaminant from water (clean-up units) and secondly as a method of de-watering crude from wet oil fields (concentrator units). It excludes usage in relation to oil spills at sea, though feasibility studies have been technically successful. It also excludes applications where dispersed water (brine) is found in oil, though articles on this application – as yet only on the fringe of commercialization – may be found in the Hydrocyclone Conferences listed in the bibliography. Operation with oil-continuous liquid is difficult since interfacial effects are larger and break-up more likely as the brine droplets are less viscous than the continuous liquid.

Table 1 lists the key stages in arriving at the present near-universal usage of hydrocyclones for removal of oil contaminants from water in the oil industry offshore and more recently onshore. Concentrators, sometimes called ‘dehydration hydrocyclones’, are used in very wet oilfields as the initial stage to reduce the water (brine) content from, say, 95% to 50% or less. Under some conditions the overflow stream inverts to become oil continuous.

The two decades since de-oiling hydrocyclones were first seen to be capable of reaching legal standards of cleanliness offshore, e.g. 40 mg kg⁻¹ maximum free oil on the UK Continental Shelf, are brief when compared with the much longer and wide-

spread employment of solid-liquid hydrocyclones as in mineral processing or china clay production. Some salient comparisons between the two categories and the consequences of the clean-up or concentrator duty are set out in **Table 2**.

Flowfield and Geometry

The dispersion of fine oil droplets and their low differential density necessitate a high radial acceleration field. Since the oil is buoyant it will migrate towards the vortex core. To understand separation performance it is helpful to stress consequences of these two points. The oil is much more sensitive to the flow pattern than solid particles so this leads to the requirement for a low turbulence, reasonably linear vortex core and low peak shear flowfield to avoid droplet break-up leading to lower oil removal efficiencies.

The overflow stream should be a small fraction of the feed, since the oil content in clean-up applications is typically below 1%. An approximate volumetric balance gives the interrelationship between the parameters of a de-contaminating hydrocyclone. If the volumetric feed concentration of oil $C_f \sim 1\%$ and the overflow and underflow concentrations C_o, C_u are assumed to be 50% and 0 respectively, then the underflow rate Q_u will be 98% of the feed rate Q_f . For a wet oil concentrator however assuming $C_f \sim 10\%$ Q_u will be $\sim 80\%$ of Q_f . The overflow (reject) stream flow rate clearly is $Q_o = Q_f - Q_u$.

Colman and Thew at the University of Southampton in the late 1970s found that a cone angle as small as $1-1\frac{1}{2}^\circ$ (total angle) produced the necessary stable vortex, with a small relatively fast moving core moving to the overflow. This reverse axial flow penetrated a long distance downstream, so that in the early work a cylindrical tailpipe was put on the end of the cone. They also found that an enlarged entry section, as illustrated on **Figure 1**, reduced the pressure drop and reduced peak shear; the left-hand side of **Figure 1** shows the approximate proportions of the

Table 1 Advances in the use of oil-water hydrocyclones

1950s and 1960s	Sporadic work on liquid-liquid hydrocyclones, especially in relation to use in the atomic energy industry
1965	Bradley produces his classic text on ‘Hydrocyclones’ clarifying the problems of liquid-liquid separation
1974	Kimber and Thew achieve 90% oil separation at Southampton University, UK
1978–80	The Southampton Group achieve > 99% separation with crude oil (Colman and Thew, 1980 Hydrocyclone conference)
1983–84	First field trials offshore
1985	First large offshore installation (15 m ³ min ⁻¹)
Late 1980s	Installations worldwide
1990s	Virtually only method of oil-water separation. Number of manufacturers grows, prices fall. Higher mechanical packing density in pressure vessels
Early 1990s	Use in concentrator mode begins
Late 1990s	‘Downhole’ trials begin

Table 2 Comparisons between solid-liquid and oil-water hydrocyclones

<i>Factor</i>	<i>Solid-liquid</i>	<i>Oil-water</i>
Differential density	Often water-quartz, 1650 kg m^{-3}	$50\text{--}300 \text{ kg m}^{-3}$
Split ratio (Q_U/Q_F)	Fixed; set by outlet orifice size	Controllable by external valves
Outlets	Usually one or both open to atmosphere	Closed system
Axial pressure gradient near the centre line	Usually very small (air core)	Substantial, overflow at lower pressure than the underflow
Pressure drop	1–5 bar	5–20 bar
Inlet pressure	1–5 barg	10–10 ² barg
Shear	May cause some size reduction due to particle-particle interaction	Likely to cause droplet break-up
Particle size	1 μm –10 mm	Usually droplets $\sim 1 \mu\text{m}$ –100 μm
Concentration (by volume)	Varies greatly; can be slurry at underflow	Typical oil contaminant concentration in feed to first stage < 0.1%, oil contaminant concentration in feed to second clean-up stage 5–10%, well-head oil concentration in feed to wet oil concentrator 5–50%
Orientation	Fixed, 'g' important	No limitation, lateral acceleration up to ~ 0.1 'g' on floaters unimportant

Southampton bi-cone design, which had twin tangential inlets to produce a linear core. The right-hand side illustrates a typical later development with a single 180° wrap-round involute inlet and a curved wall. Note the absence of a projecting vortex finder, since there is no loss of oil in any short circuit flow in the end wall boundary layer.

Both the clean-up and concentrator units use the same wall profile but the latter has a larger overflow (or reject) port.

Later systematic work by Young (1994) came up with similar proportions.

Stronger swirl increases the acceleration field, but also raises the pressure drop and too much swirl seems to increase vortex instability and shear. Using a swirl number S ($S = \pi D_R X_i (2A_i)^{-1}$, where A_i is the total inlet area measured at a point where the flow is normal to the radius from the hydrocyclone axis to the centroid of the area, X_i , and D_R is a reference diameter of the hydrocyclone), the range of values for *de-oilers* is typically 7–11 or more usually 8–10. The reference value D_R for the bi-cone design is at the junction of the two cone angles (see Figure 1), and for a curved wall at, say, the point where the tangent is at about 10° to the cyclone axis.

The axial pressure gradient near the centre line is *not* zero: see section on pressure drop later.

De-oiling hydrocyclones have shown a range of sizes but there are no large units as for solid-liquid separators, since large droplets do not exist and thus no requirement for units with a relatively small acceleration field. Size is a compromise, taking into account the factors shown in Table 3. Early installations showed D_R values rising from about 30 mm to

70 mm, but more recently this has tended to drop back to about 15–30 mm.

Installation

Unlike solid-liquid units, clean-up or concentrator hydrocyclones have hitherto almost always been installed in pressure vessels, as shown schematically in Figure 2. This allows easy fabrication of individual units (sometimes called liners) from relatively thin walled material and reduces the number of connections to be made. Several assemblies complete with instrumentation and controls are built into a skid. Some larger units have serious vibration at very high flows so that a mid-length damper is built in.

The overflow or reject stream, being a small proportion of the feed, is readily incorporated into a manifold which may double up as a mounting plate.

Though series operation is possible and has been laboratory proven, in the field the use of a single stage with many units in parallel has hitherto been worldwide. Even though the turn-down ratio (comparison of maximum and minimum usable flowrates) for an individual unit is limited – see later discussion of the influence of feed flowrate on separation – the installation of units in banks which can be valved out in turn, allows overall turn-down ratio of about four for two banks, eight for three banks and so on.

Increased cleaned water throughput of an existing installation can be achieved by the addition of more hydrocyclone units.

Apart from modularity and improved separation, clean-up hydrocyclones have other advantages over the equipment formerly used such as induced gas

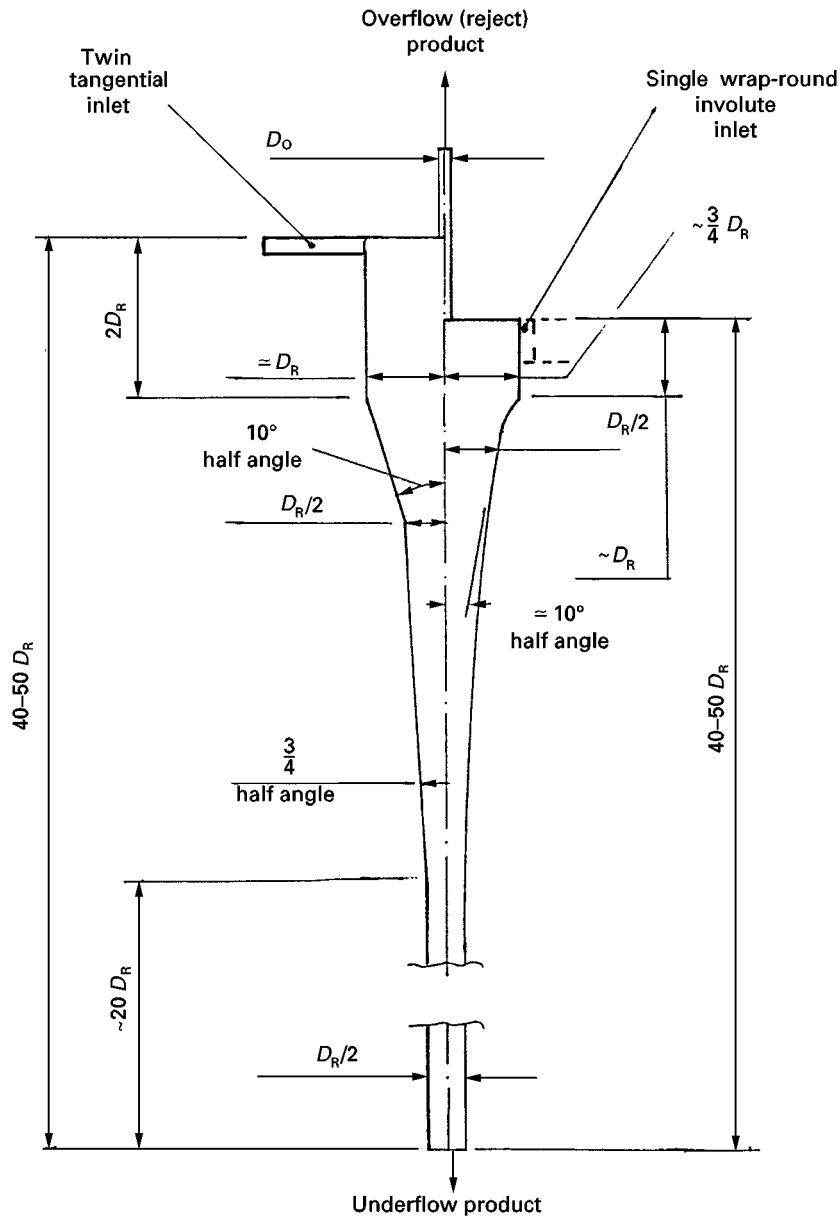


Figure 1 Hydrocyclone proportions. (left) Southampton University bi-cone design; (right) Typical later industrial development.

flotation (IGF) plant or gravity separators with plate packs. The installed size and weight of hydrocyclones has only been found to be about 10% of the older plant. Since hydrocyclones have negligible free surface effects they are insensitive to orientation and the motion of floating equipment. Unlike IGF they have no large requirement for chemicals and their cleaned underflow water does not require subsequent processing apart from occasional flocculant addition to reduce oil content below the legal limit.

As the unit residence time is only 1–2 s the hydrocyclones cannot cope with a slug of oil. Any zones of high shear upstream from these de-oiling hydrocyclones will reduce the size of oil droplets, thus worsen-

ing the separation efficiency. New installations can largely alleviate this problem by re-design to re-position flow-control valves to come after a hydrocyclone rather than upstream from it.

Performance

Though variables will often interact, for convenience their effects are discussed separately.

Separation Efficiencies

To achieve the purity required of the underflow stream from a clean-up unit, its output rate is usually

Table 3 Factors influencing the size of de-oiling hydrocyclones

Factor	Influence
Flowfield Reynolds Number, $u_i D_i/\nu$	In early development its perceived influence on separation suggested larger units. Now ignored
Pressure drop	Larger units have higher pressure drop, for the same peak radial acceleration field. Even though the reservoir pressure is often high enough to remove the need for pumps this factor tends to limit size
Separation of smaller drops *	As the hydrocyclone size reduces to a D_R of approximately 20 mm improved separation efficiency of droplets smaller than about 15 μm is achieved
Avoidance of excessive shear	For D_R values below about 10 mm experimental observation suggests that high shear causes droplet break-up and consequent loss of separation efficiency
Cost for a given flow rate	Favours few, larger units if cost for unit alone is considered
Packing density*	Units are normally installed in a pressure vessel. Higher overall throughputs can be achieved for a fixed volume pressure vessel fitted with many smaller rather than fewer larger units. This favours reduced cost for complete assembly.

*Generally dominant factors in current practice.

restricted to about 98% of the feed stream rate. This can result in the overflow reject stream having a significant water content; fortunately the oil droplets in this stream coalesce readily causing the oil and water phases to separate easily. The oil may then be pumped into an oil storage vessel or delivery line.

The inability of hydrocyclones to achieve perfect phase separation in a single step has previously been noted by Bradley (1965).

For an oil-water hydrocyclone operating in the concentrator mode, the yield of oil in the overflow product stream is the principal criterion.

Definitions for purity and yield follow below.

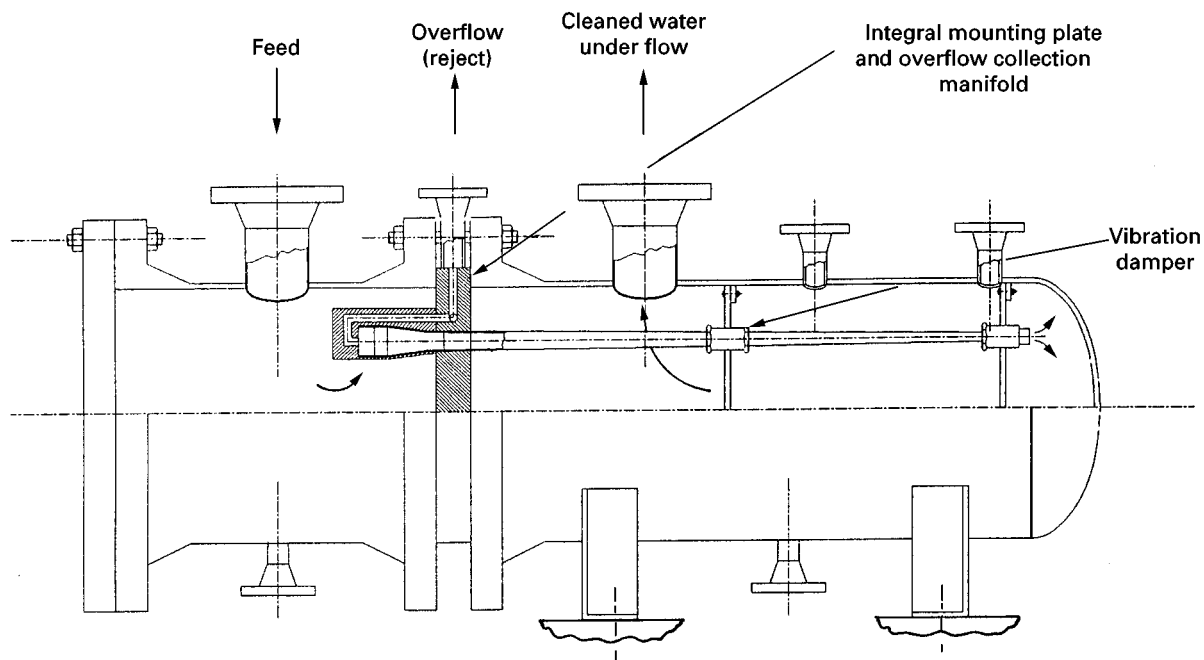
The performance of any separation unit is usually defined in terms of the fractional recovery η

of the valuable product and its purity in the product stream ε . For the clean-up units the fractional recovery η_0 is however defined by the fraction of oil in the feed which appears in the reject (overflow) stream, and ε_u for this operation is defined in terms of the oil (waste) content of the product (underflow) stream:

$$\eta_0 = \frac{Q_o \times C_o}{Q_f \times C_f}$$

and

$$\varepsilon_u = 1 - \frac{C_u}{C_f}$$

**Figure 2** Pressure vessel installation of oil-water hydrocyclones. (One unit shown.)

if the split ratio R_f and its complement F are defined by $R_f = Q_u/Q_f$ and $F = Q_o/Q_f$.

Then a relationship between the fractional recovery parameter η_0 and the underflow purity ε_u follows:

$$\eta_0 = 1 - \frac{Q_u \times C_u}{Q_f \times C_f}$$

thus $\eta_0 = 1 - R_f \times (1 - \varepsilon_u)$.

One bonus for the de-oiling duty is that the produced water, i.e. brine, is often warm. Higher temperature is beneficial as the water viscosity is reduced and the differential density increased. Possible problems arising solely from the elevated temperature, with reduced interfacial tension and easier distortion of oil drops as they are less viscous, seem unimportant. Thus values of ε_u of 0.99 or even 0.999 have been obtained, even though the differential density may only be 100 kg m^{-3} with a mean drop size $20\text{--}30 \text{ }\mu\text{m}$.

Generalized prediction of ε_u and η_0 is very difficult. Apart from the practical difficulty of predicting the feed drop size distribution, droplet break-up is influenced by interfacial tension. In the complex liquid mixtures of crude oil and produced water, interfacial tension is influenced by surface-active agents whose presence and effects are difficult to determine.

Correlation of experimental results could ideally use the Stokes Number ($St = 2Q_f\Delta\rho d^2/\pi 9D_R^3\mu$, where $\Delta\rho$ = differential density, d = characteristic droplet diameter, μ = viscosity of the continuous fluid). Strictly, this only applies to dilute dispersions with Stokesian flow with a droplet at a Reynolds Number below unity. The major problem which tends to restrict usage to laboratory investigations is in the determination of d . This is usually taken as the d_{50} diameter of a droplet that has an equal chance of reporting to underflow or overflow, but in most applications it is impractical to measure it.

Influence of Feed Characteristics

Flow rate At low flow rates the tangential velocity is too low to generate an adequate inward radial acceleration. This is reflected in the field results of Meldrum *et al.* in 1987 which have been converted from tabular results to the plot in Figure 3. These show sharply decreasing values of ε_u for a 60 mm D_R hydrocyclone on the Hutton field and for a 35 mm D_R hydrocyclone on the Murchison field for feed flows below $\sim 100 \text{ L min}^{-1}$ and 60 L min^{-1} , respectively.

Figure 3 also shows rapid falls in ε_u values for the 35 mm Murchison unit for feed flows above

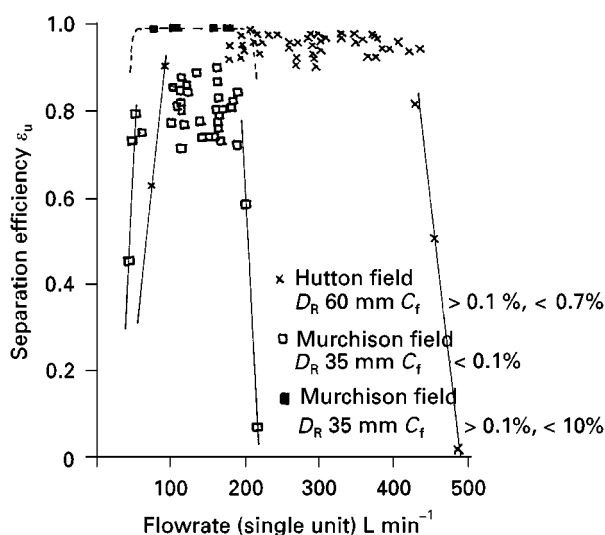


Figure 3 Field results: separation efficiency (ε_u) vs flow rate (Q_f). Calculated from Meldrum *et al.* data.

$\sim 200 \text{ L min}^{-1}$ and for the 60 mm Hutton unit above $\sim 425 \text{ L min}^{-1}$, which reflects a split ratio falling below the critical value. This is discussed fully later but essentially as flow rate rises the outlet pressures fall, and as the overflow outlet is at the lower pressure, a stage is reached where the overflow stream is so diminished that oil can only leave via the underflow.

The turn-down ratios illustrated by Figure 3 are 3 for the Murchison unit operating on a feed concentration $C_f < 0.1\%$ and 4.5 for the Hutton unit, but other fields with a larger driving pressure available have achieved values up to about 7. Pumped installations or oilfields with lower reservoir pressures might fall to about 2, for a single unit.

A plateau region separation efficiency is usual. Higher flow rates raise the acceleration field but, residence time falls, turbulent re-mixing rises and if interfacial tension is low droplet break-up may become significant. Within the plateau region, rapid transients in flow rate should not reduce separation efficiency appreciably.

Oil-water ratio Over a wide range of oil concentrations clean-up and concentrator hydrocyclones are considered to act as a flow divider, i.e. ε_u remains constant and C_u will rise in proportion to C_f if droplet size remains constant, however field results show this to give a pessimistic view as droplet sizes rise with oil content. This means that C_u may even remain constant as C_f rises.

As C_f rises the split ratio may need to be raised also. For clean-up the value of F is often maintained at 2–3%, but a rational control strategy is discussed later. In concentrator operations when C_f rises to

Table 4 Transient oil separation performance

d_f μm	ε_u Steady-state	% drop (ε_u steady state – ε_u transient)	
		5 s injection	2 s injection
50	0.93	0	1
17	0.53	4	6

d_f = mean feed drop size, BP Forties oil in cold tap water, C_f steady state $\sim 500 \text{ mg kg}^{-1}$.

5–10% the ratio F/C_f may be conservatively maintained at 2. This means the overflow stream is 50% water; for it to be, say, 70% oil (favourable result) F/C_f falls to about 1.4. A moderate transient increase in oil content, provided the F/C_f ratio remains satisfactory, has very little effect on ε_u . Table 4 shows results for a short-lived oil pulse, obtained with on-line oil content measurements compared with steady-state results.

A larger increase in C_f , but still within the acceptable range, may show a rise in ε_u if droplet size has also risen. Any further rise in C_f will exceed the capacity of the overflow and ε_u will fall substantially when F/C_f falls below about 1.2.

Droplet size Like all separation devices based on differential density, in a hydrocyclone, reduction in droplet size will give poorer results. An acceptable minimum value for d_f under favourable conditions may be as low as 5–10 μm (elevated temperature, $\Delta\rho > 150 \text{ kg m}^{-2}$, adequate interfacial tension), however the usual acceptable minimum of the feed droplets is 15–20 μm .

Droplets of 20 μm are less vulnerable to low values of interfacial tension in promoting break-up than larger ones. However, the presence of surfactants that drastically lower interfacial tension will almost certainly reduce the effectiveness of hydrocyclone separators, as shown by Colman, Thew and Corney at the First Hydrocyclone Conference (Cambridge, UK) in 1980.

In laboratory work, grade efficiency curves d_f vs ε_u have been obtained as for solid-liquid hydrocyclones, but because of the considerable difficulties in obtaining representative samples and in measurement such curves are seldom available in the field. When sampling, both isokinetic conditions and avoidance of droplet break-up are necessary and gas bubbles may complicate interpretation. A suitable technique was discussed by Colman, Thew and Corney.

Free gas Until fairly recently most clean-up hydrocyclones were installed downstream from three-phase separators. This means that the free gas content of the hydrocyclone feed was a fairly minor constituent. As

a result any gas core was relatively small in diameter. Because of the significant axial pressure gradient at the centre line this gas leaves with the overflow (oil-rich) stream.

Provided the gas content of the feed is reasonably invariant with time, laboratory tests have demonstrated that oil separation is little affected up to a threshold of 20–30% by volume free gas. This figure relates to conditions at the hydrocyclone entry. Field experience has generally confirmed this satisfactory picture except when the gas flow exhibits significant slugging. An entering gas slug does not have the angular momentum to maintain rotation of liquid and with the breakdown of inward radial acceleration, separation performance falls sharply. Amongst the thousands of units in service such a loss of performance is uncommon.

One consequence of appreciable gas leaving via the overflow is that it reduces the area for liquid to an annulus in the overflow exit port. This changes the relationship between the pressure drop and flow rate for the overflow liquid thus adversely affecting the control.

With the pressure drop in the hydrocyclone, some evolution of dissolved gas would be expected. This does occur but is too slow to be appreciable within the hydrocyclone and is manifest downstream from it, being most noticeable in the overflow stream. The evolving gas has been used to achieve post-cyclone separation of some more very fine drops in a suitable vessel possibly because the evolving gas bubbles nucleate on the oil droplets. In terms of Henry's Law the mass of gas coming out of solution in the overflow, will be proportional to $Q_o \times H (p_f - p_o)$ where p_f is the upstream feed pressure, p_o is the downstream overflow pressure and H is Henry's constant. However, the volume evolved will also depend inversely on the absolute pressure and in any case Henry's Law gives a maximum value as it relates to equilibrium conditions.

Solid particles Crude oil-brine mixtures commonly contain small amounts of reservoir solids. This problem is growing as more fields have larger produced water contents and it is made worse by the trend to produce from unconsolidated formations. The amount may range from a few hundred mg L^{-1} to about 10 g L^{-1} in worst cases. The solids may be water-wetted or oil-wetted, both usually report to the underflow unless the oil-wetted solids are very fine, in which case they may tend to be neutrally buoyant. In practice the overflow stream very seldom contains solids. Overflow blockages are rare and when they do occur they are usually associated with debris left in the system at installation or after maintenance.

Erosion, if it occurs, is usually restricted to the inlet region where velocities are higher. The use of harder materials, for example Stellite, in the inlet region has allowed long periods of satisfactory operation. A number of installations have run continuously for five years or more.

A development of the last 2–3 years is the arrival of de-sanding hydrocyclones installed ahead of the de-oiling units. These have been used prior to the choke with a containment vessel to withstand the very high pressure. Both relatively large units in appropriate steels and smaller ceramic units are entering service.

In off-shore fields the water in the oil–water mixtures may be quite corrosive, particularly if it is sour (containing H_2S). This has necessitated the use of alloy steels in the fabrication of the clean-up hydrocyclones. However, particularly for low cost, low flow land-based installations, cheaper materials may be satisfactory. Polyurethane units, possibly in a carbon steel casing or even bare are on the threshold of commercial usage.

Pressure Drop (the Cost Implications for Separation)

As in solid–liquid hydrocyclones, pressure drop $\Delta p \sim Q_f^m$ where $2.1 < m < 2.2$. In dimensionless terms defining:

$$\text{Euler Number } N_{Eu} = \frac{\Delta p}{\frac{1}{2} \rho u_f^2}$$

$$\text{Reynolds Number } N_{Re} = \frac{u_f D_i}{\nu}$$

where $u_f = Q_f/A_i$ and the inlet port diameter $= D_i$ (for multiple or noncircular inlets D_i is the diameter of the circular port with equal A_i).

Leads to the dimensionless relationship

$$N_{Eu} \sim N_{Re}^n$$

where

$$0.1 < n < 0.2$$

The use of u_f in terms of Q_f and A_i will be reflected by changes in the swirl number S .

Values of ρ and ν are based on arithmetic averages of the mixed liquids. Uncertainty in the value of the kinematic viscosity ν is not serious due to the small value of n . Typical Euler Number values are in the range 10–20 and do not seem to be affected by variations in C_f .

The de-oiling hydrocyclones have a substantial pressure gradient along the hydrocyclone axis not present in solid–liquid hydrocyclones with an air core. Thus pressure drop between the feed and the

overflow Δp_{fo} is greater than the pressure drop between the feed and the underflow Δp_{fu} , the relationship between the two being variable and set by external valves. The ratio between the two is important for control and optimization and this pressure drop ratio ($PDR = \Delta p_{fo}/\Delta p_{fu}$) varies with split ratio, R_f and also its complement F . Δp_{fo} has two principal components – one due to the radial pressure gradient and the other arising from the velocity through the overflow port. The radial pressure gradient and Δp_{fu} are both proportional to the u_f^2 and S , since $u_f = Q_f/A_i$. For a fixed geometry the $PDR = B_1 + B_2 \times F^2$ where B_1 and B_2 are constants, where $B_1 = f_1(S)$ and $B_2 = f_2(S, A_0^{-1})$. The oil concentrated overflow rate is regulated by using a fixed PDR value as set-point.

Pumped installations In younger oilfields the driving pressure stems from reservoir pressure. In older fields where pumping is necessary, this represents a cost. To reduce droplet break-up a low shear positive displacement pump should be used, however centrifugal pumps have proved satisfactory provided their speed is not too high and the duty is not too far from their best efficiency point. Fields with electrical submersible pumps have utilized de-oiling hydrocyclones satisfactorily.

Operator Control

For water clean-up units the PDR set-point is usually in the range 2–3 but for concentrators, with their larger overflows, values below 1.5 may be set. A simplified control layout is shown on Figure 4. The effectiveness of the control is restricted to some extent by the relative sizes of the underflow and overflow exit ports.

The PDR is a weak function of the feed Reynolds Number ($N_{Re} = u_f D_i/\nu$), see Figure 5. This dependence is usually ignored.

Critical split ratio (F_{CRIT}) At low oil contents it is desirable to reduce F thereby reducing the amount of the overflow stream. But below a critical value F_{CRIT} the axial pressure gradient near the centre line is inadequate to sustain the reverse flow. Though oil still gathers in the vortex core it is unable to reach the overflow outlet, becomes remixed near the inlet and leaves via the underflow so ε_u falls sharply. The effect is illustrated on Figure 6. F_{CRIT} rises with an increase in the diameter D_o of the overflow port and is therefore higher for concentrator units. Though extremely small overflow outlets will permit very small F_{CRIT} values, they are impractical as the smallest upset is too much for them to handle.

Table 5 summarizes the factors to be considered in control of the split ratio via the easily measured

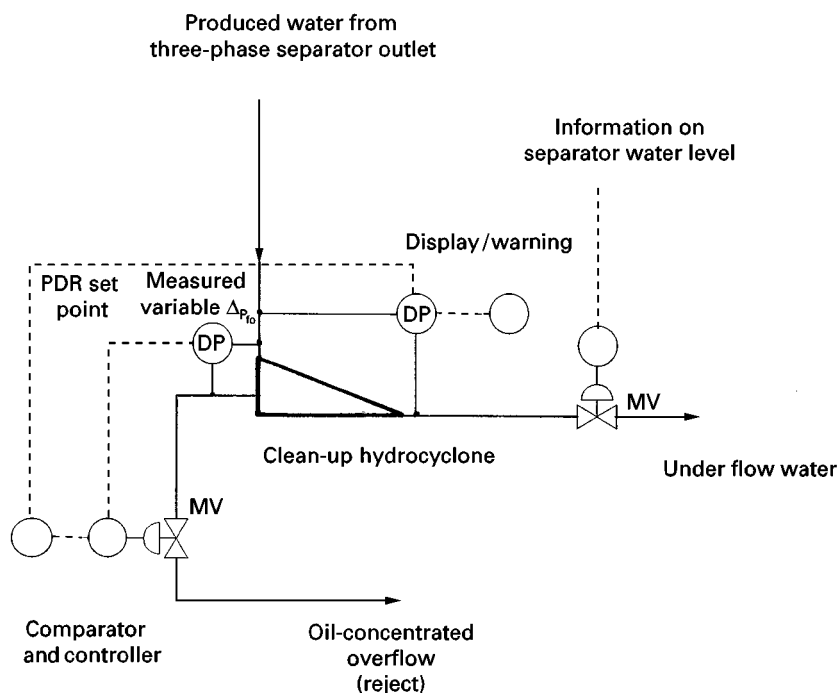


Figure 4 Simplified control layout.

variable, PDR. Hydrocyclone manufacturers will advise on the size of the overflow outlet. It may require enlargement during the life of an oilfield.

Cost Comparisons

Cost data are sparse but some information produced by BP about five years ago has been recast on Table 6 in terms of ratios. The flow rate used for deriving the information was applicable to a field producing about 16 000 m³ per day of oil.

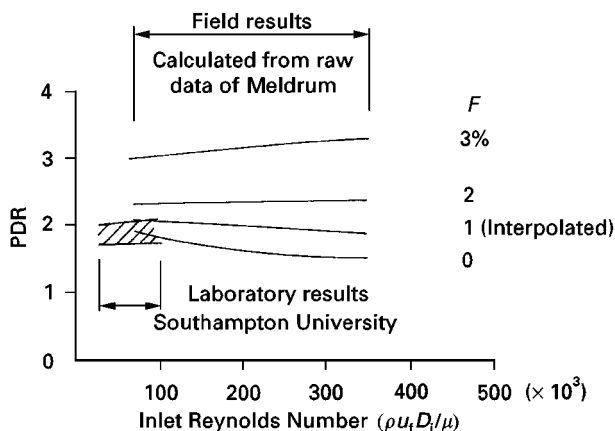


Figure 5 Pressure drop ratio (PDR) vs inlet Reynolds Number. Southampton University laboratory results and field results deduced from the data of Meldrum *et al.*

Table 6 shows that both the capital and running costs increase in the sequence hydrocyclone-IGF-filter/coalescer-centrifuge. Hydrocyclones also produce the most compact plant and are the least sensitive to orientation or lateral acceleration as encountered in installations on a floating base.

Future Developments

In 1979 an oil industry task force recommended plate pack gravity separators or IGF for produced water clean-up. Six years later the first large hydrocyclone installation – about 15 m³ min⁻¹ – was operating successfully in the North Sea, so the points below relate only to the immediate future, perhaps prior to 2003.

- Improving oil separation (in hydrocyclones) means removing smaller drops. There is probably limited scope for further optimizing geometry, though the claims for computational fluid mechanics (CFD) in rapid optimization are likely to become valid in a year or two. (Adequate representation of turbulence in confined swirling flow has proved difficult.)
- For new systems and even for some retro-fits, there is often room for worthwhile improvement by reducing shear upstream of the hydrocyclones or re-locating them. The resulting larger drops ease the separation task.

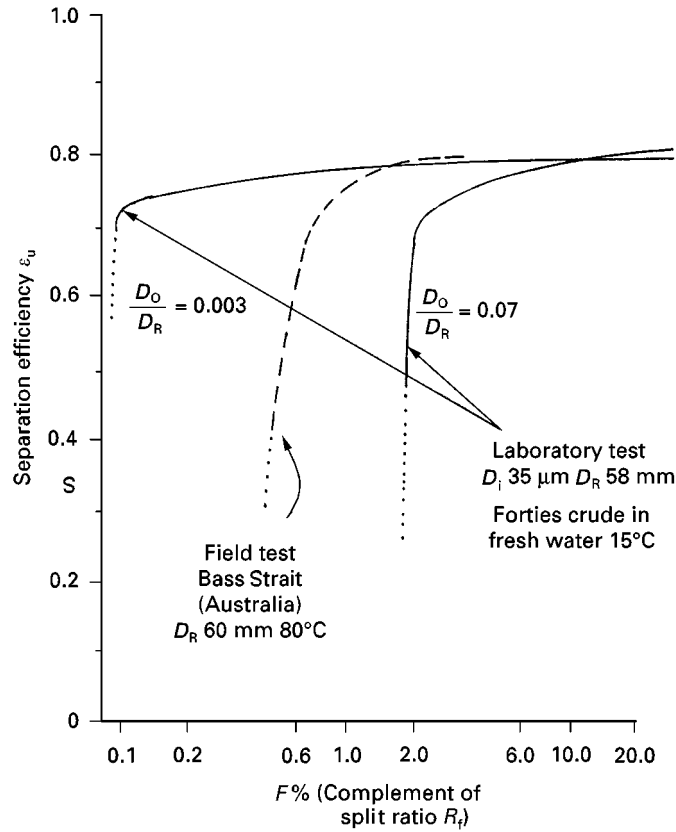


Figure 6 Separation efficiency (ϵ_u) vs complement split ratio (F). The collapse in separation consequent on too low an overflow is shown.

- If the split ratio needs frequent adjustment, a variable area overflow (two values would be adequate) simply controlled would be very useful. Laboratory tests have shown that this is readily feasible but moving parts are still not readily accepted, as they are associated with reduced reliability.
- As the cost of dealing with produced water mounts, economic/technical studies have strongly suggested hydrocyclone installation at the bottom

of the wellbore, 'downhole'. If the geology is suitable the water could be re-injected in adjacent strata. Preliminary trials using electric submersible pumps (ESP) (some concepts suggest two) have shown and are showing considerable promise. Access after installation is costly so there are problems in control and reliability, though ESP speed variation is proven. Reduced standards of separation may still be acceptable. A halfway stage to use pre-choke hydrocyclones on the sea bed is also being investigated.

Table 5 Factors affecting PDR

Factor	Correction to PDR	Comment
$F < F_{\text{CRIT}}$	Increase*	Oil is lost in underflow, $\epsilon_u \rightarrow 0$
$F/C_i < 2$	Increase*	Some oil lost to underflow (conservative criterion)
Excessive free gas in underflow	Increase*	Effective overflow area for liquids is reduced. Condition may be difficult to detect
F too high	Reduce	Δp_{io} excessive
F too high	Reduce	Too much water in overflow stream

*Opening the valve in the overflow raises the flowrates hence increasing PDR.

Table 6 Relative cost for clean-up plant ($16\,000\text{ m}^3\text{ d}^{-1}$)

Plant type	Capital cost	Running cost	Oil separation performance [†]
Hydrocyclones*	1.0	1.0	3
Induced gas flotation	1.1	1.1	4
Filter/coalescer	1.3	1.6	2
Centrifuge	4.6	4.0	1

*Capital cost is $6\text{--}7 \times$ annual running cost based on data from several North Sea fields with installations ~ 10 years old.

[†] Ranking order for oil content in cleaned flow with identical oil content and mean drop size in the feed; 1 is best.

- De-sanding hydrocyclones are now being installed upstream from the choke in some fields. There could be an energy saving if de-sanding and de-oiling could be performed in a single unit, but simultaneous optimization of both functions is unlikely. A successful laboratory research project has been reported in France, but initial field trials in West Africa were disappointing.
- Heavy oils, i.e. those with a higher density and viscosity, appear unpromising for cyclonic separation processes. Nevertheless success has been reported for commercial de-oiling units used in the concentrator mode in trials in western Canada.
- Feasibility studies and preliminary field trials are in progress on integrated de-watering plus de-oiling cyclonic separation and/or de-sanding plus de-oiling. The attraction is an ultra-compact plant suited particularly to floating installations. Though de-watering units have not yet met with widespread success, the impending arrival of compact, robust electrocoalescers to raise water droplet size prior to separator entry, could transform the situation.
- With success in dealing with petroleum it is surprising that applications to edible oils, which are about 10 times more valuable, have yet to materialize. Laboratory trials have been very satisfactory. Not only is lost oil a revenue drain but it generates a potential environmental hazard.

Further Reading

Note: The five conferences on hydrocyclones all contain several papers on oil-water hydrocyclones

- First Hydrocyclone Conference, Cambridge (UK) (1980) Priestley G and Stephens HS (eds). Cranfield: BHRA.
- Second Hydrocyclone Conference, Bath (UK) (1984) Watts GA and Pickford R (eds). Cranfield: BHRA.
- Third Hydrocyclone Conference, Oxford (UK) (1987) Wood P (ed.). Cranfield: Elsevier-BHRA.
- Fourth Hydrocyclone Conference, Southampton (UK) (1992) Svarovsky L and Thew MT (eds). Dordrecht: Kluwer.
- Hydrocyclones 96 Conference, Cambridge (UK) (1996) Claxton D, Svarovsky L and Thew MT (eds). London: MEP.
- Vortex Separation: *Fifth International Conference on Cyclone Technologies*, Warwick (UK) (2000) Svarovsky L and Thew MT. Organised and published by BHR Group, Cranfield.
- Meldrum N (1987) Hydrocyclones: a solution to produced water treatment. *Proceedings of the 19th Annual Offshore Technology Conference*, Houston, Texas, USA.
- Paige R and Ferguson M (1993) Water injection: practical experience and future potential (A BP Study). *Conference on Offshore Water and Environmental Management*. Business Seminars International, London.
- Smyth IC and Fay B (1998) Further developments of the Hydrosep™ System for downhole oil/water separation. *Conference on Downhole Production and Subsea Processing*, Aberdeen. Organised by BHR Group, London: MEP.
- Svarovsky L (1984) *Hydrocyclones*. London: Holt, Rinehart and Winston.
- Young GAB, Wakley WD *et al.* (1994) Oil-water separation using hydrocyclones: an experimental search for optimum dimensions. *Journal of Petroleum Science* 11: 37–50.

Dissolved Air

D. Shekhawat and P. Srivastava,
Michigan State University, East Lansing, MI, USA
Copyright © 2000 Academic Press

Introduction

Dissolved air flotation (DAF) is a solid-liquid separation process for the removal of fine suspended material from an aqueous suspension. The basic principle underlying DAF is Henry's law, which gives the solubility of air in water. According to Henry's law, the solubility of air in water is directly proportional to its partial pressure. A supersaturated solution of water is produced using high pressure in a saturator. The bubbles are generated by the pressure release of this water stream. These bubbles attach to

suspended material present in the aqueous stream, causing them to float to the surface, where they are collected as floc.

DAF can be carried out by vacuum or pressurized methods. In the vacuum flotation method the water to be treated is saturated with air at atmospheric pressure. The bubbles are produced by applying a vacuum to the flotation tank, releasing the air as fine bubbles. The vacuum flotation process has several disadvantages. These are (a) the amount of air available for flotation is limited by the vacuum achievable, (b) it is a batch process, and (c) it requires special equipment to produce and to maintain high vacuum. These disadvantages limit the application of vacuum flotation and it is only used in wastewater sludge thickening.

The pressure flotation process is the most widely used DAF technique. High pressure water is saturated with air. This pressurized water forms small bubbles when injected into water at atmospheric pressure. Three types of pressurization processes can be used in DAF: full flow, partial flow and recycle flow pressurization. The entire inlet stream is pressurized in full flow pressure DAF. It is commonly used when the wastewater contains large amounts of suspended solids and the pressurization process does not affect the treatment efficiency of the system. Partial flow pressurization is used where the wastewater contains moderate to low concentrations of suspended solids. In the recycle flow pressurization system, 10–25% of the clarified effluent is recycled through a pressure vessel to the flotation tank. The flocculation process is not disturbed in the recycle flow system because of intense mixing and pressurization as clear water is pumped. A recycle flow system is cost-efficient because it pressurizes only part of the water, thus requiring less compressor power. Recycle flow pressure flotation is the best-suited system for most DAF applications.

DAF is an effective alternative to sedimentation. The advantages and disadvantage of DAF relative to sedimentation are as follows:

Advantages

1. Clarification rates are higher in DAF, resulting in smaller flocculation tank volumes.
2. More concentrated sludge solids are produced in DAF than from sedimentation.
3. DAF uses lower amounts of coagulants and flocculant aids.
4. Oxygenation effects in DAF reduce odour problems.
5. DAF provides better removal of low density particles and algae, which can plug filters.

Disadvantage

1. DAF processes are more costly to operate and maintain than sedimentation processes.

Process Description

A schematic diagram of a DAF process for wastewater treatment is shown in Figure 1. Its essential elements are a flocculation tank, a flotation tank, an air compressor, an air saturator, a recycling pump and a hydrosweep system. The wastewater is pumped to the flocculation tank after being treated with coagulant/flocculent agents such as aluminium sulfate. A portion of the clarified effluent is recycled for pressurization. Compressed air is introduced into the discharge stream of the recycle pump, and the water is saturated with air at high pressure. The pressurized water stream is introduced to the flotation tank through nozzles, where fine bubbles (20–100 μm) in diameter are formed. The bubbles attach themselves to suspended solid particles, causing the agglomerates to float to the surface of the tank. The float can be mechanically skimmed from the surface, and the clarified water is taken from the bottom of the flotation tank.

Principles of Dissolved Air Flotation

DAF facilities are composed of the following four principal steps:

1. coagulation and flocculation prior to flotation
2. bubble generation
3. bubble–floc collision and attachment in the mixing zone
4. rising of the bubble–floc aggregates in a flotation tank

Coagulation and Flocculation Prior to Flotation

Coagulation and flocculation are often considered as a pretreatment step in DAF processes. Favourable

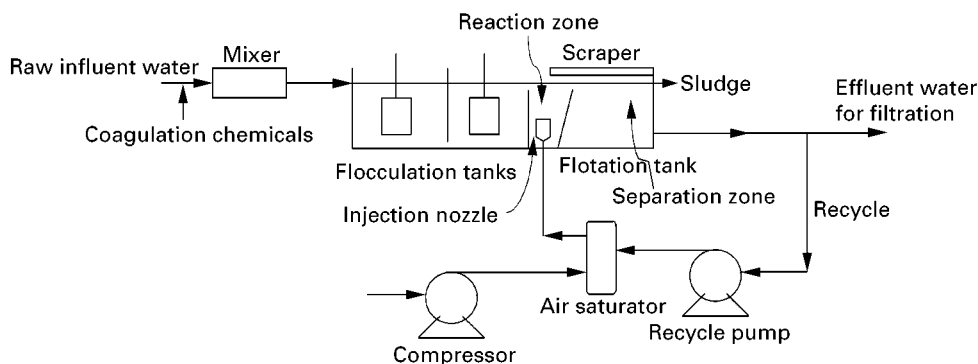


Figure 1 Schematic diagram of the dissolved air flotation process for water treatment.

conditions for bubble attachment to particles requires coagulation conditions that reduce particle charge and produce hydrophobic particles. Coagulant dosages and pH conditions that satisfy these criteria depend on the coagulant type and raw water characteristics, including particle concentration, hardness, and concentration and type of natural organic matter (NOM). Unlike in sedimentation, large floc particles are not needed in DAF. Flocculation tanks are designed to produce strong flocs with particle size distributions of 10–30 μm and short flocculation times, in the range of 10–15 min.

Bubble Generation

Small air bubbles, 100 μm or less, are formed by injection of supersaturated pressurized recycle water into a flotation tank using specially designed nozzles. The process of bubble formation involves two steps: nucleation and growth. During the first step the large pressure difference across the nozzle produces bubble nuclei spontaneously. Air bubbles grow at a fixed number of nucleation centres due to air transferred from the water. As the excess air is transferred from the dissolved to the gas phase, the bubbles grow in size. Additional bubble growth may occur as the bubbles rise due to a decrease in hydrostatic pressure or coalescence.

Measurements of bubble sizes for DAF systems indicate that bubbles maintain a steady-state size range of 10–100 μm . A reasonable estimate of average bubble diameter is 40 μm . The steady-state size depends on the saturator pressure and the injection flow rate. The injection flow must provide a rapid pressure drop and be sufficient to prevent back-flow and bubble growth on pipe surfaces in the vicinity of the injection system. To ensure small bubbles, pressure differences (saturator gauge pressures) of 400–600 kPa are recommended.

Bubble Floc Collision and Attachment in the Mixing Zone

There are three possible mechanisms for forming aggregates of bubbles and particles:

1. entrapment of preformed bubbles in large floc structures (floc size much larger than bubble size scale)
2. growth of bubbles whose nuclei formed on particles or within flocs
3. particle collision with adhesion to preformed bubbles

For DAF processes, the third mechanism is the most important.

Classically, the contact angle between the adsorbed bubble and particle has been used to characterize the extent of bubble–floc adhesion. Here the contact angle must be finite and large enough that the energy of adhesion of water to the solid particle is less than the energy of cohesion of water. A larger contact angle indicates both hydrophobicity and good adhesion. The magnitude of the contact angle, however, depends on the size of the bubbles and particles. A different view of particle–bubble attachment of colloidal particles by small bubbles is that a finite contact angle need not form. In this heterocoagulation model, the stability of charged particles and bubbles is described. Attachment requires reduction in electrical charge interactions and attraction by London–van der Waals forces as particles are transported to bubble surfaces.

Both the contact angle and the heterocoagulation models predict experimentally observed trends that two conditions are necessary for favourable flotation: charge neutralization of the particles and production of hydrophobic particles. Bubble attachment to particles requires hydrophobic particle surfaces or hydrophobic regions on the particles. For many particles, hydrophobicity can be increased by reducing the negative charge. Other particles, such as freshly precipitated or amorphous $\text{Al}(\text{OH})_3$, have polar surface groups that make them hydrophilic. This hydrophilic effect may be reduced by charge neutralization, but aluminium hydroxide particles have a polymolecular coating of water which hinders bubble adhesion.

Rising of the Bubble–Floc Aggregates in a Flotation Tank

Following bubble attachment and reduction in particle density, particle–bubble agglomerates rise to the surface of the flotation tank in the separation or clarification zone. The rise velocity of the particle–bubble agglomerate may be calculated using Stokes law.

DAF Modelling

The design and operation of DAF facilities has largely been based on experience and results from pilot-plant studies. In recent years, a conceptual model of DAF has been developed, based on a single collector collision theory in laminar flow conditions (SCC model). A kinetic model has also been presented, based on the population balance model of bubbles and flocs in a turbulent flow condition (PBT model).

For modelling purposes, DAF processes can be divided into two zones: reaction zone (regions where

the saturated recycle flow is introduced) and separation zone.

Reaction Zone Modelling

For the reaction zone efficiency (dN_{fl}/dt), defined as the reduction of number of primary particle flocs with time, floc and bubble size (d_{fl} and d_b) and concentration are defined as relevant process parameters:

$$dN_{fl}/dt = -(3/2)(\alpha_{pb}\eta_T)(\Phi_b\nu_b N_{fl})/d_b \quad [1]$$

where α_{pb} = particle bubble attachment efficiency; η_T = total single collector efficiency; d_b = bubble diameter; ν_b = bubble rise velocity; N_{fl} = floc number concentration; Φ_b = bubble volume concentration.

Particle (floc)–bubble interception is considered to be the most relevant kinetic mechanism for DAF efficiency, depending on the floc and bubble size (d_{fl} and d_b) and incorporated in η_T . This term also considers floc–bubble collision mechanisms related to Brownian diffusion, settling and drag.

A summary of these parameters, their dependence on the system variables and desirable operational conditions is given in Table 1.

Separation Zone Modelling

Assuming laminar flow conditions, the efficiency of the separation zone, ν_{flb} (defined as floc–bubble

agglomerate rising velocity), is defined by the floc–bubble agglomerate size (d_{flb}) and density (ρ_{flb}) (eqn [2]). These are dependent on the floc size–density ratio and concentration, and the size and number of bubbles comprising the floc–bubble agglomerate:

$$\nu_{flb} = g d_{flb} (p_w - p_{flb}) / 18 \mu \quad [2]$$

Eqn [3] represents a necessary prerequisite for efficient DAF, ν_{os} being the DAF overflow rate and m being the fraction of DAF tank dead space:

$$\nu_{flb} > \nu_{os} / (1 - m) \quad [3]$$

Applications of Dissolved Air Flotation

DAF is best applied to remove materials that normally settle slowly, persist in remaining in suspension or have a tendency to float. Prior to the 1960s it was mainly utilized in the area of mining and metallurgical industries. Now, DAF finds numerous applications, e.g. mineral processing, water purification, wastewater treatment, waste sludge thickening, wastewater reclamation, recycled paper de-inking, and many more. It is widely used for drinking water purification in many Scandinavian countries, South Africa, the Netherlands, the UK and others. In drinking water clarification, DAF has been applied in combination with flocculation for the removal of

Table 1 Summary of conceptual reaction zone model parameters

Parameter	Dependence	Comments
<i>Pretreatment parameters</i>		
α_{pb} (particle–bubble attachment efficiency)	1. Particle–bubble charge interactions	1. Favourable flotation; requires reduction in particle charge and hydrophobic particles
	2. Hydrophilic nature of particles	2. Increase α_{pb} to 1: optimum coagulation and charge neutralization
N_p (particle number concentration)	1. Raw water quality	1. Concentration and size of particles; concentration of NOM
	2. Coagulant type and conditions	2. Coagulants may add particles
	3. Flocculation time	3. Flocculation may reduce N_p and increase d_p
<i>Reaction zone–flotation tank</i>		
η_T (total single collector efficiency)	1. Particle–bubble collisions from diffusion and interception	1. Increase η_T : produce floc size of tens of μm
	2. Minimum η_T for d_p of $\sim 1 \mu\text{m}$	2. Short flocculation times
d_b (bubble diameter)	Controlled by pressure difference across nozzle and injection flow	1. Desire microbubbles: range 10–100 μm , median 40 μm ; smaller bubbles: better performance
		2. η_T varies as d_b^{-2} ; rate of collection of particles varies as d_b^{-1}
Φ_b (bubble volume concentration)	1. Saturator pressure	1. Increasing Φ_b increases N_p : more bubbles for collection of particles
	2. Recycle ratio	2. Increase Φ_b : more bubble volume for reducing floc density

algae and humic substances. The first water treatment plant based on the DAF process was established in South Africa in 1969. Since then it has received worldwide attention for research and development on all aspects of DAF.

The first DAF plant in the USA was set up at the Millwood water treatment plant in Westchester county (35 miles north of New York city) in August 1993. Now, several other plants based on DAF are operating or are under study in the USA. It is postulated that DAF is an emerging technology in the USA that will become more important because of existing and proposed regulations that require filtration of surface waters and increased removal of protozoa cysts such as *Cryptosporidium* and *Giardia*. Large scale pilot-plant trials of water treatment have been carried out in the UK for removal of *Cryptosporidium* using DAF. Well-operated chemical coagulation-based treatment using DAF should be capable of achieving 99% removal of *Cryptosporidium* oocysts.

DAF is also used in the forest industry, food-stuff industry, meat-processing industry, seafood industry, potato processing, pulp and paper industry, petroleum industry, poultry industry, producing refined sugar from raw juices, separation of grease, oil, fibres and other low density solids, chemical processing plants, storm water cleaning, and other similar industries.

Future Trends

There is great potential for DAF. Its use has been limited due to lack of knowledge of the process by users, designers and other regulatory agencies. The

design and operation of DAF methods are currently tested on empirical data and data from costly and time-consuming pilot-plant models. More information is needed on the performance, designs and costs of the DAF process.

See also: I/Flotation.

Further Reading

- Derjaguin BV, Dukhin SS and Rulyov NN (1984) Kinetic theory of flotation of small particles. In: Matijevic E and Good RJ (eds) *Surface and Colloid Science*, vol. 13, New York: Plenum Press, pp. 71–113.
- Edzwald JK (1995) Principles and application of dissolved air flotation. *Water Science and Technology* 31: 1–23.
- Edzwald JK, Malley JP and Yu C (1991) A conceptual model for dissolved air flotation in water treatment. *Water Supply* 9: 141–150.
- Fukushi K, Tambo N and Matsui Y (1995) A kinetic model for dissolved air flotation in water and wastewater treatment. *Water Science and Technology* 31: 37–47.
- Hall H, Pressdee J, Gregory R and Murray K (1995) *Cryptosporidium* removal during water treatment using dissolved air flotation. *Water Science and Technology* 31: 125–136.
- Ives KJ and Bernhardt HJ (eds) (1995) Flotation processes in water and sludge treatment. *Water Science and Technology* 31.
- Kitchener JA and Gochin RJ (1981) The mechanism of dissolved air flotation for potable water: basic analysis and proposal. *Water Research* 15: 585–590.
- Takahashi T, Miyahara T and Mochizuki H (1979) Fundamental study of bubble formation in dissolved air pressure flotation. *Journal of Chemical Engineering, Japan* 12: 275–280.

Electrochemistry: Contaminant Ions and Sulfide Mineral Interactions

J. T. Smit and J. Gnoinski,
Anglo American Research Laboratories (Pty) Ltd.,
Johannesburg, South Africa
R. F. Sandenbergh, University of Pretoria,
Pretoria, South Africa

Copyright © 2000 Academic Press

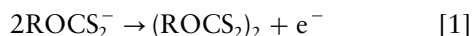
Introduction

Mineral separation by flotation is based on the selective levitation and separation of mineral particles by gas bubbles. This is carried out by the selective conversion of the surfaces of the minerals to be floated

from their typical hydrophilic nature to hydrophobic, to which the gas bubbles may attach to effect the levitation. This conversion is usually achieved by the selective attachment of collectors to the surface of the mineral or by natural processes; an example of the latter is the formation of elemental sulfur or a metal-deficient sulfide layer on sulfides.

Typical collector agents are organic substances consisting of an ionic, i.e. hydrophilic, end that attaches to the mineral and a nonionic hydrocarbon end that creates the hydrophobicity of the mineral surface. A widely used collector in selective sulfide flotation is the xanthate ion (O-alkyldithiocarbonate, ROCS_2^-).

Most of the sulfide minerals are electronic semiconductors or electrically conductive. This implies that the reactions required for the creation of a hydrophobic surface on sulfides may be electrochemical. For example, the xanthate ion may be oxidized at an anodic area of a local cell on the mineral surface to form hydrophobic dixanthogen:



The corresponding reduction reaction is the catalytic reduction of oxygen. Apart from this type of electrochemical reaction, electrochemical interaction between dissimilar sulfide minerals of different rest potentials occurs when there is electrical contact between them in a sufficiently conductive electrolyte, and this is of a galvanic nature. For contact of this nature to occur the various sulfides must be either present in composite particles, i.e. middlings, or be brought into such frequent collision contact in the flotation pulp, that significant electrical charge transfer can take place. In the laboratory these phenomena can be studied by electrically connected mineral electrodes, or stirred/fluidized beds made up of sulfide minerals only. Although these laboratory methods indicated significant electrochemical interaction, studies conducted at the authors' laboratories on simulated mineral feed of realistic plant composition showed no significant charge transfer. This was possibly due to the complexity of the flotation pulp chemistry, which makes it difficult to distinguish between the contribution of chemical and electrochemical processes to overall plant performance.

Theory and Principles of Electrochemical Interaction between Mineral Species

Reactions on mineral surfaces in which there is a change of oxidation state for the species involved are generally electrochemical in nature. This adds to the complexity of multi-mineral systems, in the sense that, apart from interactions through a common aqueous phase, by for instance dissolution-precipitation reactions, galvanic interactions through electrical contact between minerals must be considered also. Galvanic interactions between minerals will cause the more inert mineral to act predominantly as cathode, and reduction of dissolved oxygen would typically occur on its surface. This will stimulate anodic counter-reactions such as the oxidation of xanthate to dixanthogen or metal xanthates and that of metal sulfides to metal-deficient sulfides or elemental sulfur,

all of which will promote hydrophobicity on the surface of the more reactive mineral.

Similarly, contact of a less reactive sulfide mineral particle with more reactive steel, generated in abundance by industrial grinding operations, in the form of loose particles or layers smeared onto the mineral surfaces, may depress the mixed potential of the galvanic couple to such an extent that the oxidation reactions necessary for the hydrophobization of the sulfide surface will be slowed down. In extreme cases, reactions may become thermodynamically impossible.

In the following sections the role of electrochemical interactions in the separation of complex sulfide ores will be further explored. Particular attention will be paid to the use of pulp potential as a monitoring and control tool and the role of electrochemical reactions in the development of hydrophobicity.

Mixed Potential Theory

The interaction between collector reagent and mineral takes place at the mineral-solution interface. For ease of reference, and in view of the vast body of investigative work done on it, our discussion will focus on the use of xanthates as collector agents. In the case of sulfide minerals, which are generally semiconductors, the interactions with xanthate collectors involve charge transfer across the electrical double layer at the solid-liquid interfaces. Woods *et al.* suggested three ways by which the xanthate ion could confer hydrophobicity to a mineral surface. Firstly the anodic reaction leads to dixanthogen formation (see eqn [1]). Secondly they distinguish between dixanthogen produced by the anodic reaction of the xanthate ion and the xanthate ion adsorption at a lower potential which is held by electrostatic attraction:



Finally there is chemisorption for which the anodic oxidation of the xanthate ion on lead sulfide is:



The corresponding cathodic reaction typically requires the reduction of oxygen in industrial flotation systems. If it assumed that the process is Faradaic in nature, i.e. no charge accumulation can occur, the oxidation and reduction reactions will be coupled by the flow of charge. The rate of the electrochemical reactions can now be determined by considering the driving force available for the process and the kinetics of the individual processes. If the respective electrical

and ionic resistance of the mineral and solution is low, the system will with time reach a common potential called the 'mixed potential' at which the individual reactions will take place at steady state. This will typically be the case for solutions with a high salt loading and with anodic and cathodic areas in close proximity. The situation may be further complicated by the involvement of more than two half cell reactions and also by cathodic and anodic areas of varying sizes as is typically the case in galvanic interactions.

The mixed potential theory has been used to account for the collectorless flotation of sulfide minerals such as chalcocopyrite, by considering the contributions of both surface oxidation and oxygen reduction reactions to the common potential. For example, Trahar has shown that surface oxidation of sulfide minerals results in the formation of hydrophobic sulfur layers and thus enhances flotation. It has been suggested that for sulfide minerals, surface oxidation involves the progressive removal of metal atoms, leaving a hydrophobic, metal-deficient sulfide layer with a crystal lattice only marginally altered from the original structure. More recent studies by Buckley and Woods, using X-ray photoelectron spectroscopy, have confirmed that sulfur species are indeed formed on the mineral surfaces. The concepts are summarized in Figure 1.

In the presence of xanthate collector conditions for the formation of dixanthogen have been shown by Allison *et al.* to occur when the rest potential of the mineral is greater than the reversible potential of the xanthate/dixanthogen couple E_R (0.13V at pH 7.0), which for these minerals is the active collector species in xanthate-based flotation, except for galena, where the metal xanthate was indicated, as discussed by Cheng and Iwasaki (see Further Reading). The rest

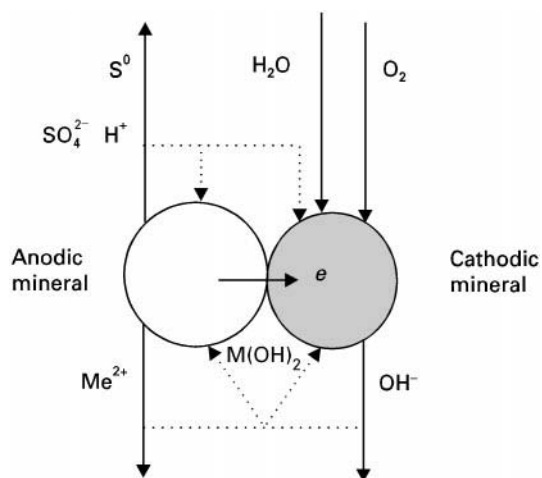


Figure 1 Generalized depiction of galvanic interaction between electrically connected particles.

Table 1 Rest potentials at various dissolved oxygen contents (Reproduced from Cheng and Iwasaki (1992) with permission Copyright Gordan and Breach Publishers.)

Mineral	Rest potential (V vs SHE) in $6.25 \times 10^{-4}M$ KEX solution	Range reported at 0–7 ppm O_2
Mild steel		– 0.515 to – 0.255
Sphalerite	– 0.15	
Stibnite	– 0.125	
Realgar	– 0.12	
Orpiment	– 0.10	
Antimonite	– 0.09	
Covellite	+ 0.05	
Bornite	+ 0.06	
Chalcocite	+ 0.06	
Chalcocopyrite	+ 0.14	0.115–0.355
Galena	+ 0.14	0.142–0.172
Molybdenite	+ 0.16	
Pyrrhotite	+ 0.21	0.055–0.290
Pyrite	+ 0.22	0.389–0.445
Arsenopyrite	+ 0.22	0.277–0.303

potential of a mineral surface, is the potential associated with a finite reaction rate in a specific solution environment (see Table 1). This is illustrated by Figure 2 from the work of Gardner and Woods, which

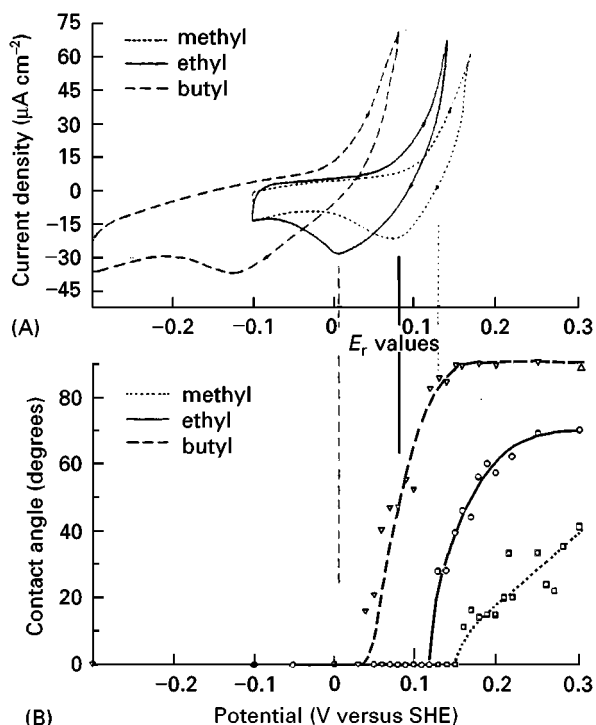


Figure 2 Pyrite electrode at 25°C in 0.05 M $Na_2B_4O_7$ solution (pH 9.2) containing 1000 ppm of three potassium alkylxanthates. (A) Cyclic voltammograms at $4 mV s^{-1}$; (B) Contact angles measured after holding the electrode at each potential for 30 s. The vertical lines are the E_r values for the xanthates. (Reproduced with permission from Gardner and Woods (1977) Copyright CSIRO Publishing.)

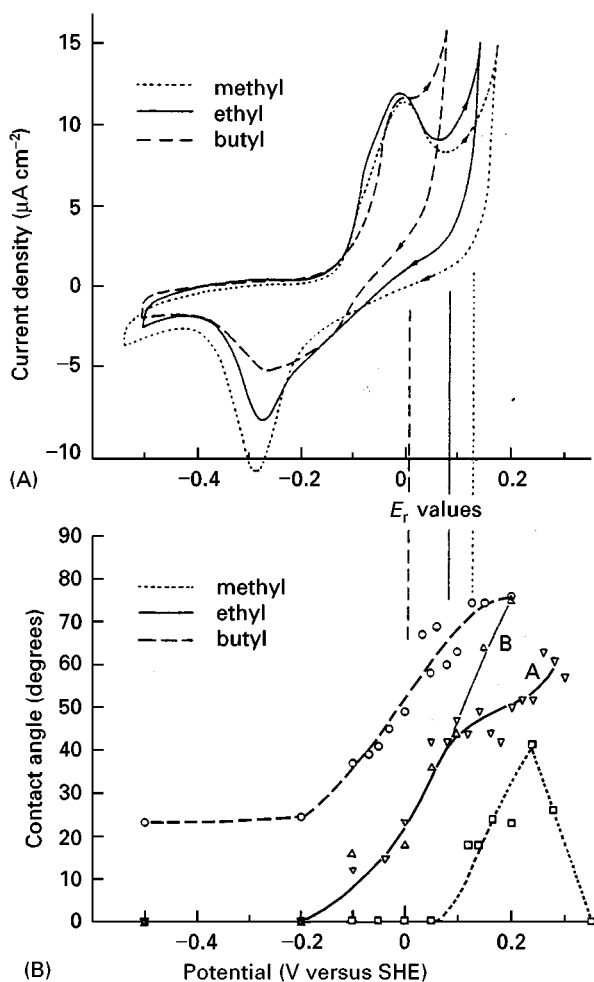


Figure 3 Galena electrode at 25°C in 0.05 M $\text{Na}_2\text{B}_4\text{O}_7$ solution (pH 9.2) containing 1000 ppm of three potassium alkylxanthates. (A) Cyclic voltammograms at 4 mV s^{-1} ; (B) contact angles measured after holding the electrode at each potential for 30 s. The vertical lines are the E_r values for the xanthates. (Reproduced with permission from Gardner and Woods (1977) Copyright CSIRO Publishing.)

clearly indicates that of pyrite hydrophobicity only develops at potentials more noble than the reversible potential for xanthate/dixanthogen reaction. For galena the response shown in Figure 3 is somewhat different, with a significant current flow occurring below E_R due to the contribution of the chemisorbed reaction. It is also interesting to observe a zero contact angle at -0.2V .

Galvanic Interaction between Sulfide Minerals in a Pulp

As indicated earlier, galvanic interactions arise between two or more dissimilar minerals, and/or metals that are in electrical contact with each other and with an electrolyte. Electrochemical reactions at the min-

eral surfaces result in coupled current and ion flows. The cathodic reaction is generally the reduction of oxygen to hydroxide, while the oxidation reaction involves the oxidation of the sulfide mineral. The current flow depends on the surface area and conductivity of the mineral as well as the chemical composition of the electrolyte.

Minerals can only be separated by flotation if they are physically separate, i.e. liberated from each other. Short periods of galvanic contact between sulfide particles are unlikely to result in the development of the longer-term hydrophobicity that would be required for flotation. Polarization studies by Gardner and Woods on lead sulfides have indicated that the formation of hydrophobic substances, in this case lead xanthate, is reversible and thus unlikely to endure long enough for bubble contact to be established. In the context of the selective flotation of sulfides it would be the middlings, where the different sulfides would still be in physical contact, that would be the most influenced by galvanic interactions.

In the case of middlings it is possible that the floatability may even be better than that of pure minerals, due to the greater spatial separation and electric potential differentiation of the anodic and cathodic sites on such composite particles compared to single mineral particles. The possibility for spatial separation will increase with increasing conductivity of the solution and will be more important in solutions of high salinity.

As an indication of the galvanic interactions that may develop between different sulfides, a list of rest potential values has been reproduced in Table 1. The rest potential values mentioned were determined at near neutral pH values and will generally decrease with increasing pH. Because of this effect, many sulfides may be depressed by an increase in pulp pH, as their potentials move further away from the dixanthogen/xanthate equilibrium potential.

This disregards any chemical changes that may occur on the mineral surfaces due to a rise in alkalinity. High pH conditions typically develop at the cathodic sites, which favour the precipitation of metal hydroxides and would encroach on the anodic reaction site if the spatial separation of the sites is not large.

Consider the flotation of a middlings particle containing chalcopyrite and pyrite. In the absence of a xanthate collector, pyrite acts as a cathode of the local pyrite-chalcopyrite cell. Oxidation of the chalcopyrite surface is the predominant reaction balanced by the corresponding reduction reaction on the pyrite surface.

Buckley and Woods demonstrated that the collectorless floatability of chalcopyrite and pyrite

middlings particles increases with the amount of quartz added. This was attributed to the adsorption of hydrophilic iron hydroxides from the sulfide mineral surfaces on the quartz surface.

The uptake of xanthate ion strongly depends on the rest potential of the sulfide mineral. For sulfide minerals with rest potentials above +0.13V, xanthate ions are oxidized at the mineral surface to dioxanthogen, which imparts hydrophobicity to the mineral surface. For bornite and chalcocite, whose rest potential was below that of the xanthate/dioxanthogen reversible couple, metal xanthate was identified. For sphalerite and stibnite, the reaction products could not be positively identified. Rao, Moon and Leja also indicated that contact between various sulfides and iron will result in the depression of the potential to such an extent that the oxidation of xanthate to dioxanthogen will no longer be possible. This is indicated in Figure 4.

During electrochemical interaction between sulfide species, ionic charge transfer takes place through the flotation liquor, while electronic charge transfer takes place through the solid interface; solid phase conductivity, as well as water conductivity is thus important. As an example, it is the experience on the Phalaborwa igneous complex that plant water conductivities range generally between 180 mS (fresh industrial

water) and extremes of *ca.* 500 ms, with a middle range of 200–300 mS.

For separate mineral particles, the solid phase charge transfer would rely on particle collision, in which the gangue particles have a shielding influence. This reduces the galvanic interactions to a point where electrochemical interactions between fully liberated minerals are unimportant in flotation plant practice, unless plant waters are highly conductive, and both pulp densities and sulfide mineral concentrations are high enough.

Reaction Products Affecting Flotation Performance

General

The reaction products of galvanic interaction may influence the flotation efficiency of composite minerals by direct depression or activation of minerals, or by affecting flotation froth characteristics. These reaction products, as will be shown, are not unique to galvanic processes, but their rate of formation may be enhanced by such interactions. The spatial separation of the anodic and cathodic reactions in galvanic interactions favours the kinetics in the sense that the reaction products formed at the

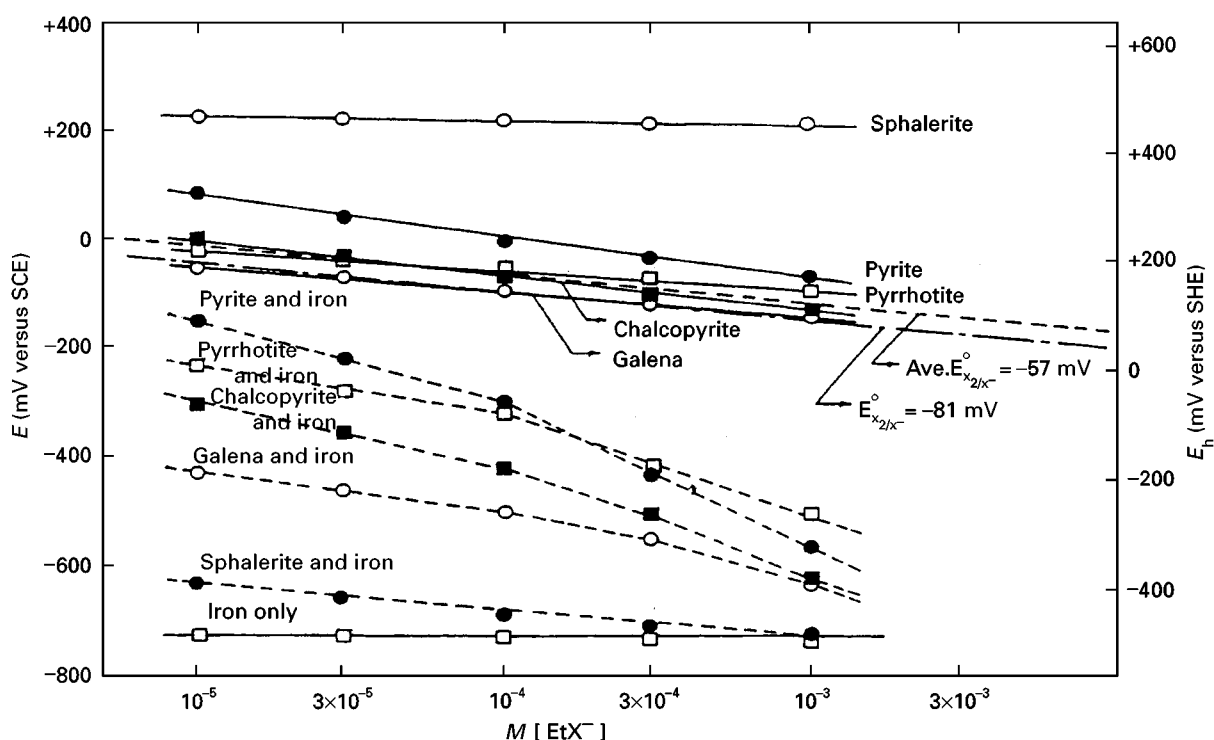
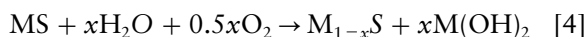


Figure 4 Mixed potentials of sulfide minerals alone and in contact with metallic iron as a function of xanthate concentration. Nonoxidizing conditions, argon purging – 400 cc min⁻¹ natural pH, 25°C. (Reproduced with permission from Rao, Moon and Leja (1976) *Flotation*, A.M. Gaudin Memorial Vol. Copyright American Institute of Mining Metallurgical and Petroleum Engineers.)

anodic and cathodic sites do not directly interact to deposit potentially reaction stifling product on the anodic site.

The reaction products of galvanic interaction between mineral species can be distinguished on the basis of their location. Firstly, the reaction product may take the form of a surface modification of the mineral, e.g. a metal-deficient sulfide layer, supported and to a greater or lesser degree stabilized, by the underlying, unaltered phase. Secondly, the product may be chemically distinct from, and physically attached to, the original mineral particle. Examples of this are elemental sulfur and ferrous hydroxide coatings. Finally, the reaction product may detach and remove itself from the original mineral, like sulfate anions, copper cations, or ferric hydroxide particulates.

The anodic reaction of sulfides is presently thought to lead to the formation of metal-deficient, sulfur-rich surface species, by releasing an active metal ion which may form a metal hydroxide ($M(OH)_2$):



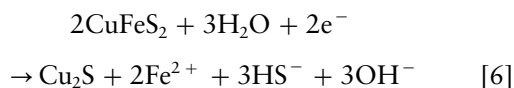
The formation of metal-deficient sulfide at the surface will tend to activate the surface and cause the metal hydroxy species to detach. However in the case of Fe^{2+} , species remain largely attached, leading to a blanketing effect that tends to hinder particle-bubble attachment. At suitable pH values, the release of reactive cations may lead to the unwanted activation of sulfide minerals, notoriously by copper ions.

As a general precaution against this reaction path, dissolved oxygen levels can be lowered. However, a lowering of pulp oxidative potential tends to lead to a general depression of flotation. An alternative is the elimination of metal-deficient sulfide species, or elemental sulfur, by reaction with aqueous sulfur dioxide:



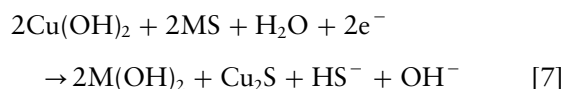
This is a possible mechanism for galena depression with sulfur dioxide in flotation, in addition to other mechanisms postulated, i.e. a lowering of copper ion activity in solution, xanthate decomposition and a lowering of the oxidative potential below that necessary for xanthate oxidation to dioxanthogen.

A reaction path for the cathodic reaction of chalcopyrite, at neutral pH values and in oxygen-starved pulps, was also proposed by Li and Iwasaki:

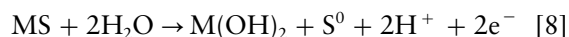


Activating Species

The release of activating species may be accelerated by galvanic interaction. Activation of sulfide species, raising their floatability above that which is achievable naturally, can occur due to an enhancement of the hydrophobicity of the mineral, or due to the insertion or attachment of ions which are more reactive towards collector reagents than the host species. In the latter case, the main, but not only, ion to consider is copper, which may attach itself to a particle as follows, by direct replacement:



The reaction path can be favoured by the presence of a suitable cathodic particulate mineral, like pyrite, reacting along the lines of the following equation:



The effect of galvanic coupling in a conducting particle will cause an electron flow, which will facilitate the simultaneous cathodic reduction of the MS surface by reaction with $Cu(OH)_2$, and the anodic oxidation of MS both reactions producing hydrophobic surface coverings of Cu_2S and S^0 , respectively.

Another example is the activation of pyrite by lead ions. In support of the assertion that true electrochemical interaction is limited to composite particles, Zhang *et al.* found, importantly, that interaction between composite particles containing pyrite and sphalerite was negligible in the absence of metal ions in solution. In their presence, sphalerite was found to successfully compete with pyrite for the activating ions, and through their action to compete more successfully for xanthate, thus depressing the floatability of pyrite. Competition for activating species thus seems to be an important factor in the interaction between minerals in flotation.

Depressing Species

The formation of hydrated, oxidized surface species like iron hydroxide and basic sulfates, increases particle hydrophilicity, and will thus depress flotation. High thiosulfate levels, which may arise when milling under relatively nonreducing conditions, e.g. fully autogenous grinding, or laboratory grinding in porcelain mills, may lead to the precipitation of insoluble thio-salts, which may also depress flotation. The generation of soluble sulfide species, especially notable in stagnant, anaerobic water reservoirs with bacterial action, may lead to mineral depression, since the

sulfide and xanthate ions compete for the same surface sites.

Froth Characteristics Affecting Species

The effect of froth structure on flotation is usually related to its stability. Stable froths have small bubbles and a high entrained water content. The solids in the entrained water are approximately at their concentrations in the pulp; consequently their overflowing concentrates will be of low grade. The presence or absence of fine, colloidal particles has a profound effect on flotation froth structure and drainage, and thus overall flotation performance. The most notable example of this is the deleterious effect that copious quantities of (naturally floatable) talc particles have on sulfide flotation, with adverse results in grade, recovery, and rates of recovery. The same froth modifying effects can be noticed when dealing with colloidal precipitates. In practice, the noticeable effects are largely limited to iron hydroxides, due to their abundance in natural systems. Thus, a change in froth structure may be noted when hydrated ferrous hydroxide particles are oxidized to (less hydrated) ferric oxide. The latter species allows a more desirable, less slimy, froth structure. As another example, it has been strongly suggested that the common practice of copper sulfate addition in flotation plants, apart from activating effects, also has strong froth structure modifying effects.

Application to Plant Practice

Collectorless Flotation

For collectorless flotation, the formation of a metal-deficient sulfide layer on the particle surface must generally be targeted. Formation of such a layer may be accelerated and spatially accentuated by galvanic interaction. When considering the flotation of sulfide minerals in the absence of collector reagents, in the context of electrochemical mineral interaction, three factors can induce floatability. First of all, floatability can be natural, i.e. due to the crystal structure and chemical bonding of a mineral. Examples of such minerals are molybdenite, stibnite, and the arsenic sulfides realgar and orpiment. Secondly, collectorless flotation can be self-induced, i.e. under the right pulp oxidative potentials, surface products will form which induce hydrophobicity. Examples of this are pyrrhotite and chalcopyrite. Rao and Finch found that pyrite/sphalerite selectivity could be enhanced by first recovering the pyrite which is naturally floatable, due to a chemically formed sulfur layer, in the absence of a collector. A third cause of floatability is mineral size. As minerals decrease in size, their

recovery into flotation froths increases due to entrainment, rather than selective attachment to froth bubbles. A good example of this is galena flotation from complex ores. At one mine site, carrying out sequential copper–lead–zinc flotation, about three-quarters of lead recovery into the copper concentrate was found to be made up of galena particles smaller than 10 μm . Since this effect is physical rather than chemical, it can only be significantly affected by a change in physical parameters, e.g. froth lamellae thickness and particle size.

In the collectorless flotation of pyrite–chalcopyrite–quartz mixtures, Johnson found a dependence of flotation behaviour on the pyrite/chalcopyrite surface area ratio, which would be consistent with electrochemical interaction. In this work it was however shown as well that copper solubilization was not enhanced in the presence of pyrite, but rather reduced; this points to copper deposition on pyrite – in other words, to activation rather than direct electrochemical interaction. Interestingly, interaction was reduced in the presence of quartz, due to adsorption of metal ions onto the quartz surfaces. In this respect, adsorption studies on other gangue minerals showed that such scavenging of potentially activating ions from solution may be substantial.

Pulp Oxidative Potential Control

Hayes and Ralston showed that the control of pulp oxidative potentials allows flotation selectivity, and is therefore a worthwhile approach in the flotation of complex sulfide ores, in addition to pH strategies. Direct electrochemical interactions between physically separated sulfide minerals, in which one affects the other's flotation behaviour directly through an anode–cathode relationship, have so far not been convincingly demonstrated on plant scale.

Galvanic and electrochemical interaction between sulfide minerals, and general chemical reactivity, is to a large degree dependent on the presence of oxygen in solution. The control of oxygen levels is thus generally the objective and result of pulp oxidative potential control. Since industrial flotation relies heavily on the use of ambient air, it has been proposed to regulate the oxygen concentrations entering flotation by admixture of nitrogen, or by partial re-circulation of process air released from the froth surface. The former approach is expensive whereas the latter depends on cells specifically designed to collect and re-circulate air leaving the top surface of the froth. Cylindrical cells seem to be most effective in this respect. The gas composition of bubbles generated by pressure differentials in flotation cells is dependent on a suite of factors, including the magnitude of

the pressure drop, dissolved substances, and nature of the nucleating surfaces. Benefits in flotation results were shown when regulating certain reagent additions on the basis of pulp oxidative potential, e.g. sulfuric acid, rather than pH. However, benefits might well be mostly due to froth structure improvements.

Trahar has shown that interactions between sulfide minerals were much decreased if they are ground separately, and only combined in the flotation cell. In this case, no mineral interaction between chalcopyrite, galena and sphalerite could be statistically proven. This demonstrates that galvanic interaction between sulfide minerals is only practically noticeable when mechanical contact exists. Grano *et al.* have also found that flotation selectivity between sulfide minerals is most sensitive to milling and preconditioning parameters, more so than to oxidative potentials during flotation itself, and mostly due to the presence of mild steel particles originating from equipment wear. For this reason, amongst others, research into comminution techniques which maximize mineral separation, whilst minimizing smearing, overgrinding, and steel consumption, must be a priority in the minerals industry. The effect of mild steel particles generated during ore comminution is mainly due to oxygen consumption, corrosion inhibitors being essentially ineffective. Full oxidation of these particles during conditioning removes their deleterious effect. Even for real ores containing significant quantities of more than one sulfide mineral, reasonable correlations exist between the behaviour of minerals in the ore and single minerals, as found by Grano *et al.* This indicates the limited extent of electrochemical mineral interactions in general practice.

Conclusion

True electrochemical interactions between sulfide minerals on industrial size plants are thought not to be of practical significance, except when physical contact between dissimilar sulfides exists (middlings), and/or at high pulp densities, high sulfide concentrations in the flotation feed, and high water conductivities. More importantly, sulfide minerals are found to interact through competitive adsorption of activating ions, the reduction of oxygen levels in the flotation pulp, and froth modifying activity of mineral oxidation products. Middlings particles, composed of two or more sulfides, do however experience electrochemical interaction, the result of which appears to be an enhancement of floatability, leading to a reduction in concentrate grades. The solution to such a problem is however more to be sought in comminution technology than electrochemical intercession.

Oxidative potential control offers advantages in industrial flotation separations, but its effect does not appear to be an interference with electrochemical mineral interactions.

Further Reading

- Allison SA, Goold LA, Nicol MJ and Granville A (1972) *Metallurgical Transactions* 3: 2613–2618.
- Buckley A and Woods R (1981) Investigation of the surface oxidation of sulfide minerals via ESCA and electrochemical techniques. Interfacial phenomena in mineral processing, Yasar B and Spottiswood DJ (eds) *Engineering Foundation* 3–17.
- Cheng X and Iwasaki I (1992) Pulp potential and its implications to sulfide flotation. *Mineral Processing and Extractive Metallurgy Review* 11: 187–210.
- Gardner JR and Woods R (1977) An electrochemical investigation of contact angle and of flotation in the presence of alkylxanthates. II. Galena and pyrite surfaces. *Australian Journal of Chemistry* 30: 981–991.
- Grano S, Ralston J and Smart RStC (1990) Influence of electrochemical environment on the flotation behaviour of Mt. Isa copper and lead-zinc ore. *International Journal of Mineral Processing* 30: 69–97.
- Hayes RA and Ralston J (1988) The collectorless flotation and separation of sulfide minerals by E_h control. *International Journal of Mineral Processing* 23: 55–84.
- Li X and Iwasaki I (1992) The effect of cathodic polarisation on the floatability of chalcopyrite in the absence of oxygen. *Minerals and Metallurgical Processing* 9: 1–6.
- Plaksin IN and Shafeev RSh (1963) Influence of surface properties of sulphide minerals on adsorption of flotation reagents. *Bulletin of the Institute of Minerals and Metallurgy* 680: 715–722.
- Rao SR and Finch JA (1987) Electrochemical studies on the flotation of sulphide minerals with special reference to pyrite-sphalerite – II. Flotation studies. *Canadian Metallurgical Quarterly* 26(3): 173–175.
- Rao SR, Moon KS and Leja J (1976) Effect of grinding media on the surface reactions and flotation of heavy metal sulphides. *Flotation*, A.M. Gaudin Memorial Vol. American Institute for Minerals Metals and Petroleum Engineering, pp. 509–527.
- Trahar WJ (1984) The influence of pulp potential in sulphide flotation. *Principles of Mineral Flotation*, The Wark Symposium. Australasian Institute of Mining and Metallurgy. Jones MH and Woodcock JT (eds), Parkville, Victoria, Australia (40): 117–135.
- Woods R, Young CA and Yoon RH (1990) Ethyl xanthate chemisorption isotherms and Eh-pH diagrams for the copper/water/xanthate and chalcocite/water/xanthate systems. *International Journal of Mineral Processing* 30: 17–33.
- Zhang Q, Xu Z, Bozkurt V and Finch JA (1997) Pyrite flotation in the presence of metal ions and sphalerite. *International Journal of Mineral Processing* 52: 187–201.

Flotation Cell Design: Application of Fundamental Principles

B. K. Gorain, J. P. Franzidis and E. V. Manlapig,
Julius Kruttschnitt Mineral Research Centre,
Indooroopilly, Queensland, Australia

Copyright © 2000 Academic Press

Introduction

The froth flotation process is commonly employed for the selective separation of a mineral species from a liquid–solid suspension of both valuable and unwanted gangue mineral particles. The valuable mineral species (which needs to be separated) is rendered hydrophobic by controlling its surface chemistry to provide the potential conditions for the attachment of the particles to air bubbles. The bubbles and particles are made to interact with each other inside a flotation machine. The flotation machine, depending on its operating conditions, provides an environment for the bubble–particle attachment and permits levitation of bubble–particle aggregates to the froth. The manner in which bubbles and particles interact with each other depends on the cell operating conditions and the type of flotation machine used.

Flotation machines, in general, may be categorized into four different classes: (i) mechanical or conventional cells; (ii) energy-intensive pneumatic cells; (iii) column cells; and (iv) froth separators. Of these, mechanical flotation cells have dominated the mineral industry since the early days of flotation and account for a significant amount of minerals processed. The aim of this article is to describe the operation and design of mechanical flotation cells.

Cell Operation

A mechanical flotation cell essentially consists of a vessel or a tank fitted with an impeller or rotor. The impeller agitates the slurry to keep particles in suspension, disperses air into fine bubbles and provides an environment in the cell tank for interaction of bubbles and hydrophobic particles and their subsequent attachment and therefore separation of valuable mineral particles from the undesired gangue mineral particles. The bubble–particle aggregates move up in the cell by buoyancy and are removed from the cell lip into an inclined drainage box called a launder (Figure 1). The launder product is commonly known as concentrate. The particles that do not attach to the bubbles are discharged out from the

bottom of the cell tank to the discharge or tailings box (Figure 1).

Hydrodynamic Zones

A mechanical flotation cell necessitates generation of three distinct hydrodynamic zones for effective flotation. The region close to the impeller encompasses the turbulent region necessary for solids suspension, dispersion of gas into bubbles and bubble–particle interaction for collection of minerals on the surface of the bubbles. Above the turbulent region lies the quiescent zone where the

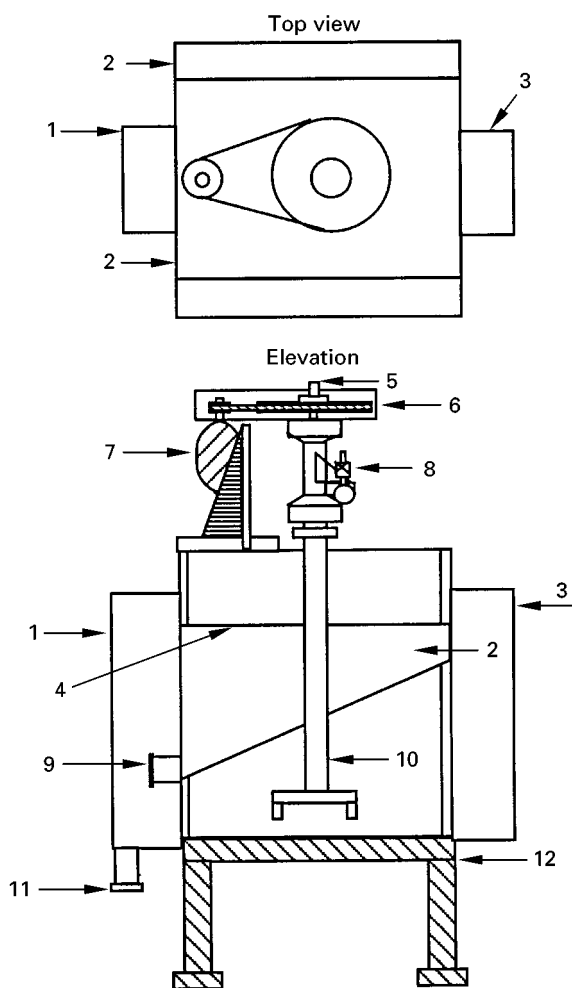


Figure 1 Schematic diagram of a mechanical flotation cell. 1, Discharge box; 2, concentrate launders; 3, feed box; 4, cell lip; 5, bearing shaft; 6, drive pulley with guard; 7, three-phase induction motor; 8, air inlet pipe with control valve; 9, concentrate launder discharge point; 10, impeller shaft; 11, tailings discharge point; 12, base support for the cell tank.

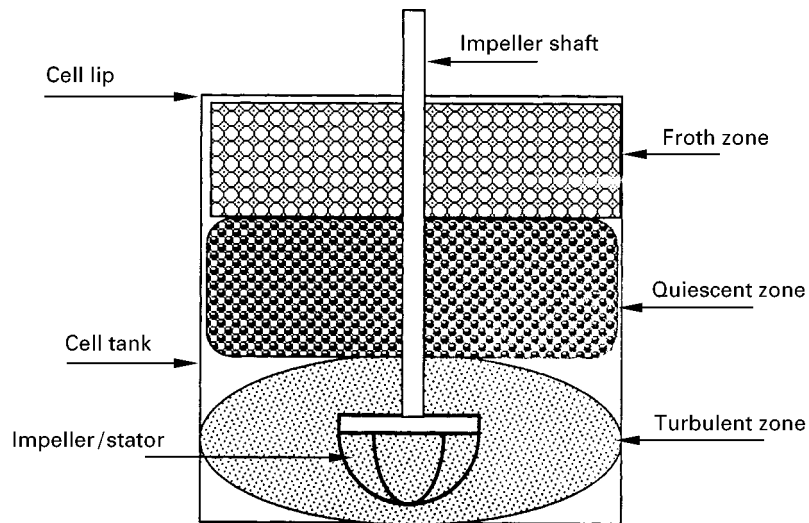


Figure 2 Hydrodynamic zones in a mechanical flotation cell.

bubble-particle aggregates rise up in a relatively less turbulent region. This region also helps in reducing the number of gangue minerals which may have been entrained mechanically or entrapped between bubbles for upgrading of valuable minerals. The region above the quiescent zone is the froth zone that serves as an additional cleaning step and improves the grade of the concentrate product. The three hydrodynamic zones in mechanical flotation cells are depicted in Figure 2.

The conflicting functional requirements in different zones in a mechanical flotation cell are a challenge in terms of the cell design and a fine balance of hydrodynamic conditions is necessary for the optimum recovery of valuable minerals in a cell.

Gas Dispersion

One of the most important hydrodynamic conditions in a mechanical flotation cell is dispersion of gas into fine bubbles. The bubble generation mechanism in

a mechanical cell is a two-stage process. Firstly, air cavities are formed at the trailing edge of the impeller blades, which is the low pressure region. Thereafter, bubbles form by shedding of vortices from the tail of the cavity, as shown in Figure 3.

The dispersion of air into bubbles can be characterized by three properties: bubble size, gas hold-up and superficial gas velocity. Mean bubble size in industrial mechanical cells varies, in general, from 0.5 to 2 mm; gas hold-up varies from 5 to 15% and superficial gas velocity varies from 0.6 to 1.5 cm s⁻¹, depending on cell operating conditions (impeller speeds and air rates) and the cell duty in plant operation – roughers, scavenging, cleaners, etc. Recent studies have shown that bubble size, gas hold-up and superficial gas velocity cannot describe the gas dispersion in a mechanical cell adequately when taken individually; but when taken together the gas dispersion properties determine the bubble surface area flux S_b in the cell, which has been shown to characterize gas dispersion very well. Typical S_b values in industrial cells vary from 30 to 60 s⁻¹. The concept of S_b has been found to be useful in metallurgical scale-up and cell optimization, design and selection.

Mode of Air Entry

In mechanical cells there are two modes by which air is introduced into the cells; one is the forced air entry mode carried out using a blower and the other is the self-induced air entry mode, in which air is sucked into the cell by vortexing. The two cell designs can be distinguished by the difference in vertical location of the impeller in the cell. In the forced air-type machine, the impeller is located close to the cell bottom with a deeper impeller submergence, and an external air blower is used to supply air under pres-

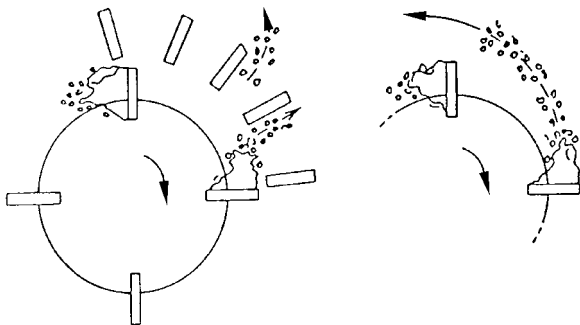


Figure 3 Schematic diagram of formation of bubbles in mechanical cells (after Grainger Allen, 1970; courtesy of Transactions of the Institute of Metallurgy, UK).

sure through the hollow shaft to the impeller region. Self-induced air machines utilize a standpipe which shrouds the drive shaft which is solid. The impeller is located almost in the midpoint of the cell which draws air through the space between the standpipe and the solid shaft.

Flow Patterns

The impeller in a mechanical flotation cell, during rotation, generates a vortex at the bottom of its blades drawing slurry from its lower section and discharging out from its upper section of the blades. Air is introduced through the impeller shaft or in the spacing between the shaft and a standpipe depending on whether the cell is forced air type or self-induced type, as described above. The dispersed air bubbles come in contact with the slurry close to the impeller discharge point. The aerated slurry flow then leaves the impeller mechanism for the surrounding tank volume. The impeller, therefore, acts as a pump drawing in slurry from below and expelling the aerated slurry to the cell volume. A typical flow pattern of a mechanical cell is shown in Figure 4.

Cell Design

The essential components of a mechanical flotation cell are described below.

Cell Tank

The profile of a cell tank is rectangular with truncated corners, U-shaped, conical or cylindrical, depending on cell type and size. Typically, mechanical cells are designed with a rectangular tank bottom for cells with volume up to 3 m³ and a U-shaped bottom for cells with volume up to about 38–45 m³. Cells larger than 38–45 m³ are typically cylindrical with either a conical or a flat bottom. Figure 5 shows a schematic of different tank designs.

In a typical plant, the mechanical cell tanks are arranged in a series called a bank. The number of cells in a bank varies depending on cell size, application and plant circuit configuration. The tailings from the first cell move on as the feed to the second cell and so on and the tailings from the last cell form the final tailings of the bank. The concentrates from different cells are combined in different ways depending on the requirements of the circuit. For example, in a cleaner bank, the concentrates from the first two cells may be combined to form the final concentrate products, whereas the concentrate product from the rest of the cells may be combined and recirculated to the feed of the cleaner bank.

Feed Box and Discharge Box

Each bank in a flotation circuit (which could also be an individual cell) is usually fitted with a feed box

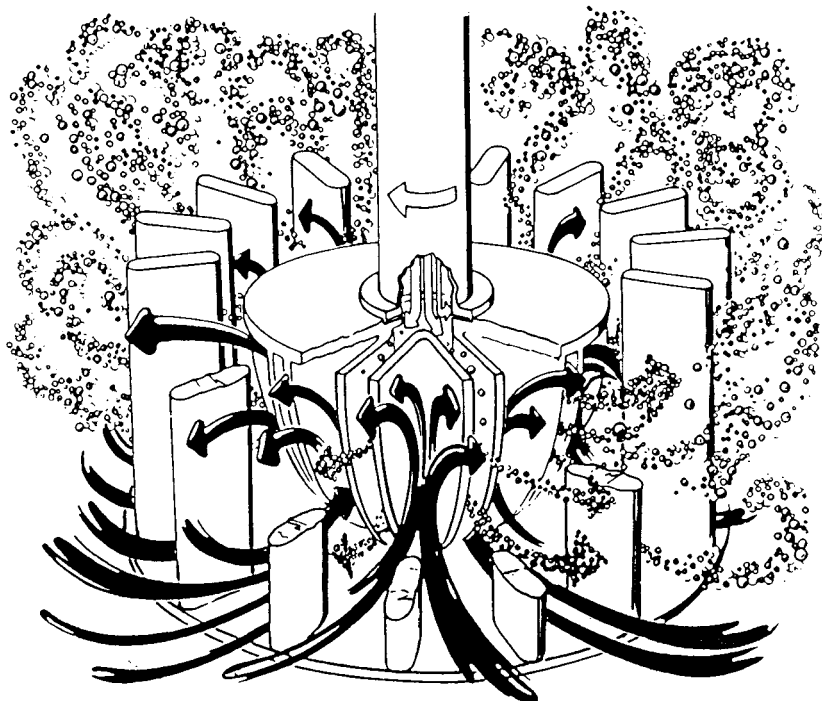


Figure 4 Typical flow patterns in a mechanical flotation cell (courtesy of Outokumpu Mintec Oy, Finland).

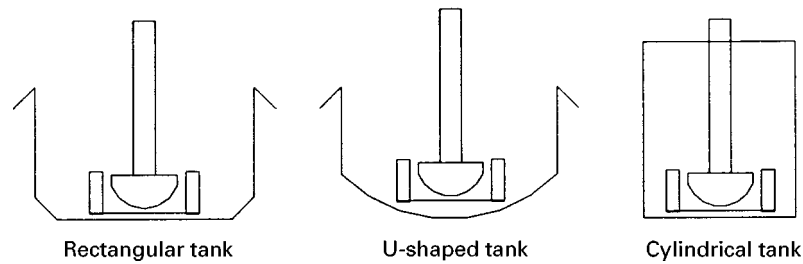


Figure 5 Typical tank designs in mechanical flotation cells.

with a rectangular opening at the bottom of the box to allow entry of slurry into the cell bank for flotation. The feed box is rectangular or half-cylindrical in shape depending on cell type and size. A tailings box or discharge box is also fitted at the end of the bank (or on the opposite side of feed box in an individual cell) to allow discharge of tailings. The discharge box is also rectangular or half-cylindrical in shape. **Figure 6** shows a typical arrangement of a feed and a discharge box in mechanical flotation cells. For some cell types and sizes, a dart valve or overflow weir are fitted in the discharge box to control pulp level in the cell tank. For other designs, a discharge box is not used and a pinch valve is fitted to the tailings outlet pipeline instead for pulp level control.

Cell Launderers

Launderers in flotation cells are located outside the overflow lip to collect and transport the froth or concentrate product out of the cell tank. Launderers are typically located on the top of the cell tank, as shown in **Figure 1**. Launderers are designed with a slope of about 10–15° for smooth transportation of froth without blockage in the launderers.

The design of launderers varies with cell size and type. The launderers are located on opposite sides adjacent to the feed and discharge boxes in rectangular cell tank designs, as shown in **Figure 1**. Launderers on three sides are also common in rectangular cells ar-

ranged in series. Large cylindrical cells have concentric launderers which can be either internal or external or both, depending on the capacity of launder necessary for froth removal.

Impellers or Rotors

The impeller or agitator, also referred to as the rotor, is considered to be the heart of a mechanical flotation cell as it provides the energy to perform the following functions necessary for the flotation process:

1. Suspension of solids in the cell tank.
2. Dispersion of air into bubbles.
3. Creation of microturbulence for effective bubble-particle collision.
4. Suction of air into the cell in self-induced type cells.

The design of an impeller varies with cell type. Most impeller designs have a flat circular disc with different shapes of blades or fingers fitted to the disc concentrically to the lower section of the disc. The shape of the blades or fingers varies from cylindrical to tapered (half-spherical). The half-spherical impeller design is more popular in the new design of cells and details of this design will be discussed later in this article. The top section of the disc connects to a drive shaft which in turn connects to the pulley/gear-motor drive assembly. The impeller is located in the centre of the cell cross-section with its

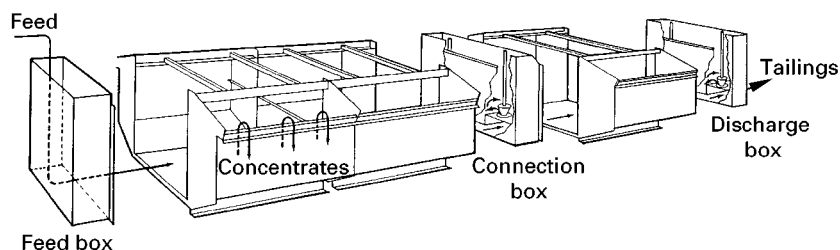


Figure 6 Schematic of a mechanical cell showing feed box and discharge box and concentrate launderers.

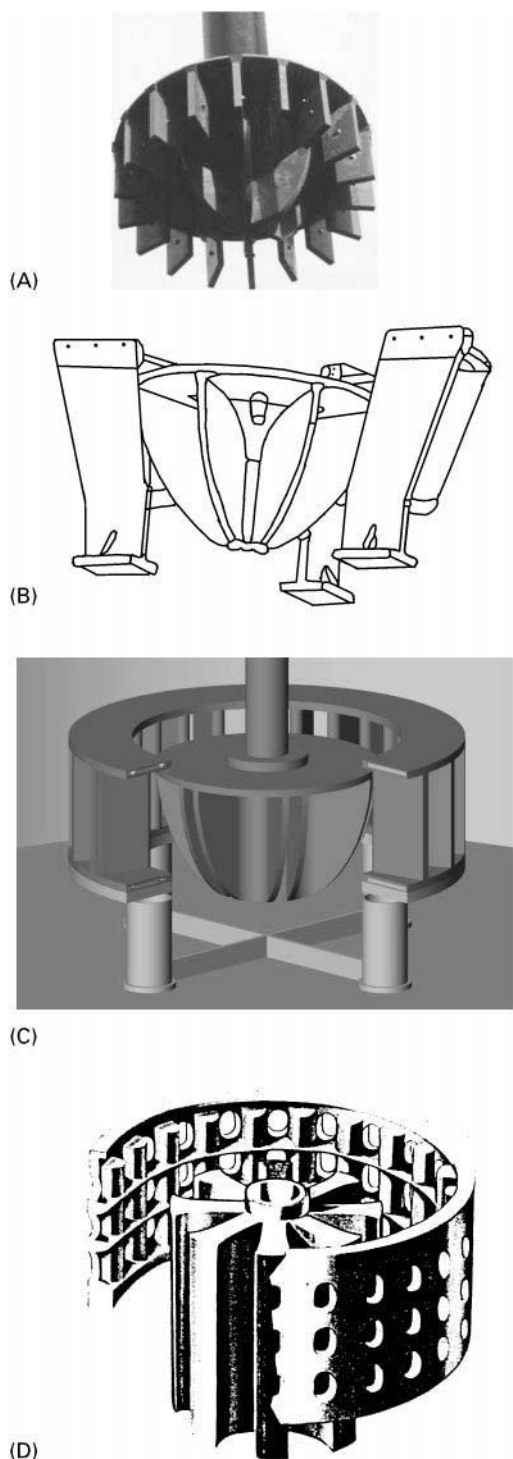


Figure 7 Shapes of different impellers and stators. (A) Bateman; (B) Dorr-Oliver; (C) Outokumpu; (D) Wemco (courtesy of Bateman Process Equipment, Dorr-Oliver, Outokumpu Mintec Oy and Baker Process, respectively).

submergence varying with cell type and mode of air entry. **Figure 7** shows the shapes of different commercially available impellers.

Stators or Diffusers

A stator or diffuser is an important component of a mechanical flotation cell, which surrounds the impeller and acts as an internal baffle useful in reducing pulp vortex in the cell. The tangential flow of the agitated slurry (due to rotation of the impeller) is transformed to a radial direction for effective dispersion of gas and solids in the cell tank. This reduction in the vortex flow helps in maintaining a stable pulp–froth interface, essential for flotation.

A stator consists of a number of blades arranged in a concentric circle with gaps between the blades to facilitate movement of slurry in the cell tank. A stator is usually mounted on the bottom of the cell tank surrounding the impeller concentrically from its bottom. In some cell designs the stator is fitted to the standpipe such that the stator shrouds the impeller from the top and hangs with an open space at the bottom: this is commonly known as an overhung stator.

The impellers and diffusers are moulded and coated with rubber or polyurethane for abrasion resistance.

Impeller Drive Assembly

The impeller connected to the shaft (hollow or solid) is driven by a three-phase induction motor with the help of V-belts, pulleys or gear box. A typical drive arrangement in a mechanical cell is shown in **Figure 1**. The size of the drive and the motor pulleys determine the speed at which an impeller operates.

Cell Types and their Designs

Most of the industrial mechanical flotation cells in the early days (before the 1970s) were of the cell-to-cell type (tanks of different cells connected in a row) for small plants and multistage cleaner floats where the pumping action of the impellers permitted the transfer of intermediate flows without external pumps. With the emergence of large flotation cells, since the early 1980s, dictated by economic considerations, open flow cells (with slurry flowing openly through a series of cells in a bank) have become prominent.

In the 1980s many mechanical cell designs were prevalent around the world. The major ones are:

1. Agitair cells from Galigher company, USA.
2. Aker machines from Aker Trondelag, Norway.
3. BCS cells from Minemet Industrie, France.
4. Booth cells from Booth Company, USA.
5. Denver cells from Denver Equipment Limited, Joy Industrial Company, USA.

6. Krupp cells from Krupp Polysius AG, West Germany.
7. Maxwell cells from Technequip Ltd, Canada.
8. Mechanobre cells from Machineoexpert V/O, USSR.
9. OK cells from Outokumpu Oy, Finland.
10. Sala cells from Sala International AB, Sweden.
11. Wedag cells from KHD Humboldt Wedag from West Germany.
12. Wemco cells, Wemco division, Envirotech, USA.

Only a handful of these cell manufacturers have survived the competitive global market by improving their products or by mergers or by diversification. Manufacturers of Wemco and Outokumpu cells, through research and development, have consistently updated their technology to remain competitive. The recent Tankcells (designated as OK-TC) and Smart-cells from the manufacturers of Outokumpu and Wemco cells, respectively, are an example. Some new designs, such as the Bateman BQ and Svedala RCS cells, have emerged in the mid 1990s. The companies which manufactured Denver and Sala cells have been procured by Svedala and their cells are marketed by Svedala's Pumps and Process division. The Agitair cells are now marketed by Baker Process (previously known as EIMCO Process Equipment Company). KHD Humboldt Wedag have stopped manufacturing mechanical cells and now market a newly developed pneumatic cell known as Pneufloat.

Presently there are five major manufacturers of mechanical flotation cells. Details of the design features of different cells are described in the sections below.

Bateman Cell

The Bateman flotation mechanism was developed in 1993 and is presently marketed by the Bateman Process Equipment Limited. The BQR series of Bateman cells have a round tank design with cell sizes varying

Table 1 Bateman cell tank dimensions for different cell sizes (courtesy of Bateman Process Equipment, South Africa)

Model	Volume (m ³)	Height (m)	Depth (m)	Installed motor (kW)
BQR 50	5	2	2	NA
BQR 100	10	2.5	2.5	45
BQR 200	20	3.2	3	55
BQR 300	30	3.6	3.4	75
BQR 400	40	4	3.75	75
BQR 500	55	4.2	4.34	115
BQR 750	75	5.2	4.5	132
BQR 1000	100	5.5	4.95	132

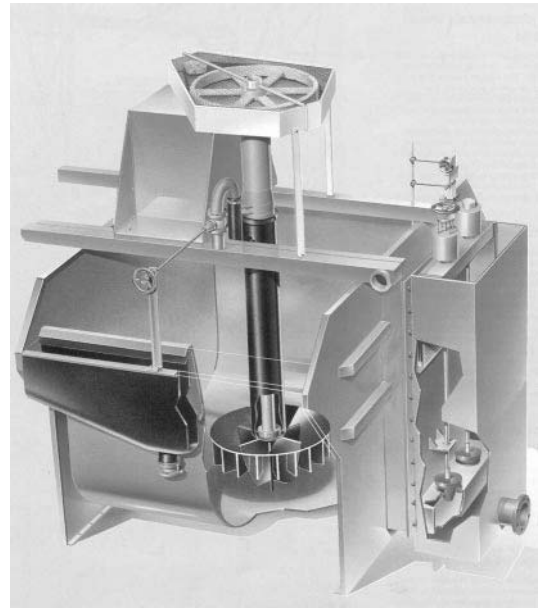


Figure 8 A schematic diagram of the Bateman flotation cell (courtesy of Bateman Process Equipment, South Africa).

from 5 m³ (BQR 50) to 100 m³ (BQR 1000). The tank dimensions of different cells of varying sizes are given in Table 1. The unit cell design Bateman cells are called HiFlo™ and HiClean™ machines.

The Bateman mechanism consists of a hemispherical-shaped impeller which is connected to a solid drive shaft. The impeller is designed with no disc on the top and the impeller blades have both the top and bottom opened. The drive shaft is shrouded with a stand pipe. The Bateman mechanism utilizes the forced air entry mode and air is supplied into the mechanism through the gap between the standpipe and the shaft. The mechanism utilizes an overhung-type stator (or diffuser) connected to the bottom of the standpipe, which is a horizontal hood with baffle plates projecting downwards (Figure 8).

Dorr-Oliver Cells

The Door-Oliver cell is marketed by Dorr-Oliver, a global corporation and member of the Krauss-Maffei Group.

The Dorr-Oliver Company Limited manufacturers flotation cells in a wide range of sizes. Cells with a volume of 0.03 m³ (DO 1) to 2.8 m³ (DO-100) have a flat-bottom tank design. Cells with volumes from 4.2 to 44 m³ come with a U-shaped tank bottom. Cells with volumes from 50 to 150 m³ are available with a round tank with a conical bottom. Details of tank dimensions for the Dorr-Oliver cells are given in Table 2.

Table 2 Dorr-Oliver cell tank dimensions for different cell sizes (taken from Dorr-Oliver flotation cell brochure; courtesy of Dorr-Oliver, Australia)

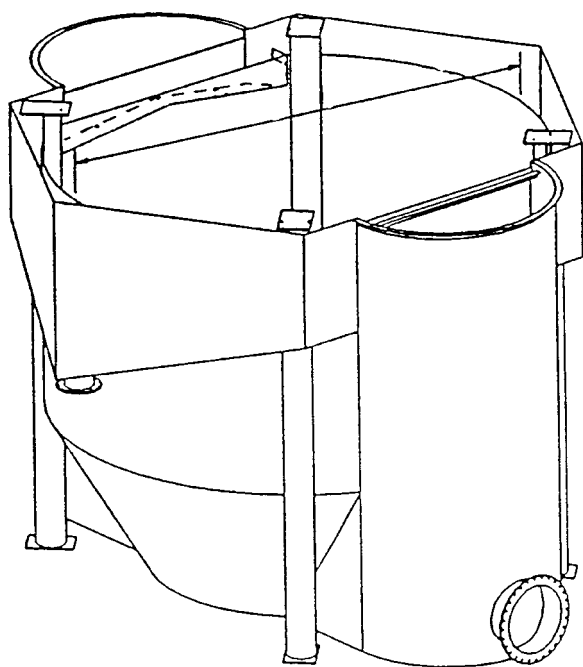
<i>DO conventional cells</i>					
<i>Model</i>	<i>Volume (m³)</i>	<i>Length (m)</i>	<i>Width (m)</i>	<i>Height (m)</i>	<i>Installed motor (kW)</i>
DO 1.0	0.03	0.3	0.3	0.33	0.55
DO 3.5	0.1	0.45	0.45	0.5	0.55
DO 10	0.3	0.65	0.65	0.66	1.1
DO 25	0.7	0.9	0.9	0.86	2.2
DO 50	1.4	1.2	1.2	0.97	4.0
DO 100	2.8	1.52	1.52	1.22	5.5
DO 150	4.2	1.83	1.83	1.53	7.5
DO 300C	8.5	2.29	2.29	1.88	7.5
DO 300	8.5	2.29	2.29	1.88	11.0
DO 500C	14	2.69	2.69	2.46	15
DO 600	17	2.95	2.69	2.46	22
DO 1000	28	3.35	3.35	2.89	30
DO 1350	38	3.81	3.58	3.22	37
DO 1550	44	3.96	3.96	3.22	45

<i>Tank design</i>				
<i>Model</i>	<i>Volume (m³)</i>	<i>Height (m)</i>	<i>Diameter (m)</i>	<i>Installed motor (kW)</i>
DO 1750	50	3.86	4.32	56
DO 3500	100	5.49	4.65	93
DO 5300	150	6.71	4.72	131

The Dorr-Oliver mechanism consists of a hemispherical-shaped impeller fitted to a hollow shaft. The mechanism utilizes the forced air entry mode in which air is introduced to the impeller through the hollow

shaft. The stators for the Dorr-Oliver cells are generally mounted on the bottom but the large cells mechanisms are designed with an overhung stator.

Figure 9 shows a schematic diagram of a large Dorr-Oliver cell with a tank design.

**Figure 9** Schematic diagram of a large Dorr-Oliver cell (courtesy of Dorr-Oliver, Sydney, Australia).

Outokumpu Cells

Outokumpu Mintec, a Finnish company which belongs to the Outokumpu Group, operates internationally and has been the manufacturer of the Outokumpu flotation cell for the last 30 years.

Outokumpu produces different flotation machines which can be categorized as:

1. OK conventional flotation machines: for rougher, scavenger and cleaner flotation.
2. OK-TC (TankCell) flotation machines: for rougher and scavenger flotation.
3. SK flotation machines: for Skim-Air Flash flotation in the grinding circuit.
4. HG flotation machines: for cleaner flotation.

The OK conventional flotation cells are available in volumes up to 38 m³. Conventional cells have a rectangular tank design for cell volumes up to 3 m³; above 3 m³ and up to 38 m³ the cells have a U-shaped tank. TankCell designs are available from a volume of 5 m³ to a volume of 160 m³ and are essentially a cylindrical

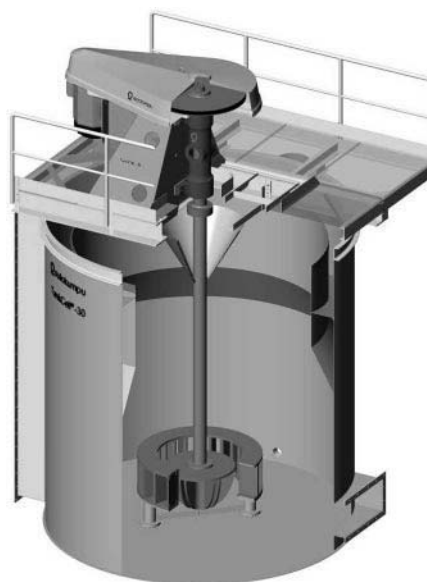


Figure 10 A schematic diagram of Outokumpu TankCell (courtesy of Outokumpu Mintec Oy, Finland).

cell with a flat bottom (Figure 10). The tank dimensions of different cells are given in Table 3.

The OK impeller mechanism is designed with a hemispherical-shaped impeller consisting of a

horizontal disc on the top which is attached to a number of narrow vertical slots tapered downwards. The impeller has separate slots for air and slurry movement. The mechanism has a forced air type entry mode in which air is brought into the impeller through a hollow shaft.

The stator in the OK mechanism is mounted on the bottom of the tank. There are two stator designs used in an Outokumpu cell: one is known as the multi-mix or conventional stator and the other is known as free-flow. The multi-mix stator is typically used for fine particle flotation, whereas the free flow stator is typically used for coarse particle flotation.

Svedala Cells

The former manufacturers of Denver flotation cells (Denver Equipment, USA) and Sala cells (Sala International in Sweden) have merged together to form the Svedala Pumps and Process Division, which is part of the worldwide Svedala Industri group. Both Denver and Sala cells are available through Svedala companies located worldwide.

The Svedala flotation cells include mechanical flotation cells in the AS range (previously known as Sala cells), in sizes from 0.03 to 16 m³; the DR range

Table 3 Outokumpu cell tank dimensions for different cell sizes (taken from Outokumpu flotation cell brochure; courtesy of Outokumpu Mintec Oy, Finland)

OK conventional cells					
Model	Volume (m³)	Length (m)	Width (m)	Height (m)	Motor installed (kW)
OK-0.5-R	0.5	NA	NA	0.84	2.75–3.75
OK-1.5-R	1.5	NA	NA	1.08	5.5–7.5
OK-3-R	3	1.52	1.52	1.21	7.5–11
OK-8-U	8	2.29	2.29	1.88	15–22
OK-16-U	16	2.95	2.69	2.46	30–45
OK-38-U	38	3.49	3.59	3.23	55–75
Model	Volume (m³)	Height (m)	Diameter (m)	Motor installed (kW)	
Tank Cells					
OK-5-TC	5	2.45	2.2	7.5	
OK-10-TC	10	2.85	2.7	15	
OK-20-TC	20	3.45	3.3	37	
OK-30-TC	30	3.9	3.9	45	
OK-40-TC	40	4.3	4.1	45	
OK-50-TC	50	4.6	4.6	75	
OK-70-TC	70	5	5	90	
OK-100-TC	100	5.3	5.6	110	
OK-130-TC	130	5.4	6.3	132	
Extra Hard Duty					
OK-100-TC-XHD	100	4.6	6.3	90	
OK-130-TC-XHD	130	4.8	6.7	110	
OK-160-TC-XHD	160	5.1	7.1	132	

Table 4 Svedala cell tank dimensions for different cell sizes (taken from Svedala flotation brochure; courtesy of Svedala, UK)

Model	Volume (m ³)	Height (m)	Diameter (m)	Installed motor (kW)
RCS 5	5	1.9	2	15
RCS 10	10	2.4	2.6	22
RCS 15	15	2.5	3	30
RCS 20	20	3	3.25	37
RCS 30	30	3.4	3.7	45
RCS 40	40	3.8	4.1	55
RCS 50	50	4.1	4.5	75
RCS 70	70	4.6	5	90
RCS 100	100	5.2	5.6	110
RCS 130	130	5.6	6.1	132
RCS 160	160	6.1	6.5	160
RCS 200	200	6.5	7	200

(previously known as Denver cells), in sizes from 0.09 to 42.5 m³; and cell-to cell machines in sizes from 0.08 to 14.2 m³.

In 1995 Svedala developed a new design of flotation cell known as the RCS Flotation machine which comes in sizes from 5 to 200 m³. The tank dimensions of different cells sizes are shown in Table 4.

The RCS Flotation machine utilizes a new DV (deep vane) mechanism. The DV mechanism consists of vertical rectangular blades or vanes tapered at the

bottom. The blades are connected to a circular horizontal disc located just above the centre of the blades. The mechanism is designed with an overhung stator with vertical vanes projecting downwards connected to the mechanism standpipe. Depending on cell application, the DV mechanism can be modified in two different ways to suit the application. The design of the mechanism which allows entry of air through a hollow drive shaft is known as the DVH mechanism (deep vane and hollow shaft), whereas the design which allows entry of air through a concentric standpipe is known as the DVS mechanism (deep vane and solid shaft).

Figure 11 shows a schematic of the Svedala RCS flotation cell, showing the DV mechanism and the cell tank design.

Wemco Cells

Wemco flotation cells are manufactured by Baker Process, which also makes Agitair cells and pyramid column cells.

There are two major Wemco designs, the Wemco 1 + 1 design and new SmartCell design (Figure 12). The 1 + 1 design comes in cell sizes from 0.57 to 85 m³. The SmartCell design comes in sizes from 8.5 to 160 m³. The Wemco 1 + 1 cell utilizes the self-induced air entry mode and consists of a rotor,

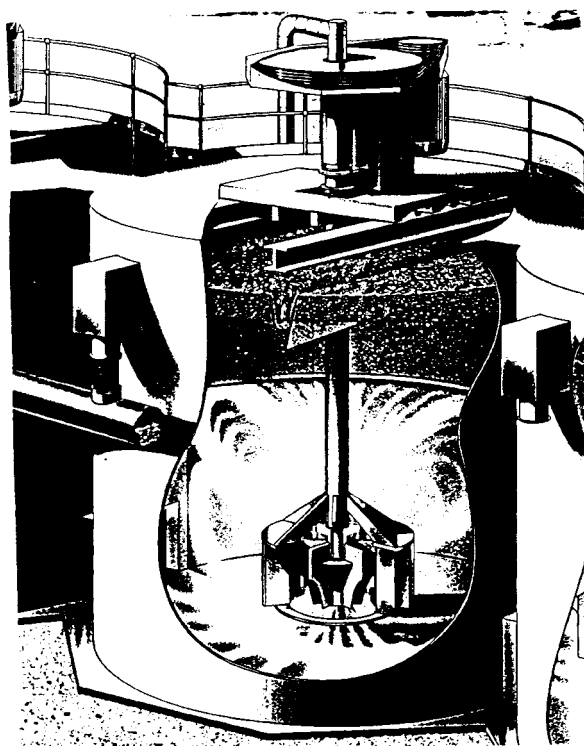
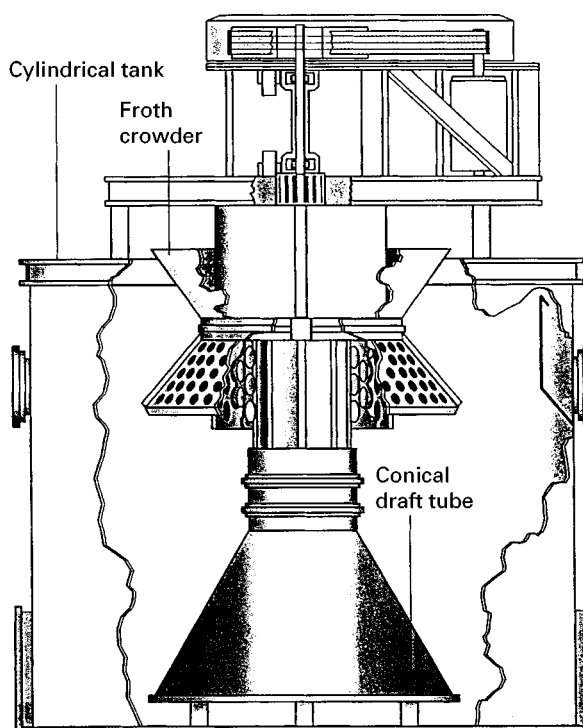
**Figure 11** A schematic diagram of Svedala RCS cell (courtesy of Svedala, UK).**Figure 12** A schematic diagram of Wemco SmartCell (courtesy of Baker Process, USA).

Table 5 Wemco cell tank dimensions for different cell sizes (taken from Wemco flotation cell brochure; courtesy of Baker Process, USA)

<i>Wemco 1 + 1</i>					
<i>Model</i>	<i>Volume (m³)</i>	<i>Length (m)</i>	<i>Width (m)</i>	<i>Height (m)</i>	<i>Installed motor (kW)</i>
44	0.57	1.12	1.12	0.57	3.75
56	1.1	1.42	1.42	1.1	5.5
66	1.7	1.52	1.68	1.7	7.5
66D	2.8	1.52	1.68	2.8	11
84	4.2	1.6	2.13	4.2	22
120	8.5	2.29	3.05	8.5	30
144	14.2	2.74	3.66	14.2	45/55
164	28.3	3.02	4.17	28.3	
190	42.5				
225	85				
<i>Wemco SmartCells</i>					
<i>Model</i>	<i>Volume (m³)</i>	<i>Height (m)</i>	<i>Diameter (m)</i>	<i>Installed motor (kW)</i>	
300	8.5	1.6	2.59	30	
500	14	2.44	2.84	30	
750	21	2.57	3.45	40	
1500	42.5	2.82	4.32	75	
2500	71	3.66	5.31	100	
4500	127	4.65	6.2	200	
5650	160	4.88	6.83	1.14	
<i>Wemco Agitairs</i>					
	<i>Volume (m³)</i>	<i>Length (m)</i>	<i>Width (m)</i>	<i>Height (m)</i>	<i>Installed motor (kW)</i>
	1.13	1.22	1.22	0.76	
	1.7	1.52	1.52	0.76	
	2.83	1.52	1.52	1.19	
	4.25	1.6	2.13	1.35	
	8.5	2.29	3.05	1.35	18.5
	14.15	2.74	3.66	1.6	30
	28.3	3.05	4.17	2.36	45

dispenser, standpipe and a hood. The larger cells are designed with a false bottom and draught tube. The SmartCell flotation machine utilizes the Wemco 1 + 1 aeration mechanism which is reconfigured and embedded with an expert control system. The dimensions of different Wemco cells are shown in Table 5.

The air and pulp circulation in the Wemco cells are determined by the rotor size, speed and submergence in the pulp. Liquid circulation and air transfer are a function of rotor speed, size and submergence.

Present and Future Trends

Traditionally, flotation machine design closely follows the trend of comminution machines in mineral-processing plants. Due to economic considerations in

the processing of low grade ores, the present comminution machines such as crushers, semi-autogenous, autogenous and ball mills are designed for very high capacities. The Cadia Hill Mine in New South Wales, Australia, which treats a copper-gold ore at the rate of 2100 tonnes per hour, utilizes a 12 m diameter SAG mill (with a 20 MW motor) and two 6.5 × 11 m ball mills (each with a 8.75 MW motor). To be compatible with the comminution circuit, large capacity 150 m³ flotation cells are used in the rougher circuit.

At present, cells as large as 300 m³ are being designed by various manufacturers. Installation of large cells has many advantages:

1. reduction in capital costs;
2. reduced size of plants;
3. reduced power consumption;
4. reduced maintenance;

5. easy control;
6. reduced reagent consumption.

However, with increase in cell size, the problem of machine design and metallurgical scale-up becomes more acute. The scale-up features that may have been tolerated on smaller cells are not applicable to larger cells. The simple similitude considerations used in terms of dimensionless numbers (power number, Froude number, air flow number, Reynolds number) are not sufficient to design large machines. The development and evaluation costs rapidly increase with cell size, which calls for a more rational and fundamental basis in cell design. Extensive research at the Julius Kruttschnitt Mineral Research Centre in Brisbane has shown that bubble surface area flux or S_b is an important criterion for metallurgical scale-up, which will gain more prominence in the future and will be considered as a parameter in conjunction with other important dimensionless numbers used in machine design and scale-up.

An increase in cell sizes also requires more effective froth transportation due to the increase in travel time of bubble-particle aggregates which results in high drop-back and low froth recovery. To address the problem of froth transportation and stability in large cells, new design features such as internal launders, double launders, high capacity launders, booster cones, froth crowders, cross-launders and beehive launders are emerging. More work will be carried out by cell manufacturers and researchers to understand froth transportation and froth recovery. The effect of the interactions of different launder designs, froth crowders and cell-operating parameters such as impeller speed, air rate and froth depth will be the subject of further investigation for better cell design and optimization of cell operation.

The design differences of various cells marketed by different manufacturers are in fact differences in impeller/stator mechanisms and air input systems (either self-induced or forced air type through a standpipe with a solid shaft or through a hollow shaft). However, the design of tanks is similar for different cell types, and resembles the cylindrical design of the old Maxwell cells. The launder and froth crowding devices in different designs are tailor-made to suit different applications.

The large new flotation cells are equipped with integrated control systems. The recent trend of installation of a few large cells in a circuit will see more control instrumentation like air flow control, variable speed drive for speed control, as well as online

measurement equipment for monitoring bubble size, superficial gas velocity, gas hold-up and bubble surface area flux, which will be used for better cell performance optimization. Froth vision equipment will also gain prominence for better control of froth in the large flotation cells.

The development of flotation cells will continue as more and more fine particle processing will be necessary in future. The large flotation machines will have to be designed to generate very small bubbles and a high degree of microturbulence for effective bubble-particle collision to remain competitive against other novel technologies like high intensity pneumatic cells. Entrainment will be a major issue in concentrators, which will need refinement of froth-washing technologies in mechanical flotation cells.

Acknowledgements

The authors would like to thank the manufacturers of Bateman, Dorr-Oliver, Outokumpu, Svedala and Wemco cells for providing sale catalogues, pictures and other information regarding their flotation cells.

Further Reading

- Bezuidenhout G (1995) The Bateman flotation machine. *XIX International Mineral Processing Congress* 3: 231-236.
- Degner VR (1988) Flotation machine design. In: Klimpel RR and Luckie PT (eds) *Proceedings of Industrial Practice of Fine Coal Processing*, SME/AIME, ch. 16, pp. 135-146. Somerset, CA.
- Grainger Allen TJN (1970) Bubble generation in froth flotation machines. *Transactions of the Institute of Mining and Metallurgy* 79: C15-C22.
- Harris CC (1986) Flotation machine design, scale-up and performance: database. In: *Advances in Mineral Processing*, ch. 37, pp. 618-638. SME/AIME.
- Nitti T and Tarvainen M (1982) Experiences with large Outokumpu flotation machines. In: *XIV International Mineral Processing Congress*, pp. VI 7.1-7.12. Toronto, Canada.
- Schubert H (1985) On some aspects of the hydrodynamics of flotation process. In: Forssberg KSE (ed.) *Flotation of Sulphide Minerals*, pp. 337-355. Amsterdam: Elsevier.
- Smith EL, Prevett MJ and Lawrence GA (1982) An improved mechanism for large flotation cells. In: *XV International Mineral Processing Congress*, pp. VI 9.1-9.19.
- Young P (1982) Flotation machines. *Ming. Mag.* 146: 35-59.

Foam Fractionation

G. Narsimhan, Purdue University,
West Lafayette, IN, USA

Copyright © 2000 Academic Press

Introduction

Foam concentration/fractionation is a separation technique in which surface-active solutes are either concentrated from a dilute solution or separated from a mixture by preferential adsorption at a gas-liquid interface created by sparging an inert gas through the solution. These gas bubbles entrain the surfactant solution and form a stable foam with a large gas-liquid interfacial area. As the foam moves through the column, the surfactant solution tends to drain due to gravity and capillary forces. This results in a decrease in the amount of liquid in the foam. The reduction in the entrained liquid is first associated with the bubbles forming the closest spherical packing, after which they will deform to a dodecahedral shape and then possibly coalesce. Consequently, there is an increase in the gas-liquid interfacial area per unit volume of the liquid. The surfactant tends to adsorb preferentially at the gas-liquid interface. At the top of the column, the foam is sent to a foam breaker where the foam is broken either mechanically or chemically. This results in either enrichment or concentration of more surface-active protein because of the recovery of adsorbed protein from the gas-liquid interface into the bulk entrained liquid. In the case of a dilute solution of a single protein,

the extent of enrichment would depend upon the relative amount of adsorbed protein compared to that in the bulk entrained liquid. In the case of a mixture of proteins in solution, the separation of a protein from the mixture would depend upon the extent of preferential adsorption of that protein at the gas-liquid interface. Since the adsorption isotherm usually leads to a much higher proportion of adsorbed protein at very low bulk concentrations, foam concentration is very effective for extremely dilute solutions.

Because of the presence of hydrophilic and hydrophobic functional groups, proteins are surface active. Therefore, foam-based separations are viable for concentration/separation of protein solutions. Foam-based separation has been applied to various proteins and enzymes. Experimental investigation has been summarized in Table 1. This review highlights the theoretical aspects of prediction of enrichment and separation of proteins and enzymes in a foam fractionation column.

Different Modes of Operation of a Foam Column

Figure 1 depicts the different modes of operation of a foam fractionation column. The simplest mode is the production of a protein-rich concentrate phase from a dilute aqueous protein solution. This can be operated as semi-batch mode (Figure 1A), in which a pool of protein solution is maintained at the bottom

Table 1 Foam fractionation of proteins

<i>Proteins separated</i>	<i>Experimental set-up</i>	<i>Reference</i>
Choline esterase	Batch	Schultz, 1937; Bader <i>et al.</i> , 1944
Pepsin, rennin	Batch	Andrews and Schultz, 1945
Sodium cholate	Batch	Bader <i>et al.</i> , 1944
Apple proteins	Semi-batch	Davis <i>et al.</i> , 1949
Bovine serum albumin	Batch	Schnepf and Gaden, 1959
		Gehle and Schugerl, 1984
Bovine serum albumin	Continuous	Ahmad, 1975a,b
		Brown <i>et al.</i> , 1990
		Uraizee and Narsimhan, 1996
Potato proteins	Batch with recycle	Weijenberg <i>et al.</i> , 1978
Catalase, amylase	Batch	Charm <i>et al.</i> , 1966
Streptokinase	Batch	Holmstrom, 1968
Lysozyme, human serum albumin	Batch	Lalchev and Exerowa, 1981
Acid phosphatase	Batch	London and Hudson, 1953
Urease, catalase	Batch	London <i>et al.</i> , 1954
Bovine serum albumin-DNA, lysozyme-DNA	Batch	Lalchev <i>et al.</i> , 1982
Placental proteins	Continuous	Sarkar <i>et al.</i> , 1987

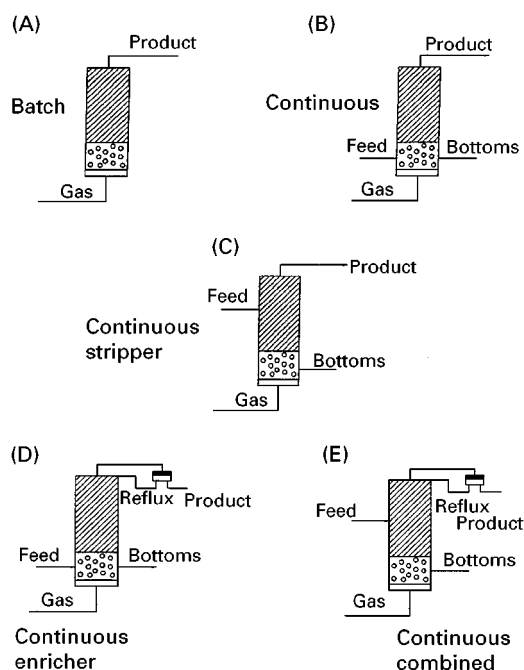


Figure 1 Different modes of operation of a foam fractionation column.

of a column and is sparged with an inert gas which forms the foam. The foam is continuously removed at the top of the column, sent to a foam breaker and the top product collected. Since the most surface-active protein is preferentially removed from the solution, the solution would progressively get depleted in that protein as time progresses. As a result, the pool would get enriched in other components in the case of mixtures. In continuous operation, a feed stream of protein solution is introduced into the pool and the bottom product withdrawn (Figure 1B). Sparging of gas bubbles mixes the liquid pool well enough so that the bottom product is at the same composition as the liquid pool. In addition, the continuous foam column can also be operated in stripping, enriching or combined modes. In the stripping mode, the object is to remove, almost completely, protein from a dilute solution. In this mode, the feed is introduced into the foam and trickles down countercurrently through the rising foam (Figure 1C). The protein concentration in the liquid below the feed-point falls with foam depth, due to it being adsorbed on to the rising bubble surface. There is a net upflow of solution through the foam maintained by entrained up-flowing liquid from the pool. If the foam column is deep enough the protein adsorbed on the bubble surface Γ_B will be in equilibrium with the feed liquid concentration c_F and the pool liquid concentration will be very low. Consequently, the bottom product is stripped of more protein than that in the simple mode of operation. In the

enriching mode (Figure 1D), the feed stream is introduced into the liquid pool and part of the top product that is obtained by collapsing the foam is refluxed into the column. Protein-rich reflux flows down countercurrently through the foam resulting in further enrichment of protein in the top product. In the combined mode (Figure 1E), the feed is introduced into the foam and the external reflux is used. Part of the column above the feed acts as an enricher, whereas the bottom part of the column acts as a stripper.

It is reasonable to assume that the residence time of the bubbles through the liquid pool is sufficiently large for protein adsorption to reach close to equilibrium so that the surface concentration of protein at the gas-liquid interface can be assumed to be close to the equilibrium value. Also, if bubble coalescence in the foam bed is negligible, the concentration of protein in the interstitial liquid can be expected to be the same as that in the liquid pool. For simple mode of operation of the foam column with a continuous feed stream consisting of a dilute protein solution, the top product concentration c_D , is related to the pool concentration c_B via:

$$c_D = c_B + \frac{6G\Gamma_B}{dD} \quad [1]$$

where G is the gas flow rate, D is the top product flow rate, d is the bubble size and Γ_B is the equilibrium surface concentration of protein at the gas-liquid interface corresponding to the pool concentration. In the above equation, the first term on the right-hand side is the contribution to the protein concentration from the bulk interstitial liquid before the foam is collapsed and the second term is the contribution from the adsorbed protein at the gas-liquid interface which is recovered into the bulk upon collapse of the foam. A mass balance around the column now gives the following equations for the top product concentration c_D and the bottom product concentration c_B respectively (Lemlich, 1968):

$$c_D = c_F + \frac{6G\Gamma_B}{d} \frac{B}{F(F-B)} \quad [2]$$

and:

$$c_B = c_F - \frac{6G\Gamma_B}{Fd} \quad [3]$$

where c_F is the feed concentration, c_B is the pool concentration, F is the feed flow rate, and B is the bottoms flow rate. In the case of binary mixture of

two proteins, the separation efficiency S , defined as the ratio of the two enrichments, is given by:

$$S = \frac{c_{D,2} c_{F,1}}{c_{F,2} c_{D,1}} = \frac{1 + \frac{6G\Gamma_2(c_{B,2})}{dc_{F,2}} \frac{B}{F(F-B)}}{1 + \frac{6G\Gamma_1(c_{B,1})}{dc_{F,1}} \frac{B}{F(F-B)}} \quad [4]$$

where the subscripts 1 and 2 refer to components 1 and 2 and $\Gamma_i (c_{B,i})$ is the equilibrium surface concentration of component i corresponding to the bulk concentration $c_{B,i}$. It can easily be seen that the separation ratio is greater than unity if component 2 is more surface active than 1. Also, in the above equation factor 6 arises because the area per unit volume of spherical bubbles of diameter d is $6/d$. If the dodecahedral shape of the bubbles in the foam is to be accounted for, factor 6 is to be replaced with 6.59. For a Langmuir adsorption isotherm, the surface concentration of proteins is related to the bulk concentration via:

$$\Gamma_i = \frac{K_i c_i}{1 + \sum_i K_i a_i c_i}, \quad i = 1, 2 \quad [5]$$

where K_i is the equilibrium constant, c_i is the bulk concentration and a_i is the area occupied by a protein molecule.

In the stripping mode, the feed stream is introduced into the foam (Figure 1C). For a long stripping column, the protein concentration of downflowing interstitial liquid will approach that of entrained liquid in the foam. The two concentrations will approach each other at the feed level. Therefore, the protein concentration of the interstitial liquid at the top can be taken to be the feed concentration. Therefore, mass balance around the foam column yields (Lemlich, 1968):

$$c_D = c_F + \frac{6.59G\Gamma_F}{d(F-B)} \quad [6]$$

and:

$$c_B = c_F - \frac{6.59G\Gamma_F}{Bd} \quad [7]$$

where Γ_F is the equilibrium surface concentration of the protein at the gas-liquid interface corresponding to the feed concentration. Since $\Gamma_F \geq \Gamma_B$, $B \leq F$, comparison of eqns [2] and [3] with eqns [6] and [7] indicates that the stripping mode yields a leaner bottom product and richer top product compared to the

simple mode of operation. The separation efficiency for a binary mixture is given by:

$$S = \frac{c_{D,2} c_{F,1}}{c_{F,2} c_{D,1}} = \frac{1 + \frac{6.59G\Gamma_2(c_{F,2})}{dc_{F,2}} \frac{1}{(F-B)}}{1 + \frac{6.59G\Gamma_1(c_{F,1})}{dc_{F,1}} \frac{1}{(F-B)}} \quad [8]$$

Analysis of Foam Column for the Prediction of Liquid Hold-up, Enrichment and Separation Factor

Various phenomena that take place in a foam column are shown schematically in Figure 2. Bubbles are formed by the sparger into the liquid pool. Proteins adsorb on to the bubbles during their formation and their passage through the liquid pool. The rate of adsorption of protein depends on the rate of diffusion of protein molecules to the gas-liquid interface as well as on the adsorption activation energy at the bubble surface. The extent of the surface coverage at the gas-liquid interface is dependent on the time of formation of the bubbles and its residence time in the liquid pool (Uraizee and Narsimhan, 1995). The foam bed consists of an assemblage of gas bubbles separated by thin liquid films, creating a large gas-liquid interfacial area. The size distribution of the bubbles depends on the type of sparger employed for bubble formation. A sintered disc with fine pores

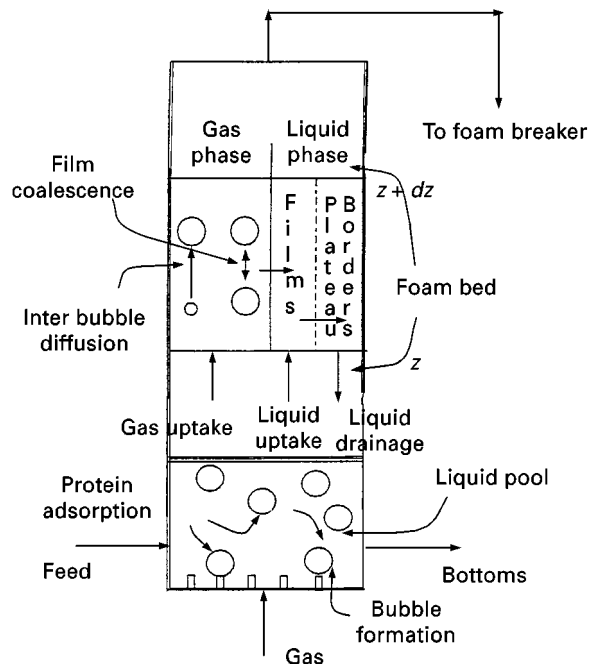


Figure 2 Schematic of various phenomena that take place in a foam column.

usually results in a wide distribution of bubble sizes whereas either capillaries or orifices of uniform sizes lead to more or less uniform bubble sizes. Since the volume fraction of liquid in a foam is usually very small, the gas bubbles are distorted and are usually approximated by a dodecahedron (Narsimhan and Ruckenstein, 1986). A typical gas bubble is shown in **Figure 3A**. The neighbouring gas bubbles are assumed to be separated by planar films of the continuous liquid phase. Where three bubbles touch, their films drain laterally into a Plateau border. This is a channel whose length is the length of a side of the touching dodecahedral bubbles, and whose walls have a sharp concave curvature of radius R_p (Figure 3B). This lateral flow is caused by a pressure drop ΔP between the liquid pressure in the film, which is essentially the air pressure in the bubble, and the pressure of the liquid in the Plateau border. If σ is the surface tension of the bubble-liquid interface, then:

$$\Delta P = \frac{\sigma}{R_p} \quad [9]$$

The liquid in the Plateau border drains under gravity. Consequently, the liquid hold-up decreases with foam height. The lateral flow out of the thin films separating the gas bubbles will cause them to thin further, possibly causing them to rupture because of instability resulting from the growth of thermal and mechanical perturbations thus leading to bubble coalescence. Coalescence leads to internal reflux of the liquid from the ruptured films into the Plateau borders and a decrease in the interfacial area because of an increase in the bubble size. The former tends to enhance separation (enrichment) whereas the latter is detrimental. The former effect is usually predominant, so that coalescence leads to higher separation (enrichment). Only when coalescence is excessive, collapse of the foam bed occurs. When there is a broad distribution of bubble sizes, diffusion of gas from smaller to larger bubbles may occur because of the difference in the capillary pressure (being

inversely proportional to bubble size) thus leading to the growth of larger bubbles at the expense of smaller ones.

In order to predict the liquid hold-up as a function of foam height, one needs to solve the balance equations for drainage of liquid from thin films into the Plateau borders. The equations describing the rate of change, with vertical position, of the volumetric hold-up of the liquid in the films, caused by their drainage into the Plateau borders and bubble coalescence is given by (Uraizee and Narsimhan, 1995):

$$-\frac{d}{dz}(\eta n_f A_f x_f) - N n_f A_f V - \frac{N}{2} n_f A_f x_f \beta = 0 \quad [10]$$

where x_f is the film thickness, n_f is the number of films per bubble, A_f is the area of the film, η is the number of bubbles entrained per unit cross-section of the foam, N is the number of bubbles per unit volume of the foam, and V is the velocity of drainage of the film and β is the coalescence frequency. η and N can be related to the superficial gas velocity G , liquid hold-up ε , and the bubble volume v through:

$$\eta = \frac{G}{v}, \quad N = \frac{1 - \varepsilon}{v} \quad [11]$$

As before, the equation describing the rate of change, with vertical position, of volumetric liquid hold-up in the Plateau borders, caused by flow from the films into the Plateau borders and bubble coalescence, and gravity drainage is given by (Uraizee and Narsimhan, 1995):

$$-\frac{d}{dz}(\eta n_p a_p l) + \frac{d}{dz} \left(\frac{4}{15} N n_p a_p u R \right) + N n_f A_f V + \frac{N}{2} n_f A_f x_f \beta = 0 \quad [12]$$

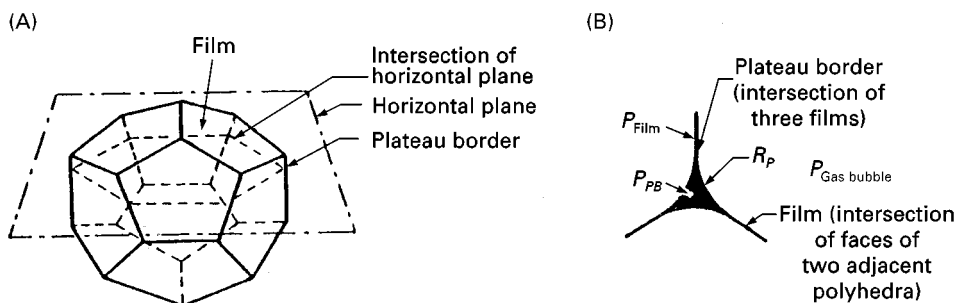


Figure 3 Schematic of a bubble in a foam column.

where n_p is the number of Plateau borders per bubble, a_p is the area of cross-section of Plateau border, R is the radius of the bubble, l is the length of the Plateau border, and u is the velocity of gravity drainage of Plateau borders. Similarly, the protein balance in the foam can be written as:

$$-\frac{d}{dz}(\eta n_p a_p l c_{p,i}) + \frac{d}{dz}\left(\frac{4}{15} N n_p u R c_{p,i}\right) + N n_f A_f V_f c_{f,i} + \beta \frac{N}{2} n_f A_f x_f c_{f,i} + \beta \frac{N}{2} n_f A_f \Gamma_i = 0, \quad i = 1, 2 \quad [13]$$

where $c_{p,i}$ and $c_{f,i}$ are the protein concentrations in the Plateau border and film respectively. In the absence of coalescence, they would be equal. However, coalescence would enrich the liquid in the Plateau border because of reflux of adsorbed protein from the ruptured thin films. In the above equation, Γ_i is related to the bulk concentration c_i via the Langmuir adsorption isotherm given by eqn [5]. In eqns [12] and [13], V and u are the velocities of drainage of films and Plateau borders, respectively. For an immobile gas-liquid interface, the velocity of drainage of films into the Plateau borders can be evaluated from the Reynolds equation:

$$V = \frac{2 \Delta P x_f^3}{3 \mu R_f^2} \quad [14]$$

where R_f is the radius of the film, μ is the viscosity, and ΔP is the pressure drop under which the film drains. The velocity of drainage of the Plateau borders for immobile gas-liquid interface is given by:

$$u = \frac{\rho g a_p}{20\sqrt{3}\mu} \quad [15]$$

where ρ is the density of the liquid.

Eqns [10], [12] and [13] are initial value problems which have to be solved with proper initial conditions at the foam-liquid interface to evaluate x_f and a_p and $c_{p,i}$ as a function of foam height.

The liquid hold-up at the foam-liquid interface ($z = 0$) can be set to the void fraction of spheres (Uraizee and Narsimhan, 1995):

$$\varepsilon_0 = N n_f A_f x_{f0} + N n_p a_{p0} l = 0.26 \quad [16]$$

As the liquid hold-up at the top of the column is much smaller than 0.26, the flow rate at the top of the

column is much smaller than the entrainment of the liquid at the foam-liquid interface. Hence, the material balance around the foam yields:

$$\frac{G \varepsilon_0}{1 - \varepsilon_0} = \frac{4}{15} N_0 n_p a_{p0} u R_0 \quad [17]$$

The inlet bubble size R_0 depends on the type of sparger and the superficial gas velocity G . The above two equations can be solved for x_{f0} and a_{p0} . Also, the protein concentration in films and Plateau borders at the foam-liquid interface can be taken as equal to the pool concentration, i.e.:

$$c_{f0} = c_{p0} = c_B \quad [18]$$

The pool concentration should satisfy the overall protein balance given by:

$$F c_F = B c_B + T c_T \quad [19]$$

where F , B and T refer to feed, bottom and top product flow rates expressed per unit area of cross-section of the foam column. The overall mass balance can be written as:

$$F = B + T \quad [20]$$

Eqns [10] to [13] can be solved with the initial conditions [16] to [20] to give the profiles of x_f , a_p and $c_{p,i}$. The liquid hold-up ε at any foam height can then be calculated via:

$$\varepsilon = N n_f A_f x_f + N n_p a_p l \quad [21]$$

The enrichment e_i for each component is given by (Uraizee and Narsimhan, 1995):

$$e_i = \frac{(N n_f A_f x_{f,i} + N n_p a_{p,i} l c_{p,i} + N n_f A_f \Gamma_i)_T}{c_{F,i} \varepsilon_T} \quad [22]$$

where $(\dots)_T$ refers to the evaluation of the quantity within the parenthesis at the top of the column. The separation factor S is then given by:

$$S = \frac{e_2}{e_1} \quad [23]$$

The above analysis assumes adsorption equilibrium for the surface concentration of proteins at the

air–water interface. Uraizee and Narsimhan (1995) have modified this analysis to account for the kinetics of adsorption of proteins on to the gas bubbles during their travel through the liquid pool before the formation of foam and demonstrated the effects of different parameters including the kinetics of adsorption and pool height on enrichment and recovery of proteins.

Effect of Operating Conditions on Enrichment and Separation

The operating conditions that can be varied in a foam column are the superficial gas velocity G , the bubble size R , the column height L , feed flow rate F , the feed concentration c_f and the mode of operation. In addition, the separation will also be influenced by the viscosity of the feed and the extent of bubble coalescence in the foam column.

Protein enrichment depends on the total amount of protein selectively adsorbed at the gas–liquid interface as well as on the liquid hold-up in the foam. Smaller liquid hold-ups result in a larger interfacial area per unit volume of the liquid and therefore in larger enrichment. At higher superficial gas velocities, more liquid is entrained by the gas bubbles from the liquid pool leading to higher liquid hold-ups in the foam column and consequently to smaller enrichment. As the bubble size increases, a larger proportion of the liquid that is entrained by the foam is distributed in the film, resulting in a faster drainage rate. On the other hand, an increase in the bubble size results in a decrease in the interfacial area per unit volume. Because of the above two opposing effects, there exists an optimum bubble size at which enrichment may be maximum (Narsimhan and Ruckenstein, 1986) for one component protein solution as shown in Figure 4. In addition, this maximum is found to be more pronounced at smaller superficial gas velocities. Narsimhan and Ruckenstein (1986) have developed a population balance model to account for the bubble size distribution in the description of drainage and coalescence in a foam bed. Their model was able to predict the change in the bubble size distribution as a result of coalescence. The results indicated collapse of the foam bed for broader inlet bubble size distribution with a coefficient of variation above a critical value. In the case of a mixture of proteins, however, the separation efficiency would depend on the preferential adsorption of one protein over the other components as can be seen from eqns [22] and [23]. As expected, the separation efficiency is higher for the protein which adsorbs the most at the gas–liquid interface with a higher value of Γ . As a result, the separation efficiency

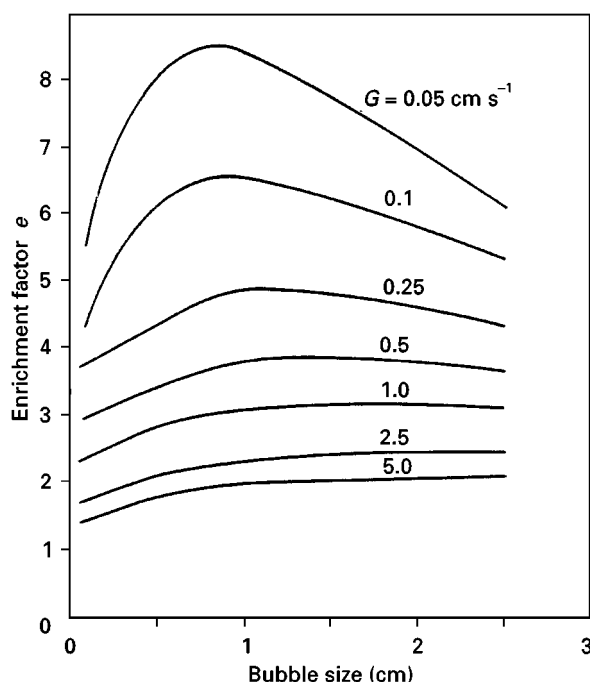


Figure 4 Effect of the inlet bubble size on the enrichment for $\mu = 10^{-2}$ P, $\mu_s = 10^{-4}$ sP, and $c_0 = 10^{-7}$ gmol mL $^{-1}$. (Reproduced with permission from Narsimhan and Ruckenstein, 1986a.)

would be higher for larger values of Langmuir adsorption parameter K_i as can be seen from eqn [5]. An increase in the viscosity of the feed would result both in a larger amount of liquid entrained by the foam as well as slower liquid drainage leading to larger liquid hold-up. Also, an increase in the viscosity of the feed would tend to stabilize the foam resulting in lower bubble coalescence. Both these effects will result in lower protein enrichment. Bubble coalescence in a foam column leads to: (i) an increase in the protein concentration due to internal reflux with subsequent increase in the surface concentration; (ii) a decrease in the liquid hold-up because of increased liquid drainage rates as a result of larger bubble sizes; and (iii) a decrease in the total surface area because of larger bubble sizes. The first effect results in more protein adsorption per unit area at the gas–liquid interface. The second effect leads to higher surface area per unit volume of the liquid. The third effect leads to a decrease in the total amount of protein adsorbed at the interface. Consequently, the first two effects lead to an increase in the enrichment and separation whereas the second and third effects lead to lower recovery. The second effect may be predominant since coalescence was found to result in an increase in protein enrichment as well as recovery (Uraizee and Narsimhan, 1995). The separation efficiency, as one would expect, depends on the relative

surface activities of proteins in a binary mixture. For larger values of Langmuir isotherm constant K_i (more surface active), the separation efficiency increases. In fact, the calculations show that the separation efficiency increases linearly with the ratio K_2/K_1 (Uraizee and Narsimhan, 1997). However, the separation efficiency was found to decrease rapidly with the feed concentration of the protein (Uraizee and Narsimhan, 1997).

Brown *et al.* (1990) measured enrichment and recovery in a continuous foam concentration column for bovine serum albumin (BSA). In their experiments, foam was generated by sparging nitrogen gas through a glass frit. As a result, the foam consisted of nonuniform size distribution of bubbles. They compared the experimental data with predictions based on a model similar to the one described above but neglecting drop coalescence. Their experimental data showed a decrease in the protein enrichment with superficial gas velocity. The model predictions agreed fairly well for the highest feed concentration of 0.1 wt% as shown in Figure 5. The experimental enrichments were found to be larger than the model predictions (even for the largest bubble size in the foam) with the deviation being larger at lower feed concentrations. This was believed to be due to the fact that drop coalescence in the foam column became increasingly important at lower feed concentrations as confirmed by experimental measurements of bubble size with the height of the column.

Uraizee and Narsimhan (1996) also observed a decrease in enrichment with gas velocity for foam concentration of BSA in their continuous foam con-

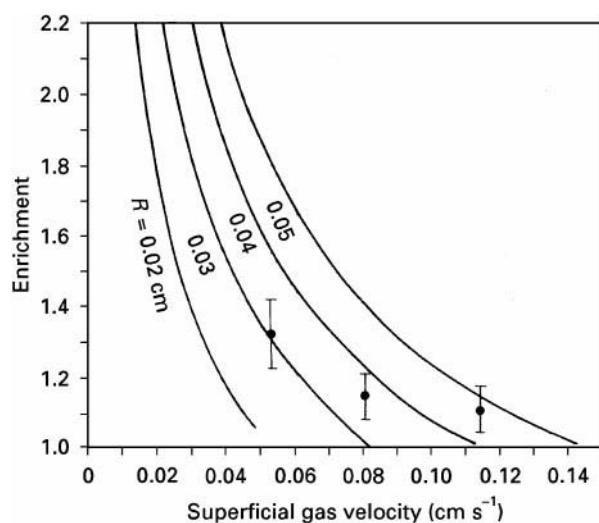


Figure 5 Effect of superficial gas velocity on protein enrichment for $c_F = 0.1$ wt%. $F = 0.02$ cm s⁻¹, $I = 0.1$ M, pH = 7, $z = 5$ cm. The curves refer to model predictions for different bubble sizes. (Reproduced with permission from Brown *et al.*, 1990.)

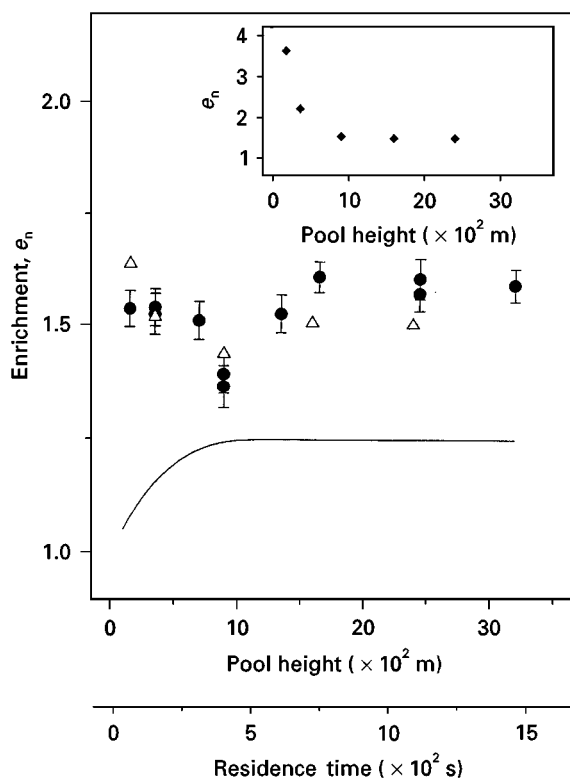


Figure 6 Comparison of experimental results with model predictions for BSA; feed concentration 0.1 wt%, bubble diameter 1.9×10^{-3} m, gas velocity 2.6×10^{-3} m s⁻¹, foam height 1.3×10^{-1} m, $F = 2 \times 10^{-5}$ m s⁻¹, pH 4.8, ionic strength 0.1 M. (●) Experimental data. (Δ) Model predictions accounting for kinetics of adsorption as well as coalescence. (—) Model predictions accounting only for kinetics of adsorption. (◆) Model prediction accounting only for coalescence assuming equilibrium surface concentration is shown in the inset. (Reproduced with permission from Uraizee and Narsimhan (1996).)

centration experiments in which the foam was generated by sparging nitrogen through a capillary bundle thus resulting in a foam of uniform bubble sizes. In their experiments, the residence time of the bubbles in the liquid pool was varied by varying the pool height. Interestingly, protein enrichment was found to increase with pool height at sufficiently high pool heights, thus indicating the importance of kinetics of adsorption of protein on to the gas-liquid interface on enrichment. At low pool heights, however, they observed an increase in protein enrichment with a decrease in pool height due to excessive bubble coalescence in the foam. Their model, which accounted both for the kinetics of protein adsorption as well as coalescence, was able to explain the increase in protein enrichment due to bubble coalescence at small pool heights and an increase in enrichment with pool heights at larger pool heights. A comparison of the experimental data with their model predictions is shown in Figure 6.

Ahmed (1975) observed an increase in the separation efficiency of albumin with the superficial gas velocity with the value reaching a plateau at sufficiently high gas velocities. Schnepf and Gaden (1959) and Ahmad (1975) reported a maximum protein enrichment at the isoelectric point of the protein which can be explained by the maximum protein adsorption at the interface due to the absence of electrostatic energy barrier for adsorption. However, this maximum was found to be considerably less pronounced at higher protein concentrations. Protein enrichment was also influenced by the change in the bubble size at different pH (Brown *et al.*, 1990). Separation efficiency of albumin was found to decrease dramatically as the foam height increased from 3 to 17 cm (Ahmed, 1975). Even though enrichment increased with foam height because of internal reflux resulting from increased drop coalescence, the top product flow rate was also found to decrease dramatically due to faster drainage. As a result, the protein separation was less at higher foam heights. Ahmed (1975) also found that the introduction of the feed stream into the foam instead of liquid pool increased the separation efficiency because the foam column was operated in the combined mode with an enricher and stripper.

In conclusion, the main attractive features of foam fractionation are its low capital and operating costs. Therefore, it can be employed as a first step for preconcentration/separation before more expensive separation methods can be used. More work is needed to establish the applicability of foam fractionation as a viable separation method for mixtures of proteins and to develop new processes based on this technique. Few experimental data are available on the adsorption isotherm and kinetics on to gas-liquid interface for mixtures of proteins. More importantly, it is necessary to probe denaturation (if any) of proteins and enzymes when subjected to foaming.

See also: II/Flotation: Bubble-Particle Capture; Froth Processes and the Design of Column Flotation Cells; Historical Development.

Further Reading

- Ahmed SI (1975) Laws of foam formation and foam fractionation. 1. The effect of different operating parameters on the foam fractionation of albumin from a solution containing organic and inorganic materials. *Separation Science* 10: 673.
- Ahmed SI (1975) Laws of foam formation and foam fractionation. 2. The influence of different association conditions on surfactants, glycerides, sugar and salts on the foam fractionation of albumins. *Separation Science* 10: 689.
- Bader R, Schultz F and Stacey M (1944) A crystalline serum mucoprotein with high choline esterase activity. *Nature* 154: 183.
- Bader R and Schultz F (1946) Fractionation by adsorption and crystallization on foam. Part II. Experiments with bile salts. *Transactions of the Faraday Society* 42: 571.
- Brown LK, Narsimhan G and Wankat PC (1990) Foam fractionation of globular proteins. *Biotechnology and Bioengineering* 36: 947.
- Charm SE, Morningstar J, Matteo C and Paltiel B (1966) The separation and purification of enzymes through foaming. *Analytical Biochemistry* 15: 498.
- Davis SG, Fellers CR and Esselen WB (1949) Application of foam fractionation procedures to the isolation of fruit juices. *Food Technology* 3: 198.
- Gehle RD and Schugert K (1984) Protein recovery by continuous fractionation. *Applied Microbiology Biotechnology* 20: 133.
- Holmstrom B (1968) Foam concentration of streptokinase from crude culture filtrates. *Biotechnology and Bioengineering* 10: 551.
- Lalchev Z, Dimitrova L, Txvetkova P and Exerowa D (1982) Foam separation of DNA and proteins from solutions. *Biotechnology and Bioengineering* 24: 2253.
- Lalchev A and Exerowa D (1981) Concentration of proteins by foaming. *Biotechnology and Bioengineering* 23: 669.
- Lemlich R (1968) Principles of foam fractionation. In: Perry ES (ed.) *Progress in Separation and Purification*, vol. 1, pp. 1–56. New York: Interscience.
- London M, Cohen M and Hudson P (1954) Some general characteristics of enzyme foam fractionation. *Biochimica Biophysica Acta* 13: 111.
- London M and Hudson P (1953) Studies on the purification of acid prostatic phosphatase. *Archives of Biochimica Biophysica Acta* 46: 141.
- Narsimhan G and Ruckenstein E (1986) Hydrodynamics, enrichment and collapse in foams. *Langmuir* 2: 230.
- Narsimhan G and Ruckenstein E (1986) Effect of bubble size distribution on the enrichment and collapse in foams. *Langmuir* 2: 494.
- Sarkar P, Bhattacharya P, Mukherjee RN and Muckerjee M (1987) Isolation and purification of protease from human placenta by foam fractionation. *Biotechnology and Bioengineering* 29: 934.
- Schnepf RW and Gaden EL (1959) Foam fractionation of proteins: Concentration of aqueous solutions of BSA. *Journal of Biochemical, Microbiological and Technological Engineering* 1: 1.
- Schultz F (1937) Adsorption on foams. *Nature* 139: 629.
- Uraizee F and Narsimhan G (1995) A model for continuous foam concentration of proteins: Effects of kinetics of adsorption of proteins and coalescence of foam. *Separation Science and Technology* 36(6): 847.

Uraizee F and Narsimhan G (1996) Effects of kinetics of adsorption and coalescence on continuous foam concentration of proteins: Comparison of experimental results with model predictions. *Biotechnology and Bioengineering* 51: 384.

Weijnenberg DC, Mulder JJ, Drinkenburg AAH and Stermerding S (1978) The recovery of protein from potato juice waste water by foam separation. *Journal of Engineering and Chemical Processing, Design and Development* 17: 209.

Froth Processes and the Design of Column Flotation Cells

I. M. Flint, Canadian Process Technologies Inc., Vancouver, BC, Canada

M. A. Burstein, NPACI Edcenter on Computational Science and Engineering, San Diego State University, San Diego, CA, USA

Copyright © 2000 Academic Press

Introduction

The function of a flotation column is selectively to separate certain suspended solid particles or liquid droplets based on their surface properties. Bubbles rise and particles (drops) settle within the vessel, and collisions are highly dependent on gravitational momentum. The vessel is a multiphase contacting/heterocoagulation device where the dispersed phase to be removed attaches to the bubbles and accumulates at the top of the column in the form of froth. The latter overflows to launders. In this quiescent system, transport, dispersion and mixing of materials are induced by the motion of gas bubbles in the continuous liquid medium.

For the purpose of designing columns, immiscible liquid droplets are considered as acting as solid spheres of an appropriate size and density: thus, a 'particle' may represent either a solid or a liquid.

Almost all flotation columns are operated in the countercurrent regime where slurry moves downwards against a continuous rising bubble swarm. This type of flow increases efficiency (selectivity) of separation as the distance between discharge ports for overflow and underflow is large. In some cases, for example for the flotation of very coarse particles, co-current columns can be considered in order to increase particle residence time and reduce loaded bubble rise time. Unless otherwise stated, all of this article is related to countercurrent columns.

Initial Design Data

The feed transport fluid must be characterized in terms of liquid flow rate and chemical composition. Component solids or immiscible liquid flow rate, material composition and size distribution must also be known. In all cases, mean values, standard

deviations and design maxima and minima are required.

Test work must be done, or approximations made, to determine the flotation characteristics of the material to be separated, including rate constants and maximum recovery for all material and particle (droplet) size fractions. Process targets must be well understood, including the desired quality of products and recovery. Data error must be minimized since it directly impacts on the accuracy of the design scale-up.

Site-specific information is also required for final designs. This includes limitations in dimensions due to plant layout, civil engineering specifications, including such items as wind loading, earthquake considerations, supporting platforms and others.

General Dimensions

Typically, columns range in height from 6 to 15 m. This height is dictated by the dimensions of the different zones within the column but is most influenced by the collection zone height.

Column cross-sections are usually round or rectangular. Cylindrical columns do not have special flow conditions at the corners. They, therefore, usually have a more uniform air and feed distribution, less tank weight due to the self-supporting nature of the structure and less wall area per unit operating volume. Rectangular columns use floor space more efficiently and are easier to baffle. The cross-sectional area is usually constant throughout the vessel and is determined by carrying capacity and residence time considerations in the collection and froth zones. Typical industrial cell cross-sectional areas range from less than 1 m² to more than 12 m².

Column Zones

The flotation column, as generally built, is composed of a number of distinct zones. Under the spargers there is a dead volume (underflow zone) which is only used to remove slurry from the vessel. The volume between the spargers and the feed port is called the collection zone. The volume between the feed port

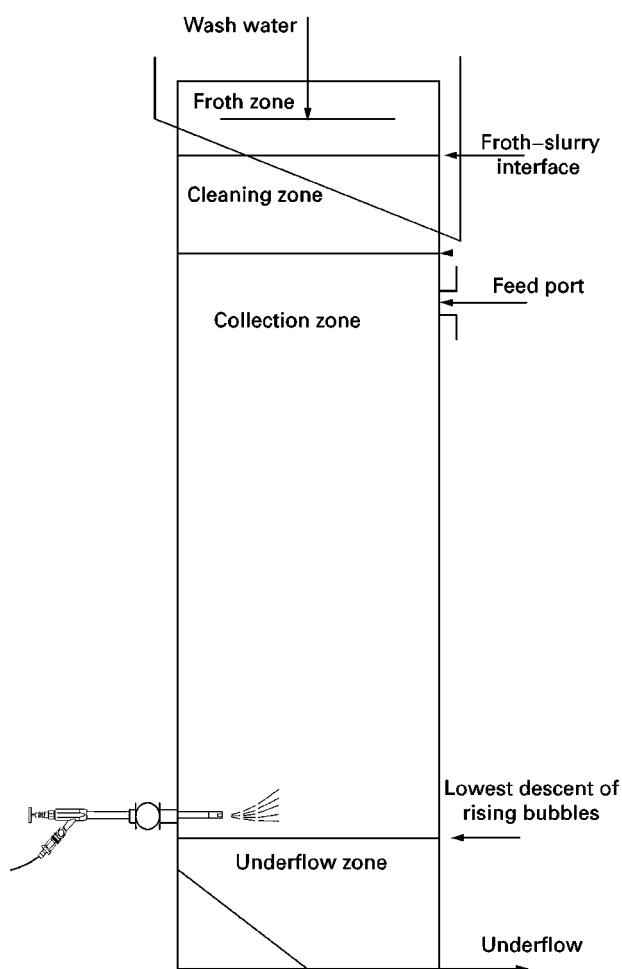


Figure 1 Column hydrodynamic zone.

and the froth interface is called the cleaning (recollection) zone and above the interface is the froth zone. The froth zone may be further divided into the washing zone, if it is under the wash water distributor, and the free drainage zone, if it is above. These zones are illustrated in Figure 1.

Underflow Zone

The physical dimensions of this zone should be minimized since its roles are to ensure that there are no small bubbles entrained by the downward flow to the underflow stream, that sloughing of the solids particles does not occur, and that the outflow from the base of the column does not create unwanted flow patterns within the active zones of the vessel. Bubble entrainment to the underflow is obvious, as in this case frothing occurs in the tailing sump or in the next open tank downstream of the column.

A zone underneath the spargers does not contribute to the floatation collection or separation. Design con-

siderations of the zone include base cone angle and placement, underflow exit port configuration and height to spargers.

Base Cone Design

In most solids separation applications, the base can be designed flat. The solids will eventually form a false bottom at the angle of repose under the specific flow conditions. Depth of the base cone should be selected considering angle of repose of particles. If sloughing of solids is considered a problem, then the column can be designed with either a real or false bottom at an angle greater than the angle of repose.

Underflow Port

Generally, the output port is designed to pull from the cross-sectional centre at the base of the vessel in order to minimize both the flow differences within the collection zone and large scale slurry circulation patterns.

The spargers are placed at a level such that the furthest descent of bubbles is above the highest expected solids settling point.

Collection Zone

The collection zone is characterized by a stream of individual bubbles rising against a descending liquid or slurry. This is the zone in which the bubble-particle attachment occurs. The capacity of the column is dictated in part by the intensity of bubble-particle collision (number of collisions per unit time), the probability of attachment, and the bubble surface area flux through the vessel (removal ability) in this zone.

When sizing a column, certain assumptions are made. These include that the column operates with dispersed bubbles that rise as a swarm without slugs. It is also assumed that the flow of bubbles, liquid and solids is uniform across the column, and that there are no large scale vortices.

There are four main collection zone design criteria which determine the vessel dimensions: floatable particle residence time, mixing characteristics, maximum gas rate and bubble loading. The resulting volume can usually be achieved with a range of height-to-diameter options. The final dimensions are also dictated by layout and economic considerations. It should be emphasized that this zone must be designed in parallel with the sparging system and froth zone as each of these parts influences the others. The placement of the column within the

operating circuit will also impact on the final design and operation.

Solids Settling

Particles settle within the column system since there is no mechanical agitation to suspend them. As such, each particle will have a specific hindered settling velocity dependent on size, density of the particle and the effective density and viscosity of the suspension with modifications due to bubble-induced mixing. Mixing enhances particle suspension, so small and/or light particles do not have their own trajectory and follow liquid flow more than in two-phase systems. The settling velocity generally has little influence on residence time for particles smaller than about 20 μm , but becomes an important design condition for larger particles.

Particle Residence Time Distribution (RTD)

Material residence time depends upon the inherent mineral settling velocity under the conditions within the column and the superficial velocity of the slurry. The total collection zone height divided by the summation of the hindered settling and slurry velocities gives a total average residence time for each particle size and density. More precisely, the particle residence time is a stochastic parameter influenced by the turbulent mixing and potential macrocirculation patterns within the column.

Elementary Processes

Flotation depends on the elementary processes of collision and attachment. In columns the probability of collision between a particle and a bubble remains virtually constant within the collection zone. There is a higher probability of attachment at the bottom of a countercurrent column since bubble surface coverage by particles is low for newly formed bubbles. This maximizes the recovery of the small proportion of particles targeted for flotation that are still present in the lower parts of the zone.

The relative movement of slurry and rising bubbles is the main source of mixing energy in columns. This results in a low intensity of the turbulence (low energy dissipation and large internal scale of turbulence) and, therefore, low relative bubble-particle velocities and accelerations. Bubble-particle collision efficiency is due to gravitational and inertial particle drift from the liquid streamlines around the rising bubble and due to the interception. The probability of particle detachment from bubbles is limited since the velocity gradient around the bubble is minimized.

Rate Constant

The floating ability of a material is generally referred to as a rate constant, similar to chemical processes, and is assumed (for simplicity) to be of first-order kinetics for each mineral component and size fraction. The value of this term is dependent on a complex function involving the collision/attachment and detachment, as well as processes occurring in other zones of the flotation column (see below). These data are generally determined through test work. As mechanism and intensities of subprocesses (collision, attachment, detachment, entrainment) in column and impeller flotation can be substantially different, the lab and pilot tests for column design and scale-up should also be made in columns. First-order flotation rates for the components can be determined from the recoveries in a continuous lab flotation column, or by simulation of kinetic tests by recycling column tails back to the feed line.

Taking into consideration separate first-order kinetic models for individual subprocesses and taking into account free bubble surface reduction in the upward direction would lead to complicated nonlinear kinetic equations. These are important in understanding the physics of the process, but cannot be used for scale-up or control, due to unavoidably high error in determining their coefficients from experimental data.

Carrying Capacity

The removal capability of the bubbles is called the carrying capacity and is the general term which characterizes the maximum amount of solids carried by the air bubbles (either in reference to the maximum capacity of the column, or to the maximum capacity per air volume). This refers to the fact that only a specific amount of particles can be attached to and removed by a certain bubble area. Thus, the maximum floatable solids removal or the surface area of attached particles is related to bubble surface area flux.

Typically, the distance between spargers and the slurry-froth interface is between 6 and 12 m. This leads to a substantial mass of particles attached to a bubble (bubble loading).

As bubbles become loaded by collected particles, the contact time between particle and bubble reduces due to the shortening of particle trajectory along the free bubble surface. This means that the rate of collection slows as loading increases, especially when the lower section of a bubble is virtually covered by attached particles. Detachment probability is also much higher for particles attached to the upper hemisphere of a bubble.

Smaller bubbles can carry more solids than larger bubbles, assuming an equal gas rate and that the loaded bubbles have sufficient buoyancy to move against slurry flow. A smaller weight of fine particles can be carried at a constant gas rate and bubble size distribution than that of coarse particles.

Carrying capacity limitations should be taken into account when estimating height-to-diameter ratio for columns working at high overflow (froth) yield. Typical carrying capacity per unit column cross-sectional area for base metal minerals flotation is $2.5 \text{ t}/(\text{m}^2 \text{ h})$ and for coal flotation $1.5 \text{ t}/(\text{m}^2 \text{ h})$.

Gas Rate and Bubble Size

Column cells are operated in the bubbly region where bubbles rise in a swarm. The flow regime in the column may change to the 'churn-turbulent' condition when coalescence is caused by gas entering a region faster than it can leave as small bubbles. As smaller bubbles have lower swarm rising velocity, the flooding occurs at a lower gas rate for fine bubble dispersions. Thus, there is a link between maximum gas rate at the flooding point and bubble size. Also, flooding is enhanced by countercurrent slurry flow; the higher its superficial velocity, the lower the gas rate at the flooding point. At bubble size ranges used for column flotation, flooding occurs typically at a superficial air velocity of $2.5\text{--}3 \text{ cm s}^{-1}$. More precise values can be calculated from the drift flux model.

It is also possible for uniform countercurrent froth flow to occur in the column even at lower superficial air and slurry rates when the bubbles are very stable (gas hold-up at both bubble and froth flow regimes can also be estimated based on the drift flux model).

Mixing

Columns are commonly sized with a dispersion method which uses the Peclet number, a dimensionless criterion, to characterize mixing. It is assumed that an axial dispersion model adequately reflects flow structure in the collection zone. It is also possible to use a tanks-in-series flow model. The Peclet number reflects the ratio between the downward path of particle and the average length of its stochastic drift due to mixing (diffusion). It is equal to UL/D , where U is the mean velocity of the phase of interest (for particles it is the sum of downward liquid velocity and a hindered settling velocity), L is the characteristic length scale for the apparatus (collection zone height of the column), and D is the turbulent dispersion (diffusion) coefficient. The latter can be determined by a tracer technique or by using one of

several approximation formulae. D ranges from 0, for perfectly mixed systems, to infinity, for plug flow. The following variables have an effect on the Peclet number: bubble size and number of bubbles (which are dependent on gas rate and surface tension), slurry rate, particle settling velocity, collection zone height and diameter. At a constant collection zone volume, a taller column is better from a flow structure perspective as less mixing is induced. Peclet number can be estimated using one of the experimental relationships, or from particle residence time distribution (RTD) similar to that in chemical reactors or separation equipment. RTD can be directly measured using a tracer method. Dispersion of the RTD can be used to calculate turbulent diffusion D and other column flow structure criteria.

The absence of an agitator limits the formation of large scale flow loops unless the column is operated in a high air rate, churn-turbulent flow or the feed distribution of either air or slurry is not even. Low mixing intensity and lack of circulation contours cause particle residence times to be highly dependent on the particle settling velocity. Reduced mixing leads to lowering of local upward flow intensities which minimizes particle entrainment to the froth. Thus, at a constant collection zone volume (slurry retention time), its increased height leads to lower mixing intensity and improved (due to this) metallurgical results up to the point when restrictions in carrying capacity limits concentrate (float product) yield. Also, higher superficial slurry velocity reduces negative influence of mixing and slime entrainment intensity.

Careful design and positioning of any baffles (horizontal or vertical), the feed system, and any internal piping that may be needed minimize local turbulence. The feed pipe must be located high enough in the column to maximize the collection zone length but also low enough to limit turbulence at the slurry-froth interface.

Entrainment

Fine and/or light hydrophilic particles may pass upwards through the collection zone by entrainment. There are two forms of entrainment. In the first, a portion of feed water containing suspended fine particles passes into the froth. This type of entrainment can be minimized by maintaining a net downward flow of water through the upper column zones. The second form of entrainment is the capture of particles in the eddies behind a rising bubble. These particles are also rejected in the froth zone operating with positive bias.

Baffling

Columns may be vertically baffled in order, both to reduce mixing and to lend additional structural support. An important condition to achieve effective operation with a baffled column is an even feed and air distribution between the compartments, otherwise detrimental circulation patterns may form between the baffled sections. This overall circulation can make a baffled column less effective in terms of flow structure than a column without baffles. Normally, baffles are installed above and below the feed distributor in a column, leaving space around feed pipe(s) and air spargers open to allow even distribution of the slurry and air bubbles, respectively.

Horizontal baffles (plates) are not typically used, though tests have confirmed their ability to improve flotation of coarse particles due to less short-circuiting in the wall part of the baffled column.

Physical Dimensions

The total volume of the collection zone is determined by residence time considerations, having also accounted for mixing and hindered settling of coarse particles, to achieve target recoveries. A formula based on an axial dispersion model and first-order flotation kinetics is typically used. A minimum diameter is then calculated to allow sufficient bubble surface area to float the required solids. The diameter and height must be larger than these minimum numbers and any combination can be used as long as the volume remains above its minimum. The volume should provide for the necessary retention time with a correction for mixing, but should not exceed it substantially. This is critical in the case of selective flotation when both components are floatable and have different but nonzero rate constants.

The selection of the vessel dimensions is an iterative process since a change in many of the variables will change the overall mixing in the vessel.

Access

Periodic maintenance is required, and access to the inside of the column may be needed. Therefore, access manholes and appropriate clearances must be maintained within the vessel.

Cleaning Zone

The purpose of this zone is to buffer the froth zone from the turbulence of the feed port. It is located above the feed port and below the interface with the froth. It is characterized by rising bubbles that may be highly loaded with solids rising from the collection zone and falling solids that have been entrained in the

bubbles' wake, or have been rejected in the froth zone by loss of bubble surface area. If a sufficient amount of wash water is used, this zone may have a net downward flow of slurry. Only a limited number of previously uncollected particles occurs in this zone due to the turbulent mixing or entrainment. Since collection of these particles can also occur in the collection zone, the height of the cleaning zone should be minimized but must be sufficient to allow damping of the feed turbulence below the froth interface.

In some circumstances the cleaning zone is the overflow point of the float product. This occurs when there is no froth zone either because a froth cannot be maintained in a solids float, or because a liquid-liquid separation is being performed. In the latter case an organic pad may be present.

Froth Zone

This zone is usually present in solid-solid or solid-liquid separations.

The froth zone in a column cell is characterized by a rising bed containing a matrix of bubbles, which are loaded with hydrophobic material, water lamellae between bubbles and Plateau-Gibbs canals. Entrained hydrophilic material may be found initially either in lamellae or in canals. Film (lamella) thinning and bubble coalescence in froth (syneresis) and drainage in Plateau-Gibbs canals are the main mechanisms of gas hold-up increase and concentrate upgrading with height in the froth. This is caused by reduction of the air-liquid interface area and subsequent particle detachment. Tracer tests indicate that, in some cases, more upgrading is observed within the froth than between slurry and lower froth layers.

Quiescent conditions in columns create a stable froth that allows the addition of wash water. This water displaces the liquid phase of the feed slurry, with entrained associated fine particles, from the froth lamellae and Plateau-Gibbs canals and allows the production of an essentially entrainment-free overflow. In some cases, addition of small amounts of water into the froth also improves the stability and rheological properties of the countercurrent froth.

A presence of highly hydrophobic, angular particles large enough to bridge the lamella between bubbles, without a population of smaller hydrophilic particles, causes froth destabilization. In this case the froth zone design is critical. In extreme cases a froth bed may not be possible.

Channelling

Uneven distribution or excessive addition of wash water can cause formation of channels in the froth

and possible froth collapse. Care must be taken in the design of the distributor to ensure even cross-sectional wash water flows.

Froth Zone Dimensions

Although the froth zone usually has the same cross-sectional area as the collection zone, it may be necked to promote crowding which increases the upward velocity in the froth. This may be done when small amounts of froth are generated, reagent conditions dictate that the froth will not be stable, or the size distribution of solid particles in the froth promotes coalescence of bubbles. It is more common to preserve the overall area and apply internal baffling and launders. Internal baffles may be added to support the froth, or to contain or localize froth collapse.

Internal Launders

Syneresis and coalescence occur within the froth zone. Thus, relative to a localized section of froth, bubble surface area is lost with time as that section travels from the slurry-froth interface to the overflow points. Furthermore, analysis of particle RTD in froth indicates that horizontal transport to the froth launder is very slow. For larger diameter columns, dead zones can form in the central part of the vessel. Columns normally do not have froth skimmers or paddles. Therefore, fast froth removal is critically important for operation and is often achieved by a series of internal froth launders.

Organic Pad

Liquid-liquid column applications may be operated with an organic pad on the top of the vessel. Organics floated in the collection zone gather at the surface of the vessel. These may overflow a weir continuously if the organics concentration is sufficient or if low concentrations of organics in the overflow stream are acceptable. Otherwise, the pad accumulates and is dumped on a regular basis. If some or all of the organic compounds present in the system are volatile, a pad may not be suitable or dumping must be frequent to prevent excessive stripping.

Air-Sparging Systems

The purpose of the sparging system is to distribute evenly the appropriate-sized bubbles near the bottom of the column. The sparging system is critical and must be designed taking into consideration many elements, including bubble size distribution, maximum air rate, bubble coalescence and induced mix-

ing; uniformity of air hold-up across the vessel, minimization of scale formation, resistance to wear, required air pressure and maintenance considerations.

There are many types of spargers used in column cells. Pneumatic (porous media or perforated) spargers form bubbles at small orifices. Pneumohydraulic spargers break up an air stream into bubbles by a water jet as an air-water mixture is distributed into the column. The air jet spargers form bubbles through the high velocity injection of air into the column. There are also a class of spargers termed external spargers that aerate the feed slurry, or portion of the underflow, and use the column as a de-aeration or bubble separation vessel rather than for particle collection. Combination of external spargers for slurry pre-aeration with microbubbles and/or dissolved air with internal spargers to facilitate microbubble buoyancy by adding larger bubbles is optimal for a wide range of applications (see below). In recent years, the general trend among major column suppliers is to use air jet and external types of spargers, although specific circumstances dictate the use of other types.

Care must be taken when designing the bubble distribution system to ensure that an even flow of bubbles is generated. Poor air distribution can cause large scale flow patterns in the column that are detrimental to performance. Macrocirculation zones can also be caused by a misalignment of the column either by bows along the length or by offsets from the vertical.

Pre-Aeration

Columns, by nature, have low turbulent momentum between the bubbles and particles, meaning that smaller particles have slow flotation kinetics in these vessels. The column is, however, a good separator of bubbles from the feed slurry, especially if wash water is added. This feature virtually eliminates hydrophilic entrainment. In order to improve the collection of fine particles, a pre-aeration system or intense flotation device can be used. These devices act by creating a turbulent zone, where the inertial momentum of both bubbles and particles is high (due to high intensity turbulence and velocity gradients) enabling higher recovery of the smallest floatable particles by microbubbles. If the pressure in the pre-aeration device is substantial, a portion of air is dissolved and then released in a column; normally, nucleation of air bubbles occurs at a solid surface, thus a collision stage of flotation process is eliminated for the cavitation bubbles.

Pre-aeration devices then feed a modified column which acts as a recollection device for the larger particles and a bubble coalescence/separation system.

Civil Engineering and Material of Construction

The final column design must be site-specific. There may be height and/or area considerations due to restrictions of space, and weight and loading considerations due to foundation requirements. In addition, some environmental considerations such as wind load, earthquake zone and rainfall intensity will affect steel thickness, foundations and attachments, braces and access platforms. As columns are normally much taller than mechanical flotation cells, they are often located outside, and these factors can play an important role in column design. There are also process considerations like per cent solids, wear factors, chemical composition of the slurry (pH, etc.) and particle size distribution which affect the physical structure, pipe sizing and materials of construction. In special cases, these units may be designed as pressurized vessels or as enclosed systems.

For example, many oil–water separation columns are pressurized or some installations use circulating inert gases to minimize oxidation. When columns are installed for oil–water separation duties, mainly on offshore platforms, a circulating hydrocarbon gas (propane) is often used instead of air.

Conclusions

Despite its simple design, the scale-up and modelling of column flotation is a complex problem. It includes analysis of three-phase three-dimensional flow in collection and cleaning zones and in the washed thick froth layer. In the last few years, a technique for column design has been developed. Its adequacy has been confirmed by many columns installed worldwide for a wide range of mineral and other applications.

Special attention should be paid to the carrying capacity of air bubbles and to secondary upgrading in the froth.

Design of air-sparging systems, feed distributors and also froth discharge systems is critically important for successful column operation.

Unconventional design and use of pre-aeration systems are the main trends in flotation column development at present.

See also: II/Flotation: Column Cells.

Further Reading

- Clift R, Grace JR and Weber ME (1987) *Bubbles Drops and Particles*. New York: Academic Press.
- Dobby GS and Finch JA (1986) Flotation column scale-up and modelling. *CIM Bulletin* 79: 89–96.
- Finch JA and Dobby GS (1990) *Column Flotation*. Oxford: Pergamon.
- Levenspiel O (1972) *Chemical Reaction Engineering*. 2nd edn. New York: Wiley.
- Lynch AJ, Johnson NW, Manlapig EV and Thorne CG (1981) *Mineral and Coal Flotation Circuits, Their Simulation and Control*. New York: Elsevier.
- Masliyah JH (1979) Hindered settling in a multi-species particle system. *Chemical Engineering Science* 34: 1166–1168.
- Ross VE and van Deventer JSJ (1988) Mass transport in flotation column froths. *Column Flotation '88. Proceedings of the International Symposium*, Phoenix, Arizona. Littleton, Colorado: Society of Mining Engineers.
- Rubinstein JB (1995) *Column Flotation, Processes, Designs and Practices*. Basel: Gordon and Breach.
- Schuhmann R. (1942) Flotation kinetics 1: methods for steady state study of flotation process. *Journal of Physical Chemistry* 46: 891–902.
- Zhou ZA, Xu Z and Finch JA (1994) On the role of cavitation in particle collection during flotation – a critical review. *Mineral Engineering* 7: 1073–1084.

Historical Development

Z. Xu, University of Alberta, Edmonton, Alberta, Canada

Copyright © 2000 Academic Press

Flotation is a versatile, surface wettability-based separation process, usually taking place in an aqueous medium. In flotation, a water-repellent (hydrophobic) target to be separated is attached to a carrier lighter than the medium in which separation occurs. The target varies from fine particulates (solid or

liquid) to ions and molecules, while the most commonly used carriers are air bubbles due to their ready availability, easy handling and very low cost. Compared to other light fluids (e.g. paraffin oil), air has the highest hydrophobicity, and its low density facilitates mass transfer of bubble-target aggregates from the bulk medium to the interface where froth forms and is collected/removed. Flotation was practised around a century ago, mainly for mineral separation applications. It is difficult, if not impossible, to pin down who should be given credit for the

Table 1 Key stages in flotation process development

Year	Concept introduced	Inventors
1860	Oil as a carrier	Haynes
1901	Gas as buoyant medium	Potter/Froment
1902	Ultraflotation/carrier flotation	Cattermole
1905	First generation flotation machines	Hoover
1908	Frother (organic compounds)	Higgins/Sulman <i>et al.</i>
1912	Activator (CuSO ₄ for sphalerite)	Bradford
1913	Depressants (SO ₂ for activated sphalerite)	Bradford
1925	Modern flotation collectors (xanthate for sulfides)	Keller

development of the flotation process in the various key stages. Nevertheless, **Table 1** provides a general picture of how flotation has evolved since its first applications in mineral processing.

As shown in this table, up until the 1930s all the ingredients required for selective flotation had been proposed, including: (i) a collector to render target particles water-repellent by its adsorption; (ii) a frother to stabilize bubbles and promote foaming; (iii) an activator to induce or enhance collector adsorption on target particles; and (iv) a depressant to destroy collector adsorption on unwanted particles; along with bubble generation in a flotation machine.

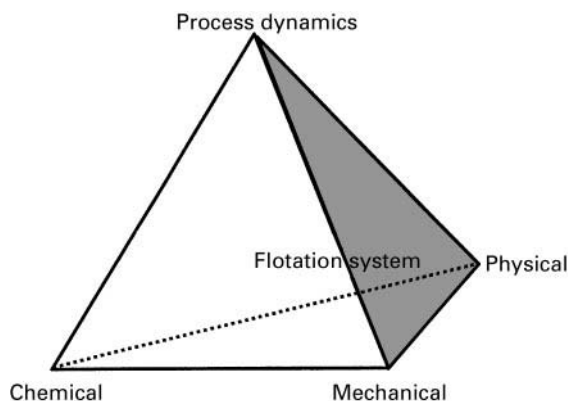


Figure 1 A flotation system shown as a tetrahedron with chemical, mechanical and physical aspects as the foundation through which process dynamics is modelled and controlled. The triangular base plane emphasizes the interrelated nature between the three foundation elements. The chemical aspect involves control of chemistry at air- and solid-aqueous interfaces by collectors, depressants, dispersants, activators, bacteria and frothers; the mechanical aspect concerns energy dissipation for bubble generation, particle dispersion, surface cleaning, hydrodynamic forces and bubble-particle contact; the physical aspect deals with the wetting phenomena and the nature of interactions between bubble-particle, bubble-bubble and particle-particle pairs in aqueous solutions involved in a flotation system.

These ingredients form one of the three foundations on which a flotation system is built. This is shown in **Figure 1** as flotation chemistry. Although neither the principles involved in flotation nor these basic ingredients have been changed since, the technology along with the fundamental understanding of the processes have evolved greatly. Developments in each of these three foundations are summarized in this article with emphasis on recent advances.

Flotation Chemistry

The search for new flotation reagents for various mineral separation systems has been one of the major aims in flotation chemistry development. Although xanthate, first used more than 70 years ago, remains the principal collector for sulfide mineral flotation, long chain surfactant has been introduced as the collector in oxide, silicate and sparingly soluble salt mineral flotation systems. The early trial-and-error approach in screening and searching for a new flotation collector has evolved into today's scientific design. Using quantum chemistry and electron density calculations, the structures of highly selective collectors have been proposed. A surfactant, with oxygen and nitrogen as the binding elements in its functional group (e.g. hydroxyoximes), was found to be a powerful and more selective collector for oxide minerals, while those with sulfur and nitrogen as the binding elements (e.g. thionocarbamate) is particularly selective for sulfide minerals. A common feature of these new collectors is their electron donor character, forming a five- to six-member closed ring structure with surface metallic elements. Many five-membered heterocyclic compounds (e.g. oxazole- or thiazole-based collectors) have recently been found to be of special selectivity in base metal ore flotation. A general correlation between flotation performance and collector chain structure (e.g. short versus long, single versus double, straight versus branched, single bond versus double bond, paraffinic versus aromatic, etc.) has also been established and a detailed list of newly developed collectors was compiled by Nagaraj in 1988. The use of a collector mixture has shown improved collecting power and selectivity, and warrants further development.

The invention of a water-soluble frother by Tveter (a polypropylene glycol ether, known as Dowfroth) was considered to be one of the major advances in frother development. Following the advent of various types of synthetic, propylene-based frothers, the effort in frother development has been directed to establishing a correlation between frother structures, frothing characteristics and their effect on recovery and selectivity. To this end, increasing branching

in frother molecules has been identified as increasing flotation selectivity, often at the cost of reduced recovery. The use of mixed frothers in a flotation system to generate air bubbles with a wide range of sizes, each suitable for particles of a given size range, has also drawn considerable attention. An increased overall recovery has been demonstrated by using a mixture of 1:1 polyglycol:methyl isobutyl carbinol (MIBC) as compared to a single frother at the same total concentration level. The synergistic effect of a collector and a frother on bubble-particle collection has also been recognized, although the practical application has not gained its fair share of attention. The stabilization of air bubbles by simple inorganic electrolyte should not be overlooked. Developed in the early 1930s for natural hydrophobic coal flotation without using a frother, salt flotation provides a different avenue for recovering natural hydrophobic minerals, as the surface active frother tends to adsorb on natural hydrophobic minerals with unfavourable orientations for flotation, consuming added chemicals and reducing their floatability. In 1995 Weissenborn and Pugh confirmed that the hydration shell around the added inorganic (ionic) species or frother's polar groups is responsible for froth stabilization.

Development in the activator appears rather limited, although most of the positively charged metal hydroxy species have been found suitable for activation in silicate flotation. In sulfide flotation, copper sulfate remains the only activator extensively used today. In contrast, development in depressants has taken on a different pace. Shortly after the introduction of sodium dichromate (for PbS) and SO₂ (for ZnS) in 1913, sodium cyanide (1922) and alkali sulfites (1923) appeared to be the popular depressants to use and remain the major depressants in modern sulfide flotation plants. Meanwhile, sodium silicate (1928) and macromolecular starch (1931) have become important depressants/dispersants in oxide, silicate and sulfide flotation systems. In addition to nonionic dextrans, cationic polysaccharides and anionic carboxymethyl cellulose have been found to be effective depressants because of their multi-anchoring nature with mineral surfaces. Recent efforts have been directed to the search for polyamines, which are effective in iron sulfide depression, driven by the environmental pressure of reducing SO₂ emission from smelters. Combined with SO₂, diethylenetriamine (DETA) has been found effectively to depress the pyrrhotite in pentlandite flotation, although the depression mechanism remains to be identified.

The control of the mineral surface property by biotreatment is an emerging area and represents a special branch in flotation reagent development.

This approach is of special importance for desulfurization in coal flotation, selective depression in base metal sulfide flotation and hydrophobization of non-sulfide minerals. The success of biotreatment in these systems lies in the extremely high selectivity of bacteria, such as *Thiobacillus*(T-)*ferrooxidans*, towards the oxidation of pyrite, without any adverse effect on the flotability of coal, resulting in a high desulfurization efficiency in coal flotation. Also reported is an improved floatability of sphalerite by pretreatment of T-ferrooxidans in an acidic medium. However, a high dose of T-ferrooxidans has been found to be detrimental to sphalerite and galena flotation. Although sulfate-reducing bacteria have a minimal effect on the floatability of molybdenite and galena, they have been found to depress the floatability of chalcopyrite and sphalerite, resulting in highly selective flotation. Brunet *et al.* (1998) reported that the combination of T-ferrooxidans, T-thiooxidans and *Leptospirillum* accelerated pyrite oxidation. The high selectivity of a bioprocess warrants the rapid growth of biotreatment in mineral flotation.

Accompanying the development of various flotation reagents is the recognition of surface reactions/adsorption and the understanding of collector/mineral interactions in selective flotation. The theory of sulfide flotation with xanthate family collectors has advanced from simple surface chemical reactions to a generalized electrochemical-chemical process. Recognizing the electrochemical nature of collector adsorption on sulfide surfaces was a quantum leap in sulfide flotation chemistry. The application of the mixed potential theory to a sulfide flotation system provides a scientific explanation for a required oxygen level to induce the floatability, and accounts for the role of pulp electrochemical potential (Eh) in sulfide flotation for a given collector chemistry. An important consequence of electrochemical involvement in sulfide flotation is the development of self-induced (also known as 'collectorless') flotation by either controlled oxidation or sulfidization of pre-oxidized sulfide minerals. The use of cyclic voltammetry allows a direct correlation between collector adsorption (determined by charge integration), under a given applied electrode potential, and contact angle, which in turn determines the floatability of sulfide minerals. An important outcome from electrochemical studies is a new mechanism for differential flotation of complex sulfides by pulp potential control. However, the controversy regarding the collector reaction product on sulfide minerals is yet to be resolved. To this end, modern spectroscopic methods are useful. Surface reactions have been studied extensively using various surface analytical techniques, including: (i) Fourier transform

infrared spectroscopy (FTIR in both *in situ* and *ex situ* modes); (ii) Raman spectroscopy; (iii) Auger and X-ray photoelectron spectroscopy (AES and XPS); (iv) fluorescence spectroscopy; (v) electron spin resonance spectroscopy; (vi) laser ionization mass spectrometry (LIMS); and (vii) time-of-flight-secondary ion mass spectrometry (TOF-SIMS). For example, the monolayer formation of polysulfide as a sulfur oxidation product on PbS has been confirmed from synchrotron XPS characterization. However, whether or not polysulfide is responsible for collectorless flotation remains to be established. Following the pioneer work on *in situ* spectroelectrochemical characterization of sulfide flotation chemistry by Leppinen *et al.* in 1988, the development of a spectroelectrochemical cell (Figure 2), combined with polarized FTIR spectroscopy, sets up an entirely new direction for sulfide flotation chemistry research. Using polarized infrared radiation, the orientation of the adsorbed molecular species can be derived, as shown in Figure 3. However, further research efforts are required to quantify the mo-

lecular orientation and to derive its practical implications in sulfide flotation practice.

In oxide and silicate mineral flotation, the interaction (i.e. adsorption of the collector, mostly surfactant) has been generally considered to be electrostatic rather than chemical in nature. An electrostatic interaction model has proven satisfactory when applied to silica and alumina flotation with ionic collectors of opposite charges from the surfaces. Progress has been made in predicting the point of zero surface charge, based on the minimum solubility theory and the sign of surface charge from the hydration energy of lattice ions. A more quantitative description of surface charge distribution has been made possible following the development of the surface triple-layer model in combination with the surface site-binding theory. Early adsorption studies have revealed the formation of surfactant hemimicelles on mineral surfaces at a bulk surfactant concentration of approximately one-hundredth of its critical micelle concentration (cmc). The formation of ionomolecular complexes has been found to enhance the floatability of oxides.

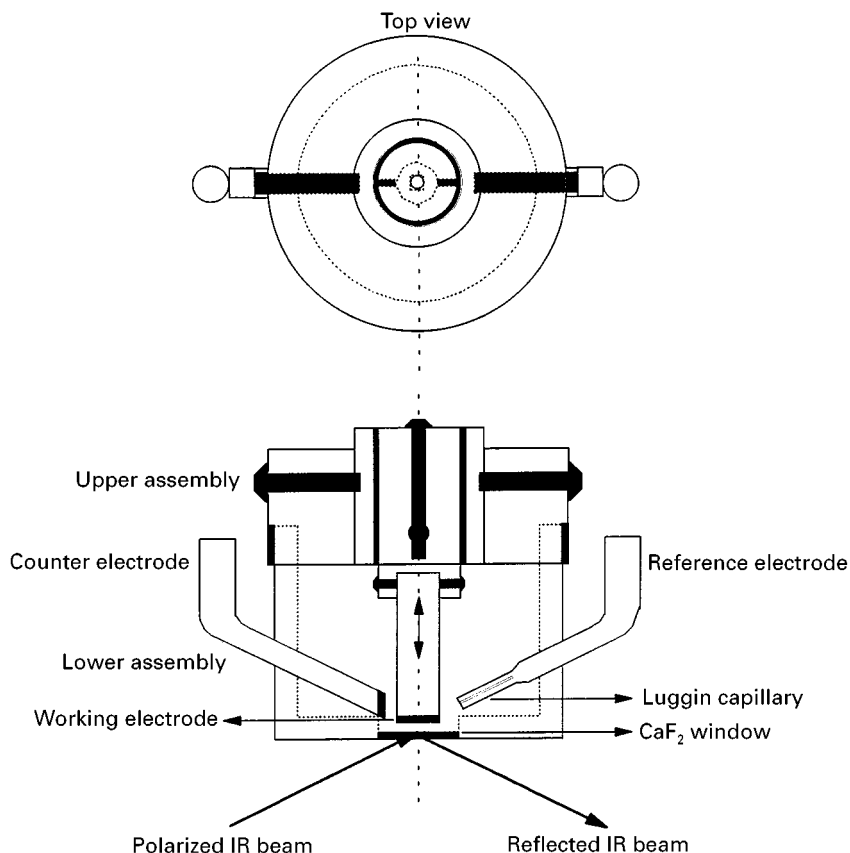


Figure 2 Schematic diagram of an *in situ* spectroelectrochemical cell suitable for studying sulfide flotation chemistry. Pushing a movable sulfide mineral working electrode against the CaF₂ window with a screw type of mechanics ensures not only elimination of bulk water films to increase the sensitivity of infrared spectroscopy, but also reproducible positioning of the electrode (after each electrode polarization) for quantitative analysis. The use of polarized infrared radiation in external reflectance mode allows identification of molecular orientation.

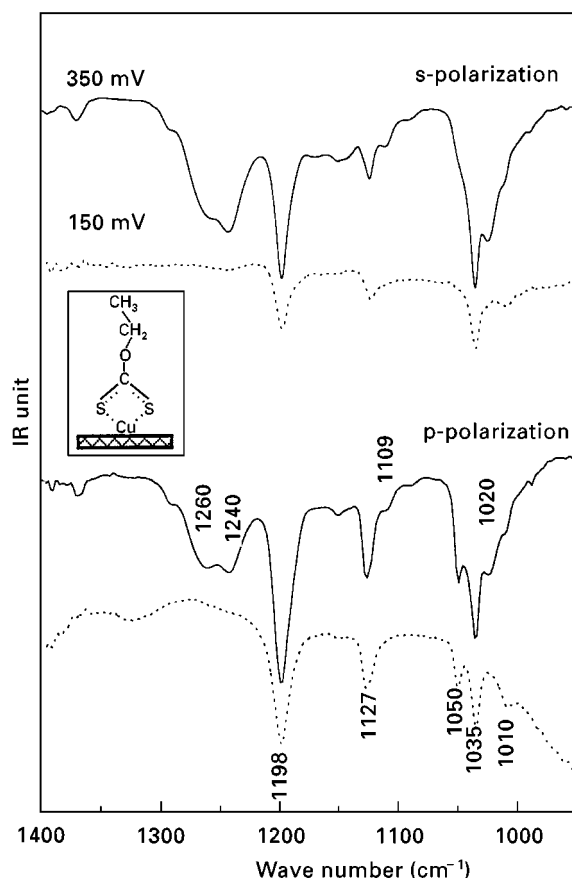


Figure 3 *In situ* infrared spectra obtained with a copper electrode polarized under electrode potentials of 150 (dotted lines) and 350 (continuous lines) mV/SHE (standard hydrogen electrode) in 2×10^{-3} mol L $^{-1}$ potassium ethylxanthate solutions. By comparing the spectra obtained with s- and p-polarized infrared beams, a near perpendicular orientation of adsorbed copper xanthate on copper electrode (inset) was derived to account for the absence of the band at 1050 cm $^{-1}$, associated with COC molecular vibrations, with the s-polarized infrared beam. In contrast, a random orientation of dixanthogen, formed under a higher applied electrode potential, was ascertained by a similar spectral feature of characteristic dixanthogen bands obtained with both polarization modes.

This is consistent with recent observations on enhanced hydrophobicity of mica surfaces in a mixed cationic amine and neutral alcohol surfactant solution. The increased overall surfactant adsorption density at the solid-liquid interface is accounted for by screening electrostatic repulsion between adjacent surfactant head groups.

Recently, a detailed study using a well-defined basal plane of crystalline sapphire in a surface forces apparatus showed that the formation of monolayer hemimicelles requires a near-cmc surfactant concentration in the surface region, while its bulk concentration has to be well below the cmc. Based on the well-known Stern-Grahame equation, this condition

cannot be satisfied in the absence of any attractive driving force of electrostatic and/or chemical nature required to preconcentrate the surfactant in the surface region to the cmc level. As a result, the lack of hydrophobic monolayer formation and hence effective flotation is anticipated.

Clearly, effective oxide flotation requires creation of a chemical environment that maximizes the surface concentration of the surfactant at as low a bulk concentration as possible. Changing suspension pH to control surface charge density in oxide flotation serves as an excellent example. Under certain circumstances, activation by hydrolysed metal ions, which provide the linkage between an anionic collector and a negatively charged mineral, is necessary to induce floatability. It should be noted that the selectivity of separation in oxide flotation is relatively poor if the electrostatic force is the only driving force for collector adsorption. This is particularly true in fine particle flotation, as heterocoagulation between different minerals often induces a secondary locking which destroys the selectivity. To this end, searching for collectors which chemically anchor on to targets remains the focus in oxide flotation systems. For sparingly soluble mineral flotation, solution chemistry calculation has been proven to be one of the most valuable tools in searching for separation windows. Since bulk solution chemistry controls the flotation response, a bulk precipitation followed by surface deposition, with a switch-on type of adsorption characteristics, has been considered to be the most favourable mechanism in flotation of soluble-type minerals, where the monolayer adsorption is hardly recognizable.

A recent trend in laboratory studies of sulfide flotation chemistry is to use a mixed mineral system. With this approach, an enhanced xanthate adsorption on anodic minerals by galvanic contact of dissimilar minerals was revealed. Also derived from this type of research is the depression of pyrite by copper sulfate addition in a sphalerite/pyrite mixed mineral system, shown in **Figure 4**, as opposed to pyrite activation in a single mineral system. A similar approach has been used in oxide and salt-type flotation systems.

In summary, our understanding of the interaction mechanism of collectors with minerals in a flotation system has evolved significantly following the development of modern instrumentation. Future advances in the fundamental understanding of flotation systems are anticipated with the introduction of the atomic force microscope in mineral flotation research. A combination of electrochemistry, *in situ* spectroscopy and surface imaging at a molecular level will enable us to pinpoint the mechanism and roles of collector-mineral interactions in flotation.

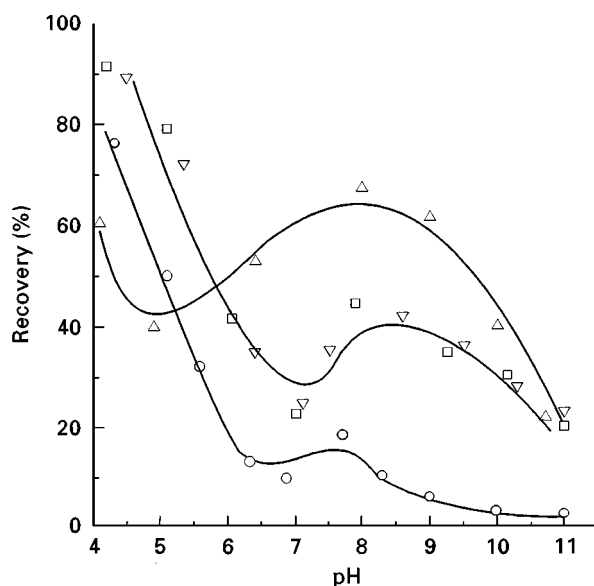


Figure 4 Flotation recovery of pyrite in the presence of 10^{-5} mol L $^{-1}$ iso-propylxanthate alone (squares) or with cupric ions (triangles), sphalerite (inverted triangles) or both (circles). The flotation of pyrite was depressed by a combination of cupric ions and sphalerite, although cupric ions alone activated pyrite flotation, illustrating the importance of studying flotation chemistry with mixed mineral systems in the context of the separation practice.

Flotation Mechanics

Bubbles are an indispensable component of froth flotation. Bubble generation in flotation machines forms the second foundation of a mineral flotation system. It is interesting to note that the development of flotation machines follows the evolution of bubble generation methods, although a flotation machine has to fulfil three basic functions: (i) generation of sufficient amount of bubbles with suitable sizes (c. 0.5–2 mm); (ii) dispersion of solid materials; and (iii) effective collision between particles and bubbles, in addition to providing a quiescent zone for froth formation. **Table 2** summarizes the major steps in the early stages of flotation machine development. Up until 1911, all available bubble generation methods had been practised in flotation machines. Driven by

an increased demand for metals and a need for cost reduction, the development of flotation machines in the subsequent 50 years was directed to the design of large volume cells, with the benefits of flexible process control and reduced capital cost, plant space, specific power and maintenance. Taking DO-3500 (Denver) as an example, cells of volume as large as 100 m 3 are now in operation. Radical changes incorporated in this new super-large cell include the use of a pump-type rotor, an overhung vane-type stator, a round tank of conical bottom and radial discharge of froth as in flotation columns. The most recognized development in flotation machines today is, however, the commercialization of flotation columns, followed by various innovative designs of aeration systems to generate microbubbles in response to slow flotation kinetics of fine particles.

The success of conventional flotation columns initiated a surge in the development of novel flotation devices, some of which are summarized in **Table 3**. Detailed analysis of these new devices shows a common feature – the generation of fine bubbles online with high energy dissipation (e.g. high turbulence in fluid). Major advances in these devices are illustrated, for example, in a fast flotation column, shown in **Figure 5**. The in-line generation of fine bubbles (feed aeration) by either a static mixer or a simple Venturi tube ensures a high bubble–particle collision efficiency. Partial recycling of tailings to the feed allows fugitive valuables to be captured, while a deep froth with wash-water addition cleans up entrained unwanted gangues. Essentially, a flotation column in this configuration is equivalent to a flotation circuit: (i) a rougher in the middle; (ii) a cleaner on the top; and (iii) a scavenger at the bottom.

The improvement of froth quality, by deep froth and froth washing in the flotation column, brought the recent development of Outokumpu's HG tank, which features an adjustable booster cone to control froth quality. A hidden feature in these newly designed flotation devices is the role of hydrodynamic cavitation. The importance of hydrodynamic cavitation in flotation is the complete elimination of the bubble–particle collision step, resulting in a 100% increase in flotation rate constant, seen in a case study using the set-up shown in **Figure 6**. The preferential nucleation of bubbles on hydrophobic particles is anticipated to contribute to improvement in flotation selectivity. With hydrodynamic cavitation, strong mechanical agitation, which is otherwise required to provide the kinetic energy necessary to overcome energy barriers for bubble–particle attachment, can be minimized. As a result, a more quiescent environment is created for enhanced froth–pulp disintegration. Along the same line of thinking, the use of

Table 2 Early developments in bubble generation and flotation machines

Year	Methods of bubble generation	Flotation acronym
1904	Electrolysis	Electroflotation
1904	Pressure reduction	Vacuum flotation
1905	Air dispersion by agitation	Mechanical cell
	Pressurization/pressure release	Dissolved air flotation
1911	Air dispersion by spargers	Pneumatic cell

Table 3 Examples of new flotation devices developed in the minerals industry since the 1980s

Device	Features	Inventors
Air-sparged hydrocyclone	Centrifugal force/porous cylinder aerator	Miller
Pneumatic cell	Slot aerator under pressure	Bahr
Packed column	Unlimited froth height	Yang
Microcell	Static mixer/tailing recycle	Yoon
Jameson cell	Self-aspiration: plunging slurry jet	Jameson
Contact cell	Feed aeration	Amelunxen
Ken Flote	Conditioning with dissolved air	Parekh <i>et al.</i>
USBM rapid cell	Static mixer	Jordan <i>et al.</i>
Rapid flotation column	Feed aeration/tailing recycle	Xu <i>et al.</i>
Next generation	Hydrodynamic cavitation	Zhou <i>et al.</i>

ultrasonication or vibroacoustic modulation, to facilitate gas nucleation and bubble–particle attachment, has been tested. A gas nucleation mechanism, most likely by hydrodynamic cavitation with innovative engineering of the cavitation tube or ultrasonic modulation, is anticipated to be the main feature of the next generation of flotation devices. A reactor–separator design as seen in Figure 5 is desirable to optimize individually bubble–particle contact and bubble–pulp separation.

Flotation Physics

It is evident that, for effective flotation, the thin liquid films between an air bubble and a target have to be thinned and ruptured (film stability), while association between different species (hetero-coagulation) needs to be avoided to separate one species from another. The physics of the flotation system (i.e.

surface forces between various phases) controls such phenomena as thin film stability and coagulation. As a macroscopic process, flotation is often analysed in terms of micro subprocesses and the knowledge about them would serve as an encyclopedia of colloidal science. Fundamental studies in flotation physics have evolved, to today's role of hydrophobic forces in flotation, from pioneer work by Wark (capillary forces), Sutherland (contact angles), Derjaguin (interparticle forces), Derjaguin and Dukin (elementary stages of flotation), Klassen (role of hydration shells in flotation), Scheludko (thin film stability) and Schultz (hydrodynamic forces).

The capillary phenomena confirmed the existence of relatively short range molecular forces, manifested in observed surface tension. The floatability of minerals has been frequently correlated to contact angles of solid against water (or, more precisely, contact angle hysteresis in flotation practice, which involves

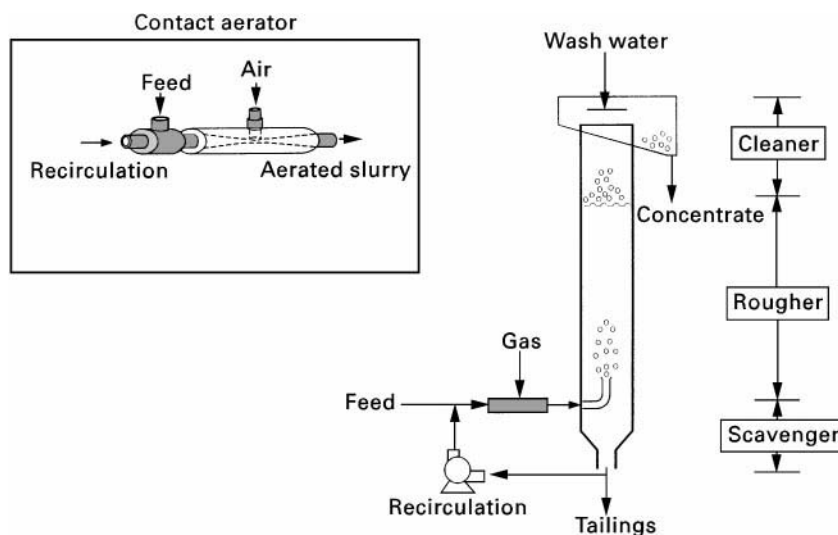


Figure 5 Schematic of a modern flotation column featuring feed line aeration (insert) and partial recycle of tailings. The main thrust of a column in this configuration is its equivalence to a virtual flotation circuit with the capability of generating fine bubbles for fine particle flotation.

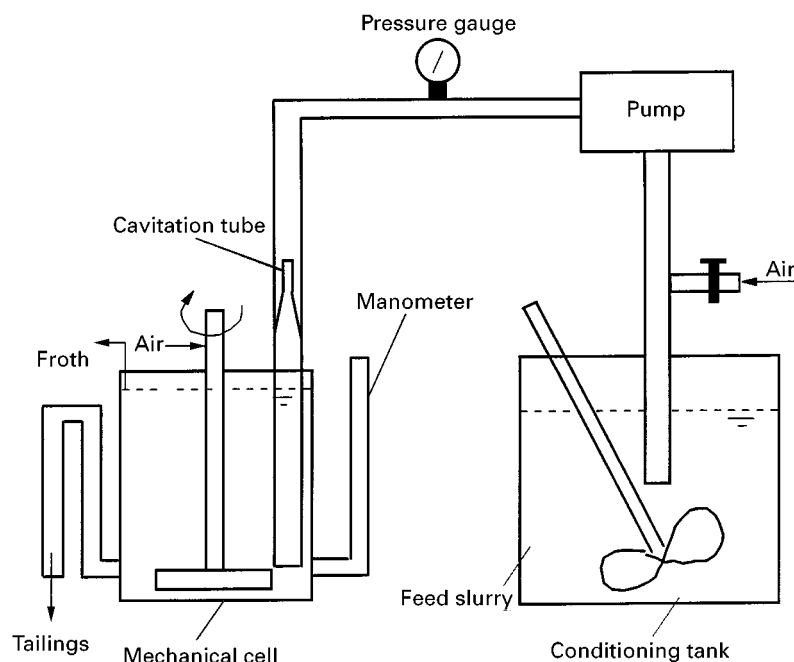


Figure 6 Schematics of a flotation system with reactor-separator design exploiting hydrodynamic cavitation in fine particle flotation. A 10-fold increase in removal efficiency of fine oil contaminants in the soil-washing process has been demonstrated in a laboratory-scale test. Using the setup at INCO's Matt separation site (Sudbury, Canada), a doubling of the pentlandite flotation rate at a comparable concentrate grade was obtained. The main attraction of this configuration is that it can be readily implemented in the existing flotation circuit by simply bridging the conditioning tank with mechanical cells using a cavitation-type reactor.

consideration of both adhesion and detachment). The contact angle phenomena manifest the competition for water molecules by solids and by water itself, assuming that the interaction between air and other phases (solid or water) is negligible. The work of cohesion of water greater than the work of water-solid adhesion is equivalent to a contact angle greater than zero as the thermodynamic criterion of floatability. However, the former provides insight into the competition between various phases. Analysis on work of adhesion and cohesion for a flotation system has contributed to the improved understanding of flotation physics. To this end, the concept of critical surface tension proposed by Zisman was adopted in a so-called Gamma flotation process, although its practical application has been limited to coal flotation or the recycling of low surface energy polymeric materials. The role of collector adsorption in flotation is to reduce the work of adhesion of target solids by exposure of weakly interactive hydrocarbon tails to water. Such a system of high solid-liquid interfacial tension is thermodynamically unfavourable, making the particles floatable.

The use of the electrostatic double layer and van der Waals forces considered in the classical colloidal stability theory (known as Deryagin-Landau-Verwey-Overbeek, or DLVO theory) has been suc-

cessful in accounting for the stability of some colloidal systems. It is now generally accepted that additional forces need to be considered to understand fully the observed phenomena in flotation systems. A typical example is that alumina is not floatable in the absence of surfactant, although a strong electric double-layer attraction between air bubbles and the solids is predicted. On the other hand, quartz dehydrated at a temperature above 1000°C is readily floatable without any collector, yet the classical DLVO theory would predict repulsive van der Waals and electrostatic forces between the two. It is clear that the additional force can be either attractive or repulsive, depending on the hydrophobic or hydrophilic nature of the solid surfaces.

Thanks to a recent breakthrough in measuring surface forces directly, the presence of additional long range attractive forces between hydrophobic surfaces and short range repulsive forces between strongly hydrated surfaces has been confirmed. The former has contributed significantly to comprehending the thin film rupture phenomena which occur in most flotation systems. The force between an air bubble and a solid surface has been directly measured with an atomic force microscope and results, shown in **Figure 7**, confirm the existence of additional attractive forces. It should be noted that the direct force

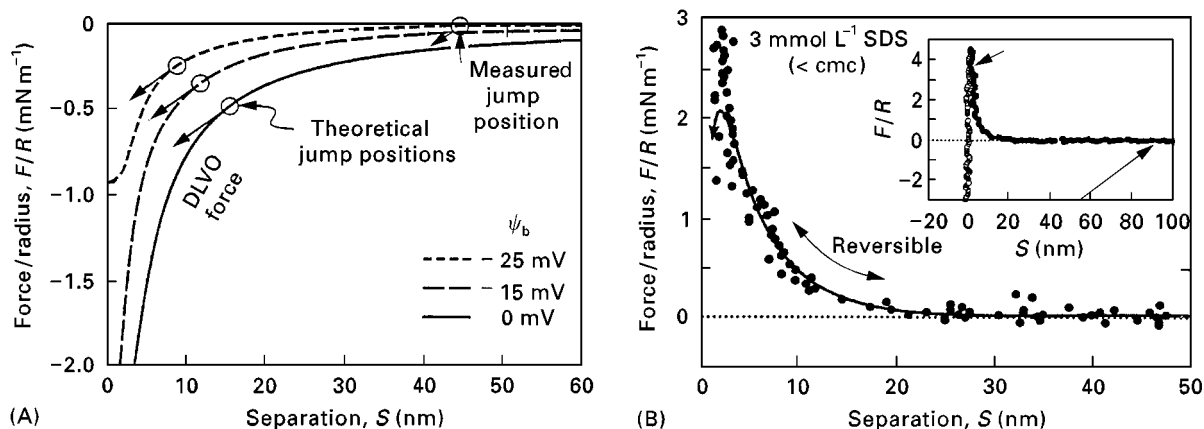


Figure 7 Forces between an air bubble and a silica particle in (A) an electrolyte solution with (B) added surfactant, measured directly with an atomic force microscope. A much greater jump in distance than predicted from the classical DLVO theory (A: shown by arrows) confirms the existence of additional attractive forces. In contrast, the presence of 3 mmol L^{-1} SDS changed the forces from a long range attraction to a long range repulsion, well-described by the DLVO theory (B), manifesting the role of surfactant in flotation.

measurement between an air bubble and a hydrophobic solid surface remains an unresolved challenge, even though it is most relevant to flotation.

Following recent advances in scientific instrumentation, such as the atomic force microscope, film balance and surface forces apparatus, flotation research has gone through a period of thermodynamic analysis of bubble-particle attachment to the understanding of intermolecular forces involved. These advances have allowed flotation subprocesses to be analysed from first principles. Bubble-particle adhesion, and hence flotation, for example requires particle-bubble contact (sliding) time greater than film rupture (induction) time controlled by wetting kinetics. An attempt has been made to derive a flotation rate equation from first principles by considering both surface forces and system hydrodynamics. The practical application of the derived equation in flotation process development remains to be explored. The empirical relations, outlined in a review by Radoev and Alexandrova (1992), remain the main source for process design and simulation.

It is important to note that chemistry, physics and mechanics, which form the three foundations of a flotation system and determine the process dynamics, are interrelated among themselves. This is emphasized in Figure 1 by a triangular relation on the base of the tetrahedron. Bubble size in a flotation system, for example, is determined by chemistry (addition of frother) which affects the physics of film stability (surface forces) balanced by mechanical forces and liquid viscosity. Only when these three factors are considered simultaneously can the flotation dynamics be optimized. An important area in flotation development is the innovations in: (i) on-stream analysis

(X-ray fluorescence analyser, ash analyser, nuclear magnetic resonance and image analysis); (ii) sensors (redox, ion-selective Eh and conductivity probes); (iii) dynamic process modelling (expert systems and artificial neural networks to mimic control actions by human operators); (iv) control (fuzzy logic and self-organizing controller); and (v) instrumentation. Details on these developments are not included in this article, and interested readers are referred to the recent review articles by Sastry and Fuerstenau (1988), Mavros and Matis (1991) and the *Proceedings of the XIX International Mineral Processing Congress* (1995).

Recent Advances in Flotation Practice

It appears unnecessary to list all of the minerals processed by flotation, since almost all minerals mined today can be separated effectively by froth flotation. In addition to developments in the three foundation areas of flotation (Figure 1), significant progress has also been made in circuit design. Following the introduction of reverse, bulk and differential flotation, the multifeed circuit, shown in Figure 8 and practised in China for processing copper sulfide, is considered to be one of the most recent advances in this regard. With the multifeed circuit, the improved recovery has been attributed largely to the autogenous carrier (piggyback) effect. The reduced reagent consumption, which creates a starving reagent addition, may have contributed to the improved concentrate grade (i.e. selectivity). In the Climax Mill (USA), the use of the multifeed circuit improved the molybdenite grade from 14 to 34% MoS_2 at comparable molybdenite recovery and

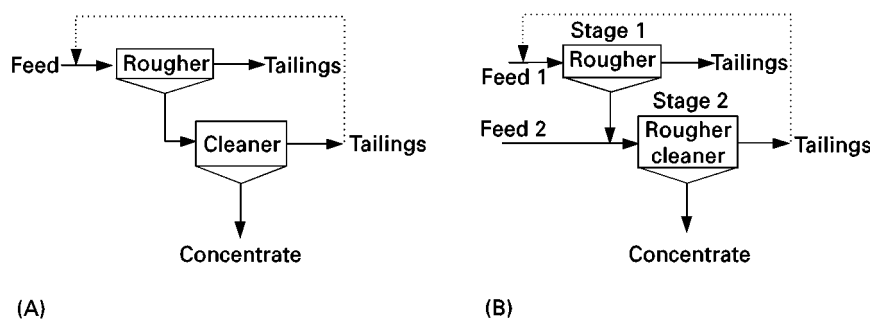


Figure 8 Comparison of (A) conventional rougher-cleaner circuit with (B) multifeed circuit. The dotted lines represent a variation of the circuits with recirculating loads. An added advantage with a multifeed circuit includes improved concentrate grade at reduced reagent consumption while maintaining the valuable recoveries.

reduced by half collector and frother consumptions. Another recent development is flash flotation which uses a coarse flotation cell (Skim-Air) in a grinding circuit to produce final concentrate from a cyclone underflow stream before further grinding (Figure 9). This approach minimizes overgrinding of valuable material richer in the cyclone underflow than in the feed stream. In addition to increased recovery, an improved throughput for the subsequent unit operations and the high dewatering efficiency of final concentrate are recognized with flash flotation. In tackling the challenge of fine particle flotation, high intensity conditioning has been developed. The improved process performance has been attributed to mechanical surface cleaning of slimes, shear-induced aggregation of target particles and, yet to be confirmed, *in situ* bubble formation on hydrophobized particles by hydrodynamic cavitation and resultant bubble-particle aggregation. Online pulp potential

control assisted by nitrogen as the carrier gas has also been engineered in flotation machines and columns as a means of improving selectivity of sulfide mineral separation.

Concluding Remarks

With generations of research efforts, flotation has matured into a process of choice for many separation tasks, including mineral separation, bitumen extraction from tar sands, soil remediation, materials recycling, de-inking, de-oiling, de-colouring, biological species fractionation and industrial effluent detoxification in the form of either froth flotation or absorptive bubble separation. Both inventions and innovations have played an indispensable role in flotation development in an evolutionary, rather than a revolutionary, fashion. Although flotation practice has always been ahead of flotation science, the gaps

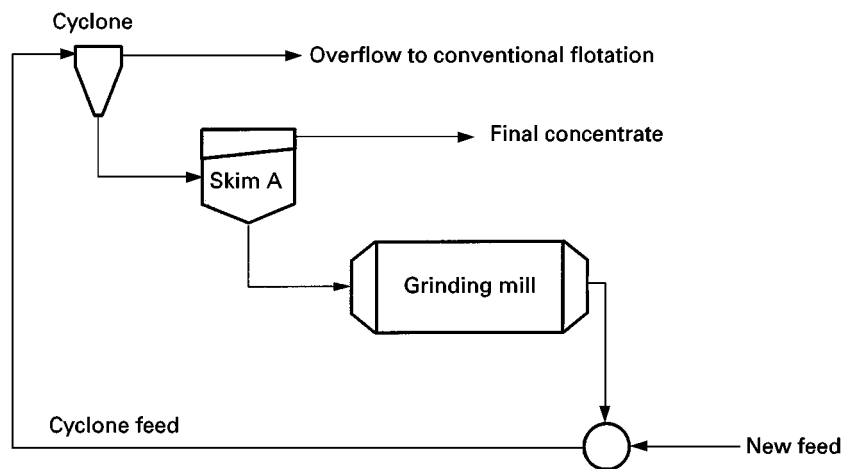


Figure 9 Schematics of a flash flotation circuit with a coarse flotation before grinding. The circuit minimizes overgrinding of valuables and improves the recovery and product quality at an increased throughput.

between the two have narrowed significantly. Improving fundamental understanding of the flotation process remains the main focus of research for the future. The areas where significant advances are anticipated include: (i) design and synthesis of more effective, environmentally friendly flotation reagents (mainly collectors, frothers and depressants); (ii) engineering of a pulp potential monitor (mineral electrodes) and control in sulfide flotation practice; (iii) development of new flotation cells to maximize separation efficiency and minimize energy consumption; (iv) understanding and utilization of biotreatment to replace both collectors and depressants; and (v) design of a better and reliable process control system based on further development of sensors and simulators. The main challenge that flotation engineers and scientists are facing is to develop viable process alternatives for fine particle flotation. Four areas of immediate interests are: (i) the development and understanding of high intensity conditioning; (ii) hydrodynamic cavitation in flotation machines; (iii) selective aggregation by coagulation, flocculation or oil agglomeration; and (iv) practical conditions for collectorless flotation of sulfide ores.

Further research is needed in the area of flotation chemistry and implementation of the outcome into process development. All of these are driven by the depletion of rich and simple mineral resources, reduction of metal prices and the increase of environmental pressures. The processing of tailings with a gravity concentrator at Laurium, from 1864 to 1920, left tailings containing 3% lead, these were reprocessed again in 1955 by flotation with a resulting tailings assay of 0.3% lead. It is not unrealistic to suggest that

the resultant tailings may be reprocessed in the future with further innovative developments, such as integration of biotreatment in flotation. To conclude, there is a long-awaited need to widen the range of flotation applications to nonmineral-processing applications, such as in material recycling and waste remediation, with revolutionary changes in flotation technology.

Further Reading

- Ives KJ (ed.) (1984) *The Scientific Basis of Flotation*. The Hague: Martinus Nijhoff Publishers.
- Jones MH and Woodcock JT (eds) (1984) *Principles of Mineral Flotation*. Victoria: AIMM.
- Laskowski JS (ed.) (1989) *Frothing in Flotation*. New York: Gordon Breach Science.
- Matis KA (ed.) (1995) *Flotation Science and Engineering*. New York: Marcel Dekker.
- Mavros P and Matis KA (eds) (1991) *Innovations in Flotation Technology*. Dordrecht: Kluwer Academic Publishers.
- Parekh BK and Miller JD (eds) (1999) *Advances in Flotation Technology*. Littleton: SME.
- Sastry KVS and Fuerstenau MC (eds) (1989) *Challenges in Minerals Processing*. Littleton: SME.
- Schulze HJ (1984) *Physico-chemical Elementary Processes in Flotation*. Amsterdam: Elsevier.
- Somasundaran P and Moudgil BM (eds) (1988) *Reagents in Mineral Technology*. New York: Marcel Dekker.
- Souninen EJ, Forssberg KSE and Buckley AN (eds) (1997) *Application of Surface Science to Advancing Flotation Technology*. Amsterdam: Elsevier.
- Wood R, Doyle FM and Richardson P (eds) (1996) *Electrochemistry in Mineral and Metal Processing*, Vol. IV. Pennington: Electrochemistry Society.

Hydrophobic Surface State Flotation

J. D. Miller, University of Utah, Salt Lake City, UT, USA
Copyright © 2000 Academic Press

Introduction

The essence of particle separation by flotation is the creation of a hydrophobic surface state, i.e. a surface that is not wetted by water, a particle surface at which bubble attachment will occur leading to flotation due to the buoyancy of the particle-bubble aggregate. (Particle flotation can also, however, be accomplished by bubble entrapment rather than by bubble attachment. For example, entrapment of air during particle aggregation/flocculation can lead to the flotation of aeroflocs.) In many instances this hydrophobicity must be

established in a selective manner, frequently by collector (surfactant) addition, so that one particle type can be separated from other particle types which are maintained in a hydrophilic state.

The extent to which a surface is hydrophobic can be described in various ways. Two of the most common laboratory methods are contact-angle measurement and bubble attachment time measurement. The contact angle measurement tends to be an equilibrium, or pseudo-equilibrium, measure of hydrophobicity, while the bubble attachment time measurement is a kinetic measure of hydrophobicity. Other measures of hydrophobicity are also possible and include bubble pick-up and microflotation experiments.

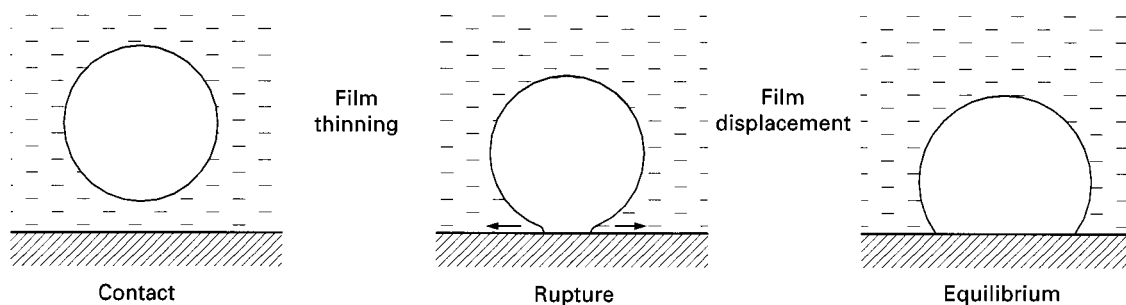


Figure 1 Bubble attachment. Sequence of events.

Bubble Attachment

Bubble attachment at a hydrophobic surface occurs due to the instability of the aqueous film that separates the bubble from the surface. As the bubble approaches the surface, to such a separation distance that the bubble may be distorted, there is a thinning of the aqueous film to the point at which rupture occurs. This time of film thinning is called the 'induction time'. After rupture, the film is displaced as it recedes across the hydrophobic surface to establish the equilibrium contact angle. The total time of film thinning and film displacement is the bubble attachment time. The sequence of events at a polished surface is depicted in **Figure 1**, where the bubble attachment time is shown to consist of the film thinning (induction) time and the film displacement time. Thus the bubble attachment time is, in part, a measure of hydrophobicity and can vary from less than a millisecond to several seconds in magnitude. Although the hydrophobicity should be an intrinsic property of the system, the bubble attachment time measurement is significantly influenced by the experimental method. For example, the bubble attachment time for a sample of naturally hydrophobic bituminous coal was found to vary by a factor of more than 50 when the results obtained for a polished surface are compared with those obtained for a particle bed as revealed in **Table 1**. Similar results have been re-

ported for chalcopyrite. The very strong effect of contact area, hydrodynamics, and surface morphology are revealed from these data. For a given experimental technique, the shorter the bubble attachment time, the greater the hydrophobicity.

Contact Angle

The equilibrium state for the attached bubble is described by the contact angle, θ , as indicated in **Figure 2**. The contact angle for this three-phase equilibrium is related to the respective interfacial tensions by Young's equation,

$$\gamma_{SG} = \gamma_{SL} + \gamma_{LG} \cos \theta$$

The attachment process should be spontaneous for all finite contact angles, but generally a contact angle of at least 20° is required for bubble attachment and flotation. The greater the contact angle, the greater the hydrophobicity. Of course contact angles much greater than 20° are desired in order to make effective flotation separations. Generally the characteristic contact angles for flotation systems rarely exceed 100° . Typical values for naturally hydrophobic minerals are given in **Table 2**. Larger contact angles are

Table 1 Measured bubble attachment times for a low-volatile bituminous coal at a polished surface and at a bed of particles (100×200 mesh)

Mode of attachment	Gas phase	Attachment time (ms)
Polished surface	Air	180–200
	N ₂	170–190
	CO ₂	140–150
Particle bed	Air	3
	N ₂	–
	CO ₂	3

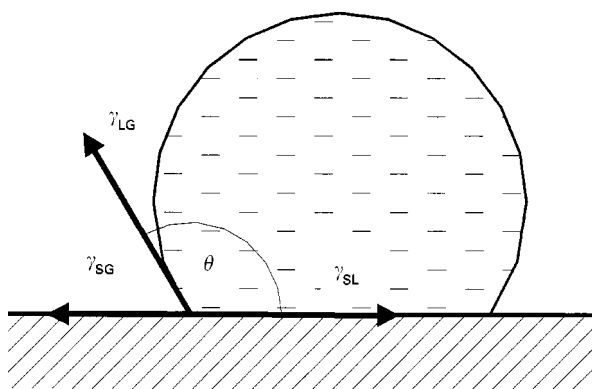


Figure 2 Equilibrium state for water drop at a hydrophobic surface.

Table 2 Naturally hydrophobic minerals and respective contact angles

Mineral	Composition	Surface plane	Contact angle (degrees)
Graphite	C	0001	86
Coal	Complex hydrocarbon		20–60
Sulfur	S		85
Molybdenite	MoS ₂	0001	75
Stibnite	Sb ₂ S ₃	010	
Pyrophyllite	Al ₂ (Si ₄ O ₁₀)(OH) ₂	001	
Talc	Mg ₃ (Si ₄ O ₁₀)(OH) ₂	001	88
Iodyrite	AgI		20

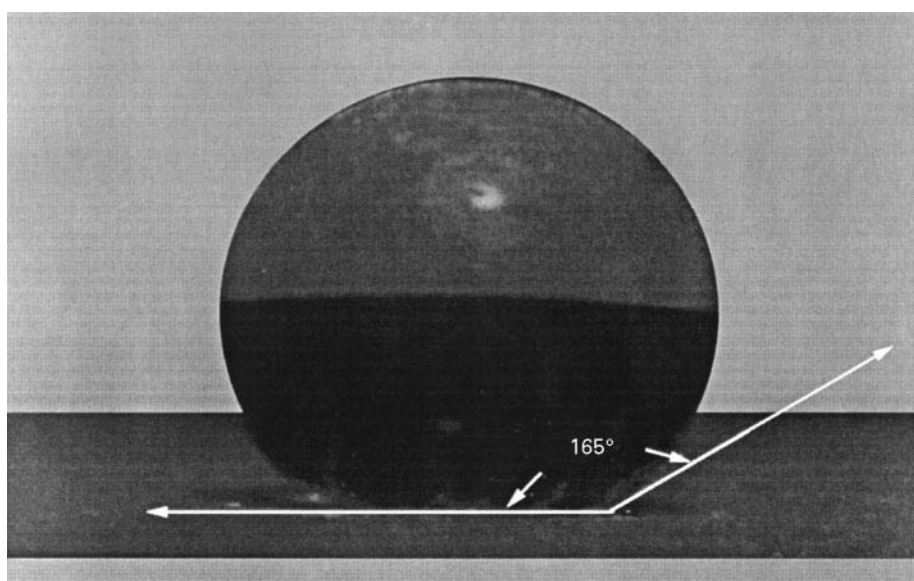
possible for specially prepared surfaces which are highly water repellant. For example, water contact angles exceeding 150° have been observed for specially prepared surfaces as shown in Figure 3.

Nonpolar Surfaces

It is evident that the hydrophobic surface state is established by nonpolar surfaces which are not extensively hydrated. Now the nonpolar surface criterion for hydrophobicity is well known and has been established for some time. Such characteristics of the hydrophobic surface state have been known since the mid-1950s. In some cases the hydrophobic surface state is due to the elemental composition of the surface; the surface is composed of elements of low polarity that do not hydrogen bond with water molecules. These elements include C, H, S, and large atoms of low polarizability. Examples include graph-

ite, coal, elemental sulfur, and iodyrite. Even the surfaces of metal sulfide minerals are reported to be hydrophobic in the absence of oxygen and can be considered to be intrinsically hydrophobic. Of course, exposure to even parts per billion of oxygen can lead to oxygen fixation and subsequent complex electrochemical reactions, the surface products of which may or may not be hydrophilic depending on solution chemistry and the extent of oxidation. In general, simply the fixation of oxygen at sulfide mineral surfaces can provide sufficient surface polarity to create a hydrophilic state. Nevertheless, under anaerobic conditions the sulfide surface is expected to be hydrophobic due to its limited ability to hydrogen bond with interfacial water molecules.

In addition to the elemental composition of the surface, the crystal structure and bonding influence the polarity of mineral surfaces. In some cases, specifically surfaces that are created by breakage of weak van der Waals bonds, a nonpolar surface is created even containing elements that normally would hydrogen bond and be hydrated by interfacial water molecules. Examples include pyrophyllite, talc, and boric acid. In this way it has been established that the hydrophobic nonpolar surface state can arise from the intrinsic properties of the elements of which the surface is composed and from bonding considerations associated with the crystal structure. Finally it should be noted that hydrophobic surfaces can be charged just as hydrophilic surfaces are and that generally maximum hydrophobicity is found at the isoelectric point, or the point of zero charge, of the surface.

**Figure 3** Water contact angle for a sessile drop of water at the surface of a newly developed water repellant material.

Water Film Stability

Of course the hydrophobic surface state must not only be described in terms of the elemental surface composition and structure but also must be described in terms of the interfacial water structure; in fact the instability of the interfacial water film accounts for bubble attachment at a hydrophobic surface. The characteristic features of interfacial water and its instability at a hydrophobic surface have not been so well described until recently. Now with the use of atomic force microscopy, surface spectroscopy, and a laser optical cavity technique, these features of interfacial water have been revealed in greater detail.

Direct force measurements during the 1980s and 1990s have revealed that attractive hydrophobic forces are usually 10 to 100 times larger than those expected from van der Waals interactions. These forces extend to distances of as much as 100–200 nm from the surface. The extent of attraction between hydrophobic surfaces is related to the degree of hydrophobicity but seems to be also independently effected by discrete features of the surface like roughness and heterogeneity.

At the same time, during the 1990s, *in situ* surface spectroscopy (sum frequency generation (SFG) and Fourier transform infrared/internal reflection spectroscopy (FTIR/IRS)) of water at hydrophobic surfaces has revealed important characteristics of interfacial water. The SFG spectral information clearly shows a distinction between water at a hydrophobic surface and water at a hydrophilic surface. Interfacial water at a hydrophobic surface is distinguished by a stronger absorption band at 3600 cm^{-1} characteristic of a dangling free OH bond. In contrast, interfacial water at a hydrophilic surface is distinguished by a diminished absorption band at 3600 cm^{-1} and a stronger signal at 3200 cm^{-1} characteristic of an ice-like structure with complete tetrahedral coordination. Based on these surface spectroscopy studies, it appears that interfacial water at a hydrophilic surface can be viewed as organized dipoles in tetrahedral coordination and oriented with respect to the polarity of the hydrophilic surface, whereas interfacial water mol-

ecules at a hydrophobic surface are not so well organized at the surface and have incomplete tetrahedral coordination with dangling free OH bonds.

It might be assumed that this *in situ* spectral data can then be used to account for film instability at a hydrophobic surface. Unfortunately, it seems that the phenomenon is not that simple. It is expected that the interfacial water structure will extend only a distance of a few molecular diameters, not more than a few nanometers or so. On the other hand, the hydrophobic attractive forces can extend to 100 nm, and even more. Thus it would seem that film instability at a hydrophobic surface involves more than just the hydrogen bonding characteristics of interfacial water.

Some researchers have attributed film instability to cavitation phenomena. The presence of nanobubbles or defects in the interfacial water region at a hydrophobic surface has been reported based on experimental results using a laser optical cavity technique. Also it should be noted that surface force measurements reveal that the range of the attractive hydrophobic force is significantly greater in gas-saturated solution than in degassed solution. It is expected that slight perturbations in the pressure field would cause these nanobubbles to coalesce and form cavities which upon further coalescence would lead to cavitation and failure of the water film at a hydrophobic surface as shown in Figure 4. In some cases, discontinuities during force measurements were observed which may be attributed to the phase transition (cavity formation) between approaching surfaces. Finally, recent FTIR/IRS spectroscopic evidence, indeed, shows that dissolved gas is accommodated at a hydrophobic surface but not so at a hydrophilic surface. Thus the presence of nanobubbles in the interfacial water region of a hydrophobic surface is supported by these spectroscopic results.

Summary

In summary, the hydrophobic surface state must be considered both with regard to the particle surface and with regard to the adjacent interfacial water

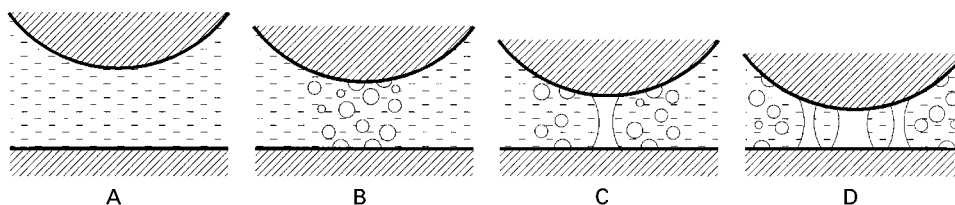


Figure 4 Schematic picture of cavitation phenomena during approach of hydrophobic sphere and hydrophobic plane in water. (A) Layers of lower medium density (adsorbed gas molecules), (B) nanobubbles formation, (C) bridging cavity formation, and (D) multiple bridging cavities, leading to film rupture and attachment.

region. The particle surface must be of low polarity which is determined by elemental composition and/or structural bonding considerations. Water film instability at a hydrophobic surface arises not only from a disrupted interfacial water structure but also from a cavitation phenomenon which involves coalescence of nanobubbles in the interfacial water region. Such is the nature of the hydrophobic surface state.

Further Reading

- Arbiter N, Fuji U, Hansen B and Raja A (1973) Surface properties of hydrophobic solids. In: Somasundaran P and Grieves RB (eds) *Advances in Interfacial Phenomena of Particulate/Solid/Gas Systems*, AIChE Symposium Series 150, vol. 71, pp. 176–182. New York: AIChE.
- Bunkin NF and Bunkin FV (1993) *Laser Physics* 3: 63.
- Bunkin NF, Kiseleva OA, Lobeyev AV, Movchan TG, Ningham BW and Vinogradova OI (1997) *Langmuir* 13: 3024.
- Chander S (1999) Fundamentals of sulfide mineral flotation. In: Parekh BK and Miller JD (eds) *Advances in Flotation Technology*, p. 129. Denver: Society for Mining, Metallurgy and Exploration.
- Drelich J, Miller JD, Li JS and Wan RY (1997) Bubble attachment time measurements at a chalcopryrite surface using a high-speed video system. In: *Proceedings of the XX International Mineral Processing Congress, Vol. 3: Flotation and other Physical Chemical Processes*, Aachen, Germany, 21–26 September 1997, pp. 53–64.
- Drost-Hansen W (1969) *Industrial Engineering Chemistry* 61: 331.
- Du Q, Freysz E and Shen YR (1994) *Science* 264: 826.
- Fokkink LGJ and Ralston J (1989) *Colloids Surfaces* 36: 69.
- Fuerstenau DW, Rosenbaum JM and Laskowski J (1983) *Colloids Surfaces* 8: 153.
- Fuerstenau MC, Miller JD and Kuhn MC (1985) *Chemistry of Flotation*, p. 35. New York: Society of Mining Engineers.
- Gaudin AM (1957) *Flotation*, 2nd edn, p. 218. New York: McGraw-Hill.
- Israelachvili J and Pashley R (1982) *Nature* 300: 341.
- Kitchener JA (1984) Surface forces in flotation – a critique, principles of mineral flotation. In: Jones MH and Woodcock JT (eds) *The Wark Symposium*, Series No. 40, pp. 65–71. Parkville, Victoria, Australia: Australian Institute of Min. Met.
- Laskowski J (1986) The relationship between flotability and hydrophobicity. In: Somasundaran P (ed.) *Advances in Mineral Processing*. Littleton, CO: Society of Mining Engineers.
- Laskowski J and Kitchener JA (1969) *Journal of Colloids and Interfacial Science* 29: 670.
- Meagher L and Craig VSJ (1994) *Langmuir* 10: 2736.
- Miller JD (1988) *The Significance of Electrochemistry in the Analysis of Mineral Processing Phenomena*. Seventh Australian Electrochemistry Conference, Sydney, Australia, February 14–19.
- Miller JD, Hu Y, Veeramasoneni S and Lu Y (1999) *Colloids Surfaces* 154: 137.
- Nalaskowski J, Hupka J and Miller JD (1999) *Physicochemical Problems in Mineral Processing* 33: 129.
- Parker JL, Claesson PM and Attard P (1994) *Journal of Physical Chemistry* 98: 8468.
- Rabinovich YI and Yoon RH (1994) *Langmuir* 10: 1903.
- Shibuichi S, Yamamoto T, Onda T and Tsujii K (1998) *Journal of Colloid Interface Science* 208: 287.
- Yamauchi G, Miller JD, Saito H, Takai K, Ueda T, Takazawa H, Yamamoto H and Nishii S (1996) *Colloid Surfaces A* 116: 125.
- Ye Y, Khandrika SM and Miller JD (1989) *International Journal of Mineral Processing* 25: 221.

Intensive Cells: Design

G. J. Jameson, University of Newcastle, Callaghan, NSW, Australia

Copyright © 2000 Academic Press

Introduction

In conventional flotation practice, the particles to be treated are dispersed in a suspension in water. Reagents are added to make the particles to be floated hydrophobic or nonwetting. The particles which are to be left behind remain in a wettable state. Air bubbles are then introduced into the slurry or pulp in a contacting device or cell, and collide with the non-wetted particles, carrying them to the surface where

they form a froth. The froth concentrate flows over a weir and out of the flotation cell, while the unwanted tailings flow out of the bottom.

The effectiveness of this type of cell lies in the ability of the bubbles rising in the liquid to collide with particles in suspension. Because the concentration or hold-up of air in the liquid is not very high – typically less than 10% by volume – the probability of a collision is correspondingly low. The low frequency of useful collisions between an individual bubble and the particles in a flotation machine can be overcome by increasing the residence time of the suspension. In this way, by using long residence times which can sometimes be as much as an hour in a

flotation bank, it is possible to achieve high recoveries of a floatable material.

In recent times, a number of flotation machines have been introduced which seek to reduce the residence time, by using new ways to bring about the contact between particles and bubbles. These are referred to as intensive flotation cells. Although the way in which the air is introduced – and the bubbles are made – differs from one type to another, they share a common feature. The collision between particles and bubbles does not take place within a liquid with a low number concentration of bubbles, or with a low gas hold-up. Rather, the air is introduced in such a way that contact is made in a device with a high air void fraction – a high ratio of gas volume to a given liquid volume. Once contact has been made, the bubbly mixture, which resembles a dense foam, passes to another vessel where the bubbles can disengage from the liquid, bearing their load of floatable particles to the supernatant froth layer.

The formation of bonds between bubbles and particles after collision is an essential step in flotation, and the topic has received much attention in flotation theory and practice. It has not always been appreciated that phenomena which take place in the froth phase above the liquid can also have a large effect on overall flotation performance. While the yield or recovery of floatable material obviously requires an efficient mechanism for contacting particles and bubbles, the grade or purity of the product is largely determined by froth-phase phenomena. When a continuous cloud of bubbles, whose surface contains selectively adsorbed hydrophobic particles, rises upwards through the froth-liquid interface, some of the liquid is trapped between the bubbles and is entrained into the froth layer. This liquid is the same composition as the main liquid in the flotation cell, so the concentration of gangue or waste particles in the liquid in the froth is approximately the same as in the liquid layer from which it arose, at least in the first instance. The presence of nonselective particles in the entrained water will reduce the grade of the concentrate product. While the bubbles are rising in the froth, the liquid layers between bubbles are draining, and gangue particles are carried downward, returning to the pulp layer. Over the last 20 years, it has become commonplace to apply clean water to the top of the froth layer, causing a continuous downward flow through the froth which tends to wash out the entrained gangue. With froth washing, flotation products of very high grade can easily be produced. (This assumes that the valuable material is completely liberated from the gangue by grinding. Any gangue which is locked into valuables

will generally float with the latter, thereby reducing the concentrate grade.)

The main objectives in the design of froth flotation equipment are always the same: to produce a device capable of achieving high grades and recoveries, with small size, minimum capital and operating costs, ease of operation and maintenance. To meet these objectives, many new cells have been tried over the years. This review will concentrate on the limited range of such cells which can genuinely be described as intensive, in that the contact time between bubbles and particles is very short, and the flotation cells are correspondingly quite small relative to the throughput. These are the air-sparged hydrocyclone (ASH), the Jameson cell, and the Ekof cell.

The Air-Sparged Hydrocyclone

The ASH was invented by Professor Jan Miller of the University of Utah, and was patented in the USA in 1981. It makes use of the centrifugal forces which arise when air is sparged through the walls of a hydrocyclone. The device consists of a cylinder with a porous wall enclosed in an external chamber (**Figure 1**). The feed slurry enters tangentially through a conventional hydrocyclone header at the top of the cyclone, to form an annular liquid layer on the inner surface of the porous wall. The slurry moves downwards through the cylinder with a strong swirling motion. Bubbles are generated at the surface of the porous wall and, because of the swirling motion, bubbles which are produced on the porous surface experience an inwardly directed centrifugal force which carries them away from the wall, to pass quickly through the annular layer, collecting floatable particles on the way, forming a froth layer in the core of the cyclone. The froth leaves through the vortex finder in the top of the cylinder, while the tailing particles whose density is greater than that of water move towards the wall and are discharged through an annular gap in the bottom of the vessel.

An important feature of the ASH is the froth pedestal in the base. This stabilizes the froth and prevents it from passing out in the tailings. The froth zone is forced to move upwards through the vortex finder, carrying the hydrophobic particles. The hydrophilic particles are carried out in the tailings slurry.

The performance of the ASH is dictated by the fluid motion in the swirl layer adjacent to the porous wall, which in turn is controlled by the kinetic energy in the inflowing slurry, and the physical dimensions of the header and the vertical cylinder.

The bubble contact time in the hydrocyclone is of the same order as that of the pulp residence time, around 10 s. There is a correspondingly high capacity

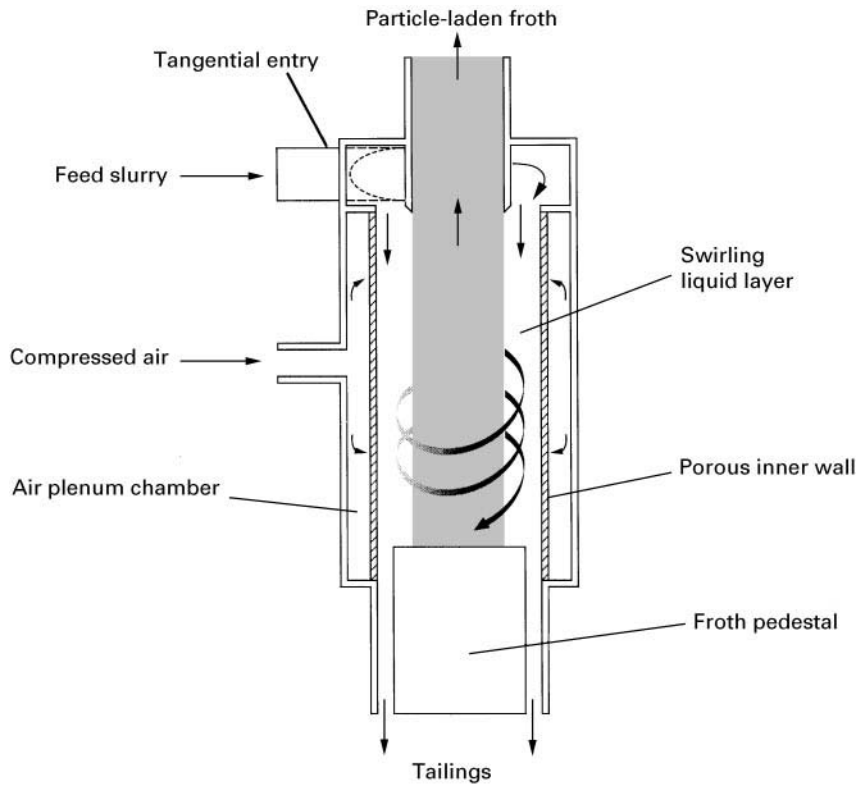


Figure 1 Schematic of the air-sparged hydrocyclone.

per unit volume, which is of the order of 100–600 tons day⁻¹ ft⁻³ of cell volume (3600–21 500 tonne day⁻¹ m⁻³) as against 1–2 tons day ft⁻³ (35–70 tonnes day⁻¹ m⁻³) for mechanical cells and columns. To date, the cells are not very large, but the capacity is quite high. Thus an ASH of diameter 5 cm and height 50 cm has a capacity of 3–18 tpd of solids.

The feed enters at conventional hydrocyclone pressures of 5–25 psi (35–170 kPa) and the air is supplied at a relatively high pressure of around 65 psi (440 kPa), which is necessary to force the air through the porous wall at the required flow rate.

An important parameter which limits the performance of flotation cells is the superficial velocity J_g , which is the volumetric flow rate of the flotation air divided by the cross-sectional area of the pulp normal to the direction of the air flow. A high J_g will lead to a high concentrate production rate, other things being equal. In conventional cells, the only force acting on the liquid in the froth is that of gravity. Because of the centrifugal field in the ASH, the drainage force on the liquid in the froth is enhanced, and high J_g s are possible. Thus, the typical air velocity in an ASH is around 1 standard L min⁻¹ cm⁻² of cylinder wall, which corresponds to a superficial velocity J_g of 17 cm s⁻¹. This figure may be compared with typical values for flotation columns, which are of the order of

0.5–4 cm s⁻¹, and mechanical cells where the figure is generally lower still – around 1 cm s⁻¹. The consequence is that the ratio of air-to-pulp flow rates can be very high, leading to high recoveries despite the short residence time. Reported values of the air-to-pulp ratio are as high as 16 : 1. In mechanical cells and flotation columns, the ratio is usually 1 : 1.

As far as contact between particles and bubbles is concerned, the ASH is clearly a very intensive flotation device. However, it is not so effective at handling the froth-phase requirements. Ideally, to obtain high grades, it is necessary to be able to apply clean washwater, which can drain through the froth and flush the gangue into the tailings stream, while leaving the hydrophobic material attached to the bubbles. For this to occur, the velocity at which water can drain through the froth under gravity must be greater than the superficial upward froth velocity in the core. Using published data, it is possible to calculate that the axial upward velocity of the froth core in an ASH is in the range 180–1300 cm s⁻¹. The diameter of flotation columns is fixed to allow for froth washing and the maximum working superficial air velocity J_g is about 4 cm s⁻¹ – far below the values attained in the ASH. Evidently it is not possible to design an ASH which can allow both intensive contact between bubbles and particles, and effective control of the

froth to obtain high grades. Accordingly, the ASH is most effective in applications where grade is unimportant, and where high recovery is desired. It is not surprising that the first large scale applications have appeared in the paper industry, for the removal of toner particles from recycled paper.

The Jameson Cell

The Jameson flotation cell was invented by Professor Graeme Jameson at the University of Newcastle, Australia, in 1986. It was developed to a practical reality at Mount Isa Mines, Mount Isa, Queensland, and was licensed to MIM Holdings of Brisbane in 1989. To date, there are 187 installations worldwide, in 19 countries. The cell is used for roughing, scavenging and cleaning, and also for removing oil haze from solvent extraction liquors. The distribution by field of use is coal 37%; copper 29%; other minerals 17%; and solvent extraction 17%.

In this cell, contact between particles and bubbles takes place in a dense foam which is produced in a vertical downcomer, as depicted in Figure 2. The pulp is introduced to the top of the downcomer as a confined liquid jet, and air is entrained into the feed and broken up into fine bubbles by the jet. A dense foam with a high void fraction is created in the

downcomer, creating a very favourable environment for collision of particles and bubbles. In fact, because of the high void fraction, of the order 50–60% by volume, the pulp is distributed in the form of thin liquid films between the bubbles, and collection occurs by migration of particles within the thin films, which are not much thicker than the diameter of the particles.

The dense mixture of bubbles and pulp discharges at the base of the downcomer, and the bubbles disengage from the pulp, rising into the froth layer. The bubble-free pulp discharges as tailings from the bottom of the cell. The froth behaves like that on top of a flotation column, in that grade and recovery can be strongly influenced by the froth depth and the application of washwater, and the upward superficial air velocity J_g . From the point of view of collection, the downcomer operates best when the ratio of air rate to feed rate is less than one-to-one on a volume basis.

The froth is treated much as in conventional columns. Washwater is usually applied if a high grade product is required. As with columns, when the air rate is altered, both steps in the flotation process – particle/bubble contact and froth entrainment – are affected. Thus an increase in air rate may cause an increase in recovery because more bubble surface area is created on which to capture particles, and because changes in the ratio of bubble to particle sizes will affect the probability of collision. At the same time, there may be an increase in entrainment of the gangue into the froth which may lead to a decrease in grade, unless steps are taken to remove the entrained gangue by changes in froth depth and washwater rate. Thus the optimum performance of the cell is related to the air superficial velocity, J_g .

The key features of the cell are:

1. The contacting environment is highly intensive, so that only short residence times are required. The total cell residence time is 1–2 min; the residence time in the downcomer is around 10 s. A short column is therefore produced which is ideal for retrofit, or installation in cramped headroom. The floor area is, however, similar to that required by conventional columns for the same throughput.
2. The bubbles formed by the impinging jet are very small, offering enhanced carrying capabilities for fine concentrate particles.
3. Air is drawn in from the atmosphere and no air compressor or blower is needed.
4. In the cleaning zone, with the use of washwater, the levels of concentrate grade approach the maximum levels possible.

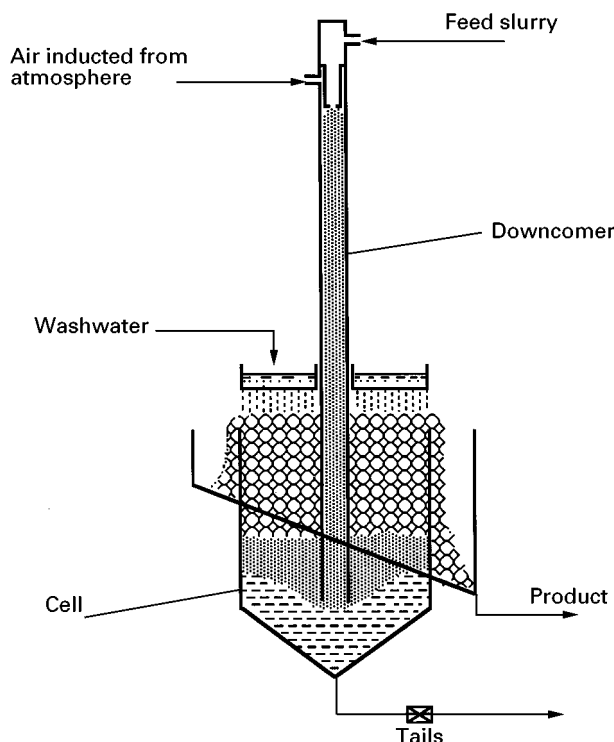


Figure 2 Schematic of the Jameson cell. The height overall is approximately 2–3 m. The cross-sectional area of the cell is directly proportional to the desired feed flow rate.

The size of bubbles produced in the flotation cell is an important determinant of cell capacity. The mass of particles which can be carried out on the surface of the bubbles is dependent on the gas-liquid interfacial area. For a given gas flow rate, the interfacial area is inversely proportional to the bubble size, so there is an advantage in making small bubbles. However, it must be kept in mind that in the disengagement zone, the buoyancy of the bubbles must be sufficient to lift particles of the largest size in the pulp to the surface of the liquid. The best compromise appears to be to make bubbles in the range 0.35–1 mm. Bubble sizings on full scale operating cells and test cells show that the Jameson cell produces an arithmetic mean bubble diameter of the order of 300–600 μm , while the Sauter (volume-to-surface) mean diameter, d_{vs} , is of the order 360–950 μm . These sizings compare very favourably with conventional columns where the Sauter mean bubble size is typically 2–3 mm.

Some general operating characteristics of the Jameson cell are now discussed.

Air Velocity in the Cell

The superficial gas velocity is the upward superficial velocity of air in a flotation cell, calculated by dividing the downcomer air rate ($\text{cm}^3 \text{s}^{-1}$) by the cross-sectional area (cm^2) of the riser part of the cell. The cell is normally circular or rectangular in section, and the appropriate cross-sectional area is simply the area normal to the direction of the flow of the froth, excluding the area occupied by the downcomer(s). The superficial velocity J_g is conveniently expressed in units of cm s^{-1} because values typically range from 0.5 to 4 cm s^{-1} in practice.

The recovery and concentrate carrying rate ($\text{g min}^{-1} \text{cm}^{-2}$) tend to increase with increasing J_g . As in conventional columns, there is a limiting upward flux of bubble surface through the pulp above which froth flooding occurs, resulting in the loss of froth-pulp interface, a very wet froth and total loss of selectivity. There is consequently a maximum air rate $J_{g\text{max}}$ defined by this limiting flux and bubble size. In flooding, the entire cell fills with froth as the only stable phase, and there is no pulp phase.

The operating J_g used in the sizing of the Jameson cell depends strongly on the application, and on the residual reagent concentrations from any upstream processes. Generally speaking, low values ($J_g = 0.4\text{--}0.8 \text{ cm s}^{-1}$) are employed in cleaning applications, and high values ($J_g = 1.0\text{--}2.0 \text{ cm s}^{-1}$) are employed in roughing or scavenging applications.

In cleaning operations, a high proportion of the feed reports to the concentrate, and the froth loading tends to be high. Consequently, the bubbles are well

coated with particles, which tend to stabilize the froth by reducing the froth coalescence rate. The drainage rate of the interstitial liquid in the froth is retarded by the relatively high concentration of particles, which has the effect of increasing the apparent viscosity of the interstitial liquid. Accordingly, it is necessary to design for lower values of J_g to allow time for the gangue to drain from the froth to obtain the required high grade. In roughing applications, however, only a small fraction of the feed reports to the concentrate and the froths formed tend to be less stable as a consequence. Also, gangue entrainment is not such a serious problem, because it can be dealt with in the downstream cleaning circuit. As a consequence of the higher coalescence rate the froth bed is shallower than that of the cleaners and a lower froth residence time will give good drainage. It is therefore usual to design a Jameson cell for a roughing application with a higher J_g than in the cleaners.

In some circumstances, high residual concentration of reagents in the feed necessitates the use of low values of J_g to avoid froth flooding. Although frother concentration is of primary importance to bubble size and hence the advent of froth flooding, circumstances have arisen where collector and frother interaction has been observed. In such a case, the frother dose should be decreased if collector dose is increased, and vice versa. Too high a frother or collector concentration can lead to froth flooding while too low a dose can lead to loss of froth stability.

Particle size can also have an influence on the maximum J_g , due to its effect on froth stability through bubble-bridging. Small particles (less than 100 μm) are easily collected at low gas rates, while recovery of coarser particles may be assisted by higher rates.

A complex system of liquid and air recirculation patterns forms in the bottom of the cell. The cell design is based on downcomer flows and downcomer placement to optimize this system to produce best grade and recovery. There is no limit on cell volume, providing the net downwards velocity of pulp, J_L , is sufficiently low to avoid the entrainment of bubbles in the underflow. When the froth and disengagement zones have the same cross-sectional area, the two important velocities are the rate of rise of the bubbles in the pulp, and the rate of drainage of liquid in the froth. The former is usually greater than the latter, so that a column sized to give the correct J_g will also give the correct J_L , and bubble entrainment in the downward flow will not be a problem.

Froth Depth

The froth phase in a Jameson cell can be controlled as in conventional columns. Shallow froth depths (less

than 200 mm) are used where high recovery is necessary and grade is of secondary importance, while deeper froths (up to 1 m) are employed to obtain maximum concentrate grade. Shallow froths result in significant entrainment of very fine ($< 10 \mu\text{m}$) gangue mineral which accompany the pulp phase. With deeper froths, significant drainage of hydrophilic gangue will take place, producing a higher grade concentrate, and a higher percentage of solids in the concentrate. Under some circumstances, the addition of washwater to the froth will assist froth mobility, and assist an otherwise immobile froth to keep moving to the overflow lip.

Air/Pulp Ratio

The air-to-pulp ratio (the ratio of the volumetric flow rates of air and pulp) in Jameson cells is usually in the range 0.3–0.9. Experiences with large (2–3 m diameter) Jameson cells indicate that operation at a low air/pulp ratio does not detract from metallurgical performance providing the superficial gas velocity J_g is maintained above 0.4 cm s^{-1} . Operation at lower air/pulp ratios has a stabilizing effect producing a finer, more uniform bubble size. A significant advantage of operation at lower air/feed ratios is that lower concentrations of frother are required.

The flux of interfacial area for a given gas rate varies directly as the gas flow rate and inversely as the bubble size. Thus the flux of bubble surface area, interfacial area per unit area of column cross-section per unit time, can be maintained with reduced superficial gas rate, providing the bubble size decreases accordingly.

The Effect of Washwater

Clean water can be applied to the top of the froth, to flush entrained material downwards, preventing it from flowing out with the flotation product. There are two measures which are used to measure and control washwater addition: the bias and the washwater ratio.

Bias is the absolute excess of the washwater applied to the froth, over the quantity of water being recovered in the concentrate, expressed as a superficial velocity J_b (cm s^{-1}): $J_b = (Q_{\text{ww}} - Q_{\text{wc}})/A_c$, where Q_{ww} , Q_{wc} are the volumetric flow rates of washwater and water in concentrate, and A_c is the cross-sectional area of the column.

The washwater ratio is defined as the ratio of the washwater addition rate, to the flow rate of water in the concentrate: $W = Q_{\text{ww}}/Q_{\text{wc}}$. The washwater ratio is a relative measure of the amount of washwater applied. If no washwater is used, the washwater ratio is zero and the bias is negative. When $J_b = 0$, $W = 1$.

A positive bias corresponds to washwater ratios greater than unity.

Although the bias does give an indication of the absolute amount of washwater being added, its use can be misleading because it does not take into account the wide variation in the absolute values of the rate of water entrainment in the concentrate. It is preferable to use the washwater ratio, which is a relative figure. In practice, it has been found that best performance is achieved when the washwater ratio is greater than 1.

Scale-Up

Scale-up of the Jameson cell is relatively simple, since the flotation capacity is proportional to the cross-sectional area of the cell, and the flow capabilities of the downcomer. Downcomers range in size from 0.2 to 0.36 m, and a large installation will have multiple downcomers. Large cells are typically 5 m in diameter, with 12–16 downcomers, and handle flow rates of $1200 \text{ m}^3 \text{ h}^{-1}$. Extensive testing has shown that the results obtained in small test units, of diameter 0.3 m, give an accurate picture of the performance of a large cell on the same feed. In many cases, test work is not required, because of the availability of data from operational plants which will allow a design to be established for a new application with an ore of similar characteristics.

Because there is a limit on the amount of air which can be supplied to a given amount of feed slurry in the downcomer, the Jameson cell can become limited by carrying capacity. Thus, if there is an excess of particles in the feed above the mass which can be carried by the available surface area of bubbles, some of the hydrophobic material will not be transferred to the concentrate. In such cases, it may be necessary to install a second cell in series with the first, to ensure a high recovery of the values. An alternative which is increasingly being used is to recycle part of the tailings. The feed pump is then sized so as to be well above the normal operating capacity. The feed pump draws from a pump box in the circuit ahead of the Jameson cell, and receives flow from two sources: new feed and recycled tails. It has been found that the recovery with recycle in the range 30–50% of the feed flow rate is equivalent to the addition of a second cell in series.

The Ekof Cell

The Ekof cell, also known as the Pneuflo cell is marketed by KHD Humboldt Wedag, of Bochum, Germany. It arose from a cell invented by Professor Albert Bahr, of Clausthal Technical University, Germany, in 1974. The Bahr cell consists of a vessel

of inverted conical form. The feed is premixed with air in a series of aerators distributed around the periphery of the vessel, in which air is injected through a porous wall into the transversely moving pulp. The bubbly pulp mixture is then fed to the vessel, where the bubbles rise and make contact with the floatable particles and carry them to the surface.

In the Bahr cell, the air-pulp mixture is introduced through pipes which enter through the wall of the vessel part-way up from the bottom of the cone, pointing vertically upwards to form a jet or plume. The jets are equispaced about the periphery of the cell. The idea was that a jet would spread out and mix with the pulp in the tank, bringing the bubbles into contact with the particles. Each jet would increase in area with vertical height, until at the surface the cross-sectional area of the jets would be about the same as that of the cell. The problem with this concept is that, as the size of the vessel and the design throughput increases, the height of the cell must increase as well. This difficulty was overcome in a later design in which the pipes delivering the air-pulp mixture are directed tangential to the cell wall, so that a low speed swirl develops. This design has been referred to as a Pneufлот cell. In both the Bahr and Pneufлот cells, the froth discharges over a lip into an annular launder which surrounds the vessel.

Because of the way the bubbles are generated, a high air pressure is needed to drive the air through the porous wall, and a relatively high feed pressure is needed to accelerate the pulp to the required speed in the aerator. In early models, froth washing was not provided, but it is available in later versions. The Bahr cell has had success especially in coal flotation.

In Pneufлот cells of the new form (Figure 3) the feed enters through a vertical pipe, and compressed air is introduced through small openings in an aerator unit at the top of the pipe. A model is also available in which the air is introduced into a Venturi. The aerated pulp is led through a central pipe to a low point in the flotation cell, and is diverted upwards by a distributor. The purpose of the distributor is to create an upward flow of bubbles which promotes flotation of coarse particles.

The latest form of Pneufлот cells is fitted with a froth crowder, which is of value when the loading of particles in the froth is low, and the froth is relatively unstable. The use of washwater is also possible in this design, as depicted in Figure 3.

Scale-up of the Pneufлот cell is not possible without testing on a pilot plant. There is no flotation time as in mechanical cells. The number of stages needed for a particular application can be determined by tests in which a Pneufлот cell is fed from an agitated tank at $6\text{--}10 \text{ m}^3 \text{ h}^{-1}$, with recycle of tailings from the cell

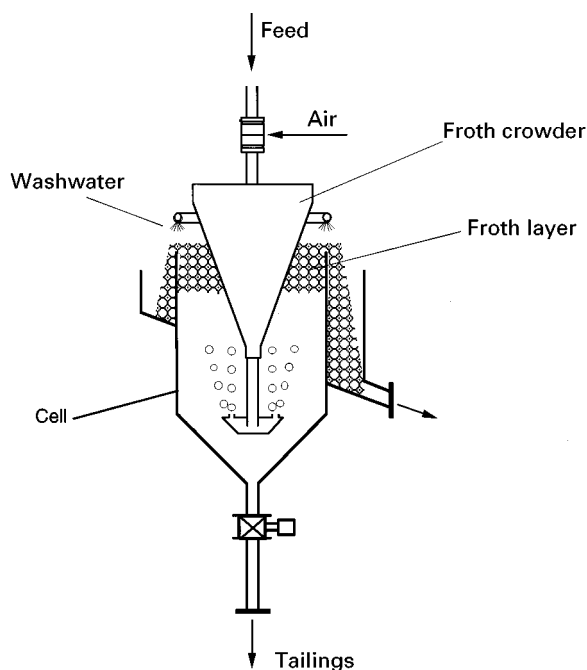


Figure 3 The essential features of the Ekof or Pneufлот cell of the new form.

back into the tank. From a plot of the concentration of the element of interest in the froth concentrate, the feed and the tailings, all as a function of time, it is possible to deduce the number of stages required by a stepping procedure.

The Pneufлот cell is in use in a number of applications, on magnesite, copper, galenafluorite, etc.

Future Developments

Further intensification of the flotation process is likely to come about in two directions. The processes of bubble contacting, bubble transfer to the pulp-liquid interface and froth drainage, are all responsive to a force field which can induce body forces on the liquid. In normal circumstances, the main body force is that of gravity. Accordingly, if the effective flotation rate per unit volume is to be increased, the logical step is to subject both the liquid and the froth to a centrifugal field. This will undoubtedly increase the mechanical complexity of the apparatus, and the saving in flotation cell volume may not warrant the extra cost of building, running and maintaining the equipment. Another possible direction for increased intensification is in the design of the initial gas-liquid contacting device. We have seen that, in both the Jameson cell and the Ekof cell, contacting takes place in a pipe or downcomer which must be of sufficient length to ensure efficient contact between bubbles and particles. It is likely that other

contactors could be devised which could bring about essentially instantaneous contact between particles and bubbles, effectively eliminating the downcomer. However, the over-riding objectives mentioned earlier – achieving high grades and recoveries, with small size, minimum capital and operating costs, in equipment which is easy to operate and maintain – will always remain the prime concerns of industrial users. In any new approaches, these objectives must be kept in view.

Further Reading

- Bahr A and Ludke H (1982) The development and introduction of a new coal flotation cell. In: *Proceedings of the XIV International Mineral Processing Congress, Toronto, Canada*, October 17–23, pp. VII-5.1–VII. 5-14. Montreal: Canadian Institute of Mining and Metallurgy.
- Bahr A, Imhof R and Ludke H (1985) Applications and sizing of a new pneumatic flotation cell. In: *Proceedings of the XV International Mineral Processing Conference, Cannes, France*; Organisé sous l'Égide de la Société de l'industrie Minérale et du Bureau de Recherches Géologiques et Minières. St-Etienne, France: Edition GEDIM, 1985–1986.
- Bahr A, Legner K, Ludke H and Mehroff F-W (1987) Five years of operational experience with pneumatic flotation in coal preparation. *Aufbereitungs Technik* 28: 1–10.
- Bahr A, Imhoff R, Changgen L and Muller W (1991) Development and progress in the application of the pneumatic flotation cell. In: Agar GE, Huls BJ and Hyma DB (eds) *Column '91, Proceedings of an International Conference on Column Flotation, Sudbury, Ontario, Canada*, 2–6 June, p. 703. Montreal: Canadian Institute of Mining, Metallurgy and Petroleum.
- Cordes H (1997) Development of pneumatic flotation cells to their present day status. *Aufbereitungs-Technik* 38: 69–78.
- Dawson W, Yannoulis GF, Atkinson BW and Jameson GJ (1996) Applications of the Jameson cell in the Australian coal industry. In: Gomez CO and Finch JA (eds) *Column '96: Proceedings of the International Symposium on Column Flotation, Montreal, Canada*, August 26–28, pp. 233–246. Montreal: Canadian Institute of Mining, Metallurgy and Petroleum.
- Evans GM, Atkinson BW and Jameson GJ (1996) Recent advances in Jameson cell technology. In: Gomez CO and Finch JA (eds) *Column '96: Proceedings of the International Symposium on Column Flotation, Montreal, Canada*, August 26–28, pp. 39–49. Montreal: Canadian Institute of Mining, Metallurgy and Petroleum.
- Finch JA (1995) Column flotation – part 4: novel flotation devices. *Minerals Engineering* 8: 587–602.
- Finch JA and Dobby GS (1990) *Column Flotation*. Oxford: Pergamon Press.
- Harbort GJ, Jackson BR and Manlapig EV (1994) Recent advances in Jameson flotation cell technology. *Minerals Engineering* 7: 319–332.
- Imhof R (1991) Device for carrying out pneumatic flotation. German patent application DE41 16 645.0.
- Jameson GJ (1988) A new concept in flotation machine design. *Minerals and Metallurgical Processing* 5: 44–47.
- Jameson GJ (1990) Column flotation method and apparatus. US patent 4,938,865.
- Jameson GJ (1994) Column flotation method. US patent 5,332,100.
- Miller JD (1981) Air-sparged hydrocyclone and method. US patent 4,279,743.
- Miller JD, Ye Y, Pacquet E, Baker MW and Gopalakrishnan S (1988) Design and operating variables in flotation separation with the air-sparged hydrocyclone. In: Forssberg KSE (ed.) *Proceedings of XVI International Mineral Processing Congress, Stockholm*, pp. 499–510. Amsterdam: Elsevier.
- Sanchez SP, Rojas FT, Fuentes GB *et al.* (1997) Ekof pneumatic flotation technology: the alternative for rougher, scavenger or cleaner flotation of metallic ores. In: Hoberg H (ed.) *Proceedings of XX International Mineral Processing Congress, Aachen, Germany*. Clausthal-Zellerfeld: GMDG Gesellschaft für Bergbau, Metallurgie, Rohstoff und Umwelttechnik.

Oil and Water Separation

B. Knox-Holmes, Baker Hughes Process Systems, Rugby, UK

Copyright © 2000 Academic Press

Development

The process of flotation needs a gas bubble to collide with, and attach to, an oil droplet; because of the hydrophobic nature of the oil droplet, a

stable gas–oil matrix is formed. The buoyancy of the oil droplet is increased by the attachment of the gas bubble, causing the oil droplet to rise rapidly through the water. Typically, one gas bubble will attach to one similar-sized oil droplet as described by Leech. As the bubbles in the froth phase burst, an oil layer is formed on the surface of the water. Oil and froth are then removed from the surface on an intermittent or continuous basis, depending on the mechanism used.

Flotation is a kinetic process. While a number of flotation models exist, Klimpel's first-order rate equation has been demonstrated to provide modelling flexibility, ease of physical interpretation and a good fit to the experimental data. The Klimpel model is written as:

$$R_0(t) = \left[1 - \left(1 - \frac{\exp(-kt)}{kt} \right) \right]$$

where $R_0(t)$ is the fractional recovery of oil at time t (s) and k is the characteristic first rate constant (s^{-1}). The key to flotation is the production of air or gas bubbles. The two major techniques are known as dissolved air flotation (DAF) and induced air flotation (IAF). IAF can be further subdivided into mechanically and hydraulically induced flotation.

Mechanically induced flotation has now been used for about 100 years to separate from a suspension in water, particles of valuable mineral from gangue. In the mining industry this process is known as beneficiation. It is now the main method of concentrating copper, molybdenum, iron, phosphate, lead and zinc ores. In the minerals industry the air is dispersed as bubbles, either through an impeller in subaeration cells or through spargers in flotation columns. These and other variants of the air addition to flotation pulps are classified as IAF. In the petroleum industry natural gas, carbon dioxide or nitrogen may be used as the flotation gas, hence the process is termed induced gas flotation or IGF. The use of these gases significantly reduces downstream corrosion problems and possible hydrocarbon degradation caused by the use of air.

Flotation techniques can remove dispersed, but not dissolved oil. As environmental legislation specifies both the limiting oil concentration and also the biological oxygen demand (BOD) in the discharged water, flotation is often the second stage of a three-stage effluent treatment process of gravity separation, flotation and biological treatment. As an example, British Petroleum's Grangemouth facility has achieved discharge concentrations of 2–3 mg L⁻¹ oil-in-water using gravity separation in American Petroleum Institute (API) separators, followed by IAF with a final biological treatment stage to remove dissolved BOD materials including ammonia, phenols and sulfides. Limits for oil-in-water discharges vary around the world, typically between 15 and 40 mg L⁻¹. A maximum BOD of 216 mg L⁻¹ daily, with a monthly average of 53 mg L⁻¹ is considered to be achievable via the application of the best available technology by the United States Environmental Protection Agency.

Process Techniques

Dissolved Air Flotation (DAF)

In this method compressed air or gas (nitrogen, carbon dioxide or methane) is dissolved into all or part, of a process liquid under pressure in a retention vessel. The gas-oil-water mixture is then sent to a flotation cell, where the pressure is reduced, causing bubbles to come out of solution. The bubbles then attach to and are possibly nucleated on the oil and suspended particles.

The solubility of a gas in water is proportional to its partial pressure and inversely proportional to the water temperature. Solubility may be characterized by Henry's law:

$$X_G = \frac{p}{H_G}$$

where X_G is the molecular fraction of the gaseous component in the liquid, p is the partial gas pressure and H_G is a constant. The release of gas following a reduction in pressure is proportional to:

$$\Delta X_G = \frac{1}{H_G}(p - p_{\text{amb}})$$

The Henry's law constants at 25°C for some gases used in DAF are given in **Table 1**.

Flotation efficiency depends on the gas used. The effectiveness of the various gases in terms of their bubble release increases in the following order: nitrogen, oxygen, natural gas (methane) and carbon dioxide. Solubility is also reduced as the dissolved solids content is increased. The amount of gas that can be dissolved ranges from 50% to 90% of its equilibrium solubility depending on the design of the pressurization system.

There are a number of ways of dissolving gas under pressure. The gas can be sparged into the liquid in a pressure vessel, liquid can be trickled over a packed bed or sprayed into an unpacked vessel, gas can be entrained with ejectors or gas can be injected into the suction side of the recycle pump.

Table 1 Henry's law constants at 25°C for various gases used in DAF

Gas	H (atm/mol fraction)
Nitrogen	9.08×10^4
Oxygen	4.38×10^4
Methane	4.13×10^4
Carbon dioxide	1.64×10^3

Full flow pressurization transfers gas to the whole feed flow at a relatively low pressure of between 30 and 40 psi. This technique is suitable when sufficient gas can be dissolved to effect flotation, and the passage of the whole flow through a centrifugal pump will not impair the subsequent flotation process through floc shearing.

Partial flow pressurization passes a proportion of the full flow through the pressurization system at 60–75 psi. This method reduces the size of the pressurization system, resulting in significant cost savings. This technique is suitable when sufficient gas can be dissolved to effect flotation, and passage of the partial flow through the pump will not impair flotation.

Recycle flow pressurization is used when a natural or chemically formed floc is to be separated from a wastewater. A portion of the clarified flotation effluent is recycled and used as the carrier of the dissolved gas. This latter technique is the most efficient and accounts for the majority of installations.

Figure 1 shows a flowsheet of a system operating with recycle flow, a flotation cell operating at atmospheric pressure, a pressurized retention vessel, feed and recycle pumps and a backpressure valve.

A level controller controls the flow into the pressurization vessel and excess gas may be vented. There is adequate residence time (typically 1–3 min) in the pressurization vessel for sufficient gas dissolution to take place (50–90% saturation). The pressurized liquid from the vessel is mixed with fresh feed, and is discharged through a back pressure valve to the flotation tank.

In the flotation tank, which may be circular or rectangular, the pressure is typically reduced to atmospheric pressure, and this reduction or let-down causes bubbles between 1 and 120 μm in diameter to come out of solution. Bubble size depends on the operation of the pressure let-down valve.

Gas bubbles may form by nucleation on an oil droplet or solid particle, or they may come out of solution and then attach to oil droplets and suspended solids by collision, or they may become trapped in a solid–chemical or oil droplet–chemical floc. Chemical usage is determined by the total chemistry of the system, and a series of bottle tests at site will be necessary to optimize performance.

Floated oil and suspended solids are removed by skimmers, while non-floatable settleings are removed from the bottom of the cell by a grit scraper. The efficiency of the removal process depends on the ratio of air to solids and/or oil in the water. Too little air and separation will not be achieved. Too much air and the additional turbulence may actually reduce separation performance by causing floc re-entrainment, resulting in a reduction in energy efficiency.

The DAF machine can be characterized by being a relatively quiescent, high retention time device (15–30 min), using small volumes of dissolved gas (35–180 L m^{-3} of throughput). Depending on gas type, dissolution pressure, stream temperature and suspended solids loading, DAF may achieve 80–95% removal of free and emulsified oil and suspended solids.

Induced Gas Flotation (IGF)

In the induced gas flotation (IGF) (or IAF) process, which resembles the design of a subaeration minerals flotation cell (see Figure 2), bubbles are induced mechanically.

IGF uses a star-shaped impeller to generate intense local turbulence. This results in subatmospheric pressures being generated in the region surrounding the impeller which causes gas to be induced from the gas space at the top of the compartment via gas inlet

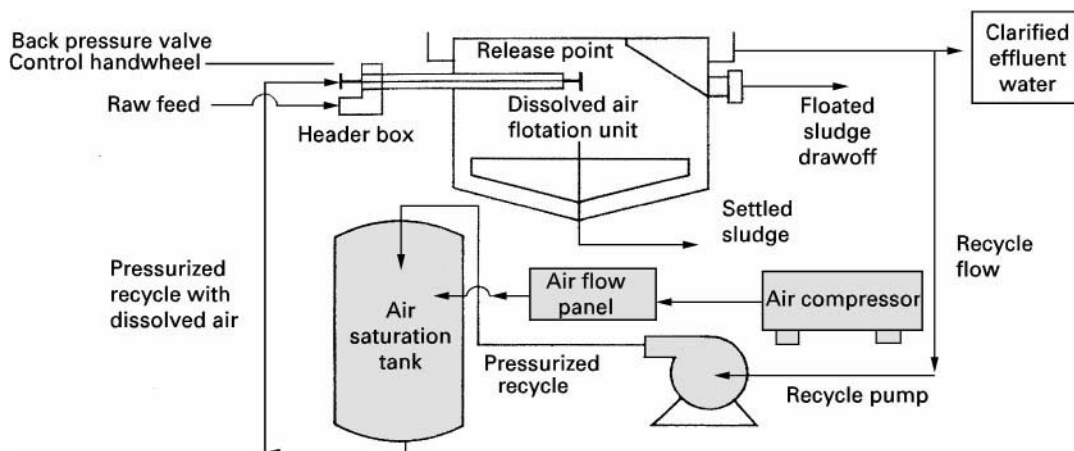


Figure 1 Flow diagram for a dissolved air flotation system. Courtesy of Baker Process.

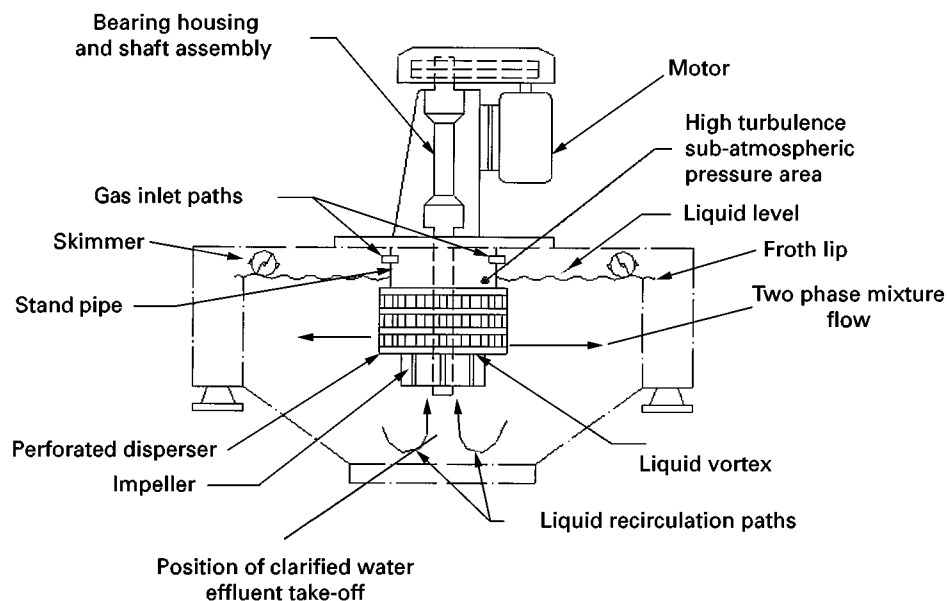


Figure 2 Transverse cross-section of mechanical induced gas flotation machine. Courtesy of Baker Process.

ducts. Impeller rotation also causes an upward circulation from the bottom of the vessel. The gas and liquid mix to form a relatively homogenous two-phase (gas-liquid) dispersion which leaves the impeller with a mainly tangential velocity. The impeller is shrouded by a perforated cylindrical disperser, which separates the intensely turbulent inner zone from the relatively quiescent outer region of the rest of the cell. The dispersion passes through the disperser, which, because of the shear resistance to the flow through its wall, reduces the size of the bubbles and improves the uniformity of their radial distribution through the main cell volume, thereby increasing the probability of a bubble-droplet collision. After attachment of the bubble to the droplet or suspended particle, separation of oil and solids occurs by flotation. The surface of the cell remains relatively quiescent as a result of the baffling effect of the disperser and hood, which minimize re-entrainment of floated oil and solids. Since the upward surface flow is uniform in the outer quiescent region surrounding the impeller, the loaded bubbles which form a froth layer at the upper surface of the cell are usually removed simultaneously from both sides of the cell.

A reduction in bubble size reduces gas flow requirements because of the more favourable surface area-to-volume ratio of the smaller bubbles. There is, however, an optimum bubble size of about $10\ \mu\text{m}$ as the collision efficiency is reduced below this size. Design considerations require a balance between impeller power input and hence total gas flow, mixing region shear turbulence, surface and flotation zone quiescence, oil droplet re-emulsification and gas bubble size.

An IAF usually has four or more cells in series with a 1 min residence time per cell. This reduces flow short-circuiting, thereby improving separation efficiency. Water enters the first active flotation cell via a feedbox, and passes from cell to cell via underflow weirs in the connecting bulkheads. Floated oil is removed separately from each cell. Dispersed oil droplet concentration in the influent should typically be no greater than 500 ppm on a long-term basis of which approximately 50% is removed by each cell, the percentage removal efficiency increasing with the influent oil droplet concentration for a fixed residence time. The treated water finally enters a quiescent discharge cell with an approximately 1 min residence time where separation continues as gas bubbles, still entrained in the water leaving the last cell, rise to the surface. Individual IGF machines are typically available in different sizes to treat feed flows of between 50 and 5000 gpm (Figure 3).

The performance of the IGF process has been extensively investigated, and proprietary predictive mathematical models derived. In the context of the trials, the most influential variables in IGF, listed in order of decreasing importance, are:

- water-treating chemical concentration;
- feed water flow rate (relates to residence time);
- impeller speed (increasing the speed will ingest more air and increase power consumption with relatively little change in fluid circulation);
- impeller submergence (distance between the liquid surface and the top of the rotor. Increased submergence increases power draw, whilst reducing

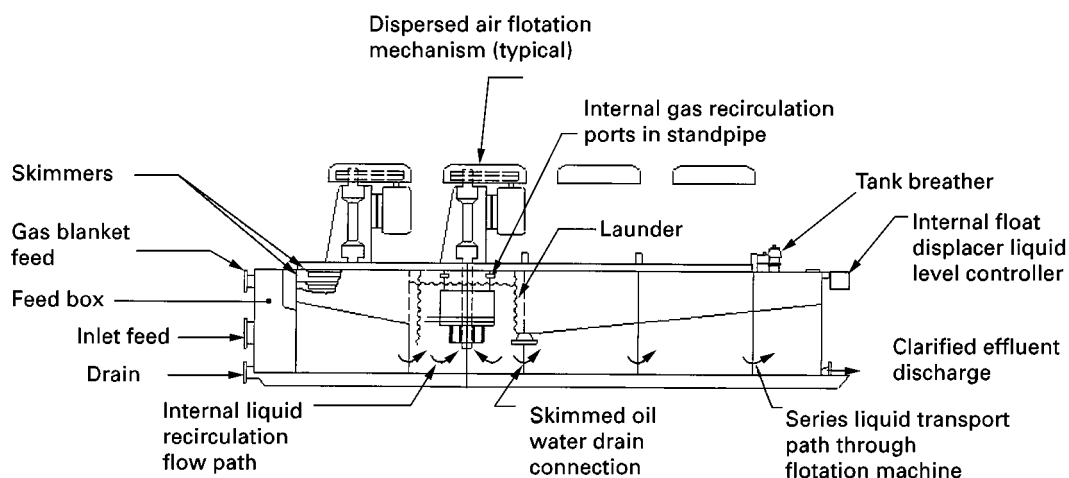


Figure 3 Longitudinal cross-section of mechanical induced gas flotation machine. Courtesy of Baker Process.

gas injection and increasing the liquid recirculation rate. Typically 200 mm);

- impeller engagement (distance from bottom of the impeller to top of draft tube. Engagement is positive if the rotor is in the tube and negative if it is above the draft tube. Influences liquid circulation. Typically 50 mm.

The order of this list may vary for different applications since removal efficiency is a strong function of the type of crude oil and the chemical composition of the feed water.

The IGF is a relatively low retention time (4–6 min) device using relatively large volumes of gas (compared to DAF) at near ambient pressure. The gas dispersion in these cells is so effective that retention times are relatively short, allowing a reduction in equipment size compared to the DAF method. The process operates at near atmospheric pressure. Both these factors give the IGF process a significant economic advantage over the DAF.

Induced Static Flotation Unit (ISF)

Since the IGF was originally developed for the mining industry, the power required by the impeller needed to be sufficient to suspend solids of perhaps 0.2–0.3 mm in diameter at concentrations of 30–40% solids. As solids removal is not the dominant process in oily water treatment, solids suspension capability can be reduced in order to achieve low turbulence in the flotation vessel at reduced power. This has led to the development of hydraulic rather than mechanical induction of bubbles (see **Figure 4**). The ISF generates bubbles hydraulically using an eductor operating under pressure, usually 60 psig rather than mechanically. Feed is added directly to

the flotation vessel. Clarified effluent water is recycled through a header, and gas is drawn from the vapour space by a Venturi effect. The resultant gas–liquid mixture is directed against a striker plate, which causes the formation of numerous small bubbles that are distributed across the full cross-section of the cell. The circular cross-section of the vessel improves the uniformity of the bubble distribution in the flotation vessel, which improves the probability of bubble–droplet collision.

Unlike the IGF, the ISF operates under pressure. Pressure operation has the advantage that hazardous (hydrogen sulfide) or environmentally sensitive gases (hydrocarbons, carbon dioxide) are contained. It has also eliminated the need for transfer pumps for the clarified water effluent and the requirement for mechanical skimmers to remove the floated oil.

The ISF design reduces the number of moving parts, while maintaining performance similar to the industry-standard mechanical units. Operation of the ISF with a centrally mounted skim trough and skim cycle timers has provided the means to reduce the skim volume to less than 1% of the forward flow in most cases. It also uses less power than the mechanical IGF. All machine adjustments are external to the vessel, thereby ensuring operator safety in hazardous applications.

The use of eductors for inducing gas to generate gas bubbles in the flotation process was first patented in the mid-1970s. Initially, ISF performance was poor compared to mechanical flotation units. The design was improved by employing a cylindrical pressure vessel, centrally mounted skimmings trough for use on floating platforms and an improved eductor configuration. The most common version of the ISF has four cells, hydraulically connected in series. Increases in the clean water recycle rate will cause

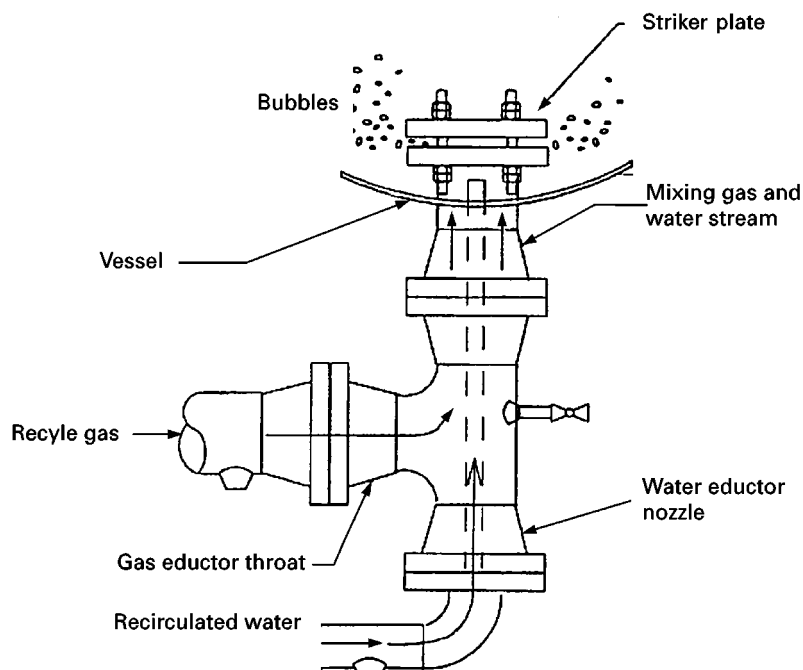


Figure 4 Eductor for hydraulic induced static flotation machine. Courtesy of Baker Process.

a progressive reduction in residence time throughout the unit, which may result in reduced bubble-droplet collision efficiency. The clean water recycle rate may be reduced by operating at a high nozzle pressure (50–100 psi).

The key features of the hydraulic flotation machine are shown in the cut-away view in Figure 5.

Comparison of DAF and Induced Processes

Dissolved and induced processes differ in a number of key parameters.

1. The amount of gas transferred to the process water is relatively small in the DAF process, approxi-

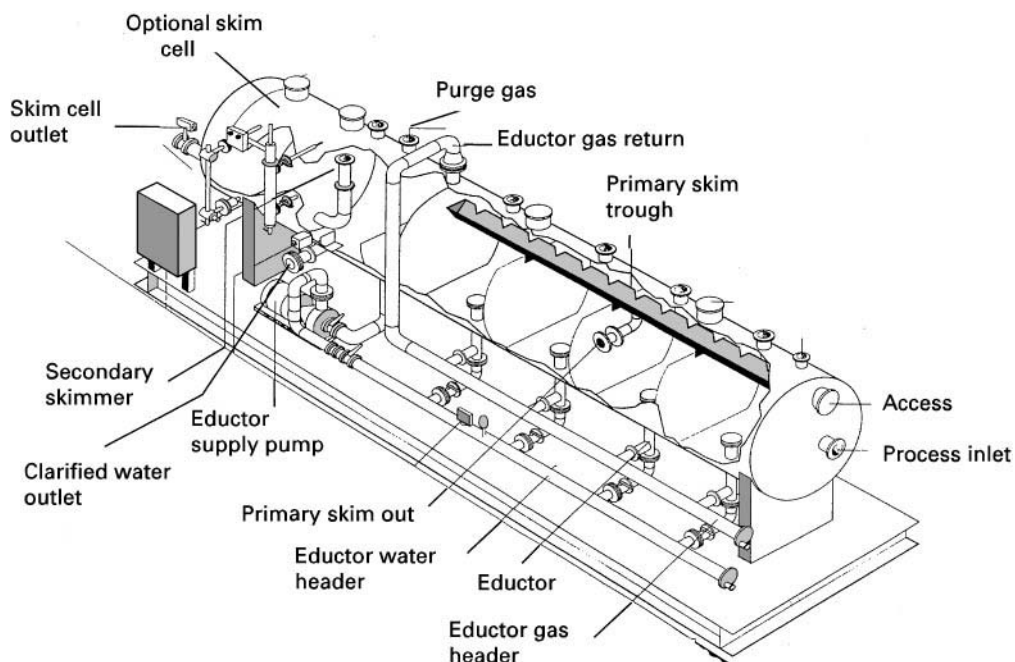


Figure 5 Hydraulic induced static flotation machine. Courtesy of Baker Process.

ately 20–40 times less than that used by the IGF process.

2. Because the DAF works by dissolution of gas in water it is sensitive to water temperature (increased temperature reducing gas solubility). By comparison, induced processes are relatively temperature insensitive. In fields where hot water or steam floods are used to recover oil, temperatures above 40°C will significantly reduce the performance of a DAF unit.
3. The means of bubble generation and mixing differs (pressure let-down in DAF vs mechanical or hydraulic induction in the IAF and ISF, respectively). Gas dissolved in the water is insignificant in process terms in the induced mechanisms since there is no pressure let-down.
4. When scaling up the process, residence time is the key variable for the IGF. For the DAF it is hydraulic loading (total process water feed divided by the vessel surface area). Hydraulic loading is related to plant floor space.

The advantages of DAF are:

1. Often lower power requirement than IGF.
2. Lower volume of skimmings as a percentage of the forward flow (1–5% for DAF systems as compared with 2–10% for mechanically induced gas systems. ISF skimmings volume compares favourably with that of DAF, being approximately 1% of the forward flow).
3. Smaller volumes of sludge may be formed than with IGF, especially where organic rather than inorganic (metallic) polyelectrolytes are used to aid flotation.
4. Better handling of suspended solids. DAF will allow the use of metal salts for coagulation and flocculation. The DAF flotation cell can also be fitted with a bottom skimmer for solid that can settle.

Advantages of induced processes are:

1. Relatively low capital cost.
2. Relatively small equipment footprint (single skid-mounted unit vs a multicomponent system).
3. Volatile organic carbons (VOC) are contained within the flotation cell. Not all DAF units use closed top flotation cells.
4. Varied flows can be handled easily.
5. Due to their high mechanical reliability, no standby capacity is required.
6. Loss of one cell will not significantly reduce separation efficiency, allowing on-line maintenance of impeller mechanisms.
7. Lower chemical consumption, since flocculation is not necessary.

In certain applications, such as removal of mineral oils from a steel rolling mill effluent, induced and dissolved process have been used in series.

Chemical Selection

From a chemical addition standpoint the two types of flotation differ due to the size of the bubble each creates:

- induced gas typically creates a relatively large gas bubble in the 10–2000 μm range;
- dissolved gas typically creates a relatively small gas bubble in the 1–100 μm range.

Dissolved Gas

In this instance, chemical treatment is used to flocculate the oil droplets and solid particles. The larger the floc, the more gas bubbles are trapped underneath the floc structure. The flotation process is significantly more quiescent than the induced processes, hence does not tend to break up flocs. Separation is therefore based on the amount of bubbles that are trapped underneath the floc, and the maintenance of uniform flow distribution to avoid floc shearing. The influent/gas bubble carrier flow distributor and mixing chamber design determines the efficiency of a DAF unit.

Ferric compounds work in a similar way to cationic polymers except where polymers are specific to the charge on the oil droplet; metal salts swamp the bulk solution leading to charge destabilization by disassociating on addition to water. As a result, the dose rate is typically higher than for a solution polymer. The solubility of metal ions is limited and hence they tend to generate weak flocs, which means that they are better used as part of a two-stage treatment, usually in conjunction with an anionic polymer. As an example, one facility described by Berne and Cordonnier uses 10 mg L^{-1} aluminium sulfate with 1 mg L^{-1} anionic polyelectrolyte. However, this does result in a large volume of sludge, 10–30 $\text{m}^3 \text{day}^{-1}$ in this case. Use of organic coagulants alone can significantly reduce sludge volumes (3–5 $\text{m}^3 \text{day}^{-1}$ in this example).

Induced Gas

The objective of chemical treatment is to change the surface charge of either the gas bubble or the oil droplet in order to cause adhesion between them after collision. The size ratio of the bubble-to-oil droplet is usually $\leq 1 : 1$. The only solids that are floated are those whose surface charge is opposite to that on the bubble surface, or those that are associated with, and contained in, the oil droplet. For this reason, induced processes may only remove 55–75% solids from the

forward flow as compared with 95–98% oil droplet removal. No attempt is made to flocculate oil droplets and solid particles, because the mixing intensity in the units will tend to break up any floc structure that has been formed.

In general, oil droplets and other suspended material will be negatively charged. Addition of cationic polymer neutralizes the charge on the oil–gas species, while a long-chain polymer collects the contaminant in preparation for removal. Most cationic polymers work best in the pH range 6–9. If the pH falls outside this range, pH adjustment of the wastewater may be required. Overall removal rates are around 90% without chemicals up to 98% with chemicals. In order to size a unit for commercial use, laboratory studies are conducted to determine the effect of variables such as rotor speed, chemical addition and feed rate on oil removal, all of which have an impact on the rate constant K . The data are then fed into proprietary models based on the Klimpel model, which contain correction factors for scaling up the equipment. The models have been validated using numerous sets of data from commercial installations. Oil–water separation is enhanced by using an emulsion breaker, a cationic high charge density, low molecular weight coagulant polymer. The polymer is distributed throughout the continuous (water) phase where it neutralizes the anionic charge at the oil–water interface. This destabilizes the emulsion, allowing oil droplets to coalesce by collision with one another.

Cationic solution polymers would usually be applied as a 1–10% solution with a dose rate of 2–30 ppm. Emulsion polymers (tightly coiled polymer molecules entrapped in solvent, activated by dilution in water) are applied at concentrations no greater than 1–2% at dose rates of 0.5–5.0 ppm.

Future Developments

Hydrocyclones and Flotation

Flotation was practised extensively on fixed offshore platforms throughout the 1970s and 1980s to clean-up produced water prior to overboard discharge. As the volumes of produced water have increased with field life, water-handling facilities have become constrained. Operators have retrofitted produced water processing capacity using hydrocyclones rather than flotation machines, because the former have a smaller footprint per volumetric flow rate of produced water treated. However, flotation oil–water separation technology has a place on offshore platforms as a polishing stage for produced water clean-up following initial treatment by hydrocyclones. One design uses what is in principle a dissolved air flotation vessel downstream of the oil–water separation hydrocyclones.

Motion Insensitive Flotation

With the increased use of floating production facilities, the motion experienced by flotation devices

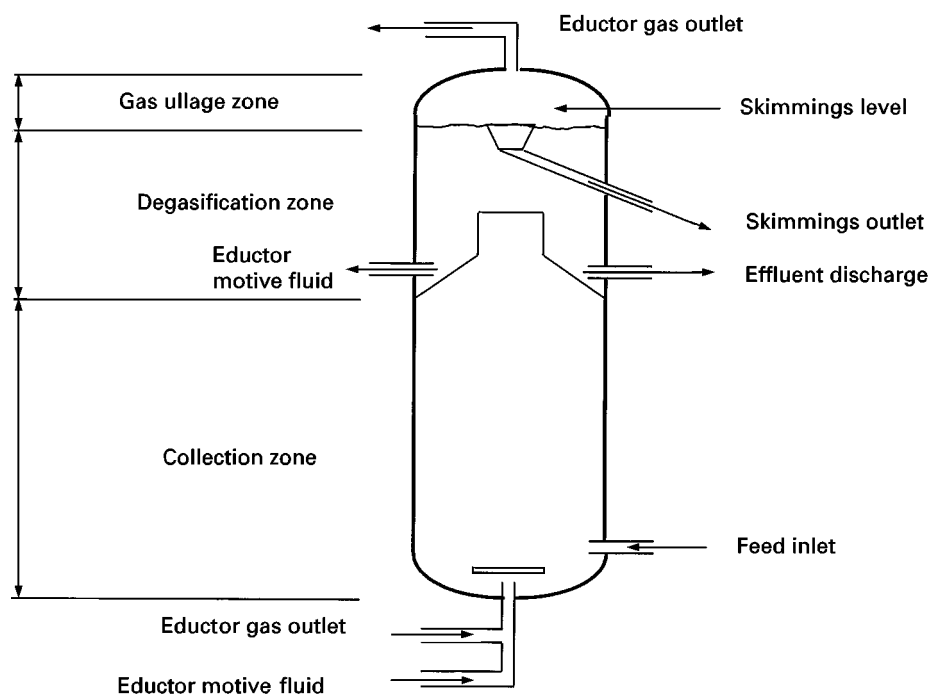


Figure 6 Single cell ISF. Courtesy of Baker Hughes Process Systems.

inhibits separation. A 2° tilt results in one end of a 12 m long flotation machine being approximately 350 mm higher than the other end of the vessel. This results in one end of the machine flooding while the other end will not remove floated oil. To overcome this problem, one manufacturer has designed a flotation column ISF machine that reduces the impact of pitch and roll to 10 mm at 2° tilt.

The method of bubble generation (eduction) is the same as that used for the four-cell ISF. Sparging was investigated as an alternative, however the bubbles were larger and moved in a linear fashion to the surface. Educated air forms smaller bubbles and exhibits random movement. Both these latter characteristics are desirable as they increase the chance of an air bubble–oil droplet collision.

Since the single-cell ISF has one rather than four cells, theory would predict that its contaminant removal efficiency would be reduced from approximately 90–98% for a four-cell unit to 80–90% for a single cell unit, primarily because the residence time in the single cell unit is some 65% of that in the traditional four cell design. In trials, however, the unit has operated successfully with inlet oil concentrations of between 50 and 1300 ppm, and suspended solids concentrations of 10–50 ppm, and has achieved oil removal efficiencies comparable to the four-cell model, taking into account the reduced residence time in the single cell. In service, actual efficiencies will depend on optimization of flow regime and chemicals (see Figure 6).

See Colour Plate 45.

See also: II/Flotation: Column Cells; Cyclones for Oil/Water Separations; Historical Development.

Further Reading

Arnold K and Stewart M (1998) *Surface Production Operations*, 2nd edn, Vol. 1, pp. 218–223. Houston, TX: Gulf.

- Berné F and Cordonnier J (1995) *Industrial Water Treatment*, pp. 80–89. Paris: Gulf.
- Bradley BW (1987) *Two Oilfield Water Systems*, pp. 171–200. Malabar, FL: Robert E Krieger.
- Degner VR (1975) Dispersed air flotation. Cell design and operation. *Water, AIChE Symposium Series*, Vol. 51, No. 151, pp. 257–264.
- Degner VR and Winter MK. Recent advances in wastewater treatment using induced air flotation. Baker Process Internal Report F8-PR-1.
- Eckenfelder WW (1989) *Industrial Water Pollution Control*, pp. 71–83. Singapore: McGraw-Hill.
- Gordon RD (1995) Refinery effluent treatment. In: Hull JB *et al.* (eds) *Strategies for Monitoring, Control and Management of Waste*, pp. 59–65. London: Mechanical Engineering Publications.
- Leech CA (1987) Oil flotation processes for cleaning oilfield produced water, pp. 1–43. *Petroleum in the Ocean Environment Conference, Oily Water Clean-up 1 Session*. American Institute of Chemical Engineers Meeting, Houston, Texas.
- Leech CA and Radhakrishnan S (1978) Performance evaluation of induced gas flotation (IGF) machine through math modelling, pp 2513–2522. *Tenth Annual Off-shore Technology Conference*, Houston, Texas.
- Liebermann NP (1997) *A Working Guide to Process Equipment*, pp. 913–939. New York: McGraw-Hill.
- Schulz J (1993) Evolution of induced flotation in oil–water separation – an historical perspective. *American Filtration Society Conference*, Houston, Texas.
- Stacy MO and Wolfenberger EE (1997) Development of a single cell induced gas flotation machine. *Produced Water Management Technical Forum & Exhibition American Petroleum Institute TECHE Chapter*, Lafayette.
- United States Environmental Protection Agency (1999) *Federal Register*, Vol. 64(8), pp. 147. Document ID FR13JA99-23.
- Zabel ThF (1992) Flotation in water treatment. In: Mavros P and Matis KA (eds) *Innovations in Flotation Technology*, pp. 431–454. Dordrecht: Kluwer.

Pre-aeration of Feed

M. Xu, Inco Technical Services Limited, Mississauga, Ontario, Canada

Z. Zhou and Z. Xu, University of Alberta, Edmonton, Alberta, Canada

Copyright © 2000 Academic Press

Introduction

Aeration of slurry is a key element in a flotation system. The extent of aeration influences the perfor-

mance of flotation machines and the overall recovery process. Flotation can, in general, be divided macroscopically into two subprocesses: selective collection of hydrophobic particles by air bubbles, and separation of bubble/particle aggregates from the pulp containing hydrophilic particles. The method and location of aeration or bubble generation control the mechanism of particle collection by either collision with and subsequent attachment to bubbles, or *in situ* bubble formation on hydrophobic particle surfaces. A flotation machine should be designed to provide an

optimal aeration condition for efficient particle collection and a suitable hydrodynamic environment for effective transfer of bubble/particle aggregates from the remaining pulp. Unfortunately, conflicting hydrodynamic environments are usually required for these two sub-processes. It is often difficult – if not impossible – to evaluate theoretically the relative contributions of individual collection mechanisms in a particular flotation device. The limited understanding of the aeration mechanisms in flotation processes is partly responsible for the development of more than 200 flotation cell designs over the years. Many of these designs are not subtle variations in basic hardware, but variations in design principles. Therefore, knowing where and how collection occurs and which aeration method is suitable for a particular application is an important step in a more scientific approach to flotation cell design.

Aeration methods used in flotation can be conveniently categorized as air dispersion and air dissolution. In the air dispersion approach, a stream of air is dispersed into slurry to achieve suitable sizes and population of bubbles. This is accomplished by shearing the air stream into bubbles under mechanical agitation as in mechanical flotation machines, or using in-line static mixers as in Microcel and packing materials as in packed columns. Air can also be dispersed through porous spargers, as used in pneumatic flotation machines or conventional Canadian flotation columns.

With the air dissolution method, on the other hand, the air is dissolved under a pressure of 3–5 atm into slurry for subsequent gas nucleation (or gas precipitation) and cavitation. Bubble formation is then achieved by either releasing gas-supersaturated slurry to atmospheric pressure as in dissolved air flotation, or decreasing the pressure of slurry by aspiration as in vacuum flotation.

Dispersed air flotation is widely used in minerals processing with relatively coarse particles (larger than 20 μm) and high slurry densities (greater than 30% solids). Other areas of applications include solid cleaning, de-inking from recycled paper and bitumen recovery from oil sands. Dissolved air flotation is suitable for municipal water and industrial effluent treatment, due to its capability of generating relatively fine bubbles of less than 100 μm required for recovering particles finer than 10 μm at a slurry density of less than 0.5% solids.

An emerging trend is to integrate the useful features of dissolved air flotation into dispersed air flotation. The combination of the two bubble-generating mechanisms has led to a new flotation cell design. Traditionally, slurry aeration and flotation separation are performed in the same vessel. Feed aeration followed

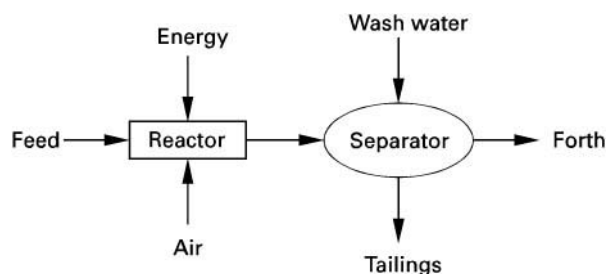


Figure 1 Schematic illustration of the concept of a flotation system consisting of a reactor and a separator.

by flotation separation in a separation vessel (a reactor–separator design), has been evolved with demonstrated higher flotation kinetics. The concept of a flotation system consisting of a reactor and a separator is illustrated in **Figure 1**. The reactor is a vigorous bubble/particle contacting device where particle collection takes place with bubbles formed by both air dispersion and nucleation/cavitation mechanisms. The separator is a quiescent bubble/pulp separation device where the hydrodynamics favour the separation of bubble/particle aggregates from the pulp with essentially no or little turbulence.

With continuing improved understanding of particle/bubble collection mechanisms and the role of aeration in flotation, it is anticipated that pre-aeration of feed will become an important component in modern flotation circuits as a means of increasing flotation kinetics and improving selectivity of fine particles. This article focuses on the fundamentals and recent developments in pre-aeration of feed used in mineral flotation.

Fundamental Basis of Feed Aeration

A theoretical analysis of aeration in a flotation system is complicated. As a result, the development of aeration techniques in flotation is largely based on phenomenological correlations. The feed aeration and subsequent particle collection during the aeration are the combination of features of dispersed and dissolved air flotation. Particle collection by air bubbles in flotation is a multi-step process, involving three phases with interactions among solid/liquid, solid/gas and liquid/gas in the presence of various inorganic and organic species under economical and mechanical constraints. At least two particle collection mechanisms have been considered in flotation.

Direct Contact of a Particle with a Bubble

In this collection process, a particle encounters a bubble, either by relative motion or the turbulence

in a flotation system. The probability of the particle being captured by the bubble (P) can be expressed as:

$$P = P_c P_a P_d \quad [1]$$

where P_c , P_a and P_d are the probability of bubble/particle collision, attachment and detachment, respectively. For a hydrophobic particle, bubble/particle collision determines the particle collection rate governed by hydrodynamic conditions. Hydrodynamic analysis showed that the collision probability between a descending particle with an ascending bubble is given by:

$$P_c = a(d_p/d_b)^n \quad [2]$$

where parameters a and n are a strong function of hydrodynamic characteristics of the system. Eqn [2] shows that the probability of particle–bubble collision is proportional to the n th ($n \geq 1$) power of the solid particle size (d_p) and inversely proportional to the same power of the bubble size (d_b). For fine particles, small bubbles have to be used to obtain sufficient particle–bubble collisions. The direct contact was analysed between a descending fine particle of $d_p = 10 \mu\text{m}$ and a rising swarm of bubbles in a flotation column. A collection zone as tall as 10 m was determined to be essential to ensure at least one collision of the particle with a bubble. This implies an inefficient collection process under conventional column flotation conditions.

To increase the particle–bubble contact frequency, a relatively high turbulence or energy dissipation rate is required, as in mechanical flotation machines. The number of particle–bubble collisions per unit volume and time in a highly turbulent flowing fluid (Z_{pb}) can be expressed as:

$$Z_{pb} = 5N_p N_b [(d_p + d_b)/2]^2 (V_p^2 + V_b^2)^{0.5} \quad [3]$$

where N_p and N_b are the number concentrations of particles and bubbles in the pulp. V_p and V_b are the mean relative velocities of the particles and bubbles (with reference to fluid), which are given collectively by:

$$V_i = 0.33\epsilon^{4/9} d_i^{7/9} (\Delta\rho/\rho)^{2/3} / \nu^{1/3} \quad [4]$$

In eqn [4], subscript i refers to bubble or particle, ϵ is the specific energy dissipation rate, $\Delta\rho$ is the difference in densities of particle i and liquid medium, ρ is the medium density, and ν is the kinematic viscosity. This equation shows that a high energy dissipation rate favours particle–bubble collision. However, vigorous agitation as in mechanical flotation machines

may break particle–bubble aggregates, thereby increasing the probability of particle detachment from bubbles and hence decreasing the overall collection rate. In addition, the back mixing (or liquid circulation) caused by increased turbulence may hinder the transport of bubble–particle aggregates out of the turbulent zone, contributing to low flotation kinetics. The incentive to separate the two functions of a flotation machine, i.e. aeration and separation, is evident, as reflected in the reactor–separator design.

In Situ Bubble Nucleation on Hydrophobic Particles

With this mechanism, gas nucleates and bubbles form selectively on hydrophobic particles. The theoretical basis of flotation by gas precipitation or nucleation was proposed in the 1960s and has recently been extended to hydrodynamic cavitation. The gas nucleation mechanism has been used to account for particle–bubble collection in dissolved air flotation. An advantage of this mechanism over a conventional particle–bubble contact mechanism is the elimination of a collision stage, a rate-limiting step in fine particle flotation. However, direct adoption of this technique to mineral flotation faces a number of challenges. Clearly, tiny bubbles in the micro and submicron range generated solely by a gas nucleation mechanism are not sufficient to float coarse mineral particles effectively. However, the collision probability of larger bubbles with the particle–tiny bubble aggregates in the quiescent region may increase. The limited number of bubbles that can be generated by gas nucleation from a supersaturated system does not provide sufficient carrying capacity to float large amounts of solids. To improve solid recovery rates, large volume slurry saturation tanks are needed, presenting extra capital and operating costs.

Alternatively, tiny bubbles and cavities can be formed by the reduction of pressure in a fast-flowing fluid, as indicated by Bernoulli's equation:

$$P_1 + (1/2)\rho U_1^2 = P_2 + (1/2)\rho U_2^2 = C \text{ (constant)} \quad [5]$$

in which U is the water flow velocity at a point where the pressure is P , and ρ is the density of liquid. If the liquid flow velocity exceeds a critical value, the pressure in the liquid stream reduces to a value where the liquid pressure falls below its vapour pressure, at which point cavities form which expand to relieve the differential pressure, a phenomenon called hydrodynamic cavitation. The presence of solids enhances hydrodynamic cavitation due to the increased turbulence and pressure fluctuations around particles in the stream. As in gas-supersaturated systems, cavities would form preferentially on hydrophobic particles

relative to energetically unfavourable hydrophilic solid-liquid interfaces. The principal advantage of exploring hydrodynamic cavitation in flotation is that gas supersaturation of slurry is not required and additional air can be introduced into the system for air dispersion. As a result, hydrodynamic cavitation can be readily implemented in mineral flotation systems.

A convenient way of aiding bubble nucleation and cavitation is by aeration in the feed slurry line. The existence of gas nuclei in water has been demonstrated in coagulation, sedimentation and filtration tests using fine coal and silica with a medium particle size of 5 and 1.5 μm , respectively. The size of gas nuclei in natural water was estimated to be 10 μm . When forcing the water through the tip of a cavitation tube at a flow velocity above 8–15 m s^{-1} , micro-size bubbles were observed to form. Numerical simulation confirmed that, at this flow velocity, a pressure close to liquid vapour pressure was attained inside the tip of the cavitation tube, suggesting the formation of bubbles by the expansion of the pre-existing gas nuclei and subsequently filled with liquid vapours. Using a light attenuation method, the onset velocity of bubble formation by hydrodynamic cavitation was found to be dependent on the diameter and length of the nozzle, slurry temperature and initial gas content. With gas-supersaturated water, for example, the onset velocity reduced from 15 to 7 m s^{-1} . Adding frother into liquid does not affect the onset of bubble formation by cavitation, but it increases the bubble stability. Sebba has reported the formation of stable bubble swarms of approximately 25–50 μm which he called aprons, generated similarly. Adding a small amount of air into the flowing liquid stream enhanced

bubble formation at a reduced liquid flow velocity, which provides a direct justification for feed aeration by hydrodynamic cavitation.

Applications of Feed Aeration

There are many new flotation devices that make use of the combined features of dispersed and dissolved air flotation. Feed slurry aeration through the concept of reactor and separator design fully exploits the combined mechanisms of bubble generation (dispersed/dissolved). Some of these flotation devices are reviewed here.

Venturi Aerated Column

The Venturi aerated column (VAC) was designed based on the concept of reactor and separator design (Figure 2). In this case, the reactor is a Venturi tube where air/slurry contact takes place. The separator is a column of length 1–2 m. The partial recirculation of tailings slurry was used to intensify the slurry jetting action, facilitating bubble size control (typically 500–800 μm) and bubble/particle interaction.

Figure 3 presents a direct comparison between a laboratory Denver cell and a single VAC cell in batch tests for a nickel sulfide ore. The VAC cell gave a higher concentrate grade at the same nickel recovery. Two VAC cells in series (as a rougher-scavenger configuration) were tested in an operating plant treating nickel sulfide ores. Compared to the mill rougher flotation, superior metallurgy was obtained with the VAC cells. With two VAC cells in series, similar metallurgical performance to the plant multi-stage

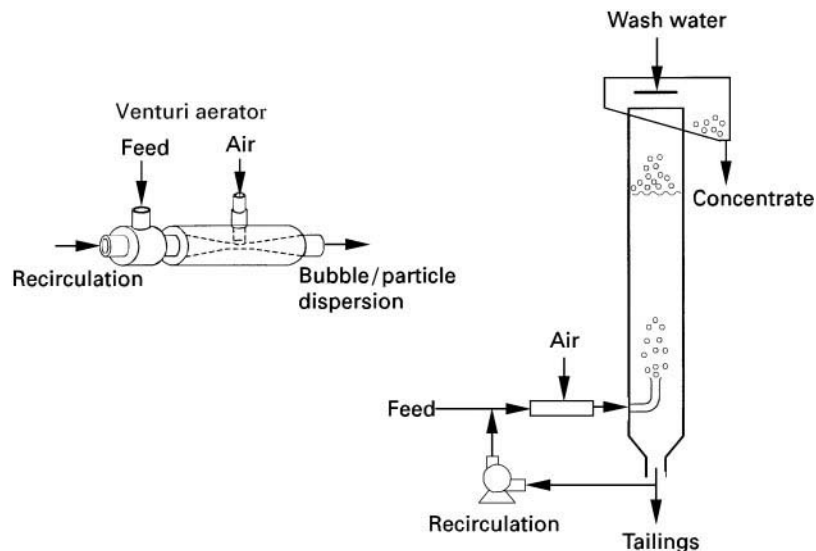


Figure 2 Schematic of a Venturi aerated column (VAC).

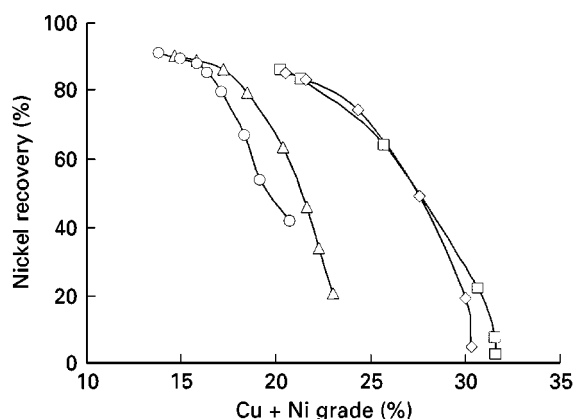


Figure 3 A direct comparison in nickel grade/recovery performance between a batch Denver cell and a batch VAC cell. Squares, column; diamonds, column (repeat); triangles, Denver; circles, Denver (repeat).

flotation circuit was achieved, as shown in **Figure 4**. The VAC cell has also been tested and found to be successful in de-inking applications of recycled paper pulp with the performance exceeding the existing plant circuit in terms of fibre recovery at comparable brightness.

Cavitation Tube

Based on the principle of nucleation, a cavitation tube (Figure 5) similar to the Venturi tube was developed and tested in association with a mechanical cell. As shown in **Figure 6** for fine silica flotation (less than $5\ \mu\text{m}$), silica recovery of 30% was obtained in the mechanical cell under conventional operating conditions (no cavitation tube). By installing a cavitation tube in the feed slurry line, silica recovery was increased significantly, depending on the slurry velocity

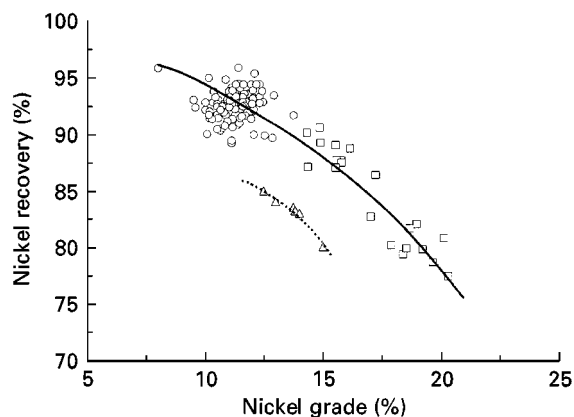


Figure 4 Comparison in nickel metallurgy between a plant rougher flotation circuit and two VAC cells in series. Squares, two VAC cells, circles, mill overall daily; triangles, mill roughers.

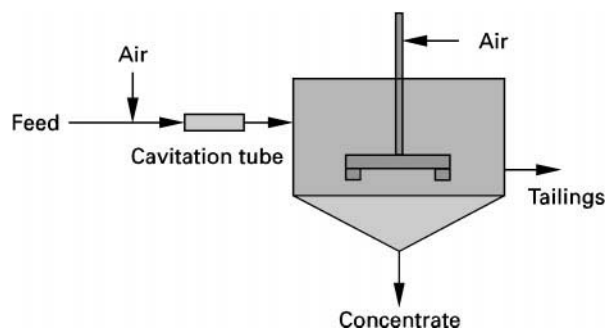


Figure 5 Schematic of a cavitation tube on the feed line before a mechanical cell.

through the nozzle. The improved recovery is clearly due to the bubble formation and particle collection by gas nucleation/cavitation. Addition of a small amount of air into the feed slurry (less than 7%) before the cavitation tube further increased silica recovery, indicating that the combined mechanisms of bubble formation by dispersed/dissolved air were beneficial to fine particle flotation. In-plant testing using a similar set-up demonstrated an improved flotation performance of Cu/Ni separation.

Other Devices and Processes Using Feed Slurry Aeration

Jameson cell The innovative design of the Jameson cell is based on the point of air addition and bubble generation. It utilized the concept of reactor and separator design. The downcomer into which air is aspirated and particle collection occurs is the reactor, while the cylindrical tank is the separator. The feed under high pressure is introduced at the top of the downcomer through a nozzle, producing a high speed slurry jet which entrains air into the downcomer. In

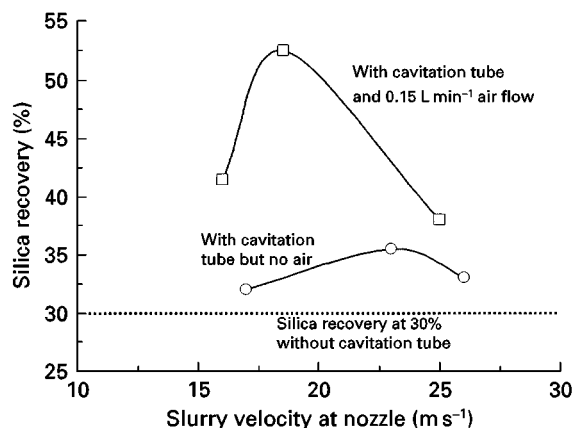


Figure 6 Fine silica recovery vs slurry velocity through the nozzle of a cavitation tube. Conditions: 1 wt.% silica ($< 5\ \mu\text{m}$); 10 p.p.m. Dowfroth 250; $1.25 \times 10^{-4}\ \text{mol L}^{-1}$ DAH; pH = 7.5–7.8; air flow rate in the mechanical cell $= 2\ \text{L min}^{-1}$.

addition to its successful use in sulfide minerals and coal flotation, the Jameson cell has also been adopted in de-inking applications for the paper industry.

Davcra cell The Davcra cell is a type of pneumatic machine, employing feed slurry aeration. Air and feed slurry are injected into the separating tank through a cyclone-type dispersion nozzle. Air dispersion and particle collection take place in the nozzle and in the highly turbulent region in the separation tank, which is separated by the quiescent zone. A limited application has been reported.

Low energy extraction process for bitumen extraction from oil sands In bitumen extraction from Athabasca oil sands, Syncrude Canada recently adopted a low energy extraction process with hydro-transport of oil sand slurries. Oil sand slurry is transported from the mine site via pipelines (3–5 km) with a relatively high slurry velocity (4 m s^{-1}). Air is injected into the pipelines. The aerated oil sand slurry is then introduced into primary separation vessels through a tangential entry feed well. Bitumen droplets attached to air bubbles float to the top of the remaining slurry to form a primary froth. Wash water is added under the froth to reduce the amount of solids reporting to the bitumen froth. Here, hydro-transport pipelines function as a reactor to increase the bubble-bitumen contact frequencies. This technique has been implemented in operation.

The Microcel, German Bahr's cell, rapid flotation cell, Contact cell, Centrifloat cell, and air-sparged hydrocyclone are other examples employing feed slurry aeration and the concept of reactor and separator design.

Concluding Remarks

With increased understanding of the role of aeration in flotation, a new trend in flotation machine design has been established. The selection of aeration in flotation is closely related to particle collection mechanisms and, to some extent, to operation and maintenance costs. Aeration in flotation has evolved from air dispersion using direct particle-bubble contact mechanism, to *in situ* bubble formation on hydrophobic particles by gas nucleation and cavitation in dissolved air flotation. The emerging trend is a combination of the two. The location of aeration has also been evolved from slurry aeration in a flotation vessel to feed aeration in a virtual reactor followed by flotation separation in a separation tank.

Flotation is an energy-dependent process and, like all the subprocesses – solid suspension, aeration, particle-bubble interaction and bubble formation – are

energy-dependent. Part of the energy dissipation in flotation systems can be attributed to the method of aeration. Ideally, as much of the input energy as possible should be directed to the main function of flotation: particle collection by bubbles. Feed aeration is associated with significant energy dissipation efficiency as the input energy is distributed evenly in slurry in contrast to mechanical cells, in which the energy is concentrated in the impeller region. The energy used for pumping, on the other hand, is a major energy requirement not needed in the existing collection processes. With the concept of feed aeration, pumping energy is utilized to force feed slurry through a hydrodynamic cavitation tube (or a Venturi tube), which facilitates the *in situ* generation of bubbles on hydrophobic particles. It is an exciting design challenge to develop energy-efficient feed aeration flotation systems.

Further Reading

- Amelunxen RL (1993) The contact cell – a future generation of flotation machines. *Engineering and Mining Journal* 194: 36–39.
- Arbiter N (1984) The flotation cell – a critique. In: Jones MH and Woodcock JT (eds) *Principles of Mineral Flotation*, pp. 301–311. Victoria, Australia: The Australasian Institute of Mining and Metallurgy.
- Arbiter N (1989) Flotation machine dynamics. In: Chander S and Klimpel RP (eds) *Advances in Coal and Mineral Processing Using Flotation*, pp. 369–372. Colorado: AIME-SME.
- Bahr A (1985) *Application and Sizing of a New Pneumatic Flotation Cell*, pp. 314–326. XV International Mineral Processing Congress, Cannes.
- Finch JA (1995) A selected review – part IV: novel flotation devices. *Minerals Engineering* 8(6): 587–602.
- Flint LR (1973) Factors affecting the design of flotation equipment. *Mineral and Science Engineering* 5(3): 232–241.
- Hu H, Zhou ZA, Xu Z and Finch JA (1998) Numerical and experimental study of a cavitation tube. *Metallurgical and Materials Trans B* 29B: 911–917.
- Jameson GJ (1988) A new concept in flotation column design. In: Sastry KVS (ed.) *Column Flotation '88*, pp. 281–285. AIME.
- Jordan CE and Susko FJ (1992) Rapid flotation using a modified bubble-injected hydrocyclone and a shallow-depth separator for improved flotation kinetics. *Mineral Engineering* 5 (10–12): 1239–1257.
- Mankowski P, Ng S, Siy R *et al.* (1999) Syncrude's low energy extraction process: commercial implementation, pp. 154–181. In: Edwards C (ed.) *Proceedings of 31st Annual Meeting of CMP*. Ottawa: CMP.
- Miller JD, Ye Y, Pacquet E *et al.* (1988) Design and operating valuables in flotation separation with the air-sparged hydrocyclone, pp. 499–510. In: Forssberg KSE (ed.) *XVI IMPC*. Stockholm, Sweden: Elsevier.

- Rubinstein J (1995) *Column Flotation: Processes, Designs and Practices*. New York: Gordon and Breach.
- Schubert H and Bischofberger C (1979) On the optimization of hydrodynamics in flotation processes. In: Laszkowski J (ed.) *Proceedings of the 13th International Mineral Process Congress*, pp. 1261–1287. Warsaw: Elsevier.
- Wills BA (1992) *Introduction to Mineral Processing Technology*, 5th edn, pp. 558–575. Oxford: Pergamon Press.
- Xu M, Quinn P and Stratton-Crawley R (1994) Graphite/chalcopyrite separation using a rapid column cell. In: Yalcin T (ed.) *Innovations in Mineral Processing*, pp. 181–186. Sudbury, Ontario, Canada.
- Xu M, Quinn P and Stratton-Crawley R (1996) A feed-line aerated flotation column. *Minerals Engineering* 8(10): 1159–1173.
- Yang DC (1988) A new packed column flotation system, column flotation '88. In: Sastry KVS (ed.) *Proceedings of the International Symposium on Column Flotation*, pp. 257–265. Phoenix, USA: SME.
- Yoon RH, Adel GT and Luttrell GH (1988) A process and apparatus for separating fine particles by microbubble flotation together with a process and apparatus for generation of microbubbles. US patent no. 5761008.
- Yoon RH and Luttrell GH (1989) The effect of bubble size on fine particle flotation. *Mineral Processing and Extractive Metallurgy Review* 5: 101–122.
- Young FR (1989) *Cavitation*. London: McGraw-Hill.
- Zhou ZA, Xu Z and Finch JA (1994) On the role of cavitation in particle collection during flotation – a critical review. *Minerals Engineering* 7 (9): 1073–1084.
- Zhou ZA, Xu Z and Finch JA (1995) The minimum recovery zone height in flotation columns from particle–bubble collision analysis. *Transactions of the Institution of Mining and Metallurgy* 104: C102–C106.
- Zhou ZA, Xu Z and Finch JA (1995) Fundamental study of cavitation in flotation. In *XIX International Mineral Processing Congress*, vol. 3, pp. 93–97. San Francisco, USA: SME.
- Zhou ZA, Xu Z and Finch JA (1996) Effect of gas nuclei on hydrophobic coagulation. *Journal of Colloid Interface Science* 179: 311–314.
- Zhou ZA, Xu Z, Finch JA and Liu Q (1966) Effect of gas nuclei on the filtration of fine particles with different surface properties. *Colloids & Surfaces* 113: 67–77.
- Zhou ZA, Hu H, Xu Z *et al.* (1997) Role of hydrodynamic cavitation in fine particle flotation. *International Journal of Mineral Processing* 51: 139–149.
- Zhou ZA, Langlois R, Xu Z *et al.* (1997) In-plant testing of a hydrodynamic reactor in flotation. In: Finch JA, Rao SR and Holubec I (eds) *Processing of Complex Ores*, pp. 185–193. Sudbury, Canada: CIM.

Reagent Adsorption on Phosphates

P. Somasundaran and L. Zhang, Columbia University, NY, USA

Copyright © 2000 Academic Press

Introduction

Adsorption of surfactants on minerals is the basic process governing flotation. It is controlled by various physicochemical processes in the pulp involving interactions among the mineral particles, surfactants, dissolved inorganics, solvent species and other additives such as polymers. Adsorption can be considered as selective partitioning of the surfactant adsorbate into the interfacial region, resulting from the more energetically favourable interactions between the adsorbate and the solid than those between the former and the species in the bulk solution. The interactions leading to adsorption include chemical bonding, electrostatic interaction, desolvation of the surfactant polar group and the mineral surface species, hydrogen bonding, van der Waals interactions, etc.

Water chemistry plays an important role in the adsorption process by affecting the surfactant–solution equilibria, the mineral–solution equilibria

and subsequently the interactions between the surfactants and the mineral particles. The interactions in mineral–solution system include dissociation, micellization and precipitation of the surfactant, dissolution of a small amount of solids followed by hydrolysis, complexation and precipitation of the dissolved species, and the interactions between dissolved mineral species with surfactant in the bulk in various forms. The dissolved species, including those introduced due to dissolution from all the minerals present in the ore and those from the water source, fresh and recycled, are the major elements that affect the water chemistry. While impurities introduced from water can be controlled to some extent, the chemical species released into the system due to dissolution from the minerals cannot be avoided. In systems containing soluble or sparingly soluble minerals where the extent of dissolution is markedly higher than that in most oxide/silicate systems, the effect of dissolved mineral species can be drastic. Understanding the mineral–solution–surfactant chemical equilibrium under different physicochemical conditions is critical for developing reagent and processing schemes for separation.

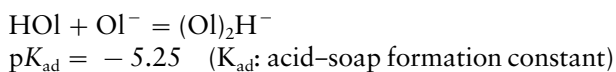
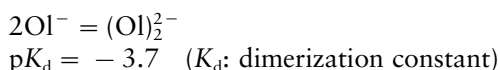
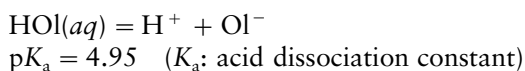
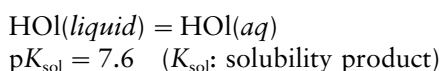
Phosphate is one of the most important minerals processed by flotation techniques. Flotation is efficient for the beneficiation of phosphate ores with silicate gangues, but those with carbonaceous gangues are difficult to separate by flotation techniques. The low selectivity has been attributed to the similarities in the surface chemical properties of the constituent minerals. These properties, in turn, are influenced by the water chemistry of the surfactant–mineral systems. In this section the effects of water chemistry on the surfactant–solution equilibrium, the mineral–solution equilibrium, the surfactant–mineral interactions in the separation of phosphate and associated minerals are discussed. Methods to manipulate and control the solution chemistry to achieve selectivity in flotation are also examined.

Water Chemistry of Flotation Reagents

Long chain fatty acids such as oleic acid are among the commonly used reagents for the flotation of oxides, silicates and salt-type minerals. Flotation of these minerals using fatty acids is affected greatly by solution properties such as pH, since weakly acidic fatty acids undergo association interactions that can influence their adsorption and flotation properties. For example, oleic acid species will undergo dissociation

to form ions (Ol^-) at high pH values and exist as neutral molecules (HOl) at low pH value. In the intermediate region, the ionic and the neutral molecular species can associate to form ion–molecule complexes ($(\text{Ol})_2\text{H}^-$). As the surfactant concentration is increased, micellization or precipitation of the surfactant can occur in the solution. In addition, surfactant species can associate to form other aggregates such as the dimer (Ol_2^{2-}) in premicellar solutions. Also, long chain fatty acids such as oleic acid have very limited solubility, which is a sensitive function of pH. The pH of precipitation of oleic acid calculated as a function of total oleate is shown in Figure 1.

The solution equilibria of oleic acid (HOl) are expressed as below:



The species distribution of oleic acid as a function of pH based on the above equilibria at a given concentration is shown in Figure 2. It can be seen from this figure that:

1. The pH of the precipitation of oleic acid at the given concentration is 7.45.
2. The activities of oleic monomer and dimer remain almost constant above the precipitation pH and decrease sharply below it.
3. The activity of the acid–soap $(\text{Ol})_2\text{H}^-$ exhibits a maximum in the neutral pH range.

The surface activities of the various surfactant species can be markedly different from each other. It has been estimated that the surface activity of the acid–soap $(\text{Ol})_2\text{H}^-$ is five orders of magnitude higher than that of the neutral molecule (HOl) and about seven orders of magnitude higher than that of the neutral molecule (HOl) and about seven orders of magnitude higher than that of the oleate monomer Ol^- .

The existence of salt will also affect the surfactant–solution equilibria by changing the surface activities of the various surfactant species, the critical micelle concentration and the solubility of the surfactant, and the solvent properties of the solution.

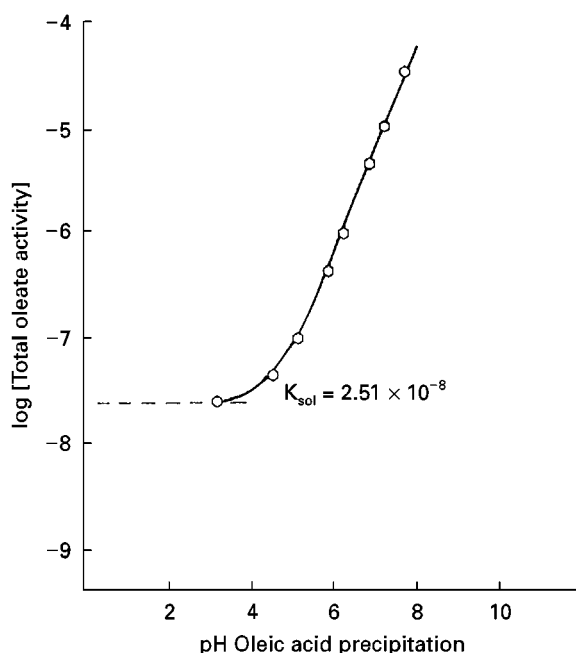


Figure 1 pH of oleic acid precipitation. (From Morgan LJ, Ananthapadmanabhan KP and Somasundaran P (1986) Oleate adsorption on hematite: problem and methods. *International Journal of Mineral Processing* 18: 39. Copyright: Elsevier Science.)

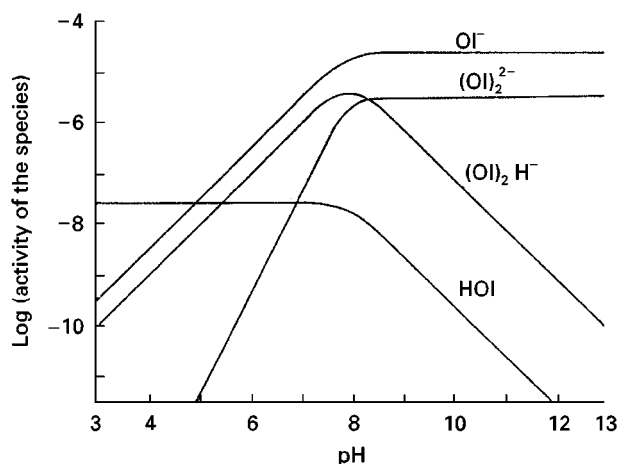


Figure 2 Oleate species distribution as a function of pH. Total oleate concentration = $3 \times 10^{-5} \text{ mol L}^{-1}$. (From Ananthapadmanabhan KP and Somasundaran P (1980) Oleate chemistry and hematite flotation. In: Yarar B and Spottiswood DJ (eds) *Interfacial Phenomena in Mineral Processing*, p. 207. New York: Engineering Foundation.)

It is clear that, to understand the adsorption of reagents on solids, the effects of concentration, pH, ionic strength and activities of the various possible reagent species on the adsorption process need to be taken into account.

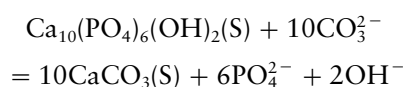
The Effect of Water Chemistry on Mineral–Solution Equilibrium

When mineral particles are in contact with water, they undergo dissolution, the extent of which is dependent on the type and concentration of chemicals in solution. The dissolved mineral species can undergo further reactions such as hydrolysis, complexation, adsorption and precipitation. The complex equilibria involving all such reactions can be expected to determine the interfacial properties of the minerals and their flotation behaviour. The equilibria that con-

trol the dissolution of calcite and apatite in water are given in Table 1.

In the case of carbonaceous phosphate minerals, apatite, calcite and dolomite will dissolve in water, followed by pH-dependent hydrolysis and complexation of the dissolved species. Since these minerals are sparingly soluble, the dissolved species have a marked effect on their interfacial properties.

It should be noted that, from theoretical considerations, depending on the solution conditions, the surface of apatite can be converted to calcite and vice versa through surface reactions or bulk precipitation of the more stable phase. The stoichiometry of the equilibrium governing the conversion of apatite to calcite can be written as:



It can be seen from this equation that, depending on the pH of the solution, apatite can be converted to calcite if the total carbonate in solution exceeds a certain value. In fact, the amount of dissolved carbonate from atmospheric CO_2 does exceed that required to convert apatite to calcite under high pH conditions.

Surface conversion due to the reaction of the dissolved species with the mineral surface can be predicted using stability diagrams for heterogeneous mineral systems. This is illustrated in Figure 3 for the calcite–apatite system. The activity of Ca^{2+} in equilibrium with various solid phases shows that the point of interception for calcite and apatite is pH 9.3. Above this pH, apatite is less stable than calcite and hence conversion of apatite to that of calcite can be expected in the calcite–apatite system. Similarly, apatite is more stable than calcite below pH 9.3. It is to be noted that Ca^{2+} in equilibrium with calcite in an open system (open to atmospheric CO_2) is significantly different from that in a closed system. Also,

Table 1 Equilibria controlling the dissolution of calcite and apatite in water

K_{sp}			K_{sp}		
<i>Calcite</i>					
CaCO ₃ (S)	$\rightleftharpoons \text{Ca}^{2+} + \text{CO}_3^{2-}$	$10^{-8.4}$	Ca ²⁺ + HCO ₃ ⁻	$\rightleftharpoons \text{CaHCO}_3^+$	$10^{0.8}$
CO ₃ ²⁻ + H ⁺	$\rightleftharpoons \text{HCO}_3^-$	$10^{10.3}$	Ca ²⁺ + CO ₃ ²⁻	$\rightleftharpoons \text{CaCO}_3(\text{aq})$	$10^{3.3}$
HCO ₃ ⁻ + H ⁺	$\rightleftharpoons \text{H}_2\text{CO}_3$	$10^{6.3}$	Ca ²⁺ + H ₂ O	$\rightleftharpoons \text{CaOH}^+ + \text{H}^+$	$10^{-12.9}$
CO ₂ (g) + H ₂ O	$\rightleftharpoons \text{H}_2\text{CO}_3$	$10^{-1.5}$	Ca ²⁺ + 2H ₂ O	$\rightleftharpoons \text{Ca}(\text{OH})_2 + 2\text{H}^+$	$10^{-22.8}$
<i>Apatite</i>					
Ca ₁₀ (PO ₄) ₆ (F,OH) ₂ (S)	$\rightleftharpoons 10 \text{ Ca}^{2+} + 6 \text{ PO}_4^{3-} + 2 (\text{F}, \text{OH})^-$				10^{-118}
PO ₄ ³⁻ + H ⁺	$\rightleftharpoons \text{HPO}_4^{2-}$	$10^{12.3}$	Ca ²⁺ + HPO ₄ ²⁻	$\rightleftharpoons \text{CaHPO}_4(\text{aq})$	$10^{2.7}$
HPO ₄ ²⁻ + H ⁺	$\rightleftharpoons \text{H}_2\text{PO}_4^-$	$10^{7.2}$	CaHPO ₄ (aq)	$\rightleftharpoons \text{CaHPO}_4(\text{s})$	$10^{4.3}$
HPO ₄ ⁻ + H ⁺	$\rightleftharpoons \text{H}_3\text{PO}_4$	$10^{2.2}$	Ca ²⁺ + H ₂ PO ₄ ⁻	$\rightleftharpoons \text{CaH}_2\text{PO}_4^+$	$10^{1.1}$
Ca ²⁺ + H ₂ O	$\rightleftharpoons \text{CaOH}^+ + \text{H}^+$	$10^{-12.9}$	Ca ²⁺ + 2F ⁻	$\rightleftharpoons \text{CaF}_2(\text{s})$	$10^{10.4}$
Ca ²⁺ + 2H ₂ O	$\rightleftharpoons \text{Ca}(\text{OH})_2 + 2\text{H}^+$	$10^{-22.8}$	Ca ²⁺ + F ⁻	$\rightleftharpoons \text{CaF}^+$	$10^{1.0}$
F ⁻ + H ⁺	$\rightleftharpoons \text{HF}$	$10^{3.1}$			

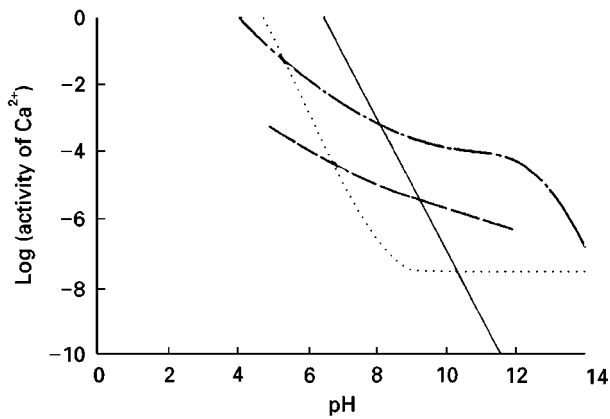


Figure 3 pH dependence of activity of Ca^{2+} in equilibrium with calcium oleate (dotted line: $\text{Ol}_T = 10^{-4} \text{ kmol m}^{-3}$), calcite (open (closed lines) and closed (dots and dashes) systems) and apatite (dashed lines). (From Ananthapadmanabhan KP and Somasundaran P (1984) The role of dissolved mineral species in calcite-apatite flotation. *Mineral and Metallurgical Processing* 1: 36.)

in the absence of atmospheric CO_2 , apatite has a wider stability region than in the open system. Atmospheric CO_2 can thus be expected to play an important role in these types of mineral-solution equilibria and in operations dependent on interfacial properties.

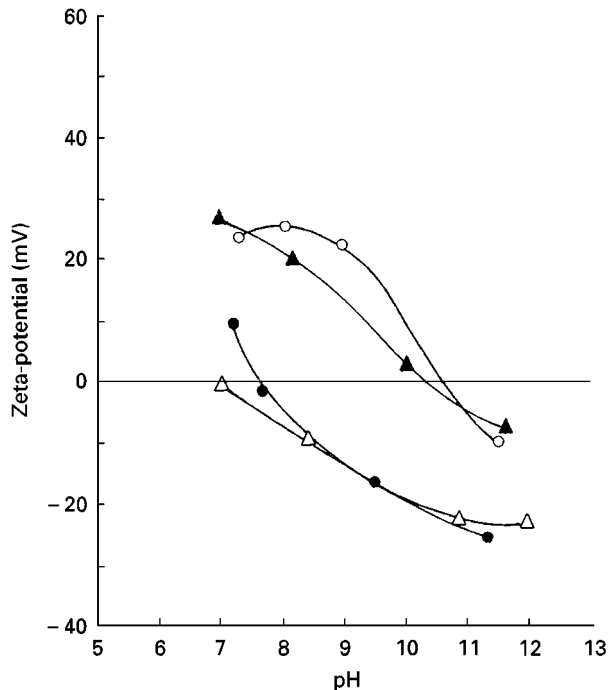


Figure 4 Illustration of the effect of supernatants on the zeta potential and isoelectric point of calcite and apatite: $2 \times 10^{-3} \text{ kmol m}^{-3} \text{ KNO}_3$. Open circles, calcite in water; open triangles, apatite in water; filled triangles, apatite in calcite supernatant; filled circles, calcite in apatite supernatant. (From Ananthapadmanabhan KP and Somasundaran P (1984) The role of dissolved mineral species in calcite-apatite flotation. *Mineral and Metallurgical Processing* 1: 36.)

The surface conversions in the calcite-apatite system have been proved experimentally; electrokinetic data obtained for the calcite-apatite system in water and in the supernatant of each other are shown in **Figure 4**. When apatite is in contact with calcite supernatant, its zeta potential is seen to shift to that of calcite and vice versa, suggesting surface conversion of apatite to calcite and calcite to apatite, respectively.

The zeta potential data obtained in mixed supernatants of calcite and apatite also show the effect of dissolved mineral species. If supernatants of calcite and apatite are combined as a 1 : 1 mixture, the two minerals have almost identical surface charge characteristics in the basic pH range (**Figure 5**).

The surface conversion of apatite and calcite is further supported by the result of electron spectroscopy for chemical analysis (ESCA) measurements. The results in **Figure 6** show that, when apatite is conditioned in the supernatant of calcite at $\text{pH} \sim 12$, its surface exhibits spectroscopic properties characteristic of both calcite and apatite. This behaviour is attributed to the precipitation of calcite on the apatite.

Dissolution equilibria of sparingly soluble minerals play a major role in determining the surface properties of these minerals and in turn, adsorption of reagents on them.

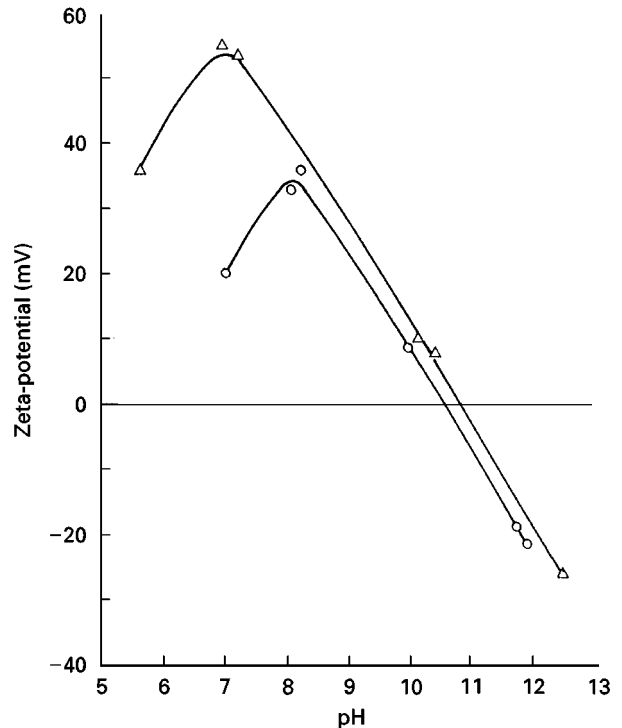


Figure 5 Illustration of the similarity in zeta potentials of calcite (circles) and apatite (triangles) in mixed supernatants. (From Ananthapadmanabhan KP and Somasundaran P (1984) The role of dissolved mineral species in calcite-apatite flotation. *Mineral and Metallurgical Processing* 1: 36.)

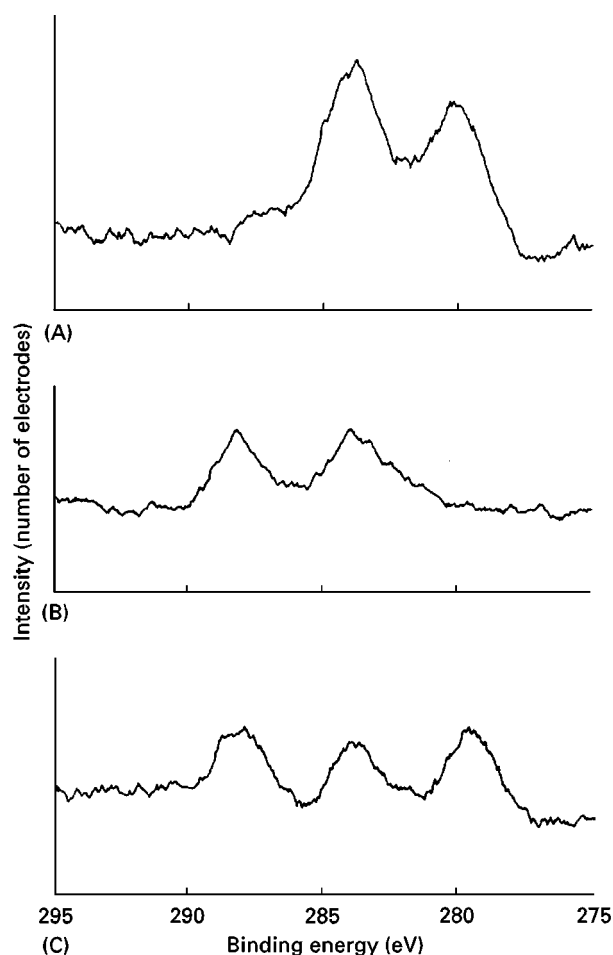


Figure 6 ESCA spectra of C(1s) peak of apatite conditioned in calcite supernatant at pH ~ 12. (A) Apatite in water; (B) calcite in water; (C) apatite in calcite supernatant. (From Ananthapadmanabhan KP and Somasundaran P (1984) The role of dissolved mineral species in calcite-apatite flotation. *Mineral and Metallurgical Processing* 1: 36.)

The Effect of Water Chemistry on Adsorption of Reagents on Minerals

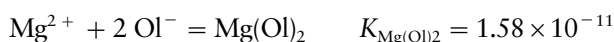
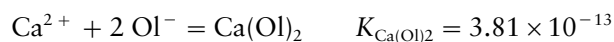
Chemical equilibria in aqueous solutions containing both the minerals and the surfactants can be expected to be much more complex than in either of the individual systems discussed above. In addition to surfactant adsorption at the solid-liquid interface, interactions between dissolved mineral species with various surfactant species can be expected. All these interactions can affect the surfactant adsorption and the subsequent flotation.

As indicated earlier, oleic acid has a very low solubility and adsorption of oleate, in some cases, is in fact precipitation of the surfactant in the interfacial region. In Figure 3, the activity of Ca^{2+} in equilibrium with various solid phases is plotted. If, at any stage, activity of Ca^{2+} in solution is greater than that

in equilibrium with Ca^{2+} -oleate, Ca^{2+} -oleate can be expected to precipitate.

Depletion isotherms of oleic acid on both francolite and dolomite has been observed to be a two-region linear isotherm with a change of slope at about $10^{-4} \text{ kmol m}^{-3}$ (Figure 7). Simultaneous analysis of the dissolved mineral species in the supernatants of the samples used in the adsorption experiments (Figure 8) shows a sharp decrease in the concentrations of both Mg and Ca species when oleate concentration exceeds $1.0 \times 10^{-5} \text{ kmol m}^{-3}$ in the case of francolite and $3.0 \times 10^{-5} \text{ kmol m}^{-3}$ in the case of dolomite. This suggests that bulk precipitation of calcium and magnesium species can occur under such conditions.

Major chemical equilibria for the precipitation of Ca and Mg species by oleate can be given as follows:



The onset of the precipitation of Ca(Ol)_2 and Mg(Ol)_2 is calculated from the solubility products given above and marked in Figure 8. The calculated oleate concentrations at the onset of precipitation are in good agreement with experimental observations.

It is postulated that, in the case of oleate adsorption on dolomite and francolite, different mechanisms govern the adsorption process. In the low concentration range ($< 10^{-4} \text{ kmol m}^{-3}$), the adsorption

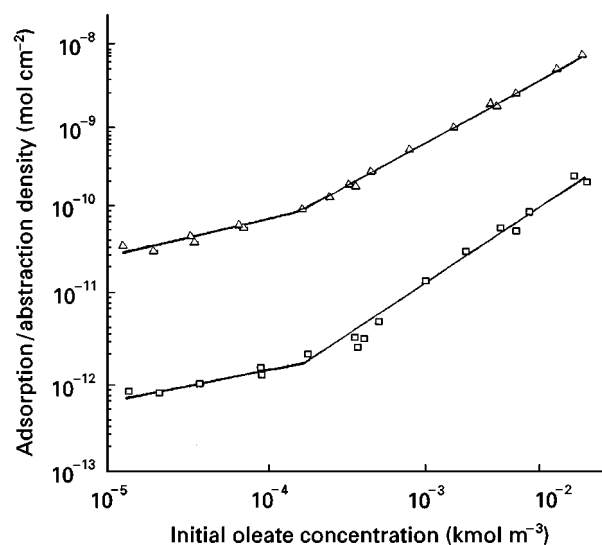


Figure 7 Depletion isotherms of ^{14}C -labelled oleic acid on francolite (squares: pH = 8.2) and dolomite (circles: pH = 9.2). Temperature, 25°C ; S/L = 0.3; $I = 3 \times 10^{-2} \text{ kmol m}^{-3} \text{ KNO}_3$. (From Somasundaran P, Xiao L and Wang D (1991) Solution chemistry of flotation of sparingly soluble minerals. *Mineral and Metallurgical Processing* 8: 115–121.)

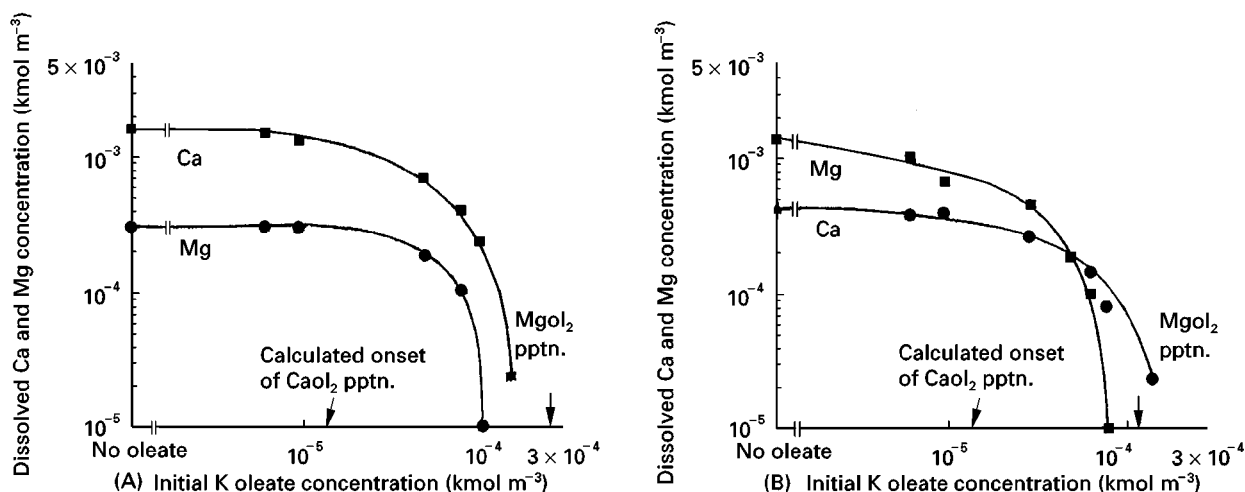


Figure 8 Dissolved Ca (squares) and Mg (circles) levels from (A) francolite (pH = 8.2) and (B) dolomite (pH = 9.2) suspensions as a function of oleate concentration. (From Somasundaran P, Xiao L and Wang D (1991) Solution chemistry of flotation of sparingly soluble minerals. *Mineral and Metallurgical Processing* 8: 115.)

of oleate on both minerals occurs mainly due to chemical bonding on surfaces without any precipitation. At an intermediate concentration of about $10^{-4} \text{ kmol m}^{-3}$, the solubility limit of Ca and Mg oleate can be reached in the interfacial region but not in the bulk solution, suggesting surface precipitation of oleate on both minerals. In the high concentration range ($> 5 \times 10^{-4} \text{ kmol m}^{-3}$), oleate depletion may be dominated in the case of both minerals by the precipitation of Ca and Mg species with oleate, on the mineral surface and in the bulk solution.

From the above discussion on apatite–calcite conversion, it is clear that a flotation separation scheme designed on the basis of the surface properties of a single mineral is not likely to perform satisfactorily. The effect of dissolved species of calcite and apatite on fatty acid flotation of both minerals has in fact been studied using mineral supernatant solutions containing various dissolved species. The flotation results are shown in **Figure 9**. Both supernatants of calcite and apatite are found to depress the calcite flotation by oleic acid in the tested pH range, with apatite supernatant exhibiting a greater depressing effect. Similar results have also been obtained for apatite flotation. The supernatants of calcite and apatite depress the apatite flotation under all tested pH conditions.

Studies on the dissolved species responsible for the observed effect revealed that, for calcite flotation, the depression role of apatite supernatant results from the combined effects of calcium species and the phosphate species in solution, while the depression role of calcite supernatant is mostly that of the calcium ion and possibly some carbonate ions. The depression due to calcium ion is caused by the de-

pletion of oleate owing to the precipitation of calcium oleate. In the case of apatite flotation, the depression is due to phosphate and carbonate species in solution. The adsorption of these ions on the surface calcium sites reduces the sites available for oleate adsorption which, in turn, lowers the hydrophobicity of the surface and so depresses the apatite flotation. Calcium oleate precipitation, in this case, does not occur to a significant extent due to the low concentration of oleic acid used in flotation. The above observations clearly show that water chemistry plays a crucial role in the flotation of apatite–calcite systems.

In addition to reagent complexation and precipitation, other reactions that occur in the bulk solution can take place in the interfacial region. For example, hemimicellization at a solid–liquid interface is a phenomenon that drastically affects the adsorption of collector reagents on solids.

Flotation is a dynamic process. In addition to the equilibrium effects associated with the water chemistry, it can also influence the adsorption kinetics of surfactants on the solid surfaces. Anionic conditioning is a unit operation that precedes rougher flotation and skin flotation of phosphates in Florida flotation plants. The effect of water chemistry on oleic acid adsorption on francolite during anionic conditioning has recently been studied in detail. In order to identify the effect of process variables on the adsorption, the experiment was carried out under both laboratory and plant conditions (**Table 2**).

The kinetics of oleic acid adsorption on francolite under both laboratory and plant conditions, using distilled water and plant water, is shown in **Figure 10**. The adsorption density and kinetics are quite different depending on the conditions and the

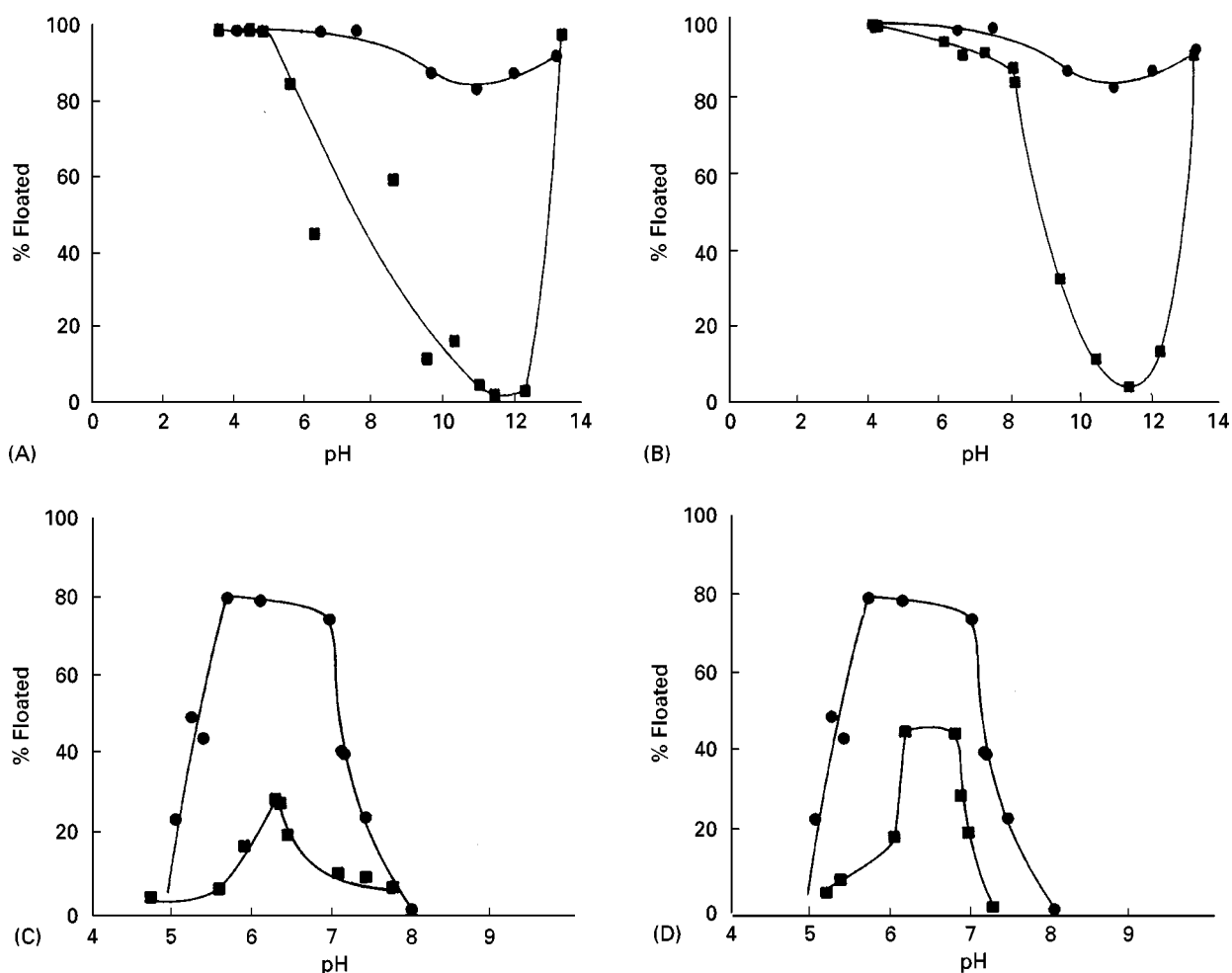


Figure 9 (A) Effect of apatite supernatant (squares) on calcite flotation. K oleate 10^{-4} kmol m^{-3} ; $I = 3 \times 10^{-2}$ kmol m^{-3} KNO_3 . Circles, water. (B) Effect of calcite supernatant (squares) on calcite flotation. K oleate 10^{-4} kmol m^{-3} ; $I = 3 \times 10^{-2}$ kmol m^{-3} KNO_3 . Circles, water. (C) Effect of calcite supernatant (squares) on apatite flotation. K oleate $= 2 \times 10^{-6}$ kmol m^{-3} ; $I = 3 \times 10^{-2}$ kmol m^{-3} KNO_3 . Circles, water. (D) Effect of apatite supernatant (squares) on apatite flotation. K oleate $= 2 \times 10^{-6}$ kmol m^{-3} ; $I = 3 \times 10^{-2}$ kmol m^{-3} KNO_3 . Circles, water. (From Ananthapadmanabhan KP and Somasundaran P (1984) The role of dissolved mineral species in calcite-apatite flotation. *Mineral and Metallurgical Processing* 1: 36.)

water. Under laboratory conditions, the adsorption in plant water is significantly lower than that in the distilled water. It is proposed that this is due to reagent loss resulting from the dissolved species in plant water precipitating the oleic acid. In contrast, under plant conditions, the adsorption behaviour of

oleic acid in plant water and distilled water is similar and adsorption densities are lower than those under laboratory conditions. The high solid/liquid ratio under plant conditions will reduce the adsorption density on the solids because of the much greater solid surface on to which the reduced total amount of

Table 2 Comparison of laboratory and plant conditions

	Laboratory conditions	Plant conditions
Conditioner	Wrist-action shaker	Lightnin Labmaster L1U08, four-bladed cruciform propeller operating at 350 rpm
pH	9.1–9.5	9.1–9.5
Water	Distilled and plant water	Plant water
Solid (%)	10 (2 g sample)	72 (1000 g sample)
Time (min)	120 (except for kinetics)	3 (except for kinetics)

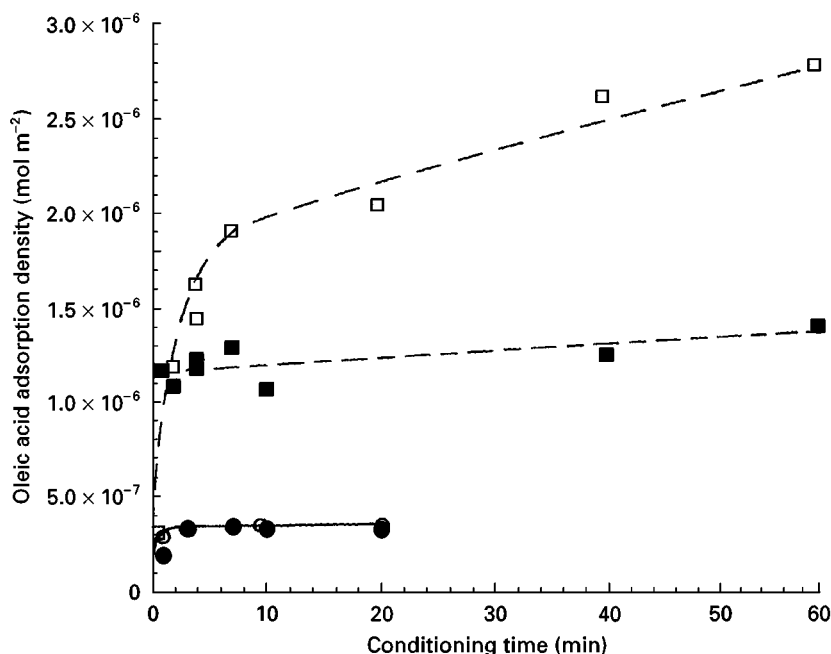


Figure 10 Kinetics of oleic acid adsorption on francolite in distilled water and plant water under laboratory and plant conditions. Open squares, distilled water in laboratory conditions; filled squares, plant water in laboratory conditions; open circles, distilled water in plant conditions; filled circles, plant water in plant conditions. Oleic acid concentration: $8.1 \times 10^{-3} \text{ mol L}^{-1}$; pH 9.1–9.5. (From Maltesh C, Somasundaran P and Gruber GA (1996) Fundamentals of oleic acid adsorption on phosphate flotation feed during anionic conditioning. *Mineral and Metallurgical Processing* 13: 157.)

reagent in the water adsorbs. This will also result in a lower reagent concentration in solution reducing the precipitation effect. The intense agitation in the plant conditioner may also remove some of the bound reagent from the surface.

The adsorption isotherms of oleic acid on francolite under laboratory and plant conditions are compared in **Figure 11**. Adsorption is markedly higher under laboratory conditions than under plant conditions. On the other hand, under plant conditions the adsorption is similar in distilled water and plant water. This suggests that the effect of dissolved species is reduced under plant conditions.

From the above discussion, it can be seen that the adsorption of surfactant on a mineral is a complicated process involving interactions such as surfactant self-association, mineral dissolution, bulk precipitation, adsorption and surface precipitation. The interactions are further complicated by the kinetic effects of the various reactions.

Understanding the effect of the water chemistry on reagent adsorption offers opportunities to manipulate such processes by optimizing the contributing factors such as alteration of the surface properties, complexation of ions which cause precipitation of the surfactant, prevention or enhancement of collector adsorption and changes in the adsorption kinetics to achieve the desired selectivity in flotation.

In the anionic flotation of phosphate, Ca^{2+} affects the grade of phosphate by activating the quartz through formation of calcium-bearing precipitates at high pH. This detrimental effect can be prevented by adding sodium silicate, which can interact with Ca^{2+} and form calcium silicate. Since calcium silicate and quartz are negatively charged, detachment of calcium silicate from quartz can occur and thus quartz flotation can be depressed.

It has been found that in carbonate/phosphate systems, with fatty acid as collector, apatite is depressed in the acid medium (pH 5.5–6.0) while carbonate is floated. The depression of phosphate at this pH is possibly due to the adsorption (or formation) of aqueous CaHPO_4 on its surface, preventing surfactant ions from approaching the surface of the phosphate particles. Free Ca^{2+} in solution can affect the formation of aqueous CaHPO_4 . From thermodynamic considerations it can be predicted that the selective flotation of carbonates from phosphates in acid media can be enhanced by minimizing free Ca^{2+} in solution and by increasing HPO_4^{2-} in the system. This can be done by (1) decreasing free Ca^{2+} concentration in the system to low values by adding suitable chemical reagents such as sulfuric acid or chelating agents such as oxalic acid, and (2) adding soluble phosphate salts to enhance the depression of the phosphate minerals. Results from experiments with

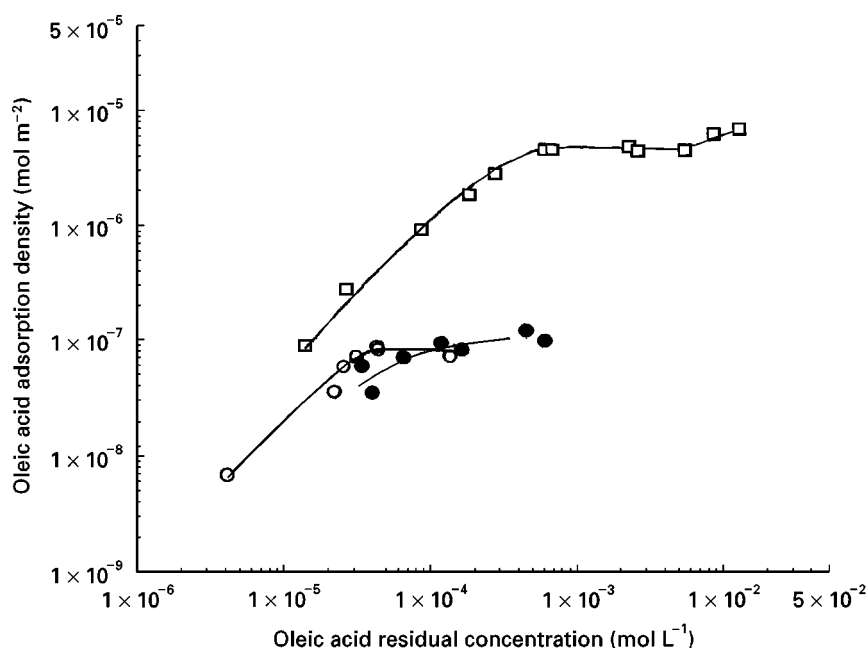


Figure 11 Adsorption isotherms of oleic acid adsorption on francolite in distilled water and plant water under laboratory and plant conditions. Squares, distilled water in laboratory conditions; open circles, distilled water in plant conditions; filled circles, plant water in plant conditions. (From Maltesh C, Somasundaran P and Gruber GA (1996) Fundamentals of oleic acid adsorption on phosphate flotation feed during anionic conditioning. *Mineral and Metallurgical Processing* 13: 157.)

natural phosphate ores are in agreement with the theoretical predictions.

Based on the oleic acid solution chemistry, a two-stage conditioning process for the flotation of dolomite from apatite has been proposed. The mixed minerals are first conditioned at pH 10 with oleic acid collector. The system is then reconditioned below pH 4.5 where dolomite is floated. The selectivity of dolomite from apatite is attributed to two factors in this process.

1. High adsorption of oleate on dolomite during the first stage at pH 10, which is maintained after reconditioning at lower pH.
2. Oleate to oleic acid transformation upon reconditioning, reducing its efficiency, and this reduction being more severe for apatite than for dolomite.

In the high pH range, oleate adsorbs on to apatite and calcite through specific interactions, while at low pH, when oleic acid is the major species, the adsorption is through weaker physical interaction. Thus, oleic acid is a poor collector compared to oleate.

Modification of collector adsorption on minerals can be used to control their flotation response. In one study, Alizarin Red S, a dye that stains calcite, was tested as a modifying agent in calcite-apatite system due to its preferential adsorption on these

minerals. Even though Alizarin Red S adsorbs more on apatite than on calcite, it depresses the flotation of apatite using oleate as collector more than that of calcite (Figure 12). In the absence of the dye, both calcite and apatite float with oleate at pH 10.5. When the dye concentration increases to $5 \times 10^{-6} \text{ mol m}^{-3}$, the flotation of calcite is very little affected with a recovery of about 90%, while apatite flotation is depressed to 5–10%. Calcite flotation is only affected at higher concentrations of dye. Alizarin Red S or its derivatives are hence promising reagents for the beneficiation of phosphate with carbonaceous gangues.

Summary

Mineral-solution equilibria, surfactant-solution chemistry, as well as interactions among dissolved species, surfactant and solids, can have a drastic effect on surfactant adsorption and flotation separation of sparingly soluble minerals. Studies on the effects of water chemistry on adsorption of surfactant on phosphate minerals such as apatite and francolite and associated minerals such as calcite and dolomite show that these interactions have marked effects on the reagent adsorption as well as flotation. Surfactant can exist in different forms in solution depending on the solution pH and the surfactant concentration. Minerals can undergo dissolution, with the extent of

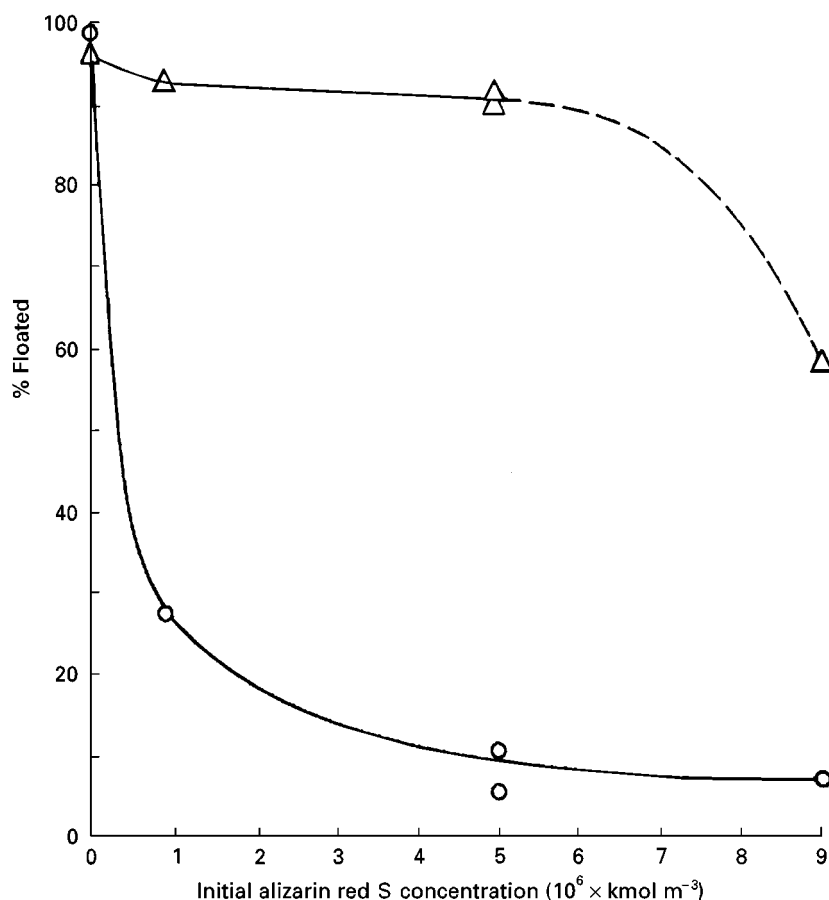


Figure 12 Flotation of calcite (triangles) and apatite (circles) from their mixture (1 : 1) at pH 10.5 as a function of Alizarin red S concentration. Alizarin red S conditioning time = 1 min; K oleate = $9 \times 10^{-5} \text{ kmol m}^{-3}$; KCl = $3 \times 10^{-2} \text{ kmol m}^{-3}$; pH = 10.5 ± 0.2 . (From Fu E and Somasundaran P (1986) *International Journal of Mineral Processing* 18: 287, with permission from Elsevier Science.)

dissolution depending upon solution conditions such as pH, ionic strength and concentration of constituent ions. The dissolved mineral species can further interact with mineral solids, leading to surface conversion of the minerals. They can also interact with surfactant, leading to surface and bulk precipitation. All these processes can significantly affect the adsorption of surfactant on minerals. A full understanding of the various interactions in surfactant-solid-solution system is essential for developing efficient separation schemes. Indeed, desired selectivity can be achieved by using appropriate additives to control dissolved species or modifying collector adsorption and by optimizing solution conditions as well as the kinetics involved.

Acknowledgement

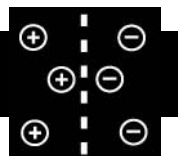
The authors acknowledge financial support of the National Science Foundation (CTS-9622781 and EEC-94-02989)

Further Reading

- Amankonah JO, Somasundaran P and Ananthapadmanabhan KP (1985) Effects of dissolved mineral species on the dissolution/precipitation characteristics of calcite and apatite. *Colloids and Surfaces* 15: 295.
- Amankonah JO, Somasundaran P and Ananthapadmanabhan KP (1985) Effects of dissolved mineral species on the electrokinetic behavior of calcite and apatite. *Colloids and Surfaces* 15: 335.
- Ananthapadmanabhan KP and Somasundaran P (1980) Oleate chemistry and hematite flotation. In: Yasar B and Spottiswood DJ (eds) *Interfacial Phenomena in Mineral Processing*, p. 207, New York: Engineering Foundation.
- Ananthapadmanabhan KP and Somasundaran P (1984) The role of dissolved mineral species in calcite-apatite flotation. *Mineral and Metallurgical Processing* 1: 36.
- Ananthapadmanabhan KP and Somasundaran P (1985) Surface precipitation of inorganics and surfactants and its role in adsorption and flotation. *Colloids and Surfaces* 13: 151.

- Ananthapadmanabhan KP and Somasundaran P (1988) Acid-soap formation in aqueous oleate solutions. *Journal of Colloid Interface Science* 122: 104.
- Dho H and Iwasaki I (1990) Role of sodium silicate in phosphate flotation. *Mineral and Metallurgical Processing* 7: 215.
- Elgillani DA and Abouzeid A-ZM (1993) Flotation of carbonates from phosphate ores in acidic media. *International Journal of Mineral Processing* 38: 235.
- Fu E, Somasundaran P (1986) Alizarin red S as a flotation modifying agent in calcite-apatite systems. *International Journal of Mineral Processing* 18: 287.
- Leja J (1982) *Surface Chemistry of Froth Flotation*. New York: Plenum Press.
- Maltesh C, Somasundaran P and Gruber GA (1996) Fundamentals of oleic acid adsorption on phosphate flotation feed during anionic conditioning. *Mineral and Metallurgical Processing* 13: 157.
- Morgan LJ, Ananthapadmanabhan KP and Somasundaran P (1986) Oleate adsorption on hematite: problem and methods. *International Journal of Mineral Processing* 18: 139.
- Moudgil BM and Chanchani R (1985) Selective flotation of dolomite from francolite using two-stage conditioning. *Mineral and Metallurgical Processing* 2: 19–25.
- Somasundaran P (1969) Adsorption of starch and oleate and interaction between them on calcite in aqueous solutions. *Journal of Colloid Interface Science* 31: 557.
- Somasundaran P and Ananthapadmanabhan KP (1986) Solution chemistry of flotation. In: Somasundaran P. (Ed.), *Advances in Mineral Processing*, p. 426. New York: AIME.
- Somasundaran P, Amankonah JO and Ananthapadmanabhan KP (1985) Mineral-solution equilibria in sparingly soluble mineral systems. *Colloids and Surfaces* 15: 309.
- Somasundaran P, Xiao L and Wang D (1991) Solution chemistry of flotation of sparingly soluble minerals. *Mineral and Metallurgical Processing* 8: 115–121.

ION EXCHANGE



Catalysis: Organic Ion Exchangers

R. L. Albright, Albright Consulting,
Southampton, PA, USA

Copyright © 2000 Academic Press

Introduction

The ion exchange polymers most often used in catalysis are insoluble materials that can be constructed from inorganic or organic monomer units. This article will present only catalysis performed by the organic ion exchangers that are insoluble solids. There are commercial ion exchangers that are liquids, but to date they have been used very little in catalysis and, therefore, will not be included in this discussion.

Insoluble ion exchangers carry out their catalytic work in a heterogeneous rather than a homogeneous fashion and are, therefore, part of the group called heterogeneous catalysts. Heterogeneous catalysts have three very significant advantages over homogeneous catalysts: first, they are not corrosive; second, they are very readily separated from the reaction mixture by a simple filtration; and third, they are

most often recyclable from one run to the next without any added treatment. Potentially, they suffer one major disadvantage over homogeneous catalysts. Intimate contact between reactants and the catalytic site is not achieved simply by mixing the heterogeneous catalyst with the reactants. In a stirred reactor, intimate contact between reactants and the homogeneous catalyst is very easily achieved and mass transport of reactants to catalyst is very rapid and almost never rate-limiting. With heterogeneous catalysis, mass transport of reactants to the catalytic site may often be the rate-limiting element, especially if the activation energy for the reaction is small and the chemical reaction is rapid. There are excellent texts and monographs on the issues surrounding heterogeneous catalysis, and the reader is referred to these for the development of a fuller understanding (see Further Reading).

Nature of Organic Ion Exchange Polymers

Chemical Composition

Organic ion exchangers are made by polymerization of organic monomers into large molecules which are made insoluble by crosslinking with a polyfunctional monomer. The nature and the level (concentration) of

the crosslinking influences the elasticity, the dimensional stability or strength of the copolymer particle, and the available space surrounding the ionogenic or catalytic site within the solvent-swelled gel phase.

Many monomers have been transformed into insoluble ion exchangers by various polyfunctional monomers, but an unabridged listing of these will not be given here. Instead, this discussion will consider only those monomer systems most used.

The most prominent insoluble copolymer matrices for constructing organic ion exchangers are those derived by the free radical copolymerization of styrene with divinylbenzene. Other matrices that have been used and are presently used to a much lesser extent are those made by the condensation polymerization of phenol (including the other hydroxylated aromatic derivatives of phenol such as catechol, resorcinol, hydroquinone, etc.) with formaldehyde and the copolymer matrices made by the free radical polymerization of the acrylate and methacrylate monomers with divinylbenzene.

The functional groups that perform the catalytic work are attached to the preformed crosslinked polymeric matrix. A vast array of chemistry allows the attachment of many different functional groups for anchoring the catalytic agent. With the aromatic polymers, electrophilic substitution reactions provide the means of functional group attachment, and with the aliphatic acrylic and methacrylic resins, the carboxyl group provides the means of functional group attachment by nucleophilic substitution reactions. A plethora of chemistry is available to build a heterogeneous catalyst upon the polymeric matrices employed to make ion exchangers.

Much of the chemistry for designing effective catalysts built upon crosslinked polymers, however, has not been pursued to a fruitful outcome. Many of the special heterogeneous catalysts have been built upon crosslinked polymers with poor mass transport in the solvent systems necessary for effective chemical transformations and, therefore, have had inferior performance to the corresponding homogeneous catalysts. This inferior performance resulting from poor mass transport has partially quenched the commercial development of what could be excellent heterogeneous catalysts when built upon the properly designed structures of the crosslinked polymers. As a result, most of the commercial effort to use ion exchangers as catalysts has been in two areas – acid- and base-catalysed reactions. Solid acids and solid bases are the two major ion exchangers employed in water demineralization and purification and have been most explored as catalysts.

The strong acid ion exchangers are sulfonated polymers of styrene crosslinked with divinylbenzene.

The solid bases are copolymers of styrene and/or vinylpyridine crosslinked with divinylbenzene and functionalized to give either a quaternary ammonium hydroxide group or a tertiary amine group. Solid bases are also prepared from copolymers of the acrylate and methacrylate monomers by crosslinking with divinylbenzene followed by attachment of the amino group to the polymer via an amide linkage.

Physical Structure

The geometry of ion exchange particles as manufactured today is spherical. The bead diameters can be varied by the method of manufacture, but the standard size of commerce is a Gaussian distribution of beads ranging in diameter from 250 μm (60 mesh US Sieve Series) to about 1000 μm (18 mesh US Sieve Series). The condensation polymers of phenol with formaldehyde may still be supplied as irregularly shaped particles, but even these polymers can be made in spherical bead form, if desired. The spherical geometry arises from the method of manufacture which is by stirring a suspension polymerization of monomer droplets dispersed in an immiscible liquid. The immiscible liquid most used is water properly formulated to maintain droplet integrity throughout the transformation of monomer into polymer.

Recently a number of manufacturers of ion exchangers have developed technology for making monosized particles in which the range of size is very narrow with a uniformity coefficient of less than 1.12. Monosized particles may have an advantage in some catalytic applications if the ion exchanger being used is a gel resin. The monosized gel beads will have an advantage over a Gaussian distribution of beads if the average diffusional path length is shorter for the monosized beads than that for the Gaussian distribution. For macroporous polymers, the bead diameter has a very small impact upon the mass transport because the ingress and egress is through a continuous pore system rather than through a solvated polymer network as in a gel polymer.

Ion exchange beads have two internal polymer morphologies: one is a gel in which the network of polymer chains is continuous throughout the bead volume; the other is a macroporous structure in which the bead is constructed from small microgel particles tending towards spherical symmetry and packed together into clusters and arrays of clusters. The macroporous bead has both a continuous pore phase and a continuous gel phase, whereas the gel bead has only a continuous gel phase. Within the gel bead, there are no pores. Porosity develops only as the polymer chains are solvated by the reaction medium and become

solvent separated. Within the macroporous polymers, there are two subgroups: those with a small specific surface area (\bar{S}) less than about 400 to 500 m² mL⁻¹ and those with a large specific surface area greater than about 600 m² mL⁻¹.

The macroporous polymers with a small specific surface area have good accessibility into the core of the bead but the number of catalytic sites on the pore surface is insufficient to provide acceptable rates of catalysis. Consequently, the working phase in these beads is primarily the gel phase of the microgel. The macroporous polymers with a large specific surface area (\bar{S}) have sufficient catalytic sites on the internal pore surface to give acceptable rates of catalysis and are, therefore, true surface phase catalysts. Table 1 shows these relationships for a family of sulfonated macroporous polymers.

In the macroreticular synthesis of macroporous polymers, large surface areas are achieved only by increasing the level of crosslinking in the polymerizing monomer mixture. The microgel of the resulting polymer is so tightly crosslinked that it is impenetrable even to molecules as small as methylene dichloride (CH₂Cl₂). For effective catalysis, the surface phase must be the working arena since the gel phase is impenetrable and also not functionalized. Consequently, mass transport and catalytic effectiveness are influenced quite differently within these three physical structures by the following:

1. Level of crosslinking
2. Bead diameter
3. Solvating nature towards the polymer by the reaction medium
4. Size of the reactants and/or products.

Mass Transport: A Critical Element in Performance

With ion exchangers as with other heterogeneous catalysts, mass transport of reactants into the catalytic site and mass transport of products from the catalytic site can become totally rate controlling. A qualitative tabulation of these interacting relationships is provided in Table 2.

For estimating the suitability or design of a macroporous polymer for effective mass transport, the equation given below, derived from the studies of Halász and Martin, has been found very useful. The appropriate pore system for good mass transport can be selected by simply knowing the molecular weight of the expected product or the largest reactant molecule.

$$d_p = 5 d_M$$

$$d_M = 0.2457 (MW_M)^{0.588}$$

where: d_p = pore diameter in Å of the pore system at 50% of the total pore volume of the macroporous polymer; d_M = random coil diameter in Å of either the product molecule or the largest reactant molecule; MW_M = molecular weight of product or largest reactant.

Functional Groups – Catalytic Agents

The most studied catalytic functional group is the sulfonic acid group (–SO₃H) attached to styrene-divinylbenzene copolymers of both gel and macroporous morphologies. Many reactions catalysed by

Table 1 Intrinsic properties of a family of sulfonated porous aromatic polymers: the relationship of surface capacity, specific surface area, crosslinking density, and the working arena

Sulfonated porous polymer	Theory weight capacity, (meq g ⁻¹)	Measured weight capacity, (meq g ⁻¹)	Rings on internal surface, (No. %)	Calculated theory wt. cap. on int. surface (meq g ⁻¹)	Crosslinking density (wt. %DVB)	Specific surface area, \bar{S}		Working phase in catalysis
						(m ² g ⁻¹)	(m ² mL ⁻¹)	
Amberlyst XN-1008 ^a	5.299	5.26	2.76	0.146	12	40	60	Gel phase
Amberlyst 15	5.210	5.00	3.72	0.197	20	55	82	Gel phase
Amberlyst XN-1005 ^b	4.854	3.50	11.95	0.683	50	120	180	Gel phase
Amberlyst XN-1010	4.749	3.60	37.92	1.827	85	615	850	Surface phase

^a Amberlyst XN-1008 is no longer marketed commercially. It has been replaced by Amberlyst 16 which has a similar specific surface area but is slightly more porous.

^b Amberlyst XN-1005 is no longer commercially available.

Table 2 Qualitative relationship between polymer morphology of ion exchanger and change in reaction system

<i>Polymer morphology</i>	<i>Change in the reaction system</i>	<i>Effect on the kinetics of catalysis</i>
Gel polymer	Increasing level of crosslinking from 2 to 12 wt.% divinylbenzene	Decreasing rate of reaction. Gel copolymers of styrene–divinylbenzene with greater than about 6% divinylbenzene perform poorly as catalysts even in good swelling solvents
	Increasing bead diameter from 250 to 1000 μm	Decreasing rate of reaction. In good solvating reaction medium, the smaller the bead diameter, the better the catalyst performance
	Poorly solvating reaction medium for catalyst	Ineffective catalysis at any particle diameter and any crosslinking level
	Increasing size of reactants and/or products	Decreasing effectiveness as a catalyst
Macroporous polymer with small specific surface area (\bar{S}) ($\bar{S} < 400\text{--}500\text{ m}^2\text{ mL}^{-1}$ bead)	Increasing level of crosslinking from 6 to 25 wt.% divinylbenzene	Moderate decline in catalytic effectiveness from compensating changes. As the crosslinking level increases, the \bar{S} increases and the microgel diameter decreases
	Increasing bead diameter from 250 to 1000 μm	For small to moderate sized molecules, almost no change in catalytic effectiveness
	Poorly solvating reaction medium for catalyst	Very small impact on catalytic performance
	Increasing size of reactants and/or products	Provided the pore system is sufficient for ingress of reactants and egress of products, only a moderate decline in effectiveness
Macroporous polymer with large specific surface area (\bar{S}) ($\bar{S} > 600\text{ m}^2\text{ mL}^{-1}$ bead)	Increasing level of crosslinking from 60 to 100 wt.% divinylbenzene	Increasing catalytic effectiveness, provided pore dimensions remain large enough to accommodate entrance of reactants and exit of products. As level of DVB increases, the surface area increases
	Increasing bead diameter from 250 to 1000 μm	Little or no impact on catalytic effectiveness
	Poorly solvating reaction medium for catalyst	No impact upon catalytic effectiveness
	Increasing size of reactants and/or products	No impact upon catalytic effectiveness provided pore system allows influx of reactants and efflux of products

homogeneous strong acids have been examined for effective catalysis by strong acid ion exchangers because of their lack of corrosiveness and their ease of separation from the reaction liquor by filtration (Table 3). Strong acid resins with crosslinking by divinylbenzene of 8 wt.% or less work well only where the reaction medium is very polar (water, dimethylformamide, N-methylpyrrolidinone or dimethyl sulfoxide) and the reactants or resulting products are small ($\text{MW} < 250\text{ Da}$).

Strong acid macroporous polymers work well in essentially all reaction media, especially the large specific surface area, strong acid macroporous polymers where the surface phase is the catalytic arena. Here solvation of the gel phase is unimportant. The surface phase sulfonic acid groups, however, are not as powerful in protonating reactants as those buried in the gel phase – the surface sulfonic acid moiety is a weaker acid than those within the gel. By placing two sulfonic acid groups on each surface ring, by

sulfonation with fuming sulfuric acid, both the acid strength and the thermal stability are increased. Sulfonated aromatic polymers with the sulfonic acid group attached directly to the aromatic ring begin to desulfonate at about 120°C , since sulfonation is acid catalysed and reversible. By attaching an electron withdrawing group, such as $-\text{SO}_2-$, $-\text{SO}_3\text{H}$, Cl, Br, F, etc., to the aromatic ring, in addition to the sulfonic acid group, the thermal stability of the strong acid resin is boosted to about 150°C .

Ion exchangers have their functional groups anchored in space relative to each other and the neighbouring groups can be used to enhance the rates of reactions of appropriately structured molecules. As an example of this effect, the rate of hydrolysis of olefinic esters is greatly enhanced by loading silver cations on to a portion of the sulfonic acid groups. At 50% loading of the cation exchanger with silver cations, the maximum rate of hydrolysis of allyl acetate is observed even though the concentration of acid

Table 3 Transformations catalysed by ion exchangers

A. Reactions catalysed effectively by strong acid resins	
Acetal and ketal synthesis	
Addition of carboxylic acids to olefins	
Alkylation of aromatic molecules, especially activated rings such as phenols, toluene, etc.	
Cumene hydroperoxide conversion to phenol and acetone	
Dehydration of alcohols into olefins	
Epoxidation of olefins with H ₂ O ₂	
Esterification	
Etherification	
Hydrolysis	
Hydrolysis of starch, cellulose and saccharides	
Olefin acylation	
Olefin alkylation	
Olefin hydration	
Olefin isomerization	
Olefin oligomerization	
Solvolysis of epoxides	
Transesterification	
B. Reactions catalysed effectively by anion exchangers	
Active methylene condensation reactions	
Aldol condensation	
Cannizzaro reaction	
Cyanoethylation	
Epoxide addition to carboxylic acids	
Michael addition reactions	
Nitrile hydrolysis to amides	
C. Reactions catalysed effectively by heterogenized solid phase transition and noble metal catalysts	
Epoxidation of olefins	
Hydroformylation	
Hydrogenation	

sites is halved. The silver ion with its propensity to complex with double bonds pulls into the resin phase a higher concentration of allyl acetate, thereby increasing the rate of hydrolysis over that of the strong acid resin without silver cations. This is a polymeric matrix effect which is not possible with a homogeneous catalyst. Polymeric matrix effects are an added advantage of solid phase over liquid phase catalysts for enhancing the catalytic effectiveness of ion exchangers.

Anion exchangers are the second most studied group of solid phase catalysts. The catalytic agents that are attached to the polymeric matrices are quaternary ammonium and tertiary amine groups. The positively charged nitrogen of the quaternary ammonium group is effective in catalysing some reactions, but most often it is the associated anion that is varied to achieve an effective catalytic agent. The positively charged nitrogen of the quaternary group is effective in catalysing epoxide addition reactions, as one example. Base catalysis is carried out with either the quaternary ammonium hydroxide or the tertiary amine group. For reactions

whose products are sensitive to the base strength, a less powerful basic anion such as carbonate or acetate can be employed when the quaternary ammonium agent is the catalyst. The quaternary ammonium resin in the hydroxide form begins to decompose when used above 60°C. Other anionic forms are stable to about 150°C. The tertiary amine resins are thermally stable to about 150°C.

Phase transfer catalysis is accomplished by anion exchangers with any one of a number of appropriate nucleophilic anions associated with the quaternary ammonium group. The appropriateness of the nucleophilic anion is controlled by the nature of the chemical reaction undergoing catalysis. Phase transfer catalysts can also be designed by attaching a quaternary phosphonium group to the polymeric matrix in place of the quaternary ammonium group. Spacer arms that move the onium group further from the crosslinked polymer backbone enhance catalytic activity in phase transfer catalysis.

Crosslinked styrene-divinylbenzene copolymers have been and continue to be actively investigated as solid supports to heterogenize homogeneous catalytic agents. These solid phase catalysts have transition metals and noble metals anchored to the solid polymeric matrix through appropriate ligands. In heterogeneous form, they promote the same chemical reactions as in solution, albeit with the imposed mass transport limitations of the solid support.

See also: II/Ion Exchange: Historical Development; Inorganic Ion Exchangers; Novel Layered Materials: Phosphates; Novel Layered Materials: Non-Phosphates; Organic Ion Exchangers; Theory of Ion Exchange. III/Catalyst Studies: Chromatography.

Further Reading

- Albright RL (1987) Basic principles of catalysis by functionalized porous organic polymers: theoretical concepts and considerations. In Stiles AB (ed.) *Catalyst Supports and Supported Catalysts*, pp. 159–186. Boston: Butterworths.
- Chakrabarti A and Sharma MM (1993) Cation exchange resins as catalyst. *State-of-the-Art Report, Reactive Polymers*, Vol. 20, pp. 1–45. Amsterdam: Elsevier.
- Ford WT (ed.) (1986) *Polymeric Reagents and Catalysts*. ACS Symposium Series 308. Washington, DC: American Chemical Society.
- Gates BC and Katzer JR (1979) *Chemistry of Catalytic Processes*. New York: McGraw-Hill.
- Hodge P and Sherrington DC (eds) (1980) *Polymer-supported Reactions in Organic Synthesis*. New York: Wiley.
- Jakovac IJ (1987) Specific reactions catalyzed by functionalized porous organic polymers. In Stiles AB (ed.) *Catalyst Supports and Supported Catalysts*, pp. 187–200. Boston: Butterworths.

- Neier W (1991) Ion exchangers as catalysts. In Dorfner K (ed.) *Ion Exchangers*, pp. 981–1027. New York: Walter deGruyter.
- Satterfield CN (1991) *Heterogeneous Catalysis in Industrial Practice*, 2nd edn. New York: McGraw-Hill.
- Sherrington DC and Hodge P (eds) (1988) *Synthesis and Separations Using Functional Polymers*. New York: Wiley.
- Thomas JM and Thomas WJ (1996) *Principles and Practice of Heterogeneous Catalysis*. New York: VCH Publishers.

Historical Development

I. Grafova, Institute for Sorption and Problems of Endoecology, National Academy of Sciences of Ukraine, Kiev, Ukraine

Copyright © 2000 Academic Press

Development of Ion Exchange Concept, Materials and Methods

The main stages in the development of ion exchange are shown in Table 1 and 2. Ion exchange gradually became an important separation method in water treatment, waste water purification, analytical chemistry, medicine, the food industry and many other areas of application.

The first systematic studies of ion exchange occurring in natural inorganic materials were performed during the period 1850–80, clays, sands and zeolites became objects of investigation and it was shown that soil treated with ammonium salts absorbs these ions, releasing an equivalent amount of calcium ions. Later, some natural materials found application for purification of water as well as for other purposes. At that time, the evidence for existence of ions in solution had not yet been elucidated and the concept of a double electric layer had not yet been proposed. Despite this the stoichiometry of ion exchange and its connection with aluminosilicates present in the soil were established. It was demonstrated that the degree of exchange increased up to a limiting value with the

increase of concentration of salt solution, while the influence of temperature on ion exchange was shown to be less significant.

At the beginning of the twentieth century complementary investigations in the areas of synthesis and application of ion exchangers took place. Industrial production of synthetic amorphous aluminosilicate ion exchange materials was started. These materials (permutites) were used for water softening and in the treatment of sugar syrups. In the first artificial sodium aluminosilicates a substitution of sodium to calcium occurred, but the ion exchanger could be regenerated in a column by treatment with saturated sodium chloride solution.

Ion exchange materials can also be obtained by oxidation and sulfonation of coals. Some types of charcoal, soft and hard brown coals, are suitable for this purpose. They can be converted into cation exchangers after treatment with fuming sulfuric acid. As a result, sulfonic and carboxylic groups (resulting from oxidation) are introduced into the coal structure, playing the role of fixed ions. Furthermore, the coal is transformed to a gel due to polycondensation reactions. The total exchange capacity of such materials is about 1.5 meq g^{-1} .

Organic Ion Exchange Materials

Later, the ion exchange properties of some organic materials were discovered, which led to the creation

Table 1 Principal practical achievements in the field of ion exchange

Year	Milestone
1850–52	Discovery of ion exchange phenomenon in soil (Thompson, Way and Roy)
1903	The first synthetic inorganic ion exchanger (Harms, Rümpler, Gans)
1935	The first ion exchange resin possessing high capacity (Adams and Holmes)
1944	Development of ion exchange resin synthesis by means of copolymerization (d'Alelio)
1947	Synthesis of zeolites (Barrer)
1950	Synthesis of ion exchange membranes (Wyllie, Sollner)
1958	Synthesis of inorganic ion exchanger based on zirconium phosphate (Amphlett)
1964	Synthesis of the first crystalline zirconium phosphate of α -type structure (Clearfield and Stynes)
1975–79	Development of ion chromatography (Small, Gjerde)
1980–present	New layered materials of α - and γ -types, organic ion exchangers; improvement of ion exchange chromatography method

Table 2 Important theoretical advances, elucidating the essence of ion exchange

<i>Year</i>	<i>Milestone</i>
1879	Helmholtz theory of electrical double layer
1911	Donnan theory of membrane equilibria
1950s	Statistical ion exchange models of Gregor, Kachalsky, Harris and Rice
1958	First edition of Helfferich's monograph devoted to ion exchange was published
1940s (2nd half)–1960s	Theories of ion exchange dynamics are developed
1960s (2nd half)–present	Theoretical models and description of new crystalline layered materials possessing ion exchange properties
1980–present	Theoretical background of ion exchange chromatography

of an ion exchange resin by Adams and Holmes. These new materials were characterized by their high capacity ($5\text{--}10\text{ meq g}^{-1}$) relative to inorganic ion exchangers. Resins were obtained by polycondensation of phenols or amines with formaldehyde, and their large-scale production began. Owing to their high degree of cross-linking the polymers had negligible solubility. The resins were hydrophilic due to the presence of ionic groups as an inseparable part of the polymer matrix: for example, for anion exchange resins amino groups inside the matrix were balanced by an equivalent quantity of anions. For cation exchangers phenolic, sulfoxylic, carboxylic or phosphonate or phosphinato groups were present inside the matrix, balanced by an equivalent quantity of cations.

A discovery by d'Alelio had great industrial significance. He invented a method of synthesis of ion exchangers based on styrene–divinylbenzene copolymers. This invention was anticipated by Staudinger's synthesis of reticular polystyrene. The first cation exchanger of this type was obtained in 1944, followed in 1948 by an equivalent anion exchanger. These resins possess high chemical and mechanical stability; their distinguishable feature is

a certain degree of control over the synthetic process. Moreover, such materials were characterized by high exchange capacity and working exchange rate. Different fixed ions can be introduced into the styrene–divinylbenzene matrix, offering a possibility to obtain resins with different cross-linking numbers and swelling behaviour. All these properties make this kind of synthetic resin of major practical significance (Table 3).

In the area of water treatment ion exchange techniques occupy a leading position worldwide and due to their increasing importance they are under continuous development. In 1951 Reents was the first to apply a mixed layer of anion and cation exchangers for the ultra-purification of water.

Emergence of cross-linked polymer electrolyte–ion exchange resins has allowed a new approach to the solution of problems of analytical and preparative chemistry: purification and separation of compounds possessing similar chemical properties. However, water treatment and waste water purification remain the main areas of application of ion exchange resins. Here exchangers capable of being universal absorbents for a wide variety of ions are mainly needed. Parallel to investigations aimed at enhancing sorption

Table 3 Main fields of application of ion exchange resins

<i>Resin type</i>	<i>Matrix type</i>	<i>Type of fixed groups</i>	<i>Application fields</i>
Strongly acidic cation exchange resins	Gel Macroreticular	Sulfonic	Water treatment; separation of rare earth elements; separation of amino acids, etc.
Weakly acidic cation exchange resins		Carboxylic	Decarbonizing of industrial water, water softening and deionization
	Gel Macroreticular		Purification of antibiotics, copper and nickel recovery
Strongly basic anion exchange resins	Gel Macroreticular	Quaternary ammonium	Different water conditioning processes; elimination of organic compounds with high molecular weight (macroreticular)
Weakly basic anion exchange resins	Gel Macroreticular	Tertiary amine or polyamine	Industrial water treatment; decolorization of sugar syrups (macroreticular)

capacity, improving the exchange kinetics, thermal stability, mechanical properties and chemical resistance, there has been a considerable development of selective ion exchangers. This requirement arose in the 1950s in connection with both the analytical problem of direct selective determination of elements in a complex mixture and the problem of extraction of metals from technological solutions during complex ore processing. The selectivity of ion exchangers is determined by two factors. The first consists of an exact correlation between the dimension of the sorbent's pores and the radius of the hydrated ion to be absorbed. The second factor is related to the formation of a coordination bond supplementary to an ionic one between the ion and the functional groups within the matrix.

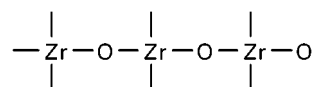
Besides development of polymeric acids and bases of different strengths, ion exchangers containing functional groups able to form chelate complexes with specific ions have also been obtained. This class of ion exchangers is characterized by high ion exchange constants and high selectivity owing to donor-acceptor interaction between adsorbent and adsorbate. In 1940, Skogseid made a macromolecular ion exchanger selective towards potassium, containing moieties analogous to dipicrylamine. Iron, uranium and rare-earth elements readily form complexes with oxygen-containing ligands. Several early transition metals like cobalt, nickel and copper give rise to stable amino complexes. Thus, anion exchangers containing amino groups (preferably those of primary amines) are selective for the latter group of elements, while exchangers containing phenolic groups are suitable for iron. Resins with carboxylic and phosphonic groups are suitable for uranium and rare-earth metals.

However, some researchers consider the ion exchange procedure of water treatment a kind of 'ecological boomerang', bearing in mind the fact that wastewater after ion exchange still contains many mineral compounds. Regeneration solutions contain them in quantities greater by an order of magnitude than the level of contaminants to be extracted. Ion exchange membranes avoid this disadvantage. The increase of mass of compounds in wastewater with respect to the quantity of extracted substances does not take place during membrane purification, providing a significant advantage for this method, when compared to distillation or sorption on ion exchangers. In 1950, the first samples of heterogeneous membranes were obtained by Wyllie and Patnode based on commercial ion exchangers reinforced by inert polymer fibres in order to provide high mechanical stability. In 1952, Manecke and Sollner reported the first homogeneous membrane, and in 1957 Gregor made the

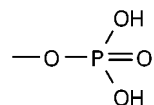
first inter-polymer membranes, where the ion-exchange and binder components are linked to each other by chemical bonds. Ultra-pure water cannot be obtained by the sole use of ion exchange membranes: nowadays one has to assemble a combination of separation methods such as filtration, microfiltration, ultrafiltration, reverse osmosis, electrodialysis with ion exchange membranes and a mono-layer of granulated ion exchange resin, and electrodialysis with ion exchange membranes filling the inter-membrane space with a mixed layer of granulated ion exchange resins.

Inorganic Ion Exchangers and Application of Inorganic Layered Materials

A reawakening of interest in inorganic ion exchangers was connected with the search for materials which can withstand high temperature, ionizing radiation and some aggressive chemicals. In 1943, Russel *et al.* discovered that insoluble zirconium phosphate is suitable for the separation of uranium and plutonium from nuclear fission products. Thus, a new class of inorganic ion exchangers was synthesized on the basis of group 4 elements, mainly of titanium and zirconium. Various kinds of functional groups can be attached to the polymer chains consisting of Ti or Zr atoms bonded to oxygen, producing different types of ion exchangers. It is a well-known fact that zirconium readily forms chains:



in solution. The behaviour of titanium is analogous. The most intense polymerization occurs in a range of pH values close to that of the hydroxide sedimentation. A polymer containing zirconyl groups together with residues of acid is obtained by addition of salt or acid to a zirconium (or titanium) salt solution. If the acid is polyprotic, then one obtains a cation exchanger containing an exchange site like:



The first material of this kind was zirconium phosphate obtained by Amphlett in 1958. It possessed a capacity of 1 meq g⁻¹ at pH 3, and 5 meq g⁻¹ at pH 11. Amorphous inorganic sorbents had a great advantage over organic resins owing to their ease of preparation.

In 1947 Barrer realized a synthesis of zeolite for the first time. He became a founder of zeolite chemistry, studying synthesis, structure, sorption and ion exchange properties of this new class of materials.

In 1964, Clearfield and Stynes synthesized the first crystalline zirconium phosphate and established its layered α -type structure $\alpha\text{-Zr}(\text{HPO}_4)_2 \cdot \text{H}_2\text{O}$, usually referred to in the literature as $\alpha\text{-ZrP}$. In 1968, the same authors reported the first γ -type zirconium phosphate, referred to as $\gamma\text{-ZrP}$. Since 1975, some organic derivatives of the latter modification have been synthesized by Yamanaka *et al.* Further development of this class of inorganic ion exchanger by Alberti *et al.* (1978) resulted in M(IV) phosphonates and organic phosphates with a layered structure of zirconium bis-monohydrogen phosphate ($\alpha\text{-ZrP}$). Some years after the first inorgano-organic sorbent was reported, Dines and Griffith described the synthesis of diphosphonates of general formula $\text{M(IV)}(\text{O}_3\text{P-R-PO}_3)$. A series of covalently pillared diphosphonates with a regular interlayer microporosity was subsequently obtained. As far as $\gamma\text{-ZrP}$ ($\text{ZrPO}_4(\text{H}_2\text{PO}_4) \cdot \text{H}_2\text{O}$) is concerned, a wide variety of layered and pillared M(IV) phosphonates were obtained in the period 1987–1990, since their structure depends on the starting material and on the nature of the $\text{O}_2\text{PRR}'$ group that replaced $\text{O}_2\text{P}(\text{OH})_2$.

Ion Exchange Chromatography

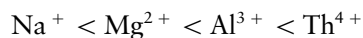
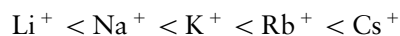
High performance in the separation of organic substances by liquid chromatography had already been achieved by the 1970s, while techniques of chromatographic separation of inorganic ions were developed to a lesser extent. In 1971, the first papers dealing with automatic spectrophotometric detection of metal ions separated by ion exchange chromatography on cation exchange resins appeared. Similarly, anions were separated on anion exchange resins. Conductometric detection was established by Small *et al.* in 1975 and Gjerde *et al.* in 1979. Finally it is necessary to mention ion exclusion chromatography applied to separate sugars and carbonic acids with an ion exchange column, but without any ion exchange interaction.

Development of Theoretical Background in the Field of Ion Exchange

Helmholtz developed the theory of the double electric layer in 1879, and this had a fundamental significance for the explanation of many phenomena related to ion exchange. According to his classic theory, the double layer consists of two electric layers, analogous

to the plates of an electric capacitor. The concept was later modified, as it had been proven that a double layer is formed at the interface between a solid phase and a solution. It consists of an immobile inner layer and a diffuse outer layer. Charge separation in this type of a system is of the order of molecular dimensions. As a result, the solid phase surface acquires an electric charge (positive or negative), while the counterions are distributed along the interface. These ions form a virtual outer plate of the diffuse layer. In fact, there is no interface but a dynamic equilibrium exists between the ions in the diffuse layer and those of the environment (the bulk solution). The existing equilibrium is disturbed upon changes in either pH or concentration of ions in the bulk solution. In this case new ions enter the diffuse layer, substituting ones already there and establishing a new ion exchange equilibrium.

The influence of valence, hydration and ion dimensions on the degree of ion exchange transformations has been established and ion selectivity series were composed by Wiegner for ion retention on aluminosilicate sorbents:



Mattson demonstrated in 1927 that aluminosilicates enriched in silica gave an increase in cation exchange capacity. Jaeger demonstrated that at higher concentrations, as well as in mixed organo-aqueous solutions, the values of the exchange potentials of ions with the same valence could be quite close, with possible inversion of the selectivity series.

Selectivity, i.e. preferable absorption of one of the counterions, is an important property of ion exchangers. Hence, the ion exchanger becomes enriched in counterions which possess small dimensions in the solvated state or which are able to enter into specific interactions with the fixed ions or with the matrix. The isotherm of ion exchange is a graphical representation of the dependence of an equivalent fraction of the counterion A in the ion exchanger, versus its equivalent fraction in solution.

In 1939 Nikolskii demonstrated that the law of mass action could be applied successfully to ion exchange:

$$(\gamma_1^{1/Z_1})/(\gamma_2^{1/Z_2}) = K(a_1^{1/Z_1})/(a_2^{1/Z_2})$$

where γ_1 and γ_2 are the quantities of ions absorbed by the resin (meq); Z_1 and Z_2 are charges of these ions in solution; a_1 and a_2 are activities of the above ions in the solution and K is the ion exchange constant.

In 1935 Kielland introduced activity coefficients for the ion exchanger phase in order to estimate deviations of ion exchange equilibria from a simple form of the law of mass action. The most clear thermodynamic approach to these equilibria was provided by Gaines and Thomas in 1953, which was not connected to model concepts.

A physical model of ion exchange processes has been gradually formed together with the accumulation of empirical data. For example, the theory of membrane equilibria created by Donnan in 1911 promoted a breakthrough after its application to ion exchange processes. The essence of Donnan theory can be briefly described as follows. An electrolyte RNa is supposed to be on one side of a membrane, and an NaCl solution on the other side. Since the membrane is not permeable for R^- ions, only sodium and chloride ion redistribution will take place in the system. However, in the above case the diffusion process is unable to equalize concentrations of all ions from both sides of the membrane. For ion exchange equilibria, an interface between liquid and solid phases is considered as a membrane, while a colloidal particle bearing the exchangeable ion is assumed to be a non-diffusing ion.

In the early 1950s, Gregor proposed an osmotic theory of exchange. According to this model, the matrix of ion exchange resin is expanded upon swelling, and thus applies pressure to the liquid inside the pores. In such a case the equilibrium is determined by a difference in the osmotic pressure between the external solution and that of the liquid inside the pores together with the elastic forces of the matrix. However, Gregor's model does not consider the formation of ion pairs, and hence does not explain selective adsorption; moreover, its accuracy is not sufficient to describe exchange in dilute solutions, which are typical for ion exchange processes.

Some years later another model of ion exchange appeared, built on a molecular background rather than the macroscopic Gregor model. The model of Kachalsky (mid-1950s) presumes that the energy of electrostatic interaction which imparts changes in free energy of the system is uniformly distributed over the polymer chain between the ionogenic groups. The model describes the resin as a linear polyelectrolyte and provides an accurate description of ion exchangers with a small number of cross-linking bonds.

A similar approach was used in the model developed by Harris and Rice at about the same time. It also uses a molecular level approach and the concept of linear polyelectrolytes, but the authors concentrated on interactions of neighbouring functional groups both in the same and in the adjacent polymer

chains, taking into account the regular distribution of fixed ions in the ion exchange resin phase. Another distinctive feature of this model is that it considers ion pair formation between the fixed ions and counterions.

Pepper has studied swelling of different absolutely dry resins in water and demonstrated that the total volume of the system undergoes shrinkage at the first step and then remains unaltered. Thus initially, the primary hydration shell is formed which consists of the so-called 'fixed' water, possessing specific properties. The water absorbed afterwards is called 'free' water and behaves like ordinary loosely bound water. The degree of swelling depends on the structure and cross-linking of the particular resin. Inorganic ion exchangers usually have a rigid crystal structure and their swelling is insignificant; layered ion exchangers undergo intralaminar swelling.

Ion exchange interactions occur at different rates in heterogeneous media; therefore studies dealing with ion exchange kinetics are of great importance. In 1947, Boyd and co-workers showed that the exchange rate is determined either by the diffusion rate inside the resin bed (gel diffusion) or by the diffusion in the layer of liquid surrounding the bed (film diffusion). When the rates of gel and film diffusions are comparable, both components determine the exchange rate. Determination of the mechanism and the limiting stage of the ion exchange process presents a rather difficult problem, because the kinetics simultaneously depend on a number of parameters, such as the concentration of adsorbate in solution, the nature of the ionic species, the type and granular composition of the ion exchanger and the relative migration rate of the interacting phases. The limiting stage of ion exchange can be approximately estimated as follows:

for gel diffusion:

$$(c\bar{D}\delta)/(cDr_0) \cdot (5 + 2K_{A/B}) \ll 1$$

for film diffusion:

$$(c\bar{D}\delta)/(cDr_0) \cdot (5 + 2K_{A/B}) \gg 1$$

and in case of mixed diffusion:

$$(c\bar{D}\delta)/(cDr_0) \cdot (5 + 2K_{A/B}) \approx 1$$

where $\bar{c} = z_i \bar{c}_i$, $c = \sum z_j c_j$ are total concentrations of exchanging ions in the solid and liquid phases

respectively; \bar{D} and D are ionic diffusion coefficients in the solid and liquid phases, respectively; δ is the thickness of the diffusion interlayer; r_0 is the radius of the ion exchanger bed; and $K_{A/B} = \bar{c}_A c_B / c_A \bar{c}_B$ is the separation coefficient for both sorts of counterions in the equilibrium state: the counterion A is present initially inside the bed, while the counterion B is initially in solution.

An equivalent exchange takes place under the following condition:

$$z_R \bar{c}_R = \sum_i^n z_{Ai} \bar{c}_{Ai}$$

where \bar{c}_R is the concentration of fixed groups inside the bed, \bar{c}_{Ai} is the concentration of i -th counterion. This is only an approximation, applicable to ion exchangers of high capacity treated with relatively dilute aqueous solutions. In all other cases, the ion exchanger absorbs a significantly higher quantity of ions than is needed for equivalence, i.e. a super-equivalent exchange occurs. An excess of counterions penetrates into the exchanger bed accompanied by a quantity of co-ions, necessary to compensate the electric charge of the former, in order to preserve a condition of electroneutrality of the bed:

$$z_R \bar{c}_R + \sum_{j=1}^n z_{Xj} c_{Xj} = \sum_{i=1}^m z_{Ai} \bar{c}_{Ai}$$

The higher the concentration of external solution, the greater is the contribution of super-equivalent exchange. Even for zeolites and highly cross-linked resins it becomes apparent at concentrations of external solution of about 0.1 N and higher. For scarcely reticulated, macroporous, highly swelling or weakly charged ion exchange resins the super-equivalent exchange has a much more pronounced effect and it becomes distinguishable at considerably lower concentrations.

A sorption without ion exchange is usually named Donnan absorption of electrolyte, because the thermodynamic description of the process is principally the same both for the system 'ion exchanger-solution' and for systems with a real semipermeable membrane as an interface separating phases in Donnan theory. However, the latter postulates that the dissociation in both phases is complete. Another situation is observed when the exchange occurs between the bed and weakly dissociated electrolyte or when ionogenic groups on the former are weakly dissociated. In that case, one deals with sorption of fragments of undissociated molecules and ion pairs and the exchange cannot be described in terms of Donnan theory. The

concept of 'super-equivalent exchange' includes the exchange of ions, absorption of electrolyte molecules without ion exchange, and other processes which could be characterized as between the above two cases.

Recent Progress in Ion Exchange

In recent years extensive research has been carried out on new crystalline inorganic and inorgano-organic layered compounds which possess ion exchange properties. Each layer in their structure can be considered as a planar macromolecule, while the substance as a whole is assumed to be a molecular crystal formed by these planar macromolecules. A reversible process of intercalation between the layers occurs due to interactions of guest species with active sites on the surface of the layer (lamella). However, the layers are unable to move spontaneously in a direction perpendicular to the plane. This is due to a certain rigidity of layers that plays an important role in intercalation reaction mechanism and energetics. Like other ion exchange materials, the charged layered solids may be strong, medium or weak cationic (or anionic).

The exchange of protons of α -ZrP phase for Li^+ , Na^+ and Ca^{2+} occurs rapidly in acidic solutions, while H^+ exchange for larger or strongly hydrated cations like NH_4^+ , Rb^+ , Cs^+ , Ba^{2+} , Mg^{2+} , Cu^{2+} and Cr^{3+} is quite slow at room temperature due to the high activation energies of interlayer expansion. Exchange can be facilitated in materials with large interlayer distances like α -Zr(HPO_4)(NaPO_4) \cdot $5\text{H}_2\text{O}$ ($d = 11.8 \text{ \AA}$) or in intercalation compounds with ethanol or alkylamines. The compounds that can be protonated are preferably used as guest species. For example, an amino derivative of cyclodextrin has been used for intercalation, increasing the interplanar distance in α -ZrP up to $d = 35.6 \text{ \AA}$. These distances for other guest species are; 14.2 \AA for ethanol, 20.4 \AA with benzimidazole, 22.8 \AA with 1-hexylamine and 23.1 \AA with lysine. The layered compounds under discussion can swell upon introduction of water or other solvents into the interlayer space. Sometimes the process leads to delamination, i.e. destruction of the crystal into separate lamellae. Withdrawal of the solvent results in reaggregation of the lamellae in thin films or membranes. Inorgano-organic derivatives, phosphonates of layered α -structure, can be obtained by introducing the corresponding acid $\text{H}_2\text{O}_3\text{PR}$ (where $\text{R} = -\text{CH}_3$, $-\text{C}_6\text{H}_5$, $-\text{O}(\text{CH}_2)_n\text{CH}_3$ etc.) into the reaction, instead of H_3PO_4 . It is also possible to synthesize those compounds by substitution of existing OH groups in the α -ZrP structure by R or OR. Another interesting group of compounds is

covalently pillared zirconium diphosphonates of general formula $M^{IV}(O_3P-R-PO_3)$. If the R group is small, then a low degree of interlayer microporosity is observed, while for pillared compounds containing fragments of 3,3(5,5)-tetramethylbiphenyldiphosphonic acid the value of interlayer porosity is raised to $375\text{ m}^2\text{ g}^{-1}$ (an average pore size of 5 \AA). Inorgano-organic derivatives have also been obtained for γ -ZrP by substitution of the interlayer $O_2P(OH)_2$ groups for O_2PRR' . Pillared phases of γ -ZrP with, for example, biphenylphosphonate groups have a volume of micropores of $320\text{ m}^2\text{ g}^{-1}$ and an average size of 5.8 \AA .

A limited number of inorganic anion exchangers is known. Layered double hydroxides (or hydrotalcite-like anionic clays) can exchange a large number of inorganic and organic anions, while layered $ZrPO_4Cl$ can selectively replace chloride anions with other monodentate anionic ligands.

Currently, ion exchange is of extreme importance for processing of irradiated nuclear fuel and treatment of spent fuel elements of nuclear power stations, where it is often combined with other techniques, e.g. extraction. The processes of sorption play an important role in deactivation of nuclear industry wastes and in purification of cooling water from nuclear reactors. Different kinds of ion exchangers are widely used for the clean-up of the world's worst nuclear accident at Chernobyl. For example, Strelko *et al.* are carrying out both research and application of highly selective inorganic granulated ion exchangers for elimination of radioactive isotopes from drinking water, milk, etc. Ion exchange is extensively used in medicine for haemosorption (or haemoperfusion) – the method of blood purification from toxic compounds by direct contact of the sorbent with the patient's blood. This method was applied for the first time by Muirhead and Reid in 1948; they directed the blood flow through a mixture of cation and anion exchangers taken in a ratio of 9:1. Haemosorption can be applied alone or in combinations with haemodialysis (when the toxins are distributed between two liquid phases, separated by a semipermeable membrane). The ion exchangers are used to regenerate dialysate from the artificial kidney apparatus. Further improvement of the haemosorption method is connected with the necessity to resolve problems of selective blood purification, as well as the problem of better sorbent compatibility with biological fluids. Another possible medical application of ion exchangers consists of the creation of drugs and pharmaceuticals with prolonged activity, offering the possibility to release an active component inside the patient's body over time and maintaining its necessary concentration.

A nontraditional application of ion exchangers in nonpolar organic media is the ultra-purification of organometallic compounds used as precursors in chemical vapour deposition. These precursors are widely utilized for synthesizing materials possessing valuable properties for micro-, opto- and acousto-electronics, and protective and optical coatings. The organometallics in question react readily with atmospheric oxygen and moisture, while at the same the requirements on their purity are quite rigorous (less than $1 \times 10^{-3}\%$ of the sum of contaminants). The above requirements can be met by treatment with a sorbent composition containing inorganic ion exchangers based on titanium and zirconium phosphates, thus replacing energy-intensive and expensive traditional methods (sublimation or distillation).

Future Developments

Undoubtedly, the future development of ion exchange as a method of separation will be directed towards ecological and biotechnological problems. The development of society parallel to scientific and technical progress will promote greater regard for natural resources. Hence, particular attention will be drawn to the application of renewable technologies and closed technological cycles including ion exchange stages or applying ion exchange materials mainly in the area of water treatment and wastewater purification, as well as in several other fields. Certainly, the use of ion exchangers in medicine will increase.

New, advanced ion exchange materials possessing desirable properties will be obtained by targeted synthesis; computer modelling and simulations as well as molecular design will be increasingly applied.

The specificity and selectivity of ion exchange will grow; i.e., the most suitable materials from the viewpoint of their origin, matrix type, the type of ionogenic groups etc. will increasingly be applied for specific cases.

The phenomenon of ion exchange discovered a century and a half ago, as well as processes established on the basis of it, are still in a process of dynamic development. The potential of ion exchange both in practical applications and from the elaboration of theoretical concepts related to ion exchange is not yet complete.

See also: II/Ion Exchange: Novel Layered Materials: Phosphates; Novel Layered Materials: Non-Phosphates; Organic Ion Exchangers; Theory of Ion Exchange.

Further Reading

- Alberti G, Casciola M, Costantino U and Vivani R (1996) Layered and pillared metal(IV) phosphates and phosphonates. *Advanced Materials* 8(4): 291.
- Amphlett CB (1964) *Inorganic Ion Exchangers*. Amsterdam: Elsevier.
- Clearfield A (ed.) (1982) *Inorganic Ion Exchange Materials*. Boca Raton, FL: CRC Press.
- Fritz JS, Gjerde DT and Pohlandt C (1982) *Ion Chromatography*. Heidelberg: Hüthig.
- Greig JA (ed.) (1996) *Ion Exchange Developments and Applications*. Cambridge: Royal Society of Chemistry.

- Helfferich F (1962) *Ion Exchange*, 2nd edn. New York: McGraw-Hill.
- Hwang S-T and Kammermeyer K (1975) *Membranes in Separations*. New York: Wiley.
- Marinsky JA and Marcus Y (eds) (1973) *Ion Exchange and Solvent Extraction*. New York: Marcel Dekker.
- Osborn GH (1961) *Synthetic Ion-Exchangers: Recent Development in Theory and Application*. London: Chapman & Hall.
- Weiss J (1994) *Ion Chromatography*, 2nd edn. Weinheim: Wiley.

Inorganic Ion Exchangers

E. N. Coker, BP Amoco Chemicals,
Sunbury-on-Thames, Middlesex, UK

Copyright © 2000 Academic Press

Summary

In the first part of this chapter, the origins of ion exchange in inorganic materials are discussed in relation to the structure of the exchanger. Thereafter, the various types of inorganic ion exchangers are introduced and categorized according to their ion exchange properties. Descriptions of particular materials follow, with special emphasis on some structure-specific and composition-specific ion exchange properties. The materials which are discussed include zeolites and zeolite-like materials, clays and other layered materials, zirconium phosphates, heteropolyoxometalates and hydrous oxides.

Types of Ion Exchange Sites in Inorganic Materials and their Origin

For the purposes of this chapter, ion exchange interactions will be defined as those involving the interchange of positively or negatively charged species (atomic or molecular) at an ion exchange site.

There are two types of chemical species which constitute the vast majority of ion exchange sites in inorganic materials:

1. structure-terminating, covalently bonded groups such as -OH
2. charge-compensating groups, electrostatically associated with, and not covalently bonded to, a charged moiety

Type 1 sites, illustrated in **Figure 1A**, are responsible for the ion exchange properties of materials such as hydrous oxides and single-layer clays. All oxidic materials have these sites to some degree, at the surfaces of particles or crystals or at defect sites within the structure. Ion exchange reactions involving these types of sites may be regarded as chemical reactions, which may display amphoteric nature.

Type 2 sites, illustrated in **Figure 1B**, are responsible for most of the ion exchange capacity of zeolites, double-layer clays and zirconium phosphates. These sites arise in structures possessing, for instance, charged layers or charged porous frameworks. The exchangeable ions are present to retain overall electroneutrality. When materials such as zeolites are concerned, a mixture of Type 1 and Type 2 sites is available, although Type 2 sites will usually greatly outnumber Type 1 sites, and the latter are often ignored. Exchange interactions involving Type 2 sites are physical in nature, as chemical bonds are neither made nor broken.

Types of Inorganic Ion Exchange Material

An important distinction between ion exchange materials is whether they exhibit capacity for cations, anions, or both. Cation exchangers, and in particular zeolites, clays and zirconium phosphates, are the most common and best understood of the ion exchangers. Anion exchangers are also important but

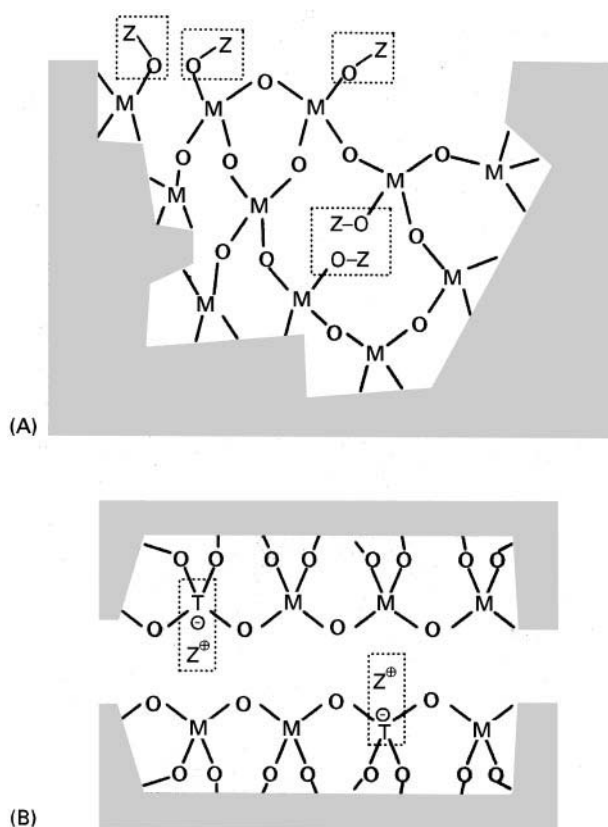


Figure 1 The two major types of ion exchange site. (A) Type 1, structure-terminating and defect groups; (B) Type 2, charge-compensating groups. M is an oxide-forming metal with oxidation state 4; T is an oxide-forming metal with oxidation state 3. The regions enclosed in dotted lines are those giving rise to ion exchange where Z^+ (or $Z-O^-$) is exchangeable. Shaded areas represent a continuation of the oxidic network.

the exchange of anions is often not fully reversible, thus the exchangers cannot be easily regenerated and the reactions are more difficult to treat thermodynamically. Multiply charged anions, in particular, may be held tenaciously by the exchanger. Examples of anion exchangers are certain clays such as hydroxy double salts (e.g. $[\text{CuNi}(\text{OH})_3]\text{Cl}$) and layered double hydroxides (e.g. hydrotalcite, $\text{Mg}_6\text{Al}_2(\text{OH})_{16}(\text{CO}_3) \cdot 4\text{H}_2\text{O}$). Amphoteric ion exchangers possess predominantly Type 1 exchange sites, e.g. hydrous oxides.

While ion exchange properties may be exhibited by both amorphous and crystalline solids, studies of the ion exchange properties of amorphous solids are often hampered by difficulties in preparing materials reproducibly and the difficulties in characterizing them fully. With crystalline materials, however, reproducible preparations can be easily verified and well-defined structural data aids in the interpretation of the results of ion exchange experiments.

Most crystalline inorganic ion exchangers are porous. This porosity may arise through the presence of void space between the layers in clay materials and layered double hydroxides, or through the intrinsic microporosity present in zeolitic materials. Many of the layered materials have the versatility to (reversibly) change their interlayer spacing and hence the size of the voids, which allows the ion exchange properties to be adjusted. The more rigid zeolite structures give rise to exchange reactions which may show extremely high selectivity to certain cations, or perform ion sieving.

Zeolites

Zeolites are microporous crystalline aluminosilicate minerals which occur naturally and may be synthesized easily in the laboratory. An introduction to the structures and properties of zeolites is given in the article by Dyer. Zeolites are used on a large scale as ion exchangers in many fields; most notable are their use as 'builders' or water softeners for laundry detergents, and their use in the decontamination of various types of waste streams. Typical applications of zeolites as ion exchangers are given in Table 1. Additionally, the ion exchange capability of zeolites can be used as a tool to modify their catalytic and sorptive properties. Some attention will be paid to structural parameters which influence the ion exchange properties of zeolites in the following paragraphs.

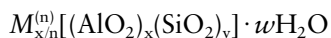
Besides the conditions under which an ion exchange reaction is performed, a number of factors may influence the ion exchange properties of zeolites, including:

- the structure of the zeolite, particularly the diameters of the windows allowing access to the pores and cavities
- the location of the ion exchange sites; different cation environments lead to different ion exchange properties. The number of charge-balancing cations required for an electroneutral material is often less than the number of available ion exchange sites, thus partial occupancy of sites is common. Some of the possible cation positions in zeolites A and X (two of the most widely used synthetic zeolite ion exchangers) are indicated in Figure 2
- the composition of the zeolite framework; varying the Si:Al ratio or changing the framework substituent elements may change, for example, the density of exchange sites, the electric field strength or the hydrophobicity of the sample as a whole

Table 1 Principal applications of zeolites as ion exchangers

<i>Application</i>	<i>Type of zeolite frequently used</i>	<i>Ion exchange process</i>
Detergent building	A (synthetic) MAP (synthetic) X (synthetic)	Removal of Ca^{2+} and Mg^{2+} from solution
Wastewater treatment	Clinoptilolite (natural) Chabazite (natural) Mordenite (natural) Phillipsite (natural)	Uptake of NH_4^+ and heavy metals from waste streams
Nuclear waste treatment	Clinoptilolite (natural) Chabazite (natural) Phillipsite (natural) Mordenite (natural) Mordenite (synthetic) Ionsiv IE-96 (synthetic) Ionsiv A-51 (synthetic)	Uptake of $^{137}\text{Cs}^+$, $^{90}\text{Sr}^{2+}$ and other radionuclides
Animal food supplement	Various (natural)	Regulation of NH_4^+ and NH_3 levels in stomach
Animal food supplement	Various (natural)	Scavenging of radionuclides following contamination of livestock
Fertilizer	Various NH_4^+ forms (natural), often those used to remove NH_4^+ from wastewater	Slow release of NH_4^+ (and other cations)

The empirical structural formula for an aluminosilicate zeolite may be given as



where the framework is constructed from the entities within the square brackets and the water molecules and charge-balancing cations (M)

occupy the interstitial space. The $x/n M^{n+}$ cations are present to counterbalance the x units of negative charge on the framework due to the presence of $x \text{ AlO}_2$ groups. In many cases, ion exchange reactions in zeolites may reach completion, that is, all of the charge-balancing cations (M) initially present are capable of being replaced by the ingoing cation.

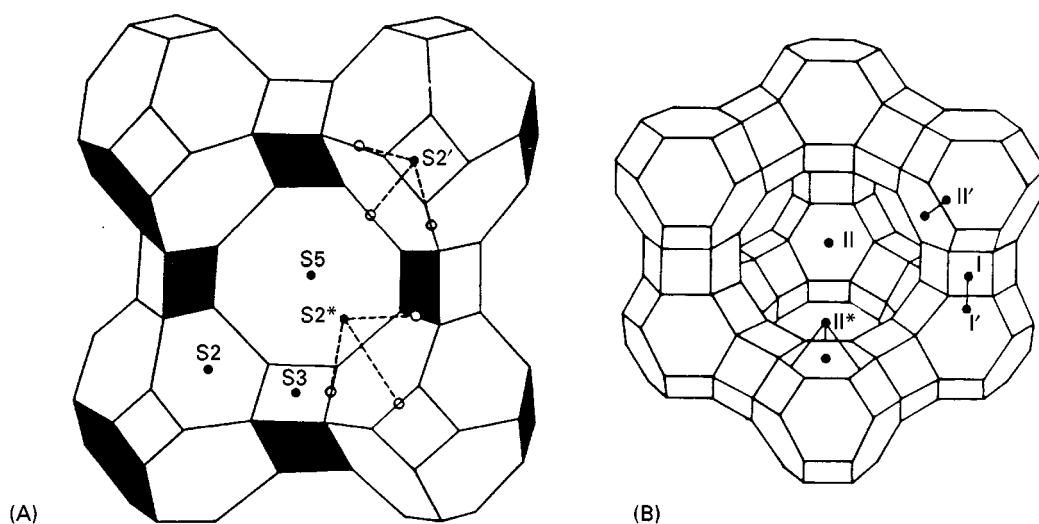


Figure 2 A representation of some of the possible positions of exchangeable cations in the structures of zeolites A (A) and X (B). Note: the two structures are not shown on the same scale. Reproduced with permission from Stucky GD and Dwyer FG (eds) (1983) *Intrazeolite Chemistry*. ACS Symposium Series, vol. 218, p. 288. Washington, DC: American Chemical Society.

Incomplete ion exchange reactions In some cases, some of the cations are constrained within the structure and are nonexchangeable. Such cations are introduced into small cavities in the structure during growth of the zeolite crystal. This situation is common with feldspars and feldspathoids, which are similar in composition to zeolites, but possess more limited porosity. Even in instances when all charge-balancing cations in the zeolite are physically exchangeable, the total theoretical exchange capacity might not be obtained practically.

There are several reasons for incomplete ion exchange; the three most important of these are given below and illustrated schematically in Figure 3.

1. The most obvious cause of partial or nonexistent exchange is ion-sieving, where the cation to be exchanged into the zeolite is too large, or has a hydration sphere which is too large and robust for it to have unrestricted access to the pores of the zeolite. Univalent cations will typically reach 100% exchange, except in limiting cases such as large cations combined with small-pore zeolites. Ion-sieving is more commonly observed with multiply charged cations, which tend to have larger hydration spheres on account of their higher charge densities. Zeolites which possess more than one ion exchange site (see Figure 2) may display ion-sieving properties depending on the thermodynamics of the exchange reactions occurring at the various sites. The sites which offer the greatest thermodynamic advantage are exchanged first, while the less favourable sites may not exchange at all.
2. Volumetric exclusion may occur if bulky (organic) cations are exchanged into zeolites of high charge density. Here, the volume occupied by the cations may reach that available in the pores of the crystal before complete exchange has occurred.
3. A third reason for limited exchange to be observed is when multivalent cations are exchanged into zeolites of low charge density. As the density of ion exchange sites decreases, the mean separation between adjacent sites increases, until a point is reached where multivalent cations are unable to satisfy two or more cation exchange sites because of the distance between them. Table 2 illustrates this point by listing the maximum exchange limits observed for several multivalent cations in samples of zeolites ZSM-5 and EU-1 possessing a range of Si/Al ratios.

It is easy to visualize the limiting factors of ion exchange under equilibrium conditions; however, practical ion exchange may have also kinetic limitations. A particular example of when the desired ion

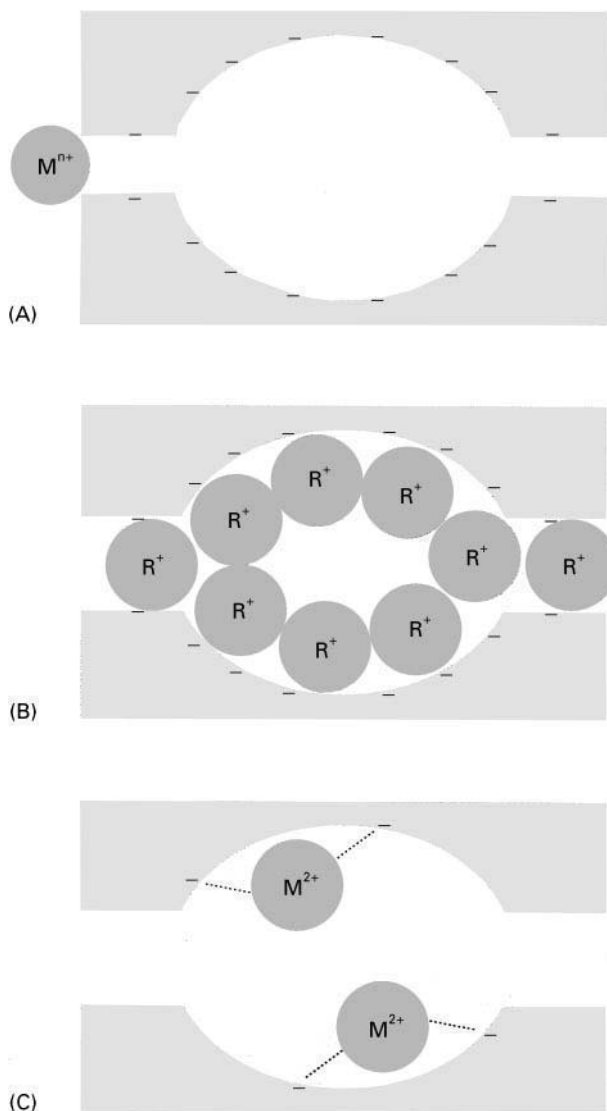


Figure 3 The principal reasons for limitations to ion exchange reactions found in zeolites. (A) Ion-sieving; (B) volume exclusion; (C) low charge density (with multivalent cations). The lightly shaded regions represent an extract of the zeolite framework. For clarity, only *ingoing* cations are shown.

exchange is kinetically limited but still capable of reaching 100% of the theoretical capacity is the softening of water.

Zeolites are used in vast quantities in the detergent industry as a water-softening additive for laundry detergents – up to 30% by weight of most modern washing powders is zeolite. The zeolite is added principally to remove calcium and magnesium and thus prevent their precipitation with surfactant molecules. Zeolite A is most commonly used, due to its high ion exchange capacity, which is a consequence of the framework possessing the maximum possible number of aluminium atoms (Si : Al = 1 : 1). Recently, zeolite

Table 2 Ion exchange limits (mole fraction) for various multivalent cations and temperatures in samples of zeolites ZSM-5 and EU-1 with varying numbers of aluminium atoms in the framework. In all cases, the ingoing cation replaces sodium

Zeolite type	Al per u.c. ^a	Ca ²⁺ (25°C)	Sr ²⁺ (25°C)	Ba ²⁺ (25°C)	La ³⁺ (25°C)	Ca ²⁺ (65°C)	Sr ²⁺ (65°C)	Ba ²⁺ (65°C)	La ³⁺ (65°C)
ZSM-5	1.1	0.28	0.31	0.36		0.50	0.51	0.52	
ZSM-5	2.0	0.31	0.36	0.56		0.54	0.64	0.76	
ZSM-5	2.4	0.36	0.48	0.67	0.39	0.50	0.67	0.77	0.48
ZSM-5	4.2	0.37	0.42	0.90		0.62	0.85	0.93	
EU-1	1.2	0.54	0.56	0.56					
EU-1	2.1	0.62	0.67	0.67		0.85	0.89	0.89	
EU-1	3.8	0.86	0.93	0.93		0.96	0.97	0.97	

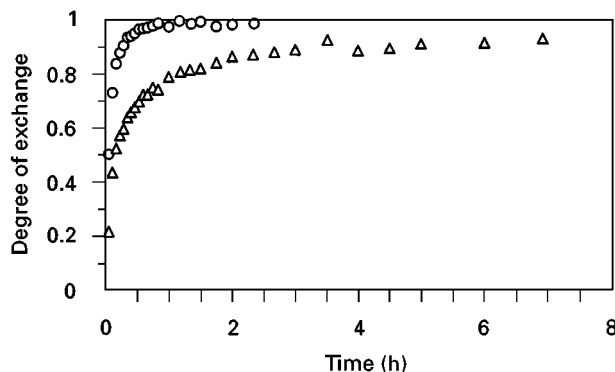
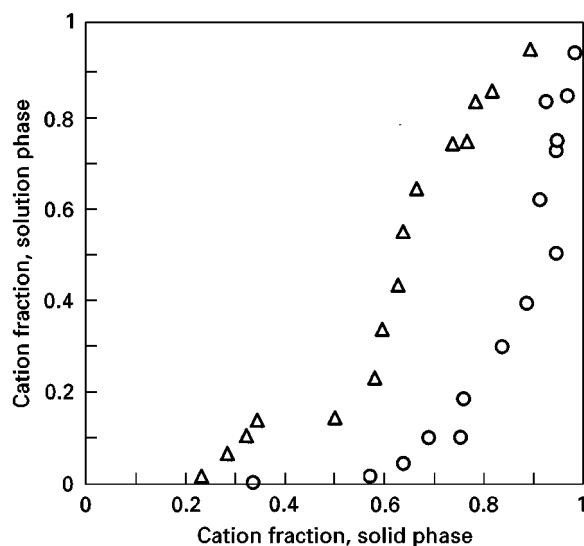
^a Number of aluminium atoms in framework per unit cell.

MAP (Maximum Aluminium P), also with Si : Al = 1 : 1, has been introduced into some detergents. Although the Mg²⁺ ion (radius 0.07 nm) is considerably smaller than the Ca²⁺ ion (radius 0.1 nm), its exchange into the zeolite is far less facile than that of Ca²⁺, due to its large, tight hydration sphere (the radii of the hydrated Ca²⁺ and Mg²⁺ cations are estimated to be 0.42 and 0.44 nm, respectively). **Figure 4** shows the kinetics of exchange of Ca²⁺ and Mg²⁺ into Na-A zeolite. The major restriction to the hydrated Mg²⁺ cation is the 0.42 nm window in zeolite A through which it must pass to gain access to the exchange sites within the structure. In order for the ion exchanger to be effective as a water softener for detergents, it must reduce water hardness within a few minutes of beginning the wash cycle. While zeolites A and MAP perform well at removing calcium from hard water quickly, their performance towards magnesium is generally poor. Despite the kinetic limitations, Ca²⁺ and Mg²⁺ are fully exchangeable into zeolite A, although selectivity is greater for Ca²⁺ (**Figure 5**). Detergent-grade zeolites possess small crystallite sizes in

order to provide acceptable kinetics of Ca²⁺ exchange.

Materials closely related to zeolites

Semicrystalline zeolites Some interest has been shown in the ion exchange properties of zeolite precursors, which are obtained by quenching a zeolite synthesis mixture before it has fully crystallized. In these semicrystalline materials, some larger windows and pores are present than in the crystalline counterpart because the structure has not fully formed. This leads to ion exchange selectivities which are different from the crystalline material. Also, their ion exchange capacities are lower than the corresponding crystalline zeolites. The materials typically show weak zeolite X-ray diffraction patterns, and are

**Figure 4** Kinetics of exchange of Ca²⁺ and Mg²⁺ for 2Na⁺ in zeolite A. Circles, Ca²⁺ exchange; triangles, Mg²⁺ exchange. Data were determined at 25°C, pH 10 and at a solution concentration of 0.05 mol equiv. L⁻¹.**Figure 5** Isotherms for Ca²⁺/2Na⁺ and Mg²⁺/2Na⁺ exchange in zeolite A. Circles, Ca²⁺ exchange; triangles, Mg²⁺ exchange. Data were determined at 25°C, pH 10 and at a solution concentration of 0.05 mol equiv. L⁻¹.

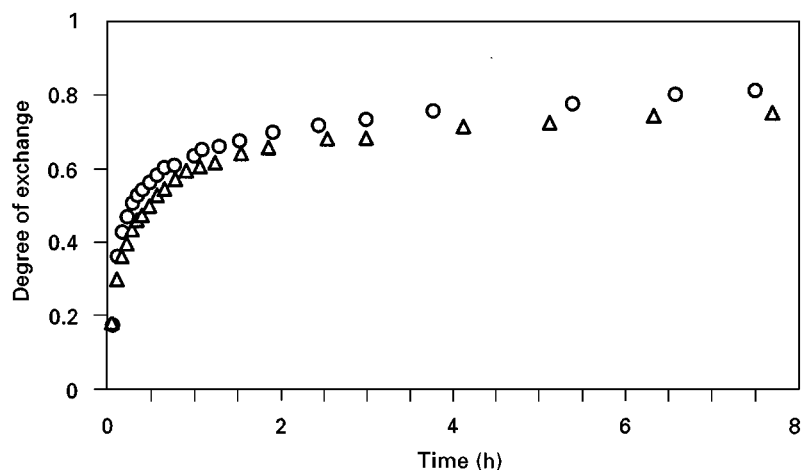


Figure 6 Kinetics of exchange of Ca^{2+} and Mg^{2+} for 2Na^+ in the semicrystalline precursor to zeolite A. Circles, Ca^{2+} exchange; triangles, Mg^{2+} exchange. Data were determined at 25°C , pH 10 and at a solution concentration of $0.05 \text{ mol equiv. L}^{-1}$.

thus not totally amorphous, but possess some short-to-medium range order. Semicrystalline precursors to zeolites have been investigated as potential water softeners with enhanced magnesium performance for detergent use. The materials show slightly limited capacities for both calcium and magnesium, but the selectivity ratio of $\text{Mg} : \text{Ca}$ is higher than that in the fully crystalline counterpart. In the kinetics of exchange, one sees the influence of the population of larger windows and pores. The rate of Mg^{2+} exchange approaches that of Ca^{2+} exchange, since the openness of the semicrystalline structure presents less limitation to the diffusion of large hydrated cations (see **Figure 6** and compare with **Figure 4**). Despite the improvement in Mg^{2+} exchange properties relative to Ca^{2+} , the performance of such zeolite precursors is probably too poor for detergent applications.

Materials with nonaluminosilicate frameworks
Zeolite-like structures composed partially or wholly of oxides other than those of Al and Si such as silicoaluminophosphates (SAPOs), metal aluminophosphates (MeAPOs), stannosilicates, zincosilicates, titanosilicates and beryllphosphates are expected to possess ion exchange properties, although few data exist in the literature. Of these materials, the titanosilicates have received the most attention. Recently, the titanosilicate TAM-5 has been developed; this exhibits high selectivity for Cs^+ in the presence of high concentrations of other alkali cations and over a pH range from below 1 to above 14. Also, high selectivity of this material for Sr^{2+} in basic media has been observed. These high selectivities, and its stability to solutions covering this pH range, has led to commercialization of

the material by UOP as Ionsiv IE-910 (powder) and Ionsiv IE-911 (granules) for use in nuclear waste treatment.

Particularly interesting ion exchange properties are shown by materials possessing high electric field strengths, which may arise with frameworks composed of oxides of elements with valencies differing from each other by more than one unit. An example is the beryllphosphate $\text{Na}_8[(\text{BeO}_2)_8(\text{PO}_2)_8] \cdot 5\text{H}_2\text{O}$, which has the same structure as the aluminosilicate zeolite gismondine (or synthetic zeolite P). Beryllium and phosphorus are strictly alternating in the structure and have valencies of $+2$ and $+5$ respectively, giving rise to a framework with alternating -2 and $+1$ nominal charges (on Be and P), as opposed to -1 and 0 for Al and Si in the aluminosilicate analogue. Due to the high electric field gradient, hard cations tend to be favoured over soft ones. Thus, magnesium is favoured kinetically over calcium; the diffusion coefficient for exchange of Mg^{2+} into $\text{Na}_8[(\text{BeO}_2)_8(\text{PO}_2)_8] \cdot 5\text{H}_2\text{O}$ is more than three times higher than that of Ca^{2+} under the same conditions (**Figure 7**), which is a reversal of the situation seen in the aluminosilicate zeolites (compare **Figures 7** and **4**). The relatively slow kinetics of exchange may be attributed to the small window size of the beryllphosphate material (the beryllphosphate unit cell is smaller than the aluminosilicate one). Univalent cations also exhibit unusual exchange characteristics with $\text{Na}_8[(\text{BeO}_2)_8(\text{PO}_2)_8] \cdot 5\text{H}_2\text{O}$, due in part to the relatively short Be–O and P–O bonds and the rigidity of the structure. High resistance is experienced by ingoing cations and large hysteresis loops are seen in, for instance, the exchange of K^+ for Na^+ , while the same reactions in the aluminosilicate analogue do not exhibit hysteresis (compare

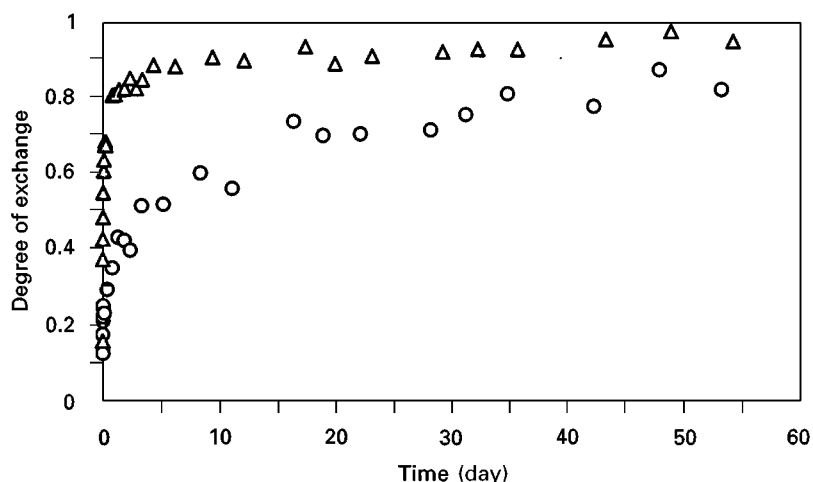


Figure 7 Kinetics of exchange of Ca^{2+} and Mg^{2+} for 2Na^{+} in $\text{Na}_8[(\text{BeO}_2)_8(\text{PO}_2)_8] \cdot 5\text{H}_2\text{O}$. Circles, Ca^{2+} exchange; triangles, Mg^{2+} exchange. Data were determined at 25°C , pH 10 and at a solution concentration of $0.05 \text{ mol equiv. L}^{-1}$. Interdiffusion coefficients (D): $D_{(\text{Ca})} = 2.0 \times 10^{-18} \text{ m}^2 \text{ s}^{-1}$; $D_{(\text{Mg})} = 6.5 \times 10^{-18} \text{ m}^2 \text{ s}^{-1}$. (Reproduced with permission from Coker EN and Rees LVC (1992) Ion exchange in beryllophosphate G. Part 2. Ion exchange kinetics. *Journal of the Chemical Society, Faraday Transactions* 88: 273–276.)

Figures 8 and 9). Hysteresis occurs when the two end-members of exchange (in this case, the pure K and Na forms) are mutually immiscible, and form separate phases which can usually be differentiated by X-ray diffraction. The two phases will be present simultaneously over a range of cation compositions (in intermediate Na/K forms), depending on the degree of immiscibility of the two end-members.

Solid-state ion exchange in zeolites The exchange of cations from one solid to another, probably mediated by the presence of small quantities of water, is referred to as solid-state ion exchange. This is a technique which is useful for the preparation of catalysts, that is, the introduction of cations which are only sparingly soluble, or which process hydration spheres which are too large to allow easy diffusion into the

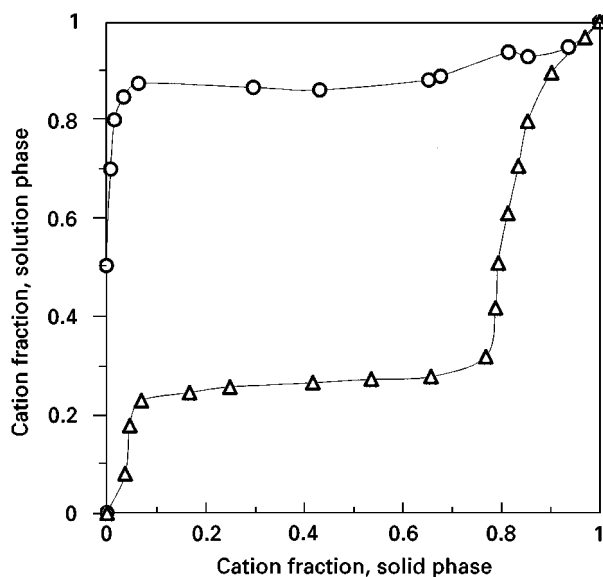


Figure 8 Isotherm for $\text{K}^{+}/\text{Na}^{+}$ exchange in $\text{Na}_8[(\text{BeO}_2)_8(\text{PO}_2)_8] \cdot 5\text{H}_2\text{O}$. Circles, forward exchange; triangles, reverse exchange. Data were determined at 25°C , pH 10 and at a solution concentration of 0.05 mol L^{-1} . (Reproduced with permission from Coker EN and Rees LVC (1992) Ion exchange in beryllophosphate G. Part 1. Ion exchange equilibria. *Journal of the Chemical Society, Faraday Transactions* 88: 263–272.)

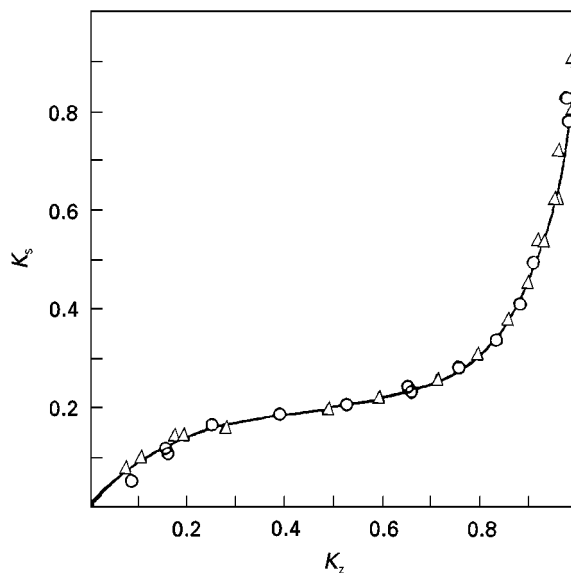


Figure 9 Isotherm for $\text{K}^{+}/\text{Na}^{+}$ exchange in zeolite P. Circles, forward exchange; triangles, reverse exchange; K_s , cation fraction in solution; K_2 , cation fraction in the solid. Data were determined at 25°C and at a solution concentration of 0.1 mol L^{-1} . (Reproduced with permission from Barrer RM and Munday BM (1971) Cation exchange reactions of zeolite NaP. *Journal of the Chemical Society A* 2909–2914.)

cavities of the zeolite from solution. The technique may involve thermal treatment (at temperatures up to 500°C) of an intimate mixture of the zeolite and the salt containing the cation to be exchanged (or another zeolite) although, in some instances, exchange has been observed to occur under ambient conditions. Another advantage of the solid-state approach to preparing catalysts is the avoidance of generating large quantities of waste exchange solution.

Clays and Other Layered Materials

Clays are one of the most abundant materials present on the earth's surface. They constitute a large component of soil, while many ceramic and building materials as well as industrial adsorbents and catalysts contain clay. Soils owe their ability to sustain plant life largely to clays which have the ability to exchange ions with their surroundings. Clays are typically composed of sheets of linked SiO_4 tetrahedra, which are connected to $\text{Al}(\text{OH})_6$ octahedra. If one sheet of silica interacts with a plane of $\text{Al}(\text{OH})_6$, then a two-tier sheet ($\text{Al}_2\text{Si}_2\text{O}_5(\text{OH})_4$) typical of kaolinite is obtained. If the octahedral plane is sandwiched between two silica sheets, then a three-tier sheet is obtained ($\text{Al}_2\text{Si}_4\text{O}_{10}(\text{OH})_2$), as found in the smectite and mica clays. The sheets are bonded to one another via covalent bonds between the silica and alumina sheets to yield a layer. It is how these layers stack together (via electrostatic and van der Waals forces only) which give clays many of their interesting properties, and gives a large degree of flexibility to the structures. Clay-like materials may be composed of oxides of elements other than silicon and aluminium.

The three principal types of clay – single-layer, nonexpandable double-layer and expandable double-layer – have been introduced by Dyer. Clays may be either cationic (exhibiting cation exchange properties) or anionic (anion exchangers). The former type is more common, accounting for the majority of naturally occurring clays; typical examples are montmorillonite and bentonite. Anionic clays, such as hydrotalcite, occur rarely in nature, but may be synthesized in the laboratory. Layered materials composed of neutral layers also exist, although they possess little or no intrinsic ion exchange capability. Table 3 lists some common types of layered material possessing cationic, anionic and neutral layers.

Pillared clays Expandable cationic clays may be converted into pillared clays by exchanging some or all of their charge-balancing cations with bulky inorganic species such as $[\text{Al}_{13}\text{O}_4(\text{OH})_{24}(\text{H}_2\text{O})_{12}]^{7+}$ or $[\text{Zr}_4(\text{OH})_{14}(\text{H}_2\text{O})_{10}]^{2+}$ and then calcining the composites to dehydrate and dehydroxylate the pillaring species, leaving hydroxy/oxide pillars. An interesting pillaring process is that involving ion exchange with a cationic 'templating' agent (cetyltrimethylammonium), followed by the synthesis of a mesoporous silica phase around the template cations. The resultant materials, in which the clay layers are propped apart by the mesoporous silica, possess surface areas up to $800 \text{ m}^2 \text{ g}^{-1}$ and interlayer spacings of 3.3–3.9 nm.

For layered materials with anion exchange properties, like layered double hydroxides, species such as $[\text{V}_{10}\text{O}_{28}]^{6-}$ and $[\text{H}_2\text{W}_{12}\text{O}_{40}]^{6-}$ may be exchanged with anions residing between the layers to increase the interlayer spacing.

Table 3 Examples of layered materials

Layer charge	Example
Neutral (no intrinsic ion exchange capability) ^a	TaS ₂ MoO ₃
Positive (anion exchange properties)	Layered double hydroxides: $[\text{M}_I^{I+} \dots \text{M}_K^{K+}(\text{OH})_2]^{x+} + [\text{X}_n^n]^{x-} \cdot z\text{H}_2\text{O}$ Hydroxy double salts: $[\text{M}_I^{I+} \dots \text{M}_K^{K+}(\text{OH})_{3(1-y)}]^{(1+3y)+} + [\text{X}_n^n]^{(1+3y)-} \cdot z\text{H}_2\text{O}$ ($\text{X}^{n-} = \text{Cl}^-, \text{NO}_3^-, \text{SO}_4^{2-}, \text{CO}_3^{2-}, \text{H}_5\text{C}_2\text{O}^-, \text{etc.}$)
Negative (cation exchange properties)	Smectite clays (low charge density) Micas M ^{IV} H-phosphates (high charge density, e.g. α -ZrP, γ -ZrP) Layered titanates Silicic acids

^aNeutral layered materials may undergo a type of ion exchange reaction via redox intercalation, whereby a neutral species is intercalated, followed by a transfer of electrons between the layer and the guest species. Thus both the layer and the intercalated species become charged.

While pillared clays usually offer advantages over normal clays in terms of their higher surface areas, higher sorptive capacities and greater ion exchange capacities, these properties begin to be diminished when the density of pillars becomes too great and the interlayer space becomes filled with pillars. Pillared clays are seldom employed as ion exchangers; their main applications lie in the fields of catalysis and adsorption.

Metal Phosphates

The most important and widespread of the metal phosphates is α -zirconium phosphate ($\text{Zr}(\text{HPO}_4)_2 \cdot \text{H}_2\text{O}$, or α -ZrP), which has an expandable layer structure. Each layer possesses a central plane of octahedral Zr atoms linked to two outer sheets of monohydrogen phosphate groups. The hydrogen form has an interlayer spacing of 0.76 nm, corresponding to a void space with diameter 0.26 nm. Although the calculated surface area of α -ZrP approaches $1000 \text{ m}^2 \text{ g}^{-1}$, in the unexpanded H form the surface area available to N_2 is only $5 \text{ m}^2 \text{ g}^{-1}$.

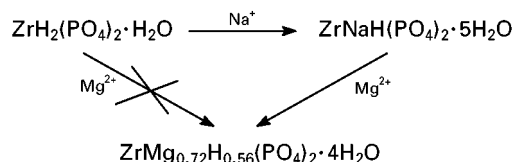
Another crystalline form of zirconium phosphate γ -ZrP ($\text{Zr}(\text{PO}_4)(\text{H}_2\text{PO}_4) \cdot 2\text{H}_2\text{O}$), is formed by a central zirconium phosphate sheet in which the PO_4 groups are linked solely to octahedral Zr atoms; this sheet is linked to dihydrogen phosphate groups to yield the γ -ZrP structure. The complex interlinking results in a more rigid framework in which only *c.* 50% of the theoretical ion exchange capacity is normally obtained.

Swelling of zirconium phosphates The interlayer cavities in α -ZrP of 0.26 nm are accessible to only small and poorly hydrated cations. A certain degree of expansion of the interlayer distance may occur concomitantly with these exchanges. Larger or more strongly hydrated ions do not readily exchange with α -ZrP. However, since the layers are held together principally by electrostatic forces, the distance between them can be increased to allow access of larger ions according to the following mechanism.

The acid form of an α -ZrP possesses H^+ cations which stabilize the negative charge on the $\text{Zr}(\text{PO}_4)_2$ units. A number of these protons may be neutralized by addition of hydroxide ions via the solution phase. This causes negative charge to build up on the layers, causing electrostatic repulsion and forcing the layers apart. Once the material has swelled, access to the exchange sites by larger and more strongly hydrated cations is possible. This view may be slightly oversimplified, since migrating OH^- ions would naturally be accompanied by cations (to preserve electroneutrality in both the solid and solution phases). It is more likely

that the above two-step process actually occurs as a one-step process driven by the neutralization reaction.

'Catalytic' exchanges in α -ZrP The interlayer spacing of α -ZrP may be too small to allow large cations access (a situation anomalous to ion-sieving in zeolites). For instance, the Mg^{2+} ion will not exchange with the protons in α -ZrP directly. However, in the presence of sodium, some magnesium exchange does occur. The process is shown conceptually below.



The hydrated Mg^{2+} ion is too bulky to reach the exchange sites between the layers of the acid form, while the smaller hydrated Na^+ ion is not. The partial exchange of Na^+ for H^+ causes a swelling of the interlayer spacing to a point which allows the hydrated Mg^{2+} to exchange.

Heteropolyoxometalates

Heteropolyoxometalates, or heteropolyacids (HPAs) and their salts are materials which are finding widespread applications as acidic and/or redox catalysts. The most common examples are those with the Keggin structure, composed of a central hetero species, typically PO_4^{3-} or SiO_4^{4-} , surrounded by 12 transition metal oxide octahedra, typically MoO_6 or WO_6 , as depicted in Figure 10. The octahedra and central hetero species are linked via shared oxygens to yield materials with the formula $[\text{XM}_{12}\text{O}_{40}]^{n-}$ where $\text{X} = \text{P}$ ($n = 3$) or Si ($n = 4$) and $\text{M} = \text{Mo}$ or W . Many other structure types are known, with up to 40 transition metal octahedra per molecule. The negative charge is balanced by protons in an HPA and by certain cations in HPA salts. The charge-balancing cations are in many cases partially or wholly exchangeable, and physical properties such as solubility, surface area and porosity may vary widely depending on the nature of the cation (Table 4).

Heteropolyoxometalates are principally used as catalysts. Due to the high solubility of many of the cationic forms of heteropolyoxometalates in aqueous media, their application as ion exchangers has been limited. Apart from ammonium phosphomolybdate and ammonium phosphotungstate which possess low solubility and have been used to scavenge radioactive caesium, and $[\text{NaP}_5\text{W}_{30}\text{O}_{110}]^{14-}$, which has been shown to have high selectivity for lanthanide and certain multivalent ions, comparatively few data are

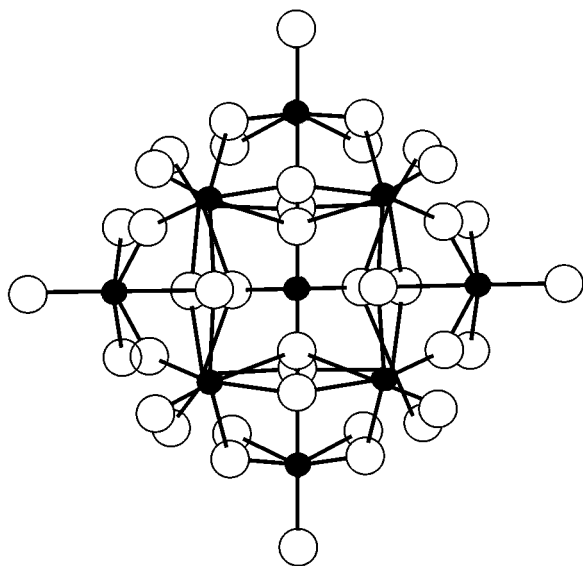


Figure 10 The structure of $[XM_{12}O_{40}]^{n-}$ where X (P or Si) is located at the centre and is surrounded by 12 metal oxide octahedra. (Reproduced with permission from Klemperer WG and Wall CG (1998) Polyoxoanion chemistry moves towards the future: from solids and solutions to surfaces. *Chemical Reviews* 98: 297–306.)

available concerning the ion exchange properties of the HPAs.

Hydrous Oxides

Hydrous oxides are amorphous metal oxides, on the surface of which exist hydroxyl groups which are

present as a necessity to terminate the structure (see Figure 1A). The general formula for a hydrous oxide is $[M^{(n)}O_{(n-x)/2}(OH)_x \cdot wH_2O]_m$, where the central cation, M , is n -valent (n is typically ≥ 3). Most of the metals in the periodic table are able to form hydrous oxides which exhibit ion exchange properties. However, for the material to be applied as an ion exchanger, it must be stable under the conditions used for exchange. In particular, solubility can be a deciding factor in the utility of hydrous oxides; stability to pHs extending from strongly alkaline to strongly acidic may be necessary. Those hydrous oxides comprised of large, low valent cations or small, multivalent cations tend to be soluble, while those intermediate between the two extremes are stable. Typical examples of acid- and alkali-stable hydrous oxides are those of Al^{III} , Ga^{III} , In^{III} , Si^{IV} , Sn^{IV} , Ti^{IV} , Th^{IV} , Zr^{IV} , Nb^V , Bi^V , Mo^{VI} and W^{VI} . Many of the materials are amphoteric, that is, they can act as either cation or anion exchangers depending on, principally, the pH of the electrolyte solution and the basicity of the metal forming the hydrous oxide (the strength of the metal–oxygen bond relative to the oxygen–hydrogen bond).

The change of a commercial alumina from cation exchanger to anion exchanger with varying pH is shown in the chapter by Dyer (Figure 8). The amphoteric nature of hydrous oxides may be illustrated schematically thus:

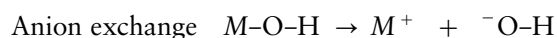
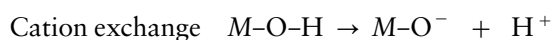


Table 4 Changes in surface properties of phosphomolybdates and phosphotungstates upon ion exchange

Approximate composition of HPA salt ^a	Surface area by N_2 BET ($m^2 g^{-1}$) ^b	Pore volume $\times 10^3$ ($cm^3 g^{-1}$)	Mean pore radius (nm)
HPMo, NaPMo, (MeNH ₃)PMo	Essentially nonporous		
(NH ₄)PMo	193	52	1.3
KPMo	40	15	0.9
CsPMo	145	6	1.4
HPW, NaPW, AgPW, (MeNH ₃)PW, (Me ₃ N)PW	Essentially nonporous		
(NH ₄)PW	128	50	1.0
KPW	90	31	0.9
CsPW	163	34	1.4
HSiW, NaSiW, KSiW	Essentially nonporous		
(NH ₄)SiW	117	40	1.0
CsSiW	150	52	1.0
RbSiW	116	40	1.0

^a PMo, PW and SiW represent $(PMo_{12}O_{40})^{3-}$, $(PW_{12}O_{40})^{3-}$ and $(SiW_{12}O_{40})^{4-}$ respectively. The charge-balancing cation indicated is assumed to be fully exchanged into the HPA, although some variation of composition is inevitable. Note that the surface properties will vary slightly depending upon the preparation and exact composition of the HPA.

^b Surface area determined using the Brunauer, Emmett and Teller isotherm approach.

Cation exchange typically takes place in alkaline solution, while anion exchange is preferred in acidic solution. Dissociation of $M-O-H$ near to its isoelectric point allows both exchange mechanisms to operate simultaneously.

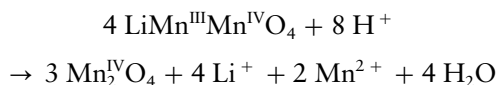
Silica, the most common and extensively studied of the hydrous oxides, is a weakly acidic cation exchanger. The physical properties of silica, particularly the porosity and surface area, vary widely depending upon the method of preparation. Generally, multivalent cations interact more strongly with the silica surface than do univalent ones, while in all cases the interactions are relatively weak and ion exchange is facile. Silica possesses between 0.5 and 0.8 hydroxyl groups per nm^2 on its surface.

Miscellaneous Materials

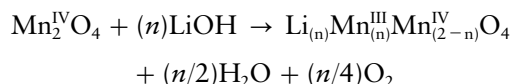
A number of specific materials have been discussed in this chapter. There are, however, numerous inorganic materials possessing ion exchange properties which have not been mentioned. In this section, a few of those materials which exhibit interesting ion exchange properties are introduced briefly. The list is far from complete, but serves to illustrate the diversity of ion exchange materials.

- Hydroxyapatites may undergo limited ion exchange reactions. While the calcium form ($\text{Ca}_{10}(\text{PO}_4)_6(\text{OH})_2$) is the most common (it is a major component of teeth and bones), pure exchange end-members of Sr^{2+} , Cd^{2+} and Pb^{2+} are known, while various cations may form intermediate mixed-cation phases. The Sr^{2+} end-member, due to a slight lattice expansion, possesses superior ion exchange properties compared to Ca-hydroxyapatite. Of the Sr-hydroxyapatites, that with a (non-stoichiometric) Sr/P ratio of 1.73 has the highest ion exchange capacity of those measured. It is interesting that the presence of HCl may assist the ion exchange reaction by formation of a chlorapatite phase. This may be an example of simultaneous anion and cation exchange.
- Copper hexacyanoferrates, $\text{Cu}_2^{\text{II}}\text{Fe}^{\text{II}}(\text{CN})_6 \cdot x\text{H}_2\text{O}$ and related compounds show quite promising exchange properties for Cs^+ , and have been investigated as agents for nuclear waste treatment. On passing caesium-containing waste through a column of $\text{Cu}_2^{\text{II}}\text{Fe}^{\text{II}}(\text{CN})_6 \cdot x\text{H}_2\text{O}$ at room temperature, decontamination factors (ratios of pre-column to post-column Cs^+ concentrations) of 10^3 can be achieved.
- Lithium manganate containing mixed-valence manganese ions exhibits unusual ion exchange properties, in that it undergoes combined ion exchange and redox reactions. Upon acid treatment of $\text{LiMn}^{\text{III}}\text{Mn}^{\text{IV}}\text{O}_4$, the Mn^{III} is oxidized to Mn^{IV}

and Li is displaced from the structure thus:



The resulting spinel structure ($\gamma\text{-MnO}_2$) is highly selective for Li, and will readily re-insert Li^+ to regain the Li-manganate spinel:



This type of exchange reaction is often referred to as the ion memory effect.

- Iodide ions may be efficiently exchanged for nitrate ion using $\text{BiPbO}_2\text{NO}_3$ in solutions of $\text{pH} \geq 13$. Under such conditions, the theoretical exchange capacity of 2 mmol g^{-1} is approached.

Conclusions

As with any commercial venture, improvements to large scale ion exchange processes will always be sought. With the advances made in structural characterization and synthetic methods, it is becoming increasingly possible to tailor the ion exchange properties of materials to specific needs. Thus, the strive for water-softening zeolites for detergents with greater capacity, selectivity and rate of exchange for Ca^{2+} and Mg^{2+} , or for exchangers with better stability over wide pH ranges coupled with high selectivity for certain ions present in waste streams will be ever-present. Recent advances have made some significant steps in these particular directions:

- The field of nuclear waste clean-up has spawned a number of interesting materials; inorganic exchangers are now available which have good structural stability in waste streams and exhibit high selectivities for Cs^+ and Sr^{2+} in the presence of large excesses of other ions over wide pH ranges.
- Zeolites continue to be used in vast quantities as water softeners in detergents. A significant recent development has been the introduction of a new detergent zeolite MAP, which offers improved performance over zeolite A.

Interesting ion exchange properties are exhibited by framework materials possessing high electric field gradients, such as the beryllophosphates. However, this particular area is deserving of more extensive exploration.

The prediction of ion exchange behaviour for a particular material is possible given data for exchange reactions in that material under

different conditions. However, the prediction of ion exchange properties on the basis of the structure of the exchanger alone may become more readily possible through the use of computer modelling.

The study of ion exchange behaviour under the influence of microwave radiation is an area which preliminary research has suggested may be interesting.

See also: **II/Ion Exchange:** Historical Development; Novel Layered Materials: Non-Phosphates; Organic Ion Exchangers; Theory of Ion Exchange.

Further Reading

Clearfield A (ed.) (1982) *Inorganic Ion Exchange Materials*. Boca Raton, FL: CRC Press.

Dyer A, Hudson MJ and Williams PA (eds) (1993) *Ion Exchange Processes: Advances and Applications*. Cambridge, UK: Royal Society of Chemistry.

Dyer A, Hudson MJ and Williams PA (eds) (1997) *Progress in Ion Exchange: Advances and Applications*. Cambridge, UK: Royal Society of Chemistry.

Greig JA (ed.) (1996) *Ion Exchange Developments and Applications*. Cambridge, UK: Royal Society of Chemistry.

Helferich F (1962) *Ion Exchange*. New York, USA: McGraw-Hill.

Slater MJ (ed.) (1992) *Ion Exchange Advances*. London, UK: Elsevier Applied Science.

van Bekkum H, Flanigen EM, Jacobs PA and Jansen JC (eds) (2000) *Introduction to Zeolite Science and Practice*, 2nd edn. Amsterdam: Elsevier.

Williams PA and Hudson MJ (eds) (1990) *Recent Developments in Ion Exchange 2*. London, UK: Elsevier Applied Science.

Multispecies Ion Exchange Equilibria

See **II/ION EXCHANGE/Surface Complexation Theory: Multispecies Ion Exchange Equilibria**

Non-Phosphates: Novel Layered Materials

See **II/ION EXCHANGE/Novel Layered Materials: Non-Phosphates**

Novel Layered Materials: Phosphates

U. Costantino, Università di Perugia, Perugia, Italy

Copyright © 2000 Academic Press

It has long been known that many polyvalent cations can be precipitated as amorphous phosphates from dilute solutions and these salts are useful in gravimetric analysis. More recently it has been recognized that many of these precipitates contain exchangeable acid protons and behave as inorganic ion exchangers. Phosphates of tetravalent metals such as Zr(IV), Ti(IV) and Sn(IV) have been found to possess high ion-exchange capacity and good stability in acid and oxidizing solutions and when exposed to high temperatures and ionizing radiation. Because of these properties, their potential uses for the purification of nuclear reactor cooling water or for the treatment of radioactive waste were investigated during the late

1950s and early 1960s, especially in nuclear centres. The ion-exchange properties of amorphous zirconium, titanium and tin phosphates were reviewed by Amphlett in 1964. However, the beginning of the chemistry of layered phosphates may be dated back to 1964, when Clearfield and Stynes refluxed zirconium phosphate gel in phosphoric acid solutions in an attempt to produce a material which was more resistant to hydrolytic attack than the original gel. The microcrystals obtained were found to possess a layered structure, called the α -type, and with the composition $\text{Zr}(\text{HPO}_4)_2 \cdot \text{H}_2\text{O}$. This compound was indeed more resistant to hydrolytic attack than the amorphous analogue. It possesses two exchangeable protons per formula weight and is an excellent intercalating agent of protophilic species and a pure solid-state protonic conductor. Moreover, it is possible to correlate the observed properties with the structural

features. These findings stimulated research on the synthesis of layered phosphates of other polyvalent metals. The progress made up to 1982 was reviewed by Clearfield, and by Alberti and Costantino, and from that date the field of layered phosphates has been continuously expanding with the discovery and resolution of the structure of new crystalline phases. It was found that zirconium (or titanium) phosphate has an isomorphous modification, named γ -type, and the composition $\text{Zr}(\text{PO}_4)(\text{H}_2\text{PO}_4) \cdot 2\text{H}_2\text{O}$. This compound, as well as having cation exchange and intercalation properties, undergoes a topotactic anion exchange reaction of the dihydrogenphosphate groups with other anions. Most recently, the preparation of a new crystalline layered phase, named λ -type, and having the composition $\text{Zr}(\text{PO}_4)\text{Cl}(\text{CH}_3)_2\text{SO}$, has opened new research possibilities. This article deals with the preparation, structure, ion exchange and intercalation properties of layered phosphates and phosphonates of polyvalent metals, mainly zirconium, and with their application. Exfoliation of layered phosphates which allows the preparation of mixed layered phosphates or thin-layer coatings on substrates such as silica and alumina or of microporous pillared layered phosphates will be described.

However, before discussing in more detail the above-mentioned materials, it is worth commenting briefly on the preparation, ion exchange properties and application of amorphous zirconium phosphate, because of its commercial availability and renewal of interest in its use in nuclear waste treatment.

Amorphous zirconium phosphate is easily prepared by adding a solution of zirconium salts to a solution of phosphoric acid in acid media ($2\text{--}4 \text{ mol dm}^{-3} \text{ HCl}$). The precipitate can be appropriately treated to obtain the exchanger in glassy, granular or powdered form. The composition is best described by the formula $\text{Zr}(\text{HPO}_4)_{2-x}(\text{OH})_{2x} \cdot n\text{H}_2\text{O}$, x ranging between 0 and 0.2. The material is stable up to 180°C (temperature at which condensation of phosphates to pyrophosphates starts) in acidic medium (e.g. $6 \text{ mol dm}^{-3} \text{ HNO}_3$), and has a remarkable resistance to strong doses of ionizing radiation. The ion exchange capacity ranges from 4 to 6 mequiv. g^{-1} . At low loading, the exchanger prefers cations with lower hydrated ionic radius and higher charge. Its use for the selective removal of ^{137}Cs and ^{89}Sr radioisotopes from aqueous nuclear wastes in ultrafiltration and fluidized bed systems has been proposed. Amorphous zirconium phosphate, because of its bio-compatibility and high insolubility, is used to fill cartridges for the removal of urea from blood in haemodialysis machines.

Layered Phosphates of Groups 4 and 14, 5 and 15 elements

Preparation

Numerous layered phosphates of the elements of the groups 4, 5, 14 and 15 of the periodic table have been synthesized and many of them are listed in Table 1, together with their interlayer distance, the free area

Table 1 Formulae and some properties of layered phosphates of groups 4, 14 and 5, 15 elements

Formula	Density (g cm^{-3})	Ion exchange capacity ($\text{mmol H}^+ \text{g}^{-1}$)	Interlayer distance (\AA)	Free area (\AA^2)*
$\alpha\text{-Ti}(\text{HPO}_4)_2 \cdot \text{H}_2\text{O}$	2.61	7.76	7.56	21.6
$\alpha\text{-Zr}(\text{HPO}_4)_2 \cdot \text{H}_2\text{O}$	2.72	6.64	7.56	24.0
$\alpha\text{-Hf}(\text{HPO}_4)_2 \cdot \text{H}_2\text{O}$	—	5.15	7.60	23.7
$\gamma\text{-Ti}(\text{PO}_4)(\text{H}_2\text{PO}_4) \cdot 2\text{H}_2\text{O}$	2.37	7.25	11.60	16.5
$\gamma\text{-Zr}(\text{PO}_4)(\text{H}_2\text{PO}_4) \cdot 2\text{H}_2\text{O}$	2.43	6.27	12.20	17.8
$\alpha\text{-Si}(\text{HPO}_4)_2$	—	8.90	7.4	—
$\alpha\text{-Ge}(\text{HPO}_4)_2 \cdot \text{H}_2\text{O}$	—	7.07	7.75	—
$\alpha\text{-Sn}(\text{HPO}_4)_2 \cdot \text{H}_2\text{O}$	3.12	6.08	7.80	21.4
$\alpha\text{-Pb}(\text{HPO}_4)_2 \cdot \text{H}_2\text{O}$	—	4.79	7.95	21.5
$\text{ZrPO}_4\text{Cl}(\text{CH}_3)_2\text{SO}$	—	—	10.2	—
$\text{VOPO}_4 \cdot 2\text{H}_2\text{O}$	2.4	—	7.41	38.5
$\text{VO}(\text{HPO}_4) 0.5\text{H}_2\text{O}$	2.8	5.81	5.70	35.7
$\text{NbOPO}_4 \cdot 3\text{H}_2\text{O}$	—	—	8.04	—
$\text{HNb}(\text{PO}_4)_2$	—	3.52	—	—
$\text{HTa}(\text{PO}_4)_2 \cdot 2\text{H}_2\text{O}$	—	2.45	9.48	46.0
$\text{HAs}(\text{PO}_4)_2$	2.88	3.52	7.98	37.1
$\text{KSb}(\text{PO}_4)_2$	3.50	—	8.47	19.6
$\text{HSb}(\text{PO}_4)_2$	—	—	—	—
SbOPO_4	4.42	—	6.34	—

*Area associated to each $-\text{OH}$ group on the plane.

surrounding the surface phosphate groups, density and calculated ion exchange capacity. It may be seen that, except for carbon, α -type phosphates of all the elements of groups 4 and 14 have been obtained. They are prepared with procedures similar to those used to obtain $\text{Zr}(\text{HPO}_4)_2 \cdot \text{H}_2\text{O}$, that is, by refluxing the amorphous precipitates in phosphoric acid ($10\text{--}12 \text{ mol dm}^{-3}$). An alternative procedure, especially used for Zr and Ti hydrogenphosphates, involves direct precipitation from solutions containing phosphoric acid and Zr (or Ti) fluoro-complexes. The degree of crystallinity of the precipitates may be controlled by modifying the velocity of removal of the complexing agent, as gaseous HF. With this method, crystals of millimetre dimensions have been obtained. Note that only Zr(IV) and Ti(IV) can form phosphate dihydrogenphosphates of γ -type. The preparation involves the slow decomposition of fluoro-complexes in an $\text{NH}_4\text{H}_2\text{PO}_4$ solution. The precipitate, e.g. $[\text{Zr}(\text{PO}_4)(\text{NH}_4\text{HPO}_4)]$, is then converted into its hydrogen form by treatment with HCl solution.

Tetravalent elements with large dimensions, such as Ce(IV) and Th(IV) do not give rise to layered phosphates of α - or γ -type. The acid phosphates of these elements have been obtained in fibrous form suitable for the preparation of fully inorganic, self-consistent papers, thin films or membranes. The acid phosphates of groups 5 and 15 elements have been obtained by dissolving the oxides in concentrated phosphoric acid and heating to 270°C . $\text{HSb}(\text{PO}_4)_2$ can be obtained by treating the potassium salt with a strong acid solution. Group 5 elements also produce non-acid layered phosphates of formula XOPO_4 ($\text{X} = \text{V}, \text{Nb}, \text{Ta}$) and structure similar to that of $\text{Zr}(\text{PO}_4)\text{Cl}(\text{CH}_3)_2\text{SO}$. Vanadyl phosphate is one of the rare examples of a layered phosphate which has a low electronic conductivity and is capable of redox intercalation reactions similar to those shown by graphite or layered dichalcogenides. Generally speaking, layered phosphates possess good chemical and thermal stability. Layered $\text{Zr}(\text{HPO}_4)_2 \cdot \text{H}_2\text{O}$ is a very insoluble compound, stable even in highly concentrated non-complexing acid solutions. The interlayer water is lost after prolonged heating at 110°C while the condensation water of monohydrogenphosphates to pyrophosphates is lost at $450\text{--}500^\circ\text{C}$. Molybdenum and some divalent cations such as Fe, Cd and Mn also form layered phosphates but their physical and chemical properties have not been investigated thoroughly.

Structural Aspects

Layered solids are molecular crystals formed by the packing of giant planar macromolecules called layers or lamellae. The bonds between the atoms present in

the layer are strong, primarily covalent, while those between the atoms of adjacent lamellae are weak, essentially of the van der Waals type. Thus, layered solids generally exhibit a high anisotropy in their physical properties. The reactivity of layered solids is shown by the intercalation reaction, that is, the reversible insertion of guest species into the interlayer region without appreciable modification of the structure of the lamellae which move apart to accommodate the guest species. Hence, the structural aspects of a layered solid are closely connected with the bidimensional structure of the layers. The Greek letter prefix that often indicates a layered phosphate is related to the layer structure. The structures of the layered phosphates listed in Table 1 will be illustrated with reference to the α -, γ - and λ -zirconium phosphates, but the phosphates of other elements have similar structures. Geometrical considerations indicate that bidimensional structures can be easily formed by concatenation through the vertices of MO_6 octahedra (M being the polyvalent metal) of suitable dimension, and of PO_4 tetrahedra. In the present case different concatenation gives rise to different layer structures.

Crystals of $\alpha\text{-Zr}(\text{HPO}_4)_2 \cdot \text{H}_2\text{O}$ are monoclinic with $a = 9.060(2) \text{ \AA}$, $b = 5.297(1) \text{ \AA}$, $c = 15.14(3) \text{ \AA}$, and $\beta = 101.71(2)^\circ$, space group $\text{P}2_1/\text{n}$. The sequence of two layers is shown in Figure 1. Each layer may be described as the concatenation of ZrO_6 octahedra and O_3POH tetrahedra. Note that each tetrahedron bridges three different octahedra and these, in turn, bridge six tetrahedra. The layer is a planar macromolecule bearing acid P-OH groups on the

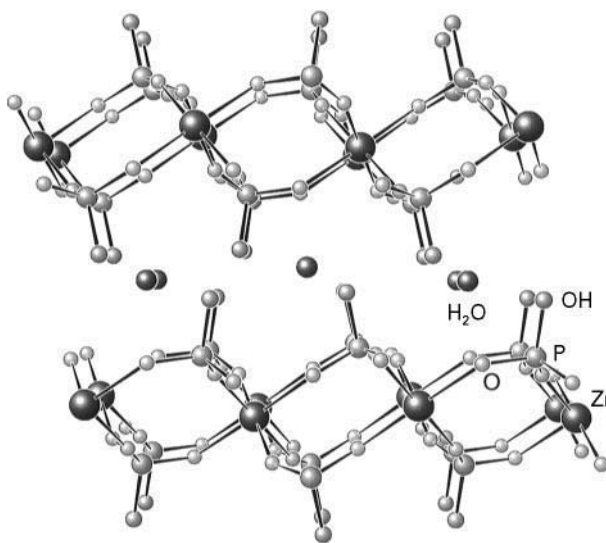


Figure 1 Computer-generated representation of the sequence of two layers of $\alpha\text{-Zr}(\text{HPO}_4)_2 \cdot \text{H}_2\text{O}$. (Crystal data from Clearfield A and Smith GD (1969) *Inorganic Chemistry* 8: 431–436.)

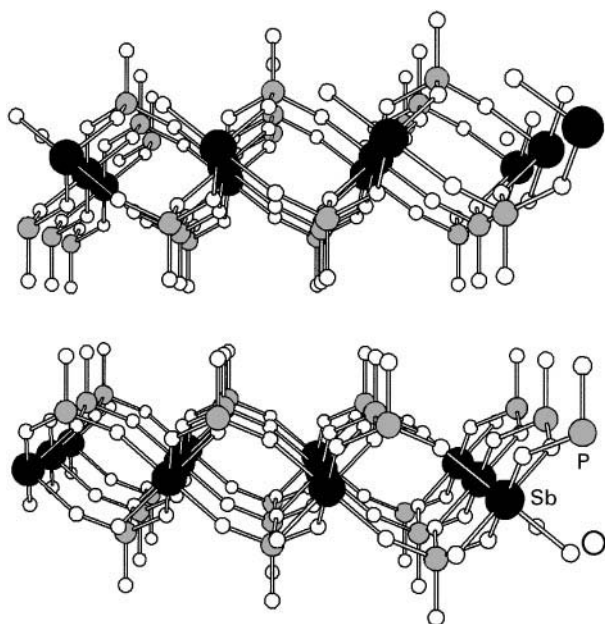


Figure 2 Computer-generated representation of the sequence of two layers of $\text{HSb}(\text{PO}_4)_2$. (Crystal data from Piffard Y, Oyetola S, Courant S and Lachgar S (1985) *Journal of Solid State Chemistry* 60: 209–213.)

surfaces. The distance between adjacent phosphate groups on one side of the layer is 5.3 \AA and the 'free area' around each P-OH group is 24 \AA^2 . The interlayer distance is 7.56 \AA and the arrangement of the pendant phosphate groups creates six-sided cavities, each containing one water molecule, in the interlayer region. This layered structure is common to the other α -layered phosphates and it is very similar to that of $\text{HSb}(\text{PO}_4)_2$, shown in Figure 2.

The second layer structure, in which two different tetrahedral species are used at the same time, is present in the γ -compound with formula $\text{Zr}(\text{IV})(\text{PO}_4)(\text{H}_2\text{PO}_4) \cdot 2\text{H}_2\text{O}$. The γ -layer consists of two ideal planes containing zirconium atoms bonded by tetrahedral PO_4 and H_2PO_4 groups (see Figure 3). The PO_4 group shares all four oxygens with zirconium atoms while the H_2PO_4 shares two oxygens with two different Zr atoms and points the remaining two OH groups towards the interlayer region. The interlayer distance is 12.2 \AA , and the free area surrounding the $\text{P}(\text{OH})_2$ groups on the surface of the layers is 35 \AA^2 .

A third layer structure of great interest can be formed by bridging four different zirconium atoms with a tetrahedral PO_4 group in a slightly different manner from γ -zirconium phosphate, and then by balancing the residual positive charge and completing the octahedral configuration of each zirconium atom with a monovalent anionic ligand, Cl^- and a neutral monodentate ligand, $(\text{CH}_3)_2\text{SO}$, as

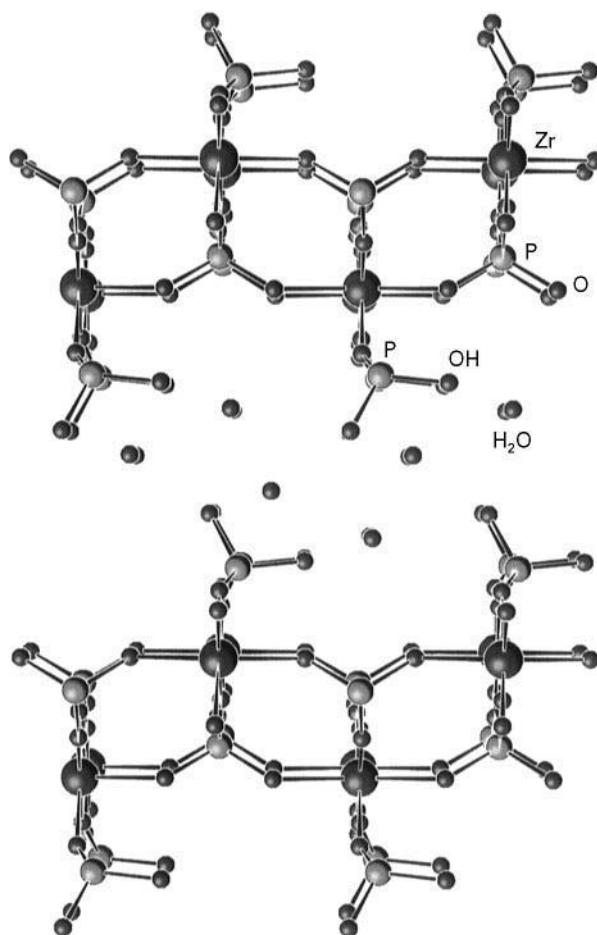


Figure 3 Computer-generated representation of the sequence of two layers of $\gamma\text{-Zr}(\text{PO}_4)(\text{H}_2\text{PO}_4) \cdot 2\text{H}_2\text{O}$. (Crystal data from Christensen A, Andersen EK, Andersen IKG, Alberti G, Nielsen N and Lehman MS (1990) *Acta Chemica Scandinavica* 44: 865–872.)

illustrated in Figure 4. Note that this structure is essentially the same as that of layered vanadyl phosphate (see Figure 5) and of uranyl phosphate.

Chemical Reactivity

Ion Exchange Properties

The protons of layered acid phosphates are able to diffuse in the interlayer region and these compounds behave as inorganic cation exchangers and proton conductors. Mainly the ion-exchange properties of $\alpha\text{-Zr}(\text{HPO}_4)_2 \cdot \text{H}_2\text{O}$ will be considered as these have been investigated extensively. However, the findings apply to the other members of the class. All these compounds are solid acids and the simplest way to completely replace the protons with other cations is by titrating the microcrystals with solutions of the hydroxide of the cation to be exchanged. The

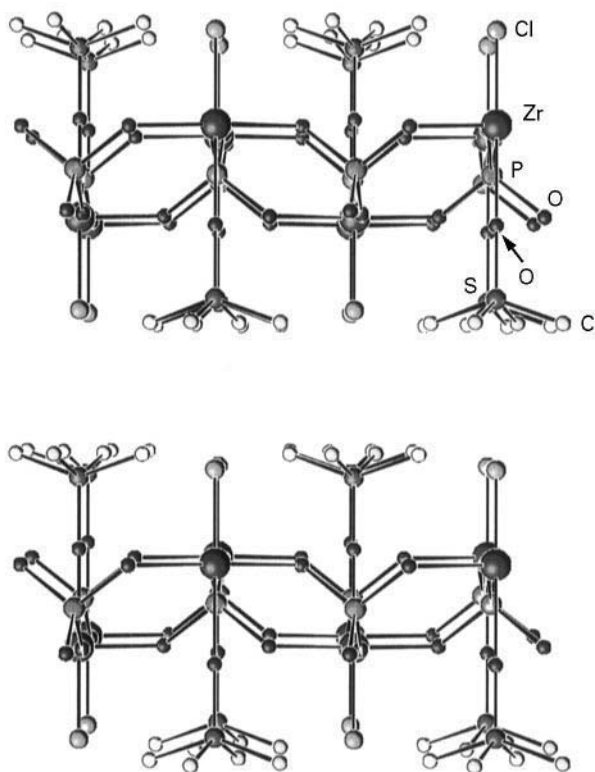


Figure 4 Computer-generated sequence of two layers of $\text{Zr}(\text{PO}_4)\text{Cl}(\text{CH}_3)\text{SO}$. (Data from Alberti G, Bartocci M, Santarelli M and Vivani R (1997) *Inorganic Chemistry* 36: 3574–3575.)

titration curves of $\alpha\text{-Zr}(\text{HPO}_4)_2 \cdot \text{H}_2\text{O}$ with alkaline metal hydroxides, in the presence of the corresponding metal chloride, are shown in Figure 6.

It may be seen that the exchange process occurs stepwise. In each plateau of the titration curve the composition of the solution, and hence also the pH, is constant. Since temperature and pressure are also

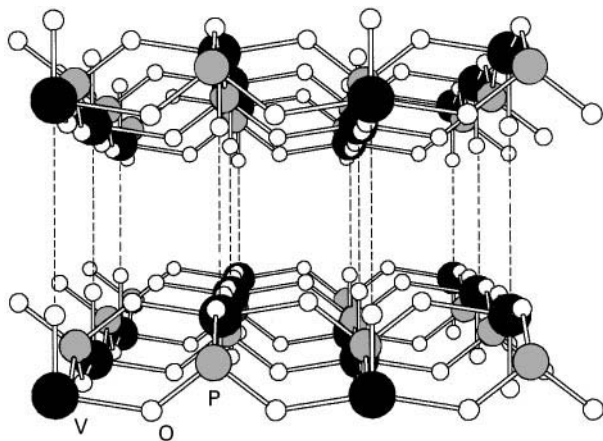


Figure 5 Computer-generated structure of the sequence of two layers of VOPO_4 . (Crystal data from Tietze HR (1981) *Australian Journal of Chemistry* 34: 2035–2038.)

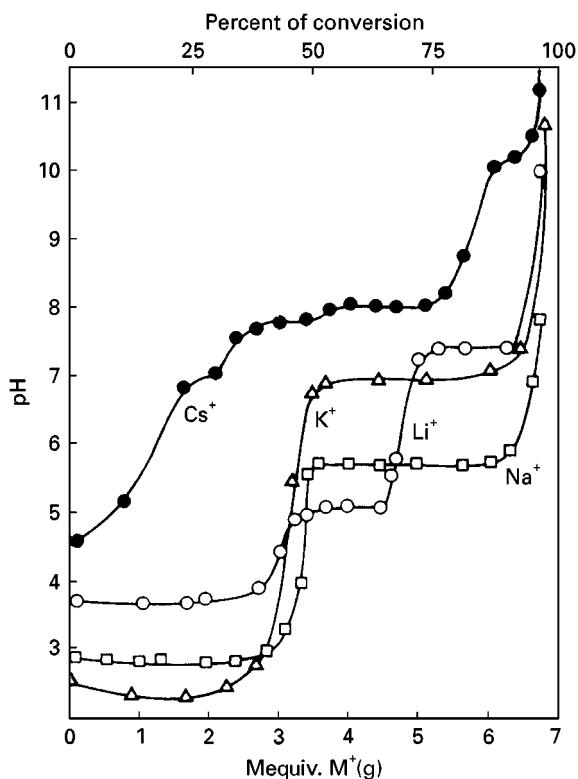
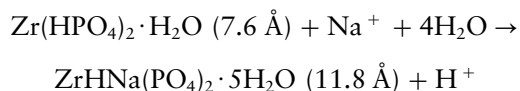


Figure 6 Potentiometric titration curves of $\alpha\text{-Zr}(\text{HPO}_4)_2 \cdot \text{H}_2\text{O}$ with the hydroxides of the indicated alkali metal ions, in the presence of the corresponding metal chlorides. (Reproduced with permission from Alberti G and Costantino U (1974) *Journal of Chromatography* 102: 5–29. Copyright: Elsevier Science Publishing, Amsterdam.)

constant, the phase rule requires the presence of two solid phases. The X-ray diffraction patterns of samples with increasing metal ion loading indeed indicate the presence of two solid phases, one transforming into the other as the exchange reaction proceeds. According to a model developed by Alberti, ion exchange in the α -phases takes place by diffusion of the cations from the external part of the layered crystals towards the bulk with an advancing phase boundary with the co-existence in the same crystallite of two phases. To illustrate the model consider H^+/Na^+ exchange (see Figure 6 and the scheme in Figure 7). Initially we observe the formation of a phase of composition $\text{ZrHNa}(\text{PO}_4)_2 \cdot 5\text{H}_2\text{O}$ and interlayer distance 11.8 Å, according to the reaction (the number in parentheses refers to the interlayer distance):



The composition of the exchanged phase does not change until half the protons of the original hydrogen

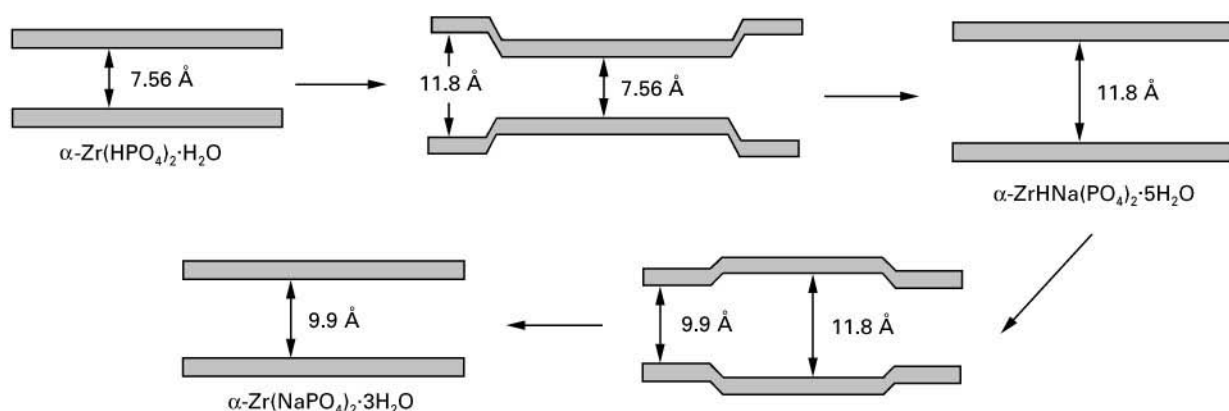
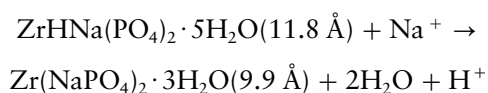
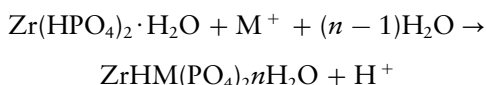


Figure 7 Schematic representation of the phases formed during the H^+/Na^+ ion-exchange process in $\alpha\text{-Zr}(\text{HPO}_4)_2 \cdot \text{H}_2\text{O}$ micro-crystals.

form have been replaced by Na^+ ions. At the end of the process only the monosodium form is present and the pH of the solution rises to a value at which the following reaction takes place:



Examination of the ion-exchange process



where M is an alkaline metal, shows the following selectivity sequence: $\text{K}^+ > \text{Na}^+ > \text{Li}^+ \gg \text{Rb}^+ \cong \text{Cs}^+$, since potassium uptake occurs at $\text{pH} \cong 2$ while H^+/Cs^+ exchange occurs at $\text{pH} \cong 7$. The different selectivity towards K^+ and Cs^+ is a direct consequence of the structural features of the host. The zeolitic cavities present in the interlayer region of $\alpha\text{-Zr}(\text{HPO}_4)_2 \cdot \text{H}_2\text{O}$, are interconnected by windows of 2.64 \AA width. Therefore, cations such as Rb^+ and Cs^+ that have an ionic diameter greater than 2.64 \AA , as well as highly hydrated divalent and trivalent cations, are not taken up unless energy is supplied to spread the layers apart. Accordingly, a facile exchange of large monovalent ions or of highly hydrated divalent or trivalent cations takes place if precursors with a high interlayer distance such as polyhydrate zirconium phosphate, $\text{Zr}(\text{HPO}_4)_2 \cdot 4\text{H}_2\text{O}$ ($d = 10.4 \text{ \AA}$) or the monosodium form $\text{ZrHNa}(\text{PO}_4)_2 \cdot 5\text{H}_2\text{O}$ ($d = 11.8 \text{ \AA}$) or some intercalation compounds with alkanols or amines (see below) are employed. A study of the ion exchange isotherms of $\text{ZrHNa}(\text{PO}_4)_2 \cdot 5\text{H}_2\text{O}$ with different monovalent and divalent cations (see Figure 8) revealed the following selectivity order $\text{Ba}^{2+} > \text{Ca}^{2+} > \text{Cs}^+ > \text{K}^+ > \text{Mg}^{2+} > \text{Na}^+ > \text{Li}^+$.

By using suitable precursors, a large number of cations of the periodic table, as well as organic cations or cationic complexes, have been intercalated via ion exchange processes into zirconium phosphate and other layered phosphates. Table 2 states the composition and interlayer distance of a selected number of phases, some of them prepared for practical applications. These layered phosphates possess good thermal resistance and are stable even when exposed to high doses of ionizing radiation.

Zirconium phosphate has been used to perform ion exchange processes in molten salts at high temperatures. Figure 9 shows the Na^+/K^+ forward and reverse isotherms obtained in molten $\text{NaNO}_3\text{--KNO}_3$ mixtures at 450°C .

Good resistance to radiation makes these phosphates particularly suitable for the uptake of dangerous radionuclides such as $^{137}\text{Cs}^+$, $^{89}\text{Sr}^{2+}$ and $^{60}\text{Co}^{2+}$.

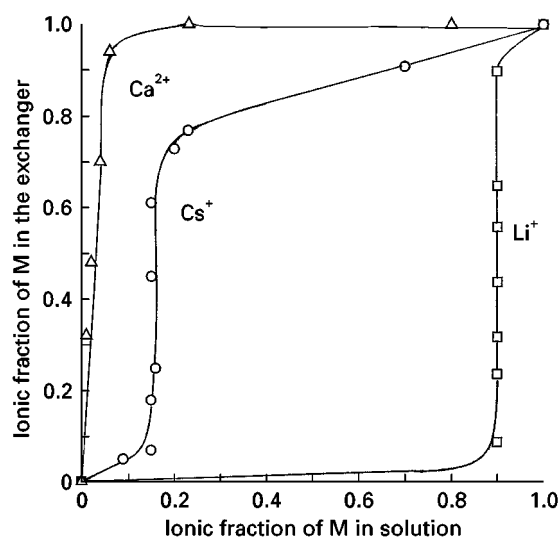


Figure 8 Forward $\text{Na}^+/\text{Ca}^{2+}$, Na^+/Cs^+ and Na^+/Li^+ ion-exchange isotherms on $\alpha\text{-ZrHNa}(\text{PO}_4)_2 \cdot 5\text{H}_2\text{O}$. Concentration: $0.1 \text{ equiv dm}^{-3}$, temperature 25°C .

Table 2 Formulae and interlayer distances of some anhydrous and hydrated salt forms of α -zirconium phosphate. Some exchanged forms with cationic complexes are also listed

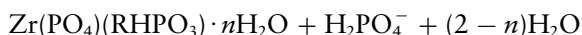
Compound	Interlayer distance (Å)	Compound	Interlayer distance (Å)
ZrHLi(PO ₄) ₂ · 4H ₂ O	10.1	Zr(UO ₂) _{0.9} H _{0.2} (PO ₄) ₂ · 5H ₂ O	10.5
Zr(LiPO ₄) ₂ · 4H ₂ O	10.0	ZrH _{0.4} Mg _{0.8} (PO ₄) ₂ · 4H ₂ O	9.8
Zr(LiPO ₄) ₂	7.05	ZrH _{0.4} Mg _{0.8} (PO ₄) ₂	7.9
ZrHNa(PO ₄) ₂ · 5H ₂ O	11.8	ZrBa(PO ₄) ₂ · 2.5H ₂ O	9.5
Zr(NaPO ₄) ₂ · 3H ₂ O	9.8	ZrMn(PO ₄) ₂ · 4H ₂ O	9.7
Zr(NaPO ₄) ₂	8.42	ZrCo(PO ₄) ₂ · 4H ₂ O	9.6
ZrHK(PO ₄) ₂ · H ₂ O	8.02	ZrNi(PO ₄) ₂ · 4H ₂ O	9.55
Zr(KPO ₄) ₂ · 3H ₂ O	10.7	ZrCu(PO ₄) ₂ · 4H ₂ O	9.6
Zr(KPO ₄) ₂	9.0	ZrZn(PO ₄) ₂ · 4H ₂ O	9.6
ZrHCs(PO ₄) ₂ · 2H ₂ O	11.3	Zr[Cr(NH ₃) ₆] _{0.25} H _{1.25} (PO ₄) ₂	10.8
Zr(CsPO ₄) ₂ · 6H ₂ O	14.2	Zr[Co(C ₅ H ₅) ₂] _{0.5} H _{1.5} (PO ₄) ₂	12.0
Zr(CsPO ₄) ₂	9.5	Zr[Pt(NH ₃) ₄] _{0.5} H(PO ₄) ₂	10.6
Zr(AgPO ₄) ₂	8.4	Zr[Cu(bpy)] _{0.5} H(PO ₄) ₂	14.5
ZrZn(PO ₄) ₂	7.66	Zr[Cu(phen)] _{0.5} H(PO ₄) ₂	15.8
ZrH _{0.5} Cr _{0.5} (PO ₄) ₂ · 4H ₂ O	11.6	Zr[Pd(dmp)] _{0.5} H(PO ₄) ₂	17.3
ZrRh _{0.66} (PO ₄) ₂ · 4H ₂ O	11.6	Zr[Fe(C ₅ H ₅) ₂] _{0.2} H _{1.8} (PO ₄) ₂	11.6
Zr(VO) _{0.5} H(PO ₄) ₂ · 3H ₂ O	9.75	Zr[Cu(NH ₃) ₄] _{0.6} H _{0.8} (PO ₄) ₂	9.6

bpy = bipyridyl; phen = phenantroline; dmp = dimethylphenantroline.

In addition, zirconium phosphates exchanged with transition metal ions are heterogeneous catalysts and supports for chromatographic separation. For the latter application it should be noted that layered acid phosphates are usually obtained as small platelets ($\sim 1 \mu\text{m}$) and very compact chromatographic columns are usually obtained. The flows are therefore slow while some particles tend to be released into the external solution. This problem may be overcome by

using larger particles, even though the rate of exchange decreases, or by supporting the layers on a suitable support such as silica gel.

Topotactic anion exchange reactions We have seen above that the majority of layered phosphates are inorganic cation exchangers. Layered phosphates of the γ -type show a typical reaction, which formally represents an anion exchange process. A topotactic exchange reaction is defined as the replacement of one group by another without alteration of the host matrix. If we consider the structure of the γ -phases we observe that the dihydrogenphosphate groups, present on the surface of the lamellae, have a net charge of -1 , delocalized over two oxygen atoms. The H_2PO_4^- is weakly bonded to the central tetravalent atom (Zr or Ti) and it may be easily replaced by other suitable groups, when the layered phosphate is equilibrated with a solution containing such groups. Topotactic exchange reactions with phosphites, hypophosphites, phosphonates or phosphinates, according to the general reaction:



are particularly efficient. R is an aliphatic or aromatic organic moiety that may bear a functional group. This simple procedure has allowed the preparation of a large number of new layered phosphate-phosphonates of γ -type with very interesting properties.

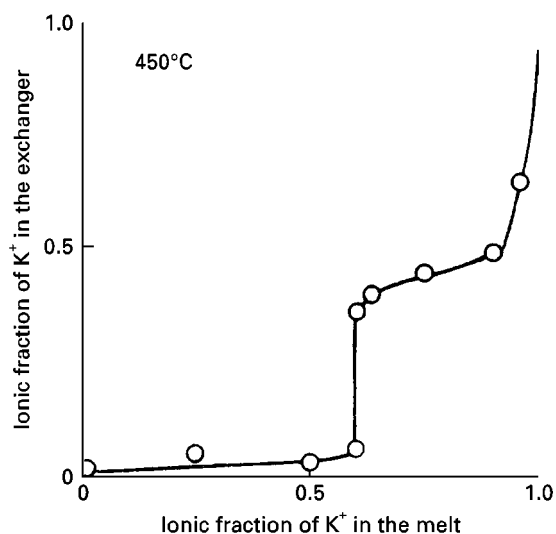
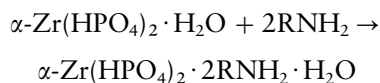


Figure 9 Forward and reverse Na^+/K^+ ion-exchange isotherms on layered α -zirconium phosphate in molten NaNO_3 - KNO_3 mixtures at 450°C . (Reproduced with permission from Alberti G and Costantino U (1974) *Journal of Chromatography* 102: 5–29. Copyright: Elsevier Publishing Science, Amsterdam.)

Intercalation Properties

Over time, research on layered phosphates has moved from the study of their ion exchange properties to that of their intercalation properties in great part determined by the presence of Brønsted acid groups in the interlayer region. Both α - and γ -zirconium phosphates are excellent intercalating agents of Lewis bases. The intercalation chemistry of the former has been more widely investigated and we will be mainly concerned with α -zirconium phosphate. Many molecules belonging to various classes of organic compounds (alkanols, glycols, alkyl and aryl amines, heterocyclic bases, aminoacids and dyes) have been intercalated. The corresponding intercalation compounds have been characterized for composition and arrangement of the guest molecules in the interlayer region. Table 3 gives the interlayer distance and composition of some typical examples of intercalation compounds.

Let us examine in more detail the intercalation of *n*-alkylamines that leads to the formation of compounds containing two moles of guest per mole of host, according to the reaction



where R is the *n*-alkyl-chain. The reaction proceeds stepwise with the formation of different phases. At low amine loading we observe the formation of a phase with interlayer distance 10.4 Å and the alkyl-chain axis is almost parallel to the layer plane (see Figure 10A). At half intercalation, the alkyl chains are arranged as a monolayer of extended molecules with the chain axes inclined by 55° with respect to the layer plane (see Figure 10B). At full intercalation *n*-alkylamines give rise to compounds in which the inorganic layer regularly alternates with a bilayer of alkylamines with the *n*-alkyl chain in *trans-trans* conformation (see Figure 10C). The terminal -NH₂ groups are protonated by the hydrogenphosphate groups.

Intercalation compounds with α,ω -alkyldiamines contain one mole of guest per formula weight. The guest molecules are arranged as a monolayer of extended chains and the terminal -NH₂ groups interact with the P-OH groups belonging to two-faced layers. Alkanols and glycols produce intercalation compounds whose composition and arrangement of guest species are similar to those found in alkyl monoamines and diamines, respectively. However, direct intercalation is prevented by the lower basicity of the alkanol OH group, compared to that of the NH₂ group. It is necessary to use as precursors pre-swelled zirconium phosphates.

Table 3 Interlayer distances and guest contents of intercalation compounds of α -zirconium phosphate

Guest molecule	mol Guest/ mol α -ZrP	Interlayer distance (Å)
Methylamine	2.0	12.1
Ethylamine	2.0	14.8
Propylamine	2.0	17.6
Pentylamine	2.0	21.5
Diethylamine	1.0	12.7
Dipropylamine	1.0	15.7
Diocetylamine	0.8	26.8
Aniline	2.0	18.4
<i>p</i> -Methoxyaniline	2.0	21.7
Benzylamine	2.0	19.1
Benzylethylamine	2.0	22.4?
Ephedrine	2.0	22.0
Histamine	1.9	20.5
Pyridine	0.95	10.9
Pyrazole	0.75	10.8
Imidazole	0.95	10.7
3-Methylpyrazole	0.98	12.1
1-Methylimidazole	0.58	10.4
Benzimidazole	1.90	20.4
Pyridazine	0.64	10.8
Pyrimidine	0.71	11.1
Pyrazine	0.78	10.8
2,2'-Bipyridyl	0.25	10.9
1,10-Phenanthroline	0.5	13.6
2,9-Dimethylphenanthroline	0.5	14.6
Ethanol		14.2
1-Propanol		16.6
1-Butanol		18.7
1-Octanol		26.7
Isopropanol		15.6
2-Methyl-1-propanol		17.5
3-Methyl-1-butanol		19.2
Benzyl alcohol		21.0
Diethylene glycol		10.5
Acetone		9.9
Acetylacetone		13.5
Acetonitrile		11.3
Urea	0.9	9.9
α -Alanine (DL)	0.5	12
Phenylalanine (DL)	1.7	23.2
Histidine (DL)	0.9	16.2
Crystal violet	0.5	22
Rhodamine	0.66	24.7

Heterocyclic bases give rise to non-stoichiometric intercalation compounds and the heterocyclic ring is positioned parallel to the layer plane. For the arrangement of other intercalated guests the reader is referred to recent reviews given in the Further Reading section. Materials with special properties have also been obtained by intercalation. Porphyrins and metalloporphyrins, thionine, methylene blue and rhodamine have been intercalated in α -zirconium phosphate and the materials obtained have been investigated for their optical properties. The possibility of intercalating dyes and of controlling, at least to

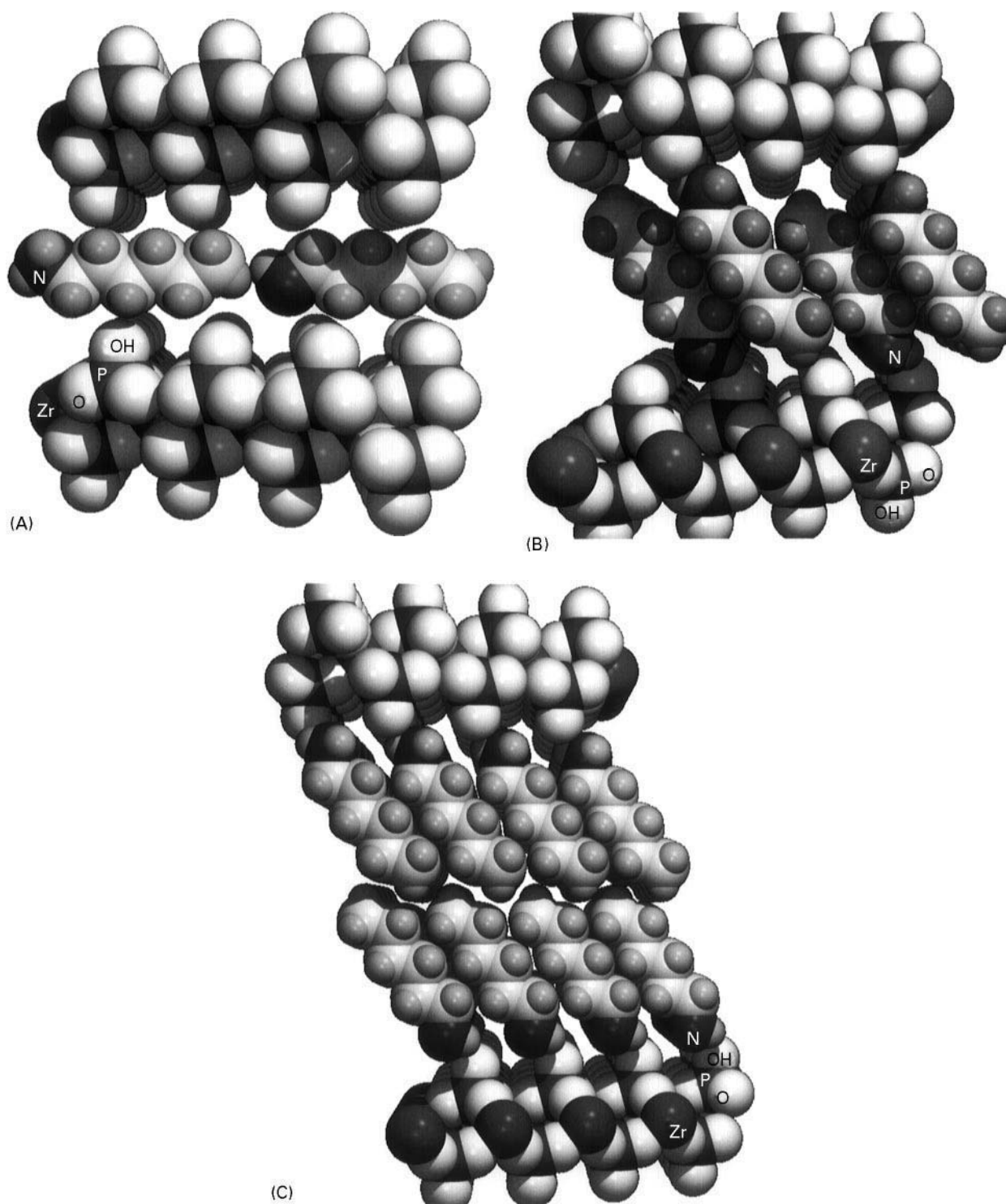


Figure 10 Arrangement of *n*-alkyl monoamines intercalated into α -Zr(HPO₄)₂ · H₂O: (A) alkyl-chain axis parallel to the layer plane. (B) Monolayer of extended molecules in *trans-trans* conformation. (C) Bilayer of extended molecules in *trans-trans* conformation.

some extent, molecular orientation is of interest in the preparation of new composite materials for non-linear optic applications. Intercalation of weak Brønsted bases was found to enhance the proton

conduction of the host and some of the compounds obtained have been used as active components in solid-state electrochemical gas sensors. Molecular and chiral recognition properties have been induced

in layered zirconium phosphate by the intercalation of suitable receptors such as aminated β -cyclodextrins, crown ethers or a Pirkle receptor.

Much attention is presently being paid to the possibility of performing reactions in the interlayer region. Polymerization, induced by chemical, thermal or photochemical treatment, of pyrrole, aniline, propargylamine or ε -aminocaproic acid intercalated in layered phosphates, produces interesting composite materials in which the inorganic layers regularly alternate with the polymers formed in the interlayer region.

Exfoliation Process

We have seen that layered polyvalent metal phosphates are obtained as molecular crystals built up by the packing of the layers which are planar macromolecules. These bidimensional macromolecules are usually very thin (5–15 Å), whereas planar dimensions are of the order of μm^2 , depending on the conditions of synthesis. If a layered crystal is exfoliated in single layers, materials with a very large surface area and with enhanced reactivity are obtained. For example, the complete exfoliation of 1 g of α -zirconium phosphate will produce material with a surface area of 950 m^2 . Furthermore, the suspension of the layers may be used to obtain thin films and pellicles or to cover suitable supports.

It is well known that layered smectite clays undergo so-called 'infinite swelling', that is, they disintegrate into single layers or packets of a few layers, when suspended in water. This phenomenon has never been observed in layered phosphates probably because of stronger layer-layer interactions. However, intercalation has made it possible to exfoliate both α - and γ -zirconium phosphates. In the case of α - $\text{Zr}(\text{HPO}_4)_2 \cdot \text{H}_2\text{O}$ and of the other α -type layered phosphates a good exfoliation has been obtained by the intercalation of short-chain alkylamines, such as methylamine or propylamine at 100% and 50% loading, respectively. This exfoliation process is shown schematically in Figure 11.

γ - $\text{Zr}(\text{PO}_4) \cdot (\text{H}_2\text{PO}_4) \cdot 2\text{H}_2\text{O}$ is best exfoliated when treated with dimethylamine. Colloidal dispersions containing highly anisotropic particles of nanoscale dimensions have a number of potential applications. After treatment with acids, flocculation allows the formation of completely inorganic pellicles or films useful in assembling the sensor layer of solid-state gas sensors, or to cover glass surfaces for chromatographic application. Composites of layered phosphates and silica gels or pillared layered phosphates have also been prepared from colloidal dispersions.

Solid dispersions of layered phosphates in silica gel Solid dispersions of α - or γ -zirconium phosphates in porous silica can be prepared starting from mixtures of a tetrapropylammonium oligosilicate solution and zirconium phosphates, previously exfoliated with amines. They are formed after gelification of the mixture with acetic acid and subsequent calcination at 650°C to remove the organic moieties. At this temperature zirconium phosphates are transformed into layered pyrophosphates, but non-condensed phosphate groups are still present on the free surfaces of the lamellae. Accordingly, the composites obtained have a large surface area (350–500 $\text{m}^2 \text{g}^{-1}$), good surface ion-exchange capacity and acid catalytic properties. Such composites may find application as stationary phases in chromatography.

Pillared layered phosphates The success obtained in the pillaring of clays to obtain microporous solids with larger pore diameters than those found in zeolites has stimulated research in preparing pillared layered structures based on metal(IV) phosphates. Synthetic strategy requires the insertion of large organic or inorganic cations (pillars) between the layers to prop them apart. If the pillars are sufficiently spaced, a microporous structure is obtained and the dimensions of the channels or diffusion paths are determined by the size of the pillars and their spacing in the interlayer region (see Figure 12).

Inorganic pillars are preferable to organic pillars because of their much higher thermal stability. To obtain thermally stable structures, pillaring has been performed with highly charged polyoxycations such as the Al_{13} Keggin ion $[\text{Al}_{13}\text{O}_4(\text{OH})_{24}(\text{H}_2\text{O})_{12}]^{7+}$, or $[\text{Zr}(\text{OH})_2(\text{H}_2\text{O})_4]^{8+}$, or inorganic clusters such as $[\text{Nb}_6\text{Cl}_{12}]^{2+}$. After suitable thermal treatment, the layered phosphates contain as pillars, aggregates of inorganic oxides which have considerable thermal stability. The problem of inserting such large pillars has often been overcome by contacting the solution of the pillaring species with colloidal dispersions containing single layers, or packets of a few layers, of tetravalent metal(IV) phosphates. This provides access to the surface POH groups, the exchange reaction and the flocculation of the pillared material. However, the problem of achieving uniform pillar spacing to obtain a narrow distribution of micropores of predictable dimensions has not been completely resolved. The topic is of great interest since materials for molecular sieving and for shape-selective catalysis might result.

Metal(IV) Phosphonates

A fundamental step in the development of the chemistry of layered phosphates was made in 1978

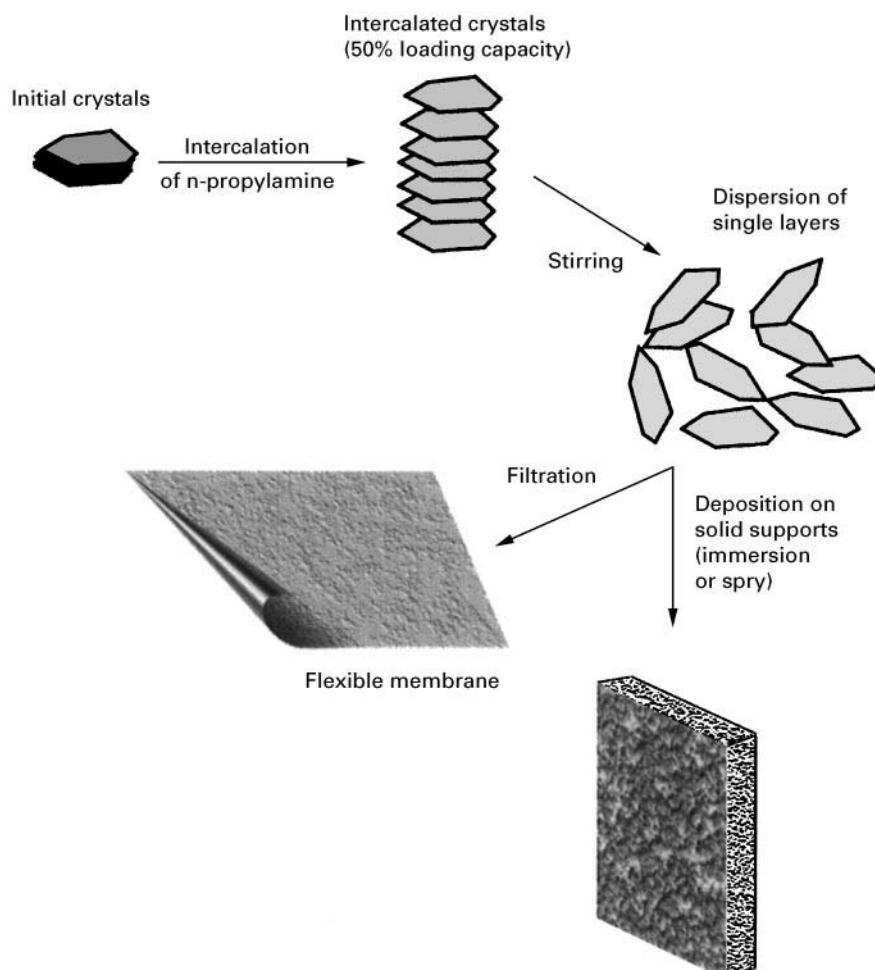


Figure 11 Schematic representation of the exfoliation of α -Zr(HPO₄)₂·H₂O microcrystals by intercalation of n-propylamine. The formation of completely inorganic films or the coating of solid surfaces is also reported.

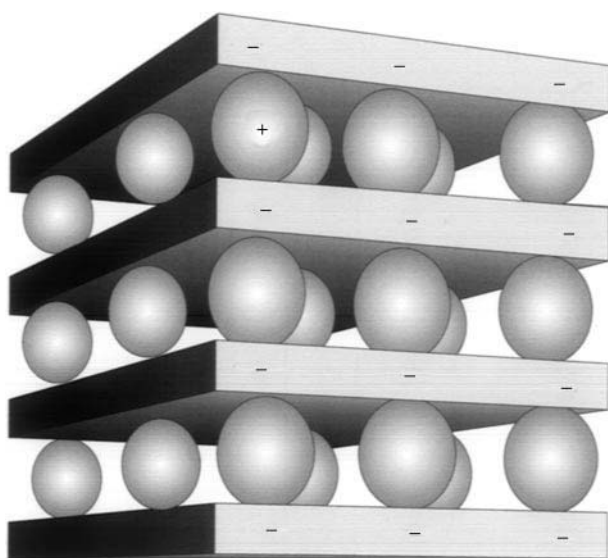


Figure 12 Schematic representation of a pillared layered structure showing the microporosity and the diffusion paths.

when the first Zr(IV) phosphonates and Zr(IV) organophosphates with formula $\text{Zr}(\text{RPO}_3)_2$ or $\text{Zr}(\text{ROPO}_3)_2$ respectively, were prepared (R being an organic group). These compounds are organic derivatives of α -Zr(HPO₄)₂·H₂O in which the -OH groups attached to the phosphorous atoms have been replaced by organic R groups, leaving the inorganic structure of the α -layer essentially unchanged.

A further development in layered metal(IV) phosphates was achieved with the resolution of the structure of the γ -phases and with the discovery that it is possible to replace interlayer dihydrogenphosphate groups by monovalent phosphonate or phosphinate anions by simple topotactic anion exchange reactions (see above).

Nowadays, a large number of metal(IV) phosphonates of α - and γ -type are known and many others can be prepared for special purposes, constituting a very large and versatile class of layered materials. A brief account of preparation procedures, structural

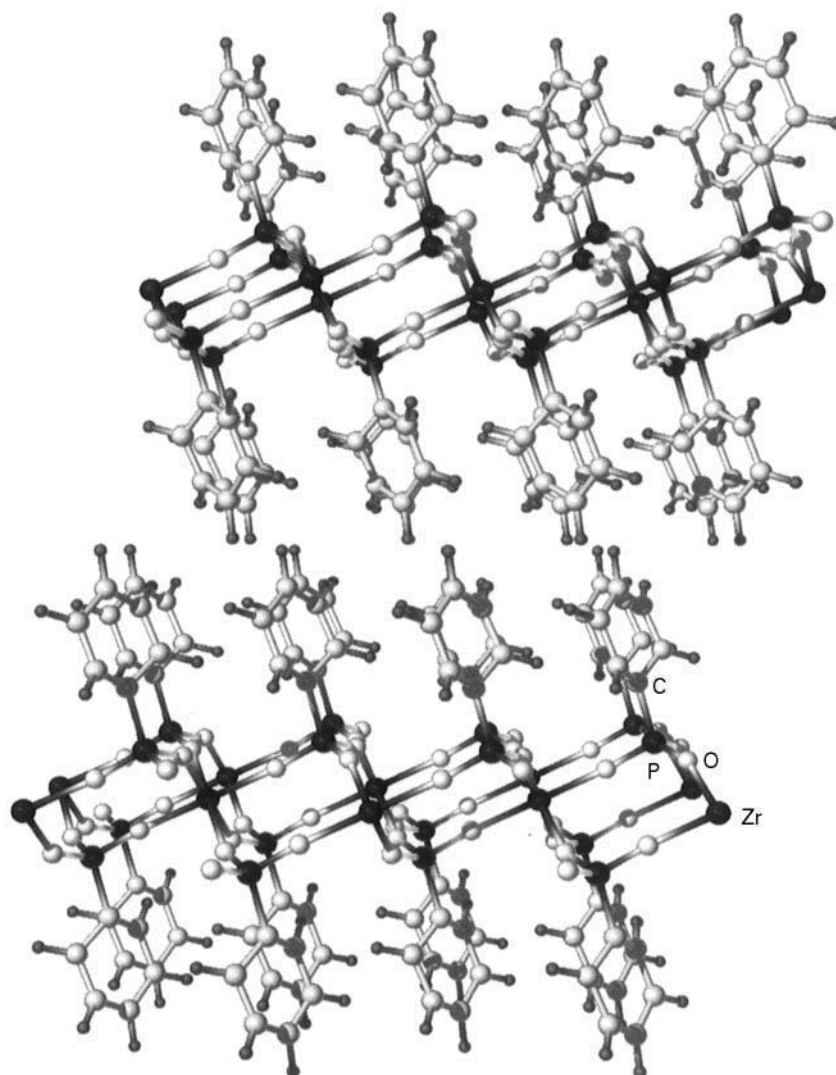


Figure 13 Computer-generated representation of the sequence of two layers of α -Zr(C₆H₅PO₃)₂. (Data from Alberti G, Costantino U, Allulli S and Tomassini N (1978) *Journal of Inorganic and Nuclear Chemistry* 40: 1113–1117, with permission from Elsevier Science.)

features and the chemistry of α - and γ -zirconium phosphonates is given.

Zirconium Phosphonates of α -Type

The preparation of Zr phosphonates is closely related to the methods employed for the preparation of α -Zr(HPO₄)₂·H₂O, i.e. refluxing of amorphous precipitates with solutions containing the chosen phosphonic acids, and the direct precipitation method in the presence of Zr fluorocomplexes and the suitable H₂O₃PR acid.

As already mentioned, the layer structure arises from the concatenation of ZrO₆ octahedra and O₃PR tetrahedra similar to that present in α -zirconium phosphate. Due to the short lateral distance between adjacent O₃P–R groups on each side of the α -layer

(5.3 Å) interpenetration of the R-groups belonging to adjacent layers cannot occur for steric reasons and a double film of R-groups is expected for all the members of this class. Therefore these organic derivatives have a layered structure similar to that of zirconium benzenephosphonate (see **Figure 13**) or zirconium carboxyethanphosphonate (see **Figure 14**), two typical compounds of the class.

A list of selected α -layered phosphonates is given in **Table 4**. Note that the compounds contain a variety of functional groups. By choosing appropriate organic groups attached to the phosphorus atom, it is possible to vary the acid properties of the phosphonates from neutral (e.g. P–CH₃) or weakly acid (e.g. P–CH₂COOH) to strongly acid (e.g. P–C₆H₄SO₃H) or even to basic (e.g. P–C₂H₄NH₂), or to anchor the amino acid chiral group. The nature of the covalently

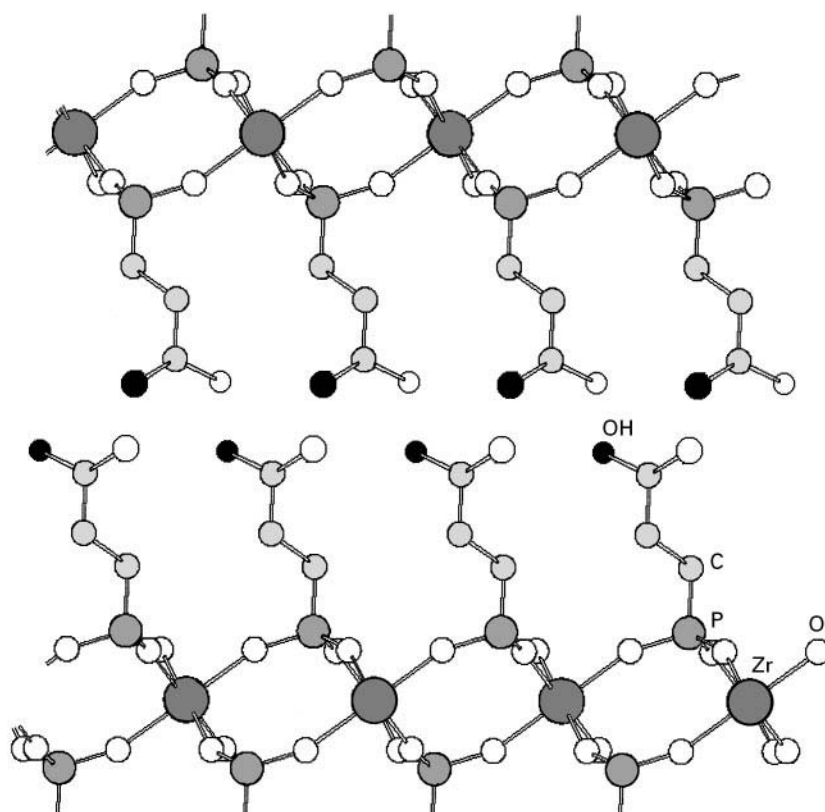


Figure 14 Computer-generated representation of the sequence of two layers of α -Zr(HOOCCH₂CH₂PO₃)₂. (Data from Alberti G, Costantino U, Casciola M, Vivani R and Peraio A (1991) *Solid State Ionics* 46: 61–68, with permission from Elsevier Science.)

attached groups depends on the imagination and ability of the chemist to synthesize the appropriate phosphonic acids.

The only limitation to synthesis is the use of organic groups with a cross-section equal to or less than 24 Å². This is the free area around each P–OH group

present on the surfaces of the layers of the parent α -Zr(HPO₄)₂. However, more voluminous groups may be attached to the α -layers if their dimensions are compensated by introducing small groups R' (R' being H, OH, CH₃) to obtain compounds of formula Zr(RPO₃)_{2-x}(R'PO₃)_x. These mixed component phases are of great interest since a very special type of complexing agent or redox couple may be fixed to the layers. A selection of the multicomponent phases prepared to date is given in Table 5.

Zirconium diphosphonates, of general formula Zr(O₃P–R–PO₃), in which adjacent inorganic layers of the α -type are covalently joined to each other by divalent organic groups, may also be obtained. These zirconium phosphates do not possess interlayer microporosity, because the distance between adjacent pillars is 5.3 Å and the van der Waals diameter of the alkyl or aryl pillar is about 4 Å. It is however possible to create microporosity in the interlayer region if some pillars are replaced by small O₃P–H groups, and if the pillar has been suitably designed. By using a pillar with bases, such as 3,3',5,5'-tetramethylbiphenyl-diphosphonic acid, a pillared compound exhibiting a high phosphite percentage and interlayer microporosity of 375 m² g⁻¹, has recently been prepared.

Table 4 Interlayer distances of some zirconium *bis*-monophosphonates and organophosphates with α -layered structure

Compound	Interlayer distance (Å)
Zr(O ₃ PCH ₃) ₂	8.9
Zr(O ₃ PCH ₂ OH) ₂ H ₂ O	10.1
Zr(O ₃ PCH ₂ Cl) ₂	10.1
Zr(O ₃ PCH ₂ CN) ₂	10.8
Zr(O ₃ PC ₃ H ₇) ₂	14.0
Zr(O ₃ P(CH ₂) ₂ COCl) ₂	13.5
Zr(O ₃ PCH ₂ COOH) ₂	11.3
Zr(O ₃ P(CH ₂) ₂ COOH) ₂	13.0
Zr(O ₃ P(CH ₂) ₃ COOH) ₂	15.0
Zr(O ₃ PCH=CH ₂) ₂	10.6
Zr(O ₃ PCH ₂ SO ₃ H) ₂	15.4
Zr[(O ₃ PO)(CH ₂ CH ₂ O) _n PO ₃]	
Zr[(O ₃ PO)(CH ₂ CH ₂ NH ₂) ₂] · 2HCl	14.3
Zr[HOOCCH(NH ₂)CH ₂ OPO ₃] ₂	14.5

Table 5 Compositions and interlayer distances of some derivatives of α -zirconium phosphate with two different pendant groups

Compound	Interlayer distance (Å)
$\text{Zr}(\text{O}_3\text{POH})_{0.66}(\text{O}_3\text{PH})_{1.34}$	6.5
$\text{Zr}(\text{O}_3\text{POH})_{1.15}(\text{O}_3\text{PC}_6\text{H}_5)_{0.85}$	12.4
$\text{Zr}(\text{O}_3\text{POH})(\text{O}_3\text{PC}_2\text{H}_4\text{COOH})$	12.9
$\text{Zr}(\text{O}_3\text{PCH}_2\text{OH})(\text{O}_3\text{PH})$	7.0
$\text{Zr}(\text{O}_3\text{PC}_2\text{H}_4\text{COOH})_{1.25}(\text{O}_3\text{PCH}_2\text{OH})_{0.75}$	13.6
$\text{Zr}(\text{O}_3\text{PC}_6\text{H}_5)(\text{O}_3\text{PH})$	10.5
$\text{Zr}(\text{O}_3\text{PC}_6\text{H}_4\text{SO}_3\text{H})_{0.85}(\text{O}_3\text{PC}_2\text{H}_5)_{1.15} \cdot 3.7\text{H}_2\text{O}$	18.5
$\text{Zr}(\text{O}_3\text{PC}_6\text{H}_4\text{SO}_3\text{H})_{0.97}(\text{O}_3\text{PCH}_2\text{OH})_{1.03} \cdot 4.9\text{H}_2\text{O}$	19.6

A computer-generated structural model of this microporous pillared compound is shown in Figure 15.

Zirconium Phosphate Phosphonates of γ -Type

The structure of the γ -layer differs from that of the α -layer since the ZrO_6 octahedra are placed in two different planes and joined to each other by PO_4 tetrahedra. Due to the fact that only three oxygens are available in phosphonate groups, pure γ -zirconium phosphonates cannot exist. However, it is possible to replace the interlayer H_2PO_4 groups by monovalent phosphonate or phosphinate anions to obtain layered inorganic-organic derivatives in which the inorganic layer regularly alternates with organic

layers. These materials are obtained from a simple topotactic reaction by contacting the original zirconium phosphate microcrystals with a solution of a suitable phosphonic acid. As we have already seen this reaction is similar to an anion exchange process. The texture of the γ -layer remains practically unchanged and it is therefore possible to predict the arrangement of the organic groups in the interlayer region by considering the interlayer distance and the dimension of the groups. Figure 16 shows the probable structure of γ -zirconium phosphate benzene-phosphonate.

Many organic derivatives have been prepared with this simple procedure including pillared compounds with regular interlayer porosity obtained by partial replacement of the dihydrogenphosphates with bivalent diphosphonate groups. A selected number of recently prepared compounds is reported in Table 6. Monophosphonic or biphosphonic acids containing crown ethers have also been used for the topotactic reaction and compounds with crown ethers covalently attached to the inorganic layers have been obtained. These materials show promise for interesting applications in ionic or molecular recognition and hence for performing selective separations. The γ -system is thus very versatile and the interlayer region can easily be engineered with a large variety of organic groups to obtain materials for application in several fields including the preparation of new stationary phases for chromatographic separation.

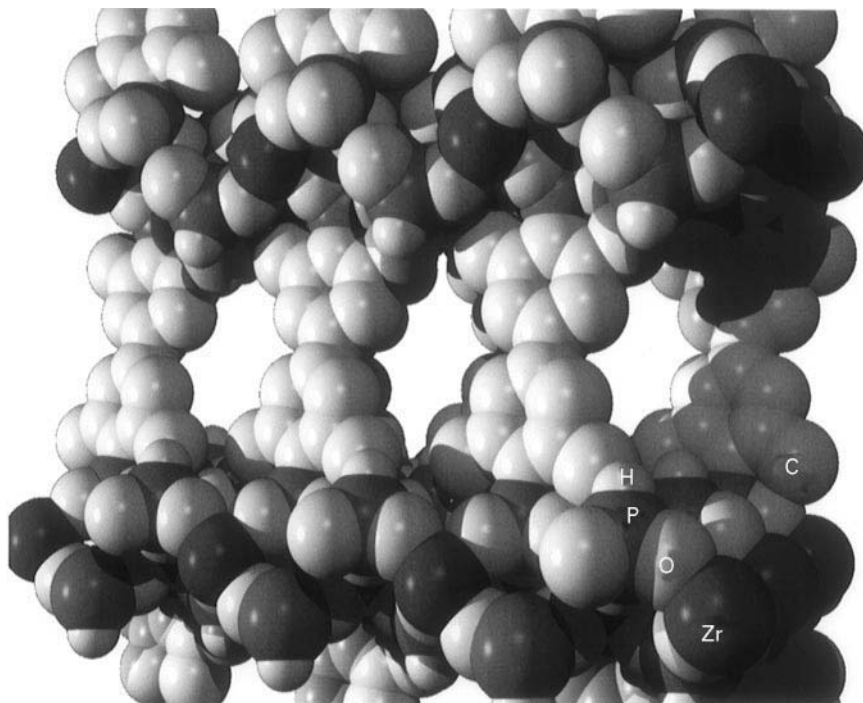


Figure 15 Computer-generated structural model of a microporous α -zirconium phosphite-diphosphonate. (Data from Alberti G, Costantino U, Marmottini F, Viviani R and Zappelli P (1993) *Angew. Chem. Int. Ed. Engl.* 32: 1357–1359.)

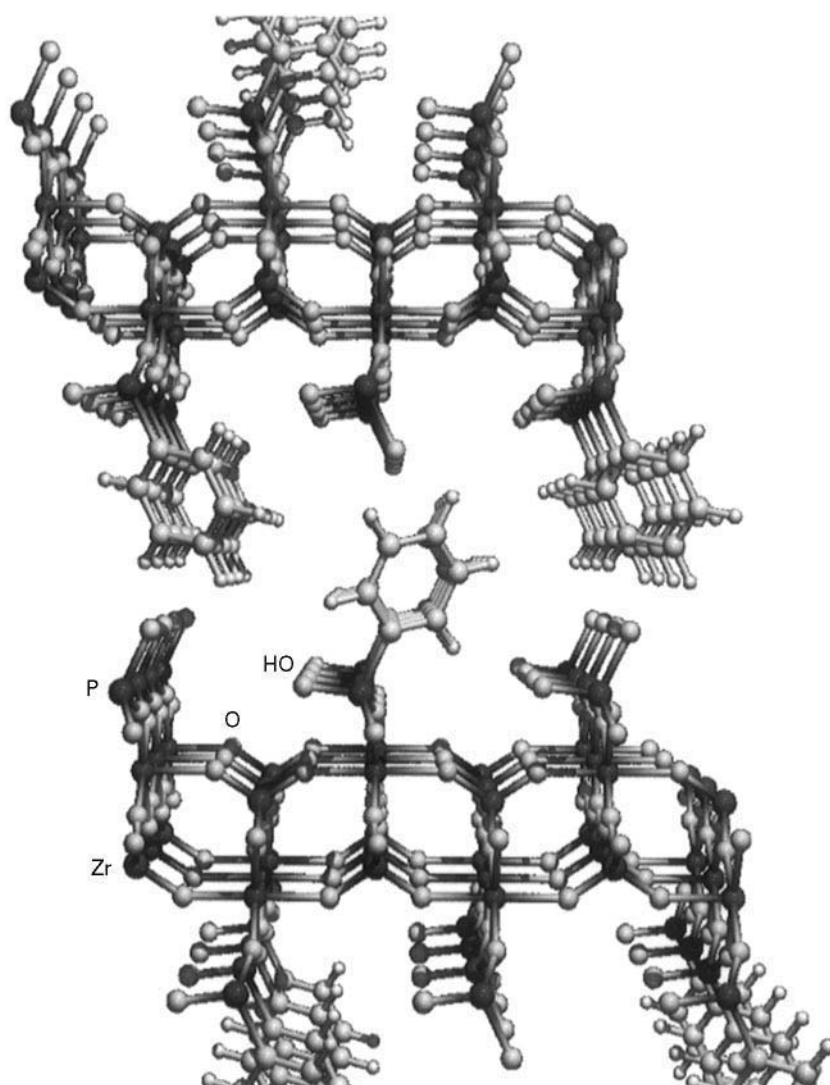


Figure 16 Computer-generated representation of the sequence of two layers of γ -zirconium phosphate-benzenephosphonate. (Data from Alberti G, Vivani R, Biswas RK and Murcia-Mascaros S (1993) *React. Polym.* 19: 1–12, with permission from Elsevier Science.)

Conclusion

The layered phosphates of polyvalent metals are obtained with different layer structures and exhibit

a rich chemistry. Many of them are inorganic ion exchangers that support the most common organic resins in processes which occur at high temperatures or in the presence of strong oxidizing solutions and

Table 6 Composition and interlayer distances of some organic derivatives of γ -zirconium phosphate obtained by topotactic exchange reactions

Acid used	Composition	Interlayer distance (\AA)
H_3PO_3	$\text{ZrPO}_4\text{O}_2\text{PHOH} \cdot 2\text{H}_2\text{O}$	12.2
H_3PO_2	$\text{ZrPO}_4\text{O}_2\text{PH}_2 \cdot \text{H}_2\text{O}$	8.8
$\text{H}_2\text{O}_3\text{PCH}_3$	$\text{ZrPO}_4\text{O}_2\text{POHCH}_3 \cdot 2\text{H}_2\text{O}$	12.8
$\text{H}_2\text{O}_3\text{PC}_3\text{H}_7$	$\text{ZrPO}_4\text{O}_2\text{POHC}_3\text{H}_7 \cdot 1.2\text{H}_2\text{O}$	15.1
$\text{HO}_2\text{P}(\text{CH}_3)_2$	$\text{ZrPO}_4(\text{H}_2\text{PO}_4)_{0.33}(\text{O}_2\text{P}(\text{CH}_3)_2)_{0.67} \cdot \text{H}_2\text{O}$	10.3
$\text{H}_2\text{O}_3\text{PC}_6\text{H}_5$	$\text{ZrPO}_4(\text{H}_2\text{PO}_4)_{0.33}(\text{O}_2\text{POHC}_6\text{H}_5)_{0.67} \cdot 2\text{H}_2\text{O}$	15.4
$\text{H}_2\text{O}_3\text{P}(\text{C}_6\text{H}_{11})$	$\text{ZrPO}_4(\text{H}_2\text{PO}_4)_{0.33}(\text{O}_2\text{POHC}_6\text{H}_{11})_{0.67} \cdot \text{H}_2\text{O}$	16.9
$\text{H}_2\text{O}_3\text{PC}_6\text{H}_5$	$\text{ZrPO}_4\text{O}_2\text{PHC}_6\text{H}_5$	15.1
$\text{H}_2\text{O}_3\text{PC}_{10}\text{H}_{21}\text{NO}_3^*$	$\text{ZrPO}_4(\text{H}_2\text{PO}_4)_{0.71}(\text{C}_{10}\text{H}_{21}\text{NO}_3\text{PO}_3)_{0.29}$	16.2

*N-(phosphonoethyl)aza crown; (12)crown-4.

strong doses of ionizing radiation. Furthermore, these inorganic ion exchangers possess a high ion exchange capacity and some peculiar selectivities. Layered phosphates are good intercalating agents of ionic or polar species. This allows the construction in the interlayer region of supramolecular assemblies with special functionalities in the fields of chromatographic supports, chemical and electrochemical sensors, ion exchange membranes, ionic and molecular recognition and catalysts. The delamination of layered phosphates has permitted the preparation of thin films and coatings and pillared layered structures with accessible microporosity. There are many more possibilities in layered phosphonate chemistry because functional groups may be inserted on alkyl chains or on aryl rings. The field of layered phosphates and phosphonates is in continuous expansion and these materials will find many applications as soon as their potential is realized.

See also: II/Ion Exchange: Catalysis: Organic Ion Exchangers; Historical Development; Inorganic Ion Exchangers; Novel Layered Materials: Non-Phosphates; Organic Ion Exchangers; Theory of Ion Exchange.

Further Reading

- Alberti G (1978) Syntheses, crystalline structure, and ion-exchange properties of insoluble acid salts of tetravalent metals and their salt forms. *Accounts in Chemical Research* 11: 163–170.
- Alberti G and Costantino U (1982) Intercalation chemistry of acid salts of tetravalent metals with layered structure and related materials. In: Whittingham MS and Jacob-

- son JA (eds) *Intercalation Chemistry*, Chapter 5, pp. 147–180. New York: Academic Press.
- Alberti G and Costantino U (1984) Recent progress in the intercalation chemistry of layered *a*-zirconium phosphate and its derivatives, and future perspectives for their use in catalysis. *Journal of Molecular Catalysis* 27: 235–250.
- Alberti G and Costantino U (1991) Intercalates of zirconium phosphates and phosphonates. In: Atwood JL, Davies JED and MacNicol DD (eds) *Inclusion Compounds*, Vol. 5, *Inorganic and Physical Aspects of Inclusion*, Chapter 5, pp. 136–176. Oxford: Oxford University Press.
- Alberti G and Bein T (eds) (1996) *Solid State Supramolecular Chemistry: Two and Three Dimensional Networks*, Vol. 7, *Comprehensive Supramolecular Chemistry*, Chapters 4 and 5, pp. 107–187. Oxford: Pergamon.
- Alberti G, Casciola M, Costantino U and Vivani R (1996) Layered and pillared metal(IV) phosphates and phosphonates. *Advanced Materials* 8: 291–303.
- Alberti G, Bartocci M, Santarelli M and Vivani R (1997) Zirconium phosphate chloride dimethyl sulfoxide, a reactive precursor of a large family of layered compounds. *Inorganic Chemistry* 36: 3574.
- Amphlett CB (1964) *Inorganic Ion Exchangers*. Amsterdam: Elsevier.
- Cheetham AK and Day P (eds) (1992) *Solid State Chemistry: Compounds*, Chapter 6, pp. 182–223. Oxford: Clarendon Press.
- Clearfield A (ed.) (1982) *Inorganic Ion Exchange Materials*, Chapters 1–3, pp. 1–132. Boca Raton, FL: CRC Press.
- Clearfield A (1990) Layered phosphates, phosphites and phosphonates of groups 4 and 14 metals. *Comments in Inorganic Chemistry* 10: 89–128.
- Clearfield A (1998) Metal phosphonate chemistry. In: Karlin KD (ed.) *Progress in Inorganic Chemistry*, Vol. 47. New York: John Wiley.

Novel Layered Materials: Non-Phosphates

R. Mokaya, University of Cambridge, Cambridge, UK
Copyright © 2000 Academic Press

Introduction

In this paper the structure and composition of layered materials (excluding those which contain phosphates) and their modified variants are described. Layered materials are made up of sheets or planes of atoms held together by interplanar forces which are weaker than intraplanar binding forces. This structural set-up allows the insertion of atomic or molecular guest species between the layers. Such insertion (or intercalation) provides a means for controlled variation of the physical and chemical properties of the host

layered material over wide ranges to yield new variants of novel layered materials. The intercalated layered materials are also described.

Layered materials may be broadly classified into three groups according to the composition of their layers and the forces that hold the layers together. The interlayer forces determine the inherent ability of the layers to resist distortions involving displacements transverse to the layer planes.

1. Type I layered materials are made up of layers of atomically thin sheets. The neutral layers are held together by van der Waals forces. Examples are graphite and boron nitride. In graphite the layers tend to be 'floppy' and are easily separated with respect to distortions transverse to the layer

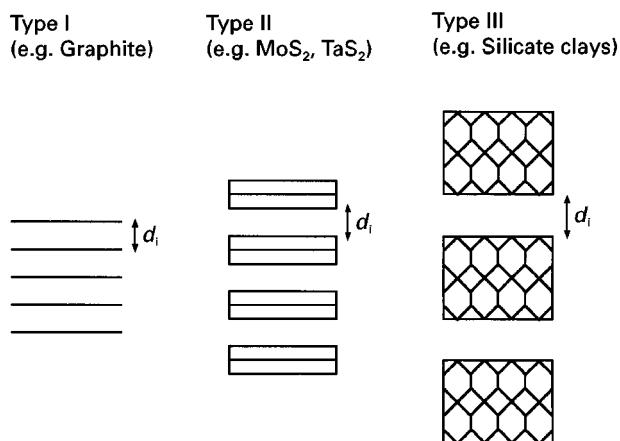


Figure 1 Schematic classification of layered solids (d_i = inter-layer distance).

- planes. Graphite is however rigid against longitudinal in-plane distortions.
2. Type II layered materials, such as dichalcogenides and lamellar oxyhalides, have layers composed of a few (usually three) distinct planes of strongly bonded atoms held together by van der Waals forces.
 3. Type III layered materials have layers made up of dense (up to seven) assemblies of strongly bonded atoms. The layers may be charged in which case the interlayer forces are ionic resulting in layered structures, such as silicate clays and layer double hydroxides, which are quite rigid to interlayer distortion or expansion.

Figure 1 gives a schematic illustration of the three classes of layered materials.

In all cases the intralayer forces are much stronger than the interlayer forces and therefore guest species can be inserted into the interlayer region between the host layers without any change to the layers themselves. This attractive feature of layered materials has been extensively exploited. Indeed, the bidimensional character of many layered materials can be gradually modified by intercalation, grafting, or pillaring with a variety of guest species to yield new classes of novel layered materials. Type I intercalation materials, such as those of graphite, form stages in which n -multilayers of the host are separated by monolayers of guest intercalant to form expanded n -stage materials. Type II materials are able to accept guest species into random interlayer sites and may ultimately form a saturated stage-1 expanded material at sufficient guest species concentrations. In contrast type III materials always form intercalation compounds with a stage 1 stacking sequence in which the host layers are separated by one or more layers of the guest

species. Novel layered materials that have found use in separation processes are mainly (intercalated or otherwise modified) type III materials and this paper is therefore devoted to such materials with only a brief mention of type I and type II intercalated materials (using graphite and dichalcogenides as examples) given below.

Type I: Graphite

Graphite is known to be intercalated by both electron donors and acceptors and to a large extent the driving force for intercalation is electronic in nature. Thus depending on the guest species, positively charged carbon layers or negatively charged carbon layers may be obtained. Graphite intercalation compounds usually exhibit a high degree of ordering and are unique among layered host materials in that the intercalation occurs such that, depending on the extent of guest species incorporation, it is possible to observe the staging phenomenon (**Figure 2**). The staging phenomenon is defined by a periodic arrangement of n graphite layers (where n is the stage index) between sequential intercalant layers. Well staged graphite intercalated materials can be prepared up to $n \sim 10$. Strong interatomic intercalant–intercalant binding relative to the intercalant–graphite binding favours a close-packed in-plane intercalant arrangement and is the driving force for the staging phenomenon. Graphite intercalation compounds (GICs) have found use as catalysts, electric conductors, recording materials (in inks and coloured leads) and as lubricants and low friction coatings.

Type II: Dichalcogenides

Dichalcogenides, sometimes denoted TX_2 , have layers made up of a sheet of metal atoms (T)

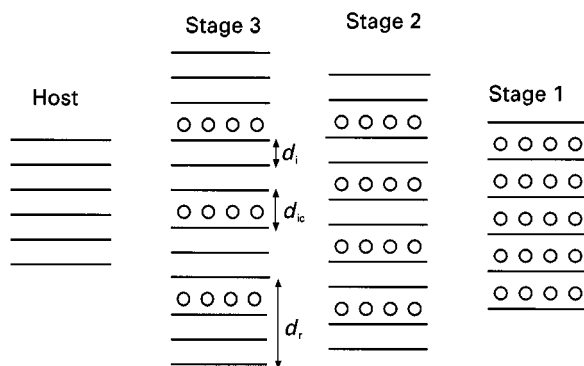


Figure 2 The staging phenomenon as exhibited by graphite (for stage 3, d_i = carbon interlayer distance, d_e = intercalate distance and d_r = repeat basal distance).

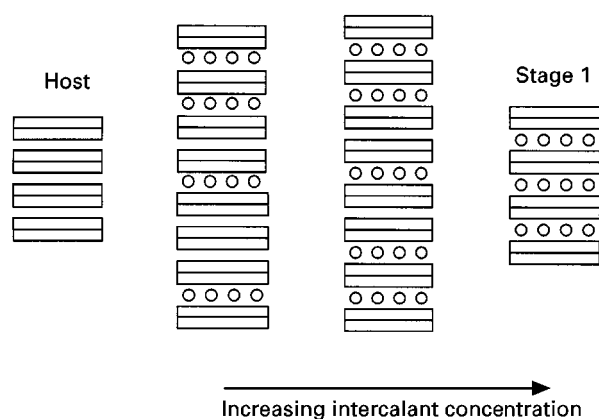


Figure 3 Schematic illustration of intercalant concentration dependent intercalation of type II layered materials.

sandwiched between two sheets of chalcogen (X) atoms. T is usually a transition metal and X may be S, Se or Te. The layers are largely neutral and separated by a van der Waals gap. As mentioned above, dichalcogenides are able to accept guest species into random interlayer sites and may ultimately form a saturated stage 1 expanded material at sufficient guest species concentrations (Figure 3). During intercalation, the guest species are inserted in the van der Waals gap and in most cases occupy interstitial sites. The intercalation is generally accompanied by charge transfer between the intercalant species and the host layers and therefore intercalation complexes are formed with electron donor species only. Such species include alkali metal atoms, transition metal atoms and organic molecules. The intercalation of metal atoms (especially alkali metal atoms) results in efficient transfer of electrons to the host compound resulting in unique electronic properties. For metal atom intercalation the increase in layer separation is not large but the weak host layer interactions are replaced by strong Coulomb (alkali metal) and covalent (transition metal) interactions yielding a quasi three-dimensional solid. The intercalation of organic molecules results in much larger layer separations. An example is the intercalation of amines in which the orientation of the amines in the van der Waals gap depends on the number of carbon atoms. Short chain amines, such as methylamine, pack parallel to the layers whereas intermediate chain amines (e.g. C_4 – C_9) orient at an angle to the layers with the nitrogen with its lone pair of electrons adjacent to the layer. The angle of inclination generally increases with chain length and for chain lengths $> C_{16}$, the amines are arranged perpendicular to the host layers and form bilayers resulting in layer separations as high as 57 Å for stage 1 intercalation.

Type III: Layer Silicates (Clays) and Layer Double Hydroxides (LDHs)

Nature of Layer Silicates (Clay Minerals)

Clays are by definition fine grained solids with particle size generally $< 2 \mu\text{m}$ and many of their properties result from their small particle size. The layers of clays are formed by condensation of sheets of linked $\text{Si}(\text{O},\text{OH})_4$ tetrahedra with those of linked $\text{M}_{2-3}(\text{OH})_4$ octahedra, where M is a divalent or trivalent cation. A 1 : 1 condensation gives two sheet minerals such as kaolinite with a general layer formula of $\text{M}_{2-3}\text{Si}_2\text{O}_5(\text{OH})_4$. A 2 : 1 condensation results in the octahedral sheet being sandwiched between two sheets of tetrahedra giving the mica type layer structure with a layer formula of $\text{M}_{2-3}\text{Si}_4\text{O}_{10}(\text{OH})_2$. In both cases the tetrahedral sheets are linked in the unit structure to octahedral sheets and to groups of coordinated cations or individual cations. The apical oxygen at the fourth corner of the tetrahedron, which is directed normal or nearly normal to the sheet, forms part of an immediately adjacent octahedral sheet in which octahedra are linked by sharing edges. The junction plane between tetrahedral and octahedral sheets consists of the shared apical oxygens of the tetrahedra and unshared OH groups that lie in projection at the centre of each six-fold ring of tetrahedra. Figure 4 shows a three-dimensional schematic illustration of layer silicates. Also possible, for example in chlorite, are four sheet clays in which the trimorphic units alternate with $\text{M}(\text{OH})_{2-3}$ sheets of octahedrally coordinated M^{2+} or M^{3+} ions.

Smectite clays, which exhibit the property of intercalation, are made up of negatively charged layers and therefore possess an ion exchange capacity which distinguishes them from the mica and pyrophyllite-talc groups of minerals (see below). The layer charge arises generally from isomorphous substitution of Si^{4+} by Al^{3+} in the tetrahedral sheet and/or Al^{3+} by Mg^{2+} , Fe^{2+} in the octahedral sheet. Some charge may also arise from broken bonds at edges of the clay crystal. Following below are ideal structural formulae of some clay silicates showing, where appropriate, isomorphous substitution:

1. Dioctahedral smectites (two-thirds of octahedral sites are occupied by trivalent cations)
 - (a) Pyrophyllite
 $[(\text{Si}_8)(\text{Al}_4)\text{O}_{20}(\text{OH})_4]$ No layer charge.
 - (b) Montmorillonite
 $[\text{M}_x(\text{Si}_8)[\text{Al}_{4-x}\text{Mg}_x]\text{O}_{20}(\text{OH})_4 \cdot n\text{H}_2\text{O}]$ Octahedral substitution.
 - (c) Beidellite
 $[\text{M}_x\text{Si}_{8-x}\text{Al}_x(\text{Al}_4)\text{O}_{20}(\text{OH})_4 \cdot n\text{H}_2\text{O}]$ Tetrahedral substitution.

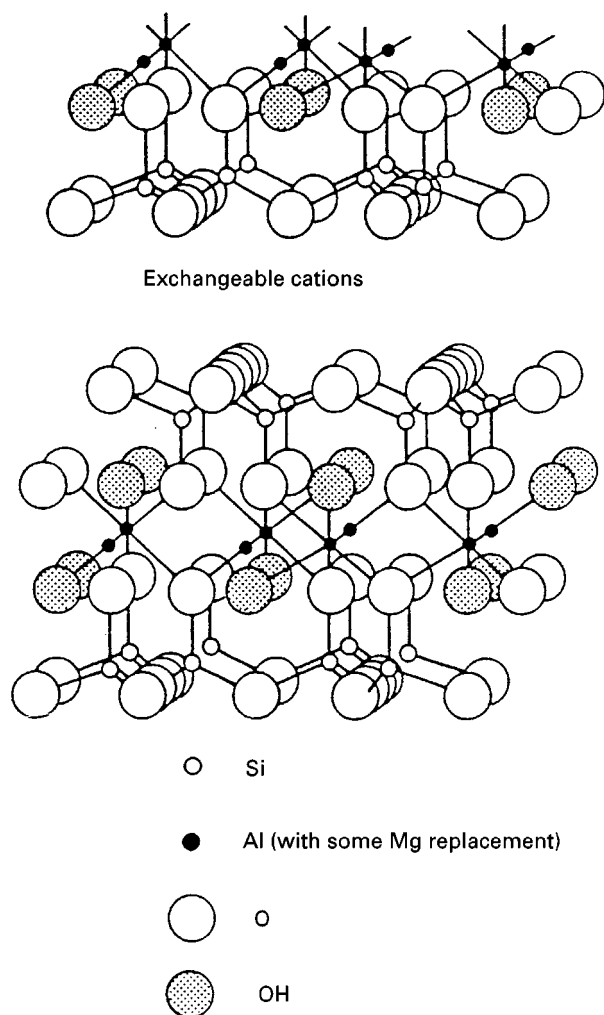


Figure 4 Three-dimensional illustration of the structure of silicate clays.

2. Trioctahedral smectites (all octahedral sites are occupied by divalent cations)
 - (a) Talc
 $[(\text{Si}_8)(\text{Mg}_6)\text{O}_{20}(\text{OH})_4]$ No layer charge.
 - (b) Hectorite
 $[M_x(\text{Si}_8)(\text{Mg}_{6-x}\text{Li}_x)\text{O}_{20}(\text{OH})_4 \cdot n\text{H}_2\text{O}]$ Octahedral substitution.

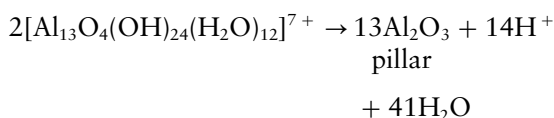
Smectite clays can intercalate other compounds in a three component system:

1. Host layer with an overall negative layer charge.
2. Exchangeable intercalates (ions) which compensate for the overall negative charge.
3. Neutral molecules (e.g. water) which occur between the layers and are associated with the interlayer cations and the layers.

Pillared Clays

Pillared clays are usually smectite clay minerals in which the interlayer cations are three-dimensional species which in some cases, after appropriate treatment, are fixed to the layers of the host clay. The shape and size of these cations allows them to function as molecular pillars which keep the layers apart at a fixed distance. The pillaring phenomenon therefore exposes much of the intercrystal basal surfaces for adsorption and molecular sieving purposes. Permanent porosity may be introduced in montmorillonite by replacing the interlayer alkali or alkaline earth cation with a variety of species such as tetraalkylammonium ions, tris-metal chelates, bicyclic amine cations and polymeric oxymetal cations. Clays pillared by oxycations or metal oxides are of greatest interest because they exhibit thermal stability in excess of 500°C and, depending on preparation methods, materials with large pore diameters and surface area (Table 1).

The most extensively studied pillared clays are those containing polymeric hydroxy-aluminium species as the pillaring cation. In this paper such Al pillared clays are used to illustrate the nature and properties generally possessed by metal oxide pillared clays. In the non-calcined so-called precursor pillared clay, layer charge is balanced by the pillaring polycations which in the case of Al pillared clays is the Keggin-like $[\text{Al}_{13}\text{O}_4(\text{OH})_{24}(\text{H}_2\text{O})_{12}]^{7+}$ ion. On calcination this ion is converted into an oxide with the layer charge balanced by the release of an equivalent number of protons, i.e.



The formation of pillars fixed to the layers of the host clay is dependent on the calcination temperature. In general the basal (0 0 1) spacing of the precursor-Al pillared clay decreases to a fixed value upon

Table 1 Pillar type and corresponding basal spacing and surface area for montmorillonite pillared clays

Pillar type	Basal spacing (Å)	Surface area (m ² g ⁻¹)
Alumina	18–19	250–400
Iron oxide	17–18	~ 280
Chromia	19–21	350–400
Zirconia	18–22	250–300
Titania	18–20; 25–29	300–350
Silica	12–13; 16–20	40–200; 150–400
Silica/alumina	16–19	350–500
Titania/silica	38–40	250–400

heating at 500°C. Heating to temperatures up to 400°C causes some contraction but does not prevent re-expansion of the clay upon exposure to moisture. However, the pillared clay obtained by calcination at 500°C usually shows no tendency to expand. This is because in the temperature range 400–500°C an irreversible contraction in the layer spacing occurs, during which the pillars are held within the host aluminosilicate sheets resulting in cross-linked materials. Therefore the precursor pillaring species dehydroxylates progressively on heating to 400°C, releasing protons which migrate into the clay structure and at 500°C condensation takes place of terminal hydroxy groups present on the polymeric ions with the lattice hydroxy groups on the clay. The oxide pillars formed become linked directly via oxygen to the aluminium and magnesium atoms in the octahedral layer resulting in a rigid cross-linked structure resistant to expansion. These changes are illustrated in Figure 5.

The microstructure of pillared clays is controlled by the wet chemistry of synthesis and, to a large

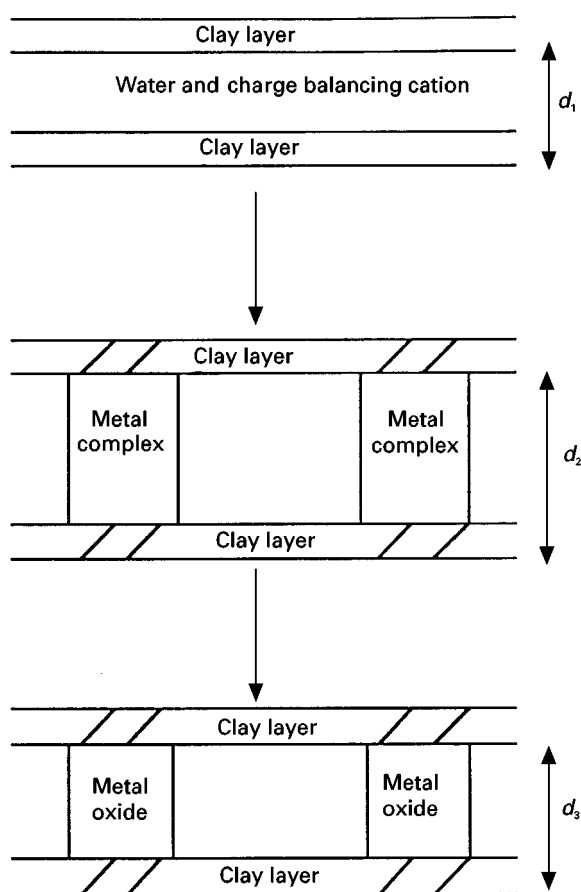


Figure 5 Schematic description of pillaring. In the case of an alumina pillared clay prepared from Ca-montmorillonite, $d_1 = 14.4 \text{ \AA}$, $d_2 = 20.5 \text{ \AA}$, $d_3 = 19.0 \text{ \AA}$.

extent, the method used to dry the precursor pillared clay. The basal spacing of the pillared clays depends on the age of the pillaring reagent, the degree of hydrolysis (polymerization) of the pillaring reagent, the amount of reactants (i.e. Al/clay ratio) and the temperature of pillaring. Pillaring of clays increases their surface area from as low as $30 \text{ m}^2 \text{ g}^{-1}$ to $500 \text{ m}^2 \text{ g}^{-1}$ (Table 1) and generates a microporous structure similar but less constrained than that of zeolites. The volume created can be used for adsorption purposes; the adsorption characteristics are known to vary with the method employed in drying the pillared clay. Air-dried pillared clays are zeolite-like products which cannot adsorb molecules of kinetic diameter 9.2 \AA (e.g. 1,2,5-triethylbenzene) but can adsorb molecules of kinetic diameter 6.0 \AA . Freeze-dried pillared clays can, however, adsorb appreciable amounts of molecules with kinetic diameter of 10.0 \AA . Freeze-dried pillared clays therefore contain a significant fraction of pore openings $> 10.0 \text{ \AA}$ whereas all the pore openings of air-dried pillared clays are $< 9.0 \text{ \AA}$. This is related to the mechanism of layer aggregation during drying. The aggregation may be face to face (for air-dried materials) or edge to face and edge to edge layer contact for freeze-dried materials. Air-dried pillared clays therefore exhibit long range lamellar order with a regular and relatively narrow pore size distribution while freeze-dried pillared clays, on the other hand, exhibit less lamellar order and a broad pore size range.

Metal oxide pillared clays in general tend to possess pores in both the micropore and mesopore size range. The ratio of micropore to mesopore volume largely depends on the interlayer spacing (pillar height) and the interpillar distance. The interpillar distance may be controlled by varying the ion exchange capacity of the host clay; this in turn determines the number of pillaring polycations required to balance the host layer charge. A low exchange capacity favours a low pillar density and vice versa. The interlayer spacing, on the other hand, may be controlled by varying the pillar type. Figure 6 gives a diagrammatic representation of two common pillar types and Table 1 gives some examples of pillar type and basal spacing for montmorillonite clay.

The porosity of pillared clays may also be varied by combining the pillaring process with other treatments such as competitive ion exchange with monocations or acid activation. Indeed acid activation of clays (see below) prior to pillaring yields a different class of materials, generally referred to as pillared acid-activated clays, with quite distinct properties.

An important characteristic of pillared clays (and clays in general) which is in some cases crucial to their

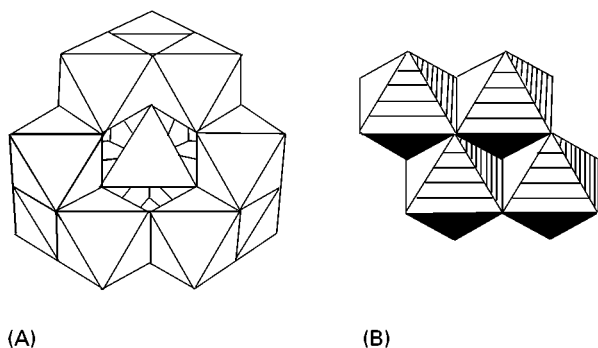
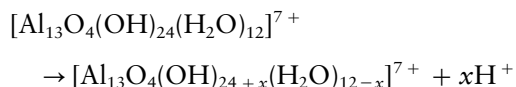


Figure 6 Diagrammatic illustration of polymeric hydroxy-Al (A) and -Ti (B) pillaring cations.

use in separation processes is that they possess considerable acidity and may be classified as solid acids. For example non-calcined precursor-alumina pillared clay possesses Brønsted acidity which arises through the following mechanisms:

1. Polarization of interlamellar water by initial exchangeable cations not replaced by the hydroxy-Al polycations. This is especially the case if the initial exchangeable cation is acidic.
2. The pillaring polymer may hydrolyse to release protons, i.e.

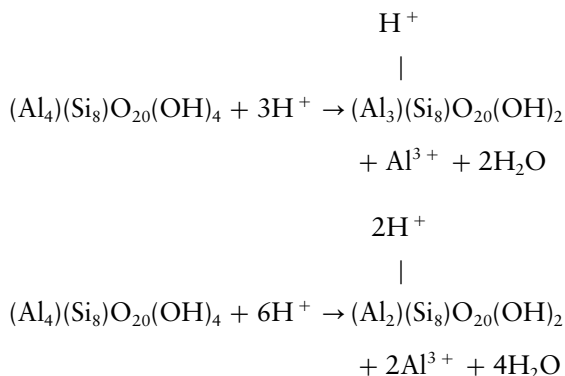


3. The OH groups of the clay lattice and the pillar may also act as Brønsted acid sites.

However, for a pillared clay calcined at temperatures above 400°C, Brønsted acidity is weaker than Lewis acidity. This is due to the migration of protons from the interlayer region into the layer structure where they neutralize the negative layer charge thus removing some Brønsted acid sites.

Acid activated clays When ‘activatable’ clay minerals are treated in acid, their chemical composition and physical properties are altered. The activation process enhances properties already present in the clay minerals and gives them certain desirable properties with respect to their applicability as adsorbents and catalysts. The clays of choice for acid activation are non-swelling bentonites containing montmorillonite as the major component. In general terms the acid activation of montmorillonites proceeds via the removal of octahedral ions and any isomorphously substituted tetrahedral ions. The changes that take place in an idealized montmorillonite with no isomorphous substitution may be

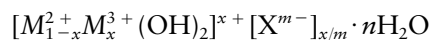
expressed as:



Layer Double Hydroxides (LDH)

Natural layer double hydroxides (or hydrotalcite-like compounds as they are sometimes called) are, unlike clay minerals, relatively rare. Where they occur they are associated with metamorphic rock formations or saline deposits. The structure of LDHs is very similar to that of brucite, $\text{Mg}(\text{OH})_2$, in which magnesium is octahedrally surrounded by six oxygen atoms in the form of hydroxide with the octahedral units extending to form infinite sheets through edge sharing. If some of the magnesium in the sheets is isomorphously substituted by a higher charge cation such as Al^{3+} , the resulting $\text{Mg}^{2+}-\text{Al}^{3+}-\text{OH}$ layer gains a positive charge. Sorption of an equivalent amount of hydrated anions occurs so as to maintain electrical neutrality; in nature the charge-balancing hydrated anion is usually carbonate. The OH groups of the positively charged brucite-like sheet are linked to the CO_3^{2-} groups either directly (via $\text{OH}-\text{CO}_3-\text{HO}$ linkages) or via intermediate water (i.e. $\text{OH}-\text{H}_2\text{O}-\text{CO}_3-\text{HO}$). The interlayer carbonate anions adopt an orientation parallel to the layers, i.e. they lie flat surrounded by loosely bound water (Figure 7). The resulting natural LDH may exist in either of two dimorphic forms, i.e. as a rhombohedral hydrotalcite or a hexagonal manasseite.

LDHs may be described by the general formula



where M represents a metal cation and X represents an anion. M^{2+} may be Mg^{2+} , Fe^{2+} , Co^{2+} , Ni^{2+} , Zn^{2+} and M^{3+} may be Al^{3+} , Cr^{3+} or Fe^{3+} . M^{2+}/M^{3+} ratios between 1 and 5 are possible but are typically $0.25 \leq x \leq 0.33$ and $0 \leq n \leq 6$. Synthetically there is a wide range of variables such as: (i) different combinations of M^{2+} and M^{3+} ; (ii) different charge balancing anions; (iii) different amounts of interlayer water; and (iv) crystal morphology and size. To form LDHs, the M^{2+} and M^{3+} cations must be of a size that can be contained in

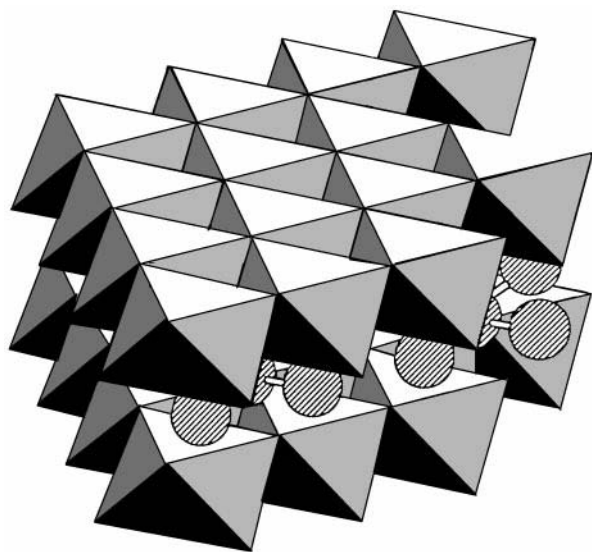


Figure 7 Illustration of the top view of LDH ($\text{Mg}_6\text{Al}(\text{OH})_{16}\text{CO}_3 \cdot 4\text{H}_2\text{O}$) lattice.

the holes (octahedral sites) between the close-packed OH groups in the brucite-like layers. This limits the possibilities to cations of ionic size between 0.5 and 0.8 Å and, in the main, excludes cations such as Be^{2+} (0.35 Å), Ca^{2+} (0.99 Å) and Cd^{2+} (0.97 Å). The formation of LDHs is not, however, limited to $\text{M}^{2+}/\text{M}^{3+}$ cations; it is, for example, possible to incorporate monovalent cations (M^+) such as Li^+ in a Li/Al material, or to have divalent/tetravalent materials such as Co/Ti.

The number of exchangeable anions in LDHs depends on the charge density on the host layers. However there are no particular restrictions on the nature of the anion. Inorganic charge-balancing anions include Cl^- , OH^- , NO_3^- , ClO_4^- and SO_4^{2-} . Organic acids such as adipic, succinic, oxalic, malonic, sebacic and terephthalic may also serve as charge-balancing species. However, as mentioned above, nature favours the carbonate ion which is tenaciously held in the interlayer region due to its relatively high polarizability and synthesis of pure LDHs with other anions requires special preparation procedures (see below). LDHs may undergo swelling in a manner not unlike that of silicate clays. For example sulfate-containing LDH may be solvated with glycol or glycerol. In general swelling of LDHs depends on the nature of the interlayer anion (charge, mass, structure), nature of the solvent (polarity, molecular dimensions) and of course the layer charge.

Pillared Layer Double Hydroxides

Pillared LDHs which possess empty interlayer/inter-pillar space are desirable but unlike pillared clays

are difficult to prepare. The difficulty is largely due to the affinity of the layers for the carbonate anion; if CO_2 is present during synthesis, the carbonate is preferentially incorporated and once in the interlayer it is held tenaciously and not easily replaced. Most of the pillaring strategies employ a CO_2 -free environment and make use of the fact that Cl^- or NO_3^- anions are easier to displace. Thus the Cl^- or NO_3^- LDH is prepared, usually under nitrogen, and these anions are then replaced with larger polyoxometalate anions such as, for example, $\text{V}_{10}\text{O}_{28}^{6-}$, $\text{Ta}_6\text{O}_{18}\text{OH}^{7-}$, $\text{Nb}_6\text{O}_{18}\text{OH}^{7-}$. Another approach has relied on the use of LDH initially synthesized with large intercalated organic anions, for example the terephthalate dianion (Figure 8) as the interlayer species. The organic anion is then displaced by the polyoxometalate species. As in clays, the pillaring of LDHs results in an increase in surface area and pore volume. The increases are however lower than in pillared clays. This is due to the high layer charge in LDHs which leads to a high pillar density which in some cases yields materials in which the pillars are 'stuffed' into the LDH and do not exist as isolated discrete pillars. An example is polyvanadate-intercalated LDH which has a surface area of *ca.* $35 \text{ m}^2 \text{ g}^{-1}$ compared to $25 \text{ m}^2 \text{ g}^{-1}$ for the unpillared material. True pillaring does occur as in the case of $\text{Zn}_2\text{Al}[\alpha\text{-SiV}_3\text{W}_9\text{O}_{40}]$ which exhibits a surface area of $155 \text{ m}^2 \text{ g}^{-1}$.

Applications of Pillared (or Intercalated) Layered Solids

The applications of expanded layered solids (LDHs or clays) are largely due to their large surface area and variation in their chemical and physical properties. These properties may be enhanced by the ability to

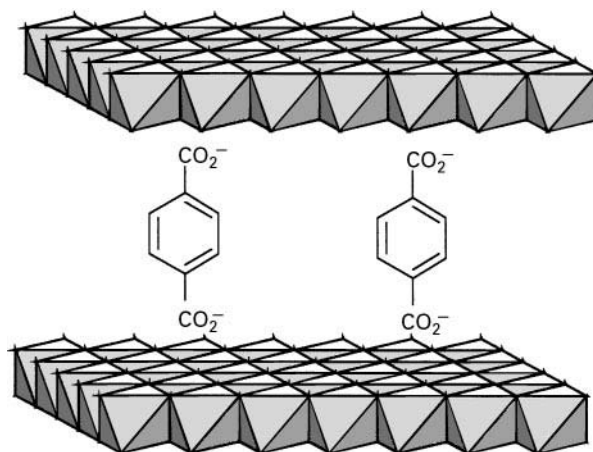


Figure 8 Illustration of terephthalate intercalated LDH.

tailor them for specific uses. In general these materials have found use as catalysts, ion exchangers and adsorbents and are also useful in gas and liquid separation processes (where they exhibit molecular sieving properties similar to those of zeolites). Some examples are:

1. Organoclays containing molecules such as $(\text{CH}_3)_4\text{N}^+$ are especially suited for certain separation processes due to their hydrophobic nature and high affinity for certain organic compounds.
2. Clays and their oxide-pillared derivatives have found use as: (i) scavengers for hazardous organics (especially from effluent streams); (ii) selective adsorbents of heavy metals from effluent streams; and (iii) purifiers for edible oils where the clays adsorb compounds such as carotenoids and chlorophyll to give the oil its clear look and taste. Indeed acid activated clays are the industry standard for the decolorizing of oil.
3. LDHs have found use as excellent acid residue scavengers.

Greater use of layered materials in separation processes can be achieved when the materials are used in the form of membranes where they act as ionic and molecular filters or sieves.

See also: **II/Ion Exchange**: Historical Development; Novel Layered Materials: Phosphates; Organic Ion Exchangers; Organic Membranes.

Further Reading

- Barrer RM (1978) *Zeolites and Clay Minerals as Sorbents and Molecular Sieves*. London: Academic Press.
- Bein T (ed.) (1992) *Supramolecular Architecture: Synthetic Control in Thin Films and Solids*. ACS Symposia Series, vol. 499.
- Dresselhaus MS (ed.) (1986) *Intercalation in Layered Materials*. New York: Plenum Press.
- Dresselhaus MS, Dresselhaus G, Fischer JE and Moran MJ (eds) (1983) *Intercalated Graphite*. MRS Symposia Proceedings, vol. 20.
- Lévy F (ed.) (1976) *Crystallography and Crystal Chemistry of Materials with Layered Structures*. Dordrecht: Reidel.
- Lévy F (ed.) (1976) *Structural Chemistry of Layer-type Phases*. Dordrecht: Reidel.
- Lévy FA (ed.) (1979) *Intercalated Layered Materials*. Dordrecht: Reidel.
- Lieth RMA (ed.) (1977) *Preparation and Crystal Growth of Materials with Layered Structures*. Dordrecht: Reidel.
- Mitchell IV (ed.) (1990) *Pillared Layered Structures: Current Trends and Applications*. London: Elsevier.
- Newman ACD (ed.) (1990) *Chemistry of Clays and Clay Minerals*, 2nd edn. London: Longman and Mineralogical Society.
- Birch R (1988) Pillared clays. *Catalysis Today* 2.
- Sequeira CAC and Hudson MJ (eds) (1992) *Multifunctional Mesoporous Inorganic Solids*. Dordrecht: Kluwer.
- Whittingham MS and Jacobson AJ (eds) (1982) *Intercalation Chemistry*. London: Academic Press.
- Yamagishi A, Amarita A and Taniguchi M (eds) (1998) *The Latest Frontiers of the Clay Chemistry*. Sendai: Smectite Forum of Japan.

Organic Ion Exchangers

C. Luca, 'Petra Poni' Institute of
Macromolecular Chemistry, Lasi, Romania

Copyright © 2000 Academic Press

Abstract

The definition and some characteristic concepts regarding organic ion exchangers are pointed out. The development of these ion exchangers, beginning with chemically modified natural products and continuing with the synthetic ones, is further presented. A classification of organic ion exchangers is proposed according to several criteria, such as the synthesis method, morphology of the three-dimensional network, their physical shape and the nature of their functional groups.

Of the general characteristics of organic ion exchangers only the exchange capacity and selectivity are briefly discussed.

Preparation and structure – chemical property relationships, and some applications with reference to strong and weak cation and anion exchangers, as well as to chelating ion exchangers – are described in more depth.

Definition

An ion exchanger generally is a solid, insoluble material that contains groups which ionize in aqueous medium.

Organic ion exchangers are three-dimensional covalent networks that contain exchangeable ions associated with fixed acid or basic groups. The term 'ion exchange resins' is also used to describe organic ion exchangers.

The ion exchangers that have fixed acid groups and carry exchangeable cations (usually H^+ or Na^+) are cation exchangers described as in the H form and Na

form, respectively. Those with fixed base groups and exchangeable anions (OH^- or Cl^-) are anion exchangers in the OH form and Cl form, respectively.

In the accepted terminology, the three-dimensional network with the fixed groups is called the matrix or framework and exchangeable ions of opposite sign, which neutralize the fixed ionic groups, are the counter-ions that are responsible for the ion exchange process.

Co-ions are mobile ions having the same sign as the fixed charges of the matrix. In fact, organic ion exchangers are crosslinked polyelectrolytes. Thus, a cation exchanger is an anionic polyelectrolyte while an anion exchanger can be regarded as a cationic polyelectrolyte.

General Aspects

The first organic ion exchanger that found technical application was a chemically modified natural product, namely a sulfonated coal, described in many patents during the 1930s.

Other exchangers were synthesized by sulfonation or phosphorylation of wood, paper, cotton, lignin and tannins, as well as by the crosslinking of pectins with formaldehyde or epichlorhydrin.

In 1935 the discovery by Adams and Holmes of ion exchange properties in the product of a reaction between phenol, or *m*-phenylenediamine, with formaldehyde started the development of synthetic organic ion exchangers. These products have a greater importance than those from a natural organic source and have found much wider technical application because of their greater chemical stability and mechanical strength as well as their very different physical and chemical structures.

Synthetic organic ion exchangers are obtained by the two principal reactions used to produce polymeric materials, namely polycondensation or addition polymerization of a mixture of co-monomers. In polycondensation, incorporation of a trifunctional co-monomer is required while in polymerization the presence of a bifunctional co-monomer is sufficient.

Most commercially available ion exchangers are from polymerization processes which create structures with higher hydrolytic and oxidative stabilities as well as better defined physical features and cross-linkings.

In the case of the polycondensation exchangers, the reaction between a co-monomer that carries base or acid groups and a crosslinking agent (formaldehyde, epichlorohydrine, etc.) is used.

In 1944, D'Alelio found that sulfonated styrene-divinylbenzene copolymers have ion exchange

properties. This finding was the beginning of the polymerization ion exchangers.

These structures are made by the polymerization of a mixture of a monovinyllic monomer with a basic or acidic group and a divinyllic monomer. The achievement of a neutral network, called the precursor or starting material, followed by the introduction of basic or acidic groups by suitable polymer-analogous reactions, is often preferred.

Usually divinylbenzene (DVB) is used as the divinyllic monomer and the quantity added, in terms of the percentage in the mixture of co-monomers, defines the degree of crosslinking of the network, although crosslinking side reactions can occur during the polymer-analogous transformations.

The structures created are called 'conventional' or 'gel'-type ion exchangers and generally have about 8% DVB for crosslinking. This amount is required to achieve a network with both mechanical strength and easy diffusion of exchangeable ions as the exchanger comes into contact with an aqueous phase when swelling of the network occurs.

Meitzner and Oline found that the copolymerization of styrene with DVB in the presence of an appropriate inert compound, called 'diluent' or 'porogene agent', gave a network with significant and measurable physical porosity in the dried state, generally containing internal pores having diameters larger than 3×10^{-9} m. This discovery led to significant progress in the field of synthetic ion exchangers, namely the development of macroporous resins. These exchangers offer the advantage that they can be used with non-aqueous solvents and have much higher sorption rates of ions and non-electrolytes than the conventional gel exchangers.

Polymerization produces exchangers in bead form, with a relatively wide distribution of size, by the suspension polymerization technique. More recently ion exchangers with uniform and controlled bead size have become available.

The polycondensation exchangers often appear as irregular-shaped particles, because they are made by bulk polycondensation followed by grinding of the bulk polymer into smaller particles. However, polycondensation exchangers can also be made in bead form by reverse-phase suspension polycondensation.

Ion exchangers in fibre form are also known, made by chemical modification of natural and synthetic fibres. Ion exchanger fibres have an improved kinetic performance when compared with the same structures in bead form.

Classification

Scheme 1 is a summary of the classification of organic ion exchangers. **Table 1** shows the most used



Scheme 1 Classification of organic ion exchangers.

acid and base functional groups on organic ion exchangers.

Characterization

Ion exchange capacity is the most appropriate characteristic of organic ion exchangers.

The total capacity indicates the number of fixed acidic or basic groups per specified amount of ion exchanger. It can be described as both weight capacity and volume capacity, having as units milliequivalents per gram of dry exchanger (meq g^{-1}) and milliequivalents per cubic centimetre of fully swollen exchanger (meq cm^{-3}), respectively. If not

otherwise stated, the capacity should be reported per gram of H form for a cation exchanger or the Cl form for an anion exchanger in the dry state. This capacity is a constant for the material and does not depend on the experimental conditions.

The effective capacity is the number of exchangeable counter-ions per specified amount of exchanger (the same units are used as above). This capacity depends on the experimental conditions and is lower than total capacity.

Another important characteristic is the selectivity which has a major role in the ion exchange processes. The selectivity is the preference of an ion exchanger for a particular counter-ion over the others, when it is

Table 1 Types of ion exchangers and their functional groups

Type	Name of fixed functional group	Chemical structure of functional group
Cation exchangers		
Strong acid	Aryl sulfonic	$-\text{C}_6\text{H}_5-\text{SO}_3\text{H}$
Weak acid	Carboxylic acid	$-\text{COOH}$
	Phenolic hydroxyl	$-\text{C}_6\text{H}_5-\text{OH}$
Intermediate acid	Phosphonic	$-\text{P}(\text{O})(\text{OH})_2$
	Phosphonous	$-\text{P}(\text{O})\text{H}(\text{OH})$
	Phosphoric	$-\text{O}-\text{P}(\text{O})(\text{OH})_2$
Anion exchangers		
Strong base	Quaternary ammonium	$-\text{N}^+$
	Phosphonium	$-\text{P}^+$
	Sulfonium	$-\text{S}^+$
Weak base	Primary amine	$-\text{NH}_2$
	Secondary amine	$-\text{NHR}$
	Tertiary amine	$-\text{NR}_2$
Amphoteric exchangers	Mixture of acid and base groups	

in contact with an electrolyte solution. The selectivity has various physical causes.

An ion exchanger tends to prefer a counter-ion with higher valence, lower solvation, higher polarizability, stronger interactions with the fixed groups or the matrix, and less participation in complex formation with the co-ions. The selectivity of an ion exchanger is improved by increasing degree of crosslinking and by decreasing solution concentration and temperature.

Types of Synthetic Organic Ion Exchangers

Strong Acid Cation Exchangers

The most important strong acid cation exchangers are those of arylsulfonic acid type.

Polycondensation structures of this type can be obtained as follows:

1. By the sulfonation of a phenol followed by the condensation of the sulfonated product with formaldehyde.
2. By the sulfonation of a preformed phenol-formaldehyde three-dimensional network.

In the first method, the addition of unsulfonated phenol to provide the trifunctionality is essential. The structures created are illustrated in **Figure 1**.

A method for the synthesis of sulfonated condensation exchangers in bead form has been developed using organic solvents as dispersion media. This is an

alternative to the grinding of bulk polymers as previously mentioned.

Most commercially available strong acid cation exchangers are those based on styrene-DVB copolymers with different morphologies of their three-dimensional networks. These products have higher capacities and better durabilities than their polycondensation predecessors. The common method for the production of these structures consists in sulfonation of the styrene-DVB copolymers with sulfonation agents such as sulfuric acid, sulfur trioxide, oleum or chlorosulfonic acid.

From the point of view of the mechanism, the sulfonation is an electrophilic substitution into an aromatic ring whereby the $-\text{SO}_3\text{H}$ group is attached in the *para*-position and a double sulfonation is probably impossible because of steric hindrance due to the polymer chain.

During the sulfonation reactions, crosslinking side reactions take place independent of the sulfonating agent, however chlorosulfonic acid apparently leads to the most crosslinks.

Side crosslinks are due to the inter-chain sulfone bridges that appear by reaction between the already attached $-\text{SO}_3\text{H}$ groups and the unreacted aromatic rings. Intra-chain sulfone bridges also can appear. The chemical structure of a sulfonated styrene-DVB copolymer is illustrated in **Figure 2**.

The pre-swelling with organic solvents of the copolymer beads before sulfonation reduces the number of sulfone bridges.

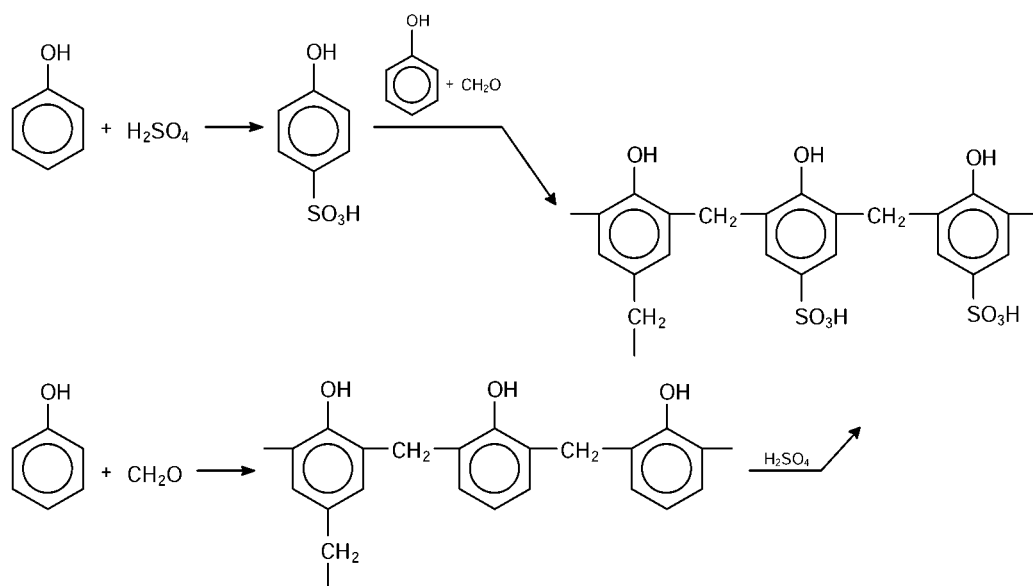


Figure 1 Preparation of sulfonated phenol-formaldehyde cation exchangers.

Addition to the styrene-DVB mixture of small amounts of a polar monomer, such as acrylonitrile, vinylpyridine, etc., improves the physical properties of the resultant ion exchanger – especially its resistance to osmotic shock because of the more uniform sulfonation reaction.

Sulfonations with the agents previously mentioned show some differences. Thus, reaction with sulfuric acid used the acid itself as a reaction medium hence a considerable excess of reagent is required. Reactions with chlorosulfonic acid or sulfur trioxide may be performed in an organic solvent, thus they need only a small excess of reagent over the stoichiometric quantities.

Sulfonations with the latter reagents take place at lower temperatures than with sulfuric acid which requires a temperature at about 100°C.

Post-sulfonation treatment of the sulfonated products is important to maintain whole beads. This can be achieved by the prevention of the changes that determine swelling, called ‘osmotic shock’, which leads to the disintegration of the beads. The gradual addition of water, or aqueous electrolyte solutions, decreases this deleterious effect.

Macroporous copolymer beads, because of their large internal surface areas, have a higher reactivity towards the sulfonation agents. They also require much lower quantities of organic swelling solvent, and are less susceptible to degradation by osmotic shock, both during preparation and in subsequent usage. In addition, they have a higher oxidation stability than the sulfonated structures of the gel type.

Strong acid cation gel-type exchangers have received major attention because of their utility in

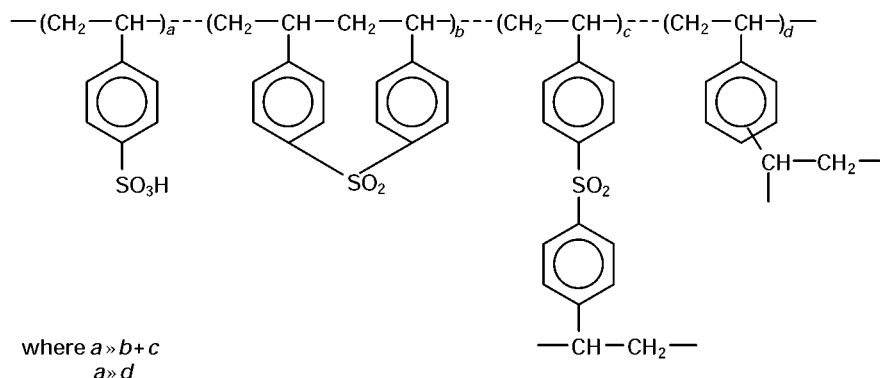


Figure 2 Chemical structure of sulfonated styrene-DVB copolymer-based cation exchanger.

water softening which is their principal use. The equivalent macroporous structures can also be used as catalysts for certain reactions, particularly in non-aqueous media, instead of sulfuric and toluene-4-sulfonic acids. The resin catalysts show some advantages compared to low molecular weight acids, such as in their regeneration and potential reuse.

Because of their very high acidity, the aryl-SO₃H groups are fully ionized throughout the pH domain of aqueous solutions. The very low preference of the sulfonic-type cation exchanger for the H ion requires the use of large quantities of mineral acids for its regeneration to the H form after the exhaustion cycle, especially in water treatment processes.

The strong acid exchanger in its H form participates in ion exchange reactions with bases like NaOH and with alkaline or neutral salts. The latter reaction is called 'salt-splitting'.

Weak Acid Cation Exchangers

The polycondensation exchangers can be prepared by the reaction of salicylic acid, or 1,3,5-resorcylic acid, with formaldehyde. In the former case, the addition of phenol is required because one *ortho*-position is not accessible to the aldehyde.

Several polymerization networks that contain -COOH groups are known. Some structures together with their preparative routes are illustrated in Figure 3. Only those with acrylic networks are commercially available.

Compared with the sulfonic group the -COOH group, has a much lower acidity and is fully ionized only in an alkaline medium as a salt form. The -COOH group also shows a very considerable preference for the H ion, unlike the -SO₃H group. This situation leads to easy regeneration of the weak acid exchangers from salt form to H form using stoichiometric quantities of mineral acids. These exchangers can react only with bases, like NaOH, and alkaline salts; they show a strong preference for Ca and Mg cations. The 'salt-splitting' reactions do not take place in the case of the weak acid cation exchangers.

The acrylic-type exchangers have a higher acidity than the methacrylic ones and can be used for the treatment of hard water containing large quantities of bicarbonates. The methacrylic type is used for special applications, such as the purification of antibiotics, where a mild pH is required.

Strong Base Anion Exchangers

Strong base anion exchangers are known only as polymerization products. Those with quaternary ammonium groups are the most common commercially

available exchangers. Their preparation is performed by the chloromethylation of gel- or macroporous-type styrene-DVB copolymers in bead form, followed by the amination of the chloromethylated copolymers with trimethylamine or dimethylethanolamine leading to the so-called strong base anion exchangers of Types I and II, respectively. Their chemical structures are shown in Figure 4.

Usually the chloromethylation is carried out with monochloromethyl ether, in the presence of a Lewis acid (ZnCl₂, AlCl₃, SnCl₄, etc.) as catalyst. The reaction takes place under mild conditions: temperature about 50°C and reaction times of 5–8 h. Generally, the -CH₂Cl groups are attached to over 90% of the *para*-positions of the styrene aromatic rings, following the chloromethylation of the mono alkylbenzene derivatives.

The main chloromethylation reaction is usually accompanied by a side alkylation reaction between pre-attached -CH₂Cl groups and non-functionalized aromatic rings. Such a side reaction determines inter-chain and/or intra-chain methylene bridges that decrease the amount of -CH₂Cl groups as well as the swelling capacity of the chloromethylated product. The latter aspect is especially prevalent in the case of gel-type copolymers. In most cases, the styrene-DVB macroporous networks show a reduction of their specific area and of the volume of their pores after chloromethylation, but an increase of the average diameter of the pores can be observed.

The use of a large excess of chloromethyl methyl ether or mixtures of chloroform or carbon tetrachloride with the halogenated ether reduces the side reaction.

An alternative route to obtain the chloromethylated styrene-DVB network is via the free-radical polymerization of chloromethylstyrene (vinylbenzyl chloride) with divinylbenzene. The first monomer is a 60 : 40 mixture of *meta*- : *para*-isomers.

The chemical structures of the two crosslinked polystyrene-based chloromethylated compounds or products are illustrated in Figures 5A and B. From these two figures one can see that the chloromethylstyrene-DVB copolymer (Figure 5A) has a more homogeneous chemical structure than the chloromethylated styrene-DVB copolymer (Figure 5B), but the former structure has the drawback of a much higher cost. For this reason chloromethylated styrene-DVB copolymers are chosen as the precursors to polystyrene-based anion exchangers.

Aminations of the chloromethylated styrene-DVB copolymers with trimethylamine and dimethylethanolamine take place easily, because the benzylic chlorine structure has a very high reactivity towards these nucleophilic reagents. Amination is performed

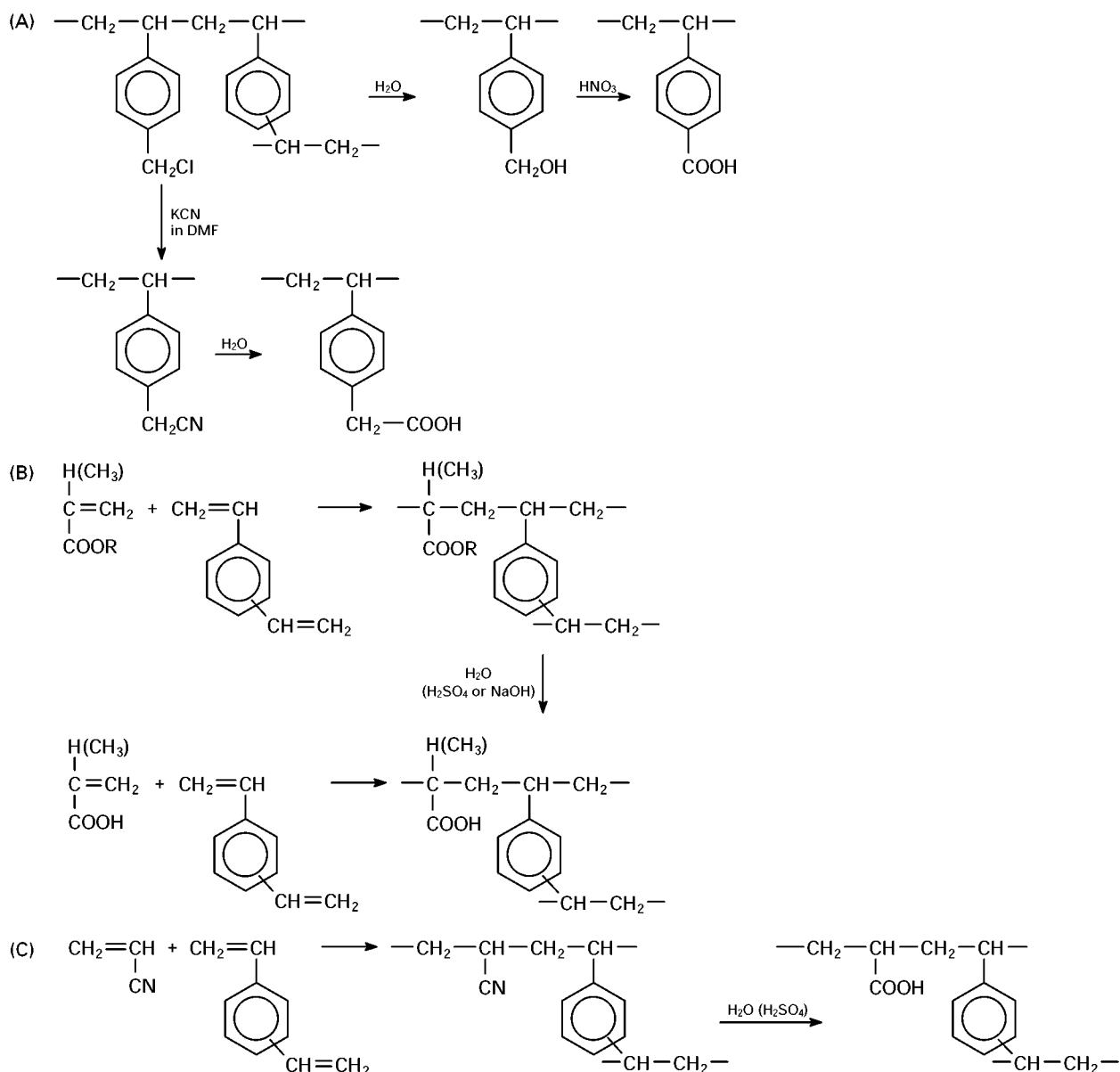


Figure 3 Some methods for the preparation of weak acid cation exchangers.

in organic or aqueous media, at a temperature of about 40–50°C, and reaction times of 6–8 h. It must also be mentioned that amination with the two amines, in contrast to the chloromethylation reaction, does not lead to crosslinking side reactions. When the reactions are carried out in water, a side reaction can occur at a very low level from the hydrolysis of a small number of $\text{—CH}_2\text{Cl}$ groups.

The chemical structures of strong base anion exchangers of Types I and II are not very stable in alkaline media because of the well-known Hofmann degradation, a property of quaternary ammonium compounds; the Type II displays a lower stability in alkaline media than Type I.

Hofmann degradation of the two structures takes place according to **Figure 6**. The degradation can lead to both loss of exchange capacity (routes A and A' in **Figure 6**) and the appearance of a weak base capacity caused by the presence of tertiary amine groups (B, B' and C in **Figure 6**).

Strong base anion exchangers have a lower thermal stability than the cation exchangers.

Other commercially available strong base exchangers are those formed with an acrylic matrix. They are usually made in bead form by free-radical polymerization of 3-dimethylaminopropyl methacrylamide with DVB followed by a quaternization reaction of the copolymer with alkyl halides as shown

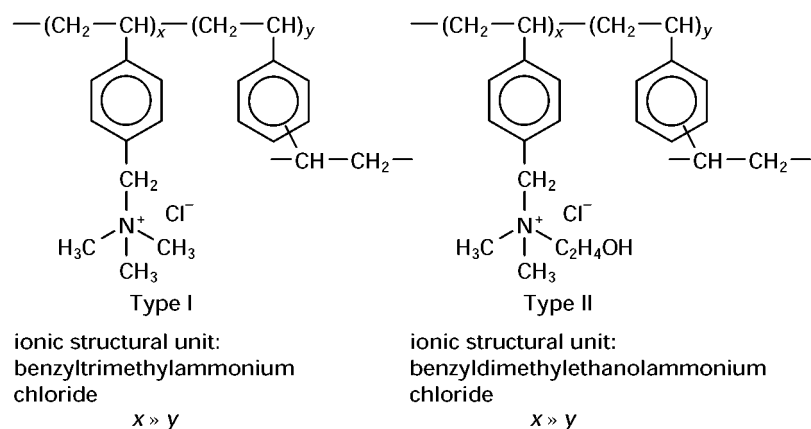


Figure 4 Classical structures of the structural units of Type I and Type II strong base anion exchangers.

in Figure 7. For the quaternization, gel- or macroporous-type copolymers can be used.

Generally, the acrylic strong base anion exchangers have a lower stability to hydrolysis, especially under acid or alkaline conditions, compared to the polystyrene-based exchangers. The hydrolysis becomes more significant when the spacer between the amide group and the quaternary group decreases in size. Thus, the product with a spacer of only one methylene group between the two functional groups has hydrolytic instability. The same phenomenon occurs in the anion exchanger prepared from 3-dimethylaminopropyl methacrylate, $\text{CH}_2=\text{C}(\text{CH}_3)\text{COO}(\text{CH}_2)_3\text{N}(\text{CH}_3)_2$, instead of the amide monomer.

In addition to the strong base anion exchangers previously presented as commercially available products, other specialized strong base exchangers are known.

In an effort to develop anion exchangers with preference for the NO_3^- anion over the SO_4^{2-} anion (an important factor for nitrate removal from potable water which invariably contains sulfate), the design of such a structure was conceived. It is the reaction product of the chloromethylated styrene-DVB copolymer with triethylamine, and can be described as a strong base anion exchanger of Type III.

Gel or macroporous 4-vinylpyridine-DVB copolymers are the precursors for strong base

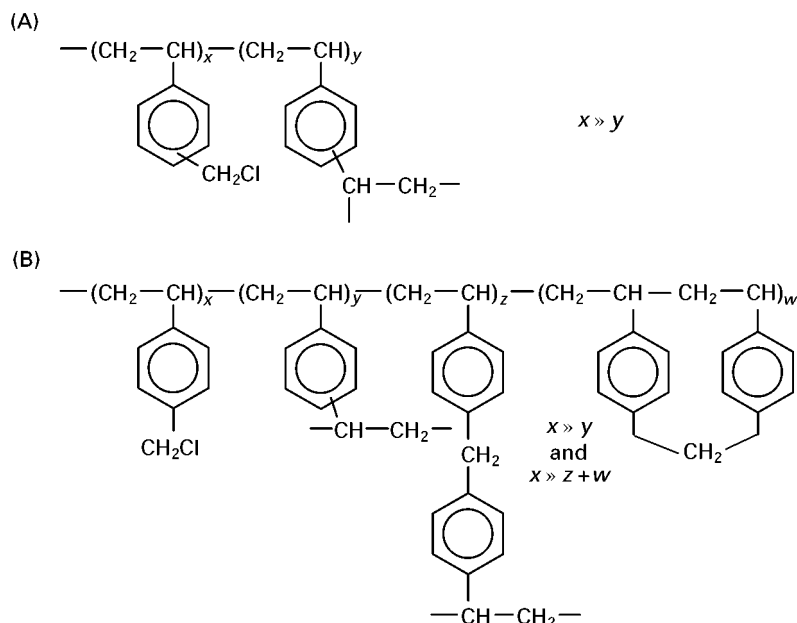


Figure 5 The two crosslinked polystyrene-based chloromethylated structures.

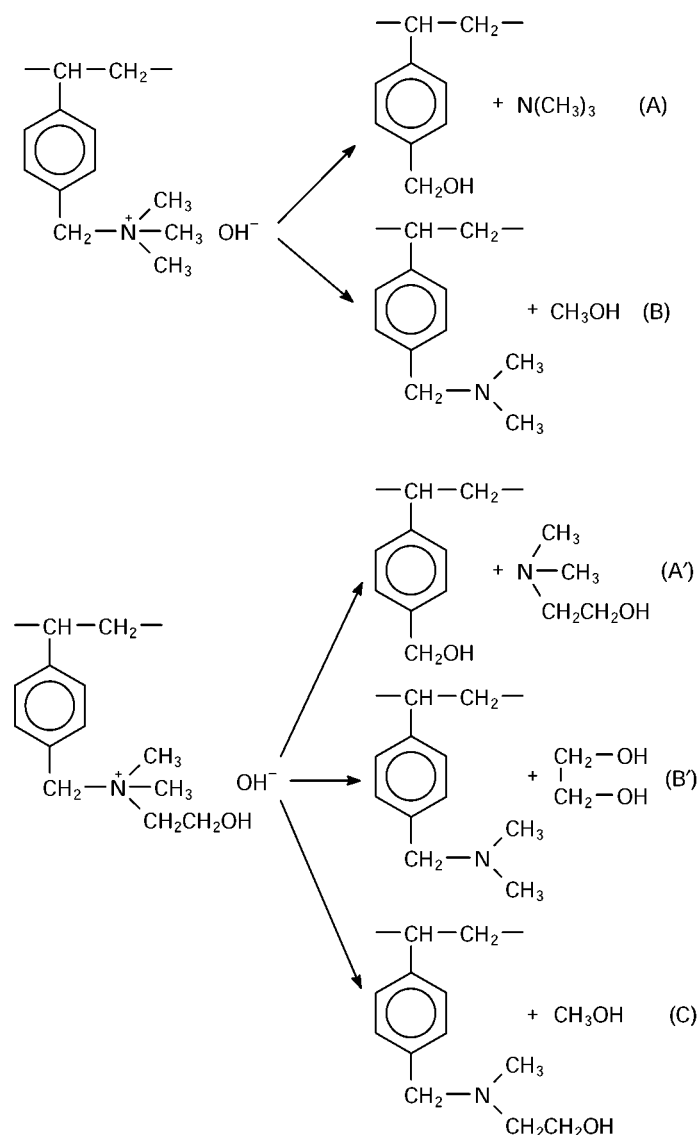


Figure 6 Hofmann degradation of Type I and Type II strong base anion exchangers.

exchangers. These exchangers are made by the well-known quaternization reaction with alkyl halides as shown in **Figure 8**.

The synthesis of this category of anion exchangers takes place by a single chemical transformation step which avoids crosslinking side reactions. However, these exchangers cannot be utilized in many fields of application because of their very low chemical stability in alkaline media.

Ion exchangers with benzyltrialkylphosphonium groups, especially benzyltri-*n*-butylphosphonium halide can be made. These structures are not used in ion exchange processes but have special applications as phase-transfer catalysts. For the improvement of their properties, structures with a spacer larger than one methylene group between the aromatic ring and

the phosphonium group have been synthesized. **Figure 9** shows the phosphonium-type structures and their preparative routes.

Commercially available exchangers of Types I and II are fully ionized in the whole pH domain of the aqueous medium, like the strong acid ones. The Type I exchanger is such a strong base that a considerable quantity of NaOH is required for its regeneration in the OH form, while the Type II exchanger, a weaker base, requires less. This aspect is an advantage of the Type II structure over Type I.

The strong base anion exchangers in their OH form react with both strong and weak acids. With the latter, the strong base anion exchanger of Type I is more effective than Type II. Because of this situation, Type I exchangers are used for soluble and

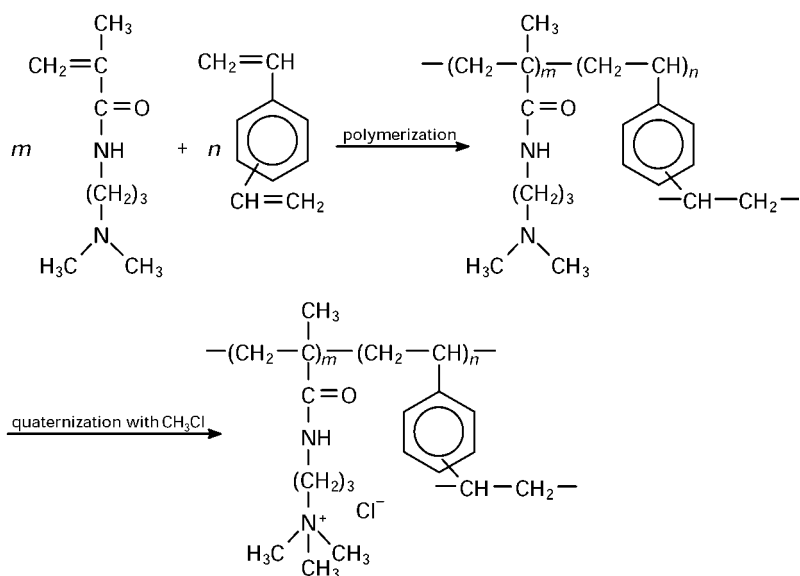


Figure 7 Preparation of an acrylic strong base anion exchanger.

colloidal silica removal from natural waters. For removal of the colloidal silica only, Type I strong base anion exchangers with special macroporous structures are effective.

Certain Type I strong base exchangers in their Cl form are used for adsorption of ionic organic compounds and are called 'scavenger' ion exchangers.

Weak Base Anion Exchangers

Commercial weak base anion exchangers are prepared by the condensation of *m*-phenylenediamine

with formaldehyde. The chemical structure of this exchanger is illustrated in **Figure 10**. In this structure, the amine groups directly attached to benzene rings have a very low basicity.

Polycondensation weak base exchangers with higher basicity were later obtained by the condensation of other reagents. An example is the epoxy structures formed by the condensation of aliphatic polyamines with epichlorohydrin. This halo-epoxy compound can react even with tertiary amine groups, thus anion exchangers containing amine and quaternary ammonium groups can be obtained as shown in **Figure 11**.

The most readily available commercial weak base exchangers are the polymerization structures based on polystyrene or acrylic matrices containing primary, secondary or tertiary amine groups, or all these groups together.

The polystyrene-based weak base exchangers are obtained by the same reaction scheme as the strong base ones with polystyrene matrices, but with the difference that dimethylamine is used in the amination step instead of trimethylamine or dimethylethanolamine. When using the secondary amine, in contrast with the tertiary amines, besides the main amination reaction which leads to the tertiary amine groups, an undesirable side reaction can also take place. This is the quaternization reaction between the pre-attached tertiary amine and $-\text{CH}_2\text{Cl}$ groups. It can take place intra- or inter-chain but both situations can occur.

The chemical structures of aminated units are shown in **Figure 12**. Both quaternization types (inter- and intra-chain) lead to anion exchangers with mixed

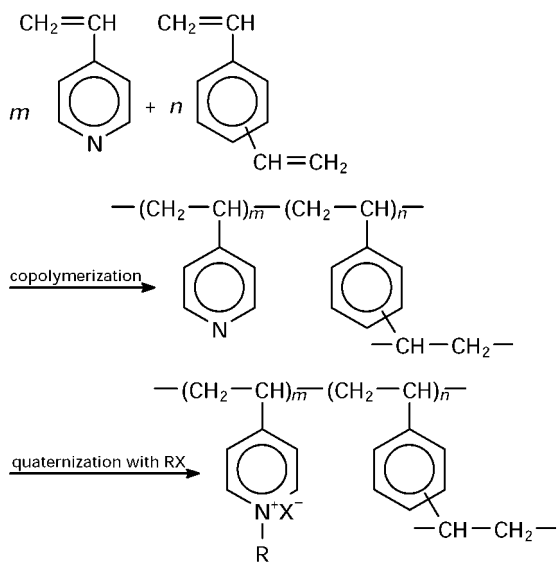


Figure 8 Preparation of strong base anion exchangers based on 4-vinylpyridine-DVB copolymer.

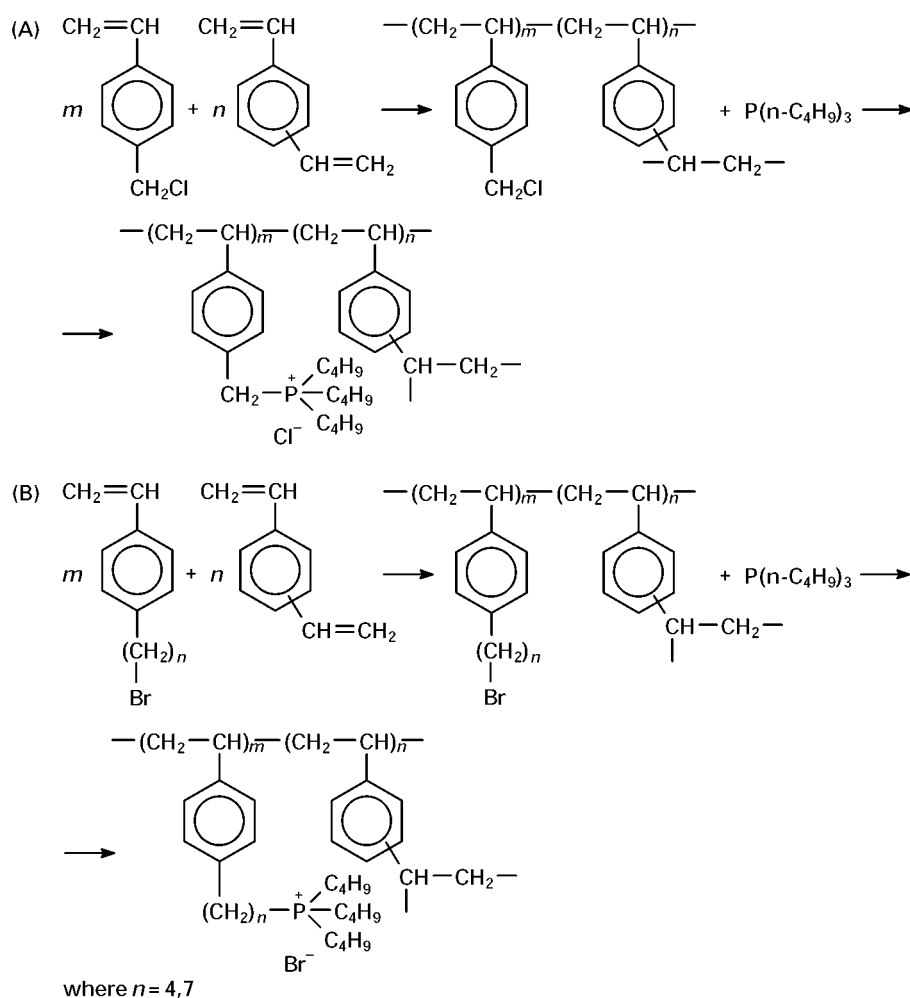


Figure 9 Preparation methods of phosphonium-type strong base anion exchangers.

functional groups and the inter-chain ones also control the degree of crosslinking.

Amination takes place quantitatively under mild conditions (30–40°C; 4–6 h) in aqueous or organic media. By using a large excess of amine, the side quaternization reaction is greatly reduced.

The most common acrylic weak base exchangers are made by the acylation of primary or secondary amines. This reaction with esters, so-called ester

aminolysis, is the most frequently used method to produce acrylic weak base exchangers.

The aminolysis of macroporous or gel-type ethyl acrylate–DVB copolymers, in bead form, with 3-dimethylamino-1-propylamine, ethylenediamine or other aliphatic polyamines, is illustrated in **Figure 13**.

The same structures can also arise from aminolysis–hydrolysis reactions of acrylonitrile–DVB copolymers. An example is shown in **Figure 14**.

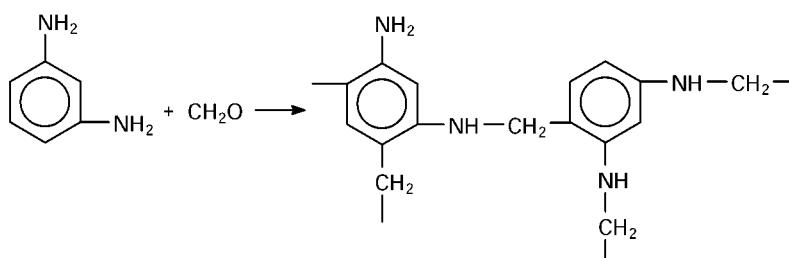


Figure 10 Chemical structure of *m*-phenylenediamine–formaldehyde weak base anion exchanger.

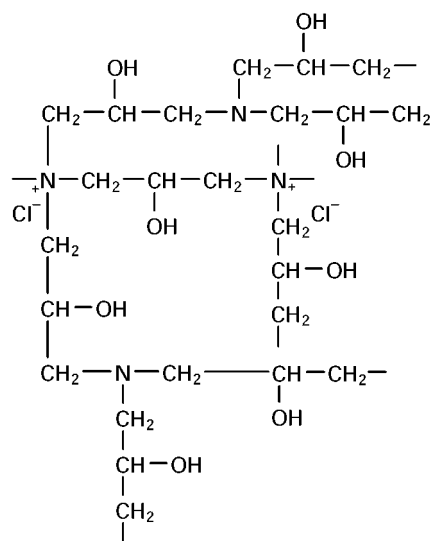


Figure 11 Chemical structure of an epoxy-type base anion exchanger.

The aminolysis and aminolysis-hydrolysis reactions take place under more stringent reaction conditions (temperature over 100°C and reaction time over 10 h) than the amination of the chloromethylated styrene-DVB copolymers.

Acrylic weak base exchangers synthesized from aliphatic polyamines have much higher exchange capacities than polystyrene-based structures.

The weak base exchangers cannot be regarded as typical ionic polymers since their amine groups are ionized only under certain conditions. Thus, an amine group in an alkaline medium is in the free-base form, but in a neutral medium it can exist in a partial ionization level, which depends upon amine basicity.

In an acid medium a high level of ionization is present and because of this, the weak base exchangers are usually used to retain strong acids in water treatment. They also can be used as insoluble acceptors of acids in different chemical reactions such as the preparation of esters from acid chlorides and alcohols, etc. For the latter aim, the best known are the 4-vinylpyridine-DVB copolymers with a low degree of crosslinking.

Scheme 2 shows some more distinctive ion exchange reactions for the four above-mentioned types of exchangers.

Amphoteric Ion Exchangers

Ion exchangers which contain both acidic and basic groups are called amphoteric resins. Usually their matrix has some structural units with acidic groups and other units with basic groups.

Very interesting amphoteric resins are the so-called 'snake-cage polyelectrolytes'. One feature distinguishes the snake-cage polyelectrolytes from other amphoteric resins, namely the acidic and basic groups are not attached to the same matrix. For example, a snake-cage polyelectrolyte is prepared by polymerization of acrylic acid (snake) into a strong base anion exchanger with quaternary ammonium groups (cage). These resins are excellent reversible sorbents for electrolytes and can be regenerated by rinsing with water. Electrolyte sorption seems to be mainly determined by the preference of the acidic groups for the cation and of the basic groups for the anion. The resins show preference for different electrolytes. This phenomenon can be used for separating electrolytes one from another.

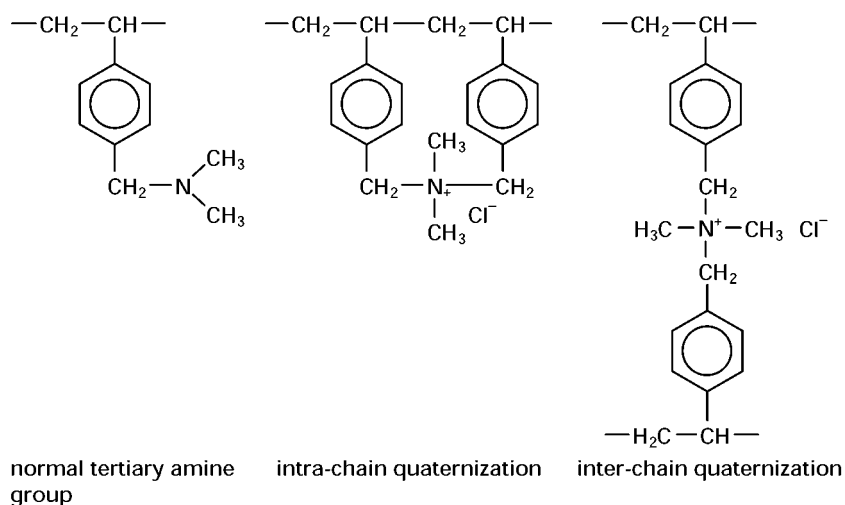


Figure 12 Chemical structure of the functional groups which can exist in a polystyrene-based weak base anion exchanger.

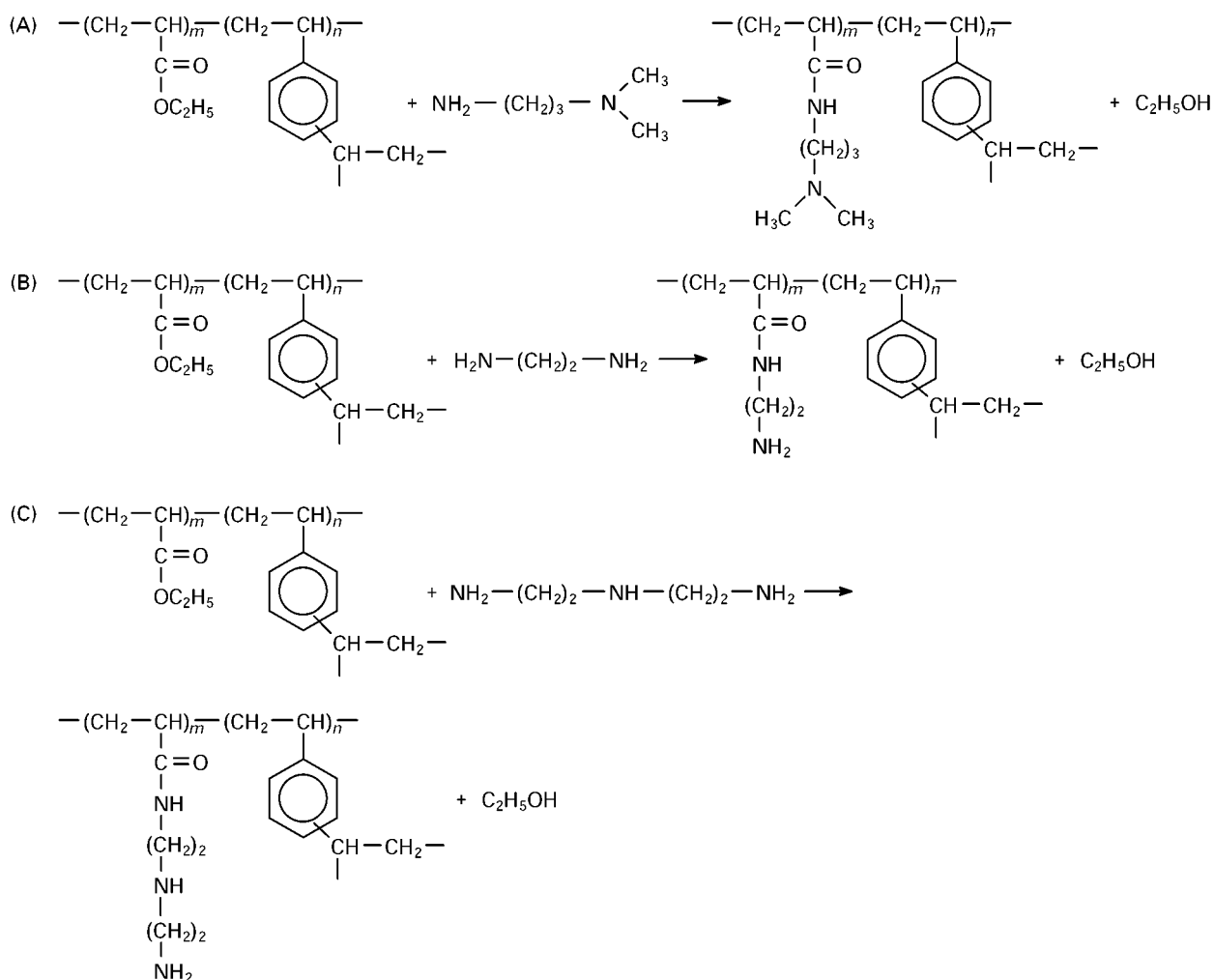


Figure 13 Acrylic-type weak base anion exchangers and their preparation methods.

The snake-cage polyelectrolytes are also used in the technique of 'ion retardation'. This technique is the separation of strong electrolytes from weak electrolytes or non-electrolytes.

Chelating Ion Exchangers

The cation binding of transition, heavy and noble metals can be performed by an ion exchange process

with strong and weak acid cation exchangers as well as with strong base exchangers; the latter are used if the metal cations are present in the form of complex anions.

However, the most promising technique for the binding of metal cations is the use of ion exchangers which contain chelating functional groups. Thus, exchangers with iminodiacetate groups can remove several ppm of Ca^{2+} , Mg^{2+} or Sr^{2+} from brine, in contrast to cation exchangers containing the

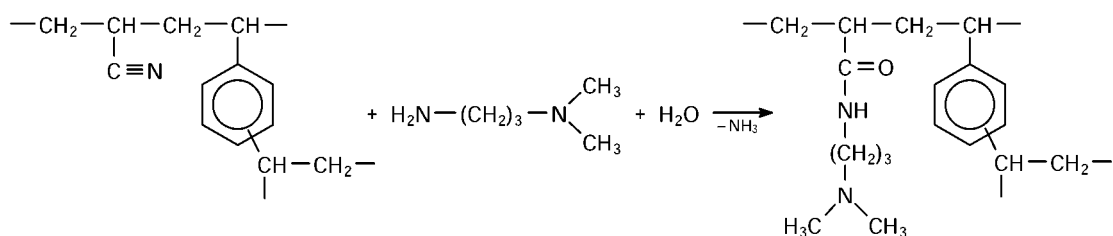
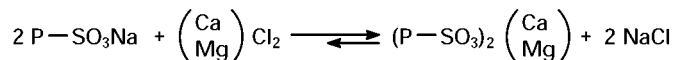
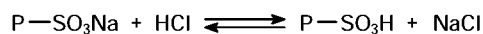
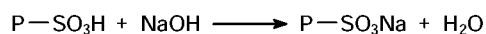
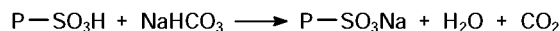
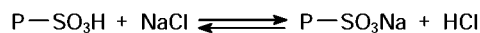
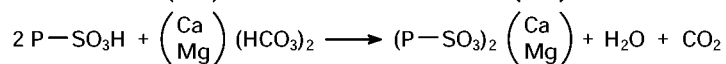
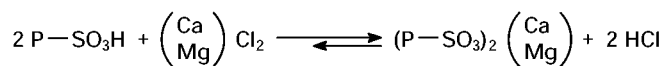
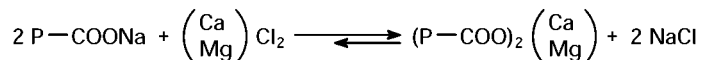
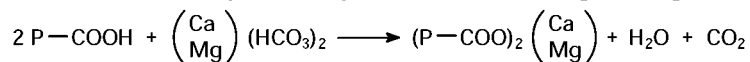
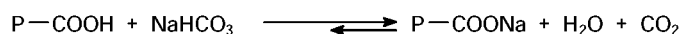


Figure 14 Preparation of an acrylic-type weak base anion exchanger from acrylonitrile-DVB copolymer.

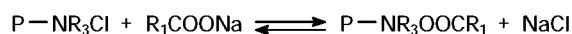
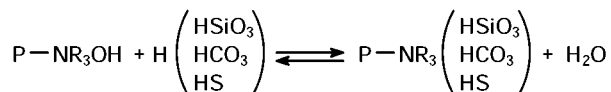
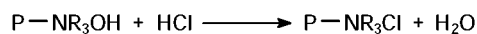
Strong acid cation exchangers



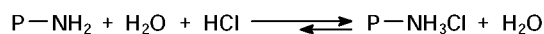
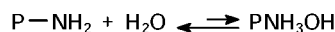
Weak acid cation exchangers



Strong base anion exchangers



Weak base anion exchangers



(P is a polymer structure unit that contains an acid or base group.)

Scheme 2 Some distinctive ion exchange reactions.

Table 2 Some chelating acid and base functional groups

Functional group	Chemical structure	Utilizations
Amine	$-\text{NH}-(\text{C}_2\text{H}_4-\text{NH})_x-\text{H}$	Removal of transitional metals
Iminodiacetic	$-\text{N}-(\text{CH}_2-\text{COOH})_2$	Selective removal of heavy metals
Isothiouonium	$-\text{S}-\text{C}(\text{NH}_2) = \text{NH}$	Selective removal of mercury and noble metals
Aminophosphonic	$-\text{CH}_2-\text{NH}-\text{CH}_2-\text{P}(\text{O})(\text{OH})_2$	Especially for decalcification of brine solutions
Phosphonic acid	$-\text{P}(\text{O})(\text{OH})_2$	Preconcentration of uranyl ions
Hydroxamic acid	$-\text{CO}-\text{NHOH}$	Selective retention for Fe(III) ions
Hydroxyamine	$-\text{CH}_2-\text{N}(\text{CH}_3)-\text{CH}_2-(\text{CHOH})_4\text{CH}_2\text{OH}$	Selective retention for boric acid

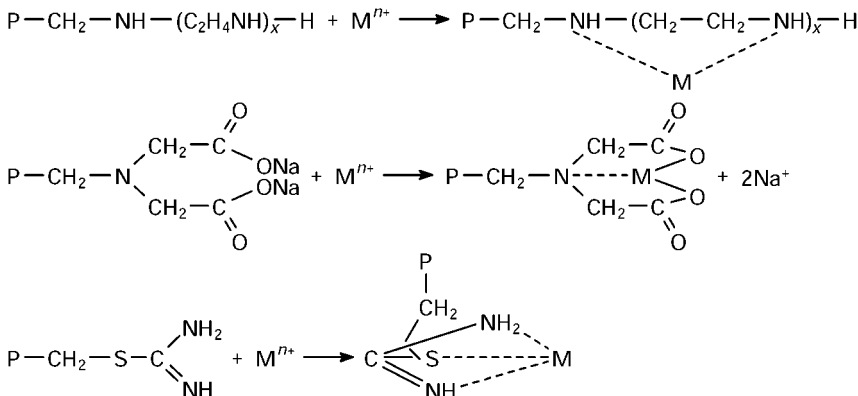


Figure 15 Classical binding of metal cations by some chelating functional groups. (P is a polymer structure unit that contains an acid or base group.)

non-chelating common acid groups. The latter exchangers show a higher selectivity for divalent cations than for Na^+ , but the difference is not very large, so that they will not be able to bind Ca^{2+} , Mg^{2+} or Sr^{2+} cations present at very low concentrations.

The high selectivity of chelating ion exchangers is attributed to the establishment of much stronger bonds than the simple electrostatic attractive forces present in the case of the common ion exchangers. Because of these bonds, the chelating processes show a high degree of irreversibility.

It must be mentioned that the chelating groups, attached to polymer networks, are groups with two or more electron donor elements, such as N, S, O and P, and they can function like the model low molecular weight chelating agents. Their preparation takes place in two main ways – polymerization or polycondensation.

Table 2 shows some functional groups, which are capable of chelating. The binding of metal cations by some chelating functional groups is illustrated in Figure 15.

The nature of metal cation binding can be modified by changing the pH of the solution to cause chemical modification of the chelating groups. Thus,

amine and isothiuronium groups can take part in the equilibria, shown in **Figure 16**. These groups will bind metal cations by a coordination process in neutral or base media via the free base forms while in an acid medium the same cations will be bound as complex anions by an anion exchange process via the salt forms.

Conclusions

The area of organic ion exchangers remains a very active one with intensive technical and scientific work on both conventional resins and entirely novel systems. Thus, organic ion exchangers with different morphologies of their three-dimensional networks and base and acid groups with various chemical structures have been prepared.

There is also a growing interest in the development of selective chelating ion exchangers for the possible application of these resins in analytical chemistry, metal recovery and wastewater treatment. The latter two applications have a great importance in economic and ecological domains. Requirements of the properties of these ion exchangers include high capacity, high selectivity and fast kinetics. Most of the

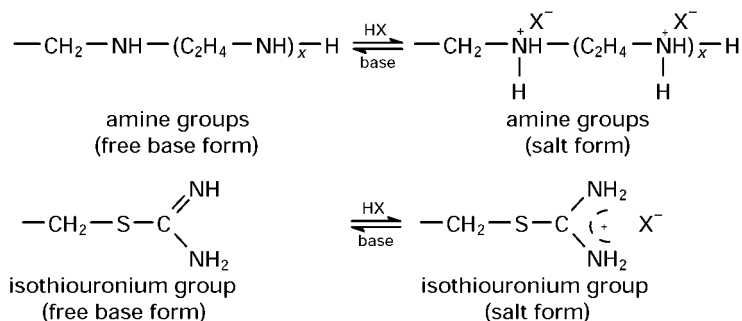


Figure 16 Chemical structure dependence of amine and isothiuronium groups on the pH of aqueous medium.

commercial resins show a high capacity but a poor selectivity towards metal ions.

The combination of the physical strength of an inorganic support with the higher ion exchange capacity and kinetics of the organic ion exchangers could, in the future, lead to an interesting class of ion exchangers with special applications.

See also: II/Ion Exchange: Historical Development; Inorganic Ion Exchangers; Organic Membranes; Theory of Ion Exchange.

Further Reading

- Albright RL and Yarnell PA (1987) *Ion-exchange Polymers: Encyclopedia of Polymer Science and Engineering*, 2nd edn, vol. 8. New York: John Wiley.
- Camps M, Chatzopoulos JM and Montheard JP (1987–88) Chloromethylation of polystyrene and styrene copolymers. *Journal of Macromolecular Science – Review of Macromolecular Chemistry and Physics* C27: 505.

- Dorfner K (1972) *Ion Exchangers*, 3rd edn. Michigan: Ann Arbor Science Publishers.
- Dorfner K (ed.) (1991) *Ion Exchangers*. Berlin: W de G de Gruyter.
- Frechet MJ and Farrall MJ (1977) *Chemistry and Properties of Crosslinked Polymers*. London: Academic Press.
- Helfferich F (1962) *Ion Exchange*. New York: McGraw-Hill.
- Hodge P and Sherrington DC (eds) (1980) *Polymer-supported Reactions in Organic Synthesis*. New York: John Wiley.
- Holliday L (1975) *Ionic Polymers*. London: Applied Science.
- Samuelson O (1963) *Ion Exchange Separations in Analytical Chemistry*. New York: John Wiley.
- Sherrington DC (1988) *Reactions of Polymers: Encyclopedia of Polymer Science and Engineering*, 2nd edn, vol. 14. New York: John Wiley.
- Strat M and Naden D (eds) (1987) *Ion Exchange and Sorption Processes in Hydrometallurgy. Critical Reports on Applied Chemistry*, vol. 15, ch. 3 and ch. 4. New York: John Wiley.

Organic Membranes

R. Wódzki, Nicholas Copernicus University,
Toruń, Poland

Copyright © 2000 Academic Press

Organic ion exchange membranes are made of insoluble polymeric foils, tubes or hollow fibres to which ion exchange groups are covalently bound. The membranes have all the properties typical of ion exchange resins and the ability to keep two different solutions physically separated. Thus, the main property of an ion exchange membrane is a selective exchange of ions and a selective permeability to ions, water or other specifically membrane-soluble species. Although optimizing all the properties would be difficult in the case of one membrane used for a variety of applications, the most desired property is always high membrane selectivity, which allows the separation of ions with low energy consumption and high transport rates. There are many additional requirements for ion exchange membranes, such as low electric resistance, high permselectivity, low free diffusion of salts (leakage), low osmotic water transport, high mechanical strength, high selectivity between ions of the same charge and high chemical stability.

Preparation

Ion exchange membranes can be classified as monopolar or bipolar. In parallel, some intermediate mem-

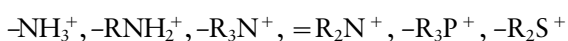
branes have been categorized as mosaic and amphoteric. The monopolar membranes can be divided into cation exchange membranes and anion exchange membranes. Combination of these membranes results in a bipolar ion exchange membrane.

The properties of any ion exchange membrane are determined by the properties of its polymer matrix and the type and concentration of the fixed ionic moieties. The polymer matrix of ion exchange membranes is usually cross-linked. The degree of cross-linking extensively influences the degree of swelling (water sorption), chemical and mechanical stability and membrane permeability by changing ionic mobility inside the membrane phase. Thus, the proper selection of membrane components, their content and the method of preparation significantly affect the membrane properties and structure. The subsequent chemical modification of the polymer matrix involves the introduction of ionogenic groups, resulting typically in the following fixed sites:

Cation exchange membranes:



Anion exchange membranes:



Monopolar Membranes

The simplest ion exchange membranes are composed of derivatives of styrene-divinylbenzene copolymers or vinylpyridine-divinylbenzene copolymers. In order to maintain their mechanical strength, these homogeneous membranes are often reinforced by backing materials. Other simple ion exchange membranes can be synthesized from finely powdered ion exchange resin and inert polymer powder applied as a bonding material. Nowadays, more advanced methods of membrane preparation are recommended. The most widely used methods are:

1. Impregnation of a basic polymer component with styrene and divinylbenzene for copolymerization followed by chemical modification (e.g. sulfonation);
2. Casting the mixed solution of poly(styrene sulfonic) acid and other inert polymer to produce an interpolymer or 'snake-in-cage' membrane;
3. Radiation grafting of a polymerizable monomer into a conventional polymer film and then introducing the ion exchange groups to the film. The films used are generally polyethylene, polypropylene and perfluoroethylene;
4. Chemical modification: this method involves direct introduction of ion exchange groups to a condensation-type polymer such as polysulfone, poly(ethylene oxide), poly(vinyl chloride), poly(vinylidene fluoride), poly(ether ether ketone). The membrane can be formed subsequently by casting the polymer solution, and then phase inversion. The procedure results in an anisotropic membrane structure with a thin skin layer and a supporting layer of sponge morphology;
5. Plasma polymerization. This relatively new method has been utilized to prepare: first, an anion exchange membrane by plasma polymerization of γ -aminopropylethoxydimethylsilane on a porous polymer film; second, a perfluorocarbon sulfonic acid membrane, by plasma polymerization of perfluorostyrene and SO_2 ; and third, a thin film sulfonic-type membrane, by plasma polymerization of ethylene and SO_2 , or acetylene and SO_2 .

Bipolar and Mosaic Membranes

Preparation methods of bipolar ion exchange membranes involve the introduction of cation exchange groups into one side of the membrane and anion exchange groups into the other side. In order to obtain the simplest bipolar membrane a separate cation exchange membrane and an anion exchange membrane can be glued together by using poly(styrene

sulfonic) acid as a binder. Other bipolar ion exchange membranes have been prepared by graft polymerization of acrylic acid on one side of the porous polymer membrane and of *N*-(2-methacryloyloxyethyl)-*N,N,N*-trimethylammonium chloride on the other side, after oxygen plasma treatment of the porous membrane. The mosaic membranes are usually prepared by casting a multiblock copolymer composed of styrene, butadiene and vinylbenzyl dimethylamine and the subsequent introduction of cation and anion exchange groups into the polymer.

Structure

The properties of ion exchange membranes depend on their microstructure, which results from the differences in properties of their ionic and neutral components. The hydrocarbon ion exchange membranes are generally composed of derivatives of styrene-divinylbenzene copolymer and other inert polymers such as polyethylene and poly(vinyl chloride). Ionic derivatives of such copolymers are finely distributed in the inert polymer-forming microdomains because of their poor mutual compatibility. This inhomogeneity causes the distribution of ion exchange groups in the membrane material to be of varied local concentration. The local distribution of fixed charges can affect all the basic membrane properties, such as electrolyte sorption, electrical conductivity and permselectivity as well as mass transport rates. Specifically, a rather unusual structure is characteristic for perfluorocarbon cation exchange membranes (with sulfonic or carboxylic acid groups), which can be classified as ionomer materials. Ionomers and ion-containing polymers with ionic sites and counterions spontaneously organized into dipole multiplets and, for some materials, into larger ion clusters containing 50 or more pairs of ions. These clusters are embedded in the perfluorocarbon membrane backbone, and are connected by narrow channels forming a continuous network.

Despite the heterogeneity resulting from the hydrophilic and hydrophobic nature of membrane components, certain additional morphology features originate from the method of preparation. So-called macroscopically homogeneous membranes can be prepared either by the polymerization of functionalized monomers or by careful modification of a homogeneous polymer film. However, depending on the method of preparation, the structural imperfection of membranes increases in the following order: interpolymer membranes, graft and block polymer membranes and membranes composed of powdered ion exchange resins embedded thereafter in an inert polymer binder.

General Physicochemical Properties

Ion exchange membranes are characterized by many of the parameters and properties described below. Independently, the basic properties describing equilibrium and transport properties of any membrane are as follows: ion exchange capacity (mol kg^{-1} of dried membrane), swelling ($\text{wt.}\%$ of water or other solvent), electrolyte sorption (mol kg^{-1} of water sorbed into membrane), distribution coefficient (ratio of solute concentration in the membrane and external solution), transference number for cations and anions (determined under standard conditions), electrical conductivity (or resistivity) and salt leakage (both determined after contacting the membrane with a standard electrolyte solution).

Co-ion Exclusion

In a cation exchange membrane, due to the system electroneutrality, the fixed anions are in equilibrium with mobile cations (referred to as counterions). In contrast, anions functioning as co-ions are more or less excluded from the membrane because their charge is identical to the fixed ion charge. This phenomenon, known as the Donnan exclusion of co-ions or electrolytes, enables the ideal membrane to transfer cations only. In the same way cations are excluded from the anion exchange membrane. The Donnan exclusion equilibrium, and thus the membrane selectivity, depends quantitatively on the concentration of the fixed ions, the valence of co- and counterions, the concentration of an equilibrating external solution, and the affinity of the exchange groups to respective counterions.

Transport Processes

The effectiveness of any membrane process is determined by the flux of species through the membrane. High fluxes arise because of high permeability of the internal aqueous membrane solution in respect to sorbed solutes. The presence and properties of transport-mediating functional ionic groups can either facilitate or hinder transport processes depending on many specific interactions between mobile species, the charged polyelectrolyte network and solvent. In general, membrane transport phenomena can be described by a general equation derived from the linear thermodynamics of irreversible processes:

$$J_i = \sum_k L_{i,k} X_k \quad (i, k = 1, 2, 3, \dots, m)$$

where J_i denotes the flux of an individual permeant, the volume of solvent, heat or electricity transferred across a membrane, and $X_{i,k}$ denotes the driving force

represented by a difference in chemical potential ($\Delta\mu$), temperature (ΔT), pressure (Δp) or chemical affinity (A). $L_{i,k}$ is the phenomenological coefficient linearly relating the flux and driving force. In practice, a general flux equation can be reduced to a description of a specific process by neglecting coupling transport phenomena. Depending on the solution and assumptions, various mathematical relations have been derived and applied to discuss transport rates of ionic substances and water through ion exchange membranes.

Permselectivity

The characteristic property of ion exchange membranes is their ionic permselectivity related to electrically driven processes and quantified by the following definitions:

$$P_{\text{CEM}} = \frac{t_{+, \text{CEM}} - t_{+}}{t_{-}} \quad \text{and} \quad P_{\text{AEM}} = \frac{t_{-, \text{AEM}} - t_{-}}{t_{+}}$$

where t is the transference number for anions ($-$) and ($+$) cations in free electrolyte or acting as counterions (cation exchange membrane (CEM) and anion exchange membrane (AEM)) in an ion exchange membrane. An ideal permselective membrane should have a P value of 1, and the permselectivity is equal to zero when the transference numbers within the membrane are the same as in an electrolyte solution. Usually, transference numbers for practical membranes attain values from 0.8 to 0.98.

Separation Ability

One of the most important uses of ion exchange membranes is the selective separation of solutes. This can be performed because of the differences in the rates at which solutes permeate through the membrane. The size of this difference depends on the separation system, i.e. on the composition of feed solution and the membrane. The criterion of separation is that the composition of the mixture emerging from the membrane cell should be different from that entering on the feed side. Consequently, the separation factor α_B^A measures the extent of selective transport of A in relation to B :

$$\alpha_B^A = \frac{J_A X_B}{J_B X_A}$$

where J_A and J_B are the fluxes (transport rates expressed as numbers of moles issuing from the membrane per unit area and time) and X_A and X_B are the mole fraction of A and B in the feed.

Membrane Processes and Applications

Many applications of ion exchange membranes in transport and separation processes have been made. Although the driving force for ions and water to penetrate through the membrane initially is primarily an electrochemical and chemical potential, it has been reported in recent years that the hydraulic permeability, temperature difference and difference in proton concentration can also be exploited. This results in some sophisticated transport mechanisms, the backgrounds and practice of which are reviewed below. The latest applications are due to developments in ion exchange membrane composition and structure. Ion exchange membranes with specific properties have been produced to meet many industrial requirements. For example, the following membranes of specific properties have been developed and commercialized: perfluorocarbon anion exchange membranes for high temperature usage and chemical stability in corrosive media, anion exchange membranes for diffusion dialysis (treatment of corrosive acidic waste waters), anion exchange membranes of high acid retention (electrodialytic concentration of dilute acids), hydrogen ion permselective cation exchange membranes (efficient electrodialysis) and monovalent cation or monovalent anion permselective membranes.

Diffusion Dialysis

Diffusion dialysis results from the difference in rates of permeation of salts and acids through anion exchange membranes. According to the scheme shown in Figure 1, this membrane allows the selective transport of anions across the membrane, ideally remaining impermeable to cations other than protons. Diffusion dialysis has been exploited to remove acids from

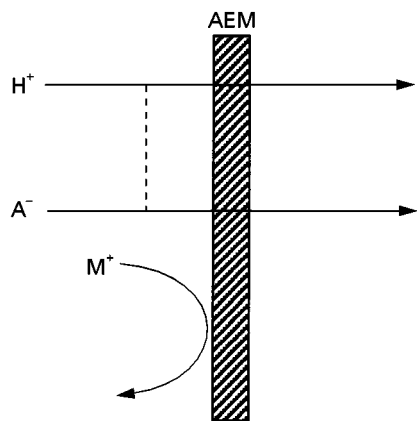


Figure 1 Scheme of diffusion dialysis of salt and acid through anion exchange membrane (AEM).

solutions containing different cation species. High quality anion exchange membranes allow this method to be applied to the recovery of sulfuric and other acids from waste solutions generated in steel, metal-refining and electroplating industries.

Donnan Dialysis

Donnan dialysis, also referred to as ion exchange dialysis, occurs after placing an ion exchange membrane between two solutions containing different electrolytes. According to the scheme depicted in Figure 2, ions can cross a membrane when their sign is opposite to the sign of the membrane-forming polyelectrolyte. At the same time, the permeation of co-ions is hindered because of their electrostatic exclusion from the membrane phase. Usually, divalent or univalent metal cations are transported from the dilute feed solution into the highly acidic stripping solution. The coupling of fluxes in this membrane system makes it possible to reach a stable flux of cations from dilute to concentrate phase. Thus, uphill transport (chemical pumping) arises as a result of the interdiffusion of different counterions.

The final distribution of ions between two membrane-adjacent solutions corresponds to the Donnan equilibrium principle, which in the typical case of M^{z+}/H^+ Donnan dialysis, takes the following form:

$$C_{M,s} = k C_{M,f} \left(\frac{C_{H,s}}{C_{H,f}} \right)^{Z_M}$$

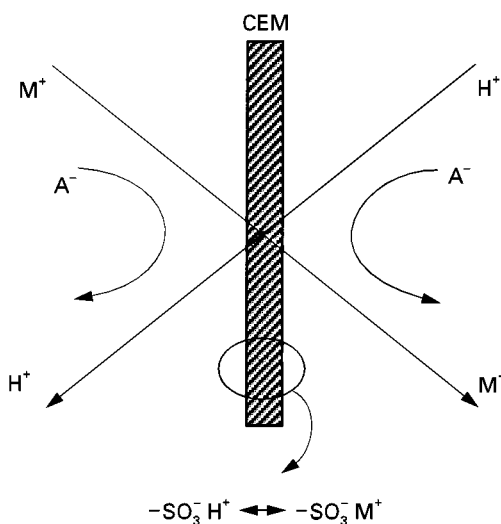


Figure 2 Scheme of Donnan dialysis of M^+ and H^+ cations through exchange membrane (CEM). (From Wódzki R, Szczepański P and Pawłowski M (1999) Recovery of metals from electroplating waste solutions and sludge. Comparison of Donnan dialysis and pertraction technique. *Polish Journal of Environmental Studies* 8(2): 111–124.)

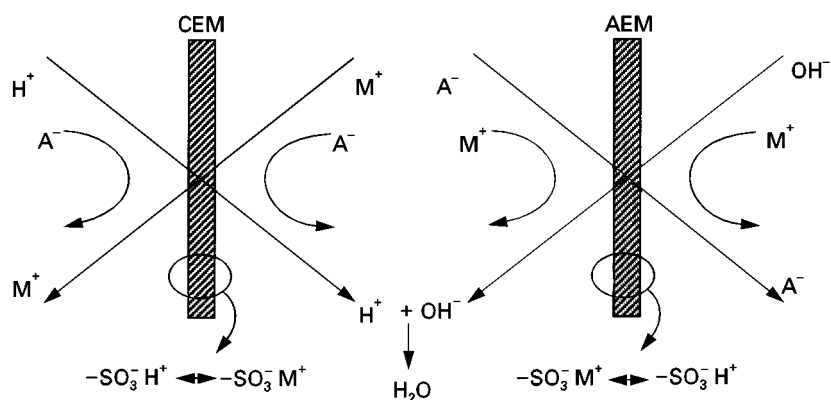


Figure 3 Scheme of neutralization dialysis of M^+ cations and A^- anions through cation (CEM) and anion exchange membranes (AEM).

Consequently, when the initial concentration (C) of metal ions (M) in the feed (f) is much lower than the concentration of counter-transported protons (H) in the stripping solution, it is possible to attain substantial enrichment of metal ions in the receiver, or alternatively, almost complete removal of these cations from the feed. Despite the many advantages, only a pilot dialyser for the nuclear industry (recovery of ^{134}Cs , ^{90}Sr and concentration of uranyl ions) has been reported as large scale implementation of this technique. On the other hand, Donnan dialysis is widely used in analytical laboratories as an efficient method for the preconcentration and separation of various cations and anions or for the treatment of complex matrices before analysis.

Neutralization Dialysis

Neutralization dialysis is a membrane process based on the coupling of two simultaneously occurring Donnan dialyses. According to the scheme shown in **Figure 3**, in this case a salt solution is separated from an external acidic and basic solution with a cation and anion exchange membrane, respectively. Protons and hydroxide ions permeate into the desalination compartment by the Donnan dialysis mechanism, which generates the counter-flow of other cations and anions. Under ideal conditions, i.e. without salt leakage and with balanced fluxes of protons and hydroxide ions, the overall process results in almost complete desalination of the internal solution. The practical use of neutralization dialysis for the demineralization of mixtures containing some organic substances (mono-, oligo- and polysaccharides) and polyelectrolytes is recommended.

Pervaporation

In pervaporation processes the application of ion exchange membranes instead of inert polymer mem-

branes is possible. During this process (**Figure 4**) an ion exchange membrane is kept in contact with a stream of the mixture of water and miscible organic solvent, whereas the second side of the membrane is kept under vacuum. Due to the strong affinity of ionic sites to water and an inertness of the polymer backbone to an organic component, water can permeate through the membrane. Thus, the permeation of water can be optimized by changing the membrane polymer, the type and content of the membrane-forming polyelectrolyte (ionomer, cross-linked copolymer, etc.), and the kind of counterions. For instance, cation and anion exchange membranes of various ionic forms have been examined for the separation of alcohol–water and pyridine–water mixtures.

Fixed-site Mediated or Carrier Transport

Analogous to liquid membrane transport mediated by the mobile carriers, ion exchange sites can be exploited as fixed carrier centres in the polymer membrane phase. The membranes exhibiting such a function are referred as fixed-site carrier membranes or reactive membranes. In general, transport phenomena in such membranes are believed to occur as a sequence of exchange reactions between permeating solute and reactive groups located along the polymer

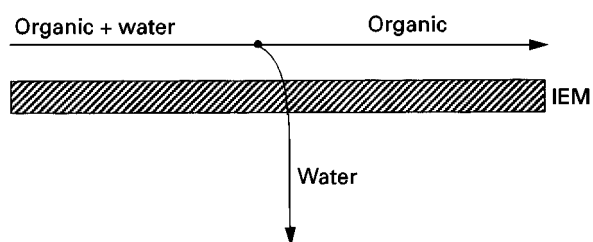


Figure 4 Scheme of water pervaporation through ion exchange membrane (IEM).

chain rather than by pure diffusion phenomena. To be effective the transport mechanism requires fixed sites to be mobile over a certain restricted area. Moreover, their concentration should exceed a certain concentration, enabling instantaneous overlapping of loaded and unloaded centres. Despite many difficulties in understanding and in the theoretical description of this type of membrane transport and separation, a number of processes have been developed. The most interesting are processes dealing with the separation of gaseous substances (CO_2), olefins and sugars. For example, a cation exchange membrane exchanged with ethylenediamine is selectively permeable to CO_2 (from a feed containing CH_4 and H_2S). On the other hand, silver ions exchanged with a cation exchange membrane form an Ag^+ -olefin complex in the membrane phase. Carrier transport of 1-hexene and 1,5-hexadiene from a decane phase through a cation exchange membrane impregnated with silver ions has been reported. Similarly, styrene permeates selectively (compared with ethylbenzene) through the Ag^+ form of cation exchange membrane. A selective transport of sugars via complexation with borate ions fixed in an anion exchange membrane has been performed and referred as carrier-relay transport. In this way, the selective transport of D-glucose, D-xylose, D-arabinose, D-mannose, D-galactose, D-fructose, L-sorbose, sucrose and D-lactose can be achieved.

Membrane Extraction-Hybrid Membrane Systems

The combinations of liquid membrane extraction (usually mediated by specific ion exchange extractant/carrier) with ion exchange membranes in some

relatively new membrane systems have been called membrane hybrid systems (MHS). The scheme of cation transport in a simple MHS is depicted in Figure 5. The MHS operation involves a series of ion exchange-diffusion processes (ion exchange membrane) as well as permeation through a liquid membrane. The presence of an ion exchange membrane at a particular interface stabilizes the liquid membrane and enhances the interfacial ion exchange reactions because of high, and specific, sorption of certain ions by the membrane polyelectrolyte. The long term and stable operation of a liquid membrane system can be achieved with the MHS idea. The selective and active transport of metal cations, inorganic anions and some carboxylic acids has been reported. It is worth noting that these systems can be regarded as biomimetic, which means that they correspond to a cellular envelope of Gram-positive bacteria composed of an ion exchange polymer membrane (cell wall) and a quasi-liquid membrane (cytoplasmic membrane).

Membrane Permeation Coupled to External Reaction

It is possible to accelerate chemical reactions by removing some products from the reaction medium before the reaction reaches its equilibrium state. Ion exchange membranes are effective in these cases. For example, fermentation processes producing ionic materials such as acetic acid can be carried out continuously as an extractive fermentation by removing the products by means of diffusion dialysis, pervaporation or electrodialysis. Ion exchange membranes can be applied to improve the kinetics of chemical reactions by the pervaporative removal of water from the reaction medium. Such a technique has been demonstrated for esterification of oleic acid with ethanol and of propionic acid with isopropanol or propanol.

In more advanced systems, membrane transport phenomena are coupled with enzyme reactions. The most representative system is composed of a cation exchange membrane layer, a porous membrane layer containing entrapped urease and an anion exchange membrane layer. Urea is decomposed into NH_4^+ and CO_3^{2-} in the enzyme layer and products permeate through the respective membrane layers without application of an electric field. A similar idea is utilized in many enzymatic membrane sensors.

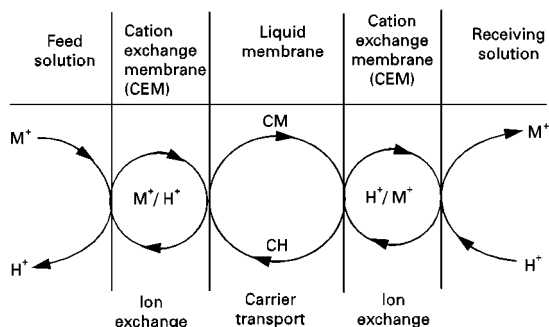


Figure 5 Scheme of membrane hybrid system composed of two cation exchange membranes and the liquid membrane containing an ionic carrier (C). Coupled countertransport of M^+ and H^+ cations. (From Wódzki R, Szczepański P and Pawłowski M (1999) Recovery of metals from electroplating waste solutions and sludge. Comparison of Donnan dialysis and pertraction technique. *Polish Journal of Environmental Studies* 8(2): 111–124.)

Ion-Exchange Membrane Separators in Power Sources, Sensors and Electrodes

A typical example is the use of an ion exchange membrane as a solid polyelectrolyte for a fuel

cell. The composite, in which anode catalyst, poly(fluorocarbon sulfonate) cation exchange membrane and cathode catalyst are combined, has been used for hydrogen-oxygen fuel cells. The only product of this cell is water, which seems to be desirable from an ecological point of view. Methanol has also been reported for the generation of electricity and utilizable industrial chemicals by the use of a membrane-containing fuel cell. Various applications of ion exchange membranes of low electrical resistance in alkali batteries are possible. Modern cation exchange membranes made of acrylic acid grafted onto polyethylene film are widely used as separators in alkaline batteries, such as a Ni-Cd secondary battery.

Water content of the ion exchange membranes and thus their physicochemical properties changes with humidity. Therefore, ion exchange membranes are usable as a working part of a hygrometer. When water content of the membrane increases with increasing humidity, the increase in the current or ionic conductivity between the electrodes on both sides of the membrane can be measured and calibrated.

The concentration of alcohol can be indirectly determined by means of a membrane with fixed alcohol-dehydrogenase or alcohol-oxylase. It has been reported that these sensors operate accurately in acidic media after coating the enzyme-fixed membrane by a cation exchange membrane (organic acids cannot approach the enzyme membrane). A similar concept is used for constructing *in vivo* operating sensors for glucose presence and concentration. Some modified electrodes are constructed by coating classic electrodes with layered ion exchange materials. A typical example is the perfluorocarbon cation exchange membrane-coated electrode to control the permeability of redox species such as $\text{Ru}(\text{bpy})_3\text{Cl}_3$ or 1,1-dihydroxymethylferrocene.

Industrial Applications

Membrane Electrodialysis

The basic principle of membrane electrodialysis is presented in Figure 6. The membranes are arranged in a series of anion and cation exchange membranes placed between an anode and a cathode. The cations migrating towards the cathode permeate the negatively charged cation exchange membrane and are retained by anion exchange membranes. The anions are transported in the opposite direction. The final result is an increase in ion concentration and ion depletion in alternate compartments. Membrane electrodialysis has been developed within the last several years, mainly for desalting brackish waters and concentrating brine from seawater. Nowadays,

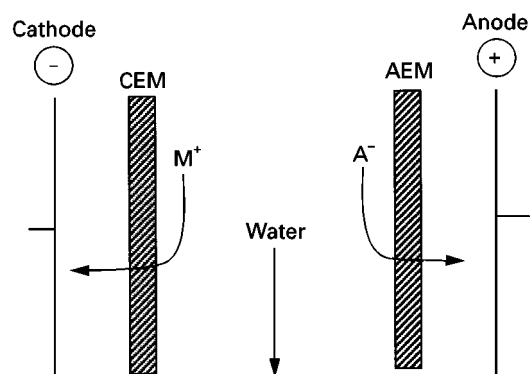


Figure 6 Basic idea of membrane electrodialysis.

electrodialysis is widely applied in environmental protection (depolluting and recycling of chemicals), in bio-industries (food, pharmacy and biotechnology) and in the treatment of drinking water. Some of these new applications have led to substantial improvements in membrane quality. For instance, special membranes with low permeability to the divalent ions in respect to the monovalent ones, membranes with very low permeability to hydroxyl ions or very low permeability to protons, are currently produced.

Membrane Electrolysis

A typical example of this kind of application is the membrane electrolysis of sodium chloride to produce chlorine, hydrogen and sodium hydroxide (membrane chlor-alkali process). A schematic diagram for this process is presented in Figure 7. Perfluorocarbon cation exchange membranes for chlor-alkali processes should have an anisotropic structure in their cross-section. The cathode side of the membrane has a thin layer of carboxylic acid groups of a given ion exchange capacity, and the anode side of the membrane has a thick sulfonic acid group layer or a carboxylic acid group layer of high ion exchange capacity. Ion exchange membranes can also be applied for the electrodialysis of water to produce hydrogen and oxygen. The technology exploiting a solid polymer electrolyte method is efficient when perfluorocarbon cation exchange membranes are used in the form of a stack with catalytic electrodes covering the membrane surfaces. Ion exchange membranes are also used as separators in organic synthesis by electrolysis. A typical example is the hydrodimerization of acrylonitrile to produce adiponitrile.

Conclusion

The technique of membrane separation can be considered as an energy-saving method because, in

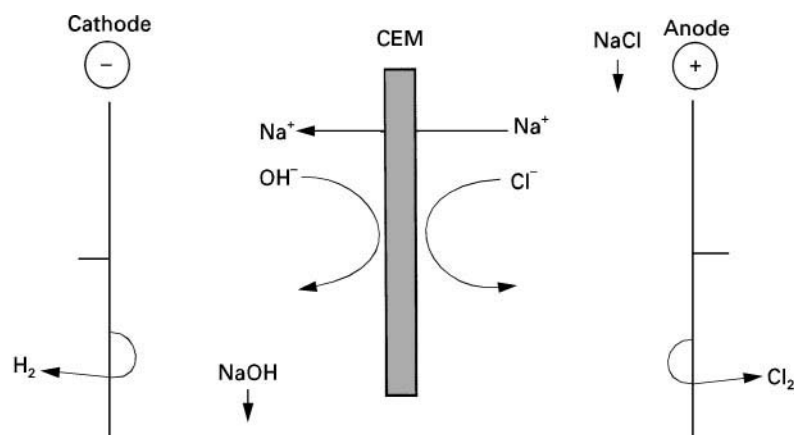


Figure 7 Chlor-alkali process (membrane electrolysis) using a cation exchange membrane (CEM).

general, it does not cause phase conversion. From this point of view, ion exchange membranes and their application technology are one of the most advanced methods enabling the embodiment of closed-loop chemical processes. As solid polyelectrolytes, the membranes are easy to regenerate, recycle and/or promote continuous usage to improve industrial processes. Environmental benefits can be achieved as well.

Since the use of ion exchange membranes has become very diverse, the requirements for membranes with new properties will increase. These requirements should result in the development of new highly functionalized ion exchange membranes. Photosynthetic membranes, biomimetic membranes, complex and specialized membrane sensors, polymerized phospholipids and polymerized crown ethers with ionic groups can be considered as new possible areas of membrane science development.

See also: **II/Ion Exchange:** Catalysis: Organic Ion Exchangers; Historical Development; Inorganic Ion

Exchangers; Organic Ion Exchangers; Theory of Ion Exchange. **III/Porous Polymer Complexes for Gas Separations: Membrane Separations.**

Further Reading

- Drioli E and Nakagaki M (1986) *Membranes and Membrane Processes*. New York: Plenum Press.
- Helfferich F (1962) *Ion Exchange*. New York: McGraw-Hill.
- Ho WS and Sirkar KK (1992) *Membrane Handbook*. New York: Chapman and Hall.
- Kesting RE (1985) *Synthetic Polymeric Membranes. A Structural Perspective*. New York: Wiley.
- Lakshminarayanaiah N (1969) *Transport Phenomena in Membranes*. New York: Academic Press.
- Lloyd DR (1985) *Material Science of Synthetic Membranes*. Washington DC: American Chemical Society.
- Selegny E, Boyd G and Gregor HP (1976) *Charged Gels and Membranes, Part I*. Dordrecht: D. Reidel.
- Strathmann H (1990) Membranes and membrane separation processes. In: Arpe H-J (ed.) *Ullmann's Encyclopedia of Industrial Chemistry*, vol. A 16, pp. 187–263. Weinheim: Verlag Chemie.

Phosphates: Novel Layered Materials

See **II / ION EXCHANGE / Novel Layered Materials: Phosphates**

Surface Complexation Theory: Multispecies Ion Exchange Equilibria

W. H. Höll, Forschungszentrum Karlsruhe,
Eggenstein-Leopoldshafen, Germany
J. Horst, Karlsruhe, Germany

Copyright © 2000 Academic Press

Introduction

Inorganic and organic ion exchangers consist of either a crystalline or a polymeric matrix and functional groups. Depending on the pH value of the liquid phase, these groups can either be protonated or dissociated. By this means exchangers are able to interact with ions from the liquid phase. There is a large variety of such interactions: they may be due to electrostatic and van der Waals forces, heteropolar and covalent binding, or coordination forces. The resulting sorption phenomena take place at the inner pores and/or surface of the exchangers.

The surface charge generates an electric potential normal to the surface. Consideration of the resulting electrostatic interactions has led to several theoretical descriptions, e.g. the Helmholtz, Gouy–Chapman and Stern models. Modern theoretical approaches consider the adsorption of counterions as a result of chemical interactions between the surface groups and dissolved species. Sorption of protons or of any other kind of ion is treated as a local equilibrium reaction. Specific (for protons and hydroxyl ions) and non-specific interactions lead to the formation of ion pairs at the surface that are designated as surface complexes. Different kinds of surface complexes can be discriminated.

Spectroscopic investigations of surfaces have given rise to the assumption that more than one single layer has to be assumed to account for the uptake of counterions. A typical approach used by many authors is the triple-layer model consisting of surface, inner and outer layers.

A further refinement of the triple-layer model is the approach developed by Horst. In this model individual sorption layers are credited to each kind of counterions. The respective theoretical approach allows the description of pure cation or anion exchange equilibria as well as of amphoteric equilibria encountered with activated alumina or activated carbon.

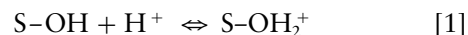
Theory

Amphoteric Reactions at a Charged Surface

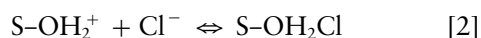
Derivation of the mathematical relationships uses a generalized exchanger whose surface contains

S–OH groups as functional sites. In aqueous systems these surface groups can be protolysed in two different ways.

In acid media the surface may be protonated according to:

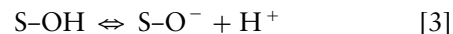


In order to maintain the condition of electroneutrality the charge on the surface has to be balanced by the negative charge of an anion, e.g.:

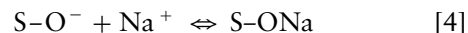


Therefore, in sufficiently acid media, a sorption of acids takes place similar to the uptake by weakly basic exchange resins.

In alkaline solutions the surface hydroxyl groups can dissociate and hand protons over to the liquid phase:



The negative surface charge has to be balanced by cations, e.g. by sodium ions:



Together the formal equation [3] and [4] represent a cation exchange on an arbitrary cation exchanger.

Each of the above models holds for the uptake of acids or the exchange of protons for other monovalent cations in arbitrary pure anion or cation exchange processes. If the state of equilibrium is considered for an amphoteric exchanger and a liquid phase containing different cations and anions, then the uptake of anions will decrease with increasing pH value until the sorption is completely suppressed. In the same direction the cation exchange of protons for cations increases. The pH regions of almost exclusive cation and anion sorption are separated by a maximum of noncharged surface groups. In this transition region sorption of both cations and anions occurs. At the point of zero charge, therefore, the surface is covered with equal amounts of equivalents of positively and negatively charged counterions.

Surface Model Assumptions

During the protonation, or dissociation, of the surface OH groups either a negative or a positive surface

potential is generated, depending on the pH and on the ionic strength of the liquid phase. Therefore, the respective counterions are subject to an attraction while the co-ions are rejected. Due to the sorption of counterions at functional groups, the surface potential is partly decreased. Unlike the description widely used in the literature, it is assumed that each kind of counterion is located at a characteristic distance from the surface. Thus, ordered double or 'Stern' layers are formed. Ion pairs between surface groups and counterions in the ordered layer are designated as surface complexes. Excess charges at the surface are balanced by counterions in the diffuse layer, which also contains co-ions. As a consequence, the surface potential continuously decreases normal to the surface to zero in the liquid phase. The equilibrium between solid and liquid phases is mainly dominated by protolytic reactions. In this way, the protons are the potential-determining species.

For a system with Cl^- and Na^+ ions the schematic arrangement of counterions and co-ions and the corresponding development of the potential are plotted in Figure 1. With respect to the radii of the hydrated species, the anion layers are assumed to be closer to the surface than those of the cations. (Cl^- and Na^+ ions are used as model counterions. Individual properties are not taken into account. Furthermore, the absolute values of the potential in the different layers are of no importance for the further mathematical derivations.)

General Sorption Equilibrium Relationships for an Amphoteric Surface

The derivation of equilibrium relationships makes use of the following assumptions:

1. The functional groups are uniformly distributed across a plane surface.

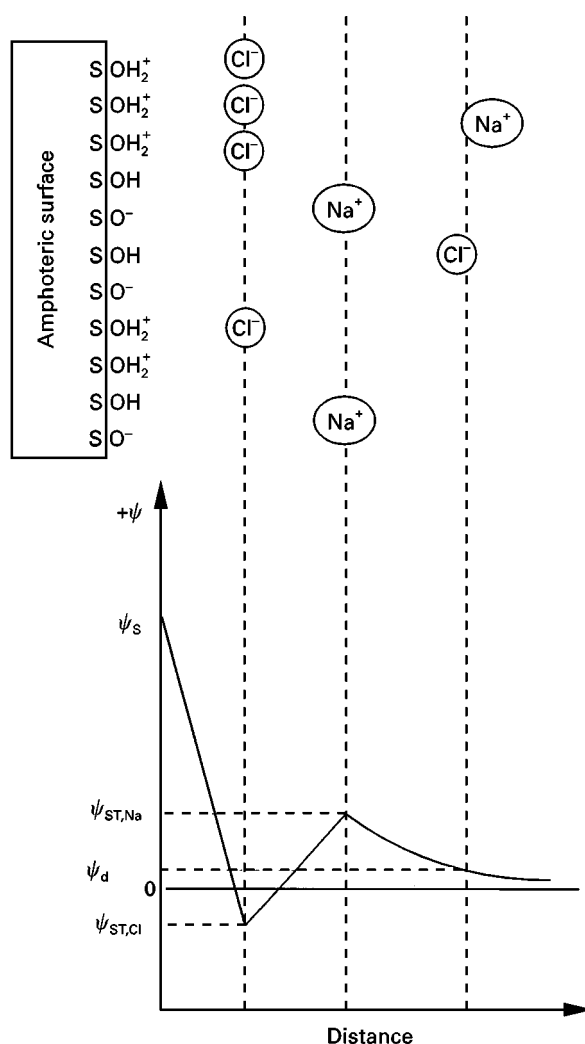
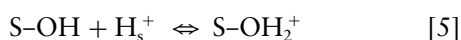


Figure 1 Schematic arrangement of ions at the amphoteric surface of activated alumina and the respective development of electrical potential.

- Activity coefficients in the exchanger phase are assumed to be 1.
- Any ion exchange develops as the replacement of one surface complex by a new one. As a consequence, an oxide valence is defined that is equal to the smallest common multiple of the valences of the counterions.

For the derivation of the equilibrium relationships a simple system with Cl^- and Na^+ ions is considered. The protolytic reactions at the surface are considered as local equilibria that can be described by the mass action law. The formation of the two surface complexes can be described by the respective formation constants, K (see Table 1 for explanation of symbols used).

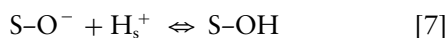
Protonation



$$K_H^+ = \frac{c(\text{S-OH}_2^+)}{c(\text{H}^+)_s \cdot c(\text{S-OH})} \quad [6]$$

where c is the concentration of the species in parentheses in mol L^{-1} .

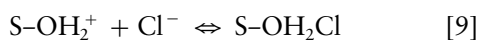
Dissociation/neutralization



$$K_H^- = \frac{c(\text{S-OH})}{c(\text{S-O}^-) \cdot c(\text{H}^+)_s} \quad [8]$$

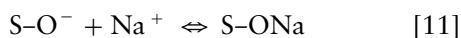
The sorption of counterions leading to two further surface complexes is considered in an analogous way.

Sorption of anions



$$K_{\text{Cl}}^- = \frac{c(\text{S-OH}_2\text{Cl})}{c(\text{S-OH}_2^+) \cdot c(\text{Cl}^-)_s} \quad [10]$$

Sorption of cations



$$K_{\text{Na}}^+ = \frac{c(\text{S-ONa})}{c(\text{S-O}^-) \cdot c(\text{Na}^+)_s} \quad [12]$$

Symbols with subscript 's' designate concentrations in the respective Stern layer. These unknown quantities can be expressed in terms of the concentrations in the

Table 1

Symbol	Unit	Definition
A_0	$\text{m}^2 \text{g}^{-1}$	Specific surface area
$\alpha(i)$	mol L^{-1}	Concentration of species i
$\alpha(i)_s$	mol L^{-1}	Concentration of species i in the Stern layer
$\alpha(i)_x$	mol L^{-1}	Concentration of species i at position x in an electrical field
$C(i, j)$	F m^{-2}	Electric capacitance of capacitor formed by the layers of species i and j
$C(\text{S}, i)$	F m^{-2}	Electric capacitance of capacitor formed by the surface and the layer of species i
F	A s	Faraday constant
K_i^{\dagger}	—	Equilibrium constant of surface reaction
L	L	Volume of liquid phase
LS	—	left-hand side expression of eqns [38] and [39]
$m(\text{H}, j)$	—	Abbreviation, defined by eqn [22]
$q(i)$	mol g^{-1}	Oxide loading with species i
q_{max}	mol g^{-1}	Maximum exchanger loading
Q_i^{\dagger}	—	Generalized separation factor
R	$\text{J mol}^{-1} \text{K}^{-1}$	Gas constant
S	g	Mass of sorbent
S-	—	Abbreviation used to designate the surface
T	K	Temperature
V	—	Sign of charge
$\gamma(i)$	—	Dimensionless loading with species i
$\gamma(i, i)$	—	Probability of the presence of two adjacent ions, i at the surface
$z(i)$	—	Valence of species i
σ_i	A s m^{-2}	Surface charge density of layer with ions i
ψ_x	V	Electrical potential at position x

liquid phase by means of the Poisson–Boltzmann relationship:

$$c(i)_x = c(i) \times \exp \left\{ -\frac{z(i)F}{RT} \times \psi_x \right\} \quad [13]$$

Here $c(i)_x$ represents the concentration of species i at position x in an electric field, $z(i)$ is the valence of species i , F is the Faraday constant, ψ_x is the electrical potential at position x , R is the gas constant, and T is the temperature in Kelvin.

The uptake of anions develops as the simultaneous sorption of protons and chloride ions. Since we have a sequence of reactions, the equilibrium of this common sorption can be expressed by the product of the respective formation constants:

$$K_{\text{Cl}}^{\text{H}} = K_{\text{H}}^+ \times K_{\text{Cl}}^- \quad [14]$$

The uptake of cations, however, develops as the competitive sorption of protons and sodium ions. As a consequence, the equilibrium of the cation exchange is expressed by the ratio of the corresponding formation constants:

$$K_{\text{Na}}^{\text{H}} = \frac{K_{\text{H}}^{-}}{K_{\text{Na}}^{+}} \quad [15]$$

By means of eqns [6]–[15] one obtains:

$$K_{\text{Cl}}^{\text{H}} = \frac{c(\text{S-OH}_2\text{Cl})}{c(\text{S-OH}) \cdot c(\text{Cl}^{-}) \cdot c(\text{H}^{+})} \times \exp \left\{ + \frac{F}{RT} (\psi_{\text{S}} - \psi_{\text{Cl}}) \right\} \quad [16]$$

$$K_{\text{Na}}^{\text{H}} = \frac{c(\text{S-OH}) \cdot c(\text{Na}^{+})}{c(\text{S-ONa}) \cdot c(\text{H}^{+})} \times \exp \left\{ \frac{F}{RT} (\psi_{\text{S}} - \psi_{\text{Na}}) \right\} \quad [17]$$

Multiplying by the volume of the liquid phase and dividing by the mass of sorbent, the concentrations of surface complexes are converted to exchanger loadings $q(\text{OH})$, $q(\text{Cl}^{-})$, and $q(\text{Na}^{+})$ respectively; $q(\text{OH})$ denotes nonionized surface groups.

As a consequence, the first factor on the right-hand sides exclusively contains quantities that can be derived from experiments. Both expressions are designated as *generalized separation factors*, Q . After introducing dimensionless loadings with species i , $y(i) = q(i)/q_{\text{max}}$, where q_{max} is the maximum exchanger loading, the following expressions are obtained:

$$Q_{\text{Cl}}^{\text{H}} = \frac{q(\text{Cl})}{q(\text{OH}) \cdot c(\text{H}^{+}) \cdot c(\text{Cl}^{-})} = \frac{y(\text{Cl})}{y(\text{OH}) \cdot c(\text{H}^{+}) \cdot c(\text{Cl}^{-})} \quad [18]$$

$$Q_{\text{Na}}^{\text{H}} = \frac{q(\text{OH}) \cdot c(\text{Na}^{+})}{q(\text{Na}) \cdot c(\text{H}^{+})} = \frac{y(\text{OH}) \cdot c(\text{Na}^{+})}{y(\text{Na}) \cdot c(\text{H}^{+})} \quad [19]$$

Similar relationships can be derived for any monovalent counterion.

The difference of electrical potentials in the exponential terms of eqns [16] and [17] needs consideration about the surface charge densities in the series of electric capacitors formed by the surface, Stern and diffuse layers. As has been shown in earlier publications, the unknown differences in the electrical potential can be expressed in terms of the loading

of the surface with Cl^{-} and Na^{+} ions. After resolving the equations for the generalized separation factor one obtains:

$$\log Q_{\text{Cl}}^{\text{H}} = \log K_{\text{Cl}}^{\text{H}} + m(\text{H}, \text{Cl}) \times [-y(\text{Cl}) + y(\text{Na})] \quad [20]$$

$$\log Q_{\text{Na}}^{\text{H}} + m(\text{H}, \text{Cl}) \cdot y(\text{Cl}) = \log K_{\text{Na}}^{\text{H}} + m(\text{H}, \text{Na}) \cdot y(\text{Na}) \quad [21]$$

The terms $m(\text{H}, i)$ are given by the following equation:

$$m(\text{H}, i) = \frac{1}{12.303} \times \frac{q_{\text{max}} \cdot F^2}{A_0 \cdot C(\text{S}, i) \cdot RT} \quad [22]$$

where A_0 is the specific surface area and $C(\text{S}, i)$ denotes the capacitance of the capacitor formed by the surface and layer i . The derivation has been given in the literature.

For a system with an arbitrary number of monovalent counterions, the following relationship can be deduced from similar considerations:

$$\log Q_i^{\text{H}} = \log K_i^{\text{H}} + \sum_{j=2}^{i-1} \{m(\text{H}, j) \cdot V(j) \cdot y(j)\} + m(\text{H}, i) \sum_i^n \{V(i) \cdot y(i)\} \quad [23]$$

$$i = 2, 3 \dots, n \text{ index of counterions}$$

$$j = 2, 3 \dots, i - 1 \text{ running index}$$

Hydrogen ions are always taken as component '1'. The factors $V(j)$ and $V(i)$ are the signs of the charge of the ions having the values of -1 for anions and $+1$ for cations. The first summation comprises counterions from index '2' to ' $i-1$ ' (closer to the surface than species ' i '). The second summation considers the counterions with indices running from ' i ' to ' n '. For a system with n counterions there are $n-1$ equations [23]. By subsequent evaluation of data all constants $\log K_i^{\text{H}}$ and $m(\text{H}, i)$ can be derived from the multicomponent system.

During the exchange of one divalent counterion for two monovalent ions, one divalent ion replaces two adjacent monovalent species at the surface, where at least one divalent species of counterion is present, the sorbent has to be assumed to have divalent functional sites in the mathematical treatment (assumption 3). As a consequence, a surface complex consisting of two sites and two monovalent counterions is defined that is replaced by a surface complex which consists of two sites with one divalent counterion. For a system with H^{+} , Na^{+} , Cl^{-} and SO_4^{2-} the generalized

separation factors are then given by the following expressions:

$$Q_{\text{II}SO_4}^H = \frac{c\{(S-OH)_2 = SO_4\}}{c\{S-OH, S-OH\} \cdot c(H^+)^2 \cdot c(SO_4^{2-})} \quad [24]$$

$$Q_{\text{II}Cl}^H = \frac{c\{S-OH_2Cl, S-OH_2Cl\}}{c\{S-OH, S-OH\} \cdot c(H^+)^2 \cdot c(Cl)^2} \quad [25]$$

$$Q_{\text{II}Na}^H = \frac{c\{S-OH, S-OH\}}{c\{S-ONa, S-ONa\} \cdot c(H^+)^2} \quad [26]$$

Here the subscript II refers to calculation under the assumption of divalent functional sites.

The probability of two adjacent monovalent counterions i at the surface is given by:

$$y(i, i) = \left(\frac{y(i)}{\sum y(j)} \right)^2 \times \sum y(j) \quad [27]$$

where $\sum y(j)$ is the sum of dimensionless loadings of all monovalent counterions with valences $+1$ and -1 .

By this means the above separation factors can be expressed as:

$$Q_{\text{II}SO_4}^H = \frac{y(SO_4) \cdot \{y(H) + y(Cl) + y(Na)\}}{y(OH)^2 \cdot c(H^+)^2 \cdot c(SO_4^{2-})} \quad [28]$$

$$Q_{\text{II}Cl}^H = \frac{y(Cl)^2}{y(OH)^2 \cdot c(H^+)^2 \cdot c(Cl)^2} \equiv [Q_{\text{II}Cl}^H]^2 \quad [29]$$

$$Q_{\text{II}Na}^H = \frac{y(OH)^2 \cdot c(Na^+)^2}{y(Na)^2 \cdot c(H^+)^2} \equiv [Q_{\text{II}Na}^H]^2 \quad [30]$$

If divalent functional sites are assumed for systems with exclusively monovalent counterions, then the equilibrium parameters $\log K_{\text{II}}^H$ and $m_{\text{II}}(H, i)$ can be transformed to the parameters for monovalent functional sites according to:

$$\log K_{\text{II}}^H = \frac{\log K_{\text{II}}^H}{2} \quad [31]$$

$$m_{\text{II}}(H, i) = \frac{m_{\text{II}}(H, i)}{2} \quad [32]$$

The subscripts I and II refer to the assumption of either monovalent or divalent functional sites. If a system contains monovalent and divalent counterions the entire calculation has to assume divalent functional sites. Equilibrium parameters derived from

systems with only monovalent counterions have to be converted corresponding to eqns [31] and [32].

Relationships for Pure Cation or Anion Exchange on Weak Electrolyte Resins

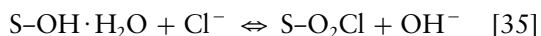
In the case of weakly acidic exchange resins there is no exchange of anions. Therefore, the terms for anions in the general equation [24] vanish. For a simple system with H^+ and Na^+ ions, eqn [21] simplifies to:

$$\log Q_{Na}^H = \log K_{Na}^H + m(H, Na) \cdot y(Na) \quad [33]$$

In a similar way, there is no exchange of cations by weakly basic exchangers. For the uptake of hydrochloric acid eqn [20] yields:

$$\log Q_{Cl}^H = \log K_{Cl}^H - m(H, Cl) \cdot y(Cl) \quad [34]$$

The uptake of anions by protonated functional groups is equivalent to the exchange of anions for hydroxyl groups:



A similar theoretical development of the exchange of OH^- for Cl^- ions leads to the equilibrium relationship:

$$\log Q_{Cl}^{OH} = \log K_{Cl}^{OH} + m(OH, Cl) \cdot y(Cl) \quad [36]$$

Relationships for Strong Electrolyte Exchangers

Relationships for the description of equilibria with strongly acidic and strongly basic resins can also be derived from the basic equation [23]. The difference, however, is that hydrogen ions cannot be assumed to be adsorbed in the innermost layer. In the case of the cation exchangers this can be explained by the fact that the exchanger is completely dissociated, even in the H^+ form. Furthermore, hydrated protons have a rather large diameter and, therefore, cannot be assumed to be located close to the surface. Similar considerations hold for strongly basic anion exchangers and hydroxyl ions. For both cases, therefore, the sequence of layers starts with the kind of counterions which in each is located the closest to the surface.

Liquid Phase Equilibrium Relationships

The liquid phase equilibrium is calculated by means of:

- the dissociation of water;
- the condition of electroneutrality; and
- mass balances for each component.

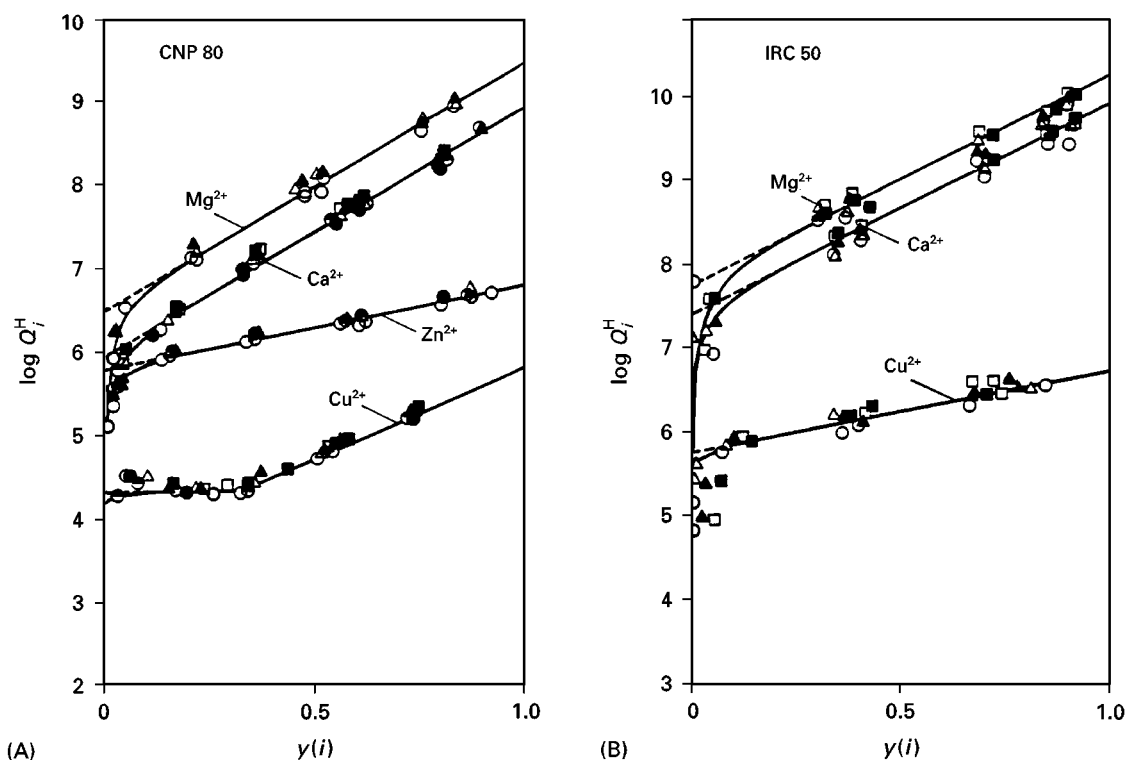


Figure 2 Development of the generalized separation factor for the weakly acidic ion exchange resins (A) LEWATIT CNP 80 and (B) AMBERLITE IRC 50 (by courtesy of Marcel Dekker Inc.).

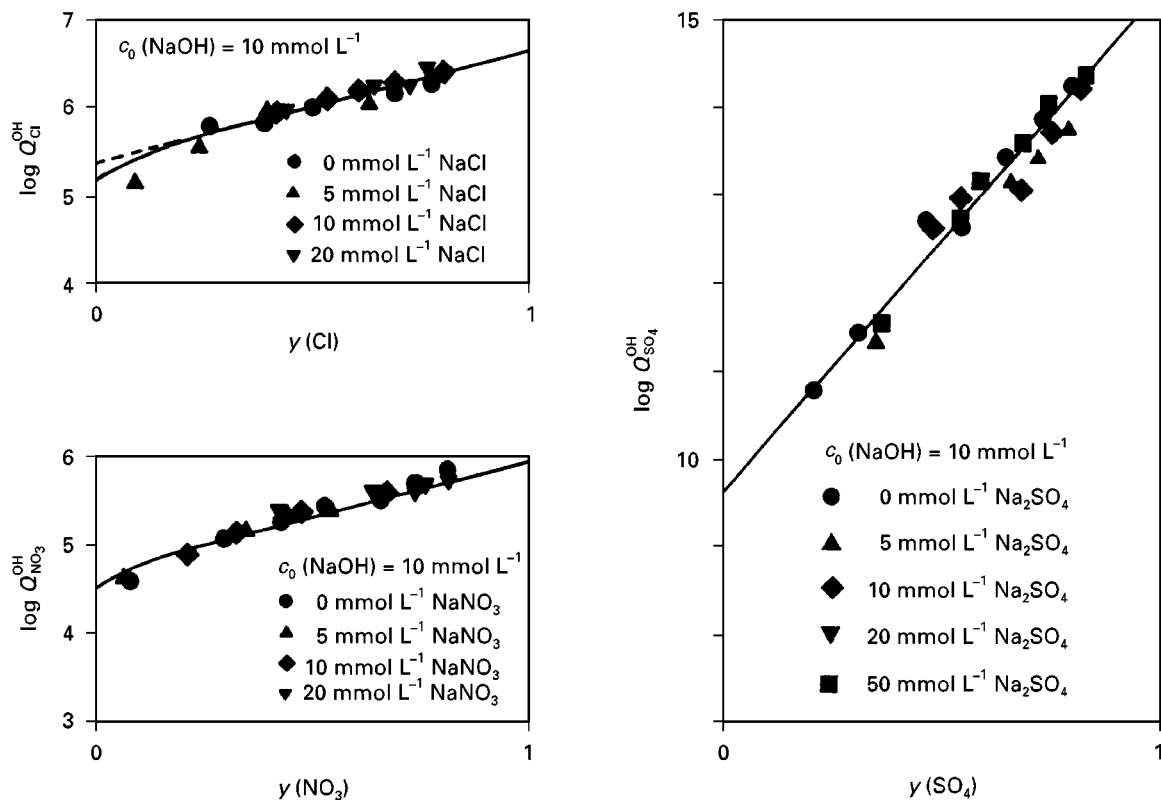


Figure 3 Development of the generalized separation factor for the weakly basic ion exchange resin AMBERLITE IRA 93 (by courtesy of Marcel Dekker Inc.).

Activity coefficients in the liquid phase can be calculated from the ionic strength using the extended Debye–Hückel relationship.

Experimental Evaluation of Equilibrium Data

General

Exchange equilibria have been determined for pure cation and anion exchangers as well as for amphoteric materials such as activated alumina and activated carbon. The pretreatment of these materials and the experimental conditions needed for obtaining proper equilibrium data have been described in detail in several publications. Cation concentrations can be measured by titration, photometric methods or by atomic absorption spectroscopy. Nitrate concentrations are measured photometrically, chloride and sulfate concentrations by ion chromatography.

In the case of pure anion or pure cation exchange, equilibria samples with increasing amounts of exchanger material are contacted with a fixed volume of the solution at constant temperature until equilibrium is obtained. Experiments with amphoteric equilibria are carried out at constant concentrations in the liquid phase and constant quantities of activated alumina or activated carbon in each of the samples. The volume/mass ratio is adjusted so that there is a substantial degree of sorption, as well as an equilibrium concentration that can be measured easily and with sufficient accuracy. Since the state of equilibrium is mainly dominated by the pH of the liquid phase, the pH value is varied in each series of samples. Details are described in the literature.

Evaluation of Data

For evaluation of equilibrium parameters the generalized separation factors have to be determined from equilibrium concentrations and resin loadings. These are then plotted against the respective dimensionless resin loading or the (algebraic) sum of resin loadings. In the case of binary systems with pure cation or anion exchange, the respective graphical representations directly yield the equilibrium parameters. The intersection of the linear relationship leads to $\log K$ and the slope of the straight line yields $m(i, j)$. Figures 2–5 show examples for different types of exchangers.

The results show that linear relationships are obtained in most cases. Systematic deviations are found for small loadings. This is attributed to the neglect of counterions in the diffuse layer. As has been demonstrated by Horst for simple systems, when this layer is considered, excellent agreement is obtained. For strongly acidic exchangers this region is compar-

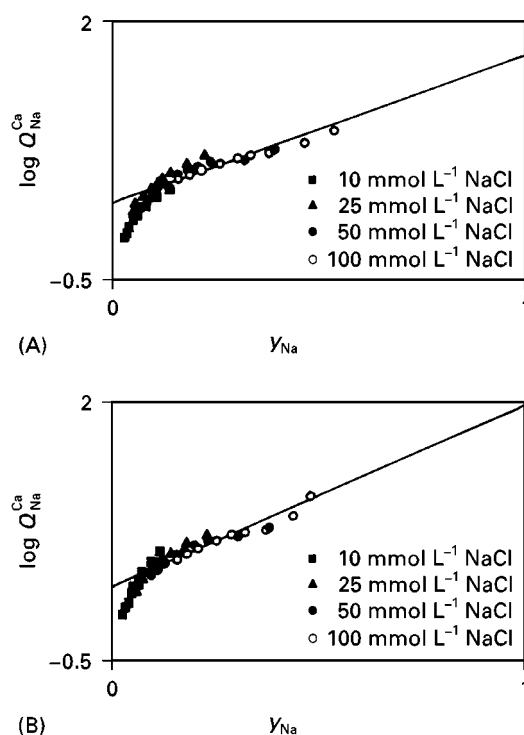


Figure 4 Development of the generalized separation factor for the exchange of calcium for sodium ions on two different strongly acidic resins. (A) Dowex HCRS; (B) LEWATIT S100.

atively larger than for other resin types. Evaluation of data for the exchange of sulfate for chloride on strongly basic exchangers shows that there are two different straight lines. There are clearly two different layers that are subsequently ‘filled’. Evaluation of data for a broad range of total concentrations up to 100 mmol L⁻¹ in the liquid phase reveals identical development of the linear relationships. For the entire range of ionic strength investigated the parameters can, therefore, be considered as ‘constant’ equilibrium constants.

Evaluation of amphoteric data requires a more sophisticated approach. The first step is the assumption of a certain sequence of layers. Evaluation of data starts with the evaluation of the equilibrium for the uptake of protons and ions in the first layer. The respective parameters are required for evaluation of the sorption of species in the next layer. Determination of the parameters for the third layer requires the sets of parameters for both the inner layers. This process has to be continued until all sets of binary parameters are derived. The sequence of a layers is assumed correctly if both the $\log K$ and $m(H, i)$ values show a steady increase with increasing distance. If this conditions is not fulfilled the calculation must be repeated with a modified sequence. Considering a system of layers H^+ , Cl^- , NO_3^- , Na^+ on activated alumina as an example, the equilibrium

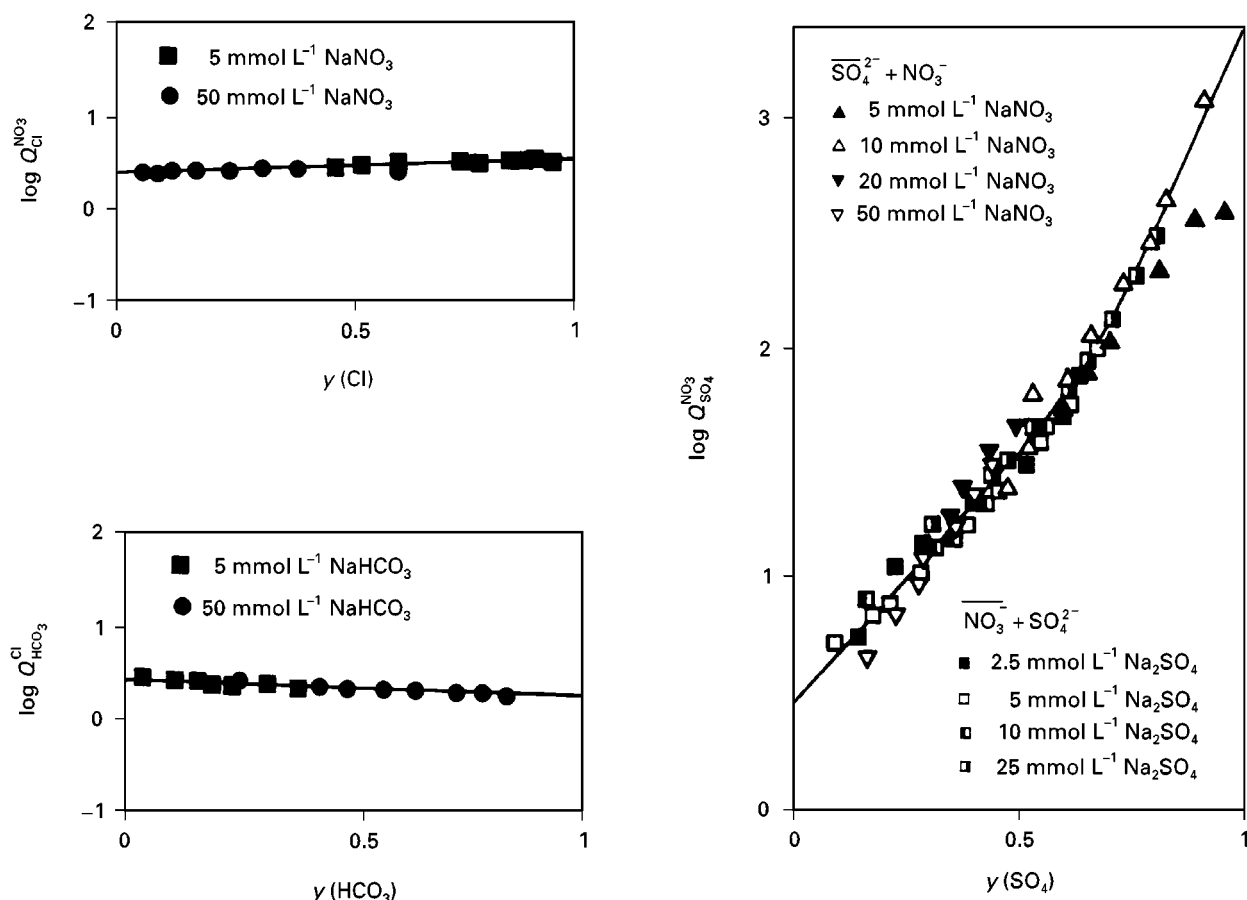


Figure 5 Development of the generalized separation factor for the strongly basic ion exchange resin AMBERLITE IRA 410 (Reprinted from Höll, Horst, Franzreb and Eberle (1993) by courtesy of Marcel Dekker Inc.).

parameters can be evaluated from the following relationships:

$$\log Q_{Cl}^H = \log K_{Cl}^H + m(H, Cl) \cdot \{ -y(Cl) \} \cdot \{ y(Na) - y(Cl) - y(NO_3) \} \quad [37]$$

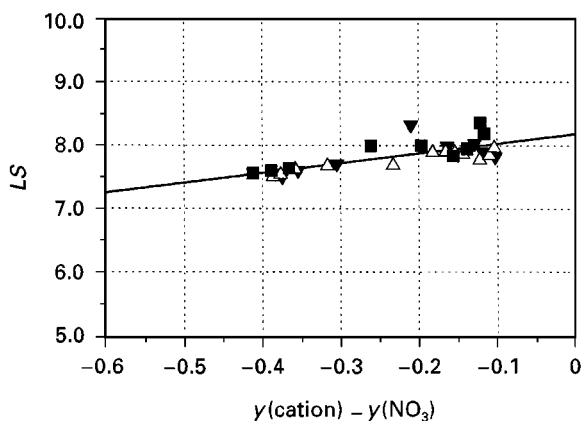


Figure 6 Development of the generalized separation factor for the uptake of nitrate by activated alumina (COMPALOX AN/V800) from a multicomponent system (cation = Na^+ or K^+). The symbols represent different experiments.

$$\begin{aligned} & \log Q_{NO_3}^H - m(H, Cl) \cdot \{ -y(Cl) \} \\ &= \log K_{NO_3}^H + m(H, NO_3) \cdot \{ y(Na) - y(NO_3) \} \quad [38] \\ & \log Q_{Na}^H - m(H, Cl) \cdot \{ -y(Cl) \} - m(H, NO_3) \\ & \cdot \{ -y(NO_3) \} = \log K_{Na}^H + m(H, Na) \cdot y(Na) \quad [39] \end{aligned}$$

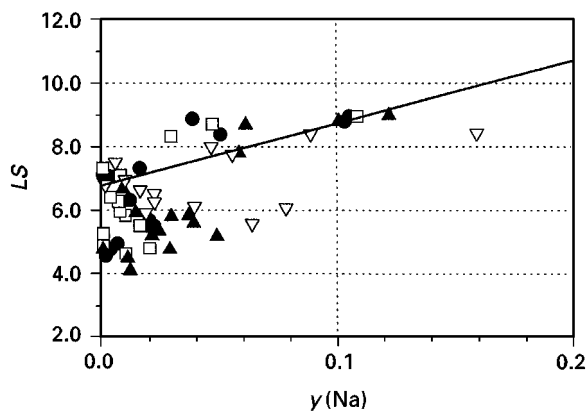


Figure 7 Development of the generalized separation factor for the sorption of sodium on COMPALOX AN/V800.

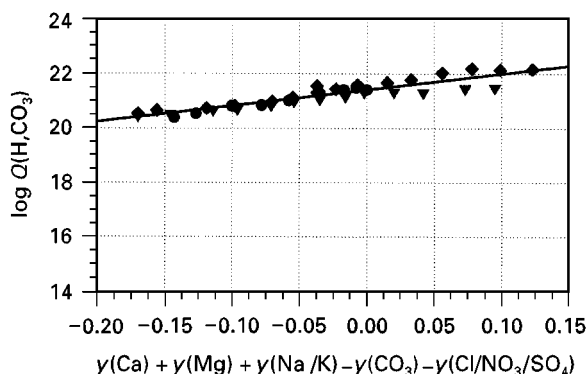


Figure 8 Development of the generalized separation factor for the sorption of carbonate species by activated carbon (NORIT ROW 0.8 Supra) from a multicomponent system.

Results of the evaluation of equilibrium data for the sorption of Cl^- , NO_3^- and Na^+ on activated alumina (COMPALOX AN/V800) are plotted in Figures 6 and 7. Although the results for the uptake of sodium ions are not satisfactory, the data demonstrate that linear relationships are obtained.

Prediction of Multicomponent Equilibria

General

Prediction of arbitrary exchange equilibria requires a set of conditions to be fulfilled:

- conservation of mass
- electroneutrality on the liquid phase
- electroneutrality on the resin phase
- adjustment of equilibrium for the exchange of ions
- dissociation equilibria in the liquid phase.

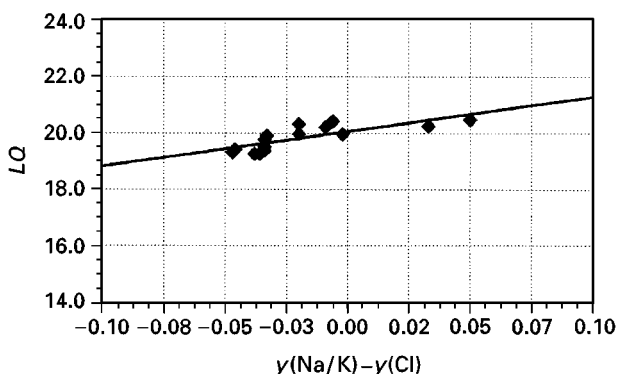


Figure 9 Development of the generalized separation factor for the sorption of chloride ions by activated carbon (NORIT ROW 0.8 Supra) from a multicomponent system. $LQ = \log Q(\text{H}, \text{Cl}) + m_{\text{II}}(\text{H}, \text{CO}_3)\gamma(\text{CO}_3) - m_{\text{II}}(\text{H}, \text{Ca})\gamma(\text{Ca}) - m_{\text{II}}(\text{H}, \text{Mg})\gamma(\text{Mg})$.

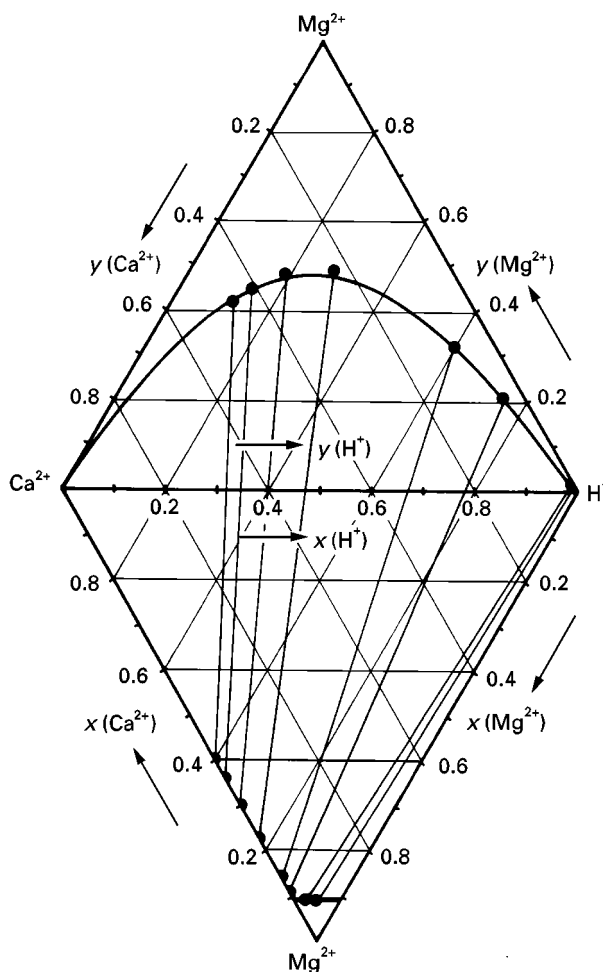


Figure 10 Comparison of experimental data and predicted equilibria for the ternary system $\text{H}^+/\text{Mg}^{2+}/\text{Ca}^{2+}$ on the weakly acidic resin LEWATIT OC 1046.

As can easily be shown, the number of equations is always greater than the number of unknown quantities. Therefore, some conditions are fulfilled automatically. The remaining set of coupled nonlinear equations must be solved by appropriate numerical methods.

Respective results for the uptake of inorganic ions by an activated carbon are plotted in Figures 8 and 9. With few exceptions, the equilibrium data satisfactorily fall on linear relationships as predicted by the theoretical approach.

Pure Cation or Anion Exchange

For prediction of multicomponent equilibria it is convenient if the binary parameters for the exchange of different counterions for the same reference ion have been deduced. For pure cation or anion exchange systems consideration of a three-component equilibrium with ions. A (reference ion), B and

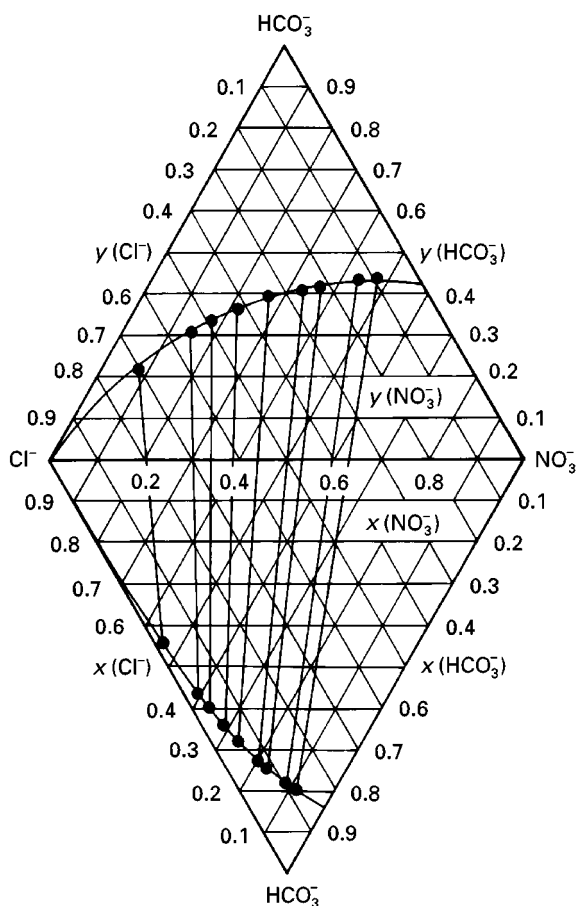


Figure 11 Comparison of experimental data and predicted equilibria for the ternary system $\text{Cl}^-/\text{HCO}_3^-/\text{NO}_3^-$ on the strongly basic resin AMBERLITE IRA 410.

C leads to the relationships:

$$\log Q_B^A = \log K_B^A + m(A, B) \cdot [\gamma(B) + \gamma(C)] \quad [40]$$

$$\log Q_C^B = \log K_C^B + m(B, C) \cdot \gamma(C) \quad [41]$$

As has been demonstrated earlier, the binary parameters for the exchange of A versus B are the same as in the pure binary case. Also, the binary parameters for the exchange of A for C have been evaluated. In the above system, therefore, the parameters for the exchange of B for C are unknown. However, they can easily be calculated: the unknown parameter $\log K_C^B$ results from the definition:

$$\log K_C^B = \log K_C^A - \log K_B^A \quad [42]$$

For derivation of the unknown slope we make use of the fact that the sequence of layers can be considered as a series of layers of an electric capacitor. Since the

definition of $m(i, j)$ contains the electric capacitance, C , we can make use of the well-known relationship for capacitances in series:

$$\frac{1}{C(A, C)} = \frac{1}{C(A, B)} + \frac{1}{C(B, C)} \quad [43]$$

Thus, one obtains:

$$m(B, C) = m(A, C) - m(A, B) \quad [44]$$

Similar relationships are obtained for systems with more than three counterions. Examples of a comparison between experimental results and equilibria predicted from binary data are given in Figures 10–12.

For amphoteric sorbents the individual equilibrium parameters are already determined during evaluation of data. Therefore, no additional calculations are required. Figure 13 shows the comparison between experimentally determined oxide loadings and developments calculated by means of the set of equilibrium parameters determined previously. The data are plotted as relative loadings ($q(i)/q_{\max}$) as a function of pH. The system contained the four components H^+ , Cl^- , SO_4^{2-} and K^+ . Obviously, sulfate ions are preferred over chloride species. The constant sulfate loadings for pH values below 5 are due to the constant initial sulfate concentration in the system. Only minor loadings with monovalent cations are observed. There is excellent agreement with the predicted loadings.

Figure 14 shows the results from one experiment with activated carbon and protons, carbonate, sulphate, calcium, magnesium and potassium as counterions. The relative loadings with both carbonate and nitrate ions decrease with increasing pH of the solution, while the loadings of calcium and potassium slightly increase. Nevertheless their uptake

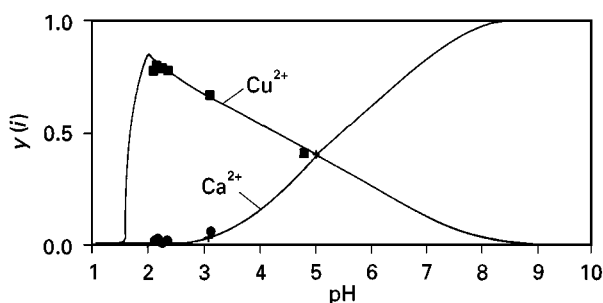


Figure 12 Comparison of experimental data and predicted equilibria for the ternary system $\text{H}^+/\text{Ca}^{2+}/\text{Cu}^{2+}$ on the chelating resin LEWATIT TP 207. $C_0(\text{HCl}) = 10 \text{ mmol L}^{-1}$; $C_0(\text{CuCl}_2) = 10 \text{ mmol L}^{-1}$. (From Horst and Höll (1997), copyright Academic Press.)

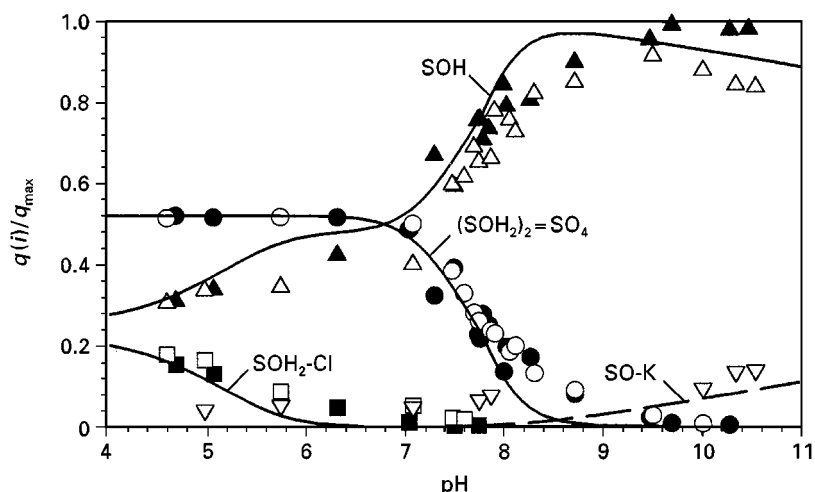


Figure 13 Comparison of experimental data and predicted loadings of activated alumina for a multicomponent system. Activated alumina: COMPALOX AN/V800.

remains small, indicating that there is only a small capacity for the uptake of cations. Again, there is good agreement with the predicted developments.

Applications

The principal advantage of the surface complexation theory lies in the fact that it can be applied to any normal or reaction-coupled ion exchange process for which other theoretical descriptions of equilibria fail.

One field of application is the prediction of multi-species exchange kinetics. This has been demonstrated by Franzreb, who included the description into the solution of the Nernst-Planck equations for

several ternary and quaternary cases. The development of systems with strong and weak exchange resins and with normal and reaction-coupled multi-species processes could be predicted with excellent accuracy.

The surface complexation theory can also be easily applied to the simplified prediction of the performance of filters in which the filter is divided into a series of equilibrium stages. By means of the porosity of the filter section the quantities of resin material and liquid phase are known. Consequently, the exchange equilibrium in each stage can be calculated. The effluent composition of the filter is given by the equilibrium in the last stage. By this means and by an appropriate assumption of the number of

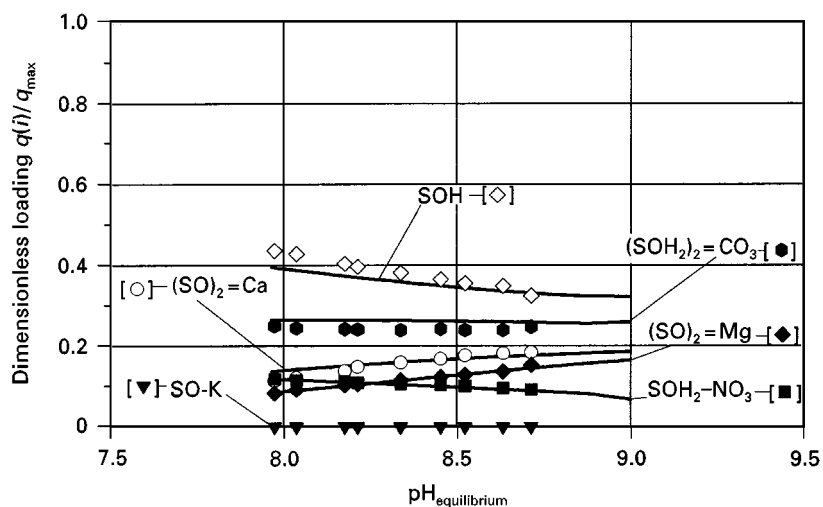


Figure 14 Comparison of experimental data and predicted loadings of activated carbon with inorganic species. Activated carbon: NORIT ROW 0.8 Supra.

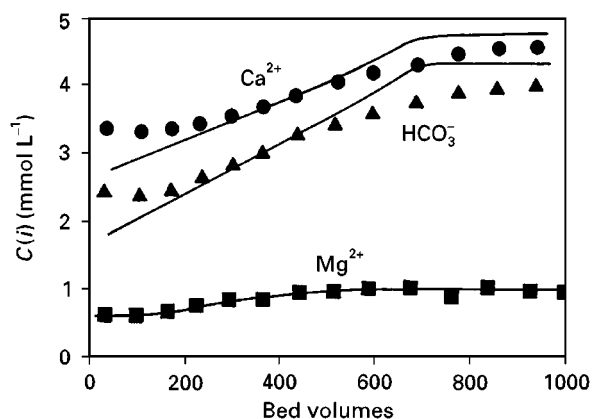


Figure 15 Comparison of experimental (●, ▲, ■) and predicted (—) breakthrough curves during softening/dealkalization of tap water. Resin: AMBERLITE IRC 50, regenerated by carbonic acid. Volume of resin, 1 L; throughput, 6.9 BV h⁻¹; feed: Ca²⁺ = 2.44 mmol L⁻¹; Mg²⁺ = 0.48 mmol L⁻¹; HCO₃⁻ = 4.42 mmol L⁻¹.

equilibrium stages a fairly good agreement between experimental and predicted concentration histories can be obtained. Figure 15 shows the comparison between experimental data and predicted developments of concentrations for a system with a weakly acidic resin which is applied for softening/dealkalization of tap water. Clearly a very satisfactory agreement is obtained.

Further Reading

Davis JA, James RO and Leckie JO (1978) Surface ionization and complexation at the oxide/water interface.

Computation of electrical double layer properties in simple electrolytes. *Journal of Colloid and Interface Science* 63: 480–499.

Franzreb M, Höll WH and Sontheimer H (1993) Liquid-phase mass transfer in multi-component ion exchange. I. System without chemical reactions in the film. *Reactive Polymers* 21: 117–133.

Franzreb M, Höll WH and Eberle SH (1995) Liquid-phase mass transfer in multi-component ion exchange. 2. Systems with irreversible chemical reactions in the film. *Industrial and Engineering Chemistry Research* 34: 2670–2675.

Höll WH, Horst J and Wernet M (1991) Application of the surface complex formation model to ion exchange equilibria. II. Chelating resins. *Reactive Polymers* 14: 251–261.

Höll WH, Horst J and Franzreb M (1993) Application of the surface complex formation model to ion exchange equilibria. III. Anion exchangers. *Reactive Polymers* 19: 123–136.

Höll WH, Horst J, Franzreb M and Eberle SH (1993) In: Marinsky J and Marcus Y (eds) *Ion Exchange and Solvent Extraction, a Series of Advances*, vol. 11, ch. 3, p. 151. New York–Basel–Hong Kong: Marcel Dekker Inc.

Horst J and Höll WH (1997) Application of the surface complex formation model to ion exchange equilibria. IV. Amphoteric sorption onto γ -aluminium oxide. *Journal of Colloid and Interface Science* 195: 250–260.

Horst J, Höll WH and Eberle SH (1990) Application of the surface complex formation model to ion exchange equilibria. I. *Reactive Polymers* 13: 209.

Stumm W (1992) *Chemistry of the Solid–Water Interface*. New York: Wiley and Sons.

Theory of Ion Exchange

R. Harjula, University of Helsinki, Helsinki, Finland

Copyright © 2000 Academic Press

Proper theoretical tools are necessary at all stages in the development of ion exchange applications. Firstly, in the laboratory, when a new application is being developed, theory is helpful in the design of new materials and necessary for the interpretation and quantification of research results. Secondly, theory is needed in the design of industrial and laboratory processes. When the process is being operated, theory is again useful to keep the process under optimal control.

Ion exchangers are used in very diverse applications in the laboratory and in industry. Considering this, and the fact that a very wide range of different substances can act as ion exchangers, it is not surprising to see in the literature that various sets of nomenclature, conventions and diverse theories exist, reflecting the special features of the applications or materials involved. For instance, one finds rather different definitions for several basic terms of ion exchange in the field of water purification compared to those used in ion exchange chromatography and even diversity in the terminology can be seen within the field of ion chromatography. It is inevitable that various theories must exist for the functioning of different types of ion exchangers, but the

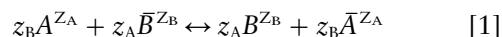
discrepancies in the most basic definitions only lead to confusion and misconception that deter the utilization of the theory.

The theory of ion exchange is a vast subject. This article presents and discusses most of the essential theory and concepts in connection with the most common applications. There is emphasis on discussing details that are important in interpreting correctly research results and in predicting and optimizing ion exchanger performance. For simplicity, the basic equations are written for cation exchange but they are applicable to anion exchange as well, with minor modifications. Theories for the prediction of cation exchange selectivity are also discussed briefly.

Basic Concepts

Ion Exchange Equilibria

A binary ion exchange reaction between ion A (charge z_A) and ion B (charge z_B) may be written as:



where superscript bars refer to the ions in a solid ion exchanger. Various equilibrium quantities are used to measure and estimate the efficiency of the ion exchanger for a given separation task. The most common of these include the following.

Selectivity coefficient (selectivity quotient)

$$k_{A/B} = \frac{\bar{C}_A^{z_B} C_B^{z_A}}{\bar{C}_B^{z_A} C_A^{z_B}} \quad [2]$$

where \bar{C} s are the concentrations of the ions in the exchanger and C s those in solution. Various concentration units are commonly used (molar, molal, equivalent fraction, etc.). When $z_A \neq z_B$, the numerical value of $k_{A/B}$ depends on the choice of the concentration units. The selectivity coefficient ($k_{A/B}$) usually changes as a function of exchanger composition ($k_{A/B} = f(\bar{C}_A)$; see Figure 1) and also as a function of the total concentration (or ionic strength) of the external solution, especially in concentrated solutions.

Corrected selectivity coefficient By making the activity (nonideality) correction for the solution phase, the so-called corrected selectivity coefficient is obtained:

$$k'_{A/B} = \frac{\bar{C}_A^{z_B} a_B^{z_A}}{\bar{C}_B^{z_A} a_A^{z_B}} = \frac{\bar{C}_A^{z_B} C_B^{z_A} \gamma_B^{z_A}}{\bar{C}_B^{z_A} C_A^{z_B} \gamma_A^{z_B}} = k_{A/B} \frac{\gamma_B^{z_A}}{\gamma_A^{z_B}} \quad [3]$$

where a_A, a_B are the activities of ions A, B in the solution. This quantity is independent of the total concentration of the external solution by definition and thus reflects the pure exchanger-ion interactions contributing to the selectivity. In dilute solutions,

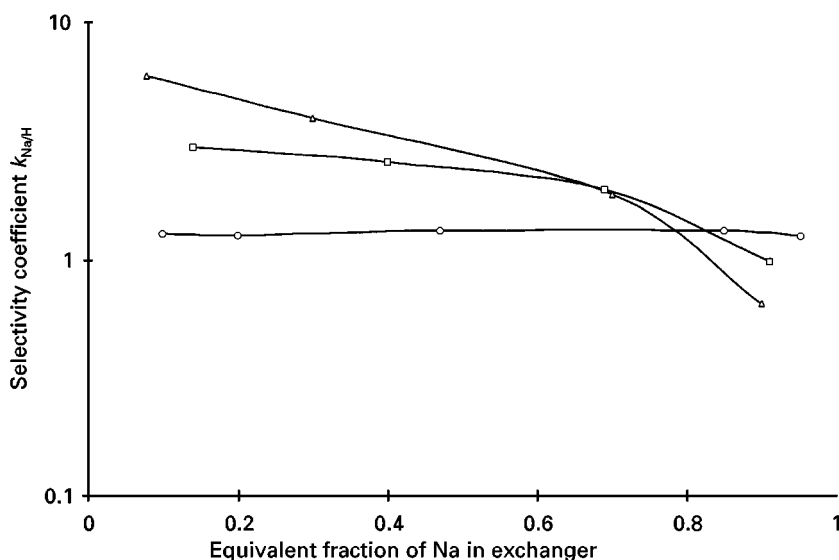


Figure 1 Selectivity coefficient $k_{Na/H}$ (see eqn [2]) for Na^+/H^+ exchange in sulfonated polystyrene/divinylbenzene (DVB) resins as a function of Na^+ equivalent fraction in resin at different degrees of cross-linking (nominal DVB content). Circles, DVB 5.5%; squares, DVB 15%; triangles, DVB 25%. (Data from Helfferich FG, 1995.)

$k'_{A/B} \approx k_{A/B}$. However, the corrected selectivity coefficient usually varies with the exchanger composition (\bar{C}_A).

Thermodynamic equilibrium constant The thermodynamic equilibrium constant $K_{A/B}$:

$$K_{A/B} = \frac{\bar{a}_A^{Z_B} \bar{a}_B^{Z_A}}{\bar{a}_B^{Z_A} \bar{a}_A^{Z_B}} = \frac{\bar{C}_A^{Z_B} \bar{C}_B^{Z_A}}{\bar{C}_B^{Z_A} \bar{C}_A^{Z_B}} \frac{\gamma_B^{Z_A}}{\gamma_A^{Z_B}} \frac{\gamma_B^{Z_A}}{\gamma_A^{Z_B}} = k'_{A/B} \frac{\gamma_B^{Z_A}}{\gamma_A^{Z_B}} \quad [4]$$

can be obtained by integrating the corrected selectivity coefficient as a function of exchanger composition. According to Argesinger *et al.* and Högfeldt *et al.*:

$$K_{A/B} = \int_0^1 \ln K_H d\bar{E}_A \quad [5]$$

where \bar{E}_A is the equivalent fraction of A in the exchanger ($\bar{E}_A = z_A \bar{C}_A / (z_A \bar{C}_A + z_B \bar{C}_B)$) and K_H is the corrected selectivity coefficient written with mole fractions (\bar{X}) as concentration units for the ions in the exchanger:

$$K_H = \frac{\bar{X}_A^{Z_B} \bar{C}_B^{Z_A}}{\bar{X}_B^{Z_A} \bar{C}_A^{Z_B}} \frac{\gamma_B^{Z_A}}{\gamma_A^{Z_B}} \quad [6]$$

Gaines and Thomas supplemented the abstract thermodynamic treatment to include the contributions of salt imbibition and water activity changes, which need to be considered when ions are exchanged in concentrated solutions.

Distribution coefficient (distribution constant, distribution ratio) Various distribution constants and coefficients are used to measure the ion exchange equilibria. In general, the distribution coefficient k_d of ion A is defined as a concentration ratio in the exchanger and solution:

$$k_d = \frac{\bar{C}_A}{C_A} \quad [7]$$

This quantity is only a constant under special conditions. In general, k_d depends on the ionic composition of the exchanger and the solution. For a binary exchange, one obtains from eqns [2] and [7] that:

$$k_d = k'_{A/B} \left(\frac{\bar{C}_B}{C_B} \right)^{\frac{Z_A}{Z_B}} \quad [8]$$

Under the special condition that A is present in the solution and in exchanger at much lower concentra-

tion than B ($C_A \ll C_B$, $\bar{C}_A \ll \bar{C}_B$), $k_{A/B}$ and \bar{C}_B are essentially constant ($\bar{C}_B \approx Q$, the ion exchange capacity) and:

$$\log k_d = \frac{1}{Z_B} \log (k_{A/B} Q^{Z_A}) - \frac{Z_A}{Z_B} \log C_B \quad [9]$$

Under these circumstances, k_d depends only on the concentration of ion B and, on a logarithmic scale, the slope of k_d equals $-z_A/z_B$, the ratio of cation charges.

Experimentally determined graphs of $\log k_d$ vs $\log C_B$ (eqn [9]) are frequently used in research to study sorption mechanisms, the charges of the exchanging species and in the estimation of exchanger performance, e.g. in water purification (estimation of processing capacity) and in ion chromatography (estimation of retention volume). Great care should be taken, however, in the interpretation of the data and in making sure that the assumptions leading to eqn [9] are valid. Because of the widespread use of distribution coefficients in ion exchange, it is useful to emphasize this point by taking a binary univalent exchange ($z_A = z_B = 1$) as an example here. For this equilibrium, eqn [9] can be further manipulated to give:

$$k_d = \frac{Q}{\frac{C_B}{k_{Cs/Na}} + C_A} \quad [10]$$

This equation now shows that, in fact, the condition for linear dependence of k_d on C_A ($\log k_d = \log (k_{A/B} Q) - \log C_B$) is that $C_A \ll C_B/k_{A/B}$. Thus, even if $C_A \ll C_B$, the dependence may not be linear if the selectivity coefficient is very large. This feature of k_d is shown as calculated examples in Figure 2. It can be seen that, if the selectivity coefficient is low, k_d falls linearly with the concentration of the macro-ion B, on a logarithmic scale with a slope of -1 , as eqn [9] implies. However, when the selectivity increases, the k_d starts to level off at lower concentrations of B and ultimately becomes independent of C_B when the selectivity is very high. In the studies of highly selective exchangers (zeolites and some other inorganic materials, chelating resins) such independence of k_d on the macro-ion concentration is often observed and every now and then the incorrect conclusion is made that the uptake of trace ions is not ion exchange but some sort of surface adsorption reaction. Figure 2 also shows an interesting feature of the link between k_d and selectivity: in dilute solutions the k_d s tend to a common value, which is determined by the ratio

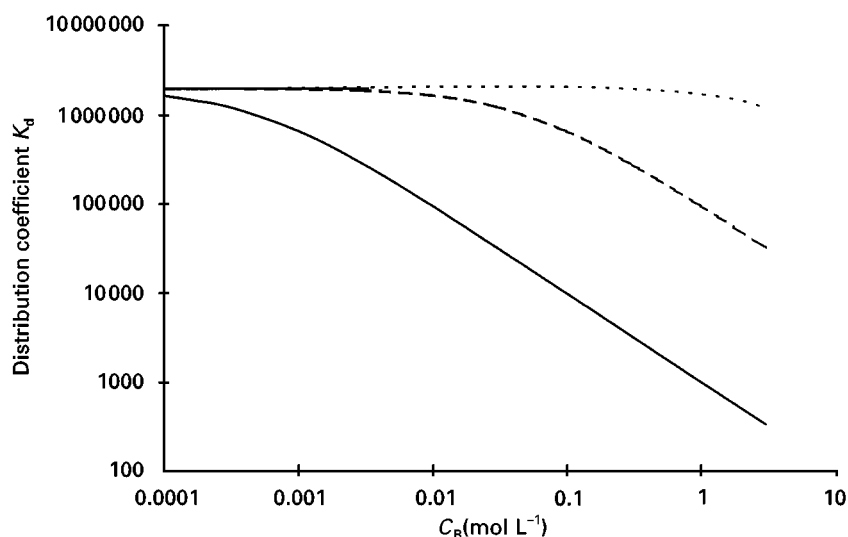


Figure 2 Calculated values (eqn [10]) for the distribution coefficient k_d for trace ion A ($C_A = 10^{-6} \text{ mol L}^{-1}$) in binary univalent A^+/B^+ exchange as a function of macro-ion concentration C_B at different values of the selectivity coefficient $k_{A/B}$. Dotted line, $k_{A/B} = 5\,000\,000$; dashed line, $k_{A/B} = 50\,000$; continuous line, $k_{A/B} = 500$. Ion exchange capacity of the exchanger 2.0 mmol g^{-1} .

of Q/C_A . The value of selectivity thus becomes unimportant in dilute solutions.

In general, eqn [9] is valid for several parallel trace ion exchange reactions ($A, C, D \dots$) in the presence of one common macro-ion B , since the ions that are present at trace level will have a negligible effect on other trace ion equilibria.

Separation factor Separation factor is usually used in ion exchange chromatography to estimate the separability of two trace ions. Considering the separation of two trace ions A and C using macro ions B as an eluent, one obtains for the separation factor ($\alpha_{A/C}$):

$$\alpha_{A/C} = \frac{\bar{C}_A C_C}{C_A \bar{C}_C} = \frac{k_{d(A)}}{k_{d(C)}} = \left(\frac{k_{A/B}}{k_{C/B}} \right)^{\frac{1}{Z_B}} \left(\frac{\bar{C}_B}{C_B} \right)^{\frac{Z_A}{Z_C}} \\ = \text{Constant} / C_B^{\frac{Z_A}{Z_C}} \quad [11]$$

In the case that $z_A \neq z_C$, the separation factor increases as the concentration of B is decreased.

Ion exchange isotherm An ion exchange isotherm is a function that represents the ionic composition of the exchanger (\bar{E}_A) as a function of the ionic composition of the solution (E_A), or vice versa, at constant temperature (Figure 3). Traditionally, the selectivity of the exchanger is estimated from the isotherm. If the isotherm is concave towards the axis representing the ion concentration in the exchanger, the ion exchanger is considered to be selective for that ion (curves a and

b in Figure 3). If the isotherm lies on the diagonal of the presentation ($\bar{E}_A = E_A$), the exchanger has no preference for either ion A or B (curve c) and a bending of the isotherm towards the E_A -axis indicates that the exchanger is nonselective. The magnitude of the selectivity coefficient cannot be always deduced from the isotherm because when $z_A \neq z_B$, the shape of the isotherm depends strongly on the total ion concentration (C_T) in the solution. This behaviour arises from the difference between the cation charges, which can be clearly seen if the equation for the selectivity coefficient is expressed in terms of equivalent fractions and rearranged:

$$\frac{\bar{E}_A^{Z_B}}{\bar{E}_B^{Z_A}} = \frac{E_A^{Z_B}}{E_B^{Z_A}} k_{A/B} C_T^{(Z_B - Z_A)} \quad [12]$$

At a given point \bar{E}_A on the isotherm (the left-hand side of eqn [12] constant), the ratio E_A/E_B must decrease as C_T is decreased when $z_A > z_B$. Thus, the relative concentration of ion A must decrease with decreasing C_T . This feature, the increased preference of an ion exchanger for the ion having a higher charge with the dilution of the solution, is called electroselectivity. It should be also noted that the ion exchanger may prefer ion A strongly even though the value of the selectivity coefficient is equal to or less than unity (see calculated examples in Figure 3).

Ion Exchange Kinetics

The rate of ion exchange is governed by the various diffusion processes in the system. In general,

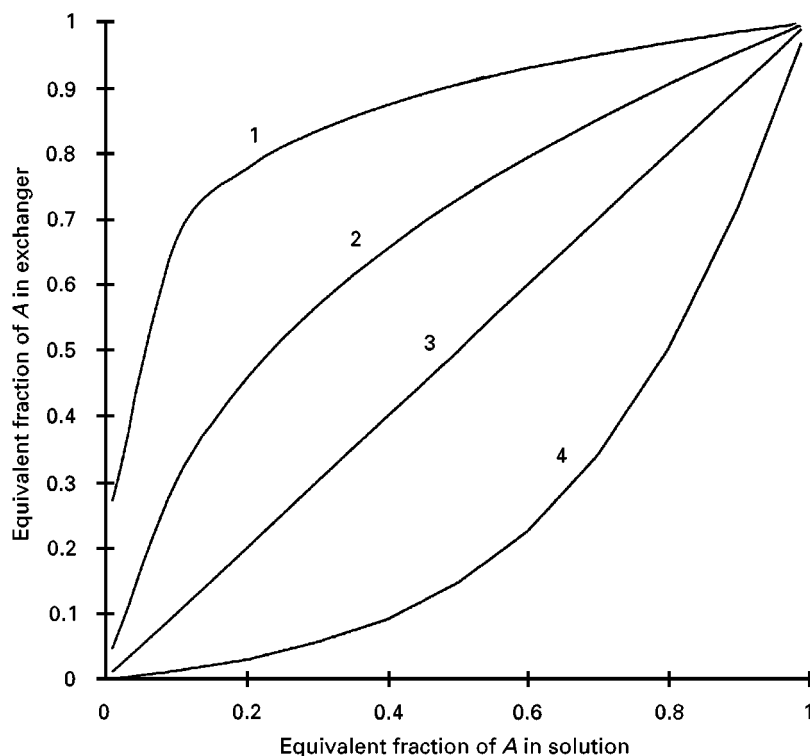


Figure 3 Calculated ion exchange isotherms for a hypothetical di-univalent (A^{2+}/B^{+}) exchange having a selectivity coefficient $k_{A/B} = 1$. The isotherms have been generated using constant total ion concentrations: 1, 0.01 mol L⁻¹; 2, 0.1 mol L⁻¹; 3, 1 mol L⁻¹; 4, 5 mol L⁻¹. The isotherms show increasing preference of the ion exchanger for ion A with increasing dilution of the solution (electroselectivity effect.)

diffusion can be described by Fick's first law. The flux of ion A (J_A) is given by:

$$J_A = -D \text{grad } C_A \quad [13]$$

where D is the diffusion coefficient. This equation describes purely statistical diffusion that is driven by the concentration gradient. In ion exchangers it is usually necessary to consider also the electric potential (ϕ) and then the flux of ion A (J_A) is given by the Nernst-Planck equation:

$$J_A = -D \left(\text{grad } C_A + z_A C_A \frac{F}{RT} \text{grad } \phi \right) \quad [14]$$

where F is the Faraday constant. Most commonly, the kinetics of ion exchange reactions are interpreted in the terms of external or internal diffusion. As the external solution is usually agitated, there is essentially no concentration gradient in the bulk of the external solution. Gradients arise, however, within a thin layer of solution adhering to the surface of the exchanger particle. Diffusion across this layer is called film diffusion. This concept, developed first by

Nernst, often satisfactorily describes the diffusion processes at solid-solution interfaces. The internal diffusion of the ions in the exchanger phase is called particle diffusion. Most often, the particle is considered homogeneous, so that the different diffusional processes within the particle (pore diffusion, matrix diffusion) are represented by a single particle diffusion coefficient. Either particle or film diffusion may be the rate-determining step for the exchange process or both may contribute to the rate in intermediate cases. In general, film diffusion may dominate at early stages of exchange (A low in exchanger, B low in solution) when the concentration gradient in the particle is large (fast rate in particle). However, as the exchange proceeds further, the concentration gradients in the particle decrease and particle diffusion may become the rate-determining step.

In the exchange process, ions A and B move in opposite directions. Therefore, generally, the so-called interdiffusion coefficient ($\bar{D}_{A/B}$) must be used in eqns [13] and [14]. For particle diffusion:

$$\bar{D}_{A/B} = \frac{\bar{D}_A \bar{D}_B (z_A^2 \bar{C}_A + z_B^2 \bar{C}_B)}{z_A^2 \bar{C}_A \bar{D}_A + z_B^2 \bar{C}_B \bar{D}_B} \quad [15]$$

Normally, the interdiffusion coefficient is not constant, but changes with the ionic composition (\bar{C}_A) of the exchanger. To calculate ion exchange rates in a given ion exchange system, the Nernst-Planck equations must be solved simultaneously for each diffusing species under boundary conditions specific to the system. In general, the resulting equations are nonlinear differential equations, which have analytical solutions only in some special cases. Such a case, for instance, is isotopic ion exchange, for which a so-called self-diffusion constant can be used. Assuming also that the solution has indefinite volume – the concentration of ion in the solution remains essentially constant – it is obtained for the half-time ($t_{1/2}$) of the exchange reaction. In the case of particle diffusion:

$$t_{1/2} = 0.030 \frac{r_0^2}{\bar{D}} \quad [16]$$

where r_0 is the radius of the exchanger particle and \bar{D} is the particle diffusion coefficient. For film diffusion:

$$t_{1/2} = 0.23 \frac{r_0 \delta Q}{DC} \quad [17]$$

where δ is the film thickness, Q the ion exchange capacity, D the film diffusion coefficient and C is the ion concentration. For particle diffusion (eqn [16]), the rate of exchange increases ($t_{1/2}$ decreases) as the particle radius decreases, being proportional to $1/r_0^2$. For film diffusion (eqn [17]), the rate increases less strongly as r_0 is decreased (the proportionality is to $1/r_0$). In film diffusion the exchange rate can also be increased by increasing the efficiency of agitation, which will decrease the film thickness. In real applications of ion exchange the exchange rates do not usually follow the simple relationships of eqns [16] and [17] and the equations are presented here just to give a simple view of the factors that can affect the ion exchange rates.

The values of film diffusion coefficients are of the same order of magnitude as the diffusion coefficients of ions in the external salt solution ($D \approx 10^{-5} \text{ cm}^2 \text{ s}^{-1}$). The values of particle diffusion coefficients depend strongly on the charge of the ion and on the structure and porosity of the exchanger matrix. In sulfonated polystyrene resins \bar{D} decreases with increasing degree of cross-linking, being in the range of 10^{-5} – $10^{-7} \text{ cm}^2 \text{ s}^{-1}$ for univalent cations. For multivalent cations, the values are much lower, falling in the range of 10^{-7} – $10^{-10} \text{ cm}^2 \text{ s}^{-1}$. In weakly acidic resins and in crystalline inorganic

ion exchangers, cation diffusion coefficients are typically 2–5 orders of magnitude lower.

Basic Ion Exchange Operations

Ion exchange reactions can be carried out as either batch or column operations. Column operation is far more common and efficient than batch operation. Batch operation is however used in research, because the experiment is simple to carry out and a large number of experiments can be carried out in parallel.

Batch Operation

In batch operation, a given amount (m) of ion exchanger is contacted with a given volume (V) of solution. The mixture is agitated until equilibrium has been attained. In typical binary batch process used for ion exchange studies (e.g. determination of $k_{A/B}$ as a function \bar{C}_A , Figure 1), the exchanger is initially in a homoionic form (e.g. the B form) and the solution initially contains only the ion A . Considering the simple uni-univalent exchange as an example, the ratio of ion concentrations at equilibrium is given by:

$$\frac{\bar{C}_A}{\bar{C}_B} = k_{A/B} \left(\frac{C_A}{C_B} \right) \quad [18]$$

In general, to achieve a high conversion to the A form in a single batch equilibration, the selectivity coefficient $k_{A/B}$ and the ratio C_A/B_B must be high. In practice, the degree of conversion to the A form is controlled by adjusting the initial concentration of A (C_{A0}) in the solution and the solution to solid ratio (V/m), often also called the batch factor (BF):

$$\bar{C}_A = (C_{A0} - C_A) \frac{V}{m} \quad [19]$$

At constant C_{A0} , the degree of conversion increases as V/m is increased (Figure 4). It is usually difficult to obtain a high conversion in a single batch equilibration, since the selectivity often decreases with increasing conversion and there is always ion B in the solution released from the exchanger. Removing B from the solution can enhance conversion. This can be achieved by equilibrating the ion exchanger successively with fresh portions of solution A .

Column Operation

There are several types of column operation, classified according to the technical design of the apparatus

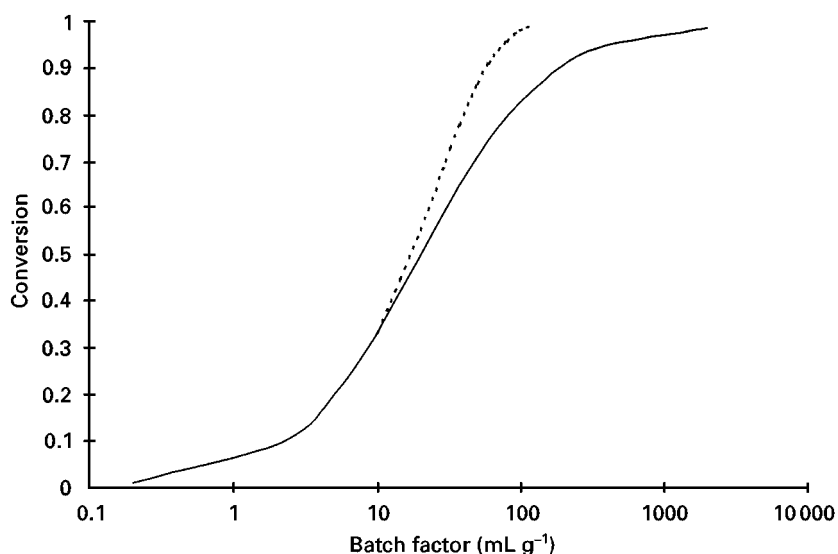


Figure 4 Batch ion exchange: calculated degree of conversion from the B^+ form to the A^+ form as a function of solution volume to exchanger mass ratio (batch factor). Selectivity coefficient $k_{A/B} = 1$, ion exchange capacity 2 mmol g^{-1} . The solid line represent the conversion in single batch equilibration. The broken line represents successive batch equilibrations with a constant batch factor of 10 mL g^{-1} .

(e.g. fixed-bed or floating-bed operation) or according to the purpose of the application (e.g. column chromatography or column separation).

Column separation Column separation usually involves elimination of undesirable ions from water (deionization, softening, decontamination). Taking the binary exchange discussed earlier as an example, a solution containing harmful ions (A) is passed through the column that contains an exchanger in the B form. The A ions are then taken up by the exchanger and B ions are released into the solution. Because B ions are constantly removed from the system, the operation is much more efficient than batch exchange in removing A ions from the solution (see eqn [18]). The column effluent is first free of ion A , but when a given amount of solution has been passed through, A starts to emerge in the effluent and its concentration increases gradually to that in the influent solution (Figure 5). The graph of the concentration of A in effluent as a function of effluent volume is called the breakthrough curve.

The area above the breakthrough curve gives the total volume of solution that has been freed from ion A . Dividing this volume by bed mass or volume gives the total processing capacity, or theoretical capacity (Q_T), of the column (L kg^{-1} or L L^{-1}). In this simple example, $Q_T = Q/C_A$ (Q = ion exchange capacity in mmol L^{-1} or mmol mL^{-1}) since at equilibrium A ions have taken up all of the ion exchange capacity. In general, Q_T is equal to k_d , which can be easily calculated in binary systems from eqn [9] for trace ions

to be separated, provided that selectivity coefficients are known. However, because ion A is considered harmful, operation is not continued until total processing capacity has been used, but the feed is discontinued when the concentration of A in the effluent reaches a measurable or a regulated value. The capacity at this point is called the processing capacity, or breakthrough capacity (Q_B). The ratio Q_B/Q_T is called the column utilization factor, F_U . For efficient separation process F_U should be maximized.

Column chromatography In column chromatography ions are separated from each other for analysis or for chemical production purposes. Considering a simple example in which ions A and C are separated for analysis, a sample solution containing A and C is passed into the column containing an exchanger in the B form. The sample volume is so low that A and C take up only a very small fraction of the column capacity near the inlet. After sample injection, an eluent solution containing ion B is passed through the column. A and C in the exchanger are exchanged for B and begin to move through the column at different velocities. At a given volume, the less preferred ion A first emerges in the eluent as a concentration peak followed by ion C . The eluent volumes at which A and C emerge, i.e. the volumes at the peak maxima, are called the retention volumes (V_R) and they can be obtained from the relation:

$$V_R = k_d V_S + V_M \quad [20]$$

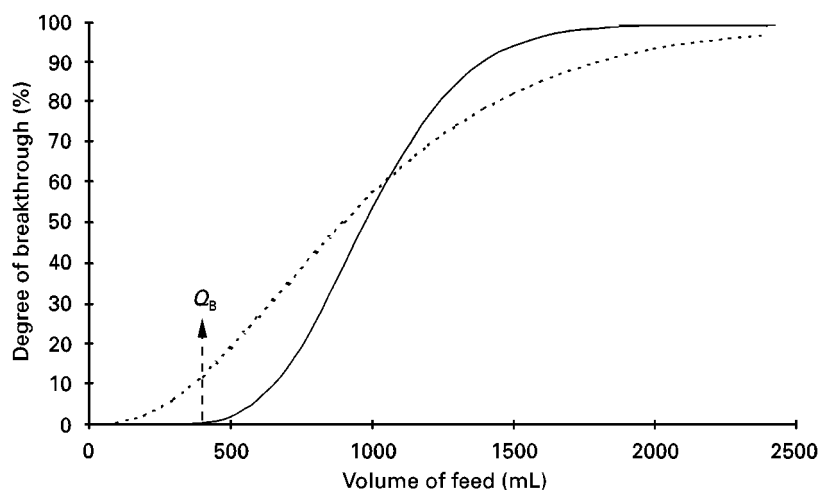


Figure 5 Examples of column breakthrough curves generated for different number of theoretical plates N (see eqns [22]–[27]). In this example, the capacity of the exchanger (Q) is 1 mmol mL^{-1} and the exchanger bed volume is 1 mL . The exchanger is initially in the B^+ form and the feed contains only ion A^+ at a concentration of $0.001 \text{ mmol mL}^{-1}$ (C_A). The total processing capacity Q_T is thus $Q/C_A = 1000 \text{ mL mL}^{-1}$ exchanger and the area above the breakthrough curves is 1000 mL for the 1 mL bed. The breakthrough capacity Q_B depends on N , which is affected by the operating conditions. Continuous line, $N = 30$; broken line, $N = 10$.

where V_S is the volume of ion exchanger bed and V_M is the free solution volume in the bed. In analytical separations A and C are present at trace levels, so k_d values are again easily calculated from eqn [9]. In analytical work, efficient operation requires that the concentration peaks of A and B are well separated (the peaks are sharp). The retention volumes V_R should not be too large, because this leads to a long analysis time and to broadening of the peaks.

Theory of Column Exchange

Most models for ion exchange column operation are based on the concept of effective plates or transfer units. Martin and Synge first used this concept for chromatography and the theory was refined by Glueckauf, who obtained for the material balance in the ion exchange column, under linear equilibrium (k_d constant):

$$\left(\frac{\partial C_i}{\partial z}\right)_v + q(k'_d + \beta) \left(\frac{\partial C_i}{\partial V}\right)_z - \frac{H}{2} \left(\frac{\partial^2 C_i}{\partial z^2}\right)_v = 0 \quad [21]$$

where z is the longitudinal coordinate in the column, q is the cross-sectional area of the bed, k'_d is the column distribution coefficient in which the exchanger phase concentration of species i is calculated per unit volume of the bed, i.e. k'_d is obtained from the k_d of eqn [7] as $k'_d = k_d (1 - \beta)$, where β is the bed void fraction. H is the effective height of the theoretical plate given by:

$$H = H_0 + H_p + H_F + H_L \quad [22]$$

H_0 , H_p , H_F and H_L are the contributions of particle size, particle diffusion, film diffusion and longitudinal diffusion to the effective height:

$$H_0 = 1.64 r_0 \quad [23]$$

$$H_p = \frac{k'_d}{(k'_d + \beta)^2} \frac{0.14 r_0^2 u}{\bar{D}} \quad [24]$$

$$H_F = \left(\frac{k'_d}{k'_d + \beta}\right)^2 \frac{0.266 r_0^2 u}{D(1 + 70r_0u)} \quad [25]$$

$$H_L = \frac{D\beta\sqrt{2}}{u} \quad [26]$$

where u is the linear flow rate. The number of theoretical plates (N) in the column is then obtained by dividing the column length L by H :

$$N = \frac{L}{H} \quad [27]$$

In general, the column performance improves as N is increased. In column separations the increase in N makes the breakthrough curve steeper (breakthrough capacity Q_T increases). In column chromatography, increase in N makes the elution peaks sharper and so increases the separation of two peaks. For a column with a constant length Z , N can be increased by decreasing the plate height H . The easiest way of doing this is to decrease the particle

radius (see eqns [23]–[25]), but there is a practical lower limit for r_0 , because the hydrodynamic pressure increases with decrease in r_0 . Another way to increase N is to decrease flow rate (eqns [24] and [25]), but a very low rate is not usually acceptable due to the effect of longitudinal diffusion (eqn [26]), which causes poor separation.

Equilibrium Theories

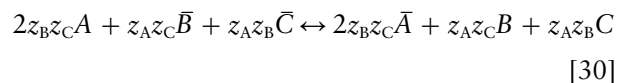
Much theoretical work has been carried out to explain the nonideality of the ion exchange systems, e.g. for the calculation of ion exchange equilibria and to understand the factors that give rise to ion exchange selectivity. For ions in solution, sufficient theories exist to calculate the nonideality (activities) in the liquid phase. For the ions in the exchanger phase, no generally valid theories exist. For the calculation of ion exchange equilibria, it is always possible to measure the nonideality of the exchanger phase, e.g. the corrected selectivity coefficient $k'_{A/B}$ as a function of exchanger ion composition at a given total solution concentration (C_T) and then use the measured function for the calculation of equilibria at other C_T values from equation:

$$k'_{A/B} \frac{\bar{E}_B^{Z_A}}{\bar{E}_A^{Z_B}} = \frac{E_B^{Z_A}}{E_A^{Z_B}} \frac{\gamma_B^{Z_A}}{\gamma_A^{Z_B}} C_T^{(Z_A - Z_B)} \quad [28]$$

In general, $k'_{A/B}$ and γ_A/γ_B are not known simultaneously, so iteration must be used to solve eqn [28]. The same approach can be extended to systems containing more than two counterions, e.g. for the ternary system the corrected selectivity coefficients $k'_{A/BC}$, $k'_{B/CA}$ and $k'_{C/AB}$ can be measured and used for the calculation of the equilibria. For instance, $k'_{A/BC}$ is defined as:

$$k'_{A/BC} = \frac{\bar{E}_A^{2Z_B Z_C} C_B^{Z_A Z_C} C_C^{Z_A Z_B} \gamma_B^{Z_A Z_C} \gamma_C^{Z_A Z_B}}{\bar{E}_B^{Z_A Z_C} \bar{E}_C^{Z_A Z_B} C_A^{2Z_B Z_C} \gamma_A^{2Z_B Z_C}} \quad [29]$$

for the exchange reaction:



$k'_{B/CA}$ and $k'_{C/AB}$ are defined accordingly. It is intrinsic to this method that it gives precise results provided that the selectivity coefficients are measured and described precisely within the exchanger composition range of interest. In practice this requires large number of measurements, which makes the method very laborious. Less effort is associated with ap-

proaches in which the solid-phase activity coefficients in multicomponent systems are estimated from the binary interaction parameters (Λ), e.g. from the Wilson equation it is obtained that:

$$\ln \bar{\gamma}_i = 1 - \ln \left(\sum_{j=1}^M \bar{X}_j \Lambda_{ij} \right) - \sum_{k=1}^M \left(\frac{\bar{X}_k \Lambda_{ki}}{\sum_{j=1}^M \bar{X}_j \Lambda_{kj}} \right) \quad [31]$$

Parameter Λ can be determined from the measurements of the corrected selectivity coefficients of the binary equilibria i/j , k/i and k/j by curve fitting. Activity coefficients obtained by eqn [31] are then used in the binary equations of thermodynamic equilibrium constant (eqn [4]) for the calculation of ion exchange equilibria. This method has given accurate results even in four-component systems (e.g. Na/K/Ca/Mg in a strong acid cation resin). Several other related approaches have been developed.

The theories above are based on the measurements of nonideality and make no assumptions about the interactions that give rise to the selectivity. Thus, they do not allow the calculation of $K_{A/B}$, $k'_{A/B}$ or $\bar{\gamma}_i$ from the fundamental data or explain the changes of $k'_{A/B}$ or $\bar{\gamma}_i$. The first theory to explain the nonideality of the exchanger phase was developed by Kielland (the graphical presentations of Figure 1 are often called Kielland plots), who considered van der Waals-type interactions and showed that for the solid-phase activity coefficients:

$$\bar{\gamma}_{AR} = c \bar{X}_{AR}^2 \quad [32]$$

$$\bar{\gamma}_{BR} = c \bar{X}_{BR}^2 \quad [33]$$

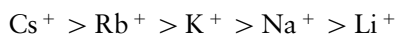
Here, AR and BR denote the salt forms of the exchanger, R being the common anion. This theory predicts that the function $k'_{A/B} = f(\bar{X}_A)$ is linear, which is in agreement with the observed behaviour in many cases. Quite often, the $k'_{A/B}$ functions are not linear, but slightly, or even strongly, curved (see Figure 1). Some of these nonlinear functions can be explained by assuming that the exchanger has several types of exchange sites, each subsite having a characteristic selectivity coefficient k'_i . The measured overall $k'_{A/B}$ decreases with \bar{X}_A as sites with higher selectivity are filled first. If these subsites behave ideally, sigmoidal curves are obtained for $k'_{A/B} = f(\bar{X}_A)$. By assuming nonideal behaviour for the subsites, the $k'_{A/B}$ functions exhibit a wide variety of different forms. This theory has been found to be consistent with the behaviour of several zeolite systems.

A related approach is to consider the different states that a given counterion may assume depending on the neighbouring counterions. In a polymer chain

(as in an organic ion exchange resin), considering the two nearest neighbours, each counterion can have three different energetic levels. As a consequence, in general $k'_{A/B} = f(\bar{X}_A)$ is a second-order polynomial function in \bar{X}_A , which is often the observed trend in organic resins (Figure 1). If two of the three energy levels are close to each other, the selectivity function is linear. Theories of this type are helpful in the calculation of ion exchange equilibria and in presenting the equilibria in a mathematical form, but they give no information about the magnitude of selectivity. In organic resins, various osmotic theories have been developed to estimate the relative magnitude of selectivity. The base in these theories is that:

$$K_{A/B} = \frac{\Pi}{RT} (z_B v_B - z_A v_A) \quad [34]$$

where Π is the osmotic pressure difference between the external solution and exchanger pore liquid and v_A and v_B are the partial molar volumes of A and B in the exchanger. The osmotic theory predicts the selectivity trend (I):



observed in strong-acid cation resins, i.e. ions with smaller hydrated radius (smaller partial molar volume) are preferred, because replacing larger ions with smaller ones will reduce the swelling pressure. The same selectivity trend can also be predicted from purely electrostatic calculations. The dielectric theory:

$$\ln K_{A/B} = \frac{-e^2}{8\pi kT} \left[\left(\frac{z_A}{r_A} - \frac{z_B}{r_B} \right) \left(\frac{1}{\varepsilon_Z} - \frac{1}{\varepsilon_S} \right) \right] \quad [35]$$

where ε_Z and ε_S are the macro-permittivities of the exchanger and solution phases, respectively, predicts that in uni-univalent exchange, the selectivity decreases as the framework charge density increases for selective exchange ($K_{A/B} > 1$). This trend is commonly observed for zeolite ion exchange.

The selectivity sequence I for alkali metal ions, shown above, is common in organic resins have a low degree of cross-linking and in zeolites with low framework charge density. Other selectivity sequences appear as the degree of cross-linking or framework charge density increases:

- II. $\text{Cs} > \text{K} > \text{Rb} > \text{Na} > \text{Li}$
- III. $\text{K} > \text{Cs} > \text{Rb} > \text{Na} > \text{Li}$
- IV. $\text{K} > \text{Cs} > \text{Na} > \text{Rb} > \text{Li}$
- V. $\text{K} > \text{Na} > \text{Cs} > \text{Rb} > \text{Li}$
- VI. $\text{K} > \text{Na} > \text{Rb} > \text{Cs} > \text{Li}$

- VII. $\text{Na} > \text{K} > \text{Rb} > \text{Cs} > \text{Li}$
- VIII. $\text{Na} > \text{K} > \text{Rb} > \text{Li} > \text{Cs}$
- IX. $\text{Na} > \text{K} > \text{Li} > \text{Rb} > \text{Cs}$
- X. $\text{Na} > \text{Li} > \text{K} > \text{Rb} > \text{Cs}$
- XI. $\text{Li} > \text{Na} > \text{K} > \text{Rb} > \text{Cs}$

Most of these sequences have been observed in ion exchangers and they can be predicted from Eisenman theory, originally developed for selective glass electrodes. The theory considers cation exchange site and cation water (hydration) interaction energies. The free energy of exchange is obtained from:

$$\Delta F_{AB}^0 = (\bar{F}_A^{\text{el}} - \bar{F}_B^{\text{el}}) - (\bar{F}_A^{\text{hyd}} - \bar{F}_B^{\text{hyd}}) \quad [36]$$

where F^{el} is the coulombic interaction energy between cation and the anionic exchange site and F^{hyd} is the hydration energy of the cation. The coulombic interaction energy for a univalent cation can be calculated for widely separated sites from:

$$\bar{F}_{\text{el}} = -332/(r_+ + r_-) \quad [37]$$

and for closely spaced sites:

$$\bar{F}_{\text{el}} = -1.56*332/(r_+ + r_-) \quad [38]$$

where r_+ is the cation radius and r_- is the radius of the anionic exchange site. The anionic field strength decreases as r_- increases. Selectivity pattern I is exhibited by exchangers having a low field strength and cations are exchanged in the hydrated state with a preference for a smaller hydrated radius. As the field strength is increased, the less hydrated cations become desolvated and the selectivity patterns start to change. At high field strength, pattern XI is exhibited and cations are exchanged as bare cations.

Conclusions

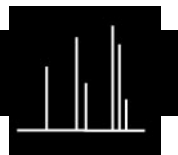
Rather simple theoretical concepts are available to describe ion exchange phenomena and applications in a qualitative manner. In some cases these concepts may give a good quantitative agreement, but generally more rigorous theories are required, considering the specific details of given systems. The application of even the simplest theories usually involves much experimental and computational effort when systems comprising more than two exchanging ions are involved.

See also: II/Ion Exchange: Historical Development.

Further Reading

- Dorfner K (1991) *Ion Exchangers*. Berlin: Walter de Gruyter.
- Franklin KR and Townsend RP (1988) Prediction of multi-component ion exchange equilibria in zeolites: a comparison of procedures. *Zeolites* 8: 367.
- Helfferrich FG (1995) *Ion Exchange*. New York: Dover Publications.
- Lehto J and Harjula R (1996) Proceedings of the Workshop on Uniform and Reliable Formulations. Nomenclature and Experimentation for Ion Exchange. *Special Issue of Reactive and Functional Polymers* 27: 93.
- Marinsky JA and Marcus Y (1966–97) *Ion Exchange, A Series of Advances*, vols 1–13. New York: Marcel Dekker.
- Mehablia MA, Shallcross DC and Stevens GW (1996) Ternary and quaternary ion change equilibria. *Solvent Extraction and Ion Exchange* 14: 309.
- Recommendations on Ion Exchange Nomenclature (1972). *Pure and Applied Chemistry* 29: 619.

MASS SPECTROMETRY



Spectrometry–Mass Spectrometry Ion Mobility

H. R. Bollan, DERA Bridgwater, Bridgwater, UK

Copyright © 2000 Academic Press

Introduction

The principle of mass spectrometry (MS) is the separation of ions in a vacuum, using an electrical or magnetic field or a combination of both. The ions may be formed through a variety of processes, but it is perhaps the fragmentation of the molecular ion that produces much of the analytical power of the technique. Mass-to-charge ratios are recorded and the structure of the parent ion may be determined from the ion molecular mass and the pattern of the fragment ions recorded. Experienced mass spectrometrists can recognize typical fragment ion patterns, however, although there are libraries available for the automated identification of mass spectra, careful judgement must be used in the final assignment of the compound's identity. The theory and uses of MS have been well documented as an analytical technique both as a stand-alone and a hyphenated technique, for example coupled with gas chromatography (GC-MS).

Less is known about the chemistry within ion mobility spectrometers, which are used in the field to monitor for contraband substances such as explosives, drugs, and on the battlefield to detect chemical warfare agents. Originally referred to as plasma chromatography, ion mobility spectrometry (IMS) is a technique concerned with the formation of ion-molecule clusters in air and their movement in an electric field, at or close to atmospheric pressure. The average ion velocity of an ion species in an electric field, v_d , is the product of that electric field, E , and

a constant of proportionality, K , i.e. $v_d = KE$. K is called the mobility of the ions, and is characteristic of a particular ion species in a specified drift gas. K may be calculated indirectly from drift time, t_d , from the equation $t_d = l_d/v_d$, where l_d is the drift length. The theory of ion mobility and reaction chemistry is covered in two monographs listed in the Further Reading section, and need not be reproduced here. Notably, the Mason–Schamp equation for mobility (an equation that attempts to reconcile fundamental properties of ions with their mobility) includes a term containing a collision integral, to which mobility is inversely proportional. The value of the collision integral is determined by the cross-section. Therefore, the mobility, and consequently the ion drift velocity, is dependent upon mass, size, shape, and polarizability. The mobilities observed for ions are weighted averages of the mobilities of all the cluster ions participating in a localized equilibrium between the ion swarm and the neutral molecules they encounter as they traverse the drift region. If the drift gas, electric field gradient, temperature, pressure, and therefore the molecular number density remain constant, mobility depends only on ion charge, reduced mass, and collision cross-section. The collision processes undergone by ions during their drift time are very complicated, and are much too complicated to go into here. However, it must be noted that these processes are affected by variations in temperature and pressure in the drift region. Ion cluster formation and fragmentation are also governed by temperature. Therefore, to simplify the situation, and to allow easy comparison between different systems, mobility of an ion is normalized for temperature and pressure, the corrected term being referred to as reduced mobility, K_0 (μ_0 in some texts).

The initial distribution of ions immediately following ionization is modified by various chemical

reactions, forming more stable ions. In clean air, these ions form what is called a reactant ion peak (RIP). Positive ion chemistry can involve proton transfer, nucleophilic attachment, hydride or hydroxide extraction, and oxidation; negative ion chemistry involves electron capture, charge transfer, dissociative capture, proton abstraction, and electrophilic attachment; both positive and negative chemistries can be subject to complex rearrangements.

When a sample atmosphere enters the ion mobility spectrometer, many competitive reactions occur and to a first approximation proton or electron affinities may define the reaction pathways. These competing species may be target or possible interference compounds. Ion mobility spectrometers respond to a broad range of compounds with various functional groups. Therefore, complicated spectra are common in ion-molecule systems based upon water chemistry, due to the relatively low proton affinity of the water molecule. Selectivity may be improved with the introduction of trace quantities of an appropriate dopant chemical into the detector carrier gas, thereby altering the degree of affinity required for reaction. This can have an effect on resolution, sensitivity, response and recovery times.

Whilst ion mobility spectrometers respond to many compounds, in the field the operator is only able to identify the compound being detected, by an ion mobility spectrometer, from its display. The efficacy of the instrument display depends upon calibration and software programming. However, as the observed peaks represent cluster ions participating in a localized equilibrium, even in the laboratory, with instrumentation capable of displaying the mobility spectra, the accurate identification of species may be difficult.

Although identification of unknowns by IMS alone is problematic, the coupling together of IMS and MS (IMS-MS) produces a powerful technique. The masses of ion-molecule clusters forming the RIP and product ion peaks are recorded either in positive or negative mode mass spectra, depending on the polarity of the ions being studied. When tuned ion analysis is performed on a specific mass in the mass spectrum, the mobility of the ion mass can be determined, i.e. its position in the mobility spectrum. With the technique enhanced, further by coupling IMS to tandem MS, the composition of ion-molecule clusters can be identified from the results of collision-induced dissociation (CID).

History

In the 1960s, Cohen (of the Franklin GNO Corporation) worked on the development of the ion mobility

spectrometer, resulting in a US patent in 1971. The instruments were developed to generate information concerning negative ions produced from specific compounds in air under atmospheric pressure conditions. This early instrumentation was to have wider application for the analysis of ultra-trace quantities of many organic molecules forming either positive or negative ions. Cohen went on to form the company PCP, and to produce commercially available IMS-MS instrumentation.

By the early 1970s, Karasek was already employing IMS as part of a hyphenated technique, using IMS-MS to determine the identity of species separated through a GC. Even without the GC in-line, it was becoming evident that IMS-MS was a powerful identification technique.

In the late 1970s and the 1980s, IMS research was directed from fundamental studies to application research, with a view to solving specific analytical problems relating to the rapid detection of volatile organic compounds in the field. Specifically, IMS was the subject of military research programmes, designed to enhance the real-time detection of chemical warfare agents. IMS-MS still played an important role in understanding the ion-molecule chemistry, which was necessary to progress the development and reliability of the field deployable IMS instrumentation. A study of the ion-molecule behaviour of selected agents and interference compounds has been made by IMS-MS. IMS-MS has also been used to support some of the IMS programmes that have been applied to more general, as well as specific, monitoring requirements. Industrial applications have been directed towards monitoring for toxic chemicals, and chemicals considered to be hazardous to man or the environment. These include acid and stack gases (e.g. hydrogen fluoride), aliphatic and aromatic amines, ketones, isocyanates, halogens, solvents, ethers, anaesthetics, fuels, nicotine, polychlorinated biphenyls, mixtures of organic compounds, organophosphorus compounds, certain hydrocarbons (e.g. benzene), perfluoroisobutene, and volatile organic compounds used in the semiconductor industry. With social pressures for a greener environment, further IMS techniques are being developed, for example, for the identification of polymers, using laser ablation-IMS, to assist with sorting plastics for recycling. The need to detect pollutants in liquid media is becoming more desirable, e.g. the detection of aniline in hexane, and of aqueous ammonia in rivers, wastewaters and drinking water treatment facilities. This problem requires a means of separating the analyte from the liquid medium, usually in the form of a selectively permeable membrane. IMS analysis proceeds once the analyte has been transferred from the liquid to the

vapour phase. IMS has also been investigated for the detection of bacteria in water and wastewater sources, using pyrolysis before introduction.

Detection of explosives is a specific and very important area of contraband detection at trace levels: RDX, TNT, PETN, NG, EGDN, HMX, EGDN, 2,4-DNT, ammonium nitrate, and tetryl detection by IMS have all been investigated. Detection of illicit drugs by IMS is another important area, which has benefited from confirmation of detected species by IMS-MS analysis. Due to legal requirements for forensic and law enforcement purposes, alleged criminals charged with the clandestine manufacture of illegal drugs in the USA must be charged with the manufacture of specific drugs in order for the case to go to court; a blanket charge of clandestine drug manufac-

ture is inadmissible. Drugs detected include heroin, cocaine, barbiturates, amphetamines, and LSD. Prescription drugs such as benzodiazepines are also detected by IMS. The pressure to be absolutely certain about the identity of target compounds emphasizes the advantages of powerful analytical techniques such as IMS-MS, which enhances the development and calibration of detection equipment.

A more specific application is of potential use to the forestry industry, which involves the identification of different timbers before processing. Fast thermolysis-IMS has proved successful for certain wood species. Wetwood, an abnormal condition of wood from both deciduous and coniferous trees caused by bacterial infection, was detected in Northern Red Oaks using this technique.

Although IMS-MS is necessarily a laboratory-based technique, it continues to play a very important part in the understanding of ion-molecule chemistry and the development of IMS equipment that, through user requirements, is becoming miniaturized. Hill continues to develop hyphenated IMS techniques, sometimes employing different ionization methods, including electrospray IMS-MS. The ion-molecule chemistry of different ionization techniques can be characterized readily by IMS-MS techniques. These fundamental studies have led the way for IMS-MS research into biomolecular sciences because, until the application of electrospray ionization, the biomolecules had been too large for successful ionization by more traditional methods employed for IMS. Clemmer and Jarrold were able to further the research by determining the conformation of biomolecules by IMS.

A chronology of the history of IMS-MS is given in Table 1.

An Ion Mobility Spectrometer–Mass Spectrometer

An ion mobility spectrometer consists of an ion-molecule reaction chamber, incorporating an ionization region, coupled to a drift region via a shutter grid. A schematic diagram is shown in Figure 1. The drift region contains a screen grid and an ion collector. A typical cell consists of metal guard rings, separated by insulators, connected to a resistance network with a high voltage attached to one end of the resistor chain, to produce a uniform electric field along the cell, usually of the order of a few hundred V cm^{-1} . Clean carrier gas is ionized by irradiation, usually with beta particles from a ^{63}Ni radioactive source, to form positive and negative reactant ions and consequently RIPs. The ion-molecule chemistry can be altered by the introduction of a dopant chemical at

Table 1 History

1890s	Studies of the ionization of air
1897	Study of the velocity of positive rays in an electric field (Thomson & Rutherford)
1900s	Langevin studies of ionized air and mathematical/chemical models for ion mobilities
1907	First mass spectrometer
1919	Determination of atomic weights using MS
1946	Time of flight mass analyser
1953	Quadrupole MS
1960s	Drift tube mass spectrometers
1965	First IMS instruments (plasma chromatographs) were developed (Franklin GNO Corporation)
1966	Studies of chemical ionization
1967	Tandem MS
1968	Electrospray ionization for MS
1970s	Research led by Cohen and Karasek using both IMS and IMS-MS techniques
1971	First IMS patent issued in the USA (Cohen MJ, US patent 3,621,239)
1974	Atmospheric pressure ionization MS
1977	IMS-MS demonstration of ion-molecule behaviour of chemical warfare agents
1982	High field asymmetric waveform IMS-MS (FAIMS-MS)
1983	IMS-MS studies of reactant ion distributions in an ion mobility spectrometer with a membrane inlet system
1984	GC-IMS Corona discharge IMS
1985	IMS-MS identification of structurally different ions of the same mass
1986	IMS-MS analysis of prescription and illicit drugs
1987	Laser desorption IMS-MS
1990	IMS-MS used to study the site of protonation in anilines IMS-MS used in the semi-conductor industry to determine cleanliness
1992	IMS-MS analysis of marijuana vapours and cigarette smoke
1994	IMS-MS confirmation of ion-molecule clusters disclosed
1997	Development of ESI-high resolution IMS-MS (Washington State University) Development of ion-trap-IMS-TOFMS systems for the elucidation of biomolecular structures

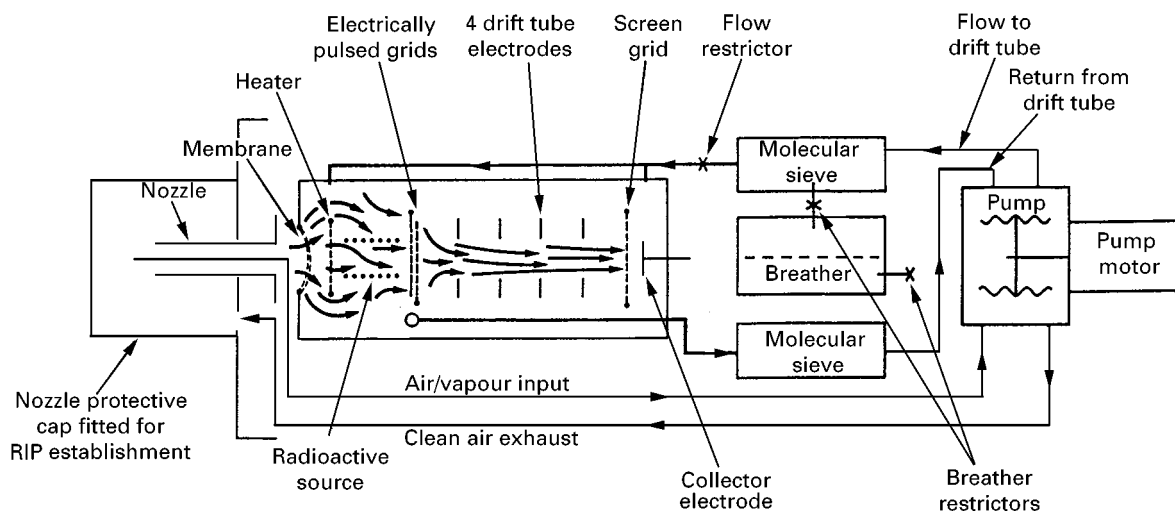


Figure 1 Schematic of an ion mobility spectrometer.

a controlled rate. Samples introduced into the ion mobility spectrometer may react to form product ions, the equilibrium concentrations of which are governed by proton affinity or electron affinity. If introduced into an electric field they will migrate according to their polarity and that of the applied field as, between collisions, individual ions have a component of acceleration in the direction of the applied field. Ions pass from the reaction region to the drift region via a shutter grid, which is pulsed open to allow a finite number of ions to enter the drift region. Operation of the shutter grid starts the timing sequence, which measures drift time. A counter-flow of clean drift gas enters the drift region near the collector electrode, which is shielded by a screen grid in order to prevent induced charge, which would lead to a distorted current peak. By monitoring the collector electrode from the instant the voltage pulse is applied to the grid, a mobility spectrum (see **Figure 2**) is generated. Mobility spectra can be generated con-

tinuously by repetitive pulsing of the grid. Typically, 25 ms is sufficient time to allow all ions to drift from the grid to the collector electrode. The signal-to-noise ratio is relatively noisy because only small ion currents are involved. The signal-to-noise ratio may be improved by averaging the signal over several scans.

In a mass spectrometer, molecules are ionized by any one of a number of techniques. These ions are then analysed using either magnetic or electric fields or a combination of both and are separated according to their mass-to-charge ratio before being detected. In mass spectrometers using magnetic field separation, a repeller plate directs ions to a set of accelerator plates, used to produce a beam of rapidly moving ions, which are directed into a uniform beam by focussing slits. Neutral molecules are drawn off by vacuum pumps. In a quadrupole mass spectrometer, an oscillating electrostatic field is set up between four rods, two diagonally opposite rods having direct current voltage applied and the other two rods having radio frequency applied. Ions acquire an oscillation in the electrostatic field set up according to the ratio of the direct current to the radio frequency amplitude. Ions of the correct m/z value undergo a stable oscillation of constant amplitude and pass through the analyser to reach the detector. Other ions undergo unstable oscillation and the amplitude of the oscillation increases until the ions strike one of the rods.

Current IMS-MS Applications

APCI-MS enables ion chemistry at pressures used in typical IMS systems to be studied, but some issues remain regarding cluster formation in the interface region and this could influence the interfacing of IMS

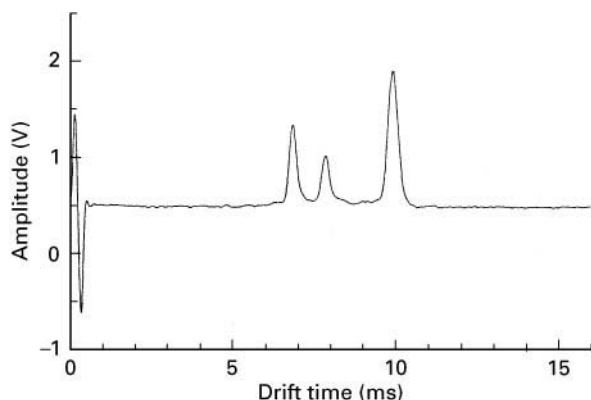


Figure 2 An ion mobility spectrum.

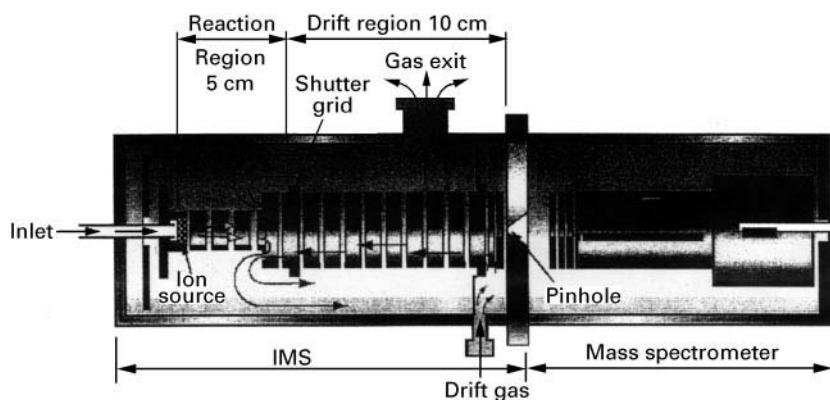


Figure 3 An ion mobility spectrometer–mass spectrometer.

(which operates close to atmospheric pressure) to MS. However, Spangler has recently published details regarding a better understanding of the behaviour at the IMS-MS interface.

An ion mobility spectrometer may be coupled to a mass spectrometer (see **Figure 3**) with sample transfer via a pinhole, typically 50 μ to 100 μ in diameter. The mass spectrometer used in conjunction with an ion mobility spectrometer enables m/z identification of the reactant and product ions. The mass spectrometer is initially programmed to scan through the chosen mass range with the IMS shutter grids continuously open. (If the ion mobility spectrometer is used in the normal pulsed mode it may take a very long time to obtain a mass spectrum, which may then not be representative.) Thus, it is possible to record ions created in an ion mobility spectrometer, and a mass spectrum of IMS sample ions is shown in **Figure 4**.

The mass spectrometer is then programmed to detect ions of one chosen mass. In this 'tuned'

ion mode (with the IMS shutter grids operating normally), a drift spectrum of the selected ion species is generated (see **Figure 5**). Thus, it is possible to associate a particular ion mass with a particular ion mobility peak. Hence, IMS-tuned MS enables the reduced mobility for ions to be determined, but the signals are weak and a significant amount of data averaging is required. Because the signals are very low, mass spectrometers used in conjunction with ion mobility spectrometers are set to pulse counting mode. Sometimes the average of thousands of spectra is necessary to produce a mobility peak. Using IMS-quadrupole MS to determine the reduced mobilities of all the ion-molecule clusters in a mobility spectrum could take from several hours to days. IMS-TOF is much faster, because it is able to scan at 50 to 60 Hz about 1000 scans per mobility spectrum. Ewing and Stone have an IMS-tuned MS for investigating the kinetic thermodynamic relationship for the ion reactions.

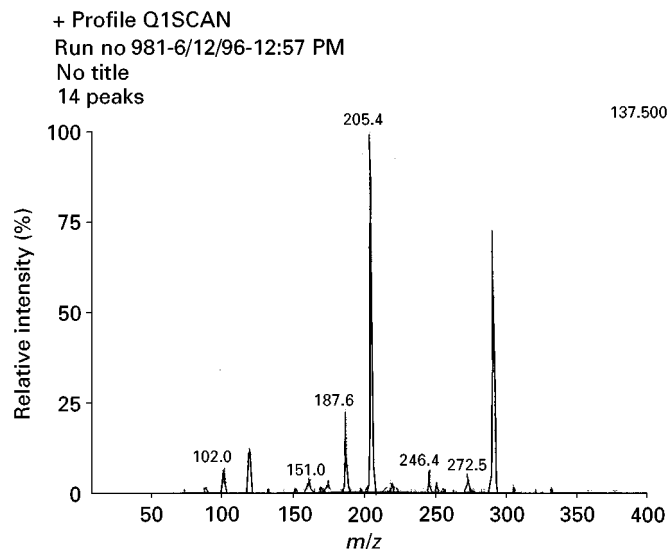


Figure 4 A mass spectrum of IMS sample ions.

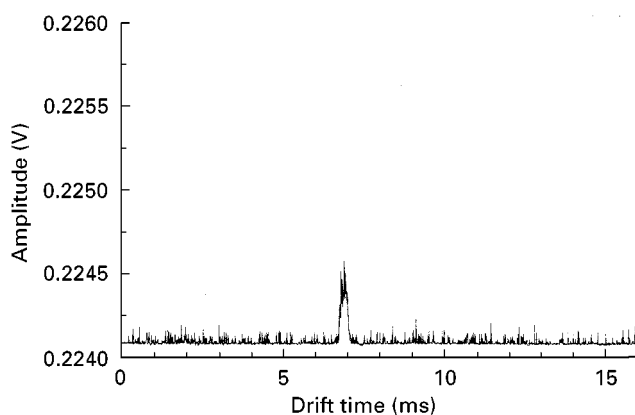


Figure 5 A drift spectrum of a selected ion species.

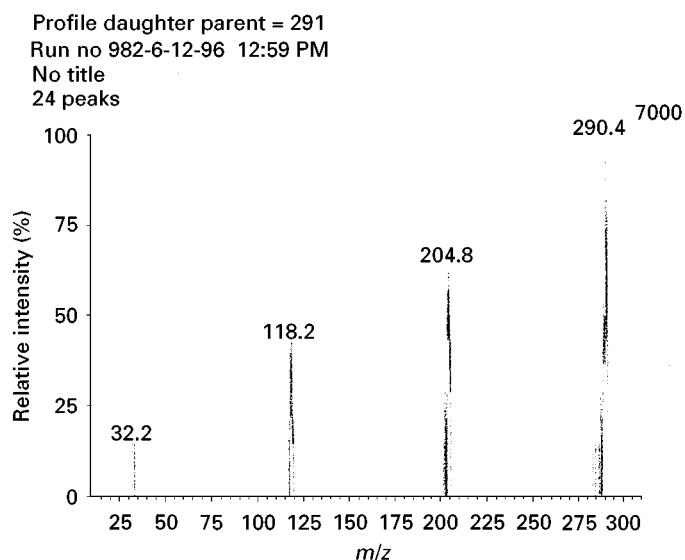


Figure 6 A mass spectrum of CID product ions.

IMS-MS-MS studies can be performed when IMS is coupled to a triple quadrupole mass spectrometer. An ion selected by the first quadrupole can be injected into a collision gas, for example argon, in a second quadrupole at 2×10^{-5} Torr (subjecting the cluster ions to CID), and then the product ions can be analysed in the third quadrupole. Figure 6 shows a mass spectrum of CID product ions. Consequently, MS-MS analysis is used extensively in assigning ion identities. IMS coupled to triple quadrupole MS enables the composite identification of the ion-molecules found in a drift tube. However, the number of ions reaching the detector in IMS-MS-MS is extremely low and a large amount of averaging is required to determine structures.

See Colour Plate 46.

See also: I/Mass Spectrometry. II/Chromatography: Gas: Gas Chromatography-Mass Spectrometry.

III/Biomedical Applications: Gas Chromatography-Mass Spectrometry; **Drugs and Metabolites:** Liquid Chromatography-Mass Spectrometry; **Explosives:** Gas Chromatography; Liquid Chromatography; Thin-Layer (Planar) Chromatography; **Forensic Toxicology:** Thin-Layer (Planar) Chromatography; **Forensic Sciences:** Capillary Electrophoresis; Liquid Chromatography; **Heroin:** Liquid Chromatography and Capillary Electrophoresis.

Further Reading

- Carr TW (ed.) (1984) *Plasma Chromatography*. New York: Plenum Publishing Corporation.
- Cohen MJ and Karasek JW (1970) *J. Chromatogr. Sci.* 8: 330.
- Eiceman GA and Karpas Z (1994) *Ion Mobility Spectrometry*. CRC Press Inc.
- Hill HH Jr, Siems WF, St. Louis RH and McMinn DG (1990) Ion mobility spectrometry. *Analytical Chemistry* 62: 1201A-1209A.
- Knighton WB and Grimsrud EP (1996) *Advances in Gas Phase Ion Chemistry*. JAI Press Inc.

MEMBRANE SEPARATIONS

Bipolar Membranes and Membrane Processes

H. Strathmann, University of Twente, The Netherlands

Copyright © 2000 Academic Press

Bipolar membranes are gaining increasing attention as an efficient tool for the production of acids and bases from the corresponding salts by electroolytic water dissociation. The process is economically very attractive and has a multitude of interesting potential applications. The large scale utilization of bipolar membranes, however, is still limited today by unsatisfactory membrane properties and by a lack of application know-how. A bipolar membrane should have adequate water dissociation capability, low electrical resistance, high permselectivity and a long useful life under operat-

ing conditions, which means that it must be stable in highly concentrated acid or alkaline solutions. The monopolar anion and cation exchange membranes which are also needed in the process should have good proton and hydroxide ion-blocking capability in addition to stability in strong bases and acids.

Although today's membranes do not meet all of these required properties, they are used successfully in a number of relevant applications.

The Principle of Electrolytic Water Dissociation

The process of electrolytic water dissociation using a bipolar membrane is illustrated in **Figure 1**, which shows a bipolar membrane consisting of cation and anion exchange layers arranged in parallel between two electrodes. If an electrical potential difference is established between the electrodes, charged species are removed from the interphase between the

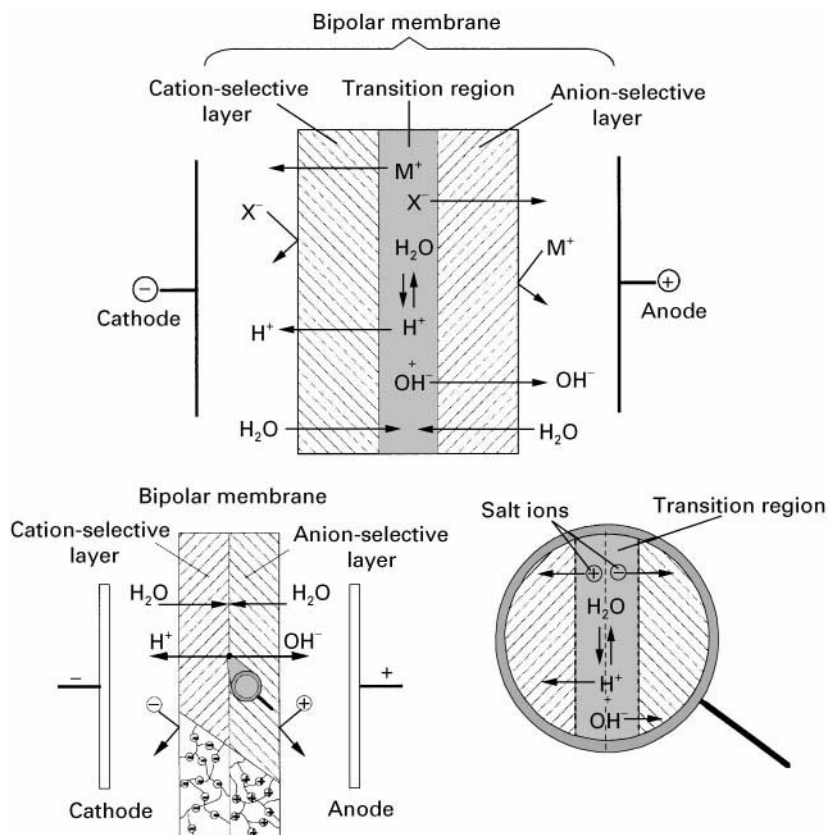
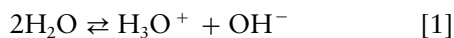


Figure 1 Schematic diagram illustrating the principle of electrolytic water dissociation in bipolar membranes.

two ion exchange layers. When all salt ions are removed from the interphase region, further transport of electrical charges can only be accomplished by protons and hydroxide ions, which are available in a concentration of *ca.* $1 \times 10^{-7} \text{ mol L}^{-1}$. Bipolar membranes resemble a laminate of a cation and an anion exchange layer with a very thin (4–5 nm) transition region in which the water dissociation occurs according to the water dissociation equilibrium given by:



The reversible energy required for the production of acids and bases in a bipolar membrane at constant temperature and pressure can be calculated by the Nernst equation for a concentration chain of solutions with different H^+ ion activities, i.e. pH values:

$$\Delta G = F \cdot \Delta U = 2.3 RT \Delta \text{pH} \quad [2]$$

Here ΔG is the reversible Gibb's free energy, ΔU the electrical potential difference between the two solutions, R is the gas constant, T is the absolute temperature, F is the Faraday constant, and ΔpH is the difference between the pH values of the two solutions separated by the bipolar membrane. For 1 mol L^{-1} acid and base solutions in the two phases separated by the membrane, ΔU is 0.8 V and ΔG is $0.02 \text{ kWh mol}^{-1}$ at 25°C .

The potential drop across the bipolar membrane measured in a water dissociation experiment is always higher than the calculated theoretical value because of irreversible effects due to the electrical resistance of the membrane and the solutions.

To utilize bipolar membranes for the production of acids and bases from the corresponding salt solution they must be combined with monopolar ion exchange membranes, as illustrated in **Figure 2**. This schematic drawing shows bipolar and cation and anion

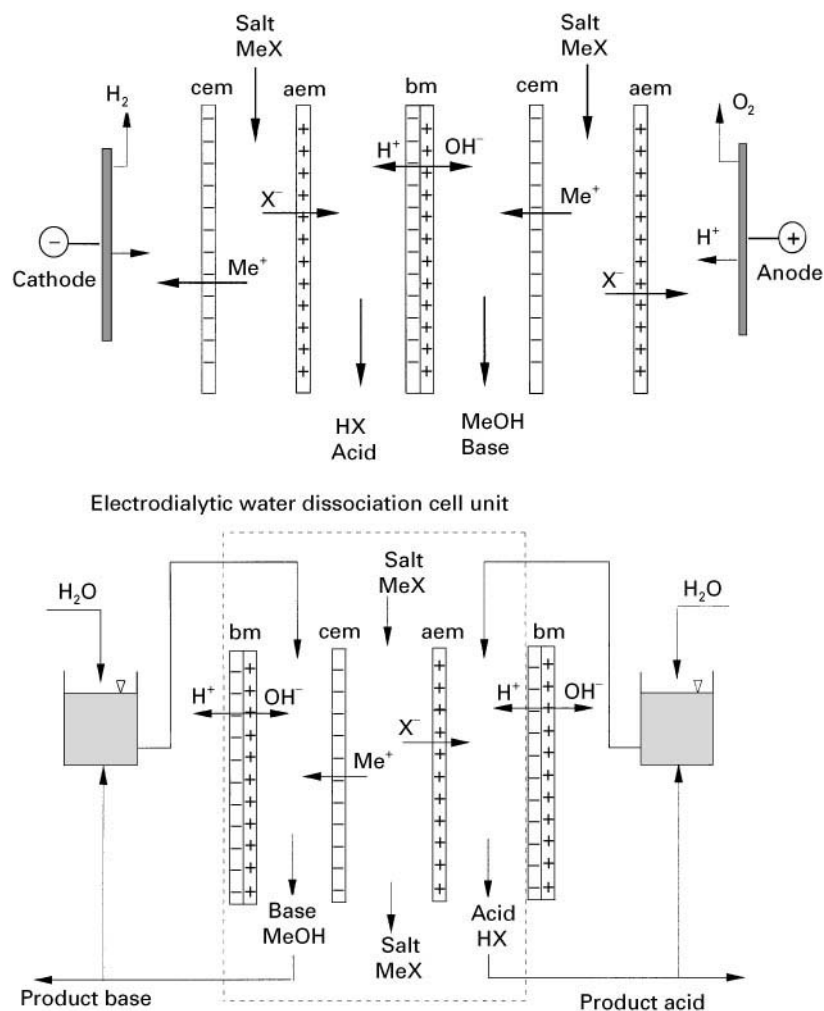


Figure 2 Schematic drawing illustrating the principle of electrodiolytic production of acids and bases from the corresponding salts with bipolar membranes.

exchange membranes arranged in parallel between two electrodes to form individual compartments. The electro dialysis cell arrangement consists of three individual compartments and three membranes, i.e. the bipolar and the cation and anion exchange membrane. As in conventional electro dialysis, a large number of the three-compartment units can be stacked between electrodes. When a salt solution is introduced in the middle compartment and an electrical potential difference between the electrodes is established, the cations in the salt solution migrate towards the cathode. They permeate the cation exchange membrane and form a base with the hydroxide ions generated in the bipolar membrane. On the other side of the bipolar membrane protons, which are generated simultaneously with the hydroxide ions, form an acid with anions migrating from the salt solution through the anion exchange membrane towards the anode. The net result of the process is the production of an acid and a base from the corresponding salt solution.

The Mechanism of Water Dissociation in Bipolar Membranes

The water dissociation rate in the bipolar membrane determines the overall efficiency of the process. It can easily be shown, however, that the dissociation rate constant of pure water is much too low to explain the experimentally determined high acid and base generation rate in bipolar membranes.

As indicated earlier, a bipolar membrane consists of a laminate of cation and anion exchange layers. The specific resistance σ of a strong acid or base ion exchange layer is in the order of 50–100 Ω cm. Assuming a thickness of 100 μ m each for the cation and anion exchange layers, the total area resistance r of the ion exchange layers of the bipolar membrane is in the order of 1–2 Ω cm².

The electrical resistance of the interphase layer of a bipolar membrane which is assumed to consist of deionized water can be calculated by:

$$r_{\text{in}} = \frac{\lambda}{\kappa} \quad [3]$$

where r_{in} is the area resistance, λ the thickness, and κ is the specific conductivity of the interphase layer. If the interphase layer contains only pure water, its specific resistance is approximately $18 \times 10^6 \Omega$ cm. Thus, the area resistance of a 1 nm thick interphase is approximately 1.8 Ω cm². The above argument however is only correct if the ion concentration in the interphase is constant and all ions which are removed

by the electric current across the bipolar membrane are replenished by the water dissociation. This means that the ion fluxes from the bipolar membrane into the outer phases cannot exceed the rate of their generation in the interphase. Thus, the maximum flux of H^+ and OH^- ions of the bipolar membrane is given by:

$$J_{\text{H}^+} = J_{\text{OH}^-} = k_d C_{\text{H}_2\text{O}} \lambda \quad [4]$$

where J is the maximum ion flux from the bipolar membrane into the outer phases, k_d is the water dissociation rate constant, $C_{\text{H}_2\text{O}}$ is the concentration of water in the interphase and λ is the thickness of the interphases. The subscripts H^+ , OH^- and H_2O refer to H^+ , OH^- ions and water, respectively.

The water dissociation rate constant k_d for pure water at 25°C is given in the literature as $2.5 \times 10^{-5} \text{ s}^{-1}$.

According to eqn [4], the maximum fluxes J_{H^+} and J_{OH^-} from a bipolar membrane that has a 1 nm thick interphase of pure water would be $1.4 \times 10^{-13} \text{ mol cm}^{-2} \text{ s}^{-1}$.

The electrical current I through the bipolar membrane is proportional to the sum of all ion fluxes and is given by:

$$I = F(J_{\text{H}^+} + J_{\text{OH}^-}) \quad [5]$$

Thus, the maximum current density through a bipolar membrane is, according to eqns [4] and [5], approximately $1.4 \times 10^{-8} \text{ A cm}^{-2}$. A current density exceeding this value would lead to a depletion of ions in the interphase and thus to a drastic increase in its electrical resistance. In practice, however, bipolar membranes can be operated at current densities in excess of 0.1 A cm^{-2} , as demonstrated in Figure 3A, which shows the current through a bipolar membrane as a function of the applied voltage. When an increasing voltage difference across a bipolar membrane is established, the current hardly increases until the voltage drop reaches a value of about 0.8 V, corresponding to the concentration potential calculated by eqn [2] for a pH value difference between the two solutions outside the bipolar membrane of about 14. A further small increase in the voltage then leads to a drastic increase in the current density to values in excess of 0.2 A cm^{-2} . Thus, the current–voltage curves determined with bipolar membranes show two plateau values that indicate a limitation in the current with increasing voltage drop across the membrane, as depicted in Figure 3B. The first plateau value indicates a limitation of the current density due to a limitation of ions in the interphase. However, at 0.8 V accelerated water dissociation begins and the current

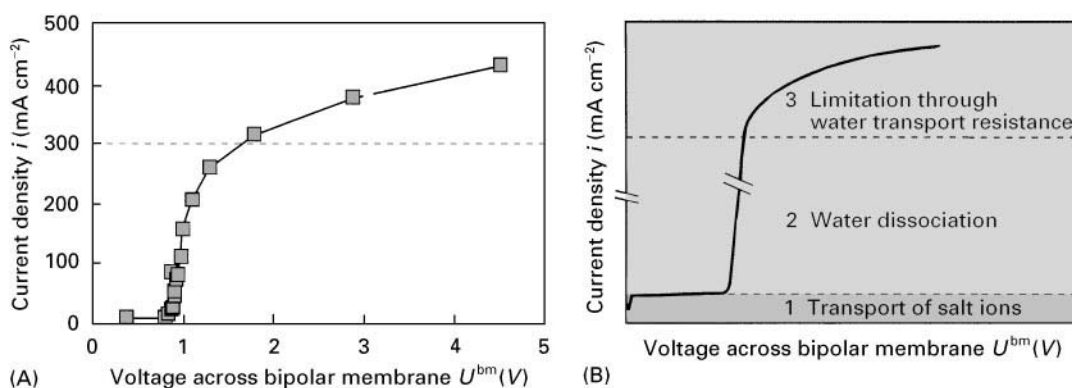


Figure 3 Schematic diagram of the current density as a function of the applied voltage (A) determined with a typical commercially available bipolar membrane and (B) three distinct areas of operation with bipolar membranes.

is no longer limited by a lack of ions until the second plateau value is reached at *ca.* 0.2 A cm^{-2} . Water dissociation is then limited by the supply of water to the interphase.

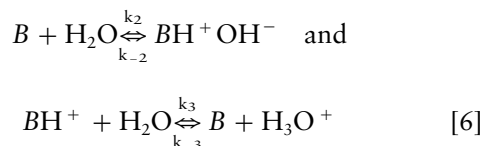
Thus, there are three distinct regions in the operation of a bipolar membrane. In the first region the current is very low and mainly transported by salt ions. In the second region, high water dissociation occurs and the current is transported by protons and hydroxide ions generated in the interphase. In the third region the production rate of protons and hydroxide ions is limited by the water transport rate into the interphase. Operation of bipolar membranes at current densities that exceed the second plateau value leads to destruction of the membrane.

The experimentally determined current densities indicate that the simple model of a bipolar membrane depicted in Figure 1 is incorrect. Either the water dissociation rate is faster by several orders of magnitude in the bipolar membrane than in free solution or the interphase is much thicker. A thick interphase, however, would lead to a high area resistance of the interphase, which is not the case. From scanning electron microscope photographs and calculations based on the Poisson and Boltzmann relation for the space charge at an interphase between differently charged ion exchange membranes, it can be concluded that the thickness of the interphase is less than 5 nm. This means that, in bipolar membranes the water dissociation is at least 10^6 times faster than in free solution.

Various mechanisms have been suggested to explain the accelerated water dissociation in bipolar membranes. One possible explanation, suggested by Wien, is that at high electric field densities the ion mobility as well as the degree of dissociation of weakly dissociated electrolytes increases with increasing field density. The increase in the dissociation constant of weak electrolytes by the electric field effect

can be expressed by an increase in the water dissociation rate constant, assuming that the recombination rate of H^+ and OH^- ions is unaffected.

Other theoretical considerations and experimental evidence support a hypothesis that the accelerated water dissociation is caused by a reversible proton transfer reaction between charged groups and water. This means that, in the presence of certain ionic groups, the water dissociation rate constant may be several orders of magnitude higher than in pure water. In the case of the bipolar membrane the anion exchange groups of the membrane polymer adjacent to the interphase layer are assumed to react with the water molecules at the membrane surface as follows:



where B is a neutral base, e.g. a tertiary ammonium group.

Both models can explain the acceleration of the water dissociation in the interphases between the anion and cation exchange layer of the bipolar membrane and serve as theoretical basis for the development of bipolar membranes.

The Preparation and Performance of Bipolar Membranes

The properties required of bipolar membranes to be useful in practical applications are low electrical resistance at high current density, high water dissociation rates, low co-ion transport rate, high ion selectivities, good thermal and, most importantly, good chemical stability since the cation-selective layer of the bipolar membrane is in direct contact with an

acid and the anion exchange layer with an alkaline solution.

Low electrical resistance of the cation and anion exchange layer of the bipolar membrane can be obtained by using a strong acid, such as sulfonic acid groups, and a strong base, such as quaternary ammonium groups as fixed charges in high concentrations in the polymer matrix. To minimize the resistance of the interphase between the cation- and the anion-selective layers the thickness of this interphase must be as thin as possible, as indicated earlier. There are various ways to prepare bipolar membranes with satisfactory properties. Most commonly, membranes are prepared as laminates with some kind of interphase which forms a transition region where the actual water dissociation takes place. In some membranes heavy metal hydroxides are deposited in the interphase to catalyse the water dissociation. However, tertiary ammonium fixed-charge groups at the surface of the anion exchange membrane seem to have the same effect.

A bipolar membrane with satisfactory properties can be prepared, e.g. as a laminate of highly permselective anion and cation exchange layers which have good alkaline and acid stability. An anion-selective layer with the required properties can be obtained by reacting chloromethylated polysulfone dissolved in *n*-methyl pyrrolidone with the monoquaternary salt of 4,4'-diazabicyclo-[2.2.2]-octane. The cation-selective layer can be prepared by introducing sulfonic acid groups as fixed charges into a polyether-ether-ketone matrix using chlorosulfonic acid. The co-ion transport and the swelling behaviour can be controlled in both layers by partial cross-linking. The properties of ion exchange membranes prepared following the above procedures are listed in Table 1.

The Performance of Bipolar Membranes

Bipolar membranes are usually characterized in terms of their water dissociation capability, their resistance

and their long-term stability. The water dissociation rate and electrical resistance of a membrane prepared by the procedure described above is shown in Figure 3A. Here the current density is shown as a function of the potential drop across the membrane. The test solutions in both compartments adjacent to the bipolar membrane are 1 molar Na₂SO₄. The results indicate that the current density is extremely low at potential differences of less than *ca.* 0.8 V. Then the current density increases up to 0.250 A cm⁻² with very little increase in voltage drop. When this value is exceeded, the resistance of the membrane increases drastically, due to limitations in the water transport into the interphase region.

Problems in Practical Applications of Bipolar Membranes

Electrodialytic dissociation of water with bipolar membranes is economically very attractive for creating acids and bases. There are, however, several severe problems in practical applications, such as the contamination of the products by salts and low current efficiency at high acid and base concentrations.

Salt contamination of the products is related to the properties of the bipolar membrane. The poor current efficiency is the consequence of the proton and hydroxide ion transport in monopolar membranes, as indicated in Figure 4, which illustrates the conversion of Na₂SO₄ into H₂SO₄ and NaOH by electrodialytic water dissociation. Figure 4(A) shows the ion transport in the bipolar membrane. What is desired is a flux of H⁺ and OH⁻ ions from the interphase of the bipolar membrane as the result of the water dissociation. However, in addition there is a flux of Na⁺ and SO₄²⁻ ions through the bipolar membrane due to incomplete permselectivity of the anion and cation exchange layers. This leads to a contamination of the base by SO₄²⁻ ions and the acid by Na⁺ ions. Since the permeability of the ion exchange layers to SO₄²⁻ and Na⁺ increases with increasing acid and base concentration, the contamination is also increasing with increasing concentration, as shown in Figure 4B. This figure shows the salt contamination in sulfuric acid and sodium hydroxide produced by water dissociation in bipolar membranes from a 1 mol L⁻¹ Na₂SO₄ solution as a function of the concentration of the acid and base produced.

The current efficiency in water dissociation with bipolar membranes is mainly affected by the properties of the anion exchange membrane which has very poor retention of the protons, as illustrated in Figure 4C. The transport mechanism of protons is based on a tunnelling mechanism, with the consequence that protons can permeate the anion

Table 1 Electrochemical properties of the cation- and anion-selective layers of a bipolar membrane prepared by the technique described above

	Anion exchange layer	Cation exchange layer
Ion exchange capacity (mmol g ⁻¹)	1.2	1.0
Membrane thickness (μm)	60	60
Area resistance (Ω cm ²)	1.05	1.31
Permselectivity (%)	97.5	98.5
Swelling (%)	8	12.5

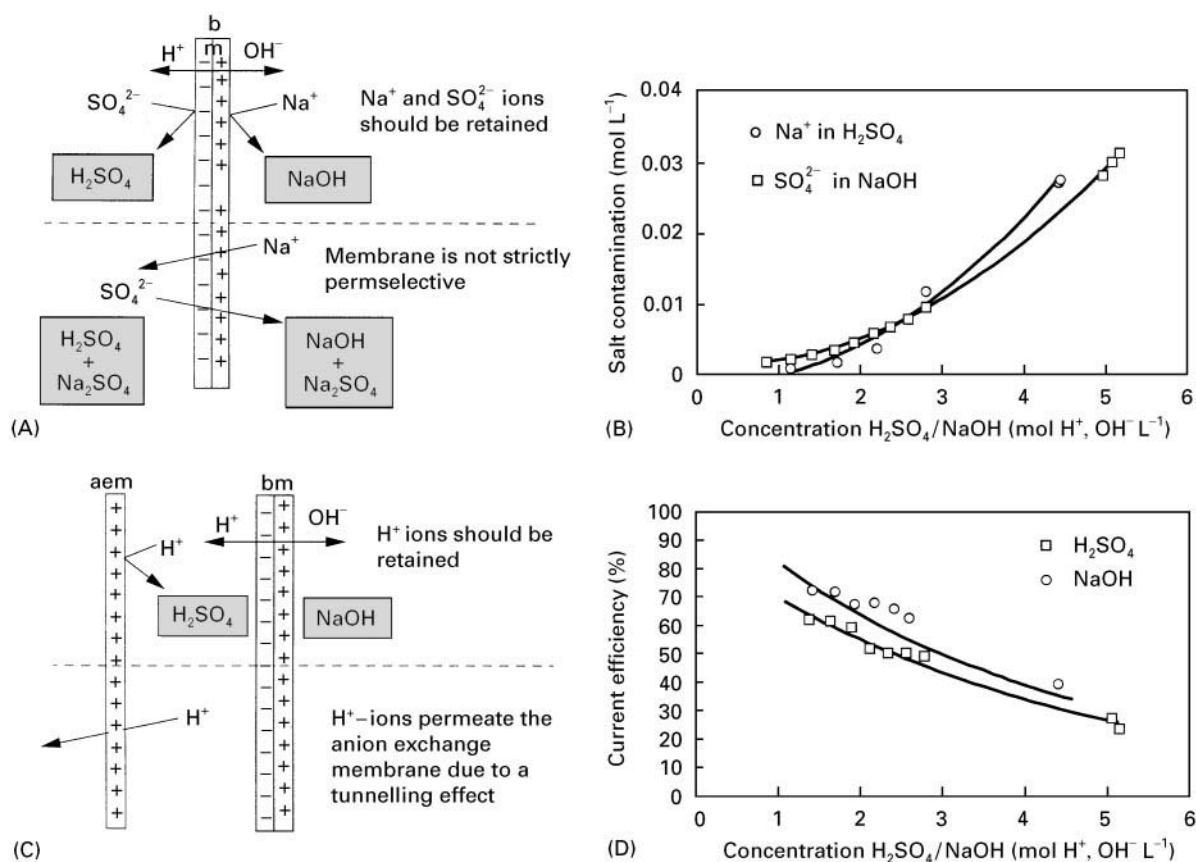


Figure 4 Schematic diagram illustrating (A) the contamination of an acid and a base by salt to incomplete permeability of the cation and anion exchange layers of a bipolar membrane; (B) experimentally determined salt contamination as a function of the acid and base concentrations; (C) the decrease in current efficiency during the production of acids and bases due to the poor acid-blocking capability of the anion exchange membrane; (D) experimentally determined current efficiency as a function of the produced acid and base concentration.

exchange membrane rather freely. The same is true for the hydroxide ions which can permeate the cation exchange membrane. The net result of the process is that protons and hydroxide ions generated in the bipolar membrane neutralize each other. The proton and hydroxide fluxes and thus the current efficiency depend on the concentration, as shown in Figure 4D. With increasing acid and base concentration, the current efficiency decreases rapidly.

Application of Bipolar Membranes

One interesting application of bipolar membranes is the production of caustic soda. Currently, caustic soda is produced as a co-product of the products of chlorine by electrolysis of salt. The worldwide demand for polyvinyl chloride and other chlorinated hydrocarbons has led to the development of a large market for chlorine. Because of environmental problems caused by chlorinated hydrocarbons and the disposal of polyvinyl chloride wastes, the demand for

chlorine is steadily decreasing, however, and it can be expected that the demand for caustic soda will soon exceed that produced in the chlorine alkaline electrolysis. Thus interest in alternative processes for obtaining caustic soda is increasing. Electrodialytic water dissociation with bipolar membranes is one of the more promising techniques for the future large scale economic production of caustic soda. However, today's bipolar membranes produce caustic soda with some salt contamination. The production of NaOH and H₂SO₄ from the corresponding salts has been investigated in great detail. Test results obtained in laboratory studies are shown in Figure 4. These tests were carried out with a 1 mol L⁻¹ solution Na₂SO₄ feed at room temperature and an applied current density of 0.1 A cm⁻². The test results indicate that up to three normal acid and base solutions can be achieved with a current utilization of 60–70%. However the produced acid and base are contaminated by salt and the salt contamination increases with increasing acid and base concentrations due to decreasing

selectivity of the bipolar membrane with increasing acid or base concentrations. Salt concentration can reach values in excess of 0.03 mol L^{-1} at 4 molar base or acid concentrations. To improve the overall efficiency of the electrodialytic dissociation processes and to obtain less salt contamination in the acids and base produced, better proton-blocking membranes have to be developed in addition to more selective bipolar membranes.

Fortunately, there are a large number of other potential applications of the electrodialytic water dissociation where the purity of the product, i.e. the produced acid or base, is not critical and traces of salts can be tolerated. Typical applications of bipolar membranes with large industrial relevance are:

- Recovery of acids and bases such as sulfuric, hydrochloric or hydrofluoric acid and sodium hydroxide from the salts generated in neutralization reactions
- The recovery of organic acids such as formic, acetic, citric, lactic and itaconic acid or certain amino acids from fermentation broths
- Adjustment of pH values in fermentation or chemical production processes without increasing the ion potential
- Regeneration of H_2SO_4 and NaOH from Na_2SO_4 obtained in industrial effluents, for example, in the production of viscose or regenerated cellulose
- Regeneration of acids and bases from scrubbers used to remove SO_2 , NO_x from contaminated air streams.

This list of potential applications of the electrodialytic water dissociation with bipolar membranes is not complete and as more efficient bipolar membranes become available, more applications will certainly be identified. In this outline three typical examples for the use of bipolar membranes are described in more detail.

Recycling H_2SO_4 and Dimethylisopropylamine from an Acid Scrubber

Alkaline or acid scrubbers are often used to remove components that are harmful to the environment, such as NO_x , SO_2 or certain amines from waste air streams. In these processes large amounts of acids or bases are consumed and salts are produced. In general, only dilute acids and bases are required in scrubbers. This makes the use of electrodialytic water dissociation with bipolar membranes a very suitable process to recover the acids or bases from the corresponding salts. The recovery of base from scrubbers used to remove SO_2 and NO_x from coal-burning power plants is described in detail in the literature.

Another similar application is the recovery of dimethylisopropylamine removed from a waste air stream by a sulfuric acid scrubber. This type of waste air stream is generated when aluminium casting moulds are made from a sand/epoxy resin mixture by injecting dimethylisopropylamine in a mixture with air as catalyst to cure the resin instantaneously. The amine is not consumed in the process and is emitted in a waste air stream containing *ca.* $0.5 \text{ g amine per m}^3$ waste air. The amine can be recovered as amine sulfate in an acid scrubber, as indicated in Figure 5. The amine can then be regenerated by adding sodium hydroxide and distilled. The net result of the process, however, is the production of large amounts of sodium sulfate.

A complete recycling of the amine, the sulfuric acid and water is achieved without the production of a salt by combining the electrodialytic water dissociation with distillation. The process is illustrated in Figure 6. The waste air stream containing the amines is fed into an acid scrubber where the free amine is converted into amine sulfate. The effluent of the acid scrubber containing about 10% amine sulfate in a mixture with sulfuric acid is then fed into the electrodialytic water dissociation apparatus

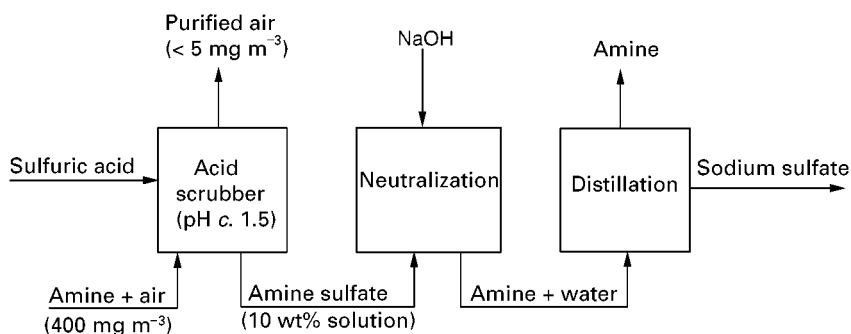


Figure 5 Schematic diagram illustrating a conventional process for recovering an amine from a contaminated air stream using an acid scrubber.

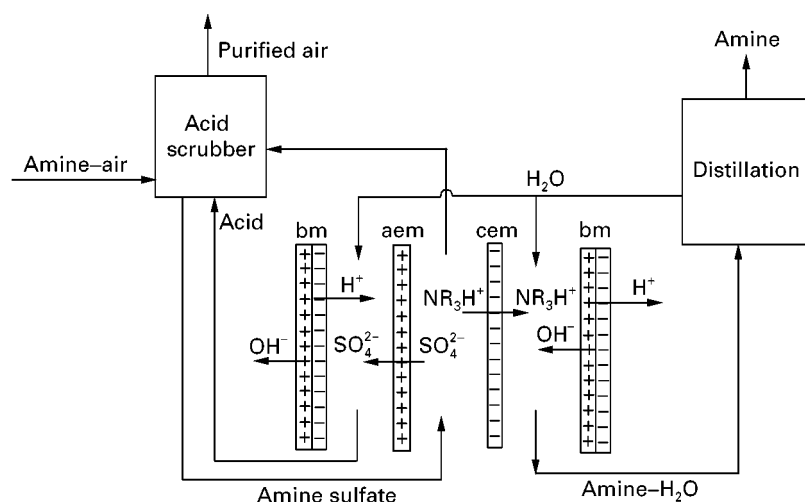


Figure 6 Schematic diagram illustrating the recovery of dimethylisopropyl amine from a waste air stream by combination of acid scrubber, diffusion dialysis and electrochemical water dissociation using bipolar membranes and distillation.

containing bipolar membranes and anion and cation exchange membranes in alternating series between two electrodes. Here the amine sulfate is converted to the free amine while the sulfate ions form sulfuric acid which is recycled to the acid scrubber. The amine–water mixture is distilled to recover the amine and the water is recycled to the electrochemical unit. Thus, the process allows complete recovery of the amine from a waste air stream by combination of an acid scrubber and electrochemical water dissociation.

Production of Itaconic Acid in a Continuous Fermentation Process

One of the more promising applications of bipolar membranes is the adjustment of the pH value of fermentation solutions to recover the organic acids from the spent medium. As an example the production of itaconic acid is described below.

Conventionally, itaconic acid is produced by a batch fermentation process. During fermentation the pH value shifts towards lower values due to the production of the acid. To avoid product inhibition the pH is maintained at a high level by addition of sodium or ammonium hydroxide which form soluble salts with the produced itaconic acid. At the end of the fermentation processes, the free acid is recovered from the spent medium by lowering the pH value by adding sulfuric acid. The adjustment of the pH values in the fermenter as well as in the spent medium is not only costly, but also creates salts mixed with the desired product and thus further purification steps are required. By applying bipolar membrane technology the production of salts can be eliminated and the itaconic fermentation can be carried out more ef-

ficiently in a continuous process, as illustrated in the production scheme depicted in **Figure 7**. The flow scheme shows a fermenter combined with an electrochemical unit fitted with bipolar membranes. The fermenter is continuously fed with substrate and its constituents passed through an ultrafiltration unit. The retained biomass is recycled to the reactor while the product containing filtrate is fed to the middle cell of a three-compartment electrochemical unit. In this cell the solution will be depleted of the ions. The cations, i.e. sodium or ammonium ions, permeate the cation exchange membrane and form, with the OH^- ions generated in the bipolar membrane, NaOH which is concentrated and then fed back into the bioreactor to adjust the pH value. The anions, i.e. the itaconate ions, permeate the anion exchange membrane and form, with protons generated at the bipolar membrane, the itaconic acid which is then concentrated and precipitated. Thus, the itaconic acid is produced in a continuous process without the addition of acids or bases, i.e. without the production of additional salts.

The Electrochemical Production of Sodium Methylate by Methanol Dissociation

Bipolar membranes may be used not only for the electrochemical dissociation of water. They can also be applied for the dissociation of alcohol and thus for the production of alcoholates, as illustrated in the following example. Methanol, like water, is both a weak base and a weak acid. Its dissociation constant, however, is somewhat less than that of water. Thus, sodium methanolate can be efficiently produced from methanol and sodium acetate in nonaqueous media by the use of bipolar membranes

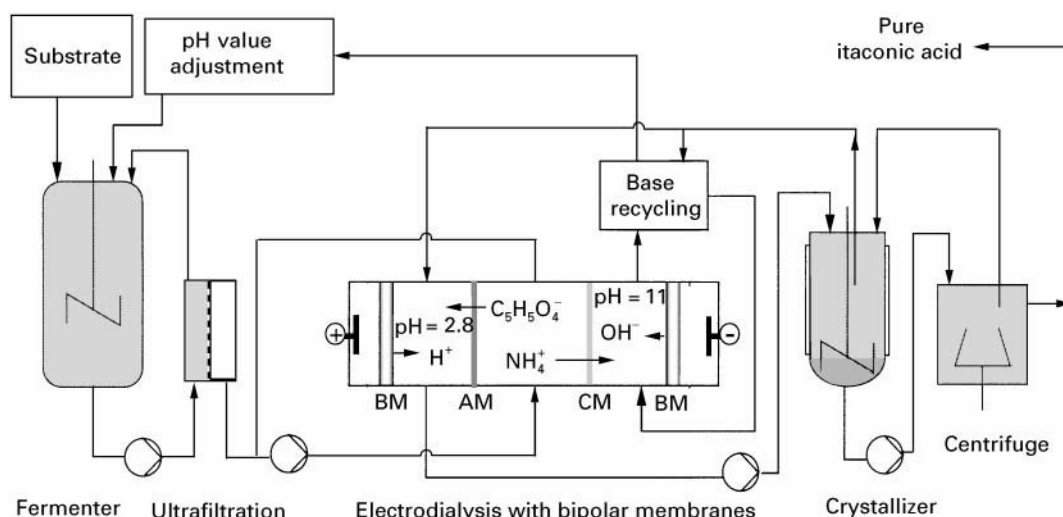


Figure 7 Schematic diagram illustrating a continuous fermentation process for the production of itaconic acid without further addition of acids or bases using bipolar membranes.

according to the reaction scheme illustrated in Figure 8, which shows a bipolar membrane electrodialysis stack consisting of two compartment cell systems in a repeating unit between electrodes. Water-free methanol and sodium acetate are fed into the cell formed by the bipolar and the cation exchange membrane which is directed towards the cathode while water-free methanol is passed through the other cell. Under the driving force of an electrical potential gradient, methanol is split in the bipolar membrane into protons and CH_3O^- ions which react with sodium ions migrating from the sodium acetate-

containing cell to form CH_3ONa . The acetate ions recombine on the other side of the bipolar membrane with the protons which were produced simultaneously with the CH_3O^- ions in the bipolar membrane to form acetic acid. Thus, sodium acetate and methanol are converted into sodium methanolate. The current efficiency decreases with increasing methylate concentration due to proton transfer from the acetic acid-containing compartment through the bipolar membrane to the sodium methanolate-containing cell. But all in all the process seems to be technically feasible.

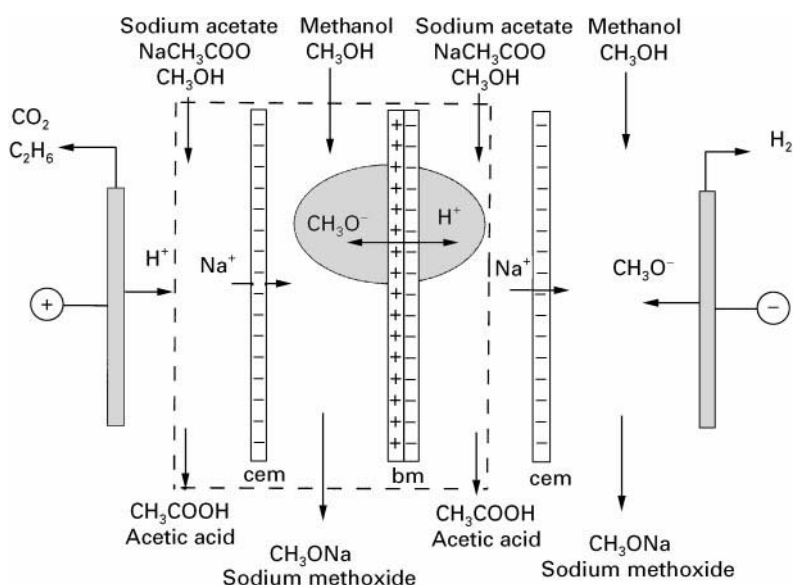


Figure 8 Schematic diagram illustrating the electrodialytic production of sodium methanolate from methanol and sodium acetate in bipolar membranes containing a two-compartment cell unit.

Conclusions

The mechanism of water dissociation in bipolar membranes can be rationalized by a hypothesis which postulates a catalytic reaction between a weak base and water. Based on this hypothesis, very stable chemical and thermal bipolar membranes can be prepared and operated efficiently at current densities in excess of 0.1 A cm^2 . The process has many potential applications. There are, however, still a multitude of problems to be solved. Some are related to the poor selectivity of the bipolar membranes and poor acid-blocking capability of the anion exchange membranes; others are caused by the lack of application know-how and practical experience.

Further Reading

- Liu KJ, Chlanda FP and Nagasubramanian KJ (1977) Use of bipolar membranes for generation of acid and base: an engineering and economic analysis. *Journal of Membrane Science* 2: 109–124.
- Mani KN (1991) Electrodialysis water splitting technology. *Journal of Membrane Science* 58: 117–138.
- Simons R (1985) Water splitting in ion exchange membranes. *Electrochimica Acta* 30: 275–282.
- Strathmann H, Kroll JJ, Rapp JJ and Eigenberger G (1997) Limiting current density and water dissociation in bipolar membranes. *Journal of Membrane Science* 125: 123–142.
- Strathmann H, Bauer B and Rapp HJ (1993) Better bipolar membranes. *Chemtech* June: 17–24.

Catalytic Membrane Reactors

M. E. Rezac, Georgia Institute of Technology, Atlanta, GA, USA

Copyright © 2000 Academic Press

Introduction

The concept of completing both a reaction and separation in a single process unit has motivated research into the development of catalytic membrane reactors. For example, it has long been recognized that palladium metal has the capacity both to permeate hydrogen and to promote a variety of reactions. Thus, harnessing both of these features in a single device seemed a logical combination. In the mid 1960s, Wood and co-workers demonstrated that the dehydrogenation of cyclohexane to cyclohexene could be increased if the hydrogen produced was removed from the reaction vessel through semipermeable palladium walls. In this case, the palladium walls also acted to catalyse the dehydrogenation reaction. A membrane reactor of this type is illustrated in Figure 1.

In Russia, Gryaznov conducted much of the research that followed. Starting in the late 1970s, Gryaznov began publishing his results on the use of palladium membrane reactors both to produce and to recover hydrogen from a myriad of dehydrogenation reactions. In the dehydrogenation reactions, hydrogen leaves the reactor by permeating through the semipermeable membrane. However, reactors can also be used in reactions where hydrogen or other reaction products enter the reaction chamber by penetration through the membrane. The commonest classes of reactions that have been successfully influenced by the use of membrane reactor technology

are listed in Table 1. Details relating to the large volume of research reported are provided in the Further Reading section. None of these membrane reactors are in commercial use. But some – the selective oxidation of methane, for example – are the subject of a very large industrial research effort. If successfully developed, this process would change the feedstock basis of a number of petrochemical processes.

Most research on the development of membrane reactors involves the use of these devices to shift equilibrium-limited reactions (often dehydrogenations). The thermodynamic equilibrium of the reactants and products at the temperature and pressure of the reaction determine the conversion achievable in any given reaction. For dehydrogenation reactions, increasing temperature and decreasing pressure promote an enhanced reaction. Unfortunately, each of these solutions has an associated cost. Increasing the reaction temperature typically results in a reduced

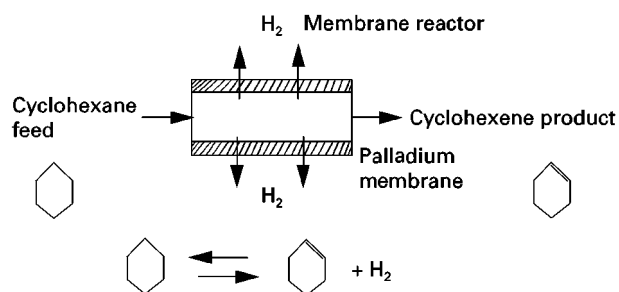


Figure 1 Schematic of a membrane reactor using hydrogen-permeable palladium membranes to shift the equilibrium of the dehydrogenation reaction cyclohexane to cyclohexene.

Conclusions

The mechanism of water dissociation in bipolar membranes can be rationalized by a hypothesis which postulates a catalytic reaction between a weak base and water. Based on this hypothesis, very stable chemical and thermal bipolar membranes can be prepared and operated efficiently at current densities in excess of 0.1 A cm^2 . The process has many potential applications. There are, however, still a multitude of problems to be solved. Some are related to the poor selectivity of the bipolar membranes and poor acid-blocking capability of the anion exchange membranes; others are caused by the lack of application know-how and practical experience.

Further Reading

- Liu KJ, Chlanda FP and Nagasubramanian KJ (1977) Use of bipolar membranes for generation of acid and base: an engineering and economic analysis. *Journal of Membrane Science* 2: 109–124.
- Mani KN (1991) Electrodialysis water splitting technology. *Journal of Membrane Science* 58: 117–138.
- Simons R (1985) Water splitting in ion exchange membranes. *Electrochimica Acta* 30: 275–282.
- Strathmann H, Kroll JJ, Rapp JJ and Eigenberger G (1997) Limiting current density and water dissociation in bipolar membranes. *Journal of Membrane Science* 125: 123–142.
- Strathmann H, Bauer B and Rapp HJ (1993) Better bipolar membranes. *Chemtech* June: 17–24.

Catalytic Membrane Reactors

M. E. Rezac, Georgia Institute of Technology, Atlanta, GA, USA

Copyright © 2000 Academic Press

Introduction

The concept of completing both a reaction and separation in a single process unit has motivated research into the development of catalytic membrane reactors. For example, it has long been recognized that palladium metal has the capacity both to permeate hydrogen and to promote a variety of reactions. Thus, harnessing both of these features in a single device seemed a logical combination. In the mid 1960s, Wood and co-workers demonstrated that the dehydrogenation of cyclohexane to cyclohexene could be increased if the hydrogen produced was removed from the reaction vessel through semipermeable palladium walls. In this case, the palladium walls also acted to catalyse the dehydrogenation reaction. A membrane reactor of this type is illustrated in Figure 1.

In Russia, Gryaznov conducted much of the research that followed. Starting in the late 1970s, Gryaznov began publishing his results on the use of palladium membrane reactors both to produce and to recover hydrogen from a myriad of dehydrogenation reactions. In the dehydrogenation reactions, hydrogen leaves the reactor by permeating through the semipermeable membrane. However, reactors can also be used in reactions where hydrogen or other reaction products enter the reaction chamber by penetration through the membrane. The commonest classes of reactions that have been successfully influenced by the use of membrane reactor technology

are listed in Table 1. Details relating to the large volume of research reported are provided in the Further Reading section. None of these membrane reactors are in commercial use. But some – the selective oxidation of methane, for example – are the subject of a very large industrial research effort. If successfully developed, this process would change the feedstock basis of a number of petrochemical processes.

Most research on the development of membrane reactors involves the use of these devices to shift equilibrium-limited reactions (often dehydrogenations). The thermodynamic equilibrium of the reactants and products at the temperature and pressure of the reaction determine the conversion achievable in any given reaction. For dehydrogenation reactions, increasing temperature and decreasing pressure promote an enhanced reaction. Unfortunately, each of these solutions has an associated cost. Increasing the reaction temperature typically results in a reduced

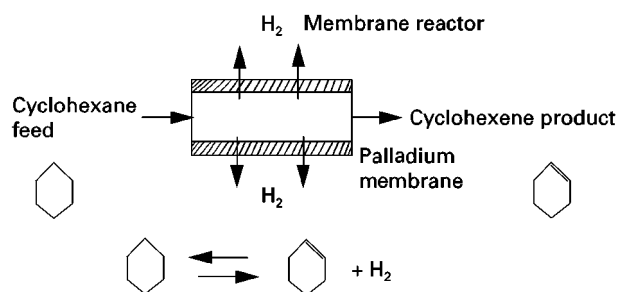


Figure 1 Schematic of a membrane reactor using hydrogen-permeable palladium membranes to shift the equilibrium of the dehydrogenation reaction cyclohexane to cyclohexene.

Table 1 Reaction classes that may be amenable to membrane reactor technology

Reaction class	Example	Role of membrane
Hydrogenation	$C_2H_2 + H_2 \rightarrow C_2H_4$ in presence of C_2H_4	Controlled addition of hydrogen
Hydrogenolysis	Cyclopentadiene + $H_2 \rightarrow$ cyclopentene + cyclopentane	Controlled addition of hydrogen
Dehydrogenation	Cyclohexane \rightarrow benzene + 3H_2	Remove hydrogen to shift equilibrium limitation
Partial oxidation	Butane + $O_2 \rightarrow$ maleic anhydride	Recovery of intermediate product of control reactant at addition rate to promote formation of intermediate product
Esterifications	$R-OOH + CH_3OH \rightarrow R-O-O-CH_3 + H_2O$	Selective water removal to shift equilibrium limit without loss of reactant
Syn gas	$CH_4 + \frac{1}{2}O_2 \rightarrow CO + 2H_2$	Selective oxidation of methane
Oxidative coupling	$2CH_4 + O_2 \rightarrow C_2H_4 + 2H_2O$	Selective oxidation of methane

catalytic selectivity for the desired product. Reducing pressure comes at the cost of adding a diluent to the reactor, paying for the additional capital to handle this component and paying the price of downstream separation.

Figure 2 provides a schematic representation of the behaviour of a conventional reactor and a theoretical membrane reactor. The conventional data are for a highly active butane dehydrogenation catalyst operating at 1 atm total pressure (pure normal butane feed). In the conventional system, the selectivity of the catalyst degrades rapidly at temperatures that are just beginning to promote reaction. Thus, the catalytic yield (defined as the product of conversion and cata-

lytic selectivity) goes through a pronounced maximum. Incorporation of an appropriately designed membrane into the reactor system results in the removal of hydrogen from the system. The catalytic selectivity does not appear to be influenced by this process, but the conversion of butane to butene is enhanced by the reduction in the hydrogen partial pressure. Thus, the yield of the membrane reactor system is markedly improved.

The ability to operate at acceptable conversions while maintaining very high catalytic selectivity is a strong driving force for the use of membrane reactor technology. By operating in a high selectivity region, the production of by-products that can act as catalyst poisons is minimized. This results in a longer catalyst life between regenerations and reduced waste production.

Possible Membrane Configurations

Incorporation of a reaction and separation zone in a single process unit allows for a variety of possible configurations. The optimum design of the equipment is closely tied to the reaction conditions and the ability of the membrane material to serve as a catalyst. Several of the more common configurations are shown in Figure 3. For illustrative purposes, the dehydrogenation of a compound to form hydrogen will be considered. The hydrogen is removed from the reaction zone to increase the equilibrium conversion. Similar configurations can be employed for the other reactions listed in Table 1. As described below, these configurations represent the most frequently employed designs, however, the list is not exhaustive and new configurations are developed and patented regularly.

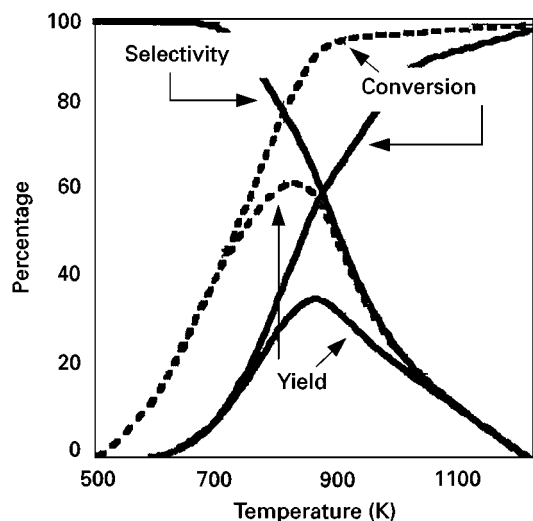


Figure 2 Influence of product hydrogen removal on the dehydrogenation of butane. Based on pure butane feed with 1.1 atm total pressure. Continuous line, conventional reactor; dashed line, membrane reactor.

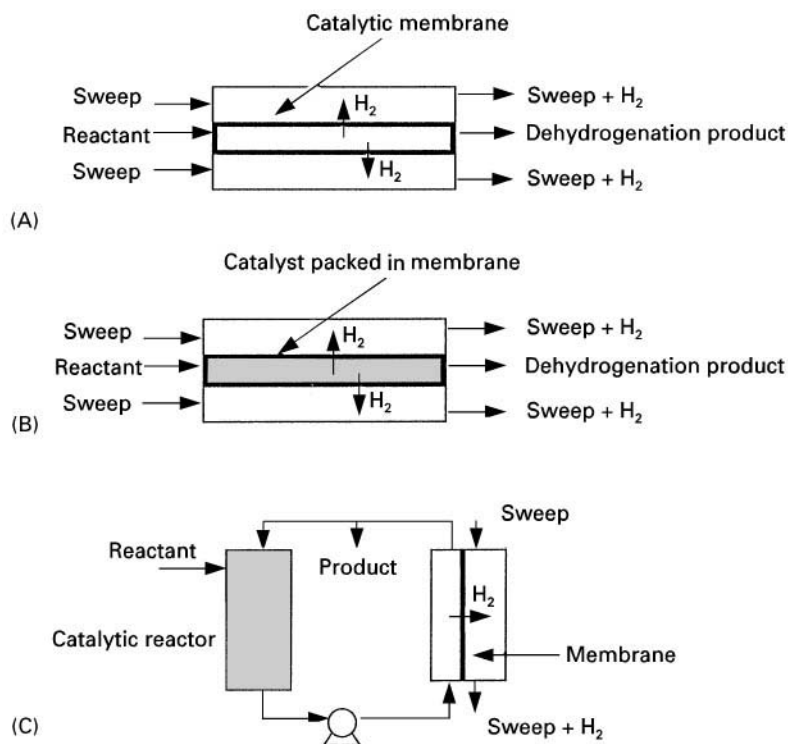


Figure 3 Common membrane reactor configurations. (A) Catalytic membrane; (B) membrane tube packed with catalyst; (C) membrane-assisted batch reactor.

Catalytic Membrane

One of the earliest catalytic membrane configurations employed was that of the reactive tube. In this configuration, the material used to construct the tube fulfills both the roles of separation medium and catalyst. Few materials have this special capability. Palladium is one. Palladium has the ability to transport hydrogen through the matrix by a process of adsorption, dissociation, diffusion, and then reassociation on the low pressure side. Palladium is also a reasonable catalyst for many of the reactions detailed in Table 1, especially hydrogenation and dehydrogenation reactions. Thus, using this material to achieve both functions was an obvious consideration.

Transport can only be achieved through a chemical potential driving force of the hydrogen from the reaction zone to the separation zone. Such a driving force has been established with the use of a sweep gas on the permeate side to keep the hydrogen concentrations low. The sweep gas may either be inert or reactive with the hydrogen. Inert sweep gases offer the advantage of being simple to employ. Unfortunately, to achieve a partial pressure difference across the membrane, the sweep gas rate must be high and the permeated hydrogen is recovered as a dilute component in the sweep gas.

Reactive sweep gases offer other engineering possibilities and challenges. The use of air as a sweep gas in catalytic dehydrogenation membrane systems has been reported. At dehydrogenation temperatures (300–600°C), oxygen can react with hydrogen to form water. This reaction is highly exothermic. In contrast, the dehydrogenation reaction is endothermic. Thus, thermal matching of the heat released by the hydrogenation of oxygen and the heat consumed by the dehydrogenation reaction would allow for an isothermal system. Because the hydrogenation reaction is rapid, the effective partial pressure on the permeate side of the membrane can be maintained near zero.

Catalytic membrane systems require that the membrane material be stable for both reaction and separation and that it operates well in both modes simultaneously.

Packed Tube

Optimization of a single material for both catalytic and separative functions is challenging. Few materials have the ability to transport the desired component and act as a catalyst for the desired reaction. Furthermore, even for materials that possess both characteristics, precise matching of the rates of reaction and

transport is difficult. To overcome these limitations, a packed membrane tube configuration has been employed. In such a configuration, a catalyst is packed in the bore of a tubular membrane. Reactants are fed into the catalyst zone and products have the potential to be transported through the membrane walls and out of the reaction zone. This configuration offers tremendous flexibility in the selection of the catalyst and membrane to be used. Both homogeneous and heterogeneous catalysts have been employed in this configuration.

Membrane-assisted Batch Reactor

The membrane-assisted batch reactor is most frequently considered for implementation because it requires the smallest process modification from traditional catalytic reactors. In this configuration, a membrane unit is added in the recycle line of a batch reactor. In so doing, the membrane has the capacity to selectively remove a product component or to selectively add a reactant. It has the advantage of allowing the pressure or temperature of the membrane and reactor unit to be controlled independently. Therefore, the properties of the membrane can be varied to optimize the separation achieved.

Membrane-assisted configurations suffer from the inability to remove product components completely as they are produced. This limits the conversion to values that are lower than those that are theoretically possible in the other configurations considered.

Available Membranes

The development of catalytic membrane reactors is limited by the availability of membranes capable of controlling the reaction environment that are stable at reaction conditions. A brief review of transport through membranes is provided and then the additional membrane requirements are summarized. Figure 4 provides a schematic of a membrane employed for the transport of a gaseous component.

Transport of a component through a solid is only possible if there are differences between the chemical potential of the component on the two faces of the solid. For gas-phase systems that operate at moderate pressures and can be considered to be ideal, transport can be described by:

$$\text{Flux}_i = P_i(p_{\text{Hi}} - p_{\text{Li}})/l \quad [1]$$

where P_i is the permeability of component i through the membrane, p_{Hi} is the partial pressure of component i on the high pressure side, p_{Li} is the partial

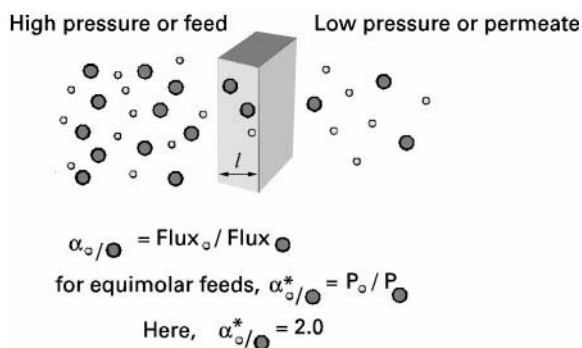


Figure 4 Schematic of transport through a solid.

pressure of component i on the low pressure side and l is the membrane thickness.

Thus, the difference in the partial pressure of the component to be transported controls the rate of transport. A high partial pressure driving force can be produced through:

- high total pressure on the feed side
- high concentration of the component of interest on the feed side
- low total pressure on the permeate side (using a vacuum)
- very low concentration of i on the permeate side using a very high dilution ratio of sweep gas

The rate at which a component is transported through a solid is defined as the flux of the component, (eqn [1]). To facilitate the comparison of a variety of materials, the properties of the material (permeability) have been separated from the process conditions (membrane thickness, pressures and concentrations). For equivalent process conditions, the material with the highest permeability will have the fastest transport.

The selectivity of a membrane for any pair of gases (A, B) is usually defined by the term $\alpha_{A/B}$, equal to the ratio of the gas permeabilities:

$$\alpha_{A/B}^* = P_A / P_B \quad [2]$$

For membrane reactors, membranes with high selectivities are required, so only the required component enters or leaves the reactor.

Specific Membranes

Certain materials have the ability to transport a single component with the complete exclusion of all others. Transport of hydrogen and oxygen through two of these materials is reviewed here.

Metals (hydrogen) Palladium and some of its alloys have the ability to transport hydrogen while

completely excluding all other compounds. The permeation of hydrogen through metals is a multistep process involving:

- chemisorption of hydrogen on to the metal surface
- dissociation of the hydrogen
- dissolution of the atomic hydrogen from the surface into the bulk of the metal
- diffusion across the metal layer
- the desorption from the bulk of the metal to the surface
- reassociation
- desorption of molecular hydrogen from the metal surface

The diffusion of atomic hydrogen across the metal layer is typically the rate-limiting step. Therefore, the transport of the hydrogen can be modelled using a Fickian diffusion equation.

Alloys of palladium have proven effective for the transport of hydrogen. Pure palladium undergoes a phase transformation in the presence of hydrogen at moderate temperatures, and a density change ensues. Even though these changes are small, they are sufficient to produce a brittle, cracked and non-selective material after only a few cycles. Therefore, few of the membranes evaluated are pure palladium and most commercial metallic hydrogen purifiers are prepared from a palladium/silver alloy containing 23% silver.

A significant limitation to the use of palladium membranes is their strong susceptibility to poisoning by sulfur compounds and CO compounds frequently found in the hydrocarbon streams of interest. Research into the development of more resistant materials is underway. However, the improved resistance has so far been attained at the cost of permeability. This issue must be resolved before these membranes can be used in the chemical process industry.

Nonporous ceramics (oxygen) Ceramic membranes have been developed which will selectively transport hydrogen or oxygen. Hydrogen has been shown to be transportable through nonporous silicon dioxide. While the transport rates are extremely slow, the selectivity to hydrogen transport is infinite, just as in defect-free palladium. Silicon dioxide has the advantage of being more resistant to the presence of sulfur compounds that act as poisons for palladium. Nevertheless, the challenge of forming this material into extremely thin layers has limited its use. Perhaps as preparation techniques continue to improve, the use of this material for the highly selective transport of hydrogen will be re-examined.

Nonporous ceramics have also been used for the transport of oxygen. Oxide-conducting materials, in-

cluding stabilized zirconia, have been used in membrane reactors. These membranes can successfully transfer oxygen while barring the transport of all other compounds. Current limitations relating to the temperatures required for operation are discussed in subsequent sections.

Nonspecific Membranes

Commercial utilization of membranes has relied almost exclusively on the use of nonspecific membrane materials. These materials have the ability to transport one component of a gas mixture in preference to a second. However, they are permeable to all components to at least some degree. Therefore, unlike palladium, which can act as a perfect separator, these membranes transport all stream components. The properties of both porous ceramics and polymeric membranes will be considered here.

Porous ceramics Porous ceramic membranes, with pore sizes ranging from a few nanometers to several microns, have been produced and are commercially available. These membranes separate by size exclusion. For the separation of gases and low molecular weight liquids, Knudsen diffusion is typically employed. For gases, Knudsen diffusion occurs for pore sizes of about 4–100 nm. For systems operating under the Knudsen diffusion regime, the separation of two molecules can be defined as:

$$\alpha_{A/B} = (MW_B/MW_A)^{0.5} \quad [3]$$

Thus, high degrees of separation selectivity are only possible if the molecular weight difference between the two components is large. These materials have been employed for the separation of hydrogen from hydrocarbon streams. The ideal separation selectivity for hydrogen over butane, for example, is 5.8. Thus, a small but measurable separation can be achieved.

The microporous nature of these membranes allows them to have very high transport rates, as compared to nonporous palladium or ceramic materials. Yet, the separation achievable is limited.

Polymers The final category of membrane materials to be considered is polymers. Polymeric membranes are employed for the separation of gas streams, the recovery of organic vapour from air, the separation of mixtures of organic liquids and filtration of particles from aqueous streams. Nonporous polymeric membranes have been considered for membrane reactor applications. Nonporous polymeric membranes separate on the basis of sorption of the component into

the polymeric matrix, diffusion across and desorption from the low pressure side.

Polymers offer several advantages when compared with the porous ceramics. For many gas pairs, the inherent selectivity of the polymeric membrane is substantially higher than that of a Knudsen diffusion-controlled ceramic. The polymeric membranes are also easier to prepare in high surface per volume modular configurations, resulting in a considerably lower price. Recent estimates put the price of commercial polymeric membranes at well under \$10 per square foot membrane area, installed. In contrast, ceramics may cost 10 times as much.

Many applications of membrane reactors, including dehydrogenation of hydrocarbons, hydrogenations and partial oxidation reactions are high temperature reactions. Conventional polymeric membranes do not have either the chemical or thermal stability to be successfully used in these reactions. However, recent advances have provided materials that can be processed using conventional solvent-based techniques and are later cross-linked to provide the chemical and thermal resistance necessary for membrane reactor applications. New polyimide-based materials provide such characteristics.

Polyimides that are thermally stable to 300°C for extended periods have been reported. When incorporated in a membrane reactor for the dehydrogenation of butane, the system performance increased markedly. With no membrane, conversions of 22% were achieved. Following addition of the membrane to the integrated system, the conversion increased to over 30%.

The development of chemically stable polymeric materials provides an opportunity to influence liquid-phase organic reactions.

Applications

While the use of membranes to influence catalytic reactions has been explored in great detail, few systems have been employed commercially. Some of the possible reasons for this slow adoption are listed below. Nevertheless, a few materials are produced through the use of membrane reactor technology. Gryaznov, for example, has reported the production of vitamin K using a single-step process utilizing a membrane reactor. The membrane was employed to control the hydrogenation of a mixture of quinone and acetic anhydride to form vitamin K. The membrane reactor process resulted in a 95% yield using an external hydrogen pressure of 1 atm. The conventional process required several processing steps and resulted in only 80% yield. This membrane reactor process is reported to be employed commercially in Russia.

Current Limitations

Some of the more important technical issues that have limited the implementation of membrane reactor technology are detailed below. In addition to technical problems, economic considerations are a concern. For many of the systems considered (Table 1), commercial production facilities using conventional reactor technology are available. If membrane reactors are to supplant these existing systems, the economic benefit must be substantial. Furthermore, the cost of the membrane reactor system must be only marginally higher than the conventional system. For most reactions, this is not currently the case.

Need for Pressure Drop

When one considers the use of membrane reactor technology for the selective removal of a product component (such as in dehydrogenations), the design of the membrane will be governed by the need for a partial pressure difference of this component. To increase the equilibrium conversion, these systems are run at low pressure with a goal of complete removal of the component as it is produced. Thus, the partial pressure of the product component is nearly zero in the reaction zone. For transport to occur, the partial pressure on the permeate side must be lower. Several techniques have been employed to attain partial achievement of these goals. These include high volumes of sweep gas on the permeate side; vacuum on the permeate side; and transforming the system to a batch reactor with continuous removal of the product component. In the last case, the partial pressure on the feed side is maintained at some finite level, and additional conversion is achieved by long residence times.

Sweep gas The use of high sweep gas ratios (nitrogen or argon is commonly employed in the laboratory) is effective in reducing the partial pressure of products in the reaction zone and enhancing conversions. For nonspecific membranes, it has been shown that two processes reduce the partial pressure of products: transport of the product from the reaction zone to the separation zone, and transport of sweep gas from the separation zone to the reaction zone. This latter process can occur because the membrane is nonselective and the partial pressure gradient of the sweep gas drives the transport. As the sweep gas permeates into the reaction zone, it acts as a diluent and provides a mechanism for an increase in the percentage conversion in the reactor. Unfortunately, the downstream separations required in these systems are significant and the economics are less favourable than simply mixing the diluent with the reactants in a conventional reactor.

Vacuum permeate An alternative method to produce a pressure drop is the use of a vacuum on the membrane permeate. This has been shown to be highly effective in laboratory settings. However, the economics are not favourable for the large scale production of inexpensive components. Nevertheless, vacuum permeate systems may prove viable for small, high value-added systems.

Batch versus continuous Continuous reactor systems are preferred; they require less down time and have higher production rates than batch systems of similar size. However, as previously detailed, if the role of the membrane is to remove a product component, the available partial pressure difference is limited and the process will always be working with a very limited pressure drop that will require very large membrane areas. Batch and semi-batch processes allow the system to develop some limited partial pressure difference before membrane separation is attempted.

Membrane Degradation

The stability of the membrane is another important consideration. Ideally, for integrated systems, the membrane should be stable in all possible reaction environments: catalyst activation, normal reaction, catalyst regeneration and any thermal cycling experienced upon transitions. This presents specific challenges for each system and there are few materials that can satisfy all of these requirements. Thus, special engineering solutions are necessary. Even if the membrane material can fulfil these specifications, the many components needed to produce a membrane reactor module may not.

Future Possibilities

Organic Separations

A great deal of research is currently focusing on the development of membranes (either polymeric, inor-

ganic, or hybrids of the two) for the selective separation of liquid organic mixtures. If this research is successful, it will allow for incorporation into liquid-phase membrane reactors.

Control of Reactant Addition for Intermediate Product Recovery

A second area of immense current research activity is the development of oxygen-permeable membranes to influence the conversion of methane to either methanol or syn gas. The goal in these processes is a mechanism for the conversion of natural gas to a transportable liquid that may be further converted to high valued products. Current research has shown that membranes can be developed and that the appropriate catalysts are available for these conversions. Many engineering challenges lie ahead. These membrane reactor processes operate in excess of 700°C (sometimes much higher). Sealing these ceramic membranes into a housing remains a limitation. Further, the thermal stresses, which develop when cycling from 25 to >700°C, may result in membrane damage. While these are complex problems, the incentive to succeed is large and numerous research efforts continue in this area.

Further Reading

- Armour JN (1989) Catalysis with permselective inorganic membranes. *Applied Catalysis* 49: 1.
- Gokhale YV, Noble RD and Falconer JL (1995) Effects of reactant loss and membrane selectivity on a dehydrogenation reaction in a membrane-enclosed catalytic reactor. *Journal of Membrane Science* 103: 235.
- Govind R and Itoh N (eds) (1989) Membrane reactor technology. *AIChE Symposium Series* 85: 268.
- Saracco G, Versteeg GF and van Swaaij WPM (1994) Current hurdles to the success of high-temperature membrane reactors. *Journal of Membrane Science* 95: 105.
- Shu J, Grandjean BPA, Van Neste A and Kaliaguine S (1991) Catalytic palladium-based membrane reactors: a review. *Canadian Journal of Chemical Engineering* 69: 1036.

Concentration Polarization

H. Wijmans, Membrane Technology and Research, Inc., Menlo Park, CA, USA

Copyright © 2000 Academic Press

Introduction

All membrane separation processes are accompanied by a phenomenon called 'concentration polarization'

in which the composition at the feed-membrane interface differs from the composition in the bulk of the feed mixture. This gradient in composition is generated by the separation performed by the membrane and, as such, cannot be avoided. However, it is important to minimize the effects of concentration polarization because the gradient in composition reduces the separation performance of the membrane and increases the potential for membrane fouling.

Vacuum permeate An alternative method to produce a pressure drop is the use of a vacuum on the membrane permeate. This has been shown to be highly effective in laboratory settings. However, the economics are not favourable for the large scale production of inexpensive components. Nevertheless, vacuum permeate systems may prove viable for small, high value-added systems.

Batch versus continuous Continuous reactor systems are preferred; they require less down time and have higher production rates than batch systems of similar size. However, as previously detailed, if the role of the membrane is to remove a product component, the available partial pressure difference is limited and the process will always be working with a very limited pressure drop that will require very large membrane areas. Batch and semi-batch processes allow the system to develop some limited partial pressure difference before membrane separation is attempted.

Membrane Degradation

The stability of the membrane is another important consideration. Ideally, for integrated systems, the membrane should be stable in all possible reaction environments: catalyst activation, normal reaction, catalyst regeneration and any thermal cycling experienced upon transitions. This presents specific challenges for each system and there are few materials that can satisfy all of these requirements. Thus, special engineering solutions are necessary. Even if the membrane material can fulfil these specifications, the many components needed to produce a membrane reactor module may not.

Future Possibilities

Organic Separations

A great deal of research is currently focusing on the development of membranes (either polymeric, inor-

ganic, or hybrids of the two) for the selective separation of liquid organic mixtures. If this research is successful, it will allow for incorporation into liquid-phase membrane reactors.

Control of Reactant Addition for Intermediate Product Recovery

A second area of immense current research activity is the development of oxygen-permeable membranes to influence the conversion of methane to either methanol or syn gas. The goal in these processes is a mechanism for the conversion of natural gas to a transportable liquid that may be further converted to high valued products. Current research has shown that membranes can be developed and that the appropriate catalysts are available for these conversions. Many engineering challenges lie ahead. These membrane reactor processes operate in excess of 700°C (sometimes much higher). Sealing these ceramic membranes into a housing remains a limitation. Further, the thermal stresses, which develop when cycling from 25 to >700°C, may result in membrane damage. While these are complex problems, the incentive to succeed is large and numerous research efforts continue in this area.

Further Reading

- Armour JN (1989) Catalysis with permselective inorganic membranes. *Applied Catalysis* 49: 1.
- Gokhale YV, Noble RD and Falconer JL (1995) Effects of reactant loss and membrane selectivity on a dehydrogenation reaction in a membrane-enclosed catalytic reactor. *Journal of Membrane Science* 103: 235.
- Govind R and Itoh N (eds) (1989) Membrane reactor technology. *AIChE Symposium Series* 85: 268.
- Saracco G, Versteeg GF and van Swaaij WPM (1994) Current hurdles to the success of high-temperature membrane reactors. *Journal of Membrane Science* 95: 105.
- Shu J, Grandjean BPA, Van Neste A and Kaliaguine S (1991) Catalytic palladium-based membrane reactors: a review. *Canadian Journal of Chemical Engineering* 69: 1036.

Concentration Polarization

H. Wijmans, Membrane Technology and Research, Inc., Menlo Park, CA, USA

Copyright © 2000 Academic Press

Introduction

All membrane separation processes are accompanied by a phenomenon called 'concentration polarization'

in which the composition at the feed-membrane interface differs from the composition in the bulk of the feed mixture. This gradient in composition is generated by the separation performed by the membrane and, as such, cannot be avoided. However, it is important to minimize the effects of concentration polarization because the gradient in composition reduces the separation performance of the membrane and increases the potential for membrane fouling.

Therefore, minimizing concentration polarization is one of the most important objectives in designing and engineering membrane separation systems.

Mathematical Description of Concentration Polarization

The velocity profile of a fluid flowing in a channel is not constant across the thickness of the channel, because of friction at the fluid-channel surface interface. The fluid velocity decreases as the distance from the channel surface decreases. The same phenomenon occurs in the channels of a membrane module, and the resulting velocity gradient adjacent to the feed side of the membrane is characteristic of all membrane processes. To facilitate mass transfer analysis, the velocity gradient is usually represented by a step function, and it is assumed that a stagnant boundary layer exists adjacent to the membrane. Any component permeating the membrane must first pass through the boundary layer as illustrated in Figure 1.

Although the boundary layer is stagnant in the direction of the feed bulk flow, the boundary layer is subject to convective flow perpendicular to the membrane surface which is generated by the permeate flux. The convective transport of a component into the boundary layer from the bulk solution is given by the product $v_p \cdot c_b$, where v_p (cm s^{-1}) is the convective velocity and c_b (g cm^{-3}) is the concentration in the bulk of the feed. The rate at which the same component leaves the boundary layer is $v_p \cdot c_p$, where c_p (g cm^{-3}) is the permeate concentration. In general, if separation is achieved, c_p does not equal c_b , and the convective flows into and out of the boundary layer, generate a mass imbalance. This imbalance then forms a concentration gradient in the boundary layer, and the concentration gradient increases until diffusion of the component down the concentration

gradient is sufficient to restore mass balance in the boundary layer.

At steady state, the sum of convective and diffusive transport in the boundary layer equals the amount permeated through the membrane. This steady state is expressed for each component by the equation:

$$v_p c_i - D dc_i/dx = J_i^w \quad [1]$$

where D ($\text{cm}^2 \text{s}^{-1}$) is the diffusion coefficient, x (cm) is the coordinate perpendicular to the membrane surface and J_i^w ($\text{g cm}^{-2} \text{s}^{-1}$) is the mass flux of i permeating through the membrane.

In liquid-phase separations (including pervaporation) concentrations are typically expressed as a weight fraction, $w_i = c_i/\rho$ where ρ (g cm^{-3}) is the density of the liquid. Assuming that the density of the feed is constant in the boundary layer:

$$v_p \cdot w_i \cdot \rho - D \cdot \rho \frac{dw_i}{dx} = J_i^w \quad [2]$$

and assuming that the feed density is equal to the density of the permeate:

$$J_i^w = w_p \cdot J_{\text{tot}}^w = w_p \cdot v_p \cdot \rho \quad [3]$$

where w_p (g g^{-1}) is the weight fraction of i in the permeate and J_{tot}^w ($\text{g cm}^{-2} \text{s}^{-1}$) is the combined mass flux of all components permeating the membrane. Combining eqns [2] and [3] and eliminating the density ρ gives:

$$v_p \cdot w_i - D \frac{dw_i}{dx} = v_p \cdot w_p \quad [4]$$

which, integrated over the thickness δ (cm) of the boundary layer, yields the polarization equation:

$$\begin{aligned} \frac{w_m - w_p}{w_b - w_p} &= \exp(v_p \cdot \delta / D) \\ &= \exp(v_p / k_{bl}) \\ &= \exp(J_{\text{tot}}^w / \rho \cdot k_{bl}) \end{aligned} \quad [5]$$

where w_m and w_b are the weight fractions of i at the membrane surface and in the bulk of the feed, respectively, and $k_{bl} = D/\delta$ (cm s^{-1}) is the mass-transfer coefficient in the boundary layer.

In gas-separation applications, concentrations are typically expressed as mole fraction n_i , which is equal

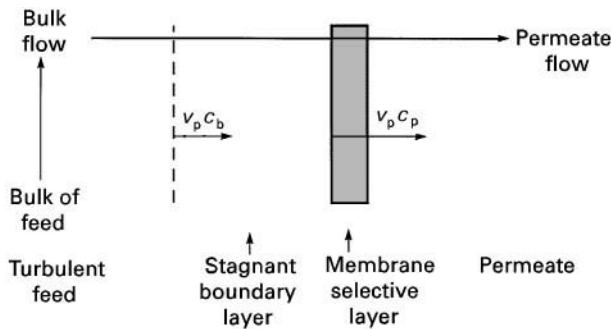


Figure 1 Schematic of the boundary layer adjacent to the membrane surface. If $c_p > c_b$, component is enriched in permeate. If $c_p < c_b$, component is depleted in permeate.

to the volume fraction, assuming the gas mixtures are ideal. Starting again with eqn [1], the mole fraction n_i can be substituted for c_i by using:

$$n_i = c_i \cdot 22\,400 \cdot T / (M_i \cdot p_f \cdot 273) \quad [6]$$

where $22\,400 \text{ (cm}^3 \text{ (STP) mol}^{-1})$ is the molar volume of an ideal gas, $T \text{ (K)}$ is the gas temperature, $M_i \text{ (g mol}^{-1})$ is the molecular weight of i , $p_f \text{ (bar)}$ is the feed gas pressure, and 273 K is the standard temperature. Also, the volume flux $J_i^v \text{ (cm}^3 \text{ (STP) cm}^{-2} \text{ s}^{-1})$ can be substituted for the mass flux J_i^w using:

$$J_i^v = J_i^w \cdot 22\,400 / M_i \quad [7]$$

Elimination of the term $M_i/22\,400$ gives:

$$v_p \cdot n_i \cdot p_f \cdot 273 / T - D \cdot p_f \cdot 273 / T \frac{dn_i}{dx} = J_i^v \quad [8]$$

Since $J_i^v = n_p \cdot J_{\text{tot}}^v$ and:

$$v_p = J_{\text{tot}}^v \cdot T / (p_f \cdot 273) \quad [9]$$

elimination of the term $p_f \cdot 273 / T$ gives:

$$v_p \cdot n_i - D \frac{dn_i}{dx} = v_p \cdot n_p \quad [10]$$

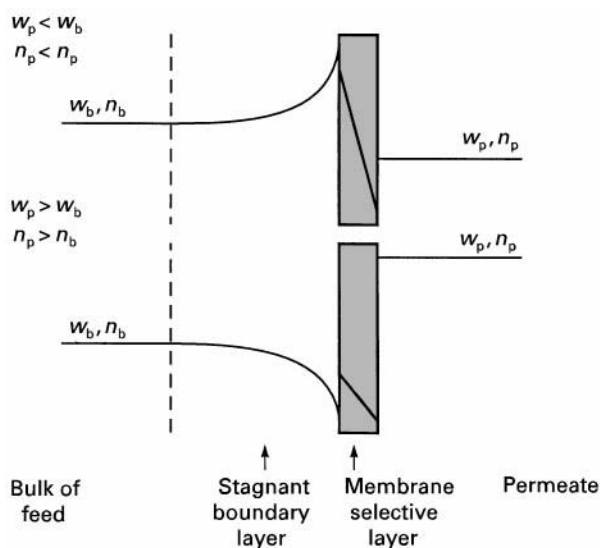


Figure 2 Schematic of the concentration polarization phenomenon. The concentration profiles in the boundary layer result from the separation achieved by the membrane. The type of concentration profile formed depends on the value of w_p relative to w_b (or n_p relative to n_b).

Integrating eqn [10] in the same way as eqn [4] gives:

$$\begin{aligned} \frac{n_m - n_p}{n_b - n_p} &= \exp(v_p \cdot \delta / D) \\ &= \exp(v_p / k_{bl}) \\ &= \exp(J_{\text{tot}}^v \cdot T / p_f \cdot 273 \cdot k_{bl}) \end{aligned} \quad [11]$$

where n_m and n_b are the mole (or volume) fraction of i at the membrane surface and in the bulk of the feed.

Eqns [5] and [11] describe the concentration profiles that develop in the boundary layer, as illustrated in **Figure 2**. Any component enriched in the permeate will be depleted in the boundary layer and any component depleted in the permeate will be enriched in the boundary layer.

Factors Determining the Extent of Concentration Polarization

The ratio of the concentration of a component at the membrane interface to the concentration in the bulk of the feed is called the ‘concentration polarization modulus’ and is a measure of the influence of concentration polarization on the separation process. The following expression for the modulus can be obtained from eqn [5]:

$$\frac{w_m}{w_b} = \frac{\exp(v_p / k_{bl})}{1 + E_o [\exp(v_p / k_{bl}) - 1]} \quad [12]$$

where $E_o = w_p / w_m$ is the intrinsic enrichment achieved by the membrane (and equal to the actual enrichment if concentration polarization were absent). An equation equivalent to eqn [12] but expressed in mole fractions can be derived from eqn [11].

Eqn [12] allows the concentration polarization modulus to be calculated as a function of v_p / k_{bl} for different values of the intrinsic enrichment factors, E_o . The ratio v_p / k_{bl} is a Peclet number and is a measure of the influence of convection relative to the influence of diffusion in the boundary layer. The results of this calculation are shown in the very informative **Figure 3**, which confirms that the concentration polarization modulus is smaller than 1 (boundary layer depletion) if the permeating compound is enriched in the permeate and larger than 1 (boundary layer build-up) if the permeating compound is depleted in the permeate. The concentration polarization modulus increasingly deviates from unity as the ratio v_p / k_{bl} increases, that is, as the flux through the membrane increases or as the turbulence

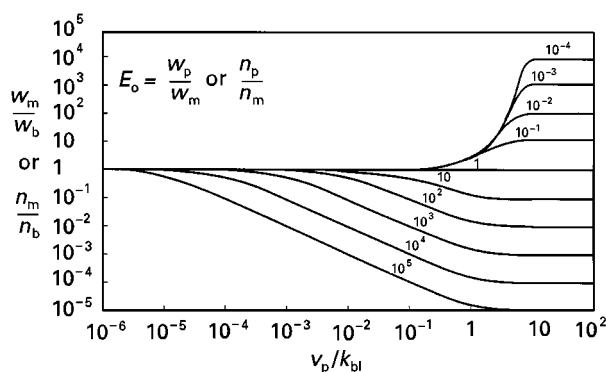


Figure 3 Concentration polarization modulus, w_m/w_b , as function of v_p/k_{bl} for a range of values of the intrinsic enrichment factor E_o . Lines calculated through eqn [12]. This figure shows that compounds that are enriched by the membrane ($E_o > 1$) are more affected by concentration polarization than compounds that are rejected by the membrane ($E_o < 1$).

of the feed fluid decreases. At high values for the ratio v_p/k_{bl} , the concentration polarization modulus, w_m/w_b , approaches the limiting value $1/E_o$. At this point, the boundary layer completely negates the separation power of the membrane permeation step. The concentration polarization modulus also increasingly deviates from unity as the intrinsic enrichment increasingly deviates from unity, that is, as the separation power of the membrane increases.

A striking feature of Figure 3 is the asymmetry with respect to enrichment and rejection. For example, when the term v_p/k_{bl} has a value of 10^{-1} , concentration polarization is essentially nonexistent for a component rejected by the membrane with an intrinsic enrichment E_o of 10^{-4} . On the other hand, concentration polarization is very severe for a component enriched by the membrane with an intrinsic enrichment E_o of 10^4 . The reason for this asymmetry is that the concentration polarization effect is generated by the difference in concentration between the permeate and the feed, $w_p - w_b = w_b(E - 1)$, where $E = w_p/w_b$ is the actual enrichment factor. It is clear that the absolute value of $w_p - w_b$ is significantly larger if $E > 1$ than if $E < 1$.

A second feature of the calculations shown in Figure 3 is that the concentration polarization modulus values are independent of the bulk concentration, w_b . This means that at a constant enrichment factor, E , the influence of concentration polarization is the same, no matter whether the component is present in the feed at a concentration of one part per hundred, one part per million, or one part per billion. Thus, concentration polarization does not necessarily affect components present at low concentrations more than components present at

higher concentrations. The primary requirement for significant concentration polarization effects is a high value for the enrichment factor, E . However, because E has an upper bound equal to $1/w_b$, a low feed concentration is a secondary requirement for severe concentration polarization effects. This confirms an empirical rule long held by membrane separation practitioners.

Transport Equations Incorporating Concentration Polarization

As pointed out in the previous sections, concentration polarization primarily affects membrane permeation by the change in composition at the membrane interface relative to the bulk of the feed mixture. To calculate the effect of concentration polarization on flux and separation, the transport equation for the membrane can be combined with eqn [5] or eqn [11] to arrive at a set of equations that predict the permeate flux and composition.

Ultrafiltration, nanofiltration and reverse osmosis are membrane processes in which a solute is separated from a solvent using a solute-rejecting membrane. Typically the permeate is essentially pure solvent, free of the solute. A simple but very effective transport equation developed for this situation is given below.

The pure solvent flux J_{solvent}^w ($\text{g cm}^{-2} \text{s}^{-1}$) of the membrane is given by:

$$J_{\text{solvent}}^w = \Delta P / R_m \quad [13]$$

where ΔP (bar) is the pressure difference applied across the membrane and R_m ($\text{bar cm}^2 \text{s g}^{-1}$) is the membrane resistance to the solvent. When a solute is present, the driving force for permeation is reduced by the osmotic pressure difference between the feed at the membrane interface and the permeate, $\Delta\pi_m$ (bar), therefore:

$$J_{\text{solvent}}^w = (\Delta P - \Delta\pi_m) / R_m \quad [14]$$

Eqn [14] is called the 'osmotic pressure model', in which the osmotic pressure is a measure of the thermodynamic work required to produce solvent from a solvent-solute mixture. Assuming that the permeate solute concentration is negligible:

$$\Delta\pi_m = a \cdot w_m^n \quad [15]$$

where a is a constant and n is an exponent equal to approximately 1 for low-molecular-weight solutes,

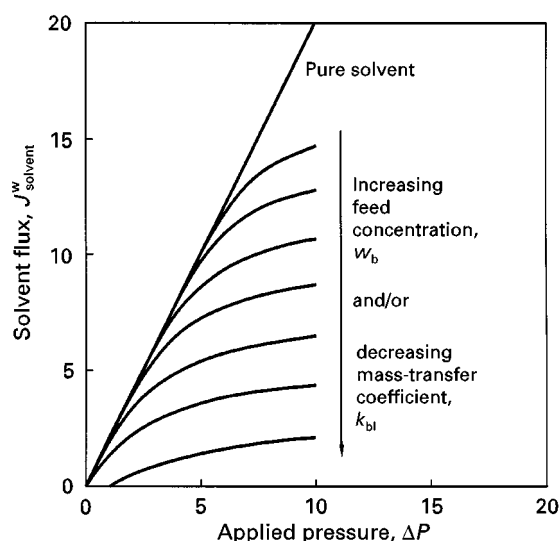


Figure 4 Solvent flux as a function of applied pressure as calculated from eqn [17]. The flux observed with solvent-solute mixtures is always less than the pure solvent flux. The deviation increases with increasing applied pressure, increasing solute concentration, and decreasing mass-transfer coefficient in the boundary layer.

but equal to 2 or higher for macromolecular solutes. Combining eqn [15] with eqn [5] and assuming $w_p = 0$ gives:

$$\Delta\pi_m = a \cdot w_b^n \cdot \exp(n \cdot J_{\text{solvent}}^w / \rho k_{bl}) \quad [16]$$

and:

$$J_{\text{solvent}}^w = (\Delta p - a \cdot w_b^n \cdot \exp(n \cdot J_{\text{solvent}}^w / \rho k_{bl})) / R_m \quad [17]$$

From eqn [17] it is clear that an increase in the flux J_{solvent}^w leads to an exponential increase in the osmotic pressure and that the flux will increase less than linearly with the applied pressure. This means that any increase in driving force ΔP will be negated at least in part by the increase in osmotic pressure. The general effect of pressure on flux predicted by eqn [17] is illustrated in **Figure 4** and is in agreement with the vast majority of experimental data. As can be seen from **Figure 4**, the flux observed with solvent-solute mixtures is always less than the pure solvent flux, and the deviation increases with increasing applied pressure, increasing solute concentration and decreasing mass transfer coefficient in the boundary layer. **Figure 4** also shows that at higher applied pressures the flux becomes essentially independent of the applied pressure. This is often observed in ultrafiltration applications and is referred to as the limiting flux. Eqn [17] predicts that under 'limiting flux' conditions the flux is independent of

the membrane resistance, which also has been confirmed experimentally.

Gel Layer Formation

When the solute is a macromolecular compound such as a protein or a polymer, there is the possibility that the solute concentration at the membrane interface exceeds the gel concentration, w_g , at which concentration the solution is no longer a fluid. A gel layer thus forms at the membrane interface which creates an additional resistance to the permeation flux which consequently decreases. The flux continues to decrease until the solute concentration at the membrane interface equals the gel concentration, at which point steady state is reached. The flux at that point can be obtained from eqn [5]:

$$J_{\text{limit}}^w = \rho \cdot k_{bl} \cdot \ln \left(\frac{w_g - w_p}{w_b - w_p} \right) \quad [18]$$

and because w_p is typically close to zero:

$$J_{\text{limit}}^w = \rho \cdot k_{bl} \cdot \ln(w_g/w_b) \quad [19]$$

The steady-state flux J_{limit}^w is called the 'limiting flux' because any increase in applied pressure will just result in a thicker gel layer and not in a higher flux. From eqn [19] it can be seen that the limiting flux as predicted by the gel layer model is independent of the applied pressure as well as the membrane resistance. Additionally, eqn [19] predicts a straight-line plot of J_{limit}^w versus $\ln(w_b)$ with a slope equal to $-\rho \cdot k_{bl}$. All these predictions have been confirmed in a vast number of ultrafiltration experiments. Interestingly, the osmotic pressure model also predicts a limiting flux with the same attributes.

Approaches to Minimize Concentration Polarization

The primary method of reducing the negative influence of concentration polarization is to maximize the mass-transfer coefficient in the boundary layer. Usually the first method used is to increase the feed velocity. This has the drawbacks of a high feed-to-residue pressure drop and the requirement of long, thin modules, which have higher capital costs than shorter, larger-diameter modules. A more efficient approach is to choose optimized feed-spacer materials and/or to create non-linear feed channels which induce mass-transfer-enhancing vortices. More complicated methods used for a feed mixture with a high viscosity and/or a high membrane fouling

potential employ spinning membranes or vibrating modules.

Further Reading

Belfort G, Davis RH and Zydney AL (1994) The behavior of suspensions and macromolecular solutions in cross flow microfiltration. *Journal of Membrane Science* 1: 96.

Brian PLT (1966) Mass transport in reverse osmosis. In: Merten U (ed.) *Desalination by Reverse Osmosis*, p. 181. Cambridge, MA: MIT Press.

Cheryan M (1998) *Ultrafiltration and Microfiltration Handbook*. Lancaster: Technomic Publishing.

Zeman LJ and Zydney AL (1996) *Microfiltration and Ultrafiltration*. New York: Marcel Dekker.

Dialysis in Medical Separations

W. R. Clark, Baxter Hemodialysis Research Lab., Wishard Hospital, Indianapolis, IN, USA

M. J. Lysaght, Brown University, Providence, RI, USA

Copyright © 2000 Academic Press

Introduction

Although haemodialysis (HD) as a therapy for uraemia (kidney failure) was first described early in the 1900s, its widespread use did not occur until the 1950s. At this time, Travenol Laboratories (now Baxter International) unveiled the 'coil' dialyser ('artificial kidney') in which tubes composed of cellophane membranes were wound around a support structure and immersed in a recirculated dialysis solution. Relative to contemporary models, the mass transfer efficiency of this type of dialyser was extremely poor, due to high mass transfer resistances in all three compartments (blood compartment, membrane, and dialysate compartment). In the early 1960s, solution mass transfer resistances were decreased with the introduction of parallel flow dialysers, in which sheet membranes were formed in a stacked configuration. The improvement in dialysate-side mass transfer with these dialysers was particularly large because the dialysis solution contacted the membrane under flow conditions as opposed to the semi-batch operation of the coil dialyser. In addition, the membranes used in these devices were thinner in structure, providing less diffusive resistance than earlier versions. Although the earliest manufactured parallel flow dialysers were not disposable, design improvements permitted the production of disposable units by the late 1960s.

The last truly major development in haemodialysers occurred more than 30 years ago when the hollow fibre artificial kidney was developed. Blood compartment mass transfer was reduced further with this design due to the high shear rate that could be achieved in the annular space of the hollow fibre. Additional benefits of the hollow fibre artificial kidney included an enhanced ability to control trans-

membrane pressure (see below) and a lower extracorporeal blood volume. This type of dialyser is now used in virtually all HD treatments.

On a global basis, approximately 800 000 patients receive chronic haemodialysis therapy for the treatment of end-stage renal disease (ESRD) and this population is growing at a rate of 8–10% per annum. This figure represents approximately 85% of the ESRD population, with the remaining patients receiving peritoneal dialysis. Numerous dialysis membrane and haemodialyser manufacturers are situated around the world, with the vast majority based in the three largest markets: United States, Western Europe and Japan.

The Haemodialysis Procedure

In addition to the dialyser, the other fundamental component of a HD system is a dialysis machine, which serves a number of purposes. First, it is equipped with a roller pump that delivers blood, usually at a rate of 200–500 mL min⁻¹, from the patient to the dialyser and back to the patient. Second, the dialysis machine prepares dialysate by mixing ('proportioning') water and a concentrated bicarbonate solution in such a ratio that the dialysis fluid produced is the same as that prescribed by a physician to meet the needs of an individual patient. The typical dialysate flow rate is 500–800 mL min⁻¹ and its major constituents are sodium, potassium, calcium and bicarbonate. The pathophysiology of uraemia is such that during the period between dialysis treatments, potassium levels in the plasma rise while calcium and bicarbonate levels fall. Consequently, the concentration of potassium in the dialysate is typically lower than that in the plasma at the beginning of the procedure while dialysate calcium and bicarbonate concentrations are typically higher. The third major function of the dialysis machine is to provide an accurate measurement of transmembrane pressure (TMP) in the dialyser, which is defined as the difference between the average pressure in the blood and

potential employ spinning membranes or vibrating modules.

Further Reading

Belfort G, Davis RH and Zydney AL (1994) The behavior of suspensions and macromolecular solutions in cross flow microfiltration. *Journal of Membrane Science* 1: 96.

Brian PLT (1966) Mass transport in reverse osmosis. In: Merten U (ed.) *Desalination by Reverse Osmosis*, p. 181. Cambridge, MA: MIT Press.

Cheryan M (1998) *Ultrafiltration and Microfiltration Handbook*. Lancaster: Technomic Publishing.

Zeman LJ and Zydney AL (1996) *Microfiltration and Ultrafiltration*. New York: Marcel Dekker.

Dialysis in Medical Separations

W. R. Clark, Baxter Hemodialysis Research Lab., Wishard Hospital, Indianapolis, IN, USA

M. J. Lysaght, Brown University, Providence, RI, USA

Copyright © 2000 Academic Press

Introduction

Although haemodialysis (HD) as a therapy for uraemia (kidney failure) was first described early in the 1900s, its widespread use did not occur until the 1950s. At this time, Travenol Laboratories (now Baxter International) unveiled the 'coil' dialyser ('artificial kidney') in which tubes composed of cellophane membranes were wound around a support structure and immersed in a recirculated dialysis solution. Relative to contemporary models, the mass transfer efficiency of this type of dialyser was extremely poor, due to high mass transfer resistances in all three compartments (blood compartment, membrane, and dialysate compartment). In the early 1960s, solution mass transfer resistances were decreased with the introduction of parallel flow dialysers, in which sheet membranes were formed in a stacked configuration. The improvement in dialysate-side mass transfer with these dialysers was particularly large because the dialysis solution contacted the membrane under flow conditions as opposed to the semi-batch operation of the coil dialyser. In addition, the membranes used in these devices were thinner in structure, providing less diffusive resistance than earlier versions. Although the earliest manufactured parallel flow dialysers were not disposable, design improvements permitted the production of disposable units by the late 1960s.

The last truly major development in haemodialysers occurred more than 30 years ago when the hollow fibre artificial kidney was developed. Blood compartment mass transfer was reduced further with this design due to the high shear rate that could be achieved in the annular space of the hollow fibre. Additional benefits of the hollow fibre artificial kidney included an enhanced ability to control trans-

membrane pressure (see below) and a lower extracorporeal blood volume. This type of dialyser is now used in virtually all HD treatments.

On a global basis, approximately 800 000 patients receive chronic haemodialysis therapy for the treatment of end-stage renal disease (ESRD) and this population is growing at a rate of 8–10% per annum. This figure represents approximately 85% of the ESRD population, with the remaining patients receiving peritoneal dialysis. Numerous dialysis membrane and haemodialyser manufacturers are situated around the world, with the vast majority based in the three largest markets: United States, Western Europe and Japan.

The Haemodialysis Procedure

In addition to the dialyser, the other fundamental component of a HD system is a dialysis machine, which serves a number of purposes. First, it is equipped with a roller pump that delivers blood, usually at a rate of 200–500 mL min⁻¹, from the patient to the dialyser and back to the patient. Second, the dialysis machine prepares dialysate by mixing ('proportioning') water and a concentrated bicarbonate solution in such a ratio that the dialysis fluid produced is the same as that prescribed by a physician to meet the needs of an individual patient. The typical dialysate flow rate is 500–800 mL min⁻¹ and its major constituents are sodium, potassium, calcium and bicarbonate. The pathophysiology of uraemia is such that during the period between dialysis treatments, potassium levels in the plasma rise while calcium and bicarbonate levels fall. Consequently, the concentration of potassium in the dialysate is typically lower than that in the plasma at the beginning of the procedure while dialysate calcium and bicarbonate concentrations are typically higher. The third major function of the dialysis machine is to provide an accurate measurement of transmembrane pressure (TMP) in the dialyser, which is defined as the difference between the average pressure in the blood and

dialysate compartments. Fluid removal requirements are quite patient-specific in this patient population such that both the rate and total volume of plasma water ultrafiltration need to be controlled accurately. Accurate control of ultrafiltration is achieved by continuous monitoring of dialyser TMP, which essentially is an ultrafiltration surrogate for a membrane of specific hydraulic permeability. Finally, monitoring components of the dialysis machine safeguards against potentially catastrophic events, such as air embolism or a massive blood leak related to a membrane defect.

Classification of Uraemic Solutes

In the properly functioning human kidney, plasma water and blood solutes are removed by ultrafiltration and convection, respectively. Solutes of molecular mass less than approximately 40 000 Da have essentially unrestrained passage through the glomerulus, the kidney's filtration unit. As such, the clearance of these solutes approximates to the plasma water ultrafiltration rate, which is about 120 mL min^{-1} for humans of normal size. By definition, ESRD is associated with absent or minimal native kidney function. As a result, blood solutes normally removed by the above filtration mechanism are retained in the blood stream with a resultant several-fold increase in their plasma concentrations.

The classification of uraemic solutes is typically based on molecular mass and three well accepted classes currently exist (Table 1). The first category, simply called 'small solutes', is comprised of nitrogenous compounds of molecular mass less than 200 Da. These solutes are by-products of protein metabolism and include the compounds urea (molecular mass 60 Da) and creatinine (113 Da), which are commonly measured in clinical medicine. The second category, referred to as 'middle molecules', consists of a diverse group of molecules in the 200 to 2000 Da range. Although this class has been widely studied from an experimental perspective, a represen-

tative solute, which is clinically measurable, has not yet been identified. Low molecular mass peptides and proteins (molecular masses 2000 to 40 000 Da) are the most recently identified class of uraemic toxins. The plasma concentrations of these compounds are typically increased 50–100-fold in ESRD. Recently, a specific toxin in this class, β 2-microglobulin (β 2M: molecular mass 11 800 Da), has been identified as a causative factor in the development of dialysis-related amyloidosis, a deposition disorder specific to the ESRD population.

Dialyser Specifications

Contemporary hollow fibre dialysers have nominal surface areas ranging from 1.0 to 2.2 m^2 , although the trend in clinical practice is to use devices at the upper end of this range. Both the length (approximately 23 cm) and inner diameter (i.d.: usually 200 μm) of hollow fibres used for clinical HD are fairly standard. The i.d. parameter represents a compromise between the desirable characteristics of a short diffusive pathlength and high shear rate with a small i.d., and a low axial pressure drop and hydraulic resistance with a large i.d. fibre. On the other hand, the variation in wall thickness is considerable, with values ranging from 6 to 55 μm . (See below for an expanded explanation.) Based on the surface area of the dialyser, the total number of fibres comprising the dialyser ranges approximately from 7000 to 12 000.

Extracorporeal Therapy Modes Used in ESRD Patients (Figure 1)

In a typical haemodialysis procedure, although transmembrane mass transfer occurs predominantly by diffusion, a modest degree of convective mass transfer is also achieved in association with the ultrafiltered plasma water. However, the recent recognition of β 2M and other low molecular mass proteins as important uraemic toxins has prompted interest in using dialytic therapies with increased convective removal capabilities for these poorly diffusible solutes. In haemodialysis, the total ultrafiltration volume and net ultrafiltration rate are determined by the degree to which a patient's plasma volume needs to be reduced and the duration of the treatment. (The total ultrafiltration requirement is dictated by the amount of fluid ingested by the patient in the period between dialysis treatments.) The total volume of plasma water ultrafiltered is approximately 3–4 L, resulting in a typical net ultrafiltration rate of $15\text{--}20 \text{ mL min}^{-1}$.

As a means to augment convective solute removal, haemofiltration (HF) was developed by Henderson,

Table 1 Classification of ureamic solutes

<i>Solute class</i>	<i>Molecular mass range (Da)</i>	<i>Examples</i>
Small solutes	< 200	Urea Creatinine
Middle molecules	200–2000	Appetite suppressant Osteoblast inhibitor
Peptides/proteins	2000–40 000	AGE-peptides β 2-Microglobulin Parathyroid hormone

Source: Vanholder R and De Smet R (1999).

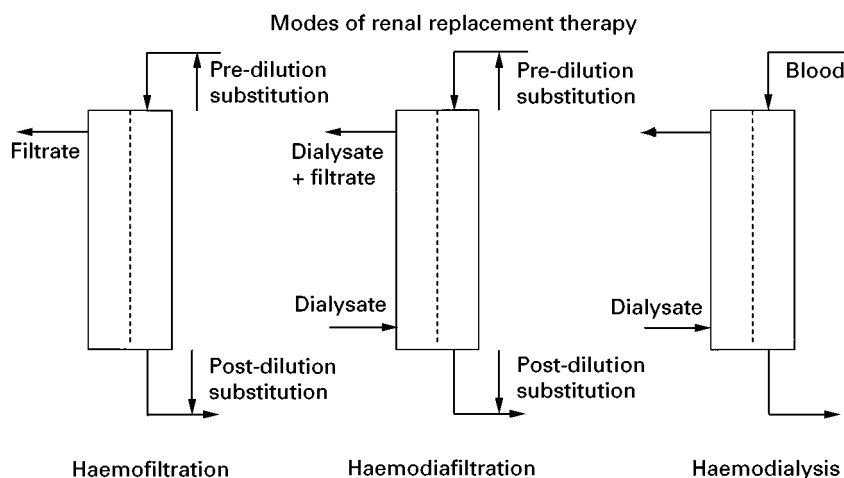


Figure 1 Extracorporeal therapy modes used in end-stage renal disease.

Lysaght and colleagues in the early 1970s. This is a purely convective therapy in which no dialysate is used but an ultrafiltration rate that far exceeds the net ultrafiltration requirements of the patient is employed. As plasma water is typically ultrafiltered at an absolute rate of at least 100 mL min^{-1} (6 L h^{-1}) in HF, the much lower net ultrafiltration rate required for fluid removal from the patient is achieved by 'replacing' most of the ultrafiltrate with a bicarbonate-based solution. For the large volume of intravenous-quality 'replacement fluid' that is required, the filtrate produced by sequential ultrafiltration of dialysate is used. This 'on-line' mechanism, in which the dialysate precursor of the replacement fluid is produced by the same HD machine that performs the HF treatment, allows very high volumes of ultrafiltrate to be produced. In HF, only dialysers with very high hydraulic permeability (see below) are used.

Although HF is a significant improvement over HD with respect to relatively large sized uraemic toxin removal, the absence of diffusion renders it only a marginal therapy with respect to small solute removal. To overcome this deficiency of HF, Canaud and colleagues approximately 15 years ago first employed online haemodiafiltration (HDF). As its name implies, this therapy is essentially a HD/HF hybrid in which both dialysate flow and high ultrafiltration rates are used. At present, HDF offers the broadest solute removal spectrum of all dialytic therapies.

Permeability Classification of Dialysis Membranes

Although numerous classification schemes have been proposed, HD membranes are traditionally classified according to water flux. The clinical parameter used to characterize the water permeability of a dialy-

ser is the ultrafiltration coefficient (K_{UF} : $\text{mL h}^{-1} \text{ mmHg}$). In fact, the only dialyser classification scheme recognized by the United States Food and Drug Administration is based on water permeability, with low and high permeability dialysers having K_{UF} values of < 8 and $\geq 8 \text{ mL h}^{-1} \text{ mmHg}$, respectively. The water permeability of a dialyser is usually derived from *in vitro* experiments in which bovine blood is ultrafiltered at varying transmembrane pressure. Based on a commonly used model which assumes that a membrane is composed of parallel cylindrical pores, the flux of plasma water through each pore is dependent on the fourth power of the radius so that small changes in mean pore size have a very large effect on water permeability.

A common misconception relating to dialyser performance is the assumption that a membrane's solute removal capabilities are necessarily correlated with its water permeability. Based on a model in which a membrane has N (straight) cylindrical pores (per unit surface area) of radius r , diffusive solute flux can be expressed as:

$$\phi = \lambda D \rho \Delta C / t \quad [1]$$

where λ is the solute partition coefficient, D is solute diffusivity, ρ is membrane porosity, ΔC is the transmembrane concentration gradient, and t is membrane thickness. (While the partition coefficient is essentially unity for solutes such as urea and creatinine, larger solutes with incomplete access to the membrane pores have λ values that are less than one.) Membrane porosity is a function of both pore size and number:

$$\rho = N \pi r^2 \quad [2]$$

For all dialysis membranes, small solutes such as urea and creatinine have free pore access ($\lambda = 1$). Therefore, small solute transport is highly dependent on membrane porosity. As eqn [2] indicates, one membrane with a large number of relatively small pores and a second membrane with a small number of relatively large pores can have equivalent porosities. Although the small solute transport properties of these two hypothetical membranes would be equivalent, the flux (water permeability) properties would greatly differ. This difference is explained by the strong dependence of ultrafiltrate flux on membrane pore size, described above.

Polymeric Composition of Dialysis Membranes

From a relatively simplistic perspective, dialysis membranes can be divided into those comprised of cellulose-based material and those comprised of synthetic materials.

Cellulosic Dialysis Membranes

The monomeric subunit of cellulosic membranes is cellobiose, a naturally occurring saccharide found in plants. Chemically, cellobiose is a ringed structure richly endowed with hydroxyl groups. The interaction of complement cascade products with these hydroxyl groups is felt to be responsible, at least partly, for the relatively pronounced complement activation observed when unsubstituted cellulosic membranes contact blood. For the past several years, a major objective among manufacturers has been the development of modified (substituted) cellulosic membranes in which a certain fraction of these hydroxyl groups are replaced with other moieties. The substitution groups diminish the degree of complement activation by at least three different mechanisms. One mechanism is the replacement of a large percentage of the hydroxyl groups with acetate groups. In the first substituted cellulosic membrane, cellulose (di)acetate, approximately 70–80% of the hydroxyl groups on the cellulosic backbone were replaced with an acetate group. Most likely because this modification eliminates a large fraction of the active surface sites for interaction with complement components, an attenuation of the intense complement activation seen with unmodified cellulose was achieved. This membrane modification also resulted in a moderate increase in pore size, yielding a slightly higher water permeability and broader solute removal spectrum for cellulose acetate in comparison to unsubstituted cellulosic membranes of similar surface area. Extrapolation of this process to total replacement of the

hydroxyl groups resulted in the cellulose triacetate fibre characterized by further attenuation of complement activation and higher water permeability.

A second cellulosic substitution mechanism is the replacement of a relatively small percentage (less than 5%) of the hydroxyl groups with a bulky chemical group, which sterically reduces the degree of interaction between complement activation products and the membrane. Examples for which this strategy is employed are Hemophan® (tertiary amine substitution) and synthetically modified cellulose (SMC; benzyl substitution group).

The evolution in cellulosic membranes has resulted in a wide spectrum of biocompatibility and flux profiles. If complement activation and neutropenia are used as the major biocompatibility criteria, regenerated cellulose is the least biocompatible while cellulose triacetate is the most biocompatible, with the other modified cellulosic membranes having intermediate profiles. However, characterization of the flux properties of these membranes is not as straightforward. For dialysers of comparable surface area, a simplistic approach is to report K_{UF} values in the following ascending order: regenerated cellulose < Hemophan®, synthetically modified cellulose < cellulose acetate < cellulose triacetate. In this simplistic scheme, a 1.5 m² dialyser having a regenerated cellulose, Hemophan®, or SMC membrane generally falls in the low flux category ($K_{UF} < 8 \text{ mL h}^{-1} \text{ mmHg}$) while comparably sized dialysers having cellulose acetate and cellulose triacetate membranes fall in the midflux ($K_{UF} 10\text{--}20 \text{ mL h}^{-1} \text{ mmHg}$) and high flux ($K_{UF} > 20 \text{ mL h}^{-1} \text{ mmHg}$) categories, respectively. However, this simplistic categorization scheme breaks down in several respects. High flux cellulose acetate membranes have now been produced and cellulose triacetate dialysers of low water permeability ($K_{UF} 9.5 \text{ mL h}^{-1} \text{ mmHg}$) are also available. Finally, the recent development of unmodified cellulosic and cellulose acetate membranes having relatively low water permeability but solute removal capabilities that include $\beta 2\text{M}$ further confounds this classification scheme and provides additional examples of a dissociation between water and solute flux.

Synthetic Dialysis Membranes

The monomeric subunits of the various synthetic membranes individually vary and all differ significantly from cellobiose. The absence of surface hydroxyl groups on synthetic membranes is one factor responsible for the reported differences in complement activation between synthetic membranes and either unsubstituted cellulosic membranes or modified cellulosic membranes of low permeability.

Subsequent to the introduction of the AN69® (sulfonated polyacrylonitrile) membrane in the early 1970s, numerous additional synthetic membranes have been introduced for clinical use. Similar to AN69®, polysulfone and polyamide were brought to the market for use in both high flux HD and haemofiltration. One obvious reason accounting for the use of these membranes in a haemofiltration mode is their significantly larger pore size and hydraulic permeability than regenerated cellulose membranes. The other reason relates to the structural differences between the synthetic and unsubstituted cellulosic membrane groups. Cellulosic membranes have relatively thin walls (generally in the 6–15 µm range) which have a uniform (symmetric) composition across their entire thickness. Although the relative thinness of cellulosic membranes is desirable with respect to diffusive solute transport, this same characteristic renders many cellulosic membranes unable to withstand the high transmembrane pressures required to perform convective therapies employing high ultrafiltration rates. The synthetic membranes have thicker walls (20 µm or more) which may be structurally symmetric (e.g. AN69®, polymethylmethacrylate (PMMA)) or asymmetric (e.g. polysulfone, polyamide, polyethersulfone). In the latter category, a very thin 'skin' (less than 5 µm) contacting the blood compartment lumen acts primarily as the membrane's separative element with regard to solute removal while the remaining thickness (stroma) imparts mechanical strength. In turn, the composition of the stroma layer is quite variable for the various synthetic membranes. For the Fresenius polysulfone membrane, the stroma is relatively homogeneous with a sponge-like structure while the Gambro polyamide membrane has, adjacent to the skin, a sponge-like stroma layer which has progressively larger pores ('macrovoids' with a finger structure) in the radially outward direction. Finally, a new synthetic (polyethersulfone) membrane developed by Membrana GmbH (formerly Akzo Nobel) has a novel configuration consisting of a sponge-like stroma layer interposed between skin layers on both the inner (blood-side) and outer (dialysate-side) aspects.

In the production of synthetic membranes made of primarily hydrophobic polymers (polysulfone, polyamide, polyethersulfone), a hydrophilic additive (polyvinylpyrrolidone: PVP) acts as a polymer alloy. PVP is used to impart sufficient hydrophilicity to the membrane to allow clinical use and, as a wetting agent, modulates surface tension and viscosity within the pore structure during membrane formulation. This latter feature explains PVP's importance in determining the overall pore size distribution of synthetic membranes.

Although synthetic membranes are employed for both haemofiltration and high flux HD, it is in the latter mode that these membranes have found their widest application. Another synthetic membrane formulation was reported in the late 1980s with the introduction of low flux versions. Low flux polysulfone and PMMA have been used clinically for several years and recently a low flux version of a polyamide/polyethersulfone copolymer has been introduced.

Effect of Membrane Composition and Structure on Dialytic Solute Removal

Small Solute Removal

Small solute removal during HD occurs almost exclusively by diffusion. To quantify a particular membrane's diffusive capabilities, its mass transfer resistance is frequently used:

$$R_O = R_B + R_M + R_D$$

In the above equation, the overall resistance to diffusive mass transfer of a particular solute (R_O) has three components: blood compartment resistance (R_B), resistance due to the membrane itself (R_M) and dialysate compartment resistance (R_D). Minimizing the mass transfer resistance in the blood compartment primarily requires the use of relatively high flow rates (i.e. shear rates) that decrease unstirred layers. Dialysate-side mass transfer resistance is likewise decreased by increasing flow rate but optimal dialysate perfusion of fibre bundles is also a consideration. Although increasing dialysate flow rate may itself improve fibre bundle perfusion (see below), another mechanism by which this can be achieved is the inclusion of spacer yarns. These devices are spacing filaments placed external to the fibres and are designed to facilitate dialysate distribution and reduce channeling. The resistance related to the membrane itself actually has two components:

$$R_M = X_M/D_M$$

where X_M is the effective diffusion path-length for a solute and D_M is the solute-specific membrane diffusivity. This equation indicates that a decrease in membrane resistance can be achieved either by a decrease in membrane thickness or an increase in membrane diffusivity, the latter of which is influenced strongly by membrane porosity.

Middle Molecule Removal

Vitamin B₁₂ (molecular mass 1350 Da) is commonly used for *in vitro* characterizations of dialysers. However, due to its extensive binding to plasma proteins, this compound is not useful *in vivo*. In fact, the removal of uraemic solutes having molecular masses which fall in the classic middle molecule category has been difficult to quantify due to the lack of an easily measured *in vivo* surrogate molecule (cf. urea and creatinine for the small solute category). Because recent evidence suggests that uraemic appetite suppression is mediated by the retention of solute(s) in this size range, an understanding of removal mechanisms for middle molecules is important. Based on dialysis practices used in the 1960s and early 1970s (i.e. relatively low flow rates and thick, low permeability cellulosic membranes), diffusive middle molecule removal was so limited that any convective removal contributed relatively substantially to total removal. However, the situation is vastly different in contemporary HD, in which higher flow rates and dialyser membranes of significantly greater diffusive permeability for middle molecules are employed.

Low Molecular Mass Protein Removal

Recent interest in increasing the extracorporeal removal of β 2M has provided insight into the general mechanisms mediating the removal of low molecular mass proteins. A number of studies published in the past 15 years support several general conclusions. First, β 2M removal by low flux unsubstituted cellulosic membranes is usually negligible, although certain exceptions do exist. Second, the primary mechanism by which β 2M is removed during high flux HD varies widely among membranes. For certain membranes, such as AN69® and particularly PMMA, removal is achieved predominantly or solely by adsorption. At the other end of the spectrum is the cellulose triacetate membrane, for which adsorption is minimal and removal occurs primarily by diffusion. High flux polysulfone and unsulfonated PAN membranes have intermediate adsorptive characteristics and achieve transmembrane β 2M removal by a combination of diffusion and convection. Third, at least for the high flux synthetic membranes, use of convection-based therapies (HF and HDF) increases β 2M removal relative to standard (diffusion-based) HD. Although many clinicians consider β 2M to be surrogate for the low molecular mass protein class of uraemic solutes, this assumption has not been conclusively proved. Nevertheless, it is reasonable to use the abundant transport data available for β 2M to provide insight into the transport charac-

teristics of other low molecular mass proteins, such as complement activation products and cytokines.

Interaction Between Biocompatibility and Flux

Measurement of complement pathway by-products is one technique used to assess the inflammatory response elicited by exposure of blood to a dialysis membrane. However, numerous previous studies have failed to account for the fact that the clinically measured complement components (C3a and C5a) are low molecular mass proteins. Therefore, the concentration of these inflammatory mediators represents the net result of the simultaneous processes of generation and any dialytic removal that may occur. In this regard, complement activation products are similar to most uraemic solutes, for which the plasma concentration is determined by both generation and net removal. The corollary of this observation is that the permeability properties and not just the polymeric composition of a dialysis membrane must be considered when evaluating complement activation data. Recent data indicate that the relatively low levels of complement activation associated with high permeability synthetic membranes is at least partially related to their ability to remove, either by adsorption or transmembrane transport, the generated inflammatory mediators.

It is simplistic to limit the discussion about membrane biocompatibility to complement activation as a number of agents have been identified as potential inflammatory mediators in chronic HD patients. A list of these putative mediators appears in Table 2. Some of these compounds, such as Lipid A and LPS fragments, potentially have their origin in dialysate, a nonsterile fluid. Due to their relatively low molecular mass, these inflammatory mediators may undergo transmembrane passage and induce cytokine

Table 2 Inflammatory mediators

Mediator	Molecular mass (kDa)
Lipid A	2–4
Lipopolysaccharide (LPS) fragments	< 8
C3a	8.9
Granulocyte inhibitory peptide (GIP) II	9.5
C5a	11
Interleukin-1	17
Tumour necrosis factor (monomeric)	17
Factor D	23
Granulocyte inhibitory peptide (GIP) I	28
Tumour necrosis factor (trimeric)	55
Lipopolysaccharide (LPS)	> 100

Source: Lonneman G (1993).

production in the blood stream, either directly via an effect on mononuclear cells or indirectly via an effect on the alternative complement pathway. Conversely, the majority of the mediators that are potentially elicited in the blood, such as C3a and IL-1, may be simultaneously eliminated during high flux therapies by an adsorptive or transmembrane mechanism, as discussed above. Other investigations have confirmed that adsorption is also important in the removal of other inflammatory mediators, such as Factor D and cytokines.

Summary

Dialysers used in contemporary HD are equipped with a wide variety of membranes and within both the cellulosic and synthetic classes, water and solute flux properties vary widely. For small and middle-sized solutes, abundant clinical data point to the importance of membrane thickness in diffusive mass transfer. The removal of low molecular mass proteins may occur largely by adsorption for some high flux membranes, particularly those of hydrophobic synthetic composition. Because many of the mediators of inflammation in dialysis patients fall in this low molecular mass protein category, the biocompatibility of a particular membrane must be interpreted in conjunction with its permeability properties.

See Colour Plate 47.

See also: **II/Membrane Separations:** Membrane Bio-separations. **III/Membrane Preparation:** Hollow Fibre Membranes; Interfacial Composite Membranes.

Further Reading

- Anderstam B, Mamoun A, Sodersten P and Bergstrom J (1996) Middle-sized molecule fractions isolated from uraemic ultrafiltrate and normal urine inhibit ingestive behavior in the rat. *Journal of the American Society of Nephrology* 7: 2453–2460.
- Cheung AK, Parker C, Wilcox L and Janatova J (1990) Activation of complement by haemodialysis membranes: polyacrylonitrile binds more C3a than cuprophane. *Kidney International* 37: 1055–1059.

- Clark WR, Macias WL, Molitoris A and Wang NHL (1995) Plasma protein adsorption to highly permeable haemodialysis membranes. *Kidney International* 48: 481–488.
- Clark WR, Hamburger RJ and Lysaght MJ (in press) The effect of membrane composition and structure on solute removal and biocompatibility in haemodialysis. *Kidney International*.
- Colton C, Henderson L, Ford C and Lysaght M (1975) Kinetics of hemodiafiltration. I. *In vitro* transport characteristics of a hollow fiber blood ultrafilter. *Journal of Laboratory and Clinical Medicine* 85: 355–371.
- Deppisch R, Gohl H and Smeby L (1998) Microdomain structure of polymeric surfaces – potential for improving blood treatment procedures. *Nephrology, Dialysis and Transplantation* 13: 1354–1359.
- Henderson L (1996) In Jacobs C, Kjellstrand C, Koch K and Winchester J (eds) *Biophysics of Ultrafiltration and Hemofiltration*, 4th edition, pp. 114–145. Dordrecht: Kluwer Academic Publishers.
- Henderson L, Colton C and Ford C (1975) Kinetics of hemodiafiltration. II. Clinical characterization of a new blood cleansing modality. *Journal of Laboratory and Clinical Medicine* 85: 372–391.
- Jindal KK, McDougall J, Woods B, Nowakowski L and Goldstein MB (1989) A study of the basic principles determining the performance of several high-flux dialyzers. *American Journal of Kidney Disease* 14: 507–511.
- Ledebo I (1998) Principles and practice of hemofiltration and hemodiafiltration. *Artificial Organs* 22: 20–25.
- Leyboldt JK, Cheung A, Agodoa L, Daugirdas J, Greene T and Keshaviah P (1997) Hemodialyzer mass transfer-area coefficients for urea increase at high dialysate flow rates. *Kidney International* 51: 2013–2017.
- Lipps B, Stewart R, Perkins H, Holmes G, McLain E, Rolfs M and Oja P (1967) The hollow fibre artificial kidney. *Transactions of the American Society of Artificial Internal Organs* 13: 200–207.
- Lonneman G (1993) Dialysate bacteriological quality and the permeability of dialyzer membranes to pyrogens. *Kidney International* (Suppl. 41) S195–S200.
- Lysaght MJ (1988) Haemodialysis membranes in transition. *Contributions to Nephrology* 61: 1–17.
- Vanholder R and DeSmet R (1999) Pathophysiologic effects of uremic retention solutes. *Journal of the American Society of Nephrology* 10: 1815–1823.

Diffusion Dialysis

T. A. Davis, Annandale, NJ, USA

Copyright © 2000 Academic Press

Introduction

Diffusion dialysis is a separation process in which an ion exchange membrane separates a source solution

and a receiving solution, usually water. Anion exchange membranes are notoriously permeable to acids, and diffusion dialysis exploits this property to separate acids from salts. A common application of diffusion dialysis is recovery of acids from waste metal pickling solutions, the strong acid solutions that are used to remove oxide coatings from metal parts before they are painted, galvanized or

production in the blood stream, either directly via an effect on mononuclear cells or indirectly via an effect on the alternative complement pathway. Conversely, the majority of the mediators that are potentially elicited in the blood, such as C3a and IL-1, may be simultaneously eliminated during high flux therapies by an adsorptive or transmembrane mechanism, as discussed above. Other investigations have confirmed that adsorption is also important in the removal of other inflammatory mediators, such as Factor D and cytokines.

Summary

Dialysers used in contemporary HD are equipped with a wide variety of membranes and within both the cellulosic and synthetic classes, water and solute flux properties vary widely. For small and middle-sized solutes, abundant clinical data point to the importance of membrane thickness in diffusive mass transfer. The removal of low molecular mass proteins may occur largely by adsorption for some high flux membranes, particularly those of hydrophobic synthetic composition. Because many of the mediators of inflammation in dialysis patients fall in this low molecular mass protein category, the biocompatibility of a particular membrane must be interpreted in conjunction with its permeability properties.

See Colour Plate 47.

See also: **II/Membrane Separations:** Membrane Bio-separations. **III/Membrane Preparation:** Hollow Fibre Membranes; Interfacial Composite Membranes.

Further Reading

- Anderstam B, Mamoun A, Sodersten P and Bergstrom J (1996) Middle-sized molecule fractions isolated from uraemic ultrafiltrate and normal urine inhibit ingestive behavior in the rat. *Journal of the American Society of Nephrology* 7: 2453–2460.
- Cheung AK, Parker C, Wilcox L and Janatova J (1990) Activation of complement by haemodialysis membranes: polyacrylonitrile binds more C3a than cuprophane. *Kidney International* 37: 1055–1059.

- Clark WR, Macias WL, Molitoris A and Wang NHL (1995) Plasma protein adsorption to highly permeable haemodialysis membranes. *Kidney International* 48: 481–488.
- Clark WR, Hamburger RJ and Lysaght MJ (in press) The effect of membrane composition and structure on solute removal and biocompatibility in haemodialysis. *Kidney International*.
- Colton C, Henderson L, Ford C and Lysaght M (1975) Kinetics of hemodiafiltration. I. *In vitro* transport characteristics of a hollow fiber blood ultrafilter. *Journal of Laboratory and Clinical Medicine* 85: 355–371.
- Deppisch R, Gohl H and Smeby L (1998) Microdomain structure of polymeric surfaces – potential for improving blood treatment procedures. *Nephrology, Dialysis and Transplantation* 13: 1354–1359.
- Henderson L (1996) In Jacobs C, Kjellstrand C, Koch K and Winchester J (eds) *Biophysics of Ultrafiltration and Hemofiltration*, 4th edition, pp. 114–145. Dordrecht: Kluwer Academic Publishers.
- Henderson L, Colton C and Ford C (1975) Kinetics of hemodiafiltration. II. Clinical characterization of a new blood cleansing modality. *Journal of Laboratory and Clinical Medicine* 85: 372–391.
- Jindal KK, McDougall J, Woods B, Nowakowski L and Goldstein MB (1989) A study of the basic principles determining the performance of several high-flux dialyzers. *American Journal of Kidney Disease* 14: 507–511.
- Ledebo I (1998) Principles and practice of hemofiltration and hemodiafiltration. *Artificial Organs* 22: 20–25.
- Leyboldt JK, Cheung A, Agodoa L, Daugirdas J, Greene T and Keshaviah P (1997) Hemodialyzer mass transfer-area coefficients for urea increase at high dialysate flow rates. *Kidney International* 51: 2013–2017.
- Lipps B, Stewart R, Perkins H, Holmes G, McLain E, Rolfs M and Oja P (1967) The hollow fibre artificial kidney. *Transactions of the American Society of Artificial Internal Organs* 13: 200–207.
- Lonneman G (1993) Dialysate bacteriological quality and the permeability of dialyzer membranes to pyrogens. *Kidney International* (Suppl. 41) S195–S200.
- Lysaght MJ (1988) Haemodialysis membranes in transition. *Contributions to Nephrology* 61: 1–17.
- Vanholder R and DeSmet R (1999) Pathophysiologic effects of uremic retention solutes. *Journal of the American Society of Nephrology* 10: 1815–1823.

Diffusion Dialysis

T. A. Davis, Annandale, NJ, USA

Copyright © 2000 Academic Press

Introduction

Diffusion dialysis is a separation process in which an ion exchange membrane separates a source solution

and a receiving solution, usually water. Anion exchange membranes are notoriously permeable to acids, and diffusion dialysis exploits this property to separate acids from salts. A common application of diffusion dialysis is recovery of acids from waste metal pickling solutions, the strong acid solutions that are used to remove oxide coatings from metal parts before they are painted, galvanized or

electroplated. Cation exchange membranes are permeable to bases, and this is utilized to recover NaOH from aluminium etching solutions.

Diffusion dialysis of acids through anion exchange membranes was reported as early as 1964, and was installed on an industrial scale by 1980. There have been many laboratory studies on membrane properties and transport of acid through such membranes. Therefore, the discussions that follow concerning the theory and practice of diffusion dialysis will focus primarily on acid transport through anion exchange membranes. Base dialysis is relatively new, and there is not a large body of knowledge about the mechanism of transport, design criteria and performance of that process. Until such information becomes available, it is reasonable to assume that the theory and practice of base dialysis parallels that of acid dialysis.

Since ion exchange membranes have an ionically charged polymeric structure, their discrimination between solutes is based on ionic charge. Anion exchange membranes are easily permeated by anions, but cations are rejected, because the positive ionic change of the membrane matrix repels the cations. Unlike other cations, hydrogen ions are an integral part of the water that pervades the membrane, and hydrogen ions seem to permeate by a different mechanism that avoids the rejection of the charged polymer structure. Anion exchange membranes transport acids while rejecting salts.

Figure 1 illustrates diffusion dialysis for recovery of HNO_3 from a solution also containing $\text{Fe}(\text{NO}_3)_2$. The anion exchange membrane is quite permeable to the NO_3^- ions, but an equivalent amount of cations must also pass through the membrane to maintain electroneutrality. Because of their double positive

charge, the Fe^{2+} ions are strongly rejected by the membrane, but the protons are transported rather easily. Thus, a useful separation of acid and salt is achieved.

Background and Theory

Transport in diffusion dialysis is described by Fick's law:

$$\text{Flux} = -U \Delta C \quad [1]$$

where ΔC is the concentration difference of the diffusing solute (the driving force for diffusion) and U is a mass transfer coefficient, expressed in units of length time⁻¹. Since the concentrations can be measured only in the bulk solutions, the measured value of ΔC is the driving force for diffusion through the membrane and the solution boundary layers next to the membrane. Therefore, an overall mass transfer coefficient U_o is needed to describe the observed flux. The reciprocal of the mass transfer coefficient is the diffusional resistance, and the diffusional resistances of the membrane and the adjacent liquid boundary layers are additive.

$$1/U_o = 1/U_m + 1/U_l \quad [2]$$

Values of U for a particular solute through a particular membrane are conveniently measured in a stirred cell with the membrane separating the source solution from the receiving solution, usually pure water. With sufficient stirring the resistance of the liquid can be minimized so that the measured value of U is essentially U_m . Acids permeate some anion exchange

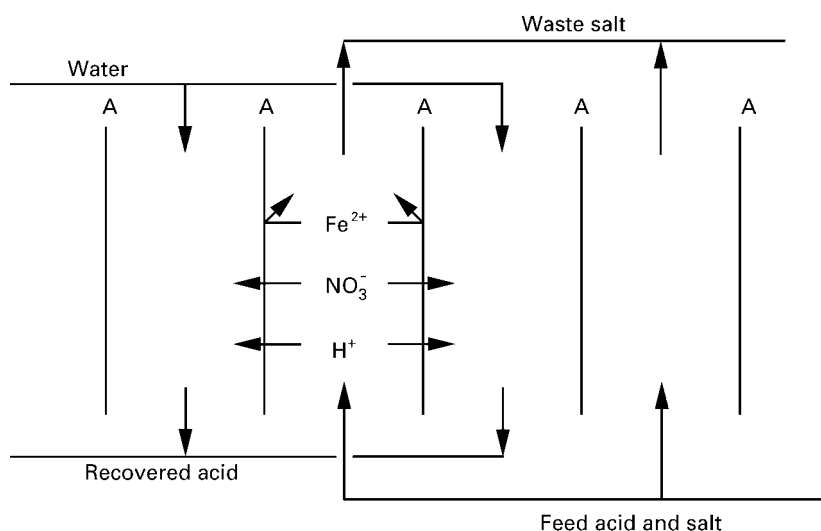


Figure 1 Diffusion dialysis to recover HNO_3 from pickling solution.

membranes rapidly, with U values of about 10^{-4} to $10^{-3} \text{ cm s}^{-1}$ while salts have U values of about $10^{-6} \text{ cm s}^{-1}$. Therefore, there is sufficient difference in the diffusion rates to achieve useful separations of acids from salts by diffusion dialysis.

Since solution velocities in commercial dialysers are slow, U_1 could be a significant part of U_0 . A rough idea of the resistance in the boundary layer can be estimated by examining the elements of the equation for diffusive flux through a film of liquid:

$$\text{Flux} = -D \Delta C/z \quad [3]$$

where D is the diffusivity of the solute through the solvent, typically about $10^{-5} \text{ cm}^2 \text{ s}^{-1}$, and z is the thickness of the film of liquid through which diffusion occurs. Spacing between membranes in a commercial dialysis apparatus is somewhat less than 0.1 cm, so liquid film thickness z would probably be about 0.01 cm. Then $D/z = 10^{-3} \text{ cm s}^{-1}$, which is a U value for the liquid film of the same order of magnitude as the typical U values for dialysis membranes.

Consequently, both the membrane and the liquid films in contact with it are likely to contribute to the resistance to diffusion in a real dialysis application, even at rather high solution velocities.

Transport of solvent through dialysis membranes can be great enough to influence diffusion dialysis performance. Osmotic forces provide a driving force to transport solvent from the dilute solution to the concentrated solution. However, the diffusing solute can drag along solvent, both in the solvation shells of the ions and by convection, in the direction opposite to that of normal osmosis. Further, osmotic pressures are caused by the concentration difference of nondiffusing solutes across the membrane, the values of which can be difficult to determine. Consequently, even the direction of solvent transport can be difficult to predict in certain circumstances, and prediction of the rate of solvent transport is quite difficult.

Mathematical analysis of dialysis is rather simple if the assumptions are made that the overall value of U is independent of C and that solvent transport is negligible. There are two typical cases that are usually encountered with dialysis in general or with diffusion dialysis.

Case 1 is an experiment done in an apparatus used to measure dialysis coefficients, i.e. U values. A sample of the membrane is placed between two chambers of equal volume in a stirred cell, with a surface area A exposed to both solutions. The source solution fills one chamber, and an equal volume V of pure water, the receiving solution, fills the other chamber. Because the volumes of the two solutions are equal, the concentration of the diffusing solute

decreases in the source solution at the same rate as it rises in the receiving solution on the other side of the membrane. The rate of concentration change, dC/dt , is related to the flux, volume and area of the membrane by the equations below. On the side containing the receiving solution:

$$dC/dt = \text{flux} \times A/V \quad [4]$$

and on the side containing the source solution:

$$dC/dt = -\text{flux} \times A/V \quad [5]$$

To integrate this equation, an expression is needed for flux in terms of concentrations on one side of the membrane. The appropriate expression can be obtained by material balance. Let C_s represent the concentration of the diffusing solute on the side with the source solution. Then the concentration of the diffusing solute in the receiving solution would be $C_r = C_0 - C_s$, where C_0 is the initial concentration of the source solution. Now an equation for solute flux can be written as follows:

$$\begin{aligned} \text{Flux} &= -U \times \Delta C = -U \times [C_s - (C_0 - C_s)] \\ &= -U \times (2C_s - C_0) \end{aligned} \quad [6]$$

The differential equation can be integrated to yield:

$$C_s = C_0(1 + e^{-2tUA/V})/2 \quad [7]$$

on the side of the source solution and:

$$C_r = C_0(1 - e^{-2tUA/V})/2 \quad [8]$$

on the side of the receiving solution.

The experiment described in case 1 is a useful technique for measuring values of U for a membrane. Sufficient stirring can reduce solution film resistance to negligible levels, and even volume changes are insignificant in short experiments. Volume changes and analytical inaccuracy can cause substantial errors if source solution concentrations are used in this determination, so determination of the U value should be based on the measured concentrations in the receiving solution.

Although the apparatus described in case 1 is useful for determining membrane properties, it is of limited commercial value as a separation process because no more than half of the diffusing solute can be removed when equal volumes are used on both sides of the membrane. A high degree of removal would require a volume of the receiving stream much larger than that of the feed, but that has limited commercial

appeal. A commercially useful separation can be achieved with countercurrent flow of the solutions through the dialyser.

Case 2 is an example of countercurrent flow of the solutions on opposite sides of the membrane. The system operates at steady state so that concentrations do not change with time, but they do change with position along the flow path of the solutions. To simplify the equations it will be assumed that there is no solvent transport through the membrane and that the source and receiving solutions have the same flow rate, F . When pure water is used for the receiving stream, the material balance is simply:

$$C_f = C_d + C_r \quad [9]$$

where the subscripts represent the feed, depleted and recovered streams respectively. The amount of solute transferred across the membrane is equal to the amount of solute appearing in the recovered stream:

$$UA \Delta C = FC_r \quad [10]$$

Because the flow rates are equal, the concentration change within a solution compartment is linear with respect to distance along the flow path, so the concentration difference across the membrane is equal to the arithmetic mean concentration difference:

$$\Delta C = (C_f + C_d - C_r)/2 \quad [11]$$

Combining this with the material balance equation yields:

$$\Delta C = C_f - C_r \quad [12]$$

which can be combined with the transfer equation:

$$UA(C_f - C_r) = FC_r \quad [13]$$

and rearranged to show the fraction of solute recovered:

$$C_r/C_f = U/(U + F/A) \quad [14]$$

In practice, the values for U are often expressed in the same units as the flow rate per unit area of membrane, $L h^{-1} m^{-2}$. For the diffusion of HCl from pickle liquor through Neosepta AFN anion exchange membrane, reported values of U are $8.6 L h^{-1} m^{-2}$ for HCl and $0.17 L h^{-1} m^{-2}$ for Fe, and a typical value for F/A might be $1 L h^{-1} m^{-2}$. With these values the HCl recovery would be $8.6/(8.6 + 1) = 0.9$, and the Fe leakage would be $0.17/(0.17 + 1) = 0.15$. Thus, 90% of the HCl is recovered, and 15% of

the Fe appears in the recovered acid. Leakage of Fe could be reduced to 8% by doubling the flow rates, but HCl recovery would drop to 81%.

The simplified equation developed above for countercurrent dialysis is only applicable when flow rates of both streams in the dialyser are equal. For those more general situations with unequal flow rates, the log-mean concentration difference would be used as the driving force in Fick's law.

Deviations from Simple Modelling

Osmotic forces play a key role in the water balance, and water transport through the membrane can invalidate the simple mathematical models described above. The following discussion is based on the recovery of acid from a steel pickling solution, which is a significant industrial application of diffusion dialysis. In the recovery of acid from a mixture with a metal salt the major driving force for osmosis is the difference in concentration of salt across the membrane. The osmotic flow of water can cause the volume of the receiving stream to decrease as much as 20% as it passes through a typical industrial dialyser. Therefore, a good mathematical model of diffusion dialysis should account for water transport through the membrane.

The presence of salt in the source solution can substantially affect the concentration of acid in the recovered stream. In diffusion dialysis of metal pickle liquors the source solution has two important components – the free acid that can diffuse through the anion exchange membrane rather easily and the metal salt that is rejected by the membrane because of repulsion of the metal cations by the fixed positive charge on the membrane matrix. There are numerous reports of countercurrent diffusion dialysis in which the acid concentration in the recovered stream is higher than the free acid concentration in the feed. Some writers have attempted to explain these observations in terms of osmotic removal of water from the receiving stream, but it seems more plausible that a concentration difference of the common anion produces a driving force for transport of protons through the membrane. That driving force is the Donnan potential (discussed in 'Membrane Separations: Donnan Dialysis') generated by the difference between the activity of anions in the two solutions. That potential difference provides a driving force for proton transport in addition to the driving force provided by the difference in concentration of the free acid.

Fick's law describes acid flux due to simple diffusion as the product of the driving force ΔC_A and the mass transfer coefficient for diffusion, U_A . A similar expression can be used to describe the acid

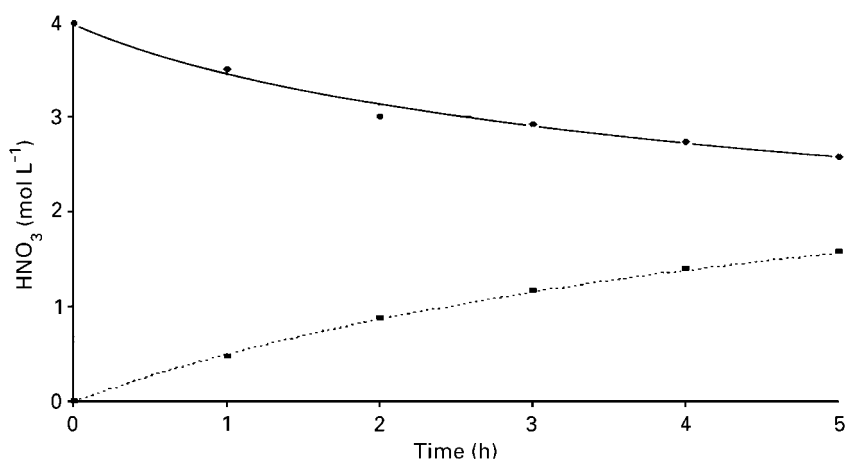


Figure 2 Diffusion dialysis of pure 4 mol L⁻¹ HNO₃ feed stream (continuous line) with a pure water-receiving stream (dotted line).

transport due to the concentration difference of the salt with a common anion, with ΔC_s as the driving force and U_s as the mass transfer coefficient. The total acid flux can be expressed as the sum of the flux due to individual driving forces as follows:

$$\text{Total acid flux} = U_A \Delta C_A + U_s \Delta C_s \quad [15]$$

This empirical equation was tested with published data by Edwards, who measured HNO₃ concentrations on both sides of a Tokuyama AFN membrane in a stirred cell. Graphs of data for three different starting compositions are shown in Figures 2–4. In each graph the data at the top connected by the continuous line show the reduction in concentration as acid diffuses from the source stream, and the data at the bottom show the increase in acid in the receiving

stream. Figure 2 shows simple diffusion of HNO₃, which is well described by the dotted line that was calculated by Fick's law with $U_A = 12.8 \text{ L h}^{-1} \text{ m}^{-2}$. But when NaNO₃ was added to the source solution, Fick's law with $U_A = 12.8 \text{ L h}^{-1} \text{ m}^{-2}$ (shown in Figure 3 by the dotted line) predicts a much slower appearance of acid than the data indicated. The equation for total acid flux with values of $U_A = 12.8 \text{ L h}^{-1} \text{ m}^{-2}$ and $U_s = 0.45 \text{ L h}^{-1} \text{ m}^{-2}$ shown by the dashed line gave a good correlation of the data. It is interesting to note in Figure 3 that the influence of the excess nitrate forced so much HNO₃ out of the source stream that its concentration fell below that in the receiving stream. The situation was reversed when NH₄NO₃ was placed in the receiving solution.

Figure 4 shows that the total acid flux equation with values of $U_A = 12.8 \text{ L h}^{-1} \text{ m}^{-2}$ and $U_s =$

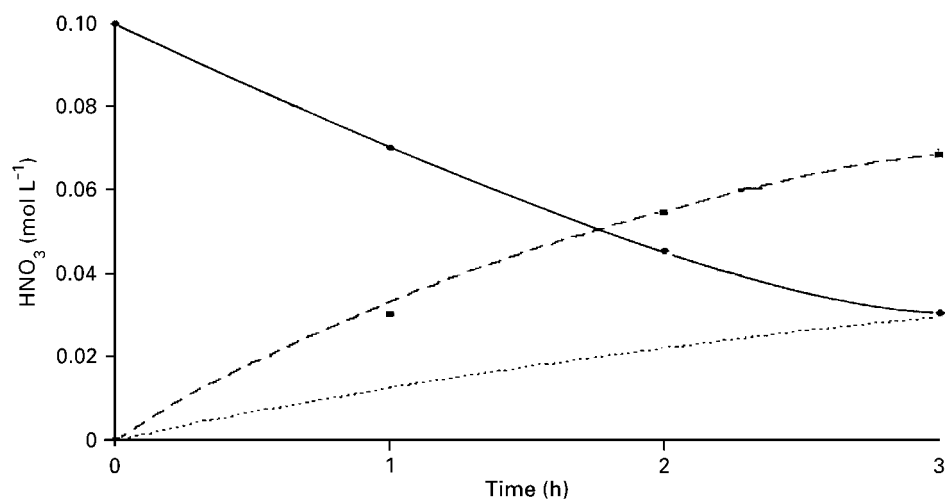


Figure 3 Diffusion dialysis of 0.1 mol L⁻¹ HNO₃ and 5 mol L⁻¹ NaNO₃ feed stream (continuous line) with a pure water-receiving stream (dashed and dotted lines). Lines calculated as described in the text.

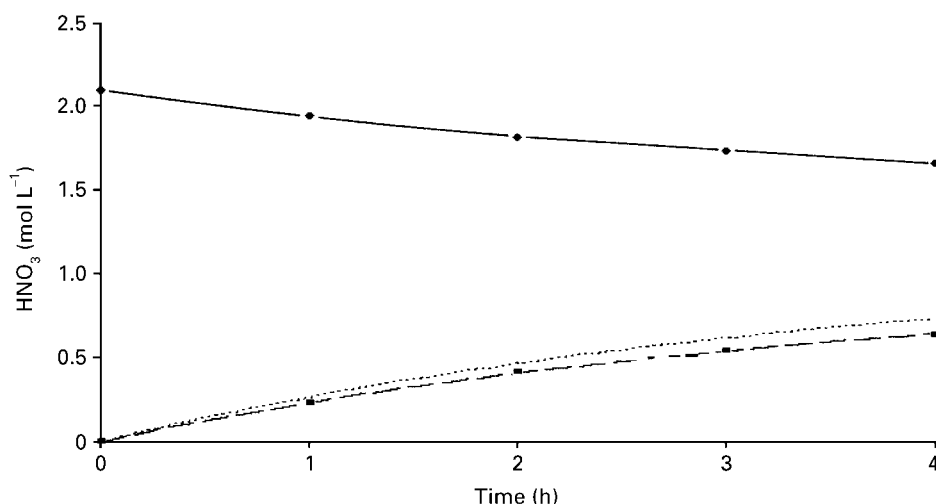


Figure 4 Diffusion dialysis of a 2.1 mol L^{-1} HNO_3 feed stream (continuous line) against a 4 mol L^{-1} NH_4NO_3 -receiving solution (dashed and dotted lines).

$0.45 \text{ L h}^{-1} \text{ m}^{-2}$ again described the data better than Fick's law and correctly showed that the appearance of acid in the receiving solution was retarded by the presence of nitrate in that solution. It should be emphasized that the total acid flux equation is empirical, but it does seem to be a useful way of accounting for the effects of salts on acid flux and would thus be useful for mathematical modelling of diffusion dialysis of acids.

Competing Processes

Diffusion dialysis, like most other membrane processes, must compete with other processes that can achieve the desired separation. Lime neutralization, sorption on ion exchange resins and bipolar membranes are competing processes for the treatment of waste acids from metal pickling. When disposal and replacement acid costs are low, lime neutralization is the most economical alternative. When the recovered acid can be used in a diluted form, sorption on ion exchange resins is attractive. When it is necessary to minimize discharge, bipolar membranes, though expensive, can be the preferred process. Diffusion dialysis offers the important advantages of very low operating costs and long membrane life that can exceed 5 years if clean, nonfouling feeds are used. Therefore, if diffusion dialysis can achieve the desired separation and if capital costs are tolerable, diffusion dialysis can be the process of choice for recovering waste acids.

Membranes for Diffusion Dialysis

Modern membranes for acid dialysis are made of anion exchange polymers which have an affinity for

acids and reject cations other than protons. The anion exchange membranes that are most permeable to acids seem to be those with a very high water content. The water content is important because the high electromobility of protons through water is attributable to a transfer mechanism that is not available to other cations. A proton can transfer from a hydronium ion to an adjacent water molecule by a mechanism which was first suggested by Grotthuss in 1806.

The major suppliers of diffusion dialysis membranes and devices are Asahi Glass, who make Selemin DMV, and Tokuyama Corporation who make Neosepta® AFN and AFX membranes. Since the membrane devices for diffusion dialysis are similar to those used in electrodialysis, any supplier of electrodialysis equipment is capable of supplying diffusion dialysis equipment as well. The supplier with the largest number of installations in the USA is Pure Cycle Environmental Technologies in Palmer, Massachusetts, and the largest supplier in Europe is Eurodia in Paris, France.

Membranes for base dialysis were parchmentized paper when the process was first developed in the 1930s. The early membranes had little selectivity between caustic and salts, but they effectively retained hemicellulose from rayon and viscose processes. Modern membranes for base dialysis are made of cation exchange polymer that rejects anions other than hydroxyl, presumably because of the Grotthuss mechanism of hydroxyl transport. The typical cation exchange membrane made for electrodialysis has low flux for base diffusion, but Tokuyama Corporation has made a special cation exchange membrane, Neosepta® CMX-SB, with acceptably high flux.

Design of Processes and Equipment

Industrial diffusion dialysis usually operates with countercurrent flow of the solutions on opposite sides of the membrane. Countercurrent flow produces the maximum concentration difference over the entire length of the membrane and allows recovery of a substantial portion of the most highly diffusive solute while minimizing the transport of the less diffusive solutes. Since fluxes in diffusion dialysis are relatively low compared to other membrane processes, the solution velocity across the membrane surface must also be slow in order to have enough residence time for adequate removal of the solute. Typical solution velocities in diffusion dialysis are about 1 cm min^{-1} . Convective effects due to density changes in the solutions can be important with such low velocities.

Dialysers for industrial applications must be robust, cleanable, efficient and economical. Industrial diffusion dialysers usually have flat sheet membranes with some type of spacer to keep the membranes apart and to form solution compartments. The membrane arrangement (without showing the spacers) and the directions of solution flows in a typical diffusion dialyser are shown in Figure 1. A single dialyser can contain hundreds of identical, vertically oriented membranes. Membranes and spacers have holes that are aligned to form manifolds, and each spacer has entry ports that connect the solution compartment to the appropriate manifold. This manifolding, which is also typical in electrodialysis, distributes the solution equally to the parallel compartments. The feed solution usually enters the bottom of the dialyser and the solvent usually enters at the top, as shown in Figure 1.

Solutions flowing through the industrial diffusion dialyser should be free of particulate matter, because the solution velocities are too slow to sweep out particles. The dialyser can be expected to perform maintenance-free for several years if the feed solution is clean and no precipitation occurs within the dialyser. A single filter on each supply line should suffice if the feed solution is inherently clean. However, primary and secondary filtration is recommended if particles are expected to be present in the feed because of the possibility of contamination during the cleaning or replacement of primary filter elements.

The low solution velocities that characterize diffusion dialysis cause extremely low pressure drops through dialysers, usually just a few kPa. Many dialysers can be fed in parallel from a single header tank positioned just above the dialysers. The solutions exiting the dialysers also enter a header tank with adjustable overflow levels. The header tanks should

have covers and filtered vents to avoid the entrance of dust. Transparent tanks or sight glasses positioned close together allow the operator to monitor visually the pressure drop through the dialyser. Density differences of the solutions should be considered in determining the actual pressure head.

In metal finishing plants the dialysis process is normally set up to run continuously to treat a small stream of the metal-laden acid in the pickling tank and return the recovered acid to the tank. This allows the dialysis to run as a steady-state process. The waste stream, which typically contains 10% of the acid and 90% of the metals from the feed, is usually neutralized to precipitate the metal as hydroxides for disposal or recovery.

It is important that the solution flow is uniformly distributed to all solution compartments that are fed in parallel. Density changes caused by solute transfer across the membranes are utilized to achieve uniform flow distribution. The feed solution, which has the highest density, enters the bottom of the dialyser and decreases in density as acid is removed. Osmotic water transport into this concentrated solution also contributes to the decrease in density. The receiving solution increases in density as it flows downward. The uniform gradation in density allows the solutions to approach plug-flow conditions in each solution compartment.

Entrapped gas can cause flow disruptions in the receiving solution compartments of acid dialysers. Water entering the top of the receiving solution compartments contains some dissolved gases (O_2 , N_2 , CO_2) that can form bubbles in the downward-flowing solution. Even if the water is not initially supersaturated with dissolved gases, the addition of solute diffusing across the membrane can lead to supersaturation within the receiving stream. The slow downward flow of solution is not sufficient to force the bubbles out the bottom of the dialyser, but it could hinder their rise in the compartments. Bubbles eventually reach such a large size that buoyancy forces exceed the forces of surface tension. Then the large bubbles rise and collect in the top of the compartment and eventually in the entry ports where they block off the flow of water into some of the receiving solution compartment. As more compartments become blocked, the solution velocity in the remaining compartments increases. But that increase in flow rate means that the residence time in those open compartments is shorter, so the performance of the dialyser deteriorates.

Removal of the dissolved gases from the water before it enters the dialyser is beneficial. Gases can be removed by heating the water in an open or vented tank, by application of a vacuum or by passing the

water through a nonwetting microfiltration device with a vacuum applied to the opposite side of the microporous membrane. Another remedy is periodically to reverse the flow of the receiving stream and force the bubbles out of the top of the dialyser into a vent tank. Flow reversal can be accomplished easily with a centrifugal pump situated in the line of the receiving solution at the entrance or exit to the dialyser. The header tanks must have sufficient surge capacity to accommodate the volume of the flow reversal. Flow reversal for a few seconds is sufficient – just long enough to displace any gas that has accumulated in the top of the receiving compartments and entry ports. These two remedies are often used together.

The heat of dilution of the acid can also cause problems of overheating in diffusion dialysis. Because the dialyser acts like a countercurrent heat exchanger, the heat released in the dialyser tends to become trapped inside. When the concentration of acid in the feed is high, the peak temperature, which occurs about halfway through the flow path, can be high enough to damage the membrane.

Limitations of Diffusion Dialysis

A necessary condition of dialysis is that the solute concentration in the recovery stream must be lower than in the feed stream in order to provide a driving force for diffusion. This is not a real limitation in applications where the diffusing solute is a waste that can be easily discarded. But this condition can be a limitation when the diffusing solute is the desired product, because the product is often recovered at a low concentration. Fortunately, the acid from steel pickling solution can be recycled to the pickling bath at the concentration at which it was recovered. Another limitation is that the nondiffusing solutes are left in the original solution in a slightly diluted state, which means that the waste volume can be considerable.

The selectivity of diffusion dialysis membranes for rejecting metal ions is influenced by the ionic charge on the metal ion. Metal ions with multiple positive charge are rejected more efficiently than ions with a single charge. However, zinc and some other metal ions form complexes with the anions of the acid. In HCl solutions, zinc forms ZnCl_3^- and ZnCl_4^{2-} complexes that behave as anions in the anion exchange membrane. These complex ions do not diffuse through the membrane as readily as Cl^- ions do, but they diffuse much faster than Zn^{2+} ions. However, zinc does not form a complex in H_2SO_4 solution, so zinc is rejected quite well in the sulfate system.

All of the halogens form complexes with some metals. Chloride complexes of Cu, Ga, Fe (ferric forms a much stronger chloride complex than ferrous), V and Zn have been reported. The existence of a chloride complex does not necessarily mean that HCl cannot be recovered from the metal salt by diffusion dialysis. Since the chloride complexes are rather bulky, they do not pass through the anion exchange membranes as easily as chloride ions do.

Applications

The first important industrial application for dialysis seems to have been for recovery of caustic from viscose, hemicellulose, wood-pulping solutions and textile-processing solutions. In the 1930s there were many patents describing dialysers that utilized diaphragms of parchmented paper and regenerated cellulose. Publications of that era described dialysis as a method for separating crystalloids (substances that form true solutions and are capable of being crystallized) from colloids (small particles in suspension).

By far the most important application for dialysis was begun during the 1940s when Dr. Willem Kolff discovered that treatment of blood by dialysis removed urea and other metabolic wastes, and he proceeded to develop the artificial kidney. The artificial kidney and other conventional dialysis processes are described in detail in 'Membrane Separations: Dialysis in Medical Separations'.

Conclusion

Diffusion dialysis utilizes membranes that contain ion exchange groups, and those were not available until the 1950s. Diffusion dialysis plants have been recovering and recycling acids in Japan since 1980, and many are being installed in the USA, particularly in metal-finishing facilities. Acids that have been recovered include HCl, HF, HNO_3 , H_2SO_4 and methanesulfonic. The recovered acid is sufficiently concentrated to be returned to the pickling tank, and the acid-free solution of metal salts requires considerably less base to precipitate the metal hydroxides. Recovery of mixed HF and HNO_3 from the pickling of stainless steel is important because these acids are expensive and cause severe pollution problems if they are discarded. Diffusion dialysis has been applied to the recovery of H_2SO_4 from aluminium anodizing baths where the trivalent aluminium cation is well rejected by the anion exchange membrane.

Base dialysis membranes have been used commercially for the recovery of NaOH from the waste

generated by the chemical milling of aluminium aircraft parts. Chemical milling is used to remove metal from aluminium parts, such as curved sections of wing or fuselage that are difficult to machine with mechanical devices. The part is dip-coated with a film of rubber, and then a selected portion of the rubber is stripped away to expose the metal surface. Then the part is immersed in boiling NaOH that rapidly and uniformly dissolves the metal from the exposed surface. The dissolved aluminium accumulates in the etch tank as NaAlO_2 , which must be discarded eventually. When the NaOH is removed from the solution by dialysis, the NaAlO_2 hydrolyses to $\text{Al}(\text{OH})_3$ and NaOH. The $\text{Al}(\text{OH})_3$ is recovered by filtration and sold as a pure product, and the released NaOH is returned to the etch tank along with the dialysed NaOH. Dialysis allows recovery of essentially all of the NaOH and completely eliminates the need for disposal of the waste etchant. An industrial installation of base dialysis has been operating success-

fully in a chemical milling plant in California since 1991.

See Colour Plate 48.

Further Reading

- Bailey DE (1993) Acid recycling system. US Patent 5 264 123.
 Davis TA (1991) Recovery of sodium hydroxide and aluminium hydroxide from etching waste. US Patent 5 049 233.
 Marshall RD and Storrow JA (1951) Dialysis of caustic soda solutions. *Industrial and Engineering Chemistry, Engineering and Process Development* 42: 2934–2943.
 Saddington AW and Julien AP (1938) Dialysis of aqueous caustic solution. US Patent 2 138 357.
 Shigekuni N and Motomura K (1979) Diffusion dialysis method. Japanese Patent 54 136 580.
 Zender J (1946) Process and apparatus for dialyzing solutions. US Patent 2 411 238.

Donnan Dialysis

T. A. Davis, Annandale, NJ, USA

Copyright © 2000 Academic Press

Introduction

Donnan dialysis is a separation process that utilizes counterdiffusion of two or more ions through an ion-exchange membrane to achieve a separation. It can also be viewed as a continuous deionization process. For example, water softening can be done with a cation-exchange membrane. Hard water flows on one side of the membrane, and NaCl brine flows on the other side. Na^+ ions from the brine diffuse across the membrane and cause the Ca^{2+} and Mg^{2+} ions to diffuse in the opposite direction. Donnan dialysis is usually performed as a continuous, countercurrent process so that a substantial portion of a cation from a dilute solution could be concentrated into a small volume. Differences in the volumes and concentrations of the two solutions can be exploited to achieve some interesting and useful separations.

Donnan dialysis can be used for changing compositions of process or analytical solutions, pollution control, and even deionization of a process stream. The deionization process, called 'neutralization dialysis',

combines Donnan dialysis through both cation-exchange and anion-exchange membranes in one apparatus with H^+ and OH^- ions exchanging for the cation and anion of a salt.

In the discussions that follow, the fundamental principles of Donnan dialysis will be presented, and some of its applications and capabilities will be described. The type of equipment and membrane arrangements appropriate for both Donnan dialysis and neutralization dialysis will be presented.

Background

The Donnan dialysis process is named after F. G. Donnan who in 1924 described the equilibrium that resulted when a semipermeable membrane separated two solutions of electrolytes, NaA on one side and KA on the other. The membrane he used was prepared by filling the pores of parchment paper with a gel of copper ferrocyanide, and he used ferrocyanide as the common anion A of the two salts. When the initial volumes and concentrations of the two salt solutions were the same, counterdiffusion of equal amounts of Na^+ and K^+ through the membrane led to an equilibrium condition where the two solutions had equal concentrations of NaA and KA. But when

generated by the chemical milling of aluminium aircraft parts. Chemical milling is used to remove metal from aluminium parts, such as curved sections of wing or fuselage that are difficult to machine with mechanical devices. The part is dip-coated with a film of rubber, and then a selected portion of the rubber is stripped away to expose the metal surface. Then the part is immersed in boiling NaOH that rapidly and uniformly dissolves the metal from the exposed surface. The dissolved aluminium accumulates in the etch tank as NaAlO_2 , which must be discarded eventually. When the NaOH is removed from the solution by dialysis, the NaAlO_2 hydrolyses to $\text{Al}(\text{OH})_3$ and NaOH. The $\text{Al}(\text{OH})_3$ is recovered by filtration and sold as a pure product, and the released NaOH is returned to the etch tank along with the dialysed NaOH. Dialysis allows recovery of essentially all of the NaOH and completely eliminates the need for disposal of the waste etchant. An industrial installation of base dialysis has been operating success-

fully in a chemical milling plant in California since 1991.

See Colour Plate 48.

Further Reading

- Bailey DE (1993) Acid recycling system. US Patent 5 264 123.
 Davis TA (1991) Recovery of sodium hydroxide and aluminium hydroxide from etching waste. US Patent 5 049 233.
 Marshall RD and Storrow JA (1951) Dialysis of caustic soda solutions. *Industrial and Engineering Chemistry, Engineering and Process Development* 42: 2934–2943.
 Saddington AW and Julien AP (1938) Dialysis of aqueous caustic solution. US Patent 2 138 357.
 Shigekuni N and Motomura K (1979) Diffusion dialysis method. Japanese Patent 54 136 580.
 Zender J (1946) Process and apparatus for dialyzing solutions. US Patent 2 411 238.

Donnan Dialysis

T. A. Davis, Annandale, NJ, USA

Copyright © 2000 Academic Press

Introduction

Donnan dialysis is a separation process that utilizes counterdiffusion of two or more ions through an ion-exchange membrane to achieve a separation. It can also be viewed as a continuous deionization process. For example, water softening can be done with a cation-exchange membrane. Hard water flows on one side of the membrane, and NaCl brine flows on the other side. Na^+ ions from the brine diffuse across the membrane and cause the Ca^{2+} and Mg^{2+} ions to diffuse in the opposite direction. Donnan dialysis is usually performed as a continuous, countercurrent process so that a substantial portion of a cation from a dilute solution could be concentrated into a small volume. Differences in the volumes and concentrations of the two solutions can be exploited to achieve some interesting and useful separations.

Donnan dialysis can be used for changing compositions of process or analytical solutions, pollution control, and even deionization of a process stream. The deionization process, called ‘neutralization dialysis’,

combines Donnan dialysis through both cation-exchange and anion-exchange membranes in one apparatus with H^+ and OH^- ions exchanging for the cation and anion of a salt.

In the discussions that follow, the fundamental principles of Donnan dialysis will be presented, and some of its applications and capabilities will be described. The type of equipment and membrane arrangements appropriate for both Donnan dialysis and neutralization dialysis will be presented.

Background

The Donnan dialysis process is named after F. G. Donnan who in 1924 described the equilibrium that resulted when a semipermeable membrane separated two solutions of electrolytes, NaA on one side and KA on the other. The membrane he used was prepared by filling the pores of parchment paper with a gel of copper ferrocyanide, and he used ferrocyanide as the common anion A of the two salts. When the initial volumes and concentrations of the two salt solutions were the same, counterdiffusion of equal amounts of Na^+ and K^+ through the membrane led to an equilibrium condition where the two solutions had equal concentrations of NaA and KA. But when

initial concentrations were different, counterdiffusion of equal amounts of Na^+ and K^+ through the membrane produced solutions with equal ratios of Na^+/K^+ on both sides of the membrane at equilibrium. This relationship of concentrations of the ions in the solutions on opposite sides of the membrane is called the 'Donnan equilibrium'.

Before proceeding with the theory, it is useful to define some terms that are often used in discussions of modern polymeric ion-exchange membranes. First, an 'ion-exchange membrane' is a plastic film with fixed ionically charged groups dispersed more or less uniformly within the film. Associated with the fixed charges are mobile charges of opposite sign called 'counterions'. The counterions are free to exchange with other counterions in the adjacent solutions. When the membrane has fixed negative charges, e.g., sulfonic acid groups, it is called a 'cation-exchange membrane', and the counterions are cations. In the external solutions, mobile anions are associated with the cations, but in the membrane the charge balance is satisfied by the fixed negative charges. Therefore, anions tend to be excluded from the interior of the cation-exchange membrane. The ions with the same charge as the fixed charge in the membrane are called 'co-ions'.

Theory

The Donnan equilibrium relationship is derived from thermodynamics. Under conditions of equilibrium the chemical potential μ_i of any dissolved species i is the same in every phase present:

$$\mu_i = \mu_i^\circ + RT \ln a_i \quad [1]$$

Here, μ_i° is the chemical potential of species i in the standard state, R is the gas law constant, T is the absolute temperature, and a_i is the activity of the particular chemical species i being considered. However, electrical potentials must also be considered when the chemical species are ionic, so the electrochemical potential η_i must be used to describe the equilibrium:

$$\eta_i = \mu_i^\circ + RT \ln a_i + z_i F \theta \quad [2]$$

where z_i is the ionic charge, F is Faraday's constant, and θ is the electrical potential. When the two liquids, phase 1 and phase 2, are at equilibrium with the membrane, there is also equilibrium between the two liquid phases, and the electrochemical potential of any mobile species i in the two phases can be equated.

$$\eta_{i1} = \eta_{i2}, \text{ or } RT \ln a_{i1} + z_i F \theta_1 = RT \ln a_{i2} + z_i F \theta_2 \quad [3]$$

It should be noted that the μ_i° terms cancel because the same standard state exists in both liquid phases. But the co-ions are not free to move through the membrane that separates the two liquid phases, so there is no opportunity for their concentrations to change. Whenever salt concentrations on opposite sides of the membrane differ, there will be a potential difference across the membrane caused by the concentration difference. This potential difference, called the 'Donnan potential', E_{Donn} , is described by rearrangement of eqn [3]:

$$\begin{aligned} E_{\text{Donn}} &= \theta_2 - \theta_1 = RT/z_i F (\ln a_{i1} - \ln a_{i2}) \\ &= RT/F \ln(a_{i1}/a_{i2})^{1/z_i} \end{aligned} \quad [4]$$

Since the Donnan potential acts on all mobile ionic species, the value of $(a_{i1}/a_{i2})^{1/z_i}$ is the same for all of the counterions in the system. In other words, the concentration difference of the co-ions causes an electrical potential that acts on the counterions.

As Donnan pointed out in his seminal description of the theory, a precise treatment of the equilibria would require the use of activities rather than concentrations of ions in the solutions. But the use of molar concentrations greatly simplifies the presentation of the theory, so that is the approach taken here. For the experiment described by Donnan where $z_i = +1$ for both Na^+ and K^+ ions, the equilibrium written with concentrations would be:

$$\begin{aligned} [\text{Na}^+]_1/[\text{Na}^+]_2 &= [\text{K}^+]_1/[\text{K}^+]_2 \text{ or } [\text{Na}^+]_1/[\text{K}^+]_1 \\ &= [\text{Na}^+]_2/[\text{K}^+]_2 \end{aligned} \quad [5]$$

Figure 1 illustrates the flow of ions in the approach to Donnan equilibrium. Two dilute salt solutions NaCl and KCl are separated a cation-exchange membrane, labelled C, which is permeable to the cations Na^+ and K^+ but impermeable to the common anion Cl^- . The concentration difference of Na^+ ions across the membrane provides a driving force for their diffusion through the membrane. There is no net flow of electric current through the membrane, so any net transfer of Na^+ to the right must be balanced by transfer of an equivalent amount of K^+ to the left. Those diffusive processes will occur until an equilibrium is established.

The equilibrium concentrations can be expressed in terms of the initial molar concentrations c_1 of NaCl on the left and c_2 of KCl on the right, x moles transported through the membrane (still the same for both cations) and the volumes V_1 and V_2 of the

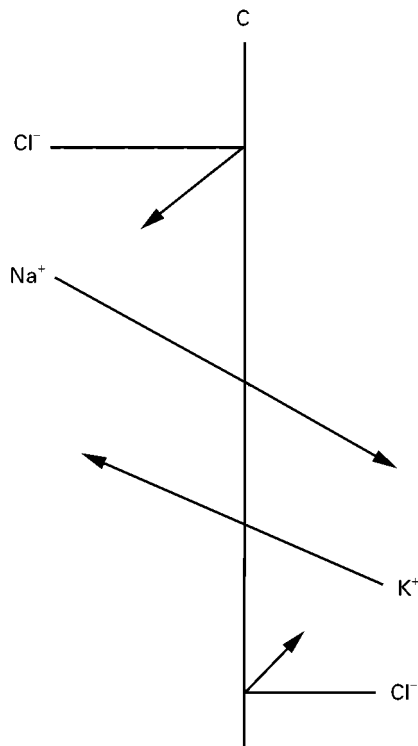


Figure 1 Donnan potential forces K^+ ions to higher concentration.

solutions, expressed in litres:

$$(c_1 - x/V_1)/(x/V_1) = (x/V_2)/(c_2 - x/V_2) \quad [6]$$

Solving this equation for x yields:

$$x = c_1 c_2 / (c_1/V_2 + c_2/V_1) \quad [7]$$

Donnan dialysis is particularly effective for recovery or removal of multivalent ions. The Donnan equilibrium for a divalent Ca^{2+} ion and a univalent K^+ is described by the equation:

$$([Ca^{2+}]_1/[Ca^{2+}]_2)^{1/2} = [K^+]_1/[K^+]_2 \quad [8]$$

For maintenance of electroneutrality in the system, the transport of x moles of Ca^{2+} ions through the membrane requires the transport of $2x$ moles of K^+ ions in the opposite direction. Thus the equilibrium is described by:

$$[(c_1 - x/V_1)/(x/V_1)]^{1/2} = (2x/V_2)/(c_2 - 2x/V_2) \quad [9]$$

For $V_1 = 10$, $V_2 = 1$ and initial concentrations of $c_1 = 0.01$ and $c_2 = 1$, the value of $x = 0.095$ is calculated by eqn [9], which means that more than 95% of the calcium would be driven through the membrane. The effect of valence is even more dramatic

when the c_1/c_2 ratio is much lower than the value used in this example.

Comparison of Donnan Dialysis with Conventional Ion Exchange

In many respects Donnan dialysis can be viewed as a continuous ion-exchange process. For instance, both processes can be used for the softening of water. In conventional ion-exchange softening, the ion-exchange resin beads are initially in the Na^+ form. When hard water flows through a column of the Na^+ form resin beads, Ca^{2+} ions in the water exchange with Na^+ ions on the resin. When the supply of Na^+ ions on the resin approaches exhaustion, the flow of hard water is stopped, the resins are regenerated by passing $NaCl$ brine through the column, and then the cycle is repeated. In contrast, water softening with Donnan dialysis is a continuous process. The Na^+ ions for regeneration are always available in the solution on one side of the membrane, and the Ca^{2+} ions are continuously removed from the feed stream. Both processes are effective for water softening. Donnan dialysis works best in a situation where a continuous flow is expected. Softening with a bed of resin beads can easily accommodate variable flow rates or even on/off operation. Since water softening is most often done in situations where flow rates fluctuate widely, the use of resin beads rather than membranes is the accepted practice.

If a particular exchange of ions can be accomplished by the cyclic process with ion-exchange resin beads or the continuous process with ion-exchange membranes, what factors might influence the selection of the membrane process over the conventional process? Because the membrane process is continuous, it operates at steady-state conditions everywhere in the dialyser. In cases where acid or base is used to drive the process, conditions of pH extremes can be avoided more easily with Donnan dialysis than with conventional ion exchange. Compared to membranes, ion-exchange beads offers a large surface area in a small volume, so the rates of mass transfer are faster with beads. But that large surface area can be a problem if components of the solution are subject to denaturation at surfaces where pH extremes exist. Donnan dialysis can be a much gentler process.

A major limitation to Donnan dialysis is that, like ion exchange, there is a need to add chemicals to recover or remove chemicals. Essentially the stripper solution in Donnan dialysis serves the same function as the regenerant solution in ion exchange. Donnan dialysis has the added limitation that osmotic water transport makes the recovered electrolyte more dilute

than it would be in the spent regenerant of an ion-exchange process. However, Donnan dialysis has the advantages that it is continuous and does not require the rinse step after regeneration. If the application is one in which the stripper solution is already available and needs to have the transported ion in it, then the Donnan dialysis can be an advantageous process.

Neutralization Dialysis

Anion- and cation-exchange membranes can be combined into a single dialyser where both acid and base drive the transport of the cation and anion of a salt as illustrated in **Figure 2**. Since the hydrogen and hydroxyl ions that drive the transport are neutralized in the feed solution, the driving force for desalting can be maintained until almost all of the acid and base are consumed. Neutralization dialysis has been used effectively for desalination of aqueous solutions of organic compounds. Research has demonstrated that the flux of salt ions increases with acid and base concentration up to about 0.1 M. Above those levels there was little benefit in raising the acid and base concentrations.

It should be noted from Figure 2 that the membrane arrangement in neutralization dialysis is different from that in electrodialysis. Here there are four membranes in a repeating sequence, two anion-exchange membranes and then two cation-exchange

membranes. It is a fortunate circumstance in neutralization dialysis that the acid only contacts cation-exchange membranes, because anion-exchange membranes are notoriously leaky to acids. Likewise, the two anion-exchange membranes that bound the base compartments resist leakage of base.

Neutralization dialysis competes with deionization with mixed bed ion-exchange resins which has lower capital cost. But neutralization dialysis has the advantage of being a continuous process that can be controlled by the flow rates and concentrations of the acid and base. Moreover, the feed solution is not exposed to such severe pH extremes as it would be in deionization with ion-exchange resins.

Membranes for Donnan Dialysis

Many ion-exchange membranes are manufactured for electro dialysis, and most of them would be potentially useful for Donnan dialysis. In addition, the Nafion[®] fluoropolymer cation-exchange membranes made by DuPont are uniquely suited to Donnan dialysis because of their ability to withstand severe thermal and chemical attack. Fluoropolymer membranes have been used to recover chromic acid, a strong oxidizing agent that attacks hydrocarbon-based membranes. Nafion[®] has been made as small tubules and fabricated into shell-and-tube dialysers.

The preparation of hollow fibres for use in analytical devices was reported in 1981. Low-density polyethylene was extruded into 300 μM i.d., 380 μM o.d. hollow fibres that were sulfonated with 10% chlorosulfonic acid in methylene chloride. A bundle of eight hollow fibres was inserted into a coiled tube and sealed with silicone rubber caulk.

Although many types of ion-exchange membranes have been used for Donnan dialysis, there seem to be no published studies comparing the performance of commercial membranes for Donnan dialysis or establishing criteria for desirable membranes. One would expect diffusional transport properties of the membranes to parallel those of electrodialysis. In Donnan dialysis, membranes with low electrical resistance would be expected to have low resistance to ion diffusion, and those with low electroosmotic water transport would be expected to have low osmotic water transport. Of course the membranes should be stable at the anticipated operating temperatures of the process and resist chemical attack by solution components. Experimental studies have established that, under typical hydrodynamic conditions, the major resistance to transport is in the boundary layer of the dilute solution rather than in the membrane; therefore, even some of the thicker commercial ion-exchange membranes could be candidates for use in Donnan dialysis.

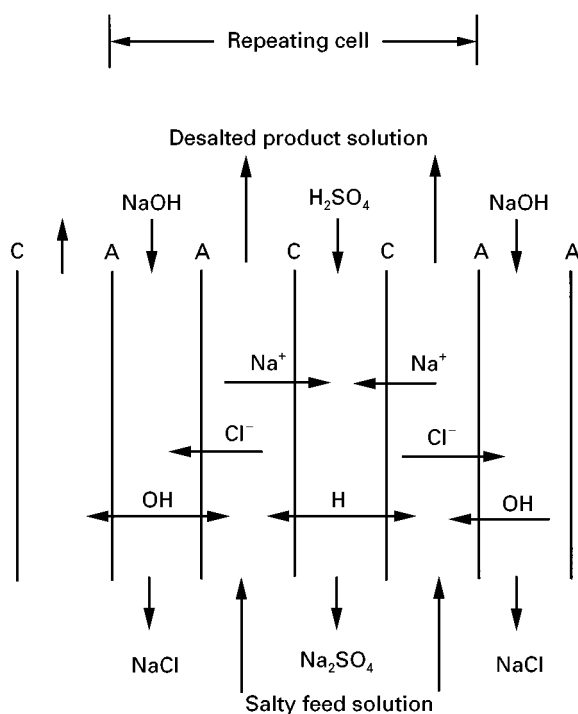


Figure 2 Neutralization dialysis for desalination. C = cation; A = anion.

Japanese researchers have made cation exchange membranes, specifically selective to the transport of uranyl ions, by forming a copolymer of 2,3-epithiopropyl methacrylate and 2-acrylamide-2-methylpropanesulfonic acid. They observed that the proportions of the monomers had a great effect on the ability of the membranes to transport uranyl ions. High transport was achieved when the 2-acrylamide-2-methylpropanesulfonic acid content was at least 34%, but very low transport occurred when that monomer comprised less than 21% of the membrane. By contrast, they found that the Selemion DLE membrane did not transport the uranyl ions under the same experimental conditions. The same researchers also made anion-exchange membranes of 2,3-epithiopropyl methacrylate-dodecyl methacrylate-methylacrylamide propyltrimethylammonium chloride terpolymer that selectively transported ferric oxalate complex anions from acidic ferric sulfate solution to a receiving solution containing sodium oxalate. These studies suggest that the development of ion-specific membranes could lead to selective separations by Donnan dialysis that cannot be economically achieved by other methods.

The amount of membrane area required for a particular Donnan dialysis application depends on the mass transfer rates that can be achieved. However, the user should be cautious about relying upon mass transfer data obtained in stirred cells to design industrial systems, because the high shear rates obtained by stirring might not be achieved in a commercial dialyser. Results reported for Donnan dialysis of uranyl ions in a countercurrent dialyzer should offer realistic mass transfer coefficients for design purposes. AM-Fion C-103 cation-exchange membranes separated solutions of 0.01 M $\text{UO}_2(\text{NO}_3)_2$ and 2 M HNO_3 . The solution compartments between the membranes were formed with 0.38-mm-thick woven screens of stainless steel. Uranyl ion fluxes were about $9 \times 10^{-10} \text{ mol cm}^{-2} \text{ s}^{-1}$. The treatment rate was about $3 \text{ L h}^{-1} \text{ m}^{-2}$, and 96% of the $\text{UO}_2(\text{NO}_3)_2$ was recovered.

Apparatus

The equipment used for Donnan dialysis is similar to that used for dialysis and diffusion dialysis. Membrane shapes include sheets, tubes, and hollow fibres. Sheet membranes have been fabricated into spiral-wound devices, but the dominant configuration for flat membranes is the plate-and-frame arrangement used in electrodialysis. Thus any supplier of electrodialysis equipment is a potential supplier of stacks for Donnan dialysis. Since the major resistance to transport usually lies in the boundary layer of the

dilute solution, equipment designers strive to achieve high shear in the feed solution. There is a major advantage to countercurrent flow of the feed and stripper solutions, because that configuration leads to maximum driving forces and maximum total transfer of the desired ions.

In a commercial dialyser, the simultaneous achievement of both high shear and countercurrent flow is difficult. High shear can be achieved by rapid stirring or by high flow rates, but the benefits of countercurrent flow can only be achieved if the residence time in the device is sufficient for a large fraction of the desired ion to be transferred through the membrane. As discussed below, studies of the effects of solution velocity on mass transfer rates show correlation with V^n where the exponent n is always less than unity. This means that increasing the solution velocity through a dialyser of a given length always results in a smaller fraction of the solute being transferred through the membrane. Therefore, an increase in solution velocity requires an increase in path length to achieve the same fraction of transfer. (This V^n relationship also applies to dialysis, diffusion dialysis, and electrodialysis.)

Process Design and Control

Most often the objective of Donnan dialysis is to both recover a target ionic species from a feed solution and raise its concentration. An increase in the concentration is achieved by the use of a small volume of a stripper solution with a diffusing ionic species that is higher in concentration than that of the target ionic species in the feed. A strip solution of about 1 M might be used with a typical 0.001 M feed solution. One might expect that a more concentrated strip solution would recover the target ionic species at a higher concentration, but stripper concentrations higher than 1 M do not seem to be beneficial. More concentrated strip solutions lead to osmotic dehydration of the gel structure of the membrane which reduces membrane permeability. Moreover, co-ion transport due to reduced Donnan exclusion at the higher concentrations allows loss of solutes from the receiving solution across the membrane, and osmotic transport of water through the membrane dilutes the strip solution.

The effects of hydrodynamics on mass transfer rates in Donnan dialysis have been studied by several researchers who correlated the data using the standard equation $\text{Sh} = k\text{Sc}^m\text{Re}^n$. The Sherwood number $\text{Sh} = KD/h$, Schmidt number $\text{Sc} = \mu/\rho D$, and Reynolds number $\text{Re} = \rho hV/\mu$ are dimensionless parameters where K is the mass transfer coefficient, D is the diffusivity of the diffusing ionic species, h is

Table 1 Dimensionless parameters for correlation of mass transfer rates in Donnan dialysis through Nafion®

Cation	Strip acid	<i>k</i>	<i>m</i>	<i>n</i>
Cu ²⁺	H ₂ SO ₄	0.48	0.33	0.28
Ni ²⁺	H ₂ SO ₄	0.166	0.33	0.475
Na ⁺ , K ⁺	HNO ₃	0.201	0.4	0.62

the characteristic thickness or diameter of the conduit, μ is the solution viscosity, ρ is specific gravity, and V is solution velocity. The coefficient k , and the exponents m and n are used to correlate the data. The results of three studies are shown in **Table 1**, and some comments about the experiments follow.

Studies with CuSO₄ and NiSO₄ were done with the feed flowing inside a fluoropolymer membrane tube a few millimetres in diameter and with H₂SO₄ stripper flowing outside the tube. The correlation parameters apply to $Re < 1000$. The following observations were made in the studies with CuSO₄ and NiSO₄. Increasing the stripper concentration from 1 to 5 M did not improve mass transfer. Increasing the solution velocity of the stripper solution produced minor increases in mass transfer. The mass transfer rate was proportional to the metal ion concentration in the feed for concentrations below 2000 mg L⁻¹ and $Re < 1000$. Studies of NaNO₃ and KNO₃ feeds with HNO₃ stripping were done with a flat sheet fluoropolymer membrane in a stirred cell with $15 > Re > 400$.

Since the flow rates in Donnan dialysis are normally rather low, one must be concerned with convective flow in the dialyser caused by density changes in the solutions as their compositions change. The use of excessively high acid concentrations in the stripper exacerbates the problem of changing densities. Osmotic transport of water into the acid stripper solution at the top of the solution compartment can cause substantial dilution of the acid, and the resulting density decrease allows the denser incoming stripper to stream downward through the diluted acid. The problem can be alleviated by mild pulsation of the solution at the top of the stripper side to improve mixing.

Applications

Although many industrial applications have been demonstrated in the laboratory and at the pilot scale, there appear to have been few industrial-scale applications of Donnan dialysis. Industrial applications have been mainly in recovering heavy metals from rinse waters of metal-finishing operations. One of the few descriptions of an industrial installation reports results of an experimental evaluation of a DuPont-made Nafion® hollow-fibre dialyser for metal recov-

ery from rinse water in a Watts nickel electroplating process with 1 M H₂SO₄ as the stripper. With typical feed concentrations of up to 1 g L⁻¹, Ni²⁺ fluxes exceeded 20 g h⁻¹ m⁻² and the recovered Ni concentration exceeded 30 g L⁻¹.

An early application of Donnan dialysis with polymeric ion-exchange membranes was described in 1967. Multiple AMFion C-103C cation-exchange membranes were assembled in a plate-and-frame dialyser with solution compartments arranged so that the feed and strip streams could flow in a pattern that was countercurrent overall. This apparatus was used to recover UO₂(NO₃)₂ from a 0.01 M feed to a final concentration of 0.28 M with 2 M HNO₃ as the stripper and to 0.46 M with 2 M H₂SO₄ as the stripper. He also used a Donnan dialyser with AMFion A-104B anion-exchange membranes to remove acid from the UO₂(NO₃)₂ feed to improve the driving force for cation transport. Complexing agents, EDTA and DPTA, were used as strippers to separate Ag⁺ and Cu²⁺ ions. The Cu²⁺ ions formed such strong complexes that the free Cu²⁺ ion concentration in the stripper was low enough to maintain a driving force until virtually all of the Cu²⁺ ions were transported across the membrane.

The use of Donnan dialysis for water softening was reported in 1970. The process is illustrated in **Figure 3**. A brine of NaCl and hard feed water flow countercurrent. The diffusion of Na⁺ ions from the

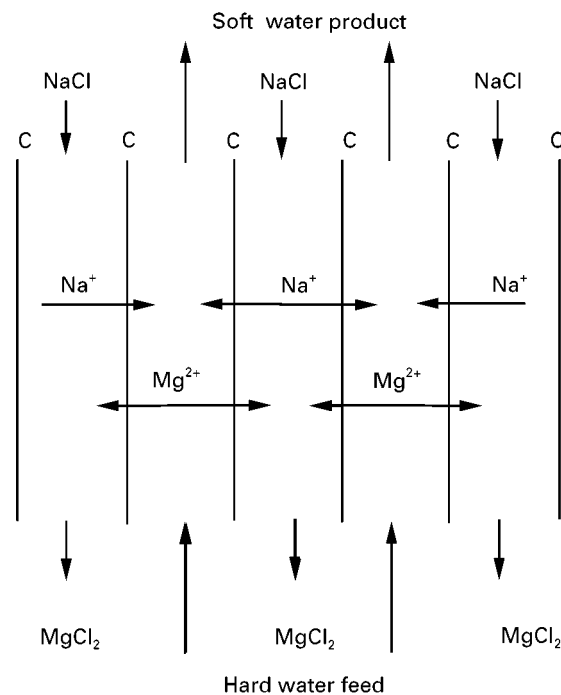


Figure 3 Donnan dialysis removes Mg²⁺ ions from hard water. C = cation.

brine causes a driving force for transport of Mg^{2+} ions from the feed into the brine. Countercurrent operation allows the large driving force to be maintained over the length of the membrane.

A hollow-fibre device has been used as a suppressor for ion chromatography. Compared to an ion-exchange column that is normally used to suppress conductance in the eluant, Donnan dialysis allowed more control over the conductivity and eliminated the need to regenerate the resins. Moreover, the resolution was improved by the use of Donnan dialysis.

The use of neutralization dialysis for desalination of cheese whey has been described.

Conclusion

Donnan dialysis can be used in many applications where ion-exchange beads are currently applied. The process might find a niche in water softening in a capacity range between that of home water softeners and the large-scale lime-soda softeners. Capital costs are higher for membranes than for resin beads, but the use of membranes offers the advantages of steady-state operation without the need for rinse-down, which produces large volumes of water that must be discarded. The capital cost of small-scale Donnan dialysis could be reduced by the availability of more ion-exchange membranes in hollow-fibre form that could be assembled into compact modules.

Further Reading

Bleha M and Tishchenko GA (1992) Neutralization dialysis for desalination. *Journal of Membrane Science* 73: 305–311.

Davis TA, Wu JS and Baker BL (1971) Use of the Donnan equilibrium principle to concentrate uranyl ions by an ion-exchange membrane process. *AIChE Journal* 17(4): 1006–1008.

Donnan FG (1924) The theory of membrane equilibria. *Chemical Reviews* 1(1): 73–90.

Grot WG (1986) *Ion Exchange Process and Apparatus*. U.S. Patent 4,591,439.

Ng PK and Snyder DD (1981) Mass transport characteristics of Donnan dialysis: the nickel sulfate system. *Journal of the Electrochemical Society* 128(8): 1714–1719.

Ng PK and Snyder DD (1983) Uranyl nitrate and nitric acid. Combined electrodialysis and dialysis for regeneration of chromic acid etching solution. *Journal of Membrane Science* 13: 327–336.

Nonaka T, Ogawa H, Morikawa M and Egawa H (1992) Uphill and selective transport of uranyl ions through 2,3-epithiopropyl methacrylate-2-acrylamide-2-methyl propanesulfonic acid copolymer membranes. *Journal of Applied Polymer Science* 45: 285–292.

Nonaka T and Fujita K (1998) Transport of ferric ions through 2,3-epithiopropyl methacrylate-dodecyl methacrylate-methylacrylamide propyltrimethylammonium chloride terpolymer membranes. *Journal of Membrane Science* 144: 187–195.

Roach ET (1985) *Evaluation of Donnan Dialysis for Treatment of Nickel Plating Rinse Water*. Final Report to U.S. Environmental Protection Agency, NTIS PB85-200046.

Stevens TS and Davis JC (1981) Hollow fiber ion-exchange suppressor for ion chromatography. *Analytical Chemistry* 53: 1488–1492.

Wallace RM (1967) Concentration and separation of ions by Donnan membrane equilibrium. *Industrial and Engineering Chemistry, Process Design and Development* 6(4): 423–431.

Electrodialysis

H. Strathmann, University of Twente, The Netherlands

Copyright © 2000 Academic Press

Electrodialysis is a process in which ion exchange membranes in combination with an electrical potential difference are used to remove ionic species from an aqueous solution. The large scale industrial utilization of the process began about 30 years ago with the development of highly selective ion exchange membranes of low electric resistance arranged in a multicell stack.

Until the mid 1970s electrodialysis stacks were operated in a unidirectional mode, that is, the polar-

ity of the electrodes was fixed. A significant step towards the efficient application of electrodialysis was the introduction of a new mode of operation referred to as electrodialysis reversal. In this operating mode the flow streams and the polarity in an electrodialysis stack are periodically reversed, which reduces membrane fouling and scaling. Costly and time-consuming membrane cleaning procedures are then unnecessary.

The main application of electrodialysis is the desalination of brackish water for domestic and industrial use. In Japan electrodialysis is also used on a large scale to concentrate sodium chloride from sea water for the production of table salt. More recently

brine causes a driving force for transport of Mg^{2+} ions from the feed into the brine. Countercurrent operation allows the large driving force to be maintained over the length of the membrane.

A hollow-fibre device has been used as a suppressor for ion chromatography. Compared to an ion-exchange column that is normally used to suppress conductance in the eluant, Donnan dialysis allowed more control over the conductivity and eliminated the need to regenerate the resins. Moreover, the resolution was improved by the use of Donnan dialysis.

The use of neutralization dialysis for desalination of cheese whey has been described.

Conclusion

Donnan dialysis can be used in many applications where ion-exchange beads are currently applied. The process might find a niche in water softening in a capacity range between that of home water softeners and the large-scale lime-soda softeners. Capital costs are higher for membranes than for resin beads, but the use of membranes offers the advantages of steady-state operation without the need for rinse-down, which produces large volumes of water that must be discarded. The capital cost of small-scale Donnan dialysis could be reduced by the availability of more ion-exchange membranes in hollow-fibre form that could be assembled into compact modules.

Further Reading

Bleha M and Tishchenko GA (1992) Neutralization dialysis for desalination. *Journal of Membrane Science* 73: 305–311.

Davis TA, Wu JS and Baker BL (1971) Use of the Donnan equilibrium principle to concentrate uranyl ions by an ion-exchange membrane process. *AIChE Journal* 17(4): 1006–1008.

Donnan FG (1924) The theory of membrane equilibria. *Chemical Reviews* 1(1): 73–90.

Grot WG (1986) *Ion Exchange Process and Apparatus*. U.S. Patent 4,591,439.

Ng PK and Snyder DD (1981) Mass transport characteristics of Donnan dialysis: the nickel sulfate system. *Journal of the Electrochemical Society* 128(8): 1714–1719.

Ng PK and Snyder DD (1983) Uranyl nitrate and nitric acid. Combined electrodialysis and dialysis for regeneration of chromic acid etching solution. *Journal of Membrane Science* 13: 327–336.

Nonaka T, Ogawa H, Morikawa M and Egawa H (1992) Uphill and selective transport of uranyl ions through 2,3-epithiopropyl methacrylate-2-acrylamide-2-methyl propanesulfonic acid copolymer membranes. *Journal of Applied Polymer Science* 45: 285–292.

Nonaka T and Fujita K (1998) Transport of ferric ions through 2,3-epithiopropyl methacrylate-dodecyl methacrylate-methylacrylamide propyltrimethylammonium chloride terpolymer membranes. *Journal of Membrane Science* 144: 187–195.

Roach ET (1985) *Evaluation of Donnan Dialysis for Treatment of Nickel Plating Rinse Water*. Final Report to U.S. Environmental Protection Agency, NTIS PB85-200046.

Stevens TS and Davis JC (1981) Hollow fiber ion-exchange suppressor for ion chromatography. *Analytical Chemistry* 53: 1488–1492.

Wallace RM (1967) Concentration and separation of ions by Donnan membrane equilibrium. *Industrial and Engineering Chemistry, Process Design and Development* 6(4): 423–431.

Electrodialysis

H. Strathmann, University of Twente, The Netherlands

Copyright © 2000 Academic Press

Electrodialysis is a process in which ion exchange membranes in combination with an electrical potential difference are used to remove ionic species from an aqueous solution. The large scale industrial utilization of the process began about 30 years ago with the development of highly selective ion exchange membranes of low electric resistance arranged in a multicell stack.

Until the mid 1970s electrodialysis stacks were operated in a unidirectional mode, that is, the polar-

ity of the electrodes was fixed. A significant step towards the efficient application of electrodialysis was the introduction of a new mode of operation referred to as electrodialysis reversal. In this operating mode the flow streams and the polarity in an electrodialysis stack are periodically reversed, which reduces membrane fouling and scaling. Costly and time-consuming membrane cleaning procedures are then unnecessary.

The main application of electrodialysis is the desalination of brackish water for domestic and industrial use. In Japan electrodialysis is also used on a large scale to concentrate sodium chloride from sea water for the production of table salt. More recently

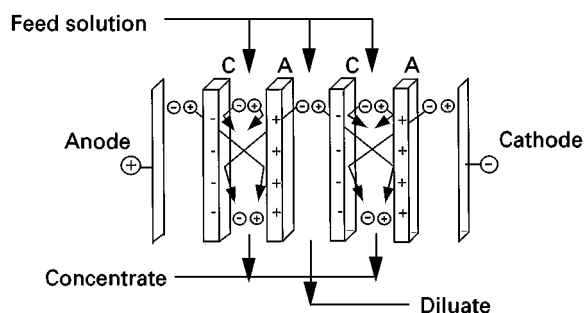


Figure 1 Schematic diagram illustrating the principle of electrodialysis.

utilization of electrodialysis in the food and chemical industry and to treat certain industrial effluent streams has become important.

The Principle of Electrodialysis

The principle of electrodialysis is illustrated in **Figure 1**. A typical electrodialysis cell arrangement consists of a series of anion and cation exchange membranes arranged in an alternating pattern between an anode and a cathode to form individual cells. If an electrolyte solution is passed through these cells and an electrical potential is established between the electrodes, the positively charged cations migrate towards the cathode and the negatively charged anions towards the anode. The positively charged cations can easily permeate the negatively charged cation exchange membrane but are retained by the positively charged anion exchange membrane. Likewise, negatively charged anions permeate the anion exchange membrane but are retained by the cation exchange membrane. The overall result is an increase in the ion concentration in alternate compartments, while the other compartments simultaneously become depleted. The depleted solution is referred to as diluate and the concentrated solution as brine or concentrate. The driving force for the ion transport in the electrodialysis process is the applied electrical potential. The total space occupied by the diluate and the concentrated solutions and the contiguous anion and cation exchange membranes make up a cell pair. The cell pair is the repeating unit in an electrodialysis stack.

The Ion Exchange Membranes

Ion exchange membranes are the key components in electrodialysis. They consist of highly swollen gel-type polymer structures carrying fixed positive or negative charges. Polymer structures carrying negatively charged groups are referred to as cation

exchange membranes, while those carrying positively charged groups are referred to as anion exchange membranes.

In a cation exchange membrane, the fixed negative charges are in electrical equilibrium with mobile cations in the interstices of the polymer. **Figure 2** shows a cation exchange membrane with fixed anions and mobile cations; the latter are referred to as counter ions. The mobile anions, called co-ions, are more or less completely excluded from the polymer matrix because their electrical charge is identical to that of the fixed ions. Because of the exclusion of the co-ions, cation exchange membranes are preferentially permeable for cations. Anion exchange membranes which carry positive fixed charges and exclude cations are preferentially permeable to anions. The extent to which co-ions are excluded from an ion exchange membrane depends on the membrane as well as on the solution properties.

The most desirable properties for ion exchange membranes are:

- High permselectivity – the membrane should be permeable to counter-ions only
- Low electrical resistance – the membrane should have high counter ion permeability
- Good mechanical and form stability – the membrane should be mechanically strong and should have a low degree of swelling in diluate solutions
- High chemical stability – the membrane should be stable over the entire pH range and in the presence of oxidizing agents and organic solvents.

The properties of ion exchange membranes are determined by the base polymer and the type and concentration of the fixed charges. The base polymer determines the mechanical, chemical and thermal

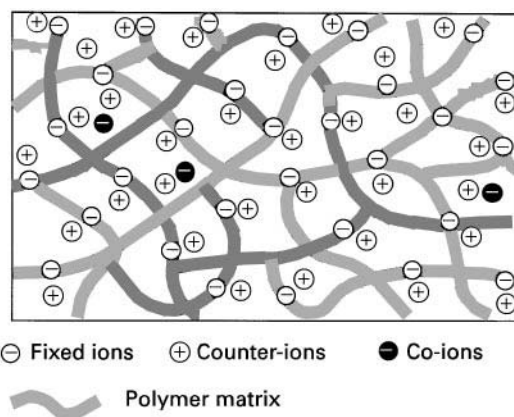


Figure 2 Schematic drawing illustrating the structure of a cation exchange membrane.

stability of the membrane. The type and concentration of the fixed ions determine the permselectivity and the electrical resistance. The moieties often used as fixed charges are $-\text{SO}_3^-$ and $-\text{COO}^-$ groups in cation exchange membranes and $-\text{R}_3\text{N}^+$ and $-\text{R}_2\text{NH}^+$ groups in anion exchange membranes. The sulfonic acid group $-\text{SO}_3^-$ is completely dissociated over the entire pH range, while the carboxylic acid group $-\text{COO}^-$ is virtually undissociated in the pH range < 3 . The quaternary ammonium group $-\text{R}_3\text{N}^+$ again is completely dissociated over the entire pH range, while the tertiary ammonium group $-\text{R}_2\text{NH}^+$ is only weakly dissociated. Accordingly, ion exchange membranes are referred to as weakly or strongly acidic or basic in character depending on the charged groups they contain.

Mass Transfer in Electrodialysis

Mass transfer in electrolyte solutions is determined by the driving forces acting on the individual ions of the solution and by the friction of the ions with other components in the solution. The driving forces can be expressed by gradients in the electrochemical potential of individual components. The friction that has to be overcome by the driving force can be expressed by the ion mobility or diffusivity.

To describe the mass transport in a system, thermodynamic and kinetic parameters must be mathematically related. Several relations are described in the literature. The one most frequently used is the Nernst-Planck equation which describes transport of ions under isobaric and isothermal conditions in an ion exchange membrane as follows:

$$J_i = m_i C_i \frac{d\eta_i}{dz} = m_i C_i \left(z_i F \frac{d\varphi}{dz} + \frac{d\mu_i}{dz} \right) \\ = m_i C_i \left(z_i F \frac{d\varphi}{dz} + RT \frac{d \ln a_i}{dz} \right) \quad [1]$$

For the definition of symbols in this and all other equations, see Table 1. J_i is the flux in the direction perpendicular to the membrane surface and z refers to the number of charges carried by an ion and indicates whether these charges are positive or negative.

A boundary condition for describing the mass transport in electrolyte solutions is the electroneutrality requirement which postulates that on a macroscopic scale there is no excess in positive or negative charges. Thus:

$$\sum_i z_i C_i = 0 \quad (i = 1, 2, 3 \dots n) \quad [2]$$

The concentration of individual ions is related to that of the salt by the stoichiometric coefficient ν which determines into how many ions a salt will dissociate in the solution. Thus:

$$C_i = \nu_i C_s \quad [3]$$

Another assumption in electrodialysis is that electrical charges are transported exclusively by ions. Thus:

$$I = \sum_i z_i F J_i \quad [4]$$

Here J_i is the flux of the individual ions and I is the total electrical current.

Transport and Transference Numbers

The transport number T_i and the transference number t_i of an ion i are given by:

$$T_i = \frac{z_i J_i}{\sum_i z_i J_i} \quad \text{and} \quad t_i = \frac{T_i}{z_i} = \frac{J_i}{\sum_i z_i J_i} \quad [5]$$

Here T_i indicates the fraction of the total current carried by the ion i , and t_i determines the number of moles of the ion i transported per mole of electrons, i.e. per Faraday.

The transference number is directly related to the ion concentration and their mobility and its sum is 1. Thus:

$$t_i = \frac{C_i m_i}{\sum_i z_i C_i m_i} \quad \text{and} \quad \sum_i t_i = 1 \quad [6]$$

The transference numbers of different salt ions in solution are not very different. In an ion exchange membrane, however, there are the fixed ions of the membrane in addition to the mobile ions of the electrolyte. The fixed ions do not contribute to the transport of electrical charges. Their transference number is therefore 0. Furthermore, the concentration of the counterions is much lower than that of the co-ions. Their concentration in the membrane determines the permselectivity of a membrane.

Membrane Permselectivity

The permselectivity of cation and anion exchange membranes is defined by:

$$\psi^{\text{mc}} = \frac{t_c^{\text{mc}} - t_c}{t_a} \quad \text{and} \quad \psi^{\text{ma}} = \frac{t_a^{\text{ma}} - t_a}{t_c} \quad [7]$$

Table 1 Definition of symbols used in mathematical equations

Symbol	Definition
η	Electrochemical potential
μ	Chemical potential
φ	Electrical potential
ν	Stoichiometric coefficient which determines into how many ions a salt will dissociate in the solution
ψ	Permselectivity of a membrane
ξ	Current utilization
Δ	Thickness of a cell
ρ	Resistance of ion exchange membranes
$\Delta\varphi$	Potential difference between solutions separated by a membrane assuming electrochemical equilibrium
ΔC	Difference in salinity of feed and product water
φ_{Don}	Donnan potential
ΔG	Energy required for production of the dilute
γ_{\pm}^m	Average activity coefficients of salt in the membrane
Δn_s	Amount of salt in moles transferred from a feed to a concentrate solution
Δp	Hydrodynamic pressure loss through the stack
Λ_s	Equivalent conductivity
γ_{\pm}^s	Average activity coefficients of salt in the electrolyte solution
Δz	Thickness of the boundary layer
a	Activity
A	Effective area
A_{min}	Minimum membrane area required for a certain plant capacity
ΔC	Concentration differences between feed and diluate
C_{co}^m	Co-ion concentration in the membrane
C_i^m	Concentration fixed ions in the membrane
C_{co}^s	Co-ion concentration in the electrolyte solution
D	Diffusion coefficient
dz	Directional coordinate perpendicular to the membrane surface
E_{des}	Energy required for desalination
E_p	Pumping energy
F	Faraday constant
I	Total electrical current
i	Current density
i_{lim}	Limiting current density
J_i	Flux of component i (individual ions)
k	Constant referring to efficiency of pumps
m	Mobility of ions in the membrane
n	Number of cell pairs in a stack
Q	Volumetric flow of the product
R	Gas constant
R	Electric resistance
T	Temperature
t	Transference number
t	Time
T_i	Transport number of component i (ions)
u	Linear flow velocity of solution in electrodialysis cells
U	Voltage drop across the electrodialysis stack
V	Volume
z	Electrochemical valence

Superscripts

' and ''	Two phases separated by the membrane
b	Boundary layer
ba	Concentrate bulk solution
bc	Concentrate bulk solution

Table 1 Continued

Symbol	Definition
bd	Diluate solution in the bulk
diff	Ion diffusion
l	Current leakage through the manifold
m	Membrane
ma	Anion membrane
mc	Cation membrane
md	Diluate solution at the membrane surface
mig	Ion migration
ms	Membrane selectivity
o	Feed
p	Product solution
s	Solution
sc	Concentrate solution
sd	Diluate concentration
se	Electrode rinse solution
sf	Feed solution
sp	Product solution
w	Water transport through the membranes

Subscripts

a	Anion
c	Cation
cou	Counterion
i	Ion
s	Salt
w	Water

The permselectivity of an ion exchange membrane relates the transport of electric charges by counterions to the total transport of electric charges through the membrane. An ideal permselective cation exchange membrane would transmit positively charged ions only, i.e. for $t_c^{\text{mc}} = 1$, $\psi^{\text{mc}} = 1$. The permselectivity approaches zero when the transference number within the membrane is identical to that in the electrolyte solution. For the anion exchange membrane the corresponding relationship holds.

Diffusion Potential, Donnan Equilibrium and Ion Exclusion

The diffusion potential can be derived by integration of eqn [1] and is given for a monovalent electrolyte when the ion activity is expressed by the salt concentration by:

$$\Delta\varphi = \varphi' - \varphi'' = \frac{RT}{F} \left(\frac{m_a - m_c}{m_a + m_c} \right) \ln \frac{C_s'}{C_s''} \quad [8]$$

An electrical potential difference is not only established between two solutions of different concentrations separated by a membrane but also between a membrane and the adjacent electrolyte solution if the ion concentration in the membrane is different from that in the adjacent solution,

which is generally the case with ion exchange membranes. This potential difference is referred to as the Donnan potential.

The Donnan potential cannot be measured directly. It can, however, be calculated from the electrochemical equilibrium of ions between the membrane and the adjacent solution. By introducing the proper relations for the electrochemical potential, the Donnan potential – the electrical potential difference between an ion exchange membrane and a solution of a monovalent salt – can be calculated to a first approximation by:

$$\Delta\phi_{\text{Don}} = \phi^m - \phi^s = \frac{RT}{F} \ln \frac{a_i^m}{a_i^s} \quad [9]$$

The numerical value of $\Delta\phi_{\text{Don}}$ is negative for the cation exchange membrane and positive for the anion exchange membrane in equilibrium with a dilute electrolyte solution.

The Donnan potential is also the basis for calculating the Donnan exclusion, which determines the co-ion concentration in a membrane. For a monovalent electrolyte, i.e. $z_i = 1$, and assuming a high fixed ion concentration in the membrane compared to the electrolyte concentration, the co-ion concentration in the membrane is given to a first approximation by:

$$C_{\text{co}}^m = \frac{C_{\text{co}}^s}{C_{\text{f}}^m} \left(\frac{\gamma_{\pm}^s}{\gamma_{\pm}^m} \right)^2 \quad [10]$$

Energy Requirements in Electrodialysis

The energy required in an electrodialysis process is the sum of two terms: firstly, the electrical energy needed to transfer the ionic components from a feed solution through the membranes into the concentrate solution, and secondly, the energy required to pump the solutions through the electrodialysis unit. Energy consumption due to electrode reactions can generally be neglected because of the large number of cell pairs usually stacked between the two electrodes.

Minimum Energy Required for Transfer of Ions from a Feed to a Concentrate Solution

In electrodialysis the minimum energy required for the transport of salt from a feed to a concentrate solution can be expressed by the Gibbs free energy of mixing. Taking into account the electrolyte concentrations in the feed, diluate and concentrate, the minimum desalting energy is given by:

imum desalting energy is given by:

$$\Delta G = zRT\Delta n_s \left[\frac{\ln \frac{C_s^{\text{sf}}}{C_s^{\text{sc}}}}{\frac{C_s^{\text{sf}}}{C_s^{\text{sc}}} - 1} - \frac{\ln \frac{C_s^{\text{sf}}}{C_s^{\text{sd}}}}{\frac{C_s^{\text{sf}}}{C_s^{\text{sd}}} - 1} \right] \quad [11]$$

Practical Energy Requirements in Electrodialysis

As discussed previously, the minimum energy required for desalting a given feed solution refers to a reversible process. In electrodialysis there are also irreversible energy losses and the total electric energy required for the transfer of ions from a feed solution to a concentrate, i.e. the actual energy used for desalination is much larger than the theoretical minimum value. This is given by:

$$E_{\text{des}} = UIt = RI^2t \quad [12]$$

The electric current required for the desalination of a feed solution is directly proportional to the concentration difference between the feed and the diluate solution. It is given by:

$$I = \frac{V^p |z_a| |z_c| \nu_s F (C_s^{\text{sf}} - C_s^{\text{sp}})}{\xi t} \quad [13]$$

The current utilization is the fraction of the total current passing through the electrodialysis stack that is used for the transfer of ions. It will be discussed in more detail later.

The electrical resistance of an electrodialysis stack is determined by the resistances of the membrane and diluate and concentrate solutions and is given to a first approximation by:

$$R = \frac{U}{I} = \frac{n}{A} \left[\frac{2\Delta}{\Lambda_s} \left(\frac{1}{C_s^{\text{sd}}} + \frac{1}{C_s^{\text{sc}}} \right) + \rho^{\text{ma}} + \rho^{\text{mc}} \right] \quad [14]$$

The electrical resistance of the solutions is inversely proportional to their salt concentrations, which are changing while passing through the stack from the feed to the product concentration. The concentration in the diluate cell is decreasing and that in the concentrate cell increasing. An electrical resistance of a stack can thus be calculated as a function of the cell thickness, i.e. the distance between two membranes. Generally, the resistances of the ion exchange membranes and the average resistance of the concentrate solution are much lower than the average resistance of the diluate and can therefore be neglected.

The electrical resistance of a stack can be calculated to a first approximation from the integral

average of the diluate concentration and is given by:

$$R = \frac{n}{A} \left[\frac{\Delta \ln \frac{C_s^{\text{sf}}}{C_s^{\text{sp}}}}{\Lambda_s(C_s^{\text{sf}} - C_s^{\text{sp}})} \right] \quad [15]$$

The superscripts sf and sp refer to the feed and the diluate at the cell outlet, which is the required product.

A combination of eqns [13] and [15] gives the energy required to remove a certain amount of salt from a feed solution. For the desalination of a monovalent salt, i.e. where z_a , z_c and ν_s are all unity, the electrical energy is given by:

$$E_{\text{des}} = \frac{n}{A} \frac{V^{\text{p}^2} F^2 (C_s^{\text{sf}} - C_s^{\text{sp}})}{\xi} \left[\frac{\Delta \ln \frac{C_s^{\text{sf}}}{C_s^{\text{sp}}}}{\Lambda_s} \right] \quad [16]$$

For a given plant capacity, salt solution and cell design, the equivalent conductivity and the number and area of cells are constant. Thus, the energy required for the desalination of a monovalent salt solution can be expressed to a first approximation by the constant factor k , by the current utilization and by the feed and the product concentration.

$$E_{\text{des}} = \frac{k}{\xi} (C_s^{\text{sf}} - C_s^{\text{sp}}) \log \frac{C_s^{\text{sf}}}{C_s^{\text{sp}}} \quad [17]$$

Pumping Energy Requirements

The operation of an electrodialysis unit requires one or more pumps to circulate the diluate, the concentrate and the electrode rinse solution through the stack. The energy required for pumping these solutions is determined by the volumes to be circulated and the pressure drop. It can be expressed by:

$$E_p = k(V\Delta p^{\text{sd}} + V^{\text{sc}}\Delta p^{\text{sc}} + V^{\text{se}}\Delta p^{\text{se}}) \quad [18]$$

Processes Affecting the Efficiency of Electrodialysis

In practical application electrodialysis is effected by concentration polarization and by incomplete current utilization. Both phenomena influence the efficiency of the process.

Current Utilization

Current utilization in an electrodialysis stack is impaired by incomplete membrane selectivity, parallel

current through the stack manifold and water transfer across the membranes due to osmosis and electroosmosis.

The ratio of the actual current needed for salt transport from a feed to a concentrate stream to that calculated theoretically is referred to as the current efficiency, which for one cell pair is given by:

$$\eta = \eta^{\text{ms}} \eta^{\text{w}} \eta^{\text{l}} \quad [19]$$

The efficiency term η^{ms} is a function of the membrane permselectivities. η^{w} is caused by convective flow due to the hydrostatic pressure difference between the diluate and concentrate cells, by transfer of water in the hydration shell of ions and by osmosis. η^{l} is determined by parallel current through the stack manifold.

The overall current utilization ξ can be defined as a function of the number of cell pairs, membrane selectivity, water transfer and manifold current flow. It is given by:

$$\xi = n(\psi^{\text{mc}} t_a + \psi^{\text{ma}} t_c) (1 - [t_w^{\text{mc}} + t_w^{\text{ma}}]) \times 0.018 (C_s^{\text{sc}} - C_s^{\text{sd}}) \eta^{\text{l}} \quad [20]$$

For relatively dilute solutions, $C_s < 0.1 \text{ mol L}^{-1}$, the efficiency loss due to water transfer is quite low. However, for higher feed solution salt concentrations the water transfer may affect the efficiency of electrodialysis quite significantly.

The current leakage through the manifold system can, in a well-designed stack, be neglected, i.e. $\eta^{\text{l}} \approx 1$.

Concentration Polarization and Limiting Current Density

Concentration polarization occurs in all mass separation processes and is the result of changes in mass transport properties at an interface. In electrodialysis, separation of ions is the result of differences in their transport numbers in solution and in the membranes. At the surface of an ion exchange membrane facing the diluate the concentration of counterions is reduced and at the surface facing the concentrate the concentration of counterions is increased because of the lower transport number of the counterions in the solution than that in the membrane. Because of the electroneutrality requirement, the co-ions in the boundary layers are transported in the opposite direction. Thus, salt concentration gradients are established in the boundary layers at membrane surfaces, which leads to an additional mass transport towards the membrane surface in the diluate and away from it in the concentrate solution. Due to turbulent mixing

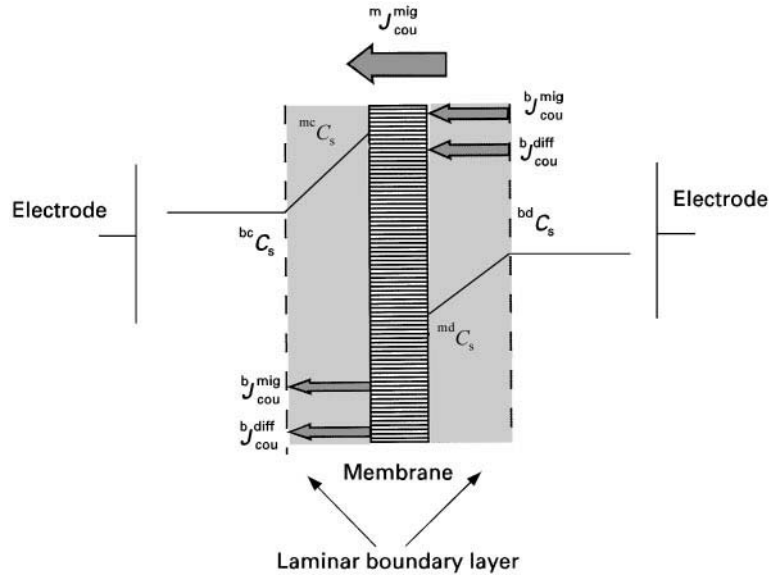


Figure 3 Schematic drawing illustrating concentration profiles of a salt in the boundary layer on both sides of an ion exchange membrane and the fluxes of cations and anions in the boundary layer and the membrane surface. For abbreviations, see Table 1.

of the bulk solutions, the concentration gradients are limited to a relatively thin laminar boundary layer at the membrane surfaces, as indicated in **Figure 3**, which shows the salt concentration profiles in the solutions near the surface of an anion exchange membrane.

The concentration profiles at the membrane surface can be determined by a mass balance based on the so-called Nernst film model, which assumes static boundary layers at the membrane surfaces, where concentration and electrical potential gradients perpendicular to the membrane surfaces are the only driving forces for the mass transport. The bulk solution between the laminar boundary layer is well mixed and has a uniform concentration. It can be assumed that the transport of ions through an ion exchange membrane is the result of migration caused only by an electrical potential gradient, while in the solution ions are transported by both migration and diffusion. In a steady state the ion flux through the membrane is identical to that through the boundary layer. For a strictly permselective membrane it is given by:

$${}^m J_{\text{cou}}^{\text{mig}} = - {}^b J_{\text{cou}}^{\text{mig}} + {}^b J_{\text{cou}}^{\text{diff}} = t_{\text{cou}}^m \frac{i}{F} = t_{\text{cou}}^b \frac{i}{F} - D_s \frac{dC_s}{dz} \quad [21]$$

The current density can be obtained from eqn [21] by integration over the boundary layer. For the boundary layer at the membrane surfaces adjacent to the diluate the current density is:

$$i = - \frac{FD_s}{(t_{\text{cou}}^m - t_{\text{cou}}^b)} \frac{{}^b dC_s - {}^m dC_s}{\Delta z} \quad [22]$$

When the hydrodynamic flow conditions are kept constant the boundary layer thickness, Δz , will be constant and the current will reach a maximum value independent of the electrical potential gradient if the salt concentration at the membrane surface, ${}^m dC_s$, becomes 0. This maximum current is referred to as the limiting current density, i_{lim} , which is given by:

$$i_{\text{lim}} = - \frac{FD_s}{(t_{\text{cou}}^m - t_{\text{cou}}^b)} \frac{{}^b dC_s}{\Delta z} \quad [23]$$

Exceeding the limiting current density in practical applications of electrodialysis can affect the efficiency of the process severely by increasing the electrical resistance of the solution and by causing water splitting, which leads to changes in the pH values of the solutions, causing precipitation of metal hydroxides on the membrane surface.

Electrodialysis Process and Equipment Design

The performance of electrodialysis in practical applications is not only a function of membrane properties but is also determined by the membrane stack and the overall process design.

Electrodialysis Stack Design

Two different stack designs are used in large scale applications today. One is the so-called sheet flow and the other is the tortuous path flow design. A typical sheet flow electrodialysis stack is shown in

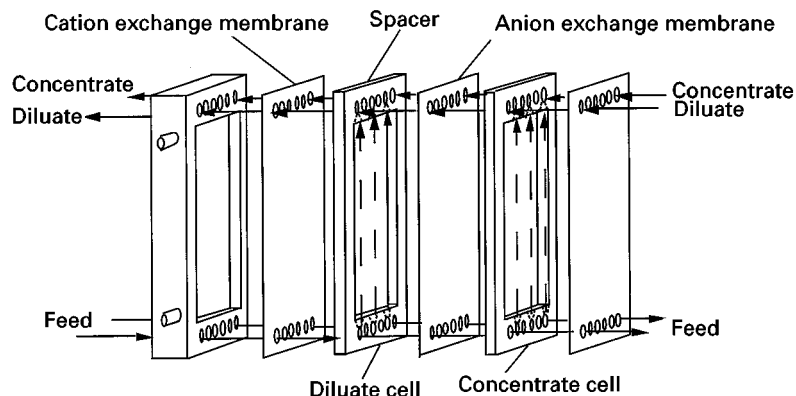


Figure 4 Exploded view of an electrodialysis stack arrangement, indicating the individual cells and the sheet flow-type spacer, also containing the manifolds for distribution of different flow streams.

Figure 4. The membranes are stacked between electrodes in such a way that the flow streams are kept separate. The gaskets that separate the membranes contain manifolds to distribute the process fluids to the different compartments. The supply ducts for the diluate and the concentrate are formed by matching holes in the gaskets, in the membranes, and in the electrode cells. To minimize the resistance of the aqueous solution, the distance between the membrane sheets is made as small as possible and is normally between 0.5 and 2 mm in industrial electrodialysis stacks. In an industrial electrodialysis system, 200–1000 cation and anion exchange membranes are installed in parallel to form an electrodialysis stack with 100–500 cell pairs. Spacers between the individual membrane sheets support the membranes and provide mixing of the flow streams.

A proper electrodialysis stack design provides the maximum effective membrane area per unit stack volume and ensures uniform flow distribution

through each compartment. The spacer screen should provide a maximum of mixing of the solutions at the membrane surfaces to reduce concentration polarization, but the pressure loss must be small.

Process Design and Modes of Operation

The efficiency of electrodialysis in a given application depends greatly on the process, design and mode of operation. Two different operating modes are currently used: the first is referred to as unidirectional electrodialysis and the second as electrodialysis reversal.

A flow diagram of a typical unidirectionally operated electrodialysis plant is shown in **Figure 5**. Feed solution pumped into the stack is converted to a diluate and a concentrate which are collected in storage tanks when the desired degree of concentration or depletion is achieved. To prevent the formation of free chlorine by anodic oxidation, the electrode cells are rinsed with a separate solution that

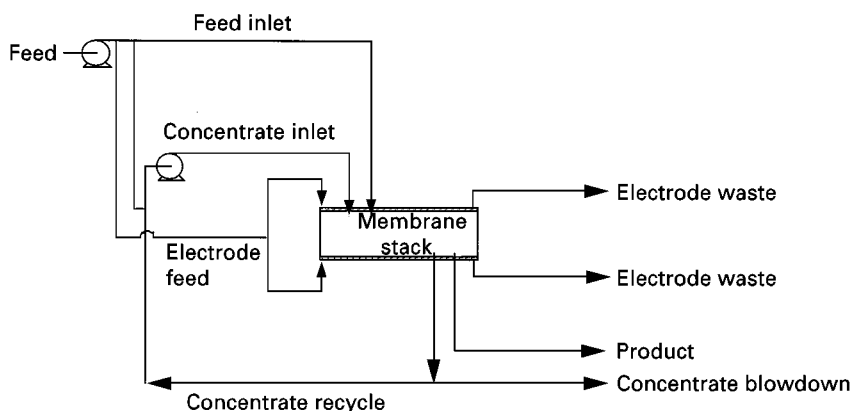


Figure 5 Flow scheme of the unidirectional electrodialysis operating mode.

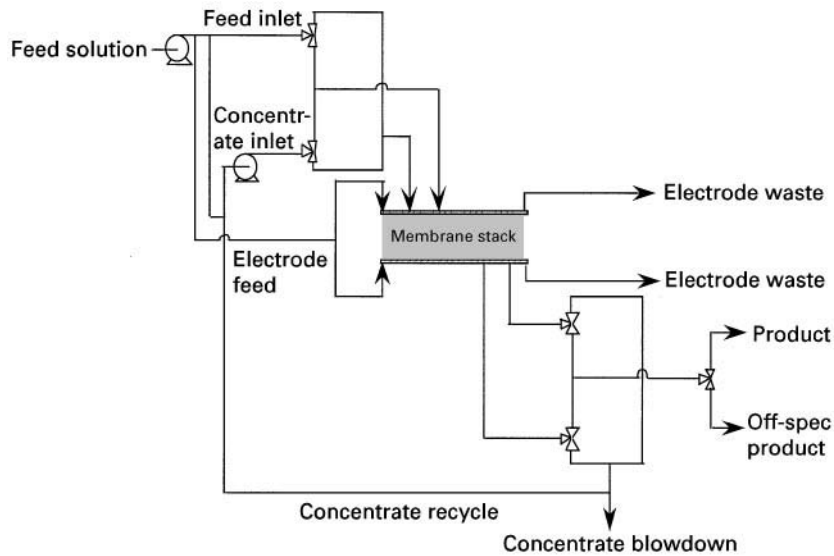


Figure 6 Flow scheme of the electrodialysis reversal operating mode.

does not contain chloride ions. Unidirectionally operated electrodialysis plants are rather sensitive to membrane fouling and scaling and often require careful feed solution pretreatment and stack-cleaning procedures.

Membrane fouling and scaling can be greatly reduced by operating in the electrodialysis reversal mode. In this operating mode, the polarity of the current is changed periodically every few minutes to a few hours. Simultaneously, the hydraulic flow streams are reversed, as shown in **Figure 6**. The advantage of the electrodialysis reversal operating mode is that precipitates that are formed in the concentrate cells are redissolved when the flow is reversed and these cells become the diluate cells. In the electrodialysis reversal operating mode there is a brief period when the concentration of the desalted product does not meet the product quality specification. Thus, a certain amount of the product will be lost to the waste stream.

Electrodialysis Process Costs

The economics of an electrodialysis process are usually expressed as cost per unit product. These costs are the sum of fixed charges associated with amortization of the investment and operating costs such as energy and labour.

Investment costs include items such as the electrodialysis stacks, pumps, electrical equipment and membranes and are proportional to the required membrane area. The minimum required membrane area for a certain plant capacity is

given by:

$$A = \frac{zFQ\Delta Cn}{i\zeta} \quad [24]$$

The required membrane area for a given capacity electrodialysis plant is proportional to the amount of ions removed from a given feed solution and inversely proportional to the applied current density.

As indicated earlier, the applied current density should not exceed a certain limiting value. According to eqn [23] this value is proportional to the diluate concentration and the mass transfer in the boundary layers at the membrane surfaces. The mass transfer depends on the boundary layer thickness, which is a function of flow velocity. For given stack and feed solution properties, the limiting current density is given by:

$$i_{\text{lim}} = {}^{\text{bd}}C_s a u^b \quad [25]$$

Here a and b are constants, the values of which are determined by a series of parameters such as the cell and spacer geometry, the solution viscosity and the transference numbers of ions in the membrane and the solution.

Eqn [25] shows that the limiting current density is proportional to the diluate concentration. However, the diluate concentration is changing during the desalting process from the concentration of the feed to that of the product. Thus, the limiting current density is decreasing along the flow path through the stack. The average limiting current density is proportional to the average concentration in the diluate cell and

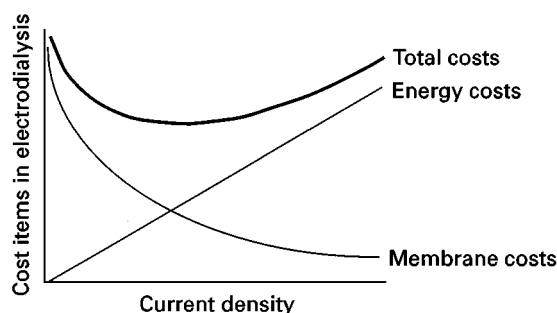


Figure 7 Membrane, energy and total costs of the actual desalination process in electrodialysis.

given by:

$$\bar{i}_{\text{lim}} = {}^{\text{bd}}\bar{C}_s a u^b = a u^b \frac{{}^{\text{bd}}C_s^{\text{co}} - {}^{\text{bd}}C_s^{\text{cp}}}{\log \frac{{}^{\text{bd}}C_s^{\text{co}}}{{}^{\text{bd}}C_s^{\text{cp}}}} \quad [26]$$

Combining eqns [24] and [26] leads to:

$$A_{\text{min}} = a' \frac{\log \frac{{}^{\text{bd}}C_s^{\text{co}}}{{}^{\text{bd}}C_s^{\text{cp}}}}{{}^{\text{bd}}C_s^{\text{co}} - {}^{\text{bd}}C_s^{\text{cp}}} \quad [27]$$

The constant a' is determined by the feed flow velocity, the stack design, etc.

The operating costs of an electrodialysis plant are mainly determined by the energy consumption which is the sum of the electrical energy required for the ion transfer and the energy necessary for pumping the solution through the stack, as indicated in eqns [17] and [18]. The energy required for the desalting process is a function of the feed solution concentration. The pumping energy depends on the flow velocities in the stack.

It should be noted that, according to eqn [12], the energy costs increase with increasing current density, while the required membrane area decreases with increasing current density. Thus the total desalination cost – which is the sum of capital, energy and operating costs – will reach a minimum at a certain current density, as illustrated in Figure 7, where the total cost of an electrodialysis process is shown schematically as a function of the applied current density.

Applications of Electrodialysis

Electrodialysis is mainly used to desalinate saline solutions such as brackish water. But other applications such as the treatment of industrial effluents, demineralization of whey and deacidification of fruit

juices are becoming increasingly important. In Japan, electrodialysis is also used in the production of table salt from sea water.

Desalination of Brackish Water by Electrodialysis

In terms of installed plant capacity, the most important application of electrodialysis is the production of potable water from brackish water. Here, electrodialysis competes directly with reverse osmosis and multistage flash evaporation. For water with a relatively low salt concentration (less than 5000 p.p.m.), electrodialysis is generally considered to be the cheapest process. Another significant feature of electrodialysis is that salts can be concentrated to comparatively high values without affecting the economics of the process severely.

Production of Table Salt

In the production of table salt from sea water, electrodialysis is used to concentrate sodium chloride up to 200 g L^{-1} prior to evaporation. This application is developed and used nearly exclusively in Japan. Key to the success of electrodialysis in this application has been the development of membranes with a preferred permeability of monovalent ions.

Electrodialysis in Waste Water Treatment

Treatment of metal ion-contaminated rinse waters produced in electroplating operations is an important application of electrodialysis. Complete recycling of the water and the metal ions can be achieved in favourable cases. A disadvantage, however, is that in electrodialysis only ions can be removed from a feed stream. Uncharged components that are also present in the rinse waters cannot be recovered.

Dump leach waters containing heavy metal ions have also been successfully treated by electrodialysis. The removal of nitrate from drinking water by electrodialysis is an application that seems to be competitive to processes such as ion exchange or reverse osmosis.

While in most of these applications the average plant capacity is considerably lower than that in brackish water desalination or table salt production, there is also a significant number of large plants installed for the treatment of refinery effluents and cooling-tower waste streams.

Concentration of Reverse Osmosis Brines

Often the disposal of large volumes of brine obtained in reverse osmosis plants is difficult and further concentration is desirable. Because of the osmotic pressure, the brine concentration cannot exceed a certain value in reverse osmosis. A further

concentration, however, may be achieved at reasonable cost by electrodialysis.

Electrodialysis in the Food and Chemical Industry

Several applications of electrodialysis in the food industries, such as the demineralization of cheese whey, have considerable economic significance and are well established today. Other applications, such as the deashing of molasses or de-acidification of fruit juices, are still in an experimental stage. In the chemical industry electrodialysis is used for the desalination of protein, dextran or sugar solutions. Here, electrodialysis is often in competition with other separation procedures such as dialysis and solvent extraction. The separation of organic acids is an application of electrodialysis that is of interest to the pharmaceutical industry.

Production of Ultra Pure Water

Electrodialysis is now being used for the production of ultra pure water for the semiconductor industry. By combining electrodialysis with mixed-bed ion exchange resins, deionized water is obtained without a chemical regeneration of the ion exchange resin. The process has been commercialized recently.

Conclusions

Electrodialysis has a long and proven history in the desalination of brackish waters. However, new applications in waste water treatment as well as in the

food and the chemical industry are becoming more and more important. There are still a multitude of problems to be solved. Some are related to the properties of the membranes and the process design, while others are caused by the lack of application know-how and practical experience.

Further Reading

- Bergsma F and Kruissink ChA (1961) Ion-exchange membranes. *Fortschritte in der Hochpolymer-Forschung* 21: 307–362.
- Helferich F (1962) *Ion-Exchange*. London: McGraw-Hill.
- Katz WE (1979) The electrodialysis reversal (EDR) process. *Desalination* 28: 31–40.
- Lacey RE (1972) Basis of electromembrane processes. In: Lacey RE and Loeb S (eds) *Industrial Processing with Membranes*. New York: John Wiley.
- Nishiwaki T (1972) Concentration of electrolytes prior to evaporation with an electromembrane process. In: Lacey RE and Loeb S (eds) *Industrial Processing with Membranes*. New York: John Wiley.
- Schaffer LH and Mintz MS (1966) Electrodialysis. In: Spiegler KS (ed.) *Principles of Desalination*, pp. 3–20. New York: Academic Press.
- Spiegler KS (1956) Electrochemical operations. In: Nachod FC and Schubert J (eds) *Ion Exchange Technology*, pp. 118–181. New York: Academic Press.
- Strathmann H (1995) Electrodialysis and related processes. In: Nobel RD and Stern SA (eds) *Membrane Separation Technology*, pp. 213–281. Amsterdam: Elsevier.
- Wilson JR (1960) Design and operation of electrodialysis plants. In: Wilson JR (ed.) *Demineralization by Electrodialysis*. London: Butterworth.

Filtration

R. Sahai, EuTech Scientific Services,
Morganville, NJ, USA

Copyright © 2000 Academic Press

Introduction

Filtration is a key processing operation in the pharmaceutical, chemical and cosmetic industries. For example, filtration may be necessary to clear process solutions before analysis or as process step in manufacturing or in the sterilization of process solutions. Analytical testing requires only laboratory-scale filtration and is usually performed by a variety of membrane types depending upon the application. Filtration in manufacturing requires large-scale filtering in engineered devices called membrane modules or cartridges.

Filtration Mechanism

Filtration is a mechanical phenomenon, which is sometimes aided by chemical manipulations of the filtration medium to make it more efficient. In any case, a driving force across the filter media is required. The following methods can be used to generate this driving force:

- Vacuum
- Pressure difference
- Centrifugal force
- Gravity pull
- Concentration difference
- Electrical potential difference
- Temperature difference
- A specific chemical attraction–repulsion

concentration, however, may be achieved at reasonable cost by electrodialysis.

Electrodialysis in the Food and Chemical Industry

Several applications of electrodialysis in the food industries, such as the demineralization of cheese whey, have considerable economic significance and are well established today. Other applications, such as the deashing of molasses or de-acidification of fruit juices, are still in an experimental stage. In the chemical industry electrodialysis is used for the desalination of protein, dextran or sugar solutions. Here, electrodialysis is often in competition with other separation procedures such as dialysis and solvent extraction. The separation of organic acids is an application of electrodialysis that is of interest to the pharmaceutical industry.

Production of Ultra Pure Water

Electrodialysis is now being used for the production of ultra pure water for the semiconductor industry. By combining electrodialysis with mixed-bed ion exchange resins, deionized water is obtained without a chemical regeneration of the ion exchange resin. The process has been commercialized recently.

Conclusions

Electrodialysis has a long and proven history in the desalination of brackish waters. However, new applications in waste water treatment as well as in the

food and the chemical industry are becoming more and more important. There are still a multitude of problems to be solved. Some are related to the properties of the membranes and the process design, while others are caused by the lack of application know-how and practical experience.

Further Reading

- Bergsma F and Kruissink ChA (1961) Ion-exchange membranes. *Fortschritte in der Hochpolymer-Forschung* 21: 307–362.
- Helferich F (1962) *Ion-Exchange*. London: McGraw-Hill.
- Katz WE (1979) The electrodialysis reversal (EDR) process. *Desalination* 28: 31–40.
- Lacey RE (1972) Basis of electromembrane processes. In: Lacey RE and Loeb S (eds) *Industrial Processing with Membranes*. New York: John Wiley.
- Nishiwaki T (1972) Concentration of electrolytes prior to evaporation with an electromembrane process. In: Lacey RE and Loeb S (eds) *Industrial Processing with Membranes*. New York: John Wiley.
- Schaffer LH and Mintz MS (1966) Electrodialysis. In: Spiegler KS (ed.) *Principles of Desalination*, pp. 3–20. New York: Academic Press.
- Spiegler KS (1956) Electrochemical operations. In: Nachod FC and Schubert J (eds) *Ion Exchange Technology*, pp. 118–181. New York: Academic Press.
- Strathmann H (1995) Electrodialysis and related processes. In: Nobel RD and Stern SA (eds) *Membrane Separation Technology*, pp. 213–281. Amsterdam: Elsevier.
- Wilson JR (1960) Design and operation of electrodialysis plants. In: Wilson JR (ed.) *Demineralization by Electrodialysis*. London: Butterworth.

Filtration

R. Sahai, EuTech Scientific Services,
Morganville, NJ, USA

Copyright © 2000 Academic Press

Introduction

Filtration is a key processing operation in the pharmaceutical, chemical and cosmetic industries. For example, filtration may be necessary to clear process solutions before analysis or as process step in manufacturing or in the sterilization of process solutions. Analytical testing requires only laboratory-scale filtration and is usually performed by a variety of membrane types depending upon the application. Filtration in manufacturing requires large-scale filtering in engineered devices called membrane modules or cartridges.

Filtration Mechanism

Filtration is a mechanical phenomenon, which is sometimes aided by chemical manipulations of the filtration medium to make it more efficient. In any case, a driving force across the filter media is required. The following methods can be used to generate this driving force:

- Vacuum
- Pressure difference
- Centrifugal force
- Gravity pull
- Concentration difference
- Electrical potential difference
- Temperature difference
- A specific chemical attraction–repulsion

Filtration is either through a membrane or bed of filter media. The chemical composition of the filter media and physical conditions to perform the filtration constitute a large number of filtration choices available today.

Membrane Filtration

Membrane filtration through a very thin filter medium is also known as 'surface filtration'. The solid particles to be separated are usually large compared to the pore size characteristic of the membrane. The pores on the surface are of irregular shapes. The rejection of particles is dependent on several factors affecting the transport through these pores into the tortuous channels. The separation is based on exclusion discrimination by physical size, charge or affinity or a combination of these properties. Large particles are rejected on the surface and do not accumulate on the surface and do not get a chance to enter into the interior of the filter.

Other types of membrane filters are screen filters and here the pores do not lead into tortuous capillary paths. The pore size is uniform but the distribution of the pores is random on the filter surface. The filter is made by bombarding a thin polycarbonate film with neutrons in a reactor. The film is then placed in a bath of etching solution which preferentially attacks the polymer along the track of the neutrons. The pore size is regulated by selecting the appropriate reagent, exposure time and temperature.

Membrane filtration can be dead end or cross-flow. In dead-end filtration all the solution is forced through the membrane. Retained particles collect on the membrane surface and in the filter greatly reducing flow. A current application of dead-end filtration is in bacterial testing where the liquid to be tested is passed through the filter retaining all bacteria on the surface. Most chromatographic filtration applications are of this type. In cross-flow membrane filtration, the feed liquid flows tangentially to the membrane surface, which prevents the build up of cake on the membrane. Both types of filtration use similar membranes.

By convention, membrane filtration or microfiltration is limited to membranes used to remove particles larger than 0.1 μm in diameter. Membranes able to remove smaller particles are called 'ultrafiltration membranes' and microsolute can be removed by reverse osmosis. Ultrafiltration and reverse osmosis are discussed elsewhere. This article is limited to the process of microfiltration.

The filtration thresholds of common membrane-filtration processes are shown in Table 1.

Table 1 Filtration threshold of common membrane-filtration processes

<i>Type of filtration</i>	<i>Impermeability of membrane</i>
Reverse osmosis	< 0.001 μm
Ultrafiltration	0.001–0.1 μm
Microfiltration	0.1–10 μm

Microfiltration

Microfiltration is used to separate suspended solids or colloidal particles between 0.1 and 10 μm in diameter from solution. Most of the chromatography applications are microfiltration based. The same type of membrane with different pore size is used for these applications. The membrane acts like a physical sieve. The fluid passes through tortuous channels while the particles are rejected on the surface of the filter. It can be easily understood as a mechanical sieve with pores leading into a capillary forming a tortuous path; within this tortuous path, there could be mechanical entrapment and adsorption (Figure 1).

Microfiltration membranes can be subjected to harsher conditions compared to ultrafiltration membranes. Membranes of different polymers in varying pore sizes are available. Even nominally the same pore-size membranes of a polymer may differ from each other in filtration characteristics because they may have different pore-size distributions, i.e. varying pore size all across the membrane. To aid in wetting, many membranes have some surfactant pretreatment and their effective pore size may be different from the real pore size. Often a membrane filter becomes more efficient as small particles are entrapped within the pores. The large particles captured on the filter can also alter the effective particle-size rejection in subsequent filtration. Filter capacity may vary depending on the solute particle-size variation in the feed. Uniform size particles result in faster clogging of filters.

Depth Filter

In depth filtration, the filter medium has larger pores than the particles it is meant to remove. The process starts out at the surface of the filter and proceeds in the cake portion of the membrane. The medium traps the particles in the interstices of the internal structure. Particles enter into the filter medium and separate by gravity settling, diffusion, and attachment to the media owing to electrostatic forces. These filters usually have a pressure drop across the filter caused by pressure, vacuum, or centrifugation. These filters usually have a long life, but

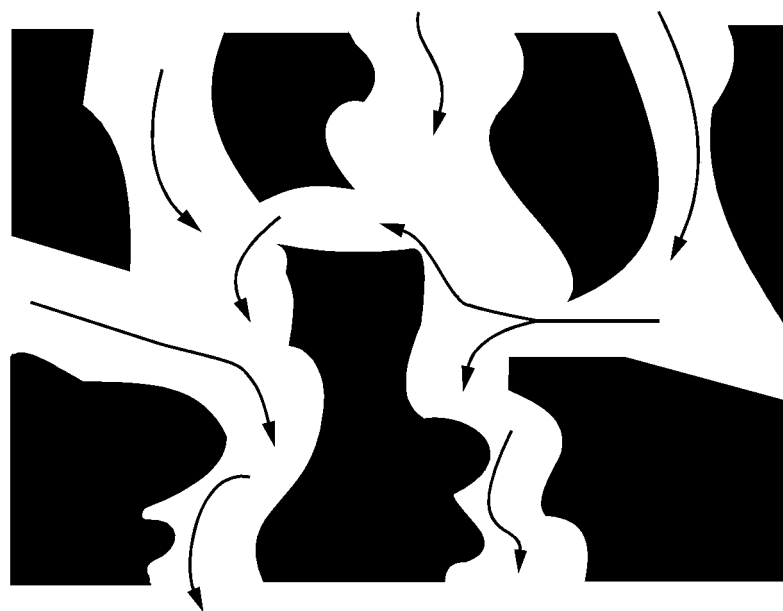


Figure 1 Tortuous path of micro- and ultrafiltration.

eventually a cake is formed over the medium stopping the flow through the filtration device. When the filter bed is full of solids and the pressure drop is very high, the entrapped solids can be back-washed. Usually less than 0.1% solids concentration is filtered through this type of filter to avoid pressure build up. There is always some liquid left behind in depth filters and some solid material still makes it through the filter medium depending upon the efficiency of the system. To use the system effectively, variations of this procedure using moving-bed filters, radial flow filters, or travelling back-wash filters can be employed. The commercial products available for this kind of filtration are application specific.

Filtration Matrices

A variety of polymers are used to manufacture filter media. Each type has specific attributes and could be best for certain applications but could be a complete failure for other applications. The same filter material from different manufacturers can differ in physical properties and in filtration characteristics. However, the chemical compatibility of the material is almost the same irrespective of the manufacturer (Table 2).

Incompatible chemicals can cause shedding, affecting pore size, as well as adding extractables. Hydrophobic membranes have to be wet before starting the filtration. In some cases, it is desirable to convert the hydrophobic membranes into hydrophilic membranes by modifying the surface. Surface reactions can also be used for changing the surface charge. The

polyvinylidene fluoride (PVDF) membranes can be treated to render them hydrophilic and can be reacted to modify the surface charge. The use of aggressive solvents should be avoided with these filters to minimize deterioration of the surface. Membranes used in filtration usually have surface-active agents incorporated in them to make the pre-wetting easier.

Filtration Devices

The filtration application dictates the type of device to be used. Industrial applications demand a high surface area, ease of cleaning and low clogging. For enhanced yield and capacity, open-channel tangential flow systems, which require two pumps for recirculation and permeation, are available from several manufacturers. Different designs are used to overcome gel formation and to continuously sweep away the contamination in the filtration process. The details of these systems are beyond the scope of this article.

The most common disposable filtration devices used in laboratories are syringe filters. The membrane is held in a polypropylene housing with an adapter for syringe attachment on one end. This adapter can be a luer lock or friction fitting. The other end is designed for easy extrusion of permeates. The filter membrane can be housed alone or with pre-filters. The membrane is bonded to the housing ultrasonically, without the use of any chemical adhesive, to avoid unwanted extractables in the filtering process. Syringe filters are disposable and used in very high volume, particularly in the pharmaceutical industry. Because the continuous use of syringe filters

Table 2 Chemical compatibility of common filter membranes with widely used solvents^a

<i>Chemical</i>	<i>Nylon</i>	<i>PTFE</i>	<i>PVDF</i>	<i>PS</i>	<i>Polypropylene</i>	<i>Regen. cellulose</i>	<i>Cellulose nitrate</i>	<i>Cellulose acetate</i>	<i>Cellulose triacetate</i>
<i>Acids</i>									
Glacial acetic acid	LC	C	C	C	C	C	NC	NC	NC
Hydrochloric acid	NC	C	C	C	C	C	NC	NC	NC
Sulfuric acid	NC	C	NC	NC	C	NC	NC	NC	NC
Nitric acid	NC	C	C	NC	C	NC	NC	NC	NC
Phosphoric acid (25%)	NC	C			C	LC	LC	C	C
<i>Bases</i>									
Ammonium hydroxide (25%)	C	C	LC	C	C	LC	C	C	C
Sodium hydroxide 3 mol L ⁻¹	C	C	C	C	C	LC	NC	NC	NC
<i>Common solvents</i>									
Acetone	C	C	NC	NC	LC	C	NC	NC	NC
Benzene	C	C	C	NC	C	C	C	C	C
Benzyl alcohol	C	C	C	ND	C	C	LC	LC	LC
Butanol	C	C	C	C	C	C	C	C	C
Carbon tetrachloride	C	C	C	NC	LC	C	C	LC	LC
Chloroform	C	LC	C	NC	LC	C	C	NC	NC
Dichloromethane	C	C	C	NC	LC	C	C	NC	NC
Dimethylformamide	LC	C	NC	NC	C	LC	NC	NC	NC
DMSO	C	C	NC	NC	C	C	NC	NC	NC
Ethanol/methanol	C	C	C	C	C	C	LC	C	C
Ethyl acetate	C	C	C	NC	LC	C	NC	NC	NC
Ethyl ether	C	C	LC	NC	C	C	NC	NC	NC
Glycerol	C	C	C	C	C	C	C	C	C
Hexane	C	C	C	NC	C	C	C	C	C
Isopropanol	C	C	C	C	C	C	LC	C	C
Methyl ethyl ketone	C	C	LC	NC	ND	C	LC	LC	LC
Tetrahydrofuran	C	C	LC	NC	C	C	NC	NC	NC
<i>Application</i>	MF	MF	MF, UF	MF, UF, RO	MF	MF, UF	MF	MF, UF, RO	MF, UF, RO

^aPTFE, polytetrafluoroethylene; PVDF, polyvinylidene fluoride; PS, polysulfone. C, compatible; LC, limited compatibility; NC, non-compatible; ND, not done; MF, microfiltration; UF, ultrafiltration; RO, reversed osmosis.

can be tiring, a mechanical device is now available which is helpful when repeated filtration is required.

Another common type of laboratory filtration is with centrifuge filters. These devices are the method of choice for molecular weight cut-off filtration and for the filtration of viscous materials. The driving force here is centrifugal force. The filter is manufactured to fit in the rotors of laboratory centrifuges. In these rotors, several filtrations can be carried out simultaneously.

Filtration Applications

In every type of filtration process, the result is always a retentate (restricted to pass through the filter media) and permeate (down stream collection). Retentate or permeate can be the desired product of the process.

Selective Filtration

Selective filtration is used to retain only a particular type of solute. Usually in these cases membranes are

modified for the desired affinity. There are several applications and products available based on ionic attraction.

Purifying Water

The constantly increasing demand for drinking water requires the sea or other sources to be converted into potable water. Most of the potable water plants use reverse-osmosis treatment. Water used in injectables, buffers and chromatography generally has very defined specifications. For most laboratory applications, water with an electrical resistance of not less than 18 MΩ is required to be pyrogen- and bacteria-free. The water used in chromatography should be free of UV/vis-absorbing and ionic impurities.

Chromatographic Applications

Filtration is required in chromatography for preparing a sample for injection. The preparation may include concentration and/or purification. Sample filtration helps in trouble-free operation of chromatography instruments and columns. The use of filtration

for processing samples and solvent is an essential part of instrument preventive maintenance programmes. The filtration of the mobile phase also results in degassing, which is essential for long pump life in high pressure liquid chromatography. The most common devices used for sample preparations are syringe filters.

Biological Applications

The use of filtration as a sterilizing technique is becoming increasingly popular. Other sterilization techniques such as autoclaving, radioactive exposure or ethylene oxide treatment can be detrimental for the product. A dead-end filtration using 0.22 μm pore-sized membrane is considered good for sterilizing by filtration. Viruses can permeate through the membrane of 0.22 μm filter. A 0.1 μm pore-size filter is used to prepare a virus-free solution.

Filtration is also used for desalting or buffer exchange of proteins and nucleic acids, deproteinizing samples, screening natural products and combinatorial products, and separation of oligonucleotide primers from nucleic acid preparations.

Selecting the Right Filtration System

Each application requires a specific filtration characteristic. Choosing the right filtration device and media are necessary when selecting the correct filtration system. The following considerations help when deciding which filter device is to be used:

- Objective of filtration.
- Sample size.
- Filter parameters required: permeability, capacity and flow rate.
- Physical conditions to which the filtration is required to be subjected.
- Tangential flow filter or dead-end filter.

The choice of filter material, pore size and physical conditions depends on the following factors:

- The chemical and physical condition of the feed.
- Size and shape of molecules.
- Zeta potential and isoelectric point. Filtration carried out at a pH close to the isoelectric point results in reduced electrostatic interactions.
- Hydrophobicity or hydrophilicity.
- Solvent in which solute is dissolved.
- Properties of the filter feed, pH, viscosity, surface tension, ionic strength, osmolarity and chemical functionality.
- Intended use after filtration of the sample

Choice is always application specific. For example, in the bacterial examination of water, the purpose is to retain all the particles on the filter surface. A dead-end filtration is used on a 0.2 μm filter. The cross-flow filter is useful for concentrating particles with the removal of solvent. In selecting the filtration system, it is necessary to always consider yield, simplicity, technical reasons and cost.

In some applications, using a combination of different filtration techniques in a certain order is the most efficient method. Sometimes it helps to pretreat the solution to be filtered. The pretreatment could include coagulation and flocculation, magnetic treatment, pH adjustments, and an electric field. A proper washing procedure is usually employed to have the most efficient filtration.

Two filters supplied by Pall Corporation are shown in Figures 2 and 3.

Filtration Validation

The validation of filtration processes includes all the equipment, physical conditions and material requirements of the process. Usually the filter manufacturer performs the basic testing to ensure the type, pore size and integrity of the filter. The filter material characteristics are covered in this article. Some of the most common tests used for this purpose are shown below.

Bubble Point

Bubble point is a function of pore size, filter medium wettability, surface tension and angle of contact. The filter membrane is wetted and a gradual increasing gas pressure is applied. The bubble starts forming from the largest pore first. The gas pressure at this time is the bubble point for the membrane. This is an indirect measurement of the size of the largest pore on the filter. It does not indicate the variability of pore sizes or irregularity of the membrane.

Water Breakthrough

The water-breakthrough test is used for hydrophobic membranes. It is similar to bubble point as this test also give information about the largest pore of the filter membrane. In this test, the minimum pressure required to permeate water from a filter membrane is measured. The water-breakthrough number is dependent on pre-wetting, temperature and pore size of the filter medium. Water is first permeated from the largest pore. This also ascertains filter usability as an aqueous barrier.



Figure 2 (See Colour Plate 49). Pall Ultipor® VF™ Grade DV50 virus filters for high protein-transmissible virus filtration. (Photo courtesy of Pall Corporation, East Hills, NY.)

Extractables

The filter devices and materials can be a source of contamination in the filtration process. The source of impurities could be additives, stabilizers, surface modifiers, detergents and monomers in the filter material. Some contaminants occur in small quantities but some detergents can make up as much as 2–3% of the dry weight of the filter. This large amount of detergent helps in efficient filtration, lower pressure requirements and permits autoclaving for sterilization. The additives and monomers can be entrapped within the body of the filter. Sometimes the source of impurities is not from the filtering material but from the housing or support of the filter. This housing material is usually plastic, and the manufacturer tests that the plastic used in containing the filter material is not going to leach out impurities under

experimental conditions. Although aggressive solvents or physical conditions may be very compatible with the filter membrane, they may affect the filter-containment system.

In some analyses, even a small amount of contaminant is enough to cause problems. Commercial filter manufacturers now certify for specific applications. For many biological applications, the manufacturer certifies the filtration material to be pyrogen-free. For chromatographic applications the filter material is certified not to add impurities to the process. The safest way to use filters for chromatography is to wash them with the same solvent used during filtration and to discard an initial volume of the filtrate. The filters used in ion analysis should be completely free of any ionic impurities. The standard operating procedure of the filtration step should clearly define the conditions and if possible include the limits of the procedure.



Figure 3 (See Colour Plate 50). Pall Ultiplex® high flow filters, providing efficient and economical high-flow filtration with reduced waste disposal costs. (Photo courtesy of Pall Corporation, East Hills, NY.)

Flow Rate

The flow rate is determined by using water or alcohol to determine the permeability to flow before any extra pressure drop produced by the filter cake. Flow rate is dependent on the hydrophobicity of the filter material, temperature of the procedure, physical thickness and pore-size distribution of the filter material. It is expressed as millilitres per minute per square centimeter. An optimum flow rate is needed for the expected life of a filter.

Capacity

Capacity of filtration is the ability to maintain an acceptable permeability. The capacity of a filter is measured until an increase of about three times in differential pressure or ~60% decrease of initial flow. It is expressed as time, volume of liquid, or by quantity of retained particles.

Pore Size

Pore size is probably the most misunderstood property of the filter membrane. The estimation of pore size depends upon the method employed to determine the porosity. The usual methods are all indirect. For

a nominal rating, a range of neutral polymers of different sizes is challenged individually on the membrane and the percentage of a particular size retained on the surface rates it for that size. It could be anywhere from 60 to 98% for a given size rating by the manufacturer. The variability of pore sizes is also polymer dependent. The pore sizes are irregular in membranes manufactured by solvent casting. The pore size is averaged to give a mean pore size assuming all pores are circular. The importance of this point is that the efficiency of the filter should be measured above this point. In actual practice, pore size is used only as a guide; retained particle size data are closer to reality in the filtration process. Most filter manufacturers give particle size retained data traceable to standards from the National Institute of Standards and Testing. In membranes manufactured by neutron bombardment, the pores are circular and same-size pores are randomly distributed along the surface of the membrane. The pore size given is the actual pore size of the membrane. In many filter membranes, detergents are used for enhancing filter characteristics; the effective pore size in these membranes is usually larger than the actual pore size.

Microbial Challenge Test

The absolute rating of a membrane is determined by challenging with test organisms (Table 3). The volume of the feed is such that it averages out to one organism per pore on the membrane surface. The absolute rated membrane is accepted if no more than one organism is present in the permeate.

A membrane with a pre-rating of 0.22 μm is acceptable for liquid filtration sterilization. The ability of a membrane to remove bacteria is dependent on the size of the pores and the thickness of the membrane. There is a finite number of specific bacteria, which can be retained by the membrane before it becomes effectively clogged.

Filtration Challenges

Despite the fact that a great deal of improvement in the filtration process and material has taken place,

Table 3 Microfiltration rating by test organisms

Microfiltration rating	Test organism
1 μm	<i>Candida albicans</i>
0.8 μm	<i>Lactobacillus</i>
0.45 μm	<i>Serratia marcescens</i>
0.2 μm	<i>Pseudomonas diminuta</i>
0.1 μm	<i>Acholeplasma laidlawii</i>

there are still some areas where any advancement will make filtration a friendlier process.

Scaling Up for Manufacturing

The filtration process development remains a challenge because the efficient separation at small volume level is not always transferable to pilot or production scale with the same efficiency and chemistry. Several manufacturers claim new scalable technologies providing similar results in large scale as applications using tangential flow with the same fibre material used throughout the development of the filtration process. Special filtration scale-up software is available commercially.

Membrane Fouling, Gel and Cake Formation

The filtration membranes may start fouling during use. This means that particles start attaching on the surface and in the internal porous structure of the membrane. Large suspended or colloidal particles usually are the cause of fouling. Fouling is a result of van der Waals forces, electrostatic attraction, or hydrogen bonding. The fouling of filter media results in a reduction in membrane permeability and uncontrolled solute removal efficiency. The pretreatment of the feed can be helpful in delaying or completely avoiding fouling. Gel formation and cake formation on the surface can be reversible and filter media can be reused. Macromolecules and some interacting small organic molecules can result in gel formation on the filtration surface.

Cleaning the Filter Media

It is not cost effective to clean the filter in laboratory-scale filtration. For large-scale filtration, usually cleaning and validation protocols are used. The cleaning process could involve cleaning with detergents or other strong chemicals. It could also involve treating with proteolytic enzymes to break down protein impurities trapped in the filter medium and EDTA to arrest activity of bacterial enzymes. Development of cleaning procedures and validation of filter media is very application specific and requires experienced people to design and implement.

Extractables

The extractables in the filter medium can create a problem in the subsequent use of the permeate. This remains a problem in some filter media where additives are used for improved performance. The origin of extractables is either in the processing or the housing device of the filter. Various kinds of extractables are found, including metals, oligomers, loose polymers, plasticizers, wetting agents, antioxidants,

resins, fillers and mould-release chemicals. The usual practice is to wash off the filter material immediately before use. The type and amount of impurity in filter media is not consistent. Each type of impurity has its own rate of extraction from the medium. Hence there is no universal filter-treatment procedure which can ensure a contamination-free permeate. The washing procedure could be under- or overdone in certain applications. The challenge exists to manufacture consistent contamination-free filter media.

Conclusion

Tremendous developments have taken place in both laboratory and large scale filtration techniques in recent years. Various new types of matrices have been exploited for filtration applications. The heavy use of filtration in industry has clearly identified the challenges that remain to be solved. Research continues on selective filtration as a cost-effective way of separation for various applications. In the next few years, we will witness improvement in both the chemical and mechanical properties of filtration equipment.

See Colour Plates 49, 50.

See also: II/Membrane Separations: Microfiltration; Ultrafiltration.

Further Reading

- Chenoweth MB (ed.) (1986) *Synthetic Membranes*. New York: Harwood.
- Cheryan M (1986) *Ultrafiltration Handbook*. Lancaster: Technomic.
- Cooper AR (ed.) (1980) *Ultrafiltration Membranes and Applications*. New York: Plenum Press.
- Crespo JG and Boddekar KW (ed.) (1994) *Membrane Process in Separation and Purification*. Dordrecht: Kluwer.
- Gutman RG (1987) *Membrane Filtration*. Bristol: IOP Publishing.
- Levy RV and Leahy TJ (1991) *Disinfection, Sterilization and Preservation*. Philadelphia: Lea and Febiger.
- Lombardi R (1998) *Membrane Filtration in Chromatography – A Trivial Pursuit*. LC–GC supplement, S47.
- Matteson MJ and Orr C (ed.) (1987) *Filtration: Principles and Practices*. New York: Marcel Dekker.
- Murkes J and Carlsson CG (1988) *Cross Filtration*. New York: John Wiley.
- Nachinkin OI (1991) *Polymeric Microfilters*. New York: Harwood.
- Osada Y and Nakagawa T (ed.) (1992) *Membrane Science and Technology*. New York: Marcel Dekker.
- Shoemaker W (ed.) (1977) *What the Filterman Needs to Know about Filtration*, p. 171. New York: American Institute of Chemical Engineers.

Gas Separations with Polymer Membranes

D. V. Laciak and M. Langsam, Corporate Science and Technology Center, Air Products and Chemicals Inc., Allentown, PA, USA

Copyright © 2000 Academic Press

Introduction

In 1996 the worldwide industrial gas market was in excess of \$29 billion (US). It continues to grow at an average rate of 4–5% per annum. Industrial gases account for some of the largest production volume chemicals (1998 US): nitrogen (843 bcf (billion cubic feet)), oxygen (698 bcf) and ammonia (19 700 million tons). Oxygen and nitrogen are separated from purified air. Ammonia is produced by the reaction of nitrogen and hydrogen. Certainly, the vast majority of industrial gases are purified using cryogenic distillation or adsorption technology. However, in the last 20 years there has been a growing interest in and an intense effort on the part of major gas producers to evaluate and develop membrane technology to produce or purify gases. By 1999 sales of gas separation membrane technology exceeded \$100 million per year. This article will describe basic concepts along with various practical aspects of polymeric gas separation membranes including permeability measurement, membrane formation, module fabrication and applications.

A polymeric membrane is defined as a thin, semipermeable barrier between two gaseous phases. Gases will permeate the membrane if a difference in their chemical potential exists between the two gaseous phases. The chemical potential difference is most often a result of pressure differences across the membrane. Thus, gases will solubilize into the membrane at the high pressure interface, diffuse across the membrane in a concentration gradient to the low pressure interface and evolve into the low pressure gas phase (Figure 1). If a mixture of gases comprised of components *i* and *j* is brought into contact with the membrane, the permeate stream will be enriched in the more permeable gas *i*, leaving the retentate enriched in gas *j*.

The realization that gases permeate through polymers is not new. Every child knows that a balloon filled with air or helium deflates over time. Indeed, this phenomenon was observed by Mitchell in 1831. Balloons made of natural rubber filled at different rates depending on the gaseous atmosphere they were placed into. Carbon dioxide filled the balloon fastest, air slowest. Thirty-five years later Graham expanded

on Mitchell's experiments and quantitatively measured the permeation rates of gases through natural rubber. He found that the permeation rate was not related to the known *gaseous* diffusion coefficients and so concluded that permeation does not proceed through microscopic pores in the rubber but must occur within the rubber itself. He also demonstrated that natural rubber could be used to produce from air a permeate which was enriched in oxygen to 46%.

A mathematical description of the permeation process was proposed by Fick. The relationship between permeation rate *J*, gas pressure *P*, membrane area *A* and membrane thickness *l*, known as Fick's first law, is governed by eqn [1], where ΔP is the pressure difference across the membrane:

$$J = P_o \cdot A \cdot \Delta P / l \quad [1]$$

The proportionality constant, P_o , is termed the permeability:

$$P_o = \frac{J \cdot l}{A \cdot \Delta P} = \frac{\text{volume gas} \cdot \text{thickness}}{\text{area} \cdot \text{time} \cdot \Delta P} \quad [2]$$

The customary unit of permeability is the barrer where:

$$1 \text{ barrer} = 10^{-10} \frac{\text{cm}^3 \cdot \text{cm}}{\text{cm}^2 \cdot \text{s} \cdot \text{cmHg}} \quad [3]$$

Permeability can also be written as the product of the gas solubility times its diffusivity, the so-called *solution-diffusion* mechanism (eqn [4]). The permselectivity (α) for two gases *i* and *j* is defined as the ratio of the permeabilities:

$$P_o = D \cdot S \quad [4]$$

$$\alpha_{ij} = P_{o_i} / P_{o_j} \quad [5]$$

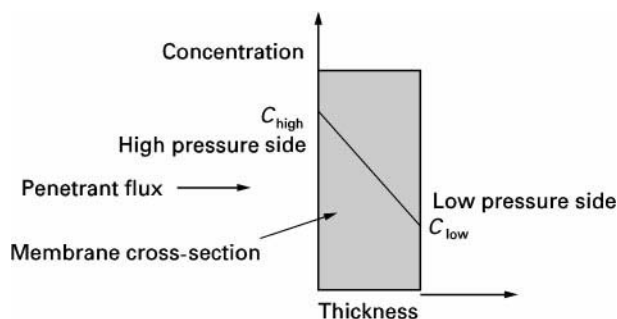


Figure 1 Schematic representation of membrane permeation.

Permeation is an activated process. The effect of temperature on permeation is given by eqn [6], where E_p is the activation energy of permeation, R is the gas constant and T is temperature:

$$P_o = P'_o \cdot \exp(-E_p/RT) \quad [6]$$

In typically encountered cases E_p is positive and the permeability increases exponentially with temperature. Additionally, E_p is related to penetrant size and therefore selectivity usually decreases with increasing temperature. This treatment is not true when dealing with gases below their critical temperature. The reader is referred to the Further Reading section for these special cases.

The above equations give a mathematical, phenomenological description of gas permeation through polymers but imply nothing of the molecular-level processes giving rise to permeation. While we speak of gas-separating polymers as being dense films, on a molecular level one must consider that the membrane is not 'solid'; that is, there are molecular-size gaps between the polymer chains. These gaps arise from packing defects in the solid state and also arise from the thermal motions of the polymer chains themselves. It is through permanent and transient gaps that gas transport is believed to occur. Solution-diffusion behaviour has proven adequate to describe permeation through rubbery polymers – those whose glass transition temperature, T_g , is below the experimental temperature. As a family, rubbery materials are highly permeable but unselective for the same molecular-level rationalization. In the rubbery state polymer chains are highly mobile, generating a high frequency of transient gaps which the penetrant gases can easily diffuse through. However, these gaps are not very selective. From a practical perspective, the purity of the product is related to the membrane permselectivity. With some exceptions, such as the

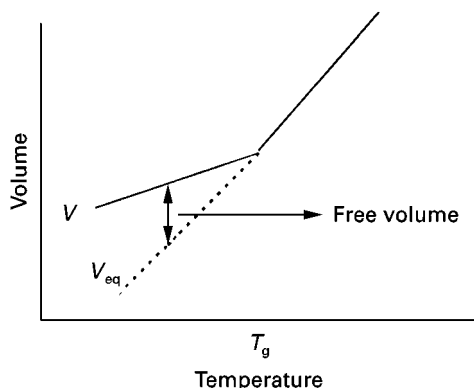


Figure 2 Schematic of free volume.

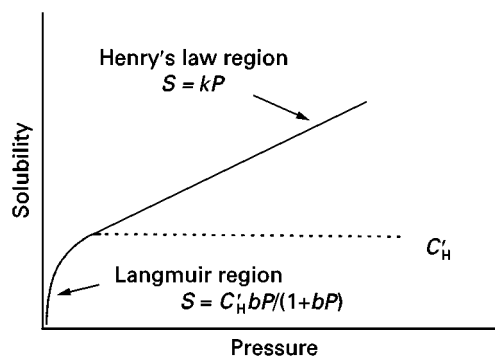


Figure 3 Dual-mode sorption isotherm.

production of oxygen-enriched air for medical applications or the recovery of C4 hydrocarbons, low-selectivity membranes and hence rubbery polymers have found limited commercial utility in the purification of industrial gases.

Dual-Mode Permeation in Glassy Polymers

Polymers in the glassy state possess 'free volume' as shown in Figure 2 – that is, a polymer quenched below its T_g to a nonequilibrium state in which its molar volume is higher than the equilibrium value. This free volume can be visualized as long-lived molecular-level gaps between the polymer chains. One aspect of free volume is that glassy polymers exhibit excess sorption capacity. Sorption in glassy polymers can be described by eqn [7]:

$$S = k_D P + \frac{C'_H b P}{1 + b P} \quad [7]$$

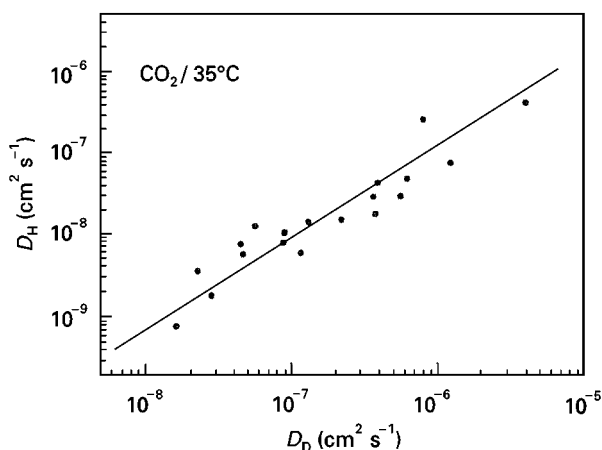


Figure 4 Coupling of Langmuir and Henry's mode diffusion coefficients.

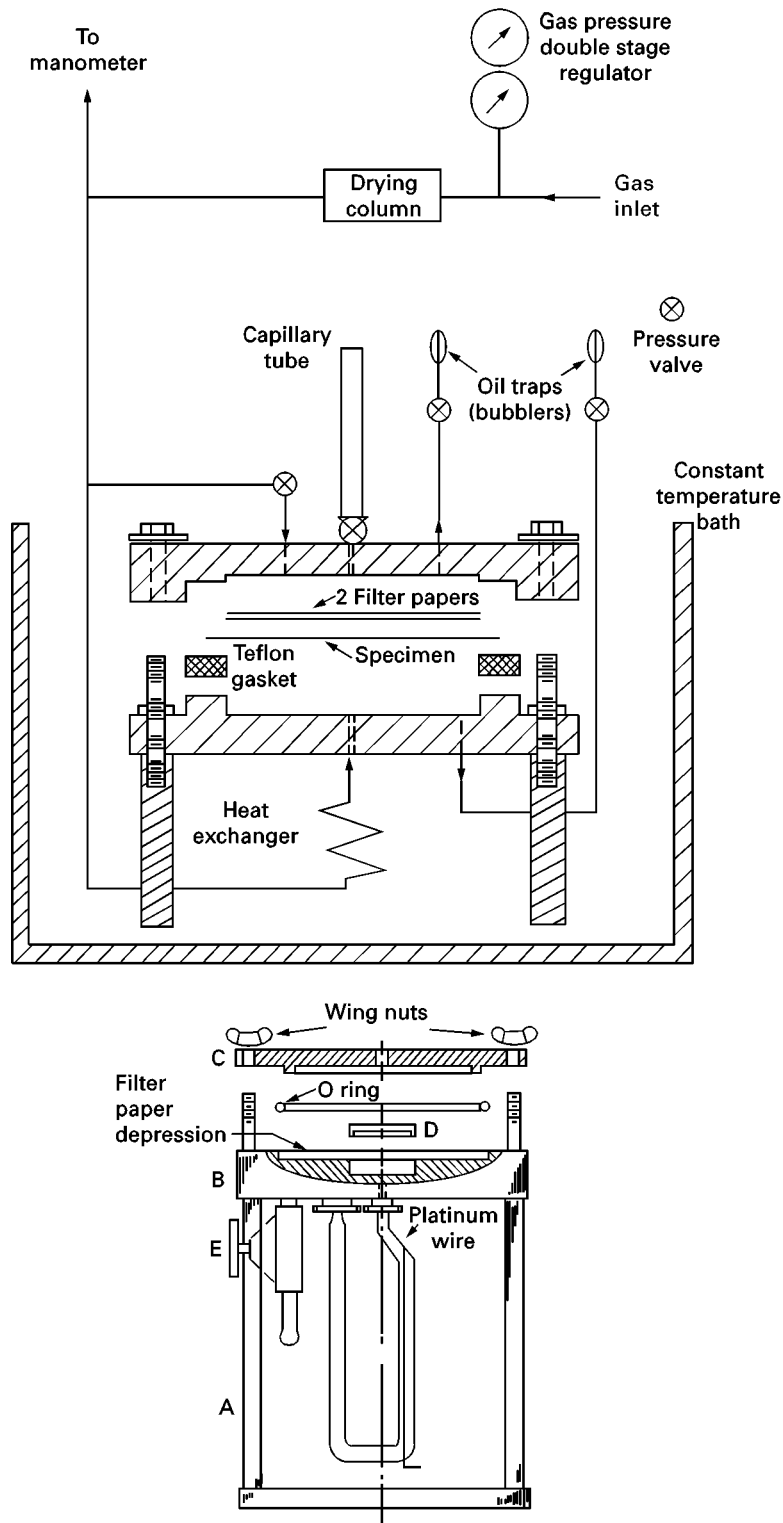


Figure 5 Permeability test cells. A, supporting legs; B, lower plate; C, upper plate; D, adapter; E, vacuum valve.

where k_D is the Henry's law solubility constant, b is the Langmuir equilibrium constant and C'_H is the Langmuir capacity and can be related to the free volume. Such sorption is often termed 'dual-mode'

behavior. A typical dual-mode sorption isotherm is shown in Figure 3. At low pressures, sorption is dominated by the Langmuir element, while at high pressure sorption is described by Henry's law.

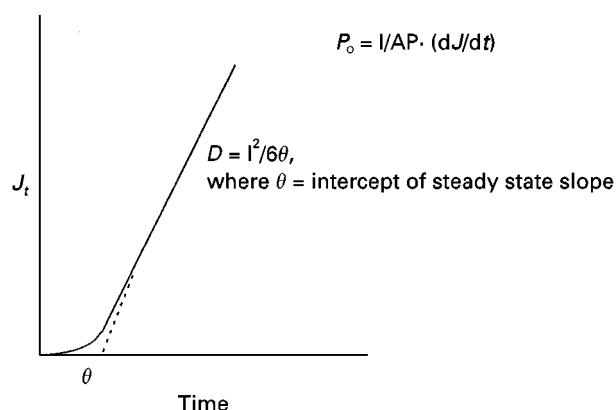


Figure 6 Time lag diffusion experiment.

Dual-mode permeation can be viewed as the simultaneous diffusion of gas molecules within and between the dense polymer phase and the Langmuir gaps or 'holes'. Dual-mode permeation then is described by the sum of permeation in these phases (eqn [8]). The two diffusion coefficients D_D and D_H appear to be strongly correlated to each other (Figure 4):

$$P_o = P_o(\text{dense}) + P_o(\text{hole}) = S_D D_D + S_H D_H$$

$$P_o = k_D D_D + \frac{C_H b D_H}{1 + bP} \quad [8]$$

Some consequences of dual-mode transport are:

1. The permeability of a dual-mode system decreases as the pressure is increased.

Table 1 Air separation characteristics of some common polymers

Polymer	P_{O_2} (barrer)	α_{O_2/N_2}
Polyacrylonitrile	0.0002	>10
Polyvinylidene chloride	0.0053	5.6
Polyethylene terephthalate	0.059	4.5
Cellulose acetate	0.78	2.8
Polystyrene	2.63	3.3
Poly(4-methyl-1-pentene)	32.3	4.1
Silicone rubber	610	2.0
Poly(trimethylsilylpropylene)	8000	1.4

2. Condensable vapours such as water and higher hydrocarbons are strongly adsorbed in the high enthalpy free volume sites and deleteriously affect permeation rates and permselectivity.
3. Strongly absorbing gases such as CO_2 can swell the membrane at high pressure.
4. The free volume, a manifestation of the non-equilibrium state of the polymer, can be decreased by annealing or upon aging.

Methods of Measuring Permeability

Conceptually, measuring the gas permeability of polymeric membranes is simple although fraught with experimental pitfalls related to establishing steady state flow. The experimental parameters are given in eqn [2]. Several methods and apparatus have been developed to conduct permeability measurements. For obtaining the permeation pure gases one

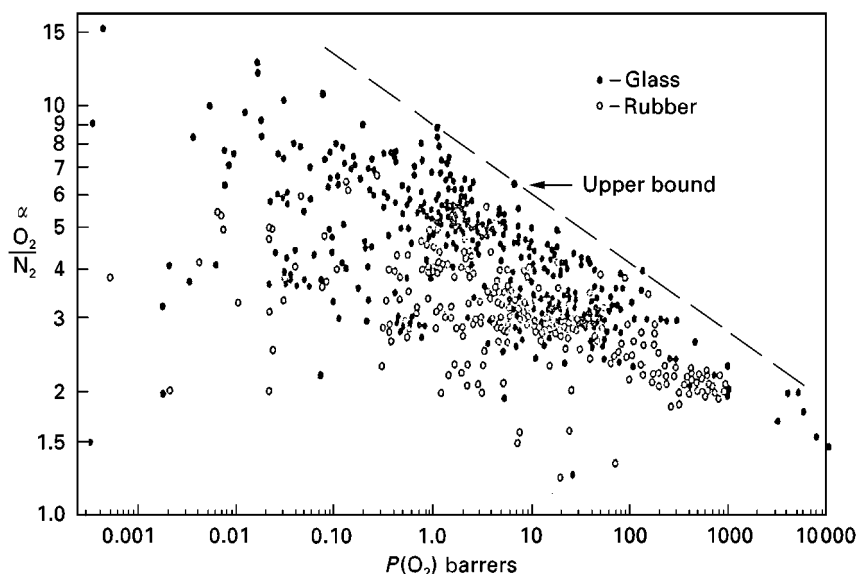


Figure 7 Upper bound representation of oxygen/nitrogen permselectivity - 1990.

Lennard-Jones kinetic diameters of various gases

Gas	He	H ₂	CO ₂	O ₂	N ₂	CH ₄
Kinetic diameter (Å)	2.6	2.89	3.3	3.46	3.64	3.8

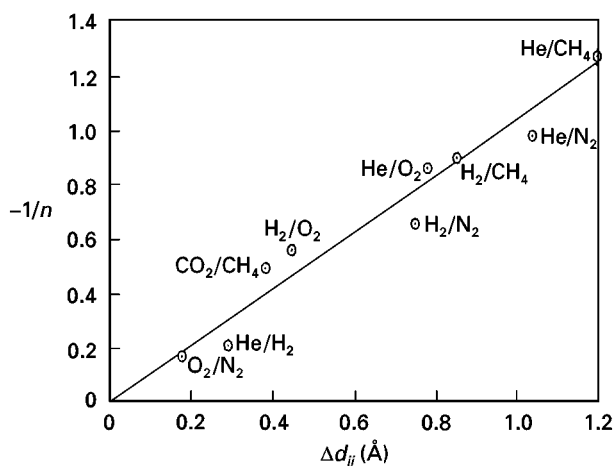


Figure 8 Relationship between the upper bound slope (n) and kinetic diameter difference of gas pairs ij .

measurers either the rate of permeability pressure rise (usually from a vacuum) in a constant volume/temperature receiver or the volume of permeate gas at a fixed pressure (Figure 5). Commercially available test cells are known as the volumetric or 'Linde cell' and the manometric or 'Dow' cell. The American Society of Testing and Materials has published a method for measuring gas permeability (ASTM Method D1434-82). It is possible to obtain the

Table 2 Upper bound parameters

$P_i = k\alpha_{ij}^n$ Gas pair (ij)	k (barrer)	n
O ₂ /N ₂	389 224	-5.800
H ₂ /CH ₄	18 500	-1.2112
CO ₂ /CH ₄	1 073 700	-2.6264
He/N ₂	12 500	-1.0242

permeability coefficient P_0 and the diffusion coefficient D through a *time lag* measurement as shown in Figure 6; subsequent calculation of the solubility term though an independent measurement of S is advised.

Measuring the permeability of gas mixtures is more complex. Usually a flow of a pre-blended source is passed over the feed side of the membrane. The steady state permeate flux can be measured by employing an inert gas such as helium to sweep the permeating components into a gas chromatograph, for example, for compositional analysis. Preferably the experiment is conducted such that back-diffusion of the helium sweep is insignificant and where the feed gas composition is not altered by permeation. Additionally, nuances in the flow patterns within test cells not specifically designed for mixed gas experiments can lead to erroneous results.

Optimization of Polymer Permeation Properties

Table 1 illustrates the range of oxygen permeability and oxygen/nitrogen permselectivity for some

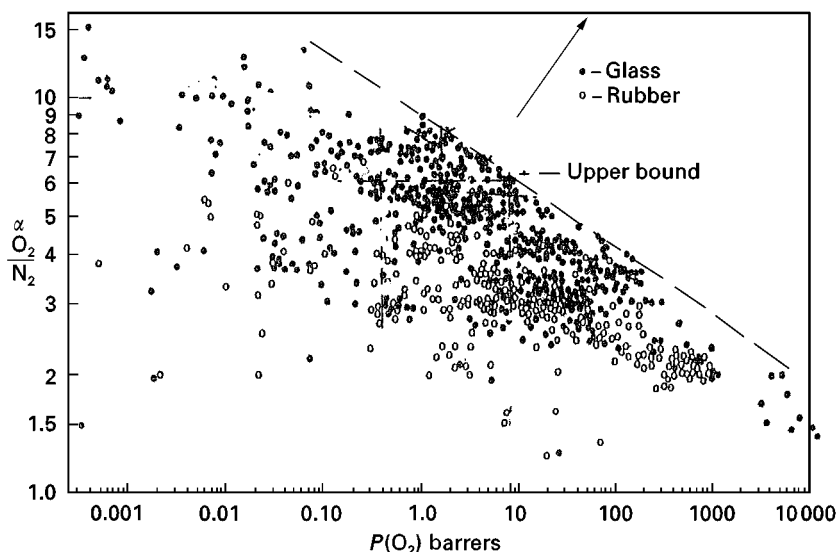
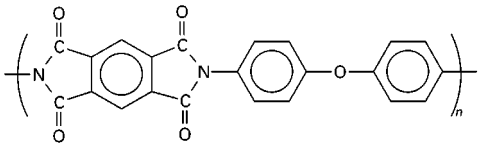
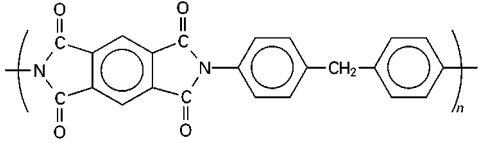
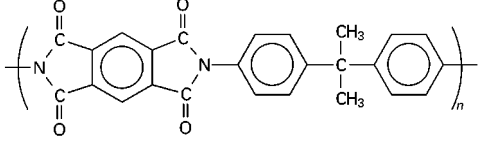
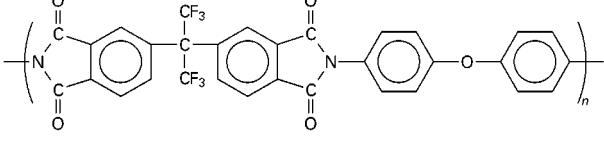
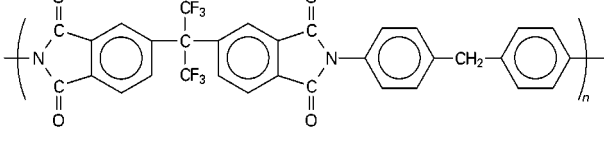
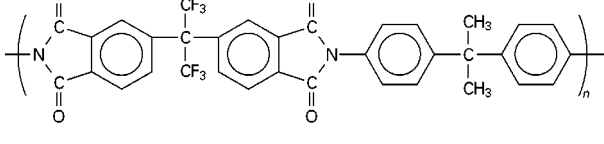
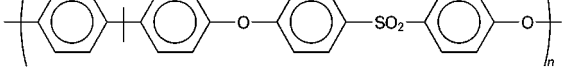
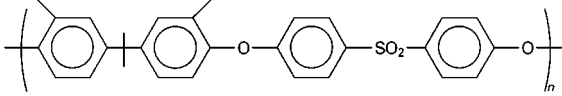
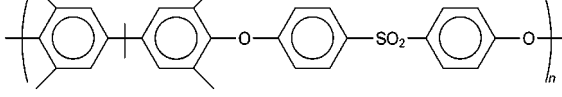


Figure 9 Upper bound representation of oxygen/nitrogen permselectivity - 1993.

Table 3 Structure–property relationships in polymer membranes

Polymer	Structure	Density (g cm ⁻³)	d-spacing (Å)	P (O ₂) (barrer)	O ₂ /N ₂
PMDA-ODA		1.40	4.6	0.61	6.1
PMDA-mDA		1.35	4.9	0.98	4.9
PMDA-IPA		1.28	5.5	7.1	4.7
6FDA-ODA		1.43	5.6	3.9	5.34
6FDA-mDA		1.40	5.6	4.6	5.70
6FDA-IPA		1.35	5.7	7.5	5.60
PSF		1.24	5.0	1.4	5.60
DMPSF		1.21	5.0	0.64	7.00
TMPSF		1.15	5.5	5.6	5.28

common polymers. Permeability spans a wide range: seven orders of magnitude. Further, as the permeability of polymers increases, their ability to differentiate between gases, the permselectivity, decreases. This correlation is valid for nearly all polymeric membranes and has been the subject of research. While long recognized, this observation was first formalized by Robeson in 1991. Working with a database of over 200 polymers, the selectivity of several gas pairs, plotted on a log-log scale against the permeability of the faster gas, exhibits a characteristic upper bound defining the combinations of permeability and permselectivity simultaneously achievable with polymeric materials (Figure 7). Upper bound performance can be described by eqn [9]:

$$P_i = k\alpha_{ij}^n \quad \text{or} \quad \alpha_{ij} = k^{-1/n} P_i^{1/n} \quad [9]$$

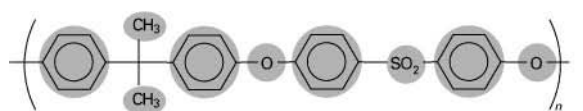
where the values of k and n , tabulated in Table 2, are calculated from the upper bound relationship for specific gas pairs. The parameter n is related to the difference in kinetic diameters of the penetrant gas pair Δd_{ij} as shown in Figure 8. This empirical treatment implies that the upper bound is a natural result of the sieving characteristic of stiff chain glassy polymers. A fundamental theory was later developed by Freeman in which the constants could be related to gas size and gas condensability and invoked just a single adjustable parameter f :

$$\ln \alpha_{ij} = -\lambda_{ij} \ln D_i + \{\ln (S_i/S_j) - \lambda_{ij}(b - f(1 - a)/RT)\} \quad [10]$$

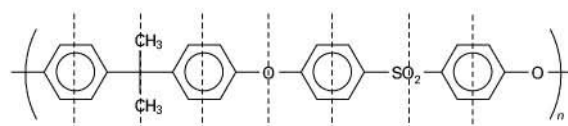
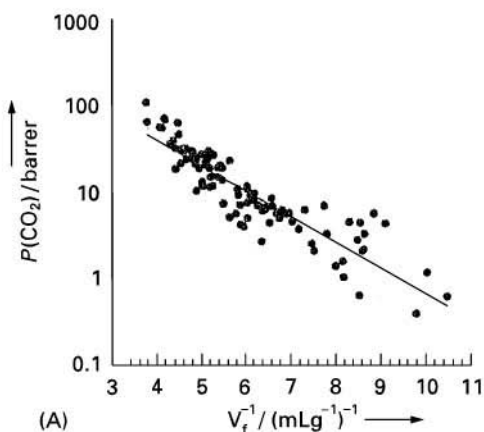
where $\lambda_{ij} = [(d_i/d_j)^2 - 1]$ and d_i is the kinetic diameter; $S_i/S_j = N(\varepsilon_i/k - \varepsilon_j/k)$, where k is the Boltzmann constant and ε is the potential energy well depth in the Lennard-Jones potential energy function. The constants a and b are derived from linear free energy relationships and are independent of gas type. Moreover a is independent of polymer and has a universal value of 0.64; b has a value of 11.5 for glassy polymers and 9.2 for rubbery polymers. The solubility selectivity among polymers is largely constant; consequently diffusivity considerations dominate upper bound permselectivity.

The optimization of polymer structure to obtain upper bound properties comprises the lion's share of polymer membrane research in the last 20 years and the reader is referred to the Further Reading section. Researchers have heuristically developed the understanding gained via the upper bound analysis. The permselectivity for gases i and j is given by eqns [4] and [5] as:

$$\alpha_{ij} = P_{O_i}/P_{O_j} = (S_i/S_j) \cdot (D_i/D_j) \quad [11]$$



Groups are defined volume of atoms within shaded areas



Groups are defined by volume of atoms between lines

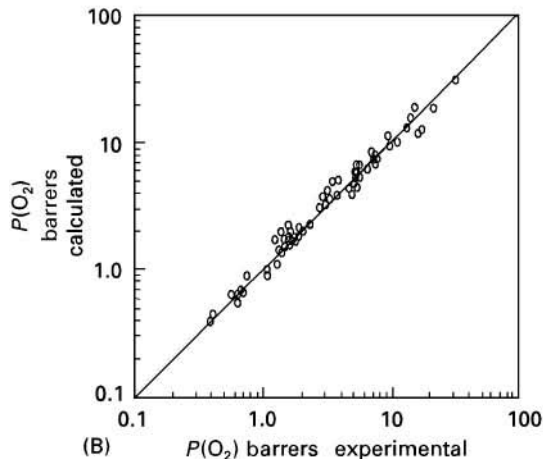


Figure 10 Structure-property relationship: (A) FFV model (Paul). (B) Robeson model.

The solubility selectivity (S_i/S_j) is nearly constant across a wide variety of polymers and for O_2/N_2 is about 2. Selectivity in glassy polymers is therefore dominated by the diffusive selectivity which in turn results from the sieving properties of the imperfectly packed polymer chains. The best trade-off in permeability properties within a polymer family is obtained when both main chain mobility is limited and intersegmental packing of polymer chains is

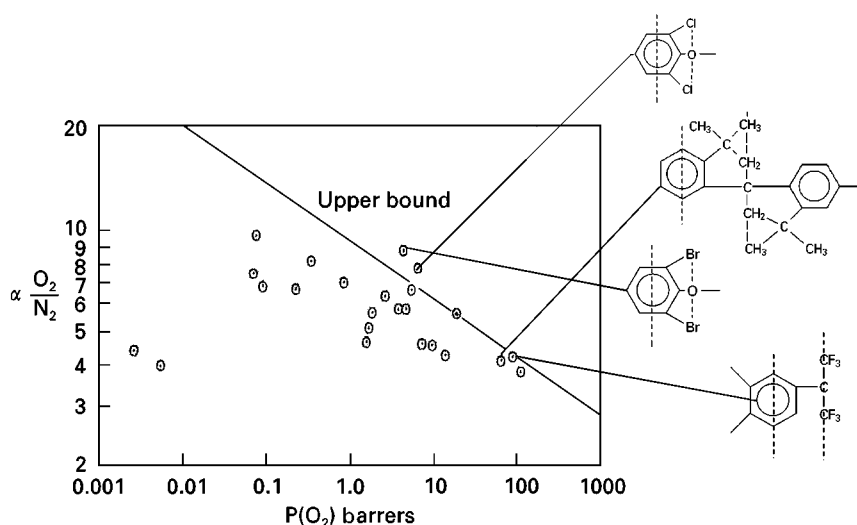


Figure 11 Structure units with imparting superior permselectivity.

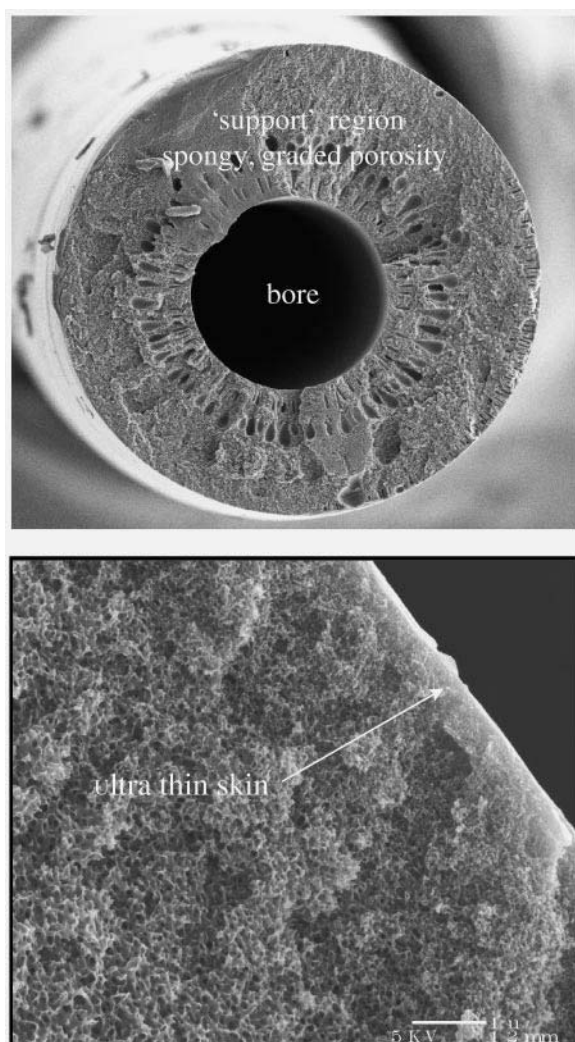


Figure 12 Cross-section of an asymmetric membrane.

inhibited. This behaviour is illustrated (Table 3) for a family of pyromellitic dianhydride (PMDA) and hexafluoro-isopropylidene dianhydride (6FDA)-based polyimides. Changes in the functionality lead to different packing arrangements as measured by density and X-ray d-spacings (average distance between polymer chains). Very small changes in chain packing result in significant changes in both permeability and selectivity. Further, groups such as 6FDA are particularly desired because they can increase permeability without a large loss of selectivity. A further example is that of *ortho*, di- versus tetra-substitution patterns on aromatic polymers. It is widely recognized that incorporation of bulky substituents leads to an increase in permeability, usually at a loss of selectivity. However, it is also noted that *ortho* di-substitution patterns result in lower permeability and higher selectivity than the symmetrically tetra-substituted analogue. Using this intuitive approach a great many new polymers were synthesized and characterized between 1990 and 1993 and as a result the empirically determined upper bound has been shifted upwards and its slope has changed (Figure 9), with many polymers lying at or near the upper bound.

Predicting Polymer Permeability

The benefit of being able to predict *a priori* the relationship between polymer structure or physical properties and permeability is obvious. One method is to correlate the permeability with the reciprocal of the fractional free volume (FFV), defined as:

$$\text{FFV} = \frac{V - V_0}{V} \quad [12]$$

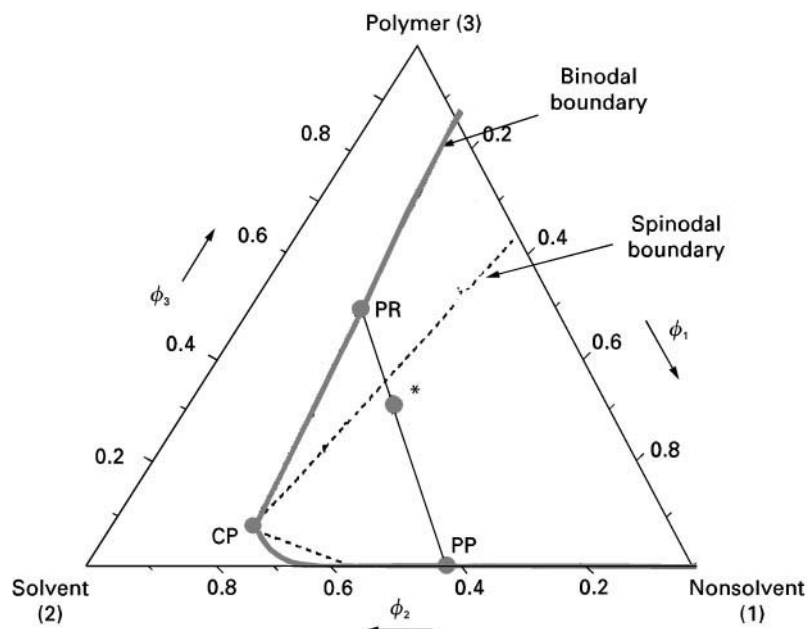


Figure 13 Phase diagram for a ternary dope system. PP, polymer-poor; PR, polymer-rich; CP, critical point.

where V is the specific volume of the polymer and V_o is the volume occupied by the polymer chains. The specific volume is obtained from experimental density measurement. Direct measurement of V_o is not possible and therefore various computational approaches have been developed. The most widely used is that developed by Bondi relating the zero point volume (the volume occupied at 0 K) to the van der Waals volume of the molecule and later modified by Park to account for the fact that different gases have access to different FFV depending on the specific gas-polymer interaction. This group contribution approach has yielded good correlations (Figure 10A) but it is not intuitively obvious how to relate polymer structure directly to free volume.

The group contribution approach by Robeson asserts that the overall polymer permeability can be represented by the sum of structural subunits that comprise the polymer in proportion to their volume fraction:

$$\ln P_o = \sum \phi_i \cdot P_i \quad [13]$$

where ϕ_i is the volume fraction of subunit i and P_i its permeability contribution. Volume fractions are calculated using molecular mechanics computer modeling and the P_o 's are experimentally determined. The P_i 's are found by regressing the set of simultaneous linear equations from eqn [13]. In addition to adequately representing the experimental data (Figure 10B), this method also identifies those subunits which exhibit upper bound properties

(Figure 11). Desirable moieties include the 6FDA, di-*ortho* substituted phenyl ethers and the spirobi-indane fragment. A superior polymer would be tetrabromo-poly(phenylene oxide); however, no one has as yet succeeded in its synthesis.

Membrane Formation

Most research on polymeric membrane materials is conducted on thin, solvent-cast, films. The practical limit to such membranes is about 25 μm for free-standing films and perhaps 1 μm if the polymer solution is cast on a microporous substrate. However, at these thicknesses the flux through the membrane is too low to be of practical value. That is to say, the economics of a membrane process utilizing these thick films would not effectively compete with established technologies such as cryogenic distillation. The enabling development for fabricating ultrathin, high flux membranes was the integrally skinned asymmetric membrane of Loeb and Sourirajan. This type of membrane is produced by inducing phase separation

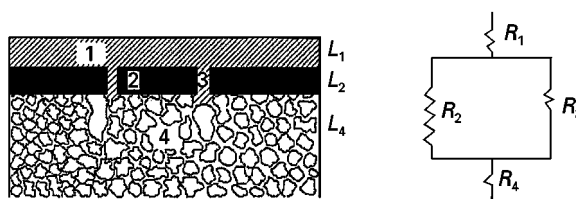


Figure 14 Series resistance model for defect repair.

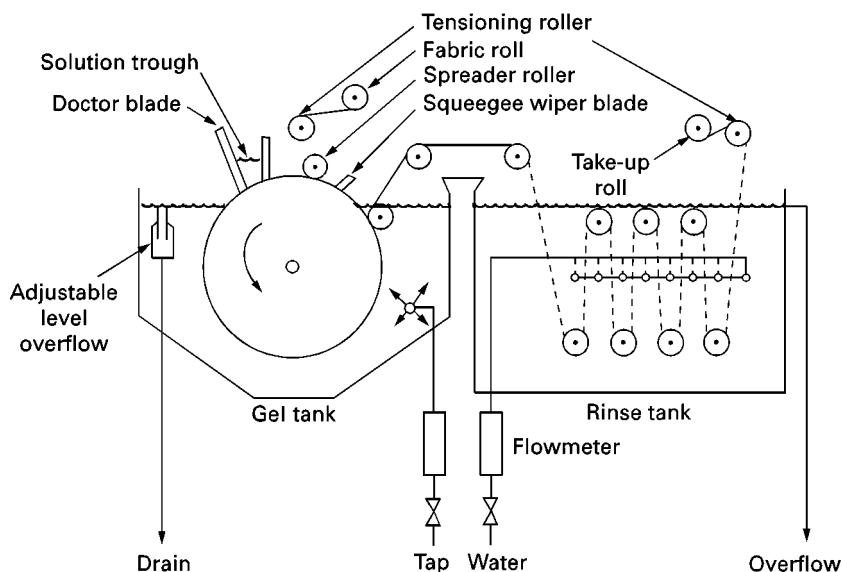


Figure 15 Flat-sheet membrane fabrication.

in a thermodynamically stable solution, usually by changing its composition through the introduction of a nonsolvent. These membranes are prepared by casting a concentrated polymer solution (dope) incorpor-

ating a water-miscible solvent into a water coagulation bath. Such membranes possess an ultrathin dense skin that gradually opens into a microporous substructure (Figure 12). The skin layer provides the

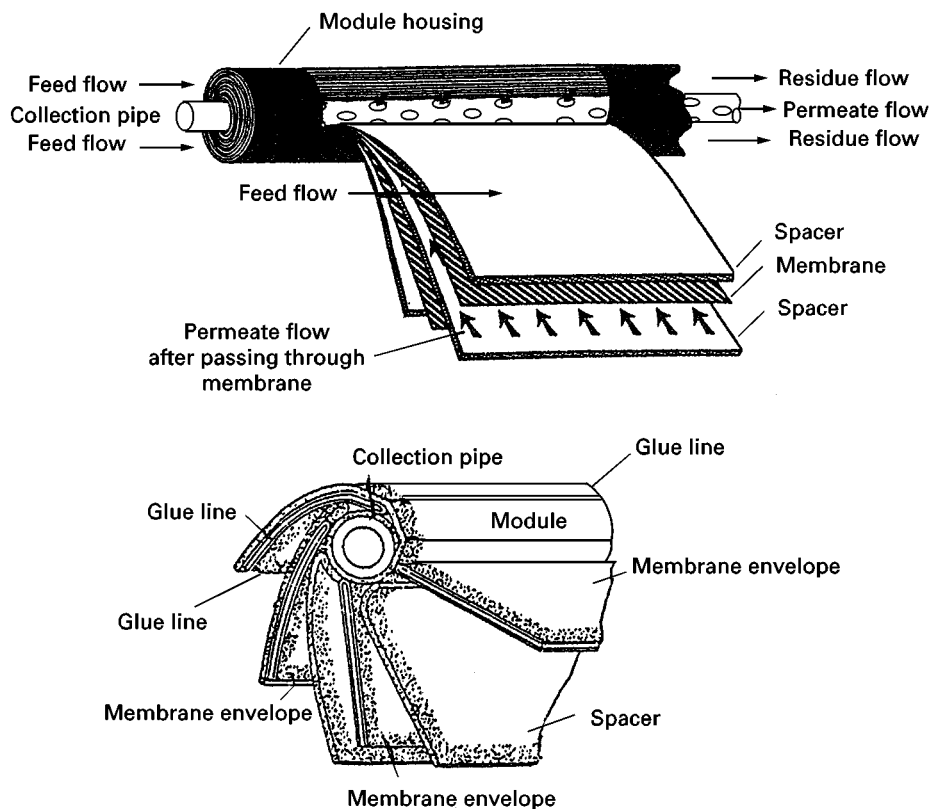


Figure 16 Spiral-wound membrane element.

separation while the thicker integral substructure provides robustness but very little resistance to gas flux.

Membrane formation processes can be grouped into three methods:

1. Dry phase inversion processes involve thermally quenching a dope or solvent evaporation in multi-component solvent system dopes.
2. Wet phase inversion processes involve quenching a cast dope in a coagulation bath.
3. Dry-wet phase inversion processes combine solvent evaporation and a quench medium.

Most commercial gas separation membranes are produced by the dry-wet process although temperature-induced phase inversion (TIPS) is also employed.

Phase diagrams illustrate the phase inversion process (Figure 13). The binodal defines the boundary of the two-phase region and is divided into two parts at the critical point (CP). A second envelope, the spinodal line, also emerges at the critical point. The phase inversion process involves bringing a dope solution into the two-phase envelope. The initially stable solution (at a composition designated by * in Figure 13) decomposes into a polymer-rich phase and a polymer-lean phase, the compositions of which are

defined by tie lines. If the decomposition takes place in the region between the binodal and spinodal a nucleation and growth mechanism of the polymer-rich and polymer-lean phases dominates, leading to structures undesirable for gas separation. Decomposition below the critical point leads to a dispersion of polymer nodules within the polymer-lean phase; decomposition above the critical point leads to a closed cellular structure of an encapsulated polymer-lean phase. The preferred inversion path is to quickly bring the dope within spinodal envelope, thus generating an interpenetrating network of polymer-lean and polymer-rich phases which vitrify into a finely porous substructure.

The thermodynamic framework for a ternary dope system lies in Flory-Huggins theory and the Gibbs free energy of mixing for a ternary system is given by:

$$\Delta G_{\text{mix}} = n_1\phi_1 + n_2\phi_2 + n_3\phi_3 + \chi_{12}n_1\phi_2 + \chi_{13}n_1\phi_3 + \chi_{23}n_2\phi_3 \quad [14]$$

where the subscripts refer to the nonsolvent (1), the solvent (2) and the polymer (3). The notations n_i and ϕ_i are the number of moles and the volume of

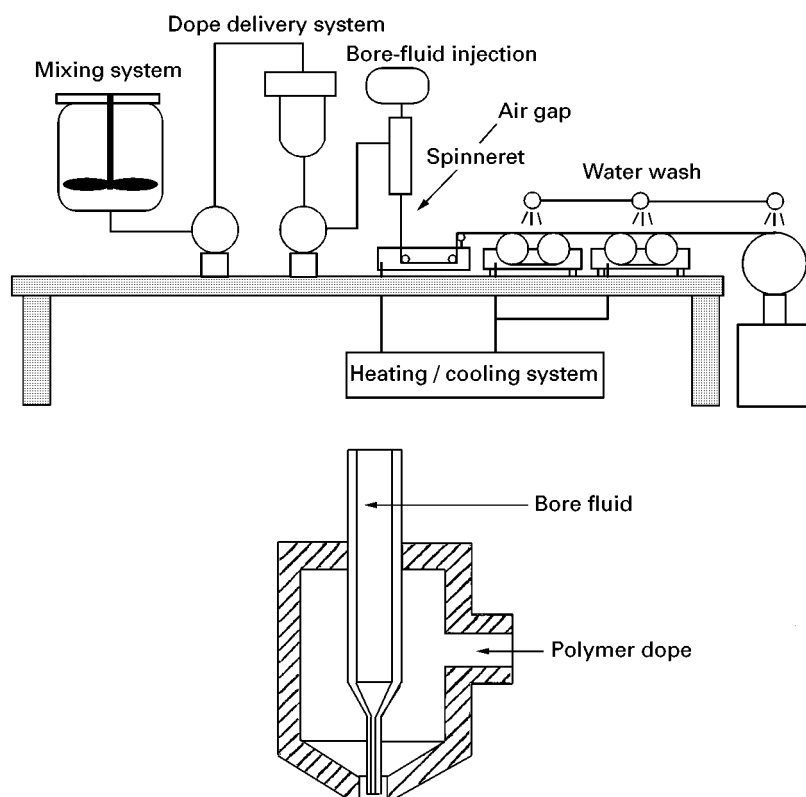


Figure 17 Hollow-fibre membrane spinning apparatus and cross-section of spinnerette.

component i and χ_{ij} is the interaction parameter accounting for the nonideality of the mixture. At equilibrium the chemical potentials (u) of the components in all the phases are equal and are given by eqn [15], which defines the binodal envelope. The composition for the spinodal line is given by the solution to eqn [16], where v_i is the pure component molar volume of species i :

$$\frac{\Delta u_i}{RT} = \frac{\delta}{\delta n_i} \frac{\{\Delta G_{\text{mix}}\}}{RT} \quad [15]$$

$$(1/\phi_1 + v_1/v_2\phi_2 - 2\chi_{12})(1/\phi_1 + v_1/v_3\phi_3 - 2\chi_{13}) \\ \times (1/\phi_1 + \chi_{23}v_1/v_2 - \chi_{12} - \chi_{13}) = 0 \quad [16]$$

Composite Membranes

The above discussion also applies to the formation of composite or multilayer membranes. Composite membranes can be categorized as either a dense, isotropic or asymmetric coating of a high performance separating layer on a microporous substrate. Composite membranes are fabricated in two operations, substrate formation followed by dip coating, allowing for the independent optimization of coating and substrate properties. Gas transport through composite membranes is described by the series resistance model by analogy to an electrical circuit. For a two-layer composite consisting of a thin layer of polymer A on a substrate of polymer B, the flux of gas i through the membrane is given by eqn [17], where l is the thickness of the respective layers:

$$J_i = \Delta P(l_B/P_{O_B} + l_A/P_{O_A}) \quad [17]$$

Regardless of their method of formation a critical element of gas separation membranes is that the skin layer must be as thin as possible in order to produce a high flux membrane. The practical limit to the skin layer thickness is thought to be in the range of 500–1000 Å. Concurrently, the skin layer must be free of manufacturing defects or pinholes. A defective surface area fraction as low as $10^{-5}\%$ can lower selectivity to an extent that the membrane is not suitable for gas separation. Conventional manufacturing processes are not capable of achieving this level of reliability. The second enabling development in commercializing gas separation membrane technology was the demonstration of a poly(dimethylsiloxane) defect repair coating to effectively ‘plug’ manufacturing pinholes and eliminate bulk flow through the defects (Figure 14). Gas permeation through this multicomponent system is described by the series resistance model analogous to an electrical

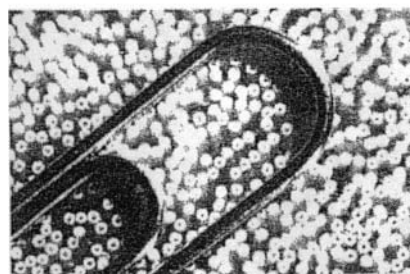
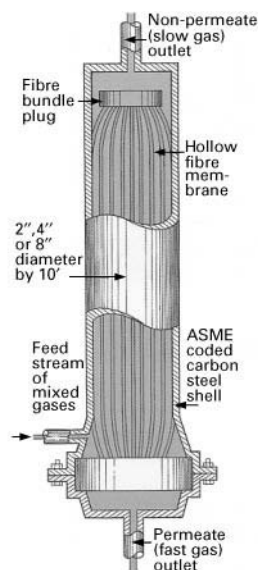


Figure 18 Hollow-fibre membrane element.

circuit. The total resistance is given by the sum resistances in the coating layer (R_c); the parallel resistance in the defective skin layer; ($R_{sk,d}$); and the resistance of the substrate R_{sub} :

$$R_{\text{tot}} = R_c + R_{sk,d} + R_{sub} \\ = R_c + \frac{R_{sk} \times R_d}{R_{sk} + R_d} + R_{sub} \quad [18]$$

After repair, the resistance of the defect, R'_d is greater than R_d and also, $R_{sk} > R'_d$, so that the effective permeability of the composite approaches the intrinsic permeability of a defect-free membrane.

Membrane Devices

Gas separation modules can be prepared from flat sheets as plate and frame assemblies and spiral-wound elements. Hollow fibres can be fine fibres ($< 1000 \mu\text{m}$ OD) or tubular. In general only fine fibres and spiral-wound elements combine

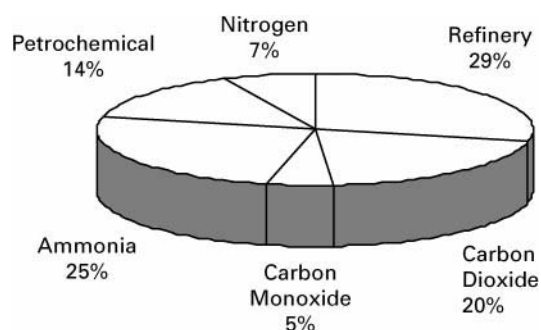


Figure 19 Membrane technology: breakdown by application.

performance and cost parameters providing economic viability. The benefits of the spiral-wound configuration include ease of fabrication and low pressure drop but manufacturing costs are high and the membrane surface area to module volume ratio is low ($\approx 700 \text{ m}^2 \text{ m}^{-3}$), leading to larger, heavier systems. Hollow fibre modules can achieve very high surface area/volume ratio ($> 5000 \text{ m}^2 \text{ m}^{-3}$) and provide a higher degree of countercurrent flow but are more difficult to fabricate and can have high pressure drop.

Flat Sheets and Spiral-Wound Elements

A schematic representation of a flat-sheet asymmetric casting device is shown in **Figure 15**. Flat-sheet membranes are typically produced on a nonwoven cloth which provides support for the nascent membrane. These nonwoven cloths are commercially available on large rolls of 24–48 inches. A thin liquid film of dope solution is metered by a doctor blade onto the nonwoven cloth while the fabric ro-

tates around a stainless steel roller. The nascent membrane is quenched in the gel tank, washed and collected on a take-up roller. A generic spiral-wound element is shown in **Figure 16**. The simplest configuration consists of a central collection pipe around which is wound and glued an envelope of flat-sheet membrane. The envelope contains the membrane and feed and permeate spacer channels. The spacer material is an extremely porous, inert material. Feed gas flows parallel to the permeate pipe; permeating gas flows into the permeate spacer and is collected in the pipe. Higher membrane areas can be achieved using the multileaved method in which two to four sheets of membrane are wrapped simultaneously.

Hollow Fibres

A second asymmetric membrane geometry is that of a hollow fibre. The ultrathin skin is present on the external surface of the fibre. Like the flat sheet, the wall of the fibre is microporous and offers low resistance to gas flow. The permeating gases collect in the bore or lumen of the fibre. A generic hollow-fibre spinning device is shown in **Figure 17**. The apparatus contains a dope reservoir, a bore fluid reservoir, pumps, coagulation baths, wash baths and a take-up winder. The dope solution and bore fluid are co-extruded through a die, resulting in a sheath of polymer around the bore fluid (typically water). This nascent fibre is then coagulated, washed and dried. Hollow-fibre devices contain thousands, even hundreds of thousands, of individual fibres within a single pressure housing (**Figure 18**). The feed gas is usually fed to the outside of the fibre (shell side) although some processes route the feed gas through the fibre

Table 4 Selected membrane applications

Category	Range of operation	Application	Gases separated
Hydrogen recovery	95% H_2 <5 MMSCFD	Ammonia synthesis purge gas Syngas ratio adjustment Hydrotreater off gas	H_2/N_2 , Ar H_2/CO
Nitrogen production	95–97% N_2 0.1–2.0 T/D	Inerting: fuel tanks; food transportation Gas and oil drilling	N_2/O_2 , CO_2 N_2/O_2 , CO_2 , H_2O
Oxygen	40% O_2	Oxygen-enriched air	O_2/N_2
Carbon dioxide removal	95 + % CH_4 <40 MMSCFD	Natural gas sweetening Enhanced oil recovery Landfill gas	CO_2/CH_4
Dehydration	Dewpoint to -40°C	Instrument air Natural gas dehydration	$\text{H}_2\text{O}/\text{air}$ or N_2 $\text{H}_2\text{O}/\text{CH}_4$
Misc.		Semiconductor process gas	Perfluorocarbon from N_2

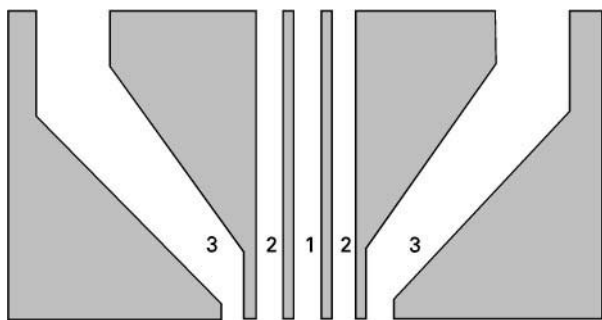


Figure 20 Triple-orifice die for co-extrusion. 1, bore fluid; 2, substrate polymer dope; 3, coating polymer dope.

bore, especially when well-defined flow characteristics are required.

Applications

The first successful commercial activity in gas separation by membranes began in 1977 with the introduction of the Prism[®] membrane system by Monsanto (now Air Products and Chemicals, Inc.), to recover H₂ from ammonia synthesis plant purge gas. Installed membrane capacity in 1977 was only 5 MMSCFD (million standard cubic feet per day) and grew to over 3500 MMSCFD by 1996. Approximately two-thirds of current installed membrane capacity is used for H₂ separation, which includes ammonia purge gas, refinery and petrochemical applications (Figure 19). Significant growth is expected for N₂ and CO₂ separations. While the specifics will vary according to application, a generic membrane system will include a compressor if the source gas is not available at pressure and pretreatment to remove condensable, corrosive or reactive components. The partial listing of applications (Table 4) represents established uses for gas separations. Expanding the slate continues to be a focus of membrane manufacturers and research institutes.

Future Trends

The concurrent need for high performance polymers and low cost membranes has resulted in research into hybrid polymer systems and improved manufacturing processes. Four areas currently being explored are:

1. *Polymer blends*: A hybrid polymer system in which expensive, high performance polymers form a continuous phase in a multipolymer blend.

Examples include Matrimid/Ultem[®] 1000 and aromatic polyimides/polysulfone.

2. *Coextruded composite hollow fibres*: An improved hollow-fibre spinning process in which a forming asymmetric substrate is simultaneously coated with a thin film of separating polymer by employing a die similar to that shown in Figure 20. This is a paradigm shift away from separate substrate fabrication and subsequent coating practices. The co-extrusion processes should lower manufacturing costs and relax price constraints on new high performance polymers.
3. *Organic/inorganic mixed matrix membranes*: A nanocomposite composite is a hybrid in which very small particles of a material with high diffusive selectivity such as a microporous carbon is dispersed with an organic polymer matrix. Such materials combine the high selectivity of the inorganic with the processability of the organic polymer matrix.
4. *Computational methods*: Molecular modelling of gas transport through rubbery polymers has already proven successful. Its application to glassy polymers is significantly more difficult, primarily because of the poorly defined nature of the glassy state, but significant progress has been made in the last several years. As our understanding of gas-polymer and polymer-polymer interactions improves and merges with advancing computer technology, widespread use of molecular dynamics should provide significant insight into gas separation with polymer membranes.

Further Reading

- Ho WS and Sircar KK (1992) *Membrane Handbook*. New York: Chapman & Hall.
- Hwang ST and Kammermeyer K (1975) *Membranes in Separations*. New York: Wiley.
- Kesting RE (1985) *Synthetic Polymeric Membranes: A Structural Perspective*, 2nd edn. New York: Wiley.
- Koros WJ and Fleming GK (1993) Membrane-based gas separations. *Journal of Membrane Science* 83: 1–80.
- Mulder M (1991) *Basic Principles of Membrane Technology*. Dordrecht: Kluwer.
- Paul DR and Yampolski YP (eds) (1994) *Polymeric Gas Separation Membranes*. Boca Raton, FL: CRC Press.
- Robeson LM (1991) Correlation of separation factor vs. permeability for polymeric membranes. *Journal of Membrane Science* 62: 165.
- Stern SA (1994) Polymers for gas separations: the next decade. *Journal of Membrane Science* 94: 1–65.

Haemodialysis

See II / MEMBRANE SEPARATIONS / Dialysis in Medical Separations

Kidney Dialysis

See II / MEMBRANE SEPARATIONS / Dialysis in Medical Separations

Liquid Membranes

L. Boyadzhiev, Institute of Chemical Engineering, Bulgarian Academy of Sciences, Sofia, Bulgaria

Copyright © 2000 Academic Press

Introduction

The separation of solutes by means of liquid membranes is based on a simple and well-established idea: two completely miscible liquid phases, separated by a third liquid, immiscible with either of them, can exchange solutes, provided there is a difference between their chemical potentials in the two phases and provided the intermediate liquid is able to transport them. In most cases the two miscible liquids, denoted hereafter as donor and acceptor phases, are aqueous solutions and the third (membrane) phase is an organic liquid. The configuration involving two organic solutions separated by an aqueous membrane is less popular.

The growing interest in the recovery and separation of solutes by means of liquid membranes may be related to the advantages of this separation method over the related separation operations – solid membranes and solvent extraction – as well as to the recent development of efficient liquid membrane techniques and contactors.

The main advantage of liquid membranes over polymer ones is the higher flux, owing to the very much higher diffusion coefficients of solutes in liquids than in solids. Moreover, some liquid membrane techniques allow a convective diffusion regime instead of a molecular one, which also increases fluxes. Another advantage of liquid membranes is the availability of a great number of substances which, when added to the liquid membrane phase, increase selectivity.

A liquid-membrane process can be regarded as a combination of extraction and a stripping process, which take place simultaneously in the same device. In solvent extraction, both the extractant amount and the distribution coefficient of the solute play essential roles for process efficiency, whereas in liquid membrane separation the selectivity is controlled by the kinetics of the transport process. In contrast to solvent extraction, in liquid membrane separation the amount of transferred solute is not proportional to the amount of the solvent used, in this case the membrane liquid. The relatively small amount of the latter permits the use of various highly efficient and selective – even expensive – carriers.

Mechanisms of Solute Transfer

Like some of the solid-membrane separation methods, the difference between the chemical potentials of the solute in the donor and acceptor solutions controls the transport of the species. In other words, the concentration difference is the driving force.

There are various mechanisms for the selective transfer of solutes in the considered three-liquid-phase system. They can be divided into two groups: nonfacilitated and facilitated, or carrier-mediated, transfer mechanisms.

In nonfacilitated processes, the membrane phase is the solvent and carrier of the solute. In facilitated processes, the membrane phase is a neutral medium, dissolving a carrier, which reacts with some molecules or ions and selectively transfers them to the acceptor phase. The carrier reacts reversibly with the solute by binding it in the donor solution or at the interface between this solution and the membrane phase; it transports it across the bulk of the membrane, and releases it at the other interface. When the transfer of

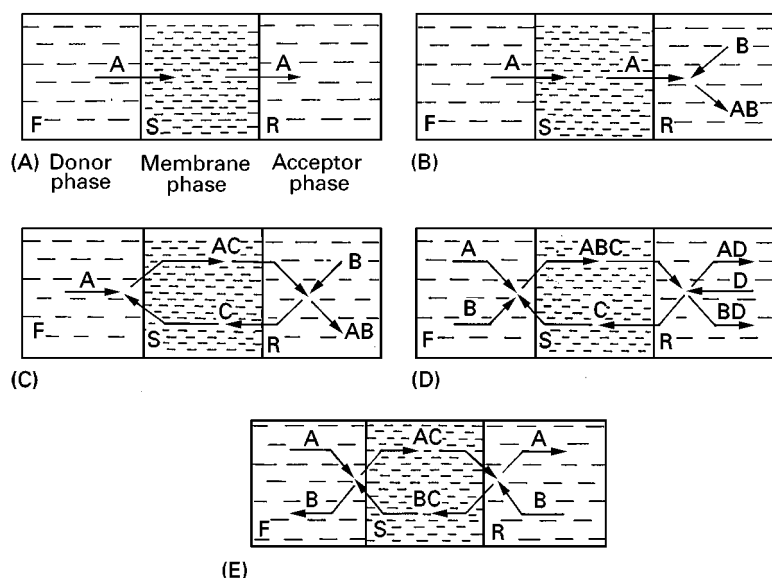


Figure 1 Basic transport mechanisms. (A) Simple nonfacilitated transport; (B) Simple uphill nonfacilitated transport; (C) facilitated uphill transport; (D) facilitated (coupled) co-transport; (E) facilitated (coupled) countertransport. See text for details.

a solute is accompanied by an equivalent transfer of one or more other solutes, it is designated as coupled transport. Depending on the direction of the accompanying transfer, the mechanisms are called co-transport and countertransport. **Figure 1** illustrates the five most popular transport mechanisms: (A) and (B) refer to nonfacilitated mechanisms, while (C)–(E) refer to facilitated mechanisms.

Nonfacilitated Mechanisms

Figure 1A shows the nonfacilitated transport of solute A from the donor solution to the membrane liquid as a result of its solubility and the low concentration in the latter. From this phase, it is transferred to the acceptor phase again for the same reasons. This process continues until the chemical potentials of the solute, i.e. its concentrations in the donor and acceptor solution, are equal. The selectivity of separation of solutes present in the donor solution mainly depends on the difference between their transfer rates, which in turn are related to their solubility in the membrane and, to a lesser extent, on the difference between their diffusion coefficients. This rather simple mechanism is of no practical interest. An example is the separation of aromatic and aliphatic hydrocarbons using water as the membrane phase.

Figure 1B shows a second example of nonfacilitated transport. The process differs from Figure 1A in that the acceptor solution has a component B which is insoluble in the membrane; it reacts irreversibly with solute A that permeates through the membrane. The reaction product AB is insoluble in

the membrane and cannot diffuse back to the donor solution. In some cases an enzyme plays the role of the reagent B, transforming transported solute into products which are insoluble in the membrane. The continuous consumption of A in the acceptor solution maintains its concentration in this phase at a low level, creating a sufficient driving force to transfer the whole amount of A from the donor solution. The solute A in the form of the product AB can reach very high concentrations in the acceptor solution, which is generally of a smaller volume than the donor solution. This transfer, apparently against the concentration gradient, is known as a simple uphill transport and it has a real practical value. A typical example is the transfer of a phenol as a neutral solute which is soluble and thus permeable through the organic membrane phase. The acceptor phase is an alkaline solution that converts the phenol to an ionized salt which is not soluble or permeable through the membrane phase.

Facilitated Transport Mechanisms

In facilitated transport mechanisms the neutral membrane liquid contains an active substance C, which selectively and reversibly reacts with the permeating solute, forming a complex AC (Figure 1C). This complex is formed at the donor interface of the membrane phase and then, due to its concentration gradient, moves to the acceptor solution membrane-phase interface. The complex AC then reacts with a reagent B. As a result of this reaction, A is irreversibly bound by B, while the carrier C is restored and goes back across

the membrane to the feed-membrane interface to bind a new portion of the solute A. Because of this shuttle mechanism, small amounts of the carrier C can transfer large amounts of the solute in the acceptor phase. An example is the recovery of nitric acid from dilute solution using a small amount of the carriers tributylphosphate or trioctylphosphine oxide. The adducts formed are unstable in strongly alkaline media (the acceptor solution), where the acid is neutralized and irreversibly converted into nitrate.

In transport processes shown in Figure 1D, sometimes called facilitated co-transport, the carrier C reversibly forms an intermediate complex not only with the solute A but also with other (one or more) constituents of the donor solution. The complex ABC so formed is transported to the acceptor solution, where it reacts with another additive, D, by forming a more stable compound. The latter, like the reagent D, is insoluble in the membrane liquid. An example of this mechanism is the transport of silver which is selectively recovered from complex polymetallic nitrate solutions. The complex, transferred across the membrane, is formed by a silver cation, a nitrate anion and two molecules of the extractant triisobutylphosphine sulfide, selective for silver. In the acceptor solution, the complex is destroyed by ammonia. The chemical reaction in the acceptor phase yields ammonium nitrate, the stable silver-ammonia complex and the regenerated carrier.

Figure 1E illustrates the third, probably most often used, facilitated transport mechanism, sometimes called facilitated countertransport. In this case, ions, initially present in the donor solution, are substituted

by other ions of the same type, present in a sufficient amount in the acceptor solution. This is actually an ion exchange process in which the ion-exchanging agent, the carrier C, transports in one direction one type of ion and in the opposite an equivalent amount of substituent. A typical example for this transfer is the recovery of some divalent metal cations, e.g. Cu^{2+} , from neutral or slightly acidic aqueous solutions by means of oleophilic chelating oximes. The latter transfers the metal ions to the strongly acidic acceptor solution and returns protons according to the scheme:



The equilibrium conditions at the two interfaces, controlled by the pH values of the aqueous phases, are chosen so that the metal-organic complex is the stable species at the donor-membrane interface, while free cations exist at the membrane-acceptor interface. This type of process is of great significance for hydrometallurgy and for the removal of heavy metals from industrial effluents.

These five types of transfer mechanisms do not exhaust all possible schemes for the selective recovery and separation of solutes by means of liquid membranes. Liquid membrane processes have been developed during the last few years on the basis of various transport and reaction mechanisms, including redox reactions. For example, the selective transfer of metals may result from the different solubility of their ions at various oxidation states. Of equal interest are some enzymatic reactions, both in the bulk of the

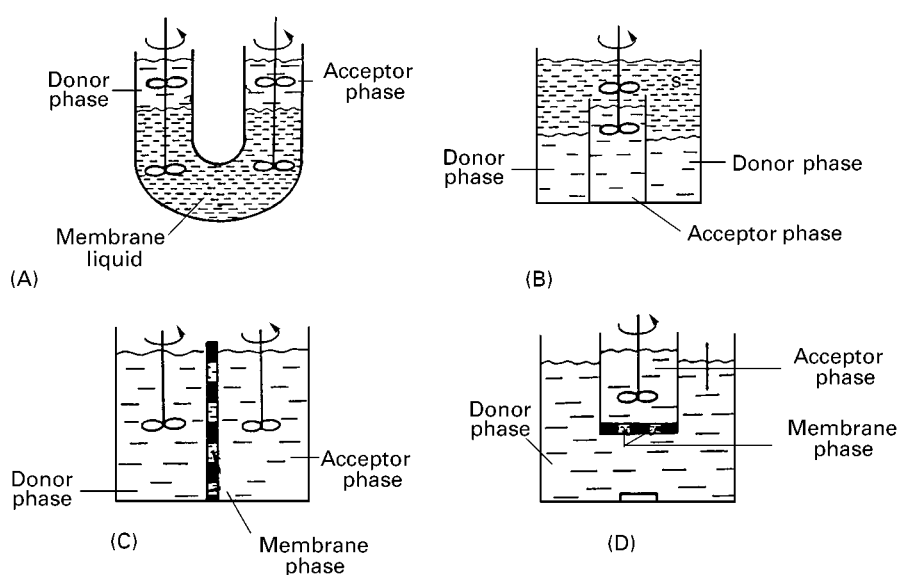


Figure 2 Bulk liquid membrane contactors for laboratory use. (A) U-tube contactor (Schulmann bridge); (B) beaker-in-beaker contactor; (C) and (D) two cells separated by supported liquid membrane.

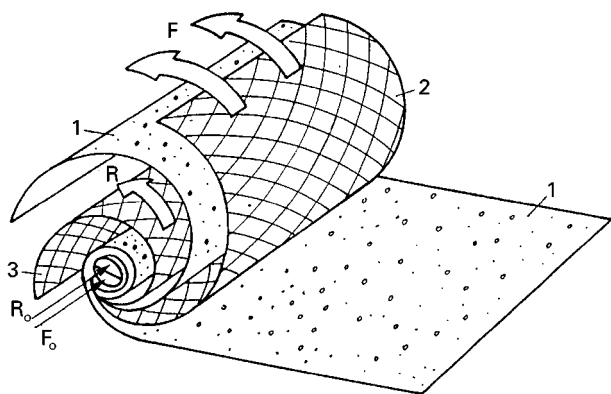


Figure 3 Spirally wound supported liquid membrane module. R, Acceptor solution; F, donor solution.

membrane and in the bulk of the acceptor solution. The reader may find further information in the Further Reading section.

Liquid Membrane Techniques

The main reason for the limited large scale application of liquid membrane processes is the lack of efficient equipment providing simultaneously large contact areas and high fluxes between the phases without deterioration of the membrane over time causing intermixing of the donor and acceptor phases. The realization of stable membranes is an extremely difficult task.

In general, liquid membrane techniques can be divided into two groups: techniques in which there is no dispersion of phases and techniques with at least one dispersed phase. The first group includes bulk liquid membranes and the supported liquid membranes, as well as some recent techniques combining elements from both techniques. The second group is mainly represented by the emulsion liquid membrane technique.

Methods Without Phase Dispersion

Simple bulk liquid membranes Several simple contact devices designed for studies of liquid-membrane processes are shown in Figure 2. In all, there is a common compartment for the membrane liquid. The other contactor space is divided into two compartments, one for the donor solution and the other for the acceptor solution. The interface between the membrane liquid and the other two solutions is free (A, B) or immobilized (C, D) by a solid porous membrane. The first device (A) is known as the Schulmann bridge. Devices of the type shown in Figure 1A and B are limited to laboratory experiments, but the con-

tactors shown in Figure 2C and D find a broader application. In these devices, the membrane liquid permeates a porous membrane, which separates the donor and the acceptor solutions. In modification (D), a cylinder with an attached porous barrier rotates and stirs the donor and acceptor phases, reducing or eliminating the mass transfer resistances in these two phases. The type of device depends on whether the membrane liquid is heavier or lighter than the other two solutions.

Supported liquid membranes The laboratory contactor shown in Figure 2C is the prototype of supported liquid membrane contactors. In these devices the membrane liquid fills the pores of a 25–100 μm thick porous membrane containing pores 0.01–10 μm in diameter. The membrane is usually made of polypropylene, polysulfone or another oleophilic polymer.

Although the membrane is quite thin, the fluxes across it are very low as a result of the total immobilization of the membrane liquid in the pores, reduced free section and pore tortuosity. This is overcome by the use of large surface area modules such as the spirally wound (Figure 3) or containing bundles of tiny porous hollow fibres, as shown in Figure 4. Hollow fibre membrane modules containing fibres with diameter of 0.2–1 mm can achieve interface areas of

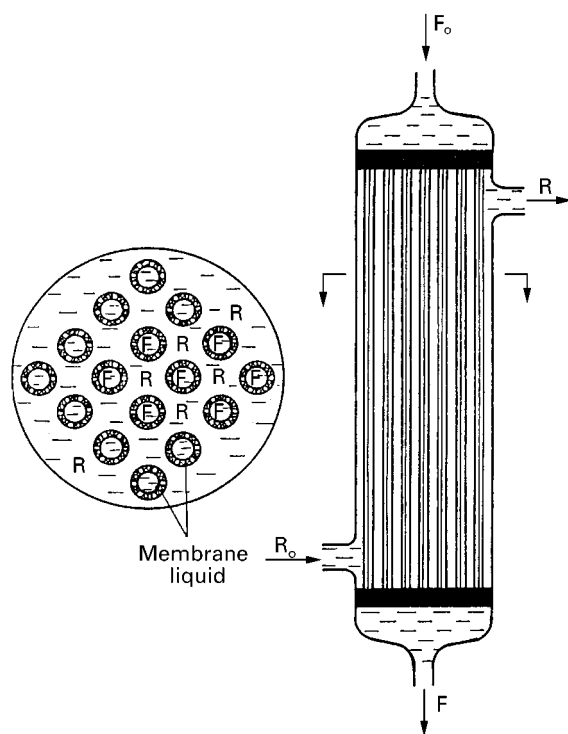


Figure 4 Hollow fibre supported liquid membrane module. R, Acceptor solution; F, donor solution; S, membrane liquid.

2000–10 000 m²/m³. In such modules, one of the aqueous phases flows in the lumen of the hollow fibres, while the other flows outside the fibres and the pores of the fibre walls are filled with the membrane liquid.

The insignificant amount of membrane liquid required in these modules (10 cm³ per 1 m² interface), often pointed out as a major advantage, is actually the chief drawback of supported liquid membrane contactors, causing their operational instability and short life. The life of the expensive modules is shortened by the inevitable solubility of the membrane liquid in the donor and acceptor phases, by its washing out or by emulsification caused by the pressure difference on both sides of the membrane, the lateral shear force, and the change of support wettability with time. In spite of numerous design improvements, e.g. periodic or continuous reimpregnation of the membrane and partial or total gelation of the membrane liquid, this technique has not been used in industrial applications.

This instability forced researchers as early as in the 1980s to look for other solutions. The combination of this technique with stable bulk liquid membranes yielded the bulk-supported liquid membranes.

Flowing liquid membranes and contained liquid membranes In these two variants of the bulk-supported liquid membrane group, as well as in numerous subsequent modifications, the membrane liquid not only fills the pores of two closely spaced porous supports separating the donor and acceptor phase, but also the space between them, as shown in Figures 5 and 6. Figure 5 shows a device introduced by Teramoto *et al.*, called the flowing liquid membrane: the spirally wound module contains one additional layer and one additional porous barrier (Figure 5) in comparison with the analogous supported liquid membrane module, shown in Figure 3. Between the two, separated by porous support spacers, flows the membrane liquid, which also fills the pores of the support which are preferentially wetted by it.

In contained liquid membranes, a technique proposed by Sirkar *et al.* in the late 1980s, the donor phase flows in the lumen of a part of the capillaries, while the acceptor phase flows in the lumen of the rest of them. As Figure 6 shows, the membrane liquid filling the space outside the hollow fibres can also be set in motion. When the hollow fibre material is wetted by the membrane liquid, the pores are filled with it. In the reverse case, they are filled with the other two phases. The module shown in Figure 6, in which the inlets and the outlets of the feed and acceptor phases are located in one end of the module case,

permits free elongation of the fibre package caused by the swelled membrane liquid.

The latter two membrane techniques provide significantly longer life of the contactors, as the inevitable losses of membrane fluid are compensated by the larger liquid volume. However, fluxes are lower because of higher mass transfer resistance due to the second porous support filled with immobilized liquid and the two additional diffusion boundary layers in the same phase. This drawback is, however, offset by the longer membrane life.

A further modification of the contained liquid membrane technique is the separation of the two hollow fibre packages in two modules – one where the donor liquid exchanges solutes with the membrane liquid and a second where the membrane

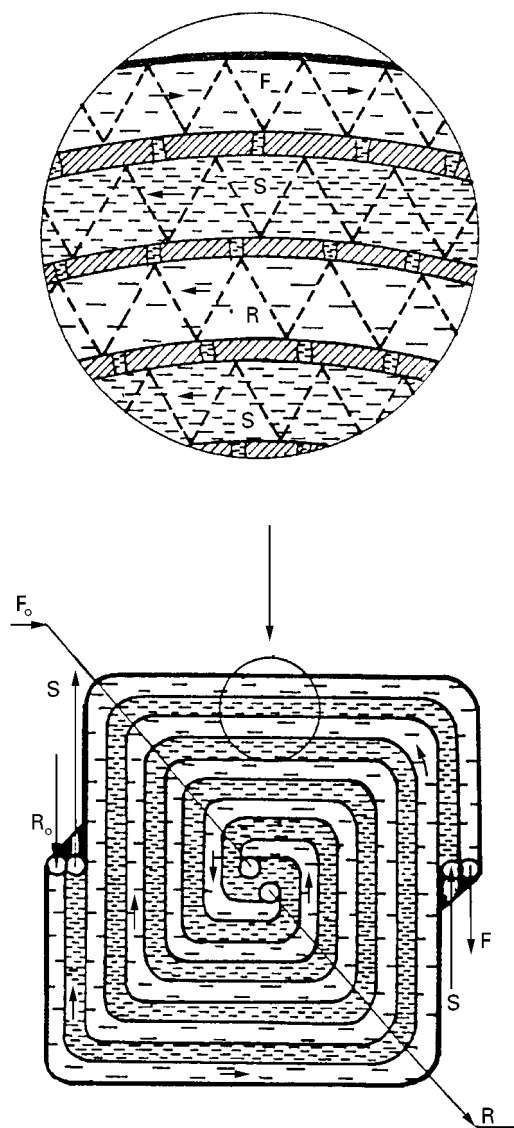


Figure 5 Spiral-type flowing liquid membrane module. R, Acceptor solution; F, donor solution; S, membrane liquid.

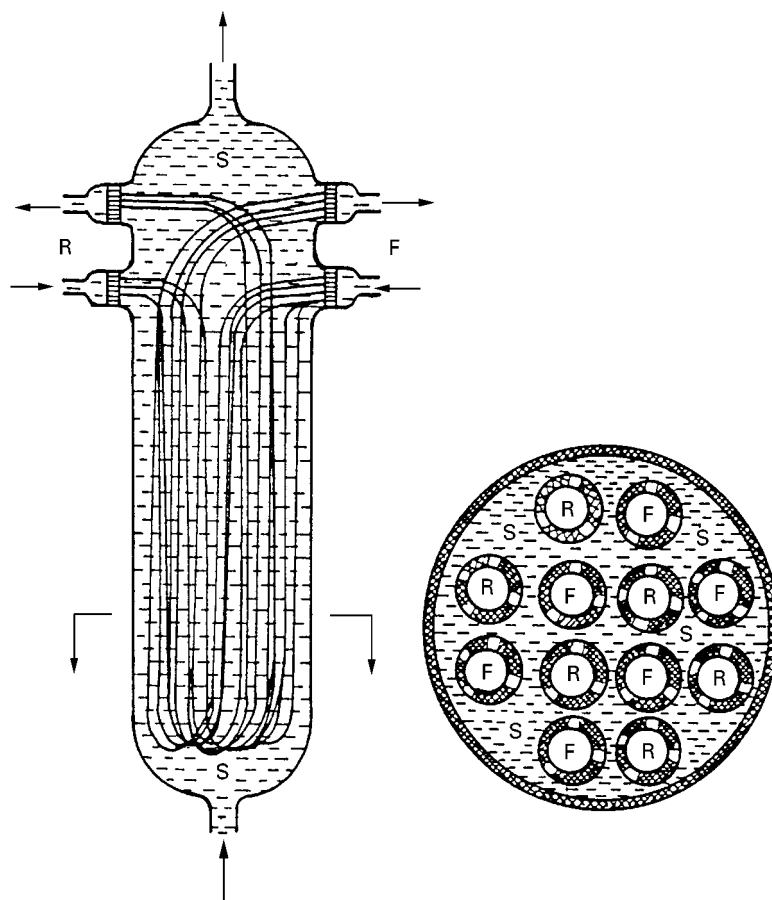


Figure 6 Contained liquid membrane contactor. R, Acceptor solution; F, donor solution; S, membrane liquid.

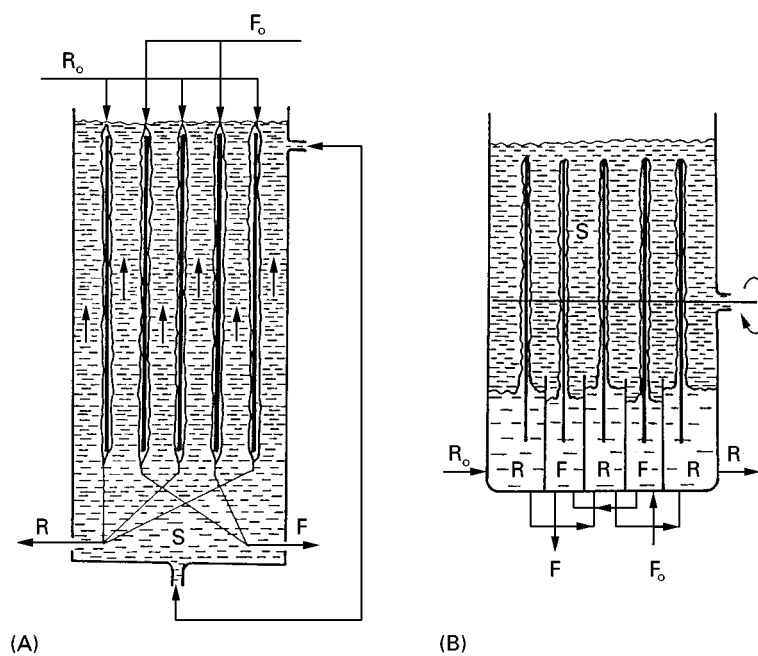


Figure 7 Liquid film pertractors: (A) falling film pertractor; (B) rotating film pertractor. R, Acceptor solution; F, donor solution; S, membrane liquid.

liquid contacts with the acceptor liquid. The membrane liquid circulates between the two devices. This technique, bearing the name two-module hollow fibre supported liquid membranes, differs little from the arrangement in a conventional extraction-stripping unit operation.

Liquid film pertraction The technique known as liquid film pertraction attempts to combine the advantages of bulk liquid membrane and supported liquid membrane. In the process all three liquids are in motion and the interfaces between the phase pairs are not immobilized, so that the transport rate in all stages of the transfer process is controlled by convective transport instead of the much slower molecular diffusion.

Two devices utilizing this technique are schematically presented in Figure 7. In the first one, called the

falling film pertraction, shown in Figure 7A, the donor and acceptor solutions flow down the surface of alternating vertical supports. The spaces between the opposite supports, covered by films of donor and acceptor liquids, respectively, are filled with the membrane phase, flowing countercurrent to the other two. By independent control of the flow rates of the feed and acceptor phases, a significant solute accumulation in the acceptor solution can be achieved.

The second technique, rotating film pertraction uses a package of rotating horizontal discs wetted only by the feed and receptor phases. This rotation generates an intensive transfer regime in all three liquids. As Figure 7B shows, the discs, alternately mounted on a shaft, are partially immersed in the corresponding wetting solutions and on rotation form mobile films which directly contact with the membrane liquid filling the spaces between the discs.

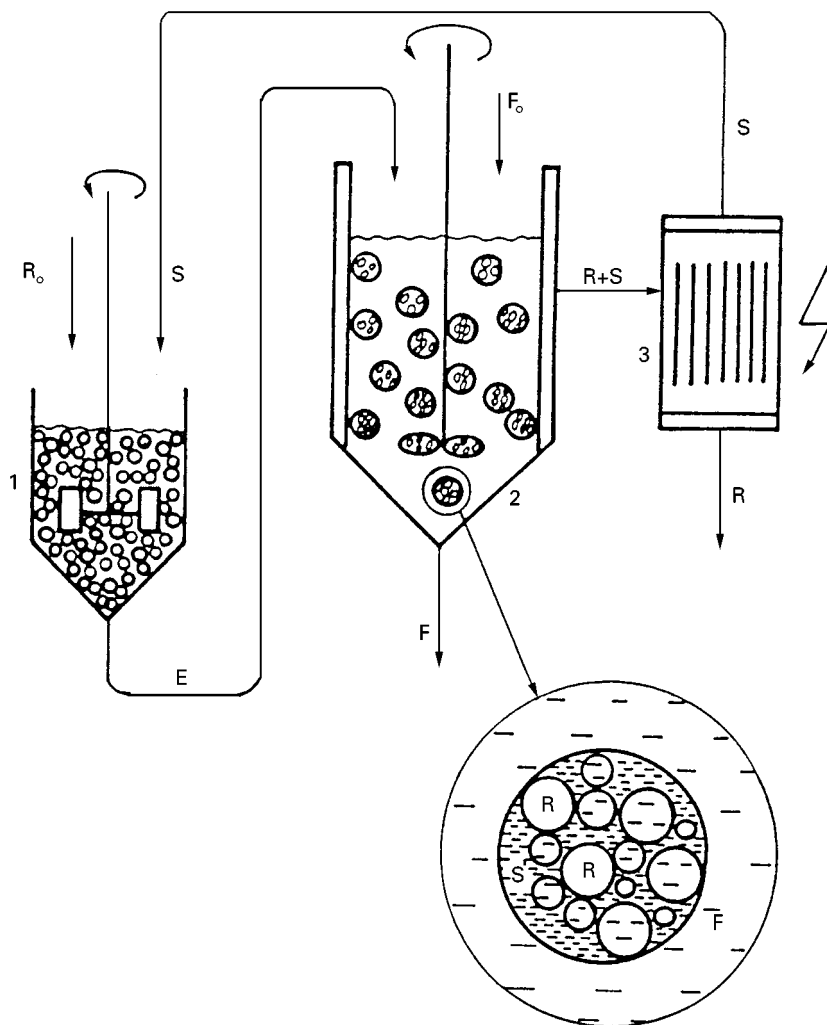


Figure 8 Separation by emulsion liquid membranes. 1, Emulsion preparation (step 1); 2, feed treatment with the emulsion (step 2); 3, break-up of enriched emulsion (step 3). R, Acceptor solution; F, donor solution; S, membrane liquid.

The advantages of these two techniques consist in the considerably larger fluxes per unit interface and in their practically unlimited life. However, the rather low ratio between the contact interface and the bulk of the solution neutralizes, the first advantage.

Methods with Phase Dispersion

Emulsion (surfactant) liquid membranes Emulsion liquid membranes were first described in 1971 by Li in a paper dealing with the separation of aromatic and aliphatic hydrocarbons by stabilized dispersion of three liquids: the above-mentioned mixture, water and an inert hydrocarbon as a recipient phase. This technique, known as emulsion (or surfactant) liquid membranes, was the first pertraction technique developed to industrial scale.

As the name implies, the three-phase system is stabilized by an emulsifier, added to the membrane liquid, in some cases its concentration in the membrane liquid reaches 5% or more. The acceptor solution is dispersed as fine (2–20 μm) droplets in the membrane phase. The thick emulsion, stabilized by the emulsifier, is dispersed in its turn in the donor solution as globules of 1–2 mm diameter and the resulting dispersion is intensely stirred for several minutes. During this contact time, the solutes, which are more soluble in the membrane phase, are transferred from the donor phase to the intermediate phase and from there to the encapsulated acceptor solution. This transfer is very fast due to the large contact areas. After termination of the second (main) process step and dispersion settling, the enriched emulsion is separated and subjected to chemical, thermal or, most often, high voltage electrocoagulation, which breaks the emulsion into two phases. The separated membrane liquid phase is fed back for a new cycle of the process and the enriched acceptor solution phase is subjected to further treatment. The scheme in Figure 8 illustrates this three-stage batch process which in some modifications is carried out as a continuous process. In this process, the recovery efficiency and the separation selectivity are controlled by the transfer kinetics, i.e. by the difference in the transfer rates of the individual solutes. As these rates depend on a great number of factors, for each case there is a specific optimum contact time, which can only be determined experimentally. A shorter than optimum contact time results in a lower solute recovery, while a longer contact time reduces selectivity and recovery efficiency. If the emulsion is too stable, this causes problems related to its break-up in the third process step. Irrespective of these drawbacks, the emulsion liquid membrane technique is most often investigated and practically applied.

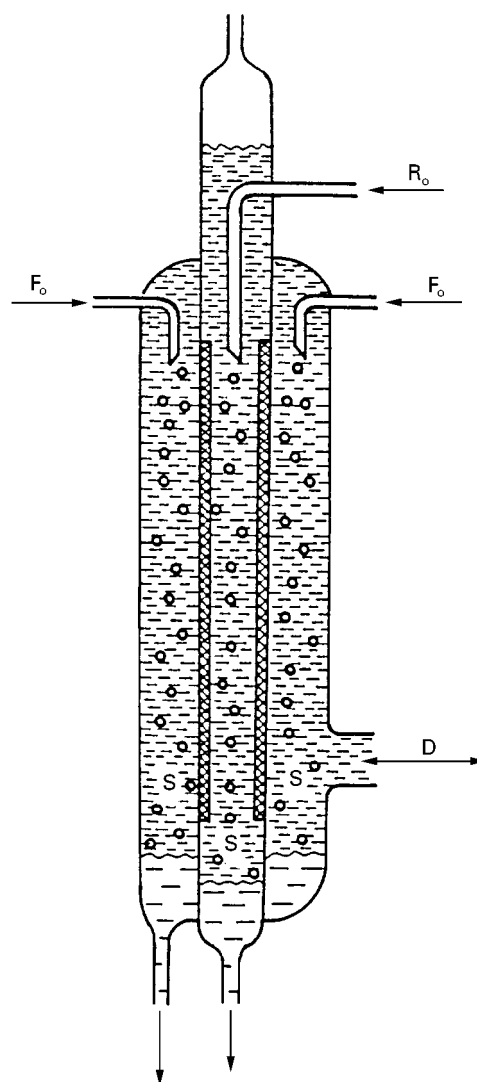


Figure 9 Two-compartment pulsating column. Applied pulsations, D, exchange the membrane liquid S between central and annular compartments across the porous wall. R, Acceptor solution; F, donor solution; S, membrane liquid.

Other techniques with phase dispersion In addition to the disadvantages listed above, the added emulsifier contaminates both the donor and acceptor phases, as in some cases its solubility in these phases exceeds that of the membrane liquid itself or of the carrier added. To avoid using surface active substances, other techniques with phase dispersion were recently proposed, two of which are illustrated in Figures 9 and 10.

Co-axially placed in the vertical tube is a second tube of porous hydrophobic material, e.g. porous polypropylene. As shown in Figure 9, both internal and annular spaces are filled with the membrane liquid which, under laterally applied pulsations, partially goes from one space to the other and back. The

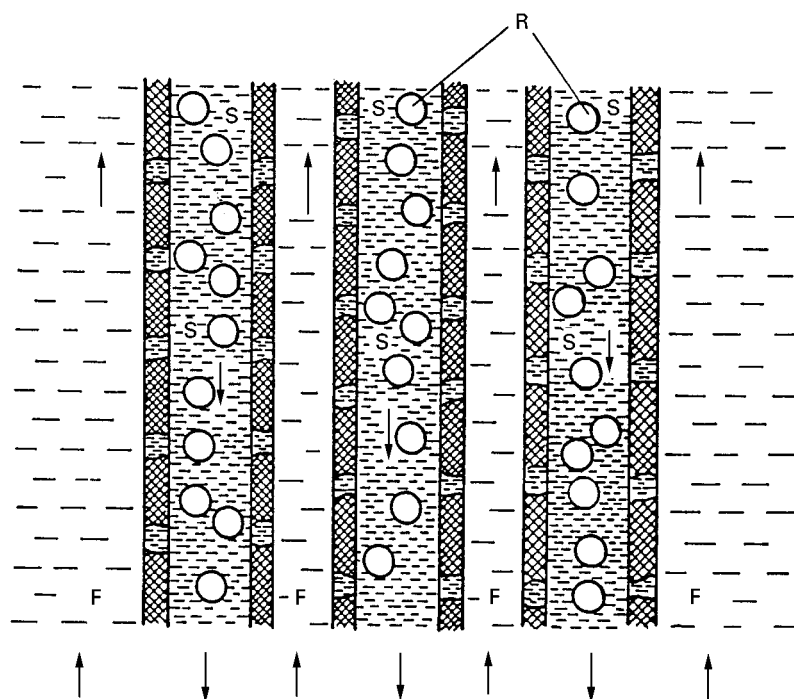


Figure 10 Combination of hollow fibre supported liquid membranes with the emulsion technique in which a nonstabilized phase R dispersed in phase S emulsion flows inside the hollow fibres.

two aqueous feed and acceptor phases are fed into the top of the central and annular space, respectively, as droplets of about 1 mm diameter. The porous filter tube does not allow intermixing of the droplets of the two aqueous phases. The aqueous droplets should be small enough to guarantee sufficient residence time of the corresponding phase in the contractor, but not too small that it penetrates into the other compartment.

The second arrangement avoiding the use of surface active substances is shown in Figure 10. The technique is a combination of hollow fibre and emulsion liquid membrane techniques without using an emulsifier for dispersion stabilization. The acceptor/membrane-phase emulsion flows in the lumen of porous capillaries wetted by the membrane liquid, filling their pores. Evidently, no intense mass transfer is possible with this technique, irrespective of the continuous wash-out of the membrane liquid by the acceptor solution dispersed in it. This drawback is, however, again compensated for by the great number of hollow fibres used and by the recirculation of the intracapillary dispersion.

Application Areas

The liquid membrane processes described above are in principle highly efficient chemical pumps selectively separating and concentrating valuable solutes. These processes have potential applications in a num-

ber of industrial areas, e.g. hydrometallurgy, electroplating and galvanic technologies, chemical and pharmaceutical industries. One of the most promising applications is in biotechnology, where pertraction, can be integrated with the basic bioprocess in order to increase process efficiency.

A very attractive feature of pertraction processes is their low investment, and in particular, their operational costs. Being a membrane operation, the separation does not involve phase transitions and therefore power consumption is very low. However, unlike solid membrane separations, the costs of lost membrane liquid and the purification of treated solutions sometimes required additionally contribute to the process costs.

The Further Reading section lists titles containing more information on various pertraction systems studied in the last 25 years.

See also: I/Membrane Separations. II/Flotation: Flotation Cell Design: Application of Fundamental Principles.

Further Reading

- Araki T and Tsukube H (eds) (1991) *Liquid Membranes: Chemical Applications*. Boca Raton, FL: CRC Press.
- Bartsch RA and Douglas Way J (eds) (1996). *Chemical Separations with Liquid Membranes*. New York: American Chemical.

- Boyadzhiev L (1990) Liquid pertraction or liquid membranes – state of the art. *Separation Science and Technology* 25: 187.
- Boyadzhiev L and Lazarova Z (1994) Liquid membranes (liquid pertraction). In: Noble RD and Stren SA (eds) *Membrane Separation Technology. Principles and Applications*, pp. 283–352. Amsterdam: Elsevier.
- Drioli E and Nakagaki M (1986) *Membranes and Membrane Processes*. New York: Plenum.
- Ho WSW and Sirkar KK (eds) (1993) *Membrane Handbook*. New York: Van Nostrand Reinhold.
- Li NN (1971) Permeation through liquid surfactant membranes. *American Institute of Chemical Engineers Journal* 17: 459.
- Noble RD and Douglas Way J (eds) (1996) *Liquid Membranes. Theory and Application*. American Chemical Society Symposium Series no 347. Washington, DC: American Chemistry Society.
- Zhang R (ed.) (1984) *Separation Techniques by Liquid Membranes* (in Chinese). Nanchang: Jiangxi Renmin.

Membrane Bioseparations

A. L. Zydney, University of Delaware, Newark, DE, USA

Copyright © 2000 Academic Press

Membrane processes are particularly well suited to the separation and purification of biological molecules since they operate at relatively low temperatures and pressures and involve no phase changes or chemical additives. Thus, these processes cause minimal denaturation, deactivation and/or degradation of highly labile biological cells or macromolecules. Although essentially all membrane processes (Figure 1) have been used for bioseparations, the greatest interest has been in the application of the pressure-driven processes of ultrafiltration (UF) and microfiltration (MF). Ultrafiltration membranes have pore sizes between 1 and 50 nm and are used for protein concentration, buffer exchange, desalting, clarification of antibiotics and virus clearance. There is also growing interest in the use of ultrafiltration for protein purification using high performance tangential flow filtration (HPTFF). Microfiltration membranes have a pore size between 0.05 and 10 μm and are thus used

for initial clarification of protein solutions, cell harvesting and sterile filtration. In addition, ultrafiltration and microfiltration of blood are used for the treatment of a variety of metabolic and immunological disorders.

The development of membrane processes for bioseparations is very similar to the design of membrane systems for nonbiological applications. However, there are some important differences including:

1. increased concerns about deactivation or denaturation of biological molecules and cells
2. very high value (on a per unit mass basis) of most biological products (particularly recombinant therapeutic proteins)
3. tendency of biological macromolecules and cells to cause significant fouling of both ultrafiltration and microfiltration membranes
4. critical importance of validation and integrity testing in bioprocessing applications

This article provides a brief review of the historical development of membrane systems for bioseparations. This is followed by a general discussion of the

	Microfiltration	Virus filtration	HPTFF	Ultrafiltration	Nanofiltration	Reverse osmosis
Components retained by membrane	Intact cells Cell debris Bacteria	Viruses	Proteins	Proteins	Nucleic acids Antibiotics	Sugars Salts
Membrane						
Components passed through membrane	Colloids Viruses Proteins Nucleic acids Sugars Salts	Proteins Nucleic acids Sugars Salts	Proteins Nucleic acids Sugars Salts	Nucleic acids Surfactants Sugars Salts	Salts Water	Water

Figure 1 Classification of pressure-driven membrane processes showing typical bioprocessing applications.

- Boyadzhiev L (1990) Liquid pertraction or liquid membranes – state of the art. *Separation Science and Technology* 25: 187.
- Boyadzhiev L and Lazarova Z (1994) Liquid membranes (liquid pertraction). In: Noble RD and Stren SA (eds) *Membrane Separation Technology. Principles and Applications*, pp. 283–352. Amsterdam: Elsevier.
- Drioli E and Nakagaki M (1986) *Membranes and Membrane Processes*. New York: Plenum.
- Ho WSW and Sirkar KK (eds) (1993) *Membrane Handbook*. New York: Van Nostrand Reinhold.
- Li NN (1971) Permeation through liquid surfactant membranes. *American Institute of Chemical Engineers Journal* 17: 459.
- Noble RD and Douglas Way J (eds) (1996) *Liquid Membranes. Theory and Application*. American Chemical Society Symposium Series no 347. Washington, DC: American Chemistry Society.
- Zhang R (ed.) (1984) *Separation Techniques by Liquid Membranes* (in Chinese). Nanchang: Jiangxi Renmin.

Membrane Bioseparations

A. L. Zydney, University of Delaware, Newark, DE, USA

Copyright © 2000 Academic Press

Membrane processes are particularly well suited to the separation and purification of biological molecules since they operate at relatively low temperatures and pressures and involve no phase changes or chemical additives. Thus, these processes cause minimal denaturation, deactivation and/or degradation of highly labile biological cells or macromolecules. Although essentially all membrane processes (Figure 1) have been used for bioseparations, the greatest interest has been in the application of the pressure-driven processes of ultrafiltration (UF) and microfiltration (MF). Ultrafiltration membranes have pore sizes between 1 and 50 nm and are used for protein concentration, buffer exchange, desalting, clarification of antibiotics and virus clearance. There is also growing interest in the use of ultrafiltration for protein purification using high performance tangential flow filtration (HPTFF). Microfiltration membranes have a pore size between 0.05 and 10 μm and are thus used

for initial clarification of protein solutions, cell harvesting and sterile filtration. In addition, ultrafiltration and microfiltration of blood are used for the treatment of a variety of metabolic and immunological disorders.

The development of membrane processes for bioseparations is very similar to the design of membrane systems for nonbiological applications. However, there are some important differences including:

1. increased concerns about deactivation or denaturation of biological molecules and cells
2. very high value (on a per unit mass basis) of most biological products (particularly recombinant therapeutic proteins)
3. tendency of biological macromolecules and cells to cause significant fouling of both ultrafiltration and microfiltration membranes
4. critical importance of validation and integrity testing in bioprocessing applications

This article provides a brief review of the historical development of membrane systems for bioseparations. This is followed by a general discussion of the

	Microfiltration	Virus filtration	HPTFF	Ultrafiltration	Nanofiltration	Reverse osmosis
Components retained by membrane	Intact cells Cell debris Bacteria	Viruses	Proteins	Proteins	Nucleic acids Antibiotics	Sugars Salts
	Membrane					
Components passed through membrane	Colloids Viruses Proteins Nucleic acids Sugars Salts	Proteins Nucleic acids Sugars Salts	Proteins Nucleic acids Sugars Salts	Nucleic acids Surfactants Sugars Salts	Salts Water	Water

Figure 1 Classification of pressure-driven membrane processes showing typical bioprocessing applications.

underlying principles governing the design of ultrafiltration and microfiltration systems, with particular emphasis on those factors that are most significant for bioseparations. The reader is referred to the Encyclopedia articles on Membrane Separations – Microfiltration and Membrane Separations – Ultrafiltration for more detailed discussions of these membrane technologies.

Historical Development

The first mention of the process now known as ultrafiltration appears to have been in an 1856 study by Schmidt on the filtration of protein and gum arabic through animal membranes. Thus, the idea of using ultrafiltration for bioseparations dates back well over 100 years. Bechhold coined the term ultrafiltration in 1906 during a systematic study of the behaviour of different pore size collodion membranes made by impregnating filter paper with acetic acid and cellulose nitrate. Zsigmondy obtained one of the first patents in membrane technology in 1922 for the preparation of flat collodion membranes from ether-alcohol solutions. The first efforts to develop microporous membranes in the USA were motivated by the need for rapid detection and analysis of biological warfare agents. This technology was subsequently transferred to the Lovell Chemical Company, which ultimately led to the establishment of Millipore Corporation.

The early historical development of ultrafiltration and microfiltration is described in an excellent review article by Ferry in 1936. The primary applications of membrane technology in the early 1900s were for a variety of biological, analytical and bacteriological assays. Ferry also described the use of membranes for enzyme concentration, analysis of bacteriophages and viruses, blood ultrafiltration to prepare cell- and protein-free ultrafiltrates, sterile filtration of biological solutions and the partial separation of albumin from globulins in blood serum. All of these bioseparations remain areas of active commercial interest even today.

Although many of the potential uses of membrane systems in bioprocessing were identified well over 60 years ago, the collodion (cellulose nitrate) membranes available at that time had inadequate chemical, mechanical and mass transport properties for the effective use of ultrafiltration on an industrial scale. The key breakthrough was the development of the asymmetric cellulose acetate reverse osmosis membrane by Loeb and Sourirajan in the early 1960s and the subsequent extension of this technique to produce asymmetric ultrafiltration membranes. These asymmetric membranes have a very thin skin (approxim-

ately 0.5 μm thick), which provides the membrane with its selectivity, and a more macroporous substructure, which provides the required mechanical and structural integrity. The thin skin results in much higher permeation rates than are obtainable with homogeneous membranes, significantly reducing the required membrane area and/or process time.

Ultrafiltration is now used throughout the downstream separation process for the purification of therapeutic recombinant proteins, blood components, natural protein products and industrial enzymes. Specific applications include protein concentration (i.e. volume reduction), desalting and buffer exchange, all of which are used to condition the product prior to, or immediately after, other separation processes or as part of the final product formulation. In addition, ultrafiltration is used extensively for the clarification of antibiotics, amino acids and other small biological molecules. Recent work has demonstrated that ultrafiltration membranes are also capable of effecting protein–protein separations using a process known as HPTFF. Microfiltration membranes are used for cell harvesting, initial clarification of cell culture media and fermentation broths, and for sterile filtration of products that are directly added to pre-sterilized containers. Sterile filters are also used to remove bacteria and particles from feedstock solutions and to reduce the overall bioburden in processes where the product will be subjected to a terminal sterilization step. Virus removal membranes are used as part of the overall viral clearance required for the production of therapeutic proteins and blood products. Virus filters can also provide a protective barrier for bioreactors through the filtration of media and buffer solutions.

Ultrafiltration and Microfiltration Principles

Membrane Selection

Membrane selection should start with the choice of a high quality vendor since robustness, reliability and reproducibility of manufacturing operations are of paramount importance in most bioprocessing applications. Consistent membrane and device characteristics can be as important to product quality, yield and economics as the inherent differences between various membranes and devices. Cellulosic membranes are attractive for many bioprocessing applications because of their low protein adsorption and low fouling characteristics. Synthetic polymers (e.g. polysulfone and polyvinylidene fluoride) are also attractive due to their greater chemical and mechanical stability. These polymers are often surface-treated to

render them more hydrophilic to reduce protein adsorption and fouling. Membranes used for sterile filtration must be steam-sterilizable, have minimal particle shedding, low extractables and must pass United States Pharmacopoeia (USP) Class VI toxicity testing.

Most manufacturers rate ultrafiltration membranes by their nominal molecular weight cutoff, which is defined as the molecular weight of a solute with a particular retention coefficient:

$$R = 1 - C_{\text{filtrate}}/C_{\text{feed}} \quad [1]$$

where C_{filtrate} and C_{feed} are the solute concentrations in the filtrate solution and feed stream, respectively. Data are typically obtained with a range of model proteins or with polydisperse dextrans. Unfortunately, the procedures used for assigning molecular weight cutoffs, including the choice of solutes, the specific buffer and flow conditions, and the chosen retention value (usually $R = 0.9$) vary widely throughout the industry. In addition, ultrafiltration systems used in bioprocessing generally require protein retention of at least 99%, and often as high as 99.9%, to minimize loss of high value products through the membrane. Data obtained with solutes having $R = 0.9$ are often of little value in determining whether a given membrane can provide these high levels of protein retention due to differences in the details of the pore size distributions.

Microfiltration membranes are typically rated by their pore size or their particle retention characteristics using the log reduction value (LRV), defined as the logarithm (base 10) of the ratio of the particle, cell or virus concentration in the feed to that in the filtrate solution. Sterilizing-grade ($0.2 \mu\text{m}$ pore size) filters are currently defined by the Health Industry Manufacturing Association (HIMA) as a filter which produces a sterile filtrate when challenged by 10^7 colony-forming units of *Brevundimonas diminuta* (formerly classified as *Pseudomonas diminuta*) per cm^2 of membrane area. This challenge uses the smallest bacteria at a concentration that exposes essentially every pore to the microorganisms. Sterile filters are often thought of as operating via a purely size-based (siev-

ing) mechanism, although bacteria can also be removed by adsorption on to the membrane surface.

The chemical compatibility of the membrane needs to be verified with the feed, regeneration chemicals and storage solutions. Sodium hypochlorite (NaOCl) is used most extensively for chemical disinfection of membrane systems in bioprocessing applications. Many membrane systems are designed for steam-in-place (SIP) sterilization, with the entire unit exposed to flowing steam as part of the completely assembled filtration system. Minimum requirements for an effective steam sterilization are 15 min exposure to steam at 121°C and 1 atm pressure. Polysulfone membranes tend to have broader chemical and thermal stability than cellulosic membranes but also require harsher chemical treatment for regeneration due to their greater fouling characteristics. Inorganic (ceramic) membranes have the greatest chemical compatibility, but they are much more expensive than polymeric membranes. The mechanical strength of the membrane is important since reverse-pressure spikes can cause membrane delamination and catastrophic yield loss.

Module Design

Dead-end, or normal-flow, filtration (Figure 2A) is used primarily for laboratory-scale separations and for systems in which the retained species are present at very low concentration. For example, dead-end microfiltration cartridges are used extensively for sterile filtration since the retained bacteria are present at very low concentration. Similar modules can be employed for virus removal applications. Almost all large scale commercial ultrafiltration devices use tangential flow filtration, also referred to as a cross-flow configuration, in which the feed flow is parallel to the membrane and thus perpendicular to the filtrate flow (Figure 2B). This allows retained species to be swept along the membrane surface and out of the device exit, significantly increasing the process flux compared to that obtained with dead-end operation.

A number of tangential flow modules have been developed for ultrafiltration and microfiltration

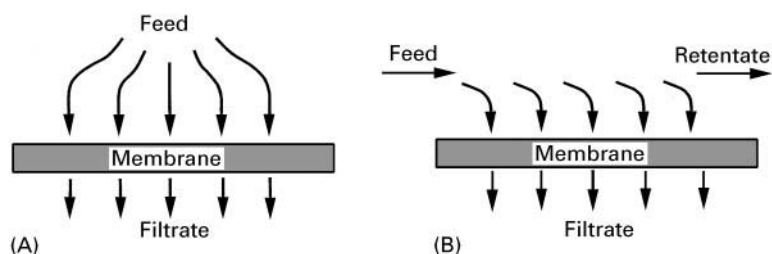


Figure 2 Comparison of (A) dead-end and (B) cross-flow configurations.

Table 1 Comparison of different module configurations

Module configuration	Channel spacing (cm)	Packing density ($\text{m}^2 \text{m}^{-3}$)	Energy costs (pumping)	Particulate plugging	Ease of cleaning
Flat sheet	0.03–0.1	300	Moderate	Moderate	Good
Hollow fibre	0.02–0.25	1200	Low	High	Fair
Tubular	1.0–2.5	60	High	Low	Excellent
Spiral wound	0.03–0.1	600	Low	Very high	Poor to fair

processes, differing primarily in the size and shape of the feed and filtrate flow channels. **Table 1** provides a general summary of the physical characteristics of the most common modules. Detailed descriptions of these modules are available elsewhere.

The small channel spacing in flat-sheet, hollow-fibre and spiral-wound modules provides high membrane-packing densities. In addition, these modules have low hold-up volumes, which facilitates the recovery of high value products. The screens used to define the flow path in spiral-wound modules and many flat-sheet cassettes are susceptible to particle plugging and this may make cleaning more difficult. Hollow-fibre membranes are self-supporting, so they can often be cleaned by simple backflushing. The large-bore tubular membranes can be cleaned by both physical and chemical methods. However, these modules operate in the turbulent flow regime which can cause cell lysis, protein denaturation or aggregation. A variety of enhanced mass transfer modules which exploit flow instabilities have also been developed for bioprocessing applications. Rotating cylinder modules which induce Taylor vortices have very high mass transfer rates, although there are concerns about the moving parts. Another attractive approach is to use helically coiled hollow fibres wrapped around a central core to induce Dean vortices.

Process Configurations

Protein concentration can be carried out using either batch or fed-batch operation (**Figure 3**). In a batch process, the entire feed volume is contained within the recycle tank. Tank design is critically important to ensure adequate mixing while avoiding air entrainment and excessive foaming. Batch operation uses a minimum of hardware and allows simple manual or automatic control. The flux rates are also higher in batch processes since the bulk concentration follows a more dilute path in going from initial to final concentration. Disadvantages of the batch configuration include less flexibility in using the same system for multiple processes, greater difficulty in designing a well-mixed system, and difficulties in obtaining high concentration factors.

The fed-batch configuration utilizes an additional tank to feed into the recycle tank (**Figure 3**). Fed-batch configurations are commonly used to obtain high concentration factors and to provide well-mixed, low-hold-up, retentate reservoirs. These systems also provide flexibility for use in multiple processes. The disadvantages of the fed-batch system include greater process time and greater number of passes of the retentate through the pumps and valves in the recycle line. The latter can lead to excessive cell lysis, protein denaturation or aggregation.

Diafiltration is commonly used for buffer exchange (for products in the retentate) and to enhance yield (for products in the filtrate). The diafiltration system looks similar to the fed-batch configuration shown in **Figure 3** except that the feed tank contains a buffer solution which is added to the recycle tank. The most common approach is constant retentate volume diafiltration in which the buffer is added at the same rate as filtrate removed.

The yield and purification obtained in ultrafiltration and microfiltration processes can be evaluated from simple mass balances on the product and impurity assuming constant rejection coefficients. The final product concentration (C_F) at the end of a batch concentration process is given as:

$$\left(\frac{C_F}{C_0}\right) = \left(\frac{V_0}{V_F}\right)^{1-S} \quad [2]$$

where V_F is the final retentate volume, V_0 is the initial retentate volume and S is the product sieving coefficient (equal to one minus the rejection coefficient). The analogous expression for a fed-batch process is:

$$\frac{C_F}{C_0} = \frac{1}{S} + \left(1 - \frac{1}{S}\right) \exp\left[-S\left(\frac{V_0}{V_F} - 1\right)\right] \quad [3]$$

The final concentration after a constant retentate volume diafiltration is:

$$\frac{C_F}{C_0} = \exp(-SN) \quad [4]$$

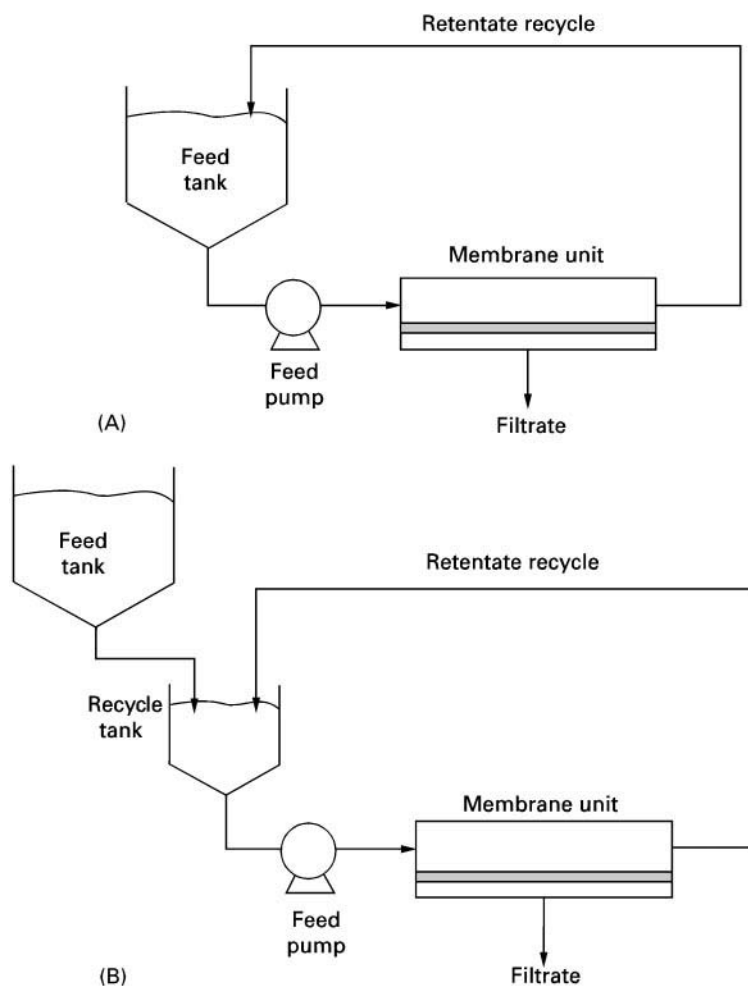


Figure 3 Comparison of (A) batch and (B) fed-batch processes for protein concentration.

where the number of diavolumes (N) is given by:

$$N = V_D/V \quad [5]$$

where V_D is the diafiltration buffer volume. Even very small sieving coefficients may result in substantial product loss when a large number of diavolumes are required in diafiltration processes. For example, a diafiltration process with a product sieving coefficient of $S = 0.01$ will result in a 10% product loss during a 10 diavolume buffer exchange.

Concentration Polarization

One of the critical factors determining the overall performance of tangential flow filtration devices is the rate of solute/particle transport in the bulk solution adjacent to the membrane. The filtrate flow causes an accumulation of partially (or completely) retained components at the upstream surface of the membrane, a phenomenon referred to as concentration

polarization. The concentration thus varies from its maximum value at the membrane surface (C_w) to its bulk value (C_b) over the thickness of the concentration boundary layer (δ). Most analyses of concentration polarization have employed the simple stagnant film model in which:

$$J = k \ln \left(\frac{C_w - C_f}{C_b - C_f} \right) \quad [6]$$

where J is the filtrate flux (typically in $\text{L m}^{-2} \text{h}^{-1}$) and k is the solute mass transfer coefficient in the particular membrane device. The accumulation of particles/solutes at the membrane surface increases the overall resistance to filtrate flow through the formation of a particle cake or gel layer and it can reduce the effective pressure driving force through the osmotic pressure of the retained solutes. At high transmembrane pressures, the wall concentration approaches a maximum value determined by the close-packed concentration of the particles or cells, the

protein solubility limit or the concentration at which the osmotic pressure of the retained solutes is essentially equal to the applied transmembrane pressure. The net result is that the flux attains a nearly constant pressure-independent value that increases with decreasing bulk concentration and increasing feed flow rate. The dependence on feed flow rate is determined by the module characteristics: approximately $1/3$ power for laminar flow in hollow fibres and open channels, $1/2$ power for screened channels, and 0.8 power for turbulent flow in tubular modules. The dependence on feed flow rate for cellular suspensions is typically greater than that for protein solutions due to shear-induced particle diffusion and inertial lift effects.

Process Control

Ultrafiltration and microfiltration processes have traditionally been performed at constant transmembrane pressure. Constant-pressure processes are very simple to control. The feed rate is ramped up to the set point and the retentate valve is then partially closed to obtain the desired transmembrane pressure. The transmembrane pressure should be gradually increased to minimize fouling. In some applications it may not be possible to maintain constant transmembrane pressure without severe reductions in filtrate flux over the course of the process due to membrane fouling. This is particularly true for cell microfiltration where the high initial flux leads to very rapid deposition of cells and cell debris on the membrane surface. Several studies have shown that higher overall throughput can often be obtained in these applications by operating at constant filtrate flux. The flux is controlled by regulating the retentate pressure control valve or by using a pump on the filtrate line.

A third method of process control that is very attractive for bioprocessing applications is to vary the filtrate flux so that the wall concentration of retained species (evaluated from eqn [6]) remains constant during the process. Control is performed using a proportional-integral-derivative (PID) loop that measures flux and controls the transmembrane pressure or filtrate flow rate to maintain a constant wall concentration throughout the process. The benefits of constant C_w control are that product yield is maximized, product quality is ensured, membrane area is minimized and process time is consistent and independent of variations in membrane permeability.

High Performance Tangential Flow Filtration

Ultrafiltration and microfiltration have traditionally been limited to separating species that differ in size by

at least 10-fold. In contrast, HPTFF enables the separation of solutes without limit to their relative size. HPTFF is able to obtain the high selectivity required for effective protein purification by exploiting several recent developments. Firstly, HPTFF is operated in the pressure-dependent regime, with the filtrate flux and device fluid mechanics chosen to minimize fouling and exploit the effects of concentration polarization. Since optimal separation in HPTFF is obtained at a specific filtrate flux, the membrane module should be designed to maintain a nearly uniform flux and transmembrane pressure throughout the module. This can be done using a co-current filtrate flow to balance the feed-side pressure drop through the module. Secondly, the buffer pH and ionic strength are adjusted to maximize differences in the effective volume of the different species. The effective volume of a charged protein (as determined by size exclusion chromatography) accounts for the presence of the diffuse electrical double layer surrounding the protein. Protein transmission through the membrane can be reduced by increasing the effective protein volume, e.g. by increasing the net protein charge (by adjusting the pH) or by increasing the double-layer thickness (by reducing the solution ionic strength). Thirdly, the electrical charge of the membrane is chosen to increase the electrostatic exclusion of all species with like charge. Thus, a positively charged membrane will provide much greater rejection of a positively charged protein than will a negatively charged membrane of the same pore size. Fourthly, protein separations in HPTFF are accomplished using a diafiltration mode to wash the impurity (or product) out of the retentate. The diafiltration maintains an appropriate protein concentration in the retentate throughout the separation, and it allows one to obtain purification factors for products collected in the retentate that are much greater than the membrane selectivity due to the continual removal of impurities in the filtrate.

Although HPTFF is still a new membrane technology, a number of recent studies have clearly demonstrated the potential of this separation technique. Several of these results are summarized in Table 2. Purification factors for the separation of bovine serum albumin (BSA) from an antigen-binding fragment (Fab) were greater than 800-fold with either protein collected in the retentate depending upon the choice of solution pH and membrane surface charge. BSA and haemoglobin have essentially identical molecular weight but different surface charge characteristics. In this case, operation at pH 7 caused a strong electrostatic exclusion of the negatively charged BSA from the negatively charged membrane. The separation of BSA monomer and dimer occurs primarily because of the difference in protein size, with the

Table 2 Purification factors and yields for HPTFF processes^a

Product (MW)	Impurity (MW)	Purification factor	Yield
BSA (68 000)	Fab (45 000)	990	94%
Fab (45 000)	BSA (68 000)	830	69%
BSA (68 000)	Hb (67 000)	100	68%
IgG (155 000)	BSA (69 000)	30	84%
BSA (68 000)	BSA dimer (136 000)	9	86%

^aBSA, Bovine serum albumin; Fab, antigen-binding fragment from recombinant DNA antibody; Hb, bovine haemoglobin; IgG, human immunoglobulin.

smaller monomer collected in the filtrate. However, electrostatic interactions are also important in this system due to the combined effects of size and charge on protein transmission and to possible differences in the charge-pH profiles for the monomer and dimer.

Validation and Integrity Testing

Membrane systems used in bioprocessing applications need to be validated to demonstrate consistent purification and yield with minimal alteration in the properties of the product. Food and Drug Administration regulations provide specific guidelines for validation of sterile filters and virus removal membranes. Validation should always be performed at the same pH, ionic strength and chemical environment as used in the actual process to ensure equivalent physical and chemical characteristics of the product and impurities. Viral clearance studies are typically performed by spiking high titre infectious viruses (with different physical characteristics) into scaled-down production systems.

Integrity testing is critical for all sterile and viral filters to ensure that the system operates at the required level of performance. Integrity tests should be performed both prior to, and immediately after, the actual process wherever possible. Integrity tests performed prior to filtration must not affect the sterility of the connections downstream of the filter. The real test for the sterile filter would be to challenge with *B. diminuta*, but the filter could not be used after this test. Thus, a number of surrogate nondestructive integrity tests have been developed. The industry standards are forward flow, pressure decay and bubble point. Each of these tests is based on the displacement of a fluid from the pores by a second fluid (or gas), with the rate of displacement providing a measure of the membrane pore size characteristics. The gas or intrusion liquid expels the wetting liquid out of the pore when the feed pressure exceeds the capillary force within the pore. The bubble point is defined as

the pressure at which the pore is first intruded by the gas. The bubble point for sterilizing grade filters can be correlated to the LRV of *B. diminuta*. Filters with water bubble points of 55 psi or greater typically yield the necessary LRV to be qualified as sterilizing-grade filters. In the forward flow test, one measures the total gas flow rate through the wetted membrane at a fixed pressure. High flow rates indicate the presence of pressure-driven flow through gas-intruded (large) pores. The pressure decay test is performed in a similar fashion, with the gas flow calculated from the rate of pressure decay. A variety of automated integrity test instruments have been developed by the different membrane manufacturers.

Bubble point tests with water-wetted membranes cannot be used to verify virus filter performance since the bubble points for these small pore size membranes would exceed the membrane pressure limits. Air diffusion and bubble point tests can be performed on these membranes using wetting fluids having lower surface tension (e.g. isopropyl alcohol). Liquid intrusion tests using two immiscible fluids (e.g. solutions of a sulfate salt and polyethyleneglycol) have been developed as integrity tests for virus filters and HPTFF membranes.

Summary

Membrane processes should continue to be of critical importance in bioprocessing applications, facilitating the cost-effective production of a wide range of biological products. Ultrafiltration has become the primary means for protein concentration and buffer exchange in the production of therapeutic proteins and industrial enzymes. Sterile filtration is used throughout the bioprocessing industry, and viral filtration is of growing importance in the production of blood products and therapeutic recombinant proteins.

The future is likely to see the continued development of high performance tangential flow filtration as a viable alternative to existing separation technologies for protein purification. There is also growing interest in the development of membrane systems for the preparation of enantiomerically enriched antibiotics, nutraceuticals and pharmaceuticals. These membrane systems use chiral ligands to separate racemic mixtures or they employ immobilized enzymes for direct production of single enantiomers in membrane reactors. Affinity membrane systems are also being actively pursued as alternatives to standard chromatographic resins for a range of adsorptive bio-separations. In this case, the membrane provides an attractive high surface area support with minimal diffusional mass transfer resistance. New advances in membrane materials, modules and processes

should lead to continued development of membrane systems for bioseparations.

See also: II/Membrane Separations: Microfiltration; Ultrafiltration.

Further Reading

- Belfort G, Davis RH and Zydney AL (1994) The behavior of suspensions and macromolecular solutions in cross-flow microfiltration. *Journal of Membrane Science* 96: 1.
- Blatt WF, Dravid A, Michaels AS and Nelsen L (1970) Solute polarization and cake formation in membrane ultrafiltration. Causes, consequences, and control techniques. In: Flinn JE (ed.) *Membrane Science and Technology*, pp. 47–97. New York: Plenum Press.
- Cheryan M (1997) *Ultrafiltration and Microfiltration Handbook*. Lancaster, PA: Technomic.
- Ferry JD (1936) Ultrafilter membranes and ultrafiltration. *Chemical Reviews* 18: 373.
- Ho WSW and Sirkar KK (eds) (1992) *Membrane Handbook*. New York: Chapman & Hall.
- Lonsdale HK (1982) The growth of membrane technology. *Journal of Membrane Science* 10: 81.
- McGregor WC (ed.) (1986) *Membrane Separations in Biotechnology*. New York: Marcel Dekker.
- van Reis R and Zydney AL (1999) Protein ultrafiltration. In: Flickinger MC and Drew SW (eds) *Encyclopedia of Bioprocess Technology: Fermentation, Biocatalysis, and Bioseparation*, pp. 2197–2214. New York: John Wiley.
- Zeman LJ and Zydney AL (1996) *Microfiltration and Ultrafiltration: Principles and Applications*. New York: Marcel Dekker.

Membrane Preparation

I. Pinnau, Membrane Technology and Research, Inc., Menlo Park, CA, USA

Copyright © 2000 Academic Press

Background

A membrane (Latin, *membrana*, skin) is a thin barrier that permits selective mass transport. Between 1850 and 1900, membranes were used to derive basic physical principles for gas and liquid transport across a barrier material (see the work of Mitchell, Fick and Graham). In these early studies it was already recognized that membranes could be used to separate fluid mixtures. Membranes used at that time included dense films of nitrocellulose, natural rubber, and palladium. The first commercial synthetic membranes

were developed by Bachmann and Zsigmondy in the early 1920s in Germany. These microporous nitrocellulose membranes were used for laboratory purposes as well as for the fast detection of bacteria in drinking water. However, until the early 1960s, membranes were not used in any industrial separation process. The major event that ultimately resulted in the widespread use of membranes for separations was the development of integrally-skinned, asymmetric cellulose acetate membranes for water desalination, by Loeb and Sourirajan at UCLA from 1958 to 1960. During a time span of only 10 years, a wide variety of membranes was developed for reverse osmosis, ultrafiltration and microfiltration applications based on modifications of the original membrane preparation method employed by Loeb and Sourirajan. Further-

Table 1 Major milestones in the development of membranes for industrial separations

Period of years	Advances
1900–1920	Development of first ultrafiltration and microfiltration membranes made from nitrocellulose (Bechhold, Zsigmondy, Bachmann).
1920–1940	Empirical studies on formation of phase inversion membranes (Bjerrum, Manegold, Elford). Development of cellulose acetate ultrafiltration membranes (Dobry, Duclaux).
1940–1960	Development of integrally-skinned asymmetric cellulose acetate membranes for water desalination by reverse osmosis (Loeb and Sourirajan).
1960–1970	Commercialization of reverse osmosis, ultrafiltration, microfiltration, and dialysis membranes.
1970–1980	Development of thin-film composite membranes made by interfacial polymerization (Cadotte, Riley). Cellulose acetate gas separation membranes (Schell).
1980–1990	Commercialization of gas separation and pervaporation membranes (Henis and Tripodi, Tusel, Bruschke).
1990–2000	Development of inorganic membranes for gas separation and pervaporation.
The next millennium	Commercialization of inorganic membranes.

should lead to continued development of membrane systems for bioseparations.

See also: II/Membrane Separations: Microfiltration; Ultrafiltration.

Further Reading

- Belfort G, Davis RH and Zydney AL (1994) The behavior of suspensions and macromolecular solutions in cross-flow microfiltration. *Journal of Membrane Science* 96: 1.
- Blatt WF, Dravid A, Michaels AS and Nelsen L (1970) Solute polarization and cake formation in membrane ultrafiltration. Causes, consequences, and control techniques. In: Flinn JE (ed.) *Membrane Science and Technology*, pp. 47–97. New York: Plenum Press.
- Cheryan M (1997) *Ultrafiltration and Microfiltration Handbook*. Lancaster, PA: Technomic.
- Ferry JD (1936) Ultrafilter membranes and ultrafiltration. *Chemical Reviews* 18: 373.
- Ho WSW and Sirkar KK (eds) (1992) *Membrane Handbook*. New York: Chapman & Hall.
- Lonsdale HK (1982) The growth of membrane technology. *Journal of Membrane Science* 10: 81.
- McGregor WC (ed.) (1986) *Membrane Separations in Biotechnology*. New York: Marcel Dekker.
- van Reis R and Zydney AL (1999) Protein ultrafiltration. In: Flickinger MC and Drew SW (eds) *Encyclopedia of Bioprocess Technology: Fermentation, Biocatalysis, and Bioseparation*, pp. 2197–2214. New York: John Wiley.
- Zeman LJ and Zydney AL (1996) *Microfiltration and Ultrafiltration: Principles and Applications*. New York: Marcel Dekker.

Membrane Preparation

I. Pinnau, Membrane Technology and Research, Inc., Menlo Park, CA, USA

Copyright © 2000 Academic Press

Background

A membrane (Latin, *membrana*, skin) is a thin barrier that permits selective mass transport. Between 1850 and 1900, membranes were used to derive basic physical principles for gas and liquid transport across a barrier material (see the work of Mitchell, Fick and Graham). In these early studies it was already recognized that membranes could be used to separate fluid mixtures. Membranes used at that time included dense films of nitrocellulose, natural rubber, and palladium. The first commercial synthetic membranes

were developed by Bachmann and Zsigmondy in the early 1920s in Germany. These microporous nitrocellulose membranes were used for laboratory purposes as well as for the fast detection of bacteria in drinking water. However, until the early 1960s, membranes were not used in any industrial separation process. The major event that ultimately resulted in the widespread use of membranes for separations was the development of integrally-skinned, asymmetric cellulose acetate membranes for water desalination, by Loeb and Sourirajan at UCLA from 1958 to 1960. During a time span of only 10 years, a wide variety of membranes was developed for reverse osmosis, ultrafiltration and microfiltration applications based on modifications of the original membrane preparation method employed by Loeb and Sourirajan. Further-

Table 1 Major milestones in the development of membranes for industrial separations

Period of years	Advances
1900–1920	Development of first ultrafiltration and microfiltration membranes made from nitrocellulose (Bechhold, Zsigmondy, Bachmann).
1920–1940	Empirical studies on formation of phase inversion membranes (Bjerrum, Manegold, Elford). Development of cellulose acetate ultrafiltration membranes (Dobry, Duclaux).
1940–1960	Development of integrally-skinned asymmetric cellulose acetate membranes for water desalination by reverse osmosis (Loeb and Sourirajan).
1960–1970	Commercialization of reverse osmosis, ultrafiltration, microfiltration, and dialysis membranes.
1970–1980	Development of thin-film composite membranes made by interfacial polymerization (Cadotte, Riley). Cellulose acetate gas separation membranes (Schell).
1980–1990	Commercialization of gas separation and pervaporation membranes (Henis and Tripodi, Tusel, Bruschke).
1990–2000	Development of inorganic membranes for gas separation and pervaporation.
The next millennium	Commercialization of inorganic membranes.

more, methods of efficiently packaging membranes into modules (plate-and-frame, spiral-wound, and hollow-fibre) were developed during this period. Around 1980, the use of membranes for separations was established as a unit operation process in the chemical process industry. Further optimization of membrane preparation and modification methods from 1980 to 1990 made membrane separations competitive in gas separation and liquid separation applications. The most important production methods that resulted in the commercial use of synthetic membranes are listed in **Table 1**. Recent attention has been directed towards the development of inorganic membranes. Optimized inorganic membranes can have significantly better separation properties compared to state-of-the-art polymeric membranes. However, currently the main limitations for large-scale commercialization of inorganic membranes are their poor mechanical strength (brittleness) and extremely high manufacturing costs.

Membrane Types

Membranes can be distinguished based on their (i) geometry, (ii) bulk structure, (iii) production method, (iv) separation regime, and (v) application, as shown in **Figure 1**. Most commonly, membranes are produced in flat-sheet or tubular (hollow-fibre) geometry. Flat-sheet membranes are either packaged in plate-and-frame or spiral-wound modules, whereas tubular membranes are packaged in hollow-fibre modules. The choice of the optimum membrane and module type depends on a wide variety of process

specific conditions. Although hollow-fibre modules offer the highest membrane area per module volume ratio, plate-and-frame and spiral-wound modules are also commonly used for large-scale separations because of their better control of fluid dynamics.

Membranes either have a symmetric (isotropic) or an asymmetric (anisotropic) structure. The structure of a symmetric membrane is uniform throughout its entire thickness, whereas asymmetric membranes have a gradient in structure. The flux of a fluid through a symmetric membrane is typically relatively low, as the entire membrane thickness contributes a resistance to mass transport. Asymmetric membranes consist of two structural elements, that is, a thin, selective layer and a microporous substructure. Typically, the bulk structure (99+%) of an asymmetric membrane is highly porous and provides only mechanical strength. Separation of a fluid mixture in an asymmetric membrane is performed in a very thin surface layer, which is typically of the order of 0.1–0.5 μm thick. The most common symmetric and asymmetric membrane types are shown in **Figure 2**.

Ideal Membranes for Separations

Membranes can be fabricated from a wide variety of organic (e.g. polymers, liquids) or inorganic (e.g. carbons, zeolites, etc.) materials. Currently, most commercial membranes are made from polymers. The properties of a membrane are controlled by the membrane material and the membrane structure. To be useful in an industrial separation process, a

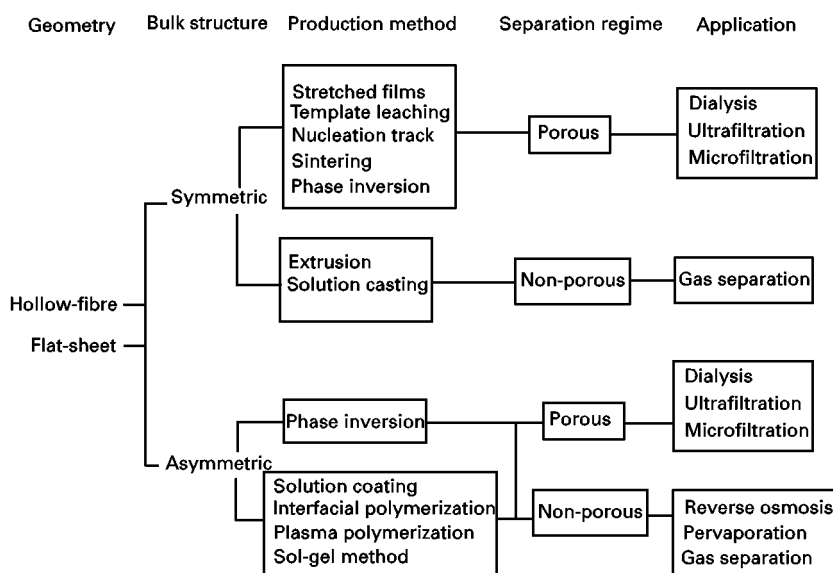


Figure 1 Classification scheme of synthetic membranes based on their geometry, bulk structure, production method, separation regime, and application.

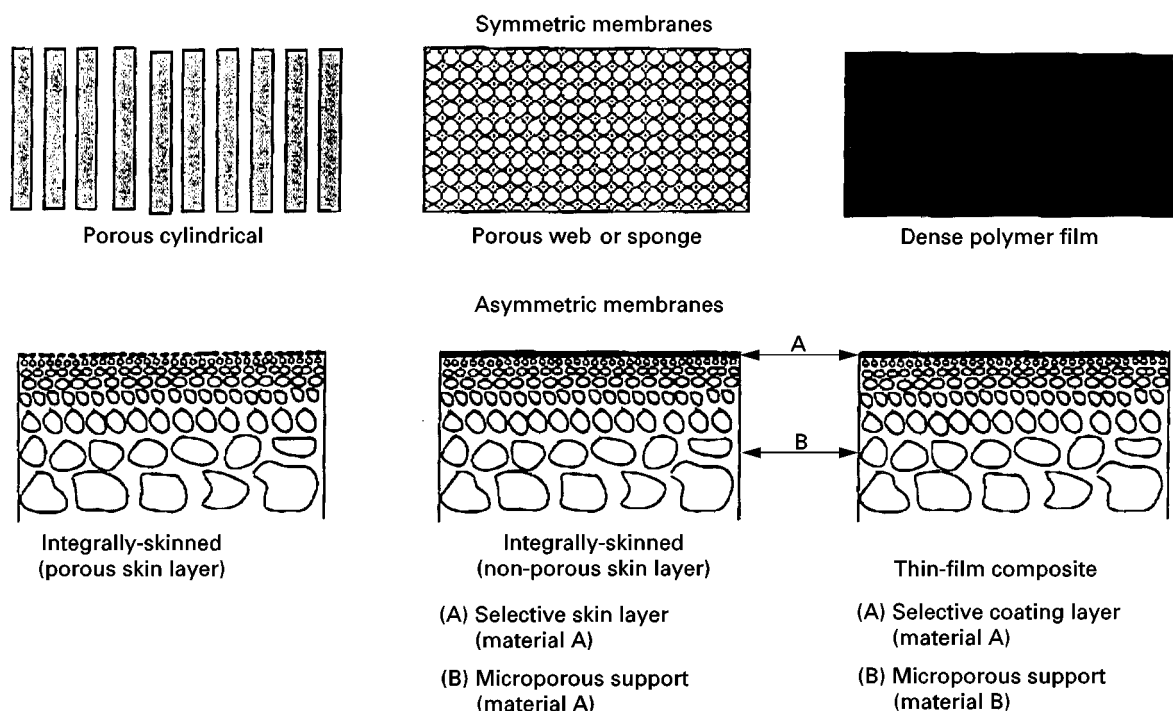


Figure 2 Schematic representation of symmetric and asymmetric membrane structures.

membrane must exhibit at least the following characteristics: (i) high flux, (ii) high selectivity (rejection), (iii) mechanical stability, (iv) tolerance to all feed stream components (fouling resistance), (v) tolerance to temperature variations, (vi) manufacturing reproducibility, (vii) low manufacturing cost, and (viii) ability to be packaged into high surface area modules. Of the above requirements, flux and selectivity (rejection) determine the selective mass transport properties of a membrane. The higher the flux of a membrane at a given driving force, the lower is the membrane area required for a given feed flow rate, and, therefore, the lower are the capital costs of a membrane system. The selectivity determines the extent of separation, and, therefore, the purity of the desired product.

Typically, porous membranes are used in dialysis, ultrafiltration, and microfiltration applications. Ideal porous membranes have high porosity and a narrow pore size distribution. Membranes having a dense, selective layer are applied in reverse osmosis, pervaporation, and gas separation processes. Permeation through dense membranes occurs by a solution/diffusion mechanism. Ideal dense membranes should have a very thin selective layer, because flux is inversely proportional to the membrane thickness. In addition, the thin separating layer must be pinhole-free, because even a very small area fraction of defects in the membrane can cause a significant decrease in selectivity.

Polymeric Membranes

Currently, most commercial membranes are made from polymers. Polymeric membranes can be fabricated by a wide variety of methods and fulfill most of the requirements of an ideal membrane listed above. Membranes are made from amorphous as well as semi-crystalline polymers by solution- or melt-processes. A list of commonly used polymers for commercial membrane separation processes is given in Table 2.

Symmetric Membranes

Dense Symmetric Membranes

Dense symmetric membranes with thicknesses greater than 10 μm can be made by melt extrusion or solution casting and subsequent solvent evaporation. Because the fluxes of fluids through dense polymer films are very low, this membrane type is rarely used for large-scale separations. Dense symmetric, ion-exchange membranes are used in electrodialysis applications for production of potable water from brackish water.

Porous Symmetric Membranes

Typically, symmetric porous membranes have cylindrical, sponge-, web- or slit-like structures, and can be made by a variety of techniques. The most

Table 2 Polymers used for production of commercial membranes

<i>Membrane material</i>	
Cellulose regenerated	D, UF, MF
Cellulose nitrate	MF
Cellulose acetate	GS, RO, D, UF, MF
Polyamide	RO, NF, D, UF, MF
Polysulfone	G, UF, MF
Poly(ether sulfone)	UF, MF
Polycarbonate	GS, D, UF, MF
Poly(ether imide)	UF, MF
Poly(2,6-dimethyl-1,4-phenylene oxide)	GS
Polyimide	GS
Poly(vinylidene fluoride)	UF, MF
Polytetrafluoroethylene	MF
Polypropylene	MF
Polyacrylonitrile	D, UF, MF
Poly(methyl methacrylate)	D, UF
Poly(vinyl alcohol)	PV
Polydimethylsiloxane	PV, GS

MF = microfiltration; UF = ultrafiltration; NF = nanofiltration; D = dialysis; PV = pervaporation; GS = gas separation.

important methods for the production of symmetric porous membranes are: (i) irradiation, (ii) stretching of a melt-processed semi-crystalline polymer film, (iii) template leaching, (iv) temperature-induced phase separation, and (v) vapour-induced phase separation.

Symmetric membranes with a cylindrical pore structure can be produced by an irradiation-etching process. These membranes are often referred to as nucleation track membranes. In the first step of this process, a dense polymer film, such as polycarbonate or polyester, is irradiated with charged particles, which cause chain scission and leave behind a sensitized track of damaged polymer molecules. These tracks are more susceptible to attack by chemical agents than the undamaged, base polymer film. In the second step, the film is passed through an etching medium, typically a sodium hydroxide solution. During this process, pores are formed by etching the partially degraded polymer along the nucleation tracks. Membranes made by this method have a very uniform pore size. The porosity and pore size of nucleation track membranes can be controlled by the irradiation time and etching time, respectively.

Membranes with a symmetric slit-like pore structure can be made from semi-crystalline polymers, such as polyethylene, polypropylene or polytetrafluoroethylene, using a melt extrusion/stretching process. In the first process step, a highly oriented film is formed by melt-extrusion of a semi-crystalline polymer and re-crystallization under high stress. The crystallites in the semi-crystalline polymer film are then

aligned in the direction of orientation. In the second step, slit-like pores, about 200–2500 Å wide, are formed between the stacked lamellae by stretching the membrane in the machine direction. The pore size of these membranes is determined by the rate and extent of stretching during the second process step. Commercial membranes made by the extrusion/stretching process are available from Hoechst-Celanese (Celgard®) and W.L. Gore (Gore-Tex®).

Template leaching is another method of producing symmetric microporous membranes by melt-processing of a semi-crystalline polymer. In this process, a leachable component, such as a high-boiling paraffin, is uniformly dispersed in a polymer melt. After extrusion and formation of a polymer film, the leachable component is extracted using a suitable solvent, and a sponge-like, microporous membrane is formed.

Symmetric porous membranes can also be made by a thermally-induced phase separation process (TIPS process). In the TIPS process, the membrane structure is formed by bringing an initially thermodynamically stable polymer solution to an unstable state by lowering the process temperature. The change in temperature causes phase separation of the initially stable solution into two phases with different compositions. The membrane structure depends primarily on the initial polymer concentration and the kinetics of the phase separation process and the local distribution of the polymer-rich phase at the point of solidification. A schematic phase diagram for a solution containing a polymer and a solvent is shown in Figure 3. The phase diagram is divided into three distinct regions: (A) stable polymer solution region, (B) meta-stable or binodal region, and (C) spinodal region. Phase separation can occur by two different mechanisms, that is, (i) nucleation and growth or (ii) spinodal decomposition. The quench paths of three different polymer-solvent solutions from temperature T_1 to temperature T_2 are illustrated in Figure 3. After lowering the initial solution temperature T_1 to T_2 , solutions A and B will be in the meta-stable region of the phase envelope and phase separation will occur by nucleation and growth. Solution A forms nuclei with composition ϕ_p^β (polymer-rich), whereas solution B will form nuclei with composition ϕ_p^α (solvent-rich). At equilibrium, both solutions phase-separate into two phases composed of ϕ_p^α and ϕ_p^β . However, the ratio of α -phase to β -phase is significantly different after phase separation of both solutions. Solution A will consist of a very small volume fraction of polymer-rich-phase (ϕ_p^β) dispersed in a large volume fraction of solvent-rich phase (ϕ_p^α). As a result of the low volume fraction of polymer, solution A will form a fine powder of precipitated polymer. On the other hand, solution B will consist of a small volume

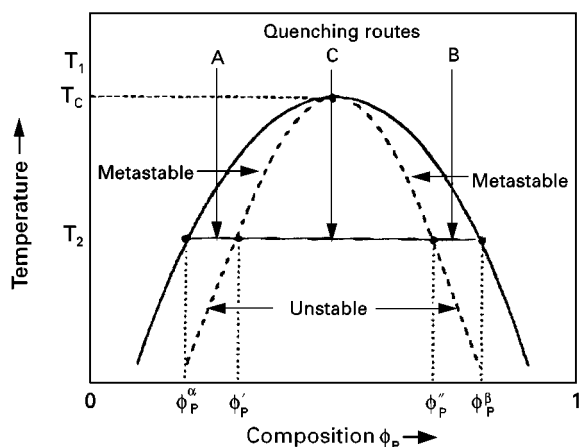


Figure 3 Schematic diagram of a binary polymer-solvent system with an upper critical solution temperature (UCST).

fraction of solvent-rich phase dispersed in a large volume fraction of polymer-rich phase. The resulting morphology is a sponge- or foam-like porous structure. A thermal quench of solution C passes directly into the unstable region of the phase diagram; therefore, phase separation occurs by spinodal decomposition. Typically, phase separation by spinodal decomposition leads to an interconnected, porous structure. The final membrane structure depends not only on liquid-liquid phase separation phenomena but also on the kinetics of the thermal quench process and the distribution of the polymer-rich phase at the point of solidification. Typically, a rapid quench rate results in a large fraction of small pores, whereas a slow quench rate produces fewer, but larger pores.

Symmetric membranes with sponge- or web-like pore structures can also be made by a vapour-precipitation/evaporation technique. Membranes made by this method are highly porous and are typically used in microfiltration applications. In its simplest form of the method, a solution containing polymer, solvents and non-solvents is cast onto a substrate and is then exposed to a water-vapour-saturated air stream. The water vapour induces phase separation in the initially stable polymer solution. After phase separation, the solvent and non-solvent components are evaporated by blowing a hot air stream across the membrane. The porosity and pore size of this membrane type can be controlled by: (i) the polymer concentration in the casting solution and (ii) the composition of the vapour atmosphere. Low polymer concentration, high humidity, and the addition of solvent-vapour to the casting atmosphere lead to membranes with high porosity and large pore size. Because membranes made by the vapour-precipitation/evaporation method have an essentially constant polymer concentration profile throughout the entire membrane thick-

ness at the onset of phase separation, the resulting membranes are porous and have a fairly symmetric structure.

Asymmetric Membranes

The most commonly used asymmetric membranes are: (i) integral-asymmetric with a porous skin layer, (ii) integral-asymmetric with a dense skin layer, and (iii) thin-film composite membranes. Integrally-skinned asymmetric membranes are typically made by a non-solvent induced phase separation process (immersion precipitation) and consist of a thin, selective layer and a porous substructure. Both skin layer and substructure are formed simultaneously during the immersion precipitation process. Porous integral-asymmetric membranes are applied in dialysis, ultrafiltration, and microfiltration applications, whereas integral-asymmetric membranes with a dense skin layer are used in reverse osmosis and gas separation applications. Thin-film composite membranes consist of a thin, selective polymer layer atop a porous support. In this membrane type, the separation and mechanical functions are assigned to different layers in the membrane. This membrane type was originally developed for reverse osmosis applications; however, nowadays thin-film composite membranes are also used in nanofiltration, gas separation, and pervaporation applications.

Integrally-Skinned Asymmetric Membranes

The first integrally-skinned asymmetric membranes were developed by Loeb and Sourirajan in the early 1960s for seawater desalination by reverse osmosis. In the original Loeb-Sourirajan technique, thin-skinned ($\sim 0.2 \mu\text{m}$) cellulose acetate membranes were made by a four-step process: (i) casting of a multi-component polymer solution, (ii) partial evaporation of a volatile solvent, (iii) immersion of the nascent polymer film into a non-solvent (water), and (iv) thermal annealing of the water-wet membrane. Membranes made by this method had water fluxes orders of magnitude higher than those of thick, isotropic cellulose acetate films while maintaining high sodium chloride rejection ($> 90\%$). The Loeb-Sourirajan method has been modified and applied to a wide variety of polymers other than cellulose acetate. In fact, the Loeb-Sourirajan process is by far the most important method for production of commercial membranes for separations.

In the simplest case, integrally-skinned asymmetric membranes are made from a binary solution containing a polymer and a solvent. Upon immersion of the cast solution into a liquid (typically water), which is

a non-solvent for the polymer but miscible with the solvent, an asymmetric structure with either a porous or non-porous skin layer is formed. The structural gradient in an integrally-skinned asymmetric membrane results from a very steep polymer concentration

gradient in the nascent membrane at the onset of phase separation. The structure of a typical membrane made by immersion precipitation having a highly porous substructure and a thin skin layer is shown in Figure 4(A) and 4(B). In the immersion precipitation process, phase separation can be induced by: (i) solvent evaporation and/or (ii) solvent/non-solvent exchange during the quench step. Typically, the formation of membranes made by the immersion precipitation method occurs over a very short time scale, typically less than a few seconds. Most commercial membranes made by the immersion precipitation method are made from multi-component solutions containing polymer, solvent(s), and non-solvent(s) or additives. The porosity, pore size, and skin layer thickness can be modified by the addition of non-solvents to the casting solution (e.g. alcohols, carboxylic acids, surfactants, etc.), inorganic salts (e.g. LiNO_3 or ZnCl_2 , etc.) or polymers (e.g. polyvinylpyrrolidone, polyethylene glycol, etc.). Even very small amounts of these solution additives can have a significant effect on the membrane structure, and hence, its separation properties. The structure of membranes made by immersion precipitation can also be altered by using multi-component quench media. For example, the addition of a solvent to the quench medium results in an increase in the surface porosity and pore size of the membrane. The formation of membranes made by the immersion precipitation process depends on a large number of material- and process-specific parameters including:

- choice of the polymer (molecular weight, molecular weight distribution)
- choice of the solvent(s) and additives
- composition of the casting solution
- choice of the quench medium
- composition and temperature of the casting atmosphere
- temperature of the casting solution and quench medium
- evaporation conditions
- casting thickness
- casting or spinning speed
- membrane support material (type of woven or non-woven)
- drying conditions.

Thin-Film Composite Membranes

Composite membranes consist of at least two structural elements made from different materials, as shown in Figure 5. A single-layer composite membrane (5A) consists of a thin, selective layer atop a microporous support. The support provides only mechanical strength, whereas the separation is

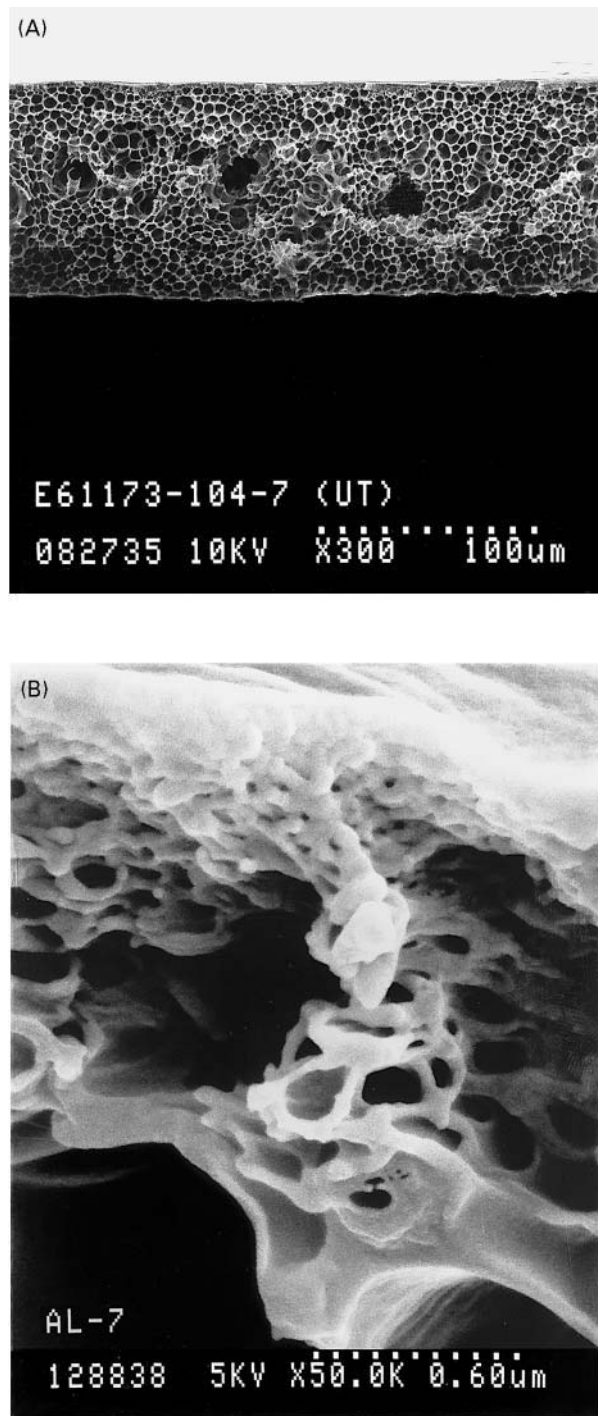


Figure 4 (A) Porous bulk structure and (B) skin layer of an integrally-skinned asymmetric polysulfone membrane made by the immersion precipitation process.

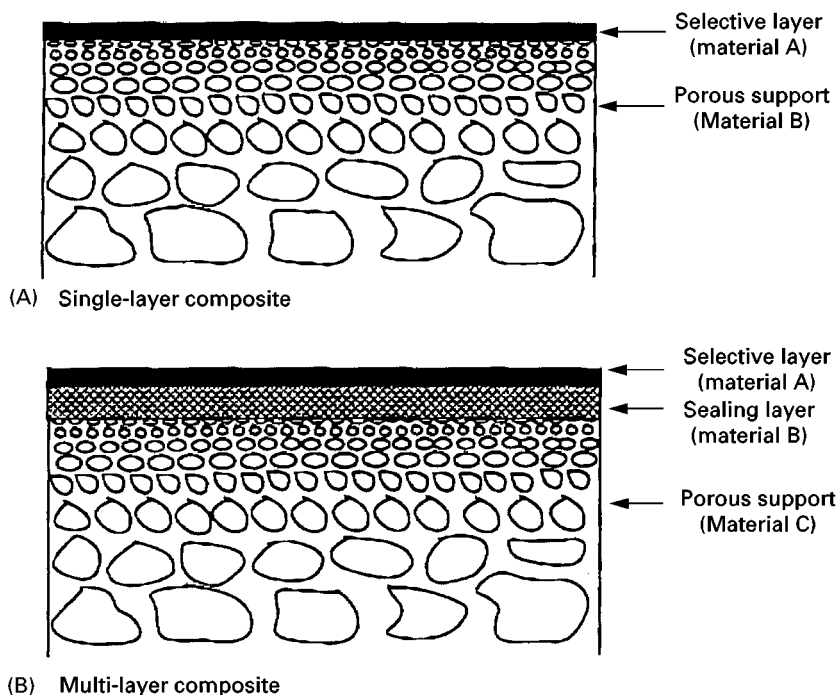


Figure 5 Schematic diagram of (A) single-layer and (B) multi-layer thin-film composite membranes.

performed by the thin top-layer. A multi-layer composite membrane (5B) consists of a porous support and several layers of different materials, each performing a specific function. Thin-film composite membranes are applied in nanofiltration, reverse osmosis, gas separation, and pervaporation applications. The selective layer can be applied by lamination, solution coating, interfacial polymerization, or plasma polymerization methods. Compared to integrally-skinned asymmetric membranes, composite membranes offer several significant advantages: (i) independent selection of materials from which the separating layer and the porous support are formed, (ii) independent preparation of the separating layer and the porous support membrane, thereby making it possible to optimize each structural element, and (iii) very expensive membrane materials (> 1000 \$/lb) can be used because only a very small amount of polymer is required for the formation of the thin separation layer (~ 1 g polymer/m² of membrane for a 1- μ m-thick selective layer).

In most cases, porous, ultrafiltration-type membranes made by the immersion precipitation process are used as mechanical support for thin-film composite membranes. Optimum porous supports for thin-film composite membranes should have the following properties: (i) porous support must be chemically resistant against the solvent or solvent mixture from which the thin separating layer is formed and (ii) the porous support should have a high surface porosity and small pore size. High surface porosity is

important because the support should not provide any significant resistance to mass transport in a composite membrane. A small pore size is required for the deposition of ultrathin, defect-free coatings.

The two most important methods for the commercial production of thin-film composite are based on interfacial polymerization and solution coating methods. The first interfacially polymerized thin-film composite membranes were developed by Cadotte at the North Star Research Institute and represented a breakthrough in membrane performance for reverse osmosis applications. The original interfacial polymerization process involved soaking a microporous polysulfone support in an aqueous solution of a polymeric amine and then immersing the amine-impregnated membrane into a solution of a di-isocyanate in hexane. The membrane was then cross-linked by heat-treatment at 110°C. The resulting polyurea membrane had better salt rejection than that of an integrally-skinned asymmetric cellulose acetate membrane and high water flux. Modifications in the chemistry of the original interfacial polymerization reaction scheme resulted in further improvement in performance of thin-film composite membranes for reverse osmosis applications.

The solution-coating method involves deposition of a dilute polymer solution onto the surface of a porous membrane and subsequent drying of the thin liquid film. The simplicity of this process is very attractive for the production of membranes on a

commercial scale. However, it is generally very difficult to produce defect-free thin-film composite membranes with a thickness of less than 1 μm by the solution coating process. These defects are caused by incomplete coverage of surface pores in the support membrane after complete evaporation of the solvent. The difficulty in completely covering surface pores results from penetration of the coating solution into the porous support membrane structure. Because capillary forces in the porous membrane tend to pull the thin liquid polymer solution into the bulk support membrane, the coating layer can be disrupted easily. Several methods have been proposed to overcome problems with the formation of the thin, selective layer by the solution-coating process. One method is to use ultrahigh molecular weight polymers for the formation of the selective layer. An alternative approach for eliminating defects in the thin selective coating layer is to fabricate multi-layer composite membranes. These membranes, shown schematically in Figure 5B, consist of: (i) a porous support, (ii) a sealing layer, and (iii) an ultrathin, selective coating. The function of the sealing layer is to plug the pores in the support membrane and to provide a smooth surface onto which the thin coating layer can be applied. In addition, the sealing layer helps in channeling the permeating components to the surface pores, thereby rendering the entire surface area available for mass transport. The sealing layer should not provide a significant mass transport resistance in a multi-layer composite membrane. Hence, the sealing layer material should be significantly more permeable than the thin, selective top-layer.

Membrane Modification Methods

The development of high-performance polymeric membranes involves the selection of a suitable membrane material and the formation of this material into a desired membrane structure. However, it is often necessary to modify the membrane material or the structure to enhance the overall performance of the membrane. Generally, the objectives for modification of pre-formed membranes are: (i) increasing flux and/or selectivity and (ii) increasing chemical resistance (solvent resistance, swelling, or fouling resistance).

The first reported membrane modification method involved annealing of porous membranes by heat-treatment. Zsigmondy and Bachmann demonstrated in the early 1920s that the pore size of pre-formed nitrocellulose membranes could be decreased with a hot water or steam treatment. Loeb and Sourirajan used the same method to improve the salt rejection of integrally-skinned asymmetric cellulose acetate reverse osmosis membranes.

During the development of integrally-skinned asymmetric cellulose acetate gas separation membranes it was found that water-wet membranes collapse and form an essentially dense film upon drying. This collapse occurs because of the strong capillary forces within the finely porous structure during the drying process. This phenomenon can be described by the well-known Young-Laplace relationship ($\Delta p = 2\gamma/r$) in the case of perfect wetting of the liquid in the pores). Hence, the capillary pressure is directly proportional to the surface tension of a liquid, but inversely proportional to the pore radius. If the modulus of the membrane material (in the swollen state) is lower than the capillary force of the liquid in the pore space, the pores will collapse and form a dense polymer film. Because water has a very high surface tension, it is often difficult to dry water-wet membranes without collapsing the membrane structure. An exchange of water with liquids having lower surface tension, such as alcohols or aliphatic hydrocarbons, results in maintaining the original membrane structure upon drying. Typical solvent-exchange methods involve replacing water first with *iso*-propanol and then with *n*-hexane. Other methods of eliminating the collapse of finely porous membrane structures include freeze-drying and the addition of surfactants to the water prior to drying of the wet membranes.

In the 1970s, commercialization of gas separation membranes was severely limited by the very poor reproducibility of making ultrathin, defect-free membranes on a large scale. Methods for production of thin-film composite membranes as well as integrally-skinned asymmetric membranes with separating layer thicknesses of less than 0.2 μm were known. However, production of these membranes without defects was not possible. Defects as small as 20 \AA over an area fraction of less than $10^{-4}\%$ can severely reduce the selectivity of gas separation membranes. However, a thin coating of a highly permeable polymer, such as polydimethylsiloxane, can render defective membranes suitable for gas separations. Modification methods developed by Browall for thin-film composite membranes and, in particular, Henis and Tripodi for integrally-skinned asymmetric membranes resulted in rapid commercialization of gas separation membranes. Surface coatings are also applicable in improving the fouling resistance of membranes for ultrafiltration or nanofiltration applications. Chemical surface modification methods of gas separation membranes include treatment with fluorine, chlorine, bromine, or ozone. Typically, these treatments result in an increase in membrane selectivity coupled with a decrease in flux. Cross-linking of polymers is often applied to improve the chemical stability (swelling

resistance) and selectivity of membranes for electrodialysis, reverse osmosis, pervaporation, and gas separation applications.

Inorganic Membranes

Ceramic Membranes

Microporous ceramic membranes for ultrafiltration and microfiltration applications can be formed from a variety of metal oxides. Specifically, aluminium and titanium oxides are preferred precursors for the production of ceramic membranes. Because ceramic membranes are chemically inert and can be operated at high temperatures, these membranes offer some significant advantages over polymeric membranes. Pore diameters in ceramic membranes for ultrafiltration and microfiltration are in the 0.01 to 10 μm range and are typically made by a slip coating-sintering process. Other techniques, such as the sol-gel method, produce ceramic membranes with pores in the range of 10 to 100 Å. In the slip coating-sintering process, a porous ceramic tube is made by pouring a dispersion of a coarse ceramic material and a binder into a mould. This mixture is then sintered at high temperature. The resulting porous tube is then coated with a mixture containing very small metal oxide particles and a binder; this mixture is called a slip suspension. Again, the mixture is sintered at high temperature to form a more finely porous layer. The slip-coating-sintering method can be used to make membranes with pore diameters between 100 to 200 Å. More finely porous membranes can be fabricated by the sol-gel technique. First, the metal oxide, dissolved in alcohol, is hydrolyzed by addition of excess water. Then, the colloidal polymeric or inorganic hydroxide solution is cooled and coated onto a preformed microporous support made by the slip coating-sintering process. The coating must be dried very carefully to avoid cracking of the thin ceramic layer. The final step of the sol-gel method involves sintering of the coating at elevated temperature, typically between 500 and 800°C. In principle, membranes made by this process can be used in a variety of applications which require membranes that are stable in harsh environment and at elevated temperature. However, reproducibility of the membrane formation process on a large commercial scale is rather poor and the membrane costs are too high for these membranes to be used in any industrial separation process.

Metal Membranes

Metal membranes have been considered for a long time for gas separation applications, specifically hy-

drogen separation. Certain noble metals, for example palladium or palladium-silver and palladium-gold alloys, are permeable to hydrogen but essentially impermeable to all other gases. In the 1950s and 1960s, Union Carbide installed a pilot membrane system containing 25- μm -thick, isotropic palladium membranes. Because the hydrogen flux through these thick palladium membranes is quite low, the membranes had to be operated at about 400°C. Although the plant generated 99.9% hydrogen, commercialization of this process was economically not feasible because of the extremely high cost of the metal membrane ($\sim \$5000/\text{m}^2$). Furthermore, contaminants in the feed stream, such as hydrogen sulfide, poison the metal which results in a dramatic decline in hydrogen flux.

Anodic Membranes

Symmetric and asymmetric microporous membranes with a conical pore shape can be made from aluminium using an anodic oxidation process. Symmetric aluminium oxide membranes having a porosity of 65% and a pore size of about 200 nm can be made. The surface pores of asymmetric aluminium oxide membranes are about 25 nm. To prepare these membranes, a thin aluminium foil is anodically oxidized in an acid electrolyte, such as sulfuric or chromic acid, thereby forming an aluminium oxide. The unaffected fraction of the metal foil is subsequently removed using a strong acid. The pore size of membranes made by anodic oxidation is determined by the voltage and the acid type.

Carbon Membranes

Microporous carbon membranes can be made by compressing ultrafine carbon particles or by pyrolysing polymeric precursors. Degradation of the base polymer upon heating leads to carbonization. The pore size and porosity of the pyrolysed membranes depend primarily on the pyrolysis temperature and the pyrolysis atmosphere. Molecular sieve membranes made from pyrolysed polyacrylonitrile and polyimide as well as selective surface flow membranes made from polyvinylidene chloride-acrylate terpolymer can have significantly better separation performance than polymeric membranes in gas separation applications. The pore sizes of microporous carbon membranes are typically in the 5 to 20 Å range.

Glass Membranes

Isotropic glass membranes with a sponge structure can be made by thermal phase separation of an initially homogenous metal oxide mixture. Microporous

glass membranes were produced by Corning (Vycor®), Schott, and PPG. Glass membranes are typically made as discs, tubes or hollow-fibres. To produce microporous glass membranes, a homogeneous melt consisting of 70 wt% SiO₂, 23 wt% B₂O₃ and 7 wt% Na₂O is formed between 1300 to 1500°C. Phase separation of the initially homogeneous glass melt occurs by lowering the temperature to about 800°C. One phase consists primarily of insoluble silicon dioxide. The other phase, rich in alkali borate, can be leached from the heterogeneous glass by treatment with a mineral acid. After removal of the alkali borate phase, a microporous silica membrane is formed.

Future Developments

During the past forty years membranes have gained significant importance in a wide variety of industrial separations. Currently, polymeric membranes are most commonly used for commercial applications. However, recent developments on inorganic membranes are very promising and such membranes may broaden the separation spectrum of membranes for separations. The wide-spread use of inorganic membranes in industrial applications is currently limited by their poor mechanical stability and very high production costs. If these problems can be solved in future work, inorganic membranes will present a new generation of high-performance membranes for the next millennium.

Further Reading

- Baker RW, Cussler EL, Eykamp W *et al.* (1991) *Membrane Separation Systems – Recent Developments and Future Directions*. Park Ridge, NJ: Noyes Data Corporation.
- Bhave RR (1991) *Inorganic Membranes*. New York: Van Nostrand Reinhold.
- Burggraaf AJ and Cot L (1996) *Fundamentals of Inorganic Membrane Science and Technology*. Amsterdam: Elsevier.
- Cabasso I (1987) In *Encyclopedia of Polymer Science and Engineering*, Vol. 9, pp. 509–579. New York: John Wiley and Sons.
- Kesting RE (1971) *Synthetic Polymeric Membranes*. New York: McGraw-Hill Book Company.
- Kesting RE and Fritzsche AK (1993) *Polymeric Gas Separation Membranes*. New York: John Wiley and Sons, Inc.
- Koros WJ and Pinnau I (1994) In: Paul DR and Yampolskii YP (eds) *Polymeric Gas Separation Membranes*, pp. 209–271. Boca Raton: CRC Press.
- Lloyd DR (1985) *Materials Science of Synthetic Membranes*. ACS Symp. Ser. 269. Washington DC: ACS.
- Mulder M (1996) *Basic Principles of Membrane Technology*, 2nd edn, Boston, MA: Kluwer Academic Publishers.
- Petersen RJ and Cadotte JE (1990) In: Porter MC (ed) *Handbook of Industrial Membrane Technology*, pp. 307–348. Park Ridge, NJ: Noyes Publications.
- Pinnau I (1994) *Polym. Adv. Techn.*, 5, 733.
- Strathmann H (1979) *Trennung von molekularen Mischungen mit Hilfe synthetischer Membranen*. Darmstadt: Dr. Dietrich Steinkopff Verlag.
- Strathmann H (1990) In: Porter MC (ed) *Handbook of Industrial Membrane Technology*, pp. 1–60. Park Ridge, NJ: Noyes Publications.

Microfiltration

I. H. Huisman, AMKM, TNO Voeding, AJ Zeist, Holland

Copyright © 2000 Academic Press

Introduction

Microfiltration is a separation technique for removing micron-sized particles, like bacteria, yeast cells, colloids, and smoke particles, from suspensions or gases. The process uses membrane filters with pores in the approximate size range 0.1 to 10 µm, which are permeable to the fluid, but retain the particles, thus causing separation. Examples of particles with sizes in the microfiltration range are presented in **Figure 1**.

Microfiltration membranes were first commercialized in the 1920s, and were at that time mainly used for the bacteriological analysis of water. After 1960 the number of successful microfiltration applications

grew rapidly, and nowadays microfiltration processes are operated in such different fields as the biotechnological, automobile, electronics, and food industry. Examples of applications are the harvesting of bacterial and yeast cells, the recovery of latex pigments from paints, and the purification of water for the electronics industry. In the food industry, microfiltration is used in the clarification of fruit juices, wine, and beer, in fat removal from whey and in removal of bacteria from milk.

Microfiltration is the largest industrial market within the membrane field, responsible for about 40% of total sales, both in Europe and in the USA. In 1997, the US microfiltration membrane market amassed revenues worth about \$400 million, growing at an average annual growth rate of 6.6%. Microfiltration can be carried out in two different operation modes: dead-end (in line) filtration and cross-flow

glass membranes were produced by Corning (Vycor®), Schott, and PPG. Glass membranes are typically made as discs, tubes or hollow-fibres. To produce microporous glass membranes, a homogeneous melt consisting of 70 wt% SiO₂, 23 wt% B₂O₃ and 7 wt% Na₂O is formed between 1300 to 1500°C. Phase separation of the initially homogeneous glass melt occurs by lowering the temperature to about 800°C. One phase consists primarily of insoluble silicon dioxide. The other phase, rich in alkali borate, can be leached from the heterogeneous glass by treatment with a mineral acid. After removal of the alkali borate phase, a microporous silica membrane is formed.

Future Developments

During the past forty years membranes have gained significant importance in a wide variety of industrial separations. Currently, polymeric membranes are most commonly used for commercial applications. However, recent developments on inorganic membranes are very promising and such membranes may broaden the separation spectrum of membranes for separations. The wide-spread use of inorganic membranes in industrial applications is currently limited by their poor mechanical stability and very high production costs. If these problems can be solved in future work, inorganic membranes will present a new generation of high-performance membranes for the next millennium.

Further Reading

- Baker RW, Cussler EL, Eykamp W *et al.* (1991) *Membrane Separation Systems – Recent Developments and Future Directions*. Park Ridge, NJ: Noyes Data Corporation.
- Bhave RR (1991) *Inorganic Membranes*. New York: Van Nostrand Reinhold.
- Burggraaf AJ and Cot L (1996) *Fundamentals of Inorganic Membrane Science and Technology*. Amsterdam: Elsevier.
- Cabasso I (1987) In *Encyclopedia of Polymer Science and Engineering*, Vol. 9, pp. 509–579. New York: John Wiley and Sons.
- Kesting RE (1971) *Synthetic Polymeric Membranes*. New York: McGraw-Hill Book Company.
- Kesting RE and Fritzsche AK (1993) *Polymeric Gas Separation Membranes*. New York: John Wiley and Sons, Inc.
- Koros WJ and Pinnau I (1994) In: Paul DR and Yampolskii YP (eds) *Polymeric Gas Separation Membranes*, pp. 209–271. Boca Raton: CRC Press.
- Lloyd DR (1985) *Materials Science of Synthetic Membranes*. ACS Symp. Ser. 269. Washington DC: ACS.
- Mulder M (1996) *Basic Principles of Membrane Technology*, 2nd edn, Boston, MA: Kluwer Academic Publishers.
- Petersen RJ and Cadotte JE (1990) In: Porter MC (ed) *Handbook of Industrial Membrane Technology*, pp. 307–348. Park Ridge, NJ: Noyes Publications.
- Pinnau I (1994) *Polym. Adv. Techn.*, 5, 733.
- Strathmann H (1979) *Trennung von molekularen Mischungen mit Hilfe synthetischer Membranen*. Darmstadt: Dr. Dietrich Steinkopff Verlag.
- Strathmann H (1990) In: Porter MC (ed) *Handbook of Industrial Membrane Technology*, pp. 1–60. Park Ridge, NJ: Noyes Publications.

Microfiltration

I. H. Huisman, AMKM, TNO Voeding, AJ Zeist, Holland

Copyright © 2000 Academic Press

Introduction

Microfiltration is a separation technique for removing micron-sized particles, like bacteria, yeast cells, colloids, and smoke particles, from suspensions or gases. The process uses membrane filters with pores in the approximate size range 0.1 to 10 µm, which are permeable to the fluid, but retain the particles, thus causing separation. Examples of particles with sizes in the microfiltration range are presented in **Figure 1**.

Microfiltration membranes were first commercialized in the 1920s, and were at that time mainly used for the bacteriological analysis of water. After 1960 the number of successful microfiltration applications

grew rapidly, and nowadays microfiltration processes are operated in such different fields as the biotechnological, automobile, electronics, and food industry. Examples of applications are the harvesting of bacterial and yeast cells, the recovery of latex pigments from paints, and the purification of water for the electronics industry. In the food industry, microfiltration is used in the clarification of fruit juices, wine, and beer, in fat removal from whey and in removal of bacteria from milk.

Microfiltration is the largest industrial market within the membrane field, responsible for about 40% of total sales, both in Europe and in the USA. In 1997, the US microfiltration membrane market amassed revenues worth about \$400 million, growing at an average annual growth rate of 6.6%. Microfiltration can be carried out in two different operation modes: dead-end (in line) filtration and cross-flow

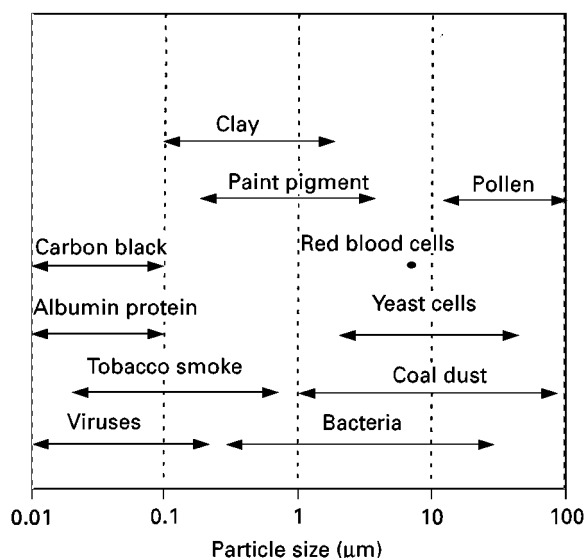


Figure 1 Particles in microfiltration size range.

(tangential flow) filtration (**Figure 2**). In *dead-end filtration* the main flow direction is perpendicular to the membrane. The suspended particles are continuously dragged towards the membrane and deposit on the surface or inside the membrane pores. The deposition of particles leads to a continuously increasing resistance to flow and thus to a continuously decreasing permeate flux rate. To reduce this deposition process, microfiltration is often carried out in the *cross-flow mode* (tangential flow) in which the main flow direction is tangential to the membrane. The flow 'scours'

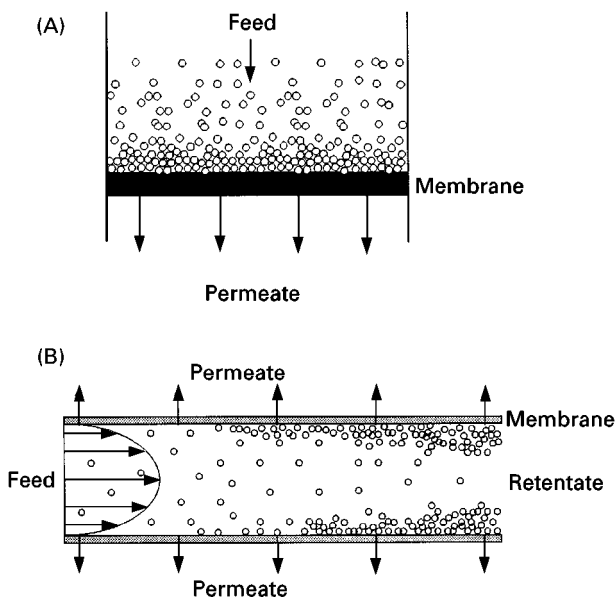


Figure 2 (A) Dead-end filtration and (B) cross-flow microfiltration using a tubular membrane.

away particles from the membrane surface, and thus limits particle deposition.

Microfiltration Membranes

Two main types of membrane filters exist: *screen filters* and *depth filters*. Screen filters contain capillary-type pores; particles are retained on the membrane surface primarily by a sieving mechanism. Depth filters contain a random, tortuous porous structure; particles are retained through adsorption and mechanical entrapment within the bulk of the filter. Screen filters are absolute: particles larger than the pore size are retained, whereas particles smaller than the pore size can pass relatively easily through the membrane. Particle retention of depth filters is not that clearly defined: retention values increase slowly over a broad particle size range and only reach 100% for very large particles. Depth filters are often used for dead-end filtration, as they can retain a high particle load.

Membrane Materials and Membrane Preparation

Microfiltration membranes are available in a wide variety of materials and methods of manufacture. Many membranes are made of polymers, such as cellulose acetate, polysulfone, and polyvinylidene fluoride (PVDF). Most of these membranes are solvent cast, through a phase inversion process. Other preparation techniques are stretching (polytetrafluoroethylene, PTFE, membranes) and track-etching (polycarbonate membranes). The track-etching process results in cylindrical pores with a very narrow size distribution.

Other microfiltration membranes available are made from glass, from ceramics, such as alumina, titania, and zirconia, and from metals, such as silver and stainless steel. Advantages of these inorganic materials are their higher stability towards extreme process conditions, such as high temperature, extreme pH values, and solvents different than water. Most metal and some ceramic membranes are produced by a sintering process, whereas other ceramic membranes are produced by sol-gel processing or by anodic oxidation. Some novel membranes are prepared by lithographic techniques.

In **Table 1**, a number of different commercial membranes and some of their key properties are presented, and in **Figure 3** SEM (scanning electron microscopy) and AFM (atomic force microscopy) images of some membranes are shown. Note that the membranes shown here are only a fraction of the total number of membrane materials and membrane manufacturers available.

Table 1 Various microfiltration membranes and their water fluxes

Manufacturer	Trade name	Material ^b	Preparation method	Pore size ^a (μm)	Water permeability at 20°C (L m ⁻² h ⁻¹ bar)
US Filter/SCT	Membralox [®]	α-Al ₂ O ₃	Sintering	0.2	2 000
Anotec	Anopore [®]	α-Al ₂ O ₃	Anodic oxidation	0.2	3 600
Carbon Lorraine		Carbon	Pyrolysis	0.2	1 500
Tech Sep	Carbosep [®]	ZrO ₂	Sintering	0.14	400
Millipore	Durapore [®]	PVDF	Phase inversion	0.22	5 900
	Fluoropore [®]	PTFE	Stretching	0.22	12 000
	MF-Millipore [®]	Mixed cellulose esters	Phase inversion	0.22	14 400
Osmonics	PCTE	Polycarbonate	Track-etching	0.2	14 600
	PES	Polyethersulfone	Phase inversion	0.2	20 500
	MCS	Mixed cellulose esters	Phase inversion	0.22	15 400
Whatman	Cyclopore [®]	Polycarbonate	Track-etching	0.2	16 000
Aquamarijn	Microsieve [™]	Silicon nitride	Photolithography	0.2	87 000

^aAll these membranes are available with pore sizes in large ranges. The pore sizes closest to 0.22 μm are mentioned here to compare water fluxes of the different membranes. ^bPVDF, polyvinylidene fluoride; PTFE, polytetrafluoroethylene.

Membrane Characterization

Originally the main goal in characterization of porous membranes was to determine the pore-size distribution. It has however been realized more recently that membrane surface properties, such as hydrophobicity, zeta potential and surface roughness, play an important factor in fouling and retention properties of membrane processes. Characterization is therefore nowadays performed by various techniques, measuring different structural and physico-chemical parameters. The relatively novel technique of AFM microscopy has been shown to provide information on many membrane properties of interest: pore size distribution, surface roughness, and adhesion behaviour. In **Table 2**, various measurement techniques are summarized.

Dead-end Microfiltration

In dead-end filtration, the fluid is forced perpendicularly through the membrane, while all or most of the particles are retained (Figure 2a). If screen filters are used, these particles build a cake layer on the surface, which causes an additional resistance to flow. If depth filters are used, these particles fill the voids within the membrane bulk, and in this way cause an increased resistance. For both types of filters, the increased resistance causes a continuous decline in flux if a constant transmembrane pressure is used (**Figure 4**). After some time, the flux has been reduced to unacceptably low levels, and the membrane has to be cleaned or replaced.

Dead-end filtration is preferred over cross-flow filtration in situations where the concentration of particles to be removed from the fluid is very low, as is

the case for sterile filtration in the pharmaceutical industry, for gas cleaning, and for guard-filters positioned as last step in a high-purity water unit. Dead-end filtration is also used in situations where backflush techniques and gas sparging are so effective that the use of a cross-flow is not necessary, as found in some wastewater-treatment plants.

Fluid Flow through Membrane Pores

The capacity of a microfiltration process is expressed as flux, J , which is the volume of permeate passing through the membrane of area A_m and per unit time:

$$J = \frac{1}{A_m} \frac{dV}{dt} \quad [1]$$

where V is the volume of permeate, and t is time: Most commercial liquid microfiltration processes operate at fluxes of typically about 10^{-4} m s^{-1} ($360 \text{ L m}^{-2} \text{ h}^{-1}$).

The driving force for this flux is the *transmembrane pressure* (most commonly written as ΔP), the pressure difference between feed side and permeate side, which results from applying either suction to the permeate side or pressure to the feed side, or both. Transmembrane pressures in liquid microfiltration are typically 5–100 kPa (0.05–1 bar). It was found phenomenologically that the flux increases linearly with the transmembrane pressure (Darcy's law):

$$J = \frac{\Delta P}{R_m \cdot \mu_0} \quad [2]$$

where μ_0 is the permeate viscosity, and R_m is the hydraulic resistance of the membrane against

permeate flow. The *permeability* of the membrane is defined as the inverse of its resistance ($1/R_m$). Microfiltration membranes have permeabilities of typically 10^{-11} m.

The permeability is related to the pore size. The exact relation between permeability and pore size depends on the geometry. For straight cylindrical pores, the Hagen–Poiseuille equation yields:

$$R_m = \frac{8l}{\varepsilon_m r_p^2} \quad [3]$$

where l is the membrane thickness, ε_m is the membrane porosity, and r_p is the pore radius. For membranes comprised of sintered spheres, the Kozeny–Carman equation may give a better approximation:

$$R_m = \frac{45(1 - \varepsilon_m)^2 l}{\varepsilon_m^3 a_m^2} \quad [4]$$

where a_m is the radius of the particles that constitute the membrane.

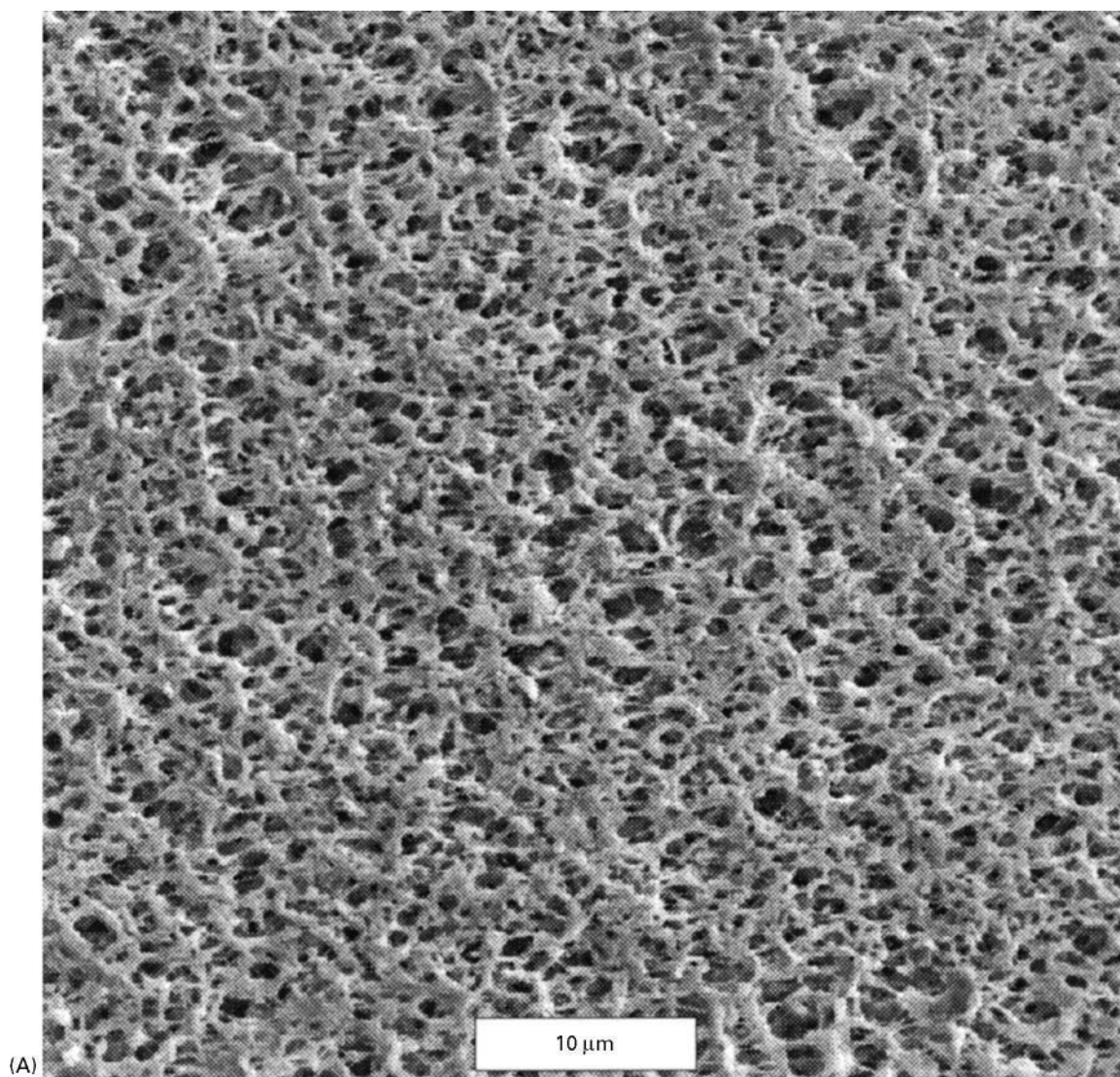


Figure 3 SEM (A–C, E–H) and AFM (D) of surfaces and cross-section of different membranes. (A) Durapore membrane, rating 0.22 μm , PVDF solvent cast membrane (Millipore). (B) Fluoropore membrane, 0.1 rating, stretched PTFE (Millipore). (C) Polycarbonate track-etched membrane (Osmonics). (D) Anopore membrane, 0.1 μm rating, anodically oxidated Al_2O_3 (Anotec). (E) Microsieve, photolithography, silicon nitride (Aquamarijn). (F) Silver membrane (Millipore). (G) AP15 glass fibre depth filter (Millipore). (H) Cross-section of a P series membrane, solvent cast polyethersulfone (Osmonics). (A), (B), (F) and (G) were kindly supplied by the Millipore corporation. (C) and (H) were kindly supplied by Osmonics; (D) was kindly supplied by the Group of Membrane Science and Technology, University of Valladolid, Spain; (E) was kindly supplied by Aquamarijn.

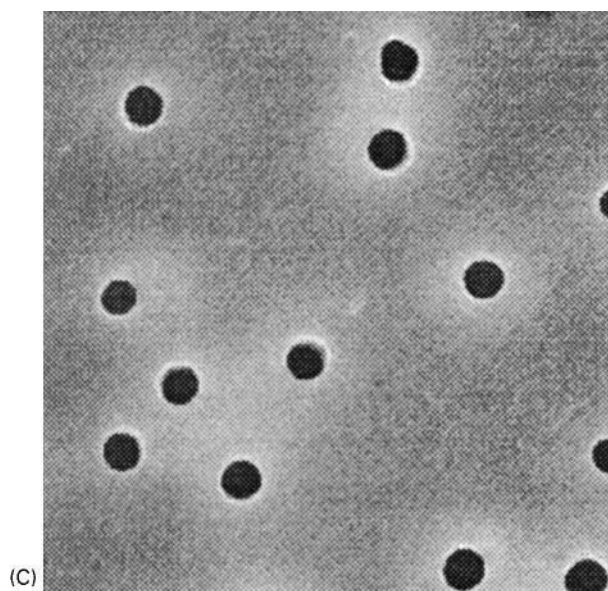
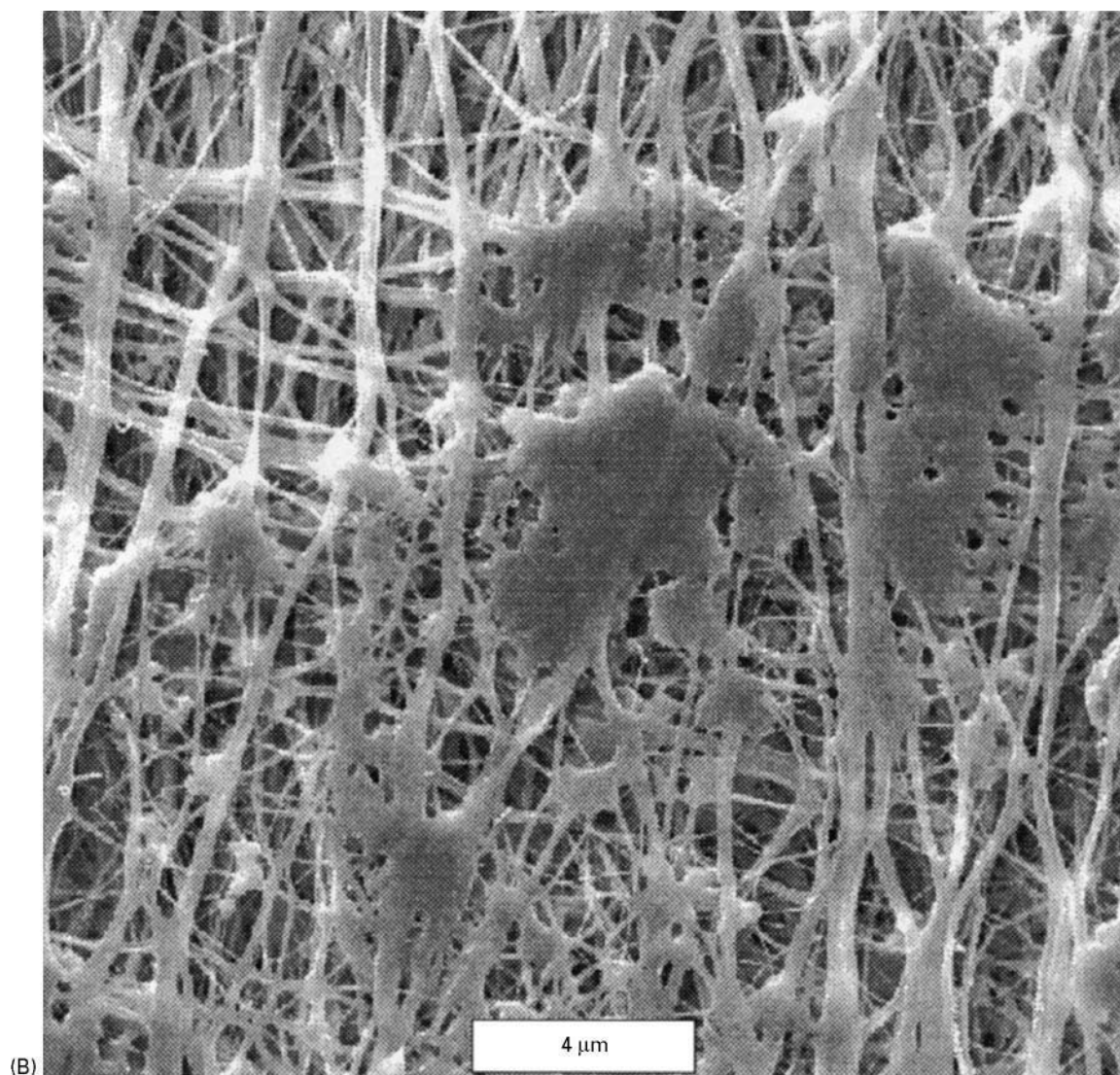


Figure 3 *Continued*

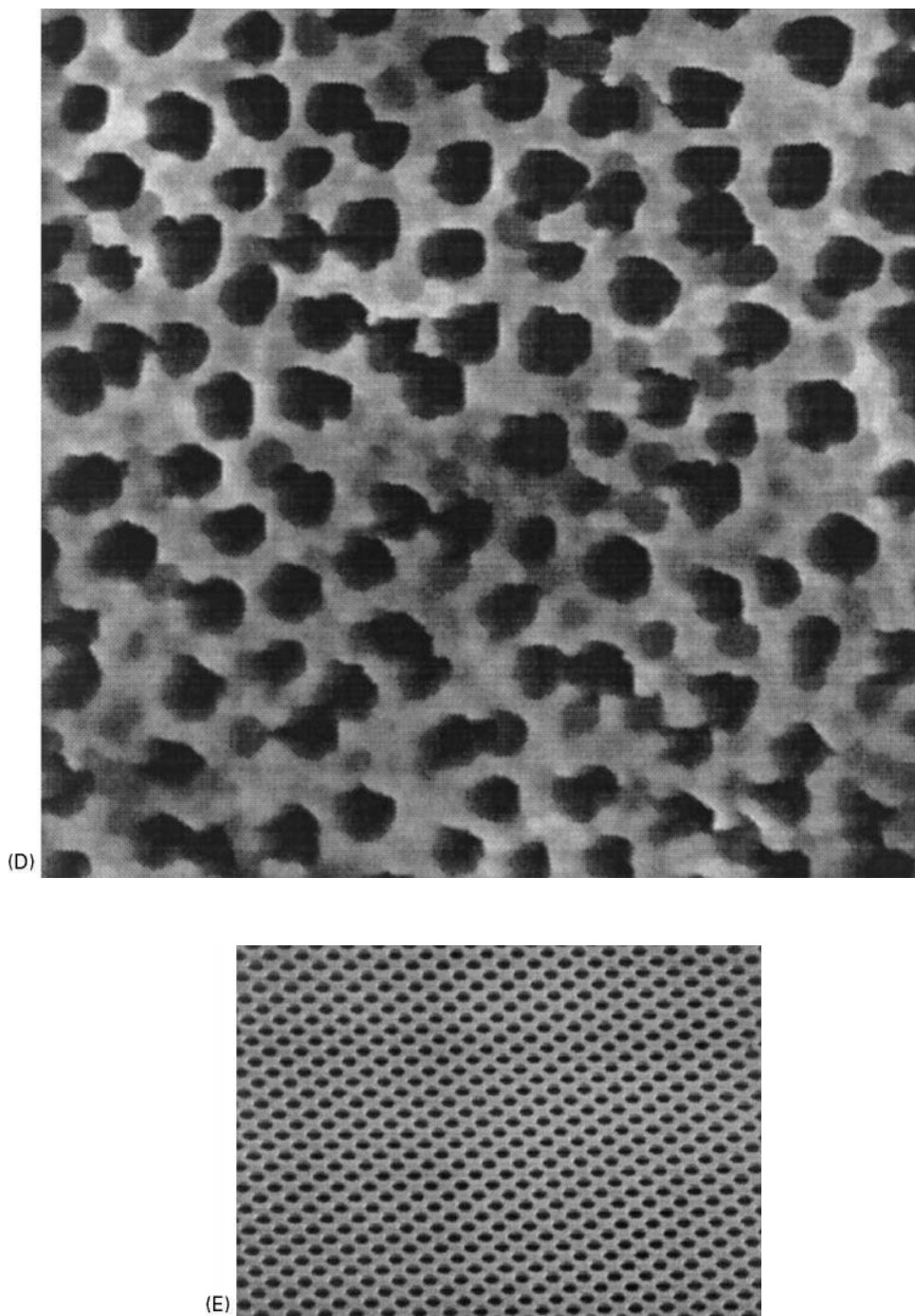


Figure 3 *Continued*

Screen Filters: Cake-layer Build-up

The flux calculated by eqns [2]–[4] is the so-called ‘pure water flux’. During filtration, fouling and cake-layer build-up continuously decrease the flux to values much lower than the pure water flux. Darcy’s law (eqn [2]) can be written for a fouled membrane as:

$$J = \frac{\Delta P}{R_{\text{tot}} \cdot \mu_0} \quad [5]$$

where R_{tot} is the total hydraulic resistance. It can be divided into the membrane resistance (R_m), the resistance caused by fouling (R_f), and the resistance caused by the cake layer (R_{cake}):

$$R_{\text{tot}} = R_m + R_f + R_{\text{cake}} \quad [6]$$

Fouling can be caused by processes such as the adsorption of macromolecules or bacteria. It is difficult

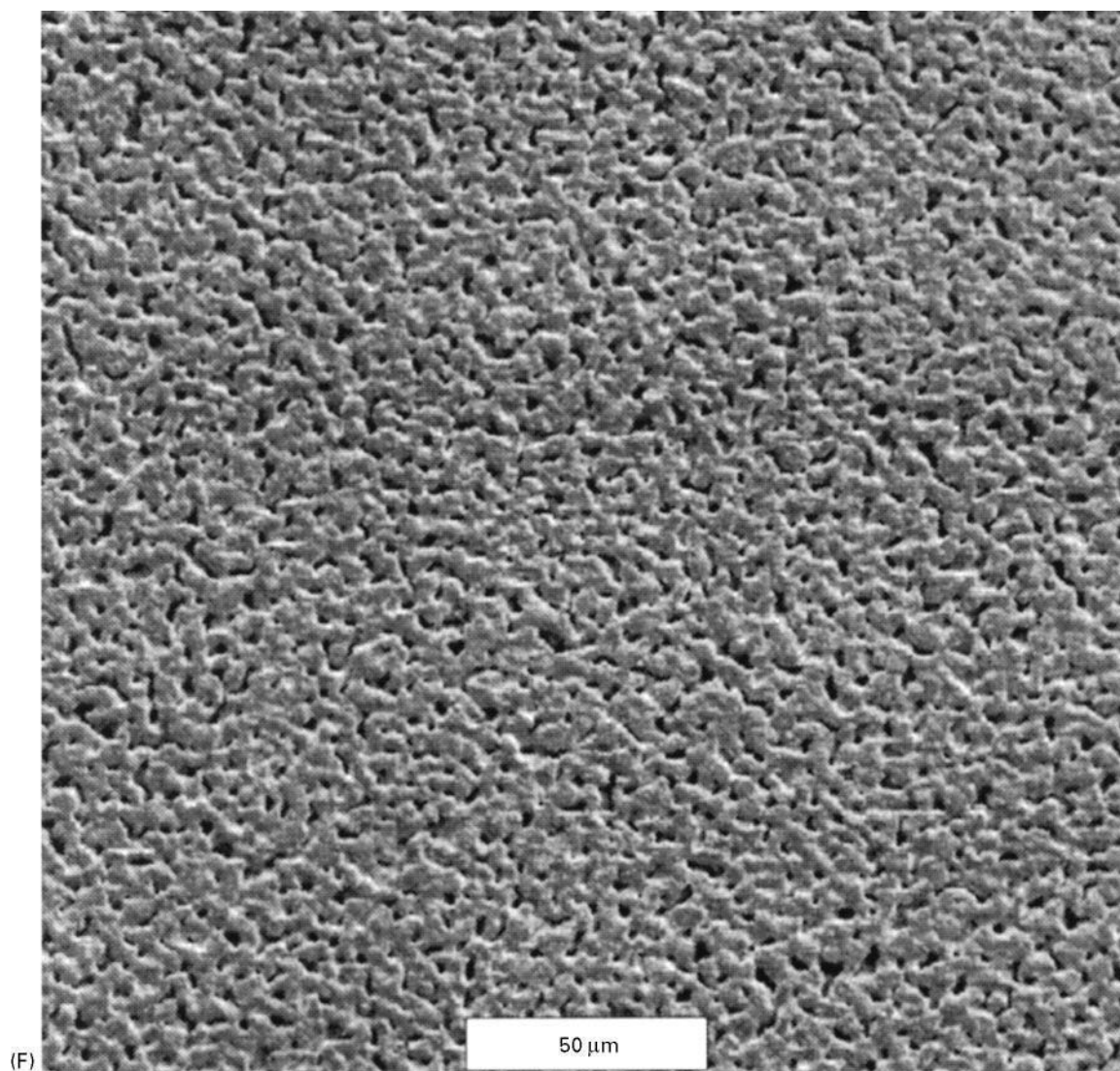


Figure 3 *Continued*

to predict the extent of fouling quantitatively; a qualitative description is given in a later section. The cake resistance can be calculated by the Kozeny–Carman equation, eqn [4], where the cake's void fraction ε , the cake-layer thickness δ_c , and the particle radius a are to be inserted for ε_m , l and a_m respectively.

The void fraction of the cake layer, ε , may depend on various parameters, such as transmembrane pressure, particle size distribution, shape, and compressibility, and the effect of particle–particle interactions. Often a value between 0.3 and 0.4 is found for ε .

A model for the time dependent dead-end filtration flux is obtained by combining eqns [4]–[6] with a mass balance describing cake layer build-up:

$$\left(\frac{d\delta_c}{dt} + J\right)\phi_b = (1 - \varepsilon) \frac{d\delta_c}{dt} \quad [7]$$

where ϕ_b is volume fraction of particles in the bulk.

If a constant ΔP is applied, the flux is given by:

$$J(t) = \frac{\Delta P}{\mu_0 R_m} \left(1 + \frac{2\hat{R}_c \phi_b \Delta P \cdot t}{(1 - \varepsilon - \phi_b) \mu_0 R_m^2}\right)^{-1/2} \quad [8]$$

where \hat{R}_c is the specific cake resistance ($= R_c / \delta_c$). Care must be taken when using eqn [8] as ε and \hat{R}_c often depend on time (cake compaction).

Depth Filters

Particle retention in depth filters is based on various mechanisms. In the case of gas cleaning, the two

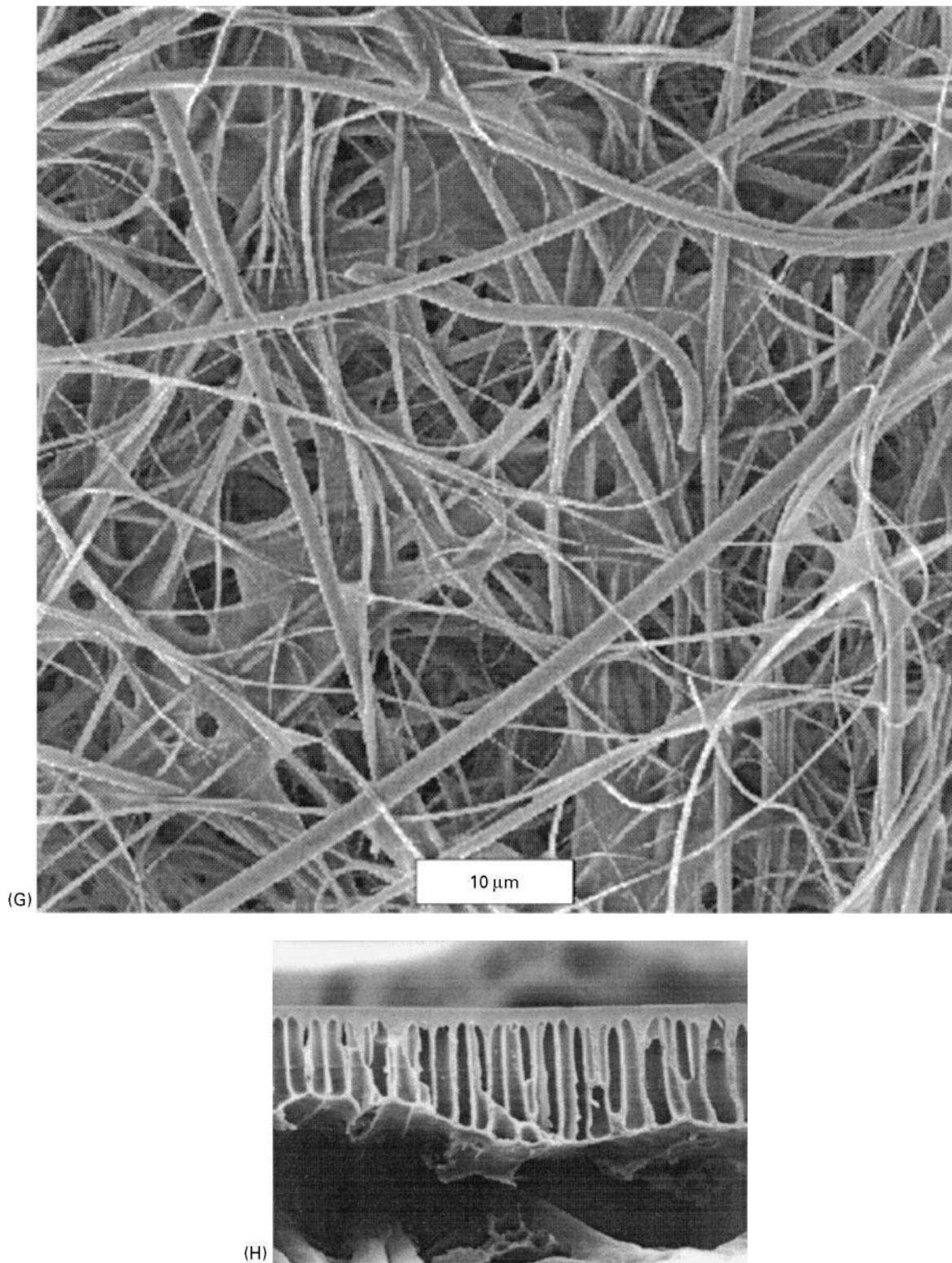


Figure 3 Continued

most important mechanisms are particle capture by *interception* and particle capture by *diffusion*. Interception occurs when a particle follows a fluid stream-

line, which at some point passes close to the filter surface at a distance less than the particle radius, thus causing contact between the particle and the filter.

Table 2 Membrane characterization methods

<i>Method^a</i>	<i>Parameters obtained</i>	<i>Description/remarks</i>
<i>Microscopic techniques</i>		
SEM, TEM, FESEM (+ image analysis)	Pore-size distribution, pore morphology (surface roughness)	'Direct' observation by microscopes. Although these methods have many advanced possibilities, they are mostly used for determining the pore-size distribution in the membrane surface. Preparation of sample necessary
AFM (+ image analysis)	Pore-size distribution, morphology, surface roughness, particle-membrane interactions	See SEM (no preparation technique is necessary)
<i>Liquid penetration methods</i>		
Bubble point method	Largest pore available	Liquids will fill larger pores at low pressures. To fill smaller pores, however, higher pressures are needed Simple method, contact angle of membrane-liquid needs to be known
Extended bubble point method	Pore-size distribution	See bubble point method
Mercury porometry	Pore-size distribution	High pressures are necessary that may damage the membrane structure
Permporometry	Pore-size distribution	Vapour condensation in pores is measured. Rather complicated method
Solute retention	Pore-size distribution ('cut-off')	Membranes with smaller pores retain solutes of smaller sizes. Simple method. More often used for ultrafiltration than for microfiltration
<i>Contact angle measurements</i>		
Sessile drop, Wilhelmy plate	Contact angle, surface tension, hydrophobicity	Direct methods that measure the contact angle liquid-air-membrane. Give qualitative information on hydrophobicity
<i>Electrokinetic methods</i>		
Electroviscous method	Zeta potential, surface charge density	Experimentally simple: measurement of water flux at various ionic strengths. Interpretation of results more difficult
Streaming potential, electroosmosis	Zeta potential, surface charge density	Direct measurements of electrokinetic effects. Interpretation of results sometimes complicated

^aSEM, scanning electron microscopy; TEM, transmission electron microscopy; FESEM, field effect scanning electron microscopy; AFM, atomic force microscopy.

Capture by diffusion occurs when the Brownian motion of the particle results in contact between the particle and the filter matrix.

Interception is the dominant capture mechanism for large particles; Brownian diffusion is the dominant capture mechanism for smaller particles. Capture is therefore least effective for intermediate size particles, leading to the existence of a 'most penetrating particle size' (Figure 5). The exact value of this most penetrating particle size depends on the membrane pore diameter and the flow velocity. It has been found, however, that capture of particles from gas streams by membranes of pore diameters of about 0.2 μm is so effective that essentially all particles are retained.

For depth filtration of liquids, the situation is different, as physicochemical (charge) effects alter the relative magnitudes of the capture mechanisms described above. If physicochemical conditions are favourable, capture efficiencies in liquids can be similar to those in gases. If conditions are less favourable, capture efficiencies for the smaller particles decrease

rapidly. Under these conditions sieving (entrapment) is the only effective particle capture mechanism, making the membrane permeable for all particles smaller than the pore size.

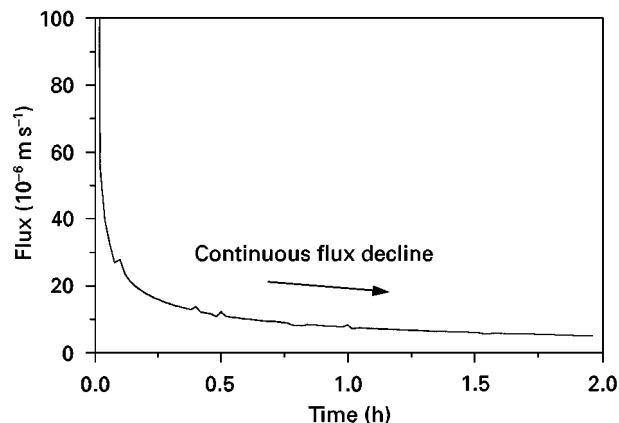


Figure 4 Flux versus time for the dead-end microfiltration of a silica particle suspension.

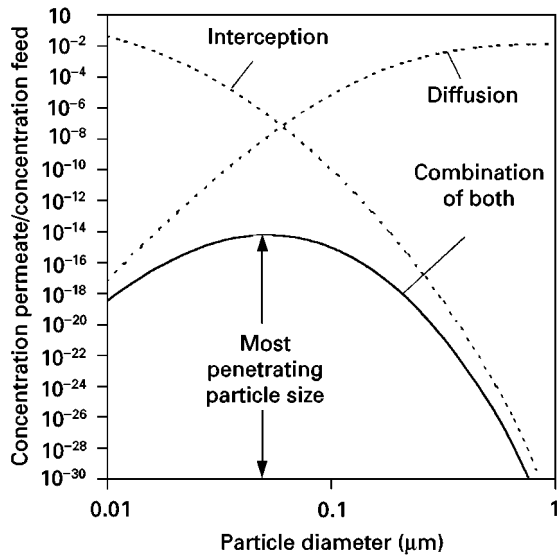


Figure 5 Schematic representation of efficiency of capture by interception and capture by diffusion versus particle size. The most penetrating particle size is obtained by combining both mechanisms.

Cross-flow Microfiltration

Dead-end microfiltration, as stated, may suffer from dramatic flux loss because of deposition of particles on the membrane surface and fouling phenomena. Therefore microfiltration is often carried out in the *cross-flow* mode (Figure 2b). The tangential flow (cross-flow) ‘scours’ away particles from the membrane surface, and thus limits cake-layer build-up and fouling. Another advantage of cross-flow filtration is the possibility for continuous operation. Cross-flow filtration is used in most industrial large-scale microfiltration plants. For cross-flow microfiltration, screen filters are mainly used.

Cake-layer Build-up and Fouling

During a cross-flow microfiltration process, a flux behaviour is often observed as shown in Figure 6. The flux declines at first rapidly with time; then the speed of flux decline decreases, and finally a *steady state* is reached where the flux does not decrease anymore. The decrease in flux is commonly ascribed to two phenomena: *cake-layer build-up* and *fouling*.

When filtering a suspension, the membrane retains suspended particles. The particle concentration near the membrane will therefore gradually increase. Cake-layer build-up will occur when the particle concentration near the membrane surface reaches the maximum packing density (0.6–0.7). Cake-layer build-up is thus caused by the particles that are retained by the membrane based on their size, independent of any specific interaction between these

particles and the membrane. Cake-layer build-up in microfiltration is a phenomenon similar to *concentration polarization* in ultrafiltration.

Fouling, on the other hand, is based on a direct contact between solutes and the membrane surface. The term ‘fouling’ includes many processes, such as adsorption and deposition of macromolecules, bacteria, or small organic molecules on the membrane surface or within the pores. Fouling increases the hydraulic resistance against permeate flow, and thus reduces the capacity of the microfiltration process. Moreover, fouling in general increases the observed retention of the membrane as it reduces the effective pore size.

If one plots the steady-state flux for crossflow microfiltration versus transmembrane pressure (ΔP) often a curve as given in Figure 7 is obtained. Three regimes can be observed. For low values of ΔP , the flux increases linearly with ΔP and often equals the pure water flux. For higher values of ΔP , the flux curve bends, because of cake-layer build-up, and fluxes become less than the pure water flux. The point where the deviation from the straight line starts is often referred to as the *critical flux*. For even higher ΔP , the flux is independent of the pressure. This pressure independent flux value is referred to as the *limiting flux*.

Factors Influencing Membrane Fouling and Cake-layer Build-up

The extent of membrane fouling and cake-layer build-up depends on many parameters, which can be grouped in three main contributors:

- properties of the membrane,
- properties of the suspension, and
- properties of the process (hydrodynamics).

Membrane properties of importance are hydrophobicity, surface charge (zeta potential), surface

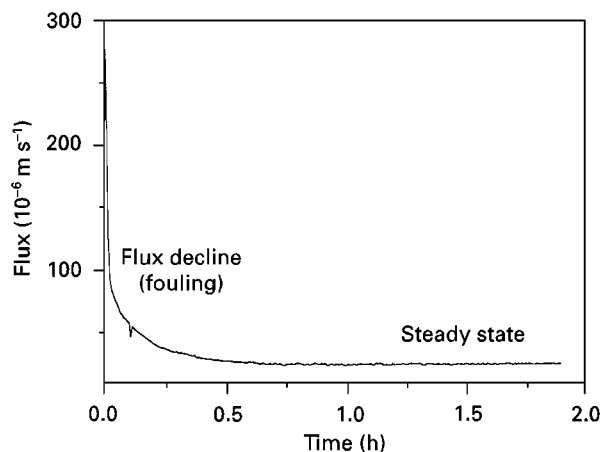


Figure 6 Flux versus time for the cross-flow microfiltration of a silica particle suspension.

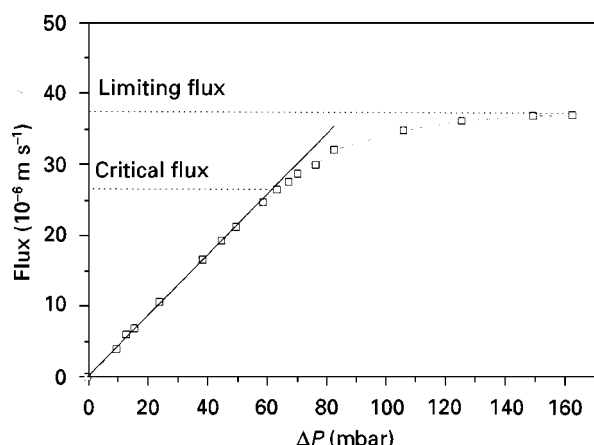


Figure 7 Steady-state flux versus ΔP for the cross-flow microfiltration of a silica particle suspension. —, water; ---□---, silica particle suspension.

roughness, and pore-size distribution. In general, macromolecular adsorption is more severe for *hydrophobic* than for hydrophilic membranes. Fouling by negatively charged colloids is less for *negatively charged membranes* than for uncharged or positively charged membranes. As most colloids in practical suspensions acquire a negative charge, negatively charged membranes are preferred in general. Membrane fouling is further reduced by choosing membranes with *smooth surfaces*, small pore sizes, and *narrow pore size distributions*.

Feed suspension properties of importance are particle concentration, particle charge (zeta potential), ionic strength, and overall composition. The amount of cake-layer build-up increases with *particle concentration*. *Charge effects* can reduce fouling by membrane-particle repulsion, and can reduce cake-layer build-up by particle-particle repulsion. Such charge effects are less pronounced at high *ionic strength*, as the ions present in solution 'shield' the charge of membrane and particles. Overall composition of the feed suspension is of great importance for the fouling behaviour. Fouling may be caused not only by the main particles retained, but also by macromolecules and small organic molecules, which 'geometrically' should pass through the pores easily.

Process properties of importance are the transmembrane pressure and the cross-flow velocity. Low fouling normally occurs at low *transmembrane pressures* and high *cross-flow velocities*. More detailed information is given in a later section.

Calculating the Limiting Flux

To calculate the limiting steady-state flux, local mass balances near the membrane surface are used. It is

then assumed that the limiting flux is reached when the amount of particles transported *towards* the membrane by the permeate flux (convection) equals the amount of particles transported *away* from the membrane by the cross-flow. The cross-flow can cause back-transport by at least four different mechanisms:

- Brownian diffusion,
- shear-induced diffusion,
- inertial lift, and
- surface transport.

In the following, these mechanisms will be explained. It is assumed throughout this section that the particles are spherical and monodisperse, and that long-term fouling and physicochemical interactions are negligible.

Brownian diffusion If back-transport is caused by Brownian diffusion the standard concentration polarization theory can be used, employing the Brownian diffusion coefficient for spherical particles:

$$D = \frac{kT}{6\pi\mu_0 a} \quad [9]$$

where k is the Boltzmann constant, T is temperature, and a is the particle radius. By numerical calculations, using a suspension viscosity that depends on the particle concentration, it can be shown that the flux is given by:

$$J = 0.0769 \left(\frac{\tau_w k^2 T^2}{\mu_0^3 a^2 L} \right)^{1/3} \phi_b^{1/3} \quad [10]$$

where τ_w is the wall shear stress and L is the membrane length.

Eqn [10] predicts fluxes of the right order of magnitude for suspensions of small particles (up to about 10 nm). It under-predicts fluxes by one or two orders of magnitude if applied to suspensions of larger particles. This discrepancy is called the 'flux paradox'. This paradox is explained by assuming that there are other mechanisms for back transport, apart from Brownian diffusion.

Shear-induced diffusion When a shear field is applied to a layer of particles, the particles will tumble over one another, leading to a more loosely packed layer. Obviously the particles must move perpendicular to the applied shear stress to achieve this. The resulting particle migration can be described by employing an effective diffusion coefficient, and is called *shear-induced diffusion*.

It can be calculated, using an empirical value of the shear-induced diffusion coefficient, that the limiting flux is given by:

$$J = 0.060 \frac{\tau_w}{\mu_0} \left(\frac{a^4(1 - 3.8\phi_b)}{\phi_b L} \right)^{1/3} \quad [11]$$

valid for $\phi_b < 0.2$, i.e. for all practical applications. Eqn [11] has been shown to give good flux predictions for suspensions of hard spherical particles, and reasonable flux predictions for complex biofluids such as milk. Although eqn [11] is derived for local viscous flow, flux calculations have also been reported to be accurate for many *turbulent* flow processes.

Inertial lift If a diluted suspension of particles flows through a duct, particles present close to the wall will migrate towards the centre, perpendicular to the streamlines. This migration, caused by complex hydrodynamic interactions, is called inertial lift. In cross-flow microfiltration, inertial lift may be able to prevent particles from depositing onto the membrane. To model this phenomenon, it is assumed that a cake layer builds up during microfiltration until the convective velocity *towards* the membrane (the flux J) equals the lift velocity, v_L , *away* from the membrane:

$$J = v_L = 0.036 \frac{\rho_0 a^3 \tau_w^2}{\mu_0^3} \quad [12]$$

The inertial lift theory neglects the influence of a particle on the motion of another particle, resulting in a flux equation which does not depend on the particle concentration. The inertial lift model is therefore only valid for very low particle concentrations. As the flux predicted by eqn [12] increases with the cube of the particle size and the square of the wall shear stress, inertial effects are expected to be important only for large particles ($> 5 \mu\text{m}$) and high cross-flow velocities ($\tau_w > 10 \text{ N m}^{-2}$).

Surface transport A particle on top of a filter cake is subject to different forces, as shown in Figure 8. The horizontal drag force caused by the cross-flow F_τ exerts a clockwise torque on the particle, and the vertical drag force caused by the permeate flux F_J exerts a counterclockwise torque. If the torque caused by the cross-flow is larger than the torque caused by the permeate flux, the particle can *roll* over the cake layer to the outlet of the membrane. This mechanism of transport is called surface transport.

Equating the clockwise torque with the anticlockwise torque, an equation for the limiting flux is

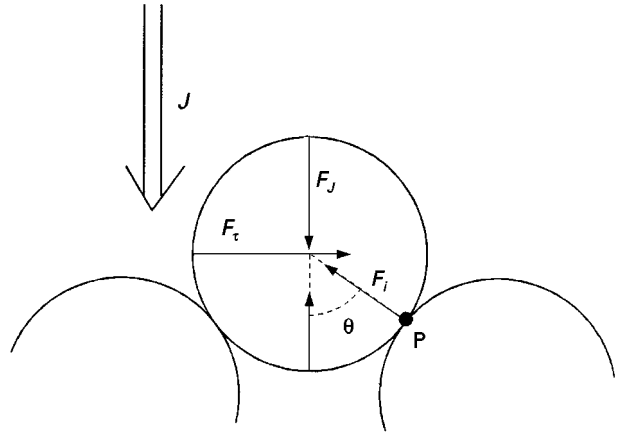


Figure 8 Torque balance for the surface transport model. F_τ = horizontal drag force caused by the cross flow; F_J = vertical drag force caused by the permeate flux J ; F_i = particle–particle interaction force; θ = angle of repose.

obtained:

$$J = \frac{2.36 a \tau_w}{\mu_0 \tan \theta (a^2 \hat{R}_c)^{2/5}} \quad [13]$$

where θ is the angle of repose (see Figure 8).

Just as for the inertial lift model, the present model neglects the influence of a particle on the motion of another particle, resulting in a flux equation which does not depend on the particle concentration. Eqn [13] overpredicts fluxes for typical microfiltration conditions by an order of magnitude or more. Two of the models described above, the Brownian diffusion model and the shear-induced diffusion model, use a *continuum approach*. The other two, the inertial lift model and the surface transport model, are based on a *single-particle approach*. The single-particle approach is only valid for low particle concentrations and large particles.

In Figure 9, the fluxes predicted by the two continuum models are given as a function of particle size for typical cross-flow microfiltration conditions. The flux predicted by the inertial lift model is plotted in the same graph to indicate the order of magnitude of inertial effects. For small particle sizes, Brownian effects dominate and the flux decreases with particle size. For intermediate particle sizes, shear-induced diffusion dominates and the flux *increases* with particle size. For large particle sizes ($> 5 \mu\text{m}$) inertial effects dominate causing the flux to increase even faster with particle size.

The combined effect of Brownian and shear-induced diffusion can be described by:

$$J_{\text{Bo + SI}} = \sqrt{J_{\text{Bo}}^2 + J_{\text{SI}}^2} \quad [14]$$

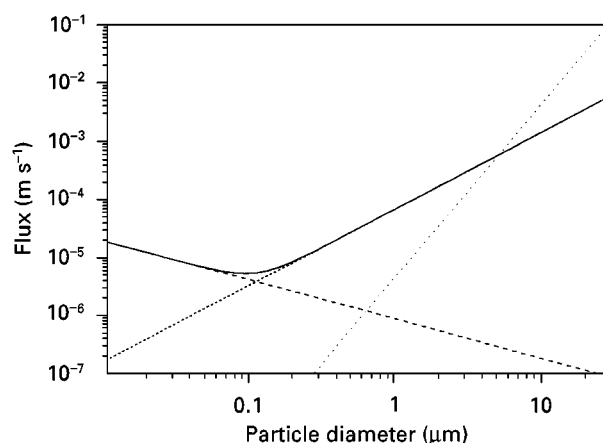


Figure 9 Flux calculated according to different models as a function of particle diameter. Calculations were performed for $\tau_w = 32 \text{ N m}^{-2}$, $\phi_b = 10^{-3}$, and $L = 1.2 \text{ m}$, using eqns [10]–[12] for the Brownian, shear-induced, and inertial-lift models, and using eqn [14] for combining Brownian and shear-induced diffusion; ---, Brownian diffusion model; ·····, shear-induced diffusion model; —, Brownian and shear-induced diffusion model; ·····, inertial lift model.

where J_{Bo} is the flux according to Brownian theory, eqn [10], and J_{Si} is the flux according to shear-induced theory, eqn [11]. Predictions according to eqn [14] are also given in Figure 9.

Calculating the Transient Behaviour of Cross-flow Microfiltration

The time dependence of the flux can be predicted using an approach as outlined in the section on dead-end filtration, yet allowing for back-transport according to the particle transport mechanisms described above. Such descriptions are rather complicated, and will not be treated here.

A simple but effective approach to model the transient behaviour of the permeate flux is the use of a combination of transient dead-end filtration theory and a cross-flow filtration model for the steady-state (limiting) flux. While the cake is initially developing, the effect of the cross-flow is small and can be neglected, so that cross-flow filtration theory can be approximated by dead-end filtration theory. Upon approaching the steady state, the cross-flow begins to arrest the cake growth and dead-end filtration theory is no longer accurate. However, near the steady state the flux shows only minor time dependence, and the flux can be approximated by its steady-state value.

The procedure to predict the total transient behaviour of the permeate flux is thus to use dead-end filtration theory (see the section on dead-end microfiltration) until the time the steady-state flux is reached and then use the steady-state flux predicted by

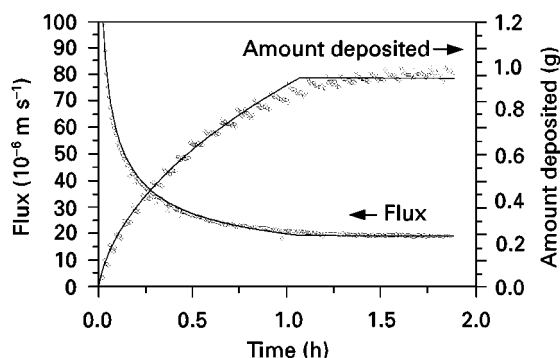


Figure 10 Flux and amount of matter deposited on the membrane as a function of time for the filtration of a suspension of $0.48\text{-}\mu\text{m}$ silica particles. Circles represent experimental values for a particle concentration of 1.7 kg m^{-3} , a transmembrane pressure of 0.42 bar and a cross flow velocity of 1 m s^{-1} ; lines represent model calculations.

a steady-state cross-flow filtration model. This approach is illustrated in Figure 10, modelling the transient flux and cake-layer build-up in the cross-flow microfiltration of a suspension of silica particles.

Process Considerations

Cross-flow microfiltration is usually carried out in the feed-and-bleed mode, shown in Figure 11. The use of a retentate recycle makes it possible to work at high cross-flow velocities (high Q_c) while having low retentate flows (i.e. high volumetric concentration factors $V_c = 1 + Q_p/Q_R$). When high concentration factors are desired, several recirculation loops may be placed in series, or in even more complicated schemes, with loops both in parallel and in series (Christmas tree design).

In many cross-flow microfiltration systems and in some dead-end systems, *backflushing* is applied to remove the fouling layer from the membrane. Backflushing is achieved by forcing the permeate periodically back through the membranes. Effective backflushing is obtained by using high counterpressures

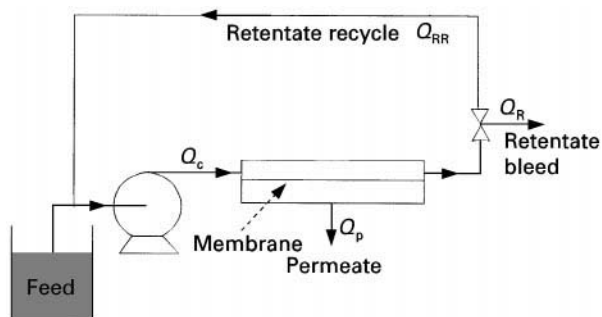


Figure 11 Feed-and-bleed operational configuration for cross-flow microfiltration.

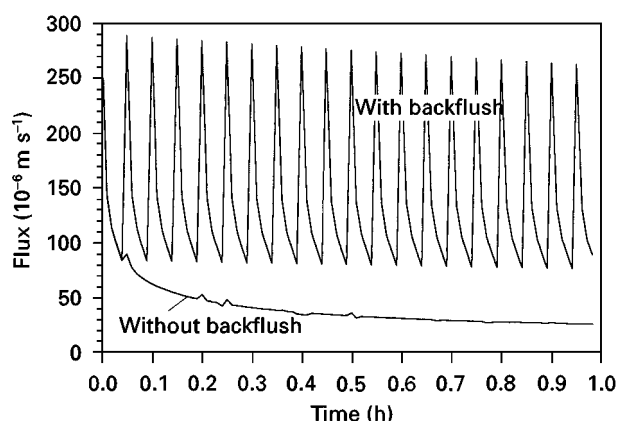


Figure 12 Microfiltration flux when filtering a particle suspension, with and without backflush.

(about 0.5 bar) for several seconds every few minutes (Figure 12).

Fouling is reduced by high cross-flow velocities and low transmembrane pressures. High cross-flow velocities cause high-pressure drops along the membrane, which cause the ΔP to be undesirably high at the entrance of the membrane module. Therefore microfiltration processes have been developed which facilitate a cross-flow both on the feed side and on the permeate side. The pressure drops on both sides are similar in magnitude, guaranteeing a *uniform transmembrane pressure*. This method of operation has been shown to be effective in many dairy applications.

Other process techniques to reduce fouling are the use of pulsed flow, gas sparging, and electric or acoustic fields, and the use of flow geometries that create secondary flows or vortices resulting in high shear rates (e.g. the use of 'turbulence promoters' or curved channels).

Conclusions

Over the last 70 years, microfiltration has developed from a small specialized technology used only in

laboratories to a multibillion dollar industry for separation and purification of liquid and gas streams. Especially since the 1980s, exciting new applications have become possible, due to improved membranes (for example, ceramics) and improved technologies (for example, backpulsing, uniform transmembrane pressure). Still, great challenges exist, for example in the processing of beverages, such as fruit juices, milk, and beer, where membrane fouling seriously impairs the economy of the process.

To overcome these problems, researchers and engineers are becoming increasingly interested in hybrid and combined processes. Combining microfiltration with good pre- and post-treatments or with other separation processes may result in better and more economic separations.

See also: II/Membrane Separations: Filtration.

Further Reading

- Belfort G, Davis RH and Zydney AL (1994) The behavior of suspensions and macromolecular solutions in cross-flow microfiltration. *Journal of Membrane Science* 96: 1–58.
- Bowen WR and Jenner F (1995) Theoretical descriptions of membrane filtration of colloids and fine particles: an assessment and review. *Advances in Colloid and Interface Science* 56: 141–200.
- Ho WSW and Sirkar KK (1992) *Membrane Handbook*. New York: Van Nostrand Reinhold.
- Howell JA, Sanchez V and Field RW (1993) *Membranes in Bioprocessing – Theory and application*, 1st edn. London: Chapman and Hall.
- Mulder M (1992) *Basic Principles of Membrane Technology*, 1st edn. Dordrecht: Kluwer Academic Publishers.
- Scott K (1995) *Handbook of Industrial Membranes*. Oxford: Elsevier Science.
- Zeman LJ and Zydney AL (1996) *Microfiltration and Ultrafiltration. Principles and Applications*. New York: Marcel Dekker.

Pervaporation

H. E. A. Bruschke and N. P. Wynn,
Sulzer Chemtech GmbH, Neunkirchen, Germany

Copyright © 2000 Academic Press

Development

In 1917 PA Kober published a paper in which he described his observation that 'a liquid in a collodion

bag, which was suspended in the air, evaporated, although the bag was tightly closed'. Kober was not the first researcher to observe this phenomenon, but the first to realize its potential for the separation of liquid mixtures which otherwise are difficult to separate, and to separate them under moderate conditions. He introduced the terms 'Pervaporation', and 'Perstillation', and the first term is now in use to describe in

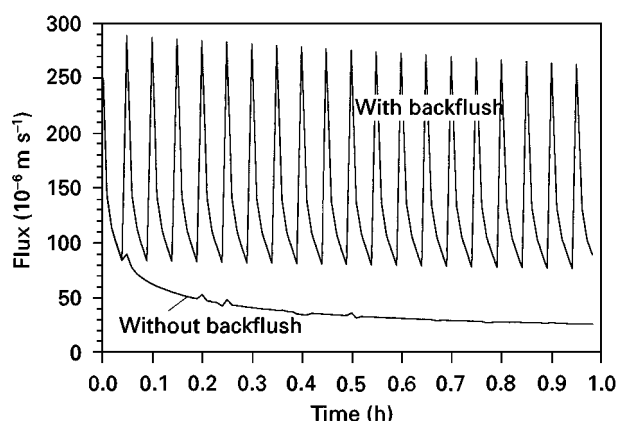


Figure 12 Microfiltration flux when filtering a particle suspension, with and without backflush.

(about 0.5 bar) for several seconds every few minutes (Figure 12).

Fouling is reduced by high cross-flow velocities and low transmembrane pressures. High cross-flow velocities cause high-pressure drops along the membrane, which cause the ΔP to be undesirably high at the entrance of the membrane module. Therefore microfiltration processes have been developed which facilitate a cross-flow both on the feed side and on the permeate side. The pressure drops on both sides are similar in magnitude, guaranteeing a *uniform transmembrane pressure*. This method of operation has been shown to be effective in many dairy applications.

Other process techniques to reduce fouling are the use of pulsed flow, gas sparging, and electric or acoustic fields, and the use of flow geometries that create secondary flows or vortices resulting in high shear rates (e.g. the use of 'turbulence promoters' or curved channels).

Conclusions

Over the last 70 years, microfiltration has developed from a small specialized technology used only in

laboratories to a multibillion dollar industry for separation and purification of liquid and gas streams. Especially since the 1980s, exciting new applications have become possible, due to improved membranes (for example, ceramics) and improved technologies (for example, backpulsing, uniform transmembrane pressure). Still, great challenges exist, for example in the processing of beverages, such as fruit juices, milk, and beer, where membrane fouling seriously impairs the economy of the process.

To overcome these problems, researchers and engineers are becoming increasingly interested in hybrid and combined processes. Combining microfiltration with good pre- and post-treatments or with other separation processes may result in better and more economic separations.

See also: II/Membrane Separations: Filtration.

Further Reading

- Belfort G, Davis RH and Zydney AL (1994) The behavior of suspensions and macromolecular solutions in cross-flow microfiltration. *Journal of Membrane Science* 96: 1–58.
- Bowen WR and Jenner F (1995) Theoretical descriptions of membrane filtration of colloids and fine particles: an assessment and review. *Advances in Colloid and Interface Science* 56: 141–200.
- Ho WSW and Sirkar KK (1992) *Membrane Handbook*. New York: Van Nostrand Reinhold.
- Howell JA, Sanchez V and Field RW (1993) *Membranes in Bioprocessing – Theory and application*, 1st edn. London: Chapman and Hall.
- Mulder M (1992) *Basic Principles of Membrane Technology*, 1st edn. Dordrecht: Kluwer Academic Publishers.
- Scott K (1995) *Handbook of Industrial Membranes*. Oxford: Elsevier Science.
- Zeman LJ and Zydney AL (1996) *Microfiltration and Ultrafiltration. Principles and Applications*. New York: Marcel Dekker.

Pervaporation

H. E. A. Bruschke and N. P. Wynn,
Sulzer Chemtech GmbH, Neunkirchen, Germany

Copyright © 2000 Academic Press

Development

In 1917 PA Kober published a paper in which he described his observation that 'a liquid in a collodion

bag, which was suspended in the air, evaporated, although the bag was tightly closed'. Kober was not the first researcher to observe this phenomenon, but the first to realize its potential for the separation of liquid mixtures which otherwise are difficult to separate, and to separate them under moderate conditions. He introduced the terms 'Pervaporation', and 'Perstillation', and the first term is now in use to describe in

general a process in which one component out of a fluid mixture selectively permeates through a dense membrane, driven by a gradient in partial vapour pressure, leaving the membrane as a vapour, and being recovered in a condensed form as a liquid.

In the years following Kober's publication a number of papers were published describing membranes and processes for pervaporation. Especially during the 1950s, the interest focused on pervaporation membranes and processes for the separation of different classes of hydrocarbons and of isomers and numerous patents were granted. Membrane materials disclosed were natural and synthetic rubbers, cellulose esters and ethers, and several treated and untreated polyolefines. None of this early membrane, however, was used in any industrial process, owing to insufficient flux and selectivity.

Pervaporation, vapour permeation and gas permeation are very closely related processes. The driving force is always a gradient in partial vapour pressure, and transport through the membrane can best be described by a so-called 'Solution-Diffusion-Mechanism'. In this mechanism it is assumed that a component of the feed having a high affinity to the membrane is easily and preferentially absorbed and dissolved in the dense membrane. Following a concentration gradient it migrates through the membrane by a diffusion process and is desorbed at the downstream side of the membrane. The separation characteristic of the membrane is thus governed primarily by the solubility of components in the membrane material and, to a lesser extent, by its diffusivity which even may counteract against the solubility separation.

In pervaporation and vapour permeation processes the partial vapour pressures of the components at the feed side are fixed by composition and temperature of the feed; they can be influenced only by increasing the temperature. Therefore, the driving force for the transport of matter through the membrane is applied by reducing the partial vapour pressure at the permeate side.

Different means have been proposed in order to effect this reduction of the permeate side partial vapour pressure:

- The permeate side of the membrane is swept with an inert gas in which the partial vapour pressure of the critical (preferential permeating) component is kept sufficiently low. If the gas stream cannot be wasted it has to be reconditioned and recycled.
- All permeating vapour is removed by means of a vacuum pump. The vapour may be condensed after recompression at the downstream side of the pump.

- The permeated vapour is condensed at sufficiently low temperatures. As the condenser surface will be installed at a certain distance to the permeate side of the membrane all non-condensable gases have to be removed from the permeate compartment in order to minimize permeate side pressure losses.

In most industrial installations the last has been proven to be the most effective and economical process.

In a pervaporation process the feed is applied as a liquid and all partial vapour pressures of the components in the feed mixture are at saturation level. Within the limits of membrane stability and process requirements, temperature and pressure on the feed side are free adjustable parameters.

In vapour permeation a vaporous feed mixture is applied, with at least the partial vapour pressure of the preferential permeating component at or close to saturation conditions. Temperature and pressure of the feed are linked by vapour-liquid equilibrium and can be chosen within these limits only.

In gas permeation all partial vapour pressures at the feed side are below saturation and the permeate can no longer be condensed. By increasing the total feed side pressure the driving force for the transmembrane transport can be adjusted.

Pervaporation treatment liquid feed mixtures is insofar unique compared with other membrane processes as the transport of matter across the membrane is coupled with a phase change from liquid to vapour. The heat of evaporation is extracted from the liquid feed and transported through the membrane, too. As a consequence the temperature of the feed is reduced, which reduces driving force and transmembrane flux. Different means such as heated modules have been proposed to replace the lost heat of evaporation. In general, the total membrane area is split into a number of segments (stages) arranged in series with intermediate heat exchangers between each two segments or stages.

Membranes and Modules

Membranes

With the much broader knowledge of membrane structure and membrane manufacture accumulated in the development of desalination membranes in the 1970s pervaporation processes gained new interest. The separation characteristic of a membrane process is determined by the difference in transport rates of the components through the membrane only, not by liquid-vapour equilibria, and azeotropic mixtures can easily be separated. Since only the heat of

evaporation of the permeate vapour is lost a single step membrane process saves energy compared with, e.g., distillation.

Two different types of pervaporation membranes were developed at about the same time in the beginning of the 1980s:

- Hydrophilic membranes, with a preferential permeation for water, used mainly for the removal of water from organic solvents and solvent mixtures, with an emphasis on azeotropic mixtures.
- Organophilic membranes for the removal of volatile organic components from water and gas streams.

In both applications composite membranes are used, allowing for very thin separation layers but with sufficient chemical, mechanical and thermal stability. Because the composite structure flat sheet configurations are preferred. The substructure of both types of pervaporation membranes is very similar: a porous support membrane with an asymmetric pore structure is laid onto a carrier layer of a woven or non-woven textile fabric and a basic ultrafiltration membrane is formed. On the free side of this porous substructure the pores have diameters in the order of 20–50 nm which widen up to the fabric side to the micrometre range. Polyester, polypropylene and similar fibres are used for the textile carrier layer; structural polymers such as polyacrylonitrile, polyetherimide, polysulfone, polyethersulfone and polyvinylidene fluoride form the porous support.

On this substructure a thin dense layer (in the range of 0.5–5 μm thick) is coated, which effects the separation. Different coating techniques are in use, most commonly a solution of the respective polymer in an appropriate solvent is spread onto the porous substructure. The solvent is then evaporated, followed by further treatment to effect cross-linking of the polymer.

In hydrophilic membranes the separating layer is made from cross-linked polyvinyl alcohol (PVA), from polyimides, or natural polymers such as chitosan or cellulose acetate (CA), with PVA dominant. For organophilic membranes, the separation layer is formed mostly from siloxanes such as polydimethylsiloxane (PDMS), or polyoctylmethyl siloxane (POMS).

In recent years new efforts have been made in academia and industry to develop new membranes for organic–organic separation. Of specific interest are the separation of olefins from paraffins, e.g. propene from propane, aromatics such as benzene or toluene from aliphatic hydrocarbons or the separation of the xylene isomers. To date, no industrialization has been achieved. The only industrial

processes in this area are the separation of the light alcohols methanol and ethanol from their mixtures with hydrocarbons, ethers and esters. The membranes in use are, however, more of the hydrophilic type, in which the more polar alcohols replace the water.

To date, only polymeric membranes have been applied in pervaporation and vapour permeation processes. Thermal, mechanical and chemical stability of the porous substructure are limiting the operation range of this type of membrane, more than the stability of the separating layer. Demand for higher operation temperatures and chemical resistance have stimulated the development of inorganic substructures, and porous ceramics in particular. These can be coated by cross-linked polymeric separating layers similar to those on polymeric substructures. In more recent developments organic separation layers are applied, either by coating the porous substructure with a layer of zeolites or by reducing the size of the pore to molecular dimensions. The separation mechanism of these membranes is even more complex than that of polymeric separating layers, as molecular sieving effects, caused by shape and size of molecules, and molecule–surface interaction decide whether a component can pass through the membrane or will be retained.

Modules

Design of modules for pervaporation and vapour permeation processes was based on the experience gained in water treatment by membranes, such as ultrafiltration and reverse osmosis processes. However, significant modifications had to be made because of the specific requirements of pervaporation and vapour permeation processes.

The partial vapour pressure at the permeate side has to be reduced in both processes to fairly low values, especially when low final concentrations have to be reached in the retentate. Therefore any pressure losses, even in the range of a few millibars have to be avoided at the permeate side. Since any feed mixture will contain organic components at high concentration, mostly at elevated temperatures, the chemical stability of all module components, such as spacer and potting material and glues is critical. To date, two types of modules are most widely applied:

- Plate modules, mainly used for dehydration applications, with permeate channels as open as applicable. Stainless steel is used as a construction material for support plates for the membranes and for spacers. The permeate channels are preferably open over the circumference of the modules which

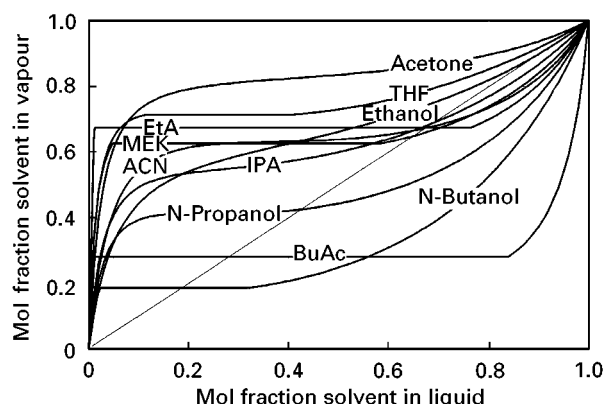


Figure 1 Vapour-liquid equilibrium curves for common pharmaceutical solvents which azeotrope with water. All can be dehydrated using pervaporation.

are assembled inside a special vacuum vessel that also house the permeate condenser. Alternative designs are very similar to plate heat exchangers, in which the supported membrane replace the heat exchanger plates. These modules are closed to the outside, with internal ducts feed and retentate, and for permeate removal.

- Spiral wound modules with stainless steel central tubes, but otherwise similar to those known from the conventional membrane processes, are mainly used for organophilic membranes. One or several of the spiral wound modules are housed inside a pressure tube and assembled in conventional skids. In a special design, the sandwich structures of membranes and permeate and feed spacer are welded together and not spirally wrapped around the central tube but arranged as flat sheets on the central tube for the removal of the permeate.

Very rarely, hollow fibres are used, generally with the feed flow inside the bore of the fibre. For the more conventional arrangement – feed flow at the shell side of the fibre – permeate pressure losses inside the bore may become detrimental for the process.

Applications

Organophilic Membranes

Organophilic membranes are mostly applied for the removal of volatile organic components (VOCs) from a gas stream such as waste air or nitrogen. The main applications are the treatment of streams originating from the evaporation of solvents in coating processes in film and tape production, purging of products such as polymers, by which unreacted monomers are removed, or from breathing of storage tanks for sol-

vents, especially from loading and unloading of petrol tanks in tank farms. In many installations the feed stream received at atmospheric pressure is compressed in order to increase the feed side partial vapour pressure. Partial condensation of the component to be removed is a wanted side effect, since then condensation on the permeate side under vacuum and at low temperature can be avoided. The permeate is simply slightly compressed by the vacuum pump and let into the inlet of the feed compressor. In specific cases the installation of a vacuum pump will not be necessary and the permeate is obtained at atmospheric pressure.

The economy of the process is usually determined by the value of the components recovered. Emission regulations in all industrial countries demand for very low final concentrations if the gas stream is released to the atmosphere, therefore the retentate from the gas purification by the membrane is either recycled or followed by an additional polishing step.

Although considerable efforts in research and development have been devoted to the removal of

Table 1 Solvents routinely dehydrated using pervaporation/vapour permeation

Isopropanol, ethanol	Standard applications for pervaporation, typically dehydrated from their azeotropes to fractions of a percent of water. Many continuous, batch and vapour permeation units are operating around the world.
Ethyl acetate, butyl acetate	Form azeotropes in the miscibility gap and were traditionally dehydrated by two distillation columns and a phase separator, however with a massive recycle. Esters decompose in contact with zeolites. Pervaporation/vapour permeation is easily the best technique for dehydration.
Acetone	Does not azeotrope with water but when distilled a large reflux is required to get a half dry product. Pervaporation is ideal for final dehydration or for debottlenecking existing distillation systems.
Tetrahydrofuran	Easily dehydrated by pervaporation down to a few hundred ppm water. Traditional caustic washing is operationally messy, requiring a redistillation of the product. Pressure swing distillation requires high pressures and large recycles.
Methyl ethyl ketone	Pervaporation is again the preferred technique. Distillation is only possible with an entrainer because the azeotropic composition is nearly identical to the miscibility limit.
N-butanol, n-propanol	Form azeotropes with high water content so the distillation/phase separation process involves massive recycle streams. Pervaporation plants are less costly to build and easier to operate.

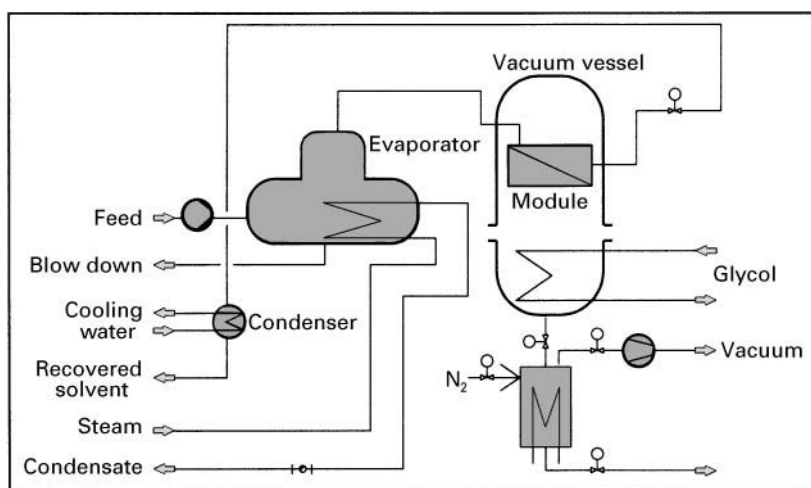


Figure 2 Typical flow diagram for recovery of solvent from mother liquors.

VOCs from aqueous stream, this technique has not yet been introduced into the industry. Potential mixtures which could be treated are more complex, the economical value of the recovered substances are low, and competing processes such as biological treatment of wastewater are cheaper. Applications may be found in the future in biotechnological processes where high-value products can be separated from a fermentation broth and be concentrated and purified in the same step.

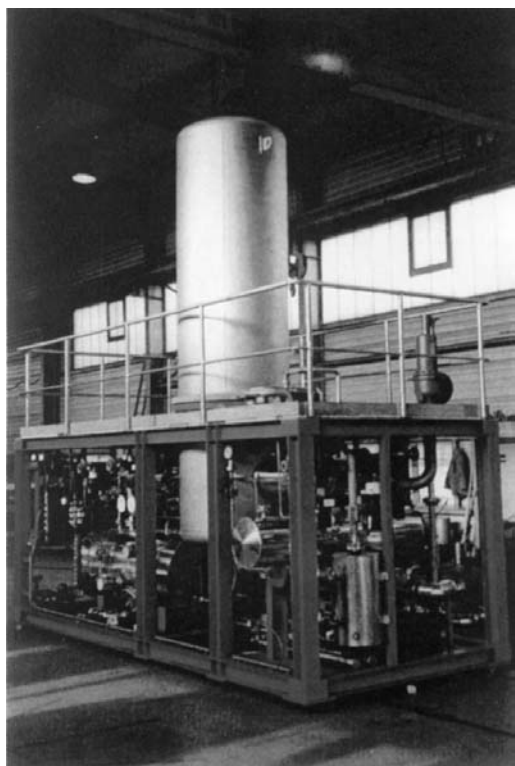


Figure 3 (See Colour Plate 51). Vapour permeation unit for recovering ink solvent.

Hydrophilic Membranes

The largest industrial installations of pervaporation and vapour permeation processes are equipped with hydrophilic membranes which are used for the removal of water from organic solvents and solvent mixtures.

Solvent dehydration Organic solvents are used for a variety of purposes in the chemical industry, e.g. for synthesis of pharmaceuticals, to precipitate materials from aqueous solutions, for cleaning purposes and for drying final products. Spent solvents nearly always contain some water. Dehydration is therefore an essential step in their recovery but difficult since most solvents form azeotropes with water. Final water removal by distillation is then impossible or complicated. Entrainer use is not an option for pharmaceutical or fine chemical production, where stringent process certification rules out adding potential sources of contamination.

Pervaporation enables solvents to be dehydrated without using any third substance or entrainer, simply, cheaply and without problems and irrespective of vapour/liquid equilibria (Figure 1). On-site solvent recovery using pervaporation and vapour permeation is thus becoming standard practice in the pharmaceutical and chemical industries (Table 1).

Often, pervaporation and vapour permeation plants are designed for operation with a number of solvents and with mixtures of solvents. Pervaporation and vapour permeation offers the following benefits when dehydrating solvents:

- No introduction of additional chemicals, complete solvent dehydration by pervaporation membranes irrespective of azeotrope formation and no possibility of contamination.

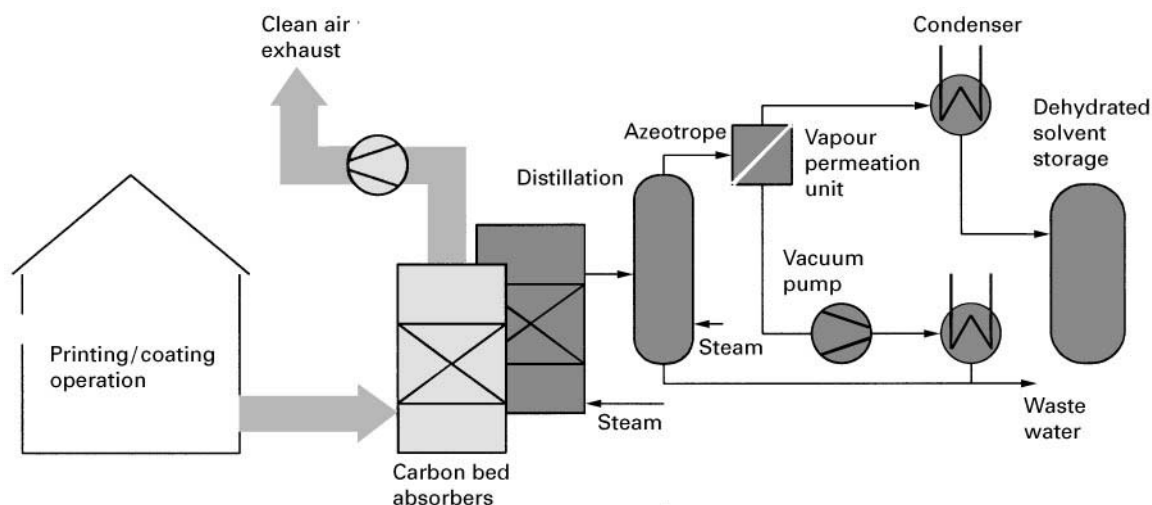


Figure 4 Carbon bed adsorption using steam regeneration and vapour permeation for final solvent dehydration.

- A choice of batch or continuous pervaporation systems, or continuous vapour permeation, depending on the duty.
- Able to dehydrate esters without any decomposition.
- Low energy consumption.

Solvent recovery from mother liquors Spent solvents (mother liquors) typically contain some water and are often saturated with dissolved material. They cannot be re-used without purification. Evaporation combined with vapour permeation is a powerful technique for purifying and dehydrating mother liquors (Figure 2).

The feed of spent solvent is evaporated and the resulting vapour is fed directly to a vapour permeation unit. Water vapour selectivity permeates the membrane and is condensed under vacuum. The water-free solvent vapour leaving the vapour permeation unit is condensed and is stored for re-use (product). A blowdown is taken from the evaporator to prevent buildup of dissolved solids. This purge can

be treated to recover valuable components. Combining evaporation with vapour permeation gives the following benefits: only vapour is fed to the membranes – no possibility of fouling and no possibility of solids carryover into the recovered solvent; both the evaporation and the vapour permeation process steps are carried out in a single unit.

Solvent recovery from carbon bed adsorbers Biodegradable solvents such as alcohols and esters are used in many specific applications in coating and printing. Typically, a solution of the coating material is applied to the surface and the solvent is evaporated into an air stream, leaving a uniform film of coat material. The use of volatile solvents speeds the drying process.

The solvent-laden air stream cannot normally be discharged. It must be cleaned up and because the solvent loading is usually quite low, carbon bed adsorbers are most commonly used. These adsorbers are periodically regenerated, using either steam or nitrogen. Solvent is then recovered from the condensate

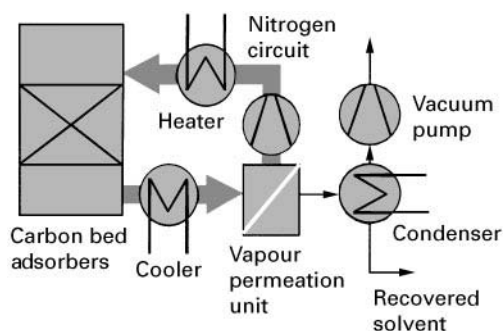


Figure 5 Use of vapour permeation to recover solvent from nitrogen desorption circuit.

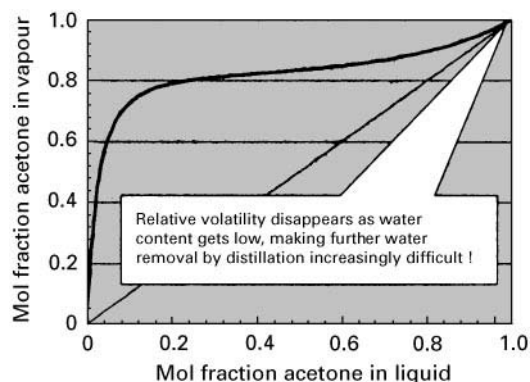


Figure 6 Vapour-liquid equilibrium diagram for acetone-water.

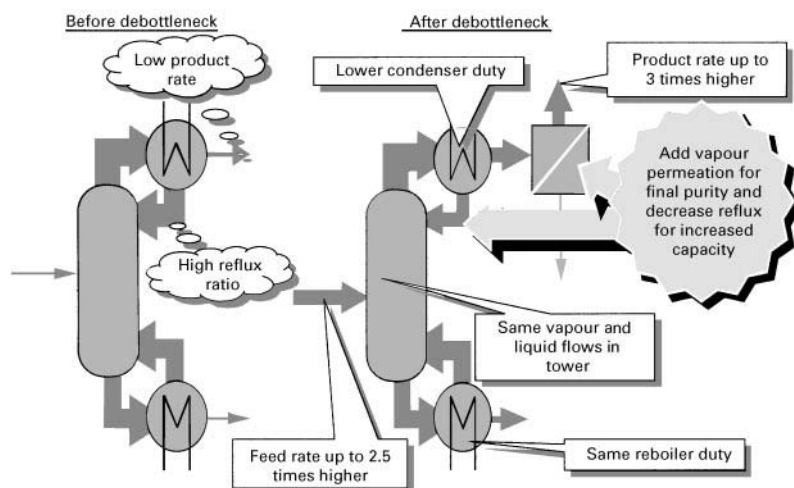


Figure 7 Debottlenecking a single pinched column using pervaporation (acetone–water example).

or nitrogen stream for re-use in the coating/printing process (Figure 3).

To evaporate quickly, the recycled solvent has to be substantially dry and because most of the organics used form azeotropes with water, distillation is not sufficient for final dehydration. Pervaporation or vapour permeation provides a dry solvent at minimal cost.

Vapour permeation for solvent dehydration in printing and coating If carbon bed adsorbers are regenerated with steam, the condensate is typically steam distilled up to the azeotrope (Figure 4). Continuous coating operations use continuous distillation to concentrate condensate from the bed regeneration. A vapour permeation system is normally connected directly to dehydrate net overhead vapour

from the distillation. This situation is shown schematically below. In this case, no additional energy is required for the final dehydration by vapour permeation.

Vapour permeation for solvent removal from circulating nitrogen If nitrogen is used to regenerate the carbon bed, solvent vapour can be continuously removed by vapour permeation through an organophilic membrane. This is much more economical than cooling the vapour to condense the solvent; because the solvent loading is low (Figure 5).

The use of vapour permeation for solvent recovery in printing and coating operations provides the following benefits: ethanol, isopropanol, ethyl acetate and other biodegradable solvents are recovered and dehydrated without entrainers and economically,

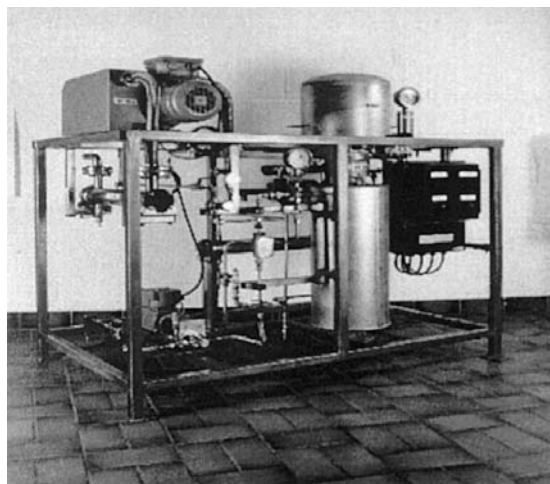


Figure 8 (See Colour Plate 52). Standard unit for batch dehydration of rinse alcohol.

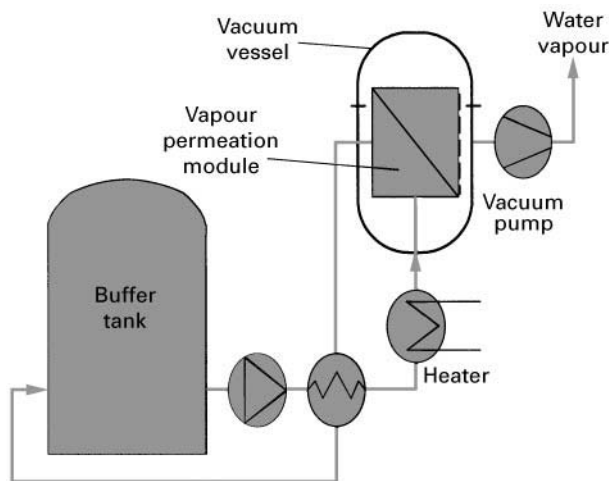


Figure 9 Batch pervaporation process for dehydration of rinse alcohol.

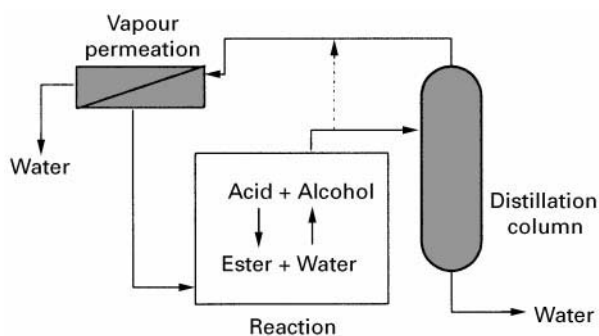


Figure 10 Water removal by distillation and vapour permeation.

even at a modest scale; solvent can be economically recovered from nitrogen streams with minimal cooling requirement.

Debottlenecking Distillations

Debottlenecking pinched distillations Distillation processes are driven by volatility differences. If these volatility differences are small, or become small under certain conditions, then columns need to operate with high reflux to achieve the desired separation. Because pervaporation/vapour permeation processes separate irrespective of volatility differences, they can

be used very effectively to debottleneck pinched distillations.

Consider for, example, the system acetone–water (Figures 6 and 7). Acetone is concentrated in the vapour phase at low concentrations so stripping of acetone from water is easy. At high concentrations this is not the case. Complete dehydration of acetone is difficult.

Debottlenecking entrainer distillation systems Existing entrainer distillation systems can also be effectively debottlenecked using pervaporation/vapour permeation. Normally, the rectification column will be operating to give a product as close to the azeotrope as possible, running with a high reflux. To debottleneck the system, reflux in the rectification column is reduced, giving more overhead product, but with a higher water content. The pervaporation unit is sized to remove enough water that the subsequent entrainer column is also unloaded. Both columns can then realize a significant capacity increase.

The pervaporation unit required for debottlenecking is relatively small since the driving force for water permeation is high. Adding a pervaporation/vapour permeation system to a pinched distillation can give providing higher product capacity and reduced re-

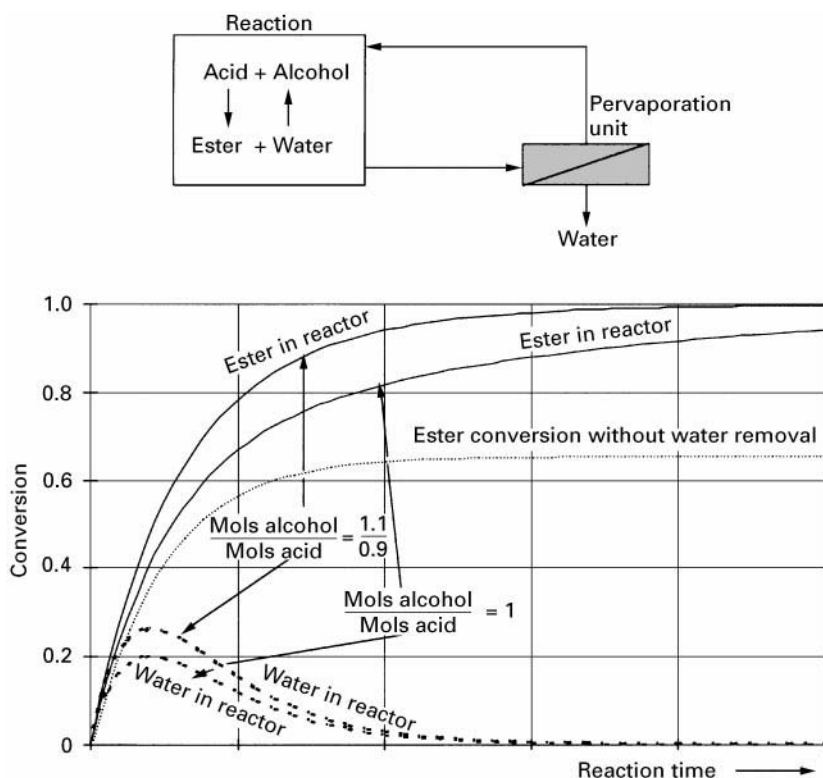


Figure 11 Progression of a batch esterification (with equilibrium constant $K = 4$) with continuous water removal by pervaporation.

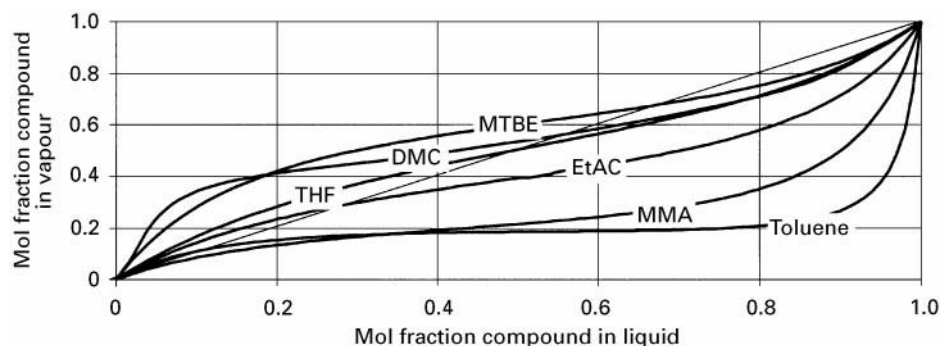


Figure 12 Some methanol azeotropes which can be separated using pervaporation vapour permeation.

flux, significantly higher products purity and reduced energy costs.

Dehydration and Purification of Rinse Alcohol

Many metal components used in the electronics industry undergo a rinse process using ethanol or isopropanol. Typically, the surface is first treated in another way to remove contaminants and then washed with water. The final rinse with alcohol displaces the water and any remaining contaminants and also wets the surface completely. The volatile alcohol then dries uniformly leaving a clean unmarked surface. Because the rinse alcohol displaces water it gradually becomes diluted and loses its drying qualities. Either fresh alcohol must be purchased or the alcohol must be dehydrated and purified to restore its performance.

The purity of the rinse alcohol is critical for component performance; wafer fabrication, for example, sets p.p.b. limits on certain metal ions (Figure 8).

Various standardized pervaporation/vapour permeation systems are now used economically and at

a site scale for dehydration and purification of rinse alcohol. A batch of used alcohol is continuously circulated from a buffer tank via a recuperator, heater and pervaporation module and water vapour is continuously removed via the vacuum pump (Figure 9). The batch is processed until the required degree of dryness is reached. Standardized units economically treat batches as small as $1 \text{ m}^3 \text{ day}^{-1}$.

Use of pervaporation and vapour permeation units to recover rinse alcohol gives the following benefits: minimal alcohol losses, very high product purities can be reached, and economical recovery at site scale.

Continuous Water Removal from Condensation Reactions

Condensation reactions such as esterifications, acetalizations and ketalizations produce water as coproduct; removal of this water from the reaction will shift the equilibrium in favour of the desired product.

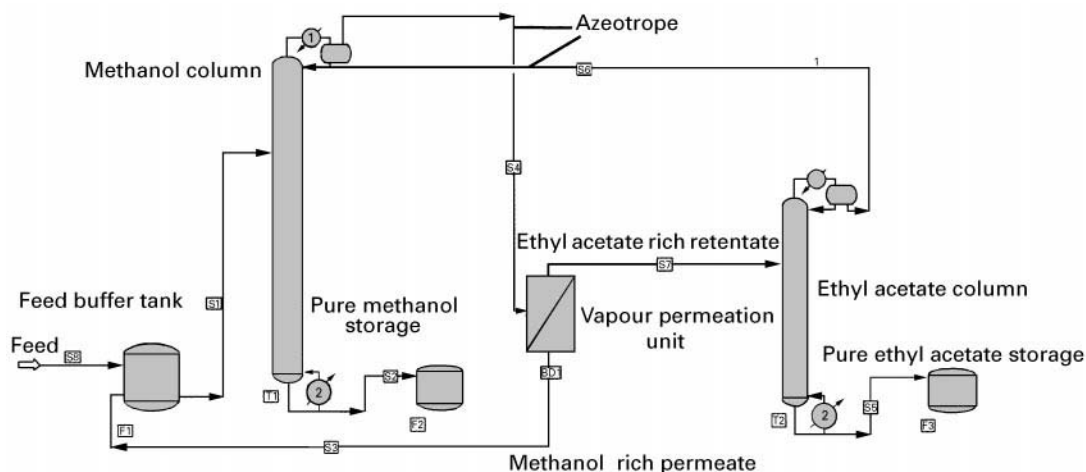


Figure 13 Methanol recovery by azeotrope breaking (methanol-ethyl acetate example).

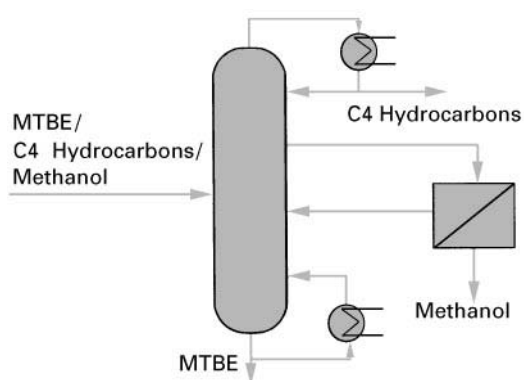


Figure 14 Methanol removal by pervaporation of column side-draw.

Distillation is often used to remove water from condensation reactions. However complete water removal is difficult because alcohols, esters and acids typically azeotrope with water. Boiling the reaction mix also removes alcohol, which is normally the most volatile component including a vapour permeation unit after the distillation step avoids the problems of azeotrope formation. Water can be completely removed (Figure 10).

Water removal by pervaporation only – membrane reactors Removing water directly from the reaction mix is more effective – the reaction can even be run under stoichiometric conditions. Reactor configuration is simpler and energy consumption is much lower (Figure 11).

Using pervaporation/vapour permeation units to continuously remove water from condensation reactions gives the following benefits: complete conversion, maximum yield, minimum reagent consumption and costs; maximizes reaction kinetics, reactor efficiency and productivity; minimizes product purification costs; works irrespective of azeotrope formation.

Methanol Recovery

Methanol is commonly used as both solvent and reactant in the chemical industry. However, it forms azeotropes with many substances, particularly esters (Figure 12). Methanol often cannot be removed from spent solvents or from reaction mixtures with simple distillation. Some quite complicated processes have been developed to get around this problem.

Industrial pervaporation/vapour permeation units are now used for separation of methanol, either stand alone or in combination with distillation.

Methanol recovery by azeotrope breaking By way of example, a separation scheme for a methanol-rich methanol–ethyl acetate mixture is shown below. The mixture is distilled to the azeotrope, taking pure methanol out as bottom product. The overhead stream is passed directly to a vapour permeation unit which permeates a methanol-rich stream. This stream is condensed and passed back to the methanol column via the feed buffer. Retentate from the vapour permeation unit, strongly depleted in methanol, can be fed directly to the ethyl acetate column. Pure ethyl acetate leaves this column as bottom product while overhead azeotrope is sent to the vapour permeation unit (Figure 13).

Many solvent or ester/methanol mixtures can be separated using a similar scheme. If the feed is close to the azeotrope then the methanol column can be dispensed with. If the capacity is small the purification column for the second component may not be required, depending on the desired purity.

Institut Français du Pétrole (IFP) has developed a process where pervaporation of methanol is used to debottleneck MTBE production. In the debutanizer columns used in MTBE processing, the MTBE–methanol azeotrope results in a concentration of methanol at a point midway between the feed tray and the reboiler (Figure 14). Pervaporating methanol out of the process from a side-draw taken at this point results in methanol free MTBE as debutanizer bottom product.

Separation systems based on pervaporation/vapour permeation of methanol offer the following benefits: problem-free separation of methanol/organic mixtures irrespective of azeotrope formation; avoids water wash for methanol removal; minimum energy costs.

See Colour Plates 51, 52.

Further Reading

- Bakish Material Corp (1985–1995) *Proceedings of the (1st to 7th) International Conference on Pervaporation Processes in the Chemical Industry*. Englewood: Bakish Material Corp.
- Böddiker KW (ed.) (1995) The early history of membrane science, *Journal of Membrane Science* 100.
- Huang RY (ed.) (1991) *Pervaporation Membrane Separation Processes, I Membrane Science and Technology, Series 1*. Amsterdam: Elsevier.
- Mulder M (1991) *Basic Principles of Membrane Technology*. Dordrecht: Kluwer Academic Publishers.

Polymer Membranes

See II / MEMBRANE SEPARATIONS / Gas Separations with Polymer Membranes

Reverse Osmosis

U. Spohn, Institute of Biotechnology,
University of Halle, Germany

This article is reproduced from *Encyclopedia of Analytical Sciences*, Copyright Academic Press 1995

Dialysis and reverse osmosis

Dialysis is a separation process with increasing areas of application in clinical, biochemical and environmental analysis. A donor and an acceptor solution are separated by a semipermeable membrane (Figure 1).

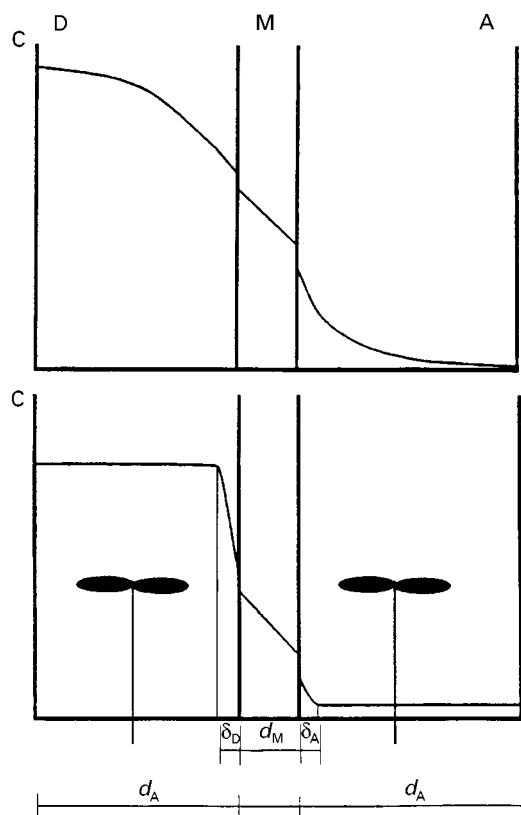


Figure 1 Dialysis between quiescent and stirred solutions. C, concentration; D, donor solution; A, acceptor solution; M, membrane; d_A , d_D and d_M ; thicknesses of the corresponding phase layers, δ_A and δ_D ; thicknesses of the diffusional boundary layers.

When the solutions have different solute activities a diffusional membrane transport from the more to the less concentrated solution takes place to establish the thermodynamic equilibrium. In most applications mass transfer to and away from the separation membrane is accelerated convectively by stirring or by the use of flow-through separation cells.

When the solutions have different solvent activities an osmotic pressure is built up, which causes a solvent flow to the solution of the lower solvent activity. This process is termed osmosis. Reverse osmosis is defined as a process during which an outer pressure is applied to force the solvent through a membrane, which is permeable to the solvent and rejects the solute. Reverse osmosis is applied to purify water for laboratory use and is very promising as a preconcentration technique in trace and environmental analysis.

Fundamentals

Thermodynamic Aspects

During dialysis the activities of the solute i in the donor and the acceptor solutions differ. The difference between the chemical potentials $\mu_{i,D}$ and $\mu_{i,A}$ is the free enthalpy per mole, which propels the dialysis. The dialysis finishes when the thermodynamic equilibrium shown in eqn [1] is reached:

$$\mu_{i,D} = \mu_{i,A} \quad [1]$$

The equilibrium constant K_i^* depends on the activity coefficients $f_{i,D}$ and $f_{i,A}$ and the absolute temperature T according to eqn [2]:

$$K_i^* = \frac{a_{i,A}}{a_{i,D}} = \frac{f_{i,A} \times c_{i,A}}{f_{i,D} \times c_{i,D}} = \exp \left[\frac{\mu_{i,D}^0 - \mu_{i,A}^0}{RT} \right] \quad [2]$$

where $\mu_{i,D}^0$ and $\mu_{i,A}^0$ are the chemical potentials of the solute under standard conditions. c is concentration and a is activity. R is the molar gas constant. An effective separation ratio K_i , which is defined

according to eqn [3], is of analytical interest:

$$K_i = \frac{c_{i,A}}{c_{i,D}} \quad [3]$$

The activity coefficients f_i depend on the solvent, the ionic strength $I = \sum z_j c_j$ of the solution and the concentrations of all nondissociated solutes. The general index, j , labels the ions in the system with the electric charge z_j . Because in most cases:

$$\mu_{i,D}^0 - \mu_{i,A}^0 = 0 \quad [4]$$

it follows that:

$$K_i^* = 1 \quad [5]$$

and:

$$K_i = \frac{f_{i,D}}{f_{i,A}} \quad [6]$$

K_i differs from unity when the dialysis equilibrium is coupled to other equilibria and/or the activity coefficients $f_{i,D}$ and $f_{i,A}$ are different. Without coupled pushing and trapping reactions the enrichment E and the purification factor P can be calculated according to eqns [7] and [8]:

$$E = \frac{c_{i,A}}{c_{i,D,0}} = \frac{(c_{i,D,0} - c_{i,D})V_D/V_A}{c_{i,D,0}} \quad [7]$$

$$P = \frac{c_{i,D,0} - c_{i,D}}{c_{i,D,0}} = \frac{(c_{i,A} - c_{i,A,0})V_A/V_D}{c_{i,D,0}} \quad [8]$$

where $c_{i,D,0}$ and $c_{i,A,0}$ are the initial solute concentrations in the donor and in the acceptor solution, respectively, and V_A and V_D are the volumes of the corresponding solutions. The maximum enrichment factor is around 0.5 for $V_A \leq V_D$. The purification factor increases up to unity with the increasing ratio of V_A to V_D .

The chemical activities of the solvent are equal at dialysis equilibrium. According to eqn [9]:

$$\mu_{L,D} = \mu_{L,A} \quad [9]$$

and because:

$$\mu_{L,D}^0 = \mu_{L,A}^0 \quad [10]$$

it follows for the solvent L that:

$$K_L^* = \exp \left[\frac{1}{RT} \{ V_{L,D} \pi_D - V_{L,A} \pi_A \} \right] \quad [11]$$

where $V_{L,D}$ and $V_{L,A}$ are the partial molar volumes of the solvent which are equal to V_L for dilute solutions, and π refers to the osmotic pressure. It therefore follows that:

$$K_L^* = \exp \left[\frac{V_L}{RT} (\pi_D - \pi_A) \right] \quad [12]$$

with the osmotic pressure difference $\pi = \pi_D - \pi_A$. A volume change is effected to equilibrate the donor and the acceptor solutions. π can be calculated for every solution according to eqn [13]:

$$\pi = - (RT/V_L) \ln a_{x,L} \quad [13]$$

where $a_{x,L}$ is the activity ($x_L \cdot f_L$) of the solvent with respect to the mole fraction x_L of the solvent. Therefore the osmotic pressure difference π has to be taken into consideration to calculate precisely almost all dialysis equilibria. The osmotic pressure difference causes a solvent flow through the separation membranes up to the state at which the hydrostatic back-pressure compensates for the osmotic pressure. e.g. in the batch-type arrangement shown in Figure 2. If the pressure p_h is greater than the osmotic pressure the osmosis will be reversed. This reverse osmosis reaches an equilibrium, which can be described by eqn [14]:

$$K_L^* = \exp \left[\frac{V_L}{RT} (\pi - p_h) \right] \quad [14]$$

Obviously the equilibrium constant decreases with increasing pressure p_h . When the solute is rejected by the membrane it can be enriched in the donor solution.

To take into consideration the electric charges z_i of the solutes and of the separation membrane the Donnan effect has to be considered. The chemical potential μ_i is extended by a term for the electric potential gradient, ϕ . When a membrane separates

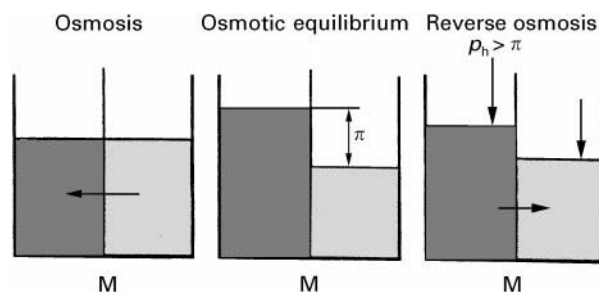


Figure 2 The principles of osmosis and reverse osmosis. M, membrane; p_h , outer pressure; π , osmotic pressure difference. ■, Aqueous salt solutions; □, water.

two solutions of a dissociating salt BA and one solution contains a rejected ion X^- , an electric potential difference $\phi = \phi_D - \phi_A$ is built up between the solutions. This Donnan potential influences the effective separation ratio K . The equilibrium constant is shown in eqn [15] with the Faraday constant F :

$$K_i^* = \exp[(\phi_D - \phi_A)z_i F/RT] \quad [15]$$

where F is the membrane area that is in contact with the solutions.

An outer electrical voltage U generates an electromigration of the anions to the positively charged anode and of the cations to the negatively charged cathode (Figure 3). The process is termed electrodialysis. If the potential difference between the electrodes U is smaller than the voltage U_D of the water decomposition a new electrochemical equilibrium is built up with the constant shown in eqn [16]:

$$K_i^* = \exp[(\phi_D - \phi_A + U)z_i F/RT] \quad [16]$$

In many practical applications the dialysis equilibrium is coupled with chemical equilibria, e.g. acid-base, redox, complexation and precipitation equilibria. It should be noted that distribution equilibria between two different solvents and phases can also be exploited to shift the overall distribution ratio K_i between the donor and acceptor solutions. The enrichment factor E can be increased by several orders of magnitude. The thermodynamics of the separation processes enable the attainable maxima of the enrichment and the purification factors to be estimated.

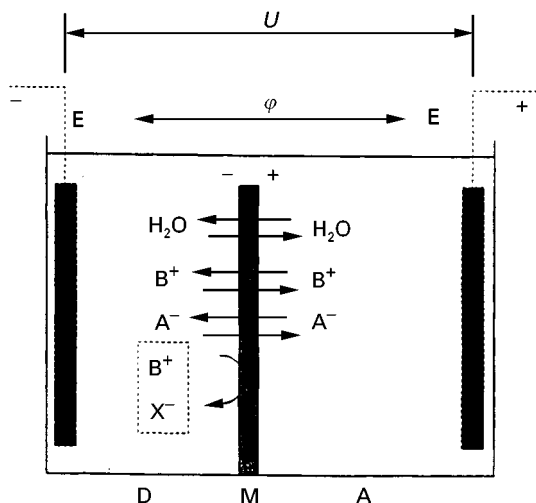


Figure 3 Domain dialysis across a microporous membrane. ϕ , Donnan potential; E, electrodes; U , outer voltage.

Mass Transport

Dialysis For quiescent donor and acceptor solutions the equilibration time ranges from minutes to several hours and is dependent on the geometrical size of the donor and acceptor chambers and the membrane permeability. In this case the equilibration is dominated by the slow diffusional analyte transport. The equilibration can be accelerated by convective mass transport according to Figure 1. Intensive stirring of both the acceptor and the donor solutions establishes diffusional boundary layers of thickness δ on the membrane. The diffusional boundary layer can also be established in flow-through dialysis cells or on rotating dialysis membranes.

The overall flux of the substance i with its molar amount n_i from the donor to the acceptor solution can be described according to eqn [17]:

$$J_i = \frac{dn_i}{dt} = kF \left(\beta_{i,D} c_{i,D} - \beta_{i,A} c_{i,A} \frac{K_{AM}}{K_{DM}} \right) \quad [17]$$

where $\beta_{i,D}$ and $\beta_{i,A}$ are the fractions of the substance i in the donor and in the acceptor solutions respectively, that can permeate through the separation membrane. K_{DM} and K_{AM} are the distribution constants between the donor solution D and the membrane M and between the acceptor solution A and the membrane, respectively. The overall mass transfer coefficient k can be derived from eqn [18]:

$$\frac{1}{k} = \frac{1}{k_D} \left(\frac{k_D \beta_D}{k_D \beta_D + k'_D (1 - \beta_D)} \right) + \frac{1}{k_M K_{DM}} + \frac{K_{AM}}{k_A K_{DM}} \left(\frac{k_A \beta_A}{k_A \beta_A + k'_A (1 - \beta_A)} \right) \quad [18]$$

where $1 - \beta_D$ is the rejected fraction of substance i , $1 - \beta_A$ is the corresponding fraction that is trapped in the acceptor solution, and k_D , k_M and k_A are the mass transfer coefficients of the permeating fractions of substance i for the donor, the membrane and the acceptor phases, respectively. k'_A and k'_D are the mass transfer coefficients for the so-called inactive form of substance i , which cannot permeate the membrane. In many cases the mass transfer across the phase boundary is to be considered additionally, e.g. for homogeneous membranes, supported liquid membranes (SLM) and gas-filled microporous membranes. Then the expression shown in eqn [19] should be added to the right term of eqn [18]:

$$a = \frac{1}{k_{pDM}} + \frac{1}{k_{pAM}} \frac{K_{AM}}{K_{DM}} \quad [19]$$

k_{pDM} and k_{pAM} are the phase transfer coefficients from the donor solution into the membrane phase and from there into the acceptor phase, respectively.

From the general equation some cases of analytical interest can be deduced.

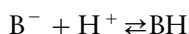
Example 1: Dialysis Through Hydrophilic and Microporous Membranes. Because $\beta_D = \beta_A = 1$, $K_{DM} = K_{AM} = 1$ and no phase transfer takes place, eqn [18] can be simplified to eqn [20]:

$$\frac{1}{k} = \frac{1}{k_D} + \frac{1}{k_M} + \frac{1}{k_A} \quad [20]$$

For large concentration gradients $(c_D - c_A)/d_M$ and very intensive stirring in the set-up shown in Figure 1 or in flow-through dialysis cells with high flow-rates the membrane diffusional transport becomes rate-determining particularly for relatively thick membranes with small pores. Eqn [21] then follows:

$$k = k_M \quad [21]$$

Example 2: Dialysis of Volatile Substances Through Hydrophobic and Microporous membranes. To separate a nonvolatile base B^- , its corresponding volatile acid BH is produced according to the equilibrium:



The donor pH value is chosen according to eqn [22] so that there is a 99.9% degree of conversion into the permeable form of the analyte:

$$\beta_{i,D} = \frac{10^{-pH}}{10^{-pH} + K_a} > 0.999 \quad [22]$$

K_a is the acid-dissociation constant of BH .

The acceptor pH value should be adjusted according to eqn [23] to trap the analyte in its nonvolatile form:

$$1 - \beta_{i,A} = \frac{K_a}{K_a + 10^{-pH}} > 0.999 \quad [23]$$

Since only the volatile part of the analyte amount can traverse the membrane, it follows that:

$$J_i = kFc_{i,D} \quad [24]$$

with:

$$\frac{1}{k} = \frac{1}{k_D} + \frac{1}{k_M K_{DM}} + \frac{K_{AM}}{k_A K_{DM}} + a \quad [25]$$

The distribution ratios K_{DM} and K_{AM} are correlated to the concentrations $\beta_{i,D} \times c_{i,1,D}$ and $\beta_{i,A} \times c_{i,1,A}$ of the volatile forms in the donor and in the acceptor solutions, respectively:

$$K_{DM} = \frac{c_{i,g,D}}{\beta_{i,D} c_{i,1,D}} \approx \frac{p_{i,D}}{\beta_{i,D} RT c_{i,1,D}} \quad [26]$$

$$K_{AM} = \frac{c_{i,g,A}}{\beta_{i,A} c_{i,1,A}} \approx \frac{p_{i,A}}{\beta_{i,A} RT c_{i,1,A}} \quad [27]$$

The right-hand terms of eqns [26] and [27] are approximations for low partial pressures $p_{i,D}$ and $p_{i,A}$. $c_{i,g,D}$ and $c_{i,g,A}$ are the concentrations of the analyte in the gas phase at the interface between the donor or the acceptor solution, respectively, and the membrane gas phase. For very small partial pressures $p_{i,D}$ and $p_{i,A}$, $K_{AM} \ll K_{DM}$ ($p_{i,D} \gg p_{i,A}$) and without hydrodynamic transport limitations, eqn [18] can be simplified to eqn [28]:

$$\frac{1}{k} = \frac{1}{k_D} + \frac{1}{k_M K_{DM}} + a \quad [28]$$

For fast-flowing donor solutions with $1/k_D \rightarrow 0$ the mass transport is determined by the gas diffusion through the membrane, the partial pressure of the analyte in the donor solution and the phase-transfer resistances. The partial pressure of the volatile analyte can be increased by decreasing the partial pressure of the water using high ionic strengths in the donor solution. For highly volatile analytes, thin and highly porous membranes, and fast-flowing solutions, the overall mass transport is controlled by the phase transfer resistance ($k = 1/a$).

Reverse osmosis The driving force of reverse osmosis is the difference between the outer pressure p_h and the osmotic pressure difference π . The mass transfer can be described according to eqn [29]:

$$J_L = PF(p_h - f_R \pi) \quad [29]$$

where J_L is the mass flux of the solvent through the separation membrane and P is the water permeability of the membrane. The osmotic pressure difference is multiplied by the reflection coefficient f_R , which is a measure of the solute rejection by the membrane. During the enrichment process in the donor solution the osmotic pressure difference π increases. The driving force decreases. When the rejection is sufficiently high, the reflection coefficient f_R approximates to unity. The rejection ratio is

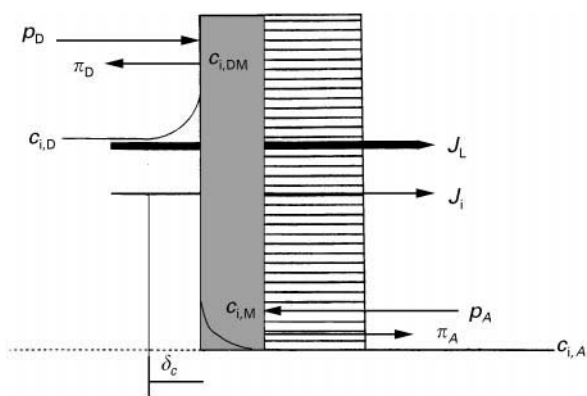


Figure 4 Reverse osmosis with concentration polarization on the asymmetric separation membrane. J_L , mass flux of the solvent; p_D , outer pressure from the donor solution; p_A , outer pressure from the acceptor solution; π_D and π_A , osmotic pressures of the donor and the acceptor solution respectively; δ_c , thickness of the polarization layer; $c_{i,D}$, solute concentration in the donor solution; $c_{i,DM}$, solute concentration on the membrane; $c_{i,M}$, solute concentration in the separation membrane. See text for further explanation.

defined by eqn [30]:

$$R = 1 - \frac{c_{i,A}}{c_{i,D,0}} \quad [30]$$

where $c_{i,A}$ is the solute concentration in the filtrate, and $c_{i,D,0}$ is the initial concentration in the donor solution. The rejected solutes accumulate on the membrane surface (Figure 4). This is the so-called concentration polarization phenomenon, which can be described approximately according to eqn [31]:

$$J_L = k_L \cdot \ln[(c_{i,DM} - c_{i,A}) / (c_{i,D} - c_{i,A})] \quad [31]$$

where $c_{i,DM}$ is the solute concentration on the membrane surface and k_L is the mass transfer coefficient.

The concentration up to the saturation level will cause the precipitation of the solute. The precipitated solute forms a secondary layer on the membrane, which reduces the solvent mass transfer J_L . Therefore the concentration polarization must be reduced by a forced convective flow.

The analytical usefulness is based on the high enrichment factor E , which can be achieved following by eqn [32]:

$$E = \frac{c_{i,D}}{c_{i,D,0}} = \frac{V_{D,0}}{V_{D,0} - V_A} \quad [32]$$

where $V_{D,0}$ is the initial volume of the donor solution.

Geometric Aspects

The geometric shape and extent both of the donor and the acceptor chambers is decisive for the effectiveness and time of the entire separation process. The geometry has to be adapted to the particular analytical task (Table 1). To minimize the separation time the thickness of the donor solution layer should be as thin as possible. The ratio of the membrane exchange area to the donor solution volume should be maximized. To maximize the enrichment factor for dialysis with enhanced selectivity the volume ratio between the donor solution and the acceptor solution has to be maximized.

In this respect, thin hollow-fibre membranes are especially useful both for enrichment and purification procedures. Thin-layer chambers with flat membranes are also useful and enable a greater variety of different membrane materials to be used. The miniaturization of the membrane exchange area up to the micro or the ultramicro scale enables reproducible sampling from quiescent or slowly flowing solutions to be performed. This is of great importance for *in vivo* sampling with microdialytic probes.

Figure 5 shows frequently used hollow-fibre and flat-membrane set-ups. Table 1 summarizes the most useful procedures for dialysis.

The Separation Membrane

The dialytic transport across thin membranes can be described in eqn [33]:

$$J_i = \frac{dn_i}{dt} = k_M F(c_{i,MD} - c_{i,MA}) \quad [33]$$

$c_{i,MD}$ and $c_{i,MA}$ are the solute concentrations in the membrane at the interfaces with the donor and the

Table 1 Dialysis procedures

Objectives in a microanalytical scale	Donor solution	Acceptor solution
Purification	Quiescent or slowly flowing, small sample volume	Flowing or stirred, large volume
Enrichment	Flowing or stirred, large sample volume	Slowly flowing or gently stirred, small volume
Reagent addition	Stirred or flowing, large reagent volume	Quiescent or slowly flowing, small volume
Separation	Quiescent or slowly flowing, small sample volume	Quiescent or slowly flowing, small volume

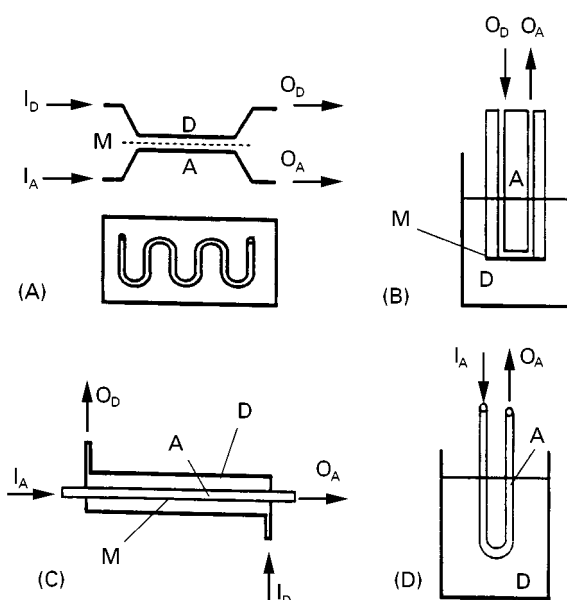


Figure 5 Frequently used dialysis set-up: (A) meander cell with a flat membrane, (B) dialysis probe with a flat membrane M, (C) hollow fibre membrane cell, (D) hollow fibre dialysis probe. I_D , I_A , inlets to the donor and the acceptor chamber; O_A , O_D , outlets from the acceptor and the donor chamber.

acceptor solutions, respectively. Linear concentration gradients can be assumed in thin membranes.

The separation membrane should be considered particularly with regard to selectivity but also with regard to the overall mass transfer kinetics. The membrane material determines the transport mechanism, which influences the selectivity of the separation process in particular. Table 2 gives an overview about the most important membrane materials and the dominant transport mechanisms. Classic dialysis through microporous membranes causes a loss of sensitivity with respect to the following detection or determination procedure. So-called selective dialysis

across gas-filled membranes or SLMs enables an analyte enrichment to be performed. The selectivity of the SLM technique can be enhanced by the addition of selectively reacting ligands to the liquid membrane phase. When charged ions are complexed and transported through these membrane systems electroneutrality must be maintained. In many cases ion pairs with selected counter ions are transported through the membrane. When the ligand is dissolved in the liquid membrane phase and the counter ion cannot transverse the membrane the analyte ion transport is coupled with a back-diffusion of an ion with the same electric charge. A similar situation can be found in ion-exchange membranes, which are used to enrich ions by Donnan dialysis.

Gas dialysis through hydrophobic and microporous membranes is a fast transport process compared with the other transport mechanisms. The diffusion constants in the gas phase are several orders of magnitude greater than in liquid and solid phases. The selectivity of the membrane transport is determined by the ratio of the partial pressure p_i of the analyte to the total pressure p in the membrane pores. In small pores the condensation and adsorption kinetics of the gases also have to be taken into account.

Gas dialysis across homogeneous membranes is generally more selective. The different solubilities of the gases in the membrane material are additional selection factors. The mass transport rate is considerably smaller than those in microporous membranes.

Applications

Dialysis

Dialysis is mainly used in flow analytical methods to purify, dilute and condition sample solutions. It can also be used to add reagents.

Table 2 Membrane transport and selectivity

Membrane material	Transport mechanisms	Factors which determine the selectivity
Hydrophillic and porous	Diffusion through micropores ($k_M = D_m \epsilon / \zeta d_M$)	Sieve effect
Hydrophobic and porous membranes, filled with an organic solvent	Diffusion through micropores	Solubility and sieve effect
As before, but with selective ligands in the solvent	Diffusion through micropores	Solubility, complexing and sieve effect, co-ion transport
Hydrophobic and gas-filled porous membranes	Gas diffusion and flow	Volatility
Ion exchange membranes	Retarded diffusion through micropores	Ion exchange and Donnan exclusion
Homogeneous and hydrophobic membranes	Solvation and diffusion of gases and hydrophobic solutes with small molecular masses	Solubility in the membrane material

ϵ , Membrane porosity; ζ , membrane tortuosity; d_M , membrane thickness; D_m , diffusion coefficient.

The dialysis module can be placed prior to or in the sample insertion unit, between the sample insertion unit and the reaction/separation zone and also into the detector zone. Figure 5A shows a typical flow-through dialysis cell, which is inserted in many online configurations with liquid chromatography (LC) and flow injection analysis (FIA), e.g. as shown in Figure 6. In Figure 6A the dialysis cell is working continuously. The acceptor stream is connected to the injection valve, which adds the prepurified sample into a nonsegmented carrier flow stream. This configuration is frequently used in LC systems. The sample substances are continuously separated from higher molecular weight substances, precipitations and microorganisms. Therefore dialysis is useful to prevent blocking and prolong the lifetime of the separation column. The continuous dialytic sample pretreatment opens up an effective way to use FIA systems for the online process monitoring of animal cell cultures and other industrial bioprocesses. In many cases food, clinical and environmental samples can be analysed without cumbersome offline sample pretreatment. To circumvent the increased detection limit, which is caused by the inherent dilution, the dialysis cell can be used as a flow-through reactor, in which the analyte is trapped as a more sensitively detectable derivate. The acceptor stream can be stopped for different times to control the reaction time. The separated analytes, e.g. phenol derivatives or aflatoxins, can also be reconcentrated on a solid-phase extraction column, which is inserted into the sampling loop of the injection valve. Also highly specific preconcentration columns, e.g. with immobilized antibodies, can be used.

In Figure 6B the dialysis membrane is contacted only during short concentration impulses with the sample solution. The probability of membrane foul-

ing and clogging is decreased considerably. The sample solution is precisely diluted. This pulsed FIA dialysis is frequently used to adapt ion-selective electrodes, biosensors and miniaturized enzyme reactors to biological sample matrices.

A very promising and expanding field of application was opened up by the so-called microdialysis technique. Miniaturized dialysis probes with tip diameters smaller than 1 mm are implanted into different tissues of living animals for sampling low molecular weight substances from the tissue fluid. The low molecular weight analytes are separated across small membrane (cellulose acetate, cut-off 1000–60 000 Da) windows into a flowing acceptor stream, as shown in Figure 5B. The enrichment factor is controlled by the flow rate ($0.5\text{--}25\ \mu\text{L min}^{-1}$). The microdialysis probes are coupled online to microcolumn LC systems, to capillary FIA set-ups and recently also to capillary electrophoresis devices. In many cases the separated substances, e.g. lactate and glucose, are converted by enzymes which are dissolved together with the cofactors and cosubstrates in the acceptor solution.

Donnan Dialysis

Donnan dialysis across ion exchange membranes is widely used as an efficient suppression technique in ion chromatography. When a cation exchange membrane separates the eluent, which is an aqueous Na_2CO_3 solution, from a reservoir of strong acid, protons are transported into the eluent. Since the membrane is impermeable to anions, the cations from the eluent must diffuse simultaneously into the suppressor reservoir. The chromatographically separated anions are combined with completely dissociated acids, which have a high equivalent conductivity. The CO_3^{2-} ions are converted to the weakly dissociated carbonic acid. In cation chromatography the eluent, e.g. aqueous hydrochloric acid, has to be suppressed. Therefore an anion exchange membrane is used to separate the eluent from a sodium hydroxide suppressor solution. The anions of the eluent are replaced with hydroxide ions to increase the conductivity in the separation peaks and to suppress the eluent conductivity by neutralization to water. Donnan dialysis across ion exchange membranes can also be used to neutralize strong alkaline and acid samples in an online sample pretreatment for ion chromatography.

Donnan dialysis is also used to enrich low molecular weight ions. When a cation exchange membrane separates a high ionic strength solution from a low ionic strength sample solution, cations are transported from the high ionic strength solution to the

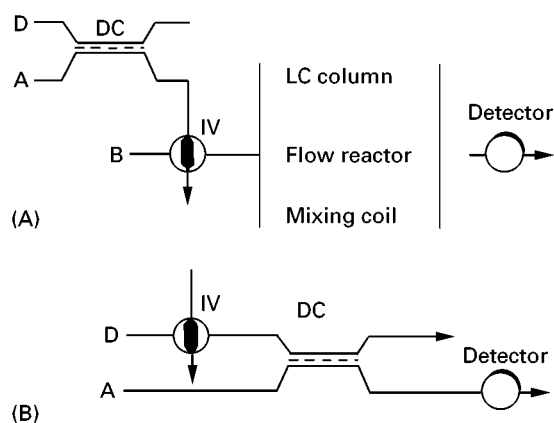


Figure 6 Continuous (A) and pulsed dialysis (B) in flow analytical set-ups. IV, injection valve; DC, dialysis cell; B, carrier solution. See text for further explanations.

Table 3 Enrichment and sample pretreatment by Donnan dialysis (Cox (1992) and cited references)

Analyte	Enrichment factor	Detection
<i>Cations</i>		
Pb(II), Cd(II), Tl(I)	> 100	FAAS
Cd(II)		DPASV
Cu(II)	> 100	FAAS
Cu(II), Zn(II)		ICP-AES
Ca(II)	22	FAAS
Fe(II), Ni(II), Cr(III)	40–80	ICP-AES
Co(II), Cd(II), Mn(II), Cu(II), Ni(II)	80–1000	IC
La(III), Nd(III)	50	ICP-AES
<i>Anions</i>		
AsO ₄ ³⁻ , PO ₄ ³⁻	5–10	CSV
Cl ⁻ , NO ₃ ⁻ , SO ₄ ²⁻ , PO ₄ ³⁻	15	IC
Pyruvate, chloroacetate	5–10	V

IC, ion chromatography; FAAS, flame atomic absorption spectrometry; ICP-AES, inductively coupled plasma-atomic emission spectrometry; ASV, anodic stripping voltammetry; DPASV, differential pulse ASV; CSV, cathodic stripping voltammetry; V, voltammetry.

low ionic strength solution. Since the membrane is almost impermeable to anions, cations from the dilute solution must diffuse back to the more concentrated solution to maintain the electroneutrality. Anions can be analogously separated by means of an anion exchange membrane.

Ions from dilute solutions, e.g. ground and drinking water samples, can be enriched into high ionic strength solutions with volumes which are smaller than the sample volume. The acceptor solutions can be adapted to whatever determination procedure is to be used. Both flat and tubular ion exchange membranes are used, as shown in Figure 5A,B and D.

Tubular ion exchange membranes with a small inner diameter are particularly useful because of their high surface area to internal volume ratios. Such concentrators can readily be combined with flow analytical set-ups, e.g. flow injection analysis-atomic absorption spectrometry (FIA-AAS) and ion chromatography (IC) systems.

Because of the high osmotic pressure difference between the donor and the acceptor solution and the porosity of the ion exchange membranes a slow water flow takes place, which can be neglected in many analytical applications (Table 3).

It should be noted that the interaction between the diffusing ions and the fixed counterions in the membrane retards the diffusion, which can be accelerated by an alternating electric field with a frequency around 1 MHz. Multiply electrically charged ions, e.g. Mg²⁺ and Al³⁺, decrease the interaction between the sample cations and the fixed counterions, whereby the diffusional transport of the sample cations is accelerated.

Selective Dialysis Across Solid and Liquid Membranes

Selective dialysis is defined here as a separation of substances from an aqueous donor phase into an aqueous acceptor phase, the phases being separated by solid and liquid membranes. The analyte transport through such membranes is based on a solvation/diffusion mechanism in a lipophilic phase. The liquid membranes have to be supported by a microporous and hydrophobic layer to enable practical applications to be performed. Again the basic set-up of the flow separation cells shown in Figure 5 can be used to apply these membranes for separation procedures that can be coupled online to LC, gas chromatography (GC) and FIA set-ups.

Thin silicon rubber membranes can be used to separate e.g. phenols and chlorphenols in a 'push-pull' procedure. The sample solution is acidified to shift the chemical equilibrium to the nondissociated phenol/chlorphenol species, which are dissolved in the silicon membrane. The phenol molecules are trapped as phenolate ions in an alkaline acceptor solution. The maximum enrichment factor is determined by the pH values in the donor and the acceptor solution.

Nonpolar organic substances can also be separated from a sample donor solution into an acceptor solution, but the enrichment factor can only be increased to values greater than 0.5 by addition of an organic solvent to the acceptor solution.

The SLMs have the advantages of faster membrane transport and easier modification of the liquid phase, which determines the transport mechanism and the separation selectivity. Dialysis across SLMs has a wide and growing field of application in

Table 4 Applications of supported liquid membranes

Analytes	Conversion with	Membrane transport	Trapping by	Detection
Mode A				
Alcohols		<i>n</i> -Heptane, supported by microporous PTFE		GC, LC, SnO ₂ -sensor
Mode B				
Amines ^a	OH ⁻	<i>n</i> -Decane, supported by microporous PTFE	H ⁺	GC, LC, ph
Phenols	H ⁺	<i>n</i> -Dodecane, supported by microporous PTFE	OH ⁻	LC, GC, ph
Carboxylates	H ⁺	<i>n</i> -Nonane, supported by microporous PVDF	OH ⁻	LC, ph
Thiolates	H ⁺	<i>n</i> -Dodecane, supported by PVDF	OH ⁻	a, GC
Mode C				
Cu(II) ^b	PAR	<i>n</i> -Pentane, which contains di-2-ethyl-hexylphosphoric acid and is supported by microporous PVDF	H ⁺	ph
Pb(II) ^c	Anions	Phenylhexane, which contains bis(1-hydroxyheptyl-cyclohexano)-18-crown-6, supported by microporous PTFE	EDTA	AAS

^aJönsson JA, Lökvist P, Audunsson G and Nilve G (1993) Mass transfer kinetics for analytical enrichment and sample preparation using supported liquid membranes in a flow system with stagnant acceptor liquid. *Analytica Chimica Acta* 277: 9–24.

^bBarnes DE and Van Staden JF (1992) Flow injection analysis in the evaluation of supported liquid membranes. *Analytica Chimica Acta* 261: 441–451.

^cIzatt RM, Bruening RL, Bruening ML *et al.* (1989) Modelling diffusion – limited, neutral – macrocycle – mediated cation transport in supported liquid membranes. *Analytical Chemistry* 61: 1140–1148.

a, amperometric; AAS, atomic absorption spectrometry; EDTA, ethylenediaminetetraacetic acid; GC, gas chromatography; LC, liquid chromatography; PAR, 4-(2'-pyridylazo)resorcinol; ph, photometric; PTFE, polytetrafluoroethylene; PVDF, polyvinylidene fluoride.

environmental, food and clinical analysis. **Table 4** summarizes some examples of application. Three modes of selective separation are used:

1. The extraction of a hydrophobic substances into the supported organic liquid phase and the following back-extraction into the aqueous acceptor stream.
2. 'Push-pull' separation. The analyte is converted into a membrane-soluble substance, which diffuses through the membrane and is trapped as a substance that is insoluble in the membrane.
3. Co-ion mediated transport on the basis of a carrier substance which is dissolved in the liquid membrane phase. The carrier molecules take up the analyte molecules or ions, whereby a hydrophobic complex or an ion-pair is formed.

Gas Dialysis

Gas dialysis can also be used for FIA procedures and other flow analytical methods to enhance their selec-

tivity. The configurations shown in Figure 5 can be used to separate and enrich volatile or nonvolatile analytes, which can be converted into a volatile substance. **Table 5** gives an overview of the applications of the gas dialysis technique to determine inorganic substances.

The application range can be extended to volatile and water-soluble organic compounds, e.g. lower alcohols (methanol, ethanol, propanol), formaldehyde, acetaldehyde, acetone, ethylene oxide, propylene oxide, ethyl acetate. Several nonvolatile species. e.g. acetate, propionate, can be separated after acidification. Gas dialysis membranes can separate aqueous solutions with very different pH values and ionic strengths, which enables also extreme sample matrices to be adapted to originally unsuitable detection procedures. Microporous PTFE or polypropylene membranes are used in most cases. However, it should be noted that, for example, surfactants and many water-soluble organic compounds can be adsorbed on the membrane surface, which then becomes increas-

Table 5 Applications of gas dialysis

Analyte	Conversion to	Trapping as or by	Detection
<i>Without conversion</i>			
ClO_2 , Cl_2 , Br_2 , I_2		A colour or chemiluminescence reaction or reduction	a, ph, c, pot
NO , NO_2		Oxidation to NO_3^-	pot (ISE)
N_2H_4		Oxidation	a, ph, c
<i>Conversion by acid-base reaction</i>			
CN^-	HCN	CN^- , $\text{Ag}(\text{CN})_2^-$	c, pot (ISE)
SCN^-	HSCN	SCN^- , colour forming reaction	pot, ph
CO_2 , HCO_3^- , CO_3^{2-}	CO_2	HCO_3^-	c, pot (ISE), ph
NH_3 , NH_4^+	NH_3	NH_4^+ , colour forming reaction or oxidation	c, pot (ISE), pH ph, ch, a
NO_2^-	NO	NO_2^- , NO_3^- or colour forming reaction	ph, pot (ISE)
H_2S , HS^- , S^{2-}	H_2S	S^{2-}	pot (ISE), a, c ph
HSO_3^- , SO_3^{2-}	SO_2	SO_2 , SO_4^{2-} or colour forming reaction	c, ph
F^-	HF	F^-	pot (ISE)
<i>Conversion by redox reactions</i>			
Cl^- , OCl^- , ClO_2^- , ClO_3^- , Br^- , BrO_3^- , I^-	Cl_2 , Br_2 , I_2	I^- , Br^- and I^- or Cl_2 , Br_2 , I_2	pot (ISE), a

a, amperometric; c, conductometric; ch, chemiluminometric; ISE, ion selective electrode; ph, photometric; pot, potentiometric.

ingly hydrophilized. Water penetrates into the membrane pores and changes the mass transfer coefficients considerably with time. In some of these situations homogeneous membranes, e.g. different silicone rubber membranes, can be used to circumvent such interferences. Silicone rubber membranes are permeable to hydrogen sulfide, hydrogen cyanide, carbon dioxide and many volatile organic compounds.

Osmosis and Reverse Osmosis

Diluted sample solutions can be concentrated by both osmosis and reverse osmosis. The concentration process is based on a pressure gradient over a membrane, which rejects the analyte molecules. High molecular weight substances are already rejected by ultrafiltration membranes. But the typical application of reverse osmosis is the separation of low molecular weight substances from aqueous solutions to purify the water or to concentrate the substances which are to be determined.

To concentrate transition and heavy metal ions from dilute aqueous solutions by osmosis the sample solution is separated from a high ionic strength solution by a membrane which is permeable only to the water. An osmotic pressure is built up, which then propels the water into the acceptor (filtrate) solution and concentrates the donor solution. In a thin-layer flow-cell, which is similar to the cell shown in Figure 5A and has a mechanically supported separation membrane (reverse osmosis membrane of cellulose

lose triacetate) preconcentration factors of up to 8–10 for copper(II), cadmium(II), manganese(II), nickel(II) and zinc(II) can be achieved in a countercurrent flow regime.

To implement reverse osmosis, an outer pressure (Figure 2) is applied to propel the water through the membrane. An interesting practical aspect is the possibility of reducing the necessary outer pressure by an osmotic pressure difference which has the same direction. This is implemented by high ionic strength acceptor solutions.

The concentration factor E (eqn [32]) increases considerably with increasing reflection factors (eqn [29]). Highly diluted sample solutions can be concentrated to values that can be determined with the available determination methods. The sample solution can be concentrated up to the precipitation of the solute. Then an additional filter layer is used, which can be exchanged and directly analysed, e.g. by X-ray fluorescence spectrometry. Transition metals could be analysed in drinking water up to the microgram per litre level. Organic contaminants, e.g. chlorobenzene and phenols in alkalized sample solutions, could also be concentrated by reverse osmosis. After this preconcentration traces of the contaminants could be analysed by LC and GC after their redissolution.

Further Reading

Cox JA (1992) Membrane methods for preconcentration of trace components of solutions. In: Zeev B and Wai CM

- (eds) *Preconcentration Techniques for Trace Elements*, pp. 301–331. Boca Raton: CRC.
- Cox JA and Twardowski Z (1980) Electric field enhancement of Donnan dialysis. *Analytical Letters* 13(A14): 1283–1291.
- Dasgupta P (1988) Approaches to ion chromatography. In: Tarter JG (ed.) *Ion Chromatography*, pp. 191–338. New York: Marcel Dekker.
- Jönsson AJ, Lökvist P, Audunsson G and Nilve G (1993) Mass transfer kinetics for analytical enrichment and sample preparation using supported liquid membranes in a flow system with stagnant acceptor liquid. *Analytica Chimica Acta* 277: 9–24.
- Robinson T and Justice JB (1991) *Microdialysis in the Neurosciences*. New York: Elsevier Science.
- Spohn U, Eberhardt R, Joks B, *et al.* (1991) Enzymatic multichannel-FIA methods for on-line fermentation monitoring and control. In: *GBF Monograph*, vol. 14, pp. 51–62. Weinheim: Verlag Chemie.
- Stec RJ, Koirtyohann SR and Taylor HE (1986) Preconcentration of trace elements from aqueous solutions by osmosis. *Analytical Chemistry* 58: 3240–3242.
- Valcarcel M and Luque de Castro MD (1991) *Non-chromatographic Continuous Separation Techniques*. Cambridge: Royal Society of Chemistry.

Ultrafiltration

M. Cheryan, University of Illinois, Urbana, IL, USA

Copyright © 2000 Academic Press

Introduction

Ultrafiltration (UF) is a filtration process that employs a membrane to fractionate liquid mixtures containing molecules that range in size from about 1000 daltons in molecular weight to 500 000 daltons. The membrane, made of either polymeric or inorganic materials, is a semipermeable barrier containing pores of a certain size distribution that are used to retain or 'reject' components of the feed mixture that are larger than the rated pore size while allowing molecules that are smaller than the pores to pass through the membrane. This separation process is very simple (Figure 1) involving only the pumping of fluids. The membrane is assembled in a particular configuration and placed in a module, and the feed stream is pumped through the module over the membrane surface in a cross-flow mode. The pressure forces solvent

(e.g. water) and solute molecules smaller than the pores on the membrane surface through the membrane into the 'permeate' stream while larger solutes are rejected and retained in the 'retentate' stream. The retentate is recycled through the module until the required degree of purification, separation or concentration is achieved.

Ultrafiltration is similar in concept to other pressure-driven membrane processes such as microfiltration, nanofiltration and reverse osmosis. However, as shown in Figure 2, the size range of the solutes that are retained by each membrane is different. Reverse osmosis (RO) membranes are designed to retain all components except for the solvent (e.g. water). It is essentially a concentration process. Owing to the osmotic pressure of the solutes retained by RO membranes, pressures needed to operate RO systems are typically 30–60 bar (450–900 lb in⁻²). Nanofiltration (NF) membranes have slightly larger pores and are designed to allow monovalent salts such as sodium chloride to pass through, but retains divalent salts, disaccharides and dissociated organic acids. Pressures are usually lower, about 15–25 bar. Microfiltration (MF) membranes retain components that are in suspension or in colloidal form, and is essentially a clarification process. Pressures are usually 1–4 bar.

Ultrafiltration, on the other hand, is designed to retain macromolecules and other solutes in the size range of 1–50 nm, or with equivalent molecular weights of 1000 to 500 000 daltons. It also operates at low pressures (2–6 bar) and can simultaneously act as a concentration, purification and fractionation process, depending on the components in the feed and the membrane properties. It has several advantages over other separation or concentration techniques. Unlike freeze concentration or evaporation, there is

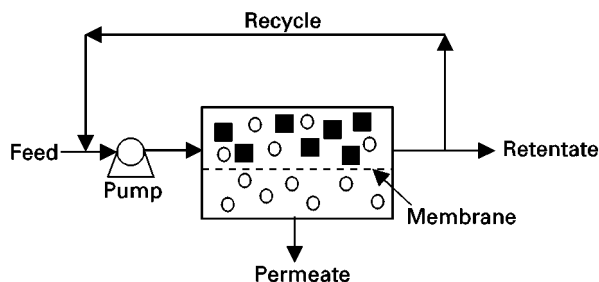


Figure 1 Cross-flow ultrafiltration. Particles in the feed that are larger than the rated pore size of the membrane are retained in the retentate stream while smaller particles pass through into the permeate. (Adapted from Cheryan (1998) with permission from Technomic.)

- (eds) *Preconcentration Techniques for Trace Elements*, pp. 301–331. Boca Raton: CRC.
- Cox JA and Twardowski Z (1980) Electric field enhancement of Donnan dialysis. *Analytical Letters* 13(A14): 1283–1291.
- Dasgupta P (1988) Approaches to ion chromatography. In: Tarter JG (ed.) *Ion Chromatography*, pp. 191–338. New York: Marcel Dekker.
- Jönsson AJ, Lökvist P, Audunsson G and Nilve G (1993) Mass transfer kinetics for analytical enrichment and sample preparation using supported liquid membranes in a flow system with stagnant acceptor liquid. *Analytica Chimica Acta* 277: 9–24.
- Robinson T and Justice JB (1991) *Microdialysis in the Neurosciences*. New York: Elsevier Science.
- Spohn U, Eberhardt R, Joks B, *et al.* (1991) Enzymatic multichannel-FIA methods for on-line fermentation monitoring and control. In: *GBF Monograph*, vol. 14, pp. 51–62. Weinheim: Verlag Chemie.
- Stec RJ, Koirtyohann SR and Taylor HE (1986) Preconcentration of trace elements from aqueous solutions by osmosis. *Analytical Chemistry* 58: 3240–3242.
- Valcarcel M and Luque de Castro MD (1991) *Non-chromatographic Continuous Separation Techniques*. Cambridge: Royal Society of Chemistry.

Ultrafiltration

M. Cheryan, University of Illinois, Urbana, IL, USA

Copyright © 2000 Academic Press

Introduction

Ultrafiltration (UF) is a filtration process that employs a membrane to fractionate liquid mixtures containing molecules that range in size from about 1000 daltons in molecular weight to 500 000 daltons. The membrane, made of either polymeric or inorganic materials, is a semipermeable barrier containing pores of a certain size distribution that are used to retain or 'reject' components of the feed mixture that are larger than the rated pore size while allowing molecules that are smaller than the pores to pass through the membrane. This separation process is very simple (Figure 1) involving only the pumping of fluids. The membrane is assembled in a particular configuration and placed in a module, and the feed stream is pumped through the module over the membrane surface in a cross-flow mode. The pressure forces solvent

(e.g. water) and solute molecules smaller than the pores on the membrane surface through the membrane into the 'permeate' stream while larger solutes are rejected and retained in the 'retentate' stream. The retentate is recycled through the module until the required degree of purification, separation or concentration is achieved.

Ultrafiltration is similar in concept to other pressure-driven membrane processes such as microfiltration, nanofiltration and reverse osmosis. However, as shown in Figure 2, the size range of the solutes that are retained by each membrane is different. Reverse osmosis (RO) membranes are designed to retain all components except for the solvent (e.g. water). It is essentially a concentration process. Owing to the osmotic pressure of the solutes retained by RO membranes, pressures needed to operate RO systems are typically 30–60 bar (450–900 lb in⁻²). Nanofiltration (NF) membranes have slightly larger pores and are designed to allow monovalent salts such as sodium chloride to pass through, but retains divalent salts, disaccharides and dissociated organic acids. Pressures are usually lower, about 15–25 bar. Microfiltration (MF) membranes retain components that are in suspension or in colloidal form, and is essentially a clarification process. Pressures are usually 1–4 bar.

Ultrafiltration, on the other hand, is designed to retain macromolecules and other solutes in the size range of 1–50 nm, or with equivalent molecular weights of 1000 to 500 000 daltons. It also operates at low pressures (2–6 bar) and can simultaneously act as a concentration, purification and fractionation process, depending on the components in the feed and the membrane properties. It has several advantages over other separation or concentration techniques. Unlike freeze concentration or evaporation, there is

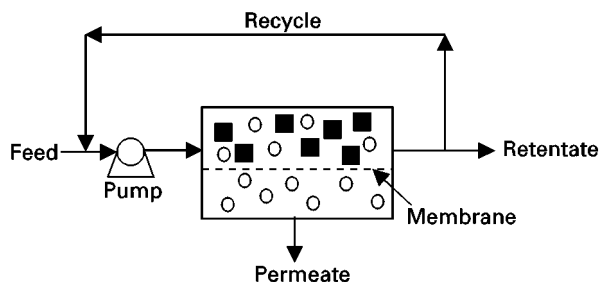


Figure 1 Cross-flow ultrafiltration. Particles in the feed that are larger than the rated pore size of the membrane are retained in the retentate stream while smaller particles pass through into the permeate. (Adapted from Cheryan (1998) with permission from Technomic.)

Size (nm)	Example	Process
0.1	Sodium chloride	Reverse osmosis
	Sucrose	
1	Vitamin B ₁₂	Nanofiltration
	Pepsin	
10	Ovalbumin	Ultrafiltration
	Immunoglobulin M	
100	Latex emulsions	Microfiltration
	Bacteria	
1000	Blood cells	
	Starch	

Figure 2 Examples of compounds of various sizes separated by different membranes. (Adapted from Cheryan (1998) with permission from Technomic.)

no change in phase of the solvent and thus energy consumption is much lower. Being a nonthermal process, there are no extremes of temperature and feed solutions can be concentrated by UF with little or no thermal damage to heat-sensitive components. Since pores are large enough to allow passage of soluble salts, acids and alkalis, the microenvironment of the solution remains largely unchanged during the process.

There are several factors that affect ultrafiltration applications: the membrane material, properties of the membrane, process engineering parameters, design of the membrane module, fouling and cleaning and process design. The most important performance parameters in UF are flux and rejection. Flux is the volume of permeate per unit time per unit membrane area. Higher flux means lower capital and operating costs. Rejection is a measure of a membrane's separating capabilities. It is defined as:

$$1 - \frac{\text{Concentration of solute in the permeate}}{\text{Concentration of solute in the retentate}}$$

Membrane Material

Membranes have been made from over 150 different polymers or inorganic materials, but only about a dozen have achieved widespread commercial use for UF. The most common are polymers such as polysulfone, polyethersulfone, polyvinylidene fluoride, polyacrylonitrile, cellulose acetate and regenerated cellulose as well as inorganic materials such as alumina, zirconia and titania. Most polymeric UF membranes are asymmetric in structure, i.e. they have a thin 'skin' 0.1–0.2 μm thick on the surface of the membrane. This skin contains the pores of the required size and determines the separation characteristics of the UF membrane. Polymer layers under the skin usually consist of voids which support the skin layer. The skin and void layer are one structure and one polymer when made by a phase-inversion process, but they could be two or more different polymers in composite membranes. The membrane is then laid on a backing such as polyester or polypropylene and then formed into the module. In some cases, such as hollow fibres, a concentrated solution of the polymer is spun or extruded to form self-supporting single polymer hollow tubes with the pores on the inside surface of the tube.

Inorganic membranes have considerably widened the range of membrane applications, particularly in food processing, waste treatment, recovery of chemicals and biotechnology applications, where high temperature, acid and/or alkali stability, steam sterilizability and cleanability are important. A macroporous substrate of a fine dispersion of the powder is first formed, e.g. by thermal sintering of an extruded paste of the powder. If a tubular geometry is used, pastes from two powders of different grain sizes may be co-extruded, with the finer grain being closer to the axis. After baking at high temperatures ($>1000^\circ\text{C}$), the inside may be coated by slip casting with the final fine grain powder. A series of such layers may be necessary to obtain the asymmetric-type ultrastructure. The membrane is finally set by a series of pressurizing, drying and baking steps. The most common ceramic materials are α -alumina, zirconia and titania. Composites of zirconia or titania membranes on alumina, carbon or stainless-steel supports are available.

Most inorganic membranes are available in tubular form, either as a single channel tube or multi-channel element, the latter containing up to 60 individual circular channels, depending on the relative diameters of the channel and the element. The inner diameter of individual channels vary from 2 to 6 mm and lengths from 0.8 to 1.2 m. As many as 99 of these elements may be put together in a single housing, resulting in

8–12 m² per module. Normal process ratings are 15 bar and 150°C.

Inorganic membranes have several desirable properties. They are inert to common chemicals and solvents and have wide temperature limits. Depending on the seals and type of housing, some inorganic membranes can be operated as high as 350°C and within wide limits of pH from 0.5 to 13.5. The biggest advantage is their extended operating lifetimes. Operating life of membranes is most affected by the frequency and nature of the cleaning regime. In contrast to polymeric membranes which typically have 9–18-month lifetimes with normal daily cleaning cycles, inorganic membranes are able to tolerate frequent aggressive cleaning regimes. Many are still operating 10–14 years after installation with the first set of membranes. One major limitation is that they are 10–30 times more expensive than polymeric membranes.

Membrane Properties

Pore size is the most important property of a UF membrane. Pores can be visualized using electron microscopy. Surface porosity (the proportion of the membrane surface occupied by pores) is less than 10% for many UF membranes. In an ideal membrane, all pores should be of the same size. In reality, there is a distribution of pore sizes, as shown in Figure 3. This makes it difficult to get a sharp separation of similarly sized molecules by UF. A common method to characterize UF membranes is to challenge the membrane with several macromolecules of known molecular sizes. Since proteins of different molecular weights are usually used as molecular markers, UF membranes are characterized in terms of their ability to retain proteins of a particular molecular weight. Figure 3 is a graphical representation of solute rejection data for ideal and real membranes. No membrane will display the sharp pore-size distribution shown for the ideal membrane. MF membranes are given 'absolute' ratings which is the largest particle that will be retained by the membrane, based on actual tests under standard conditions. In contrast, UF membranes are given 'nominal' ratings which refer to the molecular weight of a test solute (ideally it should be a globular protein) which is 90% rejected by the membrane under standard conditions. This rating is termed the molecular weight cut-off (MWCO) of the membrane.

Proteins are not ideal compounds to use for this purpose, since their molecular size can be affected by pH, ionic strength and interactions with buffer components. Proteins can have different isoelectric points, solubility and hydrophobicity, thus causing

them to interact with and foul the membrane to different extents, which affects measured rejections. In addition, proteins which differ by 10 times in MW may only differ by three times in size in their globular form. Owing to the difficulty of finding proteins that are sufficiently pure (and inexpensive) to conduct MWCO evaluations, other compounds such as polyethylene glycols (PEG) and dextrans have been used because they are water soluble and can be readily obtained with well-defined and narrow-size distributions. Since the shapes of these various compounds are different, the MWCO profile of a membrane will also differ depending on the solute test marker used. Environmental conditions such as pH and ionic strength also affect shape and conformation of molecules which can affect rejection.

Other components in the feed solution could affect the separation of the target compound. For example, with UF membranes, low-molecular-weight solutes (such as sugars and salts) have molecular sizes much smaller than the smallest pore on the membrane. These compounds will be freely permeable, i.e. they will have zero rejection, unless they interact with or bind to impermeable compounds in the feed. Changes in operating conditions will not affect their permeability. On the other hand, large solutes that are much bigger than the pores will be completely rejected (i.e. 100% rejection). Its rejection properties will also be relatively unaffected by operating conditions or if other compounds are present. However, if the solute has a size that is of the same order of magnitude as the pore, its rejection may be affected in the presence of the large molecule. This is because the large molecule forms a secondary

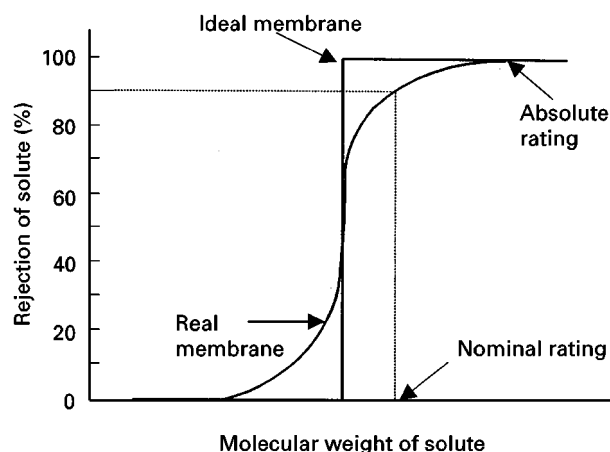


Figure 3 Typical molecular-weight profile of ideal and real membranes. Relationship shown is between molecular size of a solute in the feed stream and rejection of the solute by the membrane. (Adapted from Cheryan (1998) with permission from Technomic.)

dynamic membrane on the original membrane that inhibits passage of the smaller molecule. Operating conditions that change the shape or conformation of the solute will also affect its rejection.

As a general rule, fractionation of polymers can be accomplished if there is at least a 10-fold difference in molecular weight. Separation of similarly sized macromolecules can be enhanced by diluting the feed to minimize solute-solute interactions and solute-membrane interactions.

Other factors affecting separation are operating parameters such as pressure and cross-flow rate. These control the degree of turbulence and the thickness of the boundary layer and extent of concentration polarization (defined below), which in turn affect permeability of smaller solutes.

Operating Parameters

Separation of solutes by UF membranes occurs by a sieving mechanism. The transport of fluids through the pores is modelled as laminar flow through channels, with flux directly proportional to applied transmembrane pressure. However, it has frequently been observed that under certain operating conditions, flux becomes independent of pressure as shown in **Figure 4**. This is owing to 'concentration polarization' which is shown in **Figure 5**. Molecules or particles that are partially or completely retained by the membrane accumulate on the surface of the membrane during ultrafiltration. This build-up of solids will cause a concentration gradient within the boundary layer, resulting in back-transport of solute into the bulk stream owing to diffusion. Eventually a steady state is reached where the two phenomena balance each other. Solute concentration reaches a maximum at the 'gel concentration'. This con-

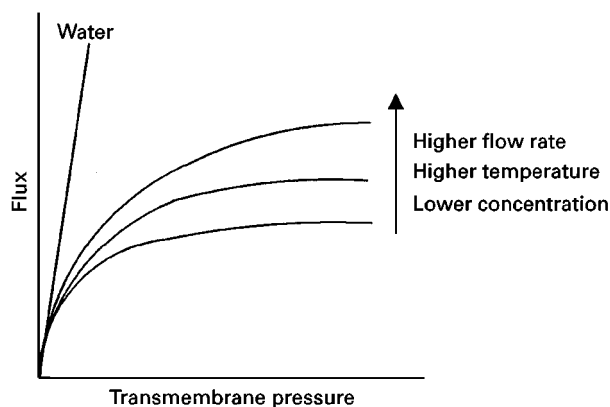


Figure 4 Effect of operating conditions on flux of an ultrafiltration system. (Adapted from Cheryan (1998) with permission from Technomic.)

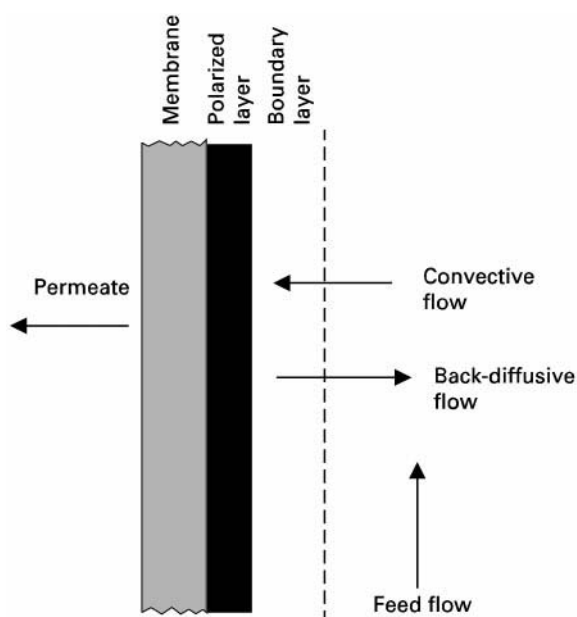


Figure 5 Concentration polarization in ultrafiltration.

solidated gel layer is the reason that pressure independence in **Figure 4** is observed. Flux is no longer controlled by pressure but by the mass-transfer characteristics of the system which in turn depends on the diffusion coefficient of the rejected molecules in the boundary layer, turbulence in the flow channel, viscosity and density of the fluid stream. Higher temperatures lead to higher flux because of its favorable effect on diffusivity and viscosity. In the pressure-independent region, flux decreases in a semi-logarithmic manner with bulk feed concentration and increases with higher turbulence (usually achieved by higher flow rates through the module).

Module Design

There are basically six different designs of membrane modules: tubular (with channel diameters greater than 3 mm), hollow fibre or capillaries (self-supporting tubes, usually 2 mm or less internal diameters), plates, spiral-wound, pleated sheets and moving modules (e.g. rotating discs or cylinders). **Figure 6** shows the more common types of modules. The selection of a particular design depends on (a) the physical properties of the feed stream and retentate, especially viscosity and osmotic pressure, (b) particle size of suspended matter in the feed, (c) fouling potential of the feed stream, and (d) sanitation requirements, such as cleanability and sterilizability. The viscosity of feed streams containing macromolecules such as polymers or proteins will increase nonlinearly with concentration above a certain value. This will require

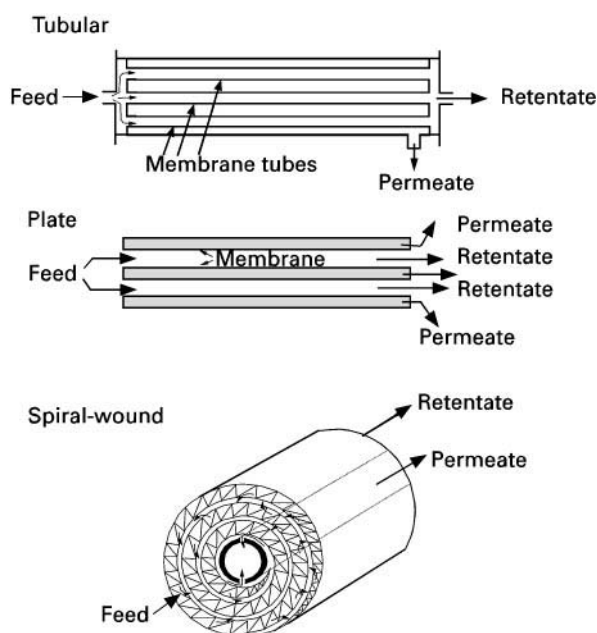


Figure 6 Schematic of ultrafiltration membrane modules: tubular, plate and spiral-wound.

high pressure drops for pumping and require the use of modules that can withstand high pressures, eliminating most hollow fibre/capillary modules. On the other hand, these modules have extremely high packing densities (surface area : volume ratios) and comparatively low energy consumption, making them useful in applications where the feed is of relatively low viscosity and low in suspended matter.

Spiral-wound modules and some plate modules incorporate a spacer in the feed channel to keep the membrane sandwich apart. This spacer can add considerable turbulence to the fluid flow and thus increase the flux. However, this spacer causes a parasitic drag and creates dead spots in the feed channel, which can cause suspended particles to block the flow channel, resulting in high pressure and cleaning problems.

Fouling and Cleaning

Fouling manifests itself as a decline in flux with time under constant operating conditions. The sieving properties of the membrane may also change. This is owing to irreversible interactions between feed components and the membrane, causing a layer of foulant on the membrane, blinding of the pores and an increased resistance to fluid flow through the membrane. Many membrane materials listed earlier are relatively hydrophobic (e.g. polysulfone, polyvinylidene fluoride) and tend to foul more than hydrophilic membrane materials (e.g. cellulose, cer-

amics). Many feed components interact strongly with membranes, e.g. oils through hydrophobic interactions with hydrophobic membranes, proteins by hydrogen bonding, charge interactions or hydrophobic interactions, and salts by precipitation or charge interaction.

A fouled membrane has to be cleaned according to the nature of the foulant. Proteins can be effectively cleaned with alkaline solutions, salts are removed with acid cleaners. The quality of the water is very important in ensuring a membrane can be effectively cleaned in the shortest time possible.

Flux can be enhanced by periodic backwashing, pulsating flows, uniform transmembrane pressure or co-current permeate flow techniques. These have been found to be effective in maintaining high fluxes with feed streams containing colloidal or suspended matter and less effective with foulants that are in solution.

Applications of Ultrafiltration

Table 1 is a listing of ultrafiltration applications. The food industry has been one of the most successful users of UF, starting from the early 1970s when it was used to treat cheese whey to recover the protein. Another successful application has been electrocoat painting, where the UF system is used to maintain the ionic balance of the painting system and to recover paint that has been washed off. Biotechnology has benefited tremendously by UF, where it finds its greatest use in the production of pyrogen-free water and for fractionation, purification and concentration

Table 1 Applications of ultrafiltration

<i>Food industry</i>	
Concentration of protein and fat for cheese manufacture; fractionation of cheese whey for whey protein concentrates; clarification of fruit juices (apple, apricot, citrus, cranberry, grape, peach, pear, pineapple); gelatin concentration and de-ashing; eggs concentration and reduction of glucose; animal blood concentration; soybean protein concentrates and isolates; clarification of protein hydrolysates; vegetable oils (degumming, deacidification, bleaching, removal of metals, dewaxing; clarifying frying oils); sugar refining; dextrose clarification; alcoholic beverages	
<i>Chemicals and wastewater</i>	
Electrocoat paint; oily wastewater; stillage from bioethanol plants; caustic and acid recovery; brine recovery; printing ink; laundry wastewater; textile industry; latex emulsions; pulp and paper industry; tanning and leather industries; fish processing; poultry industry	
<i>Biotechnology</i>	
Separation and harvesting of microbial cells; enzyme recovery; affinity ultrafiltration; membrane bioreactors	

of proteins and other macromolecules. Continued advances in membrane science and manufacture and engineering improvements to modules and systems will allow a greater penetration of this technology in a variety of industries in the future.

See also: II/Membrane Separations: Filtration; Micro-filtration.

Further Reading

- Bhave RR (ed.) (1991) *Inorganic Membranes. Synthesis, Characteristics and Applications*. New York: Van Nostrand Reinhold.
- Cheryan M (1998) *Ultrafiltration and Microfiltration Handbook*. Lancaster, PA: Technomic.
- Cheryan M and Alvarez J (1995) Membranes in food processing. In: Noble RD and Stern SA (eds) *Membrane*

- Separations. Technology, Principles and Applications*, p. 415. Amsterdam: Elsevier.
- Cheryan M and Rajagopalan N (1998) Membrane treatment of oily streams. Wastewater treatment and waste reduction. *Journal of Membrane Science* 151: 15–38.
- Ho WSW and Sirkar KK (eds) (1992) *Membrane Handbook*. New York: Chapman and Hall.
- Hsieh HP (1996) *Inorganic Membranes for Separation and Reaction*. Amsterdam: Elsevier.
- Lloyd DR (ed.) (1985) *Materials Science of Synthetic Membranes*. Washington, DC: American Chemical Society.
- Matsuura T (1994) *Synthetic Membranes and Membrane Separation Processes*. Boca Raton, FL: CRC Press.
- Mulder M (1991) *Basic Principles of Membrane Technology*. Norwell, MA: Kluwer Academic Publishers.
- Singh N and Cheryan M (1998) Membrane technology in corn refining and bio-products processing. *Starch/Stärke* 50: 16–23.

PARTICLE SIZE SEPARATION: Electric Fields in Field Flow Fractionation

See II/PARTICLE SIZE SEPARATION/Field Flow Fractionation: Electric Fields

PARTICLE SIZE SEPARATION



Electrostatic Precipitation

J. J. Harwood, Tennessee Technological University,
Cookeville, TN, USA

Copyright © 2000 Academic Press

Introduction

Electrostatic precipitators (ESPs) are the most commonly used devices for the removal of fine particles in exhaust from industrial and utility processes. Wire-plate ESPs consist of three or more sections of arrays of large (e.g., 15 m × 5 m), grounded metal collector plates between which are situated wire or other narrow, high voltage electrodes (Figure 1). Less commonly, a wire-cylinder electrode configuration is used. Particles entering the first section are quickly charged by ions generated by the plasma coronas around the wires. (Current does pass between the

electrodes, hence the term ‘electrostatic’ is not really accurate, but indicates the small current-to-electrode area.) The charged particles are drawn toward and deposit upon the collector plates, which are periodically cleaned by mechanical ‘rapping’. This method is very efficient in removing particles in the 1–>10 μm range. The most common use of ESPs is in control of exhaust from coal combustion utilities. Precipitators are also used in the cement, ore smelting, steel production, pulp and paper manufacturing, and chemical processing industries, and in waste combustion utilities. Small units are used in cleaning domestic and workplace air, and have been considered for use in animal production facilities.

M. Holfield first demonstrated the removal of particles by electrostatic charging in 1820. Holfield showed that tobacco smoke can be cleared in a bottle by applying a spark-producing voltage to a pointed electrode inserted in the bottle. In 1850, C. F. Guitard observed that a steady corona discharge is effective in dissipating smoke. Sir Oliver Lodge first attempted

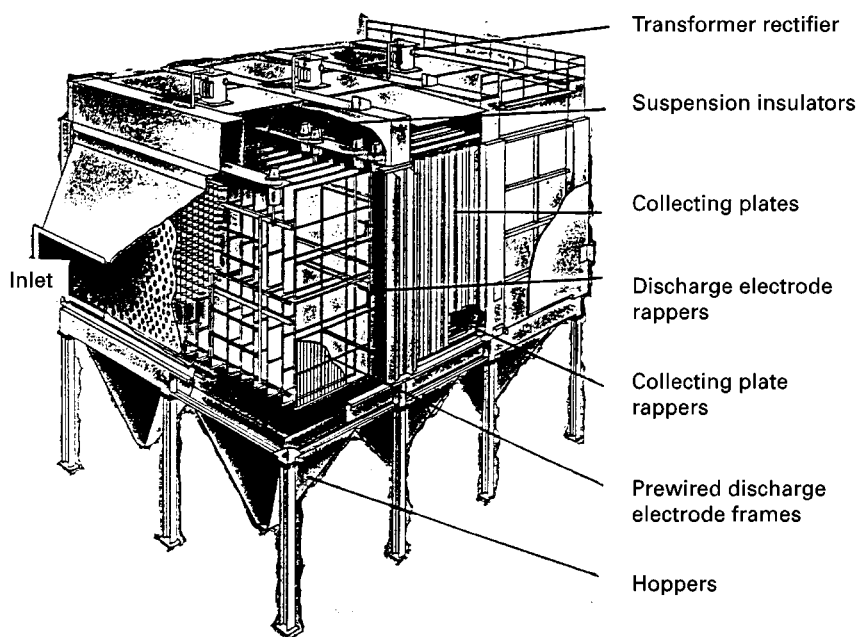


Figure 1 Rigid frame electrostatic precipitator. (Reproduced with permission. Copyright Wheelabrator Air Pollution Control Inc.)

the commercial application of this phenomenon by constructing an electrostatic precipitator to control fumes at a lead smelter. Unfortunately, lead oxide is too resistive to allow sufficient particle charging with a constant DC discharge, and the application failed. The first successful commercial application of electrostatic precipitation was by F. G. Cottrell, who designed an ESP to remove acid mist from sulfuric acid plants. Cottrell facilitated the establishment of the technique by developing the first suitable high-voltage power supplies. ESP particle control became widely used between 1910 and 1930.

Removal of small particles from gas streams is important for process, health, and environmental reasons. Centrifugal separators are used to remove particles larger than $10\ \mu\text{m}$; fabric filter 'baghouses' are used to remove finer particles and constitute a viable alternative to ESPs. Capital costs are similar for baghouses and ESPs; however, maintenance, including energy cost, is lower with ESP units.

The increased control of sulfur and nitrogen oxides in the 1970s, and recent calls for the control of very fine particles, challenge scientists and designers concerned with the ESP technique. Use of low sulfur coal reduces fly ash resistivity below that appropriate for conventional ESP operation. Treatment by the addition of limestone to coal increases the particle load on precipitators. Conventional precipitators do not efficiently remove submicron particles. As will be discussed in this chapter, researchers are developing means of adapting ESP design and opera-

tion to meet the challenges of improved environmental control.

Characteristics of Fly Ash

Hart *et al.* recently performed a comprehensive investigation of the composition and mineralogy of fly ash from three utility boilers. Using instrumental neutron activation analysis and X-ray fluorescence spectroscopy, they found Si, Al, Fe and Ca to account for more than 90% of major elements from all three boilers. Scanning electron microscopy with energy dispersive spectroscopy revealed successive ESP ashes to be composed mainly of spherical particles which decrease in average diameter with increasing distance from the boiler. Concentrations of As, Co, Cr, Ni, Mo and Sb increased from bottom ash through the sequence of ESP ashes. These trace elements are volatilized and transported to cooler regions, where they condense or are adsorbed onto fly ash particles. The major fly ash mineral phase found by these and other researchers is quartz (SiO_2) with magnetite (Fe_3O_4), anhydrite (CaSO_4), and mullite ($\text{Al}_6\text{Si}_2\text{O}_{13}$) among other minerals commonly present.

Resistivity (ρ) is the most important property of material to be collected by an ESP. The optimum range of resistivity is 10^4 – $10^{11}\ \Omega\text{-cm}$. On collection, low resistivity particles ($\rho \leq 10^3\ \Omega\text{-cm}$) release charge to the collector plate and may be re-entrained. Particles with $\rho > 10^{11}\ \Omega\text{-cm}$ insulate the collector plate, ultimately producing a sufficiently large electric field

within the dust layer to cause a counterproductive 'back corona'.

Two types of resistivity may be important in particle collection in an ESP. Ions collected at the surface of particles control 'surface resistivity', which dominates at temperatures below 250°C. As indicated in Figure 2, particle resistivity first increases with temperature, then decreases. Removal of the surface film (adsorbed water) by heating *in vacuo* at 360°C eliminates this initial increase in resistivity. Above 200°C, removal of adsorbed material no longer affects resistivity, and at higher temperatures resistivity is attributed to ions in the bulk of the particles,

'volume resistivity'. Both types of resistivity are primarily functions of Na^+ and Li^+ ion concentrations, and in some cases K^+ and I^- ions.

Two aspects of the ρ - T relationship affect ESP collection efficiency. First, the maximum resistivity of fly ash occurs within the range of temperature at which ESPs are commonly operated, 130–180°C. Second, SO_3 , produced from sulfur in coal, adsorbs onto the fly ash particles and has traditionally been responsible for lowering the resistivity of the particles to the optimum range for collection. Present use of low sulfur coals (<1% S) leads to inadequate collection.

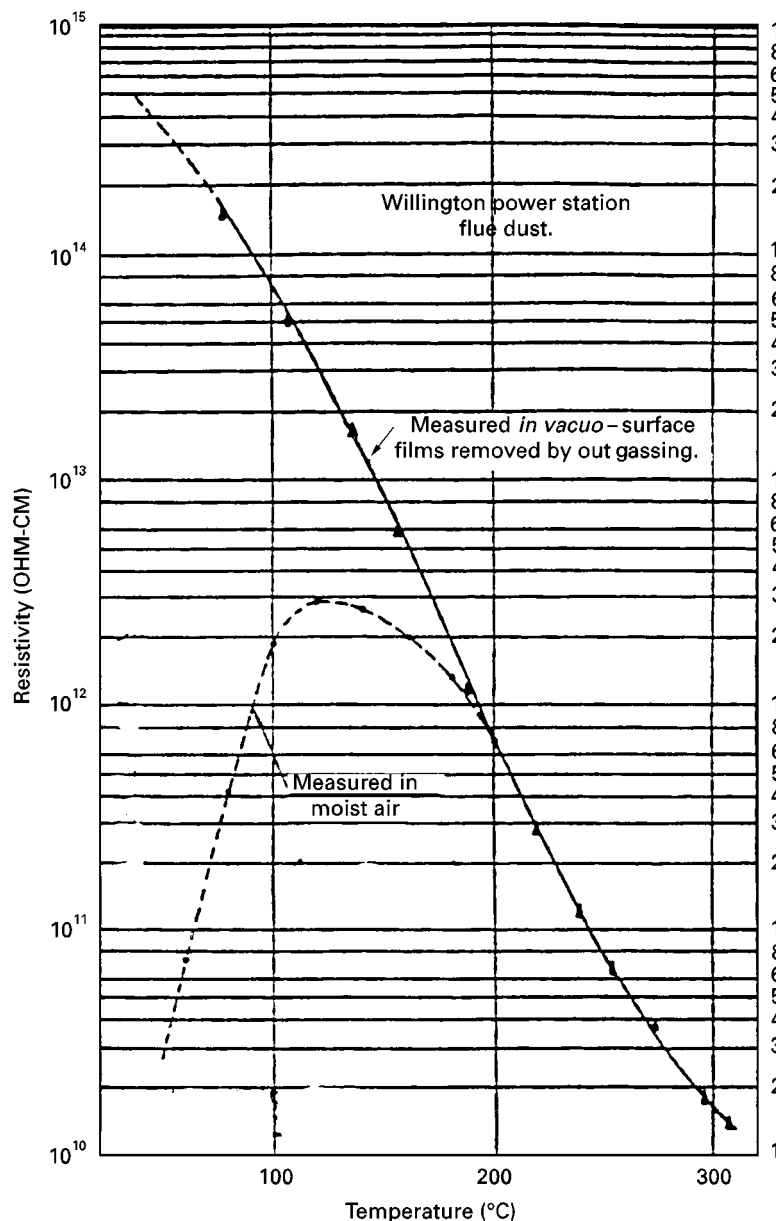


Figure 2 Effect of surface film resistivity on flue-dust resistivity. (Reproduced with permission from Busby HGT and Darby K (1963) *Journal of the Institute of Fuel* 36(268): 184. Copyright The Institute of Fuel).

Operation at non-optimal temperature can be avoided by lowering the temperature, but this requires energy input to a cooling device, and also can lead to difficulties with corrosion due to condensation. The temperature of the exhaust is normally cooled by heat exchange in an air pre-heater prior to injection into the precipitator, hence the name 'cold-side' precipitator. 'Hot-side' precipitators operate at temperatures as high as 370°C; resistivity is often reduced to a desirable level of $2 \times 10^{10} \Omega\text{-cm}$ at above 315°C. However, difficulties are encountered with the greater volume of the hot gas, and these units require more careful construction.

More commonly, resistivity of high-resistance ash is lowered by chemical conditioning.

Theoretical and Practical Aspects of Electrostatic Precipitation

Charging of Particles

The corona surrounding a discharge electrode of an ESP is a gas plasma of electrons and cations. The cations are drawn into the electrode, which is biased negative. The electrons are repelled into the interelectrode space where, within one centimetre travel, they ionize gas particles. These gas particles are drawn toward the grounded collector electrodes. On the way, many of them collide with and attach to the particles to be collected, charging them. The charged particles are then drawn towards the collector electrodes. This particle charging is efficient. Typical charging time is 5 ms; typical residence time in an ESP is 2–5 s.

Charging processes are of two types: field charging, where ions moving with the electric field charge the particles, and diffusion charging, where charging is due to collision with ions moving with random thermal motion. The types are distinguished to facilitate mathematical description. Field charging is dominant in charging particles with radius (a) greater than $0.5 \mu\text{m}$; diffusion charging is dominant with $< 0.2 \mu\text{m}$ particles. Both mechanisms are important in the intermediate size range.

The charge on an ion at time t ($q(t)$) resulting from field charging, derived by Pauthenier and Moreau-Hanot is:

$$q(t) = 12 \frac{\kappa}{\kappa + 2} \pi \epsilon_0 a^2 E_0 \frac{t}{t + \tau}$$

where κ is the relative dielectric constant; ϵ_0 is the permittivity of free space ($\text{C}^2 \text{N}^{-1} \text{m}^{-1}$); a is the particle radius (m); E_0 is the electric field (V m^{-1}); t is the

time (s) and:

$$\tau = 4\epsilon_0/N_0eb$$

where N_0 is the number density of particles (m^{-3}); e is the electronic charge (C); b is the ion mobility ($\text{m}^2 \text{s}^{-1} \text{V}^{-1}$). (This and other formulae are in the form presented in Oglesby and Nichols (see Further Reading.) The corresponding expression for diffusion charging presented by White is:

$$q(t) = \frac{akT}{e} \ln \left(1 + \frac{\pi av N_0 e^2 t}{kT} \right)$$

where k is the Boltzmann's constant (J K^{-1}); v is the rms thermal velocity of ions (m s^{-1}); T is the absolute temperature (K).

Smith and McDonald derived an expression for combined diffusion and particle charging. They divided the surface of a particle being charged into three regions: region I, where the electric field of the particle and that within the ESP duct intersect, sweeping ions onto the particle surface; region II, where the radial component of the electric field of the particle dominates; and region III, where the electric field of the particle and duct are in the same direction, sweeping ions away from the particle. Giving the electric field about the particle, E_r , as:

$$E_r = E_0 \cos \theta \left(1 + 2 \frac{\kappa - 1}{\kappa + 2} \frac{a^3}{r^3} \right) - \frac{ne}{4\pi\epsilon_0 r^2}$$

where E_r is the radial component of electric field (V m^{-1}); E_0 is the external field (V m^{-1}); r is the radial distance to point of interest (m); θ is the azimuth angle measured from the z axis (toward the discharge electrode) (rad); ne is the particle charge (C); these researchers produced a combined charging rate equation:

$$\begin{aligned} \frac{dq}{dt} &= \frac{dq}{dt_I} + \frac{dq}{dt_{II}} + \frac{dq}{dt_{III}} \\ &= (N_0 A n_s e^2 / 4\epsilon_0) \left(1 - \frac{n}{n_s} \right)^2 \\ &\quad + \frac{e\pi a^2 v N_0}{2} \int_{\theta_0}^{\pi/2} \exp \left[- \left(\frac{ne^2(r_0 - a)}{4\pi\epsilon_0 k T a r_0} \right. \right. \\ &\quad \left. \left. + \frac{[3ar_0^2 - r_0^3(\kappa + 2) + a^3(\kappa - 1)]eE_0 \cos \theta}{k T r_0^2(\kappa + 2)} \right) \right] \sin \theta d\theta \\ &\quad + \frac{e\pi a^2 v N_0}{2} \exp(-ne^2/4\pi\epsilon_0 a k T) \end{aligned}$$

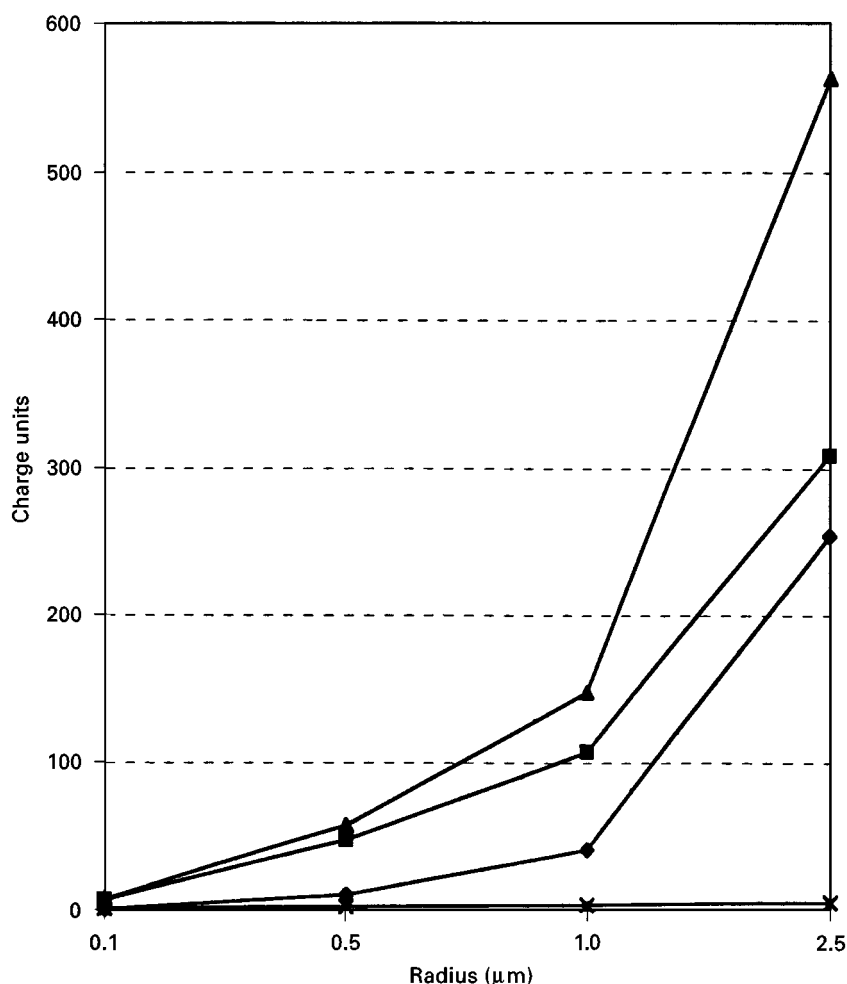


Figure 3 Modes of particle charging. —♦—, field charging; —■—, diffusion charging; —▲—, total charge; —×—, Boltzman charge AC. (Data from Kanazawa *et al.* (1993) *Journal of Electrostatics* 29: 193. Copyright: Elsevier Science.)

where A is the surface area of the particle on which ions may impinge (m^2); n_s is the saturation charge; θ_0 is the greatest angle of region from z axis (rad).

This expression agrees well with measured charging rates.

Representative saturated particle charge as a function of particle radius is presented in Figure 3.

Chemical Conditioning

Conditioning can enhance collection efficiency by reducing resistivity to prevent back corona, increasing cohesivity of the collected layer, enhancing the electric field by increasing the space charge contribution (see below), and increasing agglomeration of small particles. Some exhaust gas conditioning methods which have been used to enhance ESP performance are cooling by in-leakage of cold air, heat exchange to a waste heat boiler, evaporative spray, and chemical

conditioning. The latter has proven most popular in utility applications.

Most commonly, sulfur is combusted and the SO_2 produced is catalytically converted to SO_3 . On combination with the combustion exhaust, SO_3 hydrolyses to produce H_2SO_4 , sulfuric acid. The acid deposits efficiently on fly ash particles, decreasing the particle surface resistivity. SO_3 is added at levels of 1–10 ppm; up to 30 ppm can be added without significant increase in sulfur emission from the ESP. Significant SO_2 is produced on combustion of even low sulfur coal, but only about 1% is converted to the useful SO_3 . Knowledge of the importance of SO_3 was initially gained through experience with conditioning of smelter dusts by sulfide ores.

Ammonium salts were found to be effective when H. J. White was consulted on the problem of decreased ESP efficiency which resulted from a change in petroleum cracker catalyst. He found that replacing ammonia, released by the initial catalyst,

recovered ESP performance. As NH_3 increases collection efficiency with both low and high resistivity boiler ash, and may or may not decrease resistivity, it is thought that this conditioner functions by furnishing salt particles which increase the space charge contribution to the electric field and, by increasing dust cohesiveness, reduce rapping losses.

Characteristics of the Corona Discharge

As voltage applied to a wire discharge electrode is increased, visible discharge points, 'tufts', begin to appear dispersed along the wire. Eventually the tuft pattern stabilizes, appearing as fingers which elongate and retract at 1–10 Hz and remain at somewhat fixed locations along the wire. This stabilization of the corona is indicated by a distinct increase in the slope of the electric field vs. applied voltage curve (Figure 4). Peek determined a semi-empirical expression for the corona onset voltage (V_c) in air:

$$V_c = 3 \times 10^6 am\delta(1 + 0.03\sqrt{\delta/a})\ln(b/a)$$

where V_c is the corona onset voltage (V); a is the radius of discharge electrode (m); m is the wire roughness factor (0.5–0.9); δ is the relative air density; P is the air pressure (Pa).

This discharge produces a current density (with respect to the area of the collector electrode) in the order of 150 nA cm^{-2} . While the ionic composition of the interelectrode space has not been well studied, ionization properties indicate that this current is carried by oxygen, sulfur dioxide, and water, which are negatively charged by the electron current

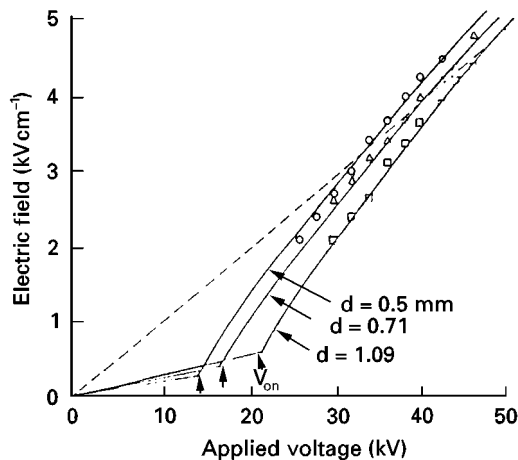


Figure 4 Electric field on the collector electrode just under the corona wire as voltage is applied; d , discharge electrode diameter. $2D = 20 \text{ cm}$; \circ , $d = 0.5 \text{ mm}$; \triangle , $d = 0.71 \text{ mm}$; \square , $d = 1.09 \text{ mm}$. (Reproduced with permission from Ohkubo *et al.* 1985.)

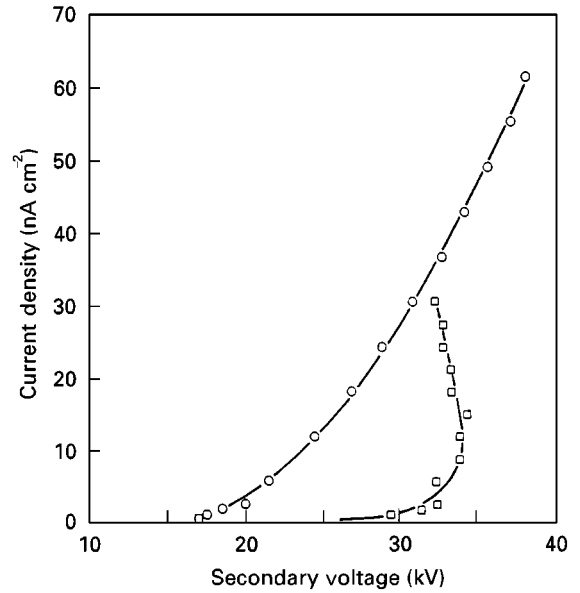


Figure 5 Pilot ESP V-I curves before and after development of severe back corona. \circ , 1 hour after startup; \square , 8 days after startup. (Reproduced with permission from DuBard and Nichols 1990.)

near the corona, and by particles ionized by these primary ions.

The Electric Field

Current vs. voltage curves (Figure 5) are commonly used in monitoring the operation of ESP. For best collection efficiency, ESP units are operated at the maximum voltage which produces a stable current. A discussion of operation monitoring of ESPs is given by DuBard and Nichols.

Much effort has been given to the task of determining the electric field within an ESP. Besides the burden of inability to solve known expressions analytically for the field in a wire-plate electrode system, this task is made difficult by uncharacterized changes in the collector electrode as the dust layer collects on it. The advent of high-speed computing has allowed satisfying solution of the field equations for a clean system.

Cristina *et al.* present a modern method of determining the electric field. These researchers use the following expressions for charge and electric potential:

$$\nabla \cdot (\epsilon \nabla \phi) = -Q$$

$$\nabla \cdot (Q \nabla \phi) = 0$$

where ϵ is the permittivity of air ($\text{C}^2 \text{ N}^{-1} \text{ m}^{-1}$); Q is the ionic charge density (C m^{-2}); ϕ is the electrical potential (V).

These equations have a unique solution for DC ion flow fields. An iterative numerical procedure

is used to balance the electric field and charge density of elements in an array of triangular elements superimposed on the inter-electrode space. These elements are each specified to have a constant ionic charge density. The contribution of space charge by ionized particulate matter is disregarded in this treatment. In the more dust-laden regions of an ESP, particulate matter is found to alter electric field slightly.

Equipotential field maps developed by this treatment show a fairly linear decrease in potential from the discharge to the collector electrode, with circular fields to about one-third distance across the channel (from 57.5 kV to 20 kV), then equipotential field lines parallel to the collector. Near the collector electrode, at about five-sixths the channel width, the potential has decreased to 5 kV. Electric fields of adjacent discharge electrodes interact, producing bell-shaped electric field patterns radiating from each wire to the adjacent collector plates.

Back Corona

In working ESPs, a portion of the applied potential is dropped across the resistive layer of the collected dust. As the dust layer thickens the resistance, hence voltage drop, across the layer increases. If the dust resistivity is high ($\rho > 10^{10} \Omega\text{-cm}$), eventually the field becomes great enough to cause electrical breakdown of gas within the dust layer, generating a back corona. Electrons are ripped from the gas, and the resulting positive ions flow into the inter-electrode space, where they attach to negatively charged particles. The diminished net charge of the particulates leads to greatly diminished collection efficiency; re-entrainment also occurs. A back corona occurs with an electrical field strength across the dust layer (resistance of layer times current) of $8\text{--}12 \text{ kV cm}^{-1}$.

A back corona can be visually observed as a glow on the collection surface. It is also characterized by an increase in corona onset voltage followed by an increase in current for a given applied voltage as compared with a correctly functioning system (Figure 5). The dust layer acts as a resistive-capacitative element in having a lag time before discharge. Both intermittent and pulse energization take advantage of this lag time to allow the application of high voltage without the occurrence of back corona.

Current Density

The electric field at ESP collection surfaces is not uniform due to both the electrode-collector geometry and to irregular resistance resulting from uneven dust layer thickness. The parameter determined in studying the situation at the collection surface is current

density, j (nA cm^{-2}). With poor distribution of current over the dust layer, collection efficiency is diminished. Re-entrainment can occur in regions of low current density, and high local currents can lead to back corona even with a low average current. Landham *et al.* measured the current density distribution in a pilot scale ESP by inserting a segmented copper electrode sensor board into a collector electrode. Conventional, intermittent, and pulse energization with both wire and barbed-strip discharge electrodes were investigated. (Barbed-strip electrodes are used by some manufacturers to force a more uniform current distribution at the collector.)

Intermittent energization (IE) is achieved by interrupting the rectifier circuit output for one to twenty half cycles of the supply power line. A baseline voltage is maintained, with relatively broad pulses superimposed. In pulse energization (PE), pulses of $1 \mu\text{s}$ to 1 ms width and up to -75 kV are superimposed on a DC voltage set just below the 'spark limit'. Both techniques have been found to save energy and to reduce the incidence of back corona. PE is more effective in countering problems with low resistivity dust. Dubard and Nichols set IE to one full AC cycle on and four off (duty cycle 0.2), and PE base voltage -20 kV with 50 Hz , $\sim 125 \mu\text{s}$ width pulses of -25 kV . Conventional full-wave rectified energization (CE) was set at about -35 kV .

These researchers found that CE and PE give Gaussian current density profiles across the sensor plate surface, while IE gives a more even, but lower magnitude distribution. Under good operating conditions (clean collector surface), PE had less collector area above dust layer breakdown current than CE or IE, with 96% useful area as compared to 83% and 86%, respectively. Under severe back corona conditions, PE maintained 84% useful area, CE 12%, and IE 54%. Similar results were obtained with both barbed-strip and wire electrodes. The results indicate a linear relationship between the increase in collector area receiving useful values of current density and collection efficiency.

Among alternative discharge electrode designs, barbed plate discharge electrodes appear more effective in producing uniform current distributions (see McKinney and Davidson). This design may also have some advantage with respect to flow turbulence.

Flow

Besides electric field and current density distribution, gas flow is important in ESP performance. ESP flow velocities vary between 0.2 and 2.0 m s^{-1} . Schwab and Johnson suggest an optimum velocity of between

1.22 and 1.52 m s⁻¹. Lower velocities diminish the turbulent mixing which brings small particles into the low flow region near the collector electrode; higher velocities overwhelm electrostatic attraction of particles to the collector electrode, and can lead to re-entrainment.

Flow within an ESP is inherently turbulent due to high gas flow velocity, which typically results in a Reynolds number of about 10 000 – five times that at which turbulent flow replaces laminar flow. Turbulence in ESPs is complicated by flow obstructions – discharge electrodes and collector stiffening baffles and connectors, and by a non-uniform flow profile at the ESP inlet. At low velocities ($\lesssim 0.5$ m s⁻¹) turbulence resulting from the ion current between discharge and collector electrodes (ionic wind) contributes significantly. The flow regime in an ESP is thus seen to be quite complicated. Baffles within the ESP duct and porous plates at the inlet and outlet are employed to create uniform flow.

Schwab and Johnson have produced a computer model based on Navier–Stokes fluid flow equations as an alternative to traditional reduced scale physical models for flow design. The model can be used to determine inlet plate perforation patterns which produce uniform flow without high flow near the duct walls.

Collection Efficiency

Most important in ESP operation is the particulate collection efficiency, η , the fraction of particulates removed. Around 1920, Deutsch and Anderson independently derived an expression for η , now commonly referred to as the ‘Deutsch equation’:

$$\eta = 1 - \exp\left(-\frac{A}{Q} \omega_e\right)$$

where A is the collector electrode area (m²); Q is the volumetric gas flow rate (m³ s⁻¹); ω_e is the effective particle migration velocity (m s⁻¹).

Efficiency is also expressed as fractional particle penetration, $P = 1 - \eta$. A/Q is the specific collection area (SCA), the parameter of importance in sizing an ESP. Assumptions of the Deutsch equation are that particles are instantaneously fully charged and accelerated, turbulent and diffusive forces cause particles to be distributed uniformly in any cross section of the precipitator, the velocity of the gas stream does not affect the migration velocity of the particles, particle motion is governed by viscous drag where Stokes’ Law applies, the effect of collision between ions and neutral gas molecules can be neglected, and there are

no disturbing effects such as erosion, re-entrainment, uneven gas flow distribution, sneakage, or back corona. A number of researchers have adjusted the Deutsch equation to account for neglected factors. Especially questionable is the assumption of complete turbulent mixing (for instance, see Zhibin and Guoquan). The Deutsch model represents one mixing extreme, with the other extreme being laminar flow (no turbulence). The Deutsch model tends to underestimate η for particles with diameter less than about 1 μ m, and overestimates the collection of larger particles.

The Matt–Öhnfeldt modification attempts to account for variation in particle size distribution:

$$\eta = 1 - \exp\left(-\frac{A}{Q} \omega_k\right)^m$$

where ω_k is the particle migration velocity (m s⁻¹); m is an exponent which depends on particle size distribution.

An m of 0.5 is commonly used with fly ash or cement dust; increasing values can be used with finer size distributions.

In comparing ESP performance under varying conditions, the migration velocity is more useful than η , being independent of ESP collection area and gas flow rate. An important consideration in using ω values is that migration velocity of large particles decreases at a much lower rate with increasing gas flow (or decreased plate size) than that of small particles, hence though small particles will be less efficiently collected, measured ω can increase with gas flow rate.

Migration of charged particles can be treated theoretically. Hall presents the expression:

$$\omega = \frac{4\pi\epsilon_0 k a E_0 E_p C D f}{6\pi\eta} \alpha$$

where k is $3\epsilon/(\epsilon + 2)$; ϵ is the dielectric constant of ash (C N⁻¹ m⁻¹); E_0 is the particle charging electric field strength (V m⁻¹); E_p is the particle collecting electric field strength (V m⁻¹); a is the particle radius (m); C is the Cunningham slip correction; D is the factor to account for diffusion charging of fines; f is the factor accounting for gas turbulence and free electron charging; η is the gas viscosity (Pa s); α is the fractional particle saturation charge.

C is used to adjust diffusion of particles with size comparable to mean-free path of gas molecules. The reader can understand that empirical estimation of ω values, from measured efficiency, is often more productive than theoretical estimation.

The Deutsch model is often used in determining a minimum specific collection area in sizing precipitators. Extrapolation from performance of pilot or other ESPs should be made only with similar designs and similar dusts.

Computer Modelling

Several comprehensive models of particle collection in wire-plate ESPs are available, including the Southern Research Institute (SRI), Research Triangle Institute Sectional (RTIS), Italian Electricity Board (ENEL), and Electric Power Research Institute (ESPM) models. As an example, the ESPM model will be briefly described (see Lawless and Altman).

In ESPM, the applied voltage for a given current density is first determined for a position directly beneath the wire:

$$V = V_c + E_c r_w \left[z - 1 - \ln \left(\frac{z+1}{2} \right) \right]$$

where E_c is the electric field at wire surface at corona onset (V m^{-1}); r_w is the radius of wire (m) and:

$$z = \sqrt{1 + \frac{j b}{\mu \epsilon_0} \left(\frac{b}{V_w} \right)^2}$$

where b is the wire-plate separation (m); μ is the ion mobility ($\text{m}^2 \text{s}^{-1} \text{V}^{-1}$).

Current densities at other plate locations are calculated as:

$$j(\theta) = j_0 \cos^n(\theta)$$

where θ is the angle from between wire and plate (rad); n is a function of j , 2 (near corona onset) to 4.

Ion mobility is based on that of SO_2 and SO_2^- . Space charge resulting from the charging of particles is treated as an equivalent ion current and used to adjust the operating voltage.

Non-dimensional parameters are used in models to add generality to results and to simplify mathematical treatment. For instance, the initial particle charging rate in an ESP model (ESPM), combining both diffusion and field charging, is:

$$\frac{dv}{d\tau} = \frac{3w}{4} \left(1 - \frac{v}{3w} \right)^2 + 1$$

where v is the non-dimensional charge; τ is the non-dimensional exposure time; w is the non-dimensional electric field.

Intermediate and saturation charging rates are modelled by different expressions. Back corona charging can be modelled with ESPM, though better understanding of this process is needed to assure accurate results.

Particle collection is modelled with a modified Deutsch expression:

$$P = \left(1 - \frac{\omega A/Q}{Nw} \right)^{Nw}$$

Nw is a parameter to adjust for turbulence: a high value approaches Deutschian total mixing, a low value approaches laminar collection (laminar when $Nw = 1$). To correct for uneven gas flow, penetration is calculated at several gas velocities and the results combined by weighted averaging. Rapping loss can be specified or estimated by applying conventional dynamics to the falling of agglomerated 'cake' during collector cleaning. The model treats each ESP section separately, 'remixing' particulates exiting from each section.

ESPM can be used to predict V-I curves, 'grade efficiency' (penetration as a function of particle diameter), and other aspects of ESP performance under varying conditions.

Innovative ESP Designs

Several new means have been developed to facilitate collection of submicron and highly resistive particles by ESPs.

Pulse energization is discussed above (see Current density). By superimposing a brief, high voltage pulse on a DC voltage set just below the back corona level, efficient fine particle charging and collection are obtained with highly resistive dusts.

Enhanced particle agglomeration can also facilitate fine particle collection. For instance, Kanazawa *et al.* have accentuated particle agglomeration with a precharging section, in which the gas stream is divided and particles in the two sub-streams given either a positive or a negative charge. On recombining the sub-streams, particles agglomerate through electrostatic attraction. Watanabe *et al.* have devised an alternative method utilizing a three sector design. Large particles are removed in the first ESP sector. A 'modified quadrupole' electrode system in the second sector applies an AC field to enhance particle collision, hence agglomeration. The third section is again a conventional ESP, which removes the agglomerated particles.

Fabric filtration is the surest means of removing fine particles. EPRI has devised the 'Compact Hybrid Particulate Collector' (COHPAC). This design simply places a baghouse after an ESP. The ESP removes much of the particulates, easing the load on the baghouse, hence reducing maintenance. The baghouse reduces pollution due to rapping loss, and is insensitive to changes in fuel.

EPRI has also developed an 'EPRICON' process which can replace conventional chemical conditioning of fly ash from low sulfur coals. In this process, a portion of the gas stream is diverted to a vanadium oxide-based catalytic unit, which efficiently converts SO_2 to SO_3 . Recombination of the treated stream with the bulk results in the necessary conditioning of the fly ash.

See also: **Particle Size Separation:** Hydrocyclones for Particle Size Separation; Sieving/Screening.

Further Reading

Busby HGT and Darby K (1963) Efficiency of electrostatic precipitators as affected by the properties and combustion of coal. *Journal of the Institute of Fuel* 36(268): 184.

Dubard JL and Nichols GB (1990) Diagnosis of electrical operation of electrostatic precipitators. *Journal of Electrostatics* 25: 75.

Hart BR, Powell MA, Fyfe WS and Ratanasthien B (1995) Geochemistry and mineralogy of fly-ash from the Mae Moh lignite deposit, Thailand. *Energy Sources* 17: 23.

Kanazawa S, Ohkubo T, Nomoto Y and Adachi T (1993) Submicron particle agglomeration and precipitation by using a bipolar charging method. *Journal of Electrostatics* 29: 193.

Landham EC Jr., Dubard JL and Piulle W (1990) The effect of high-voltage waveforms on ESP current density distributions. *IEEE Transactions on Industry Applications* 26(3): 515.

McKinney PJ, Davidson JH and Leone DM (1992) Current distributions for barbed plate-to-plane coronas. *IEEE Transactions on Industry Applications* 28(6): 1424.

McKean KJ (1988) Electrostatic precipitators. *IEE Proceedings Pt. A*. 135(6): 347.

Oglesby S Jr. and Nichols GB (1978) *Electrostatic Precipitation*. New York: Marcel Dekker Inc.

Tachibana N (1989) Back discharge and intermittent energization in electrostatic precipitation of fly ash. *Journal of Electrostatics* 22: 257.

Watanabe T, Tochikubo F and Koizumi Y *et al.* (1995) Submicron particle agglomeration by an electrostatic agglomerator. *Journal of Electrostatics* 34: 367.

Zhibin Z and Guoquan Z (1994) Investigations of the collection efficiency of an electrostatic precipitator with turbulent effects. *Aerosol Science and Technology* 20: 169.

Field Flow Fractionation: Electric Fields

S. N. Semenov, Institute of Biochemical Physics,
Russian Academy of Science, Moscow, Russia

Copyright © 2000 Academic Press

Introduction

Field flow fractionation (FFF) represents a class of separation techniques, which use a force field perpendicular to the direction of separation to control the longitudinal velocity of particles injected into the system. It is achieved by particle redistribution in the flow with a parabolic velocity profile due to the action of a transverse force. This transverse force may be due to an electric field, a centrifugal or gravity field, etc. In electric FFF (ElFFF), the transverse movement of the particles is caused by an electric field. The transverse particle velocity, U , is defined by

the expression:

$$U = b \cdot E \quad [1]$$

where b is the particle electrophoretic velocity, and E is the electric field strength in the channel interior, which is available both for the particles and the flow of the carrier liquid. The particle electrophoretic mobility is related to the particle electrokinetic potential (zeta-potential):

$$b = \frac{\varepsilon \zeta}{4\pi\eta} f\left(\frac{R}{\delta}\right) \quad [2]$$

where ε is the dielectric constant of the carrier liquid, η is the carrier liquid viscosity, ζ is the particle electrokinetic potential, R is the particle diameter, and δ is the Debye length characterizing the screening

of the electrostatic interaction in an electrolyte. $f(R/\delta)$ is a function changing monotonously from 1 for particles of $R \gg \delta$ to 1.5 for small particles, when the zeta-potentials are small. For higher zeta-potentials, this function approaches a minimum of less than one. Thus, the particle electrokinetic potential and electrophoretic mobility represent the parameters slowly changing with the particle size and depending mainly on the surface properties of the particle. For small objects like macromolecules and low-molecular-weight ions, the theory of the electrophoretic mobility is absent.

For the characteristic relaxation time, the Boltzmann transverse particle distribution is established in the system by forcing injected particles toward the wall of the channel and their thermal (diffusion) motion. In EIFFF (reported as the method for protein separation), particles of the same size with higher electrophoretic mobility or zeta-potential will accumulate more closely to the wall, while particles of lower zeta-potential will form a more diffuse layer that extends further into the flow of the carrier liquid. Proteins still represent most of the EIFFF sample materials. For particles with about the same zeta-potential, the thickness of this layer may also be different, if the particles have different diffusion coefficients, D . Particles with higher diffusion coefficient (i.e., with smaller size) will accumulate in a more extensive layer due to more intensive thermal movement. Zeta-potential is an important parameter interrelated to the particle surface charge density, and characterizing the particle surface properties and the possible exchange of substances between the particle and the surrounding liquid, e.g. in cellular processes, including transport through cell membranes, antigen-antibody interactions, and hormonal control.

EIFFF is carried out in a thin channel of rectangular cross-section with the width to thickness ratio (aspect ratio) about 100 (thickness about 10–100 microns). It allows the separation to approximate to a laminar liquid flow between infinite parallel plates, which is characterized by a parabolic velocity profile, where the fluid velocity at the channel walls is zero and reaches a maximum in the centre of the channel. Thus, if a group of particles maintain an average distance from the wall different from another group of particles, their velocities along the channel will be different and they will leave the channel at different times, related to the particle zeta-potential and size, which defines the particle diffusion coefficient. In FFF systems, the same types of fields are used as in the so-called 'direct field methods' (centrifugation, electrophoresis, etc.), but there is no requirement of complete fraction resolution in the field direction, and

field strengths may be lower. In principle, all mixtures separated by direct electrophoresis may be effectively analysed by EIFFF, if they have a size large enough to form a layer of thickness smaller than the channel thickness, even when its electrophoretic mobility is too small for electrophoretic analysis. FFF systems are elution methods and allow the collection of fractions during a separation. Since the theory of FFF dynamics is well developed, the separation times for a given sample can be directly related to the physical parameter of the particles. This parameter represents the effective particle charge q^* , which defines the thickness of the Boltzmann particle distribution $\approx \exp(q^*E \cdot x/kT)$ (x is the transverse coordinate in the channel) in the transverse electric field applied to the EIFFF channel. Using the known Einstein relationship, this effective particle charge may be defined as the ratio of the particle electrophoretic mobility multiplied by the thermal energy kT , to its diffusion coefficient:

$$q^* = kT \frac{b}{D} \quad [3]$$

In principle, this effective charge itself represents a new separation parameter, which may be used for particle and macromolecule characterization, if the theory is developed. This theory should relate the effective charge and the particle and macromolecule physicochemical parameter important in specific applications, for example, the surface density of charged groups raised in dissociation or ion adsorption. In turn, this effective charge could be used for the electrophoretic mobility or zeta-potential determination, if the particle diffusion coefficient is determined independently, and the system temperature is known. Another possibility is to separate particles with the same surface properties (i.e. zeta-potentials) but different sizes, where the sample selectivity is only due to the differences in diffusion coefficient. Of course, the real applications of EIFFF are defined by specific experimental conditions, opportunities and advantages rather than by method theory, but, without a clear physicochemical understanding of macromolecule and particle behaviour in EIFFF, the method applications will be very limited.

A focusing (or hyperlayer) mode of operation using isoelectric focusing in a pH gradient across the channel has been reported by a number of authors (see Further Reading) with a channel of trapezoidal cross section. However, the latter separation mode loses the high resolution characteristic for the FFF family due to high hydrodynamic dispersion interrelated to the shape of the cross section.

Limitations of Channel Configuration and Construction

Planar electrical FFF systems have been constructed, where the walls are defined by membranes permeable to the carrier liquid but not to the particles to be separated. In later versions these membranes are supported by porous or perforated plates. The membranes prevent the loss of the sample while allowing the passage of an electric current. Platinum wire electrodes lying outside the channel provide the transverse electric field. The carrier liquid represents a buffer, and a solution of identical composition is circulated through the chambers housing the electrodes in order to remove electrolysis products and reduce electrode polarization. Other configurations such as a hollow fibre systems and an annular porous glass channel have been reported. Presently, graphite or gold-plated glass channel walls are used, which minimize these effects. In a micro-machined channel for EIFFF, the electrode walls were of titanium and gold.

The resolution increases with the effective voltage drop across the channel, and increasing the applied voltage will have a positive effect on the resolution. Unfortunately, EIFFF is mainly carried out in aqueous solutions, and voltages above 1.7 V applied across the fluid-wall interface will cause significant electrolysis and bubble formation. Since the EIFFF system requires a stable flow velocity profile, bubbles cause serious flow disturbances, and electrolysis must be avoided. High flow velocities can limit the formation of bubbles and allow voltages above 1.7 V, but the available voltage is still small. Thus bubble formation in the electrochemical reactions at the wall electrodes is the limiting factor for the applied voltage.

Another voltage-related difficulty is the potential drop in the electric double layers near the channel walls. An electric double layer will cause most of the voltage drop to occur very close to the channel walls. As a consequence, the effective field which may be used for particle redistribution and separation, in the EIFFF system, is greatly reduced. Experimental data indicate that the effective field strength in the flow inside the channel is in the range of 0.25%–1% of the applied field depending on the composition of the buffer. Though this effect greatly reduces the performance of the EIFFF system, it is still able to perform separations. Due to the low electric field strength, Joule heating is not expected to be a significant problem in EIFFF, in contrast to electrophoresis systems.

One problem that arises in the separation in FFF systems is the symmetric parabolic velocity profile of the flow that performs the separation function. Indeed, particles with equal and opposite zeta-potential

will elute at the same time from the channel. This can be a problem for samples containing both positively and negatively charged particles. Though such particles are usually prone to coagulation or aggregation, these processes may be slowed by a steric stabilization, for example, as in polyelectrolyte solutions or particles with adsorbed polymers. The coagulation or aggregation kinetics may then be studied by EIFFF. Most samples, and especially biological samples, are of a uniform charge type. Biological samples contain mostly negatively charged particles (at least the particles of interest). For samples containing both types of particle charge, the asymmetrical flow velocity profile and an additional particle velocity asymmetry may be arranged by the application of a longitudinal electric field in a channel having walls with different zeta-potentials, which can cause electroosmotic flow with a non-uniform velocity profile.

The establishment of Boltzmann equilibrium distribution in the channel requires a relaxation time for a particle to migrate from one channel wall to the other in the applied electric field. If the drift velocity U is constant, the relaxation time will be found using eqn [1]:

$$\tau_r = \frac{w}{U} \quad [4]$$

In conventional EIFFF systems, the relaxation time typically is over 5 min, but in micro-machined EIFFF systems it may be less than 3 s.

EIFFF and Related Electrophoretic Methods

The nearest relatives of EIFFF are different electrophoresis techniques in liquids. However, electrophoresis systems often require very high field strengths for resolution, and the high voltages are limited by the Joule heating. Particle electrophoretic mobilities should also be high enough to have an acceptable resolution in common capillary lengths. Another type of electrophoresis separation system, free-flow electrophoresis, utilizes an electric field across a curtain of buffer between two vertical plates (a principle very close to FFF) and allows for continuous sample injection, but limits the detection and collection systems to the certain number of fractions. Resolution in free-flow electrophoresis is limited by fraction spreading in the fluid stream caused by the parabolic flow profile. Other methods of separating molecules and cells are needed for applications, where these limitations preclude the use of existing systems. Field flow fractionation is the solution for some applications, where particle electrophoretic mobilities are too low for the conventional

electrophoresis systems and high electric field strengths are not desirable. ElFFF has all the advantages of FFF systems, i.e., the ability to separate cells, large molecules, colloids, emulsions, and structure, which are too delicate for electrophoretic separation such as liposomes, both in the 'original' condition and after surface modification. Unlike the free-flow electrophoresis systems, elution in FFF systems is zonal and proceeds through one outlet port; for this reason, it is capable of significantly higher resolution. Therefore, anticipated applications of ElFFF systems include cell separations, characterization of emulsions, liposomes, and other particulate vehicles for intravenous drug administration with respect to size, charge, and stability, diagnostic tests for specific molecules in colloidal suspensions, quick and accurate separations of molecules, environmental water monitoring, tests for sample contamination, and further research involving zeta-potentials. ElFFF systems also find application as sample pretreatment systems by performing an initial separation on a sample, which is later collected for further testing by another analysis system.

The resolution of ElFFF is determined in the standard way for chromatography, i.e. by the comparison of the sum of the peak dispersions for two neighbouring peaks to the difference of their maxima. The resolution of ElFFF is inversely proportional to the separation distance of the electrodes; thus, the smaller the distance between the channel walls, the higher the resolution between two distinct particles, making ElFFF an ideal application for using micro-machining techniques. The resolution increases with the square root of the channel length, so the longer the channel the better the resolution, but the time required for the improved resolution increases, which is not generally desirable.

Combined Electric-Thermal FFF (El-ThFFF)

An interesting combined technique represents the application of an electric field across the channel for Thermal FFF, where a temperature gradient is used to separate the analysed particles. After a potential drop of about 2 V is applied, the ThFFF retention is apparently changed. This combination allows a more exact examination of the particle surface properties, since ThFFF, like electrophoresis, represents a surface kinetic phenomenon defined by the surface force potential. Also, this combined FFF method gives information on particle electrokinetic properties in non-aqueous solution. El-ThFFF may allow distinction between electrostatic and non-electrostatic interactions in surface layer by

programming of the electric field strength during the separation.

Conclusion

ElFFF is a method for the separation of charged particles and macromolecules according to their effective charge. This parameter is not measured by electrophoretic methods and may be obtained directly from ElFFF experiments. The effective charge may be used for the characterization of surface particle properties and macromolecule charged groups, when the required theory has been developed. ElFFF has electric field strength limitations due to electrochemical reactions at the channel walls and potential interface drop.

See also: II/Particle Size Separation: Field Flow Fractionation: Thermal; Theory and Instrumentation of Field Flow Fractionation.

Further Reading

- Andreev VP and Stepanov YV (1997) Field flow fractionation with asymmetrical electroosmotic flow. II. Charged particles. *Journal of Liquid Chromatography & Related Techniques* 20: 2873–2886.
- Andreev VP, Stepanov YV and Giddings JC (1997) Field flow fractionation with asymmetrical electroosmotic flow. I. Charged particles. *Journal of Microcolumn Separations* 9(3): 163–168.
- Caldwell KD and Gao Y-S (1993) Electrical field flow fractionation in particle separation. 1. Monodisperse standards. *Analytical Chemistry* 65: 1764–1772.
- Caldwell KD, Kesner LF, Mayers MN and Giddings JC (1972) Electrical field flow fractionation of proteins. *Science* 176: 296–298.
- Gale BK, Caldwell KD and Frazier AB (1998) A micro-machined electrical field flow fractionation (μ -ElFFF) system. *IEEE Transactions in Biomedical Engineering* 45(12): 1459–1468.
- Giddings JC, Shiundu PM and Semenov SN (1995) Thermophoresis of metal particles in a liquid. *Journal of Colloidal Interface Science* 176: 454–458.
- Liu G and Giddings JC (1991) Separation of particles in nonaqueous suspensions by thermal–electrical field flow fractionation. *Analytical Chemistry* 63(3): 296–299.
- Martin M (1998) Theory of field flow fractionation. *Advances in Chromatography* 39: 1–138.
- Martin M and Williams PS (1992) Theoretical basis of field flow fractionation. In: Dondi F and Guiochon G (eds) *Theoretical Advancement in Chromatography and Related Separation Techniques*, NATO ASI Series C: Mathematical and Physical Sciences, vol. 383, pp. 513–580. The Netherlands: Kluwer.
- Schimpf ME, Russel DD and Lewis JK (1994) Separation of charged latex particles by electrical field flow fractionation. *Journal of Liquid Chromatography* 17: 3221–3238.

Field Flow Fractionation: Thermal

S. N. Semenov, Institute of Biochemical Physics,
Russian Academy of Science, Moscow, Russia

Copyright © 2000 Academic Press

Introduction

Field flow fractionation (FFF) represents a class of separation techniques, which are one-phase methods. They are preferable for the separation and characterization of mixtures such as high molecular weight polymers which might be modified or damaged in two-phase separation methods like chromatography. FFF uses a force field perpendicular to the direction of separation to control the longitudinal velocity of particles injected into the system. It is achieved by the particle redistribution in a flow with a parabolic velocity profile due to the transverse force action. In Thermal FFF (ThFFF), the transverse movement of the particles is caused by the particle 'thermophoresis' in the temperature gradient. The transverse particle velocity, U , is defined by the expression:

$$U = b_T \cdot \nabla T \quad [1]$$

where b_T is the particle thermophoretic velocity, and ∇T is the transversal gradient of the temperature in the channel. The particle thermophoresis is commonly related to the osmotic pressure gradient produced in the surface layer due to the temperature gradient. This excess osmotic pressure is established in the particle surface layer due to accumulation of the solvent or dissolved molecules or ions in the particle surface layer. This accumulation is related to the particle surface potential Φ . This surface potential may have the electrostatic nature, when the particle surface carries electric charge, or represent some kind of dipole-dipole interaction, when ion adsorption or surface group dissociation is impossible. The latter situation should be characteristic for organic solvents, where dispersion interaction between the particle surface and solvent molecules should play the main role. The theory of thermophoresis is developed mainly for particles larger in size than the characteristic thickness of the surface layer and having moderate surface potential of several kT (k is the Boltzmann constant), which interacts with dissolved ions or molecules. These ions or molecules should be present at a concentration low enough to avoid the excluded volume effects in their accumulation in the particle surface layer. In this situation, the particle ther-

mophoretic mobility may be written as

$$b_T = \frac{3kc_0}{\eta(2+n)} \int_0^\infty y dy \left(1 + n \frac{y}{R}\right) \left[e^{-(\Phi/kT)} \left(\frac{\Phi}{kT} + 1\right) - 1 \right] \quad [2]$$

where c_0 is the solute concentration in the carrier liquid, η is the carrier liquid viscosity, R is the particle diameter, n is the particle-to-liquid thermal conductivity ratio, and y is the transverse coordinate in the surface layer. The immediate physical factor for the particle thermophoresis is the 'slip' liquid flow in the particle surface layer due to the osmotic pressure gradient, which is related to the temperature gradient in the particle surface layer established along the macroscopic temperature gradient in the liquid. Thus, the main physical events in thermophoresis take place near the particle surface, though the temperature gradient near the particle surface playing the role of the driving force for the particle is defined by the particle and liquid thermal conductivity, which are bulk properties. However, one can expect that these bulk properties will be the same for small particles and larger samples of the material, and the particle thermal conductivity can be obtained from literature data on thermal conductivity of the material or independent experimental determination. It means that particle thermophoresis is mainly related to particle surface properties. It becomes absolutely true for metal particles with very high thermal conductivity, when the parameter n in eqn [1] is very large. For metal particles, the particle thermophoretic mobility is a function of the particle surface properties only. For smaller particles with higher surface potentials, eqn [1] is not true due to intensive solute transport in the particle surface layer.

This surface transport should be compensated by the solute diffusion outside the surface layer, and which, in turn, leads to the solute concentration gradient and related electric field establishment (in electrolytes) around the particle (so-called concentration polarization). However, for a particle with moderate size and thermal conductivity having a surface potential about two to four kT , we can state that the particle thermophoretic mobility is defined by the particle surface properties and does not depend on its size. For emulsion droplets, the thermophoretic mobility in the absence of concentration polarization

is determined as:

$$b_T = -\frac{3k\epsilon_0 R \cdot \nabla T}{(2\eta + 3\eta_i)(2 + n)} \int_{-\infty}^{\infty} \left(1 + n \frac{y}{R}\right) \times \left[e^{-(\epsilon/kT) \left(\frac{\phi}{kT} + 1\right)} - 1 \right] y dy \quad [3]$$

where η_i is the viscosity of the liquid inside the droplet. For homopolymer chains, it is shown by ThFFF experiments, that chain thermophoretic mobility does not depend on chain length and branching, and one can expect that eqn [2] will define it accurately, where R will be the monomer radius. The theory of particle thermophoresis may be true, if some solutes present at low concentration, for example, salt ions, are accumulated around the monomers. However, in true polymer solutions, where no dissolved extrinsic solutes are present, excluded volume effects cannot be neglected, and eqns [2] and [3] cannot be used for the description of thermophoretic behaviour.

For calculation, the Boltzmann exponent indexes in eqns [2] and [3] may be simplified using the approximation:

$$\frac{\Phi}{kT} \approx -\epsilon \left(1 - \frac{x}{h}\right) \quad [4]$$

where ϵ is the depth of the surface potential well in kT units, and h is the characteristic width of this well. Typical orders of values for different kinds of surface potentials are present in Table 1, where A is the Hamaker constant, d is the solute radius, q is the solute electric charge, ζ is the particle zeta-potential, and λ is the Debye length.

For the characteristic relaxation time, the Boltzmann transverse particle distribution is established in the system by forcing injected particles toward the wall of the channel and by their diffusion motion. In ThFFF, particles of the same size with higher ther-

mophoretic mobility will be accumulated more closely to the wall, while particles of lower thermophoretic mobility will form a more diffuse layer that extends further into the flow of the carrier liquid. For particles with about the same thermophoretic mobility, the thickness of this layer may also be different, if particles have different diffusion coefficients, D . Particles with higher diffusion coefficient (i.e., with smaller size) will be accumulated in a more extensive layer due to more intensive thermal movement. The thermophoretic mobility related to the surface potential is an important parameter interrelated to the particle surface charge density (where it represents the electrostatic potential) and characterizing the particle surface properties and the possible exchange of substances between the particle and the surrounding liquid. Also, the separation of particles of the same material but with different sizes may be important in the characterization (molecular mass distribution) of commercial latex and polymer particles.

ThFFF is carried out in a thin channel of rectangular cross-section with a width to thickness ratio (aspect ratio) of about 100 (thickness about 10–100 microns). It allows the separation system to approximate to the laminar flow between infinite parallel plates, which is characterized by a parabolic velocity profile, where the fluid velocity at the channel walls is zero, and a maximum in the centre of the channel. Thus, if a group of particles are accumulated, maintaining an average distance from the wall different from another group of particles, their velocities along the channel will be different. As a consequence, they will leave the channel at distinct times, related to the particle thermophoretic mobility and size, which defines the particle diffusion coefficient. There are no other direct methods, where temperature gradients are used for particle, droplet or macromolecule separation. FFF systems are elution methods and allow the collection of fractions during a separation.

Table 1

Surface potential	Analytical expressions for the $\Phi(y)$, ϵ and h			The ranges of values for parameters ϵ and h	
	$\Phi(y)$	ϵ	h	ϵ	h
Van der Waals forces	$-A(d/r)^6$	A/kT	$d/3$	5–50*	10^{-8} cm (low-molecular surfactant)
Coulomb electrostatic forces	$-q\zeta'' e^{-(y/\lambda)}$	$q\zeta''/kT$	λ	0–10	10^{-7} – 10^{-4} cm** (aqueous electrolytes)
Adsorption forces	None	None	None	0–10	$\approx 10^{-7}$ cm
Structure forces	None	None	None	0–10	$\approx 10^{-5}$ cm

*The maximum values of Hamaker constant are reached for metals

**The maximum value of the Debye length is calculated for the deionized water.

Channel Configuration and Construction Limitations

In thermal FFF the temperature gradient across the channel thickness is maintained by the electrical heating of a polished metal block (usually a chrome or nickel-plated copper block) forming one wall and a cooled similar block forming the opposite wall. The plating improves resistance to corrosion, the factor limiting the range of permitted solvents and the separated particles and macromolecules. Cooling is usually accomplished by passing cold water through longitudinal holes bored in the block. To prevent thermogravitational convection, it is the upper block that is heated and the bottom one cooled. Thermocouples are mounted in the blocks to control their temperatures. In the bottom block, capillaries for the introduction and elution of the solvent and the sample are placed. The copper blocks are separated by a spacer of a polymer material with a low thermal conductivity (Mylar, Kevlar, etc.) to provide high temperature gradients. The channel constructions are described more exactly in the literature (see Further Reading). One of the main advantages of the FFF family stems from the uniform open channel geometry and the well-defined flow profile. As a consequence, retention can be related directly to the physicochemical parameters of the analyte material and carrier liquid. Possible deviations of the flow profile and the polymer parameters due to the non-uniform temperature distribution have been described.

Polymer Characterization

Progress in ThFFF instrumentation and methodology has allowed a systematic study on the thermal diffusion of polymer solutions. The success of these studies is provided by the ability of ThFFF to produce accurate values of thermal diffusion parameters using small quantities of polymer (a few hundred micrograms). The values of the thermal diffusion coefficients (parameters equal to the thermophoretic mobility) have been obtained for 17 polymer-solvent systems and are about 10^{-8} – 10^{-7} $\text{cm}^2/\text{s} \cdot \text{K}$, and their molecular masses are from about several tens to about hundred Daltons. The results show the correlation of the polymer thermophoretic mobility with several polymer and solvent parameters, the thermal conductivity of the polymer and solvent, the polymer density, and the viscosity and viscous activation energy of the carrier liquid. Studies also demonstrated a correlation of the polymer thermophoresis parameters with the solvation properties of the solvent. Though conventional diffusion in polymer solutions is well defined, the thermal diffusion of poly-

mers in liquids is not exactly understood and not well characterized. Although there are equations relating retention to experimental parameters and transport coefficients of polymers, values of polymer thermophoretic mobility are not commonly available, and a model for predicting them from physicochemical parameters is in progress only. Therefore, a calibration is necessary for characterizing the molecular weight distribution (MWD) of polymers by ThFFF (although a single calibration point can be used, when the dependence of the diffusion coefficient on molecular weight is known). Calibration is simple in the analysis of homopolymers because well-characterized molecular weight standards are available for a variety of polymers.

The characterization of copolymers presents more problems because of the overlapping effects of composition and molecular weight distribution (MWD). Often it is necessary to characterize both the MWD and the compositional distribution. In this case the commonly used method of size exclusion chromatography (SEC) is not adequate because the separation is governed by size alone. Thus, molecular weight fractions with different compositions may be eluted in SEC simultaneously. In contrast, ThFFF may separate polymers by both chemical composition and size, and is therefore capable of yielding both size and compositional information on copolymers. Separation by size in ThFFF is governed by differences in the diffusion coefficient of the polymers, while separation by chemical composition may result from differences in the thermophoretic mobility.

The results on ThFFF of random and block copolymers of polystyrene (PS) and polyisoprene (PI) in tetrahydrofuran and cyclohexane show that for random copolymers and block copolymers with a random configuration in solution, the thermophoretic mobility is a linear function of monomer composition. It may be a basis for obtaining compositional information on such copolymers by ThFFF. For copolymers with a radial segregation of monomers, thermophoresis is determined mainly by monomers located in the outer region of the polymer coil. The dependence of retention on the radial distribution of monomers provides a basis for evaluating bonding arrangements in copolymers. The further progress in copolymer characterization by ThFFF is related to progress in the theory of the polymer thermophoresis.

Particle Characterization

Though most ThFFF samples are polymers, the ability of ThFFF to retain and separate both submicron and micron size particles (latex and silica) suspended in various organic carrier liquids has also been

demonstrated by Shiundu, Lee and Giddings. In their article, the dependence of particle retention on various factors (solvent properties, amount of added electrolyte, particle size and composition, and cold-wall temperature) is evaluated and discussed.

Thermophoretic mobilities of several latex-solvent combinations have been obtained from the ThFFF retention data. The studies were carried out in polar organic solvents, cyclohexane and aqueous carriers. As a rule, the thermophoretic mobilities of particles range from 10^{-8} to 10^{-7} $\text{cm}^2/\text{s}\cdot\text{K}$, while the particle size ranges from about 0.04 to about 1 micron.

The retention of colloidal particles in ThFFF demonstrates a strong dependence on the chemical composition of the particles or their surfaces. These results are observed among both similar particles (such as latex particles) and different particles (including latex particles, and inorganic and metallic colloids). These compositional effects are observed for particles suspended in both aqueous and non-aqueous carrier liquids. Also, metal particles (e.g. palladium) are less retained than silica particles, with latex particles most retained. The resolution of particles of equal size in ThFFF experiments is also demonstrated. Surface compositional effects were also demonstrated in this study. These effects confirm the possibility of colloid particle surface analysis by thermal FFF.

Combined Electric-Thermal FFF (EI-ThFFF)

An interesting combined technique represents the application of an electric field across the channel for Thermal FFF, where a temperature gradient is also established. For details see Particle Size Separation/Field Flow Fractionation: Electric Fields.

Conclusion

ThFFF is a method for the particle and macromolecule separation in electrolyte and non-electrolyte solvents according to their interaction with the solvent molecules or/and ions of the added salt. For particles, these are surface interactions, though the particle/solvent thermal conductivity ratio is also important. Thermophoretic mobility may be cal-

culated immediately from ThFFF experimental data, when the particle or macromolecule diffusion coefficient is known. This parameter may depend on both electrostatic and non-electrostatic (dispersion) interactions and can be used for their characterization. Also, the thermophoretic mobility may be used for the characterization of surface particle and macromolecule properties, when the respective theory is developed.

See also: II/Particle Size Separation: Field Flow Fractionation: Electric Fields; Theory and Instrumentation of Field Flow Fractionation. III/Colloids: Field Flow Fractionation. Polymers: Field Flow Fractionation.

Further Reading

- Giddings JC, Shiundu PM and Semenov SN (1995) Thermophoresis of metal particles in a liquid. *Journal of Colloid Interface Science* 176: 454–458.
- Janca J (1992) *Field-Flow Fractionation. Analysis of Macromolecules and Particles*. New York: Dekker.
- Liu G and Giddings JC (1991) Separation of particles in nonaqueous suspensions by thermal electric field-flow fractionation. *Analytical Chemistry* 63(3): 296–299.
- Martin M (1998) Theory of field-flow fractionation. *Advances in Chromatography* 39: 1–138.
- Martin M and Williams PS (1992) Theoretical basis of field-flow fractionation. In: Dondi F and Guiochon G (eds) *Theoretical Advancement in Chromatography and Related Separation Techniques*, NATO ASI Series C: *Mathematical and Physical Sciences*, vol. 383, pp. 513–580. The Netherlands: Kluwer.
- Schimpf ME and Giddings JC (1987) Characterization of thermal diffusion in polymer solutions by thermal field-flow fractionation: effects of molecular weight and branching. *Macromolecules* 20: 1561–1563.
- Schimpf ME, Wheeler LM and Romero PF (1993) Copolymer retention in thermal field-flow fractionation. Dependence on composition and conformation. In: Provder T (ed.) *Chromatography of Polymers. Characterization by SEC and FFF* (ACS Symposium Series) vol. 521, pp. 63–76. Washington DC: American Chemical Society.
- Semenov SN (1997) Thermophoresis and thermal FFF in electrolytes. *Journal of Microcolumn Separations* 9(4): 287–294.
- Shiundu PM, Lee G and Giddings JC (1995) Separation of particles in nonaqueous suspensions by thermal field-flow fractionation. *Analytical Chemistry* 57(15): 2705–2713.

Hydrocyclones for Particle Size Separation

J. J. Cilliers, UMIST, Manchester, UK

Copyright © 2000 Academic Press

Introduction

The hydrocyclone is a static, continuous particle size separation device that can also be used for phase separations, including solid–liquid, liquid–liquid and liquid–gas separations and has been used for various classification duties since the 19th century.

Hydrocyclones are attractive for industrial use as they have no moving parts, a small footprint, relatively low capital and operating costs, and are simple to operate. On the other hand, their operation is rather inflexible once installed and single-stage efficiencies may be low, especially for particles finer than 10 μm .

This article describes the mode of operation of hydrocyclones, and the motion of fluid and solid particles in the classifier. Quantifying the separation is followed by the effect of the major design and operating variables on the efficiency.

Two modelling approaches are introduced: a fundamentally based model, including computational fluid dynamics (CFD), and empirical models, which are still in general use.

The article concludes with aspects of further development.

Description

Hydrocyclones are cono-cylindrical in shape, with a tangential feed inlet into the cylindrical section and an outlet at each axis. The outlet at the cylindrical section is called the vortex finder and extends into the cyclone to reduce short-circuit flow directly from the inlet. At the conical end is the second outlet, the spigot. For size separation, both outlets are generally open to the atmosphere. Hydrocyclones are generally operated vertically with the spigot at the lower end, hence the coarse product is called the underflow and the fine product, leaving the vortex finder, the overflow. **Figure 1** schematically shows the principal flow and design features of a typical hydrocyclone: the two vortices, the tangential feed inlet and the axial outlets. Except for the immediate region of the tangential inlet, the fluid motion within the cyclone has radial symmetry. If one or both of the outlets are open to the atmosphere, a low pressure zone causes a gas core along the vertical axis, inside the inner vortex.

The operating principle is simple: the fluid, carrying the suspended particles, enters the cyclone tangentially, spirals downward and produces a centrifugal field in free vortex flow. Larger particles move through the fluid to the outside of the cyclone in a spiral motion, and exit through the spigot with a fraction of the liquid. Due to the limiting area of the spigot, an inner vortex, rotating in the same direction as the outer vortex but flowing upward, is established and leaves the cyclone through the vortex finder, carrying most of the liquid and finer particles with it. If the spigot capacity is exceeded, the air core is closed off and the spigot discharge changes from an umbrella-shaped spray to a ‘rope’ and a loss of coarse material to the overflow.

The diameter of the cylindrical section is the major variable affecting the size of particle that can be separated, although the outlet diameters can be changed independently to alter the separation achieved. While early workers experimented with cyclones as small as 5 mm diameter, commercial hydrocyclone diameters currently range from 10 mm to 2.5 m, with separating sizes for particles of density 2700 kg m^{-3} of 1.5–300 μm , decreasing with increased particle density. Operating pressure drop ranges from 10 bar for small diameters to 0.5 bar for

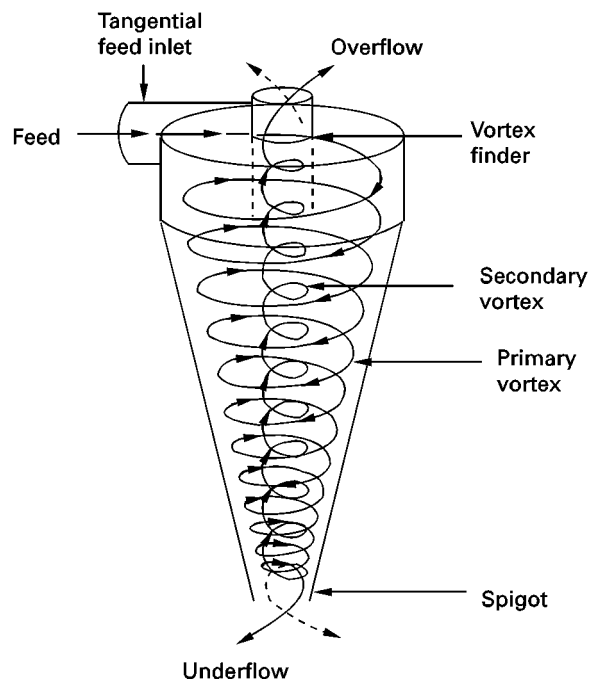


Figure 1 Principal features of the hydrocyclone.

large units. To increase capacity, multiple small hydrocyclones may be manifolded from a single feed line.

Although the principle of operation is simple, many aspects of their operation are still poorly understood, and hydrocyclone selection and prediction for industrial operation are largely empirical.

Liquid Velocity Distributions

Kelsall, in 1952, performed a classic series of experiments measuring axial and tangential fluid velocity profiles in a hydrocyclone using an ingenious experimental system with rotating objectives. The radial velocity was calculated by continuity. The velocity profiles are shown in **Figure 2**. More recently, velocity profiles measured using laser Doppler velocimetry (LDV) were found to correspond closely to those of Kelsall.

The fluid velocity in the cyclone has tangential, axial and radial components. The axial velocity is negative (downward) close to the walls in the cone and positive (upward) near the air core, increasing towards the spigot. This results in a locus of zero vertical velocity between the two vortices, which roughly follows the profile of the cyclone. Toroidal rotation in the inlet flow and interaction between the vortices result in multiple flow reversals.

The tangential velocity increases toward the axis, reaching a maximum near the air core, thereafter decreasing in a forced vortex region. It is the tangential velocity component that generates the centrifugal force, which separates coarser particles from finer ones. The radial velocity, which is two orders of magnitude smaller than the axial or tangential velocities, is directed toward the centre of the cyclone and increases toward the apex.

Particle Motion

Particles entering the cyclone move radially, depending on their mass, either outward due to tangential liquid motion, or inward due to radial fluid motion. In the radial and axial directions, the particle motion is assumed to equal the fluid motion.

Direct measurement of particle motion and solids concentrations at positions in the hydrocyclone can be performed using phase Doppler anemometry. Electrical impedance tomography has been used to measure the position of the air core and the solids concentration profile in a plane through industrial hydrocyclones.

Classification Performance and the Partition Curve

The partition curve (also called a performance curve, efficiency curve or Tromp curve) is used to quantify

hydrocyclone particle size separation performance. It quantifies the weight fraction (or percentage) of each particle size fraction in the feed reporting to the underflow product. For any particle size d , the partition number, $p(d)$, is calculated from:

$$p(d) = \frac{U \cdot u(d)}{F \cdot f(d)} \quad [1]$$

U and F are the mass flow rates of solids (in the same units) and $u(d)$ and $f(d)$ are the weight fractions of particle size d in the feed and underflow streams, respectively. The size at which the partition number equals 0.5 (or 50%) is called the cut size (d_{50}).

A fraction of fine particles always report to the underflow, hence experimentally observed partition curves do not asymptote to zero but to a minimum, called the bypass. This can be interpreted as a fraction of all particles in the feed bypassing classification and reporting directly to the underflow stream. Short-circuiting of feed material to the overflow stream may cause the partition curve not to reach a partition value of 1 (100%); this is not common. The effect of bypass on classification performance is taken into account by correcting the partition value:

$$c(d) = \frac{p(d) - r(d)}{1 - r(d)} \quad [2]$$

where $c(d)$ is the corrected partition value and $r(d)$ the fraction of material of size d bypassing classification. The particle size at which the corrected partition number is 0.5 (50%) is called the corrected cut size (d_{50c}). It is often found that the bypass equals the water recovery from the feed to the underflow (R_F), although there is no fundamental reason why this should be so.

Figure 3 schematically shows an observed and corrected partition curve.

A so-called fishhook may occur in the observed partition curve when, for particle sizes finer than that at the minimum partition value, progressively higher partition numbers are observed. This is more commonly observed for smaller diameter hydrocyclones and is thought to be the result of turbulent dispersion. In such cases the water recovery may be significantly lower than the lowest partition value observed. Applying the correcting concept to such partition curves is meaningless.

Mathematically Describing the Partition Curve

Corrected partition curves have a sigmoidal shape that can be represented using two-parameter

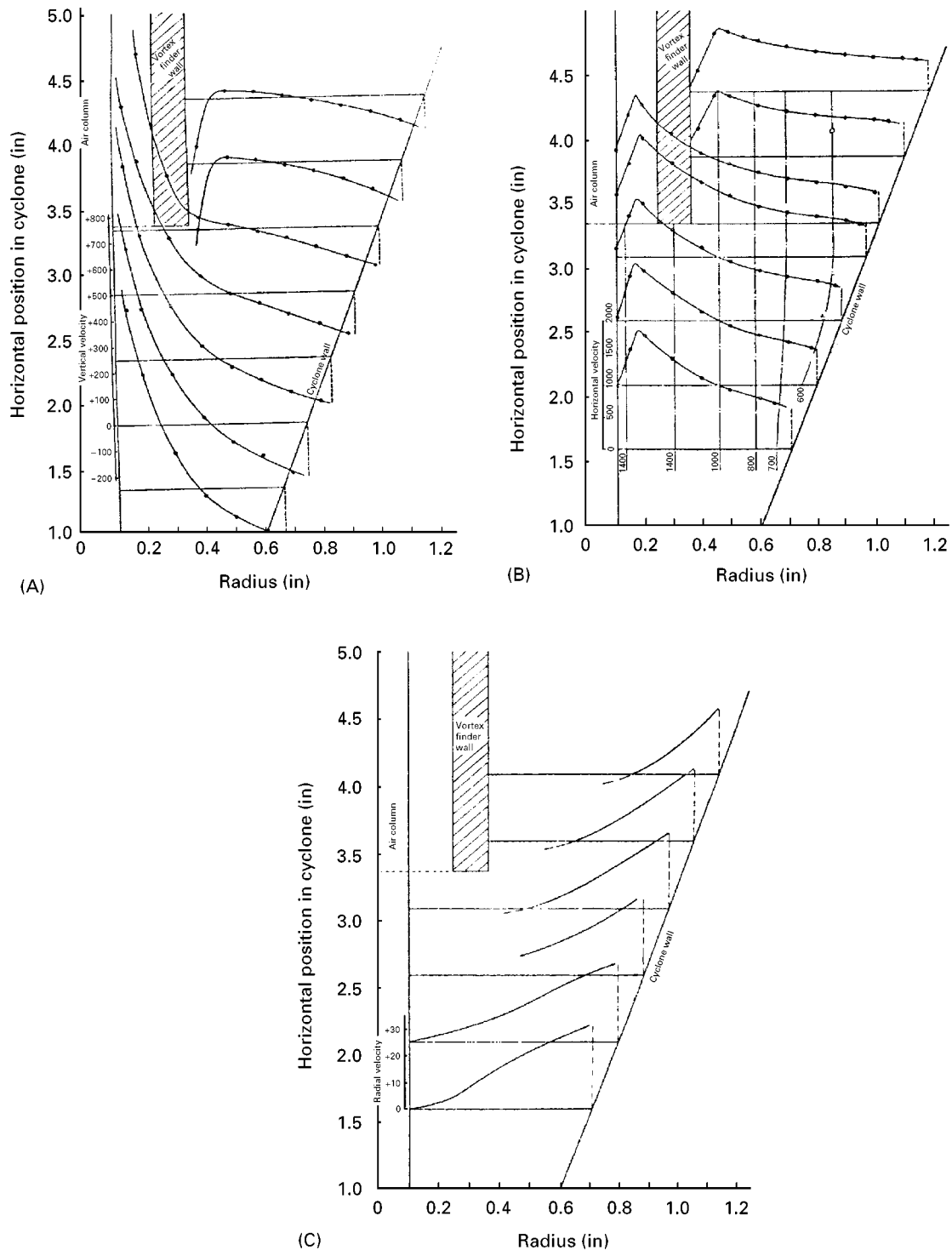


Figure 2 (A) Axial, (B) tangential and (C) radial velocity profiles in a hydrocyclone. (Reproduced with permission from Kelsall (1953).)

functions such as the exponential sum, the Rosin-Rammler and the log-logistic expressions. The two parameters determine the cut size and the sharpness of separation, respectively. The fishhook partition curve can be modelled using the sum of a corrected

partition curve and an inverted partition curve multiplied by a bypass fraction.

The observed partition curve gives a complete description of the selective separation of all sizes of solids entering a cyclone and can be used to predict

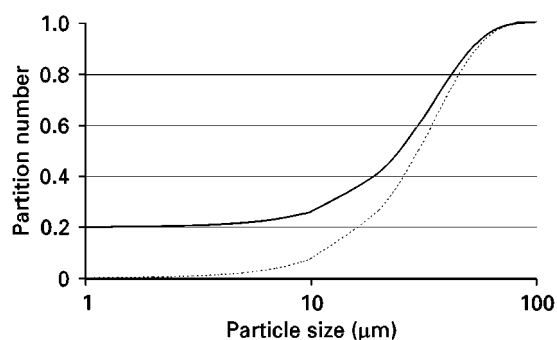


Figure 3 The observed (continuous line) and corrected (dashed line) partition curves of a hydrocyclone with a bypass of 20%.

the product size distribution and solids recovery for changes in feed size distribution. If the bypass is assumed to equal the water recovery, the liquid and volumetric balances can also be estimated.

Hydrocyclone Geometry

The hydrocyclone diameter is the main design variable, and affects both capacity and cut size. The broad operating range available for any hydrocyclone diameter is narrowed down by fixing the inlet and outlet dimensions. It is not generally possible to select independently all the design variables; however, there are reasonable ranges in relation to the hydrocyclone diameter, D_c . **Figure 4** shows the approximate cut size and throughput range that can be achieved using cyclones of different diameters.

The cone angle for classification of hydrocyclones is $15\text{--}30^\circ$, with smaller angles for finer cut sizes, and larger angles for coarser cut sizes, respectively. The free vortex height is the distance between the bottom of the vortex finder and the spigot. Increasing hydrocyclone height improves both capacity and separation efficiency, and generally varies between 3 and $8 D_c$.

The inlet opening is usually rectangular with a height to width ratio of 2 and an equivalent circular diameter of $0.14\text{--}0.33 D_c$. The inner wall, outer wall or centre of the hydrocyclone inlet may be designed to be tangential to the cyclone body, and may also scroll downwards.

The outlet dimensions are the most important physical parameters used to alter the operation. Vortex finder diameters of $0.13\text{--}0.43 D_c$ are commonly used. Spigot diameters in the range $0.1\text{--}0.2 D_c$ are used, but the ratio to the vortex finder is more important. In general, the vortex finder diameter is greater than that of the spigot. Equal diameters should be avoided.

The Effect of Operating and Design Variables

Table 1 summarizes the effect that changes to the major design and operating variables have on the capacity, cut size and sharpness of classification.

The effect of pressure drop on the sharpness of separation depends on the operating range, as an increase in pressure drop increases the throughput and hence the separation efficiency, but decreases the volumetric flow to the underflow. Of particular interest is the effect of feed solids concentration, which has a significant effect on the classification. **Figure 5** shows clearly that an increase in solids concentration increases the cut size and reduces the sharpness of separation.

Hydrocyclone Models

The modelling of hydrocyclones is performed by either describing the fluid flow and particle motion within the cyclone, or by developing empirical

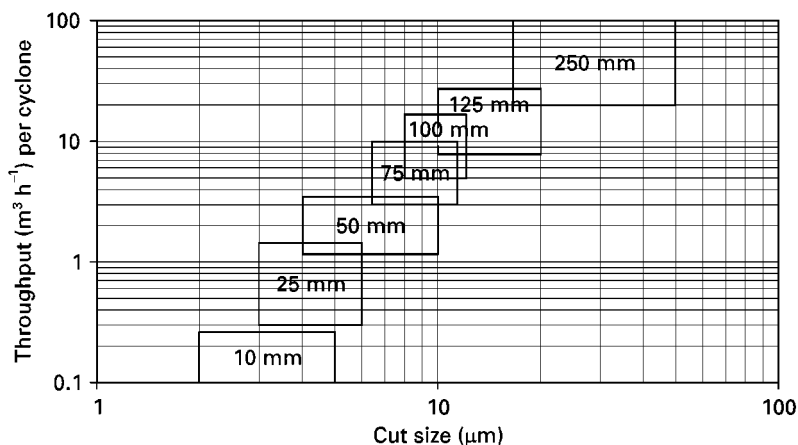


Figure 4 Cut size and throughput for different cyclone diameters.

Table 1 Cyclone design and operating variable effects^a

Increasing	Throughput (Q)	Cut size (d_{50})	Sharpness of classification
Cyclone diameter, D_c	↑	↑	↑
Vortex finder diameter, D_o	↑	↑	↑
Spigot diameter, D_u	↑	↓	↓
Feed inlet, D_f	↑	↓	↓
Cone angle	Not comparable	↑	↑
Free vortex height, h	↑	↑	↑
Pressure drop, P	↑	↓	↑ or ↓
Volumetric feed solids concentration, ϕ	↑	↑	↓

^a↑ increase; ↓ decrease.

(or semi-empirical) relationships between operating variables and measured responses. Fundamental models are appealing from a rigorous standpoint but have difficulty in describing satisfactorily the complex particle–particle and particle–fluid interactions for hydrocyclones operating at higher solids concentrations.

Empirical or semi-empirical models, which relate the parameters of the partition curve to cyclone design and operating variables, are generally used for industrial hydrocyclone modelling and simulation. A number of general models, particularly for larger diameter hydrocyclones, have been developed (see Further Reading).

Fundamentally Based Hydrocyclone Models

Early attempts at understanding the physical principles that govern size separation in hydrocyclones yielded theories based on equilibrium, residence time and crowding. More complete simulations in which

fluid and particle motion is estimated from solution of the Navier–Stokes equations have been developed more recently.

Equilibrium orbit theory It can be postulated that particles will find an equilibrium orbit in the hydrocyclone where their terminal settling velocity radially outward is equal to the radial velocity of the liquid inward. A particle will report to the spigot if its equilibrium orbit is in the downward axial liquid flow and to the vortex finder if in the upward axial flow. The cut size is defined by particles that have an equilibrium orbit that coincides with the locus of zero vertical velocity and therefore have an equal probability of reporting to either product streams. An equilibrium orbit may not be achieved due to the short residence times and high solids concentrations in the hydrocyclone.

Residence time theory This theory determines whether the residence time in the hydrocyclone allows a particle entering the cyclone at the centre of the inlet to settle to the cyclone wall and enter the boundary layer flow to the underflow.

Crowding theory At higher feed concentrations, it is found that the separation size is primarily determined by the discharge capacity of the spigot and the feed size distribution. By controlling the outlet dimensions, it is thought that any cut size within the feed size distribution can be obtained.

Computational fluid dynamics (CFD) solutions This is the preferred approach for fundamentally based modelling of hydrocyclone performance. Complete flow modelling of the hydrocyclone

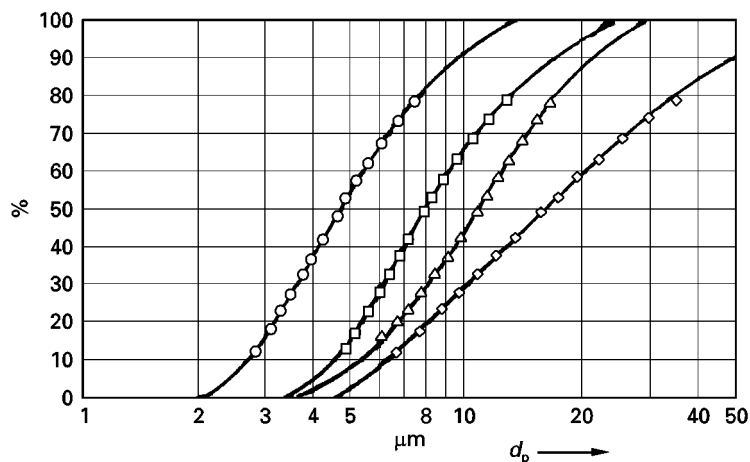


Figure 5 Effect of feed solids concentration on hydrocyclone separation. Circles, 2.68 vol%; squares, 11.11 vol%; triangles, 17.54 vol%; diamonds, 23.75 vol%. (Reproduced with permission from Braun and Bohnet (1989). Copyright: Wiley-VCH.)

involves predicting the liquid-phase velocities, the slurry concentration profile, the turbulent viscosities and the slip velocities of particles with respect to the liquid phase for a range of particle sizes before predicting the partition curve. The solution is complex, because the governing fluid flow equations are nonlinear, simultaneous partial differential equations.

Chakraborti and Miller (1992) have published an extensive review of fluid flow modelling in hydrocyclones. They describe the flow models in detail, giving particular attention to models based on the Navier–Stokes equation and the treatment of fluid turbulence. They further discuss techniques for flow measurement and visualization and give a brief summary of pressure drop correlations and measurements. This paper is an essential reference for the fluid flow modelling approach.

The general approach to develop a complete CFD-based model of a hydrocyclone must include a wide range of components. If it is assumed that variations of local density and viscosity are small for dilute slurries and that particle–particle interactions are negligible, the fluid and particle modelling can be decoupled. Liquid velocities are predicted by combining the fluid transport equations for vorticity, stream function and angular spin velocity with a modified Prandtl mixing length model, which varies both radially and axially, for the turbulent viscosity. The set of simultaneous, nonlinear partial differential equations are solved by overlaying the hydrocyclone dimensions with a rectangular grid and using appropriate boundary conditions at the solid walls and liquid–air interface, to solve for conditions within each cell of the grid. By balancing all the forces on the particle, the particle motion with respect to the fluid can be computed. The particle trajectories are found by calculating axial and radial slip velocities with respect to the fluid. Size classification performance is determined by following a particle of a given size from the inlet until it exits. This computation is repeated for each particle size across the inlet diameter yielding the partition curve.

For concentrated slurries, liquid-phase velocities are affected by local density and viscosity, which in turn are affected by local solid concentration and particle size distribution. Since particle motion determines the concentration and size distribution at each location, this being determined from liquid velocities, an iterative solution is required so that local slurry property changes can be estimated and liquid-phase velocities recalculated.

Advances in CFD methods such as computation grid generation, numerical methods and computing

resources are increasing the applicability of this modelling technique to improve designs.

Empirical Models

At present, empirical models are the most commonly used technique for hydrocyclone selection and performance prediction. Empirical hydrocyclone models use the partition curve as a basis for describing size separation. Suitable equations are developed from experimental results to relate the parameters of the corrected partition curve to physical variables. In general, empirical hydrocyclone models consist of four relationships that describe the cut size, the sharpness of separation, the water balance around the hydrocyclone and the throughput–pressure drop relationship.

An empirical hydrocyclone model was described in 1976 that is still commonly used to predict separation performance. This model was the first to document an empirical form for the sharpness of separation and therefore allow direct simulation of expected performance without any testwork. This model form is often used as a basis for the development of models that include further variables, such as, for example, angle of inclination, or for an operating range in which the model has not been tested.

The Rosin–Rammler function describes the reduced partition curve:

$$c_i = 1 - \exp(-0.693x_i^m) \quad [3]$$

where m indicates the sharpness of separation and x_i is:

$$x_i = \frac{d_i}{d_{50c}} \quad [4]$$

In SI units, and using the symbols in Table 1, the Plitt equation for the cut size is:

$$d_{50c} = \frac{50.5 D_c^{0.46} D_i^{0.6} D_o^{1.21} \exp[6.3\phi]}{D_u^{0.71} b^{0.38} Q^{0.45} (\rho_s - \rho_l)^{0.5}} \quad [5]$$

where ρ_s , ρ_l and ρ_p are the densities of the solid, liquid and pulp, respectively.

To describe the water balance, Plitt develops a relationship for the volumetric flow split between the overflow and underflow streams, S , rather than the bypass:

$$S = \frac{3.28(D_u/D_o)^{3.31} b^{0.54} (D_u^2 + D_o^2)^{0.36} \rho_p^{0.24} \exp[0.54\phi]}{p^{0.24} D_c^{1.11}} \quad [6]$$

The relationship for the sharpness of separation is given by:

$$m = 1.94 \exp[-1.58 R_v] \left[\frac{D_c^2 b}{Q} \right]^{0.15} \quad [7]$$

where R_v , the recovery of slurry to the underflow, is related to the flow split by:

$$R_v = \frac{S}{1 + S} \quad [8]$$

The relationship between the pressure drop across the cyclone and the throughput is given by:

$$P = \frac{1.88 Q^{1.78} \exp[0.55 \phi]}{D_c^{0.37} D_i^{0.94} b^{0.28} (D_u^2 + D_o^2)^{0.87}} \quad [9]$$

Roping is affected by the spigot diameter and the volumetric solids concentration in the underflow; however, there is no satisfactory method for predicting operating limit.

It must be emphasized that empirical models, although developed from an extensive database, should be used with caution.

Future Developments

The extremely wide range of hydrocyclones available and separation applications for which they can be used assures their future role in particle classification. However, significant obstacles remain before they can be used to replace more efficient methods for fine classification purposes, such as centrifuges. Classification inefficiencies, in particular the large bypass, limit their application. The potential of very small diameter hydrocyclones for sub-micron particle separation, especially in multistage configuration, is enormous, if these inefficiencies can be reduced.

Hydrocyclone modelling has advanced significantly with the use of CFD. Empirical hydrocyclone models are convenient ways of describing experimental data but do not enhance the understanding of the separation and CFD models will play a greater role in hydrocyclone simulation. Nonintrusive measurement techniques such as laser Doppler anemometry (LDA), laser Doppler velocimetry (LDV) and tomography have indicated the source of hydrocyclone inefficiencies. With increased resolution and combined with CFD models, this will improve hydrocyclone unit design.

Hydrocyclone operations will benefit from novel methods for monitoring which are currently being developed. Industrial tomography is becoming affordable, and the potential of visual and sonic techniques has been illustrated.

See also: II/Particle Size Separation: Electrostatic Precipitation.

Further Reading

- Bradley D (1965) *The Hydrocyclone*. Oxford: Pergamon Press.
- Braun T and Bohnet M (1990) Influence of feed solids concentration on the performance of hydrocyclones. *Chem. Eng. Technol.* 13: 15–20.
- Chakraborti N and Miller JD (1992) Fluid flow in hydrocyclones: a critical review. *Mineral Processing and Extractive Metallurgy Review* 11:
- Heiskanen K (1993) *Particle Classification*. London: Chapman & Hall.
- Kelsall DF (1953) A study of the motion of solid particles in a hydraulic cyclone. *Transactions of the Institution of Chemical Engineers* 30: 87–104.
- Plitt LR (1976) A mathematical model of the hydrocyclone classifier. *CIM Bulletin* December 114–122.
- Svarovsky L (1984) *Hydrocyclones*. London: Holt, Rinehart and Winston.

Instrumentation of Field Flow Fractionation

See II / PARTICLE SIZE SEPARATION / Theory and Instrumentation of Field Flow Fractionation

Sedimentation

See II / PARTICLE SIZE SEPARATION / Split Flow Thin Cell (SPLITT) Separation

Sieving/Screening

J. Skopp, School of Natural Resource Sciences,
University of Nebraska, Lincoln, NE, USA

Copyright © 2000 Academic Press

Introduction

Sieving is one of the oldest and most commonly used method of sorting materials. Yet, when improperly carried out, sieving can provide misleading information or biased separation. Sieving has widespread application to industries as diverse as mining, pharmaceutical production and agriculture. The goal is typically to control or measure the particle size distribution. Sieving may be a direct part of a production process, a quality control procedure or a sample characterization. Regardless of the purpose, an understanding of sieving is necessary to optimize and accurately use this technique.

Sieving has the clear advantage of being a simple, readily understood and relatively inexpensive method. This method also has the ability to provide reproducible results. This has tended to boost confidence in the method, even where it is not warranted. Some of this confidence is a result of ignorance as to the actual errors involved in a given sieving operation or with a particular set of sieves. While these errors can be described and measured, the difficulty of doing so largely detracts from the attractiveness of the method. Thus, most people rely on standard procedures and the reproducibility of the method to reassure themselves as to the quality of the data obtained.

Overview of Sieving Process

Sieving was the earliest means of particle size fractionation. Basically, the process of sieving is that of placing the particles to be fractionated on a pattern of openings or holes. The individual openings are referred to as the aperture. Small particles may fall through or the sieve retains the larger particles. Separation requires agitation and time. A variety of mechanisms exist to provide agitation either to the sieve or to the particles to be fractionated. Typically, commercial equipment varies in the manner in which agitation is created or the fluid used to support the particles. Either air or water may be used to support the particles as they sort on the sieve. Dry sieving has a lower practical limit of 50 μm , while wet sieving can separate smaller particle sizes when using special sieves or small volumes of particles.

We briefly examine three applications of sieving processes before continuing in more detail with a description of the sieving process, the time dependence of sieving and lastly sources of error in sieving.

Applications of Sieving

A single sieve may provide a straightforward classification (or gradation) of particles where a clear threshold is desired. Crushing operations typically seek to ensure that all particles are below such a threshold and sieves provide a convenient means of doing so. However, in some operations it is equally important to remove particles less than a given size. The first case is referred to as scalping (removing oversize particles) while the second case is referred to as removal of fines. Sometimes it is desirable to do both. Thus, it can be useful to employ a set (or nest) of sieves varying in aperture size. Unsorted particles are applied to the topmost sieve and agitation begun. As the particles sort, smaller ones pass through from upper sieves to lower ones. This cascade of particle sorting continues as the smallest particles only gradually make their way past the smallest sieve.

A nest of sieves with a sufficient variation in aperture sizes may be used to construct a particle size distribution. Such distribution may in turn be used to describe the behaviour of the material under study. A particle size distribution obtained in this way should recognize that the errors associated with the top sieve (the coarsest fraction) may be different from the errors associated with the bottom sieve (the finest fraction). This occurs in part due to differing opportunity times for the particles to pass through the sieve that they are ultimately retained upon.

A third application of sieving is the use of sieving curves to develop a morphological characterization of the material being screened. Sieving curves represent the time dependence of the sieving process and are discussed in more detail in a later section. The goal is to infer particle shape or other morphological features (e.g. agglomeration) from the speed with which sieving proceeds. Unfortunately, these techniques are still in the developmental stages.

Description of the Sieving Process

Sieve Construction

Sieves are typically constructed in one of two ways: first, through the use of a wire mesh or cloth. This

Table 1 Sieve mesh equivalent sizes: US standard testing sieves designated for wire cloth at some principal ISO sizes

Mesh number: US standard testing sieves	Sieve opening (mm)
5	4.00
7	2.80
10	2.00
14	1.40
18	1.00
25	0.710
36	0.500
45	0.355
60	0.250
80	0.180
120	0.125
190	0.090
325	0.045

results in square apertures. The diameter of the wire controls the size of the aperture and per cent of the total area that is open. Second, openings or circular holes are created by perforating a plate or flat disc. The number of perforations controls the amount of open area in this sieve. These two methods result in openings that differ in shape and in their ability to pass particles. Thus, it is important to specify which kind has been used to obtain a particular set of data.

Sieves are available in standard sizes (Table 1) from a number of companies. Sieve openings are given in a mesh number or nominal diameter of the opening. Surprisingly, no standard sieve is readily available for the 50 μm cut-off between the sand and silt separates (as defined in some systems of particle nomenclature). Consequently, sieving cannot distinguish this class boundary directly using standard sieves. However, such boundaries (or other specific sizes) can be estimated by determining the particle size distribution with a nest of sieves that bracket the desired size.

Industry standards have focused on maintaining consistency in the manufacture of sieves. This allows the comparison of sieving operations provided the materials and conditions of the sieving are also comparable. The focus of many practitioners of sieving has been on standard procedures to maintain reproducibility and consistency.

Sieve Agitation

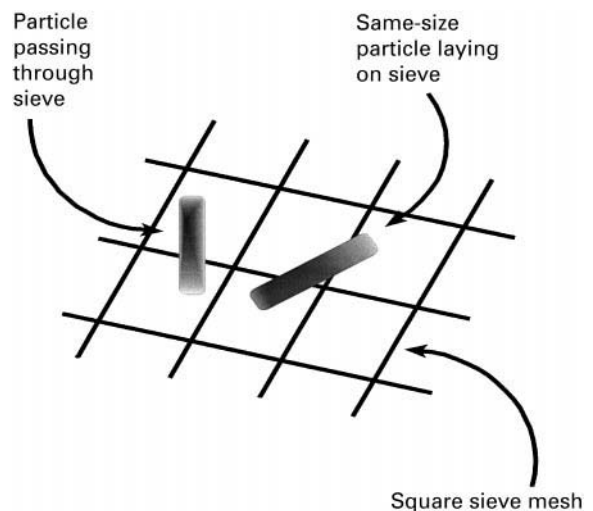
Particles placed on a sieve may not sort or pass through the openings unless some form of agitation is used. Typically, a large mass of soil placed on a sieve

will allow particles to bridge, thus restricting their passage through the openings. Agitation breaks the bridges, shuffles the particles and provides an opportunity for particles to present themselves to an opening.

An undersize particle may still fail to pass through a sieve. Figure 1 illustrates how identically shaped particles may approach the aperture at different angles. Some angles may allow passage of the particle while others may restrict passage. Agitation increases the number of times that a particle approaches the aperture and the velocity of approach and alters the orientation of the particle as it approaches the aperture. The first two factors depend on shaking intensity and competition among particles. The third factor depends on the shape of the particle and the shape of the sieve opening. These factors influence not only the speed with which fractionation occurs, but the retention of specific particles.

Alternative commercial instruments attempt to agitate the particles in different ways. Vibration is commonly used, either as a jarring action or an oscillatory motion. This motion may have a large or small amplitude and may be restricted to horizontal or vertical motion. The efficiency of separation usually increases as vibration amplitude increases, but it may reach a maximum. Efficiency declines as the increased agitation merely serves to suspend particles without giving them an opportunity to pass through an aperture.

One means of agitating particles is by displacing the fluid (air or water) surrounding the particles. In the case of air, this may involve ultrasonic oscillation or mechanical flow of air counter to the direction of sieving. In an extreme case, the sieve may be placed in

**Figure 1** How particle shape influences the efficiency of sieving by delaying passage through the sieve.

a vertical orientation as air flow lifts the particles and attempts to pass through the sieve. Particles retained on the sieve would need to be mechanically removed. Such a manipulation could be maintained in operation continuously.

Sieved Materials

The particle influences the time and efficiency of sieving. Issues relate to the sample's mass, particle size distribution, particle density, particle shape, friability, the tendency to aggregate and electrostatic properties. Specific procedures have been developed for particular materials.

Obtaining a representative sample or subsample for sieve analysis is a key step; this is a particular issue where nonuniformity is extreme or segregation of the sample may occur. It may sometimes be necessary to settle for reproducible sampling with the goal of making comparisons on a relative basis.

Sample mass influences the efficiency of sieving and the time needed for a sieving operation. At high loadings, blinding of the sieve may be more important as well as increased breakdown of friable samples.

Particle size distribution has several effects on the efficiency of sieving. These effects, if they exist, may depend on the choice of sieves. Particles which are slightly oversize may lodge in the sieve, blocking the aperture from participating in the sieving process. This 'blinding' of the sieve reduces the overall efficiency of sieving or increases the time needed to achieve separation.

Sample friability can also influence separation. Friability is the tendency of particles to break apart. The process of agitation and sieving may change the particle size distribution for friable samples. Longer sieving times or larger amplitude agitation increase these effects. Ultimately, the goal of the sieving operation must be compared to the effect of sieving on the underlying size distribution.

Time Dependence of Sieving

Sieving Curves

The mass passing through the sieve can be observed by collecting this material on a balance or strain gauge. This can be done manually or the sensor can be connected to a computer and the progress of sieving continuously monitored as a function of time. The graph of mass remaining on the sieve or the mass that has passed the sieve is referred to as a sieving curve (Figure 2). The graph shown in Figure 2 shows the mass passing through the sieve as a function of time. Note that complete separation may never be achieved.

Sieving Equations

Sieving curves like that shown in Figure 2 are the result, in part, of particle shape. Extracting this information requires a quantitative description of the sieving curve. Models describing the sieving curves can be classified as empirical or mechanistic. The most common empirical model uses a power

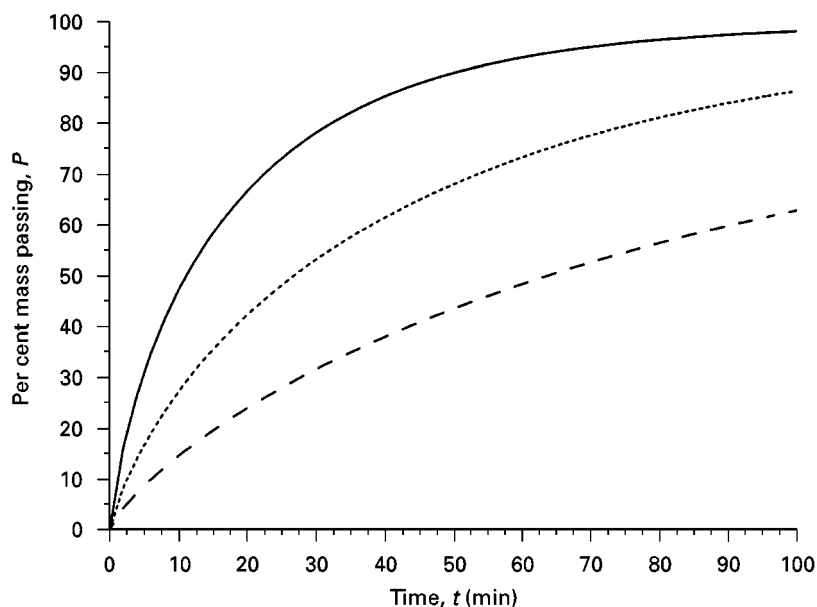


Figure 2 Example of three sieving curves modelled with the equation $P = 100\% [1 - \exp(-kt^n)]$, $n = 0.8$. Dashed line, $k = 0.025$; dotted line, $k = 0.050$; continuous line, $k = 0.10$.

function. The rate at which material passes through the sieve for short times is nearly constant and can be expressed by a power function model given as:

$$M = at^b$$

where M = cumulative mass of the material passed at sieving time t (grams), t = sieving time (seconds), b = a constant nearly equal to 1 and a = sieving rate constant, with units of $g\ s^{-1b}$. This model has had some practical utility but its validity in describing data, even for short times, is questionable and depends on how the data are truncated.

One mechanistic model starts by assuming that the probability of particle passage at time t is directly proportional to the mass of material on the sieve. Thus, the mass of material remaining (M_t) at sieving time t is described in differential form by:

$$\frac{dM_t}{dt} = -k(M_t - M_r)$$

where M_t = total mass of the material remaining on the sieve at time t (grams), M_r = material mass which does not pass the sieve (i.e. the sieve residue after infinite sieving time) (gram) and k = passage probability of the material with a given size at time t , or passage rate factor (s^{-1}).

This model assumes that, after a time, k becomes independent of time and particle size. This occurs when the smallest particles have passed through the sieve and those left on the sieve are of a size close to the sieve opening. However, the sieving constant (k) is not guaranteed to be constant. For example, it may change with the depth of material on the sieve and hence change as M changes. Thus, one difficulty in using the above equation lies in describing how k changes with experimental conditions or time.

Integrating the above equation (setting $M_r = 0$) with the application of initial conditions yields:

$$M = M_0(1 - e^{-kt})$$

where M = cumulative mass of material passed at sieving time t (grams) and M_0 = cumulative mass of the material that would pass at infinite sieving time (grams). Note that $M + M_t = M_0$. The rate constant can be determined empirically or deduced from physical principles. In the latter case k is defined as:

$$k = A[1 - 2R(1 - f_s)/D]^2$$

where A is a constant depending on the sieve and sieving conditions, R is a radius of the particle, D is the sieve opening and f_s is a grouping of factors that describe particle shape. Tests of this model have not been extensive. It should work best for longer times.

An alternative or modified proportional model has been used with some success over a wide range of sieving times. This model starts by assuming that the constant k in the differential equation above is a function of time, $k = k^*/t^m$. Then the differential equation can be written as:

$$\frac{dM_t}{dt} = -\frac{k^*(M_t - M_r)}{t^m}$$

where k^* = passage probability of the material with a given size at time t , or passage rate factor, (s^{-n}) and $n = 1 - m$ where m is a constant.

Upon solving this equation for M and substituting $1 - n$ for m , the resulting model is:

$$M = M_0(1 - e^{-k^*t^n})$$

This model appears to describe both the initial and long time sieving behaviour. It is empirical in nature, so its coefficients need to be related to particle morphology or other sample characteristics.

Sources of Error

The Sample

The major concern with sieving operations is the efficiency and time of each sieving step. This becomes particularly important when we use a nest of sieves to perform several separations simultaneously. The use of words such as effective or nominal diameters with sieves is in recognition of the imperfect separation that may occur. What is less readily recognized is that the sample may contribute to imperfect separation.

Placement of a soil sample on a sieve does not result in instantaneous separation. Several factors influence the time to achieve a fixed level of segregation. These factors include sample size, shaking intensity, particle shape, particle size and hole geometry. No one set of sieving times applies for all conditions, but for many soils with small samples (~ 100 g) a waiting time of about 3–5 min for coarse fractions and 10 min for fine fractions gives acceptable results. A typical nest of sieves (with 3 in (7.5 cm) diameter) operating for at least 15 min is desirable for separation. Since samples vary in their sieving characteristics, it is best to run a trial sample at several times. This is particularly true with a nest of sieves to ensure adequate separation past the smallest sieve opening.

The single most important factor changing the efficiency of sieving is the initial sample mass. It is faster and more efficient to split a large sample into several smaller ones. A useful rule of thumb is to keep the depth of material on the sieve to less than 1 cm. A better rule is to run a test sieving curve. In general, this will show that as the sieve opening decreases smaller masses are needed. For 8 in (20 cm) diameter sieves these typically range from 200 to 30 g for sieve openings varying from 2 mm to 45 μm .

Particle shape also influences the efficiency of sieving. Rougher surfaces with elongated shapes are expected to require longer sieving times than smooth surfaces with a more spherical shape. It may be possible to use equations like the one presented earlier to predict the sieving rate constant. However, the inverse problem of determining the particle shape from sieving curves appears to be ambiguous.

Sieve Construction and Cleaning

The manufacture of sieves is subject to error. This error takes the form of a variation in aperture opening within a sieve as well as from sieve to sieve. This error also varies with the size of the opening, with the coarser sieves generally being more consistent. It is expected that for the finer sieves (less than 100 μm), this error could approach 10%. Thus, all sieve openings represent nominal diameters. The determination of the diameter of material that passes a particular sieve must be determined by calibration, as discussed in the next section.

Sieve cleaning represents one means of ensuring the reproducibility of a sieve. This typically involves use of a brush with the coarser sieves. Finer sieves may require reverse flushing with water or use of an ultrasonic cleaning bath. Ultimately, sieves must be inspected at periodic intervals to make sure that the mesh has not been distorted or damaged in use.

Calibration

A sieve calibration is used to establish the size of separation achieved by a particular sieve. This involves the use of standard materials and microscopic examination of the material passing through the sieve. The material is placed on the sieve and sieving proceeds until the mass passing appears unchanged. The material which has passed is examined under a microscope to determine the size of particles. This

information is used to find an average equivalent volume diameter which represents the effective size of the sieve.

Conclusion

Sieving is a valuable and widely used tool for both sorting and particle size determination. It is a relatively inexpensive procedure that, with the use of standard methods, can provide reproducible results. The use of sieves for novel materials requires the determination of sieving curves under a variety of conditions such as loading. These curves are used to optimize the conditions for efficient sieving. Even where only slight variations in the material to be analysed exist, it may be desirable to determine the appropriate sieving conditions rather than relying on standard methods.

See also: II/Particle Size Separation: Hydrocyclones for Particle Size Separation.

Further Reading

- Allen T (1990) *Particle Size Measurement*, 4th edn. Powder Technology Series. London: Chapman and Hall.
- ASTM Committee E-29 on Particle Size Measurement (1985) *Manual on Test Sieving Methods*. ASTM Special Technical Publication 447B. Philadelphia, PA: ASTM.
- Beddow JK (1981) *Particulate Science and Technology*. New York, NY: Chemical Publishing.
- Beddow JK (1984) *Particle Characterization in Technology. I. Applications and Microanalysis*. Boca Raton, FL: CRC Press.
- Beddow JK (1984) *Particle Characterization in Technology. II. Morphological Analysis*. Boca Raton, FL: CRC Press.
- Fayer ME and Otten L (eds) (1984) *Handbook of Powder Science and Technology*. New York: Van Nostrand Reinhold.
- Herdan G and Smith ML (1953) *Small Particle Statistics; an Account of Statistical Methods for the Investigation of Finely Divided Materials*. Amsterdam: Elsevier.
- Irani RR and Clayton FC (1963) *Particle Size Measurement, Interpretation and Application*. New York, NY: Wiley.
- Lauer O (1966) *Grain Size Measurements on Commercial Powders; A Guide for Experts, Worked out in Alpine's Experimental Station*. Augsburg: Alpine.
- Leschonski K (1979) Sieve analysis: the Cinderella of particle size analysis methods? *Powder Technology* 24: 115–124.

Split Flow Thin Cell (SPLITT) Separation

C. Contado, University of Ferrara, Ferrara, Italy

Copyright © 2000 Academic Press

Introduction

SPLITT fractionation (SF) is a relatively new family of separation techniques primarily – but not exclusively – applicable to macromolecules and particles. The SF techniques utilize a thin ribbon-shaped flow cell and achieve fractionation by differential transport across the thin (transverse) axis of the cell. Since the cell is only a few hundred micrometres thick, the separation path – which may be less than the nominal channel thickness – is extremely short and the separative transport is correspondingly rapid. Separation is typically accomplished in only a few minutes. This is a particularly valuable feature for example for fragile species that must be fractionated rapidly to avoid degradation (e.g. biological samples). The fluid that carries dissolved or suspended components through the SPLITT cell is divided at both ends by thin flow splitter elements (see Figure 1). The inlet splitter element allows for the smooth merging of two incoming laminae, one carrying the suspended feed material and the other generally containing only the pure car-

rier liquid. Differential transport of feed components between the two laminae (after they are brought into contact) then occurs as a result of a transverse driving force or gradient. At the outlet end, the flowing liquid volume is divided at a predetermined position by a second splitter element, thus producing two sub-streams that are enriched or depleted in the desired components as a result of the differential transport.

Both preparative and analytical fractionation process can occur in the SPLITT cells, depending on the injection procedure. A continuous (CSF) process of feeding the cell is advantageous for preparative fractionation (gram, kilogram), offering rapid throughput, minimum holdup volumes, and a sharp separative cut off; examples of continuous fractionation can be found in the separation of mineralogical, industrial and food samples.

The analytical version of SPLITT fractionation (ASF) is often more practical to operate. The injection of discrete pulses can be made, if desired, to follow one another in close sequence. In this use, separation is performed for the measurement of quantitative properties of sample components and the fractionation is termed 'analytical SPLITT fractionation';

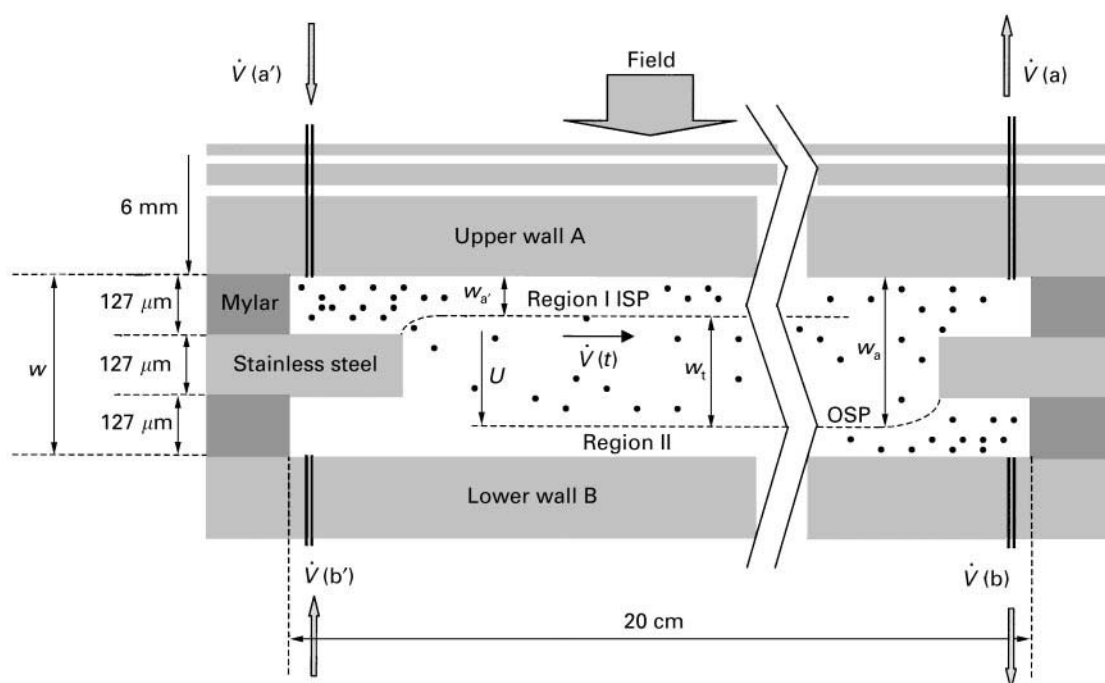


Figure 1 Side view of a generic SPLITT cell.

examples of quantitative determinations include diffusion coefficients of proteins, settling velocity and the relative content of oversized particles above a cutoff diameter in a particulate material. Moreover because of its ease of theoretical interpretation, the SPLITT cell can be used for the rapid measurement of transport-related properties such as particle size and particle size distribution. The throughput of SF is proportional to many variables such as the sample concentration in the feed stream, the volumetric flow rate of the sample stream, the applied field strength and the SPLITT cell area. For preparative applications there is obviously a trade-off between the resolution and throughput in the operation of SF: maximizing the throughput and maintaining an acceptable resolution is the common choice.

The effectiveness of the SPLITT process can be modulated by simply varying the flow rates of the inlet and outlet substreams, which determine the position of the inlet splitting plane (ISP) and the outlet splitting plane (OSP) and controlling the thickness of the transport region; sometimes, unwanted displacements of a few tens of micrometres may be difficult to discern but they are sufficient to interfere with effective separation. In some cases, the efficiency of the SPLITT process can be controlled by altering the strength of the field or gradient driving the separative transport.

The efficacy of SF separation depends instead, on the hydrodynamic integrity of the SPLITT cell. Effective separation is based in fact, on two central requirements:

- there must be no hydrodynamic mixing across stream planes; and
- the splitters must be absolutely perfectly aligned so that they are capable of splitting the film of flowing liquid evenly along the stream plane.

Success in fulfilling these requirements is not easy to judge because of the thinness of the cell and the shortness of the transport path.

The selectivity of SPLITT fractionation comes from the applied force. The principal transverse driving forces used include gravity, centrifugation, diffusion, electrical potential gradients, magnetic gradients and hydrodynamic lift forces. The geometry of all the different cells is similar to that depicted in Figure 1, except for the curvature characteristic of the centrifugal SPLITT cell.

The simplicity of the SPLITT cell leads to rather rigorous theoretical guidelines on the conditions necessary to achieve a given level of separation.

Theory

The theory of separation by SPLITT cell was formulated by J. C. Giddings in terms of experimentally controllable flow rates in the inlet and outlet substreams and it has been developed and implemented through the years; SPLITT fractionation theory can now be found in numerous publications. The separation is performed inside a thin channel, where the behaviour of a sample particle depends on the balance between the external force field and frictional forces (as for field flow fractionation techniques (FFF)), combined with the action of the fluxes operative within the cell.

In Figure 1 the sample, suspended in a suitable carrier fluid, is introduced through the top inlet a' at a predetermined volumetric flow rate $\dot{V}(a')$. At the same time, pure carrier fluid enters through the bottom inlet b' at a flow rate $\dot{V}(b')$; where the two inlet streams join to form a single stream we have the ISP. When the fluid stream reaches the end of the channel, it is mechanically divided into two fractions by the outlet splitter.

The differential displacement of the particles occurs towards wall B, based on the driving force exerted on each type of particle by the applied field and the frictional resistance offered by the carrier fluid to particle motion. Thus different types of particle occupy different laminae while the flow through the channel displaces them axially towards the outlet end.

The total volumetric flow rate \dot{V} in the channel can be written both in terms of inlet flow rates or outlet flow rates

$$\dot{V} = \dot{V}(a') + \dot{V}(b') = \dot{V}(a) + \dot{V}(b) \quad [1]$$

and since the walls A and B are parallel and their dimensions much larger than w (thickness) and b (width), the velocity profile is essentially two-dimensional (see Figure 2). The mean fluid velocity \bar{v} can be computed as \dot{V}/bw , and the velocity parabolic profile across the cell thickness is described by the equation:

$$v\left(\frac{x}{w}\right) = 6\bar{v}\frac{x}{w}\left(1 - \frac{x}{w}\right) = 4v_{\max}\frac{x}{w}\left(1 - \frac{x}{w}\right) \quad [2]$$

where v_{\max} is the maximum fluid velocity found at the midplane ($x = w/2$) of the cell.

By looking at the flow stream components (see Figure 1) it is possible to find a relation which takes into account the fluid flow proceeding in the transport layer $\dot{V}(t)$:

$$\dot{V} = \dot{V}(a') + \dot{V}(t) + \dot{V}(b) \quad [3]$$

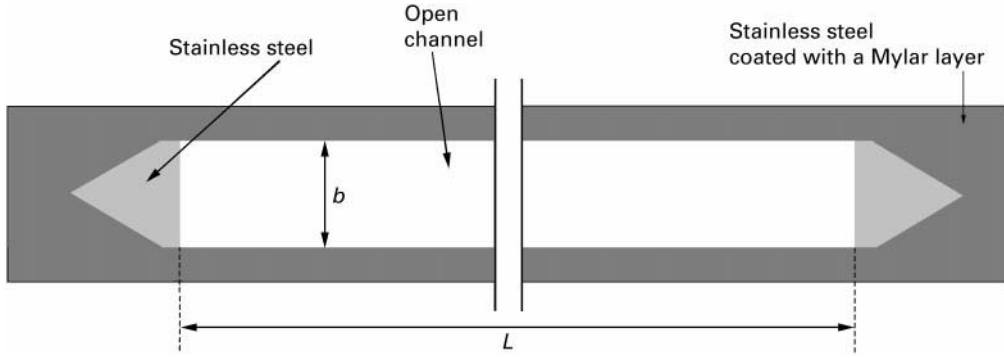


Figure 2 Upper view of the 'Splitter' used in the gravitational SPLITT cell.

$\dot{V}(t)$ can be obtained by combining eqns [1] and [3] as:

$$\dot{V}(t) = \dot{V}(a) - \dot{V}(a') = \dot{V}(b') - \dot{V}(b) \quad [4]$$

The separation of sample components is achieved, as previously described, by their different rates of transport toward the opposite wall B under the influence of the transverse field. It is important to be able to calculate the distance that a component has to travel. The ratio of sample flow rate $\dot{V}(a')$ to the total flow rate \dot{V} defines the position of the ISP as distance w_a , from wall A:

$$\frac{\dot{V}(a')}{\dot{V}} = 3\frac{w_a^2}{w^2} - 2\frac{w_a^3}{w^3} \quad [5]$$

The feed stream is then confined to the lamina thickness w_a , between wall A and the ISP.

By assuming that, during their residence in the SPLITT cell, the particles are driven from wall A to wall B at constant velocity U , the volumetric flow rate $\Delta\dot{V}$ of the lamina traversed by a particle is simply given by

$$\Delta\dot{V} = bLU \quad [6]$$

which contains the physical dimensions of the channel b , and L (length); U is the velocity of the induced transverse transport. In fact, a number of different driving forces have been utilized to implement CSF: gravitational, centrifugal, magnetic, electrical. U assumes different expressions depending on the field inducing the transverse transport, i.e.

$$U_{\text{gravitational}} = \frac{gd^2|\Delta\rho|}{18\eta_o} \quad [7]$$

$$U_{\text{centrifugal}} = \frac{\omega^2 rd^2\Delta\rho}{18\eta_o} \quad [8]$$

$$U_{\text{magnetic}} = \frac{\Delta\chi\Delta H^2 d}{48\eta_o} \quad [9]$$

$$U_{\text{electric}} = \mu E \quad [10]$$

where d is the particle diameter (assumed spherical), $\Delta\rho$ is the difference between particle density ρ_s (compact particles) and carrier density ρ_l , η_o is the viscosity of the carrier, g is the acceleration of gravity (earth field eqn [7]); ω is the angular velocity (rad s^{-1}) and r is the radius of the rotation (centrifugal acceleration eqn [8]); $\Delta\chi$ is the difference between the magnetic susceptibilities of the particles, χ_p , and the carrier, χ_l , and ΔH is the drop in magnetic field strength (eqn [9]); μ is the electrophoretic mobility and E is the electric field strength (eqn [10]). In some cases, experimental studies have been based on diffusive transport or by using hydrodynamic lift forces (which can be used in unique ways because of their nonuniformity).

In order to settle whether particles exit the channel through outlet a or b, the relative values of $\Delta\dot{V}$ and $\dot{V}(t)$ are of critical importance. For a sample introduced close to the ISP, particles exit from outlet a if:

$$\Delta\dot{V} \leq \dot{V}(t) \quad [11]$$

and from outlet b if:

$$\Delta\dot{V} > \dot{V}(t) \quad [12]$$

In the case of a SPLITT cell operating under a gravitational field, the relation which allows one to set the diameter cutoff of a spherical solid particle can be obtained by combining eqns [4], [6] and [7]. In fact, if $\dot{V}(t) = \Delta\dot{V}$ and:

$$\Delta\dot{V} = \frac{bLgd^2|\Delta\rho|}{18\eta_o} \quad [13]$$

then the diameter at which 50% of the particles exit outlet b is called the cutoff diameter d_c , expressed as:

$$d_c = \sqrt{\frac{18\eta_0(\dot{V}(a) - 0.5\dot{V}(a'))}{bL\Delta\rho g}} \quad [14]$$

in which only half of $\dot{V}(a')$ is considered (cf. eqn [4]). Once d_c has been chosen for a given channel, the difference between $\dot{V}(a)$ and $0.5\dot{V}(a')$ is set according to eqn [14]. However, the two constituents flow rates $\dot{V}(a)$ and $\dot{V}(a')$ are not uniquely defined by this equation, but some criteria useful for setting the flow rates are available in the optimization of SPLITT operations literature. In general, in order to obtain a separation with a good resolution, the practical rule which states the following necessary but not sufficient condition:

$$\dot{V}(b') \gg \dot{V}(a') \quad \text{or} \quad \dot{V}(a) \gg \dot{V}(b) \quad [15]$$

can be followed. This condition ensures that regions I and II will be narrow, which automatically increases the transport region, i.e. the cell space in which the separation process occurs. For maximum resolution, typical experimental conditions, are chosen to obtain a $\dot{V}(a')/\dot{V}(t)$ ratio within 0.1–0.3. From a theoretical point of view, the high resolution in the operative *transport mode* is, as already stated, contingent on compression of the feed sub-stream, a' , into a thin lamina near wall A, and the sharpness of the separation, as in chromatography, can be judged by the number N of the theoretical plates generated during transport. Generally, for field (gravitational) driven migrations, the effective N is given by the ratio of two energies:

$$N = \frac{Fw_t}{2kT} = \frac{\pi d^3 \Delta\rho g w_t}{12kT} \quad [16]$$

where F is the force on the particle inducing its transport, w_t the length of the transport path, and kT the thermal energy. Generally values of $N \geq 10^2$ are required to assure achievable resolution, and each type of macromolecule or particle should be checked against this criterion.

Resolution in SF can be related to channel flow rates, defining an index which measures the relative breadth of the unresolved region. It has been demonstrated that for sedimentation particles the equation of the resolving power has the following form:

$$\frac{d_1}{\Delta d} = \frac{d_1}{d_1 - d_0} \cong 2 \frac{\dot{V}(a)}{\dot{V}(a')} \quad [17]$$

where d_0 and d_1 are respectively the diameters of the particles exiting from a and b. The particles falling between these two sizes (d_1 and d_0), which are not fully resolved, exit from both outlets in different proportions, so the difference should be small. According to eqn [17] the ratio of $\dot{V}(a)$ to $\dot{V}(a')$ allows control of the range of unresolved particles which exit both outlets a and b.

Specific Applications

Determination of the Diffusion Coefficient D

CSF and ASF can be successfully applied to the separation of macromolecules such as proteins and liposomes. The transport region in this case is seen as a diffusion barrier, which acts as a dialysis membrane. In order to be able to determine the diffusion coefficient D , an important parameter useful for characterization of the sample components, the theory has to be looked at in a deeper way, with equations which explicitly contain D .

If a component enters inlet a' as a steady stream and its transport through the SPLITT system is governed by the simultaneous displacements of diffusion and parabolic flow, mass conservation requires that:

$$\frac{\partial c}{\partial t} = -v(x)\frac{\partial c}{\partial z} + D\left(\frac{\partial^2 c}{\partial x^2} + \frac{\partial^2 c}{\partial z^2}\right) \quad [18]$$

$\partial c/\partial t$ is the rate of change of concentration at an arbitrary point within the channel, x is the transverse distance into the cell measured from wall A, z is the distance into the channel along the length measured from the inlet splitter and v is the local stream velocity. In order to simplify eqn [18], it can be observed that all transverse transport in the channel occurs by diffusion and that all the components are transported along the cell (z -direction) by convection, so that the diffusion term ($D\partial^2 c/\partial z^2$) can be neglected.

Moreover, if the system operates in CSF mode, the component concentrations throughout the cell will attain a steady state, i.e. $\partial c/\partial t = 0$, so that eqn [18] reduces to:

$$\frac{\partial c}{\partial z} = \frac{D}{v(x)}\left(\frac{\partial^2 c}{\partial x^2}\right) \quad [19]$$

where $c(x, z)$ is subject to the boundary conditions:

$$\begin{aligned} c(x, 0) &= c_0 & \text{for } 0 \leq x \leq w_a \\ c(x, 0) &= 0 & \text{for } w_a \leq x \leq w \\ \partial c/\partial x &= 0 & \text{for } x = 0 \text{ and } x = w \text{ at all } z \end{aligned}$$

In order to calculate D , a dimensionless diffusion time $\tau_D = Dt^\circ/w^2$ has been developed. The parameters t° and w^2 are known because w is fixed by the geometry of the channel and t° is the elution time of a species dispersed in the total volume of the channel and is related to the total flow rate \dot{V} by:

$$t^\circ = \frac{V^\circ}{\dot{V}} = \frac{bLw}{\dot{V}} \quad [20]$$

where V° is the cell void volume expressed as a product of channel dimensions b , L and w . The dimensionless time parameter t° is thus related to D , \dot{V} , and the channel dimensions by:

$$\tau_D = \frac{Dt^\circ}{w^2} = \frac{DbL}{w\dot{V}} \quad [21]$$

Consequently D is given by:

$$D = \frac{w\dot{V}\tau_D}{bL} \quad [22]$$

This equation is used to obtain experimental D values, once τ_D is found. The total procedure requires the following steps: (i) to compute theoretically the concentration profile $c(x, L)$ over the lateral coordinate x at outlet ($z = L$) by using the Crank-Nicolson numerical method. In this way, the retrieval of a component at each outlet substream F_a (in i) and F_b (in ii) can be calculated from $c(x, L)$; (ii) to construct a graph of F_a versus τ_D for different $\dot{V}(a)/\dot{V}$ ratios; (iii) to determine experimentally the retrieval factor at outlet sub-stream a (F_a) from the relative strength of the detector signal (this value depends on the flow ratio $\dot{V}(a)/\dot{V}$ used in the experiment); (iv) to compute the correspondent τ_D value from the graph F_a versus τ_D by finding the correspondence between the experimental and theoretical F_a values; (v) to use eqn [22] to calculate D using the τ_D value, and the geometrical dimensions b , L , w and \dot{V} .

Effect of Particle Shape and Density in the Gravitational SPLITT

The SPLITT cell has been largely applied for the separation of environmental samples. Since the natural matter particles have different properties (porosity, density, shape), the basic SPLITT equations have to be revised to fit the relevant particle properties.

The basic relationship for the SPLITT cell, previously derived (see eqn [6]) can be written as:

$$\Delta\dot{V} = \dot{V}(t) = bLU_{\text{gravitational}} \quad [23]$$

By recalling the basic properties of the sedimentation process different expressions can be obtained, which contain the density parameter. During the SPLITT fractionation, under a gravitational field, the sample components are subject to two forces: the gravitational force $F_g = m_{\text{eff}}g$ and the frictional force $F_f = fU$ (m_{eff} is the effective mass, and f the friction coefficient). Usually, the stationary state is established very rapidly and the two forces balance each other out and thus:

$$U = m_{\text{eff}} \frac{g}{f} \quad [24]$$

Spherical particles In the case of compact spherical particles, by assuming that the particles do not undergo any shrinking or swelling $m_{\text{eff}} = m - m_b$ or $m_{\text{eff}} = V_s\rho_s - V_s\rho_l$, where m is the real mass and m_b the buoyant mass while V_s and ρ_s are, respectively, the volume and density of the particle and ρ_l the density of the liquid. More explicitly

$$m_{\text{eff}} = \frac{1}{6} \pi d^3 |\Delta\rho| \quad [25]$$

The $||$ accounts for positive or negative mass values in eqn [25] corresponding, respectively, to a falling or a floating particle. The friction coefficient f can be expressed by Stokes law $f = 3\pi\eta d$, where η is the viscosity of the suspension fluid, which can be approximated by the carrier viscosity, η_0 . By combining eqns [23], [24] and [25] one obtains the classical expression (see eqn [13]):

$$\dot{V}(t) = \frac{bLgd^2|\Delta\rho|}{18\eta_0} \quad [26]$$

In the case of porous particles, porosity is defined as:

$$\varepsilon = \frac{V_p}{V_s + V_p} = \frac{V_p}{V_{\text{tot}}^p} \quad [27]$$

where V_p is the volume of the pore, V_s the volume of the solid and V_{tot}^p the total volume of the particle. Then eqn [25] changes into:

$$m_{\text{eff}} = \frac{1}{6} \pi d^3 (1 - \varepsilon) |\Delta\rho| \quad [28]$$

and the correspondent eqn [26] into:

$$\dot{V}(t) = \frac{bLgd^2(1 - \varepsilon)|\Delta\rho|}{18\eta_0} \quad [30]$$

The porosity can be expressed also in terms of ‘apparent density’:

$$\rho_{\text{app}} = (1 - \varepsilon)\rho_s + \varepsilon\rho_l \quad [31]$$

from which the differential apparent density is defined as:

$$\Delta\rho_{\text{app}} = \rho_{\text{app}} - \rho_l \quad [32]$$

By combining $\Delta\rho = \rho_s - \rho_l$ with eqns [31] and [32] one has:

$$\Delta\rho_{\text{app}} = (1 - \varepsilon)\Delta\rho \quad [33]$$

which can be substituted in eqn [30].

When the ‘mass porosity’ is available:

$$p = \frac{V_p}{m} \quad [34]$$

where m is the real mass of the particle, i.e. $m = V_s\rho_s$ and by using eqn [27] one can show that:

$$\left(\frac{1}{p\rho_s + 1}\right) = (1 - \varepsilon) \quad [35]$$

which gives:

$$\dot{V}(t) = \frac{bLgd^2|\Delta\rho|}{18\eta_o} \left(\frac{1}{p\rho_s + 1}\right) \quad [36]$$

Alternatively, one can employ the ‘bulk density’, which is the ratio between the amount of the porous material, m_{tot} , and the total volume occupied by the packed particles V_{tot} including both the inter-particle volume, V_{ex} , the particle volumes, V_p^{tot} (total volume of the pores) and V_s^{tot} (total solid volume):

$$\rho_{\text{bulk}} = \frac{m_{\text{tot}}}{V_p^{\text{tot}} + V_s^{\text{tot}} + V_{\text{ex}}} = \frac{m_{\text{tot}}}{V_{\text{tot}}} \quad [37]$$

In this instance, both the ρ_{bulk} and ε_{ex} depend on the degree of packing. The relative apparent density, $\Delta\rho_{\text{app}}$ can be obtained by combining eqns [33] and [37]:

$$\Delta\rho_{\text{app}} = \frac{\rho_{\text{bulk}}}{\rho_s(1 - \varepsilon_{\text{ex}})} \Delta\rho \quad [38]$$

From eqn [33] it is apparent that, in this case, one must know the value of ε_{ex} under the same experimental conditions which ρ_{bulk} was determined. Lacking this information, it is only possible to make a rough estimate of $\Delta\rho_{\text{app}}$.

Nonspherical particles There are two main effects to be accounted for with nonspherical particles: the first is related to the particle volume expression and the second to Stokes Law. The parameter d contained in eqn [7] has to be changed depending on the kind of data available.

The first effect is accounted for by using the volume equivalent diameter, i.e. the diameter of a sphere having the same particle volume V_{sp} , i.e. $d_v = \sqrt[3]{(6V_{\text{sp}}/\pi)}$ instead of the sphere diameter, d . This quantity sometimes can be related to true geometrical dimension of the particle if its geometry is known.

An irregular shape affects the behaviour of the particle while it is moving within the fluid. Stokes Law takes account of this by substituting the diameter d with the ‘drag diameter’, i.e. the diameter of a sphere having the same resistance to the motion within the fluid

$$f = 3\pi\eta_o d_d \quad [39]$$

In order to conclude this section, an appropriate combination of all the above cases is necessary for irregular porous particles.

List of Symbols

a	= aspect ratio
b	= width of the SPLITT channel
d	= diameter of the sphere
d_c	= cutoff diameter
d_d	= drag diameter
d_v	= diameter of an equivalent sphere
D	= diffusion coefficient
E	= electrical field
f	= frictional coefficient
F_a	= retrieval of a component from outlet a
F_b	= retrieval of a component from outlet b
F_g	= gravitational force
F_f	= frictional force
g	= gravity acceleration
h	= thickness of the transport layer
h_c	= high of a cylindrical particle
L	= length of the SPLITT channel
m	= real mass of a particle
m_b	= mass corrected for buoyancy
m_{eff}	= effective mass
m_{tot}	= total mass of all particles present in the container
p	= mass porosity
r	= radius of rotation
t_r	= crossing time, i.e. the time a particle takes to pass through the cross sectional area bh in the h -direction.

U	= particle migration velocity
\bar{v}	= mean fluid velocity
v_{\max}	= maximum fluid velocity
\dot{V}	= total volumetric flow rate through cell
$\dot{V}(a')$	= volumetric flow rate at outlet a'
$\dot{V}(b')$	= volumetric flow rate at outlet b'
$\dot{V}(a)$	= volumetric flow rate at inlet a
$\dot{V}(b)$	= volumetric flow rate at inlet b
$\dot{V}(t)$	= volumetric flow rate of the transport region
V_{ex}	= external volume between particles
V_{p}	= pore volume of a particle
$V_{\text{p}}^{\text{tot}}$	= total pore volume for all the particles
V_{s}	= volume of the solid part of a particle
$V_{\text{s}}^{\text{tot}}$	= total solid volume for all the particles
V_{Sp}	= volume of a sphere
V_{tot}	= total volume occupied by all particles present in the container
$V_{\text{tot}}^{\text{p}}$	= total volume of a particle
w	= thickness of the SPLITT channel
$w_{a'}$	= thickness of the fluid lamina between wall A and ISP
w_t	= thickness of the transport region
χ_l	= magnetic susceptibility of the carrier
χ_p	= magnetic susceptibility of a particle
ε	= internal porosity
η	= suspension viscosity
η_o	= carrier viscosity
μ	= electrophoretic mobility
ρ_{app}	= apparent density
ρ_{bulk}	= bulk density
ρ_l	= density of the liquid
ρ_s	= density of the spherical particle
ω	= angular velocity
τ_D	= dimensionless diffusion time

See also: **II/Particle Size Separation:** Field Flow Fractionation: Electric Fields; Theory and Instrumentation of Field Flow Fractionation. **III/Polymers:** Field Flow Fractionation.

Further Reading

- Allen T (1981) *Particle Size Measurement*, 3rd edn. London: Chapman and Hall.
- Contado C, Dondi F, Beckett R and Giddings JC (1997) Separation of particulate environmental samples by SPLITT fractionation using different operating modes. *Analytica Chimica Acta* 345: 99–110.
- Contado C, Riello F, Blo G and Dondi F (1999) Continuous split-flow thin cell fractionation of starch particles. *Journal of Chromatography A* 845: 303–316.
- Dondi F, Contado C, Blo G and Martin SG (1988) SPLITT cell separation of polydisperse suspended particles of environmental interest. *Chromatographia* 48: 643–654.
- Fuh CB and Giddings JC (1995) Isolation of human blood cells, platelets, and plasma proteins by centrifugal SPLITT fractionation. *Biotechnology Progress* 11: 14–20.
- Fuh CB and Giddings JC (1997) Separation of submicron pharmaceutical emulsion with centrifugal split-flow thin (SPLITT) fractionation. *Journal of Microseparation* 9: 205–211.
- Fuh CB and Chen SY (1998) Magnetic split-flow thin fractionation: new technique for separation of magnetically susceptible particles. *Journal of Chromatography A* 813: 313–324.
- Fuh CB, Levin S and Giddings JC (1993) Rapid diffusion coefficient measurements using analytical SPLITT fractionation: application to proteins. *Analytical Biochemistry* 208: 80–87.
- Levin S, Myers MN and Giddings JC (1989) Continuous separation of proteins in electrical split-flow thin (SPLITT) cell with equilibrium operation. *Separation Science and Technology* 24(14): 1245–1259.
- Provder T (ed.) (1991) *Particle Size Distribution. II. Assessment and Characterization*. ACS Symposium Series 472. Washington DC: American Chemical Society.
- Yong J, Kummerow A and Hansen M (1997) Preparative particle separation by continuous SPLITT fractionation. *Journal of Microseparation* 9: 261–273.
- Zhang J, Williams PS, Myers MN and Giddings JC (1994) Separation of cells and cell-sized particles by continuous SPLITT fractionation using hydrodynamic lift forces. *Separation Science and Technology* 29(18): 2493–2522.

Theory and Instrumentation of Field Flow Fractionation

J. Janča, Université de la Rochelle, La Rochelle, France

Copyright © 2000 Academic Press

Principle

Field-flow fractionation (FFF) is one of the important analytical methodologies, suitable for the separation and characterization of particles in the submicron

and micron ranges. The effective field generates the flux of the separated particles and forms a concentration gradient of each particular species across the ribbon-shaped separation channel. The concentration gradients are counter-balanced by a diffusion flux. At equilibrium, a stable concentration distribution of each particular species is established in the direction across the channel. Simultaneously, a flow velocity profile is formed across the channel due to the viscous

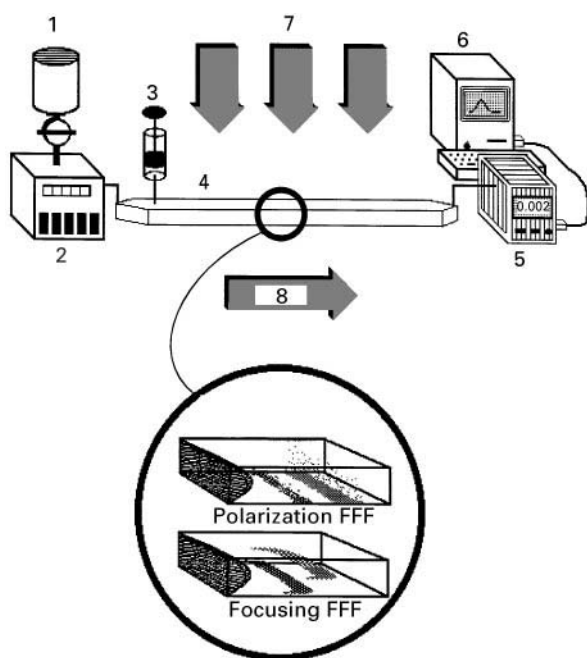


Figure 1 Schematic representation of the general principle and of the experimental arrangement of FFF: (1) carrier liquid reservoir; (2) pump; (3) injector; (4) separation channel; (5) detector; (6) computer; (7) external field; (8) hydrodynamic flow. Detail shows the schematic representation of two fundamental separation mechanisms: polarization FFF and focusing FFF.

drag in the longitudinal flow of the carrier liquid. As a result, each particle is carried along the channel with a velocity corresponding to an instantaneous position of the particle within the flow velocity profile. The carrier liquid thus elutes each species with a mean velocity which corresponds roughly to the position of the centre of gravity of the field-induced concentration distribution across the channel of that species. This principle is schematically demonstrated in Figure 1.

The separation is usually governed by the differences in size of the separated components of a poly-disperse sample. If the appropriate relationship between the retention parameters and the size of the particles is known or found empirically by using a suitable calibration procedure, the fractograms can be used to calculate the particle size distribution (PSD) and the average values of the particle size of the fractionated species. However, the intensive properties (such as the electrical charge, density, etc.) can influence the separation based on size differences.

Theory of Separation

Two distinguished separation mechanisms, either *polarization* or *focusing*, govern the separation. The separated particles can be differently compressed to

the accumulation wall of the channel according to their sizes or focused at different levels across the channel according rather to an intensive property (see Figure 1).

The polarizing field force, F , and the velocity of the field-induced migration of the fractionated particles, U , are usually constant and independent of the position in the direction of the field action:

$$F \neq 0 \text{ and } U \neq 0 \text{ within } 0 < x < w$$

where w is the thickness of the FFF channel in the direction of the field action (x -axis); $x = 0$ is situated at the accumulation wall of the channel. The steady-state concentration distributions of the sample components across the channel are exponential:

$$c_i(x) = c_i(0) \exp\left(-\frac{x}{l_i}\right)$$

where $l_i = D_i/U_i$ is the mean layer thickness, D_i is the diffusion coefficient and c_i is the concentration of the i th species. Larger particles are usually concentrated more closely to the accumulation wall. As a result, the order of the elution is from the small species to larger ones.

The focusing field force and the corresponding velocity U are position dependent:

$$\begin{aligned} F &= f(x), \quad U = f(x) \quad \text{within } 0 < x < w \\ F(x) &= 0, \quad U(x) = 0 \quad \text{for } x = x_{\max}, \quad 0 < x_{\max} < w \end{aligned}$$

The coordinate x_{\max} corresponds to the position at which the concentration distribution of a focused sample is maximal. Each sample component is focused around its proper x_{\max} position. The steady-state concentration distribution is close to the Gaussian distribution:

$$c(x) = c_{\max} \exp\left[-\frac{1}{2kT}\left(\frac{dF(x)}{dx}\right)_{x=x_{\max}}(x-x_{\max})^2\right]$$

where k is the Boltzmann constant and T is the temperature. In some cases the polarization and the focusing mechanisms can act simultaneously.

As mentioned above, a real separation channel is usually ribbon-shaped. However, two parallel infinite planes represent a good approximation of this form. The flow velocity profile established in such a hypothetical channel is parabolic under isoviscous conditions:

$$v(x) = \frac{\Delta P x(x-w)}{2L\mu}$$

where $v(x)$ is the linear velocity of a flow streamline at the position x , ΔP is the pressure drop along the channel of length L , and μ is the viscosity of the carrier liquid.

To describe conveniently the retention of the separated particulate species, the dimensionless retention ratio R is defined:

$$R = \frac{\int_0^w c(x)v(x) dx \int_0^w dx}{\int_0^w c(x) dx \int_0^w v(x) dx}$$

R is the ratio of the average velocity of a retained sample component divided by the average velocity of the carrier liquid. The integration gives the relationship for the polarization FFF

$$R = 6\lambda \left(\coth\left(\frac{1}{2\lambda}\right) - 2\lambda \right)$$

where $\lambda = l/w$. The analogous approximate relationship for the focusing FFF is:

$$R = 6 (\Gamma_{\max} - \Gamma_{\max}^2)$$

where $\Gamma_{\max} = x_{\max}/w$, is the dimensionless coordinate of the maximal concentration of the focused zone. R can be experimentally determined as the ratio of the retention volume (or the retention time) of an unretained sample component (equal to the volume of the channel) divided by the retention volume (retention time) of the retained sample component. The simple and known relationship between the λ and the particle size make it possible to calculate the PSD from the experimental retention data.

Each fractionation is based on transport processes which lead to the formation of the concentration gradients. From the thermodynamic point of view, the general entropic tendency of a closed system is to erase such gradients by molecular motion. As a result, the spreading of the zones due to dispersion processes occurs. The zone spreading can be quantitatively described by the height equivalent to a theoretical plate H :

$$H = L \left(\frac{\sigma}{V_R} \right)^2$$

where V_R is the retention volume and σ is the standard deviation of the zone of uniform size particles. The elution curve (fractogram) of a polydisperse sample thus reflects the contribution of the spreading processes superposed over the fractionation according to the PSD.

In order to calculate a true PSD from the experimental raw fractogram, a correction for the zone

spreading should be applied. It is based on the deconvolution of an experimental fractogram $h(V)$ of a polydisperse particulate sample which is a superposition of the true PSD $g(Y)$ and the spreading function $G(V, Y)$ representing the zone of uniform particles having the elution volume Y :

$$h(V) = \int_0^\infty g(Y)G(V, Y) dY$$

where V and Y are then the elution volumes. This equation, called the Tung integral equation, is the basis for all well-known correction methods and can be solved analytically under the condition that the spreading function is uniform. In this case, the convolution integral to be solved is:

$$h(V) = \int_0^\infty g(Y)G(V - Y) dY$$

In a number of practical cases, the spreading function can be approximated by the normal Gaussian function. The application of the correction of an experimental fractogram is demonstrated in **Figure 2**.

The true PSD can be expressed as a number of the particles of a given diameter n_i relative to the number of all the particles in the sample:

$$N_i = \frac{n_i}{\sum_0^\infty n_i}$$

or as the mass of the particles m_i of a given diameter d_i relative to the total mass of the sample:

$$M_i = \frac{m_i}{\sum_0^\infty m_i}$$

The PSD can be used further to calculate various average particle sizes such as the mass average particle diameter:

$$\bar{d}_m = \frac{\sum_0^\infty m_i d_i}{\sum_0^\infty m_i} = \frac{\sum_0^\infty h_i d_i}{\sum_0^\infty h_i}$$

or the number average particle diameter:

$$\bar{d}_n = \frac{\sum_0^\infty n_i d_i}{\sum_0^\infty n_i} = \frac{\sum_0^\infty h_i}{\sum_0^\infty h_i/d_i}$$

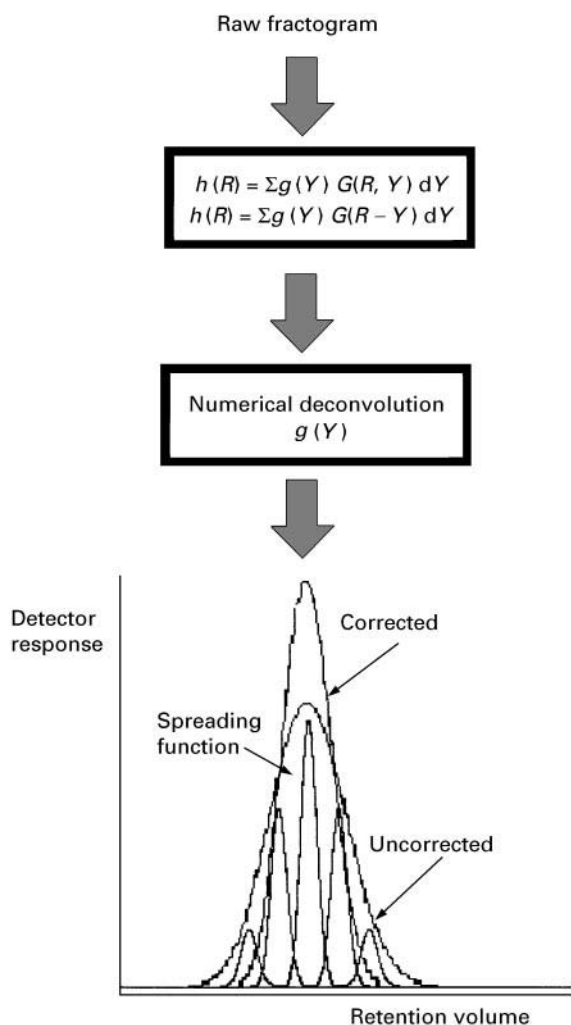


Figure 2 Schematic representation of a procedure for the treatment of a raw experimental fractogram to correct for zone broadening.

where h_i is the normalized detector response to the i th particle diameter. The polydispersity of the fractionated sample can be characterized, for example, by the index of polydispersity:

$$I = \frac{\bar{d}_m}{\bar{d}_n}$$

The above basic theory and data treatment can be applied independently of a particular FFF method or technique.

Instrumentation

Polarization FFF

In particle size separations by FFF, the nature of the applied field (physical or chemical forces) determines

each particular method or technique of polarization FFF and, consequently, the appropriate instrumentation. The most important polarization FFF methods at the present time are:

- sedimentation FFF
- flow FFF
- electric FFF
- thermal FFF

The basic experimental devices as well as specific instrumentation are described here for each particular FFF method or technique.

Independent of the method or technique, all FFF apparatuses are composed of a system of solvent delivery (reservoir, pump), injector sample (injection valve, syringe-septum, etc.), separation channel (different construction for each method), detector (refractive index detector, spectrophotometer, molar mass detector, etc.) and a data acquisition and treatment system (computer). With the exception of the FFF separation channel, all other components, and the system as a whole, are practically the same as a conventional liquid chromatography system.

Schematic representation of the separation channel for *sedimentation FFF* is shown in **Figure 3(A)**. The separation channel is coiled inside a centrifuge rotor. A delicate part of this separation unit is the rotating seal which must permit the flow-through of a carrier liquid and the connection to the injector at the entry to the channel proper and of a detector at the exit. However, this technical problem is solved and the rotors for sedimentation FFF are commercially available. On the other hand, a home-built solution is also possible providing that some technical skill is available.

If the particles to be separated are relatively large or dense and, consequently, the gravitational force is enough to generate the formation of sufficiently strong concentration gradients, the construction of the separation channel is much simpler, as shown in **Figure 3(B)**. In this case, the channel is composed of two sandwiched glass plates, one of them is provided with holes and capillaries for carrier liquid entry and exit and a thin foil in which the channel proper is cut. The whole channel must be positioned horizontally to avoid casual parasite convections which could cause the separation to deteriorate.

The channel for *flow FFF* is schematically demonstrated in **Figure 4(A)**. It is formed between two parallel, semipermeable membranes fixed on porous supports. The cross-flow of the carrier liquid is superposed perpendicularly to the flow of the carrier liquid in a longitudinal direction inside the channel. The cross-flow acts as an external field of hydrodynamic forces which generate a uniform flux of all particles.

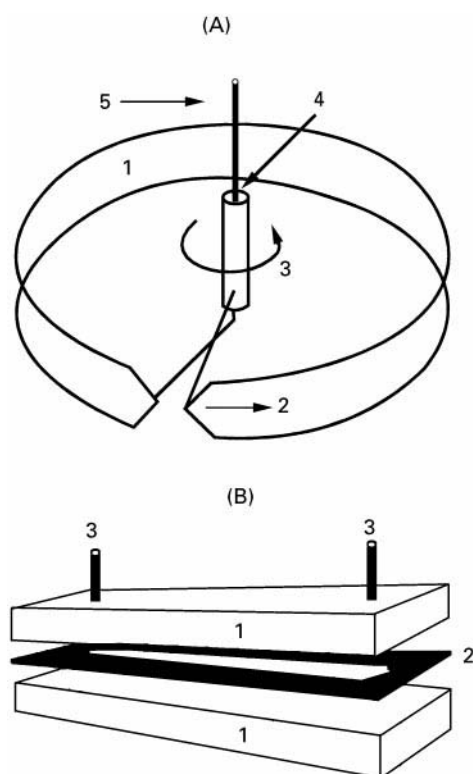


Figure 3 Simplified schemes of the construction of the sedimentation FFF channels used in a centrifuge and in natural gravitational field. (A) Sedimentation FFF channel: (1) channel; (2) direction of the flow; (3) rotation; (4) flow inlet; (5) flow outlet. (B) Gravitational FFF channel: (1) channel walls; (2) foil spacer; (3) inlet and outlet.

The carrier liquid passes through the membranes but the separated particles should not, due to the conveniently chosen porosity of the membranes. The uniformity of the cross-flow is, however, not necessary to achieve high performance separation. If only one of the main channel walls is semi-permeable, a non-uniform hydrodynamic field is generated in such an asymmetrical flow FFF channel. The dependence of the separation resolution on particle size in such a channel is different compared with a channel equipped with two semi-permeable walls, but high performance particle size separation is also achieved.

A classical type of rectangular cross-section channel has sometimes been substituted with a circular cross-section capillary with an overpressure applied inside or by applying an external cross-flow in a more standard manner, as shown in Figure 4(B). The simplicity of the construction of such a 'channel' is the main advantage of this configuration. The theoretical description of the separation is complex, however, and, moreover, the probability of the formation of parasite flows degenerating the separation is higher.

The channel for *electric* FFF is usually formed by semipermeable membranes as in flow FFF (see Figure 5). The reason for such a solution is to decouple the separation channel proper from the electrode chambers and thus to avoid the contamination of the channel by products of electrolysis (gas bubbles). However, channels of simpler construction in which the metal or graphite electrodes form the channel walls and thus are not decoupled from the separation space have been constructed and work quite well under carefully chosen experimental conditions. The channel for *thermal* FFF is constructed in such a manner to allow a temperature difference between two metallic bar walls with highly polished surfaces. The walls are separated by a spacer in which the channel proper is cut. The upper bar is heated by using appropriate electrical cartridges and the lower bar is cooled by circulating water. Both bars should be equipped with several holes to accommodate the thermocouples for temperature control. Schematic representation of a channel for thermal FFF is shown in Figure 6. In some cases, when the temperature of

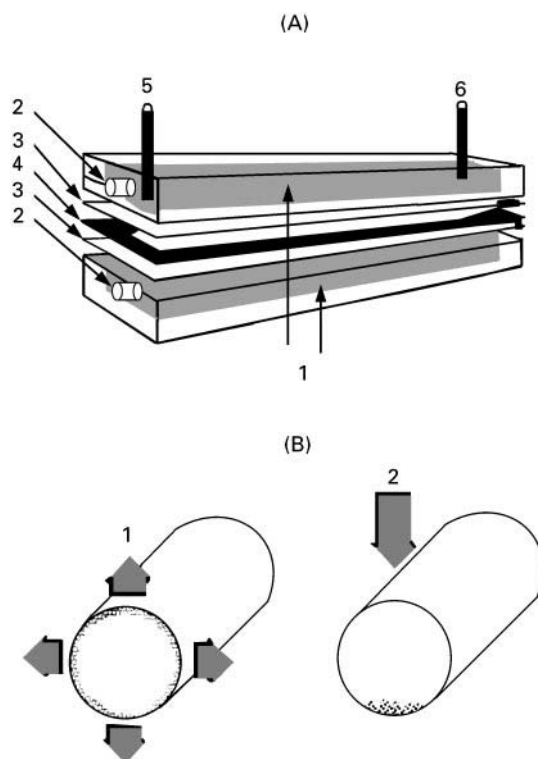


Figure 4 (A) Construction of a rectangular cross-section channel for flow FFF: (1) porous supports; (2) cross-flow inlet and outlet; (3) membranes; (4) foil spacer; (5) longitudinal flow inlet; (6) longitudinal flow outlet. (B) Circular capillary for flow FFF with: (1) overpressure applied from the inside; (2) cross-flow applied externally.

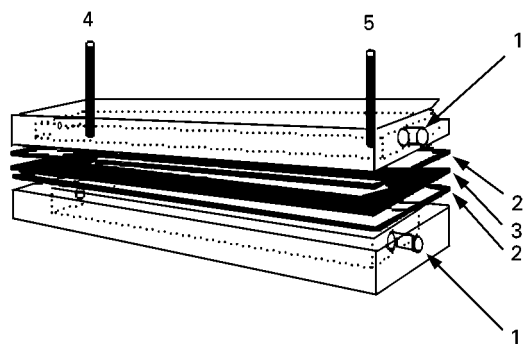


Figure 5 Construction of a channel for electric FFF: (1) electrodes and electrolyte inlet and outlet; (2) membranes; (3) foil spacer; (4) longitudinal flow inlet; (5) longitudinal flow outlet.

the heated wall is above the boiling point of the carrier liquid used, the channel must be sealed so as to operate under high-pressure conditions. The thickness of the channel can be as low as few micrometers which permits performing high-speed and high-resolution fractionations. The separation can be accomplished in just a few seconds.

Focusing FFF

Focusing FFF methods have been classified according to various combinations of the driving field forces and gradients:

- effective property gradient of the carrier liquid,
- cross-flow velocity gradient,
- lift forces,
- shear stress, and
- gradient of the non-homogeneous field action.

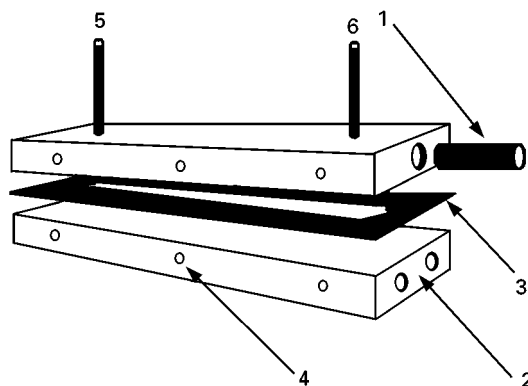


Figure 6 Construction of a channel for thermal FFF: (1) electric heating cartridge; (2) cooling liquid inlet and outlet; (3) foil spacer; (4) holes for thermocouples; (5) longitudinal flow inlet; (6) longitudinal flow outlet.

While this classification scheme is perfectly consistent with fundamental separation mechanisms and related driving forces, particular focusing FFF methods and techniques are more often called according to experimental procedure. The instrumentation will be described for each implemented focusing FFF method or technique.

The channels for sedimentation–flotation focusing field-flow fractionation (SFFFFF) or isoelectric focusing field-flow fractionation (IEFFFFF) are either of standard rectangular cross-section or of modulated cross-sectional permeability (for example, of trapezoidal or triangular cross-section), as shown in Figures 7(A) and (B). While the flow velocity profile in channels of rectangular cross-section are symmetrical (e.g. parabolic), the modulated cross-sectional permeability channels allow formation of flow velocity profiles which are not symmetrical. The advantage of these channels is that almost all zones focused symmetrically regarding the central longitudinal axis of the separation channel can be separated. If the flow velocity profile is symmetrical, the zones focused at the opposite sides regarding the central axis of the channel can be confused.

Both above-mentioned methods belong to the first category in which an effective property gradient of the carrier liquid represents the major driving force. The focusing in these cases can appear to be due to the effective property gradient of the carrier liquid in the direction across the channel combined with the primary or secondary transverse field.

It has been shown that the gradient of the effective property of the carrier liquid can be performed at the beginning of the channel. For example, the step density gradient can easily be formed by pumping the carrier liquids of various densities through several inlet capillaries into the channel. Such an arrangement can effectively be used for continuous preparative fractionation providing that the separation channel is also equipped with several outlet capillaries to continuously collect the fractions which are focused at different levels. Schematic representation of such a channel is shown in Figure 8.

The elutriation focusing field-flow fractionation (EFFFFF) method belongs to the category in which the focusing is due to the gradient of transversal flow velocity of the carrier liquid which opposes the action of the external field. The longitudinal flow of the carrier liquid is acting simultaneously. A trapezoidal cross-section as well as a rectangular cross-section channels can be used in this case. Schematic representation of such a channel for elutriation FFF is

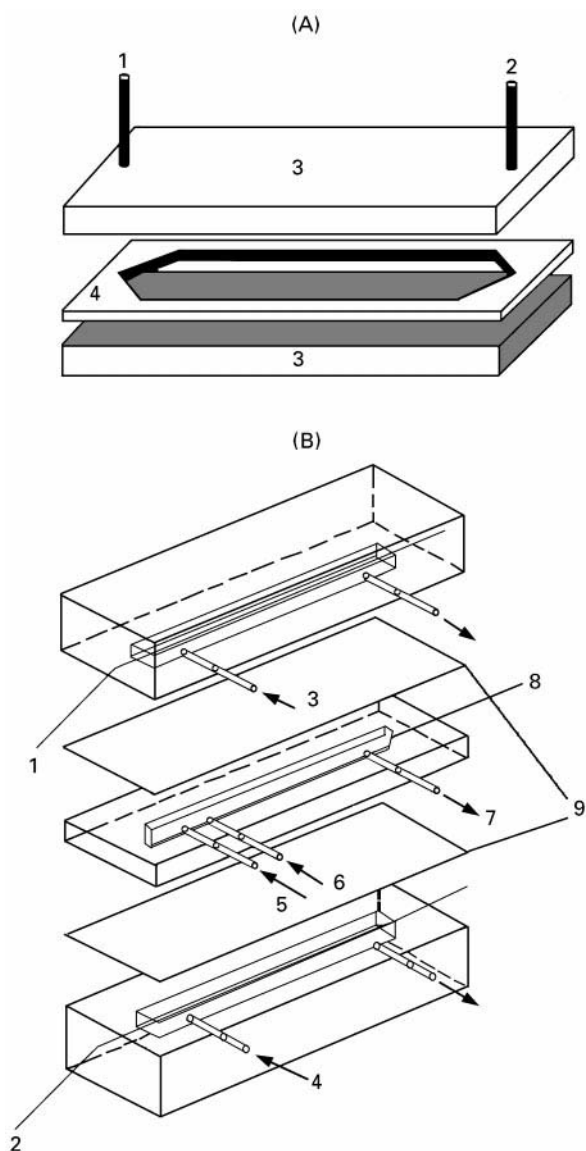


Figure 7 (A) Schematic representation of a channel for sedimentation flotation focusing FFF in coupled electric and gravitational fields: (1) flow in; (2) flow out; (3) electrodes forming the channel walls; (4) spacer. (B) Schematic representation of a trapezoidal cross-section channel for isoelectric focusing FFF: (1) Pt anode; (2) Pt cathode; (3) anolyte; (4) catholyte; (5) ampholyte; (6) sample; (7) to detector; (8) trapezoidal cross-section channel; (9) membranes.

shown in **Figure 9**. The channel shown has a trapezoidal cross-section which causes formation not only of a convenient, axially asymmetrical flow velocity profile but, providing the volumetric transversal flow-in and flow-out are equal, a linear velocity gradient is established across the channel. In combination with different constant velocities of different size-separated particles the conditions for the focusing phenomenon to appear are established.

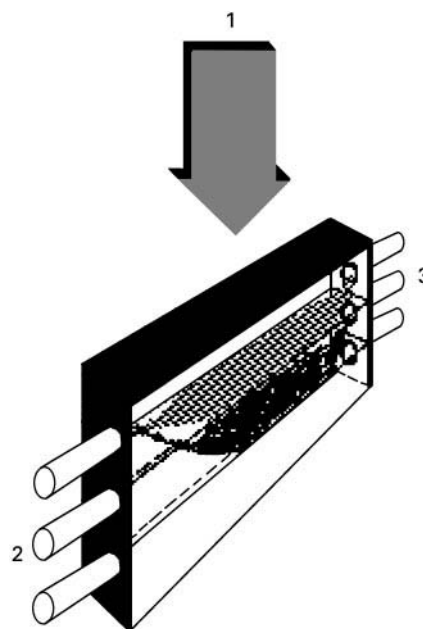


Figure 8 Continuous preparative channel for focusing FFF in preformed step density gradient: (1) gravitational field; (2) flow inlets; (3) flow outlets.

Very few experiments have been published on FFF exploiting the hydrodynamic lift forces at high carrier flow rates which, with the high shear gradient, result in the deformation of soft particles and their subsequent displacement and focusing. Similarly little has been published on FFF using a non-homogeneous high gradient external field. Although these methods can, in principle, use one of the types of channel described above for other focusing FFF methods, no experimental proof for this currently exists.

Conclusion

A large number and variety of homemade channels exist which confirms that in most cases, the construction of a channel is not extremely difficult.

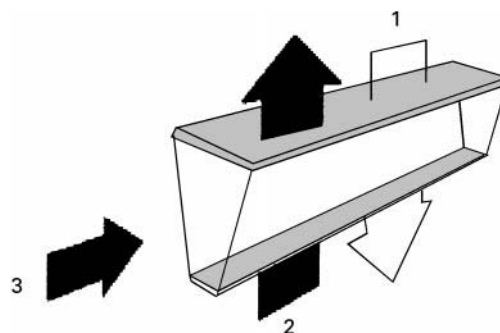


Figure 9 Schematic representation of a channel for elutriation focusing FFF: (1) field force; (2) cross-flow; (3) longitudinal flow.

However, commercial FFF apparatus is increasingly available which could further stimulate interest in applying this high performance separation methodology in routine laboratory practice.

See also: II/Particle Size Separation: Field Flow Fractionation: Electric Fields. III/Cells and Cell Organelles: Field Flow Fractionation.

Further Reading

Barth HG (ed.) (1984) *Modern Methods of Particle Size Analysis*. New York: John Wiley.

Janča J (1987) *Field-flow fractionation: analysis of macromolecules and particles*. New York: Marcel Dekker.

Janča J (1995) Isoperichoric focusing field-flow fractionation based on coupling of primary and secondary field action In: Provder T, Barth HG and Urban MW (eds) *Chromatographic Characterization of Polymers, Hyphenated and Multidimensional Techniques. Advances in Chemistry Series 247*. Washington DC: American Chemical Society.

Janča J (1999) Field-flow fractionation. In: Pethrick RA and Dawkins JV (eds) *Modern Techniques for Polymer Characterisation*. New York: John Wiley.

ACIDS



Gas Chromatography

G. Gutnikov and N. Scott, California State Polytechnic University, Pomona, CA, USA

Copyright © 2000 Academic Press

Introduction

The first separation of acids by gas chromatography (GC) coincides with the inception of GC itself. In 1952 James and Martin pioneered GC by demonstrating the separation of the C₁ to C₁₂ aliphatic acids on a stationary phase of silicone oil DC 550 containing stearic acid or H₃PO₄ and quantifying using a special titrimetric detector. Since then, the GC analysis of acids has been extended to a very wide variety of species and samples. To enable ready application of GC, the acids are usually converted to suitable volatile derivatives for resolution on efficient columns. As they are eluted they must be identified by an appropriate technique, the most definitive being mass spectrometry (MS). Various applications are presented in this article.

Derivatization

It was noted early on that separation of free acids is frequently hampered by their relatively low volatility, molecular association and, particularly, their adsorption on the stationary phase support with the resultant tailing, peak distortion and ghosting. Although special columns (FFAP, OV-351, SP-1000) have been developed since then for the separation of short and medium chain free (underivatized) aliphatic acids, the majority of carboxylic acids (especially those containing additional polar substituents) are insufficiently volatile for analysis by GC. Therefore, the carboxyl and other polar groups are usually converted to less polar derivatives to improve their chromatographic properties.

Carboxylic Acids

Both free and bound carboxyl groups are almost exclusively derivatized to volatile esters – predominantly silyl and methyl – by a variety of methods. These employ a number of silylation reagents, acid- and base-catalysed reactions, on-column pyrolysis,

diazomethane and other reagents. Each has its advantages, limitations and special applications.

Silyl esters Silylation is now one of the most extensively used techniques for esterifying free acids primarily because of its speed, convenience and the simultaneous derivatization of other polar functional groups containing an active hydrogen (–OH, –SH, –NH₂). The trimethylsilyl (TMS) group is the most commonly introduced substituent by the many silylating agents available, of which *N,O*-bis-(trimethylsilyl)trifluoroacetamide (BSTFA) is the most widely used. It reacts with all the common polar functionalities and yields volatile by-products that are usually eluted with the solvent. Even more volatile by-products are produced by substituted reagents, e.g. *N*-methyl-*N*-trimethylsilyltrifluoroacetamide (MSTFA), which are also more reactive toward the polar functional groups. Although all silylating reagents and their products are sensitive to moisture, considerably greater hydrolytic stability is exhibited by *t*-butyldimethylsilyl (TBDMS) derivatives that are best prepared with *N*-*t*-butyldimethylsilyl-*N*-methyltrifluoroacetamide (MTBSTFA), which can also serve as its own solvent. It yields excellent results with both volatile and nonvolatile carboxylic acids (Figure 1). A limitation of silylation is that bound acids such as lipids (triacylglycerols) are not converted and their derivatization to methyl (or other alkyl) esters is necessary.

Alkyl esters Methyl esters are most frequently prepared by acid-catalysed reactions with methanol. The principal advantage of this method is the concurrent esterification of free acids and the transesterification of bound ones. The most extensively used catalysts are BF₃, HCl and H₂SO₄, usually as 14%, 5% and 2% solutions, respectively. The reaction is fastest with BF₃, requiring the mixture to be boiled for 2 min for free acids and 30–60 min for lipids. With HCl and H₂SO₄ about twice the time is required. The higher concentration of BF₃ used compared to the other catalysts may be responsible not only for the faster reaction, but also for partial degradation of unsaturated acids and reported artefact formation. These problems can be reduced by prior saponification with methanolic KOH, followed by re-esterification of the free acids formed under mild conditions. Several official methods are based on this procedure.

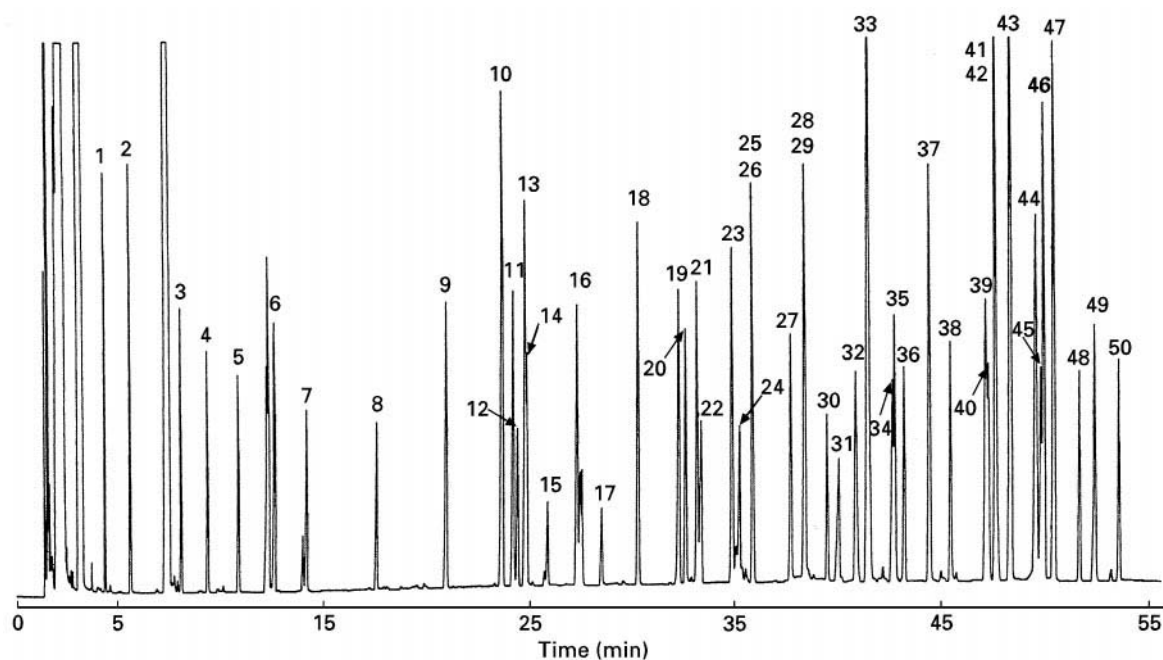


Figure 1 Chromatogram of a mixture of carboxylic acids as the *t*-butyltrimethylsilyl derivatives. GC conditions: 30 m \times 0.32 mm i.d., DB-1 fused-silica capillary column initially at 60°C for 2 min, then programmed to 280°C at 4°C min⁻¹; 0.8 L sample, injected with split ratio of 15 : 1; both injector and detector temperatures at 300°C; nitrogen as the carrier gas at 0.9 mL min⁻¹. Peaks: 1, Formic; 2, acetic; 3, propionic; 4, isobutyric; 5, butyric; 6, isovaleric; 7, valeric; 8, caproic; 9, enanthic; 10, benzoic; 11, caprylic; 12, lactic; 13, phenylacetic; 14, glycol; 15, oxalic; 16, pelargonic; 17, malonic; 18, capric; 19, succinic; 20, methylsuccinic; 21, undecanoic; 22, fumaric; 23, 5-phenylvaleric; 24, *p*-aminobenzoic; 25, lauric; 26, mandelic; 27, adipic; 28, 3-methyladipic; 29, tridecanoic; 30, phenyllactic; 31, hippuric; 32, myristic; 33, *p*-hydroxybenzoic; 34, malic; 35, suberic; 36, pentadecanoic; 37, vanillic; 38, palmitic; 39, syringic; 40, tartaric; 41, margaric; 42, α -resorcylic; 43, *p*-hydroxymandelic; 44, γ -resorcylic; 45, stearic; 46, homogentisic; 47, protocatechuic; 48, nonadecanoic; 49, citric; 50, arachidic acid. (Reproduced with permission from Kim KR, Hahn MK, Zlatkis A *et al.* (1989) Simultaneous gas chromatography of volatile and nonvolatile carboxylic acids as *tert*-butyltrimethylsilyl derivatives. *Journal of Chromatography* 468: 289.

Substituting microwave irradiation for conventional heating may substantially reduce reaction times and lipid degradation. Thus, using the BF₃-methanol reagent, a reaction time of 30 s sufficed for the transesterification of most lipids to their fatty acid methyl esters (FAMES) with less oxidation of the unsaturated species.

Base-catalysed reactions are used extensively for the transesterification of lipids because they proceed faster than those in acid media without degradation of the unsaturated fatty acids. However, they do not esterify free fatty acids. The most commonly used reagents are methanolic solutions of NaOCH₃ or KOH. Transmethylation of lipids is usually complete in 5 min at room temperature.

Strong organic bases can be used similarly and possess the great advantage of forming salts which, unlike their inorganic analogues, can be pyrolysed to methyl esters at the high temperatures of a GC injection port. This permits simple one-step determination of both free and bound acids. The organic bases that have been recommended for such

pyrolytic conversions include (*m*-trifluoromethyl-phenyl)-trimethylammonium, trimethylphenylammonium and trimethylsulfonium hydroxides. The latter reagent requires the lowest pyrolysis temperature and yields innocuous by-products. It is simply added to the sample solution, mixed and injected.

Esterification of free acids with diazomethane proceeds rapidly in high yield under mild conditions, with minimal side reactions. Special microequipment, reagents and procedures have been developed that allow its relatively safe handling despite its toxic and explosive nature. Other reagents of interest include alkyl chloroformates that can esterify free acids even in the presence of a considerable amount of water (40%). Another reagent, dimethylformamide dimethylacetal, can be simply mixed with the sample of acid and injected into the GC; the reaction occurs in the hot injection port. Silver or potassium salts of acids can be converted to esters with methyl iodide or sulfate. Many other reactions have been reported.

Short chain acids are frequently derivatized to higher esters with butanol or isopropanol and acid

catalysts in order to mitigate losses due to volatility and substantial water solubility. Higher diazoalkanes may also be used if the methyl esters are too volatile.

Enantiomers of optically active carboxylic acids have been separated following acid-catalysed esterification with a chiral alcohol such as *S*(+)-2-butanol, *R*(-)-2-octanol, or (-)-methanol or transesterification with sodium menthylate. Diastereometric esters have also been prepared from optically active acids by reaction with *O*(-)-menthyl-*N,N*-diisopropylisourea.

The above silyl and alkyl esters are most commonly detected by a flame ionization detector (FID). Greater sensitivity, however, can be achieved by forming halogenated silyl esters, e.g. chloromethyldimethylsilyl, and monitoring with an electron-capture detector (ECD). Similarly, very small amounts of volatile acids may be detected via their pentafluorobenzyl (PFB) esters with an ECD. Special derivatives for this detector include the 2-chloroethyl and trichloroethyl esters.

Other derivatives The silyl and alkyl esters described are generally also suitable for detection by MS. However, special derivatives are necessary for unsaturated fatty acids to prevent double-bond migration during fragmentation. The most widely used derivatives are those of 3-hydroxymethylpyridine (picolinyl) and 4,4-dimethyloxazoline (DMOX). Picolinyl esters must be prepared from the acid but DMOX derivatives can be prepared even from their esters.

Amino Acids

For amino acids, derivatization is indispensable for analysis by GC since they all exist in the zwitterion form. Some also contain other polar functionalities, including hydroxyl, thiol and imino groups. The different reactivities of these groups greatly complicate their concurrent derivatization. Silylation offers the best approach for a single-step attachment of the same tag to all these functional groups.

The most successful attempt to generate a single product is by silylation with MTBSTFA to form TBDMS derivatives. Reaction conditions (heating at 150°C for 2.5 h) were developed for the reproducible derivatization of amino acids in high yield. TMS derivatives of the common amino acids, except arginine, can also be prepared with BSTFA under similar conditions.

An alternative method of derivatization of amino acids entails first esterification and then acylation to produce various *N*-acyl alkyl esters (Figure 2). The most widely used of these combinations is the

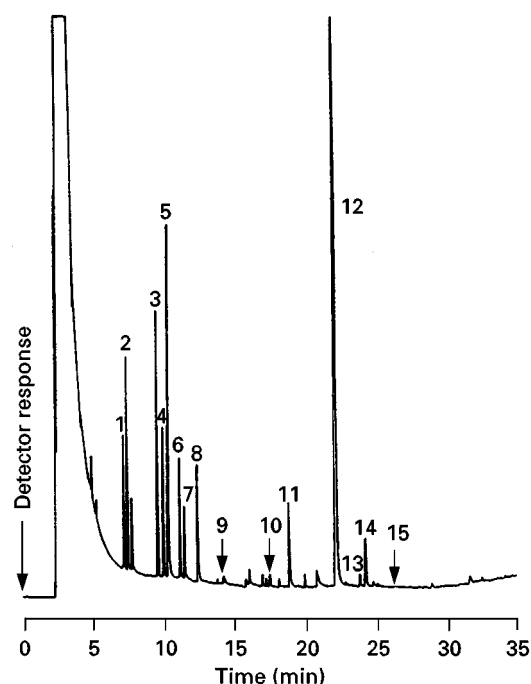


Figure 2 Separation of *N,O*-heptafluorobutyl amino acid isobutyl ester derivatives obtained from silkworm *t*-RNA after deacylation and analysed with FID. GC conditions: 25 m \times 0.4 mm i.d. capillary column coated with 5% Chromosorb R and 15% OV-101 SCOT column; carrier gas, hydrogen at a flow rate of 3 mL min⁻¹; make-up gas, nitrogen at a flow rate of 30 mL min⁻¹; hydrogen flow rate, 27 mL min⁻¹; air flow rate, 350 mL min⁻¹; temperatures: detector, 320°C; no inlet heater block; column, 80°C programmed at 4°C min⁻¹. Pulse interval, 15 μ s; attenuation, 2×10^2 ; sample size, 20 μ L. Peaks: 1, Alanine; 2, glycine; 3, valine; 4, threonine; 5, serine; 6, leucine; 7, isoleucine; 8, norleucine (l.s.); 9, proline; 10, methionine; 11, aspartic; 12, glutamic acid; 13, lysine; 14, tyrosine; 15, arginine. (Reproduced with permission from Chauhan J and Darbre A (1982) Determination of amino acids by means of glass capillary gas-liquid chromatography with temperature-programmed electron-capture detection. *Journal of Chromatography* 236: 151.

N-trifluoroacetyl-*n*-butyl ester (TAB) derivative. Esterification is performed by one of the methods described above and acylation by heating the dried product with trifluoroacetic anhydride. The selectivity of the NP detector can be exploited to monitor amino acids in the presence of interfering matrices, particularly lipids.

Enantiomeric resolution has been achieved with a chiral aliphatic alcohol and an achiral acylating agent such as *N*-trifluoroacetyl chloride. Alternatively, the amino group has been converted to diastereomeric amides, ureas, thioureas and isoindoles.

Resolution

Since many real samples are complex mixtures of acids (and other components), high efficiency

columns are essential for satisfactory resolution. This requirement has made packed columns effectively obsolete for such samples and use of capillary (or open tubular, OT) columns is becoming routine. The high efficiency of OT columns requires correspondingly less selectivity to gain the necessary separation. Therefore, relatively few different stationary phases in OT columns will adequately separate the majority of mixtures encountered.

Nonpolar stationary phases have the advantages of greater inertness, thermal stability and operation at lower temperatures. Since retention times increase with increasing polarities of the stationary phase and analyte, the least polar column affording the necessary resolution should be selected. Silyl derivatives are usually adequately separated on nonpolar polydimethylsiloxanes (e.g. DB-1, SE-30, OV-101); for greater selectivity somewhat more polar phases such as DB-5, SE-54, OV-17 or even OV-1701 may be used. On the other hand, stationary phases containing hydroxyl groups (such as the polyethylene glycols, PEGs) should be avoided because they react with silylation reagents.

Saturated and unsaturated FAMES are generally separated on more polar columns because they tend to cluster together on nonpolar phases, with the unsaturated ones preceding the saturated. On polar phases such as PEGs, the unsaturated are eluted after the saturated with minimal overlap of different chain lengths. This shift in retention behaviour is further enhanced on very polar stationary phases such as the cyanosilicones (CP-Sil-88, OV-275, DB-23) which are used for resolving *cis*, *trans* isomers and very complex mixtures.

Relatively nonpolar columns are used for the separation of diastereomeric esters formed from optically active carboxylic and amino acids. As an alternative approach, amino acid enantiomers have been separated as their alkyl *N*-perfluoroacyl derivatives on a chiral column, e.g. Chirasil-Val.

Identification

With conventional GC detectors, such as the FID and ECD, identification of the most commonly encountered acids is based on comparison of the retention times obtained with authentic standards. For unidentified acid peaks in general, retention index values or, for FAMES, equivalent chain lengths (ECL) from the literature may be helpful. The preferred solution is, however, MS detection in view of the more definitive structural information it provides. Especially for carboxylic acids, the usual data (e.g. molecular weights, fragmentation patterns, isotopic peak patterns) afforded by MS are supplemented by additional struc-

tural information, the most useful being the degree of unsaturation.

The presence of a double bond can be deduced from the molecular weight of an ester but its location cannot be ascertained due to migration during fragmentation. Hence, for reliable identification of positional isomers by GC-MS, two methods are employed: the on-site method of fixing the location of the double bond through its chemical modification, or the remote group method in which the carboxylic group is derivatized to a nitrogen-containing product which restricts double-bond migration. The remote group method is more convenient and versatile.

Chemical modification involves the addition of a reagent across the double bond of the acid ester to generate a product which gives diagnostic fragment ions. Dimethyl disulfide is a widely used reagent since it adds to a double bond in a single step at room temperature and enables identification of positional and geometrical isomers after separation on an appropriate column. But the picture is less clear with polyenoic acids, especially when the double bonds are in close proximity, and with acids containing other structural features such as cyclopropane rings. Diels-Alder reactions with cyclopentadiene derivatives can be applied similarly. The double-bond site may also be established by treating the unsaturated acid with OsO_4 and converting the resulting diol to the *bis*-TMS ethers for GC-MS analysis. Although this method is suitable for locating the double-bond sites of polyunsaturated acids, their fragmentation patterns are more complex and careful interpretation is necessary.

In derivatizing the carboxylic group, the picolinyl and DMOX compounds are the most commonly generated nitrogen-containing products. In the mass spectra of these derivatives, the saturated segments of the molecules are indicated by the regular separation of successive peak clusters by 14 amu (corresponding to the cleavage of a CH_2 group), whereas at double-bond sites the gap is only 12 amu. Furthermore, fragmentation on either side of the double bond gives two ions which are separated by 26 amu. In a branched acid derivative, the site of branching is shown by a similar gap of 28 amu.

Geometrical isomers and ring structures are more reliably identified by infrared (IR) spectrometry, which underscores the utility of GC-Fourier transform IR (FTIR)-MS in the structure elucidation of acids. However, the inherently lower sensitivity of IR requires larger sample sizes and columns with a higher load capacity.

Quantitative analysis of acids by GC-MS is carried out most sensitively by selected ion monitoring (SIM) employing an isotopically labelled analogue or a

derivative of a structurally similar acid as internal standard. The desired sensitivity of detection is a critical factor in the choice of the derivative. For increased sensitivity ion currents must be intensified by reducing fragmentation. Hence, TBDMS derivatives are preferred to those of TMS. Moreover, TBDMS derivatizes the amino acids arginine and glutamine, whereas TMS fails to do this. (However, the preferred method for quantification of amino acids involves the butyl perfluoroacyl derivatives.) Fragmentation may also be reduced by increasing molecular stability via cyclic derivatives, as illustrated by quinoxalinol compounds utilized in the GC-MS analysis of 2-oxo-acids. An excellent method of augmenting sensitivity is performing negative ion mass spectrometry via derivatives (e.g. *p*-nitrobenzyl, pentafluorobenzyl) with high electron affinity.

These methods have allowed the determination of a variety of acids by GC-MS at pg levels. Even mixtures of acids can be analysed quantitatively by monitoring several characteristic ions. Programmable SIM, which optimizes the selectivity at various points in a chromatogram and the desired sensitivity of analysis, has been invaluable in this regard.

Applications

Examples of GC analysis of acids in real-world samples are so numerous and diverse as to permit only representative cases from more significant fields to be cited.

Carboxylic acids present at abnormal levels in plasma and urine may indicate various metabolic disorders. Hence, their monitoring is vital for diagnostic purposes. GC has simplified such analysis by expediting the separation and determination of very low concentrations of acids present in these complex matrices (**Figure 3**). For example, C₂₇ and C₂₉ bile acid levels provide the basis for a screening test for a genetic condition characterized by peroxisomal dysfunction syndrome and are measured by GC-MS as methyl-silyl derivatives. Elevated levels of certain acylcarnitines may signify a potentially lethal condition caused by the deficiency of an enzyme which is essential for β -oxidation of fatty acids. Their quantification by GC-MS has been achieved by the ready conversion to volatile acyloxylactones. Metabolic products of amino acids whose presence in urine at unusually high levels may be symptomatic of

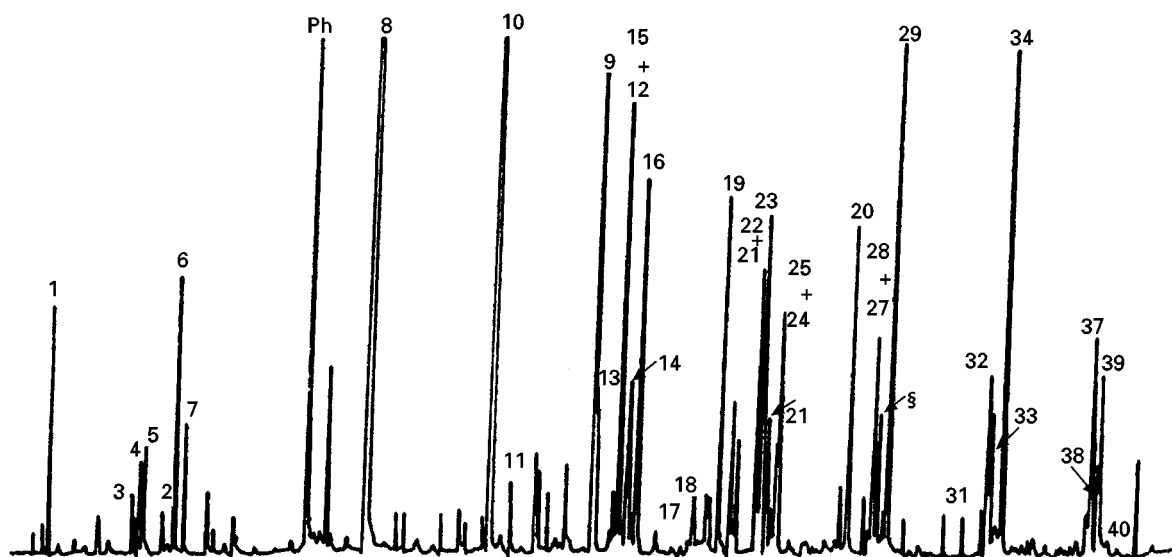


Figure 3 Chromatogram of a 3-hydroxy-dicarboxylic aciduria. GC conditions: 30 m \times 0.32 mm i.d. column coated with OV-1701; temperature-programmed from 70 to 270°C at a rate of 5°C min⁻¹. Detector: FID. Some important peaks are indicated: 1, lactic di TMS; 2, oxalic di TMS; 3, 3-hydroxy-propionic di TMS; 4, 3-hydroxybutyric di TMS; 5, 3-hydroxy-isobutyric di TMS; 6, 2-methyl-3-hydroxybutyric di TMS; 7, 3-hydroxy-isovaleric di TMS; 8, internal standard; 9, 3-hydroxy-adipic lactone mono TMS; 10, adipic di TMS; 11, hexenedioic di TMS; 12, triglycine mon TMS; 13, 4-hydroxy-phenylacetic di TMS; 14, octenedioic di TMS; 15, 3-hydroxy-adipic tri TMS; 16, suberic di TMS; 17, 3-keto-adipic enol tri TMS; 18, aconitic tri TMS; 19, citric tetra TMS; 20, hippuric mono TMS; 21, decenedioic di TMS; 22, 3-hydroxy-octenedioic tri TMS; 23, 3-hydroxy suberic tri TMS; 24, sebacic di TMS; 25, 4-hydroxy-phenyllactic tri TMS; 27, 3-hydroxy-decenedioic tri TMS; 28, 4-hydroxy-phenylpyruvic enol tri TMS; 29, 3-hydroxy-sebacic tri TMS; 31, 3-hydroxy-dodecadienedioic tri TMS; 32, 3-hydroxy-dodecenedioic tri TMS; 33, 3-hydroxydodecenedioic tri TMS; 34, 3-hydroxy-dodecanedioic tri TMS; 37, 3-hydroxy-tetradecadienedioic tri TMS; 38, 39, 3-hydroxy-tetradecenedioic tri TMS; 40, 3-hydroxy-tetradecanedioic tri TMS; Ph = phosphoric tri TMS. (Reproduced with permission from Lefevre MF, Verhaeghe BJ, Declerk DH *et al.* (1989) Metabolic profiling of urinary organic acids by single and multicolumn capillary gas chromatography. *Journal of Chromatographic Science* 27: 23.

metabolic disorders, e.g. hydroxyproline in collagen metabolism, and γ -carboxyglutamate in blood coagulation and bone metabolism. These compounds are converted to *N*-isobutyloxycarbonyl methyl derivatives prior to measurement.

Prostaglandins, which are indicators of several diseases, are a class of acidic biomolecules whose measurement in biomatrices still presents a formidable analytical challenge. They are present in urine at concentrations as low as few pg mL^{-1} and require the quantification of several structurally closely related compounds. The difficulties are further compounded by their extreme sensitivity to acids, bases and oxygen. The determination of prostaglandin E_2 has been achieved by negative ion chemical ionization (NICI)-GC-MS following methylation and derivatization of other functionalities. There are several methods reported for the determination of other prostaglandins by isotope dilution GC-MS. GC-MS has been of immense utility in elucidating the role of γ -aminobutyric acid as a neurotransmitter via its ^{15}N -labelled derivative. Catecholamines and their acidic metabolites such as homovanillic, vandilomandelic, 5-hydroxyindole-3-acetic and phenylacetic acids, are implicated as etiological factors in affective disorders. They have been determined by NICI-GC-MS via acetyl-PFB derivatives and by isotope dilution GC-MS. In clinical research, GC-MS has proved invaluable for pharmacokinetic studies of therapeutic

drugs with acidic functionalities. Such studies have been performed on methylphenidate, which is used in the treatment of children suffering from hyperkinesia, and on the butyl ester-trifluoroacetyl derivative of isotopically labelled histidine in investigations of the hereditary metabolic disorder histidinaemia. Another application is the analysis of the anti-inflammatory drug biphenylacetic acid in urine and synovial fluid by NICI-GC-MS-MS via its PFB ester. Some therapeutic drugs can lead to a build-up of toxic metabolites that must be monitored. This is exemplified by GC-MS analysis of patients' urine and plasma for 2-*n*-propyl-4-pentenoic acid, which is a product of the antiepileptic drug valproic acid.

In analytical microbiology, GC of fatty acids provides a basis for microbial chemotaxonomy and a means of identifying genus, species and even strains of microorganisms (Figure 4). The compounds profiled may be the nonvolatile C_{10} – C_{20} fatty acids present in cell membranes or the volatile acids which accumulate in the headspace. The extraction of the nonvolatile fatty acids and their derivatization to alkyl esters have been simplified by commercially available automated systems. Fatty acid profiles have permitted identification of pathogenic bacteria and even strains of yeast.

The realization that the enantiomers of a chiral compound may exhibit different bioactivities has prompted pharmaceutical and other industries to

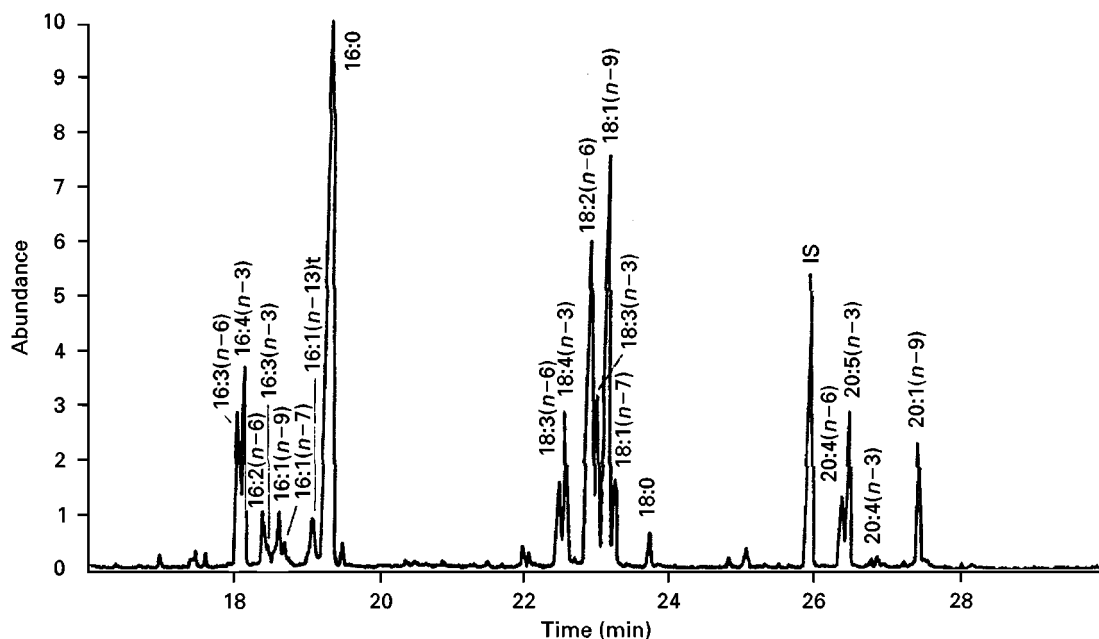


Figure 4 Reconstructed chromatogram of fatty acid methyl esters from the unicellular alga *Tetraselmis suecica* obtained by GC-MS. Chromatographic conditions: 50 m \times 0.20 mm i.d. methylsiloxane fused capillary column; column temperature, initially at 40°C for 1 min, increased to 120°C at 30°C min^{-1} and then to 310°C at 4°C min^{-1} ; helium carrier gas. (Reproduced with permission from Volkman JK, Jeffrey SW, Nichols PD *et al.* (1989) Fatty acid and lipid composition of ten species of microalgae used in mariculture. *Journal of Experimental Marine Biology and Ecology* 128: 219.

ascertain the optical purity of products and the metabolic fate of each enantiomer. As a result, industries and regulatory bodies have evinced interest in reliable methods for resolving optically active compounds. In the particular case of chiral acids, GC has proved invaluable. This is clearly illustrated by the separation of the optical isomers of the common drug ibuprofen via diastereoisomeric esters, and by a group of anti-inflammatory drugs, arylpropionic acids, which are routinely monitored in biological fluids as their *R*(-)/*S*(+)-amphetamine derivatives.

The differentiation between biogenic and non-biological urinary carboxylic acids is vital in the forensic sciences to establish the use of illicit drugs. Cannabis is the most widely used illicit drug in the world. 11-Nor- Δ -9-tetrahydrocannabinol acid (THCA) is found in urine specimens of cannabis users at few ng mL^{-1} levels as a major metabolite of tetrahydrocannabinol. THCA may be detected in urine 4–6 days after use of marijuana and even up to a month in chronic users: its determination by GC, principally as the TMS derivative, has been the focus of much research. Benzoylecgonine, which is a car-

boxylic acid produced by de-esterification of cocaine at physiological pH and temperature, and ecgonine methyl ester are the major metabolites that appear in the urine of cocaine users. Both are analysed by either GC-ECD or GC-FID, after converting the acid to the TMS derivative.

Toxic haloacids are environmentally significant and may be present in drinking water and other beverages. They are monitored by GC-MS or GC-ECD as the methyl esters. Low concentrations of pesticide and herbicide residues contaminating fruits and vegetables present another health hazard, e.g. residues of the fungicidal metal salts of alkylene-*bis*-dithiocarbamic acids. These fungicides are first converted to CS_2 for analysis by headspace GC. Traces of some widely used acidic herbicides, such as chlorinated phenoxy-carboxylic acids, are quantified in food samples by GC-MS as their methyl esters.

Carboxylic acids and derivatives are important flavour and aroma constituents of foods (Figure 5) and beverages. Volatile fatty acids that are present at low concentrations also contribute to organoleptic characteristics and can be determined by headspace GC in

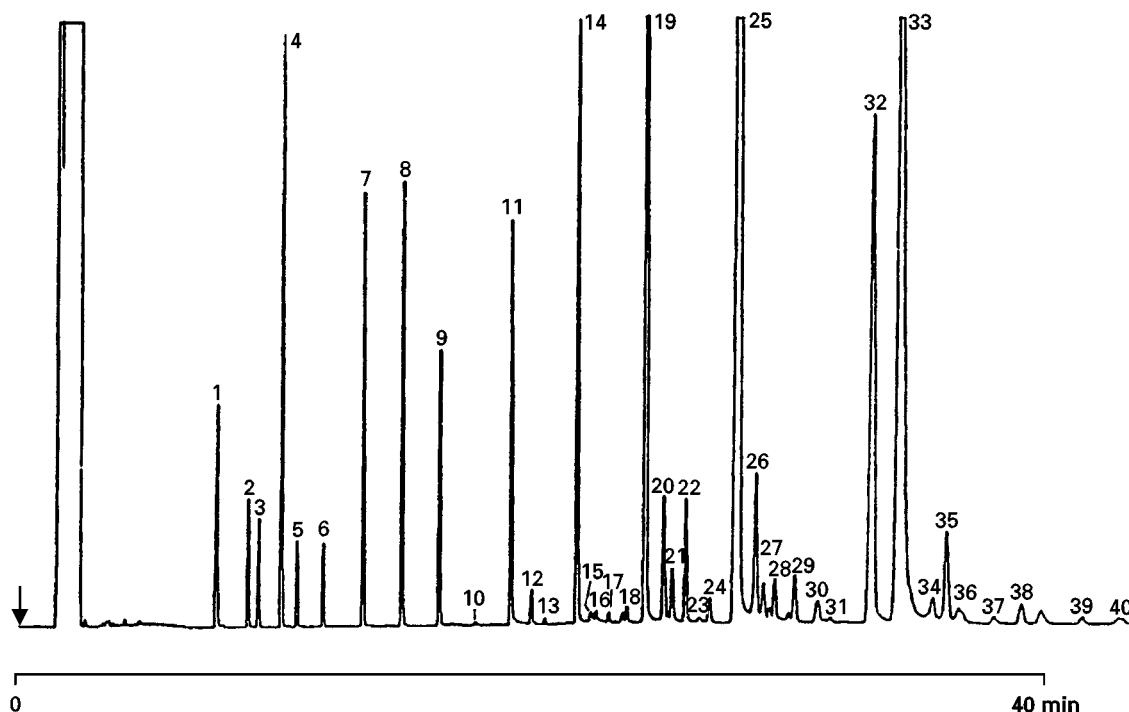


Figure 5 Gas chromatogram of free fatty acids (FFAs) from cheese spiked with an FFA reference mixture and short chain FFA (2:0, 3:0, 2- CH_3 -3:0, 5:0, 3- CH_3 -4:0 and 7:0). Chromatographic conditions: 25 m \times 0.32 mm i.d. fused silica capillary column coated with FFAP-CB; oven temperature-programmed to increase from 65 to 240°C at a rate of 10°C min^{-1} ; FID detector; helium carrier gas at a flow rate of 2 mL min^{-1} . Peaks: 1, C2; 2, C3; 3, 2- CH_3 -C3; 4, C4; 5, 3- CH_3 -C4; 6, C5; 7, C6; 8, C7; 9, C8; 10, C9; 11, C10; 12, C10:1; 13, C11; 14, C12:0; 15, C12:1; 16, C13-iso; 17, C13:0; 18, C14-iso; 19, C14:0; 20, C14:1 + C15-iso; 21, C15-anteiso; 22, C15:0; 23, C15:1; 24, C16-iso; 25, C16:0; 26, C16:1; 27, C17-iso; 28, C17-anteiso; 29, C17:0; 30, C17:1; 31, C18-iso; 32, C18:0; 33, C18:1; 34, C18:2; 35, C18:2; 36, C19:0; 37, C18:3; 38, C18:2 conjugated; 39, C20:0; 40, C20:1. (Reproduced with permission from de Jong C and Badings, HT (1990) Determination of free fatty acids in milk and cheese. Procedures for extraction, clean up and capillary gas chromatography. *Journal of High Resolution Chromatography* 13: 94.

underivatized form. Fatty acids containing unusual structural features, such as cyclopropane rings or epoxy groups, are constituents of some edible vegetable oils and are suspected of being health hazards. Hence they have been analysed in foods by capillary GC as FAMES. Such studies have provided a basis for identifying components in blends of vegetable oils with potential application to detecting adulteration. Similar studies have been carried out to determine brominated acid constituents in vegetable oils that are added to disperse flavouring constituents in citrus-based beverages. Clinical and epidemiological findings of the beneficial effects of fish oils have led to GC methods, effected on polar capillary columns, for determining ω -fatty acids such as eicosapentaenoic and docosahexaenoic acids in foods. *Trans* isomers of fatty acids have a possible link with cardiovascular diseases. Hence the occurrence of *trans* isomers in relatively large concentrations in margarines, shortenings and similar food products has stimulated development of methods for resolving geometrical isomers. The solution of this problem is very difficult by GC alone and has required the use of very long capillary columns and preliminary separation steps. It may be cited as an existing challenge to GC in the analysis of acids.

Conclusion

GC continues to be the method of choice for the analysis of acids because of its speed, efficiency and sensitivity. However, very complex mixtures still pose serious challenges. Future developments may entail use of shorter, narrower capillary columns for greater speed and, in conjunction with routine MS

detection, for more definitive identification. Automation of sample preparation, perhaps in conjunction with microwave irradiation in lieu of conventional heating, will shorten derivatization times, relieve the tedium of manual manipulations and reduce total analysis times.

See also: II/Chromatography: Gas: Derivatization; Detectors: Mass Spectrometry; Detectors: Selective. III/Oils, Fats and Waxes: Supercritical Fluid Chromatography. Triglycerides: Liquid Chromatography; Thin Layer (Planar) Chromatography. Volatile Organic Compounds in Water: Gas Chromatography.

Further Reading

- Blau K and Halket JM (eds) (1993) *Handbook of Derivatives for Chromatography*, 2nd edn. Chichester: John Wiley.
- Christie WW (1989) *Gas Chromatography and Lipids*. Ayr, Scotland: Oily Press.
- Christie WW (ed.) (1992–97) *Advances in Lipid Methodology*, vols 1–4. Dundee, Scotland: Oily Press.
- Clement RE (ed.) (1990) *Gas Chromatography – Biochemical, Biomedical, and Clinical Applications*. New York: John Wiley.
- Gutnikov G (1995) Fatty acid profiles of lipid samples. *Journal of Chromatography B* 671: 71.
- Poole CF and Schuette SA (1985) *Contemporary Practice of Chromatography*. Amsterdam: Elsevier.
- Shantha NC and Napolitano GE (1992) Gas chromatography of fatty acids. *Journal of Chromatography* 624: 37.
- Wittkoski R and Matissek R (eds) (1992) *Capillary Gas Chromatography in Food Control and Research*. Hamburg, Germany: B. Behr's Verlag.
- Zumwalt RW, Kuo KCT and Gehrke CW (1987) *Amino Acid Analysis by Gas Chromatography*, vols 1–3. Boca Raton, FL: CRC Press.

Liquid Chromatography

K. L. Ng and P. R. Haddad, University of Tasmania, Hobart, Tasmania, Australia

Copyright © 2000 Academic Press

Introduction

The determination of carboxylic acids is important in many areas of application, including environmental samples, foods and beverages, and pharmaceutical and biological materials. The modes of high performance liquid chromatography (HPLC) used most frequently in the separation of carboxylic acids are ion suppression chromatography, reversed-phase ion interaction chromatography, ion exclusion chromatography and ion exchange chromatography.

In ion suppression chromatography, a buffer of appropriate pH is added to the mobile phase in order to suppress the ionization of the carboxylic acids so that they can be retained on nonpolar stationary phases and eluted in order of increasing hydrophobicity. Ion interaction (or ion pair) chromatography has been used for the separation of carboxylic acids under isocratic or gradient conditions and involves the complete ionization of the solute and the addition to the mobile phase of an ion interaction reagent (IIR), consisting of lipophilic ions of opposite charge to the solute. Ion exclusion chromatography (i.e. the separation of partially ionized carboxylic acids on a cation exchange stationary phase using amperometry, coulometry, ultra-

violet, refractive index and both suppressed and nonsuppressed conductivity detection) is the most commonly used mode of liquid chromatography for the separation of carboxylic acids. Finally, anion exchange chromatography can be used for the separation of carboxylic acids, after conversion of these species to anions. Detection is usually achieved by suppressed or nonsuppressed conductivity or by indirect photometry.

Ion Suppression Chromatography

Background

Ion suppression chromatography is a technique for the separation of ionizable solutes which functions by suppressing the ionization of these solutes, thus increasing their retention on nonpolar stationary phases. In the separation of carboxylic acids, an acidic buffer is added to the mobile phase to suppress the ionization of the solutes, which are then separated on nonpolar polymeric or silica-based (usually C_{18}) stationary phases.

This method is only applicable to those acids for which the ionization can be suppressed using buffers having pH values in the range 3–8, since the C_{18} stationary phases are unstable outside this pH range. However, these restrictions do not apply to the use of polymeric stationary phases, which can be used for the separation of a wider variety of solutes. The mobile phase is usually an acidic buffer of the appropriate pH. Commonly used buffers include phosphoric acid, sodium or potassium phosphate, sodium hydrogen sulfate, acetic acid and citric acid. Organic modifiers such as methanol or acetonitrile can also be added to the mobile phase to improve the separation.

Manipulation of Retention of Acids in Ion Suppression Chromatography

Solute retention results from solvophobic effects occurring between the mobile phase, the stationary phase and the solutes. For the separation of monocarboxylic acids, the pH of the mobile phase influences the retention behaviour according to the following equation:

$$k' = \frac{k_0 - k_{-1} \frac{K_a}{[H^+]}}{1 + \frac{K_a}{[H^+]}} \quad [1]$$

where k_0 is the retention factor of the undissociated acid, k_{-1} is the retention factor of the conjugate base, and K_a is the acid dissociation constant in the mobile phase. This retention behaviour is illustrated in **Figure 1**, which shows the retention factor of a weak acid versus $(pH - pK_a)$. The curve is sigmoidal in shape

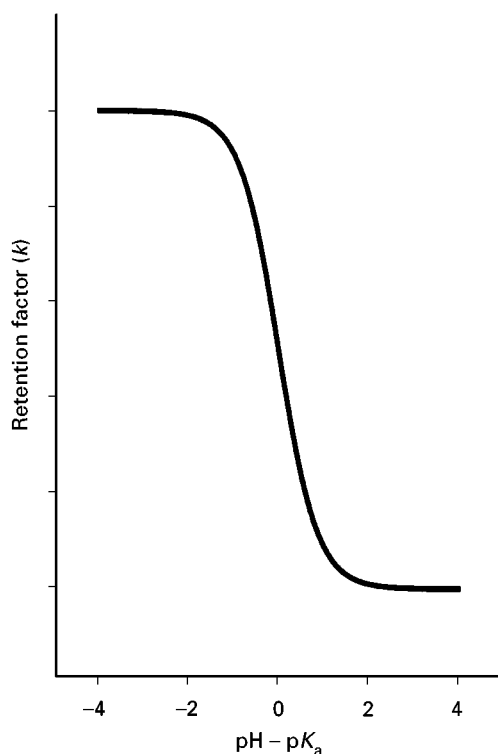


Figure 1 Plot of the retention factor of a weak monoprotic acid vs. $(pH - pK_a)$.

and the inflection point is located at the point where the pH of the mobile phase is equal to the pK_a of the solute in the mobile phase. At pH values substantially less than its pK_a value, the acid is present in its neutral form and has a large retention factor. Further decreases in mobile-phase pH show no effect on retention factor, since there will be no further change in the ionization of the acid. Conversely, mobile-phase pH values substantially greater than the pK_a value will result in complete ionization of the solute, leading to a small retention factor. At intermediate pHs, the solute charge, and hence its retention, will be dependent on the particular pH used and its proximity to the pK_a value.

In the case of dicarboxylic acids, the shape of the curve is largely determined by the difference between the two pK_a values. When pK_{a1} and pK_{a2} are very close, sigmoidal curves are obtained and the behaviour of dicarboxylic acids is almost the same as that of monocarboxylic acids. When the two pK_a values are well separated, the curve is a composite of two sigmoidal curves.

Both the ionic strength and organic modifier content of the mobile phase may be varied in order to manipulate retention in ion suppression chromatography. Increasing the ionic strength of the mobile phase causes an apparent increase in the dissociations, leading to a decrease in the retention factor.

This effect is more pronounced in nonaqueous media. In the approximate range of ionic strengths from 0 to 0.5 mol L^{-1} , the higher the ionic strength of the mobile phase, the greater the increase in ΔpK_a . The addition of organic modifiers influences retention behaviour in two ways. Firstly, increasing the organic modifier content of the mobile phase decreases the retention factor, as is generally the case in reversed-phase liquid chromatography. However, the apparent pK_a of the solute increases as organic modifier is added to the mobile phase, leading to an increase in the degree of ionization of the solute and therefore reduced retention.

Applications

The utility of ion suppression on polymeric stationary phases may be appreciated by considering the separation of the homologous series of aliphatic carboxylic acids. Neither ion exchange nor ion exclusion chromatography yields a complete separation of these species. However, ion suppression coupled with gradient elution and conductivity detection enables the separation of butyric through to stearic acid, as illustrated in **Figure 2**. The gradient used involved an increase in the percentage of organic modifier in the mobile phase and a decrease in mobile-phase pH. Carboxylic acids more hydrophilic than butyric acid are eluted in a single peak at the column void volume.

Ion Interaction Chromatography

Background

Ion interaction chromatography involves the addition of an ion interaction reagent (IIR) to the mobile

phase. The IIR is usually a lipophilic ion of opposite charge to the analyte ions. In the case of the separation of carboxylic acids, cationic IIRs such as tetraalkylammonium salts are used.

The mechanism of ion interaction chromatography is considered to begin with the establishment of a dynamic equilibrium between IIR in the mobile phase and IIR adsorbed onto the stationary phase:



where the subscripts M and S refer to the mobile and stationary phases. This results in the formation of an electrical double layer at the stationary phase surface. The adsorbed IIR ions constitute a primary layer of charge, to which is attracted a diffuse, secondary layer of oppositely charged ions. This secondary layer of charge consists chiefly of the counter-ions of the IIR. The double layer is shown schematically in **Figure 3A**. A solute anion can compete for a position in the secondary charged layer, from which it will tend to move into the primary layer as a result of electrostatic attraction and, if applicable, reversed-phase solvophobic effects. The presence of such a solute anion in the primary layer causes a decrease in the total charge of this layer, so to maintain charge balance a further IIR ion must enter the primary layer. The result is that solute retention involves the adsorption of a solute anion accompanied by the adsorption of an IIR ion, shown schematically in **Figure 3B**.

Typical stationary phases used in ion interaction chromatography include neutral poly(styrene-divinylbenzene) (PS-DVB) polymers and bonded silica materials with C_{18} , C_8 , phenyl and cyanopropyl groups as the chemically bound functionality. The

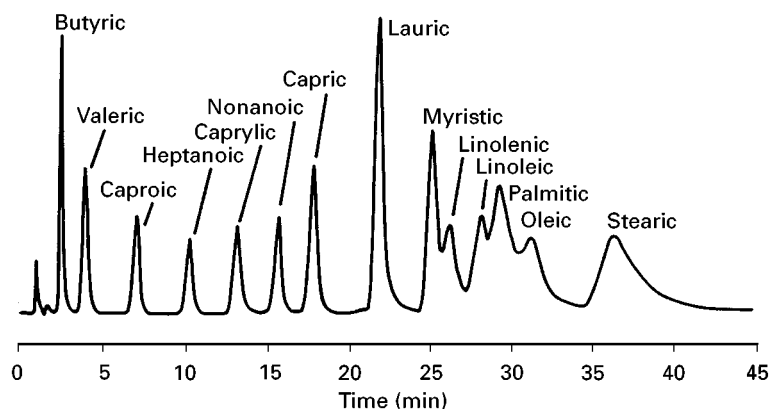


Figure 2 Gradient elution ion suppression chromatography of carboxylic acids, obtained on a polymeric reversed-phase column. A Dionex MPIC-NS1 column was used with a gradient of 100% mobile phase A ($t = 0$) to 100% mobile phase B ($t = 20$ min), with maintenance of mobile phase B after this time. Mobile phase A was 24% acetonitrile and 6% methanol in 0.03 mmol L^{-1} HCl; mobile phase B was 60% acetonitrile and 24% methanol in 0.05 mmol L^{-1} HCl with detection by suppressed conductivity. The baseline conductance for a blank gradient has been subtracted in the chromatogram shown. (Reprinted with permission from Slingsby RW (1986) Gradient elution of aliphatic carboxylic acids by ion chromatography in the ion-suppression mode. *Journal of Chromatography* 371: 373–382.)

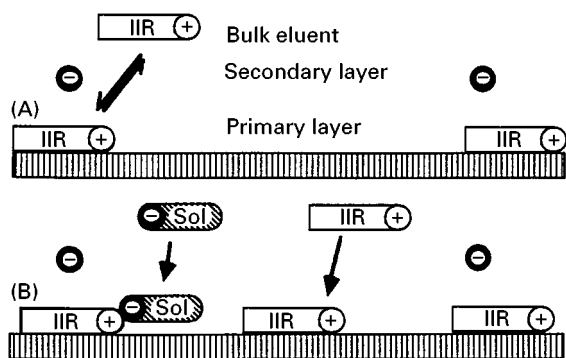


Figure 3 Schematic illustration of the ion interaction model for the retention of anionic solutes in the presence of a lipophilic cationic IIR. The solute and the IIR are labelled on the diagram. The long hatched boxes represent the lipophilic stationary phase, the black circles with negative charges represent the counter-anion of the IIR, whilst the white circles with positive charges represent the counter-cation of the solute. (Reprinted with permission from Haddad and Jackson, 1990.)

choice between stationary phases is usually based on considerations such as chromatographic efficiency, pH stability and particle size. However, the elution position of certain ions can differ between different stationary phases. Further factors to be considered in the selection of a stationary phase for ion interaction chromatography are specific interactions existing between the stationary phase and either the IIR or the solutes, and the role of residual silanol groups on silica-based stationary phases.

The most important component of the mobile phase in ion interaction chromatography is the IIR itself. The requirements of the IIR are that its charge is unaffected by mobile-phase pH, it has suitable lipophilicity to permit adsorption onto nonpolar stationary phases, and it is compatible with other mobile-phase components and the desired detection system.

In the separation of carboxylic acids by dynamic coating ion interaction chromatography, moderately hydrophobic strong base cations, such as tetrabutylammonium ions, are used as the IIR. The IIR is present at a constant, specified concentration in the mobile phase in order to maintain a desired concentration of IIR on the stationary phase. The lipophilicity of the IIR governs the degree to which it is adsorbed onto the stationary phase, which in turn governs the effective ion exchange capacity of the column and hence the retention times of solute ions.

An alternative to the above method is permanent coating ion interaction chromatography, where a very lipophilic IIR is used initially to equilibrate the stationary phase and is then removed from the mobile phase in the separation step. The coating persists for long periods of subsequent use. Permanent coating of the column is achieved by passing a solution of the

IIR (approximately 10^{-3} mol L $^{-1}$) in dilute (5%) methanol or acetonitrile through the column for about 20 min. The purpose of the organic solvent is to wet the surface of the lipophilic stationary phase in order to improve binding of the IIR.

The counter-ion of the IIR is important in dynamic coating ion interaction chromatography of anionic solutes. This counter-ion usually acts as an ion exchange competing anion and is responsible for the elution (and in many cases also the detection) of the solute anions. The nature of the counter-ion determines the type of separation which is required and the mode of detection applicable.

Manipulation of Retention of Acids in Ion Interaction Chromatography

The parameters which affect the adsorption of the IIR onto the stationary phase and hence the retention of solutes include the nature of the stationary phase, the lipophilicity of the IIR, the concentration of the IIR in the mobile phase, the ionic strength of the mobile phase, the nature and concentration of any competing ion added to the mobile phase, and the mobile-phase pH.

The first four of these factors will determine the surface concentration of the IIR on the stationary phase, and hence the surface charge density and the effective ion exchange capacity. The higher the surface concentration of IIR, the greater the solute retention. Thus, retention times will increase as the lipophilicity of the IIR is increased and as the percentage of modifier in the mobile phase is decreased. Solute retention generally increases with the concentration of IIR in the mobile phase, but there is a threshold concentration above which solute retention decreases with further increase in the concentration of IIR. The stationary phase becomes saturated with IIR and any further addition to the mobile phase results in decreased retention because of the increased concentration of the IIR counter-ion.

The nature and concentration of any competing ion added to the mobile phase will determine the retention times and elution order for solute ions. Increases in the concentration of the mobile phase competing ion will result in decreased solute retention, in the same manner as observed for ion exchange separations. Finally, the mobile phase pH may influence the charges on the competing ion and the solutes. An example of this effect is the influence of pH in an ion interaction chromatographic system using tetrabutylammonium as the IIR and phthalate as the competing anion. Increases in mobile-phase pH over the range 4.0–6.0 cause a decrease in the solute retention as a result of increased ionization of phthalate,

leading to the formation of a strong, divalent competing anion.

Applications

Carboxylic acids are usually separated by ion interaction chromatography using a reversed-phase column with quaternary ammonium salts as the IIR and water-methanol or water-acetonitrile as the mobile phase. The more lipophilic the quaternary ammonium ion, the more the acid is retained on non-polar stationary phases. Such separation systems have been used for the determination of ascorbic acid in fruits and vegetables, as well as carboxylic acids in beverages such as wine, beer and fruit juices.

Gradient elution ion interaction chromatography is also possible. The concentration of the organic modifier or the pH of the mobile phase may be varied to optimize the separation. **Figure 4** shows an example of the separation of carboxylic acids on a reversed-phase column by gradient elution using tetrabutylammonium hydroxide as the ion interaction reagent.

Ion Exclusion Chromatography

Background

Ion exclusion chromatography was first introduced by Wheaton and Bauman in 1953. In this mode of chromatography, the negatively charged, partially dissociated carboxylic acids are separated on cation exchange resins comprising silica or a polymer with chemically bound anionic sulfonate or carboxylate functional groups. This is the opposite situation to that occurring in normal ion exchange chromatography.

The chromatographic system consists of three phases: the mobile phase, the resin phase and an occluded liquid phase. The mobile phase passes through the interstitial volume existing between the beads of the ion-exchange resin. An occluded liquid phase is formed by mobile phase that becomes trapped within the pores of the resin phase. This trapped liquid acts as the stationary phase of the system. The resin phase is the solid resin network and functionalized groups, which can be considered to be a semipermeable ion-exchange membrane separating the flowing mobile phase from the stationary occluded liquid inside the resin. The three phases are illustrated schematically in **Figure 5**.

Fully ionized species (A^-) are completely excluded from the interior of the resin due to electrostatic repulsion by the fixed anionic functional groups, in accordance with the Donnan exclusion effect. Therefore, these species are not retained and are eluted at

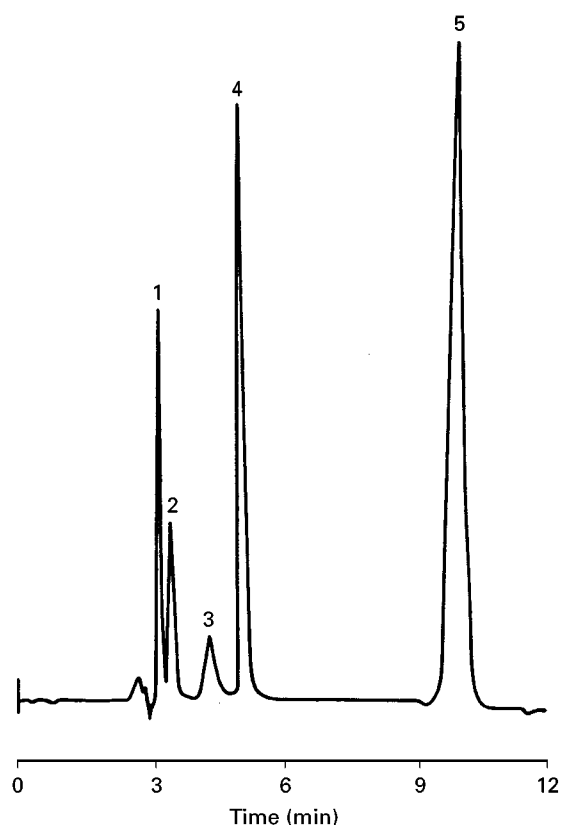


Figure 4 Ion interaction chromatography of carboxylic acids on a LiChrosorb RP-8 column with a mobile phase of aqueous tetrabutylammonium hydroxide (1 g L^{-1}) and methanol using gradient elution. Detection was at 254 nm. Carboxylic acids are: 1, ascorbic; 2, oxalic; 3, pyruvic; 4, fumaric; 5, maleic. Chromatogram courtesy of Alltech Chromatography Catalog (1997) 610.

the column void volume. Partially ionized species like weak carboxylic acids ($pK_a = 2.5\text{--}6.5$) permeate selectively into the stationary phase (the occluded liquid trapped within the pores of the resin), resulting in some retention of these species, which are then eluted some time later than the fully ionized solutes.

Ion exclusion chromatography was first performed on large particle size, high capacity, fully functionalized PS-DVB polymers. However, separations have also been performed on polymethacrylate copolymer resins, as well as on silica. Separations of carboxylic acids by modern ion exclusion chromatography are usually carried out on a cation exchange column containing sulfonated functional groups ($-\text{SO}_3^-$) or mixed sulfonate and carboxylate functional groups, with the resin most commonly being used in the hydrogen form.

Ion exclusion columns are usually quite large because most sample species are eluted with retention volumes intermediate between the interstitial volume (V_0) and $V_0 + V_i$, where V_i is the occluded (or intraparticle) liquid volume. Large columns contain more

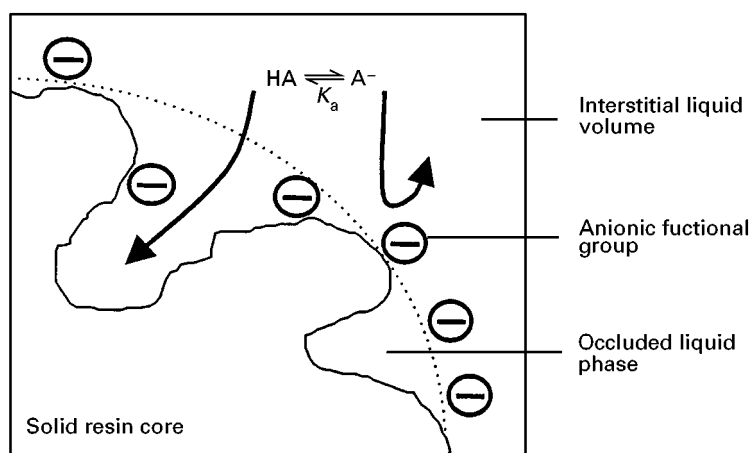


Figure 5 Schematic representation of the ion exclusion mechanism, showing the retention of a weak acid (HA) in the occluded liquid phase and the exclusion of the acid anion (A^-).

resin, thus increasing the amount of occluded liquid and hence also the capacity of the stationary phase. A typical column would be 30 cm in length, with an internal diameter of 7 mm or more.

The mobile phases used in ion exclusion chromatography are often very simple in composition. Most of the early work was performed using water as the mobile phase. However, water has limitations as stronger acids or bases show too great a degree of ionization to be retained and for weaker acids such as carboxylic acids, the separation is slow and the peaks are unsymmetrical.

In modern ion exclusion chromatography it is common to use dilute solutions of strong mineral acids for the elution of carboxylic acids. The dilute mineral acid solution suppresses the ionization of the acids so that they can partition into the occluded liquid phase, resulting in longer retention times and better separation between the stronger carboxylic acids. The choice of acid used in the mobile phase is usually determined by the form of detection being used. Sulfonic acids are used for conductivity detection without suppression since mineral acids have a high background conductance. Sulfuric acid is often used with ultraviolet detection and hydrochloric acid is used with conductivity detection after the mobile phase has been passed through a suitable suppressor. Weak acids such as benzoic acid, phosphoric acid, salicylic acid and carbonic acids have also been used as mobile phases in ion exclusion chromatography when conductivity detection is utilized.

Manipulation of Retention of Acids in Ion Exclusion Chromatography

The dominating factor which determines retention is the degree to which the acid is ionized. Separation is based on the electrostatic repulsion between the

solute ions and fixed functional groups of the resin. Therefore, ionic species are excluded from the stationary phase while partially ionized or uncharged species partition between the mobile phase and the occluded liquid within the resin pores. Assuming this is the only mechanism, the solute retention time, t_R , is given by:

$$t_R = t_0 + D_A t_i \quad [3]$$

where t_0 is the time taken for the interstitial volume of mobile phase (i.e. the volume of mobile phase flowing between the resin beads) to be eluted, t_i is the time taken for the volume of occluded liquid inside the pores of the resin to be eluted, and D_A is the distribution constant for the solute between the interstitial mobile phase and the occluded liquid. The value of D_A is dependent on the degree of ionization of the solute.

If a solute cannot enter the stationary phase because it is fully ionized (ion exclusion), $D_A = 0$. Therefore, the retention time of fully ionized solutes is equal to t_0 , whilst for an uncharged solute which is free to enter the stationary phase, $D_A = 1$, and its retention time is equal to t_i . Thus, in the separation of carboxylic acids, the retention times of the acids depend on their first dissociation constants (pK_a). Since the fraction of the ionized solute molecules increases with increasing pH, an increase in the mobile phase pH will reduce the retention time.

The retention times of monocarboxylic acids larger than acetic acid, and dicarboxylic acids larger than succinic acid, show an increase with increasing carbon number, even for solutes with similar pK_a values. This increased retention can be attributed to hydrophobic adsorption of the solutes on to the neutral, unfunctionalized regions of the polymeric resin, in a manner similar to that observed in reversed-phase

HPLC. Hydrophobic adsorption effects can be expected to increase in magnitude as the alkyl chain length of the solute is increased, leading to larger retention times. In the case of aromatic acids, the interaction of π -electrons of the benzene ring of the acid with those of the ion exchanger (such as styrene-divinylbenzene packing materials) leads to much higher retention times than expected from their pK_a values. The existence of hydrophobic adsorption effects creates the possibility for manipulation of solute retention by adding typical reversed-phase organic modifiers, such as methanol or acetonitrile, to the mobile phase.

Ion exclusion chromatography is usually carried out on a high-capacity sulfonated PS-DVB resin in the H^+ form. However, recently work has also been carried out using a polymethacrylate resin in the H^+ form with carboxylate functional groups, bare silica (where the silanol group on the surface of the silica acts as the anionic functional group) and also on silica-based cation exchangers functionalized with alkylsulfonic acid or phenylsulfonic acid groups. Since silica gel is chemically stable and inert to organic solvents, silica-based cation exchangers offer the advantage that high concentrations of organic modifiers can be used. Also, aromatic acids which adsorb strongly on to PS-DVB resin due to π -electron interactions between the aromatic ring and the solid resin network are eluted earlier when using a silica gel column.

Other factors which play a part in the retention process of carboxylic acids in ion exclusion chromatography include the addition of other mobile phase modifiers such as polyols, sugars and inclusion compounds (e.g. β -cyclodextrin), as well as resin characteristics such as the pore size, the degree of cross-linking, the ion exchange capacity and the ionic form of the resin.

Applications

The separation of carboxylic acids is the most common application of ion exclusion chromatography. When coupled with spectrophotometric detection at low wavelength (e.g. 210 nm), ion exclusion chromatography yields excellent separations and relatively clean chromatograms for a wide variety of complex sample matrices, such as urine, plasma, foods and beverages and pharmaceuticals. Figure 6 shows a chromatogram for a urine sample, without sample pretreatment. Ion exclusion chromatography has also found increasing use for the determination of anions of weak inorganic acids. It is especially attractive as an adjunct to ion exchange chromatography since the selectivities obtained by these two techniques are quite different. Solutes such as

fluoride, carbonate, cyanide, borate and sulfite have been determined using this approach. Interference from strongly ionized species is minimal because these solutes are unretained and appear at the column void volume. Ion exclusion chromatography can therefore readily separate weakly ionized solutes in samples containing high concentrations of ionic species, e.g. sea water and oil reservoir brines.

Ion Exchange Chromatography

Background

Ion exchange chromatography of carboxylic acids can be performed using an anion exchange stationary phase. The capacity of this anion exchanger is important since the capacity needs to be sufficiently high to separate carboxylic acids of similar charge, but low enough for the ionic strength of the mobile phase to permit the use of conductivity detection. The development of new high-efficiency, low- and medium-capacity columns combined with a new generation of micromembrane suppressors capable of handling concentrated mobile phases has made the determination of carboxylic acids by anion exchange chromatography a practical proposition.

One disadvantage of anion exchange chromatography is that groups of mono-, di- and tricarboxylic acids must be analysed separately. However, the use of gradient elution (water, sodium hydroxide and methanol) has made it possible to separate these compounds in a single run, as well as simultaneously separating inorganic anions (Figure 7).

Ion exchange chromatography of carboxylic acids has been performed on anion exchange resins in the hydroxyl, carbonate, sulfate, chloride, nitrate, formate, acetate or borate form. The mobile phase usually consists of an alkaline solution such as sodium hydroxide or sodium carbonate and sodium hydrogen carbonate, with detection achieved using a suppressor column and conductivity. Solutes are usually low-molecular-weight, saturated or unsaturated acids and hydroxy acids. Factors which affect retention include molecular dimensions, pK_a and specific adsorption of organic acid molecules on the organic matrix of the ion exchanger.

Manipulation of Retention of Acids in Ion Exchange Chromatography

Apart from the usual electrostatic effects which govern retention in ion exchange chromatography, one of the main factors affecting retention of carboxylic acids is the molecular adsorption of the acid on the anion exchange resin. The presence of

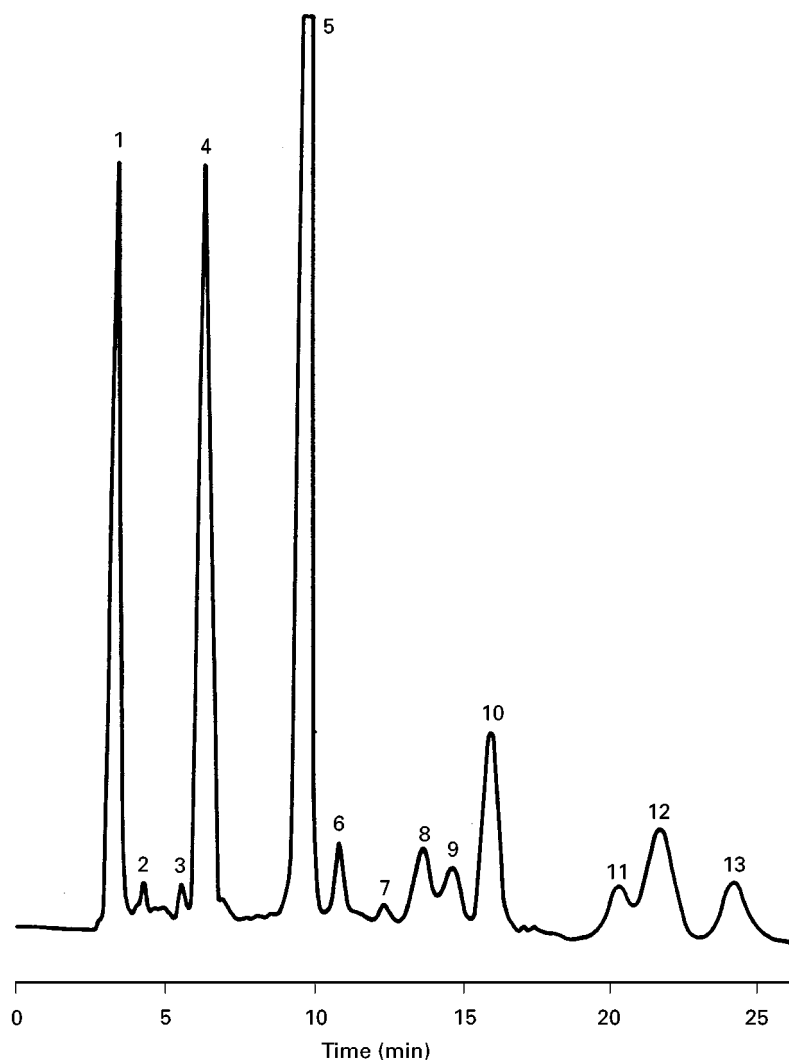


Figure 6 Analysis of human urine using ion exclusion chromatography. An Interaction ORH-801 column was used with a mobile phase comprising $10 \text{ mmol L}^{-1} \text{ H}_2\text{SO}_4$ containing 10% methanol. Detection was at 254 nm. Solute identities: 1, oxalic acid; 2, oxaloacetic acid; 3, α -ketoisovaleric acid; 4, ascorbic acid and α -keto- β -methyl-*n*-valeric acid; 5, β -phenylpyruvic acid; 6, uric acid; 7, α -ketobutyric acid; 8, homoprotocatechuic acid; 9, unknown; 10, unknown; 11, hydroxyphenylacetic acid; 12, *p*-hydroxyphenyllactic acid; 13, homovanillic acid. (Reprinted with permission from Woo DJ and Benson JR (1984) *American Clinical Products Review* Jan: 20.)

double bonds in carboxylic acids leads to higher retention factors, probably due to stronger hydrophobic interactions of the double bond with the polymeric matrix of the resin and also stronger electrostatic interactions between ionic groups. The presence of hydroxy groups in carboxylic acids increases the polarity of the acid and results in stronger interactions both with the aqueous mobile phase (leading to lower retention factors for the acids) and any alkanol substituent of the quaternary ammonium functional group of the anion exchange resin (leading to higher retention factors). Since the adsorption of carboxylic acids plays such an important role in the retention of these acids in ion exchange chromatography, the pK_a

values of the acids are also important, as are any parameters which influence the dissociation of the acid, such as the pH of the mobile phase and the concentration of any organic solvent. Additionally, the pH of the mobile phase may also affect its elution strength and hence affect retention as well.

Applications

Compared to other separation methods such as ion exclusion chromatography, anion exchange provides improved selectivity within the three groups of acids: mono-, di- and tricarboxylic acids. This is particularly true among the stronger acids such as most of

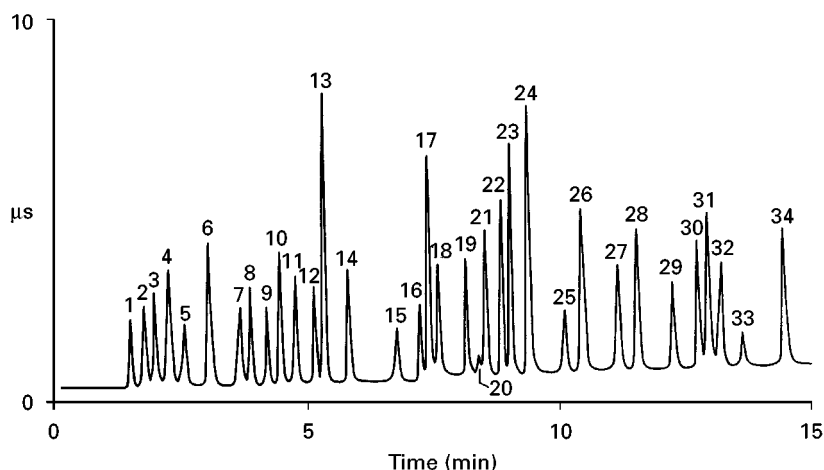


Figure 7 Example of a gradient separation of inorganic and organic acid anions by anion exchange chromatography. A Dionex IonPac AS11 column was used with a mobile phase comprising water and NaOH as a gradient. Detection was by conductivity in the suppressed mode. Solute identities: 1, isopropylethylphosphonic acid; 2, quinate; 3, fluoride; 4, acetate; 5, propionate; 6, formate; 7, methylsulfonic acid; 8, pyruvate; 9, chlorite; 10, valerate; 11, monochloroacetate; 12, bromate; 13, chloride; 14, nitrite; 15, trifluoroacetate; 16, bromide; 17, nitrate; 18, chlorate; 19, selenite; 20, carbonate; 21, malonate; 22, maleate; 23, sulfate; 24, oxalate; 25, ketomalonate; 26, tungstate; 27, phthalate; 28, phosphate; 29, chromate; 30, citrate; 31, tricarballoylate; 32, isocitrate; 33, *cis*-aconitate; 34, *trans*-aconitate. Chromatogram courtesy of Dionex Corporation Product Selection Guide (1997–98) 48.

the di- and tricarboxylic acids. Of the di- and tricarboxylic acids which are in the Krebs cycle or are commonly found in foods, there are only two groups of co-eluting acids: malic and malonic, and isocitric and *cis*-aconitic. Another advantage of anion exchange separation is the possibility of simultaneous determination of some inorganic ions, such as fluoride, chloride, and sulfate, with the carboxylic acids.

Applications of anion exchange chromatography of carboxylic acids include the quantification of short chain organic acids and inorganic anions for the biotechnology, chemical or power industries, the separation of the Krebs cycle acids in foods and beverages, and also the separation of aromatic carboxylic acids in chemical process solutions and as impurities in precursors in the polymer industry.

Conclusion

Four modes of HPLC used in the separation of carboxylic acids have been discussed. Ion suppression chromatography, using a buffer to suppress the ionization of the acids, is the simplest separation system for carboxylic acids. Ion interaction chromatography offers the greatest variety of parameters to alter the selectivity of the separation system by changing the properties of the ion interaction reagent. Ion exclusion chromatography is the most commonly used method in the separation of carboxylic acids due to its compatibility with a wide range of sample matrices. Ion exchange chromatography provides improved

selectivity within groups of acids but the technique requires the use of gradient elution.

See also: I/Ion Exchange. II/Chromatography: Liquid: Mechanisms: Ion Chromatography. Ion Exchange: Theory.

Further Reading

- Bruzzoniti MC, Mentasti E, Sarzanini C and Hajos P (1997) Ion chromatographic separation of carboxylic acids, Prediction of retention data. *Journal of Chromatography* 770: 13–22.
- Coenen AJJM, Kerkhoff MJG, Heringa RM and van der Wal Sj (1992) Comparison of several methods for the determination of trace amounts of polar aliphatic monocarboxylic acids by high-performance liquid chromatography. *Journal of Chromatography* 593: 243–252.
- Ding MY, Koizumi H and Suzuki Y (1995) Comparison of three chromatographic systems for determination of organic acids in wine. *Analytical Science* 11: 239–243.
- Haddad PR and Jackson PE (1990) *Ion Chromatography – Principles and Applications*. Amsterdam: Elsevier.
- Robards K, Haddad PR and Jackson PE (1994) *Principles and Practice of Modern Chromatographic Methods*. London: Academic Press.
- Rocklin RD, Slingsby RW and Pohl CA (1986) Separation and detection of carboxylic acids by ion chromatography. *Journal of Liquid Chromatography* 9: 757–775.
- Schmuckler G (1987) High-performance liquid ion-exchange chromatography. *Journal of Liquid Chromatography* 10: 1887–1901.
- Schwarzenbach R (1982) High-performance liquid chromatography of carboxylic acids. *Journal of Chromatography* 251: 339–358.

Thin-Layer (Planar) Chromatography

J. H. P. Tyman, Brunel University, Uxbridge,
Middlesex, UK

Copyright © 2000 Academic Press

Introduction

The thin-layer chromatography (TLC) of aliphatic and aromatic acids having a wide range of structures has proved to be of great practical value in the chemistry and biochemistry of this large group of organic compounds. This review of the TLC properties of acids is firstly conveniently divided into a discussion of qualitative aspects of the relative hR_F values of various classes of aliphatic and aromatic carboxylic acids having a wide range of structures on different layers and in different solvent systems. Some mention is made of compounds with other acidic functions. Secondly, there is a selective account of applications on the quantitative determination of acids in typical current synthetic and some natural sources.

Acyclic and Cycloaliphatic Compounds

Alkanoic, Alkanedioic, Hydroxy, Keto, Unsaturated, Arylalkanoic Acids and Other Related Acids of Biological Significance

***n*-Alkanoic acid** The separation of these acids by the technique of TLC with respect to the lower homologous fatty acids has a historic precedent in that their separation in the vapour phase on a column coated with a stationary phase was the first published example of gas chromatography.

Although it might be generally considered that gas chromatography is more suitable than TLC for the

separation of alkanoic acids, Table 1 shows some simple conditions that have been used in this series typical of a partition separation. Many of the values quoted in the ensuing tables have been adapted from extensive published information by Hanai (see Further Reading). For comparison, the hR_F values of the dibasic acids malonic, succinic, glutaric and adipic in solvent a are 9, 14, 18 and 22 respectively, and that of glycolic acid, 38. The first four acids in the table have also been examined on crystalline cellulose impregnated with sodium bicarbonate in ethanol-water (100:20) and detection by dicyclohexyl carbodiimide to separate formic acid, acetic, propionic and butanoic acids having the hR_F values 31, 37, 45 and 52 respectively.

***n*-Alkanedioic acids** The saturated dibasic acids have been more widely studied on a variety of layers and solvents, as illustrated in Table 2 which again, as with the monobasic series, shows partition separations. In cases where a considerable number of solvents have been listed, the optimum conditions for the series of compounds have been given. For comparison, the hR_F value of glycolic acid under the conditions of g was 38. In another separation on silica gel (sil G25, Macherey Nagel) with the solvent *n*-pentyl formate-chloroform-formic acid (70:15:15) and detection by bromocresol green, nonlinearity was found in that malonic, succinic, glutaric and adipic acids had hR_F values of 40, 43, 54 and 48 respectively. Folic acid, which may be regarded as a 2-acylamino derivative of glutaric acid, had an hR_F value of 0 compared with 78 for nicotinic acid on silica gel G in water as developing solvent.

Hydroxy acids It is convenient to classify this group of saturated acids as monohydroxy, monohydroxy-

Table 1 hR_F values of homologous alkanoic acids on starch and on cellulose layers

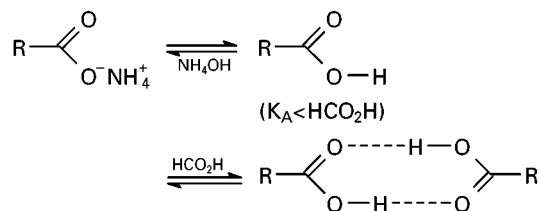
Alkanoic acid	Conditions		Detection	
	a	b	a	b
Formic	52	8	Fluorescein UV 254 nm	Methyl red
Acetic	56	19	Fluorescein UV 254 nm	Methyl red
Propionic	66	28	Fluorescein UV 254 nm	Methyl red
Butanoic	71	37	Fluorescein UV 254 nm	Methyl red
Pentanoic (valeric)	78	48	Fluorescein UV 254 nm	Methyl red
Hexanoic (caproic)	85	59	Fluorescein UV 254 nm	Methyl red

a, Ethanol-water-concentrated ammonia (78:20:13), rice starch; b, light petroleum (40–60°C)-acetone (2:1) 95% saturated with ethane-1,2-diol, cellulose and Dowex® 50 W. (With acknowledgement to Hanai, 1982.)

Table 2 hR_F values of n -alkane- α,ω -dioic acids (dibasic acids) on various layers

Dibasic acid	Conditions						
	a	b	c	d	e	f	g
Oxalic (C_2)					16	0	6
Malonic (C_3)	21	52			20	7.5	9
Succinic (C_4)	37	63	38	27	25	59	14
Gultaric (C_5)	46	71	47	32	31	74	18
Adipic (C_6)	55	82	55	37	38	84	22
Pimelic (C_7)					50	94	
Suberic (C_8)					58	100	
Azelaic (C_9)					67		
Sebacic (C_{10})					72		
Undecyl (C_{11})					82		

a, Ethanol-concentrated ammonia-water (150:8:40), cellulose (Merck 5552); b, 2-ethyl-1-butanol-formic acid-water (40:12:48); c, diethyl ether-light petroleum- CCl_4 -water-formic acid (50:20:20:8:1); polyamide 6; d, ethanol-concentrated ammonia-water (100:16:12), cellulose MN300; e, di- n -butyl ether-formic acid-water (65:25:2.2), cellulose (Merck 5716); f, toluene-propionic acid-water (47:47:4.9), silica gel (Merck 5721); g, ethanol-concentrated ammonia-water (78:13:20), rice starch. (With acknowledgement to Hanai, 1982.) The use of formic acid diminishes streaking sometimes found in the TLC of acids in neutral solvents. It is thought that in acidic solvents the formation of a dimeric intermolecularly hydrogen-bonded species is then favoured in the equilibrium with the monomeric form, while in basic solvents the monomeric anion is largely present. Acidic adsorbents may likewise simulate acidic solvents.



(Modified with permission from Hanai, 1982.)

dibasic, monohydroxytribasic, dihydroxydibasic and polyhydroxy types. Table 3 lists the hR_F values of a number of acids with this functionality. For comparison, the hR_F value of malonic acid under condition f was 40 and in the aromatic series that of mandelic acid (α -hydroxyphenylacetic acid) was 57. In general, cellulose has been used as adsorbent in examples a to e and silica gel in f. In early work, silica gel G-kieselguhr (1:1), kieselguhr impregnated with polyethylene glycol and polyamide layers were also employed. It is possible that in acidic developing solvents certain of these acids are present as intramolecularly hydrogen-bonded structures and that five-membered are likely to be more stable than six-membered rings. Thus glycolic and lactic acids would be expected to have high hR_F values whereas acids having hydrogen-bonded rings and additional acidic groups would have lower values. Under basic conditions with ammonia the solutes are more polar

and the polarity of the developing solvent has to be increased by the use of ethanol. The meso and DL forms of tartaric acid show a small difference of hR_F which can be enhanced by the use of silica gel impregnated with boric acid. It is also possible to separate the enantiomers of racemic hydroxy acids by the incorporation of a chiral additive in the adsorbent layer. The role of impregnated layers has been reviewed by Hauck *et al.* (see Further Reading).

Keto acids The hR_F values of a number of mono keto derivatives of monobasic and dibasic acids are given in Table 4. The compounds shown from top to bottom in the table are glyoxylic, pyruvic, 2-oxobutanoic, 2-oxovaleric, 2-oxoisocaproic, oxaloacetic and 2-oxoglutaric acid. The need of formic acid in high concentration to effect a separation is illustrated in d compared with f. For comparison, the hR_F values under conditions d of citric and malic acids were 44 and 56 respectively. Intramolecular hydrogen bonding may account for the higher hR_F values of the monobasic compounds. The *cis* and *trans* 2,4-dinitrophenylhydrazones of a range of keto acids have been examined.

Unsaturated monobasic dibasic and polybasic acids

The unsaturated acids are a large group which have technical and medicinal uses. The majority are either di- or tribasic. Table 5 summarizes the hR_F values of a selection of compounds. Extensive details of separations have been described by Hanai and also in early work a limited range of monobasic keto-, hydroxy acids and of dibasic acids was studied. The separation of *cis* and *trans* isomers, for example maleic and fumaric acids, appears to be generally straightforward and free of the requirement for argentation TLC, as in the case of unsaturated fatty acids. The stereochemistry of the glutaconic acid described in Table 5 was not stated. The formulae of (1) *trans*-aconitic acid, (2) itaconic acid, (3) *trans*-glutaconic acid, (4) mesaconic acid (*trans*) and (5) citraconic acid (*cis*) are depicted.

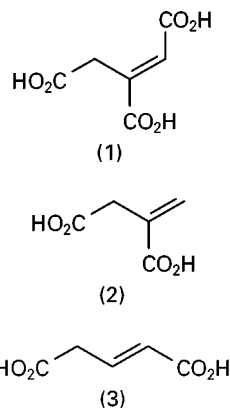
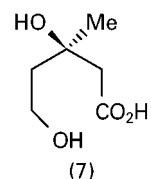
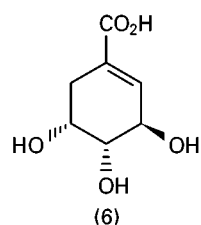
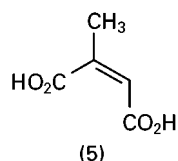
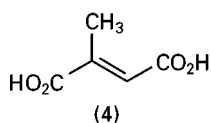


Table 3 hR_F values of hydroxyacids on various layers

Acid	Conditions					
	a	b	c	d	e	f
Glycolic, HOCH ₂ CO ₂ H		67	46	50		31
Lactic, HOCH(CH ₃)CO ₂ H (DL)	76	72	73	89		36
Malic, HO ₂ CCH ₂ CH(OH)CO ₂ H (DL)	29	30	32	35	50	26
Citramalic, HO ₂ CCH ₂ C(Me)(OH)CO ₂ H						65
Citric, HO ₂ CCH ₂ C(CO ₂ H)(OH)CH ₂ CO ₂ H	16	11	18	23	42	22
IsoCitric, HO ₂ CCH(OH)CH(CO ₂ H)CH ₂ CO ₂ H						40
Glyceric, HOCH ₂ CH(OH)CO ₂ H		60	32	24		36
Tartaric, HO ₂ CCH(OH)CH(OH)CO ₂ H (DL)		24	19	18	31	19
Quinic, 1 <i>R</i> ,3 <i>R</i> ,4 <i>R</i> ,5 <i>R</i> -Tetrahydroxycyclohexane carboxylic						18
Ascorbic						15

a, Diisopropyl ether–formic acid, (3:1), cellulose MN 300HR, detection by UV; b, ethanol–concentrated ammonia–water, (150:8:40), cellulose, (Merck 5552), detection by bromocresol green or starch–iodine reagent; c, 2-ethyl-1-butanol–formic acid–water, (40:12:48), cellulose, (Merck 5552), detection as in b; d, diisopropyl ether–formic acid–water, (65:25:10), cellulose (Merck 5716), detection by aniline–xylose, furfural; e, propanol–methyl benzoate–90% formic acid–water, (7:3:2:1), cellulose, detection by Pásková and Munk reagent; f, *n*-pentyl formate–chloroform–formic acid, (70:15:15), silG25, detection by bromocresol green. (With acknowledgement to Hanai, 1982.)



Arylalkanoic acids Prior to an account of the TLC properties of aromatic acids it is of interest to note those of the semi-aromatic group typified by phenylacetic acid and its homologues and analogues. The hR_F values of a range of these compounds are shown in Table 6. The need to use the least polar combination of solvents is illustrated by the conditions with c and d where the latter is ineffective while the former affords a separation of homologous compounds. In the case of the unsaturated compound, the separation in conditions d would almost certainly be improved with argentated silica gel.

Acidic Compounds of Biosynthetic and Biological Importance

A number of polyfunctional cyclohexanyl derivatives classifiable in several of the above groups are (6) shikimic acid, (7) mevalonic acid and (8) abscisic acid, all of which have biological significance. Their TLC properties in a number of solvents have been described.

Table 4 hR_F values of keto acids on various layers

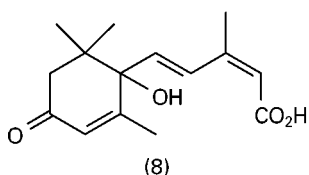
Keto acid	Conditions				
	a	b	c	d	e
OHCCO ₂ H	50		37	55	43
CH ₃ COCO ₂ H	68	25			60
CH ₃ CH ₂ COCO ₂ H	78				
CH ₃ CH ₂ CH ₂ COCO ₂ H		45			
(CH ₃) ₂ CHCH ₂ COCO ₂ H		86			
HO ₂ CCOCH ₂ CO ₂ H	18		86	53	
HO ₂ CCH ₂ CH ₂ COCO ₂ H	36		74	50	45

a, Ethyl formate–light petroleum (60–80°C)–acetic acid (50:50:7), silica gel; b, ethanol–concentrated ammonia–water (78:13:20), rice starch, detection by fluorescein and UV; c, water-saturated diethyl ether–88% formic acid (7:1), silica gel G, aniline ribose reagent; d, chloroform–methanol–formic acid (80:20:1), silica gel G, aniline ribose; e, *n*-pentyl formate–chloroform–formic acid (70:15:15), sil G25, bromocresol green. (With acknowledgement to Hanai, 1982.)

Table 5 hR_F values of unsaturated di- and tribasic acids on various layers

Acid	Conditions								
	a	b	c	d	e	f	g	h	i
Maleic	3				18	30		27	22
Fumaric	32	87	31	83	47	37	82	49	72
Itaconic	49					45	79	53	
Mesaconic (<i>trans</i>)						82	88	62	
Citraconic (<i>cis</i>)						36		39	
Glutaconic						44		56	
Hex-3-ene dicarboxylic	54								
<i>cis</i> -Aconitic	1					4	65		
<i>trans</i> -Aconitic	9	35	9	78			57		

a, Toulene-propionic acid–water, (47:47:4.9), cellulose (Merk 5716), detection by aniline-xylose, furfural; b, diisopropyl ether–formic acid (3:1), cellulose MN300HR, detection by di-chlorofluorescein; c, diethyl ether–formic acid–water, (10:2:1), cellulose (DC Fertigplatten) detection by fluorescence; d, 95% ethanol–25% ammonia–water (8:2:1), same layer and detection as c; e, diisopropyl ether–light petroleum–carbon tetrachloride–water–formic acid (50:20:20:8:1), polyamide 6, detection by K ferricyanide, ferric ammonium sulfate; f, *n*-pentyl formate–chloroform–formic acid (20:70:10), sil G25, detection by bromocresol green; g, propanol–methyl benzoate–90% formic acid–water (7:3:2:1), layer not stated but probably cellulose, detection by Pásková and Munk reagent; h, butyl formate–ethyl acetate–formic acid (82:9:9), polyamide, bromocresol green; i, diisopropyl ether–formic acid–water, (90:7:3) silica gel, bromocresol green. (With acknowledgement to Hanai, 1982 and to Copius-Peereboom, 1969.)



Shikimic acid (6), a hydroxy unsaturated cyclic compound, in the solvent g (Table 5) had an hR_F of

Table 6 hR_F values of derivatives and homologues of phenylacetic acid

Acid	Conditions			
	a	b	c	d
Phenylacetic	68	74	54	95
4-Phenylbutanoic			75	95
4-Phenylbut-3-enoic			71	95
Phenoxyacetic	64	63		
<i>trans</i> -Cinnamic			67	95

a, *n*-pentyl formate–chloroform–formic acid, (70:15:15), sil G25, bromocresol green; b, *n*-pentyl formate–chloroform–formic acid (20:70:10), sil G25; c, light petroleum–acetic acid, (49:1), silica (Eastman), bromocresol green; d, light petroleum–diethyl ether–formic acid, (45:5:1), silica (Eastman). (With acknowledgement to Hanai, 1982.)

Table 7 The hR_F values of cyclohexane- and dienecarboxylic acids (dihydro- and tetrahydro-derivatives of benzoic acid)

Compound	Conditions	
	a	b
Cyclohexanecarboxylic acid	83	92
Cyclohexa-1-enecarboxylic acid	91	95
Cyclohexa-3-enecarboxylic acid	91	95
Cyclohexa-1,4-dienecarboxylic acid	77	83
Cyclohexa-2,5-dienecarboxylic acid	77	82
Benzoic acid (cyclohexa-1,3,5-trienecarboxylic)	77	88
2-Hydroxycyclohexanecarboxylic acid	54	21

a, Benzene–dioxane–acetic acid (90:25:4), kieselgel G, detection by autoradiography; b, light petroleum–diethyl ether–acetic acid (50:50:1), as before in a. (With acknowledgement to Hanai, 1982.)

32. The hR_F value of the keto hydroxyacid, mevalonic acid, in diethyl ether–formic acid (7:1) on silica gel (Eastman) was 29 and that of abscisic acid in *n*-propanol–25% ammonia–water (80:10:10) on kieselgel (HF254) was 57. The rooting hormone, indole-3-acetic acid, under the same conditions was 45.

The hR_F values of other cyclic compounds which are metabolites of benzoic acid and also structurally related to shikimic acid are given in Table 7 alongside the reference compound benzoic acid. Isomeric compounds were not separable, although by the use of argentation TLC this may be possible.

Aromatic Acidic Compounds

Substituted Benzoic Acids

In this category the compounds under consideration are those in which the carboxyl group is directly attached to the aryl ring.

The isomeric hydroxybenzoic acids have been listed in the section on phenols. In Table 8 the TLC properties of the aminobenzoic acids are given alongside the reference compounds benzoic acid, 2-hydroxybenzoic acid, 2,4-dihydroxybenzoic acid, 3,4,5-trihydroxybenzoic acid (gallic acid) and phthalic acid.

The hR_F values of a wide range of other phenolic acids have been recorded, as have those of more complex compounds, the polycyclic series of lichen acids. In the case of *cis* and *trans* isomers of aromatic acids having an unsaturated side chain, separations do not seem to be difficult. Thus, on silica gel 60 (F₂₅₄) with diethyl ether–hexane–chloroform–acetic acid (12:38:50:0.5) the hR_F values of *cis*- and *trans*-3,4-dihydroxycinnamic acid were 18 and 27 and of the corresponding isomers of

Table 8 hR_F values of aminobenzoic acids and some hydroxybenzoic acids

Acidic compound	Conditions					
	a	b	c	d	e	f
Benzoic	53	15	72	69	79	
2-Aminobenzoic	38					
3-Aminobenzoic	28					
4-Aminobenzoic	24					
2-Hydroxybenzoic	55			72	78	54
2,4-Dihydroxybenzoic	19					30
3,4,5-Trihydroxybenzoic	4					11
Phthalic	17			55	41	

a, Ethanol–butanol–water–concentrated ammonia (40:30:15:15), rice starch, detection by UV; b, *n*-hexane–acetic acid (96:4), SIF silica gel sheet, UV; c, same as b, cellulose-TLC alumina, UV; d, *n*-pentyl formate–chloroform–formic acid (70:15:15), sil G25, detection by bromocresol green; e, *n*-pentyl formate–chloroform–formic acid (20:70:10), same as d, UV; f, 2-butanone–methyl phenyl ketone–50% acetic acid (5:5:4), poly-*N*-vinylpyrrolidone–gypsum, detection by molybdate, diazotized sulfanilic acid, phloroglucinol. (With acknowledgement to Hanai, 1982.)

4-hydroxy-3,5-dimethoxycinnamic acid, 43 and 55 respectively.

The effect of the aryl nucleus, Ar, on the hR_F value of the acid ArCO_2H is seen with benzoic, naphthalene-2-carboxylic and diphenyl-2-carboxylic acids, which are 53, 70 and 75 respectively with the solvent ethanol–butanol–water–conc ammonia (40:30:15:15) and the adsorbent, rice starch. The water-soluble vitamin, nicotinic acid (pyridine-3-carboxylic acid) on sil G25 had an hR_F value of 5 in *n*-pentyl formate–chloroform–formic acid (70:15:15), while that of benzoic acid was 69.

The hR_F values of the isometric benzenedicarboxylic and certain polybasic reference acids were the subject of early studies under a variety of conditions and are shown in Table 9.

More recent experiments on the separation of the dicarboxylic acids have been carried out with chloroform–tetrahydrofuran (2:1) on silufol in the presence of an ion pair reagent but the separations described earlier were just as effective.

The influence of the substituent position on the hR_F values of substituted benzoic acids has been studied with reference to amino, nitro, chloro, hydroxy and carboxy compounds, although nothing appears to have been described on the separation of the isomeric toluic acids. However, there has been extensive work by Guinchard *et al.* (see Further Reading) on (1) benzoic acid compared with (2) 2-chloro, (3) 3-chloro, (4) 4-chloro, (5) 2-hydroxy, (6) 3-hydroxy, (7) 4-hydroxy, (8) 2-nitro, (9) 3-nitro, (10) 4-nitro, (11) 2-amino and (12) 4-aminobenzoic acid. Figure 1

depicts the effect on the R_F of small changes in the aqueous formic acid concentration in benzene when this range of acids was chromatographed on silica gel G.

Figure 2 depicts the effect on the R_F value of the same series when run in benzene containing diethyleneglycol monoethyl ether with various concentrations of formic acid. Separation of all 12 acids can be achieved in either system with the appropriate formic acid concentration. The more polar compounds have lower R_F values than the less polar ones.

By contrast, under reversed-phase conditions with benzene as the developing solvent, Figure 3 shows the separations of a number of 2-substituted benzoic acids on silanized silica gel (RP-8) with various aqueous organic solvents (organic solvent–water, 40:60, v/v) containing 0.1 mol L^{-1} tetramethylammonium bromide. With this system the more polar solutes have higher R_F values.

An extensive range of adsorbents and solvents for a variety of aromatic carboxylic acids have been summarized by Tyman (see Further Reading).

While carboxylic acids have been the main group of acidic compounds studied, by contrast sulfonic acids RSO_3H , of both aliphatic and aromatic origin, have received little attention. 1-*N*-Acylamino-8-hydroxynaphthalene-3,6-disulfonic acid derivatives of interest for anti-human immunodeficiency virus activity have been studied on S III Chromarods with methanol or methanol–chloroform–ammonia (35:55:10) as solvents.

Sulfuric esters, ROSO_3H of substituted phenols, have been examined on silica gel G with benzene–butanone–ethanol–water (30:30:30:10). The less acidic group, for example the sulfonamides, $\text{NH}_2\text{C}_6\text{H}_4\text{SO}_2\text{NHR}$ (where R comprises a wide variety of

Table 9 The hR_F values of carboxy derivatives of benzoic acid

Acid	Conditions			
	a	b	c	d
Phthalic (1,2)	51	30	39	36
Isophthalic (1,3)	75	64	71	59
Terephthalic (1,4)	0	69	81	0
Trimellitic (1,2,4)	41	13	14	13
Pyromellitic (1,2,4,5)	0	2	2	0
Hexahydrophthalic	60	65	79	66

a, Diisopropyl ether–formic acid–water (90:7:3), silica gel; b, same as b but saturated with polyethylene glycol M 1000 kieselguhr impregnated with polyethylene glycol; c, diisopropyl ether–light petroleum–carbon tetrachloride–formic acid–water (50:20:20:8:1), polyamide; d, butyl formate–ethyl acetate–formic acid (82:9:9), same polyamide as c. (With acknowledgement to Copius-Peereboom, 1969.)

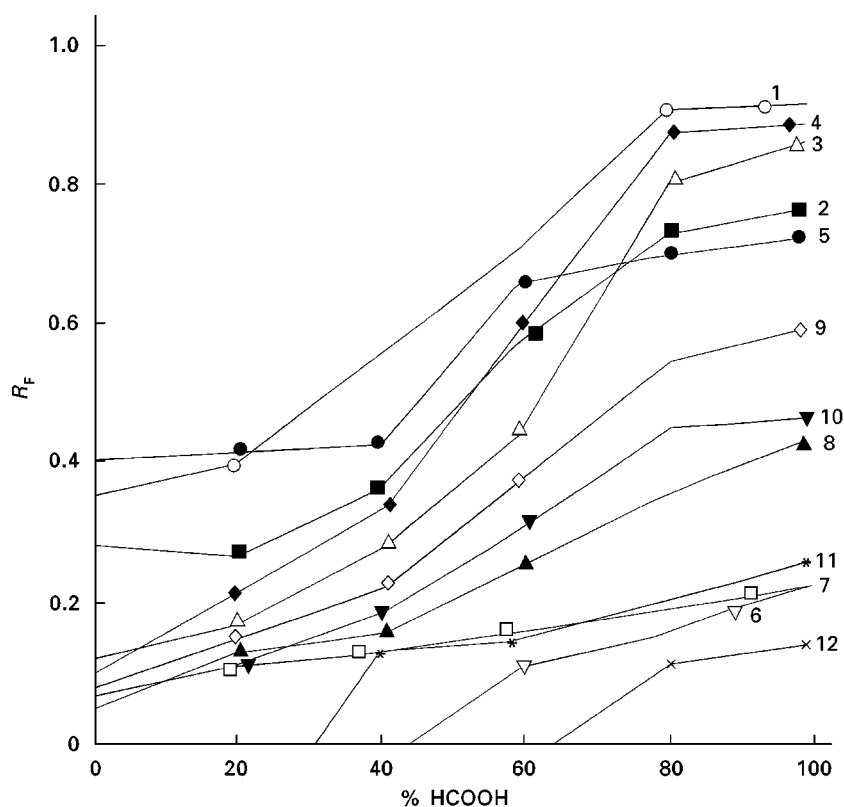


Figure 1 R_F values of aromatic carboxylic acids in benzene containing formic acid. 1, Benzoic; 2, 2-chloro; 3, 3-chloro; 4, 4-chloro; 5, 2-hydroxy; 6, 3-hydroxy; 7, 4-hydroxy; 8, 2-nitro; 9, 3-nitro; 10, 4-nitro; 11, 2-amino; 12, 4-aminobenzoic acids. (Reproduced with permission from Guinchard *et al.*, 1976.)

groups), has been examined in detail. Monoalkyl phosphate esters, ROP(O)(OH)_2 , dialkyl esters, $(\text{RO})_2\text{P(O)OH}$ and monoalkylphosphonic acids RP(O)(OH)_2 do not seem to have been examined by TLC.

Visualizing Agents for Aromatic Carboxylic Acids

In this article, reference has frequently been made to the detection of acids with bromocresol green and other systems. Some other reagents for aromatic carboxylic acids are hydrogen peroxide or alkaline potassium permanganate. Several new visualizing agents and sodium hydroxide (10% aqueous solution) were compared with respect to the minimum quantity of acid detectable (μg per spot) and the type of layer. Generally, of the three layers, silica gel 60 GF_{254} , silica gel-kieselguhr mixtures and polyamide, the first was preferred. Although the minimum detectable amount of solute varied with the 13 different solutes and the 12 different visualizing agents examined, thymol blue detected all the solutes while bromothymol blue and bromocresol green detected all but 4-hydroxybenzoic acid and 3-hydroxycinnamic acid respectively with silica gel as adsorbent.

Quantitative TLC Determination of Organic Acids in Synthetic and Natural Mixtures

Examples of the application of TLC for the quantitative determination of a variety of acids in edible, potable and polymeric products are discussed in this section. Many simple aliphatic acid aromatic acids, notably benzoic acid, citric and sorbic acids, are employed in edible materials such as preservatives while salicylic acid and its acetyl derivative appear in numerous pharmaceutical preparations. Accordingly, their quantitative determination is important and for such analyses planar methods have been widely used. Some typical quantitative applications are described in detail.

HPTLC Determination of Organic Acid Preservatives in Beverages

In a high performance TLC (HPTLC) method sorbic acid (2,4-hexadienoic acid) and benzoic acid were determined without preliminary extraction or clean-up by the chromatography of aliquots of samples and of standards on preadsorbent silica gel or C_{18} -bonded silica gel plates containing fluorescent indicator.

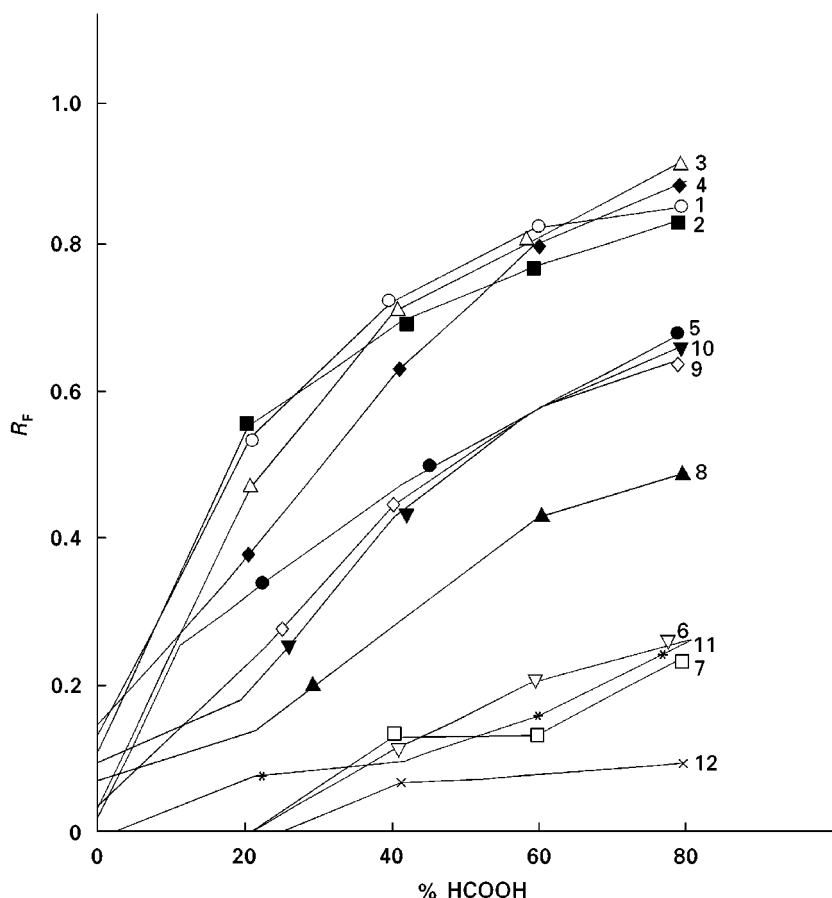


Figure 2 R_F values of aromatic carboxylic acids. 1, Benzoic; 2, 2-chloro; 3, 3-chloro; 4, 4-chloro; 5, 2-hydroxy; 6, 3-hydroxy; 7, 4-hydroxy; 8, 2-nitro; 9, 3-nitro; 10, 4-nitro; 11, 2-amino; 12, 4-aminobenzoic acid in benzene containing formic acid and diethylene glycol monoethyl ether. (Reproduced with premission from Guinchard *et al.*, 1976.)

The zones which quenched fluorescence upon UV irradiation at 254 nm were compared by scanning densitometry. This procedure was preferred to measurement of densitometry based on UV absorption.

Preadsorbent high-performance LHPKDF silica gel (Whatman) plates (20 × 10 mm) with 19 lanes were used for normal-phase experiments with the solvent *n*-pentyl formate–chloroform–formic acid (2 : 7 : 1) in which the R_F values for sorbic acid and benzoic acid were 61 and 58. For reversed-phase TLC on (Whatman) C_{18} LKC₁₈F plates (20 × 20 mm) with methanol–0.5 mol L⁻¹ sodium chloride (1 : 1), the respective R_F values for these two acids were 44 and 59. It was found necessary to apply a stream of warm air during spotting of samples with a 10 μ L Drummond digital microdispenser and, after this stage, to dry the plates. Development was then effected in a Camag twin-trough chamber to 7 cm beyond the sorbent–preadsorbent interface with normal-phase plates and to 10 cm for C_{18} plates. The plates were then dried and the areas of the dark quenched zones against a fluorescent background were scanned at the

predetermined maximum absorption (between 200 and 370 nm) with a Shimadzu Model 930 densitometer operated in the reflectance mode. From the chromatography of 0.50, 1.00, 2.00, 4.00, 6.00 and 8.00 μ L of standards for sorbic and benzoic acids containing 125–2000 ng and 1.00–16.0 μ g respectively, linear calibration plots of scan area/weight were obtained. For quantification, the sample scan area was compared with that of a closely matching standard within the linear calibration range and the corresponding weight found. Recovery analyses were carried out with beverage samples spiked with sorbic and benzoic acids, which were compared with the corresponding unfortified samples. They averaged at 98.0% for all analyses.

By the HPTLC method, sorbic and benzoic acids present separately in a variety of beverages have been directly quantified. The analysis of standards on the same TLC plate eliminates the requirement for an internal standard, as in high performance liquid chromatography (HPLC). By contrast with the HPTLC and HPLC methods, spectrophotometric

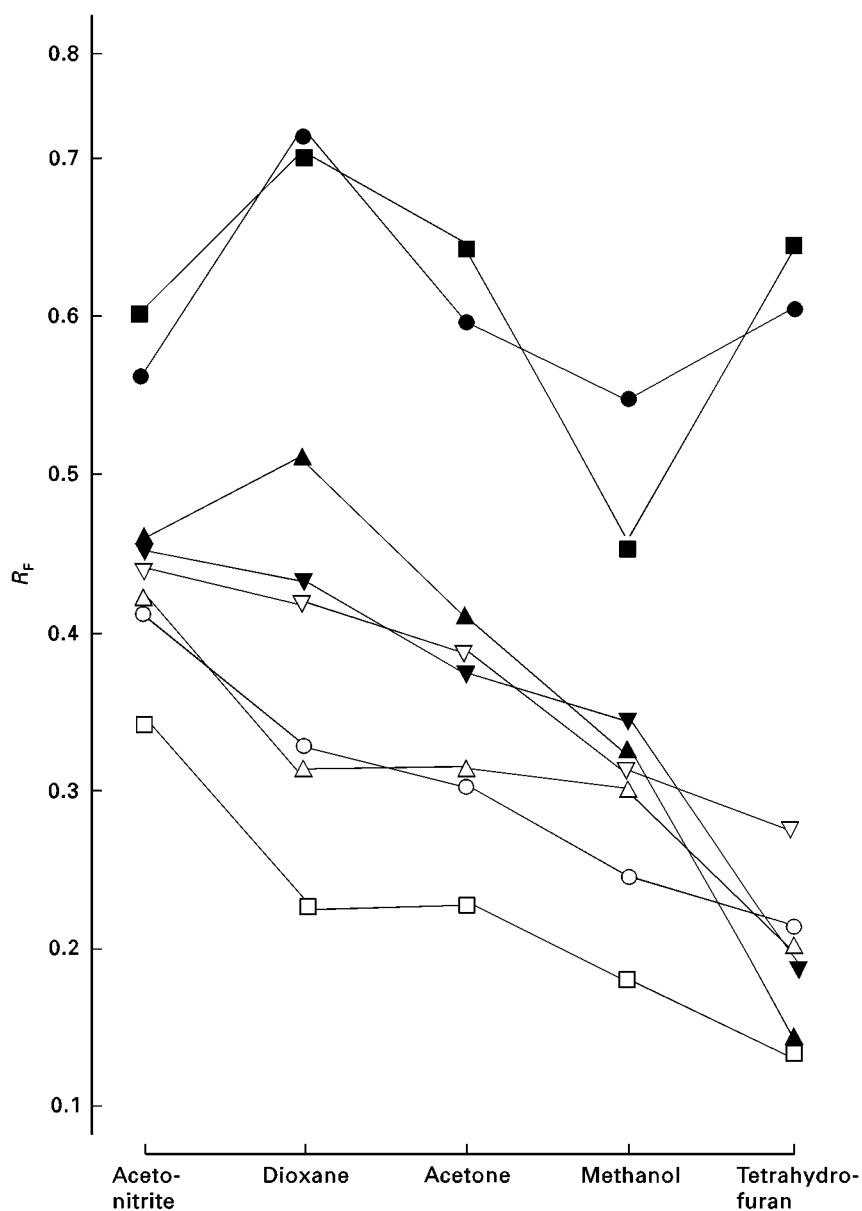


Figure 3 R_F values of 2-substituted benzoic acids in different solvents. The solvent composition, organic component–water (40:60 v/v) with addition of 0.1 mol L^{-1} tetramethylammonium bromide (pK value in parentheses): open circles, benzoic acid (4.19); filled triangles, 2-hydroxy (2.97); open squares, 2-acetoxy (3.5); filled squares, 2-carboxy (2.91/5.59); filled circles, 2-nitro (2.16); open squares, 2-methyl (3.91); open triangles, 2-amino (6.97); filled/inverted triangles, 2-chloro (2.92). (Reproduced with permission from Jost *et al.*, 1984.)

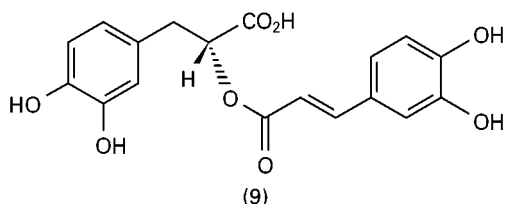
analysis requires a preliminary sample preparation by steam distillation. However, very low concentrations of benzoic acid are more amenable to HPLC analysis and when sorbic and benzoic acids are present together the method is less satisfactory due to sample streaking, even on a C_{18} -bonded silica gel layer (particularly at higher loads).

In view of these limitations, a modified method was adopted, involving solid-phase extraction (SPE) on a C_{18} cartridge followed by the preceding quantification method established on preadsorbent C_{18} plates.

The extraction procedure was validated by spiking commercial samples with known amounts of the acids in turn and demonstrating the satisfactory recovery of each. With this total method, sample interferences were eliminated and samples too low for analysis by direct spotting could be analysed. The whole TLC methodology is considered to be applicable to a wide range of solid and syrupy-type samples containing either or both of the two preservatives at concentrations as low as those measurable by HPLC.

Quantitative Fluorescence Densitometry for the Analysis of Rosmarinic Acid

Rosmarinic acid (9), a useful natural antimicrobial compound of potential interest to the food industry, occurs in eel grass (*Zostera marina*) from which it is extractable together with a number of other phenolic acids. It has been directly quantitatively and rapidly analysed by an HPTLC densitometric method which utilized the fluorescence of the material upon excitation at 366 nm.



Crushed leaves (200 mg) of the natural product were extracted with 5% acetic acid-methanol (1:2) accompanied by ultrasonication during 30 min. The extract was filtered and then employed for direct HPTLC on plates (10 × 20 cm) pre-coated with cellulose without fluorescent indicator. Samples and standard solutions (2 µL) were applied to plates as 7 mm wide bands with a Linomat IV applicator under a pressure of 2.5 bar; this was developed in a twin-trough chamber with 3% sodium chloride in 0.5% acetic acid-acetonitrile-tetrahydrofuran (100:24:1) until the solvent had migrated 4.5 cm. The dried plate was irradiated with a mercury vapour lamp and the resultant fluorescence emission measured through a cut-off filter (400 nm) by scanning with a TLC scanner II (Camag) equipped with CATS software (version 3.14).

Plots of either peak area or height/concentration were linear over concentration range 0.1–0.6 mg mL⁻¹ (i.e. 0.2–1.2 µg) and the weight of rosmarinic acid in unknown samples was readily found.

Densitometric Analysis of Gallic Acid in Fermentation Liquors

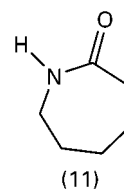
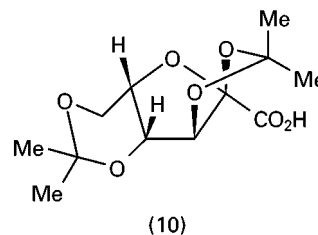
One of the ways used for obtaining gallic acid (3,4,5-trihydroxybenzoic acid), an important intermediate in synthesis for the pharmaceutical and food industries, is by the acid hydrolysis of natural gallotannins, for example from gall nuts, tara pods or sumac leaves. In an enzymatic procedure hydrolysis of these types of raw material with a fungal tannin acylhydrolase which cleaves depside bonds, the monitoring of a large number of samples by a simple and rapid TLC method was investigated as a potential alternative to HPLC analysis.

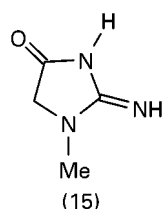
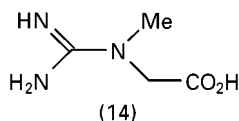
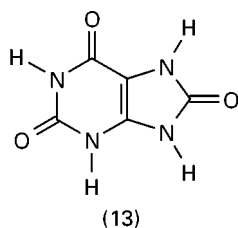
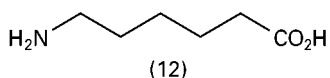
Crude samples from enzymatic solutions were diluted between one- and 100-fold with methanol and

filtered through a Minisart NML 0.45 µm filter and gallic acid used at known concentrations as an internal standard. TLC analysis was performed on glass plates (5 × 20 cm), coated with a 0.25 mm layer of RP-18 F₂₅₄ (Merck 15683); the glass plates were pre-cleaned with a single development in methanol. Samples (6 µL) were applied with a Linomat IV spotter and then developed to a distance of 12 cm, with M aqueous acetic acid-methanol (1:1) for 2 h. Densitometry was effected by spectrophotometry and a mercury light source (254 nm) in the absorbance mode, to determine extinction of fluorescence, as an area measurement, with a TLC scanner II (Camag) controlled by CATS software. Calibration plots were found to be near to linearity with between 10 and 75 µg gallic acid on the plate when the ratios of the peak area of the acid to the internal standard were between 0.3 and 1.5, although in practice ratios of areas between 0.5 and 1.25 (corresponding to gallic acid between 25 and 62.5 µg) were adopted in the analytical method. An inherent difficulty was found to be slight inhomogeneity in the coating of the fluorescent indicator: to improve on this, the plate was scanned before an assay to determine any background fluorescence, which was then subtracted to 'zero' the plate. With this proviso and by the use of the strict linearity range, the values obtained for gallic acid were 98 ± 2.1% of those found by HPLC.

Determination of Diacetonegulonic acid (DAG) in Water Samples

DAG (10) is the penultimate intermediate in the synthesis of ascorbic acid (vitamin C) and for many years was discharged in waste surface waters. This led to contamination of groundwaters and, although it is not toxic to humans, it has an inhibitory effect on the growth of grasses. Current European drinking water regulations restrict its concentration to 0.1 µg L⁻¹. A fast and efficient HPTLC method has been described.





Due to the low concentration of DAG, SPE is used for sample preparation. Because of the sensitivity of DAG to silica gel and, more particularly to acidic solutions, it was found necessary to adjust the water sample for analysis to no less than pH 4 and to effect SPE with Polyspher RP-18 (a 35 μm polystyrene-divinylbenzene polymer with C_{18} side chains) which gave a 100% recovery. For the extraction a cartridge (0.2 g) was first conditioned successively with ethyl acetate, methanol and water at pH 4 (1 cm^3 of each), after which the water sample for analysis adjusted to pH 4 (20 cm^3) was aspirated through the cartridge. The cartridge was dried in a stream of nitrogen and then eluted with ethyl acetate (2 \times 1 cm^3) and the eluate after treatment with one drop of ammonia evaporated at less than 40°C to leave 0.5 cm^3 , an aliquot of which was applied to an PTLC silica gel 60 F₂₅₄ pre-coated plate (10 \times 20 cm). In the case of original concentrations of less than 5 $\mu\text{g L}^{-1}$, the total eluate was used for TLC.

For analysis of sample volumes up to 20 μL , multiple development one-dimensionally with solvent A, chloroform-methanol (80:20) to 8 cm and then after drying, solvent B (chloroform-methanol-glacial acetic acid, 80:20:2) for 6.5 cm was carried out. Alternatively, two-dimensional development was carried out with the same two solvents, distances and drying. Spots or streaks were detected by immersion of the plate in an ethanolic solution of 4-methoxybenzaldehyde containing sulfuric acid, followed by drying and heating at 130°C for 2–3 min to form red fluor-

escent areas which were visible under UV light (366 nm) and quantified with a TLC scanner. Two-dimensional development was advocated for samples with less than 5 $\mu\text{g L}^{-1}$ DAG, while for higher concentrations, one-dimensional development was adequate. The calibration of peak area/weight DAG was linear within the range 0.125–1.5 μg . It was found that for the determination of higher concentrations it was essential to apply DAG as streaks to preserve linearity over the range of concentrations and it was then established that from 0.25 to 250 μg could be analysed with consistent accuracy.

The SPE procedure followed by TLC appears to be superior to derivatization followed by GC-MS and it was considered that very small concentrations of DAG could even be estimated visually without any instrumentation, thus generally giving an inexpensive procedure. Other application of quantitative TLC to the analysis of humic acids in natural waters, 6-aminocaproic acid (12), ϵ -caprolactam in polyamide-6 (11) and to uric acid (13), creatine (14) and creatinine (15) mixtures in biological materials have been described.

Conclusions

Acids of simple and more complex structures are components of many edible, technical and medicinal products and TLC affords an ideal approach for their analysis because no derivatization is required and a wide variety of detection methods is applicable for their qualitative and quantitative determination. It can be envisaged that the use of HPTLC, of special layers and the employment of combined techniques will continue to extend and expand the planar approach to the analysis of acidic compounds.

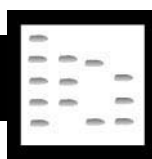
See also: II/Chromatography: Thin Layer (Planar): Densitometry and Image Analysis; Ion Pair Thin-Layer (Planar) Chromatography; Spray Reagents. III/Acids: Gas Chromatography; Liquid Chromatography.

Further Reading

- Ariga N (1972) Thin-layer chromatography of keto acid 2,4-dinitrophenylhydrazones. *Analytical Biochemistry* 1972, 49: 436.
- Barthomeuf C, Regerat F and Combe-Chevaleryer S (1993) Densitometric analysis of gallic acid in fermentation liquors. *Journal of Planar Chromatography* 6: 245–247.
- Copius-Peereboom JW (1969) Thin layer chromatography. In: Stahl E (ed.) *Foodstuffs and their Additives*, p. 653. London: G Allen and Unwin.
- Eisenbeiss A, Reuke S and Türck M (1992) Determination of diacetoneketogulonic acid in water samples by HPTLC. *Journal of Chromatography* 589: 390–393.

- Gänshirt H (1969) Synthetic pharmaceutical products. In: Stahl E (ed.) *Thin-layer Chromatography*, p. 541. London: G. Allen and Unwin.
- Guinchard C, Truong TT, Masson JD and Panouse JD (1976) Migration d'acides aromatiques en chromatographie sur couche mince de gel de silice en fonction de la teneur en eau ou en acide formique de solutions créant l'atmosphère de la cuve à chromatographie. *Chromatographia* 9: 627–629.
- Hanai T (1982) Phenols and organic acids. In: Zweig G and Sherma J (eds), *Handbook of Chromatography*, vol. 1, pp. 159–174. Boca Raton, CRC Press.
- Hauck HE, Mack M and Jost W (1996) Sorbents and precoated layers in thin-layer chromatography. In: Sherma J and Fried BJ (eds) *Handbook of Thin Layer Chromatography*, 2nd edn, p. 101. New York: Marcel Dekker.
- Jost W, Hauck HE and Herbert H (1984) Reversed-phase thin-layer chromatography of 2-substituted benzoic acids with ammonium compounds as ion-pair reagents. *Chromatographia* 18: 512–516.
- Kaštelan-Macan M, Cerjan-Stefanovics and Jalšovec D (1992) Determination of aquatic humic acids in natural river waters. *Water Science and Technology* 26: 2567–2570.
- Khan SH, Murawski MP and Sherma J (1994) Quantitative HPTLC determination of organic acid preservatives. *Journal of Liquid Chromatography* 17: 855–865.
- Klaus R, Fischer W and Hauck HE (1991) Qualitative and quantitative analysis of uric acid, creatine and creatine together with carbohydrates in biological materials by HPTLC. *Chromatographia* 32: 307–316.
- Madelaine-Dupich C, Azema J, Escoula B, Rico L and Lattes A (1993) Analysis of N-acylaminonaphthalene sulphonic acid derivatives with potential anti-human immunodeficiency activity by TLC and FID. *Journal of Chromatography* 653: 178–180.
- Petersen HW, Petersen LM, Piet H and Ravn H (1991) A new HPTLC fluorescence densitometric method for the quantitative analysis of rosmarinic acid. *Journal of Planar Chromatography* 4: 235–236.
- Petrowitz H-J (1969) Synthetic organic products. In: Stahl E (ed.) *Thin-layer Chromatography*, p. 678. London: G. Allen and Unwin.
- Sarbach Ch, Postaire E and Sauzieres J (1994) Simultaneous determination of ϵ -caprolactam and ϵ -aminocaproic acid contaminants in polyamide-6. *Journal of Liquid Chromatography* 17: 2737–2749.
- Smith MC and Sherma J (1995) Determination of benzoic acid and sorbic acid preservatives. *Journal of Planar Chromatography* 8: 103–106.
- Tyman JHP (1996) Phenols, aromatic carboxylic acids and indoles. In: Sherma J and Fried BJ (eds) *Handbook of Thin-layer Chromatography*, 2nd edn, pp. 906–907, 912–913. New York: Marcel Dekker.
- Wardas W, Pyka A and Jedrzejczak M (1995) Visualising agents for aromatic carboxylic acids in TLC. *Journal of Planar Chromatography* 8: 148–151.
- Williams RJ and Evans WC (1975) The metabolism of benzoate by *Moraxella* species through anaerobic nitrate respiration. *Biochemistry Journal* 148: 1.

AFLATOXINS AND MYCOTOXINS



Chromatography

R. D. Coker, Natural Resources Institute,
Medway University, Chatham, UK

Copyright © 2000 Academic Press

Introduction

Mycotoxins have been defined as 'fungal metabolites which, when ingested, inhaled or absorbed through the skin, cause lowered performance, sickness or death in man or animals, including birds'.

Exposure to mycotoxins can produce both acute and chronic toxic effects ranging from death to deleterious effects on the central nervous, cardiovascular and pulmonary systems, and on the alimentary tract. Mycotoxins may be carcinogenic, mutagenic, teratogenic and immunosuppressive. The ability of some mycotoxins to compromise the im-

mune system and, consequently, to reduce resistance to infectious disease, is now widely considered to be their most important effect.

The mycotoxins attract worldwide attention because of the significant economic losses associated with their impact on human health, animal productivity and both domestic and international trade. It has been estimated, for example, that annual losses in the USA and Canada arising from the impact of mycotoxins on the feed and livestock industries are in the order of US\$5 billion. In developing countries where the food staples (e.g. maize and groundnuts) are susceptible to contamination, significant additional losses amongst the human population are likely, because of morbidity and premature death associated with the consumption of mycotoxins.

It is likely that mycotoxins have plagued mankind since the beginning of organized crop production. Ergotism (St Anthony's Fire), for example, which is caused by the consumption of rye contaminated with the 'ergot alkaloids', is discussed in the Old

Testament, and reached epidemic proportions in many parts of Europe in the tenth century.

Mycotoxins of Worldwide Importance

An 'important' mycotoxin will have demonstrated its capacity to have a significant economic impact on the exposed human and/or animal population. Those moulds and mycotoxins that are currently considered to be of worldwide importance are shown in **Table 1**, and the chemical structures of the mycotoxins in **Figure 1**.

Aflatoxins

The term 'aflatoxins' was coined in the early 1960s when the deaths of thousands of turkeys ('Turkey X' disease), ducklings and other domestic animals were attributed to the presence of *Aspergillus flavus* toxins in groundnut meal imported from South America. The acute and chronic effects of the aflatoxins on a wide variety of livestock are now well documented, and include death, decreased productivity, and increased susceptibility to disease. Aflatoxin B₁ is a human carcinogen and one of the most potent hepatocarcinogens known. Human fatalities have resulted from the consumption of heavily aflatoxin-contaminated foods, frequently when wholesome food is in short supply. Aflatoxin M₁ occurs in milk, and is produced by the bovine metabolism of aflatoxin B₁ when contaminated feed is ingested by dairy cows.

Trichothecenes

T-2 toxin, deoxynivalenol (and nivalenol) belong to a large group of structurally related sesquiterpenes known as the 'trichothecenes', which occur primarily in cereals. T-2 toxin is the probable cause of 'alimentary toxic aleukia' (ATA), a disease that affected thousands of people in Siberia during the Second World War, and led to the elimination of entire villages. The symptoms of ATA include fever, vomiting, acute inflammation of the alimentary tract and a variety of blood abnormalities. The same toxin is also

associated with outbreaks of haemorrhagic disease in animals and with neurotoxic effects in poultry. An important effect of T-2 toxin (and other trichothecenes) is the immunosuppressive activity which has been clearly demonstrated in experimental animals.

Deoxynivalenol (DON) is probably the most widely occurring *Fusarium* mycotoxin. (The trivial name of 'vomitin' has also been accorded to DON because of outbreaks of emetic (and feed refusal) syndromes, amongst livestock, caused by this toxin.) The ingestion of DON has caused acute human mycotoxicoses in India, China and rural Japan. The Chinese outbreak, in 1984–85, was caused by mouldy maize and wheat. Symptoms occurred within 5 to 30 min and included nausea, vomiting, abdominal pain, diarrhoea, dizziness and headache.

Zearalenone

Zearalenone is an oestrogenic mycotoxin that is co-produced with DON, and which has been implicated, with DON, in outbreaks of acute human mycotoxicoses. In livestock, exposure to zearalenone-contaminated maize has caused hyperoestrogenism, especially in pigs, characterized by vulvar and mammary swelling and infertility.

Fumonisin

Fumonisin B₁ (FB₁) occurs in maize produced in a variety of agroclimatic zones. Two animal species, horses and pigs, are particularly targeted by FB₁. Exposure to FB₁ causes leukoencephalomalacia (LEM) in horses and pulmonary oedema in pigs. The presence of fumonisins in maize has been linked with human oesophageal cancer in the Transkei (South Africa) and China.

Ochratoxin A

Ochratoxin A (OA) causes nephropathy and immunosuppression in several animal species, and is carcinogenic in experimental animals. OA has been linked to the human disease Balkan endemic

Table 1 Moulds and mycotoxins of worldwide importance

Mould species	Mycotoxins produced	Main sources
<i>Aspergillus parasiticus</i> <i>A. flavus</i>	Aflatoxins B ₁ , B ₂ , G ₁ , G ₂ Aflatoxins B ₁ , B ₂	Edible nuts, oilseeds and cereals
<i>Fusarium sporotrichioides</i> <i>F. graminearum</i>	T-2 toxin Deoxynivalenol (or nivalenol in some areas) zearalenone	Wheat and Maize Wheat and Maize
<i>F. moniliforme</i> <i>Penicillium verrucosum</i> and <i>A. ochraceus</i>	Fumonisin B ₁ Ochratoxin A	Maize Wheat, barley, coffee beans, vine fruits

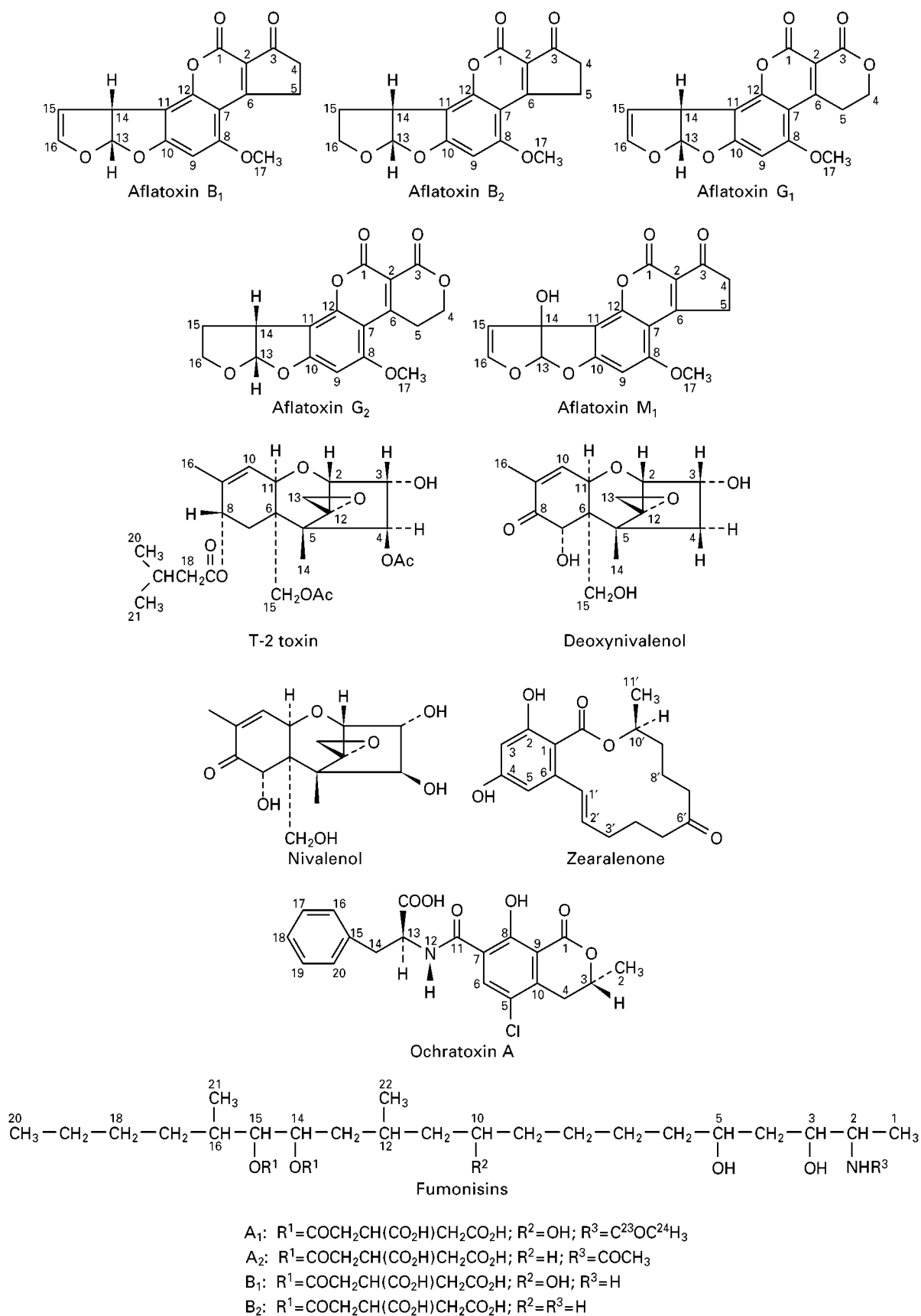


Figure 1 Mycotoxins of worldwide importance.

nephropathy, a fatal, chronic renal disease occurring in limited areas of Bulgaria, the former Yugoslavia and Romania. It has been suggested that pork products are significant human dietary sources of OA.

Control of Mycotoxins

The control of mycotoxins is summarized in Figure 2. The interventions that may be employed for the con-

trol of mycotoxins are prevention of contamination, identification and segregation of contaminated material (quality control, monitoring and legislation), and detoxification.

Preventative measures that militate against the onset of biodeterioration and, subsequently, the production of moulds and mycotoxins, may be introduced throughout the commodity system. However, the preharvest control of biodeterioration is somewhat

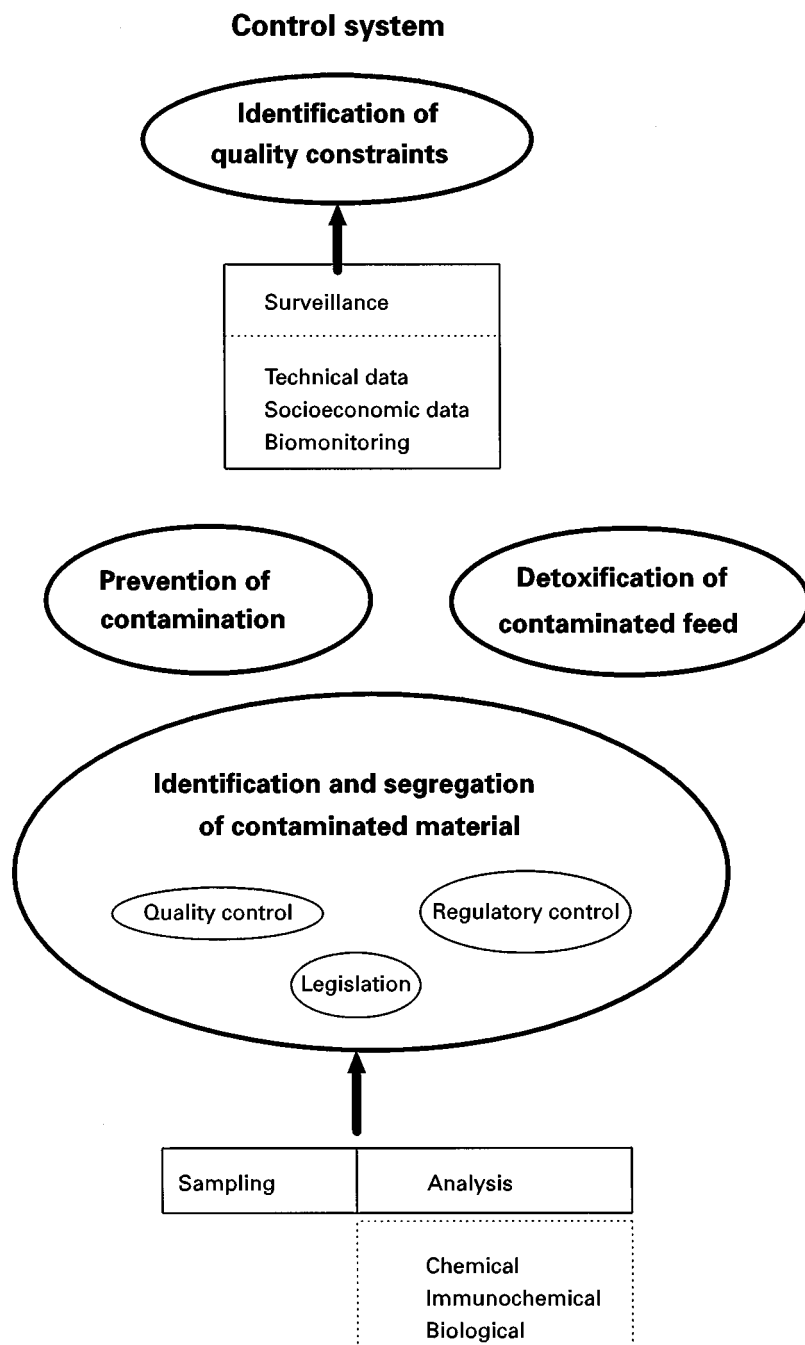


Figure 2 The mycotoxin control system.

compromised by our inability to control the climate! Attempts have been made to prevent preharvest contamination by breeding for resistance to moulds and by 'biocontrol' methods, involving the introduction, to the field, of atoxigenic strains of competing fungi. After harvest, it is important that the crop is dried to a 'safe' moisture level (which will not support the growth of moulds and mycotoxins) as quickly as possible.

The identification and segregation of mycotoxin-contaminated material may be pursued through quality control and regulatory procedures. More than 50 countries currently impose legal limits on the occurrence of mycotoxins (especially the aflatoxins) in foods and feeds.

Commercial detoxification plants, for the treatment of aflatoxin-contaminated groundnut meal, are currently operating in Senegal, France and the UK. The chemical detoxification reagent that is most widely used is ammonia, both as an anhydrous vapour and an aqueous solution.

If the package of control procedures described above is to be successfully implemented, it is essential that it is underpinned by an integrated package of sampling, sample preparation and analytical procedures.

Analysis of Mycotoxins

Worldwide, 5 parts per billion ($\mu\text{g kg}^{-1}$) is the most common maximum level of total aflatoxins permitted in foods. Similarly, aflatoxin M₁ is regulated in at least 14 countries, the permitted levels typically falling within the range 0.05 to 0.5 parts per billion. Consequently, it is essential that the analytical methods used for quality control and monitoring

(regulatory control) purposes are accurate and precise at these extremely low concentrations.

Analytical Sequence

The analysis of mycotoxins may be considered in terms of a sequence of four operations: extraction, clean-up, quantification and confirmation. Some of the more commonly used procedures associated with these operations are illustrated in Table 2.

The mycotoxin(s) under investigation must first be extracted from the complex and variable chemical milieu of the food or feed under investigation, using an appropriate extraction solvent. Commonly used solvent systems include acetone, acetonitrile, methanol, ethyl acetate, chloroform and water, either singly or as mixtures of two or more solvents. The extraction is performed either by shaking the mixture of sample and solvent for 30–45 min or by blending at high speed for approximately 3 min. The choice of solvent can significantly affect the extractability of the mycotoxin. The extraction of the aflatoxins from corn, for example, is significantly enhanced if the aqueous extraction solvent contains acetone as opposed to methanol. Supercritical fluid extraction is an emerging alternative to liquid extraction, and has been successfully applied to the extraction of aflatoxin B₁ from corn.

The crude extract, obtained after filtration of the shaken or blended mixture, is cleaned-up in order to remove as much non-mycotoxin material as possible, since the presence of extraneous compounds can seriously diminish the efficiency of the analysis. Clean-up procedures include liquid–solid extraction (defatting), liquid–liquid partitioning, chemical adsorption and chromatographic methods.

Table 2 The analysis of mycotoxins

<i>Operation</i>	<i>Commonly used procedure</i>
Extraction	Sample extracted by shaking or blending with chloroform, or mixtures of water/methanol, water/acetonitrile or water/acetone
Clean-up	Liquid–liquid partitioning or liquid–solid extraction Chemical adsorption Solid-phase extraction (SPE) Multifunctional clean-up column Chromatography Immunosorbent columns
Quantification	Thin layer chromatography (TLC) High performance thin layer chromatography (HPTLC) High performance liquid chromatography (HPLC) Gas chromatography (GC) Fluorimetry
Confirmation	Cochromatography Visual observation of colour change after derivatization Spectroscopy (with or without derivatization) Mass spectrometry

Solid-phase extraction (SPE) and immunosorbent columns are examples of recently introduced clean-up procedures that are now frequently used. SPE cartridges are available with a wide variety of polar, nonpolar and ion exchange bonded phases.

A 'multifunctional clean-up column' (MFC), composed of lipophilic, dipolar and anion exchange sites, reportedly affords the efficient clean-up of acetonitrile/water extracts within 10 s. MFC high performance liquid chromatography (HPLC) analysis methods have been applied to at least 10 mycotoxins.

The chromatographic quantification techniques used for the determination of mycotoxins in cleaned-up extracts include thin-layer chromatography (TLC), high performance TLC (HPTLC), high performance liquid chromatography (HPLC), and gas chromatography (GC). Worldwide, TLC is the most common method employed for the estimation of mycotoxins.

No assay can be considered as complete until the presence of the presumptive mycotoxin has been confirmed. This is especially important when an unusual commodity is under investigation. The ultimate confirmation involves the comparison of the physico-chemical characteristics of the presumptive mycotoxin with those of a standard compound. Such a course of action is not normally utilized as a routine procedure. Confirmatory techniques used in conjunction with HPLC include mass spectrometry and ultraviolet spectroscopy. When TLC or HPTLC are used for quantification, the formation of derivatives with characteristic chromatographic and fluorescence properties is commonly employed to confirm the presence of the presumptive mycotoxin(s).

Analytical Accuracy

The overall accuracy of the determination of mycotoxins will be governed by the combined effects of the sampling, sample preparation and analytical components of the analytical process. Undoubtedly, the sampling component is currently the greatest source of analytical error. Until effective sampling (and sample preparation) procedures have been developed for a variety of mycotoxin/commodity combinations, the accuracy and precision of methods for the determination of mycotoxins will be severely compromised.

The reliability of an analytical procedure may be expressed in terms of the accuracy, precision and limit of detection of the method. Interlaboratory precision is determined by the implementation of check-sample and collaborative studies. The level of interlaboratory precision for the determination of mycotoxins is still disappointing. A review of the reliability of mycotoxin assays, conducted in 1993,

indicated that little or no improvement in interlaboratory precision had occurred over the previous 20 years. The precision of TLC and HPLC methods were reportedly similar, whereas the precision of enzyme-linked immunosorbent assay (ELISA) methods was somewhat poorer. A series of proficiency testing exercises were carried out during 1993 and 1994 involving those European laboratories who contribute analytical data on food contamination to the World Health Organization (WHO) Global Environmental Monitoring Scheme (GEMS). The tests were performed according to the International Organization for Standardization/International Union of Pure and Applied Chemistry/Association of Official Analytical Chemists (ISO/IUPAC/AOAC) International Harmonized Protocol, and laboratories were awarded 'z scores' that signified their analytical capability. Eighty eight per cent of the laboratories obtained results of acceptable accuracy for the determination of the aflatoxins, whereas only 53% of the laboratories demonstrated acceptable accuracy for patulin (a mycotoxin produced by *Penicillium expansum* and other moulds.)

Simple Methods

Methods of quantification employing HPTLC, HPLC and GC require expensive equipment and skilled personnel. However, such procedures are not normally available in the basic analytical laboratories that exist in, for example, exporting developing countries and in some food and feed manufacturing plants.

Basic laboratory environments require simple, robust, low-cost methods that can afford reliable results in the hands of semiskilled operators. Methods that have been developed with such an application in mind include minicolumn and immunodiagnostic procedures. The minicolumn approach utilizes small glass columns packed either with selected chromatographic adsorbents or with other inorganic adsorbing materials. Minicolumns are used either to clean up the crude extract before quantification; or the mycotoxin under test is adsorbed onto the column, as a band, which is normally visually determined under ultraviolet (UV) light. Immunodiagnostic procedures take the form either of immunoaffinity columns or of solid-phase ELISA methods. Immunoaffinity columns are used to effect the sample clean-up before the mycotoxin is quantified, either by adsorption onto a Florisil 'tip' or by elution into a simple fluorimeter.

Solid-phase ELISA methods have been developed where the mycotoxin antibody is immobilized, for example, onto a card (about the size of a credit card), a plastic cup (the 'immunodot' approach) or a plastic probe. The presence of the mycotoxin, above a

predetermined level, is indicated by a visually observed colour change within small indentations within the card, cup or probe.

Chromatography of Selected Mycotoxins

The methods used for the chromatographic analysis of mycotoxins will now be further illustrated by describing the determination of the 'important' mycotoxins listed in Table 1. In each case, 'official' methods that have been approved by an appropriate internationally recognized body will be described, together with a selection of recently developed procedures.

Aflatoxins

The chromatographic methods employed for the determination of the aflatoxins ($B_1, B_2, G_1, G_2, M_1, M_2$) include TLC, HPTLC and HPLC, usually in combination with fluorescence detection. The aflatoxins exhibit an intense fluorescence when subjected to UV irradiation.

For TLC and HPTLC the intensity of fluorescence may be estimated either visually (using, for example, the 'comparison of standards' procedure) or densitometrically.

When HPLC methods are employed, the intensity of the fluorescence and the position of the excitation/emission maxima vary with the composition of the mobile phase. For example, the aflatoxins B_1 and G_1 are much less intense than aflatoxins B_2 and G_2 in aqueous or alcoholic solutions. The fluorescence excitation maximum for B_1 occurs at 355 and 363 nm in acetonitrile and water, respectively, whereas the emission maximum varies from 415 (in chloroform) to 450 nm (in water). In aqueous solutions, the sensitivity of the fluorescence detection system may be enhanced by the pre-column treatment of the aflatoxins B_1 and G_1 with trifluoroacetic acid (TFA), or by post-column treatment with either iodine or bromine solutions.

HPTLC, involving semiautomated sample application and fluorescence densitometry, is sufficiently robust to have been successfully exploited in laboratories in developing countries.

Official methods Those methods that have been approved by the AOAC and other international bodies are described in Table 3. Methods 968.22 and 971.24 have also been adopted by the International Union of Pure and Applied Chemistry (IUPAC); methods 975.36 and 972.26 by the American Association of Cereal Chemists (AACC); and methods 970.45 and 971.24 by the American Oil Chemists Society (AOCS). It is evident from Table 3 that many

of the official methods are based upon analytical procedures that were developed many years ago, using a combination of silica gel column chromatography clean-up and normal phase silica gel TLC.

Recent developments Reversed-phase HPLC, with post-column derivatization and fluorescence detection, is now widely used in the developed world for the analysis of the aflatoxins. Post-column iodination is performed within a heated reaction coil, where the column eluent is mixed with iodine-saturated water. Post-column bromination can be performed where bromide ion in the mobile phase is converted to bromine using a commercially available electrochemical cell. Sample clean-up is frequently performed using proprietary immunoaffinity or SPE columns. The AOAC Official Method 991.31, for example, utilizes the Aflatest immunoaffinity column in combination with reversed-phase C_{18} HPLC for the determination of the aflatoxins. A similar approach was reported in 1995 for the determination of aflatoxin M_1 in cheeses. Briefly, the dichloromethane extract is evaporated to dryness in a rotary evaporator, redissolved in a mixture of methanol/water/hexane (1 : 30 : 50 v/v), and subjected to liquid partitioning. The aqueous phases are then cleaned up using an immunoaffinity column containing monoclonal antibodies against aflatoxin M_1 .

Reversed-phase (C_{18}) HPLC quantification, in combination with fluorescence detection, affords an approximately 75% recovery of aflatoxin M_1 , and a limit of quantification of $0.02 \mu\text{g kg}^{-1}$. The fluorimetric excitation and emission wavelengths are 360 and 435 nm. In the EC method (92/95/EEC), the sample clean-up is performed using a combination of FlorisilTM and C_{18} SPE columns. The combination of C_{18} SPE column clean-up and HPLC quantification, with fluorescence detection, is frequently used for the determination of the aflatoxins in a variety of substrates.

HPTLC, in combination with phenyl bonded phase SPE and fluorescence densitometry, has been successfully applied to the determination of aflatoxins in a variety of commodities including corn, cottonseed, sorghum, peanut butter and palm kernels. Typically, aluminium-backed silica gel HPTLC plates are subjected to bidirectional chromatography using anhydrous diethyl ether and chloroform/xylene/acetone (6 : 3 : 1 v/v) in the first and second directions, respectively. Interfering components may be removed by carefully cutting away the upper part of the plate after the first development, before rotating the plate through 180° prior to the second development. The estimation of aflatoxin B_1 , by bidirectional HPTLC, in a variety of commodities is illustrated in Table 4. HPTLC has also been recently used for the

Table 3 Official methods for the analysis of aflatoxins; these are AOAC methods unless stated otherwise

Method no.	Date method developed	Aflatoxin	Commodity	Extraction solvent	Development solvent/mobile phase	Stationary phase	Clean-up method	^a Detection limit, LOD ($\mu\text{g kg}^{-1}$)/ Additional information
HPLC (with fluorescence detection)								
^b 980.20	1980	B ₁ , B ₂ , G ₁ , G ₂	Cottonseed products	Acetone/H ₂ O	H ₂ O saturated CHCl ₃ /(cyclohexane) CH ₃ CN (25:7.5:1) + 1.5% abs. ethanol or 2.0% isopropanol	Silica gel	Chemical adsorption and silica gel column	LOD not specified
986.16	1986	M ₁ , M ₂	Liquid milk	C ₁₈ SPE	H ₂ O/isopropanol/CH ₃ CN (80:12:8)	C ₁₈ column (pre-column derivatization)	Small silica gel column	LOD not specified
990.33	1990	B ₁ , B ₂ , G ₁ , G ₂	Corn and peanut butter	CH ₃ OH/0.1M HCl	H ₂ O/CH ₃ CN/CH ₃ OH (700:170:170)	C ₁₈ column (pre-column derivatization)	Silica gel column	5.0 10.0, total (AOAC/IUPAC method)
991.31	1991	B ₁ , B ₂ , G ₁ , G ₂	Corn, raw groundnuts and peanut butter	CH ₃ OH/H ₂ O	H ₂ O/CH ₃ CN/CH ₃ OH (3:1:1)	C ₁₈ column (post-column derivatization)	Aflatest Immunoaffinity column	10.0, total (AOAC/IUPAC method)
^c 92/95/EEC	1991	B ₁	Animal feeds	CHCl ₃	H ₂ O/CH ₃ OH/CH ₃ CN (130:70:40)	C ₁₈ column (post-column derivatization)	Florisil and C ₁₈ SPE	1.0
TLC								
^b 968.22	1968	B ₁ , B ₂ , G ₁ , G ₂	Groundnuts and their products	CHCl ₃ /H ₂ O	Acetone/CHCl ₃ (5:95 to 15:85)	Silica gel	Silica gel column	LOD not specified (IUPAC/AOAC method; CB ^d method)
970.45	1970	B ₁ , B ₂ , G ₁ , G ₂	Groundnuts and their products	CH ₃ OH/H ₂ O/hexane	Acetone/CHCl ₃ (5:95 to 15:85)	Silica gel	Centrifugation and liquid partitioning	LOD not specified (AOCS/AOAC method; BF ^d method)
971.23	1969	B ₁ , B ₂ , G ₁ , G ₂	Cocoa beans	CHCl ₃ /AgNO ₃ solution	Acetone/CHCl ₃ (5:95 to 15:85)	Silica gel	Defatting and silica gel column	LOD not specified (IUPAC/AOAC method; modified CB method)
971.24	1971	B ₁ , B ₂ , G ₁ , G ₂	Coconut, copra, copra meal	CHCl ₃ /NaCl solution	Acetone/CHCl ₃ (5:95 to 15:85)	Silica gel	Silica gel column	LOD not specified (IUPAC/AOCS/AOAC method)
972.26	1972	B ₁ , B ₂ , G ₁ , G ₂	Corn	CHCl ₃ /H ₂ O	Acetone/CHCl ₃ (5:95 to 15:85)	Silica gel	Silica gel column	LOD not specified (AACC/AOAC method; based upon CB method)
972.27	1972	B ₁ , B ₂ , G ₁ , G ₂	Soya beans	CHCl ₃ /H ₂ O	Acetone/CHCl ₃ (5:95 to 15:85)	Silica gel	Silica gel column	LOD not specified (based upon CB method)
974.16 (Method 1)	1974	B ₁ , B ₂ , G ₁ , G ₂	Pistachio nuts	CHCl ₃ /H ₂ O	Acetone/CHCl ₃ (5:95 to 15:85)	Silica gel	Silica gel column	LOD not specified (based upon CB method)
(Method 2)				CH ₃ OH/H ₂ O/hexane	Acetone/CHCl ₃ (5:95 to 15:85)	Silica gel	Centrifugation and liquid partitioning	LOD not specified (based upon BF method)
978.15	1977	B ₁	Eggs	Acetone/H ₂ O/saturated NaCl solution	2D TLC: (a) anhydrous diethyl ether/CH ₃ OH/H ₂ O (96:3:1) (b) Acetone/CHCl ₃ (1:9)	Silica gel	Chemical adsorption, liquid partitioning and silica gel column	LOD not specified

Table 3 *Continued*

<i>Method no.</i>	<i>Date method developed</i>	<i>Aflatoxin</i>	<i>Commodity</i>	<i>Extraction solvent</i>	<i>Development solvent/mobile phase</i>	<i>Stationary phase</i>	<i>Clean-up method</i>	<i>^aDetection limit, LOD ($\mu\text{g kg}^{-1}$)/ Additional information</i>
980.20	1980	B ₁ , B ₂ , G ₁ , G ₂	Cottonseed products	Acetone/H ₂ O	Acetone/CHCl ₃ (5:95 to 15:85)	Silica gel	Chemical adsorption and silica gel column	LOD not specified
980.21	1978	M ₁	Milk, cheese	CHCl ₃ /NaCl solution	For milk: CHCl ₃ /acetone/isopropanol (87:10:3) For cheese: 2D TLC: (a) diethyl ether/CH ₃ OH/H ₂ O (95:4:1) (b) CHCl ₃ /acetone/isopropanol (87:10:3)	Silica gel	Silica gel column	LOD not specified
982.24	1981	B ₁ , M ₁	Liver	CH ₂ Cl ₂ /citric acid solution	2D TLC: (a) diethyl ether/CH ₃ OH/H ₂ O (95:4:1) (b) CHCl ₃ /acetone/isopropanol (87:10:3)	Silica gel	Silica gel column	LOD not specified
993.17	1994	B ₁ , B ₂ , G ₁ , G ₂	Corn and groundnuts	CH ₃ OH/H ₂ O	CHCl ₃ /acetone (9:1)	Silica gel	Silica gel column	5.0, densitometrically 10.0, visually
Minicolumn								
975.36	1975	B ₁ , B ₂ , G ₁ , G ₂	Food and feeds	Acetone/H ₂ O	CHCl ₃ /acetone (9:1)	CaSO ₄ , Florisil, silica gel, neutral alumina	Chemical adsorption	5.0, total; almonds 10.0, total: corn, groundnuts, peanut butter, pistachio nuts, groundnut and cottonseed meals 15, total, mixed feeds Romer method (AACC/AOAC method)
979.18	1979	B ₁ , B ₂ , G ₁ , G ₂	Corn, groundnuts	CHCl ₃ /H ₂ O	CHCl ₃ /acetone (9:1)	CaSO ₄ , Florisil, silica gel, neutral alumina	Liquid partitioning	10.0 (Holaday-Velasco method)

^aThe minimum contamination level to which the method is applicable: applies to aflatoxin B₁, unless otherwise stated.^bAOAC classification. ^cEC Directive. ^dScott (1998).

determination of aflatoxin M₁ in milk. The samples were extracted with chloroform contained within a hydrated dialysis tube, before subjecting the concentrated extract to HPTLC on silica gel plates. This method gave a recovery of 96% and fluorescence densitometry gave a detection limit of 0.002 $\mu\text{g L}^{-1}$.

The excitation wavelength was 350 nm, with an emission cut-off of below 400 nm.

A recently reported novel approach to the determination of aflatoxins in corn utilizes silica or immunoaffinity column clean-up in combination with capillary electrophoresis, with laser-induced

Table 4 Estimation of aflatoxin B₁ by bidirectional HPTLC

Commodity	Extraction solvent	Clean-up method	Limit of detection (B ₁ , µg kg ⁻¹)
Peanut butter	Acetone/H ₂ O	Phenyl SPE	2.0
Corn	Acetone/H ₂ O	Phenyl SPE	1.7
Cottonseed	Acetone/0.1N HCl	Phenyl SPE	2.7
Sorghum	CHCl ₃ /H ₂ O	Florisil column	1.3

fluorescence detection. The reported limit of detection is 0.5 µg kg⁻¹ aflatoxin B₁, with an average recovery of 85% over the range 1 to 50 µg kg⁻¹.

Ochratoxins

Official methods Official AOAC methods exist for the determination of the ochratoxin A in barley, corn and green coffee. These procedures are summarized in Table 5. It is evident from Table 5 that both the TLC methods are rather old, whereas the HPLC procedure is reasonably modern. Each of the official methods utilizes the native fluorescence of ochratoxin A for detection purposes. On a silica gel TLC plate, ochratoxin A fluoresces most intensely under 365 nm UV light. If the plate is sprayed with alcoholic NaHCO₃ solution the fluorescence increases in intensity, and changes from greenish blue to blue in colour. If the TLC plate is quantified densitometrically, the optimum excitation and emission wavelengths are 310–340 and 440–475 nm, respectively. When employing HPLC, the recommended fluorescence detection wavelengths are 333 (excitation) and 460 nm (emission).

The AOAC Method 991.44 has been subjected to an interlaboratory study involving 12 European

laboratories, under the auspices of the AOAC/IUPAC/NMKL (Nordic Committee on Food Analysis). The results of the intercomparison are given in Table 6 for contamination levels, in wheat bran, rye and barley, of between 2 and 9 µg kg⁻¹ ochratoxin A. The mean recoveries varied from 64 to 72%. The method has been accepted as an official NMKL procedure.

Recent developments Recently developed HPLC methods for the determination of ochratoxin A employ silica gel SPE and immunoaffinity clean-up followed by reversed-phase C₈, C₁₈ and C₂₂ HPLC columns, in combination with fluorescence detection. The ionization of the phenolic group in the underivatized toxin is suppressed by the presence of phosphoric or acetic acids in the mobile phase.

An HPLC method (Method 1, Table 7) for the determination of ochratoxin A in roast and ground coffee uses a combination of silica gel SPE and immunoaffinity clean-up in order to ensure a good recovery (87%) of toxin. (Very low recoveries were obtained when immunoaffinity clean-up alone was used.) Fluorescence detection with excitation and emission wavelengths of 333 and 470 nm

Table 5 Official methods for the analysis of ochratoxin A; these are AOAC methods unless stated otherwise

Method no.	Date method developed	Commodity	Extraction solvent	Development solvent/Mobile phase	Stationary phase	Clean-up method	Detection limit, LOD (µg kg ⁻¹)/Additional information
TLC							
973.37	1973	Barley	CHCl ₃ /0.1 mol L ⁻¹ H ₃ PO ₄ soln	Acetone/CHCl ₃ (5:95 to 15:85)	Silica gel	NaHCO ₃ /diatomaceous earth column	LOD not specified (IUPAC/AOAC method)
975.38	1975	Green coffee	CHCl ₃	Toluene/ethyl acetate/formic acid (5:4:1) or benzene/CH ₃ OH/acetic acid (18:1:1, two sequential developments)	Silica gel	NaHCO ₃ /diatomaceous earth column	LOD not specified
HPLC							
991.44	1992	Corn and barley	CHCl ₃ /0.1 mol L ⁻¹ H ₃ PO ₄ soln	H ₂ O/CH ₃ CN/acetic acid (99:99:2)	C ₁₈ column	C ₁₈ SPE	10.0 (IUPAC/ ^a NMKL method)

^aNMKL, Nordic Committee on Food Analysis.

Table 6 Interlaboratory study of the official NMKL HPLC method for the analysis of ochratoxin A

Commodity	Coefficient of variation (%)	
	Intralaboratory	Interlaboratory
Wheat bran	21	23–28
Rye	17	20–28
Barley	12	18–31

was employed. The presence of ochratoxin A was confirmed by the HPLC determination of its methyl ester.

HPLC quantification has also been used to determine the ochratoxin A content of milk (Method 2, Table 7). The emulsion produced during the chloroform/methanol extraction was broken by refrigerated centrifugation. After clean-up, the purified extract was dissolved in methanol, by ultrasonic treatment, before application to the HPLC column. The emission and excitation wavelengths of the fluorescence detector were set at 330 and 460 nm. The presence of ochratoxin A, in the range 0.01 to 0.03 $\mu\text{g L}^{-1}$, was confirmed by ELISA.

An HPTLC method (Method 3, Table 7) has recently been developed for the determination of ochratoxin A in parboiled rice. Extraction was performed with chloroform and phosphoric acid; the clean-up involved a combination of partitioning into sodium bicarbonate solution and phenyl

bonded-phase SPE. Bidirectional HPTLC using aluminium-backed silica gel plates was employed, using diethyl ether/methanol (98:2 v/v) and toluene/ethyl acetate/formic acid (5:4:1 v/v) in the first and second directions, respectively. After removing the bottom portion of the plate, a third development was performed, in the same direction, with *n*-hexane/ethyl acetate/acetic acid (18:3:1 v/v). Fluorodensitometric detection (excitation at 365 nm) afforded a mean intralaboratory precision of 5.4% over the concentration range 10 to 200 $\mu\text{g kg}^{-1}$ ochratoxin A. The mean recovery and limit of detection were 83% and 11.6 $\mu\text{g kg}^{-1}$, respectively.

Two intercomparison studies have recently been performed, within the European Commission, Measurements and Testing Programme, on the HPLC determination of ochratoxin A. The first study, using kidney naturally contaminated at 10 $\mu\text{g kg}^{-1}$ ochratoxin A, involved 20 European laboratories. A variety of extraction and clean-up procedures were used, and recoveries ranged from 43 to 128%. The second study, involving 26 European laboratories, used wheat naturally contaminated with approximately 7 $\mu\text{g kg}^{-1}$ ochratoxin A. Again, a variety of extraction and clean-up procedures were employed. Some laboratories compared their normal clean-up method with the use of immunoaffinity columns supplied from two different sources. The recoveries and interlaboratory precision obtained using the normal and immunoaffinity clean-up methods are compared

Table 7 Contemporary methods for the analysis of ochratoxin A

Method no.	Commodity	Date method developed	Extraction solvent	Mobile phase/Developing solvent	Stationary phase	Clean-up method	Detection limit, LOD ($\mu\text{g kg}^{-1}$)
HPLC							
1 (1)	Roast and ground coffee	1997	CHCl_3 / 0.1 mol L^{-1} H_3PO_4 soln	H_3PO_4 / CH_3CN (1:1)	C_{18} column	Silica gel SPE + immunoaffinity	0.1
2 (2)	Milk	1996	CHCl_3 / CH_3OH (pH 1.6–2)	H_3PO_4 (0.008 mol L^{-1} / CH_3CN ^a (a) (60:40), (b) (90:10), (c) (60:40)	C_{18} column	Centrifugation (4°C) + silica gel SPE	0.01 $\mu\text{g L}^{-1}$ ^b 0.03 $\mu\text{g L}^{-1}$
HPTLC							
3 (3)	Rice	1996	CHCl_3 / 0.1 mol L^{-1} H_3PO_4 soln	Bidirectional HPTLC: (a) diethyl ether/ CH_3OH (98:2) (b) toluene/ethyl acetate/formic acid (5:4:1) (c) <i>n</i> -hexane/ethyl acetate/acetic acid (18:3:1)	Silica gel HPTLC plate	Liquid partitioning + phenyl SPE	11.6

^aSuccessive mobile phases.

^bQuantitation limit.

- (1) Patel S, Hazel CM, Winterton AGM and Gleadle AE (1997) Survey of ochratoxin A in UK retail coffees. *Food Additives and Contaminants* 14: 217–222.
- (2) Valenta H and Goll M (1996) Determination of ochratoxin A in regional samples of cows milk in Germany. *Food Additives and Contaminants* 13: 669–676.
- (3) Dawlatana M, Coker RD, Nagler MJ and Blunden G (1996) A normal phase HPTLC method for the quantitative determination of ochratoxin A in rice. *Chromatographia* 42: 25–28.

Table 8 Intercomparison of clean-up methods used for the HPLC determination of ochratoxin A in wheat

Clean-up method	Coefficient of variation (%) (Interlaboratory)	Recovery (%)
Normal	34	58–114
Immunoaffinity (first source)	34	58–114
Immunoaffinity (second source)	42	4–86

in Table 8. A recovery within the range 70 to 110% was considered to be acceptable. The interlaboratory coefficient of variation obtained using normal (and one immunoaffinity) clean-up methods were similar to, but slightly greater than, the values obtained by the intercomparison study of the official AOAC/IUPAC/NMKL procedure.

Deoxynivalenol

Official methods The two official AOAC methods for the determination of deoxynivalenol in wheat both date from 1986; these are outlined in Table 9. The TLC procedure (Method 986.17) involves extraction with acetonitrile/water followed by clean-up using a small column packed with a mixture of charcoal, alumina and Celite. The deoxynivalenol is observed as a blue fluorescent spot, under UV light, on the heated, aluminium chloride-treated plate. When subjected to a collaborative study the reported average recoveries were between 78 and 96%, with intra- and interlaboratory precisions (CV%) of 30–64 and 33–87% respectively.

The GC method includes extraction with water/chloroform/methanol, a silica gel column clean-up (under centrifugation) and derivatization with heptafluorobutyric acid anhydride (HFBA). Chromatography is performed on a 3% OV-101 column (using argon methane as the carrier gas) with a ^{63}Ni electron capture detector. A collaborative study of this procedure afforded an average recovery of 92% and intra- and interlaboratory precisions

(CV%) of 31 and 47%, respectively, for naturally contaminated samples.

Recent developments In 1992, an intercomparison study was reported on the determination of deoxynivalenol in wheat and corn flours. Fifteen laboratories participated, using one- and two-dimensional TLC (five participants), GC (four) and HPLC (six) procedures. Ten of the laboratories used a charcoal-based clean-up method. A mixture of acetonitrile/water was widely used as an extraction solvent. HPLC quantification was performed using UV detection at 225 nm, whereas the GC determinations employed trimethylsilyl, trifluoroacetyl and heptafluorobutyryl derivatives. For all methods the recoveries varied between 68 and 116% for wheat and 53 and 100% for corn. There was no discernible difference in the efficacy of the various quantification procedures.

Typically, TLC methods for the analysis of trichothecenes involve extraction with acetonitrile or methanol followed by clean-up using liquid partitioning and column chromatography on silica gel or Florisil. Deoxynivalenol may be visualized on the TLC plate by spraying with, for example, aluminium chloride, 4-(*p*-nitrobenzyl)-pyridine, *p*-anisaldehyde or cerium sulfate.

Recently developed methods for the determination of deoxynivalenol, T-2 toxin (and zearalenone) are summarized in Table 10.

The HPLC analysis of trichothecenes is frequently performed using gradients of methanol/water or acetonitrile/water in conjunction with C_{18} (or occasionally C_8) columns and detection by UV absorption. Electrochemical detection has also been employed, together with a variety of derivatization techniques. The extraction/clean-up step in the HPLC procedure (Method 1) includes the precipitation of milk protein, with acetic acid, pH adjustment to 7–8, ExtrelutTM column chromatography and a charcoal-alumina clean-up column. The recovery, for the concentration range 25–200 $\mu\text{g L}^{-1}$ deoxynivalenol, was low (57%)

Table 9 Official methods for the analysis of deoxynivalenol; these are AOAC methods unless stated otherwise

Method no.	Date method developed	Commodity	Extraction solvent	Development solvent or carrier gas	Stationary phase	Clean-up method	Detection limit, LOD ($\mu\text{g kg}^{-1}$)
TLC							
986.17	1986	Wheat	$\text{CH}_3\text{CN}/\text{H}_2\text{O}$	$\text{CHCl}_3/\text{acetone}/\text{isopropanol}$	Silica gel	Small column; mixture of charcoal, alumina and Celite	300
GC							
986.18	1986	Wheat	$\text{H}_2\text{O}/\text{CHCl}_3/\text{ethanol}$	CH_4/Ar (5:95)	3%OV-101 (on 80–100 mesh Chromosorb WHP)	Quick-Sep silica gel column	350

Table 10 Recently developed methods for the determination of deoxynivalenol, T-2 toxin and zearalenone

Method no.	Date method developed	Commodity	Extraction solvent	Clean-up method	Development solvent/mobile phase/carrier gas	Stationary phase	Derivatization method	Detector/detection limit, LOD ($\mu\text{g kg}^{-1}$)
HPLC								
1 (4)	1994	Cow's milk	Extrelut column	Centrifugation and charcoal/alumina column	H ₂ O/CH ₃ CN (96:4)	Reversed-phase C ₁₈ column	N/A	UV absorption (220 nm) 25 $\mu\text{g L}^{-1}$ (Deoxynivalenol only)
GC								
2 (5)	1996	Barley, mixed feed, sweet corn	CH ₃ CN/H ₂ O	Celite mixed charcoal, alumina, Celite column and C ₈ SPE	Helium (1.5% argon added for GC/MI)	Cross-linked methyl silicone capillary column	Trimethylsilylation	NICI/MS LOD not reported (T-2 and deoxynivalenol, only)
3 (6)	1996	Barley, maize	CH ₃ CN/H ₂ O	Defatting (hexane) + Florisil column	Helium	Cross-linked methyl silicone capillary column	Trimethylsilylation	EI/SIM/MS 5 $\mu\text{g kg}^{-1}$
HPTLC								
4 (7)	1998	Corn	H ₂ O/CHCl ₃	Liquid partitioning	Toluene/ethyl acetate/formic acid (6:2:1)	Silica gel HPTLC plate	N/A	Fluorodensitometry 2.6 (Zearalenone, only)

- (4) Vudathala DK, Prelusky DB and Trenholm HL (1994) Analysis of trace levels of deoxynivalenol in cow's milk by high pressure liquid chromatography. *Journal of Liquid Chromatography* 17: 673–683.
- (5) Mossoba MM, Adams S and Roach JAG (1996) Analysis of trichothecene mycotoxins in contaminated grains by gas chromatography/matrix isolation/Fourier transform infrared spectroscopy and gas chromatography/mass spectrometry. *Journal of AOAC International* 79: 1116–1123.
- (6) Ryu JC, Song YS, Kwon OS, Park J and Chang IM (1996) Survey of natural occurrence of trichothecene mycotoxins and zearalenone in Korean cereals harvested in 1992 using gas chromatography mass spectrometry. *Food Additives and Contaminants* 13: 333–341.
- (7) Dawlatana M, Coker RD, Nagler MJ, Blunden G and Oliver GWO (1998) An HPTLC method for the quantitative determination of zearalenone in maize. *Chromatographia* 47: 215–218.

but consistent; the extensive clean-up probably contributed to the loss of toxin.

GC is widely employed for the determination of trichothecenes, including deoxynivalenol, notwithstanding the inconvenience of lengthy clean-up and derivatization steps prior to quantification. Typically, either the original trichothecene, or the alcohol produced by alkaline hydrolysis, is determined. The hydroxyl group(s) of trichothecenes are normally derivatized in order to attain the required volatility and sensitivity. Trimethylsilyl (TMS) derivatives are frequently utilized for the GC of trichothecenes; heptafluorobutyl and pentafluoropropionyl derivatives are employed for electron capture detection (ECD) whereas trifluoroacetates are utilized for flame ionization (FID), ECD and mass spectrometric (MS) detection. GCMS methods have the advantage of high sensitivity together with the opportunity of using mass spectrometry for confirmation purposes. The specificity of MS detection affords the reliable detection of toxins in grains, biological fluids and other matrices. Generally, capillary GC is preferred to the use of packed columns since the efficiency

of the latter can be compromised by interferences. Capillary GC has been used for the analysis of trichothecenes in a variety of commodities.

Both GC/matrix isolation (MI)/Fourier transform infrared (FTIR) spectroscopy and GCMS have been used to analyse mixtures of trichothecenes in a variety of commodities (Method 2, Table 10). Matrix isolation was performed by adding argon to the carrier gas and trapping the effluent on the outer ring of a slowly rotating gold disc, at low temperatures. The IR-transparent argon matrix, containing the isolated trichothecenes, was then analysed by IR spectroscopy, and the presence of individual toxins confirmed by observing the characteristic MI/FTIR bands. Negative ion chemical ionization (NICI) mass spectrometry was used to quantify the high levels (67–445 mg kg^{-1}) of deoxynivalenol found in naturally contaminated sweet corn. Seven *Fusarium* mycotoxins (including deoxynivalenol, T-2 toxin and zearalenone) in barley and maize have also been determined by GC/electron impact-selective ion monitoring MS (Method 3, Table 10). 5 α -Cholestane was used as an internal

standard. The mean recovery for the seven mycotoxins was 92%.

T-2 Toxin

Official methods There are no official AOAC methods for the determination of T-2 toxin.

Recent developments Methods available for the determination of T-2 toxin include TLC, GC and HPLC.

T-2 toxin and other type A trichothecenes (characterized by a hydrogen atom or an hydroxyl group at the C8 position) are visualized on TLC plates by treatment with sulfuric acid or chromotropic acid (disodium 4,5-dihydroxynaphthalene-2,7-disulfonate dihydrate). Another approach involves the formation of the diphenylindenone sulfonyl (Dis) esters of trichothecenes and their visualization, as fluorescent spots under UV light, by spraying the TLC plate with sodium methoxide. Using this procedure 20–25 ng per spot of T-2 toxin can be detected.

The HPLC determination of T-2 toxin is compromised by the lack of the enone chromophore possessed by deoxynivalenol. The successful HPLC determination of T-2 and other Type A trichothecenes requires effective clean-up and derivatization procedures. A variety of post-column derivatization methods have been developed including those involving the UV detection of *p*-nitrobenzoate and diphenylindenone sulfonyl esters of T-2 toxin; the reported detection limits are approximately 10 and 30 ng T-2, respectively.

The capillary GC-ECD determination of T-2 toxin, and other Type A trichothecenes, afford detection limits of about 200 $\mu\text{g kg}^{-1}$ (with one chromatographic clean-up) and 50–100 $\mu\text{g kg}^{-1}$ (with two chromatographic clean-ups). A similar result has been reported using a capillary GC-FID method. T-2 toxin has also been detected in spiked wheat (in combination with deoxynivalenol), at levels of 1 $\mu\text{g kg}^{-1}$, by using a GC-NICI MS-MS method. A highly sensitive

method for T-2 in urine employs capillary GCMS (EI and NICI) with a detection limit of 2–5 $\mu\text{g L}^{-1}$. Capillary GC-PICI MS was employed after clean-up of an acetonitrile extract on an XAD-2 column and derivatization with TFA.

Recently developed GC/NICI/MS and GC/EI/MS methods for the determination of T-2 toxin, and other trichothecenes, are outlined in Table 10 (Methods 2 and 3).

Zearalenone

Official methods There are two official AOAC methods (TLC and HPLC) for the determination of zearalenone in corn (Table 11). The TLC method (976.22) dates from 1976 and has also been adopted by the AACC. The HPLC method (985.18) dates from 1985 and can also be used for the determination of α -zearalenol. No limits of detection are given for these procedures.

The official TLC method for zearalenone involves extraction with chloroform/water, clean-up by silica gel column chromatography and liquid partitioning followed by TLC using either ethanol/chloroform or acetic acid/benzene. Zearalenone fluoresces greenish-blue under 254 nm UV light; and blue under 365 nm UV light after treatment with aluminium chloride.

The official HPLC method for zearalenone and α -zearalenol involves extraction with chloroform/water (in the presence of diatomaceous earth), clean-up by liquid partitioning and chromatography on a C₁₈ column using water/acetonitrile/methanol as the mobile phase. Fluorescence detection is employed.

Recent developments A variety of HPLC methods have been developed for the analysis of zearalenone in corn together with methods for milk, blood, urine and animal tissue. Clean-up procedures include liquid partitioning and the use of silica gel cartridges. The mobile phases used for reversed-phase HPLC include

Table 11 Official methods for the analysis of zearalenone; these are AOAC methods unless otherwise stated

Method no.	Date method developed	Commodity	Extraction solvent	Development solvent/mobile phase/carrier gas	Stationary phase	Clean-up method	Detection limit, LOD ($\mu\text{g kg}^{-1}$) Additional information
TLC							
976.22	1976	Corn	H ₂ O/CHCl ₃	Ethanol/CHCl ₃ ^a (5:95)	Silica gel	Liquid partitioning	AACC/AOAC method LOD not specified
HPLC							
985.18	1985	Corn	H ₂ O/CHCl ₃	CH ₃ OH/CH ₃ CN/H ₂ O (1.0:1.6:2.0)	Reversed-phase C ₁₈ column	Liquid partitioning	LOD not specified

^aOr ethanol/CHCl₃ (3.5:96.5), acetic acid/benzene (5:95 or 10:90).

Table 12 AOAC Official First Action HPLC method for the analysis of the fumonisins

Date method developed	Commodity	Extraction solvent	Mobile phase	Stationary phase	Clean-up method	Detection limit, LOD ($\mu\text{g kg}^{-1}$)
1990	Corn	H ₂ O/CH ₃ OH	Na ₂ HPO ₄ (buffered to pH 3.3)/CH ₃ OH	C ₁₈ column	SPE SAX cartridge	10

acetonitrile/water, acetonitrile/water/acetic acid, methanol/acetonitrile/water and methanol/water. Water-saturated dichloromethane containing 2% 1-propanol has been used for normal-phase HPLC. Fluorescence detection is most commonly used; other methods include electrochemical, voltametric and UV spectroscopic detection.

An HPTLC method (Method 4, Table 10) for the determination of zearalenone in maize has recently been developed, based upon the AOAC HPLC procedure (985.15). The mean recovery is 75.3%, over the range 10 to 320 $\mu\text{g kg}^{-1}$ zearalenone.

Most of the numerous GC methods for the determination of zearalenone (and zearalenol) utilize trimethylsilyl derivatization. A recently developed GC method for the determination of zearalenone and other *Fusarium* toxins, in barley and corn, is shown in Table 10 (Method 3).

Fumonisin

Official methods An HPLC method has received Official First Action status from the AOAC International (Table 12). The procedure uses methanol/

water (3 : 1 v/v) as the extraction solvent followed by strong ion exchange (SAX) clean-up and pre-column derivatization with *o*-phthalaldehyde (OPA). The mobile phase is sodium dihydrogen phosphate solution (buffered to pH 3.3)/methanol and fluorescence detection is employed.

Recent developments Typically, the fumonisins are determined by TLC, HPLC or GCMS, using ion exchange SPE clean-up and quantification, after derivatization of the primary amino group. HPLC is by far the most widely used quantification method. A worldwide survey of methods used for the analysis of the fumonisins was reported in 1996. Of the 32 laboratories included, 91% used HPLC. TLC and GC/MS methods were each used by 3% of the laboratories. (ELISA was utilized by the remaining 3%.)

HPLC methods that are broadly similar to the AOAC Official First Action method have also been developed using other clean-up procedures (e.g. C₁₈ SPE and immunoaffinity columns) and mobile phases. The latter include mixtures of acetonitrile/methanol/acetic acid; acidified methanol; and sodium

Table 13 Recently developed methods for the analysis of the fumonisins

Method no.	Date method developed	Commodity	Chromatography type	Clean-up method	Detection limit, LOD	Additional information
HPLC						
1 (8)	1996	Corn and corn products	Ion-pair chromatography	SAX and C ₁₈ SPE	20 ng	Derivatization with OPA and <i>N</i> -acetyl- <i>L</i> -cysteine; fluorescence detection
2 (9)	1998	Corn-based feed	Reversed-phase	On-line immunoaffinity column	5 ng	Electrospray ionization MS
HPTLC						
3 (10)	1998	Rice	Silica-gel HPTLC	SAX SPE	^a 250 $\mu\text{g kg}^{-1}$	Derivatization by dipping plate into 0.17% <i>p</i> -anisaldehyde solution; fluorescence densitometry

^aLimit of quantification.

- (8) Miyahara M, Akiyama H, Toyoda M and Saito Y (1996) New procedure for fumonisins B₁ and B₂ in corn and corn products by ion pair chromatography with *o*-phthalaldehyde post column derivatization and fluorometric detection. *Journal of Agricultural and Food Chemistry* 44: 842–847.
- (9) Newkirk DK, Benson RW, Howard PC, Churchwell MI, Doerge DR and Roberts DW (1998) On-line immunoaffinity capture, coupled with HPLC and electrospray mass spectrometry, for automated determination of fumonisins. *Journal of Agricultural and Food Chemistry* 46: 1677–1688.
- (10) Dawlatana M, Coker RD, Nagler MJ and Blunden G (1995). A normal phase HPTLC method for the quantitative determination of fumonisin B₁ in rice. *Chromatographia* 41: 187–190.

hydrogen phosphate solution/methanol followed by acetonitrile/water. Although OPA is used as the derivatization reagent by the majority of laboratories, other reagents have been employed including naphthalendialdehyde, fluoronitrobenzofurazan and fluoescamine. The last reagent is unsatisfactory as it generates two peaks in the HPLC chromatogram for fumonisin B₁.

Three recently developed methods for the determination of the fumonisins in corn-based commodities are outlined in Table 13. Method 1 uses a combination of SAX and C₁₈ SPE clean-up prior to ion-pair HPLC and fluorescence detection; on-line derivatization within a reaction coil is employed. The recovery of the fumonisins ranged from 54 to 110% at 40 and 80 µg kg⁻¹, respectively. Method 2 is an automated procedure using on-line immunoaffinity clean-up, reversed-phase HPLC and electrospray ionization MS detection. The protonated molecule signal (*m/z* 722) was used to achieve a limit of quantification of 250 pg.

An HPTLC method (Method 3, Table 13), for the determination of fumonisin B₁ in rice, has recently been reported. A novel derivatization step involved the brief immersion of the HPTLC plate in a 0.16% acidic solution of *p*-anisaldehyde, followed by quantification by scanning fluorodensitometry. The response was linear over the range 0 to 5 mg kg⁻¹ (ppm).

An intercomparison study on a variety of methods for the determination of the fumonisins in maize has recently been undertaken under the auspices of the European Commission, Measurements and Testing Programme. Twenty-four laboratories participated, using their normal routine procedure for the determination of fumonisins B₁ and B₂ in the range 0.5–3.0 and 0.2–1.5 mg kg⁻¹ (ppm), respectively. All laboratories used a similar method involving extraction with methanol/water, clean-up with an SAX SPE column and HPLC fluorescence quantification of the OPA derivative. The intra- and interlaboratory precisions were high (10 and 11%, respectively, for fumonisin B₁; and 11 and 13%, respectively, for fumonisin B₂). However, the recoveries were low (70 ± 14% and 69 ± 16% for fumonisins B₁ and B₂, respectively). Interestingly, higher recoveries were

associated with extraction by shaking (85 ± 12% for fumonisin B₁) rather than by blending (62 ± 6%).

Conclusions

The continued use of a variety of chromatographic procedures for the determination of mycotoxins is envisaged. Although HPLC is the method of choice in the developed world for a wide range of applications, it is important that precise and accurate methods continue to be developed that are appropriate to the special needs of developing country laboratories.

See Colour Plate 53.

See also: II/Affinity Separation: Immunoaffinity Chromatography. **Chromatography: Gas:** Detectors: Mass Spectrometry. **Chromatography: Liquid:** Derivatization. III/Aflatoxins and Mycotoxins: Thin Layer (Planar) Chromatography. **Membrane Preparation:** Phase Inversion Membranes.

Further Reading

- Anon (1993) Some naturally occurring substances: food items and constituents, heterocyclic aromatic amines and mycotoxins. *IARC Monographs on the Evaluation of Carcinogenic Risks to Humans*, vol. 56. Lyon, France: International Agency for Research on Cancer.
- Betina V (ed.) (1993) *Chromatography of Mycotoxins: Techniques and Applications*, Journal of Chromatography Library, vol. 54. London: Elsevier.
- Coker RD (1997) *Mycotoxins and their Control: Constraints and Opportunities*, NRI bulletin 73. Chatham, UK: Natural Resources Institute.
- Coker RD and Jones BD (1988) Determination of mycotoxins. In: Macrae R (ed.) *HPLC in Food Analysis*. London: Academic Press.
- Horwitz W, Albert R and Nesheim S (1993) Reliability of mycotoxin assays – an update. *Journal of AOAC International* 76: 461.
- Miller JD and Trenholm HL (1994) *Mycotoxins in Grain Compounds Other Than Aflatoxin*. St Paul, MN: Eagan Press.
- Scott PM (1998) Natural toxins. In: Cunniff (ed.) *Official Methods of Analysis of AOAC International*, 16th edn, 4th revision. Washington: AOAC.

Thin-Layer (Planar) Chromatography

M. E. Stack, US Food and Drug Administration, Washington DC, USA

Copyright © 2000 Academic Press

The aflatoxins are toxic and carcinogenic metabolites of the moulds *Aspergillus flavus* and *A. parasiticus*.

They are often found as contaminants of peanuts, tree nuts, corn and cottonseed. They were discovered as a result of investigations into Turkey X disease in Britain, in which 100 000 turkeys and numerous other poultry died as a result of feeding on peanut meal which had been contaminated with mould.

Thin-layer chromatography (TLC) played a crucial part in the discovery and subsequent research on the aflatoxins and continues to play an important part in the analytical methods used for control of aflatoxins in food and feeds. The four major compounds are aflatoxins B₁, B₂, G₁ and G₂. Aflatoxins B₁ and B₂ have bright blue fluorescence on TLC and G₁ and G₂ are bright green-blue. Aflatoxin B₁ is found in the largest amounts in samples and is also the most toxic and carcinogenic of the four. Aflatoxin M₁ is found in the milk of animals which have ingested aflatoxin B₁.

For the structures of the aflatoxins see Figure 1. After the discovery of the aflatoxins other mycotoxins were discovered and methods of analysis using TLC have been devised for them.

Preparation of Samples

Aflatoxin contamination of food and feeds is usually in the range of ng g⁻¹ to µg g⁻¹. Sampling error is a severe problem in aflatoxin determination because only a few affected kernels can contaminate a large amount of finished product. Amounts as high as 207 000 ng g⁻¹ have been found in individual corn kernels. This is sufficient aflatoxin to produce

a level of contamination of 20 ng g⁻¹ in a batch of 10 000 kernels of grain. Sampling plans have been developed for various commodities. In general, the larger the unit size of the commodity, the larger the sample size should be. The sample should be finely ground and mixed before taking out the analytical test portion. Often the sampling error is larger than the analytical error.

Various methods of analysis have been devised. Many of these have been published in the *Official Methods of Analysis of AOAC International*, after collaborative studies by several laboratories. If the precision and accuracy of the results are acceptable the method becomes official.

The three most widely used extraction and clean-up methods for preparing aflatoxin extracts for TLC are the CB method, the BF method and the immunoaffinity column method. The CB method, named after the Contaminants Branch of the US Food and Drug Administration (FDA), uses chloroform extraction, filtering through paper, addition to a silica gel column, washing with hexane and ether, elution with chloroform-methanol (97:3 v/v), and evaporation to dryness to prepare the extract for TLC. The BF method, named after the Best Foods Company, uses methanol-water (55:45 v/v) extraction, hexane

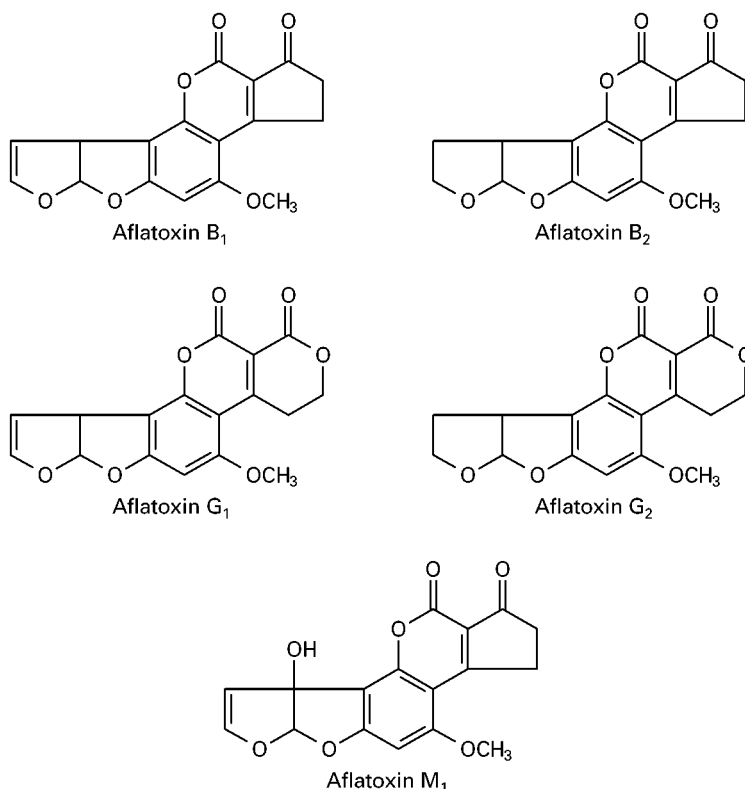


Figure 1 Structures of aflatoxins B₁, B₂, G₁, G₂ and M₁.

defatting in a separatory funnel, partition into chloroform and evaporation to dryness to prepare the extract for TLC. The immunoaffinity column method uses methanol–water (7 : 3 v/v) for extraction, filtering through paper, dilution with water, filtering through a glass microfibre filter, application to a column upon which antibodies to aflatoxins have been bound, washing with water, elution with methanol and evaporation to dryness to prepare the extract for TLC.

The advantage of the CB method is that it is precise and accurate when correctly performed. Disadvantages include the acquisition and disposal costs of the reagents used. The advantage of the BF method is that it has the lowest cost of any of the methods. The disadvantage is that it results in a somewhat dirtier extract. The advantages of the immunoaffinity column method are its simplicity of performance and the purity of the aflatoxins in the extract. Its disadvantage is the high cost of the columns.

After evaporation, in all three methods, the extract is carefully transferred using rinses of chloroform to a small vial. The solvent is again evaporated to dryness in a water bath under a stream of nitrogen. The residue is dissolved in a small amount of solvent (200 μL), usually benzene–acetonitrile (98 : 2 v/v), for spotting on TLC. Since the use of benzene is sometimes prohibited because of its toxicity, other solvents such as toluene–acetonitrile (9 : 1 v/v) may be used as well.

Aflatoxin Standards

A large source of error in the analysis is due to incorrectly prepared aflatoxin standards. In a check sample series, standards were found that contained more or less than the stated amount of aflatoxins when compared with a correctly prepared standard sent out with the study. It is very important to work with pure and accurate standards if accurate quantitative and qualitative results are to be obtained. Aflatoxin standards may be purchased from chemical distributors but need to be checked by means of TLC or liquid chromatography (LC) to ensure that they are pure. Small quantities of aflatoxin standards are sometimes available from organizations such as the FDA without cost.

Crystalline aflatoxin standards should be handled in a glove box because of their carcinogenicity and the electrostatic nature of the crystals. Because of the difficulty in handling the crystalline material, the aflatoxins are often received as dry films deposited in a precise amount in the bottom of a glass vial. The contents of the vial should be dissolved in the solvent (benzene–acetonitrile, 98 : 2 v/v) and mixed on a vor-

tex mixer for 1 min since the standards do not dissolve rapidly. After mixing, the solution is transferred to a screw-cap vial and the ultraviolet spectra measured between 370 and 330 nm. The concentration can then be calculated using the values listed in the AOAC International Official Method 971.22. The standards are applied to a TLC plate to verify the purity. The solutions must be stored in a closed and sealed vial in a refrigerator at 4–8°C. Mixtures of the four major aflatoxins can be prepared by diluting the concentrated stock solutions. The mixture most often used contains aflatoxins B_1 and G_1 at 1.0 $\mu\text{g mL}^{-1}$ and B_2 and G_2 at 0.2 $\mu\text{g mL}^{-1}$. This ratio between the four aflatoxins approximates to the ratio found in some sample extracts. The aflatoxins in benzene–acetonitrile (98 : 2 v/v) are stable when stored in a closed and sealed vial in a refrigerator at 4–8°C. Evaporation or decomposition of the aflatoxins can be detected using TLC or LC, shown by additional spots or additional peaks or an increase or decrease in the fluorescent intensity, as evidenced by unusual area integration values from the LC detector or TLC densitometer.

Spotting, Development and Examination of the TLC Plate

The plates most often used for aflatoxin analyses are 20 \times 20 cm glass plates, pre-coated with a 0.25 mm layer of silica gel 60 (E. Merck, Darmstadt); plates from other manufacturers may work equally well. Spotting should be done in subdued incandescent light to avoid photodecomposition of the aflatoxins. Using a 10 μL syringe, on an imaginary line 4 cm from the bottom of the plate and 1 cm apart, 2, 5 and two 10 μL spots of the sample extract are applied together with 2, 5 and 10 μL spots of mixed aflatoxin standards; 5 μL of the standard is applied on top of one of the 10 μL spots of sample extract. It is possible to spot four samples on to each plate.

The plate is developed for less than 90 min with acetone–chloroform (1 : 9 v/v) until solvent is within 4 cm of the top of the plate. It may be necessary to adjust the acetone–chloroform ratio to obtain optimum resolution. The plate is removed from the tank and air-dried in the hood in the dark.

Plates are examined under long wave ultraviolet light at 365 nm in a cabinet equipped with a filter for protecting the eyes from the ultraviolet light. Aflatoxins appear in order of decreasing R_F : B_1 , B_2 , G_1 and G_2 . G_1 and G_2 are slightly greener than the blue B_1 and B_2 . The R_F values for the aflatoxins in the sample spots should be the same as those of the standard spots. The aflatoxins in the sample spot upon which the standard is superimposed should

coincide exactly with the standard spots. The intensity of the fluorescence of each of the sample spots may be compared with that of the standard spots to estimate the amount of aflatoxin present in the extract. Separate estimates need to be made for B₁, B₂, G₁ and G₂. If the spots of the smallest portion of the sample are more fluorescent than the strongest standard spot it is necessary to dilute the sample extract and re-chromatograph. The plate may be run on a densitometer equipped with an ultraviolet light source set at 365 nm and an ultraviolet filter before the photomultiplier detector. Connecting the TLC densitometer to a computer permits the integration, calculation, printing, and storage of results. If more accurate quantitative results are necessary, the extract can be re-diluted to a concentration approximately equal to that of the standard and re-chromatographed in the same manner as above. The concentration of each aflatoxin in the extract can be calculated using the formula:

$$\text{ng g}^{-1} = (S \times Y \times V)/(X \times W)$$

where $S = \mu\text{L}$ of standard spot equal to sample; $Y = \text{concentration of standard in ng } \mu\text{L}^{-1}$; $V = \mu\text{L}$ of final dilution of sample extract; $X = \mu\text{L}$ of sample spot equal to standard; and $W = \text{grams of sample that the extract represents}$.

Not all blue fluorescent spots in the extracts are necessarily aflatoxins. Sample extracts may contain interferences, especially at the R_F values of G₁ and G₂. Respotting with an alternative solvent system such as the top phase benzene-ethyl alcohol-water (46 : 35 : 19 v/v) or with benzene-methanol-acetic acid (90 : 5 : 5 v/v) often resolves the aflatoxins from the interferences. Other solvents which are sometimes used are: ether-methanol-water (96 : 3 : 1 v/v), chloroform-acetone-water (88 : 12 : 1.5 v/v), or chloroform-acetone-isopropanol-water (88 : 12 : 1.5 : 1 v/v).

Two-Dimensional TLC

Another powerful technique for resolving the aflatoxins from interferences is two-dimensional TLC. In this technique two spots of aflatoxin standards and one spot of sample extract are spotted on the plate, as shown in Figure 2. The plate is first developed with ethyl ether-methanol-water (96 : 3 : 1 v/v) in the first direction. After development and air drying, the plate is redeveloped in the second direction with acetone-chloroform (1 : 9 v/v). After development and air drying the plate is examined under ultraviolet light at 365 nm for aflatoxin spots. A blue spot should appear at the intersection of imaginary lines from the two standard spots. The

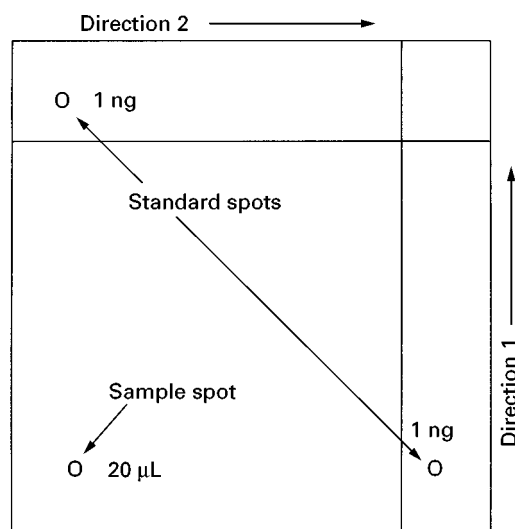


Figure 2 Two-dimensional TLC plate for aflatoxin analysis.

two-dimensional technique works well for difficult materials such as eggs and spices.

Confirmation of Identity of Aflatoxins

To confirm the identities of aflatoxins B₁ and G₁ a technique has been devised which uses derivative formation on the TLC plate. The sample extracts and standards are spotted on the origin line of the plate and 1 μL amounts of trifluoroacetic acid are then added to each spot. After reacting for 5 min, the trifluoroacetic acid is removed by blowing air at 35–40°C on the plate for 10 min. The trifluoroacetic acid catalyses the addition of water across the double bond in the terminal furan ring of aflatoxins B₁ and G₁ to form the derivatives called aflatoxin B_{2a} and G_{2a}, which give lower R_F values than the parent compounds. The plate is developed with chloroform-acetone (85 : 15 v/v). Upon examination of the plate under ultraviolet light at 365 nm, sample and standard will have low R_F blue and green spots of the derivatized aflatoxins. Since aflatoxin B₂ and G₂ do not have the unsaturated double bond, they will be unaffected by the test and will appear at their normal R_F values. For additional confirmation the plates can be sprayed with sulfuric acid-water (1 : 3 v/v), which causes the aflatoxin spots to change from blue or blue-green to yellow fluorescence.

Mass Spectrometric Confirmation of the Aflatoxins

The aflatoxins may be confirmed by negative ion chemical ionization-mass spectrometry. The aflatoxin is first purified using preparative TLC. The entire extract is applied along the origin line of a TLC

plate which is developed using chloroform–acetone (9 : 1 v/v). After drying, the silica gel is scraped from a band containing the aflatoxin B₁. If the silica gel is scraped into a sintered glass funnel the aflatoxin can be eluted with chloroform–methanol (2 : 1 v/v). After evaporation and re-dissolving in acetone, the aflatoxin can be introduced into the inlet probe of the mass spectrometer and spectra of sample and standard aflatoxin compared.

Methods of Analysis for Aflatoxin M₁

When cows consume aflatoxin in their feed, a small percentage of it is metabolized and excreted in the milk in the form of aflatoxin M₁. Aflatoxin M₁ is also toxic and carcinogenic, so methods have been developed to detect it in milk. Since infants and children are major consumers of milk products, the levels of concern for M₁ in milk are set quite low by various countries, in the range of 0.05–0.5 µg L⁻¹. Analyses of milk and cheese samples at these low levels are more difficult. One method of analysis uses partition from the milk into chloroform and silica gel column clean-up before the TLC determination. Another method used extraction from the milk on to a C₁₈ solid-phase extraction column and clean-up on a silica gel column before TLC or LC determination. An immunoaffinity column clean-up can also be used.

TLC is accomplished on 10 × 10 cm or 20 × 20 cm, 0.25 mm layer thickness silica gel 60 plates developed with chloroform–acetone–isopropanol (87 : 10 : 3 v/v). Other solvent systems which have been used are ether–methanol–water (95 : 4 : 1 v/v) and ether–hexane–methanol–water (87 : 10 : 4 : 1 v/v).

A two-dimensional TLC method for aflatoxin M₁ has been developed for liver but also works for milk and cheese extracts. The plate is spotted in a similar manner to the two-dimensional plate for aflatoxin B₁ and developed in the first direction with ether–methanol–water (95 : 4 : 1 v/v) and after development and drying is developed in the second direction with chloroform–acetone–isopropanol (87 : 10 : 3 v/v). The developed plate is examined under ultraviolet light at 365 nm for a blue spot at the intersection of imaginary lines from the two standard spots.

The confirmatory technique using trifluoroacetic acid works for aflatoxin M₁ as well but is performed using two-dimensional TLC and requires heating the plate in an oven at 75°C for the reaction to occur.

TLC Determination of Other Mycotoxins

Mycotoxins can be generated by a large number of mould species. Several books review the incidence

and toxicity of the most common mycotoxins. The interest of the regulatory authorities has been focused on relatively few of these metabolites that cause problems in human and animal health. The mycotoxins of regulatory interest are currently the aflatoxins, ochratoxin A, patulin, fumonisins, deoxynivalenol, other trichothecenes and zearalenone. TLC procedures are described below for these mycotoxins.

Ochratoxin A

Ochratoxin A (Figure 3) is a metabolite of some *Aspergillus* and *Penicillium* species. It is found as a contaminant of barley, corn, wheat, oats and coffee. It has also been found in meat, human blood and human milk. Ochratoxin A causes porcine nephropathy, notably in some Scandinavian countries when contaminated barley is fed to swine. Ochratoxin A is extracted from samples with chloroform in the presence of phosphoric acid and cleaned up using partition into sodium bicarbonate and C₁₈ solid-phase extraction. In a similar manner to the TLC of aflatoxin discussed above, ochratoxin A is spotted on a plate pre-coated with a 0.25 mm layer of silica gel 60 (E. Merck, Darmstadt) and developed with benzene–methanol–acetic acid (18 : 1 : 1 v/v) or toluene–ethyl acetate–formic acid (5 : 4 : 1 v/v). After drying, the plate is examined under long and short wave ultraviolet light (365 and 254 nm). Ochratoxin A ($R_F = 0.65$) fluoresces brightest under long wave ultraviolet light and is usually accompanied by the less toxic ochratoxin B ($R_F = 0.5$) which fluoresces brightest under short wave ultraviolet light. The fluorescence of the ochratoxins can be enhanced by spraying the plate with alcoholic sodium bicarbonate solution which changes them to their more fluorescent salt forms. The ochratoxins can be confirmed by ester formation using boron trifluoride in ethanol and re-chromatographing using the same conditions as above. The ethyl esters appear at lower R_F values than the parent compounds under long and short wave ultraviolet light.

Patulin

Patulin (Figure 3) is a lactone metabolite of several moulds, including *Penicillium expansum*, which causes brown rot in apples. Patulin is often found in apple juice, especially juice from fallen apples. Patulin can be extracted from apple juice with ethyl acetate and cleaned up using silica gel column chromatography. After evaporation, the extract is dissolved in chloroform and spotted on silica gel plates and developed with toluene–ethyl acetate–formic acid (5 : 4 : 1 v/v). After drying, the plate is sprayed

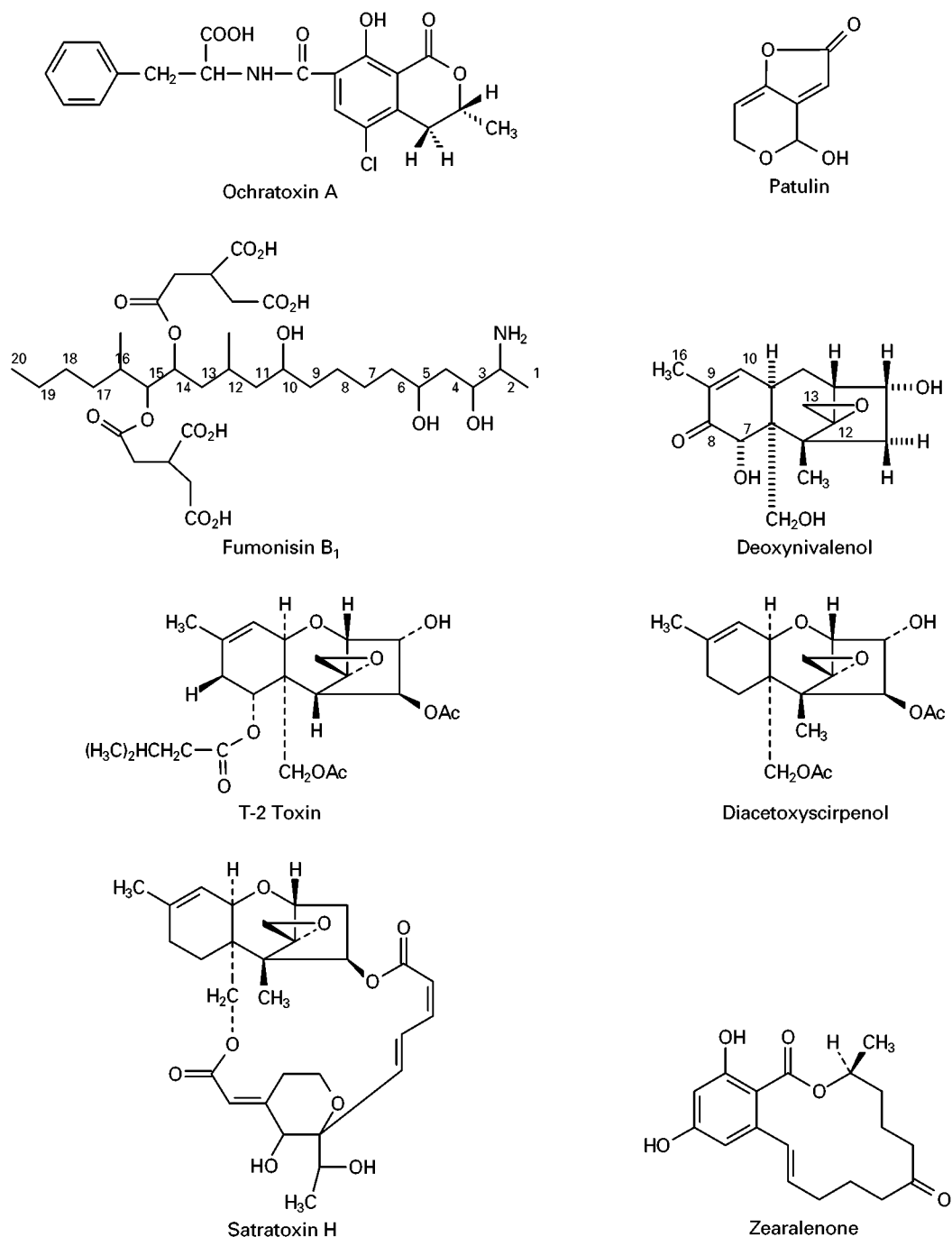


Figure 3 Structures of ochratoxin A, patulin, fumonisin B₁, deoxynivalenol, T-2 toxin, diacetoxyscirpenol, satratoxin H and zearalenone.

with 3-methyl-2-benzothiazolinone hydrazone-HCl (MBTH) solution and heated for 15 min in an oven at 130°. Under ultraviolet light at 365 nm, patulin ($R_F = 0.5$) appears as a yellow-brown fluorescent spot. The amount of patulin in the sample can be determined by comparing the intensity of fluorescence of the standard and sample spots. Other TLC developers, such as hexane-anhydrous ether (1 : 3 v/v), chloroform-methanol (95 : 5 v/v), and

chloroform-acetone (9 : 1 v/v) can be used to confirm the identity of the patulin. After development, plates are sprayed with MBTH to reveal the patulin.

Fumonisin

Fumonisin B₁ (Figure 2) and B₂ are metabolites of *Fusarium moniliforme* and *F. proliferatum*. They are common natural contaminants of corn and have

caused deaths in horses and swine. Small amounts have been found in cornmeal and breakfast cereals. In order to ensure that they are not present in food in excessive amounts, methods of analysis have been developed. Most methods use LC after formation of derivatives of the primary amine function with reagents such as *o*-phthalaldehyde. However, a reversed-phase TLC determination has been devised. The fumonisins, dissolved in acetonitrile–water (1 : 1 v/v), are spotted at the origin of a 10 × 10 cm C₁₈ plate and developed with methanol–1% KCl in water (3 : 1 v/v). After drying, the plates are sprayed with 0.1 mol L⁻¹ sodium borate (pH 8–9) followed by fluorescamine (0.4 mg mL⁻¹ in acetonitrile). After a 1 min delay, further spraying with 0.01 mol L⁻¹ boric acid–acetonitrile (2 : 3 v/v) is carried out. Examination under 365 nm ultraviolet light reveals fluorescent yellow spots of fumonisin B₁ ($R_F = 0.5$) and fumonisin B₂ ($R_F = 0.1$).

Deoxynivalenol

Deoxynivalenol (Figure 2), also called vomitoxin, is a trichothecene metabolite of *F. graminearum*, an organism which causes a disease in barley and wheat called head blight or scab. Deoxynivalenol is found as a contaminant of barley, wheat, corn and rye and causes adverse health effects in animals and humans, including feed refusal and vomiting in swine. An advisory level of 1 µg g⁻¹ has been set for finished wheat products. Methods for analysis have been devised using LC and TLC. The TLC method uses acetonitrile–water (84 : 16 v/v) extraction and clean-up using a charcoal–alumina–Celite (7 : 5 : 3 v/v) column. The extracts and standard deoxynivalenol are dissolved in methanol and spotted near the 20 cm edge of a 20 × 10 cm Linear-K High Performance (Whatman, Clifton NJ) or equivalent silica gel plate and developed with chloroform–acetone–2-propanol (8 : 1 : 1 v/v). After drying the plate is sprayed with aluminium chloride solution (20 g AlCl₃·6H₂O in 100 mL methanol–water: 1 : 1 v/v) and then heated in an oven at 120° for 7 min. Under 365 nm ultraviolet light, deoxynivalenol appears as a blue fluorescent spot at $R_F = 0.78$. Spots may be scanned with a densitometer.

Other Trichothecenes

The trichothecenes are a large group of fungal metabolites produced by various species of *Fusarium*, *Myrothecium*, *Stachybotrys*, *Verticimonosporium*, *Cylindrocarpon*, *Trichoderma* and *Tricothecium*. They have been implicated in numerous farm-animal poisonings. A human disease called alimentary toxic

aleukia occurred in the former Soviet Union during World War II when grains were eaten after they had lain out in the field under snow during the winter. *Fusarium* moulds isolated from these grains were shown to produce large amounts of T-2 toxin (Figure 3) and related derivatives. T-2 toxin and related compounds can be analysed by silica gel TLC using chloroform–methanol (9 : 1 v/v) as the developer. Since the trichothecenes are colourless and do not fluoresce, it is necessary to spray the developed plate with sulfuric acid–methanol (1 : 1 v/v), heat for 10 min at 100°C and examine the plate under 365 nm ultraviolet light. Trichothecenes of the T-2 group will appear as blue fluorescent spots, T-2 at $R_F = 0.64$, diacetoxyscirpenol (Figure 3) at $R_F = 0.60$, neosolaniol at $R_F = 0.39$, dihydroxydiacetoxyscirpenol at $R_F = 0.32$ and HT-2 toxin at $R_F = 0.31$.

Other trichothecenes of the nivalenol group do not form fluorescent derivatives with sulfuric acid but instead give a dark pink to brown spot when the plate is examined under visible light. A more useful detection procedure for these compounds is spraying with 4-(*p*-nitrobenzyl)-pyridine (NBP: 1% in chloroform), heating for 30 min at 150°C and spraying with tetraethylenepentamine (TEPA). Under visible light a plate developed with chloroform–methanol (9 : 1 v/v) will have blue spots of fusaranon-X at $R_F = 0.36$, and dihydronivalenol at $R_F = 0.07$. A plate developed with benzene–acetone (1 : 1 v/v) will have tetraacetylnivalenol at $R_F = 0.62$, crotocin at $R_F = 0.59$, dihydronivalenol at $R_F = 0.07$ and nivalenol at $R_F = 0.09$.

Another type of trichothecene is a series of macrocyclic di- and trilactonic derivatives of verrucarol. These have been implicated in a disease of horses and other farm animals called stachybotryotoxicosis. Recently they are suspected of contributing to the death of some infants exposed to the air in mouldy houses. Since they contain an ultraviolet-absorbing functional group, they can be detected by using silica gel plates which fluoresce under 254 nm ultraviolet light. The satratoxins appear as dark spots on a white background. If developed with chloroform–2-propanol (99 : 1 v/v) roridin E will appear at $R_F = 0.85$, verrucarin J at $R_F = 0.45$, satratoxin F at $R_F = 0.40$, satratoxin G at $R_F = 0.20$ and satratoxin H (Figure 3) at $R_F = 0.15$.

Zearalenone

Zearalenone (Figure 3) is a metabolite of the mould *F. graminearum* also called by its perfect name *Gibberella zeae*. Zearalenone is found in barley, wheat and corn and causes hyperoestrogenism in swine, resulting in infertility and spontaneous abortions. It

sometimes co-occurs with deoxynivalenol. Zearalenone can be extracted from grain with chloroform and cleaned up using a silica gel column, followed by defatting by partitioning between hexane and acetonitrile. For TLC the samples and standards are dissolved in benzene and spotted on a silica gel and developed with ethanol–chloroform (5 : 95 v/v) or acetic acid–benzene (5 : 95 v/v). Under 254 nm ultraviolet light, zearalenone appears as a greenish-blue fluorescent spot at $R_F = 0.5$. If the plate is sprayed with an aluminium chloride solution and heated for 5 min at 130°C, zearalenone will appear under 365 nm ultraviolet light as a blue fluorescent spot.

Summary

TLC methods have been developed to analyse for a variety of mycotoxins in the commodities in which they occur. TLC densitometric determinations provide precise quantitative data at ng g^{-1} to $\mu\text{g g}^{-1}$ levels. The major advantages of TLC over LC are its low cost and its use as a screening tool. The commercial availability of precoated TLC plates, including silica gel, reversed-phase and high performance plates has resulted in expanded applications in the mycotoxin field. The role of TLC in the analysis of mycotoxins will continue for the foreseeable future.

See also: II/Chromatography: Thin-Layer (Planar): Historical Development; Preparative Thin-Layer (Planar)

Chromatography. III/Aflatoxins and Mycotoxins: Chromatography. Immunoaffinity Extraction.

Further Reading

- Bullerman LB and Draughon FA (eds) (1994) *Fusarium moniliforme and Fumonisin symposium*. *Journal of Food Protection* 57: 513–546.
- Cole RJ and Cox RH (eds) (1981) *Handbook of Toxic Fungal Metabolites*. New York: Academic Press.
- Eaton DE and Groopman JD (eds) (1994) *The Toxicology of Aflatoxins*. San Diego: Academic Press.
- Purchase IFH (ed.) (1974) *Mycotoxins*. Amsterdam: Elsevier.
- Rodricks JV (ed.) (1976) *Mycotoxins and Other Fungal Related Food Problems*. Advances in Chemistry Series 149. Washington, DC: American Chemical Society.
- Rodricks JV, Hesseltine CW and Mehlman MA (eds) (1977) *Mycotoxins in Human and Animal Health*. Park Forest South, IL: Pathotox.
- Scott PM (ed.) (1995) Chapter 49, Natural toxins. In: Cunniff P (ed.) *Official Methods of Analysis of AOAC International*, 16th edn., Gaithersburg, MD: AOAC International.
- Stack, ME (1996) Toxins. In: Sherma J and Fried B (eds) *Handbook of Thin-layer Chromatography*. New York: Marcel Decker.
- Steyn PS (ed.) (1980) *The Biosynthesis of Mycotoxins*. New York: Academic Press.
- Touchstone JC (ed.) (1982) *Advances in Thin Layer Chromatography*. New York: Wiley.
- Whitaker TB, Springer J, Defize PR *et al.* (1995) Evaluation of sampling plans used in the United States, United Kingdom, and the Netherlands to test raw shelled peanuts for aflatoxin. *Journal of AOAC International* 78: 1010–1018.

AIR LIQUEFACTION: DISTILLATION



R. Agrawal and D. M. Herron, Air Products and Chemicals, Hamilton Boulevard, Allentown, PA, USA

Copyright © 2000 Air Products and Chemicals, Inc

Oxygen, nitrogen and argon, the major components of air, have been separated by distillation at cryogenic temperatures for nearly a century. Air was commercially liquefied as early as 1895 by Carl von Linde and also by William Hampson. Linde separated oxygen from air by distillation in a single column in 1902. A commercial plant producing pure nitrogen was already in operation by 1904. The first double-col-

umn distillation system, the predecessor to current double-column processes, was commissioned in 1910 by Linde. Argon was produced on an industrial scale by 1913. Today the major industrial companies supplying products from air distillation and liquefaction and also the equipment for this purpose are: AGA, Air Liquide, Air Products and Chemicals, the BOC Group, Linde, Messer Group, Nippon Sanso and Praxair.

The composition of dry and impurities-free air is given in Table 1. The critical temperature and normal boiling point (at 101.3 kPa) for each component is also listed. In this table, and in the rest of this chapter, concentration in p.p.m. refers to parts per million on a volume basis. The gases listed in Table 1 are used in

Table 1 Composition of air and thermodynamic properties of its constituent gases

<i>Constituent gas</i>	<i>Concentration (mol%)</i>	<i>Boiling temperature (°C)^a</i>	<i>Critical temperature (°C)</i>
Nitrogen	78.12	− 195.8	− 146.9
Oxygen	20.95	− 182.9	− 118.8
Argon	0.93	− 185.9	− 122.4
Neon	18 p.p.m.	− 246.1	− 228.8
Helium	5.3 p.p.m.	− 268.9	− 267.9
Krypton	1.1 p.p.m.	− 153.4	− 63.8
Xenon	0.08 p.p.m.	− 108.1	− 16.6

^a Boiling temperature at 101.3 kPa.

a wide range of industrial and medical applications. Typical industries using these gases include: ferrous and nonferrous metals, chemicals, petroleum, food, paper, glass, textile and electronics. Oxygen is generally used as an oxidant while nitrogen and argon are used to provide inert atmospheres. Krypton is used in light bulbs, lasers, sputtering of electronic components and high energy physics. Neon is used in fluorescent lighting, infrared detection equipment and experimental physics at cryogenic temperatures. Xenon is used in electronic flashlights, as an anaesthetic and in a new application where an on-board xenon ion propulsion system is used for positioning a satellite. Helium is not generally recovered from air due to its low concentration.

The history of air distillation started with oxygen production followed by recovery of other constituents. Therefore, the distillation processes to produce oxygen are described first here followed by argon and then nitrogen. These topics are followed by liquefaction processes and finally a brief description is given of the major equipment used in cryogenic air separation and liquefaction processes.

Distillation

Distillation of Air to Recover Oxygen

The basic steps of any cryogenic air distillation process are shown in **Figure 1**.

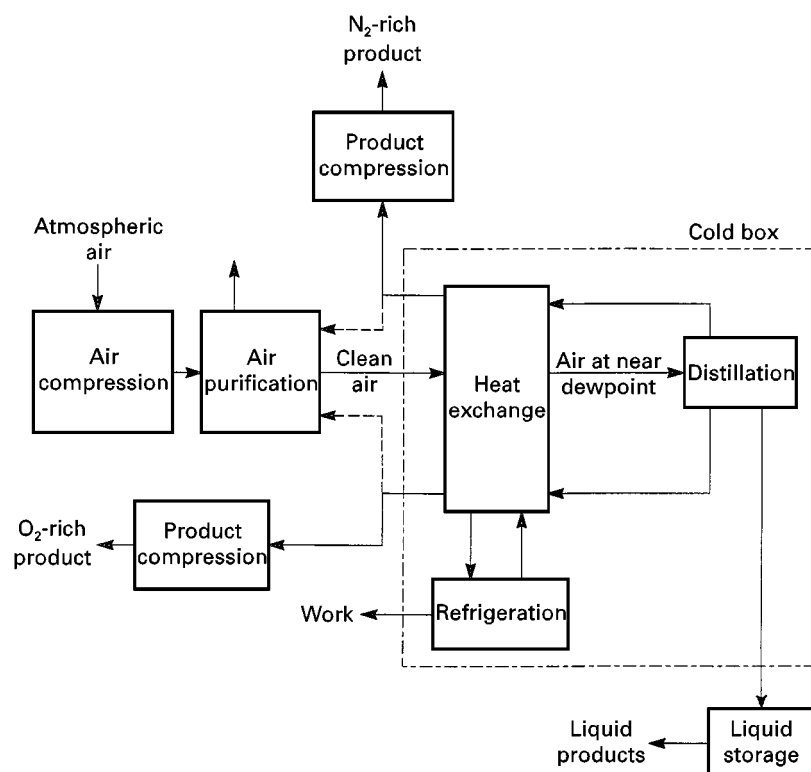


Figure 1 Basic steps in a cryogenic air distillation plant.

Air is first compressed in a multistage compressor and cooled to near ambient temperature. Given the boiling point temperatures of nitrogen and oxygen in Table 1, it is clear that air has to be cooled to extremely low temperatures before it can be distilled. It follows that a number of impurities present in air and which would freeze at such cryogenic temperatures must be removed to avoid plugging of heat exchange and separation equipment. Typical impurities that are not listed in Table 1 but are present in air include: water (after compression air is saturated); carbon dioxide (about 375 p.p.m.); hydrocarbons such as acetylene (0.1–1 p.p.m.), methane (2–10 p.p.m.) and some higher hydrocarbons in varying concentrations (ethylene, propylene, ethane, etc.); carbon monoxide; nitrogen oxides and sulfur compounds. Therefore, in the second step, compressed air is sent through a purification system at least to remove impurities such as water, carbon dioxide, acetylene, nitrogen oxides and sulfur compounds.

In the third step, the compressed and cleaned air is cooled to near its dewpoint by heat exchange. Finally, the cooled air is sent to an appropriate distillation column system. Here air is distilled into at least two product streams – one stream is enriched in oxygen and the other is enriched in nitrogen. Both of these streams are then warmed to near ambient temperature by countercurrent heat exchange with the incoming air. When a product stream is required at a higher pressure, it is further compressed. Liquid products such as liquid oxygen, liquid nitrogen or liquid argon can also be produced from the distillation column system and sent to liquid storage for later distribution.

The heat exchanger and the distillation system are enclosed in a well-insulated enclosure called the cold box. Despite the insulation, there is heat leakage and therefore, refrigeration is provided to the cold box to keep the inside equipment cold. For this purpose, modern cryogenic plants employ turbo-expanders that are also enclosed in the cold box. These turbo-expanders produce work out of the cold box and keep all the equipment at the desired cryogenic temperatures.

Now that the basic steps that are common to all the air distillation plants have been described, attention will be paid to the distillation of air after it is cooled to near its dewpoint temperature. The distillation of air is at the heart of an air separation plant and its arrangement varies with the number, quantity and purity of products being produced.

The early developments in air distillation to produce oxygen were propelled by the invention of the oxyacetylene blow torch for welding and steel cutting. In 1902, Carl von Linde introduced the first air distillation process using a single distillation column.

A simplified sketch of this single column arrangement is shown in Figure 2.

Compressed, cleaned and cooled air that is near its dewpoint temperature is first condensed in a reboiler-condenser located in the bottom (sump) of the distillation column. The condensed liquid air is then reduced in pressure across a valve and fed to the top of the distillation column. The stream provides both the feed and the liquid reflux. From Table 1 it can be seen that, of the three major components in air, nitrogen is the most volatile, oxygen the least volatile and argon is of intermediate volatility. As a result, the liquid descending the distillation column becomes enriched in oxygen. The vapour needed for distillation is provided by boiling the oxygen-enriched liquid in the sump by heat exchange against the condensing air in the reboiler-condenser. A portion of the vapour rising from the sump is collected as gaseous oxygen product while the rest is allowed to travel up the distillation column. As vapour ascends the distillation column, it becomes enriched in nitrogen and finally leaves from the top of the column as a nitrogen-enriched waste stream. If needed, a liquid oxygen product stream is collected from the sump of the distillation column. Even when liquid oxygen is not a desired product, a very small quantity of liquid oxygen is continuously withdrawn from the bottom of the distillation column to avoid accumulation of hydrocarbons in the sump. Both the gaseous oxygen product stream and nitrogen-rich vapour stream are then warmed to near

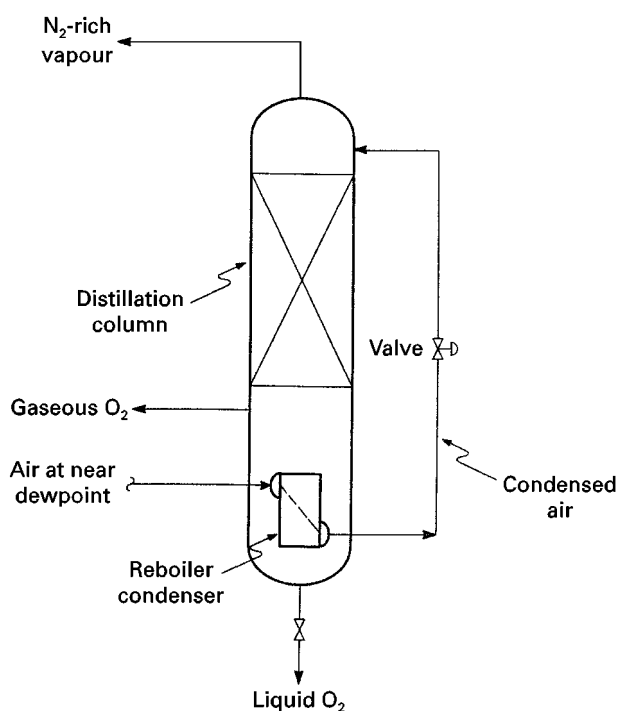


Figure 2 A single column to produce oxygen.

ambient temperature by heat exchange against the incoming air stream (Figure 1). While the early plants produced oxygen at a purity of 80–90%, the single-column process can provide oxygen at any desired higher purity. Generally, the purity of oxygen used in metal welding and cutting is 99.5% or greater.

The problem with the single distillation column process shown in Figure 2 is that the recovery of oxygen is low. The reason is that the minimum concentration of oxygen in the nitrogen-rich vapour stream leaving the top of the distillation column is limited to that value which is in equilibrium with the liquid air that is fed at the top. Since the concentration of oxygen in air is fairly high, a sizeable fraction of the oxygen in the feed air leaves in the nitrogen-rich vapour stream. To illustrate this for a distillation column operating at 1.4 atm and producing 99.5% oxygen, the pressure of feed air is about 5 atm and a vapour stream in thermodynamic equilibrium with the liquid air stream (at 1.4 atm) will be 6.9% oxygen. A typical oxygen recovery from such a distillation column would only be in the neighbourhood of 14 mol of oxygen per 100 mol of feed air.

It is clear that, for higher recoveries of oxygen, the concentration of oxygen in the nitrogen-rich vapour stream leaving the top of the distillation column must be low. In other words, both product streams should be relatively pure. This requires that the liquid reflux to the top of the distillation column should also be relatively pure. It seems that Georges Claude was the first to provide the solution by using his dephlegmation equipment in 1903. However, it was Carl von Linde's double distillation column of 1910 that revolutionized the industry and is still the workhorse of the modern cryogenic oxygen plants.

A typical double distillation column configuration is shown in Figure 3.

In this arrangement, compressed, cleaned and cooled air is now sent to a high pressure distillation column that operates at about 6 atm. As the vapour rises up this high pressure column, it is enriched in nitrogen and at the top of the column, the concentration of oxygen has been reduced to an extremely low level. The nitrogen vapour is condensed by heat exchange in a reboiler-condenser. Of this condensed nitrogen stream, about 60% is returned back to the top of the high pressure column as liquid reflux; approximately 40% of the flow is sent to the top of a low pressure column that operates at around 1.4 atm. The liquid descending the high pressure column becomes enriched in oxygen to produce crude liquid oxygen leaving the bottom (typically around 35% oxygen). This crude liquid oxygen is reduced in pressure across a valve and fed to an intermediate location in the low pressure column. In the low pres-

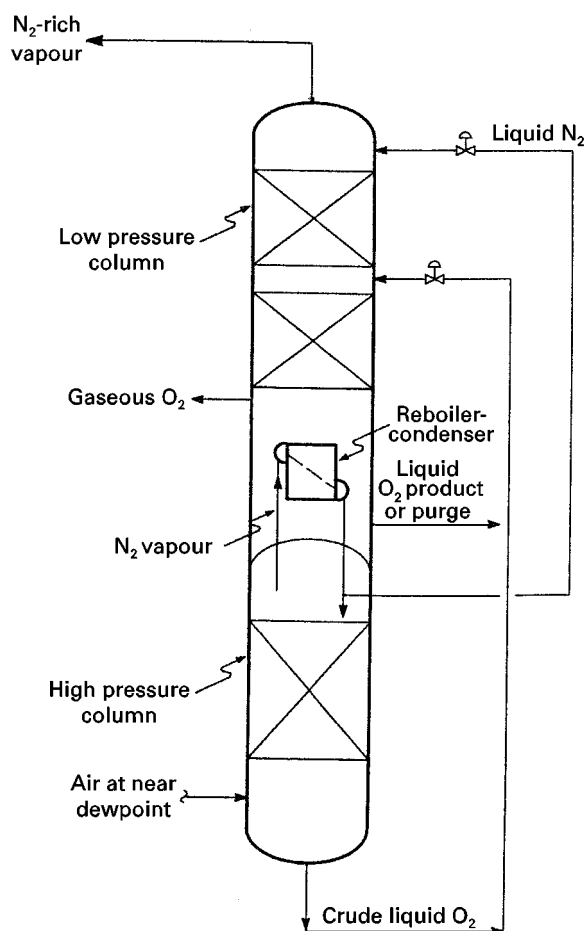


Figure 3 A double-column arrangement to produce oxygen.

sure column, crude liquid oxygen is distilled to produce a nitrogen-rich vapour stream at the top and an oxygen product stream at the bottom. The boil-up at the bottom of the low pressure column is provided by vaporizing the liquid oxygen stream in the sump by heat exchange against the condensing nitrogen vapour stream from the top of the high pressure column. A portion of the vapour from the reboiler-condenser is recovered as gaseous oxygen product while the rest rises to perform distillation in the low pressure column. When needed, some liquid oxygen can also be recovered from the sump as product.

In a double-column arrangement, the main purpose of the high pressure column is to distil and provide two saturated liquid streams from the feed air – a liquid nitrogen reflux and a crude liquid oxygen feed. It is in the low pressure column that the crude liquid oxygen is distilled to provide the needed oxygen product stream. The liquid nitrogen stream provides the much needed liquid reflux at the top of the low pressure column. By using sufficient stages of separation in the high pressure column, the concentration of oxygen in the liquid nitrogen stream can

often be reduced to p.p.m. level. Therefore, the concentration of oxygen in the nitrogen-rich vapour stream from the top of the low pressure column is reduced to extremely low levels. This not only allows the potential to recover the nitrogen-rich vapour stream as a useful product stream, but also makes very high recoveries of oxygen possible. For a double-column process, production of 99.5% oxygen in excess of 20.5 mol per 100 mol of feed air (maximum oxygen content being 20.95 mol) is quite common.

For most uses, gaseous oxygen is needed at pressures greater than atmospheric pressure. This pressure can range from about 2 atm absolute pressure for glass-making to pressures in the range of 30–80 atm for the gasification of hydrocarbons such as coal and petroleum residuum. One obvious method to deliver pressurized oxygen is to compress gaseous oxygen to the desired pressure after it exits the cold box. However, safety considerations tend to make the equipment associated with oxygen compressors expensive. In certain applications, where both oxygen and nitrogen are needed at higher pressures, one has the option of increasing the pressure of the distillation columns and directly produce both products at elevated pressures. Unfortunately, the low pressure column is seldom operated at pressures greater than 8 atm absolute. This is because the pressure of the high pressure column is typically greater than two to three times the pressure of the low pressure column and distillation in the high pressure col-

umn must be conducted at a pressure that is sufficiently lower than the critical pressures of nitrogen and oxygen. A third method that is becoming more popular is the use of a pumped liquid oxygen process. This method is also sometimes referred as internal oxygen compression. A schematic of such a plant is shown in Figure 4.

In the pumped liquid oxygen process of Figure 4, air is compressed in a multistage air compressor (MAC) to about 6 atm absolute pressure, cooled to near ambient temperature and then sent to a molecular sieve purifier. About 70% of the cleaned air is directly fed to the cold box for cooling in the main heat exchanger. From an intermediate location of the main heat exchanger, corresponding to 100°C to –130°C, approximately 10–20% of this flow is withdrawn and expanded in a turbo-expander to a pressure slightly above atmospheric pressure and fed to an intermediate location of the low pressure column. The work extracted from the turbo-expander provides the needed refrigeration for the cold box. The air that remains after the withdrawal of expander feed is cooled to near the dewpoint temperature and is fed to the bottom of the high pressure column. The arrangement of the double distillation column process is the same as discussed in Figure 3, with only two differences. The first is that the liquid nitrogen stream from the top of the high pressure column is cooled in a subcooler heat exchanger against the nitrogen-rich vapour streams.

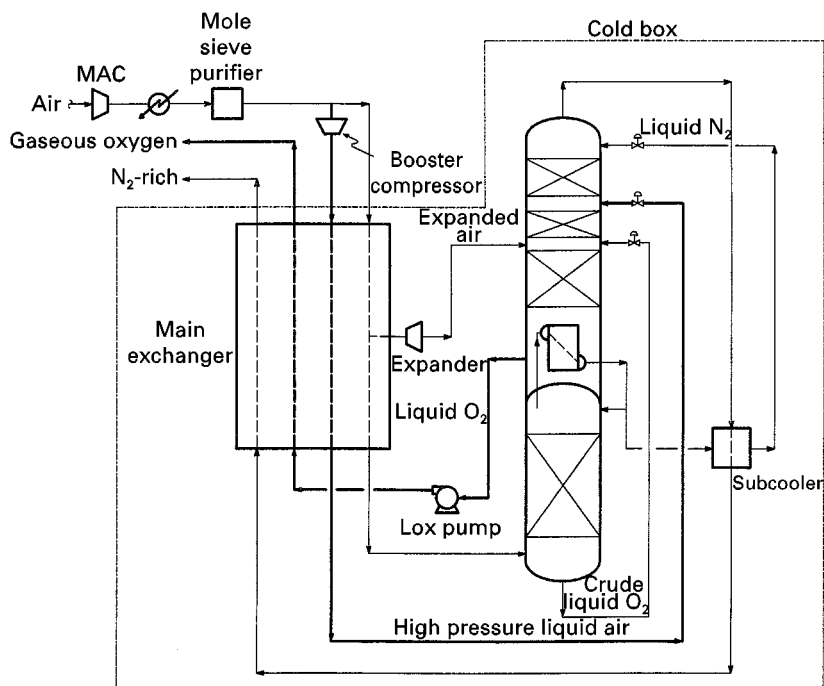


Figure 4 Pumped liquid oxygen flowsheet.

This increases the fraction of liquid in this stream as its pressure is reduced to that of the low pressure column. This technique, which is commonly used in any oxygen plant to increase liquid nitrogen reflux to the low pressure column, has the beneficial effect of increasing the purity and recovery of products.

The second major difference is the withdrawal of oxygen product from the low pressure column as liquid and its subsequent vaporization. The liquid oxygen is pumped in a liquid oxygen pump to the desired oxygen product pressure. This pumped liquid oxygen is then vaporized in the main heat exchanger. In order to maintain refrigeration balance, it is essential that another stream be condensed through heat exchange as the pumped liquid oxygen is being vaporized. For this purpose, about 30% of the cleaned air is further boosted to a higher pressure in a booster compressor. The pressure of the boosted air is chosen such that it would easily condense through heat exchange with the vaporizing oxygen stream. Generally the pressure of the condensing air stream is much greater than the oxygen stream. The condensed liquid air from the main heat exchanger is appropriately fed to either one or both of the distillation columns. The warmed gaseous oxygen stream provides the desired pressurized oxygen product.

While the early oxygen plants produced only a few tons of oxygen per day, modern plants are capable of producing in excess of 3000 tons per day of oxygen in a single train.

Distillation of Air to Recover Argon

After nitrogen and oxygen, argon is the most abundant component in air. Its inert property is quite attractive for metals and several other material-processing applications. Within a very short time of the discovery of the double-column system, argon was distilled from air in 1913. The distillation arrangement to produce argon in modern plants was generally described in a German patent by 1935.

The arrangement for argon production starts with an examination of the argon concentration profile in the low pressure column of a double-column process. From the normal boiling temperatures listed in Table 1, it is readily observed that the volatility of argon is between that of nitrogen and oxygen and, furthermore, it is closer to oxygen than nitrogen. As a result, the concentration of argon in the liquid nitrogen stream from the high pressure column (Figures 3 and 4) is at p.p.m. level and virtually all the argon is contained in the crude liquid oxygen. Therefore, the bulk of the argon in air enters at an intermediate point on the low pressure column. When oxygen containing less than 0.5% argon is produced, argon is forced to escape from the top of the low

pressure column in the nitrogen-rich vapour stream. However, the liquid nitrogen reflux stream is virtually free of argon and tends to drive argon down the low pressure column. Consequently, the concentration of argon in the vapour phase at an intermediate location between the crude LOX feed and the oxygen product withdrawal point reaches levels approaching 20%. A typical vapour-phase argon concentration profile in the low pressure column is shown in Figure 5. The build-up of argon provides an opportunity to withdraw a side vapour stream from near the location where a peak in argon concentration occurs and to distil it further in a side distillation column to produce concentrated argon.

A typical argon recovery arrangement is shown in Figure 6. An argon-rich vapour stream containing between 10 and 25% argon, p.p.m. levels of nitrogen and the rest oxygen is withdrawn from an intermediate location of the bottom section of the low pressure column and is fed to the bottom of a side argon column. The flow of this vapour stream is about 20% of the feed air. As vapour ascends the side argon column, it is depleted in oxygen. The development of structured packing for cryogenic distillation columns has allowed the modern cryogenic plants to use in excess of 175 theoretical stages of separation in the side argon column. As a result, the vapour at the top of this column can contain only p.p.m. levels of oxygen. This vapour stream is condensed in a reboiler-condenser; most of it is returned back as reflux to the side argon column and a small portion is recovered as a crude argon stream. The liquid to vapour flow ratio in this column is in the neighbourhood of 0.97. The liquid from the bottom of the side argon column is

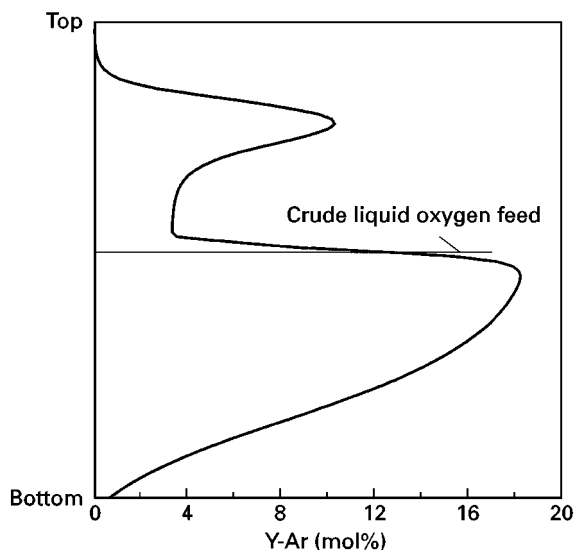


Figure 5 Vapour-phase composition in the low pressure column.

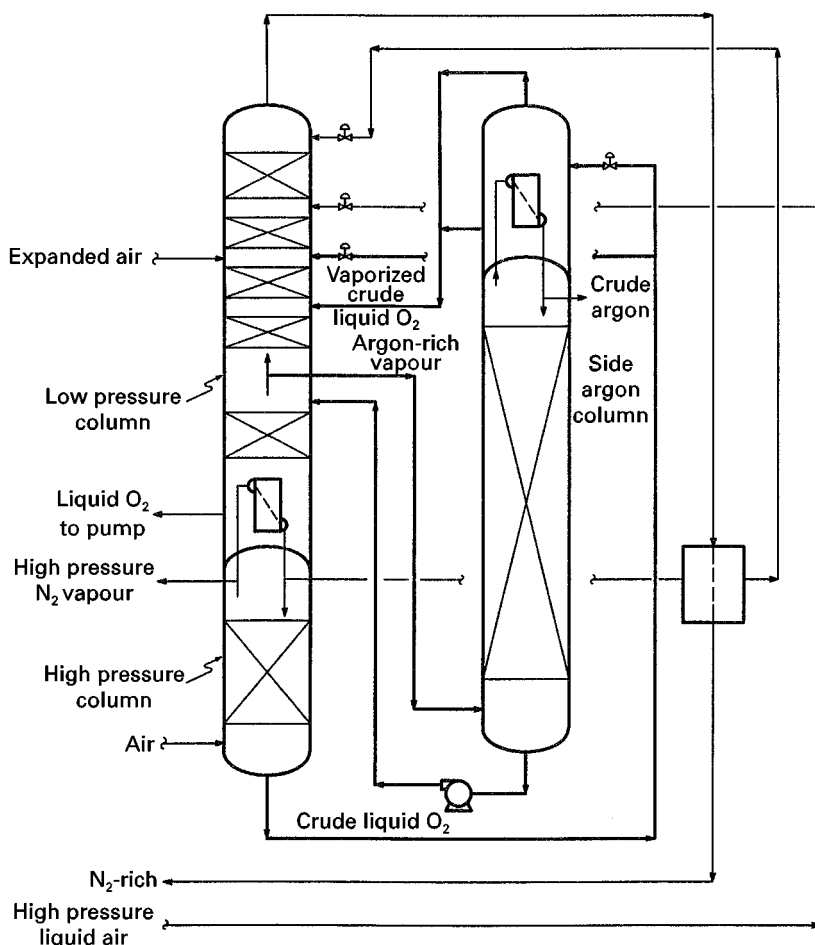


Figure 6 Distillation arrangement for argon separation from air for the process shown in Figure 4.

pumped back to the argon-rich vapour draw location of the low pressure column. Condensation at the top of the side argon column is provided by boiling a portion of the crude liquid oxygen at nearly the low pressure column pressure, as shown in Figure 6. The vaporized crude liquid oxygen stream is fed to the low pressure column a few stages of separation below the location where the unboiled crude liquid oxygen is fed. The recovery of argon from cryogenic air is easily in the range of 70–85% and occasionally, if needed, it can be as high as 95% of the total argon contained in the feed air.

While the concentration of oxygen in the crude argon recovered from the arrangement in Figure 6 is below 5–100 p.p.m., the nitrogen concentration is much higher, as nearly all the nitrogen contained in the argon-rich vapour stream shows up in the crude argon. Generally, the argon product specification requires that the nitrogen concentration also be below 5 p.p.m. Therefore, the crude argon stream is subsequently distilled in a pure argon column with separation stages both below and above the feed. Boil-up and condensing duties for this column are extremely

low and are easily provided by using side streams that are withdrawn from one or more appropriate process streams, shown in Figure 6, such as crude liquid oxygen, high pressure liquid air or high pressure nitrogen vapour. A waste vapour stream containing all the nitrogen is withdrawn from the top of the pure argon column and pure liquid argon product is collected and sent to a storage tank from the bottom of this column.

Distillation of Air to Recover Nitrogen

In most industrial applications, nitrogen is used as an inert gas. Cryogenic air separation can easily produce nitrogen gas with concentrations of oxygen below 5 p.p.m. Until the 1950s, the demand for nitrogen was low. Supply could easily be met by withdrawing a portion of nitrogen vapour from the top of the high pressure column as a co-product of a double-column process for oxygen production (for example, see Figure 6). Generally, up to 30% of the feed air can be recovered as high pressure nitrogen product from the top of the high pressure column. When needed, a portion of the nitrogen-rich vapour stream from the top

of the low pressure column can also be recovered as a useful product.

In the 1960s industrial demand for nitrogen increased, and this led to a need for plants that were designed solely for nitrogen with no co-production of oxygen. For most applications, nitrogen product is required at a pressure between 6 and 10 atm. There are two basic schemes for nitrogen separation from air: one uses a single column while the other uses two columns (similar to the double-column process for oxygen production). The single-column process is used for relatively small size nitrogen plants (up to about 500 tons per day of nitrogen) and two-column processes are used for larger size plants. Cold boxes can now be designed to produce as much as 10 000 tons per day of nitrogen in a single train.

A single-column process for nitrogen separation is shown in **Figure 7**.

Feed air is compressed to a pressure in excess of about 5 atm absolute, cleaned of impurities in the molecular sieve purifier and cooled to near its dew-point in the main heat exchanger by heat exchange against the returning streams. The cooled air stream is then fed to the bottom of a single column. Sufficient separation stages are used in this column to attain the desired purity at the top of this column. A portion of the nitrogen vapour from the top is withdrawn and warmed in the main heat exchanger to provide the desired nitrogen product. The rest of

the nitrogen vapour stream is condensed in a reboiler-condenser and returned as reflux to the column. The ratio of liquid to vapour flow rates in the column is in the neighbourhood of 0.6. The crude liquid oxygen stream from the bottom of the column is reduced in pressure and vaporized in the reboiler-condenser. The vaporized stream is partially warmed in the main heat exchanger and then expanded in a turbo-expander to near atmospheric pressure to provide the needed refrigeration for the plant. The expanded stream is then warmed to near ambient temperature in the main heat exchanger and eventually discharged as an oxygen-rich waste stream. The concentration of oxygen in the waste stream is approximately 35%. The flow rate of the nitrogen product stream is about 40–50 mol per 100 mol of the feed air.

The main problem with the single-column process is that the crude liquid oxygen leaving from the bottom of the column is at best, in thermodynamic equilibrium with the feed air. This means that there is a lower limit to the concentration of nitrogen in the crude liquid oxygen stream. This limits the recovery of nitrogen. For higher recoveries of nitrogen and more efficient processes, it is essential that the crude liquid oxygen stream be further distilled to recover the contained nitrogen. **Figure 8** shows such a two-column process.

The major difference between this process and the single-column process of **Figure 7** is that now

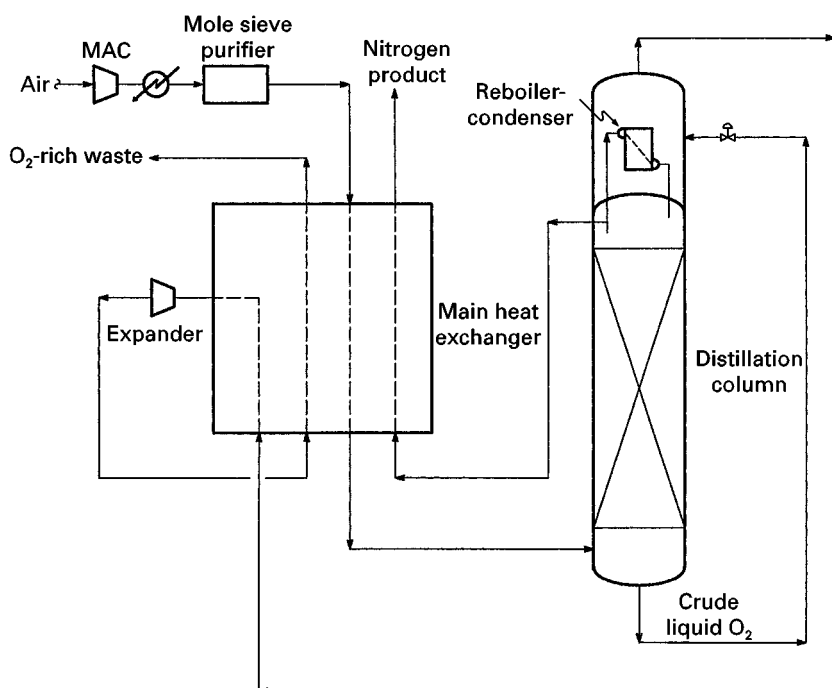


Figure 7 A single distillation column process for nitrogen production.

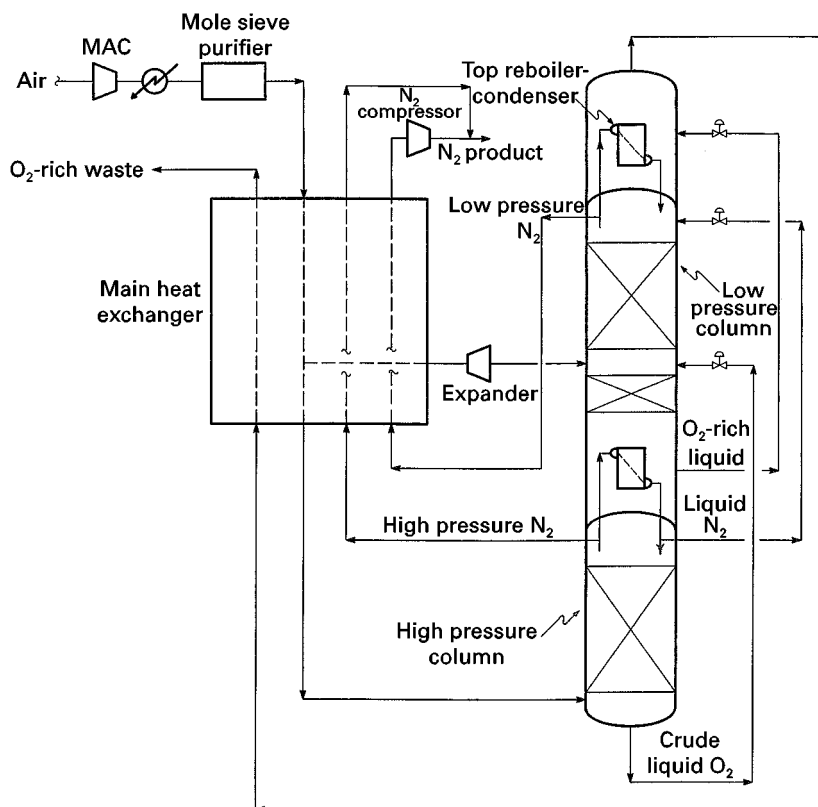


Figure 8 A two-column process for nitrogen production.

crude liquid oxygen from the bottom of the high pressure column is fed to an intermediate location of a low pressure column for further distillation. A low pressure nitrogen vapour stream is recovered from the top of the low pressure column as a second product stream. Another portion of this low pressure nitrogen stream is condensed in the top reboiler-condenser and returned as the major reflux stream to the top of the low pressure column. Optionally, a minor nitrogen reflux stream can also be provided to the low pressure column from the high pressure column. An oxygen-rich liquid stream containing about 70% oxygen is withdrawn from the bottom of the low pressure column, reduced in pressure and vaporized in the top reboiler-condenser. The vaporized stream is then warmed in the main heat exchanger and eventually discarded as a waste stream. Note that the refrigeration for the plant is met by expanding a portion of the gaseous feed air stream to the low pressure column in a turbo-expander. In this process, the feed air is compressed to about 8–9 atm absolute and the pressure of the low pressure column is about 3 atm absolute. A nitrogen compressor is generally used to compress the low pressure nitrogen product stream and then it is combined with the high pressure nitrogen product stream. The typical flow rate of the

combined nitrogen product stream is about 72 mol per 100 mol of the feed air stream. This two-column nitrogen generator and its variations are particularly attractive for enhanced oil recovery where a very large quantity of nitrogen is injected in the wells to maintain pressure.

Ultrahigh Purity Nitrogen and Oxygen Production for the Semiconductor Industry

The fast-growing semiconductor industry uses bulk nitrogen and oxygen gases in the manufacturing of computer chips. The acceptable level of impurities in the supply of these bulk gases has been continually declining over the last decade. Currently, impurities are limited to few parts per billion (p.p.b.) and levels are expected to drop down to parts per trillion levels as wafer sizes increase. The cryogenic distillation process is the only known method of present that, in conjunction with other adsorption and catalytic processes, can meet the stringent demands of ultrahigh purity (UHP) gases.

In addition to the constituent components listed in **Table 1**, air typically consists of several impurities at p.p.m. levels. Hydrogen is a light impurity that is in the range of 1–5 p.p.m.; carbon monoxide is also present at the same levels. There are several

impurities that are heavier than oxygen – methane and higher hydrocarbons and nitrogen oxides are all present in p.p.m. concentrations. When nitrogen is distilled in one of the typical processes discussed earlier, it contains almost all the hydrogen, helium and neon and a major fraction of the carbon monoxide contained in the air. Similarly, a typical high purity oxygen contains all the unacceptable heavier impurities – krypton, xenon, methane and higher hydrocarbons, for example. Clearly the conventional distillation methods need modification to be able to supply the UHP gases.

One early method used to produce UHP nitrogen was to pass the nitrogen from a typical cryogenic distillation process over a bed of a nickel supported on silica to remove the trace levels of oxygen, hydrogen and carbon monoxide. This method is now used for back-up systems since the regular supply of UHP nitrogen is produced directly from the cold box to the semiconductor fabrication plant without any further compression. The pressure of the supply UHP nitrogen is generally 8–10 atm absolute. The feed air after compression is heated to a temperature of about

200°C and passed over a noble metal catalyst such as platinum to oxidize all the carbon monoxide and hydrogen. The exhaust gas is then cooled and passed through the molecular sieve unit. In an alternative process, a separate noble metal catalyst is not used but instead, layers of adsorbent catalysts are supplied within the molecular sieve unit to remove hydrogen and carbon monoxide to p.p.b. level. The impurities-free air is then cooled in the main heat exchanger and distilled in a column similar to the one shown in Figure 7. A large number of separation stages (60–100) are used in this main distillation column to reduce the oxygen concentration in the resulting nitrogen product stream to a level of a few p.p.b.

In addition to stage count, another major difference between the processes of Figures 7 and 9 is the manner in which crude liquid oxygen from the main distillation column is treated. In the UHP nitrogen process of Figure 9, crude liquid oxygen is fed to the top of a short column containing three to six stages of separation. The boil-up at the bottom of this column is provided by condensing a portion of the nitrogen vapour stream from the top of the main (high pressure) distillation column. The nitrogen and oxygen concentration in the vapour leaving the top of the short column is similar to that in air – this stream is called synthetic air. The pressure of the synthetic air is generally greater than 4 atm absolute. To recover

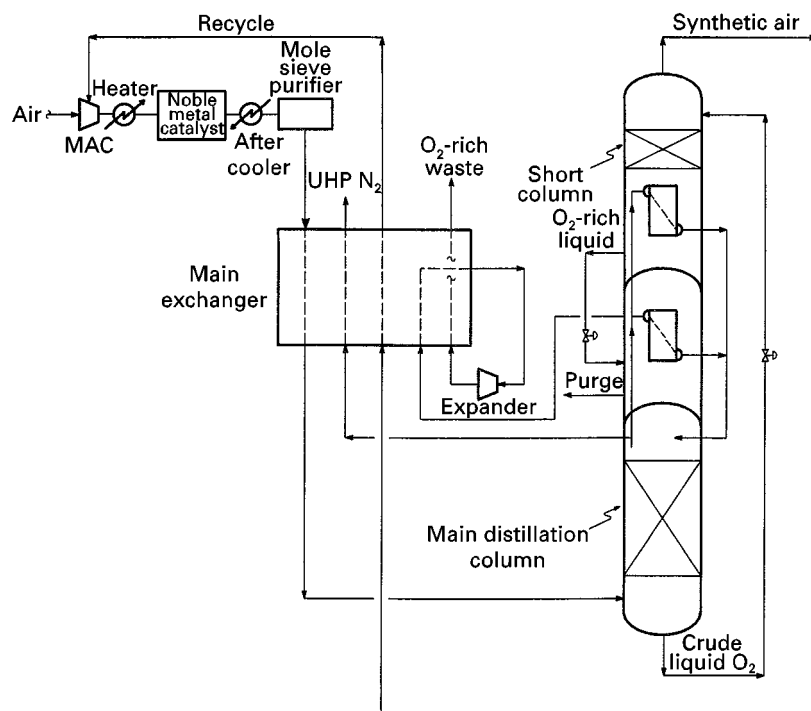


Figure 9 A UHP nitrogen scheme.

the pressure energy, this stream is recycled after further boosting its pressure to that of the main distillation column. In **Figure 9**, synthetic air is fed to an interstage of the main air compressor. This configuration saves the capital cost associated with a separate booster recycle compressor.

Not all the liquid at the bottom of the short column is vaporized; instead, an oxygen-rich liquid containing about 60–70% oxygen is withdrawn. The pressure of this liquid is reduced by 1–2 atm and then it is vaporized in a separate reboiler-condenser to produce another portion of the liquid nitrogen reflux for the main distillation column. A liquid purge stream is taken from this reboiler to prevent the accumulation of hydrocarbons to unsafe levels. The vaporized oxygen-rich stream is then expanded to provide the needed refrigeration for the plant and is eventually discharged as a waste stream.

The reason for modifying the distillation scheme of **Figure 7** to that of **Figure 9** stems from the fact that, in a UHP nitrogen process, the distillation pressure is quite high. In **Figure 7**, high pressure distillation causes the waste stream to vaporize in the reboiler-condenser at a pressure greater than 4 atm. When a large portion of the feed air (in this case 60%) is sent to the turbo-expander at such a high pressure, excess refrigeration is produced. The consequence is that the pressure energy of the waste stream is not utilized effectively and the process becomes inefficient. In contrast, the UHP nitrogen distillation scheme in **Figure 9** recovers nearly half of the crude liquid oxygen stream as a recycle synthetic air stream, thereby reducing the flow to the turbo-expander. In other words, the production of excess refrigeration is avoided and efficient operation is maintained by sending only that portion of the crude liquid oxygen stream needed for the refrigeration to the turbo-expander.

There are several other distillation schemes used for the production of UHP nitrogen. However, all the efficient schemes are based on modification of the scheme in **Figure 7**, such as is shown in **Figure 9**.

Generally, UHP oxygen is required in much smaller quantities (generally 1–5% of the UHP nitrogen production rate). It is essential that not only the concentration of a lighter impurity such as argon be in the p.p.m. to p.p.b. level but also that the concentration of heavier impurities, such as krypton, xenon and hydrocarbons, be no more than a few p.p.b. in the UHP oxygen stream. In contrast to this, a standard-grade oxygen from the process shown in **Figure 4** contains about 0.5% argon and all of the heavier impurities such as methane, krypton and xenon are contained in the feed air.

A UHP oxygen distillation scheme that is a modification to the distillation configuration of **Figure 9** is shown in **Figure 10**.

This modification results from an observation that, as the feed air ascends the main distillation column, all the impurities that are heavier than oxygen are rapidly reduced to nearly zero within a few separation stages. The concentration of oxygen, however, is still at significant levels. Thus, a heavies-free liquid stream is withdrawn from about 10–15 separation stages above the vapour feed air location of the main distillation column. This heavies-free liquid stream contains about 10–20% oxygen and, after pressure reduction to near atmospheric pressure, is fed to the top of the UHP oxygen column. Since the feed to this column only contains components that are more volatile than oxygen, the purpose of the column is essentially to distil off these components from oxygen. Depending on the desired purity of UHP oxygen, 60–100 separation stages are used. Since the amount of UHP oxygen to be produced is low compared to the amount of UHP nitrogen, the boil-up at the bottom of the UHP oxygen column is met by cooling crude liquid oxygen in the sump of this column. The vapour from the top of this column is typically mixed with the discharge stream from the turbo-expander. About 25% of the heavies-free liquid feed to the UHP oxygen column is recovered as UHP liquid oxygen product from the bottom of the column. It is a true credit to the cryogenic distillation industry that the stringent purity demanded by the semiconductor industry can be met without post-treatment.

Liquefaction

Liquid nitrogen and liquid oxygen are produced and stored in a back-up system to supply gases (after vaporization of the stored liquid) in the event of the cryogenic air separation plant shut-down. Liquid may also be supplied in tankers from a central plant location to an end-use site where the consumption of nitrogen and oxygen is not high and economically it is not justifiable to build a dedicated plant. Liquid nitrogen is also used as a source of refrigeration in such applications as food freezing.

In 1895, Carl von Linde built the first industrial-scale air liquefier. His liquefier used a Joule–Thompson (JT) valve to create refrigeration. His genius was the realization that, for the same pressure ratio across a JT valve, the amount of cooling (drop in temperature) increases rapidly as the absolute pressure of air is increased. Therefore, such a liquefier operated at about 125 atm while the pressure across the JT valve dropped to approximately 5 atm. In 1902,

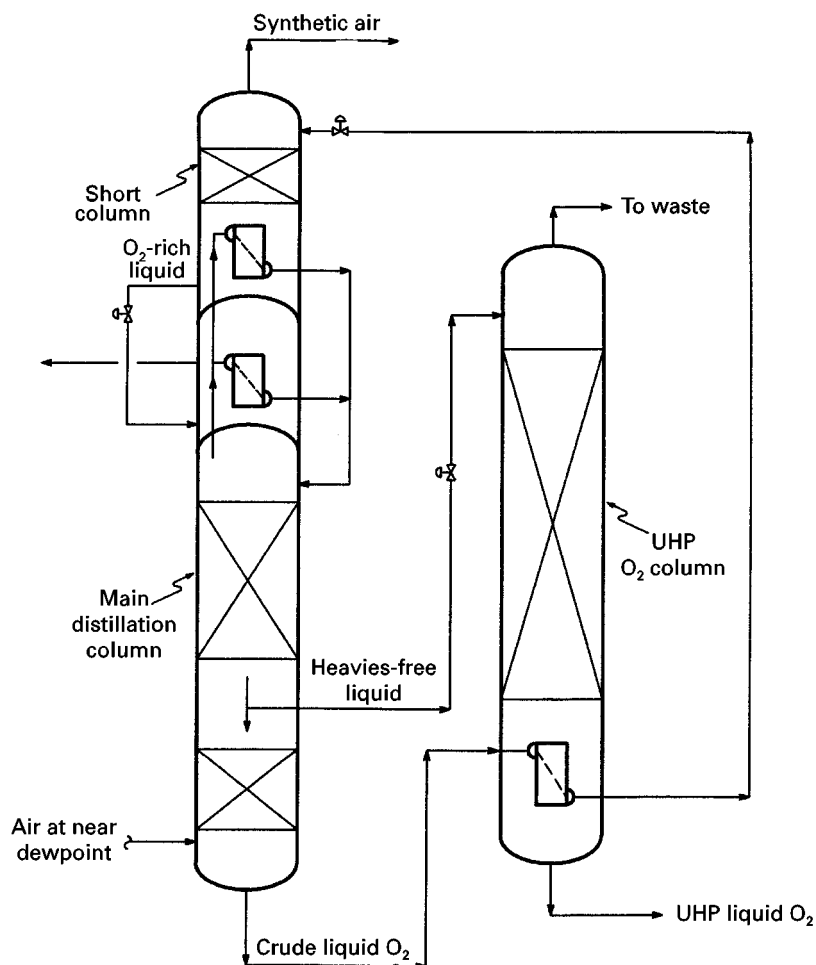


Figure 10 A distillation scheme for UHP oxygen production.

Georges Claude demonstrated that it was possible to lubricate a piston expander with petroleum ether at cryogenic temperatures. He then built an air liquefier using his piston expander. Since this liquefier did not rely on a JT valve to supply all the refrigeration, it was much more efficient than the liquefier built seven years earlier by Linde. In 1935, Kapitza built a piston expansion engine with gas lubrication and in 1939 he built an air liquefier with an expansion turbine. Most modern liquefiers use expansion turbines.

Although the early 'masters' of cryogenics were interested in liquefying air, the focus of modern liquefiers is mainly to liquefy nitrogen. This is due to the dominant use of liquid nitrogen for refrigeration supply. Liquid oxygen is generally produced by supplying some liquid nitrogen as reflux to the low pressure column of a double-column process and by withdrawing an equivalent amount of liquid oxygen from the bottom of this column. The gaseous nitrogen needed for the nitrogen liquefier is provided by any of the suitable air distillation processes described earlier.

Liquefiers that are capable of producing in excess of 1000 tons per day of liquid nitrogen and oxygen are now in operation.

A two-expander nitrogen liquefier is shown in **Figure 11**.

Make-up nitrogen from an air distillation cold box is compressed to about 6 atm in a make-up compressor and is further compressed to a pressure in excess of 27 atm in a recycle compressor. The pressurized nitrogen leaving the recycle compressor is further boosted to a pressure in excess of 45 atm in compressor 1 and compressor 2, and then fed to a heat exchanger for cooling. A portion of the high pressure nitrogen stream is withdrawn near the warm end of the heat exchanger and expanded in a warm expander to provide a portion of the refrigeration needed for the liquefaction. A second portion of the high pressure nitrogen stream is withdrawn from an intermediate location of the heat exchanger and expanded in a cold expander to provide the refrigeration in the cold part of the heat exchanger. The remaining

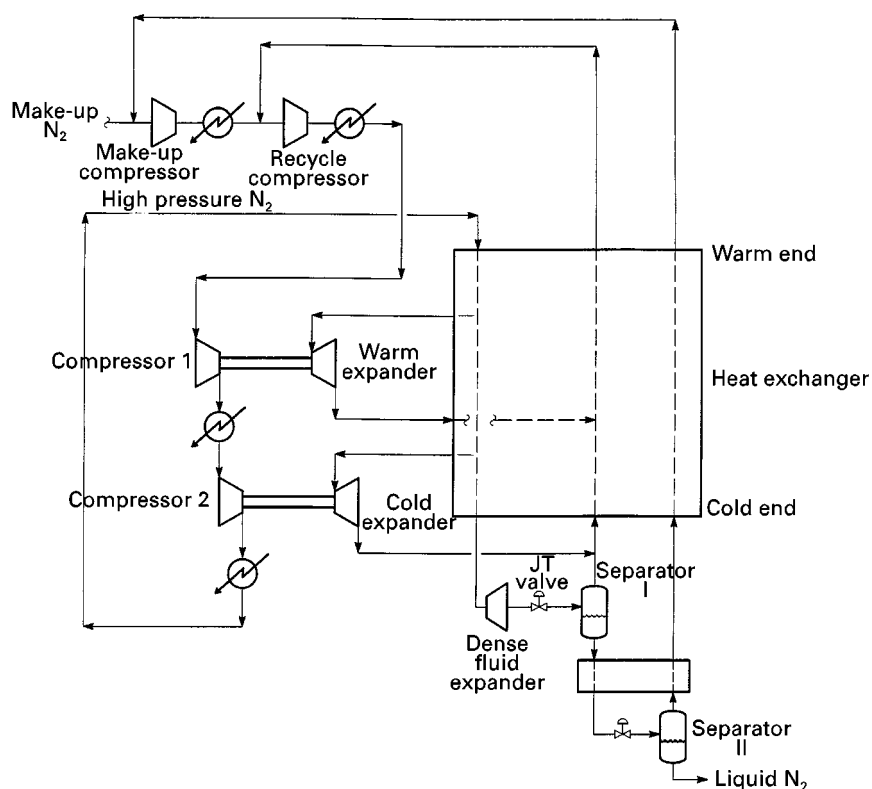


Figure 11 A nitrogen liquefier.

portion of the high pressure nitrogen stream exits the cold end of the heat exchanger at a temperature below -170°C and is sent to an optional dense fluid expander. The pressure drop across this dense fluid expander is maximized, subject to the constraint that very little vapour forms in the exhaust. The pressure of this stream is further reduced to about 6 atm in a JT valve and the resulting two-phase stream is separated in separator I. The vapour from this separator and the exhaust streams from the cold and warm expanders are mixed at appropriate temperatures, warmed and returned to the recycle compressor. The liquid from separator I is further cooled and reduced to near atmospheric pressure through another JT valve. The resulting liquid is collected as liquid nitrogen from separator II and the vapour is recycled to the make-up compressor.

The liquefier shown in **Figure 11** is quite efficient. The use of a dense fluid expander contributes to increased efficiency but its use is optional. The working pressure range of the modern brazed plate and fin aluminium heat exchangers now approaches 100 atm. For increased efficiency, the pressure of the high pressure nitrogen stream is increased to maximum feasible values. Recently, processes using more than two gaseous expanders have been suggested for incrementally higher efficiencies.

In **Figure 11**, if none of the expanders are used then the liquefaction process reduces to the one proposed by Carl von Linde. On the other hand, if the warm expander and the dense fluid expander are removed, then the resulting process is similar to the one used by Georges Claude.

Equipment

Machinery

The selection of a compressor depends on the volumetric flow rate, the operating pressures, the compressor efficiency, its capital cost and the cost of energy. Because of their lower installation cost, centrifugal compressors are chosen over reciprocating compressors when volumetric flow rates and pressure allow their use. Axial compressors are used for large volumetric flow rates. Reciprocating machines are used at very high pressures and small volumetric flows.

For most air plants in the size range of 30–3000 tons per day of oxygen, centrifugal compressors containing three or four stages are used for compressing the feed air. Interstage cooling is provided with cooling water to approximate isothermal compression. A large fraction of the water contained in the feed air

is condensed in these interstage coolers. Most of these compressors are electrically driven; however, steam or gas turbines are occasionally used when economically justified. Air is passed through one or two stages of filtration to remove particulates prior to entry in a MAC. For plants that are larger than 3000 tons per day of oxygen, a combination of axial and centrifugal compressors is used. At the other end of the scale, for small size plants in the size range of less than 30 tons per day of oxygen, inexpensive screw compressors are used. These guidelines for oxygen plants can easily be translated to nitrogen plants, because for the same production rates, a nitrogen plant requires only 30–50% of the feed air flow required by an oxygen plant.

When gaseous oxygen is to be compressed, a centrifugal compressor is used for low to moderate pressures while a reciprocating compressor is used for higher pressures. When oxygen is needed at fairly high pressures, the initial stages of compression may be centrifugal. The design of an oxygen compressor requires careful selection of materials and seals, and total prevention of rubbing contacts to avoid ignition in the presence of high pressure oxygen. Furthermore, an oxygen compressor is generally enclosed in a building with an external barrier to increase the safety of plant personnel. Special test and start-up procedures are also used for oxygen compressors.

Expanders are used to provide refrigeration by extracting work from an expanding fluid. In the expansion process, the temperature of the expanded fluid is reduced. An air separation or a liquefaction plant generally uses a single-stage radial inflow turbine as a standard. For small plants, the work energy from the expander is either dissipated in an oil brake or through an ambient air blower. For medium to large size separation plants and liquefiers, it is essential that the work energy from an expander be recovered to increase process efficiency. This is done by either loading an expander with an electric generator or a compressor for some other process fluid. When an expander is directly coupled to a compressor, the arrangement is called a compander. As seen from Figure 11, companders are widely used in liquefiers. Expanders used in the cryogenic air separation and liquefaction industry typically have isentropic efficiencies in the range of 85–90%. The dense fluid expanders are essentially reverse-running liquid pumps (Figure 11).

Front-end Purification

The compressed air from a main air compressor must be cleaned of impurities such as water, carbon dioxide and some hydrocarbons to avoid plugging at

cryogenic temperatures. The original plants used recuperative heat exchangers which were later replaced by regenerators in 1930 upon their invention by Matthias Fränkl. Around the mid-1950s, owing to the introduction of large brazed aluminium plate and fin heat exchangers, the regenerators were replaced by reversing heat exchangers. Recuperators, regenerators and reversing heat exchangers all operated to freeze the impurities within the device – complete removal of these trace components was never achieved. Beginning in the early 1980s, reversing exchangers were replaced with ambient temperature adsorption beds. Today almost all cryogenic air separation plants use molecular sieve vessels to remove impurities.

A typical two-bed adsorption system for air purification is shown in Figure 12. Each vessel is filled with 13X (Na-X zeolite) molecular sieve. This sieve has an excellent capacity for carbon dioxide and water removal. Sometimes an additional layer of alumina is used at the entrance for bulk water removal to decrease the energy demand during regeneration. While one bed is on stream, the other bed is being regenerated. In Figure 12, bed A is on stream and bed B is being regenerated. A bed is on stream for a pre-specified period until carbon dioxide is about to break through the bed. At this point the feed air is directed to another bed. The pressure of the spent bed is reduced to near atmospheric pressure and a hot dry gas in the temperature range of 150–200°C is passed through the bed to desorb the adsorbed impurities. After the impurities have been removed, the bed is cooled by a flow of cool dry gas and it is then ready to be brought on

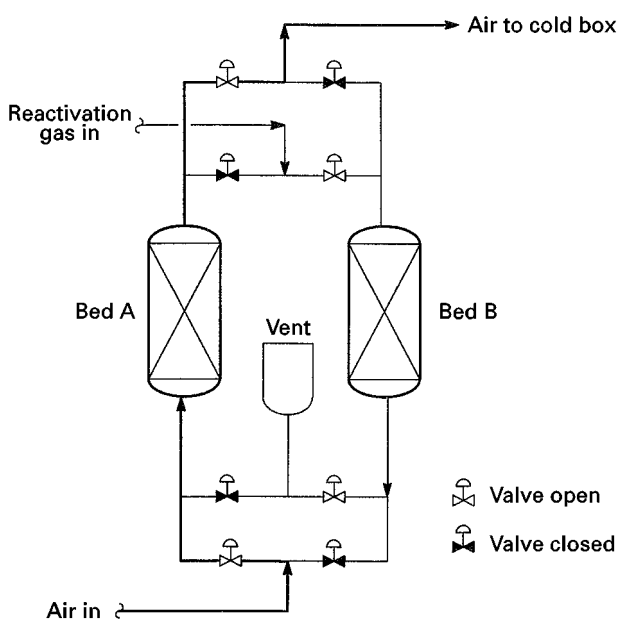


Figure 12 A front-end system for air purification.

stream. The dry gas used for regeneration is generally a portion of the gas exiting the cold box. Regeneration gas flow rate is typically in the range of 10–20% of the feed air flow. For oxygen plants, the regeneration gas is a portion of the nitrogen stream.

Heat Exchangers

Around the mid-1950s, large brazed aluminium plate and fin heat exchangers were commercially introduced. They readily became the heat exchangers of choice for cryogenic air separation and liquefaction plants. In this type of heat exchanger, corrugated fins are sandwiched between plates to form a passage for gas flow. The use of fins provides increased surface area for heat transfer. Typical fin heights range between 5 and 9 mm; fin spacing can be as low as 1 fin per mm. A heat exchanger block is formed by stacking passages. Generally, flow through individual passages is countercurrent with a warming stream in one passage and a cooling stream in the adjacent passage. A heat exchanger block can easily handle multiple warming and cooling streams. Plate and fin heat exchangers are applied in virtually all the heat exchanger services of an air separation plant. They are used as main heat exchangers, reboiler-condensers and subcoolers. The maximum size and pressure rating of these heat exchangers depend on the manufacture; however, heat exchangers 1200 mm wide by 1200 mm stack height by 6000 mm long with a pressure rating up to 50 atm can easily be found. For large size plants, multiple heat exchangers are used in parallel and careful attention is paid to the flow distribution in the manifolds.

Distillation

Until the 1980s almost all air distillation was performed in columns containing sieve trays. Due to the close relative volatility between argon and oxygen and the purity of the products, columns with over 100 separation stages are not uncommon. Therefore, tray spacing is generally 150 mm or less. Pressure drop across a large number of trays in the low pressure column increases the pressure of the boiling fluid in the low pressure column sump. This increases the pressure of the condensing nitrogen at the top of the high pressure column. In turn, the pressure of the air at the discharge of the main air compressor is increased. This leads to an increase in power consumption. As a result, there is an incentive to use a liquid–vapour contact device with lower pressure drop.

Today, most modern cryogenic air separation plants use low pressure drop structured packing in one or more of the distillation columns. The pressure drop through structured packing is only one-fifth to one-tenth that of a trayed column. The use of struc-

tured packing has led to more than 3% power savings for a typical oxygen plant. It has also allowed the use of over 175 stages of separation in the side argon column of Figure 6 for the production of argon with less than 5 p.p.m. oxygen through distillation. This eliminates the need for a second deoxidation (Deoxo) process using hydrogen and a catalyst, thereby making pure argon production much simpler.

Cold Boxes

The cryogenic equipment is enclosed in an insulated enclosure termed a cold box. A rectangular cold box consists of a steel frame with panels of sheet metal. It also provides structural support for the equipment. Cylindrical cans with insulation are also used in certain applications. Mineral wool was used for insulation prior to the late 1940s. Starting around 1948, a powdered insulation called perlite was increasingly used. The advantage of perlite is that installation costs are lower and cold boxes can be insulated with greater uniformity, leading to reduced heat leak and improved plant efficiency.

Materials of Construction

Early plants used copper or copper alloys to fabricate vessels and piping. Austenitic stainless steels were occasionally used. In the later 1950s, with the development of welding techniques for aluminium, its use became the most popular. This occurred because aluminium and aluminum alloys are easily available and are low cost and light weight. Cryogenic liquid containers are also constructed from low carbon 9% nickel steel.

Safety

Many materials react with pure oxygen, so great care is taken in the selection and clean-up of materials that come into contact with oxygen. Potential ignition sources must be minimized. All impurities that come into contact with oxygen, especially unsaturated hydrocarbons, must be reduced to safe levels. To avoid hydrocarbon build-up, generally a small purge stream is taken from the sumps where oxygen-rich liquids are being boiled. The combustion hazard increases as pure gaseous oxygen is compressed to higher pressures and therefore, special care should be taken in the compression and handling of high pressure oxygen gas.

See also: II/Distillation: Energy Management; Historical Development; Instrumentation Control Systems; Multi-component Distillation; Theory of Distillation; Vapour–Liquid Equilibrium: Theory.

Further Reading

- Agrawal R (1995) Production of ultra high purity oxygen: a distillation method for the co-production of the heavy key component stream free of heavier impurities. *Industrial Engineering Chemical and Research* 34: 3947.
- Agrawal R and Thorogood RM (1991) Production of medium pressure nitrogen by cryogenic air separation. *Gas Separation and Purification* 5: 203.
- Agrawal R and Woodward D (1991) Efficient cryogenic nitrogen generators – an exergy analysis. *Gas Separation and Purification* 5: 139.
- Agrawal R, Woodward DW, Ludwig KA and Bennett DL (1992) Impact of low pressure drop structure packing on air distillation. In: *Distillation and Absorption*. IChemE Symposium Series no. 128, A125.
- Isalski WH (1989) *Separation of Gases*. Oxford: Oxford Science Publications Clarendon Press.
- Latimer RE (1967) Distillation of air. *Chemical Engineering Progress* 63: 35.
- Linde W and Reider R (1997) How it all began. In: *The Invisible Industry*. Cleveland, Ohio: The International Oxygen Manufacturers Association.
- McGuinness RM (1998) Oxygen Production. In: Baukal CE (ed.) *Oxygen-enhanced Combustion*, Ch. 3. Boca Raton: CRC Press.
- Scott RB (1988) *Cryogenic Engineering*. Boulder, Colorado: Met-Chem Research.
- Scurlock RG (1992) *History and Origins of Cryogenics*. Oxford: Clarendon Press.
- Springmann (1977) The planning of large oxygen plants for steel works. *Linde Report in Science and Technology* 25: 28.
- Thorogood RM (1986) Large gas separation and liquefaction plants. In: Hands BA (ed.) *Cryogenic Engineering*, Ch. 16. London: Academic Press.
- Timmerhaus KD and Flynn TM (1989) *Cryogenic Process Engineering*. New York: Plenum Press.
- Venet FC, Dickson EM and Nagamura T (1993) Understand the key issues for high purity nitrogen production. *Chemical Engineering Progress* 89: 78.
- Wilson KB, Smith AR and Theobald A (1984) Air purification for cryogenic air separation units. *IOMA Broadcaster* January, pp. 15–20.

AIRBORNE SAMPLES: SOLID PHASE EXTRACTION



D. J. Eatough, Brigham Young University,
Provo, Utah, USA

Copyright © 2000 Academic Press

Introduction

Organic material in the atmosphere may exist in either the gas phase or in particles. For the purposes of this chapter, atmospheric organic material will be divided into three classes, defined by the phase distribution of the organic material in the atmosphere. Gas phase compounds will include those organic compounds which are present only in the gas phase. This will include essentially all non-aromatic organic material with fewer than about 12–14 carbon atoms. Nonvolatile organic material will include those compounds which are present in particles and whose concentrations in the gas phase are negligible compared to the particulate material. Semi-volatile organic material includes those compounds which are present in equilibrium between the gas and particulate phases in the atmosphere and for whom the concentrations in both phases are significant. The collection of gas phase and nonvolatile organic material is relatively straightforward. However, the

accurate determination of the phase distribution of semi-volatile organic material requires the use of diffusion denuder technology.

Correct assessment of the contribution of fine particulate carbonaceous material to various atmospheric processes is dependent on the accurate determination and characterization of fine particulate organic material as a function of particle size. Several studies have shown that about one-third of the mass of fine particulate matter (dia. $<2.5\ \mu\text{m}$) collected on filters in remote desert regions of the Southwest U.S. is organic compounds and elemental carbon. Similar fractions of carbonaceous material are found in particles collected on filters in western urban areas. In the eastern United States sulfate is the major component of filter collected airborne fine particles. However, organic material comprises one-fourth or more of the fine particulate mass. In the Northwest, organic material has been found to be the dominant fine particulate component. However, unless proper sampling procedures are used to collect particulate material, the composition of organic material in fine particles will be significantly underestimated due to losses from the semi-volatile particulate organic fraction during sample collection, i.e. a 'negative' sampling artifact.

Several studies have also indicated the presence of a 'positive' artifact in the determination of particulate organic compounds collected on a quartz filter, due to the adsorption of gas phase organic compounds by the quartz filter during sampling. Data obtained using sampling systems with two quartz filters in series suggest that quartz filters collect at least some gas phase organic compounds. In addition, particulate material collected on a filter can also absorb some gas phase organic compounds. The adsorption of organic compounds by a second quartz filter has been shown to be reduced, but not eliminated, in samples collected in the Los Angeles Basin if a multi-channel diffusion denuder with quartz filter material as the denuder collection surface precedes the quartz filters. This artifact can be eliminated by the use of activated charcoal at the denuder surface. Recent experiments have shown that the quartz filter artifact can result both from the collection of gas phase organic compounds and from the collection of semi-volatile organic compounds lost from particles during sampling. Thus, results available to date suggest that both a 'positive' and a 'negative' artifact can be present in the determination of particulate phase organic compounds using two tandem quartz filters.

Collection of Gas Phase Organic Material

A well validated technique for the collection of gas phase organic material for subsequent analysis is the use of SUMMA stainless steel canisters. If the canisters are properly cleaned before use and analysed within a few weeks of sample collection, valid results can be obtained for most gas phase compounds.

A second method which has frequently been used to collect gas phase organic materials consists of the use of a filter to remove particulate material, followed by a sorbent bed to collect the gas phase organic compounds. This approach is not valid if (1) the gas phase organic material is oxygenated or polar and therefore capable of being absorbed by a quartz filter or by organic material collected by the particle removing filter, or (2) the gas phase organic material is semi-volatile and therefore, may be present on and lost from particles during sampling (see following section). The absorption of organic material by various types of filters has been reviewed. Teflon has been suggested to be relatively inert to absorption artifacts, but this filter is not amenable to the determination of total carbon. Glass fibre and cellulose membrane filters both absorb significant quantities of gas phase organic material. Quartz membrane filters are suitable for the determination of total carbon, but they also can absorb significant quantities of gas phase

organic material. This is illustrated in **Figure 1** which shows the analysis of total carbon for a filter which was preceded and not preceded by a charcoal based diffusion denuder to remove gas phase material. The large peak seen in the absence of a diffusion denuder is gas phase organic material collected by the quartz filter. A similar peak (plus some higher temperature material) is seen on a second quartz filter which is not preceded by a denuder.

Materials which have been validated as sorbents for the removal of gas phase organic compounds include polyurethane foam (PUF), poly(oxy-m-terphenyl-2',5'-ylene), Tenax, copolymers of styrene and divinylbenzene (XAD), Chromosorb and charcoal. Of these sorbents, Tenax is best suited for the collection of very low molecular weight organic material and Chromosorb or XAD are effective for collection over a wide range of molecular weights. A caution is that many of the sorbents can produce spurious results due to reactions during sample collection and each of the sorbents can be difficult to clean for the detection of trace substances. Thus, for example, a PUF cartridge produces mutagenic compounds upon extraction with methanol and Tenax forms decomposition products during sampling.

Collection of Non-Volatile Organic Material

Compounds which are sufficiently volatile that they exist essentially only in the gas phase can be collected on any filter suitable for total particle collection, such as quartz or Teflon filters. Quartz filter are usually used when the determination of total carbonaceous material in addition to the identification of specific compounds is desired. However, if only specific compound identification is desired, the use of Teflon filters avoids the complication associated with the absorption of gas phase material by the filter. However, if the target species include compounds which are reactive or unstable, they may be altered by chemical reactions associated with the sampling process. Examples of potential problems are given in the following sections.

Collection of Semi-Volatile Organic Material

To address the issues of both 'positive' and 'negative' artifacts in the sampling of particulate phase organic compounds, several groups have constructed and tested sampling systems employing diffusion denuders, filters and sorbent filters. The data obtained to date with these sampling systems show that particulate

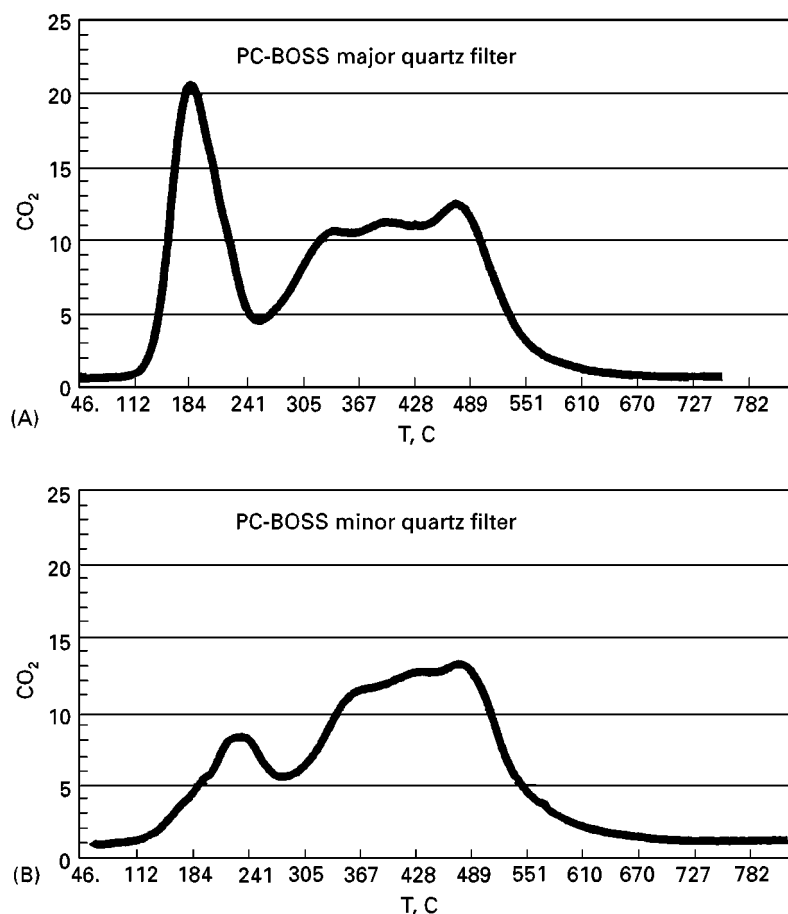


Figure 1 Temperature-programmed volatilization analysis of quartz filters (A) not preceded and (B) preceded by a denuder with charcoal impregnated filter surfaces. The large initial peak seen in (A) but not in (B) is due to the absorption of gas phase organic material by the quartz filter not preceded by a diffusion denuder to remove gas phase organic compounds.

phase organic compounds have been significantly underestimated by the collection of particles with only a filter. The collection of gas phase compounds by a quartz filter may produce a significant 'positive' artifact (Figure 1), but a much larger negative error usually results from the loss of 20–80% of the particulate phase semi-volatile organic material during sampling. This sampling artifact must be considered in the collection of semi-volatile particulate organic compounds. Accurate collection procedures for semi-volatile organic compounds must meet the following two criteria:

1. Organic compounds initially present in the gas phase which can be adsorbed onto particles or the filter must be distinguished from semi-volatile organic compounds lost from particles during sampling.
2. Organic compounds initially present in the particulate phase and lost from particles during sampling must be captured during sampling separate

from compounds which are present in the gas phase in the atmosphere.

These two criteria cannot be met by any sampling procedure in which the particulate phase organic compounds are collected before the collection or separation of gas phase organic compounds because the gas phase organic compounds and organic compounds volatilized from particles become indistinguishable. Thus, it is necessary first to remove the gas phase organic compounds and then to collect the particulate phase organic compounds with a sampler which will collect all organic material, gas and particle. This can be accomplished using diffusion denuder sampling technology.

The BOSS and BIG BOSS Diffusion Denuder Samplers

Diffusion denuder sampling systems for the determination of total fine particulate organic material have been developed at Brigham Young University.

The objectives which guided the development of these sampling systems were:

1. The sampling system should have a flow rate sufficient to enable measurement of low concentrations of particulate carbonaceous material and to allow the detailed chemical characterization of particulate organic material, e.g. flow rates of from 30 to 300 L min⁻¹ were considered desirable.
2. The sampler should have a diffusion denuder capable of removing all gas phase semi-volatile organic compounds which are in equilibria with compounds in the particulate phase in the atmosphere.
3. The diffusion denuder of the sampler should be effective in removing all gas phase compounds which can be adsorbed by a quartz filter or by collected particles during sampling.
4. The capacity of the diffusion denuder for the removal of gas phase organic compounds should be high enough that samples can be collected at the target flow rates over sampling periods of several days to weeks.
5. Particle losses during the passage of sampled air through the diffusion denuder should be small.
6. The sampler after the diffusion denuder should collect both particles and any semi-volatile organic material lost from particles during sampling with high efficiency.
7. The collection materials used in the sampler should be compatible both with the determination of total carbonaceous material and with the detailed chemical characterization of particulate organic material.

The BOSS (BYU Organic Sampling System) requires two different samplers as shown schematically in Figure 2:

1. A charcoal impregnated filter (CIF), multi-channel, parallel plate diffusion denuder followed by a filter pack containing quartz and CIF filters. The denuder removes gas phase organic compounds. The quartz filter after the denuder collects fine (<2.5 μ m) particles. The organic compounds collected by the CIF sorbent filter in this sampler are semi-volatile organic compounds lost from the particles during sampling and a small fraction (about 5%) of the gas phase organic material not collected by the diffusion denuder.
2. A quartz filter followed by a CIF diffusion denuder and a CIF sorption filter. The quartz filter collects particles and any gas phase organic compounds which can be absorbed by quartz, both those ori-

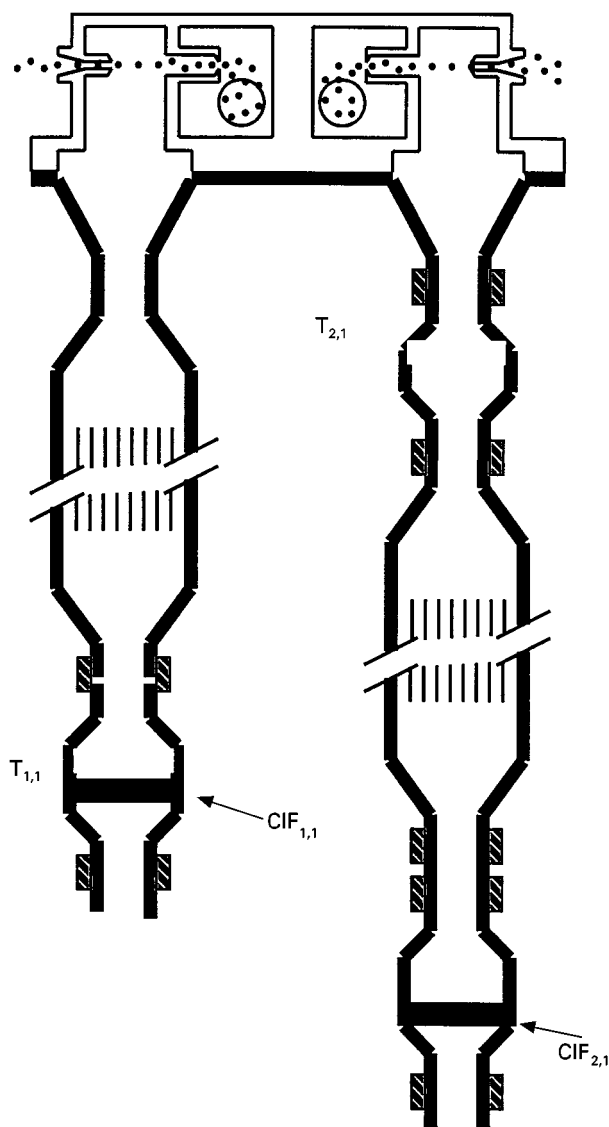


Figure 2 Schematic of the BOSS. Non-volatile particulate carbonaceous material is determined from analysis of $T_{1,1}$. Semi-volatile carbonaceous material lost from particles is determined from analysis of $CIF_{1,1}$, corrected for the denuder inefficiency determined from analysis of $CIF_{2,1}$.

ginally in the gas phase and those lost from the particles during sampling. The denuder then removes gas phase compounds passing the quartz filter. Any gas phase compounds not removed by the denuder are then collected by the CIF sorbent filter. This system is used to determine independently the gas phase organic compounds not collected by the denuder to correct the data obtained with the CIF filter of Sampler 1.

The various 47 mm diameter filters of the BOSS are contained in Teflon filter packs (University Research Glass, Model 2000-30F) with the filter packs holding

the quartz filter in Sampler 2, Figure 2, being modified so that the outlet is identical to the inlet to allow for convenient connection to the diffusion denuder (University Research Glass, Model 2000-30FB). The diffusion denuder is based on a design originally reported by Fitz (1990). Each denuder is comprised of 17 (4.5×58 cm) strips of Schleicher and Schuell charcoal impregnated filter paper which are separated at the long edges by 2-mm rods. The multi-parallel plate array of filter strips is contained within a (5×5 cm) square aluminium tube. The entire assembly is nominally 90 cm in length to accommodate 58 cm sorbent filter strips and two nominally 15 cm long flow straightening sections ahead of and behind the denuding section. The multi-channel diffusion denuder is designed to have acceptable efficiency for the removal of gas phase organic material in the denuder, negligible loss of particles to the denuder during sampling, and high capacity for the collection of gas phase organic material. The total capacity of the CIF multi-channel denuder has not been directly measured. However, no degradation of the efficiency of the denuder for the collection of gas phase organic compounds was seen during continuous operation at 40 L min^{-1} for over two months or for sampling at 180 L min^{-1} for continuous periods equivalent to seven and fourteen days in the Los Angeles Basin, for ten days in the Mohave Desert, or for twelve days at Research Triangle Park, NC.

The CIF (Schleicher and Schuell, Inc.) strips in the diffusion denuder are used as received from the manufacturer. The 47 mm CIF (Schleicher and Schuell, Inc., No. 508) filters are cleaned with dichloromethane and dried at 200°C before use. Alternately, a 47 mm Carbon EMPORE (3M) filter may be used. The Carbon EMPORE filters may be used as received from the manufacturer, however, flow through these filters is limited to about 7 L min^{-1} . The 47 mm quartz filters (Pallflex, 2500 QAT-UP) are pretreated by firing at 800°C for four hours prior to sample collection. The flow through the two samplers of the BOSS, Figure 2, is controlled at about 40 L min^{-1} . A version of the BOSS using a shortened denuder (27 cm CIF strips) with a flow of from 4 to 20 L min^{-1} has also been described. The CIF or Carbon EMPORE filters may also be replaced with an XAD sorbent bed. The XAD (Rohn & Haas) is cleaned by first sonicating 10 times with CH_3OH to remove very fine particles and then Soxhlet extracting for 24 hours sequentially with CH_3OH , CH_2Cl_2 and $\text{C}_2\text{H}_5\text{OC}_2\text{H}_5$.

The efficiency of removal of gas phase organic compounds by the CIF denuder (or by an annular denuder configuration) is described by eqn [1]:

$$C/C_o = 0.819e^{-22.5(D_j L W/4Fd)} \quad [1]$$

where C_o and C are the concentrations of organic compounds entering and exiting a section of the denuder, respectively, D_j is the diffusion coefficient of the gas phase organic compound(s) at the experimental conditions, L and W are the length and effective width of the denuder section, F is the flow and d is the space between the denuder surfaces. A plot of the log of the amount collected in equal length sections of a denuder versus the distance from the start of the denuder through the section should be linear with a slope of $-22.5 D_j W/4Fd$. The expected deposition gradient was observed for organic material collected by a CIF based denuder containing two parallel sheets of the charcoal impregnated filter material. The slope of the line describing the deposition pattern for the collection of ambient gas phase organic compounds gives an average diffusion coefficient for the collected gases of $0.052 \pm 0.008 \text{ cm}^2 \text{ s}^{-1}$. This diffusion coefficient gives a calculated effective average molecular weight of 160 ± 25 . This average molecular weight is consistent with the majority of the organic material which has been shown to be collected by the diffusion denuder. The deposition pattern was also consistent with the measured efficiency of the CIF denuder for the removal of gas phase organic compounds.

The importance of the particulate organic compounds which have not been identified in past studies where particles are collected on a filter will be dependent on the chemical composition and the size distribution of the particulate organic compounds, both those lost from the particles during sampling and those remaining on the particles after sampling. A high-volume, multi-component diffusion denuder sampling system (BIG BOSS) for the determination of the size distribution and chemical composition of fine particulate organic compounds using diffusion denuder sampling technology has been developed and tested.

The BIG BOSS uses a variety of size selective virtual impactor inlets to control the particle size of the particles introduced to the diffusion denuder sampler. The inlet system is a modification of a high-volume, multi-jet virtual impactor. The nominal total flow through all systems of the BIG BOSS is $0.9 \text{ m}^3 \text{ min}^{-1}$ inlet flow. This flow is divided among four systems, each with a coarse particle minor flow stream and a fine particle major flow stream. Two of the four systems have an inlet cut of $2.5 \mu\text{m}$. The other two systems are designed to operate with an inlet cut of 0.8 and $0.4 \mu\text{m}$ (see Tang, 1994).

The PC-BOSS Denuder Sampler

The combination of the technology used in the previously described BIG BOSS sampling system and the

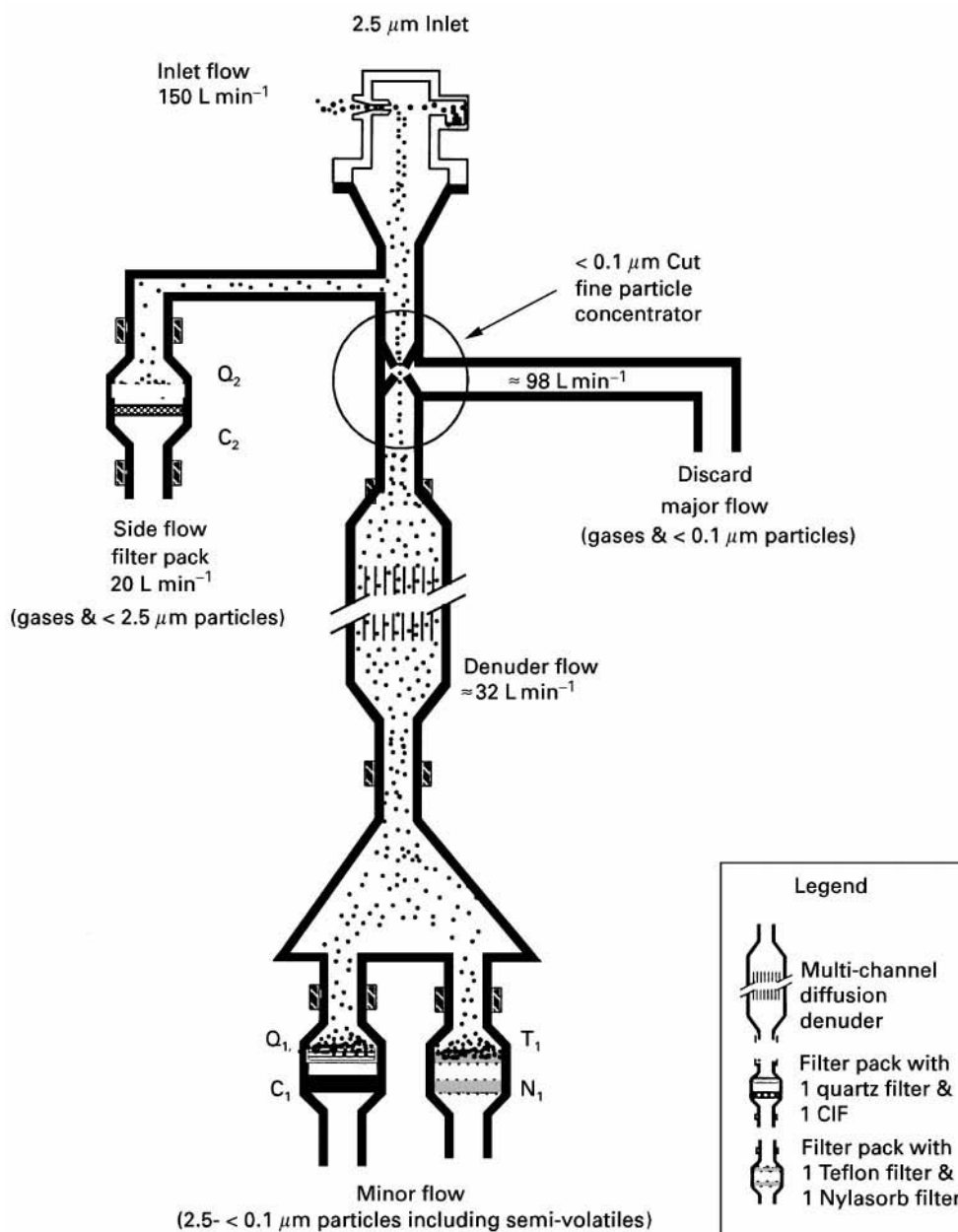


Figure 3 Schematic of the PC-BOSS. The composition of fine particulate matter is determined from analysis of the two filter packs after the denuder. The efficiency and losses of the fine particle concentrator is determined by comparison of sulfate on Q_2 with that on Q_1 or T_1 .

Harvard particle concentrator results in the Particle Concentrator-Brigham Young University Organic Sample System (PC-BOSS) shown schematically in **Figure 3**. The system has been optimized to meet the following criteria: (1) removal of at least 75% of the gas phase material before the sampled aerosol is passed through the diffusion denuder, (2) efficiency, >99% for the removal of SO_2 , HNO_3 and gas phase semi-volatile organic material, (3) determination of particle mass, carbonaceous material and nitrate with

a diffusion denuder sampler, (4) operation on less than 20 amps of 110 V power.

The inlet to the sampler is a Bendix cyclone with a particle cut of $2.3 \mu\text{m}$ aerodynamic diameter at an inlet flow of 150 L min^{-1} . Following the inlet, 20 L min^{-1} is diverted to a filter pack to provide data for calculating the efficiency of and losses in the PC-BOSS particle concentrator. The remaining flow enters the virtual impactor particle concentrator. The design and evaluation of the particle concentrator has

been previously described. The particle concentrator separates most of the gas phase material into the major flow and leaves particles larger than the cut point (about $0.1\ \mu\text{m}$) along with a significantly reduced fraction of the gas phase material in the minor flow. The performance of the particle concentrator for collection of ambient samples with the PC-BOSS was evaluated as a function of the minor to major flow ratio, and the distance between the accelerator and receiver slits of the virtual impactor. The optimum design uses a single particle concentrator with a 9.5 cm long slit and a distance between the accelerator and receiver slits 1.5 times the slit width of 0.32 mm. The minor flow (25% of the total $150\ \text{L min}^{-1}$ flow) containing concentrated particles enters the BOSS diffusion denuder. The denuder is followed by two parallel filter packs (Figure 3). The filter pack containing a 47 mm quartz filter (Pallflex, pre-fired) followed by a 47 mm charcoal impregnated filter is used to determine fine particulate carbonaceous material, including semi-volatile organic material lost from the particles during sampling. The second filter pack contains 47 mm Teflon (Gelman Zefluor) and nylon (Gelman Nylasorb) filters to determine mass, sulfate and nitrate, including any nitrate lost from particles during sampling.

The IOVPS and IOGAPS Denuder Samplers

Researchers at Lawrence Berkeley Laboratories have developed an annular denuder sampling system, the Integrated Organic Vapour/Particle Sampler (IOVPS) with an XAD-IV based diffusion denuder for the measurement of SVOC. This diffusion denuder sampler is similar in design and operation to the BOSS systems described above. The IOVPS is shown schematically in Figure 4. An advantage of the IOVPS sampler is that the gas phase material collected by the denuder can be easily recovered for organic compound chemical characterization and quantitation. Current disadvantages of the sampler are the total carbonaceous material is not determinable in the denuder or post-filter XAD sorbent beds (Figure 4) and the capacity of the denuder limits the length of time over which the denuder may be used from hours to days.

The denuder of the IOVPS system is prepared by adhering very fine mesh XAD to a glass multi-annular denuder surface. The adhesion of the finely ground XAD to the sandblasted glass is strong enough that the coating is resistant to removal by handling, solvent washing and air sampling. Quantitation of gas phase organic compounds removed by the IOVPS denuder is accomplished by extraction with a suitable solvent and analysis by GC or GC/MS. The collection efficiency of these denuders for various gas phase

organic compounds has been shown to be close to that predicted by eqn [1]. A 5-channel denuder with 1 mm spacing in the annulus and a coating length of 38 cm has been used for most applications of the IOVPS denuder.

The capacity of the IOVPS XAD based denuder is dependent on two factors: (1) the capacity of the XAD surface for a given compound and (2) the time required to elute a dilute concentration of a given gas down the XAD column length. The dominant factor appears to be the movement of collected gas phase material down the XAD column. As a result, studies using the IOVPS denuder have generally been limited to chamber studies where the sampling period is short or to ambient studies where the sample collection occurred only over a few hours. By increasing the length and surface area of the denuder (including using parallel denuders) prototype systems have been developed by Lawrence Livermore Laboratory and the Atmospheric Environment Service of Environment Canada (IOGAPS, Integrated Organic Gas and Particle Sampler) which are capable of sample collection for up to 48 hours. Comparisons of results obtained from 24 hour IOGAPS and sequential 4 hour IOVPS data where the annulus width of the IOGAPS was 1.5–3.0 mm with a residence time of 2.6 s indicated there was about 10% breakthrough of naphthalene in the IOGAPS. A redesign with an annulus width of 1.0–1.4 mm is expected to eliminate this problem.

Particle losses to the wall of the IOVPS denuder has been evaluated in several studies. The results are essentially identical to those reported above for the BOSS and BIGBOSS samplers. With face velocities of around $20\ \text{cm s}^{-1}$ through the denuder, losses are less than 2%. At higher face velocities of 35 to $50\ \text{cm s}^{-1}$, the losses increase to about 5–7%. These losses are comparable to that seen for conventional annular denuders.

Other Diffusion Denuder and Related Samplers

Diffusion denuder sampling techniques have also been developed and used by several other investigators to determine fine particulate organic material. The focus of these studies has been on the determination of specific organic compounds. Krieger and Hites have used short sections of capillary gas chromatographic columns as a diffusion denuder and determined concentrations of gas and particulate phase polychlorinated biphenyl (PCB) and polyaromatic hydrocarbon (PAH) compounds. Coutant *et al.* have described the development of a circular multi-channel diffusion denuder for the study of PAH in ambient air. However, results on field studies using the sampling system have not yet been published. The

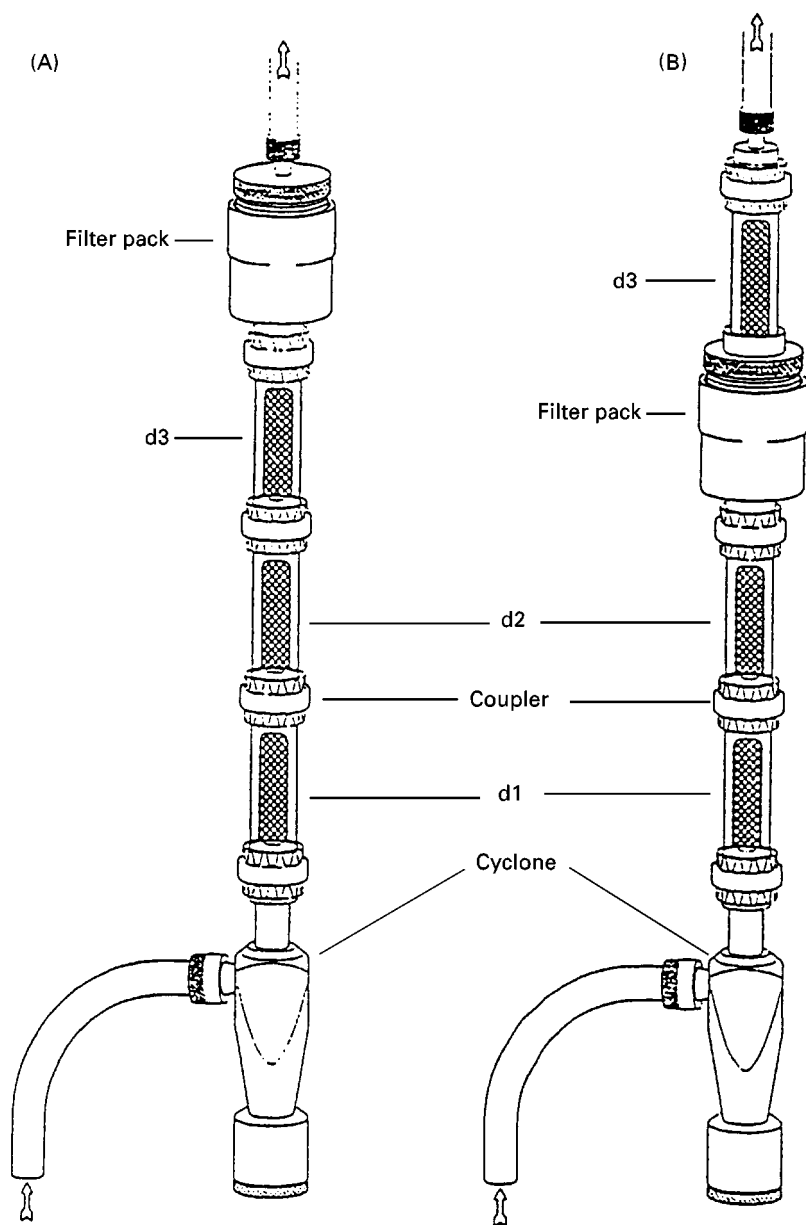


Figure 4 Schematic of the IOVAPS (from Gundel, 1999). The denuders contain XAD as the gas phase organic sorbent. Non-volatile particulate carbonaceous material is determined from analysis of the filters in either of the filter packs. Semi-volatile carbonaceous material lost from particles is determined from analysis of the denuder d3.

Atmospheric Environment Service of Environment Canada has been involved since 1984 in the development and use of a diffusion denuder sampler for the determination of PCBs and chlorinated hydrocarbons. The instrument uses a silicone gum/Tenax-coated, multi-tube, annular, diffusion denuder to remove the target organic compounds. Turpin *et al.* have developed a sampling system which corrects for the loss of semi-volatile organic compounds during sampling by removal of most of the gas phase material from the particles in a diffusion separator sampling system. The system has been evaluated for the

collection of PAH. All of the systems which have been described by other research groups collect samples at a flow rate of a few L min^{-1} . One advantage of the use of the diffusion denuder sampling systems described above is that the attainable high flow rate, 200 L min^{-1} , allows for more collected material and a wider range of analyses on the collected samples.

Residence Time in the Denuder

The efficiency of a diffusion denuder sampler for the removal of gas phase material can be improved by

increasing the residence time of the sampled aerosol in the denuder. However, the residence time can only be increased within limits. Since the diffusion denuder reduces the concentration of gas phase semi-volatile organic material, semi-volatile organic material present in the particles passing through the denuder will be in a thermodynamically unstable environment and will tend to outgas SVOC during passage through the denuder. The residence time of the aerosol in the denuder should be short enough to prevent significant loss of particulate phase SVOC to the denuder. Various studies have suggested that the residence time in the denuder should be less than about 2 s. The residence times in the various denuder designs described above are about 1.5, 0.2, 0.2 and 1.4 s for the BOSS (or PC-BOSS), BIG BOSS, IOVPS and IOGAPS denuders, respectively.

Changes in Chemical Composition during Sampling

The preceding sections have outlined sampling systems designed to identify correctly the atmospheric gas and particulate phase distribution of collected organic material. An additional sampling artifact which has been little considered in the collection of atmospheric sampling is the potential alteration of organic compounds as a result of the sampling process. These alterations appear to result from the movement of ambient air containing oxidants and other reactive compounds past the collected particles. The addition of NO_2 (<1 p.p.m.) or O_3 (<200 p.p.b.) to the sampled air stream (0 to 5°C) for a high volume sampler reduced the concentrations of benzo(a)pyrene and benzo(a)anthracene from a few up to 38%, with the observed reduction increasing with increased concentration of the added gases. Spiking a filter with an amine resulted in an increase in measured concentrations of nitrosoamines in both the filter and a following XAD sorbent bed for a mid-volume sampler. Similar results have been obtained for the exposure of a deuterated amine on a filter to NO_x . When Tenax columns spiked with deuterated styrene and cyclohexane were exposed to p.p.m. concentrations of ozone or halogens, oxygenated and halogenated compounds were shown to be formed. Similar oxidation of aldehydes and PAN during sampling has been observed. Collected PAH compounds can be oxygenated and/or nitrated on a filter but 1-nitropyrene has been shown to be resistant to additional nitration. These various chemical transformations of collected organic compounds can be eliminated by removal of the gas phase oxidants, NO_x , HNO_3 , etc., prior to collection of the particles. The PC-BOSS denuder described above should be

effective in eliminating most of chemical transformation artifacts since reactive gases are removed by the charcoal denuder which precedes the particle collection filter.

Application of Diffusion Denuder Samplers to the Determination of Semi-Volatile Organic Material

The application of diffusion denuder samplers to the determination of gas and particulate phase semi-volatile organic material is illustrated with results from three different studies, one each using the BIG BOSS, PC-BOSS and IOVPS samplers.

Semi-volatile organic compounds lost from particles during sampling and subsequently collected by an XAD-II trap and semi-volatile organic compounds retained by the quartz filters during sampling have been chemically characterized for <2.5 μm particles in BIG BOSS samples collected at Azusa in the Los Angeles Basin. The XAD-II sorbent beds included significant concentrations of aliphatic, acidic and aromatic organic compounds. Similar compounds were also detected in the GC-MS analysis of the filter extracts. However, the compounds retained by the filter were of higher molecular weight. The distribution of compounds lost from particles during sampling and remaining on the particles during sampling is illustrated by the GC/MS results for paraffinic compounds (Figure 5).

The pattern seen in Figure 5 is typical of results obtained for all classes of compounds and all samples studied to date. For those compounds which have been characterized, the envelopes of each class of compounds remaining in the particles and lost from the particles overlap. For each compound class, the more volatile compounds predominate in the material lost from the particles and collected in the XAD-II bed during sampling. In contrast, the higher molecular weight organic compounds are retained by the particles during sampling. For example, particulate n-tetradecane and n-pentadecane are found only in the XAD-II bed and not in the particles after sampling (Figure 5). Hydrocarbons lower in molecular weight than these two compounds are found in comparable concentrations in the XAD-II beds of both Samplers 1 and 2 of the BOSS (Figure 2) indicating they originate mainly from the breakthrough of some fraction of the gas phase component of these species. In contrast, n-tetracosane and higher molecular weight aliphatic hydrocarbons are retained by the particles during sampling and are not found in the XAD-II sorbent beds (Figure 5). Compounds of intermediate molecular weight, e.g. n-decosane, are partially lost and partially retained by the particles. Also illustrated

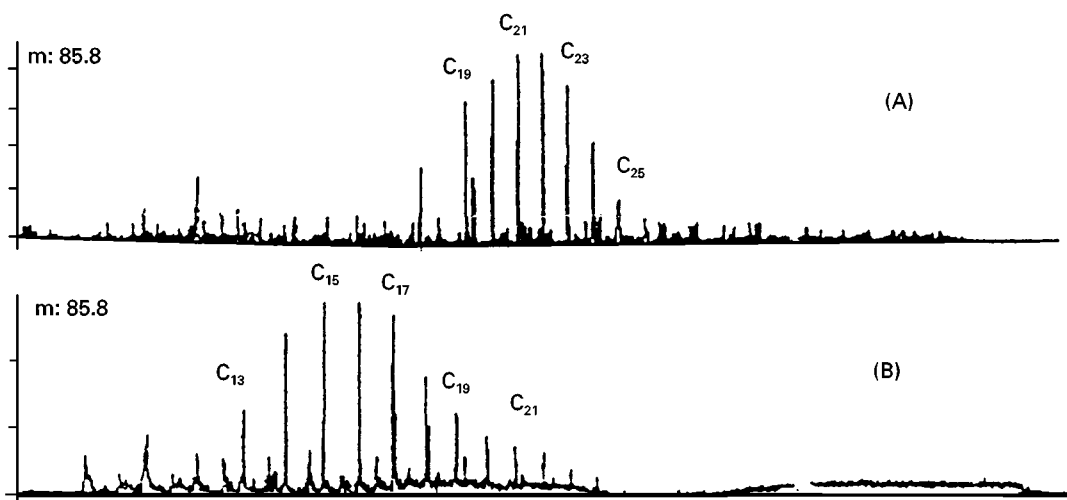


Figure 5 GC/MS data ($m/z = 85$) for paraffinic compounds; (A) retained by particles and (B) lost from particles during collection on a filter (from Tang, 1994).

by the GC-MS data is the increased tendency for lower molecular weight semi-volatile organic compounds to be retained by the particles during sample collection as the polarity of a given molecular weight compound increases. For example, *n*-heptadecane (MW 226) is largely lost from particles during sampling (Figure 5). However, lauric acid (MW 214) and fluoranthene (MW 202) are largely retained by the particles during sampling.

Results for the determination of PAH compounds in indoor air obtained with the IOVPS and with a conventional filter-sorbent sampler are given in Figure 6. As indicated in Figure 6(A), about 90% of the phenanthrene, pyrene and chrysene are present in the gas phase. However, about 60% of the more volatile phenanthrene (MW 178) and pyrene (MW 202) are lost from the filter of the filter pack during sample collection. In contrast, the loss of the less volatile chrysene (MW 228) was negligible. These

results are comparable to those given above for the Azusa study with the BIG BOSS.

Recent studies have indicated that the U.S. Environmental Protection Agency (EPA) PM_{10} air quality standard does not provide adequate human health protection because the fine particle ($PM_{2.5}$) component of PM_{10} is related to observed health effects at concentrations substantially below the PM_{10} standard. As a result, EPA has promulgated a $PM_{2.5}$ air quality standard. In order to implement the new $PM_{2.5}$ standard, a Federal Reference Method (FRM) for fine particulate monitoring has been proposed (see Schaefer, 1997). The $PM_{2.5}$ FRM is a single filter pack sampling method with gravimetric determination of the collected mass.

For the reasons outlined above, the FRM will tend to not measure semi-volatile fine particulate constituents. The amount of semi-volatile material is expected to be a substantial fraction of the total $PM_{2.5}$

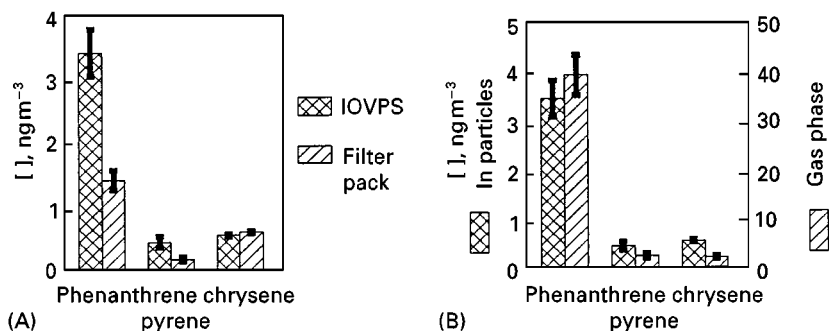


Figure 6 Retention and loss of particulate PAH compounds during sampling. (A) The lower concentrations determined by a filter pad, compared to IOVPS, is due to losses from particles during sampling. (B) Concentrations of both particle and gas phase PAH with the IOVPS.

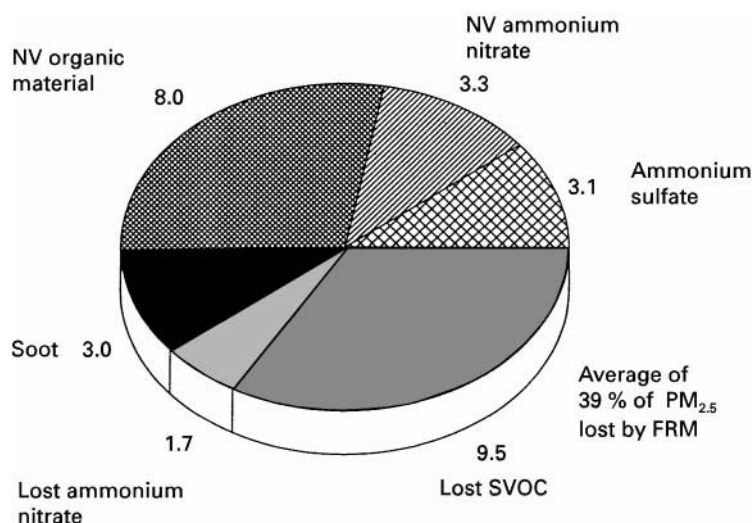


Figure 7 Average composition of PM_{2.5} in Riverside CA, including semi-volatile ammonium nitrate and organic material lost during sampling from particles collected on a filter.

mass observed in many urban areas. As a result, the proposed Federal Reference Method may under-determine fine particulate mass. A comprehensive field study to evaluate the PC-BOSS and compare with results obtained by other PM_{2.5} sampling methods, including the FRM has been conducted in Riverside, California. Riverside was chosen for the study because high particulate pollution resulting from summer inversions is expected. Both annual and 24 hour maximum concentration of PM₁₀ exceeded the federal standards in 1995 and high concentrations of particulate semi-volatile ammonium nitrate and organic materials are expected to be present in this area.

The average result for the determination of the composition of fine particulate matter in Riverside during August and September 1997 are given in **Figure 7**. Substantial amounts of both ammonium nitrate and semi-volatile organic material were lost from the filters of both the PC-BOSS and the PM_{2.5} FRM. The average loss of ammonium nitrate (34%, 1.7 $\mu\text{g m}^{-3}$) was smaller than that for the semi-volatile organic material (54% of total fine particulate organic material, 9.5 $\mu\text{g m}^{-3}$). As a result of the loss of these species, the PM_{2.5} FRM lost an average of 39% of the fine particulate material during the collection of the sample.

The results obtained in these three examples illustrate the importance of correctly sampling for semi-volatile particulate organic material.

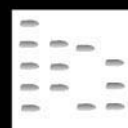
See also: II/Extraction: Solid-Phase Extraction. **Membrane Separations:** Filtration. III/Atmospheric Analysis: **Gas Chromatography:** Supercritical Fluid Chromatography. **Solid-Phase Extraction with Discs.**

Further Reading

- Chow JC (1995) Measurement methods to determine compliance with ambient air quality standards for suspended particles. *J. Air & Waste Management Assoc.* 45: 320–382.
- Cui W, Eatough DJ and Eatough N (1998) Fine particulate organic material in the Los Angeles Basin – I: Assessment of the high-volume Brigham Young University Organic Sampling System, BIG BOSS. *J. Air & Waste Manage. Assoc.* 48: 1024–1037.
- Ding Y, Lee ML and Eatough DJ (1998) The determination of total nitrite and n-nitroso compounds in atmospheric samples. *J. Environ. Anal. Chem.* 69: 243–255.
- Eatough DJ (1999) BOSS, the Brigham Young University Organic Sampling System: Determination of particulate carbonaceous material using diffusion denuder sampling technology. In: Douglas Lane (ed.) *Gas and Particle Phase Partition Measurements of Atmospheric Compounds*, Vol. 2, 233–285. Gordon and Breach Science Publishers.
- Eatough DJ, Obeidi F, Pang Y *et al.* (1999) Integrated and real-time diffusion denuder samplers for PM_{2.5} based on BOSS, PC and TEOM technology. *Atmospheric Environment* 33: 2835–2844.
- Eatough DJ, Tang H, Cui W and Machir J (1995) Determination of the size distribution and chemical composition of fine particulate semivolatile organic material in urban environments using diffusion denuder technology. *Inhal. Toxicol.* 7: 691–710.
- Fitz DR (1990) Reduction of the positive organic artifact on quartz filters. *Aerosol Sci. Technol.* 12: 142–148.
- Fraser MP, Cass GR, Simoneit BRT and Rasmussen RA (1998) Air quality model evaluation data for organics. 5. C₆–C₂₂ nonpolar and semipolar aromatic compounds. *Environ. Sci. Tech.* 32: 1760–1770.

- Gundel LA and Lane DA (1998) Direct determination of semi-volatile organic compounds with sorbent coated diffusion denuders. *J. Aerosol Sci.* 29: S341-S342.
- Gundel LA, Lee VC, Mahanama KRR, Stevens RK and Daisey JM (1995) Direct determination of the phase distributions of semi-volatile polycyclic aromatic hydrocarbons using annular denuders. *Atmos. Environ.* 29: 1719-1733.
- Hart KM and Pankow JF (1994) High-volume air sampler for particle and gas sampling. 2. Use of backup filters to correct for the adsorption of gas-phase polycyclic aromatic hydrocarbons to the front filter. *Environ. Sci. Technol.* 28: 655-661.
- Kamens RM, Odum J and Fan Z-H (1995) Some observations on times to equilibrium for semivolatile polycyclic aromatic hydrocarbons. *Environ. Sci. Technol.* 29: 43-50.
- Lane DA and Johnson ND (1993) Vapor and particle phase measurements of polycyclic aromatic compounds (PAC) in ambient air. *Poly. Arom. Comp.* 13 (Supplement): 511-518.
- McDow SR and Huntzicker JJ (1990) Vapor adsorption artifact in the sampling of organic aerosol: face velocity effects. *Atmos. Environ.* 24: 2563-2571.
- Pankow JF (1989) Overview of the gas phase retention volume behavior of organic compounds on polyurethane foam. *Atmos. Environ.* 23: 1107-1111.
- Pankow JF (1988) Gas phase retention volume behavior of organic compounds on the sorbent poly(oxy-m-terphenyl-2',5'-ylene). *Anal. Chem.* 60: 950-958.
- Pellizzari ED and Krost KJ (1984) Chemical transformations during ambient air sampling for organic vapors. *Anal. Chem.* 56: 1813-1819.
- Schaefer G, Hamilton W and Mathai CV (1997) Implementing the NAAQS and FACA subcommittee for ozone, particulate matter and regional haze. *Environ. Man.* Oct 1997: 22-28.
- Tang H, Lewis EA, Eatough DJ, Burton RM and Farber RJ (1994) Determination of the particle size distribution and chemical composition of semi-volatile organic compounds in atmospheric fine particles with a diffusion denuder sampling system. *Atmos. Environ.* 28: 939-947.
- Turpin BJ and Huntzicker JJ (1994) Investigation of organic aerosol sampling artifacts in the Los Angeles basin. *Atmos. Environ.* 28: 3061-3071.
- Williams EL and Grosjean D (1990) Removal of atmospheric oxidants with annular denuders. *Environ. Sci. Technol.* 24: 811-814.

ALCOHOL AND BIOLOGICAL MARKERS OF ALCOHOL ABUSE: GAS CHROMATOGRAPHY



F. Musshoff, Institute of Legal Medicine, Bonn, Germany

Copyright © 2000 Academic Press

The use of alcoholic beverages is probably the most ancient social habit worldwide, but alcohol abuse has generated severe problems. Chronic and/or acute alcohol intoxication has been demonstrated to be connected with serious pathologies, suicides, homicides, fatal road and industrial accidents and many criminal offences. Alcoholism is a widespread social, medical and economic problem in a large section of the population of nearly all ethnic groups. Therefore, it is of great importance to have diagnostic tools (biological markers) to detect excessive alcohol consumption and alcoholism. This article deals with gas chromatographic techniques to determine excessive alcohol consumption. The following parameters are described: ethyl alcohol and congeners, ketone bodies, ethyl glucuronide, fatty acid ethyl esters and condensation products like salsolinol.

Ethyl Alcohol

The most obvious and specific test for heavy drinking is the measurement of blood, breath or urine alcohol (ethyl alcohol). However, this simple test cannot distinguish between acute and chronic alcohol consumption, unless it can be related to an increased tolerance of alcohol. According to the American National Council on Alcoholism (NCA), the first-level criteria for the diagnosis of alcoholism are blood alcohol exceeding 1.5 g L^{-1} without gross evidence of intoxication, over 3 g L^{-1} at any time, or over 1 g L^{-1} in routine examination. The determination of alcohol has already been the subject of many reviews. The most important facts are summarized here.

As a first step, various pitfalls and analytical problems such as interference in alcohol analysis induced by cleaning the skin with ethanol or isopropanol before expert venepuncture should be borne in mind. The stability of ethanol during storage is a problem. The main factors affecting alcohol determination in stored blood are the duration and temperature of storage, with negligible losses in the frozen state, and the presence of a preservative. Three mechanisms accounting for these changes are: oxidation (highly

temperature-dependent, needing oxygen from oxyhaemoglobin), the growth of microorganisms metabolizing ethanol (inhibited by sodium fluoride at $\geq 0.5\%$, w/v) and diffusion from containers owing to closure failure. A further potentially interfering factor, especially in autopsy cases, is ethanol production in (postmortem) tissues by bacteria and yeasts. Freezing seems to be the best precaution in order to maintain the original alcohol levels.

Gas chromatography (GC) is *par excellence* the all-purpose technique for the determination of volatile molecules, such as alcohols and related compounds. Almost all GC methods for ethanol determination allow the simultaneous measurement of a wide range of other volatile analytes (alcohols, aldehydes, ketones, glycols, etc.). Although some of the earlier techniques have become obsolete, the incorporation of advances such as headspace chromatography have extended the popularity of chromatography. The analytical conditions of the

most interesting methods are summarized in Tables 1 and 2. The following classification has been used.

Direct Injection

Methods using direct injection of whole blood suffer from the adsorption of undesirable compounds (proteins and other macromolecules) on the column and, consequently, in most procedures prior dilution or centrifugation have been used.

With Extraction

For a prior extraction step organic solvents such as *n*-propyl acetate, *n*-butanol or dioxan are used.

With Distillation

Sample and internal standard in sodium tungstate/sulfuric acid are subjected to distillation. The distillate is injected into the column and detection is performed by thermal conductivity or flame ionization.

Table 1 Direct injection gas chromatography. Representative overview of standard procedures for the determination of ethyl alcohol

Specimen (mL or g) ^a	Diluent (mL)	Column (m × mm I.D.)	Packing (mesh)	Oven temperature (°C)	Carrier gas (mL min ⁻¹)	Detection	Internal standard
Blood (0.5)	Int. standard solution (0.5)	1.8 × 6	30% Carbowax 20M on Chromosorb W (60–80)	100	Nitrogen (35)	FID	Isobutanol
Blood (0.01)	Int. standard solution (0.1)	1.5 × 4.8	10% Carbowax 400 on Chromosorb W (80–100)	75	Nitrogen (75)	FID	<i>n</i> -Propanol
Blood	Int. standard solution	2 × 3	(1) 0.2% Carbowax 1500 on Carbopack C (80–100)	120		FID	<i>n</i> -Propanol
Urine	(0.5 µL)		(2) 30% Carbowax 20M on Chromosorb W HP (60–80)	100	(20)		Isobutanol
Serum							
Plasma							
(0.5 µL)							
Serum (0.1)	Int. standard solution + Triton-X-100 (0.1)	3 × 3.2	Porapak Q (80–100)	155	Nitrogen (18)	FID	Acetonitrile
Serum (0.2)	Int. standard solution (0.2) Sodium tungstate 0.2 mol L ⁻¹ (0.2) Copper (II) sulfate 0.2 mol L ⁻¹ (0.2)	30 × 0.25	Methylsilicone-bonded phase (0.25 µm)	35	Helium	FID	<i>n</i> -Propanol
Blood	Water (50-fold sample vol.)	15 × 0.53	Polyethylene glycol (1.0 µm)	40	Helium (25)	FID	
Blood	Int. standard solution	1.8 × 2	Porapak S (80–100)	165	Nitrogen (45)	FID	Acetonitrile
Urine	(twofold)						
Serum							
Plasma							
Blood	Sodium tungstate	2 × 3	Porapak Q (80–100)	180	Nitrogen (30)	FID	Isopropanol
(0.1–0.3)	12.5% (0.2) Sulfuric acid 0.33 mol L ⁻¹ (0.2)						
Blood (0.2)	Int. standard solution (0.8)	1.2 × 4	5% Carbowax 20M on Supelcoport (100–120)	100	Helium (30)	FID	<i>n</i> -Butanol

^amL for serum/plasma/urine or g for blood.

Selection according to Tagliaro *et al.* (1992) Chromatographic methods for blood alcohol determination. *Journal of Chromatography* 580: 161.

Table 2 Headspace gas chromatography. Representative overview of standard procedures for determination of ethyl alcohol

Specimen (mL or g) ^a	Incubation		Packing (mesh)	Oven temperature (°C)	Carrier gas (mL min ⁻¹)	Detection	Internal standard
	Temperature (°C)	Time (min)					
Blood (0.02)	60	3	Porapak Q (80–100)	150	Nitrogen (30)	FID	<i>n</i> -Propanol
Blood	60	30	5% Carbowax 20M on Carbopack B (60–80)	65–110	Nitrogen (30)		<i>n</i> -Propanol
Serum (0.5)							
Blood (0.2)	60	20	(1) 0.2% Carbowax 1540 on Carbopack C (60–80) (2) 15% Polyethylene glycol on Celite (60–100)	85–100		FID	<i>tert</i> -Butanol
Blood (0.2)	20–40	30	0.2% Carbowax 1500 on Carbopack C (80–100)	125	Nitrogen (20)	FID	<i>n</i> -Propanol
Blood	20–40	30	Methylsilicone	35–40	Helium (25)	FID	<i>n</i> -Propanol
Blood (0.5)	55	12	(1) Methylsilicone (megabore) (2) DB-wax (megabore)	45	Helium (7.5)	FID	<i>n</i> -Propanol
Blood	40	18	(1) 0.2% Carbowax 1500 on Carbopack C (80–100) (2) 5% Carbowax 20M on Carbopack B (60–80) (3) 15% Carbowax 20M on Chromosorb W	100	Nitrogen (20)	FID	<i>n</i> -Propanol
Urine (0.1)							
Plasma	25	—	Porapak S (80–100)	165	Nitrogen (45)	FID	

^amL for serum/plasma/urine or g for blood.Selection according to Tagliaro *et al.* (1992) Chromatographic methods for blood alcohol determination. *Journal of Chromatography* 580: 161.

Headspace Methods

The most important advantage is the prevention of column contamination.

Methods requiring solvent extraction or distillation should be considered obsolete mainly because they are time- and sample-consuming and not susceptible to automation. Direct injection and headspace GC are the only techniques in general use that can be fully and easily automated. The description of direct injection technique is mostly connected with the dilution of the sample (mostly with aqueous solutions containing the internal standard) and with the injection of small volumes. Additional protection from contamination can be obtained with a glass sleeve inserted in the injection port or with a pre-column glass insert filled with a silanized glass wool plug. Triton X-100 has been reported to improve the performance of the direct injection of serum by acting as a protein-dispersing agent. Protein precipitation, which can be carried out in conjunction with the addition of the sample with the internal standard, has been proposed as a simple means of overcoming the problems related to the injection of whole blood. Headspace GC for blood alcohol analysis was the subject of a review in 1975 by Machata who made many contributions to

the development of this technique. Chromatograms are shown in **Figure 1**. Headspace analysis prevents any contamination of the column and injector with involatile material and is preferred in routine laboratories. Also, reproducibility is often better than in direct injection (typical within and between-run coefficients of variation < 1.5% and < 2.5%, respectively). Analytical problems arise concerning the choice of the sample equilibration temperature; oxidation of ethanol takes place at temperatures exceeding 40°C, but higher temperatures increase the air–blood partition coefficient and, consequently, the sensitivity. The conversion of ethanol into acetaldehyde is reportedly inhibited by the addition of sodium nitrite or sodium dithionite. Increased sensitivity due to a salting-out effect is obtained using sodium chloride, sodium nitrite, potassium carbonate, sodium fluoride and ammonium sulfate. In such non-ideal solutions, the vapour pressures of volatile components at a fixed temperature have been reported to depend on the water content of the sample.

An additional advantage of headspace technique is the complete elimination of matrix-related effects, which prompted its use for the analysis of tissues, stool samples or other biological material. A new procedure is the headspace–solid-phase microextraction

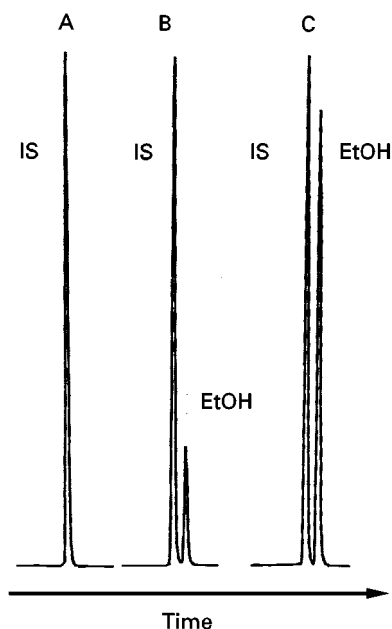


Figure 1 Representative headspace gas chromatograms determining alcohol concentrations in human serum samples. A, Blank (serum); B, 0.48 g L^{-1} ; C, 1.95 g L^{-1} . Retention times: EtOH, 1.65 min; t-butanol, 2.2 min.

(HS-SPME) technique, based on the adsorption of analytes directly from the headspace on to a coated fused silica fibre. Various fibres for different analytes are available and a $65 \mu\text{m}$ Carbowax/divinylbenzene coating is used for alcohols.

Alcohols can be efficiently separated with different GC columns and the choice is often only based on practical considerations such as total analysis time, cost, column life and the possibility of using the same column for different analyses. Carbowax 20M is superior to Carbowax C coated with Carbowax 1500 for the determination of acetaldehyde and methanol and is also superior to adsorption chromatography on Porapak Q and Chromosorb 102. Separation is generally carried out under constant temperature conditions; temperature programming has been used for the simultaneous determination of less volatile compounds. Detection is universally carried out by a flame ionization detector (FID). Capillary chromatography (Carbowax 20M) allows a higher separation performance and easier coupling with mass spectrometry, which is preferred for the determination of lower volatile alcohols.

Congeners

Besides ethanol, alcoholic beverages contain up to 800 flavour compounds and some of these congeners can be found in sufficient quantities to allow their detection in the blood of the consumer. There are

characteristic differences in the congener content of alcoholic beverages. A close correlation between the consumed amount of a congener alcohol and the resulting blood level can be helpful for the evaluation of allegations concerning alcohol intake in forensic cases, especially when determining types of drinks and when estimating the time of drinking (Figure 2). The sensitivity of conventional headspace GC is sufficient for blood ethanol determinations down to 0.01 g L^{-1} , but for the detection of congener alcohols the limits of detection had to be improved to 0.01 mg L^{-1} . Some procedures contain special sample preparation steps, which include homogenization by ultrasound and/or ultrafiltration. As the long chain alcohols are partly or completely bound to glucuronic acid, incubation with β -glucuronidase is necessary. Using a temperature programme and capillary columns the loading capacity can be enhanced by a cryofocusing technique.

Methanol is an important congener of most alcoholic beverages. Metabolism of methanol via liver alcohol dehydrogenase is inhibited by ethanol levels exceeding 0.4 g L^{-1} . Consequently, excessive and prolonged drinking results in high blood methanol levels. Increased blood methanol levels are frequently found in drunken drivers and alcoholics. On the basis of these findings, blood methanol levels exceeding 10 mg L^{-1} have been suggested to be an indicator of alcoholism. Additionally higher concentrations of acetone and propanol-2 have been proposed as an indication of drinking behaviour. This phenomenon is caused by reciprocal formation through the alcohol dehydrogenase system. If the sum of the concentrations exceeds 9 mg L^{-1} , heavy drinking is suspected. However, due to the effects of metabolic disorders (ketosis, diabetes, hunger, physical stress), the significance has been regarded as very low.

Ketone Bodies

In many forensic cases alcohol abusers have been found dead and the cause of death cannot be ascertained. In order to examine the possible role of ketoacidosis as the cause of death the concentrations of ketone bodies (acetone, acetoacetate, D- β -hydroxybutyrate) have to be determined in postmortem blood specimens. The phenomenon of ketoacidosis is often seen as typical in periods of abstinence with low intake of food. It is due to the accumulation of D- β -hydroxybutyrate and acetoacetic acid. The accumulation is probably the result of various factors such as volume depletion and starvation, which have a lipolytic effect.

A routine procedure is a coupled enzymatic headspace GC method (Figure 3). This procedure is based

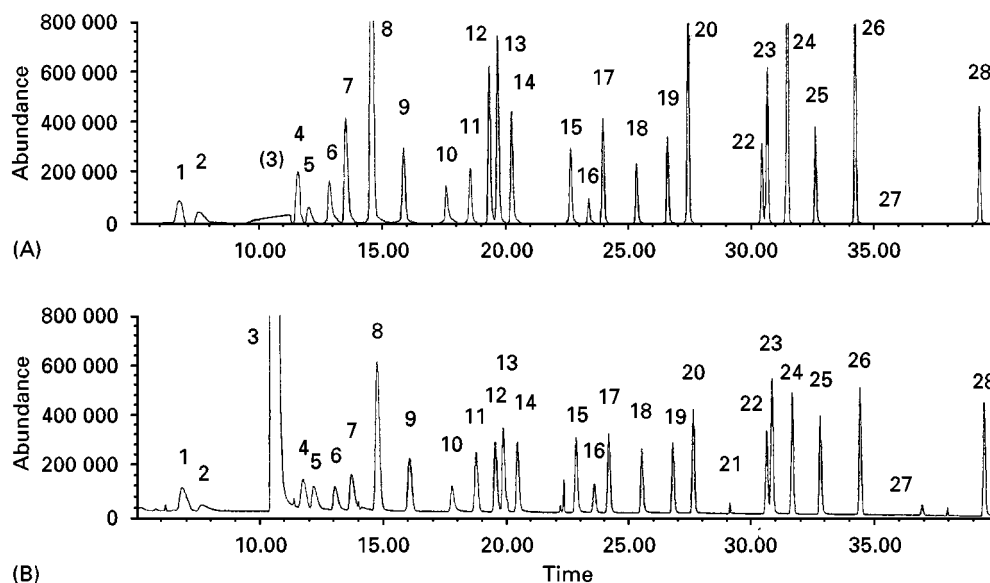


Figure 2 Total ion chromatograms ((A) selected ion monitoring and (B) full scan mode) of a standard solution of 28 substances relevant in congener analysis in concentrations of 2 mg L^{-1} (methanol 10 mg L^{-1} , acetaldehyde 0.5 mg L^{-1}). 1, Acetaldehyde; 2, methanol; 3, ethanol; 4, propionaldehyde; 5, acetone; 6, propanol-2; 7, methyl acetate; 8, *t*-butanol (internal standard); 9, *i*-butyraldehyde; 10, propanol-1; 11, *n*-butyraldehyde; 12, methyl ethyl ketone; 13, ethyl acetate; 14, butanol-2; 15, *i*-butanol; 16, *i*-valeraldehyde; 17, 2-methylbutyraldehyde; 18, butanol-1; 19, *n*-valeraldehyde; 20, 1,1-diethoxyethane; 21, 3-hydroxybutanone-2; 22, 3-methylbutanol-1; 23, 2-methylbutanol-1; 24, *i*-butyl acetate; 25, pentanol-1; 26, butyl acetate; 27, ethyl lactate; 28, hexanol-1. GC parameter: HP 5890 II GC with HP MSD 5972, equipped with a DB 624 column ($60 \text{ m} \times 0.32 \text{ mm}$, $\text{df} = 1.8 \text{ }\mu\text{m}$); helium flow 1 mL min^{-1} ; injector 150°C ; detector 200°C ; oven initially 30°C for 8 min, 3°C min^{-1} up to 180°C . (Reproduced with permission from Roemhild W (1998) Congener analysis by means of 'headspace'-GC/MS. *Blutalkohol* **35**: 10.)

on enzymatic dehydrogenation of *D*- β -hydroxybutyrate into acetoacetate and subsequent decarboxylation of this compound into acetone. Three portions are taken from each sample. One portion is heated to 60°C in a headspace sampler, which gives the free acetone. Acetoacetate is converted into

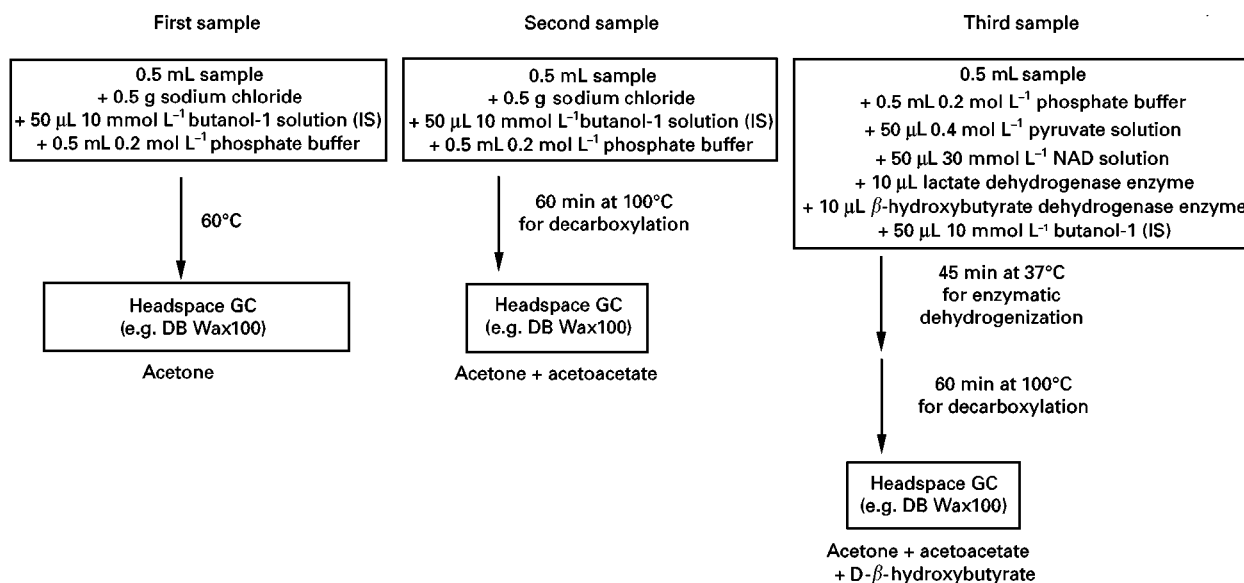


Figure 3 Schematic presentation of a standard procedure for determination of ketone bodies in blood specimens. Three portions are taken from each sample to determine free acetone and the sums of acetone + acetoacetate and acetone + acetoacetate + *D*- β -hydroxybutyrate.

acetone by decarboxylation at 100°C in the second portion. This part gives the combined amount of acetone and acetoacetate. In the third portion, D- β -hydroxybutyrate is first enzymatically dehydrogenized into acetoacetate by D- β -hydroxybutyrate dehydrogenase and then decarboxylated into acetone. Quantification of acetone then yields the molar equivalent of the total ketone bodies. Omission of the enzymatic stage of the analysis allows quantification of the molar equivalent of acetone and acetoacetate present, and the subtraction of this value from total ketone quantitation allows calculation of the D- β -hydroxybutyrate concentration.

The reported ketone body concentrations vary a lot. It was held that if the ketone body concentration of the blood exceeds 531 $\mu\text{mol L}^{-1}$ and if there is no other plausible cause of death in a group of alcohol abusers, the term ketoalcoholic death should be used. In another study it was pointed out that very high levels, above 10 mmol L^{-1} , are indicative of profound alcoholic ketoacidosis.

Ethyl Glucuronide

Ethyl glucuronide (EtG) is a minor metabolite of ethanol and is formed from ethanol by conjugation with uridine diphosphate (UDP)-glucuronic acid. EtG has been detected in human urine, serum and clipped hair samples of ethanol consumers. The formation of EtG depends on the serum ethanol concentration. It was shown that serum EtG concentrations higher than 5 mg L^{-1} may indicate alcohol misuse, especially if the serum ethanol concentration is less than 1 g L^{-1} . The EtG concentration declines exponentially with a half-life of 2–3 h and testing for EtG is restricted to a period of about 6–18 h after drinking, depending on the ethanol dose and individual metabolism. In forensic cases testing is predominantly indicated when the ethanol determination gives nega-

tive results and consumption is denied. For retrospective studies detection of EtG in hair samples also seems to be possible. However, if excessive ethanol consumption over a period of months or years provokes a stimulation of glucuronyltransferase in the liver, the extent of the EtG formation might be an indicator of ethanol abuse.

For the determination of EtG in serum the sample is precipitated with acetone or methanol and the dried supernatant is derivatized by addition of acetic anhydride and pyridine. A mass spectrum of the triacetyl derivative is shown in Figure 4. Hair samples are extracted with methanol, including treatment by ultrasound prior to derivatization. On an OV-1 capillary column, the retention index is 1920. Gas chromatography–mass spectrometry (GC-MS) was performed with an electron energy of 70 eV and gave the following m/z values (intensities higher than 20% in parentheses): 85 (53), 88 (41), 101 (38), 113 (66), 114 (42), 115 (100), 117 (47), 130 (25), 157 (73), 142 (25) and 143 (28); there is no parent peak. An m/z value of 303 (1%, M-45) indicates that EtG is decarboxylated.

Fatty Acid Ethyl Esters

Fatty acid ethyl esters (FAEE) are formed by an enzyme-mediate esterification of ethanol with fatty acids or fatty acyl-coenzyme A. It has been shown that FAEE and the FAEE synthase are predominantly present in those organs most often damaged by ethanol abuse, notably the pancreas and liver. This has led to speculation that FAEE, lipids more hydrophobic than triglycerides, are mediators of ethanol-induced organ damage. Following ethanol consumption by humans, FAEE have also been found in serum lipoproteins. Recently it was reported that the concentration of FAEE in the blood closely parallels the concentration of blood ethanol. In serum samples of

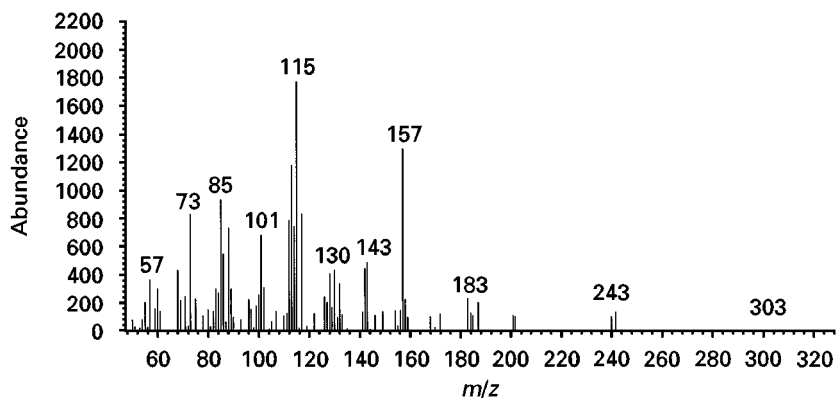


Figure 4 Mass spectrum of the triacetyl derivative of ethyl glucuronide.

subjects who had blood ethanol concentrations $> 1.5 \text{ g L}^{-1}$, FAEE concentrations ranged up to 2500 nmol L^{-1} and were still detectable 24 h after ethanol ingestion. However, serum FAEE may evolve into both a short-term and long-term marker of ethanol ingestion. In forensic cases the determination of a recent intake of ethanol may be necessary. A negative blood ethanol with a positive FAEE test is consistent with ethanol intake 4–24 h before blood collection. Additionally it has been reported that FAEE are present in significantly higher amounts in postmortem adipose tissues obtained from individuals with a history of chronic alcohol abuse, with ethanol-induced organ damage at autopsy and zero blood ethanol at the time of death (mean \pm SEM equals $300 \pm 46 \text{ nmol g}^{-1}$) compared to those from a control group without a history of chronic ethanol ingestion, without ethanol-related organ damage and with zero blood ethanol at the time of death ($43 \pm 13 \text{ nmol g}^{-1}$; Figure 5).

Studies on FAEE frequently involve isolating the compounds by liquid–liquid extraction and thin-layer chromatography (TLC) prior to identification and quantification. The isolation of FAEE by these methods is especially suitable for adipose tissue. Sample material (1–2 g) is extracted in acetone (10% w/v) and the lipids are separated by TLC on silica gel using a petroleum ether/diethyl ether/acetic acid (75:5:1) solvent system. Fatty acid ethyl esters, $R_F = 0.5$, are identified by comparison with standards and eluted from the silica gel with acetone. The reproducibility of this procedure is sometimes a problem and the method often results in low yields. The small amounts of the very hydrophobic FAEE present in human plasma after ethanol ingestion are commonly lost during extraction. As with fatty acids, FAEE moieties which contain two or more double bonds can be oxidized within minutes on a dried TLC plate and are thereby lost prior to quantification. To enhance the recovery of the relatively small amounts of FAEE, an effective solid-phase extraction (SPE) method for isolation is preferred. Extraction of FAEE from serum is initiated by the addition of acetone/hexane solution. After being dried and re-suspended in hexane the extract is applied to an aminopropyl silica SPE column with simultaneous elution of FAEE and cholesteryl esters from the column with hexane. The FAEE can then be separated from cholesteryl esters, if necessary, by chromatography on an octadecylsilyl (ODS) SPE column and elution with isopropanol/water (5:1, v/v). Recently a relationship between various levels of alcohol consumption and the appearance of fatty acid methyl esters (FAME) in postmortem tissue samples have been reported. In addition, this connection is suppos-

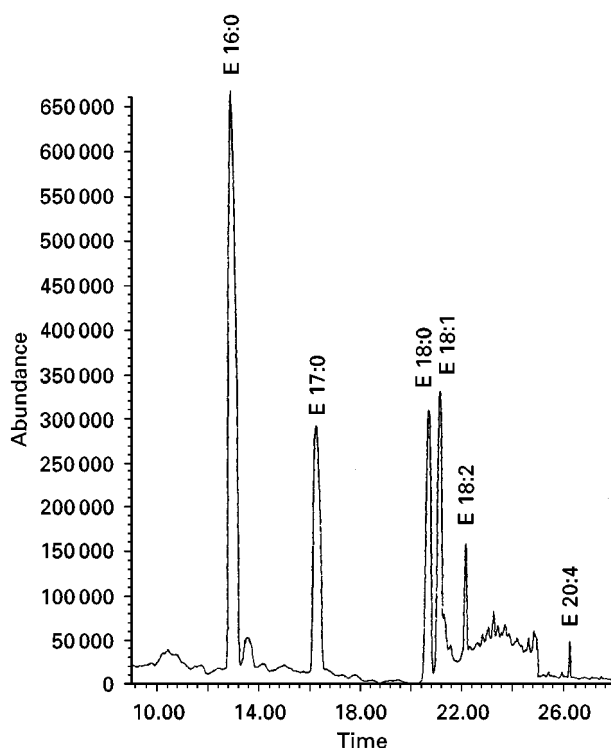


Figure 5 Analysis of FAEE from human plasma. Lipids from sera of patients with markedly elevated blood ethanol levels were extracted into hexane and applied to an aminopropyl silica column. Lipids eluted from the column were dried under nitrogen to a small volume and an aliquot injected into a gas chromatograph – mass spectrometer (WCOT Supelcowax capillary column). The peaks identified as FAEEs are labelled: E 16:0, ethyl palmitate; E 17:0, ethyl heptadecanoate; E 18:0, ethyl stearate; E 18:1, ethyl oleate; E 18:2, ethyl linoleate; E 20:4, ethyl arachidonate. (Reproduced from Bernhardt TG *et al.* (1995) Purification of fatty acid ethyl esters by solid-phase extraction and high-performance liquid chromatography. *Journal of Chromatography B* 675: 189, with permission from Elsevier Science.)

edly caused by the accumulation of the congener alcohol, methanol, during chronic alcohol abuse.

The GC analysis of FAME after esterification of lipids was the subject of an excellent review by Eder in 1995 and the comments are applicable to FAEE. The most critical step in the GC analysis of FAME is sample introduction. The classical split injection technique, which is the most widely used procedure, has the potential disadvantage of boiling-point discrimination. Cold injection of the sample, either on-column or by programmed-temperature vaporization, does not present this problem and is therefore preferred. Separation of FAME can be carried out with nonpolar, polar and very polar stationary phases. The polarity influences the retention times, especially those of polyunsaturated FAME. The resolution capability is highest in columns with very polar phases. However, very polar phases have a shorter lifetime

Table 3 Selection of procedures for determination of tetrahydroisoquinolines (TIQ) and tetrahydro- β -carbolines (THBC)

<i>Sample material</i>	<i>Analytes</i>	<i>Work-up procedure</i>	<i>Packing (mesh)/column (m \times mm I.D.)</i>	<i>Limit of detection</i>
Tissue and body fluids	Various TIQs and catecholamines	Al ₂ O ₃ extraction; fluoracylation; GC with electrochemical detection (GC-ECD)	3–5% OV-17, SE-30, SE-54, XE-60 or GE XF-1150 on Gas Chrom Q (80–100) (6 ft \times 2)	0.2–50 pg per sample
Brain	Salsolinol	Liquid–liquid reextraction; fluoracylation; GC-ECD	3% OV-1 on Gas Chrom Q (100–120) (6 or 8 ft \times 2)	10 pg per sample
Urine	TIQs	Liquid–liquid reextraction; trimethylsilyl (TMS) derivatives; GC with mass spectrometry (MS)	3% OV-1 on Gas Chrom Q (100–120) (6 ft \times 2)	
Blood, platelets, plasma and brain	Various THBCs	Liquid–liquid reextraction; heptafluorobutyl (HFB) derivatives; GC-MS	2% SP-2250 (4 ft \times 2) or SE-30 (15 \times 0.3) on Chromosorb W-HP (100–120)	1 pmol per sample
Brain and biological fluids	Salsolinol and others	Al ₂ O ₃ extraction with deuterated standards; fluoracylation; GC-MS	1% OV-17 (2.5 \times 2) or SE-54 (25 \times 0.2)	1 pmol per sample
Biological fluids and foods	THBCs	Liquid–liquid extraction with deuterated standards; fluoracylation; GC-MS	SE 52 W COT (20 \times 0.25)	0.3 pmol mL ⁻¹
Brain	Nor salsolinol	Amberlite extraction; propionyl derivatives; GC-MS	2% SP-2250 on Chromosorb W-HP (100–120) (4 ft \times 2)	1 ng g ⁻¹
Brain and foods	TIQ and <i>N</i> -methyl-TIQ	Liquid–liquid extraction; HFB derivatives; GC-MS	3% OV-17 on Shimalite (80–100) (2 \times 2.5) or OV-1 or OV-101 or DB-17 (25 \times 0.2 mm)	0.25 ng per sample
Brain and foods	Various THBCs	Liquid–liquid extraction; pentafluorobenzyl (PFP) derivatives; GC-MS	SE 52 WCOT (20 \times 0.35 mm)	0.1–0.5 ng per sample
Brain and foods	1-methyl-THBC	Liquid–liquid extraction; TFA derivative; GC-MS with negative CI	OV-1701 (25 \times 0.25)	10 fg per sample
Urine	Various THBCs and TIQs	Combined liquid–liquid and solid-phase extraction; carbomethoxy/propionyl derivatives; GC-MS	OV-1 (12 \times 0.2 mm)	100 pg mL ⁻¹
Urine	1-methyl-THBC	Liquid–liquid extraction; derivatization with (<i>R</i>)-(-)-2-phenylbutyryl chloride (PBC)-enantiomeric composition; GC-NICI-MS	RTX-cross-bonded SE-30 (30 \times 0.25 mm)	
Plasma and urine	Salsolinol and others	Solid-phase extraction over phenylboronic acid (PBA) cartridges; two-step derivatization (TMS-PBC)-enantiomeric composition; GC-MS	BGB-silaren (30 \times 0.32 mm)	100 pg mL ⁻¹
Urine	Salsolinol	Extraction and derivatization in one step by Schotten–Baumann two-phase reaction utilizing pentafluorobenzoyl-chloride	DB-5 (30 \times 0.25)	10 fmol mL ⁻¹
Brain	THBC and 1-methyl-THBC	Liquid–liquid extraction; TFA derivatives; GC-NCI-MS	RTX-cross-bonded SE-30 (30 \times 0.25 mm)	20 pg per sample
Urine	Salsolinol and norsalsinol	Solid-phase extraction (PBA); propionyl derivative; GC-MS	OV-1 (12 \times 0.2 mm)	100 pg per sample

TFA, trifluoroacetyl; CI, chemical ionization; NCI, negative chemical ionization; TMS, trimethylsilyl.

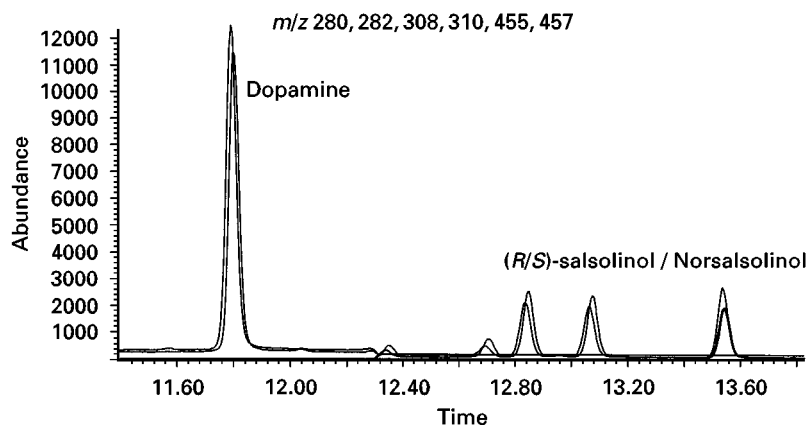


Figure 7 Identification of dopamine, (R)-(+)- and (S)-(–)-salsolinol and norsalsolinol in an authentic urine sample of a chronic alcoholic.

extensively documented. Salsolinol, which might be formed *in vivo* by ring cyclization of dopamine with acetaldehyde, is one of the most discussed tetrahydroisoquinolines. Several studies have been done to improve analytical techniques for identification in human urine, plasma, brain and cerebrospinal fluid samples. Poor assay specificity and possible artefact formation of the alkaloids during work-up and storage have been suggested to be responsible for controversial reports on the detection of these compounds in mammalian tissues and fluids after alcohol intake. The variability of reported levels of Salsolinol might also be a result of variables, including dietary conditions during the experiments or the duration of ethanol ingestion and analytical problems associated with the detectability of the analytes. The presence of TIQ and THBC compounds has been established using (radioenzymatic) TLC methods, high performance liquid chromatography coupled with electrochemical or fluorescence detection, or GC procedures mostly combined with mass spectrometry (Table 3). Recently, it has been considered that the (R)-(+)- and (S)-(–)- enantiomers of salsolinol do not exert identical biological activities. Thus, methods for the determination of the enantiomeric composition of endogenous salsolinol have been developed (Figures 6 and 7). More experimental work is necessary to determine whether alcohol really has an influence on the biosynthesis of salsolinol or other condensation products and if the (S)-(–)-salsolinol enantiomer is a sufficient clinical marker to distinguish between alcoholics and nonalcoholics.

Conclusion

Several chemical abnormalities associated with excessive alcohol consumption are useful in the diag-

nosis of alcoholism. Additionally, in forensic cases information can be helpful to evaluate allegations concerning alcohol intake, especially when determining the types of drinks and estimating the time of drinking. In these problems GC procedures measuring the concentration of ethyl alcohol and congeners or EtG can be helpful. The determination of ketone bodies is a diagnostic tool in a prospective postmortem toxicology analysis in alcoholics for considering a ketoalcoholic death. Further studies are necessary to determine the connection between alcohol abuse and the formation of FAEE and condensation products. Further investigations could lead to important pathophysiological bases of alcohol drinking behaviour and ethanol-induced organ damage and ultimately to better forms of prevention and therapy.

See also: II/Chromatography: Gas: Headspace Gas Chromatography. **Detectors:** Mass Spectrometry. **III/Clinical Diagnosis:** Chromatography. **Forensic Sciences:** Liquid Chromatography.

Further Reading

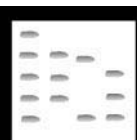
- Bonte W (1987) *Begleitstoffe alkoholischer Getränke*. Lübeck: Schmidt-Römhild.
- Bonte W (1990) Contributions to congener research. *Journal of Traffic Medicine* 18: 5.
- Eder K (1995) Gas chromatographic analysis of fatty acid methyl esters (review). *Journal of Chromatography B* 671: 113.
- Laposata M (1997) Fatty acid ethyl esters: short-term and long-term serum markers of ethanol. *Clinical Chemistry* 43: 1527.
- Machata G (1975) The advantage of automated blood alcohol determination by head space analysis (review). *Zeitschrift für Rechtsmedizin* 75: 229.

- Musshoff F and Daldrop T (1998) Determination of biological markers for alcohol abuse (review). *Journal of Chromatography B* 713: 245.
- Pounder DJ, Stevenson RJ and Taylor KK (1998) Alcoholic ketoacidosis at autopsy. *Journal of Forensic Sciences* 43: 812.
- Ruz J, Fernandez A, De Castro MDL and Valcarcel M (1986) Determination of ethanol in human fluids I. Determination of ethanol in blood, II. Determination of ethanol in urine, breath and saliva (reviews). *Journal of Pharmaceutical and Biomedical Analysis* 4: 545.
- Schmitt G, Aderjan R, Keller T and Wu M (1995) Ethyl glucuronide: an unusual ethanol metabolite in humans. Synthesis, analytical data, and determination in serum and urine. *Journal of Analytical Toxicology* 19: 91.
- Tagliaro F, Lubli G, Ghielmi S, Franchi D and Marigo M (1992) Chromatographic methods for blood alcohol determination (review). *Journal of Chromatography* 580: 161.
- Thomsen JL, Felby S, Theilade P and Nielsen E (1995) Alcoholic ketoacidosis as a cause of death in forensic cases. *Forensic Science International* 75: 163.

ALCOHOLIC BEVERAGES: DISTILLATION

See III/WHISKY: DISTILLATION

ALDEHYDES AND KETONES: GAS CHROMATOGRAPHY



H. Nishikawa, Gifu Prefectural Institute of Health and Environmental Sciences, Gifu, Japan

Copyright © 2000 Academic Press

Introduction

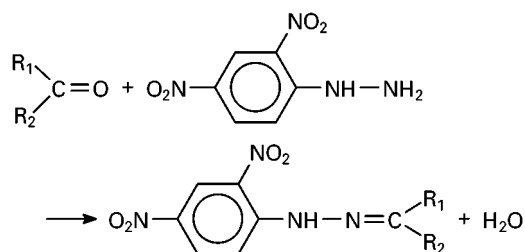
Simple aldehydes, such as formaldehyde, acetaldehyde and acrolein, are known to be hazardous air pollutants. Aldehydes are emitted from incomplete burning of various organic compounds and from various chemicals, and are formed by photochemical reaction with hydrocarbons in the atmosphere.

Volatile ketones are used as solvents in various chemical plants and laboratories and are emitted into the atmosphere. The toxicity of ketones is, in general, not as high as that of aldehydes. Carbonyl compounds are significant in environmental chemistry, i.e. in rainwater and as a photochemical oxidant.

Separation of aldehydes and ketones is very important for the determination of volatile aldehydes. Usually, analysis of aldehydes is performed by derivatization and gas chromatography (GC) or high performance liquid chromatography (HPLC). Selective and sensitive gas chromatographic methods for separation of aldehydes and ketones are described below.

2,4-Dinitrophenylhydrazone Derivatization

2,4-Dinitrophenylhydrazone (DNPH) derivatives of aldehydes and ketones have been used in gas chromatography for many years. The reaction procedure of aldehyde or ketone is as follows:



Kallio *et al.* analysed 15 carbonyl compounds (aldehydes and ketones) known to be flavour components by derivatization/GC with DNPH. The DNPHs of the carbonyl compounds were prepared by shaking 100 µL of each compound with 100 mL of a saturated solution of DNPH in aqueous 2 mol L⁻¹ hydrochloric acid and allowing the mixture to stand at room temperature overnight. The precipitated DNPHs were dissolved in ethyl acetate, then analysed by GC-FID or dissolved in benzene and analysed by GC-ECD (electron-capture detector). Packed columns with silicone stationary phases were used. Relative retention times of DNPHs of aldehydes and ketones on one of these columns are listed in Table 1

Table 1 Relative retention times (*R*) of 2,4-dinitrophenylhydrazones of carbonyl compounds

Carbonyl compound	2% SE-30 column 200–270°C ^a <i>R</i>
Formaldehyde	0.52
Acetaldehyde	0.71
Propenal	0.84
Acetone	0.84
Propanal	0.86
2-Methylpropanal	0.94
2-Butanone	1.00
3-Methylbutanal	1.13
2-Butenal	1.16
Hexanal	1.42
Furfural	1.62
	1.58 ^b
Heptanal	1.63
Octanal	1.83
Benzaldehyde	1.97
Nonanal	2.03

^aPerkin-Elmer F-11 gas chromatograph equipped with a coiled glass column, 6 ft long and 1/8 in i.d.

^bRelative retention times of secondary peaks.

Reproduced with permission from Kallio H *et al.* (1972) Gas-liquid chromatographic analysis of 2,4-dinitrophenylhydrazones of carbonyl compounds. *Journal of Chromatography* 65: 355.

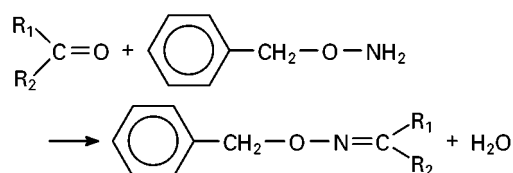
and a typical chromatogram of DNPHs of carbonyl compounds is shown in Figure 1. The peaks of the DNPHs of propanal, propenal and acetone are not separated under these conditions. The sensitivity was of the order of nanograms of carbonyl compounds when FID was used and five-hundred times greater with an ECD.

Saito *et al.* reported an improved GC method with DNPH for the determination of trace low molecular weight aliphatic carbonyl compounds in auto exhaust. They used a glass capillary column, 30 m × 0.27 mm i.d., coated with OV-17 and operated isothermally at 210°C. Aldehydes and ketones in the exhaust were selectively collected by passing 600 ml min⁻¹ of exhaust gas through two impingers which were connected in series and which contained hydrochloric acid saturated with DNPH. The derivatives were extracted twice with chloroform in a separating funnel. After concentration by evaporation under a stream of nitrogen, anthracene was added as internal standard, and 1 µL of the solution was injected into a GC equipped with an FID. Six aliphatic aldehydes and three aliphatic ketones were analysed (Figure 2). The derivatives of C₃ carbonyl compounds, propionaldehyde, acetone and acrolein, were completely separated, and simultaneously determined with formaldehyde and acetaldehyde. The minimum

detectable concentrations of formaldehyde, acetaldehyde and acrolein were 85, 140 and 190 ppb, respectively, for a 10 L gas sample with a relative standard deviation of less than 8%. Using this method, formaldehyde, acetaldehyde, propionaldehyde, isobutyraldehyde, acetone, acrolein, methyl ethyl ketone and methyl isopropyl ketone (or butyraldehyde) were measured in gasoline engine exhaust gas.

Benzylloxime Derivatization

Derivatization of simple aldehydes and ketones to benzylloximes was developed by Magin. The reaction proceeds as follows:



The GC used for the analysis of these derivatives was equipped with a nitrogen-selective detector and

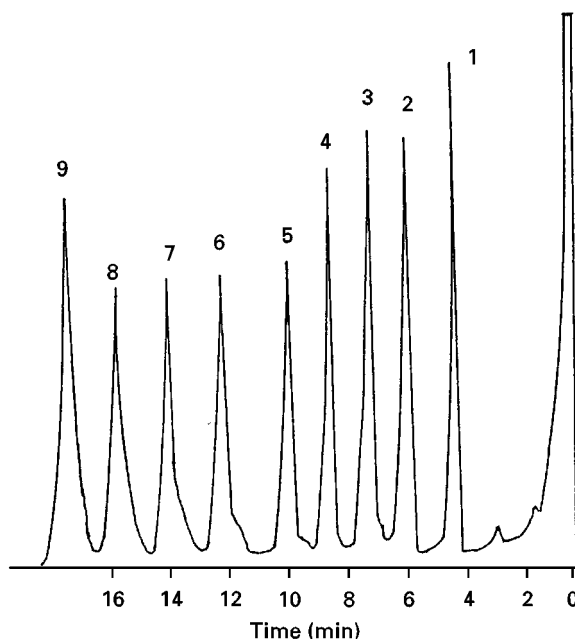


Figure 1 Chromatogram of a mixture of 2,4-dinitrophenylhydrazones of carbonyl compounds on a 2% SE-30 column. 1, Formaldehyde; 2, acetaldehyde; 3, acetone; 4, 2-butanone; 5, 2-butenal; 6, hexanal; 7, heptanal; 8, octanal; 9, nonanal. Programmed temperature analysis from 200 to 270°C (4°C min⁻¹) on a Perkin-Elmer F-11 chromatograph equipped with a hydrogen flame ionization detector. Injected sample: 1.0 µL of ethyl acetate containing about 1000 ng of each of the derivatives. Attenuation 128, range 1. (Reproduced with permission from Kallio H *et al.* (1972). Gas-liquid chromatographic analysis of 2,4-dinitrophenylhydrazones of carbonyl compounds. *Journal of Chromatography* 65: 355.)

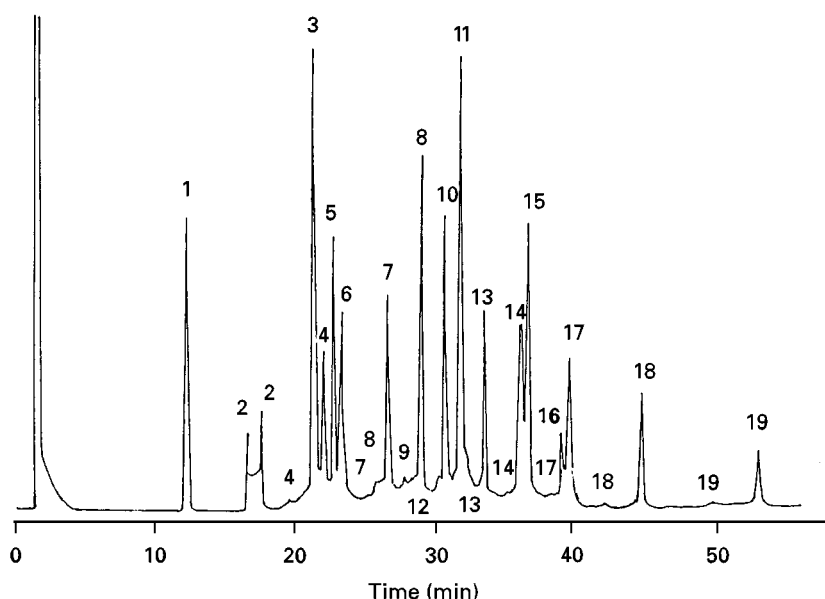


Figure 2 Chromatogram of the 2,4-dinitrophenylhydrazones of carbonyl compounds. 1, Formaldehyde; 2, acetaldehyde; 3, acetone; 4, propionaldehyde; 5, isobutyraldehyde; 6, acrolein; 7, methyl ethyl ketone; 8, butyraldehyde; 9, methyl isopropyl ketone; 10, diethyl ketone; 11, methyl *t*-butyl ketone; 12, isovaleraldehyde; 13, methyl propyl ketone; 14, methyl *s*-butyl ketone; 15, methyl isobutyl ketone; 16, valeraldehyde; 17, crotonaldehyde; 18, methyl butyl ketone; 19, capronaldehyde. (Reproduced with permission from Saito T *et al.* (1983) Determination of trace low molecular weight aliphatic carbonyl compounds in auto exhaust by gas chromatography with a glass capillary column. *Bunseki Kagaku* 32: 33.)

a glass capillary column (12 m \times 0.4 mm i.d.) coated with a 0.4 μ m film of free fatty acid phase (FFAP); helium was used as the carrier gas. The column temperature programme was 100–180°C at 2°C min⁻¹; the temperature was kept at 180°C to the end of the analysis. The retention times of the benzyloximes of a number of aldehydes and ketones (1–7 carbon atoms) are shown in Table 2. The results show almost complete separation under these conditions.

Magin also reported the application of the benzyloxime-GC analysis of aldehydes and ketones to the semi-quantitative analysis of simple monocarbonyls in cigarette smoke. The smoke was passed through a silica gel column to trap the carbonyls, followed by elution with water. About 15 mL of eluted solution was collected in a screw-capped bottle, and the benzyloximes of the carbonyls were prepared. Separation was accomplished by a temperature-programmed 12 m glass capillary FFAP column. An internal standard (hexanal) was added both as a reference for retention time determination, and as an aid in estimating the amounts of the individual carbonyls in the smoke samples. Levels of some carbonyls in the cigarette whole smoke samples are shown in Table 3. One problem with this method was that acetaldehyde, one of the major carbonyl compounds in cigarette smoke, could not be determined since peaks corresponding to the benzyloxime derivative of acet-

aldehyde appeared in the reagent blanks. Mass spectra of these peaks were identical to the spectra of the genuine acetaldehyde derivatives, but the source

Table 2 Adjusted retention times of *O*-benzyloxime derivatives

Aldehydes	Retention time (min)	Ketones	Retention time (min)
Formaldehyde	6.5	Acetone	12.6
Acetaldehyde	9.9	2-Butanone	14.2
Propanal	11.7	2-Pentanone	16.1
Butanal	17.6		
Pentanal	22.5	3-Pentanone	16.8
Hexanal	30.0	4-Heptanone	22.1
Heptanal	36.5		
Octanal	43.5	Cyclopentanone	34.5
		Cyclohexanone	38.4
Isobutanal	13.9	Cycloheptanone	45.0
Isopentanal	20.0		
		3-Methyl-2-butanone	14.4
Propenal	15.9	3-Methyl-2-pentanone	15.4
2-Butenal	27.9		
2-Hexenal	44.0	4-Methyl-2-pentanone	15.2
Methacrolein	17.9	5-Hexen-2-one	25.9
Benzaldehyde	67.7		

Perkin-Elmer Model 3920 gas chromatograph equipped with glass capillary column, 12 m long and 0.4 mm i.d. Reproduced with permission from Magin DF (1979) Preparation and gas chromatographic characterization of benzyloximes and *p*-nitrobenzyloximes of short-chain (C1–C7) carbonyls. *Journal of Chromatography* 178: 219.

Table 3 Levels of selected carbonyls in the whole smoke of some cigarettes

Carbonyl	Cigarette A (filter)	Cigarette B (filter, low delivery)	Cigarette C (non-filter)
Formaldehyde	31 (10–50)	10 (9–10)	21 (12–30)
Acetone	400 (325–475)	137 (130–144)	330 (310–350)
Propanal	61 (37–100)	37 (30–40)	50 (50–53)
Acrolein	23 (13–37)	3 (3–4)	22 (20–25)
Methacrolein	17 (14–38)	18 (18–19)	27 (20–32)
Butanal	20 (9–29)	13 (12–13)	18 (17–20)

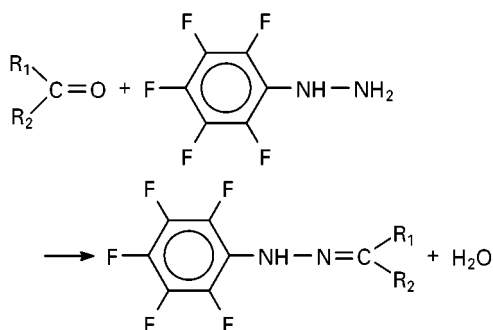
Levels are tabulated as average; values in parentheses indicate the range. The values are given in μg per cigarette.

Reproduced with permission from Magin DF (1980) Gas chromatography of simple monocarbonyls in cigarette whole smoke as the benzyloxime derivatives. *Journal of Chromatography* 202: 255.

in the blanks was unknown. Another problem was the lack of reproducibility from run to run. For this reason, the method was described as semi-quantitative.

Pentafluorophenylhydrazone Derivatization

A sensitive and selective GC analysis of lower aliphatic carbonyl compounds as their pentafluorophenylhydrazones was described by Hoshika and Muto.



The general procedure for the preparation of the pentafluorophenylhydrazone derivatives was as follows: 0.5×10^{-3} mol of lower aliphatic carbonyl compound was added, using a 100 μL microsyringe, to 1 mL methanol containing 1.01×10^{-3} mol pentafluorophenylhydrazine (PFPH). The mixture was allowed to stand overnight at room temperature. A 1 μL volume of the solution was injected into the GC. The acetone, acrolein and propionaldehyde derivatives were separated on a 30 m \times 0.25 mm i.d. glass capillary column coated with polyethylene glycol 20 M at 130°C with an FID. This temperature compares favourably with the 200°C column temperature necessary with DNPH derivatives.

A procedure for the GC determination of low molecular weight carbonyl compounds in aqueous

solution as their pentafluorophenylhydrazones and its application to such compounds produced by photolysis of α -amino acids were reported by Kobayashi *et al.* (Figure 3). The calibration graphs for formaldehyde, acetaldehyde and isobutyraldehyde showed good linearity in the range 10–40 μg . Solutions of DL-alanine, DL-valine, DL-leucine or DL-isoleucine in phosphate buffer containing mercury (II) chloride were irradiated in a quartz vessel with a 20 W blacklight lamp (300–400 nm) as a light source for 300 h and the mixtures were measured by this method. Two peaks corresponding to formaldehyde and acetaldehyde were observed for valine.

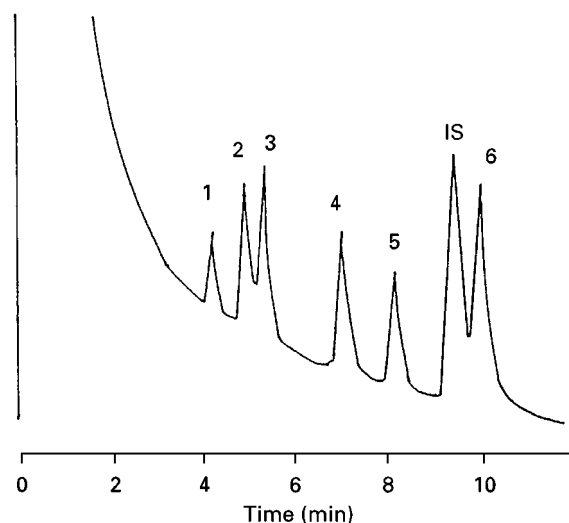
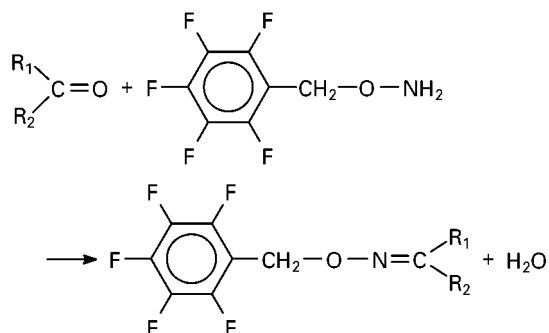


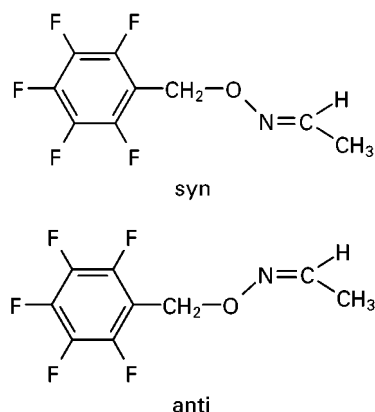
Figure 3 Chromatogram of some carbonyl compounds as their pentafluorophenylhydrazones. Conditions: 3% XE-60, 2.0 m glass column, temperature-programmed from 105 to 130°C at 2°C min⁻¹, FID. 1, Formaldehyde; 2, acetaldehyde; 3, acetone; 4, isobutyraldehyde; 5, diethyl ketone; IS, *p*-xylylene dichloride; 6, methyl isobutyl ketone. (Reproduced with permission from Kobayashi K *et al.* (1979) Gas chromatographic determination of low-molecular-weight carbonyl compounds in aqueous solution as their pentafluorophenylhydrazones. *Journal of Chromatography* 176:118.)

Pentafluorobenzoyloxime Derivatization

Pentafluorobenzoyloxime (PFBOA) was synthesized by Nambara *et al.* as a new derivatizing agent for GC of ketones using electron-capture detection. Kobayashi *et al.* reported a GC analysis of low molecular weight carbonyl compounds in aqueous solution as their *O*-pentafluorobenzoyloximes. The reaction procedure of aldehyde or ketone is as follows:



The retention times of 13 *O*-pentafluorobenzoyloxime (*O*-PFBO) derivatives of carbonyl compounds relative to the internal standard obtained on XE-60 and other columns are shown in Table 4. When some carbonyl compounds react with PFBOA, two peaks are obtained, corresponding to *syn*- and *anti*-isomers formed by the condensation reaction with PFBOA:



Good linearity of response was obtained for formaldehyde, acetaldehyde, isobutyraldehyde and diethyl ketone in the range 1–50 μg in 0.5 mL of aqueous solution. The utility of PFBOA was compared with that of PFPH. The formation of the *O*-PFBO derivatives of aldehydes was easily achieved with a much lower concentration of PFBOA than that required for PFPH. The derivatization of aldehydes with PFBOA is complete in 20 min at room temperature, but the reaction with ketones proceeds slowly (within 24 h). The PFBO derivatives are much more volatile than the corresponding pentafluorophenylhydrazones and therefore the separation can be carried out at lower temperatures (70–100°C). It was shown that the PFBO derivatives are stable in ethyl acetate at room temperature for several days.

Table 4 Relative retention times of the *O*-pentafluorobenzoyloximes of carbonyl compounds

Parent compound	Stationary phase and column temperature (each column: 2 m \times 3 mm i.d.)			
	3%XE-60 (90°C)	3%XF-1105 (100°C)	3%SE-30 (80°C)	2%OV-17 (70°C)
PFBOA	0.62	0.69	0.88	0.65
HCHO	0.19	0.27	0.29	0.19
CH ₃ CHO	0.32, 0.34 ^a	0.48, 0.51 ^a	0.57, 0.59 ^a	0.43
C ₂ H ₅ CHO	0.47, 0.51 ^a	0.80	1.05	0.72
<i>n</i> -C ₃ H ₇ CHO	0.80	1.41	1.83, 1.92 ^a	1.30, 1.38 ^a
iso-C ₃ H ₇ CHO	0.57	1.01	1.32	0.88
<i>n</i> -C ₄ H ₉ CHO	2.72	1.91, 1.99 ^a	2.55, 2.72 ^a	1.76, 1.94 ^a
CH ₃ COCH ₃	0.40	0.70	0.88	0.65
CH ₃ COC ₂ H ₅	0.61	1.13	1.50	1.04
CH ₃ CO-iso-C ₃ H ₇	0.73	1.48	2.08	1.24, 1.43 ^a
CH ₃ CO-iso-C ₄ H ₉	1.16	2.36	3.38	2.08
C ₂ H ₅ COC ₂ H ₅	0.85	1.74	2.43	1.61
C ₂ H ₅ CO- <i>n</i> -C ₃ H ₇	1.27	2.70	3.95	2.61
CH ₂ ClC ₆ H ₄ CH ₂ Cl ^b	1.00	1.00	1.00	1.00

^aDouble peaks.

^bInternal standard (α, α' -dichloro-*p*-xylene). PFBOA, Pentafluorobenzoyloxime. Shimadzu Model GC-4APF gas chromatograph equipped with an FID.

Reproduced with permission from Kobayashi K *et al.* (1980) Gas chromatographic determination of low-molecular-weight carbonyl compounds in aqueous solution as their *O*-(2,3,4,5,6-pentafluorobenzyl) oximes. *Journal of Chromatography* 187: 413.

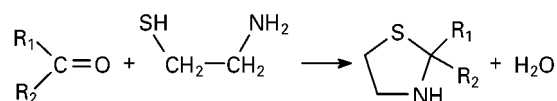
Aldehydes in air are important as pollutants and photochemical products because they are irritants to the skin, eyes and nasopharyngeal membranes. Trace amounts of formaldehyde in air was determined as the PFBO derivative using GC-ECD by Nishikawa *et al.* Sub-ppb levels of formaldehyde in air could be determined in this way. Although the FID or ECD can be used with PFBO derivatives, the FID has poor sensitivity and in some cases the peaks of the derivatives suffer interference from co-existing materials with both detectors. In the case of analysis of samples with a complex matrix such as exhaust gas or emission gas, the thermionic detector (TID) is more effective. The TID is very sensitive and selective to nitrogen compounds such as oximes and can therefore be used with advantage for the analysis of aldehydes as PFBOA derivatives in automobile exhaust and emission gas. Gas (2–30 L) was collected by bubbling the exhaust through two impingers connected in series. Each impinger contained 10 mL of the absorption solution (300 mg L⁻¹ PFBOA·HCl in ethanol). The sample gas was drawn at a rate of 0.5 L min⁻¹. After sampling, the absorbed solution was made up to 20 mL with ethanol and was allowed to stand for 80 min at room temperature. A 10 mL portion of the solution and 20 mL of distilled water were mixed well and the mixture was passed through a Sep-Pak C₁₈ cartridge. The cartridge was eluted with 1.5 mL hexane and the eluate was analysed with an SE-52 fused silica column (25 m × 0.25 mm i.d.) at 130°C with an FTD. The relative retention times for aldehyde and ketone derivatives are shown in Table 5. Except for formaldehyde, acetone and di-

ethyl ketone, each derivative has syn- and anti-isomers and the double peaks appear for the isomers. The peaks of the formaldehyde, acetaldehyde, propionaldehyde and butyraldehyde derivatives were completely separated from those of the ketones. Although the first peak of propionaldehyde was not separated from the first peak of acrolein, the second peak of propionaldehyde was separated from the second peak of acrolein. Therefore, it can be judged whether the first peak of propionaldehyde contained the peak of acrolein or not. The calibration graphs obtained show good linearity over the range 0–5 µg for formaldehyde, 0–4 µg for acetaldehyde, 0–15 µg for propionaldehyde and 0–13 µg for butyraldehyde in 1 mL of the absorption solution. The determination limits ranged from 14 ppb (v/v) for formaldehyde to 67 ppb for propionaldehyde when a 30 L gas sample was used.

This method is very selective, without interference from ketones, and is well-suited to analyse simple aldehydes in various exhaust gas samples. The PFBO method was applied to analysis of carbonyl compounds in clothes, river water, seawater, tap water, indoor air samples and environmental air samples.

Thiazolidine Derivatization

Hayashi *et al.* developed a method to determine formaldehyde and methyl glyoxal in foods and beverages. This method is known as the cysteamine method. Volatile aliphatic aldehydes and ketones react with 2-aminoethanethiol (cysteamine) to form thiazolidine compound as follows:



Only one derivative is formed from each aldehyde or ketone; the reaction proceeds rapidly under mild conditions and the derivatives can be readily separated on a capillary column. The derivatives can be detected selectively with a nitrogen–phosphorus detector (NPD). Carbonyl compounds in the headspace gases above heated pork fat were analysed as thiazolidine derivatives by Yasuhara and Shibamoto (Figure 4). A GC with a 30 m × 0.25 mm i.d. DB-Wax fused silica capillary column and an NPD was used for the qualitative and quantitative analysis of the carbonyl compounds in the samples. The column temperature was held at 50°C for 2 min and then programmed to 190°C at 3°C min⁻¹. Nine aldehydes and four ketones were analysed as thiazolidine derivatives in traps containing aqueous cysteamine or

Table 5 Relative retention times of *O*-pentafluorobenzoyloxime derivatives

Parent compound	Relative retention time
Formaldehyde	1.00
Acetaldehyde	1.30, 1.34 ^a
Propionaldehyde	1.75, 1.79 ^a
Butyraldehyde	2.52, 2.58 ^a
Acrolein	1.76, 1.88 ^a
Crotonaldehyde	— ^b
Acetone	1.63
Methyl ethyl ketone	2.20, 2.24 ^a
Methyl isopropyl ketone	2.69, 2.75 ^a
Diethyl ketone	3.00
Methyl propyl ketone	3.03, 3.14 ^a

GC conditions: SE-52 capillary column (25 m × 0.25 mm i.d.), temperature 130°C.

^aDouble peaks; ^bno peaks appeared.

Reproduced with permission from Nishikawa H *et al.* (1987) Determination of aldehydes in exhaust gas and thermal degradation emission using volatile derivatization and capillary GC with flame thermionic detector. *Bunseki Kagaku* 36: 381.

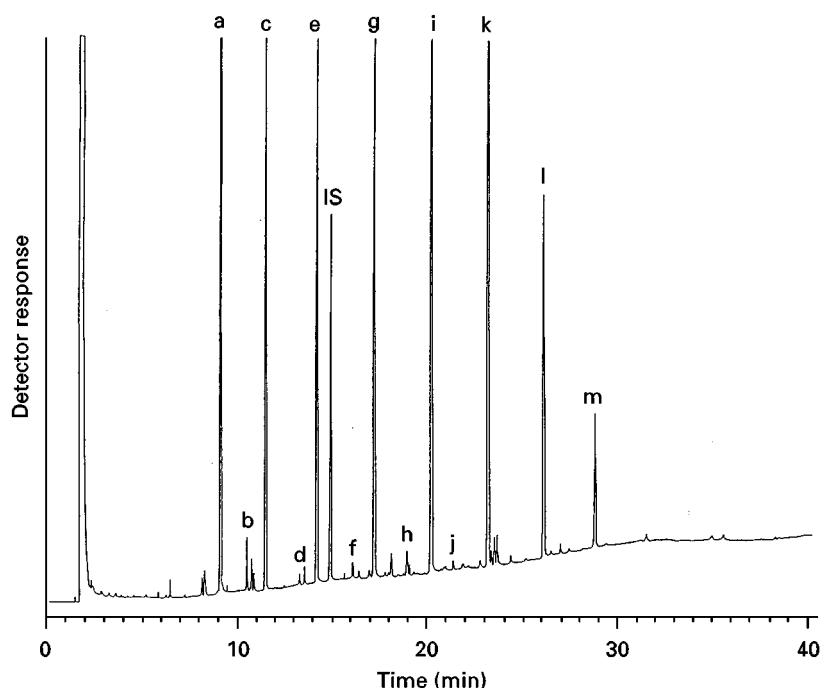


Figure 4 Chromatogram of the thiazolidine derivatives of carbonyl compounds produced from heated pork fat. a, Acetaldehyde; b, formaldehyde; c, propionaldehyde; d, 2-pentanone; e, butyraldehyde; f, 2-hexanone; g, valeraldehyde; h, 2-heptanone; i, hexylaldehyde; j, 2-octanone; k, heptaldehyde; l, octaldehyde; m, nonylaldehyde; IS, N-methyl acetamide. (Reproduced with permission from Yasuhara A (1991) Analysis of lower aldehydes in air. *Journal of Environmental Analytical Chemistry* 1: 253.)

aqueous sodium bisulfite. The major compounds produced from the samples were pentanal, hexanal and heptanal. Generally, aqueous cysteamine was more efficient at trapping carbonyl compounds than was aqueous sodium bisulfite but formaldehyde and acetaldehyde were trapped better by sodium bisulfite. Acrolein and malonaldehyde were analysed as 1-methyl-2-pyrazoline and 1-methyl-pyrazole, respectively, from the trap containing methylhydrazine. Good separation of volatile aldehydes and ketones was obtained by this method.

The cysteamine derivatization method has been applied to the determination of trace amounts of carbonyl compounds in automobile exhaust, air samples, the headspace of heated food oils, foods and beverages.

Conclusion

The DNPH-GC and PFBO-GC methods are now widely used for the derivatization and gas chromatographic analysis of aldehydes and ketones. The PFBO-GC and cysteamine-GC methods will become more common. These reactions proceed under mild conditions and the derivatives are well separated with a capillary column at comparatively

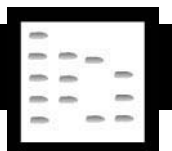
low temperatures. The GC-MS measurement of these derivatives will be utilized for analysis of trace amounts of aldehydes and ketones in a variety of samples.

See also: II/Chromatography: Gas: Derivatization; Detectors: Selective.

Further Reading

- Afgran BK, Chau ASY (1989) *Analysis of Trace Organics in the Aquatic Environment*. Florida: CRC Press.
- Kallio H, Linko RR and Kaitaranta J (1972) Gas-liquid chromatographic analysis of 2,4-dinitrophenylhydrazones of carbonyl compounds. *Journal of Chromatography* 65: 355.
- Katz M (ed.) (1977) *Methods of Air Sampling and Analysis*. Washington, DC: American Public Health Association.
- Izard C and Libermann C (1978) Acrolein. *Mutation Research* 47: 115.
- Nishikawa H and Sakai T (1995) Derivatization and chromatographic determination of aldehydes in gaseous and air samples. *Journal of Chromatography A* 710: 159.
- Yasuhara A (1991) Analysis of lower aldehydes in air. *Journal of Environmental Chemistry* 1: 253.

ALKALOIDS



Gas Chromatography

M. Muzquiz, SGIT-INIA, Madrid, Spain

Copyright © 2000 Academic Press

Introduction

Alkaloids are an important class of compounds that have pharmacological effects on the human body. These compounds can be found in natural products such as plants, and the type and amount of these alkaloids varies greatly, depending on the portion of plant analysed and the stage of maturation. Although alkaloids have traditionally been isolated from plants, an increasing number are to be found in animals, insects, marine invertebrates and microorganisms.

There is no clear definition of what constitutes an alkaloid, but these compounds do share the following characteristics: they are basic components that contain nitrogen; they are mostly complex components, derived biosynthetically from various amino acids; and they show pronounced pharmacological effects on various tissues and organs of humans and other animal species.

Pelletier defines an alkaloid as 'a cyclic compound containing nitrogen in a negative oxidation state which is of limited distribution in living organisms'. This definition includes both alkaloids with nitrogen as part of a heterocyclic system as well as the many exceptions with extracyclic bound nitrogen (**Figure 1**).

Although a wealth of information is available on the pharmacological effects of these compounds, little is known about how plants synthesize these substances or about how this synthesis is regulated. Alkaloids belong to the broad category of secondary metabolites. This class of molecule has historically been defined as a naturally occurring substance that is not vital to the organism that produces them. Alkaloids have traditionally been of interest only due to their pronounced and various physiological activities in animals and humans. A picture has now begun to emerge that alkaloids do have important ecochemical functions in the defence of the plant against pathogenic organisms and herbivores and are found to play an important role in plant interactions with animals and higher and lower plants. Alkaloids are now generally considered to be part of an elaborate system of

chemical defence in plants; indeed, the same seems to be true in vertebrates, invertebrates and microorganisms. Alkaloids have now been isolated from such diverse organisms as animals, insects, marine organisms, microorganisms and lower plants, although it is not yet clear whether *de novo* alkaloid biosynthesis occurs in each organism.

In the past ten years there has been an increasing interest in the isolation and determination of alkaloids in plant materials, in pharmaceutical products, and in other samples of biological interest. In addition, numerous alkaloids have been synthesized and chemically characterized. The active agents of around 13 000 plant species are known to have been used as drugs throughout the world. Some are used as pure compounds for therapeutic purposes (such as the narcotic and analgesic, morphine; the analgesic and antitussive, codeine; and the chemotherapeutic agents, vincristine and vinblastine) or as teas and extracts. Plant constituents have also served as models for modern synthetic drugs, such as atropine for tropicamide, quinine for chloroquine, and cocaine for procaine and tetracaine. Alkaloids can also be found in the stimulants caffeine in coffee and tea and nicotine in cigarettes. Currently, much work is being done to discover new alkaloid molecules for different applications such as new antiviral and tumour treatments.

However, many alkaloids are toxic substances and it is important to evaluate these. The vegetables Solanaceae, which contain steroidal glycoalkaloids, and Leguminosae, which contain quinolizidine alkaloids, are the principal food crops that contain alkaloids. Grain legumes are extremely important owing to their significance in human and animal nutrition. They also conserve the soil and fix nitrogen, and are used as sources of timber, fuel oils, etc. Plants of the Leguminosae rank second in economic importance only to those of the Gramineae, and the demand for legumes is likely to escalate as humans begin to utilize more marginal agricultural lands to provide food for the increased population. The largest legume subfamily is the Papilionaceae, which embraces approximately 440 genera and 12 000 species in 32 tribes, as recently reclassified by Polhill. Over 450 alkaloids have been reported to occur in plants of the Leguminosae, with the majority of such compounds occurring in papilionaceous species. Quinolizidine alkaloids (QA), contained in lupins, are the largest single group of legume alkaloids. Since lupin seeds contain

up to 50% protein and up to 20% lipids, they are of interest in terms of animal and human nutrition. *Lupinus luteus*, *L. albus* and *L. angustifolius* have

been consumed for centuries in European countries, while *L. mutabilis* (tarwi) is an important component of the South American diet.

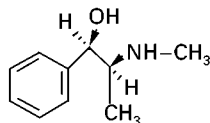
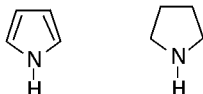
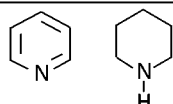
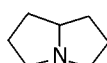
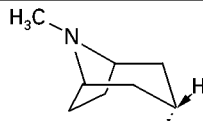
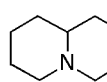
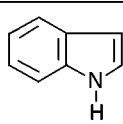
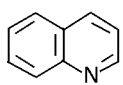
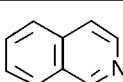
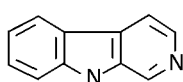
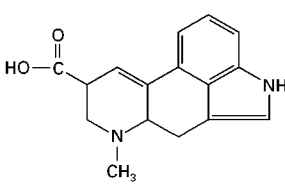
Alkaloids with a nonheterocyclic N			Ephedrine		
Alkaloids with a heterocyclic N	Mononitro-heterocycles	Simple heterocycle	Pyrrole		
			Pyridine Pyrrolidine		
		Complex heterocycle	Heterocycle sharing N	Pyrrolizidine Piperidine	
				Tropane	
				Pyridicoline	
			Heterocycle with N condensed with an aromatic ring	Indole	
				Quinoline	
				Isoquinoline	
			Two condensed heterocycles	Carbonylic (indole + pyridine)	
				Lysergic (indole + quinoline)	

Figure 1 Chemistry classification of alkaloids.

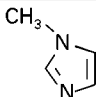
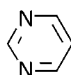
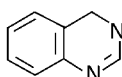
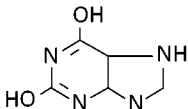
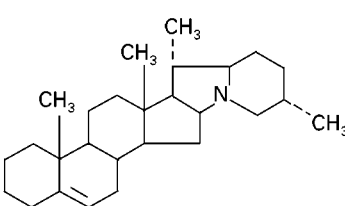
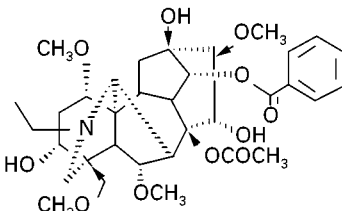
Alkaloids with a heterocyclic N	Dinitro-heterocycle	Simple heterocycle	Imidazole	
			Pyrimidine	
		Complex heterocycle	Quinazoline	
			Xantic bases	
	Alkaloids with special structure	Steroid		
		Diterpenoid		

Figure 1 Continued

This article aims to provide an overview of various aspects of separation of alkaloids by gas chromatography (GC). Although a number of phytochemical methods have been developed for the qualitative and quantitative determination of alkaloids, one of the most popular methods for the evaluation of complex alkaloid mixtures is capillary gas-liquid chromatography combined with mass spectrometry (MS). Depending on the task high performance liquid chromatography (HPLC), thin-layer chromatography (TLC), colorimetry, NMR, radioimmunoassay, capillary electrophoresis and enzyme-linked immunosorbent assay (ELISA) are additional helpful analytical techniques.

GC-MS Method for Analysis of Alkaloids

Capillary gas chromatography (CGC) analysis has been described for several classes of alkaloids. A ma-

jor advantage of GC over other methods is its enhanced sensitivity and high resolution. Another advantage is its easy coupling to a mass spectrometer, which allows the identification of new and minor compounds of a mixture without laborious isolation procedures. This makes it a particularly attractive method for thermally stable mixtures. The analysis of pyrrolizidine alkaloids, tropane alkaloids, steroidal alkaloids, quinazoline alkaloids, quinolizidine alkaloids, diterpenoid alkaloids and lycopodium alkaloids has been described by a number of authors.

Capillary gas chromatography was the method of choice and was officially accepted at the 6th International Lupin Conference in Chile (1990) as a method of determination of quinolizidine alkaloids in lupins. As an example, we will describe the methodology for the analysis of these compounds.

Sample Preparation for Chemical Analysis of Alkaloids

Successful chemical analysis of alkaloids depends on the sampling method and pretreatment of the sample. It is therefore important to know the chemistry of the compounds to be analysed. As described by Roberts and Wink, a basic character is no longer a prerequisite for an alkaloid and the chemistry of the nitrogen atom allows for at least four groups of nitrogenous compounds:

1. Secondary and tertiary amines, which are more or less protonated and therefore hydrophilic at $\text{pH} < 7.0$, or the more general case where they are lipophilic and unprotonated at $\text{pH} > 8.0$. This is the classical alkaloid type.
2. Quaternary amino compounds, which are very polar, charged at all pH values, and have to be isolated as salts, e.g. berberine and sanguinarine.
3. Neutral amino compounds, which include the amide-type alkaloids such as colchicine, capsaicin, and most lactams, e.g. ricinine.
4. *N*-oxides, which are generally highly water soluble, are frequently found in many alkaloid classes. The pyrrolizidine group of alkaloids is rich in this particular alkaloid type.

A conventional alkaloid extraction process involves successive removal of nonalkaloids and alkaloids by organic solvents from acidified and basified aqueous solutions of an ethanol extract. The extraction of alkaloids is generally based on the fact that they normally occur in the plant as salts and on their basicity, in other words on the differential solubility of the bases and salts in water and organic solvents (Figure 2).

The techniques used for sample preparation are liquid-liquid extraction, solid-phase extraction and, more recently, supercritical fluid extraction.

Liquid-liquid solvent extraction This technique is the most commonly used method for sample treatment and is based on the observation that alkaloids can usually be removed from the sample by extracting them into a water-immiscible solvent. The method relies on the relative solubility of alkaloids in the extracting solvent and the sample matrix.

Although such techniques are usually satisfactory, difficulties can be found when they are applied to chromatography where the limits of quantification are often in the ppb range. This is principally caused by the solvents being nonselective and therefore tending to extract endogenous material from the matrix, which results in spurious peaks in the chromatogram.

An example of quinolizidine alkaloid liquid-liquid extraction is provided in Figure 3.

Solid-phase extraction for sample preparation

Sample clean-up is required when impurities in the sample matrix interfere with analyte measurement. The interest in this technique led to the commercial introduction of small disposable cartridges packed with relatively large particles of various bonded silicas. The particle size allows the use of minimum pressure to force the sample and wash solutions through the column. Indeed, it is common practice to suck the solution through the packings rather than to use pressure.

There are many advantages of solid-phase extraction including: (1) the possible use of large sample sizes in pretreatment; (2) the technique is quick and automated; (3) the low consumption of solvents used; (4) the use of selective sorbents and solvents; (5) the possible achievement of a high pre-concentration of the component of interest, enabling high sensitivities to be obtained; (6) there is good reproducibility in GC; and (7) the technique is inexpensive.

In developing assays using solid-phase extraction, it is necessary to take into account several factors when deciding on the choice of sorbent to be used in a particular assay for alkaloid analysis.

The most important consideration of the technique is that the compounds of interest must be capable of being readily absorbed from the matrix. In some cases, pretreatment of the sample is necessary, especially in cases of protein binding. This can usually be solved by the addition of perchloric or trichloroacetic acid to denature the proteins. In addition, it may be necessary to adjust the pH of the sample to ensure that the compound is in the correct ionic form to achieve efficient retention by the packing. Proteins can also be removed by the addition of organic solvents such as acetonitrile or methanol.

After removing the majority of the interfering substances, the final step of the technique is efficient elution from the bonded silica. This step must ensure that the compounds of interest are desorbed in the least volume of eluent, since it is usual to evaporate the solution to dryness and reconstitute the residue in a small volume prior to chromatographic analysis. The evaporation step generally precludes the use of inorganic salts in the final wash solution, with the exception of those compounds that are readily volatile.

Quinolizidine alkaloid solid-phase extraction is illustrated in Figure 4.

Analytical supercritical fluid extraction At present, and in view of increasing environmental concerns of

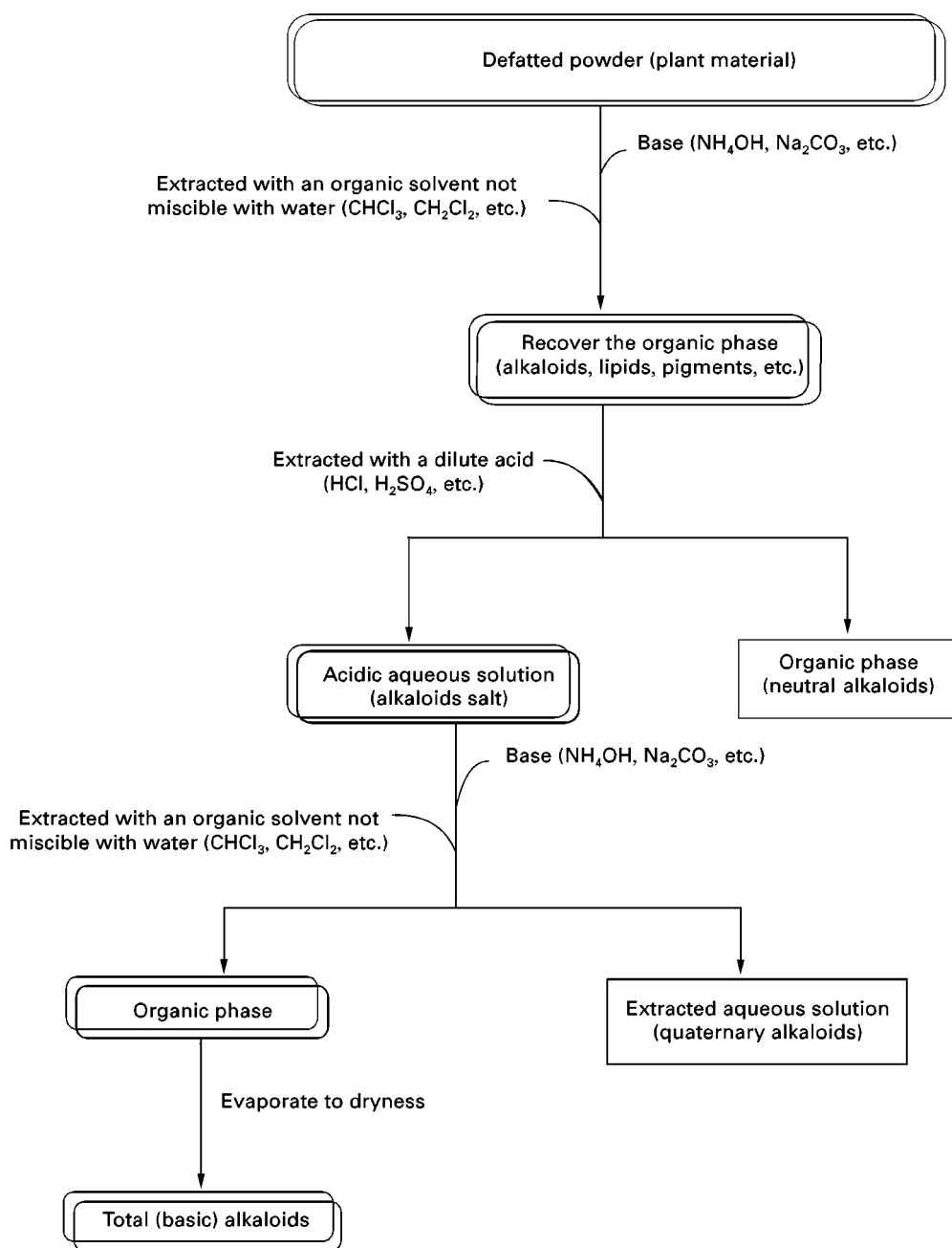


Figure 2 Extraction of alkaloids.

the use of liquid solvents in the extraction of natural products, there has been growing interest in alternative and reliable sample extraction techniques using supercritical fluids. Supercritical fluids have been widely used for the extraction of alkaloids on both analytical and industrial scales and for many years for the selective extraction of selected compounds from bulk samples. The extraction of caffeine from coffee is a well-known process performed on an industrial scale. The aim here is to remove a specific component

(i.e. caffeine) from large quantities of the bulk matrix in order to increase its commercial value.

Analytical-scale supercritical fluid extraction (SFE) is concerned more with extraction of analytes of interest from a bulk matrix as a sample preparation step prior to characterization by other analytical methods such as GC. It is therefore potentially very useful for the extraction of natural products prior to structural characterization. SFE is gaining acceptance as an alternative to Soxhlet extraction. Much of the

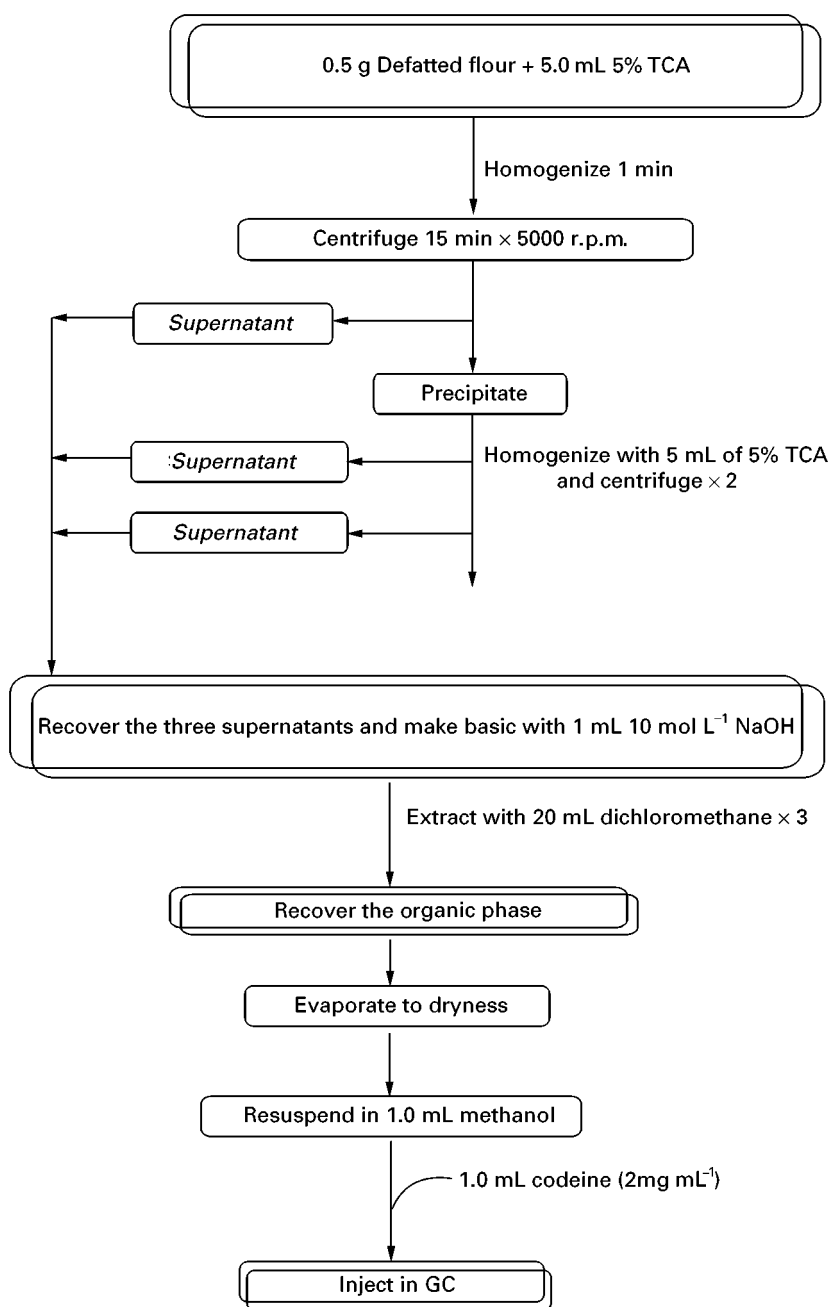


Figure 3 Extraction of quinolizidine alkaloids (Muzquiz *et al.* 1994).

current interest in using analytical-scale SFE stems from the need to replace conventional liquid extraction methods with sample preparation methods that are more efficient, easier to automate, faster and safer to use. Many of the properties of supercritical fluids such as carbon dioxide have facilitated advances in these areas. Thermally labile compounds can be extracted at low temperatures and greatly reduced extraction times. Extracts can also be analysed online by coupling the SFE directly with a gas chromatograph (SFE-GC).

Determination of Alkaloids by Gas-Liquid Chromatography-Mass Spectrometry

Methods for the unequivocal identification and quantification of alkaloids in various, often complex, matrices are of great interest. For this purpose chromatography is widely used. Originally thin-layer chromatography (TLC) was the major method applied for both qualitative and quantitative analysis of alkaloids. Although TLC is still a major tool in alkaloid analysis, in recent years high performance liquid

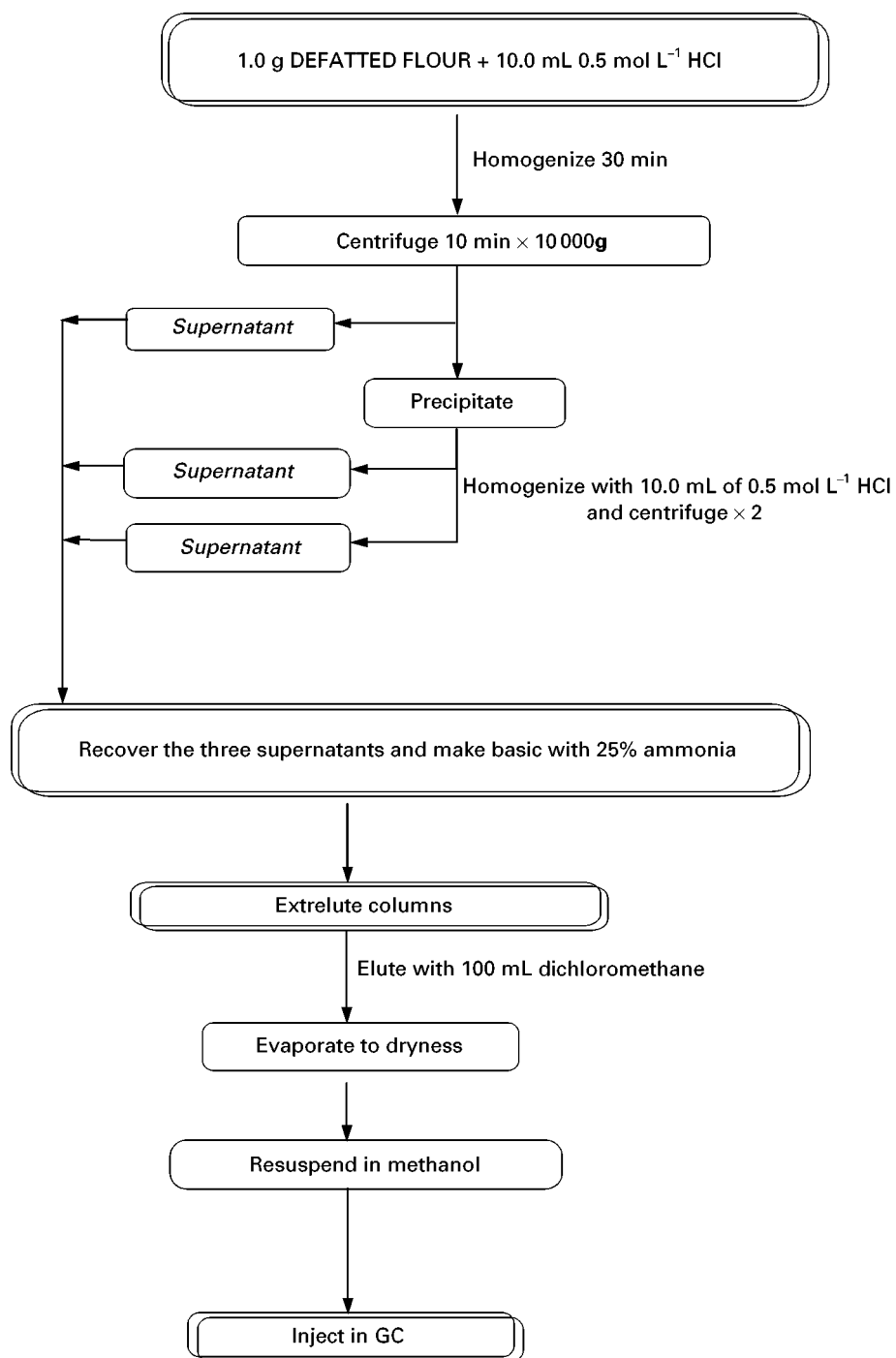


Figure 4 Extraction of quinolizidine alkaloids (Wink *et al.* 1995).

chromatography (HPLC) has also developed as an important method for the quantitation of alkaloids. However, more and more applications of capillary (CGC) for complex alkaloids have been reported recently.

Combined gas chromatography-mass spectrometry (GC-MS) has been increasingly used over the

last decade for the convenient analysis of alkaloids. This sensitive technique is applicable to the qualitative analysis of individual components of crude alkaloid fractions and is normally able to resolve alkaloid diastereoisomeric pairs. GC-MS is particularly suitable for work of a chemotaxonomic nature, since in such studies it is desirable to identify all the alkaloids

that may have accumulated at a specific time and site in a specific part of a species, rather than only the most abundant compounds present. Also, the use of GC-MS may enable the experimenter to rule out the presence of a particular alkaloid group in the plant material being examined. Impressive separations of alkaloids have been obtained using the high column efficiencies achieved in CGC.

Until 1980 most GLC applications for separating alkaloid mixtures involved packed columns. However, better results can be obtained using the new generation of fused silica capillary columns with bonded phases. The advantage of using small internal diameter columns is not only the higher plate number per unit length, but also the improved lower level of detection due to reduced band broadening. Much more important than efficiency however, is the selectivity that can be introduced into the chromatographic system. The reason for this is that even the best capillary column still has a limited peak capacity (maximum 1000), which is certainly insufficient for unravelling the complex profiles that have to be dealt with in natural product research.

Some GC systems used for the analysis of alkaloids are indicated in Table 1. The column selectivity can be adapted to the specific problem by selecting the most suitable stationary phase. Stationary phase selection, however, has no influence on the peak capacity. In addition to universal inlets such a split, splitless, cool on-column and temperature-programmed vaporization, a number of selective inlets are available in CGC.

In the case of QA the capillary columns used (dimensions 15 m \times 0.23 mm to 30 m \times 0.32 mm) have a high number of theoretical plates ($> 70\,000$), which allow the separation of complex mixtures and even of enantiomers, epimeric at C11 or C6, such as sparteine and α -isosparteine, lupanine and α -

isolupanine, 13-hydroxylupanine and 23-epihydroxylupanine, anagyrine and thermopsine, 13 α -tigloyloxylupanine and 13 β -tigloyloxylupanine, and of *cis* and *trans* isomers, such as 13 α -angeloyloxylupanine and 13 α -tigloyloxylupanine, as well as the *trans*- and *cis*-cinnamic acid esters.

As a liquid phase several silicone derivatives (0.1 μ m or 1 μ m films) are employed; good resolutions have been obtained using DB-1 or DB-5 columns, but equivalent products of other manufacturers also work. Split injection techniques are usually appropriate. On-column injection does not provide significant advantages for most applications.

Helium is routinely used as carrier gas, but hydrogen or nitrogen will also work. The injector temperature is usually set at 250°C, that of the detectors at 300°C. Furthermore, even nanogram amounts of alkaloids can be detected by the FID (flame ionization detector) or more sensitively and specifically by a nitrogen-specific detector (NPD).

Hydroxylated QA, such as 13-hydroxylupanine or 3-hydroxylupanine, may be derivatized by trimethylsilyl prior to injection to avoid tailing and to achieve better quantification. Care should be taken not to use the NPD for these derivatives, since the detector would soon be destroyed.

Some authors give relative retention indices for QA. However, Kováts retention indices (RI) give better comparative information and are helpful in identifying individual alkaloids in a GC profile.

Additionally, since this method can be combined with mass spectrometry (GC-MS) it is easy to identify the individual compounds present. Among the spectroscopic methods, mass spectroscopy is definitely the most powerful technique and should therefore take an important place in any laboratory. The problems of interfacing both techniques have been completely

Table 1 Some GC systems used for the analysis of alkaloids

Alkaloid	Column type, length (m) \times i.d. (mm)	GC conditions			Carrier gas
		Injector	Temperature program (°C)	Detector	
Pyrrolizidine	WCOT DB-1 25 m \times 0.25 mm	250°C	120–290 (8°C min ⁻¹)	FID, NPD	He
Quinolizidine	SPB-1 30 m \times 0.25 mm	240°C	150–235 (5°C min ⁻¹)	FID, NPD	He
Tropane	DB-1 15 m \times 0.25 mm	250°C	150–270 (6°C min ⁻¹)	FID, NPD	He
Morphinan	DB-5 15 m \times 0.25 mm	280°C	180–270 (30°C min ⁻¹)–320° (40°C min ⁻¹)	MSD	He
Aconitum	DB-5 15 m \times 0.25 mm	320°C	250–320 (16°C min ⁻¹)	MSD	He
Amaryllidaceae	DB-1 15 m \times 0.25 mm	260°C	200–250 (4°C min ⁻¹)	FID, NPD	He
Solanum	RT _x -1 15 m \times 0.53 mm	270°C	210–260 (1°C min ⁻¹)	FID	He
Ephedra	HP-5 25 m \times 0.20 mm	220°C	90–124 (3°C min ⁻¹)–280 (20°C min ⁻¹)	NPD	He

WCOT, Wall coated open tubular column.

overcome by direct coupling (no interface) or the use of an open split interface. Low and high resolution mass spectrometers are the most universal detection devices for CGC. They are capable of electron impact

or chemical ionization and can be operated in the full scan mode for identification of unknowns or in the ion-monitoring mode for quantification of target compounds.

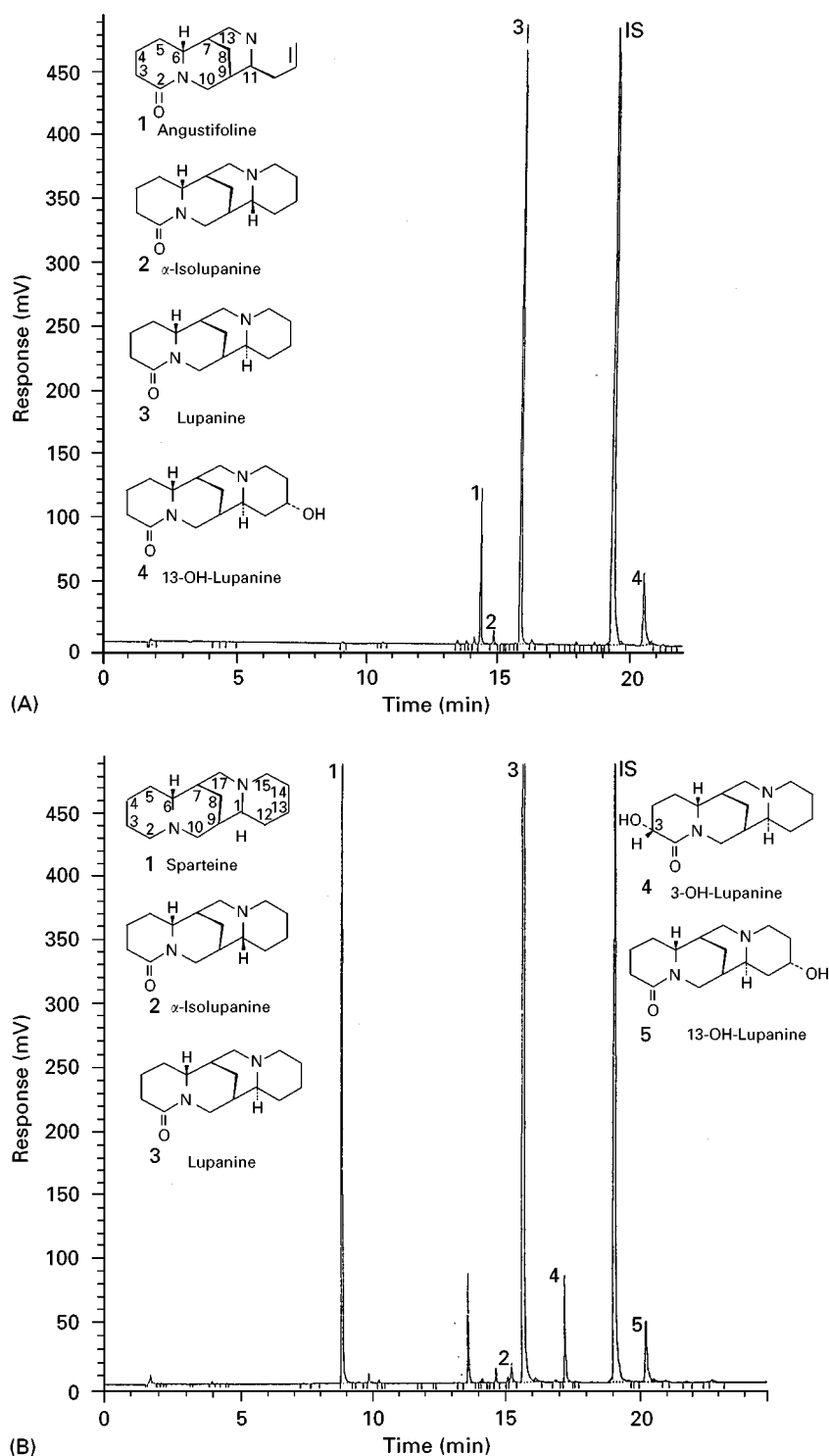


Figure 5 Separation of an alkaloid extract from *L. angustifolius* (A) and *L. mutabilis* (B) bitter seeds by capillary GC. Injector, 240°C; detector 300°C; oven 150–235°C, 5°C min⁻¹; carrier gas, helium; detection of alkaloids by nitrogen-specific detector (NPD) and mass-selective detector.

Mass spectrometry is widely used today, since QA usually provide distinctive fragmentation patterns in the electron impact mode (EI-MS). Chemical

ionization (CI-MS), field desorption (FD-MS) and fast atom bombardment (FAB-MS) are suitable for identifying molecular ions of QA esters and of

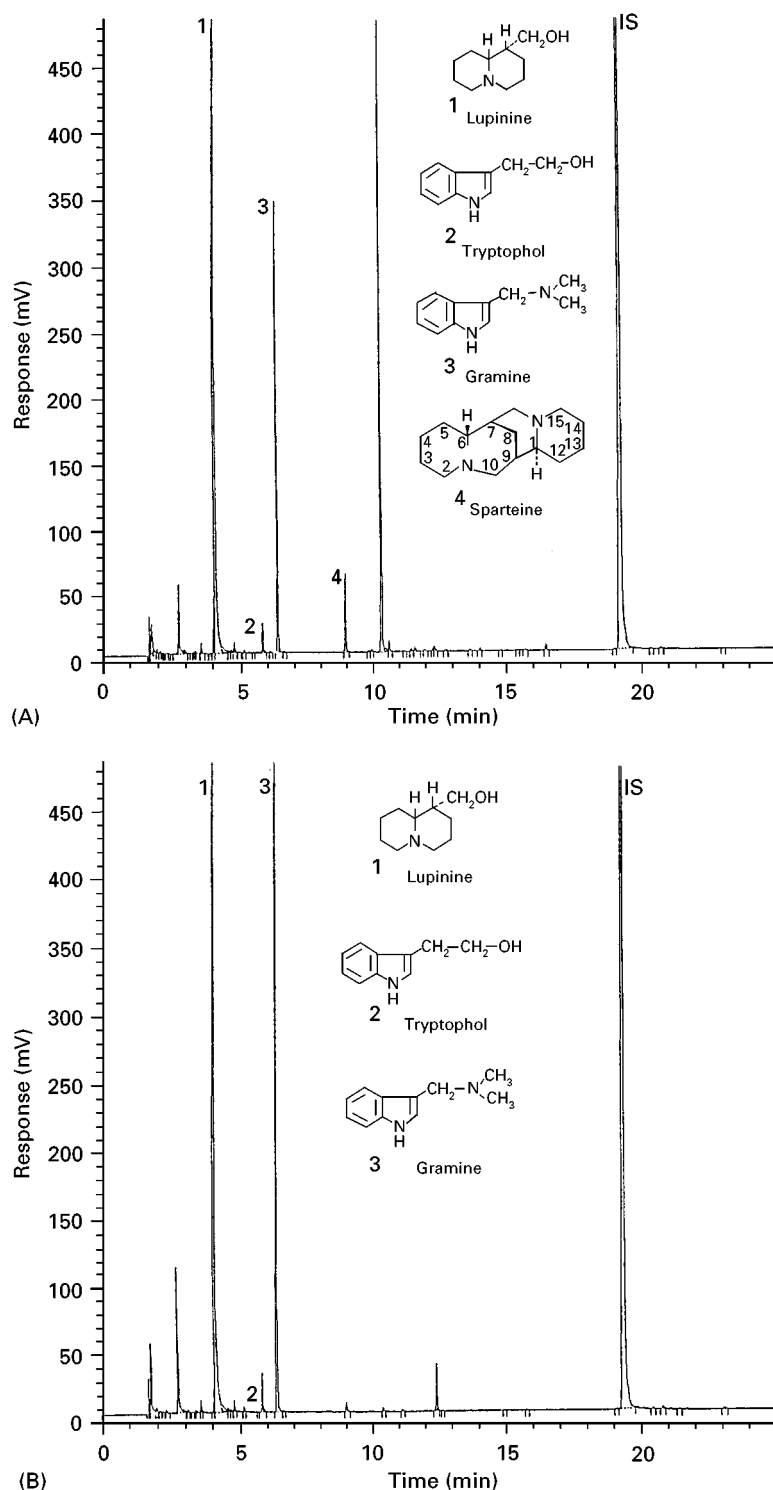


Figure 6 Separation of an alkaloid extract from *L. luteus* (A) and *L. hispanicus* (B) bitter seeds by capillary GC. Injector, 240°C; detector 300°C; oven 150–235°C, 5°C min⁻¹; carrier gas, helium; detection of alkaloids by nitrogen-specific detector (NPD) and mass-selective detector.

tricyclic alkaloids, whose molecular ions are usually obscure or absent in EI-MS spectra. A major advantage of MS is the possibility it gives of combining the high resolution power of capillary GC with the sensitivity of and information provided by EI- or CI-MS. Work using GC-MS was very much facilitated after 1980 by the development of new GC capillary columns, the development of new methods to position the GC column exit near the MS ion source and, most importantly, by improved data processing.

Alkaloid extracts of many legumes contain piperidine alkaloids such as ammodendrine, *N*-methylammodendrine, hystrine or smipine. These alkaloids also derive biogenically from lysine via cadaverine. Simple indole and quinolizidine alkaloids, such as gramine and lupanine may also be encountered. Even combinations of both indole and quinolizidine units are possible, as in the case of *Lupinus hispanicus*.

Separation and identification of QA by GC-MS is shown in Figures 5–7.

Conclusion and Future Developments

Gas chromatography is a versatile tool in the analysis of natural products with a wide area of application. It

is capable of extracting a wide range of diverse compounds from a variety of sample matrices.

Clear advantages of GC are the high sensitivity of the most common detection method, the FID, and the fact that the detector response of similar compounds will be about the same (i.e. peak areas may be directly compared for quantification). By using a nitrogen-specific detector (NPD) sensitivity for alkaloids can be even further improved while at the same time introducing selectivity.

No systematic studies to determine which column is best suited for alkaloid analysis have been reported, but from the methods described to date it is clear that thinly coated apolar columns are preferred for the analysis of underivatized alkaloids. The length of the columns used varies considerably and it is advisable to test the stability of a compound under GC conditions with a short column. A longer column may be used later if the desired chromatographic resolution has not been achieved.

A wealth of information can be obtained by the analysis of alkaloids by GC coupling to MS. Coupled techniques (GC-MS) have demonstrated their analytical potential. The large amounts of data produced by capillary GC, especially when coupled to a mass spectrometer, can now be handled by a personal

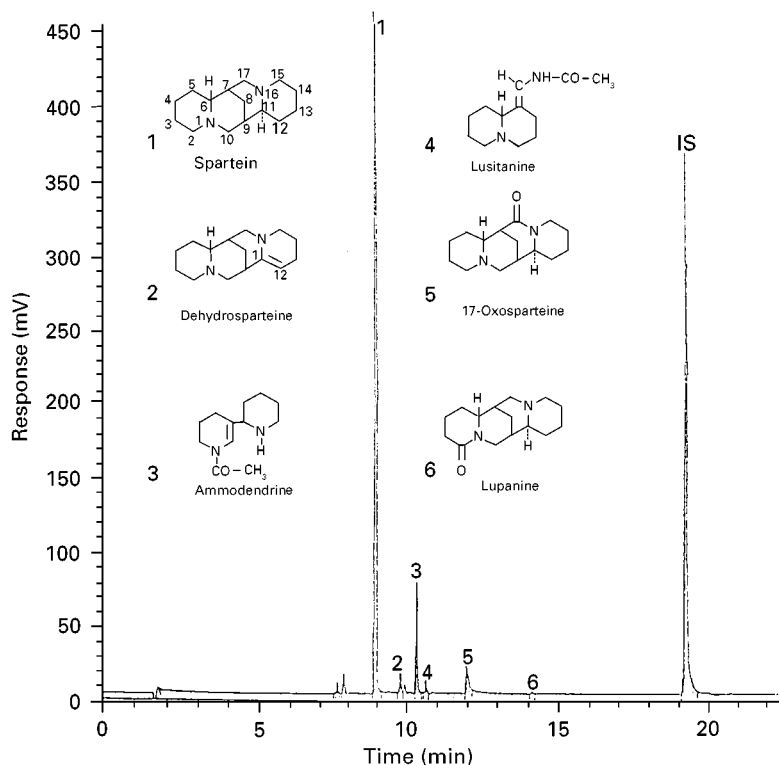


Figure 7 Separation of alkaloid extracts from *Chamaecytisus proliferus* by capillary GC. Injector, 240°C; detector 300°C; oven 150–235°C, 5°C min⁻¹; carrier gas, helium; detection of alkaloids by nitrogen-specific detector (NPD) and mass-selective detector.

computer. The data can be acquired, manipulated and displayed in real time and can be stored for record purposes.

Looking to the future, it is reasonable to expect continued evolutionary development: new selective detectors, more complex analysers for automated sample processing, increasing use of coupled techniques, columns with immobilized phases of a wider range of selectivity, etc. It is hoped that further research and development will encourage the use of GC-MS in the areas of alkaloid analysis that still await investigation.

Acknowledgements

The author gratefully acknowledges M. Martin-Pedrosa, T. Ortega, C. Cuadrado and C. Burbano for their helpful comments.

See also: II/Chromatography: Gas: Detectors: General (Flame Ionization Detectors and Thermal Conductivity Detectors); Detectors: Mass Spectrometry; Detectors: Selective. III/Alkaloids: Liquid Chromatography; Solid-Phase Extraction; Solid-Phase Microextraction; Supercritical Fluid Extraction; Thin-Layer (Planar) Chromatography. Extraction: Analytical Extractions.

Further Reading

- Bruneton J (ed.) (1995) *Pharmacognosy Phytochemistry Medicinal Plants*. Paris: Technique and Documentation Lavoisier.
- Cheeke PR (ed.) (1989) *Toxicants of Plant Origin*. vol. 1: *Alkaloids*. Boca Raton, FL: CRC Press.

- Dagnino D and Verpoorte R (1994) Gas chromatography in the analysis of alkaloids. In: Linskens HF and Jackson JF (eds) *Modern Methods of Plant Analysis*. Berlin: Springer-Verlag.
- David F and Sandra P (1992) Capillary gas chromatography-spectroscopic techniques in natural product analysis (Review paper). *Phytochemical Analysis* 3: 145–152.
- D'Mello JPF, Duffus CM and Duffus JH (eds) (1991) *Toxic Substances in Crop Plants*. Cambridge: Royal Society of Chemistry.
- Kutchan TM (1995) Alkaloid biosynthesis. The basis for metabolic engineering of medicinal plants. *Plant Cell* 7: 1059–1070.
- Modey WK, Mulholland DA and Raynor MW (1996) Analytical supercritical fluid extraction of natural products (Review paper). *Phytochemical Analysis* 7: 1–15.
- Papadoyannis IN and von Baer D (1993) Analytical techniques used for alkaloid analysis in legume seeds. In: Van der Poel AFB, Huisman J and Saini HS (eds) *Recent Advances of Research in Antinutritional Factors in Legume Seeds*. Wageningen: EAAP.
- Pelletier SW (ed.) (1984) *Alkaloids: Chemical and Biological Perspectives*. New York: John Wiley and Sons.
- Roberts MF and Wink M (eds) (1998) *Alkaloids. Biochemistry, Ecology, and Medicinal Applications*. New York and London: Plenum Press.
- Tomás-Barberán FA (1995) Capillary electrophoresis: a new technique in the analysis of plant secondary metabolites (Review paper). *Phytochemical Analysis* 6: 177–192.
- Verpoorte R and Niessen WMA (1994) Liquid chromatography coupled with mass spectrometry in the analysis of alkaloids. *Phytochemical Analysis* 5: 217–232.
- Wink M (1993) Quinolizidine alkaloids. *Methods in Plant Biochemistry*.

High Speed Countercurrent Chromatography

See III/MEDICINAL HERB COMPOUNDS: HIGH SPEED COUNTERCURRENT CHROMATOGRAPHY

Liquid Chromatography

R. Verpoorte, Leiden/Amsterdam Center for Drug Research, Leiden, The Netherlands

Copyright © 2000 Academic Press

Definition and Classification of Alkaloids

Alkaloids represent a wide variety of chemical structures (Figure 1). More than 16 000 are known and most

are derived from higher plants. Alkaloids have also been isolated from microorganisms, marine organisms like algae, dinoflagellates and puffer fish and terrestrial animals like insects, salamanders and toads.

An alkaloid has been defined by Pelletier as a cyclic organic compound containing nitrogen in a negative oxidation state which is of limited distribution among living organisms. From the analytical chemical point of view, the most important trait of alkaloids is their

basicity arising from a heterocyclic tertiary nitrogen atom. Notable exceptions are colchicine and the xanthines (e.g. caffeine), with pK_a values between 1 and 2. Alkaloids are biosynthetically derived from

amino acids, such as phenylalanine, tyrosine, tryptophan, ornithine and lysine. The biogenesis of alkaloids is used for their classification, as this is directly linked with their molecular skeleton, e.g. the two

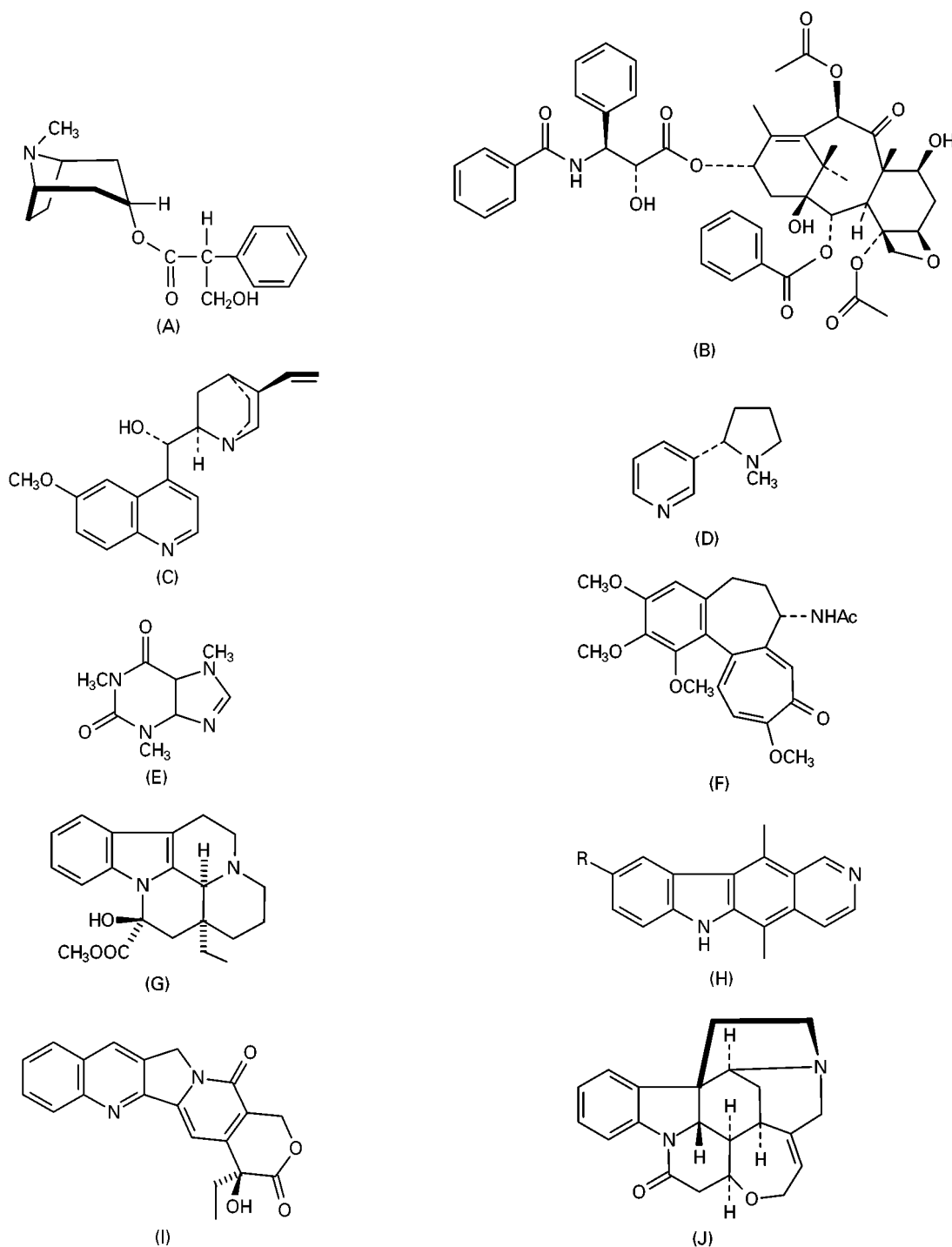


Figure 1 Structures of alkaloids. (A) L-hyoscyamine; (B) taxol; (C) quinine; (D) nicotine; (E) caffeine; (F) colchicine; (G) vincamine; (H) R = H ellipticine; R = OH 10-hydroxyellipticine; (I) camptothecin; (J) strychnine; (K) reserpine; (L) H-20 α tetrahydro alstonine; H-20 β ajmalicine; (M) emetine; (N) berberine; (O) galanthamine; (P) sanguinarine; (Q) R = H morphine; R = CH₃ codeine; (R) R = H *d*-tubocurarine; R = CH₃ *d*-chondrocurarine; (S) solasodine.

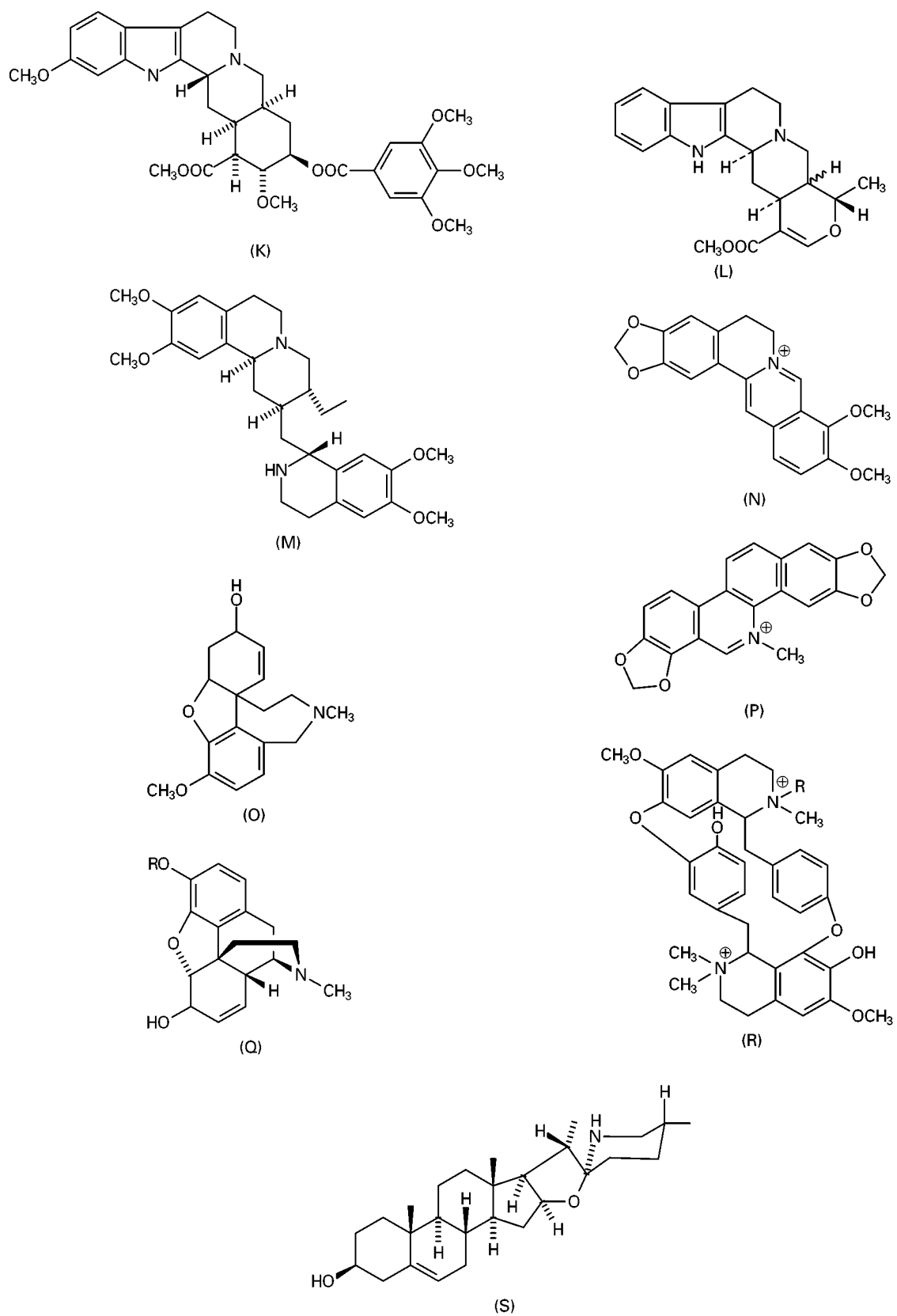


Figure 1 Continued

Table 1 Alkaloids of pharmaceutical interest

<i>Indole alkaloids</i>	<i>Tropane alkaloids</i>
Ajmalicine	Cocaine
Ajmaline	Scopolamine
Camptothecin	Atropine (<i>d/l</i> -hyoscyamine)
Ergocornine	
Ergocristine	<i>Terpenoid alkaloids</i>
Ergocryptine	Aconitine
Ergonovine	Solasodine
Ergosine	Taxol
Ergotamine	Tomatidine
Harmaline	Veratrine
9-Hydroxyellipticine	
Lysergic acid	<i>Miscellaneous</i>
Physostigmine	Caffeine
Psilocybin	Colchicine
Reserpine	Ephedrine
Rescinnamine	Lobeline
Serotonin	Mescaline
Strychnine	Muscarine
Yohimbine	Nicotine
Vincamine	Pilocarpine
Vinblastine	Saxitoxin
Vincristine	Sparteine
	Tetrodotoxin
<i>Quinoline alkaloids</i>	Theobromine
Quinine	Theophylline
Quinidine	
<i>Isoquinoline alkaloids</i>	
Apomorphine	
Berberine	
Boldine	
Chelerythrine	
Codeine	
Emetine	
Galanthamine	
Heroin	
Morphine	
Narceine	
Noscapine	
Papaverine	
Sanguinarine	
Thebaine	
Tubocurarine	

largest groups are indole alkaloids (more than 4100 compounds) and isoquinoline alkaloids (more than 4000 compounds). Other important groups are tropane alkaloids (*c.* 300 compounds), steroidal alkaloids (*c.* 450 compounds), pyridine and pyrrolizidine alkaloids (about 250 and 570 compounds, respectively).

The botanical origin of the alkaloids is also used as a classification method, e.g. *Papaver* (opium) alkaloids, *Cinchona* alkaloids, *Rauvolfia* alkaloids, *Catharanthus* alkaloids, *Strychnos* alkaloids, ergot alkaloids, cactus alkaloids and *Solanum* alkaloids. As secondary metabolites, alkaloids probably play a role in defending organisms against pests and

diseases. For example, for some types of alkaloids, insect antifeedant activity has been established. Thus, many alkaloids have strong biological activities. Their effect in humans can be explained by structural relationships with important signal compounds (neuro-transmitters) like dopamine, acetylcholine, noradrenaline and serotonin. Consequently, some alkaloids are used as medicines or in pharmacological studies (Table 1). In addition to pure compounds, crude plant extracts containing alkaloids are used (phytotherapy). Another area where alkaloids play a major role is in drugs of abuse, e.g. mescaline, cocaine, morphine and its semisynthetic derivative, heroin. Alkaloids are also of interest in the analysis of doping (e.g. strychnine, ephedrine, caffeine) and poisons (e.g. strychnine, pyrrolizidine alkaloids, coniine, nicotine, aconitine, tetrodotoxin).

Due to their various applications, the analysis of alkaloids is of great importance. The very different types of (ab)use of the alkaloids mean that the type of analyses also varies. Alkaloids must be analysed in a broad variety of matrices, such as plant material, tablets, drug seizures, urine and blood. Each requires different sample clean-up methods and chromatographic selectivities. Liquid chromatography is the most commonly used method since the instability and low volatility of alkaloids mean that gas chromatography has a limited applicability. Because the extracts are often complex and 'dirty', thin-layer chromatography is useful in analysing alkaloid-containing plant extracts.

Chemical Properties and Artefact Formation

Most alkaloids have basic properties with pK_a values of about 6 to 12, but usually 7–9. The free base is soluble in organic solvents and not in water. Protonation of the nitrogen in the free base usually results in a water-soluble compound. This behaviour is the basis of the selective isolation of alkaloids by liquid/liquid partitioning processes. Quaternary alkaloids are poorly soluble in organic solvents but soluble in water at any pH.

Many alkaloids are difficult to crystallize in the form of the free base, but do crystallize as a salt. Alkaloids are usually colourless; only some highly conjugated compounds are coloured or show strong fluorescence (e.g. berberine and serpentine).

Alkaloids are not very stable; in particular, N-oxidation is quite common. Stability is influenced by solvents, as well as heat and light. Halogen-containing organic solvents such as chloroform and dichloromethane are widely used in alkaloid research.

Chloroform in particular is a very suitable solvent, because of its relatively strong proton donor character. However, this solvent easily causes the formation of artefacts, e.g. (*N*-)oxidation occurs easily. Dichloromethane may result in the formation of quaternary *N*-dichlorometho-compounds. Similar compounds are formed with the minor impurities present in chloroform. Peroxides in ethers may also cause *N*-oxidation.

Alkaloids are more stable in toluene, ethyl acetate and alcoholic solutions. Carbinolamine functions are often found in alkaloids, either formed during the coupling of a carbonyl group and an amine in the biosynthesis, or as products formed from rearrangements of *N*-oxides. Carbinolamines readily react with alcohols (e.g. *O*-methyl pseudostrychnine formed from pseudostrychnine with methanol). Ketones such as acetone and methylethylketone are well-known artefact formers. Berberine, for example, may react with acetone. Ammonia and acetone may react during column chromatography, yielding condensates that give a Dragendorff-positive reaction. Ammonia may also react with aldehydes present in plant materials, giving rise to artificial alkaloids, e.g. the pyridine-type alkaloid gentianine is formed from sweroside during extraction.

Extraction

Due to the more lipophylic character of alkaloids as free bases, they can be extracted under neutral or basic conditions (e.g. after basification of the plant material or biofluid to pH 7–9 with ammonia, sodium carbonate or sodium bicarbonate) with organic solvents (such as dichloromethane, chloroform, ethers, ethyl acetate and alcohols). Strongly basic alkaloids can only be completely extracted at higher pH (>10), e.g. tryptamine. As a general rule of thumb, for the extraction of an alkaloid one should choose a pH of $pK_a + 2$. On the other hand, alkaloids containing phenolic groups are protonated at higher pH, and thus not extracted by organic solvents under such conditions (e.g. morphine).

Alkaloids can be extracted in protonated form (after acidification to pH 2–4 with diluted acids like phosphoric acid, sulfuric acid, citric acid) with water or alcohols (e.g. methanol).

Alkaloids can be further purified by liquid–liquid extraction or liquid/solid extraction. In liquid–liquid extraction the alkaloids are, after basification, extracted from an aqueous solution with an immiscible organic solvent or from an organic solvent with an aqueous acid solution. To avoid the formation of lipophylic ion pairs, phosphoric acid, sulfuric acid and citric acid are preferred over acetic acid and

hydrochloric acid. By using a back-extraction from aqueous solution to organic and back to aqueous, or from organic to aqueous and back to organic solution, alkaloids can easily be separated from neutral and acidic compounds.

Alkaloids can be extracted from acidic aqueous solutions with organic solvents by using ion-pairing reagents (e.g. alkylsulfonic acids). It should be noted that common anions such as Cl^- , Br^- , I^- and acetate also form ion pairs which are readily soluble in organic solvents.

Solid-phase extraction using adsorption or ion exchange can also be used. For adsorption of the alkaloids in the free form, reversed-phase materials, such as chemically bonded C_8 and C_{18} on silica, are widely used. A suitable solvent system is a mixture of methanol and water; the crude extract is fractionated by stepwise elution of the adsorbent with a solvent of decreasing polarity. XAD-2 is also used for the concentration of alkaloids, e.g. from biological fluids. Various cation exchange materials can be used for the selective extraction of alkaloids.

For preparative purposes purifications based on the precipitation of alkaloids are employed. A crude extract of the alkaloids is made with aqueous acid; subsequently the alkaloids are precipitated with reagents such as Mayer's reagent (1 mol L^{-1} mercury chloride in 5% aqueous potassium iodide) or Reinecke's salt (5% ammonium reineckate in 30% acetic acid) at pH 2, or picric acid (saturated aqueous solution) at pH 5–6. After collection by filtration or centrifugation, the precipitate is dissolved in an organic solvent (acetone:methanol:water; 6:2:1). The complexing group is then removed by means of an anion exchanger. Quaternary alkaloids cannot be purified by means of liquid–liquid extraction, therefore precipitation is particularly suited for their purification.

Thin-layer Chromatography

Thin-layer chromatography (TLC) is widely used as a versatile method in the analysis of alkaloids. It offers the advantage of a broad range of polarities being separated in one single analysis, which is of interest in plant materials and metabolism studies. The most widely used stationary phase is silica; alumina plates are rarely employed nowadays. Reversed-phase materials, such as chemically bonded C_{18} on silica, are also applied but silica is still used most widely.

Strongly basic alkaloids will show severe tailing on silica gel plates, due to the acidic properties of silica. The use of mobile phases which contain

Table 2 Some common thin-layer chromatography systems for the analysis of alkaloids

<i>Solvent system (all with silica plates)</i>	<i>Commonly used ratios</i>	<i>Polarity range</i>
Cyclohexane–chloroform–diethylamine	5 : 4 : 1–(0) : 9 : 1	lp-mp
Chloroform–acetone–diethylamine	5 : 4 : 1	mp
Chloroform–methanol–ammonia	8 : 1 : 1	mp
Chloroform–methanol/ethanol	99 : 1–1 : 1	lp-mp, wb
Ethyl acetate–isopropanol–25% ammonia	100 : 2 : 1, 80 : 15 : 5, 45 : 35 : 5	lp-mp
Ethyl acetate–methanol	9 : 1–1 : 1	lp-mp, wb
Toluene–ethyl acetate–diethylamine	7 : 2 : 1	lp-mp
Toluene–acetone–ethanol–25% ammonia	20 : 20 : 3 : 1	mp
Dichloromethane–diethyl ether–diethylamine	20 : 15 : 5	mp
Acetone–methanol–25% ammonia	40 : 10 : 2, 95 : (0) : 5	mp-p
Methanol–25% ammonia	95 : 5	lp-p
<i>n</i> -Butanol–acetic acid–water	4 : 1 : 1	lp-p
Methanol–1 mol L ⁻¹ aq. M NH ₄ NO ₃ –2 mol L ⁻¹ aq. ammonia	7 : 1 : 2	lp-p
Methanol–0.2 mol L ⁻¹ aq. M NH ₄ NO ₃	3 : 2	lp-p

lp, Low polarity compounds; mp, medium polarity compounds; p, polar compounds; wb, weakly basic compounds.

a base such as ammonia or diethylamine will overcome this problem. A more elaborate method is the use of TLC plates impregnated with a basic solution.

For the analysis of highly polar quaternary alkaloids and *N*-oxides, solvent systems consisting of methanol and aqueous salt solutions are useful. In Table 2 some widely used TLC systems are summarized. For the detection of alkaloids a large number of methods have been reported. Besides quenching ultraviolet (UV) light on fluorescent plates and fluorescence, general reagents for selectively detecting alkaloids are Dragendorff's reagent (orange-brown spots) and potassium iodoplatinate (brown-violet-purple spots; Table 3). Dragendorff's reagent may cause false-positive reactions with, for example, compounds containing conjugated carbonyl or lactone functions. The iodoplatinate reagent has less risk of false-positive reactions and is more selective due to a broader spectrum of colours observed for individual alkaloids.

Highly selective reagents have been reported for the visualization of various classes alkaloids (Table 4). These are based on different colorations under strongly oxidative conditions.

Liquid Chromatography

High performance liquid chromatography (HPLC) is a major tool for the analysis of alkaloids. Most separations are done on reversed-phase (RP) materials (C₈-, C₁₈- and phenyl-bonded phases on silica). Although extensive tailing due to the interaction of the basic nitrogen and residual acidic silanol groups may occur on the RP materials. In particular, strong bases show this problem. Several solutions have been found

to circumvent this. First, special RP materials have been developed for basic compounds. These materials have an altered silica surface, a high load of the alkyl groups or they have undergone a rigorous endcapping treatment to reduce the number of free silanol groups. Often the plate numbers observed for alkaloids on an HPLC column are considerably lower than those measured with the usual neutral test compounds. Polymeric (e.g. polystyrene-based) stationary phases do not have the problem of residual silanol groups; however, plate numbers observed with such columns are not usually better than those found with specially made RP silica materials. Phenyl-type RP columns are also successful in the separation of alkaloids.

Another way of reducing the tailing is through modification of the eluent. By adding long chain alkylamines (e.g. hexylamine) in low concentrations

Table 3 Detection reagents for alkaloids on thin-layer chromatography plates

<i>Dragendorff's reagent (modification according to Munier)</i>
(A) 1.7% bismuth subnitrate in 20% aq. tartaric acid solution
(B) 40% potassium iodide in water
A and B are mixed (5 : 2) and the spray reagent is prepared by mixing 50 mL of the stock solution with 100 g tartaric acid and 500 mL water.
Colours observed after spraying: orange-brown spots for alkaloids
<i>Potassium iodoplatinate reagent</i>
The reagent is prepared freshly by mixing 3 mL of 10% aq. hexachloroplatinic acid solution with 97 mL water and 100 mL of 6% aqueous potassium iodide solution.
Colours observed after spraying: brown-violet-purple spots for alkaloids

Table 4 Selective colour reactions for the detection of alkaloids on thin-layer chromatography plates

<i>Spray reagent</i>	<i>Commonly used for the detection of</i>
0.2 mol L ⁻¹ ferric chloride in 35% perchloric acid and heat	Indole alkaloids, isoquinoline alkaloids
1% ceric sulfate in 10% sulfuric acid	Indole alkaloids
1% <i>p</i> -dimethylaminobenzaldehyde in ethanol, followed by exposure to hydrochloric acid vapour	Ergot alkaloids
Sulfuric acid and heat	Various alkaloids

(typically 1 mmol L⁻¹) to the mobile phase, tailing can be considerably reduced. Also, addition of amines like triethylamine or tetramethylammonium can be helpful in reducing tailing. Moreover, alkaloids have been analysed on aminopropyl- and cyanopropyl-type of columns, in both normal and reversed-phase modes.

In liquid chromatography of alkaloids, the pH of the mobile phase must be strictly controlled, as stationary phases are unstable at a pH above 8, usually a pH between 2 and 4 is used, i.e. the alkaloids are present in the protonated form. Ion suppression systems are quite common. Because of the preference for the lower pH range of the eluent, ion pairing is used with C₄–C₈ alkylsulfonates at a concentration of 25–100 mmol L⁻¹ for the analysis of alkaloids. Increasing length of the alkyl chain causes longer retention.

Some general features of RP HPLC systems for the analysis of alkaloids are given in Table 5.

The number of applications of ion exchange chromatography for the separation of alkaloids is limited. In general, cation exchange columns will also affect the selectivity of the separation through nonionic interactions, e.g. through the stationary phase matrix. Usually an elevated temperature is used to improve peak shape.

A large number of liquid–solid separations on silica have been reported (Table 6). The systems applied are similar to those reported for TLC.

UV is most widely used for detection. Particularly for the groups of indole and isoquinoline alkaloids,

strong and specific UV chromophores are found. These can greatly assist in identifying compounds, e.g. in using HPLC with diode array detection. The pH of the solvent as well as the solvent itself may have an effect on the UV spectra, e.g. causing shifts of maxima and minima. Some alkaloids can be detected by means of their fluorescence. Some type of alkaloids have poor UV absorption properties, e.g. tropane alkaloids, pyrrolizidine alkaloids and steroidal alkaloids require detection at lower wavelengths (200–220 nm). Electrochemical detection has been applied, enabling the selective attenuation of interfering compounds. Mass spectrometry is a major tool in the identification and structure elucidation of alkaloids. In combination with gas chromatography and liquid chromatography, it is very useful in the qualitative and quantitative analysis of complex mixtures of alkaloids. Solvent systems suited for liquid chromatography–mass spectrometry should only contain volatile compounds (e.g. ammonium acetate, ammonium formate).

Countercurrent Chromatography

The preparative isolation of alkaloids can be achieved by means of modern countercurrent chromatography. Because of the ionic nature of the alkaloid systems with a controlled pH are preferred for the separation. Improved efficiency can be obtained by using ion pair gradients, e.g. solvent two-phase systems consisting of chloroform–methanol–aqueous

Table 5 General outline of reversed-phase high performance liquid chromatography systems for the separation of alkaloids

<i>Stationary phase</i>	<i>Mobile phase</i>
C ₈ , C ₁₈ or phenyl-bonded phase with low percentage of free silanol groups	<p><i>Ion suppression mode</i></p> <p>Methanol (acetonitrile)–water containing c. 0.01–0.1 mol L⁻¹ phosphate buffer, ammonium carbonate or sodium acetate (pH 4–7)</p> <p><i>Ion pair mode</i></p> <p>Methanol (acetonitrile)–water containing c. 25–100 mmol L⁻¹ alkylsulfonate and 1% acid (e.g. acetic acid), pH 2–4</p>

Table 6 General outlines of normal-phase high performance liquid chromatography systems for the separation of alkaloids

Stationary phase	Mobile phase		
Silica gel	Dichloromethane, Chloroform, Diethyl/isopropyl ether, Tetrahydrofuran, or Ethyl acetate	Methanol or Isopropanol	Ammonia, Diethylamine or Triethylamine (c. 1% of the mobile phase)

phosphate or citrate buffer, pH c. 4, containing perchlorate, acetate or chloride as the ion pairing agent. High loadability and different selectivity compared with column chromatography are important features of countercurrent chromatography.

See also: III/Alkaloids: Gas Chromatography; Thin Layer (Planar) Chromatography. **Natural Products:** High-Speed Countercurrent Chromatography.

Further Reading

- Baerheim Svendsen A and Verpoorte R (1983) *Chromatography of alkaloids. Part A: Thin-layer chromatography*. Amsterdam: Elsevier Science Publishers.
- Manske RHF and Holmes HL (eds) *The Alkaloids*, Volume 1–5 (1950–1995), Manske RHF (ed.) Volume 6–16 (1955–1977), Manske RHF and Rodrigo R (eds) Volume 17–20 (1979–1981), Brossi A (ed.) Volume 21–40 (1983–1992), Cordell GA (ed.) Volume 40– (1992–) New York: Academic Press.
- Cordell GA (1981) *Introduction to Alkaloids. A Biogenetic Approach*. New York: John Wiley.

- Glasby JS (1975) *Encyclopedia of Alkaloids*, vols 1 and 2. New York: Plenum Press.
- Hesse M (1974) *Progress in Mass Spectrometry*, vol. 1, parts 1 and 2. *Mass Spectrometry of Indole Alkaloids*. Weinheim, Verlag Chemie.
- Hesse M and Bernhard HO (1975) *Progress in Mass Spectrometry*, vol. 3. *Mass Spectrometry of Alkaloids*. Weinheim: Verlag Chemie.
- Pelletier SW (ed.) (1983) *Alkaloids: Chemical and Biological Perspectives*, vols 1–6. New York: John Wiley.
- Popl M, Fährnich J and Tatar V (1990) *Chromatographic Analysis of Alkaloids*. New York: Marcel Dekker.
- Sangster AW and Stuart KL (1965) Ultra-violet spectra of alkaloids. *Chemical Reviews* 65: 69–130.
- Southon IW and Buckingham J (1989). *Dictionary of Alkaloids*. London: Chapman & Hall.
- Verpoorte R and Baerheim Svendsen A (1984) *Chromatography of alkaloids. Part B: Gas-liquid chromatography and high-performance liquid chromatography*. Journal of Chromatography Library. Volume 23B. Amsterdam: Elsevier Science Publishers.
- Verpoorte R (1986) Methods for the structure elucidation of alkaloids. *Journal of Natural Products* 49: 1–25.

Thin-Layer (Planar) Chromatography

J. Flieger, Medical Academy, Lublin, Poland

Copyright © 2000 Academic Press

Introduction

In 1938, Izmailow and Schraiber pioneered the thin-layer chromatography (TLC) method for the analysis of plant material containing alkaloids. The subject matter of their scientific research was an extract of a plant rich in tropane alkaloids. Later on, the method was developed by Bekesy, who applied it to the separation of ergot alkaloids. Since then, numerous papers exploring the detection, isolation and quantitative determination of alkaloids by TLC have been pub-

lished. It has been stated that no other method has delivered so much information on alkaloids.

From the chemical point of view, alkaloids form a very diverse group of organic nitrogen compounds of a basic character (with the exception of some derivatives of purine and colchicine). They have tertiary or quaternary amino groups in their molecules and only a few contain secondary amino groups. Considering the fact that analytical problems connected with alkaloids are mostly concerned with their physicochemical properties, they are commonly divided according to the type of chemical structure into tropane, quinoline, indole, diterpene and others. Another useful classification is based on botanical groups (e.g. tobacco, lupine, ergot, strychnos, vinca and catharanthus alkaloids), and this is

especially valuable as far as chemotaxonomical studies are concerned.

In early work, alkaloids were predominantly isolated from the natural plant material. TLC was then used for qualitative and quantitative analysis of plants and the study of the biosynthesis of alkaloids. Because of their powerful physiological properties alkaloids have become important therapeutic compounds and many of them have been prepared synthetically or by partial synthesis. As a consequence, many derivatives have been formed that do not occur in nature. TLC is particularly well suited for checking the processes of synthesis as well as for establishing the progress of reactions and finally testing of products in pharmaceutical preparations. The importance of alkaloids is also fundamental in toxicological analysis; many are used as narcotics and hallucinogenic drugs, as doping substances and as poisons. The presence of alkaloids in drugs of abuse and their metabolites in biological fluids such as urine and blood has also been tested by means of TLC.

Preparation of Samples

Various sample preparation procedures have been developed for pharmaceutical formulations, plant and biological materials. Due to the fact that, in most of them, alkaloids occur as salts together with complex mixtures of nonalkaloid compounds such as inorganic salts or substances of lipophilic character, their pre-separation by a suitable extraction procedure is necessary.

While in the case of the analysis of solutions, alkalinized (or acidified) samples and extraction with an organic solvent such as chloroform or diethyl ether is usually sufficient, isolating alkaloids from a plant material is a multistage process and may be conducted using several methods.

Most often preparative isolation is carried out by liquid-liquid extraction. Plant material with a high liquid content should be initially extracted with light petroleum or water containing diluted hydrochloric acid to remove lipids. The release of alkaloidal bases occurs under the influence of the addition of a mineral base, commonly ammonia. Then they are extracted by means of water-immiscible organic solvents or water-alcohol mixtures.

For efficient extraction in the above cases described, alkaloids should be present in the extractable form in at least 95%, so pH adjustment of the sample to $\text{pH} = \text{pK}_a + 2$ is sufficient.

Further purification is achieved by re-extracting alkaloids from organic solvents into an aqueous phase of the opposite pH, where the alkaloids are present as salts.

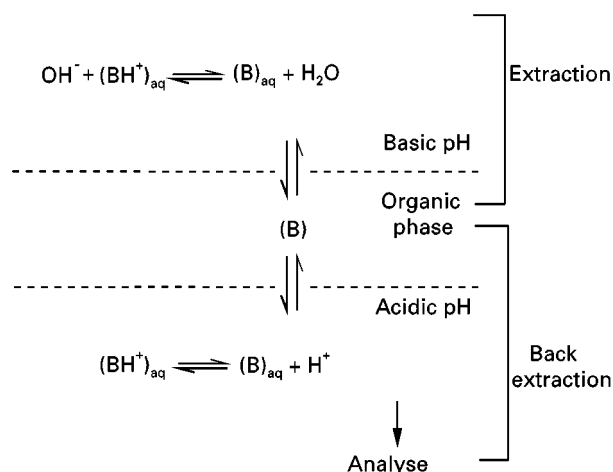


Figure 1 Scheme for the back-extraction procedure of a basic drug (B) (after Adamovics JA (1990) *Chromatographic Analysis of Pharmaceuticals*. New York and Basel: Marcel Dekker, Inc.)

This back-extraction procedure for basic compounds (B) is shown schematically in **Figure 1**.

A liquid extraction technique used to increase extraction efficiency and selectivity is an ion pair extraction originally used to extract strychnine from syrup.

Purification of crude plant extracts from non alkaloidal compounds may be carried out by precipitating the alkaloids with picric acid, Reinecke's salt or Mayer's reagent or by using ion exchange or a small adsorption column. Solid-phase extraction (SPE) is gaining in popularity. Specific sorption conditions under which alkaloids are strongly retained lead to preconcentration of free bases (on aluminium oxide), their salts (on phosphoric acid impregnated silica) or as an ionic form (on ion exchangers).

It should be emphasized that, in the case of silica gel, quaternary alkaloids are more strongly retained than ternary ones with an aqueous buffer-methanol mobile phase. Such differences also create the possibility of separating these two groups of alkaloids.

One of the latest methods of isolating groups of alkaloids from solid samples is supercritical fluid extraction (SFE). The method increases the efficiency of extraction and shortens the overall time of analysis.

While considering the problems of extraction, isolation and purification of alkaloids, one should be cautious about the possibility of undesirable reactions and artefact formation. One reason may be impurities present in the solvents applied. Thus, peroxides (in ethers) cause oxidation, ethyl chloroformate (in chloroform) forms ethylcarbamates of alkaloids; halogen-containing compounds; bromochloromethane and dichloromethane (in chloroform) cause quaternization of tertiary alkaloids, while cyanogen

chloride (in dichloromethane) is the cause of nitrilation of primary and secondary amines. Decomposition may also be caused by a photochemical reaction, especially in chloroform solutions. Finally there may be a reaction with a solvent itself, mainly with chloroform, but also with ketones or strong alkali. The fact that the chloroform used as a component of the mobile phase may present a quenching effect should also be emphasized.

Development Techniques

Adsorbents used in TLC may be either commercial products or home-made plates (now seldom employed). High quality chromatograms can be achieved with HPTLC plates which were introduced in the 1980s.

Plates may be developed in a linear, circular or anticircular mode. The most common technique in TLC of alkaloids is ascending, single, one-dimensional development in tanks saturated with the vapour of the solvent system.

Preconditioning the plate with the vapours, thus preventing demixing of the mobile-phase components, can also be performed in sandwich-type chambers produced by Camag (Vario-KS) and Chromdes (DS). In some cases, especially where compounds differ in polarity, repeated development of the plate with the same solvent or solvents of increasing strength or the continuous development technique has some advantages. In other cases, programmed multiple development with the same solvent may be successfully applied. Also useful is two-dimensional development, which is especially valuable for separating a greater number of alkaloids in a given section of the plate.

Great differences in the polarity of alkaloid molecules make gradient elution advantageous. This technique may be developed in both glass chambers and in horizontal chambers as well as with overpressured layer chromatography.

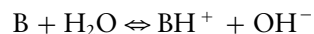
Worth noticing is one technique related to TLC – thin-layer electrophoresis, which has been used as a two-dimensional combination with TLC for the separation of ergot alkaloids.

Separation Methods

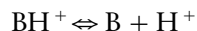
It is obvious that the kind of adsorbent used and solvent system composition determine the separation mechanism occurring in the chromatographic process. The adsorbent also determines the method of sample preparation. Thus, for adsorption and partition chromatography, alkaloids are mostly applied as bases in organic polar solvents; for ion exchange

sorbents they are applied in the form of salts in aqueous solution.

Choosing the optimal chemical character of the stationary and mobile phase is especially important in the case of alkaloids because of the ionization ability of their molecules. Dissociation of bases in aqueous solution can be expressed by the following equation:



or, in the case of the conjugated acid BH^+ , by:



with a dissociation constant (acidic) K_a .

The dependence of the molar ratio of nondissociated molecules $[B]$ to the total concentration of an alkaloid $[B] + [BH^+]$ on the pH of the mobile phase is shown in the curves presented in Figure 2. The pK_a values of chosen alkaloids are summarized in Table 1.

For TLC of alkaloids, numerous chromatographic systems have been reported. Some are presented in Table 2, together with their practical applications.

Adsorption Chromatography

Silica gel is the most frequently used solid-phase in adsorption chromatography. The weakly acidic properties of its surface may be the reason for the chemisorption of alkaloids, especially when neutral nonpolar solvents are used.

Tailing of spots may occur and the danger in using a neutral mobile phase is the formation of double spots, resulting from partial deprotonation of molecules if alkaloids are applied as salts. This is why

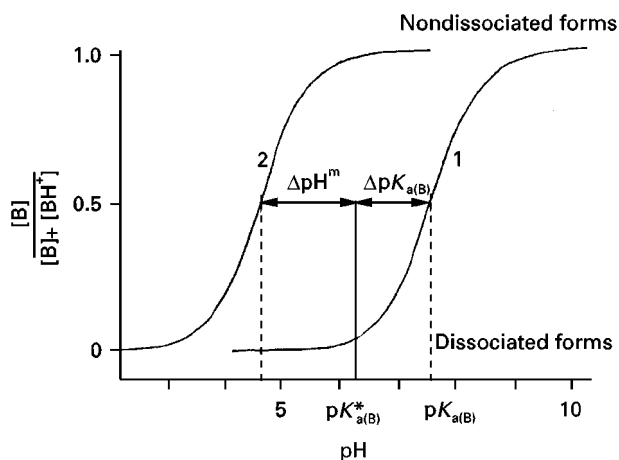


Figure 2 Dependence of the degree of dissociation of an alkaloid (B) on pH of buffer in mixed solvent ($\Delta pK_{a(B)} < 0$ and $\Delta pH_m > 0$). 1, solution in water; 2, solution in mixed solvent $pK_{a(B)}^* = pK_a$ in 50% (w/w) methanol (after Popl M, Fährnich J and Tatar V (1990) *Chromatographic Analysis of Alkaloids. Chromatographic Science*. New York and Basel: Marcel Dekker, Inc.).

Table 1 Values of pK_a for the dissociation of alkaloids in water

<i>Alkaloid</i>	pK_a	<i>Alkaloid</i>	pK_a
Aconitine	8.35	Methylecgonine	9.16
Arecaidine	9.07	Morphine	8.21
Arecoline	7.41	Narceine	3.30
Atropine	9.85	α -Narcotine	6.37
Benzoylecgonine	11.80	Nicotine	8.02
Berberine	11.73		($pK_{a2} = 3.12$)
Brucine	8.16	Nicotyrine	4.76
	($pK_{a2} = 2.50$)	Papaverine	6.40
Caffeine	1.00	<i>d,l</i> -Pelletierine	9.40
Cinchonidine	8.40	Pilocarpine	6.87
	($pK_{a2} = 4.17$)	Piperine	1.98
Cinchonine	8.35	Protopine	5.99
	($pK_{a2} = 4.28$)	Quinidine	8.77
Cocaine	8.39		($pK_{a2} = 4.20$)
Codeine	8.21	Quinine	8.34
Colchicine	1.85		($pK_{a2} = 4.30$)
α -Coniine	10.90	Retronecine	8.88
Cytisine	8.12	1-Scopolamine	7.55
	($pK_{a2} = 1.20$)	Solanine	7.54
Emetine	8.43	Sparteine	11.96
	($pK_{a2} = 7.56$)		($pK_{a2} = 4.80$)
Ergometrine	6.73	Strychnine	8.26
Harmine	7.61		($pK_{a2} = 2.50$)
Heliotridine	10.55	Thebaine	8.15
Heroine	7.60	Theobromine	1.00
1-Hyoscyamine	9.65	Theophylline	1.00
		Tropacocaine	9.88
Isopilocarpine	7.18	Tropine	10.33
		Yohimbine	7.45
			($pK_{a2} = 3.00$)

Reproduced with permission from Popl *et al.* (1990).

silica gel is most often used in combination with basic mobile phases or the gel is impregnated with basic buffers or basic compounds (KOH, NaOH, NaHCO_3). Colchicine is the exception to these rules and, because of its neutral character, can be analysed in neutral solvent systems in combination with silica gel plates.

There are fewer applications using alumina. Basic alumina is most often used. The weakly basic character of the surface allows the use of neutral solvent systems as mobile phases. Depending on the nature of the alkaloids examined, neutral or acidic alumina may sometimes be more suitable.

As presented in detail in Table 2, solvent systems used in adsorption chromatography are either binary or ternary mixtures of chloroform, benzene, ethyl acetate and others. Alkalification of the mobile phase is achieved by the addition of ammonia, diethylamine, triethylamine or triethanolamine. Very interesting methods for choosing a suitable solvent were proposed in the late 1960s, and were based on the weighted average values of dielectric constants, and by the introduction of homogenous azeotropic

mixtures (methanol-chloroform-methyl acetate, methanol-acetone-chloroform, methanol-benzene). When choosing the proper solvent strength, especially in complex eluent mixtures used for the analysis of alkaloids, the x_e , x_d , x_n parameters developed by Snyder are useful. They refer to the possibility of a solvent acting as a proton acceptor, proton donor or the one exhibiting strong dipole interaction. All possible compositions of quaternary, ternary and binary solvent mixtures have been described by the Prisma model. It may be applied either in normal or reversed-phase systems with the aim of optimizing the conditions of separation.

Pseudo-reversed-phase Chromatography

Chromatographic systems composed of silica gel and buffered aqueous organic mobile phases have been successfully used in recent years to isolate and separate alkaloids. The retention mechanism occurring here, described as pseudo-reversed phase, is fairly complex. An important role is played by the hydrophobic

Table 2 Examples of the most popular chromatographic systems for TLC of the main alkaloid groups

Compounds separated	Applications	Adsorbent	Solvent system
<i>Phenylethylamine derivatives</i>			
Ephedrine and its derivatives	Qualitative identification of ephedrine	Silica gel	Butanol–acetic acid–water (6 : 3 : 1)
		Silanized silica gel	1 mol L ⁻¹ acetic acid–3% potassium chloride
	Determination of ephedrine in Herba Ephedrae	Silanized silica gel impregnated with anionic and cationic detergents	1 mol L ⁻¹ acetic acid–methanol (80 : 20)
		Silica gel	Isopropyl ether–acetone–tetrahydrofuran (15 : 3 : 2)
Colchicine and related compounds	Determination of ephedrine in bulk drugs	Silica gel	<i>n</i> -Butanol–water–formic acid (7 : 2 : 1)
	Determination of colchicine in bulk drugs, dragees (BP)	Silica gel	Chloroform–acetone–ammonium hydroxide (5 : 4 : 0.2 or 25 : 20 : 0.4)
	Analysis of colchicine in tablets and plant material: <i>Colchicum autumnale</i> seeds, <i>Iphigenia indica</i>	Aluminium oxide	Chloroform–methanol (80 : 0.5)
	Separation of colchicine and 3-demethylocolchicine, demecolcine in Turkish <i>Colchicum</i> and <i>Merendera</i> species	Silica gel	Benzene–ethyl acetate–butylamine (5 : 4 : 1 or 7 : 2 : 1)
<i>Imidazole alkaloids</i>			
Pilocarpine	Qualitative identification of pilocarpine	Silica gel	Chloroform–acetone–diethylamine (5 : 4 : 1)
	Determination of pilocarpine in ocular system	Aluminium oxide	Chloroform–acetone–water (5 : 4 : 1)
		Silica gel	Chloroform
	Determination of pilocarpine nitrate in bulk drugs (EP)	Silica gel	Methanol–1% potassium dihydrogen phosphate (pH 6 : 9 : 1)
	Separation of pilocarpine, isopilocarpine, pilocarpic acid and isopilocarpic acid in eye drops	Silica gel	Chloroform–methanol–ammonium hydroxide (85 : 14 : 1)
<i>Indole alkaloids</i>			
Strychnos alkaloids	Determination of strychnine in biological specimens	Silica gel	Ethanol–chloroform–28% ammonium hydroxide (53 : 30 : 17)
	TLC analysis of strychnine and brucine in plant extract from <i>Strychnos nux vomica</i>	Silica gel	Dichloromethane–methanol–water–formic acid–diethanolamine (72.3 : 25 : 2.5 : 0.1 : 0.1)
	Separation of strychnine and brucine	Aluminium oxide	Methanol–4 mol L ⁻¹ ammonium hydroxide (9 : 1)
Yohimbine type Rauwolfia alkaloids and related bases	Determination of reserpine in <i>Rauwolfia serpentina</i> and <i>R. cubana</i> stem bark	Silica gel	Benzene–ethanol (9 : 1 or 8 : 2)
	Isolation of alkaloids from <i>Mitragyna speciosa</i>	Cellulose	Chloroform–methanol (19 : 1 or 9 : 1)
		RP-18	Ethyl acetate–cyclohexane–diethylamine (210 : 90 : 1)
	TLC analysis of extract from <i>Uncaria</i>	Silica gel	Butanol–acetic acid–water (60 : 15 : 25)
	Determination of serpentine and ajmalicine in <i>Catharanthus roseus</i>		Methanol–water (4 : 2)
		Silica gel	Chloroform–acetone (5 : 4)
	TLC analysis of ajmaline stereoisomers, vincine, vincamine	Silica gel	Ethyl acetate–isopropanol–ammonium hydroxide (100 : 2 : 1)

Table 2 *Continued*

<i>Compounds separated</i>	<i>Applications</i>	<i>Adsorbent</i>	<i>Solvent system</i>
Ergot alkaloids	Determination of ergotamine tartrate in bulk drugs and dihydroergotamine mesylate (USPXXI, EP, BP)	Silica gel	Dimethylformamide-ether-chloroform-ethanol (15 : 70 : 10 : 5) Chloroform-ethanol (9 : 1)
	Qualitative identification of hallucinogen ergot alkaloids from <i>Ipomoea Tricolor Cav</i>	Silica gel	Ethanol-tetrahydrofuran-ethyl acetate (1 : 1 : 8) Water-ethanol-ether (5 : 35 : 60) Acetonitrile-ethanol-toluene (85 : 10 : 5) Water-ethanol-ether (1 : 7 : 12) Acetonitrile-ethanol-toulene (17 : 2 : 1)
	Quantitative analysis of ergot alkaloids: lysergol, ergometrine, agroclavine, ergotamine, ergocristine, ergotamine, ergocristinine	Silica gel (circular U-RPC)	
	Qualitative identification of ergot alkaloids	Silica gel	Stepwise gradient elution: 1 Chloroform-diethylamine (12 stages, 7 steps) 2 Chloroform-acetone-diethylamine (11 stages, 5 steps)
<i>Pyridine and piperidine alkaloids</i>			
Tobacco alkaloids	Rapid TLC identification of cytisine and nicotine	Silica gel	Dichloromethane-methanol-10% ammonium hydroxide (83 : 15 : 2)
	Determination of nicotine, nor nicotine, anabasine, nicotyrine, 2,2-dipiridyl	Silica gel (OPLC)	Ethyl acetate-methanol-water (12 : 35 : 3)
Tropane alkaloids	Quantitative determination of atropine in Chinese medicine	Silica gel	Chloroform-acetone-methanol-ammonium hydroxide (70 : 10 : 15 : 1)
	Determination of atropine in pharmaceutical preparations: bulk drugs and injections (USPXXI)	Silica gel	Chloroform-diethylamine (9 : 1)
	Qualitative identification of atropine, scopolamine, tubocurarine in African arrow poison	Silica gel	Chloroform-cyclohexane-diethylamine (3 : 6 : 1)
	TLC analysis of <i>Belladonna</i> tinctura (atropine, scopolamine)	Silica gel with micro-crystalline cellulose (5 : 2)	Chloroform-acetone-methanol-ammonium hydroxide (73 : 10 : 15 : 2)
	Analysis of <i>Hyoscyamus</i> extract	Silica gel	Methanol-ammonium hydroxide (98 : 2) Chloroform-butylamine (9 : 1) Ethyl acetate-formic acid-ammonium hydroxide (10% : 83 : 15 : 2) Water-methanol-sodium acetate buffer (0.2 mol L ⁻¹ aqueous: 28 : 12 : 60 : 1)
Pseudotropine alkaloids	Determination of cocaine and local anaesthetics	Silica gel	Two-dimensional: 1 Cyclohexane-benzene-diethylamine (75 : 15 : 10) 2 Chloroform-methanol (8 : 1) Chloroform-ethanol (1 : 1) Butanol-ethanol (95 : 1)
	Identification of alkaloids in <i>Erythroxylum hypericifolium</i> leaves	Aluminium oxide	
<i>Quinoline alkaloids</i>			
Cinchona alkaloids	Quantitative analysis of 17 cinchona alkaloids	Silica gel	Chloroform-acetone-methanol-25% ammonium hydroxide (60 : 20 : 20 : 1)
	TLC analysis of cinchona alkaloids as pure substances	Silica gel	Chloroform-diethylamine (9 : 1) Chloroform-methanol-ammonium hydroxide (25% : 85 : 14 : 1) Kerosene-acetone-diethylamine (23 : 9 : 9)

Table 2 Continued

Compounds separated	Applications	Adsorbent	Solvent system
			Toluene–diethyl ether–diethylamine (20 : 12 : 5)
	Determination of quinidine and dihydroquinidine in serum	Silica gel	Ethyl acetate–ethanol– <i>n</i> -butanol–ammonium hydroxide (56 : 28 : 4 : 0.5)
	Preparative TLC quinoline alkaloids from <i>Orixa japonica</i> stems	RP-18 Silica gel	Methanol–water (2 : 1) Benzene–ethyl acetate (4 : 1)
	Determination of quinine hydrochloride, quinidine sulfate in bulk drugs (EP, BP)	Silica gel	Diethylamine–ether–toluene (10 : 24 : 40)
	Determination of cinchonine in bulk drugs	Silica gel sprayed with 0.1 mol L ⁻¹ methanolic potassium hydroxide	Ammonium hydroxide–methanol (1.5 : 100)
<i>Isoquinoline alkaloids</i>			
Protoberberine and protopine alkaloids	Determination of berberine in biological matrix	Silica gel	Ethyl acetate–methyl acetate–methanol–water (27 : 23 : 6 : 5)
	Separation of berberine in presence of quaternary alkaloids in plant extracts	Silica gel (OPLC)	Ethyl acetate–tetrahydrofuran–acetic acid (6 : 2 : 2)
	Quantitative analysis and qualitative identification of protoberberine alkaloids	Silica gel	Two-step development in twin trough chamber: 1 Ethyl acetate–methanol–ammonium hydroxide (10 : 10 : 1) 2 Benzene–ethyl acetate–isopropanol–methanol–water (20 : 10 : 5 : 5 : 1) Second trough containing 5 mL conc. NH ₃
	Quantitative analysis of berberine in capsule	Silica gel	Ethyl acetate–acetone–formic acid–water (20 : 17 : 4 : 2)
	TLC analysis of protopine and allocryptopine from Turkish <i>Papaver curviscapum</i>	Silica gel	Benzene–ethanol–ammonium hydroxide (8 : 2 : 0.03) Benzene–acetone–methanol (7 : 2 : 1) Toluene–acetone–methanol–ammonium hydroxide (45 : 45 : 7 : 3)
	Determination of berberine in bulk drugs	Silica gel sprayed with 0.1 mol L ⁻¹ methanolic potassium hydroxide	Ammonium hydroxide–methanol (1.5 : 100)
	Determination of sanguinarine, chelidonine, protopine, allocryptopine in <i>Chelidonium majus</i>	Silica gel	Toluene–methanol–diethylamine (60 : 5 : 2) saturated with formamide
Morphine alkaloids	Analysis of morphine alkaloids in opium	Silica gel	Benzene–ethanol (17 : 1 or 9 : 1) Benzene–dioxane–ethanol–ammonium hydroxide (50 : 40 : 5 : 5) Toluene–acetone–ethanol (96%)–ammonium hydroxide (25%) (45 : 45 : 7 : 3) Hexane–chloroform–diethylamine (50 : 30 : 7) Ethyl acetate–methanol–ammonium hydroxide (85 : 10 : 5 or 75 : 20 : 5) Chloroform–triethanolamine (95 : 5) Chloroform–methanol–water (7 : 5 : 1) Butanol–ammonium hydroxide–water–methanol (20 : 1 : 4 : 2)
	Determination of morphine and semisynthetic derivatives	Silica gel	

Table 2 Continued

Compounds separated	Applications	Adsorbent	Solvent system
Isoquinoline bases	Determination of Dabsyl derivatives of morphine in urine	Silica gel	Chloroform-ethanol-triethanolamine (30 : 2 : 0.05)
	Determination of papaverine, codeine, eupaverine	RP-18 (IP-TLC)	Water-acetone (20 : 80, 100 : 0) with 0.1 mol L ⁻¹ of ion reagent-sodium alkylsulfonate
	Determination of emetine and tubocurarine	Silica gel	Ethyl acetate-isopropanol-ammonium hydroxide (25% : 9 : 7 : 2)
	TLC analysis of emetine hydrochloride in bulk drugs (USPXXI, BP)	Silica gel	Chloroform-diethylamine (9 : 1)
	TLC analysis of codeine in bulk drugs (EP)	Silica gel	Ammonium hydroxide-cyclohexane-ethanol (6 : 30 : 72)
	TLC analysis of papaverine hydrochloride in bulk drugs (EP)	Silica gel	Diethylamine-ethyl acetate-toluene (1 : 2 : 7)
	Determination of codeine, chlorpheniramine, phenylephrine, paracetamol (acetaminophen) in syrup and tablets	Silica gel	Butanol-methanol-toluene-water-acetic acid (3 : 4 : 1 : 2 : 0.1)
Benzylisoquinoline alkaloids	Determination of alkaloids in <i>Anisocycla cymosa</i> roots and plant extract	Silica gel	Chloroform-methanol-diethylamine-ammonium hydroxide (8 : 2 : 2 : 0.5) Benzene-acetone-ammonium hydroxide (15 : 15 : 1)
	Determination of bisbenzylisoquinoline alkaloids in <i>A. jollyana</i> leaves	Silica gel	Chloroform-toluene-methanol-acetone-ethyl acetate-ammonium hydroxide (270 : 30 : 80 : 30 : 3)
Aporphine alkaloids	Analysis in plant material	Aluminium oxide	Toluene-chloroform-methanol-ammonium hydroxide (100 : 150 : 40 : 3)
		Silica gel	Cyclohexane-ethyl acetate (3 : 2) Cyclohexane-acetone (9 : 1) Petrol ether-acetone (7 : 3) Chloroform-methanol (9 : 1)
Various isoquinoline alkaloids	Determination of cocaine, heroin and local anaesthetics in street drugs	Silica gel	Benzene-chloroform-triethanolamine (9 : 9 : 4) Ethyl acetate-isopropanol-28% ammonium hydroxide (40 : 30 : 3)
	Analysis of major drugs of abuse in urine	Silica gel	Ethyl acetate-cyclohexane-methanol-ammonium hydroxide (conc.)-water (70 : 15 : 8 : 2 : 0.5) Ethyl acetate-cyclohexane (50 : 60)
<i>Diterpene and steroidal alkaloids</i>			
Diterpene	Determination of aconitine nitrate in bulk drugs	Silica gel spray 0.1 mol L ⁻¹ potassium hydroxide methanol	Ammonium hydroxide-methanol (1.5 : 100)
	Determination of aconitine, 3-deoxyaconitine, mesaconitine in <i>Wutou</i> and <i>Aconitum</i>	Silica gel	Cyclohexane-ethyl acetate-ethylenediamine (8 : 1 : 1)
	Isolation of norditerpenoid alkaloids from extract of roots of <i>Delphinium tatsienense</i> TLC of 8 diterpenoid alkaloids from <i>Aconitum septentrionale</i>	Aluminium oxide (neutral)	Gradient elution: hexane, hexane-diethyl ether (25 : 75), diethyl ether, diethyl ether-methanol
		Silica gel (centrifugal TLC)	Diethyl ether-75% methanol-0.3% diethylamine
		Silica gel (preparative TLC)	Diethyl ether-5% methanol
		Silica gel	Hexane-chloroform (6 : 4)
		Aluminium oxide (centrifugal TLC)	Chloroform-methanol (8 : 2 or 97 : 3) Gradient of hexane, ether and methanol

Table 2 *Continued*

<i>Compounds separated</i>	<i>Applications</i>	<i>Adsorbent</i>	<i>Solvent system</i>
Steroidal alkaloids	Isolate ecdysteroids from the herba of <i>Silene tatarica</i>	Silica gel (droplet countercurrent chromatography)	Ethyl acetate-methanol-ammonium hydroxide (17 : 5 : 3) Dichloromethane-ethanol (17 : 3) Chloroform-methanol-acetone (6 : 2 : 1) Methanol-water (13 : 7)
Veratrum alkaloids	Determination of veratrum alkaloids jervine, veratroylzygadenine, rubijervine, isorubijervine, veromine in <i>Veratrum</i> root and tincture	Silica gel Aluminium oxide	Benzene-ethanol-diethylamine (80 : 16 : 4) Benzene-ethanol (95 : 5)
Solanum alkaloids	Determination of solanum alkaloids (solanidine) from spiked milk and α -solasonine, α , β -solamargine from <i>Solanum ptycanthum</i>	Silica gel	Methanol-chloroform-1% ammonium hydroxide (2 : 2 : 1)
<i>Miscellaneous heterocyclic systems</i>			
Pyrrolizidine alkaloids	TLC analysis in plant material	Silica gel	Dichloromethane-methanol-ammonium hydroxide (85 : 15 : 2 or 75 : 23 : 2 or 79 : 20 : 1) Chloroform-methanol (4 : 1) Chloroform-methanol-ammonium hydroxide (60 : 10 : 1 or 17 : 38 : 0.25) Chloroform-methanol-28% ammonium hydroxide (85 : 14 : 1)
Lupin alkaloids	TLC of lupanine and 7-hydroxylupanine from <i>Cytisophyllum seccilifolium</i>	Silica gel impregnated with 0.1 mol L ⁻¹ NaOH Silica gel	
Carbazole alkaloids		Silica gel	Benzene-chloroform (1 : 1)
Xanthine alkaloids	Qualitative identification and preparative TLC of alkaloids from <i>Bosistoa floydi</i> leaf	Silica gel	Chloroform-ethyl acetate (3 : 2)
Purine bases	Determination of purine bases in urine	Silica gel	Two-dimensional: 1 Chloroform-methanol (4 : 1) 2 Butanol-chloroform-acetone-ammonium hydroxide (4 : 3 : 3 : 1)
	Determination of caffeine, theophylline and 15 drugs in Chinese herbal preparations	Silica gel	Dichloromethane-methanol-water (183 : 27 : 5) Ethyl acetate-toluene-dimethylformamide-formic acid (75 : 70 : 4 : 2) Dichloromethane-methanol (183 : 27) Ammonium hydroxide-acetone-chloroform-butanol (1 : 3 : 3 : 4)
	Determination of caffeine and theobromine in bulk drugs (EP)	Silica gel	
	Determination of theophylline in capsules (USPXXI) in tablets with ephedrine hydrochloride and phenobarbital (USPXXI, EP)	Cellulose Silica gel	Methanol-water Chloroform-acetone-methanol-ammonium hydroxide (50 : 10 : 10 : 1)
Quinolizidine	Qualitative identification	Silica gel Aluminium oxide	Chloroform-cyclohexane-butylamine (5 : 4 : 1) 1.5% Methanol in chloroform

BP, British Pharmacopoeia; EP, European Pharmacopoeia, USPXXI, The United States Pharmacopoeia, Twenty-first Revision.

interactions of siloxane groups with the non-polar fragments of the separated alkaloids, as well as by ion exchange interactions. In the retention of alkaloids a dominant role is played by the ion exchange mechanism which is due to the weak cation exchange prop-

erties of silica gel at pH = 2–8 and the fact that aromatic amines chromatographed in an aqueous mobile phase are weakly protonized at pH = pK_a – 1. The selectivity of such systems depends then, primarily, on the pH of the mobile phase but

also on the kind of organic modifier, which is usually methanol or acetonitrile.

Reversed-phase Chromatography

Nonpolar adsorbents have rarely been applied in TLC of alkaloids, perhaps because of the low efficiency of such systems, which is caused by the interaction of alkaloid molecules with silanol groups present on the adsorbent surface in addition to the hydrocarbon chains. In reversed-phase chromatography on silanized silica gel, alkaloids as easily ionized compounds require specific conditions of analysis such as suppression of dissociation, ion suppression or the application of specific ion pair reagents.

The suppression of dissociation is achieved with a mobile phase of a suitable pH ($\text{pH} \geq \text{pK}_a$) for the specific solvent, in accordance with the curve shown in Figure 2.

Reversed-phase conditions may also be obtained by impregnating silica gel with paraffin or silicone oil. Additionally, chemically bonded reversed phases with polar groups (cyano- and amino-layers) have been employed. Their properties depend on the kind of compounds to be separated and on the composition of the mobile phase.

Ion Pair Chromatography

The use of ion pair chromatography (IP-TLC) of alkaloids may be carried out on normal and reversed phases. This technique has been applied to analyse basic drugs, including alkaloids, on silica gel using normal-phase systems. The best results are obtained by applying chloride and bromide as counterions of at least 0.1 mol L^{-1} concentration in the spreading slurry or in the solvent.

Reversed-phase IP-TLC is far more widely used. The counterion reagents which may be present in the mobile phase and serve for impregnation in the nonpolar stationary phase may be di-(2-ethylhexyl) orthophosphoric acid (HDEHP), camphoric and camphorosulfonic acids, sodium dodecylsulfate and simple hydrophilic anionic reagents such as perchloric acid, oxalic acid and trichloroacetic acid. The acidic environment of the mobile phase ensures ionization of the acidic counterions and enables the creation of an ion pair with the alkaloids protonized under these conditions. The behaviour of some isoquinoline bases using RP-18 plates and alkylsulfonates as counterions has also been investigated.

Although retention and separation selectivity in IP-TLC depend on many factors, optimization of such chromatographic systems is basically concerned with pH changes, concentration and the chain length

of the counterion or the concentration of organic modifier in the mobile phase.

Partition Chromatography

In the past, partition chromatography conducted on paper was a perfect model for establishing optimum extraction systems for alkaloid isolation. In paper chromatography, the system allowing partition conditions is mainly composed of cellulose with an aqueous solvent or an aqueous buffer solution of pH 3–7, depending on the nature of the alkaloids. Silica gel combined with an aqueous phase or a water-saturated organic solvent also allows for the domination of the partition mechanism, thanks to deactivation of the surface silanol groups. The aqueous phases in such systems are often alkalized with aqueous ammonium hydroxide or acidified with hydrochloric acid.

Partition conditions, similar to paper chromatography, may be obtained by impregnating cellulose or silica gel with a solution of formamide in ethanol and using mobile phases immiscible with the stationary phase, such as chloroform, benzene, cyclohexane or their mixtures.

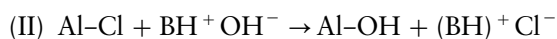
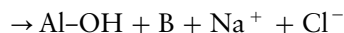
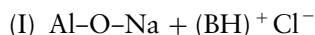
Ion Exchange Chromatography

Ion exchange techniques are applied for both crude fractionation and separation and determination of alkaloids.

The typical ion exchange sorbents used for TLC of alkaloids have been as follows: anion exchangers AG 1-X4 and Cellex D, and cation exchangers with cellulose (alginic acid and sodium carboxymethylcellulose), paraffin (Rexyn 102) and polystyrene (Dowex 50-X4) matrices.

While choosing the best eluent for ion exchange chromatography, pH values should be carefully considered. They are closely correlated with the number of charges in the alkaloid molecules and at the same time decide the retention values. The trends for most alkaloids fit the type of curves shown in Figure 3.

One of the popular adsorbents which may function as an ion exchanger is aluminium oxide (Al_2O_3) with an aqueous mobile phase. Depending on the kind of aluminium oxide used, a cation- or anion-exchanging mechanism may occur. Thus, in aqueous alcoholic solution basic alumina functions as a cation exchanger (I), but acidic alumina acts as an anion exchanger (II). With neutral alumina, both types of reactions may take place depending on the conditions used:



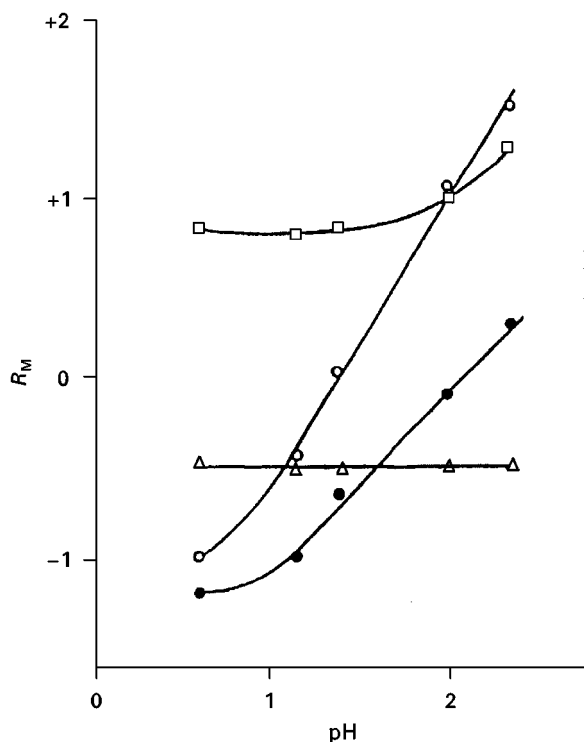


Figure 3 R_M versus pH curves for some alkaloids on alginic acid thin layers (after Lepri L, Desideri PG and Lepori M (1976) Chromatographic Behaviour of Alkaloids of Thin Layer of Cation Exchangers. Journal of Chromatography 123, 175. Amsterdam: Elsevier).

Adsorbents Impregnated with Metal Salts

The use of silica gel and aluminium oxide impregnated with metal salts (cadmium and zinc nitrate) for the separation of some alkaloids has been studied.

For steroid alkaloids, the impregnation of the stationary phase with silver salts – so-called argentation TLC – has been applied. This technique is based on the formation of π -complexes with the separated compounds during the chromatographic process.

Detection of Alkaloids

Only a few alkaloids are directly visible on the chromatogram as coloured spots and visualization methods have to be applied to detect them. In order to detect the compounds under UV light, fluorescing indicators are added to the adsorbent.

Alkaloids become visible in short wavelength UV light ($\lambda = 254$ nm), where they appear as dark zones on a fluorescent background. This is considered to be a nonselective method of detection because, on the layer containing a fluorescent indicator, the emission is quenched in regions where all aromatic organic

compounds absorb the UV light with which the plates are irradiated.

Some alkaloids, such as indoles, quinolines, isoquinolines and purines, cause pronounced quenching of fluorescence, but some (e.g. tropine alkaloids) only weakly quench UV light. Sometimes compounds can be detected under a UV lamp due to their own luminescence. Excitation is usually performed using long wavelength radiation of $\lambda = 365$ nm. Alkaloids absorb radiation and then usually emit it in the visible region of the spectrum, where they appear as bright-coloured luminous zones of blue, blue-green or violet, for example, *Rauwolfia radix*, *Chinae cortex*, *Ipecacuanhae radix*, *Boldo folium*, and of yellow, e.g. *colchicine*, *sanguinarinae*, *berberine*.

Other methods of physical detection make the most of the chemical properties of alkaloids. As basic compounds, these properties can be detected using pH indicators applied to the chromatogram by dipping it or spraying it with 0.01–1% indicator solutions.

Bromocresol Green with pH transition from 3.8 to 5.4 is applied for many alkaloids; Bromocresol Purple (pH = 5.2–6.8) is predominantly applied for ephedrine.

Another nonselective detection method for alkaloids as lipophilic substances is the treatment of a chromatogram with iodine vapour or dipping into or spraying with 0.5–1% iodine solutions. Molecular iodine is enriched in the chromatogram zones and colours them brown. Emetine and cephaeline, the two major alkaloids of *ipecacuanha*, begin to glow after treatment with iodine vapour. In this case, the molecular iodine which acts as a quencher must be removed by heating, before the yellow (emetine) and blue (cephaeline) fluorescent zones become visible.

Although the methods described are usually fairly sensitive and allow a detection limit of less than 1 μ g, sometimes they are insufficient. That is why they have to be supplemented by specific reactions with a number of detection reagents (Table 3).

The most popular reagents which react with tertiary and quaternary nitrogen atoms present in alkaloid molecules are Dragendorff's reagent and potassium iodoplatinate. Alkaloids containing primary and secondary amino groups treated with dimethyl sulfate give quaternary nitrogen atoms, permitting effective detection with these reagents too.

Dragendorff's and iodoplatinate reagents exist in various modifications. The replacement of water in these reagents by acetic acid or ethyl acetate, diethyl ether–methanol or hydrochloric acid increases the sensitivity of the reaction and significantly improves the sharpness of spots. Spraying 10% sodium nitrate solution after the use of Dragendorff's reagent causes

Table 3 Selection of detection reagents for postchromatographic derivatization of alkaloids

Reagent	Substances detected	Reaction	Method	Result
Ammonia vapour	Alkaloids, e.g. morphine, heroin, 6-mono-acetylmorphine	Morphine and heroin form fluorescent oxidation products	Heat the chromatogram in the drying cupboard to 110–120°C for 25 min and place it for 15 min in a twin-trough chamber, whose second trough contains 10 mL of 25% ammonia solution. Then immerse for 2 s in a solution of liquid paraffin– <i>n</i> -hexane (1 : 2)	Morphine, 6-monoacetylmorphine and heroin appear as blue fluorescent zones on a dark background under UV light ($\lambda = 365$ nm). In each case the detection limits are 2 ng of substance per chromatographic zone. The fluorimetric determination is carried out in UV light $\lambda_{\text{exc}} = 313$ nm, $\lambda_{\text{fl}} = 390$ nm
Formaldehyde reagent (1,2-naphthoquinone-4-sulfonic acid)–perchloric acid	Alkaloids, e.g. codeine, morphine, heroin, 6-mono-acetylmorphine	The reaction mechanism has not been elucidated. It is possible that formaldehyde reacts by oxidation, as in Marquis reaction	Dry the chromatogram in a stream of warm air for 5 min, immerse in the reagent solution for 4 s and heat to 70°C for <i>c.</i> 10 min	Morphine alkaloids yield blue chromatogram zones on a pale blue background. The detection limits are 10–20 ng of substance per chromatogram zone. The absorption photometric analysis can be performed at reflectance $\lambda = 610$ nm
2-Methoxy-2,4-diphenyl-3(2H)-furanone (MDPF)	Alkaloids from <i>Colchicum autumnale</i> (Colchicine)	MDPF reacts directly with primary amines to form fluorescent products	Free the chromatogram from mobile phase in a stream of warm air (45 min), immerse in the reagent solution for 4 s and then heat to 110°C for 20 min	Colchicine appears as a yellow fluorescent zone on a dark background in UV light (365 nm). The detection limit is 10 ng per chromatogram zone. The fluorimetric analysis is carried out with excitation at $\lambda_{\text{exc}} = 313$ nm, and evaluation at $\lambda_{\text{fl}} > 390$ nm
2,4-Dinitrophenyl-hydrazine	Alkaloids	Reagent reacts with carbonyl groups with the elimination of water to yield hydrazone and with aldoses or ketoses to yield coloured osazones	Immerse the chromatogram in the dipping solution for 2 s or spray and then dry in a stream of warm air (10–20 min at 110°C)	Substances yield yellow to orange-yellow chromatogram zones on an almost colourless background
2,6-Dichloro-quinone-4-chloroimide	Isoquinoline alkaloids	Reagent reacts with phenols or anilines which are not substituted in the <i>p</i> -position	Dry the chromatogram for 5 min in a stream of warm air, immerse in the dipping solution for 5 s and then heat to 110°C for 2 min	Cephealine produces a blue colour immediately on immersion, while emetine only does so on heating. On storage this colour slowly changes to brown (background light brown). The detection limits are <i>c.</i> 10 ng per chromatogram zone. The absorption photometric analysis was made at $\lambda = 550$ nm
α -Phthalaldehyde (OPT, OPA)	Ergot alkaloids	In the presence of 2-mercaptoethanol, α -phthalaldehyde reacts with primary amines to yield fluorescent isoindole derivatives	Immerse the dried chromatogram for 1 s in the reagent solution and then heat to 40–50°C in the dry cupboard for 10 min	Substance zones are produced that mainly yield blue (or yellow) fluorescence under long wavelength light ($\lambda = 365$ nm)
Phosphomolybdic acid	Morphine	Morphine can be oxidized with phosphomolybdic acid, whereby a portion of the Mo(VI) is reduced to Mo(IV) which forms blue-grey oxides with the remaining Mo(VI)	Dry the chromatogram in a stream of warm air and immerse for 2–3 s in the reagent solution, or spray the layer with it	Blue zones appear on a yellow background immediately or after a few minutes

Table 3 *Continued*

<i>Reagent</i>	<i>Substances detected</i>	<i>Reaction</i>	<i>Method</i>	<i>Result</i>
Trichloroacetic acid	Alkaloids from, e.g. <i>Veratrum colchicum</i>	The reaction mechanism has not yet been elucidated	Dry the chromatogram in a stream of cold air and immerse for 1 s in the reagent solution or spray with it and then heat at 120°C for 10 min	Light blue fluorescent zones appear mainly under long wavelength UV light ($\lambda = 365$ nm). The fluorescence can be stabilized and intensified by dipping the plate into a solution of liquid paraffin- <i>n</i> -hexane (1 : 2)
Sulfuric acid	Alkaloids	The reaction mechanism has not yet been elucidated	Dry the chromatogram in a stream of warm air for 10 min, immerse in the dipping solution for 1–2 s or spray with the spray solution, dry in a stream of warm air and then heat to 95–140°C for 1–20 min	Under long wavelength UV light ($\lambda = 365$ nm) characteristic substance-specific yellow, green, red and blue fluorescent chromatogram zones usually appear, and are often recognizable in visible light
7-Chloro-4-nitrobenzo-2-oxa-1,3-diazole (NBD-chloride reagent)	Alkaloids	NBD reacts with nucleophilic compounds to yield the corresponding 7-substituted 4-nitrobenzofurazan derivatives	Dry the chromatograms. Immerse in dipping solution of sodium acetate in methanol–water for 1 s. Dry in a stream of warm air and dip after cooling in NBD-chloride reagent in ethanol and then heat to 100°C for 2–3 min. Alternatively the chromatogram can be sprayed with the appropriate spray solutions	Under UV light ($\lambda = 365$ nm) the chromatogram zones fluoresce greenish-yellow, olive brown or violet. The plate background also fluoresces, but appreciably less. The detection limits are 100–800 ng substance per chromatogram zone
<i>tert</i> -Butyl hypochlorite	Alkaloids	The reaction mechanism has not yet been elucidated	Dry the chromatogram, immerse in dipping solution of reagent in carbon tetrachloride or cyclohexane for 1 s (or spray or expose to its vapours) then immerse in dipping solution of chloroform, paraffin oil and triethanolamine (6 : 1 : 1) for 1 s and dry in hot air	The analysed compounds appear in long wavelength UV light (365 nm), yellow to violet fluorescent zones, on a dark background. The detection limit for morphine is 10 ng and for papaverine 1 ng per chromatogram zone
Formaldehyde-sulfuric acid (Marquis reagent)	Alkaloids, e.g. morphine, codeine, heroin, 6-monoacetyl-morphine	Morphine reacts with formaldehyde in acidic solution to yield a cyclic ketoalcohol, which is transformed into the coloured oxonium or carbenium ion in acidic conditions	Dry the chromatogram in a stream of warm air for 5 min, immerse in the dipping solution for 6 s and heat to 110°C for 20 min	Morphine alkaloids yield reddish chromatogram zones (codeine yielded blue on a pale pink background). If a quantitative fluorimetric analysis is to follow, the chromatogram is exposed to ammonia vapour for 20 min and immersed for 2 s in 20% dioctyl sulfosuccinate in chloroform. After drying, morphine alkaloids appear as pink to red fluorescent zones on a blue fluorescent background under UV light ($\lambda = 365$ nm). The fluorimetric analysis is carried out at $\lambda_{\text{exc}} = 313$ nm, $\lambda_{\text{fl}} = 560$ nm

Table 3 *Continued*

<i>Reagent</i>	<i>Substances detected</i>	<i>Reaction</i>	<i>Method</i>	<i>Result</i>
Iron (III) chloride-perchloric acid (FCPA reagent)	Indole alkaloids, e.g. from <i>Rauwolfia</i> , <i>Tabernaemontana</i> , <i>Mitragyna</i> , <i>Strychnos</i> , <i>Synclisia</i> , <i>Cinchona</i>	The reaction mechanism has not yet been elucidated	Free the chromatogram from mobile phase in a stream of warm air (45 min), immerse in the dipping solution for 4 s. Dry and heat to 110°C for 20 min	Variously coloured chromatogram zones are produced on a colourless background. For instance, strychnine appears as a red and brucine as a yellow chromatogram zone on a colourless background. The detection limit for both is 10 ng per chromatogram zone. The light absorption in reflectance was measured at $\lambda = 450$ nm
Hydrochloric acid vapour	Alkaloids, e.g. papaverubines	The reaction mechanism has not yet been elucidated	Free the chromatogram from mobile phase (first in a stream of cold air for a few minutes, than at 100°C for 5 min), place in the free trough of the prepared twin-trough chamber for 5 min and then evaluate	Alkaloids are visible after irradiation with unfiltered UV light from a mercury lamp

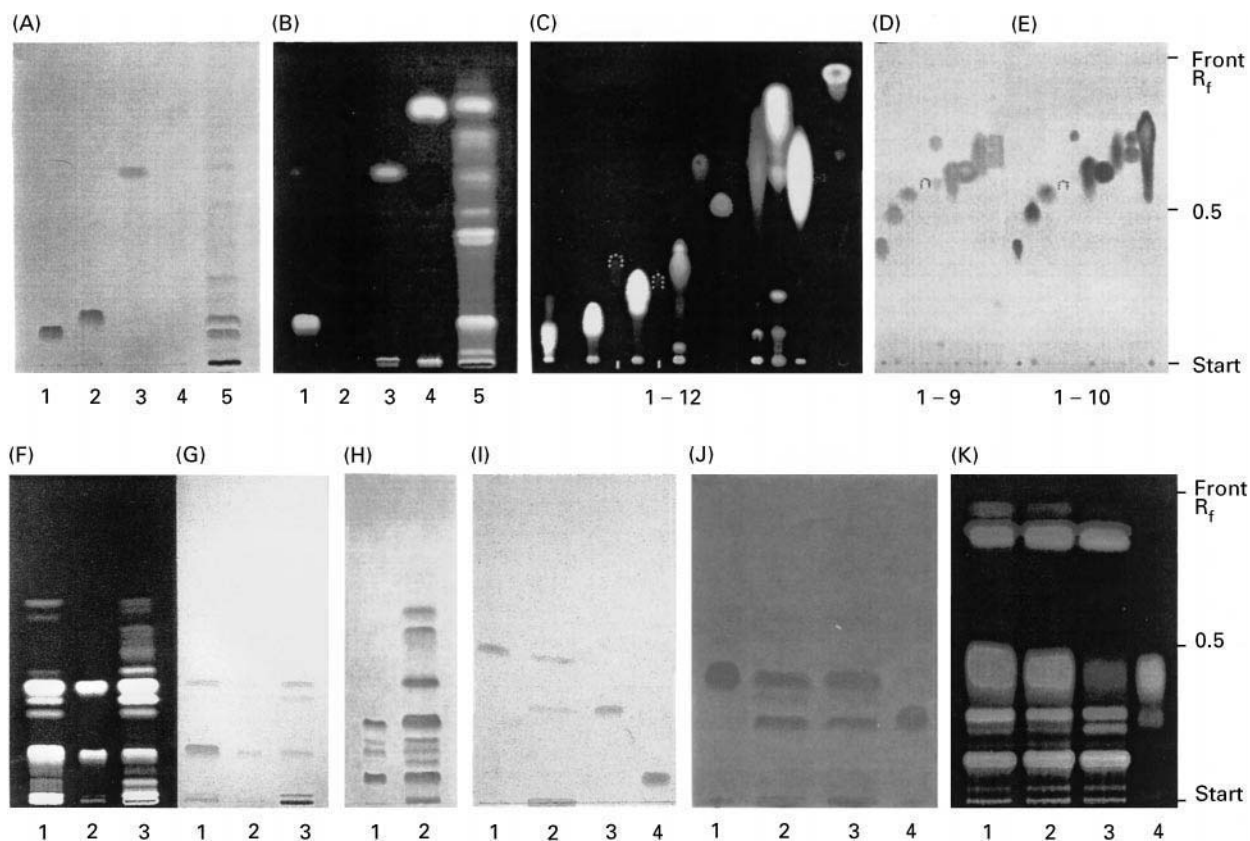


Figure 4 (See Colour Plate 54). The chromatograms of the separated alkaloids developed on silica gel or alumina in solvent systems 1–4, detected with different reagents. Solvent systems: 1, toluene–ethyl acetate–diethylamine (70 : 20 : 10); 2, chloroform–diethylamine (90 : 10); 3, toluene–chloroform–ethanol (28.5 : 57 : 14.5); 4, 1-propanol–water–formic acid (90 : 9 : 1). For identification of compounds, reagents used and obtained results, see Table 4. (Reproduced with permission from Wagner H and Bladt S (1996) *Plant Drug Analysis. Thin-layer Chromatography Atlas*. Berlin: Springer.)

Table 4 Symbols used in Figure 4

Symbol	Detection	Solvent system	Reference compounds	Result
A	Marquis reagent → vis	1	Morphine (1), codeine (2), papaverine (3), noscapine (4), opium extract (5)	Morphine and codeine are immediately stained violet; papaverine: weak violet; noscapine: weak yellow brown
B	Natural products, polyethylene glycol reagent (NP/PEG) → UV 365 nm	1		Morphine, papaverine, noscapine give a blue fluorescence in UV 365 nm; codeine does not fluoresce
C	Sulfuric acid reagent → UV 365 nm	1	Serpentine (1), quinine (2), cinchonine (3), quinidine (4), cinchonidine (5), cephaeline (6), emetine (7), yohimbine (8), noscapine (9), hydrastine (10), berberine (11), sanguinarine (12)	The fluorescence of quinine and quinidine is a radial blue; cinchonine and cinchonidine: deep violet, berberine and sanguinarine: bright yellow
D	Dragendorff reagent → vis		Strychnine (1), yohimbine (2), physostigmine (3), nicotine (4), veratrine (5), emetine (6), papaverine (7), lobeline (8), aconitine (9), narcotine (10)	Alkaloids give orange-brown, stable colours
E	Dragendorff reagent followed by sodium nitrite → vis	1		The zones become dark brown
F	Iodine/CHCl ₃ reagent → UV 365 nm	1	<i>Cephaelis accuminata</i> (1), cephaeline: $R_f \sim 0.2$; emetine: $R_f \sim 0.4$ (2).	Cephaeline fluoresces bright blue and emetine: yellow-white
G	→ vis	1	<i>Cephaelis ipecacuanha</i> (3)	Cephaeline gives red and emetine weak yellow zones
H	10% H ₂ SO ₄ followed by iodoplatinate reagent → vis	2	China alkaloid mixture (1) <i>Cinchona succirubra</i> (2)	The violet-brown zone of quinine is followed by the grey-violet zone of cinchonidine, a weak red-violet zone of quinidine and brown-red cinchonine (1) In <i>Cinchona succirubra</i> extract additionally three red-violet zones appear in the R_f range 0.4–0.6 (2)
I	van URK reagent → vis	3	Ergocristine (1), <i>Secale cornutum</i> (2), ergotamine (3), ergometrine (4)	Secale alkaloids appear as blue zones in the R_f range of 0.05–0.4
J	UV 254 nm	1	Strychnine (1), <i>Strychni semen</i> (2), <i>Ignatii semen</i> (3), brucine (4)	Strychnine and brucine are characterized in UV 254 nm by their strong quenching zones
K	UV 365 nm	4	<i>Chelidonii herba</i> different trade samples (1–3), sanguinarine (4)	The major alkaloid coptisin at $R_f \sim 0.15$ (bright-yellow) is followed by berberine, chelerythrine, sanguinarine (broad yellow) and chelidonine (weak yellow-green) in the R_f range of 0.75–0.85

the colour of alkaloid zones to be intensified or stabilized and increases the sensitivity to 0.01–0.1 µg.

Modification, where a chromatogram is sprayed with 10% sulfuric acid after the use of Dragendorff's

reagent, also causes an increase in the sensitivity of the reaction. Potassium iodoplatinate reagent gives preliminary identification, due to the fact that different colours are obtained with different alkaloids.

Table 5 Examples of prechromatographic derivatization of alkaloids

Prechromatographic derivatization	Reagent used	Special applications
Oxidation	10% Chromic acid in glacial acetic acid Potassium dichromate Dehydration by heating the applied sample on silica layer	Strychnine and brucine
Reduction	Sodium borohydride solution	Not specified
Iodination	Iodine vapour saturated chamber (18 h)	Quinoline, isoquinoline, indole alkaloids
Nitration	Concentrated nitric acid	Brucine
Dansylation	Dansyl chloride and twice bigger volume of 8% sodium bicarbonate solution	Morphine, 6-monoacetylmorphine, morphine-6-nicotinate

Table 6 Systematic analysis of alkaloids on TLC plates

Chemical skeleton	Plant drug	Botanical origin	Major alkaloid	Fluorescence in UV light (366 nm)	Colour with iodoplatinate reagent	hR _F values							
						S ₁	S ₂	S ₃	S ₄	S ₅	S ₆	S ₇	S ₈
Tropane	Fol. Belladonnae	<i>Atropa belladonna</i> L., Solanaceae	Atropine		Violet-blue	38	40	16	5	12	0	10	17
	Rad. Belladonnae												
	Fol. Hyoscyami	<i>Hyoscyamus niger</i> L., Solanaceae	Homatropine		Violet-blue	37	45	15	5	23	4	24	15
	Fol. Stramonii	<i>Datura stramonium</i> L., Solanaceae	Apoatropine		Violet-blue	54	67	40	20	26	15	40	16
	Rad. Scopoliae	<i>Scopolia carniolica</i> Jacq., Solanaceae	Scopolamine Scopoline		Violet White	56 60	60	19	3	34	30	0	52
	Fol. Duboisiae	<i>Duboisia myoporoides</i> R. Br., Solanaceae	Tropacocaine		Violet	65	90	56	34	45	58	78	35
	Fol. Cocae	<i>Erythroxylon coca</i> Lamarck, Erythroxylaceae	Cocaine		Violet	73	90	65	36	58	84	77	62
Indole	Semen Calabaris	<i>Physostigma venenosum</i> Balfour, Papilionaceae	Physostigmine		Pink	65	>90	32	4	44	59	50	46
	Rad. Rauwolfiae	<i>Rauwolfia serpentina</i>	Reserpine	Green-yellow	White	72	80	20	0	46	63	35	69
	Rad. Serpentinae	Bentham, Apocynaceae	Serpentinine	Dark brown	Red-brown	24	15	0	0	4	0	0	0
	Semen Strychni	<i>Strychnos nuxvomica</i> L., Loganiaceae	Serpentine Ajmaline Strychnine	Yellow-green Blue	Yellow-brown Beige Yellow	53 47 53	56	8	0	10	0	3	12
	Cortex Yohimbehe	<i>Pausinystalia yohimbe</i> Pierre, Rubiaceae	Yohimbine	Green-blue	Light yellow	63	62	18	3	37	33	15	60
			Ergocristinine	Violet-blue	Light brown	61	57	13	0	20	0	27	70
			Ergotamine	Violet-blue	Pink	24	16	0	0	3	10	5	59
			Ergometrine	Violet-blue	White	14	6	0	0	2	3	0	64
			Ergometrinine	Violet-blue	Violet-blue	42	25	3	0	8	12	10	62
			Ergocristine	Violet-blue	Beige-light brown	51	38	14	5	13	46	15	70
			Ergotaminine	Violet-blue	Pink	24	51	0	0	14	42	15	68
			Dihydroergotamine	Violet-blue	Brownish	21	12	0	0	3	7	0	61
			Dihydroergocristine	Violet-blue	Brownish	12	30	3	0	7	15	7	69
Isoquinoline	Opium	<i>Papaver somniferum</i> L., Papaveraceae	Thebaine		Red-brown	65	90	51	16	50	71	76	40
			Narceine		Deep-blue	3	0	0	0	3	0	0	0
			Morphine		Deep-blue	10	8	0	0	3	3	0	34
			Papaverine	Yellowish	Yellow	67	90	42	3	47	85	84	70
			Codeine		Pink-violet	38	53	16	4	26	12	27	35
			Noscapine	Blue	Light-yellow	72	90	51	10	57	81	79	72
			Hydrastinine	Steel blue	Violet-blue	66	90	58	41	50	0	25	0
			Dihydromorphinone		Brownish yellow	24	23	8	1	11	5	8	16
			Dihydrocodeine	Blue	Violet-blue	38	54	18	6	28	10	30	25
			Dihydrocodeinone		Violet	51	65	21	4	30	48	43	18
	Fol. Boldo	<i>Peumus boldus</i> Monimiaceae	Boldine	Violet	Beige	16	16	3	0	5	24	6	58
Quinoline	Cortex Chinae	<i>Cinchona succirubra</i> , P. Rubiceae	Quinidine	Blue	Light yellow	34	40	15	0	25	12	18	50
			Quinine	Blue	Yellow-white	19	26	7	0	17	9	18	43
			Cinchonine		Beige-brown	38	44	17	7	27	0	22	40
Imidazole	Fol. Jaborandi	<i>Pilocarpus microphyllus</i> Stapf e.a.; Rutaceae	Pilocarpine		Light brown	41	52	9	0	13	32	25	55

Table 6 Continued

Chemical skeleton	Plant drug	Botanical origin	Major alkaloid	Fluorescence in UV light (366 nm)	Colour with iodoplatinate reagent	hR _F values							
						S ₁	S ₂	S ₃	S ₄	S ₅	S ₆	S ₇	S ₈
Pyridine	Semen Arecae Herba Lobeliae	<i>Areca catechu</i> L., Palmae	Arecoline		Violet	66	90	56	34	48	0	0	0
		<i>Lobelia inflata</i> L., Lobeliaceae	Lobeline		Red-brown	68	90	48	14	48	55	60	55
Quinolizidine		<i>Sarothamnus</i> <i>Scoparius</i> ; Leguminosae	Sparteine		Violet	70	90	68	68	55	0	55	5
Dihydroindole	Fol. Catharanti	<i>Catharantus roseus</i> Apocynaceae	Aspidospermine		White	65	90	54	20	49	50	60	65
Aporphine	Rhizoma Corydalis	<i>Corydalis cava</i> L., Schweigg et Koerte Papaveraceae, Fumariaceae	Bulbocapnine	Blue	White	65	>90	35	7	54	78	70	48
Isoquinoline	Rad. Ipecacuanhae	<i>Cephaelis</i> <i>ipecacuanha</i> Rubiaceae	Emetine Cephaeline	Blue Violet-blue	Red-brown White	67 56	90 63	40 19	6 2	45 23	38 25	58 17	50 37
Miscellaneous alkaloids													
Derivatives of diterpene	Aconiti Tuber	<i>Aconitum napellus</i> L., Ranunculaceae	Aconitine		Red-brown	68	>90	35	3	49	36	60	65
Xanthine	Herba Ephedrae	<i>Ephedra sinica</i> Stapf. Ephedraceae	Ephedrine		Light-grey	47	41	4	0	4	11	0	57
Colchicine	Semen Colchici	<i>Colchicum autumnale</i> L., Liliaceae	Colchicine		Light brown								

TLC systems

S₁, Silica gel G, activated: chloroform–acetone–diethylamine (5 : 4 : 1).S₂, Silica gel G, activated: chloroform–diethylamine (9 : 1).S₃, Silica gel G, activated: cyclohexane–chloroform–diethylamine (5 : 4 : 1).S₄, Silica gel G, activated: cyclohexane–diethylamine (9 : 1).S₅, Silica gel G, activated: benzene–ethyl acetate–diethylamine (7 : 2 : 1).S₆, Aluminium oxide G, activated: chloroform.S₇, Aluminium oxide G, activated: cyclohexane–chloroform (3 : 7) + 0.05 diethylamine.S₈, Silica gel G, impregnated with 0.1 mol L⁻¹ sodium hydroxide, activated: methanol.(Reproduced with permission from Svendsen AB and Verpoorte R (1983) *Chromatography of Alkaloids*. Journal of Chromatography Library. Amsterdam: Elsevier.)

For particular alkaloids, specific reagents can be used; for instance, Marqui's reagent (formaldehyde–sulfuric acid) or Fröhde's reagent (sulfomolybdic acid–sulfuric acid) for morphine. König's reaction can be used to detect nicotine and related alkaloids; Wachtmeister's reagent (*bis*-diazotized benzdine–sulfuric acid) is applied for alkaloids belonging to the protoberberine and protopine group.

The Vitaly reaction is specific for the tropane alkaloids, and reaction with 4-dimethylaminobenzaldehyde for indole alkaloids. Some examples of applications of different reagents are illustrated in Figure 4 and Table 4.

The use of π -acceptor reagents producing colour spots (TCNQ: 7,7,8,8-tetracyano-quinodimethane; TNF: 2,4,7-trinitrofluorenone; TetNF: 2,4,5,7-tetranitro-9-fluorenone; DDQ: 2,3-dichloro-5,6-dicyanoquinone; DNFB: 2,4-dinitrofluorobenzene) for the detection of alkaloids has been employed.

Initial derivatization during sample preparation or *in situ* on the layer after the application of the sample is called prechromatographic derivatization and comprises oxidation, reduction, iodination, nitration and dansylation (Table 5).

Starting chromatographic separation with sample derivatization allows better-quality results to be obtained, especially as far as reproducibility and

lowering the detection limits are concerned. Morphine as a dansyl derivative is an example of fluorescence stabilization and intensity augmentation as a result of treatment of the chromatogram with a 20% solution of liquid paraffin in *n*-hexane.

A similar phenomenon is observed for codeine, morphine, monoacetylmorphine and heroin with the aid of hydrophilic liquids, such as a 20% solution of dioctyl sulfasuccinate in ethanol as a fluorescence intensifier.

Enhanced sensitivity can be achieved by impregnating the layer, by adding the reagent to the solvent or by spraying the plate after development. In addition to the reagents mentioned above, fluorescence intensifiers such as triethanolamine, glycerol and Triton X-100 are quite popular.

Identification and Quantification

The forte of TLC is qualitative analysis. It is possible to identify unknown alkaloids owing to the large amount of R_F data available from the literature and the ability to perform a chemical reaction using a wide spectrum of different reagents *in situ*. For some alkaloid drugs, a compilation of TLC data has been elaborated and stored in computer-based information systems.

Many authors make an identification based on R_F values in a number of chromatographic systems. One scheme has been described in which the analysis of a series of alkaloids by eight TLC systems, combined with observations under UV light ($\lambda = 366$ nm) and colour reactions with iodoplatinate reagent (Table 6) is used.

For precise identification, UV or infrared spectra after elution have become indispensable. Together with the melting point and optical rotation values, they are sufficient for the identification and comparison of isolated pure substances. Other spectral methods such as nuclear magnetic resonance or mass spectrometry have frequently been used to identify alkaloids.

Although quantitative determination in TLC is more difficult and requires more effort, it is becoming increasingly important nowadays. There exist two forms of quantitative analysis: direct and indirect. The first method is based on the elution of spots with a suitable solvent and determination in solution, followed by spectrophotometric, fluorometric or acid-base potentiometric titration. The second possibility utilizes adsorption of UV and visible radiation or luminescence of alkaloids, and is performed by the means of photodensitometry, densitometry and fluorimetry *in situ*. This latter technique requires the use of an optical scanner, which is a relatively expensive piece of equipment.

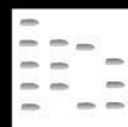
See Colour Plate 54.

See also: II/Chromatography: Thin-Layer (Planar): Layers; Modes of Development: Forced Flow, Overpressured Layer Chromatography and Centrifugal; Spray Reagents. III/Alkaloids: Gas Chromatography; Impregnation Techniques: Thin-Layer (Planar) Chromatography; Liquid Chromatography.

Further Reading

- Adamovics JA (1990) *Chromatographic Analysis of Pharmaceuticals*. New York: Marcel Dekker.
- Bieganowska ML and Petruczynik A (1994) Thin-layer reversed-phase chromatography of some alkaloids in ion-association systems. *Chemia Analityczna* 39: 139.
- Camag Bibliography Service *Thin-layer Chromatography*. Cumulative CD, Version 1.00. Camag 1997.
- Deyl A, Macek K and Janak J (1975) *Liquid Column Chromatography. A Survey of Modern Techniques and Applications*. Amsterdam: Elsevier.
- Golkiewicz W, Gadzikowska M, Kuczyński J and Jusiak L (1993) Micropreparative chromatography of some quaternary alkaloids from the roots of *Chelidonium majus* L. *Journal of Planar Chromatography* 6: 382.
- Jork H, Funk W, Fischer W and Wimmer H (1990) *Thin-layer Chromatography, Reagents and Detection Methods*. Weinheim: VCH.
- Lepri L, Desideri PG and Lepori M (1976) Chromatographic behaviour of alkaloids of thin layer of cation exchangers. *Journal of Chromatography* 123: 175.
- Niederwiesser A and Pataki G (1972) *Progress in Thin Layer Chromatography and Related Methods*. Michigan: Ann Arbor Science.
- Popl M, Fähnrich J and Tatar V (1990) *Chromatographic Analysis of Alkaloids. Chromatographic Science*. New York: Marcel Dekker.
- Rönsch H and Schreiber K (1967) Analytische und präparative Dünnschichtchromatographische Trennung von 5 α -gesättigten BZW. Δ^5 -ungesättigten Steroidalalkaloiden und-sapogeninen an silbernitrat-haltigen Adsorptionsschichten. *Journal of Chromatography* 30: 149.
- Smith RM (1996) Supercritical fluid extraction of natural products. *LC/GC International, the Magazine of Separation Science*, Vol. 9, p. 8. Chester, UK: Advanstar Communications.
- Soczewiński E and Flieger J (1996) Thin Layer Chromatography of Alkaloids. *Journal of Planar Chromatography* 9, 107.
- Svendsen AB (1989) Thin layer chromatography of alkaloids. *Journal of Planar Chromatography* 2: 8.
- Svendsen AB and Verpoorte R (1983) *Chromatography of Alkaloids*. Amsterdam: Elsevier.
- Touchstone JC (1992) *Practice of Thin Layer Chromatography*. New York: John Wiley.
- Wagner H and Bladt S (1996) *Plant Drug Analysis. Thin Layer Chromatography Atlas*. Berlin: Springer.

ALLERGENS IN PERFUMES: GAS CHROMATOGRAPHY- MASS SPECTROMETRY



S. C. Rastogi, National Environmental
Research Institute, Røskilde, Denmark

Copyright © 2000 Academic Press

Perfumes (fragrance substances) are used in the formulation of consumer products to provide pleasure to the user and/or to mask malodours of some other ingredients in the products. Perfumes are also used in aromatherapy. A typical perfume may be composed of 10–300 substances selected from a battery of over 3000 synthetic and natural fragrance materials. It has been shown that approximately 2% of the general population is allergic to perfumes. Furthermore, perfumes have also been shown to be one of the major cause of allergic contact dermatitis from the use of cosmetics and toiletries. Besides cosmetics, the use of many other consumer products such as perfumed laundry detergents and dishwashers have also been implicated as the cause of perfume allergy in contact eczema patients.

Perfume allergy in contact eczema patients is diagnosed by patch-testing with a fragrance mix containing 1% each of geraniol, eugenol, isoeugenol, cinnamic alcohol, cinnamic aldehyde, α -amylcinnamic aldehyde, hydroxycitronellal and an extract from oakmoss – oakmoss absolute. However, only 50–80% of perfume allergy cases are diagnosed by this test. For the management of allergy, it is important to identify the fragrance allergen responsible for contact eczema in a patient, as this makes it possible for the patient to avoid the use of products containing the sensitizing allergen(s). To establish the identity of the fragrance substance responsible for perfume allergy in a contact eczema patient, it is recommended that the product(s) used by a patient should be analysed for the contents of fragrance allergens followed by patch-testing the patient with the relevant fragrance allergens present in the product.

Gas chromatography-mass spectrometry (GC-MS) is frequently used for the analysis of fragrance substances in essential oils. This approach is used for the identification and semiquantitative determination of the fragrance substances of interest in essential oils. In 1995, GC-MS was used for the identification and quantification of 10 selected fragrance substances including the seven chemically defined substances of fragrance mix in perfumes, eau de toilette,

deodorants, creams, lotions, shampoos and other perfumed consumer products which may contain both natural as well as synthetic fragrance materials. The method was later modified slightly so that quantitative analysis of many more fragrance substances in perfumes or in perfumed products could be performed. This method, described in the present article, has been applied to the analysis of perfumes in various consumer products. To demonstrate the potential of the method for perfume analysis, example of analysis of fragrance substances in a deodorant and in an eau de toilette are presented here. Sample preparation methods for the GC analysis of fragrances in various types of consumer products is also described. The quantitative data on fragrance substances in various consumer products are reported in the publications described in the Further Reading section.

Target Fragrance Substances

The analytical method has been developed for the quantification of 21 fragrance substances which in relatively high concentrations are commonly used in the composition of perfumes, or which are established contact allergens:

- 1 geraniol: CAS registration number 106-24-1;
- 2 eugenol: 97-53-0;
- 3 isoeugenol: 97-54-1;
- 4 linalool: 78-70-6;
- 5 linalyl acetate: 115-95-7;
- 6 citronellol: 106-22-9;
- 7 cinnamic alcohol: 104-54-1;
- 8 cinnamic aldehyde: 104-55-2;
- 9 hydroxycitronellal: 107-75-5;
- 10 α -amylcinnamic aldehyde: 122-40-7;
- 11 α -hexylcinnamic aldehyde: 101-86-0;
- 12 α -isomethylionone: 127-51-5;
- 13 coumarin: 91-64-5;
- 14 piperonal: 120-50-7;
- 15 benzyl alcohol: 100-51-6;
- 16 benzyl acetate: 140-11-4;
- 17 benzyl benzoate: 121-51-4;
- 18 benzyl salicylate: 118-51-8;
- 19 Lillal®: 80-54-6;
- 20 Lyrall®: 31906-04-4;
- 21 Hedione®: 24851-98-7.

Approximately 1.0% (w/v) solutions of all of the substances in ethanol served as stock solutions. The stock solutions were stored in closed vials at 4°C and were used within 1 month.

Sample Preparation

Perfumes, Eau de Toilette, Aftershave and Deodorant Sprays

These products were approximately diluted in ethanol so that the concentrations of target fragrance substances were $\leq 0.1\%$. Depending on the concentrations of the target fragrance substances in a sample, it may be necessary to analyse several dilutions of the sample.

Shampoos, Creams, Lotions, Lipsticks, Face Powders and Deodorant Sticks

Perfumes from 1 g sample were extracted in 10 ml methanol at 60°C (to facilitate the extraction) followed by removal of matrix components by silica gel column chromatography. The extract was loaded on a 7 × 1.8 cm silica gel column, and the fragrance fraction was eluted with methanol. The perfume extract was stored at 4°C and analysed within 24 h.

Soap Bar and Laundry Detergents

Perfumes from 1 g sample dissolved in 50 ml water were extracted in 10 ml ethyl acetate employing liquid-liquid extraction. The perfume extract in ethyl acetate was centrifuged to remove any solid or aqueous contamination. The perfume extract was stored at 4°C and analysed within 24 h.

Dishwashing liquid

The method used for the extraction of perfumes from dishwashing liquids was the same as for shampoo.

GC-MS Analysis

MS Conditions

Electron impact ionization at 70 eV was used, scanning m/z 29–250 in 0.6 min.

Results

The method described here has been applied to the determination of 21 target fragrance substances in consumer products. The chromatographic separation of these 21 compounds employing GC is shown in Figure 1. Day-to-day variation of retention times of the fragrance substances is $< 0.5\%$. The detection limits of all of the target substances are ≤ 1 p.p.m.,

the calibration curves for all of the target substances are linear (coefficient of correlation > 0.995) in the tested concentration range 10–2000 p.p.m., the relative standard deviations of the determination of all of the substances are $< 11\%$. The recovery of all of the target substances from the spiked samples is 82–116%, and day-to-day variations of quantitative analysis for all of the substances are within 5%.

The reconstructed ion chromatogram obtained by GC-MS analysis of fragrance substances in a deodorant (undiluted) is shown in Figure 2. The fragrance substances in the product were identified by comparing the retention times of the GC peaks with those of the reference materials, as well as by comparing the spectra of the GC peaks with the reference spectra of standard compounds in the mass spectrum library. Followed by GC-MS identification, quantification of target fragrance substances in the sample is carried out with external standards.

Most consumer products contain many more fragrance substances other than the target compounds. The identification of these substances was only performed by comparing the mass spectrum of a GC peak with the mass spectra of reference compounds in the MS library. In this case, both the spectrum fit and spectrum purity of match of the unknown spectrum with those of library spectra were > 900 . An example of identification of fragrance substances in an eau de toilette is shown in Figure 3A–E, where the results are divided in six windows for the clarity of peak identification. Confirmation of the identification of these substances and their quantification were performed where a reference material was available.

In some cases it is not possible to identify all the peaks because of the absence of mass spectra of the compounds in the mass spectral library.

Discussion

For the analysis of perfumes on a routine basis, GC-MS identification of the fragrance substances followed by quantification employing GC-flame ionization detection (FID) was found to be a more suitable approach. The main reason for this is that the use of GC-FID allows relatively rapid production of validated data. Thus, several relevant analysis recommended by quality assurance/quality control (QA/QC) protocol for a set of samples can be easily performed by GC-FID. Fulfilling the requirements of QA/QC protocol for the analysis by GC-MS is time-consuming, because it requires tuning and calibration of the MS at regular intervals and frequent cleaning of the ion source. The detection limits of the target

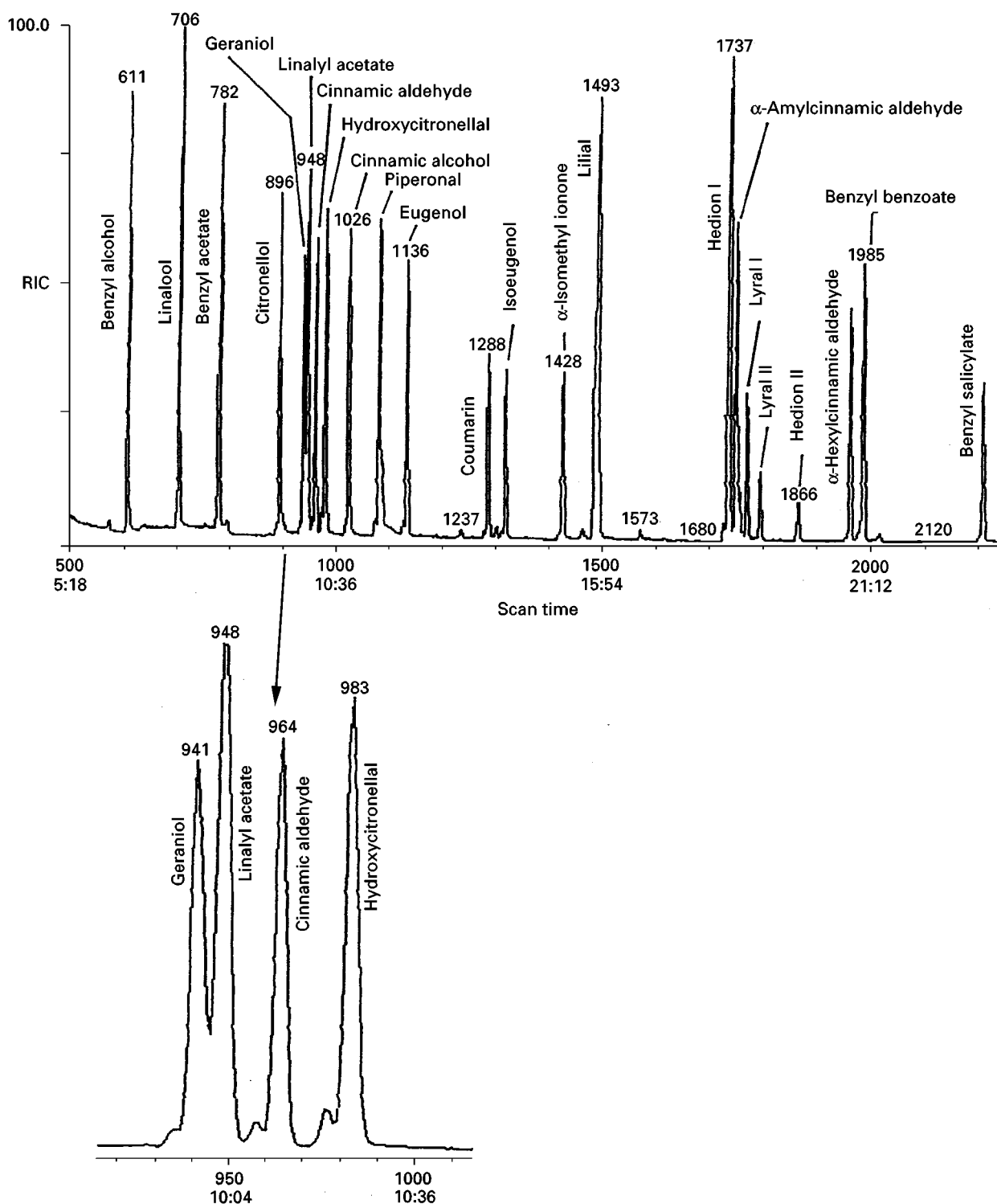


Figure 1 GC-MS analysis of a mixture containing 83–117 p.p.m. of the 21 target fragrance substances. 50 m × 0.32 mm, 1.2 μm film thickness Chrompack fused silica capillary columns coated with CP-Sil-5CB, were used. 1 μL split injection; helium carrier gas flow 30 ml min⁻¹, column-head pressure 20 psi; injector temperature 300°C; column temperature program: 40–140°C in 4 min, thereafter 5°C min⁻¹ to 280°C, 5 min at 280°C. 2 μL injection volume was used when the content of perfume in a sample was relatively low.

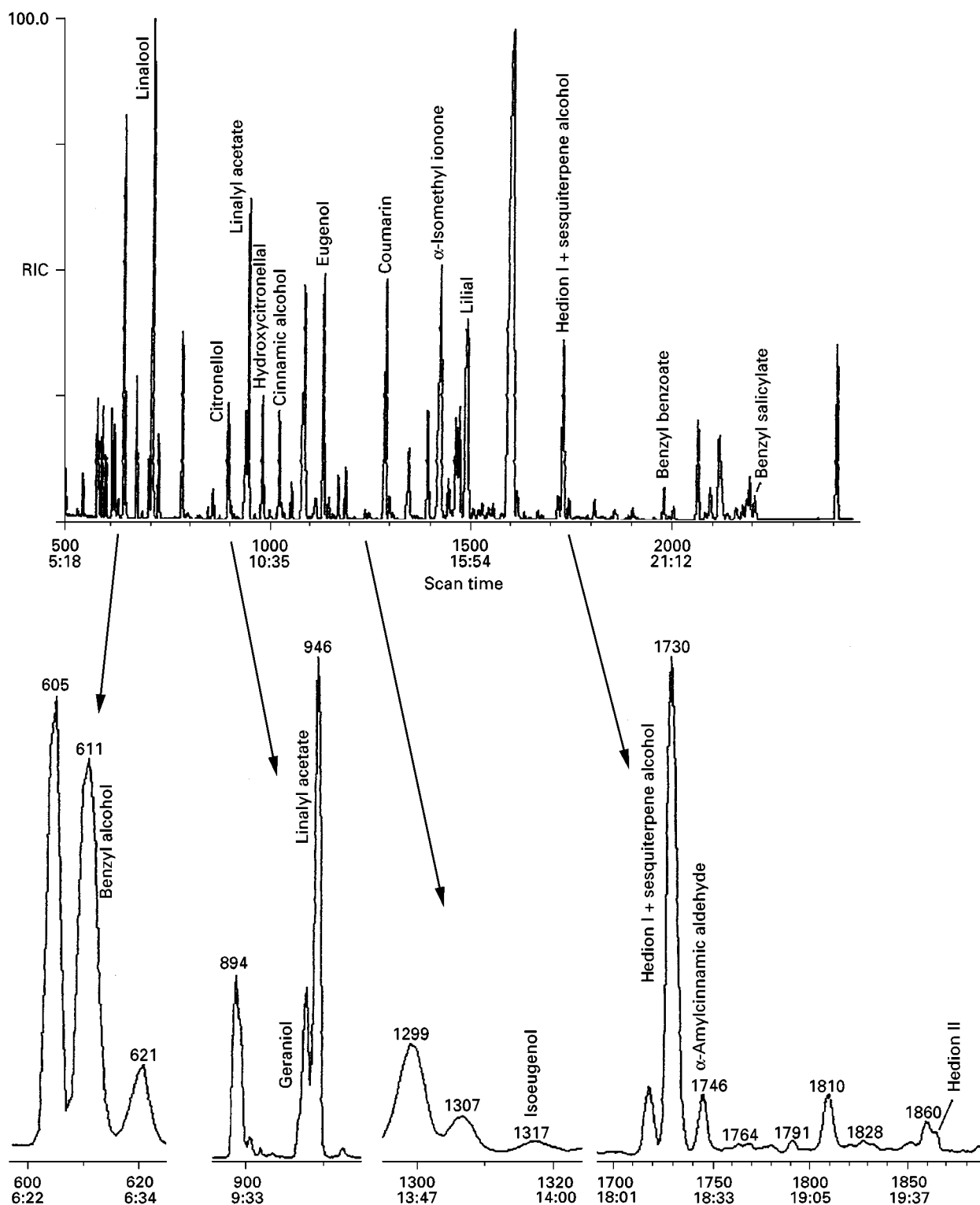


Figure 2 GC-MS analysis of the target fragrance in an undiluted deodorant. The following were present among the target fragrance substances: 102 p.p.m. benzyl alcohol, 1028 p.p.m. linalool, 141 p.p.m. citronellol, 136 p.p.m. geraniol, 614 p.p.m. linalyl acetate, 205 p.p.m. hydroxycitronellal, 183 p.p.m. cinnamic alcohol, 408 p.p.m. eugenol, 1051 p.p.m. coumarin, 7 p.p.m. isoeugenol, 319 p.p.m. α -isomethylionone, 291 p.p.m. Lilial®, 199 p.p.m. Hedion®, 68 p.p.m. α -amylcinnamic aldehyde, 101 p.p.m. benzyl benzoate and 112 p.p.m. benzyl salicylate. Quantification of Hedion® was performed by the analysis of 1 : 10 dilution of the sample, where no interference by the sesquiterpene alcohol present in the sample was observed.

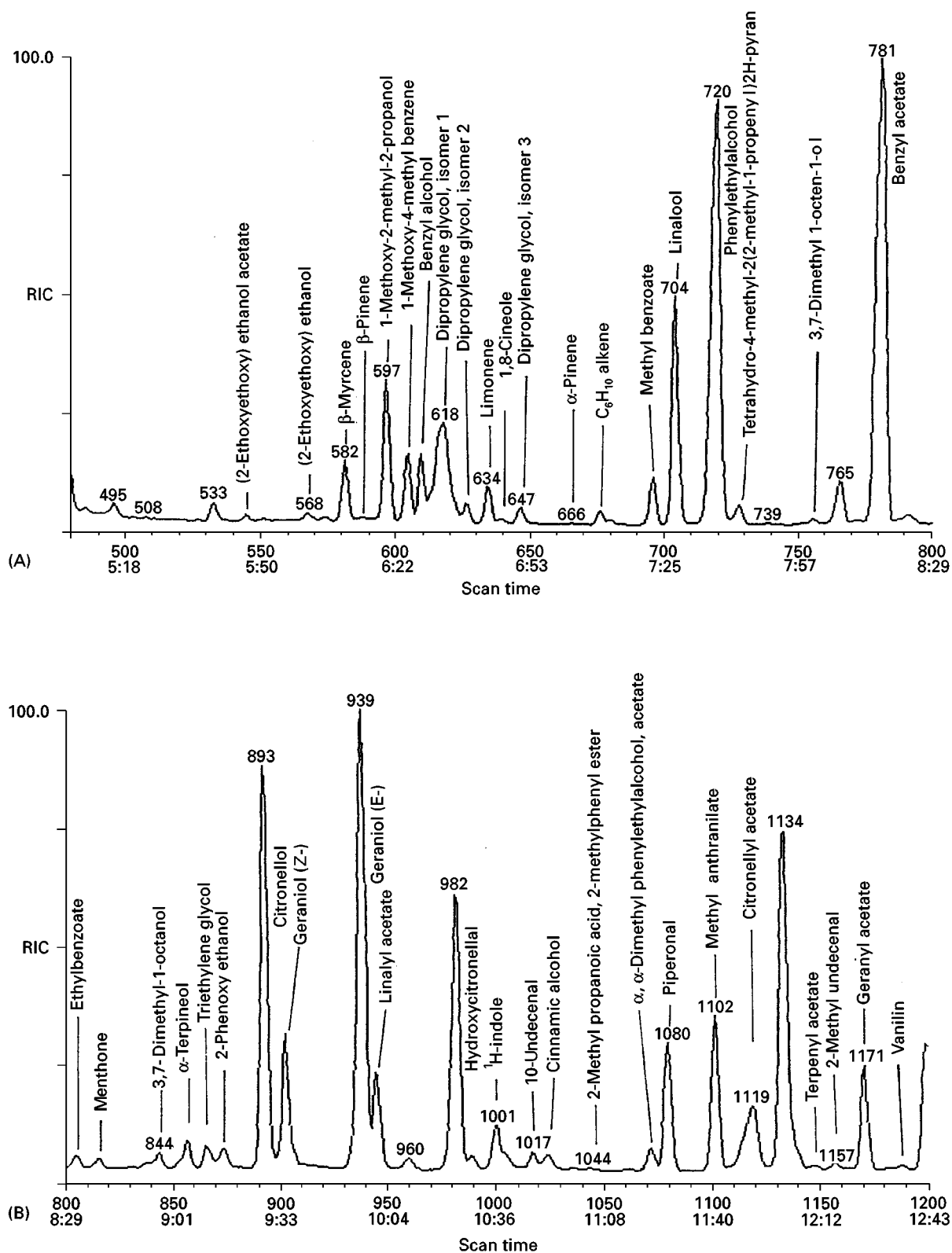


Figure 3 GC-MS analysis of an eau de toilette, diluted 1 : 10 in ethanol. The reconstituted ion chromatogram is divided in six windows (A-F) for the clarity of the compounds identified in the sample. Peaks with no name could not be identified.

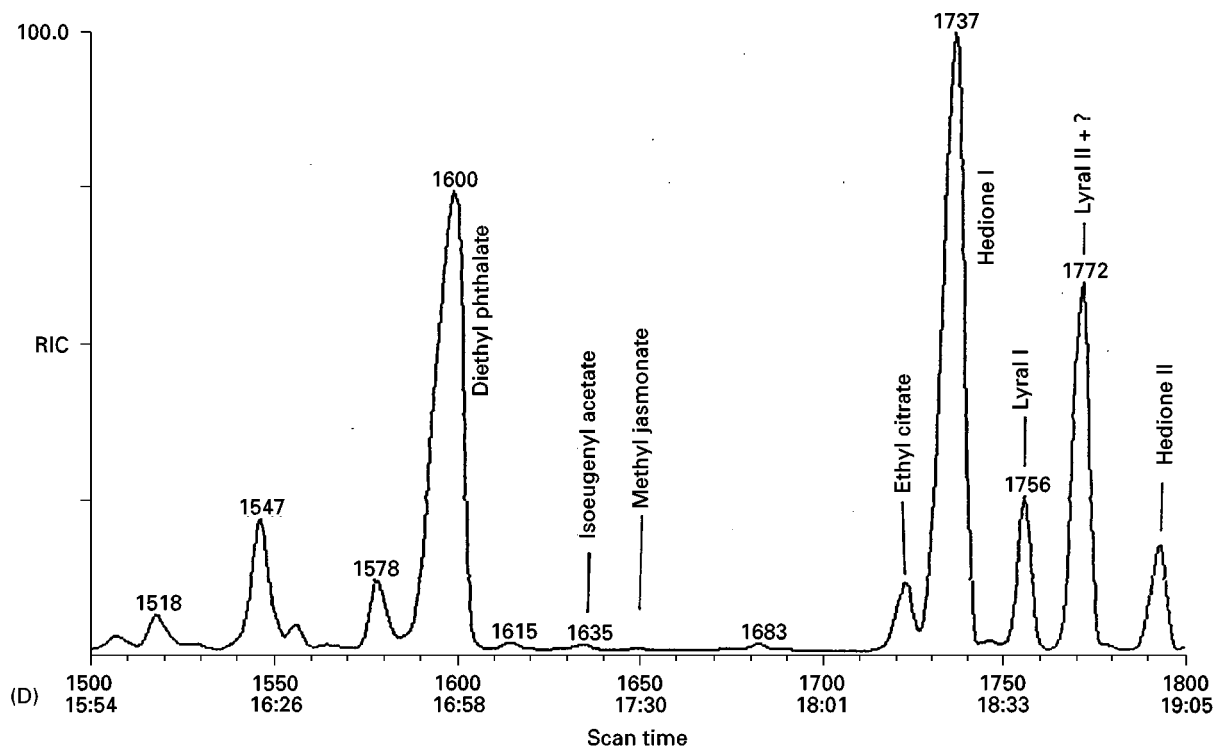
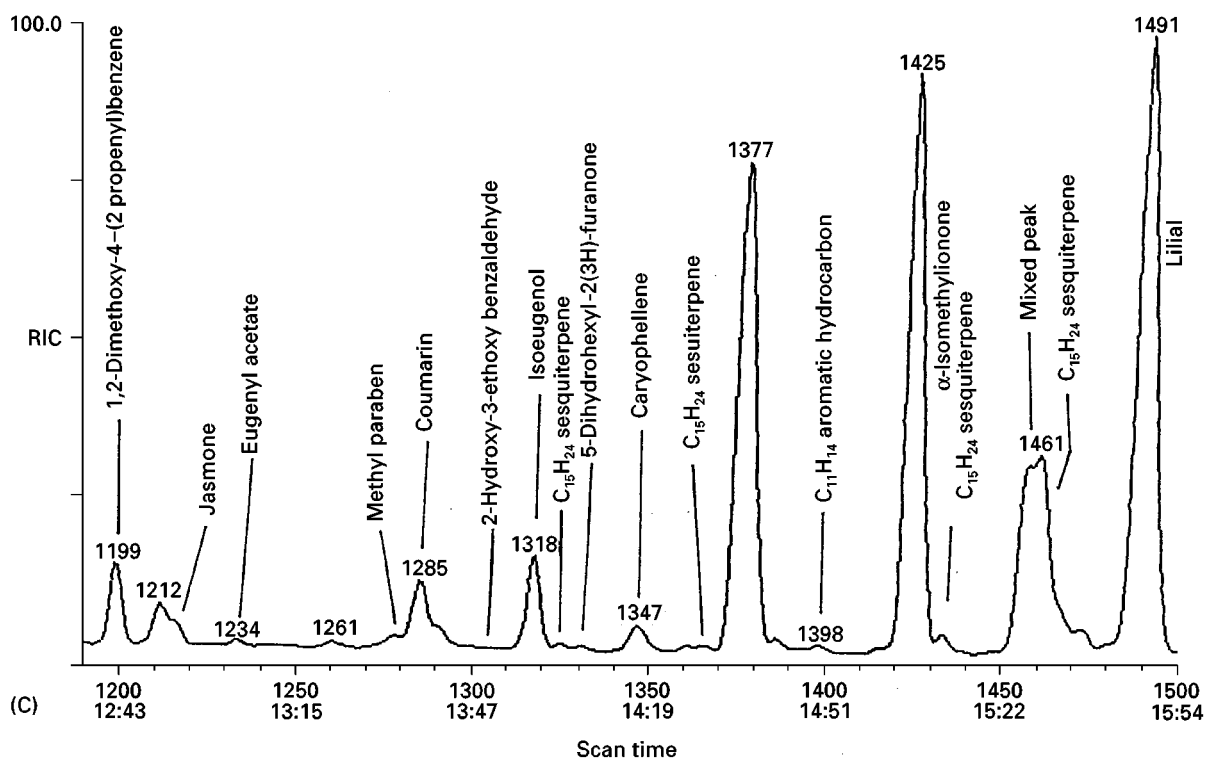


Figure 3 Continued

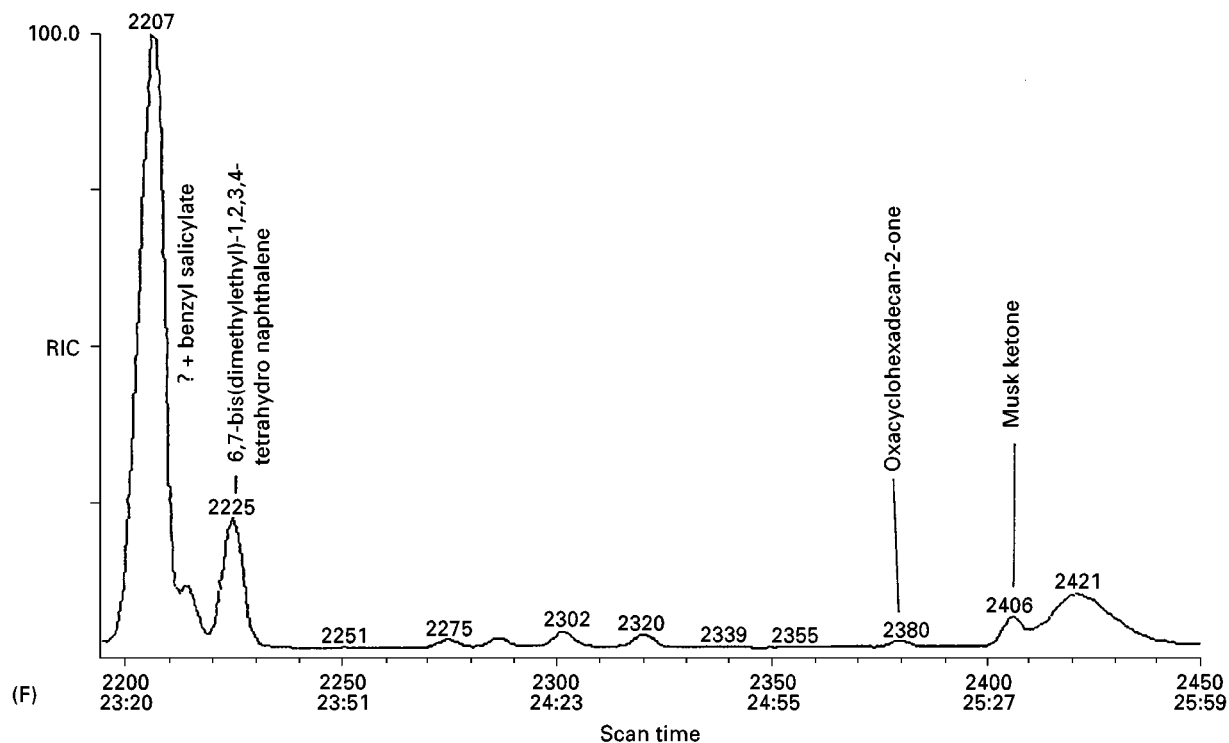
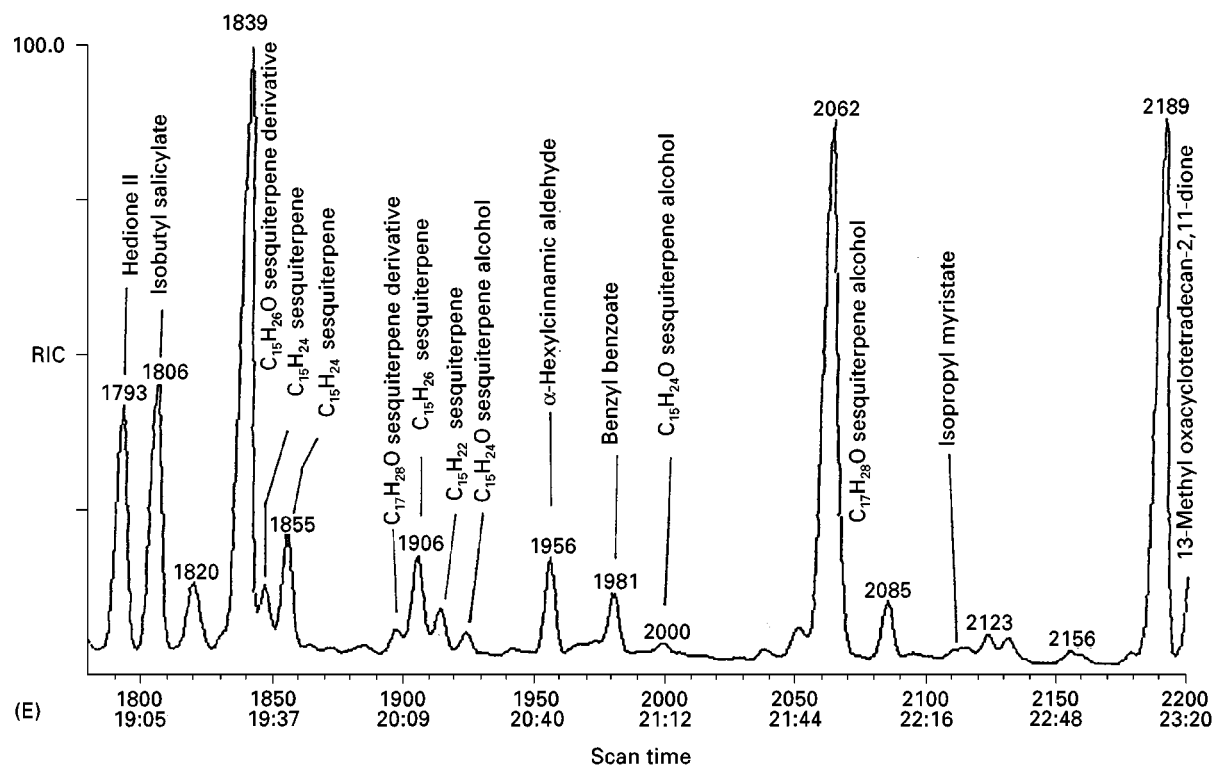


Figure 3 Continued

substances by GC-FID, however, are 2–5 p.p.m. So, unless the quantification was required at 1 p.p.m. level, GC-FID was chosen for the determination of fragrance substances after prior identification by GC-MS.

Most of the fragrance substances in use, including the target fragrance substances, have a molecular weight < 250 Da. Therefore, the MS scan was performed only up to m/z 250. Occasionally, for example in the identification of musk ketone, it is necessary to scan masses up to 300.

Not all the fragrance ingredients in all tested products could be identified or quantified, in some cases due to interferences. Occasionally the GC peak of a relatively high amount of dipropylene glycol present in a sample overlapped the peak by benzyl alcohol; a C_{11} -alkyne interfered with the analysis of Lilial®; high amounts of triethyl citrate and/or a sesquiterpene alcohol ($C_{15}H_{26}O$) interfered with the analysis of Hedione® and relatively high amounts of Hedione® interfered with the analysis of α -amylcinnamic aldehyde. An unidentified compound was found to interfere with the analysis is benzyl salicylate. In most cases these problems could be solved by analysing diluted samples.

By using GC-MS, identification of 226 substances in deodorants has recently been reported. A structure–activity relationship (SAR) analysis of contact allergens revealed that 84 of the identified compounds possess at least one structural alert (chemical group) having sensitizing potential, and 70 belong to, or are susceptible to metabolize into, the chemical groups having sensitizing properties: aldehydes, ketones and α,β -unsaturated aldehydes, ketones or esters. The combination of GC-MS and SAR analysis could be helpful in the selection of substances for supplementary investigations regarding sensitizing properties.

Analysis of as many fragrance ingredients as possible in a perfumed product is of great importance for clinicians to establish the identity of contact allergens in each case. This information is also important for clinical research to investigate cross-reactions of fragrance allergens. The quantitative data on the fragrance ingredients in consumer products make a basis for exposure assessment that is a help for establishing threshold concentrations of fragrances for the elicitation of contact allergy.

Conclusions

Chemical analysis of perfumes and perfumed products is of great importance for the diagnosis and management of perfume allergy. The GC-MS/GC-

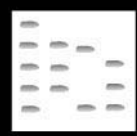
FID method described here for the analysis of fragrance substances in consumer products has proved to be valuable to identify allergens in patients with contact eczema from the use of perfumes and perfumed products. Using GC-MS in combination with SAR it has been possible to identify several fragrance substances in perfumes which possess sensitizing potential.

See also: II/Chromatography: Gas: Column Technology; Derivatization; Detectors: General (Flame Ionization Detectors and Thermal Conductivity Detectors); Detectors: Mass Spectrometry; Detectors: Selective; Headspace Gas Chromatography; Theory of Gas Chromatography. III/Flavours: Gas Chromatography: Sulphur Compounds: Gas Chromatography.

Further Reading

- Calkin RR and Jellinek JS (1994) *Perfumery Practice and Principles*. New York: Wiley.
- De Groot AC and Frosch P (1997) Adverse reactions to fragrance. A clinical review. *Contact Dermatitis* 36: 57–86.
- Frosch PJ, Pliz B, Andersen KE *et al.* (1995) Patch testing with fragrances: results of a multicenter study of the European Environmental and Contact Dermatitis Research Group with 48 frequently used constituents of perfumes. *Contact Dermatitis* 33: 333–342.
- Frosch PJ, Johansen JD and White IR (eds) (1998) *Fragrances: Beneficial and Adverse Effects*. Berlin: Springer-Verlag.
- Johansen JD, Rastogi SC and Menné T (1996) Contact allergy to popular perfumes; assessed by patch test, use test and chemical analysis. *British Journal of Dermatology* 135: 419–422.
- Larsen W, Nakayama H, Lindberg M *et al.* (1996) Fragrance contact dermatitis: a worldwide multicenter investigation (part I). *American Journal of Contact Dermatitis* 7: 77–83.
- Pybus DH and Sell CS (eds) (1999) *The Chemistry of Fragrances*. Cambridge: Royal Society of Chemistry.
- Rastogi SC (1995) Analysis of fragrances in cosmetics by gas chromatography-mass spectrometry. *Journal of High Resolution Chromatography* 18: 653–658.
- Rastogi SC, Johansen JD and Menné T (1996) Natural ingredients based cosmetics: content of selected fragrance sensitizers. *Contact Dermatitis* 34: 423–426.
- Rastogi SC, Johansen JD, Frosch P *et al.* (1998) Deodorants on the European market: quantitative chemical analysis of 21 fragrances. *Contact Dermatitis* 38: 29–35.
- Rastogi SC, Leppoitevin JP, Johansen JD *et al.* (1998) Fragrances and other materials in deodorants: search for potentially sensitizing molecules using combined GC-MS and structure activity relationship (SAR) analysis. *Contact Dermatitis* 39: 293–303.

AMINES: GAS CHROMATOGRAPHY



H. Kataoka, S. Yamamoto and
S. Narimatsu, Okayama University, Tsushima,
Okayama, Japan

Copyright © 2000 Academic Press

Aliphatic and aromatic mono-, di- and polyamines are naturally occurring compounds formed as metabolic products in microorganisms, plants and animals, in which the principal routes of amine formation include the decarboxylation of amino acids, amination of carbonyl compounds and degradation of nitrogen-containing compounds. Accordingly, amines are important indicators of a wide variety of biochemical, clinical, toxicological and fermentation processes. Amines are also widely used as raw materials or as intermediates in the manufacture of industrial chemicals, e.g. pesticides, medicines, dyestuffs, rubbers, polymers, surfactants, cosmetics and corrosion inhibitors. Many of them are discharged into the atmosphere and water from anthropogenic sources such as foods, cattle feeds, livestock buildings, waste incineration, sewage treatment, automobile exhaust, cigarette smoke and various industries. Furthermore, many amines have an unpleasant smell and are hazardous to health as sensitizers and irritants to the skin, eye, mucous membranes and respiratory tract. Some amines are also suspected to be allergenic, mutagenic or carcinogenic substances due to their adsorption in living tissue. Amines are not only toxic of themselves but can also become toxic *N*-nitrosamines through chemical reactions with nitrosating agents such as nitrite or nitrate.

Gas chromatography (GC) has been widely used for amine analysis because of its inherent advantages of simplicity, high resolving power, high sensitivity, short analysis time and low cost. In addition, a wide variety of detectors can be used: nitrogen-phosphorus (NPD), electrolytic conductivity (ELCD) and chemiluminescent (CLD) detectors offer increased selectivity for specific amines. Furthermore, the combined technique of GC-mass spectrometry (MS) can provide structural information for the unequivocal identification of amines. Sub-nanogram detection limits can be achieved using these detectors. However, GC separation of free amines at very low concentrations generally has inherent problems related to the difficulty in handling low molecular

mass amines because of their high water solubility, high volatility and ready oxidation under chromatographic conditions. Furthermore, amines tend to be strongly adsorbed and decomposed on the columns and give tailing peaks, ghosting phenomena and low detector response. The adsorption tendency in the analytical system, i.e. in sample vessels, injector, glass wool and GC column, is in the order primary > secondary > tertiary amines, and tailing becomes increasingly severe as the basicity of the amines increases. In addition, it is generally more difficult to chromatograph aliphatic than aromatic amines.

A common method of overcoming these problems is to convert such polar compounds to relatively non-polar derivatives more suitable for GC analysis. A number of derivatives such as acyl, silyl, dinitrophenyl, permethyl, Schiff base, carbamate, sulfonamide and phosphonamide compounds have been used for this purpose.

Another successful approach has been to employ less reactive column packing materials to reduce the interaction with solutes, for example, the use of porous polymers and the deactivation of supports by treatment with alkali. Wall-coated (WCOT), support-coated (SCOT) and porous-layer (PLOT) open tubular capillary columns, which minimize column-solute interactions, have also been used for this purpose. Free amines can be analysed after addition of alkali, either by direct injection or by headspace sampling, or they can be extracted into an organic solvent before analysis. Direct or headspace analysis of samples minimizes sample preparation, thereby reducing the possibility of contamination. Solid-phase microextraction (SPME), with integrated sampling, extraction, concentration and sample introduction in a single step, has recently been used for amine analysis by coupling with GC.

This article is concerned with the general aspects of direct GC separation of underivatized aliphatic and aromatic amines, and various characteristics with respect to columns are considered in more detail below.

Column Development

Packed-column GC is generally simpler to set up than capillary GC, because of the ability to apply the stationary phase easily to the solid support and modify it appropriately to the particular analysis

required. Deactivation of the glass surface can be effected using a suitable silylating reagent to limit the effect of adsorption on the wall of the column. However, the general difficulty in the chromatography lies in absorptivity on the solid support leading to tailing. The adsorption of amines by the support material has been attributed to the presence of free silanol groups on the silica surface participating in hydrogen bonding with the free electron pair of the nitrogen atom of the amine. Simple treatment with KOH reduces the adsorption to a minimum, allowing good peak shape and optimum performance.

Glass and fused silica capillary columns have also been used for the analysis of free amines. The inherent strength and flexibility of fused silica make it easier to use and less fragile than glass capillary columns. Furthermore, fused silica provides a more inert surface for improved performance and less adsorption. The analysis of free amines on packed columns has now largely been replaced by analysis on fused silica capillary columns that are commercially available with a range of stationary phases. The packed and capillary GC columns reported in the past 30 years for amine analysis are summarized in Tables 1 and 2.

Packed Columns

Three types of packing can be used to separate amines: graphitized carbon coated with a stationary phase and deactivated, coated and uncoated porous polymers, and conventional columns packed with a deactivated diatomaceous earth coated with a sta-

tionary phase. The columns are usually deactivated with KOH, trimethylchlorosilane (TMCS) or ammonia in the carrier gas. Carbowax graphitized carbon and porous polymer packings are well suited for separating C_1 – C_{10} compounds, but retention times for larger molecules are excessive; deactivated and coated conventional packings are better suited to the analysis of higher molecular weight amines.

Graphitized carbon packings Graphitized carbon packings are generally used for free amine analysis after coating with a stationary phase. Sterling FT-G and Vulcan, sold by Supelco as Carbowax A and Carbowax B, respectively, have been used for the analysis of C_1 – C_{16} aliphatic amines with suitable amounts of KOH and polyethylene glycol (PEG), e.g. PEG 20M and PEG-1500. A 4.8% PEG 20M/0.3% KOH on Carbowax B column is recommended for the analysis of C_1 – C_4 aliphatic amines in aqueous solution at nanogram level. This column offers complete separation of the C_2 – C_3 amine isomers and is less affected by water than the other packed columns. However, the preparation of the column seems to be difficult for routine analysis. A 1.5% UCON 50-HB-2000 on Carbowax B packing deactivated with 0.8% KOH has also been used to separate a mixture of aliphatic, aromatic and cyclic amines, and rapid separation of nine amines without ghosting was obtained by temperature programming and treatment of glass wool in the column ends with dimethylchlorosilane (DMCS). On the other hand, 4% Carbowax 20M on 0.8% KOH-deactivated Carbowax B packing has

Table 1 Packed columns for analysis of free amines

Column packing	Type	Length (m)	Amine	Detection
1.3% PEG 20M/0.3% KOH on Sterling FT-G	GC	2.0	AL	FID
0.5% PEG-1500/0.2% KOH on Sterling FT-G	GC	1.4	AL	FID
4% PEG 20M/0.8% KOH on Vulcan	GC	1.4	AL	FID
4.8% PEG 20M/0.3% KOH on Carbowax B	GC	1.8	AL	FID
1.5% UCON 50-HB/0.8% KOH on Carbowax B	GC	1.83	AL, AR	FID
4% Carbowax 20M/0.8% KOH on Carbowax B	GC	1.7–3.75	AL	FID, NPD
Tenax GC	PP	1.52	AL	FID
Chromosorb 103	PP	1.5–3.3	AL	FID, NPD
Chromosorb 102/5% TMCS/5% KOH	PP	2.0	AL	NPD
5% Squalene/2% KOH on Chromosorb 103 or 104	PP	3.0	AL	CLD
4% Carbowax 20M/1% KOH on Corning glass	PC	1.8	PO	FID
10% Carbowax 20M/2% KOH on Chromosorb W AW	PC	1.5–1.9	AL	FID, NPD
5% PEG-1000/0.5% Na_3PO_4 on Chromosorb G	PC	2.0	AL	SID
5% PEG-HT/1% KOH on Umiport HP	PC	2.0	AR	FID
3% SP-2250 on Supelcoport	PC	1.83	AR	NPD
5% SP-2401-DB on Supelcoport	PC	1.83	AR	NPD
1.5% SP-2250/1.95% SP-2401 on Supelcoport	PC	1.83	AR	NPD
3% Silar 5CP on Supelcoport	PC	1.83	AR	NPD

GC, Graphitized carbon; PP, porous polymer; PC, partition column; AL, aliphatic amine; AR, aromatic amine; PO, polyamine; FID, flame ionization detection; NPD, nitrogen–phosphorus detection; surface ionization detection; CLD, chemiluminescence detection.

Table 2 Capillary columns for analysis of free amines

Column			Amine	Detection
Stationary phase	Type	Length (m)		
10% PEG 400	WCOT/G	99	AR	FID
5% PEG 400/2% KOH	WCOT/G	40	AR	FID
Supelcowax 10	WCOT/G	10	AL, AR	FID
SP-2250	WCOT/G	30	AR	NPD
SP-2100	WCOT/G	30	AR	NPD
Carbowax 20M	WCOT/G,F	25–37	AR	FID, NPD, MSD
SE-54	WCOT/G,F	30	AR, DR	FID, NPD
SE-52	WCOT/G,F	30	AR	NPD, ELCD, PID
SE-30	WCOT/G,F	30	AR	FID, NPD
CAM	WCOT/F	30	AL	FID
HP-20M	WCOT/F	25	AR	FID
Carbowax Amine	WCOT/F	30	AL, AR	FID
PoraPLOT Amines	PLOT/F	25	AL	FID, ELCD
CP-Sil-19CB	WCOT/F	10	AL, AR	FID
DB-35ms	WCOT/F	25	AR	FID
DB-5ms	WCOT/F	30	AL, AR	FID, MSD
HP-5	WCOT/F	25–30	DR	FID, MSD
HP-101	WCOT/F	25	AL, AR	FID
HP-1	WCOT/F	10–30	AL, AR	FID, NPD
DB-1	WCOT/F	30	AL, DR	FID, MSD
OV-1	WCOT/F	25	DR	MSD
SBP-1	WCOT/F	30	AL, AR	FID
CBJ-17	WCOT/F	30	DR	NPD

WCOT, Wall-coated; PLOT, porous layer; G, glass; F, fused silica; AL, aliphatic amine; AR, aromatic amine; DR, basic drug; FID, flame ionization detection; NPD, nitrogen-phosphorus detection; ELCD, electrolytic conductivity detection; MSD, mass selective detection; PID, photoionization detection.

been specifically developed for monitoring low molecular weight aliphatic amines at p.p.m. levels in water. Heterocyclic amines can also be separated on this packing, but aromatic amines exhibit excessively long retention times. By using this column and an NPD, low molecular weight amines in sea water were determined. In order to reduce the appearance of ghost peaks, 15% ammonia solution was injected on to the hot (150–200°C) column after each sample run. As shown in **Figure 1**, 23 amines were separated within 25 min (**Figure 1A**), and 12 amines were selectively detected in sea water (**Figure 1B**).

A general characteristic of Carbowax-based columns is that sample components are separated by carbon number and are eluted in the order $C_1 \rightarrow C_2 \rightarrow C_3$, and so forth. This is seen in the separation of methylamine, dimethylamine, trimethylamine and ethylamine. Both C_2 amines (dimethylamine and ethylamine) are eluted before the C_3 amine (trimethylamine). On these packings, it is necessary to use small samples to prevent tailing due to overloading. Furthermore, the column must be conditioned by injecting a number of relatively large amounts of water when analysing amines in aqueous solution. This treatment converts any K_2CO_3 in the column to

KOH, making the column more basic and improving its inertness for amines. Acidic compounds in the sample are irreversibly adsorbed by the KOH. In addition, a certain amount of stationary phase is hydrolytically decomposed and appears as a water peak in the chromatogram when water passes through the column. Therefore, conditioning is needed to clean the column and minimize the water peak when standards and sample are subsequently injected. These packed columns should not be exposed to air, since the packing will adsorb carbon dioxide and lose its deactivation. Furthermore, the water used should be distilled or deionized, and freshly boiled to remove CO_2 .

Porous polymer packings Porous polymers possessing large surface area are often used as column packing in GC without coating with a stationary phase. Tenax GC and Chromosorb 103 were specifically developed to separate low molecular weight aliphatic amines. Although Chromosorb 103 proved inconsistent and difficult to handle, and tended to expand on heating, leaving gaps in the column upon cooling, these effects could be minimized by paying scrupulous attention to packing. By using Chromosorb 103,

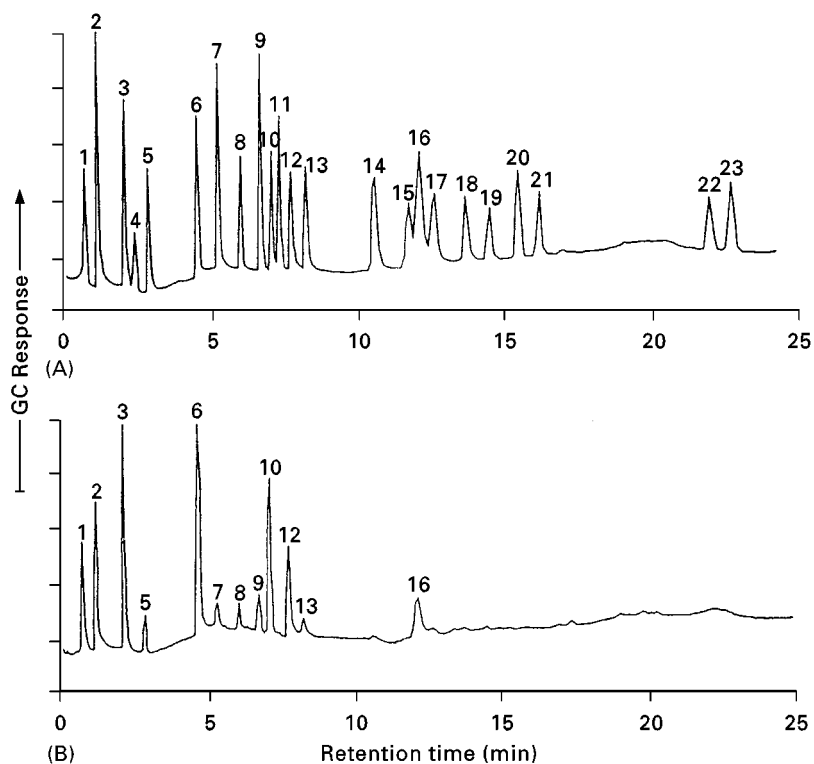


Figure 1 (A) Amine standards and (B) a sea water sample. GC conditions: packed column, 4% Carbowax 20 M and 0.8% KOH on Carbowax B ($2\text{ m} \times 2.5\text{ mm i.d. glass}$); column temperature, initially hold at 85°C for 2.5 min, increase to 150°C at $32^\circ\text{C min}^{-1}$ for 6 min and then to 220°C at $10^\circ\text{C min}^{-1}$; injector and detector temperatures, 200 and 220°C , respectively; He carrier gas flow rate, 22 mL min^{-1} ; detector, NPD. Peaks: 1, ammonia; 2, monomethylamine; 3, dimethylamine; 4, ethylamine; 5, trimethylamine; 6, 2-propylamine; 7, 1-propylamine; 8, *tert*-butylamine; 9, diethylamine; 10, *sec*-butylamine; 11, 2-butylamine; 12, pyrrolidine; 13, 1-butylamine; 14, piperidine; 15, triethylamine; 16, pyridine; 17, 2-amylamine; 18, 1-amylamine; 19, pyrrole; 20, dipropylamine; 21, cyclohexylamine; 22, tripropylamine; 23, dibutylamine. (Reproduced with permission from Yang *et al.* (1993) *Analytical Chemistry* 65: 572.)

11 aliphatic amines were isothermally separated without the ghosting observed with alkali-washed support packings. The use of longer columns resulted in increased analysis time that could not be reduced with a higher final temperature owing to excessive column bleed. Amines tail on other porous polymers, but performance can be improved by coating them with a stationary phase and TMCS. By using 5% squalene/2% KOH on Chromosorb 103 or 104 and GC-CLD, low molecular weight aliphatic amines have been determined. A column packed with Chromosorb 102 treated with 5% TMCS and coated with KOH has been used to determine methylamines in biological materials at low concentration by headspace GC-NPD. Use of headspace sampling avoids the possibility of interference from other water-soluble biological substances.

Partition columns A partition column consists of a support, generally a diatomaceous material, coated with a stationary phase. However, the support tends to interact with active analytes, such as amines, caus-

ing the peaks to tail, unless it is made strongly basic by adding KOH or an amine or by using an amine as the stationary phase. This alkaline deactivation of diatomaceous supports appears to be more effective than silanization for the analysis of amines. The major disadvantage of alkali-washed packings lies in the thermal instability of the liquid phases that prevents temperature-programmed analysis. Generally, Chromosorb W (white and light weight) and Chromosorb P (pink) supports are used as support materials; polytetrafluoroethylene supports are widely regarded as very inert, but they do not appear to be especially inert to amines. The stationary phase must be compatible with the basic material. Polyglycols, such as Carbowax and certain hydrocarbons, have been used successfully with basic materials.

Although a 10% Carbowax 20M/2% KOH on Chromosorb W AW packing was used for separating aliphatic mono- and diamines, many of the higher boiling anilines apparently did not elute from the column. Other PEG packings, such as PEG-1000 on Chromosorb G and PEG-HT on Uniport HP, have

also been used for the analysis of aliphatic and aromatic amines. Di- and polyamines in tissue samples were analysed using Corning glass beads coated with 4% Carbowax and 1% KOH. This column gave a good separation and a nearly complete recovery of these amines.

Aromatic amines are generally less basic than aliphatic amines and consequently present less of an adsorption problem. Although they can be separated on the highly basic columns described above, the analysis is generally carried out with a silicone stationary phase on an acid-washed, dimethylchlorosilane (AW-DMCS) treated support. The SP-2250 and SP-2401-DB packings were specially developed for separating amines at low concentrations. When analyte concentrations are very low, even AW-DMCS treatment is inadequate, and it is necessary to use a specially deactivated column or derivatize the analytes. The 3% SP-2250 column partially resolved all the anilines, but some peak tailing was evident, especially for aniline. The 5% SP-2401-DB (containing KOH) and 1.5% SP-2250/1.95% SP-2401 gave no improvement in peak shape, in spite of the greater polarity, compared to SP-2250. In addition, several compounds were not resolved on these columns. The Silar 5CP column partially resolved all the anilines except for 3- and 4-chloroanilines, and gave good peak shape for all the compounds. As shown in Figure 2, the best separation of 19 anilines was obtained using a 3% SP-2250 on Supelcoport.

Capillary Columns

Capillary columns offer a significant improvement in separation, in comparison to conventional packed columns, and have been used for the separation of complex mixtures and components closely related chemically and physiologically. As shown in Table 2, various glass and fused silica capillary columns have been used for free amine analysis. Fused silica capillary columns provide strength, flexibility and a more inert surface for improved performance and less adsorption. Cross-linked or bonded-phase columns can be washed with solvents, prolonging their lifetime. Furthermore, the advance of commercially available cross-linked and bonded-phase capillary columns and precise temperature-controlled GC ovens has meant that the retention times are extremely reproducible. This is critical when using automated data-handling equipment for identification and quantification. Typically, 10–30 m long columns, coated with either non-polar or polar stationary phases, have been used for amine analysis. Many of the phases used today are specifically manufactured by the column supplier, and give excellent performance, low bleed and high efficiency. However, there is the drawback that a col-

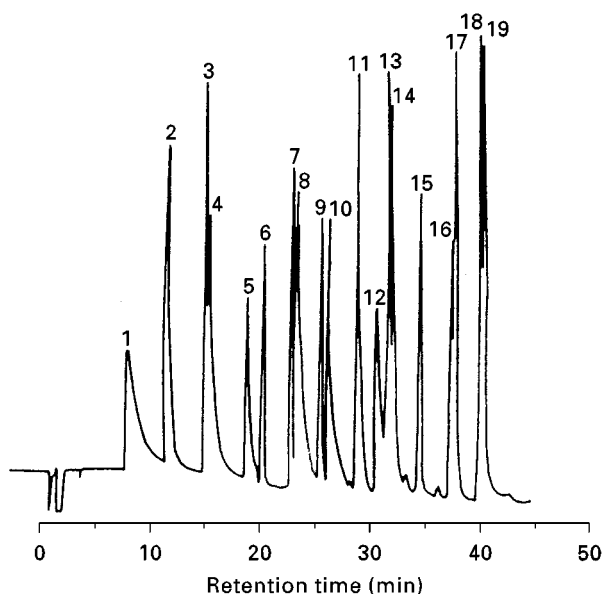


Figure 2 Aniline compounds on packed column. GC conditions: column, 3% SP-2250 on Supelcoport (1.83 m \times 2 mm i.d. glass); column temperature, 4°C min⁻¹ from 80 to 230°C; injector and detector temperatures, 250 and 300°C, respectively; He carrier gas flow rate, 30 mL min⁻¹; detector, NPD. Peaks: 1, aniline; 2, 2-chloroaniline; 3, 3-chloroaniline; 4, 4-chloroaniline; 5, 4-bromoaniline; 6, 3,4-dichloroaniline; 7, 2,4,6-trichloroaniline; 8, 2-nitroaniline; 9, 2,4,5-trichloroaniline; 10, 3-nitroaniline; 11, 4-chloro-2-nitroaniline; 12, 4-nitroaniline; 13, 2,6-dichloro-2-nitroaniline; 14, 2-chloro-4-nitroaniline; 15, 2-bromo-6-chloro-4-nitroaniline; 16, 2,6-dibromo-4-nitroaniline; 17, 2-chloro-4,6-dinitroaniline; 18, 2,4-dinitroaniline; 19, 2-bromo-4,6-dinitroaniline. (Reproduced with permission from Riggins *et al.* (1983) *Analytical Chemistry* 55: 1862.)

umn from one supplier may not give the same separation as the nominally equivalent column from another supplier.

Glass capillary columns In early work, glass capillaries were employed for the separation of aromatic amines using alkaline PEG as the stationary phase. Although a disadvantage of this phase is its tendency to deteriorate at temperatures slightly above 200°C, it has been used for the separation of methylanilines and methylpyridines in coal-tar light oil. Carbowax 20M columns have been used for the determination of airborne aromatic amines with an NPD. The necessary inertness of glass capillary columns may be achieved by deactivation with octamethylcyclotetrasiloxane (OMCTS). The glass or fused silica columns were silanized using OMCTS and trifluoropropyl(methyl)cyclosiloxane, and coated with various phases (SE-30, SE-52, SE-54). Test mixtures containing about 1 ng of such difficult substances as primary mono- and diaminoalkanes gave symmetrical peaks on some of these phases. As shown in

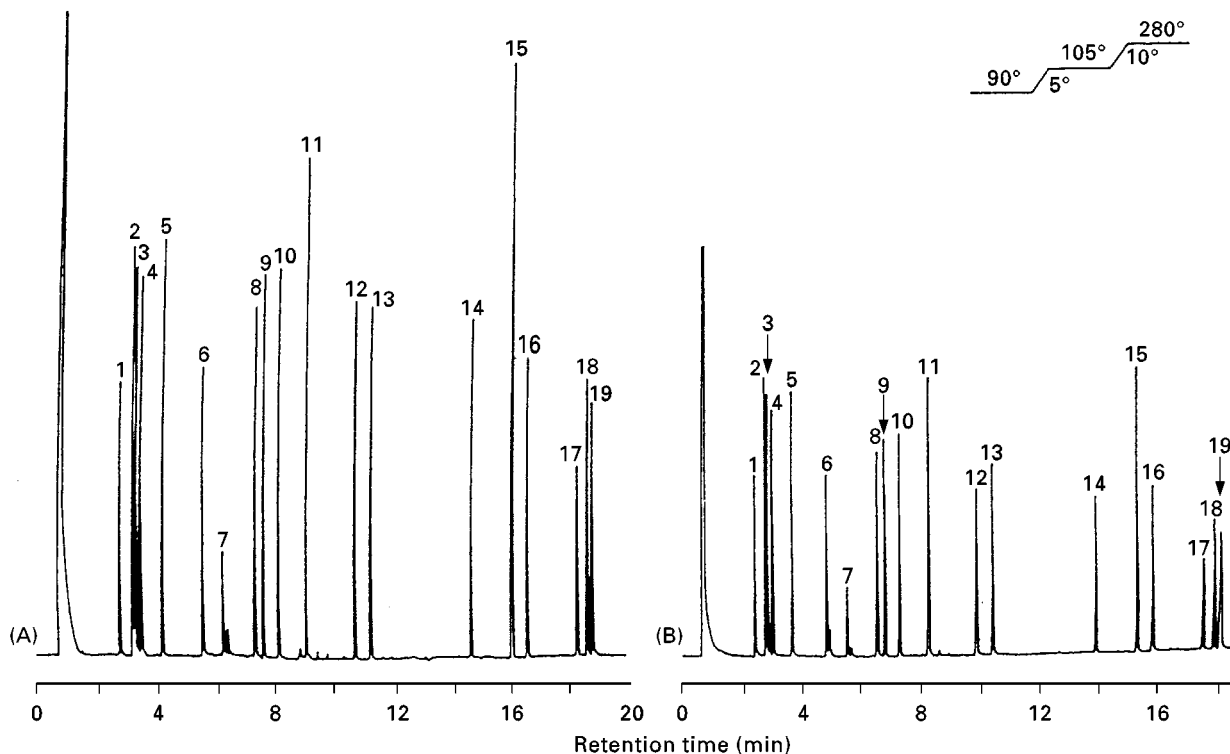


Figure 3 Drug standard mixtures on (A) AR glass and (B) fused silica capillary columns coated with SE-54 and with flame ionization detector. Temperature programmes are shown within the figure. Peaks: 1, amphetamine; 2, phentermine; 3, propylhexedrine; 4, methamphetamine; 5, ethylamphetamine; 6, propylamphetamine; 7, ephedrine; 8, phenmetrazine; 9, phendimetrazine; 10, amfetramone; 11, benzocaine; 12, phenacetin; 13, methyl phenidate; 14, procaine; 15, methaqualone; 16, cocaine; 17, codeine; 18, ethylmorphine; 19, morphine. (Reproduced with permission from Blomberg *et al. Journal of Chromatography* 239 (1982) 51).

Figure 3, the separation of some underivatized drugs is equally good on alkali-resistant (AR) glass and fused silica capillaries, although alkali-resistant (AR) glass has a basic character that can be reduced by careful leaching.

On the other hand, interesting results dealing with the separation of free amines and other nitrogen compounds were reported in glass capillary columns with stationary phases polymerized *in situ*.

Fused silica capillary columns For the analysis of amines, capillary columns with a nonimmobilized PEG-type stationary phase have been specially prepared and are commercially available. For the analysis of volatile amines, aromatic and heterocyclic amines and other amino substances, CAM, CP-Wax, HP-20M, Carbowax 20M and Carbowax Amine capillary columns have been recommended. These columns are generally deactivated with KOH to elute basic compounds with good peak shapes and responses. Three types of fused silica capillary columns, Supelcowax 10 (PEG), CP-Sil-19CB (methylphenylcyanopropylsilicone) and HP-1 (methylsilicone) have also been used for the separation of aliphatic and aromatic amines. Ammonia as a carrier gas can dras-

tically affect the retention factors and improve the peak symmetry for aliphatic amines. A porous polymer fused silica capillary column, PoraPLOT Amine, has been used to separate very volatile amines. By using this column and ELCD, C_1 – C_6 amines in aqueous and methanolic solution were analysed. The separation of aniline and its halogen and nitrogen derivatives in waste water were evaluated using several glass and fused silica capillary columns of polysiloxane type (SE-30, SE-52, SE-54, SP-2100) and NPD. Each of the capillary columns gave excellent peak shape for all the anilines, but failed to resolve at least one compound pair (e.g. the SE-30 completely resolved 3- and 4-chloroaniline that co-eluted on SE-54, but failed to resolve the 2,6-dibromo-4-nitroaniline and 2,4-dinitroaniline which were completely resolved on SE-54). Figure 4 shows a chromatogram of an aniline mixture on an SE-54 fused silica column. The NPD sensitivities for many anilines are substantially better with the SE-54 capillary column (Figure 4) than with the 3% SP-2250 packed column (Figure 2), primarily because less peak tailing is observed at low concentration. Interestingly, the fused silica and glass capillary SE-54 columns gave different elution patterns for the various anilines. Using both SE-54 and SE-30

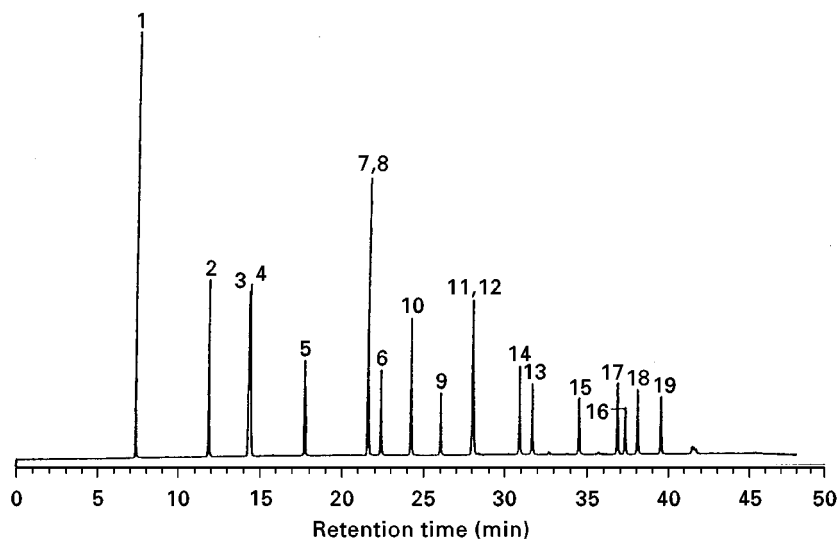


Figure 4 Aniline compounds on fused silica capillary column. GC column, SE-54 (30 m \times 0.25 mm i.d.); He carrier gas flow rate, 30 cm s⁻¹; split ratio, 10 : 1. Other conditions and peak numbers are the same as Figure 2. (Reproduced with permission from Yang *et al.* (1993) *Analytical Chemistry* 65: 572.)

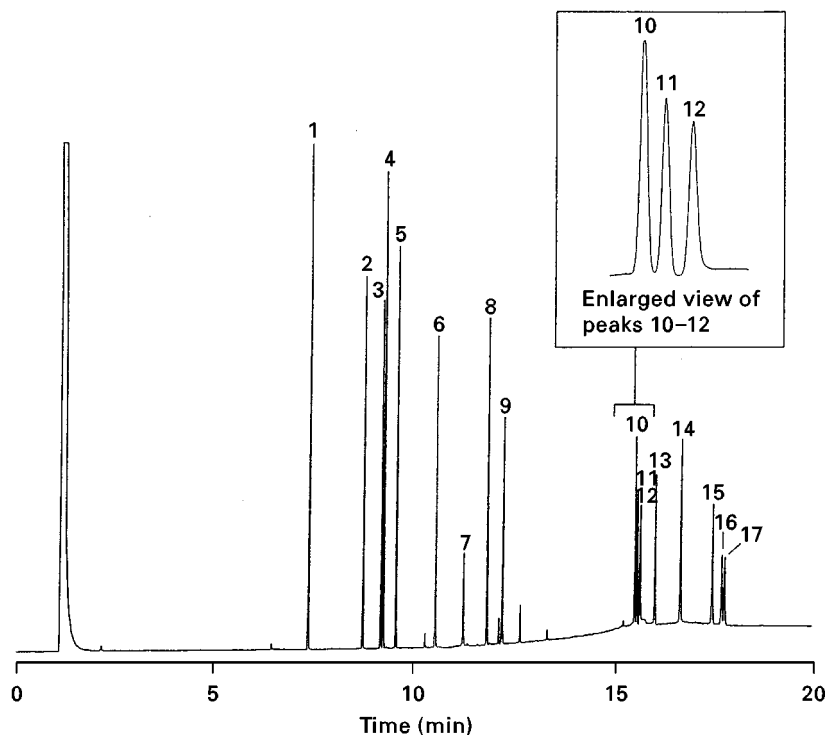


Figure 5 Aromatic amines on fused silica capillary column. GC conditions: column, DB-35ms (25 m \times 0.20 mm i.d. glass); column temperature, initially hold at 50°C for 2 min, increase to 340°C at 20°C min⁻¹ and then hold at 340°C for 10 min; injector and detector temperatures, 280 and 320°C, respectively; He carrier gas flow rate, 35 cm s⁻¹; splitless injection; detector, NPD. Peaks: 1, *o*-toluidine; 2, 4-chloroaniline; 3, 2-methoxy-5-methylaniline; 4, 2,4,5-trimethylaniline; 5, 4-chloro-2-methylaniline; 6, 2,4-diaminotoluene; 7, 2,4-diaminoanisole; 8, 2-aminonaphthalene; 9, 2-methyl-5-nitroaniline; 10, 4,4'-oxydianiline; 11, 4,4'-methylenedianiline; 12, benzidine; 13, 2-aminoazotoluene; 14, *o*-toluidine; 15, 4,4'-thiodianiline; 16, 3,3'-dimethoxybenzidine; 17, 3,3'-dichlorobenzidine. (Reproduced with permission from Catalog and Technical Reference, C407, J & W Scientific, California.)

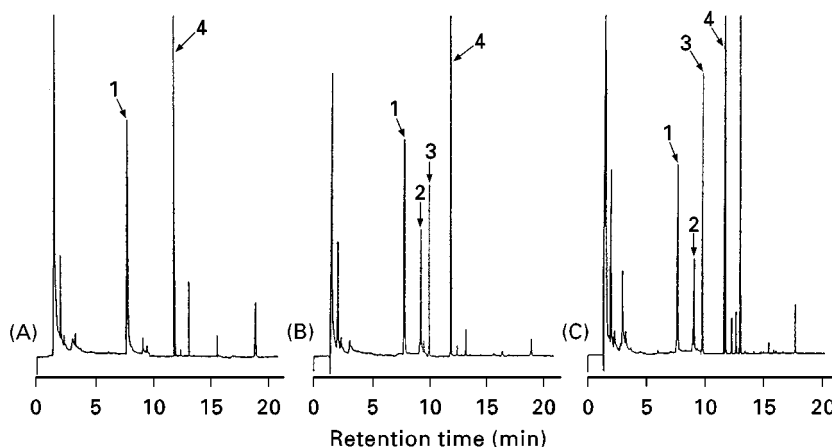


Figure 6 Chromatograms obtained from hair samples. (A) Normal hair; (B) normal hair with standard amphetamines added; (C) abuser's hair. GC conditions: column, CBJ-17 (30 m \times 0.53 mm i.d. fused-silica, Shimadzu); column temperature, initially hold at 100°C for 5 min, increase to 220°C at 10°C min⁻¹ and then hold at 220°C for 3 min; injector and detector temperatures, 220°C; He carrier gas flow rate, 4 mL min⁻¹; split ratio, 2 : 1; detector, NPD. Peaks: 1, α -phenethylamine (internal standard); 2, amphetamine; 3, methamphetamine; 4, *N*-propyl- β -phenethylamine (internal standard).

fused silica capillary columns, all 19 anilines can be resolved.

A polysiloxane capillary column specially designed for the analysis of basic compounds using new deactivation technologies has been developed. This proprietary deactivation provides both the inertness (basicity) and surface energies required to coat a 5% diphenyl/95% dimethylpolysiloxane stationary phase successfully. Using this column, C₃–C₁₀ primary amines can be separated as symmetrical peaks. This column allows lower limits of detection for basic compounds such as substituted anilines and benzidines. Since the column is virtually identical in polarity to the widely used ordinary columns with the same stationary phase, it can be directly substituted and run under the same temperature conditions. DB-5ms and DB-35ms columns certified for use with MS have been developed for the analysis of aliphatic and aromatic amines. These columns have very low bleed characteristics and excellent inertness. As shown in **Figure 5**, 17 aromatic amines were completely separated using a DB-35ms column.

Lower aliphatic tertiary amines in environmental samples were analysed by headspace GC with a mass selective detector (MSD) using a polymethylsiloxane column. The SPME method has gained popularity as a solvent-free, reliable and flexible tool for sampling a variety of volatile and semi-volatile compounds. By combining SPME with GC, these compounds can be simply and rapidly extracted, concentrated and introduced into the GC system. Using headspace SPME and GC-MSD on polysiloxane-type fused silica capillary columns such as DB-1, OV-1, SPB-1, HP-1 and HP-5, amphetamine, methamphetamine and related

stimulants in urine can be analysed at the ng mL⁻¹ level. Recently, headspace SPME and GC-NPD using a slightly polar capillary column CBJ-17 (**Figure 6**) has developed as a method for determining amphetamines in human hair.

Future Prospects

Much of the early work on the separation of free amines was done with columns packed with PEG and KOH on diatomaceous earths. Although this approach was reasonably successful, the analysis of free amines on packed columns has now largely been replaced by analysis on fused silica capillary columns. Application of capillary columns is expected to increase as further developments in these columns, e.g. shorter inactive columns with smaller internal diameters giving ultra-high column efficiency and speed, higher temperature phases and exterior coating for the fused silica tubing, permit the analysis of both high temperature and highly volatile amines. Furthermore, simple, rapid and automatic analysis of free amines in various samples will be achieved by combination with convenient sample preparation techniques such as SPME.

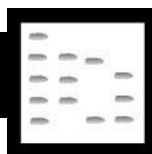
See also: II/Chromatography: Gas: Column Chromatography; Detectors: Selective.

Further Reading

Clement RE (ed.) (1990) *Gas Chromatography. Biochemical, Biomedical, and Clinical Applications*. New York: John Wiley.

- Grant DW (ed.) (1996) *Capillary Gas Chromatography*. New York: John Wiley.
- Grob RL (ed.) (1995) *Modern Practice of Gas Chromatography*, 3rd edn. New York: John Wiley.
- Heftmann E (ed.) (1992) *Chromatography*, 5th edn. Part B: *Applications*. (Journal of Chromatography Library, Vol. 51B). Amsterdam: Elsevier.
- Hyver KJ and Sandra P (eds) (1989) *High Resolution Gas Chromatography*, 3rd edn. Delaware: Hewlett-Packard.
- Kataoka H (1996) Derivatization reactions for the determination of amines by gas chromatography and their applications in environmental analysis. *Journal of Chromatography A* 733: 19.
- Kataoka H (1997) Methods for the determination of mutagenic heterocyclic amines and their applications in environmental analysis. *Journal of Chromatography A* 774: 121.
- Pawliszyn J (1997) *Solid Phase Microextraction: Theory and Practice*. New York: Wiley VCH.
- Riggin RM, Cole TF and Billets S (1983) Determination of aniline and substituted derivatives in waste water by gas and liquid chromatography. *Analytical Chemistry* 55: 1862.
- Yang X-H, Lee C and Scranton MI (1993) Determination of nanomolar concentrations of individual dissolved low molecular weight amines and organic acids in seawater. *Analytical Chemistry* 65: 572.

AMINO ACIDS



Gas Chromatography

S. L. MacKenzie, Plant Biotechnology Institute,
Saskatoon, Saskatchewan, Canada

Copyright © 2000 Academic Press

During the 1950s and 1960s, significant progress was made in the development of automated amino acid analysers based on separation by ion exchange. However, such instruments were dedicated to the task of amino acid analysis and were of limited application to the analysis of other types of compounds. Furthermore, they were expensive. During the same period, gas chromatography (GC) was being rapidly developed following the demonstration in 1952 by James and Martin that fatty acids could be assayed by GC. There followed a vast expansion in the application of GC to the analysis of other types of compounds. Amino acids were a logical target. In the intervening years, methods have been developed for assaying amino acids in protein hydrolysates and physiological fluids, and for determining the proportions of amino acid enantiomers in racemic mixtures. Some landmark developments are listed in Table 1.

Proteic and Physiological Amino Acids

Derivative Development

Amino acids are not sufficiently volatile or stable at the temperatures required for analysis by GC. Thus, they must be converted to derivatives having the desired characteristics. It was to be no simple task to derivatize or mask the several functional groups in even the 20 proteic amino acids. Carboxy, amino,

hydroxy and sulfhydryl groups all need to be converted to eliminate internal zwitterionic charges and hydrogen bonding, and thus increase the volatility of the derivatives. It was thought in those early years that the molecular mass also required to be reduced but it was later realized that this was not an absolute requirement. As new reagents became available, it was found that volatility could be significantly increased while increasing the derivative mass. Apart from the multiplicity of functional groups, it is also necessary that each group should be quantitatively converted.

The first report of amino acid analysis by gas liquid chromatography was published in 1956. Hunter, Dimick and Corse oxidized isoleucine and leucine with ninhydrin to form volatile aldehydes. These were resolved using a 10 ft long silicone oil–celite column operated isothermally at 69°C. Peaks were detected at about 44 and 48 min (**Figure 1**). The aldehydes were generated using 2–5 mg of each amino acid. Either of the leucines could be assayed in the presence of 10-fold quantities of the other. However, only about eight simple amino acids yield volatile aldehydes.

From this simple but momentous beginning, there followed, in the next two decades, a proliferation of reaction schemes to prepare stable, volatile amino acid derivatives. Various oxidation, hydrocracking, pyrolysis and reduction reactions were explored but significant progress was to evolve from those procedures which focused on substituting the exchangeable protons of the reactive groups. In 1957, Bayer, Reuther and Born separated glutamic acid, leucine, methionine, norleucine, norvaline, phenylalanine, sarcosine and valine methyl esters on a silicone oil–sodium caproate packing. The use of an acyl ester constituted the first report of a key component in

Table 1 Advances in gas chromatography of amino acids

1956	First GC analysis (Hunter, Dimick and Corse)
1959	Acyl amino acid alkyl esters separated (Youngs)
1965	Resolution of alanine, leucine and valine enantiomers (Gil-Av, Charles and Fischer)
1962–79	Development of derivatization and separation procedures for the proteic amino acids (Gehrke)
1971	First single column separation of all proteic amino acids (Moss, Lambert and Diaz)
1971–76	Further improvements in resolution
1977	Development of Chirasil Val® (Frank, Nicholson and Bayer)
1989	Use of cyclodextrins for enantiomer resolution (König, Krebber and Mischnick)
1991	4 min analysis of proteic amino acids (Hušek)

a derivatization strategy which would eventually prove to be successful. One year later, Bayer reported that good resolution could be achieved using *N*-trifluoroacetyl (TFA) amino acid esters. This work represented the first use of *N*-TFA derivatives, representatives of a class of compounds which would feature strongly in later developments.

In the next decade, *N*-formyl and -acetyl derivatives were combined with a variety of alkyl esters such as methyl, ethyl, propyl, isopropyl, isobutyl, amyl and isoamyl. The work of Youngs in 1959 was the first in which *N*-acyl derivatives were combined with alkyl amino acid esters. *N*-acetyl ethyl and butyl esters of six simple amino acids were separated on

hydrogenated vegetable oil. This approach was to provide the foundation for developments leading, over the next several years, to the quantitative resolution of all the amino acids in a protein hydrolysate. In 1964 Karmen and Saroff showed that excellent yields of *N*-TFA amino acid methyl esters were obtained when the esters were first prepared and then acylated. This general protocol remains in use.

The use of *N*-TFA derivatives in combination with amino acid alkyl esters was first reported by Ettre in 1962. Starting in the same year, Gehrke and his colleagues systematically studied the derivatization and chromatography of the *N*-TFA *n*-butyl amino acid esters. TFA derivatives were used in amino acid chemistry by Weygand as early as 1952 but were first applied in the context of GC analysis in 1960. In the first report, 22 naturally occurring amino acid derivatives were resolved in less than 45 min using a 2 m column packed with Gas Chrom A coated with 1% neopentyl succinate. Subsequently, the esterification reaction was simplified by using direct esterification instead of methylation followed by interesterification. Direct on-column injection and an all-glass system were demonstrated to avoid degradation of some derivatives. Rigorous exclusion of water is necessary both for complete derivatization and to prevent hydrolysis of derivatives once formed. These and other procedures developed by Gehrke formed a solid quantitative foundation for subsequent studies by others.

Continued refinement of both the reaction chemistry and the columns culminated in the complete separation of the 20 proteic amino acids in 1971. Seventeen amino acids were resolved using a 4 mm i.d. × 1.5 m glass column packed with 0.65% ethylene glycol adipate (EGA) on 80–100 mesh Chromosorb W-AW. The derivatives of arginine, histidine, tryptophan and cystine were separated from those of the other amino acids on a 4 mm i.d. × 1.5 m glass column packed with a mixed stationary phase of 2% OV-17 and 1% OV-210 coated on 100–200 mesh Supelcoport. In particular, histidine could be directly assayed. The two columns were operated simultaneously, resulting in an analysis time of 15–30 min. In 1979, the same derivatives were separated on a single EGA liquid phase but no significant improvement over other available procedures was obtained.

Gehrke also conducted a thorough assessment of possible sources of contamination. As detection sensitivity increased, contamination became a significant problem. At the nanogram level, contamination was shown to derive from laboratory reagents such as butanol, methylene chloride and water, and from human sources such as dandruff, fingerprints, hair, saliva and skin fragments.

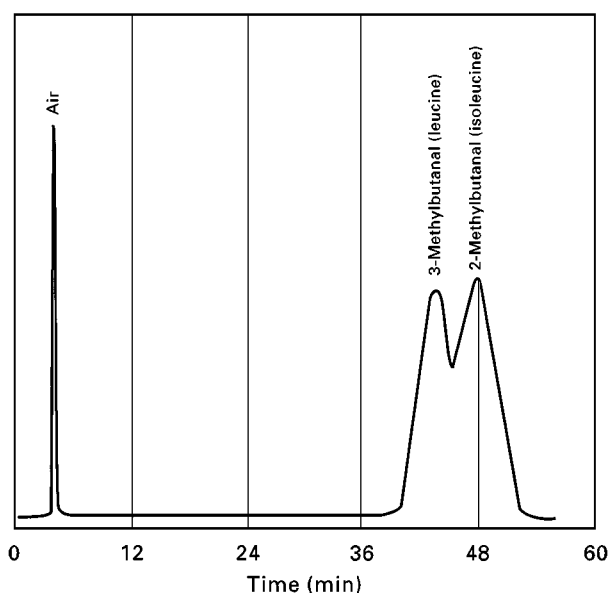


Figure 1 Separation of 3-methylbutanal and 2-methylbutanal using a 10ft column filled with a silicone-celite mixture. (Reproduced with permission from Hunter IR, Dimick KP and JW Corse (1956) Determination of amino acids by ninhydrin oxidation and gas chromatography. *Chemistry and Industry* 294–295.)

The stationary phases used during the early years of development fell into three main classes: silicones, polyglycols and polyesters. Because it was difficult to separate even the proteic amino acids on a single phase, mixed phases were common. Eventually, however, the silicone phases, in nonpolar or slightly polar forms, became favoured and were essential for quantitative elution of arginine, cystine and histidine derivatives. Dual- and triple-column procedures were to give way in the search for a single column separation of the proteic amino acids. The first such resolution was achieved in 1971 by Moss, who prepared the *N*-heptafluorobutyl (HFB) *n*-propyl esters. These were resolved on a 10 × 1/4 in glass column packed with 3% OV-1 coated on 80–100 mesh HP Chromosorb W (Figure 2). No quantitative data were provided. There followed other variations on the same theme. The *N*-HFB isoamyl (1973), isobutyl (1974) and isopropyl (1979) esters provided similar resolutions but with subtle separatory advantages depending on the relative proportions of specific amino acids present. Resolution was primarily a function of the ester, while the acyl group mainly moderated the volatility.

The search for a single-column resolution of the proteic amino acids was paralleled by a search for a single reaction which would derivatize all the functional groups present in amino acids. Trimethylsilylation was introduced as early as 1961 by Rühlman and Giesecke who reacted trimethylchlorosilane with amino acid salts. Six amino acids were separated in less than 30 min. A fuller account in 1963 reported that tyrosine and histidine derivatives tended to decompose in the presence of moisture or oxygen. The early reagents were generally silylated amines or monosubstituted amides and double derivative formation was a significant problem. However, newer

reagents, for example *bis*-(trimethylsilyl)trifluoroacetamide, were considerably more potent and derivatization became quantitative. In more recent work (1993), all 22 proteic amino acids, including glutamine and asparagine, which would not be present in protein hydrolysates, have been quantitatively resolved as the *N*(*O*)-*tert*-butyldimethylsilyl derivatives in 41 min on a DB-1 column. The derivatives are formed in 30 min at 75°C.

Other approaches have also been used in the search for the simplest derivatization commensurate with reproducibility and stability, and with good chromatographic characteristics. Reaction with dichlorotetrafluoroacetone forms stable 2,2-*bis*(chlorodifluoromethyl)-4-subst-1,3-oxazolidine-5-one derivatives. All the proteic amino acids and more than 30 other α -amino acids have been studied. However, a second reaction with HFB anhydride is required and analysis of the diaminodicarboxylic acids histidine and tryptophan required a second column.

Alkoxy carbonyl alkyl esters, specifically the isobutoxycarbonyl methyl esters, were first prepared by Makita in 1976. Twenty proteic amino acid derivatives were separated using a dual-column system but the derivatization procedure involves multiple extraction. Arginine was first converted to ornithine. At that time, this procedure offered no significant advantage over the other protocols available. However, the method was subsequently improved so that, in 1996, all the proteic amino acid derivatives were resolved as single peaks in 9 min using a DB-17 capillary column. Serum amino acids could be assayed without any prior clean-up except for deproteinization. The isobutoxycarbonyl derivatives have also been effectively combined with *tert*-butyldimethylsilyl esters.

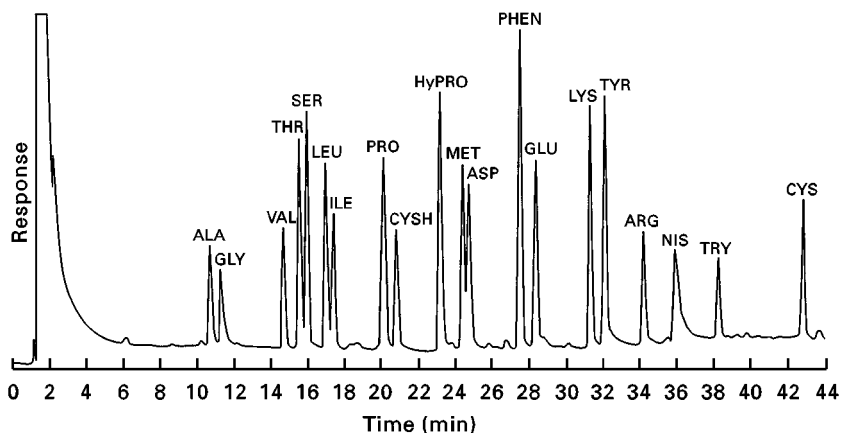


Figure 2 Separation of *N*(*O*, *S*)-heptafluorobutyl *n*-propyl amino acids. (Reproduced with permission from Moss CW, Lambert MA and Diaz FJ (1971) Gas-liquid chromatography of twenty protein amino acids on a single column. *Journal of Chromatography* 60: 134–136.)

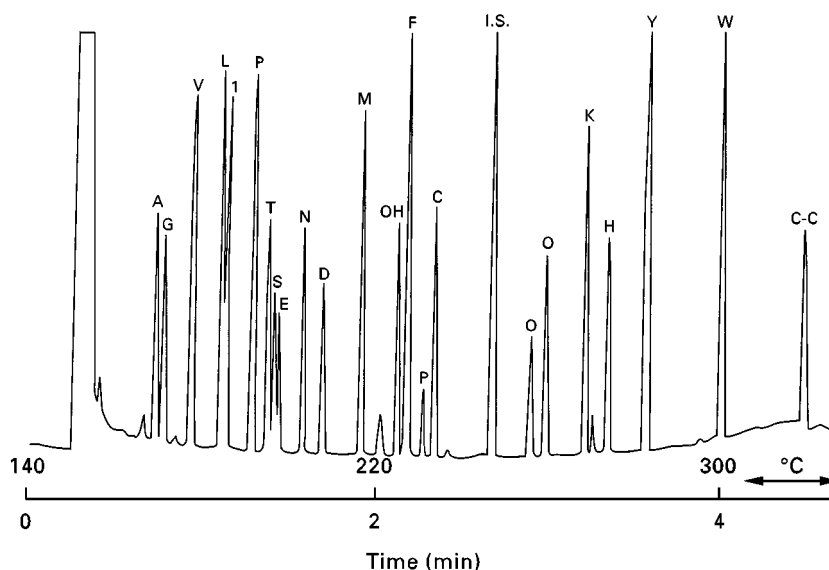


Figure 3 Analysis of *N*(*O*, *S*)-ethoxycarbonyl amino acid ethyl esters on a 10 m × 0.25 mm i.d. capillary column coated with OV1701. (Reproduced with permission from Hušek P and Sweeley CC (1991) Gas chromatographic separation of protein amino acids in four minutes. *Journal of High Resolution Chromatography* 14: 751–753.)

In 1991, Hušek prepared derivatives in the same general class but using ethyl chloroformate which reacts with all the functional groups found in amino acids. The *N*(*O*, *S*)-ethoxycarbonyl ethyl esters are formed in seconds in an aqueous medium. The derivatives were resolved in less than 5 min using a moderately polar OV1701 capillary column (Figure 3).

A variety of derivatization options are now available. The *N*-HFB isoamyl, isobutyl or isopropyl esters are equally effective for the relatively simple task of assaying the standard proteic amino acids. However, procedures requiring only a single derivatization step are more convenient and are preferred. Either the isobutoxycarbonyl methyl esters or the ethoxycarbonyl ethyl esters can be quickly prepared and resolved in less than 10 min using moderately polar capillary columns.

The several hundred amino acids which are present in physiological fluids cannot be resolved by any single method. Each method has advantages in a specific context. Frequently, however, the target is a single or a few structurally related amino acids. In such a context, any of the methods cited above may be appropriate, depending on the specific separations required. However, methods based on alkoxycarbonyl alkyl esters are more convenient to implement. Furthermore, some physiological samples, such as sera, can be assayed directly after deproteinization.

Very few amino acids are not amenable to being analysed by GC. Furthermore, the resolving power of capillary column chromatography cannot be matched by any other separatory medium. GC remains the

method of choice for assaying amino acids in complex physiological samples.

Resolution of Optical Isomers

The determination of the configuration of amino acids and the relative proportions of the *D* and *L* forms is important in both natural and synthetic contexts. Proteins in living organisms commonly contain only the *L*-amino acids but *D*-amino acids occur in antibiotics (e.g. antiamoebin, gramicidin, valinomycin), bacterial cell wall peptidoglycans and in animals and insects. They have also been detected in human urine and blood. On death, the *L*-amino acids racemize, but so slowly that a racemic mixture is only produced over a geological time scale. The racemization rate is a function of temperature and the structure of each amino acid. Aspartic acid, which has a racemization half-life of about 15 000 years at 20°C, is most commonly used for archaeological dating, but there is considerable controversy over the results obtained.

Animal bones and shells and certain sediments contain proteins, for example, collagen and conchiolin. Extraction of the residual protein and determination of the enantiomer ratio of aspartic acid following hydrolysis can, when combined with knowledge of the thermal history of the sample, be used to determine the age of the fossil. Racemization age dating is generally more sensitive and less expensive than the radiocarbon method. Typical examples of the use of this technique have been analysis of Apollo 12 lunar material and dating of the Dead Sea scrolls.

Amino acids also racemize under various conditions such as prolonged acid hydrolysis and during solid-phase peptide synthesis. Chemical procedures such as asymmetric synthesis require proof of enantiomeric purity, especially if the product is to be used for pharmaceutical purposes. Configurational analysis of peptide antibiotics and establishing retention of configuration during peptide synthesis are other contexts in which it is important to determine the enantiomeric composition of amino acid samples.

Enantiomeric amino acid mixtures are resolved using two approaches. The first is to derivatize (acylate or esterify) with optically active reagents to form diastereoisomers or diastereomers which are resolved on an optically inactive stationary phase. The reagents must be of high optical purity and conversion must be quantitative. The second approach is to derivatize with optically inactive reagents, for example the *N*-TFA isopropyl esters, and then conduct the separation on columns containing optically active stationary phases.

Most amino acid optical isomers result from asymmetry at the α -carbon atom and depend on the presence of an α -hydrogen atom. However, some contain two optically active centres. Thus, the *threo* and *erythro* forms of the hydroxy amino acids and isoleucine and *allo*-isoleucine can be resolved on conventional columns. Similarly, isovaline, which contains one asymmetric centre but no α -hydrogen, has also been resolved. The mechanism has been postulated to depend on the formation of transient diastereomeric hydrogen-bonded association complexes but other factors such as dipole-dipole interactions and dispersion forces may also play a role.

Resolution of Diastereomers

All four diastereomers cannot be resolved using optically inactive stationary phases: the DD + LL and DL + LD enantiomer pairs usually coelute. The elution order depends on the specific derivatives. A diastereomer can be formed by esterification or by acylation.

Optically Active Esterification Reagents

Initial studies focused on forming active esters of *N*(*O*)-acyl amino acids and these were subsequently to be the most widely used derivatives. In 1965, Gil-Av reported the first resolution of amino acid diastereomers by GC (Figure 4). The 2-butyl and 2-octyl amino acid esters of alanine, glutamic acid, leucine, phenylalanine, proline and valine were resolved on capillary columns coated with either poly(trifluoropropylmethylsiloxane) or poly(propylene glycol) operated isothermally at 140 or 180°C. In the same year, Pollock reported the resolution of the *N*-TFA 2-butyl esters of 13 amino acids but those of aspartic acid, serine and threonine were only partially resolved. A study by Westley (1968) concluded that the resolution was directly proportional to the size of the groups attached to the alcoholic asymmetric carbon and to the proximity of the branching to the asymmetric centre. Thus 3,3-dimethyl-2-butanol gave superior resolution. In 1968, Pollock extended his study to the resolution of all the proteic amino acids except arginine, histidine and cystine. Three years later, 37 amino acid diastereomers were resolved as the *N*-TFA 2-butyl esters.

In 1977, König separated the *N*-pentafluoropropionyl (PFP) (+)-3-methyl-2-butyl esters of all the

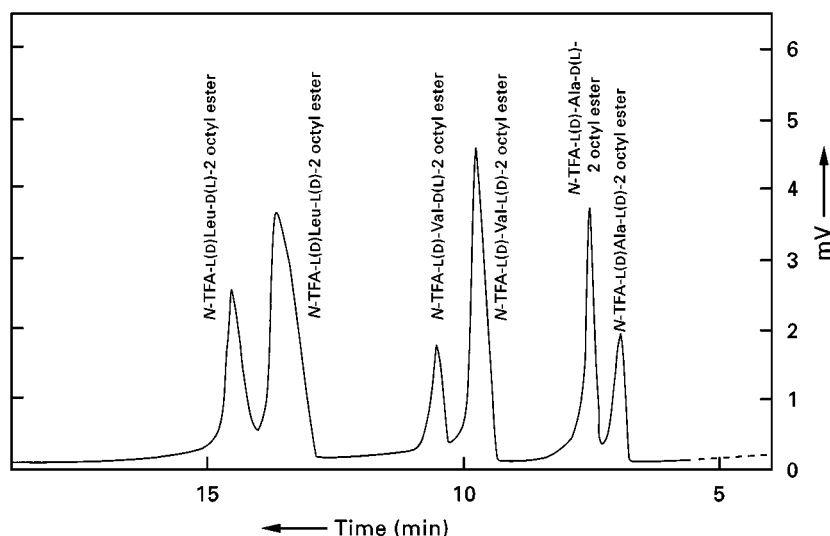


Figure 4 Resolution of diastereomers of *N*-trifluoroacetyl amino acid (*N*-TFA) 2-octyl esters. (Reproduced with permission from Gil-Av E, Charles R and Fischer G (1965) Resolution of amino acids by gas chromatography. *Journal of Chromatography* 17: 408–410.)

common proteic amino acids, including arginine, histidine and tryptophan. Excellent resolution was obtained using a 25 m column coated with SE30 and temperature programming from 85 to 220°C at 2°C min⁻¹.

Optically Active Acylation Reagents

A variety of carbonyl chlorides have been used to generate optically active dipeptides. *N*-TFA-L(-)-prolyl chloride was first used in 1965 by Halpern and Westley who separated the isomers of alanine, leucine, methionine, phenylalanine, proline and valine. The reagent was chosen because it was thought that the cyclic nature of the derivative would preclude racemization via an oxazolinone mechanism. This reasoning was later shown by Bonner to be incorrect but the problem was overcome by modifying the derivatization procedure. The reagent subsequently came into fairly common use. It was extensively studied by Iwase and Murai who combined TFA, PFP and HFB forms with methyl, *n*-propyl, *n*-butyl, *tert*-butyl and cyclopentyl esters. By assessing the resolution of alanine, valine, leucine and isoleucine, they concluded that the esters of *n*-alkyl alcohols gave better resolution than branched or cyclic chain alcohols.

König introduced a second asymmetric centre into amino acid methyl esters using the chiral reagent L- α -chloroisovaleryl chloride. Formation of the 3-methyl-2-butyl esters enabled resolution of all the proteic amino acid diastereomers, including arginine, on an SE-30 capillary column in less than 1 h. A separate analysis was required for the basic amino acids. Nevertheless, the diastereomer approach was to be overtaken by the more direct and absolute method of enantiomer resolution on chiral phases.

Resolution of Enantiomers on Optically Active Columns

In 1966, Gil-Av demonstrated the first resolution of amino acid enantiomers on an optically active stationary phase. The *N*-TFA-2-butyl esters of alanine, valine and leucine were resolved on an *N*-TFA-L-isoleucine lauryl ester phase coated on a capillary column. However, phases of this type quickly gave way to dipeptide phases such as *N*-acyl-L,L-dipeptide alkyl esters which were first introduced by Feibush and Gil-Av in 1967 and which produced better resolution.

In 1970 Nakaparskin and colleagues separated 17 amino acid enantiomers on an *N*-TFA-L-val-L-val-cyclohexyl ester phase (val-val). In earlier studies, stainless-steel columns up to 500 ft long were used.

Consequently, analysis times were prolonged and the cystine, serine and threonine derivatives were degraded. In addition, dipeptide stationary phases such as val-val were functional over a limited temperature range or a limited maximum operating temperature. Columns were usually operated in isothermal mode.

König addressed the problem of temperature stability by introducing the *N*-TFA-L-phenylalanyl-L-leucine cyclohexyl ester which could be operated at 140°C. A later modification, the *N*-TFA-L-phenylalanyl-L-aspartic acid *bis*-(cyclohexyl) ester, was stable over the range 96–165°C and allowed the use of temperature programming. In addition, the introduction of glass capillary columns reduced degradation of the amino acid derivatives. The high boiling *N*-PFP isopropyl esters of aspartic acid, methionine, phenylalanine, glutamic acid, tyrosine, ornithine and lysine were eluted using a 20 m column. However, the diamide phases still left room for improvement in thermal stability and in peak resolution.

Another generation of phases was introduced by Frank, Nicholson and Bayer who linked the diamide moiety, L-valine *tert*-butylamide, to a polysiloxane backbone. Later termed Chirasil Val®, phases of this general type became predominant and are still in use. Early versions of this phase resulted in the overlap of D- and L-proline, D-isoleucine and L-*allo*-isoleucine, and L-threonine and D-*allo*-isoleucine. Nevertheless, the enantiomers of all the other proteic amino acids were resolved as the *N*-PFP *n*- or isopropyl esters in about 30 min by temperature programming from 90 to 190°C (Figure 5). Acid treatment of the glass capillary followed by methanol washing was necessary rigorously to exclude basic sites and thus to obtain satisfactory elution of cysteine, serine, threonine and tyrosine and to obtain a sharp peak for arginine. The relative retention times of the amino acids can be manipulated by including polar modifiers such as cyanopropyl and phenyl groups but the effect varies with specific amino acids. The L-valine *tert*-butyl moiety was subsequently grafted to chloropropionyl-methyl phenylmethyl silicone, a modified OV-225, and to Silar 10C, but no overall improvement was achieved.

Chirasil-Val® was further improved by the incorporation of 15% phenyl groups substituted for methyl groups in the dimethylsiloxane units and the introduction of fused silica capillary columns. Thermal stability, ease of handling and separation efficiency were improved. The product is commercially marketed as Heliflex™ Chirasil-Val®.

Later improvements included the enhancement of enantioselectivity and thermal stability by immobilization of the Chirasil-Val® by radical or thermal

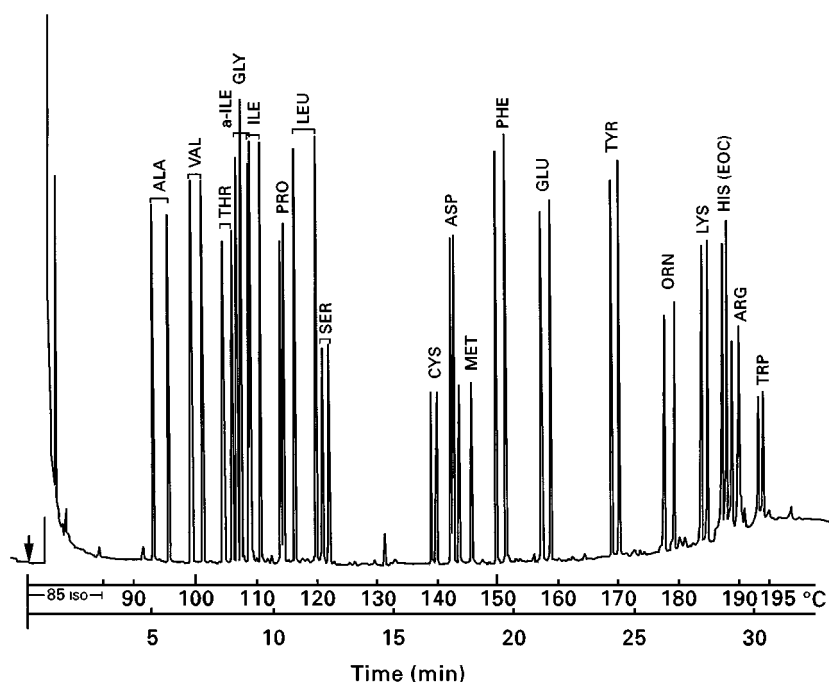


Figure 5 Resolution of a racemic mixture of proteic amino acids as the *N*-(*O*, *S*)-pentafluoropropionyl *n*-propyl esters. (Reproduced with permission from Bayer E, Nicholson G and Frank H (1987) Separation of amino acid enantiomers using chiral polysiloxanes: quantitative analysis by enantiomer labeling. In Gehrke CC, Kuo KCT and Zumwalt RW (eds) *Amino Acid Analysis by Gas Chromatography*, Volume II, pp. 35–53. Boca Raton, FL: CRC Press.)

reactions. Chiral polysiloxanes with regular repeat units, e.g. trifluoroethyl ester-functionalized polysiloxanes supporting *L*-val-*tert*-butylamide or *L*- α -naphthylethylamine liquid phases, have shown improved enantioselectivity. Backbone modification achieved by replacing one methyl group per dialkylsiloxane unit with a pentyl or hexyl group improved resolution of arginine and tryptophan *N*-TFA *n*-propyl esters but the overall separation of the other amino acids was not significantly affected. However, satisfactory results have been obtained by varying the proportion of *L*-val-*tert*-butylamide on the polysiloxane backbone. A ratio of about 6–7 dimethylsiloxane units per chirally modified dialkyl siloxane unit is effective for the complete resolution of all components present in a chiral mixture of the 20 proteic amino acids in about 35 min on a 20 m \times 0.3 mm glass capillary column.

Most studies on amino acid enantiomer resolution on Chirasil-Val® type columns have used *N*-perfluoroacyl alkyl ester derivatives. However, other derivatives may present advantages in specific contexts. For example, the *N*-alkyloxycarbonyl alkylamide derivatives of proline are completely resolved on a Chirasil-Val® column. Similarly, König demonstrated the utility of isocyanate derivatives for resolving the enantiomers of *N*-methyl and β -hydroxy amino acids.

A radically different approach to enantiomer resolution has become possible with the development of cyclodextrins as stationary phases. Although suitable for liquid chromatography, the high melting point of cyclodextrins rendered them unsuitable for GC without further modification. König reduced the melting point and increased stability by introducing hydrophobic moieties by both partial and complete alkylation and acylation of the hydroxy groups. γ -Cyclodextrin substituted with 3-*O*-butyl and 2,6-di-*O*-pentyl residues was found to resolve most of the common amino acid enantiomers as the *N*-TFA methyl esters. Histidine enantiomers were only partially separated and arginine did not elute from the column. However, proline, 3,4-dihydroxyproline and pipecolic acid enantiomers were resolved, strongly suggesting that hydrogen bonding is not involved in the separatory mechanism. Atypical amino acids such as *N*-methyl and β -amino acids were also resolved.

More recently (1994), Abe explored capillary columns coated with four types of cyclodextrin derivatives of 6-*O*-*tert*-butyldimethylsilyl-2,3-di-*O*-acetyl or *n*-butyl- β - and γ -cyclodextrin. Depending on the phase, all proteic amino acid enantiomers except for those of tryptophan were resolved as the *N*-TFA isopropyl esters. Variants such as 2,6-di-*O*-pentyl-3-*O*-propionyl- γ -cyclodextrin have also been used to

separate a number of amino acid enantiomers. Molecular modelling has positively correlated the GC elution order of proline derivatives on 2,6-di-*O*-methyl-3-*O*-trifluoroacetyl- β -cyclodextrin with the energies of the host-guest complexes.

Several satisfactory methods now exist for the resolution of amino acid enantiomers. Typically, 0.1% of a minor enantiomer can be precisely determined and, depending on the context and the specific method used, it is possible to assay as little as 0.01% or less.

Detectors

By far the majority of GC amino acid analyses have been conducted using flame ionization detectors (FID). These have the advantage of being sensitive and economical, but are nonspecific and provide no structural information.

Selective detectors confer distinct analytical advantages but are most often used to address special, nonroutine analytical problems. For example, the ability to detect a specific atom or molecular property can simplify sample preparation. Thus, by using a nitrogen/phosphorus-selective detector, contaminating compounds not containing nitrogen or phosphorus are simply not detected in most samples. Furthermore, it can reasonably be assumed that those peaks which have been detected contain nitrogen. In addition, problems caused by overlapping peaks are reduced. Selective detectors can also provide additional sensitivity. The ultimate detector is a mass spectrometer which can, depending on the context,

provide all of these advantages and also provide detailed structural information.

A number of selective detectors have been used to assay amino acids. Their use will be illustrated using some examples.

A nitrogen/phosphorus-specific detector, operated in the nitrogen mode, has been used to assay free amino acids in conifer tissues. All the proteic amino acids and several biologically important nonproteic amino acids were assayed at the low picomole level as the *N*-HFB isobutyl esters. Comparison of the FID chromatogram with the NPD chromatogram enabled identification of those compounds which did not contain nitrogen (Figure 6). Similarly, 1-aminocyclopropane-1-carboxylic acid, a precursor of the plant hormone ethylene, has been assayed as the *N*-benzoyl *n*-propyl derivative in the leaves and xylem sap of tomato plants. More recently (1997), 21 proteic and 33 nonproteic amino acids have been resolved in less than 30 min as the *N*-isobutoxycarbonyl methyl esters at a detection limit of 6–150 pg per injection. Small urine samples were analysed without prior clean-up and with no detectable influence from any non-nitrogen-containing compounds present.

Flame photometric detection (FPD) is useful for analysing sulphur-containing amino acids but has rarely been used in that context. Amino acid phosphorylation is an important biochemical regulatory mechanism and is also important for correlating protein structure and function. The *O*-phosphoamino acids, specifically *O*-phospho serine, threonine and tyrosine, have been assayed as the *N*-isobutoxycarbonyl methyl esters using FPD. The detection limits

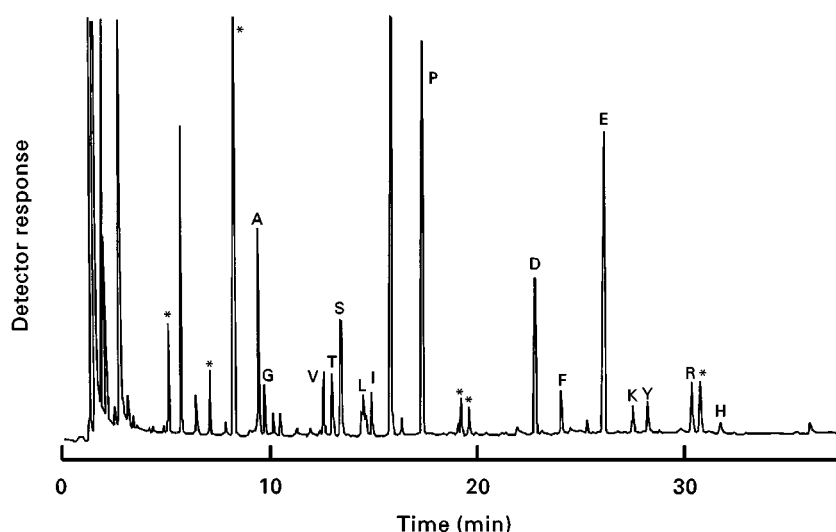


Figure 6 Resolution of White Spruce leaf-free amino acids as the *N*-(*O*, *S*)-heptafluorobutyl isobutyl esters using a flame ionization detector. Peaks marked by asterisks were shown not to contain nitrogen by comparison with an analysis of the same sample using a nitrogen-selective detector. (Reproduced with permission from MacKenzie SL (1986) Amino acid analysis by gas-liquid chromatography using a nitrogen-selective detector. *Journal of Chromatography* 358: 219–230.)

ranged from 0.18 to 0.3 pmol, reflecting a sensitivity about 200 times greater than FID detection. The method has been applied to the determination of O-phosphoamino acids phosphorylated by protein kinase both *in vitro* and *in vivo* without radiolabelling. Other amino acids did not interfere. The secondary amino acids, proline, pipercolic, thioproline, hydroxyproline and hydroxypipercolic acids, have also been assayed using FPD. Detection limits for the N-dimethylthiophosphoryl methyl esters were 0.1–0.7 pmol per injection.

Electron capture detectors are particularly useful for detection of the strongly electronegative perfluoroacyl derivatives of amino acids, but few studies have been conducted. Typically, as little as 1.4 pmol of tyrosine has been detected in a standard amino acid mixture. γ -Aminobutyric acid and five other aliphatic acids have been assayed in small volumes of supernatants from brain homogenates following sequential reaction with isobutyl chloroformate and pentafluorophenol.

Mass spectrometric detection provides structural as well as quantitative information. It is most frequently used either to confirm the structure of derivatives during the development of new protocols or to identify unknown compounds. Detection limits are frequently in the femtomole range. Electron impact (EI) ionization is most commonly used but both positive and negative ion chemical ionization have also been applied. Selected ion monitoring (SIM) of diagnostic ions is often used to increase sensitivity.

Typical examples of the structural information role of a mass spectrometric detector are the identification of O-phosphoamino acids in urine hydrolysates, the identification of amino acid ethyl esters in wines, the determination of amino acid composition in small peptides, and the assaying of γ -aminobutyric acid in mouse brain synaptosomes following therapy with the antiepileptic drug valproic acid. The versatility of GC-mass spectrometry (GC-MS) is further illustrated by the identification of 3-OH-4-methyldecanoic acid, a fungal cyclodepsipeptide, and by the simultaneous analysis of branched-chain carboxylic, α -oxo, α -hydroxy and α -amino acids in the urine of patients suffering from maple syrup urine disease. GC-MS has also been used to characterize binding media from medieval polychrome sculptures. Animal glues, casein, egg and drying oils were identified as components of the binders of paint and ground layers.

The expense of mass spectrometers mitigates against their use as routine analytical detectors and many real sample analyses by GC-MS (as distinct from the analysis of standard mixtures) have been directed to addressing analytical problems which cannot be resolved using other types of detectors.

The ratios of the stable isotopes of C and N are used in the assessment of *in vivo* protein turnover studies, and in identifying the sources and history of organic matter. Both natural abundances and the ratios obtained after enrichment with singly or multiply labelled amino acids or other compounds such as ^{13}C -glucose, pyruvate or acetate have been determined. The ratios may be determined after online combustion following GC and introduction of the resultant gases into a conventional isotope ratio mass spectrometer. This approach has been used to study ^{15}N : ^{14}N isotopic ratios in plasma-free amino acids and, by eliminating many preparative steps, requires only about 500 μL -of plasma, whereas preparatory methods may require as much as 60 mL.

Alternatively, the intact labelled compounds can be introduced directly into the mass spectrometer. For example, by combining stable isotope dilution with the use of EI and SIM to monitor the $[\text{M}-57]^+$ peak, homocysteine sulfinic acid, homocysteic acid, cystine sulfinic acid and cysteic acid have been shown to be agonistic to N-methyl-D-aspartate receptors in brain tissue. This approach also enabled the identification and quantitation of these compounds in normal human serum. Similarly, endogenous and newly synthesized concentrations of the neurotransmitter amino acids γ -aminobutyric acid, glutamate and aspartate have been assayed in brain slices following incubation with ^{13}C -labelled precursors.

Future Developments

The techniques for derivatizing and separating the standard amino acids in protein hydrolysates are mature and there is no significant room for improvement. Given the existence of quantitative derivatization protocols which proceed very rapidly, it is doubtful whether the development of on-column derivatization would constitute a significant advantage. Similarly, proteic amino acids can now be assayed in less than 10 min, so, given the availability of reliable automatic injectors, a reduction in analysis time is not of significant value.

Physiological samples may contain several hundred amino acids and these cannot, at present, all be resolved on any one single column. Frequently, however, only a subset is of interest. Thus, although the simultaneous derivatization and separation of all the proteic amino acids and as many as 50 of the more common nonproteic amino acids are now possible, it is likely that procedures targeted at specific subsets will remain important in specific contexts. The sensitivity of the FID detector is adequate for most analytical purposes but mass spectrometric detectors

will remain important for specialized applications requiring femtomole sensitivity.

See also: III/Amino Acids: Liquid Chromatography; Thin-Layer (Planar) Chromatography. **Amino Acids and Derivatives: Chiral Separations. Amino Acids and Peptides: Capillary Electrophoresis.**

Further Reading

Gehrke CW, Roach D, Zumwalt RW *et al.* (eds) (1968) *Quantitative Gas-liquid Chromatography of Amino Acids in Proteins and Biological Substances: Macro, Semimicro and Micro Methods*. Columbia, MO: Analytical Biochemical Laboratories.

Hušek P and Macek K (1975) Gas chromatography of amino acids. *Journal of Chromatography* 113: 139.

König WA (1987) *The Practice of Enantiomer Separation by Capillary Gas Chromatography*. Heidelberg: Hüthig.

MacKenzie SL (1981) Recent developments in amino acid analysis by gas-liquid chromatography. In: Glick D (ed.) *Methods of Biochemical Analysis*, vol. 27, p. 1. New York: Interscience.

Weinstein B (1966) Separation and determination of amino acids and peptides by gas liquid chromatography. In: Glick D (ed.) *Methods of Biochemical Analysis*, vol. 14, p. 203. New York: Interscience.

Zumwalt RW, Kuo KCT and Gehrke CW (eds) (1987) *Amino Acid Analysis by Gas Chromatography*. Boca Raton, FL: CRC Press.

Liquid Chromatography

I. Molnár-Perl, L. Eötvös University,
Budapest, Hungary

Copyright © 2000 Academic Press

The first approach to the automatic liquid chromatography (LC) of amino acids (AAs) – known today as ion exchange chromatography (IEC) – was published by Spackman *et al.* in 1958. In over 40 years later, it now takes less than 5 min (**Figure 1**) to separate and quantitate the essential protein AAs instead of 2 days. Early separations were carried out by post-column derivatization.

Over the last 20 years LC has offered unlimited possibilities in both the preparative and analytical scale. The wide choice and sophisticated columns, detectors, derivatization procedures, development of modern instrumentation and data-handling systems reduce time and costs, and give versatility and automation in Good Laboratory Practice (GLP)- controlled conditions for selectivity, sensitivity and reproducibility. It is the responsibility of the researcher to choose the most appropriate method for the given task. The most popular LC method for analysis of both free AAs (present in many natural matrices, biological fluids and tissues, feed and foodstuffs) and of those constituents of protein hydrolysates is now reversed-phase (RP) chromatography after pre-column derivatization of the AAs.

Numerous methods for derivatization are available in the literature. This article will discuss the advantages and drawbacks of the commonly used derivatives.

Current trends in AA analysis identify the best conditions for enantiomer separation and the development of LC-mass spectrometry (LC-MS).

LC of Underivatized AAs

To attain one of the main advantages of LC – separating the ‘classical 20’ as underivatized AAs – has appealed to chromatographers. In spite of a number of efforts, the simultaneous LC of underivatized AAs has remained of secondary importance. Determination of a few selected AAs, such as tryptophan or sulfur-containing AAs, has proved to be fruitful for special tasks.

The aim of various investigations was to render unnecessary the time-consuming derivatization techniques. However, the characteristics of the free AAs are considerably different from each other and their various structural properties did not permit their easy resolution. Thus, in attempting to achieve better separation of free AAs, further means of discrimination were needed. For this purpose special techniques have been introduced, such as the use of various phase systems, ion pair and ligand exchange chromatography, column-switching techniques or anion exchange chromatography with electrochemical detection.

The solvent-generated ion exchange phase system ensured the gradient elution of 19 AAs (**Figure 2A**): some, but not all, are baseline-separated. A simple isocratic method using aqueous, copper acetate/alkyl-sulfonate additives containing acetate buffer (pH 5.6) as mobile phase, a conventional RP column and UV detection (230–240 nm) at different temperatures and varying the concentrations of additives was unable to separate the classical 20 protein amino acids. Significant improvement in the separation can be obtained by column switching (**Figure 2B**), as well as by using an anion exchange column, a quaternary

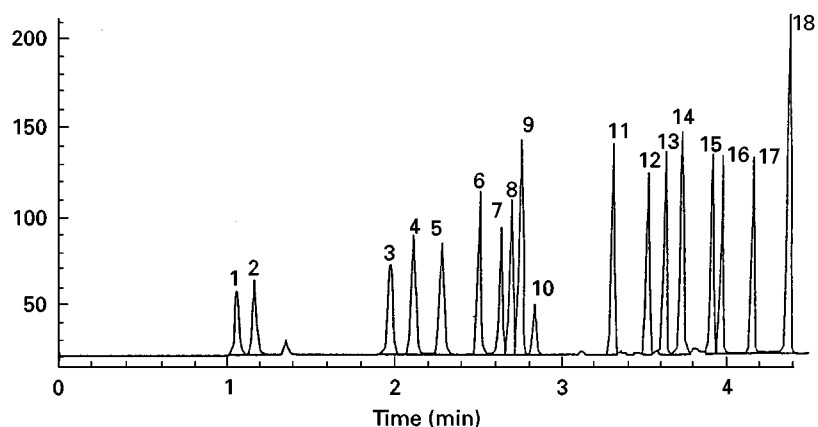


Figure 1 Separation of the phenylthiocarbamyl AAs separated on TSKgel Super-ODS (for details see Table 3). Peaks: 1, ASP; 2, Glu; 3, Ser; 4, Gly; 5, His; 6, Arg; 7, Thr; 8, Ala; 9, Pro; 10, NH_4^+ ; 11, Tyr; 12, Val; 13, Met; 14, Cys; 15, Ile; 16, Leu; 17, Phe; 18, Lys. (Reproduced with permission from Tosohaas, *The Bioseparation Specialist*, (1995) Catalogue p. 157, Figure 9/2.)

gradient mobile phase and pulsed amperometric detection (Figure 2C). For tryptophan and the sulfur-containing AAs (cysteine/cystine, methionine, glutathione, etc.), the fast isocratic elution of the underivatized samples has gained wide acceptance and is a powerful tool in their quantitation.

Tryptophan can be measured directly, within 8 min, in neutralized alkaline hydrolysates of feed and foodstuffs, using an RP column, 5% methanol containing acetate buffer (pH \sim 4.0) and UV detection at 280 nm. The pulsed amperometric detection of sulfur-containing AAs, at the low pmol level, was carried out with an Au working- and an Ag/AgCl reference electrode, subsequent to their separation on both cation exchange and on RP columns, applying as mobile phase $0.1 \text{ mol L}^{-1} \text{ HClO}_4/0.15 \text{ mol L}^{-1} \text{ NaClO}_4/5\% \text{ ACN}$.

LC of Derivatized AAs

Derivatization studies have concerned the optimization of parameters, such as the yield and stability of derivatives, to separate and quantitate all AAs with a simple and fast elution procedure.

Post-column Derivatization (Table 1, Figure 3)

Post-column derivatization was the first development of IEC in the area of RP/high performance liquid chromatography (HPLC), in its pioneer period. It took time to develop pre-column derivatization concepts which resulted in considerable advantages.

Drawbacks of the post-column techniques (Table 1) are long elution times and the need for costly devices, such as a delivery system for the derivatizing reagent (one or more extra pumps); (a) mixing chamber for the column effluent and the re-

agent(s); special thermostable reactors (packed bed, air-segmented and/or coil reactors) ensuring the necessary delay for quantitative reactions accompanied with as small band broadening as possible. Last but not least, the mobile phase was probably incompatible with the derivatizing reagent. The preferred mobile phase might be inappropriate for the optimum conditions of derivatization reaction. The early and current stages of post-column methods can be illustrated by elution followed by post-column reaction with ninhydrin (NH₂YD; Figure 3A), with *o*-phthaldialdehyde/ β -mercaptoethanol (OPA/MCE; Figure 3B), or with 1,2-naphthoquinone-4-sulfonyl chloride (NQS; Figure 3C). All three types of derivatives have been separated in most cases on ion exchange resin columns from the early 1970s. Recent post-column methods are without exception, slow separations (Table 1). However, the efficiency of the recently published methods of NH₂YD derivatives using short columns is superior, determining 59 compounds in 150 min and 40 compounds in 120 min respectively.

Pre-column Derivatization (Tables 2 and 3; Figures 4–6)

Pre-column derivatization offers numerous advantages. It requires less equipment and allows the evaluation of the derivatives in an easier way from the point of view of their selectivity, sensitivity, various means of detection, derivatization yield, stability and storability. All of these phenomena can be controlled and improved by use of modern instrumental techniques and computerization, both individually and simultaneously. Potential disadvantages in pre-column derivatization as procedures can be completely avoided: contamination from the reagents (due to their insufficient purity) and loss of analyte

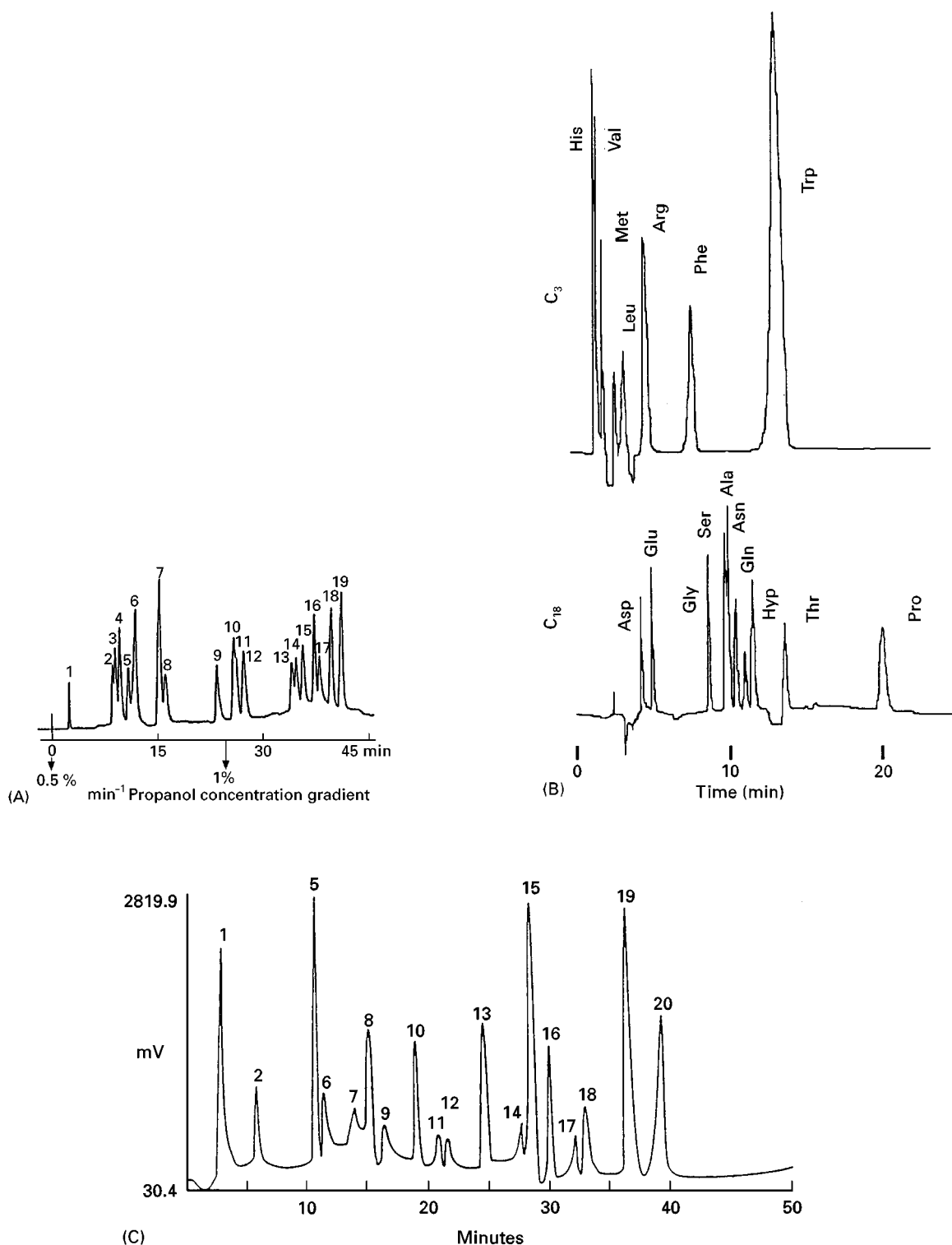


Figure 2 LC of underivatized AAs. (A) Separation of a test mixture using *n*-propanol gradient. Column: 250 × 3 mm, RP-8; temperature = 25°C. Peaks: 1, CySO₃H; 2, Asp; 3, Ser; 4, Glu; 5, Thr; 6, Gly + Pro; 7, Ala; 8, Cys; 9, NH₄⁺; 10, Tyr; 11, Val; 12, Met; 13, Ile; 14, Phe; 15, Leu; 16, His; 17, Lys; 18, Trp; 19, Arg. (Reproduced with permission from Kraak JC *et al.* (1977) *Journal of Chromatography* 142: 671.) (B) Chromatogram of standard AAs using a column-switching technique. First column, Inertsil C₃; second column, Inertsil ODS-2. (Reproduced with permission from Hanai T and Hirukawa M (1988) *Journal of Liquid Chromatography* 11: 1741.) (C) Chromatogram of AAs obtained by pulsed amperometric detection. Peaks: 1, Arg; 2, Lys; 3, Gln; 4, Asn; 5, Thr; 6, Ala; 7, Gly; 8, Ser; 9, Val; 10, Pro; 11, Ile; 12, Leu; 13, Met; 14, system peak; 15, His; 16, Phe; 17, Glu; 18, Asp; 19, Cys; 20, Tyr. (Reproduced with permission from Frankenberger WT Jr and Martens DA (1992) *Journal of Liquid Chromatography* 15: 423.)

Table 1 Advances in the LC of post-column derivatized AAs, obtained with α -phthalaldehyde/ β -mercaptoethanol (OPA/MCE), with ninhydrin (NHYP) or with 1,2-naphthoquinone-4-sulfonate (NQS)

Author and date	Column size cm × mm, μ m			Type	Eluents (elution temperature °C)	Detector UV (nm) FEx/Em	Reagent (°C)	Analyte (nmol L ⁻¹)	RSD %	Matrix	No. of AAs/ elution time (min)
Moore, 1958	150	0.9	40	Amberlite IR-120, IE	Citrate buffers, 0.2 mol L ⁻¹ : pH 3.25 for first day (30°C), and pH 4.25 for the second day (55°C)	UV 440, 570	NHYD (-)	100–3000	—	AAs in hydrolysates	20/ 24–48 h
Grunau, 1992	15	3	5	Pickering 'fast run'	Pickering Eluents A (Li280), B (Li750), C (RG003) (42°C)	UV 570	NHYD (130°C)	20	—	Plasma AAs	59/ ~150
Iwase, 1995	6	4.6	3	2622, Hitachi, IE	Five eluents: PF-1–PF-4, PF-RG, cont. Li salts, ethanol, benzyl alcohol, thiodiglycol, Brij-35 buffer with pH 2.8, 3.7, 3.6, 4.1, -; (gradient programme: 28–40°C)	UV 440,570	NHYD (130°C)	50	< 3	Plasma AAs	40/120
Roth, 1973	25	6		Aminex 6, IE	Citrate buffers: pH 3.20, 4.25 and 6.40 for 40, 60 and 70 min (34°C for 100 min, then raised to 55°C)	F —	OPA/MCE (55°C)	10	—	Model study	14/170
Elrifi, 1986	60	9	—	IE	Pierce Pico-Buffer system, Li citrate buffers; pH of A,B,C,D and E = 2.9, 3.1, 3.5, 3.4 and 2.3; temperature gradient: 0–44 min (34°C), 44–128 min (63°C)	F* No data	OPA/MCE (40°C)	0.63–45.0	—	AAs in foods	23/128
Haginaka, 1988	30 +guard 3	4.6 4.6	5 5	ODS-5	A: 15 mmol L ⁻¹ Na octane sulfonate/ 21 mmol L ⁻¹ H ₃ PO ₄ /9 mmol L ⁻¹ NaH ₂ PO ₄ /CH ₃ OH (20/20/20/1, v/v), pH 2.8; B: as A, except (1/1/1/6, v/v), pH 4.2 (60°C)	F 340/450	OPA/MCE (60°C)	0.25–2.5	< 4.5	AAs in hydrolysates	18/ ~120
Møller, 1993	15 +guard 2	3 3	5 5	Pickering, IE	A: 0.24 mol L ⁻¹ Li citrate, pH 2.27, B: 0.64 mol L ⁻¹ Li citrate pH = 7.50 (50°C)	F 340/448	OPA/MCE (4°C)	0.6	< 11	Physio-logical AAs	39/180
Saurina, 1994	15	4.6	5	Spherisorb ODS 2	A: 20 mmol L ⁻¹ H ₃ PO ₄ + 20 mmol L ⁻¹ NaH ₂ PO ₄ + 15 mmol L ⁻¹ SDS; B: 25 mmol L ⁻¹ H ₃ PO ₄ + 25 mmol L ⁻¹ NaH ₂ PO ₄ + 18.5 mmol L ⁻¹ SDS/ProH (4:1, v/v); (50°C)	UV 305	NQS (65°C)	32	< 5	AAs in food + feed ^a	18/105

No data available; IE, ion exchange resin; ^ahydrolysates.

from incomplete interaction, undesirable side reactions and sample handling losses.

Although numerous pre-column derivatization techniques have been introduced in the last 30 years, none complies with the criteria of an ideal procedure: providing rapid and quantitative interaction in aqueous media, permitting mild conditions, ensuring interaction with both primary and secondary AAs and resulting in single and stable derivatives in the case of all AAs.

OPA Derivatives (Table 2 and Figure 4)

The pioneering work of Roth (1971) on the very fast reaction of AAs in aqueous solutions with ophthalaldehyde mercaptoethanol (OPA/MCE), detectable by

both UV and fluorescence, without the need to remove excess reagent, represented a great advance. Because of the different stability of the isoindoles obtained from the reaction of AAs with OPA/MCE, pre-column derivatization with 3-mercaptopropionic acid (MPA) and several *N*-alkyl-L/D-cysteines was proposed. The OPA/MPA and OPA/*N*-acetyl-L-cysteine (NAC) reagents provide more stable isoindoles compared to those formed with OPA/MCE, and the optical resolution of enantiomeric amino acids with OPA/NAC, as well as with other *N*-alkyl-L/D-cysteine reagents, has opened a new area in enantiomer separation of AAs. Due to robotic autosamplers which provide excellent reproducibility for even moderately quantitative interactions, most AA analyses are

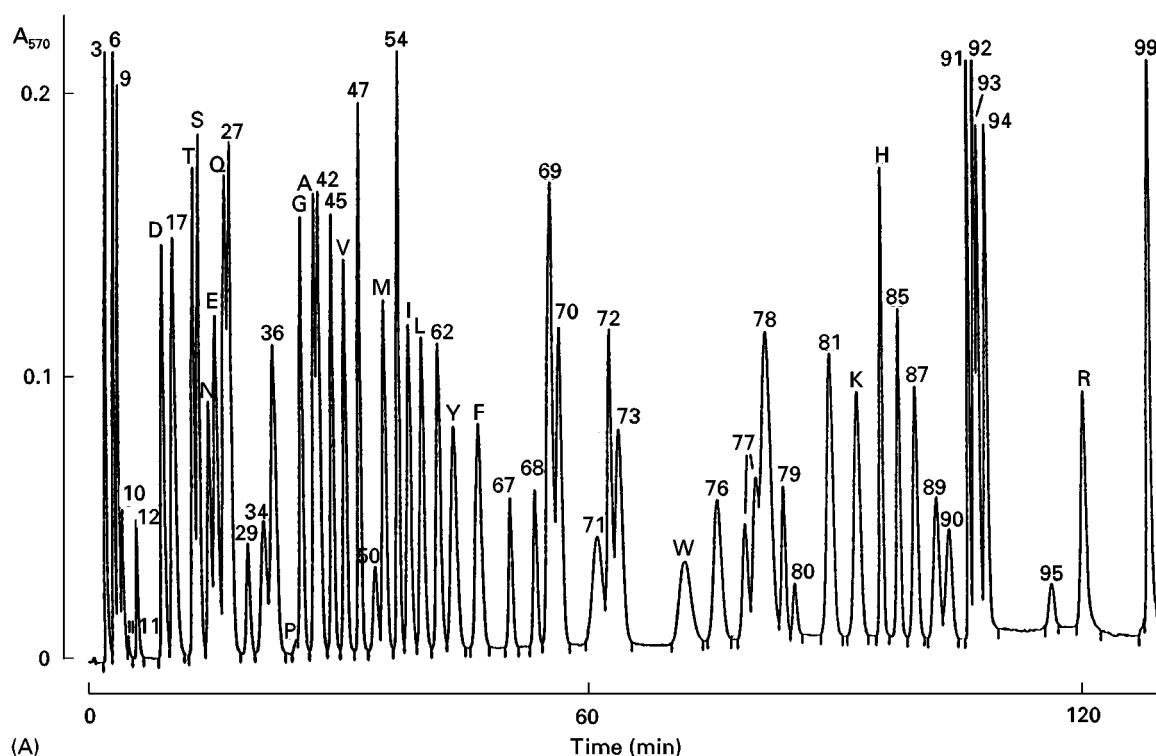


Figure 3 LC of post-column derivatized AAs (for details see Table 2). (A) Chromatographic profile of 59 AAs and related compounds. Peaks: 3, *o*-phospho-DL-serine; 6, taurine; 9, *o*-phosphoethanolamine; 10, *N*^z-(1-D-mannityl)-L-glutamine (mannopine); 11, urea; 12, β -ciano-L-alanine; D, L-aspartic acid; 17, *o*-acetyl-L-serine; T, L-threonine; S, L-serine; N, L-asparagine; E, L-glutamic acid; Q, L-glutamine; 27, L-homoserine; 29, sarcosine; 34, DL- α -amino adipic acid; 36, *S*-methyl-L-cysteine; P, L-proline; G, glycine; A, L-alanine; 42, L-citrulline; 45, L- α -aminobutyric acid; V, L-valine; 47, L-cystine; 50, α -methyl-DL-methionine; M, L-methionine; 54, L-cystathionine; I, L-isoleucine; L, L-leucine; 62, L-norleucine; Y, L-tyrosine; F, L = phenylalanine; 67, β -alanine; 68, DL-aminoisobutyric acid; 69, DL-homocystine; 70, δ -aminolevulinic acid; 71, 5-hydroxy-L-tryptophan; 72, γ -aminobutyric acid; 73, DL-kynurenine; W, L-tryptophan; 76, ethanolamine; 77, δ -hydroxylysines (DL- and DL-allo); 78, ammonia; 79, *e*-amino-*n*-caproic acid; 80, creatinine; 81, L-ornithine; K, L-lysine; H, L-histidine; 85, 3-methyl-L-histidine; 87, 1-methyl-L-histidine; 89, L-carnosine; 90, L-anserine; 91, L-canavanine; 92, *S*-methyl-DL-methionine; 93, L- α -amino- β -guanidinopropionic acid; 94, L-leucinamide; 95, *N*^{G1}-dimethyl-L-arginine; R, L-arginine; 99, L-homoarginine. (Reproduced with permission from Grunau JA and Swiader JM (1992) *Journal of Chromatography* 594: 165.) (B) Separation of OPA/MCE derivatives by gradient IEC chromatography. (Reproduced with permission from Møller SE (1993) *Journal of Chromatography* 613: 223.) (C) Determination of AAs by ion pair liquid chromatography with post-column derivatization using 1,2-napthoquinone-4-sulfonate (NQS). Peaks: 1, Asp; 2, Ser; 3, Glu; 4, Gly; 5, Thr; 6, Ala; 7, Pro; 8, Tyr; 9, Met; 10, Ile; 11, Phe; 12, Leu; 13, Nle; 14, Trp; 15, His; 16, Orn; 17, Lys; 18, Arg. Line = elution gradient profile. (Reproduced with permission from Saurina J and Hernández-Cassou (1994) *Journal of Chromatography* 676: 311.)

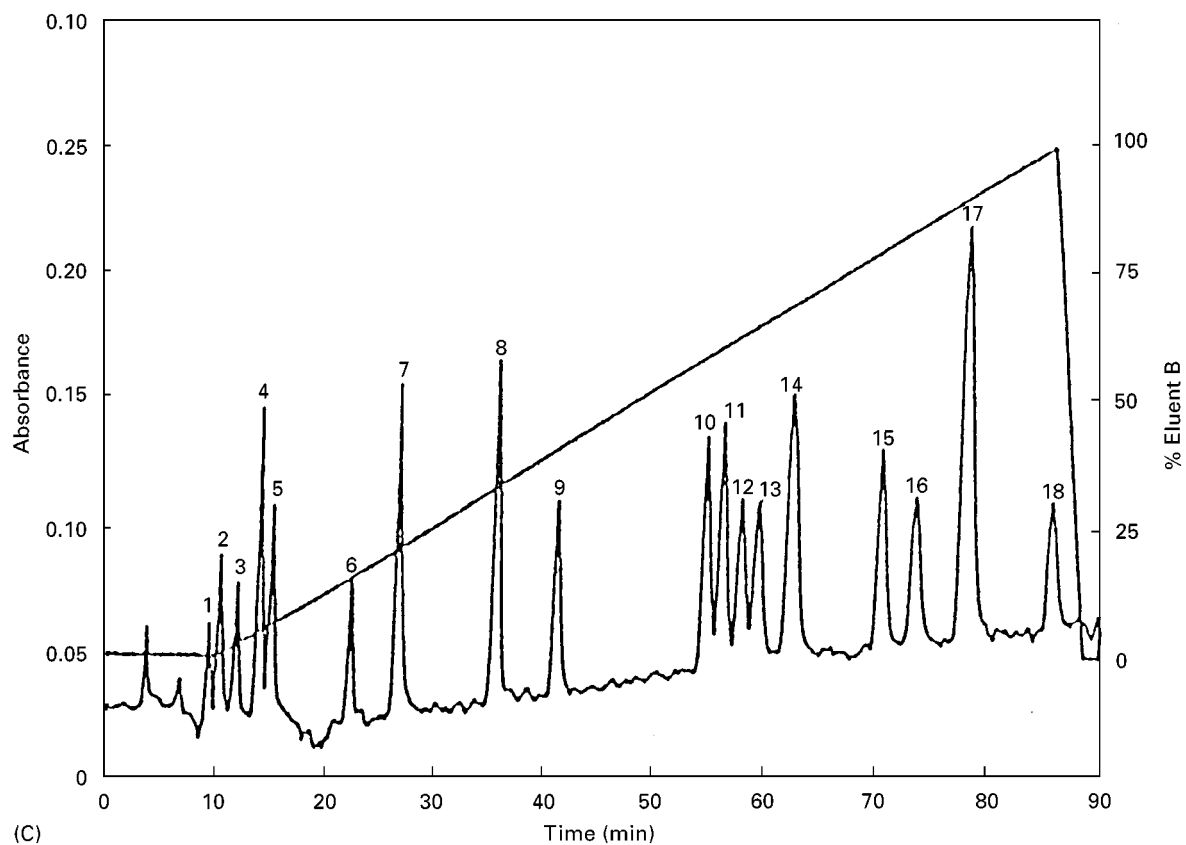
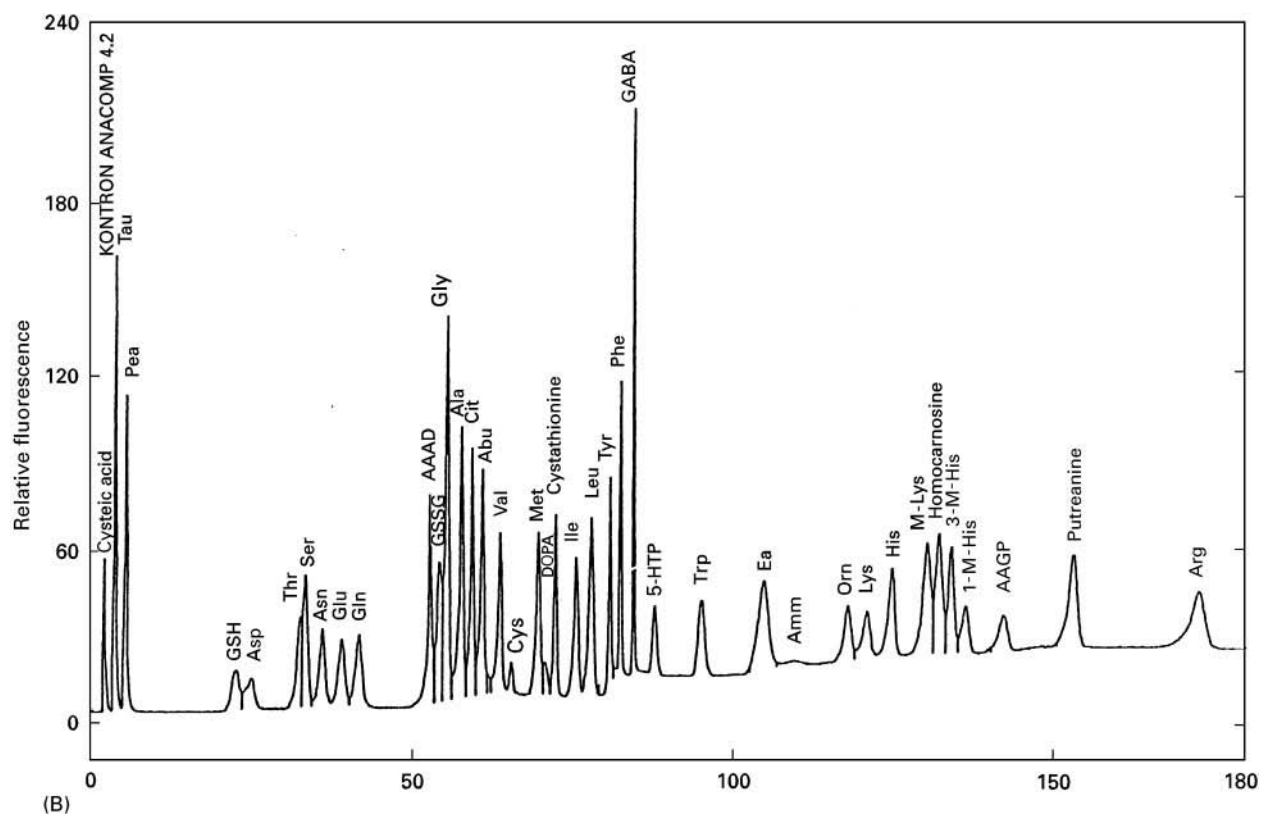


Figure 3 Continued

Table 2 Advances in the LC of pre-column derivatized AAs, obtained with OPA/MCE, OPA/3-ethanethiol (OPA/ET), OPA/mercapropionic acid (OPA/MPA), OPA/*N*-acetyl-L-cysteine (OPA/NAC), with OPA/isobutyryl-L/D-cysteine (OPA/NIBC) or with OPA/MPA/fluorenylmethylchloroformate (OPA/MPA/FMOC)

Author and date	Column size			Type	Eluents (elution temperature °C)	Detector UV (nm) FEx/Em	Reagent (°C)	Analyte (pmol L ⁻¹)	RSD %	Matrix	No. of AAs/elution time (min)
	cm	×	mm, μm								
Jones, 1983	75 +guard 45	4.6 2.1	3 40	Ultrasphere ODS	A: THF/CH ₃ OH/NaAc (pH 7.2) = (5:95:900, v/v) B: CH ₃ OH; (—)	F 305–395 420–650	OPA/ MCE (—)	0.1–80	<1.5	AAs in hydrolysates	48/50
Fekkes, 1995	12.5	4.6	5	Spherisorb ODS-2	A: (pH 6.72–6.77 and B: (pH 5.95–6.00): 250 mmol L ⁻¹ Na ₂ HPO ₄ / 250 mmol L ⁻¹ propionic acid/ACN/THF/H ₂ O = (20:20:7:2:51, v/v) C: ACN/CH ₃ OH/DMSO/H ₂ O = (28:24:5:43, v/v); (25–35°C)	F 337/452	OPA/ MCE (3°C)	50	<2	Plasma AAs	40/49
Hill, 1979	30	3.9	—	μ-Bondapak C-18	A: 12.5 mmol L ⁻¹ Na ₂ HPO ₄ (pH 7.2) B: A eluent/ACN in gradient; (—)	F 229/470	OPA/ ET (—)	5	—	AAs in human serum	20/40
Eslami, 1987	50	4.5	3	ODS IBM	Buffer: ~2 mol L ⁻¹ Na ₂ HPO ₄ (pH 7) A: ACN/H ₂ O/buffer = (50:425:25, v/v) B: ACN/H ₂ O/buffer = (275:200:25, v/v); (22°C)	F 330/480	OPA/ ET (—)	40–100	—	Model study	22/14
Godel, 1984	25	4	4	Supersphere CH-8	A: 12.5 mmol L ⁻¹ Na ₂ HPO ₄ (pH 7.2) B: 12.5 mmol L ⁻¹ Na ₂ HPO ₄ (pH 7.2)/ ACN-(1:1, v/v); (—)	F 330/445	OPA/ MPA (—)	1–10	<4.2	AAs in biological fluids	28/40
van Eijk, 1993	15 +guard 1	4.6 4	2–3	Spherisorb ODS-2	A: 12.5 mmol L ⁻¹ Na ₂ HPO ₄ (pH 7.0) + 7 mL THF/1 l eluent B: 12.5 mmol L ⁻¹ Na ₂ HPO ₄ (pH 7.0)/ ACN/THF = (57:43:7, v/v); (35°C)	F 335/440	OPA/ MPA (—)	35	<3	Plasma AAs	30/28
Teerlink, 1994	10 + guard 1	4.6 2	3	Microsphere ODS	A: 4.5 mmol L ⁻¹ K ₂ HPO ₄ (pH 6.9) + 2 mL THF/1L B: 4.5 mmol L ⁻¹ K ₂ HPO ₄ (pH 6.9)/CH ₃ OH/ACN = (50:35:15, v/v); (—)	F 230/389	OPA/ MPA (—)	100	<3.2	Plasma AAs	25/17
Schuster, 1989	20 20	2.1 4.6	5 5	Hypersil ODS	Protein hydrolysates, A: 30 mmol L ⁻¹ NaAc cont. 0.5% THF (pH 7.2); ACN/0.1 mol L ⁻¹ NaAc = (4:1, v/v); (42°C) Plasma AAs, A: 60 mmol L ⁻¹ NaAc cont. 0.6% THF (pH 8.0); B: ACN/0.1 mol L ⁻¹ NaAc/ CH ₃ OH = (14:4:1, v/v); (43°C)	UV 338/266 F 230/455 266/310	OPA/ MPA/ FMOC (4°C)	UV: 2–5 F: 0.02–0.05	<2.5	AAs in protein hydrolysates Plasma AAs	19/20 38/60

Table 2 Continued

Author and date	Column size			Type	Eluents (elution temperature °C)	Detector UV (nm) FEx/Em	Reagent (°C)	Analyte (pmol L ⁻¹)	RSD %	Matrix	No. of AAs/elution time (min)
	cm	×	mm, μm								
Bartók, 1994	10	4	3	Hypersil ODS	A: 18 mmol L ⁻¹ NaAc (pH 7.2) + 0.02% (v/v) TEA + 0.3% THF (v/v) B: ACN/CH ₃ OH/NaAc 0.1 mol L ⁻¹ (pH 7.2) = (2:2:1, v/v); (40°C)	F 340/450 264/313	OPA/MPA/FMOC (4°C)	50	<1.1	Plant AAs	21/8

Indications as in Table 1.

performed with OPA derivatives. The essential shortage of an OPA/S_H-group reagent (reactive toward the primary AAs only) was eliminated by Shuster's principle – the automatic two-step pre-column derivatization method applying the OPA/MPA/fluorenylmethyl chloroformate (FMOC) reagent, which also ensures derivatization of the secondary AAs. A high speed elution of OPA/MPA/FMOC derivatives was shown recently (Table 2, Figure 4: 19 compounds/8 min). Evaluating the improvements between the corresponding early and recent procedures, in the newer methods shorter, thermostated columns of smaller particle size with autosamplers are now used, giving greater sensitivity and reproducibility.

Phenylthiocarbamyl (PTC), FMOC, 1-*N,N'*-Dimethylaminonaphthalene-5-sulfonyl (DANS) and Dimethylaminoazobenzenesulfonyl (DABS) Derivatives (Table 3, Figures 1, 5 and 6)

Judging by the number of publications in the last decade, the interest in the PTC and FMOC deriva-

tives has proved to be lasting, while the application of DANS and DABS derivatives is decreasing. However, in the direct enantiomer separation of AAs, the use of DANS derivatives is preferred.

The reaction of AAs with *phenylisothiocyanate* (Table 3, Figures 1 and 5), in water-free media at ambient temperature is quantitative and fast (10 min), resulting in the highly stable single PTC derivatives (except for cyst(e)ines in hydrolysates which elute in one to four peaks). The excess reagent is removed by vacuum, and the PTC derivatives can be stored in the freezer for an unlimited time, and for a day after dissolution in buffer at 4°C. UV detection at 254 nm allows their quantitation in the low pmol range. The short PicoTag and the short TSK gel columns can separate 17 AAs within 12 min and 4.5 min, respectively.

The first LC separation of the strongly fluorescent DANS AAs has been used earlier in protein chemistry and in thin-layer chromatography. The decreased popularity of this technique in LC can be

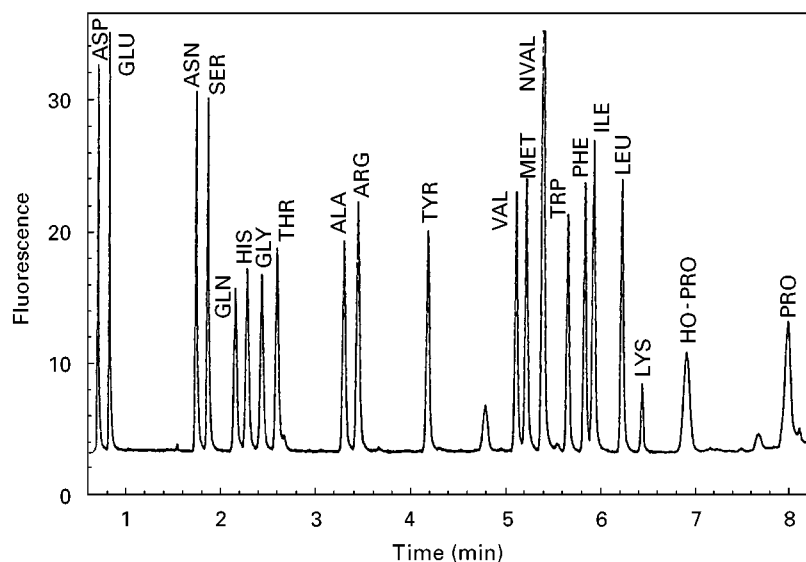


Figure 4 High speed RP-HPLC analysis of the OPA/MPA/9-fluorenylmethyl chloroformate derivatives. (Reproduced with permission from Bartók T *et al.* (1994) *Journal of Liquid Chromatography* 17: 4391.)

Table 3 Advances in the LC of pre-column derivatized AAs, obtained with phenylisothiocyanate (PITC), 5-dimethylaminonaphthalene-1-sulfonyl-Cl (DANS), 4-dimethylaminoazobenzene-4-sulfonyl-Cl (DABS) or with 9-fluorenylmethyl chloroformate (FMOC)

Author and date	Column size <i>cm × mm, μm</i>		Type	Eluents (elution temperature °C)	Detector UV (nm), (°C) FEx/Em	Reagent	Analyte (pmol L ⁻¹)	RSD %	Matrix	No. of AAs/elution time (min)
Koop, 1982	25	4.6	5	Ultrasphere ODS	A: 70 mmol L ⁻¹ NaH ₂ PO ₄ (adjusted to pH 6.45 with TEA) B: ACN; (27°C)	UV 254 PITC (—)	6000	—	AAs in protein hydrolysates	18/130
Tosohaas, 1995	10	4.6	2	TSKgel Super-ODs	A: 50 mmol L ⁻¹ NaAc (pH 6.0)/ACN = (97:3, v/v) B: 50 mmol L ⁻¹ NaAc (pH 6.0)/ACN = (40:60, v/v); (40°C)	UV 254 PITC (—)	250	—	Model study	17/4.5
Shang, 1996	15	3.9	5	PicoTag ODS	A: NaAc (pH 6.4) B: ACN; A and B performed in gradient (38°C)	UV 254 PITC (—)	5	< 1.9	AAs in kelp	17/12
Bayer, 1976	50	3	10	LiChrosorb, RP 8	Eluent 10 mmol L ⁻¹ Na ₂ HPO ₄ /CH ₃ OH = (50:20, v/v) to which 1.5 mL CH ₃ OH/min is added (45°C)	F 340/510 DANS (amb)	0.1	—	Model study	17/40
Martins, 1996	15	3.9	4	Nova Pak C 18	A: 30 mmol L ⁻¹ phosphate buffer (pH 7.4) + 5 mL CH ₃ OH + 6.5 mL THF adjusted to 100 mL with distilled water B: CH ₃ OH/H ₂ O = (70/30, v/v); (25°C)	F 338/445 DANS (40°C)	60	—	AAs in polypeptides	17/35
Chang, 1983	—	—	5	—	A: 25 mmol L ⁻¹ NaAc (pH 6.5) containing 4% dimethylformamide B: ACN (40°C)	UV 436 DABS (70°C)	5	—	AAs in protein hydrolysates	17/40
Yang, 1993	15	4.6	5	Hypersil ODS	A: 25 mmol L ⁻¹ NaAc (pH 6.35) containing 4% dimethylformamide B: ACN (40°C)	UV 436, 580 DABS (70°C)	50	—	AAs in polypeptides	17/40
Einarsson, 1983	50 500	4.6 2.26	3 5	Spherisorb ODS-2	Eluent: 20 mmol L ⁻¹ NaAc buffer (pH 4.08–4.31)/ACN gradient; (—)	F 265/315 FMOC (—)	(—)	< 6.6	AAs in protein hydrolysates, in urine	17/10 and 33/100
Qu, 1996	15	4.6	5	Hypersil ODS	A: 30 mmol L ⁻¹ phosphate buffer (pH 6.5) in 15% CH ₃ OH (v/v) B: 15% CH ₃ OH (v/v) C: 90% ACN (v/v); (38°C)	F 270/316 FMOC (—)	125	< 1.0	AAs in protein hydrolysates, biological samples	15/35
Bank, 1996	15	4.6	5	Micropak ODS-80TM	A: 20 mmol L ⁻¹ citric acid/NaAc buffer (pH 2.85); B: 20 mmol L ⁻¹ NaAc (pH 4.5)/CH ₃ OH = (80:20, v/v); A, and B both, cont. 0.01% (w/v) NaN ₃ + 5 mmol L ⁻¹ (CH ₃) ₄ NCl; C: ACN; (40°C)	F 254/630 FMOC (—)	50	< 3.6	AAs in protein hydrolysates	21/35

Indications as in Table 1.

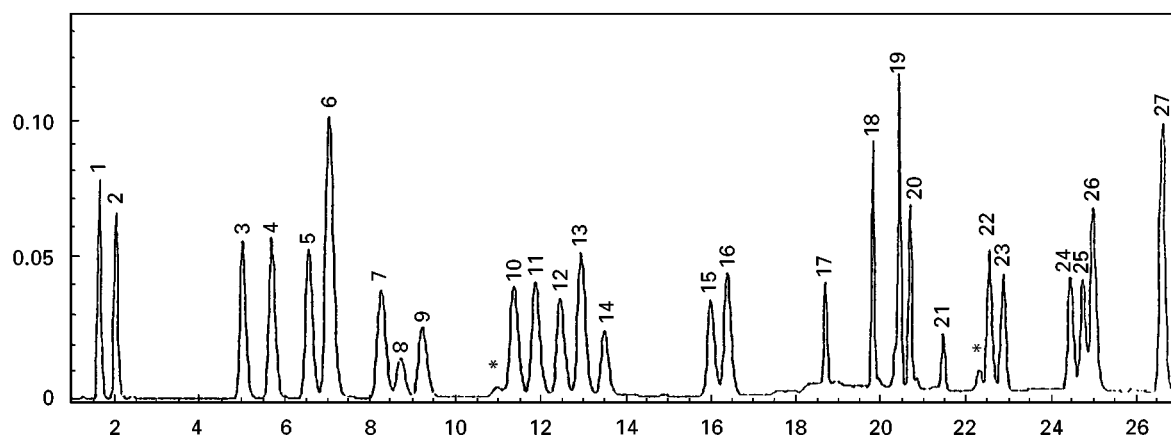


Figure 5 Separation of 27 phenylthiocarbamyl AAs. Column 150 + (20 guard) \times 4 mm, C_{18} Hypersil 5 μ m, temperature, 50°C, eluent A: 0.05 mol L⁻¹. NaAc pH 7.2; B: A eluent/acetonitrile/methanol = 46/44/10 (pH = 7.2), flow rate: 2.1 mL min⁻¹. Peaks: 1, aspartic; 2, glutamic acids; 3, hydroxyproline; 4, serine; 5, glycine; 6, asparagine; 7, β -alanine; 8, glutamine; 9, homoserine; 10, γ -aminobutyric acid (GABA); 11, histidine; 12, threonine; 13, alanine; 14, 1-amino-1-cyclopropane carboxylic acid (ACPCA); 15, arginine; 16, proline; 17, homoarginine; 18, tyrosine; 19, valine; 20, methionine; 21, cyst(e)ine; 22, isoleucine; 23, *n*-leucine; 24, phenylalanine; 25, tryptophan; 26, ornithine; 27, lysine. *system peaks. (Reproduced with permission from Vasanits A and Molnár-Perl (1998) *Journal of Chromatography* 832:109.)

explained by its two main disadvantages: long reaction times, or elevated temperatures for derivatization, and generation of fluorescent side products (DANS hydroxide, DANS amide) and interference from excess reagent. The disturbing effect of these compounds cannot be completely eliminated and they elute between the AA derivatives. No significant improvement has been obtained and cannot be expected.

DABS AAs were first separated applying pre-column labelling. Derivatization was performed in $\text{Na}_2\text{CO}_3/\text{NaHCO}_3$ buffer, at pH \sim 8.9 with DABS chloride dissolved in acetone under continuous stirring at 80°C for 10 min. DABS AAs can be

stored for 4 weeks in solution at 25°C, without any changes. In spite of the unique stability of DABS AAs in aqueous media, and the improvement in their chromatographic conditions, the use of DABS AAs is dwindling.

FMOC was introduced in 1983, as a fluorescent labelling agent, reacting rapidly with both primary and secondary AAs, under mild conditions (borate buffer, pH 7.7–8.0) to give stable derivatives. The excess reagent is extracted by pentane. Recent derivatization studies have shown that, depending on the time (2 and 40 min) and pH (8.0 and 11.4), considerable differences can be found. At pH \sim 8, acidic AAs manifest low responses, and slow reaction

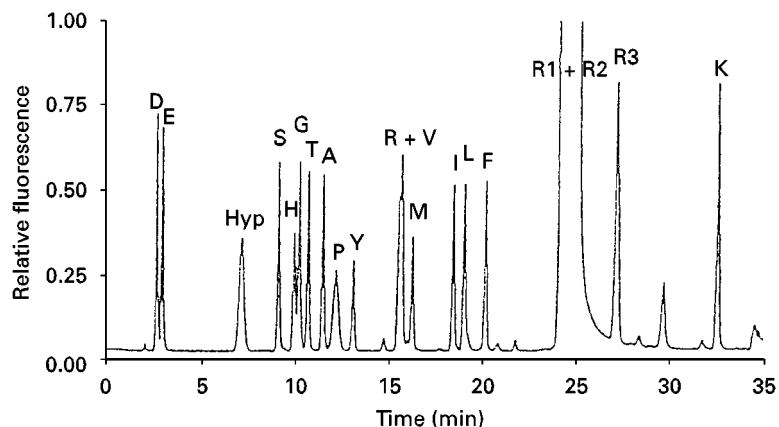


Figure 6 (for details see Table 3) HPLC of AAs derivatized with 9-fluorenylmethyl chloroformate (FMOC). Peaks labelled with one-letter abbreviations for protein AAs, as well as: Hyp, hydroxyproline; R1, FMOC-hydroxylamine; R2, FMOC-hydroxyde; R3, reagent peak present in blank derivatization. (Reproduced with permission from Qu K *et al.* (1996) *Journal of Chromatography* 723: 219.)

Table 4 Advances in the chiral separation of amino acids by LC: applying chiral mobile-phase additives (CMA), chiral stationary-phase columns (CSP) and chiral derivatization reagents (CDR), such as OPA/ NAC^a and OPA/NIBC^b

Author and date	Column size cm × mm, μm		Type	Eluents (elution temperature °C): chiral recognition method	Detector UV (nm) FEx/Em	Reagent (°C)	Analyte (pmol L ⁻¹)	RSD %	Matrix	No. of AAs/elution time (min)
Takeuchi, 1992	15	0.35	5	Develosil ODS-5	A: 40 mmol L ⁻¹ AmmAc + 27 mmol L ⁻¹ γ-CD/ACN = (3:1, v/v) B: AmmAc/ACN = (72:28, v/v); (25°C) CMA	F 315/539	DANS (-)	(-)	Model study	1 pair/30
Marchelli, 1996	10 15	8 4	5 5	Radialpak C18	Isocratic: ACN/30 mmol L ⁻¹ NaAc (pH 7.0), containing 0.5 mmol L ⁻¹ N2-S-2'-hydroxypropyl-S-phenyl-alaninamide + 5 mmol L ⁻¹ Cu(II) Ac = (2:8, v/v); (21.5°C) CMA	F 330/560	DANS (-)	(-)	Model study	3 pairs/130
Galli, 1994	15	4	5	LiChrosorb Si 100 ^c	Isocratic: ACN/10 mmol L ⁻¹ NaAc (pH 7.52), containing 25 mmol L ⁻¹ Cu(III) Ac = (7:3, v/v); (60°C) CSP	UV 254	DANS DABS (-)	(-)	Model study	3 pair/30 4 pair/30
Iida, 1997	15	6	5	Home made ^d	A: 100 mmol L ⁻¹ AmmAc (pH 6.5), B: 100 mmol L ⁻¹ AmmAc (pH 6.5)/CH ₃ OH = 50:50 (v/v); A and B both contain 1 mmol L ⁻¹ butanesulfonate; (20–30°C) CSP	UV 254	PTC (-)	1000 (-)	Protein sequencing	18 pairs + 1 single/ 150
Nimura, 1986	20	6	5	Develosil ODS-5	A: 50 mmol L ⁻¹ NaAc B: ACN (25°C) CDR ^c	F 360/405	OPA/ NAC (-)	5000 < 2.3	D- and L-AAs in protein hydrolysates	14 pairs/70
Brückner, 1995	25+ guard 2	4 2.1	5	Hypersil ODS	A: 23 mmol L ⁻¹ Na acetate (pH 5.95) B: ACN/CH ₃ OH = (60:5, v/v); (25°C) CDR ^d	F 230/445	OPA/ IBLC (IBDC) (-)	1–1000 < 2	D- and L-AAs in food hydrolysates	17 pairs + 5 single/70

Indications as in Tables, as well as: CD cyclodextrin; ^aN-acetyl-L-cysteine; ^bIBL (D) C, isobutyl-L(D)-cysteine; ^c[(S)- and (R)-phenylalanine-amide were covalently bonded to LiChrosorb Si100 silica gel; home made^d silica support treated with PITC + β-CD; DANS, dansyl; DABS, dabsyl; PTC, phenylthiocarbonyl.

is experienced; histidine and tyrosine give their mono- and disubstituted derivatives in varying ratios. With longer reaction times, the amount of disubstituted histidine decreases and that of tyrosine increases, together with interfering hydrolysis products of the reagent. At pH ~ 11.4 faster reaction and less interfering hydrolysis products are found. After 40 min reaction time, the monosubstituted histidine and the disubstituted tyrosine are formed in quantitative yield. Also 30% less hydrolysis product is obtained, favouring the resolution of the neighbouring alanine. The separation of the FMOC derivatives and

the presence of interfering substances are shown in Figure 6.

Chiral Separations (Table 4 and Figure 7)

The knowledge of the distribution of AA enantiomers in different matrices, and/or the enantiomeric purity of AAs, is of primary importance in the quality control of peptide syntheses for pharmaceuticals/medicines, as well as in various plant products and in high AA-containing foods, including baby formulas.

For separation and quantitation of enantiomers, HPLC is the method of choice. The application of the three main approaches for enantiomer separation is shown in Table 4 and Figure 7, including direct, chiral mobile-phase additive (CMA) and chiral stationary phase (CSP) and indirect methods (chiral derivatization reagent CDR).

Direct Methods

Applying either γ -cyclodextrin (γ -CD) or Cu(II) salts together with N^2 - S -(N^2 - R -)2'-hydroxypropyl- S -

phenylalanineamide as CMA is very time-consuming (Figure 7A): the separation of three AA pairs requires more than 2 h. Thus, CMAs can be regarded as an inferior approach in the chiral recognition of AA enantiomers, due to the need for a continuous supply of the often expensive CMA and to the disadvantageous chromatographic conditions. Bonded N^2 - S -(N^2 - R -)2'-hydroxypropyl- S -phenylalanine-amide, CSP, allows the comparison of the CMA and CSP protocols for the same enantiomer separations. The CSP method resolved four pairs of

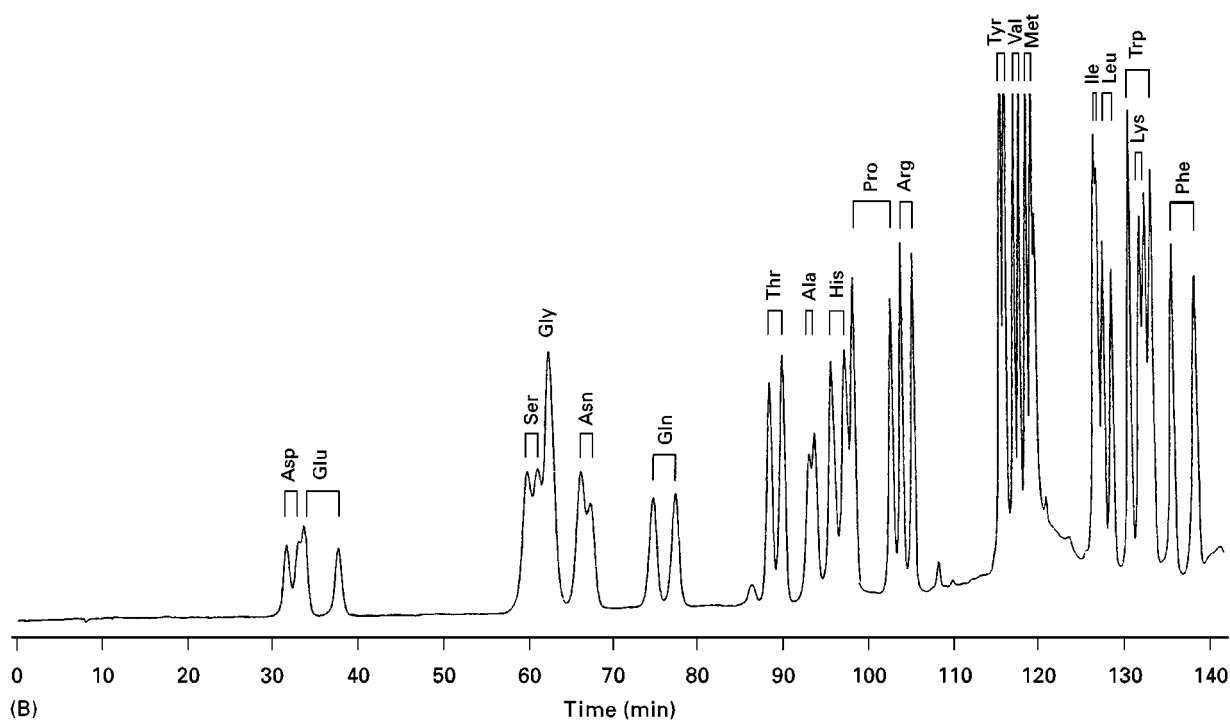
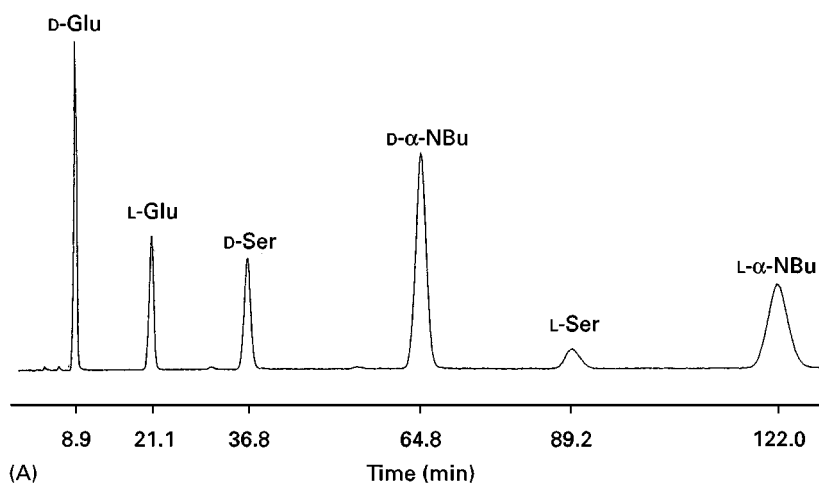


Figure 7 LC separation of AA enantiomers. (A) Enantiomeric separation of a mixture of three dansyl AAs. (Reproduced with permission from Marcelli R *et al.* (1996) *Chirality* 8: 452.) (B) Separation of 37 phenylthiocarbamyl AAs. (Reproduced with permission from Iida T *et al.* (1997) *Analytical Chemistry* 69: 4463.) (C) Aminogram of fir honey derivatized with (a) OPA/IBLC and (b) OPA/IBDC. (Reproduced with permission from Brückner H *et al.* (1995) *Journal of Chromatography* 697: 229.)

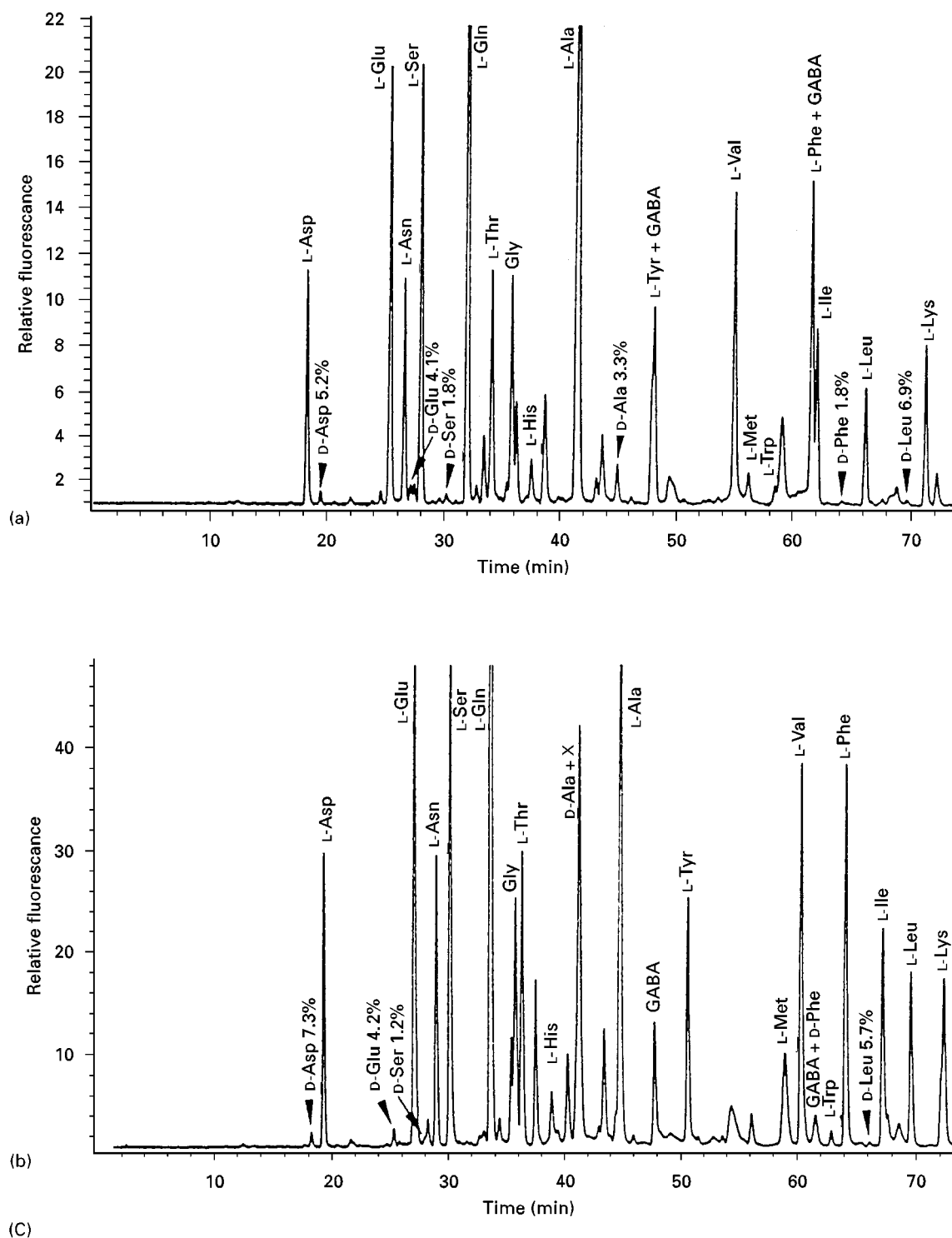


Figure 7 Continued

dansylated AAs within 30 min, attesting to the superiority of CSP over CMA. Recently, the elution of the PTC AAs on a new CSP (Figure 7B) permitted the partial separation of 18 AA pairs within 150 min.

Indirect Methods

Spectacular results have been achieved with the separation of AAs derivatized by CDRs (Figure 7C). Performing the separation with both OPA/N-L(D)-

acetyl-cysteinyl and with OPA/N-L(D)-isobutyrylcysteinyl AA derivatives gave excellent resolution of enantiomers. Consequently, the CDR technique is the primary importance in a number of practical applications of the separation of enantiomeric AAs. The interaction of AAs with the enantiomerically pure reagents takes place at ambient temperature, without racemization, resulting in the formation of stable diastereomer derivatives.

Online LC-MS

In the case of AAs, thermospray ionization has been displaced by the milder techniques of electrospray (ES) and atmospheric pressure chemical ionization (APCI), converting analyte molecules without fragmentation into ions. The analyte should contain the AAs in a stable form: either in the free condition or in the form of stable derivatives, such as phenylthiohydantoin (PTH) or PTCs. Significantly reduced flow rates are essential ($100\text{--}300\text{ nL min}^{-1}$) for stable ES and APCI operation. In automated Edman microsequencing, the ES-MS of PTH derivatives. The protonated molecules were measured with a linear response in the $50\text{--}1000\text{ fmol}$ level.

Future Trends

Efforts are needed to extend the life time, plate number and reproducibility of columns, and to standardize testing methods. The extended use of thermostated columns is desirable in order to obtain reproducibility in absolute and relative retention times. LC-MS will be more widely used in laboratories as the cost of these instruments falls to the level of GC-MS, and/or an all-purpose interface becomes available.

See also: II/Chromatography: Liquid: Derivatization; Mechanisms: Reversed Phase.

Further Reading

- Blau K and Halket J (eds) (1993) *Handbook of Derivatives for Chromatography*. Chichester: John Wiley.
- Brückner H, Langer M, Lüpke M, Westhauser T and Godel H (1995) Liquid chromatographic determination of amino acid enantiomers by derivatization with o-phthalaldehyde and chiral thiols. *Journal of Chromatography* 697: 229.
- Deyl Z, Hyanek J and Horakova M (1986) Profiling of amino acids in body fluids and tissues by means of liquid chromatography. *Journal of Chromatography* 379: 177.
- Grunau JA and Swiader JM (1992) Chromatography of 99 amino acids and other ninhydrin reactive compounds in the Pickering lithium gradient system. *Journal of Chromatography* 594: 165.
- McClung G and Frankengerger WT Jr (1988) Comparison of reversed-phase high performance liquid chromatographic methods for precolumn-derivatized amino acids. *Journal of Liquid Chromatography* 11: 613.
- Molnár-Perl I (1998) Amino acids. In: Deyl Z, Tagliaro F and Teserova E (eds) *Advanced Chromatographic and Electromigration Methods in BioSciences*. Amsterdam: Elsevier.
- Snyder LR, Kirkland JJ and Glajch JL (1997) *Practical HPLC Method Development*. New York: Wiley Interscience.
- Spackman DH, Stein WH and Moore S (1958) Automatic recording apparatus for use in the chromatography of amino acids. *Analytical Chemistry* 30: 1190.
- Zhou J, Hefta S and Lee TD (1997) High sensitivity analysis of phenylthiohydantoin amino acid derivatives by electrospray mass spectrometry. *Journal of the American Chemical Society of Mass Spectrometry* 8: 1165.

Thin-Layer (Planar) Chromatography

R. Bhushan, University of Roorkee,
Roorkee, India

J. Martens, Universität Oldenburg, Oldenburg,
Germany

Copyright © 2000 Academic Press

Introduction

Thin-layer chromatography (TLC) is a simple and inexpensive technique permitting a number of samples to be handled simultaneously, thus yielding a higher precision than sequential analysis. The inert character of the thin-layer material makes it ideally

suitable for use with strong corrosive reagents and one can perform many kinds of chemical reactions on the plate, both from the points of view of detecting and locating the spot and of achieving improved separation. Certain groups of interest can be chemically bonded to the reactive groups of support material, e.g. silanization for reversed-phase studies. Impregnation of the adsorbent with a variety of reagents adds an additional feature for influencing the adsorption characteristics without covalently affecting the inert character of the adsorbent. TLC is also successful in providing direct resolution of enantiomers of a variety of compounds by the proper manipulation of the support material. The analysis of amino

acids and derivatives and the resolution of enantiomers of amino acids by TLC techniques using a wide variety of adsorbents and impregnating agents, the possibility of obtaining relationships between the chromatographic behaviour and chemical structure and the many practical applications drawn from the literature are described in detail in the following sections.

Adsorbents and Thin Layers

A variety of adsorbents such as silica gel, alumina, polyamide and cellulose are available commercially and are used to make thin layers for TLC. Alumina and silica gel are used with or without a suitable binder such as gypsum or starch. Mixtures of two adsorbents or adsorbents impregnated with certain reagents such as 8-hydroxyquinoline or different metal ions have also been used successfully to improve resolution.

Cellulose layers have several advantages: they are stable, they can be used with various specific reagents and they give reproducible data. They are particularly recommended for quantitative evaluation by densitometry. The drawbacks of cellulose layers are that corrosive reagents cannot be used and the sensitivities of detection reactions of certain amino acids are lower than on silica gel layers.

The best known and most widely used adsorbents for TLC purposes are from Merck, but other products can be used satisfactorily. Pre-coated plates are widely available and increasingly used for the investigation of amino acids and their derivatives. For example, ready-made cellulose layers from Macherey-Nagel (Germany) containing MN cellulose-300 in appropriately bound form are one of the best-known products. Chiralplate from the same firm and Chir from Merck, for the separation of enantiomers of amino acids and their various derivatives, contain a coating of reversed-phase silica gel impregnated with a chiral selector and copper ions. Using home-made thin-layer plates is possible and it is recommended that one should not change the brand of adsorbent during a particular set of experiments.

Application of mixed layers of cellulose and the ion exchanger Amberlite CG-120 and a double layer consisting of a 2 cm band of cellulose + cation exchanger (45 + 5 g) in aqueous CM-cellulose (0.05%), with the remaining portion of the layer prepared from cellulose SF suspension, have also been effectively used. A newly synthesized support named aminoplast comparable with that of starch and cellulose has been reported. Nevertheless, silica gel continues to be the most widely used and successful material.

Preparation of Thin-layer Plates

Most thin-layer work is done on layers prepared from water-based slurries of the adsorbents. Even with the same amount and type of binder, the amount of water used for a given slurry varies with kinds and brands of adsorbents. For example, in the case of cellulose the amount of powder to be mixed with water varies depending on the supplier: Serva, Camag and Whatman recommend the use of 60–80 mL, 65 mL and 25 mL water for 10 g of their cellulose powders, respectively. These slurries may be prepared by shaking a stoppered flask or by homogenizing for a few seconds with a mechanical mixer. On the other hand, for the preparation of an aluminium oxide slurry (acidic, basic or neutral), it is recommended that 35 g of aluminium oxide is used with 40 mL water for spreading equipment, and 6 g of adsorbent in 15 mL ethanol–water (9:1) mixture for pouring directly on to the plate without a spreading apparatus. A slurry of 120 g of alumina G in 110 mL of water has been used successfully to make 1 mm-thick layers for preparative TLC. In general, cellulose powders contain impurities that are soluble in water or organic solvents, and these should be removed by washing the cellulose several times with acetic acid (0.1 mol L^{-1}), methanol and acetone and drying before use. The layer is made by turbo-mixing MN (Machery-Nagel) cellulose 300 (15 g) for 10 min in distilled water (90 mL) and then spreading it to give a 0.25 mm thick layer. The layers are left overnight to dry.

A slurry of silica gel G (50 g) in distilled water (100 mL) is prepared and spread with the help of a Stahl-type applicator on five glass plates of $20 \times 20 \text{ cm}$ to obtain 0.5 mm thick layers. The plates are allowed to set properly at room temperature and then dried (activated) in an oven at an appropriate temperature ($60\text{--}90^\circ\text{C}$) for 6 h or overnight. The plates are cooled to room temperature before applying the samples.

The same method has been used successfully to prepare plates with silica gel, silica gel polyamide, cellulose and these adsorbents impregnated with a variety of reagents including di-(2-ethylhexyl) orthophosphoric acid (HDEHP), tri-octyl-phosphine oxide (TOPO), 8-hydroxyquinoline, dibenzoyl methane and several metal salts. Brucine and tartaric acid are also mixed in slurries of silica gel as impregnating reagents to resolve enantiomers of amino acids and their PTH derivatives. Mixtures of H_2O – EtOH and other organic solvents can also be used, depending on the nature of the impregnating reagents. Citrate and phosphate buffers have also been used for slurring silica gel in place of water. It is customary to use 0.25

or 0.50 mm thick layers in activated form, but for preparative purposes 1–2 mm layers are best.

Development of Chromatograms

Standard solutions of amino acids are prepared in a suitable solvent such as 70% EtOH or 0.1 mol L⁻¹ HCl in 95% ethanol. These solutions are generally applied as tight spots, 1–2 cm from the bottom of each layer, using a glass capillary or Hamilton syringe. In the beginning a higher concentration, e.g. 500 ng or more, is applied; however, the detection limits are determined for the system developed by repeating the experiment with lower concentrations.

The chromatograms are generally developed in rectangular glass chambers, which should be paper-lined for good chamber saturation and pre-equilibrated for 20–30 min with solvent before use. The time taken depends on several factors such as the nature of the adsorbent, the solvent system and the temperature. The developed chromatograms are dried in an oven between 60 and 100°C, and the cooled plates are usually sprayed with ninhydrin reagent. Heating at 90–100°C for 5–10 min produces blue to purple zones of all amino acids except proline (yellow spot).

The same method is adopted for both one- and two-dimensional modes. The locating reagent is used after the second run, and a more polar solvent is generally used to develop the chromatogram in the second dimension.

Separation of Amino Acids

Silica gel and cellulose are the commonest adsorbents for one- or two-dimensional resolution of amino acids. These have been used as such (untreated) or impregnated with some other reagent employing a large number of solvents. Some of the successful systems for one- and two-dimensional resolution of amino acids are given in Table 1 and Table 2. Table 3 shows a comparative account of the separation of amino acids (R_F values) on silica gel, cellulose and ion exchange thin layers using *n*-butanol–acetic acid–water (3 : 1 : 1). The data are of great value for separating and detecting amino acids by one-dimensional TLC and based on it the amino acids have been grouped for the separation of 18-component mixtures (separation I) and essential amino acid mixtures (separation II) by calculating

Table 1 Solvent systems for TLC of amino acids on silica gel

<i>Solvent system</i>	<i>Ratio v/v</i>
<i>Silica gel</i>	
96% Ethanol–water	7 : 3
<i>n</i> -Propanol–water	7 : 3
<i>n</i> -Butanol–acetic acid–water	4 : 1 : 1
<i>n</i> -Propanol–34% NH ₄ OH	7 : 3
<i>n</i> -Propanol–water	1 : 1
Phenol–water	3 : 1
Propan-2-ol–water	7 : 3
Butyl acetate–methanol–acetic acid–pyridine	20 : 20 : 5 : 5
<i>n</i> -Butanol–formic acid–ethanol	3 : 1 : 1
<i>n</i> -Butanol–acetic acid–chloroform	3 : 1 : 1
<i>n</i> -BuOH–HOAc–EtOAc–H ₂ O	50 : 20 : 30 : 20
<i>n</i> -Propanol–H ₂ O	7 : 3
<i>n</i> -BuOH–H ₂ O–HOAc	40 : 7 : 5
<i>Cellulose</i>	
Propan-2-ol–butanone–1 mol L ⁻¹ HCl	60 : 15 : 25
2-Methylpropan-2-ol–butanone–acetone–methanol	20 : 1 : 14 : 5
Butanol–acetic acid–H ₂ O	4 : 1 : 5
Methanol–H ₂ O–pyridine	20 : 5 : 1
Propanol–8.8% NH ₃	4 : 1
Chloroform–MeOH–17% NH ₃	20 : 20 : 9
Butanol–acetone–Et ₃ NH–H ₂ O	10 : 10 : 2 : 5
Phenol–water	3 : 1
Ethyl acetate–pyridine–HOAc–H ₂ O	5 : 5 : 1 : 3
<i>n</i> -Butanol–acetic acid–H ₂ O–EtOH	10 : 1 : 3 : 0 : 3 or 4 : 1 : 10 : 1
Ethanol–conc. HCl	30 : 1
<i>n</i> -BuOH–HOAc–H ₂ O	4 : 1 : 1
Pyridine–acetone–NH ₄ OH–H ₂ O	26 : 17 : 5 : 12
Propan-2-ol–formic acid–H ₂ O	25 : 3 : 2

Table 2 Solvent systems for two-dimensional TLC

First	Second
<i>Silica gel</i>	
<i>n</i> -Butanol–HOAc–H ₂ O (4 : 1 : 5, v/v, upper phase)	Phenol–water (15 : 1, w/w)
Chloroform–MeOH–17% NH ₃ (2 : 2 : 1)	Phenol–H ₂ O (3 : 1)
<i>n</i> -Butanol–HOAc–H ₂ O (4 : 1 : 5, upper phase)	CHCl ₃ –MeOH–17% NH ₃ (2 : 2 : 1)
Butanone–pyridine–H ₂ O–HOAc (70 : 15 : 15 : 2)	CHCl ₃ –MeOH–17% NH ₃ (2 : 2 : 1)
<i>Cellulose</i>	
Propanol–HCOOH–H ₂ O (40 : 2 : 10)	<i>t</i> -Butanol–methylethyl ketone–0.88 NH ₃ –H ₂ O (50 : 30 : 10 : 10, v/v)
Propan-2-ol–butan-2-ol–1 mol L ^{−1} HCl (60 : 15 : 25 by vol.)	2-Methyl propanol–butan-2-one–acetone–MeOH–H ₂ O–(0.88) NH ₃ (10 : 4 : 2 : 1 : 3 : 1) or 2-methylpropanol–butanone–propanone–methanol–H ₂ O (40 : 20 : 2 : 1 : 14.5, v/v)

the resolution possibilities of each pair of acids (Table 4).

Amino acids chromatographed in the presence of trichloroacetic acid (used in deproteinizing serum samples) show anomalous behaviour, and this interference can be almost completely removed by predevelopment (twice) in ether saturated with formic acid. The migration sequences for the separation of 18 amino acids on reversed-phase thin layers including C₁₈ chemically bonded silica gel and on cellulose in *n*-propanol–H₂O (7 : 3, v/v) have generally

been found to be the same. Sorbents with ion exchange properties such as diethylaminoethyl (DEAE)–cellulose have also been used as the stationary phase for TLC separation of the main protein amino acids with *n*-butanol–acetic acid–water (5 : 1 : 6, upper phase) and pyridine–water (4 : 1) in one- and two-dimensional modes.

Locating the spots of amino acids After drying the chromatogram it may be viewed under ultraviolet light if the absorbent had a fluorescent indicator, or

Table 3 hR_F ($R_F \times 100$) values for amino acids on different layers

	A	B	C	D	E		
					FX _A	FX _B	FX _C
Ala	41.9	29.0	32.4	28.8	50.9	51.2	53.6
Ser	26.9	16.1	26.4	24.1	67.1	64.1	67.1
Tyr	50.0	36.1	49.4	45.9	11.9	13.9	15.5
Glu	34.4	22.6	30.0	28.2	34.5	29.4	30.6
Asp	26.3	14.8	25.3	21.8	71.5	68.2	68.6
Arg	25.6	11.0	12.9	10.0	1.8	2.2	2.2
Gly	29.4	14.8	25.9	23.5	55.6	52.4	53.6
Leu	75.0	63.9	51.8	48.8	21.8	17.8	19.4
Ile	73.1	60.0	49.4	47.1	27.8	22.2	23.3
Try	55.6	36.1	54.1	51.8	1.8	2.2	2.2
Met	41.0	22.5	47.3	43.5	28.0	27.2	25.0
Val	63.1	48.4	43.5	41.2	42.5	35.0	34.4
Lys	18.1	7.1	10.0	7.1	7.5	5.0	5.6
His	20.0	7.1	11.7	7.1	10.6	8.9	10.0
Phe	67.5	54.8	52.4	50.0	14.4	11.1	11.7
Thr	32.5	21.3	30.0	27.6	67.1	60.0	57.2
Cys	6.9	3.2	14.1	7.1	55.9	50.0	57.9
Pro	43.8	33.5	24.1	21.2			
Time for 17 cm (h)	7	11	4.5	7.5	6.5	6	2

A, Baker Flex cellulose sheets; B, Baker Flex microcrystalline cellulose sheets; C, Whatman K6 silica gel plates; D, Whatman high performance silica gel plates; E, Fixion ion exchange sheets (Na⁺ form); FX_A, no prior treatment; FX_B, layer pre-equilibrated with equilibration buffer for 16 h; FX_C, layer pre-equilibrated as for FX_B but at 45°C. Solvent for A–D, 2-butanol–acetic acid–water (3 : 1 : 1); solvent for E and run buffer, 84 g citric acid + 16 g NaOH + 5.8 g NaCl + 54 g ethylene glycol + 4 mL conc. HCl (pH 3.3); solvent equilibration buffer, run buffer diluted 30 times (pH 3.8).

Table 4 Group separation of amino acids

<i>System as in Table 3</i>	<i>Group</i>	<i>Amino acids resolved</i>
A	I	Leu, Phe, Try, Ala, Glu, Ser, Lys, Cys, Tyr
	II	Leu, Phe, Try, Thr, Lys
B	I	Leu, Phe, Tyr, Val, Glu, Asp, Lys
	II	Leu, Phe, Val, Try, Thr, Lys
C	I	Try, Ile, Val, Ala, Ser, Cys, Lys
	II	Try, Ile, Val, Thr, Lys
D	I	Try, Ile, Val, Ser, Glu, Arg, Lys
	II	Try, Ile, Val, Thr, Lys
FX _A	I	Thr, Gly, Val, Glu, Met, Leu, Phe, His, Lys, Arg
	II	Thr, Val, Met, Leu, Phe, His, Lys, Try
FX _B	I	Asp, Thr, Gly, Val, Met, Leu, Thr, His, Lys, Try
	II	Thr, Val, Met, Leu, Phe, His, Lys, Try
FX _C	I	Asp, Thr, Gly, Val, Met, Leu, Thr, His, Lys, Try
	II	Thr, Val, Met, Leu, Phe, His, Lys, Try

Group I, 18-component mixture of amino acids; Group II, Mixture of essential amino acids.

the compounds – such as dansyl amino acids – fluoresce. Solvent fronts indicate regularity of solvent flow. Ninhydrin is the most commonly used reagent for the detection of amino acids, and a very large number of ninhydrin reagent compositions have been reported in the literature. The reagent may be made slightly acidic with a weak acid following the use of an alkaline solvent and vice versa. Constancy of colour formed may be attained by the addition of complex-forming cations (Cu^{2+} , Cd^{2+} or Ca^{2+}) and specific colours may be produced by the addition of bases such as collidine or benzylamine. Some of the ninhydrin compositions and their applications are described below.

1. A solution of ninhydrin (0.2% w/v in acetone) is prepared with the addition of a few drops of collidine or glacial acetic acid. The chromatogram is dipped or sprayed with the solution and dried at 60°C for about 20 min or at 100°C for 5–10 min. Excessive heating causes a dark background. Most amino acids give a violet colour, while aspartic acid gives bluish-red, and proline and hydroxyproline give a yellow colour; the sensitivity limit is 1 µg.
2. Ninhydrin (0.3 g) in *n*-butanol (100 mL) containing acetic acid (3 mL) is sprayed on a dried, solvent-free layer, which is then heated for 30 min at 60°C or for 10 min 110°C. Detection limits range from 0.001 µg for alanine to 0.1 µg for proline and aspartic acid.
3. Ninhydrin (0.3 g), glacial acetic acid (20 mL) and collidine (5 mL) are made up to 100 mL with ethanol or ninhydrin (0.1%, w/v) in acetone–glacial acetic acid–collidine (100 : 30 : 4%).
4. A solution of cadmium acetate (0.5 g) in water (50 mL) and glacial acetic acid (10 mL) is made up (500 mL) with acetone. Portions of this solution are taken and solid ninhydrin is added to give a final concentration of 0.2% w/v. The chromatogram is sprayed and heated at 60°C for 15 min. The results are noted immediately and again after 24 h, at room temperature. Alternatively, the layer is impregnated thoroughly with the reagent and the colours are allowed to develop in the dark at room temperature for 24 h. This reagent gives permanent colours, mainly red but yellow for proline. Sensitivity is 0.5 nmol.
5. Ninhydrin (1.0 g) in absolute ethanol (700 mL), 2,4,6-collidine (29 mL), and acetic acid (210 mL) has been used for spraying on solvent-free cellulose layers. The chromatogram is then dried for 20 min at 90°C.
6. Development of ion exchange resin layers in ninhydrin (1% w/v) in acetone containing collidine (10% w/v) at room temperature for 24 h, or at 70°C for 10 min has also been recommended.
7. Spray of ninhydrin (0.1% or 0.2% w/v in acetone on chromatograms followed by heating at 60 or 90°C for 10–20 min has also been used.
8. Polychromatic reagent consists of firstly, ninhydrin (0.2% w/v) in ethanol (50 mL) + acetic acid (10 mL) + 2,4,5-collidine (2 mL) and secondly, a solution of copper nitrate (1.0% w/v) in absolute ethanol. The two solutions are mixed in a ratio of 50 : 3 before use. Replacement of ethanol by methanol also gives polychromatic amino acid detection by joint application of ninhydrin and primary, secondary or tertiary amines. The layers are first sprayed with diethylamine, dried for 3 min at 110°C, cooled, and then sprayed with 0.2% w/v methanolic ninhydrin and heated for 10 min at 110°C, when the spots of amino acids appear on

a pale blue background. Use of ninhydrin (0.27 g), isatin (0.13 g), and triethylamine (2 mL) in methanol (100 mL) gives spots of amino acids on a yellow background.

Several other reactions have also been used for the detection of specific amino acids (Table 5). Oxalic acid (ethanolic 1.25% w/v), dithio-oxamide (ethanolic-saturated) and dithizone followed by ninhydrin have been used to aid identification and detection of amino acids with various specific colours. Acetylacetone-formaldehyde gives yellow spots under UV light. Using isatin-ninhydrin (5 : 2) in *n*-butanol or modifying ninhydrin detection reagent by addition of D-camphor, and various acids improves identification of amino acids. Spraying of layers with 1,3-indanedione or *o*-mercaptobenzoic acid prior to ninhydrin improves sensitivity limits and colour differentiation. 3,5-Dinitrobenzoyl chloride can be used to detect amino acids at a 3–4 µg level, and synchronization of timing is achieved by coupling pneumatic nebulization with optical fibre-based detection in a chemiluminescence TLC system to detect dansyl-amino acids. Chromatograms sprayed with ninhydrin (0.3 g ninhydrin in 100 mL *n*-butanol plus 3 mL of glacial acetic acid), air-dried for 5 s, resprayed and heated in an oven at 110°C for 10 min gives the best sensitivity, stability and colour differentiation compared with different recipes of ninhydrin and fluorescamine sprays.

Separation of Amino Acid Derivatives

Separation and identification of derivatives of amino acids such as dinitrophenyl (DNP), PTH, dansyl and dimethylamino azobenzene isothiocyanate (DABITC), is very important, particularly in the primary structure determination of peptides and proteins. The preparation of PTH, dansyl, and DNP amino acids, and the methods for their identification after separation from the *N*-terminal of peptides and proteins, are available in literature.

PTH Amino Acids

The PTH amino acids are sensitive to light, and optically active derivatives racemize easily. Both manual and automated, and liquid-phase and solid-phase Edman degradation methods (coupling of the NH₂ group of an amino acid at the *N*-terminal end of a polypeptide or a free molecule with phenyl isothiocyanate) are currently used for small and large polypeptides to establish their primary structure. An automated sequencer can deliver several PTH amino acids in 24 h and these are required to be identified rapidly to match the output.

Table 5 Detection reactions for specific amino acids

<i>Amino acid</i>	<i>Reagent</i>
Arg	8-Hydroxyquinoline
Arg	α -Naphthol, urea, Br ₂
Asp	Ninhydrin, borate solution, HCl
Cys, Met	NaN ₃ , iodine
Gly	<i>o</i> -Phthalaldehyde, KOH
His	Sulfanilic acid
Ser, Thr, Tyr	Sodium metaperiodate, Nessler reagent
Try	<i>p</i> -Dimethylaminobenzaldehyde

TLC has been used for the identification of PTH amino acids since Edman and Begg used it in their classical work describing the automatic sequencer. Various TLC systems with different kinds of adsorbents, such as alumina, silica gel and polyamide, have been reported. The results of some TLC systems used for resolution and identification of PTH amino acids are given below.

Two-dimensional TLC has been carried out using plates coated with polyamide containing three fluorescent additives when all PTH amino acids show coloured spots under UV light. About 0.1 nmol of PTH amino acid can be detected. Typical results are given in Table 6. A compilation of solvent mixtures useful in the TLC of PTH amino acids on various supports is given in Table 7.

Resolution and identification of PTH amino acids on silica or polyamide layers, as discussed above, do not discriminate between derivatives of Leu/Ile and cannot resolve complex mixtures without two-dimensional chromatography. Difficulties in resolving combinations of PTH Phe/Val/Met/Thr and PTH Asp and Glu are also observed. Use of chloroform-acetic acid (27 : 3, v/v) and chloroform-methanol (30 : 4, v/v) has been found to be extremely satisfactory for discriminating between PTH Asp and PTH Glu, as the difference in their *hR_F* values is around 10 units. The difficulties in resolving and identifying various combinations of PTH amino acids can be overcome by the use of certain solvent systems, given in Table 7.

Detection of PTH amino acids The methods of detection include firstly, spraying a dilute solution of fluorescein on a plain layer of silica gel when the spots are visible as dark areas against a yellow background in UV light; secondly, exposing the dried chromatograms to iodine vapours to locate the spots as light brown compact zones; and thirdly, use of iodine-azide solution when bleached spots on a light brown background are observed. The iodine azide method is considered less sensitive and causes difficulties in demarcating the exact spots and measuring the

Table 6 Characteristic colours of PTH amino acids on polyamide plates containing mixed fluorescent additive 3

PTH amino acid	Colour after	
	Second treatment	Alkaline treatment
Valine	Red	Red
Proline	Red	Red
Alanine	Red	Red
Glycine ^a	Red	Brownish red
Serine	Red	Brownish red (blue)
Asparagine ^a	Red	Greenish brown (bluish green) ^b
Aspartic acid	Red	Brownish red (dark brown)
Methionine ^a	Red	Brownish red
Leucine	Red	Brownish red
Isoleucine	Red	Red
Lysine	Red	Red
Tyrosine ^a	Red	Red (bluish green) ^b
Threonine ^a	Red	Bluish green (blue)
Glutamine ^a	Red	Greenish brown (white yellow)
Glutamic acid	Red	Red
Phenylalanine ^a	Red	Greenish red (white blue) ^b
Tryptophan ^a	Red	Greenish red (white blue) ^b
Histidine ^a	Red	Blue (light blue) ^b
Arginine ^a	Red	Purple (blue) ^b
Cysteic acid	Red	Brownish red (dark brown)

^aSpots appear yellow, except glycine (pink); ^bFluorescent. Solvents: toluene-*n*-pentane-acetic acid (6 : 3 : 2, v/v) and acetic acid-water (1 : 3, v/v) for first and second dimension, respectively. Alkaline treatment: spray 0.05 mol L⁻¹ NaOH in methanol-water (1 : 1, v/v), heating at 150°C for 30 min, UV.

correct R_F . Characteristic changes in the colours of some derivatives are observed by heating the plate after spraying with an alkaline solution when the

Table 7 Various solvent systems for TLC of PTH amino acids

	Ratio
<i>Polyamide</i>	
<i>n</i> -Heptane- <i>n</i> -BuOH-HOAc	40 : 30 : 9
Toluene- <i>n</i> -pentane-HOAc	60 : 30 : 35
Ethylene chloride-HOAc	90 : 16
Toluene- <i>n</i> -pentane-HOAc	60 : 30 : 35
EtOAc- <i>n</i> -BuOH-HOAc	35 : 10 : 1
<i>n</i> -BuOH-MeOH-HOAc (+ 30 mg butyl fluorescent reagent per litre)	19 : 20 : 1
<i>Silica gel</i>	
Heptane-CH ₂ Cl ₂ -propionic acid	45 : 25 : 30
Xylene-MeOH	80 : 10
CHCl ₃ -EtOH and	98 : 2
CHCl ₃ -EtOH-MeOH (in the same direction)	89.25 : 0.75 : 10
CHCl ₃ - <i>n</i> -butyl acetate	90 : 10
Diisopropyl ether-EtOH	95 : 5
CH ₂ Cl ₂ -EtOH-HOAc (or on cellulose)	90 : 8 : 2
Petroleum ether (60–80°)-acetic acid	25 : 3
<i>n</i> -Hexane- <i>n</i> -butanol	29 : 1
<i>n</i> -Hexane- <i>n</i> -butyl acetate	4 : 1
Pyridine-benzene	2.5 : 20
MeOH-CCl ₄	1 : 20
Acetone-dichloromethane	0.3 : 8

plate with mixed fluorescent additives is used (Table 6). A rapid colour-coded system due to ninhydrin spray is mentioned in Table 8; the colours produced allow easy identification of those amino acids that have nearly identical R_F values, for example, Lys and Ser degradation products, Ala/Met/Phe, and Tyr/Thr. The method is significant because it gives positive identifications of PTH Ser/Lys/Glu/Asp and their respective amides, which cannot be identified by gas chromatography (GC).

Dansyl Amino Acids

Derivatization of free amino group of amino acids with 5-methylaminonaphthalene-1-sulfonyl (dansyl) chloride has become increasingly popular for *N*-terminal determinations in proteins and for manual Edman degradation. In addition, dansylation has also been used as one of the most sensitive methods for quantitative amino acid analysis.

Two-dimensional TLC on polyamide sheets using water-formic acid (200 : 3, v/v) for the first-direction run and benzene-acetic acid (9 : 1, v/v) for development at right angles to the first run has mostly been employed in conjunction with the Edman dansyl technique for sequencing peptides. These solvents cannot resolve Dns-Glu/Asp, Dns-Thr/Ser, and α -Dns-Lys/ ϵ -Dns-Lys/Arg/His. However, a third run in ethyl

Table 8 Characteristic colours of PTH amino acids following ninhydrin application

<i>PTH derivative</i>	<i>Colour properties</i>	<i>NH₄OH colour change</i>
Proline	UV, colourless	Light blue after heating
Alanine	Purple	Deeper colour
Glycine	Orange	
Serine	UV, purple	
Serine breakdown	Faint orange	Weak red
Asparagine	Yellow	More intense
Carboxymethylcysteine	UV, purple	
Methioninesulfone	Light tan	
Methionine	Faint tan	
Lysine	Very faint pink	Weak blue after heating
Tyrosine	UV, yellow before spray	Intense yellow
Threonine	Colourless	Light tan
Glutamine	Dark green	Dark blue
Phenylalanine	UV, colourless	Faint yellow
Tryptophan	UV, yellow before spray	Deep yellow
Aspartic acid	UV, pink	Darker
Glutamic acid	Grey	Dark blue

Silica gel plates, without fluorescent indicator, developed in heptane–CH₂Cl₂–propionic acid (45 : 25 : 30) and xylene–MeOH (80 : 10), sprayed with iodine–azide and 1.7% ninhydrin in MeOH–collidine–HOAc (15 : 2 : 5), heated at 90°C for 20 min; colour changes by blowing a saturated ammonia atmosphere over ninhydrin plate.

acetate–acetic acid–methanol (20 : 1 : 1) in the direction of solvent 2 resolves Dns-Glu/Asp, and Dns-Thr/Ser. A further run in the direction of solvent 2 and 3 using 0.05 mol L⁻¹ trisodium phosphate–ethanol (3 : 1, v/v) resolves the monosubstituted basic Dns amino acids. Use of molarity ammonia–ethanol (1 : 1, v/v) as a third solvent for two-dimensional chromatograms, for the separation of basic dansyl amino acids in particular, has been effective. Most of the TLC systems reported up to 1978 required more than two runs for complete resolution of all Dns amino acids. A few solvent systems to yield separations of basic, acidic and hydroxyl derivatives in the presence of other amino acids without resorting to the third solvent system and *R_F* values are given in Table 9. Additionally, a large number of solvent systems for one- or two-dimensional resolution of dansyl amino acids on silica gel or polyamide have been summarized in Table 10. Bhushan and Reddy reviewed the TLC of dansyl, and DNP amino acids and evolved several successful and effective solvent systems for the resolution of almost all the dansyl amino acids on silica gel plates (Tables 11 and 12).

Detection of dansyl amino acids In all cases, dansyl amino acids, being fluorescent, have been detected under a UV lamp (254 nm).

DABITC Derivatives of Amino Acids

DABITC reacts with the NH₂-terminal end of an amino acid in basic media to give a 4-dimethylamino

azobenzene thiohydantoin (DABTH) amino acid via a DABTC derivative, in a manner similar to the Edman method, where a PTH amino acid is obtained by the reaction of phenylisothiocyanate (PITC). The presence of excess free amino acid does not, in any case, interfere with the analysis.

Two-dimensional TLC on polyamide sheets by ascending solvent flow is used to identify all DABTH amino acids except DABTH-Ile/Leu. No phase equilibrium is necessary; H₂O–acetic acid (2 : 1, v/v) is used for the first dimension and toluene–*n*-hexane–acetic acid (2 : 1 : 1, v/v) is used for the second. For discrimination between DABTH-Ile/Leu, one-dimensional separation on polyamide using formic acid–ethanol (10 : 9, v/v) or one-dimensional separation on silica gel (Merck) using chloroform–ethanol (100 : 3, v/v) is carried out. The successful identification of DABTH amino acids relies on skilful running of the small polyamide sheet and interpretation of the pattern of spots.

Detection of DABITC derivatives of amino acids The use of DABITC reagent during amino acid sequencing of proteins has distinct advantages over the use of dansyl chloride; for example, the colour difference between DABITC, DABTC derivatives and DABTH-amino acids greatly facilitates direct visualization and identification. DABTH amino acids are coloured compounds having absorption maxima at 520 nm in acid media ($\epsilon = 47\,000$). Thus, using the visible region, the quantitation and

Table 9 R_F values for Dns amino acids in various solvent systems on polyamide sheets

<i>Dns amino acid</i>	<i>R_F</i> in solvent systems									
	<i>A</i>	<i>B</i>	<i>C</i>	<i>D</i>	<i>E</i>	<i>F</i>	<i>G</i>	<i>H</i>	<i>I</i>	<i>J</i>
1. Ala	0.53	0.48	0.49	0.69	0.69	0.57	0.81	0.68	0.43	0.76
2. Arg	0.05	0.03	0.03	0.91	0.39	0.09	0.76	0.22	0.01	0.06
3. Asp	0.08	0.07	0.10	0.69	0.38	0.10	0.88	0.37	0.12	0.19
4. Cys	0.03	0.03	0.04	0.19	0.43	0.22	0.78	0.09	0.03	0.06
5. Glu	0.15	0.10	0.15	0.66	0.88	0.02	0.88	0.34	0.05	0.30
6. Gly	0.32	0.21	0.32	0.69	0.63	0.48	0.80	0.48	0.28	0.69
7. His	0.07	0.05	0.13	0.96	0.76	0.32	0.84	0.36	0.06	0.18
8. Ile	0.77	0.54	0.65	0.40	0.57	0.71	0.78	0.76	0.60	0.84
9. Leu	0.70	0.49	0.59	0.34	0.57	0.71	0.78	0.75	0.54	0.80
10. Lys (mono)	0.35	0.21	0.38	0.22	0.09	0.63	0.72	0.58	0.09	0.79
11. Lys (di)	0.53	0.37	0.48	0.78	0.69	0.35	0.82	0.40	0.39	0.76
12. Met	0.52	0.36	0.51	0.43	0.59	0.68	0.80	0.62	0.55	0.81
13. Phe	0.57	0.38	0.53	0.31	0.43	0.68	0.77	0.62	0.51	0.81
14. Pro	0.85	0.66	0.71	0.55	0.74	0.46	0.84	0.75	0.69	0.90
15. Ser	0.12	0.07	0.16	0.81	0.71	0.49	0.82	0.42	0.10	0.44
16. Thr	0.15	0.10	0.26	0.81	0.74	0.57	0.82	0.56	0.16	0.56
17. Tyr	0.63	0.47	0.61	0.00	0.00	0.84	0.73	0.65	0.58	0.91
18. Val	0.72	0.56	0.61	0.47	0.67	0.71	0.81	0.80	0.61	0.88
19. Dns-OH	0.00	0.01	0.00	0.51	0.54	0.16	0.74	0.00	0.04	0.04
20. Dns-NH ₂	0.51	0.38	0.47	0.71	0.17	0.96	0.49	0.60	0.40	0.91

Solvent systems: A, benzene–acetic acid (9 : 1, v/v) ; B, toluene–acetic acid (9 : 1, v/v); C, toluene–ethanol–acetic acid (17 : 1 : 2, v/v) ; D, water–formic acid (200 : 3, v/v); E, water–ethanol–ammonium hydroxide (17 : 2 : 1, v/v); F, ethyl acetate–ethanol–ammonium hydroxide (20 : 5 : 1); G, water–ethanol–ammonium hydroxide (14 : 15 : 1, v/v); H, *n*-heptane–*n*-butanol–acetic acid (3 : 3 : 1, v/v); I, chlorobenzene–acetic acid (9 : 1, v/v); J, ethyl acetate–methanol–acetic acid (20 : 1 : 1).

Table 10 Various solvent systems for TLC of dansyl amino acids

<i>Solvent systems</i>	<i>Ratio</i>
1. HCOOH	1.5%
Benzene–acetic acid	9 : 1
2. Formic acid	1.5%
Benzene–acetic acid	4.5 : 1
3. H ₂ O–pyridine–HCOOH	93 : 35 : 3.5
Benzene–acetic acid	4.5 : 1
4. NH ₄ Cl + NH ₃ + ethanol	80 g + 22 mL + 10 mL
Benzene–pyridine–HOAc	75 : 2 : 6
5. H ₂ O–propanol–formic acid	100 : 5 : 2
Benzene–acetic acid	9 : 1
6. Ethyl acetate–MeOH–HOAc	20 : 1 : 1
Benzene–HOAc–BuOH	90 : 10 : 5
7. Formic acid	1.5%
Benzene–acetic acid	9 : 2
8. Benzene–anhydrous HOAc, followed by	9 : 1
EtOAc–MeOH–anhydrous HOAc in the same direction	10 : 1
Formic acid	1.5%
9. H ₂ O–pyridine–HCOOH	93 : 35 : 3.5
Benzene–acetic acid	4.5 : 1
10. Formic acid	3%
Benzene–acetic acid	9 : 1
11. Me–acetate– <i>iso</i> -PrOH–NH ₃	9 : 7 : 4
CHCl ₃ –MeOH–HOAc	15 : 5 : 1
CHCl ₃ –EtOAc–MeOH–HOAc	45 : 75 : 22.5 : 1
Pet ether– <i>t</i> -BuOH–HOAc	5 : 2 : 2
12. CHCl ₃ –MeOH	9 : 1
13. CCl ₄ –2-methoxyethanol	17 : 3
14. Benzene–pyridine–acetic acid	80 : 20 : 2

Solvents at serial no. 1–8 : two-dimensional TLC on polyamide layers.

Solvents at serial no. 9–14 : one-dimensional TLC on silica gel layers.

Table 11 R_F Values of 10 dansyl amino acids on silica gel thin layers (Sl. no. = serial number)

Sl. no.	Dansyl amino acid	Solvent system				
		S_1	S_2	S_3	S_4	S_5
1.	Dansyl-L-alanine	62	61	60	50	27
2.	Dansyl-L-isoleucine	80	92	85	85	49
3.	Dansyl-L-leucine	83	85	80	89	65
4.	Dansyl-L-methionine	86	64	62	55	31
5.	Dansyl-L-proline	60	84	72	30	39
6.	<i>N</i> - <i>O</i> -dansyl-L-tyrosine	55	73	40	60	18
7.	<i>N</i> - α -dansyl-L-tryptophan	51	53	46	40	21
8.	Dansyl-L-phenylalanine	77	76	74	52	40
9.	Dansyl-L-valine	72	88	65	48	35
10.	Dansyl-L-norvaline	75	81	68	45	37

S_1 , *n*-heptane–BuOH–HOAc (20 : 8 : 3, v/v); S_2 , dichloromethane–MeOH–propionic acid (30 : 1 : 0.5, v/v); S_3 , chloroform–HOAc–ethyl acetate (24 : 5 : 4, v/v); S_4 , chloroform–MeOH–ethyl acetate (23 : 8 : 2, v/v); S_5 , chloroform–propionic acid–ethyl acetate (23 : 6 : 4, v/v); R_F values are average of five determinations.

identification of these derivatives become more convenient and sensitive (10 pmol on a polyamide plate). Exposure to HCl vapours turns all yellow spots to red or blue on polyamide sheets.

DNP Amino Acids

Use of DNP amino acids, formed by condensation of 1-fluoro-2,4-dinitrobenzene (FDNB) with the free amino group of an amino acid, was first described by Sanger in 1945, who identified DNP amino acids by paper chromatography. Since then many modifications in the methods of obtaining derivatives of

Table 12 R_F Values of 10 dansylamino acids on silica gel thin layers

Sl. no.	Dansyl amino acid	Solvent system				
		A_1	A_2	A_3	A_4	A_5
1.	<i>N</i> - α -dansyl-L-asparagine	56	75	53	30	35
2.	Dansyl-L-aspartic acid	66	72	60	64	30
3.	α -Dansyl-L-arginine	7	12	3	2	3
4.	<i>N</i> - <i>N</i> -didansyl-L-cystine	84	83	68	85	18
5.	Dansyl-L-cysteic acid	82	80	25	15	11
6.	Dansyl-L-glutamic acid	80	90	84	74	55
7.	Dansyl-L-glutamine	62	77	63	41	40
8.	<i>N</i> -dansyl-L-lysine	16	20	10	6	8
9.	<i>N</i> -dansyl-L-serine	72	85	72	58	32
10.	Dansyl-L-threonine	76	88	76	68	45

A_1 , Dichloromethane–MeOH–propionic acid (21 : 3 : 2, v/v); A_2 , ethyl acetate–MeOH–propionic acid (22 : 10 : 3, v/v); A_3 , chloroform–MeOH–HOAc (28 : 4 : 2, v/v); A_4 , chloroform–acetone–HOAc (20 : 8 : 4, v/v); A_5 , chloroform–acetone–propionic acid (24 : 10 : 5, v/v) R_F values are the average of five determinations.

Table 13 R_F Values of DNP amino acids on silica gel thin layers

Sl. no.	<i>N</i> -DNP-L-amino acid	Solvent system				
		S_1	S_2	S_3	S_4	S_5
1.	Phenylalanine	53	48	85	70	55
2.	Isoleucine	68	82	96	97	60
3.	Tyrosine	25	30	60	52	36
4.	Alanine	40	36	68	50	42
5.	Glycine	28	17	35	25	27
6.	Leucine	65	73	93	90	52
7.	Tryptophan	48	33	53	47	34
8.	Methionine	45	40	75	57	42
9.	Valine	62	65	90	85	47
10.	Proline	41	45	74	60	38
11.	Norvaline	61	62	88	83	45

		Solvent system				
		A_1	A_2	A_3	A_4	A_5
12.	<i>N</i> -DNP-L-serine	51	68	70	70	70
13.	<i>N</i> -DNP-lysine	21	26	11	7	27
14.	<i>N</i> -S-di-DNP-L-cysteine	82	87	77	85	85
15.	<i>N</i> -DNP-L-glutamic acid cyclohexyl-amine salt	67	80	83	92	82
16.	<i>N</i> -DNP-L-aspartic acid	38	70	75	60	60
17.	<i>N</i> -DNP-L-asparagine	30	64	45	38	55
18.	<i>N</i> -DNP-L-arginine	10	6	5	3	18
19.	<i>N,N</i> -di-DNP-L-cystine	48	70	55	65	82

S_1 , *n*-heptane–*n*-butanol–acetic acid (20 : 4 : 1, v/v); S_2 , chloroform–propionic acid (26 : 2, v/v); S_3 , chloroform–acetic acid (21 : 1, v/v); S_4 , chloroform–ethanol–propionic acid (30 : 2 : 1, v/v); S_5 , benzene–*n*-butanol–acetic acid (34 : 1 : 1, v/v); A_1 , chloroform–methanol–acetic acid (25 : 5 : 1, v/v); A_2 , chloroform–propionic acid–methanol (15 : 10 : 1, v/v); A_3 , *n*-heptane–butanol–acetic acid (16 : 8 : 4, v/v); A_4 , *n*-butanol–ethyl acetate–acetic acid (20 : 8 : 2, v/v); A_5 , *n*-butanol–methanol–propionic acid (18 : 8 : 2, v/v). R_F values are average of five determinations.

amino acids for sequence analysis and in identification of such derivatives have been reported, and the use of DNP amino acids for sequencing purposes is rapidly going out of practice. Nevertheless, the importance of DNP amino acids has not yet disappeared.

Kirchner presented considerable information on the analysis of DNP amino acids based on the literature available up to 1970. In one of the earlier methods, thin-layer plates (20 × 20 cm × 0.25 mm) were prepared from a mixture of 10 g of cellulose MN-300 and 4 g silica gel H (Merck), homogenized in 80 mL of water, dried overnight at 37°C and developed in the first dimension with two solvents successively: *iso*-propanol–acetic acid–H₂O (75 : 10 : 15) for 15 min and *n*-butanol–0.15 mol L^{−1} ammonium hydroxide (1 : 1, upper phase). The dried chromatograms were developed in 1.5 mol

L⁻¹ sodium phosphate buffer (pH 6.0) in the second dimension.

In almost all methods reported, the separation has been carried out in groups of water-soluble and ether-soluble DNP amino acids, and for each group mostly two-dimensional TLC has been performed. A few solvent systems for one-dimensional resolution of DNP amino acids on silica gel plates are shown in Table 13.

Detection of DNP amino acids The DNP amino acids have been visualized by UV light (360 nm with dried plates, or 254 nm with wet ones) or by their yellow colour, which deepens upon exposure to ammonia vapours. Thin layers of silica gel usually give an intense purple fluorescence for DNP amino acids under UV light, which masks the presence of very faint spots and decreases the colour contrasts. The cellulose-silica mixed layer gives much lower fluorescence and preserves the colour contrasts between various derivatives. Because of the photosensitivity of these derivatives, it is advisable to carry out their preparation and chromatography in the absence of direct illumination.

Resolution of Amino Acids and Derivatives on Impregnated Layers

The technique of incorporating a suitable reagent with the adsorbent, prior to applying the samples to the plates, originated from simple TLC and can be termed impregnated TLC. The reagents and methods used for impregnation are not to be confused with locating/spray reagents because the latter are required for the purpose of identification even on impregnated plates.

Methods for Impregnation

Of the various methods used for impregnation, one is mixing of the impregnating reagent with the inert support. A second approach is the immersion of the plates into an appropriate solution of the impregnating reagent carefully and slowly so as not to disturb the thin layer. Alternatively, a solution of the impregnating material is allowed to ascend or descend the plate in the normal manner of development; this method is less likely to damage the thin layer. Exposing the layers to the vapours of the impregnating reagent or spraying the impregnating reagent (or its solution) on to the plate have also been employed; spraying provides a less uniform dispersion than the other methods. Another approach is to have a chemical reaction between the inert support and a suitable reagent: the support is chemically modified before making the plate, the compounds of interest are bonded to the reactive groups of the layer.

The impregnating agent participates in various mechanisms in the resolution process, including ion-pairing, complex formation, ligand exchange, coordination bonds, charge transfer, ion exchange and hydrogen bonding.

Amino acids Resolution of amino acids has been reported to be very rapid and improved by using copper sulfate, halide ions, zinc, cadmium and mercury salts, and alkaline earth metal hydroxides as impregnating materials and some of the results are described in Tables 14–17. The chromatograms developed in these systems provide compact spots, without lateral drifting of the solvent front. C₁₈ layers impregnated with dodecylbenzene sulfonic acid are helpful in confirming the presence of an unknown amino acid in a sample and the migration sequence on these impregnated plates is reversed, probably due to an ion exchange mechanism. Separation of α -amino acids with butan-1-ol-acetic acid-water (3 : 1 : 1, v/v), butan-1-ol-acetic acid-chloroform (3 : 1 : 1, v/v), and butan-1-ol-acetic acid-ethyl acetate (3 : 1 : 1, v/v), on plain and nickel chloride impregnated plates has been reported; the partition and adsorption coefficients for the amino acids under study were determined on both untreated and Ni²⁺ impregnated silica gel in a batch process and correlations were drawn between TLC separation of amino acids on the impregnated gel with adsorption/partition characteristics. The results indicate a predominant role of partitioning in the separation. Application of antimony (V) phosphate-silica gel plates in different aqueous, nonaqueous and mixed solvent systems has also been reported. Some impregnated TLC systems for resolution of amino acids are summarized in Table 18.

PTH amino acids As mentioned above, certain difficulties in resolving or identifying various PTH amino acid combinations have successfully been removed and multicomponent mixtures separated with metal impregnated silica gel layers, while other reagents such as (+)-tartaric acid and (–)-ascorbic acid have been used for the resolution of enantiomeric mixtures. The methods reported provide very effective resolution and compact spots (by exposure to iodine vapours) and can be applied to the identification of unknown PTH amino acid; some of these are given in Tables 19–21. Some of the successful solvent systems for TLC of PTH amino acids on impregnated plates are summarized in Table 22.

High performance TLC (HPTLC)/overpressured TLC (OPTLC) Improvements in the solid-phase materials for TLC have resulted in an increase in

Table 14 hR_F of amino acids in presence of halides

Sl. no.	Amino acid	Control plate	Amino acids pretreated with			Plates impregnated with		
			Cl^-	Br^-	I^-	Cl^-	Br^-	I^-
1.	Gly	07	08	09	12	07	08	09
2.	Tyr	30	35	40	47	29	30	31
3.	Pro	12	15	19	22	08	09	10
4.	Thr	15	14	15	19	13	14	16
5.	Cys	22	22	25	27	19	20	22
6.	Leu	32	40	47	50T	50T	55T	60T
7.	Met	23	35	36	37	22	23	24
8.	Ile	30	38	44	44	30	30	31
9.	Ala	15	19	13	16T	16T	16	16
10.	Try	35T	40	50T	53	30	31	34
11.	Phe	36T	41	48	48	365	37	38
12.	Val	19	32	25	29	25	26	26
13.	Asp	08	13	14	15	08	09	10
14.	Ser	09	13T	13	14T	08	08	09
15.	His	01	03	04	05	02	02	02
Time (min)		50	64	67	67	50	50	50

Solvent system: *n*-butanol–acetic acid–chloroform (3 : 1 : 1, v/v); temperature $25 \pm 2^\circ C$.

T = tailing.

separation efficiency, sample detectability limits and reduced analysis time. HPTLC can be used with advantage for the separation of PTH amino acids but separation of all 20 common PTH amino acids was

Table 15 hR_F values for amino acids on copper sulfate and polyamide mixed silica gel plates

Amino acid	A	B	C
L-Leucine (Leu)	65	63	71
D,L-Isoleucine (Ile)	66	72	81
D,L-Tryptophane (Try)	63	68	75
D,L-Methionine (Met)	64	64	72
D,L-Valine (Val)	64	60	77
L-Lysine-HCl (Lys)	16T	12	33
L-Histidine-HCl (His)	22T	20	39
D,L- β -Phenylalanine (Phe)	64	65	82
D,L-Threonine (Thr)	50	51	67
D,L-Alanine (Ala)	46	45	64
D,L-Serine (Ser)	40	43	56
L-Tyrosine (Tyr)	58	61	71
L-Glutamic acid (Glu)	41	48	58
D,L-Aspartic acid (Asp)	28	25	44
L-Arginine HCl (Arg)	24T	19	39
Glycine (Gly)	36	46	49
L-Proline (Pro)	37	36	58
L-Cysteine HCl (Cys)	20T	17	29
D,L-2-Aminobutyric acid (Aba)	51	54	61
L-Ornithine	27T	23	35

The values are average of two or more identical runs, 10 cm in 35 min. A, untreated silica gel plate; B, copper sulfate-impregnated silica gel; C, polyamide mixed silica gel layers; T, tailing Solvent, methanol–butyl acetate–acetic acid–pyridine (20 : 20 : 10 : 5, v/v).

not achieved initially. A continuous multiple development on silica gel was able to separate 18 samples and standards simultaneously using five development steps with four changes in mobile-phase and scanning densitometry; typical results are given in Table 23. PTH-Leu/Ile/Pro have been identified by HPTLC using multiple wavelength detection. OPLC using chloroform–ethanol–acetic acid (90 : 10 : 2) for polar, and dichloromethane–ethyl acetate (90 : 10) for nonpolar PTH amino acids has been successful in their separation and quantitation; the method is claimed to be superior to HPTLC in having relatively increased migration distance, resulting in the resolution of complex mixtures containing a large number of derivatives. OPTLC and HPTLC on RP-8, RP-18, and home-made ammonium tungstophosphate layers have also been used for the analysis of DNP amino acids.

Separation of 18 amino acids on cellulose, silica gel and chemically bonded C_{18} HPTLC plates has been achieved. All of these plates contain a preadsorbent zone except the cellulose. Quantification is carried out by scanning standard and sample zones at 610 nm. hR_F values of amino acid standards on reversed-phase and on normal-phase layers in different solvents are given in Tables 24 and 25, respectively.

Resolution of Enantiomeric Mixtures of Amino Acids and Derivatives

The measurement of specific rotation is a common and accepted method for evaluating the enantiomeric

Table 16 hR_F values of 15 amino acids on silica gel impregnated with Zn, Cd and Hg salts

	A	B	C	D	E	F	G	H	I	J
Thr	25	55	42	41T	35	36	42	33	50	40
Ser	12	38	39	28T	32	29	31T	15	40	31T
Gly	10	35	29	23T	28	25	28	16	35	27T
Lys	03	13	07	05	51	08	05	04	10	05
Ala	30	48	40	31	38	36	38	20	5	35
Tyr	60	60	52	50	48	45	51	62	55	56
Ile	55	67	56	52	50	48	54	50	60	53
Leu	50	65	55	55	52	50	56	47	64	55
Cys	00	00	00	00	00	00	00	00	00	00
Met	45	62	48	48	48	42	48	39	54	45
Glu	18T	43	38	36T	34	27	38T	18	36	34T
Try	57	60	53	51	51	44	54	45	60	47
Phe	54	67	57	55	55	46	57	58	68	52
Val	50	63	45	50	52	42	56	47	57	45
Arg	07	19	13	13	09	11	11	10	15	08

Solvent, butyl acetate–methanol–acetic acid–pyridine (20 : 20 : 5 : 5, v/v). Developing time, 30 min. Detection limit, 10^{-4} mol L $^{-1}$. Solvent front, 10 cm. A, plain silica gel; B, C, D, 0.5%, 0.2%, 0.1% Zn $^{2+}$ -C-impregnated, respectively; E, F, G, 0.5, 0.2, 0.1% Cd $^{2+}$ -impregnated, respectively; H, I, J, 0.5, 0.2, 0.1% Hg $^{2+}$, respectively. T = tailing.

purity of chiral compounds. The determination of enantiomeric excess (*ee*) values is influenced by the presence of impurities and changes in concentration, solvent and temperature, and requires the $[\alpha]_D$ value for the pure enantiomer. The availability of a reliable optically pure standard depends on the analytical method by which it had been resolved from the enantiomeric or racemic mixture of the compound in question. Though TLC provides a direct method for resolution and analytical control of enantiomeric

purity, there are few reports on TLC separation of enantiomers.

In general, the following approaches for the resolution of enantiomers have been used.

Indirect method

This method involves reaction of the enantiomeric mixture with a suitable chiral reagent to make the corresponding diastereomeric derivatives prior to chromatography; the choice of chiral selector is

Table 17 hR_F values of amino acids on untreated plates and plates impregnated with metal sulfates

Aminoacids	Unimpregnated plate	Plate impregnated with							
		Mn $^{2+}$	Fe $^{2+}$	Co $^{2+}$	Ni $^{2+}$	Cu $^{2+}$	Zn $^{2+}$	Cd $^{2+}$	Hg $^{2+}$
Asp	21	51	54	50	62	58	52	59	64
Glu	25	51	63	55	59	61	54	58	65
Phe	45	64	74	67	72	74	69	68	65
Tyr	46	66	73	68	72	70	72	68	71
Lys	7	15	21	22	18	18	16	32	25
Orn	28	15	23	23	19	23	20	28	T
Arg	30	20	25	30	28	28	25	35	33
Ala	30	50	52	53	60	55	49	58	73
Val	48	60	70	58	71	65	59	65	70
Ser	29	45	57	48	57	52	44	56	48
Hypo	26	42	52	47	48	50	43	57	45
Gly	20	43	58	48	52	40	45	54	55
Leu	50	67	72	69	75	71	74	69	SF
Cys	SF	24	37	32	34	35	30	34	40

T, Tailing; SF, migrates with solvent front. hR_F values are the average of at least five determinations.

Table 18 TLC of amino acids on impregnated silica gel layers

Solvent system	Ratio (v/v)	Impregnation
<i>iso</i> -Amyl alcohol–H ₂ O–HOAc H ₂ O–EtOAc–MeOH	6 : 5 : 3 64.3 : 5.7 : 30	Pyridinium tungstoarsenate Silanized silica and triethanol amine. SDS, sodium di-octylsulfonate, dodecyl benzene sulfonic acid Dodecyl benzene sulfonic acid Ammonium tungstophosphate and dodecyl benzene sulfonic acid Ammonium tungstophosphate
0.1 mol L ⁻¹ HOAc in aq. 50% MeOH Aq. MeOH + I ₂ (KCl or HOAc added)		
Aq. NH ₄ NO ₃ or HNO ₃ or H ₂ O–HOAc–MeOH (79 : 1 : 20) H ₂ O		Polyamide Kieselguhr or cellulose
H ₂ O–butanol–anhyd. HOAc	4 : 4 : 2	
<i>n</i> -Butanol–acetic acid–water	4 : 1 : 5	Starch–agar (1 : 1)
Propan-2-ol–EtOAc–acetone–methanol– <i>n</i> -pentyl alcohol–aq. 26% NH ₃ –water in first direction; and Butanol–acetone–propan-2-ol– formic acid–water in second direction	9 : 3 : 3 : 1 : 1 : 3 : 3 18 : 8 : 8 : 3 : 6	Cellulose
1 mol L ⁻¹ NH ₄ NO ₃ –0.1 mol L ⁻¹ HNO ₃ MeOH–butyl acetate–HOAc–pyridine	4 : 4 : 2 : 1	Ammonium tungstophosphate Copper sulfate and polyamide
<i>n</i> -Butanol–acetic acid–CHCl ₃	3 : 1 : 1	Cl ⁻ , Br ⁻ , I ⁻
<i>n</i> -Butanol–acetic acid–ethanol	3 : 1 : 1	Hydroxides of Mg, Ca, Ba, Sr
Butyl acetate–MeOH–HOAc–pyridine	4 : 4 : 1 : 1	Zn ²⁺ , Cd ²⁺ , Hg ²⁺

limited due to the feasibility of its reaction with the analyte.

Direct method

1. This method uses a chiral stationary phase; it may be due to either natural chirality of the material as such, like cellulose, or some sort of synthesis of the phase.
2. Chiral discriminating agents are added to the mobile phase.

3. A suitable chiral reagent is incorporated, such as acid, base, an organic compound or a metal complex with the adsorbent during plate making, or at a stage before developing the chromatogram.

DL-amino acids Separation of D,L-tryptophan on a crystalline cellulose-coated plate in 1980 seems to be one of the first TLC reports. Applying the principle of ligand exchange, (2*S*, 4*R*, 2'*RS*)-4-hydroxyl-1-(2'-hydroxy dodecyl)-proline was used as the chiral

Table 19 hR_F values of PTH amino acids on Fe²⁺, Co²⁺, Ni²⁺ and Zn²⁺ impregnated silica plates

Sl. no.	PTH-amino acid	Alone	Fe ²⁺		Co ²⁺		Ni ²⁺		Zn ²⁺	
			0.2%	0.3%	0.05%	0.1%	0.1%	0.2%	0.2%	0.3%
1.	Alanine	60	42	41	57	51	38	40	50	43
2.	Aspartic acid	0	0	0	0	0	0	0	0	0
3.	Glycine	39	26	21	44	38	29	30	32	27
4.	Glutamic acid	0	0	0	0	0	0	0	0	0
5.	Isoleucine	90	84	75	72	90	65	71	81	72
6.	Leucine	95	87	71	82	81	70	76	85	76
7.	Lysine	23	8	6	15	17	7	4	10	8
8.	Methionine	70	54	47	81	62	58	51	57	58
9.	Phenylalanine	75	61	49	77	68	52	55	66	58
10.	Proline	97	89	89	84	76	83	90	96	89
11.	Serine	13	5	5	11	9	11	12	8	5
12.	Tyrosine	96	867	69	68	95	85	78	83	78
13.	Tryptophan	95	91	70	91	97	77	82	88	81
14.	Threonine	86	78	57	94	83	60	63	78	70
15.	Valine	85	75	73	96	79	57	58	76	67

Solvent, chloroform–ethyl acetate (29 : 3, v/v); developing time 35 min; solvent front, 10 cm.

Table 20 R_F values of PTH amino acids on untreated plates and plates impregnated with sulfates of Mg, Mn, Fe and Co

PTH amino acid	S1 (heptane–butylacetate, 15 + 5)					S2 (heptane–propionic acid, 20 + 4)					S3 (benzene–ethyl acetate, 15 + 3) ^a	
	PS ₁	M ₁	M ₂	M ₃	M ₄	PS ₂	M ₁	M ₂	M ₃	M ₄	PS ₃	M ₄
Methionine	28	30	26	32	31	43	45	30	32	35	62	78
Phenylalanine	30	35	29	37	34	50	52	36	38	40	67	80
Tryptophan	63	61	51	60	57	71	67	55	55	57	82	94
Valine	49	46	40	51	47	66	62	52	50	55	73	85
Isoleucine	62	62	50	62	59	77	72	61	60	62	78	65
Trysine	66	64	53	64	61	80	74	64	64	65	84	89
Threonine	57	52	45	56	53	63	64	53	53	53	72	83
Alanine	23	25	23	26	25	32	34	27	25	29	50	67
Serine	55	55	42	55	51	48	46	38	49	40	70	44
Leucine	69	65	54	63	56	76	71	62	60	67	80	96
Lysine	06	04	02	03	05	06	10	04	06	07	18	35
Glycine	17	15	13	15	15	17	20	15	15	18	37	55
Glutamic acid	04	06	05	06	06	04	04	06	06	05	0	14
Aspartic acid	05	07	06	07	07	05	08	07	07	06	0	22
Proline	44	33	31	34	32	44	42	35	35	45	79	96

^aCompounds moved to solvent front on plates impregnated with sulfates of Mg, Mn and Fe. PS₁, PS₂, PS₃, untreated plates; M₁, M₂, M₃, M₄, treated with sulfates of Mg, Mn, Fe, and Co, respectively. R_F values are the average of at least five determinations. Developed in 30–40 min at 25°C ± 2°C, and exposed to iodine vapours to locate the spots.

selector to resolve several racemic α -amino acids on reversed-phase 18-TLC plates first immersed (1 min) in a 0.25% copper(II) acetate solution (MeOH–H₂O, 1 : 9, v/v), dried, and then immersed in a 0.8% methanolic solution of the chiral selector (1 min); the results are shown in Table 26. Ready-to-use *Chiral-plates*[®] are now marketed by Macherey-Nagel, Duren, Germany, and *Chir*[®] plates are marketed by Merck, Germany. Resolution of DL-methyl Dopa, and DL-Dopa is very successful on Chiralplates using

methanol–H₂O–acetonitrile (50 : 50 : 30, v/v) as the mobile phase and ninhydrin as the detecting reagent (Figure 1). The R_F values for L-Dopa and D-Dopa were reported to be 0.47 and 0.61, respectively, and the system is capable of resolving enantiomers in trace amounts, with the lowest level of detection of the D-enantiomer in L-Dopa samples being 0.25%. The resolution of enantiomers of α -substituted α -amino acids, and racemic mixtures of natural and nonnatural amino acids, N-methylated and

Table 21 R_F Values of PTH amino acids on silica plates impregnated with zinc salts

PTH amino acid	S1 (heptane–butylacetate, 15 + 5)				S2 (heptane–propionic acid, 20 + 4)				S3 (benzene–ethyl acetate 15 + 3)			
	L ₁	L ₂	L ₃	L ₄	L ₁	L ₂	L ₃	L ₄	L ₁	L ₂	L ₃	L ₄
Methionine	17	22	18	25	33	33	29	33	42	57	48	58
Phenylalanine	22	25	25	28	37	38	35	36	47	60	52	60
Tryptophan	36	41	41	51	40	50	40	55	67	74	61	82
Valine	40	35	44	42	52	53	54	52	54	68	64	69
Isoleucine	50	46	55	54	50	62	63	63	62	79	74	74
Trysine	55	48	59	56	62	64	75	65	64	84	79	78
Threonine	47	40	52	48	53	51	52	56	57	72	72	67
Alanine	23	17	21	22	29	27	23	27	35	44	38	44
Serine	49	45	42	50	38	36	37	39	52	66	60	64
Leucine	55	51	55	59	61	50	67	60	65	81	77	76
Lysine	03	02	03	03	04	05	04	07	6	7	6	8
Glycine	15	10	12	13	16	15	15	15	24	29	25	31
Glutamic acid	0	04	0	04	03	02	02	04	0	0	0	0
Aspartic acid	0	05	0	05	04	03	03	05	0	0	0	0
Proline	38	25	32	30	40	40	40	42	70	77	83	72

L₁, L₂, L₃, L₄ plates impregnated with Cl[−], SO₄^{2−}, CH₃COO[−] and PO₄^{3−} of zinc, respectively. Other conditions as in Table 20.

Table 22 TLC of PTH amino acids on impregnated silica gel layers

<i>Solvent system</i>	<i>Ratio (v/v)</i>	<i>Impregnation^a</i>
CHCl ₃ -H ₂ O-EtOAc	28 : 1 : 1	Zn ²⁺ , Cd ²⁺ , Hg ²⁺
CHCl ₃ -MeOH-Benzene	19 : 1 : 9	
CCl ₄ -HOAc	19 : 1	
CHCl ₃ -Benzene-EtOAc	25 : 5 : 3	Fe ²⁺ , Co ²⁺ , Zn ²⁺
CHCl ₃ -EtOAc	29 : 3	Fe ²⁺ , Co ²⁺ , Ni ²⁺
<i>n</i> -Heptane- <i>n</i> -butyl acetate	15 : 5	Cl ⁻ , CH ₃ COO ⁻ , PO ₄ ³⁻ of zinc, or SO ₄ ²⁻ of Mg ²⁺ , Mn ²⁺ , Fe ²⁺ , Co ²⁺
<i>n</i> -Heptane- <i>n</i> -propionic acid	20 : 4	
Benzene-EtOAc		
CHCl ₃ - <i>n</i> -butyl acetate	10 : 5	
CHCl ₃ -EtOAc	25 : 2	

^aVarious concentrations of each of the impregnating reagent have been used.

N-formylated amino acids, and various other derivatives of amino acids has also been achieved on Chiralplates; typical results are presented in **Tables 27 and 28**. A novel chiral selector from (1*R*, 3*R*, 5*R*)-aza-bicyclo[3,3,0]-octan carboxylic acid has been synthesized and used as a copper(II) complex for the impregnation of reversed-phase 18 plates for ligand exchange TLC separation of amino acids and the results were comparable to those on Chiralplates®.

Chiral selectors such as (–)-brucine and Cu-L-proline complex are used to resolve enantiomers of amino acids (**Table 29**), and (+)-tartaric acid and (–)-ascorbic acid for the resolution of enantiomeric PTH amino acids (**Table 30**). The chiral selectors are mixed with silica gel slurry.

Resolution of tryptophans and substituted tryptophans on cellulose layers developed with copper sulfate solutions has shown that excess of Cu²⁺ ions decreases the chiral discrimination of the system, and development with aqueous α-cyclodextrin (1–10%) plus NaCl solutions (0.1, 0.5, 1.0 mol L⁻¹) showed the best results with aqueous 4% α-cyclodextrin–1 mol L⁻¹ NaCl solution; the results are comparable to Chiralplate®. It has been observed that chiral effects are essentially additive (for cellulose and α-cyclodextrin) and there is a strong temperature dependence for the chiral separations.

α- and β-cyclodextrins, hydroxypropyl-β-cyclodextrin and bovine serum albumin in the mobile phase

have provided enantiomeric separations of amino acids and derivatives. Chiral monohalo-s-triazines have been used for the TLC resolution of DL-amino acids. Racemic dinitropyridyl-, dinitrophenyl- and dinitrobenzoyl amino acids are separated on reversed-phase-TLC plates developed with aqueous-org mobile phases containing bovine serum albumin as a chiral agent.

Dansyl-DL-amino acids Reversed-phase TLC plates from Whatman are developed before application of dansyl amino acids in buffer A (0.3 mol L⁻¹ sodium acetate in 40% acetonitrile, and 60% water adjusted to pH 7 by acetic acid). After fan-drying, the plates are immersed in a solution of 8 mmol L⁻¹ *N,N*-di-*n*-propyl-L-alanine and 4 mmol L⁻¹ cupric acetate in 97.5% acetonitrile, 2.5% water for 1 h or overnight and left to dry in air. After applying the samples, the plates are developed in buffer A with or without *N,N*-di-*n*-propyl-L-alanine (4 mmol L⁻¹) and cupric acetate (1 mmol L⁻¹) is dissolved in it. The enantiomers are detected by irradiating with UV light (360 nm) to yield fluorescent yellow-green spots. Use of 25% acetonitrile is preferred for glutamic and aspartic acids and serine and threonine derivatives. *N,N*-di-*n*-propyl alanine can be prepared by the following procedure: L-alanine (17.8 g) is dissolved in ethanol (200 mL) and 10% palladium on activated charcoal catalyst (3 g) and

Table 23 Optimum experimental conditions for the separation of PTH amino acids by continuous multiple development HPTLC

<i>Step</i>	<i>Mobile phase</i>	<i>Plate length (cm)</i>	<i>Time (min)</i>	<i>PTH amino acid identified</i>
1.	CH ₂ Cl ₂	3.5	5	Pro
2.	CH ₂ Cl ₂ -propan-2-ol (99 : 1, v/v)	7.5	10	Pro, Leu, Ile, Val, Phe
3.	CH ₂ Cl ₂ -propan-2-ol (99 : 1, v/v)	7.5	10	Pro, Leu, Ile, Val, Phe, Met, Ala/Try, Gly, Lys, Tyr, Thr
4.	CH ₂ Cl ₂ -propan-2-ol (97 : 3, v/v)	7.5	10	Pro, Met, Lys, Tyr, Thr, Ser, Glu
5.	C ₂ H ₅ COOCH ₃ -CH ₃ CN-CH ₃ COOH (74.3 : 20 : 0.7, v/v)	7.5	10	Asn, Glu/Gln, Asp, Cm-Cys, His, Arg

Table 24 R_F Values of amino acid standards on reversed-phase layers

Amino acid	TLC system					
	1	2	3	4	5	6
Aspartic acid	30	59	72	60	83	73
Arginine	28	4	35	28	86	82
Serine	55	36	69	50	82	73
Glycine	50	38	62	45	69	54
Tyrosine	91	77	88	68	77	67
Alanine	78	59	71	63	71	54
Glutamic acid	82	70	86	67	83	69
Proline	56	69	64	40	65	46
Cystine	11	12	39	33	85	84
Methionine	90	74	75	59	75	61
Lysine	31	84	27	24	74	79
Tryprophan	90	77	85	63	72	63
Valine	90	74	75	59	75	61
Threonine	78	52	68	50	72	57
Histidine	21	3	29	23	77	68
Phenylalanine	90	76	83	65	72	61
Leucine	90	77	81	62	75	63
Isoleucine	91	77	81	62	74	61

Layers: 1, 2, Whatman C-18; 3, 5, Merck RP-18; 4, 6, Merck RP-18W. Mobile phases: 1, 3, 4, *n*-Butanol–glacial acetic acid–water (3 : 1 : 1, v/v); 2, 5, 6, *n*-propanol–water (7 : 3, v/v).

propionaldehyde (43 mL) is added. The mixture is hydrogenated for 48 h at 40–50°C at an initial hydrogen pressure of 50 psi; the catalyst is removed using

Table 25 R_F Values of amino acid standards on normal-phase layers

Amino acid	TLC system			
	1	2	3	4
Aspartic acid	28	27	26	58
Arginine	18	18	17	2
Serine	26	30	27	40
Glycine	26	32	28	43
Tyrosine	46	58	53	78
Alanine	38	32	32	55
Glutamic acid	69	56	50	64
Proline	45	32	28	50
Cystine	10	11	9	30
Methionine	60	59	51	72
Lysine	15	13	10	4
Tryptophan	55	63	57	82
Valine	60	56	49	68
Threonine	34	32	32	53
Histidine	14	14	11	17
Phenylalanine	68	61	55	80
Leucine	79	61	55	78
Isoleucine	78	59	54	77

Layers: 1, Cellulose; 2, 4, Whatman silica gel; 3, Merck silica gel. Mobile phases: 1, Butan-2-ol–glacial acetic acid–water (3 : 1 : 1, v/v); 2, 3, *n*-butanol–glacial acetic–water (3 : 1 : 1, v/v); 4, *n*-propanol–water (7 : 3, v/v).

Table 26 Enantiomeric resolution of amino acids by TLC

Amino acid	R_F value (configuration)		Mobile phase
	R	S	
Isoleucine	0.37 (2 <i>R</i> , 3 <i>R</i>)	0.44 (2 <i>S</i> , 3 <i>S</i>)	A
Phenylalanine	0.38	0.45	A
Tyrosine	0.34	0.26	B
Tryptophan	0.39	0.45	A
Proline	0.40	0.59	B
Glutamine	0.53	0.37	A

Development distance: 14 cm; saturated chamber. A, MeOH–water–MeCN (1 : 1 : 4, v/v); B, MeOH–water–MeCN (5 : 5 : 3, v/v).

a sintered glass filter and the filtrate is evaporated to dryness. The reaction product (*N,N*-di-*n*-propyl-L-alanine) is crystallized from chloroform, and the purity may be confirmed by TLC, and carbon, hydrogen, nitrogen analysis.

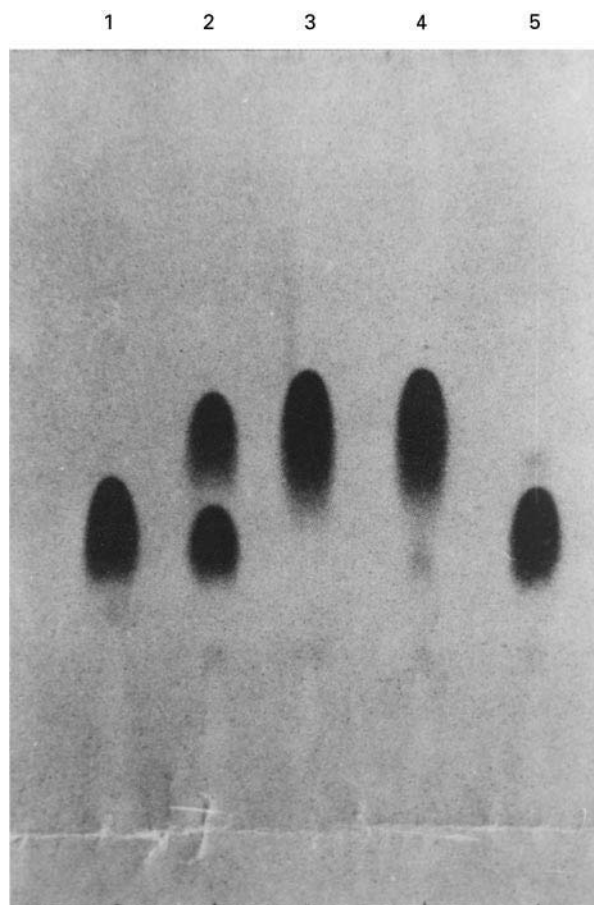
**Figure 1** Chromatogram showing separation of different D- and L-dopa samples on Chiralplate. From left to right: 1, L-dopa; 2, D,L-dopa; 3, D-dopa; 4, 3% L-dopa in D-dopa; 5, 3% D-dopa in L-dopa. Developing solvent, methanol–water–acetonitrile (5 : 5 : 3, v/v). Developing time 45–60 min. Detection 0.1% ninhydrin spray reagent.

Table 27 Enantiomeric resolution of α -dialkyl amino acids by TLC

Parent amino acid	R ₁	R ₂	R _F value	Configuration	Mobile phase
Asp	CH ₂ CO ₂ H	CH ₃	0.52 (D)	0.56 (L)	A
Glu	(CH ₂) ₂ CO ₂ H	CH ₃	0.58 (L)	0.62 (D)	A
Leu	CH ₂ CH(CH ₃) ₂	CH ₃	0.48	0.59	A
Phe	CH ₂ C ₆ H ₅	CH ₃	0.53 (L)	0.66 (D)	A
Ser	CH ₂ OH	CH ₃	0.56 (L)	0.67 (D)	B
Try	CH ₂ -3-indolyl	CH ₃	0.54	0.65	A
Tyr	CH ₂ -(4-OH-C ₆ H ₄)	CH ₃	0.63 (D)	0.70 (L)	A
Val	CH(CH ₃) ₂	CH ₃	0.51	0.56	A
α -Amino butyric acid	CH ₂ CH ₃	CH ₃	0.50	0.60	A
Phe	CH ₂ C ₆ H ₅	CHF ₂	0.63	0.70	A
Phe	CH ₂ C ₆ H ₅	CH ₂ -CH=CH ₂	0.57	0.63	A
Phe	CH ₂ C ₆ H ₅	CH ₂ CH ₂ SCH ₃	0.57	0.62	A

Mobile phase: A, methanol–water–acetonitrile (1 : 1 : 4, v/v); B, methanol–water–acetonitrile (5 : 5 : 3, v/v). Development distance 13 cm; saturated chamber.

In a two-dimensional reversed-phase TLC technique for the resolution of complex mixture of dansyl-*dl*-amino acids, the Dns-derivatives are first separated in nonchiral mode using 0.3 mol L⁻¹ sodium acetate in H₂O–acetonitrile (80 : 20, pH 6.3) to which 0.3 mol L⁻¹ sodium acetate in H₂O–aceto-

Table 28 Enantiomeric resolution of racemates by TLC

Racemate	R _F value	Configuration	Mobile phase
Valine	0.54(D)	0.62(L)	A
Methionine	0.54(D)	0.59(L)	A
Allo-isoleucine	0.51(D)	0.61(L)	A
Norleucine	0.53(D)	0.62(L)	A
2-Aminobutyric acid	0.48	0.52	A
<i>o</i> -Benzylserine	0.54(D)	0.65(L)	A
3-Chloroalanine	0.57	0.64	A
<i>S</i> -(2-Chlorobenzyl)-cysteine	0.45	0.58	A
<i>S</i> -(3-Thiabutyl)-cysteine	0.53	0.64	A
<i>S</i> -(2-Thiopropyl)-cysteine	0.53	0.64	A
<i>cis</i> -4-Hydroxyproline	0.41(L)	0.59(D)	A
Phenylglycine	0.57	0.67	A
3-Cyclopentylalanine	0.46	0.56	A
Homophenylalanine	0.49(D)	0.58(L)	A
4-Methoxyphenylalanine	0.52	0.64	A
4-Aminophenylalanine	0.33	0.47	A
4-Bromophenylalanine	0.44	0.58	A
4-Chlorophenylalanine	0.46	0.59	A
2-Fluorophenylalanine	0.55	0.61	A
4-Iodophenylalanine	0.45(D)	0.61(L)	A
4-Nitrophenylalanine	0.52	0.61	A
<i>o</i> -Benzyltyrosine	0.48(D)	0.64(L)	A
3-Fluorotyrosine	0.64	0.71	A
4-Methyltryptophan	0.50	0.58	A
5-Methyltryptophan	0.52	0.63	A
6-Methyltryptophan	0.52	0.64	A
7-Methyltryptophan	0.51	0.64	A
5-Bromotryptophan	0.46	0.58	A
5-Methoxytryptophan	0.55	0.66	A
2-(1-Methylcyclopropyl)-glycine	0.49	0.57	A
<i>N</i> -Methylphenylalanine	0.59(D)	0.61(L)	A
<i>N</i> -Formyl- <i>tert</i> -leucine	0.48(+)	0.61(–)	A
<i>N</i> -Glycylphenylalanine	0.51(L)	0.57(L)	B

A, Methanol–water–acetonitrile (1 : 1 : 4, v/v); B, methanol–water–acetonitrile (5 : 5 : 3, v/v). Development distance, 13 cm; saturated chamber.

Table 29 Resolution data for enantiomers of amino acids from brucine-impregnated plates

Sl. no.	D-L-amino acid	hR_F pure L	D	L
1.	Alanine	53	18	53
2.	γ -Aminobutyric acid			
3.	Isoleucine	35	16	35
4.	DOPA			
5.	Leucine			
6.	Methionine	29	18	29
7.	Norleucine			
8.	Phenylalanine	40	27	40
9.	Serine	50	12	50
10.	Threonine	29	16	29
11.	Tryptophan	31	17	31
12.	Tyrosine	29	22	29

Silica plates impregnated with (–)-brucine, developed in *n*-butanol–acetic acid–chloroform (3 : 1 : 4, v/v), up to 10 cm.

nitrile (70 : 30) is added to give a final acetonitrile concentration of 38% or 47%. For the second dimension, the mobile phase is 8 mol L^{–1} N,N-di-*n*-propyl-L-alanine and 4 mmol L^{–1} copper(II) acetate dissolved in 0.3 mol L^{–1} sodium acetate in H₂O–acetonitrile (70 : 30, pH 7); the plates are developed in the second dimension using a temperature gradient. The method is reported to be applicable to the resolution of amino acids in a protein hydrolysate with quantitation by densitometry.

β -Cyclodextrin (β -CD) plates have been used successfully for the resolution of enantiomers of dansyl amino acids and β -naphthylamide amino acids. The plates are prepared by mixing 1.5 g of β -CD bonded silica gel in 15 mL of 50% methanol (aqueous) with 0.002 g of binder and acetate in 50/50 MeOH–1% aqueous triethyl ammonium acetate (pH 4.1). Some of the results are shown in Table 31.

Table 30 hR_F of pure and resolved enantiomers of PTH amino acids, for tartaric acid-impregnated plate

D,L Mixture of PTH amino acids	hR_F of pure L	D (resolved)	L (resolved)
Met	83	18	83
Phe	85	15	85
Try	95		95
Val	80	21	80
Ile	92	15	92
Tyr	95	16	95
Thr	85	30	85
Ala	55	12	55
Ser	84	10	84

Solvent, chloroform–ethyl acetate–water (28 : 1 : 1, v/v). Development time, 35 min, solvent front, 10 cm, room temperature, 25 ± 1°C. Impregnation with (+)-ascorbic acid resolved D,L mixtures of PTH-Met, Phe, Val, Ala, Ser.

A macrocyclic antibiotic, vancomycin, has been used as a chiral mobile-phase additive for the separation of 6-aminoquinolyl-*N*-hydroxy succinimidyl carbamate (AQC) derivatized amino acids and dansyl amino acids on chemically bonded diphenyl-Freversed-phase plates. Both the nature of stationary phase and the composition of the mobile phase have a strong influence on the enantiomeric resolution; typical results are given in Table 32. Another macrocyclic antibiotic, erythromycin, has been used as a chiral impregnating reagent for the resolution of 10 dansyl-DL-amino acids on silica gel plates (Figure 2); hR_F values and solvent combinations are shown in Table 33. Resolution of dansyl-DL-amino acids has recently been reported (Table 34) on thin silica gel plates impregnated with (1*R*, 3*R*, 5*R*)-azabicyclo[3,3,0]octan-3-carboxylic acid, which is an industrial waste material and a proline analogue non-proteinogenic α -amino acid.

Quantitation

TLC is supplemented with spectrophotometric methods for the quantitation of amino acids and their PTH and DNP derivatives.

Amino Acids

The scraped layer corresponding to each spot is extracted with 70% ethanol in a known minimum volume, and ninhydrin reaction is performed followed by spectrophotometry. Six to eight standard dilutions in an appropriate concentration range for each amino acid are prepared; 2 mL of amino acid solution and 2 mL of buffered ninhydrin are mixed in a test tube, heated in a boiling-water bath for 15 min, cooled to room temperature and 3 mL of 50% ethanol is added. The extinction is read at 570 nm (or 440 nm for proline) after 10 min. Standard plots of concentration versus absorbance are drawn for each amino acid. Materials consist of standard solutions of amino acids, acetate buffer (4 mol L^{–1}, pH 5.5), ethanol (50%), methyl cellosolve (ethylene glycol monomethyl ether), and ninhydrin reagent (0.9 g ninhydrin and 0.12 g hydrantin dissolved in 30 mL methyl cellosolve and 10 mL acetate buffer, freshly prepared). The concentration of the unknown sample is read from the standard plots. TLC densitometry can be used to determine 0.5 mg L^{–1} of phenylalanine in blood as an indicator of phenylketonuria.

PTH Amino Acids

The quantitation of PTH amino acids is carried out *in situ* or after elution. For *in situ* determination, the fluorescence-quenching areas of PTH derivatives are usually measured against the fluorescent background

Table 31 Separation data for enantiomeric compounds on β -CD-bonded-phase plates

Compound, D,L mixture	R _F		Mobile phase ^a	Detection method
	D	L		
Dns-leucine	0.49	0.66	40/66	Fluorescence
Dns-methionine	0.28	0.43	25/75	Fluorescence
Dns-alanine	0.25	0.33	25/75	Fluorescence
Dns-valine	0.31	0.42	25/75	Fluorescence
Alanine- β -naphthylamide	0.16	0.25	30/70	Ninhydrin
Methionine- β -naphthylamide	0.16	0.24	30/70	Ninhydrin

^aVolume ratio of methanol to 1% triethylammonium acetate (pH 4.1).

at 254 nm. While using a Turner fluorometer fitted with a door for scanning chromatoplates, the position of the scanner, the standardization of time between scanning and the end of chromatography, the loading volume, the developing distance and the layer thickness are the important influencing factors for reproducibility. The quantitation of PTH amino acids is also carried out by measuring their UV absorbance after they have been eluted from the layer. The scraped layer is extracted with methanol overnight, centrifuged for 30 min at 300 rpm, and the spectra of the extracts are recorded in the range from 320 nm to about 230 nm. To obtain reproducible UV absorbances the layers must be washed with methanol prior to development, and with chloroform after the separ-

ation has been carried out. The quantitation of PTH amino acids has also been practised as follows: the developed chromatograms are exposed to iodine vapours and the brownish spots scraped off, eluted with 95% ethanol or ethyl acetate, and the iodine removed by warming the sample tubes in a warm-water bath. The optical densities are read at 269 and 245 nm, appropriate blank determinations are carried out, standard plots are drawn, and the concentration of the unknown sample is calculated.

Table 32 RP-TLC enantiomeric separation using vancomycin as chiral mobile-phase additive

Compound	hR _F		Vancomycin concentration (mol L ⁻¹)
	L	D	
AQC-allo- <i>iso</i> -leucine	14	21	0.025
AQC-methionine	19	23	0.025
AQC- <i>nor</i> -leucine	13	16	0.025
AQC- <i>nor</i> -valine	21	25	0.025
AQC-valine	23	27	0.025
Dansyl-glumatic acid	21	23	0.04
Dansyl-leucine	03	09	0.04
Dansyl-methionine	05	12	0.04
Dansyl- <i>nor</i> -leucine	03	07	0.04
Dansyl- <i>nor</i> -valine	05	12	0.04
Dansyl-phenylalanine	03	05	0.04
Dansyl-serine	15	20	0.04
Dansyl-threonine	13	17	0.05
Dansyl-tryptophan	01	03	0.04
Dansyl-valine	06	10	0.04

Mobile phase, acetonitrile–0.6 mol L⁻¹ NaCl (2 : 10). Plates developed at room temperature (22°C) in cylindrical glass chambers. Time, 1–3 h for 5 × 20 cm plates. Visualization, UV. AQC, 6-Aminoquinolyl-*N*-hydroxysuccinimidyl carbamate, a fluorescent tagging agent; reaction mixture of AQC and amino acid was used without purifying the derivatives.



Figure 2 Chromatogram showing resolution of Dns-DL-phenylalanine, valine and leucine. From left to right: 1, Dns-DL-phenylalanine; 2, Dns-L-phenylalanine; 3, Dns-DL-valine; 4, Dns-L-valine; 5, Dns-DL-leucine; 6, Dns-L-leucine. Developing solvent, aq. 0.5 mol L⁻¹ sodium chloride + acetonitrile (15 + 1). Developing time 20–25 min. Detection 254 nm.

Table 33 hR_F Values of enantiomers of dansyl amino acids resolved on plates with erythromycin

Dansyl DL-amino acid	Pure L	hR_F from DL mixture		Solvent system 0.5 mol L ⁻¹ aq. NaCl-MeCN-MeOH (v/v)
		D	L	
Serine	64	68	64	10 : 4 : 1
	30	36	30	15 : 1 : 1
Glutamic acid	45	56	45	22 : 1 : 0.5
	56	65	56	22 : 1 : 0
	52	59	52	26 : 1 : 0
Phenylalanine	50	65	50	15 : 2 : 0
	20	27	20	15 : 1 : 0
Valine	22	30	22	15 : 1 : 0
Leucine	24	32	24	15 : 1 : 0
Tryptophan	38	47	38	18 : 1 : 0.25
Methionine	56	63	56	25 : 2 : 0.5
Aspartic acid	50	63	50	28 : 1.5 : 0.5
α -Amino- <i>n</i> -butyric acid	42	51	42	12 : 1 : 0
Norleucine	63	71	63	16 : 1 : 0 : 0.4 HOAc

Temperature $25 \pm 2^\circ\text{C}$. Solvent front, 10 cm. Time, 20–25 min. Visualization, UV, 254 nm.

DNP Amino Acids

Use of direct fluorimetric quantitation (fluorescence quenching) *in situ* has been recommended. Silica gel G plates are developed in chloroform–benzyl alcohol–acetic acid (70 : 30 : 3 v/v) and *n*-propanol–ammonia (7 : 3 v/v) and polyamide plates are developed in benzene–acetic acid (4 : 1 v/v). The spots are scanned using a Camag/Turner scanner, after being dried in a stream of air, at the scanning speed of 20 mm min⁻¹ and an excitation wavelength of 254 nm. Alternatively, the layer is scraped off the plate and extracted for 5 min, with 1 mL 0.05 mol L⁻¹ Tris buffer, pH 8.6, at room temperature. Then the slurry is removed by centrifugation and the clear liquid is

evaluated by measuring the optical density at 360 nm or at 385 nm for DNP proline. For a blank, a similar extract is obtained from a clear spot on the same layer.

Future Developments

TLC and HPLC are often looked at as competitive methods, but each has its own advantages. In HPLC, finding suitable separation parameters is frequently costly in terms of time and materials; therefore, a combination of the two by first optimizing the particular separation parameter with TLC is a step leading to considerable time-saving and cost for an analysis. TLC is suitable as a pilot technique for the

Table 34 Results from resolution of dansyl DL-amino acids

Dansyl DL-amino acid	Pure L	hR_F from DL mixture		Solvent system 0.5 mol L ⁻¹ aq. NaCl-MeCN (v/v)
		D	L	
Phenylalanine	50	65	50	15 + 2
Valine	38	49	38	15 + 1.5
Tryptophan	23	34	23	20 + 0.5
Aspartic acid	55	67	55	15 + 2
	61	70	61	18 + 2
	52	60	52	15 + 1
	30	52	30	20 + 0.5
Leucine	64	68	64	10 + 4 + 1 MeOH
				9 + 3 + 0.5 MeOH
Norvaline	56	61	56	17 + 2 + 0.4 MeOH
				16 + 2 + 0.25 MeOH

Temperature $25 \pm 2^\circ\text{C}$. Solvent front, 10 cm. Time, 25–30 min. Visualization UV, 254 nm.

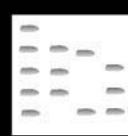
investigation of appropriate separation conditions, particularly because with TLC various phase systems can be checked at the same time without expensive apparatus. TLC will continue to serve as a useful method for daily routine control analyses to identify and determine the purity of a variety of compounds, including enantiomers, with ease and speed, and can be readily modified for new situations. A wide choice for separation conditions will always be available as various phase systems can be checked simultaneously.

Further Reading

- Bhushan R and Martens J (1996) Amino acids and derivatives. In: Sherma J and Fried B (eds) *Handbook of Thin Layer Chromatography*, 2nd edn. New York: Marcel Dekker.
- Bhushan R and Martens J (1997) Direct resolution of enantiomers by impregnated TLC. *Biomedical Chromatography* 11: 280.

- Bhushan R and Reddy GP (1987) TLC of phenylthiohydantoins of amino acids: a review. *Journal of Liquid Chromatography* 10: 3497.
- Bhushan R and Reddy GP (1989) TLC of DNP- and dansyl-amino acids: a review. *Biomedical Chromatography* 3: 233.
- Grassini-Straza G, Carunchio V and Girelli M (1989) Flat bed chromatography on impregnated layers: review. *Journal of Chromatography* 466: 1–35.
- Günther K, Matrens J and Schickendanz M (1984) TLC enantiomeric resolution via ligand exchange. *Angewante Chemie International Edition in English*. 23: 506.
- Kirchner JG (1978) *Thin Layer Chromatography*, 2nd edn. New York: John Wiley.
- Rosmus J and Deyl Z (1972) Chromatography of N-terminal amino acids and derivatives. *Journal of Chromatography* 70: 221.
- Sherma J (1976 to 1996) Thin Layer Chromatography or Planar Chromatography: Review every two years. *Analytical Chemistry*. Washington, DC: American Chemical Society.

AMINO ACIDS AND DERIVATIVES: CHIRAL SEPARATIONS



I. D. Wilson, AstraZeneca Pharmaceuticals,
Macclesfield, UK
R. P. W. Scott, Avon, CT, USA

Copyright © 2000 Academic Press

Introduction

It is an interesting feature of life that in general its building blocks, whilst often containing chiral centres, are generally composed from optically pure single enantiomers. An excellent, and well known, example of this is provided by the amino acids as those found in mammals are all of the L-form. This being the case, why is there a need to resolve the enantiomers of amino acids?

The chiral separation of amino acids is important for a number of reasons. Perhaps the major reason for the pharmaceutical industry is the need for optically pure amino acids, of the required configuration, in order to prepare synthetic peptides, both for testing and as potential new drugs. In this case methods are needed to determine optical purity, and measure amounts of the unwanted enantiomer at the 0.1% level and for large-scale isolation for subsequent synthetic work. Another pharmaceutical example is provided by the sulphhydryl drug penicillamine where the

D-enantiomer is used to treat arthritis but the L-form is highly toxic, and the optical purity of the drug therefore clearly becomes an issue.

Another interesting reason for wishing to examine the ratio of different amino acid enantiomers is that, as a result of their slow racemization with time, it provides another means of dating archaeological samples. Other applications include the determination of the nature of the amino acids found in microbial peptides and polypeptides where D amino acids are not uncommon (e.g. as constituents of certain antibiotics).

Chiral separations involve the resolution of individual enantiomers that are chemically identical and only differ in the spatial distribution of their individual atoms or groups. As each isomer will contain the same interactive groups, the intermolecular forces involved in their retention will also be the same. Consequently, unless a second retention mechanism is invoked, in addition to those involving intermolecular forces, both enantiomers will exhibit identical retention times on all stationary phases and remain unresolved. A variety of chromatographic separation strategies have been developed to obtain the resolution of amino acids. These include gas, thin-layer and column liquid approaches. In the case of liquid chromatography these methods have

included enantiomer separation via chiral stationary phases (CSPs; for a detailed treatment of the various stationary phase types the reader is directed to the Further Reading and relevant encyclopaedia entries), chiral mobile phases (generated by the addition of a chiral selector to the eluent) or derivatization with a chiral reagent to form diastereoisomers. The methodology used will depend to a large extent on the problem to be solved (e.g. analysis or preparative isolation) and each of these methodologies for amino acids are detailed below.

Derivatization of Amino Acids to Form Diastereoisomers

One of the earliest strategies to be implemented for the separation of amino acid is the formation of diastereoisomeric derivatives using an optically pure chiral derivatizing reagent. These can then be separated relatively easily on conventional stationary phases with achiral eluents. The major difficulty with this approach is ensuring that the reagent is indeed 100% optically pure and that racemization (of either reagent or amino acid) does not occur during the derivatization reaction. Clearly, if attempting to determine optical purity at the 0.1% level, even a 99.9% pure reagent is not sufficient. However, if these conditions can be met, the methodology is easy and robust. A huge range of chiral derivatizing reagents have been prepared and many of these can be used for amino acids. These applications would include the use of, for example, substances such as Marfey's reagent (1-fluoro-2,4-dinitrophenyl-5-L-alanine amide), 2,3,4,6-tetra-O-acetyl-D-glucopyranosyl isocyanate (GITC) and similar compounds, or the fluorescent 1-(9-fluorenyl)ethylchloroformate (FLEC). In addition, it is possible to form highly fluorescent diastereoisomeric isoindoles from amino acids using O-phthalaldehyde and a chiral thiol. Whilst these examples are among the most common chiral derivatizing reagents, there are many others.

Chiral Selectors in the Mobile Phase

An alternative to forming covalent derivatives is to employ chiral mobile phase additives that will act as chiral selectors interacting selectively with the different enantiomers of the amino acids to effect a separation.

For amino acids, separation by chiral ligand exchange has been of considerable importance. In this context a chiral mobile phase can be generated by adding a chiral selector such as L-proline (or another amino acid such as L-arginine, L-histidine or substances such as *N,N*-di-isopropyl-L-alanine or *N*-(*p*-tol-

uenesulfonyl)-L-phenylalanine, etc.) and copper(II) ions to an aqueous/organic solvent. Factors which affect the complex formation include the metal (as indicated above, this is usually copper but zinc, nickel and mercury have also been used albeit with inferior resolution), the metal ion/ligand ratio (usually 2 : 1), the concentration of the metal/ligand complex and pH. For practical applications the pH of the mobile phase would normally be recommended to be in the range of 7–8 in order to be able to carry out chromatography on conventional reversed-phase columns (this pH preserves the integrity of the columns and higher pH values cause the precipitation of the copper complexes).

As well as chiral ligand exchange, some use has been made of the ability of the cyclodextrins to form inclusion complexes with amino acid derivatives. The cyclodextrins are produced by the partial degradation of starch followed by the enzymatic coupling of the glucose units into crystalline, homogeneous toroidal structures of different molecular size. The three most widely characterized are the α -, β - and γ -cyclodextrins which contain six (cyclohexamylose), seven (cycloheptamylose) and eight (cyclo-octamylose) glucose units, respectively. These cyclic, chiral, torus-shaped macromolecules contain the D(+)-glucose residues bonded through α -(1 \rightarrow 4) glycosidic linkages. The mouth of the torus-shaped cyclodextrin molecule has a larger circumference than at the base and is linked to secondary hydroxyl groups of the C2 and C3 atoms of each glucose unit. The cyclodextrins provide a ubiquitous means of separating enantiomers either as mobile-phase additives or when used to make chiral stationary phases (see below) and an example of this would be the use of β -cyclodextrin as chiral mobile phase additive for the resolution of dansylated amino acids on a conventional reversed-phase column (C_8).

Chiral Stationary Phases for the Separation of Amino Acid Enantiomers and their Derivatives

There are a number of types of chiral stationary phase that are used for the separation of amino acids and their derivatives and these include ligand exchange phases, protein-based phases, the Pirkle-type phases, molecular imprints, coated cellulose and amylose derivatives, macrocyclic glycopeptide phases, and cyclodextrin-based CSPs.

Amino Acid Enantioseparation via Chiral Ligand Exchange Phases

The separation of amino acids on chiral ligand exchange columns represents one of the earliest

methods for the resolution of these compounds, both free and as derivatives (e.g. dansylated). The original work was performed by Rogozhin and Davankov using resins containing optically active bi- and trifunctional α -amino acids loaded with a metal ion such as copper(II). More recently, more efficient columns have been prepared by bonding chiral amino acid ligands to silica gel. It is also the case that by using a long-chain alkyl-substituted chiral selector such as *N*-decyl-1-histidine to the mobile phase a 'dynamically coated' CSP can be prepared from a normal reversed-phase column. In such cases it is still necessary to continue to supply a small amount of the chiral selector in the mobile phase to ensure that the ligand leached from the stationary phase is constantly topped up. As with ligand exchangers used as mobile phase additives, the mechanism of retention involves the formation of complexes between the ligand (generally based on L-proline), a metal ion (usually copper(II)) and the amino acid itself. Separations are made using reversed-phase types of eluents. Because of the ease of use of ligand exchange chromatography with chiral mobile phases on standard reversed-phase columns, these may be more useful than dedicated stationary phases.

Amino Acid Enantioseparation via Protein-Based Stationary Phases

The protein-bonded stationary phases were some of the first to be developed and usually consist of natural proteins (e.g. bovine serum albumin, α_1 -acid glycoprotein, ovomucoid, etc.) bonded to a silica matrix. Proteins contain a large number of chiral centres of one configuration and are known to interact strongly with small chiral compounds for which they can exhibit strong enantiomeric selectivity. Some specific interactive sites on the protein provide the chiral selectivity, but there are many others that generally contribute to retention. Protein columns based on bovine serum albumin have been employed for the separation of the enantiomers of certain aromatic amino acids and various derivatives, including dansyl, *N*-(9-fluorenylmethoxycarbonyl)- (Fmoc), *N*-(fluorescein thiocarbamoyl)- (FITC) *N*-(2,4-dinitrophenyl) and *N*-benzoyl. The use of the reagent *N*-(chloroformyl)carbazole to provide highly fluorescent derivatives has enabled the resolution of the enantiomers of all of the protein amino acids often with high separation factors. Proteins have also been described as showing remarkable enantioselectivity towards *N*-acylated amino acids.

The mobile phases employed for this type CSP are generally composed of phosphate buffers (0.1–0.2 M) modified with a limited amount of propan-1-ol. The pH range normally employed is be-

tween 4.5 and 8.0 and for example, in the case of the *N*-benzoyl-derivatized amino acids, increasing pH results in decreased retention. In general the lower the buffer concentration (from 0 to 0.1 M) the better the retention; however, an effect of increased buffer concentration (above 0.2 M) has been observed for *N*-benzoyl derivatives. An increase in organic modifier concentration reduces the hydrophobic interactions of the solutes with the column resulting in shorter retention times. Whilst very useful for the determination of, for example, enantiomeric purity, protein phases tend to have rather limited sample loading capacity.

The Pirkle-Type Stationary Phases

The so-called Pirkle stationary phases (named after their inventor W. M. Pirkle) consist of relatively small molecular weight chiral substances covalently bonded to silica. Each bonded moiety contains a limited number of chiral sites (sometimes only one). Nevertheless, on account of their small size, there will be a larger number of interactive groups bonded to the silica and thus the probability of the solute interacting with a chiral centre is still very high. In addition, as the interacting molecule is relatively small, the extra-chiral contributions to retention are also comparatively small, and consequently the chiral interactions themselves represent a higher proportion of the total. It follows that chiral selectivity becomes a more dominant factor controlling retention with the Pirkle phases.

The Pirkle phases have also been used very successfully for the separation of many free and derivatized amino acids. The separation of the *p*-bromophenyl derivatives of the enantiomers of a number of amino acids is shown in Figure 1. The stationary phase was a naphthyl urea Pirkle stationary phase multiply-bonded to the silica. All of the enantiomers were separated and the analysis time was less than 50 min. Elution was achieved by progressively increasing the dispersive character of the mobile phase. Consequently, the chiral selectivity was probably dominated by polar interactions.

Amino Acid Enantioseparation via Coated Cellulose and Amylose Derivatives

Another useful type of chiral stationary phase for amino acids and their derivatives is based on the polymers of cellulose and amylose. Usually the polymers are derivatized to increase chiral selectivity or improve stability. The derivatized cellulose or amylose polymer is coated (not bonded) to a silica support. The fact that the chiral material is not bonded to the silica makes the material somewhat labile with respect to certain solvents.

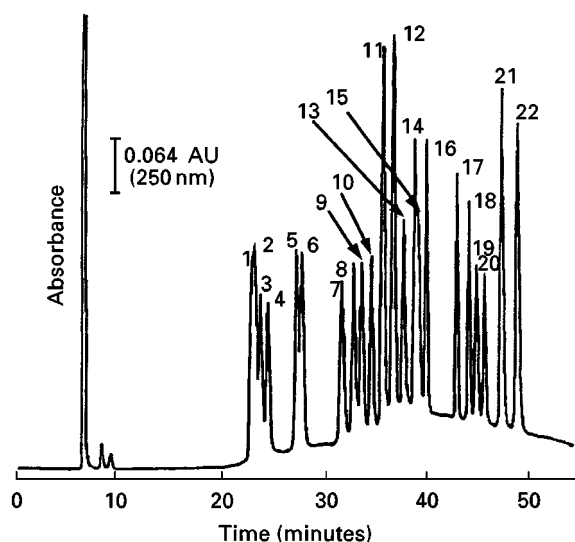


Figure 1 The separation of a series of amino acid derivatives. The column was 10-cm long, 6 mm i.d. One mobile phase component (A) was 50 mM phosphate buffer (pH 6.0) and the second component (B) pure acetonitrile. The gradient used was isocratic for 12 min 30% (B), then programmed from 12 to 29 min from 30% (B) to 47% (B), then from 29 to 49 min 47–67% (B) and, finally, from 49 to 57 min, 67–93% (B). The flow rate was 1 mL min⁻¹. 1, L-serine; 2, D-serine; 3, L-threonine; 4, D-threonine; 5, L-alanine; 6, D-alanine; 7, L-valine; 8, D-valine; 9, L-methionine; 10, D-methionine; 11, L-leucine and isoleucine; 12, D-leucine and isoleucine; 13, L-tyrosine; 14, L-phenylalanine; 15, D-tyrosine; 16, D-phenylalanine; 17, L-tryptophan; 18, D-tryptophan; 19, L-lysine; 20, D-lysine; 21, L-cystine; 22, D-cystine. (Courtesy of Iwaki K, Yoshida S, Nimura N and Kinoshita T (1987) Optical resolution of enantiomeric amino acid derivatives on a naphthylethylurea multiple-bonded chiral stationary phase prepared via an activated carbamate intermediate. *Journal of Chromatography* 404: 117–122.)

Both cellulose and amylose contain five chiral centres per unit and thus the polymeric material offers a large number of chirally interactive centres and high probability of interaction. There are basically two common types of cellulose and amylose derivatives that are used as stationary phases. The first type are simple esters usually formed from the acid chlorides such as acetyl chloride or benzoyl chloride. The more stable, and probably the more popular derivatives, are the carbamates which can be synthesized from the appropriate isocyanate. The most useful cellulose- and amylose-based chiral stationary phases are probably those derivatized with the different substituted tris(3,5-dimethylphenylcarbamates). An example of the separation of *N*-benzyloxycarbonyl alanine ethyl esters on cellulose tris(3,5-dimethylphenylcarbamate) is shown in Figure 2.

The column was 25-cm long, 4.6-mm i.d., and the mobile phase was hexane–2-propanol (90 : 10 v/v). The stationary phase was operated in the normal

phase mode, consequently, retention and selectivity was again controlled by differential polar interactions.

Amino Acid Enantioseparation via Macrocyclic Glycopeptide Stationary Phases

There are three commonly used macrocyclic glycopeptides and they are the antibiotics vancomycin, teicoplanin and avoparcin all of which were introduced as chiral stationary phases by Armstrong. They contain a large number of chiral centres, together with molecular cavities in which solute molecules can enter and interact with neighbouring groups. Vancomycin, for example, contains 18 chiral centres surrounding three ‘pockets’ or ‘cavities’ which are bridged by five aromatic rings. Strong polar groups are proximate to the ring structures that can offer strong polar interactions with the solutes. This type of stationary phase is stable in mobile phases containing 100% organic solvent.

The macrocyclic glycopeptides have a higher loading capacity than the traditional protein phases and are more stable. They can also tolerate a much wider range of solvents than the cellulose and amylose phases.

The macrocyclic glycopeptide stationary phases can also be used very effectively for the separation of amino acids and their derivatives. The separation of the isomeric bromophenylalanines as their Fmoc derivatives formed by reacting them with 9-fluorinylmethylchloroformate is shown in Figure 3. The two enantiomers are very well separated indicating that the chiral selectivity of the teicoplanin stationary phase was extremely high. It should be noted, that the ‘pure’ (*S*) enantiomer actually contained a significant amount of the (*R*) enantiomer. The macrocyclic glycopeptide stationary phases often exhibit high selectivity for chiral substances of biological origin, perhaps due to their being biological products themselves.

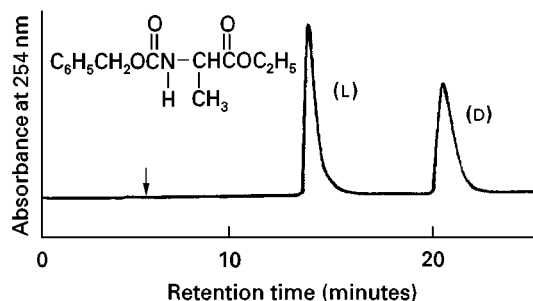


Figure 2 The separation of *N*-benzyloxycarbonyl alanine ethyl ester on cellulose tris(3,5-dimethylphenylcarbamate).

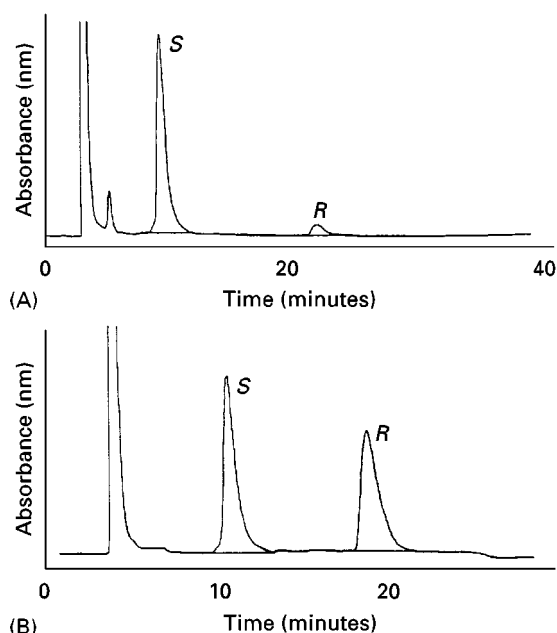


Figure 3 The separation of the enantiomers of 2-bromophenylalanine and 3-bromophenylalanine. (A) A 'pure' sample of the *S* enantiomer of Fmoc 2-bromophenyl alanine. (B) A racemic mixture of Fmoc 3-bromophenylalanine. The separation was carried out on a CHIROBOTIC T (teicoplanin) column, 25-cm long, 4.6-mm i.d., packed with 5 μ m particles. The mobile phase was programmed from methanol–1% triethylamine acetate (pH 4.5) (40 : 60 v/v) to methanol–1% triethylamine acetate (pH 4.5) (60 : 40 v/v) over 20 min. The flow rate was 1.0 mL min⁻¹ and the sample was injected as a solution in acetone. (Courtesy of Chirotech Technology Ltd.)

Amino Acid Enantioseparation via Cyclodextrin-Based Chiral Stationary Phases

In addition to the use of cyclodextrins as mobile phase additives discussed above, they have also been widely used for the preparation of CSPs. For this the three cyclodextrins, α , β and γ are bonded to a suitable support such as silica. An example of their use for the separation of three racemic *N*-*t*-Boc-amino acids is shown in Figure 4. It is seen that a very clean separation of the enantiomers is obtained. Other examples include the use of β -cyclodextrin columns for the resolution of dansylated amino acid derivatives and α -cyclodextrin columns for the separation of a variety of natural and synthetic amino acids and their derivatives.

Amino Acid Derivative Enantioseparation via Molecular Imprints

Molecular imprinted polymers (MIPs) are produced by preparing a polymer (usually prepared from a methacrylic acid, styrene or 4-vinylpyridine monomer template cross-linked with ethylenedimethylmethacrylate) in the presence of an imprint, or template, molecule. When the template is subsequently

removed it leaves a cavity capable of 'recognizing' and selectively rebinding the imprinted compound. This property allows discrimination between enantiomers and has been used as the basis for the development of CSPs for the highly selective separation of amino acid derivatives (e.g. dansyl, anilide, BOC-1-amino acid anilides, etc.) and a number of examples of this type of separation have been published. A typical example would be the use of a molecular imprint to the amino acid derivative L-phenylalanine anilide for the resolution of a mixture of the two enantiomers of the print molecule. In this case the more retained enantiomer is the L-form of the amino acid derivative as it exhibits a greater affinity for the stationary phase. In general the imprinted polymers are most selective for the particular print molecule used to prepare them. However, there are examples of the separation of enantiomers of non-imprint molecules as well.

Conclusions

As shown above there are various means for separating the enantiomers of amino acids and their

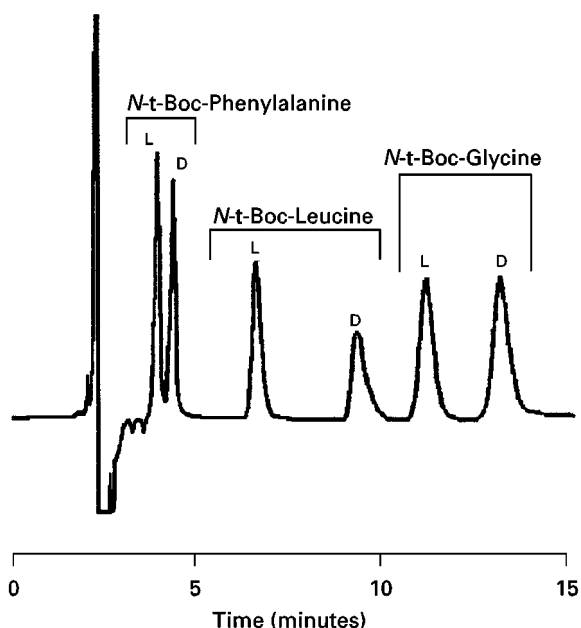


Figure 4 The separation of the enantiomers of three *N*-*t*-Boc-amino acids. The column used was 25-cm long packed with Cyclobond 1 RSP and operated at a mobile phase flow rate of 1.0 mL min⁻¹ at a temperature of -220°C . The mobile phase was 7% v/v acetonitrile–93% v/v% buffer (1% triethylamine, pH 7.1) and the separation was monitored with a UV detector at 225 nm. (Courtesy of San Chung Chang, Wang LR and Armstrong DW (1992) Facile resolution of *N*-tert-butoxycarbonyl amino acids: the importance of enantiomeric purity in peptide synthesis, *Journal of Liquid Chromatography* 15: 1411–1429.)

derivatives. These range from indirect methods such as the formation of diastereoisomeric derivatives or direct methods that exploit the spatial characteristics of different enantiomers by making them interact with a chiral stationary or mobile phase. This selectively enhances the standard free entropy of distribution of one amino acid enantiomer compared to the other and can provide adequate chiral selectivity to permit enantiomeric resolution. By one or other of these approaches the separation of the enantiomers of the majority of naturally occurring amino acids can be achieved by liquid chromatography.

See also: II/Chromatography: Liquid: Derivatization. III/Chiral Separations: Capillary Electrophoresis; Cellulose and Cellulose Derived Phases; Chiral Derivatization; Countercurrent Chromatography; Crystallization; Cyclodextrins and Other Inclusion Complexation Approaches; Gas Chromatography; Ion-Pair Chromatography; Ligand Exchange Chromatography; Liquid Chromatography; Molecular Imprints as Stationary Phases; Protein Stationary Phases; Synthetic Multiple Interaction ('Pirkle') Stationary Phases; Supercritical Fluid Chromatography; Thin-Layer (Planar) Chromatography.

Further Reading

- Ahnoff M and Einarsson S (1989) Chiral derivatisation. In: J Lough (ed.) *Chiral Liquid Chromatography*, pp. 39–80. Glasgow: Blackie.
- Allenmark S, Bromgren B and Boren B (1984) Direct liquid chromatographic separation of enantiomers on immobilized protein stationary phases. IV. Molecular interaction forces and retention behaviour in chromatography on bovine serum albumin as a stationary phase. *Journal of Chromatography* 316: 617–624.
- Allenmark S (1991) *Chromatographic Enantioseparation: Methods and Applications*, 2nd edn. Chichester: Ellis Horwood.
- Armstrong DW, Li W and Chang CD (1990) Polar-liquid, derivatised cyclodextrin stationary phases for the capillary gas chromatography separation of enantiomers. *Analytical Chemistry* 62: 914–923.
- Armstrong DW, Tang Y, Chen S, Zhou Y, Bagwill C and Chen JR (1994) Macrocyclic antibiotics as a new class of chiral selectors for liquid chromatography. *Analytical Chemistry* 66: 1473–1484.
- Beesley TE and Scott RPW (1998) *Chiral Chromatography*. New York: John Wiley.
- Iwaki K, Yoshida S, Nimura N and Kinoshita T (1987) Optical resolution of enantiomeric amino acid derivatives on a naphthylethylurea multiple-bonded chiral stationary phase prepared via an activated carbamate intermediate. *Journal of Chromatography* 404: 117–122.
- Kempe M and Mosbach K (1995) Separation of amino acids, peptides and proteins on molecularly imprinted stationary phases. *Journal of Chromatography A* 691: 317–323.
- Lam S (1989) Chiral ligand exchange chromatography. In: Lough J (ed.) *Chiral Liquid Chromatography*, pp. 83–101. Glasgow: Blackie.
- Okamoto Y (1986) Optical resolution of β -blockers by HPLC on cellulose triphenylcarbamate derivative. *Chemical Letters* 1237–1240.
- Okamoto Y, Kaida Y, Aburantani R and Hatada K (1989) Optical resolution of amino acid derivatives by high-performance liquid chromatography on tris(phenylcarbamate)s of cellulose. *Journal of Chromatography* 477: 367–376.
- Pirkle WH and House DW (1979) Chiral high pressure liquid chromatographic stationary phases. 1. Separation of the enantiomers of sulfoxides, amines, amino acids, alcohols, hydroxyacids, lactones and mercaptans. *Journal of Organic Chemistry* 44: 1957–1960.
- San Chun Chang, Wang LR and Armstrong DW (1992) Facile resolution of *N*-tert-butoxycarbonyl amino acids: the importance of enantiomeric purity in peptide synthesis. *Journal of Liquid Chromatography* 15: 1411–1429.
- Skidmore MW (1993) Derivatization for chromatographic resolution of optically active compounds. In: Blau K and Halket J (eds) *Handbook of Derivatives for Chromatography*, 2nd edn., pp. 215–252. Chichester: John Wiley.

AMINO ACIDS AND PEPTIDES: CAPILLARY ELECTROPHORESIS

+



-

P. Bohn, Institut für Instrumentelle Analytik/
Umweltanalytik, Universität des Saarlandes,
Saarbrücken, Germany

Copyright © 2000 Academic Press

Introduction

Advancement in modern biotechnology is mainly attributed to a detailed understanding of the structural features of proteins. This is predominantly accom-

plished by sequencing techniques and the analysis of amino acid composition. Irregularities in the structural characteristics of proteins, e.g. after translation of the protein, are determined by fragmentation to smaller peptides. Progress in the field of synthetic peptides utilizing synthesis based on these partial sequences depends on their immunological potential. The design of new specialized biomolecules such as hormones or neurotransmitters will have considerable pharmaceutical applications.

The large number of analytes and the small quantities present in biological samples have increased the demand for specific and sensitive analytical techniques. Capillary electrophoresis (CE) is capable of handling small sample volumes down to microlitre size with only a few nanolitres injected. High efficiencies, short analysis time and easy enantiomeric assays make CE an indispensable tool in the modern analysis of peptides and amino acids.

Amino Acids

Physicochemical Properties

In choosing an electrophoretic system it is important to consider both matrix and the structural features of the analytes. Whereas 18 amino acids are found after the hydrolysis of proteins, more than 50 derivatives are present in physiological fluids.

Amino acids are small, highly polar species. The individual species only differ in the residues *R*. Except for glycine this situation induces a chiral centre at the α -C-atom where two enantiomers (*R*-, *S*-) can be distinguished. Classifying these residues *R* by their impact on electrophoretic behaviour means a differentiation by their polarity or the generation of charge. Due to their zwitterionic nature, amino acids possess isoelectric points (pI); pH values equal to pI yield molecules without net charge and therefore no migration occurs in an electrical field. At pH values above the pI the molecules are negatively charged and migrate against the electroosmotic flow (EOF) towards

the anode, whereas lower pH values induce cations which migrate with the EOF towards the cathode.

Most amino acids lack suitable physical characteristics that can be exploited for detection. Only few species possess aromatic groups with high absorptivity, e.g. try, phe and tyr. In order to analyse native amino acids three strategies can be pursued. UV detection can be used at low wavelengths. A second approach is the application of indirect detection techniques. Detection concepts involving derivatization technology, especially fluorescence labelling, can also improve detection sensitivity.

Electrophoretic Systems – Separation Strategies

Analysis of native amino acids Direct UV detection at wavelengths below 220 nm takes advantage of the absorptivity of the carbonyl bond. Detection at such nonspecific wavelengths requires highly transparent buffers. Borate and phosphate are convenient electrolyte systems. Selectivity is mainly achieved by the optimization of pH because the analysis is performed with the native species.

In order to obtain cationic analytes, pH has to be adjusted to values lower than the first dissociation step ($pK \sim 2$). The stability of fused-silica capillaries is restricted to pH values above 2.5. Thus basic conditions with analytes migrating counter to the EOF are preferred. This separation mode benefits by prolonging the effective separation distance, keeping the electrical field strength constant so that higher resolution is achieved. Limits of detection are in the range of about $10^{-4} \text{ mol L}^{-1}$ (Figure 1).

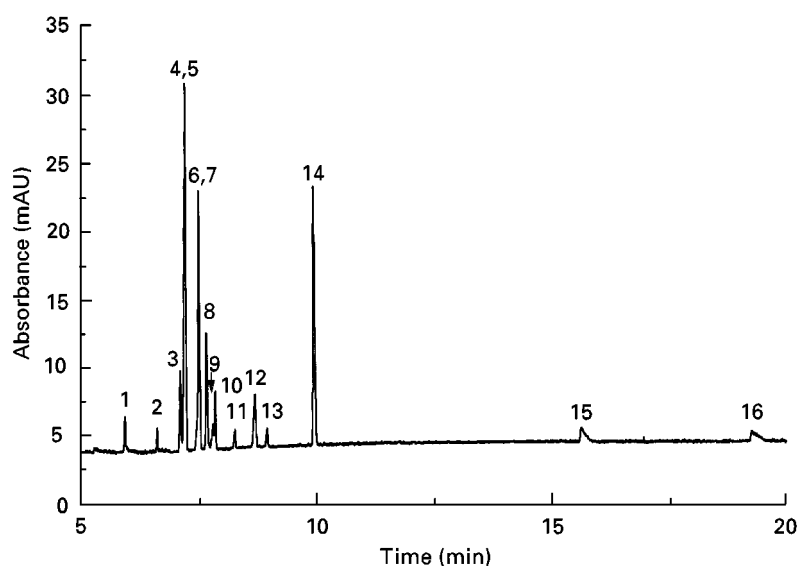


Figure 1 Separation of amino acids and dipeptides in an infusion solution using direct detection at low wavelength. Capillary: fused silica 75 μm i.d., 65/73.5 cm; buffer: borate 40 mmol L^{-1} , pH = 11.0; $E = 408 \text{ V cm}^{-1}$, 191 nm; injection 50 mbar, 5 s. 1, Lys; 2, Pro; 3, Try; 4, Leu; 5, Ile; 6, Gly-Glu; 7, Val; 8, Phe; 9, His; 10, Met; 11, Ala; 12, Thr; 13, Ser; 14, Gly-Tyr; 15, Glu; 16, Asp.

Indirect UV detection was evolved for the analysis of small inorganic ions but it is also an efficient technique for analysis of a broad range of nonabsorbing components. This methodology is performed very easily with CE using a UV-absorbing electrolyte. With respect to dissociation behaviour, mobility and absorptivity the background electrolyte (BGE) has to be chosen carefully. As mentioned above, basic conditions should be applied to generate anionic species of amino acids. Therefore the BGE has to be negatively charged under alkaline conditions. Beside generating the background signal the nature of the electrolyte used has great influence on separation selectivity. Best resolution can be achieved with electrolytes of moderate mobility, e.g. salicylic acid ($\mu_{\text{pH}=11.5} = -6 \times 10^{-4} \text{ cm}^2 \text{ V}^{-1} \text{ s}^{-1}$). Salicylate at low mmol L^{-1} concentrations may also be used for indirect fluorescence detection. Concentration limits are in the range of $10^{-5} \text{ mol L}^{-1}$ (Figure 2).

Another approach to a universal, high sensitivity detection scheme is mass spectrometry (MS). Beside the very low limits of detection which are achievable, this technique provides information about molecular mass and structure. The compatibility of capillary zone electrophoresis (CZE) to MS can be attributed to the low flow rates in CZE. The main problem in coupling CZE to MS is the buffer. Further developments on suitable volatile buffers and interface types will extend the scope of applications.

Analysis of derivatized amino acids Many of the chemical reactions for labelling originate from peptide synthesis where they were used as protective groups or sequencing agents.

As a consequence of derivatization, amino acids change from small ionic species to large hydrophobic molecules. Differences in mobilities decrease. A sufficient separation selectivity is mainly achieved by micellar electrokinetic capillary chromatography (MEKC).

Many reagents have been investigated to improve sensitivity as well as suitability for fluorescence detection. Depending on the separation problem, further requirements have to be considered. The reagent must react quantitatively and reproducibly with primary and secondary amines to form stable products. Side reactions and fluorescence of the tag itself can interfere with the analysis. The choice of derivatizing agent is limited by these prerequisites.

The commonest applied systems are discussed below (Figure 3).

The classical agent ninhydrin is not used for derivatization in CE because the aldehydes formed cannot be separated.

O-phthaldialdehyde (OPA) was one of the first reagents developed for pre-column derivatization in liquid chromatography (LC). Strongly absorbing isoindoles with fluorescence properties are formed in a rapid reaction. The stability of the derivatives mainly depends on the amino acid and the reducing agent, e.g. thiols. Unfortunately, secondary amines are not derivatized. An increase in stability and detection sensitivity has been achieved by using naphthalene-2,3-dicarboxaldehyde (NDA) or 3-(4-carboxybenzoyl)-2-quinolinecarboxaldehyde (CBQCA).

Phenylthiohydantoins (PTH) of amino acids are generated during Edman degradation of peptides. Maximum absorbance is found at 254 nm but the

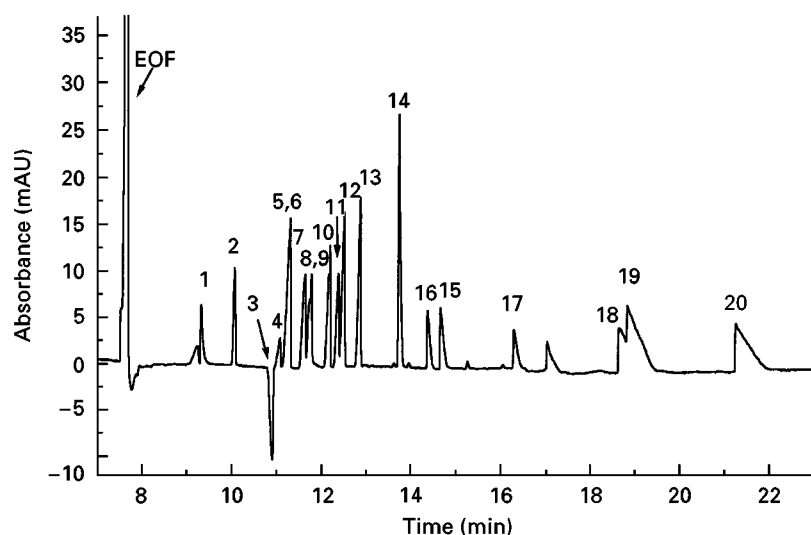


Figure 2 Separation of amino acids and dipeptides using indirect detection. Capillary: fused silica $75 \mu\text{m}$ i.d., 86.5/95 cm; buffer: salicylic acid 5 mmol L^{-1} ; pH = 11.5; $E = 316 \text{ V cm}^{-1}$, 214 nm; injection 50 mbar, 5 s. 1, Lys; 2, Pro; 3, Try; 4, Gly-Glu; 5, Leu; 6, Ile; 7, Val; 8, His; 9, Met; 10, Ala; 11, Thr; 12, Asn; 13, Ser; 14, Gly; 15, Tyr; 16, Ac-Tyr; 17, Cys-Cys; 18, Ac-Cys; 19, Glu; 20, Asp.

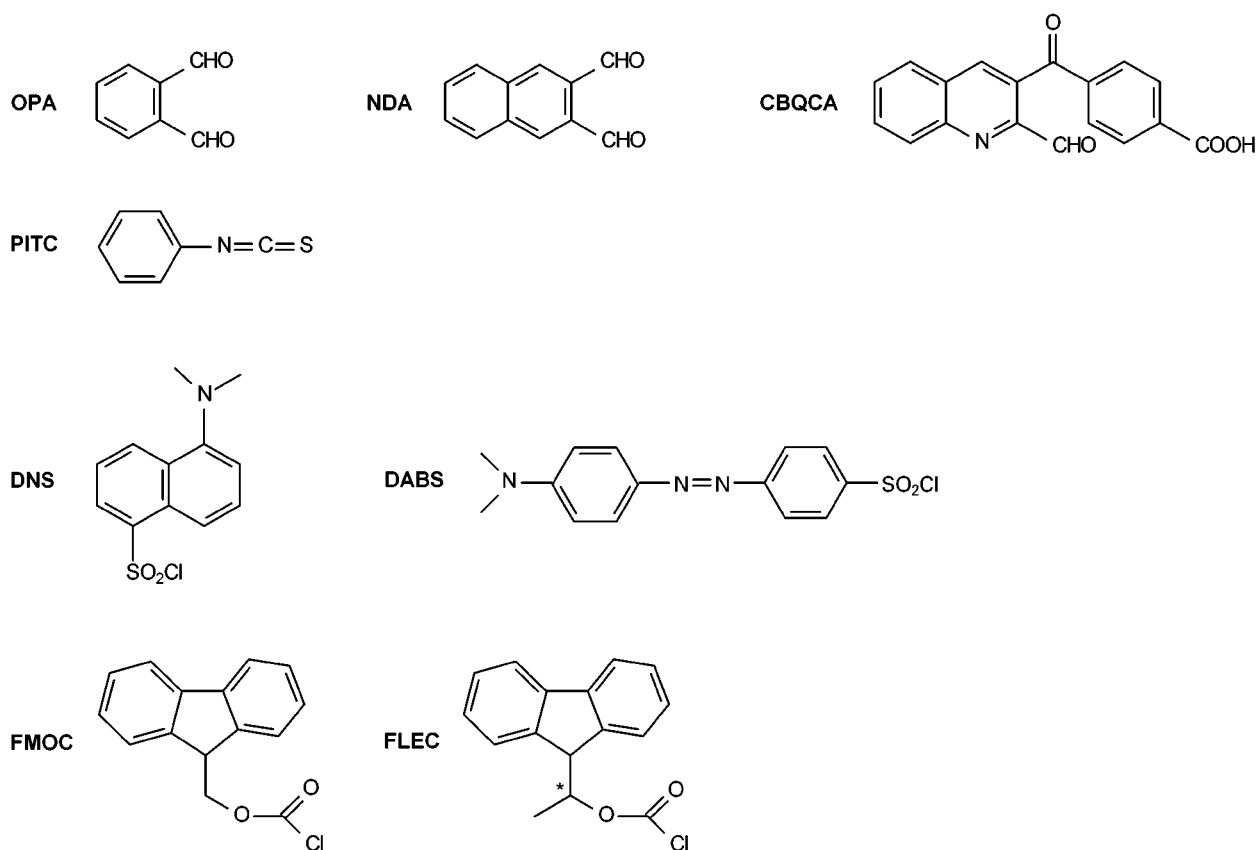


Figure 3 Structures of derivatizing reagents. OPA, o-Phthalaldehyde; NDA, naphthalene-2,3-dicarboxaldehyde; CBQCA, 3-(4-carboxybenzoyl)-2-quinolinecarboxaldehyde; PITC, phenylisothiocyanate; DNS, 5-dimethylaminonaphthalene-1-sulfonyl chloride; DABS, dimethylaminoazobenzenesulfonyl chloride; Fmoc, 9-fluorenylmethyl chloroformate; FLEC, (*R*) (*S*)-1-(fluorenyl) ethyl chloroformate.

derivatives lack fluorescence. Analysis is performed using phosphate or borate buffers under alkaline conditions. Surfactants such as sodium dodecyl sulfate (SDS) give a micellar pseudo-stationary phase allowing the partition process. In contrast to cationic surfactants, e.g. dodecyltrimethylammonium bromide (DTAB), analytical systems using anionic surfactants benefit from a wider migration time window. This can be mainly attributed to their counterosmotic migration behaviour (Figure 4).

Sulfonyl chlorides can convert primary as well as secondary amines. Well-known representatives are dansyl (DNS) and dabsyl (DABS) chloride. In order to separate all DNS amino acids, acidic buffers are used to reduce the EOF. In addition, neutral surfactants such as TWEEN 20 have been applied. The main disadvantage is the prolonged analysis time of about 70 min. Faster separations can be achieved using SDS with the penalty of a decrease in resolution. In some cases resolution can be enhanced by operating at lower temperatures (Figure 5).

Carbonyl chlorides such as fluorenylmethyl chloroformate (Fmoc) are more reactive than sulfonyl

chlorides. Fmoc amino acids fluoresce strongly and are stable at room temperature. Detection sensitivities in the nmol L⁻¹ range can be achieved.

Beside fluorescence detection, further improvements in sensitivity and specificity can be obtained with laser-induced fluorescence (LIF) techniques. A prerequisite is the match of emission wavelengths of the derivatized analyte with the spectral lines of the lasers. Great effort has been invested in the development of new fluorophores such as TRTC, CTSP, TBQCA, IDA and CBQ (Table 1).

Unfortunately, most of them are not commercially available.

Different derivatization techniques are applied: pre-column tagging is the commonest method. Several attempts have been made to transfer post-column methodology from LC to CE. A further promising technique is derivatization in the capillary because it simplifies automation. Reagent and sample are injected in succession. With the tandem mode a plug of reagent is injected into the column followed by the sample. A second technique is the introduction of an additional plug of reagent after the sample (sandwich

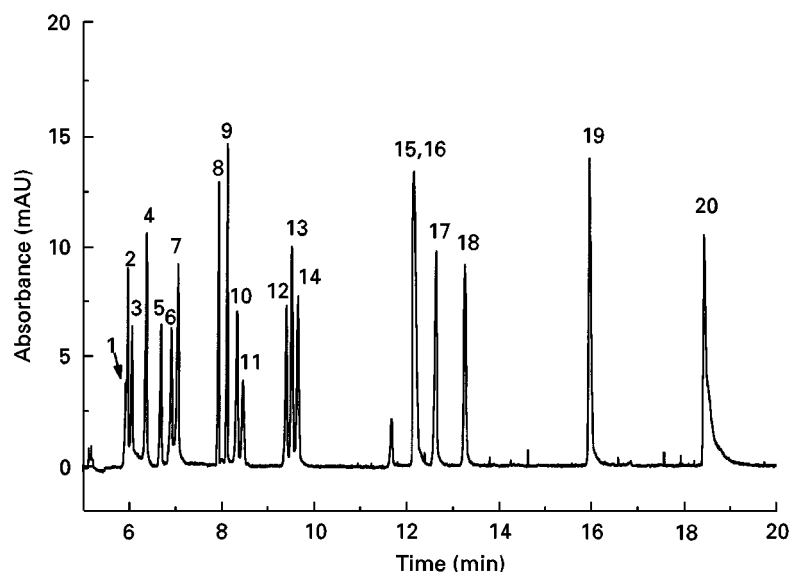


Figure 4 Separation of 20 PTH amino acids by MEKC. Capillary: fused silica 50 μm i.d., 59/67.5 cm, buffer: phosphate 25 mmol L^{-1} ; SDS 25 mmol L^{-1} ; pH = 9.0; $E = 444 \text{ V cm}^{-1}$, 260 nm; injection 50 mbar, 5 s. 1, Thr; 2, Asn; 3, Ser; 4, Gln; 5, Asp; 6, Gly; 7, Ala; 8, His; 9, Glu; 10, Tyr; 11, Cys; 12, Pro; 13, Val; 14, Met; 15, Leu; 16, Ile; 17, Try; 18, Phe; 19, Lys; 20, Arg.

mode). After a specified time for reaction, the separation can be performed.

Chiral analysis Assays of enantiomeric purity are easily performed by CE by simply adding the chiral selector to the running buffer. Two different methodologies are applied to achieve resolution. First, chiral distinction can be established by the formation of non-covalently bonded diastereomers.

The most widely applied cyclodextrins form host-guest complexes with one of the enantiomers preferentially. Compared to migration in the bulk phase, the complexed species possesses a different mobility. The separation occurs due to different complex stabilities resulting in different migration velocities. Enhancement of enantioselectivity is primarily attributed to cavity size (α -, β -, γ -cyclodextrin (CD)) and derivatization of the hydroxy moieties of

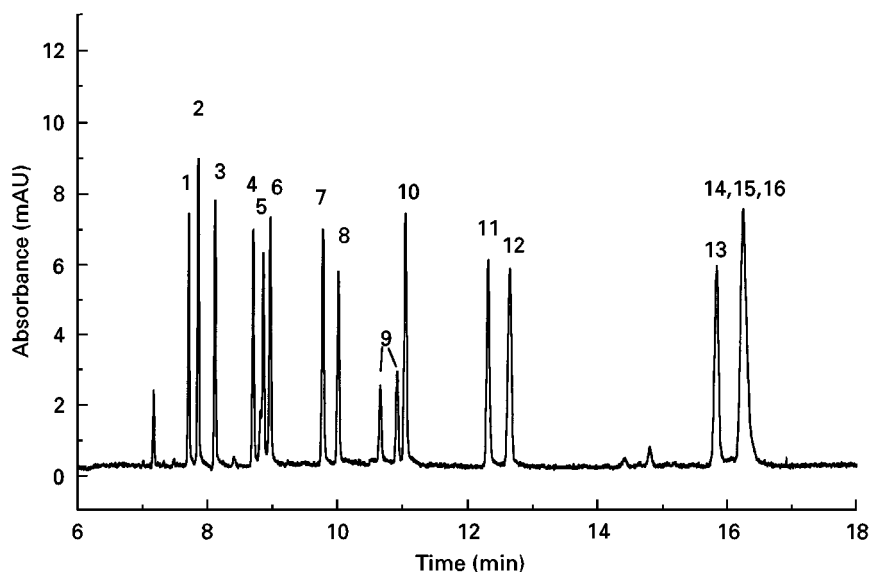


Figure 5 Separation of DNS amino acids by MEKC in an infusion solution. Capillary: fused silica 50 μm i.d., 50/57.5 cm, buffer: borax 20 mmol L^{-1} SDS 102.5 mmol L^{-1} ; pH = 9.1; $E = 435 \text{ V cm}^{-1}$, 214 nm; $T = 7.5^\circ\text{C}$; injection 50 mbar, 5 s. 1, Thr; 2, Ser; 3, Ala; 4, Gly; 5, Glu; 6, Val; 7, Pro; 8, Met; 9, Ile; 10, Leu; 11, Phe; 12, Try; 13, Arg; 14, His; 15, Tyr; 16, Di D-Lys.

Table 1 Examples of derivatizing reagents and detection wavelengths

	ε (mol L ⁻¹ cm ⁻¹)	$\lambda_{\text{abs/ex}}$ (nm)	λ_{em} (nm)	Remark
OPA		334	455	Presence of reducing agents (thiols), strong absorbance, strongly fluorescence, unreacted OPA not fluorescent, derivatives lack of stability, reaction rapid
NDA		462	490	Reaction rapid, increased stability compared to OPA, recently commercially available
CBQCA		450		
PITC		254		Peptide sequencing by Edman degradation, cyclic thiohydantoin; no fluorescence properties
DNS	14 100	254	570	Problems with derivatization by-products
DABS		420-450		
FMOC-Cl		265	315	Fluorogenic derivatives with primary/secondary amines, strong absorbance
FLEC		265	310	Converts enantiomers to diastereomers
TRTC	> 100 000	540	567	Ex at 540 nm matches with emission line of low cost HE laser
CTSP	82 000	663	687	Semiconductor laser
TBQCA		465	550	
IDA	33 100	409	482	
CBQ		466	544	

OPA, *o*-Phthalaldehyde; NDA, naphthalene-2,3-dicarboxaldehyde; CBQCA, 3-(4-carboxybenzoyl)-2-quinolinecarboxaldehyde; PITC, phenylisothiocyanate; DNS, 5-dimethylaminonaphthalene-1-sulfonyl chloride; DABS, dimethylaminoazobenzenesulfonyl chloride; FMOC, 9-fluorenylmethyl chloroformate; FLEC, (*R*)-(*S*)-1-(1-fluorenyl)ethyl chloroformate; TRTC, tetramethylrhodamine isothiocyanate; CTSP, pyronin succinimidyl ester; TBQCA, 3-(4-tetrazolebenzoyl)-2-quinolinecarboxaldehyde; IDA, 1-methoxycarbonylinodolizine-3,5-dicarbaldehyde; CBQ, 3-(*p*-carboxybenzoyl) quinoline-2-carboxaldehyde.

the cyclodextrin (methyl-, hydroxypropyl-, sulfo-butyl-CD). Whereas compounds with a single aromatic core fit into α -CDs, β -CDs mainly form complexes with polynuclear aromates such as tyr or try. Larger structures are accommodated by γ -CDs. Most of the enantiomeric separations are performed using phosphate or borate electrolytes with native β - or γ -CD or mixed MEKC-CD systems which additionally contain a surfactant, mostly SDS.

Additives like urea or small amounts of organic solvents can improve the resolution.

Chiral surfactants such as *N*-dodecanoyl-L-serine (SDVal) or *N*-dodecanoyl-L-glutamate (SDGlu) have been investigated. These amino acids with hydrophobic alkyl chains are applied in a mixture with nonchiral surfactants, e.g. SDS.

Metal ions of copper(II), zinc(II) or cobalt(III) can be added to the electrolyte containing an L-isomer of an amino acid, e.g. L-proline, L-histidine or a dipeptide, e.g. aspartame. These metal-amino acid or metal-dipeptide complexes preferentially form a ternary complex with one enantiomer of the amino acid in the sample. Separation occurred due to different complex stabilities resulting in different mobilities for the individual enantiomers.

As a second approach, a racemic mixture of amino acids is derivatized with an optically pure reagent yielding covalent-bonded diastereoisomers. Reagents like GITC (2,3,4,6-tetra-*O*-acetyl- β -D-glucopyran-

osyl isothiocyanate) allow the application of non-chiral separation techniques. Detection sensitivity can be improved simultaneously by using reagents like FLEC ((*R*) or (*S*)-(1-fluorenyl)ethyl chloroformate) containing chromophores or OPA with a chiral thiol.

Peptides

Peptides are compounds of great medical interest due to their physiological role as hormones and neurotransmitters. Furthermore, considering peptides as subunits of proteins, peptide mapping after chemical or enzymatical cleavage allows characterization of the protein and to reveal metabolic disorders.

Physicochemical Nature of Peptides

The characteristics of peptides are situated between those of amino acids and high molecular weight proteins. Oligopeptides containing up to 15 amino acids behave similarly to amino acids. Short peptide chains cannot create a complicated conformation. In contrast, very long polypeptides with chain lengths up to approximately 100 units behave like small proteins. They exhibit characteristic features of secondary and tertiary structure.

Peptides exist in aqueous solution as amphoteric ions. Therefore peptides possess isoelectric points (pI). The peptide has net electroneutral properties at

the pI. The zwitterionic characteristics are influenced predominantly by the acidity of the medium. In acidic media the carboxyl group ($pK_a \sim 2.7\text{--}2.9$) is protonated and the peptide behaves as a cation. In alkaline media the protonated ammonium group is eliminated and the zwitterionic form is converted into an anion. The degree of dissociation is determined by the dissociation constants of the functional groups yielding different net charges.

A further feature to be considered in electrophoretic behaviour is the sequence of the amino acids. The dissociation constants of the individual residues are affected by the arrangement of the amino acids in the chain. Mass-to-charge ratios are altered and the peptide exhibits a different mobility.

Prediction of Electrophoretic Mobility of Peptides

A theoretical model of electrophoretic migration underlying the experimental approach can be very useful for the optimization of analytical conditions. It supports predicting peptide mobilities under different experimental conditions such as pH. If selectivity between closely migrating species has to be implemented, the model facilitates adjustment of the separation environment.

Furthermore, considering technical processes and purity control of peptide synthesis or enzymatic digestion of proteins, a defined relationship between apparent mobility and physicochemical parameters supports the identification of unknown species. Variation in the sequence of peptides can also be easily determined.

The mathematical description of the migration process is based on the contribution of two forces. The electrical field accelerates an ion with a force proportional to its charge. In addition, the ion is influenced by a retarding force which results from the viscosity of the medium and is connected to a size parameter.

For permanently ionized small ions a prediction of migration is easily achieved by applying Stoke's law which correlates mobility with $q \times r^{-1}$ and $q \times M^{-1/3}$ (q , charge and M , molecular mass). With larger, more complex aggregates like peptides both the charge and a suitable size parameter has to be ascertained. For computing the charge, the sequence of amino acids has to be considered as the environment of a residue affects the extent of ionization, e.g. neighbouring amide bond or acidic/basic residues at terminal amino or carboxylic groups. This means that the ionization constants of the free amino acids have to be adjusted. During the development of a theoretical understanding of migration phenomena, many approaches have been made considering mass, surface, radius and the number of units in a peptide chain as size parameter.

The following equation results from the semi-empirical approach by Offord relating electrophoretic mobility μ of peptides with their charge q and their molecular mass M :

$$\mu = k \times q \times m^{-2/3}$$

This linear relationship has been validated by experimental research; a large set of analytes covering collagen fragments, tryptic digest of human growth hormone (33 peptides), motilin fragments (24 peptides) and many additional peptides differ widely in charge and amino acid sequence. Nowadays several computer programs are available which are capable of calculating the charge-to-mass ratio just requiring the amino acid sequence.

Electrophoretic Systems – Separation Strategies

To optimize the separation of peptides, the experimental conditions have to be adjusted to emphasize differences in the charge-to-mass ratios of the analytes.

Apart from external parameters like electrical field, capillary dimensions (length, inner diameter) and temperature, separation is mostly influenced by the electrolyte. Intrinsic variables like type of buffer, mobility, ionic strength, pH and buffer additives determine electrophoretic and electroosmotic mobility.

In the first place selectivity in the analysis of peptides is controlled by pH. Altering the acidity of the separation medium affects both the charge of the peptide and the ionization of the capillary wall, resulting in the change in EOF.

The hysteresis-like course of the EOF shows the greatest variation in the pH range of approximately 5–7, i.e. near the dissociation constant of the silanol groups. For pH values below 3 or greater than 9, the influence of the superimposed EOF can be neglected and the migration of the peptide is almost independent from the EOF.

In acidic media (pH ~ 2) both basic and acidic residues of the peptide are protonated. Selectivity is attributed to the number of positive-charged ammonium groups in the chain resulting in different charge densities. Analytes migrate with the EOF. In high pH buffers (pH ~ 10), deprotonation of terminal and side chain ammonium groups (His) induces negatively charged species (presence of carboxylate groups) which migrate in the opposite direction to the EOF. At higher pH values the side chain amino groups of arg and lys are the only ones affected.

Optimization of pH values below 2 and above 12 is difficult to achieve since the limiting values of mobility are reached. Furthermore, due to the high conductivities of protons and hydroxyl ions, high currents

accompanied by Joule heating are generated. For practical purposes selectivity control for peptides with a majority of acidic moieties is mainly achieved in the range of pH 3–6 while basic residues are mostly affected at pHs around 10.

Additionally, isoelectric points of the peptides have to be included in the optimization strategy.

If peptides are obtained by chemical or enzymatic digests of proteins the cleaving agent has to be considered, e.g. trypsin cuts at the C-terminal side of lys and arg respectively. Thus fragments contain an excess of acidic residues. Selectivity can be easily affected in acidic media. Cleavage at aromatic or aliphatic side chains is performed with chymotrypsin or pepsin, yielding fragments with both acidic and basic residues and optimization can be extended to the full pH range (Figure 6).

Frequently used electrolytes for peptide mapping are phosphate, citrate and acetate as acidic buffers while borate or TRIS/Tricine are mainly applied under basic conditions. Phosphate and citrate are buffers that can be used over a broad pH range due to their multiple association constants. Borate exhibits very low conductivity compared to phosphate and other buffers. Buffer concentrations in the range of 10 mmol L^{-1} to approximately 100 mmol L^{-1} can be used. The electrolytes used should not possess any UV absorbance at low wavelengths.

An increase in ionic strength generates sharper peaks (zone focusing) due to the drop of the electrical field at the sample–electrolyte boundary and sample loading capacity can be increased. High ionic strengths induce high electrical currents and the in-

crease of Joule heating can give rise to band broadening.

Dispersive effects caused by the interaction with the capillary wall are usually not a problem with peptides but larger species can exhibit characteristics similar to proteins in that they tend to adsorb at the capillary wall.

High ionic strength, extreme pH values and buffer additives competing in adsorption with the peptides are strategies of optimization which can be adapted from protein analysis. At extreme pH values, peptides and the capillary wall are equally charged so electrostatic repulsion diminishes adsorption. Coated capillaries have been used to suppress this phenomenon.

High salt content in the sample may destroy the separation efficiency of the electrophoretic system so sample preparation steps must remove the high ionic strength in the sample.

Enhancement in selectivity can be attained if an additional equilibrium is superimposed on to the electrophoretic process. Mostly the additives used for this are complexing agents which interact with specific groups of the peptide.

As for amino acids, metal ions can be employed for the separation of peptides and histidine-containing peptides especially interact with zinc salts. Separation of two histidine dipeptides (L-L, D-L) can be attributed to favourable steric arrangement of the histidine residues in one isomer.

Cyclodextrins form dynamic inclusion complexes with hydrophobic parts of the peptide, e.g. with amino acid residues containing aromatic rings like phenylalanine. The mass of a complexed analyte is

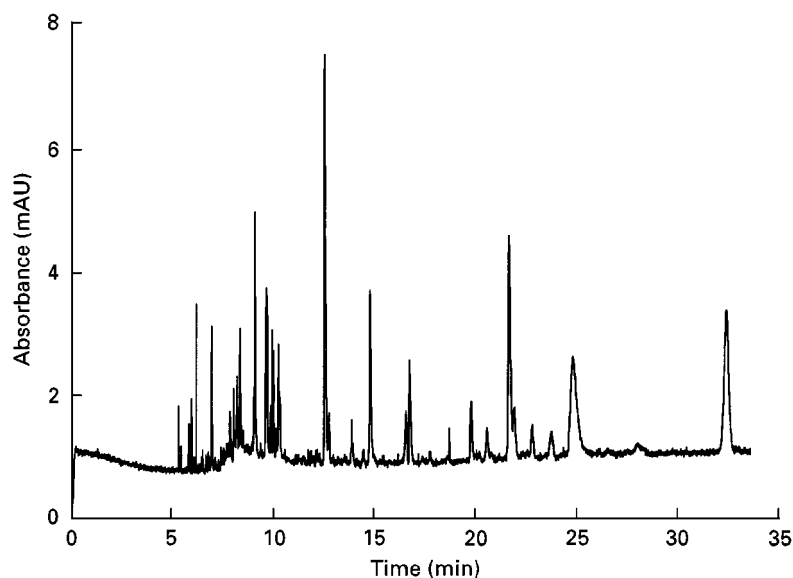


Figure 6 Tryptic digest of a haemoglobin variant separated by CZE. Capillary: poly(vinyl alcohol) coated fused silica capillary $50 \mu\text{m}$ i.d., $50/57 \text{ cm}$, buffer: phosphate 50 mmol L^{-1} ; pH = 2.5; $E = 526 \text{ V cm}^{-1}$, 214 nm ; injection 0.5 psi , 5 s .

increased in this way and lower charge-to-mass ratio results in decreased mobility.

Ion-pairing reagents like short chain alkylsulfonic acids are particularly applied to adjust selectivity for hydrophobic peptides. Concentrations below the critical micellar concentration are used. The mechanism is based on the interaction between the hydrophobic surface of the peptides and the hydrophobic alkyl chain. Depending on the hydrophobicity of a peptide, different amounts of alkylsulfonic acid are attracted. Charge-to-mass ratios of the individual peptides are influenced to a different extent leading to the separation of the species.

A second approach to impart selectivity to large peptides with identical mobilities but different hydrophobicities is the use of ion-pairing reagents above their critical micellar concentration (CMC). This technique may also be used for peptides differing in neutral amino acids such as ala, val, leu or ile. MEKC takes advantage of the partitioning of the peptides between the electrolyte and the pseudo-stationary phase of the micelles. Hydrophilic moieties of the peptide interact with the outer polar sections of the micelle whereas hydrophobic parts are situated in the inner hydrophobic sphere. These peptide-micelle aggregates possess a different mobility compared to the electrophoretic mobility of the peptide in free solution.

Types of surfactants employed are divided into anionic, cationic and nonionic micelle-forming reagents. Because of the different charges, different migration directions are obtained. Negatively charged SDS, one of the most frequently used additives, migrates counter to the EOF and is used in concentrations up to approximately 150 mmol L^{-1} .

Common positively charged reagents are cetyl, dodecyl and hexadecyltrimethylammonium salts. These reagents invert the EOF at concentrations below the CMC so that as a consequence the polarity of the applied electrical field has to be reversed.

The addition of organic solvents such as methanol, ethanol, acetonitrile or tetrahydrofuran can provide selectivity for closely migrating peptides. These changes can be mainly attributed to solvation of side chains and variations in dissociation of the functional groups of the peptide. Additionally the EOF is modified due to altering the ζ -potential and the increase in buffer viscosity which generates a lower EOF and lower currents. In this way separations have been established for peptides differing in only a single neutral amino acid.

Peptides, especially large peptides with protein-like characteristics, sometimes tend to adsorb at the capillary wall. Beside the possibilities for avoiding dispersive effects mentioned above, the addition of amino-

or diamino compounds like diamino-pentane, butane or morpholine can diminish the peptide-wall interaction. Competing equilibria in the electrostatic attraction between analyte-silanol and amine-silanol groups suppress the adsorption of the peptide. Another approach to reduce adsorption is derivatization of the silanol groups with an uncharged polymer (coated capillaries).

Detection Techniques

The detection of peptides suffers from the same difficulties as described for amino acids. Additionally only a few amino acids (phe, try, tyr and to a lesser extent his, arg, gln, asn) provide residues with strong chromophores.

Measuring UV absorbance at low wavelengths ($< 220 \text{ nm}$) is the commonest mode of detection to give limits of detection of about $1 \mu\text{g mL}^{-1}$ ($\sim 10^{-5}$ – $10^{-6} \text{ mol L}^{-1}$) which are sufficient for most applications. Spectra obtained by a photodiode array detection support identification of impurities in peptide synthesis due mainly to the absence of the characteristic absorbance of aromatic residues at 220 nm (Figure 7).

Indirect techniques can be applied as for amino acids.

Detection of trace amounts of peptides requires more sensitive methods and sensitivity can be improved by fluorescence methods.

This approach faces the same difficulties as UV absorbance detection in that only try and, to a lesser extent, tyr and phe exhibit native fluorescence when excited at 280 nm (Xe-lamp). However, this 'natural specificity' facilitates selective identification of try-containing peptides. In addition, indirect fluorescence detection using salicylic acid for anionic charge peptides (basic buffers) or quinine for the positive mode (acidic buffer) have been applied.

To accomplish lower detection limits for a broader range of species derivatization techniques have to be applied and all the agents described for amino acids can be used for the derivatization of peptides.

Increased interest is being paid to mass spectrometric techniques for the characterization of peptides, especially soft ionization techniques like electron spray ionization (ESI). A promising approach towards nonfragmented peptides is the matrix-assisted laser desorption ionization with time-of-flight mass spectrometers (MALDI-TOF).

Concluding Remarks

CE has proved to be a versatile method for the high efficient separation of complex mixtures of amino

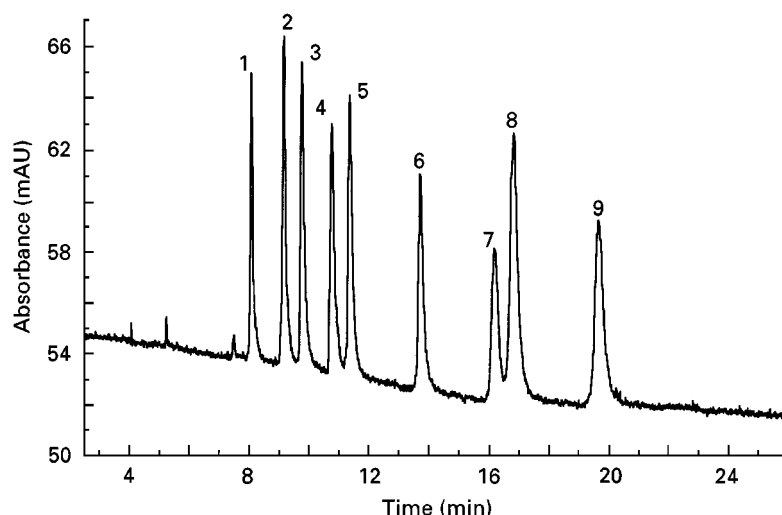


Figure 7 CZE separation of a peptide mixture. Capillary: ethylene/vinyl acetate dynamically coated with polyvinyl alcohol 75 μm i.d., 25/45 cm, buffer: phosphate 50 mmol L^{-1} ; pH = 2.5; $E = 155 \text{ V cm}^{-1}$, 200 nm; injection 50 mbar, 5 s. 1, Bradykinin; 2, angiotensin II; 3, α -MSH; 4, TRH; 5, LH-RH; 6, leucin enkephalin; 7, bombesin; 8, methionin; 9, oxytocin.

acids and peptides due to the manifold separation modes that can be applied. Short analysis times, easy manipulation of separation conditions and small injection volumes (nanolitres) are further advantages.

The field of biomedical and clinical amino acid and peptide analysis is still under investigation, especially as the transfer and adaptation of the separation modes to a broader range of real samples has to be established. Thus monitoring of *in vivo* processes, e.g. analysis of neurotransmitters in cerebrospinal fluid after online microdialysis, could be realized.

This is directly related to further improvements in reproducibility and detection strategies.

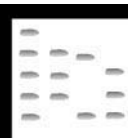
The most promising techniques that will fulfil the demands of trace analysis in biological fluids are CE-LIF and CE-MS.

Future trends are micro-fabricated CE devices implementing CE technology on a microchip and multiple capillary arrays allowing simultaneous analysis of up to 96 samples. Thus, a down-scaling of the analytical process and the performance of high throughput analysis could be achieved.

Further Reading

- Bardelmeijer HA, Waterval JCM, Lingeman H *et al.* (1997) Pre-, on- and post-column derivatisation in capillary electrophoresis (review). *Electrophoresis* 18: 2214.
- Blau K and Halket JM (eds) (1993) *Handbook of Derivatives for Chromatography*, 2nd edn. Chichester: John Wiley.
- Camilleri P (ed.) (1993) *Capillary Electrophoresis – Theory and Practice*. Boca Raton: CRC Press.
- Cifuentes A and Poppe H (1997) Behavior of peptide in capillary electrophoresis (review). *Electrophoresis* 18: 2362.
- Landers JP (ed.) (1994) *Handbook of Capillary Electrophoresis*. Boca Raton: CRC Press.
- Novotny MV, Cobb KA and Liu J (1990) Recent advances in capillary electrophoresis of proteins, peptides and amino acids (review). *Electrophoresis* 11: 732.
- Smith JT (1997) Developments in amino acid analysis using capillary electrophoresis (review). *Electrophoresis* 18: 2377.
- Szökő E (1997) Protein and peptide analysis by capillary zone electrophoresis and micellar electrokinetic chromatography (review). *Electrophoresis* 18: 74.

ANAESTHETIC MIXTURES: GAS CHROMATOGRAPHY



A. Uyanık, Ondokuz Mayıs University,
Kampus-Samsun, Turkey

Introduction

Today, anaesthetists normally use mixtures of nitrous oxide and oxygen as a background anaesthetic and carrier to introduce a potent volatile liquid

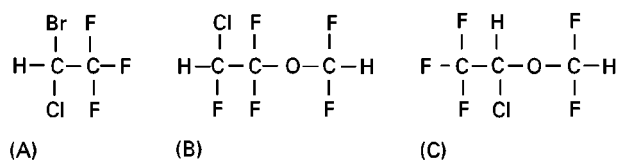


Figure 1 Molecular structures for the volatile liquid anaesthetics (A) halothane, (B) enflurane and (C) isoflurane.

anaesthetic such as halothane (2-bromo-2-chloro-1,1,1-trifluoroethane), isoflurane (1-chloro-2,2,2-trifluoroethyl difluoromethyl ether) or enflurane (2-chloro-1,1,2-trifluoroethyl difluoromethyl ether: **Figure 1**) to produce a state of anaesthesia and analgesia and to sedate a patient. Monitoring the patient's inhaled and exhaled breath during surgery is very important as a measure of the anaesthetic uptake and the depth of the anaesthesia. In operating theatres, therefore, physical methods of analysis (e.g. dedicated infrared analysers) are employed on account of their speed of response and continuous display facilities, though most can reliably handle only one component at a time. However, there is still the need to analyse such mixtures for all the major components, either in the course of research programmes involving different agents and different combinations such as inhaled or exhaled mixture analysis, blood and body fluid analysis, anaesthetic pollution studies, thermal decomposition studies or as a back-up to confirm the performance of the dedicated analysers. The major gases present in such mixtures, in addition to air, are carbon dioxide, nitrous oxide and halothane, isoflurane or enflurane (or cyclopropane, which is still in use in some places). If all the components (gases and vapours) need to be detected, gas chromatography is extremely powerful in the separation and quantification of the components, in comparison with the other techniques available.

Instrument Requirements and Procedures

There is no rigid boundary separating the basic instrumental requirements for conventional gas analysis and anaesthetic mixture analysis by gas chromatography. All the theoretical and practical knowledge and basic equipment of conventional gas analysis applies to anaesthetic mixtures and this simplifies the practice of the technique in this specialized field. A dual-column gas chromatograph fitted with a gas sampling valve (operated at room temperature), and equipped with a thermal conductivity detector (TCD) or preferably both TCD and flame ionization detector (FID) is most suitable for all the anaesthetic gas mixture analysis encountered. If a septum-type inlet system is also present, it should be placed next to the gas switching valve.

Sample Handling and Injection

Sample handling and injection techniques are greatly influenced by the source of the analysed samples such as liquid samples containing anaesthetics (e.g. blood, urine, sperm, tissue), low concentration gas samples (e.g. anaesthetics in pollution studies) and high concentration gas samples (e.g. inhaled and exhaled gas mixtures).

Direct injection of a liquid sample to the chromatographic column is very simple, but it is a rather crude approach and has serious disadvantages such as contamination of the sample port, column and detector, alterations in the baseline characteristics and interference by water vapour. The problems associated with the presence of the liquid in the chromatographic system are avoided by the technique of headspace analysis, whereby the vapour above the sample is injected under controlled conditions. Headspace sampling is rapid and is suitable for direct determination of the partial pressure of anaesthetics in blood.

Low concentration samples of liquid anaesthetics trapped in an adsorbent-filled cartridge (integrated sampling or passive dosimeter) in pollution studies are introduced into a gas chromatographic system via a gas sampling valve. Trapped anaesthetics are desorbed from the adsorption cartridge and transferred by the carrier gas to the main chromatographic column by heating the adsorption cartridge rapidly.

Low concentration (spot sampling) and high concentration samples in the gaseous state may be introduced to a gas chromatographic system by a gas-tight syringe (0.1–5.0 mL) with the usual septum-type inlet system. However, this is not a reproducible sample introduction method and creates problems of reliability where quantification of the components is needed. In addition to this, polymeric material such as rubber (e.g. on the barrel of a disposable syringe), plastics, and even glass itself adsorb liquid anaesthetics (~1–3%) on the contact surface. Adsorption on glass surfaces becomes more important when dealing with mixtures at lower concentrations (**Figure 2**). Therefore, syringe injection should be avoided in quantitative studies.

If gas samples are to be taken repeatedly to produce reproducible quantitative data, a gas sampling valve fitted with the desired size of sampling loop (0.25–10 mL) should be used at a constant temperature and filling pressure (usually ambient). It should be noted that, when using a concentration-sensitive detector such as TCD, the sample size and column diameter relationship must be taken into consideration to avoid column overloading. Several commercial gas sampling valves are available in various configurations. Some operate on the slider with the

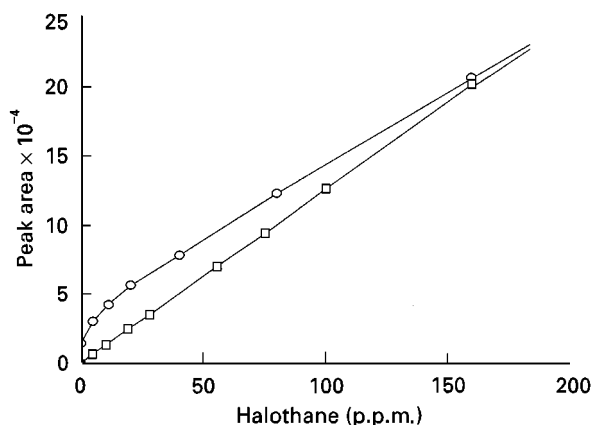


Figure 2 Adsorption of halothane on glass surface at lower concentrations. Squares, cylinder preparation; circles, syringe dilution.

O-ring principle, while others operate by rotation of a Teflon® (polytetrafluoroethylene) or polyimide rotor in various flow paths. The analyst should be aware that some polymeric materials (e.g. silicone rubber O-rings) adsorb anaesthetic vapours to some extent (halothane > isoflurane > enflurane). Gas switching valves made of a stainless-steel body and Teflon® rotor or O-rings are the most suitable choice for anaesthetic purposes. It is important to note that gas sampling valves must not be used with flow control of the carrier gas, as this restricts the filling rate and hence the rate of flushing of the loop, resulting in tailing peaks. Pressure control is used instead.

Choice of Column

The column has an essential role in the separation process. Optimization of the separation process by suitable choice of chromatographic column, therefore, is the main starting point of any gas chromatographic analysis. Selection of a column is often made on the basis of the nature of the samples and the number of components to be analysed.

Capillary columns have been little used, and mainly for liquid anaesthetic analysis without gas components. The reason for this is the unfavourable retention factors of low boiling compounds on capillary columns operated at room temperature.

Packed columns may be subdivided as liquid partition and solid adsorbent columns. Almost all the anaesthetic gas analysis reported so far has been performed on packed columns of various lengths, either single or combined, commonly with 1/8 in and 1/4 in o.d. Liquid partition columns are generally employed to separate the high boiling or heavier components such as liquid anaesthetics, while solid adsorbent columns are used for the permanent gases (CO_2 , O_2 and N_2).

Synthetic porous polymer beads, which have been in widespread use as solid adsorbent packing material, are available commercially under a variety of trade names (Chromosorb Century Series, Porapak). Columns packed with porous polymer beads are more versatile and capable of separating each of the individual groups of components such as light gases and liquid anaesthetics at different temperatures as well as their complex mixtures with suitable temperature and column arrangements. No special treatment is required to obtain symmetrical peaks as they are chemically inert to the anaesthetic substances under the chromatographic conditions employed (usually 20–220°C). The combined effects of increasing viscosity of the carrier gas and expansion of the stationary phase as the temperature rises result in a very marked decrease in the carrier flow (Figure 3), e.g. a temperature rise from ambient to 200°C decreases the flow of the carrier from around 50 mL min⁻¹ to 20 mL min⁻¹ at 40 psig (2.7 bar) He inlet pressure, with a 2 m, 80–100 mesh Chromosorb 101 column. Nevertheless, the chromatography remains adequate and gives peaks for the liquid anaesthetics which are easily integrated. The size of the particles, expressed in mesh size, is very important in the column efficiency as the separation is provided by the surface and structure characteristics of the packing material. When the size of the particles is reduced, the column efficiency is increased and so is the inlet pressure because of the high pressure resistance of the column. At the present time, 80/100 mesh is the most widely used fraction; however, in instances where higher efficiency is needed, 100/120 mesh is frequently used.

Column Tubing Materials

Since most anaesthetic mixtures contain at least one volatile liquid component other than the permanent

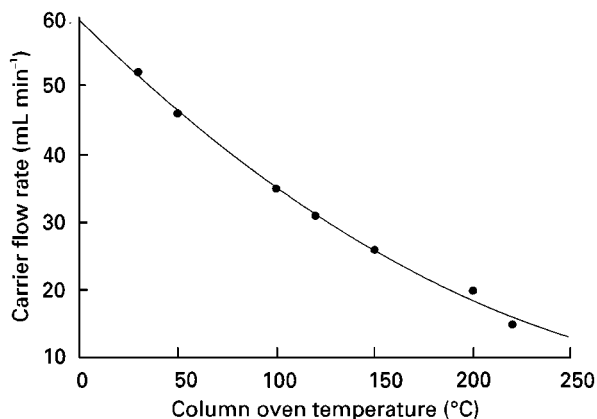


Figure 3 Relationship of temperature to flow rate of a porous polymer packing (80/100 mesh). Flow rate = $3.86 \times 10^{-4} T^2 - 0.283 T + 59.6$.

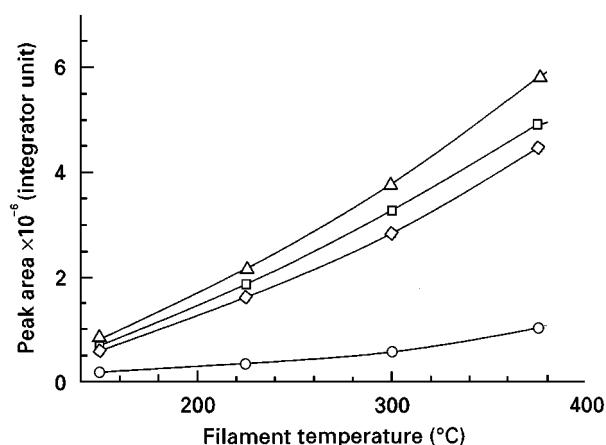


Figure 4 Variation of the hot-wire TCD responses with detector filament temperature. Circles, halothane; squares, nitrous oxide; triangles, carbon dioxide; diamonds, air.

gases, operating temperatures with solid adsorbent columns are considerably higher (e.g. 150–220°C) than those required for the separation of the permanent gas alone. Therefore, many of the commonly

used tubing materials for permanent gas analysis at lower temperatures may not safely be used in anaesthetic gas analysis. For example, anaesthetic vapours (particularly halothane) tend to decompose in contact with metals (or metal/metal oxide) such as aluminium (~200°C) and copper (>250°C) at elevated temperatures, producing a number of halogenated products. Relatively inert materials such as glass and stainless steel may safely be used as column tubing materials for anaesthetic separation purposes at high operating temperatures. Since mixtures contain large amounts of oxygen, heated septum-type injection ports should have a glass liner to prevent metal–liquid anaesthetic contact at higher temperature settings.

Choice of Detectors

The most commonly used detectors in anaesthetic gas analysis are TCD, FID and electron capture detector (ECD).

TCD is concentration-sensitive and has been the most widely used in chromatographic analysis for the determination of gases, and for any applications in explosion hazard areas. If inorganic gases, besides

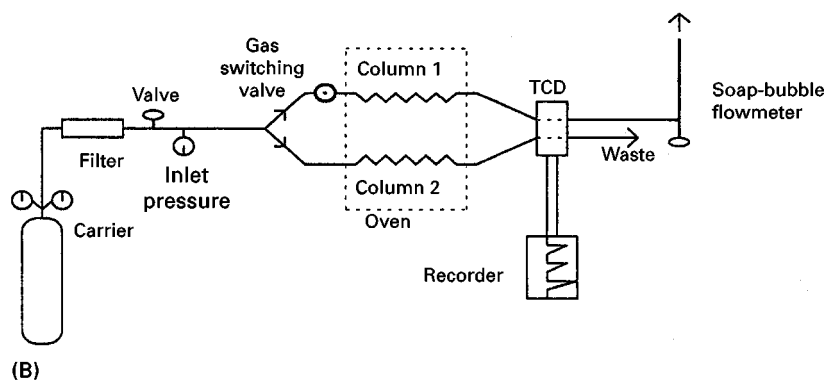
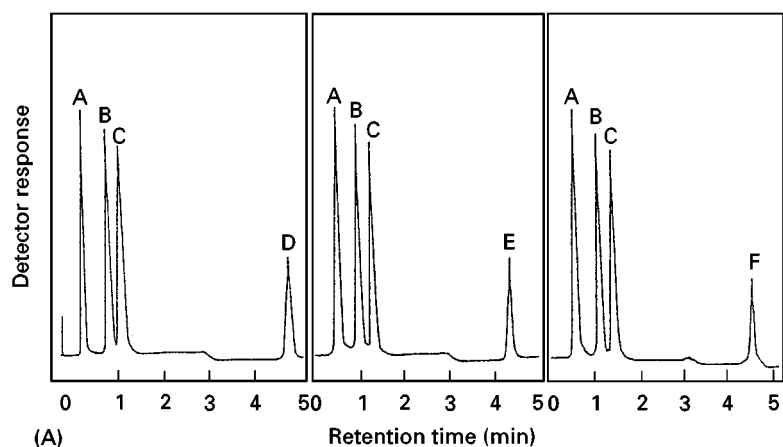


Figure 5 (A) Gas chromatograms for the single-column separation of anaesthetics by temperature programming (linear or non-linear). A, Air; B, carbon dioxide; C, nitrous oxide; D, halothane; E, isoflurane; F, enflurane. (B) Simple set-up of a temperature-programmed (linear or nonlinear) dual-column chromatograph.

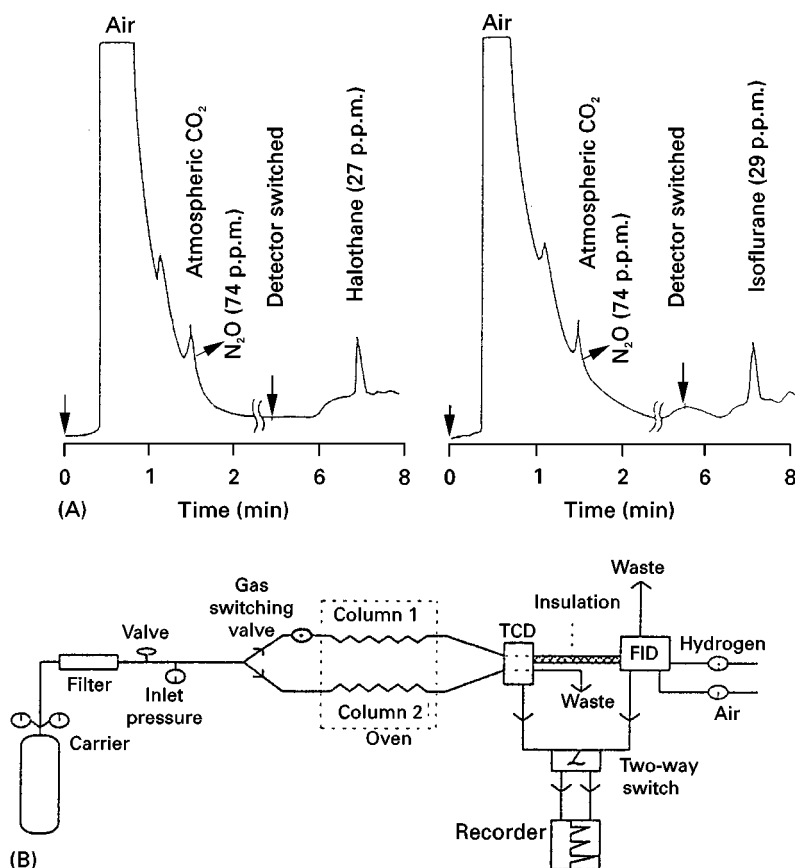


Figure 6 Chromatograms for dual detector chromatography (A) halothane (left) and isoflurane (right) in atmospheric air. (B) Simple set-up of a dual detector chromatograph.

liquid anaesthetics, need to be analysed, TCD is the detector of choice due to its universal response to almost all substances and its very large linear dynamic range. Because of its relatively poor sensitivity, it is unsuitable for the determination of low concentrations (<40 p.p.m.) without employing extreme detector conditions and large sample volumes. The nondestructive character of the TCD enables it to be used in dual-column chromatography by utilizing two channels simultaneously or in series with another detector such as the FID. Sensitivity of the hot-wire TCD depends on the temperature difference between filament and cell wall temperature (Figure 4), and higher chromatographic responses are obtained at higher filament temperatures.

The ECD is very sensitive to electrophilic species such as polyhalogenated anaesthetics and also to nitrous oxide, but its linear dynamic range is limited to a range of about 10^4 and it can easily be saturated. For this reason, it is generally employed for the low concentration determination of liquid anaesthetics and nitrous oxide. Since oxygen and water influence the detector sensitivity, these compounds must be rigor-

ously removed from the carrier and make-up gases. Contamination also causes serious interference. The detector must be held at an elevated temperature, always with a steady flow of carrier gas, and must be regularly baked out to ensure cleanliness. All these factors make ECD a difficult detector in anaesthetic gas analysis.

The very widely used FID is a mass-sensitive detector, with the disadvantage compared to the TCD that it is destructive. It responds to virtually all organic components but does not respond to the permanent gases. In the great majority of studies where only the determination of the volatile liquid anaesthetics is needed (e.g. blood and body fluid analysis), FID is used. If the analysis includes nitrous oxide in addition to liquid anaesthetics, the ECD alone may be chosen. For low concentration analysis, TCD and FID may be connected in series to determine the permanent gases and the liquid anaesthetics.

Choice of Carrier Gas

Choice of the carrier gas depends on the detector employed. For FID and ECD, carrier gas is not critical

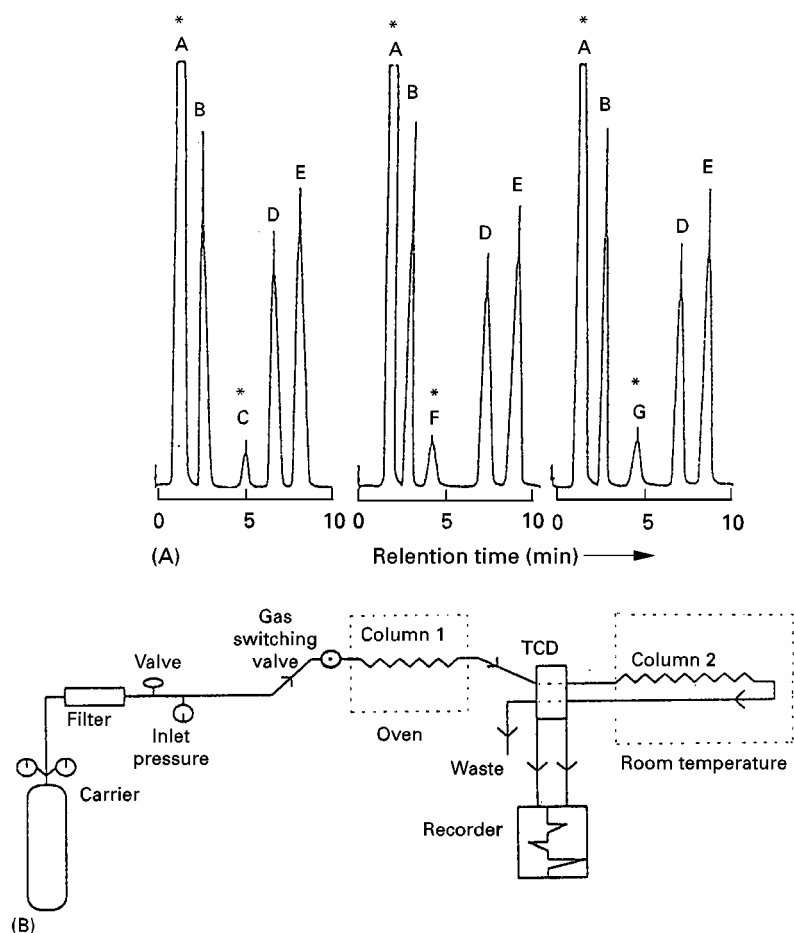


Figure 7 (A) Gas chromatograms for the dual-column separation of A, combined peak; B, air; C, halothane; D, carbon dioxide; E, nitrous oxide; F, isoflurane; G, enflurane; *, converted peaks. (B) Simple set-up of a temperature-programmed (linear or nonlinear) single-column chromatography.

and nitrogen may be used for most chromatographic purposes in anaesthetic analysis. For the operation of the TCD, hydrogen and helium give the highest sensitivities, but helium is preferred on safety grounds.

Tactics for the Anaesthetic Gas Analysis

It is usually required to measure a number of the components in an anaesthetic mixture (e.g. vapours and permanent gases), and a single column in a single isothermal run rarely meets this need. Although isothermal operation is preferred whenever possible, temperature programming may be used to improve the separation process. The magnitude of the temperature range depends on the sample components and the nature of the column packing materials. The disadvantage of temperature programming is that time is required at the end of an analysis to return the initial column temperature.

Using temperature as a variable is not, however, the only approach. Improved separations can be achieved by employing mixed column packing materials in various proportions and column lengths (e.g. porous polymers and molecular sieves) and multicolumn (parallel or serially) arrangements operating in tandem or at different temperatures with single or multidetector systems. Utilizing these approaches in various multicolumn and detector combinations allows the analyst to separate most mixtures of anaesthetics and permanent gases. Figures 5–7 show the various arrangements with examples of the chromatograms obtained.

Quantitative Analysis

To be able to carry out quantitative work, the gas chromatograph must be calibrated with accurately prepared mixtures of known composition. Dynamic methods for calibration such as gas stream

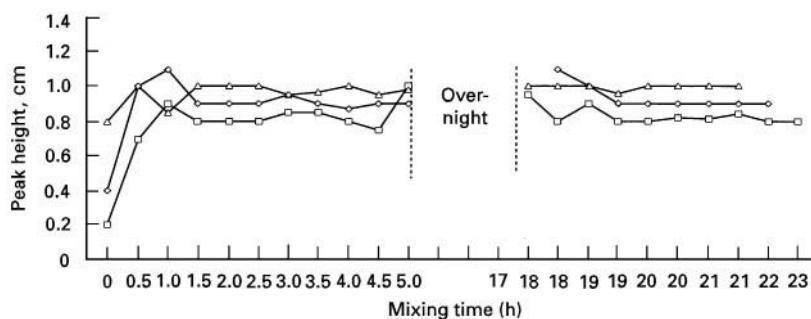


Figure 8 Mixing time for halothane prepared in helium. Squares, 1.1% halothane at 8.5 bar; diamonds, 1.2% halothane at 5.0 bar; triangles, 1.4% halothane at 3.1 bar.

mixing, permeation, diffusion and evaporation generate continuous flows of mixtures of known composition and are generally employed in studies where large volumes of standards at low concentrations are needed. Static methods for producing standard gas mixtures are appropriate when relatively small volumes of mixtures are required at moderately high concentration levels and have been widely used in calibrating gas chromatographic instruments. The preparation of calibration mixtures in gas cylinders involves either volumetric or gravimetric mixing. Gravimetric methods in which the concentrations are determined from the mass of each component present in the cylinders irrespective of the temperature and pressure of the mixture represent the nearest approach to an absolute method, provided the mixture is homogenous. The mixing rate is inversely proportional to the total pressure and is rapid if thermal or mechanical agitation of some kind is introduced to cause turbulence in the gas (usually the cylinder is rolled in a horizontal position). Without mechanical mixing, equilibration is likely to take several days (Figure 8). Syringe dilution methods (even with all-glass syringes) are not suitable for calibration purposes, particularly at lower concentrations, due to the adsorption of the liquid anaesthetics (see Figure 2).

Quantitative evaluation may be performed either by peak height or by peak area. The most commonly used method is based on direct calibration with standard samples which bracket the anticipated values in the unknown sample. The correlation peak value versus concentration generally exhibits a linear plot. The basic condition for successful quantitative analysis is a high degree of constancy of operating conditions and the accuracy of the analysis is significantly affected by apparatus parameters, characteristics of the detector and the skill of the analyst.

Conclusions

It may be concluded that there is no lack of knowledge, equipment and method to perform gas chromatographic separation and quantitative evaluation of all types of anaesthetic mixtures from one to multicomponent mixtures (including light gases and gaseous anaesthetics) in this extensively described well-established field. Nevertheless, the time required for analysis means that gas chromatography is mainly used for anaesthetic research purposes. Separations taking 5–10 min are not acceptable to medical personnel who would require a time scale an order of magnitude less for analysis of patient's breath in an operating theatre. However, there is room for future improvements to simplify the column systems, developing fast and continuous methods with automated samplers to be able to monitor anaesthetic concentrations during surgery.

See also: II/Chromatography: Gas: Gas-solid Gas Chromatography; Headspace Gas Chromatography; Detectors: General (Flame Ionization Detectors and Thermal Conductivity Detectors); Detectors: Mass Spectrometry; Detectors: Selective; Sampling Systems. III/Gas Analysis: Gas Chromatography.

Further Reading

- Cowper CJ (1995) The analysis of hydrocarbon gases. In: Adlard ER (ed.) *Chromatography in the Petroleum Industry*. Amsterdam: Elsevier Science.
- Cowper CJ and DeRose AJ (1983) *The Analysis of Gases by Gas Chromatography*. Oxford, UK: Pergamon Press.
- Grant WJ (1978) *Medical Gases, their Properties and Uses*. Buckinghamshire, England: HM + M.
- Hill DW (1980) *Physics Applied to Anaesthesia*, 4th edn. London: Butterworths.
- ISO (1981) International Standard 6142. *Gas Analysis – Preparation of Calibration Gas Mixtures – Weighing Methods*, 1st edn. ref. no: ISO 6142-1981 (E).
- Stephen CR and Little DM (1961) *Halothane*. Baltimore, MD: Williams & Wilkins.

ANALYTICAL APPLICATIONS: DISTILLATION



J. D. Green, BP Amoco Chemicals, Hull, UK

This article is reproduced from *Encyclopedia of Analytical Science*, Copyright © 1995 Academic Press.

Distillation is a widely used technique in chemical analysis for characterizing materials by establishing an index of purity and for separating selected components from a complete matrix. The technique is even more widely used in preparative chemistry and throughout manufacturing industry as a means of purifying products and chemical intermediates. Distillation operations differ enormously in size and complexity from the semi-micro scale to the 'thousands of tonnes per annum' production operations. For analytical purposes the scale employed is usually bench-level.

Numerous quoted standard specifications refer to distillation ranges as criteria of purity or suitability for use, or as indicators of performance. Published standards for analytical reagents in the AnalaR range and similar documentation by the American Chemical Society refer to distillation ranges as criteria of purity for appropriate materials.

Distillation is the process that occurs when a liquid sample is volatilized to produce a vapour that is subsequently condensed to a liquid richer in the more volatile components of the original sample. The volatilization process usually involves heating the liquid but it may also be achieved by reducing the pressure or by a combination of both. This can be demonstrated in a simple laboratory distillation apparatus comprising a flask, distillation head, condenser and sample collector (**Figure 1**). A thermometer is included in the apparatus as shown to monitor the progress of the operation. In its simplest form this procedure results in a separation into a volatile fraction collected in the receiver flask and a nonvolatile residue in the distillation flask. When a distillation column is incorporated in the equipment (**Figure 2**), the evaporation and condensation processes occur continuously. This results in a progressive fractionation of the volatiles as they pass up the column. The most volatile components emerge from the top of the column initially and the less volatile components emerge later. By changing the receivers throughout the course of the distillation a separation or fractionation is effected. Eventually, all the volatiles will have passed over into the sample collectors and any

involatile residue present will remain in the distillation flask.

Principles

The underlying principles are conveniently illustrated by reference to a vapour-liquid equilibrium diagram (**Figure 3**). The diagram relates to a binary mixture containing components P and Q. The lower curve gives the composition of the liquid boiling at various temperatures whilst the upper curve gives the composition of the vapour in equilibrium with the boiling liquid. Points x and y therefore give the boiling points of the individual components P and Q respectively. For example, point A shows that at X degrees the vapour has a composition of approximately 90% P, whilst point B shows that the boiling liquid with which it is in equilibrium, has a composition of approximately 80% P. In a continuous distillation process, such as occurs in a distillation column, liquid of composition C (90% Q, 10% P) vaporizes to vapour of composition D which condenses to liquid of composition E. Subsequently liquid E becomes vapour F and liquid G (composition: 50% Q, 50% P). This continuous process of vaporization and condensation occurs in the distillation column until a volatile fraction leaves the top of the column and is removed from the process by being collected in the collection flask. At the same time the liquid in the distillation flask becomes progressively more concentrated in the involatile component.

Distillation techniques may be classified into several different types including:

- Distillation at atmospheric pressure
- Distillation under reduced pressure
- Steam distillation
- Molecular distillation (short-path distillation)
- Azeotropic distillation
- Isopiestic distillation

Distillation at atmospheric or reduced pressure produces a separation according to the general principles discussed in the introduction.

Steam distillation is a means of distilling that part of a sample that is volatile in steam at a lower temperature than would otherwise be the case. This method is typically used for removing phenols from an aqueous sample. A means of introducing steam into the distillation flask must be provided.

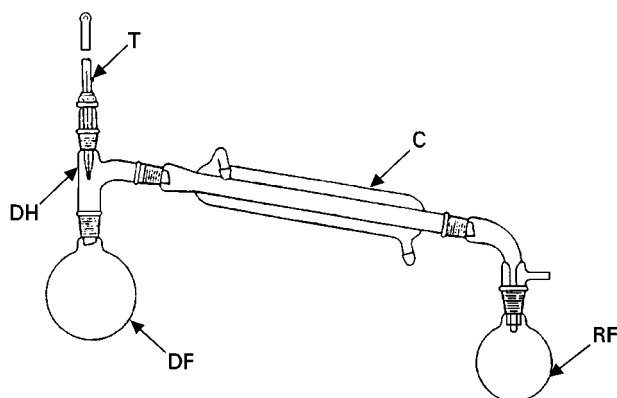


Figure 1 Simple distillation apparatus comprising distillation flask (DF), distillation head (DH), thermometer (T), condenser (C) and receiver (or collection) flask (RF). (Reproduced by permission of Longman Scientific & Technical from Furniss *et al.*, 1989.)

Molecular distillation, sometimes termed short-path distillation, is used principally for compounds normally having high boiling points. In such cases, very low pressures are needed to achieve the desired low boiling points. The apparatus is constructed such that the condensing surface is located only a short distance from the distilling liquid and the pressure is reduced so that the process is governed to a large extent by the mean free path of the molecules involved. Hence the terms short-path distillation and molecular distillation.

Azeotropic distillation occurs when a mixture of two materials distils at constant composition. This technique is commonly used to remove water from samples. As an example, toluene may be added to a complex sample containing water, the distillation

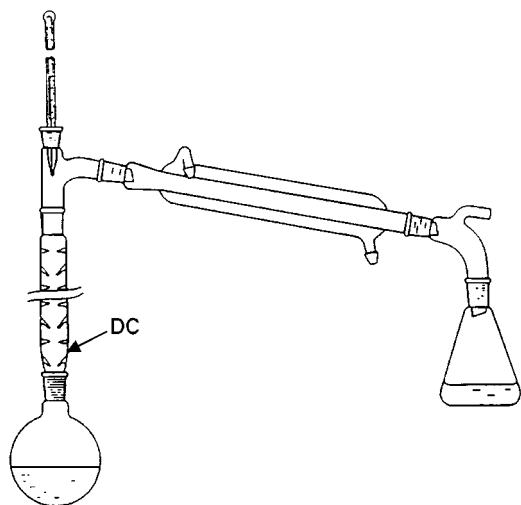


Figure 2 Distillation apparatus including distillation column (DC). (Reproduced by permission of Longman Scientific & Technical from Furniss *et al.*, 1989.)

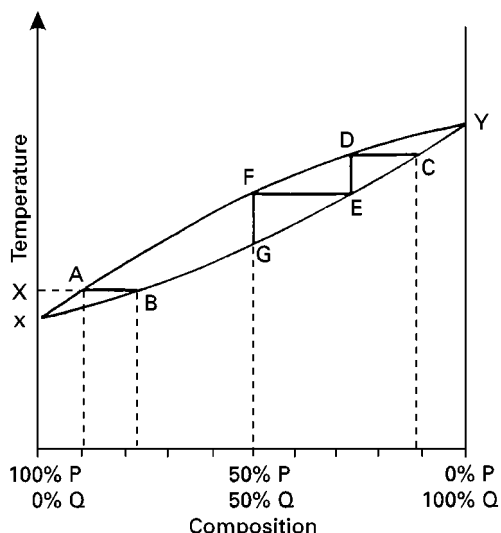


Figure 3 Vapour-liquid diagram for a binary mixture of components 'P' and 'Q', illustrating the principles of distillation (see text for details).

process results in the toluene-water azeotrope distilling. The distillate can then be examined to determine the water content of the original sample.

Isopiestic distillation is a convenient way of producing metal-free aqueous samples of volatile acids. The 'crude' acid is placed in an open container, such as a beaker, in a desiccator containing also an open beaker of pure water. The acid vaporizes and subsequent condensation in the pure water produces an aqueous sample of the volatile acid without any of the involatile contaminants such as metals.

The alternative terms 'flash' distillation and 'fractional' distillation are sometimes used to describe some of the above procedures carried out in a particular way. Flash distillation effects a crude separation into volatiles and residue, whilst fractional distillation produces a series of 'cuts' of different volatility (or boiling point) ranges.

Additionally, there are other forms of sample purification and separation that are either a type of distillation or are related to a distillation process:

- Simultaneous distillation/extraction (see application section)
- Dean and Stark distillation (see application section)
- Simulated distillation (gas chromatographic technique)

Analytically, distillation is used for two principal purposes, firstly as a criterion of purity and secondly as a means of preparing a sample for analysis. Many specification tests include reference to a distillation range within the limits of which a stated percentage

of the material of interest distills. Alternative distillation may be used to separate volatiles from a sample prior to a suitable analytical technique being employed on the distillate or on the residue. Standard tests are documented that involve distillation as a sample pretreatment method prior to titrimetry, potentiometry and spectrophotometry.

It is of course essential, if meaningful comparative results are to be obtained, that the design and use of the apparatus are standardized for such determinations.

Apparatus

A wide variety of apparatus is available to satisfy the different distillation techniques. The appropriate design of apparatus depends upon the type of distillation to be performed, considering, for example, whether a vacuum is required or steam is needed. Descriptions of apparatus are to be found in a number of different texts (see the Further Reading). Standards referring to the design and use of distillation apparatus have been published by the British Standards Institute and the American Society for Testing and Materials. Simulated distillation, which is a gas chromatographic technique, is dealt with in a [recent] review by Robillard *et al.* and referred to in several standards.

Apparatus may be discussed in terms of the distillation flask, the distillation column, the condenser and the collecting flask(s). By far the most effort has been expended in the design and operation of the distillation column, which is at the heart of the separation efficiency. The form of the column, its size and the packing used are very influential upon the results that are achievable. A summary of some different types of columns is given in **Table 1** and of packings in **Table 2**.

Once apparatus has been chosen carefully to compare with previously used apparatus or to conform to standards, the operation of the equipment must be considered. The following factors are among the most important to be controlled:

- The heating of the distillation flask must be carefully controlled.
- The distillation column must be operated so that it does not become flooded.
- The reflux ratio, that is the ratio of material returning via reflux to the distillation column or the distillation flask compared to the amount presented to the condenser in unit time must be carefully controlled. The higher the reflux ratio, the purer the material collected from the distillation. Reflux ratios are controlled in simple distillation appar-

Table 1 Types of distillation column

Column type	Description/comments
Duflon	An open tube into which a glass spiral fits closely
Hempel	A simple tube normally filled with a suitable packing (rings/helices) and having a side-arm near the top
Oldershaw	A column with fixed but perforated plates that maintains a fixed amount of liquid on each plate
Podbielniak	A simple tube with a wire packing to provide large contact area between liquid and vapour to effect high efficiencies
Spinning band	A tube fitted with a closely fitting spiral of PTFE or metal gauze that can be rotated at typical speeds of 600 to 3000 rev min ⁻¹ as the vapour-liquid equilibrium is maintained in the column
Vigreux	A tube having pairs of indentations down its length that slope downwards and provide a large and designed surface area to enhance the liquid-vapour equilibrium

atus by adjustment of the heating rate and by maintaining stable thermal conditions throughout the apparatus.

Applications

Documentation of analytical applications of distillation is widely dispersed. However, there are numerous references to distillation as a means of characterizing materials and as means of sample pretreatment in the lists of BSI standards, the ASTM methods documentation, the analytical methods of the Institute of Petroleum and those of other worldwide standards organizations. **Table 3** gives a selection of standards involving distillation originating from various standards organizations.

Table 2 Distillation column packings

Packing	Description
Balls	Mostly made of glass. Columns have a tendency to flood easily
Helices	Made from metal or glass, although metal may be packed mechanically to produce a more uniform column
Rings	Usually made of glass of an appropriate size for the column but can be made of porcelain, stainless steel, aluminium, copper or nickel. Depending upon design they can be termed Raschig, Lessing or Dixon rings
Wire packings	Produced as 'Heli-Grid' and 'Heli-Pak' packings especially for use with Podbielniak columns

Table 3 Applications of distillation in analysis

<i>Application</i>	<i>Standards^a</i>
<i>Water/moisture determination</i>	
Petroleum products	AASHTO T55; ASTM D95; BS 4385; CNS K6339
Crude oil	ASTM D4006
Wool	ASTM D2462
Wood/wood products	TAPPI T208 OM
Coal/coke	BS 1016
Spices	BS 4585; ISO 939
Animal feeds/feedstuffs	AACCH 44-50
Fats/oils	AACCH 44-51; BS 684; ISO 934
Paints and pigments	CGSB 1-GP-71 Meth 24-1
Fruits/vegetables	SASO 436
Soaps/detergents	CGSB 2-GP-d11M Meth 13-2; ISO 4318
Tobacco	CNS N4133; ISO 6488
Pulp and paper	CNS P3025
Plastic moulding materials	DIN 53713
<i>Water quality assessment</i>	
Phenol index	BS 6068 Sect. 2.12; ISO 6439
Ammonium content	BS 6068 Sect. 2.7; ISO 5664
<i>Hydrocarbons, purity</i>	
Road tars	ASTM D20; IP27
Petroleum products	AASHTO T115; ASTM D86; BS 7392; CNS K6109; IP 123
Creosote/creosote oil	AASHTO T62; ASTM D246; CNS K6070
Bituminous coatings	AASHTO T78 & T110; ASTM D255
Aromatic hydrocarbons	ASTM D580; CNS K6255
Volatile organic liquids	ASTM D1078
<i>Organic liquids, distillation range and characterization</i>	
Amyl acetate	BS 552
Analytical reagents	Anala standards for laboratory chemicals
Butyl acetate	BS 551
Chloroform	BS 4774
Diethyl ether	BS 579
Perchloroethylene	BS 1593
Isopropyl acetate	BS 1834
4-Methylpentan-2-one	BS 1941
2-Ethoxyethanol	BS 2713
Oil of lime	CNS K5089
Citronella oil	CNS K6063
Formic acid	ISO 731 Part VII
Phenols	ISO 1897 Parts 12 & 13
Caprolactam	ISO 8661
<i>Miscellaneous application of distillation</i>	
Ethyl acetate	BS 553
White spirit	IP 123
<i>N-determination</i>	
Sulfuric acid/oleum	ISO 914
Urea	ISO 1592
Ammonium nitrate	ISO 3330, 3331
Fertilizers	BS 5551; ISO 5314 & 5315
<i>Available fluorine in:</i>	
Hexafluorosilicic acid	BS 6445; ISO 6677
Fluorspar	ISO 5439
Arsenic in ores	CNS M3094
<i>Volatiles content</i>	
Aerosols	CNS Z6052
Fire residues	ASTM E1385

^aSources: AASHTO, American Association of State Highway Transport Offices; ASTM, American Society for Testing and Materials; BS, British Standards Institution; CGSB, Canadian General Standard Board; CNS, Chinese National Standards; DIN, Deutsche Institut für Normung; ISO, International Organization for Standardization; SASO, Saudi Arabian Standards Organization; TAPPI, Technical Association of the Pulp and Paper Industry; IP, Institute of Petroleum.

Distillation is used widely to determine the moisture or water content of a variety of samples from petroleum products to cereal feeds. The technique used is one of azeotropic distillation using a codistillate such as toluene. Table 3 includes a selection of the available methods. Dean and Stark provided a particular design of apparatus that can be used for determining water content following azeotropic distillation with an immiscible organic solvent. As the azeotropic distillate condenses, the water separates from the immiscible organic and can be estimated directly in a specially graduated collection arm.

Some methods for the determination of water quality involve distillation, for example the determination of a 'phenol index', nitrate content or ammonium content.

The determination of nitrogen by the Kjeldahl method involves a preliminary distillation of the sample. Thus methods for the determination of ammoniacal and total nitrogen in ammonium nitrate, urea, sulfuric acid and fertilizers for industrial purposes involve a preliminary distillation followed by titrimetry.

Methods for the determination of available fluorine involve distillation prior to a potentiometric or spectrometric method.

The determination of distillation range is a method of establishing the purity of materials. Specific standard methods are available, for example, for methanol, ethylene glycol and propylene glycol. Many unpublished in company methods are used for products and intermediates to validate purity standards and to establish the suitability of materials for subsequent use.

As trace analysis of residual compounds in consumables has become more important, methods of extracting these compounds have been developed. A method known as simultaneous distillation extraction developed from the original work of Likens and Nickerson has been particularly popular and effective for extracting the volatiles from foods and plant materials, and the herbicide and pesticide residues in agricultural products. The method involves steam distilling the compound of interest from an aqueous suspension of the crude sample while the condensed steam is continuously extracted with an immiscible organic solvent refluxing within the apparatus. The design of the apparatus allows the volatiles that are extracted from the condensed water to be flushed into the flask containing the organic solvent. After a previously determined time of extraction, the apparatus may be disassembled and the organic solvent removed by evaporation from the now concentrated extract. Further analytical techniques can be used to identify and quantify the components of the residue according to the particular requirements.

A common application of distillation in the separation sciences is the purification and recovery of solvents especially from HPLC and GPC usage. There is a range of equipment supplied for recycling of solvents and useful sources of information can be found on the internet, for example the web pages for B/R Instruments and Recycling Sciences are included in the Further Reading.

The applications of distillation in analysis are widespread, with the technique being used to characterize materials and as a means of preparing samples prior to analysis. Standard apparatus and methods are described for many specific applications. Reference to the general texts and the standards detailed in the Further Reading will provide a source of information for future applications.

See also: II/Distillation: Energy Management; Historical Development; Laboratory Scale Distillation; Multicomponent Distillation; Vapour-Liquid Equilibrium: Theory.

Further Reading

AnalaR Standards for Laboratory Chemicals. AnalaR Standards (1984) (AnalaR is a registered trademark of Merck Ltd.).

Annual Book of American Society for Testing and Materials. Philadelphia: ASTM.

B/R Instruments Corporation – www.brinstruments.com

BSI Standards Catalogue. London: British Standards Institute. Distillation Principles – <http://lorien.ncl.ac.uk/ming/distil/distil0.htm>

Furniss BS, Hannaford AJ, Smith PWG and Tatchell AR (1989) *Vogel's Textbook of Practical Organic Chemistry*, 5th edn. pp. 168–197. Harlow: Longman Scientific & Technical.

Godefroot M, Sandra P and Verzele MJ (1981) *Chromatography* 203: 325.

Likens ST and Nickerson GB (1964) *American Society of Brewing Chemists, Proceedings*, 5.

Methods for Analysis & Testing (1993) IP Standards for Petroleum & Related Products, 52nd edn. London: Wiley, Institute of Petroleum.

Perrin DD and Armarego WL (eds.) (1988) *Purification of Laboratory Chemicals*, 3rd edn, pp. 5–12. Oxford: Pergamon Press.

Reagent Chemicals, 8th edn. (1993) American Chemical Society.

Recycling Sciences Inc. – www.rescience.com

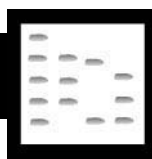
Robillard MV, Spock PS and Whitford JH (1991) *An Overview of Methodology and Column Technology for Simulated Distillation Analysis*. Bellefonte, PA: Supelco.

Stichlmair J and Fair J (1998) *Distillation – Principles and Practice*. New York: John Wiley.

ANION EXCHANGERS FOR WATER TREATMENT: ION EXCHANGE

See III / WATER TREATMENT / Anion Exchangers: Ion Exchange

ANTIBIOTICS



High-Speed Countercurrent Chromatography

H. Oka, Aichi Prefectural Institute of Public Health, Nagoya, Japan,
Y. Ito, National Institutes of Health, Bethesda, MD, USA

Copyright © 2000 Academic Press

Introduction

Development of antibiotics requires considerable research effort in isolation and purification of the

desired compound from a complex matrix such as fermentation broth and crude extract. The purification of antibiotics by liquid-liquid partition dates back to the 1950s when the countercurrent distribution method (CCD) was used for separation of various natural products such as peptide antibiotics, aminoglycoside antibiotics and penicillin. However, CCD had serious drawbacks such as bulky fragile apparatus, long separation times and excessive dilution of samples. In the early 1970s an efficient continuous countercurrent separation method called countercurrent chromatography was introduced followed by the advent of high speed countercurrent chromatography (HSCCC) a decade later. Because of its high partition efficiency and speedy separation,

HSCCC has been widely used for separation and purification of natural products including a number of antibiotics as listed in Table 1. Being support-free chromatographic systems, HSCCC and CCD share important advantages over other chromatographic systems by eliminating complications arising from a solid support such as sample loss and decomposition.

Selection of Two-Phase Solvent System

Among the purification of natural products, the isolation of antibiotics is one of the most difficult tasks since the crude sample often contains, in addition to numerous impurities, a set of closely

related components that tend to exhibit similar partition behaviour in a given solvent system. Consequently, successful separation necessitates a painstaking search for a suitable solvent system, which often requires days, weeks and even months of hard trial. Once a suitable solvent system is found, however, the separation is usually completed within several hours.

HSCCC utilizes two immiscible solvent phases, one as a stationary phase and the other as a mobile phase. Solutes are subjected to a continuous partition process between these two phases along the column space free of a solid support, hence the separation is almost entirely governed by the difference between their partition coefficients.

Table 1 Separation of antibiotics by HSCCC

<i>Sample</i>	<i>Amount</i>	<i>Solvent system</i>	<i>Mobile phase</i>
Daunorubicin derivatives		Chloroform/ethylene chloride/hexane/methanol/water (1:1:1:3.5:1)	UP
Gramicidins A, B, and C	100 mg	Benzene/chloroform/methanol/water (15:15:23:7)	UP
Siderochelin A	400 mg	Chloroform/methanol/water (7:13:8)	UP
Efrotomycin	670 mg	Carbon tetrachloride/chloroform/methanol/water (5:5:6:4)	UP
Pentalenolactone	50 mg	Chloroform/methanol/water (1:1:1)	UP
Bu 2313B	200 mg	<i>n</i> -Hexane/dichloromethane/methanol/water (5:1:1:1)	LP
A 201E	350 mg	Carbon tetrachloride/chloroform/methanol/water (2:5:5:5)	UP
Tirandamycin A and B	134 mg	<i>n</i> -Hexane/ethyl acetate/methanol/water (70:30:15:6)	UP
Actinomycin complex	83 mg	Ether/hexane/methanol/water (5:1:4:5)	UP
Benzanthrins A and B (quinone antibiotics)	620 mg	Carbon tetrachloride/chloroform/methanol/water (4:1:4:1)	UP
Coloradocin	400 mg	Chloroform/methanol/water (1:1:1)	UP
Candicidin (polyene macrolide antibiotics)	100 mg	Chloroform/methanol/water (4:4:3)	?
2-Norerythromycins (macrolide antibiotics)	500 mg	<i>n</i> -Heptane/benzene/acetone/isopropanol/0.01 mol L ⁻¹ citrate buffer (pH 6.3) (5:10:2:3:5)	UP
Niddamycins (macrolide antibiotics)	200 mg	Carbon tetrachloride/methanol/0.01 mol L ⁻¹ potassium phosphate buffer (pH 7) (2:3:2)	UP
Tiacumicins (macrolide antibiotics)	200 mg	Carbon tetrachloride/chloroform/methanol/water (7:3:7:3)	UP
Coloradocin (macrolide antibiotics)	400 mg	Chloroform/methanol/water (1:1:1)	UP
Sporaviridin complex	100 mg	<i>n</i> -Butanol/diethylether/water (10:4:12)	LP
Dunaimycin (macrolide antibiotics)		<i>n</i> -Hexane/ethyl acetate/methanol/water (8:2:10:5)/(70:30:15:6)	UP
Bacitracin complex	50 mg	Chloroform/ethanol/water (5:4:3)	LP
Bacitracin complex	50 mg	Chloroform/ethanol/methanol/water (5:3:3:4)	LP
Mycinamicins	Analytical works	<i>n</i> -Hexane/ethyl acetate/methanol/8% aq. ammonia (1:1:1:1)	LP
Colistins	Analytical works	<i>n</i> -Butanol/0.04 mol L ⁻¹ TFA (1:1) containing 1% glycerol	LP
Pristinamycins (macrolide antibiotics)	1 mg	Chloroform/ethyl acetate/methanol/water (3:1:3:2)	UP
Pristinamycins (macrolide antibiotics)	1 mg	Chloroform/ethyl acetate/methanol/water (2.4:1.6:3:2)	UP
Ivermectin	25 mg	<i>n</i> -Hexane/ethyl acetate/methanol/water (19:1:10:10)	LP
Colistin	20 mg	<i>n</i> -Butanol/0.04 mol L ⁻¹ TFA (1:1)	LP

Generally speaking, the two-phase solvent system should satisfy the following requirements:

1. *Retention of the stationary phase.* Since the system eliminates the solid support, the retention of the stationary phase in the separation column entirely depends upon the hydrodynamic interaction between the two solvent phases in the rotating column under a centrifugal force field. While the hydrodynamic motion of the two phases is highly complex, the retention of the stationary phase may be predicted by the following simple procedure to measure the settling time of the two phases under gravity: Place 2 mL of each phase of the equilibrated two-phase solvent system into a 5 mL capacity graduated cylinder (alternatively, a 13 mm o.d. and 100 mm long glass test tube equipped with a plastic cap may also be used) which is then sealed with a stopper. Gently invert the cylinder five times to mix the contents and immediately place it on flat surface to measure the time required for the mixture to settle into two layers. This settling time should be considerably less than 30 s for stable retention of the stationary phase.

2. *Partition coefficient (K).* The partition coefficient is the key parameter for HSCCC. It is usually expressed by the analyte concentration in the stationary phase divided by that of the mobile phase. For a successful separation, the K value of an analyte should be close to 1. If $K \ll 1$, the analyte will elute close to the solvent front resulting in loss of peak resolution. On the other hand, if $K \gg 1$, the analyte will remain in the separation column for a long period of time, producing an excessively broad peak. In order to separate two components, the ratio between their partition coefficients, which is called separation factor (α), should be 1.5 or greater for a standard semipreparative multilayer coil HSCCC equipment providing a moderate partition efficiency of about 800 theoretical plates.

HSCCC Separation of Antibiotics

As mentioned earlier, HSCCC has been successfully applied to the separation of a variety of antibiotics (Table 1). The list includes peptide antibiotics, which are strongly adsorbed on the silica gel used as the stationary phase in column chromatography. Sample loading capacity of HSCCC widely varies from 1 mg to 10 g, depending on the tube diameter and the length of the multilayer coil used as the separation column. Two-phase solvent systems may be selected according to the hydrophobicity of the analytes, i.e. *n*-butanol solvent systems for hydrophilic groups, chloroform systems for moderately hydrophobic groups, and *n*-hexane systems for the most hydropho-

bic groups. Below, we describe the HSCCC separation of selected antibiotics including sporaviridins, bacitracins, colistins and ivermectins, especially focusing on the procedures for optimization of two-phase solvent systems.

The apparatus used in the following separations was a HSCCC-1A prototype multilayer coil planet centrifuge (Shimadzu Corporation, Kyoto, Japan) with a 10 cm orbital radius which produces a type-J synchronous planetary motion at 800 rpm. The multilayer coil was prepared by winding about 160 m of PTFE (polytetrafluoroethylene) tubing onto the column holder. Unless otherwise indicated, all separations were performed under the following conditions: speed of revolution: 800 rpm; stationary phase: organic phase; flow rate: 3 mL min⁻¹; elution mode: head to tail.

Sporaviridins

Sporaviridins (SVD, Figure 1) are basic water-soluble antibiotics produced by *Kutzneria viridogrisea* (formerly) *Streptosporangium viridogriseum* and they are active against Gram-positive bacteria, acid-fast bacteria and trichophyton. As shown in Figure 2, they consist of six components each having a 34-membered lactone ring and seven monosaccharide units, one pentasaccharide (viridopentaose) and two monosaccharides.

The SDV complex is soluble only in polar solvents such as water, methanol and *n*-butanol, and is extracted with *n*-butanol from the fermentation broth. Therefore, a two-phase solvent system containing *n*-butanol as a major organic solvent was mainly examined. We found that the SVD sample was entirely partitioned into the upper organic phase in a *n*-butanol/water binary two-phase solvent system (Table 2). This result indicated that the hydrophobicity of the *n*-butanol phase must be decreased to obtain a suitable partition coefficient. A nonpolar solvent such as *n*-hexane or diethyl ether was added to the *n*-butanol solvent system as a modifier. Initially, the volume of *n*-butanol was fixed at 10 mL while that of the diethyl ether was varied, and a two-phase system composed of diethyl ether/*n*-butanol/water (10:4:10) was selected. Next, the volumes of *n*-butanol and diethyl ether were fixed while that of water was varied from 11 to 14. At a solvent ratio of 10:4:12, almost evenly dispersed partition coefficients among the six components were obtained as shown in Table 2. Therefore, this solvent system was selected for the separation of the SVD components.

The preparative HSCCC separation of six components from the SVD complex was performed. In this experiment the retention of the stationary phase, elution time, and elution volume were 75%, 3.5 h and

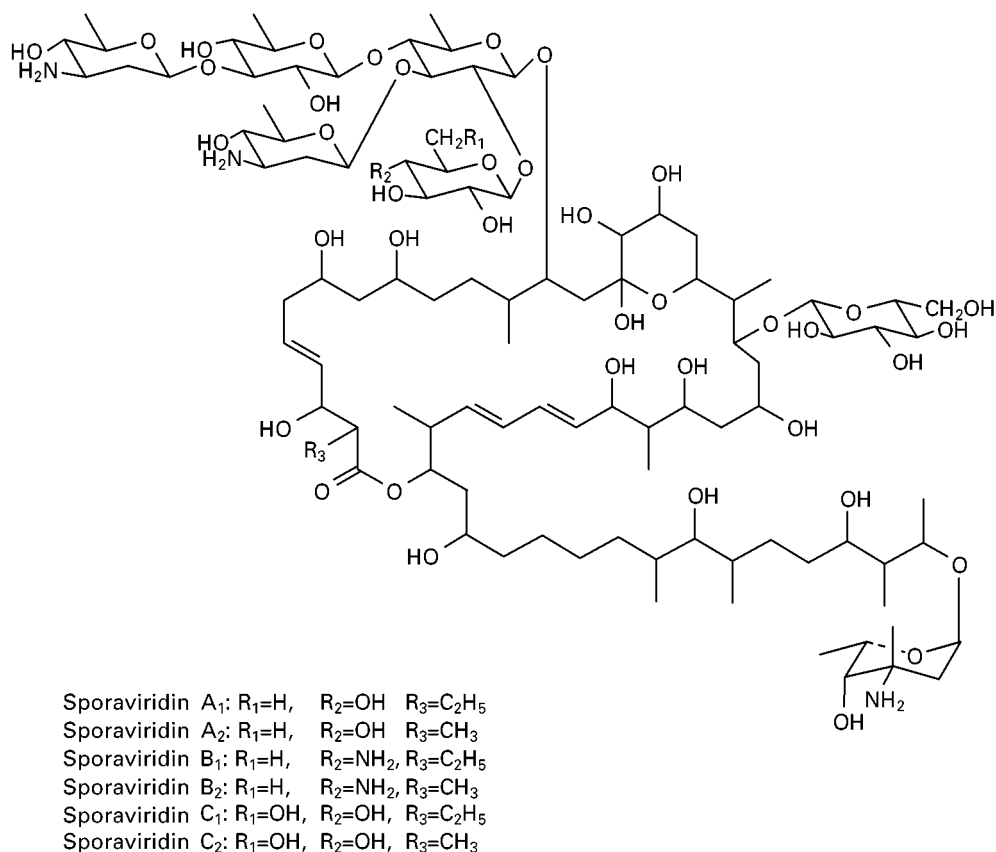


Figure 1 Structures of sporaviridins. (Reproduced with permission from Oka H *et al.* (1998).)

500 mL, respectively. The six components were eluted in an increasing order of their partition coefficients yielding high purity of components A₁ (1.4 mg), A₂ (0.6 mg), B₁ (0.7 mg), B₂ (0.5 mg), C₁ (1.1 mg), and C₂ (1.4 mg) from 15 mg of the SVD

complex. HPLC analyses of the purified components are illustrated in **Figure 3**.

Bacitracins

Bacitracins (BCs) are peptide antibiotics produced by *Bacillus subtilis* and *Bacillus licheniformis*. They exhibit an inhibitory activity against Gram-positive bacteria and are most commonly used as animal feed

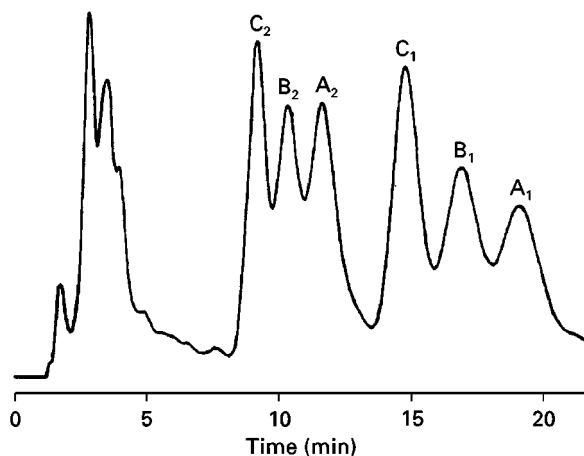


Figure 2 HPLC separation of sporaviridins. Column, Cosmosil 5C18 (5 μ m, 4.6 \times 150 mm); mobile phase, methanol/1 mol L⁻¹ ammonium chloride (74:26); flow rate, 1 mL min⁻¹; detection, 232 nm. (Reproduced with permission from Oka H *et al.* (1998).)

Table 2 Partition coefficients of SVD components with *n*-butanol systems

<i>n</i> -Butanol/ diethyl ether/water	Partition coefficients (UL ⁻¹)					
	C2	B2	A2	C1	B1	A1
10:0:10	2.96	6.41	6.65	4.87	8.81	9.09
10:3:10	0.96	2.17	2.78	1.84	3.34	4.19
10:4:10	0.50	1.12	1.59	1.04	1.85	2.91
10:5:10	0.38	0.78	1.11	0.74	1.25	2.12
10:6:10	0.39	0.90	1.19	0.81	1.39	1.70
10:7:10	0.24	0.63	1.10	0.59	1.08	1.82
10:4:11	0.31	0.89	1.24	0.70	1.50	2.00
10:4:12	0.38	1.09	1.41	0.80	1.85	2.32
10:4:13	0.37	1.05	1.51	0.73	1.58	2.10
10:4:14	0.29	1.09	1.17	0.57	1.22	1.74

Reproduced with permission from Harada K-I *et al.* (1990) and Oka H *et al.* (1998).

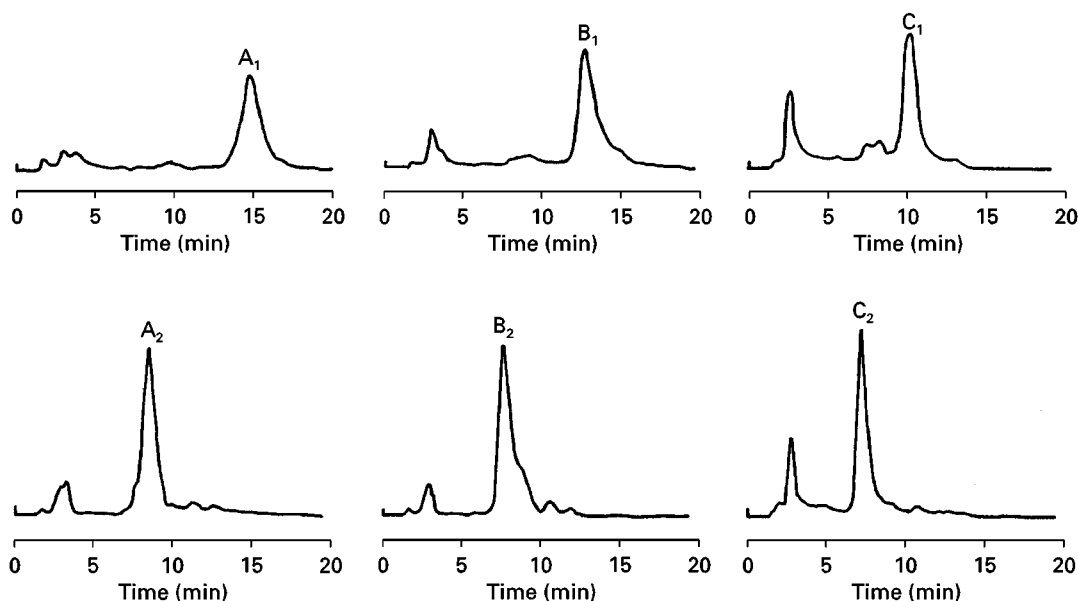


Figure 3 HPLC separation of sporaviridin components. For experimental conditions, see legend to Figure 2. (Reproduced with permission from Oka H *et al.* (1998) and Harada K-I *et al.* (1990).)

additives. Over 20 components are present in the bacitracin complex (Figure 4) among which BC-A and BC-B are the major antimicrobial components. BC-F is a degradation product and has nephrotoxicity. Only the structures of BC-A and -F have been determined (Figure 5).

We examined three groups of two-phase solvent systems containing *n*-butanol, ethyl acetate or chloroform as a major organic solvent, and ethanol and/or methanol as a modifier against water in each group. The *n*-butanol system produced suitable *K* values for

peaks 13–18 whereas those for peaks 20–22 are too large. The ethyl acetate system represented by ethyl acetate/ethanol/water showed a long settling time, suggesting poor retention of the stationary phase in the column. The most promising results were obtained from the chloroform, ethanol and/or methanol, water systems as summarized in Table 3. Among all combinations for the solvent volume ratio, chloroform/ethanol/ methanol/water (5:3:3:4) and chloroform/ethanol/water (5:4:3) gave the most desirable *K* values.

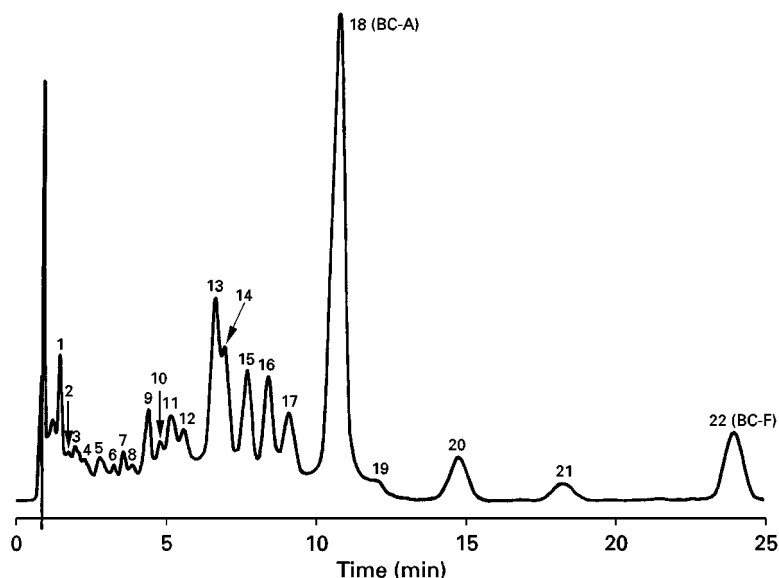


Figure 4 HPLC separation of bacitracins. Column Capcel Pak C₁₈ (5 μ m, 4.6 \times 150 mm); mobile phase, methanol/0.04 mol L⁻¹ sodium dihydrogen phosphate (6:4); flow rate, 1.3 mL min⁻¹; detection, 234 nm. (Reproduced with permission from Oka H *et al.* (1998) and Harada K-I *et al.* (1991).)

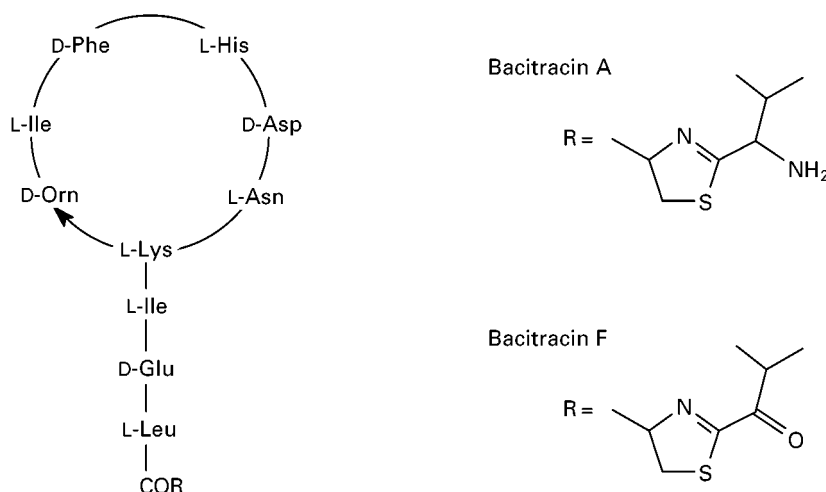


Figure 5 Structures of bacitracins A and F. (Reproduced with permission from Harada K-I *et al.* (1991) and Oka H *et al.* (1998).)

Figure 6 shows the countercurrent chromatogram of bacitracin components using the chloroform/ethanol/methanol/water (5:3:3:4) system. A 50 mg amount of the bacitracin complex was loaded into the HSCCC column. The retention of the stationary phase was 72.7% and the elution time was about 3 h. All components were eluted in an increasing order of their partition coefficients, yielding 5.5 mg of BC-A from peak 18 and 1.5 mg of BC-F from peak 22.

Ivermectins

Ivermectins B₁ are broad spectrum antiparasitic agents widely used for food-producing animals such as cattle and pigs. They are derived from avermectins B₁, the natural fermentation products of *Streptomyces avermitilis*. Avermectins B₁ have double bonds between carbon atoms at 22 and 23, whereas the ivermectins B₁ have single bonds in these positions (Figure 7). The ivermectins B₁ are a mixture of two major homologues, ivermectin B1a (> 80%) and ivermectin B1b (≤ 20%), but a crude ivermectin complex also contains various minor compounds (Figure 8A).

Table 3 Partition coefficients of the bacitracin components

Chloroform ethanol/ methanol/ water	Partition coefficients (UL^{-1})						
	Peaks	3, 14	17	18	20	21	22
5:2:3:4		7.20	2.46	4.17	0.64	0.65	0.48
5:2:1:4		∞	∞	33.27	1.62	1.38	0.75
5:3:3:4		3.35	1.40	2.37	0.57	0.47	0.45
5:3:0:3		11.1	3.20	5.34	0.32	0.35	0.27
5:4:0:2		3.19	1.05	2.00	0.25	0.26	0.21
5:4:0:3		5.49	1.46	2.20	0.16	0	0.16
5:4:0:4		6.10	2.04	2.68	0.14	0	0.10

(Reproduced with permission from Harada K-I *et al.* (1991) and Oka H *et al.* (1998).)

We selected a two-phase solvent system composed of *n*-hexane, ethyl acetate, methanol and water. This solvent system is conveniently used for the separation of components with a broad range of hydrophobicity by modifying the volume ratio between the four solvents. In the *n*-hexane/ethyl acetate/methanol/water (8:2:5:5) system first examined, the *K* values of the components corresponding to peaks 1–7 were 0, 0.46, 0.61, ∞, 1.86, 3.06, and 4.38, respectively.

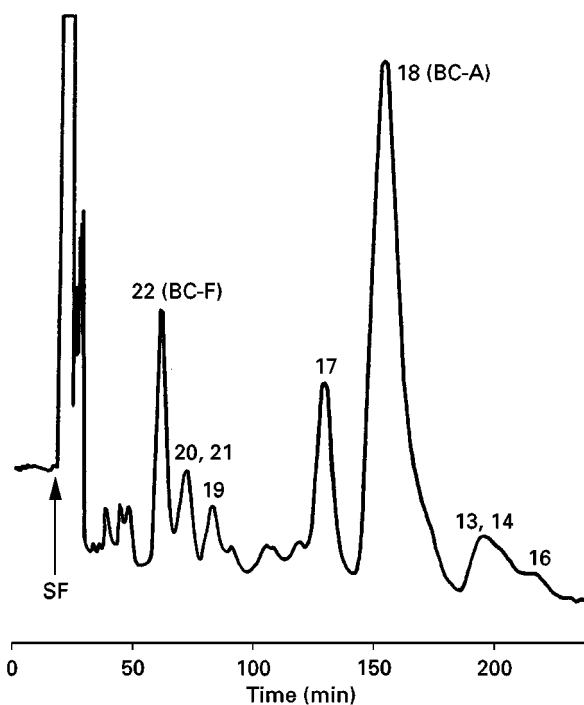


Figure 6 HSCCC separation of bacitracin components. Apparatus, HSCCC-1A; revolution, 800 rpm; solvent system, chloroform/ethanol/methanol/water (5:3:3:4); mobile phase, lower organic phase; flow rate, 3 mL min⁻¹; detection, 254 nm. (Reproduced with permission from Harada K-I *et al.* (1991) and Oka H *et al.* (1998).)

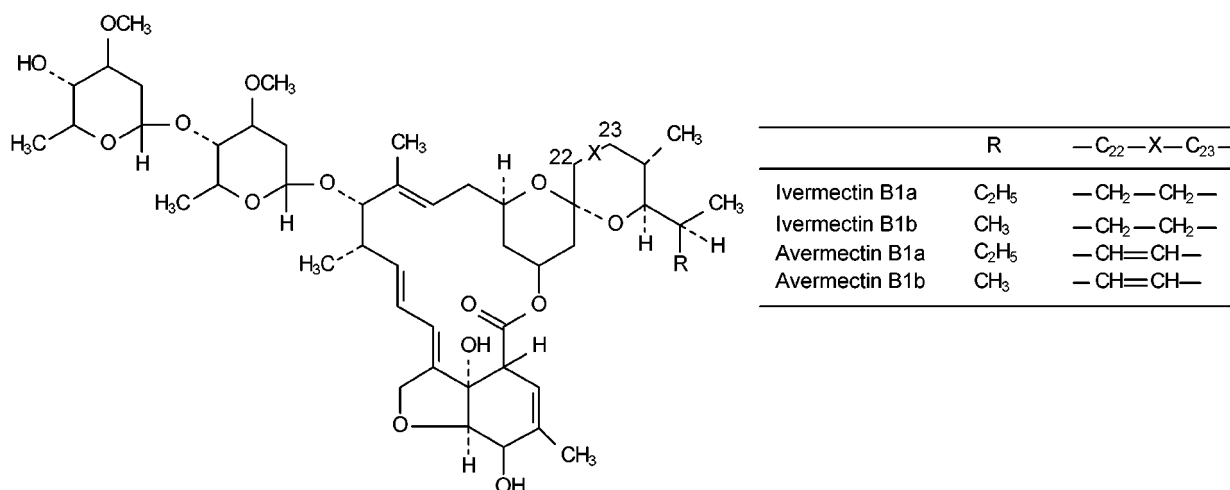


Figure 7 Structures of ivermectins and avermectins. (Reproduced with permission from Oka H *et al.* (1996, 1998).)

This indicates that the component corresponding to peak 6 (ivermectin B1a) is mostly partitioned in the upper organic phase (Table 4). Although the *n*-hexane/ethyl acetate/methanol/water (9:1:5:5) system somewhat improved the *K* value of peak 6, it was still too large and the α value between peaks 6 and 7 is smaller than 1.5. Finally a slightly less polar solvent mixture at the volume ratio of 19:1:10:10 yielded the best *K* value, as indicated in Table 4. The settling time of this solvent system was 7 s, promising excellent retention of the stationary phase. In addition, the volume ratio between the two phases is nearly 1, indicating that either phase can be used as the mobile phase without wasting the solvents. Therefore, the above solvent was selected for separation of ivermectin components.

A 25 mg quantity of crude ivermectin was separated using the above solvent system at a flow rate of 2 mL min⁻¹. The retention of the stationary phase was 67.6% and the total separation time, 4.0 h. The HSCCC elution curve of the ivermectin components monitored at 245 nm is shown in Figure 9, where all components are separated into three peaks, A, B and C. HPLC analysis of each peak fraction and the column contents revealed that both HPLC and HSCCC systems elute all components in the same order: HPLC peaks 3, 5, and 6 correspond to HSCCC peaks A, B and C, respectively, while HPLC peak 7 was still retained in the HSCCC column. This separation yielded 18.7 mg of 99.0% pure ivermectin B1a (Figure 8B), 1.0 mg of 96.0% pure ivermectin

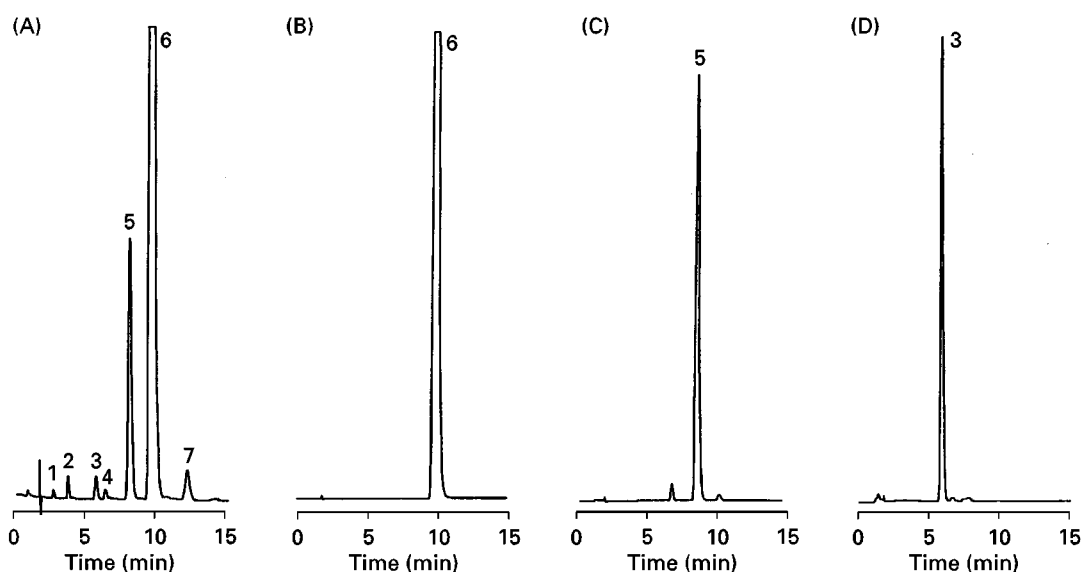


Figure 8 HPLC separation of ivermectin components. Column, TSK GEL-80 TsC₁₈ (5 μ m, 4.6 \times 150 mm); mobile phase, methanol/water (9:1); flow rate, 1 mL min⁻¹; detection, 245 nm. (A) Crude ivermectin; (B) Fraction II (ivermectin B1a); (C) Fraction IV (ivermectin B1b); (D) Fraction VI (avermectin B1a). (Reproduced with permission from Oka H *et al.* (1998).)

Table 4 Partition coefficients of the ivermectin components (K = peak area of upper phase divided by peak area of lower phase.)

Solvent system	Peak no.						
	1	2	3	4	5	6	7
<i>n</i> -Hexane/ethyl acetate/methanol/water (8:2:5:5)	0	0.46	0.61	∞	1.86	3.06	4.38
<i>n</i> -Hexane/ethyl acetate/methanol/water (9:1:5:5)	0	0.15	0.33	∞	1.17	2.31	3.21
<i>n</i> -Hexane/ethyl acetate/methanol/water (19:1:10:10)	0	0	0.18	0.48	0.79	1.36	2.83

(Reproduced with permission from Oka H *et al.* (1996, 1998).)

B1b (Figure 8C) and 0.3 mg of 98.0% pure avermectin B1a (precursor of ivermectin) (Figure 8D).

Colistin

Colistin (CL) is a peptide antibiotic produced by *Bacillus polymyxa* var. *Colistinus* that inhibits the growth of Gram-negative organisms. CL is a mixture of many components (Figure 10) where two main components are colistins A (CL-A) and B (CL-B). As shown in Figure 11, CLs-A and -B are linear-ring peptides that differ only in their *N*-terminal fatty acid. CL is used as a feed additive for domestic animals such as calf and pigs for preventing bacterial infection and/or improving feed conversion efficiency. CL is soluble in water, slightly soluble in alcohols, but insoluble in nonpolar solvents such as hexane and chloroform. From this property, we selected *n*-bu-

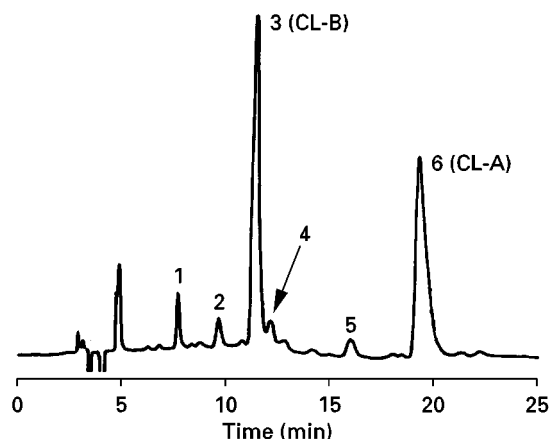


Figure 10 HPLC separation of commercial CL. Column, Chromatorex Ph ($5\ \mu\text{m}$, $4.6 \times 250\ \text{mm}$); mobile phase, acetonitrile/ $0.01\ \text{mol L}^{-1}$ TFA aqueous solution (24:76); flow rate, $1.0\ \text{mL min}^{-1}$; detection, $210\ \text{nm}$. (Reproduced with permission from Ikai Y *et al.* (1998) and Oka H *et al.* (1998).)

tanol and water as a basic solvent system. However, this combination was not suitable by itself, because the CL components were entirely partitioned into the aqueous phase. In order to partition the CL components partly into the *n*-butanol phase, various salts (NaCl and Na_2SO_4) or acids (HCl , H_2SO_4 and CF_3COOH or TFA) were added as a modifier. The desired effect was produced from TFA where the partition coefficients of CL components rose as the concentration of TFA in the solvent system was increased. This effect may be explained as follows: as shown in Figure 11, CLs-A and -B have five free amino groups in L-diamino-butyric acid (L-Dab), and these amino groups dissociate in the aqueous phase under neutral to acidic conditions. Since TFA forms an ion pair with these amino groups, the hydrophobicity of the CL components increases with the concentration of TFA resulting in their partition toward the organic phase. In order to determine the optimal concentration of TFA in the solvent system, K values of five components were measured at various TFA concentrations. As shown in Figure 12, the K value of each component increases with the TFA concentration, and at $40\ \text{mmol L}^{-1}$ TFA concentration, K values of CL-A and CL-B reached 1.5 and 0.6, respectively. At this TFA concentration, the α values between the adjacent peaks are all greater than 1.5, promising a good separation for all components. The settling time of the solvent system was 28 s, which is within the acceptable range. Therefore, we selected a solvent system of *n*-butanol/ $40\ \text{mmol L}^{-1}$ TFA aqueous solution (1:1) for the HSCCC separation.

Using the above solvent system, a 20 mg quantity of commercial CL was separated by HSCCC. The retention of the stationary phase was 45%. The

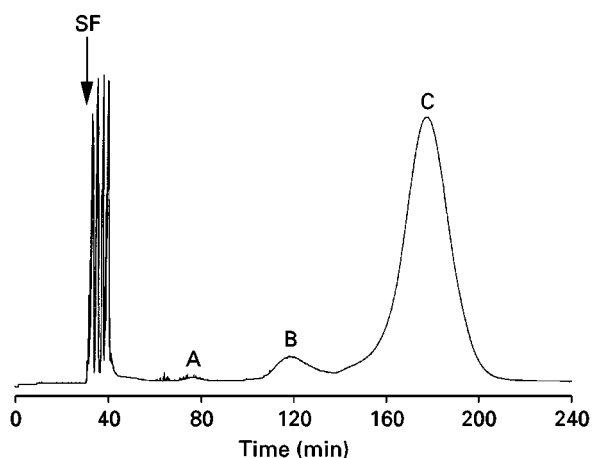


Figure 9 HSCCC separation of ivermectin components. Apparatus, HSCCC-1A; revolution, 800 rpm; solvent system, *n*-hexane/ethyl acetate/methanol/water (19:1:10:10) mobile phase, lower aqueous phase; flow rate, $2\ \text{mL min}^{-1}$; detection, $245\ \text{nm}$. (Reproduced with permission from Oka H *et al.* (1996, 1998).)

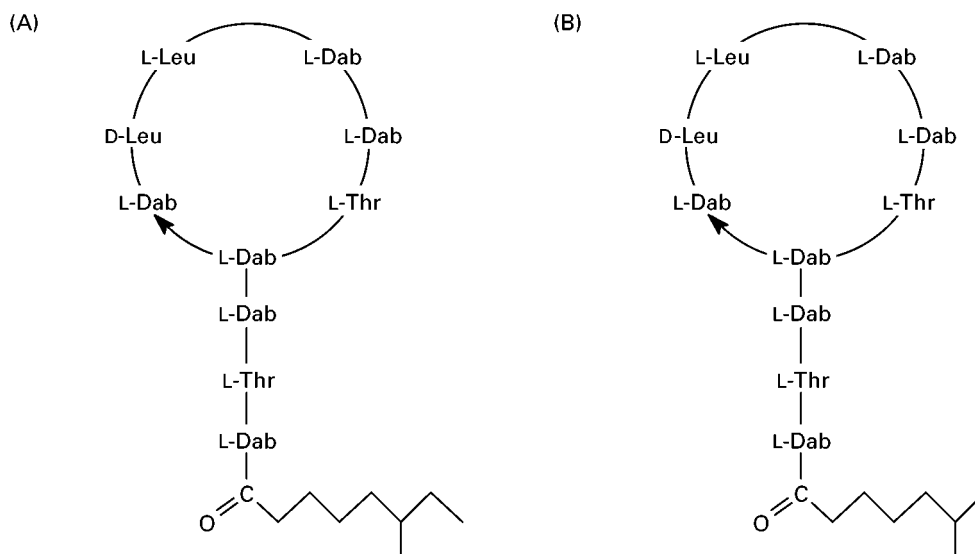


Figure 11 Structures of colistin components. (Reproduced with permission from Ikai Y *et al.* (1998) and Oka H *et al.* (1998).)

elution curve monitored at 220 nm is shown in **Figure 13**. According to the results of HPLC analysis and the elution curve, all collected fractions were combined into five large fractions as shown in **Figure 13**. The yields of CL-A and CL-B were 9 mg each and those of other minor components were 0.5–1.0 mg. HPLC analysis was performed for each fraction; as shown in **Figure 14**, the fractions of CLs-A and -B each produced a peak with a purity of over 90%.

Conclusions

Because it is a support-free partition system, HSCCC has an important advantage over other chromatographic methods in that it eliminates various com-

plications such as adsorptive loss and deactivation of samples as well as contamination from the solid support. As shown by our examples, HSCCC can isolate various components from a complex mixture of antibiotics by carefully selecting the two-phase solvent system to optimize the partition coefficient (K) of the target component(s). Compared with CCD and other countercurrent extraction methods, HSCCC can yield higher partition efficiencies in a shorter elution time. The HSCCC system can also be applied to microanalytical-scale separations without excessive dilution of samples. We believe that HSCCC is an

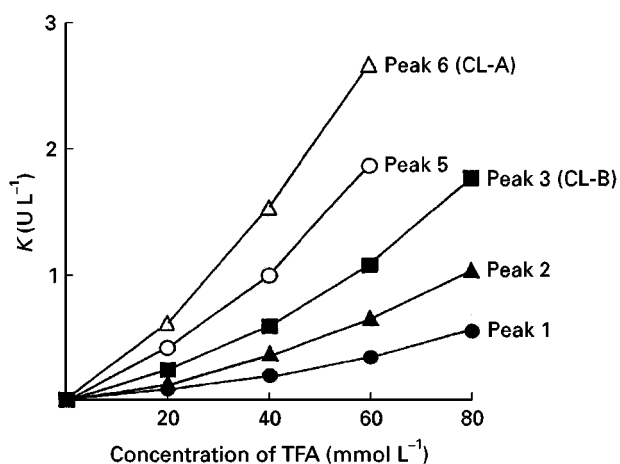


Figure 12 Effect of TFA concentration on the partition coefficients of CL components. (Reproduced with permission from Ikai Y *et al.* (1998) and Oka H *et al.* (1998).)

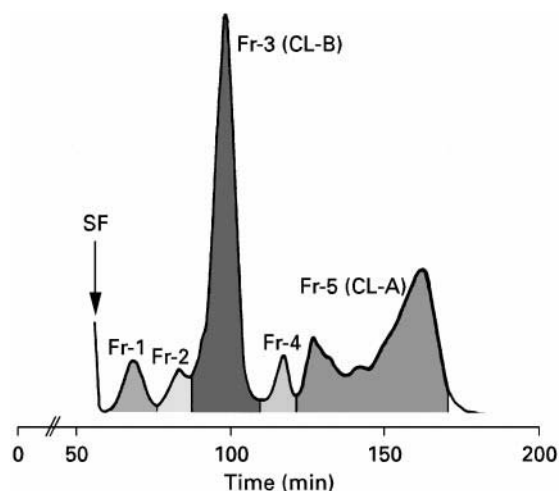


Figure 13 HSCCC separation of commercial CL. Apparatus, HSCCC-1A; revolution, 800 rpm; solvent system, *n*-butanol/0.04 mol L⁻¹ TFA aqueous solution (1:1); mobile phase, lower aqueous phase; flow rate, 2.0 mL min⁻¹; detection, 220 nm. (Reproduced with permission from Ikai Y *et al.* (1998) and Oka H *et al.* (1998).)

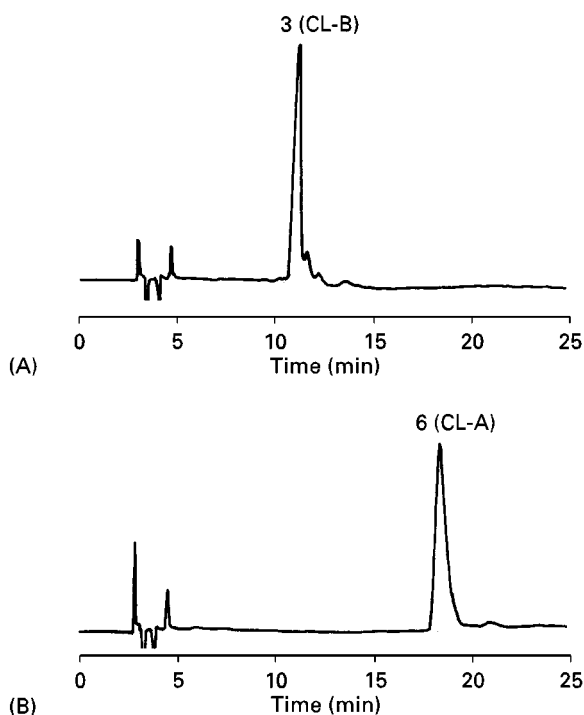


Figure 14 HPLC analysis of CL components of HSCCC fractions. (A) CL-A (Fraction 5); (B) CL-B (Fraction 3). (Reproduced with permission from Oka H *et al.* (1998).)

ideal method for separation and purification of antibiotics.

See also: II/Chromatography: Countercurrent Chromatography and High-Speed Countercurrent. Chromatography:

Instrumentation. **Chromatography: Liquid:** Countercurrent Liquid Chromatography. **III/Antibiotics:** Liquid Chromatography. Supercritical Fluid Chromatography.

Further Reading

- Harada K-I, Kimura I, Yoshikawa A *et al.* (1990) Structural investigation of the antibiotic Sporaviridin. XV. Preparative-scale preparation of Sporaviridin components by HSCCC. *Journal of Liquid Chromatography* 13: 2373–2388.
- Harada K-I, Ikai Y, Yamazaki, Y *et al.* (1991) Isolation of bacitracins A and F by high-speed counter-current chromatography. *Journal of Chromatography* 538: 203–212.
- Ikai Y, Oka H, Hayakawa J *et al.* (1998) Isolation of colistin A and B using high-speed countercurrent chromatography. *Journal of Liquid Chromatography* 21: 143–155.
- Ito Y and Conway WD (1996) *High-Speed Countercurrent Chromatography*. New York: Wiley.
- Oka H, Ikai Y, Kawamura N *et al.* (1991) Direct interfacing of high speed countercurrent chromatography to frit electron, chemical ionization, and fast atom bombardment mass spectrometry. *Analytical Chemistry* 63: 2861–2865.
- Oka H, Ikai Y, Hayakawa J *et al.* (1996) Separation of ivermectin components by high-speed counter-current chromatography. *Journal of Chromatography A* 723: 61–68.
- Oka H, Harada K-I, Ito Y and Ito Y (1998) Separation of antibiotics by countercurrent chromatography. *Journal of Chromatography A* 812: 35–52.

Liquid Chromatography

T. Itoh and H. Yamada, Kitasato University, Tokyo, Japan

Copyright © 2000 Academic Press

Introduction

High performance liquid chromatography (HPLC) has been widely used for the analysis of antibiotics because it is superior to conventional microbiological assays in terms of specificity, sensitivity and analysis time. In this article, HPLC conditions for the analysis of a variety of antibiotics are summarized. For analysis of biological samples, not only extraction methods but also derivatization methods are described, if necessary. Since it is not possible to list HPLC methods for all antibiotics in clinical use, only a few have been chosen from each class. Where a stereoisomer exists

for the antibiotic of interest, the HPLC conditions that are able to resolve stereoisomers are described.

Aminoglycosides

Aminoglycosides are analysed by reversed-phase HPLC. However, derivatization is usually necessary owing to very poor UV or visible absorption. For detection of aminoglycosides without derivatization, electrochemical, refractive index or mass spectrometric detection may be used.

Amikacin

For determination of amikacin (Figure 1, structure 1), the serum sample is loaded onto the silica gel column, followed by addition of *o*-phthalaldehyde (a derivatizing reagent). The column is eluted with 95% ethanol (pH 10) and the eluent is heated at 50°C. After cooling, the mixture is injected onto an ODS

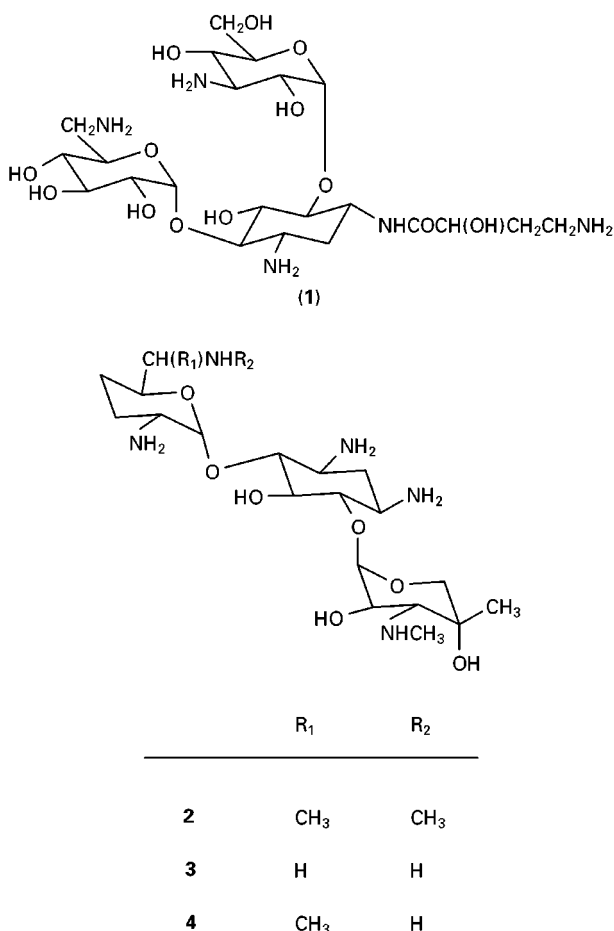


Figure 1 Chemical structures of amikacin (1) and gentamycins C₁ (2), C_{1a} (3) and C₂ (4).

column. Mobile phase is methanol–water–acetonitrile (65 : 30 : 5) containing 0.2% tripotassium ethylenediamine tetraacetic acid (EDTA). Amikacin is detected fluorometrically at 350 nm for excitation and 420 nm for emission. The detection limit is 1 µg mL⁻¹. In order to resolve amikacin from its three isomers, a similar method is used except that the mobile phase is methanol–water (7 : 3). Tobramycin may be analysed with the same method.

Pre-column derivatization of amikacin is also conducted by addition of 1-fluoro-2,4-dinitrobenzene to plasma or urine, leading to formation of a stable chromophore, which can be detected at 360 nm. An ODS column is used with a mobile phase consisting of acetonitrile–water (68 : 32). The detection limit is 1 µg mL⁻¹. Amikacin may be extracted from serum using a cation exchange solid-phase extraction column prior to derivatization.

Gentamycin

Gentamycin in plasma is extracted with a cation exchange solid-phase extraction column (carboxy-

propyl-bonded silica column). Gentamycin is eluted with a 1 : 1 mixture of acetonitrile–0.2 mol L⁻¹ borate buffer (pH 10.5) and is derivatized with 9-fluorenylmethyl chloroformate. Derivatized gentamycin is analysed on an ODS column with a mobile phase consisting of acetonitrile–water (9 : 1). The derivatives are detected fluorometrically at 260 nm excitation, 315 nm emission, with a detection limit of less than 50 ng mL⁻¹. Gentamycins C₁, C_{1a} and C₂ are resolved (Figure 1, structures 2, 3 and 4, respectively).

o-Phthaldialdehyde, dansyl chloride, fluorescamine, 1-fluoro-2,4-dinitrobenzene or 2,4,6-trinitrobenzenesulfonic acid may also be used as derivatizing reagents.

Glycopeptides

Various glycopeptide antibiotics are separated with an ODS column. The mobile phase composition is either 7–32% acetonitrile (7% for 1 min, then increase to 34% over 13 min) in 0.1 mol L⁻¹ phosphate buffer (pH 3.2) or 5–35% acetonitrile (5% for 1 min, then increase to 35% over 13 min) in 0.025 mol L⁻¹ phosphate buffer (pH 6.0). Glycopeptides are detected at 220 nm.

Vancomycin

Serum is deproteinized with an ice-cold mixture of 10% trichloroacetic acid–acetone (2 : 1) and the supernatant is injected into an ODS column. The mobile phase consists of 50 mmol L⁻¹ sodium dihydrogen phosphate (pH 3.3)–acetonitrile (4 : 1) containing 1 mmol L⁻¹ sodium dodecyl sulfate. Vancomycin is detected at 235 nm with a detection limit of 1 µg mL⁻¹.

Macrolides

Clarithromycin

Clarithromycin (Figure 2, structure 5) and its major metabolite (14-hydroxyclearithromycin) are analysed with a C₈ column. The mobile phase consists of acetonitrile–methanol–water (39 : 9 : 52) containing 0.04 mol L⁻¹ sodium dihydrogen phosphate with the pH being adjusted to 6.8 using sodium hydroxide. The eluent is monitored by electrochemical detection with a quantification limit of 30 ng mL⁻¹. Plasma and urine are extracted with ethyl acetate–hexane (1 : 1).

Erythromycin

Erythromycin A (the major and most active component, Figure 2, structure 6), erythromycin B,

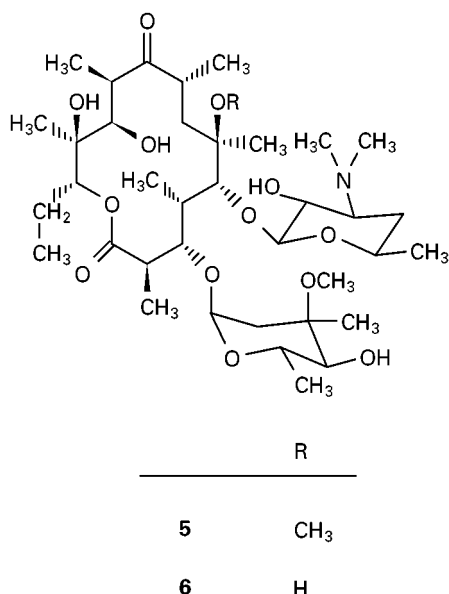


Figure 2 Chemical structures of clarithromycin (5) and erythromycin A (6).

erythromycin C and related compounds in commercial preparations are analysed with an ODS column using a mobile phase consisting of acetonitrile–methanol–0.2 mol L⁻¹ ammonium acetate–water (45 : 10 : 10 : 35, pH adjusted to 7.0–7.8). Erythromycins are detected at 215 nm.

Erythromycin and its metabolites in biological fluids are analysed with an ODS column using a mobile phase consisting of acetonitrile–methanol–0.2 mol L⁻¹ sodium acetate (pH 6.7, 40 : 5 : 55). Erythromycin is detected with a dual-electrode electrochemical detector with a detection limit of 10 ng mL⁻¹ in plasma. Erythromycin is extracted from plasma with ether, and urine is deproteinized with acetonitrile. Other related erythromycins and degradation products are also resolved.

Ivermectin

Ivermectin in tissue is analysed with an ODS column using a mobile phase of acetonitrile–water (9 : 1) at 65°C. Ivermectin is detected fluorometrically at 272 nm excitation, 465 nm emission, with a detection limit of 0.25 ng g⁻¹. Tissue sample is loaded onto a C₈ solid-phase extraction column, eluted with acetonitrile, and the eluate dried under a stream of N₂. The dried residue is dissolved with ethyl acetate–hexane (2 : 3), loaded on a silica column, and eluted with methanol–ethyl acetate (1 : 1). The eluate is dried under a stream of N₂ and treated with trifluoroacetic anhydride and methylimidazole. The analyte thus obtained is injected into an HPLC.

Penicillins and Cephalosporins

Many penicillins and cephalosporins are chiral, partly due to the chirality of the side chain. The D-epimers of ampicillin (see Figure 3, structure 13), cephalexin (Figure 3, structure 17) and cephaloglycin are more active than the corresponding L-epimers. Stereoisomers also exist for amoxicillin (Figure 3, structure 14), azidocillin, cefamandole, cefsulodin and cefibuten (Figure 3, structure 16). For these β -lactams, commercial preparations contain only a single isomer.

For some β -lactams, commercial preparations contain both epimers. These include carbenicillin (7), clometocillin, moxalactam (18), phenethicillin (11), propicillin (12), sulbenicillin (8), temocillin (9) and ticarcillin (10) (see Figure 3). Epimers of these β -lactams are resolved by reversed-phase HPLC.

Ampicillin

In order to separate ampicillin (Figure 3, structure 13) from penicilloic acid, phenylglycine and 6-aminopenicillanic acid, an ODS column is used with a mobile phase consisting of 35% acetonitrile in an aqueous solution of 3.5 mmol L⁻¹ sodium dodecyl sulfate and 0.2 mol L⁻¹ formic acid. Ampicillin and other compounds are detected at 254 nm. For separation of ampicillin from its degradation products, an ODS column is used with a mobile phase of 22.5% methanol in an aqueous solution of 5 mmol L⁻¹ tetrabutylammonium hydrogen sulfate and 5 mmol L⁻¹ ammonium sulfate (pH 2.6). Ampicillin and the degradation products are detected at 238 nm.

Ampicillin is analysed in biological fluids with an ODS column using a mobile phase consisting of 0.06 mol L⁻¹ phosphate buffer (pH 4.6)–methanol (425 : 75). Ampicillin is detected at 225 nm with a limit of accurate determination of 0.5 μ g mL⁻¹ in urine, plasma or saliva. Samples are deproteinized with perchloric acid.

In order to increase sensitivity, ampicillin and its metabolites in urine are subjected to postcolumn alkaline degradation following separation with an ODS column. Urine is diluted with water and injected directly. The mobile phase is an aqueous mixture of 5 mmol L⁻¹ sodium heptylsulfonate, 1 mmol L⁻¹ sodium dihydrogen phosphate and 9 mmol L⁻¹ phosphoric acid–methanol (1.5 : 1, pH 3.0). Degradation of ampicillin and its metabolites is conducted with 0.75 mol L⁻¹ sodium hydroxide, 2 mmol L⁻¹ mercuric chloride and 10 mmol L⁻¹ EDTA, and the degradation products are detected at 300 nm. The limits of accurate determination are 0.5 μ g mL⁻¹ for ampicillin and 1–2 μ g mL⁻¹ for the metabolites.

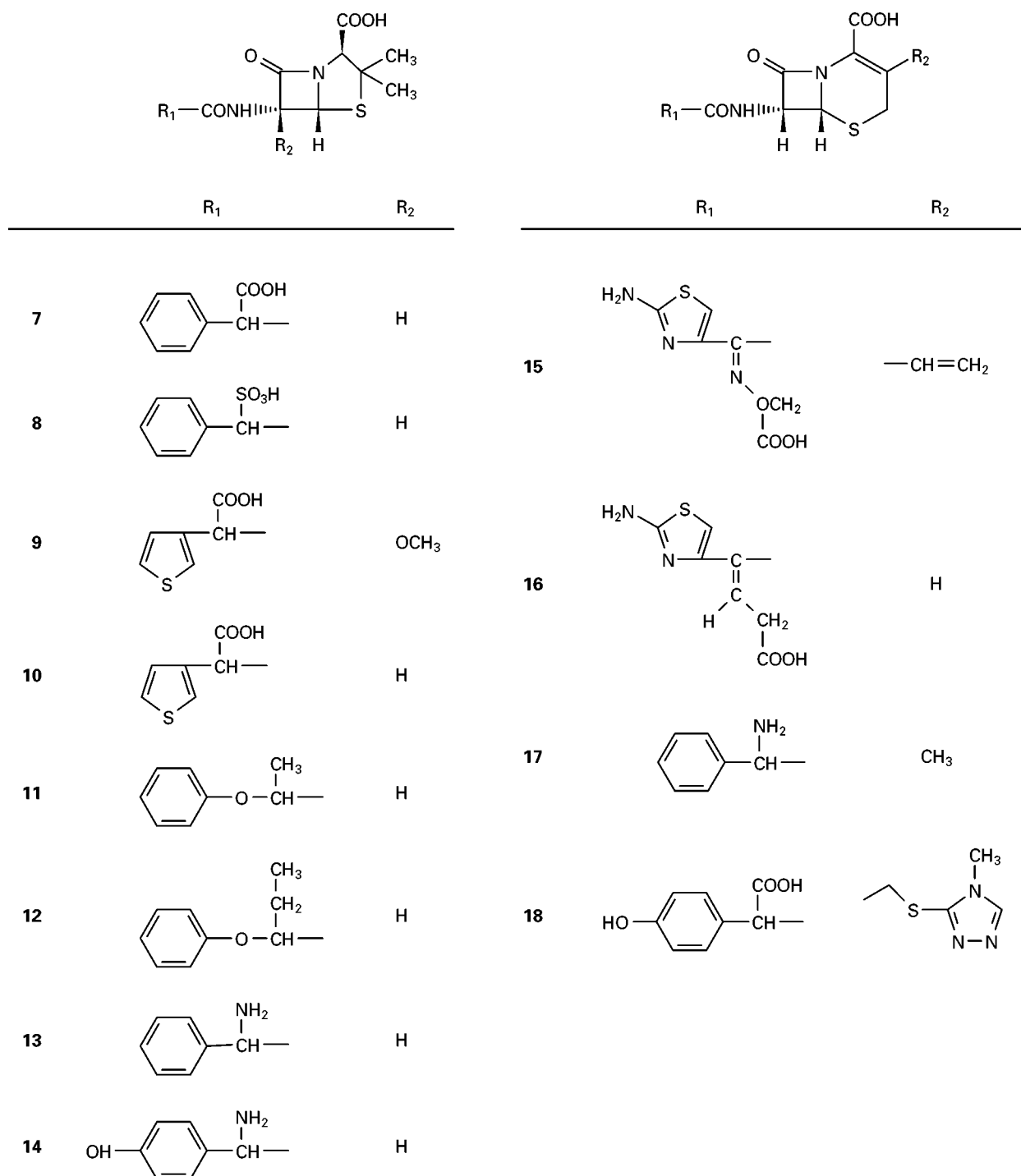


Figure 3 Chemical structures of carbenicillin (7), sulbenicillin (8), temocillin (9), ticarcillin (10), phenethicillin (11), propicillin (12), ampicillin (13), amoxicillin (14), cefixime (15), ceftibuten (16), cephalixin (17) and moxalactam (18).

Carbenicillin, Sulbenicillin and Ticarcillin

These epimeric, di-anionic β -lactams are similar in physicochemical properties and are analysed under very similar conditions. For analysis of carbenicillin (Figure 3, structure 7), plasma and urine samples are

loaded onto an anion exchange solid-phase extraction column. Carbenicillin epimers are eluted with 10% lithium chloride-methanol (3 : 2) and injected into an HPLC. Analysis is on an ODS column with a mobile phase consisting of 0.05 mol L⁻¹ ammonium acetate-methanol (9 : 1). Carbenicillin

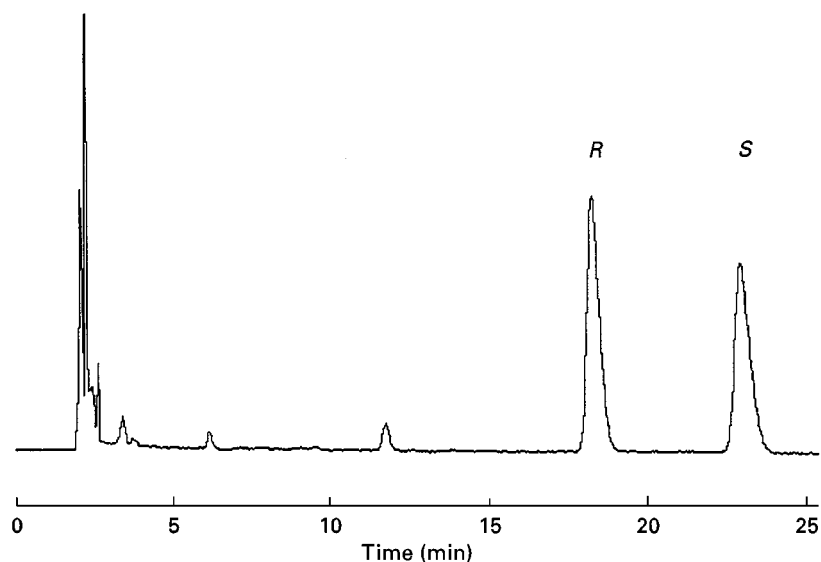


Figure 4 Chromatogram of human plasma spiked with carbenicillin. Five hundred microlitres of human plasma was spiked with 20 μL of an aqueous solution of carbenicillin (5.2 mg mL^{-1}). R, R-epimer, S, S-epimer.

epimers are detected at 254 nm. The epimers are resolved to the baseline with the R-epimer being eluted prior to the S-epimer (Figure 4).

Similar methods can be applied for the analysis of sulbenicillin (Figure 3, structure 8) and ticarcillin (Figure 3, structure 10). For sulbenicillin, the mobile phase consists of 0.05 mol L^{-1} phosphate buffer (pH 7.0)–methanol (8 : 1). The epimers are resolved to the baseline with the S-epimer being eluted faster than the R-epimer. The detection limit is $0.5 \mu\text{g mL}^{-1}$ for each epimer. For ticarcillin, the mobile phase consists of 0.05 mol L^{-1} phosphate buffer (pH 7.0)–methanol (12 : 1). The epimers are resolved to the baseline with the R-epimer being eluted faster than the S-epimer.

Cefixime

Cefixime (Figure 3, structure 15) is determined on an ODS column with a mobile phase consisting of acetonitrile–water (2.75 : 7.25) containing 0.01 mol L^{-1} ammonium acetate and 0.01 mol L^{-1} tetra-*N*-butylammonium bromide. Cefixime is detected at 290 nm.

For analysis of cefixime in serum, an ODS column is used with a mobile phase consisting of 0.3% potassium dihydrogen phosphate–acetonitrile (88.5 : 11.5). For urine analysis, the mobile phase is a mixture of 0.15% potassium dihydrogen phosphate–acetonitrile (77 : 23) containing 0.1% phosphoric acid. Cefixime is detected at 254 nm with a detection limit of $0.1 \mu\text{g mL}^{-1}$.

Ceftibuten

Although commercially available formulations contain only the *cis* isomer (Figure 3, structure 16),

HPLC methods for determination of both *cis* and *trans* isomers have been developed because isomerization is observed *in vivo*.

Ceftibuten and its *trans* isomer are separated with an ODS column using a mobile phase consisting of 100 mmol L^{-1} ammonium acetate–methanol (92 : 8). Both isomers are detected at 262 nm.

An HPLC method for ceftibuten isomers is also developed for plasma and urine samples. Samples are deproteinized with ethanol and injected into an ODS column with a mobile phase composed of PIC A (tetrabutylammoniumphosphate)–acetonitrile–methanol (50 : 6 : 3). Both isomers are detected at 256 nm with a detection limit of $1 \mu\text{g mL}^{-1}$ for each isomer.

Cephalexin

Cephalexin epimers are separated with an ODS column using a mobile phase of 0.1 mol L^{-1} phosphate buffer (pH 3.5)–methanol (95 : 5). The epimers are detected at 254 nm. The two epimers are separated to the baseline with the L-epimer being eluted prior to the D-epimer.

Cephalexin epimers in serum and urine are analysed using a TSK-gel ODS-80 TM column after deproteinization with methanol. Mobile phase compositions are 10 mmol L^{-1} ammonium acetate–methanol (4 : 1) for determination of the D-epimer, and 10 mmol L^{-1} phosphate buffer (pH 3.0)–methanol (9 : 1) containing 10 mmol L^{-1} ammonium acetate and 10 mmol L^{-1} pentanesulfonic acid for determination of the L-epimer. The epimers are detected at 260 nm.

Other β -Lactams

Epimers of phenethicillin (PEPC, **Figure 3**, structure 11), propicillin (PPPC, **Figure 3**, structure 12) and clometocillin are analysed with a Zorbax C₈ column. The mobile phase is composed of methanol–water–5% 0.2 mol L⁻¹ phosphate buffer (pH 7.0) and the epimers are detected at 254 nm. Ratios of methanol in the mobile phase are 37.5, 45 and 50% for PEPC, PPPC and clometocillin, respectively. Epimers are resolved close to the baseline, and the D-epimers elute faster than the corresponding L-epimers.

The same HPLC conditions can be used for the analysis of ampicillin, amoxicillin and azidocillin, except that the methanol content is varied between 10 and 40%. The L-epimer elutes faster for ampicillin, whereas the D-epimer elutes faster for amoxicillin and azidocillin. The less active epimers are not detected in the commercial preparations of these penicillins.

Epimers of PEPC and PPPC are also resolved with an ODS column. The mobile phase consists of 100 mmol L⁻¹ ammonium acetate–methanol (62 : 38 and 58 : 42 for PEPC and PPPC, respectively) with a UV detection at 220 nm. PEPC and PPPC epimers are baseline separated (**Figure 5**).

Bacampicillin and cefotiam hexetil are the prodrugs of ampicillin and cefotiam, respectively, which are commercially available as mixtures of two epimers due to chirality of the prodrug moiety. For separation of bacampicillin isomers, an ODS column is used with a mobile phase consisting of 20 mmol L⁻¹ ammonium acetate–methanol (45 : 55). The isomers are detected at 220 nm. For separation of the isomers of cefotiam hexetil, an ODS column is used with a mobile phase consisting of 50 mmol L⁻¹ phosphate buffer (pH 3.0)–acetonitrile (73 : 27). The isomers are detected at 262 nm. Baseline separation of the isomers of bacampicillin and cefotiam hexetil are observed.

Semisynthetic cephalosporins are extracted from biological fluids and chromatographed with an ODS column. Urine samples are merely centrifuged and diluted with distilled water. Serum samples are mixed with 0.4 mol L⁻¹ HCl and extracted with CHCl₃–*n*-pentanol (3 : 1). The organic phase is re-extracted into phosphate buffer (pH 7), which is injected into the HPLC. The mobile phase is 0.01 mol L⁻¹ acetate buffer (pH 4.8)–methanol (15 : 85) with detection wavelengths of 254, 245, 234, 275, 270, 240 and 240 nm for cefuroxime, cefoxitin, cefotaxime, cefazolin, cefamandole, cephalotin and cefoperazone, respectively.

Cephalosporins in serum are also analysed with an octyl column using a mobile phase of methanol–12.5 mmol L⁻¹ phosphate buffer (pH 2.6, 1 : 4). Cefaclor, cefadroxil, cefixime, cephalixin and cephadrine are simultaneously analysed and detected at 240 nm. The detection limits are 0.1 μ g mL⁻¹ for cefixime and 1.0 μ g mL⁻¹ for other cephalosporins. Serum is deproteinized with acetonitrile.

Cephalosporins with a tetrazole ring are analysed from plasma with an ODS column using a mobile phase consisting of 0.05 mol L⁻¹ phosphate buffer (pH 6.6)–methanol with ratios of 3 : 1 and 2 : 1 for cefamandole and cefoperazone, respectively. For cefotiam and cefmetazole, a mixture of phosphate buffer–tetrahydrofuran (20 : 1) is used as a mobile phase. Cephalosporins are detected at 254 nm with a limit of detection of 1 μ g mL⁻¹ for all cephalosporins.

In order to increase sensitivity, ampicillin, amoxicillin, cephalixin and cephadrine in plasma are assayed after formation of fluorescent degradation products. Plasma is deproteinized with 10% trichloroacetic acid and the supernatant is heated under various conditions to form degradation products. The degradation products are extracted with an organic solvent and injected into a Nucleosil C₁₈ column at

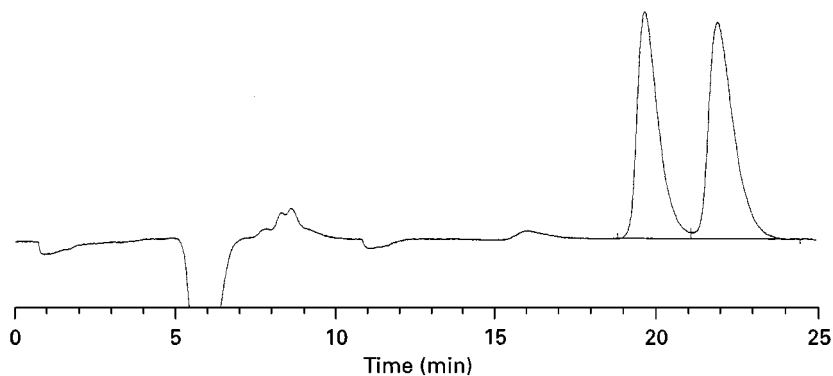


Figure 5 Chromatogram of phenethicillin. One hundred microlitres of an aqueous solution of phenethicillin (22 μ g mL⁻¹) was directly injected onto HPLC.

Table 1 HPLC conditions for β -lactams

β -Lactam	Stationary phase	Mobile phase	Detection
Benzylpenicillin	ODS	Methanol–0.05 mol L ⁻¹ ammonium carbonate (1 : 3)	UV (254 nm)
Benzylpenicillin	ODS	Phosphate buffer (pH 6.0)–acetonitrile (4 : 1)	UV (225 nm)
Cefsulodin	ODS	16.8 mmol L ⁻¹ dibasic ammonium phosphate–acetic acid–methanol (100 : 1.68 : 5.98) containing 5 mmol L ⁻¹ triethylamine	UV (260 nm)
Cefsulodin	ODS	Aqueous solution (containing 38.8 mmol L ⁻¹ ammonium acetate, 0.292 mmol L ⁻¹ dibasic ammonium phosphate and 9.363 mmol L ⁻¹ triethylamine)–acetonitrile–methanol–dimethylformamide–acetic acid (1000 : 7.06 : 1.05 : 1.31 : 0.30)	UV (260 nm)
Moxalactam	ODS	Methanol–0.05 mol L ⁻¹ monobasic potassium phosphate (5 : 95) adjusted to pH 6.5	UV (254 nm)
Moxalactam	ODS	Methanol–0.005 mol L ⁻¹ tetra- <i>n</i> -butylammonium phosphate (1 : 3) adjusted to pH 6.0	UV (254 nm)
Moxalactam	ODS	0.1 mol L ⁻¹ Ammonium acetate–acetonitrile (95 : 5) adjusted to pH 6.5	UV (270 nm)
Moxalactam	ODS	0.1 mol L ⁻¹ Sodium phosphate–methanol (84 : 16) adjusted to pH 3.2	UV (254 nm)
Temocillin	ODS	Methanol–0.1 mol L ⁻¹ phosphate buffer (pH 7.0, 1 : 9)	UV (230 nm)
Temocillin	Octyl silane	Methanol–0.1 mol L ⁻¹ phosphate buffer (pH 7.0, 16 : 84)	UV (230 nm)
7-Ureidoacetamido cephalosporins	ODS	0.01 mol L ⁻¹ Diammonium hydrogen phosphate containing 5–20% methanol	UV (254 nm)

55°C. The mobile phase consists of methanol–water (3 : 2) with a fluorescent detection at 345 nm (excitation) and 420 nm (emission) for ampicillin, cephalexin and cephadrine. For amoxicillin, the mobile phase is methanol–water (55 : 45) with a fluorescent detection at 355 nm (excitation) and 435 nm (emission). Detection limits are 0.5 ng mL⁻¹ for ampicillin, 2 ng mL⁻¹ for cephalexin and 10 ng mL⁻¹ for amoxicillin and cephadrine. For sensitive determination of β -lactams, pre-column derivatization with imidazole–metal salt reagent or formaldehyde, or post-column derivatization with *o*-phthalaldehyde or fluorecamine may be applied.

HPLC conditions for several other β -lactams are summarized in Table 1. Epimers of these β -lactams are separated using the conditions listed in Table 1, except for benzylpenicillin.

Fluoroquinolones

Among fluoroquinolone antibiotics, lomefloxacin, ofloxacin and temafloxacin are used clinically as the racemates (see Figure 6, structures 19, 20 and 21, respectively). Therefore, enantiospecific HPLC methods are described below for these fluoroquinolones. Non-chiral HPLC conditions for the chiral as well as other non-chiral fluoroquinolones are summarized in Table 2. Detection limits listed in Table 2 are mostly those for plasma or serum analysis.

Lomefloxacin

Lomefloxacin enantiomers are extracted from plasma at pH 7 with a mixture of chloroform–isopentyl alcohol–diethyl ether (71.25 : 3.75 : 25) and derivatized with *S*-(+)-(1-naphthyl)ethylisocyanate to form diastereomers. Derivatized diastereomers are analysed with a Radial Pak normal-phase column using a mobile phase of hexane–chloroform–methanol (64.5 : 33 : 2.5). Diastereomers are detected fluorometrically at 280 and 470 nm for excitation and emission. The limit of accurate quantification is less than 10 ng mL⁻¹ for each enantiomer.

Ofloxacin

Serum and urine samples are diluted with 0.1 mol L⁻¹ phosphate buffer (pH 7.0) and extracted with dichloromethane. Ofloxacin enantiomers in the extract are reacted with L-leucinamide to form diastereomers. The diastereomers are extracted with 1 mol L⁻¹ HCl, and injected into an ODS column. The mobile phase is 0.2 mol L⁻¹ phosphoric acid (with the pH adjusted to 1.85 with tetraethylammonium hydroxide)–acetonitrile (4 : 1) with fluorescence detection at 298 nm excitation and 458 nm emission. The derivative of the *S*-(–)-enantiomer elutes prior to that of the *R*-(+)-enantiomer with baseline separation. Detection limits are 3 and 80 ng mL⁻¹ for plasma and urine, respectively.

Ofloxacin enantiomers are also analysed using a chiral stationary phase (bovine serum albumin

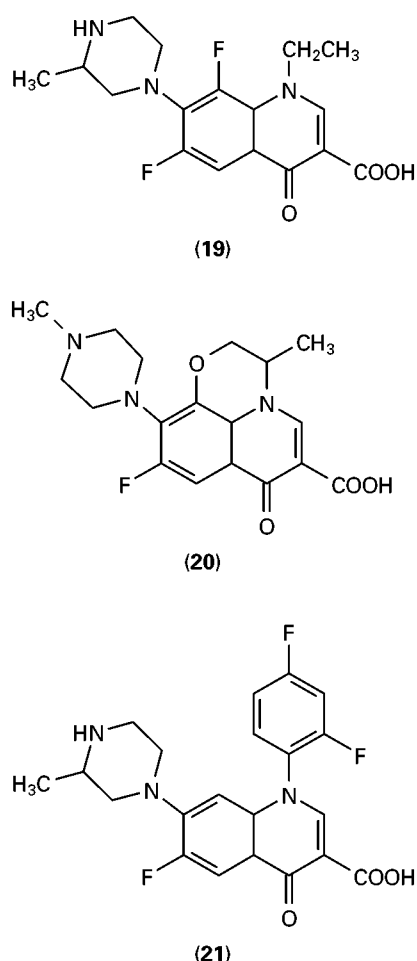


Figure 6 Chemical structures of lomefloxacin (19), ofloxacin (20) and temafloxacin (21).

covalently bonded to silica) without derivatization. Mobile phase is 0.2 mol L⁻¹ phosphate buffer (pH 8.0)–2-propanol (97 : 3). Enantiomers are detected fluorometrically at 298 nm excitation, 458 nm emission. Resolution and sensitivity are poorer than those for the above derivatization method.

For clinical use, ofloxacin has been changed to levofloxacin which is the pharmacologically active *S*-(–)-enantiomer.

Temafloxacin

Temafloxacin enantiomers in biological fluids are extracted with methylene chloride and analysed by two types of HPLC method with derivatization. For the first method, temafloxacin enantiomers are reacted with *S*-(–)-*N*-1-(2-naphthylsulfonyl)-2-pyrrolidine carbonylchloride to form diastereomers, which are injected into a silica gel column. The mobile phase is hexane–methyl acetate–methanol–ammonia water (150 : 100 : 10 : 1) with UV detection at 280 nm. The detection limit is 5 ng mL⁻¹ for each diastereomer with a separation coefficient of 1.05.

For the second method, temafloxacin is reacted with acetic anhydride to form acetylated temafloxacin followed by reaction with isobutylchloroformate to form carbonylamidated derivatives. These double-derivatized temafloxacin enantiomers are analysed with an ovomucoid conjugated silica gel column using a mobile phase of 0.02 mol L⁻¹ phosphate buffer (pH 7.0)–acetonitrile (92 : 8). The enantiomers are detected at 280 nm. The detection limit is 5 ng mL⁻¹ for each enantiomer with a separation coefficient of 1.50, indicating a better resolution by the second method.

Sulfonamides

Various sulfonamides are analysed with an ODS column using a mobile phase composed of acetic acid–triethylamine–water–acetonitrile–methanol (0.4 : 0.2 : 710 : 100 : 100) and detection at 254 nm. Sulfonamides in formulations are extracted or dissolved using dimethylformamide, methanol or the mobile phase.

Sulfonamides in body fluids are analysed with an ODS column using a mobile phase consisting of acetonitrile–water (1 : 9, changing to 9 : 1 in 10 min). Detection is either UV at 254 nm or with a mass spectrometer. Sulfonamides are extracted with hexane–dichloromethane–ether (1 : 1 : 1) at pH 3.0–3.2.

Sulfamethoxazole

Sulfamethoxazole and its acetylated metabolites in body fluids are analysed with an ODS column using a mobile phase consisting of methanol–1% acetic acid (1 : 4, pH 2.9). Sulfamethoxazole and the metabolites are detected at 230 nm with a detection limit of less than 1 µg mL⁻¹. Plasma is extracted with ethyl acetate, and urine is deproteinized with acetonitrile.

Sulfamethoxazole in body fluids are also analysed with an ODS column using a mobile phase consisting of 0.067 mol L⁻¹ phosphate buffer (pH 6.7)–methanol (5 : 1). Sulfamethoxazole is detected at 260 nm with a detection limit of 0.5 µg mL⁻¹.

Sulfasalazine

Sulfasalazine is decomposed in the colon to generate two biologically active drugs, i.e. sulfapyridine and 5-aminosalicylic acid. Sulfasalazine in commercial preparations is analysed with an ODS column using a mobile phase consisting of 10–15% 2-propanol in 0.01 mol L⁻¹ phosphate buffer (pH 7.7), and detected at 254 nm. A silica column is also used for analysis of sulfasalazine and its degradation products in commercial preparations with a mobile phase of chloroform–acetonitrile–*n*-butanol (4 : 1 : 1).

Table 2 Non-stereospecific HPLC conditions for chiral as well as non-chiral fluoroquinolones

Fluoroquinolone	Stationary phase	Mobile phase	Detection ¹	Detection limit
Enoxacin	ODS	30% Methanol in an aqueous solution of 0.05 mol L ⁻¹ potassium dihydrogen phosphate and 2% acetic acid	UV (265 nm)	3 pmol
Ciprofloxacin	ODS	An aqueous solution of 18 mmol L ⁻¹ potassium dihydrogen phosphate and 0.13 mmol L ⁻¹ heptane sulfonic acid-methanol-phosphoric acid (7 : 3 : 0.01)	Fluorescence (ex. 278 nm, em. 475 nm)	200 ng mL ⁻¹
Lomefloxacin	ODS	An aqueous solution of 0.2% sodium acetate trihydrate, 0.2% citric acid monohydrate and 0.1% triethylamine (pH 4.8)-acetonitrile (80 : 23)	Fluorescence (ex. 280 nm, em. 430 nm)	50 ng mL ⁻¹
Nalidixic acid	ODS	Water-methanol-cetrimonium bromide (50 : 50 : 0.12)	(UV 313 nm)	1 µg mL ⁻¹
Nalidixic acid	Amino-cyano	Methanol-0.1 mol L ⁻¹ citrate buffer (pH 3, 95 : 15)	(UV 254 nm)	0.1 µg mL ⁻¹
Norfloxacin	Anion-exchange	0.05 mol L ⁻¹ phosphate buffer (pH 7)-acetonitrile (4 : 1)	(UV 273 nm)	0.1 µg mL ⁻¹
Norfloxacin	ODS	Acetonitrile-0.01 mol L ⁻¹ phosphate buffer (pH 2.5) containing 1 mmol L ⁻¹ triethylamine (11 : 89)	(UV 279 nm)	20 ng mL ⁻¹
Ofloxacin	ODS	0.5% Sodium acetate (pH 2.5)-acetonitrile (87 : 13)	(UV 300 nm)	100 ng g ⁻¹ tissue
Ofloxacin	ODS	Tetrahydrofuran-0.06 mol L ⁻¹ phosphate buffer (pH 2.6) containing 3% triethylamine (5.5 : 94.5)	Fluorescence (ex. 282 nm, em. 450 nm)	20 ng mL ⁻¹
Pefloxacin	ODS	An aqueous solution of 0.2% sodium acetate, 0.2% citric acid and 0.1% triethylamine-acetonitrile (86 : 14)	Fluorescence (ex. 330 nm, em. 440 nm)	50 ng mL ⁻¹
Sparfloxacin	ODS	5% Acetic acid-acetonitrile-methanol (70 : 15 : 15)	UV 364 nm	5 ng mL ⁻¹
Temafloxacin	ODS	53% Acetonitrile in an aqueous solution of 40 mmol L ⁻¹ phosphoric acid, 10 mmol L ⁻¹ sodium dihydrogen phosphate, 0.2% sodium dodecyl sulfate and 5 mmol L ⁻¹ <i>N</i> -acetylhydroxamic acid	Fluorescence (ex. 280 nm, em. 389 nm)	10 ng mL ⁻¹
Temafloxacin	ODS	19% Acetonitrile in an aqueous solution of 5 mmol L ⁻¹ tetrabutylammonium bromide, 10 mmol L ⁻¹ sodium hydrogen phosphate	Fluorescence (ex. 275 nm, em. 450 nm)	10 ng mL ⁻¹
Fleroxacin	ODS	10% Acetonitrile in an aqueous solution of 5 mmol L ⁻¹ tetrabutylammonium bromide, 10 mmol L ⁻¹ sodium hydrogen phosphate	Fluorescence (ex. 277 nm, em. 445 nm)	2.5 ng mL ⁻¹
Fleroxacin	ODS	Phosphate buffer (pH 3)-acetonitrile-methanol (85 : 7.5 : 7.5) containing tetrabutylammonium hydroxide and triethylamine	Fluorescence (ex. 290 nm, em. 470 nm)	5 ng mL ⁻¹

¹ex., excitation; em., emission.

Sulfasalazine in plasma is extracted with isoamyl acetate and analysed with an ODS column using a mobile phase of 0.01 mol L⁻¹ phosphate buffer (pH 7.7)-acetonitrile (83 : 17). Sulfasalazine is detected at 365 nm with a limit of detection of 5 ng.

Sulfasalazine, sulfapyridine, 5-aminosalicylate and their metabolites in plasma are analysed with

a methylsilane column using a mobile phase of methanol-0.05 mol L⁻¹ phosphate buffer (pH 7.4) containing 0.1% tetrabutylammonium hydrogen sulfate (22.5 : 77.5). The eluants are monitored fluorometrically at 320 nm excitation, 389 nm emission, with a detection limit of 0.5 µg mL⁻¹. Plasma is deproteinized with methanol.

Tetracyclines

Various tetracyclines are analysed with an octyl column using a mobile phase of methanol–acetonitrile–0.01 mol L⁻¹ aqueous oxalic acid solution (pH adjusted to 2.0 with 28% aqueous ammonia, 1 : 1.5 : 5) and detection at 360 nm.

Tetracycline (TC), chlortetracycline (CTC), doxycycline, minocycline, oxytetracycline (OTC), impurities of these tetracyclines including 4-epitetracycline, anhydrotetracycline and 4-epianhydrotetracycline (a nephrotoxic degradation product) are resolved with an ODS column using a gradient system (see Figure 7 for chemical structures). The mobile phase is an aqueous solution of 1 mmol L⁻¹ tetraammonium ethylenediamine tetraacetate and 50 mmol L⁻¹ diethanolamine (pH adjusted to 7.3 with 85% phosphoric acid) containing 2–10% isopropanol. Tetracyclines are detected at 254 nm. Impurities of tetracycline are also analysed with an ODS column using a mobile phase consisting of methanol–acetonitrile–0.2 mol L⁻¹ aqueous oxalic acid solution (pH adjusted to 2.0 with 28% aqueous ammonia, 1 : 1 : 3.5). Tetracycline and impurities are detected at 400 nm.

TC, CTC and OTC in plasma and urine are analysed with an ODS column using a mobile phase consisting of 0.01 mol L⁻¹ phosphate buffer (pH 2.4)–acetonitrile (7 : 3 or 6 : 4). Tetracyclines are detected at 355 nm with a detection limit of 1 µg mL⁻¹. Extraction of tetracyclines from biological fluids into

ethyl acetate is improved by formation of phenylbutazone–tetracycline ion-pairs.

Other Antibiotics: Azole Antifungals

Itraconazole and its active metabolite (hydroxyitraconazole) in serum are analysed with a Lichrospher RP8 column using a mobile phase of acetonitrile–water (62 : 38) containing 0.05% diethylamine. The pH of the mobile phase is adjusted to 6.0 with 30% acetic acid. Itraconazole and hydroxyitraconazole are detected at 258 nm with detection limits of 10 and 7 ng mL⁻¹, respectively. Serum is extracted with heptane–isoamyl–alcohol (9 : 1).

Itraconazole and hydroxyitraconazole in plasma and tissue are also analysed with an ODS column using a mobile phase of water–acetonitrile–diethylamine (42 : 58 : 0.05). The pH of the mobile phase is adjusted to 2.45 with 85% phosphoric acid. Itraconazole and hydroxyitraconazole are detected fluorometrically at 260 nm excitation and 365 nm emission. Detection limits of itraconazole are 5 ng mg⁻¹ and 5 ng mL⁻¹ for tissue biopsy and plasma, respectively. Itraconazole in tissue or plasma is extracted with methanol.

Fluconazole in plasma is analysed with an octyl column using a mobile phase of water–acetonitrile (72 : 28). Fluconazole is detected at 260 nm with a detection limit of 0.4 µg mL⁻¹. Plasma is deproteinized with acetonitrile.

Miconazole in plasma is analysed with an ODS column using a mobile phase of methanol–acetonitrile–0.01 mol L⁻¹ phosphate buffer (pH 7.0, 36 : 36 : 28). Miconazole is detected at 230 nm with a detection limit of 5 ng mL⁻¹. Plasma is treated with an octadecyl solid-phase extraction column prior to HPLC analysis.

Econazole in serum is determined with an ODS column using a mobile phase of 0.01 mol L⁻¹ potassium dihydrogen phosphate–methanol (3 : 7), with the pH being adjusted to 4.5. Econazole is detected at 220 nm with a detection limit of 40 ng mL⁻¹.

Sulconazole in plasma is analysed with an ODS column using a mobile phase of acetonitrile–0.01 mol L⁻¹ phosphate buffer (pH 8, 66 : 34). Sulconazole is detected at 229 nm with a detection limit of less than 0.5 µg mL⁻¹.

Some of the azole antifungals are used clinically as the racemates, and the enantio-specific HPLC conditions with a chiral stationary phase, tris(chloromethylphenylcarbamate)s of cellulose, are reported. The mobile phase is *n*-hexane–2-propanol (85 : 15) for separation of enantiomers of enilconazole, econazole, miconazole and ornidazole, and *n*-hexane–2-propanol (9 : 1) for bifonazole enantiomers. A similar

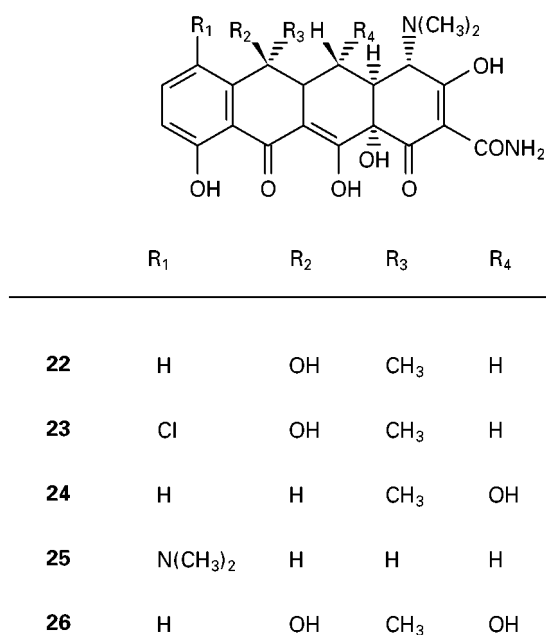


Figure 7 Chemical structures of tetracycline (22), chlortetracycline (23), doxycycline (24), minocycline (25) and oxytetracycline (26).

type of cellulosic chiral stationary phase (Chiralcel-OD) with a mobile phase of *n*-hexane-2-propanol (9 : 1) is used for separation of sulconazole enantiomers.

Conclusion

Since there is an enormous volume of information on the separation of antibiotics in the literature, readers should be able to find HPLC conditions for almost any antibiotic of interest. Readers are also encouraged to consult the official compendia for analysis of bulk or formulated drugs. For analysis of biological samples, the samples may be directly injected with a column switching technique instead of employing liquid-liquid or solid-phase extraction. For sensitive detection, drugs may be subjected to pre- or post-column derivatization, especially with a fluorescent chromophore. Diastereomeric derivatization is useful for analysis of chiral drugs. Mass spectrometric (MS) detection is another way to increase sensitivity. Indeed, cephem and macrolide antibiotics are analysed with HPLC-MS to detect minute amount of drugs. For cephem antibiotics, capillary HPLC has been coupled with mass spectrometric detection.

See also: II/Chromatography: Liquid: Derivatization; Detectors: Fluorescence Detection; Instrumentation.

Further Reading

Foster RT, Carr RA, Pasutto FM and Longstreth JA (1995) Stereospecific high-performance liquid chrom-

atographic assay of lomefloxacin in human plasma. *Journal of Pharmaceutical and Biomedical Analysis* 13: 1243-1248.

Griggs DJ and Wise R (1989) A simple isocratic high-pressure liquid chromatographic assay of quinolones in serum. *Journal of Antimicrobial Chemotherapy* 24: 437-445.

Itoh T and Yamada H (1995) Diastereomeric β -lactam antibiotics: analytical methods, isomerization and stereoselective pharmacokinetics. *Journal of Chromatography A* 694: 195-208.

Kirschbaum JL and Aszalos A (1986) High-performance liquid chromatography. In: Aszalos A (ed.) *Modern Analysis of Antibiotics*, pp. 239-322. New York: Marcel Dekker.

Lehr KR and Damm P (1988) Quantification of the enantiomers of ofloxacin in biological fluids by high-performance liquid chromatography. *Journal of Chromatography* 425: 153-161.

Margosis M (1989) HPLC of penicillin antibiotics. In: Giddings JC, Grushka E and Brown PR (eds) *Advances in Chromatography*, pp. 333-362. New York: Marcel Dekker.

Matsuoka M, Banno K and Sato T (1996) Analytical chiral separation of a new quinolone compound in biological fluids by high-performance liquid chromatography. *Journal of Chromatography B* 676: 117-124.

Stead DA and Richards RME (1996) Sensitive fluorimetric determination of gentamicin sulfate in biological matrices using solid-phase extraction, pre-column derivatization with 9-fluorenylmethyl chloroformate and reversed-phase high-performance liquid chromatography. *Journal of Chromatography B* 675: 295-302.

Supercritical Fluid Chromatography

F. J. Señoráns and K. E. Markides,
Uppsala University, Uppsala, Sweden

Copyright © 2000 Academic Press

Introduction

The analysis of antibiotics is of primary importance for drug monitoring in pharmacokinetic and health studies, as well as for the quality control of drug production and of numerous food products. As a consequence, the demand for new methods of determination of antibiotics of very different types is continuously increasing. The main methods employed for these analyses include immunoassays and chromatography, as well as various chemical techniques. Among the chromatographic methods, high performance

liquid chromatography (HPLC) is the most commonly used, followed by thin-layer chromatography and gas chromatography (GC), while supercritical fluid chromatography (SFC) is still being introduced to this area of application.

In SFC the mobile phase is a fluid subjected to pressures and temperatures near or above the critical point of that fluid, to enhance and control the mobile-phase solvating power. This fact determines that the mobile-phase properties (e.g. diffusivity, density, viscosity) are intermediate between those of gases and liquids and can be varied and controlled by small changes in the pressure or temperature of the systems. The most common fluid used in SFC is carbon dioxide, which has a critical temperature of 31°C, allowing the separation of thermally labile compounds under mild conditions. In general, antibiotics are compounds with intermediate to high polarity, while

supercritical carbon dioxide only has an adequate solvating power for nonpolar compounds. For that reason, the elution of more polar solutes requires the addition of a more polar organic solvent (for example, 5–30% methanol), the so-called modifier, that increases the polarity of the mobile phase and has a solvating effect on silica-based packed columns. With this technique it is possible to separate antibiotics in complex samples at lower temperatures than GC and in shorter times than liquid chromatography. The use of low concentrations of additives in the modifier (for example, 0.1% trifluoroacetic acid and/or 0.1% triethylamine) is also used to control the separation conditions to an even greater extent, especially retention, peak shape and enantioselectivity.

SFC can be divided into two categories based on column type – open tubular and packed – with differences in selectivity, detection and need for modifier addition to the carbon dioxide characterizing the two types. Both types have been employed in the separation of drugs in very different samples. Separations of antibiotics and related compounds are best performed using packed columns, although there are some applications that do well on open tubular columns. Packed columns can be used with UV detection and a wide range of packing materials, from pure silica, to phenyl, diol, amino, octadecyl-modified silica or chiral materials such as cyclodextrins, derivatized cellulose or amylose. For these silica-based columns, the peak symmetry is improved and the retention times of the antibiotics are shortened when a modifier is added to the carbon dioxide, due to the solvating effect on the free silanol groups of the silica (cf. end-capping in HPLC). In general, the separation of antibiotics in SFC is affected by the number, location, nature and conformation of the individual functional groups, which can define the need or not, as the case may be, of a modifier and additive. Nevertheless, the determination of antibiotics by SFC is not so straightforward as other pharmaceutical separations and until now it has not been thoroughly developed.

The area that has been developed the most is probably the chiral separation of antibiotics and related compounds, where the combination of a temperature that is milder and more selective than GC and an efficiency better than HPLC results in enhanced resolution, which is especially valuable.

Another area where supercritical fluids have a niche is the monitoring of food products for antibiotic residues. This area is of increasing importance due to the concern for the effect on human health that abuse of these drugs can have. In this case, the main advantage of supercritical fluids is in the sample preparation from these complex matrices, when supercritical fluid extraction coupled to SFC can be used.

SFC versus HPLC for the Determination of Antibiotics and Related Drugs

The main problem posed in the separation of antibiotics is their broad range of structures that covers almost the whole range of organic chemistry. This includes carbohydrate, macrocyclic lactones, quinones, peptides and heterocyclic compounds, although antibiotics in general are relatively polar, nonvolatile and thermally labile drugs. For that reason, liquid chromatography has increasingly been chosen as the method of analysis, and SFC is gaining greater acceptance with the extended use of packed columns combined with organic modifiers and additives that allow the separation of the more polar solutes.

GC commonly provides the highest resolution in the shortest analysis time, but it also requires high temperatures and often derivatization of the drugs. HPLC methods have lower resolution and longer analysis times. The SFC technique can provide the same resolution as GC and short run times, but with the added benefit that it does not need high temperatures (Figure 1). Typical temperatures are as low as 50–80°C in packed-column SFC.

The packed columns used for SFC of polar drugs are similar to the columns used in HPLC, although back-pressure is not a problem in SFC, allowing columns to be coupled in series to achieve high resolution systems, even for polar analytes. When it comes to detection, the commonest systems for antibiotics determination are UV (Figure 2), or mass spectrometry (MS). In comparing packed-column SFC and LC, the ultraviolet detector can be operated at lower wavelengths in SFC, because of the lack of background absorbance from the solvent and the mass spectrometric ionization techniques work best with volatile mobile phases also favouring SFC (Table 1).

Characteristics of the Separation of Antibiotics using Supercritical Fluids

The main properties of SFC which significantly affect antibiotic separation are related to the high solvating power of supercritical fluids and their low viscosity, which yields high resolution power and throughput. This fact has two main consequences on this type of separation. Firstly, as already pointed out above, compounds like antibiotics can be analysed at lower temperatures than in gas chromatography, and in shorter times than in liquid chromatography, as a result of good solvating capacity. Secondly, SFC is able to resolve complex mixtures of not very volatile compounds, allowing the direct injection of samples

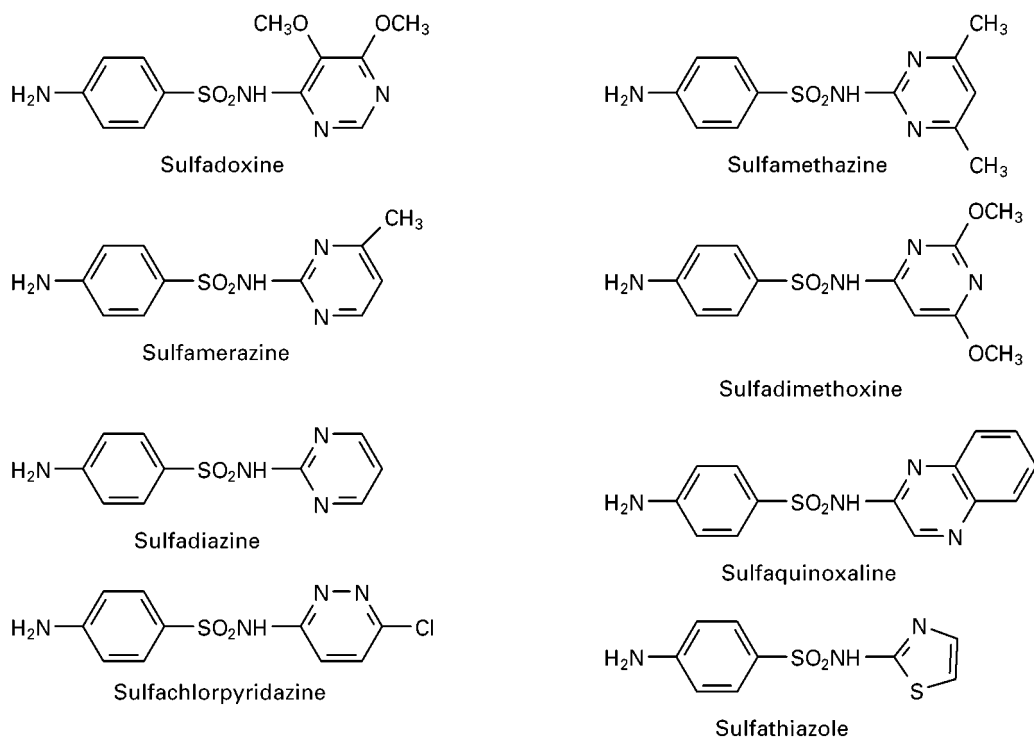


Figure 1 Structures of eight sulfonamides determined by SFC (see chromatogram shown in Figure 2).

that contain antibiotics with little or no sample pre-treatment.

Some antibiotics may be degraded or lost during exposure to light, heat or extreme values of pH. In SFC, all these factors are avoided, providing separation under mild conditions that preserves the integrity of the sample.

Antibiotic determination presents some difficulties due to the complexity of the sample matrix and the relatively low concentration of the antibiotics in these samples. The whole procedure, including extraction and fractionation, is not only time-consuming and prone to error, but may degrade labile antibiotics and create artefacts. Consequently, new approaches have been developed in the last few years that avoid several or all of these questionable sample preparation steps by using multidimensional systems or even direct injection in SFC.

The analysis of antibiotics in human serum has been performed with both open tubular and packed-column SFC. With open tubular columns, it is possible to determine the antibiotic content with a simple liquid-liquid extraction. The use of a flame ionization detector has, however, not demonstrated satisfactory detection limits to date. Better results have been obtained with SFC and mass spectrometric detection, which thus provides a very useful method for the determination of low levels of impurities in macrolide

antibiotics, and presents an alternative approach to several LC-MS methods.

Online SFE-SFC for the Analysis of Antibiotics

Online supercritical fluid extraction (SFE)-SFC can be used for the analysis of antibiotics in complex samples, resulting in time savings and less exposure to organic solvents. Multidimensional systems take advantage of two orthogonal separation techniques with complementary characteristics, for example one extraction and one chromatographic step, where the first step is aimed at producing a clean and undiluted sample containing the compounds of interest, and the second step provides a high resolution separation of the target analytes.

The main advantages of these online systems is that a fast and automatic sample preparation reduces or avoids the errors of the manual steps. Also, solvent consumption is less, which reduces toxic hazards and disposal costs. As is often the case in chromatography, the largest source of error in the quantitative analysis of antibiotics and the most time-consuming steps occur in the sample preparation and extraction stages.

Supercritical fluid techniques have a number of advantages for use in multidimensional chromatographic

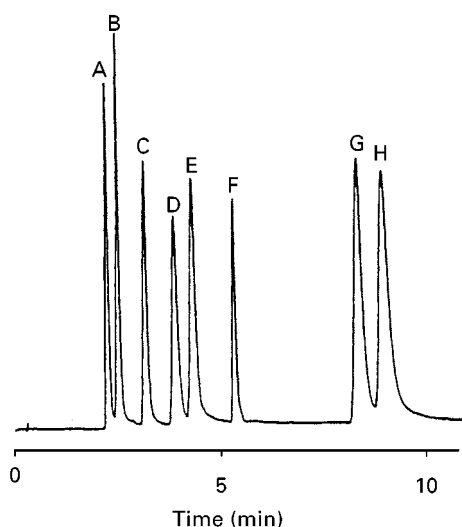


Figure 2 Chromatogram obtained from SFC of a mixture of sulfonamides with UV (wavelength 270 nm). Peak identification: A, sulfadoxine; B, sulfamethazine; C, sulfamerazine; D, sulfadimethoxine; E, sulfadiazine; F, sulfaquinoxaline; G, sulfachlorpyridazine; H, sulfathiazole. Chromatographic conditions: column packed with 5 μm particle amino-bonded Spherisorb (100×4.6 mm i.d.), column temperature 90°C , CO_2 flow rate of 4 mL min^{-1} , pressure 361 bar. Mobile phase was CO_2 modified initially with 15% methanol and after 4 min with 25% methanol. Reproduced with permission from Perkins JR, Games DE, Startin JR and Gilbert JJ (1991) Analysis of sulfonamides using supercritical fluid chromatography and supercritical fluid chromatography-mass spectrometry. *Journal of Chromatography* 540: 239.

systems. The commonest multidimensional system, LC-GC, is limited to the determination of thermally stable and volatile solutes, while SFC can substitute the first fractionation step, as well as the second step of high resolution chromatography. In the case of SFE-SFC, the transfer is performed without changes in the mobile phase, which minimizes losses of analytes and reduces technical complexity

Analysis of Aqueous Matrices

Recently, new methods for the direct injection of water samples on to an adsorbent with solvent venting and online SFE-SFC of the target solutes have been developed.

In this procedure, the liquid sample is introduced in the SFE cell filled with a suitable adsorbent, which retains the solutes while the aqueous solvent is vented with an inert gas. The venting of the water improves the performances and flexibility of both the separation and the detection steps. After elimination of solvent, the analytes are extracted with supercritical carbon dioxide, and focused in a cryogenic trap, providing a solute enrichment before automatic online injection into the SFC column. In addition to its speed, this method provides a preconcentration step

for the analysis of trace levels of residues in biofluid samples and also allows class-selective extractions based on the tuneable polarity of the extracting agent, which thus represents an additional clean up stage and further reduces interface from the matrix.

This coupling has to date been applied to separations in open tubular columns of compounds in water samples, and may provide a breakthrough development for the future, with the use of packed capillary column SFC-MS for polar analytes. Although this method has not yet been applied to the determination of antibiotics, it could provide an automatic way of analysing drugs in biological fluids directly, i.e. with no separate extraction step.

Analysis of Antibiotic Residues in Food

Antibiotics have been used in animal feed for several decades to control infections and promote growth (Figure 3). Recently, increasing concern about antibiotic resistance has led to the prohibition of the use of some antibiotics for this purpose in several countries. Consequently, there is a growing interest in new and improved methods of analysis for antibiotics and their residues in food, and LC-MS is a common technique used to achieve this goal.

In solid and heterogeneous matrices such as food, sample preparation is the most time-consuming step in the routine determination of analytes in trace amounts, for instance, antibiotic residue levels. It remains the largest source of error in quantitative analytical methods. For this reason, the development of methods with less sample pretreatment requirements and with the possibility of automation is desirable.

For this application, SFC in combination with the universal flame ionization detector, or with highly sensitive mass spectrometric detection, shows a good balance between high resolution and good sample throughput, that can minimize the need for sample clean-up and be an optimal procedure in specific cases. An example of separation of veterinary antibiotics by SFC with UV detection prior to online SFC-MS can be seen in Figure 4.

An alternative approach is the online coupling of SFE and SFC for solid or semi-solid samples, allowing the extraction of the fraction of interest and the online transfer of the solutes from the liquid or solid matrix directly to the chromatograph, reducing solvent usage and the need for clean-up.

Chiral Separation of Antibiotics

The stereochemistry of an antibiotic is a prominent issue in the development, approval and clinical use of

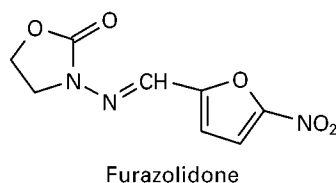
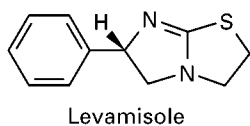
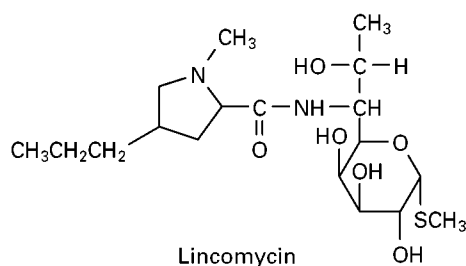
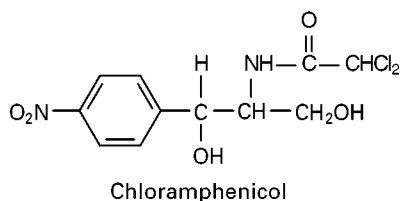
Table 1 Determination of antibiotics by supercritical fluid chromatography

Column type	Sample	Comments	Detector	Reference
Packed (1 mm i.d., 5 µm particles) and open tubular (50 µm i.d.) columns	Sulfonamides and tetracyclines	100°C 8% Isopropanol as modifier	UV	Schmidt S, Blomberg, LG and Campbell ER (1988) <i>Chromatographia</i> 25: 775
Packed column 150 × 4.6 mm 5 µm particle amino silica	Erythromycin A Cephalosporins	65°C 2–8% Methanol as modifier	MS UV	Lane SJ (see Markides and Lee, 1988)
Packed column 100 × 4.6 mm 5 µm particle amino-bonded Spherisorb	Sulfonamides, veterinary drugs	75–90°C 15–25% Methanol as modifier	MS UV	Perkins JR, Games DE, Startin JR and Gilbert JJ (1991) <i>Journal of Chromatography</i> 540: 239
Packed column 250 × 4.6 mm 10 µm particle Chiralcel OB	Lactams	25°C Chiral separation	Diode array	Caude and Macaudiere (see Markides and Lee, 1988)
Open tubular 10 m × 50 µm i.d. SB-biphenyl-100	Cyclosporine A FK 506 (Tacrolimus) Rapamycin	70°C Whole blood extracts	FID	Wong <i>et al.</i> (1994) <i>Journal of Liquid Chromatography</i> 17: 2093
Open tubular 5 m × 50 µm i.d. DB-5	Macrolide antibiotic Midecamycin A ₁	100°C Standard solutions	MS	Ramsey <i>et al.</i> (1995) <i>Analytical Proceedings</i> 32: 455
Different packed columns 250 × 4.6 mm 5 µm particles	Sulfonamides	50–100°C Great influence of temperature on resolution	UV	Combs MT, Ashraf-Khorassani M and Taylor LT (1997) <i>Journal of Chromatographic Science</i> 35: 176

This summary is not intended to be a comprehensive review of all antibiotic separations by SFC; it aims to provide general information on the main applications in this field.

these drugs. For the separation of enantiomers, SFC with chiral stationary phases is very convenient due to its high resolution and relatively low analysis temperature.

Chiral separations in SFC can be carried out using open tubular columns with immobilized cyclodextrins or, more recently, by packed columns with most of the same phases commonly used in LC, since the

**Figure 3** Structures of some veterinary antibiotics analysed by SFC.

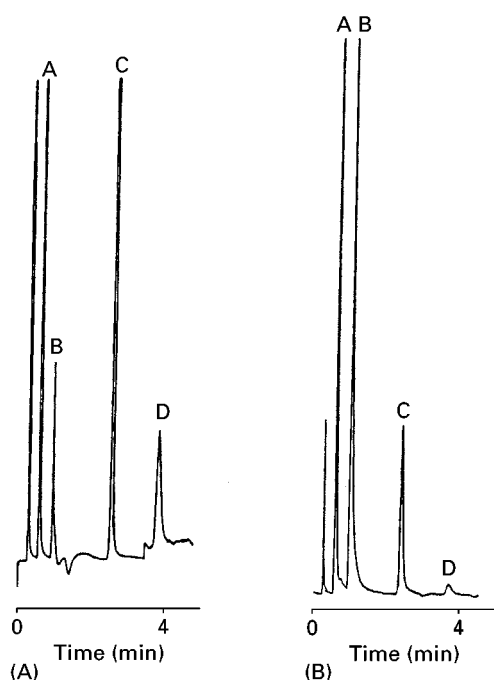


Figure 4 Chromatograms obtained from SFC of a mixture of veterinary antibiotics with UV (A, wavelength 215 nm; B, wavelength 230 nm). Peak identification: A, levamisole; B, furazolidone; C, chloramphenicol; D, lincomycin. Chromatographic conditions: column packed with 5 μ m particle amino-bonded Spherisorb (100 \times 4.6 mm i.d.), column temperature 75°C, CO₂ flow rate of 4 mL min⁻¹, pressure 351 bar. Mobile phase was CO₂ modified with 15% methanol. Reproduced with permission from Perkins *et al.* (1991).

chiral selector is covalently bound to the packing material. The latter method frequently requires the addition of a modifier and is more common in the separation of drugs.

Several examples of the SFC of antibiotic enantiomers can be found in the literature, although the technique is not as commonly used as LC. Packed columns with chiral stationary phases are normally employed with carbon dioxide modified with methanol or ethanol as mobile phase, under supercritical or subcritical conditions (i.e. at room temperature). Further applications can be expected from the use of packed capillary columns for chiral separations, which may provide better resolution and shorter analysis times than the equivalent LC separation.

Future Developments

Current developments in new types of columns, equipment and detectors for SFC show that this technique has great potential for expansion and will achieve a broader use in the future with the advent of new instruments for packed capillary columns and adaptation of the routine use of MS-detectors, which

will be very valuable in the accurate determination of high and low concentration of antibiotics in samples where high resolution and mild conditions are imperative.

It is becoming more frequent to use solvents under subcritical conditions, which is blurring the boundary between SFC and LC – a fact that is already being used in chiral separations and will probably become more frequent in separations of antibiotics and related drugs.

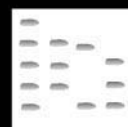
Another probable source of improvement is the use of new detectors with higher sensitivity than UV and flame ionization detection and at the same time compatible with the use of modifiers in packed capillary column SFC. An example is the new amperometric detectors which avoid the problems observed in the quantitation of some drugs by SFC.

The development of new generations of commercial equipment for SFE-SFC and SFC-MS that are more user-friendly and robust than the present ones would also contribute to a wider use of this technology in quality control and research of pharmaceutical compounds.

Further Reading

- Agarwal VK (ed.) (1992) *Analysis of Antibiotic/Drug Residues in Food Products of Animal Origin*. New York: Plenum Press.
- Ahuja S (ed.) (1992) *Chromatography of Pharmaceuticals*. Washington, DC: American Chemical Society.
- Jinno K (ed.) (1992) *Hyphenated Techniques in Supercritical Fluid Chromatography and Extraction*. Amsterdam: Elsevier.
- Lee ML and Markides KE (eds) (1990) *Analytical Supercritical Fluid Chromatography and Extraction*. Provo, UT: Chromatography Conferences.
- Markides KE and Lee ML (1988) *SFC Applications*. Provo, UT: Brigham Young University Press.
- Medvedovici A, Sandra P, Toribio L and David F (1997) Chiral packed column subcritical fluid chromatography on polysaccharide and macrocyclic antibiotic chiral stationary phases. *Journal of Chromatography A* 785: 159.
- Perkins JR, Games DE, Startin JR and Gilbert J (1991) Analysis of veterinary drugs using supercritical fluid chromatography and supercritical fluid chromatography-mass spectrometry. *Journal of Chromatography* 540: 257.
- Señoráns FJ and Markides KE (2000) On line SFE-SFC for the analysis of fat soluble vitamins and other lipids from water matrices. In: Williams JR (ed.) *Methods in Molecular Biology: Supercritical Fluid Methods and Protocols*. Totowa, NJ: Humana Press.
- Xie LQ, Markides KE and Lee ML *et al.* (1993) Bioanalytical application of multidimensional open tubular column supercritical fluid chromatography. *Chromatographia* 35: 363.

ARCHAEOLOGY: USES OF CHROMATOGRAPHY IN



C. Heron and R. Stacey, University of Bradford, UK

Copyright © 2000 Academic Press

History

Although recent advances in analytical methods have accelerated the study of these materials, the analysis and identification of ancient organic residues has a long history. An early example, in the 1920s, was the use of wet chemical techniques by the chemist Alfred Lucas to study organic material from pottery and mummified human remains from the tomb of Tutankhamun. Over the last 20 years or so, the analysis of organic residues has grown into a recognized field in its own right. Examples of organic residues include the debris associated with the remains of food and other natural products as a result of their manipulation in pottery containers (e.g. cooking of food), the balms in the wrappings of mummified bodies and traces of colouring dyes impregnated in ancient textiles. Given the amorphous character of organic residues, the most effective approach to their identification lies in their chemical composition. Characterization of organic residues generally relies upon the principles of chemotaxonomy, where the presence of a specific compound or distribution of compounds in an unknown sample is matched with its presence in a contemporary natural substance. The use of such molecular markers is not without its problems, since many compounds are widely distributed in a range of natural materials, and the composition of an ancient residue may have changed significantly during burial. In general, molecular markers belong to the compound class defined as the lipids, a heterogeneous group of molecules which includes fats and oils and molecules with common solubilities, such as the constituents of resins and waxes.

Early work in this field relied heavily on either thin-layer chromatography (TLC) or gas chromatography (GC) alone to characterize residues. Today, combined GC-mass spectrometry (GC-MS) and, to a lesser extent, high-performance liquid chromatography-MS (LC-MS) are demonstrating considerable value in identifying ancient organic matter. The wider availability of these techniques and, in particular, the introduction of GC-isotope ratio mass spectrometry (GC-IRMS), is contributing to more

specific identifications than was possible before. GC-IRMS allows the ratios of abundances of stable isotopes of elements such as carbon and nitrogen to be determined for individual compounds introduced via a gas chromatograph. Stable isotope ratios are of particular importance to studies of foodwebs due to the characteristic isotope signatures of plants utilizing different photosynthetic pathways. These distinctive ratios are passed along the food chain to herbivores and carnivores. The method requires very small samples and is being applied to trace organic residues in pottery vessels to establish their origin with a high degree of precision.

Methods

Analysis of archaeological material presents a number of challenges, including the small amount of sample available, the presence of complex molecular mixtures from more than one source, chemical alteration due to processing or degradation, and contamination. Furthermore, every sample is unique. These factors mitigate against simple interpretations of analytical results.

Recent developments in instrumental chromatographic techniques have enabled trace amounts of organic residues to be detected. Hence it is possible to analyse molecules surviving in an inorganic matrix such as pottery or soil, or surviving in morphological organic remains such as lipids in seeds or bone. Insoluble or polymeric fractions of residues that are not themselves volatile enough for conventional analysis can be broken up by pyrolysis, thereby allowing separation and identification of the fragments. Pyrolysis-GC-MS has been successfully applied to the recognition of biopolymers in fossil and recent higher plant resins, and to macromolecular debris remaining from the burning of food in archaeological pottery vessels.

Preparation of ancient lipids and natural products normally involves solvent washing of samples. Prefractionation of the lipid residue can be undertaken using microscale column chromatography or TLC. Prior to analysis, unhindered acid functionalities are derivatized by treatment with diazomethane. Trimethylsilylation using *N,O*-bis(trimethylsilyl) trifluoroacetamide (BSTFA) + 1% trimethylchlorosilane (TMCS) is used for the derivatization of hindered carboxyl groups and alcohols. In some cases an

internal standard is added to the sample to quantify yield.

GC remains a useful screening technique prior to GC-MS and can provide fingerprint chromatograms, whereby a complex set of peaks in a mixture can be matched to those in reference samples. Nevertheless, since molecular alteration is likely, this approach must be exercised with caution. Combined GC-MS provides valuable structural information on each of the components separated, and permits identification of molecular modification.

Applications

Residues Associated with Pottery

Fragments of broken and discarded pottery vessels are one of the most common classes of archaeological find. These sherds offer few immediate clues as to their original content and use – a significant point of enquiry in archaeology. During use, however, pottery vessels are known to accumulate residues of foods processed in them. If these residues survive long-term burial then they offer potential for determining artefact use. The residues occur as both charred or burnt deposits, which can be observed on the surface of the pottery, and as absorbed residues whereby organic components migrate into the pores of the vessel fabric. The porous microstructure of the fabric offers some protection to the residue from the effects of biodegradation and leaching during burial. The lipid constituents of these residues preserve rather well, and these can be extracted (by solvent washing of powdered sherd) from excavated sherds and analysed by GC and GC-MS.

A gas chromatogram from a typical degraded fat residue recovered from an archaeological sherd of Iron Age date (c. 100 BC) is shown in **Figure 1B**. The residue is rich in acylglycerols and free fatty acids and is typical of a partially hydrolysed lipid. This can be compared with the composition of fresh mammalian depot fat (**Figure 1A**), which is dominated by intact triacylglycerols. The monoacylglycerols, diacylglycerols and free fatty acids in the degraded fat result from the hydrolytic processes which begin as the pot is used (e.g. during boiling of food) and continue during burial. Furthermore, lipid residues are depleted in unsaturated fatty acids (such as oleic acid; C_{18:1}). This illustrates the problems in making simple comparisons between ancient lipids and fatty acid compositions of modern fats and oils.

Fractionation of the lipid to obtain minor constituents, such as sterols, can assist in determining a plant

or animal source (or indeed whether lipids from both are present). Odd and branched-chain fatty acids may also be present. These are characteristic components of bacteria. They are, however, also introduced into ruminant adipose tissue by bacteria in the rumen and migrate throughout the animal's body, contributing to all the tissues. The presence of appreciable levels of these components, both in the free state and as components of the acylglycerol fraction, supports the view that the predominant source of lipid in the example shown derives from a ruminant animal.

Identification of thermal degradation products may give clues to vessel use. The long chain ketones in **Figure 1** are formed by a high temperature reaction of fatty acids that is catalysed by the mineral matrix of the pottery fabric. Thus vessel use may be further understood by linking the molecular composition of the residues with exposure to high temperatures during formation, for example, during cooking. Recent research suggests that animal fats (such as adipose tissue, dairy products and fish/marine mammal oils) and plant tissues (notably the waxy compounds coating the surfaces of leaves) have the ability, under favourable burial conditions, to survive.

Pottery sherds may also exhibit the remains of organic surface treatments or sealants preserved as surface deposit. These are often resins, waxes or tars. GC analysis of one such deposit, a burnt surface residue on a neolithic potsherd, from Ergolding Fischergasse, Germany (mid 4th millennium BC), led to its identification as beeswax (**Figure 2**). The chromatograms shown compare wax ester distributions in fresh beeswax (*Apis mellifera*) with the fraction extracted from the surface deposit removed from the neolithic sherd. The principal wax esters in both samples are even-carbon-numbered aliphatic chains of saturated alcohols and fatty carboxylic acids with total carbon numbers in the range C₄₀ to C₅₀, with the C₄₆ wax ester the most abundant. The unsaturated wax esters present in the natural beeswax are absent from the neolithic residue. This is due to the deleterious effects of burial, during which the double bond is rendered susceptible to oxidation or reduction reactions. Natural beeswax also contains a considerable alkane component (in the range C₂₁–C₃₃), yet this was severely depleted in the archaeological sample, suggesting its combustion when the beeswax was burned. The sealing and water-repelling properties of beeswax suggest that it may have been used to seal the vessel to enable it to hold liquids. It is possible, however, that the vessel was used to store the beeswax for other uses. The identification of this commodity also implies the availability of honey to

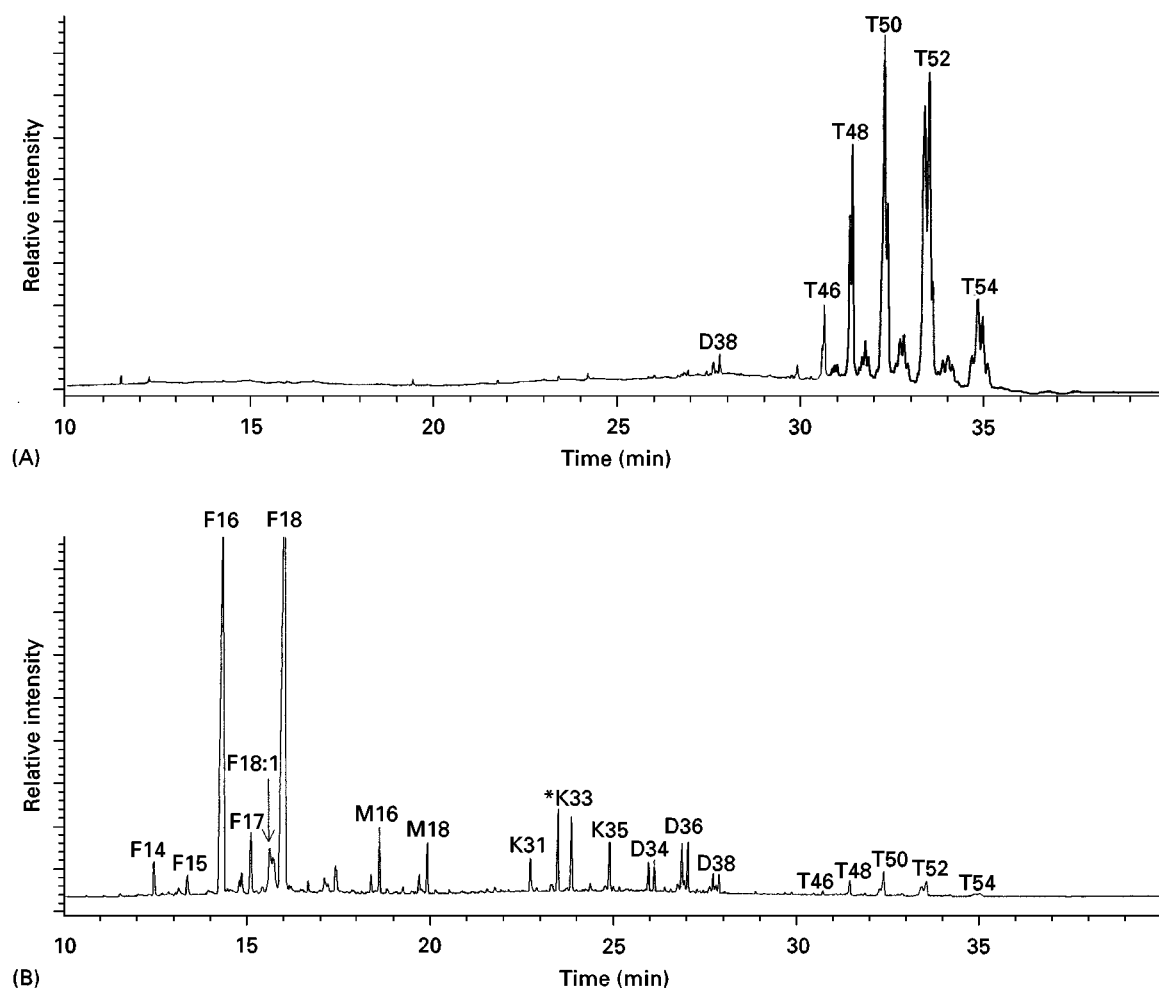


Figure 1 Partial gas chromatograms showing the compositions of (A) fresh beef fat and (B) the lipid residue extracted from an Iron-Age cooking vessel from Easingwold, Yorkshire, UK. The peak identities were established by GC-MS and are as follows: F14–F18 denote saturated fatty carboxylic acids with 14–18 carbon atoms respectively; F18:1 denotes a monounsaturated fatty acid with 18 carbon atoms; M16 and M18 are monoacylglycerols with 16 and 18 fatty acyl carbon atoms respectively; K31, K33 and K35 are mid-chain ketones with 31, 33 and 35 carbon atoms respectively; D34 and D36 represent diacylglycerols with 34 and 36 fatty acyl carbon atoms respectively. T46–T54 are triacylglycerols with 46–54 fatty acyl carbon atoms respectively. * Internal standard.

Analytical conditions: gas chromatography was carried out on a Hewlett Packard 5890 series II gas chromatography, equipped with a flame ionization detector. Samples were introduced by on-column injection into a 60 cm \times 0.32 mm i.d. retention gap of deactivated polyimide-clad fused silica capillary tubing connected to the analytical column via a capillary connector. The carrier gas was helium at a constant flow of 1 mL min⁻¹. The temperature of the oven was programmed from 50 to 340°C at a rate of 10°C min⁻¹ following a 2-min isothermal hold at 50°C after injection, with the final temperature held for 8 min.

The combined GC-MS was performed using a Hewlett Packard 5972A quadrupole mass selective detector in conjunction with a Hewlett Packard 5890 series II gas chromatograph. Samples were introduced via a splitless injector at 340°C with a 3-min purge time. Helium carrier gas was at constant pressure of 10 psi. Mass spectra were recorded over a mass range of 50–700 μ m. The MSD interface temperature was 340°C, and the temperature was programmed from 50 to 340°C at a rate of 10°C min⁻¹ following a 2-min isothermal hold at 50°C after injection, with the final temperature held for 12 min.

In both cases, the analytical column was a polyimide-clad 12 m \times 0.22 mm i.d. fused silica capillary coated with BP1 stationary phase (immobilized poly(dimethylpolysiloxane), OV-1 equivalent, 0.1 μ m film thickness, SGE, UK).

neolithic communities in Europe. GC-MS has also been used to identify beeswax residues associated with medieval ceramics, and in lamps from late Minoan Crete where the wax was burned as a fuel.

Analysis of a large number of vessels from an archaeological site enables correlation between resi-

due type and pottery form and fabric, providing general assessments of use within assemblages.

Amorphous Residues and Adhesives

Amorphous organic substances can survive in other contexts, such as on stone tools, or as isolated

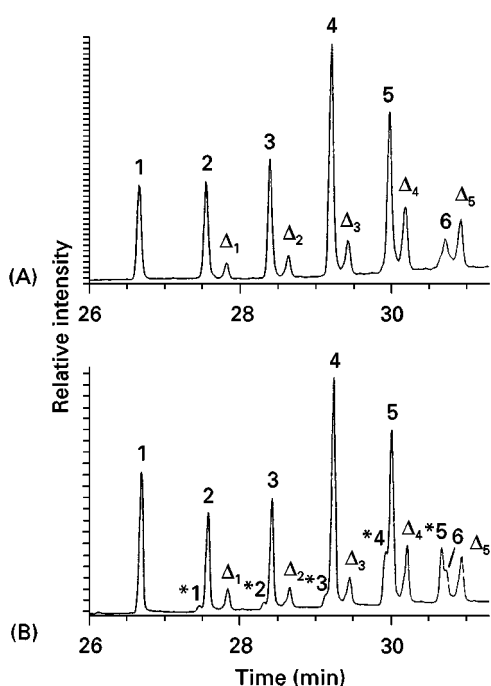


Figure 2 Partial gas chromatograms comparing the wax ester distribution in (A) Neolithic deposit on a potsherd from Ergolding Fischergasse, Germany with (B) authentic beeswax (*Apis mellifera*). Peak identities: 1–6 are wax esters in the range C_{40} (peak 1) to C_{50} (peak 6) comprising mostly hexadecanoic (palmitic) acid esterified with alcohols of increasing chain length (C_{24} to C_{34}). Peaks Δ_1 to Δ_5 represent co-elution of hydroxymonoester isomers and are seen in both samples. In contrast, peaks $*_1$ to $*_5$ are only present in the authentic sample and represent wax esters comprising an unsaturated (octadecanoyl) fatty acid moiety. Their absence in the ancient samples is not unexpected given the susceptibility of the double bond to oxidation or reduction reactions. Reproduced with permission from Heron C, Nemcek N, Bonfield KM *et al.* (1994). The chemistry of Neolithic beeswax. *Naturwissenschaften* 81: 266–269. Courtesy of Springer Verlag.

aggregates. An example is birch bark tar, which has been used as multipurpose natural product for at least 10 000 years, and its use continues to the present day in some parts of eastern and south-eastern Europe. The tar is obtained by heating fresh birch bark (*Betula* sp.) at temperatures of 250–350°C. Spectroscopic and chromatographic investigations of the material began during the 1960s, and a variety of techniques such as TLC, infrared and nuclear magnetic resonance (NMR) spectroscopy were used to identify birch bark tar on flint implements, lithics, ceramic and lumps of tar with human tooth impressions. More recent analysis has revealed that the tar was used to glue flint tips to arrows belonging to Ötzi – the ‘ice man’ discovered in the Tyrolean Alps in 1991. The tar has also been identified on potsherds, stone implements and worked bone from Ergolding Fischergasse (mid 4th millennium BC).

Many of the early analyses have recently been confirmed by GC-MS, including lumps with tooth impressions, interpreted as a very early form of chewing gum.

Figure 3 compares fresh birch bark tar with samples from the Mesolithic site of Star Carr (Yorkshire, UK). The triterpenoids of the outer bark of *Betula* sp. are derivatives of lup-20(29)-ene and, to a lesser extent, olean-2-enes. The triterpenoid composition is modified slightly by heating the bark and by some 9000 years of water-logged burial, but the identity and relative abundance of these biomarkers is sufficient to characterize the archaeological samples. Tars produced from other bark and wood samples have a very different molecular composition. For example, softwoods produce diterpenoid compounds and are easily distinguishable, while the barks and tars of other trees such as hazel, rowan and willow produce triterpenoids but with different carbon skeletons or relative abundance of the lup-20(29)-enes. Analysis by GC-MS enables identification of the molecular markers of the heating of the bark and post-depositional alteration (Figure 4).

Bitumen represents the fraction of sedimentary organic matter which is soluble in organic solvents. The liquid or semi-solid varieties of bitumen were widely used in the Near East and Middle East in antiquity, serving as a multipurpose glue and water-proofing material, a building mortar, medicinal agent and as one of the constituents of the organic preparations applied to mummified bodies in Ancient Egypt. Compounds consistent with a bituminous substance include saturated hydrocarbons which have linear (alkylated alkanes) or cyclic (steranes, terpanes) carbon skeletons. These molecules largely derive from microscopic plants deposited in the sediments as well as bacterial inputs. It has proved possible to identify molecular and isotopic characteristics of the bitumen, which enables archaeological finds to be assigned to a particular source of bitumen. At the site of Susa, Iraq (dating from the beginning of the 4th millennium BC), bitumen was deliberately mixed and heated with mineral elements, to produce a substance known as bitumen mastic – a product ideal for fashioning decorative objects by sculpture.

Understanding Archaeological Sites

In addition to extant residues, chromatographic analyses can be used to identify the remains of ancient human activities that are invisible to the archaeological excavator. Identification of β -stanols, which are faecal biomarkers, in soil samples from archaeological sites have enabled identification of specific site features such as cess pits. The approach may also be used on a large scale to look at issues of waste

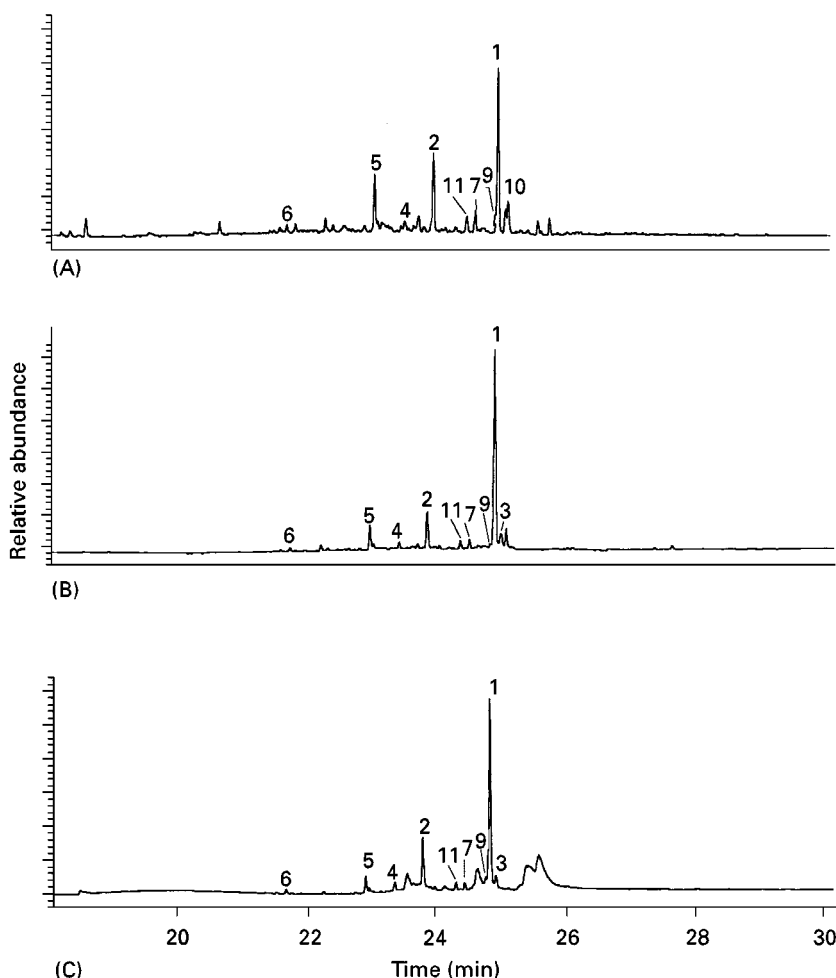


Figure 3 Partial gas chromatograms obtained by analysis of the solvent-soluble portions of samples of birch bark tar (*Betula pendula*) (peak identities were confirmed by GC-MS and are identified in Figure 4). (A) Birch bark tar prepared from fresh bark in the laboratory (350°C); (B) mesolithic sample from Star Carr ('resin cake'); (C) mesolithic sample from Star Carr (hafting glue). Reproduced with permission from Aveling EM and Heron C (1998). Identification of birch bark tar at the mesolithic site of Star Carr. *Ancient Biomolecules* 2(1): 69–80. Reproduced with permission of the copyright owners OPA (Overseas Publishers Association) N.V.

disposal and manuring patterns and early results suggest that the identification of specific sources of faecal matter may be possible.

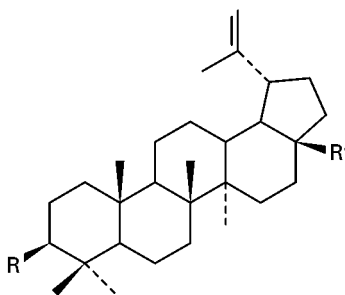
Other Applications

These examples cover only a small part of the spectrum of archaeological approaches making use of chromatographic techniques. It should be emphasized that high performance liquid chromatography has been used not only for the separation of amino acids and peptides (for the purposes of dating, amino acid racemization studies and isotopic investigations), but also in the study of ancient wine residues in pottery containers from the Old World, the analysis of ancient dyes, the identification of alkaloids (such as caffeine and theobromine characteristic of cacao in Mayan archaeological ceramics from Mexico) and in

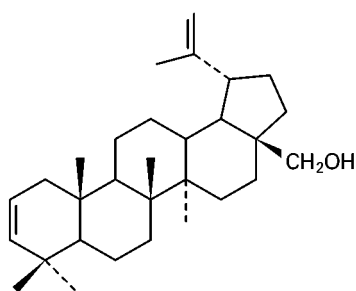
tracing alteration products of purine and pyrimidine bases in nucleic acid extracts of animal and plant remains.

Summary

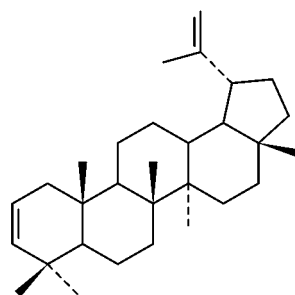
Today, chromatography is embedded in the battery of analytical approaches used to interrogate the surviving materials and residues of past societies. The acceleration of research in biomolecular archaeology in the last decade can largely be attributed to the availability of increasingly sophisticated analytical techniques. GC-MS is becoming the routine approach for the characterization of lipids and natural products, and compound-specific carbon isotope determinations are proving their value in identifying the origin of residue components. Chromatographic



Peak number	R	R'	Compound name
1	OH	CH ₂ OH	Betulin (lup-20(29)-en-3 β ,28-diol)
2	OH	CH ₃	Lupeol (lup-20(29)-en-3 β -ol)
3	OH	COOH	Betulinic acid (3 β -hydroxylup-20(29)-en-28-oic acid)
4	O=	CH ₃	Lupenone (lup-20(29)-en-3-one)
7	O=	CH ₂ OH	Betulone (lup-20(29)-en-3-one-28-ol)
9	OH	CHO	Betulinic aldehyde (3 β -hydroxylup-20(29)-en-28-al)



Peak 5: Lupa-2,20(29)-dien-28-ol



Peak 6: Possibly Lupa-2,20(29)-diene

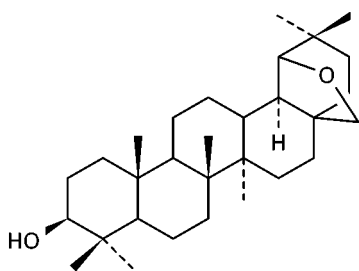
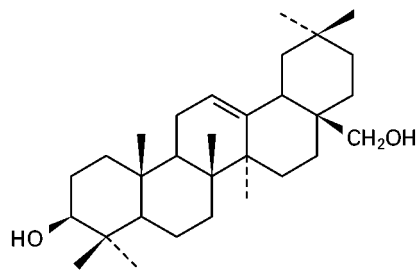
Peak 10: Allobetulinol
(19 β ,28-epoxy-3 β -hydroxy-18 α (H)-oleanane)Peak 11: Erythrodiol
(Olean-12-ene-3 β ,28-diol)

Figure 4 Structures of birch bark triterpenoids identified in Figure 3. (Reproduced with permission from Gundel LA and Lane DA (1999).)

techniques are contributing ever more to our understanding of the relationship between past human populations and their use of plant and animal resources, and of myriad ways in which artefacts were used.

See Colour Plate 55.

See also: **II/Chromatography: Gas:** Derivatization; Detectors: Mass Spectrometry; Pyrolysis Gas Chromatography. **Chromatography: Liquid:** Detectors: Mass Spectrometry. **III/Alkaloids:** Liquid Chromatography; Gas Chromatography; Thin-Layer (Planar) Chromatography. **Amino Acids:** Gas Chromatography; Liquid Chromato-

graphy; Thin-Layer (Planar) Chromatography. **Amino Acids and Derivatives: Chiral Separations. Lipids:** Gas Chromatography; Liquid Chromatography; Thin-Layer (Planar) Chromatography.

Further Reading

- Connan J and Deschesne O (1996) *Le Bitume à Suse: Collection du Musée du Louvre*. Paris, France: Département des Antiquités Orientales, Musée du Louvre.
- Evershed RP, Dudd SN, Charters S *et al.* (1999) Lipids as carriers of anthropogenic signals from prehistory.

Philosophical transactions of the Royal Society of London B 354: 19–31.

Summary of recent pioneering work in lipid analysis of archaeological materials.

Heron C and Evershed RP (1993) The analysis of organic residues and the study of pottery use. In: Schiffer MB (ed.) *Archaeological Method and Theory V*, pp. 247–286. Tucson, AZ: University of Arizona Press.

Lambert JB (1997) *Traces of the Past: Unravelling the Secrets of Archaeology Through Chemistry*. Reading, MA: Addison-Wesley.

Mills JS and White R (1994) *The Organic Chemistry of Museum Objects*. Oxford: Butterworth-Heinemann.

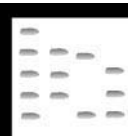
Orna MV (ed.) (1996) *Archaeological Chemistry: Organic, Inorganic and Biochemical Analysis*. ACS Symposium Series 625. Washington, DC: American Chemical Society.

Pollard AM and Heron C (1996) *Archaeological Chemistry*. Cambridge: Royal Society of Chemistry. Includes a chapter on the identification of natural products (resins, pitch and waxes) from European prehistoric sites.

AROMAS: GAS CHROMATOGRAPHY

See III / FRAGRANCES: GAS CHROMATOGRAPHY

ART CONSERVATION: USE OF CHROMATOGRAPHY IN



S. L. Vallance, Royal Society of Chemistry,
London, UK

Copyright © 2000 Academic Press

Introduction

Analytical science plays a vital role in the conservation of our artistic heritage and chromatography is one of the most valuable techniques available to the conservation scientist.

In order to design the optimum safe conservation/restoration treatment plan, which takes account of the nature of the original materials used by the artist, conservators require a detailed knowledge of the materials used. The microscopic samples characteristic of work in this area are notoriously problematic to deal with and the sensitivity of the analytical technique is paramount.

The question why are some painted works in better condition than others of a similar age? is an important one for the conservator and specific information regarding the nature of the media used in such works may offer some insight as to why variations in the ageing characteristics of individual paintings occur.

Paint Media

Artists have traditionally used a diverse range of materials as binding media for their pigments: natural

oils, gums and proteinaceous materials such as egg, milk and collagen glues have all been incorporated into paint layers.

Oil painting was popular in northern Europe from before the 13th century and analytical evidence suggests that linseed oil was favoured, whilst in Italy, where oil painting was introduced in the 15th century, walnut oil was initially preferred. The oils most widely used in western European art are linseed, walnut and poppy, though the use of other oils, such as tung and safflower, has become more common in recent years.

Plant gums are commonly found as adhesives and binders. Gum arabic is primarily used as a painting medium, but others such as gum tragacanth (a medium for painting on linen) and cherry gum (which results in an enamel-like effect when mixed with egg or casein emulsions) are used less frequently. There is documentary evidence to suggest that gums have been employed as binding media and sizing materials for centuries: gum was used as a replacement for sun-dried oil as early as the 12th century.

Proteinaceous media include gelatine, milk and egg proteins. Animals and fish collagen glues are widely used as strong adhesives for wood, binders in the preparation of grounds, size for canvas, and pigment binders in decorative paints. Casein (a mixture of related phosphoproteins found in milk products), egg albumin (glair) and egg yolk (tempera) have traditionally found uses as pigment binders, temporary

varnishes and sealant over primers or grounds: in addition, casein provides one of the strongest natural adhesives known, much used by joiners and cabinet makers in the past.

The choice of binding medium is determined by a number of factors, predominantly the nature of the pigments being used, coupled with the effect desired by the artist, plus historical factors like location and the period of the piece. A variety of materials have enjoyed periodic popularity due to artistic trends and scientific progress.

Analysis of Paint Media

The analyses of oil-based media are well documented, but any information on the nature of other paint media has been obtained primarily via microscopic staining methods or crude solubility tests. Existing methods of analysis provide the basis for the separation of the general categories of binding media (oil, gum and protein) by qualitative means: for example, oil and protein layers can be distinguished by the differential staining of cross-sections, whilst colorimetric spot tests can be used for the identification of polysaccharide gums.

The applicability of these microanalytical techniques *in situ* can be advantageous, but the results can be misleading or inaccurate and for this reason these techniques are best used in conjunction with other analytical methods.

Such simple qualitative techniques, including paper and thin-layer chromatography (TLC), are adequate where merely the general category of binding medium is required, or where the material contains unique constituents (e.g. hydroxyproline in gelatine). However, only quantitative chromatographic techniques will enable differentiation between the similar binding media where they have no distinctive composition, such as in egg and milk proteins.

Gas Chromatography

Conservation scientists have routinely used gas chromatographic (GC) methods for the analysis of proteinaceous, oil and gum media for many years. The technique is highly sensitive – an important factor in the analysis of small samples – and a selection of derivatizing agents is available for use.

GC analysis of trimethylsilyl derivatives of amino acids in protein hydrolysate has been widely reported. The carboxyl group of an amino acid is easier to silylate than the amino group, which results in the formation of two products upon silylation: under mild conditions, the silyl ester is the major product

formed using hexamethyldisilazane as the silylating agent. Silylation of the amino group usually requires a stronger donor and silylation with either *N*-trimethylsilyldiethylamine or *N,O*-bis(trimethylsilyl)acetamide yields the silylamine-silyl ester.

Volatile butyl ester derivatives of amino acids found in the protein hydrolysate of binding media from paint layers and priming removed from 16th- and 18th-century easel and wall paintings have been used for GC analysis. Derivatization is achieved in two stages: the carboxyl functions are first converted into butyl esters by the addition of butanol (with dissolved hydrogen chloride), then the amino groups are acetylated with trifluoroacetic anhydride. The samples, dissolved in ethyl acetate, are separated on a temperature-programmed capillary column. Calculation of the relative peak areas of each amino acid revealed a distinctive profile for each of the binding media.

The existence of an amino acid profile was established for each of the protein media types, confirming their identity by the characteristic amino acid ratios seen for each. Proteinaceous material from the gesso, ground and paint layers of a selection of Italian works was hydrolysed under acid conditions, then deionized on a small ion exchange column. The samples were then successfully methylated (carboxyl function) and acetylated (amino function), yielding the highly volatile *N*-acetylmethyl esters of the amino acids, which were separated on a packed column. Results are shown in Table 1.

Loss of analytes is a problem associated with acid hydrolysis. The acid hydrolysis of proteinaceous samples in the presence of carbohydrates may lead to the elimination of amino acids as humins, which cause darkening of the hydrolysate and the formation of insoluble matter. A major contributory factor in the production of humins (a mixture of coloured compounds which resemble natural melanins) is the presence of tryptophan and amino sugars (e.g. galactosamine) or carbohydrates in the sample, which degrade during acid hydrolysis.

GC has been used to quantify the fatty acid content of eggs. The use of a tempera medium can be confirmed by the absence of azelate in the presence of both palmitate and stearate nondrying oils (i.e., oils which thicken but do not dry to a skin). Samples removed from aged paint films were saponified before methylation with diazomethane, then injected directly on to a wide-bore column. The presence of the methyl esters of saturated palmitic and stearic acids, with variable amounts of unsaturated oleic acid, was revealed. This method is also applicable for the analysis of oil-based media, the palmitate : stearate ratio proving the means of differentiation.

Table 1 Percentage amino acid composition (calculated from peak areas)

Amino acid	Amino acid percentage, peak areas							
	Laboratory aged samples				Samples from paintings			
	Test 1	Test 2	Test 3	Test 4	Sample 1	Sample 2	Sample 3	Sample 4
Alanine	3.9	10.2	5.1	10.0	2.3	10.9	7.5	14.4
Valine	4.4	4.6	6.9	2.4	19.0	1.5	4.8	1.3
Glycine	1.5	4.1	7.4	19.4	3.3	17.5	3.3	27.9
Isoleucine	2.3	3.1	5.2	1.1	4.0	0.6	2.6	0.4
Threonine	4.1	4.9	5.4	2.2	0.1	1.4	4.2	1.4
Leucine	16.4	15.5	11.8	4.0	10.6	3.9	13.0	4.7
Serine	5.8	9.8	7.0	2.9	8.1	2.6	7.9	3.6
Proline	21.0	7.7	5.4	19.6	14.4	20.6	6.3	8.3
Aspartic acid	8.0	15.6	11.1	5.1	7.4	4.6	11.6	7.0
Hydroxyproline				14.2	0.2*	15.7		13.7
Methionine	0.4	0.1	1.1	0.3		0.0	0.2	0.2
Glutamic acid	14.9	11.3	13.2	8.6	18.1	11.6	18.1	13.1
Phenylalanine	5.4	8.0	9.1	3.9	11.8	4.1	13.6	2.8
Lysine	11.2	4.4	10.7	5.6	0.4	4.2	6.1	0.7

Test 1, casein ground; test 2, glair/chalk mix; test 3, egg yolk/chalk mix; test 4, rabbit skin glue/chalk mix; sample 1, upper red layer from the façade of San Petronio, Bologna; sample 2, gesso ground from Bellini's *The Madonna of the Meadow*; sample 3, unpigmented priming from Bellini's *The Madonna of the Meadow*; sample 4, ground layer from Baccafumi's *Tanaquil*. Reproduced from White (1984) with permission.

A mixed medium such as tempera contains both fatty acids and amino acids and GC has been employed to analyse both components simultaneously. Samples of mixed proteinaceous and oil media were hydrolysed under acid conditions, and derivatized to yield the volatile *N*-(*O*, *S*)-ethoxycarbonyl ethyl esters, which were then separated by capillary GC. This method has also been used for the analysis of amino acids alone.

Volatile ethyl chloroformate derivatives of amino acids in the hydrolysate of samples of proteinaceous media have been analysed to study the effects of pigments and ageing on the actual analysis/characterization of proteins from art objects, the results being interpreted via statistical methods.

GC is the method of choice for the analysis of natural gum media from works of art, though to date there has been relatively little work published in this area. An obvious problem associated with the use of many analytical techniques for this type of analysis is the insufficient sensitivity of the method for the microscopic samples available to the conservation scientist. However, progress has been made in the analysis of gum media by GC, often in conjunction with TLC.

Trimethylsilyl derivatives of sugars from the hydrolysed samples of surface coating taken from a wooden Egyptian sarcophagus (dating from the 21st dynasty) were analysed using a combination of GC and TLC, revealing the presence of gum tragacanth. The same

procedure was also employed for the analysis of the paint medium itself and disclosed the use of a mixture of gum tragacanth and honey.

Samples of media taken from Asian wall paintings were also found to contain polysaccharide material when analysed by GC and TLC. Gum sample hydrolysates were acetylated prior to analysis and characterization of the media, but the actual method of sample preparation was lengthy and tedious, requiring 12 h for hydrolysis and a further 5 h for derivatization.

Results obtained for the GC analysis of samples of gum from trees of the *Acacia* genus growing in the vicinity of the Tomb of Nefertari revealed that they were lacking in rhamnose, which usually indicates gum tragacanth, whilst the remainder of the sugar content matched that of gum arabic from other sources. When samples of media from paintings in the tomb were analysed by GC, the same sugar profile was observed: it was therefore concluded that the paint medium was in fact gum arabic.

Twilley's comprehensive analytical studies of natural gums and their artistic applications employed a variety of techniques, including the GC analysis of trimethylsilyl sugar derivatives. In addition, GC was used for the analysis of reference samples of aged ink, thus enabling the characterization of ink samples taken from a number of ancient manuscripts.

GC with a mass selective detector following a simple 'one-pot' hydrolysis and derivatization procedure was used for the characterization of a number of suspected gum media samples taken from the paint and ground layers of tempera works by William Blake. The results frequently indicated the presence of mixed gum media (typically comprising gums arabic, tragacanth and karaya) with the addition of cane sugar. Figure 1 shows the chromatograms of four

standard gum media samples, whilst Figure 2 shows the chromatograms obtained for samples of priming and paint media removed from two works by Blake, *Spiritual Form of Nelson Guiding Leviathan* (1805–9) and *Body of Christ Borne to the Tomb* (1799–1800).

GC has also facilitated the analysis of coatings, such as resins, waxes, lacquers and varnishes removed from works of art. Coatings are often applied

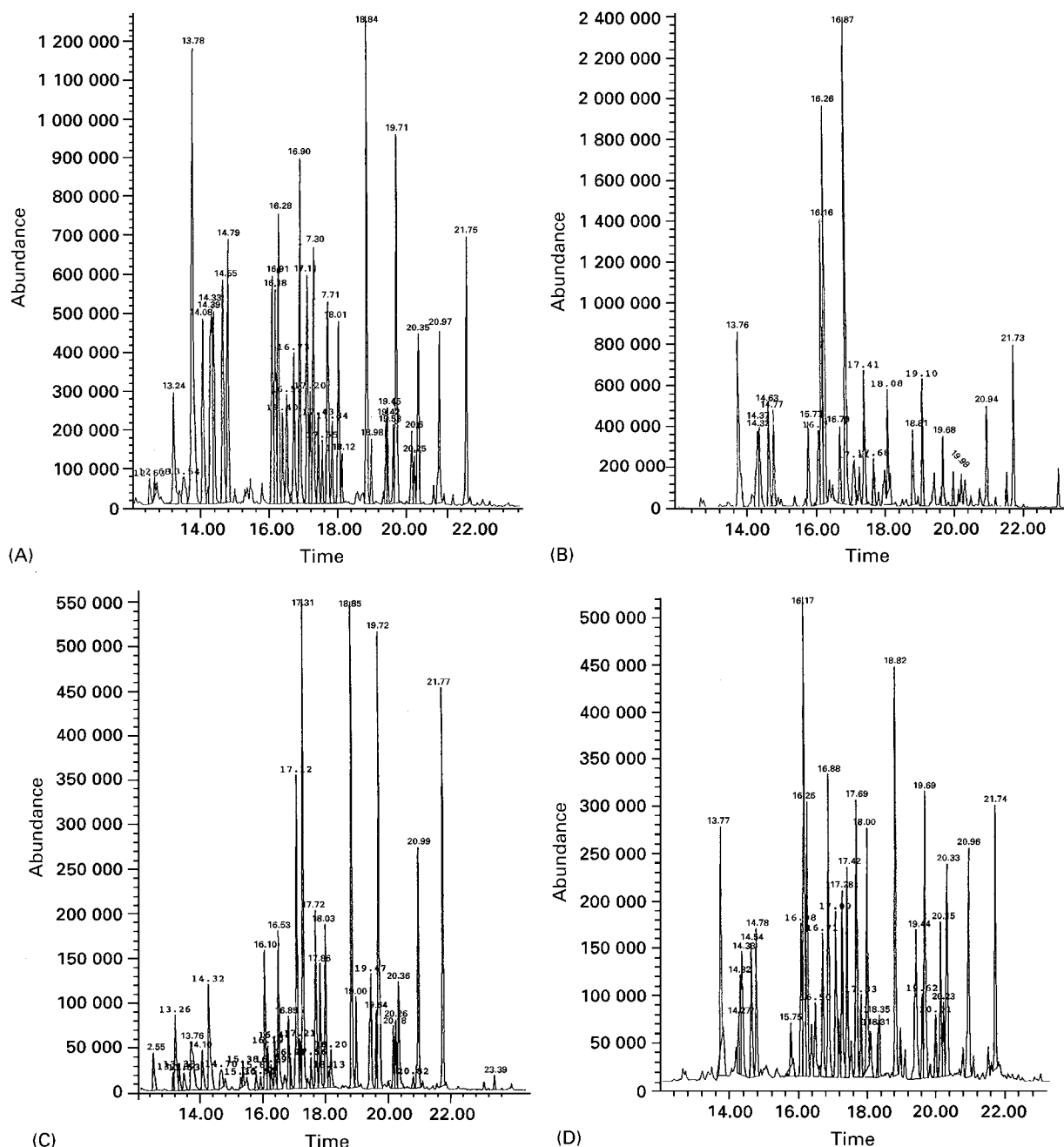


Figure 1 Chromatograms of four standard gum media samples: (A) gum arabic; (B) gum tragacanth; (C) karaya gum; (D) cherry gum.

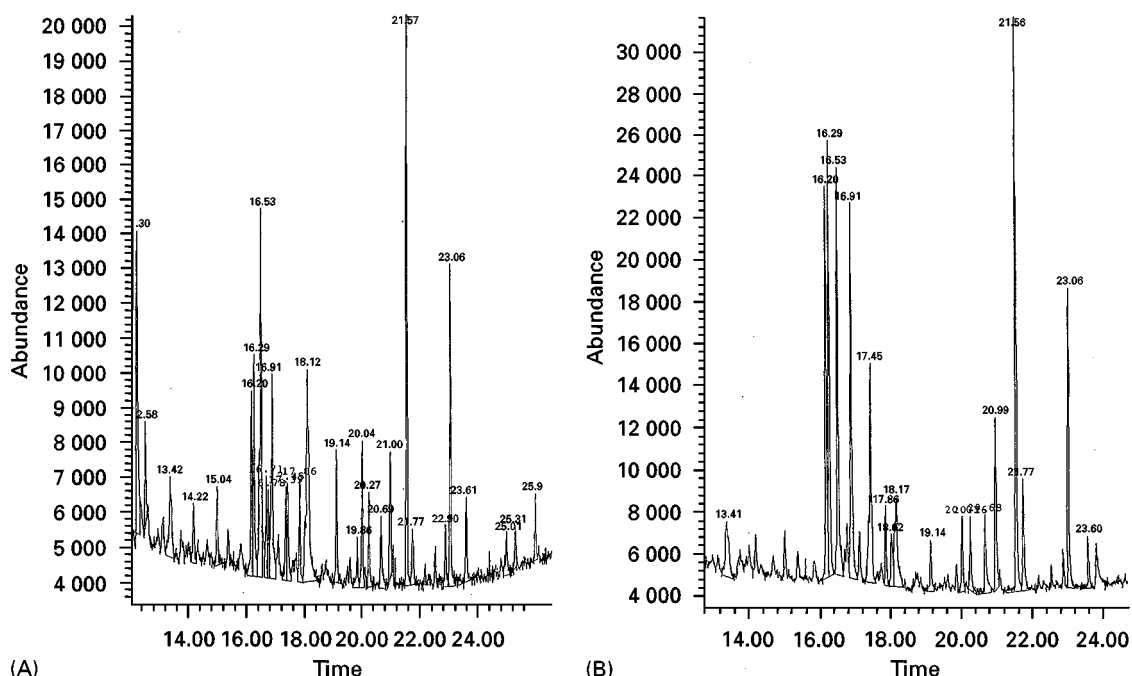


Figure 2 Chromatograms of samples removed from two works by William Blake: (A) white priming sample from *Spiritual Form of Nelson Guiding Leviathan* (1805–9); (B) green paint sample from *Body of Christ Borne to the Tomb* (1799–1800).

in an attempt to protect them from weathering and contamination and, though not classed as media themselves, their characterization may provide important evidence when determining the reasons for the ageing/degradation of works of art.

Varnish samples are commonly saponified prior to methylation, then the components separated on a capillary column with a linear temperature programme. Using mass spectrometry as a detection technique, two major peak groups can be seen, corresponding to the diterpenoid and triterpenoid components.

Waxes are stable materials comprising hydrocarbons and esters and, because of the virtual absence of polar groups, they can be analysed directly by high temperature capillary GC without the need for derivatization.

Reversed-phase High Performance Liquid Chromatography

The speed and sensitivity of reversed-phase high performance liquid chromatography (RP-HPLC) has led to significant developments in the analysis of proteins: RP-HPLC is now one of the most widely used techniques for the analysis of amino acids, since pre-column derivatization is possible with a selection of derivatizing agents and a variety of detection techniques can be employed. RP-HPLC lends itself well to conservation science, being particularly suitable for the analysis of the extremely small samples removed from works of art.

Phenylthiocarbamyl derivatives of amino acids in the hydrolysate of proteinaceous media samples have been separated on a C_{18} column using a ternary solvent system as the mobile phase (water–acetonitrile–acetate buffer).

Following hydrolysis of proteinaceous material removed from a series of Italian 15th-century painted panels, Halpine used phenyl isothiocyanate (PITC) for the derivatization of the amino acids, which were then separated on a C_{18} column using a binary solvent system of acetonitrile and acetate buffer (Table 2). The addition of nor-leucine as an internal standard facilitated the quantification of the amino acid components in the proteins, which in turn resulted in the characterization of a number of animal glue and egg/glue media. However, PITC-amino acid derivatives degrade in solution, so must be stored at low temperature prior to analysis.

PITC derivatives have also been analysed by RP HPLC when attempting to identify media samples which had been removed from a variety of French and Italian stone and wooden sculptures, frescoes and statues. Proteinaceous material was extracted from the matrices with sodium hydroxide and the subsequent analysis indicated the presence of gelatine and egg proteins.

9-Fluorenylmethyl chloroformate (FMOC) is a useful derivatizing agent for amino acids since it favours mild, aqueous conditions, reacts with both primary and secondary amino acids and is stable at room

Table 2 Percentage amino acid composition

Amino acid	Percentage amino acid composition							
	Control samples				Samples from panels			
	Control 1	Control 2	Control 3	Control 4	Sample 1	Sample 2	Sample 3	Sample 4
Aspartic acid	1.0	9.1	5.6	7.9	5.5	*	10.2	5.2
Glutamic acid	2.3	11.1	9.3	13.0	5.9	6.4	9.8	4.1
Hydroxyproline	12.3	0.6	0.3	—	11.7	9.9	3.8	5.9
Serine	3.8	11.1	10.7	9.4	5.7	5.7	8.4	8.9
Glycine	27.7	10.9	7.8	5.2	26.9	24.7	15.8	18.6
Histamine	0.8	1.3	1.5	1.6	*	*	*	1.2
Arginine	5.7	5.3	5.9	4.0	4.1	*	4.3	3.0
Threonine	2.6	5.6	6.6	3.9	3.9	*	4.8	6.6
Alanine	11.1	8.6	10.2	8.8	11.8	11.2	10.0	12.8
Proline	16.9	5.4	5.9	4.0	11.6	12.4	6.7	10.3
Tyrosine	1.2	2.7	3.6	2.4	*	*	1.1	1.8
Valine	3.3	6.6	7.8	7.5	4.2	5.3	5.5	7.2
Methionine	1.3	1.7	2.0	4.8	*	6.7	1.3	0.3
Isoleucine	1.9	4.3	5.0	5.8	3.6	11.7	4.7	4.6
Leucine	3.9	8.5	10.0	9.0	1.5	6.0	7.2	7.1
Phenylalanine	2.0	3.3	3.7	5.9	3.7	*	3.3	2.4
Lysine	2.0	4.0	4.5	5.7	*	*	3.0	*

*Too small to quantify; control 1, rabbit skin glue ground with blue pigment; control 2, egg yolk with red pigment; control 3, egg yolk with blue pigment; control 4, egg albumin; sample 1, light blue paint; sample 2, dark blue paint; sample 3, light brown paint; sample 4, green paint. All paint samples removed from Cosimo Tura's *The Annunciation with Saint Francis and Saint Louis of Toulouse* (c. 1475). Reproduced from Halpine (1992) with permission.

temperature for up to 2 weeks. The FMOc moiety is both highly fluorescent and a good UV chromophore, so absorption and emission detection techniques can be used. Detection methods are an important concern in conservation science in view of the very small samples available – FMOc is particularly useful since fluorescence is usually far more sensitive than UV absorption. Standard proteinaceous media and museum sample hydrolysates have been characterized as FMOc derivatives.

Other Chromatographic Techniques

Ion Exchange Chromatography

Ion exchange chromatography was first used for the analysis of samples from works of art in 1969 when the successful analysis of antique and modern art specimens was reported. The eluted amino acids were detected by optical density with ninhydrin, then the percentage amino acid composition was calculated for each sample. Samples of gelatine, casein, glair, tempera and even animal horn were characterized using this method.

The use of ion exchange chromatography in this particular area is problematic: the method of sample preparation is both lengthy and complex, pH gradients are difficult to control precisely and the required

sample size of paint is relatively large when put into the context of a specimen to be removed from a valuable work of art. Furthermore, museums and galleries are notoriously short of both money and space, thus specific single-purpose equipment is deemed unaffordable by many institutions.

Thin-layer Chromatography

TLC has been used on many occasions, particularly in the analysis of natural gum media – it is often used in conjunction with GC for such analyses but can provide useful information when used alone.

TLC has been used to characterize gum media taken from a 16th-century manuscript: hydrolysed gum samples were separated on silica plates, facilitating the subsequent identification of gum arabic.

Samples of binding media from paint layers were removed from three ancient Egyptian epitaphal stelae on wooden supports, then TLC was used to investigate the nature of the media, revealing the presence of gum tragacanth.

Pyrolysis–Gas Chromatography

Pyrolysis–gas chromatography (Py-GC) has been employed in the analysis of natural gum media from works of art. The distinctive pyrograms obtained for a series of standard gum samples enabled their identification and it was discovered that by pyrolysing the

complex gum-pigment mixed samples at 400°C, differences in peak patterns between standard samples and mixed samples were minimized. Sample identification is aided by the use of computational methods of pattern recognition.

Conclusions

When preparing to analyse a sample removed from a work of art, conservation scientists must select a technique which gives the maximum amount of information for the minimum amount of sample and sample preparation: it appears that RP-HPLC using FMOc as the amino acid derivatizing agent is the optimum analytical technique for the characterization of proteinaceous binding media, whilst GC is routinely used for oil-based media.

At present, GC analysis of silylated sugar residues is arguably the best method for the identification of natural gum media, and the use of mass spectrometry as the detection technique offers superior sensitivity and flexibility for these complex samples. However, this seems to be the least investigated area of analysis and significant developments in methodology which will further improve the sensitivity of the technique can be anticipated: this is of particular importance in the analysis of gum media since samples invariably contain no more than 10% binding medium, resulting in minute amounts of actual analyte in the samples. It is possible that microbore HPLC techniques may find a use in conservation science, since they are obviously suited to the minuscule samples routinely provided for analysis.

Simple qualitative techniques such as TLC may be sufficient to indicate the basic media type used in works of art, but as more and more works require some form of conservation or restoration treatment it is becoming increasingly important that the conservator has as much information as possible relating to the nature of the materials used in the work, in order to avoid damaging irreplaceable objects of artistic importance.

Chromatographic techniques provide reliable and accurate methods of analysis, suitable for use with the microscopic samples typically seen in this field of work. Further work should lead to simplification of methods of sample preparation – any improvements which mean that the size of samples required for analysis is reduced and that analyte losses are minimized would be welcomed by the conservation community.

See Colour Plates 59, 60.

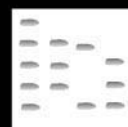
See also: II/**Chromatography: Gas:** Derivatization; **Chromatography: Liquid:** Derivatization. III/**Amino Acids:** Gas Chromatography; Liquid Chromatography;

Thin-Layer (Planar) Chromatography. **Paints and Coatings: Pyrolysis:** Gas Chromatography. **Pigments:** Liquid Chromatography; Thin-Layer (Planar) Chromatography. **Polysaccharides:** Liquid Chromatography.

Further Reading

- Birstein VJ (1975) On the technology of Central Asian wall paintings: the problem of binding media. *Studies in Conservation* 20: 8.
- Derrick MR and Stulik DC (1990) Identification of natural gums in works of art using pyrolysis-gas chromatography. *ICOM Committee for Conservation, 9th Triennial Meeting, Dresden, 26–31 August 1990: Preprints* (ed. Grimstad K), p. 9.
- Erhardt D, Hopwood W, Baler M and von Endt D (1988) A systematic approach to the instrumental analysis of natural finishes and binding media. *Preprints of Papers presented at the 6th Annual Meeting*. American Institute for Conservation of Historic and Artistic Works. Washington, DC: pp. 67–84.
- Flieder F (1968) Mise au points des techniques d'identification des pigments et des liants inclus dans la couche picturale des eluminures de manuscrits. *Studies in Conservation* 13: 49.
- Grzywacz CM (1994) Identification of proteinaceous binding media in paintings by amino acid analysis using 9-fluorenylmethyl chloroformate derivatization and reversed-phase high-performance liquid chromatography. *Journal of Chromatography A* 676: 177.
- Halpine SM (1992) Amino acid analysis of proteinaceous media from Cosimo Tura's *The Annunciation with Saint Francis and Saint Louis of Toulouse*. *Studies in Conservation* 37: 22.
- Keck S and Peters T (1969) Identification of protein-containing paint media by quantitative amino acid analysis. *Studies in Conservation* 14: 75.
- Kenndler E, Schmidt-Beiwel K, Mairinger F and Pöhm M (1992) Identification of proteinaceous binding media of easel paintings by gas chromatography of the amino acid derivatives after catalytic hydrolysis by a protonated cation exchanger. *Fresenius Journal of Analytical Chemistry* 342: 135.
- Masschelein-Kleiner L, Herlan J and Tricot-Marckx F (1968) Contribution à l'analyses des liants, adhésifs et vernis anciens. *Studies in Conservation* 13: 105.
- Mills JS and White R (1994) *The Organic Chemistry of Museum Objects*, 2nd edn. London: Butterworth Heinemann.
- Nowik H (1995) Acides amines et acidgras sur un même chromatogramme un autre regard sur l'analyse de liants en peinture. *Studies in Conservation* 40: 120.
- Twilley JW (1984) The analysis of exudate plant gums in their artistic applications: an interim report. *American Chemistry Society Advances in Chemistry Series* 205: 357.
- Vallance SL, Singer BW, Hitchen SM and Townsend JH (1998) The development and initial application of a gas chromatographic method for the characterization of gum media. *Journal of the American Institute for Conservation* 37(3): 294.
- White R (1984) The characterization of proteinaceous binders in art objects. *National Gallery Technical Bulletin* 8: 5.

ATMOSPHERIC ANALYSIS: GAS CHROMATOGRAPHY



A. C. Lewis, University of Leeds, Leeds, UK

Copyright © 2000 Academic Press

Introduction

The determination of both naturally produced and anthropogenic organic species in the atmosphere is a key area in atmospheric chemistry research. Nearest to the earth's surface, within the boundary layer of the troposphere, the determination of hydrocarbon species is important because of their ability to react rapidly with NO_x in the presence of sunlight to form photochemical smog. At the other extreme of the atmosphere in the stratosphere, remote measurements of very long-lived halogenated species are required because of their critical impact on ozone destruction. Species such as methane, present throughout the atmosphere, have importance as greenhouse gases and influence global climate and temperature change.

The wide range of both short- and long-lived species that are of interest in atmospheric science coupled to extremely low concentrations and a requirement often for *in situ* automated analysis has led to the development of many novel chromatographic techniques and methodologies. While some atmospheric species such as organic acids, peroxides and aldehydes have been determined using high performance liquid chromatography, the majority of species are analysed using capillary gas chromatography. The range of compounds that are of interest has resulted in almost every kind of detector finding a role within atmospheric analysis.

This article only deals with the analysis of species found in the gas phase, although many species present in the atmosphere are bound to particles or are in aerosol form. A vast number of methodologies for analysis of these species exist, although in common with gas phase species, gas chromatography plays a vital role in their analysis.

The range of techniques that are in use is so broad that a complete review of analytical methods is impractical. Many individual methods, however, have common components or key procedural steps and these will be discussed. A general outline of a typical atmospheric determination can be broken down into the following steps: sample acquisition, preparation, separation and detection. The first two stages, acquisition and preparation, often prove to be the most

challenging. A number of chromatograms obtained from atmospheric analysis are also presented in Figures 1–4. Figures 1 and 2 were obtained from an urban environment and Figures 3 and 4 came from a single field campaign held on the west coast of Ireland to study clean marine air.

Sample Acquisition

The initial step of sample acquisition is a far from trivial task in atmospheric measurements, and segregates a major grouping of techniques into either *in situ* or post-acquisition analysis. The ability to store an atmospheric sample is critical to the decision on whether analysis may be performed back in the laboratory or on-site immediately following acquisition. Stable species such as methane, carbon monoxide and chlorinated fluorocarbons may be stored successfully in sample vessels for many weeks without affecting sample integrity, and widespread measurements of these species have therefore been performed. Atmospheric degradation products, such as peroxyacetyl nitrate (PAN , $\text{CH}_3\text{C}(\text{O})_2\text{ONO}_2$), are so unstable, however, that analysis must be performed immediately. For many other important reactive species such as alkenes, monoterpenes and dimethyl sulphide, the storage of samples has been shown to lead to a degree of analyte losses due to reaction with co-sampled pollutants such as ozone and oxides of nitrogen. To overcome these problems of reaction during storage, many forms of scrubber (e.g. potassium iodide and glycerol to remove ozone) have been tested to remove such species without affecting sample integrity.

Much atmospheric sampling is performed using canister methods, filled either by vacuum release or by pumping sample into the canister using stainless steel or Teflon diaphragm pumps. For any sample to be stored successfully there must be minimal interaction with the canister walls and coating methods such as electropolishing, silica or Teflon coating are currently in use. The preparation and cleaning of canisters require careful attention and high vacuums are often applied together with elevated temperatures for periods of hours or even days. A similar method to canister samples is the use of collapsible Teflon or Tedlar sample bags. These bags may be filled by pump and returned to a laboratory for analysis using very similar procedures to those used with canister

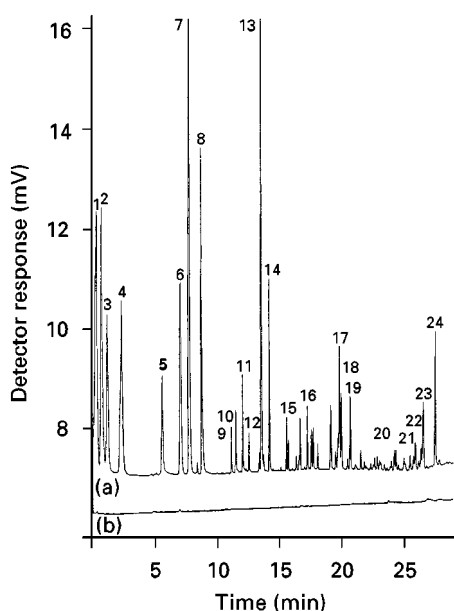


Figure 1 Low molecular weight hydrocarbons including methane determined using an online activated charcoal adsorbent trap in a programmed temperature vaporization injector. Column 50 m, 0.53 mm i.d. $\text{Al}_2\text{O}_3/\text{NaSO}_4$ PLOT (Chrompack) 10 μm film thickness. Desorption temperature was at 16°C s^{-1} from -20°C to 400°C , and column temperature programmed from 45°C to 200°C . Chromatograms showing (a) the separation of C_1 – C_6 components of Leeds city-centre air, and (b) a blank following desorption. Peaks: 1 = methane, 2 = ethane, 3 = ethene, 4 = propane, 5 = propene, 6 = 2-methylpropane, 7 = ethyne, 8 = *n*-butane, 9 = *trans*-2-butene, 10 = 1-butene, 11 = isobutene, 12 = *cis*-2-butene, 13 = 2-methylbutane, 14 = *n*-pentane, 15 = 1,3-butadiene, 16 = pentenes, 17 = 2-methylpentane, 18 = 3-methylpentane, 19 = *n*-hexane, 20 = methyl hexanes and hexenes, 21 = heptane, 22 = methylcyclopentane, 23 = benzene, 24 = toluene. Reproduced with permission from Lewis AC and Bartle KD 1996. A simplified method for the determination of atmospheric hydrocarbons. *LC-GC International* 9: 297–304.

samples. While generally of lower unit cost, the bag method often produces a greater degree of sample artefact and analyte losses.

Some low volatility species are less suitable for sampling using canister methods because of the increased possibility of analyte condensation on to the walls of the container. For this reason a second method of sample acquisition is widely used based on use of a solid-phase adsorbent as an analyte trap. The adsorbent used in the trap may be chosen to introduce an element of selectivity to the trapping mechanism, although in practice a trap-all approach is commonly used. Adsorbent traps allow for instrument automation that is not always possible with canister methods and such traps now form the basis of many national monitoring programmes in the urban environment, as well as automated instruments for research in very clean air.

A huge range of adsorbents is currently available from high surface area ($>1000 \text{ m}^2 \text{ g}^{-1}$) carbon-based materials with strong retention characteristics to lower surface area ($<50 \text{ m}^2 \text{ g}^{-1}$) polymers such as Tenax TA. While being relatively low cost compared to sample canisters, care is often required in the cleaning and preparation of sample tubes. Samples may be introduced to the adsorbent tubes either dynamically over short periods of time (typically minutes) or via diffusional sampling over longer periods (typically several days). Carbon-based adsorbents are suitable for a wide range of species ranging from volatile hydrocarbons and CFCs to organic nitrates. Polymeric materials are used mainly for the concentration of low volatility species such as aromatics and monoterpenes in air, although compounds as large as two and three ring polycyclic aromatics may also be successfully trapped and desorbed from the gas phase.

Sulfur species trapping is often performed via chemisorption on to gold wool traps that provide a stable matrix for the sample to be stored for reasonable periods of time.

The complete retention of all target analytes on the adsorbent bed must be carefully evaluated and calculation of retention volume (often referred to as breakthrough volume) is essential. For sampling very volatile species (for example ethane or ethene) the retention volume for an adsorbent system is often the critical factor in determining system sensitivity. Trapping at sub-ambient temperatures is commonly employed to increase the maximum sample volume, often using liquid nitrogen or carbon dioxide. For operation of any instrument in a field location, the supply of these coolants may be a problem and modern instruments often now employ Peltier coolers.

Sample Preparation and Injection

Removal of Water

The inevitable presence of water in atmospheric samples and its removal prior to sample analysis is a complex area. In certain circumstances its presence may be both beneficial, e.g. with canister samples where it occupies the active sites on the canister walls, or detrimental, e.g. where it affects analysis in some way. Alumina porous layer open tubular (PLOT) columns are particularly affected by moisture in the sample, and large changes in stationary phase affinity occur when water is introduced. Detectors such as mass spectrometers are also extremely sensitive to water introduced with the sample and high background noise may result. Even the flame

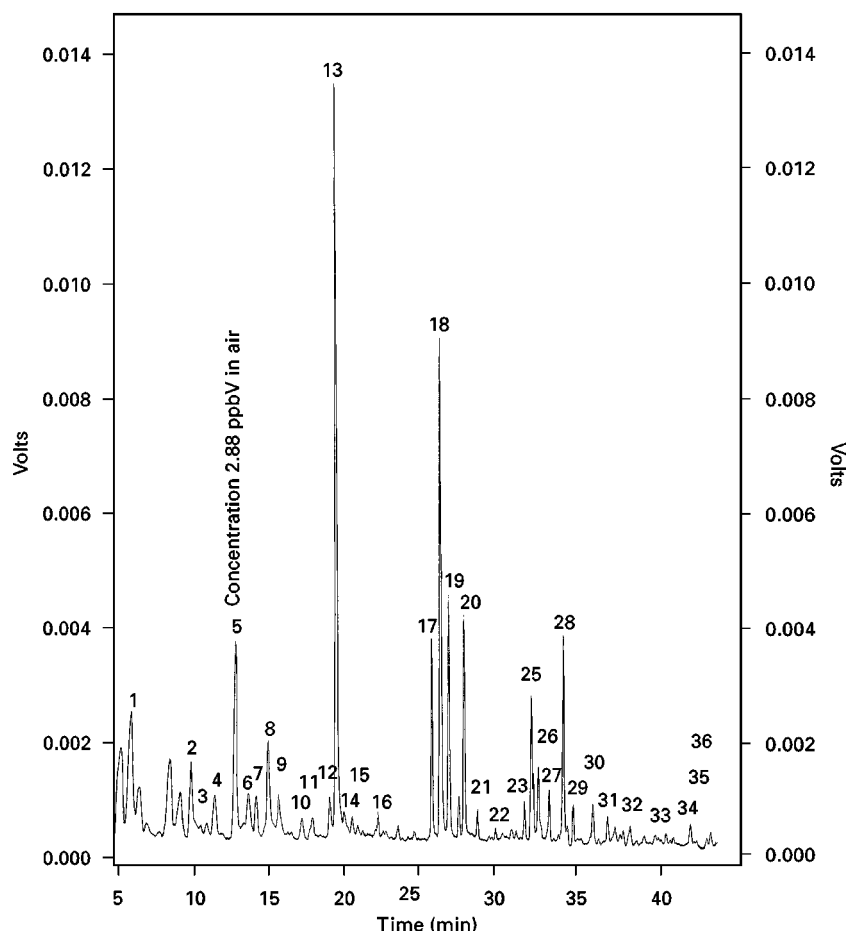


Figure 2 Aromatic hydrocarbon species determined using an online Tenax TA adsorbent trap in a programmed temperature vaporization injector. Column 60 m, 0.53 mm i.d., poly(dimethylsiloxane) 3 μ m film thickness. (Restek RTX-1). Desorption temperature was at 16°C s⁻¹ from 0°C to 220°C, and column temperature programmed from 35°C to 240°C.

1. unresolved volatile material	13. toluene	25. <i>p</i> -ethyltoluene
2. hexane	14. 2- and 4-methylheptane	26. 1,3,5-trimethylbenzene
3. methyl cyclopentane	15. 3-methylheptane	27. <i>o</i> -ethyltoluene
4. 2,4-dimethylpentane	16. octane	28. 1,2,4-trimethylbenzene
5. benzene	17. ethylbenzene	29. decane
6. 2-methylhexane	18. <i>m</i> - and <i>p</i> -xylene	30. 1,2,3-trimethylbenzene
7. 3-methylhexane	19. styrene	31. indane
8. 2,2,4-trimethylpentane	20. <i>o</i> -xylene	32. 1,4-dimethyl 2-ethylbenzene
9. heptane	21. nonane	33. dimethylethylbenzenes and undecane
10. methyl cyclohexane	22. isopropylbenzene	34. 1,2,3,5-tetramethylbenzene
11. 2,4- and 2,5-dimethylhexane	23. propylbenzene	35. naphthalene
12. 2,2,3-trimethylpentane	24. <i>m</i> -ethyltoluene	36. dodecane

(Reproduced with permission from Lewis AC *et al.* (1996) Atmospheric monitoring of volatile organic compounds using programmed temperature vaporisation injection. *Journal of High Resolution Chromatography* 19: 686–690.)

ionization detector can be affected by injection of water, and the flame may be extinguished when water elutes from the column.

Many forms of selective water removal exist, the simplest of which is the use of condensation traps or stripping coils. Losses of low boiling molecular species are insignificant although condensation of higher boiling organic material may arise at low condensa-

tion temperatures. Inorganic adsorbents are also commonly used, notably potassium carbonate and magnesium perchlorate. Adsorbents such as these, however, have limited capacity and often require frequent regeneration or replacement. A combination of initial condensation and second stage adsorbent scrubber often provides sufficient capacity to dry a sample stream of air for many hours or days. Con-

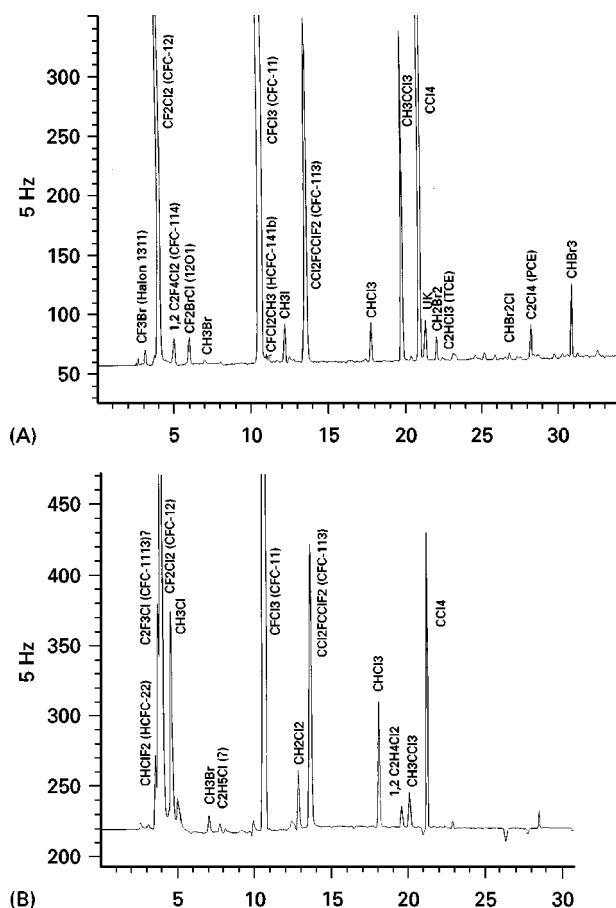


Figure 3 CFCs and halon species in clean marine air determined using an online Carbosieve micro adsorbent trap and direct injection to capillary GC. Detection by dual ECD/oxygen-doped ECD. Column 60 m, 0.33 mm i.d., 1 μ m film DB-1 (J&W). (A) Stage 1: standard ECD; (B) Stage 2: oxygen-doped ECD. (Reproduced with permission from Bassford M, and Simmonds PG, University of Bristol, Cantocks Place, Bristol.)

tinuous drying may be achieved using permeation membranes such as Nafion. These forms of driers operate by means of a concentration gradient across a membrane that is permeable only to highly polar material such as water. A counter-current of dry gas is passed around the outside of the membrane as a sheath gas and carries moisture away to waste. However, this type of drier is unsuitable for samples where the quantitation of polar materials is required.

Direct loop injection High concentration atmospheric species require the least amount of sample preparation, often only the removal of excess water from the sample. Methane, carbon monoxide and N_2O analyses are performed simply by filling a known volume injection loop, followed by direct injection into the analytical column. Backflushing is

often then performed to remove the remaining components from the analytical column. A further example of direct loop injection is in the analysis of PAN where, due to thermal decomposition of the sample, analysis must be performed *in situ*. It is performed using direct loop injection to a cooled isothermal pre-column followed by a short analytical capillary column coupled to an electron capture detector. An ancillary measurement of carbon tetrachloride is often gained from using this approach.

Sample concentration methods Whether an atmospheric sample is collected using adsorbent or canister techniques, several stages of sample preparation are required prior to injection into the analytical column. The sheer size of sample – often many litres – precludes any form of direct injection except in the case of the high concentration species described earlier, making sample concentration a vital step prior to injection.

Canister samples require complete concentration prior to introduction to the capillary column.

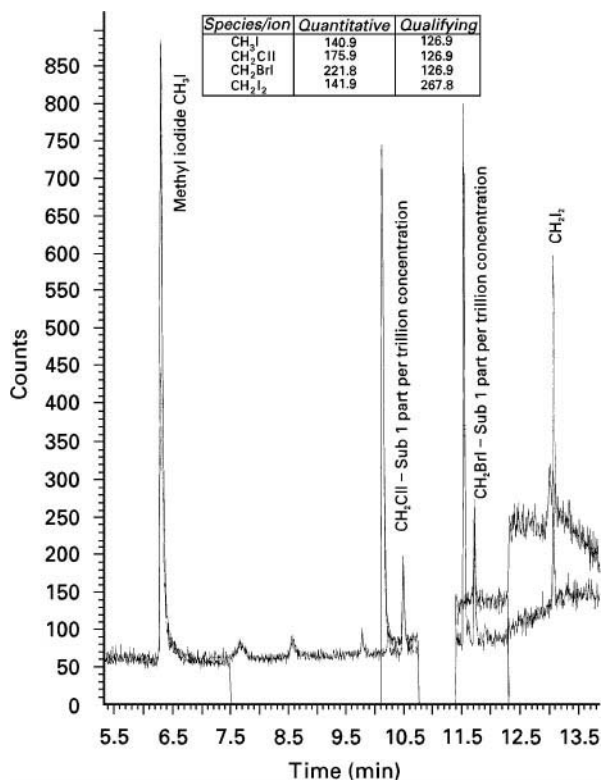


Figure 4 GC-SIM/MS of natural halocarbons (CH_3I , CH_2ClI , CH_2BrI and CH_2I_2) in marine air. PLOT column trap cooled with liquid nitrogen. Flash heating to capillary GC. Column 60 m, 0.33 mm i.d., 1.8 μ m film DB-VRX (J&W). Detection by single ion monitoring HP mass selective detector. (Reproduced with permission from Carpenter, L and Sturges, WT, School of Environmental Sciences, University of East Anglia, Norwich, UK.)

Analytes are removed from the canister via either internal canister pressure (for pumped-in samples) or vacuum pump (for atmospheric pressure samples) over a cryogenic trap. Liquid nitrogen is most commonly used but liquid argon has been used to reduce the amount of oxygen retained in the focusing stage. The concentration zone may consist of a packed tube containing either an absorbent such as Tenax TA or glass beads or it may simply be empty stainless steel tubing. Since the concentration stage is at such low temperatures, the majority of water vapour in the sample must be removed prior to focusing in order to stop blockage of lines with ice. Once a sufficient volume has been collected on the focusing trap, the trap is generally flash heated either electrically or by using hot water. This results in a very sharp band of compounds being introduced to the head of the analytical column.

With adsorbent tube analysis the collected analytes are generally thermally desorbed either directly on to the analytical column (in the case of programmed temperature vaporization injection), or on to a focusing cold trap. The desorption temperature is generally defined by the maximum temperature that the adsorbing material can support. For polymeric adsorbents this may be relatively low ($<250^{\circ}\text{C}$) while carbon-based materials may support desorption at temperatures of 500°C or higher.

If a programmed temperature vaporization (PTV) injector is used, the desorption may be sufficiently rapid ($>15^{\circ}\text{C s}^{-1}$) so that initial column focusing is sufficient to obtain well-resolved peaks. If the desorption from an adsorbent tube is relatively slow then a focusing step is used, with a similar concentration mechanism to that used with canister samples. Once again, water must be removed from the sample since it may affect the column or the detection system.

While the majority of species are thermally desorbed from the trap to the analytical column, a few types of compounds require solvent extraction prior to syringe injection. Organic nitrates fall into this class along with higher molecular weight polycyclic aromatic compounds that may suffer from incomplete or slow thermal release.

Separation of Atmospheric Samples

While a number of specific applications utilize packed columns (notably in the analysis of methane, CO and N_2O), current methods for the separation of atmospheric components are performed almost exclusively using capillary column gas chromatography.

The few applications remaining where packed columns are in use, generally employ molecular sieve packings for the separation of permanent gas species.

With the introduction of Al_2O_3 PLOT columns, fast high resolution analysis of even the highest volatility species has been made possible and many applications that previously used packed column GC are now being performed using capillary columns.

Where only one species is to be determined simple isothermal separations may be used, often in conjunction with a column backflush step. The analysis of PAN is an example of this where a short backflushing pre-column is used prior to a 10 m analytical column. A simple two-dimensional separation has also been proposed for PAN using heart-cutting.

The wide magnitude of analyte volatilities encountered imposes limits on the range of species that can be successfully separated on a given column. PLOT columns are used widely for the analysis of $\text{C}_1\text{--C}_7$ hydrocarbons and some high volatility halogenated compounds. The retention characteristics of this type of column are not favourable for the analysis of oxygenated compounds, and water often plays a significant role in degrading the quality of any PLOT column separation. Very strong retention of higher boiling species leads to extensive peak broadening coupled with lengthy analysis times.

Analysis of higher molecular weight species, including volatile organic compounds (VOCs), CFCs and hydrogen-containing chlorofluorocarbon replacements (hCFCs), aromatic and monoterpene compounds, has commonly been performed with nonpolar (methylpolysiloxane) or slightly polar (5% phenyl methylpolysiloxane) 1–5 μm -thick film capillary columns, 0.32 mm i.d. by 50 m long. Wide bore, 0.53 mm i.d. columns are often used where desorption is direct from a preconcentration trap to the analytical column. For the analysis of complex hCFC mixtures in the atmosphere, columns as long as 100 m have been reported.

To improve retention of volatile VOCs on thick film siloxane columns, without use of sub-ambient cooling, operation with columns containing films up to 15 μm thick have been reported. Band broadening effects through stationary phase diffusion become significant with films of this thickness and this approach has not been widely adopted. The highest molecular weight gas phase species such as naphthalene, fluorene and anthracene may be separated efficiently only on thinner film non-polar columns with film thicknesses of typically 0.25–0.5 μm .

Organic nitrate species in the atmosphere may also be determined using capillary GC with either charcoal adsorbent traps, extracted with aromatic organic solvent or via direct cryofocusing from a canister sample. Lengthy analysis times can result due to the necessity of using combinations of columns to achieve full separation of target analytes although commonly

moderate polarity 50% phenyl/50% methyl polysiloxane columns are used.

Detection Systems

Even the highest resolution capillary columns often have insufficient peak capacity to resolve all components in a typical atmospheric sample. Since selectivity in trapping is not always possible, selectivity in detection is a useful tool in the simplification of atmospheric analysis.

The flame ionization detector (FID) is by far the most commonly used detector in atmospheric analysis by GC since it offers high sensitivity, extremely wide linearity and good reliability. Using well-cleaned fuel gases coupled to low noise electrometer circuitry it is possible to determine amounts down to 1 pg s^{-1} . With a typical sample volume of 1 L, detection limits for individual species may be in the low parts per trillion range (10^{-12}). Calibration can be performed with relative ease but the complexity of samples can make peak identification difficult. Methods for alkene/aromatic analysis utilizing selective response from the photoionization detector (PID) have been proposed although they are not in widespread use.

Mass spectrometry offers obvious solutions to problems of compound identification but the operation of currently available bench-top MS in full scan mode often has insufficient sensitivity for trace level measurements. Spectral information obtained from GC/MS of atmospheric hydrocarbons often leads to highly similar fragmentation patterns and assists little in the identification of isomeric species. Similarly, identification of monoterpene species can only be confirmed through a combination of both spectral information and retention time data.

While MS of hydrocarbon species in clean air is often unsuccessful when operating in full scan mode there is sufficient sensitivity and resolution to allow for detection of long-lived CFC species. Long-term monitoring of these species has been performed by GC-ion trap detection in the worldwide MS-GAGE (global atmospheric gases experiment) network. In single ion mode, femtogram sensitivities can be achieved and this approach has been used for field monitoring of naturally produced trace level iodo- and bromo- compounds.

More commonly used for CFC measurements in the atmosphere is the electron-capture detector (ECD) that offers high sensitivity to certain species plus high selectivity over hydrocarbon compounds. GC-ECD measurements require careful calibration due to the great variation in response to halogenated species, although their high stability allows gas standards to

be used over many years. Some halogen-containing species of interest (e.g. CH_3Cl , CHF_2Cl , CH_2Cl_2) have a relatively poor ECD response and the use of the oxygen-doped ECD to enhance their response has been successful and is demonstrated in Figure 3. The determination of some nitrogen-containing species is also performed using ECD, notably in the areas of organic nitrate analysis and the determination of PAN. Organic nitrate analysis using ECD is often complicated by the co-elution of halogenated compounds, so often a nitrogen-specific detector such as the chemiluminescence detector is used in parallel.

Detection of CO is generally performed using the reduction gas detector (RGD) where hot HgO reduction with one CO molecule releases one Hg molecule from a catalytic bed. The Hg molecule released is then detected by UV absorption.

The analysis of sulfur compounds in the atmosphere, in particular dimethyl sulfide (DMS), has often been performed using a combination of GC with sulfur selective detection to overcome problems of insufficient chromatographic resolution. Flame photometric detection (FPD) has been used extensively in the past although signal quenching by co-eluting hydrocarbons results in drastically reduced sensitivity. The *Hall* detector or electrolytic conductivity detector (ELCD) has also been used for atmospheric determinations although it requires regular maintenance making it unattractive for an automated instrument. Emerging methods are now taking advantage of significant advances in bench-top atomic emission detectors (AED). The multielemental nature of the AED offers significant advantages in atmospheric measurements both in terms of sensitivity (sulfur $- 2 \text{ pg s}^{-1}$), and where concurrent emission line measurements for carbon and hydrogen may provide information on empirical formulae of unknown species. The sulfur chemiluminescence detector, which is a more recent technique that offers extremely high sensitivity and selectivity, may yet find an important role in atmospheric sulfur analysis.

The analysis of oxygenated species in the atmosphere is one of the least studied areas using gas chromatography. It is an area of fundamental significance where species may be present in the atmosphere as direct emissions or as degradation products of olefins. While most aldehydes and ketones may be successfully separated using GC, sample preparation and analyte detection are the key problem areas. Sample preparation is an area where new adsorbents may provide selective concentration of polar species simplifying the chromatogram produced. Detection of oxygenates is a further difficulty due to their often very low response in both ECD and FID. Use of elemental specific detection such as AED offers

some potential in atmospheric oxygenate analysis although AED sensitivity for oxygen is only around 100 pg s^{-1} . Detectors such as the helium ionization detector (HID), which produce a nonselective high sensitivity response to these types of compounds, may in future allow on-line measurements of oxygenates with GC, assuming sufficient chromatographic resolution or trapping selectivity can be obtained.

Future Work

Gas chromatography has an important role to play in monitoring mankind's emissions into the atmosphere and exploring the natural balance of biogenically released materials. New developments in injection technology and adsorbent materials will allow a greater number of species to be determined automatically in field locations. Development in column technology to reduce the effect of moisture on chromatographic separation and broaden the range of volatilities that may be separated on a given column will also bring significant benefits. Improvements in detector sensitivities and reliability (notably bench-top MS) will determine which of the many available detectors become standard in the next generation of atmospheric instruments.

See Colour Plates 56, 57, 58.

See also: II/Chromatography: Gas: Detectors: General (Flame Ionization Detectors and Thermal Conductivity Detectors); Detectors: Mass Spectrometry; Detectors: Selective. III/Environmental Applications: Gas Chromatography-Mass Spectrometry.

Further Reading

- Cao X-L and Hewitt CN (1993) Passive sampling and gas chromatographic determination of low concentration of reactive hydrocarbons in ambient air with reduction gas detector. *Journal of Chromatography* 648: 191–197.
- Ciccioli C, Cecinato A, Brancaleoni A, Frattoni M, and Liberti A (1992) Use of carbon adsorption traps com-

bined with high resolution gas chromatography-mass spectrometry for the analysis of polar and non-polar C_4 – C_{14} hydrocarbons involved in photochemical smog formation. *Journal of High Resolution Chromatography* 15: 75–84.

- Grimsrud EP (1992) The electron capture detector. In: Hill HH and McMinn DG (eds) *Detectors for Capillary Chromatography*, pp 83–106. New York: John Wiley.
- Helmig D and Greenberg JP (1994) Automated *in situ* gas chromatography-mass spectrometric analysis of ppt level volatile organic trace gases using multistage solid-adsorbent trapping. *Journal of Chromatography A* 677: 123–132.
- Kruschel BD, Bell RW, Chapman RE, Spencer MJ, and Smith KV (1994) Analysis of ambient polar and non-polar volatile organic compounds (VOCs) by thermal desorption, high resolution gas chromatography-mass spectrometry (TD/HRGC/MS). *Journal of High Resolution Chromatography* 17: 187–190.
- Lewis AC, McQuaid JB, Seakins PW, Pilling MJ, Bartle KD and Ridgeon P (1996) Atmospheric monitoring of volatile organic compounds using programmed temperature vaporisation injection. *Journal of High Resolution Chromatography* 19: 686–690.
- O'Brien JM, Shepson PB, Muthuranu, Hao C, Niki H, Hastie DR, Taylor R and Roussel PB (1995) Measurement of alkyl and multifunctional organic nitrates at a rural site in Ontario. *Journal of Geophysical Research* 100: 22795–22804.
- Penkett SA, Blake NJ, Lightman P, Marsh ARW, Anwyl P and Butcher G (1993) The seasonal variation of non-methane hydrocarbons in the free troposphere over the north Atlantic ocean possible evidence for extensive reaction of hydrocarbons with the nitrate radical. *Journal of Geophysical Research* 98: 2865–2885.
- Simmonds PG, Derwent RG, McCulloch A, O'Doherty S and Gaudy A (1996) Long-term trends in concentrations of halocarbons and radiatively active trace gases in Atlantic and European air masses monitored at Mace Head, Ireland 1987–1994. *Atmospheric Environment* 30: 4041–4063.
- Swan HB and Ivey JP (1994) Analysis of atmospheric sulphur gases by capillary gas chromatography with atomic emission detection. *Journal of High Resolution Chromatography* 17: 814–820.

BACTERIOPHAGES: SEPARATION OF



P. Serwer, The University of Texas Health Science Center, San Antonio, TX, USA

Copyright © 2000 Academic Press

Introduction

Bacteriophages are viruses that infect bacteria. Historically, interest in bacteriophages was first

generated by the possibility of using bacteriophages as biological antibiotics. This interest is periodically revived when difficulties are encountered with the use of chemical antibiotics. Interest in bacteriophages was also generated by both the short life cycle and the simple (short) genome of bacteriophages. These characteristics were useful in developing the science of molecular genetics. Bacteriophages were a favourite

for asking questions about transfer of biological information via DNA replication, transcription (copying of RNA from DNA) and translation (using the information in RNA to assemble proteins). Today, bacteriophages are used to carry small pieces of the DNA of higher organisms. The purpose is to determine the nucleotide sequence of the pieces and, ultimately, the nucleotide sequence of the whole genome of higher organisms. Basic science uses bacteriophages as models for understanding how separate molecules assemble to form a complex structure. The questions asked in these studies are fundamental: How do biological motors work? How is specificity maintained in intermolecular binding? How is accuracy assured during assembly? To what extent is biological form determined by either pathway of assembly or energetics of the final structure? Are errors corrected during assembly of biological macromolecules? Are separate biochemical processes integrated in the context of the interior of a cell? Pursuit of the answers to all these questions requires purification of bacteriophage particles.

Purification of both bacteriophages and bacteriophage-like particles is also needed for other types of study. Bacteriophage-like particles are present in both lakes and oceans. Some are true bacteriophages. Others are viruses that infect algae, rather than bacteria. Environmental biologists detect and sometimes purify these particles without knowing what they are. Purification helps establish what they are, both biologically and chemically. Finally, bacteriophages are model viruses. Study of the evolution of bacteriophages helps in the understanding of the evolution of other viruses, including pathogenic viruses. A major advantage of studying bacteriophages is their comparatively short life cycle. For example, bacteriophage T7 has a 13 min life cycle at 37°C and a 25 min life cycle at 30°C. The host cell is *Escherichia coli*. Most other bacteriophages that infect *E. coli* have life cycles less than 60 min at 37°C. Thus, studies of evolution are achieved more quickly than they are with any other organism. Also, the short life cycle of bacteriophages reduces the time needed to grow them.

Growth of Bacteriophages

Bacteriophages are grown in either gelled or liquid solutions of nutrients. Gels are made of the polysaccharide, agar. Gel-embedded infected cells are used to count viable bacteriophage particles. The procedure is to embed bacteriophages in the gel, together with host cells. The number of host cells is much greater than the number of bacteriophages. This gelled mixture is incubated to replicate the cells and infect them. A bacteriophage particle infects a growing host cell

while in the gel. The cell bursts at the end of the infection. Light-scattering (turbidity) decreases when the infected cell bursts. All progeny of a single bacteriophage particle remain in a restricted region of the gel. This region is comparatively clear (nonturbid). The clear region is called a plaque. A viable bacteriophage particle is assayed by the formation of a single plaque on a glass or plastic Petri dish or plate which holds the gel with plaques. Plaques are counted after incubating viable bacteriophage particles with host cells. The number of viable bacteriophage particles per plate is small enough (usually 100–2000) so that overlapping plaques do not cause difficulty in counting. The number of plaques is multiplied by a dilution factor, if the bacteriophage particles had been diluted before assay. Bacteriophage plaques are illustrated in Figure 1.

Incubation of a host–bacteriophage mixture in a gel can also be used to prepare large numbers of bacteriophage particles before purification. The bacteriophages produced are sometimes called a plate stock. Preparing of bacteriophage particles via large volume (> 100 mL) plate stocks is not efficient (in time and cost), in comparison to preparing bacteriophage particles via infection in liquid culture. However, some bacteriophages which do not grow well in liquid cultures grow comparatively well when prepared as a plate stock. Thus, plate stocks are sometimes used for the growth of bacteriophage particles before purification. To remove bacteriophage particles from the gel of a plate stock the gel is minced

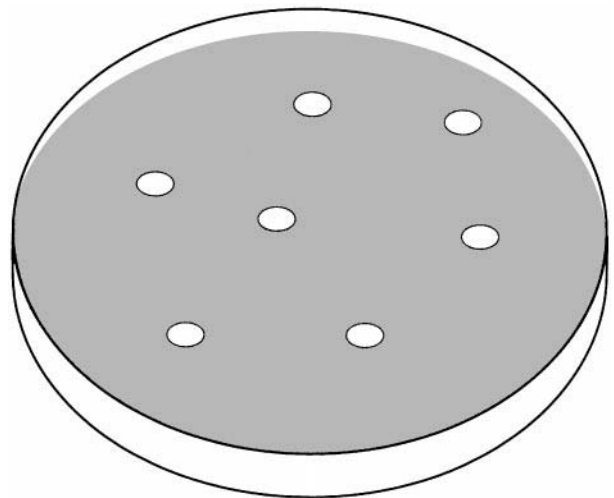


Figure 1 Plaques of bacteriophage T7. A Petri plate is filled with a 1% agar gel in an enriched growth medium. Subsequently, 0.7% molten agar in the same enriched medium is mixed with both host bacteria and bacteriophage particles. This mixture is spread on the 1.0% gel. The plate is incubated at 37°C. A plaque forms at the position of a single bacteriophage particle.

with either a glass rod or a spatula and the minced gel is incubated with buffer. The bacteriophage particles diffuse out of the gel, into the buffer during this process. Centrifugal pelleting is then used to remove the pieces of gel, together with pieces of the host bacterium. Some bacteriophages are pelleted with the gel. Thus, the pelleted pieces of gel are resuspended in buffer and then pelleted a second time. This process is called washing. Washing is typically performed two or three times. The supernatant solutions are pooled to produce a clarified plate stock.

Details of plate stock preparation vary slightly among the various bacteriophages. A bacteriophage best prepared by plate stock is bacteriophage G. Bacteriophage G is the largest bacteriophage (known to the author) that can be grown in culture. Bacteriophage G has a double-stranded DNA genome 670 kilobase pairs long. Bacteriophage G can be grown in liquid cultures, but results are erratic and greater success has been achieved with plate stocks. Typically, plate stocks of bacteriophage G are clarified by centrifugation at 5000 rpm in a 250 mL bottle (or the equivalent; centrifugal force at the bottom of the bottle is 3800 g). This speed is doubled (centrifugal force is quadrupled) in the case of smaller bacteriophages that don't sediment as quickly as bacteriophage G. Pelleting the bacteriophage particles (or aggregates of them) works against the objective of clarifying a plate stock.

Maintaining the stability of the bacteriophage particles is an objective at all stages of purification. Known bacteriophages are stabilized by the presence of divalent cations. Magnesium is usually used. Thus, magnesium should be present in the buffer. The presence of $0.001 \text{ mol L}^{-1} \text{ MgCl}_2$ is usually sufficient for stability. Some salt (usually NaCl) should also be present. Some bacteriophages increasingly adsorb to fragments of host cell, as the salt concentration is lowered. Thus, salt concentrations are sometimes raised from the typical 0.1 mol L^{-1} to 0.5 mol L^{-1} or more. Adsorption to host cell debris can either inactivate a bacteriophage particle or cause it to pellet with the fragments of gel.

Storage

Plate stocks are also sometimes preferred when a new bacteriophage is isolated. The new bacteriophage might have been isolated from the wild. It might also have been produced by genetic modification of a previously isolated bacteriophage. A plate stock made with a single plate is a rapid and simple way of preserving this new strain. Preservation is completed by freezing a clarified plate stock. Freezing (typically at -70°C) is used to prevent inactivation during storage for periods of years to decades. A cryoprotectant

is added before freezing. Glycerol (10%) can be used as a cryoprotectant. Alternatively, a high molecular weight cryoprotectant can be used. A high molecular weight cryoprotectant sometimes used is 10% dextran, average molecular weight = 10 000. High molecular weight cryoprotectants are less likely to enter a bacteriophage particle. Therefore, high molecular weight cryoprotectants are less likely to cause bacteriophage particles to burst from osmotic shock during thawing. Osmotic shock during thawing occurs because freezing causes nonuniformity in the concentration of cryoprotectant. If the bacteriophage particle is in a region of comparatively low cryoprotectant concentration, an outward osmotic pressure gradient will develop. This is a demonstrated cause of inactivation of bacteriophage T4 by freeze-thawing.

Growth in Liquid Culture

A bacteriophage is usually grown in liquid culture, when the purpose is either chemical or physical characterization of either the bacteriophage or its nucleic acid. In this case, amounts in the 1–50 mg range may be needed. Either simple, well-defined media or enriched media are used. A simple, well-defined medium might have glucose as the primary (sometimes only) source of both carbon and energy. The medium is typically buffered with phosphate. The medium is supplemented with ammonium chloride to provide nitrogen for proteins. Other salts are also added. Both magnesium sulfate and calcium chloride are added after sterilization by autoclaving. Apparently, some requirements, such as iron, are present in sufficient quantity as contaminants. Alternatively, an enriched, but less well-defined, medium can be used. The major components of an enriched medium are often both tryptone and an extract of yeast cells.

Some bacteriophages are more easily (and more inexpensively) grown in minimal medium. This is true for some lytic double-stranded DNA bacteriophages, for example. A lytic bacteriophage always produces progeny when it infects a cell. The counterpart of a lytic bacteriophage is a lysogenic bacteriophage. A lysogenic bacteriophage may or may not produce progeny. The lysogenic bacteriophage genome both remains in and replicates with the host, if progeny are not produced. This state is called lysogeny. Lysogeny can simplify growth of some bacteriophages, as described below. Growth of a lytic bacteriophage, but not a lysogenic bacteriophage, encounters the following problem: cells are infected at a low ratio of bacteriophage particles to host cells, typically 0.01–0.1. Multiple cycles of infection occur. Therefore, the concentration of cells during the final (and most critical) cycle of infection is hard to control. Overgrowth of

cells can result in a suboptimal yield, because of inadequate aeration. Undergrowth of cells can result in suboptimal yield, because of the low concentration of cells. The more rapidly cells grow, the more difficult controlling their concentration during the last cycle is. Cells grow more slowly in minimal medium (typical doubling time = 1.5–2.0 h for *E. coli* at 30°C) than they do in enriched medium (typical doubling time = 30–40 min for *E. coli* at 30°C). Thus, the infection is more easily controlled in minimal medium. None the less, other factors are also involved. Some experimentation with growth medium is required to optimize conditions of growth, when these conditions have not been previously optimized.

Growing lysogenic bacteriophages is usually easier than growing lytic bacteriophages. Lysogenic bacteriophages can be made to leave a state of lysogeny and enter a lytic cycle. Some mutants will do this when the temperature is raised. Thus, growth of lysogenic bacteriophages (bacteriophages λ and P22, for example) can be simplified. Host cells in a state of lysogeny are grown to an optimal concentration. The temperature is raised to induce the lytic cycle. The temperature is then lowered to an optimal temperature for growth. This process is useful for producing bacteriophage particles in large amount. It is also useful for producing other components of bacteriophage-infected cells. For example, some components of bacteriophage-infected cells retain their metabolic activity when infected cells burst (lyse is a frequently used synonym for burst). These activities include packaging of double-stranded DNA in bacteriophage capsids. Thus, a fragment of foreign DNA can be cloned by, first, incorporating the fragment in a bacteriophage genome, and, then, packaging the DNA *in vitro* by incubating the DNA in an extract of lysed, infected cells. Extracts of lysed, bacteriophage-infected cells can sometimes be used for incorporating the foreign DNA, as well as packaging it. An extract can be made by use of a lytic bacteriophage, as well as a lysogenic bacteriophage. The process is, however, less time- and resource-consuming with a lysogenic bacteriophage.

Equipment for Large-Scale Growth of Bacteriophages in Liquid Culture

Small scale (1–1000 mL) liquid cultures are grown in typical laboratory glassware. A flask is sometimes used, with aeration by shaking. Alternatively, a bottle is used with aeration via a bubbler and forced air. The latter alternative is simpler, less expensive and less space-consuming. A reliable shaker is needed in the former case; a source of forced air is needed in the latter. A reliable and reliably clean source of forced

air is an aerator designed for use with tropical fish. The use of forced air is scalable to at least a 15 L culture. Shaking is scalable to roughly a 1 L culture.

The control of temperature can be achieved via several routes. A temperature-regulated fermentor with forced air can be used. The cost and inconvenience can, however, be dramatically lowered by using a bottle in a temperature-controlled water bath. Even a bottle in a temperature-controlled, water-filled sink can be used. In the latter two cases, a bottle with sterile medium and bubblers is aerated via forced air.

First Stage of Purification

The targeted degree of purification varies with the intent of the investigator. The minimal purification is removing large fragments of the host cell. Pelleting in a centrifuge is used. This stabilizes the bacteriophages by preventing adsorption of the bacteriophages to fragments of host cell membrane. Pelleting is typically done immediately after lysis for small (< 1 L) cultures. Pelleting is sometimes delayed until after precipitation of bacteriophage particles for large cultures. The precipitation is performed by both raising the salt concentration (typically to 0.5 mol L⁻¹) and adding a high molecular weight polyethylene glycol. Details vary among the different bacteriophages. The precipitation concentrates bacteriophage particles for subsequent steps in purification. Alternatively, bacteriophage particles can be concentrated by pelleting, without precipitation. The newer centrifuges can pellet bacteriophages in increased volume and decreased time. Bacteriophages in eight 50 mL tubes can now be pelleted in 1–4 h. The time depends on how rapidly the bacteriophage particles sediment at any given speed of centrifugation.

Subsequent Stages of Purification

Concentration and partial purification of bacteriophage particles are achieved in the first stage of purification. The subsequent stages can, in theory, be essentially any procedure of purification used for other biological macromolecules. However, in practice, the simplest, highest yielding, highest volume procedure has been found to be centrifugation. Three types of centrifugation are used, sometimes in tandem. The details of procedure vary with both the properties of the bacteriophage and the purposes of the investigator.

Buoyant Density Centrifugation

Buoyancy is a familiar concept to anyone who has learned to swim. Buoyancy can be used to purify any

macroscopic object by placing the object in solution that continuously varies in density. Gravity will drive the particle to the region of the density gradient that has a density equal to the density of the particle (isodense region). This concept also works for bacteriophages. However, bacteriophages are small. They are so small that ultracentrifugation is needed to drive them to an isodense region (a process called buoyant density centrifugation). Thermally driven motion (diffusion) randomizes the position of the bacteriophage particles in the absence of centrifugation. Even if diffusion did not occur, the bacteriophage particles would take impractically long to find their isodense region, if centrifugal force were not applied. Buoyant density centrifugation is performed by mixing bacteriophage particles with a solute that will form a density gradient when centrifuged ('before' column of the first row of **Figure 2**; the sample is grey). The density gradient forms because the solute, like the bacteriophage particles, is driven in the direction of the centrifugal force. The motion caused by centrifugal force eventually achieves equilibrium with thermal motion. The result is a density gradient. The bacteriophage particles are driven to an isodense region of the gradient ('after' column of the first row of **Figure 2**; the sample is black). Comparatively small ions (or molecules), like caesium cations, form the

most linear density gradients. Caesium chloride is the most frequently used compound for fractionating bacteriophages by buoyant density centrifugation.

The word isodense means same density. But, what is the density of a bacteriophage particle? Can this density vary with position in a density gradient? This density not only can, but does, vary with position in a density gradient. The density varies because the anhydrous components of the bacteriophage are not the only components, from the perspective of buoyant density. The bacteriophage also contains both water- and density-forming solute. The concentration of water inside the bacteriophage is not necessarily the same as the concentration outside the bacteriophage. The bacteriophage nucleic acid sometimes binds a large amount of solute-free water, for example. But, this concentration does vary with the concentration of water outside of the bacteriophage. Analysis of this situation is beyond the scope of this article. This analysis is not critical for achieving practical results. However, it is critical for interpreting densities in terms of a particle's composition.

Many studied bacteriophages consist only of a protein capsid that contains a nucleic acid genome. The capsid has a density of roughly 1.3 g mL^{-1} when centrifuged to an isodense region in a caesium chloride density gradient. Double-stranded DNA has a density of roughly 1.7 g mL^{-1} . Both these densities vary slightly with detailed composition. Double-stranded DNA bacteriophages are, in general, roughly 50% DNA, 50% protein. The density of these bacteriophages is 1.5 g mL^{-1} . This density is halfway between the density of protein and the density of DNA. This relationship is, however, not an intrinsic feature of densities. Its source is roughly equal hydration of DNA and protein in caesium chloride density gradients. These two hydrations are usually not equal.

Buoyant density centrifugation has the following limitation. Low molecular weight contaminants (molecules of RNA, unassembled proteins) diffuse so rapidly that they contaminate the bacteriophages, even though their density is different. Thus, bacteriophage purification procedures often have one stage at which particles are fractionated by size.

Rate Zonal Centrifugation

Rate zonal centrifugation fractionates particles by both size and shape. The procedure is to layer a sample in a restricted zone on top of a pre-poured density gradient. The density gradient is then centrifuged. All particles migrate into the density gradient, because the density gradient has only densities much lower than the densities of the particles being centrifuged (illustrated in the second row of **Figure 2**). The

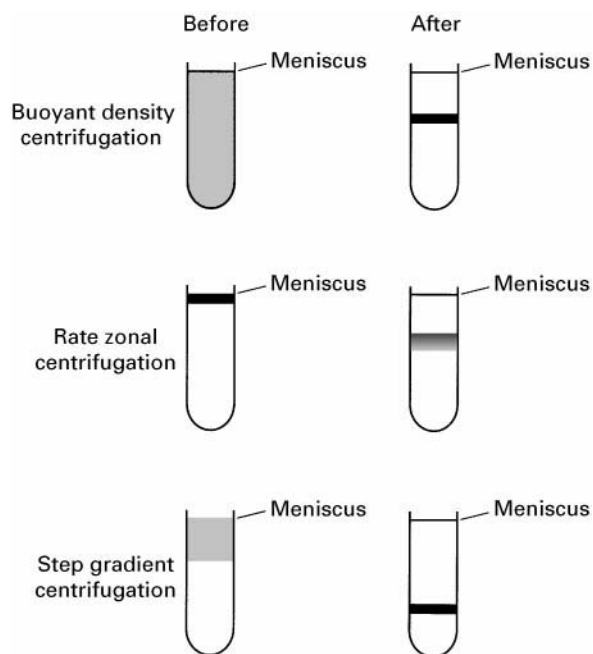


Figure 2 Purification of bacteriophage particles by ultracentrifugation. The three rows illustrate the three types of ultracentrifugation described in the text. The appearance of a centrifuge tube before centrifugation is shown in the column labelled before. The appearance of the same centrifuge tube after centrifugation is indicated in the column labelled after.

particles are fractionated primarily by size and shape. The larger a particle is, the more rapidly it sediments. The more spherically symmetrical a particle is, the more rapidly it sediments. Bacteriophages sediment much more rapidly than unassembled proteins and RNA. Thus, bacteriophages are separated from these particles by a single rate zonal centrifugation in a sucrose gradient. Some fragments of host cells co-sediment with bacteriophage particles. However, these fragments have a variable rate of sedimentation. The bacteriophage particles have a unique rate of sedimentation. Therefore, separation from most of these fragments occurs.

Rate zonal centrifugation has the following limitation. The sample occupies a small region of the centrifuge tube at the start of fractionation. Furthermore, the sample becomes less concentrated during fractionation. Thus, the amount of sample is more limited when compared to the amount fractionated by buoyant density centrifugation. During buoyant density centrifugation, the sample occupies the entire centrifuge tube at the start of fractionation. The sample becomes more concentrated during fractionation. Thus, rate zonal centrifugation is usually not the procedure of choice. However, some bacteriophages (including bacteriophage G) are not stable when centrifuged in caesium chloride density gradients. Rate zonal centrifugation is a reasonable alternative in this case. Unstable bacteriophages have been stabilized by including polyethylene glycol in the density gradient used for rate zonal centrifugation.

Combined Buoyant Density and Rate Zonal Centrifugation

Advantages of buoyant density centrifugation are combined with advantages of rate zonal centrifugation when the following hybrid procedure is used. A comparatively broad zone of sample is layered on a pre-formed caesium chloride density gradient (before column of the third row of Figure 2). The caesium chloride density gradient had been formed before centrifugation, by successfully layering 3–5 caesium chloride solutions. These solutions decrease in density, from bottom to top. The rapid diffusion of a caesium cations converts the discontinuous gradient (called a step gradient) into a more continuous gradient. The step gradient with layered sample is centrifuged until bacteriophage particles reach an isodense position in the gradient (after column of the third row of Figure 2). Thus, the advantages of buoyant density centrifugation are achieved: increase in the sample's concentration and fractionation by density. On the other hand, the advantage of rate zonal centrifugation is also achieved: separation of bacteriophage particles from rapidly diffusing components of the cell.

The advantages of a caesium chloride step gradients make them a method of choice for purifying many bacteriophages. A single centrifugation is sometimes sufficient to achieve the purity needed. Alternatively, a buoyant density centrifugation can be performed after centrifugation in a step gradient. Increase in concentration of the sample is achieved by combining bacteriophages from several step gradients in a single buoyant density gradient.

Nondenaturing Gel Electrophoresis

Bacteriophage particles can be fractionated by electrophoresis through gels. This procedure is called nondenaturing gel electrophoresis because the bacteriophage particles are intact (infective) during electrophoresis. In contrast, other procedures of electrophoresis are used to analyse the components of disassembled bacteriophage particles. The gels used for nondenaturing electrophoresis must have pore sizes large enough to admit bacteriophage particles (30–90 nm in radius). Polyacrylamide gels can be made dilute enough to achieve the needed pore sizes. However, these polyacrylamide gels are very weak and difficult to handle. Agarose gels achieve the needed pore sizes with gels that are easy to handle. Agarose has been the gel-forming compound most frequently used to fractionate bacteriophages (and other viruses) by nondenaturing gel electrophoresis.

Gel electrophoresis fractionates any spherical particle by two properties of the particle: the average electrical surface charge density (σ), and the radius. The value of σ is the sole determinant of the electrophoretic mobility (= velocity/electrical field) in the absence of the gel, within experimental accuracy. For example, a dimer of a bacteriophage capsid has an electrophoretic mobility indistinguishable from that of a capsid monomer, when the electrophoretic mobility is extrapolated to a gel concentration of zero. In theory, the value of σ will be the sole determinant of gel-free electrophoretic mobility, for all conditions likely to be encountered during the analysis of bacteriophage particles. Changing the value of the particle's radius will, however, change its electrophoretic mobility during electrophoresis through a gel. The larger the radius is, the more retarded the particle will be by the fibres that form the gel.

The fractionation by σ is independent of fractionations achieved by either buoyant density or rate zonal fractionation. Thus, nondenaturing gel electrophoresis can differentiate particles not differentiated by any procedure of centrifugation. The result has been the finding that at least one bacteriophage (T7) exists in more than one state. The different states appear to have evolved to improve the survivability of T7.

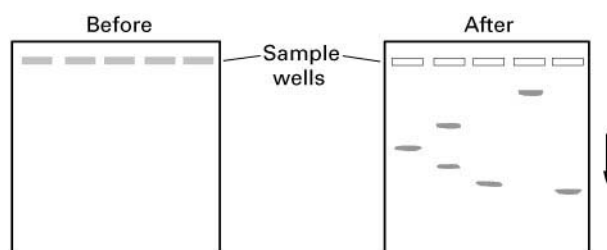


Figure 3 Nondenaturing gel electrophoresis. A horizontal gel with samples loaded is illustrated in the before panel. The same gel with stained, fractionated bacteriophages is shown in the after panel. The arrow indicates the direction of electrophoresis.

In practice, gel electrophoresis can be performed by the following procedure:

1. An agarose gel is cast in a horizontal orientation (before column in **Figure 3**). The gel has sample wells for placing the sample (indicated in **Figure 3**).
2. The gel is submerged beneath an electrophoresis buffer. The pH should be close to the pK_a of the buffer. The gel chosen should not adhere to the bacteriophage particles. Agarose can be purchased at several levels of purity. Several agarose derivatives and mixtures can be purchased. Some nonagarose polysaccharides can also be used for electrophoresis.
3. The sample is placed in a sample well. The sample contains an uncharged compound (glycerol, sucrose, a polyethylene glycol, for example), in order to prevent the sample from floating.
4. An electrical potential is placed across the gel. The electrical field and time of electrophoresis are chosen, based on the following:
 - (a) The most rapidly migrating particle should not migrate out of the gel.
 - (b) The separation between particles should be sufficient so that each particle forms a separate band.
 - (c) Bacteriophage particles should not disrupt during electrophoresis.
 - (d) The time of electrophoresis should be short enough so that band broadening is not a problem.
 - (e) The electrical current should be low enough so that rise in temperature does not destabilize bacteriophage particles.

The bacteriophage particles are visualized by either light scattering or staining, after electrophoresis (illustrated in the after column of **Figure 3**). Ethidium is a stain used for DNA; Coomassie blue is a stain used for protein. Preparative fractionation should use light

scattering, to avoid stain-induced changing of the bacteriophage particles.

Large scale fractionation of bacteriophage particles is almost never done by gel electrophoresis. Gel electrophoresis is used primarily for analysis, not purification. The reasons are the following:

1. Like rate zonal centrifugation, nondenaturing gel electrophoresis begins with the sample in a small volume. The sample is diluted during fractionation.
2. Recovery of particles after gel electrophoresis is not as good as recovery after fractionation in solution.
3. The bacteriophage particles are contaminated with both agarose and contaminants of agarose, after fractionation.
4. The bacteriophage particles are exposed to products of the electrolysis of water. The result is an unnecessary source of possible damage of bacteriophage particles.

Concluding Remarks

The purification of bacteriophages by centrifugation is a routine procedure. The most difficult requirement is the obtaining of centrifuges. Challenges are encountered primarily when a bacteriophage is unstable during exposure to the conventional conditions of centrifugation. A further challenge is encountered when bacteriophage particles are purified for the purpose of high resolution analysis of structure. This latter challenge is heterogeneity of bacteriophage particles that appear homogeneous when fractionated by centrifugation. Nondenaturing gel electrophoresis can reveal heterogeneity. However, nondenaturing gel electrophoresis has not been useful for preparative fractionation. Thus, a challenge for the future is the development of preparative procedures of nondenaturing gel electrophoresis. This last challenge would be met by development of a procedure of continuous-flow gel electrophoresis. Continuous-flow preparative gel electrophoresis is possible, in theory. Hopefully, it will be achieved in practice.

See also: **II/Electrophoresis: Agarose Gels. Centrifugation: Theory of Centrifugation.**

Further Reading

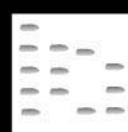
Alberts B, Bray D, Lewis J *et al.* (1994) *Molecular Biology of the Cell*, 3rd edn. New York: Garland.

- Proctor LM (1997) Advances in the study of marine viruses. *Microscopy Research and Techniques* 37: 136–161.
- Serwer P, Khan SA and Griess GA (1995) Non-denaturing gel electrophoresis of biological nanoparticles: viruses. *Journal of Chromatography A* 698: 251–261.
- Stafford WF and Schuster TM (1995) Hydrodynamic methods. In: Glasel JA and Deutscher MP (eds.) *Introduction to Biophysical Methods for Protein and Nucleic Acid Research*. San Diego, CA: Academic Press, pp. 111–145.
- Stent GS and Calendar R (1978) *Molecular Genetics: An Introductory Narrative*, 2nd edn. San Francisco, CA: WH Freeman.
- van Holde KE, Johnson WC and Ho PS (1998) *Principles of Physical Biochemistry*. Upper Saddle River, NJ: Prentice Hall.
- Yamamoto KR, Alberts BM, Benzinger R *et al.* (1970) Rapid bacteriophage sedimentation in the presence of polyethylene glycol and its application to large-scale virus purification. *Virology* 40: 734–744.

BALSAMS AND RESINS: THIN-LAYER (PLANAR) CHROMATOGRAPHY

See III / ESSENTIAL OILS / Thin Layer (Planar) Chromatography

BASES: THIN-LAYER (PLANAR) CHROMATOGRAPHY

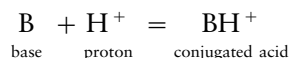


L. Lepri and A. Cincinelli, University of Florence, Florence, Italy

Copyright © 2000 Academic Press

Introduction

According to the Brønsted–Lowry definition (1923) a base is a proton acceptor:



The stronger the base, the larger is its K_b and consequently the smaller is its pK_b and the larger is the pK_a of the conjugated acid.

There are various types of bases, including natural and synthetic compounds, and they occur in a vast array of products, extending from the alkaloids, sulfa drugs (sulfonamides), dyes (azines, indoles), herbicides (simazine, atrazine, promazine), biogenic amines to numerous other groups.

This chapter includes only aliphatic and aromatic amines and their derivatives, heterocyclic bases and miscellaneous compounds (nitrosamines, amides, hydrazines). Thin-layer chromatography is used extensively for the analysis of bases and can achieve separations of complex mixtures comparable to column liquid chromatography.

Aliphatic Amines

The first attempts to separate aliphatic amines were performed on silica gel using chloroform–ammonia (39 : 1), chloroform–methanol–17% ammonia (2 : 2 : 1), butanol–acetic acid–water (4 : 1 : 5) and phenol–water (8 : 3) as eluents. However, highly volatile amines cannot be chromatographed with an ammoniacal solvent. A systematic collection of data on the chromatographic behaviour of a large number of aliphatic amine hydrochlorides, with particular emphasis on eluents, adsorbents and detection reagents, was published by Prandi (see hR_F values in Table 1, columns 1, 2 and 3).

Silica gel is particularly useful for the adsorption chromatography of amines that have different polarities but does not resolve the fatty amine series. In particular, the R_F values increase as the aliphatic chain length increases but this increase becomes smaller with increasing chain length.

Reversed-phase partition chromatography on paraffin oil–saturated silica gel is useful for the separation of fatty amines. $R_M[\log(1/R_F)^{-1}]$ values for such amines increase as the length of the aliphatic chain increases and there is a linear relationship between R_M and the number of carbon atoms in the molecule.

Table 1 Retention data (R_F)* of aliphatic amine hydrochlorides under different experimental conditions^a

Amine	Silica gel ^b		Po-s Kieselguhr ^c	Silica gel + chlorophenol ^d	Sil C ₁₈ -50 + 4%HDBS ^e	AWP ^f
	Eluent A	Eluent B	Eluent C	Eluent D	Eluent E	Eluent F
Methylamine	3	6	—	26	92	69
Dimethylamine	4	7	—	31	—	—
Trimethylamine	—	43	—	35	—	—
Ethylamine	7	16	—	46	85	75
Diethylamine	16	32	—	50	—	—
Triethylamine	—	75	—	53	—	—
Ethanolamine	4	10	—	—	—	—
Diethanolamine	5	16	—	—	—	—
Triethanolamine	18	36	—	38	—	—
Ethylethanolamine	11	23	—	—	—	—
Ethyl-diethanolamine	30	52	—	—	—	—
2-Ethylhexylethanolamine	65	93	—	—	—	—
Propyldiethanolamine	52	69	—	—	—	—
Propylamine	16	35	—	57	—	—
Di- <i>n</i> -propylamine	51	80	—	—	—	—
Isopropylamine	17	36	—	63	—	—
Diisopropylamine	33	66	—	—	—	—
Propanolamine	4	8	—	—	—	—
Triisopropanolamine	52	85	—	—	—	—
Allylamine	—	—	—	60	—	—
Diallylamine	—	—	—	66	—	—
Butylamine	22	48	—	—	55	65
Di- <i>n</i> -butylamine	63	95	—	80	—	—
Tri- <i>n</i> -butylamine	—	—	—	85	—	—
Isobutylamine	31	58	—	—	62	70
Diisobutylamine	85	99	—	—	—	—
3-Methoxypropylamine	18	43	—	—	—	—
Pentylamine	29	55	—	—	34	60
Isoamylamine	30	56	—	—	45	62
2-Methylbutylamine	36	68	—	—	—	—
Hexylamine	34	65	86	—	24	53
Cyclohexylamine	33	63	—	76	—	—
3-Amino-2,2'-dimethylbutane	51	90	—	—	—	—
2-Amino-3-methylpentane	47	78	—	—	—	—
2-Amino-4-methylpentane	42	73	—	—	—	—
Heptylamine	36	70	82	—	14	elongated spots
Octylamine	37	74	78	—	7	3
2-Ethylhexylamine	54	88	—	—	—	—
Di-2-ethylhexylamine	100	100	—	—	—	—
tert-Octylamine	52	87	—	—	—	—
Nonylamine	39	77	74	—	—	—
Decylamine	40	78	70	—	1	0
Undecylamine	42	79	65	—	—	—
Dodecylamine	44	79	58	—	0	0
Tridecylamine	47	80	50	—	—	—
Tetradecylamine	50	82	43	—	0	0
Pentadecylamine	52	83	38	—	—	—
Hexadecylamine	55	85	30	—	—	—
Heptadecylamine	58	85	24	—	—	—
Stearylamine	60	85	18	—	—	—
1,2-Diaminoethane	2	4	—	22	82	49
1,2-Diaminopropane	3	10	—	—	81	58
1,3-Diaminopropane	—	—	—	—	84	36
1,4-Diaminobutane	—	—	—	—	84	32
1,5-Diaminopentane	—	—	—	—	85	26
1,6-Diaminohexane	—	—	—	—	79	19
1,7-Diaminoheptane	—	—	—	—	72	17
1,8-Diaminooctane	—	—	—	—	56	16
N-(3-Aminopropyl)cyclohexylamine	5	18	—	—	—	—

Table 1 *Continued*

Diethylenetriamine	0	0	–	17	–	–
Spermidine	–	–	–	–	81	10
Spermine	–	–	–	–	72	2
Tetraethylenepentamine	0	0	–	–	–	–

* $hR_f = R_f \times 100$.

^aEluents: A and B = chloroform–methanol–17% ammonia in the 82.5 : 15.5 : 2 (A) and 70 : 26 : 4 (B) ratios; C = acetone–17% ammonia (70 : 30 v/v); D = *n*-butanol–acetic acid–water (35 : 5 : 10); E = 1 M acetic acid + 1 M HCl in 30% methanol; F = 2 M NH_4NO_3 .

^bSilica gel G (Merck); detection reagents: 1% ninhydrin solution in ethanol–acetic acid (95 : 5); 1% potassium permanganate + 1% potassium persulfate (1 : 1); 25% iodine methanolic solution; 5% sodium nitroprusside in acetaldehyde–2% sodium carbonate (1 : 1 v/v) solution. Sample volume; 10 μL of a 0.5% water–alcohol solution of the amine hydrochloride.

^cParaffin oil–saturated Kieselguhr G (Merck) layers were prepared by immersing the plates in a 5% solution of the oil in acetone.

^dHome-made plates were prepared by spreading a slurry of 50 g of silica gel G (BDH) in 2% *o*-chlorophenol solution (100 mL). The plates were dried for 24 h at 60°C before use. Detection agent: 3 g ammonium thiocyanate and 1 g cobalt chloride in 20 mL of distilled water (blue spots).

^eThe Sil C₁₈-50 impregnated layers (Macherey-Nagel) were prepared by immersing the plates in a 4% dodecylbenzenesulfonic acid (HDBS) solution in 95% ethanol.

^fHome-made plates were prepared by spreading a slurry of 4 g ammonium tungstophosphate (AWP) and 2 g calcium sulfate hemihydrate in 50 mL of distilled water after stirring 10 min with a magnetic stirrer. Detection agent: 1% ninhydrin solution in a 5 : 1 (v/v) mixture of pyridine and glacial acetic acid.

Sources: Adapted from Prandi C (1978) Thin-layer chromatography of aliphatic amines. *Journal of Chromatography* 155: 149–157; Srivastava SP, Dua VK and Chauhan LS (1980) Chromatographic behaviour of aliphatic amines on phenol-impregnated thin layers. *Journal of Chromatography* 196: 225–235; Lepri L, Desideri PG, Heinler D and Giannessi S (1982) High-performance thin-layer chromatography of nitrogen compounds on layers of RP-18 and Sil C₁₈-50 untreated or impregnated with dodecylbenzenesulfonic acid and of ammonium tungstophosphate. *Journal of Chromatography* 245: 297–308.

Cellulose and aluminium oxide have also been used as adsorbents. The phenomenon of multiple-spot formation of amines on cellulose thin layers when using neutral or weakly acidic eluents is caused by the presence of carboxyl groups in the cellulose. Partial hydrolysis of the amine hydrochloride, volatilization of the liberated hydrochloric acid and the presence of charged groups in silica gel and alumina layers have also resulted in double-spot formation for specific compounds.

Phosphate and acetate-buffered silica gel and impregnated plates have been used. Hydrogen bond formation between the impregnated plates and aliphatic amines influences their chromatographic behaviour on metal salt-impregnated plates and on phenol-impregnated silica-gel layers.

The hR_f values of some amines, obtained on silica gel impregnated with a 2% solution of *o*-chlorophenol using a butanol–acetic acid–water (35 : 5 : 10) mixture as eluent are reported in Table 1 (column 4). No correlation exists between the $\text{p}K_a$ value of the conjugated acid of an amine and its R_M value; it therefore seems that the chromatographic behaviour of such compounds is due to hydrogen bond formation between the amine and silica gel as well as *o*-chlorophenol.

Reversed-phase thin-layer chromatography of several aliphatic mono- and polyamines has been performed on layers of silanized silica gel untreated and

impregnated with anionic and cationic surfactants. Ion-exchange and/or partition contribute to the retention of the amines depending on the type of stationary phase, the percentage of surfactant and the apparent pH of the eluent.

Table 1 (column 5) shows the retention data obtained on Sil C₁₈-50 plates impregnated with a 4% dodecylbenzenesulphonic acid solution in 95% ethanol and eluted with 1 M acetic acid + 1 M hydrochloric acid in 30% methanol. On these plates the retention of polyamines is governed chiefly by an ion-exchange mechanism while aliphatic monoamines can be differentiated according to the number of carbon atoms in their side chain.

Aliphatic amines have been studied on layers of weak and strong ion exchangers, Dowex 50-X4 (Na^+ and H^+), sodium carboxymethylcellulose and Rexyn 102 (Na^+), using hydrochloric acid and various buffer and salt solutions as eluents.

The use of ammonium tungstophosphate (AWP) as a layer material is particularly promising since on this exchanger different affinity sequences in comparison with the above-mentioned results are found (see Table 1, column 6). The behaviour of polyamines is of interest since it seems to be correlated to the distance between the protonated amino groups involved in the ion-exchange process and, in the case of 1,2-diaminoethane and 1,2-diaminopropane, to the steric hindrance of the methyl group.

Quantitative analysis of the diamine hydrochloride recovered from acid-hydrolysed copolyamides prepared from diamine-diacid has been carried out on silica gel G eluting with phenol-*n*-butanol-formic acid-water (5:2:1:2 v/v) or phenol-formic acid-water (74:1:25 v/v). Densitometric scanning was performed using a Shimadzu spectrophotometer at 560 nm after spraying the plates with a 0.2% solution of ninhydrin in ethanol and heating at 90°C for 15 min.

Specific procedures have been developed for alkanolamines. The high performance TLC (HPTLC) behaviour of closely related diethanolamines was studied on silica-gel layers eluted with binary solvents (methanol-chloroform, methanol-dichloromethane, methanol-acetone, acetone-chloroform) and on four types of reversed-phase, chemically bonded, silica gel with methanol-water as mobile phase. Alkanolamines, in particular ethanolamines and iso-propanolamines, are used extensively in hydraulic brake fluids and cutting oils as corrosion inhibitors; the derivatives with fatty acids are used as emulsifiers and detergents. Their separation and identification is performed on neutral silica gel using methylene chloride-95%-ethanol-ammonia (0.880) in the proportions 43:43:15 v/v as eluent. A solution of 0.2% ninhydrin, then alizarin in acetone, is employed to locate the separated alkanolamines. The method has been applied to commercial formulations.

Phenylalkylamines

The structures of alkylamines with an aromatic ring in the side chain are shown in **Figure 1**. The phenylethylamine group comprises a range of natural and synthetic compounds, some of which are used in drug formulations, and includes catecholamines and other biogenic amines which are excreted in the urine. The separation of these compounds by TLC and overpressured-layer chromatography (OPLC) is very important as shown by the numerous studies dealing with the determination of phenylethylamines in pharmaceutical preparations, with their identification as drugs of abuse and with the determination of catecholamines, their metabolites and their precursors in urine. These studies are carried out on silica gel, cellulose thin layers or using reversed-phase chromatography on different ready-for-use plates of silanized silica gel untreated and impregnated with anionic and cationic detergents.

The chromatographic behaviour of these compounds has also been studied on strong and weak ion-exchangers and on layers of AWP, an inorganic synthetic ion exchanger which has been used in the separation of other nitrogen compounds.

Table 2 (column 1) lists the hR_F values of 19 phenylethylamines on reversed-phase OPTI-UPC₁₂ plates eluted with 1 M HCl + 3% KCl in water. The presence of potassium chloride in the eluent accounts for the compactness of the spots. Among the diastereoisomers, the differences in the retention allow the separation of norephedrine from norpseudoephedrine.

The Sil C₁₈-50 plates impregnated with 4% N-DPC and eluted with 0.5 M Na₂CO₃ in 30% methanol (**Table 2**, column 2) show considerable differences in the affinity sequence of phenylethylamines with respect to the untreated layers and an improvement in the separation of both the two diastereoisomers of norephedrine and the two isomers of phenylethylamine.

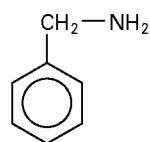
On layers of RP-18 + 4% dodecylbenzenesulfonic acid (HDBS) (**Table 2**, column 3), the retention of the compounds depends on the concentration of hydrochloric acid in the eluent and can be ascribed to the cation-exchange process between the protonated amino group and the surfactant adsorbed on the layer.

A peculiar behaviour is observed on AWP + CaSO₄· $\frac{1}{2}$ H₂O plates (**Table 2**, column 4) since the steric hindrance of the phenyl group on the carbon atom bound to the amino group allows a complete separation ($\alpha = 1.86$) between the two isomeric phenylethylamines.

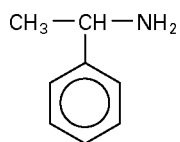
The use of *o*-benzenesulfonamido-*p*-benzoquinone in methanol or acetone has been described as a means to detect and distinguish the 3,4-methylenedioxyamphetamine of the 'Ecstasy' group on silica gel 60 F₂₅₄ plates with ethyl acetate-acetone-methanol-25% ammonia (20 + 20 + 8 + 2) solution as eluent.

Derivatized Amines

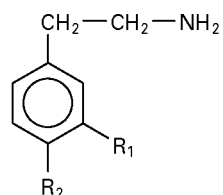
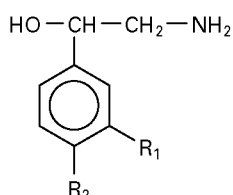
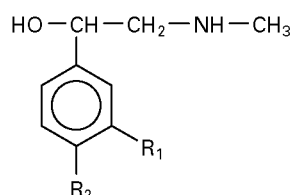
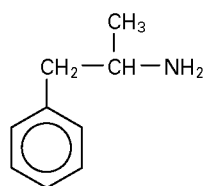
Direct chromatography on thin layers of primary and secondary amines is frequently difficult due to the strong adsorption of the NH₂ or NH groups to the adsorbents employed. Derivatives are often used to overcome these difficulties. A series of reagents has been recommended for the formation of derivatives of primary and secondary amines in order to assist in separating, identifying and determining such compounds on thin layers. The formulae of the most important reagents are shown in **Figure 2**. The chromatographic behaviour of derivatized amines with some common reagents is shown in **Table 3**. Most of these derivatives are intensely coloured (i.e., DADB-, PABS-, DBAB-) or give fluorescent spots (NBD-); in some cases, however, the detection can be considerably improved by exposure of the plates to iodine vapour or by spraying the chromatogram with 0.01 M sulphuric acid (DBAB-amides).



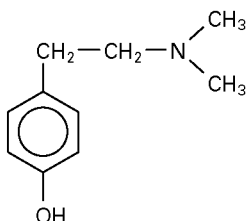
Benzylamine



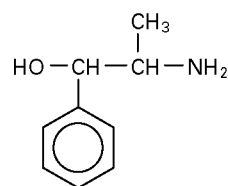
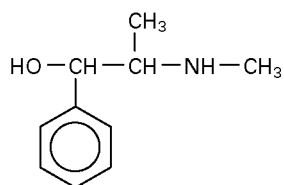
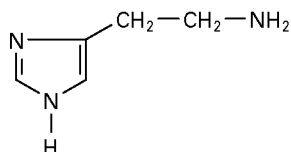
1-Phenylethylamine

2-Phenylethylamine $R_1=R_2=H$ Tyramine $R_1=H$; $R_2=OH$ Dopamine $R_1=OH$; $R_2=OH$ 3-Methoxytyramine $R_1=OCH_3$; $R_2=OH$ 3,4-Dimethoxyphenethylamine $R_1=R_2=OCH_3$  β -Hydroxyphenethylamine $R_1=R_2=H$ Octopamine $R_1=H$; $R_2=OH$ Noradrenaline (norepinephrine) $R_1=R_2=OH$ Normetanephrine $R_1=OCH_3$; $R_2=OH$ Synephrine $R_1=H$; $R_2=OH$ Adrenaline (epinephrine) $R_1=R_2=OH$ Metanephrine $R_1=OCH_3$; $R_2=OH$ 

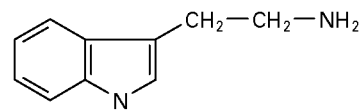
Amphetamine (Benzedrine)



Hordenine

Norephedrine (*erythro*)
Nor- ψ -ephedrine (*threo*)Ephedrine (*erythro*)
 ψ -Ephedrine (*threo*)

Histamine



Tryptamine

Figure 1 Structures of phenylalkylamines.

The procedure used for PABS-amides does not allow characterization of the movement of individual compounds by ordinary R_F values, as the chromatography is continued after the solvent front has reached the upper edge of the plate. Therefore, the hR_X values reported in Table 3 (column 2) represent relative

values with respect to the derivative of *n*-butylamine taken as 100.

The dansylated derivatives of ammonia, 1,3-diaminopropane, 1,4-diaminobutane, 1,5-diaminopentane, spermidine, spermine and histamine were separated on silica-gel 60 plates eluted with

Table 2 Retention data (R_F) of phenylalkylamines under different experimental conditions^a

Compound	OPTI-UPC ₁₂ ^b	Sil C ₁₈ -50 + 4% N-DPC ^c	RP-18 + 4% HDBS ^d	AWP ^e	Dowex 50 X4 ^f (H ⁺)	Rexyn 102 ^g (Na ⁺)
	Eluent A	Eluent B	Eluent C	Eluent D	Eluent E	Eluent F
Benzylamine	—	—	—	—	28	43
1-Phenylethylamine	28	26	30	42	25	51
2-Phenylethylamine	27	18	24	28	18	38
Tyramine	47	44	66	42	23	31
Dopamine	61	16	75	42	30	21
3-Methoxytyramine	26	46	62	21	—	—
3,4-Dimethoxyphenethylamine	10	34	44	6	—	—
β -Hydroxyphenethylamine	47	38	44	46	—	—
Octopamine	74	70	78	56	41	30
Noradrenaline	84	25	87	57	49	20
Normetanephine	55	70	77	40	—	—
Synephine	54	52	74	48	—	—
Adrenaline	68	26	88	—	—	—
Metanephine	35	52	72	27	—	—
Amphetamine	18	14	24	17	20	43
Norephedrine	28	29	32	41	—	—
Norpseudoephedrine	23	21	32	44	—	—
Ephedrine	16	16	29	27	—	—
Pseudoephedrine	13	15	31	26	—	—
Hordeine	16	13	54	17	—	—
Histamine	—	—	—	—	47	15
Tryptamine	—	—	—	—	4	23

^aEluents: A = 1 M HCl + 3% KCl in water; B = 0.5 M Na₂CO₃ in water-methanol (30%); C = 1 M CH₃COOH + 1 M HCl in water-methanol (40%); D = 1 M NH₄NO₃ in water; E = 4 M HCl; F = 0.2 M acetate buffer.

^bOPTI-UP C₁₂ plates (Antec).

^cThe plates were impregnated with 4% *N*-dodecylpyridinium chloride in ethanol.

^dThe plates were impregnated as described in Table 1.

^e4 g Ammonium tungstophosphate + 2 g calcium sulfate hemihydrate in 50 mL of distilled water.

^fHome-made Dowex 50-X4 (H⁺) layers were prepared by mixing 3 g of the resin (200–400 mesh) with 6 g of microcrystalline cellulose in 40 mL of water.

^gHome-made Rexyn 102 (Na⁺) layers (Fisher) were prepared by mixing 3 g of the resin (200–400 mesh) with 6 g of microcrystalline cellulose in 40 mL of water.

Sources: Adapted from Lepri L, Desideri PG and Coas V (1973) Chromatographic and electrophoretic behaviour of primary mono- and diamines on layers of weak and strong ion exchangers. *Journal of Chromatography* 79: 129–137; Lepri L, Desideri PG and Heimler D (1985) High performance thin-layer chromatography of phenylethylamines and phenolic acids on silanized silica and on ammonium tungstophosphate. *Journal of Chromatography* 347: 303–309.

chloroform–triethylamine (5 : 1 v/v). Putrescine, cadaverine, spermidine and spermine can be quantitatively determined in human urine; higher amounts of the last two amines were found in the urines of cancer patients compared to the values of these substances in normal urine. Dansyl amines can be determined by *in situ* fluorescence on silica gel and, sometimes, on polyamide layers. In favourable cases as little as 10^{−12} moles/spot of a DANS-derivative can be visualized on a normal thin-layer plate.

The separation and quantification of dansylated biogenic amines in vegetables have been recently performed on 20 × 20 cm silica-gel HPTLC plates with stepwise gradient elution using the Personal OPLC BS50 overpressured-layer chromatography apparatus (Kovács *et al.*, 1998).

Another reagent (NBD-Cl), which itself is not fluorescent but forms fluorescent derivatives with primary and secondary aliphatic amines, seems to have advantages compared to dansyl chloride since it does not produce fluorescent products with phenols, thiols and anilines, or as a consequence of hydrolysis reactions.

Two-dimensional (2D) TLC allows the separation of nearly every mixture of interest. A comparative study of the chromatographic properties of derivatized biogenic amines with dansyl chloride, dansyl chloride and 4-chloro-7-nitrobenzoxazole shows that the dansyl chloride should be preferred in terms of both sensitivity and, to a lesser extent, resolution on silica gel by 2D-TLC. Dansylated and dansylated products were found to have similar TLC characteristics and were adequately resolved by eluting in the

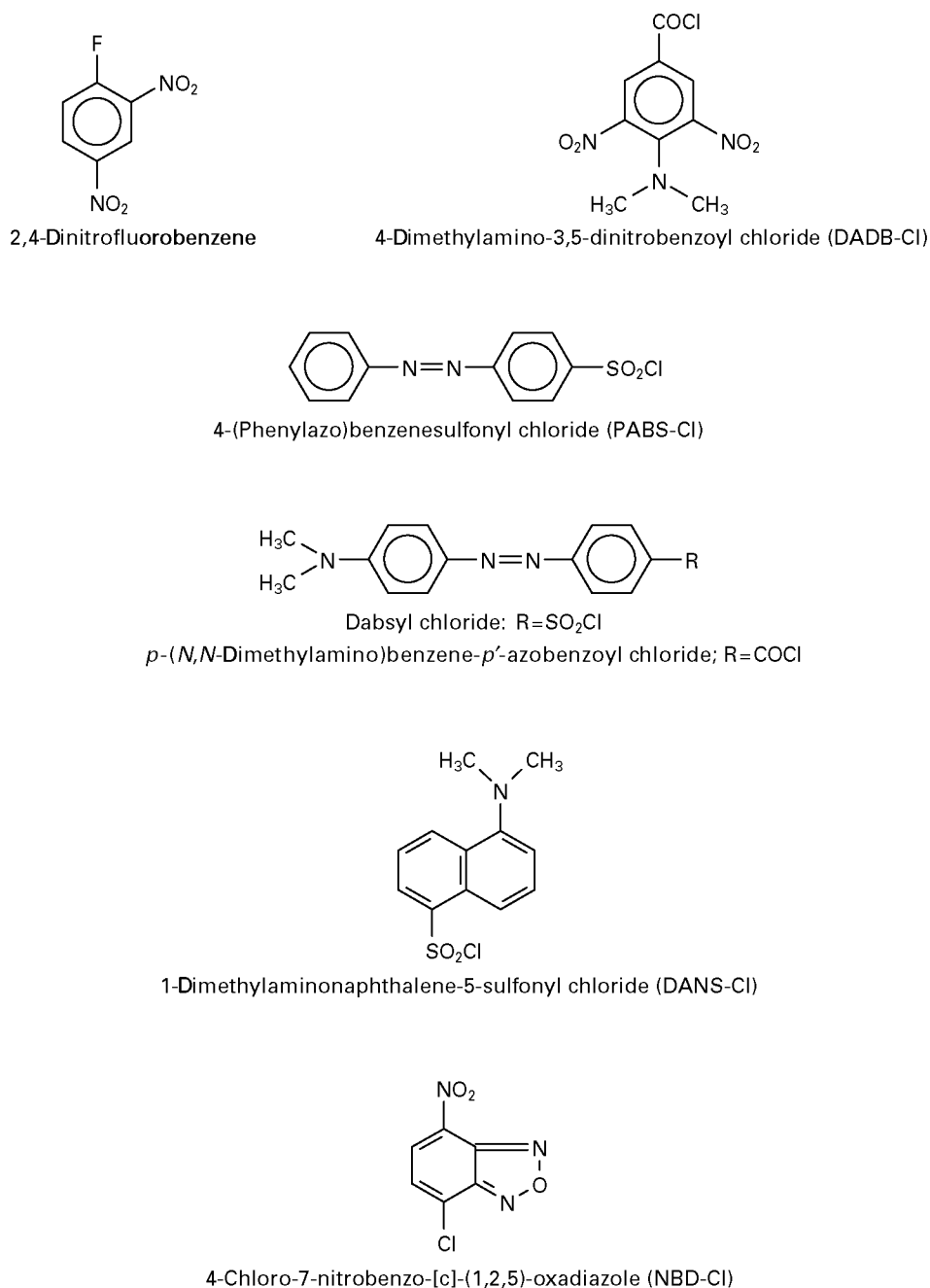


Figure 2 Structures of the reagents used for derivative formation.

first direction with ethyl acetate–cyclohexane (3 : 2 v/v) and in the second with benzene–triethylamine (5 : 1 v/v). The plates were developed in the dark.

Aromatic Amines

Table 4 shows the hR_F values of several primary aromatic amines under different experimental conditions. Such compounds have been studied on silica-

gel G or alumina using organic and aqueous–organic solutions as eluents.

Further studies concern the chromatographic behaviour of aromatic amines on silica gel impregnated with silver compounds as π -complexing metal and manganese, cadmium and zinc salts as complexing agents. On silica gel impregnated with manganese salts, the pK_a values of the conjugated acids of sixteen isomeric methylanilines and chloroanilines

Table 3 Retention data (hR_F or hR_X^* for eluent B) of derivatized amines under different experimental conditions^a

Amine	DADB- ^b Silica gel + Carbowax Eluent A	PABS- ^c Alumina Eluent B	NBD- ^d Silica Eluent C	DBAB- ^e Silica gel G Eluent D	DNP- ^f Silica gel HF ₂₅₄ Eluent E
Ammonia	–	–	45	–	3
Methylamine	15	47	57	17	30
Dimethylamine	44	116	–	19	34
Ethylamine	24	71	63	30	59
Diethylamine	58	143	–	36	69
<i>n</i> -Propylamine	33	87	–	36	75
Di- <i>n</i> -propylamine	65	150	–	44	–
Isopropylamine	39	92	–	40	74
Diisopropylamine	–	–	–	47	–
Allylamine	–	81	–	39	62
Diallylamine	–	147	–	–	–
<i>n</i> -Butylamine	42	100	71	42	81
Di- <i>n</i> -butylamine	68	>150	–	48	–
Isobutylamine	50	106	71	43	82
Diisobutylamine	–	>150	–	48	–
<i>sec</i> -Butylamine	–	104	–	–	–
<i>tert</i> -Butylamine	–	105	–	–	–
<i>n</i> -Amylamine	50	108	–	–	85
Di- <i>n</i> -amylamine	–	>150	–	51	–
Isoamylamine	51	113	–	47	86
<i>n</i> -Hexylamine	–	115	–	47	88
Di- <i>n</i> -hexylamine	–	–	–	57	–
Cyclopentylamine	–	100	–	–	–
Cyclohexylamine	–	105	–	51	–
Dicyclohexylamine	–	–	–	56	–
Octylamine	–	120	–	–	90
Di- <i>n</i> -octylamine	–	–	–	64	–
Decylamine	–	127	–	–	92
Benzylamine	–	87	–	–	67
Dibenzylamine	–	141	–	–	–
1-Phenylethylamine	–	86	–	–	–
2-Phenylethylamine	26	83	–	–	66
Ephedrine	–	57	–	–	–
Amphetamine	–	94	–	–	–
β -Phenylisopropylmethylamine	–	126	–	–	–
Mescaline	–	15	–	–	–
Tryptamine	3	–	55	–	–
Tyramine	8	–	48	–	–
3-Methoxytyramine	–	–	48	–	–
Histamine	–	–	30	–	–
Putrescine	–	–	31	–	–
Cadaverine	–	–	34	–	–
Spermidine	–	–	27	–	–
Spermine	–	–	30	–	–

* $hR_F = R_F \times 100$; $hR_X = R_X$ values $\times 100$ (relative to the hR_X of *n*-butylamine derivative taken equal to 100).

^aEluents: A = *n*-hexane–ethyl acetate (7 : 3); B = 25 mL ethyl acetate and 100 mL petroleum ether (62–82° from Shell) saturated with water; C = toluene–acetic acid (4 : 1 v/v); D = cyclohexane–methyl ethyl ketone (70 : 30); E = pentane–benzene–triethylamine (45 : 45 : 10).

^b4-Dimethylamino-3,5-dinitrobenzoyl-; home-made plates were prepared by spreading a mixture of 10 g of Carbowax 400 (Fluka) and 40 g of silica gel G (Merck) in 80 mL of water.

^c4-(Phenylazo)-benzenesulfonyl-; microchromatoplates (40 \times 76 mm) coated with alumina (Fluka, D5).

^d4-Chloro-7-nitrobenzo-[c]-(1,2,5)-oxadiazole; silica 60 (250 μ m) TLC plates (20 \times 20 cm) were obtained from Sigma.

^e*p*-(*N,N*-Dimethylamino)benzene-*p'*-azobenzoyl.

^f2,4-Dinitrophenyl.

Sources: Adapted from Wirotama IPG and Ney KH (1971) Dunnschicht chromatographie von aminen als 4-dimethylamino-3,5-dinitrobenzoyl amide. *Journal of Chromatography* 61: 166–168; Jart A and Bigler AJ (1967) Thin-layer chromatographic separation of primary and secondary amines as 4-(phenylazo) benzene sulfonamides. *Journal of Chromatography* 29: 255–258; Price NPG and Gray DO (1993) Mapping of derivatised biogenic amines by two-dimensional thin-layer chromatography. A comparative study. *Journal of Chromatography* 635: 165–170; Churáček J (1970) Einige neue reagenzien zur chromatographischen identifizierung von säuren, alkoholen und aminen. *Journal of Chromatography* 48: 241–249; Ilert HJ and Hartmann T (1972) Dünnschichtchromatographie der 2,4-dinitrophenyl derivate wasserdampf-flüchtiger amine und ihre anwendung auf die trennung pflanzlicher amine. *Journal of Chromatography* 71: 119–125.

Table 4 Retention data (R_F) of primary aromatic amines under different experimental conditions^a

Amine	Silica gel G		Silanized silica + 4% <i>N</i> -DPC ^b			AG-1 XA(CH ₃ COO ⁻) ^c		p <i>K</i> _a
	Eluent A	Eluent B	Eluent C	Eluent D	Eluent E	Eluent F	Eluent G	
Aniline	–	–	22	72	92	–	–	4.58
<i>o</i> -Toluidine	42	17	16	61	77	–	–	4.39
<i>m</i> -Toluidine	29	10	14	68	79	–	–	4.69
<i>p</i> -Toluidine	20	5	14	75	81	–	–	5.12
2,4-Dimethylaniline	–	–	7	53	71	–	–	–
2,6-Dimethylaniline	–	–	11	21	50	–	–	–
<i>o</i> -Aminophenol	24	0	–	–	–	46	83	4.72
<i>m</i> -Aminophenol	13	0	–	–	–	30	83	4.17
<i>p</i> -Aminophenol	1	0	–	–	–	70	84	5.49
<i>o</i> -Anisidine	42	15	18	66	78	58	83	4.49
<i>m</i> -Anisidine	30	9	20	53	70	44	83	4.20
<i>p</i> -Anisidine	2	2	26	85	86	74	84	5.29
<i>o</i> -Chloroaniline	75	66	–	–	–	12	40	2.64
<i>m</i> -Chloroaniline	51	40	–	–	–	15	64	3.34
<i>p</i> -Chloroaniline	41	22	6	14	44	18	75	3.98
<i>o</i> -Bromoaniline	78	69	6	13	17	10	27	2.60
<i>m</i> -Bromoaniline	58	44	4	10	28	10	55	3.51
<i>p</i> -Bromoaniline	47	27	5	9	37	12	69	3.91
<i>o</i> -Nitroaniline	55	52	5	7	17	4	8	– 0.29
<i>m</i> -Nitroaniline	44	36	9	10	28	21	31	2.50
<i>p</i> -Nitroaniline	37	29	6	9	23	2	7	1.02
<i>o</i> -Aminobenzoic acid	47	44	–	–	–	–	–	–
<i>m</i> -Aminobenzoic acid	28	12	–	–	–	–	–	–
<i>p</i> -Aminobenzoic acid	37	29	–	–	–	–	–	–
<i>o</i> -Phenylenediamine	0	0	37	81	86	67	83	4.47
<i>m</i> -Phenylenediamine	0	0	49	96	96	71	84	4.88
<i>p</i> -Phenylenediamine	0	0	60	95	97	79	84	6.08
2,4-Dichloroaniline	–	–	6	15	44	–	–	–
2,4-Dinitroaniline	–	–	3	5	15	0	0	– 4.53
2,4-Diaminotoluene	–	–	34	92	94	72	83	–
2,5-Diaminotoluene	–	–	–	–	–	79	84	–
2,6-Diaminotoluene	–	–	50	95	96	73	83	–
3,4-Diaminotoluene	–	–	10	23	34	67	83	–
2,4-Diaminoanisole	–	–	–	–	–	72	83	–
2-Amino-4-nitrophenol	–	–	–	–	–	1	10	–
2-Amino-5-nitrophenol	–	–	–	–	–	1	2	–
4-Amino-2-nitrophenol	–	–	–	–	–	22	65	–
2-Amino-4,6-dinitrophenol	–	–	–	–	–	0	0	–
4-Nitro- <i>o</i> -phenylenediamine	–	–	–	–	–	8	16	–
2-Amino-4-chlorophenol	–	–	–	–	–	3	41	–
2-Amino-3,4,6-trichlorophenol	–	–	–	–	–	0	1	–
α -Naphthylamine	–	–	3	9	38	–	–	–
4-Aminodiphenylamine (DPA)	–	–	2	31	53	–	–	–
2-Amino-DPA	–	–	2	11	23	–	–	–
3-Methoxy-4-amino-DPA	–	–	2	29	55	–	–	–
4-Methoxy-4'-amino-DPA	–	–	2	45	56	–	–	–
4,4'-Diamino-DPA	–	–	28	97	97	–	–	–
2,4-Dinitro-4'-amino-DPA	–	–	2	3	26	–	–	–
Benzidine	–	–	6	65	81	–	–	–
<i>o</i> -Tolidine	–	–	2	26	73	–	–	–
<i>o</i> -Dianisidine	–	–	2	7	49	–	–	–

^aEluents: A = dibutyl ether ethylacetate–acetic acid (15 : 5 : 1); B = dibutyl ether–acetic acid–*n*-hexane (20 : 1 : 4); C = 0.1 M CH₃COONH₄ + 0.1 M NH₄OH in water–methanol (20%) (pH = 9.20); D and E = 0.1 M and 2 M, respectively, CH₃COOH in water–methanol (20%); F = 0.1 M acetate buffer; G = 1 M acetic acid.

^bHome-made layers prepared by spreading a mixture of 20 g of silanized silica gel 60HF (Merck) with 4% *N*-dodecylpyridinium chloride in 50 mL of 95% ethanol.

^cHome-made AG1-X4 (CH₃COO⁻) plates prepared by mixing 2 g of the resin (200–400 mesh) and 6 g of microcrystalline cellulose in 40 mL of water.

Sources: Adapted from Gillio-Tos M, Previtera SA and Vimercati A (1964) Separation of some aromatic amines by thin-layer chromatography. *Journal of Chromatography* 13: 571–572; Lepri L, Desideri PG and Heinler D (1979) Soap thin-layer chromatography of sulfonamides and aromatic amines. *Journal of Chromatography* 169: 271–278; Lepri L, Desideri PG and Coas V (1974) Chromatographic and electrophoretic behaviour of primary aromatic amines on anion-exchange thin layers. *Journal of Chromatography* 90: 331–339.

were correlated with their R_M values using benzene-ethyl acetate-acetic acid (2 + 2 + 1 v/v) as mobile phase. Separations via charge-transfer complexes with nitro compounds (picric acid, 2,4,6-trinitrophenyl-*N*-methylnitramine and 2,4-dinitrochlorobenzene) have also been reported.

Reversed-phase planar chromatography has been performed on silanized silica gel untreated or impregnated with cationic and anionic surfactants. The aromatic amines, which are in the free base form at the pH of the eluent, exhibit a high affinity towards the silanized silica gel and are more strongly retained in the presence of *N*-dodecylpyridinium chloride on the stationary phase.

As the pH of the eluent decreases, a sharp increase in the R_F values is observed on the impregnated layers (see Table 4, columns 3–5). Such behaviour is correlated with the protonation of one or more of the amino groups present in the aromatic amines. On the basis of hR_F values many interesting separations of isomers can be carried out.

Primary aromatic amines can be separated, with difficulty, on polystyrene-based cation exchangers in aqueous-organic solutions and also by elution with concentrated mineral acids owing to the high affinity of such exchangers towards compounds which contain one or more aromatic nuclei. Therefore weak cation exchangers, i.e., carboxymethylcellulose (H^+ or Na^+ form) and alginic acid, or synthetic inorganic exchangers such as ammonium molybdophosphate and tungstophosphate, have been used for separating such compounds. Better results can be achieved using polystyrene-based anion exchangers as shown by the hR_F values obtained on AG-1X4 (CH_3COO^-) plates (see Table 4, columns 6 and 7).

As regards the influence of the pH of the eluent, not that the protonated forms of the amines exhibit a lower affinity towards the exchanger than the free base forms.

An equation similar to that suggested for alkaloids can be used for studying quantitatively the influence of eluent pH on the chromatographic characteristics of aromatic amines:

$$(1/R_F) - 1 = (1/R_{F_{alk}} - 1)(K_a/K_a + [H^+]) + (1/R_{F_{ac}} - 1)([H^+]/(K_a + [H^+]))$$

where K_a is the dissociation constant of conjugated acid of the base and $R_{F_{ac}}$ and $R_{F_{alk}}$ are the R_F values of the protonated and the free base form of the amines, respectively.

The detection of aromatic amines has been accomplished with fluorescamine in glacial acetic acid (1 mg mL^{-1}), 5% *p*-dimethylaminobenzaldehyde in

a 5 : 1 mixture of ethanol and glacial acetic acid, 0.2% chloranil in chlorobenzene or 9-chloroacridine in 95% ethanol.

Diazotization and coupling can be carried out directly on the layer, i.e., the plates can be exposed to nitrogen dioxide to diazotize the amines and then sprayed with a solution of 0.1 M β -naphthol and 0.1 M triethylamine in benzene.

Derivatives of aromatic amines have also been used for separating and identifying these compounds. Therefore, 2,4-dinitrophenyl derivatives and dansyl derivatives have been studied on silica gel with different solvent systems.

Fifty-four aromatic amines used as antioxidants and/or antiozonants for elastomers have been separated on silica gel with a concentrating zone using benzene-ethyl acetate-acetone (100 : 5 : 1 v/v) and benzene-*n*-hexane (50 : 50 v/v) as eluents. The detection reagent is *N*-chloro-2,6-dichloro-*p*-benzoquinone monoimine in buffered alkaline medium.

Heterocyclic Bases

Heterocyclic compounds containing one or more nitrogen atoms have been extensively investigated on thin-layer chromatography as detailed in Table 5. Almost all the heterocyclics are chromatographed on polar stationary phases (silica gel, alumina, cellulose, polyamide) and, to a lesser extent, on hydrophobic layers obtained by impregnating polar adsorbents with nonpolar substances or by using silanized silica gel plates. Chemically modified and impregnated layers with cationic and anionic surfactants are also used.

Among the various types of 'simple' nitrogen heterocyclics, the separation of pyridines, indoles, quinolines and pyrimidines is of interest. The indole group of compounds is conventionally divided into the so-called simple derivatives and the indole alkaloids and dyes. A number of simple indole derivatives play important roles in physiological processes. Alkaline and acidic systems are employed on both silica gel and silanized silica for the separation of these compounds (see Table 6).

The two-dimensional technique on Sil C_{18} -50 plates can be performed by eluting in the first direction with *n*-hexane-ethyl acetate-acetic acid (72 : 27 : 1 v/v) and in the second direction with 0.1 M ammonia in 40% methanol. This technique allows the separation of 20 indole derivatives; the spots can be identified from their positions on the chromatogram and also from their colours obtained after spraying with 1% *p*-dimethylaminobenzaldehyde solution in concentrated hydrochloride acid-methanol (1 : 1) and heating the plates at 50°C for 20 min.

Table 5 Methods used for the separation of various types of nitrogen heterocyclics

Compound	Layer	Eluent
Azines	Alumina	Benzene–Chloroform (1 : 1)
Azines	Silica gel with or without a fluorescent indicator (F ₂₅₄)	CCl ₄ –EtOH–Me ₂ CO (50 + 1 + 2); <i>n</i> -PrOH– <i>n</i> -hexane in different ratios
Azines	Cellulose MN-300 F ₂₅₄ , Aminoplast	CH ₃ OH–H ₂ O–CH ₃ CN (30 + 20 + 5); CH ₃ OH–aqueous ammonia (30 + 20); CH ₃ OH–aqueous acetic acid (30 + 20)
Azines	Silica gel F ₂₅₄ impregnated with 5% paraffin oil in <i>n</i> -hexane	Water–organic solvents
Azines	RP-2, RP-8, RP-18	H ₂ O–CH ₃ OH in different proportions
Benzodiazepines	Silica gel and silica gel F ₂₅₄	CHCl ₃ –Me ₂ O–iPrOH and <i>n</i> -hexane–Me ₂ CO in different ratios; CHCl ₃ –Me ₂ CO (80 + 20); benzene; BuOH–CHCl ₃ –NH ₄ OH (50 + 50 + 1); BuOH–C ₆ H ₆ –NH ₄ OH (50 + 50 + 1 and 40 + 10 + 30); CHCl ₃ –MeAc (90 : 10); C ₆ H ₆ –iPrOH–25% NH ₄ OH (85 + 15 + 1)
Benzodiazepines	RP-18, KC18F	Acetate or phosphate buffer + CH ₃ OH or CH ₃ CN in different proportions
Benzodiazepines	Silica gel impregnated with oleyl alcohol	NaOH–aqueous buffer solutions (pH 9–9.5) saturated with oleyl alcohol
Benzoquinoxalinone derivatives	Silica gel 60 F ₂₅₄	CH ₂ Cl ₂ + EtAc (17 + 3)
Benzimidazoles and Benztriazoles	Cellulose F ₂₅₄ , starch F ₂₅₄	H ₂ O + CH ₃ OH or CH ₃ CN in different proportions
Carbazoles	Silica gel	Benzene; EtAc–MeOH–HCOOH–Pyridine (7.5–7.5–7.5–10); EtOH
Carbazoles	Alumina	Petroleum ether (40–60°C)–CHCl ₃ (10 : 1); petroleum ether–HAc (10 : 1)
Cyclic amidines	Silica gel F ₂₅₄	CH ₃ OH + CHCl ₃ or benzene in different ratios
Imidazolines	Silica gel	Benzene–Me ₂ CO–25% NH ₄ OH (4 : 17 : 1)
Imidazoles	Silica gel	CHCl ₃ –Me ₂ CO–HAc (34 : 4 : 3) EtAc saturated with NH ₄ OH
Indoles	Silica gel	BuOH–HAc–H ₂ O (2 : 1 : 1); Me ₂ O–HAc (100 : 1); phenol–H ₂ O (4 : 1); iPrOH–25% NH ₄ OH–H ₂ O (20 : 1 : 2) BuOH–EtOH–cyclohexylamine (76 : 3 : 6); Me ₂ CO–CHCl ₃ –HAc–H ₂ O (8 : 8 : 4 : 1); MeCOEt–CHCl ₃ –conc. NH ₄ OH (40 : 10 : 1); MeCOEt–CH ₃ OH–conc. NH ₄ OH; EtAc–iPrOH–conc. NH ₄ OH (45 : 35 : 20) BuOH–HAc–H ₂ O (12 : 3 : 5); benzene–dioxane–H ₂ O (1 : 1 : 1); benzene–pyridine–H ₂ O (1 : 1 : 1)
Indoles	Cellulose	CHCl ₃ –EtAc–HAc (7 : 2 : 1); CHCl ₃ –cyclohexane–BuOH–HAc–H ₂ O (1 : 1 : 1 : 1 : 0.2)
Indoles	Polyamide	H ₂ O–CH ₃ OH–HAc (59 : 40 : 1); 0.1 M NH ₄ OH in 40% methanol; <i>n</i> -hexane–EtAc–HAc (72 : 27 : 1); 0.1 M NH ₄ OH + 0.1 M NH ₄ Cl in 40% methanol; 0.5 M NH ₄ OH + 0.5 M NH ₄ Cl in 40% methanol; <i>n</i> -hexane EtAc–HAc (67 : 32 : 1)
Indoles	Sil C ₁₈ -50; Sil C ₁₈ -50 + 4% N-DPC	1 M NH ₄ NO ₃
Indoles	AWP	Octanol–petroleum ether (110–115°C) (1 : 5)
Indole esters	Silica gel	1 M NH ₄ OH + 1 M NH ₄ Cl in water or in various mixtures with methanol
Nitroimidazoles	Silica gel G F ₂₅₄ impregnated with a 5% solution of silicone oil in diethyl ether	
Piperazines	Silica gel	EtAc–CH ₃ OH (4 : 1); CHCl ₃ –CH ₃ OH–HAc (14 : 2 : 1)
Piperidines	Alumina	CHCl ₃ saturated with NH ₄ OH
Pyrazoles	Silica gel	EtAc (saturated with H ₂ O); CHCl ₃ –Me ₂ CO (7 : 3); MeCOEt
Pyrazolones	Silica gel	Cyclohexane–CHCl ₃ –EtOH (4 : 10 : 1); cyclohexane–MeCOEt (4 : 5)
Pyrazolidines	Alumina	
Pyridines	Silica gel	Benzene–MeOH (25 : 1); EtAc–MeOH–HAc (15 : 4 : 1); diethylether–dimethylformamide (99 : 1)
Pyridines	Silica + Ag ₂ O	Me ₂ CO–C ₆ H ₆ (2 : 3); MeCOEt–iPrOH (4 : 1); CHCl ₃ –CH ₃ OH (3 : 2)

Table 5 Continued

Pyridine derivatives	Silanized silica gel untreated or impregnated with sodium dodecylsulphate as ion-pairing reagent	Phosphate buffer solution-CH ₃ OH (1 : 1) with the buffer pH adjusted to the appropriate value (pH 3 to 10)
Pyrimidines	Silica gel	CHCl ₃ -CH ₃ OH (3 : 1)
Pyrimidines	Dowex 50-X4 (H ⁺)	0.25-4 M hydrochloric acid
Pyrimidines	Carboxymethylcellulose (Na ⁺), Dowex 50-X4 (Na ⁺)	Water; 0.1 and 0.5 M acetate buffer
Pyrroles	Silica gel	<i>n</i> -Hexane-CHCl ₃ (9 : 1); diethylether-2% HAc in <i>n</i> -hexane (1 : 1)
Pyrrole acids	Silica gel	CHCl ₃ -96% HAc (1 : 1); benzene-CH ₃ OH-HAc (45 : 8 : 4)
Quinolines	Silica gel	EtAc-iPrOH-NH ₄ OH (9 : 6 : 4); benzene-EtAc (1 : 1)
Quinolines	Silica gel 60HF ₂₅₄ , aluminium oxide, Florisil	Binary mixtures of <i>n</i> -heptane with polar modifiers (iPrOH; dioxane, EtAc, tetrahydrofuran MeCOEt, Me ₂ CO, iPr ₂ O, CH ₂ Cl ₂)
Thioindigoid thiazolidinones	Silica gel H	EtOH; CH ₃ CN; Et ₂ O; CH ₃ OH
Triazoles	Alumina	<i>n</i> -Hexane-benzene (1 : 1); 1% adipate in xylene-formic acid (49 : 1)

Tryptophan and some of its indole metabolites in urine (5-hydroxytryptophan, tryptamine, serotonin, indolyl-3-acetic acid and 5-hydroxyindolyl-3-acetic acid) have been separated by TLC, stained with van Urk's Salkowski reagent, and determined by scanning densitometry using indolyl-3-butyric acid as internal standard. Sep-Pak C₁₈ cartridges are used for extraction of metabolites from urine. The detection limits are 2 µg mL⁻¹ 5-hydroxytryptophan, 1.75 µg mL⁻¹ 5-hydroxyindolyl-3-acetic acid, 1.5 µg mL⁻¹ tryptophan, 0.8 µg mL⁻¹ indolyl-3-acetic acid, 0.9 µg mL⁻¹ indolyl-3-butyric acid, 1.75 µg mL⁻¹ serotonin and 1.25 µg mL⁻¹ tryptamine.

The chromatographic behaviour of several pyridine derivatives, some diazines and their sulfides, dimers and trimers has also been studied on both silica gel and silanized silica (see Table 7). The retention of azines and diazines in adsorption TLC on silica gel with *n*-propanol-*n*-hexane eluents can be calculated by the relationship adopted by Kowalska for reversed-phase chromatography:

$$R_F = A + B(X_1)^{1/2} + CX_2$$

where X₁ and X₂ are the volume fractions of alcohol and hydrocarbon, respectively, and A, B, and C the equation constants. In the reversed-phase systems on RP-2, RP-8 and RP-18 plates, R_M values were found to be linearly dependent on methanol concentration (binary methanol-water mixtures) showing the dependence of the retention values on the hydrophobicity and chemical structure of the analysed compounds.

A large number of pyrimidines (nucleobases included) have been studied on plates of silanized silica gel with different characteristics. The layers were also impregnated with anionic surfactants in order to

evaluate the role of the ion-exchange process on the chromatographic behaviour of these compounds (Table 8). The hR_F sequences of the pyrimidines under the various conditions are related to solvophobic effects, their acid-base characteristics, and the association of the species in solution.

Seven different thin-layer chromatographic systems were investigated to separate 19 pairs of the *E-Z* geometrical isomers of pyrimidine, purine and pyrazole derivatives with potential cytokinin activity. These systems employed silica, silanized silica, silanized silica/Cu(II) cation, chemically bonded RP-8 and RP-18 as stationary phases and a variety of binary mobile phases. The best performance was observed on silica gel with *n*-hexane-ethyl acetate 1 + 9 v/v as mobile phase.

For the location of heterocyclic bases, Dragendorff's reagent is usually employed; other detection agents are tetracyanoethylene and iodine-azide solutions.

Pyrazoles can be visualized with sodium nitroprusside; pyrazolones with 1% mercuric nitrate, iodine-potassium iodide or 10% ferrocyanide-12.5% hydrochloric acid (1 : 1); and imidazoles with iodo-platinate reagent. Indoles can be detected with Ehrlich's, van Urk's and Prochazka's reagents, or *o*-phthalaldehyde-sulfuric acid solution (0.15% w/v). A specific and sensitive fluorescent detection method was proposed for the analysis of nitroimidazoles (titanium (III) chloride followed by spraying with diazotized sulfanilic acid).

Miscellaneous Nitrogen Compounds

Because of the possible presence of nitroso carcinogens in foods, the separation and determination of

Table 6 Retention data (hR_F) of indole derivatives under different experimental conditions^a

Indole derivative	Silica gel G		Sil C ₁₈ -50/UV ₂₅₄		
	Eluent A	Eluent B	Eluent C	Eluent D	Eluent E
Indole	84	73	16	13	97
Skatole	87	78	–	–	–
3-Hydroxymethylindole	84	45	–	–	–
Indole-3-aldehyde	81	20	25	18	60
Indole-3-acetaldehyde	86	46	32	22	96
Indole-3-ethanol	–	–	29	23	74
Indole-3-acetone	–	–	24	18	95
Indole-3-acetonitrile	85	46	23	17	95
Indole-2-carboxylic acid	–	–	34	78	63
Indole-3-carboxylic acid	–	–	–	–	–
Indole-5-carboxylic acid	–	–	69	89	75
Indole-3-acetic acid	31	28	62	84	61
Indole-3-propionic acid	38	34	22	77	75
Indole-3-butyric acid	40	38	14	69	81
Indole-3-glyoxylic acid	–	–	61	82	0
Indole-3-lactic acid	–	–	59	80	4
Indole-3-acrylic acid	33	29	15	24	64
5-Hydroxyindole-3-acetic acid	19	4	78	92	18
Indole-3-acetamide	–	–	41	36	34
Indole-3-ethylacetate	–	–	9	7	98
Indole-3-glyoxylamide	–	–	25	20	52
Isatin	75	27	42	40	78
Gramine	77	0	–	–	–
Tryptamine	77	0	47	2	0
Serotonin	65	0	62	8	0
Tryptophan	23	0	64	67	0
5-Hydroxytryptophan	14	0	–	–	–

^aEluents: A = methyl acetate-isopropanol-25% ammonium hydroxide (9 : 7 : 4); B = chloroform-96% acetic acid (95 : 5); C = water-methanol-acetic acid (59 : 40 : 1); D = 0.1 M NH₄OH in 40% methanol; E = *n*-hexane-ethyl acetate-acetic acid (72 : 27 : 1).

Source: Adapted from Stahl E and Kaldeuoe H (1951) Trace analysis of physiologically active, simple indole derivatives. *Zeitschrift für Physiologische Chemie* 323: 183–191; Lepri L, Desideri PG and Heinler D (1983) High-performance thin-layer chromatography of indole derivatives on layers of Sil C₁₈-50 untreated or impregnated with N-dodecylpyridinium chloride and on ammonium tungstophosphate. *Journal of Chromatography* 260: 383–389.

N-nitrosamines are of interest. Silica gel, magnesium silicate, cyano- and diol-bonded silica have been used as stationary phases to separate these compounds. Alkyl- and aryl nitrosamines can be separated on silica gel with *n*-hexane-diethyl ether-dichloromethane (4 : 3 : 2 v/v) and cyclic nitrosamines with the same solvent mixture in a ratio of 5 : 7 : 10 (v/v).

The chromatographic behaviour of 26 compounds derived from 1,1-diphenylhydrazine was investigated by normal and reversed-phase chromatography. The same techniques were used for the separation of several thiosemicarbazides and 1,2,4-triazoline-3-thiones on silica gel, alumina, and C₁₈-modified silica-gel layers, and nonaqueous and aqueous eluents.

Amides are physiologically active compounds and a knowledge of possible interactions of the amide

group and of different substituents under conditions close to those in physiological systems is highly important.

The separation of formanilide and ten para-substituted acetanilides was investigated on starch and cellulose layers, as an alternative to RP-18, using aqueous mobile phases with methanol, acetonitrile, acetone and 1-propanol as modifiers. Because R_M values are related to the partitioning of solute molecules in the given system, they can be regarded as a measure of solute hydrophobicity.

The retention behaviour of three series of aromatic amides was investigated on silica gel with eight binary solvent mixtures (benzene-CHCl₃ 20 : 30 v/v; benzene-ethyl acetate 45 : 5 v/v; benzene-acetone 45 : 5 v/v; benzene-dioxane 45 : 5 v/v; heptane-ethyl acetate 40 : 10 v/v; carbon tetrachloride with ethyl acetate, acetone or dioxane in a 45 : 5 v/v ratio). The

Table 7 Retention data (R_F) of various heterocyclic bases under different chromatographic conditions^a

Compound	Silica gel G				RP-2	RP-8	RP-18
	Eluent A	Eluent B	Eluent C	Eluent D	Eluent E	Eluent E	Eluent E
Pyridine	29	54	20	–	70	55	56
2,2'-Bipyridyl	–	–	40	–	72	53	52
2,2',2''-Tripyridyl	–	–	35	–	66	46	41
2-Methylpyridine	30	54	–	–	–	–	–
3-Methylpyridine	35	55	–	–	–	–	–
4-Methylpyridine (γ -picoline)	27	48	0	26	61	49	46
γ,γ' -Bipicolyl	–	–	24	20	60	49	43
2,4-Dimethylpyridine	28	49	–	–	–	–	–
2,6-Dimethylpyridine	36	59	–	–	–	–	–
2,4,6-Trimethylpyridine	26	51	–	–	–	–	–
2-Ethylpyridine	42	62	–	–	–	–	–
2- <i>n</i> -Propylpyridine	47	64	–	–	–	–	–
2-Hydroxypyridine	6	20	–	–	–	–	–
3-Hydroxypyridine	23	53	–	–	–	–	–
4-Hydroxypyridine	0	2	–	–	–	–	–
2-Aminopyridine	27	50	–	–	–	–	–
3-Aminopyridine	18	45	–	–	–	–	–
4-Aminopyridine	5	14	–	–	–	–	–
Pyridine-2-carbinol	18	45	–	–	–	–	–
Pyridine-3-carbinol	13	39	–	–	–	–	–
Pyridine-4-carbinol	4	39	–	–	–	–	–
Pyridine-2-aldehyde	51	67	–	–	–	–	–
Pyridine-3-aldehyde	33	58	–	–	–	–	–
Pyridine-4-aldehyde	36	56	–	–	–	–	–
Pyridine-2-carboxylic acid	2	4	–	–	–	–	–
Pyridine-3-carboxylic acid	6	6	–	–	–	–	–
Pyridine-4-carboxylic acid	5	5	–	–	–	–	–
Pyridine-2,6-dicarboxylic acid	3	5	–	–	–	–	–
2-Acetylpyridine	57	69	–	–	–	–	–
2-Benzoylpyridine	62	71	–	–	–	–	–
2-Fluoropyridine	62	69	–	–	–	–	–
2-Chloropyridine	61	70	–	–	–	–	–
2-Bromopyridine	63	72	–	–	–	–	–
3-Chloropyridine	56	65	–	–	–	–	–
3-Bromopyridine	57	67	–	–	–	–	–
3-Iodopyridine	58	70	–	–	–	–	–
Pyrazine	–	–	10	13	73	54	57
2,2'-Bipyrazyl	–	–	24	40	73	52	51
Quinoline	–	–	33	65	78	58	57
2,2'-Biquinolyl	–	–	70	67	74	53	45
6,6'-biquinolyl sulfide	–	–	5	36	73	36	31
8,8'-Biquinolyl sulfide	–	–	47	78	–	–	–
Quinoxaline	–	–	32	54	82	56	56
2,2'-Biquinoxalyl	–	–	54	83	70	43	32
Thieno[2,3- <i>b</i> ; 4,5- <i>b'</i>]biquinoxalyl	–	–	8	–	74	51	39
2-Methylquinoxaline	–	–	20	55	74	55	49
3,3'-Dimethyl-2,2'-biquinoxalyl	–	–	34	59	67	41	28

^aEluents: A = ethylacetate; B = acetone; C = chloroform–ethanol–acetone (50 + 1 + 2); D = *n*-propanol–*n*-hexane (45 + 55); E = methanol–water (90 + 10).

Source: Adapted from Petrowitz HJ, Pastuska G and Wagner E (1965) Thin layer chromatography of some pyridines and quinolines. *Chemiker-Zeitung* 89: 7–12; Baranowski I and Swierczek S (1994) A study of the retention of azines and diazines in RPTLC with bonded alkyl stationary phases. *Journal of Planar Chromatography – Modern TLC* 5: 399–405.

anilides used were: *N*-substituted amides of 2,2-dimethylpropanoic acid; *N*-substituted benzamides and α -phenylacetamides, with –F, –Cl, –Br, –CF₃, –CH₃, –C₂H₅, –OCH₃, –CN, –N(CH₃)₂ or –N(C₂H₅)₂

as substituent at the *para* position. Spots were observed under UV light at $\lambda = 254$ nm.

Dialkylaminoethyl dialkylamido fluorophosphates, which exhibit choline esterase-inhibiting effects, were

Table 8 Retention data (R_F) of pyrimidine derivatives under different experimental conditions^a

Pyrimidine derivative	OPTI-UPC ₁₂		Sil C ₁₈ -50 + 4% HDBS	
	Eluent A	Eluent B	Eluent C	Eluent D
4-Amino-2-hydroxypyrimidine (cytosine)	54	42	7	24
3-Methylcytosine	53	19	8	25
5-Hydroxymethylcytosine	61	52	11	33
5-Methyl-2,4-dihydroxypyrimidine (thymine)	30	29	78	79
1-Methylthymine	13	19	71	73
2,4-Dihydroxypyrimidine (uracil)	55	51	86	86
4,6-Dihydroxypyrimidine	70	75	83	84
4,6-Dihydroxy-2-methylpyrimidine	63	66	72	74
5-Nitouracil	57	52	84	87
5-Hydroxymethyluracil	63	60	87	90
6-Methyluracil	31	30	80	83
5,6-Dimethyluracil	14	19	67	76
5-Aminouracil	64	64	73	96
6-Aminouracil	54	58	84	85
Uracil-5-carboxylic acid	87	87	84	94
Uracil-6-carboxylic acid (orotic acid)	68	73	90	89
Orotic acid methyl ester	20	29	77	80
Uracil-6-acetic acid	68	71	90	90
6-Chlorouracil	34	56	69	78
5-Chlorouracil	41	47	68	77
5-Bromouracil	36	40	63	73
5-Iodouracil	27	31	57	66
6-Chloromethyluracil	29	34	62	71
5-Trifluoromethyluracil	40	47	60	66
6-Chloro-1,3-dimethyluracil	3	7	44	48
5-Hydroxyuracil (isobarbituric acid)	66	68	91	93
2-Thiouracil	48	56	70	77
4-Phenyl-2-thiouracil	3	17	23	28
5-Methyl-2-thiouracil	28	34	65	70
6-Hydroxy-2-thiouracil (2-thiobarbituric acid)	68	72	83	85

^aEluents: A = 3% KCl in water; B = 0.5 M Na₂CO₃ in water; C = 1 M acetic acid in water-methanol (20%); D = 1 M acetic acid + 0.5 M HCl in water-methanol (20%).

Source: Adapted from Lepri L, Coas V, Desideri PG and Zocchi A (1988) Planar chromatography of purines, pyrimidines and nucleosides on untreated and detergent-impregnated silanized silica plates. *Journal of Planar Chromatography – Modern TLC* 1: 317–324.

separated on silica-gel plates developed with methanol-pyridine-formamide, 80 + 15 + 5 (v/v) and detected with ninhydrin.

The lipophilicity of fused-ring nitrogen heterocyclic was determined by reversed-phase TLC on paraffin oil impregnated Silkoplat plates (Labor, MIM) using acetonitrile-aqueous solutions of different pH as eluents.

Lastly, amino-PAHs have been identified in sewage sludge after separation of the DMF extracts on a silicic acid column into three groups: carbazoles, aminoarenes and azaarenes. RP-18 F₂₅₄ (Merck) layers were developed with acetonitrile + water (9 : 1 v/v), observed under UV illumination at $\lambda = 254$ and 365 nm and then sprayed with specific reagents for detection of the amino group. Aminonaphthalene, aminoquinoline and/or aminoisoquinoline, amino-fluorene, aminoanthracene and/or aminophenanthrene,

aminopyrene, aminophenylanthracene and aminochrysene were found in the sludge.

Concluding Remarks

This article demonstrates the current possibilities for the separation of selected organic bases. Most attention has been devoted to the advantages of TLC, retention mechanisms, structure, sample preparation, mobile and stationary phases, usual modes of development and detection procedures, and also two-dimensional techniques.

Quantification of organic bases mainly by *in situ* densitometry has been described. The development of HPTLC and the potential for other innovations such as overpressured thin-layer chromatography (OPTLC) with this group of compounds is of considerable interest.

See also: II/Chromatography: Thin-Layer (Planar): Densitometry and Image Analysis; Layers; Modes of Development: Conventional; Modes of Development: Force Flow, Overpressured Layer, Chromatography and Centrifugal; Spray Reagents. III/Amines: Gas Chromatography. Impregnation Techniques: Thin-Layer (Planar) Chromatography. Pharmaceuticals: Basic Drugs: Liquid Chromatography.

Further Reading

Airaudo ChB, Gayte-Sorbier A, Aujoulat P and Mercier V (1988) Thin-layer chromatography of amine antioxidants and antiozonants used in elastomers. *Journal of Chromatography* 437: 59–82.

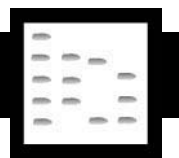
Fatér Z, Tasi G, Szabady B and Nyiredy Sz (1998) Identification of amphetamine derivatives by uni-dimensional multiple development and two-dimensional HPTLC combined with postchromatographic derivatization. *Journal of Planar Chromatography—Modern TLC* 11: 225–229.

Kovács A, Simon-Sarkadi L and Mincsovcics E (1998) Stepwise gradient separation and quantification of dansylated biogenic amines in vegetables using personal OPLC instrument. *Journal of Planar Chromatography—Modern TLC* 11: 43–50.

Klimes J and Kastner P (1993) Thin-layer chromatography of benzodiazepines. *Journal of Planar Chromatography—Modern TLC* 6: 168–180.

Seiler N (1971) Identification and quantification of amines by thin-layer chromatography. *Journal of Chromatography* 63: 97–112.

BILE ACIDS



Gas Chromatography

A. K. Batta and G. Salen,

UMD-NJ Medical School, Newark, NJ and VA Medical Center, East Orange, NJ, USA

Copyright © 2000 Academic Press

Introduction

Bile acids, a group of steroidal acids with a carboxyl group in the side chain, are the major end products of cholesterol catabolism, formed in the liver, conjugated with amino acids, glycine and taurine, and secreted into the bile. In most animal species, bile acids contain 24 carbons, with the terminal side chain carbon in the form of a carboxyl group; however, certain reptiles have 27-carbon bile acids as the major biliary bile acids. Primary bile acids are formed via the 5β -saturation of cholesterol double bond by hepatic enzymes, epimerization of 3β -hydroxyl group to α -configuration and further insertion of 7α - and/or 12α -hydroxyl group, shortening of the side chain by three carbons and oxidation of the terminal carbon to a carboxyl group. Structures of some of the bile acids found in animal species are shown in Figure 1. Bile acids facilitate the absorption of dietary lipids, including fat-soluble vitamins and cholesterol, via their detergent action. The detergent properties of bile acids result from their unique structure with a non-polar steroid skeleton and a polar carboxyl group and α -oriented hydroxyl groups, further increased by hepatic conjugation with glycine and taurine (Figure 1).

Bile acid conjugates form micelles with phospholipids that solubilize cholesterol in the bile. The primary bile acids, cholic acid and chenodeoxycholic acid, are effectively reabsorbed from ileum during their enterohepatic circulation, but approximately 5% that escape reabsorption seep into the colon, and are subjected to modification to secondary bile acids by intestinal bacteria. These modified bile acids, in particular the 7α -dehydroxylated bile acids, lithocholic acid and deoxycholic acid, are the major faecal bile acids and are also significantly absorbed from the colon and circulate in the enterohepatic circulation, with deoxycholic acid as one of the major plasma and biliary bile acids in humans. Whereas only small amounts of bile acids are excreted into the urine, approximately 500 mg per day is excreted in faeces and forms a major catabolic pathway for the elimination of body cholesterol.

In hepatobiliary and intestinal diseases, the hepatic synthesis and clearance of bile acids and their intestinal absorption are abnormal, which disturbs both cholesterol synthesis and its metabolism, causing increased plasma, urinary and faecal concentrations of bile acids. This results in accumulation of precursors of cholesterol or bile acids and clinical malformations ensue. Early diagnosis of such conditions is often possible from bile acid analysis in bile, serum, urine and faeces. On the other hand, bile acids have therapeutic applications in conditions of abnormal cholesterol biosynthesis and metabolism, and chenodeoxycholic acid, and its 7β -hydroxy epimer, ursodeoxycholic acid, are used for medical treatment of gallstones while ursodeoxycholic acid is also being

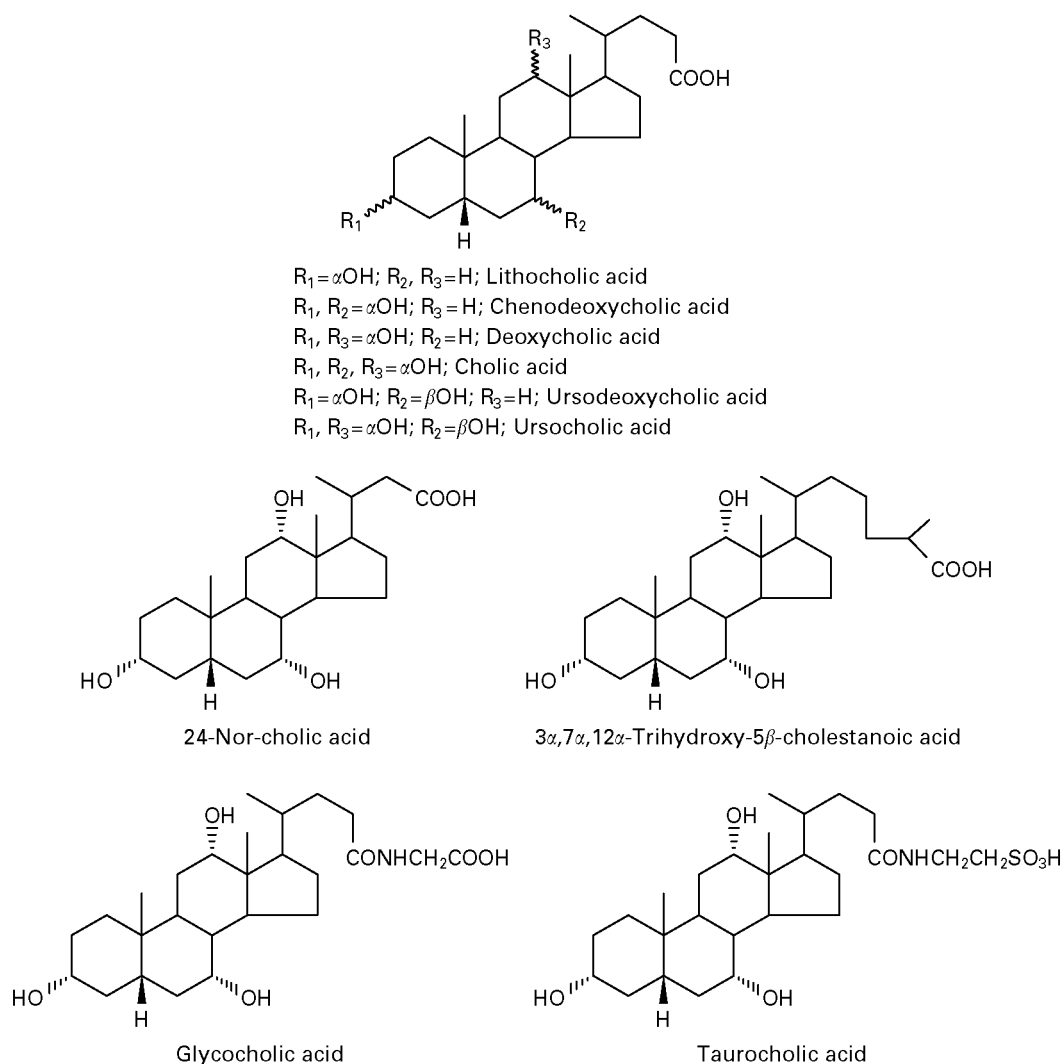


Figure 1 Structures of bile acids and their derivatives.

used in clinical trials for a variety of hepatobiliary diseases, including primary biliary cirrhosis, primary sclerosing cholangitis and hepatitis C, and is suggested to suppress colon polyp formation in experimental animals. Thus, bile acid analysis is an important diagnostic tool for diseases of the liver and intestine, and for monitoring bile acid therapy in such diseases. Of the several methods employed for bile acid analysis in biological fluids, gas chromatography (GC) has proven to be the most versatile and is sensitive enough to quantitate nanomole to picomole amounts present in biological specimens.

Choice of Column

For more than a decade, since the first application of GC for bile acid analysis by Vanden Heuvel *et al.* in

1960, GC was performed using metal or glass-packed columns. Introduction of capillary or open tubular columns was a major landmark in the development of GC. The separation of serum bile acids using capillary columns was first demonstrated by Laatikainen *et al.* in 1975 (Table 1). Coupled with the fact that the retention times are highly reproducible, capillary columns have fast become columns of choice for most chromatographic applications for bile acids. The usual capillary column is 25–50 m long with an internal diameter of 0.22–0.25 mm. The inner wall is coated with the liquid phase, which may vary from nonpolar (e.g. methyl silicones, such as OV-1, CP-Sil-5 CB and SE-30) to more polar (like phenylmethyl- and cyanopropylsilicone, e.g. CP-Sil-19 CB) depending on the need. Usually peaks are very sharp; however, the dead volume must be very small and

Table 1 Important advances in gas chromatography of bile acids

1960–61	Vanden Heuvel <i>et al.</i>	First application of gas chromatography for bile acid analysis. Bile acid methyl ester-trifluoroacetates were analysed on packed columns
1965	Grundy <i>et al.</i>	Comprehensive method for faecal bile acid analysis using packed columns. Bile acids were isolated free from faecal fatty acids, sterols and other contaminants before chromatography. Method often used as a standard to which other methods are compared
1975	Laatikainen <i>et al.</i>	Introduction of capillary columns for serum bile acid analysis
1987	Child <i>et al.</i>	Simultaneous quantitation of faecal bile acids, sterols and fatty acids
1998	Batta <i>et al.</i>	Bile acid analysis was greatly simplified. Bile acids were derivatized and quantitated directly in the stool sample and the multiple steps of removal of sterols and fatty acids were avoided

only microgram or nanogram quantities of compounds can be injected in order to get appropriate peak shapes.

New instrumentation and use of splitless injectors have greatly reduced the dead volume while increasing the sensitivity, so that capillary columns are ideal for chromatography of trace compounds in biological fluids. Quantitation of bile acids in a sample is carried out by comparison of peak areas with those of known amounts of reference compounds in a range where a linear detector response is obtained. Usually a known amount of an internal and/or external standard is added to the sample to facilitate quantitation. Often a mass spectrometer is used as a detector for GC, and gas chromatography–mass spectrometry (GC-MS) has the added advantage that the mass fragmentation can give insight to the structure of the compound. The sensitivity of GC-MS is several-fold increased by using selected-ion monitoring, when picomole quantities of bile acids can be detected. Selection of the right internal standard is important for quantitation of bile acids using the mass spectrometer in the selected-ion mode. Often isotope-labelled bile acids (polydeuterated) are used, the advantage being that such compounds mix with the bile acid to be quantitated and are similarly extracted from the biological source. Otherwise, a bile acid with different GC retention time is employed, and peak heights are calibrated using known amounts of the compounds to be quantitated. The mass ion selected for quantitation is usually a high mass ion and with significant abundance.

Extraction of Bile Acids

Bile acids are present from 1–2 $\mu\text{g mL}^{-1}$ in plasma and urine to significant amounts in the intestinal content and as much as 80 mg mL^{-1} in the gall bladder bile. They are present in unconjugated form as well as conjugated with glycine and taurine or as sulfate/glucuronides, often in association with proteins, sterols and their esters, free or esterified fatty acids, bile pigments and water-soluble small mole-

cules, which may interfere in their analysis. It is often necessary to isolate and at least partially purify bile acids before preparation for GC. Plasma bile acids mainly exist as glycine and taurine conjugates and unconjugated bile acids are present in only small proportions. Plasma is usually passed through Sep-pak, a reversed-phase C_{18} cartridge, when proteins and most of the cholesterol are removed and bile acids and their conjugates are eluted with methanol. Other methods of concentrating bile acids include lipophilic anion exchange gel, diethylaminohydroxypropyl Sephadex LH-20 and, more recently, size exclusion chromatography using Sephadex G-75 gel. Some of these ion exchange resins are also employed for separation of various conjugated bile acids so that conjugation pattern is determined in the sample. The bile acid fraction obtained by any of these methods is treated with strong alkali (4 mol L^{-1} sodium hydroxide, 115°C at 15 psi pressure) to hydrolyse the conjugates; neutral sterols are extracted out with solvents and the free bile acids are then extracted with ether or ethyl acetate after acidification. Under these conditions, the glucuronides and sulfate esters are also hydrolysed, and a pre-step of solvolysis may not be necessary. As an alternative to alkaline hydrolysis, bile acid conjugates may be hydrolysed with the enzyme, cholesteryl glycerol hydrolase, while β -glucuronidase plus sulfatase is used to hydrolyse glucuronides and sulfates. In order to correct for losses during extraction, an internal standard is added before the hydrolysis step, while an external standard (usually 5 α -cholestane) corrects for detector responses of the various compounds. The appropriate internal standard is a bile acid that is not present in the bile acid mixture to be quantitated. Nor-deoxycholic acid and nor-cholic acid are usually used as internal standards, but other compounds like hyodeoxycholic acid and 7 α , 12 α -dihydroxy-5 β -cholanoic acid have also been employed.

Biliary bile acids are present predominantly as the glycine and taurine conjugates. Since they are present in high concentrations in the bile, only a few microlitres of bile are usually required for quantitation by

GC. Also, since bile contains only 1–2% of cholesterol, it is much easier to obtain pure bile acids free from cholesterol. Urinary bile acids are also present mainly in conjugated form, and only a few milligrams per day are excreted. However, in hepatobiliary diseases like primary biliary cirrhosis, urine may become a major pathway for bile acid excretion and sulfate conjugation of bile acids is increased. Again, bile acids need to be deconjugated before GC analysis and methods similar to those for plasma can be used to obtain urinary bile acid composition.

Faecal bile acids are mainly found in unconjugated form and the bile acid pattern is highly complex, due to bacterial deconjugation and extensive metabolism during intestinal transit. Most abundant of these secondary bile acids are deoxycholic acid and lithocholic acid, which are reabsorbed from the colon and further modified by hepatic enzymes and circulate in enterohepatic circulation. Whereas scores of metabolites of bile acids are formed in the colon, bile acids in the jejunum remain predominantly conjugated due to the absence of bacteria in the small intestine, and they therefore mirror biliary bile acids. A major difficulty in quantitative analysis of faecal bile acids is their strong binding with the bacterial debris in the stool, and quantitative extraction is difficult. Furthermore, in addition to bile acids, stool contains neutral sterols, including cholesterol and its bacterial metabolites and plant sterols and their bacterial metabolites, and also fatty acids. Several methods have been reported for bile acid extraction from faeces, and most are quite complex. Thus, one method involves continuous Soxhlet extraction of aliquots of homogenized stool with chloroform–methanol; the extracted bile acids are subjected to methyl ester formation followed by preparative thin-layer chromatography. Grundy *et al.* extracted neutral sterols from homogenized stool, deconjugated any bile acid conjugates with alkali and finally extracted bile acids with chloroform–methanol after acidification of the solution. After evaporation of solvents, the residue was chromatographed over Florisil and the purified bile acid fraction was subjected to methyl ester formation and then to preparative TLC to separate fatty acids. Bands due to bile acids were isolated and used for GC. In other methods, stools have been extracted with ammoniacal alcohol, methanol–hydrochloric acid, acetic acid–toluene, and bile acids extracted after removal of neutral sterols.

Derivatization of Bile Acids

Derivatization of Carboxyl Group

The carboxyl group in bile acids is most often converted into the methyl ester. Treatment with

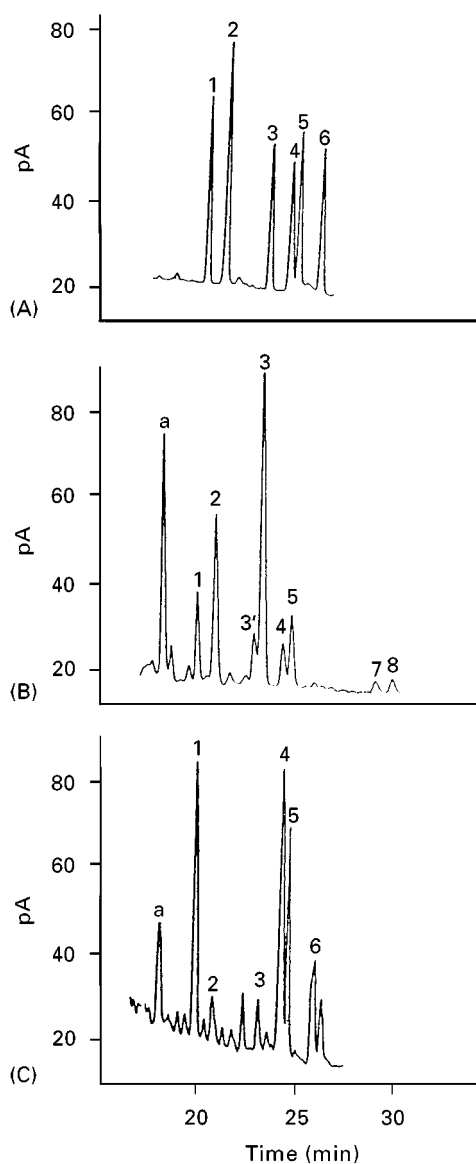


Figure 2 Gas chromatography of bile acids. Chromatographic conditions are described in Table 2; CP-Sil-5 CB capillary column was employed. (A) *n*-Butyl ester-trimethylsilyl ether derivatives of standard bile acids. Peak identification, derivatives of: 1, nor-cholic acid; 2, lithocholic acid; 3, deoxycholic acid; 4, chenodeoxycholic acid; 5, cholic acid; 6, ursodeoxycholic acid. (B) Faecal bile acids in a healthy volunteer. Dried stool (10 mg) containing 20 μ g nor-cholic acid as internal standard was directly subjected to *n*-butyl ester followed by trimethylsilyl ether formation, dissolved in 200 μ L hexane and 1 μ L was injected into the GC column. Peak identification: 1–6, same as in (A); a, sitosterol, 3', isodeoxycholic acid; 7, 3-keto, 12 α -hydroxy-5 β -cholanoic acid; 8, 12-ketolithocholic acid (C) Plasma bile acids in a patient with lipid storage disease, sitosterolemia. Plasma (1 mL) containing 10 μ g nor-cholic acid as internal standard was used. Bile acids were enzymatically deconjugated and bile acids obtained by passing through Sep-pak. Bile acids were derivatized as *n*-butyl ester-trimethylsilyl ethers, dissolved in 100 μ L hexane and 5 μ L was injected into the GC column. Peak identification: 1–6, same as in (A); a, sitosterol.

Table 2 GC retention indices of bile acids as their methyl ester-trimethylsilyl ether derivatives^a

Bile acid methyl ester-trimethylsilyl ether	Retention index ^b	
	CP-Sil-5 CB	CP-Sil-19 CB
Lithocholic acid	3157	3339
Deoxycholic acid	3221	3373
Chenodeoxycholic acid	3244	3397
Cholic acid	3261	3381
Ursodeoxycholic acid	3279	3439
Hyodeoxycholic acid	3256	3422
Hyocholic acid	3340	3445
β -Muricholic acid	3310	3468
Nor-cholic acid	3140	
Nor-deoxycholic acid	3106	
Homocholic acid	3346	
3 α ,7 α ,12 α -Trihydroxy-5 β -cholestanoic acid	3468	

^aA Hewlett-Packard model 6890 gas chromatograph equipped with a flame ionization detector and an injector with a split/splitless device for capillary columns was used. A chemically bonded fused silica CP-Sil-5 CB or CP-Sil-19 CB capillary column (25 m \times 0.22 mm i.d.) was employed and helium was used as the carrier gas. The column temperature was kept at 100°C for 2 min, then increased at a rate of 35°C min⁻¹ to a final temperature of 278°C.

^bRetention indices (Kovats values) were determined by previous injection of an alkane mixture under identical GC conditions.

diazomethane in ether converts bile acids instantly into their methyl esters. However, small amounts of methyl ethers are formed as artefacts, so alternative methods are often employed. Methyl esters are quantitatively formed with methanol-sulfuric acid or anhydrous methanolic hydrochloric acid. Alternatively, 2,2-dimethoxypropane-hydrochloric acid may be used for derivatization. In addition to methyl esters, ethyl, *n*-propyl, isobutyl and *n*-butyl esters have all been employed, the advantage being that the retention times of the bile acid derivatives are increased and, sometimes, resolution is improved. In particular, much better separations from neutral sterols can be obtained and, as shown in Figure 2, chemical removal of neutral sterols may be completely unnecessary with the use of butyl esters.

Derivatization of Hydroxyl Groups

The derivative of choice for the hydroxyl group is the trimethylsilyl ether and a variety of silylating reagents are commercially available for quantitative derivatization of even hindered and tertiary hydroxyl groups. Thus, *N,O*-bis(trimethylsilyl)acetamide, in combination with trimethylchlorosilane, can convert relatively unhindered hydroxyl groups into their trimethylsilyl ether derivatives and, when mixed with trimethyliodosilane, the reagent is highly potent and

can silylate hydroxyl groups in all positions. Bis(trimethylsilyl)trifluoroacetamide is equally reactive as *N,O*-bis(trimethylsilyl)acetamide but the reagent and the by-products are more volatile. The older silylating reagent, a mixture of 1,1,1,3,3,3-hexamethyldisilazane, trimethylchlorosilane and pyridine (3 : 1 : 9) is still commonly used for derivatization. Retention volumes of several common bile acid methyl ester-silyl ether derivatives on capillary

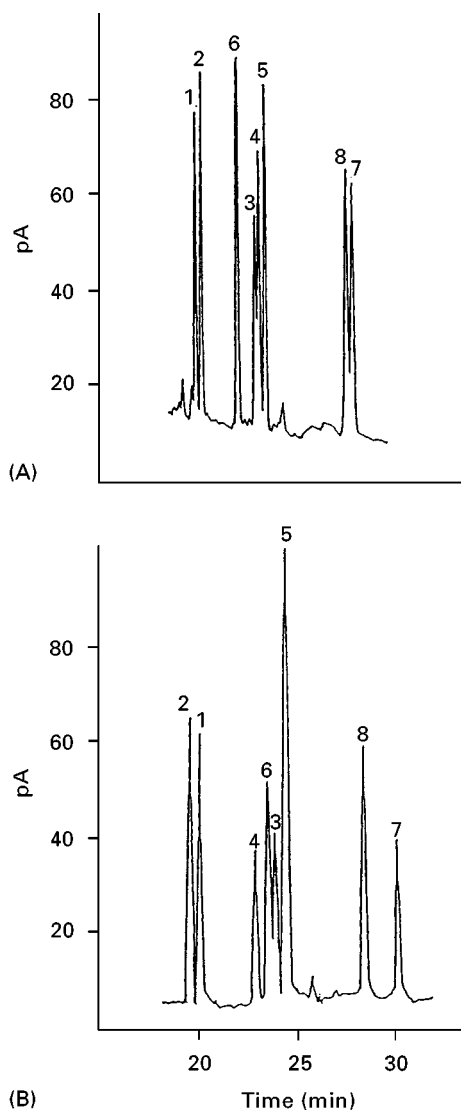


Figure 3 Gas chromatography of 6-hydroxylated bile acids. Chromatographic conditions are described in Table 2. (A) CP-Sil-5 CB capillary column; (B) CP-Sil-19 CB capillary column. Peak identification, derivatives of: 1, 3 α ,6 β ,7 α -trihydroxy-5 β -cholanoic acid; 2, 3 α ,6 β ,7 α ,12 α -tetrahydroxy-5 β -cholanoic acid; 3, 3 α ,6 α ,7 α -trihydroxy-5 β -cholanoic acid; 4, 3 α ,6 α ,7 α ,12 α -tetrahydroxy-5 β -cholanoic acid; 5, 3 α ,6 β ,7 β -trihydroxy-5 β -cholanoic acid; 6, 3 α ,6 β ,7 β ,12 α -tetrahydroxy-5 β -cholanoic acid; 7, 3 α ,6 α ,7 β -trihydroxy-5 β -cholanoic acid; 8, 3 α ,6 α ,7 β ,12 α -tetrahydroxy-5 β -cholanoic acid.

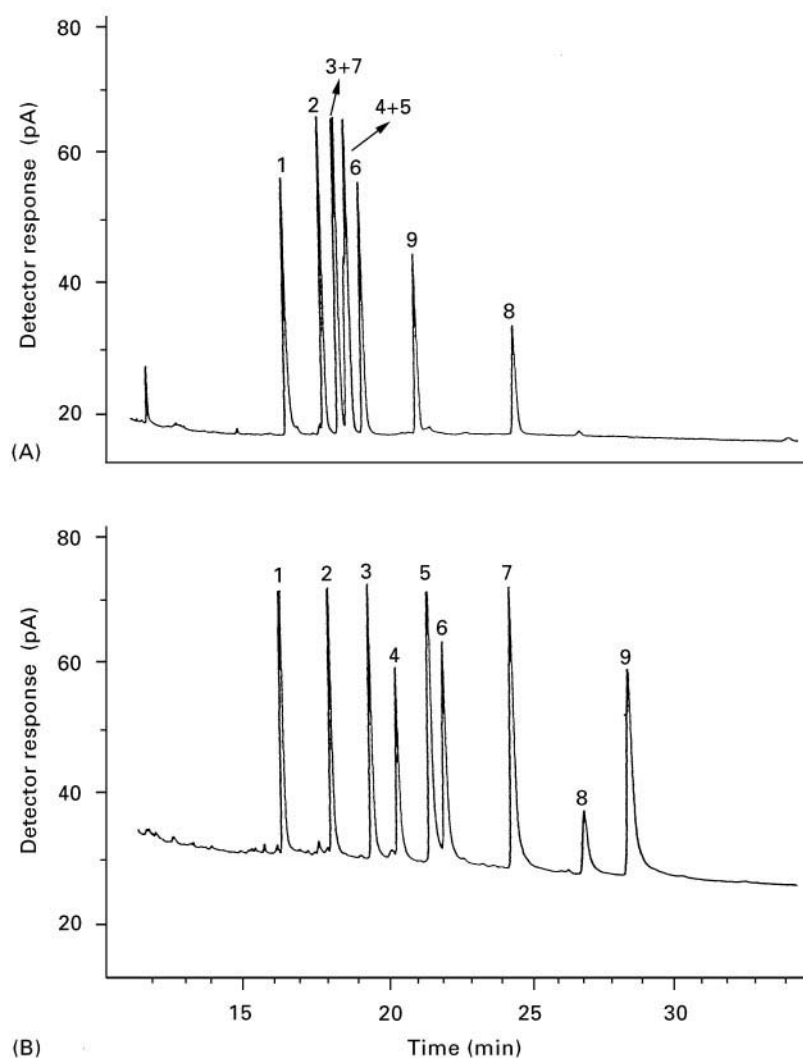


Figure 4 Gas chromatography of acetate-methyl esters and trimethylsilyl ether-methyl esters of bile acids. Chromatographic conditions are described in Table 2; CP-Sil-5 CB capillary column was employed. (A) Trimethylsilyl ether-methyl esters of bile acids. (B) Acetate-methyl esters of bile acids. Peak identification: 1, lithocholic acid; 2, deoxycholic acid; 3, chenodeoxycholic acid; 4, cholic acid; 5, 3 α ,6 α -dihydroxy-5 β -cholanoic acid; 6, ursodeoxycholic acid; 7, 3 α ,6 β ,7 α -trihydroxy-5 β -cholanoic acid; 8, 3 α ,6 α ,7 β -trihydroxy-5 β -cholanoic acid; 9, 3 α ,6 β ,7 β -trihydroxy-5 β -cholanoic acid.

columns of low and medium polarity are given in Table 2, while the chromatographic resolution of these derivatives of a number of bile acids with additional hydroxyl group at C₆ (present in several animal species and in patients with hepatobiliary diseases) is shown in Figure 3. Although trimethylsilyl ethers have gained general applicability in bile acid analysis, other silylating groups sometimes have advantages. Thus, dimethylethylsilyl and dimethylpropylsilyl ether derivatives have longer retention times than the corresponding trimethylsilyl ethers, while *t*-butyldimethylsilyl ether derivatives are very stable, and also show significantly longer retention times, so that often better resolutions can be obtained. Hydroxyl groups can

also be protected as acyl derivatives and formate, acetate and trifluoroacetate derivatives have all been employed for GC. These derivatives are often more stable than the silyl derivative and sometimes show better resolution, as seen in Figure 4. A one-step derivatization of the hydroxyl and carboxyl groups with heptafluorobutyric anhydride, also resulting in simultaneous hydrolysis of the glycine and taurine conjugates of the bile acids, has been reported.

Derivatization of Oxo Groups

Oxo bile acids are formed by bacterial modification of bile acids during their intestinal transit and are therefore found in the intestinal content. Quantitation of

oxo bile acids is beset with problems. Thus, oxo bile acids, in particular, 3-oxo bile acids, are vulnerable to rigorous alkaline hydrolysis conditions and therefore the much milder enzymatic hydrolysis of conjugates is preferred when oxo bile acids are suspected. Oxo bile acid methyl esters can be chromatographed without further derivatization (the hydroxyl groups in the partially oxidized compounds must be derivatized); however, sometimes artefacts are produced and it may be better to protect the oxo groups as the *O*-methyloxime or the dimethylhydrazone derivatives.

Summary

Detection and quantitation of bile acids are important in health and disease. Bile acid synthetic defects may arise from both defective cholesterol synthesis and metabolism; bile acid therapy may correct some of these abnormalities. GC has proved to be of vital importance in determination of bile acids in biological fluids. However, a complete GC analysis generally takes a long time. By appropriate column and derivatization selection, analysis time can be significantly reduced, but sample preparation for GC analysis is usually time-consuming. Combination of GC and mass spectrometry greatly aids in the characterization of unknown bile acids. In attempts to get additional information, Child *et al.* have developed a method to quantitate sterols and fatty acids together with bile acids in stool samples. Advantage is taken of the greatly increased retention times of the *n*-butyl ester-acetates of bile acids, so that sterol acetates are eluted earlier than all bile acids present and a group separation of faecal fatty acids, sterols and bile acids is achieved. In a further advancement of the method, Batta *et al.* have prepared *n*-butyl esters of bile acids directly in faecal samples, followed by trimethylsilyl ether formation. They showed that

faecal bile acids could be quantitatively derivatized and eluted from the faeces and bile acids could be quantitated in the presence of other faecal components. The method is also applicable to plasma bile acid measurement. Figure 2 shows plasma and faecal bile acids in a healthy volunteer determined as the *n*-butyl ester-trimethylsilyl ether derivatives. Since the extra steps of extraction of bile acids and their purification are eliminated, the method can easily be adapted for routine screening of samples for bile acid analysis.

See also: II/Chromatography: Gas: Detectors: Mass Spectrometry; Derivatization; Solid Phase Extraction. III/Acids: Gas Chromatography; Liquid Chromatography; Thin-layer (Planar) Chromatography. Extraction: Supercritical Fluid Extraction.

Further Reading

- Batta AK, Salen G, Rapole KR, Batta M, Earnest D and Alberts D (1998) Capillary gas chromatographic analysis of serum bile acids as the *n*-butyl ester-trimethylsilyl ether derivatives. *Journal of Chromatography (B)* 706: 337–341.
- Child P, Aloe M and Mee D (1987) Separation and quantitation of fatty acids, sterols and bile acids in faeces by gas chromatography as the butyl ester-acetate derivatives. *Journal of Chromatography* 415: 13–26.
- Grundy SM, Ahrens Jr EH and Mietinnen TA (1965) Quantitative isolation and gas-liquid chromatographic analysis of total faecal bile acids. *Journal of Lipid Research* 6: 397–410.
- Kuksis A (1976) Gas chromatography of bile acids. In: Marinetti GV (ed.), *Lipid Chromatographic Analysis*, vol. 2, pp. 479–610. New York: Marcel Dekker.
- Sjovall J, Lawson AM and Setchell KDR (1985) Mass spectrometry of bile acids. In: Clayton RB (ed.) *Methods in Enzymology* 111: 63–113. New York: Academic Press.

Liquid Chromatography

K. Saar, Aventis Research & Technology,
Frankfurt, Germany

S. Müllner, Enzyme Technology, Düsseldorf, Germany

Copyright © 2000 Academic Press

Introduction

Bile acids, the major components of the bile fluid, play a significant role in lipid metabolism. After formation in the liver and storage in the gall bladder, the bile is secreted in the duodenum. Due to their

chemical structure, all bile acids tend to form micelles and serve as natural detergents. In addition, bile acids are co-factors of pancreatic lipases and are pivotal for the digestion and absorption of fats and fat-soluble vitamins.

The primary bile acids cholic acid and chenodeoxycholic acid are synthesized in the liver and during their enterohepatic circulation various modifications occur. Conjugation with the amino acids taurine or glycine as well as deconjugation, sulfation, glucuronidation and modification by intestinal

bacteria lead to numerous secondary bile acid structures. The biliary and serum bile acid pattern as such as well as the detection of several secondary bile acids in serum can serve as disease markers and are of interest in therapeutic monitoring.

In healthy individuals the bile acid concentrations in the gall bladder and in duodenal bile are in the upper micromolar up to millimolar range. The determination of faecal bile acids is, however, not hampered by their overall concentration but by the complex pattern of primary and secondary derivatives as well as by the nature of the matrix. Bile acid patterns in serum, which are for healthy individuals in the upper nanomolar concentration range, are much harder to determine.

A number of gastrointestinal disorders and hepatic or biliary diseases, e.g. liver cirrhosis and hepatitis, lead to increased serum and urinary bile acid levels and result in significant changes in the bile acid pattern. Since bile acids are the major products of cholesterol metabolism, they play an important role in research and development of lipid lowering drugs and therapies.

This is the reason why simple, reproducible and sensitive methods for detection, separation and quantitation of bile acid patterns in all kinds of biological matrices and body fluids are of increasing importance in the pharmaceutical industry as well as for clinical chemistry.

Liquid Chromatographic Methods

With enzyme-based assays or other analytical methods like radioimmunoassays either total bile acid concentrations or single bile acids can be detected. Gas-liquid chromatography is a commonly used method for bile acid analysis, however, it does not allow the detection of conjugated bile acids. Therefore, in order to achieve relevant diagnostic data with regard to changes in the bile acid pattern, other specific separation techniques have to be employed.

In early studies on liquid chromatography of bile acids, silica gel was a commonly used stationary phase. Other materials such as aluminium oxide or neutral polymers were also used for separations under gravity pressure. Various solvent systems, e.g. mixtures of light petroleum, butanol, glacial acetic acid and other organic solvents have been described, mostly in combination with thin-layer chromatography (TLC) as a detection method. With the systems described, the separation of different groups into conjugated/nonconjugated bile acids is possible, however poor sensitivity and insufficient selectivity are major drawbacks and make them unsuitable for routine diagnostics.

High Performance Liquid Chromatography (HPLC) Analysis

Separation

The development of sophisticated HPLC instrumentation and of precise pumps with low pulsation as well as improved sensitivity of the detection systems along with new column materials have made this technique well suited for routine laboratory work. Over the last 20 years, a number of different HPLC methods for determination of bile acids in all kinds of biological fluids have been published, each of them with special advantages and disadvantages.

Early HPLC work was based on polar column materials like silica gel and others. However, these were just adaptations from TLC and LC studies to higher pressure and were again limited in selectivity and reproducibility due to the nature of the matrix as well as the solvents used. It took the development of reversed-phase materials like octadecylsiloxane-modified silica to make HPLC the most commonly used analytical method in the bile acid field. Using nonpolar C_{18} materials, conjugated as well as nonconjugated bile acids can be separated satisfactorily. Reversed-phase materials tolerate most organic solvents and are stable over a pH range from 0 to 7. They also tolerate high pressures without changes in the column bed, and custom-made packing materials guarantee the required reproducibility of the analytical results. Therefore it comes as no surprise that almost all of the HPLC methods published for bile acid separation are based on reversed-phase applications.

The solvent systems described are normally based on organic solvents, e.g. acetonitrile or methanol, mixed with a buffer system. Buffers are based either on ammonium salts, ammonium acetate or ammonium carbamate, or on alkali phosphates.

Detection

The major challenge in bile acid analysis is their detection, particularly of unconjugated bile acids. Various methods have been described based on detection systems like UV absorption, refractive index, fluorescence, electrochemistry and enzymatic or chemical post-column derivatization. The most common and sensitive methods will be discussed here. Electrochemical and refractive index detection, due to their limitations in sensitivity and reproducibility, play only a marginal role in bile acid analysis.

UV detection The amino acids glycine and taurine make the whole group of conjugated bile acids detectable by UV absorption at 200 nm (**Figure 1**). This method limits the components of the mobile phase to

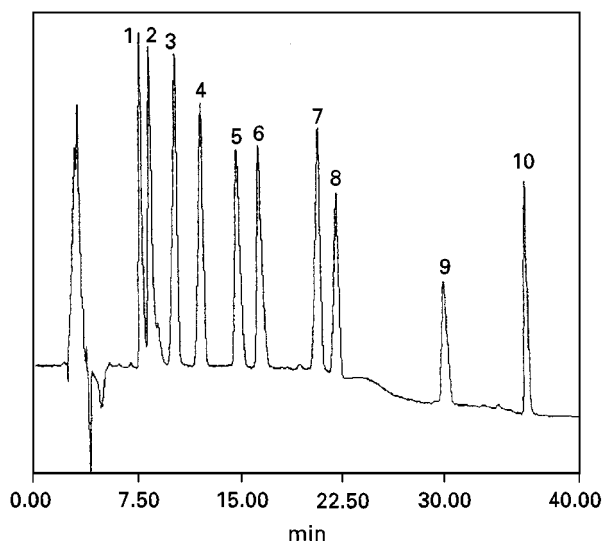


Figure 1 Separation of 10 conjugated bile acids by reversed-phase HPLC and UV detection at 200 nm: 1, taurocholic acid; 2, tauroursodeoxycholic acid; 3, glycocholic acid; 4, glycourso-deoxycholic acid; 5, taurochenodeoxycholic acid; 6, taurodeoxycholic acid; 7, glycochenodeoxycholic acid; 8, glycodeoxycholic acid; 9, tauroolithocholic acid; 10, glycolithocholic acid.

solvents with low UV absorption. As detection at low wavelength is sensitive to all kinds of impurities, efficient sample preparation especially of biological material with low bile acid concentration is recommended. Also high purity reagents for the preparation of buffers and ultra pure organic solvents are required. Taking this into consideration, all methods based on RP-HPLC with UV detection allow qualitative and quantitative separation of all conjugated bile acids with biological relevance by gradient elution. The detection limits are in the range from 40 to 60 ng and show some individual characteristics for the respective bile acids.

Lacking a characteristic chromophore and due to their chemical structure, unconjugated bile acids cannot be determined by UV detection with sufficient sensitivity under conditions comparable to their conjugated counterparts. One solution to this problem might be the addition of an ionic compound like hyamine®, tetrabutylammonium phosphate or decyltrimethylammonium bromide as counter ion to the mobile phase. Separation and detection are then based on the formation of ion pairs. Some reports suggest that this method increases the sensitivity as well as the selectivity of separation and detection so that UV determination of unconjugated bile acids in a range of 20–30 ng is possible. In contrast to that, detection limits for the conjugated forms are about three-fold lower. However, since other detection methods provide higher sensitivity and efficiency, ion pair chromatography is rarely used in bile acid analysis.

Fluorescence detection A method to increase sensitivity in determination of bile acids is fluorescence labelling and fluorescence detection. Two different systems to generate fluorescent bile acid derivatives are commonly used.

A relatively old method to quantify total bile acid concentrations is enzymatic detection by 3 α -HSD. Since all natural bile acids possess a hydroxyl group in the 3 α -position, by enzymatic dehydrogenation and via formation of nicotinamide adenine dinucleotide (NADH), spectrometric detection at 340 nm is possible. Going back to this principle, 'column reactors' containing immobilized 3 α -HSD have been developed. When connected with the separation unit, usually a C₁₈ column, each substance is enzymatically transformed and as one of the reaction products, NADH can be determined by fluorescence detection at 350–460 nm. This method allows detection of nearly all free bile acids having a 3 α -hydroxyl group independent from conjugation, but is not suitable for derivatives where the 3 α -hydroxyl group is esterified, e.g. by sulfation or glucuronization. In the analysis of biological samples, other steroids with free 3 α -hydroxyl group can influence the results. Application of the post-column derivatization method needs additional instrumentation for introduction of the enzymatic reagent.

On the other hand, several fluorescent agents for pre-column derivatization have been reported. One of the most reproducible and sensitive methods is based on 4-bromomethyl-6,7-dimethoxycoumarin (BMC) as derivatizing agent. BMC reacts with carboxyl groups by formation of fluorescent esters detectable at 340–460 nm. Therefore, unconjugated and glycine-conjugated bile acids can be labelled as well as all kinds of bile acid esters at the 3 α -hydroxyl group. Despite the high sensitivity – concentrations of less than 5 ng can be detected – the method has disadvantages. One major problem results from the fact that taurine-conjugated bile acids cannot be detected, due to the lack of a carboxyl group necessary for an ester bond. Samples containing high amounts of these conjugates, e.g. gallbladder bile, have to be treated with choloylglycylhydrolase for deconjugation before the total amount of the free acids can be measured, or an additional method for detection of taurine conjugates has to be employed. Though the BMC reagent will react with all components possessing a free carboxyl group, e.g. fatty acids, bile acids can be well separated and quantified by choosing an appropriate elution system and adequate sample pretreatment. The BMC derivatization reaction works with dicyclohexanocrown ether (DCCE). Because of that, potassium salts of the bile acids have to be prepared so that a further sample preparation step

can be carried out. An alternative, very sensitive method with a detection limit of less than 1 ng has been suggested, based on the formation of naphthyl ester derivatives. This labelling procedure also needs some careful preparation steps in order to obtain a good analytical sample for fluorescent detection. Nevertheless, pre-column fluorescence labelling seems to be suitable especially for samples containing low total bile acid concentrations, but also for samples with unconjugated bile acids as major components as in serum (Figure 2).

Detection by mass spectrometry The most sensitive technique by far for bile acid detection is the coupling of a suitable HPLC system with a mass spectrometer. Detection limits range from 1 to 5 pg. However, the prerequisite for the production of valid and reproducible data is high quality equipment, resulting in high initial costs. LC-MS coupling is the method of choice for the specific determination of low bile acid concentrations in all biological matrices or tissues. Mass spectrometry requires very small sample volumes and flow rates. For the HPLC separation a microsystem able to produce constant flow rates in the range of microlitres per minute is recommended. The use of standard HPLC systems is possible, but a precise flow-splitting device has to be used. This has the advantage that the main part of the eluate can be utilized for further determinations, e.g. UV detection, in order to achieve additional data for quantification. A high performance system allowing the baseline separation of all bile acids of interest is necessary to obtain best results from MS detection. Both isocratic and gradient elution are possible, and all kinds of bile acids, despite conjugation or other modification, can be detected. After sample pretreatment and purification to remove interfering substances no further steps such as deconjugation, derivatization or enzymatic treatment are required.

Different mass spectrometry systems are reported to be suitable for LC-MS coupling. HPLC-thermospray MS methods were reported earlier, but seem to be less sensitive and reproducible compared to other methods. Fast atomic bombardment (FAB) MS and electrospray ionization (ESI) MS have been interfaced with HPLC and good results in reproducibility and sensitivity have been reported.

A special type of a mass detection system is the evaporative light-scattering mass detector (ELSD). A special feature of this detection method is that the eluate coming from the column is evaporated, and nonvolatile components such as bile acids are determined by measurement of the light deflected. The detection unit consists of a photodiode and a laser beam. When nonvolatile compounds pass through

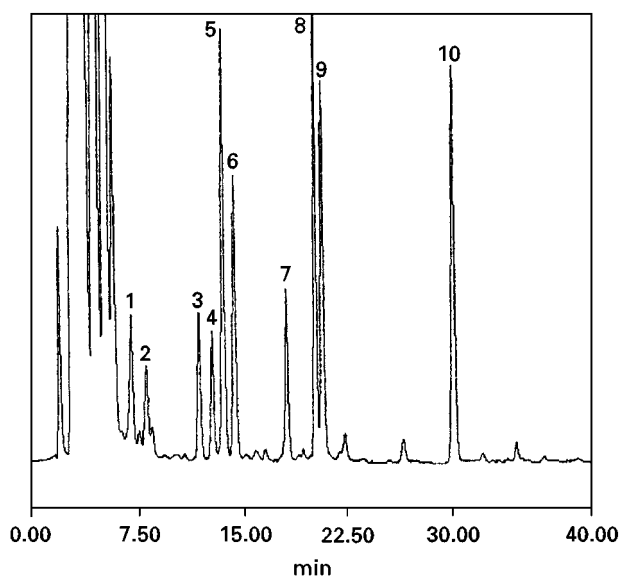


Figure 2 Separation of 10 unconjugated and glycine conjugated bile acid derivatives (pre-column fluorescence derivatization with bromomethoxycoumarin) by reversed-phase HPLC and fluorescence detection: 1, glyoursodeoxycholic acid; 2, glycocholic acid; 3, glycochenodeoxycholic acid; 4, glycodeoxycholic acid; 5, ursodeoxycholic acid; 6, cholic acid; 7, glycolithocholic acid; 8, chenodeoxycholic acid; 9, deoxycholic acid; 10, lithocholic acid.

the laser, light scattering appears and can be detected. The signal is dependent on the molecular mass of the separated substance. The ELSD technique seems to be moderately sensitive with respect to UV detection but detects all bile acids and their derivatives as well as other analytes of interest. However, isocratic elution systems are required and, therefore, ELSD detection is only applicable in niche areas of application.

Detection of Bile Acids in Biological Samples

Bile The determination of the bile acid pattern in gallbladder or intestinal bile does not need a time-consuming sample pretreatment or enrichment. The bile fluid of mammalian individuals consists mainly of glycine- and taurine-conjugated bile acids in relatively high concentrations compared to other body fluids such as serum or urine samples. Therefore, HPLC separation with UV detection is the commonly used method for analysis of samples derived from bile. In the bile fluid of healthy individuals only small amounts of protein are present and do not interfere with bile acid detection. Therefore, no deproteination procedure is necessary. However, in order to remove small amounts of protein as well as cell debris and larger particles, the addition of methanol followed by a centrifugation step is recommended. For conventional analysis, dilution with the mobile phase and filtration through a microfilter is sufficient as sample pretreatment. The use of a guard column in the HPLC

system is recommended when larger sample quantities are to be analysed.

Faeces Problems in the analysis of bile acids in faeces are not caused by the total amount of bile acids but by the complexity of the faecal matrix. Since the primary bile acids in gallbladder bile and in the intestine are modified by the intestinal microflora during enterohepatic circulation, in faeces mainly secondary unconjugated bile acids are found. Time-consuming extraction procedures have been suggested, e.g. Soxhlet extraction or the use of alcoholic alkali solutions. Homogenization of the material in a mixture of chloroform and methanol using an ultraturrax mixer, followed by further purification with solid-phase extraction cartridges for sample pretreatment as described for serum preparation, seems to be able to extract most faecal bile acids quantitatively. Methods for pre-column fluorescence labelling, e.g. with bromomethoxycoumarin derivatives, are reported. For these derivatization procedures, sample pretreatment with choloylglycylhydrolase for deconjugation is recommended. In addition, detection with an evaporative light-scattering detector can be applied, with the advantage that a mass sensitive detection system is not limited by modifications in bile acid structure. However, the method suffers from nonspecific matrix products influencing the signal to noise ratio and hampering bile acid detection.

Serum and urinary samples The extraction, detection and quantification of bile acids in serum samples of healthy individuals is the most ambitious goal in the field of bile acid analysis. However, since changes in serum pattern can be characteristic for several metabolic and cancer diseases, considerable efforts have been made to develop methods of high sensitivity and reproducibility as tools for diagnostic purposes. Due to the nature of the matrix and to total bile acid concentrations in the low micromolar range, a sophisticated sample pretreatment procedure is absolutely necessary. The commonly used method for extraction and purification of serum samples employs solid-phase extraction as described by Setchell *et al.* Reversed-phase C₁₈ cartridges are activated with methanol and water as recommended by all manufacturers of these columns. Sodium hydroxide solution is added to the serum samples and is followed by a 15–30 min heating step where samples are incubated at 64°C to suppress protein binding. The resulting solution is passed through the activated C₁₈ cartridge where the bile acids should be retained while the matrix components are found in the eluted solution. Washing steps with water, in some cases followed by nonpolar organic solvents such as n-hexane,

are carried out. Bile acids are recovered by elution with methanol. In most cases, eluted samples are dried and redissolved in a small volume of the mobile phase used for HPLC separation. In some reports an additional purification step by anion exchange cartridges is described.

Despite the fact that this sample preparation method has been commonly used over a number of years it suffers from several disadvantages. The major problem is the relatively strong binding of bile acids to serum proteins. Incubation at higher temperatures leads to protein denaturation but does not release the bile acid binding sufficiently and reproducibly. Another approach is the enzymatic digestion of serum proteins. However, this method seems to be limited, since the products of the protein digestion, small peptides and amino acids, interfere with further HPLC detection. Recent work describes a deproteinization procedure by adding serum samples slowly to acetonitrile and incubating them in an ultrasonic bath for some minutes. This efficiently prevents co-precipitation of proteins and bile acids and secures reliable and validated analytical data. Another point has to be considered if solid phase extraction is applied as a sample pretreatment. C₁₈ column materials are offered by several manufacturers and differ in their quality and their respective features. For instance, endcapped and non-endcapped C₁₈ phases are offered commercially. These materials can differ in the quantity and the selectivity of bile acid retention. This leads to remarkable differences in bile acid pattern for the sample when different C₁₈ cartridges are used. Therefore, the results obtained can only be validated when exactly the same material, i.e. same specifications, batch, etc., is used.

An interesting method for automation of the sample pretreatment procedure has been described by Yoshida *et al.* The online purification, concentration and separation of bile acids in serum samples is performed by an HPLC device equipped with three columns. First samples are injected on to a hydroxyapatite column to remove serum proteins. For further purification and concentration, a second pre-column (Serumout-25®) is used. After washing and elution from this column the bile acids are injected via an injection valve to the reversed-phase separation column. This strategy of sample pretreatment might be of value for high throughput assays, e.g. in clinical diagnostics. However, it leaves the problem of protein binding unsolved and, therefore, lack of sensitivity and efficiency is expected.

In urinary samples almost the same problems as in serum bile acid analysis occur. In contrast to blood samples, the urine from healthy individuals does not contain proteins and is available in much

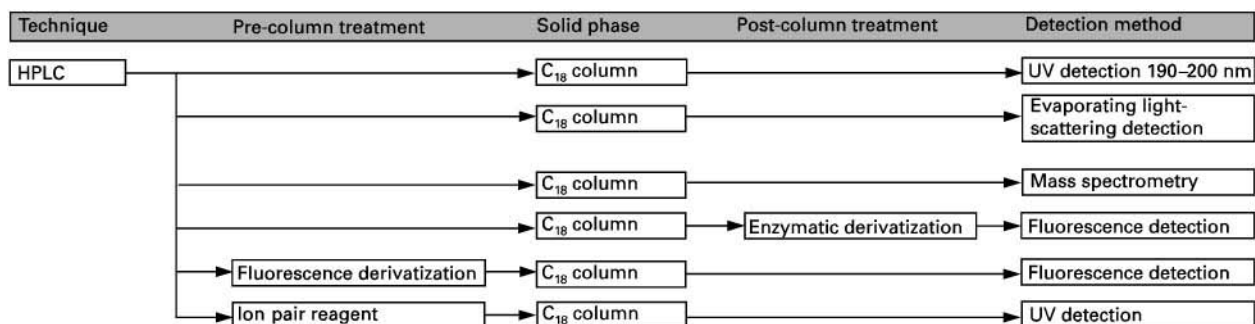


Figure 3 Separation methods for bile acids by liquid chromatography.

higher quantities. For these samples the standard purification procedure using C₁₈ solid-phase extraction is suitable.

Due to the low concentration range of the bile acid pattern in serum and urine, the methods of choice for quantitative and reproducible determination are pre-column fluorescence derivatization and HPLC-MS coupling.

Conclusion

With regard to the liquid chromatographic methods described for bile acid analysis, especially with regard to their determination in biological matrices, several approaches for qualitative and quantitative determination have been described. A critical evaluation of the advantages and disadvantages of these methods results in the conclusion that there are specific limitations for every application (**Figure 3**). Since cumbersome derivatization steps as well as laborious and unsuitable sample pretreatment play a key role in the value of the analytical results, technologies are needed where direct analysis of the bile acid pattern, especially in serum, is feasible. Only HPLC-MS coupling presently allows such analysis, but costly equipment and highly skilled personnel requirements limit this method to highly specific problems and makes it unsuitable for routine work.

Presently, HPLC of bile acids is state-of-the-art and only incremental improvements can be expected

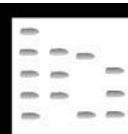
from new column materials and microcolumns (\varnothing 1–2 mm). The future will be in the area of low cost, high throughput HPLC-MS devices for routine use.

See also: **II/Chromatography:** Liquid: Derivatization. Detectors: Evaporative Light Scattering; Detectors: Fluorescence Detection; Detectors: Mass Spectrometry; Detectors: Ultraviolet and Visible Detection. **III/Bile Acids:** Gas Chromatography.

Further Reading

- Güveli DE and Barry BW (1980) Column and thin-layer chromatography of cholic, deoxycholic and chenodeoxycholic bile acids and their sodium salts. *Journal of Chromatography* 202: 323–331.
- Roda A, Gioacchini AM, Cerre C and Baraldini M (1995) High-performance liquid chromatography-electrospray mass spectrometric analysis of bile acids in biological fluids. *Journal of Chromatography B* 665: 281–294.
- Setchell KD and Worthington J (1982) A rapid method for the quantitative extraction of bile acids and their conjugates from serum using commercially available reverse-phase octadecylsilane bonded silica cartridges. *Clinical Chimica Acta* 125: 135–144.
- Street JM, Trafford DJH and Makin HLJ (1983) The quantitative estimation of bile acids and their conjugates in human biological fluids. *Journal of Lipid Research* 24: 491–511.
- Yoshida S, Murai H and Hirose S (1988) Rapid and sensitive on-line purification and high-performance liquid chromatography assay for bile acids in serum. *Journal of Chromatography* 431: 27–36.

BILE COMPOUNDS: THIN-LAYER (PLANAR) CHROMATOGRAPHY



K. Saar, Aventis Research & Technology,
Frankfurt, Germany

S. Müllner, Enzyme Technology, Düsseldorf, Germany

Copyright © 2000 Academic Press

Introduction

Gall bladder bile is, like other physiological fluids, of very complex nature. It is produced by liver

hepatocytes of healthy human beings in a volume of 500–1000 mL per day. The major function of the bile fluid is to support digestion and resorption of lipids and lipophilic substances during intestinal passage. In this respect, bile acids and their different conjugates are the most important components. Bile acids are steroids of amphophilic nature and, owing to their chemical structure, tend to form micelles and serve as physiological detergents. It is this feature that makes bile acids so important in their role in emulsifying fatty food components. In addition, bile acids serve as enzyme cofactors and support fat digestion by activating lipases and other factors of lipid metabolism. Humans, together with some other animals, possess a gall bladder in which bile fluid is stored. The human gall bladder has a capacity of 15–20 mL of concentrated bile. When bile is needed for digestion excretion into the gut is triggered by cholecystokinin, a gastrointestinal hormone which causes ejection of gall bladder contents. In the gall bladder bile is concentrated five- to ten-fold, leading to increased concentrations of all major bile components. Total bile production as well as bile composition are highly dependent on amount and composition of food. For example, according to differences in eating, the pH values of human bile range from 6.5 to 8.5. Other animals, such as rats, secrete bile fluid directly into the intestine.

The most important bile components are the bile acids and their different amino acid conjugates. Bile acids are synthesized in the liver from cholesterol and therefore play an additional key role in cholesterol homeostasis. Products of this process are the so-called primary bile acids cholic acid and chenodeoxycholic acid. In the bile fluid mainly glycine and taurine conjugates of these primary bile acids as well as those of deoxycholic acid are present. However, after secretion into the gut primary bile acids are modified by the intestinal microflora. Primary bile acids and all their derivatives produced during intestinal passage undergo enterohepatic circulation, by which bile acids are reabsorbed nearly completely and are transported back to the liver. Only a very small part of the bile acid pool, 2–8%, is excreted with the faeces. Nevertheless, the bile of healthy individuals contains more primary than secondary bile acids. As changes in total bile acid amount as well as in the bile acid pattern are of importance for diagnostic purposes, simple and fast methods for the analysis of these biological compounds are required (Figure 1).

Many drugs and drug metabolites are secreted into the bile, and this, in addition, makes bile analysis important for the understanding and controlling of pharmacokinetic mechanisms during drug development. Several methods using high performance liquid

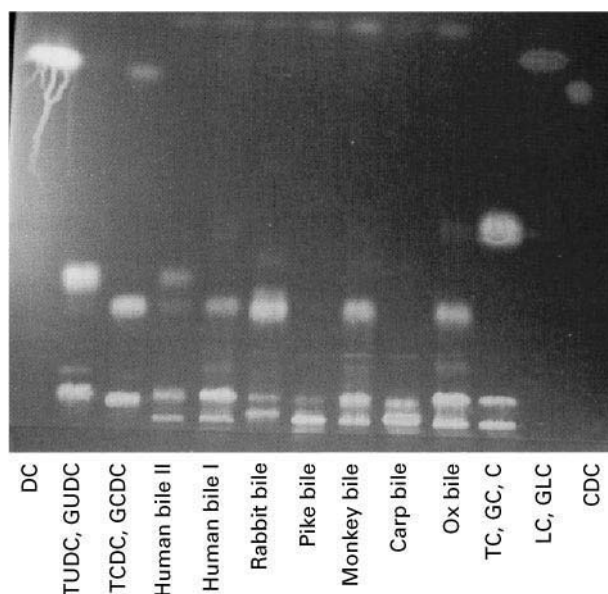


Figure 1 Thin-layer chromatogram of gall bladder bile from several animals, and of human T-drainage bile; comparison with selected standard bile acids. C, cholic acid; DC, deoxycholic acid; CDC, Chenodeoxycholic acid; GC, glycocholic acid; GCDC, glycochenodeoxycholic acid; TC, taurocholic acid; TCDC, taurochenodeoxycholic acid; TUDC, tauroursodeoxycholic acid; GUDU, glyoursodeoxycholic acid; LC, lithocholic acid; and GLC, glycolithocholic acid. (From Müller *et al.* 1992.)

chromatography (HPLC) and thin-layer chromatography (TLC), have been described for the analysis of pharmacologically interesting substances and their metabolites in bile, but as the analytical conditions are always dependent on the chemical nature of the drug and its concentration, they will not be considered here. Another bile component, cholesterol, has become increasingly important during recent decades. The role of increased serum cholesterol concentrations in diseases such as atherosclerosis, leading to stroke and cardiac infarction, for example, is the subject of debate, but when added to other risk factors its involvement is undisputed. Cholesterol concentrations in gall bladder bile range from 1 to 15 g L⁻¹ in humans. Increased bile cholesterol concentrations in most cases cause the formation of gallstones through cholesterol crystallization. The development of drugs influencing either serum or bile cholesterol concentrations is one of the most important areas in pharmaceutical research. Therefore, also in this field fast and simple methods for the detection and quantification of cholesterol in bile are necessary (Figure 2).

Bile fluid also contains high concentrations of phospholipids, especially lecithin, in amounts of 2–4 g L⁻¹. However, whether increases or decreases in phospholipid concentration are significant for

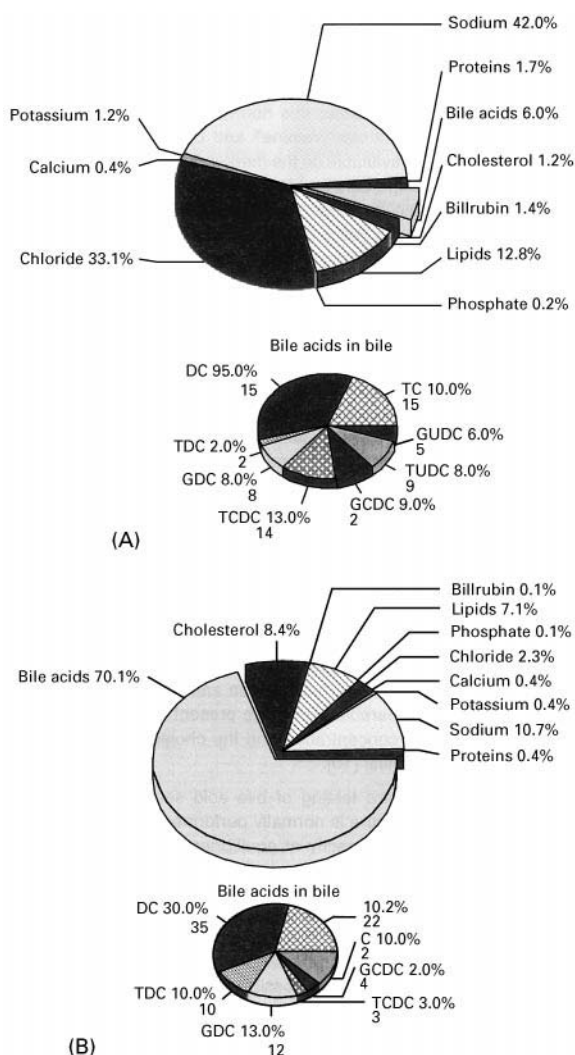


Figure 2 Composition of (A) human T-drainage bile (water content 95.5%) and (B) bovine gall bladder bile (water content 81.5%). (From Müller *et al.* 1992.)

differential diagnosis of certain enterohepatic diseases is not known. Nevertheless, the analysis of phospholipid pools and pattern in bile can be of value for metabolism and kinetic studies in drug development. Several TLC-based methods for separation and detection are known. Other bile components, such as bile pigments, proteins (e.g. alkaline phosphatase) and electrolytes, have to be analysed by other analytical methods (e.g. enzyme assays or spectrometric methods). In general, biliary protein concentration is negligible in healthy individuals (Figure 3).

Thin-Layer Chromatography

Bile Acid Separation

In contrast to other analytical technologies such as HPLC and gas chromatography, which are also com-

monly used for bile acid analysis, TLC is a very simple and nearly universal method. No highly sophisticated and expensive instrumentation is needed for reliable semiquantitative analysis. If precise quantification is essential, a TLC scanner equipped with a computer software system for fast and easy data registration and evaluation is recommended. Whereas HPLC analysis is limited by the fact that only one sample can be analysed at a time, TLC allows multiparallel analysis of probes in combination with an almost unlimited number of detection and visualization methods.

Several solvent systems for the separation of bile acids in biological fluids are described. With respect to bile, bile acid concentrations are in the millimolar range and therefore no detection problems occur, which makes TLC well suited for bile and bile acid analysis. In addition, time-consuming sample pretreatment procedures can be generally avoided for standard analysis of bile acids. However, dilution of the bile samples with phosphate-buffered saline increases the sensitivity of the selected detection (Figure 4).

For bile acid pattern analysis a satisfactory separation of the main components, the glycine- and taurine-conjugated bile acids, is necessary. In general, silica gel TLC plates are used for routine analysis since high quality materials are commercially available in several sizes and from several suppliers and, in contrast to reversed-phase plates for example, at a relatively low price. Our experience in this field leads us to suggest the use of silica gel pre-coated on glass plates with a concentration zone to improve separation, bile acid band shape and overall resolution. Solvent systems suitable for the separation of bile acids on silica gel are shown in Table 1. Many methods for bile acid separation have been described in the literature, and only a selection are shown here.

System 2 leads to the most satisfactory results in resolution and band shape. With this system the glycine and taurine conjugates of deoxycholic acid and of chenodeoxycholic acid can be separated with good resolution. The TLC plates have to be developed six times in the same solvent mixture for bile acid separation and this requires more time compared with the other solvent systems described, but if quantification by TLC scanning is followed system 2 is the method of choice. Solvent system 3 provides a simple and fast method for the separation of conjugated and unconjugated bile acids with sufficient overall resolution to allow quantification. The advantage of this system is the simultaneous separation of cholesterol, which migrates faster than the bile acids. Chamber saturation before analysis increases resolution and improves band shape. With system 4, a solvent

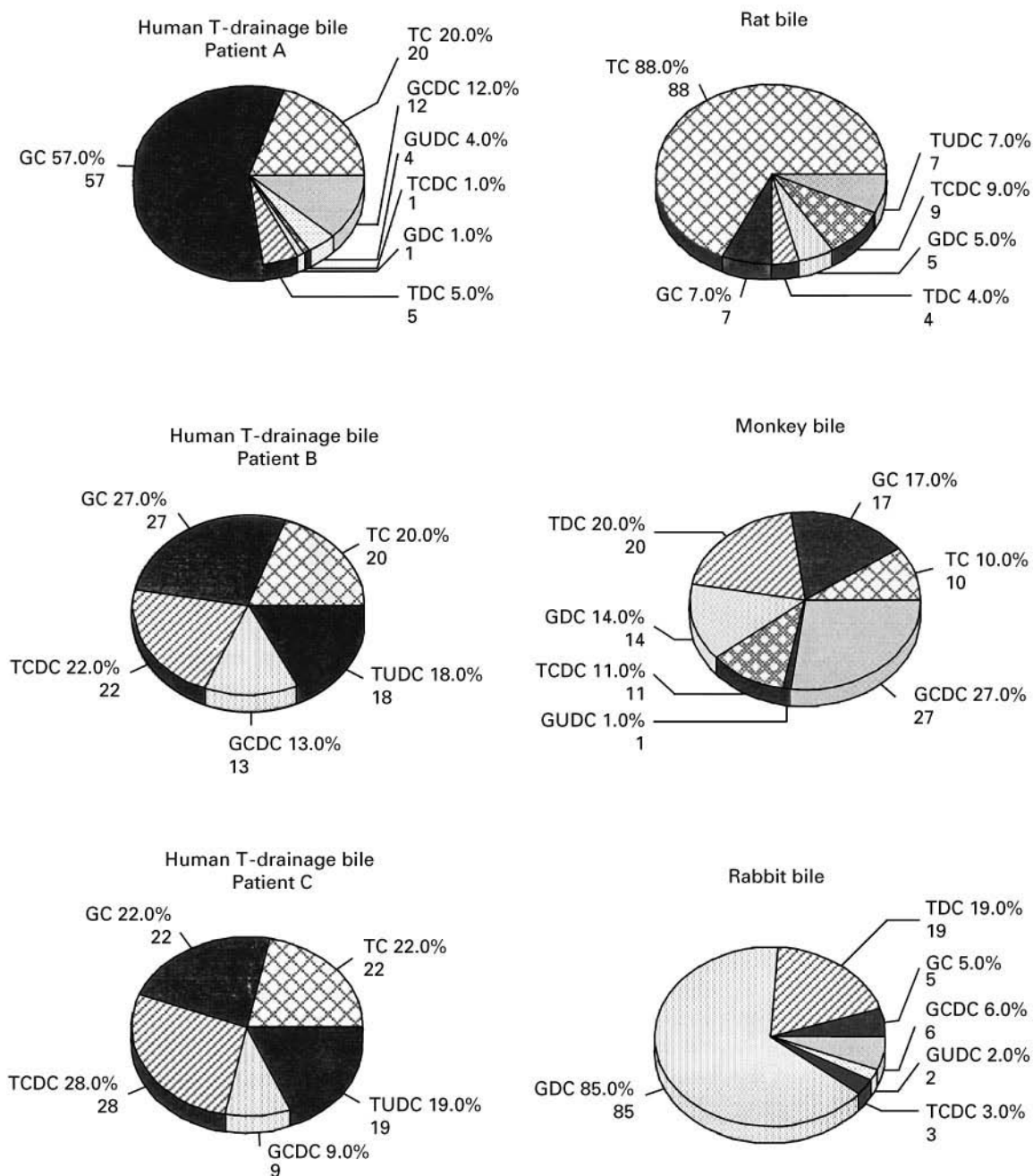


Figure 3 Bile acid patterns obtained from three samples of human T-drainage bile and from the bile of other animals. Key as for Figure 1, plus GDC, glycodeoxycholic acid and TDC, taurodeoxycholic acid. (From Müller *et al.* 1992.)

mixture for the separation of conjugated bile acids on reversed-phase TLC plates is provided. TLC conditions are similar to an HPLC method described for the separation of conjugated bile acids, and may be helpful in comparison of sample analysis by different analytical techniques or in cases where simultaneous separation of bile acids and drug metabolites is required.

In all the separation systems described temperature plays an important role in resolution.

Although room temperature (20–22°C) allows satisfactory separation employing the systems described, in some cases decreasing the temperature improves separation and band shape. Depending on the sample concentration and composition the influence of temperature on separation resolution should be taken

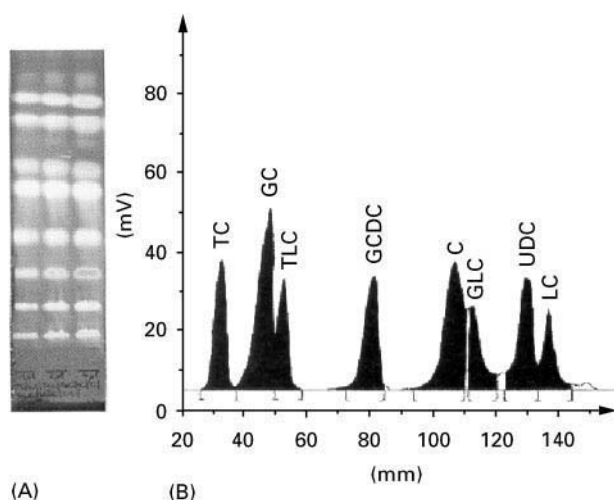


Figure 4 (A) Thin-layer chromatogram of increasing amounts (1, 2 and 4 μL of 4 mg mL^{-1} solutions) of bile acid standards TC, GC, TLC, GCDC, C, GLC, UDC and LC. (B) Fluorescence scan of the left lane of the chromatogram. Key as for Figure 1. (From Müller *et al.* 1992.)

into account as a critical factor for optimization of the chosen solvent system.

Numerous detection methods for bile acid visualization on TLC plates after separation have been described and two principally different systems are in use. Detection methods using reagents which form coloured complexes have the advantage that bands can be visualized directly. A universal detection re-

agent for a vast amount of biological substances is anise aldehyde dissolved in sulfuric acid. Spraying or dipping of the developed TLC plates followed by incubation at 125°C generates spots of different colour which are stable for some time. However, the low specificity of this reagent may cause problems in the analysis of samples with a high content of other components or analytes. Spots can also be visualized under ultraviolet (UV) light, which increases sensitivity. Individual bile acids can be identified by their different colours (Figure 5).

Molybdotophosphoric acid is another reagent often used for detection of biological components and forms blue bands on a yellow ground. Since colour intensity of the visualized spots is not stable over a long period of time, quantification must follow immediately after development of the colour.

The sensitivity of detection of bile acids on TLC plates can be increased dramatically by using a reagent system which forms fluorescent bands. HClO_4 has been described as giving reproducible fluorescent spots with bile acids on TLC plates, provided a 5% solution of this derivatizing agent is used and UV light of 365 nm excitation wavelength is employed after spraying and appropriate treatment at higher temperature.

According to our experience a reagent mixture of manganese dichloride and sulfuric acid is preferred for detection, owing to the reproducible results and its convenience in use. Plates are dipped in the reagent

Table 1 Solvent systems for bile acid separation

<i>System 1</i>		
Unconjugated bile acids	Isooctane Diethyl ether n-Butanol Acetic acid Mixture 10 + 2.5 + 1 + 1 (v/v)	Room temperature
<i>System 2</i>		
Glycine- and taurine-conjugated bile acids	Chloroform 2-Propanol 2-Butanol Acetic acid Double-distilled water Mixture 30 + 20 + 10 + 2 + 1 (v/v)	Room temperature 2 × 15 cm followed by 4 × 7 cm
<i>System 3</i>		
All bile acids	Chloroform Methanol Acetic acid Mixture 85 + 20 + 9 (v/v)	Room temperature Chamber saturation
<i>System 4</i>		
Glycine- and taurine-conjugated bile acids	Acetonitrile (90%) 0.01 M Ammonium carbamate pH 7.3 Mixture 55 + 45 (v/v)	Room temperature Separation on RP8 plates

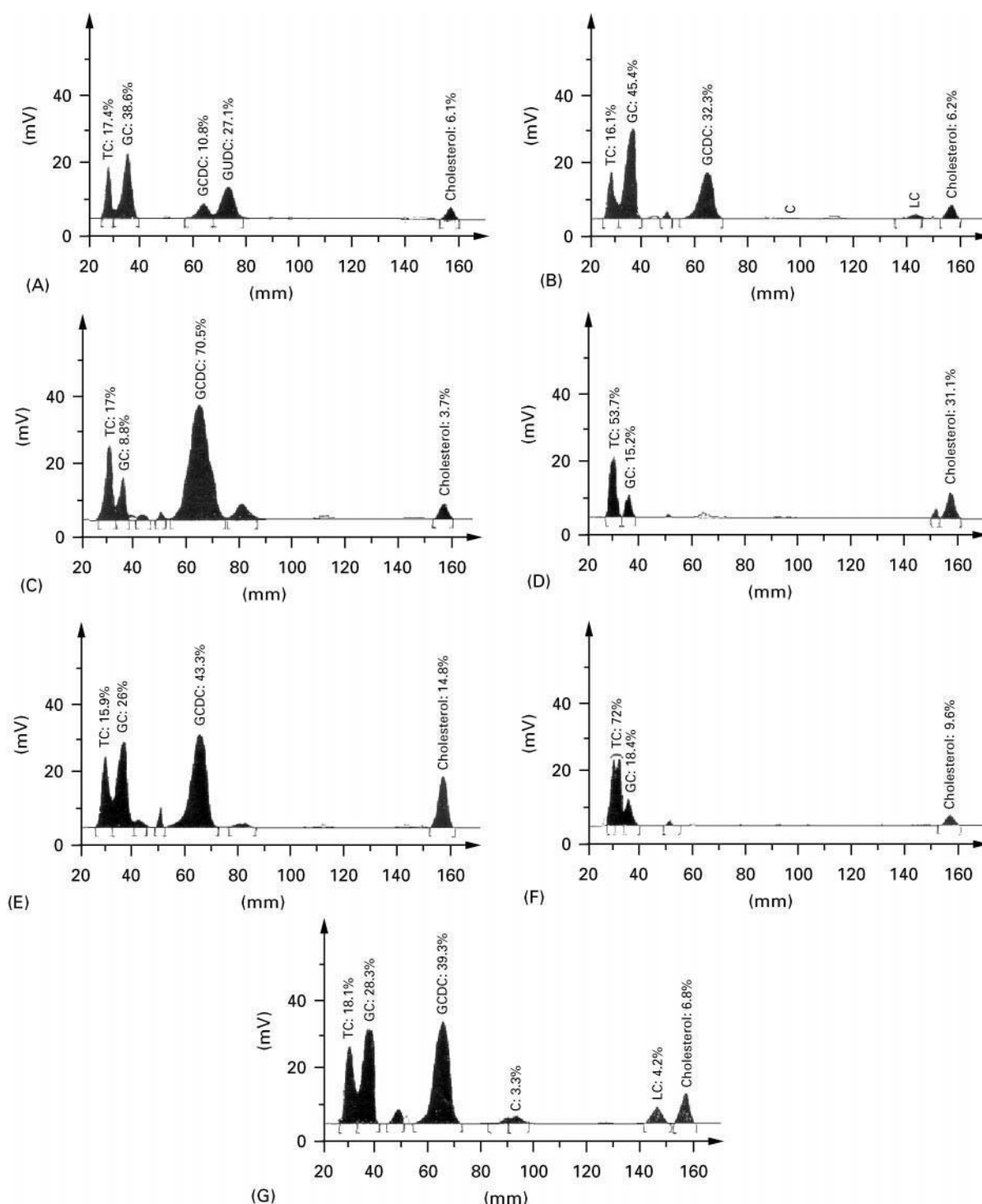


Figure 5 Fluorescence scans of bile specimens from Figure 1: (A) human bile II; (B) human bile I; (C) rabbit bile; (D) pike bile; (E) monkey bile; (F) carp bile; (G) ox bile. Key as for Figure 1. (From Müller *et al.* 1992.)

and heated to 110°C for 10–15 min. Bile acids react with the reagent with the formation of yellow or brown coloured spots. Under UV light (365 nm) blue or yellow fluorescing bands can be detected. Bile acids can be differentiated by their respective colour. The detection sensitivity for the bile acids under UV con-

ditions is 2–5 ng and is therefore about 1000-fold higher compared to visible light (Figure 4).

Cholesterol

Cholesterol and cholesterol esters are important bile components. Several solvent systems for the

Table 2 Solvent systems for separation of cholesterol and cholesterol esters on silica gel plates

<i>System 1</i>	Room temperature
Chloroform	Chamber saturation
Methanol	
Acetic acid	
Mixture 85 + 20 + 9 (v/v)	
<i>System 2</i>	Room temperature
Chloroform	
Acetone	
Mixture 85 + 15 (v/v)	
<i>System 3</i>	Room temperature
Cyclohexane	
Diethyl ether	
Mixture 50 + 50 (v/v)	
<i>System 4</i>	Multiple plate development
Methanol	
Diethyl ether	
n-Hexane	

separation of these steroids exist, but only some of them are suitable for the analysis of cholesterol in complex biological fluids. In **Table 2** four commonly used methods are shown. The mixture of chloroform and acetone is described for the detection of cholesterol in serum samples and can successfully be adapted to bile analysis. In system 4 three organic solvents with decreasing polarity are suggested for three consecutive development steps and can be used in automated multiple development devices.

If simple and fast one-step analysis of cholesterol and bile acids is required, solvent system 1 combined with the above described manganese detection reagent should be used, since cholesterol can be separated and identified easily by fast migration and its orange fluorescence. Other staining reagents containing either trichloroacetic acid or 8-anilinonaphthalene-sulfonic acid ammonium salt have been shown to react with cholesterol to fluorescent bands, and numerous other universal detection systems are described in the literature. Adaptation to bile analysis seems to be possible in most cases.

Use of the NCS reagent (1,2-naphthochinone-2-sulfonic acid sodium salt) leads to purple bands which can be easily detected and quantified with detection limit at 5 ng cholesterol.

Phospholipids

As for the other bile components, several solvent systems for separation of phospholipids are known. However, most of them were not developed for the analysis of bile samples, but for other biological ma-

terials or mixtures of purified standard compounds. Due to the fact that the most abundant phospholipid in bile samples is lecithin, three solvent systems able to separate phosphatidylcholine, phosphatidylethanolamine, phosphatidylserine and phosphatidylglycerol are shown in **Table 3**.

Some of the most commonly used and versatile detection reagents described in the sections above are also suitable for phospholipid detection both under UV and visible light. Detection with the 2,7-difluorescein reagent increases sensitivity and allows reliable and satisfactory quantification. Detection by a reagent mixture containing ammonium molybdate, sulfuric acid and ascorbic acid results in blue bands which can be easily detected and quantified by a TLC scanning device at a wavelength of 620 nm.

Conclusion

For decades, TLC has proven its advantages as a fast, inexpensive, reliable as well as highly reproducible technology in the analysis of bile, bile acids and bile acid derivatives. Especially in bile acid and cholesterol analysis several separation and detection systems have been developed which have shown convincing sensitivity and overall resolution.

Solvent systems allowing the simultaneous detection of bile acids, cholesterol and drug metabolites in a one-step analysis give a significant time advantage at reduced cost. In addition, the separation system and overall conditions can easily be adapted to the respective analytical problem in most cases.

Although the quantitative detection of phospholipids in bile does not play a key role in bile

Table 3 Solvent systems for phospholipid separation on silica gel plates

<i>System 1</i>	Room temperature
Chloroform	
Methanol	
Ammonia (conc.)	
Mixture 60 + 35 + 3 (v/v)	
<i>System 2</i>	Room temperature
Petroleum ether	
Chloroform	
Methanol	
Acetic acid	
Mixture 30 + 50 + 15 + 10 (v/v)	
<i>System 3</i>	Room temperature
Cyclohexane	
Isopropanol	
Double-distilled water	
Mixture 30 + 40 + 6 (v/v)	

analysis at the moment, there is still a need to develop accurate TLC methods for detailed separation of these lipids. Further investigations on the use of new TLC materials in the quantitative analysis of bile components are needed, as well as the adaptation of TLC methods to automated devices. Nevertheless, compared to other analytical tools TLC is the method of choice for fast routine use.

See also: **II/Chromatography: Thin-Layer (Planar):** Densitometry; Layers; Mass Spectrometry; Spray Reagents. **III/Bile Acids:** Liquid Chromatography; Gas Chromatography. **Clinical Diagnosis: Chromatography. Lipids:** Liquid Chromatography; Gas Chromatography; Thin-Layer (Planar) Chromatography. **Neonatal Meta-**

bolic Disorders: Detection: Thin-Layer (Planar) Chromatography.

Further Reading

Jork H, Funk W, Fischer W and Wimmer H (eds) (1989) *Dünnschichtchromatographie*, vol. 1a. Weinheim: VHC Verlagsgesellschaft.

Müllner S, Hofmann R, Saar K and Karbe-Thönges B (1992) Economic assay for the evaluation of bile acid sequestrants using ox bile and quantitative TLC analysis. *Journal of Planar Chromatography* 5: 408–416.

Rivas-Nass A and Müllner S (1994) The influence of critical parameters on the TLC separation of bile acids. *Journal of Planar Chromatography* 7: 276–285.

BIOANALYTICAL APPLICATIONS: SOLID-PHASE EXTRACTION



D. A. Wells, Sample Prep Solutions Company,
Maplewood, MN, USA

Copyright © 2000 Academic Press

Introduction

The quantification of drugs and metabolites in biological fluids (e.g. plasma, serum and urine) is one of the most active research fields in clinical and pharmaceutical analysis. Drug bioanalysis is important in clinical chemistry to demonstrate optimal drug therapy, because plasma drug concentrations relate to the therapeutic or toxic effects of a drug. Knowledge of the plasma drug concentration is used to determine why a patient does not respond to drug therapy or why a drug causes an adverse effect. Dosage adjustment by the physician is then warranted. Drug bioanalysis is important in pharmaceutical research to determine the pharmacokinetics and metabolic biotransformation of new drug molecules. It is a technique used throughout the development of all new drugs. In particular, during drug discovery, bioanalysis yields essential data that is used in the decision-making process of whether or not a new molecule should be a candidate for further development.

This chapter discusses the utility of solid-phase extraction (SPE) in comparison with other drug sample preparation techniques for bioanalysis. Several applications of SPE will be summarized in the clinical setting for therapeutic drug monitoring, and in the pharmaceutical research setting for drug discovery and development. The separation and detection techniques used for bioanalysis will be

examined, contrasting the use of high-pressure liquid chromatography (HPLC) in the clinical setting and the rapid proliferation of HPLC combined with tandem mass spectrometry (liquid chromatography/mass spectrometry/mass spectrometry or LC/MS/MS) for specific and sensitive detection of drugs for pharmaceutical bioanalysis.

Drug Sample Preparation Techniques

A reliable analytical method is achieved with efficient sample preparation, adequate chromatographic separation, and a sensitive detection technique. Detailed and exact guidelines exist for the validation of bioanalytical methods, which meet requirements agreed to by the Food and Drug Administration. The sample preparation step is an important component of each overall bioanalytical method, as it

- often concentrates an analyte to improve its limits of detection,
- removes unwanted matrix components that can cause interferences upon analysis, thus improving method specificity, and
- frees the analyte from matrix components so that it can be placed into a solvent suitable for injection into the chromatographic system.

Liquid/liquid extraction

A common sample preparation procedure used to isolate drug analytes from biological matrices is liquid/liquid extraction (LLE). It is quite effective at removing salts and proteins; water-soluble endogenous components often remain in the aqueous phase.

The organic phase containing the extracted analyte is isolated, evaporated to dryness, and reconstituted in liquid chromatographic mobile phase for analysis. One of the benefits of LLE is that with proper selection of solvent and pH, very clean extracts can be obtained with good selectivity for the target analytes. However, the disadvantages of LLE are that

- it is a very labour intensive procedure,
- it requires large volumes of organic solvents which can be expensive to purchase and dispose,
- exposure of personnel to these solvents can be hazardous to health,
- it cannot easily be automated,
- emulsions have been demonstrated to occur,
- evaporative losses can occur upon dry-down with volatile analytes.

Despite its drawbacks, LLE continues to be used for drug bioanalysis when there is adequate labour and its associated costs are not prohibitive, and the sample throughput can be adequately met.

Protein precipitation

A fast and simple method of sample preparation is protein precipitation, also referred to as 'dilute and shoot'. This nonselective technique involves adding a water-miscible organic solvent (e.g. acetonitrile) or inorganic acid (e.g. trichloroacetic acid, 10%) to the biological matrix (usually in a 3 : 1 or 4 : 1 ratio, v/v), centrifuging or filtering to remove precipitated proteins and injecting an aliquot of the diluted supernatant. This technique is often performed in pharmaceutical drug discovery laboratories as the first attempt to prepare samples for bioanalysis. Satisfactory analyses have been demonstrated with this rapid sample preparation approach, but it has disadvantages. This technique dilutes the sample by a factor of four or five, so it is useful only when sample levels are relatively high, typically in the low $\mu\text{g mL}^{-1}$ range. Also, matrix components are not efficiently removed, and thus may co-elute with the analyte in the isolated supernatant or filtrate. When present, these contaminants have been shown to interfere with detection techniques and lower the signal for the analyte of interest. This approach thus lacks selectivity and problems can arise from column fouling since the precipitation efficiency is not complete.

Solid-phase extraction

Solid-phase extraction has, during the last 18 years, become recognized as a preferred technique for extracting drug analytes from complex biofluids using adsorption chemistry. The attraction of the analyte for a solid phase adsorbent ('sorbent') is exploited to

the exclusion of other compounds through a selective wash step. Elution of the analyte is achieved with an organic solvent that disrupts the attraction to the solid sorbent. Solvent exchange is followed by analysis on a chromatographic system. The traditional format for SPE has been single disposable columns and cartridges. Its advantages are that multiple samples can be prepared in parallel, low volumes of solvents are used and procedures can be readily automated. The technology has been improved in recent years with the introduction of more selective solid sorbent chemistries, disc-based SPE devices, smaller bed mass sorbent loading, on-line SPE techniques and introduction of the 96-well plate format for improved productivity.

An on-line SPE technique has recently shown great utility. A commercial device (ProspektTM (Spark Holland)) combines an autosampler and a solvent delivery unit to aliquot liquid samples into the flow path of solvent. An SPE cartridge is preconditioned and is in-line with the solvent flow. The cartridge retains target analytes while a weak solvent elutes unretained salts and polar matrix components. An optimized sequence of solvents, each with increasing solvent strength, is used to wash out weakly retained components. A final elution with LC mobile phase elutes the analytes of interest from the SPE cartridge and onto an analytical column for chromatographic separation followed by detection.

The autosampler within this device can be preloaded with up to 160 samples and the entire tray can be analysed in an automated procedure. Its advantages are: unattended sample prep and analysis, minimized adsorptive losses, since sample transfers are not performed as in off-line techniques, and trace enrichment of analyte occurs. Some disadvantages are that analysis is serial (although a sample is always being analysed while another is being extracted and prepared for injection) and sample stability may be an issue for some drugs as a result of extended storage times in the autosampler.

Therapeutic Drug Monitoring

Therapeutic drug monitoring (TDM) is an established clinical specialty in which laboratory specialists quantify drug concentrations for the purpose of evaluating therapeutic response. Examples of drugs that are frequently subjected to TDM are antibiotics, antiarrhythmics, antiasthmatics, antidepressants, antiepileptics, and antineoplastics. These drugs possess a narrow range of therapeutic and safe plasma concentration. Therapeutic index (TI) is defined as the ratio between the maximum and minimum plasma concentrations of the drug's therapeutic

range. A narrow range is defined as a ratio of 2 to 3. A TI below 2 infers that the dose that yields a subtherapeutic response is close to the dose that produces toxicity. Most drugs have a TI of greater than 2.

The preferred technique for drug analysis is use of an immunoassay analyser (e.g. fluorescence polarization immunoassay, FPIA) because it is relatively quick, can be automated, and requires minimal technician training for execution. However, newer drugs requiring plasma quantification often do not have an immunoassay developed, so chromatography is almost always used at first. Drugs whose metabolites play a role in their efficacy and clinical interpretation also need to be determined by chromatography, which analyses multiple components simultaneously. Immunoassays are often not selective enough to distinguish between parent drug and metabolite, and interferences can adversely affect results for some drugs. Another difficulty facing clinical laboratories is that more accurate quantitation and detection requirements must be satisfied owing to lower dosages being administered. The proliferation of new drugs also increases the potential for concomitant administration. When the issue of cost is considered, in addition to the drawbacks listed above for immunoassays, chromatographic techniques can become quite attractive. Most often for clinical bioanalysis, detection methods involve ultraviolet or fluorescence detection coupled with liquid chromatographic separation.

Antidepressants

Tricyclic and newer antidepressant drugs are one of the most frequently monitored classes of therapeutic drugs in the clinical setting. Drug concentrations are monitored in patients for compliance and to ensure that therapeutic blood levels are reached. Also, patients sometimes take multiple antidepressant drugs, often from different physicians, which can be determined from a LC analysis. Immunoassays frequently cross-react with these drugs (e.g., imipramine, amitriptyline, desipramine and fluoxetine) and their metabolites. SPE has been used in some immunoassay kits to measure specifically one tricyclic drug. Overall, LC is advantageous because of its ability to monitor simultaneously multiple drugs and to resolve potential interferences from concomitantly administered drugs.

Solid-phase extraction methods for antidepressant drugs abound in the literature. These drugs are basic and can be adsorbed to reversed-phase sorbents such as C18 and C8 by both reversed-phase attraction and secondary interactions via cationic adsorption to silanols on the silica surface. Polar sorbents such as cyanopropyl, in which the cationic adsorption be-

comes primary, have also been used successfully. Methods for these drugs typically involve a solvent exchange of organic eluent for aqueous/organic mobile phase. Evaporative losses are always a concern with this step, but can be avoided by use of SPE discs, in which elution is accomplished with a small volume of mobile phase solution.

Corticosteroids

The measurement of steroids (prednisone, cortisone, prednisolone, cortisol, corticosterone, methylprednisolone) in blood is often inaccurate owing to interference from sample matrix and cross-reactivity with chemically similar steroids. For example, antiserum for cortisol is nonspecific and cannot differentiate between cortisol, its metabolites and therapeutically administered steroids. Again, SPE is a preferred technique for drug sample preparation. An efficient method has been reported using C8 sorbent discs, which allows for elution in mobile phase compatible solution for direct injection, eliminating the need for a tedious dry-down and reconstitution step. Steroids are released from proteins by incubation at room temperature with a HCl solution. Neutralization is accomplished by addition of a sodium borate solution. Following centrifugation, the supernatant is loaded onto conditioned C8 discs. A dilute methanol-water solution acts as an efficient wash to remove adsorbed proteins. Elution is performed with acetonitrile, followed by water. The resulting mixture is compatible with mobile phase for direct injection.

Cyclosporin

Cyclosporin, an immunosuppressant drug, has many metabolites and is commonly monitored for drug concentrations in the blood of patients who have received an organ transplant. Monoclonal antibody-based immunoassays are in use for this assay, as well as LC methods. Technology for immunoassay detection is constantly being improved, and the tests in use now are reliable. However, LC methods also function quite well, and the issue of antibody versus LC method often rests with cost analysis for a clinic. LC methods rely on SPE using whole blood and, when coupled with automation, can be quite cost effective. An advantage of LC is that it can simultaneously measure several metabolites.

The extraction procedures for cyclosporin are commonly reversed phase. Note that whole blood is preferred to avoid temperature-dependent cyclosporin redistribution. Mixing with acetonitrile-water haemolyses blood, and aliquots of the supernatant are loaded onto conditioned extraction columns. Wash steps may involve a weak concentration of

acetonitrile in water and elution is achieved with methanol or ethanol, or with an alcohol–water solution.

Antiepileptics

Plasma concentrations of antiepileptic drugs are often monitored during therapy, since a therapeutic range has been well defined. These drugs include phenytoin and carbamazepine and their metabolites, phenobarbital and newer agents such as lamotrigine. Solid-phase extraction is commonly performed using reversed-phase sorbents such as C8 and C18. The wash is performed with water, since the more hydrophilic drug lamotrigine is removed from the sorbent bed at low organic concentrations in water. Elution is efficiently accomplished with acetonitrile. Again, the use of the disc SPE formats can allow elution in volumes small enough to eliminate the evaporation step; a small elution volume of acetonitrile is mixed with water and the resulting solution is injected directly onto the liquid chromatograph.

Pharmaceutical Drug Discovery and Development

The discovery and development of new drug entities can be a perplexing task for analytical chemists. Drug molecules that demonstrate activity in receptor assays may exhibit structural characteristics that make them poor candidates for absorption *in vivo*, and other times they may be so rapidly metabolized as to limit their duration of activity in the body. Drugs may be difficult to separate on chromatographic columns, or be so labile that analytical techniques become a challenge. Once these challenges are overcome, the determination of drug concentrations in blood and urine yields the data used to understand the time course of drug action, or pharmacokinetics, in animals and man. Modern requirements for bioanalytical assays include specificity to determine parent drug from metabolites, sensitivity to detect concentrations of ng mL^{-1} and often lower, and speed.

The mainstay for detection following chromatographic separation was formerly ultraviolet or fluorescent detection. These techniques have served the analytical needs well over the years, but newer analytical instrumentation, namely the maturing of MS interfaces to LC, has allowed analytical chemists to use a more powerful detection technique for their routine analyses. The development of more potent drugs has also placed greater emphasis on the determination of lower concentrations of drugs, down to the pg mL^{-1} range. The answer to the analytical need for greater sensitivity, specificity and speed has been LC coupled with tandem mass-spectrometry (LC/MS/MS).

An application illustrating efficient sample preparation required prior to LC/MS/MS analysis is the determination of leukotriene LTE_4 in urine. Leukotrienes are biologically important molecules derived from arachidonic acid by the action of the enzyme 5-lipoxygenase. LTE_4 is difficult to analyse because it is unstable under a variety of conditions. The unique capabilities of MS have yielded detailed structural and metabolic information about these compounds. The extraction of LTE_4 from 5 mL human urine is accomplished by pH adjustment to 4.5 before loading onto a conditioned C18 SPE column or disc. A wash of 5% formic acid is used, followed by elution with a small volume of methanol. The eluate is evaporated and then reconstituted in mobile phase for analysis by LC/MS/MS. This extraction method is simple, yet selective for LTE_4 in human urine. Concentration range tested was 50 pg mL^{-1} to 10 ng mL^{-1} .

A recent advance in improving the throughput of drug development, made possible by LC/MS/MS techniques, is the simultaneous determination of mixtures of drug candidates in single analytical samples as a means to select optimal target drugs. In this case, animals are dosed with several test compounds at once; pooled plasma from multiple animals dosed with single compounds also has been shown. The specificity and sensitivity of the MS detection techniques now available have made this advancement possible. The data generated by this approach have been reported to yield meaningful pharmacokinetic data.

High Throughput Applications of SPE in Bioanalysis

The introduction and utilization of liquid chromatography interfaced with tandem MS techniques has resulted in a dramatic change in sample preparation techniques for drug bioanalysis. The speed of LC/MS/MS, in which run times are typically 1–3 min, allows more samples to be analysed per unit time than traditional HPLC analysis techniques, which require about 10–30 min per sample. The ability of the instrumentation to analyse samples faster than ever before, combined with the emergence of combinatorial chemistry techniques for drug discovery, have put more drugs into the drug development pipeline. The greater number of drugs under evaluation places increased demands on the resources available for pharmacokinetic drug metabolism support. As a result, sample preparation has become the rate-limiting step in achieving higher throughput in bioanalysis.

The pharmaceutical industry has responded to the challenge of higher throughput sample preparation by using a recent advance, SPE in a 96-well microtitre plate format. This technique utilizes single blocks or

plates that have 96 wells containing discs or packed beds of sorbent particles arranged in an 8-row \times 12-column rectangular matrix. Although the plates can be processed manually, instrumentation is preferred for processing liquids through the SPE plates. The advent of high throughput sample preparation formats, in combination with the specificity, sensitivity and speed of LC/MS/MS analytical techniques, have created a superior combination for the analytical chemist to meet the demands for faster sample processing and data generation to support the drug development process.

Conclusion

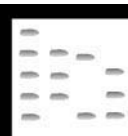
The future of drug bioanalysis using SPE is promising as more and more laboratories increase the usage of LC/MS/MS instrumentation and justify the need for high throughput SPE. LC/MS/MS instrumentation is now common in pharmaceutical laboratories and clinical laboratories are slowly beginning to demonstrate utility for mass spectrometry for certain drug classes, e.g. tacrolimus (FK506, an immunosuppressant). The 96-well plate format is finding its way into many bioanalytical applications; when coupled with automation, there is currently no faster sample preparation method. Individual SPE cartridges will continue to have a role in sample preparation, but 96-well plates will proliferate in pharmaceutical applications. More bioanalytical applications will adopt smaller sorbent mass products, as the productivity gains from reduced solvent volume are realized, especially using automation. As the sorbent mass in plates decreases, the number of applications that demonstrate elimination of the evaporation step by using small elution volumes of mobile phase compatible solution for direct injection will increase.

See also: **II/Extraction:** Solid-Phase Extraction. **III/Drugs and Metabolites:** Liquid Chromatography – Mass Spectrometry. **Solid-Phase Extraction with Discs.**

Further Reading

- Brewer E and Henion J (1998) Minireview. Atmospheric pressure ionization LC/MS/MS techniques for drug disposition studies. *Journal of Pharmaceutical Science* 87(4): 395–402.
- Hartmann C, Smeyers-Verbeke J, Massart DL and McDowall RD (1998) Review: Validation of bioanalytical chromatographic methods. *Journal of Pharmaceutical and Biomedical Analysis* 17: 193–218.
- Hoja H, Marquet P, Verneuil B *et al.* (1997) Applications of liquid chromatography-mass spectrometry in analytical toxicology: a review. *Journal of Analytical Toxicology* 21: 116–126.
- Lensmeyer GL, Darcey BA and Wiebe DA (1991) Application of a novel form of solid phase sorbent (Empore membrane) to the isolation of tricyclic antidepressants from blood. *Journal of Chromatographic Science* 29: 444–449.
- Lensmeyer GL, Onsager C, Carlson IH and Wiebe DA (1995) Use of particle-loaded membranes to extract steroids for HPLC analyses. Improved analyte stability and detection. *Journal of Chromatography A* 691: 239–246.
- McDowall RD, Doyle E, Murkitt GS and Picot VS (1989) Review: Sample preparation for the HPLC analysis of drugs in biological fluids. *Journal of Pharmaceutical and Biomedical Analysis* 7(9): 1087–1096.
- Wells DA (1999) 96-Well plate products for solid-phase extraction. *LC/GC* 17(7): 600–610.
- Wong SHY (1989) Review: Advances in liquid chromatography and related methodologies for therapeutic drug monitoring. *Journal of Pharmaceutical Biomedical Analysis* 7(9): 1011–1032.
- Wu Y, Lily Y-T, Henion JD and Krol GJ (1996) Determination of LTE₄ in human urine by liquid chromatography coupled with ionspray tandem mass spectrometry. *Journal of Mass Spectrometry* 31: 987–993.

BIOGENIC AMINES: GAS CHROMATOGRAPHY



R. Draisci, Laboratorio di Medicina Veterinaria, Istituto Superiore di Sanità, Roma, Italy
P. L. Buldini, CNR Lamel, Bologna, Italy
S. Cavalli, Laboratorio Applicazioni, Dionex Milano, Italy

Copyright © 2000 Academic Press

Introduction

The term 'biogenic amine' was proposed by Guggenheim in 1940 in order to define the low-molecular-

weight organic bases, produced by the decarboxylation of amino acids, that possess biological activity. Biogenic amines are receiving increasing interest because they are often present in foods, such as cheese, meat, and fish where they are used as a useful indicator of spoilage and markers of food quality. They occur naturally in the central nervous system, where they play an important role as neurotransmitters. Their presence in metabolic pathways in health and disease has been studied because of their biological activity as reported by Parvez *et al.*, and they are

Table 1 GC of biogenic amines with FID detection

Analyte	Chromatographic column	Carrier, type and flow rate	Injector temperature and program	Matrix	Sample treatment	Reference
Aliphatic monoamines, aliphatic polyamines, catecholamines, indolyl amines, imidazolyl amines (57 amines)	Dual fused silica capillary DB-5 DB-17, length 30 m, i.d. 0.25 mm, film thickness 0.11 μm	He	260°C, 260°C \rightarrow 4°C min ⁻¹ \rightarrow 280°C	Biological fluids	Two-phase isobutyloxy carbonylation, SPE purification and derivatization with <i>N</i> -methyl- <i>N</i> -(butyldimethylsilyl)-trifluoroacetamide	Kim <i>et al.</i> (1997)
Histamine, tyramine, putrescine, cadaverine, adrenaline, noradrenaline, tryptamine, dopamine, agmatine, spermine, spermidine, phenylethylamine	Fused silica capillary SE-54, length 25 m, i.d. 0.31 mm, film thickness 0.52 μm	He, 50 ml min ⁻¹	310°C, 125°C \rightarrow 10°C min ⁻¹ \rightarrow 300°C	Foods	Liquid-liquid extraction, SPE purification, derivatization with trifluoroacetic anhydride	Laleye <i>et al.</i> (1987)
Cadaverine, 1,3-diaminopropane, putrescine, isoputrescine, spermine, spermidine	Fused silica capillary cross-linked methyl siloxane deactivated by silanization, length 35 m, i.d. 0.20 mm, i.d. 0.20 mm, i.d. 0.20 mm, film thickness 0.11 μm	He, 0.5 ml min ⁻¹	300°C, 120°C \rightarrow 7°C min ⁻¹ \rightarrow 260°C	Biological fluids	SPE purification, derivatization with heptafluorobutyric anhydride	Muskiet <i>et al.</i> (1984)
1,3-Diaminopropane, putrescine, cadaverine, 3-aminopropylcadaverine, spermidine, <i>sym</i> -homospermidine, <i>sym</i> -norspermidine, spermine, <i>sym</i> -norspermine, thermospermine, canavalamine	0.5% KT-300 on Unipore HP packing, length 0.5 m, i.d. 3 mm	N ₂ , 80 ml min ⁻¹	285°C, 130°C \rightarrow 10°C min ⁻¹ \rightarrow 280°C	Plants	Ion exchange resin separation, derivatization with ethylchloroformate	Yamamoto <i>et al.</i> (1984)
Adrenaline, dopamine, noradrenaline, 5-hydroxytryptamine	5% OV-17 on Chromosorb W HP 80-100 mesh packing, length 1 m, i.d. 3 mm	N ₂ , 36 ml min ⁻¹	265°C isothermal	Biological tissues	Derivatization with pentafluorobenzoyl chloride and pyridine in acetonitrile	Bock and Waser (1981)

Reproduced with permission by Kim KR *et al.* (1997).

reported to be responsible for diseases related to their biological activity.

Muskiet *et al.* investigated a comparison of the popular high performance liquid chromatographic (HPLC) methods, whose chief advantage is a reduced sample pre-treatment, and other chromatographic techniques, such as gas chromatography, for the separation and determination of biogenic amines. In chromatographic methods, two main steps are neces-

sary: (a) the separation of amines from the matrix and (b) their determination. Pre-column derivatization is very often required for selectivity and sensitivity enhancement.

Sample Preparation

The first step is the most critical in terms of obtaining an adequate recovery for amines, because of the

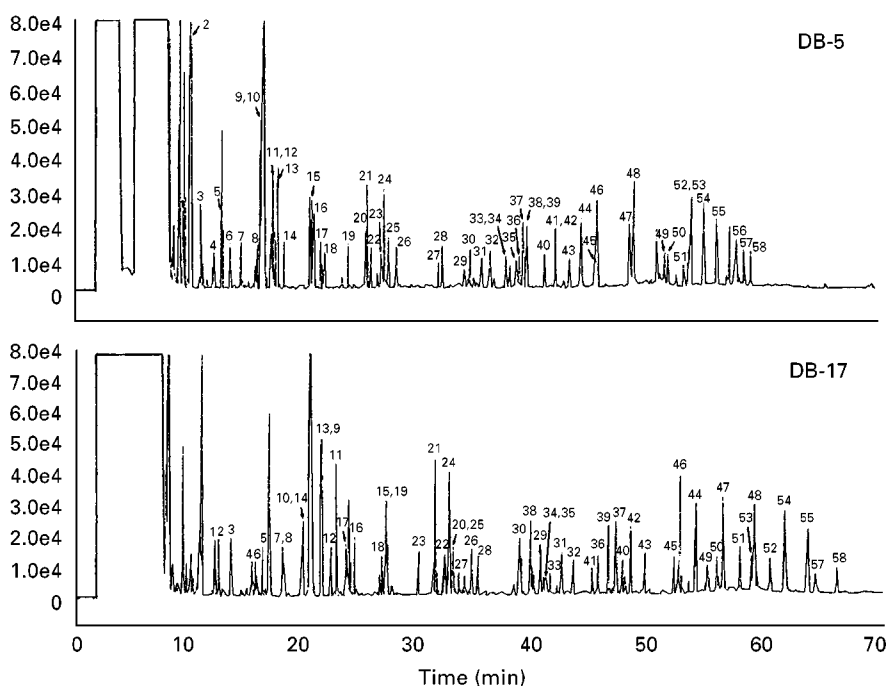


Figure 1 Dual chromatograms of amines as *N(O)*-isobOC, *O*-TBDMS derivatives separated on DB-5 and DB-17 (both 30 m \times 0.25 mm I.D., 0.11 μ m film thickness) dual-capillary column system. GC conditions are described in the text. Peaks: 1 = ethyl-methylamine; 2 = *tert*-butylamine; 3 = diethylamine; 4 = *sec*-butylamine; 5 = isobutylamine; 6 = diisopropylamine; 7 = *n*-butylamine; 8 = dipropylamine; 9 = pyrrolidine; 10 = isoamylamine; 11 = morpholine; 12 = piperidine; 13 = *n*-amylamine; 14 = diisobutylamine; 15 = thiazolidine; 16 = *n*-hexylamine; 17 = dibutylamine; 18 = cyclohexylamine; 19 = *n*-heptylamine; 20 = diphenylamine; 21 = *o*-toluidine; 22 = benzylamine; 23 = *n*-octylamine; 24 = *m*-toluidine; 25 = *p*-toluidine; 26 = β -phenethylamine; 27 = dihexylamine; 28 = *n*-decylamine; 29 = 2,4-dichlorobenzylamine; 30 = dicyclohexylamine; 31 = 1,3-diaminopropane; 32 = 3,4-dichlorobenzylamine; 33 = β -hydroxyphenethylamine; 34 = norephedrine; 35 = ephedrine; 36 = putrescine; 37 = 3,4-dimethoxyphenethylamine; 38 = diethanolamine-1; 39 = dibenzylamine; 40 = cadaverine; 41 = diethanolamine-2; 42 = histamine; 43 = 1,6-diaminohexane; 44 = tryptamine; 45 = 1,7-diaminoheptane; 46 = tyramine; 47 = 3-methoxytyramine; 48 = 5-methoxytryptamine; 49 = synephrine; 50 = octopamine; 51 = metanephrine; 52 = 3,4-dihydroxybenzylamine; 53 = normetanephrine; 54 = dopamine; 55 = spermidine; 56 = serotonin; 57 = epinephrine; 58 = norepinephrine. (Reproduced with permission from Kim KR *et al.* (1997).)

complexity of the matrices usually considered. All matrices pose different problems depending on their complexity so many clean-up techniques have been proposed making use of different extraction procedures, i.e. liquid-liquid, solid-phase extraction (SPE), etc. and a variety of solvents (perchloric, trichloroacetic, and hydrochloric acids and/or both polar and non-polar organic solvents).

In the second step, account must first be taken of the amine pre-column derivatization; this is often, if not always, necessary for enhancing the analyte response and selectivity. The other aim of pre-column derivatization is to obtain derivatives, which are both volatile and sufficiently stable for subsequent analyses. Gas chromatographic analysis of the amines requires one or more appropriate derivatization procedures to block active protons in amino and other polar groups and acylation, silylation, benzoylation, sulfonylation, phosphorylation and alkylloxycarbonylation have been used. Baker *et al.* have given an example of a complete study of the derivatization process in biogenic amines determination.

Chromatography

Separations are mostly performed on capillary columns whose length ranges from 15 to 30 m. The silica capillary columns are coated with different film thickness of methylsiloxane, methylphenylsiloxane, or cyanopropylphenylsiloxane polymers or polyethylene glycols. Only a few examples in the past reported the use of packed columns. Both isothermal and programmed temperature conditions are used.

Detection

Among the different detectors used in gas chromatography for biogenic amine analysis, the four detectors most commonly used are: flame ionization detector (FID), electron-capture detector (ECD), nitrogen-phosphorus detector (NPD) and mass spectrometry (MS).

Flame Ionization Detector (FID)

Some biogenic amines such as aliphatic mono-, di- and polyamines do not exhibit structural features that

permit their specific detection, in this case a non-specific detector such as flame ionization (FID) can be used, but the lack of sensitivity and/or selectivity may require the use of other detectors coupled with FID as shown in Table 1.

Bock and Waser acylated, via a single-step reaction, some biogenic amines for their specific and quantitative gas chromatographic assay. The retention times were found to be inversely proportional to their molecular weights and also to the number of the pentafluorobenzoyl groups. FID and ECD detector responses were compared; FID was selected for nanogram range and ECD for picogram range determinations, in order to optimize linearity and accuracy. The structure of the derivatives was confirmed by GC-MS technique.

Yamamoto *et al.* proposed a routine method for the determination of polyamines as their *N*-ethyloxycarbonyl derivatives. The sample preparation is simple and reproducible and the derivatives are stable. Also in this case, the identity of the derivatives was confirmed by GC-MS technique.

Muskiet *et al.* prepared extracts of acid-hydrolysed biological fluids by pre-purification with silica gel to give recoveries of better than 90%. The isolated compounds were derivatized and simultaneously determined by a capillary gas chromatographic method. FID and NPD detector responses were compared showing that NPD is both more selective and sensitive than FID.

Laleye *et al.* developed trifluoroacetylation for quantifying biogenic amines on a microgram scale in foods.

One of the most recent and notable applications of FID detector is the determination of 57 amines described in the paper of Kim *et al.* In their work they demonstrated the wide applicability of the FID supported by the simultaneous use of two capillary columns of different polarity, such as DB-5 and DB-17 for resolving all the considered amines, as shown in Figure 1. The proposed method is based on two-phase isobutyloxycarbonylation with a pH shift. The resulting derivatives are separated by SPE and the remaining hydroxyl groups are derivatized for dual capillary column gas chromatographic analysis. Response is linear in the 0.2–12-ppm range.

Electron-Capture Detector ECD

Examples of the use of the electron-capture detection (ECD) are given in Table 2.

Staruskiewicz and Bond developed a procedure for the quantitative determination of putrescine and cadaverine in foods. The amines were extracted with methanol and a dry residue of their hydrochloride salts was prepared. The salts were derivatized and both the reagent excess and reaction by-products were removed by means of an alumina column, minimizing in this way the solvent fronts and interfering extraneous peaks, some of which adversely affected the ECD response. The recovery of diamines was within the range 97 to 102%. Gas chromatographic separation was performed and the retention time for the derivatives of putrescine and cadaverine was found to be 4.3 and 5.7 min, respectively. When

Table 2 GC of biogenic amines with ECD detection

Analyte	Chromatographic column	Carrier, type and flow rate	Injector temperature and program	Matrix	Sample treatment	Reference
Histamine, <i>tele</i> -methylhistamine, <i>m</i> -, <i>p</i> -tyramine, 3-methoxytyramine, putrescine, cadaverine, tryptamine, spermine, spermidine, 2-phenylethylamine, 5-hydroxytryptamine	Fused silica capillary SE-54, length 15 m, i.d. 0.25 mm	He, 2 mL min ⁻¹	250°C, 105°C → 25°C min ⁻¹ → 240°C	Foods	Liquid-liquid extraction, derivatization with pentafluorobenzoyl chloride-benzene-acetonitrile	Baker <i>et al.</i> (1987)
Cadaverine, putrescine, spermine, spermidine	3% OV-17 on Chromosorb W HP packing length 1.5 m, i.d. 3 mm	He, 60 mL min ⁻¹	120°C → 15°C min ⁻¹ → 280°C	Biological fluids	SPE purification, derivatization with heptafluorobutyric anhydride	Fujihara <i>et al.</i> (1983)
Cadaverine, putrescine	3% OV-225 on Gas Chrom Q 100-120 mesh packing, length 1.8 m, i.d. 2 mm	He, 28 mL min ⁻¹	200°C, 180°C isothermal	Foods	Liquid-liquid extraction, derivatization with pentafluoropropionic anhydride, SPE purification	Staruszkiewicz and Bond (1981)

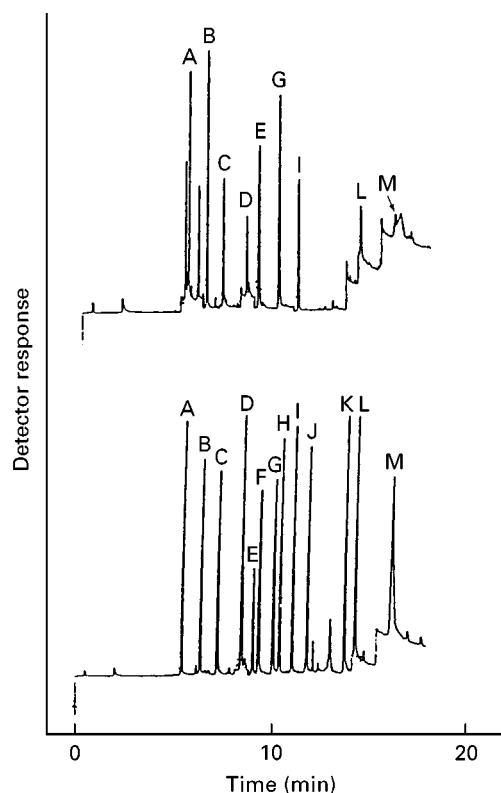


Figure 2 Gas chromatogram of extracts of bioactive amines from (top) cheese sample and (bottom) a solution of authentic standards. Extraction and derivatization were as described in the text. Derivatives of 2-phenylethylamine (A); 2-(4-chlorophenyl)ethylamine, internal standard (B); *tele*-methylhistamine (C); histamine (D); putrescine (E); tryptamine (F); cadaverine (G); *m*-tyramine (H); *p*-tyramine (I); 3-methoxytyramine (J); 5-hydroxytryptamine (K); spermidine (L); and spermine (M). Attenuation changes were programmed in to ensure that all peaks remained on scale for the purpose of illustration. (Reproduced with permission from Baker GB *et al.* (1987).)

compared to a nitrogen-specific detector, the ECD had greater sensitivity. Less than 1 ppm of diamine in the food can be quantitated with a coefficient of variation lower than 3.0%.

Fujiyama *et al.* developed a sensitive and selective method for the estimation of polyamines in biological fluids after their separation from other compounds and derivatization. These derivatives are well resolved within 15 min with detection limit of 0.1 pmol for putrescine and cadaverine and 0.02 pmol for spermine and spermidine.

Baker *et al.* proposed a method based on extractive derivatization of the amines with a perfluoroacylating agent under basic aqueous conditions. Polyamine recovery was virtually quantitative, whilst for the other amines the recoveries ranged from 70 to 85%. Derivatives showed good chromatographic properties and ECD was used for enhancing sensitivity of biogenic amines in food samples. The derivative structures

were confirmed by GC-MS. The detection limits (peak/noise ratio = 2) of the different types ranged between 5 and 20 pg on-column and calibration curves were linear over two orders of magnitude.

A typical chromatogram obtained with this technique is shown in Figure 2, that is relative to the determination of perfluoroacetyl derivatives in foods. The method of Baker *et al.* resulted in a reference paper for all later authors using the ECD.

Nitrogen-Phosphorus Detector (NPD)

Another very specific detector for amines is the nitrogen-phosphorus detector (NPD). The most recent papers relative to the use of this detector for biogenic amine determination are reported in Table 3.

One of the first comparisons between FID and another detector (NPD) appeared in the paper of Muskiet *et al.* These authors prepared extracts of acid-hydrolysed biological fluids by pre-purification with silica gel. The isolated compounds were derivatized and simultaneously determined by capillary gas chromatography with nitrogen-phosphorus detection. Their comparison between typical chromatograms obtained with FID and NPD is shown by an example in Figure 3.

Perez-Martin *et al.* also compared FID and NPD results, but contrary to Muskiet *et al.* they considered both detector responses as equivalent. These authors treated seafoods with trichloroacetic acid and then extracted the resulting solution with benzene under highly basic conditions. Retention times are 1.03 min for dimethylamine and 1.35 min for trimethylamine.

Hessels *et al.* developed a capillary gas chromatographic method with NPD for the determination of the *N'*-acetylspermidine catabolite in biological fluids and compared it with the GC-MS method of Van den Berg *et al.*, shown in Table 4. The results were within a relative standard deviation of 3%.

One of the most recent applications of NPD for polyamines profiling is the work of Dorhout *et al.* that used capillary gas chromatography with NPD for the determination of polyamines, *N*-acetylated polyamines and the polyamine analogues *N'*,*N''*-bis(ethyl)norspermine and 1,19-bis(ethylamino)-5,10,15-triazanonadecane in biological samples. The suggested method provided for the use of four internal standards and pre-purification steps comprising deproteinization and isolation on silica at pH 9.0 with 70–90% recoveries depending on polyamine type. The precision is better than 7%, while the detection limits (peak/noise ratio = 2) of the different components ranged from 0.4 to 0.7 pmol. Figure 4 shows a typical chromatogram obtained with the method described in the Dorhout work.

Table 3 GC of biogenic amines with NPD detection

Analyte	Chromatographic column	Carrier, type and flow rate	Injector temperature and program	Matrix	Sample treatment	Reference
Putrescine, cadaverine, spermine, spermidine, 1,3-diaminopropane	Fused silica capillary methyl silicone phase, length 37.5 m, i.d. 0.20 mm, film thickness 0.11 μm	He, 0.6 mL min^{-1}	260°C, 120°C \rightarrow 5°C min^{-1} \rightarrow 260°C \rightarrow 2°C min^{-1} \rightarrow 280°C	Biological tissues	Deproteinization, SPE purification and derivatization with heptafluorobutyric anhydride	Dorhout <i>et al.</i> (1997)
Polyamines, <i>N</i> -acetylspermidine	Fused silica capillary HP 17, length 25 m, i.d. 0.20 mm, film thickness 0.17 μm		260°C, 180°C \rightarrow 3°C min^{-1} \rightarrow 270°C	Biological fluids	Alkalization, liquid-liquid extraction and SPE purification	Hessels <i>et al.</i> (1991)
Trimethylamine, dimethylamine	4% Carbowax 20M + 0.8% KOH on Carbowax B and Chromosorb 103 packing, length 1.8 m, i.d. 2 mm	N ₂ , 25 mL min^{-1}	250°C, 115°C isothermal	Seafoods	Liquid-liquid extraction	Perez-Martin <i>et al.</i> (1987)
Cadaverine, 1,3-diaminopropane, putrescine, isoputrescine, putrescine, spermine, spermidine	Fused silica capillary cross-linked methyl silicone and siloxane deactivated, length 35 m, i.d. 0.20 mm, film thickness 0.11 μm	He, 0.5 mL min^{-1}	300°C, 120°C \rightarrow 7°C min^{-1} \rightarrow 260°C	Biological fluids	SPE purification, derivatization with heptafluorobutyric anhydride	Muskiet <i>et al.</i> (1984)

Reproduced with permission from Muskiet FAJ *et al.* (1984).

Mass Spectrometry (MS)

The actual trend in biogenic amine gas chromatographic analysis is to establish a complete profile of all the important amines by using a single method, thus the widest used detector is mass spectrometry (MS) (Table 4). This technique was formerly used in conjunction with other detectors for confirmation purposes only.

The advantage of MS over other detection systems is based on the possibility of identifying compounds with a high degree of specificity. This can be realized using high resolution capillary gas chromatography combined with the monitoring of characteristic ions in the mass spectrum of a compound (GC-MS). GC-MS can afford characteristic ratios of ion intensities or the m/z value of a particular ion. These parameters may be changed in a predictable manner by derivatization processes in order to provide additional proof of identity.

Duncan *et al.* compared the results obtained using both HPLC with electrochemical detection and GC-MS in the single-ion monitoring mode (SIM) when applied to dopamine and norepinephrine (noradrenaline) determination, after a single-step alumina extraction, in a selection of food and beverage

samples. The results provided an opportunity for qualitative and quantitative comparison of these two techniques and discussion of their respective merits and limitations.

The specificity associated with SIM is responsible for a significant reduction in the complexity of data obtained when using a GC-MS system. The use of appropriate deuterated internal standards eliminates the influence of the original sample matrix, minimizing sample pre-treatment, and allows precise multi-component quantitation at low levels.

Davis *et al.* preferred to use GC-MS in the multiple-ion detection mode (MID) after derivatization with two different reagent systems and precipitation of protein with sulfosalicylic acid prior to extraction, in order to analyse a large number of biogenic amines and their metabolites in a single run.

Van den Berg *et al.* described the identification of a metabolite of spermidine by GC-MS in biological fluids of normal healthy humans and cancer patients. The quantification was based on stable isotope dilution mass fragmentography monitored at m/z 185 and 188.

Fujihara *et al.* measured putrescine metabolism in biological fluids. Putrescine was decomposed by oxidative deamination to form ammonia that was

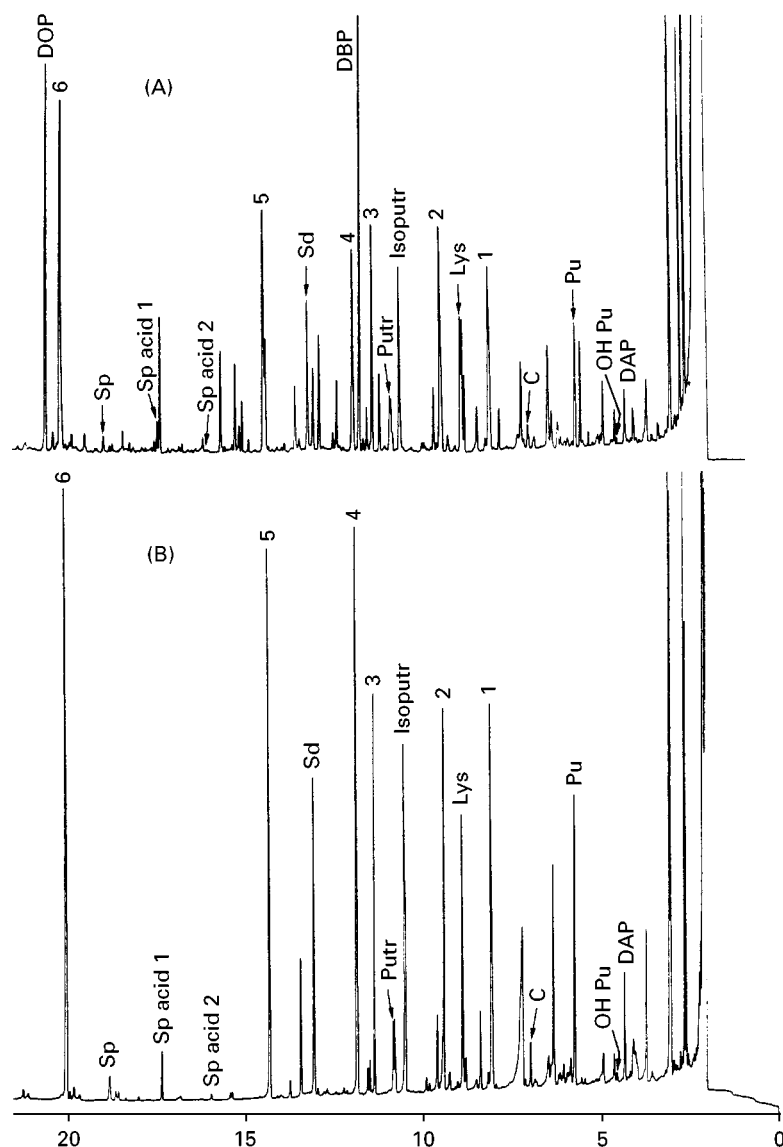


Figure 3 Comparison between typical chromatograms obtained with flame-ionization (A) and nitrogen-phosphorus (B) detectors after capillary gas chromatography of methyl-heptafluorobutyryl-derivatized extracts of acid-hydrolyzed urine from a normal man. *Abbreviations:* DAP, 1,3-diaminopropane; OH Pu, 2-hydroxyputrescine; Pu, putrescine; C, cadaverine; 1, 1,6-diaminohexane; Lys, lysine; 2, 1,7-diaminoheptane; *Isoputr*, isoputrescine; *Putr*, putrescine; 3, *N*'-methylisoputrescine; DBP, dibutylphthalate (plasticizer, tentatively identified by gas chromatography-mass spectrometry); 4, *bis*(3-aminopropyl)amine; *Sd*, spermidine; 5, *N*-(3-aminopropyl)-1,5-diaminopentane; *Sp acid 2*, *N*, *N*'-bis(2-carboxyethyl)-1,4-diaminobutane; *Sp acid 1*, *N*-(3-aminopropyl)-*N*'-(2-carboxyethyl)-1,4-diaminobutane; *Sp*, spermine; 6, *N*, *N*'-bis(3-aminopropyl)-1,5-diaminopentane; DOP, dioctylphthalate (plasticizer). 1 through 6 are added internal standards. Time axis, minutes. (Reproduced, with permission, from Muskiet FAJ, van den Bergh GA, Kingma AW, Fremouw-Ottenvangers DC and Halie R (1984) Total polyamines and their non- α amino acid metabolites simultaneously determined in urine by capillary gas chromatography, with nitrogen-phosphorus detector; and some clinical applications. *Clinical Chemistry* 30: 687.)

determined by GC-MS. Its quantification was based on mass fragmentography synchronously monitored at m/z 195, 211 and 212. The method is inferior to isotope mass spectrometry, but its speed, reproducibility (better than 0.5%) and sensitivity are superior.

Shafi *et al.* applied GC-MS in the negative ion chemical ionization mode (NICI) for the determination of biogenic amines. After derivatizing the amines and separating them by solvent extraction, they hydro-

lysed the phenolic esters and converted the free hydroxyl groups to trimethylsilyl esters and analysed these derivatives by GC-MS-NICI. The molecular ion of these derivatives (together with the isotope peaks) carried more than 60% of the ion current, which made the method highly specific and gave a potential limit of detection below the picogram level.

This technique has the advantage that the silylating reagent may be changed in order to shift both the m/z

Table 4 GC-MS of biogenic amines

Analyte	Chromatographic column	Carrier, type and flow rate	Injector temperature and program	Matrix	Sample treatment	Reference
<i>p</i> -Tyramine, <i>p</i> -octopamine, <i>p</i> -synephrine, dopamine, noradrenaline, adrenaline, 5-hydroxytryptamine	Fused silica capillary HP 1, length 12.5 or, 25 m, i.d. 0.20 mm, film thickness 0.2 μ m	He, 40 mL min ⁻¹	250°C, 100°C → 10°C min ⁻¹ → 300°C	Biological tissues	Liquid-liquid extraction and derivatization with 5-ditrifluoromethylbenzoyl chloride and isopropyl dimethylsilyl- <i>N</i> -methyltrifluoroacetamide	Shafi (1995)
Indole ethylamines	Fused silica capillary OV 1, length 12 m, i.d. 0.20 mm, film thickness 0.33 μ m		260°C, 100°C → 40°C min ⁻¹ → 300°C	Biological fluids	Formaldehyde addition, hydrolysis, derivatization with methyl chloroformate, liquid-liquid extraction and SPE purification	Musshoff <i>et al.</i> (1993)
Phenolamines, catecholamines, 5-hydroxytryptamine, phenylalanine, tyrosine, dopamine, <i>p</i> -tyramine, <i>p</i> -synephrine, <i>p</i> -octopamine, adrenaline, noradrenaline	Fused silica capillary SGE BP1, length 12 m, i.d. 0.20 mm, film thickness 0.25 μ m	He	250°C, 100°C → 10°C min ⁻¹ → 300°C	Biological tissues	Liquid-liquid extraction and derivatization with butyldimethylsilyl chloride and ditrifluoromethylbenzyl bromide	MacFarlane <i>et al.</i> (1991)
<i>p</i> -tyramine, <i>m</i> -, <i>p</i> -synephrine, <i>m</i> - <i>p</i> -octopamine, dopamine, 5-hydroxytryptamine, noradrenaline, adrenaline, dihydroxybenzylamine	Fused silica capillary HP1, length 12.5 m or 25 m, i.d. 0.20 mm	He	250°C, 100°C → 10°C min ⁻¹ → 300°C	Biological tissues	Extraction-derivatization with difluoromethylbenzoyl chloride, liquid-liquid extraction, derivatization with bistrimethyl silylacetamide (or <i>t</i> -butyldimethylsilyl chloride and imidazole) SPE purification	Shafi <i>et al.</i> (1989)
Putrescine	3% OV-1 on Chromosorb W AW DMCS 80-100 mesh packing, length 2 m, i.d. 3 mm	He, 60 mL min ⁻¹	280°C, 280°C isothermal	Biological fluids	Derivatization of the ammonia resulting from metabolism with pentafluorobenzoyl chloride	Fujiyama <i>et al.</i> (1986)
Spermidine	Fused silica capillary CP-Sil-19, length 25 m, i.d. 0.32 mm, film thickness 0.20 μ m	He, 1 mL min ⁻¹	250°C, 200°C → 10°C min ⁻¹ → 260°C	Biological fluids	Liquid-liquid extraction, derivatization with acetyl chloride	Van den Bergh <i>et al.</i> (1986)
Dopamine, adrenaline, noradrenaline, phenylethylamine, phenylethanolamine, tryptamine, <i>m</i> -, <i>p</i> -tyramine, <i>m</i> -, <i>p</i> -octopamine	Fused silica capillary DB-1, length 60 m, i.d. 0.32 mm	He	140°C → 10°C min ⁻¹ → 240°C	Biological fluids	Deproteination and derivatization with methanolic hydrogen chloride (or trifluoroethanol) and pentafluoropropionic anhydride	Davis <i>et al.</i> (1986)
Dopamine, norepinephrine (noradrenaline)	3% OV-17 packing, length 0.7-1 m	He, 30 mL min ⁻¹	222°C, 146°C → 200°C	Foods, beverages	SPE purification, derivatization with trifluoroacetic anhydride and trifluoroethanol	Duncan <i>et al.</i> (1984)

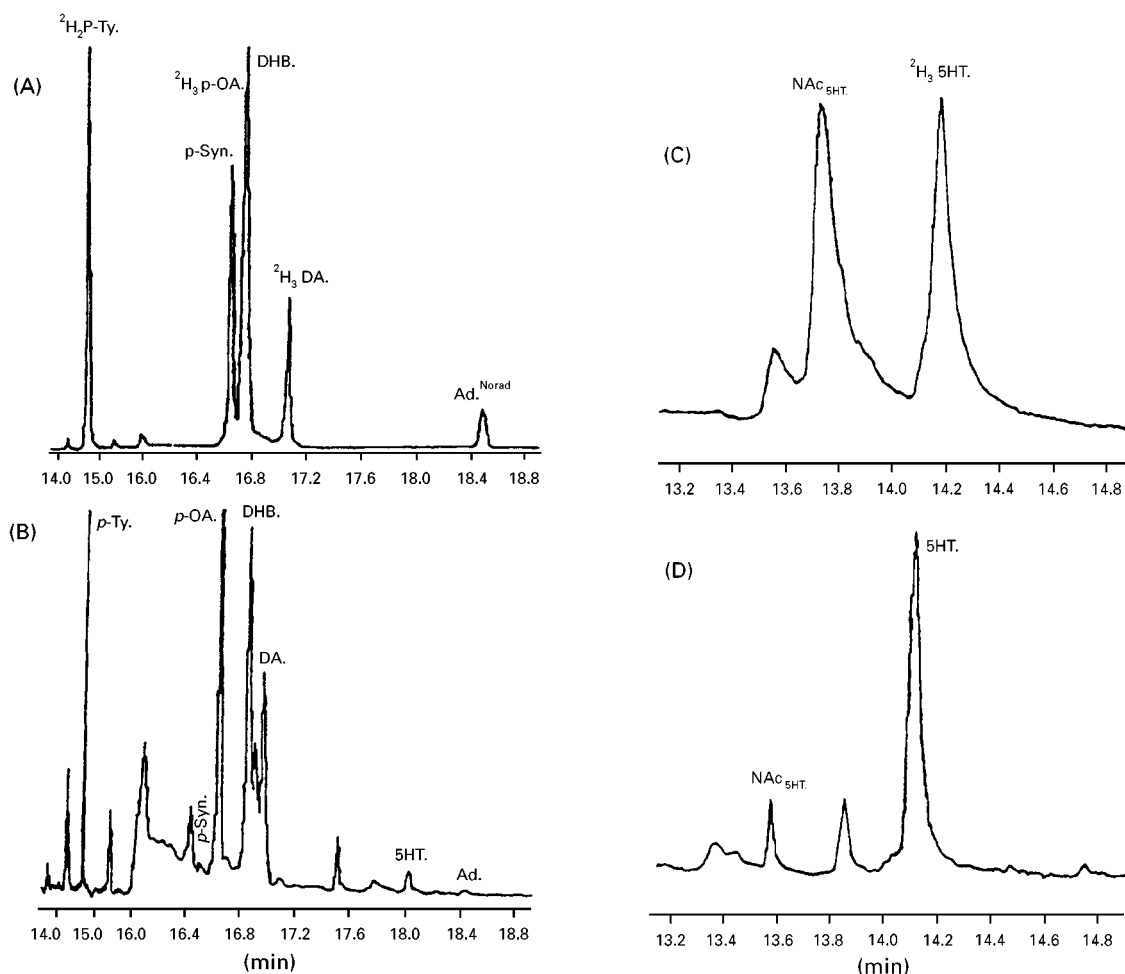


Figure 4 (A) NICI SIM trace of DTFMB-IPDMS derivatives of deuterated and undeuterated biogenic amines (each 20 ng) and (B) the corresponding endogenous biogenic amines from a single brain of American cockroach after addition of deuterated internal standards (20 ng). (C) NICI SIM trace of Pr-PFP derivatives of deuterated and undeuterated biogenic amines (each 20 ng) and (D) the corresponding endogenous biogenic amines from a single brain of American cockroach after addition of deuterated internal standards (20 ng). (Reproduced, with permission, from Shafi N (1995) Identification and quantitative determination of biogenic amines and their metabolites by gas chromatography negative ion chemical ionisation mass spectrometry (GC-NICIMS) *Journal of the Chemical Society of Pakistan* 17: 103.)

value of the molecular ion and the retention time of the derivative to ensure that its identification is unequivocal. In the same laboratories MacFarlane *et al.* used a similar procedure, but they state that the ion current was generally carried by four or five large ions.

Musshoff *et al.* derivatized the compounds formed by reaction of formaldehyde with biogenic amines in biological fluids in order to avoid the simultaneous formation of these compounds via condensation. These derivatization products are stable and can be well purified from most of the interfering matrix compounds by liquid-liquid and solid-phase extraction. They have good GC-MS properties, therefore the retention times, together with the diagnostic mass fragments (at least three) and the specific ion ratios, can be used for separation and identification.

Shafi summarized the use of different derivatizing agents, whose scope was shifting both the m/z value and the retention time in order to ensure the unequivocal identification of amines (Figure 5). In each case, the principal ion in the mass spectrum was the molecular ion, which carried almost all of the ion current under negative ion chemical ionization conditions; the sensitivity of this method of derivatization was 1 pg of biogenic amine on-column.

The possibility of easy determination of biogenic amines by other chromatographic techniques, such as HPLC, has reduced the interest in updating the existing gas chromatographic methods.

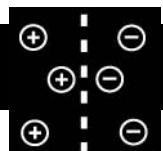
See also: II/Chromatography: Gas: Column Technology; Derivatization; Detectors: General (Flame Ionization

Detectors and Thermal Conductivity Detectors); Detectors: Mass Spectrometry; Detectors: Selective. **Extraction:** Solid-Phase Extraction.

Further Reading

- Baker GB, Coutts RT and Holt A (1994) Derivatization with acetic anhydride: applications to the analyses of biogenic amines and psychiatric drugs by gas chromatography and mass spectrometry. *Journal of Pharmacological and Toxicological Methods* 31: 141.
- Baker GB, Wong JTF, Coutts RT and Pasutto FM (1987) Simultaneous extraction and quantitation of several bioactive amines in cheese and chocolate. *Journal of Chromatography* 392: 317.
- Bock UEG and Waser PG (1981) Gas chromatographic determination of some biogenic amines as their pentafluorobenzoyl derivatives in the picogram range and its applicability to biological materials. *Journal of Chromatography* 213: 413.
- Davis BA, Durden DA and Boulton AA (1986) Simultaneous analysis of twelve biogenic amine metabolites in plasma, cerebrospinal fluid and urine by capillary column gas chromatography-high-resolution mass spectrometry with selected-ion monitoring. *Journal of Chromatography B* 374: 227.
- Dorhout B, Kingma AW, de Hoog E and Muskiet FAJ (1997) Simultaneous determination of polyamines N-acetylated polyamines and the polyamine analogues BE-3-3-3 and BE-4-4-4-4 by capillary gas chromatography with nitrogen-phosphorus detection. *Journal of Chromatography B* 700: 23.
- Duncan MW, Smythe GA, Nicholson MV and Clezy PS (1984) Comparison of high-performance liquid chromatography with electrochemical detection and gas chromatography-mass fragmentography for the assay of salsolinol, dopamine and dopamine metabolites in food and beverage samples. *Journal of Chromatography B* 336: 199.
- Fujihara S, Nakashima T and Kurogochi Y (1983) Determination of polyamines in human blood by electron-capture gas-liquid chromatography. *Journal of Chromatography B* 277: 53.
- Fujihara S, Nakashima T and Kurogochi Y (1986) Determination of $^{15}\text{NH}_3$ by gas chromatography-mass spectrometry. Application to the measurement of putrescine oxidation by human plasma. *Journal of Chromatography B* 383: 271.
- Guggenheim M (1940) *Die biogenen Amine*. Basel: Karger.
- Halász A, Baráth A, Simon-Sarkadi L and Holzapfel W (1994) Biogenic amines and their production by microorganisms in food. *Trends in Food Science and Technology* 5: 42.
- Hassels J, Kingma AW, Sturkenboom MCJM, Elzinga H, van den Bergh GA and Muskiet FAJ (1991) Gas chromatographic determination of N-acetylispoptreanine- γ -lactam, a unique catabolite of N¹-acetylspermidine. *Journal of Chromatography B* 563: 1.
- Kim KR, Paik MJ, Kim JH, Dong SW and Jeong DH (1997) Rapid gas chromatographic profiling and screening of biologically active amines. *Journal of Pharmaceutical and Biochemical Analysis* 15: 1309.
- Laleye LC, Simard RE, Gosselin C, Lee BH and Giroux RN (1987) Assessment of Cheddar cheese quality by chromatographic analysis of free amino acids and biogenic amines. *Journal of Food Science* 52: 303.
- MacFarlane RG, Midgley JM and Watson DG (1991) Biogenic amines: their occurrence, biosynthesis and metabolism in the locust, *Schistocerca gregaria*, by gas chromatography-negative-ion chemical ionisation mass spectrometry. *Journal of Chromatography B* 562: 585.
- Muskiet FAJ, van den Bergh GA, Kingma AW, Fremouw-Ottenvangers DC and Halie R (1984) Total polyamines and their non- α -amino acid metabolites simultaneously determined in urine by capillary gas chromatography, with nitrogen-phosphorus detector; and some clinical applications. *Clinical Chemistry* 30: 687.
- Muskiet FAJ, Dorhout B, van den Bergh GA and Hessels J (1995) Investigation of polyamine metabolism by high-performance liquid chromatographic and gas chromatographic profiling methods. *Journal of Chromatography B* 667: 189.
- Musshoff F, Daldrup TH and Bonte W (1993) Gas chromatographic-mass spectrometric screening procedure for the identification of formaldehyde-derived tetrahydro- β -carbolines in human urine. *Journal of Chromatography B* 614: 1.
- Parvez S, Nagatsu T and Parvez H (ed.) (1983) *Methods of Biogenic Amine Research*. Amsterdam: Elsevier.
- Perez-Martin RI, Franco JM, Molist P and Gallardo JM (1987) Gas chromatographic method for the determination of volatile amines in seafoods. *International Journal of Food Science and Technology* 22: 509.
- Shafi N (1995) Identification and quantitative determination of biogenic amines and their metabolites by gas chromatography negative ion chemical ionisation mass spectrometry (GC-NICIMS). *Journal of the Chemical Society of Pakistan* 17: 103.
- Shafi N, Midgley JM, Watson DG, Smail GA, Strang R and MacFarlane RG (1989) Analysis of biogenic amines in the brain of the American cockroach (*Periplaneta americana*) by gas chromatography negative ion chemical ionisation mass spectrometry. *Journal of Chromatography B* 490: 9.
- Staruszkiewicz WF Jr and Bond JF (1981) Gas chromatographic determination of cadaverine, putrescine and histamine in foods. *Journal of the Association of Official Analytical Chemists* 64: 584.
- Van den Berg GA, Kingma AW, Elzinga H and Muskiet FAJ (1986) Determination of N-(3-acetamidopropyl) pyrrolidin-2-one, a metabolite of spermidine, in urine by isotope dilution mass fragmentography. *Journal of Chromatography B* 383: 251.
- Yamamoto S, Iwado A, Hashimoto Y, Aoyama Y and Makita M (1984) Gas chromatography-mass spectrometry of polyamines as their N-ethyloxycarbonyl derivatives and identification of sym-homospermidine and sym-norspermine in mosses and ferns. *Journal of Chromatography* 303: 99.

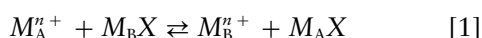
BIOLOGICAL SYSTEMS: ION EXCHANGE



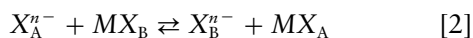
R. J. P. Williams, Imperial College,
London, UK

Copyright © 2000 Academic Press

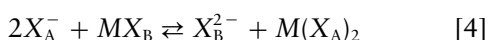
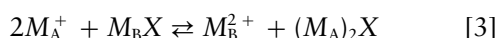
There are two very different processes which are described under the heading of ion exchange within biological systems. The first is exchange in an aqueous environment of two different ions, M_A and M_B , held by a molecule in free solution, or in a precipitate, or on a membrane surface:



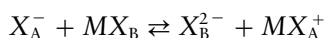
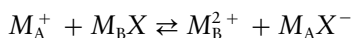
Here, M is a metal cation and X is an anion, often an organic molecule which can be as large as a protein or DNA. Exchange of anions is also possible, as in the equilibrium:



Both eqns [1] and [2] have been written for exchanging ions of equal charge type n . This is not a necessary condition, so we can also consider:



Again, the charge balance shown so far in the equations is not essential, so we must also examine the situation of electrogenic exchange:



where charge distribution is associated with MX changes. Before considering the second way in which ion exchange can occur across a membrane, we give one or two examples of ion exchange to and from a bound condition in a single aqueous solution.

Exchange of Major Cations and Anions in Cells

The major small cations and anions in cells which undergo ready exchange are shown in Table 1. They may associate with one another in rapid exchange or

bind to surfaces of proteins, other polymers, precipitates or membranes and exchange rapidly or slowly.

Consider a magnesium protein such as Mg^{2+} parvalbumin, where parvalbumin is a common anionic metal-ion-binding protein in muscle cells. When the protein, which is magnesium bound in the cell, is exposed to calcium, the reaction of exchange occurs: Ca^{2+} parvalbumin is formed and Mg^{2+} is freed. If the initial protein complex had been Na^{+} parvalbumin, then replacement by Ca^{2+} would have been electrogenic, unless of course two Na^{+} ions had been bound originally.

A second example of exchange on the surface of a polymer is provided by polynucleotides such as RNA and DNA. These polymers have anionic phosphate backbones and their negative charges are balanced, not entirely randomly, by exchanging cations, including particularly K^{+} , Mg^{2+} and ammonium derivatives. The positive charge, like the negative charge, in an exchanging system can also be carried on a large molecule and in biology there are many polyamines and positively charged proteins, such as histones, which bind DNA. They can bind and exchange anions such as HPO_4^{2-} and SO_4^{2-} .

A further example of biological metal ion exchange in one aqueous solution now involving a solid precipitate is the case of bone, which we can write as $(Ca^{2+})_2(OH^{-})PO_4^{3-}$ for simplicity. Bone scavenges many other cations by exchange and contains considerable amounts of Mg^{2+} and even Al^{3+} in place of Ca^{2+} . Bone also exchanges Ca^{2+} for protons (H^{+}). This mineral is additionally an anion-exchanging solid in which some OH^{-} is replaced by F^{-} (a process used in the protection of teeth). To some extent, a pair of $OH^{-} + PO_4^{3-}$ can be replaced by $2CO_3^{2-}$ anions. Notice that exchange can be electrogenic when charge is left on the surface of the bone mineral.

The last example of this relatively simple exchange is at the surface of membranes. All biological membranes carry negative charge due to covalently bound phosphate or carboxylate groups. Since the charges are quite close-packed, the membranes have a considerable affinity for cations and all membranes have associated K^{+} and Mg^{2+} (mainly internally) and Na^{+} and Ca^{2+} (mainly externally) associated with their surfaces. The outermost coats of cell walls in Gram-negative bacteria are also anionic and are stabilized by exchangeable cation, often Ca^{2+} , incorporation.

Table 1 Major small cations and anions of cells

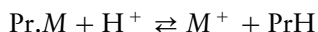
Cation	Anion
Na^+ largely rejected	Cl^- largely rejected
K^+ cytoplasmic	HPO_4^{2-} cytoplasmic
Mg^{2+} cytoplasmic	SO_4^{2-} cytoplasmic
Ca^{2+} rejected (vesicular)	HCO_3^- balanced
RNH_3^+ cytoplasmic	RCO_2^- cytoplasmic
	ROPO_3^{2-} cytoplasmic

H^+ (pH 7); OH^- (pH 7).

Exchange of Trace Elements

Major exchange of trace elements (Table 2) occurs from many carrier or buffer proteins. For example, iron is carried in the blood stream of higher animals by the protein transferrin in the form of Fe^{3+} , in co-association with the carbonate anion, CO_3^{2-} . The uptake into the cell involves the transfer of the whole protein to a vesicle, the lysozyme, which is much more acidic than blood. There the protein loses both iron and CO_3^{2-} , which are exchanged for bound protons. The iron is processed further into the cell as Fe^{2+} , only to be reoxidized in a precipitate inside a protein matrix, ferritin, where it is stored as $\text{Fe}(\text{OH})_3$. From this small particle, iron exchanges into the cytoplasm, to give a great variety of compounds (see Figure 1) for the case of bacteria.

A second example of cytoplasmic ion exchange of trace elements involves both copper and zinc bound to sulfur-containing proteins. The proteins release copper or zinc (M) to the cytoplasm in equilibrium with free hydrogen ions:



where Pr is a protein such as metallothionein. This equilibration ensures constant levels of Zn^{2+} and Cu^+ in the cytoplasm.

Trace anions are also carried in the blood stream by special proteins and are then transported into cells. The proteins which transfer SO_4^{2-} , SeO_4^{2-} and MoO_4^{2-} are known to be similar to transferrin.

Table 2 Trace cations and anions of cells

Cation	Anion
Mn^{2+} vesicular	SeO_4^{2-} cytoplasmic
$\text{Fe}^{2+}/\text{Fe}^{3+}$ cytoplasmic (precipitate)	MoO_4^{2-} cytoplasmic
Co^{2+} cytoplasmic	I^- cytoplasmic
Ni^{2+} vesicular	NO_3^- cytoplasmic
Cu^{2+} rejected	
Zn^{2+} cytoplasmic	

Many of the ions are held in complexes with organic agents.

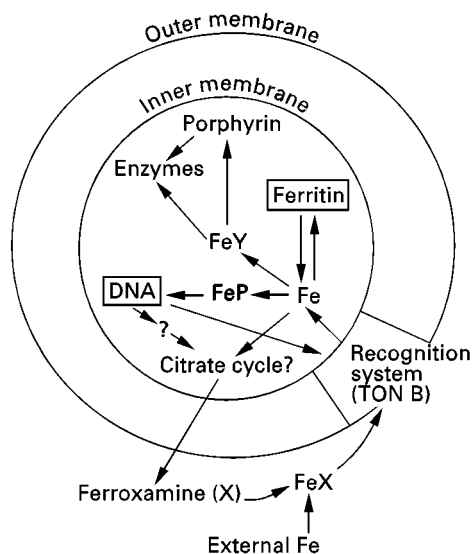


Figure 1 An outlined scheme of the variety of ion exchange reactions in the uptake of iron. Iron is captured as Fe^{3+} outside the cell by a small organic molecule, ferroxamine (X). FeX is passed through membranes (TON B) using energy, and is then exchanged in a variety of paths. Some involve proteins, P; some enzymes catalyse for example the citrate cycle. Some iron is exchanged into new small organic molecules, porphyrins, to make new enzymes. Finally, much is stored in a bound small particle of $\text{Fe}(\text{OH})_3$, called ferritin.

Ion Exchange across Membranes

A different form of ion exchange is that which occurs across a membrane separating two aqueous phases (Figure 2). Once again, the simplest exchange is of two ions, cations such as Na^+/K^+ , $\text{Mg}^{2+}/\text{Ca}^{2+}$ or of anions such as OH^-/Cl^- , where there is equal charge maintenance but change of concentration on both sides of the membrane. There are other possibilities than exchange of equally charged ions, such as the exchange of $2\text{Na}^+/\text{Ca}^{2+}$ or $2\text{Cl}^-/\text{HPO}_4^{2-}$, when only concentration changes are again involved on exchange. The further possibility is that the exchange process is electrogenic, when charge differences are built up across a membrane. Simple examples are the exchanges of $\text{H}^+/\text{Ca}^{2+}$ or $\text{OH}^-/\text{HPO}_4^{2-}$.

In the case of electrogenic exchange, an electrical potential develops across the membrane. Such potentials exist across most membranes of all cells but to different degrees. The development of such ion exchange potentials has led to the successive evolution from simple cells to nerves and then to the brain. In these cells Na^+/K^+ exchange carries the electrolytic current.

Examples of exchange of ions across membranes are numerous in biological systems. One of the best known is the $2\text{Na}^+/\text{Ca}^{2+}$ exchange in many slow

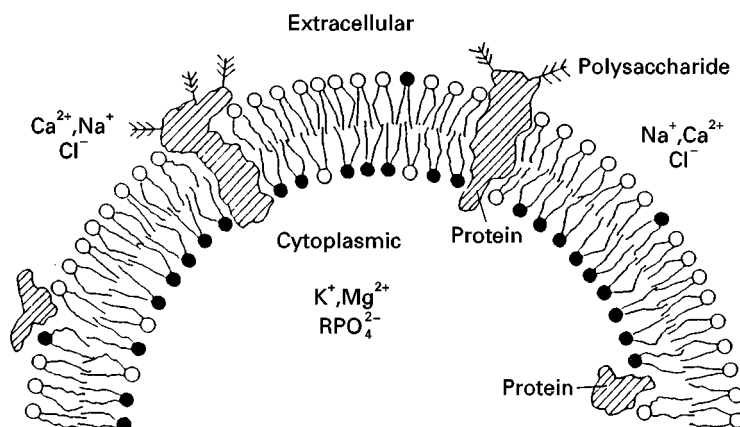


Figure 2 The distribution of the major anions, Cl^- and RPO_4^{2-} and cations, Na^+ , K^+ , Ca^{2+} and Mg^{2+} across a biological cell membrane. Filled circles, charged (negative) phospholipids; open circles, uncharged lipids.

muscle cells. This exchange occurs after muscle action is triggered by the invasion of Ca^{2+} and is used to restore the resting state of a muscle such as that of the heart. An example of electrogenic exchange is found in the nerve when 2K^+ ions enter the cell in exchange for 3Na^+ , thus creating a membrane potential (Figure 3). However, this process costs energy and was a later development in evolution. We turn to the energetics of such exchange processes below.

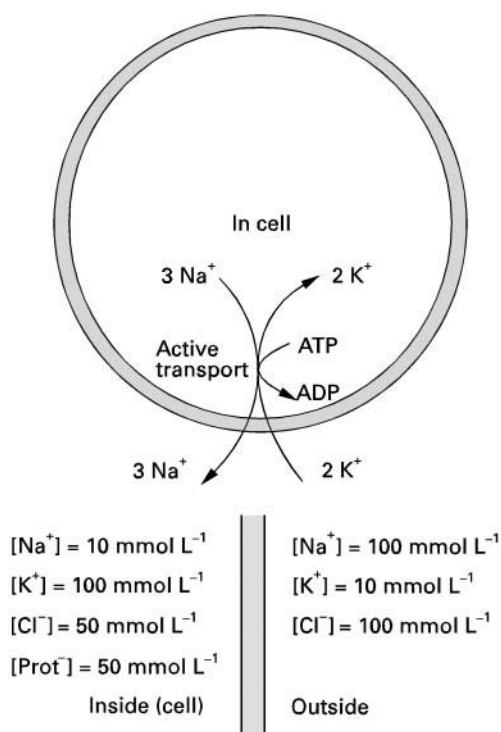


Figure 3 The adenosine triphosphate (ATP) pump in mammalian cells. It exchanges 3Na^+ for 2K^+ and is electrogenic. The concentration of ions inside and outside human cells is shown below.

The Natural Environment and Ion Exchange

To appreciate the value of ion exchange in biological systems, we must look at the environment of cells and the nature of cellular organic chemicals. The major fluids surrounding cells are the sea, fresh water and artificially maintained body fluids for multicellular species such as humans living in air. All of these fluids are aqueous electrolyte solutions containing elements as ions, as shown in Figure 3. The composition of the sea is given in Figure 4. The major feature of the internal cellular solution, that is, the solution protected by the cell's membrane, called the cytoplasm, is that it contains many organic molecules and anions. Both the environmental fluids and the cytoplasm have an osmotic pressure which, unless counter measures are taken to exclude many of the ions of the environment, will be greater for the cytoplasm due to the organic molecules present there. Hence all cells are in danger of bursting through osmotic stress. Due to the anionic nature of the organic molecules in the cell and the fact that the membranes themselves are also anionic due to the phospholipid head groups, they are also in danger of breakdown due to internal electrostatic repulsion between the anions. Various ways of overcoming these problems have been observed in different biological cells and they frequently involve ion-exchange.

Osmotic stress can be overcome by protecting the outer membrane by a cell wall. This wall, built from anionic organic cross-linked polymers, is commonly found in bacteria and plant cells. The anionic wall is exposed to the environment and acts as an ion-exchange resin accepting especially Ca^{2+} and Mg^{2+} ions, which considerably strengthen the wall by cross-linking the organic polymers in it. These cations freely exchange with the environment, so that the wall

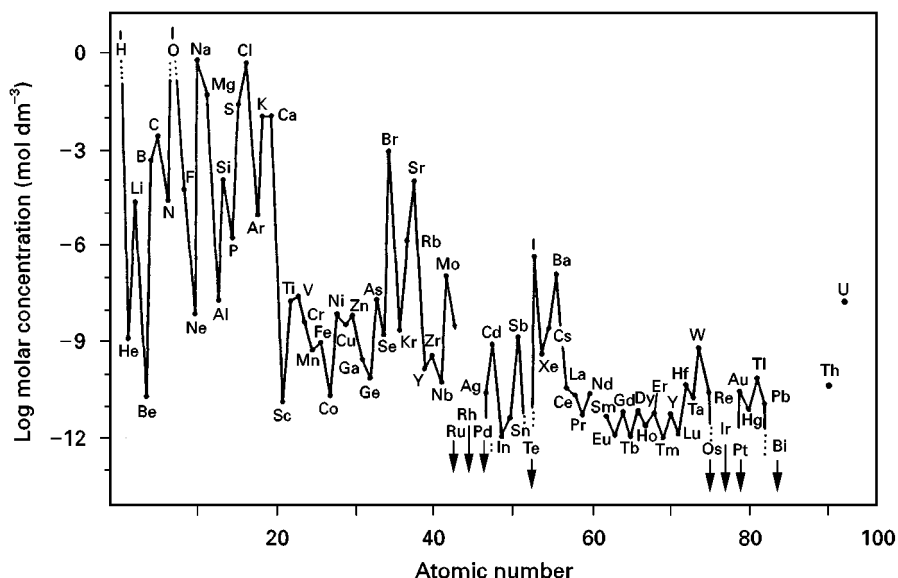


Figure 4 The concentrations of elements in various ionic forms in the sea. Surfaces of cells exchange ions with all these species but clearly those up to atomic number 20 dominate. However, a biological cell exchanges and picks up more than 20 elements, including molybdate and iodide (from Cox 1995, with permission).

does not have a fixed chemical composition and acts much like an artificial ion exchange resin.

All cells, bacterial, plant and animal, also overcome osmotic stress by the selective admission and rejection of ions of the environment. The major ions of the environment are Na^+ and Cl^- , and in the case of the sea they are quite highly concentrated. Both must be prevented from equilibrating between the environment and the cytoplasm if the cell is not to burst. However, to maintain approximate electrical neutrality there has to be counterions to the anionic organic constituents of the cell. Hence, all cells admit K^+ and Mg^{2+} ions and reject Na^+ and Cl^- ions to a greater or lesser degree (Table 3). Of course, this arrangement of ions across the cell membrane costs energy, so the forced exchange of ions must use an energy source internal to the cell.

Before describing the modes of employing energy in pumping ions across membranes so as to establish

nonequilibrium conditions, we need to observe that cells have to move many substances other than Na^+ , K^+ , Mg^{2+} and Cl^- (Table 3). Firstly, they need to exclude Ca^{2+} , since at the concentration of the environment these ions would precipitate cell anions such as carboxylates and phosphates. Secondly, the cytoplasmic level of anions such as phosphate is too low and that of sulfate is too high in the environment, especially in the sea, so that their cellular concentrations must be controlled. Thirdly, the cell must be able to take in anions (or cations) useful as food for synthesis of organic molecules and these include nitrate, small organic phosphates and carboxylates and ammonium or small amine cations. Fourthly, there are a variety of trace elements in the environment, all of which are required in selected amounts in the cell; for example, cations such as those of iron and manganese and anions such as selenate and molybdate. Finally, we have not mentioned the universal presence

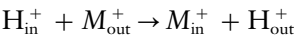
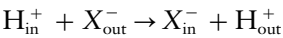
Table 3 Pumped gradients of metals and their complexes

Metal	Inward to cytoplasm	Outward to	Organelle or vesicle
Na^+		Free ion	Outside
Mg^{2+}	Free ion		
H^+	Free ion and many ligands	Free ion and many ligands	Vesicles, outside
K^+	Free ion		
HPO_4^{2-}	Free ion	Several organic phosphates	Mitochondria
Cl^-	Free ion	Free ion	Outside
Fe^{3+}	Ferroxamines, etc.		
	Transferrin	Citrate	Mitochondria
Co^{2+}	Vitamin B_{12}		
Ca^{2+}		Free ion	Reticula, outside

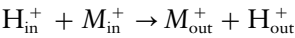
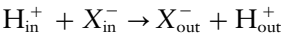
of the proton H^+ which is in constant exchange with many anionic surfaces. Very much of the energy of biological reactions is expended in ion exchange across membranes.

Energized Ion Exchange

There are two major sources of energy open to cells. One is a gradient of protons, H^+ (a pH gradient), developed from the action of light or from the oxidation of organic molecules (Figure 5), while the second comes from the hydrolysis of pyrophosphate bound to nucleotides such as adenosine triphosphate (ATP). The proton gradient can be used in direct ion exchange with other ions, X , across the membrane to accumulate them:



or to develop unfavourable gradients for protection by removing X or M from the cell to the environment:



The first is termed a symport and the second an antiport. In every case, movement across the membrane can be aided by carriers, M or X in the membrane, or by utilizing channels. Channels are controlled, gated pores through membranes.

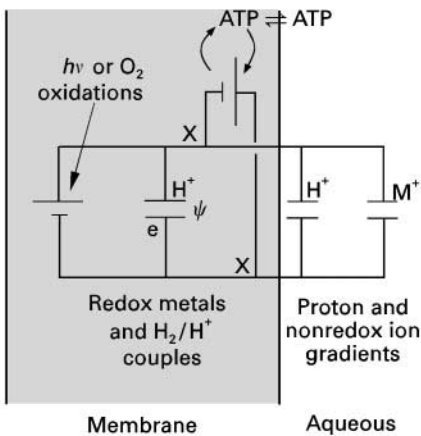
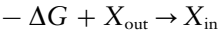
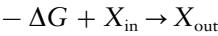
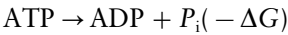


Figure 5 A simplified picture of the production of a proton gradient and then of ATP by the action of light or oxidation of organic molecules inside a membrane. The gradient or ATP is then connected (X) to aqueous phases when ion (M) exchange across membranes can be driven, indicated by \rightleftharpoons , the symbol for a condenser.

Table 4 Examples of ATP-driven ion exchange pumps in cell membranes

Pump	Function
K^+/Na^+	K^+ moves in; Na^+ moves out. Nerve conduction
H^+/Ca^{2+}	Ca^{2+} moves out. Fast (skeletal) muscle recovery
H^+/M	Trace element input or rejection

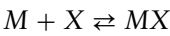
The use of ATP is that its hydrolysis energy ($-\Delta G$) can pump ions across membranes:



It is now known that the action of ATP pumps frequently involves ion exchange so that transfer of one cation or anion is coupled to transfer of a second ion in the opposite direction, giving ion exchange while building energized ion gradients. Examples are given in Table 4.

Selectivity of Ion Exchange

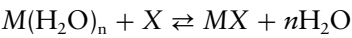
The selectivity of ion exchange interactions depends on the relative binding strengths of ions to a site, where the site may be a molecule free in the cytoplasm, a carrier molecule in a membrane, a surface of a membrane or a precipitated phase, or part of a channel or a pump for moving ions across membranes. The affinity for the site can usually be expressed in a very simple form as a binding stability constant, K , for the equilibrium:



where $K = [MX]/[M][X]$.

The concentration of X is here treated in mass action equations and takes a similar form for surface sites or sites in free solution. In the case of surface sites, the equation takes the form of a Langmuir isotherm.

Selectivity of binding depends on the size and charge of an ion in the first instance. It would be expected that small highly charged ions of opposite sign would bind together best, but this expectation is not fully borne out in practice, since competition for a site also depends on constraints due to hydration of the ions:



Since small, highly charged ions are the most strongly hydrated, making for competition between H_2O and

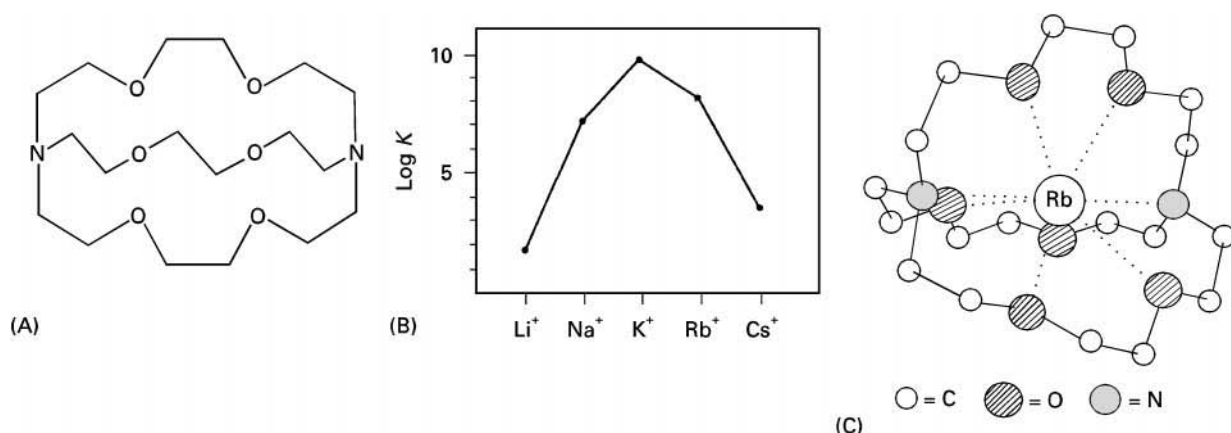


Figure 6 The molecule shown at (A) can bind the monovalent ions selectively because of how it wraps around them (C). The hole in the middle selects the size of the ion, as shown by the binding constants (B). The best binding is for potassium. Such molecules can pick up cations and transfer them across membranes, exchanging the ion for other ions according to binding strengths and concentrations. Many antibiotics are based on such exchange possibilities.

X, there is the possibility of matching ions, M , of different charges and sizes with particular kinds of designed exchange site, X . Controlling factors now for cations, M , are the charge on X and the steric restrictions present in X or induced in MX on binding. Real examples illustrate the point that the binding of cations M to sites X can be in almost any order. The case of the preferred selection of K^+ over the smaller and larger ions Li^+ , Na^+ , Rb^+ and Cs^+ illustrates the point in **Figure 6**. In all cells the K^+ channel virtually excludes Na^+ . Similarly, the Ca^{2+} pump of most cells excludes Mg^{2+} . In both bases the larger ion is preferred due to the size of the cavity and the accepting anion, X .

For trace element metal ions such as those of iron (Fe^{2+} , Fe^{3+}), zinc (Zn^{2+}) or copper (Cu^+ , Cu^{2+}), facts other than charge and size influence selectivity. They are the ability to form covalent bonds depending on the electron affinity of the cation and stereochemical preferences of the metal ions due to their polarizability. Again, examples illustrate these points.

A very important distinction between the bindings of the major metal ions, Na^+ , K^+ , Mg^{2+} and Ca^{2+} and the trace elements, is that the binding units X for the former generally employ organic molecules containing oxygen (O) donor centres only, while for the trace elements the group X may utilize nitrogen (N) or sulfur (S) donors. Examples are given in **Table 5**. Amongst the trace elements the strength of binding follows the general series of divalent M^{2+} ions:



The additional selectivity factor arises due to the stereochemical preferences of these ions.

We can now consider the cytoplasm of a cell as a solution of ion exchange centres, often proteins, which can all bind M but with different affinities.

Together with the fact that the amounts of ions, M , in the cytoplasm varies from $10^{-1} \text{ mol L}^{-1}$ (Na^+ , K^+) to $10^{-17} \text{ mol L}^{-1}$ (Fe^{3+}), this chemical selectivity leads to a virtually complete fixation of the M distribution on different X centres. However, it must not be forgotten that these associations are not permanent and exchange takes place all the time. Many sites will only be occupied preferentially, not specifically, by a given cation. This is particularly important when the environment becomes polluted.

The selective uptake of anions follows similar properties based on size, charge and steric constraints. However, covalent attachment is much less significant than hydrogen bonding. The ability to form hydrogen bonds by anions appears to be related to surface charge density. Thus, F^- and OH^- readily form H bonds when compared with Cl^- , Br^- or SH^- . Once again, the anions exchange quite rapidly with organic surfaces.

Ion Exchange and Cell Compartments

The selectivity of binding to carriers, to channels and channel parts of pumps in membranes leads to

Table 5 Preferred metal/nonmetal ion association

Metal	Preferred nonmetal association
Na^+ , K^+	Low association, preference for O-donor
Mg^{2+} , Ca^{2+}	Moderate association with O-donor anions such as carboxylates and phosphates
Fe^{2+} , Co^{2+}	Strong association with mixture of N- and O-donors
Cu^{2+} , Zn^{2+}	Strong association with S-donor such as thiolates

Exchange is fast for Na^+ , K^+ but progressively slower down the table.

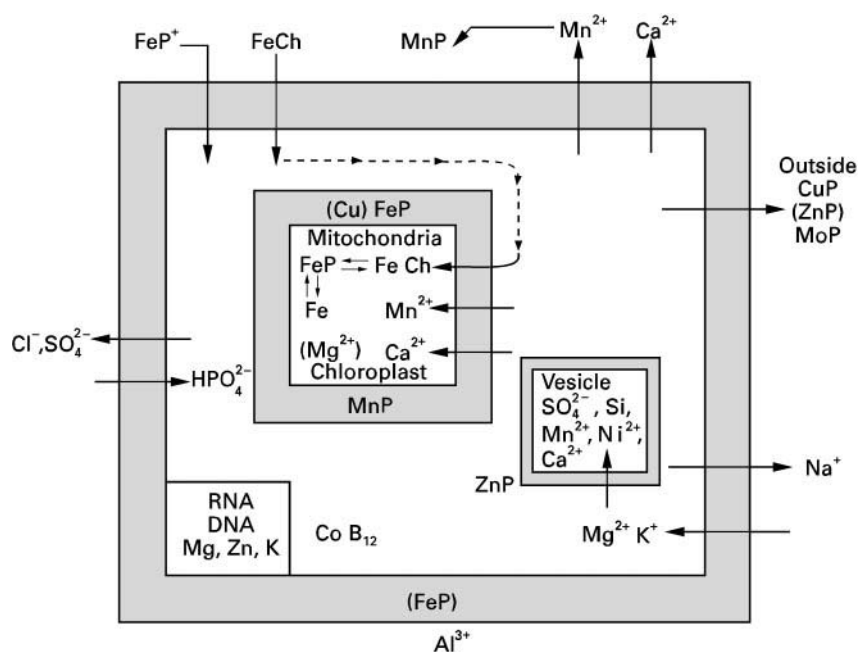


Figure 7 Some of the distributions of elements in eukaryotic cells. Iron is often in membranes, while Cl^- , Ca^{2+} and Na^+ are concentrated away from the cytoplasm; K^+ and Mg^{2+} concentrate inside cells, Mn^{2+} is to be found in vesicles, but copper is more usual outside cells. Zinc is everywhere and cobalt is rare everywhere. Aluminium may be rejected. P, Protein; Ch, chelating agent. Many movements are due to ion exchange.

separate movement of elements in cells and then positions them in particular zones of vesicles. Within these zones, ion exchange of the selected M ions at X occurs, so that selectivity of association is manipulated by the input of energy. Some cell compartments and their selective element contents are shown in Figure 7.

The setting-up of such ion gradients across membranes has great value, not only in that it allows specific reactions to occur in particular parts of space but also that, under stimulus, the ions can be released from their storage sites into the cytoplasm. There is then ion exchange signal. A particularly important example concerns the storage and subsequent release of calcium ions from vesicles into the cytoplasm, causing manifold changes in metabolism and mechanical structure. Simple examples are muscle contraction and hormone release.

We can look upon a mineral phase as a compartment where minerals such as amorphous silica (often in plants), calcium carbonate and calcium hydroxyphosphate are the obvious examples. These precipitates, by exchanging ions, can buffer solutions holding ions in their neighbouring solutions in fixed amounts.

Ion Exchange and Organs

As well as the local problems of ion exchange, large-bodied organisms, such as human beings, must con-

trol ion levels throughout their whole body. They do this by managing uptake and rejection of ions selectively. Thus it is necessary to ingest sufficient but not too much of many ions such as Na^+ , K^+ , Cl^- and HPO_4^{2-} . The monitoring and rejection organ is the kidney. The kidney membranes act as complicated ion exchange systems. However, the brain apparently requires special ionic conditions, since cerebrospinal fluids of quite different composition from blood.

Ion Exchange and Pollution

Many unusual elements enter environmental waters due to mining and industrial processing of minerals. Several of these elements are toxic and we note especially lead and mercury. There is considerable interest today in the removal from cells of poisonous elements such as Hg^{2+} , Pb^{2+} and AsO_4^{3-} . Once again, even in bacteria, special proteins recognize these ions and either transfer them directly across membranes or release them to specialized pumps for energized movement out of the cell. While bacteria have evolved detoxifying processes, higher animals have not, so humans have to take action to remove the offending elements. The application of a drug may force the offensive element to exchange from the site where it causes damage, becoming bound to the drug when it is excreted.

Conclusion

While ion exchange appears to be an extremely simple idea, it is used in remarkably complicated ways in living organisms. Of course, we do not know how life began but perhaps the earliest step in the direction of the development of these organized chemical systems was the formation of an ion gradient across a membrane. Once such a gradient had formed, possibly of the proton, ion exchange could be used to move some elements out of cells and others into cells. These ions could be inorganic or organic. The movements became more complicated as more membrane containments developed in evolution. Within each compartment ions could bind to form complexes or precipitates by exchange processes. We know that cells have many different kinds of ion gradient through this exchange: some relate to energy storage and some to messages by release of the gradients. Recently evolved systems are calcium triggering of muscle and sodium/potassium currents in nerves. The restoration of the gradients is very frequently energized by ion exchange across membranes. This leads us to the tantalizing problem of the movement of ions in the brain. Are ion exchange processes deeply involved in storage, memory, and in thinking? We know that the brain is an electrolytic device and hence ion movements are always active. Clearly, we could speculate at length on this topic, but what is really required is more experimental evidence concerning ion exchange in organisms and especially in the brain.

See also: **II/Ion Exchange:** Inorganic Ion Exchangers; Theory of Ion Exchange.

Further Reading

- Aidley DJ and Stanfield PR (1996) *Ion Channels*. Cambridge: Cambridge University Press.
- Allen TJA, Noble D and Reuter H (eds) (1989) *Sodium-Calcium Exchange*. Oxford: Oxford Science Publications.
- Birch NJ (1993) *Magnesium and the Cell*. London: Academic Press.
- Bockris J O'M and Reddy AKN (1970) *Modern Electrochemistry*, vols 1 and 2. London: Plenum Press.
- Cheung WY (ed.) (1982) *Calcium and Cell Function*, vols I-IV. New York: Academic Press.
- Cox PA (1995) *The Elements on Earth*. Oxford: Oxford University Press.
- Frausto da Silva JJR and Williams RJP (1996) *The Biological Chemistry of the Elements*. Oxford: Oxford University Press.
- Gennis RB (1989) *Biomembranes*. New York: Springer.
- Kaim W and Schwederski B (1994) *Bioinorganic Chemistry. Inorganic Elements in the Chemistry of Life*. Chichester: Wiley.
- Mitchell AR (1995) *The Clinical Biology of Sodium*. Oxford: Pergamon Press.
- Phillips CGS and Williams RJP (1966) *Inorganic Chemistry*, vol. 1, ch. 7, pp. 231-265. Oxford: Oxford University Press.
- Stryer L (1988) *Biochemistry*, 3rd edn. New York: W.H. Freeman.
- Townshend A (ed.) (1995) *Encyclopedia of Analytical Science*, vol 4, pp. 2261-2365. London: Academic Press.
- Walton HF and Rocklin RD (1990) *Ion Exchange in Analytical Chemistry*. Boca Raton, FL, USA: CRC Press.

BIOLOGICALLY ACTIVE COMPOUNDS AND XENOBIOTICS: MAGNETIC AFFINITY SEPARATIONS



I. Šafařík and M. Šafaříková,
Institute of Landscape Ecology, Academy of
Sciences, České Budějovice, Czech Republic

Copyright © 2000 Academic Press

Introduction

Isolation and separation of specific molecules is used in almost all areas of biosciences and biotechnologies. Separation technology is thus one of the most important areas for further study and development. New separation techniques, capable of treating dilute solutions or solutions containing only minute amounts of

target molecules in the presence of vast amounts of accompanying compounds in both small and large-scale processes, even in the presence of particulate matter, are necessary.

In the area of biosciences, isolation of biologically active compounds and xenobiotics is usually performed using a variety of chromatography procedures, affinity chromatography being one of the most important. Affinity ligand techniques currently represent the most powerful tool available for downstream processing both in terms of their selectivity and recovery. The strength of column affinity chromatography has been shown in thousands of successful applications, especially on a laboratory

scale. The disadvantage of standard column procedures is the impossibility of such systems to cope with samples containing particulate material so they are not suitable for use in the early stages of the isolation/purification process where suspended solid and fouling components are present. In this case magnetic affinity batch adsorption, applications of magnetically stabilized fluidized beds or magnetically modified two-phase systems have shown their usefulness.

The basic principle of magnetic affinity separation is very simple. Magnetic carriers bearing an immobilized affinity ligand or magnetic biopolymer particles are mixed with a sample containing target compound(s). Samples may be crude cells lysates, whole blood, plasma, urine, cultivation media, water, soil extracts and many others. Following an incubation period when the target compound(s) bind to the magnetic affinity particles, the whole magnetic complex is easily and rapidly removed from the sample using an appropriate magnetic separator. After washing, the isolated target compound(s) can be eluted and used for further work.

Magnetic separation techniques have several advantages in comparison with standard separation procedures. The separation process can be performed directly in crude samples containing suspended solid material. Due to the magnetic properties of the magnetic affinity particles (and the diamagnetic properties of the majority of the contaminating molecules and particles present in the treated sample) they can be relatively easily and selectively removed from the sample. In fact, magnetic separation is the only feasible method for recovery of small magnetic particles (diameter ca. 0.1–1 μm) in the presence of biological debris and other fouling material of similar size. Moreover, the power and efficiency of magnetic separation procedures is especially useful for large-scale operations. The magnetic separation techniques are also the basis of various automated procedures, especially magnetic particle-based immunoassay systems for the determination of a variety of analytes. The basic equipment for laboratory experiments is very simple. Magnetic particles of various types are easily available, as well as magnetic separators. A short description is given below.

Equipment and Materials

Magnetic carriers with immobilized affinity ligand or magnetic particles prepared from a biopolymer exhibiting affinity for the target compound(s) are used to perform the isolation procedure. Magnetic separators are necessary to recover magnetic particles from the system.

Magnetic carriers and adsorbents are commercially available and can also be prepared in the laboratory. Such materials are usually available in the form of magnetic particles prepared from various synthetic polymers, biopolymers or porous glass, or magnetic particles based on inorganic magnetic materials such as surface-modified magnetite can be used. In fact, many of the particles behave like paramagnetic or superparamagnetic ones responding to an external magnetic field, but not interacting themselves in the absence of a magnetic field. This is important due to the fact that magnetic particles can be easily resuspended and remain in suspension for a long time. The diameter of the particles is from ca. 50 nm to ca. 10 μm . Magnetic particles having a diameter larger than ca. 1 μm can be easily separated using simple magnetic separators, while separation of smaller particles (magnetic colloids with a particle size ranging between tens and hundreds of nanometers) may require the use of high-gradient magnetic separators.

Commercially available magnetic particles can be obtained from a variety of companies. In most cases polystyrene is used as a matrix, but carriers based on cellulose, agarose, silica, porous glass or silanized magnetic particles are also available. Particles with immobilized affinity ligands are available, oligodeoxythymidine, streptavidin, antibodies, protein A and protein G being used most often. Magnetic particles with such immobilized ligands can serve as generic solid phases to which native or modified affinity ligands can be immobilized (e.g. antibodies in the case of immobilized protein A, protein G or secondary antibodies, biotinylated molecules in the case of immobilized streptavidin or adenylated molecules in the case of immobilized oligodeoxythymidine). In exceptional cases, enzyme activity may decrease as a result of usage of magnetic particles with exposed iron oxides. In this case encapsulated microspheres, having an outer layer of pure polymer, are safer. In **Table 1** is given a list of companies producing and selling magnetic particles of various types.

In the laboratory, magnetite (or similar magnetic materials such as maghemite or ferrites) particles are usually surface modified by silanization. This process modifies the surface of the inorganic particles so that appropriate function groups become available, which enable easy immobilization of affinity ligands.

Biopolymers such as agarose, chitosan, κ -carrageenan and alginate can be easily prepared in a magnetic form. In the simplest way, the biopolymer solution is mixed with magnetic particles and after bulk gel formation the magnetic gel formed is broken into fine particles. Alternatively, biopolymer solution containing dispersed magnetite is dropped into a mixed hardening solution or a water-in-oil suspension

Table 1 Examples of commercially available magnetic particles suitable for magnetic affinity separations

Manufacturer/supplier	Name of particles	Diameter (μm)	Polymer composition/surface modification	End groups/activation possibility	Immobilized ligands
Advanced Biotechnologies, Epsom, UK	XM200 Microsphere	3.5	Polystyrene	-COOH	Oligo (dT), antibodies, streptavidin, protein A
Bangs Labs, Fishers, IN, USA	Magnacil	0.5-3.5	Silica	Silica	
	Magnetic Microspheres	~ 1	Styrene-divinyl benzene copolymer	-COOH, -NH ₂	Streptavidin, protein A, antibodies
Cortex Biochem, San Leandro, CA, USA	MagaCell		Cellulose	-OH	Streptavidin, protein A, protein G, oligo (dT), DEAE, CM, PEI
CPG, Lincoln Park, NJ, USA	MPG	5	Porous glass	-SiOH, glyceryl, -NH ₂ , hydrazide	Streptavidin, avidin
Dynal, Oslo, Norway	Dynabeads M-280	2.8	Polystyrene	Tosyl activated	Streptavidin, oligo (dT), antibodies
	Dynabeads M-450	4.5			
	Dynabeads M-500	5.0			
Immunotech, Marseille, France	Iobeads	~ 1			Antibodies, avidin
Merck, Darmstadt, Germany	Biobeads	1	Polystyrene		Streptavidin
		1-3	Silica		
Novagen, USA	Magnetight				Oligo (dT)
PerSeptive Biosystems, Farmingham, MA, USA	BioMag	0.5-1.5	Silanized iron oxides	-COOH, -NH ₂	Antibodies, protein A, protein G, streptavidin, biotin
Prolabo, Fontenay-Sous-Bois, France	Estapor	~ 1	Polystyrene	-COOH, -OH, -NH ₂	
Promega, Madison, WI, USA	MagneSphere Paramagnetic Particles				Streptavidin
ProZyme, San Leandro, CA, USA	Magnetic beads	1.4	Styrene-divinyl-benzene copolymer		Streptavidin, protein A, protein A/G, protein G
		2.2			
		2.3			
Qiagen	Ni-NTA Magnetic agarose beads	20-70	Agarose		Nitrilotriacetic acid
Quantum Magnetix, USA	Magnetic particles	0.05			Streptavidin, DEAE, CM, C18, protein A, silica
		0.25			
Scigen, Sittingbourne, UK	M 100	1-10	Cellulose	-OH	Streptavidin, biotin, oligo (dT)
	M 104				
	M 108				
	Magnetic agarose	1-5	Agarose		
Seradyn, Indianapolis, IN, USA	Sera-Mag	1		-COOH	Streptavidin, oligo (dT)
Spherotech, Libertyville, IL, USA	SPHERO magnetic particles	1-4.5	Polystyrene	-COOH, -NH ₂	Streptavidin, biotin, antibodies

technique is used to prepare spherical particles. Basically the same procedures can be used to prepare magnetic particles from synthetic polymers such as polyacrylamide or poly(vinylalcohol).

In one of the approaches used, standard affinity chromatography material is post-magnetized by pumping the water-based ferrofluid through the column packed with the sorbent. Magnetic material accumulates within the affinity adsorbent pores thus modifying the chromatography material into magnetic form.

Some affinity ligands (usually general binding ligands) are already immobilized to commercially

available carriers (see Table 1). To immobilize other ligands to both commercial and laboratory-made magnetic particles, standard procedures used in affinity chromatography can be employed. Usually functional groups available on the surface of magnetic particles such as -COOH, -OH or -NH₂ are used for immobilization; in some cases, magnetic particles are already available in the activated form (e.g. tosyl activated).

Magnetic separators are necessary to separate the magnetic particles from the system. In the simplest approach, a small permanent magnet can be used, but various magnetic separators employing strong

rare-earth magnets can be obtained at reasonable prices. Commercial laboratory scale *batch magnetic separators* are usually made from magnets embedded in disinfectant-proof material. The racks are constructed for separations in Eppendorf microtubes, standard test tubes or centrifugation cuvettes. Some have a removable magnetic plate to facilitate washing of separated magnetic particles (Figure 1). Other types of separators enable separations from the wells of microtitration plates and the flat magnetic separators are useful for separation from larger volumes of suspensions (up to ca. 500–1000 mL).

Flow-through magnetic separators are usually more expensive and more complicated, and *high-gradient magnetic separators* (HGMS) are typical examples (Figure 2). Laboratory-scale HGMS are constructed from a column packed with fine magnetic-grade stainless-steel wool or small steel balls placed between the poles of an appropriate magnet. The suspension is pumped through the column, and magnetic particles are retained within the matrix. After removing the column from the magnetic field, the particles are retrieved by flow and usually by gentle vibration of the column.

Basic Principles of Magnetic Affinity Separations

In general, magnetic affinity separations can be performed in two different modes. In the *direct method* an appropriate affinity ligand is directly coupled to the magnetic particles or biopolymer exhibiting affinity towards target compound(s) is used in the course of preparation of magnetic affinity particles. These particles are added to the sample and target compounds then bind to them. In the *indirect method* the free affinity ligand (in most cases an appropriate antibody) is added to the solution or suspension to enable the interaction with the target compound. The resulting complex is then captured by appropriate

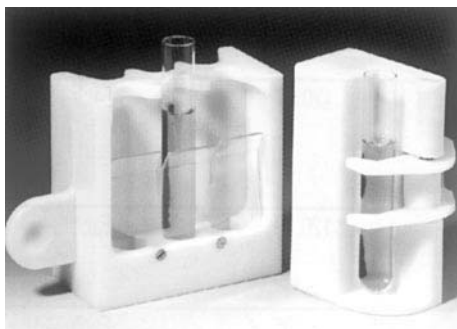


Figure 1 (See Colour Plate 61). Examples of test-tube magnetic separators (Dynal, Norway). Left, Dynal MPC-6; right, Dynal MPC-1. Courtesy of Dynal, Oslo, Norway.

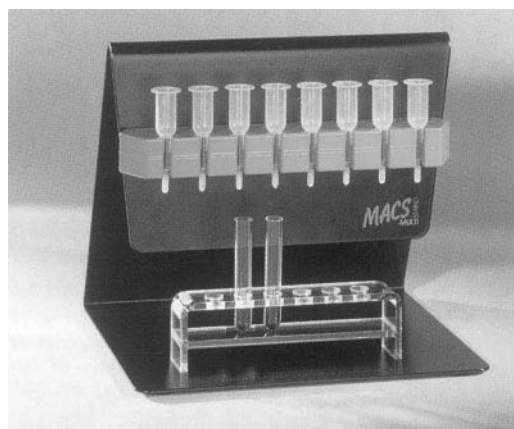


Figure 2 (See Colour Plate 62). A typical example of laboratory-scale high-gradient magnetic separators. OctoMACS Separator (Miltenyi Biotec, Germany) can be used for simultaneous isolation of mRNA. Courtesy of Miltenyi Biotec, Germany.

magnetic particles. In case antibodies are used as free affinity ligands, magnetic particles with immobilized secondary antibodies, protein A or protein G are used for capturing the complex. Alternatively, the free affinity ligands can be biotinylated and magnetic particles with immobilized streptavidin or avidin are used to capture the complexes formed. In both methods magnetic particles with isolated target compound(s) are magnetically separated and then a series of washing steps are performed to remove the majority of contaminating compounds and particles. The target compound is then usually eluted, but for specific applications (especially in molecular biology, bioanalytical chemistry or environmental chemistry) they can be used still attached to the particles, such as in the case of polymerase chain reaction, magnetic ELISA, etc.

The two methods perform equally well, but, in general, the direct technique is more easily controlled. The indirect procedure may perform better if affinity ligands have poor affinity for the target compound.

In some cases, nonspecific binding of accompanying compounds can be observed due to the specific properties of the magnetic particle material. In this case, pretreatment with the magnetic carrier without immobilized affinity ligand or with immobilized nonspecific molecules will usually help. The nonspecific binding can be also minimized by adding a nonionic detergent both in the sample and in the washing buffers after isolation of the target.

In most cases, *magnetic batch affinity adsorption* is used to perform the separation step. This approach represents the simplest procedure available, enabling the whole separation to be performed in one test-tube or flask. If larger magnetic particles (with diameters

ca. $> 1 \mu\text{m}$) are used, simple magnetic separators can be employed. If magnetic colloids (diameters ranging between tens and hundreds of nanometers) are used as affinity adsorbents, high-gradient magnetic separators have usually to be used to remove the magnetic particles from the system.

Alternatively, *magnetically stabilized fluidized beds* (MSFB), which allow continuous separation, can be used. The use of MSFB is an alternative to conventional column operation, such as packed bed or fluidized bed, especially for large-scale purification of biological products. Magnetic stabilization enables the expansion of a packed bed without mixing of solid particles. High column efficiency, low pressure drop and elimination of clogging can be attained.

Biocompatible two-phase systems, composed for example from dextran and polyethylene glycol, are often used for isolation of biologically active compounds, subcellular organelles and cells. The separation of the phases can be accelerated by the addition of fine magnetic particles or ferrofluids to the system followed by the application of a magnetic field. Magnetically enhanced phase separation usually increases the speed of phase separation by a factor of about 10 in easy systems, but it may increase by a factor of many thousands in difficult systems.

Examples of Magnetic Affinity Separations of Biologically Active Compounds and Xenobiotics

Magnetic affinity separations have been successfully used in various areas, such as molecular biology, biochemistry, immunochemistry, enzymology, analytical chemistry and environmental chemistry. Tables 2–4 show some selected applications of these techniques.

At present, magnetic affinity separation techniques are used especially in molecular biology for the isolation of RNA, DNA and oligonucleotides. Almost all the procedures employ the same basic principle, based on the hybridization of immobilized oligonucleotides and target structures. There are several companies offering oligodeoxythymidine immobilized on magnetic particles, which can be effectively used for rapid isolation of highly purified, intact poly A⁺ mRNA from eukaryotic total RNA. Poly A⁺ mRNA has been successfully isolated from various samples, such as cells, animal and plant tissues, blood, cells isolated by immunomagnetic separation, paraffin-embedded tissues, etc. Also cells and tissues containing high RNase activities can be used for mRNA isolation. The separated mRNA can be eluted from the beads by lowering the ionic strength of the elution buffer and used for further applications (Northern blotting, dot-blot hybridization, hybridization probes) or used still bound to magnetic particles (cDNA synthesis, construction of solid-phase cDNA library, etc.). Enzymatic downstream applications are usually not inhibited by the presence of magnetic particles. The covalent binding of oligodeoxythymidine to magnetic particles makes it possible to regenerate the specific adsorbent and to reuse it up to four times.

Isolation of DNA and RNA can be simply performed using biotinylated specific nucleic acids or oligonucleotides immobilized on magnetic particles with immobilized streptavidin. Usually large binding capacity can be achieved resulting in excellent reaction kinetics and high efficiency of the procedure. In addition, magnetic silica particles have been used for simple isolation of DNA and RNA from various biological samples and also to purify DNA fragments after agarose gel electrophoresis.

Table 2 Typical examples of magnetic separations of nucleic acids

Nucleic acid	Magnetic system used	Typical examples
RNA	Magnetic particles with immobilized oligo (dT) ₂₅	Eukaryotic poly A ⁺ mRNA, viral poly A ⁺ RNA
	Magnetic particles with immobilized specific oligonucleotides	tRNA
DNA	Dynabeads DNA DIRECT	PCR-ready DNA
	Biotinylated cloned genomic DNA immobilized on Dynabeads Streptavidin	cDNA
	Dynabeads M-280 Streptavidin with immobilized biotinylated oligonucleotide complementary to the lacZ region	M13 single-stranded DNA
	Magnetic particles with immobilized pyrimidine oligonucleotide	Double-stranded target DNA (triple helix formation)
	COOH-terminated magnetic beads (under specific concentrations of polyethylene glycol and salt)	Double-stranded DNA, PCR products, M13 single-stranded DNA
	Magnetic silica particles	DNA

Table 3 Selected examples of magnetic affinity separation of proteins

<i>Isolated protein</i>	<i>Magnetic system used</i>	<i>Typical examples</i>
Enzymes	Sub-micron ferrite particles with immobilized soybean trypsin inhibitor	Trypsin
	Ferrofluid-modified 5'-AMP-Sepharose 4B	Alcohol dehydrogenase
	Magnetic agarose beads with immobilized dye	Lactate dehydrogenase
	Magnetic chitin	Lysozyme
	Dynabeads with immobilized polyclonal antibodies	Angiotensin-converting enzyme
	Iminodiacetic acid coupled to magnetic agarose and charged with Zn^{2+}	Angiol-TEM- β -lactamase
	Alginate-magnetite beads	Pectinase
Antibodies	Magnetic affinity aqueous two-phase system	Hexokinase
	Magnetic particles with immobilized antibodies against human IgG	Human IgG antibodies
	Magnetic particles with immobilized protein A or protein G	Antibodies
Lectins	Human serum albumin immobilized onto ferromagnetic dactron	Antibodies against human serum albumin
	Magnetic cross-linked chitosan	<i>Solanum tuberosum</i> lectin
Receptors	Dynabeads M-450 sheep anti-mouse IgG ₁ with immobilized monoclonal antibody	Human transferrin receptor
	Magnetic particles with immobilized oligonucleotide containing EcdR binding sequence	Ecdysteroid receptor (EcdR) from <i>Drosophila melanogaster</i>
Other proteins	Magnetic particles with immobilized DNA/RNA fragment containing the specific binding sequence	DNA/RNA binding proteins
	Magnetic particles with immobilized <i>m</i> -aminophenylboronic acid	Glycated haemoglobin
	Organomercurial-agarose magnetic beads	Transcriptionally active chromatin restriction fragments with accessible histone H3 thiols
	Ni-NTA Magnetic agarose beads	6xHis-tagged proteins

Table 4 Selected examples of magnetic separation of low-molecular-weight biologically active compounds and organic and inorganic xenobiotics

<i>Type of compound</i>	<i>Magnetic system used</i>	<i>Typical examples</i>
Biologically active compounds	Magnetic particles with immobilized aldosterone antiserum	Aldosterone
	Molecularly imprinted polymer containing magnetic iron oxide	(S)-propranolol
	Magnetic charcoal	Separation of free antigens in radioimmunoassays
Organic xenobiotics	Magnetic particles with immobilized Cu-phthalocyanine	Polyaromatic hydrocarbons, triphenylmethane dyes
	Magnetic polyethyleneimine microcapsules	Carcinogens
	Magnetic particles with immobilized specific antibodies	Pesticides, polyaromatic hydrocarbons, TNT, PCBs
	Bacterial cells adsorbed to magnetite	Chlorinated hydrocarbons and pesticides
	Magnetic charcoal	Water-soluble dyes, pesticides
Inorganic xenobiotics	Magnetic chitosan	Cu^{2+} ions
	Cells of <i>Enterobacter</i> spp. immobilized on magnetite	Ni^{2+} ions
	Magnetic cross-linked cell walls of <i>Saccharomyces cerevisiae</i>	Ions of heavy metals
	Magnetotactic bacteria	Ions of heavy metals
	Solvent extractants on magnetic microparticles	Radionuclides

In the case of protein separation no simple strategy for magnetic affinity separations exists. Various affinity ligands have been immobilized on magnetic particles, or magnetic particles have been prepared from biopolymers exhibiting affinity for target enzymes or lectins, as shown in Table 3. Immunomagnetic particles, i.e. magnetic particles with immobilized specific antibodies against the target structures, have been used for the isolation of various antigens, both molecules and cells and can thus be used for the separation of specific proteins. Enzyme isolation is usually performed using immobilized inhibitors, cofactors, dyes or other suitable ligands, or magnetic beads prepared from affinity biopolymers are used. A general procedure, especially from the point of view of recombinant oligohistidine-tagged proteins, is based on the application of metal chelate magnetic adsorbents. Another general procedure employs immobilized protein A or protein G for the specific separation of immunoglobulins from ascites, serum and tissue culture supernatants.

Magnetic separation of low-molecular-weight biologically active compounds has been used in the course of their determination by various types of immunoassays. Usually immunomagnetic particles directly capture the target analyte, or magnetic particles with immobilized streptavidin are used to capture the complex of biotinylated primary antibody and the analyte. The separated analyte is then determined using an appropriate method.

Isolation and separation of organic and inorganic xenobiotics from environmental and clinical samples using magnetic techniques may find useful applications in the near future. Immobilized copper phthalocyanine dye has an affinity for planar organic compounds, such as polyaromatic hydrocarbons with three and more fused aromatic rings in their molecules, and for triphenylmethane dyes, both groups representing real or potential carcinogens and mutagens. Immunomagnetic separation of xenobiotics such as pesticides, TNT or PCBs is used as a first step in the course of their immunoassay.

Magnetic solid-phase extraction (MSPE) enables preconcentration of target analytes (e.g. environmental contaminants) from large volumes of solutions or suspensions using relatively small amount of magnetic specific adsorbent. This procedure can substitute the standard liquid-liquid and solid-phase extraction procedures.

Future Perspectives

The isolation and separation of biologically active compounds and xenobiotics using magnetic affinity techniques are a relatively new approach and still

under development. Due to the commercial availability of magnetic affinity particles and kits these techniques are currently used mainly in molecular biology (especially for separation of nucleic acids) and as parts of the kits for the determination of selected analytes using magnetic ELISA and related techniques (especially determination of clinical markers and environmental contaminants). Up to now small-scale separations prevail and thus the full potential of these techniques has not been fully exploited.

It can be expected that further development will be focused on two areas. The first one will be oriented to the laboratory-scale application of magnetic affinity separation techniques in biochemistry and related areas (isolation of a variety of both low- and high-molecular weight substances of various origins directly from crude samples thus reducing the number of purification steps) and in biochemical and environmental analysis (application of immunomagnetic particles for separation of target analytes from a mixture followed by their detection using ELISA and related principles). Such a type of analysis enables portable assay systems to be constructed for the detection and determination of environmental contaminants directly on site or for near-patient analysis of various disease markers. Alternatively, fully automated systems for the detection of clinical markers will be constructed.

In the second area, larger-scale (industrial) systems will be developed and used for the isolation of biologically active compounds directly from the crude culture media, wastes from food industry, etc. It is not expected that large amounts of low-cost products will be isolated using magnetic techniques, but attention will be directed to the isolation of minor, but highly valuable components present in raw materials. Of course, prices of magnetic carriers have to be lowered, and special types of low-cost, biotechnology-applicable magnetic carriers prepared by simple and cheap procedures have to become available. Magnetic separations could thus be the technique for the 21st century.

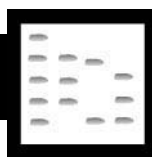
See Colour Plates 61, 62.

See also: I/Affinity Separation. II/Affinity Separation: Immunoaffinity Chromatography. Extraction: Solid-Phase Extraction; Solvent Based Separation. III/Catalyst Studies: Chromatography: Isolation Magnetic Techniques; DNA. Immunoaffinity Extraction: RNA. Appendix 1/Essential Guides for Isolation/Purification of Cells: Essential Guides for Isolation/Purification of Enzymes and Proteins: Essential Guides for Isolation/Purification of Nucleic Acids. Appendix 2/Essential Guides to Method Development in Affinity Chromatography.

Further Reading

- Biomagnetic Techniques in Molecular Biology* (1998) Technical Handbook, 3rd edn, 184 pp. Oslo: Dynal.
- Cell Separation and Protein Purification* (1996) Technical Handbook, 2nd edn, 165 pp. Oslo: Dynal.
- Häfeli U, Schütt W, Teller J and Zborowski M (eds) (1997) *Scientific and Clinical Applications of Magnetic Carriers*, 628 pp. New York: Plenum Press.
- Lundeberg J and Larsen F (1995) Solid-phase technology: magnetic beads to improve nucleic acid detection and analysis. *Biotechnology Annual Review* 1: 373–401.
- Moffat G, Williams RA, Webb C and Stirling R (1994) Selective separations in environmental and industrial processes using magnetic carrier technology. *Minerals Engineering* 7: 1039–1056.
- Šafařík I and Šafaříková M (1997) Overview of magnetic separations used in biochemical and biotechnological applications. In: Häfeli U, Schütt W, Teller J and Zborowski M (eds) *Scientific and Clinical Applications of Magnetic Carriers*, pp. 323–340. New York: Plenum Press.
- Šafařík I and Šafaříková M (1999) Use of magnetic techniques for the isolation of cells. *Journal of Chromatography B* 722: 33–53.
- Sinclair B (1998) To bead or not to bead. Applications of magnetic bead technology. *The Scientist* 12(13): 17–19.

BIOMEDICAL APPLICATIONS



Gas Chromatography – Mass Spectrometry

V. Garner, Stockport, UK

Copyright © 2000 Academic Press

Introduction

The tremendous technological developments that have followed the initial interfacing of gas chromatographs with mass spectrometers together with the phenomenal advances in computerized data handling have provided an analytical technique that finds practically universal application. The biomedical sciences afford an enormous range of applications of this instrumentation where its full potential as a primary method for the separations and identification of extremely complex mixtures is clearly demonstrated.

The applications can be grouped into three broad categories based upon the nature of the analytes:

- Small volatile molecules, e.g. metabolites, xenobiotics (drugs, toxins, etc), food components
- Large labile molecular species, e.g. biomacromolecules and even whole cells
- Isotopomers (molecules differing only in isotopic composition), e.g. tracer studies, isotopic labelling, breath gas diagnostics, natural abundance studies

The analysis of small volatile molecules, perhaps after derivatization, is the major application area; particular biomedical applications in clinical chemistry

and occupational hygiene are illustrated below. Others are exemplified under the headings sport, environment, food and forensics. The analysis of biomacromolecules and whole cells is another rapidly expanding field but using other mass spectrometric and separatory techniques (electrospray, atmospheric pressure and matrix assisted laser desorption ionization; see also LC–MS, CE–MS). Gas chromatography–mass spectrometry (GC–MS) of pyrolysates can provide information about otherwise intractable materials.

The elucidation of mechanisms and biochemical pathways using tracer and labelling techniques is an example of the third category of applications which is also a rapidly expanding area with the wider availability of stable as opposed to radioactive labelled compounds. The ability to separate and distinguish between components in a complex mixture that differ solely in their isotopic composition allows exogenous materials to be distinguished from endogenous species; it also provides a means of improving quantitation (via isotope dilution) and allows dynamic studies of metabolism or dysfunction to be undertaken. It is this latter area of GC–SIRMS (GC–stable isotope ratio MS) that will be emphasized.

Analysis of Small Volatile Molecules

Instrumentation

The majority of instruments utilize capillary columns thereby allowing relatively simple connection to the mass spectrometer. Earlier systems used packed columns that required some form of separator in order

to reduce the amount of carrier gas entering the mass spectrometer ionization chamber. A 5% poly(diphenyldimethylsiloxane) stationary phase is frequently used because of its wide general applicability and stability. Samples can be introduced using an autoinjector or manually by syringe; headspace gases, solutions in volatile solvents, solid-phase microextraction (SPME) systems and thermal desorption with cryofocussing can all be used. In some cases it is necessary or advisable to derivatize the sample in order to enhance its thermal stability.

Mass spectrometers of any type can be coupled, from huge magnetic sector machines to time-of-flight systems and the small 'bench-top' quadrupole or ion trap instruments. When the mass spectrometer is op-

erated in positive ion mode with electron impact ionization at 70 eV spectra generated can be compared with those in the extensive databases organized by NIST and Wiley. Using computerized file-handling techniques, spectra can be compared very rapidly and a list of possible compounds can be compiled. The mass spectrometer can also be operated in negative ion mode which allows improved sensitivity with particular analytes especially with chemical ionization.

Applications

Figure 1 shows typical results from a GC-MS study using a bench-top quadrupole system. The sample was obtained by extraction of serum taken after administration of an oestradiol prodrug. The upper

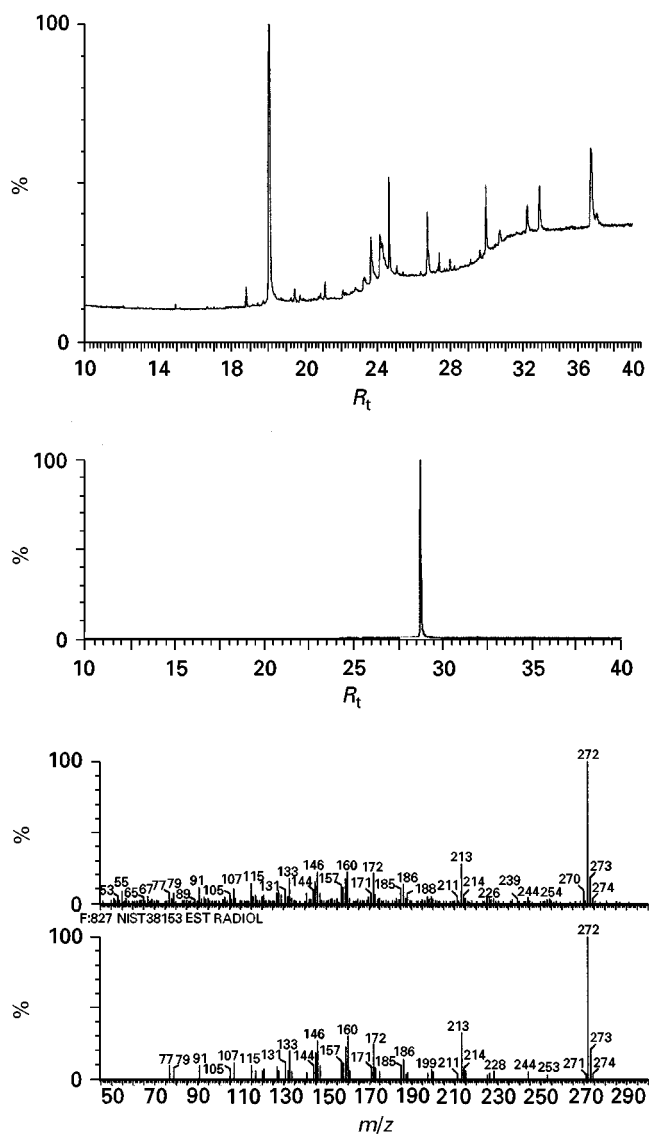


Figure 1 GC-MS of serum extract following oestradiol prodrug administration: (top) total ion chromatogram; (middle) mass chromatogram for $m/z = 272$; (bottom) mass spectrum for peak at $R_t = 28.76$ min and NIST library spectrum for oestradiol.

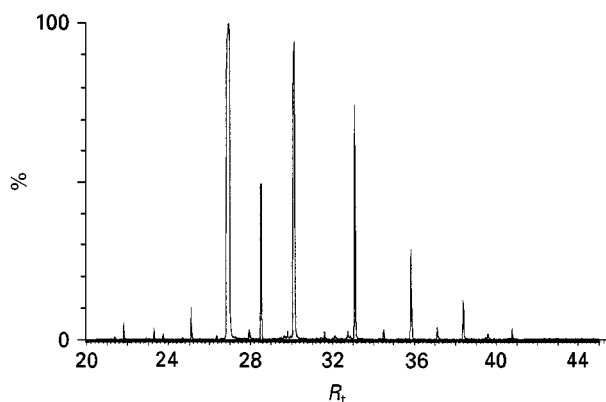


Figure 2 Mass chromatogram for $m/z = 74$ identifying FAMES.

trace shows the total ion chromatogram (TIC), the second trace shows the mass chromatogram for $m/z = 272$ which is diagnostic for oestradiol. The mass spectrum obtained for this component and the NIST library match are the lower traces.

Use of mass chromatograms of diagnostic ions allows facile recognition of homologous series such as fatty acid methyl esters (FAMES). **Figure 2** shows the mass chromatogram for $m/z = 74$ for the FAME derivatives prepared from an archeological sample; this valuable information assisted in the interpretation of the pottery artifact.

The signal at $m/z = 74$ is due to methyl ethanoate formed in the mass spectrometer by a McLafferty rearrangement shown in **Figure 3**. This process can occur with any FAME having an available hydrogen atom at position 4 and thus provides a useful diagnostic ion.

Selected ion recording (SIR) measures the ion current for a restricted range of ions instead of the whole spectrum. This is of particular use in biomonitoring studies for example where the analyte is well characterized from the chromatographic and spectrometric point of view, affording improved sensitivity and precision.

Figure 4 is a graphical representation of the data from an occupational health study of urinary amines: paired samples of urine taken at the beginning and end of a working day were analysed for a particular aromatic amine. A protocol was used that freed the amine from excreted conjugates followed by ex-

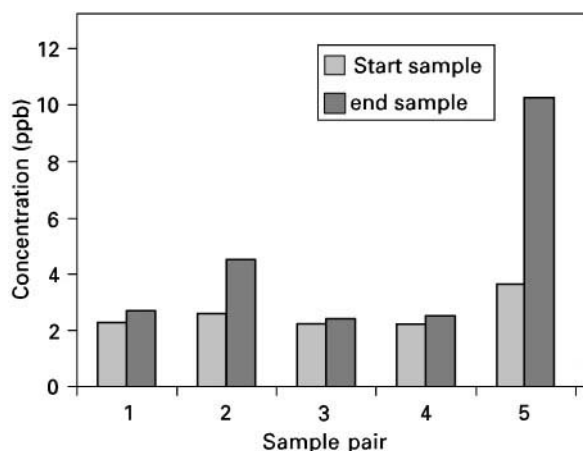


Figure 4 Urinary amine concentrations of paired samples.

traction and derivatization. The graph emphasizes the difference between the amounts of amine in the paired samples; although the values were well below regulatory limits, those from the fifth pair led to a change in working practice for that donor.

Amines can be converted into perfluoroacyl derivatives which are more stable thermally and chemically; such derivatives give improved sensitivity in electron-capture detectors and this is also manifest in negative ion chemical ionization mass spectrometry. This approach can be adopted for the analysis of materials that form relatively stable gas phase anions in the mass spectrometer. **Figure 5** shows data from another typical example: prostanoids such as $\text{PGF}_{2\alpha}$ are converted into the t-butyldimethylsilyl ether/pentafluorobenzoyl ester derivatives. Under negative ion chemical ionization conditions using either methane or ammonia as reagent gas, the ester function is lost in a fragmentation reaction to form a fragment ion at $m/z = 695$ corresponding to the silyl ether carboxylate anion shown in the figure. This ion shows satellites due to silicon and carbon isotopes at 696 and 697 that are in accord with calculated distributions. Detection levels for this analyte are in the low $\text{pg } \mu\text{L}^{-1}$ (ppm) range for full scan data and $\text{fg } \mu\text{L}^{-1}$ (ppb) range with selected ion recording.

The final example of this first group of applications involving small volatile species crosses the boundary into analysis of large intractable materials and concerns a pyrolysis study. Occasionally there may be insufficient sample to carry out a normal extraction prior to GC-MS analysis, this is particularly so with conserved archeological material and microscopic biopsy samples. In such circumstances, microscale sealed vessel pyrolysis GC-MS can be applied: **Figure 6** shows the TIC obtained from a hair sample (2 mg) taken from an Egyptian mummy. The individual components of the pyrolysate can be identified

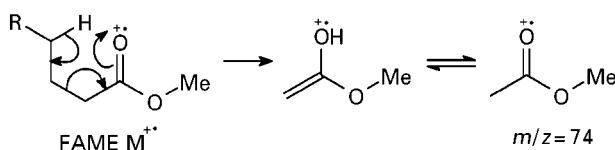


Figure 3 McLafferty rearrangement in a FAME $\text{M}^{+\bullet}$ to form $m/z = 74$.

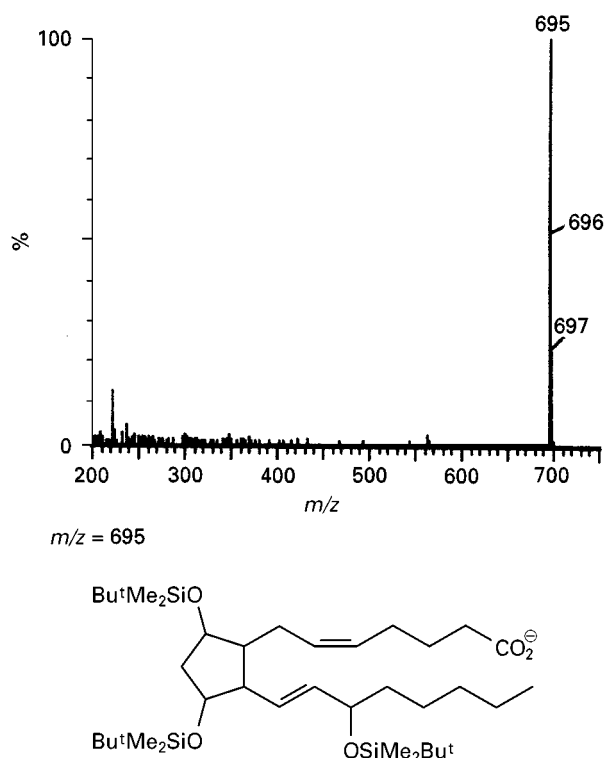


Figure 5 Mass spectrum of derivatized $\text{PGF}_{2\alpha}$ in negative ion chemical ionization and structure of anion corresponding to $m/z = 695$.

by comparison with library spectra and interpreted in terms of the mummification process.

This pyrolysis method can be applied to other complex analytes including whole cells in order to investigate occluded materials or for the identification of chemical modification of biopolymers such as starch.

The quantitative analysis of halogenated dibenzodioxins and -furans in biological (and environmental) matrices is a good example of the combination of high resolution GC (HRGC) and MS (HRMS) technologies using the isotopes of chlorine and carbon

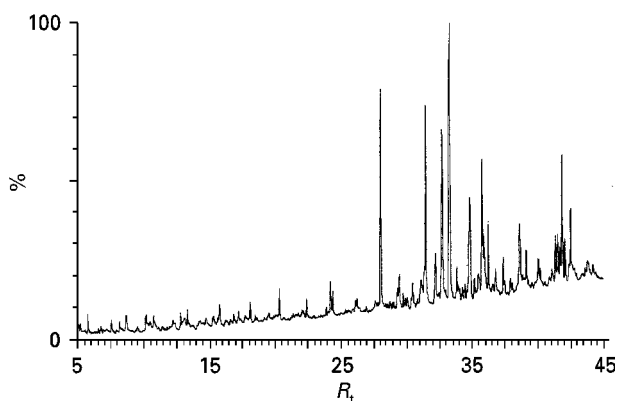


Figure 6 Total ion chromatogram from GC-MS of pyrolysis products from archaeological hair sample.

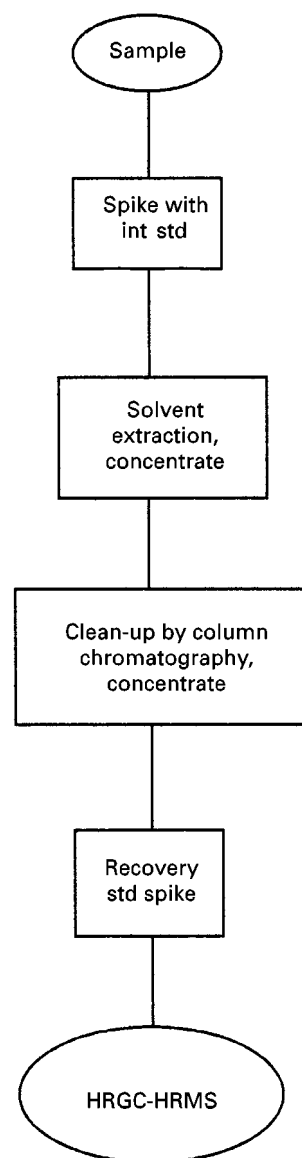


Figure 7 Protocol for pretreatment of dioxin/furan samples prior to HRGC-HRMS.

to facilitate identification and quantification. Prior to any instrumental analysis, the flesh, vegetation or other material has to be prepared according to a quality assured protocol that is summarized in Figure 7.

Intrinsic to the procedure is the use of standards: the first standard to be added is $^{13}\text{C}_{12}$ -2,3,7,8-tetrachlorodibenzodioxin upon which quantitation is based. Another standard, $^{13}\text{C}_{12}$ -1,2,3,4-tetrachlorodibenzodioxin is added after the chemical manipulation of the sample is complete and immediately prior to GC-MS analysis. Comparison of the signals from the two standards then allows the efficiency of the extraction process to be assessed. Typical data sets are shown in Figures 8 and 9: both show four traces, the upper two traces are the high resolution

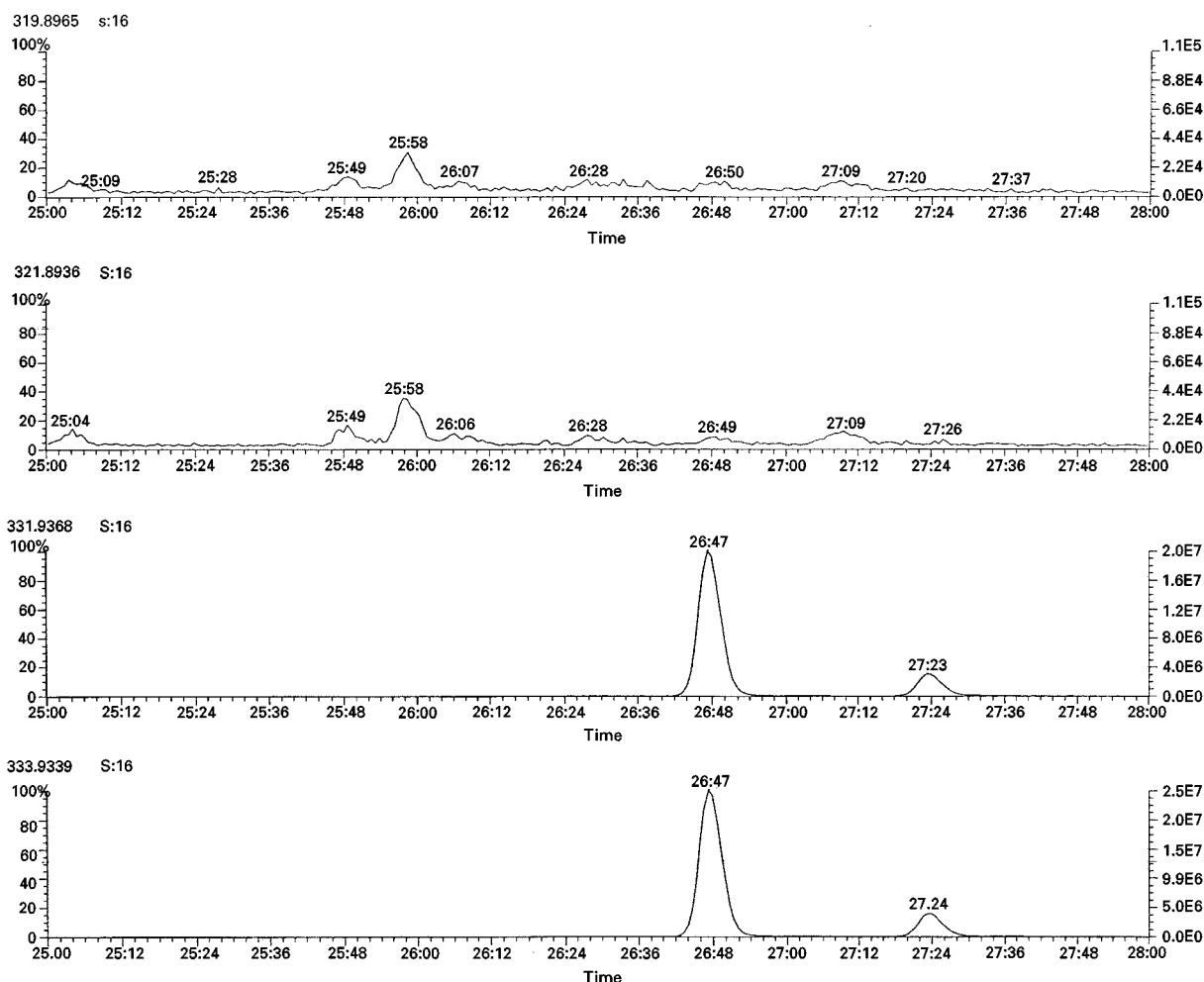


Figure 8 HRGC–HRMS SIR data from dioxin/furan analysis of meat extract.

SIR data for $m/z = 319.8965$ and 321.8936 corresponding to the molecular ions of tetrachlorodibenzodioxins (TCDD), i.e. $C_{12}H_4(^{35}Cl)_4O_2$ and $C_{12}H_4(^{35}Cl_3^{37}Cl)O_2$ respectively. The lower two traces in each case correspond to the ions of $m/z = 331.9368$ and 333.9339 for the ^{13}C -isotopomers, i.e. $^{13}C_{12}H_4(^{35}Cl)_4O_2$ and $^{13}C_{12}H_4(^{35}Cl_3^{37}Cl)O_2$ for the two standards.

The data shown in Figure 8 represents TCDD levels below regulatory limits whereas those in Figure 9 (from an environmental sample) were significantly higher.

Analysis of Isotopomers

The above example shows the dual benefits of high resolution instrumentation and isotope dilution to effect precise quantification and identification. There are many other examples of this type of application that relies upon analysis of the intact analyte molecule in the mass spectrometer. The

second group of applications follows a different approach in which isotopomeric components are initially separated then converted into light gases, carbon dioxide, hydrogen and nitrogen. It is these latter materials that are investigated in the isotope ratioing mass spectrometer whereby the ratios of carbon, hydrogen, oxygen and nitrogen isotopes are determined with much greater precision.

Instrumentation

The design of the mass spectrometer is extremely simple comprising an electron impact ionization source, a very stable magnetic analyser and triple Faraday cup collector (Figure 10A).

The combustion interface incorporates a furnace containing heated copper oxide which converts organic chemicals in the column effluent into carbon dioxide and water; a cold trap is used to remove the water vapour. Conversion of the individual components into the same chemical species such as carbon dioxide removes some of the variables that arise from

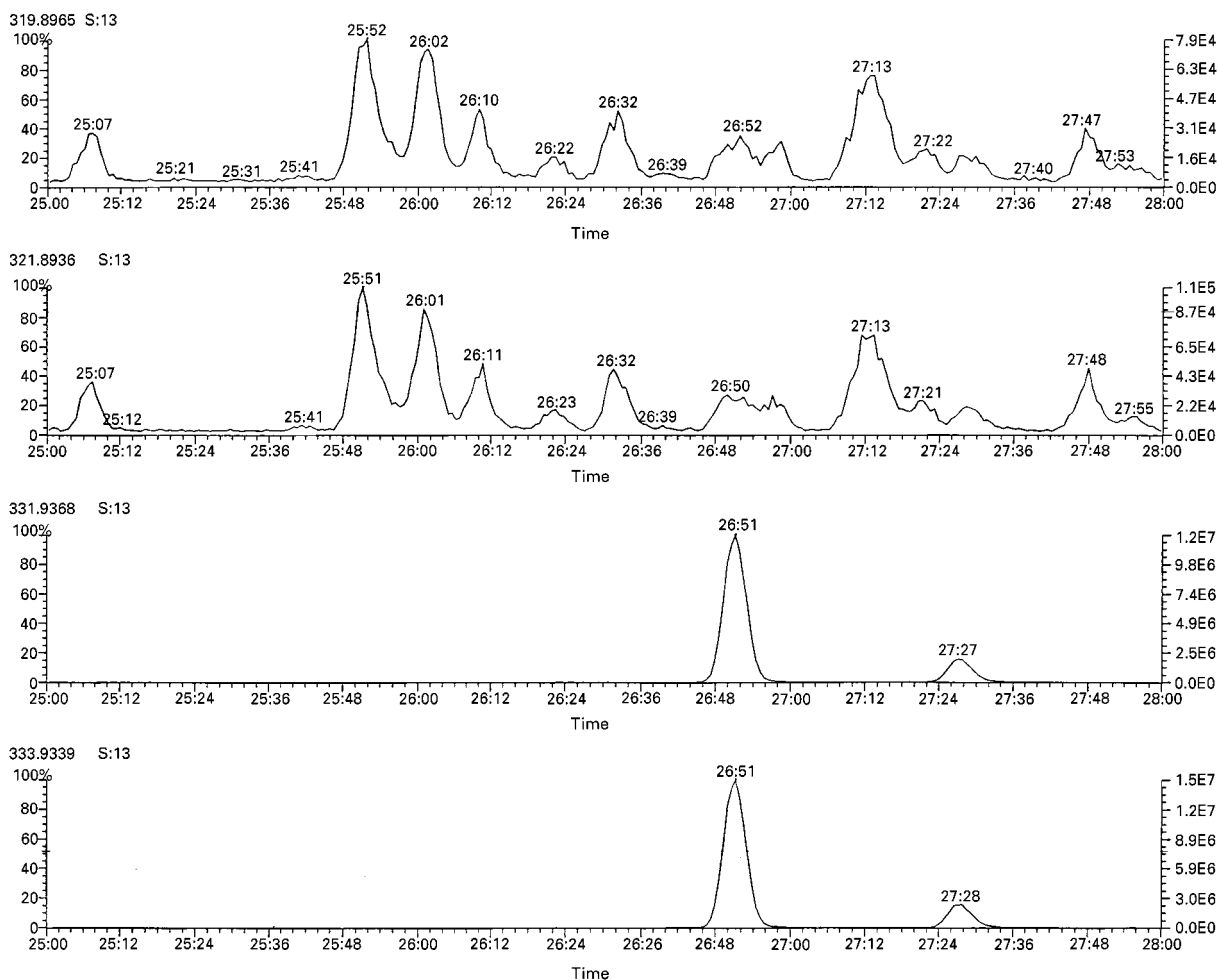


Figure 9 HRGC–HRMS SIR data from dioxin/furan analysis of an environmental sample.

different sample behaviour and isotopomeric distribution commonly observed in electron impact ionisation. Simultaneous recording of the ion beams at $m/z = 44, 45$ and 46 (corresponding to $^{12}\text{C}^{16}\text{O}_2$, $^{13}\text{C}^{16}\text{O}_2$ and $^{12}\text{C}^{16}\text{O}^{18}\text{O}$ respectively for carbon dioxide) using three separate Faraday collectors minimizes background signal fluctuation. These differences result in a dramatic improvement in the stability of the signal allowing determination of isotopic ratios at about 10^{-5} at%.

Figure 10B shows a graphical output from the three collectors for three reference gas pulses and one sample.

The units used to express the relative difference in isotopic abundances are either atoms% (at%) or delta (δ , per mil or ‰).

$$\text{At\%} = \left(\frac{\text{no. of minor atoms}}{\text{no. of major atoms}} \right) \times 100$$

$$\delta = \frac{(\text{sample ratio} - \text{reference ratio})}{\text{reference ratio}} \times 1000$$

Applications

The use of stable isotopes such as ^2H , ^{13}C , ^{15}N or ^{18}O instead of the radioactive analogues removes all risks associated with radiation but the introduction of an isotopic substitution at the site of a rate-limiting reaction can introduce kinetic isotope effects. Thus an artificial change to the natural isotopic distribution could in theory alter the kinetics of the biochemical process and thereby affect the overall metabolic rate. Many theoretical calculations and experimental observations have been made: the greatest differences occur with hydrogen replacement with a maximum relative rate ratio ($k_{\text{H}}/k_{\text{D}}$) of 18. The differences with other isotopic replacements are much smaller: $^{12}\text{C}/^{13}\text{C}$ up to 1.25; $^{14}\text{N}/^{15}\text{N}$, 1.14; $^{16}\text{O}/^{18}\text{O}$, 1.119 and $^{32}\text{S}/^{34}\text{S}$, 1.05. This particular risk is however even smaller than that with the corresponding radiolabels whose values are $^1\text{H}/^3\text{H}$, 60 (max) and $^{12}\text{C}/^{14}\text{C}$, 1.5.

Breath Gas Testing Using $^{13}\text{CO}_2$

The basic principle is illustrated in **Figure 11**.

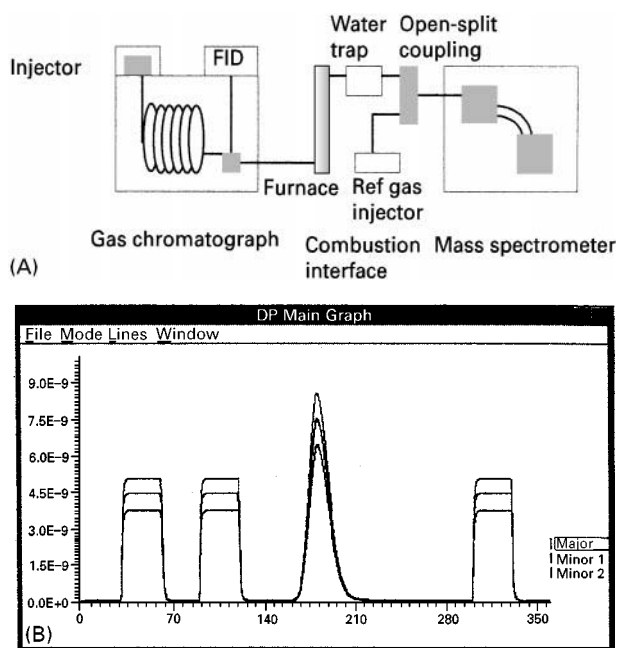


Figure 10 (A) Schematic representation of a GC-SIRMS system (B) Graphical output from SIRMS of two reference gas pulses, sample, reference gas pulse.

Oral administration of either a solution of the ^{13}C -labelled substrate in water or fruit juice or a suspension in a flavoured colloidal preparation is usually preferred to intravenous injection to emphasize the 'non-invasive' approach. Breath gas is the easiest means of sample collection. However, there are others including saliva, urine, faeces, milk, hair, nails

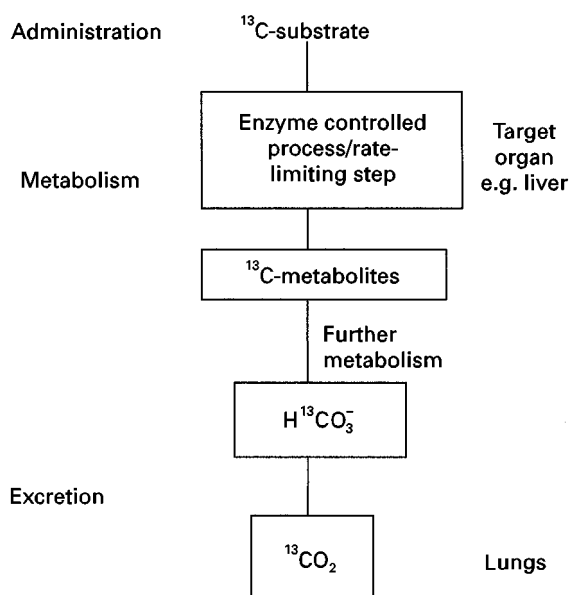


Figure 11 Schematic diagram of procedure for breath gas testing.

or blood, gastric fluid or muscle. These latter requiring clinical intervention.

The ^{13}C -urea breath test for *Helicobacter pylori* A characteristic of this bacterium is its high urease activity; this is exploited by administering a solution of ^{13}C -urea (1 mg kg^{-1} body weight, ca. 75 mg for an average adult) and investigating the effect on the level of $^{13}\text{CO}_2$ in the breath after a short time interval of about 20–30 min. If the bacterium is present, the urea is converted into bicarbonate which appears in the breath as $^{13}\text{CO}_2$; in its absence the isotopic distribution remains unchanged (Figure 12).

Typical results from a group of untreated and treated patients are shown in Figure 13: differences between the pre- and post-breath samples (referring to ^{13}C -urea administration) of more than 3‰ are taken to indicate infection.

Other metabolic breath tests Introduction of a variety of ^{13}C -labelled substrates into a test meal that is ingested by the patient can be used to monitor particular metabolic functions *in vivo* without the need for invasive surgery and the collection of biopsy samples and subsequent *in vitro* biochemical investigation. Thus gastric emptying rates can be measured using octanoic acid labelled at position 1 with ^{13}C ; abnormalities in the cytochrome P450 pathway in liver metabolism can be determined using a variety of substrates shown in Figure 14 with typical data shown in Figure 15.

These data show that measurements taken after a time interval of one hour (after dosing with the labelled substrate) allow unambiguous detection of abnormality. A similar distinction is possible for lipid malabsorption using a range of ^{13}C -labelled triacyl glycerides. The results summarized in Figure 16 are from a study of absorption of ^{13}C -dodecanoic acid introduced intraduodenally.

Tracer studies

The facile determination of carbon isotope ratios in specific compounds extends the scope of tracer studies to include assessment of metabolic rates for a wide variety of substrates. Thus administration of specifically labelled lipids, amino acids and carbohydrates followed by GC-SIRMS analysis of fractionated serum samples allows not only the identification of

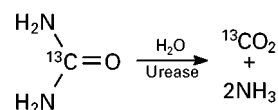


Figure 12 Chemical basis of the *Helicobacter pylori* breath test.

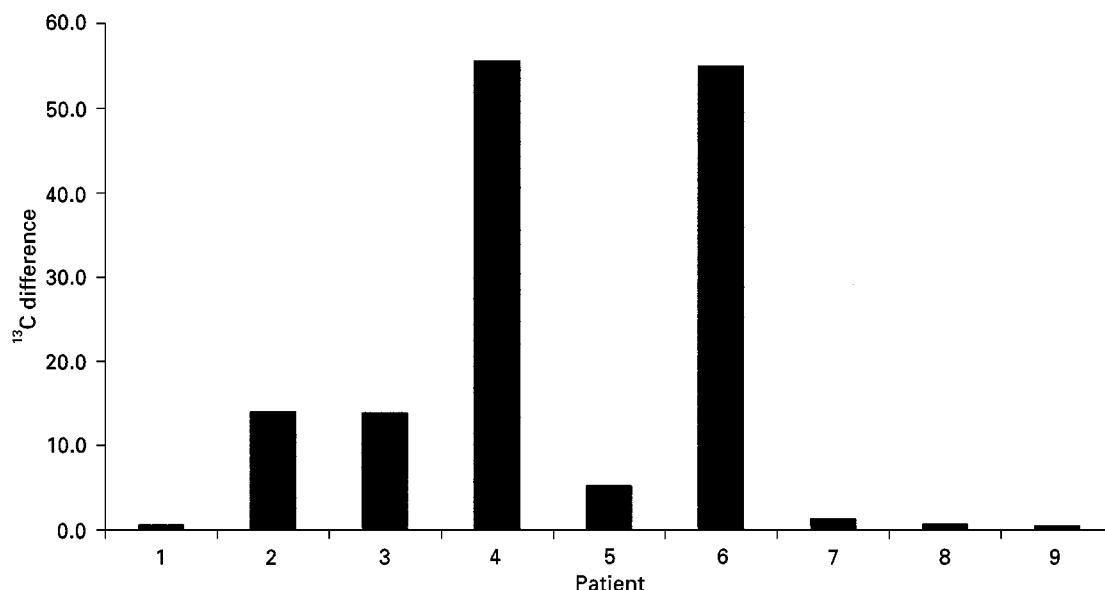


Figure 13 Typical results from *Helicobacter pylori* breath tests.

metabolic products but also the measurement of turn-over rates of those substrates. The sensitivity of the system is such that measurements can be made using enriched substrates (as opposed to fully labelled compounds). **Figure 17** summarizes the results of a study using ¹³C-enriched maize sugar administered at 1 g kg⁻¹ body weight then timed blood samples purified and analysed for enrichment of plasma glucose by GC-SIRMS.

The data demonstrated that even at relatively low levels of enrichment, the appearance rate could be measured.

Natural abundance measurements

Primary and secondary kinetic isotope effects, although small, lead to fractionation of isotopomers and the observed natural variations in isotopic abundances. These temporal and geographical variations can be measured using SIRMS and used to

detect adulteration and authenticity of foodstuffs and identify migration patterns of insects.

The variation in ¹³C content of a variety of natural materials is summarized in **Figure 18**. Plants convert carbon dioxide into carbohydrates by two main photosynthetic mechanisms: the Calvin–Benson cycle or the Hatch–Slack pathway. Plants such as rice, wheat, potatoes, beet or brassicas utilize C₃ intermediates and result in depleted ¹³C content (i.e. delta values are more negative) whereas maize, sugar cane and tropical fruits use C₄ intermediates that demonstrate higher ¹³C content. The differences are large enough to be translated through the food web and be measured by GC-SIRMS.

The average δ-¹³C value of honey, produced from flowers of C₃ plants by bees, is significantly lower than that of high fructose corn syrup (HFCS, produced from maize, a C₄ plant). Hence, it is possible not only to identify adulteration of honey with HFCS but also to determine its extent.

Many natural products, e.g. vanillin, are also available as synthetic products from chemical or biochemical syntheses; the distinction between natural, nature-identical and synthetic can be determined using GC-SIRMS. The natural product obtained by extraction has a generally higher δ-¹³C value (ca. –20‰) compared to fossil fuel derived material (ca. –30‰) or fermentation product (ca. –35‰).

The method can be used to distinguish exogenous materials from their endogenous counterparts; this is particularly useful in the detection of anabolic steroids' administration in meat products, animals, racehorses or athletes where conventional GC–MS

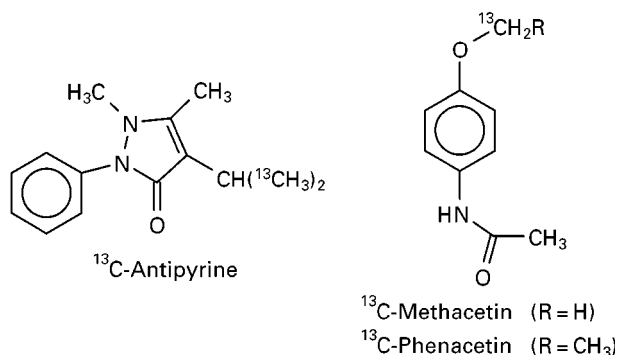


Figure 14 Substrates for breath tests of liver metabolism.

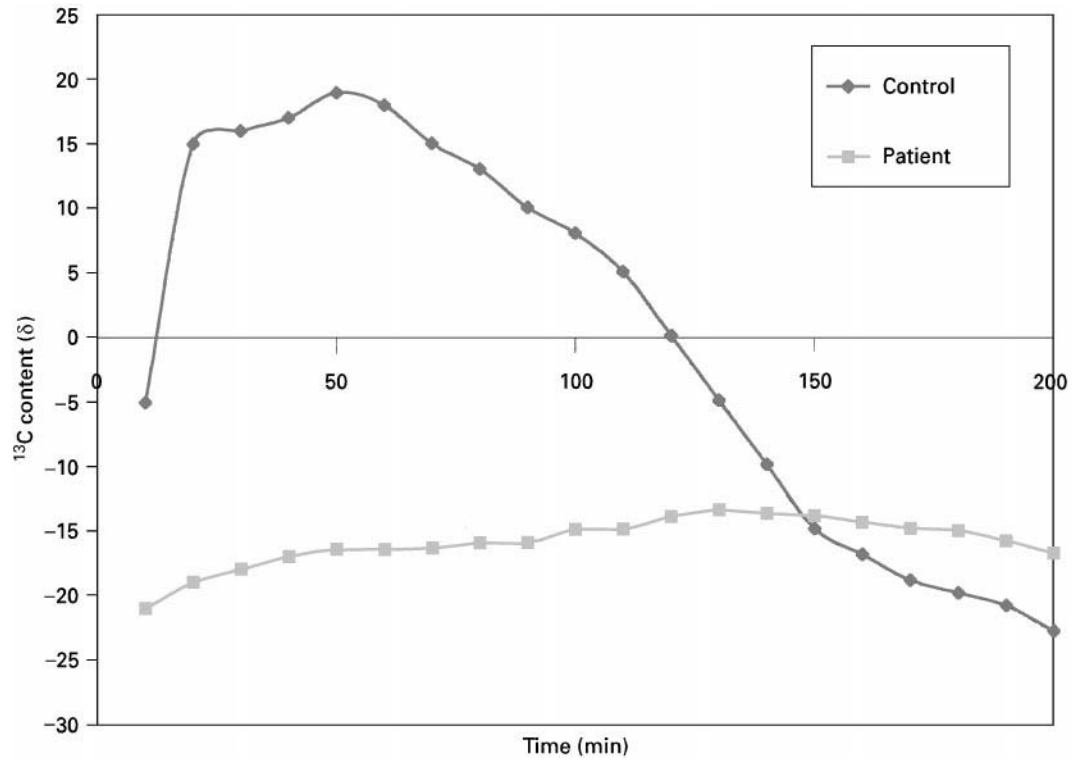


Figure 15 Comparison of data from patient and control for liver metabolism.

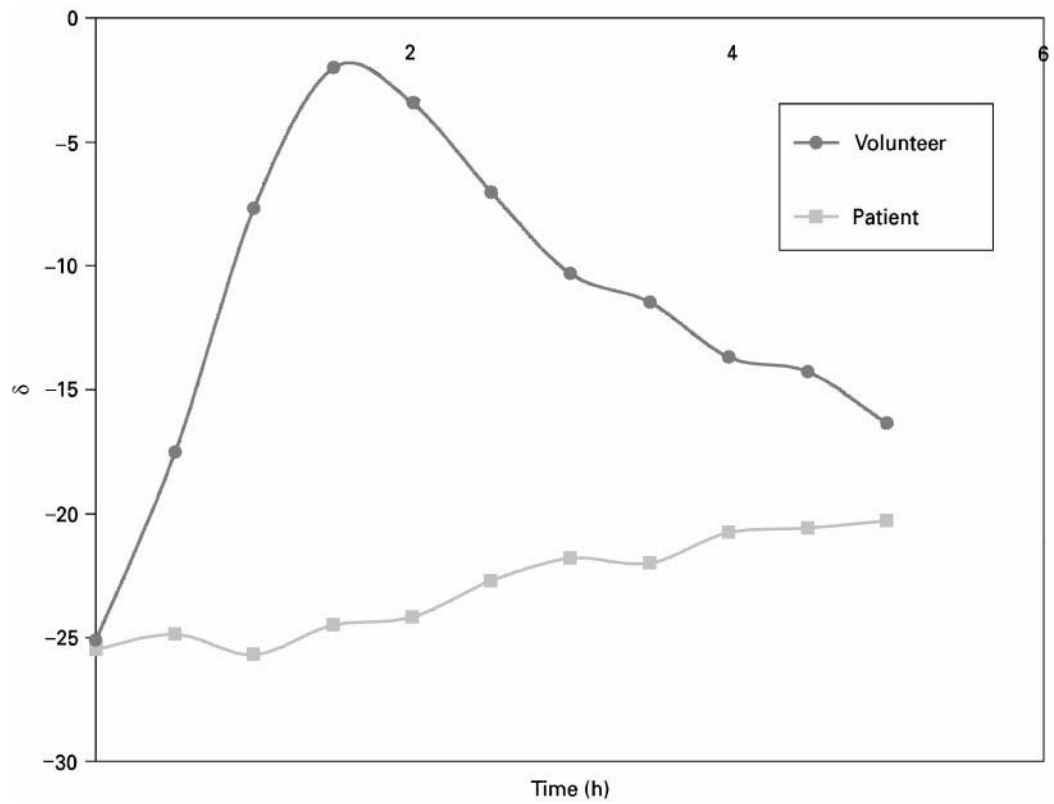


Figure 16 Appearance data for breath gas analysis following ^{13}C -dodecanoic acid administration in a study of lipid malabsorption.

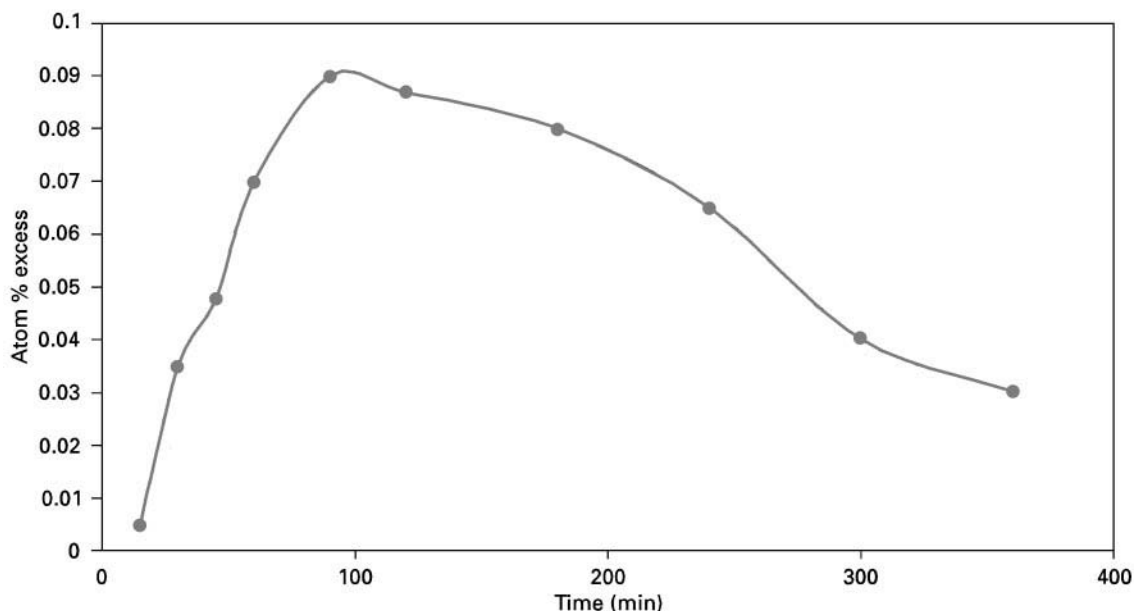


Figure 17 Appearance rates from a GC-SIRMS study of plasma glucose.

protocols have been shown to be inadequate. When the carbon isotope ratios for the major metabolites of testosterone, for example, are normalized to an endogenous reference compound such as cholesterol, the differences between testosterone-treated and untreated animals is statistically significant.

It is not only carbon that shows variability in its isotopic distribution; hydrogen and oxygen also show geographical variability that is correlated to rainfall latitude. Continuous-flow pyrolysis measurements of δD and $\delta^{18}O$ have been used to study animal migration patterns using a development of the technology described above. The use of helium as a carrier gas means that there is a large signal generated for He^+ at $m/z = 4$ and this needs to be totally resolved from the relatively small signal at $m/z = 3$ due to HD^+ . This is further complicated by the presence of ions at

$m/z = 3$ due to H_3^+ arising from an ion molecule reaction in the mass spectrometer source. This latter problem is overcome by application of a correction factor calculated from data from reference gas pulses.

The sample (e.g. insect wings, ca. 1 mg) is pyrolysed in a helium stream in a furnace containing quartz chips and nickel carbide at about $1000^\circ C$. The pyrolysis products, hydrogen, carbon monoxide and nitrogen, are separated using a packed column (1.5 m, molecular sieve 5 Å) then introduced into the mass spectrometer.

Reference pulses of hydrogen and carbon monoxide are introduced prior to the sample peaks and used to calculate the δD and $\delta^{18}O$ values for m/z 3/2 and m/z 30/28 and 29/28 (for carbon monoxide). A typical data set is:

	Sample 1	Sample 2	Sample 3
Latitude	30°	40°	50°
δD precipitation	-15‰	-33‰	-80‰
δD sample	-78‰	-92‰	-125‰
$\delta^{18}O$ sample	$+5.7\text{‰}$	$+3.8\text{‰}$	$+0.3\text{‰}$

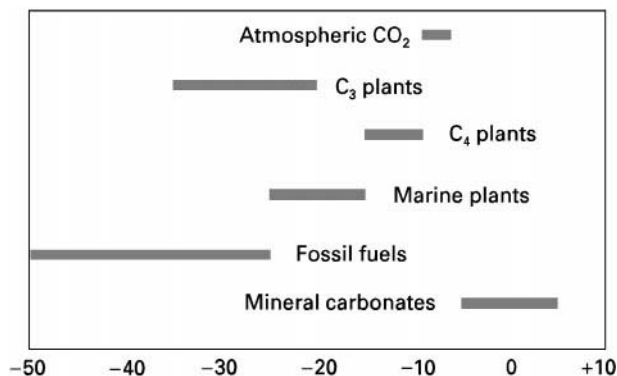


Figure 18 Natural variation in ^{13}C content (‰) of natural materials.

Conclusion

GC-MS will continue to provide much high quality and fundamental analytical information that will allow the biomedical sciences to develop along the avenues described above for some time. Improvements in the technology of extraction and sampling will allow progressively smaller samples to be used.

The availability of relatively inexpensive and safe isotopically labelled substrates and precursors will benefit tracer studies and allow improved precision in quantitative measurements of a wide variety of analytes. GC-SIRMS will facilitate dynamic studies of metabolism and migration. The capacity to distinguish exogenous from endogenous materials is bound to be a significant and expanding area of application that will find great use in the identification of abuse, adulteration and authenticity.

Acknowledgements

The following are acknowledged: Nick Ordsmith and Keith Hall from Hall Analytical Laboratories Ltd. Andy Phillips from Micromass Ltd. Nick Bukowski from ThermoQuest.

See also: II/Chromatography: Gas: Detectors: Mass Spectrometry. III/Drugs of Abuse: Solid-Phase Extraction.

Further Reading

Chapman JR (1993) *Practical Organic Mass Spectrometry. A Guide for Chemical and Biochemical Analysis*, 2nd edn. Chichester: John Wiley.

Johnstone AW and Rose ME (1996) *Mass Spectrometry for Chemists and Biochemists*. 2nd edn. Cambridge: Cambridge University Press.

Krumbiegel P (1991) *Stable Isotope Pharmaceuticals for Clinical Research and Diagnosis. (Drug Development and Evaluation)*, vol.18. Jena: Fischer.

McLafferty FW and Turecek F (1993) *Interpretation of Mass Spectra*. 4th edn. Sausalito: University Science Books.

Thin-Layer (Planar) Chromatography

See III/CLINICAL CHEMISTRY: THIN LAYER (PLANAR) CHROMATOGRAPHY

BITUMENS: LIQUID CHROMATOGRAPHY



K. Dunn, G. V. Chilingarian and T. F. Yen,
University of Southern California, Los Angeles,
CA, USA

Copyright © 2000 Academic Press

Introduction

Great confusion exists in the literature on the definition of the term *bitumen*. It occurs in the earth's crust in various forms: firstly, in a dispersed state, in trace quantities; and secondly, as accumulations, where bitumen either impregnates the rock or occurs in a pure or nearly pure form. In the first half of the 20th century, the term bitumen was applied to crude oil and its natural derivatives (maltha, asphalt, ozokerite). In this original meaning, bitumens are called naphthides. The term bitumen is also used for asphalts and asphalt-like manufactured substances utilized in road construction, including products from the processing of coals and/or oil shales. In crude oils, in distillate cuts beginning with kerosene, and in distillation residues, there is a group of high molecular weight heteroorganic compounds that are lumped under the name of resins and asphaltenes. Their content may be as large as 40% in heavy crude oils.

Carbon and hydrogen constitute 80–95% of the resin and asphaltene molecules, with oxygen always present. Sulfur, nitrogen and metals are also usually present. The content of resins in crude oil (2–40%) exceeds by far (from 3 to 40 times) the content of asphaltenes (trace to 6%; usually <1%). Carboids and carbenes, which resemble asphaltenes, differ from them by having a higher oxygen content. However, they are absent in crude oils and distillate cuts. In small quantities, they are found in residues from vacuum distillation, in cracked tars, and in native and petroleum asphalts.

Bitumens and the related heat-treated asphalt are a very complex mixture of compounds with a wide range of molecular weights, which are difficult to isolate into classes of pure compounds. Resins are semi-liquid (sometimes almost solid) dark brown to black substances which have a specific gravity around 1 and a molecular weight of 500–2000 (usually 600–1000). Asphaltenes, on the other hand, are dark, amorphous powders and have a specific gravity greater than 1 and molecular weights of 1000–10 000 (average 5000). Using various methods, the observed molecular weights suggest that asphaltenes form molecular aggregates or colloids, even in dilute

Table 1 Unit molecular weight of asphaltenes

Method	Particle weight	Researcher
Viscosity	900–4000	Fischer and Schrem (1959)
High angle X-ray	805–3360	Yen <i>et al.</i> (1961)
Light absorption	1000–4000	Markhasin <i>et al.</i> (1966)
Electron microscopy	3440–5430	Dickie <i>et al.</i> (1969)
VPO	2950–8130	Dickie and Yen (1967)
VPO	2000–4600	Dickie and Yen (1967)
VPO	1220–2160	Speight <i>et al.</i> (1985)
Cryoscopic, naphthalene	1700	Hilman and Barnett (1937)
Cryoscopic, phenathrene	2500	Boyd and Montgomery (1962)
Cryoscopic, benzene	5000–6000	Katz (1934)

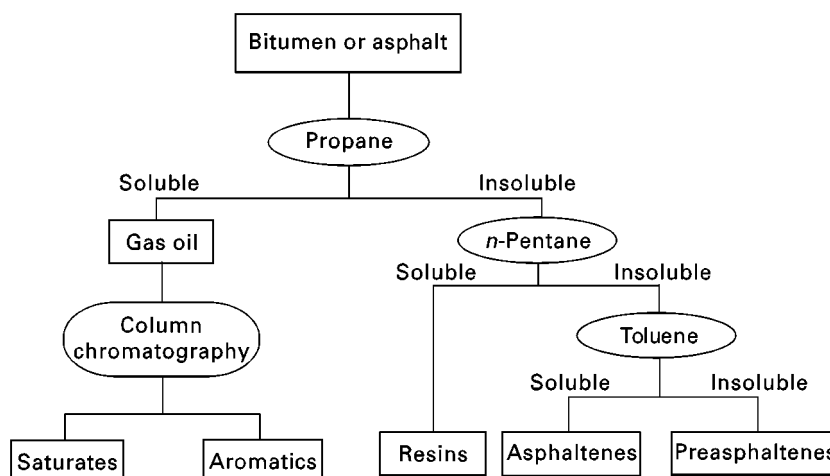
solutions. The results are influenced by solvent polarity, asphaltene concentration and the temperature used. Different molecular weights of asphaltenes can be obtained by different instruments. For example, the data obtained from solution viscosity and cryoscopic method are low, whereas those obtained from the ultracentrifuge and electron microscope are high. Vapour pressure osmometry (VPO) is considered to be the most accurate method at present when a good solvent is used to disperse the asphaltenes. Because the solvent affects the degree of asphaltene aggregation, the true molecular weights of asphaltenes are generally much lower than those measured. Some of these results are listed in **Table 1**.

The asphaltene content is a variable value depending on the relative amounts and characteristics of the source material and on the procedure adopted for separation. The physical and chemical characteristics are of considerable importance: the higher boiling point components of crude oil can precipitate in certain solvents, whereas the lower boiling point components (cyclic and aromatic compounds) are soluble in solvents. Most of the studies on bitumens and asphalts are concentrated on groups of compounds with

particular physical and chemical properties. Depending on the solubility in certain solvents, asphalt or bitumen is generally fractionated into four main fractions: saturates, aromatics, resins and asphaltenes. The polarity of these fractions increases in the following order: saturates < aromatics < resins < asphaltenes. A detailed scheme for bitumen fractionation is shown in **Figure 1** and explained as follows:

1. Gas oil is propane-soluble and *n*-pentane-insoluble.
2. Resins are *n*-pentane-soluble but propane-insoluble.
3. Asphaltenes are toluene-soluble but *n*-pentane insoluble.
4. Preasphaltenes are insoluble in both *n*-pentane and toluene.

Asphaltenes are multipolymer systems containing a great variety of building blocks. The statistically average molecule contains a flat sheet of condensed aromatic systems that may be interconnected by sulfide, ether, aliphatic chains or naphthenic ring linkages. Gaps and holes appear as defect centres in the aromatic systems most likely involving free radicals. Heterocyclic atoms may be coordinated to transition

**Figure 1** Fractionation scheme of bitumen or asphalt.

metals such as vanadium, nickel and iron. Approximately five of these sheets are associated by π - π interaction. They are stacked one above the other: the distance between the sheets ranges from 0.36 to 0.38 nm, giving an overall height for a stack of 1.6–2.0 nm; the average sheet diameter appears to be 0.85–1.5 nm. The hypothetical structure of an asphaltene is shown in Figure 2.

Resins are considered smaller analogues of asphaltenes with a much lower molecular weight. The resins contain aromatic compounds substituted with longer alkyl chains and a greater number of side chains attached to the rings than asphaltenes. The combination of the saturated and aromatic characteristics of resins stabilizes the colloidal nature of asphaltenes present in the oil.

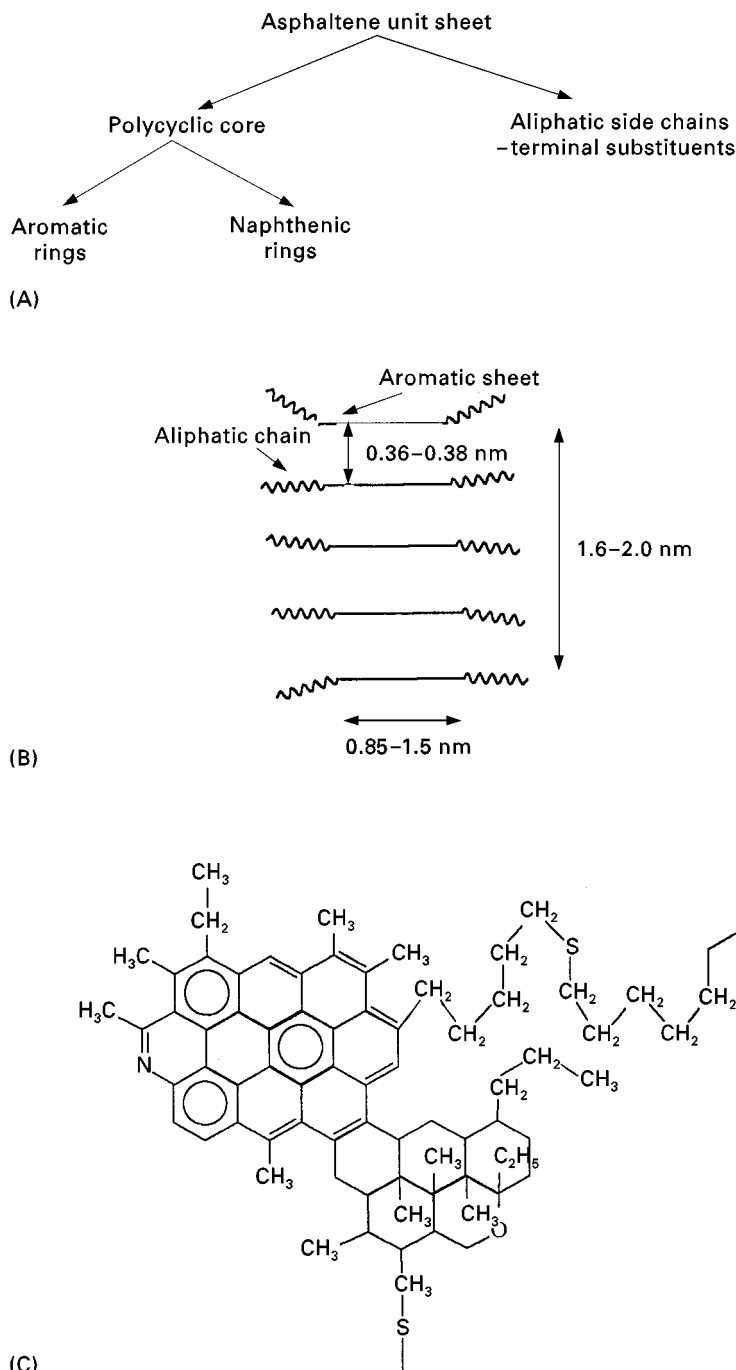


Figure 2 (A) The classification of asphaltene structure. (B) The structure of asphaltene stack. (C) The structure of one sheet of asphaltene stack.

The gas oils constitute the lowest molecular fraction of the asphalt and serve as the dispersion medium for the peptized asphaltenes. Structurally, gas oils consist mostly of naphthenic–aromatic nuclei with a greater proportion of side chains than the resins. Alkyl naphthenes predominate and straight chain alkanes are rarely present. The naphthenic content is 15–50%, with naphthenics containing two to five nuclei per molecule.

The fractionation techniques for crude oil involve solvent fractionation and precipitation, column chromatography, ion exchange and complexation methods. No matter what method is used, the important step is the isolation of asphaltenes. Of course, all these separation processes are carried out on the heavy fractions of petroleum only; usually the volatile fractions have been removed by distillation.

The most popular method of column chromatography is the fractionation into saturates, aromatics, resins and asphaltenes (SARA). Solvent fractionations have been used in the industry since 1930, becoming widely accepted between 1950 and 1970. Recently, centrifugal thin-layer chromatography (TLC) has been used to separate crude oil successfully. This method reduces the separation time and cost, as well as preserving each fraction for further study. TLC with flame ionization detector (TLC-FID) can achieve quantitative analysis quickly and simply. The combination of solvent fractionation by silica gel and ion exchange chromatography can achieve a more detailed separation showing the complexity of petroleum. The polar fraction of the crude oil is separated by ion exchange. For chromatographic methods for

bitumen or asphalt separation (SARA method, centrifugal TLC, TLC-FID and the combination of silica gel chromatography and ion exchange) are described in detail in the following sections.

The SARA Method

Background

The SARA method enables the separation of bitumen into groups. The method is an extension of column chromatography in order to permit more standardized separation. Two packed columns are employed: Firstly, a SARA column (ion exchange resins) and secondly, an activated silica gel column. The resin fractions are irreversibly retained in the SARA column, whereas the gas oil (saturates and aromatics) fraction remains in the solvent after elution of this column. The gas oil fraction can be further separated into saturates and aromatics by the activated silica gel column. A flow diagram of the SARA method is given in Figure 3. Although the SARA method has been considered as a standard separation technique for asphaltenes, there are some drawbacks to prevent it from becoming popular: it is time-consuming (it takes at least 1 week) and there is incomplete recovery (resin fraction is difficult to recover).

Separation Procedure

Separation of asphaltenes The asphaltene fraction is separated by a precipitation process. The bitumen and asphalt samples can be dissolved first in toluene to form dispersions for precipitation by another

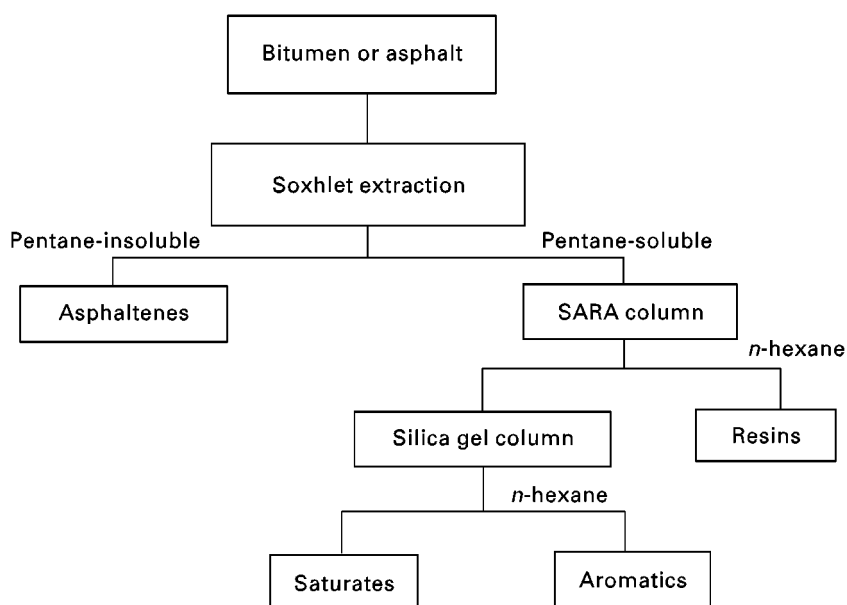


Figure 3 Flow chart of SARA separation method.

liquid. Asphaltene precipitation occurs when an excess of *n*-pentane is added to the toluene dispersion. A toluene-*n*-pentane volumetric ratio of 1 to 50 is required to ensure the precipitation of asphaltenes. After the precipitation process, the toluene dispersion can be separated into two fractions: pentane-insoluble (asphaltenes) and pentane-soluble (maltenes). To purify asphaltenes, the precipitation process is followed by Soxhlet extraction. *n*-Pentane is used during Soxhlet extraction until it becomes clear. This requires over 48 h. The maltene fraction can be further separated by column chromatography.

Separation of saturates and resins The SARA column is dry-packed under vibration with various packings, purged with nitrogen and equilibrated with *n*-pentane. The column contains four discretely packed zones with a sequence of H^+ cation exchange resin, OH^- ion exchange resin, clay-coated with ferric chloride, and OH^- ion exchange resin, as illustrated in Figure 4. The maltenes present in the sample are dissolved by the *n*-pentane, placed in the top reservoir and carried into the column. The leaching process is continued by recycling until the eluate is

colourless. Liquid must always be present in the top reservoir. All operations are carried out under nitrogen. The result of the separation is that the gas oils (saturates and aromatics) collect in the bottom flask, whereas the resins remain in the column. The gas oils can be further fractionated into saturates and aromatics on a silica gel column using *n*-hexane as the eluent, with the saturates being eluted first. The cut-off point of elution between saturates and aromatics can be distinguished by UV examination. Under the UV light, the saturates are colourless, whereas the aromatics exhibit a yellow-green colour.

Separation of resins In the analytical SARA separation, the resin content is obtained from the mass balance, by deducting the weights of asphaltenes and gas oils from the original weight of the sample. This method is easy and rapid to quantify the resin content in the bitumen or asphalt sample; however, the fact that resins cannot be collected for further study is a drawback. The resin fraction retained in the SARA column may be semiquantitatively recovered (approximately 90%) by exhaustive elution of the packing with chloroform. For complete recovery of

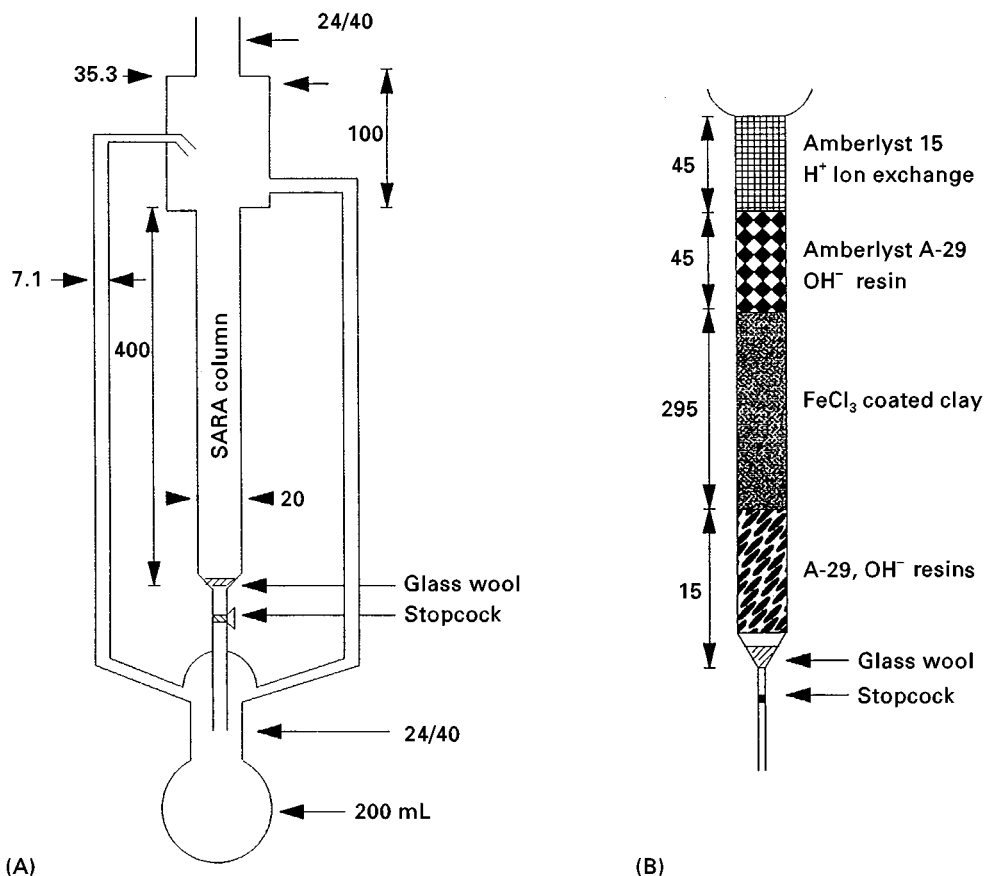


Figure 4 Preparative SARA column. (A) Recycle column for separating resins and oils; (B) SARA column packing sequence. All dimensions are in millimetres. (Modified after Atgelt *et al.*, 1979.)

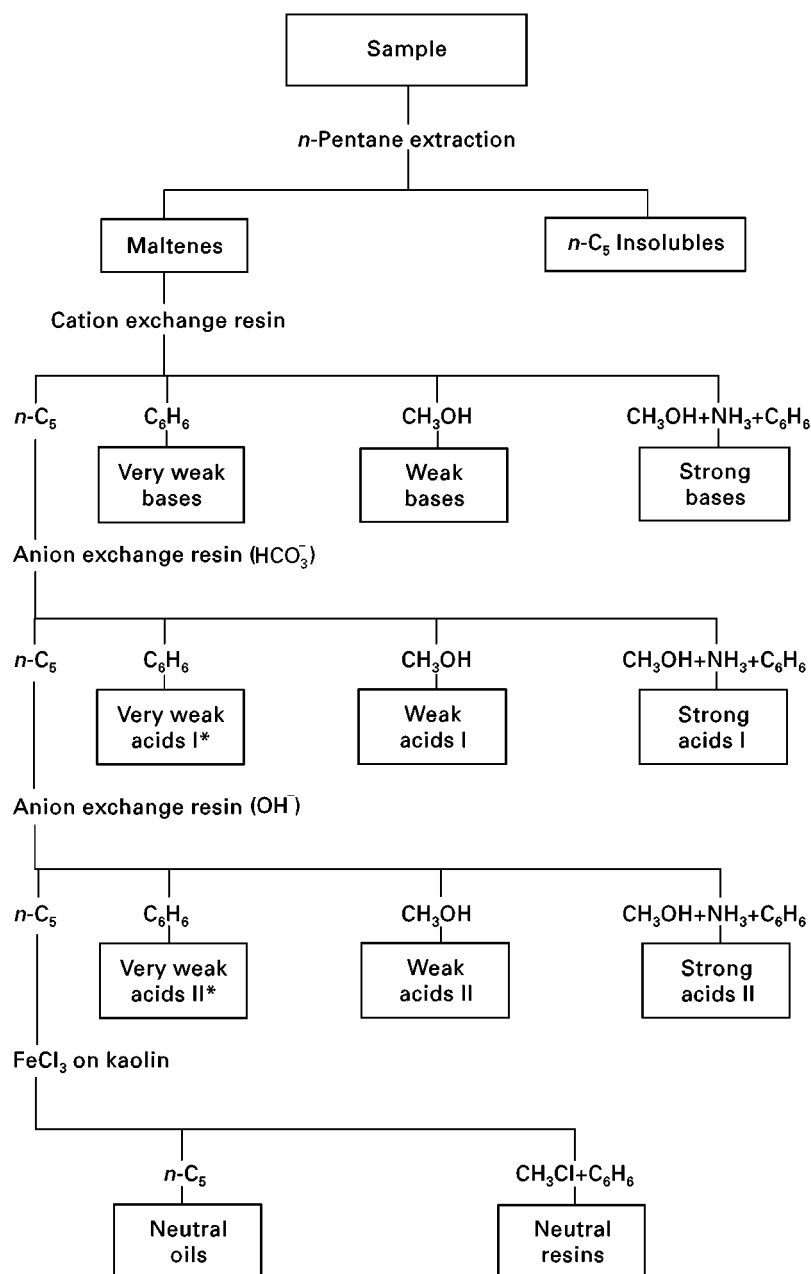


Figure 5 Stepwise separation of resins. *Acids I are stronger than the corresponding acids II. (Reproduced with modification from Jewell, 1979.)

resins, individual cation/anion columns for stepwise separation are used. This separation process, shown in **Figure 5**, includes cation exchange, HCO_3^- anion exchange, OH^- anion exchange, and clay- FeCl_3 complexation. This scheme provides 10 groups of resins, and this demonstrates the great complexity of petroleum composition.

Separation using the SARA method is a time-consuming process. The extraction time varies with the amount and nature of the sample and especially with the content of asphaltenes and other insolubles pres-

ent. Petroleum residues are commonly extracted overnight, whereas samples of tar sands, shale oils and coal liquids may require 3–4 days.

Centrifugal Preparative Thin-layer Chromatography

Background

Hydrocarbon-type fractions from bitumen, heavy crude and distillation residues can be separated by

TLC. This is a rapid, effective and inexpensive method which has the potential to become the major tool for semi-quantitative analysis of composition of the heavy hydrocarbon mixtures. The application of TLC to the separation of petroleum products has been successfully employed by many investigators (e.g., Lian *et al.*, 1992). A conventional TLC method can differentiate (and characterize) among heavy and residue fractions from petroleum, coal liquids, tar sands, bitumens and asphalts. A preparative, centrifugally accelerated, radial, thin-layer chromatograph (the Chromatotron) is suitable not only for quantitative determination of bitumens and asphalts, but also for the collection of various fractions. It is very important to select the appropriate solvents or solvent mixtures for separation into four fractions. Figure 6 shows the solubility parameters of common solvents in relation to those required to dissolve the various asphalt fractions.

Separation Procedure

One type of centrifugal TLC equipment for analysis of the constituents of hydrocarbon mixtures and especially for determination of the composition of bitumen is illustrated in Figure 7. The preliminary preparation (such as rotor coating, sample preparation and application to the rotor) is important in order to achieve good results. Proper preparation of the sample and the appropriate selection of solvent to

dissolve the sample is very important. Details are discussed in the following sections.

Rotor preparation The glass rotor should meet certain requirements: chemical resistance to solvents and developing reagents, ability to withstand temperatures needed for reaction in the rotor, mechanical strength, thickness uniformity and low cost. Silica gel 60 HF254 + 366 (with a binder) can be used as an adsorbent coated on the rotor as a thin layer. The thickness of the adsorbent layer determines the proper flow rate of mobile phase and solvent volume. Table 2 shows the interrelationships of adsorbent layer thickness, solvent volume and flow rate.

Sample preparation and application The process of adding the sample to the Chromatotron rotor is one of the most important steps to ensure the success of the separation. The solvent used must be highly volatile and nonpolar because solvents with a high boiling point or high polarity are difficult to remove from the adsorbent during sample introduction. Sample injection is performed by means of a pump operated at a low flow rate in order to add a large volume of sample to the rotor and to achieve vaporization of the solvent. Sample introduction as a narrow initial band can enhance the resolution greatly. It is necessary to wait for the solvent to vaporize completely before starting the elution process. If a small

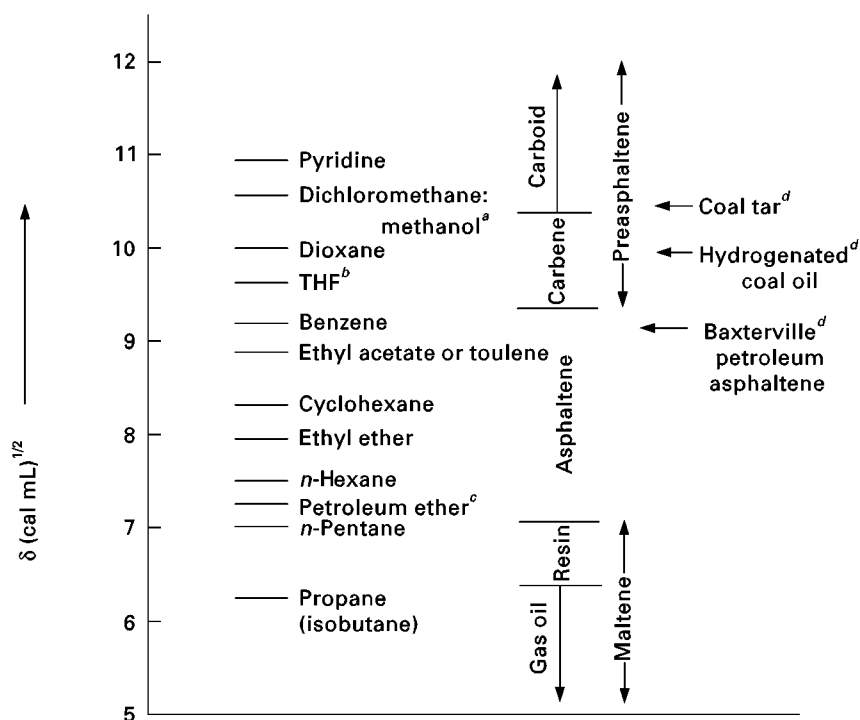


Figure 6 Solubility parameters of common solvents in relation to the values required for dissolution of asphalt fractions. ^a95:5 (v/v); ^btetrahydrofuran; ^cestimated, mixture; ^dcalculated value.

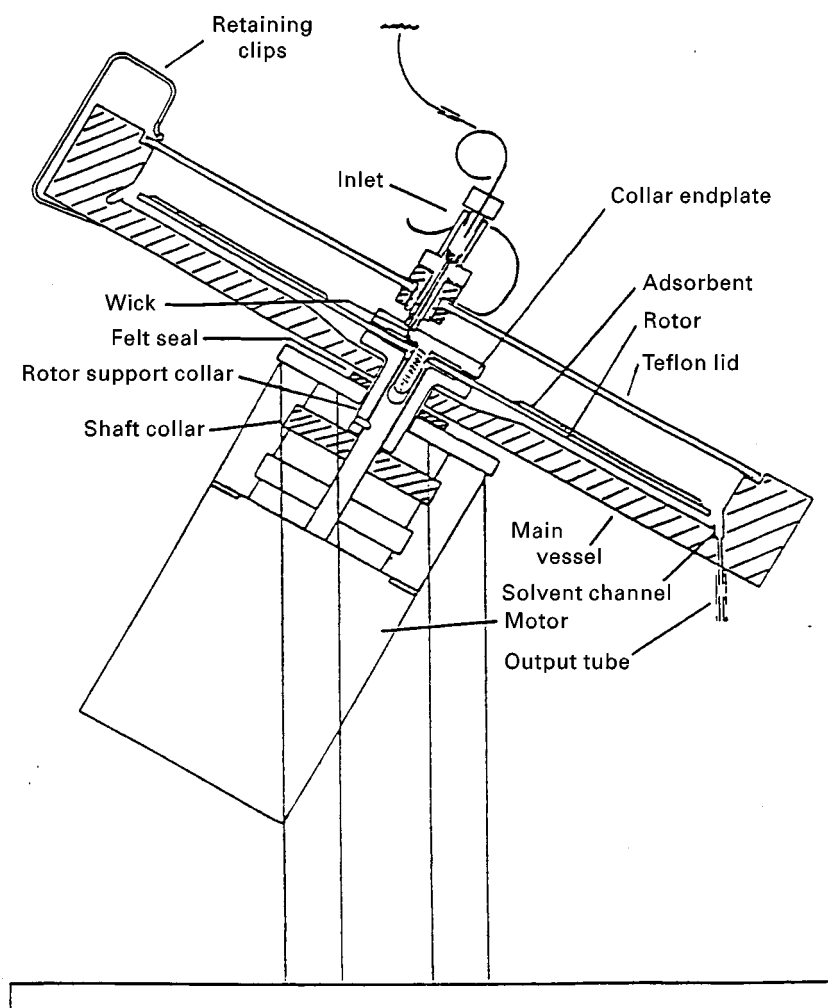


Figure 7 Schematic diagram of the Chromatotron. (Courtesy of Harrison Research.)

amount of solvent is retained in the adsorbent after introduction of the sample, it will adversely affect the separation process due to spreading of the sample in the rotor.

Chromatotron The Chromatotron is a glass rotor coated with a thin layer of adsorbent. The mobile phase and solutions of compounds are introduced to the adsorbent through an inlet, which delivers them close to the centre of the rotor. A motor drives the

rotor at a constant speed, which establishes radial elution of solvent and sample, forming concentric bands of separated substances that move to the edge of the rotor and are channelled by an output tube for collection. The four steps used in the procedure are:

1. Petroleum ether elution of saturated and mono- and diaromatic hydrocarbons.
2. Petroleum ether-ether mixture (80/20, v/v) elution of polyaromatic compounds and resin-1 fraction. This solvent is most suitable for ensuring that the aromatic hydrocarbons form a separate concentric band.
3. Ethyl acetate elution of resin-2 fraction.
4. Tetrahydrofuran elution of asphaltenes.

Table 2 Interrelationships among the thickness of the adsorbent layer, solvent volume and flow rate using the Chromatotron

Thickness of adsorbent layer (mm)	Flow rate (mL min ⁻¹)	Solvent volume (mL)
1	2-4	5
2	6-8	10
4	8-10	20
6	>10	30

The method can be used for both qualitative and quantitative purposes; the complete process is summarized in **Figure 8**. It is very important to determine the cutoff points for the separation process for collecting four high purity fractions. There are two

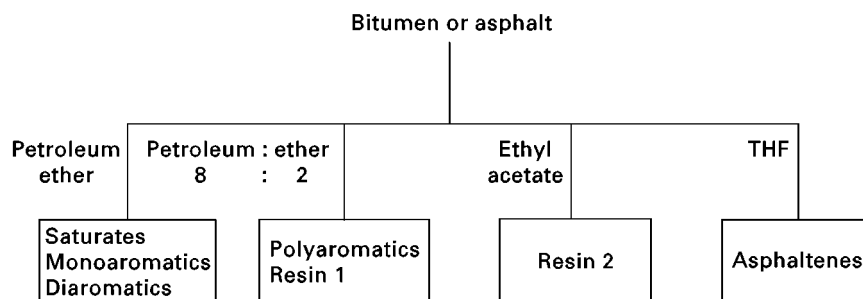


Figure 8 Characterization of bitumen or asphalt by preparative method using the Chromatotron.

methods which can be used to identify the cutoff points:

1. UV examination: this method is useful for estimating the cutoff point between the saturates and aromatics. To identify this point, the rotor can be examined by illumination with UV light at 254 nm. The aromatics will exhibit a yellow-green colour, whereas the saturates are colourless.
2. Spot test: a spot test can be used to identify the cutoff points of saturates, aromatics and resins. Spots obtained using a freshly prepared sulfuric acid-formaldehyde solution (98 + 2, v/v) have the following colours: saturated compounds, colourless; monocyclic aromatics, reddish brown; dicyclic aromatics and polycyclic aromatics, dark green.

Thin-layer Chromatography with Flame Ionization Detection

Background

The fingerprinting of asphalt and its components can be made by TLC-FID much more rapidly and simply than by classical column chromatography and preparative TLC. TLC-FID involves separation of solvent-extractable organics on silica-coated quartz rods called Chromarods into saturates, aromatics and polar component classes combined with semiquantitative detection by automated FID.

Separation

The working principle of a commercially available instrument, the Iatroscan TH-10, designed to scan the adsorbent-coated Chromarods, is illustrated in Figure 9. A set of up to 10 coated rods is mounted on rod holders used for both chromatography and subsequent scanning. The samples to be analysed are dissolved in a solvent and applied near one end of the coated rods, which are then developed using suitable solvents, as in conventional TLC. Thereafter the developing solvent is removed by evaporation, and finally the coated rods are scanned in the FID device. The fractions resolved on each of the Chromarods are

thereby successively vaporized/pyrolysed and the ionizable carbon is detected at the collector electrode. The FID signals from each fraction are amplified and recorded as separate peaks.

In as much as the bitumens comprise a complex mixture of various substances which are impossible to isolate, a compositional analysis technique is generally used whereby a sample is separated into four fractions by performing multistage development with eluting solvents of varying polarities. The solvent elution sequence for asphalt separation is firstly, hexane for separating saturates; secondly, toluene for separating aromatics; and thirdly, dichloromethane-methanol (95/5, v/v) for separating resins. The order of eluted components from the top of the rods is: saturates, aromatics, resins and asphaltenes.

Analysis

TLC-FID is a fast, multiple-analysis method which can be performed simultaneously on 10 samples. The total elapsed time for the analysis is less than 2 h (compared to about 2 days per sample with the SARA procedure). It is, however, destructive and does not yield fractions for further examination.

Linearity of response versus concentration is important in obtaining quantitative results. The sample size, the flow rate of hydrogen fed to the FID and the speed of scanning all have an effect on the linearity of response versus concentration, baseline stability of the FID signal and reproducibility of response values.

Silica Gel and Ion Exchange Chromatography – Separation of Polar Fractions

Background

The separation and study of polar compounds in crude oil and bitumens is of considerable importance in the fields of petroleum recovery and processing. Numerous methods for separation of polar compounds

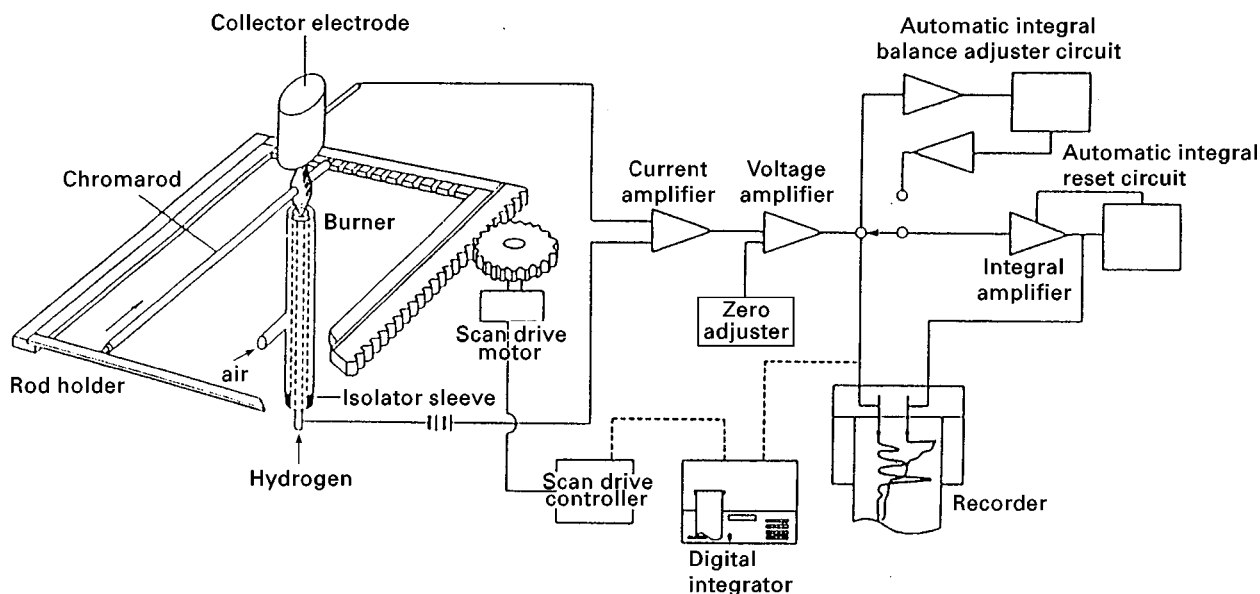


Figure 9 Construction of a coated-rod TLC scanner, latroscan TH-10 Mk III. (Modified from Mukherjee, 1991.)

from crude oil and bitumens have been developed. Among these, the most widely used is the method developed by the Bureau of Mines and American Petroleum Institute. The acid and base fractions of heavy petroleum distillates or residues are isolated by ion exchange chromatography, the neutral nitrogen compounds by complexation chromatography on ferric chloride and saturates, and mono-, di- and polyaromatics by adsorption chromatography on activated alumina or on a combined alumina-silica gel column. The definition of acids or bases by ion exchange methods is based on the hydrogen donating or accepting tendency of the molecules. In as much as many polar compounds are amphoteric, their definition as acids or bases depends on the analytical sequence employed. Although this method is rather complex and tedious, it is used to separate the polar fractions from crude oil and bitumens.

Separation Procedure

There are two stages in the separation: firstly, silica gel chromatography and secondly, ion exchange

chromatography. The first stage separates the crude oil or bitumen into four fractions (I-IV: **Figure 10**). The polar fraction obtained from the first stage is further split into subfractions by the second-stage chromatography.

Silica gel chromatography Fractionation of crude oil or bitumen is carried out by solvents with increasing polarity through a column using Baker reagent grade, 60-200 mesh silica gel. The silica gel is thermally activated before use. The sample (10-20 g) is dissolved in 200 mL tetrahydrofuran (THF) and then filtered. The volumetric ratio of the sample to the adsorbent is about 1:35. The columns are eluted with *n*-hexane, toluene, 4:1 (v/v) toluene-methanol and 2:1 (v/v) toluene-methanol, to obtain fractions I, II, III and IV, respectively. Figure 10 shows the overall separation scheme. All samples must be evaporated to a constant weight by (rotary) evaporation and using a vacuum oven. Recovery of fraction IV is generally lower than 5% and, therefore, this fraction has not been considered for further study. The most polar

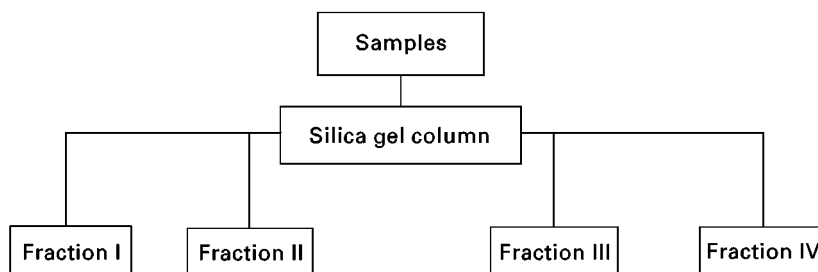


Figure 10 Solvent fractionation scheme using a silica gel column for crude oil and shale oil.

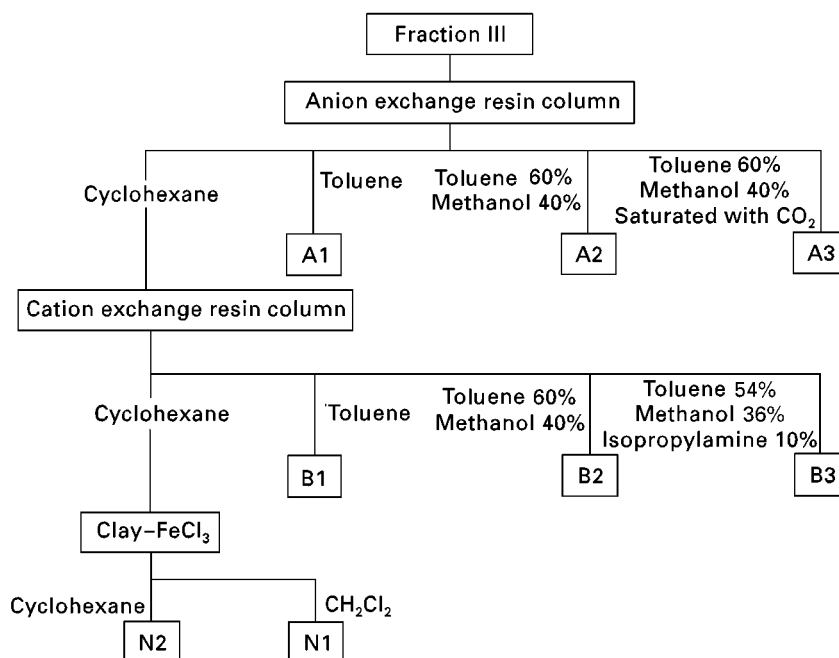


Figure 11 Separation of fraction III (see Figure 10) to subfractions by ion exchange chromatography: A, acid; B, base; and N, neutral.

groups are present in fraction III because of the high interfacial tension compared with those for fractions I and II. Fraction III is further fractionated by ion exchange chromatography.

Ion exchange chromatography The polar material (fraction III) obtained using the silica gel column is mixed with cyclohexane. There are three further stages of separation: anion exchange, cation exchange and clay-FeCl₃ complexation. In order to obtain acidic fractions from the polar material, a strongly basic anion exchange resin is used and an eluting scheme is employed, based on increasing polarity of the solvent. This scheme includes four elution steps: cyclohexane; toluene; a 3:2 mixture of toluene-methanol; and a 3:2 mixture of toluene-methanol saturated with CO₂. The first fraction eluted by cyclohexane from the anion exchange resin is further fractionated by passing it through a strongly acidic cation exchange resin. The same elution scheme as in the first elution step is used, with a slight modification for the cation exchange elution in that the fourth step uses a 5.4: 3.6:1.0 mixture of toluene-methanol-isopropylamine. Three basic fractions result from these fractionations.

A column packed with clay-FeCl₃ is employed to separate further the material obtained from the cyclohexane elution in the second stage. The solvents used to obtain the neutral fractions are cyclohexane and dichloromethane. The volumetric ratio of sample to adsorbent is around 1:10 for the three adsorbents

used. Two neutral fractions can be obtained at this last stage of separation process. A detailed diagram of the scheme is given in Figure 11.

Conclusion

The SARA separation method is at present the most comprehensive and most widely used method for the study of heavy oil fractions. Despite its shortcomings (tedious, time-consuming and possible losses), it can be viewed as a standard by which other methods should be evaluated. Preparative, centrifugal, TLC with the Chromatotron is capable of isolating crude oil and bitumen in the amounts required for further identification by other instrumental techniques.

TLC-FID has a great potential of becoming a standard method for quantitative evaluation of crude oil and bitumen. It is rapid, accurate, requires only small samples and does not involve tedious procedures in comparison to the SARA method. Solvent fractionation using silica gel rods simply separates crude oil and bitumen into four fractions. With automatic instrumentation, the method can be used routinely for industrial purposes. The combination, of fractionation by solvents and ion exchange followed by complexation, is a good method for studying the composition of crude oil and bitumen. Ion exchange processes rely on the great selectivity for acidic and basic components in the crude oil. The complexation process enables the neutral nitrogen compounds to be separated. This scheme provides 10

resin fractions, which demonstrates the great complexity of crude oil composition.

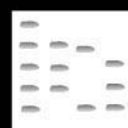
The choice of a procedure primarily depends on the information required. Combining different separation steps and/or short-cuts to achieve a specific purpose is possible.

See also: II/Chromatography: Liquid: Mechanisms: Ion Chromatography. Chromatography: Thin-layer (Planar): Modes of Development: Conventional. III/Crude Oil: Liquid Chromatography. Flame Ionization Detection: Thin-Layer (Planar) Chromatography. Flash Chromatography. Metal Complexes. Petroleum Products: Liquid Chromatography.

Further Reading

- Atgelt KH, Jewell DM, Latham DR and Selucky ML (1979) *Chromatography in Petroleum Analysis*, pp. 186–214. New York: Marcel Dekker.
- Boyd ML and Montgomery DS (1962) Structural-group analysis of the asphaltene and resin components of Athabasca bitumen. *Fuel* 41: 335–350.
- Dickie JP and Yen TF (1967) Microstructures of the asphaltic fractions by various instrumental methods. *Analytical Chemistry* 39: 1847–1852.
- Dickie JP, Haller MN and Yen TF (1969) Electron microscopic investigation on the nature of petroleum asphaltics. *Journal of Colloid Interface Science* 29: 375–484.
- Eremenko NA (1990) *Petroleum Geology Handbook*. Los Angeles, CA: OSI.
- Hilman ES and Barnett B (1937) The composition of cracked and uncracked asphalts. *Proc. Am. Soc. Testing Materials*, 37: 558.
- Hirsch DE, Hopkins RC, Coleman HJ *et al.* (1972) Separation of high-boiling petroleum distillates using gradient elution through dual-packed (silica gel–alumina gel) adsorption columns. *Analytical Chemistry* 44: 915.
- Jewell DM (1979) *Chromatography in Petroleum Analysis*, pp. 284–285. New York: Marcel Dekker.
- Jewell DM, Weber JH, Bunger JW *et al.* (1972) Ion-exchange, coordination and adsorption chromatographic separation of heavy-end petroleum distillates. *Analytical Chemistry* 44: 1391.
- Katz M (1934) Alberta bitumen. *Canadian Journal of Research* 10: 435–451.
- Lian H, Lee CZH, Wang YY and Yen TF (1992) Characterization of asphalt with the preparative Chromatotron. *Journal of Planar Chromatography* 5: 263–266.
- Mukherjee KD (1991) *Handbook of Thin-layer Chromatography*, pp. 339–350. New York: Marcel Dekker.
- Sadeghi KM, Sadeghi MA, Wu WH and Yen TF (1989) Fractionation of various heavy oils and bitumen for characterization based on polarity. *Fuel* 68: 782–787.
- Shue FF and Yen TF (1981) Concentration and selective identification of nitrogen and oxygen-containing compounds in shale oil. *Analytical Chemistry* 53: 2081–2084.
- Suatoni JC and Swab RE (1976) Preparative hydrocarbon compound type analysis by high performance liquid chromatography. *Journal of Chromatographic Science* 14: 535.
- Speight JG, Wernick DL, Gould KA *et al.* (1985) Molecular weight and association of asphaltene, a critical review. *Rev. Inst. Fr. Pét.* 40: 51–62.
- Wang YY and Yen TF (1990) Rapid separation and characterization of fossil fuels by thin-layer chromatography. *Journal of Planar Chromatography* 3: 376–380.
- Weinberg VA, White JL and Yen TF (1983) Solvent fractionation of petroleum pitch for mesophase formation. *Fuel* 62: 1503–1510.
- Yen TF (1990) Asphaltenic materials. In: *Encyclopedia of Polymer Science and Engineering*, 2nd edn, pp. 1–10. New York: John Wiley.
- Yen TF and Chilingarian GV (1994) Asphaltenes and asphalts 1. In: *Developments in Petroleum Science* 40A. New York: Elsevier Science.
- Yen TF, Erdman JG and Pollack SS (1961) Investigation of the structure of petroleum asphaltenes by X-ray diffraction. *Analytical Chemistry* 33: 1587–1594.
- Yen TF, Shue FF, Wu WH and Tzeng D (1983) Ferric chloride-clay complexation method. Removal of nitrogen-containing components from shale oil and related fossil fuels. *ACS Symposium Series* 230: 457–466.

CARBAMATE INSECTICIDES IN FOODSTUFFS: CHROMATOGRAPHY AND IMMUNOASSAY



G. S. Nunes, Federal University of Maranhão/UFMA, São Luís-Ma, Brazil

D. Barceló, CID/CSIC, Barcelona, Spain

Introduction

Pesticides have received special attention over the years, due mainly to the problems of environmental and food contamination. Analytical methods for determining pesticide residues have their main application in the control of food for human consumption,

especially in the control of fruit and vegetables produced using direct applications of pesticides. Moreover, the determination of pesticide residues in food is fundamental in monitoring and regulatory programmes. Pesticide residue levels higher than the maximum residue level (MRL) are monitored through two different but complementary approaches: regulatory monitoring focusing on raw agricultural commodities that measure the levels in individual lots for compliance with legal tolerances, and total diet study, in which dietary intakes of pesticides are determined by analysis of fruit and vegetables.

Carbamates constitute a family of pesticides registered for use on several crops in South America, Europe and the USA. Their use for pest control has progressively increased in recent years, along with organophosphates (OPs), as alternatives to organochlorine (OC) insecticides. Owing to their broad spectrum of biological activity, carbamates can be used as insecticides, miticides, fungicides, nematocides and molluscicides. **Table 1** shows the structures of the most extensively used carbamates, including some *N*-methylcarbamate (NMC) insecticides. Carbamate residues are of concern because of the acute toxicity of some compounds – aldicarb and carbofuran exhibit an LD₅₀ (the dose of a compound that causes death in 50% of the organisms to which it has been administered) in rats of 1 and 8 mg kg⁻¹, respectively. Some carbamate residues are suspected carcinogens and mutagens. Such insecticides act as inhibitors of the acetylcholinesterase enzymes, and a number of adverse effects have been reported in the literature.

Several analytical methods have been proposed for the separation and quantification of carbamate residues in food samples. The carbamate pesticides are thermally labile and not readily amenable to gas chromatography (GC), making the use of the liquid chromatographic (LC) techniques preferable. In general, the time and expenses involved in classical analytical methods (i.e. sampling, sample preparation and laboratory analysis) have substantially limited the number of samples that can be analysed in food research and surveys. In addition, the quantity of chemicals and toxic solvents that are used sometimes offer a risk factor considerably greater than that of the pesticide residue to be determined. These disadvantages have emphasized the need for developing fast, easy, robust, sensitive and cost-effective methods capable of being used in the field. Instrumental techniques that combine these characteristics are slowly starting to appear in pesticide residue analysis. They include the immunoassay (IA) techniques, immunoaffinity chromatography and electrochemical/optical biosensors. To avoid the general drawbacks of the classical methods, significant developments have

taken place in extraction/clean-up procedures, and in the final determination of pesticide residues in foodstuffs.

This article examines recent progress, focusing primarily on simplified and miniaturized analytical methods for determining carbamate insecticides in foodstuffs, including fast and simple extraction/clean up strategies, and the use of IA techniques for detection prior to laboratory analysis.

Chromatographic Methods for Carbamate Analysis

LC Methods

Standard LC methods for carbamate determination based on Krause's method generally consist of reversed-phase HPLC with gradient elution followed by two post-column reactions to yield fluorescent species (**Figure 1**). The carbamates are hydrolysed with an alkaline solution (usually sodium hydroxide) to a methylamine that is sequentially derivatized in the presence of *o*-phthaldehyde (OPA) and mercaptoethanol (MERC) to create the fluorescent product. Two high pressure pumps are used to introduce the post-column reagents. To separate the main NMCs and their metabolites, a cycle time of 45–60 min is required. Limits of detection (LODs) in water analysis are in the range of 1 to 4 ng, which is equivalent to 2.5 to 10 p.p.b. in the water injected. However, if a preconcentration step is carried out before chromatographic separation, the LOD value is lower.

The sensitivity and selectivity of Krause's method have allowed its use for the determination of residues of NMCs in fruits and vegetables with great accuracy. Unfortunately, such methods involves extraction with methanol, and large amounts of sample and solvent are used. The clean-up, starting with successive liquid–liquid partition (LLP) steps, and finishing with elution of the target compounds on a Celite®/charcoal adsorbent column, is mainly responsible for the slowness and tediousness of the method, making the analysis of a large number of samples impractical. Usually, it is satisfactorily used as a reference method in collaborative studies and also to carry out validation of new methods. Different procedures for clean-up of crop extracts by employing either glass adsorbent columns and commercially available solid-phase extraction (SPE) cartridges have been compared and a specific solid-phase elution protocol employing a solvent polarity gradient proposed. A schematic outline of the method is illustrated in **Figure 2**. The extraction is carried out with methanol, and a LLP step is only necessary if a UV detector is to be used. In most cases, recoveries of the more polar compounds

Table 1 Carbamates commonly used in crop protection and some of their breakdown products

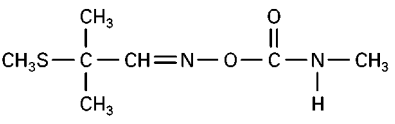
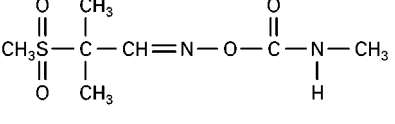
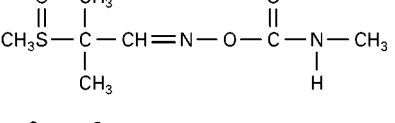
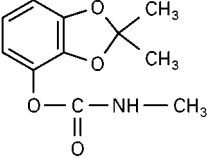
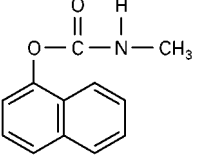
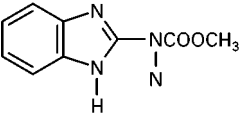
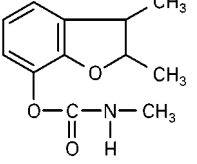
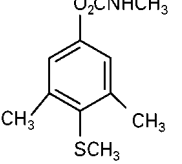
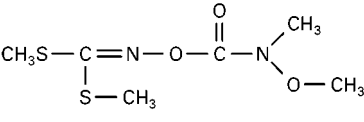
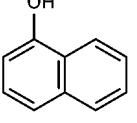
Compound name	Chemical structure	Class	IUPAC name
Aldicarb		Insecticide	2-Methyl-2-(methylthio)propionaldehyde <i>o</i> -methylcarbamoyloxime
Aldicarb sulfone		Insecticide (metabolite of aldicarb)	2-Methyl-2-(methylsulfonyl)propanal <i>o</i> -[(methylamino)carbonyl]-oxime
Aldicarb sulfoxide		Insecticide (metabolite of aldicarb)	2-Methyl-2-(methylsulfinyl)propanal <i>o</i> -[(methylamino)carbonyl]-oxime
Bendiocarb		Insecticide	2,3-Isopropylidenedioxyphe-nyl methylcarbamate
Carbaryl		Insecticide	1-Naphthyl methylcarbamate
Carbendazim		Insecticide	2-Methyl benzimidazol-2-ylcarbamate
Carbofuran		Insecticide	2,3-Dihydro-2,2-dimethylbenzofuran-7-yl-methylcarbamate
Methiocarb		Insecticide, acaricide, molluscicide	4-Methylthio-3,5-xylyl methylcarbamate
Methomyl		Insecticide	<i>S</i> -Methyl <i>N</i> -(methylcarbamoyloxy) thioacetimidate
1-Naphthol		Insecticide (metabolite of carbaryl)	1-Naphthalenol

Table 1 Continued

Compound Name	Chemical structure	Class	IUPAC name
Oxamyl	$ \begin{array}{c} \text{O} \quad \quad \text{O} \quad \text{H} \\ \parallel \quad \quad \parallel \quad \\ (\text{CH}_3)_2\text{N}-\text{C}-\text{C}=\text{N}-\text{O}-\text{C}-\text{N}-\text{CH}_3 \\ \\ \text{SCH}_3 \end{array} $	Insecticide, nematocide, acaricide	<i>N,N</i> -Dimethyl-2-methylcarbamoyloxime-2-(methylthio)acetamide
Pirimicarb		Insecticide	2-Dimethylamine-5,6-dimethylpyrimidine-4-dimethylcarbamate
Propoxur		Insecticide	2-Isopropoxyphenyl- <i>N</i> -methylcarbamate

are higher if the partitioning step is omitted and fluorimetric detection is employed.

A series of tests to assess the feasibility of using activated carbon membranes in the clean-up of vegetables (green peppers) for the analysis of NMC pesticides by HPLC with post-column derivatization and fluorescence detection have been carried out. These tests showed that the membranes were effective in retaining sample interferences in both offline (with a 22 cm diameter activated carbon membrane) and online (extract injected directly in the HPLC system) methods. Solid-phase extraction with bonded-silica adsorbents, including octyl (C_8), ethyl (C_2), octadecyl (C_{18}) and cyclohexyl (CH), has also been successfully developed as an alternative to LLP clean-up. Elution patterns and recovery from various adsorbent materials were determined for 17 OPs, nine carbamates and

three other pesticides in a sample matrix of rice grain. The method performance was comparable to conventional clean-up procedures.

Following the general tendency toward miniaturization, a new method for NMC determination in fruits and vegetables has been proposed. This method eliminates the need for delivery pumps to introduce the hydrolysis/derivatization reagents, since they are already present in the mobile phase. For this purpose, a Kromasil-100 C_{18} column (which tolerates basic conditions) and a borate buffer mobile phase were chosen. A simplified LC-fluorescence (FS) method for the determination of traces of carbamates in grains, fruits and vegetables has been described. Here, the sample size and solvent volumes were considerably reduced, and a clean-up on aminopropyl-bonded Sep Pak® cartridge was performed in order to separate the target compounds from the coextractives. Recovery of the pesticides and limits of detection in different food matrices varied from 60 to 103% and from 1 to 4 ppb. A complete analytical methodology for the determination of some NMCs in vegetable, fruit and feed crop samples has been developed in which the pesticides are extracted, cleaned on an aminopropyl-bonded SPE column, and then determined by LC-FS.

Depending on the detection technique, not only the method selectivity, but also the method sensitivity, can be changed considerably. For example, by using LC with UV detection, the presence of coextractives can severely limit the analyte determination, resulting in poor method sensitivity when analysing real samples compared with standard solutions. Despite this, and considering that the maximum residue levels for foodstuffs are higher than those for water samples,

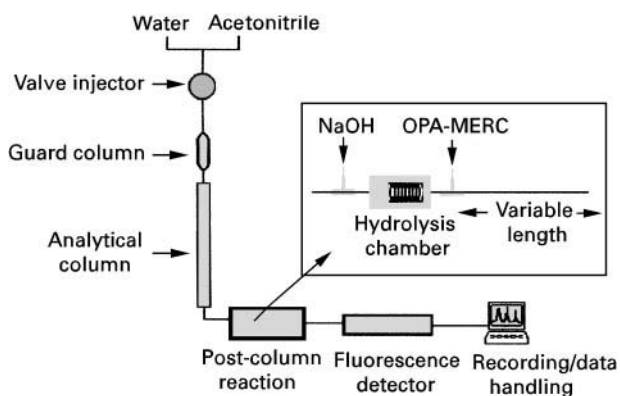


Figure 1 Liquid chromatography system with post-column reactions and fluorimetric detection for determination of *N*-methylcarbamate pesticides.

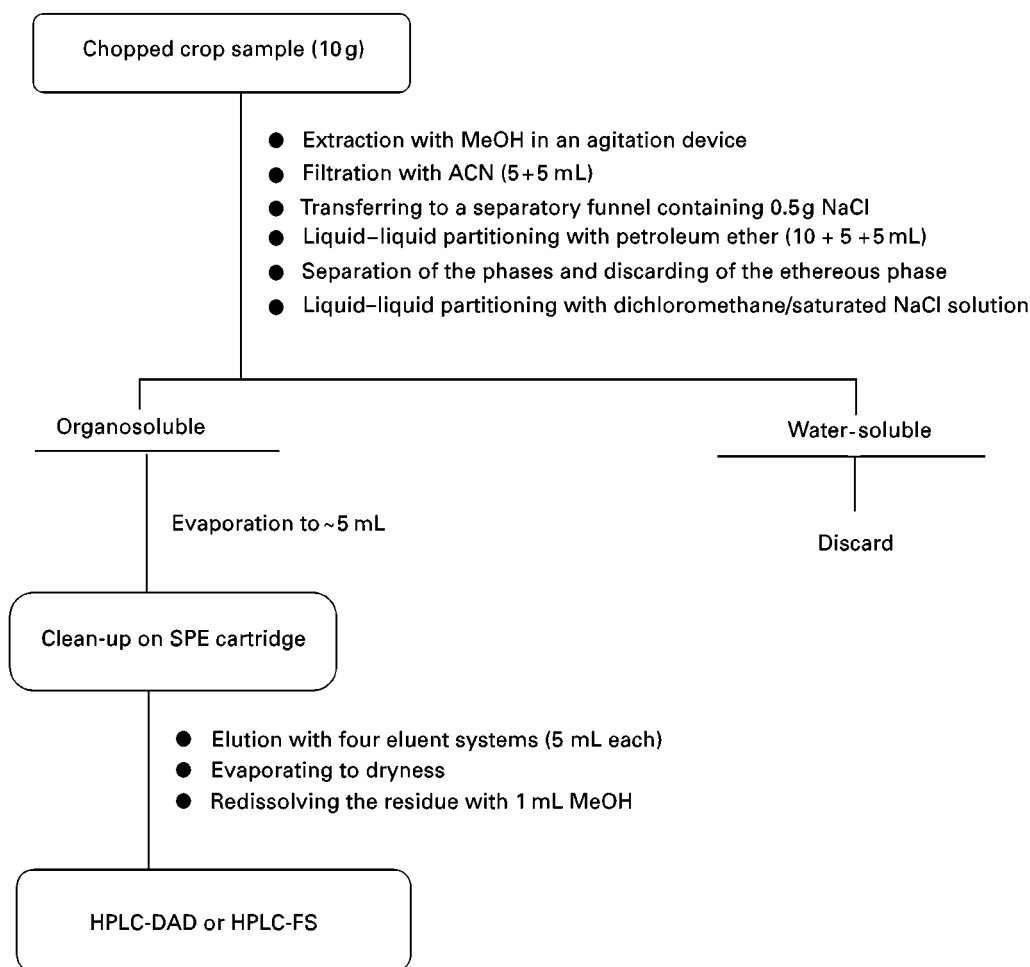


Figure 2 Block diagram of a scheme for extract preparation for HPLC analysis *N*-methylcarbamate pesticides in fruit and vegetables. If fluorimetric detection is performed, the LLP step can be omitted. Elution through an SPE column was carried out according to the method described by Nunes GS, Ribeiro ML, Polese L and Barceló D (1998) Comparison of different clean up procedures for the determination of *N*-methylcarbamate insecticides in vegetable matrices by high-performance liquid chromatography with UV detection. *Journal of Chromatography* 795: 43–51.

a simple and rapid method has been proposed to analyse eight carbamate insecticides and 10 of their main metabolites in apples, pears and lettuce. The clean-up procedure is based on that of the De Kok method, which uses solid-phase cartridges, and the amounts of solvents and sample are substantially reduced. It was found that matrix interferences could be minimized by diluting the final extract, but the method sensitivity is also reduced.

GC Methods

The relationship between the mode of detection and the required extraction procedure for this mode has resulted in the emergence of numerous sample preparation procedures. Using GC-mass spectrometry (MS) and LC-FS techniques, the extraction of 199 pesticides from fruits and vegetables with acetonitrile, and removal of the coextractives with a minia-

ture charcoal-Celite clean-up column have been carried out. Good recovery data obtained by spiking pears, carrots and bananas at the 0.1–0.5 p.p.m. demonstrated the excellent performance of this method.

Various types of detectors have been evaluated for the analysis for the carbamate insecticides by GC. Among these, the nitrogen-phosphorus detector (NPD), the flame photometric detector (FPD) with either a phosphorus or sulfur filter, the electron-capture detector (ECD) and the mass spectrometric detector (MS), either in electron impact mode (EI) or in positive chemical ionization (PCI) mode, have been tested. Sensitivity, linearity and selectivity of the different detectors have been detailed and application to real samples, including foodstuffs, has also been presented. Although the thermolability of the carbamates is considered the major limitation as regards to the use of GC techniques, it has been shown that

thermal degradation of some carbamates and metabolites does not occur under certain conditions, as was demonstrated by the fragmentation patterns of the studied compounds. GC-NPD methods for the monitoring of residues of some carbamates in real samples have been also described. A comparison has been made of GC and LC techniques for the analysis of the most popular (in terms of amount produced and applied) pesticide classes, such as carbamates, phenylureas, triazines, phenoxy acid herbicides and chlorinated phenols. Sample concentration and detection have been discussed in relation to their influence on the performance of the particular separation technique. GC methods, when applicable, have the advantages of greater separation efficiency, higher speed of analysis and the availability of a wide range of highly sensitive detectors. On the other hand, LC is often the choice when polar, nonvolatile and/or thermolabile compounds need to be analysed, as it is in the case of carbamates.

Supercritical Fluid Chromatography/Extraction

Supercritical fluid chromatography (SFC) is a technique that in many ways is a hybrid of GC and HPLC. It is recognized as a valuable technique for the analysis of thermally labile compounds such as carbamates. A few applications have been reported for SFC in the field of pesticide determination in food. The versatility in separation, the possibility of using different detectors (LC or GC detectors), and the prospect of directly coupling with supercritical fluid extraction (SFE), make this analytical technique very attractive. SFE using CO₂ has been examined for separating carbamates from interfering coextractives prior to analysis either by LC-MS or by GC with ion trap mass spectrometry (ITMS) detection. Pre-extraction of ground meat with acetonitrile before SFE left behind over 99% of the fat and fibre. SFE of the acetonitrile extracts with pelletized diatomaceous earth further reduced the amount of coextractives 10-fold, removing the interferences that would have appeared in the fluorescence mode.

Simplification of Multiresidue Methods

Official laboratories that investigate and analyse pesticide residues usually utilize the established multiresidue methods (MRM) of analysis. One of the most commonly used MRM for pesticide analysis in fruit and vegetables samples is the AOAC (Association of Official Analytical Chemists) method. It involves an aqueous acetone extraction and laborious clean-up

employing LLP procedures using organic solvent of limited water capacity, to achieve the removal of the coextractives present in the sample extract and/or solid-phase clean-up with silica or Florisil. Finally, analyte determination is performed by GC or HPLC with selective detectors.

More than 300 pesticides and pesticide-related compounds can be determined by the well-known MRMs described in the official literature, such as the AOAC method, the German MRM S19 (Deutsche Forschungsgemeinschaft, DFG), and the method adopted by the National Food Administration of Sweden. They all have several disadvantages, such as their inefficiency as screening methods, since they are too time-consuming and labour-intensive, the large amount of solvents used, and, in addition, newly developed groups of pesticides are becoming more polar and/or thermodegradable, making difficult their analysis by conventional chromatographic techniques.

During the past two decades, research has gone in the direction of reduction of organic solvent toxicity, elimination of the partition step and elimination of the column clean-up. A rapid and efficient multiresidue extraction procedure has been reported using ethyl acetate and sodium sulfate, followed by gel permeation chromatography (GPC) on an SX-3 column. Its effectiveness to analyse OC and OP insecticides was confirmed. Several other methods based on it have arisen using specific detectors that have decreased the number of interfering chromatographic peaks.

LC-MS Techniques

Confirmation of the presence of carbamates in real samples has been performed by HPLC-MS with various interfaces, but in general most of these studies have been performed with standard solutions. **Table 2** summarizes the development of LC-MS techniques for the analysis of different pesticides, including carbamate insecticides. Up to the present, few food analysis applications have been reported. Atmospheric pressure chemical ionization (APCI) techniques for the mass spectral analysis of several NMCs have been evaluated and the results compared with those obtained using ionspray (ISP) and thermospray (TSP) interfaces. The results were also compared with EI ionization and methane CI spectra obtained with a particle beam (PB) interface. These methods were applied to the confirmatory analysis of three representative carbamate pesticides, spiked at the 0.1 ppm level in green peppers.

Multiresidue confirmations of pesticides from different classes using APCI techniques have also been performed. It was observed that the fragmentation of the carbamates studied was highly voltage-dependent. An increase in the potential of the sampling

Table 2 MS interfaces most commonly used for LC analysis of pesticides, including carbamate insecticides

<i>Spectrometry interface</i>	<i>Pesticides studied</i>	<i>Sample type</i>	<i>LOD (ng)</i>
APCI, ISP, TSP and CI	NMCs	Aqueous solutions Green peppers Ground water	— Full-scan mode: 0.8–10 SIM mode: 0.01–1
APCI (in positive- and negative-ion modes), TSP, and PB-MS	17 pesticides in five chemical classes (triazines, phenylureas, carbamates, organophosphorus and miscellaneous)		
TSP	Anilides, carbamates, <i>N</i> -heterocyclic, organophosphorus, and phenylureas)	Aqueous solutions	—
TSP (with online and offline SPE procedures)	Nitrogen- and phosphorus-containing pesticides	Aqueous solutions	SIM mode: 0.04–0.6
TSP	3 <i>N</i> -methylcarbamates, 3 <i>N</i> -methylcarbamoyloximes, 2 substituted urea pesticides, and 1 ester of a substituted carbamic acid	Aqueous solutions	—
TSP (with either filament- and discharge-assisted ionization modes)	19 carbamates and 12 of their known degradation products	Aqueous solutions	—
TSP	16 carbamates from four chemical subclasses (oxime-NMCs, aryl-NMCs, <i>N</i> -phenylcarbamates and methyl esters of substituted carbamic acids)	Aqueous solutions	—
FIA-PB-PCI	14 carbamates	Aqueous solutions	—
FIA-PB-EII-CI (with either negative- and positive-ion modes)	33 carbamates and 14 of their degradation products	Surface water	—
APCI	11 carbamates	Food samples	0.3–10
ES	20 carbamates	Fruits and vegetables	—
ES	<i>N</i> -Heterocyclic compounds, phenylureas and carbamates	Fruits and vegetables	—

APCI, atmospheric pressure chemical ionization; CI, chemical ionization; DCI, desorption chemical ionization; EII, electron impact ionization; ES, electrospray interface; FIA-PB-PCI, flow injection analysis-particle beam-positive chemical ionization; ISP, pneumatically assisted electrospray ionization; LOD, limit of detection; SIM, selected-ion monitoring; SPE, solid-phase extraction; TSP, thermospray interface.

cone strongly affected the formation of diagnostic daughter ions. The dependence of the ion abundances in the TSP mass spectra of several pesticides has been studied with regard to the vaporizer and the gas-phase temperatures and under collision-activated dissociation conditions. Fragmentation pathways under certain experimental conditions were investigated for some of the carbamate pesticides. Both vaporizer and source jet temperatures were monitored. APCI, ESP, fast-atom bombardment, Cf-252 plasma desorption and collision-activated dissociation spectra were then performed for the pesticides to confirm proposed pathways and to gain additional information.

Through an interlaboratory study involving nine laboratories, it was concluded that, in TSP-LC-MS systems, the thermospray tip temperature plays a major role in adduct formation and ion fragmentation of thermally labile carbamate pesticides. As a result, this temperature needs to be carefully controlled. This effect has been confirmed by investigating the influence of three LC eluent additives (ammonium acetate, ammonium formate and nicotinic acid) and the vaporizer temperature on ion formation. The performances of different thermospray interfaces (which exhibit wide differences in source geometry) used in

carbamate analysis have also been compared, and the so-called suppression effects on the ion formation have been studied in coeluted compounds. Thermally labile carbamates gave unsatisfactory results with regard to spectral compatibility between the interfaces. These differences are due to thermally assisted hydrolysis reactions that occur in the various vaporizer designs. Different approaches using desorption chemical ionization (DCI) and flow injection (FIA)-particle beam (PB)-ammonia PCI-MS were further evaluated. The mass spectra using FIA-PB-PCI-MS exhibit higher relative abundances for fragment ions, and the ion intensities are strongly dependent on the ion source pressure. Another study, employing EI ionization and ammonia/methane with positive/negative chemical ionization, has shown ammonia to be the best reagent gas. Using ammonia gave less fragmentation and better quantitative results than methane for the analysis of 33 carbamates and 14 of their degradation products.

LC-APCI-MS and LC-post-column fluorimetry for the determination of carbamates in foodstuffs were compared. It was observed that, despite its great potential in detection and confirmation, in general LC-APCI-MS is less sensitive for quantitation

purposes, which agrees with previous reports. The feasibility of using reversed-phase LC-MS with an electrospray interface for measuring traces of NMC insecticides in 10 different types of fruit and vegetables has been evaluated. Extraction with methanol, followed by clean-up on a Carbograph 1 extraction cartridge, provided an average recovery higher than 80% for all compounds. It was noticed that changing from methanol to acetonitrile as the organic modifier resulted in a significant decrease in ion signal for the carbamates. The presence of coextractives derived from the crop samples in the electrosprayed solution did not interfere significantly with the ionization process of the compounds studied. The photochemical behaviour of pesticides in a photolysis reactor coupled online with an LC-ESP-MS system has been investigated this system has been used successfully to trace confirmatory analysis of carbamates in foodstuffs.

Recently an analytical method for confirmation of aldicarb and its metabolites in fruit and vegetable samples has been optimized. Aldicarb is one of the NMCs most commonly used for insect control in tropical countries in different agricultural fields. Figure 3 illustrates schematically the metabolic pathway of aldicarb under environmental conditions, and shows the formation of the mass fragments used to identify the parent and metabolic compounds. Initial metabolic attack is rapid and complete oxidative conversion to aldicarb sulfoxide is followed by a much

slower oxidation to the sulfone. It is interesting to consider the rapid degradation of aldicarb after its application, because in some cases the parent compound is not present in the studied matrix. Since that the toxicity could be effectively more acute if the metabolites were present in more elevated concentrations, their confirmation in real samples by LC-MS is of crucial importance. Such compounds have been analysed by LC-APCI-MS using the selected ion monitoring (SIM) mode based on five channels. Figure 4 shows a typical total ion chromatogram and the five selected ions used to identify the compounds in orange extracts. Here, the fragmentation was assisted by the addition of ammonium formate in the mobile phase (acetonitrile/water) and ion adducts did not appear in the mass spectra, resulting in a sensitive method free from interferences.

Thin Layer Chromatography Methods

Thin-layer chromatography (TLC) is used for the qualitative and quantitative analysis of a wide variety of compounds, including pesticides. Among the carbamate insecticides analysed by TLC can be found those most commonly used in crop protection, such as carbaryl, carbofuran, methomyl, bendiocarb, propoxur, aldicarb and carbendazim. Since the 1980s, only a few papers concerning carbamate analysis by TLC have been published. Thin-layer chromatographic procedures have been developed for the separation of several carbamates, such as

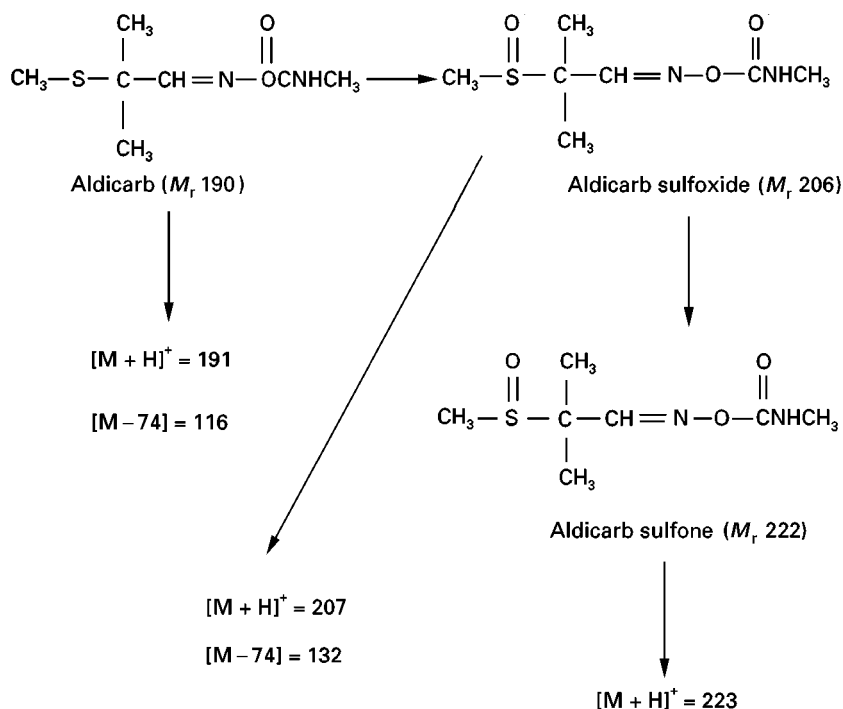


Figure 3 Metabolic pathway of aldicarb to its degradation products under environmental conditions, and mass fragments used for the LC-MS confirmation of the compounds.

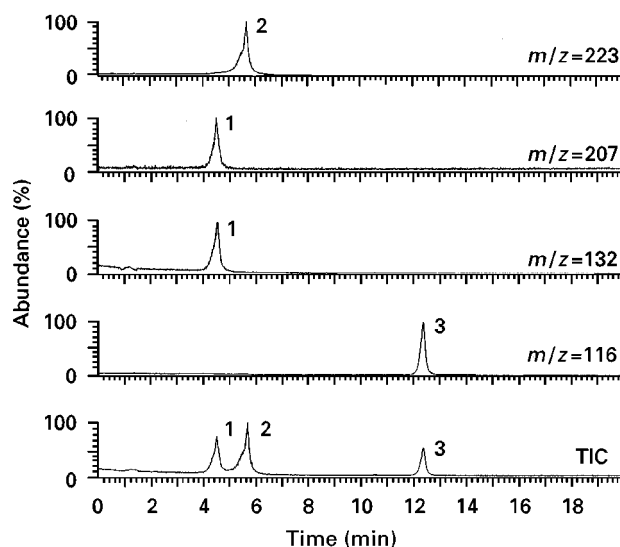


Figure 4 Mass spectra for (1) aldicarb sulfoxide (2), aldicarb sulfone and (3) aldicarb present in a spiked orange extract. Peak confirmation by SIM mode of five selected channels on the total ion chromatogram (TIC). Final extract 20-fold concentrated (see sample preparation in Figure 2). Chromatographic separation of the compounds was carried out using a C_{18} RP-LC column and a water/acetonitrile mixture, both containing 0.1% ammonium formate as mobile phase.

carbaryl, bendiocarb, carbofuran, 2-isopropyl-phenyl-*N*-methylcarbamate (MIPC) and 2-*sec*-butyl-*N*-methylcarbamate (BPMC). Suitable schemes using plates coated with silica gel containing 1% zinc acetate as support, and benzene/ethyl acetate (50:10) as solvent have been developed for carbamate analysis in various matrices, such as aqueous biological fluids and food samples, mainly fruit juices. Residues of carbofuran and its two metabolites have been extracted with HCl, partitioned into CH_2Cl_2 , chromatographed on silica gel and detected with KOH-*p*-nitrobenzenediazonium fluoroborate. Sequential TLC has been used for the detection and determination of carbaryl in water samples. More recently, the chromatographic behaviour of carbamate pesticides and related compounds has been examined on thin layers of alumina, barium, sulfate, calcium carbonate, calcium phosphate, calcium sulfate, cellulose and silica Gel G[®].

Immunoassay (IA) Methods for Carbamate Determination

In the last few years, the number of enzyme-linked immunosorbent assay (ELISA) methods for the determination of pesticides has increased, but there is still a lack of IA methods for pesticide residue determination in food and crop samples. IA techniques can provide complementary and/or alternative approaches in reducing the use of expensive equipment

and analysis time while still maintaining reliability and sensitivity. Moreover, IA can be used as a screening method in order to detect food contamination. The relatively short analysis time allows for the screening of a large number of samples which is a major advantage.

IA has been shown to have potential as a screening method for the detection of pesticides in food samples. A rapid bioluminescence method was used for screening several OP and NMC insecticides in processed baby food. Among the 155 samples tested, there were 23 suspected positives (14.2%) that were further analysed by HPLC; this resulted in confirmation of the presence of carbaryl in 18 of the samples.

The utility and applicability of an analytical method depends in great part on the absence of matrix interferences. In this regard, ELISA is not different from other detection techniques, and the sample preparation prior to analysis is still a critical point for pesticide residue determination by IA methods. A competitive ELISA has been developed for quantification of methyl 2-benzimidazolecarbamate in fruit juices. Matrix effects are minimized by diluting the samples before IA. Rapid methods based on water or acetonitrile extraction have been evaluated for screening carbofuran and aldicarb sulfone in mean and liver using commercial ELISA kits. The final extracts are diluted in order to eliminate the effect of the solvent, which is more pronounced than the natural compound effects in some cases. Attempts have been made to minimize the matrix and organic solvent effects in ELISA for carbaryl by diluting the crop extracts in the assay buffer, but it was observed that the effect of the solvent residue in the diluted extracts on the assay was still higher than the matrix effect. The direct application of IA to vegetable/fruit juices diluted in the assay buffer is possible, without large losses in the method sensitivity. As an example, **Figure 5** shows some calibration curves for carbaryl in assay buffer and in lemon juices diluted in assay buffer. In this case the absence of matrix effect, after sample dilution and pH adjustment, indicates good IA performance. Unfortunately, in most cases the recoveries of IA-based methods have proved to be lower than those of methods that do not employ any prior sample treatment.

Different experimental approaches to ELISA quantification of NMC insecticides in fruit juices, without any sample pre-treatment other than dilution, have also been developed. For carbaryl and carbofuran residue determination in fruit juices, high affinity monoclonal antibodies (MABs) have been used. Offline SFE and ELISA have been used for the determination of nine pesticides, including four carbamates, in foodstuffs consisting of baby food and Food and

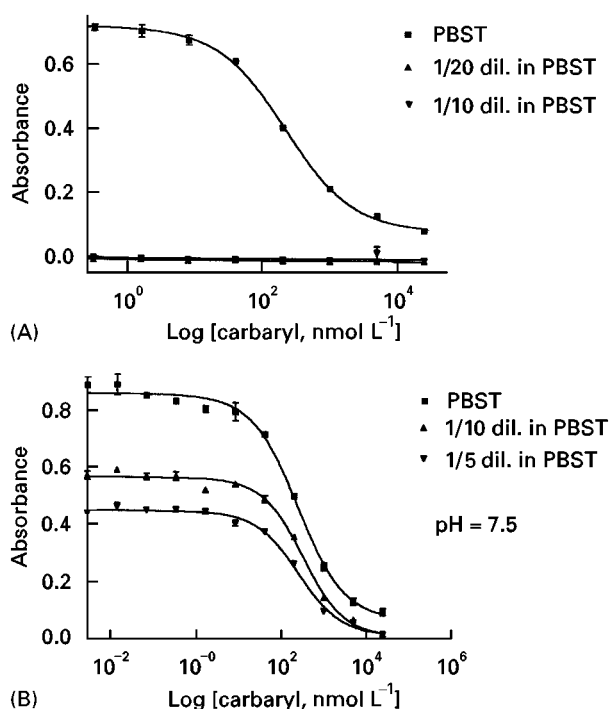


Figure 5 Matrix effect of lemon juice on the enzyme-linked immunosorbent assay (ELISA) for carbaryl analysis. Calibration curves were constructed with PBST buffer and PBST-diluted lemon juices. (A) Natural pH of the diluted samples; (B) pH adjusted with an alkaline solution. PBST, (Reproduced with permission from Nunes GS (1999) Analysis of *N*-methylcarbamate insecticides by chromatographic techniques, immunoassay (ELISA) and amperometric biosensors. Institute of Chemistry IUNESP, Anaraquara, São Paulo, 230 pp [doctorate thesis].

Drug Administration (FDA) Total Diet Study (TDS) samples. The benefits of SFE-ELISA included replacement of harmful organic extraction solvents, rapid extractions with a relatively inexpensive extractant, and a reduced number of steps in the determination of the target compounds.

In contrast to conventional chromatographic techniques for pesticide analysis in foods, IA methods have not yet been extensively characterized. The validation of the proposed ELISA against another validated method has been the primary objective in only a few published papers. As for any analytical method, quality control and assessment of material and equipment stability are required. In addition, IA evaluation involves defining working ranges, sensitivity, precision, accuracy, linearity, specificity and matrix effects.

Immunoaffinity Chromatography

Immunoaffinity chromatography (IC) has been widely used for the determination of various analytes in the medical field; however, the use of antibodies immobilized on an appropriate support to pre-concentrate pesticides from environmental samples is only

a recent development. In the analysis of pesticides in food matrices, the use of IC is still more limited. IC is based on the highly selective interaction of antigens with their antibodies, which are immobilized on a support material called an immunosorbent. The production of antibodies against pesticides is based on the conjugation of hapten to a large immunogenic carrier molecule (typically bovine serum albumin or keyhole limpet haemocyanin), and subsequently the complex is injected into a suitable vertebrate (rabbit, mouse, rat, sheep). Since antibody-antigen interactions occur over short distances, steric effects are involved in the coupling reaction. These steric effects are what make antibody-antigen interactions so selective, and only the antigen that produced the immune response, or very closely related molecules, will be able to bind to the antibody. Thus, theoretically, when the sample is run through the immunosorbent the analytes are selectively retained and subsequently eluted free of the coextratives (Figure 6). Once the analytes have been separated from interferences, they can be determined by conventional chromatographic techniques. The use of IC as a separation tool before pesticide analysis is thus extremely attractive.

Among the carbamate pesticides, only carbofuran has been separated from natural components of crop samples by IC and a highly sensitive online IC with coupled-column LC-MS was used to analyse some fruit and vegetable samples.

Current Trends and Conclusions

A tremendous amount of work has been done and much more is under way in the field of pesticide analysis in food samples. In the chromatographic field several new techniques for pesticide analysis, such as immunoaffinity chromatography and LC-MS with various interfaces, have appeared. These have undoubtedly contributed to increased separation efficiency and improved sensitivity. It is expected that the bioanalytical techniques for pesticide analysis will become a common analytical alternative because of their demonstrated advantages, especially in the analysis of carbamates in food samples. The capacity that these compounds show in inhibiting a certain class of enzymes (the cholinesterases) must be further explored. Development of approaches based on the coupling of the chromatographic separation with biodection systems is a promising alternative.

Sample handling is the bottleneck in the analysis of carbamate insecticides in foodstuffs, since in many cases a complex clean-up step is needed before chromatographic separation. The use of biological techniques, such as immunoassays and biosensors,

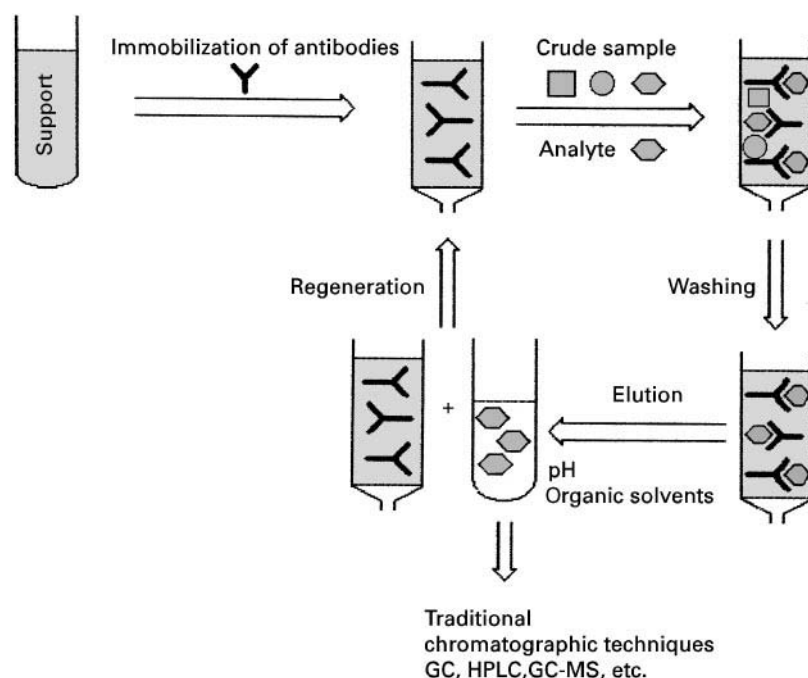


Figure 6 Schematic separation of analytes by immunoaffinity chromatography for pesticide determination in food matrices.

can overcome some of these limitations. In the LC-MS techniques, the use of an atmospheric pressure chemical ionization interface is at present the best alternative since it offers high selectivity and sensitivity for the trace determination of carbamates.

See also: **II/Affinity Separation:** Immunoaffinity Chromatography. **Chromatography: Gas:** Detectors: Mass Spectrometry. **Chromatography: Liquid:** Detectors: Mass Spectrometry. **Extraction:** Supercritical Fluid Extraction. **III/Immunoaffinity Extraction. Multi-residue Methods: Extraction. Pesticides:** Extraction from Water; Gas Chromatography; Supercritical Fluid Chromatography; Thin-Layer (Planar) Chromatography.

Further Reading

Barceló D and Hennion M-C (eds) (1997) Trace determination of pesticides and their degradation products in water. In: *Techniques and Instrumentation in Analytical Chemistry*, vol. 19. Amsterdam: Elsevier Science.

FAO (1993) *Agriculture Towards 2010*. C 93/24, Document of the 27th Session of FAO Conference, Rome.

Harlow ELD *Antibodies: A Laboratory Manual*, ch. 5, Cold Spring Harbor, NY: Cold Spring Harbor Laboratory.

Hassal KA (1983) *The Chemistry of Pesticides: Their Metabolism, Mode of Action and Uses in Crop Protection*. New York: Macmillan.

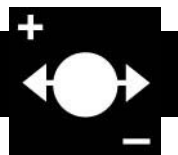
Lopez-Avila V, Charan C and Van Emon J (1995) Immunoassays for residue analysis. In: Beier RC and Stanker LH (eds) *Food Safety*, ACS Symposium Series 621, p. 438. American Chemical Society.

National Library of Medicine (1992) Carbaryl. *Hazardous Substances Databank* 4: 293-297.

Sawer LD, McMahon BM, Newsome WH and Parker GA (1990) In: Helrich K (ed.) *Official Methods of Analysis, Association of Official Analytical Chemists, Agricultural Chemicals, Contaminants, Drugs*, vol. 1, p. 274. Arlington, VA: Association of Official Analytical Chemists.

Sherma J (1989) *Analytical Methods for Pesticides and Plant Regulations*, vol. 17, San Diego, CA: Academic Press.

CARBOHYDRATES



Electrophoresis

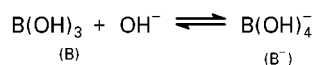
O. Grosche, Universität des Saarlandes,
Saarbrücken, Germany

Copyright © 2000 Academic Press

Introduction

Electrophoresis has been an important tool for carbohydrate analysis since its early stages of development. Moving with time from paper electrophoresis to polyacrylamide slab gel electrophoresis and then to the sophisticated high performance capillary

Step 1. (pH > 9)



Step 2. Equilibria of complexation

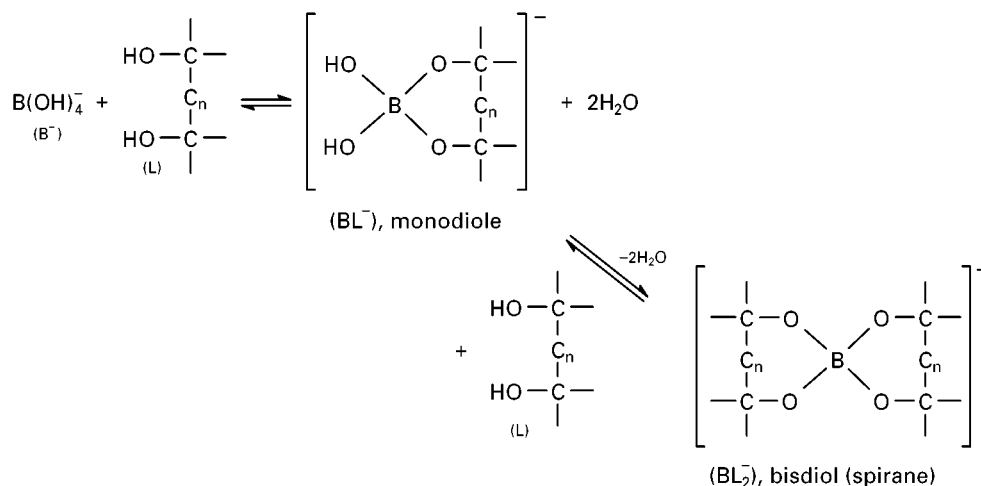


Figure 1 Boric acid as a Lewis acid forms borate in water. Borate reacts with polyol compounds to mono- or bisdiol complexes.

electrophoresis (HPCE), its influence in many chemical, biochemical and biomedical fields has grown constantly. New detection techniques and buffer systems have been developed to make use of the advantages offered by HPCE, such as low sample and buffer volumes, fast separations and high efficiencies. Today, sample volumes in the range of single cell liquids can be analysed. The development of highly sensitive detectors and new derivatization procedures has constantly lowered the detection limit. In the light of these advantages, the following article will focus on capillary electrophoresis.

The Electrophoretic System

Electrolyte Systems

The presence of an ionic charge is the usual prerequisite for migration in an electrophoresis system. Only some saccharides, such as aldonic acids, uronic acids, sialic acids, aminosugars or sulfated sugars of chondroitin, dermatan, keratan and heparin, possess charged functional groups in their structures. The separation of uncharged molecules requires the conversion into charged species by complex formation or derivatization.

The most commonly used systems in planar electrophoresis are those with borate buffers, but other inorganic acids can form complexes with uncharged saccharides. In HPCE, systems are based mainly on sugar-borate complexes and to a lesser extent on sugar-metal cation complexes. Boric acid in aqueous

media acts as a Lewis acid to form the tetrahedral anion B(OH)_4^- . At pH 8–10, the formation of mono- and diesters with the carbohydrates is most effective, but depends largely on the structure of that particular sugar (Figure 1).

The complexation of metal cations also depends on the structure of the carbohydrate. In addition, the ionic radius is crucial for the stability of the complex. Complexation is possible with alkaline metals, Cu^{2+} , Pb^{2+} , Zn^{2+} , Ni^{2+} and Cd^{2+} . For alkaline earth metal buffers, the separation efficiencies decrease in the following order: $\text{Ba}^{2+} > \text{Sr}^{2+} > \text{Ca}^{2+} \gg \text{Mg}^{2+}$. Another way to introduce an ionic charge is by the deprotonation of the hydroxyl functions of the sugars. For this purpose, high pH values (sodium hydroxide solutions, pH > 12) are necessary.

Carbohydrates can also be separated by micellar electrokinetic chromatography (MEKC). In this case, the separation is caused by the different distribution coefficients of the sugars between the free solution and the interior of the migrating micelles of a charged detergent (sodium dodecyl sulfate).

Detection Systems

Precolumn derivatization Most carbohydrate species do not possess strong chromophores in their structures. This condition does not allow their direct sensitive detection by UV absorption. To overcome this difficulty, carbohydrates can be tagged with suitable fluorophores or chromophores. If the tag also provides the charge necessary for electrophoresis,

uncharged carbohydrates can also be separated without the use of complexing buffer systems as well. In principle, derivatization of the hydroxyl groups should be a good approach for the tagging of carbohydrates, but the derivatization of sugars with different reactivities would lead to multiple tagging of the molecule. This would consequently cause a distribution of different products rather than a single derivative. Therefore, other functional groups of the sugar molecule must be considered. The carbonyl group in the open chain form of reducing sugars is the most widely used functional group for the attachment of the label. In amino sugars or acidic compounds, the amino group or the carboxyl group provides potential for derivatization.

Since it is required to produce only one species of derivative in precolumn derivatization, the label must not possess more than one reactive function for the attachment to the carbohydrate. Another requirement is the high molecular absorptivity (UV detection) or photoluminescence efficiency (fluorescence detection) of the tag. Although laser-induced fluorescence detection (LIF) exhibits the lowest detection limits, it is difficult to find a suitable reagent for the respective laser system. The label has to be matched to the laser system used with respect to excitation wavelength and emission intensity. Table 1 compares the detection limits of the different systems after derivatization.

The different labelling agents can be divided into three groups according to their set charge in the separation system: positive, negative or uncharged. Table 2 gives examples of some commercially available derivatization agents and the wavelengths used in different detection systems. Recently, they have found their way into standard chemical catalogues (Fluka, Sigma, Aldrich, ICN). The positively charged compounds usually contain heterocyclic nitrogen functions, e.g. 2-aminopyridine or 6-aminoquinoline. They can be protonated at lower pH values and are commonly used for separation in phosphate buffer solutions (pH 2.5–4). Depending on their pK_a values, these amino compounds can also be used as uncharged labels in high pH buffers. Chromophores with strongly acidic groups, like aminonaphthalene trisulfonic acid (ANTS), remain negatively charged over a wide pH range. Multiple sulfonic acid func-

tions introduce several negative charges to the molecules, which results in high mobility and low adsorption of the derivatives to the capillary surface. All that these compounds have in common, is that they contain a single amino function, which allows the attachment to the carbonyl function of the reducing sugar by reductive amination. In this one-pot reaction, the open chain form of the sugar reacts with the amine to a Schiff's base. To accelerate the reaction and to shift the equilibrium to the product side, the imino function is reduced by sodium cyanoborohydride to the respective secondary amine (Figure 2). An exception to this is the reaction of reducing carbohydrates with 1-phenyl-3-methyl-pyrazolone (PMP). In this case, the acidic hydrogens of PMP and the aldehyde functionality condense under slightly basic conditions.

A disadvantage of precolumn derivatization is the higher structural similarity of the compounds and the higher complexity of sample preparation. Another problem is the varying reactivity of carbohydrates, especially of monosaccharides, with the derivatizing agent. Optimized reaction conditions have to be determined for every sample mixture. The reproducibility of the sample preparation is crucial for the quantification of the compounds.

Indirect detection Indirect detection modes have been applied for the analysis of compounds whose structures lack the necessary physical properties for direct detection. The key element is the use of a background electrolyte, which provides a high, continuous signal. The analyte ion displaces the background electrolyte ion and leads to a change in the UV absorption signal. Therefore, the background electrolyte needs to have the same type of ionic charge as the analyte. The attainable detection limit is given by

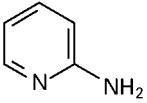
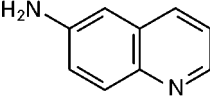
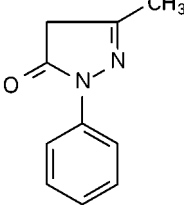
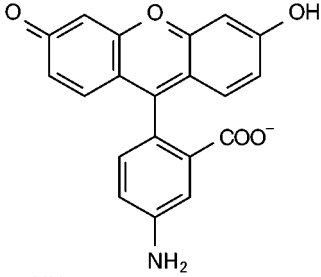
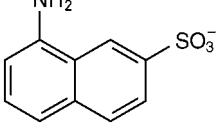
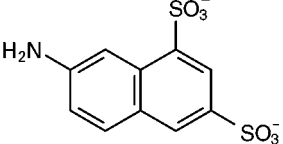
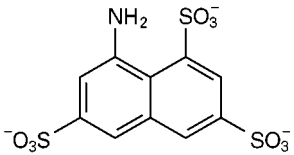
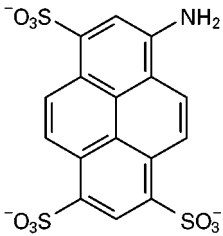
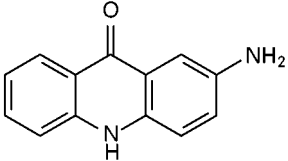
$$C_{\text{lim}} = \frac{C_M}{DR \cdot TR}$$

C_M represents the concentration of the background electrolyte, DR is the dynamic reverse and TR is the transfer ratio. DR is defined as the ability to measure a small change on top of a large signal and is equal to the signal/noise ratio of the background signal. TR is defined as the number of molecules of the background ions displaced by the charged analyte. It can be seen,

Table 1 Detection limits of monosaccharides after derivatization

Detection	Absolute amount (mol)	Concentration (mol L ⁻¹)	Weight concentration
UV derivatization	10 ⁻¹³ –10 ⁻¹¹	10 ⁻⁶ –10 ⁻⁴	ca 10 ppm
Fluorescence derivatization	10 ⁻¹⁶ –10 ⁻¹¹	10 ⁻⁹ –10 ⁻⁴	ca 10 ppb
Derivatization for LIF	10 ⁻²¹ –10 ⁻¹⁷	10 ⁻¹³ –10 ⁻⁹	ca 1 ppt

Table 2 Examples for derivatization agents and used detection wavelengths

Structure	Name	λ_{ex}	λ_{em}
	2-Aminopyridine (2-AP)	240, 320	400
	6-Aminoquinoline (6-AQ)	355	550
	1-Phenyl-3-methyl-5-pyrazolone (PMP)	245	–
	5-Aminofluorescein	257	471
	1-Aminonaphthalene-7-sulfonic acid	229	482
	7-Aminonaphthalene-1,3-disulfonic acid (ANDS)	325	520
	8-Aminonaphthalene-1,3,6-trisulfonic acid (ANTS)	223, 325	520
	8-Aminopyrene-1,3,6-trisulfonic acid (APTS)	325	520
	2-Aminoacridone (AMAC)	488	520

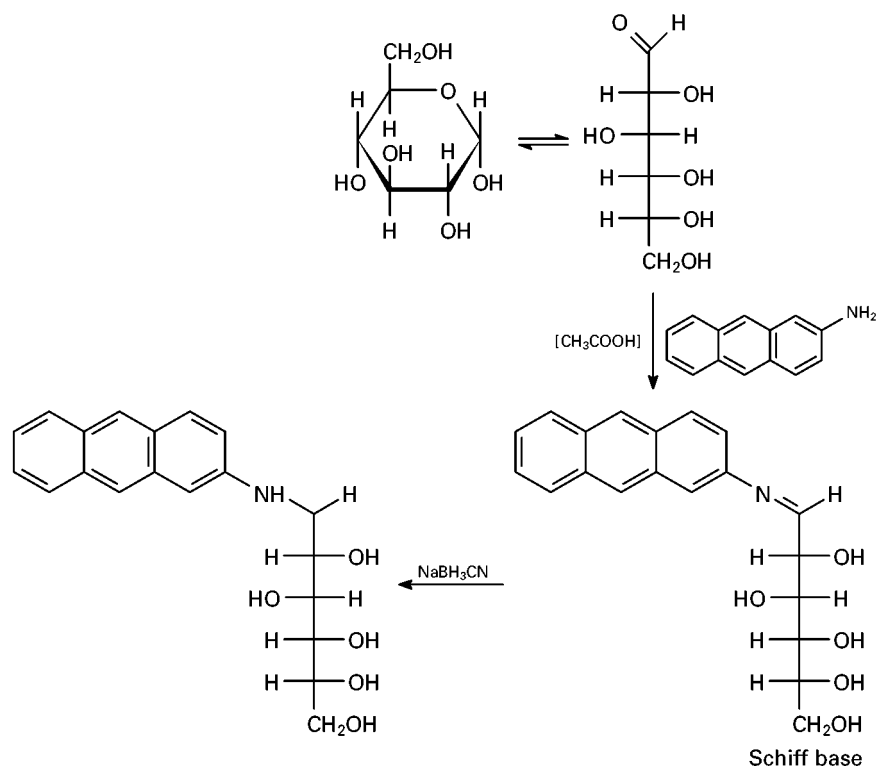


Figure 2 The open chain of the reducing carbohydrate reacts with the amino compound to a Schiff base, which is reduced to a secondary amine by sodium cyanoborohydride.

that C_M should be as low as possible while still generating a high DR . The TR should be close to unity.

Either indirect laser-induced fluorescence detection or UV detection can be applied to the separation of underivatized carbohydrates. Coumarin (LIF) and sorbic acid (UV), for example, have been used as background electrolytes with deprotonated carbohydrates at high pH values. In indirect detection, the concentration of the background electrolyte should be low. Thus, the use of a borate buffer (required concentrations between 0.1 and 0.25 mol L⁻¹) is excluded. Furthermore, the deprotonation of the carbohydrates at high pH values is limited by the increasing concentration of hydroxide anions, which compete with the background electrolyte ions in the displacement mechanism.

Direct detection Different modes of direct detection have been applied to HPCE separations of underivatized carbohydrates. First, low wavelength UV (below 200 nm) can be used to detect carbohydrates which have a sufficient molar absorption coefficient, especially those compounds having carboxyl or other UV-absorbing groups. Mixed oligosaccharides of heparin and heparan sulfate, chondroitin sulfate and dermatan sulfate can be detected at 232 nm. The poor absorption coefficients of many carbohydrates in the range 190 to 280 nm, limits this detection mode.

Amperometric detection Another method is pulsed amperometric detection (PAD) with gold or platinum electrodes, using a strongly alkaline buffer, which has been adapted from the HPLC-PAD systems. These systems require a specialized pulse sequence and therefore expensive instrumentation. Other systems have used ultramicroelectrodes, equipped with a 25- μm copper wire at a constant potential. These systems permit the realization of a linear range over three magnitudes and a limit of detection for mono- and disaccharides in the femtomole range. However, using PAD systems, the running buffer must not contain any electroactive species that might oxidize on the working electrode and cause a strong background signal or poison the electrode surface. Thus, amperometric detection excludes the use of borate buffers, which are essential for the separation of many neutral and native saccharides.

Refractive index detection The determination of the refractive index (RI) has shown its potential in HPLC, although it is not very sensitive and its detection limit falls below that of low wavelength UV. To overcome the problems with the low volume flow in capillary electrophoresis (CE), a sub-nanolitre laser-based refractive index detector has been developed. The detection is based on the change of interferences caused by the change of the refraction index. However, the

adaptation of RI detection of HPCE gives some problems, caused by the joule heating, which introduces changes in the temperature of the liquid and, with this, changes in the refractive index.

Capillaries with partially increased inner diameter

Theoretically, the limit of detection is reduced with the increasing inner diameter of the capillary, due to the increased lightpath through the solution. This is limited by the increasing current with constant field strength, on moving to greater diameters. High currents lead to joule heating effects and contribute to additional band broadening. Capillaries, which are widened locally at the detection window, can help to decrease the detection limit. In this case, the capillary is partially etched with hydrofluoric acid at the detection window. The reaction is controlled by temperature. The diameter widens drastically at the 'hot spot' only. The reaction rate with the capillary wall at other locations is relatively low. Using this procedure, 25- μm capillaries can be widened up to 75 or 150 μm , easily. Recently, detection cells with elongated light-path (high sensitivity cells, z cells) have become commercially available.

Applications and Separation Methods

Monosaccharides

The analysis of monosaccharides, the basic units of carbohydrates, is crucial for many areas of biochemistry, pharmacology, biotechnology and food science.

Several approaches have been made to influence the resolution of the HPCE separation of monosaccharides.

The most common buffer system is based on the complexation of the carbohydrates with an alkaline borate buffer. **Figure 3** demonstrates the separation of a mixture of several aldopentoses and aldohexoses. The sugars were tagged by reductive amination with 2-aminoanthracene. A counter-electroosmotic separation with normal polarity and fluorescence detection was performed. In this case, the intrinsic mobilities of the analytes are lower than the mobility of the electroosmotic flow (EOF). The analyte molecules are transported against their migration direction to the cathodic end of the capillary. The fastest compound is detected last. Five monosaccharides were baseline separated, while one pair (arabinose/mannose) co-migrate. The stability of the carbohydrate complex with the borate ion, which depends on the structure of the monosaccharide, has the dominating influence on the separation. Due to these differences, fucose (desoxyhexose) is separated from the unresolved pair mannose (hexose) and arabinose.

To underline the differences in the migration mechanisms, **Figure 4** shows a co-electroosmotic separation of the same mixture in an acidic medium. At a pH of 2.0, the amino function of the analyte is protonated and leads to a co-electroosmotic migration, i.e. in the same direction as the electroosmotic flow. The fastest compound is detected the first. Due to the low dissociation of the silanol groups at the capillary surface, the EOF is very low at this pH.

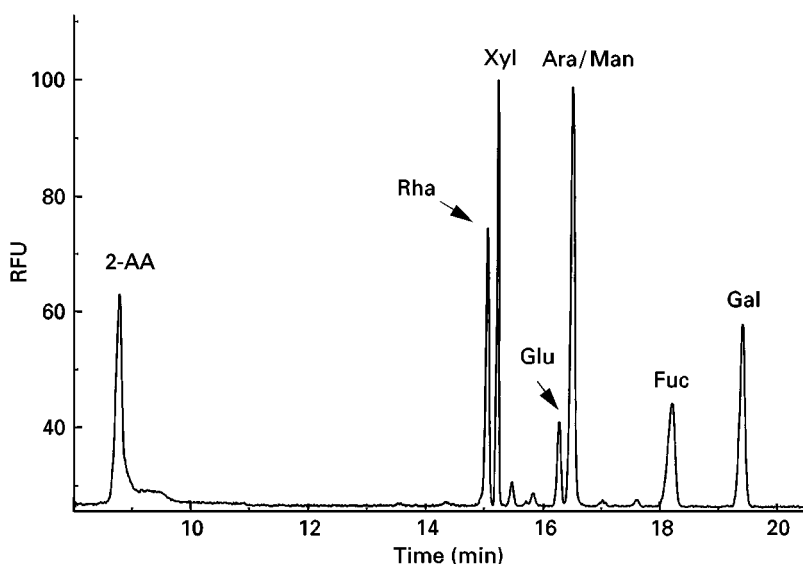


Figure 3 Counter-electroosmotic separation of 2-AA-labelled monosaccharides rhamnose (Rha), xylose (Xyl), glucose (Glu), arabinose (Ara), mannose (Man), fucose (Fuc), galactose (Gal) and 2-aminoanthracene (2-AA). Buffer: borate 250 mM, pH 10.5; $U = 30$ kV; capillary-fused silica, i.d. = 50 μm , $l = 88$ –100 cm; inj. 6s 100 mbar.

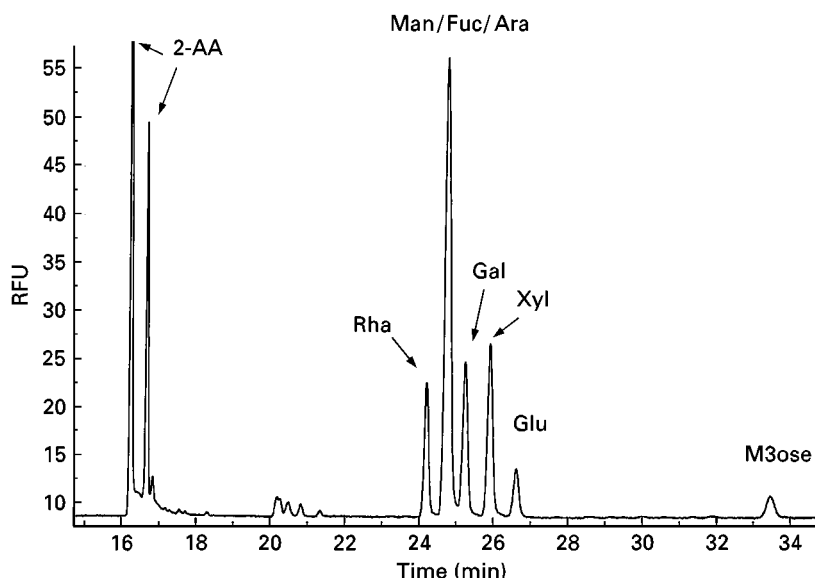


Figure 4 Co-electroosmotic separation of 2-AA-labelled monosaccharides rhamnose (Rha), xylose (Xyl), glucose (Glu), arabinose (Ara), mannose (Man), fucose (Fuc), galactose (Gal), maltotriose as standard (M3ose) and 2-aminoanthracene (2-AA). Buffer: phosphate 100 mM, 20% (v/v) iPropOH, pH 2.0; capillary fused silica, $l = 49\text{--}60$ cm, i.d. = $50\text{ }\mu\text{m}$; $U = \text{ramp } 2.5\text{ kV min}^{-1}$ from 5 to 30 kV; inj. 6s 100 mbar.

To enhance resolution, an organic modifier (isopropanol) was added. The co-electroosmotic separation leads to a different electropherogram. Here, other parameters, such as the hydrodynamic radius of the analytes, have the dominating influence on the migration mechanism. The differences in mobility of mannose, fucose and arabinose are too small to lead to a separation, while the resolution of the epimers glucose and mannose is increased compared to the borate buffer system.

It is also possible to separate a monosaccharide mixture by micellar electrokinetic chromatography (MEKC). In this system, the dominating mechanism is the dynamic distribution of the uncharged analytes between free solution and the migrating micelles of the detergent (often SDS). Here, other properties of the analytes, such as differences in their hydrophobicity, effect the separation.

Figure 5 shows the separation of a monosaccharide mixture in a trisborate/SDS buffer. Unlike the results of the previous separation systems, the peaks of mannose and arabinose show a sufficient resolution.

Table 3 gives some examples of the buffer systems and tags used so far to analyse monosaccharide mixtures. The use of borate buffers dominates. Other systems have also been used, but have not yet found their way into standard applications.

Linear Oligo- and Polysaccharides

Oligo- and polysaccharides can be classified either as homo- or heteropolymers, depending on whether

they consist of one type or more than one type of monosaccharide unit that alternate in the repetitive sequence. High molecular weight polysaccharides are usually analysed through their degradation products (chemical or enzymatic cleavage). The systems described for the separation of monosaccharides can be easily applied to the separation of oligosaccharides. With few exceptions, the mobilities decrease with increasing molecular weight of the analytes. The use of divalent metal ions for complexation is not favourable for analysing carbohydrates, as it leads to insufficient separation efficiency.

The composition of oligosaccharide mixtures should be considered when selecting the separation system. The use of a borate buffer focuses on the structural differences of the oligosaccharides and should be used for separation of heterogeneous oligosaccharides with the same degree of polymerization. For homologous oligosaccharides, the use of permanently charged labels in a co-electroosmotic system is favourable. Here, the charge-to-mass ratio is the dominant parameter responsible for the migration differences. The influence of the electroosmotic flow should be reduced to a minimum to ensure good resolution of the compounds with higher molecular mass.

Figure 6 shows the counter-electroosmotic separation of 2-AA labelled maltooligosaccharides in the borate buffer system. As the molecular weight increases, the differences in migration time decrease very fast. This can be explained by a lower degree of

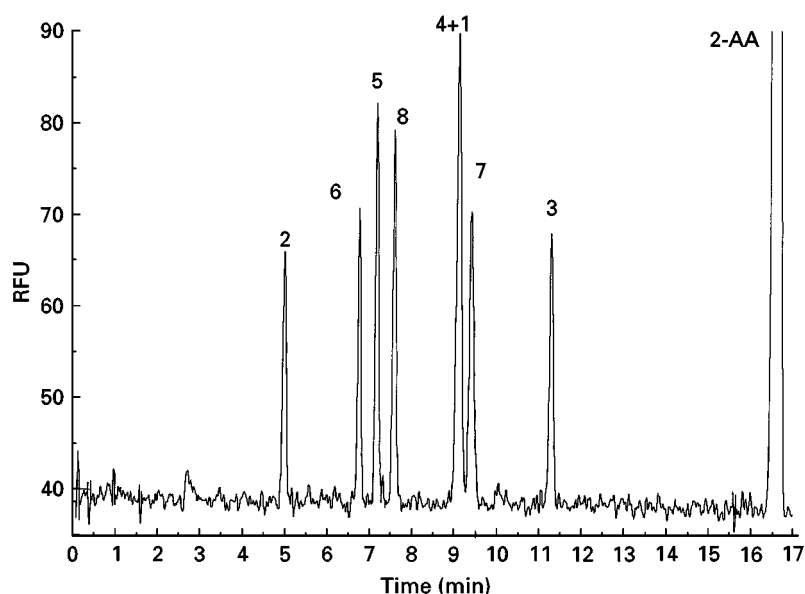


Figure 5 MEKC separation of 2-AA-labelled monosaccharides. 1, rhamnose; 2, cellobiose; 3, xylose; 4, ribose; 5, glucose; 6, mannose; 7, arabinose; 8, galactose; 2-AA, 2-aminoanthracene. Buffer: trisborate 100 mM/urea 4 M/SDS 100 mM, pH 8.3; capillary-fused silica, $l = 48\text{--}60$ cm, i.d. = 25 μm ; $U = 30$ kV.

structural change, going step by step to higher degrees of polymerization. Also, the ratio of $\mu_{\text{analyte}}/\mu_{\text{EOF}}$ decreases with increasing degree of polymerization. With a higher degree of polymerization, the mobility

differences decrease drastically and lead to insufficient resolution.

For higher degrees of polymerization (> 7), the use of charged labels at low EOF is to be preferred.

Table 3 Examples of the separation mode, buffer systems and detection methods for different carbohydrates

Analytes	Detection	Separation mode	Derivatization	Buffers
Monosaccharides	Direct UV	CZE	2-AP	200 mM borate, pH 10.5
Monosaccharides	Direct Fluorescence	CZE	2-AA	200 mM borate, pH 10.5
Monosaccharides	Indirect UV	CZE	–	6 mM sorbate, pH 12.1
Monosaccharides	Indirect LIF	CZE	–	50 μM fluoresceine, pH 12.2
Monosaccharides	Direct LIF	CZE	APTS	25 mM borate, pH 10.0
Monosaccharides	Amperometric detection	CZE	–	100 mM NaOH, pH 13
Monosaccharides	RI detection	CZE	–	100 mM borate, pH 9.0
Maltooligosaccharides $\text{DP}_{\text{max}} < 25$	Direct UV	CZE	2-AP	100 mM phosphate, pH 2.5
Maltooligosaccharides	Direct LIF	CZE	ANTS	50 mM phosphate, pH 2.5
Branched xyloglucans	Direct UV	CZE	2-AP	100 mM phosphate, 50 mM tetrabutylammonium bromide, pH 4.75
Dextrans $\text{DP}_{\text{max}} < 25$	Direct fluorescence	CZE	2-AA	100 mM phosphate, pH 2.0
Low molecular weight heparin	Direct UV	CZE	–	10 mM borate, 50 mM sodium dodecyl sulfate
Polygalacturonic acid $\text{DP}_{\text{max}} < 70$	Direct LIF	CGE	ANTS	100 mM Tris, 25 mM borate, pH 8.5
Hyaluronic acid $\text{DP}_{\text{max}} < 400$	Direct LIF	CGE	APTS	Polyacrylamide gel, 18% T, 3% C
Glycoforms of ribonuclease A	Direct UV	CZE	–	25 mM citric acid, 12.5 mM tris, 0.03% aminodextran (mol. wt 10 000)
				20 mM phosphate, 50 mM sodium dodecyl sulfate, 5 mM borate, pH 7.2

DP_{max} , maximum degree of polymerization (baseline separation); CZE, capillary zone electrophoresis; CGE, capillary gel electrophoresis.

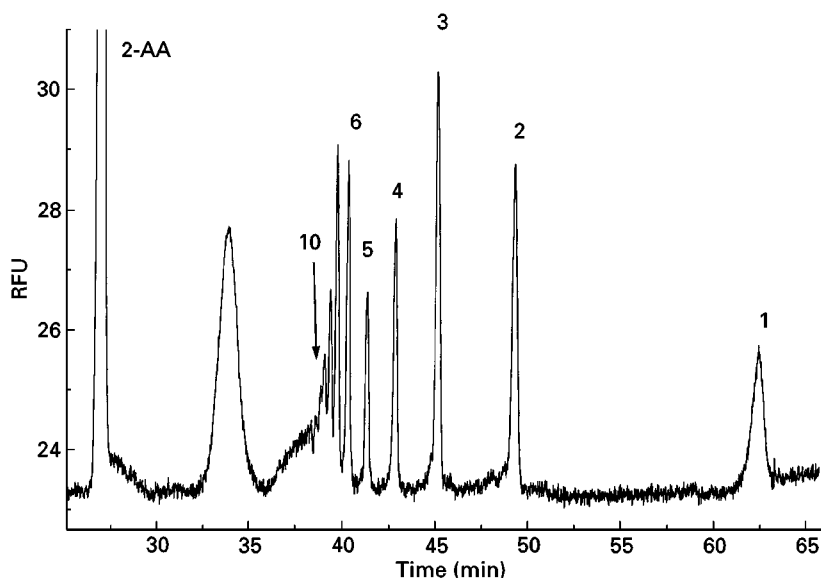


Figure 6 Counter-electroosmotic separation of the starch hydrolysate Dextrin 10 (numbers indicate the degree of polymerization). Buffer: borate 300 mM, pH 10.5; capillary fused silica, $l = 108\text{--}120$ cm, i.d. = $50\text{ }\mu\text{m}$; field = 30 kV; inj. 6s 100 mbar.

It can be seen in **Figure 7** that protonation of the amino function of the 2-aminoanthracene-labelled aminoglycans leads to a higher resolution of the oligosaccharide peaks. With a higher number of monosaccharide units, the mobility differences decrease less than those in the borate system. Increasing charge of the label can increase the mobility of the molecules. This has proved to be the case with naphthalene di- and trisulfonic acid derivatives especially. By derivatizing with aminonaphthalene trisulfonic acid, it is possible to separate more than 30 malto-oligomers within 10 min.

To improve the resolution of homologue oligosaccharides with a higher degree of polymerization, two different approaches have been attempted. First, the use of coated capillaries (polyether, polyvinyl alcohol) showing very low or virtually no electroosmotic flow can lead to an increase in resolution. The disadvantages of these systems are the limited pH range in which they can be used and the high cost of the capillary material.

A similar approach to that for the separation of oligonucleotides involves using gel-filled capillaries. Gel-filled capillaries can have a sieving effect on the

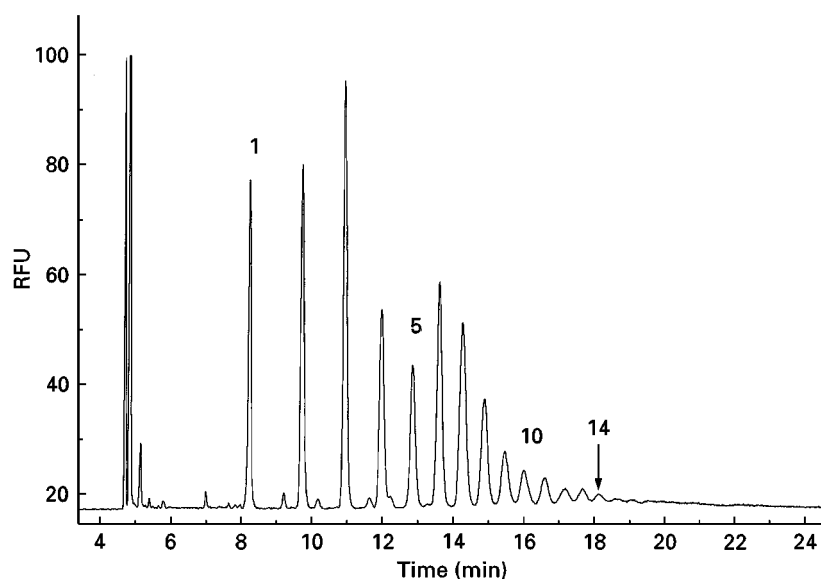


Figure 7 Co-electroosmotic separation of the starch hydrolysate Dextrin 10 (numbers indicate the degree of polymerization). Buffer: phosphate 100 mM, pH 2.0; capillary-fused silica, $l = 49\text{--}60$ cm, i.d. = $50\text{ }\mu\text{m}$; $U = 25$ kV; inj. 5s 100 mbar.

analytes. This size discrimination can be used to increase the differences in mobility. Unfortunately, the use of gel-filled capillaries is accompanied by many difficulties such as poor gel-to-gel reproducibility, bubble formation, quenching effects by the matrix, and the collapse of the gel matrix buffer. Another problem is the relatively low mobility of the formerly uncharged molecules, which are tagged by a charged label. The use of gel-filled matrices can increase the migration time to an unacceptable extent.

For structures consisting of charged monosaccharide species, such as polyuronic acids, the use of a mixture of aminodextran and linear polyacrylamide (LPAA) as buffer additive is successful. In this case, the retention mechanism cannot be due to the sieving effect of the matrix only. The system is, rather, based on size-dependent electrostatic interactions between the protonated amino functions of the aminodextran and the dissociated carboxylic groups of the uronic acids.

Table 3 gives some examples of the systems used so far.

Branched Oligosaccharides

Branched oligosaccharides can be produced by enzymatic digestion of branched heteropolysaccharides, for example xyloglucan polysaccharides. In combination with a charged label, some information about the branching of the compounds can be achieved. If only the label is charged, the compounds migrate in order of increasing size, as shown before. With similar molecular weight, the less branched oligosaccharides migrate faster than the more branched ones. For branched xyloglucan oligosaccharides, a mobility index system has been introduced to describe the migration behaviour of the branched compounds with respect to their linear homologues. The equation below shows how the mobility index (MI) can be calculated:

$$MI = 100n + 100 \left(\frac{\log \mu_s - \log \mu_{n+1}}{\log \mu_n - \log \mu_{n+1}} \right)$$

μ_s is the electrophoretic mobility of the branched analyte, and μ_n and μ_{n+1} are the electrophoretic mobilities of the two homologues with n and $n+1$ repetitive units, which migrated before and after the branched fragment. This index system can only be applied if the following requirements are fulfilled. First, the system must consist of homopolymers or heteropolymers with a strictly repeating sequence. Second, the logarithmic mobilities of the homologues must show a logarithmic dependence on the degree of polymerization, which is not always the case.

Glycoconjugates

Glycoproteins Glycoproteins function as enzymes, transport proteins, receptors, hormones and structural proteins. The carbohydrate content of glycoproteins can vary from less than 1% to more than 60% by weight. Protein glycosylation can occur at two or more positions in the amino acid sequence. The glycans at a single position may be heterogeneous or may be missing from some molecules. This leads to populations of glycosylated species of a single protein (glycoforms). The relative proportions of glycoforms are found to be reproducible, depending on the glycosylation conditions (environment of the reaction, physical state and type of organism), the manufacturing process and the isolation procedures.

On the one hand, glycoform separation and mapping has to cope with the problems introduced by the protein moiety, such as interactions of the protein with the capillary wall in low pH electrolyte systems. In this case, a hydrophilic coating of the capillary surface can avoid adsorption phenomena. On the other hand, the UV absorption coefficients at 200 nm are sufficient for the detection of the compounds without precolumn derivatization. Common buffer systems are phosphate, TRIS/boric acid or borate buffers, depending on the separation mode and the pH range.

Glucosaminoglycans Glucosaminoglycans (mucopolysaccharides) are unbranched polysaccharides of alternating uronic acid and hexosamine residues, for example, heparin, chondroitin sulfate, dermatan sulfate or hyaluronic acid. After exhaustive treatment with polysaccharide lyases, disaccharides can be obtained bearing unsaturated uronic acids. These compounds can be detected directly at 232 nm. To enhance sensitivity, they can also be labelled. Since the mucopolysaccharides are already charged over a wide pH range, it is not necessary to introduce a charge by a tag or complexation. The use of SDS micelles can increase the resolution.

Glycolipids Some lipids contain oligosaccharide moieties as an integral part of their structure. Since these contain a hydrophilic head and a hydrophobic tail, they form micellar systems. Temperature, concentration of the analyte and ionic strength of the electrolyte system are crucial for the size and mobility of the micelles. Thus, the separation of some glycolipids as monomeric species is impeded. The investigations made so far have been based on phosphate buffer systems and low wavelength UV detection.

Further Directions

Capillary electrophoresis has proven potential for carbohydrate analysis. High efficiencies and short analysis times are its advantages compared with other analytical separation methods. A variety of different separation modes can be applied to separate complex carbohydrate mixtures. It has been shown that, depending on the properties of the sample, different separation methodologies can be applied and optimized.

The electrophoretic analysis of carbohydrates is still under development. In particular the analysis of biochemical compounds, such as glycoconjugates, is still a challenge and can give new information about cell mechanisms, structure of antibodies, etc. This article has focused on the basic aspects of capillary electrophoresis of carbohydrates. The carbohydrates described were confined to simple model compounds. For more specific information, the Further Reading list should be consulted.

See also: III/Ion Analyses: Capillary Electrophoresis.

Further Reading

- El Rassi Z (1994) Capillary electrophoresis of carbohydrates. *Advances in Chromatography* 34: 177–250.
 El Rassi Z and Nashabeh W (1995) High performance capillary electrophoresis of carbohydrates and glyco-

conjugates. *Journal of Chromatography Library* 58: 267–360.

- Hase S (1996) Precolumn derivatization for chromatographic and electrophoretic analyses of carbohydrates A. *Journal of Chromatography A* 720 (1 + 2): 173–182.
 Kakehi K and Honda S (1996) Analysis of glycoproteins, glycopeptides and glycoprotein-derived oligosaccharides by capillary electrophoresis. *Journal of Chromatography A* 720 (1 + 2): 377–393.
 Lee KB, Loganathan D, Merchant ZM and Linhardt RJ (1990) Carbohydrate analysis of glycoproteins. A review. *Applied Biochemistry and Biotechnology* 23 (1): 53–80.
 Linhardt RJ and Pervin A (1996) Separation of negatively charged carbohydrates by capillary electrophoresis. *Journal of Chromatography A* 720 (1 + 2): 323–335.
 Oefner P, Chiesa C, Bonn G and Horvath C (1994) Developments in capillary electrophoresis of carbohydrates. *Journal of Capillary Electrophoresis* 1 (1): 5–26.
 Olechno JD and Nolan JA (1997) Carbohydrate analysis by capillary electrophoresis In: *Handbook of Capillary Electrophoresis*, 2nd edn, pp. 297–345. Cleveland, OH: CRC Press.
 Paulus A and Klockow A (1996) Detection of carbohydrates in capillary electrophoresis. *Journal of Chromatography A* 720 (1 + 2): 353–376.
 Voegel PD and Baldwin RP (1997) Electrochemical detection in capillary electrophoresis. *Electrophoresis* 18 (12–13): 2267–2278.

Gas Chromatography and Gas Chromatography–Mass Spectrometry

A. Fox, M. P. Kozar and P. A. Steinberg,
 University of South Carolina,
 Columbia, SC, USA

Copyright © 2000 Academic Press

Overview of Derivatization of Sugars for GC, GC-MS or GC-MS-MS Analysis

Table 1 overviews many of the important events in chromatographic and mass spectrometric analysis of sugar monomers. These will be discussed at appropriate points in this review. It was not until the years 1961–1963 that gas chromatography (GC) was applied to the quantitative analysis of mixtures of neutral and amino sugar monomers, even though individual sugars had been derivatized earlier. Carbohydrate analysis by GC lagged behind the analysis of many other compounds because of the difficulty in producing volatile derivatives. Two schools of

thought developed, relating to whether the anomeric centre should be retained or destroyed in derivatization. Both persist to this day. Sugars exist in equilibrium between ring and straight chain forms. If the anomeric centre is not eliminated, derivatization fixes the sugars in the anomeric ring forms. Thus, two to four peaks will be produced from each L or D sugar (two from furanose and two from pyranose anomers). Interpretation of chromatograms becomes complicated and quantitation difficult. Acidic sugars (i.e. generally with carboxyl groups) require additional derivatization steps. The carboxyl moiety may be converted to a lactone, ester or reduced to an alditol.

The Alditol Acetate Procedure

The alditol acetate procedure was the first developed in which the anomeric centre is eliminated. The anomeric centre is converted by borohydride reduction (although later borodeuteride was introduced)

Table 1 Important advances in analysis of carbohydrates

1960–1965	Fundamental articles on preparation of sugar derivatives for gas chromatography (GC)
1970s	Introduction of gas chromatography–mass spectrometry (GC-MS) for structure analysis of carbohydrates
Late 1970s–early 1980s	Introduction of selected ion monitoring (SIM) GC-MS for trace analysis of derivatized carbohydrates
1980s	Development of anion exchange liquid chromatography/pulsed amperometric detection of native sugars
1990s	Introduction of liquid chromatography–electrospray mass spectrometry for analysis of underivatized sugars
1995–1996	Introduction of gas chromatography–tandem mass spectrometry for trace analysis of derivatized sugars
1995–1996	Introduction of liquid chromatography–tandem mass spectrometry for identification of native sugars

to an alcohol prior to acetylation (to produce a volatile derivative). Unfortunately, borate derived from the added borohydride, or borodeuteride, inhibits the subsequent acylation step. The classical procedure employs a multi-step evaporation with methanol–acetic acid to remove borate as tetramethyl borate gas in between the reduction and acetylation steps (Figure 1).

In the 1960s, sodium acetate and pyridine were introduced as catalysts for acetylation, pyridine being more efficient than sodium acetate. However, in both cases borate must be removed prior to acetylation. Subsequently, several catalysts (including methylimidazole) were described that allowed acetylation without removal of borate or moisture. Unfortunately, many catalysts (including both pyridine and methylimidazole) often generate side-reaction products (from reaction with acetic anhydride) that produce chromatograms contaminated with extraneous peaks. Furthermore, in the presence of moisture

and/or borate, acetylation can be somewhat unpredictable. When using sodium acetate as a catalyst following removal of borate and moisture, these problems do not occur but unfortunately, the process to remove borate and moisture is tedious to perform. An automated evaporator has been developed to perform the multiple cycles of methanol–acetic acid addition/evaporation for borate removal in the alditol acetate procedure. More recently, an automated derivatization instrument has been developed to automate the entire alditol acetate procedure.

The Trimethylsilyl Procedure

Also in the early 1960s, other workers described a simple one-step trimethylsilyl derivatization of hydroxyl groups. This remains one of the most common procedures used for GC analysis. Derivatization is readily achieved. However, complex chromatograms are produced due to anomer formation noted above. Also, analysis must be prompt since the derivatives

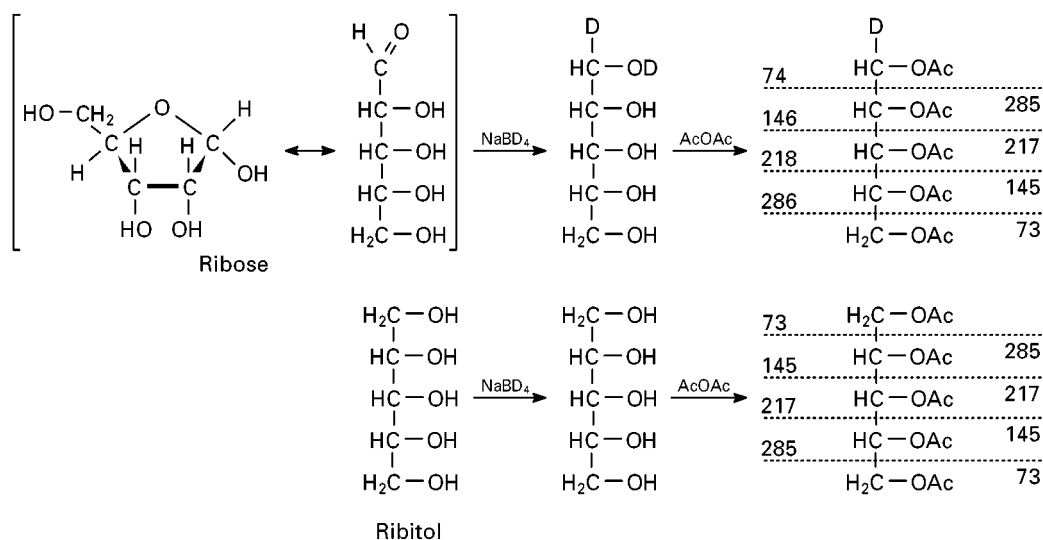


Figure 1 An example of an alditol acetate derivatization reaction employing sodium borodeuteride in the reduction step. Differences in the mass spectra of ribose and ribitol illustrate the distinctness of mass spectra of alditols and aldoses.

decompose in the presence of moisture, complicating clean-up of complex samples.

The Aldonitrile Acetate and O-Methyloxime Acetate Procedures

Procedures developed in the 1970s involving destruction of the anomeric centre were particularly concerned with proceeding directly to the final acylation step. Such procedures generally employed acetylation as the final acylation step due to the stability of acetylated sugar derivatives. Such methods included the aldonitrile acetate and the O-methyloxime acetate procedures. To generate the former, the aldehyde is reacted with hydroxylamine to produce an oxime which is converted to a nitrile on acetylation. O-methyloxime acetates, on the other hand, are prepared by destruction of the anomeric centre by reaction with O-methyl-hydroxylamine, also followed by acetylation. Unfortunately, O-methyloxime acetates display a new isomeric centre and two products, syn- and anti, are generated for each sugar.

An advantage of both aldonitrile and O-methyloxime acetate methods is that aldoses produce distinct peaks from alditols. However, substitution of borodeuteride for borohydride reduction (in alditol acetate formation) labels the aldose group, whilst alditols remain unlabelled. Thus, aldoses and alditols can be distinguished by gas chromatography–mass spectrometry (GC-MS) analysis. Alternatively, alditols do not contain an anomeric centre and can be acetylated without prior derivatization steps (e.g. reduction) and are simply analysed. This also allows discrimination of alditols from aldoses. For further details see the section on GC-MS analysis of alditol acetates, below.

The Trifluoroacetyl Procedure

Trifluoroacetyls, like trimethylsilyl derivatives, are also formed by a simple one-step derivatization procedure. However, as with trimethylsilyl derivatives, multiple peaks are generated for each sugar and are unstable on exposure to moisture. Therefore, samples must be analysed soon after derivatization. As noted above, acetate derivatives are generally stable indefinitely.

Chiral Derivatives

Methods developed have followed two approaches: after conventional derivatization (e.g. permethylation) enantiomers (L and D isomers) can be separated on chiral (e.g. cyclodextrin) GC columns; alternatively, glycosidation with chiral reagents (e.g. an optically active alcohol such as butanol) produces diastereoisomers that can be resolved on conventional nonchiral capillary columns.

Choice of Derivatives for Instrumental Detection

Most reports in the 1960s and 1970s employed the flame ionization detector (FID). While the FID is useful as a GC detector, it lacks specificity. The use of the mass spectrometer (MS) or tandem mass spectrometer (MS-MS) as a GC detector dramatically expands the capability of the analysis. GC-MS, using electron impact ionization (EI) or chemical ionization (CI) followed by positive ion detection, employs the same derivatives as in FID but provides specificity that the FID lacks.

There have been a few reports using the electron-capture detector (ECD) offering the possibility of increased sensitivity if a halogenated (electron-capturing) derivative such as trifluoroacetyl, pentafluoropropyl or heptafluorobutyl is employed. Unfortunately, such derivatives are unstable in the presence of moisture. Furthermore, compounds other than sugars may be converted to halogenated derivatives, resulting in increased background. Thus, it is unclear whether the increased sensitivity can be utilized. An unusual derivative not widely used is the O-pentafluorobenzyl oxime acetate derivative. For this derivative, pentafluorobenzyl oxime replaces the aldehyde as the electron-capturing group prior to acetylation. Unlike other halogenated derivatives, the O-pentafluorobenzyl oxime acetate is stable to moisture. Alternatively, such derivatives might be appropriate for use with MS in the negative ion mode. Like ECD, negative ion chemical ionization (NI-CI) GC-MS also necessitates an electron-capturing derivative. Use of GC-MS-MS might take further advantage of the increased sensitivity of NI-CI since background is essentially eliminated.

The first benchtop GC-MS instruments were introduced in the late 1970s and had only EI capability. Later instruments could perform both EI and CI with both positive and negative ion detection capabilities. In the past 3–4 years, comparably priced benchtop GC-MS-MS instruments, also with EI-CI and positive/negative ionization capability, have been introduced. Most GC-MS and GC-MS-MS analyses of sugars are still performed with EI in positive ion detection mode. These instruments are simple to operate and maintain and are run by Windows-based PCs.

Preparation of Alditol Acetate Derivatives of Sugars Present in Complex Matrices

Steps in the analysis of complex sugar mixtures include release of the sugar by hydrolysis, addition of internal standard, derivatization and instrumental

analysis. Examples of analyses performed with the alditol acetate procedure will be used here to illustrate these steps.

Hydrolysis

There have been numerous articles on the selection of hydrolysis conditions. Parameters requiring consideration include temperature, duration and the type and strength of acid (primarily hydrochloric, sulfuric and trifluoroacetic acids). Optimization is highly dependent on the sugar(s) of interest to be released from a particular polymeric matrix. If the hydrolysis conditions are too gentle, there is an inadequate release of the sugar monomers. Conversely, if the conditions are too harsh, then destruction of certain sugars occurs. Neutral sugars are often easier to release and destroy than aminosugars. Invariably, a compromise must be made in the analysis of a mixture of neutral and aminosugars in a complex matrix. It must also be recognized that it is not the absolute amount of polymeric sugar present in the matrix that is being determined, but the amount released as monomers under the selected hydrolysis conditions.

Following hydrolysis and prior to derivatization, the acid must be removed. Trifluoroacetic and hydrochloric acids are generally removed by evaporation. Under these conditions further destruction of sugars is possible. Sulfuric acid can be removed by neutralization with a solution of barium hydroxide or a suspension of barium carbonate. Unfortunately, on neutralization with a barium hydroxide solution, it is difficult to remove the sugar from the precipitate of barium sulfate. The use of barium carbonate is not practical because a coat of barium sulfate forms, protecting a large portion of the particulate barium carbonate from reacting. Thus, large quantities of barium carbonate are needed for neutralization. A simple alternative involves neutralization with a solution of an organic base (*N,N*-diethylmethylamine) in chloroform. Sugars remain in the aqueous phase and sulfate is removed in the organic phase.

Choice of Internal Standard

There is a great deal of variability of sugar monomers that can be present in complex biological matrices. Quantitation of each sugar present in a profile is desirable, but it is not practical to select one internal standard for each sugar. Generally, internal standards are selected for groups of sugars based on structural similarities. On SP-2330 columns, neutral sugars elute much earlier than aminosugars. Relative standard deviations (RSD) for multiple samples on GC analysis for late-eluting aminosugars are high if an early eluting neutral sugar (e.g. arabinose) is used as the internal standard. Selection of a late-eluting

aminosugar (e.g. methylglucamine) as an internal standard for aminosugars dramatically increases precision. However, on less polar columns, such as the DB-5ms, certain high molecular weight neutral sugars (e.g. heptoses) tend to elute in the same region as aminosugars (e.g. aminohexoses). In the analysis of heptoses, when using arabinose as the internal standard (by comparing relative peak areas), the RSD for D-glycero-D-mannoheptose and L-glycero-D-mannoheptose was found to be 25.3% and 30.7%, respectively. Using methylglucamine, RSD was lowered to 11.0 and 7.2%. This suggests that, when selecting an internal standard, the relative retention time of the eluting sugars, rather than similarity in structure, may be more critical. Heptoses are highly characteristic of Gram-negative bacteria.

The aldoses L-glycero-D-mannoheptose and D-glyceroheptose are not available commercially. On reduction they are converted into their respective heptitols. However, the ketose heptulose, which is available commercially, on reduction generates both L-glycero-D-mannoheptitol and D-glycero-D-mannoheptitol. Hydrolysates of *Escherichia coli* contain L-glycero-D-mannoheptose but not D-glycero-D-mannoheptose. Thus, by comparing chromatograms of standards containing heptulose and hydrolysates of *E. coli* (as alditol acetates) it is possible to identify the two heptose peaks. Figure 2 shows a typical separation of a mixture of neutral and amino sugar standards (including both heptose peaks) on a DB-5ms fused silica capillary column and a hydrolysate of *E. coli* (containing L-glycero-D-mannoheptose but not D-glycero-D-mannoheptose).

The Automated Derivatization Instrument for Preparation of Alditol Acetates

The manually performed alditol acetate derivatization procedure described elsewhere has been used for many years. This multi-step procedure can now be performed sequentially by a computer-controlled instrument. The procedure, which previously took 2½ working days, is performed in an automated fashion, requiring a total of 90 min manual work. The samples are processed in four stages:

1. evacuation/hydrolysis (3 h 15 min, automated);
2. prederivatization clean-up (1 h, manual);
3. alditol acetate derivatization (23 h, automated);
4. post-derivatization clean-up (30 min, manual).

The core of the machine, where chemical manipulations and reactions are performed, consists of a custom-built manifold with 21 glass chambers, to each of which a test tube is attached. The manifold is seated in a movable heating block. A series of electrically driven solenoid valves are attached in-line with

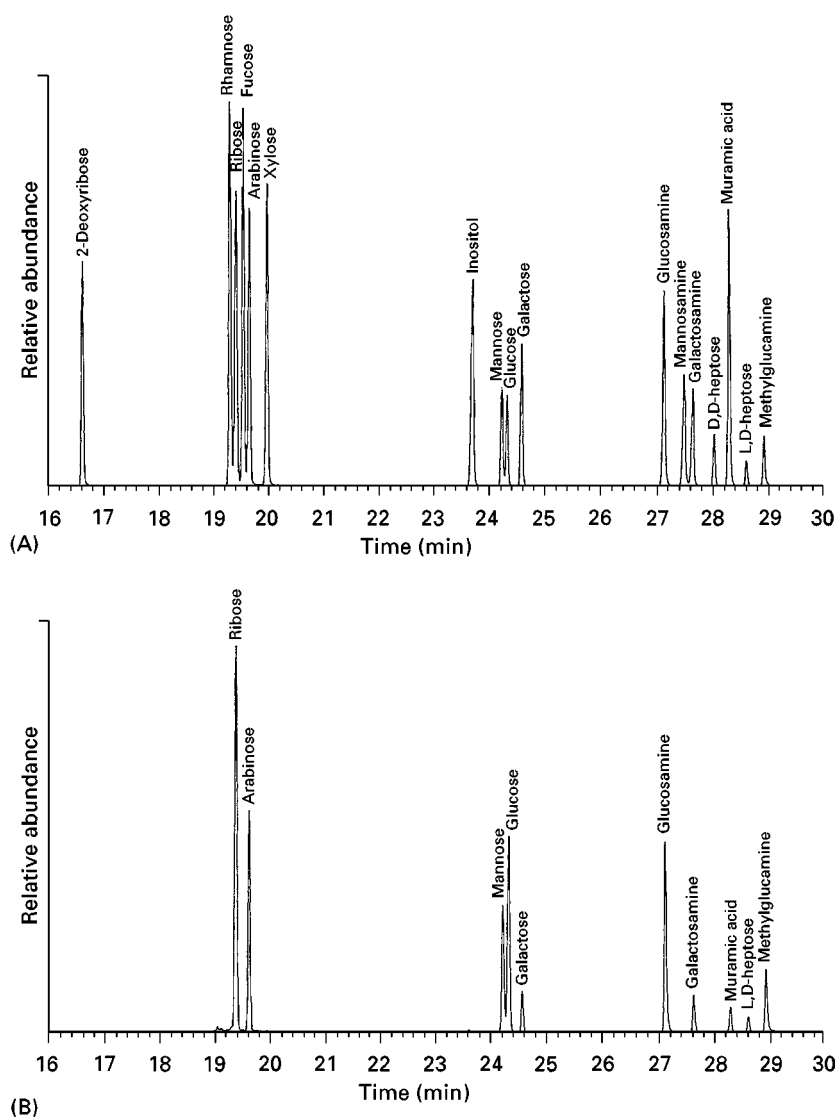


Figure 2 Selected ion monitoring (SIM) GC-MS chromatograms of alditol acetates (A) sugar standards and (B) hydrolysate of *Escherichia coli*. The following m/z were monitored: 160 (deoxyribose); 171 (rhamnose and fucose); 145 (ribose, arabinose and xylose); 199 (inositol, 199); 290 (mannose, glucose and galactose); 318 (glucosamine, galactosamine, mannosamine); 362 (D,D-heptose and L,D-heptose); 168 (muramic acid); 327 (methylglucamine).

the manifold. A set of solvent valves control the input of solvent and/or nitrogen gas to each sample chamber. A set of gas valves controls output to atmosphere or vacuum. Additionally, closure of all valves allows the samples to be sealed in a closed chamber.

Computer control of the individual stages of the derivatization process is a major feature of the system. Ten mg of each sample, in 1 mL of 2 mol L⁻¹ sulfuric acid, is placed in each of the custom test tubes. The samples are attached to the manifold and the program started. Oxygen is evacuated by repeated alternate exposure of nitrogen and vacuum. After evacuation, the program sets the heating block to 100°C for hydrolysis. Heating continues for 3 h under nitrogen.

Following hydrolysis, internal standards are added, the samples are removed from the instrument, neutralized with 2 mL 50% N,N-dioctylmethylamine (Fluka, Buchs, Switzerland) in chloroform, and then centrifuged. The aqueous phase containing the sugar monomers is removed and passed through C₁₈ columns (J&W, Folsom, CA) into 21 new sample tubes via the evacuated 21-chamber manifold described above. Aqueous sodium borodeuteride 200 µL (25 mg mL⁻¹) is then added to each sample.

The derivatization procedure is entirely under computer control. After a 2 h delay, in which sample reduction occurs at room temperature, methanol–acetic acid (200:1 v/v) is added by activation of a solenoid valve connected to a reagent reservoir. The

program then sets the heating block to 60°C, and evaporation under N₂ occurs for 30 min. This step (solvent addition and evaporation) is automatically repeated several times to remove borodeuteride as tetramethyl borate gas. After the last addition, the system is evacuated by activation of the attached vacuum pump, and the samples are dried for 4 h at room temperature. Acetic anhydride is then added to the samples from another reservoir, and the samples acetylated for 13 h at 100°C. Finally, the samples are evaporated to dryness under N₂, and chloroform is added from a third reservoir.

The final post-derivatization clean-up (taking 30 min) is performed manually but also uses the 21-sample manifold, alleviating the necessity for additional equipment. Samples are passed through a pair of connected Chem-Elut columns (Varian, Walnut Creek, CA), the first pre-treated with 2 mol L⁻¹ acetic acid and the second with 14.8 mol L⁻¹ ammonium hydroxide. The chloroform eluent is evaporated under N₂, and samples reconstituted for analysis.

Instrumental Analysis of Alditol Acetate Derivatives

Columns of GC Analysis

There was a great deal of work in the early days in the selection of packed columns for separation of a complex mixture of neutral and amino sugars by GC. This work was readily extrapolated to the vastly improved fused silica columns introduced later. As an example, excellent capillary GC separation of neutral and aminosugar mixtures is obtained on relatively polar SP-2330 columns. However, aminosugars require high final temperatures and/or extended run times for elution and this column tends to display poor temperature stability under such conditions. Furthermore, irreversible adsorption of aminosugars is a significant problem, causing poor sensitivity of the aminosugars relative to neutral sugars. More recently, nonpolar DB-5ms columns have been used which have not exhibited these problems. In complex mixtures, sugars are observed as sharp peaks with almost baseline resolution. It would be highly desirable if a commercial column were developed that displayed the stability of the DB-5ms column but had the resolving capacity of the SP-2330 column.

GC-MS Analysis of Alditol Acetates (Total Ion Spectra and SIM)

Using total ion GC-MS, carbohydrate monomers can readily be identified by their characteristic ion spectra. Once the sugar has been identified, a particular ion or set of ions characteristic of that monomer

can be chosen for selected ion monitoring (SIM). Once retention time has been established, SIM chromatograms allow for clean, easily quantifiable peaks for each monomer. Figures 3 and 4 compare total ion and SIM GC-MS analysis of two bacterial hydrolysates (*Bacillus subtilis* strains 168 and W23). In the total ion chromatograms there are a number of tiny background peaks (e.g. the glucose and methylglucamine peaks both have shoulders). The extraneous peaks are eliminated in the SIM chromatograms. Furthermore, sensitivity is dramatically increased in SIM analysis. This is illustrated in that galactosamine is readily detected in the SIM – but not the total ion chromatogram – for strain 168. In such analyses, generally µg amounts of sugars are present but, in our experience, SIM GC-MS can be used to detect as little as 100–250 ng in complex samples (10–20 mg of starting sample). However, background peaks become increasingly more of a problem as the concentration of sugar is decreased.

As noted above, a native sugar forms 2–4 anomers upon acylation, thus creating multiple peaks from a single sugar and complicating chromatograms. The anomeric centre is usually first destroyed. If hydroxylamine and O-methylhydroxylamine are used in the acylation of carbohydrate monomers, aldononitrile acetates and O-methyloxime acetates, respectively, generate distinct chromatographic peaks for aldoses and alditols. This is not the case for alditol acetates.

Sugars are generally reduced using sodium borohydride or borodeuteride prior to acylation to eliminate anomer formation. For example, during reduction of aldoses the C₁ aldehyde is converted to an alcohol (i.e. aldose to an alditol), whereas alditols remain chemically unchanged. Using sodium borohydride, in the formation of alditol acetates, aldoses and alditols cannot be differentiated. However, when using sodium borodeuteride, two deuteriums are added to the aldehyde moiety, one of which remains after acylation. Thus, there is a one mass unit shift in ions containing C₁. Fragments lacking C₁ generate ions of the same *m/z* for deuterated and nondeuterated samples.

As an example, *B. subtilis* W23 is readily discriminated from *B. subtilis* 168 by the presence of a ribitol containing polysaccharide (teichoic acid). Total ion and SIM chromatograms of carbohydrates derived from these two bacterial strains are shown in Figures 3 and 4 respectively. During hydrolysis, ribitol is released from the teichoic acid. Unfortunately, RNA releases ribose upon hydrolysis which is converted to ribitol upon reduction, thus hindering the detection of ribitol originating from teichoic acid. However, ribitol from teichoic acid is also partially

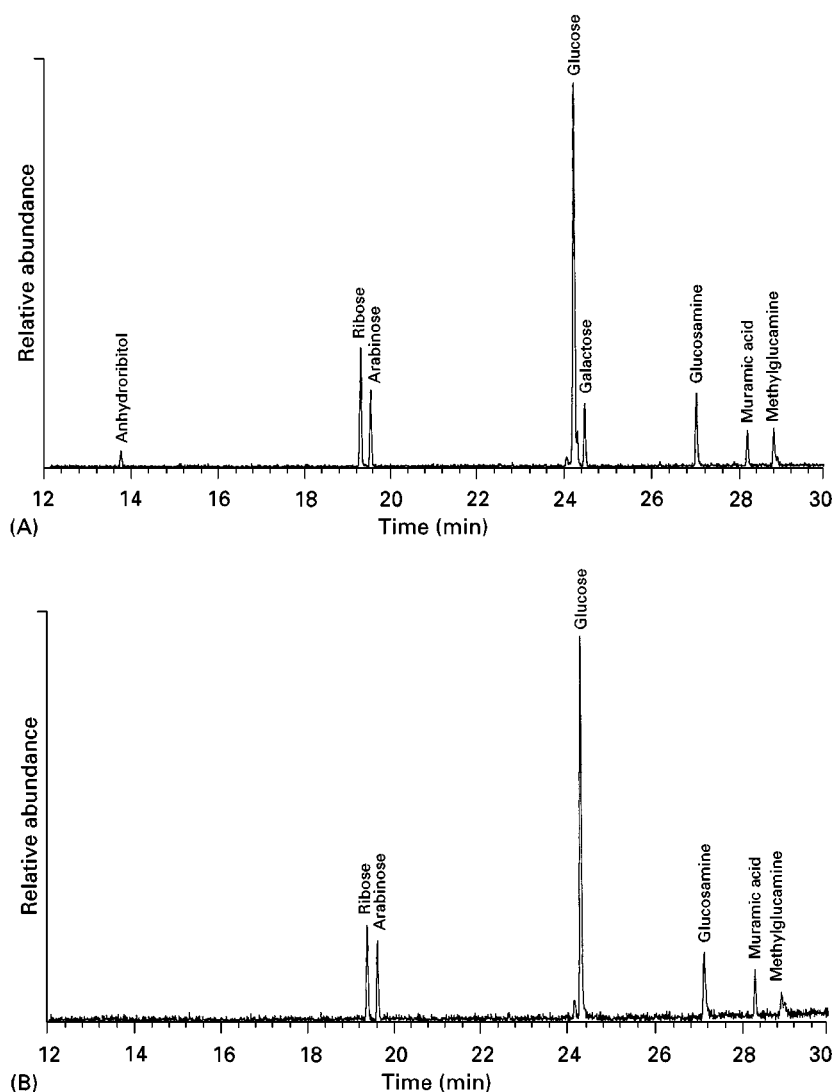


Figure 3 Total ion GC-MS chromatograms of alditol acetates of hydrolysates of *Bacillus subtilis* (A) strain W23 and (B) strain 168. Ribose is present at 1.13% of the dry weight of the sample of W23 analysed (total 10 mg), i.e. 113 μg .

converted to anhydrosorbitol during hydrolysis. Strain W23 can therefore be readily distinguished from strain 168 by the presence of anhydrosorbitol. The mass spectrum of anhydrosorbitol and its structure are shown in Figure 5. The molecular weight of anhydrosorbitol is 260; m/z 187 (M-73, breakage between C_4 and C_5 , which leaves the ring intact), m/z 127 (loss of acetic acid, 60) and m/z 85 (loss of ketene, 42).

On examination of SIM chromatograms, the ribitol/ribose peak cannot be used to distinguish the two organisms. However, this can be accomplished by full scan (GC-MS) analysis. As noted above, on borodeuteride reduction, aldoses (e.g. ribose) gain two deuteriums, one of which remains after acylation, while alditols (e.g. ribitol) remain unchanged. For aldoses, pairs of peaks are generated, from the

C_1 end labelled with deuterium and the other, unlabelled end. For alditols, C_1 is not labelled, resulting in single peaks. Thus, the mass spectrum of ribose contains pairs of ions of nearly equal abundance (i.e. m/z 115/116, 145/146, 187/188 and 217/218) generated from the two ends of the molecule, while ribitol would be dominated by single ions (i.e. m/z 115, 145, 187 and 217). Therefore, for strain W23 where ribitol, in addition to ribose, is present, the mass spectrum contains a greater abundance of the lower mass ion of each pair than for strain 168 (where ribose alone is present). Figure 6 clearly demonstrates that standard ribose has a mass spectrum indistinguishable from the ribose peak derived from the hydrolysate of strain 168. However, the peak for strain W23, containing a mixture of ribose and ribitol, is readily distinguished by the dominance of

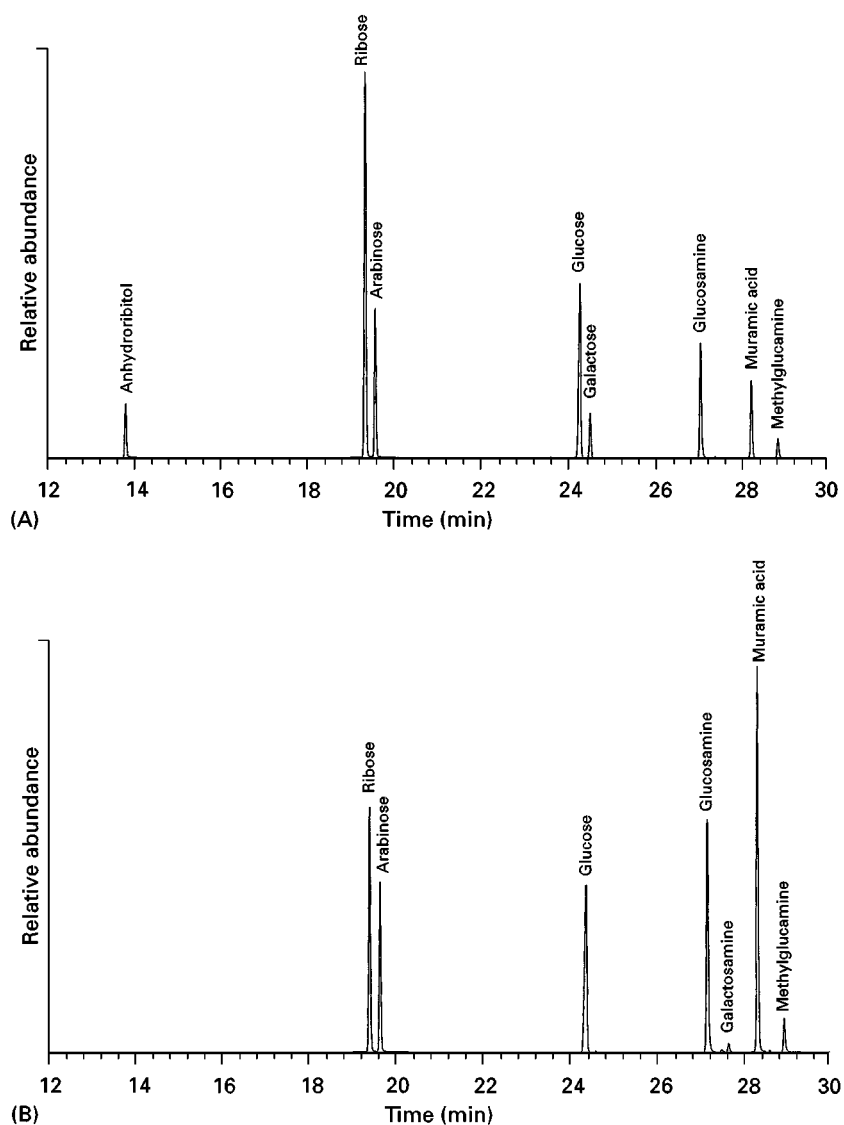


Figure 4 Selected ion monitoring GC-MS chromatograms of alditol acetates of hydrolysates of *Bacillus subtilis* (A) strain W23 and (B) strain 168. Same ions as Figure 2 plus 187 (anhydrosorbitol).

115 over 116, 145 over 146, 187 over 188 and 217 over 218.

The base peak in EI mass spectra of alditol acetates is generally dominated by the acetylinium ion (m/z 43). Many primary fragments are produced by cleavage between sequential carbon atoms. Secondary fragmentation results from losses of acetic acid (m/z 60), acetoxyl groups (m/z 59) and ketene (m/z 42). Generally, mass spectra of aminosugars are relatively simple since cleavage preferentially occurs between the carbon with attached acetamido group and adjacent acetylated carbons.

Mass spectra of stereoisomers of alditol acetates contain ions of the same m/z . On casual observation the mass spectra appear similar. However, certain isomers display differences in relative ion abundances

which can be quite striking. Aminodideoxyhexoses, quinovosamine and fucosamine (found in legionellae), have been noted to display distinct mass spectra. Differences in mass spectra among isomers are accentuated by the use of borodeuteride. Aldoses are asymmetric since there is an aldehyde on C_1 . Asymmetry is retained after borodeuteride but not borohydride reduction since C_1 is labelled. It has been proven that all eight hexoses can be differentiated by a combination of distinct mass spectra and/or retention times.

Muramic acid, 3-O-lactyl glucosamine, is an unusual sugar which additionally contains a carboxyl group in ether linkage. A lactam (a cyclic amide) is formed by internal dehydration between its carboxyl and amino groups on derivatization. In contrast to

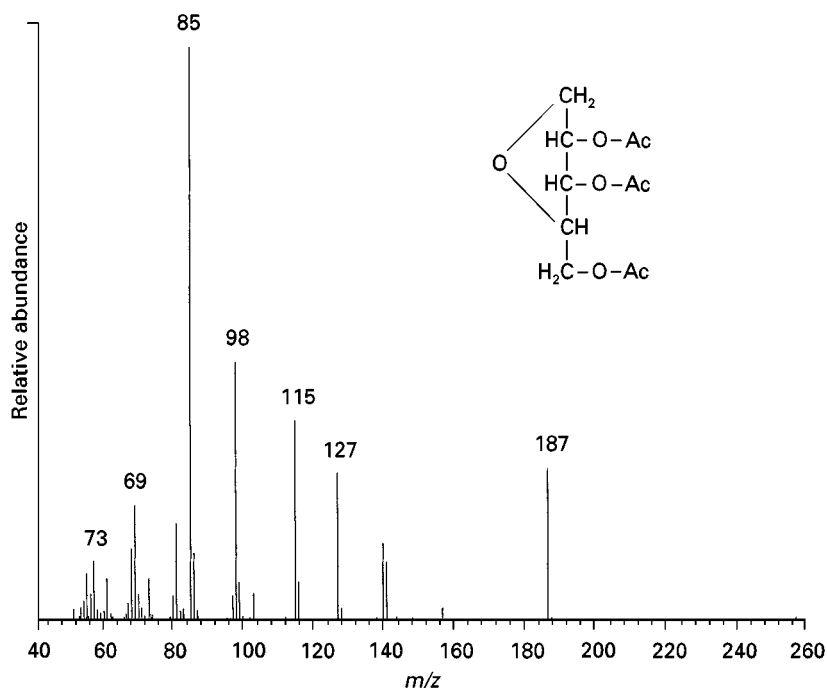


Figure 5 Mass spectrum of alditol acetate of anhydrosorbitol derived from hydrolysate of *Bacillus subtilis* W23.

acetylation of other aminosugars, which produce amides, muramicitol pentaacetate (acetylated muramic acid) has an imido group in which two acyl groups, lactyl and acetyl respectively, are linked to the nitrogen atom. Formation of the imido moiety requires harsh conditions (higher temperatures and longer heating times).

Naturally occurring O-methylated sugars exist in bacteria and in eukaryotes. The fragmentation pattern of methylated sugars is distinctive. Fragmentation between the O-methylated carbon and the adjacent acetylated carbon atoms dominates the spectra. Additional secondary ions can be produced by loss of methanol (m/z 32) and formaldehyde (m/z 30).

GC-MS-MS Analysis of Alditol Acetates (Multiple Reaction Monitoring and Product Ion Spectra)

High resolution chromatographic separations coupled with selective clean-up steps are important in improving the specificity of the detection of chemical markers (e.g. muramic acid as a marker for bacterial infection) in complex matrices. However, chromatographic separation is not sufficient to eliminate extraneous peaks when nonselective detectors are employed. The use of the mass spectrometer as a selective GC detector (i.e. GC-MS analysis in SIM), helps greatly in diminishing background noise by focusing only on ions that are present in the compound of interest. However, even when using SIM, it is not uncommon to find extraneous background peaks. The tandem mass spectrometer, as a GC detector,

provides even greater specificity in detecting trace amounts of chemical markers in complex matrices. Tandem mass spectrometry has the added advantage of generating a total ion spectrum from a selected precursor ion (product ion spectrum). The resulting product ion spectrum can be used for a definitive identification of the compound of interest at trace levels.

Multiple reaction monitoring (MRM) and generation of product ion spectra both involve three discrete mass analysis steps. The first stage involves selection of a precursor ion. This instrumental clean-up removes other ions. The precursor ion is then fragmented by collision-induced dissociation (CID) using an inert gas. In the third stage, all precursor ions can be collected (product ion spectrum) or a single product ion is selected for monitoring (MRM). Both SIM GC-MS and MRM GC-MS-MS analysis allow excellent quantitation of such chemical markers, but the latter provides much greater confidence in trace analysis.

Two types of GC-MS-MS instruments are primarily used in such analysis: ion traps and triple quadrupoles. In triple quadrupole instruments, the three stages of analysis are performed using three distinct quadrupole mass analysers. There is some decrease in sensitivity due to loss of ions in transmission through the three quadrupoles. In ion trap tandem mass spectrometers, the three stages occur in the same mass analyser. This dramatically simplifies the instrument and its cost. Furthermore, sensitivity of MS-MS

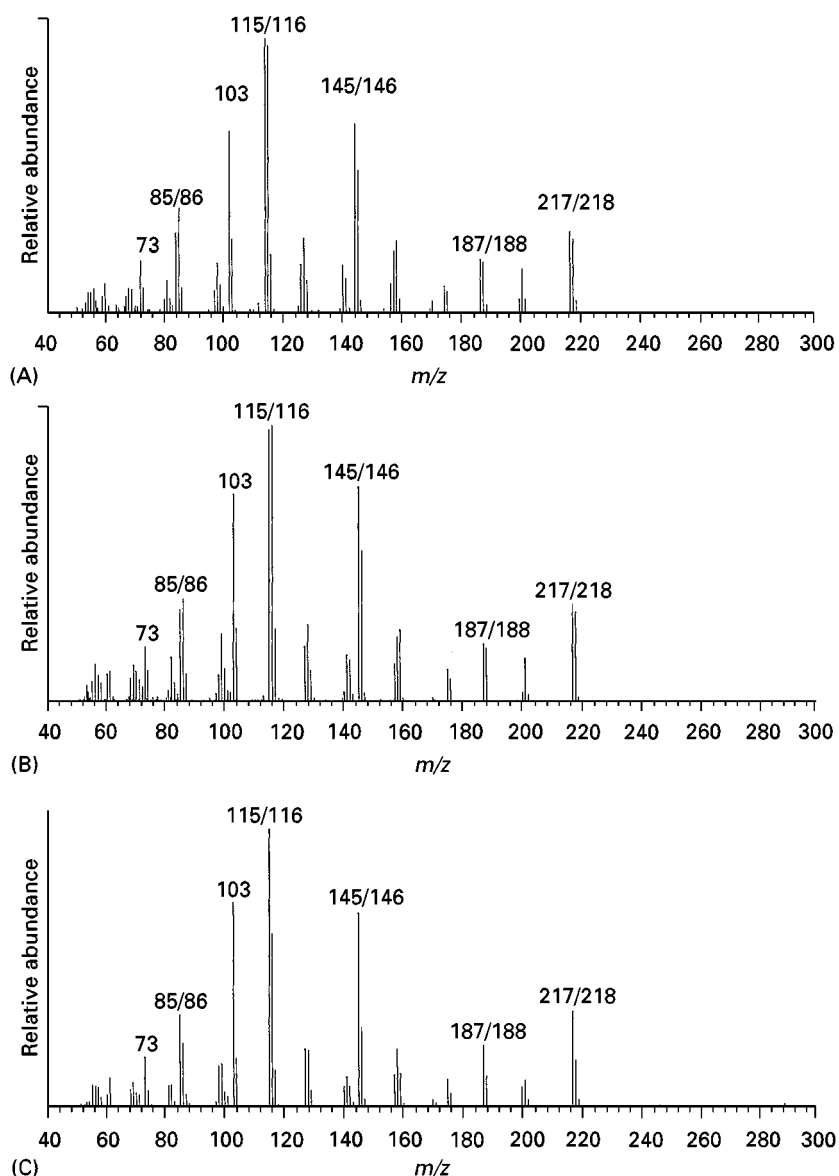


Figure 6 Mass spectra of alditol acetates (A) ribose standard (B) ribose present in hydrolysate of strain 168 (C) a mixture of ribitol and ribose present in hydrolysates of *Bacillus subtilis* W23. Ions derived from the C₁ end are labelled with deuterium (e.g. m/z 146). Ions generated from the C₆ end are not labelled and thus m/z is one less (e.g. m/z 145).

analysis is improved, particularly in product ion spectrum mode. However, in trace quantitative analysis of carbohydrates, in MRM mode, it has been observed that the ion trap is less precise than the triple quadrupole. However, the low cost, ease of use of the ion trap and its power for absolute identification (product ion spectrum) make its use extremely attractive for diagnostic applications.

It is important to note that heavy isotope-labelled internal standards for many sugars are unavailable as pure compounds. Whole ^{13}C -labelled bacterial cell hydrolysates may be used as a cheap alternative source. As an example, in quantitative studies, both methylglucamine and ^{13}C -labelled muramic acid have

been used as internal standards in the analysis of muramic acid (a unique chemical marker for bacteria not found elsewhere in nature). While quantitation is better with the latter, there is a possibility of contamination of the ^{13}C -labelled muramic acid with non-labelled muramic acid. Thus, at the detection limit of the procedure, where the major issue is to prove the presence or absence of muramic acid, methylglucamine is preferred. At higher levels, where quantitation is the major issue, ^{13}C -labelled muramic acid is preferred. Obviously an internal standard with both characteristics would be optimal and this is currently under investigation. Isomuramic acid has been described as a natural component of the

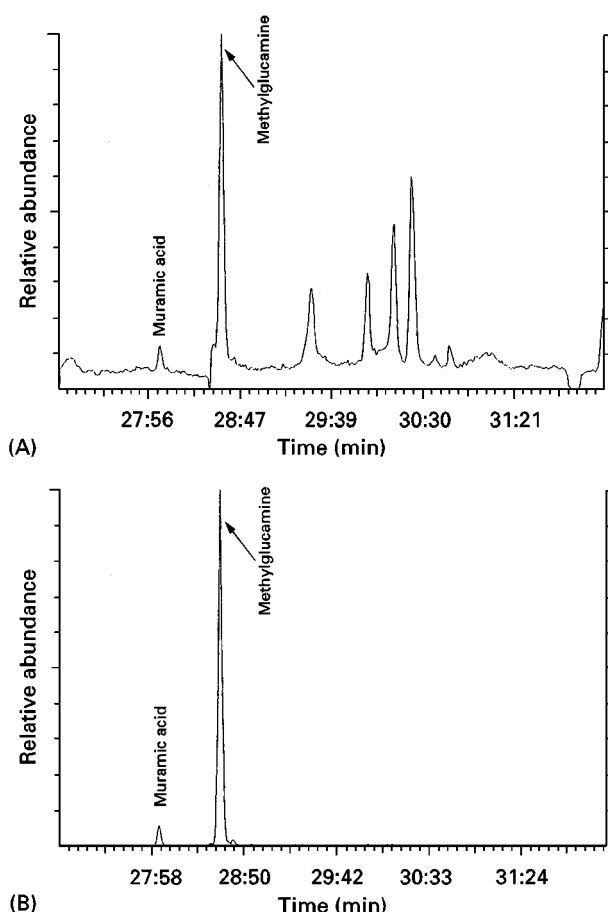


Figure 7 GC-MS-MS shows chromatograms of cerebrospinal fluid from a patient with bacterial meningitis. (A) Full scans (precursor ion m/z 403 for muramic acid and m/z 327 for methylglucamine) would have a similar appearance to a SIM GC-MS chromatogram (m/z 403 and m/z 327 respectively); (B) multiple reaction monitoring (m/z 403 to m/z 198 transition). 250 μ L of cerebrospinal fluid was analysed and found to contain a total of 13.6 ng muramic acid. Methylglucamine 500 ng (internal standard) was present in the sample.

lipopolysaccharide of certain bacteria and also has been chemically synthesized. Whether muramic acid and isomuramic acid can be adequately chromatographically resolved has not yet been addressed.

Application of GC-MS-MS in Trace Analysis

Ion trap GC-MS-MS has been used for absolute identification of trace levels of muramic acid in human body fluids. This is the only report to date using GC-MS-MS to detect muramic acid or any other marker for bacteria in a human/animal body fluid or tissue. Product ion mass spectra (upon MS-MS analysis) of muramic acid peaks (≥ 30 ng mL $^{-1}$) found in infected human body fluids were identical to those of pure muramic acid. An illustration of the detection of muramic acid in human cerebrospinal fluid is shown (approximately 5 ng mL $^{-1}$). A powerful feature of

the ion trap is the utility of the product ion spectrum for absolute identification of trace levels in complex matrices. This is likely to have particular utility for studies of clinical specimens to determine the presence of bacteria (that are difficult to culture) or their nonviable cell wall components (not detectable by culture). Sterile body fluids and tissues from healthy humans or animals do not generally contain muramic acid.

Figure 7 shows GC-MS-MS chromatograms of cerebrospinal fluid from a patient with bacterial meningitis. The full scan (precursor ion m/z 403 from muramic acid and m/z 327 for the internal standard, methylglucamine) would be similar in appearance to a SIM GC-MS chromatogram (m/z 403 and m/z 327 respectively). Muramic acid is readily detected, but there are clearly numerous background peaks, particularly in the m/z 327 window. For comparison, using multiple reaction monitoring (m/z 403 to m/z 198 transition) background peaks are eliminated. The sample contained a total of 13.6 ng of muramic acid. Figure 8, for comparison, shows full scan and MRM

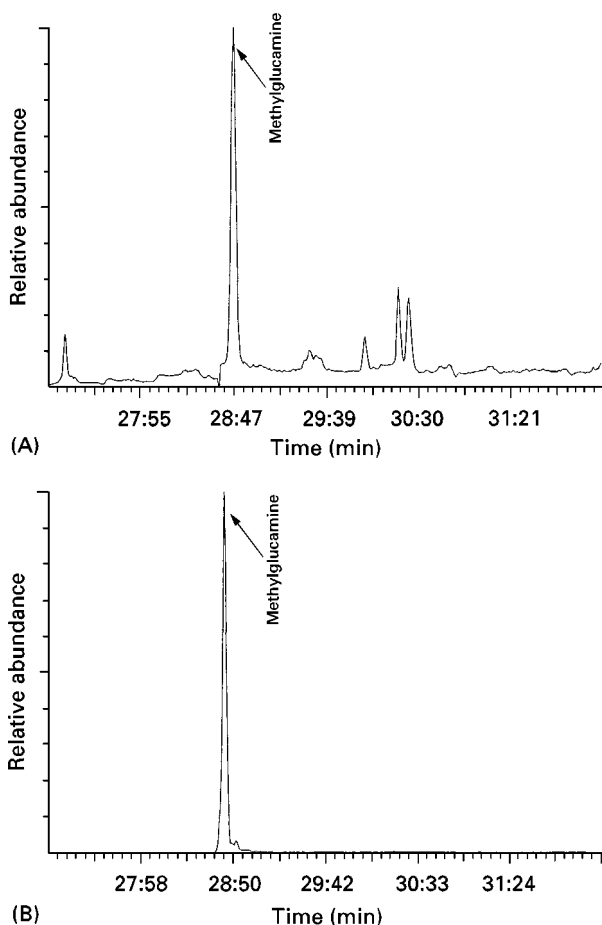


Figure 8 GC-MS-MS chromatograms of uninfected cerebrospinal fluid from a patient with otitis media. (A) Full scan of precursor m/z 403 (equivalent in appearance to SIM GC-MS); (B) multiple reaction monitoring (m/z 403 to m/z 198 transition).

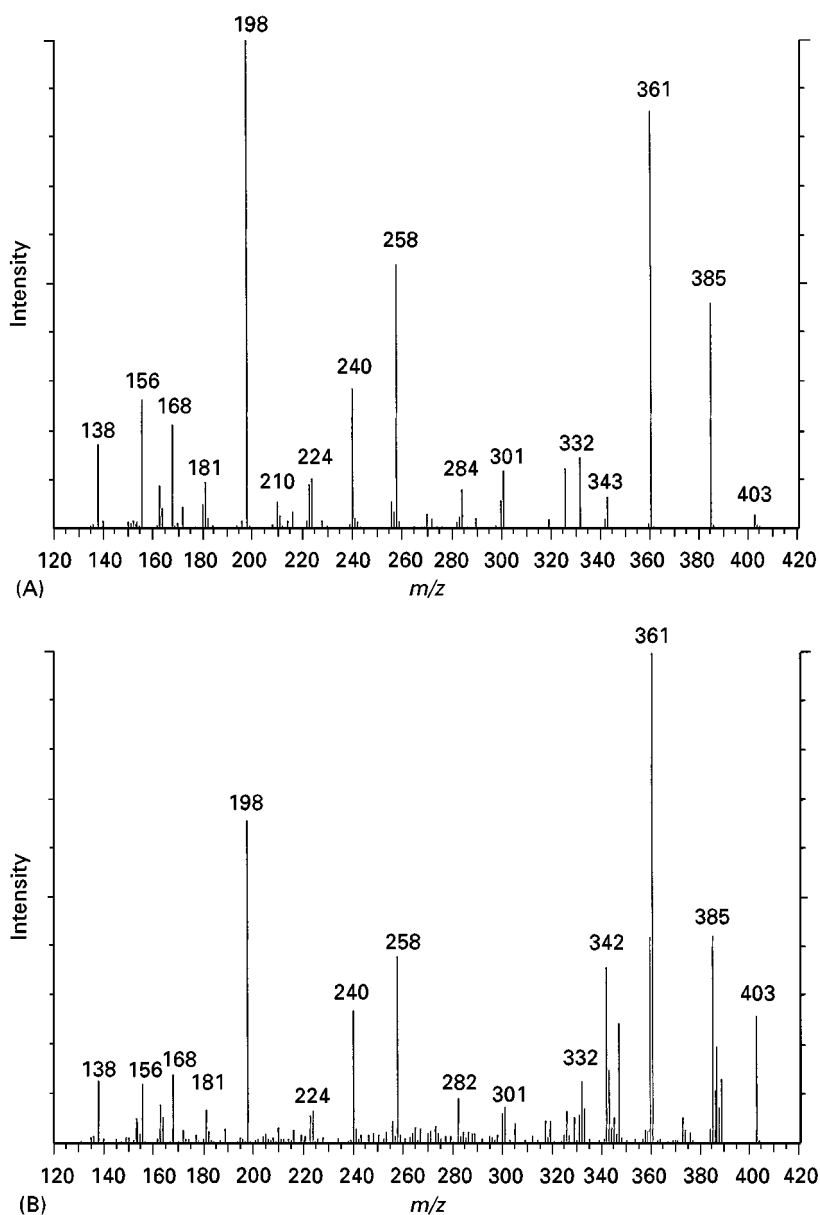


Figure 9 Product ion spectrum (GC-MS-MS) of m/z 403 (A) muramic acid standard (250 ng total) and (B) cerebrospinal fluid from patient with bacterial meningitis (2.7 ng in 400 μ L of cerebrospinal fluid analysed).

of cerebrospinal fluid from a patient with otitis media (inner-ear infection). In this instance, culture indicated the absence of bacteria in the sample. As expected, there is no peak at the retention time of muramic acid; this serves as a negative control.

A product ion spectrum of muramic acid present in a cerebrospinal fluid (2.7 ng total) and a muramic acid standard (250 ng) are compared in **Figure 9**. Muramic acid is clearly categorically identified from the spectrum of the patient's sample, although background ions are obvious. Clearly, this represents an analysis close to the detection limit, for GC-MS-MS of this type of complex biological sample.

MRM analysis has great utility for determining the levels of bacterial contamination for clinical and environmental analyses. For example, muramic acid levels have been demonstrated to serve as a useful measure of biocontamination of air. This has relevance to our understanding of the 'sick building phenomenon' and assessing the quality of indoor air. The product spectrum is of limited use in the analysis of environmental samples, since bacteria are invariably present. However, as noted above, it is a powerful tool for absolute detection of bacteria in human body fluids and tissues which are sterile in the absence of infection.

Gas Chromatography and Liquid Chromatography

In the 1980s successful analysis of underivatized sugars using high performance liquid chromatography was introduced. Eliminating derivatization dramatically reduces sample handling and chemical manipulation. After separation on anion exchange columns (particularly the PA1 column) sugars are detected with a pulsed amperometric detector (PAD). This LC system has been successfully used for the separation and identification of amino, neutral and acidic sugars. Chromatography is performed in concentrated NaOH. At high pH, interaction of ionized hydroxyl groups with the anion exchange resin produces excellent sugar separations. The electrochemical (PAD) detector also detects carbohydrates with excellent sensitivity at alkaline pH. Unfortunately, in the analysis of sugars in complex matrices, the nonselective PAD detector often has inadequate specificity to discriminate sugars of interest from background noise.

When chromatography is performed in conjunction with the mass spectrometer (e.g. GC-MS or LC-MS), the increased selectivity of detection allows analysis of less purified samples. For example, whole cell hydrolysates can be analysed. With LC-PAD analysis, structural components such as glycoproteins or polysaccharides must be purified prior to analysis. LC-MS-MS has been used for quantitation of sugars in complex environmental matrices. LC-MS and LC-MS-MS for the analysis of carbohydrates show great promise but are still in the developmental stage. Currently, GC-MS and GC-MS-MS have considerably lower detection limits than LC-MS and LC-MS-MS. Automation of sugar derivatization for GC eliminates many of the advantages of LC-based techniques over the GC-based ones but the only derivatization procedure for carbohydrate analysis by GC that has been automated, at this time, is the alditol acetate procedure.

Conclusions

GC-MS and GM-MS-MS are mature techniques which may be used in the analysis of carbohydrate monomers in complex samples. In SIM GC-MS and MRM GC-MS-MS, sugars are readily detected and quantitated in complex samples, although use of MRM dramatically lowers the detection limit. Using total ion (MS) and product ion spectra (MS-MS), identification at trace levels is readily performed. The detection limit is much lower for the latter when the ion trap GC-MS-MS is used. Substantial improvements have been made to sample preparation, including simplification and computer-controlled automation of derivatization reactions for GC analysis. This is likely to help GC-based techniques to remain competitive with their LC competitors where derivatization

is usually eliminated. The limit of detection is still currently much lower with GC-based procedures.

See also: II/Chromatography: Gas: Detectors: Mass Spectrometry. III/Carbohydrates: Electrophoresis; Liquid Chromatography; Thin-Layer (Planar) Chromatography. **Polysaccharides:** Liquid Chromatography.

Further Reading

- Biermann C and McGinnis G (eds) (1989) *Analysis of Carbohydrates by GLC and MS*. Boca Raton: CRC Press.
- Conboy JJ and Henion J (1992) High performance anion-exchange chromatography coupled with mass spectrometry for the determination of carbohydrates. *Biological Mass Spectrometry* 21: 397.
- Fox A and Black G (1994) Identification and detection of carbohydrate markers for bacteria: derivatization and gas chromatography–mass spectrometry. In: Fenselau C (ed.) *Mass Spectrometry for the Characterization of Microorganisms*, p. 107. Washington, DC: American Chemical Society.
- Fox A, Schwab JH and Cochran T (1980) Muramic acid detection in mammalian tissues by gas–liquid chromatography–mass spectrometry. *Infection and Immunity* 29: 526.
- Fox A, Wright L and Fox K (1995) Gas chromatography tandem mass spectrometry for trace detection of muramic acid, a peptidoglycan marker in organic dust. *Journal of Microbiological Methods* 22: 11.
- Gunner SW, Jones JKN and Perry MB (1961) Analysis of sugar mixtures by gas–liquid partition chromatography. *Chemistry and Industry (London)* 255.
- Hardy MR, Townsend RR and Lee YC (1988) Monosaccharide analysis of glycoconjugates by anion exchange chromatography with pulsed amperometric detection. *Analytical Biochemistry* 170: 54.
- Lönngren J and Svenssen S (1974) Mass spectrometry in structural analysis of natural carbohydrates. In: Tipson R and Horton D (eds) *Advances in Carbohydrate Chemistry and Biochemistry*, Vol. 29, p. 41. Amsterdam: Academic Press.
- Rocklin RD and Pohl CA (1983) Determination of carbohydrates by anion exchange chromatography with pulsed amperometric detection. *Journal of Liquid Chromatography* 6: 1577.
- Sawardeker JS, Sloneker JH and Jeanes A (1965) Quantitative determination of monosaccharides as their alditol acetates by gas–liquid chromatography. *Analytical Chemistry* 37: 1602.
- Simpson RC, Fenselau CC, Hardy MR *et al.* (1990) Adaptation of a thermospray liquid chromatography/mass spectrometry interface for use with alkaline anion exchange liquid chromatography of carbohydrates. *Analytical Chemistry* 62: 248.
- Sweeley CC, Bentley RS, Makita M and Wells WW (1963) Gas–liquid chromatography of trimethylsilyl derivatives of sugars and related substances. *Journal of the American Chemical Society* 85: 2497.

Liquid Chromatography

C. Corradini, Istituto di Cromatografia det CNR,
Roma, Italy

Copyright © 2000 Academic Press

Introduction

The development of selective and sensitive methods for analyses for carbohydrates is one of the most challenging areas of analytical chemistry. The main difficulties in the analysis of carbohydrates arise from their considerable number of isomeric forms due to the various possible configurations of the monosaccharides. Oligo- and polysaccharides are composed of different combinations of them, forming linear or branched polymeric species, many of which may differ only in the position of attachment and anomeric configuration of the glycosidic linkages. Moreover, complex carbohydrates can also be characterized by the presence of various nonglycosyl substituents, which include acetyl, pyruvyl, methyl and sulfate esters and ether, amine and phosphate groups. Finally, methods of analysis for carbohydrates require special attention as they play an important role in many diverse research and industrial domains such as biochemistry, clinical chemistry, biology, pharmacy, biotechnology and food science.

Over the last 25 years, high performance liquid chromatography (HPLC) has been the method of choice for the determination of carbohydrate species, and as a result a large number of HPLC methods have been developed to determine a wide variety of carbohydrate samples.

Alkyl or aminoalkyl bonded silica and polymeric phases, protonated or metal-loaded cation exchange resins in conjunction with refractive index (RI) or low wavelength UV detection, as well as high-performance anion exchange chromatography at high pH (HPAEC), coupled with pulsed amperometric detection (PAD) are the methods commonly used. These different approaches are considered in more detail later.

Polar Phases

Polar silica-based packings, as well as unmodified silica are suitable stationary phases for the separation of sugars and other carbohydrates by hydrophilic interaction chromatography (HILIC), a name proposed in 1990 by Alpert to indicate all chromato-

graphic methods driven by polar interactions, which involve partitioning between the more hydrophobic mobile phase and a layer of mobile phase enriched with water and partially immobilized on the stationary phase. Since 1975 aminopropylsiloxane-bonded silica columns have been used widely for this type of chromatography. The fundamental mechanism governing separation of carbohydrates using amino-propylsiloxane-bonded phases is partition between the mobile phase and the water-enriched solvent associated with the stationary phase.

The most common bonded phases are manufactured by reaction of microparticulate silica (having an average particle diameter of 3 or 5 μm) with organosilanes (for example, 3-aminopropyltrimethoxysilane), to form siloxane bonds. Improvements in column efficiency can be achieved using spherical particles of silica gel, which form more homogeneous beds than those obtained employing irregularly shaped particles.

For separations on aminoalkylsiloxane-bonded silica columns, acetonitrile–water mixtures are usually employed as the mobile phase. The proportion of acetonitrile ranges from 80 to 90% by volume for chromatography of sugars and other carbohydrates of low molecular weight. For example, a mobile phase consisting of 85% acetonitrile in water is useful for the separation of monosaccharides. A low percentage of water in the mobile phase is necessary to increase the interactions between sugars and the amino groups bonded to the stationary phase, improving selectivity and monosaccharide separation. On the other hand, 80% acetonitrile in water allows good separation of di- and trisaccharides differing sufficiently in structure, such as sucrose, maltose, lactose and raffinose. For chromatographic analysis of oligosaccharides of degree of polymerization (dp) above 3, mobile phases containing acetonitrile in lower proportions are required. Under these conditions separations are currently carried out at room temperature and with flow rates from 1 to 2 mL min^{-1} . An example of the effective separation of oligosaccharides obtained by lowering the acetonitrile content in the eluent is shown in **Figure 1**, where about 30 distinct peaks of a partial hydrolysate of (1 \rightarrow 4)- α -D-glucan from amylose are separated using a mixture of acetonitrile–water (57 : 43, v/v). Although acetonitrile is the most common organic component of the mobile phase, the use of ethyl acetate, together with acetone or methanol have also been proposed.

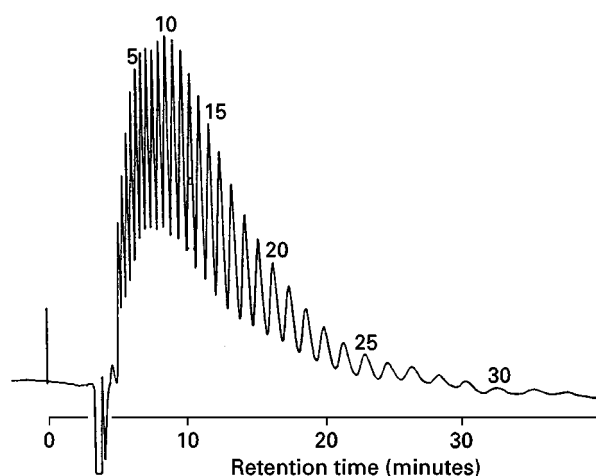


Figure 1 Chromatogram of partial hydrolysate of (1 → 4)- α -D-glucan (amylose). Chromatographic conditions: column, ERC-NH-1171 (200 \times 6 mm ID); eluent, acetonitrile–water (57 : 53); flow rate, 1 mL min⁻¹, detector, Shodex RI SE-32 at 1×10^{-5} RI units full scale; temperature ambient. (Reproduced from *Journal of Chromatography* (1985), 321: 151, with the permission of Elsevier Science Publishers.)

Aminopropylsiloxane-bonded silica packings have been widely used in HILIC of sugars and other carbohydrates. However, they have the drawback of limited life, due to the formation of glycosylamines by reaction of the amino groups bonded to the stationary phase with reducing sugars (formation of Schiff's bases). The formation of glycosylamines results in both deactivation of the column and loss of the sugar analytes with an undesirable effect on quantitative analysis. An alternative to the use of these columns is the addition of a small amount (0.01–0.02%, v/v) of a diamino or polyamino compound to the eluent used in HPLC on a silica column, which results in modification of the silica to give it characteristics of an amino propylsiloxane-bonded phase. This approach can be accomplished with various amine modifiers, which must carry at least two amino groups, one being required to bond the modifier to the silica gel via hydrogen bond formation, and one which has to be free to interact with the carbohydrate analytes. Usually *in situ* modified silica columns show a longer life than aminopropylsiloxane-bonded columns, because the amine adsorbed on the silica surface is continuously regenerated by the amine added to the mobile phase. Various polyfunctional amines have been proposed as modifiers, including ethylenediamine, 1,4-diaminobutane, tetraethylenepentamine (TEPA) and piperazine.

Another approach is to replace aminopropylsiloxane-bonded columns with a silica-based packing carrying bonded amide, cyano, diol, polyol or cyclodextrins as alternative stationary phases. These phases have similar selectivity to amino-type phases

and do not form Schiff's bases with reducing sugars. Polymer-based columns have also been proposed, increasing application in HILIC of carbohydrates. Although diol-bonded silica, as well as vinylpyridinium polymers have proven to be capable of greater selectivity in carbohydrate separations, aminopropylsiloxane-bonded columns are the most frequently used in HILIC of carbohydrates. A list of some HPLC columns commonly employed in the HILIC of carbohydrates is given in Table 1.

Cation Exchangers

HPLC analyses of carbohydrates are most frequently carried out on cation exchange stationary phases consisting of sulfonated polymer-based materials, which can be obtained in various degrees of cross-linking and various particle sizes.

Cation exchangers based on poly(styrene-divinylbenzene) (PS-DVB) copolymers are the most common stationary phases used for carbohydrate separations. Copolymer-based columns offer many advantages for the analysis of carbohydrates and alditols. The PS-DVB copolymers exhibit excellent physical strength, pH stability over a wide range and are not easily subjected to degradation by oxidation, hydrolysis or elevated temperature. Carbohydrate separations on column packed with a cation exchanger PS-DVB resin can be affected by the degree of cross-linking and type of counterion.

PS-DVB resins are relatively rigid gel-type media and separation can take place when the analytes penetrate at least partially into the matrix. The lower the cross-linking, the more open the structure and more permeable it is to higher molecular weight carbohydrates. For example, a 4% cross-linked resin is suitable to resolve oligosaccharides of high molecular weight, whereas smaller oligosaccharides can be well resolved on an 8% cross-linked resin.

As mentioned earlier, the selectivity of cation exchange columns depends to a large extent on the ionic form of the packing material. Loading of sulfonated resins with various cations produces substantial changes in retention of neutral carbohydrates in several ways, such as the formation of coordination complexes, ion–dipole interactions, ionic hydration and hydrogen bonding. When the resins are loaded with Ca^{2+} , Ag^+ , Pb^{2+} , La^{3+} , marked differences in the retention and selectivity are observed and the mechanism of retention involves the formation of coordination complexes between the carbohydrates and the fixed-metal ions. However, the separation of oligosaccharides is predominantly governed by size-exclusion mechanisms and oligomers elute in order of decreasing molecular weight. The first systematic

Table 1 Examples of silica-based columns and chromatographic conditions employed in carbohydrate separation

<i>Column (particle size, μm) (Supplier)</i>	<i>Functional group</i>	<i>length × ID (mm)</i>	<i>Mobile phase</i>	<i>Temperature (°C)</i>	<i>Flow rate (mL min⁻¹)</i>	<i>Detector</i>	<i>Applications</i>
Adsorbosil (5 μm) (Alltech)	Amino	250 × 4.6	Acetonitrile– water (85 : 15)	Ambient	1.0	ELSD	Glucose sucrose lactose melezitose maltotriose
Adsorbosphere (5 μm) (Alltech)	Amino	250 × 4.6	Acetonitrile– water (85 : 15)	Ambient	1.5	RI or ELSD	Fructose glucose sucrose maltose lactose
Alltima NH ₂ (5 μm) (Alltech)	Amino	250 × 4.6	Acetonitrile– water (gradient)	Ambient	1.5	ELSD	Maltooligosaccharides
Amino, Spheri-5 (5 μm) (Brownlee)	Amino	250 × 4.6	Acetonitrile– water (75 : 25)	Ambient	1.0	RI	Monodisaccharides
Nucleosil carbohydrate (5 μm) (Macherey- Nagel)	Amino	250 × 4.6	Acetonitrile– water (79 : 21)		1.0	RI	Monooligosaccharides
Hypersil APS-2 (5 μm) (ThermoQuest)	Amino	100 × 3.0	Acetonitrile– water (80 : 20)	Ambient	0.5	RI	Monodisaccharides
Supelcosil LC-NH ₂ (5 μm) (Sigma)	Amino	250 × 4.6	Acetonitrile– water (75 : 25)	Ambient	1.0	RI	Ribose arabinose galactose sucrose maltose isomaltose melezitose raffinose
Ultrasil NH ₂ (10 μm) (Beckman)	Amino	250 × 4.6	Acetonitrile– water (75 : 25)	Ambient	1.0	RI	Mono-, di-, trisaccharides
Lichrospher DIOL (10 μm) (Merck)	Diol	250 × 7.0	Acetonitrile– water (gradient)	Ambient	1.0	ELSD	Monosaccharides dextrins
Zorbax NH ₂ (5 μm) (Du Pont)	Amino	250 × 4.6	Acetonitrile– water (75 : 25)	Ambient	1.0	RI	Fructose glucose sucrose maltose lactose
Zorbax OH (10 μm) (Du Pont)	Diol	250 × 6.0	Acetonitrile– water (90 : 10)	Ambient	1.0	ELSD	Monosaccharides
Zorbax ODS (10 μm) (Du Pont)	C ₁₈	250 × 4.6	Water	60–70°C	1.0	ELSD	dp 2–5
Spheri-5 ODS (5 μm) (Brownlee)	C ₁₈	100 × 4.6	Water	Ambient	0.5	RI	glucose dp 2–5

study of the chromatography of sugars and alditols on a cation exchange resin was published in 1975 by Goulding, who showed that the complexing cations Ca^{2+} , Ag^+ , Sr^{2+} , Ba^{2+} and La^{3+} gave longer retention times than the alkali-metal cations. This effect

can be attributed to coordination between the metal ions and -OH groups of sugars and alditols and their retention can be correlated with the ability to form relatively strong chelate complexes of the adjacent hydroxyl groups of sugars and alditols with the fixed

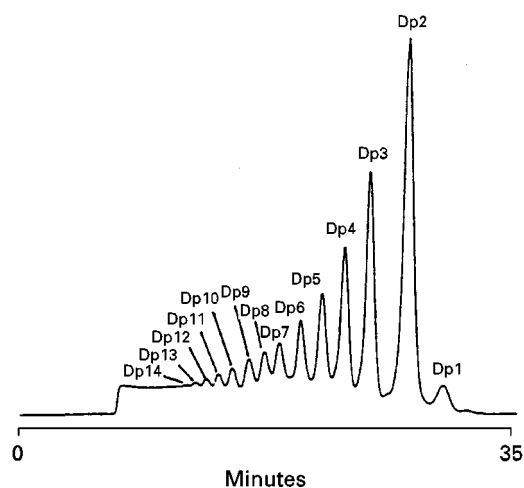


Figure 2 Separation of maltooligosaccharides from dp 14 to dp 2. Chromatographic conditions: column, Rezex RSO-Oligosaccharide (200 × 10 mm ID); mobile phase, water; flow rate, 0.4 mL min⁻¹, temperature, 75°C; detector, RI (with permission of Phenomenex, Torrance, CA, USA).

cation of the resin. For example, stronger binding will occur in sugars where the configuration of the hydroxyl groups at C-1, C-2 and C-3 of the pyranose ring have an axial-equatorial-axial sequence that can form relatively strong tridentate complexes than the binding of sugars, which form complexes with only a pair of axial-equatorial hydroxyl groups. In sulfonated cation-exchange resins carrying Li⁺, Na⁺, and H⁺, there is no evidence that these counterions interact directly with carbohydrates, and their effects can be interpreted simply by ionic hydration. Cation exchange resins carrying calcium ions are the most commonly used for chromatography of sugars allowing good separations of monomeric sugars (pentoses, hexoses), alditols and di-, trisaccharides (Figure 2). Cation exchange resins carrying silver ions give better separation of maltooligosaccharides up to a degree of polymerization of 13 glucose units (see Figure 3).

Carbohydrate separations on cation exchange resins loaded with various metal ions can be carried out with deionized water as the mobile phase. However, when chromatographic runs are performed at room temperature, peaks are broadened or eluted as a doublet owing to the separation of the two anomeric forms of reducing carbohydrates. As is well known, for each of the ring modifications of a free sugar, two isomers (α and β isomers or anomers) can exist, because a new asymmetric centre is created by ring closure at the reducing carbon atom (see Figure 4). The two anomers can be selectively retained on cation exchange resins loaded with various metal ions. For example, when glucose is chromatographed at room temperature on a sulfonated PS-DVB

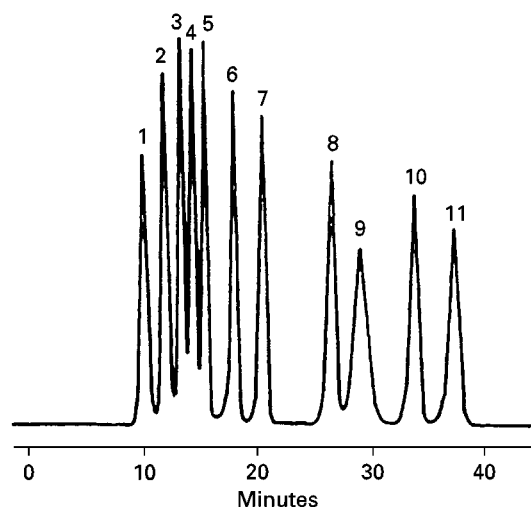


Figure 3 Separation of monosaccharides and alditols. Chromatographic conditions: column, Rezex RPM-Monosaccharide (300 × 7.0 mm ID); mobile phase, water; flow rate, 0.6 mL min⁻¹, temperature, 75°C; detector, RI (with permission of Phenomenex, Torrance, CA, USA).

resin column in the hydrogen form, the reducing monosaccharide is eluted as a single peak (Figure 5A), whereas with the same column in the calcium form, almost baseline separation of α and β anomers is achieved, indicating that a ligand exchange mechanism is also involved (Figure 5B).

The most common approach to avoid the formation of doublets is to increase column temperature. By heating the HPLC column in the calcium form to 85°C, the rate of interconversion between the α and β anomers of glucose is accelerated, and it is eluted as a single peak. Separations are usually performed with a column temperature ranging from 80 to 85°C, though lower temperatures (65°C) may be used. Higher temperatures give faster diffusion and narrower peaks. Conversely, increasing temperature is normally accompanied by a decrease in retention. Organic modifiers such as acetonitrile may be added to the eluent up to a concentration of 30% (v/v) without causing any damage to the PS-DVB matrix. For example, the addition of acetonitrile increases retention of the analytes and may improve resolution of sugar alcohols.

Sulfonated resins in the protonated form are useful for profiling not only monosaccharides and sugar alcohols, but may be useful for analysis of a wide range of organic acids, alone and in combination with carbohydrates, short-chain alcohols, aldehydes and ketones. Selectivity can be altered by changing the pH as well as the type of mineral acid (H₂SO₄ or HCl at mmol concentration), used as the eluent. Employing these columns, amino sugars may also be separated. Sugars of food interest and sugar alcohols,

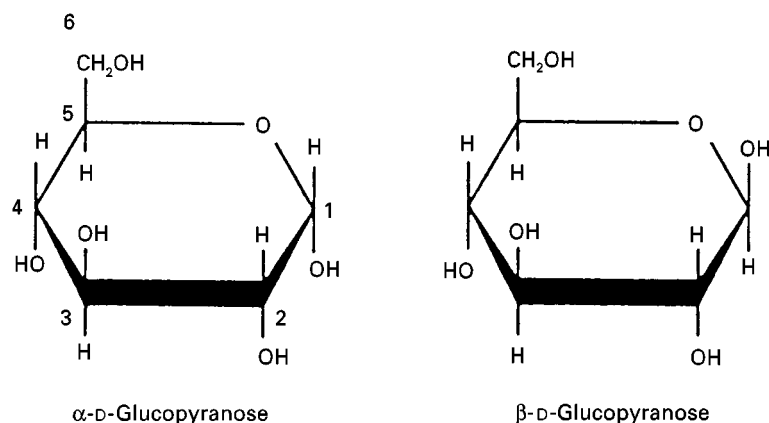


Figure 4 Anomeric configurations of D-glucose.

including sorbitol and mannitol may be separated using pure water as the mobile phase. An example is shown in **Figure 6**, where a mixture of lactose, galactose, mannitol, sorbitol and xylitol are separated on a sulfonated cation exchange resin in protonated form. Furthermore, a separation of lactose, glucose and galactose in a lactose-hydrolysed milk sample is shown in **Figure 7**. Both separations were performed by isocratic elution with water at room temperature. Under these conditions sugar alcohols, as well as reducing sugars are eluted as single sharp peaks.

Tables 2 and **3** list some of the commercially available columns containing sulfonated styrene-divinylbenzene resins in various ionic forms.

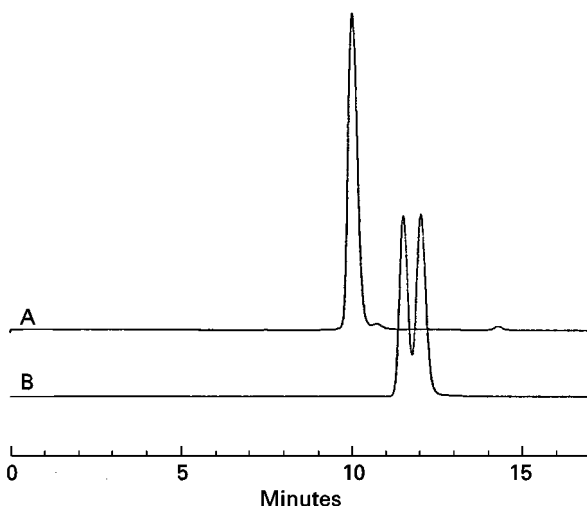


Figure 5 Elution of D-glucose at room temperature. Chromatographic conditions of chromatogram (A) column, PL Hi-Plex H (hydrogen form); dimensions, 300×7.7 mm; mobile phase, water; flow rate, 0.6 mL min^{-1} ; temperature, 25°C ; detection, refractive index detection. Chromatographic conditions of chromatogram (B) column, PL Hi-Plex Ca (calcium form); other conditions as chromatogram A. Both columns from Polymer Laboratories (Shropshire, UK).

Anion Exchangers

Anion exchange chromatography is not a technique commonly associated with analysing neutral carbohydrates. It has been shown that the hydroxyl groups in carbohydrates can form reversible anionic complexes with borate, which can be separated on an anion exchange column. However, this technique is not currently applied to HPLC of mono- and oligosaccharides.

Anion exchange chromatography is basic media allows the separation of carbohydrates without addition of any borate to the mobile phase. The pK_a of neutral carbohydrates usually fall in the range of 12–14, and at high pH their hydroxyl groups are either partially or completely ionized, enabling this class of compounds to be separated as anions by high performance anion exchange chromatography (HPAEC). Moreover, alkaline conditions allow the detection of carbohydrates by PAD at a gold electrode. The compatibility of PAD with gradient elution coupled with the high selectivity of specifically tailored anion exchange stationary phases, allows mixtures of underivatized simple sugars, oligo- and polysaccharides to be separated with good resolution in a single run, and quantified down to picomole levels. Under these conditions, separations cannot be performed using classical silica-based columns due to their poor stability at high pH levels. The columns commercially available are packed with polymer-based anion exchangers produced by proprietary manufacturing processes. These packings include electrostatically latex-coated polymer-based anion exchangers and macroporous polymer-based resins functionalized with quaternary ammonium groups, which have unique selectivity for sugar alcohols.

Monosaccharide separations are usually performed under isocratic conditions and the elution order is inversely correlated with pK_a . Alditols are

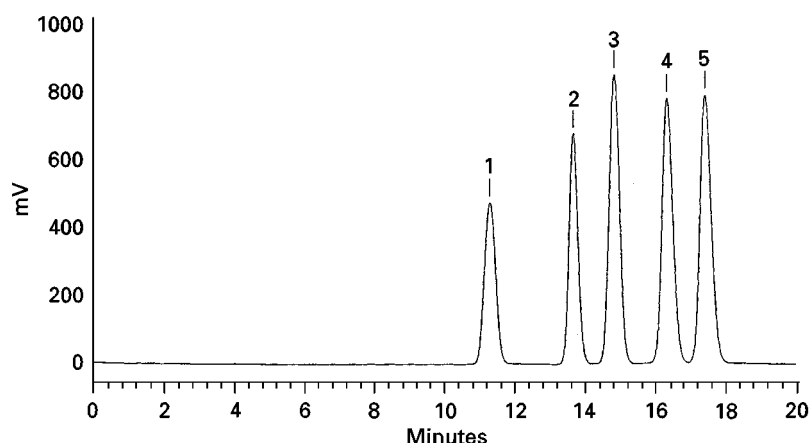


Figure 6 Separation of (1) lactose, (2) galactose, (3) mannitol, (4) sorbitol and (5) xylitol on a sulfonated cation-exchange resin in the hydrogen form. Chromatographic conditions: column, PL Hi-Plex H ($8\ \mu\text{m}$, $300 \times 7.7\ \text{mm}$ ID Polymer Laboratories Ltd, Shropshire, UK); mobile phase, water; flow rate, $0.4\ \text{mL min}^{-1}$ at room temperature; detector, refractive index detection.

less retained than the corresponding reducing sugars as can be readily understood on the basis of acidity. Since the anomeric hydroxyl group is the most acidic among all the OH groups, replacing it with an ordinary OH group (which is less acidic) would naturally result in less retention. For oligosaccharides, retention increases dramatically with increasing molecular mass. HPAEC, followed by PAD detection, has been found to resolve positional isomers of neutral oligosaccharides, which are defined as having the same number, type, sequence, and anomeric configurations as monosaccharides, but differing in the

linkage position of a single sugar. Correlation of retention times with the structure of different oligosaccharides may suggest that at least two factors are involved in determining the superior resolution of oligosaccharides by HPAEC: the relative acidity of the hydroxyl groups and the accessibility of oxyanions of the saccharides to the functional groups of the stationary phase.

Addition of a modifier, such as sodium acetate, allows the elution of oligosaccharides in more reasonable times. Acetate anion is used as a strong 'pusher' because it offers rapid equilibration, allowing a

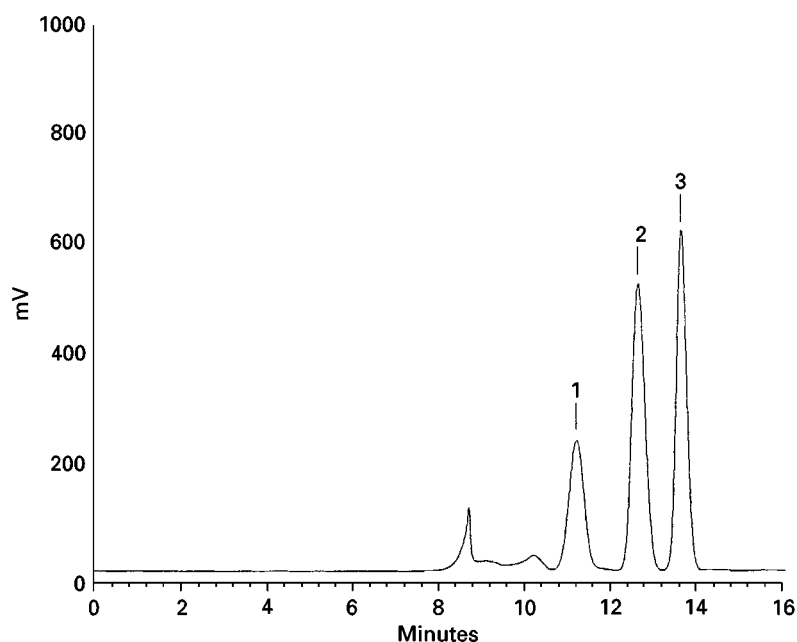


Figure 7 Separation of (1) lactose, (2) glucose and (3) galactose in an UHT lactose-hydrolysed milk. Chromatographic conditions as in Figure 6.

Table 2 Examples of polymeric-based ion-exchanger columns and chromatographic conditions employed in carbohydrate separation

<i>Column (Supplier)</i>	<i>Matrix (PS-DVB) *</i>	<i>Length × ID (mm)</i>	<i>Mobile phase</i>	<i>Temperature (°C)</i>	<i>Flow rate (mL min)⁻¹</i>	<i>Detector</i>	<i>Applications</i>
Cation exchange (Alltech)	Sulfonated (calcium form)	300 × 6.5	Water	90	0.5	RI	Maltotriose, sucrose, glucose, galactose, fructose, mannitol, arabitol, sorbitol
Aminex HPX-87N (Bio-Rad)	(PS-DVB) sulfonated (sodium form)	300 × 7.8	Water	85	0.6	RI	Monosaccharides
Aminex HPX-87K (Bio-Rad)	Sulfonated (potassium form)	300 × 7.8	Water	85	0.6	RI	Monosaccharides
Aminex HPX-87C (Bio-Rad)	Sulfonated (calcium form)	300 × 7.8	Water	85	0.6	RI	Monosaccharides, sugar alcohols
Aminex HPX-87P (Bio-Rad)	Sulfonated (lead form)	300 × 7.8	Water	85	0.6	RI	Cellobiose, glucose, xylose, galactose arabinose mannose
Aminex HPX-42A (Bio-Rad)	Sulfonated (silver form)	300 × 7.8	Water	85	0.4	RI	Oligosaccharides to dp 11
Aminex HPX-87H (Bio-Rad)	Sulfonated (hydrogen form)	300 × 7.8	0.005 N sulfuric acid	50 – 65	0.6	RI	Glucose, ribose, fructose, organic acids
Supelcogel C-611 (Supelco)	Ion-exchange resin containing two different cations	300 × 7.8	10 ⁻⁴ N NaOH	60	0.5	RI	Sucrose, glucose, fructose, mannitol, sorbitol, ribose
Nucleogel sugar Pb (Macherey-Nagel)	Sulfonated (calcium form)	300 × 6.5	Water	80	0.4	RI	Sucrose, maltose, glucose, xylose, galactose, arabinose, mannose
Nucleogel ION 300 OA (Macherey-Nagel)	Sulfonated (hydrogen form)	300 × 7.8	Sulfuric acid 0.01 N	30	0.6	RI	Sucrose, glucose, citric acid, fructose, tartaric acid, malic acid, glycerol acetic acid, lactic acid, methanol, ethanol
Nucleogel Sugar Na (Macherey-Nagel)	PS-DVB sulfonated (lead form)	300 × 7.8	Water	85	0.4	RI	Mono oligosaccharides
IOA-1000 (Alltech)	Sulfonated (hydrogen form)	300 × 7.8	0.005 sulfuric acid	65	0.3 – 0.4	RI	Maltotriose, maltose, glucose, fructose, organic acids

*PS-DVB = polystyrene-divinylbenzene copolymer.

faster elution of strongly retained components without compromising selectivity and does not interfere with amperometric detection. **Figure 8** is the chromatogram of a sample of starch hydrolysate containing over 20 linear homologous maltooligosaccharides. The separation was obtained by increasing sodium acetate content in the mobile phase by linear gradient elution. On the other hand, under isocratic

elution, alditols and mono- and disaccharides can be separated in a single run (**Figure 9**).

As has been shown by several authors in comparative studies, the use of HPAEC-PAD for quantification of neutral monosaccharides, aminosaccharides, glucuronic acids, linear and branched oligosaccharides in complex matrices, is usually superior to HPLC-RI and HPLC-UV in terms of sample

Table 3 Columns with a selectivity comparable to Aminex columns

<i>Aminex column</i>	<i>Sarasep (length × ID mm) (Interchim)</i>	<i>Nucleogel (length × ID mm) (Macherey-Nagel)</i>	<i>Polyspher (length × ID mm) (Merck)</i>	<i>Sugar-Pak (length × ID mm) (waters)</i>	<i>Rezex (length × ID mm) (Phenomenex)</i>	<i>Supelcogel (length × ID mm) (Sigma)</i>
HPX-87N	–	Sugar Na (300 × 7.8)	CH NA (300 × 7.8)	–	RNM (300 × 7.8)	–
HPX-87K	–	–	–	–	RKP (300 × 7.8)	K (300 × 7.8)
HPX-87C	Car-Ca (300 × 7.8)	Sugar Ca (300 × 7.8)	CH CA (300 × 6.5)	SC-1011 SC 1821 (300 × 8.0)	RCM (300 × 7.8)	Ca (300 × 7.8)
HPX-87P	Car-Pb (300 × 7.8)	Sugar Pb (300 × 7.8)	CH PB (300 × 7.8)	SP-0810 (300 × 7.8)	RPM (300 × 7.8)	Pb (300 × 7.8)
HPX-42A	–	–	–	–	RSO (300 × 7.8)	Ag (300 × 7.8)
HPX-87H	Car-H WA-1 (300 × 7.8)	ION 300 OA (300 × 7.8)	OA HY (300 × 6.5)	–	RHM (300 × 7.8)	C-610 H (300 × 7.8)

preparation and sensitivity. In the last five years many significant developments in carbohydrate analysis by HPAEC-PAD have been reported.

Alkylsilica Packings

Octadecylsiloxane bonded silica materials, usually designed for reversed-phase (RP) chromatography are

nonpolar stationary phases having relatively strong hydrophobic character. The choice of an RP column with pure water as the eluent is an easy method for HPLC analysis of carbohydrates. However, the mechanism governing retention of carbohydrates is not reversed-phase partition but a form of hydrophobic chromatography, involving van der Waals interactions between carbohydrates and the alkyl chains of

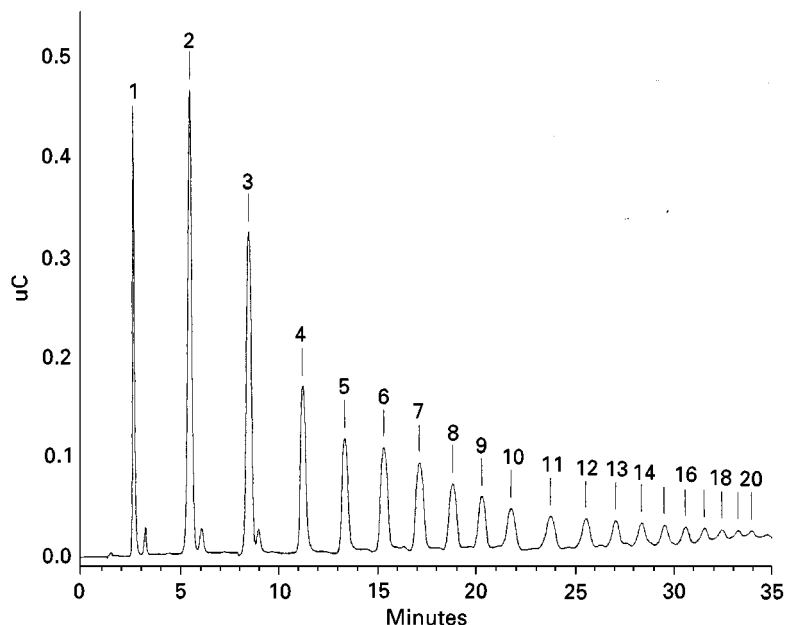


Figure 8 Separation of linear maltooligosaccharide oligomers of up to 20 residues. Chromatographic conditions: column, CarboPac PA 100 (250 × 4.0 mm ID) connected to a CarboPac PA 100 guard column (50 × 4.0 mm ID), all from Dionex, Sunnyvale, CA, USA; eluent A, 50 mM sodium acetate in 120 mM sodium hydroxide; eluent B, 300 mM sodium acetate in 120 mM sodium hydroxide; flow rate, 1.0 mL min⁻¹ at room temperature; detector, PED in pulsed amperometric mode. Maltooligosaccharides were eluted by a linear gradient from eluent A to eluent B in 35 minutes. Numbers over peaks indicate dp values.

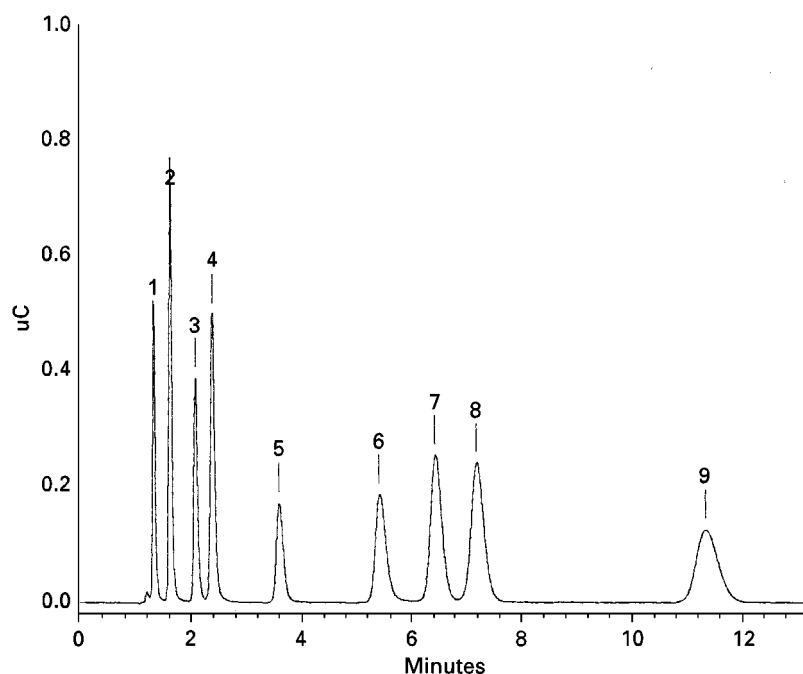


Figure 9 Separation of glycerol (1) xylitol, (2) sorbitol, (3) mannitol, (4) lactitol, (5) maltitol, (6) glucose, (7) fructose, (8) and sucrose, (9) by isocratic elution. Chromatographic conditions: column, CarboPac PA 10 (250 \times 4.0 mm ID) connected to a CarboPac PA 10 guard column (50 \times 4.0 mm ID), all from Dionex, Sunnyvale, CA, USA; mobile phase, 65 mM sodium hydroxide; flow rate, 1 mL min⁻¹ at room temperature; detection, PED in pulsed amperometric mode.

the bonded phase. The first HPLC separation of carbohydrates employing octadecylsiloxane-bonded silica columns was carried out in 1981 using a DextropakTM (Waters) column specifically developed for the separation of underivatized oligosaccharides. However, separation of monosaccharides was poor. Furthermore, a drawback of the reversed-phase column in carbohydrate separation is the undesired resolution between α and β anomers of the saccharides, which complicates the chromatograms.

Different approaches have been proposed to avoid unwanted double peaks. The most widely used approach is to reduce the oligosaccharide samples with sodium borohydride. In this way for each reducing saccharide the corresponding alditol is eluted as a single peak. As reported earlier, another approach to avoid the formation of doublets is to increase column temperature, which increases the rate of interconversion between the α and β anomers. Cheetham and Teng reported that modification of a Dextropak C₁₈ column by adding nonionic Triton X-100 detergent or tetramethylurea to the eluent, avoids the elution of anomeric doublets. The elution of broad peaks or doublets due to resolution of anomers can be precluded by the addition of triethylamine to the eluent. However, under these conditions, some risk of silica degradation is likely.

This drawback may be overcome by the use of reversed-phase packings obtained by introducing oc-

tadecyl groups into hydrophilic porous polymers having hydroxyl groups on the surface. Koizumi *et al.* have described the use of an AsahipakTM ODP-50 column packed with C₁₈-bonded vinyl alcohol copolymer gel for the separation of glucooligomers, which were selectively eluted as single peaks using sodium hydroxide at pH 11 as the mobile phase. Under these conditions, the rate of interconversion between the α and β anomers of saccharides was accelerated satisfactorily, avoiding the elution of anomeric doublets. The same polymeric column has been used to separate cyclodextrins and branched cyclodextrins. Columns packed with C₁₈-bonded phases have also found application in ion-pair chromatography with tetrabutylammonium in a buffered medium, for analysis of oligosaccharides containing an acid or sulfate group.

Detection

One shortcoming in the HPLC of carbohydrates is the often inadequate sensitivity and selectivity in the detection process, particularly when they are at a much lower concentration than other compounds present in complex matrices. The analysis of neutral carbohydrates is difficult due to their absence of a chromophore. RI detection is the most popular detection technique for carbohydrates in HPLC but a serious drawback is that it can only be used to monitor

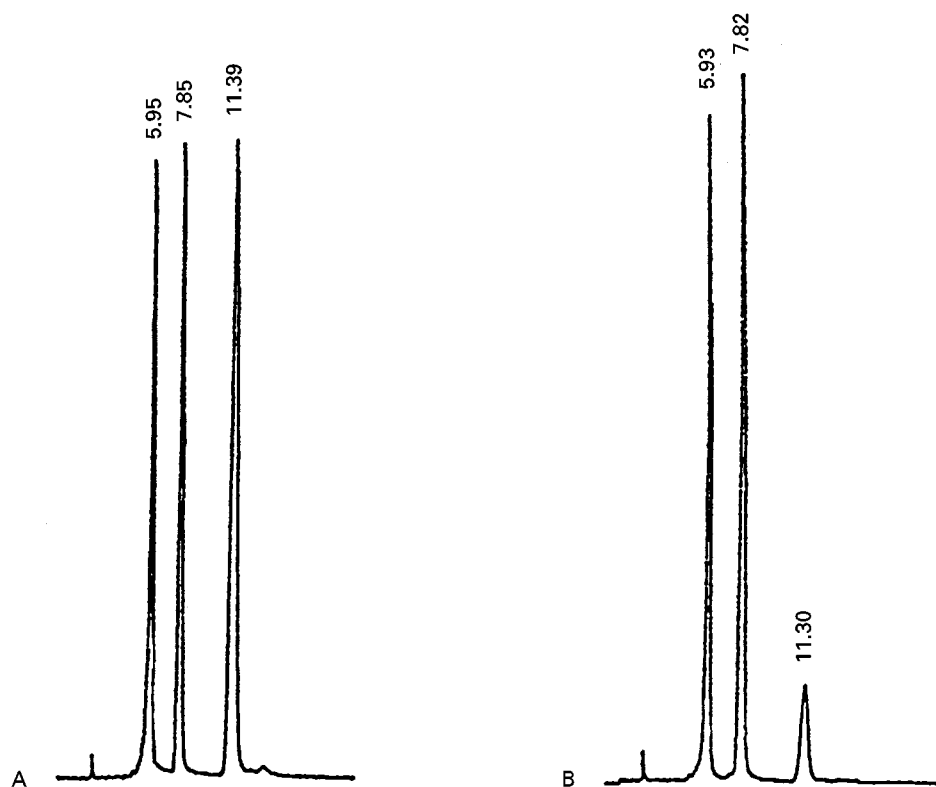


Figure 10 Detection of sugars in fruit juices by ELSD. Chromatographic conditions: column, LiChrosorb Diol ($5\ \mu\text{m}$, $250 \times 4.6\ \text{mm ID}$, from Merck); mobile phase, dichloromethane–methanol (82:18 v/v); flow rate, $1\ \text{mL min}^{-1}$ at room temperature; detector, ELSD; evaporator, 50°C ; air inlet pressure, 20 psi. Chromatogram A: fructose ($t_r = 5.95$), glucose ($t_r = 7.85$), sucrose ($t_r = 11.39$) in a blood orange juice. Chromatogram B: fructose ($t_r = 5.93$), glucose ($t_r = 7.82$), sucrose ($t_r = 11.30$) in a grapefruit juice.

isocratic separations. As a substitute for RI, the evaporative light-scattering detector (ELSD) can be used with gradient elution, thus performing better chromatographic separations. In addition, ELSD provides rapid stabilization before operation and improves baseline stability and better sensitivity. The direct detection of analytes is achieved through three consecutive stages, which are independent of each other. The first stage consists in the nebulization of the column effluent with air or nitrogen to produce a finely divided spray, which passes through a heated chamber to vaporize the eluent. During the second stage, solutes less volatile than the eluent create a particle stream that intersects a collimated light beam (mono- or polychromatic, depending on the apparatus design), producing light scattering. The scattered light is then detected by a photomultiplier (or photodiode), where the output is proportional to the amount of solute present over a wide concentration range. Description of the technical performance and configuration of the current commercial ELSD detectors for both HPLC and supercritical fluid chromatography (SFC), have recently been reported by Henry, Dreux *et al.* and Lafosse *et al.* Owing to the nature of light scattering detection, ELSD is especially

suitable for solutes which are characterized by a lower volatility than the eluent used for the chromatographic separation. A wide variety of solvents may be used as eluents; highly volatile mobile phases are preferred either as pure solvents or as a combination of two or more. Nevertheless, carbohydrates are more soluble in water than in organic solvents and therefore water is frequently a constituent of the mobile phase.

By coupling the HPLC system with an ELSD detector, carbohydrate separations on bare silica, as well as diol and polyol, bonded phases can be performed by isocratic or gradient elution from mixtures of dichloromethane–methanol. With these organic eluents, separation of mono-, di- and oligosaccharides can be achieved by gradient elution without baseline drift and with a good sensitivity; an example of the analysis of sugars using a diol silica-based column coupled with ELSD detection is reported in **Figure 10**. Fructose, glucose and sucrose are separated from a blood orange juice and a grapefruit juice using a mixture of dichloromethane–methanol (82:18 v/v) as the mobile phase. The detection limit is 20 ng for all analysed sugars. Furthermore, the stationary phase employed avoided Schiff's base

formation with reducing sugars and periodic regeneration of the column was not needed. The high chemical stability of the column is demonstrated comparing the reproducibility of the retention times reported in chromatogram A with those reported in chromatogram B, which was performed 100 injections apart. The use of ELSD detection is less favourable when employing metal-bearing cation exchange columns, where carbohydrates are eluted with plain water at high temperature (80–95°C). Since these cationic resin–water systems cause an increase in detector noise at the temperature of the separation. On the other hand, Dreux and Lafosse demonstrated the usefulness of ELSD detection in oligosaccharide and polysaccharide analysis obtained on octadecylsiloxane-bonded silica columns with gradient elution at increasing methanol content in water.

Only few carbohydrates exhibit significant absorbance in the low UV, such as acidic disaccharides released from glycosaminoglycans by enzymatic digestion, which carry an unsaturated uronic acid residue at the nonreducing end that enables their UV detection at an absorbance maximum of 232 nm. Neutral carbohydrates can be analysed by UV detection at wavelengths lower than 200 nm but under these conditions they are subject to interference from other compounds with similar absorption properties. Furthermore, in this UV region acetonitrile also absorbs strongly and therefore the UV detector is unsuitable for use in HILIC of underivatized carbohydrates, where separations are usually performed employing mobile phases rich in this solvent. This drawback can be overcome by either pre- or postcolumn derivatization. The most common chemical derivatization methods allow the conversion of carbohydrates into derivatives that can be detected with an online ultraviolet, visible, or fluorimetric detector. Besides an improvement in the detection properties, the chemical reaction can also enhance the selectivity of the total analytical method. For example, pre-column derivatization of oligosaccharides with a hydrophobic chromophore is the most common approach to enhance the resolution and detection of oligosaccharides into their components by RP-HPLC.

A wide variety of methods have been developed for pre- and postcolumn derivatization of carbohydrates. Comparative advantages and disadvantages of these two approaches have been reviewed by Giese and Honda (see Further Reading).

Although prechromatographic and postcolumn chemical derivatization methods allow the conversion of carbohydrates into either photometrically or fluorimetrically active adducts that can be detected with high sensitivity, the simplicity of sensitive direct

detection in HPLC will always be preferred whenever possible.

In HPLC, polar aliphatic compounds containing electroactive groups can be directly detected by pulsed electrochemical detection (PED), a generic term introduced by LaCourse to indicate all detection strategies based on the application of multi-step potential-time waveforms at noble metal electrodes for electrochemical detection.

Amperometric detection is used to measure the current or charge generated by the oxidation or reduction of analytes at the surface of a working electrode in a flow cell. For several classes of molecules, which include carbohydrates and aliphatic alcohols and amines, amperometric detection can only be performed if a repeating sequence of three potentials is applied for specific times to the working electrode. Amperometric detection under the control of a three-step potential-time waveform is known as PAD.

This detection mechanism was first applied in 1981 for the detection of aliphatic alcohols at Pt electrodes and then proposed for the direct determination of carbohydrates when in 1983 Rocklin and Pohl coupled the first commercial detector dedicated to PAD with HPAEC.

In pulsed amperometric detection mode, the working electrode is held at an analytical potential E_1 for a time t_1 . At this potential the CHOH groups of carbohydrates are oxidized. The current is measured at the end of the E_1 pulse to allow the charging current to decay, resulting in more accurate measurement of the electroactive species. If only a single potential is applied, the detector response would steadily decrease as the electrode surface became fouled. The electrode surface is oxidatively cleaned by a positive potential E_2 ($E_2 > E_1$) for a time t_2 . The voltage on the electrode is then reversed to a strongly reducing potential E_3 for a time t_3 to convert the gold oxide layer at the surface of the electrode back to native gold, thus renewing the surface.

Selection of the potentials for detection, cleaning and conditioning are based on current (i)-potential (E) response from cyclic voltammetry (CV) recorded for triangular waveforms ($E - i$). Extensive studies on the optimization of waveforms for pulsed amperometric detection of carbohydrates have been published recently by LaCourse. Carbohydrates can be detected by PAD at Au electrodes in highly alkaline media. For separations which are not carried out under adequately alkaline conditions, as in the analysis of monosaccharides, the detection requirement of a strong alkaline medium can be satisfied by post-column addition of NaOH (generally in the range 300–500 mM) by means of a pump, a hydraulic device, or membrane reactor.

Conclusions: Summary of Main Trends

A wide variety of HPLC methods are available to analyse carbohydrates from various complex matrices. Aminopropylsiloxane-bonded silica of small particle diameter (3 µm), amine-bonded vinyl alcohol copolymer packings, diol- and cyclodextrin-bonded silica, as well as macroporous cross-linked vinylpyridinium polymers, are some of the columns of choice for high selectivity in the HILIC of carbohydrates. Furthermore, a large number of columns may be selected to separate carbohydrates on cation exchange resins carrying different counterions. Employing these columns the chromatographic separation is governed by a combination of size exclusion and ligand exchange mechanisms. In oligosaccharide separations, size exclusion is the primary mechanism which involves the binding of hydroxyl groups of the sugars with the fixed counterion of the resin, thus they elute last.

On the other hand, RP-HPLC with plain water as the eluent may be useful for the separation of various underivatized oligosaccharides. The mechanism governing this HPLC method produces separations that complement those given by cation exchange columns and therefore the two techniques should be used in conjunction in isolation and analysis of carbohydrates.

Column instability and low detection sensitivity are the major disadvantages using these HPLC methods. However, column and detection technologies to analyse carbohydrates are in continuous development.

Mono- and oligosaccharides are detected without any derivatization by PAD, which is sensitive and selective for detection of these analytes. The use of HPAEC is now widely accepted as a powerful analytical tool for carbohydrate analysis. However, HPAEC methods require dedicated columns and instrumentation.

See also: II/Chromatography: Liquid: Detectors: Evaporative Light Scattering; Detectors: Refractive Index De-

tectors; Instrumentation; Mechanisms: Reversed Phases. III/Polysaccharides: Liquid Chromatography.

Further Reading

- Alpert AJ (1990) Hydrophilic-interaction chromatography for the separation of peptides, nucleic acids and other polar compounds. *Journal of Chromatography* 499: 177.
- Cheetham NHW and Teng G (1984) Some applications of reversed-phase high-performance liquid chromatography to oligosaccharide separation. *Journal of Chromatography* 336: 161.
- Churms SC (1990) Recent developments in the chromatographic analysis of carbohydrates. *Journal of Chromatography* 500: 555.
- Dreux M and Lafosse M (1995) Evaporative light scattering detection of carbohydrates in HPLC. In: El Rassi Z (ed.) *Carbohydrate Analysis – High Performance Liquid Chromatography and Capillary Electrophoresis*. Amsterdam: Elsevier.
- El Rassi Z (1995) *Carbohydrate Analysis – High Performance Liquid Chromatography and Capillary Electrophoresis*. Amsterdam: Elsevier.
- Giese R and Honda S (1996) Chromatographic and electrophoretic analyses of carbohydrates (Special Issue). *Journal of Chromatography* 720.
- Goulding RW (1975) Liquid chromatography of sugars and related polyhydric alcohols on cation exchangers – The effect of cation variation. *Journal of Chromatography* 103: 229.
- Herbreteau B (1992) Review and state of sugar analysis by high performance liquid chromatography. *Analisis* 20: 355.
- Honda S (1984) High-performance liquid chromatography of mono- and oligosaccharides. *Analytical Biochemistry* 140: 1.
- Hurst WJ (1997) *Seminars in Food Analysis – HPAEC-PAD in Food and Beverage Analysis*. London: Chapman and Hall.
- LaCourse WR (1993) Pulsed electrochemical detection at noble metal electrodes in high performance liquid chromatography. *Analisis* 21: 181.
- Lee YC (1990) High-performance anion-exchange chromatography for carbohydrate analysis. *Analytical Biochemistry* 189: 151.

Thin-Layer (Planar) Chromatography

J. F. Robyt, Laboratory of Carbohydrate Chemistry and Enzymology, Iowa State University, Ames, IA, USA

Copyright © 2000 Academic Press

Introduction

Carbohydrates are some of the more difficult compounds to separate from each other. They primarily

differ in the number of carbon atoms, the configuration of the chiral centres and the size of the molecules, that is to say whether they are di-, tri- and oligosaccharides. If two carbohydrates have any one of the three characteristics in common, they can be difficult to separate. There are some carbohydrates that differ by having a special functional group, for example a carboxyl group (giving uronic, onic and aric acids),

an amino or acetyl-amino group (giving amino and *N*-acetyl amino sugars), or a phosphoric acid ester group (giving carbohydrate phosphates). Nevertheless, because carbohydrates play such an important role in living systems and comprise a large number of important naturally occurring products, methods for separating them were some of the earliest chromatographic procedures developed.

Early chromatographic methods in the 1950s for separating carbohydrates used paper as the solid support. In the early 1960s Thoma introduced thin-layer chromatography (TLC) for separating carbohydrates. The use of TLC, however, was not particularly easy and convenient at that time, as each laboratory had to prepare its own thin-layer plates. This led to a wide variation in the quality of the plates and in the results that were obtained, even within a single laboratory. The results were difficult to reproduce from day to day and particularly from laboratory to laboratory. It was not until reproducible thin-layer plates were commercially developed and produced at a reasonable price, primarily by Whatman and Merck in the late 1970s, that TLC became a viable and valuable procedure.

TLC has now become the principal method of choice for the separation of carbohydrates. High performance liquid chromatography (HPLC) has displaced TLC in many laboratories, although for carbohydrates and other materials, TLC is much preferred over HPLC. When compared with HPLC, TLC is much less expensive, easier to perform, uses simple equipment, uses much less sample, and the detection of the carbohydrates directly on the plate is more sensitive. TLC is also more reproducible. With HPLC, once a sample has been added to a column, the column is irreversibly modified. Because of the high cost of the HPLC columns, many hundreds of samples must be separated and analysed in series on the same column to make the procedure economically feasible; whereas sample placed on to a TLC plate is separated in its own little column or lane, which is not affected by other compounds that have previously been adsorbed and separated on the support material. Further, approximately 18 samples can be simultaneously separated on a single 20 × 20 cm TLC plate, which can include standards. A simple comparison of the migration positions with the migration positions of the standards can be used for qualitative identification.

TLC Support Material, Solvents and Detection Methods

The principal support material found most useful for valuable in the separation of carbohydrates is silica

gel, a stable and inert substance. The silica gel thin layer is usually uniformly 250 µm thick over the TLC plate. The resolution of carbohydrates is achieved by the selection of a specific solvent system. Many solvent systems have been empirically developed. The particular solvent used depends on whether the carbohydrates are monosaccharides, disaccharides, trisaccharides or oligosaccharides, or whether they contain a charged group such as a uronic acid, an amino sugar or a carbohydrate phosphate.

A relatively simple solvent that has found valuable use in the separation of a number of mono-, di- and trisaccharides is acetonitrile–water (85 : 15, v/v). This solvent is frequently the first choice when separating unknown carbohydrates in a sample. Solvents for the separation of more complex mixtures can then be developed using other organic compounds in combination with the acetonitrile–water system. Many solvent systems contain three components: water, a water-soluble component and a water-insoluble component. The three components are combined in various proportions so as to give a homogeneous solution. For maximum resolution, the technique of multiple ascents is frequently employed. In this technique, the solvent is allowed to ascend to the top of the TLC plate, whereupon the plate is removed from the developing tank and the solvent is completely evaporated from the plate. The plate is then put back into the TLC tank for a second, third and/or fourth ascent. **Figure 1** illustrates the separation of relatively complex mixtures of carbohydrates using this technique with acetonitrile–water (85 : 15, v/v) solvent.

A very sensitive detection system has recently been developed in which most carbohydrates can be detected in the 50–2000 ng range, directly on the TLC plate. The method uses a detecting reagent, consisting of 0.3% (w/v) of *N*-(1-naphthyl)ethylenediamine and 5% (v/v) concentrated sulfuric acid in methanol. The TLC plate is removed from the developing tank, dried and rapidly dipped into the reagent. The plate is dried and placed in an oven at 120°C for 10 min. Carbohydrates give blue-black spots on a white background. Most carbohydrates can be detected by using this reagent, with the exception of 2-amino-2-deoxy sugars, 2-*N*-acetylamino-2-deoxy sugars and sugar alcohols. This is primarily due to the requirement of forming furfurals from the carbohydrates by dehydration with the sulfuric acid. An older method used sulfuric acid charring, in which a 25% (v/v) solution of sulfuric acid in methanol was sprayed on to the TLC plate, dried and then heated at 120°C for 10 min. This is a much less sensitive method, with detection in the 10–100 µg range. Further, the

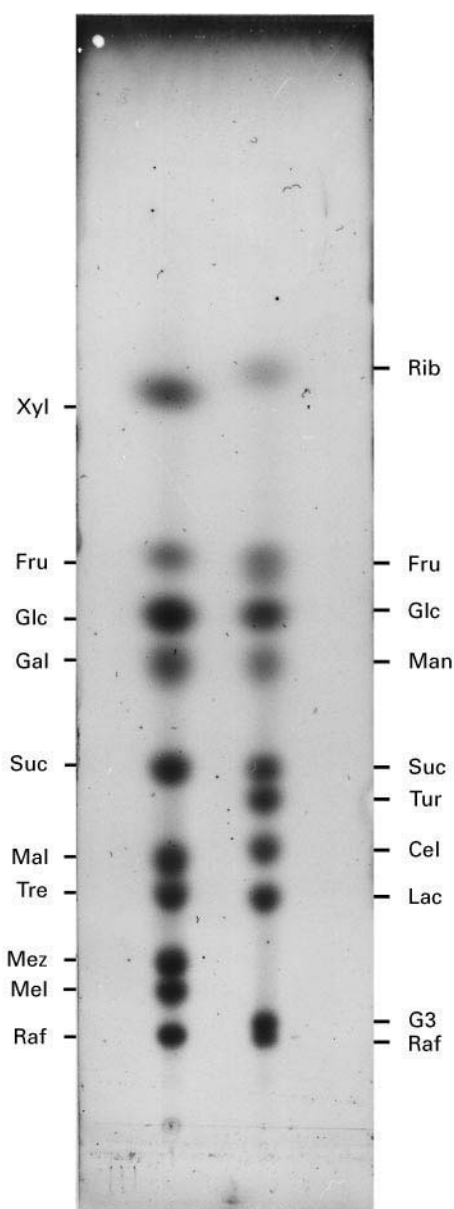


Figure 1 Separation of various mono-, di- and trisaccharides on Whatman K5 TLC plates (18.5 cm solvent path length for each ascent), using four ascents of acetonitrile–water in volume proportions of 85 : 15 at 20–22°C. The carbohydrates were detected by using the *N*-(1-naphthyl)ethylenediamine–sulfuric acid–methanol dipping reagent.

spraying technique is much less environmentally friendly than a dipping technique.

The separation of radiolabelled carbohydrates permits several sensitive techniques to be used to detect and quantify the carbohydrates directly on the TLC plate, such as a TLC radioactive scanner or a PhosphoImager. Both can be used to detect and quantitate ^{14}C , ^{35}S , or ^{32}P radioactive isotopes, although the PhosphoImager is several orders of

magnitude more sensitive and relatively easy to use quantitatively.

TLC Separation of Homologous Series of Oligosaccharides

The separation of oligosaccharides is important in a wide variety of applications, such as analysis of carbohydrates in foods, analysis of oligosaccharides from glycoproteins and glycolipids, the analysis of enzymatic synthesis of oligosaccharides and the analysis of the hydrolysis of polysaccharides. Many of these analyses involve the separation of a homologous series of oligosaccharides containing one or possibly two kinds of glycosidic linkages and as many as 20–30 monosaccharide residues of the same type in the oligosaccharides. The separation of a homologous series of saccharides, containing 2–30 monosaccharides residues, linked β -1 \rightarrow 2, β -1 \rightarrow 3, α -1 \rightarrow 4, and α -1 \rightarrow 6, has been reported, using silica-gel plates developed with butanol-1–ethanol–water. The development time was however, several hours for one ascent.

Much faster systems, using Whatman K5 plates or Merck silica gel 60 plates and multiple ascents with acetonitrile–water systems, have been developed for the separation of maltodextrins (α -1 \rightarrow 4 linked glucosaccharides) and isomaltodextrins (α -1 \rightarrow 6 linked glucosaccharides). The separation of maltodextrins was achieved using acetonitrile–ethyl acetate–propanol-1–water in volume proportions of 85 : 20 : 50 : x . The amount of water (x) can be varied from 50 to 70 parts by volume, depending on the desired number of saccharides to be separated. The largest saccharides can have 20 D-glucose residues. Likewise, using up to four ascents can increase the number of saccharides separated. **Figure 2** illustrates the separation of maltodextrins using one to four ascents of 85 : 20 : 50 : 60 volume proportions at 20–22°C.

Isomaltodextrins migrate more slowly than an equivalent maltodextrin mixture, primarily because of differences caused by the α -1 \rightarrow 6 glycosidic linkage vs the α -1 \rightarrow 4 glycosidic linkage. To obtain an equivalent separation for the isomaltodextrins, the water content (x) of the solvent system has to be increased to 90 or 100 volume proportions. **Figure 3** illustrates the separation of isomaltodextrins using one to four ascents of acetonitrile–ethyl acetate–propanol-1–water in the volume proportions of 85 : 20 : 50 : 90 at 20–22°C.

The power of TLC separations of saccharides, using these solvents, is illustrated in **Figure 4** in which complex saccharides are separated from mixtures produced by the action of two different enzymes

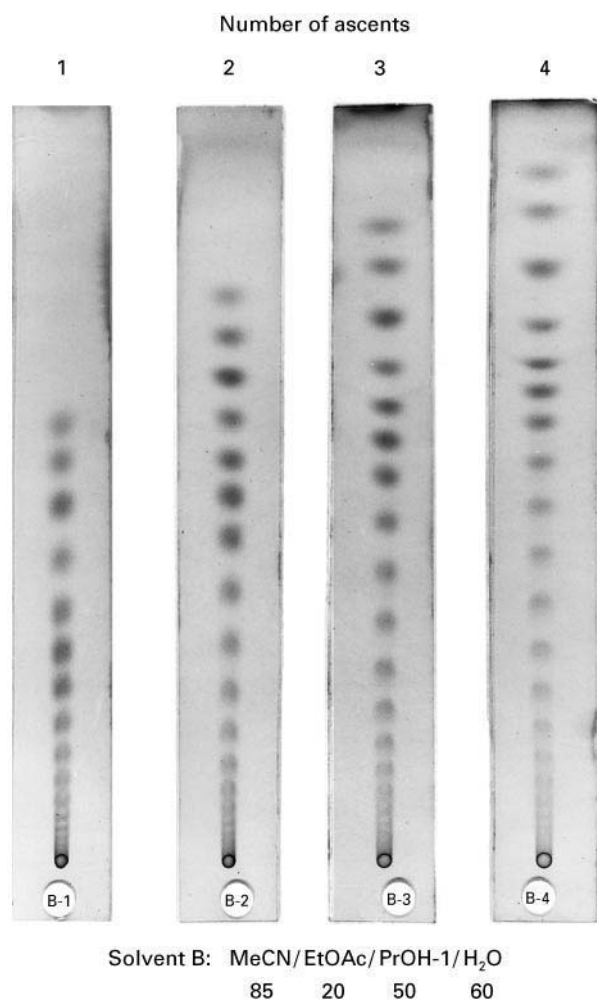


Figure 2 Separation of D-glucose and maltodextrins on Whatman K5 TLC plates (18.5 cm solvent path length for each ascent), using 1–4 ascents of acetonitrile–ethyl acetate–propanol-1–water in volume proportions of 85 : 20 : 50 : 60 at 20–22°C. The numbers at the top of each chromatogram indicate the number of solvent ascents. The carbohydrates were detected using the *N*-(1-naphthyl)ethylenediamine–sulfuric acid–methanol dipping reagent. Reproduced with permission from Robyt and Mukerjea (1994).

acting on polysaccharides. The saccharides were separated by using four ascents of acetonitrile–ethyl acetate–propanol-1–water in volume proportions of 85 : 20 : 50 : 50 at 20–22°C on a Whatman K-5 plate. Lane 1 on the plate is a set of maltodextrin standards, containing D-glucose, maltose, maltotriose and so forth down to maltodextrins with 14 D-glucose residues; lane 2 shows an equivalent set of maltodextrin saccharides that were obtained by the action of isoamylase acting on shellfish glycogen; lane 3 shows the separation of products that resulted from the action of porcine pancreatic α -amylase acting on potato amylopectin. Saccharides marked B6, B7 and B8

contain six, seven and eight D-glucose residues, respectively having one α -1 \rightarrow 6 glycosidic linkage and five, six and seven α -1 \rightarrow 4 glycosidic linkages. These saccharides migrate in between the maltodextrins, for example, BB6 migrates behind G6 and faster than G7, B7 migrates behind G7 and faster than G8, and so forth. Saccharides marked BB9, BB10 and BB11 contain nine, 10 and 11 D-glucose residues, respectively, with each having two α -1 \rightarrow 6 glycosidic linkages and seven, eight and nine α -1 \rightarrow 4 glycosidic linkages. Saccharides containing one D-galactose residue will usually migrate more slowly than an equivalent saccharide containing all D-glucose

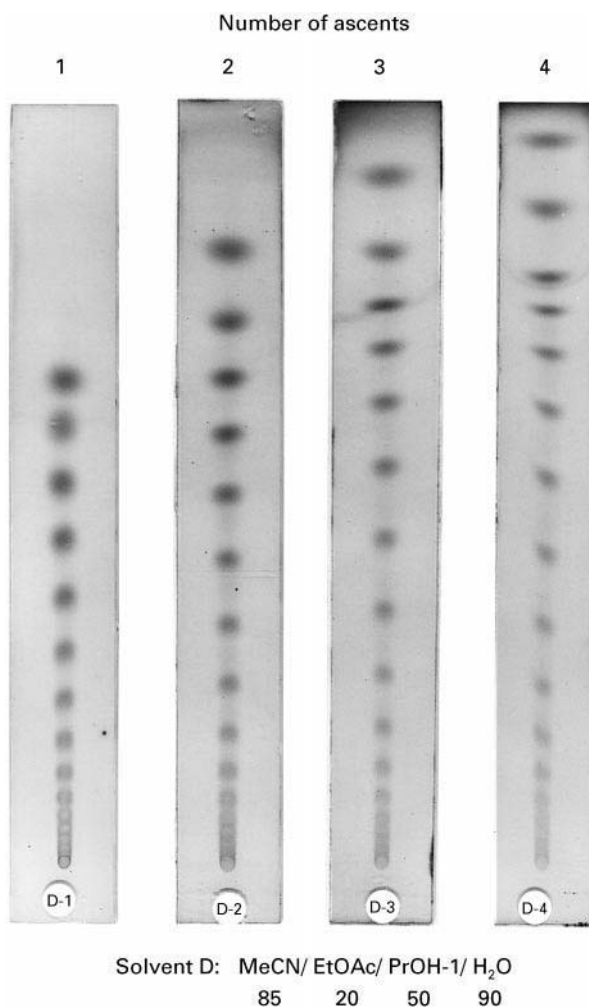


Figure 3 Separation of D-glucose and isomaltodextrins on Whatman K5 TLC plates (18.5 cm solvent path length for each ascent), using 1–4 ascents of acetonitrile–ethyl acetate–propanol-1–water in volume proportions of 85 : 20 : 50 : 90. The numbers at the top of each chromatogram indicate the number of solvent ascents. The carbohydrates were detected using *N*-(1-naphthyl)ethylenediamine–sulfuric acid–methanol dipping reagent. Reproduced with permission from Robyt and Mukerjea (1994).

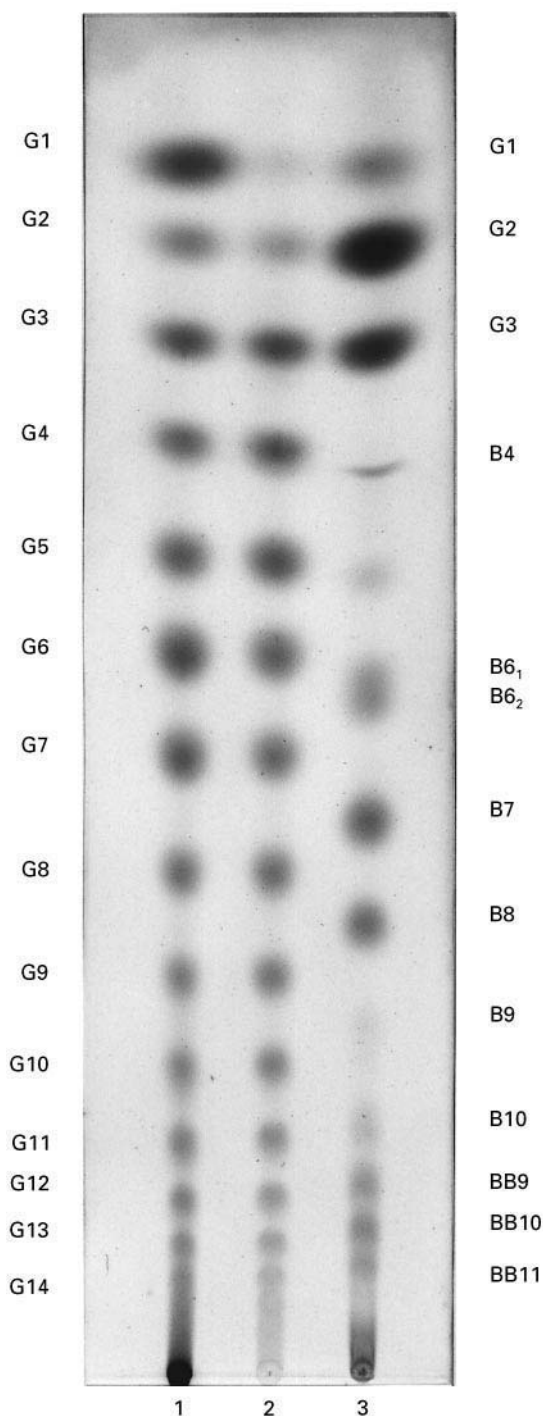


Figure 4 Separation of maltodextrins and maltodextrins, containing one and two α -1 \rightarrow 6 linkages. Lane 1, glucose and maltodextrin standards; lane 2, maltodextrins resulting from the action of isoamylase reaction with shellfish glycogen; lane 3, α -amylase action on amylopectin. Whatman K5 TLC plate (18.5 cm solvent path length for each ascent) was irrigated four times with acetonitrile-ethyl acetate-propanol-1-water in volume proportions of 85 : 20 : 50 : 50 at 20–22°C. The carbohydrates were detected using the *N*-(1-naphthyl)ethylenediamine-sulfuric acid-methanol dipping reagent. Reproduced with permission from Robyt and Mukerjea (1994).

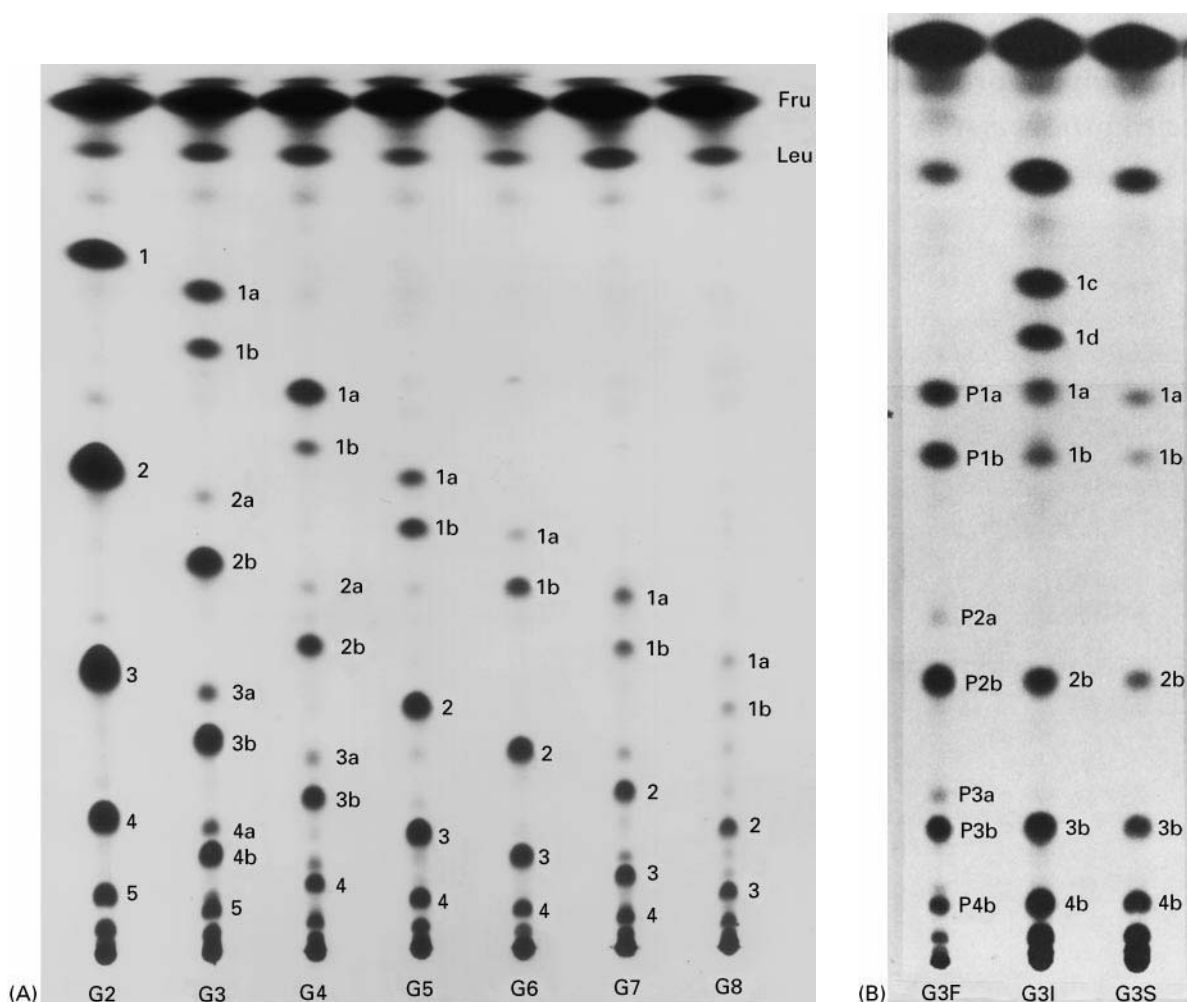
residues. Compare the migration of lactose with cellobiose in Figure 1.

To illustrate the tremendous power that TLC has in separating carbohydrate oligosaccharides with very similar structures, **Figure 5A** shows the chromatographic separation of saccharides formed by the action of *Leuconostoc mesenteroides* B-512FM dextransucrase transfer of D-glucose from sucrose to malto-oligosaccharide acceptors having two to eight D-glucose residues. Two different products were formed by the transfer of D-glucose to the reducing end of the acceptor saccharide to form an α -1 \rightarrow 6 linkage (product-1a) and transfer of D-glucose to the non-reducing end of the acceptor saccharide to form α -1 \rightarrow 6 linkage (product-1b). Products 2a, 2b, 3a, 3b and so forth are products resulting from the transfer to C₆ of reducing-end glucose residue and to C₆ of the nonreducing-end glucose residue, and so forth of the first, second and third acceptor products. These complex products were separated using four ascents of ethyl acetate-ethanol-water (2 : 2 : 1, v/v/v) on a Whatman K5 TLC plate.

Figure 5B shows the separation of an even more complex mixture of products, containing the same number of D-glucose residues, but differing from each other by the location of the transferred D-glucose residue and the types of linkages, either α -1 \rightarrow 6 or α -1 \rightarrow 3. D-Glucose was transferred from sucrose to maltotriose by the action of three enzymes (F, I and S). Enzyme I gave four initial products, 1a–1d; 1a had D-glucose transferred to C₆ of the reducing-end glucose residue of maltotriose; 1b had D-glucose transferred to C₆ of the nonreducing-end glucose residue of maltotriose; 1c had D-glucose transferred to C₃ of the reducing-end glucose residue of maltotriose; and 1d had D-glucose transferred to C₃ of the nonreducing-end glucose residue of maltotriose. Enzymes F and S only gave two initial products, 1a and 1b. All three enzymes gave higher products: 2a, 2b, 3a, and so forth.

Separation and Detection of Sugar Alcohols on TLC

One of the more difficult separations of carbohydrates is that of separating aldoses from their corresponding alditols (sugar alcohols). Alditols can be separated from their aldoses on TLC by using two ascents of acetonitrile-ethyl acetate-propanol-1-water in volume proportions of 85 : 20 : 20 : 15. As previously mentioned, alditols are not readily detected by the sulfuric acid-based reagents described above. The best detection system is an alkaline silver nitrate-sodium thiosulfate dipping system that will detect alditols in the range of 500 ng to 1 μ g. The dry TLC plate is dipped into a silver nitrate-acetone



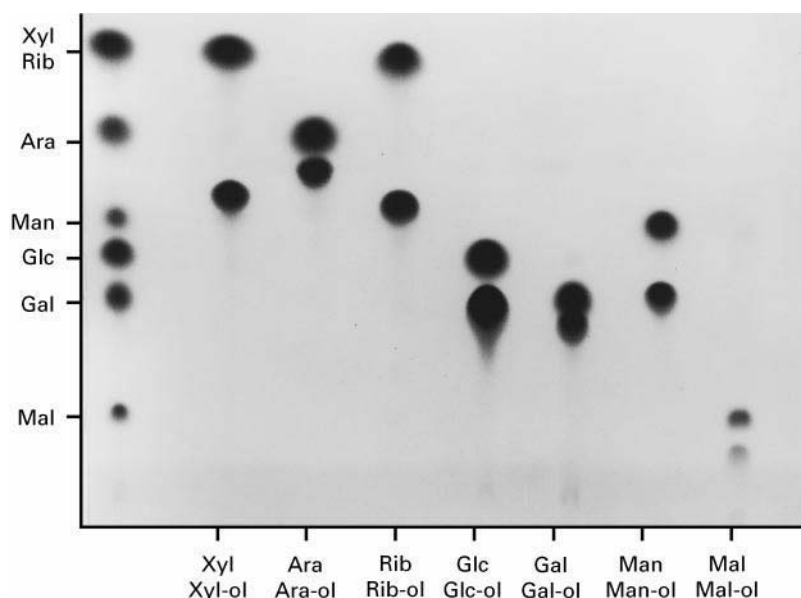


Figure 6 Separation of alditols (sugar alcohols) from their corresponding aldoses on Whatman K5 TLC plates (18.5 cm solvent path length for each ascent) using two ascents of acetonitrile–ethyl acetate–propanol–water in volume proportions of 85 : 20 : 20 : 15 at 20–22°C. The carbohydrates were detected by using the alkaline silver nitrate dipping reagents. Reproduced with permission from Han and Robyt (1998).

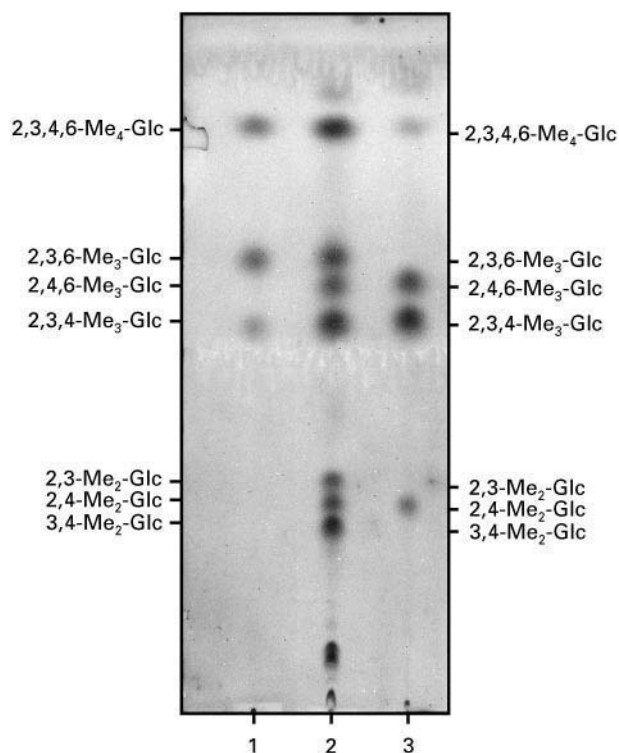


Figure 7 Separation of *O*-methylated D-glucoses. Lanes 1 and 3 are standards; lane 2 is the analysis of a complex, highly branched D-glucan. Whatman K6 plates were irrigated (18.5 cm solvent path length for each ascent) at 20–22°C, using two ascents of acetonitrile–chloroform–methanol in volume proportions of 3 : 9 : 1. The carbohydrates were detected by using the *N*-(1-naphthyl)ethylenediamine–sulfuric acid–methanol dipping reagent. Reproduced with permission from Mukerjee *et al.* (1996).

acid hydrolysis. The number of methyl groups and their location on the resulting monosaccharides indicate the positions of the linkages to the monosaccharides in the oligosaccharides or polysaccharides and whether or not the saccharides are branched. For example, if a gluco-polysaccharide contains 1 → 4 glycosidic linkages with 1 → 6 branch linkages, there would be three kinds of methylated monosaccharides: 2,3,6-tri-*O*-methyl-D-glucose (major), 2,3,4,6-tetra-*O*-methyl-D-glucose (minor from the nonreducing-end D-glucose residues) and 2,3-di-*O*-methyl-D-glucose (minor from the branched D-glucose residues). The use of TLC to separate and analyse these methylated monosaccharides has greatly simplified methylation analysis of oligo- and polysaccharides. Further, because of the sensitivity of detecting the methylated monosaccharides (lower limits of 25–50 ng range) directly on the TLC plate, micro amounts of saccharide (10 µg) can be methylated and analysed. **Figure 7** illustrates the chromatography of methylated D-glucoses on Whatman K6 TLC plates, using two ascents of acetonitrile–chloroform–methanol in volume proportions of 3 : 9 : 1 at 20–22°C. The methylated carbohydrates are detected by dipping the plate into the *N*-(1-naphthyl) ethylenediamine–sulfuric acid–methanol reagent described above, followed by heating for 10 min at 120°C.

Quantitative Determination of Carbohydrates

The easiest method of detecting and quantitating carbohydrates on a TLC plate is to use ¹⁴C-labelled

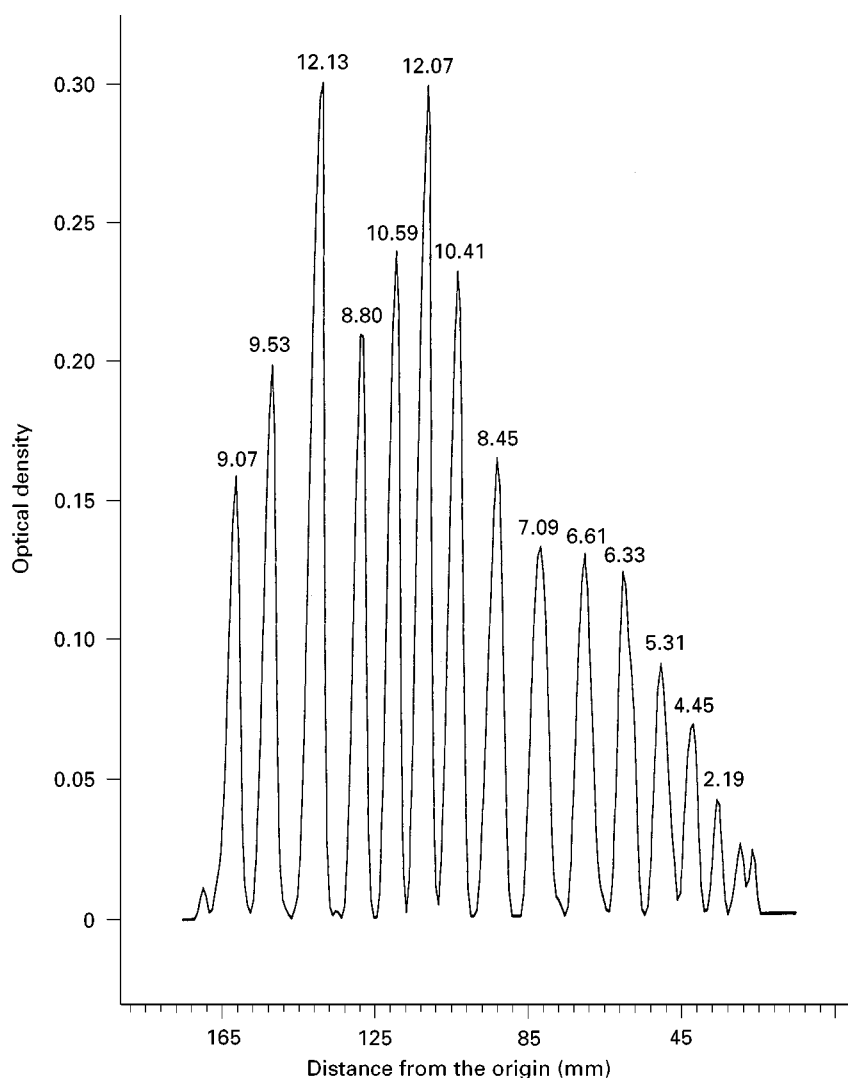


Figure 8 Densitometric scan of TLC number 3 shown in Figure 2, using a Bio-Rad imaging densitometer. The relative weight per cents for each of the carbohydrates are shown at the top of each peak. The first peak is D-glucose, followed by maltodextrins: maltose, maltotriose, maltotetraose, and so forth, down to a maltodextrin with 14 D-glucose residues.

carbohydrates. The radioactivity can be detected and quantitated directly on the plate using a phosphorimager. The use of radioactively labelled carbohydrates, however, is limited to carbohydrates that can be obtained in radioactive form and therefore limited in the kinds of experiments that can be performed. The more usual case is the chromatography of nonlabelled carbohydrates. The detection of carbohydrates on a TLC plate, using a sulfuric acid-based reagent, such as *N*-(1-naphthyl)ethylenediamine reagent described above, can be quantified using a scanning densitometer. Absolute, quantitative amounts can be determined using various amounts of the monosaccharide involved in the saccharides as standards, for example, D-glucose, D-mannose, or

sucrose, and so forth. However, for many purposes, the relative amounts of the individual saccharides in a mixture are sufficient. In this instance, the individual saccharides that are separated in a mixture can be scanned, the densities of the compounds summed and the percentage of the individual compounds computed by dividing the individual densities by the sum of the densities. Figure 8 shows a density scan of chromatogram no. 3 in Figure 2.

Preparative Separation of Carbohydrates Using TLC

By using the same solvent systems as is used in analytical TLC separations, but substituting TLC plates

that have a much thicker silica gel layer (1000–2000 μm), preparative separations of carbohydrates can be obtained. Approximately 25–50 μL of a 20–30 mg sample of a mixture of carbohydrates is streaked along a sample application line, 15 mm above the bottom of a 20 \times 20 cm TLC plate. The plate is developed in the usual way. After development, 15 mm strips are cut off from each end of the chromatogram and dipped into the detecting reagent. The strips are lined up with the plate and the locations of the desired compounds are marked. The silica gel area containing the compound is scraped from the plate into approximately 2 mL of water. The suspension is mixed and the silica gel removed by filtration or centrifugation. The aqueous extract can then be concentrated to dryness by evaporation, and the compound redissolved if necessary.

Points to Consider to Obtain Good Separations

1. A relatively small (1–25 μL) measured amount of sample should be carefully added on to the TLC plate, keeping the size of the spot as small as possible. The use of a microlitre syringe pipette, such as a Hamilton syringe, is desirable. When many samples are to be added to the TLC plate, a multi-spotting instrument can conveniently be used to make very small, uniform spots with a minimum of effort. The multi-spotter is also convenient when a relatively large volume, for example 10–25 μL , of sample is to be added.
2. Be sure that the developing tank is tightly sealed during development (vacuum grease can be used with glass-to-glass surfaces). The solvent and vapour should be in equilibrium before beginning the development.
3. Allow the solvent to ascend to the *top* of the TLC plate to give the maximum path length for the solvent. The old idea that the TLC plate should be removed from the solvent *before* the solvent has reached the top or *just as* the solvent reaches the top of the plate is not valid, if the chamber is tightly sealed. In fact, it is best to allow 5–10 min extra, after the solvent reaches the top of the TLC plate, before removing the plate. This ensures that the plate has been completely saturated with the solvent over the entire surface of the plate.
4. Use no more than 15 mm margin from the bottom of the plate to the point of sample application, so as to give the maximum path length for the solvent. Also, be sure only to use pencil to mark the TLC plates.
5. In multiple ascending chromatography, dry the plates thoroughly between each ascent. The use of

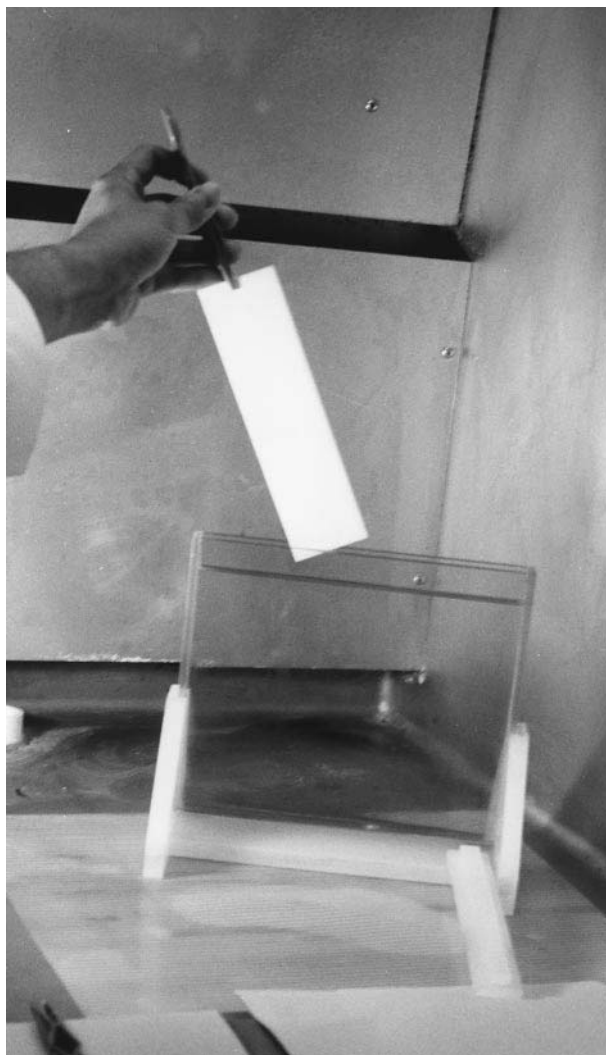


Figure 9 Glass chamber and holder used to dip the TLC plates into the detecting reagent.

a hair-dryer is a fast and convenient method for drying plates.

6. In developing the chromatogram, rapidly and carefully dip the irrigated plate into the detecting reagent to obtain a uniform amount of reagent over the entire plate. The use of a narrow 1.5 \times 22 \times 22 cm glass chamber is convenient for dipping. A stand and a lid have to be fabricated from polypropylene or similar material to hold the chamber (Figure 9).

Conclusions and Future Prospects

TLC has become a powerful analytical tool for separating compounds with very similar chemical and

physical properties, such as carbohydrates. The development of reliable and reproducible commercial TLC plates has placed it at the forefront of separation methods that can be used for both qualitative and quantitative determinations. Further, the use of relatively simple and inexpensive materials permits a wide range of laboratories, from the high-school teaching laboratory to quality control and research laboratories, to analyse and compare compounds easily, quickly and with high sensitivity. The use of relatively inert materials, such as silica gel on glass, allows chemical reactions to be conducted directly on the plate where the compounds have been separated. These reactions provide qualitative identification of the compounds by specific colour production and the quantitative determination of the compounds by the use of scanning densitometry. The latter is particularly important for carbohydrates as they do not lend themselves to the usual physical detection and quantifying methods, such as ultraviolet or visible absorbance, light scattering or refractive index. The development of a wide variety of solvents has also permitted the separation of carbohydrates that differ from each other in subtle aspects of configuration of chiral centres, differences in the kinds of glycosidic linkages present, and differences in the size of the compounds.

Future developments in TLC of carbohydrates may come slowly as much progress has been made in the last 50 years. But, as in most areas of endeavour, need is the necessity of invention. Developments will undoubtedly be made in new solvents that will separate new kinds of mixtures of carbohydrates obtained from natural products and from chemical and enzymatic modification reactions. There will probably be detection methods developed that will give greater sensitivity in the submicro range of carbohydrates on the plate. The latter will then also provide for the development of new physical instrumentation using lasers for scanning density, reflectance and fluorescence in quantifying carbohydrates directly on the plate.

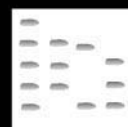
See also: II/Chromatography: Thin-Layer (Planar): Layers; Preparative Thin-Layer (Planar) Chromatography; Radioactivity Detection; Spray Reagents. III/Carbohydrates: Electrophoresis; Gas Chromatography and Gas

Chromatography-Mass Spectrometry; Liquid Chromatography.

Further Reading

- Block RJ, Durrum EL and Zweig G (1958) *A Manual of Paper Chromatography and Paper Electrophoresis*, 2nd edn, pp. 170–214. New York: Academic Press.
- Churms SC (1982) In: Zweig G and Sherma J (eds). *Handbook of Chromatography: Carbohydrates*, vol. I, pp. 137–153. Boca Raton, FL: CRC Press.
- Fu D and Robyt JF (1990) Acceptor reactions of maltodextrins with *Leuconostoc mesenteroides* B-512FM dextranase. *Archives of Biochemistry and Biophysics* 321: 379–387.
- Fu D and Robyt JF (1991) Maltodextrin acceptor reactions of *Streptococcus mutans* 6715 glucosyltransferases. *Carbohydrate Research* 217: 201–211.
- Gauch R, Leuenberger U and Baumgartner E (1979) Quantitative determination of mono-, di-, and trisaccharides by thin-layer chromatography. *Journal of Chromatography* 174: 195–210.
- Han NS and Robyt JF (1998) Separation and detection of sugars and alditols on thin-layer chromatograms. *Carbohydrate Research* 313: 135–137.
- Huber CN, Scobell HD, Tai H and Fisher EE (1968) Thin-layer chromatography of the malto-oligo and megalosaccharides with mixed support and multiple irrigations. *Analytical Chemistry* 40: 207–209.
- Jeanes A, Wise CS and Dimler RJ (1951) Improved techniques in paper chromatography of carbohydrates. *Analytical Chemistry* 23: 415–418.
- Koizumi K, Utamura T and Okada Y (1985) Analysis of homogeneous D-gluco-oligosaccharides and -polysaccharides (degree of polymerization up to about 35) by high performance liquid chromatography and thin-layer chromatography. *Journal of Chromatography* 321: 145–157.
- Mukerjee R, Kim D and Robyt JF (1996) Simplified and improved methylation analysis of saccharides, using a modified procedure and thin-layer chromatography. *Carbohydrate Research* 292: 11–20.
- Robyt JF and Mukerjee R (1994) Separation and quantitative determination of nanogram quantities of maltodextrins and isomaltodextrins by thin-layer chromatography. *Carbohydrate Research* 251: 187–202.
- Su D and Robyt JF (1993) Control of the synthesis of dextran and acceptor-products by *Leuconostoc mesenteroides* B-512FM dextranase. *Carbohydrate Research* 248: 339–348.

CAROTENOID PIGMENTS: SUPERCRITICAL FLUID CHROMATOGRAPHY



V. Sewram, Programme on Mycotoxins and Experimental Carcinogenesis (PROMEC), Medical Research Council, Tygerberg, South Africa
M. W. Raynor, Advanced Technology Center, Matheson Gas Products, Longmont, CO, USA

Copyright © 2000 Academic Press

Introduction

Carotenoids are one of the main classes of natural pigments and are found in a large number of fruits and vegetables (oranges, tomatoes, carrots) and in leaves where their presence is masked by chlorophylls until autumn. They are also found in some animal products (eggs, milk) and seafoods. Typically, carotenoids contain eight isoprenoid units bonded such that the units are reversed at the centre of the molecule. With this arrangement, many carotenoids are symmetrical in nature. The pigmentation of these tetraterpenes is a result of the chromophore created by the series of conjugated double bonds. The structural formula of all carotenoids is derived from that of lycopene, starting with different structural modifications which include hydrogenation, cyclization, oxidation or dehydrogenation. The oxygenated derivatives are known as xanthophylls and bear either the epoxy, carbonyl or hydroxy ester functions on their extremity or terminal ring, while the hydrocarbon carotenoids are referred to as carotenes. The structures of some basic carotenoids are given in **Figure 1**.

Carotenoids have been used for many years in the food industry as colouring material. These compounds also have many biochemical roles, including the important functions of light harvesting and photoprotection in photosynthesis. In humans, the primary use of carotenoids, whether taken as carotenoid-containing food or as dietary supplements, is the prevention or correction of vitamin A deficiency. However individual carotenoids are capable of forming different *cis/trans* geometrical isomers and this in turn is known to affect their biochemistry in certain situations. In fresh plant tissue, all the double bonds have the all-*trans* configuration (most stable structural form); however, isomerization to the *cis* configuration results in a loss of nutritional value. Hence the determination of these isomers is necessary for the quality control of fresh foodstuffs in order to assess the pro-vitamin A activity of foods and for the evaluation of the effects on food-processing on fresh-

ness. Feeding studies have also shown that *cis* isomers of β -carotene have lower pro-vitamin A activities when compared to the all-*trans* form. β -Carotene, besides having the highest pro-vitamin A activity of the carotenoids, has also been reported to have anti-neoplastic activity, perhaps due to their antioxidant and free radical quenching activity, not only at the stage of onset of the disease but also on existing tumours. Hence the importance of the constituents, in terms not only of colour but also nutrition, explains why attempts have been made to characterize and determine these pigments which occur together in mixtures that can be resolved only with the mildest and most selective analytical methods. While the existence of carotenes and xanthophylls was known before 1906, it was not until Tswett developed column chromatography that much was known about the carotenoids. Subsequently, chromatographic methods have improved drastically from countercurrent distribution, gas chromatography (GC), thin-layer chromatography, gravity column chromatography through to high performance liquid chromatography (HPLC).

Recently, a number of studies have been performed involving the separation of carotenoids by either supercritical (SFC) or subcritical fluid chromatography, showing that SFC with carbon dioxide as the mobile phase can provide an alternative to the traditional HPLC methods used. A brief history of the SFC of carotenoids up to the present is summarized in **Table 1**. Supercritical fluids have lower viscosities than liquids and thus solute diffusion coefficients are higher than in conventional solvents. Furthermore, the low critical temperature of some fluids enables many heat-sensitive compounds to be separated without degradation. Manipulation of various parameters such as temperature, pressure, mobile phase, modifiers and stationary-phase type makes complex separations possible. These aspects are considered in more detail in subsequent sections.

Effect of Mobile Phase and Modifiers on Carotene Separations

Supercritical CO₂ has been the most commonly used mobile phase in SFC. It is nontoxic and also has a low critical temperature (31°C), which enables the separation of thermally labile compounds such as carotenoids at low column temperatures. Furthermore, it

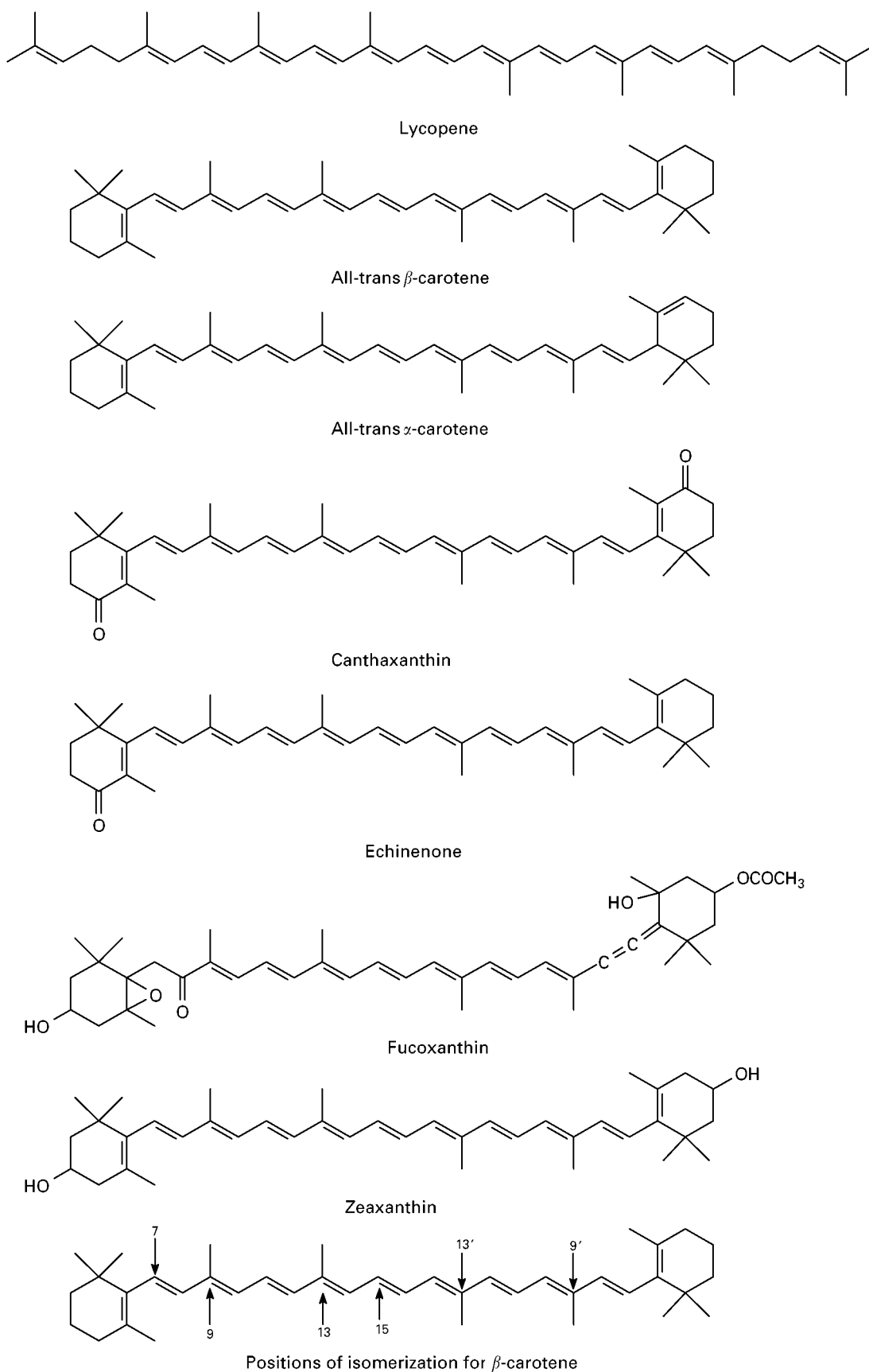


Figure 1 Chemical structures of some basic carotenoids.

Table 1 Advances in SFC of carotenoid pigments

Date	Development
1968	Separation of α - and β -carotene by packed-column SFC (Giddings <i>et al.</i>)
1983	Separation of lycopene and α - and β -carotene (Gere)
1989	Separation of geometrical isomers of α - and β -carotene by open tubular SFC (Schmitz <i>et al.</i>)
1991	Understanding of the effect of temperature, pressure, modifier and stationary-phase type on carotene separations (Lesellier <i>et al.</i> , Aubert <i>et al.</i>)
1994	Investigation of spectral shifts of carotenoids in supercritical CO ₂ (Hui <i>et al.</i>)

is compatible with a wide range of HPLC and GC detectors. Nitrous oxide exhibits a polarity similar to CO₂ but has only received limited use because of its oxidizing properties. Nevertheless, both of these mobile phases have been investigated with β -carotene as a probe molecule. Interestingly, the retentive properties of the polar amino stationary phase for β -carotene are largely affected by the CO₂ and N₂O mobile phases, in comparison to the nonpolar octadecylsilyl stationary phase, which is not appreciably affected by these mobile phases.

In cases where increased solubilizing power is required to elute components of interest, modifiers have been successfully added to the supercritical fluid. The resulting effect is reduced solute retention, improvement of chromatographic efficiency and, in some cases, altered elution order. One of the advantages of supercritical CO₂ is that it is chemically compatible and miscible with a large number of modifiers. The effects of a range of modifiers – methanol, acetonitrile, tetrahydrofuran, dichloromethane and trichlorotrifluoroethane – on the SFC of carotenes have been studied using binary and ternary mixtures with CO₂ containing 3–20% (v/v) of the modifiers. Addition of each of these modifiers produces a concentration-dependent decrease in the capacity factors (k') of the carotenes. The effectiveness of the modifiers has not been directly correlated with their densities nor with their polarities, and this suggests that specific interactions between the solutes and the modifiers are important.

Minimal retention is obtained with the strongest modifier, dichloromethane, which is closest to the dipole–dipole interaction of Snyder's triangle. Furthermore, increasing the dichloromethane concentration in the CO₂ results in an overall decrease in retention of the carotenes and also a decrease in selectivity, probably due to reduced interactions between the solutes and the stationary phase, as all the carotenes have high affinities for this solvent. A plot of $1/k'$ against modifier concentration is linear for

a mixture of tetrahydrofuran–methanol in CO₂ whereas, for more polar modifiers, the line curves slightly downwards due to increased solvent polarity, which indicates that solute–solvent interactions are important. On the other hand, an exponential curve is observed for the nonpolar modifiers, suggesting that the solubility of the carotenes is enhanced by an amount independent of the concentration of the modifier.

The selectivity between the *trans* and *cis* isomers is unaffected by the modifiers, whereas the selectivity between the α - and β -all-*trans* compounds diminishes with increasing percentage of modifier. With a CO₂–methanol–acetonitrile mixture, the selectivity between *trans* and *cis* isomers falls as the proportion of acetonitrile is increased, for both the α - and β -carotenes. This phenomenon has been used to advantage in optimizing the separation of the components of a carrot extract, as shown in Figure 2. With methanol–carbon dioxide, the peaks were not well resolved; however, replacing some of the methanol with acetonitrile allowed an additional component in the extract to be resolved and eluted before all-*trans* α -carotene.

Effect of Stationary Phase Type on Retention and Selectivity of Carotenoids

Both open tubular and packed columns have been employed in the separation of carotenoids. Several β -carotene isomers have been separated on an SB-Cyanopropyl-25 (25% cyanopropyl–75% methylpolysiloxane) stationary phase employing supercritical CO₂ with 1% ethanol as the mobile phase. Separation of the isomers of α -carotene however requires the use of a SB-cyanopropyl-50 (50% cyanopropyl–50% methylpolysiloxane) stationary phase. A mixture of β -carotene, echinenone, canthaxanthin, astacene and fucoxanthin has also been separated on open tubular columns with cross-linked poly(cyanopropyl)methylsiloxane and Carbowax stationary phases. However, the more polar carotenoids did not elute.

One of the problems with immobilized polar stationary phases in open tubular columns is their instability towards higher concentrations of polar modifiers. Consequently, both polar and nonpolar packed columns have been investigated for SFC of carotenoids. The retention mechanism in normal-phase columns is based on the lattice-fluid model where the important property of the mobile phase in β -carotene retention is absorptivity as well as solubilizing power. Elution of carotenoids from normal-phase alumina and silica particles can be compared to that of normal-phase LC; however, the materials are strong

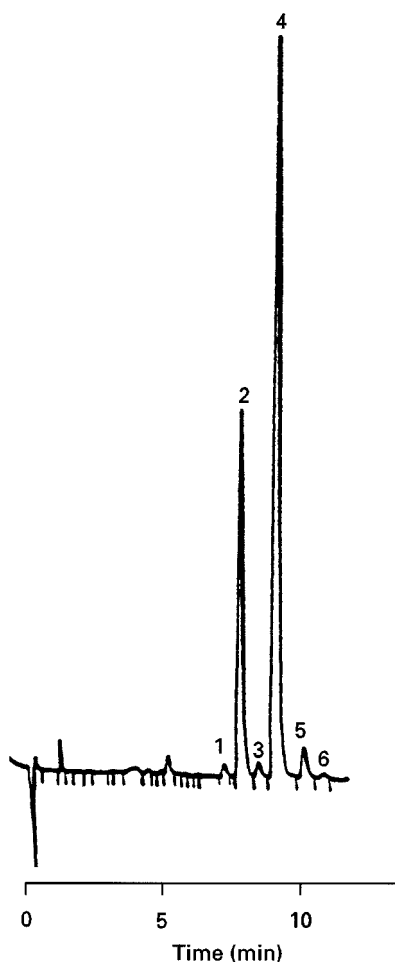


Figure 2 Separation of a carrot extract by supercritical fluid chromatography using an Ultrabase UB 225 column (250×4.6 mm i.d.); mobile phase, CO_2 -methanol-acetonitrile (85 : 0.75 : 14.25, v/v/v); pressure, 15 MPa; temperature, 22°C ; flow rate, 3.0 mL min^{-1} ; detection, 450 nm. Peak identification: 1, γ or ζ -all-*trans*-carotene; 2, all-*trans*- α -carotene; 3, *cis*- α -carotenes; 4, all-*trans*- β -carotene; 5, *cis*- β -carotene; 6, *cis*- β -carotene. Reproduced with permission from Aubert *et al.* (1991).

adsorbents and can prove too adsorptive for CO_2 to elute the more polar analytes. The reversed-phase packings modified with C_8 and C_{18} exhibit dipole-dipole interactions from the surface silanols in addition to the desired dispersion characteristics and have been successfully applied to carotenoid analysis.

The retention of β -carotene on octadecylsilyl (ODS) columns is well correlated to its solubility in the mobile phase. Both the type and the percentage carbon loading of the stationary phase influence the separation of the carotenes by SFC. Among factors that determine the performance of a column, such as the shape and size of the particles, the pore size, the specific surface area and the percentage surface coverage, the kind of function that is bonded to the support is particularly important.

The effect of the stationary phase can be evaluated from overall variations in retention factors or from variations in the extent of separation of different pairs or groups of compounds, such as first, α - and β -carotenes (the isomers not being separated) and second, *cis* and *trans* isomers of β -carotene, or *cis/trans* α - and β -carotenes.

The relationship between the retention factor in SFC and carotene solubility in the mobile phase can be given by the following equations (as long as the same kind of fluid is used as a mobile phase):

$$\ln k^R = \ln \phi + \ln C_{\text{st}}^0 + \frac{(\mu_{\text{ss}}^0 - \mu_{\text{st}}^0)}{RT} - \ln S \quad [1]$$

$$S = a_{\text{m}}^{\text{sat}} C_{\text{m}}^0 \quad [2]$$

where ϕ is the volume ratio of the stationary and mobile phases, C_{st}^0 is the standard (surface or volume) concentration in the stationary phase, μ_{ss}^0 is the chemical potential of the pure solid solute at standard pressure, μ_{st}^0 is the chemical potential of the solute in the stationary phase as it moves toward infinite dilution and standard concentration and pressure, $a_{\text{m}}^{\text{sat}}$ is the activity of the solute at saturation in the solvent and C_{m}^0 is the standard concentration of the solute in the mobile phase. The first, second and third terms on the right-hand side of eqn [1] are constant for a particular column, solute and temperature. If the property of the stationary phase is independent of the nature and pressure of the mobile phase, the solute capacity factor is a function of only the solute solubility in the mobile phase, regardless of the kind of solvent.

The effect of the nature of the stationary phase on carotene retention should be more significant in SFC compared with LC because the interaction between a solute and a supercritical fluid is generally small. In fact, some researchers have reported that solute retention in SFC is sensitive to the properties of the stationary phase. Where the stationary phase is prepared with a monofunctional alkylsilane, there is one-to-one bonding between the reagent and the silanol groups, giving a 'brush-type' structure. Di- and trifunctional silanes can bond to more than one silanol group on the silica support, to give essentially the same type of brush-type stationary phases as monofunctional silanes. However, they can also polymerize in the presence of traces of water. Under suitable conditions, a stationary phase can also be prepared in which each alkylsilane that is bonded to the surface of the silica gives rise to an arborescent-polymeric structure that is not brush-like and differs from column packings in which the support

Table 2 Effect of different stationary phases on the selectivity and resolution of carotene isomers

Column	L (mm)	V ₀	Porosity ε (%)	Type of bonding	t _r α- carotene (min)	k ^R α- carotene	Separation of α- and β-carotenes	Selectivity of trans/cis β-carotene isomers	Resolution of trans/cis β-carotene isomers	Separation of α- and β- carotene trans/cis isomers
Ultrapase UB 225	250	2.463	59	M	11.22	12.58	Yes	> 1	> 1.5	Yes
Spheri-5 ODS-5A	250	2.456	59	P(A)	11.40	12.85	Yes	> 1	> 1.5	Yes
LiChrospher 100 RP 18	250	2.150	68	D	8.35	10.57	Yes	> 1	> 1.5	Yes
LiChrospher 100 PR 18e	250	2.187	70	D	9.60	12.05	Yes	> 1	> 1.5	Yes
Nucleosil C ₁₈	250	2.866	69	P(A)	7.38	6.66	Yes	> 1	> 1.5	Yes
ChromTech CT-Sil C ₁₈	150	1.545	62	—	4.89	8.36	Yes	> 1	> 1.5	Yes
Superspher 100 RP ₁₈	250	2.106	67	D	8.16	8.02	Yes	> 1	> 1.5	Yes
Spherisorb ODS-2	100	1.029	62	P(A)	3.75	9.73	Yes	> 1	> 1.5	Yes
Supelcosil LC-PAH	150	1.768	71	P(A)	2.05	2.37	Yes	> 1	< 1.5	No
Erbasil C ₁₈	150	1.656	66	P(A)	3.60	5.40	Yes	> 1	< 1.5	No
Suplex pKb-100	150	1.623	65	—	2.38	3.27	Yes	> 1	> 1.5	No
Ultracarb 5-ODS 20	150	1.789	72	—	10.32	16.20	Yes	> 1	> 1.5	No
Zorbax ODS	250	2.678	64	M	4.98	4.50	Yes	= 1	< 1.5	No
Ultrasphere ODS	250	2.520	61	M	2.48	1.86	No	= 1	—	No
Vydac 201 HS	150	1.760	70	M	5.43	8.13	No	= 1	—	No
Partisil 5 ODS-3	250	2.803	67	M	7.70	7.17	No	= 1	—	No
μBondapak C ₁₈	300	2.908	70	—	6.29	5.42	No	= 1	—	No
Vydac 210 TP	150	1.680	67	P(A)	1.60	1.73	Yes	> 1	< 1.5	No
Perkin-Elmer HC-ODS/PAH	250	0.327	88	P(A)	1.25	2.05	Yes	> 1	< 1.5	No
Vydac 218 Tp	250	2.898	70	P(A)	3.28	2.32	Yes	> 1	> 1.5	No
Hypersil 15C ₁₈	150	2.635	63	M	7.01	6.90	No	= 1	—	No
Synchrompak SCD-100	150	1.874	75	M	1.68	1.59	Yes	> 1	< 1.5	No

M, monofunctional C₁₈ groups; D, difunctional C₁₈ groups; P(A), arborescent-polymeric C₁₈ groups; — exact nature unknown.

itself is polymeric. Arborescent-polymeric C₁₈-bonded stationary phases appear to be particularly suitable for separating closely related compounds that differ in the degree of planarity of their structures and have successfully been applied to SFC separation of *cis* and *trans* α- and β-carotenes. Table 2 lists the different columns that have been evaluated for their separating capabilities of the different classes of carotenes. Particular attention should be paid to the estimation of the retention (R) factor (*k'*) for the analytes because this parameter characterizes the stationary phase independently of factors such as size and porosity of the column. It has been found that on arborescent-polymeric columns, the separation of α- and β-carotenes is incomplete if the retention (R) factor for α-carotene is below 6. One also needs to be aware that, unlike a polar stationary phase, an ODS stationary phase is not appreciably affected by the nature of the mobile phase and that β-carotene, being much larger than the alkyl chains grafted on the silica surface, is less affected by the residual silanol groups on the silica surfaces.

Effect of Temperature and Pressure on Carotenoid Separations

The solubility of a substance in a supercritical fluid is the sum of two factors: the volatility of the substance (which is a function of temperature) and the solvating effect of the supercritical fluid (which is a function of fluid density). Hence, solubility is controlled experimentally by selecting appropriate temperatures and pressures which are important for controlling retention in SFC. These parameters influence the solvating power, efficiency and selectivity. At constant pressure, an increase in temperature decreases the density and consequently the solvating power. The temperature also influences the diffusion coefficients of the solutes in the supercritical fluid. With increasing temperature, diffusion coefficients increase and higher chromatographic efficiency results. However, one needs to exercise caution in this regard as carotenoids are thermally labile and will decompose at high temperatures. With pure carbon dioxide, the capacity factor (*k^R*) increases in proportion to the temperature

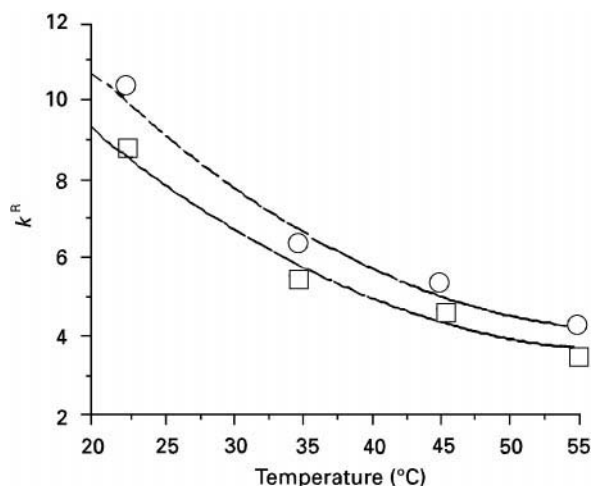


Figure 3 Dependence of k^R values of carotenoids on temperature at constant pressure (25 MPa). Column, Spheri-5 ODS-5A; mobile phase, CO₂-methanol (80 : 20 v/v); flow rate, 3.0 mL min⁻¹; detection, 450 nm. Squares, all-*trans* α -carotene; circles, all-*trans* β -carotene. Reproduced with permission from Aubert *et al.* (1991).

(at constant pressure) and can be explained by the resulting decrease in the density of the mobile phase. On the other hand, as shown in Figure 3, when the carotenoids are eluted with carbon dioxide containing 12% methanol, k^R decreases with increasing temperature between 22 and 55°C, while the resolution between the all-*trans* α - and β -carotenoids decreases as the temperature is increased. Although the optimum temperature for this separation is between 22 and 25°C, and the mobile phase is therefore subcritical, this is of little consequence because there is no discontinuity in the physical properties of the fluid at the critical point.

At constant temperature, an increase in pressure produces an increase in density. Increasing the pressure increases the mobile-phase viscosity, thus decreasing the mass transfer term C and the diffusion coefficient. In SFC, density (or pressure programming) is the primary method for developing separation. It is analogous to temperature programming in GC, and eluent composition programming in LC. Increasing the pressure at constant temperature leads to decreased capacity factors, which can be explained by the enhanced solubility of the solutes with increasing density of the mobile phase. Figure 4 illustrates the dependence of k^R values of carotenoids on pressure at constant temperature. In this work, the pressure was varied between 100 and 250 bar, at 22°C and the capacity factors were observed to decrease less rapidly at pressures above 200 bar. This is probably due to the nonlinearity of the P - T curve of carbon dioxide, which at 22°C becomes less compressible. In practice, it is preferable to avoid working at pressures

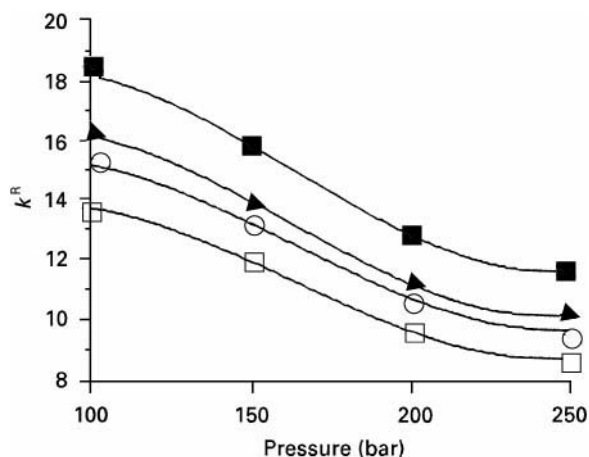


Figure 4 Dependence of k^R values of carotenoids on pressure (P) at constant temperature (22°C). Column, Spheri-5 ODS-5A; mobile phase, CO₂-methanol (80 : 20 v/v); flow rate, 3.0 mL min⁻¹; detection, 450 nm. Open squares, all-*trans* α -carotene; circles, *cis* α -carotenoids; triangles, all-*trans* β -carotene; filled squares, *cis* β -carotenoids. Reproduced with permission from Aubert *et al.* (1991).

where the fluid is very compressible, as the pressure drop along the column is associated with a density gradient and reduced efficiency.

Detectors in SFC with Reference to Carotenoid Analysis

SFC is compatible with a wide range of detection methods. The two basic types of detectors are the ionization detectors and optical detectors. Most commercial open tubular SFC systems provide a flame ionization detector (FID) as standard and it is therefore the most widely used detector for carotenoids. However, detection of carotenoids in supercritical fluids following chromatographic separation has also been achieved using mass spectrometry (MS) and UV/Vis detectors. SFC-MS provides detailed information on the molecular structure of eluted carotenoids and greatly aids peak identifications. Due to the thermal instability of these compounds, 'soft' chemical ionization is recommended. Use of methane as the chemical ionization reagent gas and a low source temperature of 100–120°C results in minimal fragmentation, even for thermally labile carotenoids. For more routine analysis, online UV-Vis monitoring (especially using photodiode array detection) is now the standard procedure for the analysis of carotenoids by HPLC and is the preferred detection system for the SFC analysis of carotenoids, with a number of high pressure, temperature-regulated flow cells being available. The effects of pressure and temperature on the absorption spectra of carotenoids dissolved in supercritical carbon dioxide are discussed in the following section.

Behaviour of Electronic Absorption Spectra in Supercritical CO₂

When using UV-Vis detection for SFC of carotenoids, attention must be paid to spectral shifts that occur in supercritical fluids, in comparison to those measured in liquid solvents. This is particularly relevant as the effect can influence qualitative and quantitative results. The shape of the absorption spectra of all-*trans*- β -carotene, 15-*cis*- β -carotene and the xanthophylls, zeaxanthin, cathaxanthin and astaxanthin, which are nonacidic oxygen derivatives of the carotenes, are similar in both supercritical CO₂ and hexane. The λ_{\max} of the five carotenoids however shifts to a shorter wavelength (hypsochromic shift) in supercritical CO₂. Figure 5 shows the absorption spectra of all-*trans*- β -carotene in supercritical CO₂ and in hexane. Table 3 lists the maximum absorbance wavelength of the selected carotenoids in supercritical CO₂ and in hexane. Due to the relatively low solubilities of the xanthophylls in supercritical CO₂ below 5000 psi pressure, comparison of the spectra has been carried out at 6000 psi and 35°C. While solvent-induced shifts of the visible (¹Bu⁺) spectra of carotenoids in a range of polar and nonpolar organic solvents commonly used for HPLC are well established, changes in the supercritical CO₂ density have also been observed to shift the λ_{\max} . Density is related to both pressure and temperature, hence a change in either of the two variables is known to affect the absorption maxima of carotenoids. An increase in pressure increases the visible λ_{\max} of all-*trans*- β -carotene. Over the pressure range of 1500–6000 psi (at a constant temperature of 35°C), the position of this λ_{\max} shifts 7.0 nm to longer wavelength (430.0 to 437.0 nm) in a nonlinear manner.

The effect of variation in temperature on λ_{\max} has also been assessed in the range 25–50°C at a constant

Table 3 The maximum absorbance wavelength of carotenoids in hexane and in supercritical CO₂ (6000 psi at 35°C)

Carotenoid	λ_{\max} (nm)	
	Hexane	CO ₂
All- <i>trans</i> - β -carotene	450.0	437.0
Lycopene	472.0	456.0
Astaxanthin	474.0	453.0
Canthaxanthin	464.0	452.0
Zeaxanthin	448.0	436.0

pressure of 3000 psi and over this range only a 2.0 nm shift is observed. Thus, changes to both pressure and temperature can induce shifts in the (¹Bu⁺) λ_{\max} of all-*trans*- β -carotene in supercritical CO₂, although the former is much more significant. In addition to the main absorption peak in the visible region, *cis*-isomers of carotenoids exhibit a peak in the UV region, termed the *cis*-peak, which originates from the ¹Ag⁺ transition. The electronic absorption spectrum of 15-*cis*- β -carotene in supercritical CO₂ shows a clear *cis*-peak in the region 250–350 nm. Unlike the behaviour of the main λ_{\max} in the visible region, the position of the *cis*-peak maxima does not alter as a function of temperature and pressure, but remains fixed, suggesting that the energies of the ¹Bu⁺ and ¹Ag⁺ states of carotenoids may not respond in the same manner to alternations in density.

Future Developments

As SFC continues to evolve, it will probably be increasingly applied to carotenoid analysis, particularly in view of the thermal instability of these compounds. Development of more selective stationary phases and application of micro-packed columns for SFC are key areas where improvements are likely. Micro-packed columns with internal diameters of 200–400 μ m offer increased efficiencies, shorter run times and increased ease of interfacing with ionization detectors. Further, mobile phases such as the fluoro-carbons have shown potential in similar applications and are therefore likely to be investigated for SFC of carotenoids.

Further Reading

Aubert M-C, Lee CR, Krstulovic AM *et al.* (1991) Separation of *trans/cis*- α - and β -carotenes by supercritical fluid chromatography. (I) Effects of temperature, pressure and organic modifiers on the retention of carotenes. *Journal of Chromatography* 557: 47.

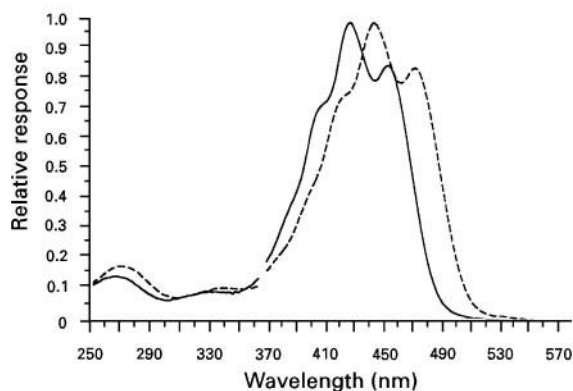
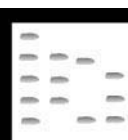


Figure 5 Absorption spectra of all-*trans*- β -carotene in supercritical CO₂ (continuous line) and in hexane (dashed line). Supercritical conditions: mobile-phase CO₂, temperature 35°C, pressure 3000 psi. Reproduced with permission from Hui *et al.* (1994).

- Giddings JC, McLaren L and Myers MN (1968) Dense-gas chromatography of nonvolatile substances of high molecular weight. *Science* 159: 197.
- Hui B, Young AJ, Booth LA *et al.* (1994) Detection of carotenoids on supercritical fluid chromatography (SFC). A preliminary investigation on the spectral shifts of carotenoids in supercritical carbon dioxide. *Chromatographia* 39: 549.
- Lesellier E, Tchaplal A, Péchard M-R *et al.* (1991) Separation of *trans/cis* α - and β -carotenes by supercritical fluid chromatography. (II) Effect of the type of octadecyl-bonded stationary phase on retention and selectivity of carotenes. *Journal of Chromatography* 557: 59.
- Lesellier E, Tchaplal A, Marty C and Lebert A (1993) Analysis of carotenoids by high-performance liquid chromatography and supercritical fluid chromatography. *Journal of Chromatography* 633: 9.
- O'Neil C and Schwartz SJ (1992) Chromatographic analysis of *cis/trans* carotenoid isomers. *Journal of Chromatography* 624: 235.
- Sakaki K, Shinbo T and Kawamura M (1994) Retention behaviour of β -carotene on polar and nonpolar stationary phases in supercritical fluid chromatography. *Journal of Chromatographic Science* 32: 172.
- Schmitz HH, Artz WE, Poor CL *et al.* (1989) High-performance liquid chromatography and capillary supercritical fluid chromatography separation of vegetable carotenoids and carotenoid isomers. *Journal of Chromatography* 479: 261.
- Tee E-S and Lim C-L (1991) The analysis of carotenoids and retinoids: a review. *Food Chemistry* 41: 147.

CATALYST STUDIES: CHROMATOGRAPHY



B. Mile, Llandaff, Cardiff, Wales, UK

Copyright © 2000 Academic Press

Introduction

Catalysis is a branch of chemical kinetics of great industrial and commercial importance. Heterogeneous catalysts are certain particulate solids of high surface area ($1\text{--}300\text{ m}^2\text{ g}^{-1}$) that increase the rates of attaining equilibria. This is achieved by the temporary attachment of reactant molecules by moderate chemical bonds to active sites on their surfaces. Catalysts themselves are not consumed during the process, although their activity is eventually lost by surface degradation. Over 90% of the world's manufactured chemicals involve catalysis at one or more stages. The market is about $\text{£}7 \times 10^9$ per annum, with £200 return on each pound spent on a catalyst.

Background to Heterogeneous Catalysis and Contributions from Gas Chromatography

The invention of gas chromatography (GC) in 1952 and its development since then have been widely reviewed. Before looking at the applications of GC to catalysis, it is necessary to summarize the major stages in the concepts of catalysis and the often independent technological achievements of industrial

scientists and engineers. Tables 1 and 2, respectively, contain the important concepts and terms and the major technical advances in catalysis.

Catalysis has a much longer history than GC – indeed life itself may originate from the catalysed conversion of the primitive atmosphere into bioorganic molecules on the surfaces of clay minerals. The ancients used enzymatic catalysts unknowingly in fermentation to make wine and vinegar. It is salutary that these natural catalysts far outperform any of our synthetic catalysts at ambient pressures and temperatures. Silver, regarded for at least three millennia as having preservative and curative powers and long used for storing wines and wound treatments, has now re-emerged in the sterile surface coating, Amenitrop, whose active antibacterial and antiviral ingredients are silver thiosulfate complexes.

In catalysis empirical technology and industrial innovation have almost always outpaced scientific theory and understanding, but this is less so today; exceptions include the Haber process for ammonia production. Nevertheless, it has always been true that basic studies provide the intellectual framework and accelerate technical developments, i.e. they 'catalyse' progress!

The scientific study of catalysis started soon after the beginnings of chemistry and at the time when phlogiston theory still held some sway. In 1835 Berzelius coined the term 'catalysis' (which is Greek for *to loosen*) after realizing that research findings in the first decades of the nineteenth century demonstrated

Table 1 Terms and characteristics used in catalysis

Term	Characteristics
Heterogeneous catalysts	Large surface area solids that accelerate the rate of attaining equilibrium; they are themselves chemically unchanged by the reaction and therefore do not affect the final equilibrium yields
Active sites	Those unique sites on the surface where the catalytic event takes place. They are usually the steps, edges and kinks of the flat unreactive terraces, and often represent only a few percent of the total surface atoms. Interestingly, catalysis is chemistry at imperfections and discontinuities.
Specific activity	Rate of reaction per unit area of catalyst under standard reactant concentrations. Activity is sometimes defined empirically by the temperature needed for a reaction to reach an arbitrary rate of conversion.
Turnover frequency (TOF)	Number of product molecules formed per second per active site (10^{-2} to 10^2 s $^{-1}$ for synthetic catalysts, compared with 10^3 to 10^7 for enzymes).
Structure sensitive/insensitive reactions	Rate dependent on particle size and crystal face/rate invariant to size and face.
Selectivity	The fraction of reacted molecules converted to a desired product
Durability	How long the catalyst remains active

the accelerating effects of small amounts of materials that themselves were chemically unchanged by the reaction. He is sometimes erroneously quoted as suggesting an almost occult catalytic force, whereas in fact he clearly stated the new 'force' is 'a manifestation of the electrochemical affinities of matter' Michael Faraday had a clear concept of catalysis in 1834 even before Berzelius' presentation of the term to the Swedish Academy of Sciences. It is tempting to associate the discovery of catalysts with the alchemists vain search for the philosopher's stone to transmute base metals into gold; in some respects the traces of 'catalyst stone', which transform 'useless' raw materials into useful products, are more valuable than a stone for making ornamental gold. The appellation 'black art' still lingers, perhaps with some justification, since most industrial catalysts are still formulated by recipes that are incompletely understood and retain an aura of mystery.

The burgeoning nineteenth century chemical industry quickly appreciated the utility and exploitability of catalysts and the lead chamber and contact processes developed rapidly, as did the hydrogenated hardening of vegetable oils and the synthesis of indigo. Perhaps the most important catalyst ever developed, because it averted world famine, was that for the high pressure synthesis of ammonia by Fritz Haber in 1909, and its commercialization by Badische Aniline and Sodafabrik. The technical development of the iron catalyst, which remains largely unchanged, exemplifies the rewards of painstaking research, a full appreciation of thermodynamics and the courage to build large scale industrial plants operating at the then unprecedented pressure of 300 atmos-

pheres at 450°C. The process is a *tour de force* of chemical engineering linked with outstanding science.

The molecular understanding of catalysis really begins in the twentieth century, as have the majority of the catalysts and processes now in use. This is especially true of the petroleum and petrochemical industry, which in the 1960s and 1970s had annual growth rates of 15%. The outstanding development in the interwar years was the Houdry process for the catalytic cracking of heavy petroleum fractions into volatile gasoline components (C₂–C₁₃). The immediate postwar period saw developments such as: (1) platforming catalysts for upgrading gasoline research octane numbers (RONs) by isomerization of straight into branched alkanes and the dehydrogenation of cyclohexanes to aromatics; and (2) steam reforming of methane, naphtha and fuel oil feedstocks into synthesis gas, a carbon monoxide/hydrogen mixture important for ammonia and methane production. The recent development of vehicle exhaust catalytic converters based on rhodium-promoted platinum–alumina for converting carbon monoxide, nitrogen oxides and unburnt hydrocarbons into harmless products is a remarkable achievement for catalysis science, especially in view of the varying gas compositions and temperatures that have to be sustained.

The realization by Langmuir that catalysis involved short-range chemical bonds, which dictated that reactions occurred in surface monolayers, and Taylor's suggestion that catalysis occurred only at unique active sites, together with the discovery of the importance of atomic clusters with specific geometric arrangements by Balandin, were seminal to the growing

Table 2 Important stages and concepts in heterogeneous catalysis

Date	Event
The beginning!	Life originates on the surfaces of clay minerals
Prehistory	Enzymes for making wine and vinegar, sterile silver
1834/1835	Berzelius coins the term catalysis Faraday appreciates the occurrence of catalysis
1830–80	Industrial: H ₂ SO ₄ by lead chamber, contact catalysts; synthetic dyes by mercury catalysis; hardening of oils
1900	Start of modern kinetics by Bodenstein and Ostwald
1900–14	Gasification of coal; syn-gas manufacture
1909	Haber's catalytic synthesis of ammonia
1918	Langmuir's monolayer and Rideal Ely mechanisms
1920s →	Petroleum industry: continuous processing; catalytic cracking; platforming catalysts
1923	Fischer–Tropsch hydrocarbons from syn-gas
1925	Taylor proposes catalysis occurs only at active sites
1925–36	Houdry catalytic cracking process to increase octane number of gasoline
1929	Balandin's proposal of catalysis on multiplet sites
1938	Brunauer–Emmet–Teller (BET) adsorption isotherm
1939–45	Synthetic substitutes for natural products like rubber
1941	Use of oriented metal films by Beeck and Schwab
1941	Fluidized-bed technology
1950–1970s	Explosive growth of the petrochemical industry
1952	Gas chromatography introduced
1955	Zeigler Natta stereoregular polymerization catalysts
1955	Sasol gasification of coal in South Africa
1956	Gas chromatographic reactors introduced
1960	Steam reforming of methane and naphtha to synthesize gas for ammonia and methanol manufacture
1964	Oxychlorination to make vinyl chloride monomer
1965	Microcatalytic chromatographic reactor introduced
1965	Sohio process for acrylonitrile and acrylic acid
1970 →	Surface science studies of surface–substrate intermediates and surface atom arrangements and restructuring
1976 →	Catalytic converters for exhausts emission control
1985 → 1990s	Control of and blending of refinery streams by GC Improvements in exhaust catalytic converters Development of catalytic power generators Hygiene catalysts: sterile coatings, oven cleaning ICI Hydcat process for hypochlorite removal from waste streams Immobilized enzymes – pharmaceutical production Zeolites and aluminium phosphate (ALPO) catalysts developed

detailed understanding, as were the applications of the absolute theory of reaction rates.

Outline of Conventional GC in Catalysis Research

Since many of the developments in catalysis listed in Table 2 predate the invention of GC in 1952, its contributions have inevitably been since then. However, all the important characteristics of catalysts defined in Table 1 require analysis of complex gas mixtures. Thus inevitably the use of this powerful analytical technique in catalyst research is now endemic and pervasive; so much so that it is now used almost routinely in catalyst laboratories and on catalyst testing rigs. It is the technique *sine qua non* for multicomponent analysis, especially when allied to mass spectrometry and spectroscopic methods. It has revolutionized the analysis of complex volatiles in the same way that liquid and paper chromatography have caused a sea change in the analysis of complex involatile bioorganic molecules. It has replaced previous tedious and time-consuming methods such as fractional distillation, which have largely been abandoned since its advent (but see later for a discussion of the online infrared methods now in an advanced state of development). The complex nature of catalysis product streams is illustrated by the chromatograph of a gasoline in Figure 1.

The acceleration of reaction rates by catalysts arises because of the lowering of the energy barriers through the formation of surface compounds. The energy released by the making of surface bonds facilitates the scission or rearrangement of bonds in the substrate molecule, as depicted in Figure 2. The surface bonds must be of intermediate strength; if they are too strong permanent bonding to the surface occurs, and if they are too weak the perturbations are too small. This gives rise to an optimum value of the enthalpy of formation of the surface intermediate and the so-called 'volcano' plots when catalyst activity is plotted against bond enthalpy.

GC cannot give direct information about these crucial surface intermediates, although ingenious experiments using radiolabelling experiments and normal kinetic analysis and numerical modelling can lead to information about their nature. Major advances in surface spectroscopic techniques have occurred since the 1960s allow the observation and quantitation of minuscule amounts (10^{-3} monolayers) of stable and metastable surface species.

However, there has sometimes been a short-sighted overemphasis of the results of these powerful and expensive techniques and a neglect of those from cheaper methods of final product analysis such as GC.

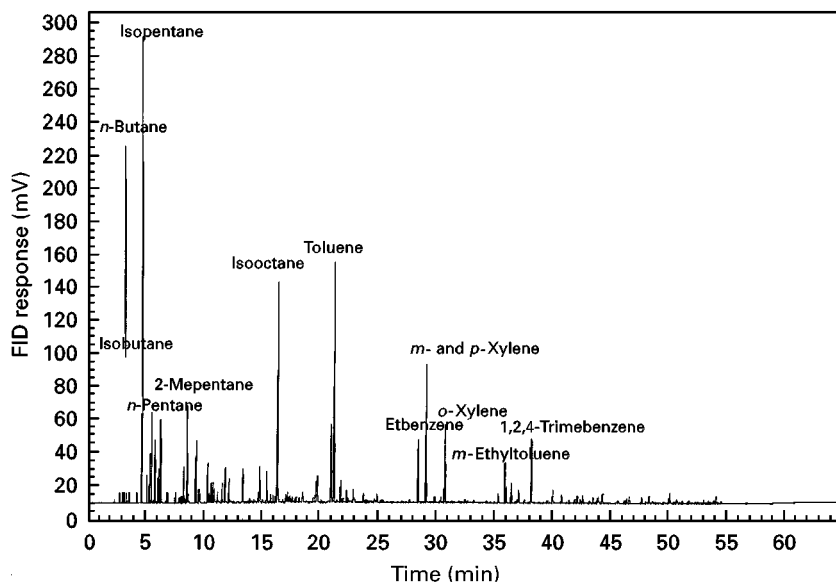


Figure 1 Chromatogram of a gasoline fraction (courtesy of Dr R. Malpas, Shell Research Ltd, Thornton Research and Technology, Centre).

There is the danger that the moieties seen by surface spectroscopies are mere spectators and not the active participants. Prudent researchers interlink surface science results with those from stable final product time profiles and conventional rate studies on the same catalyst. This problem has been highlighted in an elegant demonstration that the rates of ethene hydrogenation were invariant to the levels of the much studied surface ethylidenes. This underlines the essential importance of stable product analytical methods in catalyst research and evaluation. These are integral components for the study of catalysis in

the multifarious reactor types in use, namely: batch, continuous stirred tank slurry, fixed and fluid bed, trickle bed, catalytic gauze and spinning basket.

The high sensitivity of GC (detection limits of 0.1 to 1 ppm) enables very low conversions to be studied. This reduces the problems of poisoning by products of secondary reactions. GC is used routinely and extensively in laboratory research to find new catalysts and processes for existing and new products. It is also used in all the scale-up stages to full plant operation. The output of the plant is constantly monitored by GC and other methods of analysis and the results used to trim operating conditions to meet product specifications when there are changes in feedstock composition, flow rates, and reactor temperatures and pressures.

Conventional reactor studies can be readily automated by using multiple sample loop valves activated by signals from minicomputers, which also acquire and process the compositional data and GC conditions in digital modes. A semiautomatic pulsed small reactor system with a simple timing device for sampling at prescribed times and early data acquisition and processing methods was described as early as 1960.

A commercial laboratory rig incorporating GC is now marketed for catalytic studies at pressures of several hundred atmospheres and temperatures up to 350°C (Chemical Data Systems, Pittsburgh, USA). The pulse of products from the high pressure micro-reactor is depressurized in a multiple loop valve so that its pressure is compatible with that of the carrier gas stream into which it is injected. The unit is

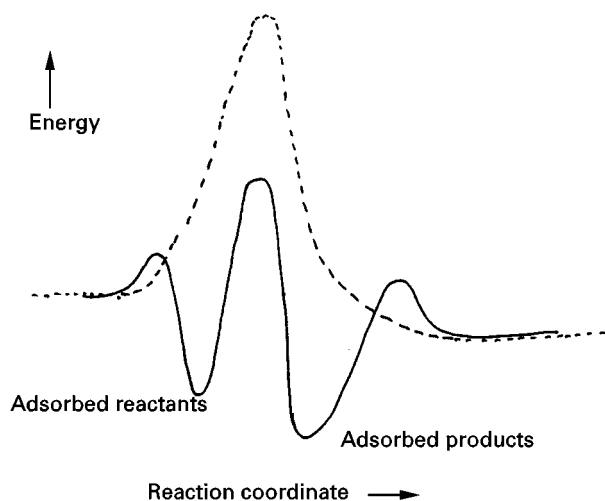


Figure 2 Energy diagram for a reaction occurring homogeneously and heterogeneously.

semiautomatic and data acquisition, processing and control is by a personal computer (PC).

The very ease of using GC routinely often means that the technique is not mentioned in the title of research papers in the open literature, in much the same way that the use of NMR is often assumed and not noted in papers on synthetic organic chemistry. Perusal of recent issues of journals such as the *Journal of Catalysis* and the *Journal of Applied Catalysis* indicate that about 40% have used GC for product analysis, while a BIDS search of the years 1991–97 shows the linking of GC with catalysis in about 90 papers each year.

It is worth emphasizing that process improvement is more common than purposeful or serendipitous invention and discovery. This is because large companies prefer to expand and advance by steady or even marginal changes associated with low risk rather than to initiate new high risk processes requiring large capital investment and many years of negative cash flows and long payback periods. An example is hydrocracking, which was not considered worthwhile by most of the oil companies until Chevron (California, USA) brought the first hydrocracking plant on stream in the mid-1960s – competition is as much the mother of invention as necessity! The scale of operations provides the motivation for marginal improvements; a catalyst that increases the yields of a product by 1% can earn £1 million per annum if product turnover is £100 million p.a. It is in such marginal improvements that GC can prove so valuable because of the ease of measuring such small changes in product yields.

GC has played a role in the development of devices to protect the environment from the complex chemical wastes from the chemical semiconductor and electroplating industries. It was used in the development of the remarkable ‘three-way’ catalytic converter fitted into motor vehicle exhausts. The simultaneous oxidation of carbon monoxide and unburnt hydrocarbons alongside the reduction of nitric oxide in the same catalyst bed exposed to widely different exhaust compositions and temperatures from ambient to 1000°C is a major chemical and engineering achievement. Even the humble kitchen stove has been rendered self-cleaning by incorporating manganese dioxide/zeolites/ferrites into its glass enamel coatings. The application of catalysis and GC in environmental protection is increasing in importance.

Microcatalytic Chromatographic Technique

The microreactor is probably the most direct link between GC and catalysis and has been widely used

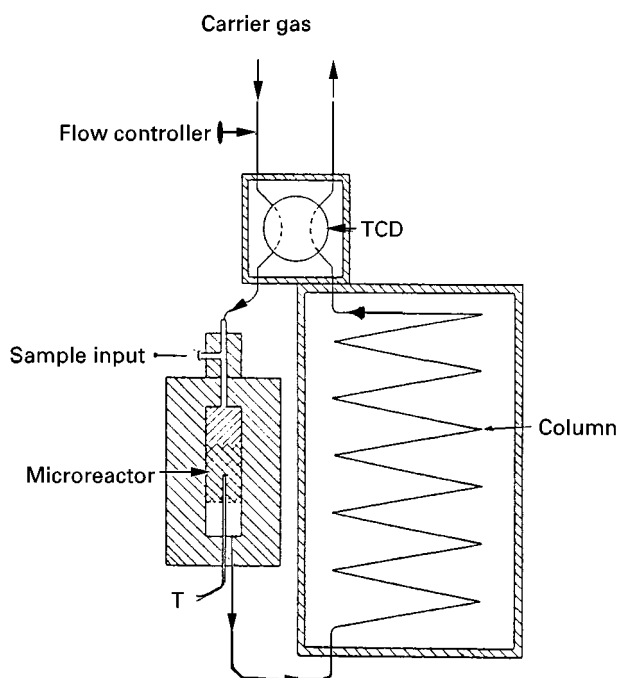


Figure 3 Schematic of a microcatalytic chromatographic reactor. TCD, thermal conductivity detector.

for catalyst research since it was first described in 1955. A schematic of the system is shown in **Figure 3**. The principle of this ‘one shot’ technique is simple. A small catalytic reactor is placed as near as possible to the entrance of a GC column. Small pulses of reactant are injected into an inert or reactive carrier gas stream just before the reactor. Reaction takes place in the catalyst bed and the unconverted reactant pulse together with volatile products are swept into the GC column where the components are separated in the usual way and then detected by a rapid response microthermal conductivity detector. A useful adjunct, employed even in the earliest studies, is to place a Geiger detector in the exit stream from the thermal conductivity detector so that the radioactivity of each peak can be determined. This extends the method to include tracer experiments using ^{14}C - and tritium-labelled compounds. The advantages and disadvantages of the microreactor are listed below.

Advantages

1. Rapid surveys of new or modified catalyst are possible, enabling rapid assessment of whether the changes in catalyst formulations have been beneficial or detrimental (but see item 6 below). The rate of acquisition of results ultimately depends on the speed of analysis; because of its relatively slow speed, the interval between successive pulses can be tens of minutes in packed columns but less

in the high speed wall coated open-tubular columns (WOTC) now available.

2. The high sensitivity of GC enables very small reactant pulses to be used with a consequent reduction in the risk of poisoning active sites by trace impurities.
3. Radioactive tracer experiments are straightforward, enabling the path of individual reaction sites in reactant molecules to be tracked into the product molecules.
4. By careful analysis of the changes in product yields with changes in flow rate (contact time) and sample size, the rate expression of the reaction can be established and rate constants and Arrhenius parameters estimated (but see Disadvantage 2).
5. The technique is particularly well suited for kinetic isotope experiments. Alternate pulses of a deuterated and protonated reactant can be injected into the microreactor so that their reactions are compared on exactly the same catalyst sample under identical conditions. Very accurate measures of primary and secondary kinetic isotope effects (the ratio k_D/k_H) can be obtained and subtle mechanistic detail unravelled.
6. Poisoning effects can sometimes be monitored if the activity of the catalyst is found to diminish with successive pulses, an aspect that can be enhanced by using longer contact times or larger pulses.
7. The developments in data acquisition, storage and processing, coupled together with the use of highly reproducible and readily automated loop sampling valves, benefit and facilitate the use of the microcatalytic reactor for mechanistic and kinetic studies and for catalyst screening.

Disadvantages

1. Steady-state conditions are often not achieved in the short contact times used in microreactors. This can be useful for kinetic studies, but is a disadvantage for screening tests of a new catalyst or a new formulation since the catalyst will usually operate commercially in a continuous flow configuration, where steady-state or pseudo steady-state conditions prevail.
2. Accurate measures of the residence time of the reactant pulse in the catalyst bed are essential for reliable kinetic measurements. The time cannot be calculated simply from the outlet gas volumetric flow rate and the bed volume because of the considerable pressure drop between the reactor and the end of the GC column, which varies with flow rate. The corrected residence time t_r is determined from the following equation derived by application of the gas laws to the exiting carrier gas flow

rate:

$$t_r = \frac{2aL}{3V_0} \frac{P_r T_0}{P_0 T_r} \frac{(P_i/P_r)^{3/2} - 1}{(P_i/P_r)^2 - 1}$$

where L is the reactor length and a its cross-section; V_0 , P_0 and T_0 are the volume flow rate, pressure and temperature at the end of the GC column; P_i and P_r are the pressures at the inlet and outlet of the reactor.

Nonlinear first-order plots result if the uncorrected residence time is used, whereas excellent linearity is obtained by using corrected residence times.

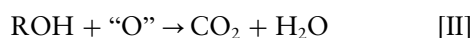
3. If the carrier gas is itself a reactant, its depletion in the gas pulse leaving the reactor can result in artefacts because of changes in detector sensitivity when the pulse components pass through the detector. This can be avoided by split stream techniques. In microreactor studies of the dehydrochlorination of 1,2-dichloroethane, air was used as the carrier gas to eliminate the build-up of carbonaceous poisons when inert carrier gases were used. The problem of different amounts of oxygen feeding into the flame ionization detector (FID) flame at different flow rates was overcome by splitting the stream leaving the GC column, so that the air supply to the flame could be held constant by venting different amounts of excess air through a control valve in the column exit stream. Peak broadening and overlapping occurs in the catalyst bed and in the dead volume between the end of the reactor and the beginning of the GC column, leading inevitably to some loss of resolution.
4. The data obtained are inherently integral despite the small contact times used, so that the technique is not readily adapted to give differential reaction kinetics.
5. Most catalyst laboratories will probably use microcatalytic chromatographic reactors in the near to medium-term future, especially since high speed numerical computer methods are now available to model the differential equations of flow and reaction in these reactors. These results place rigorous and stringent tests on the reaction mechanisms proposed and reliable estimates of rate parameters for some of the rate-determining steps can result. These numerical modelling techniques are much better than the use of the approximate though complicated rate expressions, which contain functions of many rate parameters often conjoined and requiring much ingenuity and chemical intuition to untwine. However, the necessity for intricate valving, pressure and temperature corrections, and computer control and data acquisition

and processing, leads to a loss of the essential simplicity of the microreactor technique. These elaborations may lead researchers into using conventional catalytic reactors with proscribed switching of the reacted gas streams into multi-loop sampling valves linked to GC and GC-MS analysers.

Chromatographic Catalytic Reactors (CCR): the Use of Fluid Logic Modules

A GC catalytic reactor deliberately combines the chromatographic separation of components with a catalytic function in the same reactor bed. The technique, first described in 1956, is a variant of the microcatalytic reactor just discussed. The reactor, in conjunction with pulse techniques, can be used for yield enhancement by displacing equilibria and for preserving primary products from secondary reactions with one of the reactants. The yields of primary products from a conventional catalytic reactor are ultimately limited, either thermodynamically through the value of the equilibrium constant, or kinetically by consumption of primary products, which often react more rapidly with one of the reactants, such as oxygen, than does the other reactant, such as an alkene or alkane. Both these limitations can be avoided in a chromatographic catalytic reactor (CCR). The equilibrium limitation arises because the catalyst accelerates the second-order back-reactions as much as it does the forward reaction. The back-reactions may be minimized by chromatographically separating the products from each other. **Figure 4** illustrate the case for the simple equilibrium, $A = B + C$. The back-reaction can only occur in the initial regions of the column where there is overlap between the B and C peaks. If the bed is long enough, then complete conversion of A into B and C is possible. The laws of thermodynamics are not broken because the equilibrium limitation is circumvented by an energy input to

maintain the gas flow and peak separation. By CCR it has been possible to achieve virtually complete dehydrogenation of cyclohexane to benzene at temperatures where the equilibrium constant was $10^{-3} \text{ mol L}^{-1}$. The yields of useful primary products such as alcohols and epoxides are often low because of their rapid secondary reactions. The secondary reactions can be reduced chromatographically by holding back the primary product on the catalyst surface while the reactant pulse rapidly sweeps down the column because of its lower retention. **Figure 5** illustrates the simplified situation for the reaction sequence given below:



The occurrence of reaction [II] can be reduced by rapid separation of the reactant pulse containing oxygen from the ROH formed and retained in the catalytic chromatographic column. By using a silica-supported silver oxide CCR, large quantities of crotonaldehyde have been preserved in the catalytic oxidation of but-1-ene. The lifting of both the thermodynamic and kinetic limitations is enhanced by using narrow injected pulses. Injectors based on fluid logic modules, which have no moving parts and none of the intrinsic delays of actuating the opening and closing of solenoid valves, are ideal for this task and have previously been used for fast GC analysis. Pulses down to 10 ms have been generated and further reductions are possible.

Process Monitoring and Control

The wealth of detail given by GC about the composition of streams leaving reactors and purification units such as distillation columns can, in principle, be used for manual, semiautomatic or fully automatic process

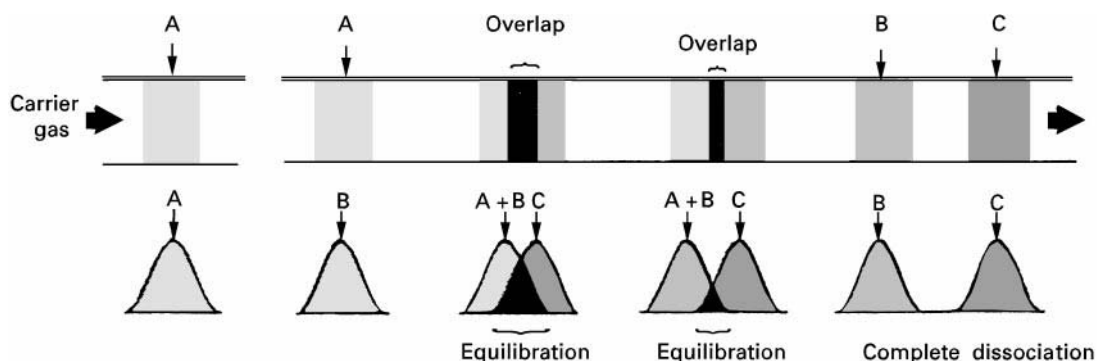


Figure 4 Illustration of how the equilibrium, $A \rightarrow B + C$, is displaced in a GCC reactor.

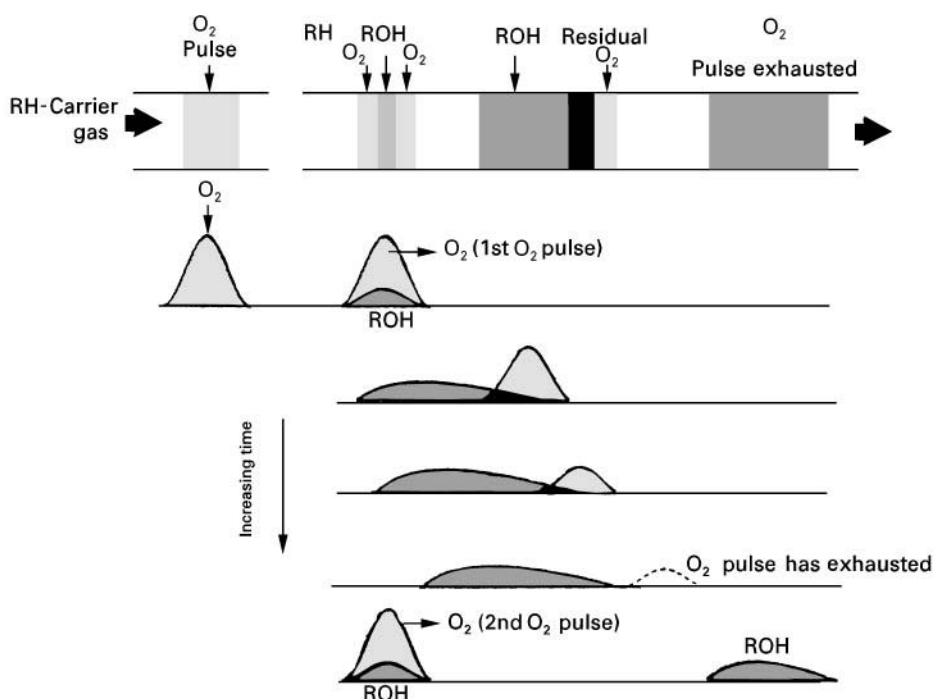


Figure 5 Illustration of how a primary product, ROH, is preserved from secondary reactions with oxygen in a GCR.

control. Automatic GC has been applied to determine gasoline components and a linear algorithm has been developed relating Reid vapour pressures, boiling points and ASTM distillation curves to component indices with good correlations and repeatability. The method has been developed further to enable the RON of a gasoline to be determined automatically by GC analysis with a standard deviation of only 0.09 for RON values in the range 90 to 100. The method has not yet been taken to the point of closing a control loop so that a reactor or a distillation column is controlled by GC, although this closure is feasible.

GC suffers as the control element because of the time needed for analysis. The response time of the plant must be longer than the time for analysis, which is usually tens of minutes, and there is a clear need to develop faster GC based on short narrow-bore open-tubular columns and variants. It is relevant that a method called the 'optical octane dipstick' is now being used in many refineries. This uses a nondispersive near-infrared analyser (NIR) to determine the absorbance at five wavelengths. Apparently a very good measure of RON is obtained from an algorithm linking these absorbencies to ASTM/RONs determined in a standard Petter engine. Clearly this spectroscopic method is faster than GC but can only be used for a narrow range of RONs and composition. The more detailed compositional description by GC analysis could outweigh its present relative slowness. The NIR control units already in use pave the way

forward by posing a challenge to the analyst to speed up chromatographic methods. If the challenge can be met, then the closing of control loops for catalytic reactors based on GC will follow.

Current Trends and Future Prospects

Table 3 lists some of the recent developments that are close to commercial realization together with more speculative, but possible, advances in the new millennium. GC will play an important part in the catalyst

Table 3 Current trends and future prospects

Gas turbines for electricity generation powered by catalytic combustion of natural gas and biomass
Better electrochemical catalysts with high durability for fuel cells based on methanol and eventually hydrocarbons
Production of propene oxide by the catalytic partial oxidation of propene
Home and hospital hygiene based on catalyst-containing surface coatings
Treatment of commercial and domestic waste
Search for power generation from renewable resources and sunlight-activated catalytic dissociation of water into hydrogen and oxygen
Enzymes immobilized on rugged supports may provide ways of fixing nitrogen at ambient temperatures and also of achieving commercial chiral synthesis
Closing of control loops for catalytic reactors, distillation columns, etc., based on GC analysis of product streams and neural control networks

theories and technologies that will be needed to bring these ideas to fruition. The tasks are challenging, even formidable, and require the commitment of scientists and engineers as well as the provision of vast funds for research, development and capital investment by governments and industry.

Further Reading

- Carberry JJ (1976) *Chemical and Catalytic Reaction Engineering*. New York: McGraw-Hill.
- Choudry VR and Doraiswamy R (1971) *Industrial Engineering and Chemical Product Research and Development* 10: 218.
- Durand JP, Boscher Y and Dorbon M (1990) *Journal of Chromatography* 404: 49.
- Emmett PH (1957) *Advances in Catalysis*, vol. 9, p. 645. New York: Academic Press.
- Hall WK, MacIver DS and Weber HP (1979) *Industrial and Engineering Chemistry* 52: 425.
- Guichon G and Gonnard F (1979) *Analytical Chemistry* 51: 379.
- Mile B, Adlard ER, Roberts GM and Sewell PA (1988) *Catalysis Today* 2: 685.
- Mile B, Ryan TA, Tribeck TD, Zammitt MA and Hughes GA (1994) *Topics in Catalysis* 1: 153.
- Mile B, Howard JA, Tomietto M, Joly HA and Sayari (1996) *Journal of Materials Science* 31: 3080.
- Petroff N, Hoscheit A and Durand D (1993) *Hydrocarbon Processing (International Edition)* 72: 103.
- Rideal EK and Taylor HS (1919) *Catalysis: Theory and Practice*. London: Macmillan.
- Rooney JJ (1985) *Journal of Molecular Catalysis* 31: 147.
- Somorjai GA (1984) *Chemical Society Review* 13: 321.
- Zelter MS (1993) *Hydrocarbon Processing (International Edition)* 72: 103.

CATALYST STUDIES: CHROMATOGRAPHY



Isolation: Magnetic Techniques

I. Šafařík and M. Šafaříková, Institute of Landscape Ecology, Academy of Sciences, České Budějovice, Czech Republic

Copyright © 2000 Academic Press

The first experiments with magnetic separation of cells date from the 1950s when lymphocytes were magnetically separated after *in vitro* phagocytosis of iron granules. The real boom in the application of magnetic labels for cell isolation came in the 1980s and since then an enormous amount of work has been done in both the development and application of this technique.

Magnetic separation of cells has several advantages in comparison with other techniques. In general, the magnetic separation procedure is gentle, facilitating the rapid handling of delicate cells in an unfriendly environment. It permits the cells of interest to be isolated directly from crude samples such as blood, bone marrow, tissue homogenates, stools, food, cultivation media, soil and water. The cells isolated by magnetic separation are usually pure, viable and unaltered. Magnetic separation is a simple, fast and

efficient procedure and the whole separation process can be performed in the same tube. Large differences between magnetic permeabilities of the magnetic and nonmagnetic materials can be exploited in developing highly selective separation methods. The separation procedure can easily be scaled up if large quantities of living cells are required.

Principles of Magnetic Separation of Cells

Two types of magnetic separation can be distinguished when working with cells. In the first type, cells to be separated demonstrate sufficient intrinsic magnetic moment so that magnetic separations can be performed without any modification. There are only two types of such cells in nature: magnetotactic bacteria containing small magnetic particles within their cells and red blood cells (erythrocytes) containing high concentrations of paramagnetic haemoglobin. In the second type, cells of interest have to be tagged by a magnetic label to achieve the required contrast in magnetic susceptibility between the labelled and unlabelled cells. The attachment of magnetic labels is usually attained by the use of affinity ligands of various types, which can interact with target structures on the cell surface. Usually antibodies

microbial pathogens) and parasitology (isolation and detection of protozoan parasites). No doubt many new processes and applications in other fields of biosciences and biotechnologies will be developed in the near future.

See Colour Plates 63, 64, 65, 66.

See also: II/Centrifugation: Analytical Centrifugation; Large-Scale Centrifugation. III/Cells and Cell Organelles: Field Flow Fractionation.

Further Reading

- Cell Separation and Protein Purification* (1996) Oslo, Norway: Dynal. 165 pp.
- Häfeli U, Schütt W, Teller J and Zborowski M (eds) (1997) *Scientific and Clinical Applications of Magnetic Carriers*. New York: Plenum Press.
- Olsvik Ø, Popovic T, Skjerve E *et al.* (1994) Magnetic separation techniques in diagnostic microbiology. *Clinical Microbiology Reviews* 7: 43–54.

Recktenwald D and Radbruch A (eds) (1998) *Cell Separation Methods and Applications*. New York: Marcel Dekker. 352 pp.

Šafařík I and Šafaříková M (1999) Use of magnetic techniques for the isolation of cells. *Journal of Chromatography B* 722: 33–53.

Šafařík I, Šafaříková M and Forsythe SJ (1995) The application of magnetic separations in applied microbiology. *Journal of Applied Bacteriology* 78: 575–585.

Ugelstad J, Olsvik Ø, Schmid R *et al.* (1993) Immunoaffinity separation of cells using monosized magnetic polymer beads. In: Ngo TT (eds) *Molecular Interactions in Bioseparations*, pp. 229–244. New York: Plenum Press.

Ugelstad J, Prestvik WS, Stenstad P *et al.* (1998) Selective cell separation with monosized magnetizable polymer beads. In: Andrä W and Nowak H (eds) *Magnetism in Medicine: A Handbook*, pp. 471–488. Berlin: Wiley-VCH Verlag.

Uhlén M, Hornes E and Olsvik Ø (eds) (1994) *Advances in Biomagnetic Separations*. Natick: Eaton Publishing.

CELLS AND CELL ORGANELLES: FIELD FLOW FRACTIONATION



P. J. P. Cardot, S. Battu,
T. Chianea and S. Rasouli,
Université de Limoges, Limoges, France

Copyright © 2000 Academic Press

Introduction

Analysis and sorting of living cells and purification of cell organelles are important procedures in the life sciences. There is a wide range of techniques and methodologies available, which can be divided into three main groups. The techniques in the first groups are based on physical criteria such as species size, density and shape, and include centrifugation, elutriation and field flow fractionation. Those in the second group are linked to cell surface characteristics, while flow cytometry techniques make up the third group. At a fundamental level, field flow fractionation (FFF) exploits the physical characteristics of the cells or cell organelles. However, cells or cell organelles exhibit some specific characteristics that can be described by a multipolydispersity matrix. The different physical characteristics of these biological materials require different FFF techniques and modes of operation. Special care must be taken if biological integrity and viability are to be preserved.

Specific Cell Characteristics

Cellular materials range in size from 1 µm to 50 µm. Cell populations are classified by a set of morphological, functional and biophysical characteristics. The biophysical characteristics are of particular interest in FFF. Usually, separations in FFF are influenced (but not directed) by surface properties of the sample components (to avoid particle–particle or particle–separator interactions). These properties can be modulated by the use of appropriate carrier-phase modifiers (surfactants). In terms of FFF separations, mass, size and density appear to be the major first order parameters. However, size is generally defined by the radius or the diameter of a sphere whose volume is identical to that of the cell. Size can therefore be deduced accurately if the cell of interest is perfectly spherical. However, this is not usually the case, and the sphericity index, I , is then used:

$$I = \frac{4.84(V^{2/3})}{S}$$

In this equation V is the cell volume and S is its surface area can be difficult to determine. In terms of cell population, these dimensions are averages and should be associated with a variance. These general

considerations are also valid for cell density. Each measurable cell characteristic is therefore associated with an average value and its related variance. A probe of this 'diversity' is of great significance, even in a highly purified cell population. Polydispersity is historically defined in polymer chemistry as the ratio of the percentage of the standard deviation to the average value.

Any cell population can therefore be described by a set of values (average, variance) that leads to a polydispersity index. Cells are different from polymers in that each measurable characteristic of a cell can be associated with polydispersity, so polydispersity can apply to mass, size, volume or density. This matrix of parameters (average, variance) can be used to define a 'multipolydispersity matrix'. The dimensions of the multipolydispersity index depend on the information available. For example, the human normal red blood cell (HNRBC) is the best known cellular material. Its average volume has been measured as 95 ± 5 fL, and its surface area has been calculated as 138.0 ± 5 μm^2 . The HNRBC is known for its discoid shape, which generates other measurable dimensions. Its average diameter is 8.1 ± 0.43 μm , and minimum and maximum thicknesses of 1.0 ± 0.3 μm and 2.4 ± 0.15 μm have been measured. An average sphericity index of 0.77 has been calculated. The density was found to vary from 1.035 to 1.102, with an average value of 1.051. Using these data, it is possible to describe the HNRBC population using a preliminary multipolydispersity matrix, as shown in Table 1.

More complex properties such as cell/nucleus ratio or surface electric charge density (ζ potential, used for dielectric cell purification) can later be added to this basic matrix. In FFF, the sample (i.e. cell surface) characteristics are most important in the development of any separation process. The separator material is chosen so as to avoid or limit particle-separator interactions, which can lead to limited recovery and viability, separator ageing or poisoning. In this domain a general set of empirical rules emerged. If the cell surface is hydrophilic (blood and yeast cells) a hydrophobic material should be used for the separator. The lower the surface energy of the cell, the less non-specific cell-separator interactions occurred, and vice

versa. The interactions between the environmental material and the cells can now be assessed by the general 'biocompatibility' rules.

However the HNRBC population found in circulating blood is not a homogenous, and contains red blood cells (RBCs) of different ages. This suggests that a morphologically homogenous population can be considered to contain different sub-populations. An HNRBC suspension contains cells of equal volume, and cells of equal density, shape or mass. This complex definition of 'population' characteristics is described in Figure 1A. If a set of common parameters is defined, the HNRBCs that meet these limitations may represent only a minor proportion of the whole population. By considering some aspects of this multipolydispersity matrix, rules for cell separation based on biophysical characteristics can be found. Figure 1B shows a three-dimensional graphical representation of the multipolydispersity of the circulating blood cells (platelets, HNRBC, lymphocytes, monocytes, granulocytes) based on the characteristics of size and density. It is obvious that if a size driven cell separation technology could be used, all these populations could be isolated. An isolation technique based only on density would be more complex, as some blood cell population densities overlap. However a size and density driven separation (whose balance has not so far been assessed) would allow selective isolation.

FFF Techniques for Cell Separations

The Different Techniques

The requirements of different fields have led to a wide variety of FFF techniques. Four major technologies have emerged. The first uses fields generated by gravity, either simple earth gravity or centrifugally generated multigravitational fields. It is now generically described as sedimentation FFF (SdFFF for multigravity fields and GFFF for gravity induced fields). The basic technology is the same, although a more complex instrumental design is required for SdFFF, as shown in Figure 2A and B. However, the very simple GFFF designs and procedures can be upgraded for SdFFF separations. This group was historically the most successful in biological applications. Channel cleaning, decontamination and sterilization procedures are common and can be performed simply, as described later. There are many channel wall materials available, and a wide diversity of sample injection technologies or procedures.

The second group encompasses fields generated by a flow, where the accumulation wall is made of a semipermeable membrane of adapted cut-off. This

Table 1 Multipolydispersity matrix for HNRBC

	Average	Standard deviation	Polydispersity (%)
Volume (fL)	95	5	10
Density	1.051	0.08	3
Sphericity	0.77	0.15	11

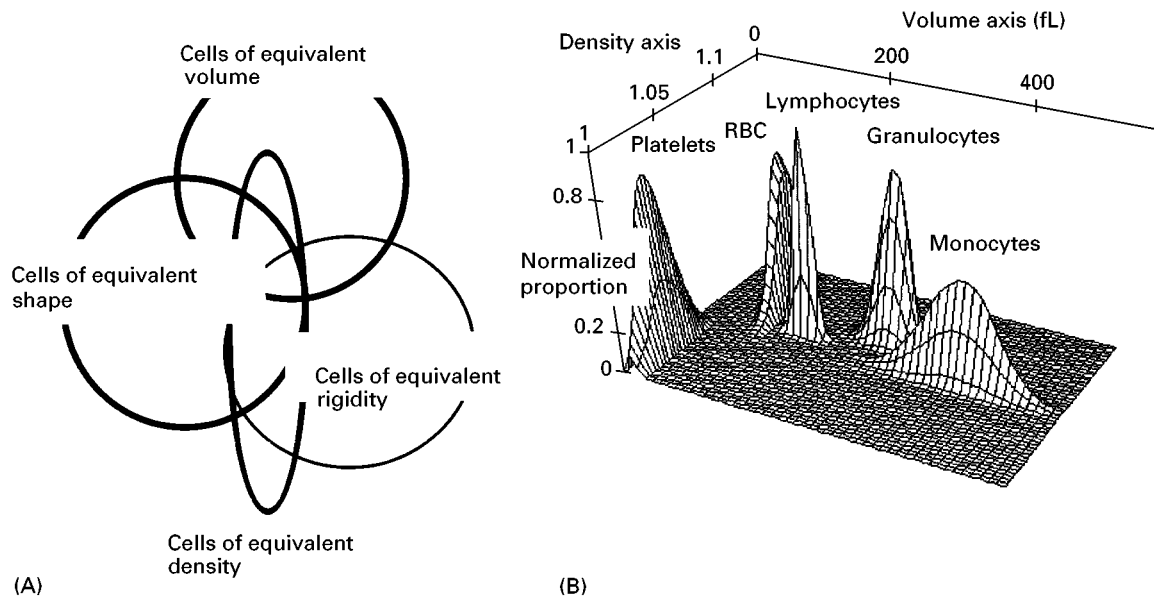


Figure 1 Multipolydispersity matrix. (A) The definition of a homogenous population is complex. A cell population with homogenous morphological characteristics is actually a complex mixture of sub-populations with different biophysical characteristics. (B) Three-dimensional plot of circulating blood cells (normalized dimensions) as a function of size and density (from bibliographic data). Red blood cells and lymphocytes have the closest characteristics.

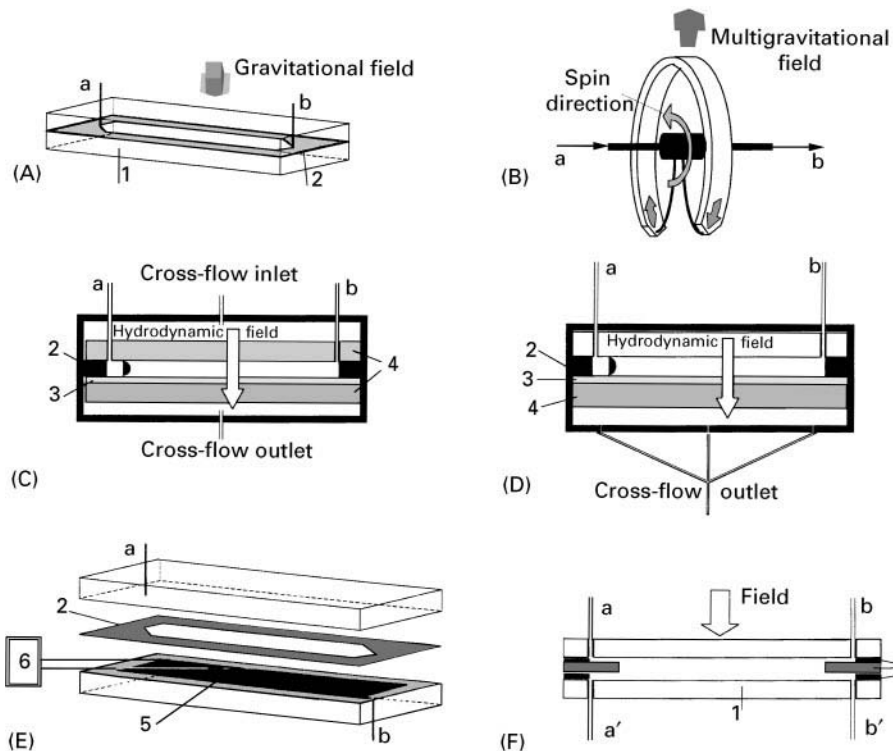


Figure 2 The different FFF techniques. (A) Gravitational FFF device; (B) Sedimentation FFF device; (C) symmetrical flow FFF device; (D) asymmetrical flow FFF device; (E) experimental layout of DEP-GFFF device; (F) schematic view of SPLITT-FFF device. 1, Channel wall (accumulation wall); 2, Mylar® spacers; 3, semipermeable membrane (accumulation wall); 4, frit; 5, interdigitated electrode; 6, power amplifier and source of signal; a, inlet (sample and carrier phase); b, outlet (to detector and fraction collection); a' and b', secondary inlet and outlet.

group is of interest because of the possibility of separating species by buoyancy (particle suspension and carrier phase with identical density), such as cell organelles or macromolecules. Two flow-generated FFF techniques were developed. Symmetrical flow FFF (FFFF) uses two independent flows, one to create the external field and the second to sweep the species along the channel (Figure 2C). Asymmetrical flow FFF (AFFFF) uses the same flow along and across the channel, as shown in Figure 2D. However, sample injection procedures are more limited and complex membrane-sample interactions may occur. Fortunately, the wide range of membranes available has made the technique very versatile. The in-channel pressure needed to create the transverse flow-generated field by means of off-channel restrictors has led to rather sophisticated fraction collection devices.

The third group uses electric fields either as the main transverse field (electric FFF) or as dielectric fields combined with gravity (DEP-GFFF) to obtain a hyperlayer focusing elution mode, as shown in Figure 2E. The fourth group encompasses continuous separation devices based on the general SPLITT concept, as shown in Figure 2F.

General Features Linked to Cell Elution Process

The osmotic and pH properties of the biological media must be preserved. Buffer solutions of known pH and ionic strength are used. For example the classical isotonic phosphate buffered saline (PBS) solution. Compared with other FFF elution carried phases, only limited surfactants can be used. Sucrose solution and albumin are both possibilities, the latter being the most versatile carrier phase modifier, usually at a concentration of 0.1% (v/w). The surfactant effect of albumin limits particle-particle interactions as well as particle-wall ones. Albumin adsorption occurs, on relatively hydrophobic channel wall materials, leading to channel ageing or poisoning. Rigorous cleaning and channel regeneration procedures are therefore recommended.

As the general purpose of cell elution in FFF is to limit particle-wall interactions, the commonly used 'stop flow injection procedure' can cause problems. The procedure involves injecting sample at the inlet of the channel in the absence of a flowing stream but while an external field is applied. The species are concentrated near the accumulation wall at the beginning of the channel. The procedure is essential if species are eluted according to the 'Brownian' elution mode, but this is not the case for cells. With cells the risk of generating particle-particle or particle-wall interactions is increased. Specific instrumental modifications of the inlet geometry (directly on the accumulation wall) or low flow-injection procedures will

limit the risk. However, flow injections may enhance selectivity because of the different speeds at which sample components reach the steric hyperlayer focused position in the channel thickness. Elution of cellular material in a steric mode is associated with reduced recovery and possibly with reduced selectivity. Examples of the steric hyperlayer elution mode of HNRBCs and duracytes are given in Figure 3.

Cell Elution Methodology and Detection

Decontamination and Sterilization of FFF Separator

This is necessary to prevent bacterial contamination, but the use of sodium azide should be avoided as it is a cellular toxic. Safe and effective decontamination processes can be considered as an additional step in the cleaning procedure.

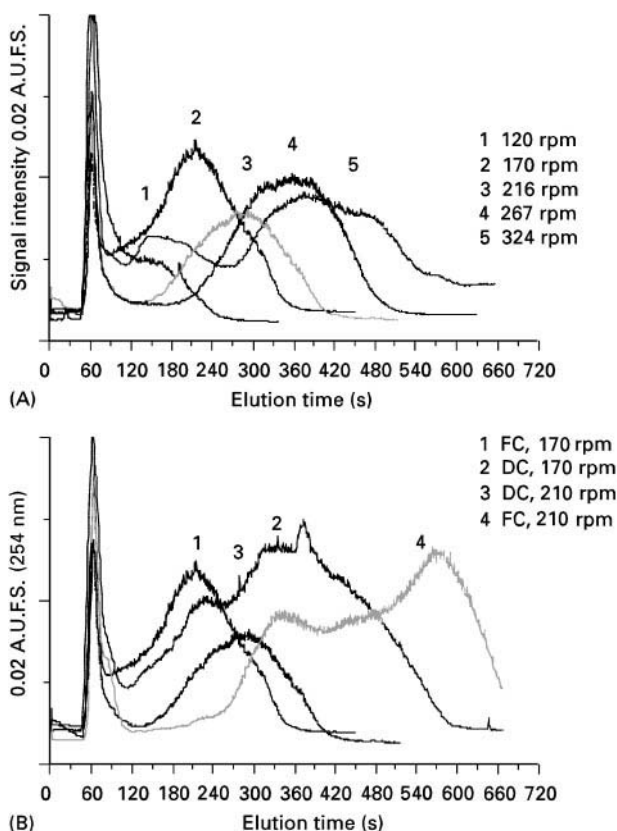


Figure 3 Red blood cells with different elution characteristics in sedimentation field flow fractionation. (A) Fractograms (elution signal) of fresh RBCs. Channel walls made of hydrophobic materials, channel dimensions 0.5 cm wide, 0.025 cm thick, 58 cm long. The channel distance from rotor axis, 10.7 cm. Photometric detection at 254 nm. Sample injection in the established flow (flow rate of 0.5 mL min⁻¹). (B) Fractograms showing retention differences between fresh RBCs and duracytes. RBCs and duracytes are similar in size, but duracytes are rigid fixed RBCs of higher density. FC, fresh red blood cell; DC, duracytes.

The cleaning procedure involves flushing the channel (ten times the void volume) with a hypo-osmotic carrier phase to destroy the cells, then with a classical deproteinization agent (ten times the void volume) to desorb and destroy the cell and surfactant proteins adsorbed in the FFF separator. Finally the system is flushed again with the hypo-osmotic carrier phase.

Decontamination is performed by allowing a hypochloride solution (3–6°C) to flow through the whole FFF system. The volume used should be three to four times the void volume of the FFF device. Prior to injection the channel should be flushed with ethanol and rinsed with the sterile mobile phase. Decontamination and sterilization can be simultaneous if a 5°C hypochloride solution is used with a 70°C ethanol solution.

Cell Detection, Viability and Recovery

At the outlet of the channel it is necessary to obtain eluted material that retains its integrity, that is the diagnosis of the whole particle. Photometric devices operated in the light scattering mode can be used to follow elution. After fraction collection off-line analyses methods such as microscopy, granulometric or flow cytometry analyses are recommended. Cell specific staining is also possible. Cell viability can be diagnosed by means of specific tests, and recovery must also be clearly defined.

Conclusions

The choice of FFF separation techniques for purification of cell or cell organelle populations is influenced by their possible elution modes. Micron sized species eluted under the steric hyperlayer model can be separated using sedimentation techniques if their density differs from that of the carrier phase medium. This is also possible for 'nonbuoyant' sub-micron sized cell organelle species eluted according to the 'Brownian' elution mode.

If species are to be separated according to their size, FFF techniques that use a flow generated external field are preferred. If differences in surface characteristics are important, electrical-based FFF techniques

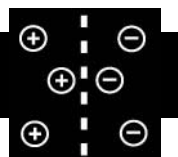
should be chosen. For large sample volume preparations, SPLIT techniques are useful, whatever the external field. The major technical goal in cell separation is not the set-up of the separator, but the construction of a chain of knowledge. The separator is designed according to the sample characteristics as well as the mode of operation. Cleaning and sterilization procedures, and detection and viability procedures, are linked to the nature of the material to be purified. This 'biotechnological' process is of major importance for FFF separations in the life sciences.

See also: **II/Particle Size Separation:** Field Flow Fractionation: Electric Fields; Theory and Instrumentation of Field Flow Fractionation. **III/Colloids:** Field Flow Fractionation. **Polymers:** Field Flow Fractionation. **Proteins:** Field Flow Fractionation. **III/Catalyst studies:** **Chromatography:** Isolation: Magnetic Techniques.

Further Reading

- Bernard A, Paulet B, Colin V and Cardot PhJP (1995) Red blood cell separations by gravitational field flow fractionation: instrumentation and applications. *Trends Anal. Chem.* 14(6): 266–273.
- Caldwell KD, Cheng ZQ and Hradecky P (1984) Separation of human and animal cells by steric field flow fractionation. *Cell Biophysics* 6: 233–251.
- Giddings JC (1993) Field flow fractionation analysis of macromolecular, colloidal and particulate materials. *Science* 260: 1456–1465.
- Nilson M, Kallio PT, Bailey JE, Bulow L and Wahlund KG (1999) Expression of *Vitreoscilla* hemoglobin in *Escherichia coli* enhances ribosome and tRNA levels: a flow field flow fractionation study. *Biotechnology Progress* 15(2): 158–163.
- Williams PS, Zborowski M and Chalmers JJ (1999) Flow rate optimization for the quadrupole magnetic cell sorter. *Analytical Chemistry* 71: 3799–3807.
- Yang J, Huang Y, Wang XB, Becker FF and Gascoyne PRC (1999) Cell separation on microfabricated electrode using dielectrophoretic/gravitational field-flow fractionation. *Analytical Chemistry* 71: 911–918.
- Yue V, Kowal R, Neargarder L *et al.* (1994) Miniature field-flow fractionation system for analysis of blood cells. *Clinical Chemistry* 40(9): 1810–1814.

CHELATING ION EXCHANGE RESINS



R. J. Eldridge, CSIRO Molecular Science,
Clayton South, Victoria, Australia

Copyright © 2000 Academic Press

Introduction

The useful role of ion exchange is to separate a solution at a low initial concentration C_i into a small

theories and technologies that will be needed to bring these ideas to fruition. The tasks are challenging, even formidable, and require the commitment of scientists and engineers as well as the provision of vast funds for research, development and capital investment by governments and industry.

Further Reading

- Carberry JJ (1976) *Chemical and Catalytic Reaction Engineering*. New York: McGraw-Hill.
- Choudry VR and Doraiswamy R (1971) *Industrial Engineering and Chemical Product Research and Development* 10: 218.
- Durand JP, Boscher Y and Dorbon M (1990) *Journal of Chromatography* 404: 49.
- Emmett PH (1957) *Advances in Catalysis*, vol. 9, p. 645. New York: Academic Press.
- Hall WK, MacIver DS and Weber HP (1979) *Industrial and Engineering Chemistry* 52: 425.
- Guichon G and Gonnard F (1979) *Analytical Chemistry* 51: 379.
- Mile B, Adlard ER, Roberts GM and Sewell PA (1988) *Catalysis Today* 2: 685.
- Mile B, Ryan TA, Tribeck TD, Zammitt MA and Hughes GA (1994) *Topics in Catalysis* 1: 153.
- Mile B, Howard JA, Tomietto M, Joly HA and Sayari (1996) *Journal of Materials Science* 31: 3080.
- Petroff N, Hoscheit A and Durand D (1993) *Hydrocarbon Processing (International Edition)* 72: 103.
- Rideal EK and Taylor HS (1919) *Catalysis: Theory and Practice*. London: Macmillan.
- Rooney JJ (1985) *Journal of Molecular Catalysis* 31: 147.
- Somorjai GA (1984) *Chemical Society Review* 13: 321.
- Zelter MS (1993) *Hydrocarbon Processing (International Edition)* 72: 103.

CATALYST STUDIES: CHROMATOGRAPHY



Isolation: Magnetic Techniques

I. Šafařík and M. Šafaříková, Institute of Landscape Ecology, Academy of Sciences, České Budějovice, Czech Republic

Copyright © 2000 Academic Press

The first experiments with magnetic separation of cells date from the 1950s when lymphocytes were magnetically separated after *in vitro* phagocytosis of iron granules. The real boom in the application of magnetic labels for cell isolation came in the 1980s and since then an enormous amount of work has been done in both the development and application of this technique.

Magnetic separation of cells has several advantages in comparison with other techniques. In general, the magnetic separation procedure is gentle, facilitating the rapid handling of delicate cells in an unfriendly environment. It permits the cells of interest to be isolated directly from crude samples such as blood, bone marrow, tissue homogenates, stools, food, cultivation media, soil and water. The cells isolated by magnetic separation are usually pure, viable and unaltered. Magnetic separation is a simple, fast and

efficient procedure and the whole separation process can be performed in the same tube. Large differences between magnetic permeabilities of the magnetic and nonmagnetic materials can be exploited in developing highly selective separation methods. The separation procedure can easily be scaled up if large quantities of living cells are required.

Principles of Magnetic Separation of Cells

Two types of magnetic separation can be distinguished when working with cells. In the first type, cells to be separated demonstrate sufficient intrinsic magnetic moment so that magnetic separations can be performed without any modification. There are only two types of such cells in nature: magnetotactic bacteria containing small magnetic particles within their cells and red blood cells (erythrocytes) containing high concentrations of paramagnetic haemoglobin. In the second type, cells of interest have to be tagged by a magnetic label to achieve the required contrast in magnetic susceptibility between the labelled and unlabelled cells. The attachment of magnetic labels is usually attained by the use of affinity ligands of various types, which can interact with target structures on the cell surface. Usually antibodies

against specific cells surface epitopes are used, but other specific ligands can also be employed. The newly formed complexes have magnetic properties and can be manipulated using an appropriate magnetic separator.

The magnetic separation process for the purification of target cells usually consists of the following three fundamentals steps:

1. The suspension containing cells of interest is mixed with magnetic labels. Incubation time is usually not longer than 30–60 min. Then the magnetic complex formed is separated using a magnetic separator and the supernatant is discarded or used for another application.
2. The magnetic complex is washed several times to remove unwanted contaminants. The selected cells with attached magnetic labels can be used directly, e.g. for cultivation experiments. Alternatively, cells can be disrupted and the cell content analysed using various methods.
3. If necessary, a variety of detachment procedures can be used to remove the magnetic labels from the separated cells. After detachment, the magnetic label is removed from the suspension in a separator and free cells are ready for further applications and analyses.

Necessary Equipment

Magnetic labels and magnetic separators are necessary to be able to perform efficient cell separation. Typical examples are given below.

Magnetic Labels

With the exception of erythrocytes and magnetotactic bacteria, the cells to be isolated have to be magnetically labelled in order to be amenable to magnetic treatment. Magnetic labelling can be performed with magnetic and superparamagnetic particles (*c.* 1 μm and more in diameter), magnetic colloids (*c.* 50–200 nm), magnetoliposomes or with molecular magnetic labels. In most cases the magnetic properties of the labels are caused by the presence of small particles of magnetite (Fe_3O_4) or maghemite ($\gamma\text{-Fe}_2\text{O}_3$); in some cases, chromium dioxide particles or ferrite particles have been used.

Magnetic and superparamagnetic particles Magnetic and superparamagnetic particles (typical diameter *c.* 1–5 μm) attached to the target cells can easily be removed from a suspension with a simple magnetic separator. Since there is usually no magnetic re-

manence the particles are not attracted to each other and therefore they can be easily suspended into a homogeneous mixture in the absence of any external magnetic field. Magnetic particles typically comprise fine grains of iron oxides dispersed throughout the interior of a polymer particle (in many cases of a monosized type), the surface chemistry of which can be modified to provide a range of different linking methods. Alternatively, silanized particles of magnetic iron oxides or magnetic porous glass can be used for the same purpose.

A number of particulate magnetic labels can be purchased commercially. Up to now, in most applications, monosized polymer particles marketed as Dynabeads (Dynal, Oslo, Norway) in various forms have been used. Dynabeads are prepared from monosized macroporous polystyrene particles which are magnetized by an *in situ* formation of ferromagnetic material inside the pores. Other commercially available magnetic particles can be successfully used for cell separation. A selection of these products can be found in Table 1.

Colloidal magnetic labels Colloidal magnetic labels (typical size *c.* 50–200 nm) are prepared by a variety of methods which result in flocks composed of polymer (typically dextran, starch or protein) and magnetite and/or other iron oxide crystals. A standard procedure for the synthesis of superparamagnetic dextran nanospheres is performed by precipitation of iron oxide in the presence of the polysaccharide. To such materials, ligands (usually antibodies, lectins, streptavidin or biotin) are coupled so they can be used for cell separation. Using high gradient magnetic columns, the labelled cells are easily separated. Magnetic particles isolated from magnetotactic bacteria (50–100 nm) composed of magnetite covered by a stable lipid membrane can also be used successfully.

Magnetoliposomes Magnetoliposomes are magnetic derivatives of ordinary liposomes prepared by incorporation of colloidal magnetic particles into the lipid vesicles. When magnetoliposomes are associated with antibodies they can label and/or selectively concentrate the target cells.

Molecular magnetic labels Molecular magnetic labels are usually lanthanides (especially erbium), ferritin and magnetoferritin. Erbium in the form of erbium chloride (ErCl_3) has been used for magnetic labelling of a variety of cells. Different Er^{3+} binding sites, such as carboxyl groups in glycoproteins or the Ca^{2+} receptor sites on the cell wall are responsible for the binding of erbium ions.

Table 1 Selected examples of commercially available magnetic particles and colloidal magnetic labels used or usable for magnetic separation of cells

Name	Diameter (μm)	Polymer composition/surface modification	End groups and activation possibility	Immobilized compounds	Manufacturer/supplier
BioMag	~ 1	Silanized iron oxides	$-\text{COOH}$ $-\text{NH}_2$	Secondary Abs, anti-CD Abs, anti-fluorescein Ab, protein A, protein G, streptavidin, biotin	Perseptive Biosystems, Framingham, MA, USA
Dynabeads M-280	2.8	Polystyrene	Tosyl-activated	Secondary Abs, anti-CD Abs, Abs against <i>Escherichia coli</i> O157, <i>Salmonella</i> , <i>Listeria</i> , <i>Cryptosporidium</i> , streptavidin, oligo(dT)	Dynal, Oslo, Norway
Dynabeads M-450	4.5				
Dynabeads M-500	5				
Estapor	~ 1	Polystyrene	$-\text{COOH}$ $-\text{NH}_2$		Prolabo, Fontenay-sous-Bois, France
Ferrofluids	0.135 0.175	Modified hydrophilic protein	$-\text{COOH}$ $-\text{NH}_2$	Secondary Abs, protein A, streptavidin	Immunicon, Huntingdon Valley, PA, USA
M 100 M 104 M 108	1–10	Cellulose	$-\text{OH}$		Scigen, Sittingbourne, UK
MACS Microbeads	0.05	Dextran	$-\text{OH}$	Secondary Abs, anti-CD Abs, streptavidin, biotin	Miltenyi Biotec, Bergisch Gladbach, Germany
Magnetic microparticles	1–2	Polystyrene, cellulose, polyacrolein	$-\text{COOH}$ $-\text{NH}_2$	Secondary Abs, protein A, protein G, streptavidin	Polysciences, Warrington, PA, USA
Magnetic nanoparticles	0.09–0.6	Starch, dextran, chitosan	$-\text{OH}$, $-\text{COOH}$	Streptavidin, biotin, protein A	Micro caps, Rostock, Germany
MagNIM	0.05 0.25 0.5		$-\text{COOH}$ $-\text{NH}_2$	Secondary Abs, Ab against <i>E. coli</i> O157, streptavidin, protein A	Cardinal Associates, Santa Fe, NM, USA
Magnetic particles	~ 1	Polystyrene	$-\text{COOH}$ $-\text{NH}_2$	Secondary Abs, Protein A, streptavidin,	Bangs Laboratories, Fishers, IN, USA
MPG	5	Porous glass	$-\text{NH}_2$, hydrazide, glyceryl	Streptavidin, avidin	CPG, Lincoln Park, NJ, USA
XM200 Microsphere	3.5	Polystyrene	$-\text{COOH}$	Secondary Abs, protein A	Advanced Biotechnologies, Epsom, UK

Ferritin is a naturally occurring, soluble iron storage protein in mammals. For magnetic modification of cells cationized horse spleen ferritin (ferritin coupled with *N,N*-dimethyl-1,3-propanediamine) exhibiting a net positive charge at pH 7.5 is usually used. Under these conditions the cationized ferritin readily forms ionic bonds with the anionic sites on the

cell membrane. Magnetic derivatives of ferritin called magnetoferritin, prepared by controlled reconstitution conditions, have also been used for cell labelling.

Magnetic Separators

A variety of magnetic separators is available on the market, starting with very simple concentrators for

one test tube and ending with complicated fully automated devices. In many cases, especially when working with larger labels, very cheap home-made magnetic separators can be used successfully.

Batch magnetic separators Batch magnetic separators are usually made from strong rare-earth permanent magnets embedded in disinfectant-proof material. The racks are designed to hold various sizes and numbers of tubes. Some of the separators have a removable magnet plate to facilitate easy washing of magnetic particles (**Figure 1**). Test tube magnetic separators enable separation of magnetic particles from volumes ranging between about 5 μL and 50 mL. It is also possible to separate cells from the wells of standard microtitration plates. Magnetic complexes from larger volumes of suspensions (up to approximately 500–1000 mL) can be separated using flat magnetic separators. More sophisticated magnetic separators are available, e.g. those based on the quadrupole and hexapole magnetic configuration.

Flow-through magnetic separators Flow-through magnetic separators are characterized by the flow of the liquid and suspended cells through the separation system. These systems are usually more expensive and more complicated in comparison with batch separators, but for preliminary experiments simple devices can also be used.

Laboratory-scale high gradient magnetic separators (HGMS; **Figure 2**) are composed of small columns loosely packed with fine magnetic-grade stainless steel wool which are placed between the poles of strong permanent magnets or electromagnets. Magnetically labelled cells are pumped through the column, labelled cells are retained on the steel wool, the field is removed and cells are retrieved by flow and usually by gentle vibration of the column. Automation of the separation process has led to the develop-

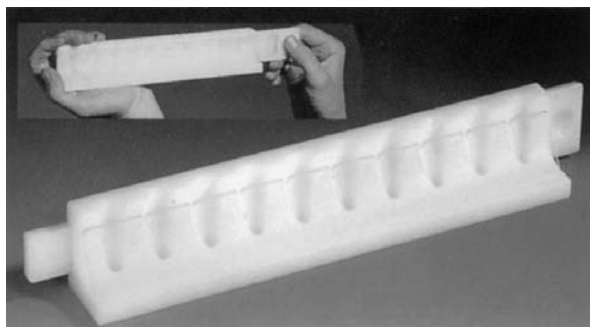


Figure 1 (See Colour Plate 63). Example of a magnetic separator (Dynal MPC-M) for work with microcentrifuge tubes of the Eppendorf type, with a removable magnet plate to facilitate easy washing of magnetic particles. Courtesy of Dynal, Oslo, Norway.

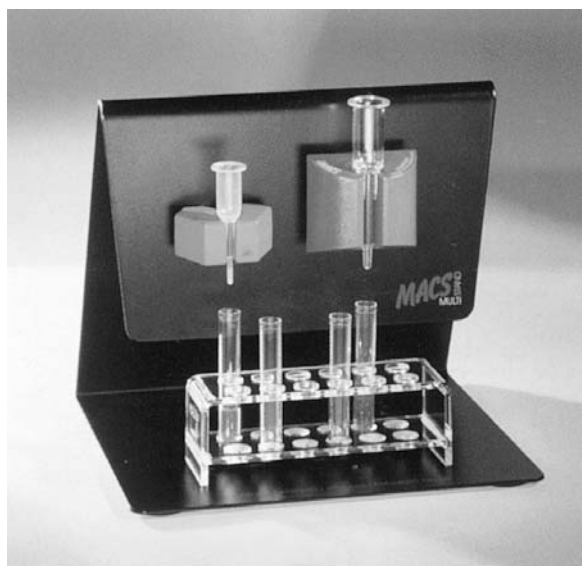


Figure 2 (See Colour Plate 64). Examples of laboratory-scale high gradient magnetic separators. Left: MiniMACS separation unit; right: MidiMACS separation unit, both with inserted columns. Courtesy of Miltenyi Biotec, Bergisch Gladbach, Germany.

ment of computer-controlled magnetic cell sorters, such as CliniMACS (**Figure 3**) and AutoMACS, both produced by Miltenyi Biotec, Germany.

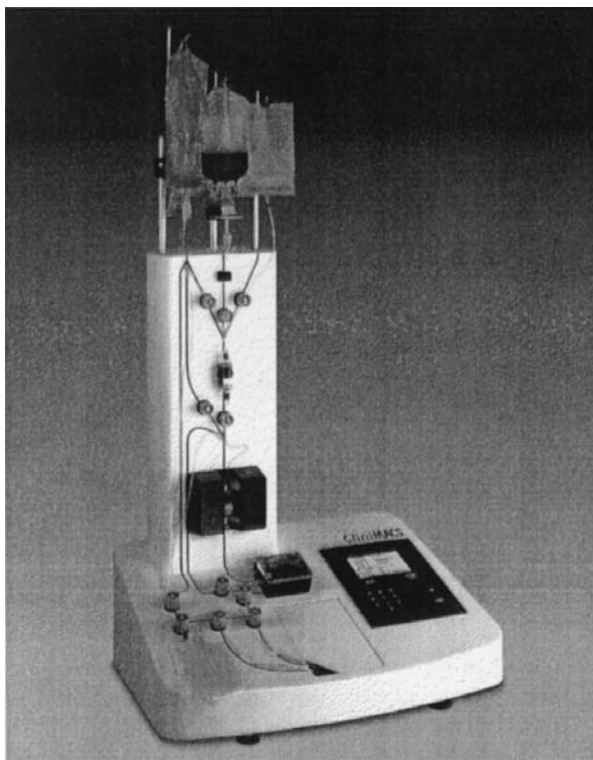


Figure 3 (See Colour Plate 65). Computer-controlled magnetic cell sorter CliniMACS. Courtesy of Miltenyi Biotec, Bergisch Gladbach, Germany.

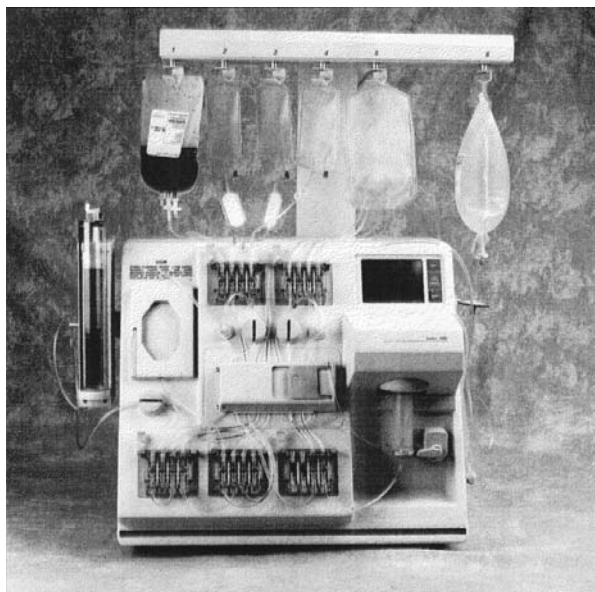


Figure 4 (See Colour Plate 66). The Isolex 300i Cell Selection System. Courtesy of Nexell Therapeutics, USA.

A continuous magnetic sorter based on an electrophoresis counter-flow chamber has been developed. The injected magnetic particles are deviated in the inhomogeneous magnetic field and focused into a stream that is completely separated from the streams of the undeviated particles.

The Isolex 300i Magnetic Cell Separator, produced by Nexell Therapeutics, USA, is intended for the isolation of stem cells from blood or bone marrow. The whole process is done automatically and the device represents a flexible platform for future applications in cell separation (Figure 4).

Procedures for Performing Magnetic Separation of Cells

Magnetic separation of cells is usually performed in one of the following formats:

1. Direct method. The affinity ligand is coupled to the magnetic particles, which are then added directly to the cell sample. During incubation the magnetic particles will bind the target cells which can be then recovered using a magnet.
2. Indirect method. Target cells are first sensitized with a suitable primary affinity ligand. After incubation, excess unbound affinity ligand is removed by washing the cells and then magnetic particles with an immobilized secondary affinity ligand with affinity for the first ligand are added. The magnetic particles will bind the target cells, which can then be recovered using a magnetic separator.

Another differentiation of magnetic separation techniques is based on the selection of the magnetically labelled cells.

1. Negative selection. Negative selection is a method by which a cellular subset is purified by removing all other cell types from the sample. Both the direct and indirect method are applied for negative selection. The advantage is that the purification process does not involve any direct contact of magnetic labels with the cells to be isolated.
2. Positive selection. The target cells are isolated from the cell suspension. Both the direct and indirect method can be used. The separated magnetically labelled cell complexes can be further characterized directly, but in many cases it is necessary to remove larger magnetic particles from the positively selected cells after their isolation.
3. Depletion of cells. Depletion is a method by which one or more unwanted cellular subsets is removed from a cell suspension. Both the direct and the indirect procedure can be applied for this purpose.

Immunomagnetic Separation

Immunomagnetic separation (IMS) is the most often used approach for the isolation of cells. Most often, a monoclonal antibody is used for IMS, but also polyclonal antibodies are used successfully. IMS can be performed in all the formats mentioned above.

In the direct method the appropriate antibody is coupled to the magnetic particles and colloids, which are then added directly to the sample. Ideally, the antibody should be oriented with its Fc part towards the magnetic particle so that the Fab region is pointing outwards from the particle. Several procedures are available for direct binding of antibodies (Table 2).

The indirect method is also used very often. The cell suspension is first incubated with primary antibodies which bind to the target cells. Not only purified primary antibodies have to be used, crude antibody preparations or serum can also be used. After incubation, the unbound antibodies are usually removed by washing. Then magnetic particles with immobilized secondary antibody are added to bind the labelled cells. Target cells – primary antibody complexes – can be also captured by protein A or protein G immobilized on magnetic carriers. Alternatively, biotinylated or fluorescein-labelled primary antibodies and magnetic particles with immobilized streptavidin or anti-fluorescein antibody are used to capture the target cells.

The indirect method is generally more efficient in removing target cells from a suspension because free antibodies will find their target antigen more easily

Table 2 Selected procedures for binding of antibodies on magnetic particles and colloids

Adsorption of antibodies on hydrophobic magnetic particles (especially those made of polystyrene)
Covalent binding of antibodies on activated magnetic particles (e.g. tosyl-activated), or on magnetic particles carrying appropriate functional groups (e.g. carboxy, amino, hydroxy, hydrazide) using standard immobilization procedures
Immobilization of secondary antibodies (i.e. antibodies against primary antibodies) on magnetic particles followed by binding of primary antibodies
Immobilization of biotinylated antibodies on magnetic carriers with immobilized streptavidin
Immobilization of antibodies on magnetic particles with immobilized protein A and protein G
Immobilization of antibodies tagged with oligo dA on magnetic particles with immobilized oligo dT
Immobilization of antibodies on magnetic carriers with immobilized boronic acid derivative via their carbohydrate units on the Fc part

than antibodies bound to magnetic particles. The indirect technique is recommended when the target cell has a low surface antigen density or a cocktail of monoclonal antibodies is used. The direct method is usually faster and requires less antibody than the indirect method. Also, the direct method is advantageous when one does not want to cover all antigen sites with antibody.

Typically, 95–99% viability and purity of the positively isolated cells can be achieved with a typical yield of 60–99%. Depletion efficiency often reaches 99.9% and leaves remaining cells untouched. Sequential depletions are markedly more efficient.

Magnetic particles usually do not have any negative effect on the viability of the attached cells. Many types of magnetic particles are usually compatible with subsequent analytical techniques such as flow cytometry, electron and fluorescence microscopy, polymerase chain reaction (PCR), fluorescence *in situ* hybridization (FISH) or cultivation in appropriate nutrient media. In some cases, however, it is necessary to remove larger immunomagnetic particles from the cells after their isolation. The detachment process can be performed in several ways (Table 3).

Incubation time for cell separation is usually 5–60 min while the binding of primary antibodies to secondary coated magnetic particles usually takes 30 min or less. In positive isolation, the purity of cells generally decreases with time, although the yield increases.

Nonspecific interactions of nontarget cells with hydrophobic magnetic particles can be expected. These

interactions can be partially eliminated using bovine or human serum albumin, casein and nonionic tensides such as Tween 20.

Magnetic Separations using other Labels

Antigens Antigens immobilized on magnetic particles can be used for the isolation of antibody expressing or antigen-specific cells. This approach has been successfully used for selection of antigen-specific hybridoma cells or human antibody-producing cell lines.

Lectins Lectins immobilized on magnetic carriers can interact with saccharide residues on the cell surfaces. A typical example of this approach is the application of immobilized *Ulex europaeus* I lectin which binds to terminal L-fucosyl residues present on the surface of human endothelial cells. Magnetic beads can be released from the isolated cells using a free competing sugar.

Oligosaccharides Oligosaccharides immobilized on magnetic particles can be used for the rapid isolation of specific lectin-expressing cells. Target cells bound to the magnetic particles can be released using a free competing saccharide structure.

Bacteriophage *Salmonella*-specific bacteriophage immobilized to a magnetic solid phase has been used for the separation and concentration of *Salmonella* from food materials.

Table 3 Selected typical procedures for detachment of cells after immunomagnetic separation

Incubation of rosetted cells overnight in cell culture medium with subsequent mechanical forces such as firm pipetting, flushing the suspension 5–10 times through a narrow-tipped pipette
Trypsin, chymotrypsin and pronase have general applicability for proteolytic detachment of isolated cells
Detachment with a polyclonal antibody that reacts with the Fab fragments of primary monoclonal antibodies on magnetic beads. This principle is commercialized by Dynal, Norway (DETACHaBEAD)
Using synthetic peptides which bind specifically to the antigen-binding site of primary antibodies (Baxter Healthcare, Deerfield, IL, USA)
Antibodies immobilized via carbohydrate units on the Fc part to the magnetic particles with immobilized $-B(OH)_3$ groups are dissociated with sorbitol
A complex primary antibody–DNA linker can be split enzymatically using DNase
<i>Cryptosporidium</i> oocysts were successfully released from the immunomagnetic particles by decreasing the pH of the suspension (adding HCl)

Erbium ions, ferritin and magnetoferritin have been used for magnetic labelling of both prokaryotic and eukaryotic cells. Magnetotactic bacteria can be introduced into granulocytes and monocytes by phagocytosis which enables their magnetic separation. Submicron magnetic particles of $\gamma\text{-Fe}_2\text{O}_3$ adhere to the surface of *Saccharomyces cerevisiae*, making the cells magnetic and amenable to magnetic separation.

Magnetotactic bacteria, due to the presence of ferromagnetic material in their cells, can be magnetically separated without any labelling. Erythrocytes can be separated by the high gradient magnetic separation technique after conversion of diamagnetic erythrocytes containing oxyferrohaemoglobin into paramagnetic red blood cells by the oxidation of the iron atoms in the cell haemoglobin to the ferric state (methaemoglobin). Erythrocytes, infected by *Plasmodium*, contain paramagnetic hemozoin, that is a component of malarial pigment. The paramagnetic moment of hemozoin is of sufficient magnitude to enable the separation of malaria-infected (hemozoin-bearing) erythrocytes.

Magnetic Separations in Microbiology, Cell Biology, Medicine and Parasitology

IMS and, in some cases, lectin-magnetic separations are often used in the above-mentioned disciplines. In microbiology they are especially used for the detection of pathogenic microorganisms. IMS enables the time necessary for detection of the target pathogen to be shortened. Target cells are magnetically separated directly from the sample or the pre-enrichment medium. Isolated cells can then be identified by standard, specific microbiological procedures. IMS is not only faster but also usually gives a higher number of positive samples. Also sublethally injured and stressed microbial cells can be very efficiently isolated using IMS. The most important microbial pathogens can be detected using commercially available specific immunomagnetic particles; they are used for the detection of *Salmonella*, *Listeria* and *Escherichia coli* O157. New immunomagnetic particles for the detection of other microbial pathogens are under development.

Removal of cancer cells is one of the most important applications of IMS in the area of cell biology and medicine. The first experiments were performed in the 1970s and since then an enormous number of applications have been described. Cancer cells are usually removed from bone marrow prior to its autologous transplantation and using IMS they are detected in blood. Elimination of graft-versus-host disease (GvHD) in allogenic bone marrow transplan-

tation requires an effective removal of T cells from the bone marrow of the donor. A direct method enabled a 10^3 times depletion of T cells.

Magnetic particles are being increasingly used for isolation of human cell subsets directly from blood and other cell sources. B lymphocytes, endothelial cells, granulocytes, haematopoietic progenitor cells, Langerhans cells, leukocytes, monocytes, natural killer cells, reticulocytes, T lymphocytes, spermatozoa and many others may serve as examples. Cells from other animal and plant species have been successfully separated, too.

Not only whole cells, but also cell organelles can be isolated from crude cellular fractions. Dynal (Oslo, Norway) has developed Dynabeads M-500 Subcellular, which are able to isolate rapidly more than 99% of target organelles.

In the area of parasitology *Cryptosporidium* and *Giardia* are the parasites where IMS is of interest. Two commercially available kits can be used for this purpose. Both products are used in the method 1622: *Cryptosporidium* in Water by Filtration/IMS/FA (December 1997 Draft) of the US Environmental Protection Agency. In very low turbidity samples (clean waters), IMS has demonstrated significantly better results than the standard procedures. When water samples were turbid, the recovery efficiency of IMS diminished.

Future Developments

Magnetic separation of cells is a simple, rapid, specific and relatively inexpensive procedure, which enables the target cells to be isolated directly from crude samples containing a large amount of nontarget cells or cell fragments. Many ready-to-use products are available and the basic equipment for standard work is relatively inexpensive. The separation process can be relatively easily scaled up and thus large amount of cells can be isolated. New processes for detachment of larger magnetic particles from isolated cells enable use of free cells for *in vivo* applications. Modern instrumentation is available on the market, enabling all the process to run automatically. Such devices represent a flexible platform for future applications in cell separation.

IMS play a dominant role at present but other specific affinity ligands such as lectins, carbohydrates or antigens will probably be used more often in the near future. There are also many possibilities to combine the process of cell magnetic separation with other techniques, such as PCR, enabling the elimination of compounds possibly inhibiting DNA polymerase. New applications can be expected, especially in microbiology (isolation and detection of

microbial pathogens) and parasitology (isolation and detection of protozoan parasites). No doubt many new processes and applications in other fields of biosciences and biotechnologies will be developed in the near future.

See Colour Plates 63, 64, 65, 66.

See also: II/Centrifugation: Analytical Centrifugation; Large-Scale Centrifugation. III/Cells and Cell Organelles: Field Flow Fractionation.

Further Reading

- Cell Separation and Protein Purification* (1996) Oslo, Norway: Dynal. 165 pp.
- Häfeli U, Schütt W, Teller J and Zborowski M (eds) (1997) *Scientific and Clinical Applications of Magnetic Carriers*. New York: Plenum Press.
- Olsvik Ø, Popovic T, Skjerve E *et al.* (1994) Magnetic separation techniques in diagnostic microbiology. *Clinical Microbiology Reviews* 7: 43–54.

Recktenwald D and Radbruch A (eds) (1998) *Cell Separation Methods and Applications*. New York: Marcel Dekker. 352 pp.

Šafařík I and Šafaříková M (1999) Use of magnetic techniques for the isolation of cells. *Journal of Chromatography B* 722: 33–53.

Šafařík I, Šafaříková M and Forsythe SJ (1995) The application of magnetic separations in applied microbiology. *Journal of Applied Bacteriology* 78: 575–585.

Ugelstad J, Olsvik Ø, Schmid R *et al.* (1993) Immunoaffinity separation of cells using monosized magnetic polymer beads. In: Ngo TT (eds) *Molecular Interactions in Bioseparations*, pp. 229–244. New York: Plenum Press.

Ugelstad J, Prestvik WS, Stenstad P *et al.* (1998) Selective cell separation with monosized magnetizable polymer beads. In: Andrä W and Nowak H (eds) *Magnetism in Medicine: A Handbook*, pp. 471–488. Berlin: Wiley-VCH Verlag.

Uhlén M, Hornes E and Olsvik Ø (eds) (1994) *Advances in Biomagnetic Separations*. Natick: Eaton Publishing.

CELLS AND CELL ORGANELLES: FIELD FLOW FRACTIONATION



P. J. P. Cardot, S. Battu,
T. Chianea and S. Rasouli,
Université de Limoges, Limoges, France

Copyright © 2000 Academic Press

Introduction

Analysis and sorting of living cells and purification of cell organelles are important procedures in the life sciences. There is a wide range of techniques and methodologies available, which can be divided into three main groups. The techniques in the first groups are based on physical criteria such as species size, density and shape, and include centrifugation, elutriation and field flow fractionation. Those in the second group are linked to cell surface characteristics, while flow cytometry techniques make up the third group. At a fundamental level, field flow fractionation (FFF) exploits the physical characteristics of the cells or cell organelles. However, cells or cell organelles exhibit some specific characteristics that can be described by a multipolydispersity matrix. The different physical characteristics of these biological materials require different FFF techniques and modes of operation. Special care must be taken if biological integrity and viability are to be preserved.

Specific Cell Characteristics

Cellular materials range in size from 1 µm to 50 µm. Cell populations are classified by a set of morphological, functional and biophysical characteristics. The biophysical characteristics are of particular interest in FFF. Usually, separations in FFF are influenced (but not directed) by surface properties of the sample components (to avoid particle–particle or particle–separator interactions). These properties can be modulated by the use of appropriate carrier-phase modifiers (surfactants). In terms of FFF separations, mass, size and density appear to be the major first order parameters. However, size is generally defined by the radius or the diameter of a sphere whose volume is identical to that of the cell. Size can therefore be deduced accurately if the cell of interest is perfectly spherical. However, this is not usually the case, and the sphericity index, I , is then used:

$$I = \frac{4.84(V^{2/3})}{S}$$

In this equation V is the cell volume and S is its surface area can be difficult to determine. In terms of cell population, these dimensions are averages and should be associated with a variance. These general

The cleaning procedure involves flushing the channel (ten times the void volume) with a hypo-osmotic carrier phase to destroy the cells, then with a classical deproteinization agent (ten times the void volume) to desorb and destroy the cell and surfactant proteins adsorbed in the FFF separator. Finally the system is flushed again with the hypo-osmotic carrier phase.

Decontamination is performed by allowing a hypochloride solution (3–6°C) to flow through the whole FFF system. The volume used should be three to four times the void volume of the FFF device. Prior to injection the channel should be flushed with ethanol and rinsed with the sterile mobile phase. Decontamination and sterilization can be simultaneous if a 5°C hypochloride solution is used with a 70°C ethanol solution.

Cell Detection, Viability and Recovery

At the outlet of the channel it is necessary to obtain eluted material that retains its integrity, that is the diagnosis of the whole particle. Photometric devices operated in the light scattering mode can be used to follow elution. After fraction collection off-line analyses methods such as microscopy, granulometric or flow cytometry analyses are recommended. Cell specific staining is also possible. Cell viability can be diagnosed by means of specific tests, and recovery must also be clearly defined.

Conclusions

The choice of FFF separation techniques for purification of cell or cell organelle populations is influenced by their possible elution modes. Micron sized species eluted under the steric hyperlayer model can be separated using sedimentation techniques if their density differs from that of the carrier phase medium. This is also possible for 'nonbuoyant' sub-micron sized cell organelle species eluted according to the 'Brownian' elution mode.

If species are to be separated according to their size, FFF techniques that use a flow generated external field are preferred. If differences in surface characteristics are important, electrical-based FFF techniques

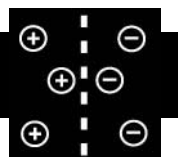
should be chosen. For large sample volume preparations, SPLIT techniques are useful, whatever the external field. The major technical goal in cell separation is not the set-up of the separator, but the construction of a chain of knowledge. The separator is designed according to the sample characteristics as well as the mode of operation. Cleaning and sterilization procedures, and detection and viability procedures, are linked to the nature of the material to be purified. This 'biotechnological' process is of major importance for FFF separations in the life sciences.

See also: **II/Particle Size Separation:** Field Flow Fractionation: Electric Fields; Theory and Instrumentation of Field Flow Fractionation. **III/Colloids:** Field Flow Fractionation. **Polymers:** Field Flow Fractionation. **Proteins:** Field Flow Fractionation. **III/Catalyst studies:** Chromatography: Isolation: Magnetic Techniques.

Further Reading

- Bernard A, Paulet B, Colin V and Cardot PhJP (1995) Red blood cell separations by gravitational field flow fractionation: instrumentation and applications. *Trends Anal. Chem.* 14(6): 266–273.
- Caldwell KD, Cheng ZQ and Hradecky P (1984) Separation of human and animal cells by steric field flow fractionation. *Cell Biophysics* 6: 233–251.
- Giddings JC (1993) Field flow fractionation analysis of macromolecular, colloidal and particulate materials. *Science* 260: 1456–1465.
- Nilson M, Kallio PT, Bailey JE, Bulow L and Wahlund KG (1999) Expression of *Vitreoscilla* hemoglobin in *Escherichia coli* enhances ribosome and tRNA levels: a flow field flow fractionation study. *Biotechnology Progress* 15(2): 158–163.
- Williams PS, Zborowski M and Chalmers JJ (1999) Flow rate optimization for the quadrupole magnetic cell sorter. *Analytical Chemistry* 71: 3799–3807.
- Yang J, Huang Y, Wang XB, Becker FF and Gascoyne PRC (1999) Cell separation on microfabricated electrode using dielectrophoretic/gravitational field-flow fractionation. *Analytical Chemistry* 71: 911–918.
- Yue V, Kowal R, Neargarder L *et al.* (1994) Miniature field-flow fractionation system for analysis of blood cells. *Clinical Chemistry* 40(9): 1810–1814.

CHELATING ION EXCHANGE RESINS



R. J. Eldridge, CSIRO Molecular Science,
Clayton South, Victoria, Australia

Copyright © 2000 Academic Press

Introduction

The useful role of ion exchange is to separate a solution at a low initial concentration C_i into a small

volume of concentrate and a much larger volume of depleted solution. In favourable cases the concentration C_e of the target species in the regeneration effluent approaches the regenerant concentration C_r . The concentration factor achieved is then given approximately by:

$$R \equiv C_e/C_i \approx C_r/C_i \quad [1]$$

One usually wants to separate a single valuable species from the other constituents of the initial solution, and the ion exchanger must then be selective for the target species. (Separation can also be achieved by selective desorption, but selective adsorption is preferable because more of the available resin capacity is occupied by the target ion.) The affinity of a resin for a single ion M , under given conditions, can be represented by a distribution coefficient, defined by:

$$D \equiv \frac{\text{amount of } M \text{ on unit mass of resin}}{\text{amount of } M \text{ in unit volume of solution}} \quad [2]$$

Selectivity between two ions can be expressed by a separation factor, defined by:

$$\alpha \equiv C_e^T \cdot C_d^U / C_d^T \cdot C_e^U \quad [3]$$

where C^T represents the concentration of the target and C^U that of an unwanted species, while C_e refers to the regeneration effluent and C_d to the depleted solution.

Common strong acid resins show a small degree of selectivity between singly and doubly charged cations, and even within these categories. Table 1 shows some selectivity values from the literature for a typical strong acid cation exchanger. These are rational equilibrium constants for the reaction:



defined by:

$$K \equiv A_M \cdot a_{\text{Na}}^n / A_{\text{Na}}^n \cdot a_M \quad [5]$$

where A_M is the activity (on the rational scale) of M^{n+} bound to the resin phase and a_M the activity (molal scale) of the salt MX_n in the solution phase. A_{Na} and a_{Na} are the activities of the analogous sodium species. The observed values are too small to allow

one cation from a mixture to be selectively concentrated by a large factor.

Weak acid resins tend to be more selective than strong acid. Table 1 also lists some selectivity coefficients (not constants), defined by:

$$K' = M_M \cdot m_{\text{Na}}^2 / M_{\text{Na}}^2 \cdot m_M \quad [6]$$

for adsorption of divalent cations M^{n+} on a carboxyl resin initially in the Na^+ form. Here M_M is the molal concentration of M^{n+} in the resin phase and m_M its molality in the solution phase. Although K' and K are only roughly comparable, the carboxyl resin is clearly more selective among these four divalent cations.

Chelating Resins

Ion exchangers incorporating chelating groups have higher selectivity among cations than conventional strong or weak acid resins. (In one sense, adsorption of a di- or trivalent cation by any resin is a chelation process, since the ion is coordinated by two or more ligands linked by a chain of covalent bonds, but the term chelating resin is more usually reserved for resins containing discrete chelating groups, each attached to a single monomer unit. A given cation may be coordinated by one or more of these chelating units.) Technical aspects of their use were outlined by Waitz in 1979. A review and a monograph emphasizing analytical applications were published by Warshawsky and Marhol, respectively, in 1982. A comprehensive review by Sahni and Reedijk appeared in 1984, and a shorter update by Beauvais and Alexandratos in 1998.

Resins with an enormous variety of chelating ligands have been synthesized in the laboratory, but few have been manufactured commercially. Essentially any complexing agent used in analytical chemistry can be coupled to a resin, although the challenge to the synthetic chemist is to avoid sacrificing ligand groups such as thiol or primary amino groups in the coupling reaction. Many published syntheses have been too complex to be economic on an industrial scale or have yielded resins of low stability, but new resin structures continue to be reported. In this review we can consider only a few illustrative examples.

Table 1 Selectivities of strong and weak acid cation exchangers^a

Ion	Na^+	K^+	Mg^{2+}	Ca^{2+}	Zn^{2+}	Ni^{2+}	Cu^{2+}	Pb^{2+}
K	1.00	1.5	4.3	11	4.8	6.1	5.9	39
K'	1.00			14	98	38	550	

^aRational selectivities K of a sulfonated polystyrene resin (8% cross-linked); molal selectivities K' of a methacrylic acid resin (5% cross-linked, degree of ionization 0.85, background electrolyte 1 mol L⁻¹ NaNO₃), relative to Na^+ .

Table 2 Some commercial chelating resins

Chelating group	Examples
Amidoxime	Duolite ES 346 ^a , Diaion CR-50 ^b
Aminophosphonate	Duolite ES 467, Lewatit OC 1060 ^c
Iminodiacetate	Dowex A-1 ^d , Diaion CR-10, Duolite ES 466, Lewatit TP 208
Diphosphonate	Diphonix ^e
Bis(2-picolyl)amine	Dow 3N (Dowex XFS 4195)
2-Picolyl-2'-hydroxypropylamine	Dow 2N (Dowex XFS 43084)
Oligoamine	Diaion CR-20, Lewatit E 304, Sumichelate MC10 ^f

^a Rohm and Haas; ^b Mitsubishi Chemical; ^c Bayer; ^d Dow Chemical; ^e Eichrom Industries; ^f Sumitomo Chemical.

Early chelating resins based on phenolic polymers were largely displaced by styrene-divinylbenzene resins, functionalized via chloromethylation, because of their greater stability. More recently, acrylic polymers have gained ground, with glycidyl methacrylate being a favoured monomer because ligands are easily coupled by reaction with its epoxide group, although possible hydrolysis of the ester link at extremes of pH limits the applicability of these resins. Sherrington, Driessen and their co-workers have used this strategy to prepare a suite of chelating resins containing nitrogen heterocycles. Similarly, Chanda and Rempel have coupled a wide range of chelating groups to polybenzimidazole beads activated with epichlorohydrin.

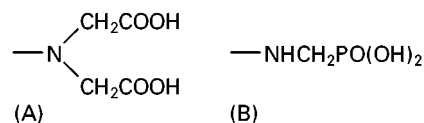
Table 2 lists some commercially available chelating resins. The order of preference for iminodiacetate resins is typically:

Univalent cations: Ag > Li > Na > K > Rb > Cs
 Divalent cations: Hg > U(VI) > Cu > Pb > Ni
 > Cd ≈ Zn > Co > Fe > Mn
 > Ca > Mg > Ba > Sr
 Trivalent cations: Cr > In > Fe > Ce > Al > La

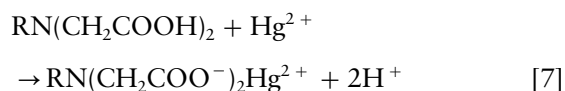
Structures for the iminodiacetate and aminophosphonate groups are shown in **Figure 1**. Some selectivity coefficients (no definition given) for iminodiacetate resins, recalculated from Waitz, are collected in **Table 3**.

Iminodiacetate Resins: Mercury

Iminodiacetate resins are clearly more selective among the transition metals than are weak acid

**Figure 1** Chelating functionalities: (A) iminodiacetic acid and (B) aminophosphonic acid.

resins. Adsorption of all metal cations decreases with decreasing pH, and uptake of moderately preferred ions such as Ni²⁺ and Zn²⁺ becomes negligible at pH 1–2, but Hg²⁺ and Cu²⁺ are still strongly adsorbed. For Hg²⁺ in sulfuric acid, $D \approx 2 \text{ L g}^{-1}$ at pH 1. The advantage of this high selectivity is illustrated by some results for treatment of a highly acidic, mercury-containing smelter wastewater. Simulated wastewater containing Hg(II), Zn(II), Fe(III), Cd(II) and Pb(II) salts at pH 1.5 was treated with an iminodiacetate resin in bench-scale column runs. **Table 4** and **Figure 2** show the composition of the column effluent over 157 bed volumes. Uptake of Hg(II) was close to 100%, while most of the other cations were not significantly adsorbed. Adsorption of mercury can be represented by:



It appears that a small amount of Pb(II) is adsorbed initially, then displaced by Hg(II). Fe(III) is adsorbed more strongly than Pb(II), but still less strongly than Hg(II). Uptake of iron can essentially be eliminated by reducing Fe(III) to Fe(II), which is not significantly adsorbed at this low pH.

Regeneration with Complexation

Chelating resins are commonly regenerated with mineral acid, but in some cases the resin's affinity for the target metal is too great for this to succeed. In the Hg(II)-iminodiacetate system desorption with nitric acid failed because of the very strong complexation of Hg(II). Concentrated NaCl solution was an effective regenerant because Cl[−] ions convert Hg²⁺ to a series of chlorocomplexes (**Figure 3**). In other words, Hg²⁺ is adsorbed more strongly than H⁺, but can be displaced even by Na⁺ because it is simultaneously complexed by Cl[−]. In this example, both adsorption and desorption steps are selective for Hg(II) over

Table 3 Selectivities at pH 4 of an iminodiacetate chelating resin, relative to Ca²⁺

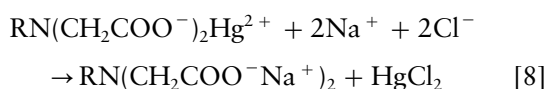
Ion	Ca ²⁺	Fe ²⁺	Co ²⁺	Cd ²⁺	Zn ²⁺	Ni ²⁺	Pb ²⁺	Cu ²⁺	Hg ²⁺
K ^{''}	1.00	4.0	6.7	15	17	57	1200	2300	2800

Table 4 Selective removal of Hg(II) on a chelating resin^a

	<i>Hg(II)</i>		<i>Zn(II)</i>		<i>Fe(III)</i>		<i>Cd(II)</i>		<i>Pb(II)</i>	
	<i>mg L⁻¹</i>	%	<i>mg L⁻¹</i>	%	<i>mg L⁻¹</i>	%	<i>mg L⁻¹</i>	%	<i>mg L⁻¹</i>	%
Feed	11.8	100	78	100	37	100	1.7	100	4.6	100
<i>Bed volumes</i>										
23	<0.015	< 0.1	73	94	1	3	1.6	94	4.0	87
47	0.015	0.1	74	95	7	19	1.7	100	5.5	120
77	0.015	0.1	78	100	14	38	1.7	100	5.0	109
111	0.030	0.3	78	100	17	46	1.7	100	4.7	102
157	0.035	0.3	76	97	28	76	1.7	100	4.9	107

^aMetal concentrations before and after treatment of a simulated smelter wastewater (pH 1.5) with an iminodiacetate resin. Reproduced with permission from Becker NSC and Eldridge RJ (1993) *Reactive Polymers* 21: 5.

most elements, although Fe(III) shares the ability of Hg(II) to adsorb as a cation and desorb as a chloro-complex. The regeneration reaction can be written:



Alkaline Earths

The formation of chelate complexes is often regarded as an exclusive property of transition metal cations, but both iminodiacetate and aminophosphonic resins chelate alkaline earth cations and consequently are highly selective for them relative to the alkali metal cations. Separation factors achievable with iminodiacetate resins are reported to be 50–60 for Mg/Na and 500–600 for Ca/Na at pH 7–10;

for aminophosphonate resins $\alpha_{\text{Na}}^{\text{Mg}} \approx 1000$ and $\alpha_{\text{Na}}^{\text{Ca}} \approx 20\,000$. These resins are very effective in softening applications, including, as an extreme case, the removal of low levels of unwanted divalent cations from brine in caustic chlorine plants, despite the great excess of sodium ions.

Amidoxime Resins: Uranium from Seawater

The possibility of recovering valuable metals from the oceans presents a challenge to designers of chelating resins. Uranium is present in seawater at about 14 nmol L^{-1} ($3 \mu\text{g L}^{-1}$), predominantly as the tricarbonyluranate(VI) anion $\text{UO}_2(\text{CO}_3)_3^{4-}$. Recovery by ion exchange would require an extremely selective sorbent, since seawater also contains Na^+ at

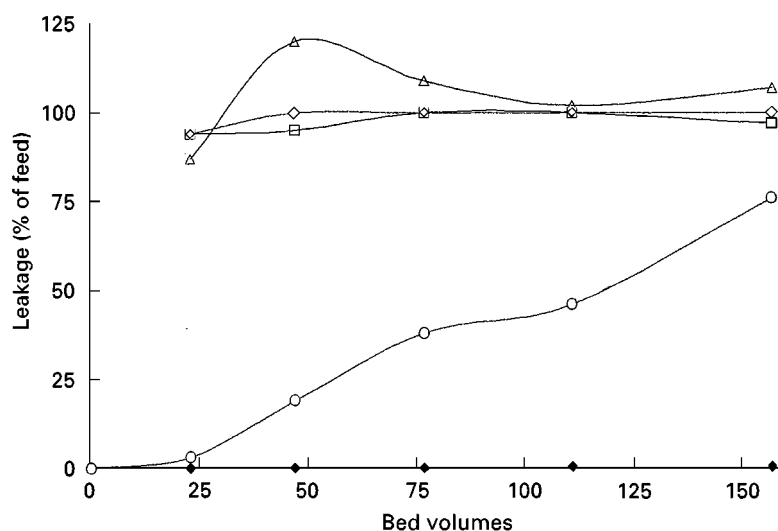


Figure 2 Separation of metal cations on an iminodiacetate resin at pH 1.5. Triangles, Pb(II); open diamonds, Cd(II); squares, Zn(II); circles, Fe(III); filled diamonds, Hg(II). (Reproduced with permission from Becker NSC and Eldridge RJ (1993) *Reactive Polymers* 21: 5.)

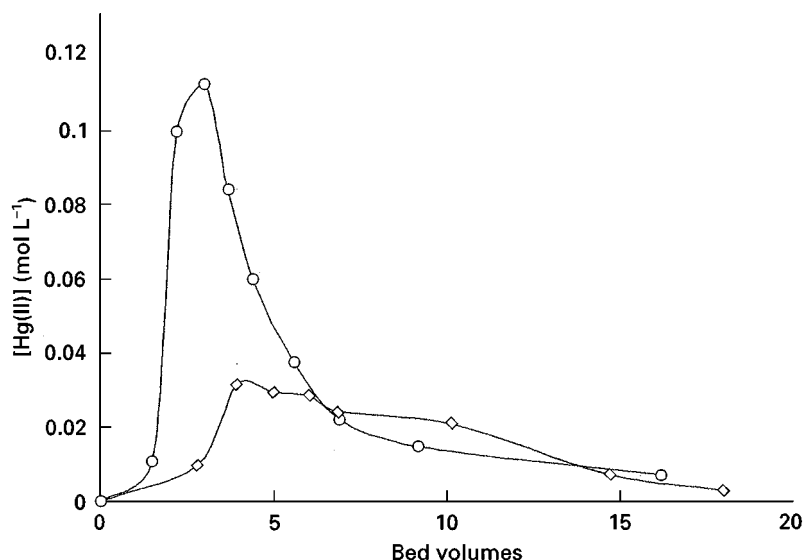
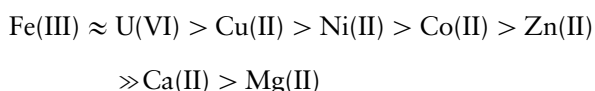


Figure 3 Regeneration of a chelating resin may require a complexing eluant: desorption of Hg(II) from an iminodiacetate resin with 3 mol L⁻¹ sodium chloride (circles) or 2 mol L⁻¹ nitric acid (squares). (Reproduced with permission from Becker NSC and Eldridge RJ (1993) *Reactive Polymers* 21: 5.)

0.6 mol L⁻¹, Mg²⁺ at 0.4 mol L⁻¹ and transition metal ions such as Fe³⁺, Cu²⁺ and Zn²⁺, at 10–100 nmol L⁻¹. Iminodiacetate resins fail to adsorb significant amounts of uranium from seawater, since their UO₂²⁺/Mg²⁺ selectivity coefficient is only ~ 600. During the 1980s, amidoxime resins derived from polyacrylonitrile (**Figure 4**) were extensively investigated by several research groups, particularly in Europe and Japan, and shown to adsorb up to about 1 mg U g⁻¹ resin from spiked seawater. Distribution coefficients decrease in the order:



from ~ 300 L g⁻¹ for Fe(III) and U(VI) to ~ 20 mL g⁻¹ for Mg(II). UO₂²⁺ cations are believed to be complexed by two deprotonated amidoxime groups, which displace the carbonate ligands. Adsorption rates are higher for resins incorporating hydrophilic cross-linkers or comonomers. Hydrochloric acid at 0.5–1 mol L⁻¹ is an effective regenerant, but causes some hydrolysis of the amidoxime groups.

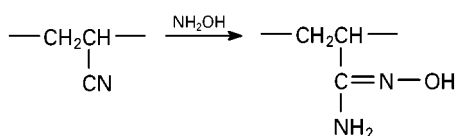


Figure 4 Synthesis of an amidoxime resin from polyacrylonitrile.

In one experiment with unspiked seawater, an experimental amidoxime resin adsorbed 1 mg g⁻¹ uranium ($D \approx 300$ L g⁻¹). Fe³⁺, Cu²⁺ and Zn²⁺ were concentrated by similar factors. Isolation of pure uranium would therefore need selective regeneration or post-treatment of the regeneration effluent.

Amidoxime resins are also highly selective for Ga(III) at high pH and have been used to recover gallium from Bayer liquor. Again, capacity loss is a problem.

Oligoamine Resins

Many of the transition metal cations are strongly coordinated by uncharged nitrogen-containing ligands. Consequently, chelating resins possessing strongly electron-donating nitrogens will selectively remove Cu²⁺, for example, from solutions containing alkali and alkaline earth cations. Since the resin is uncharged, the adsorbed cations must be accompanied by mobile counterions to maintain electroneutrality. SenGupta has exploited this effect to adsorb anions such as phosphate, selenite, oxalate and phthalate on copper-loaded picolylamine resins (Dow 2N or 3N). These coordinating anions displace anions, such as sulfate, that are associated with adsorbed Cu(II) only by electrostatic attraction. Loss of copper from the resin during ligand exchange is extremely small.

Even conventional weak base resins – usually used as anion exchangers – are capable of separating transition metals from alkaline earths. Uptakes of

Cu(II) have been demonstrated at pH 5 on the phenolic weak base resin Duolite A7 and the acrylic weak base Amberlite IRA35 comparable to their anion exchange capacities ($1\text{--}2\text{ meq g}^{-1}$). Uptake of Ni(II) or Zn(II) was smaller. Regeneration with mineral acid was efficient. An aminophenol resin of similar structure to Duolite A7 was found to adsorb Cu(II), presumably accompanied by sulfate ions, from CuSO_4 solutions at pH 4–7. Other transition metal ions (Fe^{2+} , Co^{2+} , Ni^{2+} , Zn^{2+} , Cd^{2+} and Hg^{2+}) were scarcely adsorbed in this pH range, but in the protonated form (pH ≈ 2) the resin became highly selective for Fe^{3+} .

The transition metal affinity of resins having aliphatic oligoamine substituents increases with chain length (number of amino groups in each chelating group). It has been reported that acrylic oligoamine resins (Figure 5) can adsorb significant amounts of Cu^{2+} , Ni^{2+} , Zn^{2+} or Cd^{2+} from solutions containing ethylenediaminetetraacetic acid (EDTA), provided alkaline earth cations are also present. Transition metal uptakes were highest on resins derived from tetraethylenepentamine or pentaethylenhexamine.

Diphonix

A similar coordination mechanism operates in the adsorption of some metal ions from highly acidic solution on phosphonic acid resins, for example actinide ions on Diphonix[®], one of very few new chelating resins to be introduced commercially in the 1990s. The chelating groups in this resin are contributed by vinylidene-1,1-diphosphonic acid monomer units, but the resin also contains acrylic acid and styrenesulfonic acid units (Figure 6). As with the amidoxime resins described above, hydrophilic monomers are essential for high reaction rates. Diphonix is the outcome of work at the Argonne National Laboratory on 1,1-diphosphonic acid ligands and at the University of Tennessee on ion exchangers possessing two or more types of functional group, operating by different mechanisms. It was developed primarily for actinide separations in highly acidic media, but also strongly adsorbs divalent transition metal cations at pH 1–2 and trivalent cations at pH 0–2.

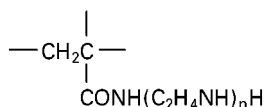


Figure 5 Acrylic oligoamine resin.

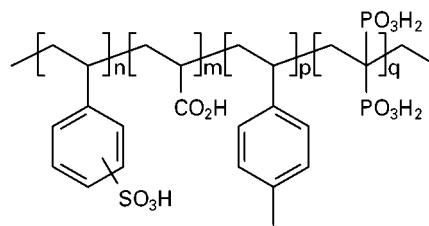
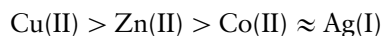
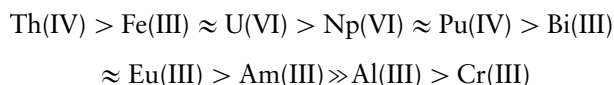


Figure 6 Structure of Diphonix[®].

In pH 1 nitric acid distribution coefficients on Diphonix decrease in the order:



from $\sim 3\text{ L g}^{-1}$ to $\sim 500\text{ mL g}^{-1}$. For these ions a double-logarithmic plot of the distribution coefficient against $[\text{H}^+]$ has slope $-n$, where n is the cation charge. This indicates that adsorption occurs by simple exchange of M^{n+} for H^+ . In 1 mol L^{-1} nitric acid, the order of selectivity is:



with D as high as 900 L g^{-1} for Th(IV) and 200 L g^{-1} for Fe(III) and U(VI), decreasing to 400 mL g^{-1} for Al(III) and 80 mL g^{-1} for Cr(III). Uptake of the strongly preferred ions shows little pH dependence, indicating adsorption without displacement of H^+ on phosphonic acid groups that are not significantly ionized under these conditions. To maintain electroneutrality, the complexed metal ions must be associated with anions from solution, either free or in mixed-ligand complexes containing phosphonic acid groups and small ion ligands such as Cl^- . The less preferred ions show simple ion exchange behaviour over a limited pH range, but uptake increases at high acid concentrations, indicating a change in mechanism.

The very high affinity of Diphonix for Fe(III) makes it very suitable for removing iron from acidic copper electrolytes in copper production by electrowinning. The process has been demonstrated in pilot-scale trials at copper refineries, with no decrease in resin performance over hundreds of cycles. Fe(III) is desorbed by reducing it to Fe(II).

Circumventing Limitations to Selectivity

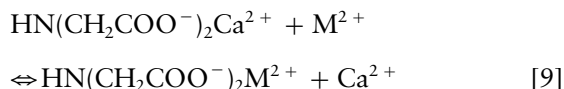
The selectivity between two cations of a chelating resin should in principle be equal to that of the chelating ligand itself, but this is seldom true in practice. For example, iminodiacetate resins are very much less

Table 5 Comparison of an iminodiacetate resin with the iminodiacetate ion^a

Ion	Ca ²⁺	Fe ²⁺	Co ²⁺	Cd ²⁺	Zn ²⁺	Ni ²⁺	Pb ²⁺	Cu ²⁺	Hg ²⁺
<i>K''</i>	1.00	4.0	6.7	15	17	57	1200	2300	2800
<i>K_m</i>	1.00	1600	2.3 × 10 ⁴	600	2.8 × 10 ⁴	4.7 × 10 ⁵	7 × 10 ⁴	9 × 10 ⁷	1.5 × 10 ⁹

^aSelectivities for divalent cations (relative to Ca²⁺) of an iminodiacetate chelating resin (*K''*) and the iminodiacetate ion (*K_m*).

selective than the free iminodiacetate ion, as shown in Table 5, which compares equilibrium constants for the reaction:

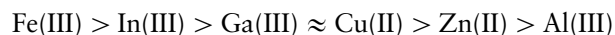


with the corresponding values from Table 3 for iminodiacetate resins. There are several reasons for the discrepancy. In the first place the resin is heterogeneous on a molecular scale. Its chelating groups are located in environments that may vary in polarity, dielectric constant or steric crowding, depending for example on their closeness to cross-links. This variation in chemical environment affects the binding constant for different metal ions to differing extents, degrading the selectivity of the resin. Secondly, the high local concentration of ligands in the resin may lead to a mixture of 1 : 1, 2 : 1 and higher complexes. At loadings less than 100%, the number of ligands coordinated to each metal ion is almost impossible either to control or to measure. Thirdly, the exchange reaction itself changes the properties of the resin. Selectivities of simple ion exchangers are well known to vary with the extent of loading, and the same will be true of chelating resins, especially when adsorbed metal ions are coordinated by ligands attached to different polymer chains, reversibly creating additional cross-links. The result of these factors is not merely reduced selectivity of polymeric resins relative to low molecular weight ligands, but in some cases the order of selectivity is reversed (Table 5).

The mixed composition and additional cross-link effects can be eliminated by designing the resin to accommodate the maximum coordination number of the cation with a single multidentate ligand. Resins containing EDTA moieties are an example. These were synthesized by Takeda *et al.* at Asahi Chemical in 1985, with *m*-divinylbenzene as the essential building block. Addition of bromine across one double bond before polymerization allowed the introduction of an iminodiacetate group on each carbon of the pendant C₂ chains. However, even in these resins, ligands still experience a range of chemical environments.

Oligoamine weak base resins suffer an additional source of heterogeneity since the amine (diethylenetri-

riamine (DETA), for example) can attach to the precursor resin (chloromethylated polystyrene-co-divinylbenzene) through either primary or secondary nitrogens, and can react with multiple chloromethyl groups, introducing additional covalent cross-links. This effect was eliminated in experimental resins: the primary nitrogens of DETA were blocked by forming Schiff base adducts, followed by amination exclusively through the secondary nitrogen and subsequent hydrolysis of the Schiff base groups to recover the primary amino groups (Figure 7). The latter were then converted by further reaction to iminodiacetate, aminophosphonate or other chelating groups. The selectivity sequence of the *bis*(iminodiacetate) derivative is:



with distribution coefficients decreasing from ~ 10 L g⁻¹ at pH 1 for Fe(III) to ~ 10 mL g⁻¹ for Al(III) at pH 2. The resin readily separates Ga(III) and In(III) from Zn(II) and Al(III) in acid solution, but Fe(III) and Cu(II) must first be removed (by precipitation as sulfides, for example). For most trivalent rare earth cations, *D* ≈ 100–500 mL g⁻¹ at pH 2, with the highest values being observed for the medium atomic

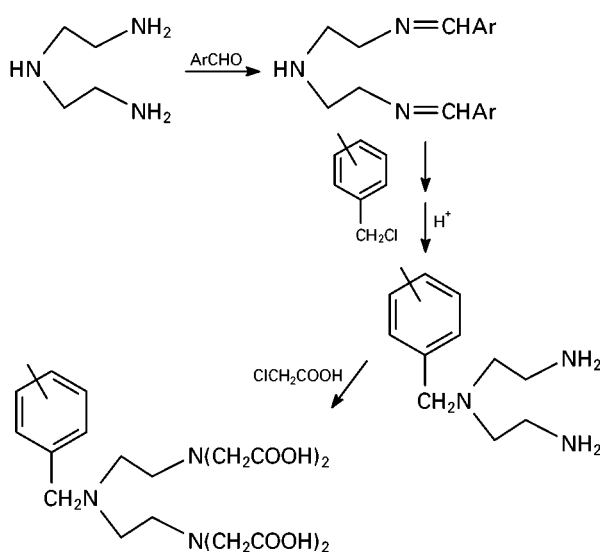


Figure 7 Synthesis of diethylenetriamine resin coupled exclusively through the secondary nitrogen, and conversion to a *bis*(iminodiacetic acid) derivative.

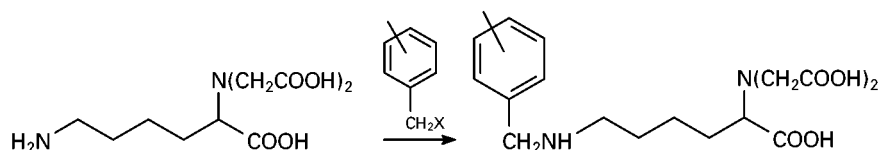


Figure 8 Lysine- N^{α},N^{α} -diacetic acid resin.

weight lanthanides (Sm-Dy). The selectivity is great enough to permit chromatographic separation of pairs of lanthanides (La/Pr or Nd/Sm).

The effect of inhomogeneity can be minimized by introducing spacer groups between the chelating groups and the polymer backbone. A highly selective nitrilotriacetate-like resin was synthesized by functionalizing a polystyrene matrix with lysine- N^{α},N^{α} -diacetic acid (**Figure 8**). This resin shows high selectivity for trivalent ions such as Ga(III) and In(III) over divalent cations. When loaded with Fe(III) it can be used to adsorb As(III) and As(V) oxyanions by ligand exchange.

Sulfur Ligands

In the quest for high affinity and high selectivity, many sulfur-containing ligands have been investigated, including thiol, thioether and thiocarbonyl groups, as well as sulfur–nitrogen heterocycles. Thiol resins are available from several manufacturers. Although falling outside the above definition of chelating resins, they can be regarded as the prototype of resins containing thiocarbonyl, thioether or dithiocarboxylate groups, or multiple ligands such as thiol/amino combinations. Thiol resins have been used for adsorption of mercury(II) and are effective in the presence of competing ligands such as Cl^- . However, regeneration is difficult, requiring concentrated acid, and the thiol group is prone to oxidation.

Sulfur-containing ligands tend to have high affinity for platinum group metals (PGM). Isothiuronium resins (**Figure 9**), first prepared in the 1960s by Koster and Schmuckler and subsequently commercialized in both gel (Srafion) and macroporous (Monivex) versions, adsorb PGM from strongly acidic solution and require complexing agents for regeneration. Adsorption is believed to be by simple ion exchange when the functional groups are fully protonated, but this not

achievable in the gel resin, and adsorption then involves both electrostatic and complexing interactions.

Isothiuronium resins have been used in laboratory- and pilot-scale PGM separations from HCl leach solutions, with thiourea or thiocyanate as regenerant. However, new sulfur–nitrogen resins are still being reported for heavy metal and PGM applications. Polybenzimidazole functionalized with dithiooxamide was found to be strongly selective for Pd(II) and Pt(IV) over first-row transition metals in acidic solution. Other researchers report similar behaviour with resins containing, for example, thiosemicarbazide, dithizone, thiadiazole or thiotetrazolium substituents.

Kinetics

Adsorption and desorption rates are an important consideration in ion exchange, as well as equilibrium behaviour. Complexation rates benefit from small particle size, high porosity and, as noted above, high hydrophilicity. Capturing the rate advantage of small size requires a solution to the problem of handling fine particles. Incorporating a magnetic component is one strategy that has been demonstrated. Resins can also be made in nonconventional formats, such as graft copolymers or fine fibres, to keep diffusion paths short. A range of fibrous sorbents was developed under the name Fiban, derived from polyacrylonitrile fibres or polypropylene fibres grafted with styrene, including a chelating material containing imidazoline groups derived from polyacrylonitrile. These sorbents could be used to form filaments or nonwoven fabrics. Similarly, others have reported amidoxime sorbents made from polyacrylonitrile fibre and woven into cloth for use in uranium recovery, and polyacrylonitrile-g-glycidyl methacrylate fibres (Tiopan) functionalized with ligands including thiosemicarbazide, 8-mercaptoquinoline and 2-aminothiazole.

Conclusion

Ingenious syntheses of chelating resins continue to be reported. However, large scale applications for such materials are limited, and few are likely to be produced

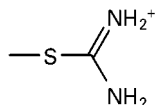


Figure 9 Isothiuronium group.

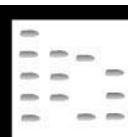
industrially. The main markets appear to be in the production of low volume, high value elements: precious metals, rare earths with valuable optical properties and raw materials for electronic devices. Applications in lower value fields such as waste management or by-product recovery should benefit from novel resin formats designed for improved resin/liquid contacting.

See also: **II/Ion Exchange:** Historical Development; Novel Layered Materials: Non-Phosphates; Novel Layered Materials: Phosphates; Organic Ion Exchanger; Organic Membranes; Theory of Ion Exchange.

Further Reading

- Beauvais RA and Alexandratos SD (1998) Polymer-supported reagents for the selective complexation of metal ions: an overview. *Reactive and Functional Polymers* 36: 113–123.
- Chanda M and Rempel GL (1990) Polybenzimidazole resin based new chelating agents. Palladium(II) and platinum(IV) sorption on resin with immobilized dithiooxamide. *Reactive Polymers* 12: 83–94.
- Chiarizia R, Horwitz EP, Alexandratos SD and Gula MJ (1997) Diphonix® resin: a review of its properties and applications. *Separation Science and Technology* 32: 1–35.
- Hirotsu T, Katoh S, Sugasaka K, Takai N, Seno M and Itagaki T (1987) Adsorption of uranium on cross-linked amidoxime polymers from seawater. *Industrial and Engineering Chemistry Research* 26: 1970–1977.
- Hoffmann H and Martinola F (1988) Selective resins and special processes for softening water and solutions: a review. *Reactive Polymers* 7: 263–272.
- Marhol M (1982) Chelating resins and inorganic ion exchangers. In Svehla G (ed.) *Wilson and Wilson's Comprehensive Analytical Chemistry*, Vol. XIV, ch. 6, pp. 377–399. Oxford: Elsevier.
- Naden D and Streat M (eds) (1984) *Ion Exchange Technology*. Chichester: Ellis Horwood.
- Sahni SK and Reedijk J (1984) Coordination chemistry of chelating resins and ion exchangers. *Coordination Chemistry Reviews* 59: 1–139.
- Suzuki TM and Matsunaga H (1991) Metal selective polymer resins for the separation and concentration of rare metals. *Trends in Inorganic Chemistry* 2: 33–47.
- Warszawsky A (1982) Selective ion exchange polymers. *Die Angewandte Makromolekulare Chemie* 109/110: 171–196.
- van Berkel PM, Punt M, Koolhaas GJAA, Driessen WL, Reedijk J and Sherrington DC (1997) Highly copper(II)-selective chelating ion-exchange resins based on bis(imidazole)-modified glycidyl methacrylate copolymers. *Reactive and Functional Polymers* 32: 139–151.
- Zhao D, SenGupta AK and Zhu Y (1995) Trace contaminant sorption through polymeric ligand exchange. *Industrial and Engineering Chemistry Research* 34: 2676–2684.

CHEMICAL WARFARE AGENTS: CHROMATOGRAPHY



P. A. D'Agostino, Medicine Hat, Alberta, Canada

Copyright © 2000 Academic Press

Introduction

The development and application of analytical methods for the analysis of chemical warfare agents have received increased attention, due in large part to the recently ratified Convention on the Prohibition of the Development, Production, Stockpiling and Use of Chemical Weapons and their Destruction (commonly referred to as the Chemical Weapons Convention or CWC). After considerable effort the CWC was opened to signature in 1993, with the treaty coming into force on 29 April 1997. The treaty has been ratified by 120 states, all of which agree not to develop, produce, stockpile, transfer or use chemical weapons and agree to destroy their own chemical weapons and production facilities. A strong compli-

ance-monitoring regime involving site inspections was built into the CWC to ensure that the treaty remains verifiable. The Organisation for the Prohibition of Chemical Weapons, or OPCW, based in The Hague, has responsibility for implementation of the treaty. Routine OPCW inspections have or will take place at declared sites, including small scale production, storage and destruction sites, and challenge inspections will take place at sites suspected of non-compliance.

An analytical capability will be required to help verify compliance with the treaty, since inspectors will have the option to take and analyse suspect samples to help establish compliance or noncompliance. Gas chromatography is the current method of choice for the separation and analysis of chemical warfare agents, with this technique being employed in the field-portable gas chromatographic-mass spectrometric (GC-MS) instrumentation in use by the OPCW inspectorate.

Chemical warfare agents are a group of toxic chemicals that have been defined in the CWC as 'any chemical which through its chemical effect on life processes can cause death, temporary incapacitation or permanent harm to humans or animals...'. Poisonous or toxic compounds have been utilized in an effort to gain military superiority throughout history but it is only during the past century that chemical warfare agents have been produced and used on a large scale. Tear gas grenades were used in 1914 by the French at the outbreak of World War I, but it was not until the Germans first used chlorine near Ypres in 1915 that the world entered the modern era of chemical warfare. Other chemical warfare agents such as phosgene and mustard were used by both sides in World War I.

The use and development of chemical warfare agents continued after World War I despite the signing of the 1925 Geneva Protocol, which bans the first use of chemical weapons. Mustard was used by the Italians against the Abyssinians (Ethiopia) during 1936–1937, and just prior to World War II, the Germans discovered and produced the first nerve agent, tabun. Nerve agents were made into weapons by the Germans but neither side made use of their chemical weapons stock. More effective nerve agents, such as VX, were developed in the 1950s, mustard was used in the Yemen War (1963–1967), and allegations of chemical warfare agent use were reported in South-East Asian conflicts. Nerve and mustard agents were used by Iraq in the 1980s war between Iran and Iraq, and were considered a real threat to United Nations armed forces during their action against Iraq (1990–1991). More recently, sarin was used against the population of a Kurdish village in 1993 and again in 1995 by terrorists in the Tokyo underground transit system. Proliferation of chemical weapons and their use will hopefully decrease over the coming years as the CWC proceeds towards its goal of worldwide chemical weapons destruction.

Chemical Warfare Agent Categories

Chemical warfare agents have been classified into nerve, blister, choking, vomiting, blood, tear and incapacitating agent categories based on their effect on humans. The most significant chemical warfare agents in terms of military capacity and past use are the nerve and blister agents. For these reasons the analysis of these compounds will be emphasized over the other groups. The choking, blood and vomiting agents are for the most part obsolete chemical agents that were employed during World War I. The tear agents were used during the Vietnam War but their primary use, because of their inability to produce

high casualties, remains in riot control and for the training of military personnel in chemical defence. Incapacitating agents have been included as the USA did develop an agent in this category.

The compounds listed in Table 1 represent the most common chemical warfare agents, grouped by category with their Chemical Abstracts registry numbers, and is not intended to be exhaustive. It has been estimated that more than 7000 compounds are controlled under the CWC, although in practical terms the actual number of chemical warfare agents, precursors, degradation products and related compounds that are contained in the OPCW GC-MS database is in the hundreds. The structures of some common nerve and blister chemical warfare agents are illustrated in Figure 1.

Gas Chromatographic Methods

Chemical warfare agents have often been referred to as warfare gases and, in the military, the phrase 'gas, gas, gas' has become synonymous with attack by chemical warfare agents. In fact, many chemical warfare agents exist as liquids at ambient temperatures but have varying degrees of volatility and pose a significant vapour hazard as well as a liquid contact hazard. This physical characteristic has made the analysis of chemical warfare agents amenable to gas chromatography (GC) with a variety of detectors including mass spectrometry (MS).

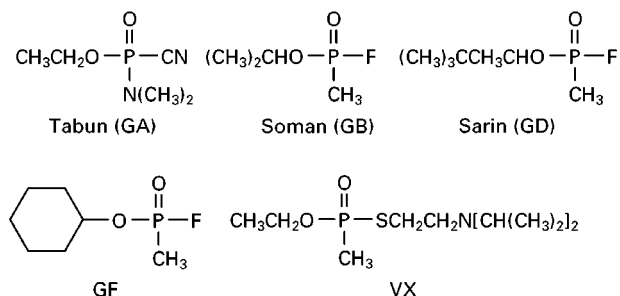
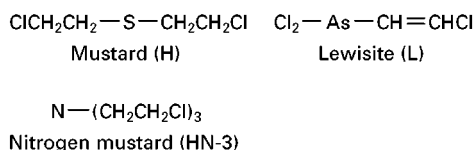
The OPCW, an important end-user of analytical techniques for chemical warfare agents, requires the use of two or more spectrometric techniques and the availability of authentic reference standards for the unambiguous identification of these controlled compounds. For this reason, the combined use of GC–Fourier transform infrared spectrometry (FTIR) has received increased attention as newer technologies have led to detection limits approaching those routinely reported during GC-MS analysis. For analyses involving low levels of chemical warfare agents in the presence of high levels of interfering chemical background, tandem mass spectrometry (MS-MS) is receiving increased attention.

GC Retention Behaviour

Packed column GC was routinely employed in the past for the analysis of chemical warfare agents, but with the advent of fused silica capillaries this technology has been used less frequently. Capillary column GC has become the most frequently employed analytical separation method for the screening of samples contaminated with chemical warfare agents. Separation of chemical warfare agents may be achieved with fused silica columns coated with poly-

Table 1 Common chemical warfare agents

Full name (trivial name(s))	Chemical Abstracts no.
(a) <i>Nerve</i> (reacts irreversibly with cholinesterase; this results in acetylcholine accumulation, continual stimulation of the body's nervous system and eventual death)	
<i>O</i> -Isopropyl methylphosphonofluoridate (sarin, GB)	107-44-8
<i>O</i> -Pinacolyl methylphosphonofluoridate (soman, GD)	96-64-0
<i>O</i> -Cyclohexyl methylphosphonofluoridate (GF)	329-99-7
<i>O</i> -Ethyl <i>N,N</i> -dimethylphosphoramidocyanidate (tabun, GA)	77-81-6
<i>O</i> -Ethyl <i>S</i> -2-diisopropylaminoethyl methylphosphonothiolate (VX)	50782-69-9
(b) <i>Blister</i> (affects the lungs, eyes and produces skin blistering)	
Bis(2-chloroethyl)sulfide (mustard, H)	505-60-2
Bis(2-chloroethylthio)ethane (sesquimustard, Q)	3563-36-8
Bis(2-chloroethylthioethyl)ether (T)	63918-89-8
Tris(2-chloroethyl)amine (HN-3)	555-77-1
2-Chlorovinyl dichloroarsine (lewisite, L)	541-25-3
(c) <i>Choking</i> (affects respiratory tract and lungs)	
Chlorine	7782-50-5
Carbonyl dichloride (phosgene, CG)	75-44-5
(d) <i>Vomiting</i> (causes acute pain, nausea and vomiting in victims)	
Diphenylarsinous chloride (DA)	712-48-1
10-Chloro-5,10-dihydrophenarsazine (adamsite, DM)	578-94-9
Diphenylarsinous cyanide (DC)	23525-22-6
(e) <i>Blood</i> (prevents transfer of oxygen to the body's tissues)	
Hydrogen cyanide (HCN, AC)	74-90-8
(F) <i>Tear</i> (Causes tearing and irritation of the skin)	
[(2-chlorophenyl)methylene]propanedinitrile (CS)	2698-41-1
2-Chloro-1-phenylethanone (CN)	532-27-4
Dibenz[b,f][1,4]oxazepin (CR)	257-07-8
(g) <i>Incapacitating</i> (prevents normal activity by producing mental or physiological effects)	
3-Quinuclidinyl benzilate (BZ)	6581-06-2

Nerve agents**Blister agents****Figure 1** Structures of common chemical warfare agents.

siloxane or other films and retention index data relative to *n*-alkanes and *n*-alkylbis(trifluoromethyl)phosphine sulfides (M-series) have been reported for many chemical warfare agents and related compounds under temperature programming conditions. Retention indices relative to *n*-alkanes have been reported for 100% dimethyl-polysiloxane (e.g. J&W DB-1), (95%)-methyl-(5%)-diphenyl-polysiloxane (e.g. J&W DB-5), (86%)-dimethyl-(14%)-cyanopropylphenyl-polysiloxane (e.g. J&W DB-1701) and other films. In general, the best separations have been achieved with a moderately polar film such as (86%)-dimethyl-(14%)-cyanopropylphenyl-polysiloxane. **Table 2** lists typical retention index data for several common chemical warfare agents on three different liquid phases under temperature programming conditions.

The use of retention indices relative to *n*-alkanes by the OPCW during on-site inspections is anticipated in the near future to differentiate between controlled compounds that exhibit similar electron impact mass spectrometric (EI-MS) data during GC-MS analysis,

Table 2 GC retention index data for common chemical warfare agents (relative to *n*-alkanes)

Compound name	GC retention index ^a		
	DB-1	DB-5	DB-1701
<i>O</i> -Isopropyl methylphosphonofluoridate (sarin, GB)	792	824	966
<i>O</i> -Pinacolyl methylphosphonofluoridate (soman, GD) ^b	1008	1045	1188
	1013	1049	1193
<i>O</i> -Ethyl <i>N,N</i> -dimethylphosphoramidocyanidate (tabun, GA)	1078	1132	1340
<i>O</i> -Ethyl <i>S</i> -2-diisopropylaminoethyl methylphosphonothiolate (VX)	1664	1710	1881
Bis(2-chloroethyl)sulfide (mustard, H)	1124	1173	1326
Bis(2-chloroethylthio)ethane (sesquimustard, Q)	1623	1689	1923
Bis(2-chloroethylthioethyl)ether (T)	1910	1983	2241

^aGC retention indices determined with three J&W 0.25 μ m films with the following temperature program: 50°C (2 min), then 10°C min⁻¹ to 300°C (5 min).

^bRetention data for both enantiomer pairs.

but different GC retention behaviour. Application of GC retention indices during the analysis of VX-contaminated samples is likely since the EI-MS data for VX and a number of VX-related compounds are remarkably similar. The EI data for these compounds lack a molecular ion and contain a base ion at m/z 114 due to $(\text{CH}_2\text{N}(\text{iPr})_2)^+$ and additional ions related to the $-\text{SC}_2\text{H}_4\text{N}(\text{iPr})_2$ substituent.

Chiral stationary phases have been developed for the resolution of stereoisomers of several chiral nerve agents, most notably soman. The use of multiple columns of differing polarity during one analysis has also been successfully employed during chemical warfare agent analysis and the term 'retention spectrometry' was coined to describe this technique.

Conventional GC Detectors

Most of the GC detectors commonly applied to pesticide residue analysis have also been applied to the screening of samples for chemical warfare agents. Detection limits are typically in the nanogram to picogram range. Flame ionization detection (FID) is routinely used for preliminary analyses, as this technique provides a good indication of the complexity of a sample extract. **Figure 2** illustrates GC-FID chromatograms obtained using a J&W DB-1 capillary column for three different munitions grade mustard formulations, HT, HS and HQ. HT is typically 60% distilled mustard (H) and 40% bis(2-chloroethyl-

thioethyl)ether (T) by weight, while HQ is usually 75% distilled mustard and 25% sesquimustard (Q) by weight. HS is crude mustard-containing 15% carbon tetrachloride. Munitions grade samples typically contain additional sample components that may provide synthetic procedure or source information. These samples contained several other sulfur-containing impurities, including 1,4-thioxane, 1,4-dithiane (two common mustard degradation products) and several longer chain blister agents (chromatographic peaks 8, 9 and 10 in **Figure 2**).

Figure 3 illustrates the application of capillary GC-FID for the characterization of tabun and related impurities in a munitions grade sample used for military chemical agent detector evaluation. The volatile organic content of this munitions grade tabun was estimated on the basis of the FID response of the individual components. Tabun accounted for 81% of the sample. The impurities, isopropyl *N,N*-dimethylphosphoramidocyanidate (isopropyl analogue of tabun), ethyl *N,N,N',N'*-tetramethylphosphorodiamidate, *N,N,N',N'*-tetramethylphosphorodiamidic cyanide and the cluster of pyrophosphates, represented approximately 5%, 4%, 2% and 5%.

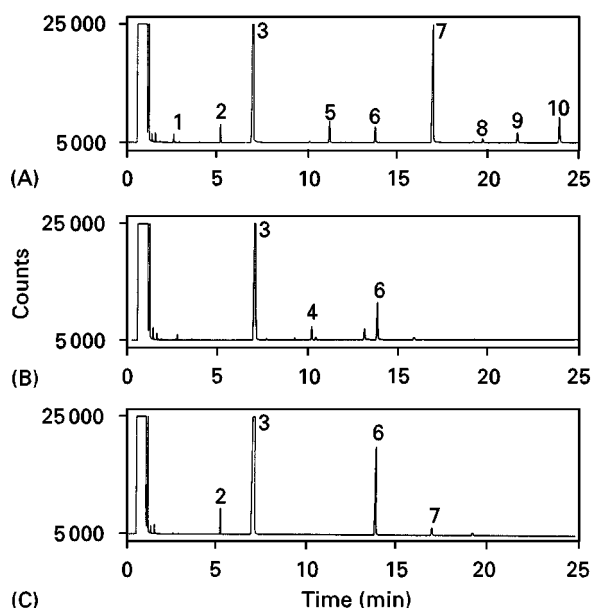


Figure 2 Capillary column GC-FID chromatograms of three munitions grade mustard samples: (A) HT, (B) HS and (C) HQ. Identified compounds include: 1, 1,4-thioxane; 2, 1,4-dithiane; 3, mustard (H); 4, bis(2-chloroethyl)disulfide; 5, 2-chloroethyl (2-chloroethoxy)ethyl sulfide; 6, sesquimustard (Q); 7, bis (2-chloroethylthioethyl)ether (T); 8, 1,14-dichloro-3,9-dithia-6,12-dioxatetradecane; 9, 1,14-dichloro-3,6,12-trithia-9-oxatetradecane; and 10, 1,16-dichloro-3,9,15-trithia-6,12-dioxahaptadecane. (GC column: 15 m \times 0.32 mm ID J&W DB-1, temperature programme: 50°C (2 min), then 10°C min⁻¹ to 280°C (5 min), 2×10^{-10} A full scale.)

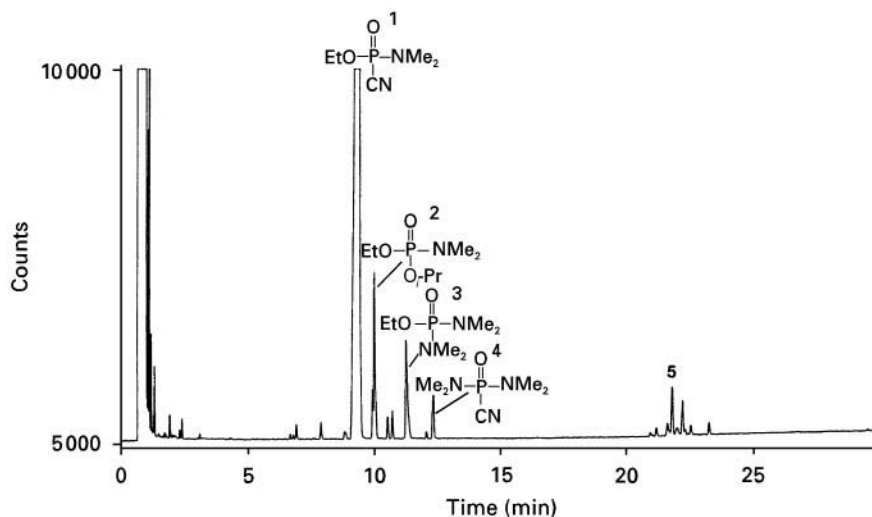


Figure 3 Capillary column GC-FID chromatogram of munitions grade tabun (GA) sample. Compounds identified include: 1, tabun (GA); 2, ethyl isopropyl *N,N*-dimethylphosphoramidocyanidate; 3, ethyl *N,N,N',N'*-tetramethylphosphorodiamidate; 4, *N,N,N',N'*-tetramethylphosphorodiamidiccyanide; and 5, pyrophosphates. (GC-column: 15 m \times 0.32 mm ID J&W DB-5, temperature programme: 50°C (2 min), then 10°C min⁻¹ to 280°C (5 min), 5×10^{-11} A full scale.)

The need for higher specificity and sensitivity has led to the application of element-specific detectors such as flame photometric detection (FPD), thermionic detection (TID), atomic emission detection (AED) and electron capture detection (ECD). The simultaneous use of FID with one or more element-specific detectors has also been demonstrated during dual or tri-channel GC analysis using conventional and thermal desorption sample introduction. While these detectors may provide strong collaborative evidence for the presence of chemical warfare agents, they cannot be used for full confirmation. Use of GC with one or more spectrometric technique such as MS is required to confirm the presence of chemical warfare agents.

Mass Spectrometry

Mass spectrometry is the method of choice for the detection and characterization of chemical warfare agents, their precursors, degradation products and related compounds. Extensive use has been made of GC-MS and the mass spectra of numerous chemical warfare agents and related compounds have been published, with the most common chemical warfare agent mass spectra being available in the OPCW, commercial or defence community databases.

Samples collected for chemical warfare agent analysis typically fall into one of the following general categories: (a) munitions or munition fragments (e.g. neat liquid or artillery shell casing); (b) environmental (e.g. soil, water, vegetation or air samples); (c) artificial materials (e.g. paint or rubber); and (d) biological media (e.g. blood or urine). The ease of analysis

depends on the amount of preparation required to obtain a suitable sample or extract for GC analysis. In the simplest case where neat liquid can be obtained the sample requires dilution with a suitable solvent prior to GC-MS analysis. Environmental and other samples generally require (at a minimum) solvent extraction and concentration prior to analysis, with an exception being direct thermal desorption analysis of samples using a GC equipped with a thermal desorption device that may be loaded with the actual sample. Recommended methods for sample preparation have been published by The Ministry of Foreign Affairs of Finland as part of their contribution to Chemical Disarmament.

Figure 4 illustrates the capillary column GC-MS chromatogram obtained for the extract of a soil sample containing VX and several related compounds. Seven components were identified in the sample following ultrasonic extraction of 1 g of soil with dichloromethane. Extraction of chemical warfare agents from biological samples is generally more difficult. Bonierbale, Debordes and Coppet recently demonstrated a method for the extraction of VX from rat blood as part of a study designed to follow the hydrolysis of VX. Figure 5 illustrates a typical mass chromatogram for the blood extract containing VX, malathion and diisopropylaminoethanethiol.

The data acquired in Figures 4 and 5 and most MS data obtained by OPCW inspectors during inspections have been obtained under EI-MS conditions. However, many of the chemical warfare agents in particular the organophosphorus nerve agents such as VX, and the longer chain blister agents related to

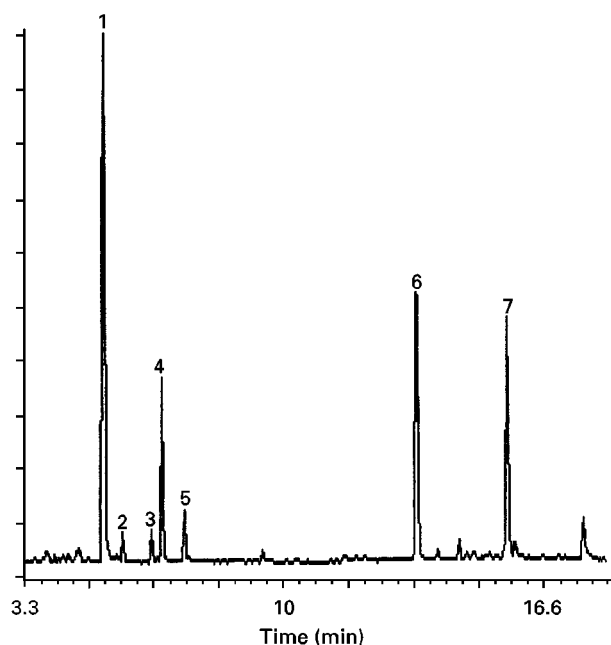


Figure 4 Capillary column GC-MS (EI) chromatogram of dichloromethane extract of soil sample contaminated with VX. VX and six other compounds were identified: 1, diethyl methylphosphonate; 2, *N,N*-diisopropylethylamine; 3, 2-(diisopropylamino)ethyl methyl sulfide; 4, *O,S*-ethyl methyl methylphosphonothiolate; 5, *O,S*-diethyl methylphosphonothiolate; 6, VX; and 7, bis[2-(diisopropylamino)ethyl] disulfide. (GC column: 15 m \times 0.32 mm ID J&W DB-1701, temperature programme: 50°C (2 min) then 10°C min⁻¹ to 280°C (5 min).)

mustard, such as Q and T, do not provide molecular ion information during EI-MS. This hinders confirmation of these compounds and makes identification of novel chemical warfare agents or related impurities difficult.

Considerable effort has been devoted to the use of chemical ionization (CI) as a complementary ionization technique. This milder form of ionization generally affords molecular ion information for the chemical warfare agents and has been used extensively for the identification of related compounds or impurities in chemical warfare agent munitions samples and environmental sample extracts. The identity of these related compounds is important because the origin of samples, synthetic process information or degree of degradation (weathering) may be deduced based on this 'fingerprint' data.

Isobutane, ethylene and methane gases were initially demonstrated as suitable CI gases for the acquisition of organophosphorus nerve agent CI-MS data. More recently, the efficacy of ammonia CI-MS for organophosphorus nerve agents and related compounds has been demonstrated and many laboratories now employ this complementary confirmation technique. Ammonia CI not only offers abundant

molecular ion data, but also affords a high degree of specificity as less basic sample components are not ionized by the ammonium ion.

Capillary column GC-MS-MS offers the analyst the potential for highly specific, sensitive detection of chemical warfare agents as this technique significantly reduces the chemical noise associated with complex sample extracts. The specificity of product scanning with moderate sector resolution, as well as the specificity of ammonia CI, were demonstrated with a hybrid tandem mass spectrometer during analysis of painted panel samples circulated during an international round robin verification exercise.

The painted panel extract was contaminated with numerous hydrocarbons. Only two of the three longer chain blister agents, sesquimustard (Q) and bis(2-chloroethylthioethyl)ether (T), could be identified during capillary column GC-MS (EI) analysis (Figure 6A). The arrow indicates the chromatographic retention time of the third blister agent, 2-chloroethyl (2-chloroethoxy)ethyl sulfide (O). The specificity of ammonia CI (Figure 6B) was clearly demonstrated during this analysis. All three longer chain blister agents were determined in the presence of high levels

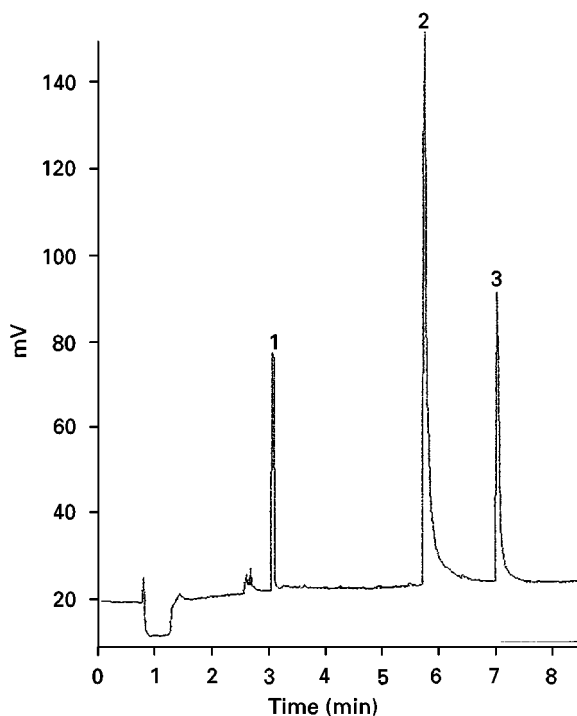


Figure 5 Capillary column GC-MS (EI) chromatogram of 374 $\mu\text{mol L}^{-1}$ VX incubated for 2 h in the presence of rat plasma. Extracted sample components: 1, 3 $\mu\text{mol L}^{-1}$ malathion; 2, VX; and 3, diisopropylaminoethanethiol. (GC column: 25 m \times 0.32 mm ID CP 8CB; temperature programme: 100°C (0.5 min), then 30°C min⁻¹ to 210°C (1 min) followed by 30°C min⁻¹ to 300°C (3 min).)

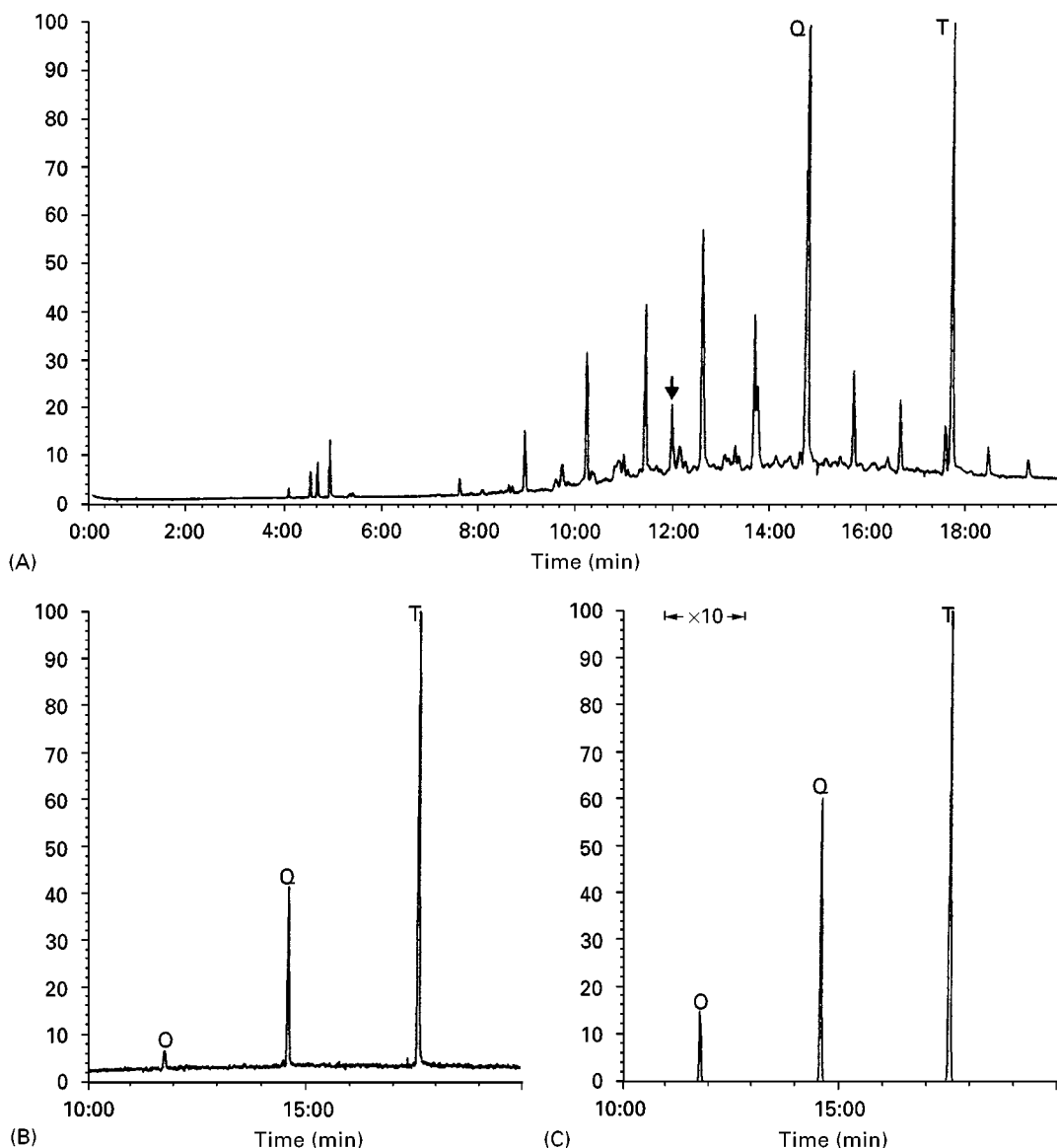


Figure 6 Capillary column (A) GC-MS (EI), (B) GC-MS (ammonia CI) and (C) GC-MS/MS (EI) chromatograms obtained during analysis of international round robin painted panel extracts. Sequimustard (Q) and bis(2-chloroethyl (2-chloroethoxy)ethyl sulfide) (T) were detected during EI analysis. The downward arrow in (A) indicates the retention time of 2-chloroethyl (2-chloroethoxy)ethyl sulfide (O). This compound (O) was masked by the organic content of the sample during EI analysis and only detected following (B) ammonia CI and (C) MS-MS analysis. (GC column: 15 m \times 0.32 mm ID J&W DB-1701, temperature programme: 40°C (2 min), then 10°C min⁻¹ to 280°C (5 min).)

of interfering hydrocarbons, as the hydrocarbons were not sufficiently basic to ionize. Similarly, it was possible to use the resolution of hybrid tandem mass spectrometry to discriminate between ions at m/z 123 arising from the longer chain blister agents from those ions at m/z 123 arising from the hydrocarbon background. The resultant GC-MS-MS chromatogram (Figure 6C), where only m/z 123 ions due to the blister agents were transmitted into the collisional activated dissociation cell, was virtually free of chemical noise and all three components were detected.

The three longer chain blister agents were well resolved with the J&W DB-1701 capillary column, with all three components exhibiting similar product spectra during GC-MS-MS analysis.

Hydrolysis Products of Chemical Warfare Agents

Both the nerve and blister agents undergo hydrolysis in the environment and methods are required for retrospective detection and confirmation of these hydrolysis products. Hydrolysis products are significant as they are generally compounds that would not be

routinely detected in environmental samples and their presence strongly suggests the prior presence of chemical warfare agents. The degradation products of the chemical warfare agents, in particular the nerve agents, are nonvolatile hydrolysis products that must be derivatized prior to GC analysis. A variety of derivatization techniques including methylation, *t*-butyldimethylsilylation and trimethylsilylation have been investigated to allow GC analysis of, in particular, the organophosphorus acids related to the nerve agents (e.g. alkyl methylphosphonic acids and methylphosphonic acid).

Mustard and longer chain blister agents hydrolyse to their corresponding diols, with thiodiglycol being the product formed following hydrolysis of mustard. These compounds may be analysed by GC-MS directly provided the sample is loaded onto the column using 'cool' on-column injection. Figure 7 illustrates a typical GC-MS(EI) chromatogram obtained for products formed following hydrolysis of a sample containing both HT and HQ. The principal hydrolysis products of H, Q and T – thiodiglycol, bis(2-hydroxyethylthio)ethane, and bis[(2-hydroxyethylthio)ethyl] ether, respectively – are well resolved with the J&W DB-1701 capillary column. Molecular ion

information for the longer chain hydrolysis products, were obtained under ammonia CI conditions.

Use of thermospray mass spectrometry and, more recently, the use of atmospheric pressure ionization techniques (e.g. electrospray (ESI), ionspray and atmospheric pressure CI), has enabled the direct mass spectrometric analysis of the hydrolysis products of chemical warfare agents. Both techniques may be interfaced to liquid chromatography for component separation, with thermospray having been largely superseded by atmospheric pressure ionization (API) for most LC-MS applications. Examples of LC-ESI-MS methods for the direct analysis of chemical warfare agent hydrolysis products are relatively few, and only recently has this technique been demonstrated for the analysis of the nerve agents as well. These new LC-ESI-MS methods complement existing GC-MS methods for the analysis of chemical warfare agents and their hydrolysis products and will likely replace some GC-MS methods currently in use for the analysis of contaminated aqueous samples.

Safety and Disposal

Chemical warfare agents are extremely hazardous and lethal compounds. They can only be used in designated laboratories by personnel trained in safe-handling and decontamination procedures and with immediate access to medical support. Safety and standard operating procedures must be developed and approved before any chemical warfare agents are handled. Chemical warfare agents can only be used in laboratory chemical hoods with a minimum face velocity of 100 linear feet per minute equipped with emission control devices that limit exhaust concentration to below 0.0001 mg m^{-3} . Personnel handling chemical warfare agents should wear rubber gloves, lab coats and full faceshields, and a respirator (gas mask) must be kept within easy reach. Sufficient decontaminants to destroy all chemical warfare agent being handled must be on hand before commencing operations.

Blister agents such as mustard can be destroyed with 10% hypochlorite or strong bleach solutions. The nerve agents can be destroyed using saturated methanolic solutions of sodium or potassium hydroxide. Decontaminated chemical warfare agents must be disposed of in an environmentally approved method according to local legislation.

Conclusion

Capillary column GC is the chromatographic method of choice for the separation and analysis of chemical warfare agents. This technology is employed in the

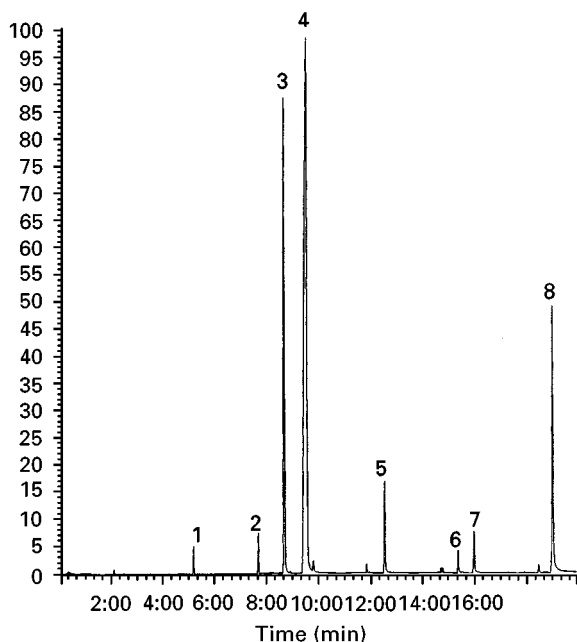


Figure 7 Capillary column GC-MS(EI) chromatogram of the hydrolysis products of a munitions grade mustard sample containing HT and HQ. Eight compounds were identified: 1, 1,4-dithiane; 2, mustard (H); 3, hemisulfur mustard; 4, thiodiglycol (hydrolysis product of H); 5, 2-chloroethyl (2-hydroxyethylthio)ethyl ether; 6, 2-chloroethyl (2-hydroxyethylthio)ethyl sulfide; 7, bis(2-hydroxyethylthio)ethane (hydrolysis product of Q); and 8, bis[(2-hydroxyethylthio)ethyl] ether (hydrolysis product of T). (GC column: $15 \text{ m} \times 0.32 \text{ mm ID}$ J&W DB-1701, temperature programme: 40°C (2 min), then $10^\circ\text{C min}^{-1}$ to 280°C (5 min).)

field-portable GC-MS instrumentation currently in use by the OPCW inspectorate. Use of GC with one or more spectrometric technique such as mass spectrometry is required to confirm the presence of chemical warfare agents. For this reason many analyses are carried out by GC-MS under electron impact or chemical ionization conditions. For analyses involving low levels of chemical warfare agents in the presence of high levels of interfering chemical background, GC-MS-MS is receiving increased attention.

Atmospheric pressure ionization (e.g. electrospray (ESI), ionspray and atmospheric pressure CI) techniques may be used for the direct mass spectrometric analysis of the hydrolysis products of chemical warfare agents in aqueous samples. Examples of LC-ESI-MS methods for these analyses are relatively few, and only recently has this technique been demonstrated for the analysis of the nerve agents as well. These new LC-ESI-MS methods complement existing GC-MS methods for the analysis of chemical warfare agents and their hydrolysis products and will likely replace some GC-MS methods currently in use for the analysis of contaminated aqueous samples.

See also: II/Chromatography: Gas: Column Technology; Detectors: Mass Spectrometry; Detectors: Selective. Chromatography: Liquid: Detectors: Mass Spectrometry.

Further Reading

Bonierbale E, Debordes L and Coppet L (1997) Application of capillary column gas chromatography to the study of

hydrolysis of the nerve agent VX in rat plasma. *Journal of Chromatography B* 688: 255–264.

Compton JAF (1988) *Military Chemical and Biological Agents*. Caldwell, NJ: The Telford Press.

D'Agostino PA (1995) Chemical warfare agents – analysis and characterization. In: Townshend A and Worsfold PJ (eds.), *Encyclopedia of Analytical Science*, pp. 599–608. London: Academic Press.

D'Agostino PA, Hancock JR and Provost LR (1999) Packed capillary liquid chromatography-electrospray-mass spectrometry analysis of organophosphorus chemical warfare agents. *Journal of Chromatography A* 840: 289–294.

Gander TJ (1996) *Jane's NBC Protective Equipment*. London: Butler and Tanner Inc.

Ivarsson U, Nilsson H and Santesson J (1992) *A Briefing Book on Chemical Weapons*. Ljungforeytagen Oregro.

Kaipainen A, Kostainen O and Riekkola M-L (1992) Identification of chemical warfare agents in air samples using capillary column gas chromatography with three simultaneous detectors. *Journal of Microcolumn Separations* 4: 245–251.

Kientz ChE (1998) Review: Chromatography and mass spectrometry of chemical warfare agents, toxins and related compounds: state of the art and future prospects. *Journal of Chromatography* 814: 1–23.

Methodology and Instrumentation for Sampling and Analysis in the Verification of Chemical Disarmament (1977–1994) Helsinki: The Ministry of Foreign Affairs of Finland.

Somani SM (1992) *Chemical Warfare Agents*. New York: Academic Press.

Witkiewicz Z, Mazurek M and Szulc J (1990) Review: Chromatographic analysis of chemical warfare agents. *Journal of Chromatography* 503: 293–357.

CHIRAL SEPARATIONS

Amino Acids and Derivatives

See III / AMINO ACIDS AND DERIVATIVES: CHIRAL SEPARATIONS

Capillary Electrophoresis

B. J. Clark, University of Bradford, Bradford, UK

Copyright © 2000 Academic Press

Background

Since its commercial inception in 1988 capillary electrophoresis (CE) has increasingly offered the separ-

ation scientist a very wide range of application (biopolymers to cations), with ultra-high efficiency. It is generally cost-effective, easy in use, with low sample and buffer requirements and has the capability for automation. For these reasons CE has expanded considerably and is now used as an orthogonal and complementary technique alongside well-established analytical procedures. Of all its

application fields, the separation of compounds with one or more chiral centres has been particularly successful. Analytical chiral separations increased in importance throughout the 1980s: considerable interest was generated in the resolution of stereoisomers of food additives, agrochemicals, petrochemicals and pharmaceuticals. During this time the analyst was presented with numerous procedures to examine chiral compounds. Chromatography and, particularly, high performance liquid chromatography (HPLC) with immobilized chiral stationary phases used as column packings was the most successful for separation of enantiomeric mixtures, albeit at considerable cost.

However, chiral separations by chromatography do not give a unique solution to all difficulties relating to the resolution of chiral compounds. Thus, with CE analysts have another tool at their disposal, with all the benefits of the technique to be exploited. Two major processes of separation are undertaken in enantiomeric separations. The commonest procedure is where the enantiomers are resolved directly as diastereoisomers in the conditions of a chiral environment present in the capillary. The transient diastereoisomers are formed *in situ* and resolved on the basis of their different physicochemical properties. Alternatively, conventional CE separations follow after off-line diastereomeric derivatives are produced through reaction of the analyte with optically active reagents, in a procedure which is commonly referred to as an indirect method. An example is the resolution of the diastereomeric pairs of D, L-tryptophan with (+)-diacetyl-L-tartaric anhydride which are resolved on a polyacrylamide-coated, conventional silica capillary. Certain precautions are necessary within this procedure; primarily, a reagent of very high optical purity (100%) is required for specific reaction with the individual enantiomers. Variability in purity of a reagent sample would result in diastereomeric interference and errors in the determination of the analytes. Incomplete reaction and differences in the speed of reaction are also problems which must be addressed when carrying out the derivatization.

Over the last 10 years, a number of CE modes have been examined for separation of stereoisomers. Of these, capillary zone electrophoresis (CZE) in conjunction with chiral additives in the buffer phase is the most frequently used for charged chiral compounds. For neutral chiral analytes (and charged compounds), micellar electrokinetic chromatography (MEKC) has been applied through a chiral surfactant or a chiral additive and achiral surfactant, as additives to the buffer in a conventional silica capillary, when operated at the critical micelle concentration. In contrast to these applications where the selector

acts in free solution, some success with constraining the chiral selector within the capillary has been achieved. Two approaches have been considered – attaching the selector to the capillary wall or trapping it within a gel (in capillary gel electrophoresis), although in practice, limited applications have been reported so far. The most recent proposal for optical separations is through electrochromatography, where a chiral stationary phase is packed into the silica capillary and the mobile phase moves under electroosmotic flow (EOF).

Chiral Selector in the Buffer Phase

Ligand Exchange

CE enantiomeric resolution was first established, through a procedure named ligand exchange. This is based on metal chelate complexation with copper or zinc at the centre of the complex. It was directed towards amino acids, which as dansyl-labelled derivatives were resolved through initially interacting copper (Cu(II)) and L-histidine in the run buffer and then forming a ternary metal complex with an enantiomer of a chiral amino acid. In an enantiomeric mixture the metal complexes can have differential stability, and therefore mobility differences between the enantiomers result. In the case above, a neutral pH buffer was used, which gives a positively charged metal-histidine interaction and the enantiomer forming the higher stability complex migrates faster. One drawback of this procedure is the requirement that the amino acid in the metal-amino acid interaction has to be of very high purity to stop enantiomeric impurities being introduced into the assay. Following the initial research, the same group impressively resolved 14 racemic amino acids by this procedure where the complex was Cu(II)-aspartame. At present the procedure is limited to amino acids, with some extension to peptides and additional separations, and most applications appeared in the early years of CE.

Cyclodextrins

The interest in cyclodextrins (CDs) in the chemical, cosmetic, food and drug industries has grown considerably. In the pharmaceutical field incorporation within the CD has led to improvements in bioavailability, pharmacokinetics and stability. However, to the analyst, their major influence has been in enantiomer stereoselectivity, which originates from the chirality of the glucose units and involves stereochemical interaction through hydrophobic inclusion, hydrogen bonding and often steric repulsion, when the CD is used as an additive in an aqueous CE buffer. The CDs, produced enzymatically from starch, are

comprised of 6–8 D-(+)-glycopyranose units as α -, β - and γ -CD. The molecules are shaped as truncated cones, with relatively hydrophilic exteriors, due to secondary C2 and C3 hydroxy groups at the top and primary C6 hydroxy groups at the bottom of the cone. The rigid structure presents an internal hydrophobic cavity, which will accommodate ring-structured enantiomers. Therefore, for chiral recognition of enantiomers, the most favourable chemical structure is where the hydrophobic centre, such as a cycloalkane or aromatic group (which generally interacts most closely with β -CD), gives a close cavity fit. But one of the enantiomers gives a poorer steric fit, which results in differential binding constants between the enantiomers. Typically, a small molecule with a single aromatic ring will include with a tight fit into the β -CD cavity. Additionally, hydrogen-bonding sites are required for interaction with the secondary hydroxyls on the rim of the cavity and at least one repulsive interaction with the CD. Generally, for interaction with the CDs the chiral molecule's hydrophobic centre should be close to the chiral centre (Figure 1).

CDs are generally reasonably straightforward to work with in CE. They are commercially available, ultraviolet transparent and, during method development, the concentration and the buffer conditions, such as pH, can easily be changed, without the need for long equilibration times. One area of slight difficulty is solubility which, although adequate in water or organic solvent for α and γ (14.5 and 23.2 g per 100 mL in water), is only 1.85 g per 100 mL with the commonly used β -CD. Other general properties are

that CDs are neutral molecules and that the difference in electrophoretic mobility in mixtures has to occur from the charge on the chiral analytes. In method development it is important to optimize the enantiomeric separation, and there are three main areas of interest, two of which revolve around solvation effects, influenced through varying the pH and the organic additive concentrations. The CD concentration is also important: a theoretical model, has been described which indicates a maximum concentration for enantiomeric resolution. Other researchers have confirmed this and extended discussions to chiral separation models which include the function of pH and organic additives in the buffer. Other parameters shown to have an influence on resolution include buffer concentration and internal diameter of the capillary.

It was clear, however, in method development and in stereoselective HPLC assays with chiral additives that the solubility of the native CDs was a limiting factor, particularly with β -CD. As a result a large number of CD derivatives have been synthesized and tested and are now commercially available for use in CE. These range from the electrophoretically neutral methylated β -CD and hydroxypropyl β -CD to charged species, such as methylamino β -CD and sulfobutylated β -CD. In the former case solubility is improved manifold and, in the latter case, in addition to improved solubility the charge on the CD gives electrophoretic mobility to uncharged and neutral chiral compounds. Apart from these advantages the derivatized CDs often have different enantioselectivities over the native CDs (Figure 2). The first enantioseparations with CDs were carried out in 1985 as an extension to isotachopheresis, where the CD was added to the leading buffer. However Fanali is credited with one of the first uses of β -CD for the resolution of ephedrine alkaloids by CZE.

With a better understanding of the implications of chiral compounds in everything from the chemical to food and pharmaceutical industries, stereospecific synthesis has developed to a point where very few racemic compounds will be used in the future. However, the analyst still has a role to play in checking the enantiopurity of the synthetic product. Detection levels are regularly at < 0.5% m/m and the order of migration can often dictate whether low enantiomer levels are detected. Most favourable conditions generally exist when the minor enantiomer precedes the major component. One option to control the migration order is to operate with anionic, cationic or neutral coated silica capillaries. A typical example is shown in Figure 3 of a cationic coating, a polyamine on the surface and α -CD, which gives a limit of quantitation of < 0.05% m/m for D-tryptophan, in

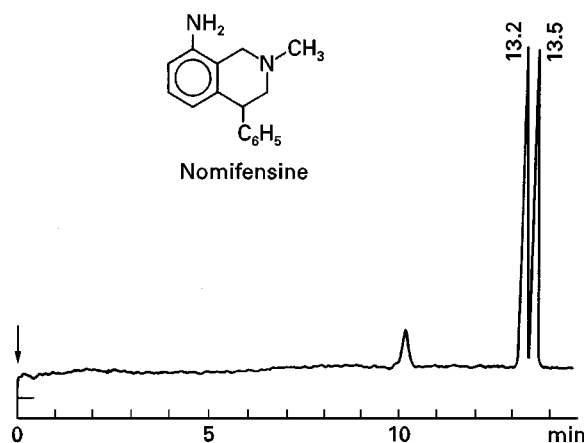


Figure 1 Capillary-zone electrophoresis resolution with β -cyclodextrin (β -CD) of the drug nomifensine maleate (65 mg L^{-1}) which has the hydrophobic group close to the chiral centre. The buffer was 20 mmol L^{-1} sodium tetraborate (pH 12.5) containing 20 mmol L^{-1} β -CD. The capillary was 37 cm (30 cm to detector) \times $50 \text{ }\mu\text{m}$ i.d. The applied voltage was 20 kV, detection wavelength 284 nm and temperature 30°C .

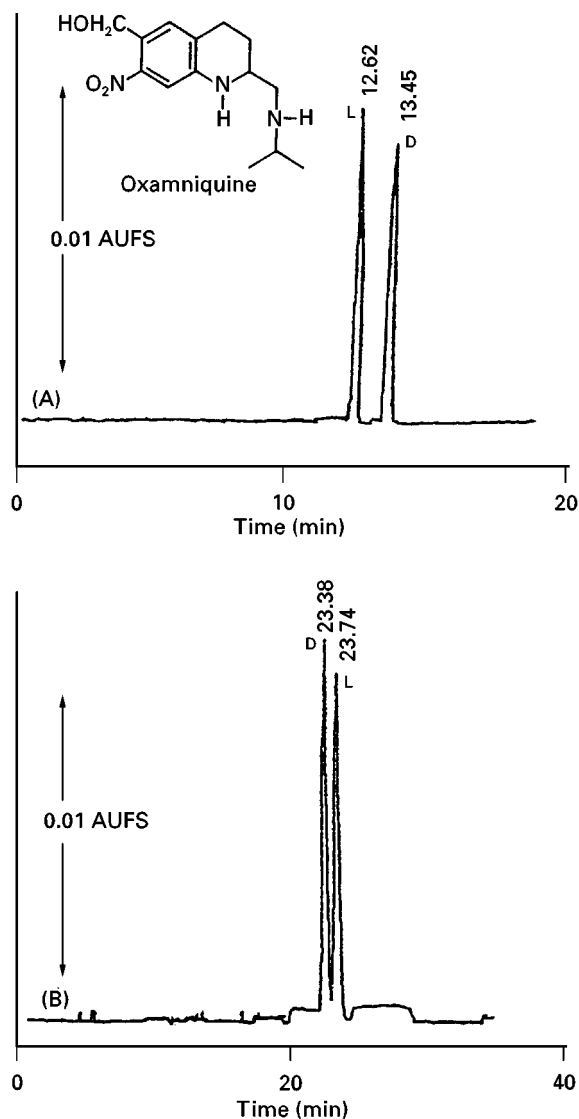


Figure 2 The resolution of oxamniquine by capillary-zone electrophoresis with neutral cyclodextrins. Resolution was at pH 2.25 with hydroxypropyl β -CD, but there was no resolution with β -CD at this pH. The β -CD gives resolution at pH 12, but with reversed migration order. (A) 50 mmol L⁻¹ disodium hydrogen phosphate (pH 12) with 25 mmol L⁻¹ β -CD; applied voltage 15 kV; (B) 50 mmol L⁻¹ sodium dihydrogen phosphate (pH 2.25) containing 40 mmol L⁻¹ hydroxypropyl β -CD; applied voltage 20 kV. The temperature was 30°C and detection wavelength 246 nm.

the presence of the L-enantiomer. During these runs the polarity is reversed over the conventional direction of operation. The coated capillaries mentioned above are commercially available and have been shown to be stable if used within the suggested limits. The anionic (sulfonic acid) coated capillaries are of particular interest in chiral and conventional separations as they give a consistent EOF over the range pH 3–9 and therefore are more controlled in operation.

Crown Ethers

Crown ethers act in a similar manner of enantiomer inclusion as CDs and contain a central cavity, although the mechanism is based on ionic and hydrogen bonding. They are macrocyclic polyethers, soluble in both aqueous and organic solvents, which form stable complexes with enantiomers, which have a primary amine or alkylamine functionality. For resolution, differential stability of the host–guest complex is required. This is reliant on the spatial arrangement between the amine and its hydrogen bonds with the ether oxygens. 18-Crown-6-tetracarboxylic acid is the easiest to obtain commercially and has been used to resolve a number of primary amines and racemic amino acids on a silica capillary, by addition of the crown ether into the buffer phase at low concentration, under CZE conditions. By this means a few chiral separations have been achieved which have not been fully successful by other means, such as chiral peptides. Crown ethers have also been used in combination with CDs for complex mixtures. In general, however, crown ethers have not been

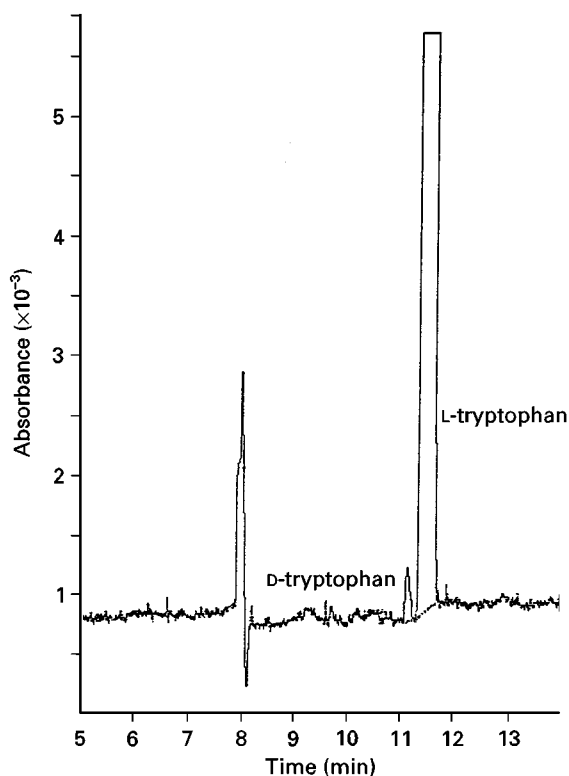


Figure 3 Detection of D-tryptophan at 0.05% m/m in L-tryptophan (LOD ($3 \times s/n$) 0.01% m/m) with a polyamine coated capillary (eCAP™ with polyamine regeneration solution) to give a positive charge on the capillary. Capillary was 37 cm (30 cm to detector) \times 50 μ m fused silica and buffer 40 mmol L⁻¹ tris-phosphoric acid containing 75 mmol L⁻¹ α -CD. The applied voltage was -10 kV, detection wavelength 241 nm, injection time 2 s and operating temperature 30°C.

extensively used because they need to be applied under controlled conditions as they are highly toxic and they are limited to amines and alkylamines. However, in the applications reported they give highly efficient resolutions of certain chiral compounds.

Other Chiral Additives

Apart from the CDs, linear oligosaccharides are potential chiral discriminators in CE, and maltodextrin mixtures, corn syrups and pure malto-oligosaccharides have all been used to resolve non-steroidal anti-inflammatory drugs (NSAIDs). Polysaccharides have also been discussed in these reports, with applications of heparin, a naturally occurring mammalian mucopolysaccharide (anticoagulant), in the resolution of chiral drugs. The molecule is chiral, highly anionic and helical and has been used in the chiral discrimination of antimalarials and antihistaminics. In **Figure 4**, oxamniquine is resolved with a large resolution factor with 2% w/v heparin. Thus heparin and some of the other polysaccharides with their high separation efficiencies appeared to be good alternatives to CDs. There is one drawback: because of their heterogeneous character, batch-to-batch and different source material can result in changes in the resolution and therefore method robustness would be questionable for regular assay for industry.

Proteins provide another alternative based on successes in HPLC and particularly separations with α_1 -acid glycoprotein (AGP) and bovine serum albumin (BSA) for chiral drug separations. BSA has

been cross-linked with glutaraldehyde to form a polymer matrix. However, BSA has a high ultraviolet background and as such needs to be used in indirect detection mode or where the gel is only partially loaded on to the capillary and stops just before the detection window. AGP, ovomucoid (egg white) and fungal cellulose have all been used, with some success. The major problem with the fungal cellulose is absorption on to the capillary wall if used with uncoated capillaries, although adding materials such as polyethylene glycol or methyl cellulose into the electrolyte does alleviate wall interaction.

Micellar Electrokinetic Capillary Chromatography

Neutral compounds present a problem in CE since they have no differential mobility because of their lack of charge and are carried without separation by the EOF. One solution is to operate with surfactants, which form micelles above a certain concentration, and then differentiate between the compounds on the basis of both electrophoretic migration and micellar partitioning. This technique has been so successful that it is now one of the commonest procedures used in CE. Initially the emphasis was on achiral compounds, but it was quickly extended to chiral compounds by the introduction of either chiral surfactants or chiral additives, such as CDs. Surfactants are long chain molecules, characterized by a hydrophobic tail pointing inwards and a hydrophilic head pointing outwards into the aqueous buffer. Micelles are amphiphilic aggregates of surfactant molecules which form above a surfactant concentration, known as the critical micelle concentration (CMC) (**Table 1**). There are four classes of surfactants – anionic,

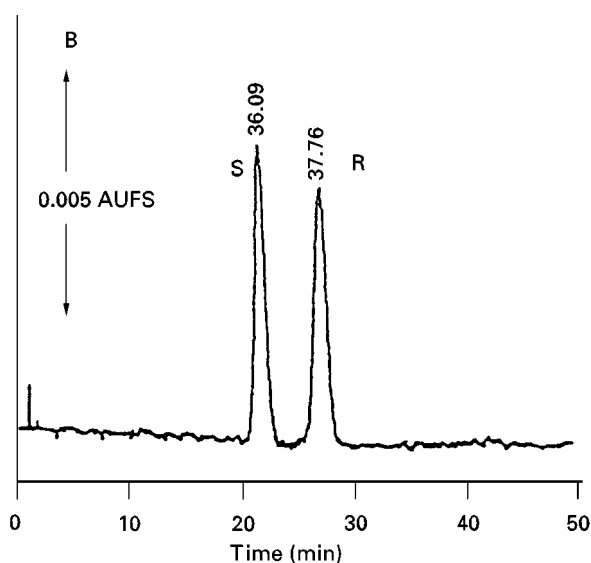


Figure 4 The resolution of oxamniquine by capillary-zone electrophoresis with heparin in the electrolyte solution. The electrolyte was 50 mmol L⁻¹ sodium dihydrogen phosphate (pH 3.0) containing 2% m/v heparin. The capillary was 71 cm (50 cm to detector) \times 50 μ m i.d., the applied voltage 20 kV, temperature 30°C and the detection wavelength 246 nm.

Table 1 The critical micelle concentrations of chiral surfactants and achiral surfactants

Surfactant	Critical micelle concentration (mmol L ⁻¹)
<i>Chiral</i>	
Sodium cholate	14
Sodium taurocholate	13
Sodium deoxycholate	5
Sodium taurodeoxycholate	4
Sodium <i>N</i> -dodecanoyl-L-valinate	6 (40°C)
<i>Achiral</i>	
Sodium dodecyl sulfate (SDS)	8
Sodium decane sulfate	40
Tetradecyltrimethylammonium bromide (TTAB)	4
Cetyltrimethylammonium bromide (CTAB)	1

cationic, zwitterionic and nonionic – which can be both synthetic and naturally occurring. The synthetic group includes the anionic sodium dodecyl sulfate (SDS) and cationic cetyltrimethylammonium bromide (CTAB).

A slightly different process, microemulsion electrophoretic chromatography, has recently been developed. In this process a combination of oil–water–surfactant and co-surfactant such as an alkyl chain alcohol is used as a pseudo-stationary phase.

Chiral Surfactants

These can be synthetic optically active amino acid derivatives and natural surfactants, such as glycyrrhizic acid, β -escin, bile salts and digitonin. Digitonin is nonionic, but has been used as a mixed micelle with SDS to give the electrophoretic mobility, to resolve chiral amino acids. These materials are generally water-soluble and can be added easily at micelle concentrations to the electrolytes in MEKC, although viscosity increases should be noted. Initially enantiomeric separations were directed towards neutral chiral compounds such as benzoin, and warfarin, a heart drug, which were selectively resolved with materials such as sodium *N*-dodecanoyl-L-valinate (SDVal) and *N*-dodecanoyl-L-glutamate (SDGlu). But it was soon realized that charged chiral compounds could also be resolved. Sodium taurocholate (STC) or the taurodeoxycholate (STDC) has been used under acidic conditions for the resolution of dansylated-DL-amino acids and for carboline derivatives and 2,2'-dihydroxy-1,1'-dinaphthyl used under neutral conditions for the drug diltiazem (Figure 5).

Chiral Selector with an Achiral Surfactant

This mode can give added selectivity to resolution of both neutral and charged chiral molecules, as the solutes are distributed between chiral selector such as a CD, the aqueous phase and the micelle (Figure 6). As a result, the chiral analytes will move in and out of the micelle/CD, with the CD moving with the EOF and the micelle (depending on polarity) moving according to charge. Racemic amino acids, β -blocker drugs, Trogers base and the drug terbutaline have all been resolved with this procedure. In the case of terbutaline either 5 mmol L⁻¹ di-O-methyl- β -cyclodextrin or 15 mmol L⁻¹ β -cyclodextrin was successfully used with 15 mmol L⁻¹ SDS. Other approaches have been to carry out competitive separations with CD-MEKC, where an additive, such as D-camphor-10-sulfonate, is introduced into the buffer and competes for inclusion with the chiral analytes. With this procedure an improved resolution of Trogers base was obtained. Overall, this form of

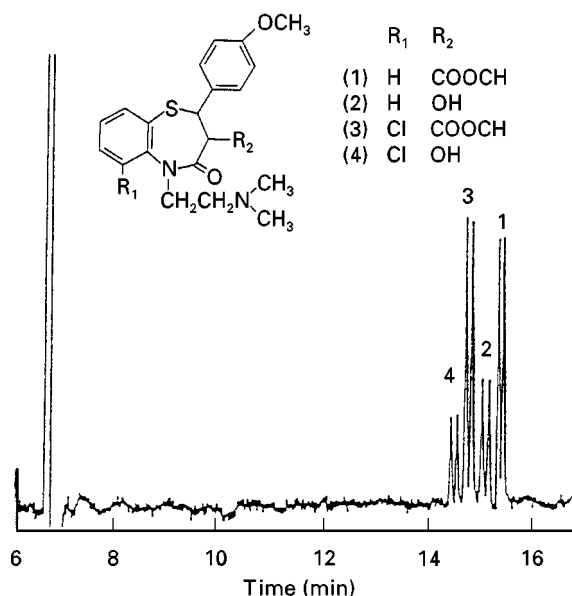


Figure 5 The use of bile salts to resolve the enantiomers of diltiazem and related substances by chiral micellar electrokinetic chromatography (MEKC). The electrolyte was 20 mmol L⁻¹ disodium hydrogen phosphate–sodium tetraborate (pH 7.0) containing 50 mmol L⁻¹ sodium taurodeoxycholate. The capillary was 65 cm (50 cm to detector) \times 50 μ m i.d. Applied voltage was 20 kV, detection wavelength was 210 nm and temperature was 25°C.

separation of chiral analytes has become quite popular, particularly as there are many derivatized CDs to choose from, and many examples have been published. Of the native CDs, γ -CD has shown the greatest success, which is the opposite of the case with the conventional addition of CDs to the buffer phase. In this case the larger inner diameter of the cavity of the γ -CD allows not only the chiral molecules to be included but also the surfactant.

Capillary Electrochromatography (CEC)

There is much current interest in electrochromatography, which is a hybrid technique between HPLC and CE, operating with packed capillaries. It is based on partitioning the analytes between the stationary phase (in packed capillaries) and the mobile phase (electrolyte) under CE conditions with a high applied voltage. The procedure benefits from the large range of HPLC stationary phases and some specific phases which are beginning to be developed for CEC. It links the high efficiency of CE with the range of separations possible with reversed-phase HPLC. For transport of the analytes in CEC, EOF is still present, but now the effective EOF is mainly generated from the packed bed of stationary phase rather than at the walls of the capillary. This results from the electrical double layer

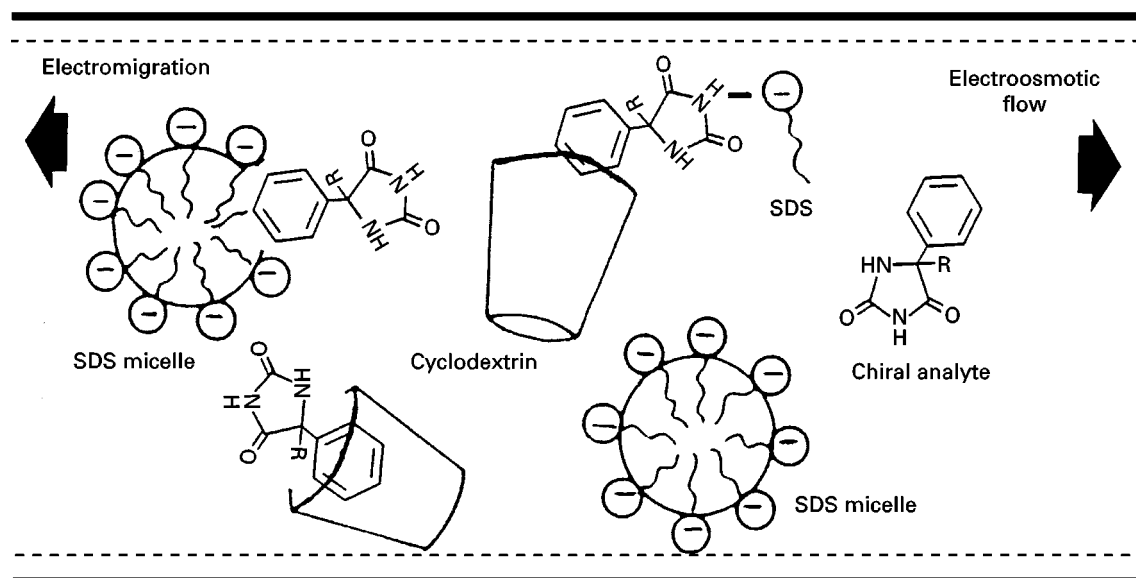


Figure 6 Schematic of the chiral analyte 5-alkyl-5-phenyl hydantoin distributed between the cyclodextrin, the aqueous phase and the micelle. SDS, Sodium dodecyl sulfate.

on the surface of the particles in contact with the mobile phase and produces a ζ potential. The potential of CEC was first demonstrated in 1987, showing the presence of the partitioning effects and, for charged analytes, the continued effect of electromigration. In terms of the separation conditions in CEC and HPLC, the stationary and mobile phases are very similar, but the separation efficiency can be much improved. Many applications of electrochromatography are currently being studied and the range of capillary packing materials continues to expand.

Chiral stationary phases are being examined by a number of researchers. In one of the first reports of chiral separations by CEC 5 μm AGP, immobilized on to silica, was packed into a 50 μm internal diameter capillary. Cationic and neutral enantiomers were resolved by this method, which included benzoin and the drugs cyclophosphamide and hexobarbital. This early work did not illustrate large improvements in peak efficiency over other procedures as the capillary packing methods required improvement, but it did illustrate the potential.

CDs have also been used as immobilized silica-based materials and the neutral CD hydroxypropyl- β -CD silica was used in resolution of the basic drug mianserin. In method design with the CDs, the choice of the background electrolyte has played an important part and pH, organic modifier and differences in field strength have all been considered. The direction of flow past the detector was shown to be dependent on the background electrolyte used. For β -cyclodextrin and a phosphate buffer the direction of flow is

towards the cathode, but with triethylammonium acetate the flow is reversed. This can be beneficial in controlling the order of retention in CEC. The pH change in the electroosmotic mobility can be used to obtain a suitable overall retention time. Organic modifiers such as methanol and acetonitrile in the electrolyte have an effect on both the retention and enantioselectivity. The results from studies with CD-bonded silica phases indicate that a range of parameters and additives can affect the retention and enantioresolution in CEC, as they do with chiral stationary phases in HPLC.

Other stationary phases which have been shown to give enantioseparations are the cellulose and amylose derivatives which have been coated on to silica. These stationary phases are known as Chiralcel and Chiralpak phases (Daicel, Japan), respectively. These materials have been successful in HPLC for enantioselectivity with a wide range of chiral compounds and have recently been utilized as packing materials for CEC (Figure 7). Generally in CEC good resolution has been achieved for a number of chiral compounds resolved by HPLC, with improvements in separation efficiencies in many cases.

Future Developments

Capillary electrophoresis has had a major impact on the resolution of chiral compounds by the methods discussed above. The method is now regularly used to assay enantiomeric compounds in many fields with generally better efficiency than in HPLC and with

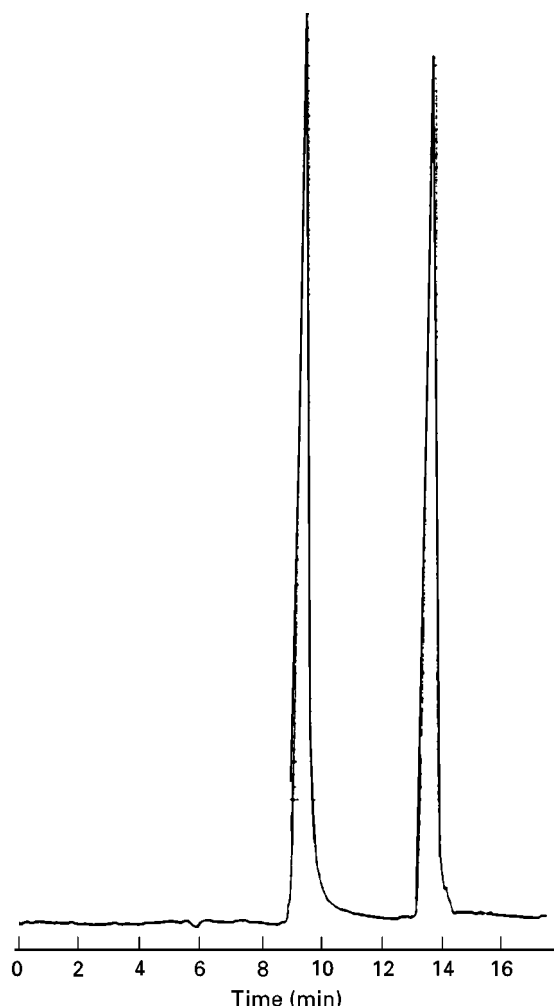


Figure 7 Electrochromatographic resolution of methylphenyl barbitone by a Chiralcel OJ (Daicel, Japan) chiral stationary phase. The cellulose ester derivative commercially coated on to silica was packed into a 30 cm (21 cm packed and 22 cm to detection window) \times 75 μ m i.d. fused silica capillary. The mobile phase was acetonitrile–water (70 : 30 v/v), applied voltage 15 kV and temperature 25°C.

shorter overall migration times. Many different areas are showing considerable research interest, such as electrochromatography, where in the future commercially available columns may prevail over in house methods of packing capillaries with chiral stationary phases. Generally, commercial interest in the area of capillary packings is likely to increase as more ‘tailor-made’ phases are introduced.

Further Reading

- Chankvetadze B, Endresz G and Blaschke B (1996) Charged cyclodextrin derivatives as chiral selectors in capillary electrophoresis. *Chemical Society Reviews* 141–153.
- Clark BJ (1994) Separations of enantiomeric compounds by chiral selectors in the mobile or solvent phase. In: Subramaninan G (ed) *A Practical Approach to Chiral Separations*, p. 311. Weinheim, Germany: VCH.
- Kuhn R and Hoffstetter-Khun S (1993) *Capillary Electrophoresis: Principles and Practice*. Berlin: Springer-Verlag.
- Lelievre F, Yan C and Zare RN (1996) Capillary electrochromatography: operating characteristics and enantiomeric separations. *Journal of Chromatography A* 723: 145–156.
- Nishi H and Terabe S (1995) Optical resolution of drugs by capillary electrophoretic techniques. *Journal of Chromatography A* 694: 245–276.
- Rabel SR and Stobaugh JF (1993) Applications of capillary electrophoresis in pharmaceutical analysis. *Pharmaceutical Research* 10: 171–175.
- Schmitt T and Engelhardt H (1995) Optimisation of enantiomeric separations in capillary electrophoresis by reversal of the migration order and using different derivatized cyclodextrins. *Journal of Chromatography A* 697: 561–570.
- Wren SAC (1993) Theoretical aspects of chiral separation in capillary electrophoresis. *Journal of Chromatography A* 603: 235–241; 609: 363–367; 636: 57–62.

Cellulose and Cellulose Derived Phases

J. Dingenen, Janssen Research Foundation, Belgium

Copyright © 2000 Academic Press

Introduction

The properties of cellulose derivatives for the separation of enantiomers were recognized in 1966 by Lüttringhaus and Peters. The full potential of microcrystalline cellulose triacetate (CTA) was definitely established by Hesse and Hagel in 1973. Meanwhile,

microcrystalline cellulose tribenzoate became commercially available. Another milestone in the development of cellulose- and amylose-based phases was the work of Okamoto and co-workers who in 1984 introduced polysaccharide derivatives coated on a macroporous silica. Currently such materials are certainly the most universally applicable type of commercially available chiral stationary phases. Then, in 1988 Francotte and co-workers introduced cellulose esters of aromatic acids in the form of almost spherical, partially crystalline particles with a relatively

good mechanical stability. The last few years have also seen a lot of research in grafting cellulose and amylose derivatives on to a silica matrix.

Recently, different types of polysaccharide phase (Chiralcel AD, Chiralcel AS, Chiralcel OD and Chiralcel OJ) wall-coated open tubular (WCOT) columns have also been used for supercritical fluid chromatography applications.

Here, the properties and possibilities of different types of polysaccharide phases used for enantiomer separation are discussed.

Microcrystalline Cellulose Triacetate

By a heterogeneous acetylation procedure, cellulose can be acetylated so that the mutual arrangement of the carbohydrate chains within their crystalline regions is maintained. CTA obtained by this acetylation technique has only weak chiral recognition abilities. Only in its swollen state is triacetyl cellulose capable of separating enantiomers. An ethanol–water (95 : 5, v/v) mixture is the most frequently used swelling agent for CTA. When dry CTA is boiled for 15 min in the ethanol–water mixture, a volume increase of about 40% is observed.

Microcrystalline CTA is a material that can be used to separate a broad variety of enantiomers belonging to many different classes of organic compounds (thiazoline-2 thiones, barbiturates, hydrocarbons, oxiranes, flavanones, γ - and δ -lactones, metal complexes, etc.) Its high loading capacity makes it an extremely useful material for preparative chromatographic purposes.

Mobile-Phase Design

A lot of different solvents, e.g. acetone, chlorinated alkanes and acetonitrile, cannot be used because they dissolve CTA more or less completely. In tetrahydrofuran, CTA forms a gel. In some other solvents, like for example, 1,4 dioxane and dimethoxyethane, CTA swells too strongly. Different investigators found as a general rule that the retention factors of the investigated analytes increased when, respectively, methanol, ethanol or propanol was used as the eluent. However, the highest selectivity factors are often found with ethanol as the eluent. Successful separations are also obtained by using other low molecular weight alcohols, ethers, hydrocarbons and mixtures of these eluents. Examples are methanol-2-propanol (80 : 20; v/v); ethanol-*tert*-butyl methyl-ether–water (86 : 10 : 4, v/v) and *n*-hexane-2-propanol–water (70 : 27 : 3, v/v).

In general, a significant influence on the retention factor and enantioselectivity is observed when ethanol as the eluent is modified with methanol, 2-

propanol, different amounts of water, or is completely replaced by methanol or 2-propanol.

If compounds bearing an ionizable group have to be analysed, buffer systems should be tried. CTA seems to withstand the use of buffers in the range between pH 5 and 10 for a long time without any significant loss of chromatographic properties. Eluents with a high water content at high or low pH values should be avoided because CTA can be hydrolysed under these conditions.

Empirically, it has been found that, on CTA successful enantiomer separations can be expected if the analytes possess an aromatic or nonaromatic ring close to the chiral centre or if the products have an asymmetric atom on a rigid ring structure.

Also it is known from experience that compounds bearing an ionizable group, like for example, a hydroxyl, carboxyl or amino group, are generally poorly resolved on CTA.

Derivatization of these functional groups into the corresponding ester, amide or carbamate derivative often improves the selectivity. For alcohol, an esterification reaction with a *P*-substituted benzoic acid chloride (F, Cl, Br, CN, NO₂, OCH₃) has been successfully applied to solve a number of different separation problems.

CTA is attractive for chiral separations because it can be synthesized from a low cost natural product. The wide range of products that can be separated, together with its high loading capacity, certainly makes it a material that should be considered as a valuable tool in the development of chiral separation methods. Besides the usefulness of CTA in the field of enantiomer separations, this material is also suitable for the separation of positional isomers.

Microcrystalline Cellulose Tribenzoate

As early as 1969, Safanova and Klenkova had described the heterogeneous benzylation of microcrystalline cellulose. Rimböck *et al.* later described a method for preparing this material using an ultrasonic field to accelerate the reaction. Nowadays, a methanol–water solution containing about 40% of the pre-swollen material is commercially available.

Comparable with CTA, different solvents or solvent combinations also cause different degrees of swelling of this material. Dichloromethane or tetrahydrofuran cannot be used as the eluent because tribenzoylcellulose is soluble in these solvents.

With microcrystalline cellulose tribenzoate, a stationary phase for chromatographic enantiomer separations has been introduced, which allows the resolving of different classes of organic compounds.

Cellulose tribenzoate, compared to some other types of chiral stationary phases, offers the advantage that, besides analytical separations, preparative work can also be performed without a great deal of effort.

Benzoyl Cellulose Beads (in the Pure Polymeric Form)

Francotte and co-workers developed this type of chiral stationary phase. These materials are cellulose esters of aromatic acids in the form of almost spherical, partially crystalline particles with a good mechanical stability.

To characterize these phases, a broad variety of product classes on experimental batches of benzoyl- and *p*-methylbenzoyl cellulose beads have been examined. Methanol, ethanol and *n*-hexane-2-propanol were used as the eluent and the results obtained were compared with data measured under the same experimental conditions on the corresponding physically coated materials (Chiralcel OB and Chiralcel OJ).

In general, much higher retention values are observed on the pure cellulose derivatives compared to the values measured on the corresponding coated stationary phases. This observation is logical, because the physically coated phases only contain about 20 weight percent of the cellulose derivative. For the investigated product series, in most cases smaller retention values were measured for methanol than for ethanol as the mobile phase. Furthermore, most products also demonstrated the highest resolution values when methanol was used as the eluent.

For some of the substances tested, practically no difference in resolution was observed between the pure cellulose material and the coated phases, while other product classes were always better separated on the commercially available columns.

Mobile-Phase Effects

A chromatogram of the Mesuximid enantiomer separation that clearly illustrates the separation power of this type of materials is depicted in **Figure 1**.

For Mesuximid, using *n*-hexane-2-propanol as the mobile phase, the investigation of the effect of the polar modifier concentration on the retention factor demonstrate that, below a certain polar modifier concentration, the retention factor strongly increases. This can be an indication that competition between the polar modifier and the solute for hydrogen-binding sites on the stationary phase might be the determining factor in the retention process.

Although the retention factor is strongly influenced by the polar modifier concentration, the effect on the

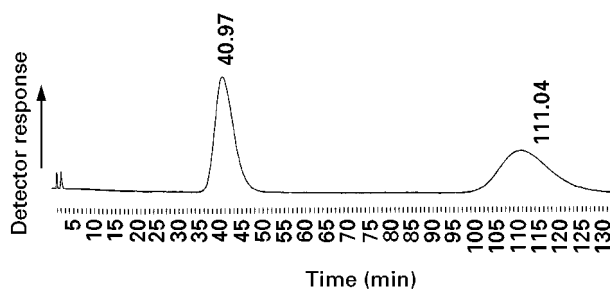


Figure 1 Benzoyl cellulose beads in the pure polymeric form: effect of polar modifier concentration on the retention factor. Column: 125 × 4 mm i.d. filled with 10 μ m *p*-methylbenzoyl cellulose beads. Mobile phase: *n*-hexane-2-propanol in different ratios. Flow rate: 1 mL min⁻¹. Sample: Mesuximid.

selectivity factor in the studied range of polar modifier content remains rather small.

The benzoyl cellulose derivatives in the pure polymeric form allow the separation of a broad variety of compounds. In many cases, results are obtained which are comparable with the values measured on the corresponding physically coated phases. Furthermore, these materials are very useful as stationary phases for preparative chromatographic applications.

Physically Coated Cellulose and Amylose Derivatives

This type of chiral stationary phase, developed by Okamoto and commercialized by Daicel Chemical Industries, can be considered to be the most universally applicable type of chiral stationary phase for both analytical and preparative chromatographic applications. Many different column types are available on the market. However, experience suggests that, with four different types of phases, a wide range of racemates, belonging to a broad variety of product classes, can be separated. The most interesting phases in our view are:

1. Cellulose derivatives:
 - (a) Chiralcel OD (3,5 dimethylphenyl carbamate derivative)
 - (b) Chiralcel OJ (*para*-methylbenzoyl derivative)
2. Amylose derivatives:
 - (a) Chiralpak AD (3,5 dimethylphenyl carbamate derivative)
 - (b) Chiralpak AS [(*S*)- α -methylbenzyl carbamate derivative]

The analytical phases are coated on a 10 μ m wide pore silica. However, some types of phases are also available on a 5 μ m silica matrix. Furthermore, two phases, which are specifically designed for reversed-phase applications, have been brought on to the market. An overview of the different types of commercially available coated phases is given in **Table 1**.

Table 1 Commercially available silica-coated phases for enantioseparation

<i>Cellulose esters</i>	<i>Type of absorbent</i>
Chiralcel OJ	<i>p</i> -Methylbenzoyl
Chiralcel OJ-R	For reversed-phase application
Chiralcel OB	Benzoyl
Chiralcel OB-H	Coated on a 5 μ m silica matrix
Chiralcel OA	Acetyl
Chiralcel OK	Cinnamoyl
Chiralcel CA-1	Acetyl
<i>Cellulose carbamates</i>	
Chiralcel OD	3,5-Dimethylphenyl
Chiralcel OD-H	Coated on a 5 μ m silica matrix
Chiralcel OD-R	For reversed-phase applications
Chiralcel OD-RH	For reversed-phase applications
Chiralcel OC	Phenyl
Chiralcel OG	<i>p</i> -Methylphenyl
Chiralcel OF	<i>p</i> -Chlorophenyl
<i>Amylose carbamates</i>	
Chiralpak AD	3,5 Dimethylphenyl
Chiralpak AS	(<i>S</i>)- α -Methylbenzyl

Mobile-Phase Design and Parameter Optimization

Different investigators have suggested that the mechanism of chiral recognition on cellulose and amylose derivatives is based on:

1. Hydrogen bonding
2. Dipole-dipole interaction
3. Charge transfer complex formation (π - π interactions)
4. Possible inclusion into chiral cavities or channels of the chiral stationary phase

Whatever the type of interaction involved, the mobile phase must be considered as a dynamic part of the system, capable of interacting with both the enantiomeric solute and the chiral stationary phase. For solutes where hydrogen bonding plays an important role in the selective chiral interaction process, proton-donating polar modifiers can compete with the solute for the hydrogen-bonding sites of the stationary phase. In other cases, π - π interactions between an aromatic moiety on the solute and the chiral stationary phase seems to be the most important interaction force.

Most of the separations on physically coated cellulose and amylose columns have been performed with mobile phases consisting of *n*-hexane or *n*-heptane as the major component, mixed with various aliphatic alcohols. The choice of solvent combination is principally based on recommendations for use by the manufacturer. Concerns about the stability of these columns combined with the relatively high cost

discouraged the use of other solvent combinations than those recommended by the manufacturer. However, in the last few years, other aprotic solvents, e.g., acetonitrile, methyl-tertiary-butyl ether and ethyl acetate have been applied on certain types of the derivatized polysaccharide columns. Certainly in the field of preparative chromatographic enantiomer separations. These alternative solvents widen the application range of this type of stationary phase.

For method development on this type of phase screening experiments on 50 \times 4.6 mm ID pre-columns filled with respectively Chiralcel OJ, Chiralcel OD, Chiralpak AD and Chiralpak AS are convenient. In use such column are rapidly equilibrated, give fast separations and have in many cases more than sufficient separation power for initial method development work. As a general rule, pure ethanol at a flow rate of 0.5 mL min⁻¹ is used as the eluent of choice to perform the first experiments.

Pure ethanol is chosen based on the experience that, for a lot of products, below a certain amount of polar modifier in an *n*-hexane or *n*-heptane based mobile phase, the retention factors strongly increase. In general, the effect of the polar modifier on the retention factor decreases upon increasing modifier content. An indication that the competition between the solute and the polar modifier in the eluent for the hydrogen-bonding sites of the stationary phase is a saturable process and a maximum effect on the retention factor will be reached within a certain range of polar modifier concentration (for our type of compounds, mostly situated between 15 and 20%). If, in the screening experiments, the analytes are insufficiently retained or no separation is observed, ethanol is mixed with *n*-heptane or *n*-hexane in different ratios. Once a suitable *n*-heptane-ethanol ratio has been found to reach a *k'* value between 3 and 6, ethanol is replaced by the same molar amount of one of the other lower aliphatic alcohols (1- or 2-propanol, primary, secondary or tertiary butanol). In many cases, large effects on the resolution values can be observed when ethanol as polar modifier is replaced by another alcohol.

Experience shows that pure methanol or mixtures of ethanol and methanol or ethanol and 2-propanol are often very useful to improve a separation.

On these phases it has been observed that the retention factors of a range of 2,3-dihydro-1,4-benzodioxin-2-carboxylic acid esters increased with increased chain length of the alcohol used for chromatography on a Chiralcel OB column. This effect might be based on a reduced capability of the larger alcohols to compete with the solute for hydrogen-binding sites on the stationary phase.

The higher retention values measured for the branched alcohols compared to their corresponding linear analogues may be due to steric influences, which result in a reduced tendency of these alcohols to interact by hydrogen bonding with the polysaccharide phase.

The observed decrease in retention factor with increasing chain length of the ester group could be an indication that hydrophobic effects also contribute to the interaction mechanism between the solute and the chiral stationary phase.

For the lower members of the homologue series of the 2,3-dihydro-1,4-benzodioxin-2-carboxylic acid esters, practically no difference in resolution values can be observed between the different polar modifiers. Depending on the type of alcohol used, the resolution rapidly decreases for the pentyl ester and the higher homologues. Only for *n*-butanol as polar modifier, is the decrease in resolution value rather limited. For ethanol the lowest resolution values are observed for the whole product series. There are indications that, for the investigated solutes, hydrogen-bonding forces certainly play an important role in the chiral recognition process.

This type of experiment clearly demonstrates that, when *n*-hexane or *n*-heptane-alcohol mixtures are used, testing different alcohols as polar modifier during method development should be performed, because in many cases, large differences in enantioselectivity may be observed.

It is also interesting to note that, by changing the polar modifier phase, an inversion of the elution order can occur, as illustrated in the following example. On a Chiralcel OD column, it was possible to separate the investigated compound (R89439) in its two enantiomers using a mixture of *n*-hexane-ethanol in an 80 : 20 volume ratio. The desired enantiomer eluted as the first peak under these experimental conditions, as illustrated in **Figure 2A**. When the ethanol as polar modifier was partially replaced by methanol, a reversal of elution order was observed, as illustrated in **Figure 2B**.

Some investigators have suggested that binding a polar modifier to sites near the chiral cavities might alter the steric environment of these cavities. If the environment of these cavities changes, it can certainly have an influence on the steric fit of the chiral solutes in these cavities, which may in part be responsible for the observed phenomenon of reversal in elution order. It is furthermore interesting to note that a reversal of elution order can often be achieved by the changeover of a carbamate-type phase towards a benzoate-type phase. This knowledge can be very useful when a small amount of one enantiomer has to be determined besides a large excess of the other enan-

tiomer, because it is easier to quantify a small peak in front of a large one than in the opposite situation. Based on experience, it is also important to mention that sometimes even small variations in experimental conditions can have a tremendous effect on the resolution of enantiomers on this type of stationary phases.

The often observed strong influence of small differences in experimental conditions on the resolution, certainly has to be considered when robust and reproducible methods have to be developed on this type of phases, for regulatory (Good Laboratory (GLP), Good Manufacturing (GMP)) purposes.

An example of the use of aprotic modifiers, which can also affect the separation on these phases, is as follows. About 40 g of a diastereomeric mixture had to be separated into its four enantiomers. Very good separation was obtained on an amylose 3,5-dimethyl-phenyl carbamate (Chiralpak AD) column using pure ethanol, pure methanol or a mixture of ethanol and 2-propanol in a 90 : 10 volume ratio. Unfortunately, the solubility of the diastereomeric mixture in the alcohol used was very poor. We therefore decided to study the behaviour of ethanol-acetonitrile mixtures, because the solubility of the product was a lot better in acetonitrile.

The results of these experiments are summarized in **Table 2** and graphically represented in **Figure 3**.

As illustrated in **Figure 3**, the addition of an aprotic modifier to the polar organic solvent has a clear effect on the retention behaviour and the enantioselectivity, especially for the most retained enantiomers. The investigated solute molecule contains different hydrogen-bonding groups, which can strongly interact with the carbamate functionality of the stationary phase. Combined with poor solubility of the substance in the lower molecular weight alcohols, this makes these solvents less suitable to displace the solute from the stationary phase and probably explains the high retention values observed for pure methanol or ethanol.

The addition of acetonitrile improves the solubility of the product. This at first simplifies the transfer of the solute into the mobile phase and furthermore gives the protic solvent a better chance to compete for the hydrogen-bonding sites of the stationary phase, which may explain the observed systematic decrease in retention factors with increasing acetonitrile concentration. Below a certain concentration of protic solvent in the eluent, the strong hydrogen-bonding properties of the solute predominate again, resulting in an increase in retention factor. Using a mixture of ethanol and acetonitrile in a 30 : 70 volume ratio allowed the separation of the diastereomeric mixture in its four enantiomers without difficulty.

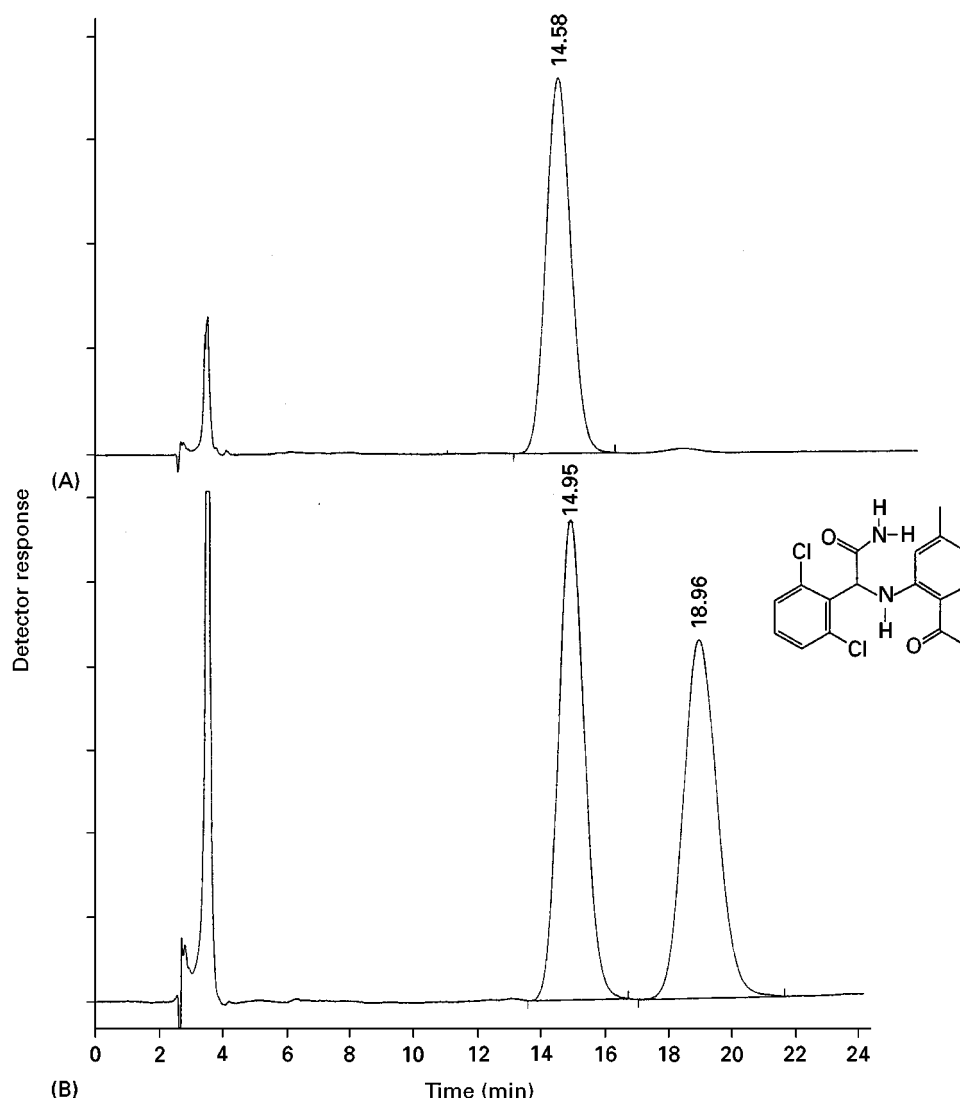


Figure 2 Effect of mobile-phase composition on the elution order. Column: 250 × 4.6 mm. Chiralcel OD (cellulose 3,5 dimethylphenyl carbamate). Mobile phase: (A) *n*-hexane–ethanol (80 : 20; v/v); (B) *n*-hexane–ethanol–methanol (80 : 5 : 15; v/v). Flow rate: 1 mL min⁻¹. Sample: R89439 (racemate plus pure enantiomer).

Table 2 Effect of the addition of acetonitrile on retention behaviour and enantioselectivity

Acetonitrile (%)	<i>k'</i> 1	<i>k'</i> 2	<i>k'</i> 3	<i>k'</i> 4	α (1–2)	α (3–4)
0	2.94	6.43	11.97	28.24	2.187	2.359
5	1.80	3.6	8.67	14.30	2	1.649
10	1.25	2.7	7.55	10.25	2.16	1.358
15	0.95	2.08	6.34	8.03	2.189	1.267
20	0.66	1.59	5.47	6.62	2.409	1.210
30	0.50	1.25	5.26	5.26	2.50	1.0
40	0.46	1.1	5.05	5.05	2.391	1.0
50	0.45	1.04	5.72	5.72	2.311	1.0
70	0.90	1.73	9.38	12.05	1.922	1.285
80	1.31	2.67	16.86	27.0	2.038	1.601

Basic or acidic additives can also have major effects on the separations. Thus, for some basic or acidic substances, it is often necessary to add respectively a base or an acid to improve the peak shape. Based on the manufacturer's recommendations, it is possible to use up to 1% of di- or triethylamine to reduce the tailing of basic substances. Acetic or trifluoroacetic acid can be used for the analysis of acidic substances.

The usefulness of these mobile-phase additives, is shown in the following example. For the enantiomer separation of [(±) 2,6-dichloro- α -(4-chlorophenyl)-4-(4,5-dihydro-3,5-dioxo-1,2,4-triazin-2-(3H)-yl) benzene acetonitrile] (diclazuril) initially a method was used in which the acidic NH-group in the 3,5-dioxo-1,2,4 triazin part of the molecule was methylated with diazomethane. The derivatized product

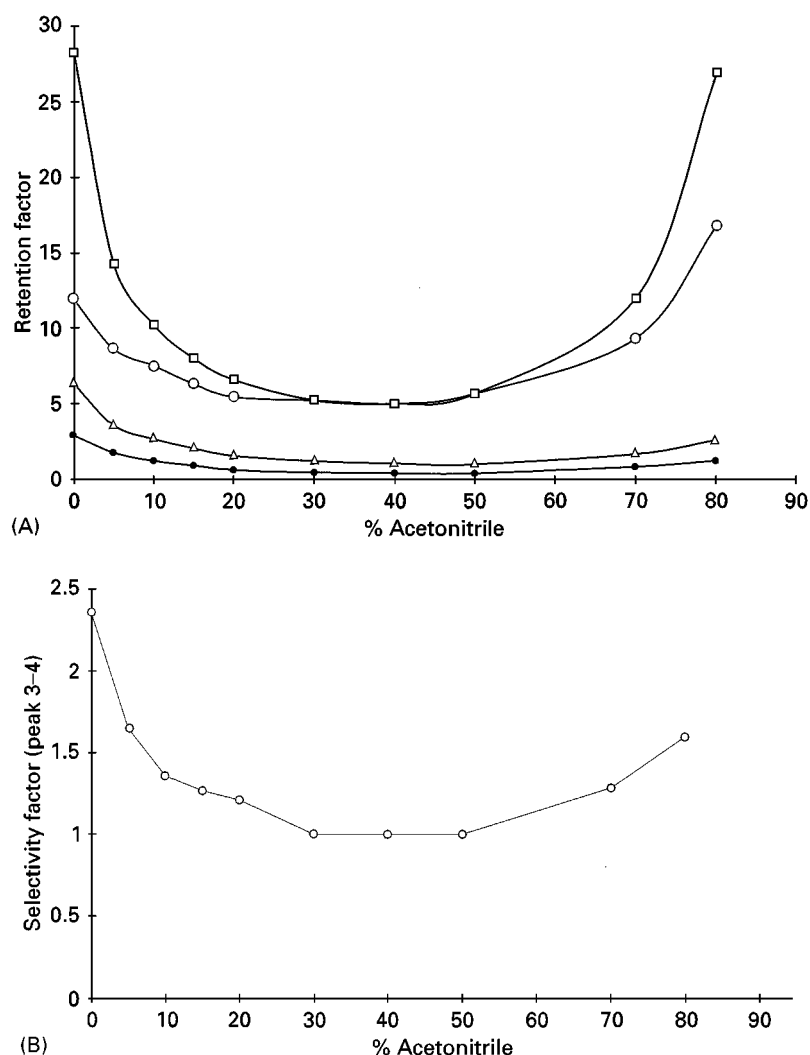


Figure 3 Effect of acetonitrile on (A) the retention factor; (B) enantioselectivity. Column: 250 \times 4.6 mm Chiralcel AD (amylose 3,5 dimethylphenyl carbamate). Mobile phase: ethanol-acetonitrile in different ratios. Flow rate: 1 mL min⁻¹. Filled circles, k'_1 ; triangles, k'_2 ; open circles, k'_3 ; squares, k'_4 .

could easily be analysed on an amylose 3,5 dimethylphenyl carbamate (Chiralpak AD) column, using ethanol-*n*-hexane in an 80 : 20 volume ratio.

A chromatogram of this separation is illustrated in Figure 4A.

As can be seen from Figure 4A, reaction with diazomethane results in different reaction products, with both nitrogen alkylated and oxygen alkylated compounds observed. Because direct analysis of this product on the cellulose- or amylose-based stationary phases, using the classical eluents, was not possible, due to the presence of the acidic NH-group in the 3,5-dioxo-1,2,4-triazin part of the molecule (which resulted in a retardation of the substance on the stationary phase), the effect of the addition of trifluoroacetic acid was examined. The result of such an

experiment on a micro-LC column is shown in Figure 4B.

The use of an amine as tailing reducer is illustrated in the following example. A few grams of a chiral amino alcohol had to be separated in its two enantiomers. Only partial separation could be obtained on a Chiralcel OD (cellulose 3,5-dimethylphenyl carbamate) column using a mixture of *n*-hexane and 2-propanol in a 70 : 30 volume ratio. Because a severe tailing was observed, we investigated the effect on the addition of triethylamine as mobile-phase additive. A small quantity of 0.1 vol% of triethylamine improved the peak shape and the resolution. However, a much better result was observed when the triethylamine content was increased to 0.5 vol%. Thereafter, triethylamine was replaced for the same

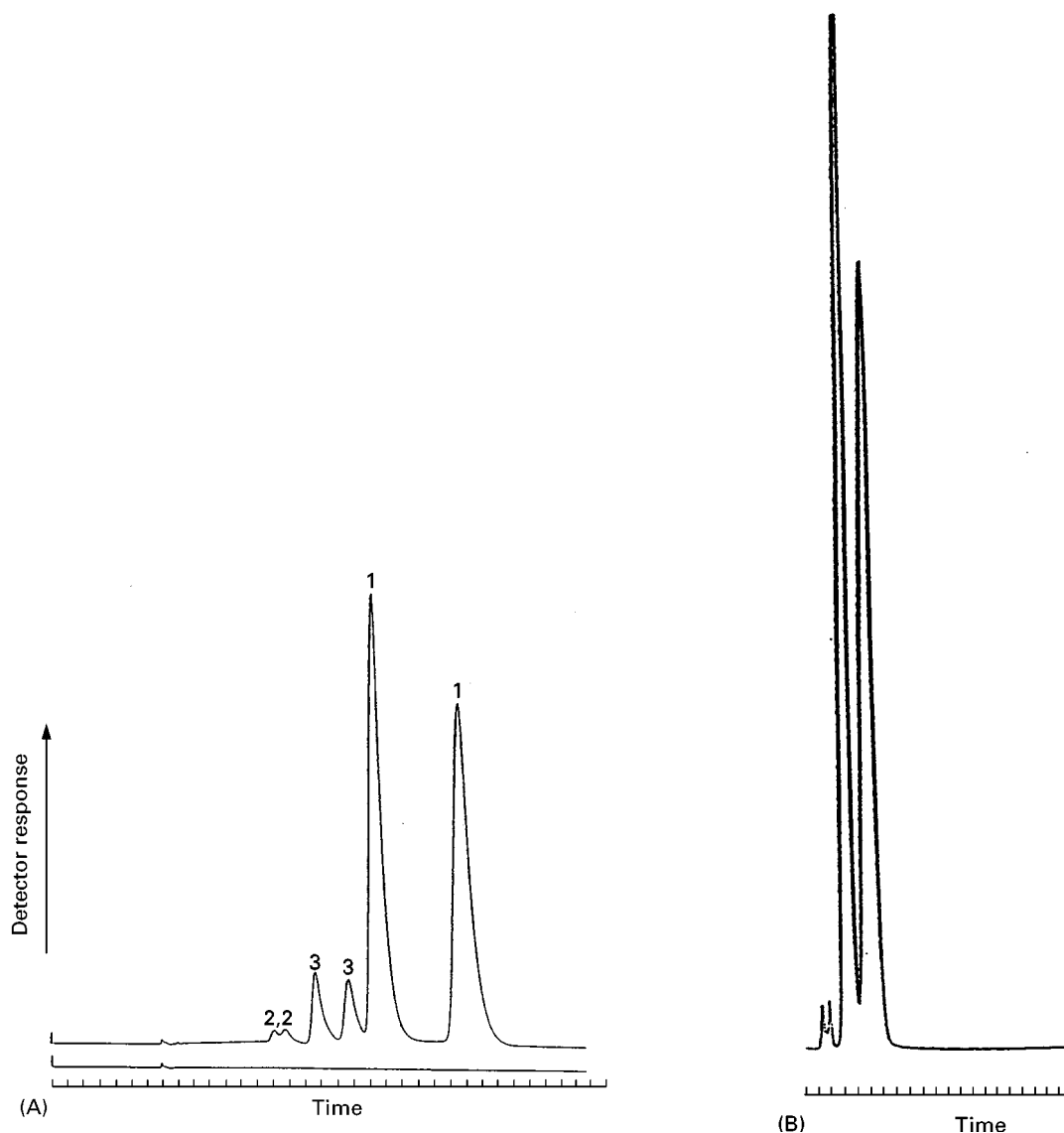


Figure 4 (A) Separation of diclazuril after derivatization with diazomethane. Column: 250×4.6 mm i.d. Chiralpak AD (amylose 3,5 dimethylphenyl carbamate). Mobile phase: ethanol-*n*-hexane (80 : 20; v/v). Flow rate: 0.5 mL min^{-1} . Detection: UV (290 nm). Injection volume: $10 \text{ }\mu\text{L}$. Temperature: ambient. Peak 1: Enantiomers of *N*-methylated product. Peaks 2 and 3: Enantiomers of *O*-methylated product. (B) Separation of diclazuril using trifluoroacetic acid as mobile-phase additive. Column: 150×0.32 mm i.d. Chiralpak AD. Mobile phase: ethanol-1% trifluoroacetic acid. Flow rate: $5 \text{ }\mu\text{L min}^{-1}$. Detection: UV (280 nm). Injection volume: 60 nL . Temperature: ambient.

amount of diethylamine. The addition of 0.5% diethylamine resulted in the highest resolution value.

Therefore, the first experiment on the preparative column was performed with a mobile phase containing 0.5 vol% of diethylamine. The obtained result was rather poor. The enantiomers eluted as relatively broad peaks, which were only partially resolved. Because for preparative chromatographic application we prefer to work with triethylamine instead of diethylamine, the method was therefore further optimized using triethylamine as tailing reducer. To reach

maximum resolution on the preparative column, the amount of 2-propanol had to be reduced from 30% to 10 vol%, while the triethylamine concentration had to be increased to 2 vol%.

Using this method, it was possible to inject 250 mg of the product. The optimized method enabled sufficient amount of the pure enantiomers to be prepared in a reasonable amount of time.

The solute structure will also clearly have a direct effect on the separation. Thus, the chiral recognition process on polysaccharide phases results from

differences in the summation of binding energies originating from:

1. hydrogen bonding
2. dipole-dipole interactions
3. charge transfer (π - π) complex formation
4. steric interactions

It is not possible to generalize which type of interaction forces plays the key role in the solute-chiral stationary phase complex formation. Hydrogen bonding certainly has a strong role in the selective chiral interaction process.

Based on the knowledge that on polysaccharide phases different mechanisms play a role in the chiral recognition process and small variations in experimental conditions or solute structure can strongly affect the enantioselectivity, it is clear that small changes in the molecular structure of a specific type of compounds that are in general well separated can often be a challenge to find an acceptable separation method for some of the members of such a product series.

The effect of small structural changes on the retention behaviour and the enantioselectivity is illustrated in the following examples.

In the first example, a few imidazole derivatives bearing an ester function on the imidazole ring were investigated on a Chiralcel OC (cellulose phenyl carbamate) as well as on a Chiralcel OD (cellulose 3,5-dimethylphenyl carbamate) column, using *n*-hexane-2-propanol as the mobile phase. On the Chiralcel OC column a mixture of *n*-hexane-2-propanol in a 90 : 10 volume ratio was used. Because with this mobile-phase composition the products were not sufficiently retained on the Chiralcel OD column, the amount of polar modifier had to be reduced to 5 vol% on this column type. On both column types the retention factor strongly decreased with increasing chain length of the ester group attached to the imidazole ring. Also steric effects seem to play a role, because on both columns the smallest retention value is measured for the 2-propyl ester.

When the resolution values are considered, a clear difference was to be observed between both column types. For the 1-propyl and 2-propyl esters, baseline resolution is obtained on both stationary phases. However, the observed differences for the ethyl and methyl ester are striking. On the Chiralcel OC column the ethyl ester is still baseline-resolved, while the methyl ester is only partially separated, whereas on the Chiralcel OD column, the methyl ester is very well separated and the ethyl ester did not display any separation at all. Certainly there is an indication that small but nevertheless influential contributions play

an important role in the chiral recognition process, which of course makes it not always that easy to predict whether a new product in a series of comparable structures will be separated or not on a particular type of stationary phase.

The next example also demonstrates that it is not always easy to predict whether a product within a series will be separated on a certain type of polysaccharide phase.

Some tetramisol derivatives were investigated on three different carbamate-type phases (Chiralcel OC, Chiralcel OF and Chiralcel OD) using *n*-hexane-2-propanol in a 70 : 30 volume ratio. For the investigated compounds, the highest retention is measured on the Chiralcel OF (*p*-chlorophenyl carbamate) column, while the smallest values are observed on the Chiralcel OD column. However, on the three different column types the *meta*-substituted derivative has always the most strongly retained.

Although the products were most strongly retained on the Chiralcel OF column, not one of the 10 investigated substances was fully baseline-resolved. Two of the *ortho*-substituted compounds and the unsubstituted tetramisol were best resolved on the Chiralcel OC column, while for the *meta*- and *para*-substituted derivatives the highest resolution value was in general measured on the Chiralcel OD column.

It is quite clear therefore from the different examples that small changes in solute structure or experimental conditions can have a strong influence on the chromatographic behaviour. This phenomenon makes it often difficult to predict whether a product will be separated on a certain type of polysaccharide phase or not. Therefore, even when a good mobile-phase composition has been found on a particular column, it is always advisable to test this solvent mixture on another column of the same type (carbamate or benzoate).

Achiral derivatization can be exploited to improve resolution as it is well known from experience that compounds bearing an ionizable group, e.g. a carboxyl, hydroxyl or amino group, are often poorly resolved on the polysaccharide type of phases. Derivatization of these functional groups to the corresponding ester, carbamate or amide derivatives frequently improves the separation.

For alcohol, for example, an esterification reaction with a *para*-substituted benzoic acid chloride has proven to be effective in solving difficult separation problems. The effect of an esterification reaction on the retention behaviour and the enantioselectivity is illustrated by means of the next examples.

The hydroxyl function of two completely different compounds was derivatized to yield the following

types of esters:

- | | | |
|------------------------------|---|---------|
| 1. Benzoyl | } | Benzoyl |
| 2. <i>p</i> -Fluorine | | |
| 3. <i>p</i> -Chlorine | | |
| 4. <i>p</i> -Bromine | | |
| 5. <i>p</i> -Trifluoromethyl | | |
| 6. <i>p</i> -Methyl | | |
| 7. <i>p</i> -Methoxy | | |
| 8. <i>p</i> -Nitro | | |
| 9. <i>p</i> -Cyano | | |
| 10. 1-Naphthoyl | | |
| 11. 2-Naphthoyl | | |
| 12. 9-Anthracoyl | | |

The different esters were respectively investigated on a Chiralcel OD, Chiralcel OJ, Chiralpak AD and Chiralpak AS column using pure ethanol as the eluent.

These compounds were retained more on the benzoate type of phase than on the carbamate type of stationary phase. Also, the resolution is significantly higher on the Chiralcel OJ column than on the other columns. The favourable results on the benzoate type of column inspired us to investigate the difference between ethanol and methanol as the mobile phase for this type of compound. For methanol much higher retention factors are measured than when ethanol is the eluent. In general, about twice as high resolution values are measured for methanol.

In the foregoing example, the best results for the different esters were obtained on a benzoate type of column. This is certainly not a general rule. Another alcohol [4,4-dimethoxy-1-(phenylmethyl)-3 piperidinol] was derivatized to yield a similar series of esters. This homologue series was also investigated on the four different types of polysaccharide phases, using ethanol as the eluent.

On the Chiralcel OJ column only the 2-naphthoyl derivative was partially separated. On the Chiralcel OD column only the 2-naphthoyl and the 9-anthracoyl ester were partially resolved, while on the Chiralpak AS column only the 9-anthracoyl ester showed partial resolution. However, on the Chiralpak AD column most of the products were separated. What is striking in this particular example is the partial separation of the native alcohol, while the benzoyl- and *p*-fluorobenzoyl esters do not show any separation at all.

For further synthesis applications, alcohols are frequently converted to the mesylated and tosylated derivative. When we are confronted with the preparative chromatographic separation of a racemic alcohol, we always investigate the mesylated or tosylated alcohol before carrying out other derivatization work, because we have experienced that in many

cases, these compounds are easier to separate than the native alcohol. For very difficult separations we eventually had to synthesize the naphthylsulfonyl derivative.

Temperature is well known to affect chiral isolation. Thus, on chiral stationary phases, specific interaction mechanisms are involved in the separation process. Therefore, this type of phase often displays slow mass transfer characteristics.

Temperature, together with the mobile-phase velocity, certainly has to be considered as a factor that can be used to influence this mass transfer process.

In the next example, we examined the combined effects of temperature and flow velocity variations on enantioselectivity, column efficiency and resolution. The enantiomers of the investigated racemate were difficult to separate. Only partial separation could be achieved with *n*-hexane-ethanol in a 90 : 10 volume ratio on a Chiralcel OJ column, using our standard experimental conditions of flow rate and temperature. To investigate this separation problem further, the temperature was varied between 5 and 40°C and flow rates between 0.25 and 2 mL min⁻¹ were tested.

A good linear relationship between the logarithm of the α value and the temperature has been observed. The α value steadily increased with decreasing temperature. However, the most significant parameter to indicate the separation between two products is the resolution value. This parameter is determined by both thermodynamic and kinetic contributions.

Although two completely different measuring principles have been used, comparable patterns are observed for the two resolution values. Both figures indicate that only for temperatures below 15°C and a flow rate of 0.25 mL min⁻¹ can a nearly baseline separation be obtained. Although it was not possible to obtain a full baseline separation of the enantiomers, the optimized analysis method was sufficiently accurate to follow up the investigations that were performed to develop a stereospecific synthesis method.

As this example indicates, during method development and optimization experiments, the factored temperature certainly has to be investigated. Besides essential information for analytical purposes, it also gives chromatographers performing preparative chromatographic separations a good idea of whether it is possible to work at higher temperatures without losing efficiency. Due to the limited choice of possible mobile-phase compositions, the major problem one has to deal with in preparative chromatographic work on polysaccharide phases is the solubility of the product to be separated in the eluent used. Because solubility in most cases increases with increasing temperature, the ability to work at higher temperatures

often improves throughput in preparative chromatographic separations.

The experiments performed also demonstrate that the flow velocity is a parameter that can be used to optimize a separation process.

Separation of Diastereomers

Although diastereomers are in general easy to separate under normal or reversed-phase chromatographic conditions, it often happens, especially when the chiral centres are located far away from each other, that it is not always easy to separate these compounds. When we are confronted with such a problem, we always investigate the possibilities of microcrystalline cellulose triacetate or tribenzoate and the physically coated derivatized polysaccharides. We have experienced that this approach can be a solution in many cases. An example of such a separation is described in the next example.

A racemic alcohol was derivatized with optically pure (1*S*)-camphor sulfonic acid chloride. It was not possible to separate the obtained diastereomers under normal-phase conditions on bare silica or amino-modified silica. Under the reversed-phase conditions which we generally apply in our laboratories it was not possible to separate the isomers. We did some experiments on different derivatized polysaccharide phases. On a 50 × 4.6 mm i.d. Chiralpak AD (amylose 3,5-dimethylphenyl carbamate) using ethanol as the

eluent, the diastereomers were very well separated. Because with pure ethanol the retention factors were relatively high, the effect of the addition of acetonitrile was investigated. A few chromatograms of these experiments are depicted in **Figure 5**. Using a mixture of 95 vol% ethanol and 5 vol% acetonitrile, it was easy to isolate a large pure amount of both diastereomers.

Reversed-Phase Applications

As mentioned before, two types of polysaccharide phases which are specifically designed for reversed-phase applications are currently on the market. This type of phase is extremely interesting for the direct injection of aqueous solutions (ionic products, plasma samples, etc.). Furthermore, the columns are useful in column-coupling techniques (for example, an octadecylsilica column followed by a polysaccharide column) to solve difficult separation problems. The manufacturer recommends on this type of column to use a mobile phase consisting of an aqueous solution of a sodium, ammonium or potassium salt in combination with methanol, ethanol or acetonitrile as the organic modifier. The choice of the cationic part of the salt seems not to have a significant effect on the separation. However, a significant difference in separation has been observed with various anions. Anions, such as ClO_4^- and PF_6^- in general show good separation. Also the salt concentration can strongly affect the retention time and the resolution.

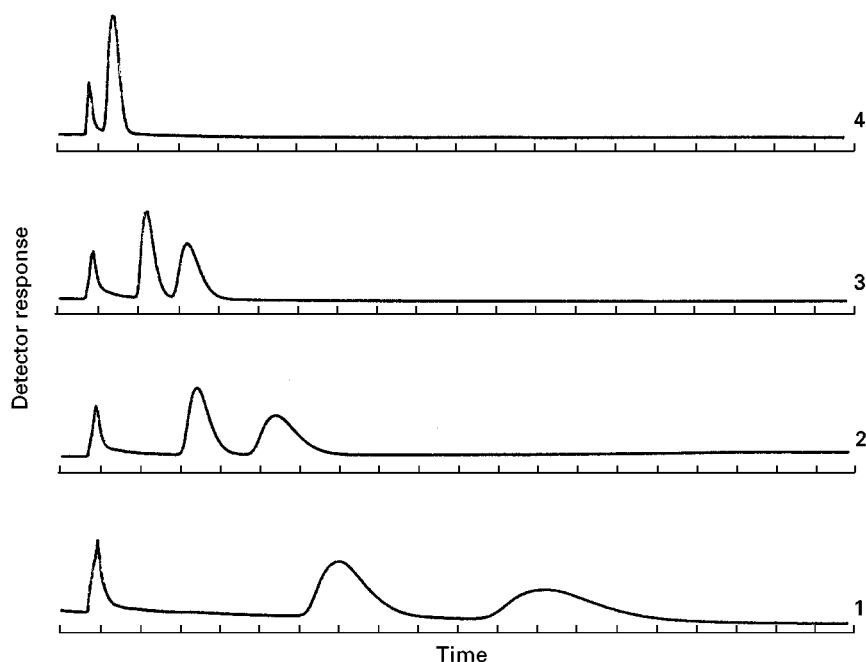


Figure 5 Diastereomer separation. Column: 50 × 4.6 mm i.d. Chiralpak AD (amylose 3,5 dimethylphenyl carbamate). Flow rate: 1 mL min⁻¹. Mobile phase: 1, ethanol; 2, ethanol–acetonitrile (95 : 5; v/v); 3, ethanol–acetonitrile (90 : 10; v/v); 4, acetonitrile.

Mobile-phase design and parameter optimization

Triethylamine salts are very popular as tailing reducers in reversed-phase applications. We have therefore investigated the usefulness of these salts on the polysaccharide-type phases. Experience with cyclodextrin and derivatized cyclodextrin columns taught us that a salt concentration of 50 mmol L⁻¹ in general is high enough to obtain good peak shapes for basic substances. Experimental work was started with this salt concentration. Afterwards, specific experiments performed to investigate the effect of the tailing reducer concentration on the chromatographic parameters confirmed that 50 mmol L⁻¹ was a good choice. In a concentration range between 10 and 50 mmol L⁻¹ the highest resolution values were always measured for the highest salt concentration. However, this concentration also resulted in the strongest retardation of the compounds.

In a first set of experiments, the difference in chromatographic behaviour of a few products under normal-phase and reversed-phase conditions was investigated on a Chiralcel OJ-R and Chiralcel OD-R column. The columns were first equilibrated with ethanol. Thereafter, a mixture of *n*-hexane–2-propanol in a 70 : 30 volume ratio was pumped through the column until equilibrium was reached and the different products were analysed. After rinsing the columns with ethanol, the column was equilibrated with a mixture consisting of 70 vol% methanol and 30 vol% of a 50 mmol L⁻¹ triethylamine solution in water adjusted with sulfuric acid to a pH value of 2.5.

In general the products are better retained when reversed-phase conditions are applied. It was also striking that for most of the investigated products there was a large difference in resolution values between the two modes of operation.

Type of tailing reducer Experiments on cyclodextrin and derivatized cyclodextrin columns have shown us that, for the analysis of basic compounds, the anionic part of the tailing reducer has a clear effect on enantioselectivity. To investigate this effect, we selected some imidazole derivatives.

To perform the experiments, a 55 mmol L⁻¹ solution of triethylamine in analytical grade water was prepared and 2 L portions of this solution were adjusted to a pH value of 2.5 with respectively hydrochloric, trifluoroacetic, methanesulfonic, camphorsulfonic, sulfuric and phosphoric acid. After pH adjustment the solution was further diluted to obtain a solution which contains exactly 50 mmol L⁻¹ triethylamine.

As eluent a mixture composed of 70 vol% of methanol and 30 vol% of the triethylamine solution was used. On the Chiralcel OJ-R and on the Chiralcel

OD-R column, the retention values for phosphate or sulfate anion are markedly higher than the values measured for the other anions. The lowest values were in most cases measured for chloride as the counterion.

On both column types, the anionic part of the tailing reducer has a clear effect on enantioselectivity (Figure 6). In general, the best results are obtained for phosphate or sulfate as the anion, although for some products better results were obtained using another type of anion.

The Chiralcel OJ-R column is much more suitable for the separation of the investigated compounds than the Chiralcel OD-R column.

Type of polar modifier In experiments using a mixture of methanol and triethylamine in a 70 : 30 volume ratio, high retention times were observed for some compounds. Therefore, it was interesting to investigate the effect of the addition of acetonitrile on retention time and enantioselectivity. To perform these experiments, a mixture of 70 vol% methanol and 30 vol% triethylamine adjusted to pH 2.5 with phosphoric acid was prepared and thereafter mixed with different amounts of acetonitrile. The different chromatograms obtained during these experiments are shown in Figure 7.

As Figure 7 clearly illustrates, acetonitrile strongly affects retention of the investigated compound. Although the resolution steadily decreases with increasing acetonitrile content, the *k'* value of the second eluting peak could be reduced by a factor of 38 with a full baseline resolution of the enantiomers as a result.

Because the elution power of acetonitrile is significantly higher than for methanol, we generally prefer to start new experiments with a methanol–water–tailing reducer mixture. If the compounds of interest are too strongly retained with this eluent, methanol is systematically replaced by acetonitrile until an acceptable compromise between the retention factor and the resolution value is found.

pH In the analysis of ionizable compounds, pH can certainly have a strong effect on the chromatographic behaviour. We therefore investigated for the product series summarized in Table 2 the effect of pH variations in the range between 2.5 and 4.5 on a Chiralcel OJ-R using a mobile phase composed of methanol–acetonitrile and a 50 mmol L⁻¹ triethylamine solution in water adjusted to the desired pH value with phosphoric acid. For one of the products investigated, the different chromatograms obtained during these experiments are depicted in Figure 8.

Figure 8 shows that the retention factors steadily increase with increasing pH value, reaching

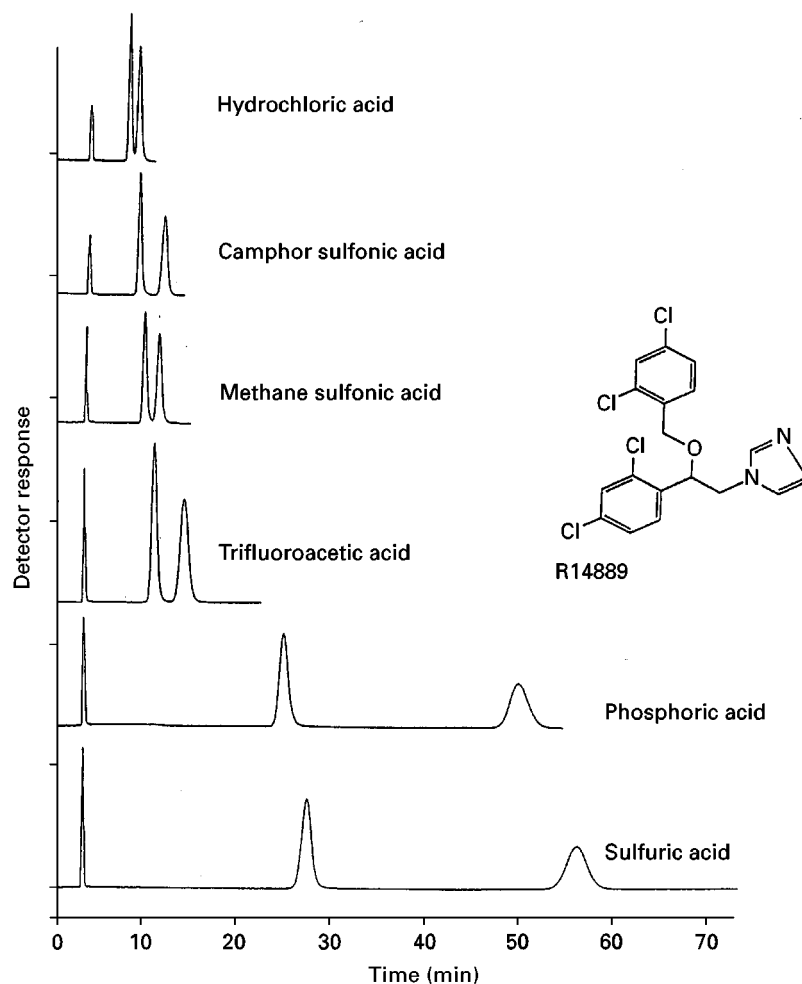


Figure 6 Effect of the anionic part of the tailing reducer on the resolution. Column: 250×4.6 mm i.d. Chiralcel OJ-R (*p*-methylbenzoyl cellulose). Flow rate: 1 mL min^{-1} . Mobile phase: 50 mmol L^{-1} triethylamine adjusted to a pH value of 2.5 with different acids-methanol (30 : 70; v/v).

maximum at pH 4 and decreasing again above this pH value. A similar pattern was also observed for the resolution value.

The different experiments that have been performed clearly indicate that, for ionizable compounds, pH can have an important effect on the enantioselectivity, which of course makes it a parameter to be investigated thoroughly during method development and optimization.

Chemically Bonded Polysaccharide Phases

Over the last few years, various attempts have been made to graft derivatized polysaccharides on to a silica matrix, without losing the chiral recognition properties of these materials. One of the major problems encountered was the limited amount of polysaccharide that could be chemically bonded. For the time being, only the French company Chiralsep (La Fresnaye) has a few chemically bonded polysacchar-

ide-based columns (Chirose-bond C1 and Chirose-bond C3) on the market.

We were able to test a few experimental chemically bonded polysaccharide phases. At first we compared a chemically bonded *p*-methylbenzoyl cellulose column with the corresponding physically coated material (Chiralcel OJ) using the classical alcohol-based mobile phases. Whereas on the coated phases most of the investigated compounds were partially or completely resolved with pure ethanol as the eluent, this was not the case on the chemically bonded material. For most of the compounds investigated it was necessary to dilute ethanol with *n*-hexane to obtain an acceptable resolution value. The experiments performed certainly prove that the chiral properties of the derivatized polysaccharide were not lost during the grafting process. However, compared to the coated phases, smaller retention factors were measured on the chemically bonded material. This is

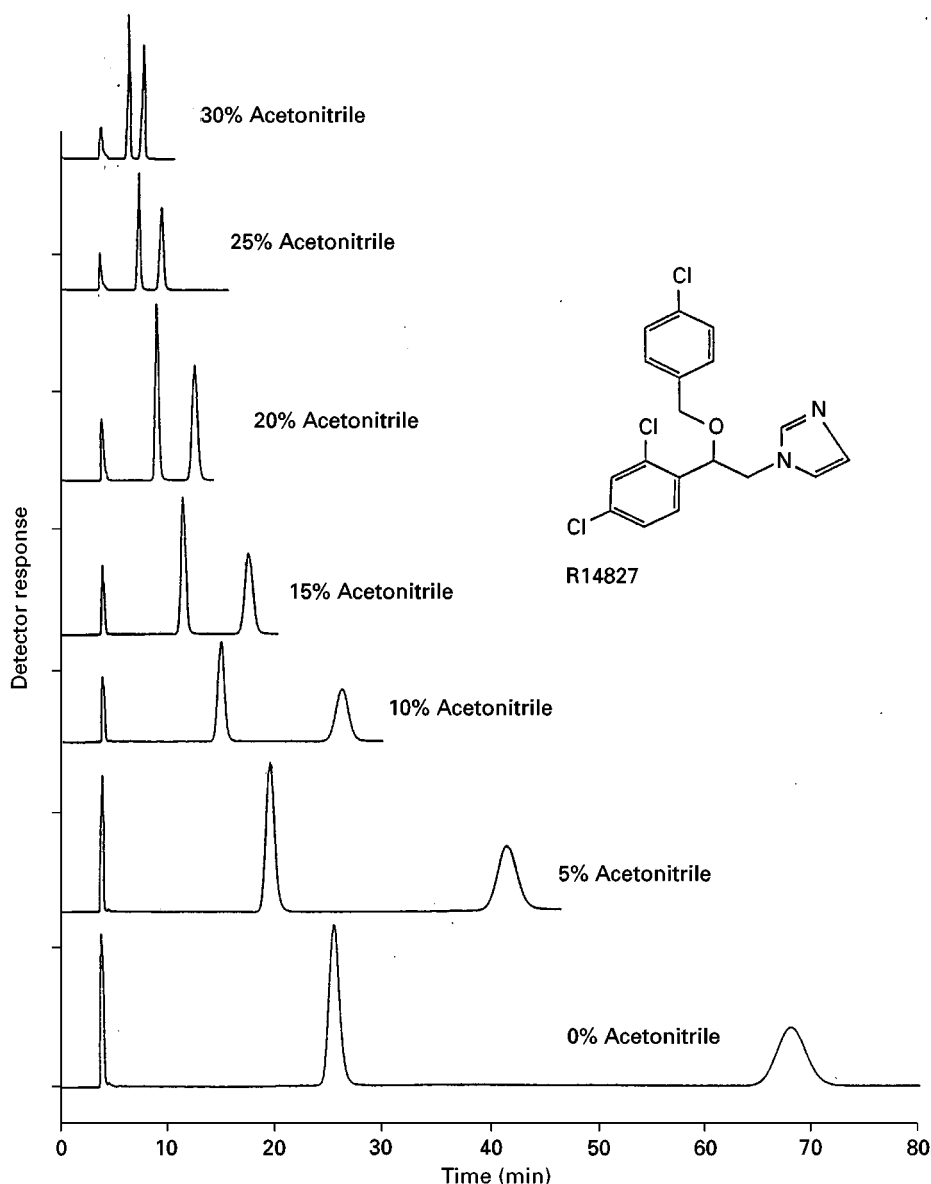


Figure 7 Effect of type of polar modifier on chromatographic behaviour. Column: 250 × 4.6 mm i.d. Chiralcel OJ-R (*p*-methylbenzoyl cellulose). Flow rate: 1 mL min⁻¹. Mobile phase: 50 mmol L⁻¹ triethylamine adjusted to a pH value of 2.5 with phosphoric acid-methanol (30 : 70; v/v) + acetonitrile in different ratios.

possibly an indication that only a small quantity of the chiral moiety was chemically bonded on to the silica matrix. Also, some differences in enantioselective properties could be observed between both phases. Phenoperidine, for example, was not resolved with pure ethanol on the coated phase while on the chemically bonded column this product was very well separated, as illustrated in **Figure 9**.

A few experiments under reversed-phase conditions were also performed on the chemically bonded *p*-methylbenzoyl cellulose column. Methanol or ethanol in combination with a 0.5% ammonium acetate solution in water was used as the mobile phase.

For all the investigated compounds, the smallest retention and selectivity values were measured for ethanol as the organic modifier. For some products, extreme differences in resolution could be observed between the different experimental conditions applied. For an amino alcohol, the chromatograms obtained using methanol and ethanol as organic modifier are graphically compared in **Figure 10**.

Although only a limited number of experiments were performed, we can conclude that the tested chemically bonded polysaccharide phase has a high potential for reversed-phase applications.

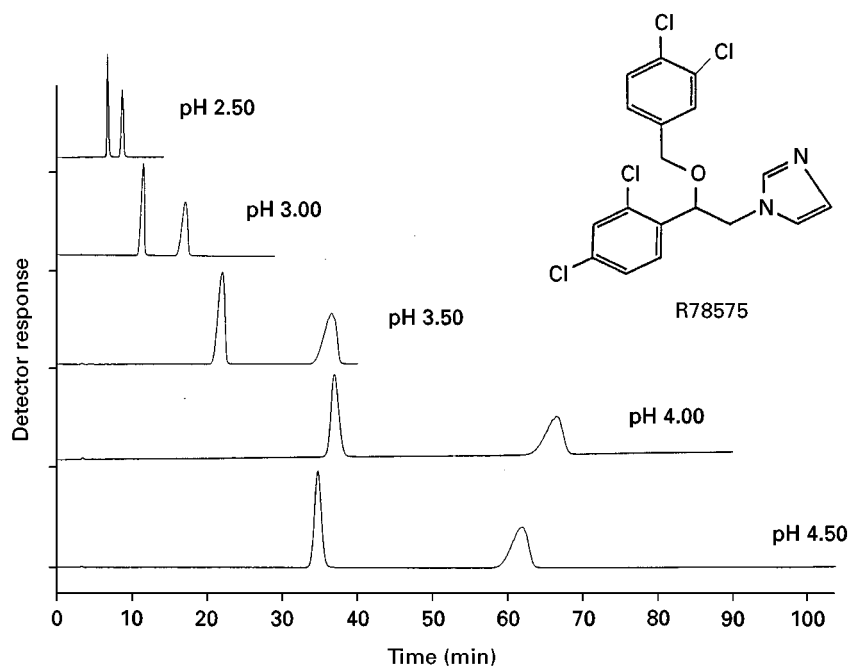


Figure 8 Effect of pH variations on the chromatographic behaviour. Column: 250×4.6 mm i.d. Chiralcal OJ-R (*p*-methylbenzoyl cellulose). Flow rate: 1 mL min^{-1} . Mobile phase: 50 mmol L^{-1} TEA adjusted to the indicated pH values with phosphoric acid-methanol-acetonitrile (30 : 40 : 30; v/v).

Besides these experiments, a series of 37 racemates belonging to different product classes were investigated on chemically bonded equivalents of respective-

ly Chiralcel OJ, Chiralcel OD, Chiralpak AD and Chiralpak AS originating from a different source to the column used in the foregoing experiments.

For the first tests, pure ethanol was used as the mobile phase. Using this eluent, the largest number of products were separated on the chemically bonded equivalent of Chiralcel OJ. Twenty compounds were partially or completely resolved on this column, compared to six products on the cellulose 3,5-dimethylphenyl carbamate column, 14 products on the amylose 3,5-dimethylphenyl carbamate column and eight compounds on the chemically bonded equivalent of Chiralpak AS. However, the number of products that were separated on the chemically bonded *p*-methylbenzoyl cellulose column was only 69% of the number of products resolved on the physically coated Chiralcel OJ column, using the same eluent. Because for the same eluent composition similar retention factors were measured on the chemically bonded columns and their physically coated equivalents, we may conclude that the amount of cellulose or amylose grafted on to the silica matrix has to be the same order of magnitude as the amount present on the physically coated phases.

Other solvents were also used on these columns. After extensive use of dichloromethane, which normally dissolves cellulose and amylose derivatives, the properties of the columns were tested again and compared with the results obtained on a fresh column. Practically no difference in retention or resolution

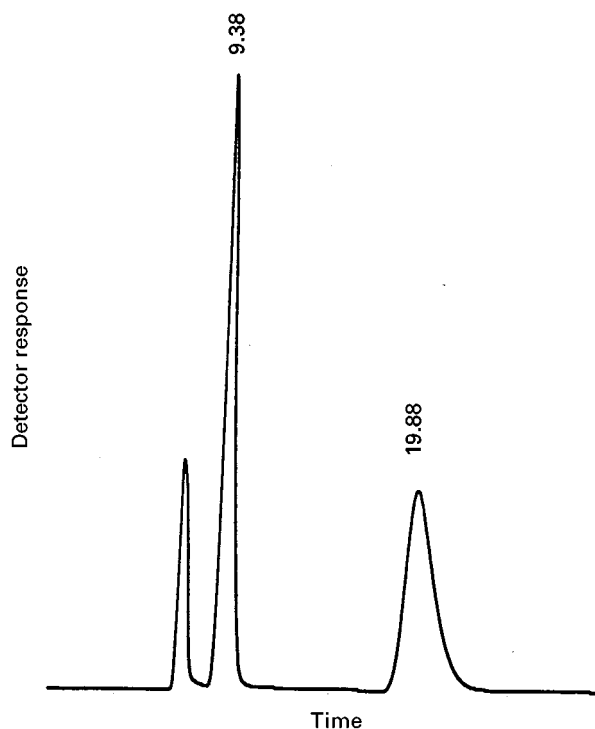


Figure 9 Separation of phenoperidine. Column: 250×4.6 mm i.d. chemically bonded *p*-methyl benzoyl cellulose. Flow rate: 1 mL min^{-1} . Mobile phase: ethanol.

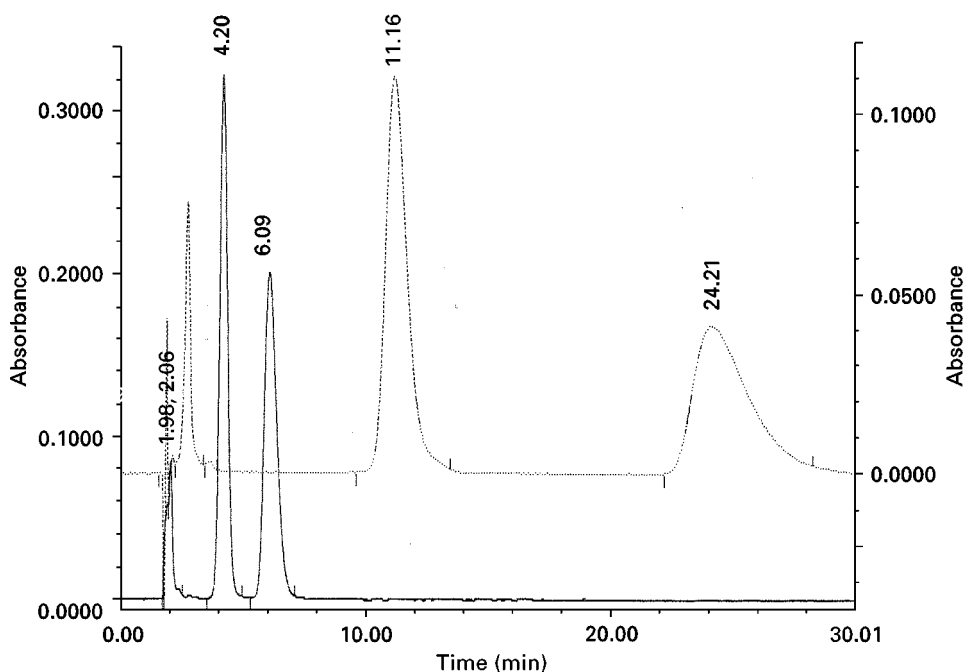


Figure 10 Separation of an amino alcohol under reversed-phase conditions. Column: 250 × 4.6 mm i.d. chemically bonded *p*-methylbenzoyl cellulose. Flow rate: 1 mL min⁻¹. Mobile phase: continuous line, 0.5% ammonium acetate in HPLC-grade water-ethanol (50 : 50; v/v); dotted line, 0.5% ammonium acetate in HPLC-grade water-methanol (50 : 50; v/v).

values could be observed before and after the use of dichloromethane. This is an indication that the polysaccharide derivative was perfectly bonded on to the silica matrix.

Some of our products were also investigated under normal-phase conditions on the Chirose-bond C1 column of Chiralsep. Most compounds eluted as relatively broad peaks with a severe tailing. From the 22 investigated compounds, only three products were fully baseline-resolved. The addition of a small amount of triethylamine did not solve the tailing problem. For only one of the investigated compounds was a very good resolution observed on the Chirose-bond C1. The results of these experiments are summarized in **Table 3**.

The ability to use dichloromethane for this compound is interesting for preparative chromatographic purposes, because the solubility of this product in the commonly used solvents (alcohol, or alcohol-*n*-hexane mixtures) is rather poor.

Some of the chemically bonded polysaccharide phases which have been tested certainly have a high potential. The possibility of using a broader pallet of solvents or solvent combinations especially widens for preparative chromatographic work the field of application.

Conclusions

Different types of derivatized cellulose and amylose stationary phases are nowadays commercially available. With a limited number of these phases it is possible to separate a broad variety of products. Furthermore, these phases are also extremely useful for preparative chromatographic applications.

Although differences in chromatographic behaviour between the tested chemically bonded phases and their physically coated equivalents have been observed, we might expect that, after further optimization of the grafting process, these phases will certainly enlarge the field of application of the derivatized cellulose and amylose materials.

Table 3 Use of dichloromethane on chemically bonded cellulose derivative

Mobile-phase composition	<i>k'</i> ²	α	Resolution
<i>n</i> -Hexane-2-propanol (45 : 55; v/v)	3.93	2.15	5.88
<i>n</i> -Hexane-2-propanol-dichloromethane (40 : 50 : 10; v/v)	3.14	1.97	4.63

See also: **II/Chromatography: Liquid:** Chiral Separations in Liquid Chromatography: Mechanisms. **III/Chiral Separations:** Amino Acids and Derivatives; Capillary Electrophoresis; Chiral Derivatization; Countercurrent Chromatography; Crystallization; Cyclodextrins and Other Inclusion Complexation Approaches; Gas Chromatography;

Ion-pair Chromatography; Ligand Exchange Chromatography; Liquid Chromatography; Molecular Imprints as Stationary Phases; Protein Stationary Phases; Supercritical Fluid Chromatography; Synthetic Multiple Interaction ('Pirkle') Stationary Phases; Thin-Layer (Planar) Chromatography.

Further Reading

Allenmark S (1991) *Chromatographic Enantioseparation, Methods and Applications*, 2nd edn. London: Ellis Horwood.

Beesley TE and Scott RPW (1998) *Chiral Chromatography*. Chichester: Wiley.

Hesse G and Hagel R (1973) A complete separation of a racemic mixture by elution chromatography on cellulose triacetate. *Chromatographia* 6: 277–283.

Johns DM (1989) Binding to cellulose derivatives. In Lough WJ (ed.) *Chiral Liquid Chromatography*, pp. 166–175. Glasgow: Blackie.

Shibata T and Mori K (1989) In Krstulović (ed.) *Polysaccharide Phases in Chiral Separations by HPLC, Applications to Pharmaceutical Compounds*, pp. 336–398. Chichester: Ellis Horwood.

Chiral Derivatization

S. Görög, Chemical Works of Gedeon, Richter Ltd, Budapest, Hungary

Copyright © 2000 Academic Press

Introduction

The Importance of Enantiomeric Separations

The separation of enantiomers of chiral compounds by chromatographic methods and related techniques is one of the important tasks in modern analytical chemistry, especially in the analysis of compounds of biological and pharmaceutical interest. However, analysis of this kind is also required in food analysis and the analysis of pesticides, flavours and fragrances. The reasons for this are as follows:

- As a consequence of the existing or potential differences between the biological–pharmacological activities of the antipodes of racemic drugs, analytical methods are required for their simultaneous determination in biological samples, thus enabling one to follow the fate of the enantiomers of the administered drug (candidate) in the animal or human organism.
- Asymmetrical syntheses are in the focus of interest in various fields of organic chemistry especially in the synthesis of drugs administered as the pure enantiomer. In these cases and also if the preparation of the enantiomers is carried out by classical resolution techniques, analytical methods are necessary for the determination of their enantiomeric purity.

Possibilities for Enantiomeric Separations

Since in achiral environment the physicochemical properties of the antipodes of racemates are identical, their separation is not possible if the generally used, achiral separation systems – ordinary high-perfor-

mance liquid chromatography (HPLC) and gas chromatography (GC) columns, thin-layer chromatography (TLC) plates, capillary electrophoresis (CE) capillaries, etc., with ordinary mobile phases – are used. The main possibilities for the separation of enantiomers are:

- Transformation of the enantiomers to covalently bonded diastereomeric derivatives by reacting them with homochiral derivatizing reagents prior to their chromatographic separation using achiral stationary phases or and mobile phases. The detailed description of this general method, which is often referred to as an indirect method, is described here.
- Incorporation of the chiral reagent in the mobile phase for the dynamic formation of diastereomeric adducts, ion pairs or complexes with the enantiomers to be separated during the chromatographic run. In this case also, achiral stationary phases are used.
- Separation of the enantiomers on chiral stationary phases (HPLC, GC and TLC). Although in principle this general method does not require derivatization, the separation can be improved in many cases by modifying the enantiomers using pre-column achiral derivatization. These aspects are also briefly discussed here.

Covalent Chiral Derivatization of Enantiomers and Separation of the Diastereomeric Derivatives on Achiral Columns

Introductory Remarks: the Role of Covalent Chiral Derivatization in Enantiomeric Separations

The derivatization of enantiomers using homochiral reagents to form their diastereomeric derivatives

separable on achiral GC or HPLC columns or TLC plates was the first, widely used general method in the chiral analysis of drugs and related materials. After the introduction of newer chromatographic and capillary electrophoretic techniques briefly mentioned above, the importance of enantioseparations based on covalent chiral derivatization has naturally decreased to some extent. However, this general method is still a method of choice widely used especially in HPLC. The reasons for this are the large number of commercially available homochiral reagents and well-established reactions enabling diastereomeric derivatives with excellent separation and detection possibilities to be formed and the possibility of tailor-made separations using inexpensive, achiral columns, i.e. being in possession of the *R*- and *S*-forms of the reagent, it is possible to have the peak of the enantiomeric impurity eluting before the main peak.

The importance of covalent chiral derivatization can be characterized by the large number of publications (above 300) from the early 1970s up to the present time. References to the most important publications from this field can be found in chapters in books and review papers listed in Further Reading which cover the literature until 1993. The relatively large number of papers published after 1993 describing new applications of previously described derivatization reagents, moreover the introduction of new reagents is an indication that this branch of chiral analysis has retained some of its importance to the present day (see figure legends).

Important Features of Chiral Derivatization Reactions and Reagents

The presence of a suitable functional group in the molecule of the analyte The prerequisite of the use of any kind of enantioseparation based on covalent, chiral derivatization is the presence of at least one functional group (amino, hydroxyl, carboxyl, epoxy, thiol, etc.) in the molecule of the chiral compound which is capable of reaction with the reactive group of the derivatizing reagent.

Good chromatographic properties of the derivatives The optimization of the chromatographic parameters of retention time, peak shape and separability of the enantiomers from other components of the complex mixture by proper selection of the column (usually reversed-phase but in some cases normal phase columns), and the composition and pH of the eluent is done in the usual ways for achiral HPLC.

Sufficient separation of the diastereomers formed This is also influenced by the above-mentioned sol-

vent composition and column selection, but in this case it is even more important to select a proper derivatizing reagent enabling diastereomers to be formed with sufficiently different molecular fine structures for their chromatographic separation. If the number of the chiral centres in the analyte is more than one, the reagent should enable the separation of all stereoisomers. An example for this is the separation of (*S,R*), (*R,S*), (*S,S*) and (*R,R*) nadolol in **Figure 1**.

The structural features which influence the separation of the diastereomers are:

- The distance between the two chiral centres. In the majority of cases this is two to four atoms but there are many exceptions to this rule.
- Conformational rigidity of the diastereomers favours resolution. Bulky groups in the vicinity of one of the chiral centres or the incorporation of one of them into a ring system are especially advantageous. For example, in the case of one of the most widely used chiral derivatizing reagent, GTC (2,3,4,6-tetra-*O*-acetyl- β -D-glucopyrasonyl isothiocyanate, see later) the chiral centres of the reagent are in the pyrane ring. The exchange of the acetyl groups to the bulkier benzoyl groups improves the resolution. The position and bulkiness of the remote functional groups also influences the separation of the diastereomers. In these instances, however, the direction of the influence is difficult to predict. As an example, the investigation leading to the highly efficient derivatizing agent for the amino group (+)-2-methyl-2 β -naphthyl-1,3-benzodioxole-4-carboxylic acid chloride is mentioned. It was found that the difference between the bulkiness of the two substituents at C-2 favourably influences the separation and with the isomeric 5-carboxylic acids only poor separation is achievable.
- The formation of hydrogen bonds. For example, in the case of propranolol the secondary amino group of the molecule is transformed by chiral isocyanates or isothiocyanates to diastereomeric urea or thiourea derivatives. The formation of a hydrogen bond between the carbonyl or thiocarbonyl group of the latter and the free hydroxyl group of propranolol plays an important role in the separation: the resolution deteriorates with etherification of the hydroxyl group.

Selection of the elution order This is especially important if the aim of the analysis is the determination of trace level enantiomeric impurity in a drug which is administered as the pure enantiomer. In order to have the impurity peak appear before the main peak the

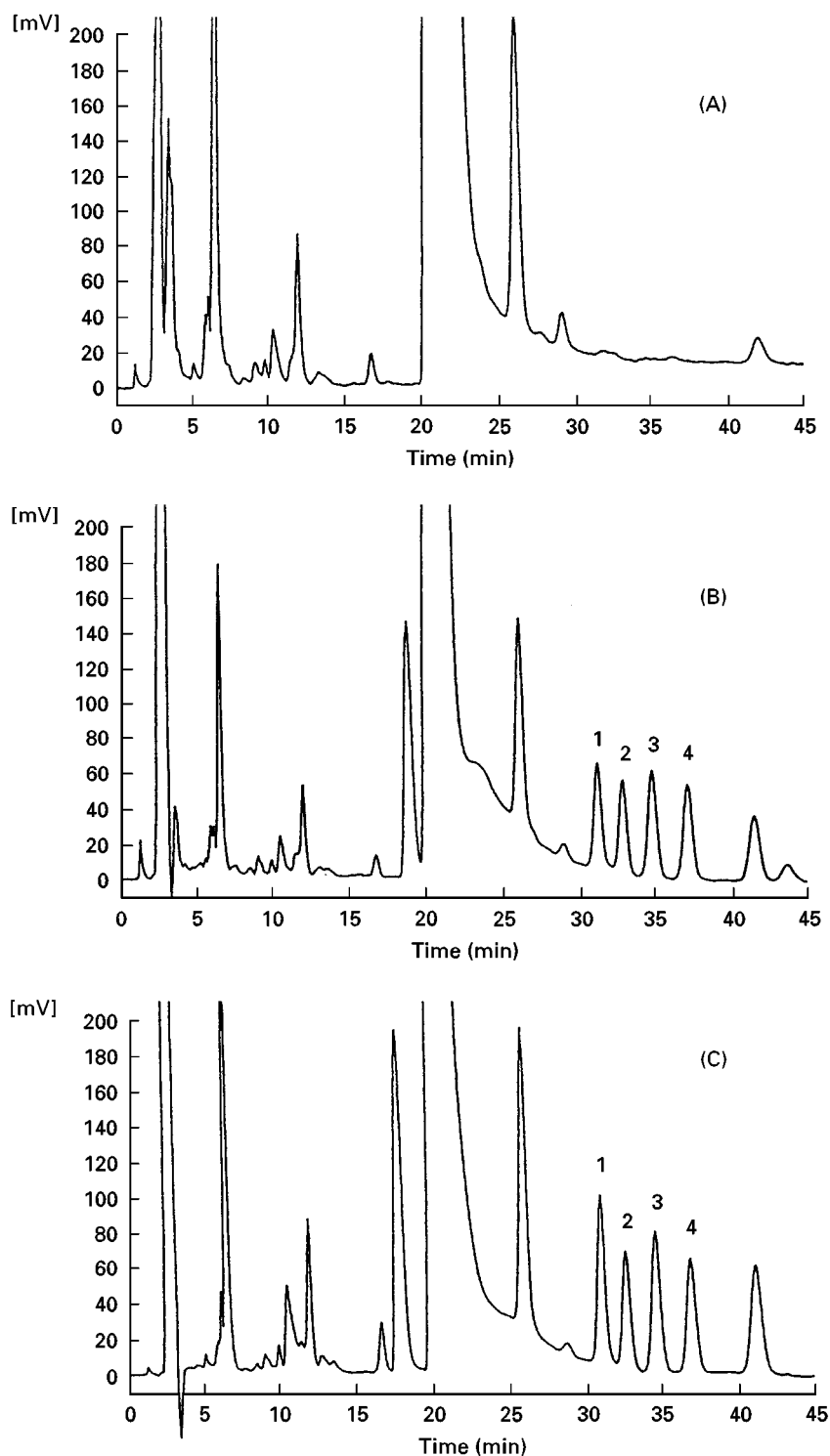


Figure 1 Resolution of the four diastereomers of the two racemates of nadolol as urea derivatives after reaction with (*R*)-(–)-1-(naphthyl)ethyl isocyanate and their determination in dog plasma extracts. Column YMC-AM-303 ODS(250 × 4.6 mm, 5- μ m); mobile phase, water–acetonitrile (60:40, v/v); flow rate, 1 mL min⁻¹; temperature, 40°C; UV detection at 285 nm. (A) Blank control dog plasma; (B) plasma spiked with 50 ng ml⁻¹ of each diastereomer; (C) plasma obtained 2 h after oral administration of 1 mg kg⁻¹ of racemic nadolol. Peaks: 1, (*S,R*)-nadolol; 2, (*R,S*)-nadolol; 3, (*R,R*)-nadolol; 4 (*S,S*)-nadolol. Reproduced with permission from Hoshino M, Yajima K, Suzuki Y and Okahira A (1994) *Journal of Chromatography B* 661: 281, copyright Elsevier.

proper chromatographic system (normal- or reversed-phase) has to be selected; it is even more advantageous to select a derivatizing agent that is available in both the *R* and *S* forms. Curves a and b in Figure 2 demonstrate this: the elution order of amino acids changes upon changing from *R* to *S* reagent in their derivatization with the *o*-phthalaldehyde-*N*-butyryl-cysteine reagent.

Unidirectional derivatization reaction taking place under mild conditions The most widely used reactions are completed at room temperature within 1 h and the reaction mixture can be injected directly into the chromatograph. The necessity of heating or extraction of the reaction mixture does not preclude a reaction being used and nor does the occurrence of side reactions, provided that their products do not interfere with the detection and quantification of the peaks of the main products and the side reactions do not show stereospecificity.

Enantiomeric purity and stability of the derivatizing reagent The enantiomeric purity of the reagent is one of the most important factors determining the success of the determination of the enantiomeric purity of the analyte. It is evident that when using a homochiral reagent containing its antipode as an impurity, the latter also reacts with the main component of the analyte. This results in a diastereomeric derivative which has the same retention time as that originating from the reaction of the main component of the reagent and the impurity of the analyte. It is therefore difficult to estimate if the satellite peak originates from the impurity of the reagent or from that of the analyte. If the aim of the study is the determination of the enantiomeric purity of a drug administered as pure enantiomer and the test limit for the antipode is 0.5%, the enantiomeric purity of the reagent should be at least 99.9%. If the requirement for the enantiomeric purity of the drug is higher, the purity of the reagent should be even higher. If the aim is the determination of commensurable amounts of enantiomers (e.g. in biological samples), 1–2% of the enantiomeric impurity in the reagent is tolerable.

The enantiomeric purity of the reagent can be checked if the enantiomers of the analyte (or at least one of them) are available in enantiomerically pure form. The relative peak area of the diastereomeric impurity after the reaction with the reagent will be characteristic of enantiomeric impurity of the reagent.

The enantiomeric stability of the reagent is also an important prerequisite to obtain reliable results. For

example, *N*-trifluoroacetyl-(*S*)-(–)-prolyl chloride or anhydride, were found to racemize upon storage. Reagents which are available commercially at the present time fulfil this requirement.

The absence of kinetic resolution and racemization The absence of kinetic resolution, e.g. difference between the reaction rates of the two enantiomers with the reagent and the enantiomeric stability of the analyte and its diastereomeric derivative are important prerequisites of the applicability of a reagent to a given purpose. These can be checked by comparing the peak areas of the diastereomers during and after the reaction with a racemate. The peak area should be close to unity.

Good chromophoric or fluorophoric properties of the reagent Although the primary aim of derivatization in chiral chromatography is the formation of easy to separate diastereomeric derivatives it is advantageous if, at the same time, the reagent improves the detectability of the separated enantiomers by introducing chromophoric or fluorophoric groups into their molecules. A typical example for such 'dual-purpose' fluorophoric reagents is (–)-2-[4-(1-aminoethyl)phenyl]-6-methoxybenzoxazole. The detection limit for the enantiomers of 2-phenylpropionic acid after derivatization with this reagent is as low as 10 fmol (1.5 pg). Many more examples of this type are presented in the next section.

It is important to note that the UV or fluorescence characteristics of the diastereomers formed are not necessarily equal and therefore have to be checked during the validation of a new method by comparing the spectra and band intensities of the diastereomers.

Covalent Enantiomeric Derivatization of Some Important Functional Groups

Derivatization of amines The reagents suitable for the chiral derivatization of amines can be categorized as follows:

Activated carboxylic acids These are usually carboxylic chlorides and the reaction with primary and secondary amines leads to diastereomeric carboxamides. The classical reagent *R*(+)- α -methoxy- α -(trifluoromethyl)phenylacetyl chloride is still in use for the preparation of gas chromatographically separable diastereomers. Some others ('dual-purpose' reagents with strong UV absorption or fluorescence) include 1-(4-nitrophenylsulfonyl)-*L*-prolyl chloride, dansyl-*L*-proline activated by triethylamine/diethyl phos-

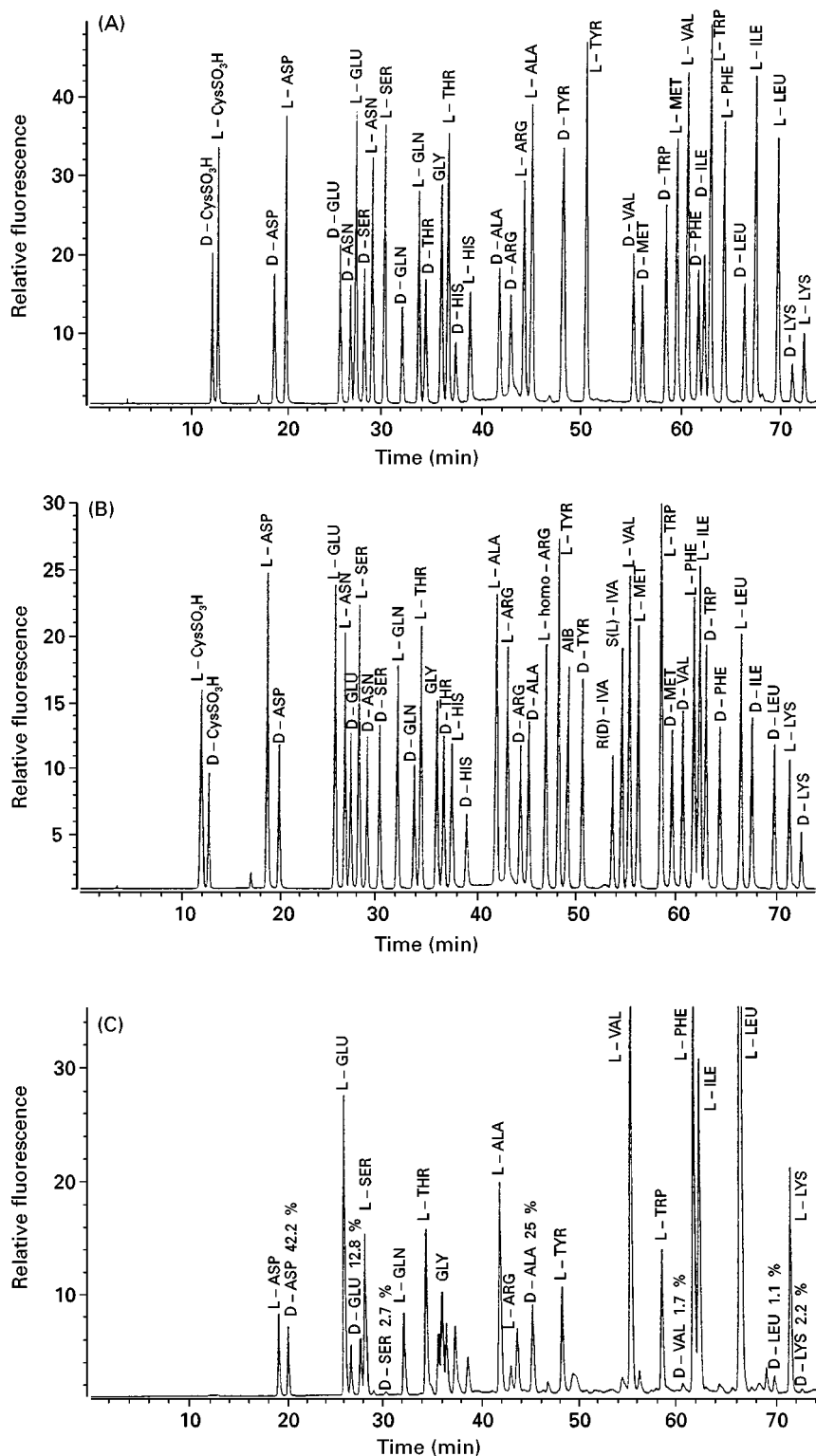


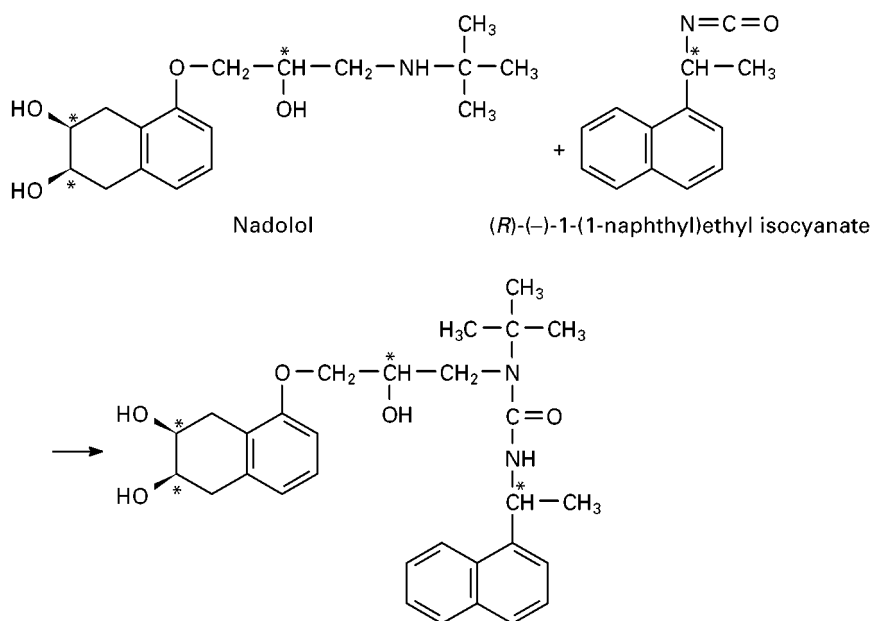
Figure 2 High-performance liquid chromatographic (HPLC) elution profile of the mixture of L and D-amino acids (L : D = 2 : 1), glycine and L-homo-arginine (internal standard) derivatized as the isoindoles with (A) *o*-phthalaldehyde-*N*-isobutryl-D-cysteine and (B) *o*-phthalaldehyde-*N*-isobutryl-L-cysteine; (C) amino acids from an ethanolic extract of *Lactobacillus acidophilus*, derivatization with *o*-phthalaldehyde-*N*-isobutryl-L-cysteine. Column, Hypersil ODS (250 × 4 mm, 5 μm); mobile phase, gradient elution; A = 23 mM sodium acetate (pH 5.95); B = methanol-acetonitrile (600 : 50 v/v), linear gradient from 0% B to 53.5% B in 75 min; flow rate 1 mL min⁻¹; fluorescence detection, 230 nm excitation, 445 nm emission. Reproduced with permission from Brückner H, Haasmann S, Langer M, Westhauser T and Godel H (1994) *Journal of Chromatography A* 666: 259, copyright Elsevier.

phorocyanidate, *N*-[4-(6-methoxy-2-benzoxazolyl)] benzoyl-L-phenylalanine or -proline, activated by 2,2'-dipyridyl disulfide/triethylphosphine, *N*-benzyloxycarbonyl-L-phenylalanine, activated by acetic anhydride(+) -2-methyl-2 β -naphthyl-1,3-benzodioxole-4-carboxylic acid chloride, (*S*)-(+) -naproxen chloride, (*S*)-(+) -flunoxaprofen chloride, (*S*)-(+) -benoxaprofen chloride, etc. Their strong fluorescence enables the enantiomers of chiral drugs such as tranilcypromine, tocainide, carvedilol, baclofen and propranolol to be determined. (The isocyanate, isothiocyanate and chloroformate derivative of these compounds have also been introduced as chiral derivatizing agents as shown in the subsequent sections.)

An on-line solid-phase derivatization reagent is fluorenylmethyloxycarbonyl-L-proline (Fmoc-L-proline), bonded to beads of a styrene-divinylbenzene copolymer as the active ester of a 4-hydroxy-3-nitrobenzophenone moiety. By positioning the HPLC column after the reaction column, the transformation of chiral amines (e.g. amphetamine) to their highly fluorescent diastereomeric Fmoc-L-prolyl derivatives and their separation was achieved.

formate is that it is suitable for the derivatization of the tertiary amine promethazine via demethylation of the dimethylamino moiety.

Isocyanates These reagents form diastereomeric urea derivatives with chiral primary and secondary amines. (*R*)-(-)- and (*S*)-(+)-1-(1-naphthyl)ethyl isocyanate and (*R*)- α -methylbenzyl isocyanate are among the classical chiral derivatizing reagents. Isocyanate derivatives of the drugs mentioned in one of the previous sections as the carboxylic chlorides and (*R*)-*N*-3,5-dinitrobenzoyl)phenyl glycine have also been used for the derivatization of β -blockers and other amines. Eqn [1] shows the reaction between nadolol and (*R*)-(-)-1-(1-naphthyl)ethyl isocyanate, while the separation of the four diastereomers of the two racemates is depicted in Figure 1. It is remarkable that by selecting a suitable reagent and proper chromatographic conditions not only can the four diastereomers be separated but the interference from dog plasma can also be eliminated.

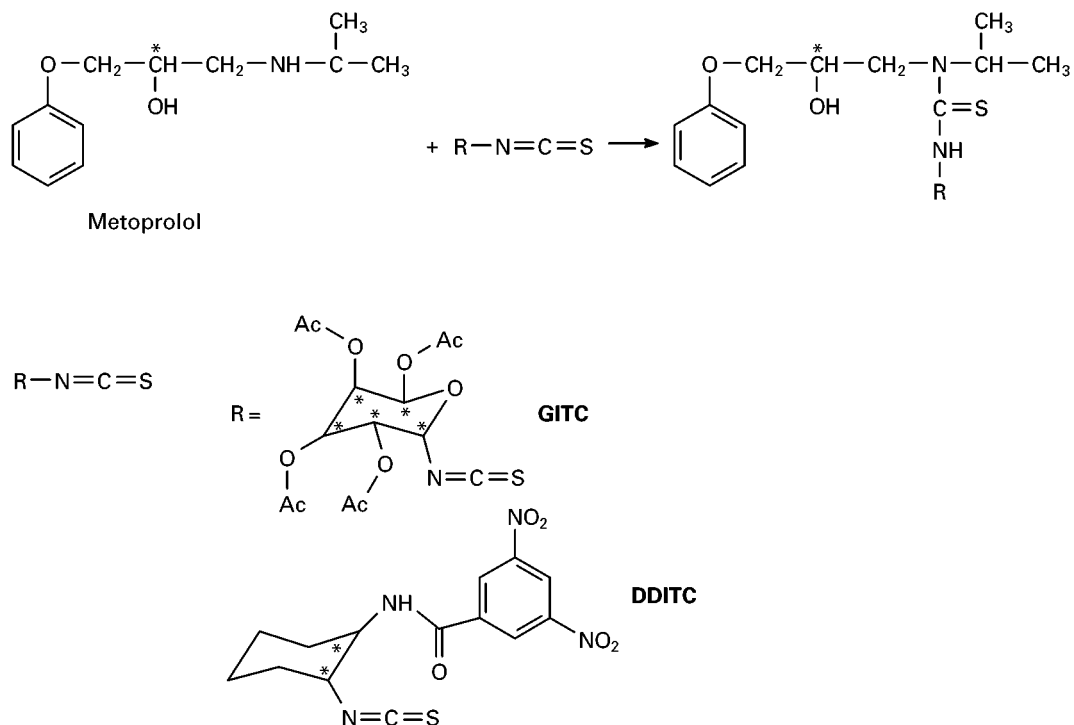


Chloroformates The above-mentioned Fmoc group has been incorporated into another types of chiral reagents: (+)-1-(9-fluorenyl)ethyl chloroformate is one of the most widely used derivatization reagents for the chiral HPLC of amino acids, β -blockers, to form the corresponding carbamate derivatives.

An interesting feature of another widely used reagent of the chloroformate type, (-)-menthyl chloro-

Isothiocyanates Of the isothiocyanates forming thiourea derivatives with primary and secondary amines, GITC is most widely used. If the four acetyl groups are replaced by benzoyl groups the sensitivity of the detection is greatly improved. Other reagents of this type leading to highly fluorescent derivatives include (*R*)-(-)- and (*S*)-(+)-4-(3-isothiocyanatopyrrolidin-1-yl)-7-nitro-2,1,3-benzoxadiazole and its 7-(*N,N*-dimethylaminosulfonyl) analogue as well as DDITC ((1*R*,2*R*)- and (1*S*,2*S*)-*N*-[(2-isothio-

cyanato)cyclohexyl]-3,5-dinitrobenzoylamide, which excels with the high chemical stability, high UV activity and the excellent separability of the diastereomeric derivatives. The equation of the reaction of GITC and DDITC with the β -blocker metoprolol and the separation of the derivatives are depicted in eqn [2] and Figure 3, respectively.

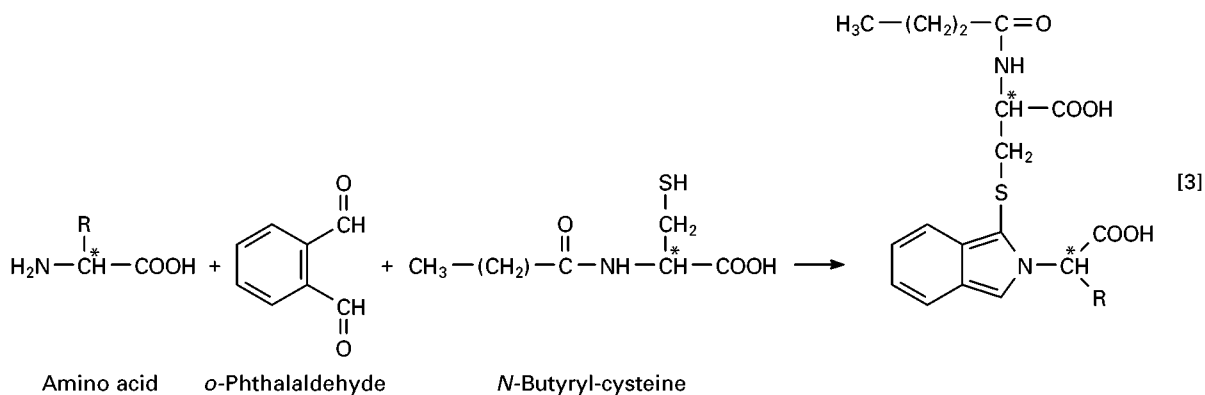


N-Haloarylamino acid derivatives Marfey's reagent (1-fluoro-2,4-dinitrophenyl-5-L-alaninamide) is one of the most generally used reagents in the analytical control of racemization during peptide synthesis. The peptides are split either by hydrochloric acid or enzymatically. The nucleophilic attack of the α -amino group of the amino acids on the C-F bond activated by the two nitro groups on the aromatic ring results in a smooth reaction to form diastereomeric aniline derivatives with good UV detectability (see eqn [4]). The

valinamide analogue of the Marfey reagent gives even better resolution.

***o*-Phthalaldehyde + chiral thiols** This dual derivatization reaction leading to fluorimetrically highly active isoindole derivatives is another generally used method in the chiral analysis of amino acids (see eqn

[3]). As the chiral thiol *N*-acetyl-L-cysteine is most widely used but the use of 2,3,4,6-tetra-*O*-acetyl-1-thio- β -D-glucopyranoside and *N*-isobutyryl-L-cysteine (and D-cysteine) have been found to be advantageous in the resolution of the diastereomers. The reaction of amino acids with *o*-phthalaldehyde and the latter reagent is shown in eqn [3], while in Figure 1 the separation of as many as 36 enantiomers of 18 amino acids and amino acid analogues as well as glycine is depicted together with a practical application.



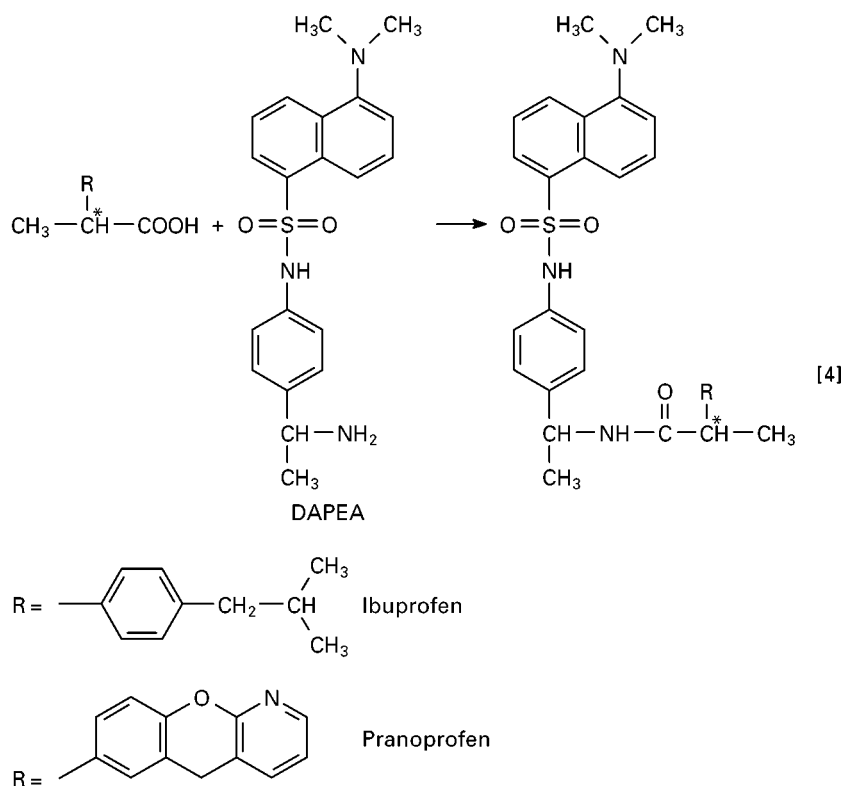
Enzymatic deamination Chiral HPLC of a mixture of amino acid enantiomers with and without selective oxidative deamination of D-amino acids with the aid of the enzymes D-amino acid oxidase and catalase enables D-amino acids to be identified in the mixture.

Derivatization of the carboxyl group

Esterification with chiral alcohols (+)- or (-)-2-octanol, (+)-1-phenylethanol, (-)-menthol, (+)- or (-)-2-butanol are the classical reagents for the chiral analysis of carboxylic acids. The reactions usually require harsh conditions and for this reason the danger of racemization should be taken into consideration.

Amidation with chiral amines Prior to their reactions with chiral amines the carboxyl group should

UV or fluorometric properties are also in use, e.g. (*R*)- α -methyl-4-nitrobenzylamine, (*R*)-(+)-1-(1-naphthyl)ethylamine, (-)-1-(1-anthryl)ethylamine, *R*-(-)- and (*S*)-(+)-amphetamine, (1*R*,2*R*)-(-)- or (1*S*,2*S*)-(+)-2-amino-(4-nitrophenyl)-1,3-propanediol, L-leucinamide, L-alanine- β -naphthylamide, L- or D-O-(4-nitrobenzyl)tyrosine methyl ester, (-)-2-[4-(1-aminoethyl)-phenyl]-6-methoxybenzoxazole and other related derivatives where the 1-aminoethyl group is replaced by L-leucyl or D-phenylglycyl groups, drug-related amines (flunoxaprofen amine, benoxaprofen amine and naproxen amine), (*R*)- and (*S*)-1-(4-dansylaminophenyl)ethylamine, etc. The reaction of ibuprofen and pranoprofen with the last reagent and the separation of the diastereomeric carboxamide derivatives are shown in eqn [4] and Figure 4, respectively.



be activated. Possibilities for this are, e.g. reaction with thionyl chloride to form carboxylic chlorides, with chloroformates to form mixed anhydrides, with 1,1-carbonyldiimidazole to form reactive *N*-acylimidazoles and with the classical coupling agent dicyclohexylcarbodiimide to form the reactive *N*-acylurea derivatives. The classical but still widely used amine reagent is (*S*)-(-)- α -methylbenzylamine, but several others with excellent separation power,

Derivatization of the alcoholic and phenolic hydroxyl groups The most frequently used general method for the derivatization of the hydroxyl group of chiral alcohols and phenols is esterification. A great variety of chiral carboxylic acids have been used for this purpose such as *R*(+)- and *S*(-)- α -methoxy- α -(trifluoromethyl) phenylacetic acid (Mosher's acid), *R*(+)-*trans*-chrysanthemic acid, (-)-menthenyloxyacetic acid for the gas chromatographic or HPLC

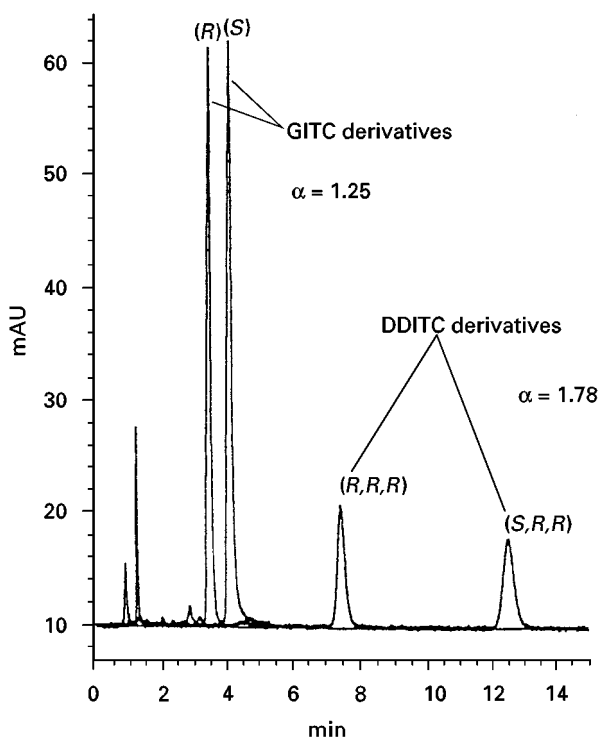


Figure 3 Resolution of (*R,S*)-metoprolol derivatized as (*R,R*)-DDITC- and GITC-thioureas. Column, Hypersil ODS (125 × 4 mm, 5 μm); mobile phase, acetonitrile-20 mM ammonium acetate 55:45, v/v; flow rate 1 mL min⁻¹ detection at 254 nm. Reproduced with permission from Kleidnigg OP, Posch K and Lindner W (1996) *Journal of Chromatography A* 729: 33, copyright Elsevier.

separation with UV detection and (–)-(1*S*,2*R*,4*R*)-*endo*-1,4, 6,7,7-hexachlorobicyclo[2.2.1]-hept-5-ene-2-carboxylic acid and (*S*)-(+)-2-*tert*-butyl-2-methyl-1,3-benzodioxolo-4-carboxylic acid for HPLC separation with fluorimetric detection, etc. Dicyclohexylcarbodiimide can be used as the coupling agent, but the use of *in situ* transformation of the acids to their chlorides by the addition of thionyl chloride is more widespread. The direct enzymatic D-(+)-glucuronidation reaction of phenols has also been described.

Acyl chlorides, anhydrides and acyl cyanides can be used directly. For example (–)-camphanic acid, *R*(+)- α -methoxy- α -(trifluoromethyl)phenylacetyl chloride, β -naphthylsulfonyl-L-prolyl chloride, flunoxaprofen chloride, (*R,R*)-*O,O*-diacetyl- (or di-*p*-toluoyl-) tartaric anhydride and (–)-2-methyl (or methoxy)-1,1'-binaphthalene-2'-carbonyl cyanide lead to well-separable, UV or fluorimetrically active diastereomeric ester derivatives with chiral alcohols.

As an illustration, the reaction of delmopinol and its analogue used as the internal standard in the determination of the drug in plasma with the reagent (*R,R*)-*O,O*-di-*p*-toluoyl-tartaric anhydride is shown in eqn [5]. The separation is depicted in Figure 5.

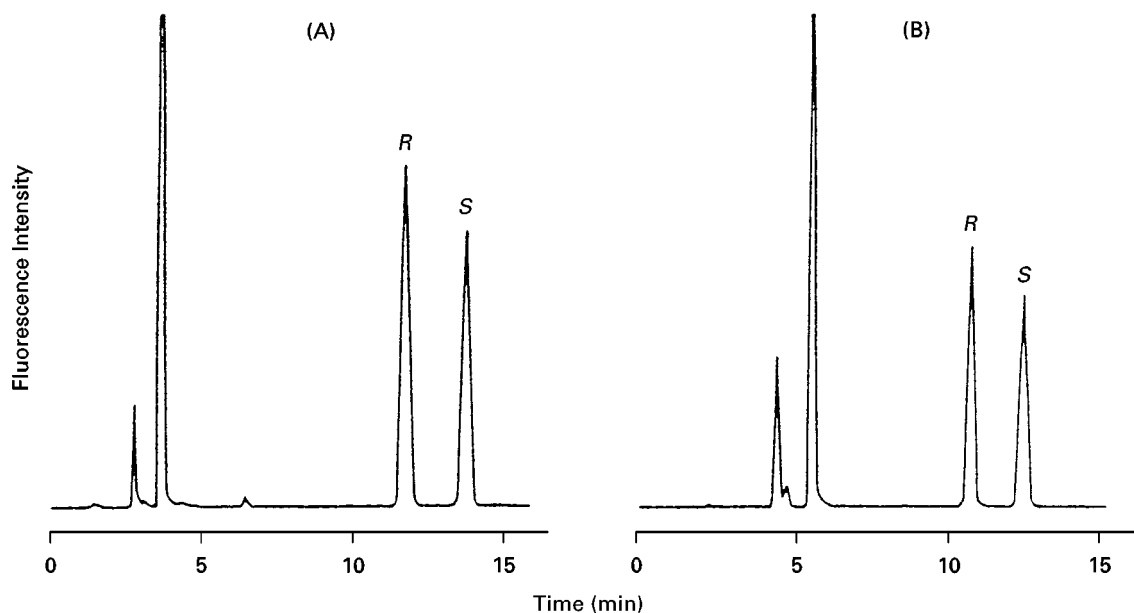
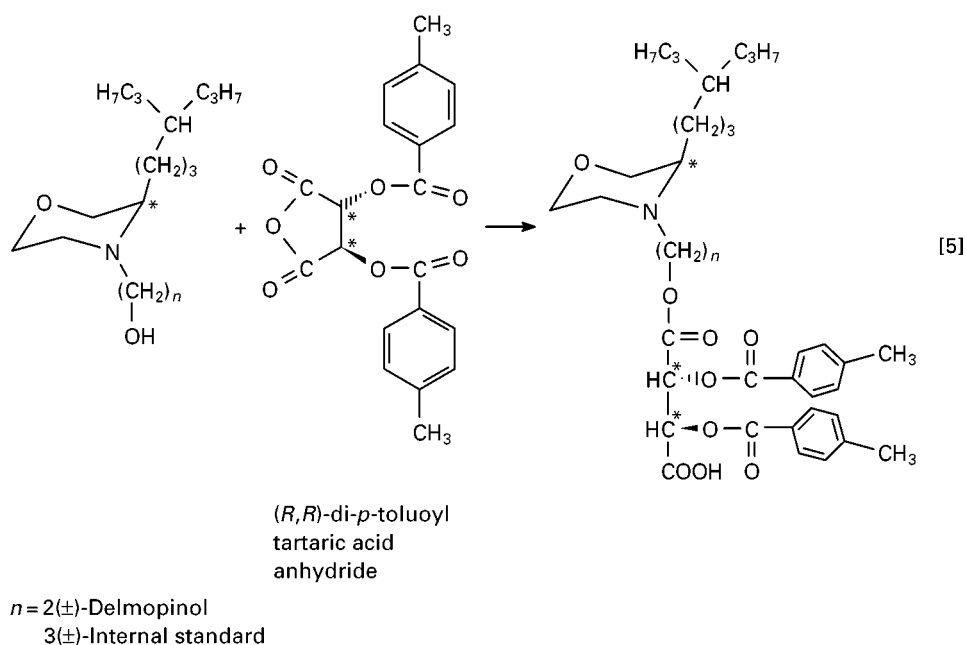


Figure 4 Resolution of (A) (*R,S*)-ibuprofen and (B) (*R,S*)-pranoprofen as the carboxamides formed with (*S*)-1-(4-dansylaminophenyl)ethylamine. Column ODS-80TM (150 × 4.6 mm, 5 μm); mobile phase: 50 mM sodium acetate (pH 6.5)-acetonitrile (A) 30:70, v/v and (B) 45:55, v/v, and flow rate 1 mL min⁻¹; fluorescence detection, 338 nm excitation, 535 nm emission. Reproduced with permission from Iwaki K, Bunrin T, Kameda Y and Yamazaki M (1994) *Journal of Chromatography A* 662: 87, copyright Elsevier.



Further derivatization reactions include the use of (*R*)-1-(1-naphthyl)ethyl isocyanate for the derivatization of, e.g. diacylglycerol derivatives to form the corresponding carbamates. The lower reactivity of the hydroxyl group compared with the

amino group can be overcome by using a suitable catalyst (4-pyrrolidinopyridine). (–)-Menthyl chloroformate, which has already been mentioned, has also found application here as a reagent for amines; the reaction products with chiral alcohols are carbonates.

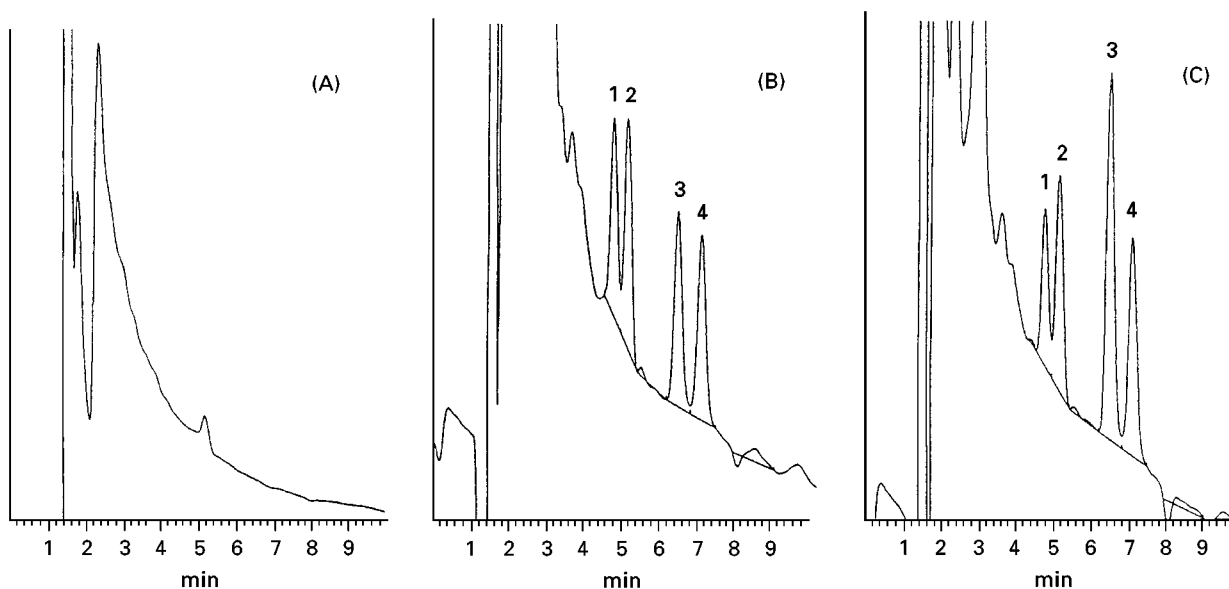


Figure 5 Resolution of (–)- and (+)-delmopinol (peaks 1 and 2) and (–)- and (+)-internal standard (peaks 3 and 4) and their determination in human plasma extracts. Derivatization with (*R,R*)-*O,O'*-di-*p*-toluoyl tartaric acid anhydride to form the esters. (A) Blank plasma; (B) plasma spiked with 6 ng of each enantiomer; (C) authentic plasma sample. Column, Hypersil ODS (125 × 4 mm, 5 μm); mobile phase, 100 mM ammonium acetate–acetonitrile 35:65, v/v, pH 5.7; flow rate, 0.8 mL min^{–1}; electrochemical detection. Reproduced with permission from Egginger G, Blaschke E, Lindner W and Olsson A-M (1994) *Journal of Chromatography A* 666: 275, copyright Elsevier.

Derivatization of the aldehyde group The importance of this kind of chiral derivatization reactions is much smaller than those described for amines, carboxylic acids and alcohols. For example, aldoses can be transformed with L-cysteine methyl ester to diastereomeric thiazolidine derivatives which can be separated by GC after trimethylsilylation. The two aldehyde groups of gossypol were transformed with (*R*)-(-)-2-amino-1-propanol to the diastereomeric Schiff's bases separable by HPLC.

Derivatization of epoxides The oxirane ring of chiral epoxides is opened by sodium sulfide to form a vicinal hydroxythiol derivative. In the second step of the derivatization reaction the thiol group reacts with *o*-phthalaldehyde and a chiral amino acid to form the diastereomeric isoindole derivative mentioned in the section dealing with the derivatization of the amino group. Another ring-opening reagent is 2-propylamine. The secondary amino group of the 1,2-amino alcohol is then reacted with 2,3,4,6-tetra-*O*-acetyl (or benzoyl)- β -D-glucopyranosyl isothiocyanate to form the diastereomeric thiourea derivatives.

Derivatization of the thiol group The formation of diastereomeric isoindole derivatives from chiral amino acids, chiral thiols and *o*-phthalaldehyde (already mentioned in the section dealing with the derivatization of the amino group; see eqn [4]) can also be used for the enantioseparation of thiols. Reagents of other types are (*R,R*)-dinitrobenzoyldiaminocyclohexyl isothiocyanate and *N*-[(2-isothiocyanato)cyclohexyl]-pivalinoyl amide which transform the thiol compound to their diastereomeric dithiocarbamate derivatives.

Derivatization of Enantiomers With Achiral Reagents to Improve Their Chromatographic Properties and Their Separation on Chiral Columns

Introductory Remarks

Chiral columns enable the direct separation of enantiomers. In many cases the chromatographic properties of the enantiomers can be improved by transforming them to suitable derivatives using achiral reagents.

Pirkle-Type Chiral Columns

The purposes of using pre-column derivatization are:

- Blocking of the polar groups of the analyte (amino, carboxyl, hydroxyl groups) to avoid strong interactions with the polar groups of the chiral selector thus improving the separation.
- The introduction of aromatic rings into the analyte to enable π - π interactions to take place between the aromatic moieties of the chiral selector and the analyte which play a dominant role in the resolution of the enantiomers.
- Improve UV detectability.

To fulfil these requirements amino groups in the analyte are usually transformed to aromatic acyl derivatives by 4-nitro- or 3,5-dinitrobenzoyl chloride or to aromatic urea or thiourea derivatives by means of phenyl-, 4-fluorophenyl-, 4-methoxyphenyl-, 3,5-dinitrophenyl- or 1-naphthyl-isocyanates and isothiocyanates. Carboxyl derivatives are derivatized after activation with thionyl chloride or carbodiimides to form anilides, 3,5-dimethylanilides, 3,5-dinitroanilides, naphthylmethanilides, etc. The derivatizing agents for the hydroxyl group are benzoyl chloride, 3,5-dinitrobenzoyl chloride, 1-naphthyl chloride to form ester derivatives and 1-naphthyl- or 3,5-dinitrophenyl isocyanates to form the corresponding carbamates.

Cyclodextrin-Bonded Phases

In the case of enantiomeric HPLC separations on cyclodextrin-bonded stationary phases the necessity of pre-column achiral derivatization is not as general as with the Pirkle-type phases. The introduction of the aromatic ring into analytes often improves their separation. Amino acids are usually derivatized with dansyl chloride, 3,4-dinitrobenzoyl chloride, *o*-phthalaldehyde/2-mercaptoethanol, etc., or with highly fluorescent reagents such as 9-fluorenylmethyl chloroformate, 9-fluorenylmethoxycarbonylglycine chloride, 6-aminoquinolyl-*N*-hydroxysuccinimidyl carbamate, etc.

α_1 -Acid Glycoprotein Column

In most instances no derivatization is necessary to obtain good enantioseparation. In the case of carboxylic acids, separation is improved by the addition of ion pairing agents to the eluent. For some basic drugs anionic reagents in the eluent also improves the column efficiency, peak symmetry and resolution.

Covalent derivatization is only seldom used. Acetylation or formylation of the amino and hydroxyl groups, esterification of the carboxyl group

with 2-propanol have been found in some instances to improve the separation.

Functionalized Cellulose Phases

In the overwhelming majority of cases enantiomers can be separated on these columns without derivatization. In a few instances esterification of the carboxyl group and the introduction of a benzoyl group into the molecule have been found advantageous.

Conclusions and Future Trends

It is indisputable that the direct chromatographic enantioseparations based on chiral stationary phases has greatly surpassed the importance of indirect separations based on covalent chiral derivatization. The fact that the overwhelming majority of papers reporting on the development and application of chiral separations are from these fields does not necessarily reflect the real of the contribution of covalent chiral derivatization in the solution of practical problems in pharmaceutical and biomedical analysis. In some areas (e.g. the determination of small concentrations of D-amino acids in various biological samples, etc.) the well-established classical methods are still in use. It is also remarkable that the combination of chiral derivatization with the use of chiral stationary phases has proved to be suitable for the solution of very delicate problems (separation of several enantiomers and diastereomers of drugs with more than one chiral centre). It should also be noted that the combination of chiral chromatography with fluorescence derivatization enables the limit of detection of enantiomeric impurities to be decreased to the 10 ppm. level. These tendencies are expected to continue in the near future.

See also: II/Chromatography: Liquid: Derivatization. III/Chiral Separations: Amino Acids and Derivatives;

Capillary Electrophoresis; Cellulose and Cellulose Derived Phases; Chiral Derivatization; Countercurrent Chromatography; Cyclodextrins and Other Inclusion Complexation Approaches; Gas Chromatography; Ion-Pair Chromatography; Ligand Exchange Chromatography; Liquid Chromatography; Molecular Imprints as Stationary Phases; Protein Stationary Phases; Supercritical Fluid Chromatography; Synthetic Multiple Interaction ('Pirkle') Stationary Phases; Thin-Layer (Planar) Chromatography.

Further Reading

- Ahnoff M and Einarsson S (1989) Chiral derivatization. In: Lough WJ (ed.), *Chiral Liquid Chromatography*, pp. 39–80. Glasgow: Blackie.
- Allenmark SG (1989) *Chromatographic Enantioseparation: Methods and Application*. Chichester: Ellis Horwood.
- Arvidsson E, Jansson SO and Schill G (1991) Enantiomeric derivatization. In: Ahuja S (ed.) *Chiral Separations by Liquid Chromatography*, pp. 126–140. Washington: American Chemical Society.
- Gal J (1993) *Indirect methods for the chromatographic separation of drug enantiomers*. In: Wainer IW (ed.), *Drug Stereochemistry. Analytical Methods and Pharmacology*, pp. 65–106. New York: Marcel Dekker.
- Görög S (1990) Enantiomeric derivatization. In: Lingeman H and Underberg WJM (eds), *Detection-Oriented Derivatization Techniques in Liquid Chromatography*, pp. 193–216. New York: Marcel Dekker.
- Görög S and Gazdag M (1994) Enantiomeric derivatization for biomedical chromatography. *Journal of Chromatography B* 659, 51–84.
- Skidmore MW (1993) Derivatization for chromatographic resolution of optically active compounds. In: Blau K and Halket J (eds), *Handbook of Derivatives for Chromatography*, pp. 215–252. Chichester: Wiley.
- Souter RW (1985) *Chromatographic Separation of Stereoisomers*. Boca Raton: CRC Press.
- Stevenson D and Wilson ID (eds) (1989) *Chiral Separations*. New York: Plenum Press.
- Zief M and Crane LJ (eds) (1987) *Chromatographic Chiral Separations*. New York: Marcel Dekker.

Countercurrent Chromatography

Y. Ma and Y. Ito,
National Institutes of Health,
Bethesda, MD, USA

Copyright © 2000 Academic Press

Introduction

Countercurrent chromatography (CCC) is a generic term for support-free liquid/liquid partition chro-

matography, which can be used for the separation of a variety of enantiomers by dissolving a chiral selector (CS) in the liquid stationary phase. The method eliminates the time-consuming procedure which involves chemically bonding the chiral selector to a solid support for chiral chromatography. It also provides an important advantage over the conventional methods in that the same column can be used for the separation of various enantiomers simply by

dissolving the suitable chiral selector in the liquid stationary phase.

In the past various hydrostatic CCC systems, such as droplet CCC, rotation locular CCC (RLCCC) and centrifugal partition chromatography (CPC), have been used for the separation of chiral compounds. None of those techniques, however, is considered satisfactory for preparative purposes in terms of sample size, resolution and/or separation time. Recently, the hydrodynamic CCC system termed high speed CCC has remarkably improved the technique so that highly efficient separations can be achieved in a short elution time. This technique has been successfully applied to the separation of racemates using a Pirkle-type chiral selector. In this method analytical (milligram) and preparative (gram) separations can be performed simply by adjusting the amount of chiral selector in the liquid stationary phase in the standard separation column. Gram quantities of enantiomers can be obtained by pH-zone-refining CCC, a new preparative separation technique recently developed for the separation of ionizable compounds (see pH-zone-refining CCC). In addition, the present method allows computation of the formation constant of the chiral-selector complex, one of the most important parameters for studies on the mechanism of enantioselectivity.

Standard High speed CCC Technique for Chiral Separation

The separations are performed using a commercial high speed CCC centrifuge equipped with a set of multilayer coil separation columns. The two-phase solvent system is selected in such a way that the target

analyte has a partition coefficient ranging from 0.5 to 1 in the CS-free solvent system. When the organic phase is used as the stationary phase, the chiral selector may be made hydrophobic by attaching a long hydrocarbon chain to enhance both solubility and retention in the stationary phase.

In each separation, the column is first filled about half way with the CS-free stationary phase. This is followed by introduction of the CS-containing stationary phase (about 60% of the total column capacity) by discharging the excess amount of CS-free stationary phase from the other end of the column. In this way some amount of CS-free stationary phase (about 10% of the stationary phase retained in the column) remains at the end of the column during separation to absorb carried-over CS from the mobile phase which would contaminate the eluted fractions. After the sample solution is injected through the sample port, the mobile phase is pumped into the column while the column is rotated at the required speed, usually 800–1000 rpm. If desired separation can be carried out by successive injection of samples without replenishing the CS-containing stationary phase.

Figure 1 shows the separation of four pairs of dinitrobenzoyl (DNB)-amino acid enantiomers by the standard CCC technique using a two-phase solvent system composed of hexane/ethyl acetate/methanol/10 mM HCl with *N*-dodecanoyl-L-3,5-dimethylanilide as a CS in the organic stationary phase. Because of its high hydrophobicity ($K > 100$), this CS has high solubility in the organic stationary phase and is almost entirely partitioned into the stationary phase. All analytes were well resolved in 1–3 h. This chiral selector is similar to the 'Pirkle'

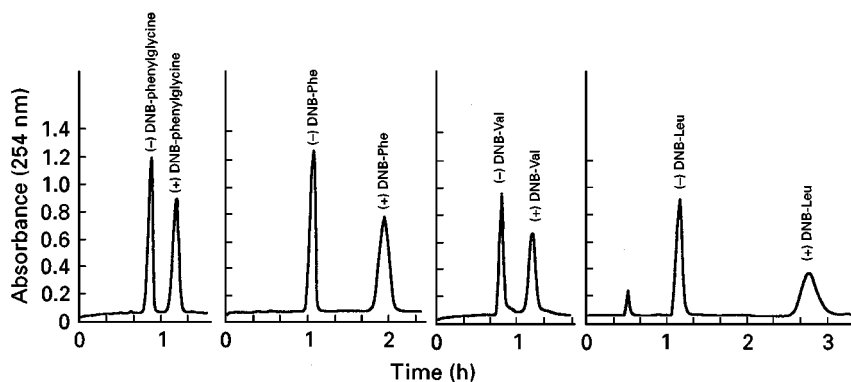


Figure 1 Separation of four racemic pairs of DNB-amino acids by the standard high speed CCC technique. Experimental conditions: apparatus: multilayer coil high speed CCC centrifuge with a semipreparative column of 1.6 mm i.d. and 330 mL capacity; solvent system: hexane/ethyl acetate/methanol 10 mM HCl (8 : 2 : 5 : 5, v/v/v/v), *N*-dodecanoyl-L-proline-3,5-dimethylanilide (CS) (2 g) was added to the organic stationary phase (200 mL) as a chiral selector; samples: from left to right, (±)-DNB-phenylglycine, (±)-DNB-phenylalanine, (±)-DNB-valine, and (±)-DNB-leucine, 5–10 mg of each dissolved in 5 mL of solvent consisting of equal volumes of each phase; flow rate: 3.3 mL min⁻¹; revolution: 800 rpm; analysis of fractions: optical rotation and circular dichroism; stationary phase retention: 65% of the total column capacity.

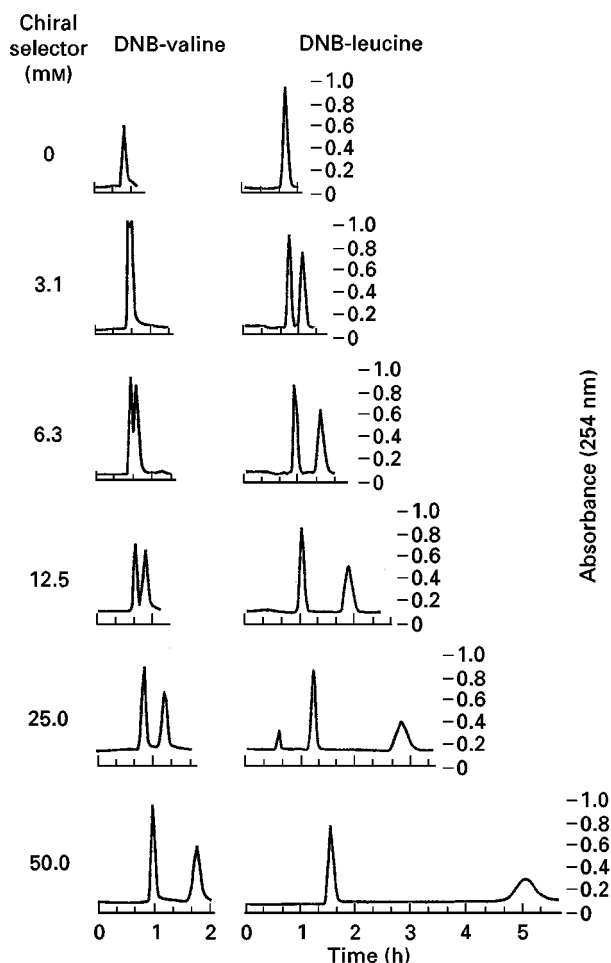


Figure 2 Effects of the amount or concentration of CS on the separation of DNB-amino acid racemates. In all resolved chromatograms, the first peak represents (–)-enantiomer and the second peak (+)-enantiomer. Experimental conditions: apparatus and column: see the Figure 1 caption; sample: racemic DNB-amino acid mixture consisting of DNB-valine and DNB-leucine, each 5–10 mg dissolved in 2 mL of solvent (1 mL of each phase); solvent system: hexane/ethyl acetate/methanol/10 mM HCl (8 : 2 : 5 : 5, v/v/v/v); stationary phase: upper organic phase with CS ranging from 0 to 4 g in 200 mL as indicated; mobile phase, lower aqueous phase; flow rate: 3 mL min^{–1}; revolution: 800 rpm.

chiral stationary phase which has been introduced for the HPLC separation of racemic DNB-amino acid *t*-butylamides. For CCC separation an *N*-dodecanoyl group was covalently attached to the CS molecule to increase its hydrophobicity so that it is almost entirely partitioned into the organic stationary phase.

The effect of the CS concentration in the stationary phase on the peak resolution was investigated by a series of experiments as shown in Figure 2. As the CS concentration was increased, the separation factor and peak resolution were increased as indicated by eqn [6]. The results clearly imply an important technical strategy for the present method: the best peak

resolution is attained by using a saturated solution of the CS in the stationary phase in a given column, and the resolution is further improved by using a longer and/or wider-bore coiled column which can hold a greater amount of CS in the stationary phase.

The preparative capability of the system was investigated on the separation of DNB-leucine enantiomers by varying the CS concentration in the stationary phase. The results shown in Figure 3 indicate that the sample loading capacity is mainly determined by the CS concentration in the stationary phase, i.e. the higher the CS concentration, the greater the peak resolution and sample loading capacity. As mentioned earlier, the standard HSCCC column (typically 300 mL in capacity) can be used for both analytical and preparative separation simply by adjusting the CS concentration in the stationary phase.

pH-Zone-refining CCC for Chiral Separation

pH-Zone-refining CCC is a powerful preparative technique that yields a succession of highly concentrated rectangular solute peaks with minimum overlap where impurities are concentrated at the peak boundaries. This technique has been applied to the resolution of DNB-amino acid racemates using a binary two-phase solvent system where the retainer acid and chiral selector were added to the organic stationary phase and the eluent base to the aqueous mobile phase. Figure 4 shows a typical chromatogram of a DNB-leucine racemate obtained by pH-zone-refining CCC. The pH of the fraction (dotted line) reveals that the peak is evenly divided into two pH zones with a sharp transition. Compared with the standard CCC technique, the pH-zone-refining CCC technique allows separation of large amounts of analyte in a shorter elution time.

Determination of Formation Constant of CS–Enantiomer Complex

The present technique has an advantage over conventional HPLC by allowing the determination of the formation constant (K_f) for the CS–enantiomer complex which is useful for developing the CS for chiral chromatography.

In a schematic view of the portion of the separation column in Figure 5, enantiomers (A_+ and A_-) are partitioned between the organic stationary phase (upper half) and the aqueous mobile phase (lower half). In the organic stationary phase enantiomers form a CS complex $[CSA_{\pm}]$ according to their formation constants ($K_{f\pm}$). In this situation:

$$D_{\pm} = ([A_{\pm}]_{\text{org}} + [CSA_{\pm}]_{\text{org}})/[A_{\pm}]_{\text{aq}} \quad [1]$$

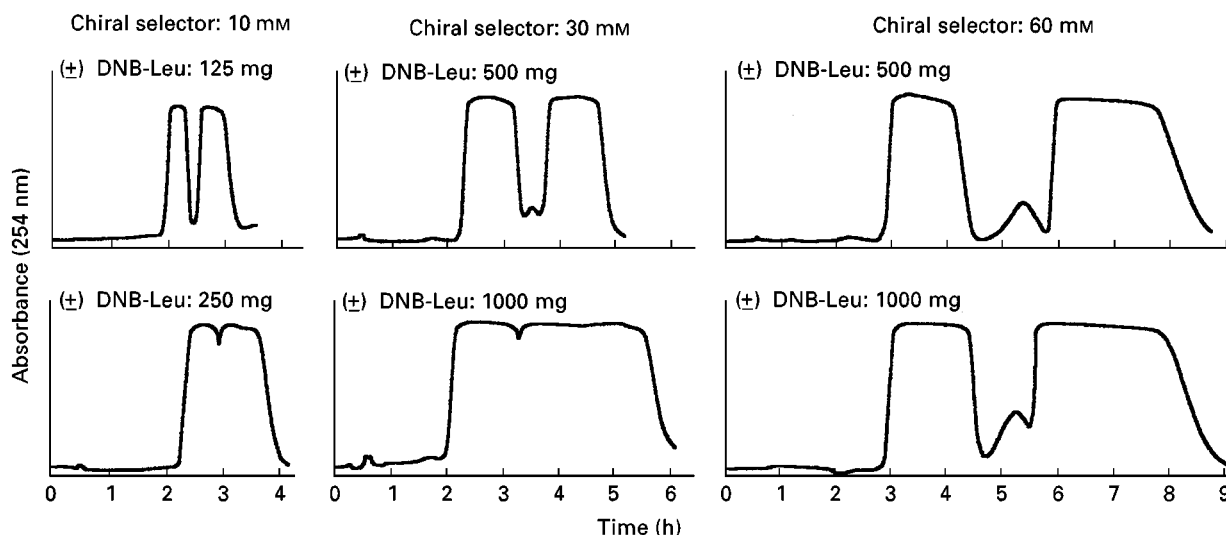


Figure 3 Preparative separation of DNB-leucine racemate by high speed CCC. Experimental conditions: solvent system: hexane/ethyl acetate/methanol/10 mM HCl (6 : 4 : 5 : 5) where the organic stationary phase containing CS at 10 to 60 mM as indicated; samples: (±)-DNB-leucine 125–1000 mg dissolved in 10–45 mL of solvent. (For other conditions, see the Figure 1 caption.)

$$D_0 = [A_{\pm}]_{\text{org}}/[A_{\pm}]_{\text{aq}} \quad [2]$$

$$K_{f\pm} = [\text{CSA}_{\pm}]_{\text{org}}/[\text{CS}]_{\text{org}}[A_{\pm}]_{\text{org}} \quad [3]$$

where D_0 is the partition coefficient of the analyte in a CS-free solvent system (this is also called the parti-

tion ratio) and D_{\pm} is the partition coefficient in a CS-containing solvent system. From these equations, the partition coefficient of the analyte is given by the following equation:

$$D_{\pm} = D_0(1 + K_{f\pm}[\text{CS}]_{\text{org}}) \quad [4]$$

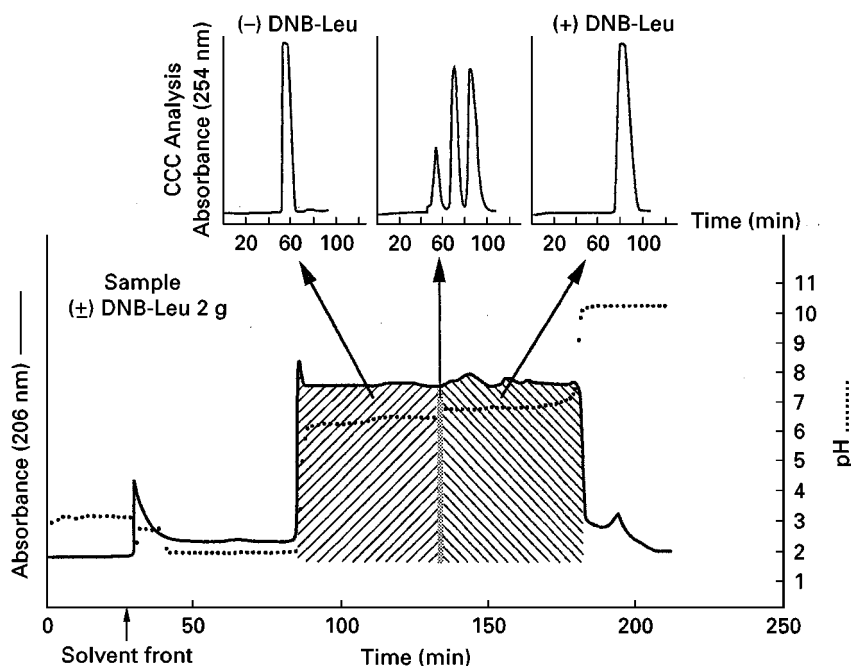


Figure 4 Separation of DNB-leucine racemate by pH-zone-refining CCC. Experimental conditions: apparatus: see the Figure 1 caption; solvent system: methyl t-butyl ether/water; stationary phase: upper organic phase to which trifluoroacetic acid (40 mM) and CS (40 mM) were added; mobile phase: lower aqueous phase to which aqueous ammonia was added to 20 mM; sample: (±)-DNB-leucine 2 g; flow rate: 3.3 mL min⁻¹; revolution: 800 rpm; analysis: chirality by analytical HSCCC (see Figure 1) and pH by a portable pH meter. Note that the analysis of the fraction from the mixing zone (middle chromatogram) shows three peaks corresponding to (-)-DNB-leucine, impurity and (+)-DNB-leucine from left to right.

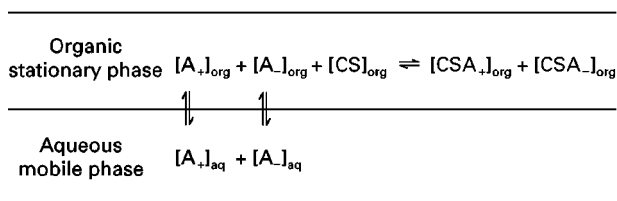


Figure 5 Schematic diagram of simple chemohydrodynamic equilibrium between the racemates (A_{\pm}) and chiral selector (CS) in the separation column.

Here, $[CS]_{org}$ is the difference between the initial concentration of the CS and the concentration of the CSA_{\pm} complex, i.e.:

$$[CS]_{org} = [CS]_{initial} - [CSA_{\pm}]_{org} \quad [5]$$

When $[A_{\pm}]_{org} \ll [CS]_{initial}$, $[CS]_{org}$ approaches $[CS]_{initial}$ hence, eqn [4] may be rewritten:

$$D_{\pm} \approx D_0(1 + K_{f\pm}[CS]_{initial}) \quad [6]$$

The validity of eqn [6] has been examined by a series of experiments, the results of which indicated that the separation factor (D_+/D_-) is increased as expected by increasing the concentration of chiral selector in the stationary phase (Figure 2).

For computation of K_f , eqn [6] can be modified into a more convenient form:

$$(D_{\pm} - D_0)/D_0 \approx K_{f\pm}[CS]_{initial} \quad [7]$$

where D_{\pm} and D_0 can be computed from the chromatograms obtained with and without the chiral selector in the stationary phase.

Using eqn [7] the formation constant ($K_{f\pm}$) has been determined by a series of experiments where small amounts (0.1–0.2 mg) of enantiomers were separated at various CS concentrations in the stationary phase. **Figure 6** is drawn by plotting the $(D_{\pm} - D_0)/D_0$ values from each enantiomer against the initial CS concentration in the stationary phase where the formation constant is computed from the slope of the straight line. These results indicate that the method is useful for computing the formation constants of various analyte-CS pairs.

General Chemodynamic Model in Chiral CCC

This second model deals with more generalized condition where the ionic analytes are dissociated in the aqueous mobile phase. This approach can be useful for predicting the feasibility of chiral resolution by pH-zone-refining CCC.

In Figure 5, which shows the chemodynamic equilibrium in a portion of the separation column, if the analytes are ionizable (e.g. acids) they will be partially dissociated to form anions $[A_{\pm}]_{aq}$ which are almost insoluble in the organic phase.

In this equilibrium state, the following set of equations is given for each racemate:

$$D_{\pm} = ([A_{\pm}H]_{org} + [CSA_{\pm}H]_{org}) / ([A_{\pm}H]_{aq} + [A_{\pm}^-]_{aq}) \quad [8]$$

$$D_0 = [A_{\pm}H]_{org} / [A_{\pm}H]_{aq} \quad [9]$$

$$K_a = [A_{\pm}H]_{aq} / [A_{\pm}^-]_{aq} [H^+]_{aq} \quad [10]$$

$$K_{f\pm} = [CSA_{\pm}H]_{org} / [CS]_{org} [A_{\pm}H]_{org} \quad [11]$$

where D_{\pm} , D_0 , K_a , and $K_{f\pm}$ represent the partition coefficient, the partition ratio, the dissociation constant, and the CS-complex formation constant for each racemate, respectively. From these equations, we obtain:

$$pH_{Z\pm} = pK_a + \log\{D_0/D_{\pm}(1 + [CS]_{org}K_{f\pm}) - 1\} \quad [12]$$

In pH-zone-refining CCC, the peak resolution is mainly determined by the difference in pH between

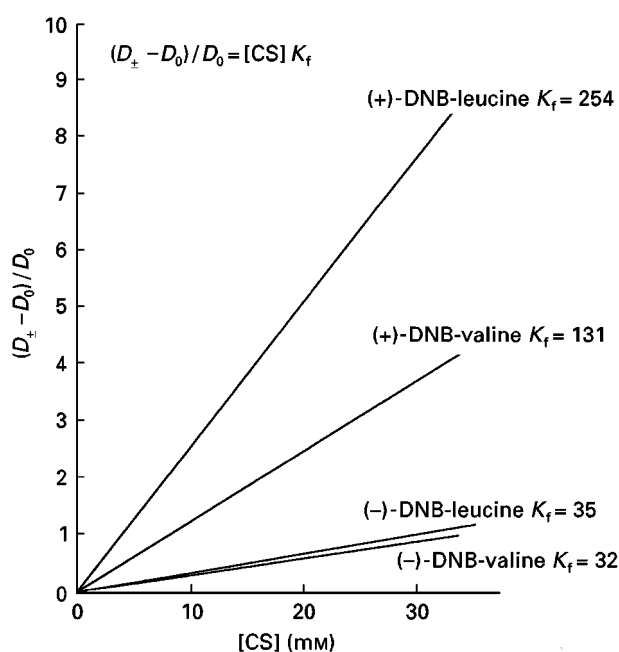


Figure 6 Determination of formation constant of CS-DNB-amino acids by the standard HSCCC technique. The diagram was produced by plotting $(D_{\pm} - D_0)/D_0$ (eqn [7]) against the initial CS concentration in the organic stationary phase. The slope of each line indicates the formation constant (K_f) of the corresponding enantiomer.

the two zones, i.e.:

$$\Delta p H_{Z\pm} = \log\left\{\frac{[CS]_{org/Z+} K_{f+} + 1 - D_0/K_r}{[CS]_{org/Z-} K_{f-} + 1 - D_0/K_r}\right\} \quad [13]$$

where $[CS]_{org/Z+}$ and $[CS]_{org/Z-}$ are the free CS concentrations in the A_+ and A_- zones, respectively. When $K_{f+} > K_{f-}$, $[CS]_{org/Z+} < [CS]_{org/Z-} < [CS]_{initial}$. Eqn [13] indicates that chiral resolution can be improved by increasing D_0/K_r and/or choosing the CS with a large K_{f+}/K_{f-} value. It also implies that increasing the CS concentration will yield higher peak resolution.

Advantages of Chiral CCC

Countercurrent chromatography can be applied to the separation of enantiomers by dissolving a suitable chiral selector in the liquid stationary phase in analogy to binding the CS to the solid support. The HSCCC technique has the following advantages over the conventional chromatographic technique using a solid stationary phase:

1. The method permits repetitive use of the same column for a variety of chiral separations by choosing appropriate chiral selectors.
2. Both analytical and preparative separations can be performed in a standard CCC column by adjusting the amount of CS in the liquid stationary phase. The method is cost effective especially for large scale preparative separations.
3. The separation factor and peak resolution can be improved by increasing the concentration of CS in the stationary phase.

4. The method is very useful for investigation of the enantioselectivity of the chiral selector including determination of formation constant and separation factor.

5. pH-Zone-refining CCC can be applied to chiral separation allowing a large scale separation in a shorter separation time.

See also: II/Chromatography: Chromatography: Instrumentation. **Chromatography: Liquid:** Column Technology. **III/Chiral Separations:** Amino Acids and Derivatives; Capillary Electrophoresis; Cellulose and Cellulose Derived Phases; Countercurrent Chromatography; Crystallization; Cyclodextrins and Other Inclusion Complexation Approaches; Gas Chromatography; Ion-Pair Chromatography; Ligand Exchange Chromatography; Liquid Chromatography; Molecular Imprints as Stationary Phases; Protein Stationary Phases; Supercritical Fluid Chromatography; Synthetic Multiple Interaction ('Pirkle') Stationary Phases; Thin-Layer (Planar) Chromatography. **Zone Refining Countercurrent Chromatography.**

Further Reading

- Ma Y and Ito Y (1995) Chiral separation by high-speed countercurrent chromatography. *Analytical Chemistry* 67 (17): 3069-3074.
- Ma Y, Ito Y and Foucault A (1995) Resolution of gram quantities of racemates by high-speed countercurrent chromatography. *Journal of Chromatography A* 704: 75-81.
- Ma Y, Ito Y and Berthod A (1998) Chiral separation by high-speed countercurrent chromatography. In: Menet JM and Thiebaut D (eds), *Countercurrent Chromatography*. New York: Marcel Dekker.

Crystallization

A. Collet, École Normale Supérieure de Lyon, Lyon, France

Copyright © 2000 Academic Press

Methods for obtaining optically active compounds in enantiopure form are commonly classified into three categories: utilization of chiral pool starting materials (stereoselective multistep synthesis), creation of chirality from achiral precursors (asymmetric synthesis) and separation of racemates into their enantiomer constituents (resolution). This last method can be carried out in a variety of ways: crystallization processes, chromatography of racemates on chiral stationary phases and kinetic resolution mediated by chiral reagents or enzymes.

The crystallization methods comprise several variants: (1) direct crystallization of enantiomer mixtures, (2) separation of diastereoisomer mixtures – the so-called classical resolution – and (3) crystallization-induced asymmetric transformation. The first two were discovered by Louis Pasteur in 1848 and 1853, respectively. The third was first reported in 1913. At the turn of the 21st century, these methods are in wide use in laboratory-scale separations as well as in industry for the preparation of pharmaceutical and agrochemical active principles. To cite but a few examples, hundreds to thousands of tonnes of commercially important materials such as (–)-menthol, (S)-(+)-naproxen, L- α -methyldopa, D-phenylglycine and the pyrethroid insecticide deltamethrin are produced by such methods.

In the context of enantiomer separations crystallization techniques are attractive for several reasons. Firstly, in many instances they are more straightforward and more economical than any other method. Secondly, these methods, once considered old-fashioned, have, during the past two decades, been greatly improved in their rationale and efficiency, as a consequence of a better knowledge of the properties upon which separations by crystallization are based: identification of racemate types, utilization of phase diagrams describing solid-liquid equilibria. Thirdly, these methods apply not only to the resolution of racemates (i.e. 1 : 1 mixtures of *d* and *l* enantiomers), they can also be used for obtaining pure enantiomers from nonracemic (partially resolved) mixtures, regardless of their origin. And finally, the so-called crystallization-induced asymmetric transformation overcomes the inherent 50% yield limitation of a resolution, permitting up to 100% of a racemic material to be converted into one enantiomer in a single stage.

Enantiomer Mixtures

This section deals with crystallization methods allowing pure enantiomers to be prepared from partially resolved mixtures or from racemates without the help of any chiral auxiliary reagent.

Phase Diagrams of Enantiomer Systems

We call enantiomer systems mixtures containing the two mirror-image *d* and *l* components in any ratio, either without solvent (binary (*d*, *l*) mixtures), or in the presence of a solvent (ternary (*d*, *l*, Σ) mixtures). Depending on the nature of the crystal phases which may coexist with the liquid (melt or solution), three categories of enantiomer systems have been identified.

In the first category, which represents 5–10% of cases, the enantiomers crystallize separately from one another (homochiral crystallization, spontaneous resolution). A solid (*d*, *l*) system then consists of a mechanical mixture of *d* and *l* crystals in a ratio corresponding to their respective mole fractions (*x*; 1 − *x*). The melting point phase diagram shows a simple eutectic at *x* = 0.5 (racemate composition). Such a (*d*, *l*) system is said to be a conglomerate of enantiomers (Figure 1A). In a conglomerate, the racemate has a melting point about 30 K lower than those of its pure enantiomers. Its solid-state infrared spectrum is identical with the solid-state spectrum of a pure enantiomer, because the infrared spectrometer does not make a difference between right- and left-handed crystals. Since most binary mixtures of enantiomers

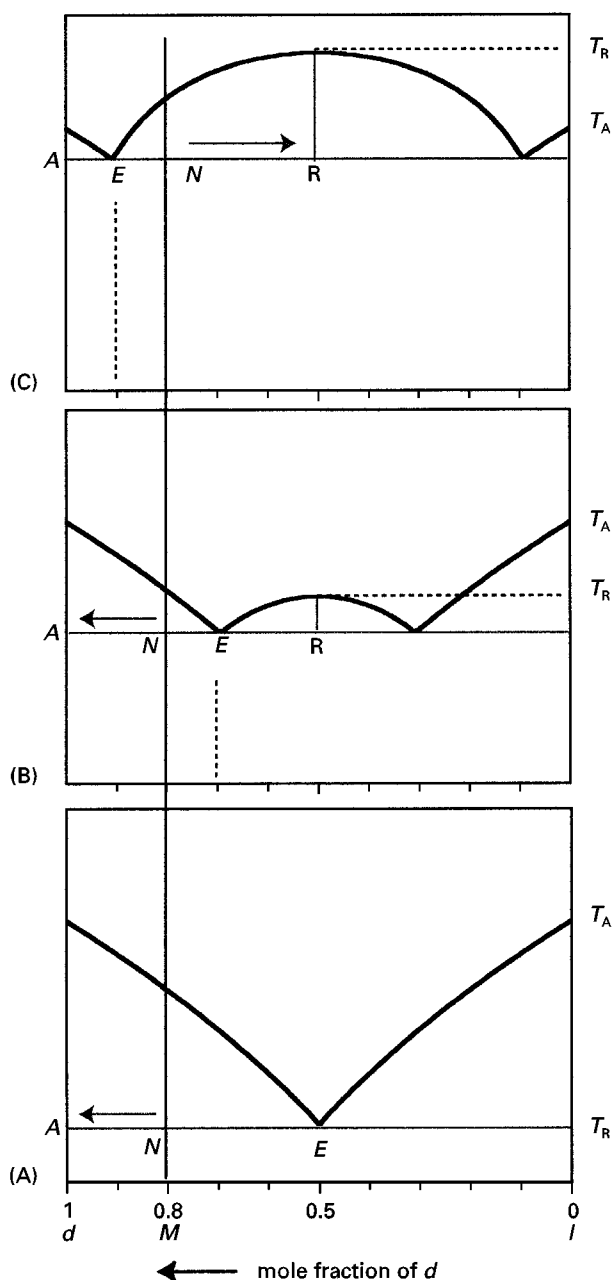


Figure 1 Binary melting point phase diagram for enantiomer systems. (A) Conglomerate; (b) racemic compound with $T_R < T_A$, eutectic at $x = 0.3$ and 0.7 ; (c) racemic compound with $T_R > T_A$, eutectic at $x = 0.1$ and 0.9 . On recrystallization, a solid mixture *M* in which the mole fraction of the major enantiomer (here *d*) is 0.8 (enantiomeric excess $ee = 60\%$) can give this enantiomer in pure form in cases (A) and (B), the maximum yield being given by the ratio NA/EA ; in case (C) only the racemic compound can be obtained (see text).

behave ideally in the liquid state, the liquidus curves of a conglomerate phase diagram can generally be accurately calculated by means of the Schröder-van Laar equation, where T_A and ΔH_A are the temperature and enthalpy of fusion, respectively, of a pure

enantiomer, and R is the gas constant. This equation gives the melting temperature T of a mixture in which x represents the mole fraction of the major enantiomer:

$$\ln x = \frac{\Delta H_A}{R} \left(\frac{1}{T_A} - \frac{1}{T} \right)$$

In the second, main category of enantiomer systems, representing 90–95% of cases, the d and l enantiomers crystallize together to form an ordered 1:1 compound, called a racemic compound (heterochiral crystallization). Typical binary phase diagrams corresponding to this case are shown Figure 1(B) and (C). The melting point T_R of the racemic compound can be either lower or higher than that of the pure enantiomers (however, on average, the difference between T_R and T_A rarely exceeds ± 20 K). The solid-state infrared spectrum of a racemic compound is different from that of a pure enantiomer. This is a simple way of distinguishing between a racemic compound and a conglomerate (in addition to the melting point criterion). In such systems, a partially resolved solid consists of a mechanical mixture of two crystal phases, the racemic compound, in amount $r = 2(1 - x)$, and the enantiomer in excess, in amount $ee = 2x - 1$. In Figure 1(B) and (C) the liquidus curves for the enantiomer branches are calculated by means of the Schröder–van Laar equation, while the racemic compound branch is calculated by a similar equation first given by Prigogine and Defay, where T_R and ΔH_R are the temperature and enthalpy of fusion, respectively, of the racemic compound:

$$\ln 4x(1 - x) = \frac{2\Delta H_R}{R} \left(\frac{1}{T_R} - \frac{1}{T} \right)$$

In the last category of enantiomer systems, called pseudoracemates, there is almost no chiral discrimination between the d and l species which co-crystallize more or less at random within the same lattice to form a solid solution. In a pseudoracemate, a partially resolved sample consists of a single crystal containing the d and l enantiomers in a ratio (x ; $1 - x$). Such systems are, fortunately, not common. They may occur with rod-shaped or quasi-spherical molecules (e.g. camphor). They do not lend themselves easily to separation by crystallization techniques, and for this reason they will no longer be considered here.

Solubility Rules Derived from Binary-phase Diagrams

In the absence of temperature- or solvent-dependent polymorphism, the solubility rules that govern the

behaviour of enantiomer mixtures on crystallization can be simply derived from the binary phase diagrams depicted in Figure 1. The component which can be obtained upon crystallization will be either the racemic compound, or the enantiomer in excess, depending on the composition of the starting mixture with respect to the closest eutectic of the phase diagram. Thus, recrystallization of mixture M , having $x = 0.8$ ($ee = 60\%$) can give the major enantiomer in pure form in cases (A) and (B). The maximum possible yield is given by $NE/EA - 60\%$ in case (A), and only 33% in case (B). In case (C), recrystallization of M can only afford the racemate in a maximum yield NE/RE . In this case the enantiomeric enrichment takes place in the liquid, but under equilibrium conditions the highest attainable purity is that of the eutectic. In other terms, in a partially resolved conglomerate, it is always possible to recover the major enantiomer in a yield equal to the ee of the starting material, whereas in a racemic compound the outcome of the crystallization will depend on the enantiomeric composition of the starting material and on that of eutectic; even in relatively favourable cases such as that depicted in Figure 1(B), the maximum possible yield will be lower than the ee of the starting material.

Ternary Phase Diagrams

For applications in which accurate quantitative data are required (e.g. optimization of large-scale recrystallizations), it is preferable to utilize ternary (solubility) phase diagrams (d, l, Σ). Solubility phase diagrams are 3D triangular prisms where each face is a binary melting point phase diagram, (d, l), (d, Σ) and (l, Σ). It is customary to convert this 3D representation into a 2D one by keeping one of the variables fixed, most often the temperature. Accordingly, a horizontal slice of the prism generates the usual triangular isotherm describing the solid–liquid phase equilibria at given T . This is illustrated in Figure 2(A), for a conglomerate. In order to facilitate the use of such triangular isotherms, it is convenient to adopt a system of cartesian axes (C, E), where C represents the concentration and E the excess of enantiomer, expressed in the same dimensionless unit (generally in weight %); C and E are defined as follows:

$$C = \frac{d + l}{d + l + \Sigma} \times 100 \quad E = \frac{d - l}{d + l + \Sigma} \times 100$$

Typical ternary isotherms for a conglomerate and a racemic compound are shown in Figure 2(B) and (C), respectively. In a conglomerate the solubility of the racemate is normally twice the solubility of each

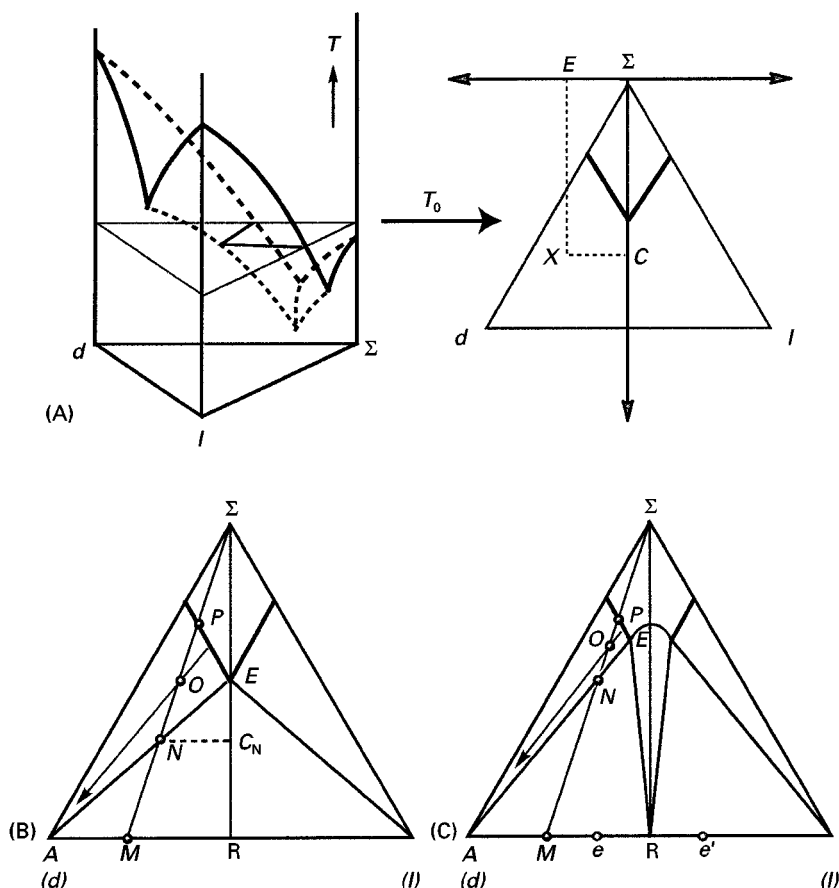


Figure 2 (A) 3D-representation of a $\{d, l, \Sigma\}$ system and the corresponding 2D-isotherm, for a conglomerate. The composition of a ternary system X is conveniently defined by its cartesian coordinates (C, E) . Note that $E/C = ee$, the usual enantiomeric excess, defined as $ee = (d - l)/(d + l)$; (B) and (C) represent ternary isotherms that correspond roughly to the binary phase diagrams (A) and (B) of Figure 1. On recrystallization, mixture M will only afford the major enantiomer in pure form if the composition of the ternary system is comprised between N and P , the maximum yield being obtained for system N (see text). In diagram (C), e represents the ee of the ternary eutectic E .

individual enantiomer, unless special circumstances, such as common ion effects or aggregation phenomena, decrease or increase the solubility ratio with respect to its normal value. **Figure 2(B)** and **(C)** roughly correspond to the binary phase diagrams of **Figure 1(A)** and **(B)**, respectively. On recrystallization of mixture M , the major enantiomer d can be obtained between N and P , for instance from system O . However, the best yield Y in pure d will be obtained from system N , at concentration C_N (in weight %):

$$Y = \frac{NE}{AE} \times \frac{100}{C_N}$$

For a conglomerate the above calculated yield is the same as that derived from the binary phase diagram, $Y = NE/AE$. For a racemic compound, Y calculated from the ternary isotherm is usually very close to that derived from the binary phase diagram because in such systems the ee of the eutectic does not change

significantly with temperature, except in the case of polymorphism or of solvation.

This is why information on the type of enantiomer system and, in particular, on the location of the eutectics in racemic compound phase diagrams is of great importance when the purification of partially resolved mixtures by crystallization techniques is undertaken. When the phase diagram of the considered system is not favourable (e.g. as in **Figure 1C**), recrystallization should be avoided and it may be advisable to postpone the purification to a next step, or to seek derivatives having more favourable phase diagrams. These concepts are particularly useful for the final purification of enantiomers prepared by asymmetric synthesis or chiral chromatography.

Direct Crystallization of Racemates

Separation of enantiomers by direct crystallization of their racemate is an attractive method, because no

costly chiral auxiliary is required. Such resolutions only apply to conglomerates. Essentially two main types of methods are then available. In the first of these the two enantiomers are allowed to crystallize simultaneously from a solution or melt which is always close to the racemic composition. In the second, called entrainment, the crystallization of a single enantiomer is promoted from a supersaturated solution or supercooled melt which is not allowed to come to equilibrium.

Simultaneous Crystallization

Although hand-sorting of the *d* and *l* crystals (as originally performed by Pasteur on sodium ammonium tartrate) can occasionally be a useful technique, the localization of the crystallization of each enantiomer on suitably disposed *d* and *l* seeds represents an improvement of greater practical interest. In small-scale preparations, one can utilize a small number of *d* and *l* seeds sufficiently separated from one another in the same crystallizer, and the large crystals which are eventually formed are collected manually. Large-scale applications utilize pairs of crystallization chambers, each one being loaded with a large amount of seeds of one enantiomer. The system is then continuously fed with a circulating, slightly supersaturated, racemic solution. Such processes have been proven to be valuable for continuous large-scale productions such as those developed by Haarmann & Reimer for (–)-menthol (resolved as its benzoate), and Merck for L- α -methyldopa (resolved as its nitrile precursor).

Entrainment

The entrainment method takes its origin in experiments performed by Gernez in 1866, showing that a supersaturated solution of sodium ammonium tartrate, when seeded with a particle of (+) salt, only yielded crystals of that salt. The resolution by entrainment is a batch process, which rests on the control of the crystallization rates of the two enantiomers, and implies the utilization of ternary phase diagrams, such as that shown in Figure 3. A solution *M*, supersaturated with respect of both enantiomers, and containing a small excess (*E* g%) of one of them (here, *l*) is seeded with crystals of that enantiomer. Crystallization is then allowed to proceed until the solution has reached composition *N*. At this point, the rotation of the solution is approximately equal and opposite in sign to that of the starting solution, and the *l* enantiomer that has crystallized amounts to twice its excess in the original solution *M* (i.e. $\approx 2E$ g%). At this stage, the crystals are separated off, and the same

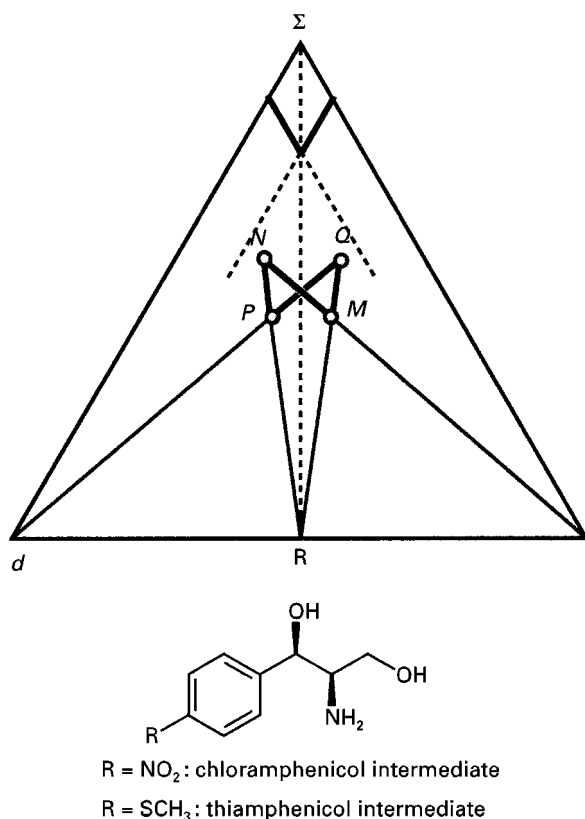


Figure 3 Principle of the entrainment process. In the cycle *MNPQ*, *MN* and *PQ* correspond to the crystallization of enantiomers *l* and *d*, respectively; *NP* and *QM* correspond to the loading of racemic material. In commercial processes, 20–90 crystallizations are commonly performed.

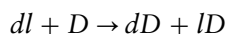
weight of racemic material is added to the filtrate and dissolved by heating. This results in a new supersaturated system of composition *P*, symmetrical to *M*, where the *d* enantiomer is now in the same excess as was the *l* in the previous experiment. Seeding with the *d* form and crystallization up to *Q* then yields $\approx 2E$ g% of *d*, and addition of the same weight of racemate allows the return to *M*, and so forth.

In practice, the economics of the process depends on the amount of material collected after each crystallization, which should represent at least 10–15% of the solute, and on the number of cycles which can be performed; this number is limited by the build-up of impurities which follows the addition of fresh racemate at each step, and which may eventually disturb the crystallization kinetics. The Roussel-Uclaf and Zambon processes for the manufacture of the chloramphenicol and thiamphenicol intermediates shown in Figure 3 are well-known industrial applications of resolution by entrainment. The method is also of great value for laboratory-scale resolutions, especially at the 100 g to kg scale.

For low-melting conglomerates, the entrainment can also be effected without solvent, in a supercooled melt. Such processes are easily understood by means of the melting point phase diagrams, by considering the metastable extension of the liquidus curves below the eutectic temperature.

Diastereoisomers

The most widely used method for the separation of enantiomers, often called classical resolution, rests on the crystallization of diastereoisomers formed from a racemate (dl) and an enantiopure reagent (say, D), called a resolving agent:



It is convenient to designate with letters p (positive) and n (negative) the diastereoisomers resulting from reaction of the two constituents of like sign and opposite signs, respectively. In this convention, no account is taken of the sign of rotation of the diastereoisomers themselves, which, if needed, can be specified by adding a $+$ or $-$ subscript to the p and n descriptor. Accordingly, the above reaction yields a mixture of p (dD) and n (lD) diastereoisomers, which, for instance, can both be dextrorotatory, i.e. p_+ and n_+ . The opposite enantiomer (L) of the resolving agent would then afford with the same racemate the diastereoisomer pair p_- (lL) and n_- (dL), mirror image of p_+ and n_+ (Marckwald principle). Note that the reciprocal resolution of DL by, for instance, d , would yield a mixture of p_+ (dD) and n_- (dL).

Diastereoisomeric salts, formed from simple acid-base reactions, are central to such resolutions, although covalent diastereoisomers (esters, amides, etc.) are also occasionally resolvable by crystallization. To cite but a single example, the DSM company resolves DL-phenylglycine by crystallization of its diastereoisomeric salts with (+)-10-camphorsulfonic acid, to produce the D-enantiomer required for the manufacture of the antibiotic ampicillin, at a scale of more than 1000 tonnes per year.

Diastereoisomeric inclusion complexes, in which the resolving agent is a chiral crystalline host lattice, represent an interesting alternative for the resolution of substances that cannot form salts, or do not possess functional groups suitable for formation of covalent diastereoisomers.

Phase Diagrams and Solubility Rules

Diastereoisomers p and n are distinct compounds and exhibit different structures in the crystal state. It fol-

lows that all physical properties involving the crystal themselves and the crystal/liquid or crystal/gas equilibria, such as melting points, solubilities, sublimation properties, crystal densities, etc., are different for the p and n species of a given pair. However, the possibility of separating p and n diastereoisomers by crystallization of their 1 : 1 mixture, resulting from the reaction of a racemate with a resolving agent, does not depend only on the properties of the pure p and n compounds: it rests primarily on the existence of favourable solid-liquid phase equilibria for the binary (p, n) or ternary (p, n, Σ) systems. The phase diagrams of diastereoisomer systems (Figure 4) are basically similar to those of enantiomer systems. There exist, however, several important differences between them: (1) the phase diagrams of diastereomer mixtures are not symmetrical; (2) in contrast to enantiomers, diastereoisomers preferentially form eutectics or solid solutions (Figure 4(A) and (C), respectively); (3) the occurrence of 1 : 1 (pn) addition compounds depicted in Figure 4(B) is by far less than that of (dl) racemic compounds.

Only diastereoisomer systems forming eutectic phase diagrams are suitable for resolution by crystallization. In the solubility isotherm of Figure 4(A), 1 : 1 (p, n) mixtures will afford the pure less soluble diastereoisomer (here p) if the crystallization is carried out between N and P , for instance from solution O . The best yield however will be obtained from solution N . This yield is given by:

$$Y = \frac{NE}{Ep} \times \frac{100}{C_N}$$

where C_N is the concentration of solution N . Since the p/n ratio in the ternary eutectic is usually close to that of the binary eutectic, Y is not very different from RE/AE in the melting point phase diagram. The best systems are those in which the eutectic is close to the edge of the phase diagram, and the maximum value of $Y = 50\%$ is approached when E is closed to one of the pure components. The occurrence of such good systems has been estimated at 20–25% of diastereoisomer mixtures. It is important to recognize that in such cases one or two crystallizations are normally sufficient to obtain the less soluble diastereoisomer in pure form.

Systems in which a 1 : 1 [p, n] compound exists, as in Figure 4(B), are totally unsuitable for resolution because crystallization of a 1 : 1 mixture will afford the 1 : 1 compound. Some resolution is possible with systems forming a solid solution, as shown in Figure 4(C), providing that the solubility difference between the pure components is sufficiently large. Most

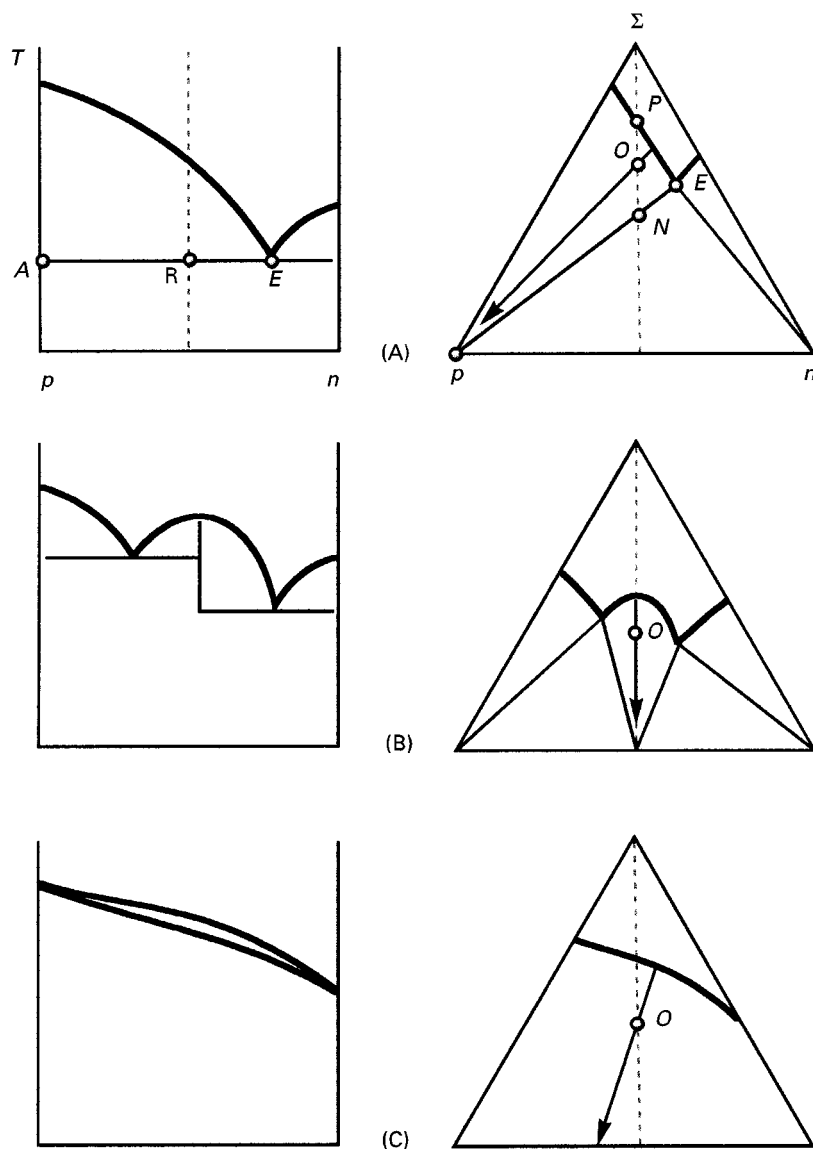


Figure 4 Melting point (left) and solubility (right) phase diagrams for diastereoisomer systems. (A) eutectic; (B) 1 : 1 addition compound; (C) solid solution. The arrows indicate the nature of the solid obtained from crystallization of a system of composition O .

often, however, the enrichment is very modest and utilization of systematic fractional crystallization techniques is required. These techniques are very tedious and time-consuming and this is why resolution of (p, n) systems forming solid solutions is not recommended unless alternative methods cannot be found. Note that diastereoisomeric lattice inclusion complexes are more prone to form solid solutions than the other types of diastereoisomers and often need repeated crystallizations to reach good enrichments. In such cases rather than purify the diastereoisomers, it may be advisable to complete the purification on the partially resolved enantiomers, along the lines indicated above.

Resolving Agents

In order to set up practical process for the separation of diastereoisomeric salts, initially a system forming a eutectic must be selected. This leads to the choice of the resolving agent and of the solvent. Next the crystallization conditions are optimized by means of phase diagrams along the lines discussed above. A classical resolving agent is a chiral acid or base available in bulk quantities at low price, and which has a propensity to form crystalline diastereoisomers when combined with racemic bases or acids. **Table 1** lists some of the most common resolving agents for salt formation. Other, more specialized, resolving agents for the separation of

Table 1 Common resolving agents

Acids	Bases
Tartaric acid (+), (–)	α -Methylbenzylamine (+), (–)
Dibenzoyltartaric acid (+), (–)	Ephedrine (+), (–)
Mandelic acid (+), (–)	2-Amino-1-butanol (+), (–)
Camphoric acid (+)	Quinine (–)
Malic acid (+), (–)	Quinidine (+)
10-Camphorsulfonic acid (+), (–)	Cinchonine (+)
α -Bromo- π -camphorsulfonic acid (+), (–)	Cinchonidine (–)
Glutamic acid (+), (–)	Brucine (–)
Aspartic acid (+), (–)	Yohimbine (+)
ω -Camphanic acid (+), (–)	Dehydroabietylamine (+)
1,1'-Binaphthyl-2,2'-diyl-hydrogen phosphate (+), (–)	N-Methyl-D-glucamine (–)

diastereoisomers by chromatography or for analytical purposes (nuclear magnetic resonance spectroscopy) are not mentioned here. For important commercial applications, it may be appropriate to design new resolving agents: for example, the *N*-alkyl-D-glucamine family (prepared from D-glucose) has been developed by Syntex as a substitute for cinchonidine for the large-scale resolution of naproxen (over 1000 tonnes per year). There are no clear guidelines allowing the prediction of a good resolving agent for a given substrate. This is not really a serious problem because the number of available resolving agents, being very limited, generally allows systematized protocols to identify the best ones very quickly.

Salts usually need polar solvents to crystallize, and a statistical survey of solvents used in over 800 such resolutions indicate that anhydrous or aqueous acetone and alcohols (ethanol, methanol, 1- and 2-propanol, 1-butanol), and water feature in 80% of cases. The presence of water may be necessary whenever the salts crystallize as hydrates. This is why 95% ethanol (rather than absolute ethanol) is to be preferred during the selection of a resolving agent.

Interesting achievements in the area of chiral host lattices have been reported during the last decade. A small number of chiral substances that form diastereoisomeric crystalline inclusion complexes with a variety of guests have been identified. In addition to the alkaloid brucine, which has been utilized for resolving, at least partially, chiral halogenoalkanes (including CHFCIBr) and, more recently, acetylenic alcohols and cyanohydrins, several new hosts have been discovered, among which readily available diols prepared from tartaric acid seem to have the greatest potential as resolving agents.

Crystallization-induced Asymmetric Transformations

The 50% yield limit of a resolution can be exceeded if the diastereoisomers can be equilibrated in the solu-

tion (i.e. $dD \rightleftharpoons lD$) at a rate faster than the crystallization of the least soluble one. Such a phenomenon was first reported by Leuchs in 1913; he isolated in 94% yield a single diastereoisomeric salt after reaction of an easily racemizable racemic acid with brucine. In addition to the requirement that the diastereoisomers must epimerize easily, processes of this type can only be successful if the diastereoisomer system belongs to the eutectic type. In **Figure 5**, the starting material has composition *O* (overall concentration C_0). In the liquid phase, the composition of the diastereoisomer mixture in chemical equilibrium is indicated by *L*, which in the case shown is slightly shifted towards the *n* species. The final equilibrium state is featured by *N*, representing the overall composition of the system at the end of the process. System *N* consists of pure solid *p* in equilibrium with liquid *L*. The yield in diastereoisomer *p* is proportional to LN/Lp , and can be derived from C_0 and the composition of the liquid in equilibrium (C_{eq}):

$$Y = \frac{(C_0 - C_{eq})}{(100 - C_{eq})} \times \frac{100}{C_0}$$

Accordingly, yields approaching 100% can only be obtained in poor solvents, in which C_{eq} is very small. Typically, $C_{eq} = 2$ g% and $C_0 = 20$ g% would give a *Y* of nearly 92%. In contrast to the case of a classical resolution, the yield does not depend directly on the location of the eutectic. However, it is the distance between the eutectic *E* and the equilibrium solution *L* which provides the driving force for the process, and this is why, again, a eutectic close to the edges of the phase diagram is preferable.

There are many examples of such processes in industry. They can be performed on diastereoisomeric salts (e.g. phenylglycine camphorsulfonate) as well as on covalent diastereoisomers (e.g. in the Roussel-Uclaf synthesis of the insecticide deltamethrin).

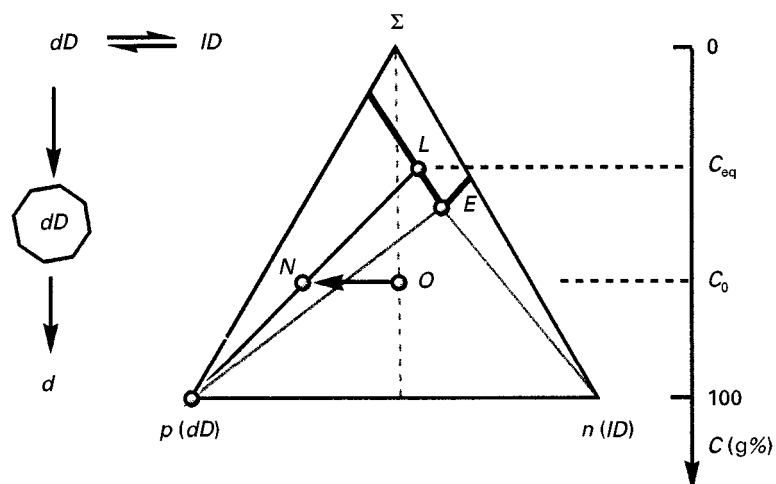


Figure 5 Crystallization-induced asymmetric transformation of diastereoisomers. In the solubility isotherm shown, *L* represents the composition of the liquid in which the two diastereoisomers are in chemical equilibrium (here with a slight excess of *n*). This liquid is itself in physical equilibrium with the solid, consisting of pure *p*. After completion of the chemical and physical equilibrations, the starting system *O* will be converted into the final system *N*, consisting of solid *p* in equilibrium with liquid *L*.

Crystallization-induced asymmetric transformations of enantiomers forming conglomerates can also be carried out by combining entrainment techniques with simultaneous racemization of the substrate in the solution. Although a number of examples have been described, and a number of patents have been filed, only a few processes of this type have reached commercial application.

Future Prospects

The understanding of phase equilibria in enantiomer and diastereoisomer systems is a central question, not only in view of its practical relevance to separation processes, but also because it may shed light on some of the mechanisms governing molecular recognition in condensed matter. Among the numerous unsolved questions, that of the prediction of racemate types is perhaps one of the most challenging. Recently, it has been shown that, in theory, conversion of racemic compounds into conglomerates could be achieved for some racemates by crystallization under high pressure. An experimental verification of this prediction would be of great importance in extending the possibilities of resolving racemates by direct crystallization.

See Colour Plate 67.

Further Reading

Ahuja S (ed.) (1997) *Chiral Separations, Applications and Technology*. Washington, DC: American Chemical Society.

Collet A (1989) Optical resolution by crystallization methods. In: Krstulovic AM (ed.) *Chiral Separations by HPLC*. Chichester, UK: Ellis Horwood.

Collet A (1996) Optical resolution. In: Reinhoudt DN (ed.) *Comprehensive Supramolecular Chemistry*, vol. 10. Oxford: Pergamon.

Collet A, Brienne M-J and Jacques J (1980) Optical resolution by direct crystallization of enantiomer mixtures. *Chem. Rev.* 80: 215.

Collet A, Ziminski L, Garcia C and Vigné-Maeder F (1995) Chiral discrimination in crystalline enantiomer systems: facts, interpretations, and speculations. In: Siegel JS (ed.) *Supramolecular Stereochemistry*. NATO ASI Series. Dordrecht: Kluwer.

Collins AN, Sheldrake GN and Crosby J (eds) (1994) *Chirality in Industry*. Chichester, UK: Wiley. Ibid. (1997) *Chirality in Industry II*.

Eliel EL, Wilen SH and Mander N (1994) *Stereochemistry of Organic Compounds*. New York: John Wiley.

Jacques J, Collet A and Wilen SH (1981) *Enantiomers, Racemates, and Resolutions*. New York: John Wiley. Ibid. (1994) *Reissue with corrections*. Malabar, Florida: Krieger.

Toda F (1996) Diol, bisphenol, and diamide host compounds. In: MacNicol DD, Toda F and Bishop R (eds) *Comprehensive Supramolecular Chemistry*, vol. 6. Chichester, UK: Pergamon.

Weber E (1996) Shape and symmetry in design of new hosts. In: MacNicol DD, Toda F and Bishop R (eds). *Comprehensive Supramolecular Chemistry*, vol. 6. Chichester, UK: Pergamon.

Wilen SH, Collet A and Jacques J (1977) Strategies in optical resolutions. *Tetrahedron* 33: 2725.

Cyclodextrins and Other Inclusion Complexation Approaches

J. Dingenen, Janssen Research Foundation, Belgium

Copyright © 2000 Academic Press

Introduction

Cyclodextrins are cyclic nonreducing oligosaccharides containing from six to twelve glucose units in a C-1 chair conformation, bonded through α -(1,4) linkages (Figure 1). The glycopyranose units are arranged in the shape of a hollow truncated cone. The larger opening of the molecule is surrounded by the secondary (C-2 and C-3) hydroxyl groups, while the primary (C-6) hydroxyl groups constitute the smaller end of the cone.

Since all the primary and secondary hydroxyl groups are located at the outside of the molecule, the exterior faces are hydrophilic. The interior cavity, essentially comprised of methylene linkages and glycosidic oxygen bridges, is relatively hydrophobic in comparison with polar solvents such as water. Furthermore, the glycosidic oxygen bridges produce a high electron density, giving the interior of the cavity a slightly Lewis-base character.

The three smallest cyclodextrin homologues are readily commercially available:

- α -cyclodextrin (cyclohexamylose);
- β -cyclodextrin (cycloheptamylose);
- γ -cyclodextrin (cyclooctamylose);

The basic property of cyclodextrins is their ability to form selective inclusion complexes with a broad variety of organic and inorganic molecules.

The formation of inclusion complexes is in general determined by the ability of the guest molecule to closely fit the cavity of the cyclodextrin. However, the polarity of the guest molecule also plays an important role.

Inclusion complexes are usually formed in the presence of water or in water mixed with organic modifiers.

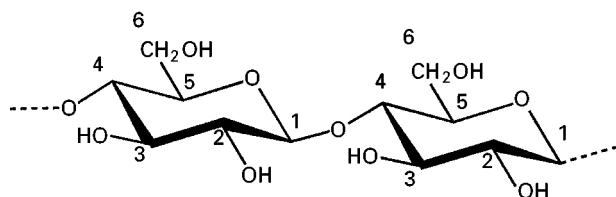


Figure 1 Numbering of carbon atoms in the cyclodextrin ring structure.

One of the first effective uses of cyclodextrins in chromatography was as mobile phase additive in thin-layer chromatography. In the mid-1980's a process was developed to produce stable cyclodextrin high performance liquid chromatographic (HPLC) phases. Nowadays, native α -, β - and γ -cyclodextrin, as well as a variety of derivatized cyclodextrin HPLC columns are commercially available. Also many cyclodextrin-based capillary gas chromatography (GC) columns are on the market. With the growing importance of capillary electrophoresis in chiral separations, the use of native cyclodextrin and cyclodextrin derivatives as an electrolyte additive steadily increases.

Cyclodextrins in HPLC Applications

Native cyclodextrin HPLC columns were deliberately designed to be used in the reserved-phase mode of operation, in order to take full advantage of the host-guest complexation capabilities of the molecule.

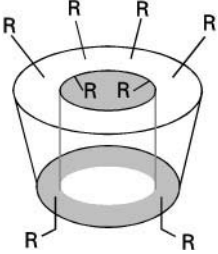
In a more recent and somewhat different experimental approach, the inclusion properties are suppressed by using a non-hydrogen bonding, polar organic solvent (e.g., acetonitrile) as the main component of the mobile phase. Acetonitrile has the tendency to occupy the cavity and seems to enhance hydrogen bonding between the hydroxyl groups on the cyclodextrin and hydrogen bonding groups on the chiral analyte.

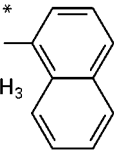
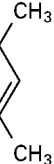
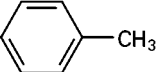
In this so-called polar organic mode of operation, the addition of small amounts of glacial acetic acid and triethylamine is used as a tool to enhance enantioselectivity. On the other hand, the addition of a hydrogen bonding solvent such as methanol allows reduced retention of strongly retained molecules. This technique produces some unusual enantioselectivities that certainly enhance the usefulness of native cyclodextrin phases.

Furthermore, a variety of cyclodextrin derivatives has been immobilized on a chromatographic support, which can be used under normal as well as under reversed-phase conditions. The most popular commercially available derivatized cyclodextrin chiral selectors are listed in Table 1.

Mobile Phase Design and Parameter Optimization

Because complex stability constants usually have greater values in water or water-organic organic solvent mixtures than in a pure organic medium, native cyclodextrin columns are predominantly used in the reserved-phase mode. Ethanol, propanol, 1,4-dioxane, dimethyl sulfoxide, dimethyl formamide,

Table 1 Commercially available derivatized cyclodextrin phases


<i>R</i>	<i>Trade name, Advanced Separation Technologies</i>	
$\begin{array}{c} \text{O} \\ \parallel \\ -\text{C}-\text{CH}_3 \end{array}$	Cyclobond® I 2000 Ac	Acylated
$\begin{array}{c} \text{OH} \\ \\ -\text{H}_2\text{C}-\text{CH}-\text{CH}_3 \\ * \end{array}$ <p>*<i>RS</i> or <i>S</i></p>	Cyclobond® I 2000 RSP Cyclobond® I 2000 SP	Hydroxypropyl ether
$\begin{array}{c} \text{O} \\ \parallel \\ -\text{C}-\text{NH}-\text{C}^*-\text{CH}_3 \\ \\ \text{O} \end{array}$  <p>*<i>R</i> or <i>S</i></p>	Cyclobond® I 2000 RN Cyclobond® I 2000 SN	Naphtylethyl carbamate
$\begin{array}{c} \text{O} \\ \parallel \\ -\text{C}-\text{NH}-\text{C}_6\text{H}_3(\text{CH}_3)_2 \\ \\ \text{O} \end{array}$ 	Cyclobond® I 2000 DMP	3,5-Dimethylphenyl carbamate
$\begin{array}{c} \text{O} \\ \parallel \\ -\text{C}-\text{C}_6\text{H}_4-\text{CH}_3 \\ \\ \text{O} \end{array}$ 	Cyclobond® I 2000 PT	<i>p</i> -Toluoyl

methanol and acetonitrile have been used as organic modifiers. However, methanol and acetonitrile are most commonly used. It is difficult to predict in advance which of these two modifiers will produce the best separation in any given case. In many cases, pH and ionic strength of the aqueous part of the mobile phase are even more important than the choice of the organic modifier.

The following factors influence enantioselectivity.

Ionic strength With an eluent composed of a mixture of 5 millimolar tetrabutylammonium hydrogen-sulfate (TBAHS) in water and methanol in an 80–20 volume ratio, experiments were performed on a β -cyclodextrin Astec column (Cyclobond®) and a similar Merck column Merck (Chiradex®). The only difference between both stationary phases is the chemistry used to attach the β -cyclodextrin to the silica matrix.

In these initial experiments, especially on the Cyclobond® column, a poor peak shape for different products was observed. This effect was less pronounced on the Chiradex® column but it also occurred for some products. The origin of the poor peak shapes can have different causes, as for example an insufficient shielding of residual silanol groups. Therefore, the effect of the tailing reducer concentration was investigated.

Figure 2 illustrates the effect of the tailing reducer concentration on the retention factor and the resolution of miconazole (R14889). In this figure, the resolution factor based on the location of the valley point between two peaks is used. The resolution parameter (Auflösung (*g*)) is defined to evaluate the degree of separation between two partially resolved enantiomers. This measuring principle is based on the location of the valley point between two adjacent peaks. It is a useful and, from a measurement viewpoint,

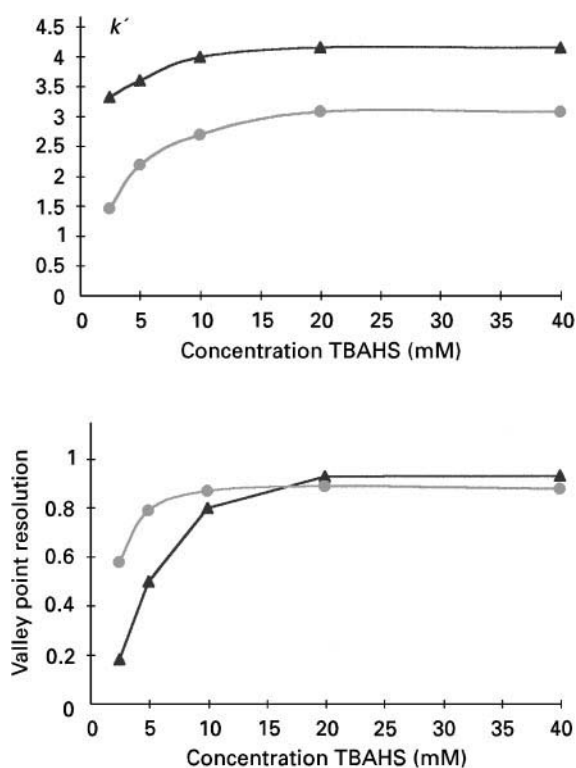
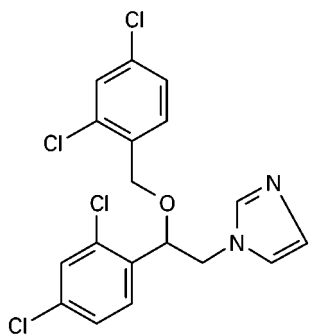


Figure 2 Influence of tailing reducer concentration on the retention factor and valley point resolution ▲, Cyclobond®; ●, Chiradex®. Experimental conditions: column: 25 cm × 4.5 mm ID chemically bonded cyclodextrin phase; mobile phase: TBAHS in water at different concentrations–methanol (80–20, v/v); flow rate: 1 mL min⁻¹. Solute:



easy evaluation technique for characterizing the separation degree between two peaks.

If we analyse **Figure 2**, it is easy to conclude that ionic strength has a strong effect on the chromatographic behaviour of the investigated chiral molecule. It is furthermore perfectly clear that the influence of ionic strength on the retention factor is more pronounced on the Chiradex® than the Cyclobond® column. However, for both types of stationary phase a constant value is observed above a tailing reducer concentration of 20 mmol. At low TBAHS concentration, the smallest resolution values are measured on

the Cyclobond® column. Also, the ionic strength required to reach the highest resolution value is different for both columns.

Further experiments dealing with the effect of ionic strength on peak shape and chromatographic behaviour have demonstrated that for each individual column type–tailing reducer combination it can be very helpful to investigate this parameter thoroughly. However, to save time, we nowadays start our chiral method development work on cyclodextrin-based columns with tailing reducer concentrations between 30 and 50 mmol, because we have experienced that with these values there is in general a good chance of being successful.

Type of tailing reducer The acetic acid salt of triethylamine is popular as tailing reducer in reversed-phase chromatography. Instead of using acetic acid to adjust the pH value of an aqueous triethylamine solution, we investigated the usefulness of some other organic and inorganic acids. At first we did not expect any influence of the type of counterion on enantioselectivity, but some preliminary experiments showed a distinct effect, worthwhile to investigate further. Therefore, we examined about 30 products belonging to different product classes. As mobile phase, a mixture of 20 vol% of methanol and 80 vol% of 50 mmol aqueous triethylamine solution adjusted to a pH value of 2.5 with respectively hydrochloric, hydrobromic, phosphoric, perchloric, sulfuric, trifluoroacetic and oxalic acids was used.

For all the investigated products, the largest retention factors were observed for the triethylamine solution adjusted to the desired pH value with sulfuric and oxalic acids. Also with sulfate as counterion, the largest number of investigated products was partially or completely resolved. Compared to the other acids, with trifluoroacetic and perchloric acid a smaller number of products were separated. To further investigate the observed effect, we repeated the same experiments for a series of azoles, which differed only slightly in structure. For these substances, the effect of the counterion on resolution is illustrated in **Figure 3**. See also **Table 2**.

For this product series, the results confirm the initial observations. Furthermore, **Figure 3** clearly demonstrates that even small change in molecular structure, as for example the number or position of the chlorine atoms on one of the phenyl groups of the molecule, can have a tremendous effect on the enantioselectivity.

Although for the investigated series of azoles pH adjustment with sulfuric acid in general resulted in good peak shapes and high resolution values, one peculiarity was observed. Under these experimental

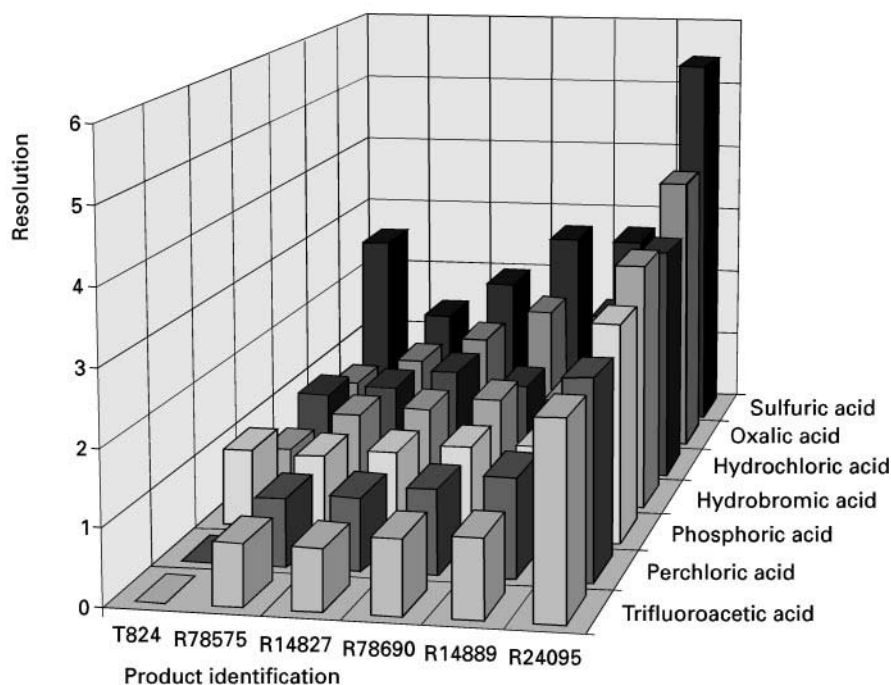


Figure 3 Azoles: effect of the counterion on resolution. Experimental conditions: column: 25 cm \times 4.6 mm ID Cyclobond® (Astec); mobile phase: 50 mM triethylamine in water adjusted to pH 2.5 with different acids–methanol (80–20, v/v); flow rate: 1 mL min⁻¹, solutes; see Table 2.

conditions, R78575 was strongly retained and both enantiomers eluted as broad peaks with an irregular shape (Figure 4). On the other hand, pH adjustment of the triethylamine solution with the other acids resulted in normal peak shapes (Figure 5). This is an indication that minor differences in structure, or small variations in experimental conditions, can have a tremendous effect on the chromatographic behaviour of enantiomers.

A comparable set of experiments was subsequently performed using tetrabutylammonium hydroxide instead of triethylamine as tailing reducer. In this set of experiments, oxalic acid was excluded and perchloric acid could not be used owing to the formation of an insoluble salt with tetrabutylammonium hydroxide in the water–methanol mixture. For the whole test series of 24 different substances, sulfuric acid could be identified as the counterion that generated the highest resolution values. From a practical point of view, it is certainly an advantage that sulfate is the anion of choice. For temperatures between room temperature and 50°C the corrosion of stainless steel (316 or equivalent) is negligible for dilute sulfuric acid solutions, while the chemical resistance of this material for chloride ions (even in low concentrations), is rather limited.

In conclusion, the anionic part of the tailing reducer has a clear effect on enantioselectivity, as illus-

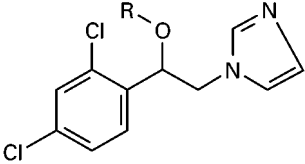
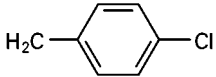
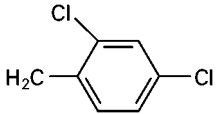
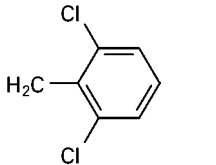
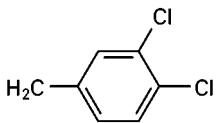
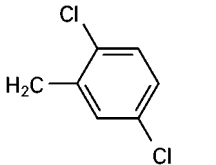
trated previously. The influence of the counterion on the retention factor and resolution of the investigated compounds can possibly be related to a difference in ability of the counterion to compete with the organic guest molecule for the hydrogen bonding sites of the cyclodextrin host.

To complete the experiments concerning the influence of the type of tailing reducer, we also found it necessary to do some tests in which the anionic part of the tailing reducer was kept identical while the cationic part was varied. In these experiments, a 30 mmol solution of tetramethyl-, tetraethyl-, tetrapropyl- and tetrabutylammonium hydroxide solution was adjusted with sulfuric acid to a pH value of 2.5 and used as mobile phase in an 80–20 volume ratio with methanol as organic modifier.

The smallest resolution values are observed for tetramethylammonium hydroxide and the highest values for tetrabutylammonium hydroxide, but compared with the influence of the anionic part of the tailing reducer the differences are far less pronounced. However, for the investigated test series, the tailing factor measured at 10% of the peak height gradually decreases with increasing chain length of the alkylammonium hydroxide.

pH Whatever type of silica-based reversed phases are used, these materials always display some acidic

Table 2 Structures of the investigated azole derivatives

 Azoles	
Product	R
T824	H
R14827 (econazole)	
R14889 (miconazole)	
R24095 (isoconazole)	
R78575	
R78690	

surface area properties owing to residual hydroxyl groups on the silica surface. During the analysis of basic substances not only hydrophobic interactions take place, but also acid-base interactions between these acidic groups and basic functions in the analyte can be expected to occur. This type of interaction often results in increased retention combined with peak tailing. One of the possibilities to solve this problem is to adjust the pH below the pK_a value of the sample that has to be analysed. At pH values lower than $pK_a - 2$ the basic function is protonated and a salt is formed which no longer has basic properties.

Because the cyclodextrin columns are used under reversed-phase conditions, it is certainly worthwhile to investigate the effect of pH on enantioselectivity. For some monobasic molecules, the effect of pH on the retention factor is depicted in Figure 6.

Figure 6 clearly illustrates that the retention factor of the investigated products follows a typical reversed-phase pattern. At higher pH values the degree of protonation of the analyte diminishes. As a result the chance for hydrophobic interactions with the stationary phase increases and higher retention values are measured. When the pH is equal to the pK_a value of the sample, the number of protonated and nonprotonated molecules is equal. Small changes in pH around this value will immediately have an effect on the retention factor. Even the effect of small structural changes, causing some differences, in hydrophobic nature of the nonprotonated solute molecules, can be clearly observed.

R8110 has the smallest retention factor owing to the presence of a fluorine atom on the phenyl group, giving the molecule a more polar character than the other two members of the test series. The largest retention factors are measured for R7405 bearing an ethyl group on the ester function attached to the imidazole ring instead of a methyl group for R7315.

To better visualize the effect of pH variations on enantioselectivity we often use for the graphical

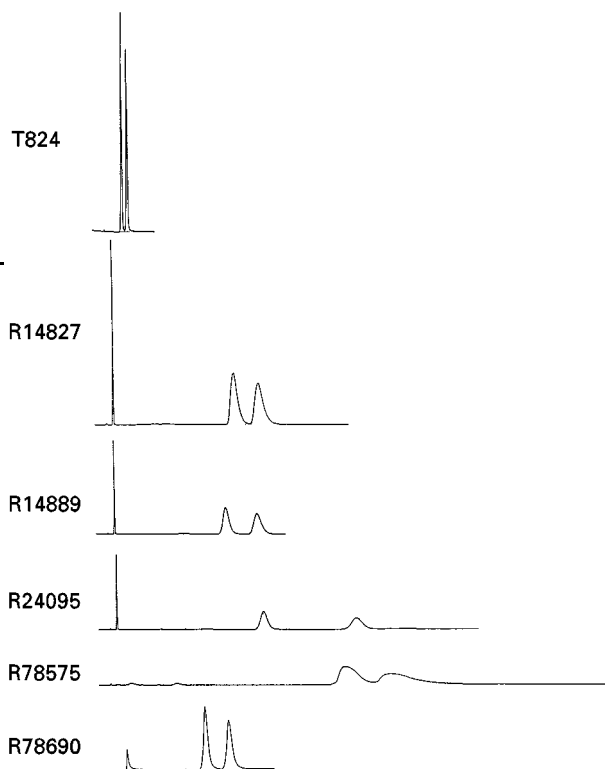


Figure 4 Peak shape of the different azoles. Experimental conditions: column: 25 cm \times 4.6 mm ID Cyclobond® (Astec); mobile phase: 50 mM triethylamine in water adjusted to pH 2.5 with sulfuric acid-methanol (80–20, v/v); flow rate: 1 mL min⁻¹; solutes: see Table 2.

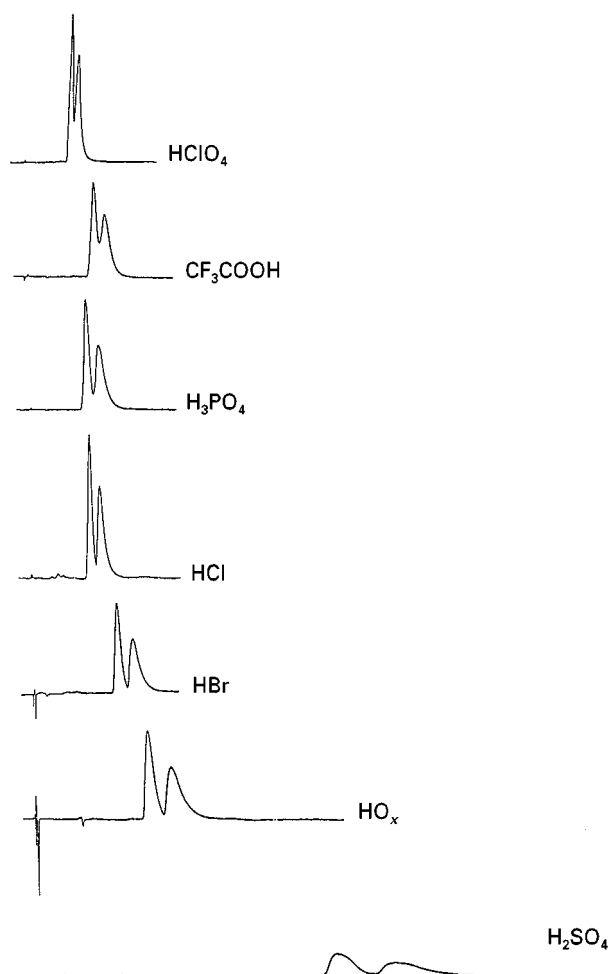
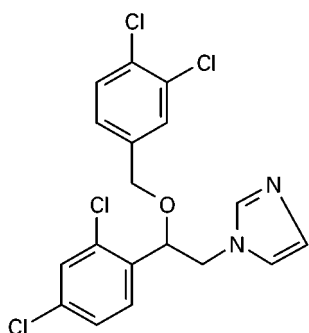


Figure 5 Peak shape of R78575. Experimental conditions: column: 25 cm \times 4.6 mm ID Cyclobond® (Astec); mobile phase: 50 mM triethylamine in water adjusted to pH 2.5 with different acids-methanol (80–20, v/v); flow rate: 1 mL min⁻¹; solute:



representation of experimental data the degree of protonation of the solute molecules instead of pH values. For monobasic substances the ratio between protonated and nonprotonated molecules at a certain pH value can be easily calculated:



$$K_a = \frac{[\text{R-NH}_2] \cdot [\text{H}^+]}{[\text{R-NH}_3^+]}$$

$$\text{p}K_a = \text{pH} + \log \frac{[\text{R-NH}_3^+]}{[\text{R-NH}_2]}$$

(Henderson-Hasselbalch equation)

$$\text{p}K_a - \text{pH} = \log \frac{[\text{R-NH}_3^+]}{[\text{R-NH}_2]}$$

From:

$$10^{(\text{p}K_a - \text{pH})} = \frac{[\text{R-NH}_3^+]}{[\text{R-NH}_2]}$$

and:

$$[\text{R-NH}_3^+] + [\text{R-NH}_2] = 100$$

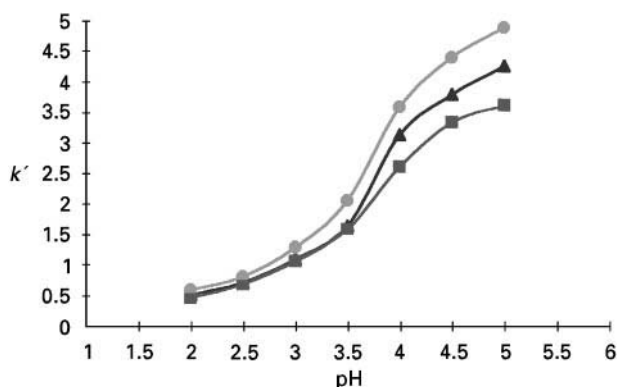
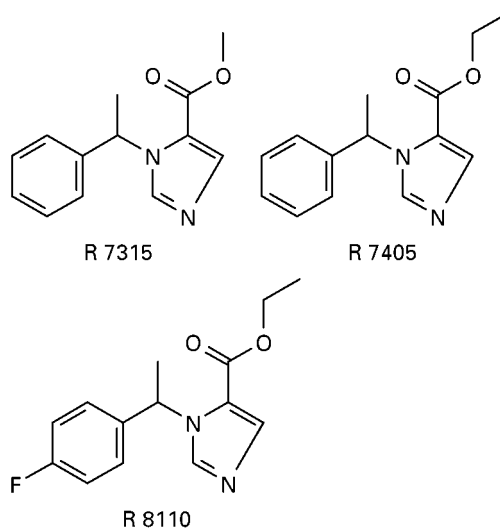


Figure 6 Effect of pH on retention factor. \blacktriangle , R7315; \bullet , R7405; \blacksquare , R8110. Experimental conditions: column: 25 cm \times 4 mm ID Chiradex® (Merck); mobile phase: 50 mM triethylamine in water adjusted to different pH values with sulfuric acid-methanol (80–20, v/v); flow rate: 1 mL min⁻¹; solutes:



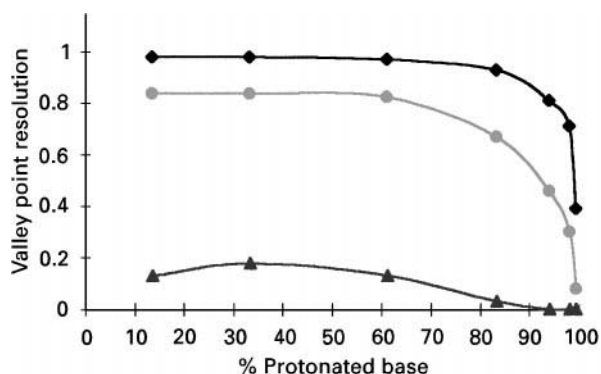
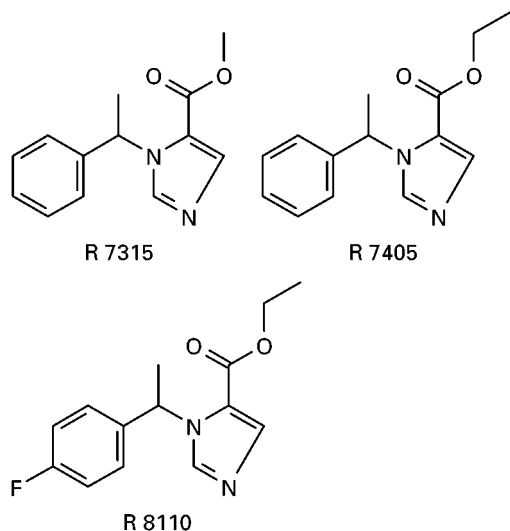


Figure 7 Effect of degree of protonation of the analyte on resolution. ◆, R7315; ●, R7405; ▲, R8110. Experimental conditions: column: 25 cm \times 4 mm ID Chiradex® (Merck); mobile phase: 50 mM triethylamine in water adjusted to different pH values with sulfuric acid-methanol (80–20, v/v); flow rate: 1 mL min⁻¹; solutes:



it is possible to easily calculate for each pH value the ratio between protonated and free base. For R7315, R7405 and R8110 the valley point resolution versus the percentage protonation is depicted in Figure 7.

For the investigated product series, it is clear that under the experimental conditions applied above a certain degree of protonation of the solute molecules the enantioselectivity strongly decreases. Probably due to an increase in hydrophilic character of the protonated molecules, the strength of the hydrophobic interactions between the analyte and the cavity of the cyclodextrin molecule diminishes, with a reduced enantioselectivity as a result. Within the investigated pH range, triethylamine ($pK_a = 10.72$) always remains fully protonated. Therefore, competition for hydrophobic interactions with the cyclodextrin cavity between the tailing reducer and the solute molecules has to be considered as nonexistent and can be excluded as a possible reason for reduced enantioselectivity at higher pH values.

Besides investigations on the effect of pH using triethylamine as basic substance in the aqueous part of the mobile phase, experiments have also been performed with different tetraalkylammonium hydroxides adjusted to the desired pH value with sulfuric acid. Within the same pH range, tetrabutylammonium hydroxide and triethylamine displayed comparable patterns when the valley point resolution was plotted against the percentage of protonation of the solute molecules.

For a dibasic substance (R60844) with respectively pK_a values of 5.4 and 6.7 the protonation pattern versus pH, together with the valley point resolution for two types of mobile phase additives, is given in Figure 8.

Although for the dibasic product R60844 both basic functions remain fully protonated up to a pH value of 4, the resolution continuously increases between pH 2 and 4. However, above pH 4 the enantioselectivity rapidly decreases.

For the different product series that have been examined we have observed that under the same experimental conditions, in general, higher resolution values are obtained with triethylamine than with

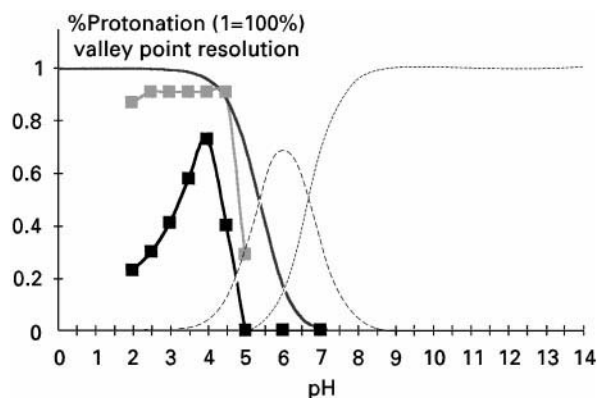
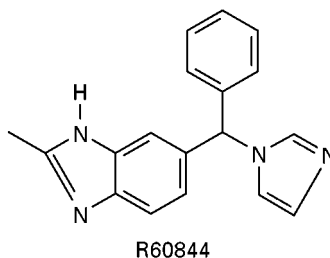


Figure 8 Effect of pH on the degree of protonation and resolution of a dibasic substance. —, Alpha 0; ---, alpha 1; - - - -, alpha 2; ■, TBA-OH; □, TEA. Experimental conditions: column: 25 cm \times 4 mm ID Chiradex® (Merck); mobile phase: 50 mM triethylamine in water adjusted to different pH values with sulfuric acid-methanol (80–20, v/v); and 30 mM tetrabutylammonium hydroxide in water adjusted to different pH values with sulfuric acid-methanol (80–20, v/v); flow rate: 1 mL min⁻¹; solute;



tetrabutylammonium hydroxide as mobile phase additive.

In conclusion, the stability of the inclusion complexes formed between the solute molecule and the cyclodextrin seem to be dependent on the charge of the guest molecule. Therefore, the retention as well as the degree of separation of molecules bearing an ionizable acidic or basic group can be affected by changing the pH. However, the effect of pH variations is not so easy to predict.

In the experiments performed, some products (R7315, R7405, T824, etc.) display the highest resolution values when they are present as free base or as a partially charged molecule. Other products (R60844, most of the azoles) reach maximum resolution when they are completely or nearly completely protonated. For some products the effect of pH variations within a range of 2–3 pH units is small, while for others extreme effects can be observed. Furthermore, for different types of tailing reducers the resolution versus pH profiles can have a different shape.

Therefore, the different experiments that have been performed to investigate the effect of pH on enantioselectivity clearly demonstrate that besides host-guest complexation interactions between the solute molecule and the cyclodextrin cavity, the hydroxyl groups at the outside of the cyclodextrin molecule together with reversed phase and other less predictable types of interactions certainly play an important role in the chiral recognition process.

Because small changes in pH can have a tremendous influence on the enantioselectivity, it is certainly advisable to thoroughly investigate this parameter during method development and optimization work on cyclodextrin columns.

Temperature In equilibrium-based processes, temperature plays an important role. For all investigated compounds, a very good linear relationship between the natural logarithm of the retention factor and the inverse of temperature is observed. For the products R7315 and R7405 only small differences in slope are measured. Indications that for both products the enthalpy values for solute-stationary phase transfer are very similar. The effect of temperature on the valley point resolution is given in Figure 9.

Only for R23979 was a valley point resolution of one measured for the whole temperature range between 1 and 40°C meaning that for this product the effect of temperature variation is of the same magnitude for both enantiomers. For R60844 and R7315 practically no influence on the resolution was observed between 1 and 15°C. Above that temperature, for both products the resolution value starts to decrease in a similar way. The continuous decrease of

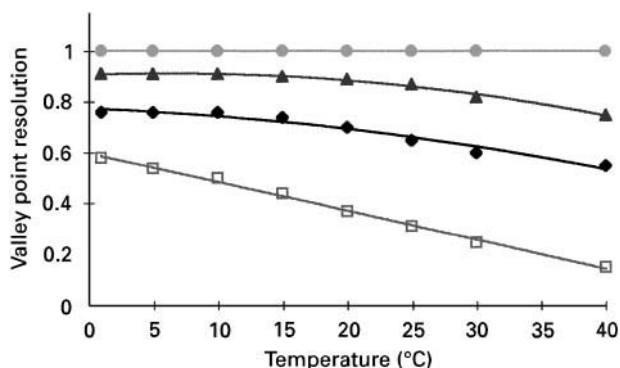
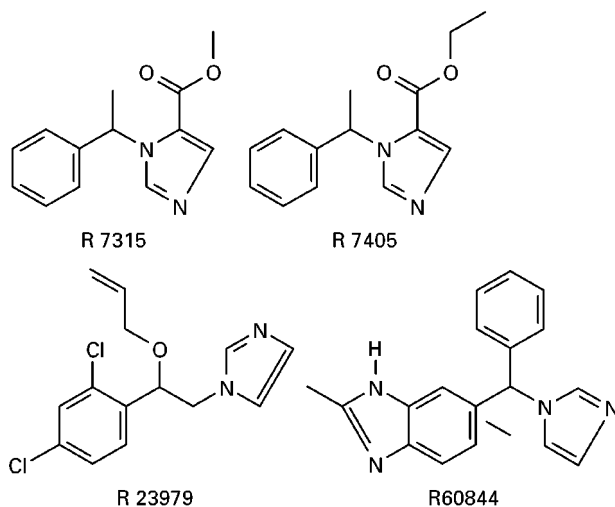


Figure 9 Influence of temperature on the retention factor. ◆, R7315; □, R7405; ▲, R60844; ●, R23979. Experimental conditions: column: 25 cm × 4 mm ID Chiradex® (Merck); mobile phase: 30 mM triethylamine hydroxide in water adjusted to different pH values with sulfuric acid-methanol (80–20, v/v); flow rate: 1 mL min⁻¹; temperature range: 1–40°C; solutes:



the resolution value with increasing temperature observed for R7405 can be considered as a logical behaviour, because for R7405 and R7315 the smallest retention factors are measures – an indication that the binding forces between the stationary phase and these solutes are smaller than for the other products investigated. As a result, the effect of a temperature increase on the resolution is more pronounced for these compounds. However, we did not expect to observe a different effect of temperature variations for R7315 and R7405, because for both products only minor differences in enthalpy values were measured. Therefore, temperature variations probably have the same influence on both enantiomers of R7405, while the enantiomers of R7315 are affected in a different way.

In conclusion, temperature variations have an influence on the retention factor as well as on the resolution value. However, the effects observed differ from one product to another. Therefore, this parameter

has to be investigated on an individual basis during method development and optimization work.

Type and concentration of organic modifier It is known that for the reversed-phase analysis of several alkylbenzenes on chemically bonded cyclodextrin columns the type of alcohol, together with its concentration in the mobile phase, strongly influences the retention behaviour of these substances.

To investigate the effect of type of alcohol on enantioselectivity, we performed some experiments in which the normally used modifier (methanol) was replaced by the same amount of ethanol 1-propanol. For all the investigated substances, the retention factor strongly decreased with increasing chain length of the alcohol used.

The retention factors measured for an ethanol-based mobile phase are about 30–50% lower than the values observed for methanol as organic modifier. A decrease of approximately the same magnitude could be observed when ethanol was replaced by 1-propanol. Therefore, in extreme cases the retention factor drops to about 20% of the value measured for methanol, when this solvent is replaced by the same amount of 1-propanol. With increasing chain length the hydrophobicity of the alcohol increase, which enhances the chance for competition between the solvent and the analyte molecules to interact with the hydrophobic cyclodextrin cavity.

Because a strong decrease in retention time of the solutes could be observed when ethanol or 1-propanol was used as organic modifier, these solvents seem to have a greater affinity for the cyclodextrin cavity than methanol. Therefore, they will be more effective for displacing strongly retained substances from a cyclodextrin column. The manufacturers of cyclodextrin columns in fact use this property, because they recommend regenerating their columns by passing several column volumes of pure ethanol through the column, followed by pure water and then methanol.

In general, an increasing water content in the mobile phase increases both the retention and the enantioselectivity. However, for practical applications the retention factors are generally too long when mobile phases with a high water content are used, and a compromise has to be found. For our product classes we therefore use a mixture of 80 vol% of aqueous phase and 20 vol% of methanol as a typical starting mobile phase composition. If the products are too strongly retained or do not elute at all, the amount of methanol is systematically increased.

Flow rate Due to the very specific type of interactions, which play a major role in chiral recognition

processes, chiral stationary phases often display slow mass transfer characteristics. Therefore, on chiral stationary phases, flow rate can have a strong effect on the enantioselectivity. For difficult separations, lowering the flow rate certainly has to be considered as a tool to enhance enantioselectivity.

Derivatized Cyclodextrins

Native cyclodextrin columns cannot be used effectively for the separation of enantiomers under normal phase chromatographic conditions. On the other hand, different naturally occurring chiral molecules that have been derivatized are extensively and very successfully used in the normal phase mode of operation.

Triacetylcellulose, obtained by heterogeneous acylation of cellulose, was one of the first commercially available derivatives. However, the later developed and commercialized aromatic cellulose and amylose derivatives (benzoates, carbamates), compared with triacetylcellulose, are much more universally applicable. Owing to the broad applicability of the cellulose and amylose derivatives similar cyclodextrin-based stationary phases have been developed.

In our laboratories we investigated the possibilities of the derivatized cyclodextrin columns under normal as well as reversed-phase chromatographic conditions. We also compared these phases with the corresponding cellulose derivatives.

Our first experiments on the functionalized cyclodextrin phases were performed under normal phase conditions. A series of 42 products covering a broad range of organic chemistry were investigated on the *S*-naphthylethyl carbamate, the *para*-toluoyl and 3,5-dimethylphenyl carbamate cyclodextrin derivative, using *n*-hexane-2-propanol in different ratios as the mobile phase.

The results obtained were rather poor. Of the whole test series only six products were partially or completely resolved on the 3,5-dimethylphenyl carbamate column. The situation was even worse on the two other columns tested. Therefore, we decided to switch immediately to the reversed-phase mode of operation. The initially used test series of 42 products was first investigated on the three above-mentioned cyclodextrin columns with a mobile phase consisting of 0.5% ammonium acetate in water and methanol in a 30–70 volume ratio. This mobile phase composition was chosen after some preliminary experiments, which demonstrated that higher water content caused a tremendous increase in retention times. Compared with the results under normal phase conditions, the number of products separated and the degree of separation were much better on all the investigated

column types. Because earlier experiments on the native cyclodextrin phases have demonstrated that an acidic pH generally results in better separations, a 20 mM tetrabutylammonium hydrogensulfate solution (pH 2.3) was thereafter used as tailing reducer.

Owing to the well-known reversed-phase effect of retention decrease with lowering pH values, the methanol content in the mobile phase had to be reduced to 40 vol% instead of the 80 vol% used in the experiments with ammonium acetate as tailing reducer. Under these experimental conditions, the largest number of products was separated on the *S*-naphthylethyl carbamate column, although the results on the other two columns only differed slightly. It was also interesting to observe that some products, which could not be separated on native cyclodextrin, were completely resolved on one of the derivatized phases. In the next set of experiments, a 20 mM solution of respectively tetramethyl-, tetraethyl- and tetrabutylammonium hydroxide was adjusted with sulfuric acid to a pH value of 2.5 and used in combination with 70 vol% of methanol as the mobile phase. The effect of the cationic part of the tailing reducer is not clear. With tetraethylammonium hydroxide the largest number of products are partially or completely resolved, but the resolution values are in general somewhat higher with tetramethylammonium hydroxide, although the differences with the two other alkylammonium hydroxides are minimal. Only for one member of the test series was tetramethylammonium hydroxide required to obtain partial resolution.

On native cyclodextrin columns, we could clearly demonstrate the influence of the anionic part of the tailing reducer. Therefore, a similar test was done on the 3,5-dimethylphenyl carbamate cyclodextrin derivative, using 20 mM tetramethylammonium hydroxide adjusted to pH 2.5 with respectively trifluoroacetic, hydrochloric, phosphoric, (*D*)-camphorsulfonic and sulfuric acids, (*D*)-Camphorsulfonic acid has been deliberately chosen to investigate eventual additional effects by introducing chirality in the mobile phase. After pH adjustment, the aqueous phase was mixed with methanol in a 30–70 volume ratio. Some products were also tested with a 50–50 mixture of aqueous phase and methanol. Comparable with the observations on the native cyclodextrin column, and also on the functionalized cyclodextrin, pH adjustment with sulfuric acid resulted in the largest number of separations. For all the other acids, the number of partially or completely resolved products dropped to about 50% or less of the value observed for sulfuric acid. However, three products which could not be separated with one of the different acids

tested were partially resolved when (*D*)-camphorsulfonic acid was used to adjust the pH of the tetrabutylammonium hydroxide solution.

Comparison of derivatized cyclodextrins and the corresponding cellulose derivatives Because derivatized cellulose and amylose columns are extensively used in our laboratories for both analytical and preparative chromatographic applications, it seemed worthwhile to compare these phases with the corresponding cyclodextrin derivatives. At present only two cellulose phases are commercially available which can be used equally well under reversed-phase and normal phase conditions, namely Chiralcel® OD-R (3,5-dimethylphenyl carbamate and Chiralcel® OJ-R (*para*-methylbenzoate) (Daicel, Japan). We compared these phases with Cyclobond®-DMP and Cyclobond®-PT columns (Advanced Separation Technologies), respectively.

The first experiments were performed under normal phase conditions, using *n*-hexane–2-propanol in a 70–30 ratio as the mobile phase. If products eluted too fast with this mobile phase composition, the amount of 2-propanol was reduced to respectively 20 or 10 vol%. A total of 21 different products were examined. The results of these experiments are summarized in Table 3.

From this data it is clear that for the investigated product classes the cellulose derivatives are far superior compared to the corresponding cyclodextrin phases when normal phase conditions are applied. We thereafter examined the same product series under reversed-phase conditions using a mixture of 70 vol% of methanol and 30% of a 50 mM triethylamine solution adjusted to pH 2.5 with sulfuric acid. The results of these experiments are summarized in Table 4.

When we compare this data with the results obtained under normal phase conditions, we have to conclude that in the reversed phase mode of

Table 3 Derivatized cyclodextrins versus the corresponding cellulose derivatives under normal phase conditions

Column type	Good separation $\beta > 0.90$		Partially resolved ^a		Total	
	Number	%	Number	%	Number	%
Chiralcel OD-R	9	42.9	6	28.6	15	71.4
Cyclobond I-DMP	2	9.5	3	14.3	5	23.8
Chiralcel OJ-R	13	61.9	5	23.8	18	85.7
Cyclobond I-PT	–	–	2	9.5	2	9.5

^aFor the partially resolved peaks, the resolution on the cellulose derivatives is always much higher than on the cyclodextrin derivatives.

Table 4 Derivatized cyclodextrins versus the corresponding cellulose derivatives under reversed phase conditons

Column type	Good separation $\beta > 0.90$		Partially resolved ^a		Total	
	Number	%	Number	%	Number	%
Chiralcel OD-R	2	9.5	10	47.6	12	57.1
Cyclobond I-DMP	2	9.5	5	23.8	7	33.3
Chiralcel OJ-R	14 ^b	66.7	–	–	14	66.7
Cyclobond I-PT	–	–	3	14.3	3	14.3

^aFor the partially resolved peaks, the resolution on the cellulose derivatives is always much higher than on the cyclodextrin derivatives.

^bAll products are fully baseline resolved ($\beta = 1.00$).

operation fewer products are separated on the cellulose derivatives, although on the Chiralcel® OJ-R column all separated products are fully baseline resolved. The smallest resolution value equals 2.5 while the largest value is greater than 12.5, while under normal phase conditions the highest resolution value observed equals 6.3.

On the cyclodextrin derivatives a few more products are separated but the increase in number is certainly not spectacular. Furthermore, in many cases where partial resolution has been indicated in the table the chromatograms only showed a small deviation in the peak shape, indicating the early beginning of separation.

For a series of products which under comparable experimental conditions are all very well separated on the native cyclodextrin column, the results on the different cyclodextrin and cellulose derivatives using 50 mM triethylamine adjusted to pH 2.5 with sulfuric acid and methanol in a 30–70 volume ratio as mobile phase are illustrated in Figure 10.

Because only one substance of the test series is separated on the Cyclobond-PT column, and most of the products are only partially resolved on the Cyclobond-DMP column, while all these products are perfectly baseline resolved on native cyclodextrine, it is clear that other parameters must play a role in the chiral recognition process on the derivatized phases.

As a general conclusion it can be stated that for the type of substances investigated the derivatized cyclodextrin columns are, in both modes of operation (normal as well as reversed phase), less universally applicable than the corresponding cellulose derivatives.

Hydroxypropyl- β -Cyclodextrin Derivative

A hydroxypropyl- β -cyclodextrin column (experimental phase of the Chromatography Research group of Merck Darmstadt) in the reversed-phase mode of operation has been extensively investigated. The result on this type of material were completely comparable with the data obtained on the native cyclodextrin columns. However, for the whole range of products the degree of separation was in general

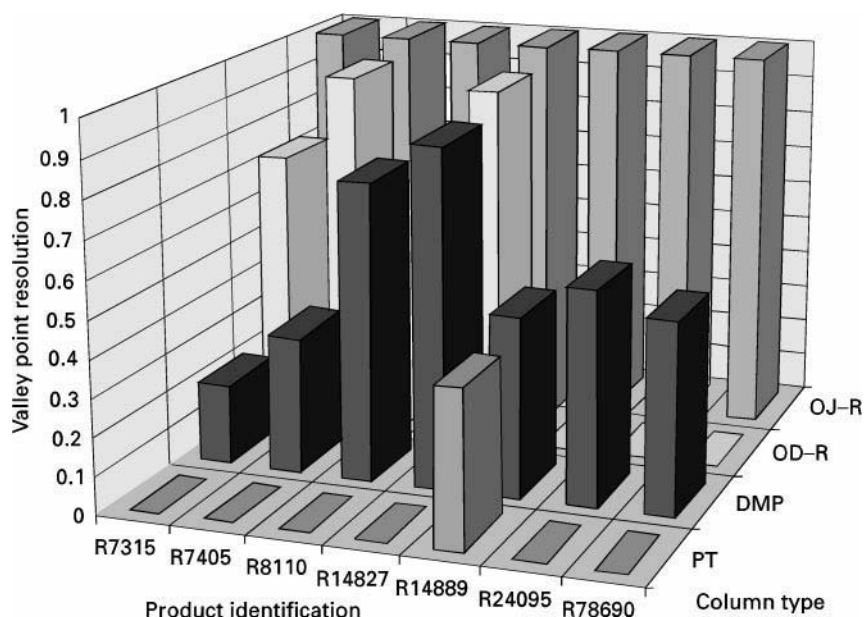


Figure 10 Derivatized cyclodextrin columns versus the corresponding cellulose derivatives. Experimental conditions: column: 250 mm \times 4.6 mm ID (Cyclobond®-DMP, Cyclobond®-PT, Chiralcel® OD-R, Chiralcel® OJ-R); mobile phase: 50 mM triethylamine adjusted to pH 2.5 with sulfuric acid-methanol (30–70, v/v); flow rate: 1 mL min⁻¹.

better on the hydroxypropyl column. To investigate new products, we therefore always start our experiments on a hydroxypropyl- β -cyclodextrin column instead of using the classical native β -cyclodextrin type of material.

γ -Cyclodextrin

A test series of 28 products, which also have been investigated on β -cyclodextrin, have been examined on a γ -cyclodextrin column using a mobile phase consisting of 80 vol% of a 50 mM triethylamine solution in water adjusted to pH 2.5 with sulfuric acid and 20 vol% of methanol. On the β -cyclodextrin column, 22 products were partially or completely resolved. On the γ -derivative only nine products could be resolved.

Compared with the results obtained on the β -cyclodextrin column, it is clear that from a general point of view the γ derivative is less suitable for the separation of the investigated product series. Nevertheless, it remains an additional tool that might help to solve a separation problem when experiments on other types of cyclodextrin columns fail.

Dynamically Generated Cyclodextrin Phases

Instead of using the commercially available chemically bonded cyclodextrin phases, it is also possible to perform enantiomer separations on a reversed-phase column after addition of cyclodextrin or cyclodextrin derivatives to the mobile phase. A number of experiments have been performed with hydroxypropyl- β -cyclodextrin as mobile phase additive. This derivative was initially chosen because it is readily soluble in water.

To investigate the possibilities of a dynamically generated cyclodextrin phase, a test series of 22 products was examined on three different types of reversed-phase packing material. RP Select B (Merck), Hypersil BDS (Shandon) and Aluspher RP Select B (Merck) were selected as stationary phases. An aqueous solution containing 50 mM triethylamine and 50 mM of hydroxypropyl- β -cyclodextrin adjusted to pH 3 with sulfuric acid combined with methanol in an 80–20 volume ratio was used as the mobile phase.

Compared with the data obtained on a chemically bonded hydroxypropyl- β -cyclodextrin column using the same eluent, the chemically bonded column gives, in general, better results than the dynamically coated reversed-phase materials. Furthermore, alumina as stationary phase matrix seems to be less effective. However, in a few exceptional cases the Aluspher Select B column gives as good or even better results than the silica-based materials.

Cyclodextrin Phases in Preparative Chromatographic Applications

The importance of preparative chromatographic enantiomer separations in industry is continuously growing. Therefore it was very interesting to investigate the usefulness of cyclodextrin phases in preparative chromatographic applications.

On an experimental hydroxypropyl- β -cyclodextrin phase (Merck Darmstadt), several products which showed a good resolution on the corresponding analytical material were investigated on a preparative scale. An example of a preparative chromatographic separation is illustrated in Figure 11.

On the hydroxypropyl- β -cyclodextrin phase, in general a loading capacity of 2 mg g^{-1} of packing material was used. However, in some other cases we were able to load up to 4 mg of product per gram of stationary phase, which from a preparative chromatographic point of view certainly can be considered as a reasonable value for this type of application.

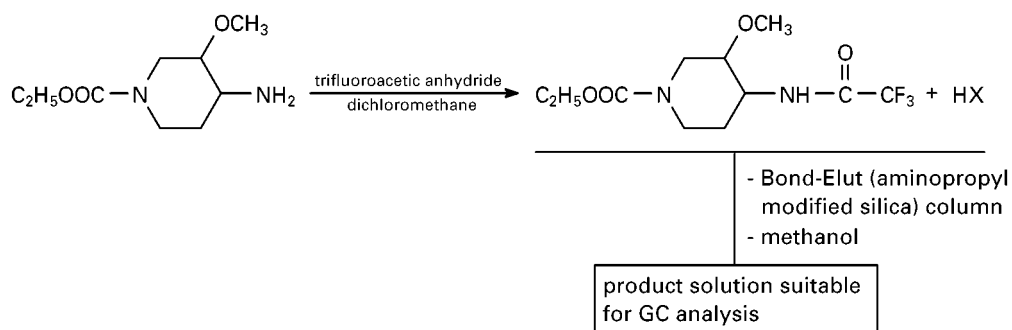
Cyclodextrins as Stationary Phases in Gas Chromatography

For the preparation of cyclodextrin-based capillary columns for gas chromatographic applications, two complementary methods have been developed and are commercially used. In the first method, alkylated cyclodextrins are diluted with polysiloxanes and immobilized on the inside wall of a fused silica capillary. In the other method, pentyl and hydroxyalkyldimethylcyclodextrins are coated on the inside wall of a fused silica capillary. Different well-known chromatography companies offer cyclodextrin-based capillary columns:

- Chrompack: diluted cyclodextrins;
- Macherey-Nagel: undiluted n-pentylated or acylated cyclodextrins;
- Advanced Separation Technologies: a broad variety of undiluted cyclodextrin derivatives (permethylated, hydroxypropyl, trifluoroacylated, butyrylated, dialkylated).

Different types of compounds (amines, epoxides, alkanes, alcohols, lactones, sugars, etc.) can be separated on cyclodextrin-based capillary columns.

The usefulness of these materials is illustrated by means of the separation of the four isomers of a piperidine derivative. Gas chromatography on cyclodextrin-based columns was tried after acetylation with trifluoroacetic anhydride using the following procedure:



An advantage of this derivatization procedure was that all types of salts (used to investigate the possibilities of diastereomeric salt formation as a stereoselective synthesis method) could be acylated without prior liberation of the free base.

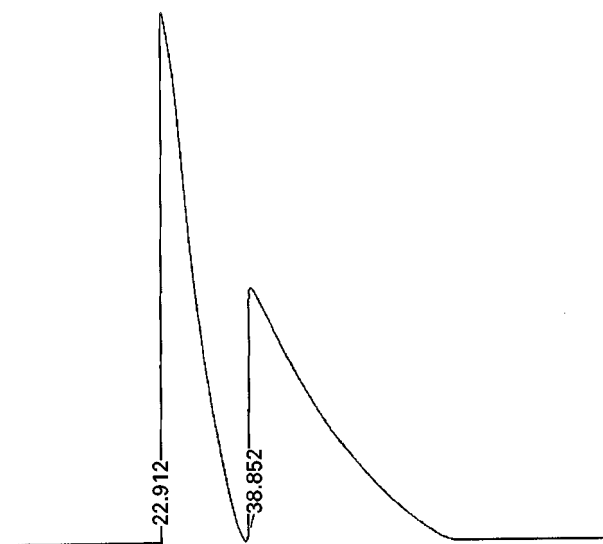
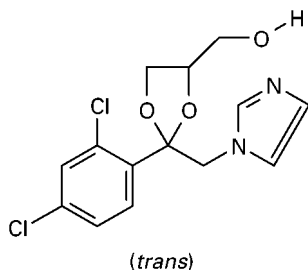


Figure 11 Preparative chromatographic separation on a β -cyclodextrin columns. Experimental condition: column: 80 mm ID dynamic axial compression column (Prochrom); stationary phase: 500 g 10 μm chemically bonded hydroxypropyl- β -cyclodextrin (experimental phase Merck Darmstadt; packing pressure 80 bar; mobile phase: 50 mM triethylamine adjusted with 50 mM sulfuric acid to pH 2.5–methanol (80–20, v/v); flow rate: 150 mL min⁻¹; detection: UV, wavelength 220 nm, range 2.56 AUFS; sample size: 1 g dissolved in 50 mL of concentrated sulfuric acid; solute:



The first experiments were done on a 15 m \times 0.32 mm ID Chiralsil-Dex[®] column (Chrompack). On this type of column, it was only possible to separate the *cis* and *trans* isomers.

Thereafter, chromatographic experiments were performed on four different cyclodextrin phases from Advanced Separation Technologies:

- ChiralDEX[®] B-PH: (*S*)-2-hydroxypropyl permethylated β -cyclodextrin;
- ChiralDEX[®] B-DA: (2,6-di-*O*-*n*-pentyl)- β -cyclodextrin;
- ChiralDEX[®] B-TA: (2,6-di-*O*-*n*-pentyl-3-*O*-trifluoroacetyl)- β -cyclodextrin;
- ChiralDEX[®] G-TA: (2,6-di-*O*-*n*-pentyl-3-*O*-trifluoroacetyl)- γ -cyclodextrin.

Chromatograms of the different experiments are illustrated in **Figure 12** and **Figure 13**. The largest differentiation between *cis* and *trans* isomers was observed on the permethylated hydroxypropyl- β -cyclodextrin column (ChiralDEX[®] B-PH). However, the best separation of all isomers individually was observed on the trifluoroacetylated β -cyclodextrin column (ChiralDEX[®] B-TA).

Noticeable is the time required to perform an analysis. Compared with the analysis method on the crown ether column, a GC analysis is more than six times faster, although one has to take into account that on the crown ether column the diastereomeric salt could be analysed as such, while for the gas chromatographic method the product has to be derivatized prior to chromatography.

Cyclodextrins in Capillary Electrophoresis

In the pharmaceutical industry the importance of capillary electrophoresis is continuously growing. It is a technique which is increasingly used for determination of the optical purity of intermediates and final products. Many different optically pure compounds

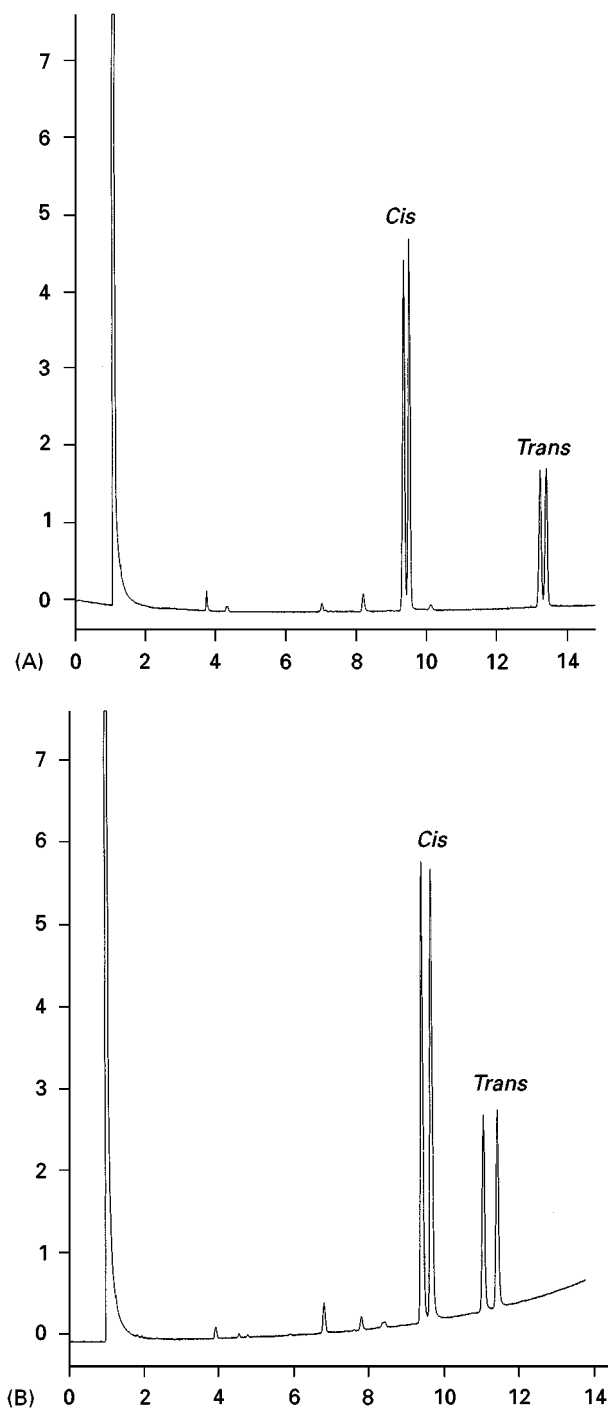


Figure 12 Capillary GC analysis on cyclodextrin stationary phases. Experimental conditions: column: (A) 15 m \times 0.32 mm ID Chiraldex® B-PH ((*S*)-hydroxypropyl- β -cyclodextrin (Astec)); (B) 15 m \times 0.32 mm ID Chiraldex® B-DA (dipentylated β -cyclodextrin (Astec)); carrier gas: helium (linear velocity 25 cm s⁻¹); temperatures: column 150–200°C (3°C min⁻¹), injector 210°C, detector 210°C; detection: FID; injection: 1 μ L split (split ratio 1/100).

can be used to generate the required chiral environment. Cyclodextrins of course are also very suitable as an electrolyte additive.

The different types of cyclodextrins, which are most frequently used are:

- α -cyclodextrin;
- β -cyclodextrin;
- γ -cyclodextrin;
- (2-hydroxy)propylated β -cyclodextrin;
- (2-hydroxy)propylated γ -cyclodextrin;
- Heptakis (2,6-di-*O*-methyl) β -cyclodextrin;
- Heptakis (2,3,6-tri-*O*-methyl) β -cyclodextrin;
- carboxymethylated β -cyclodextrin.

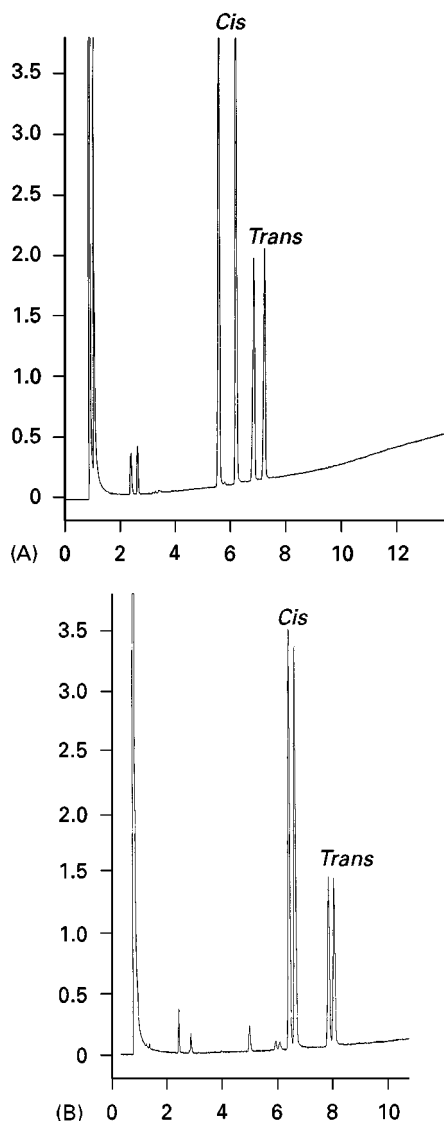


Figure 13 Capillary GC analysis on cyclodextrin stationary phases. Experimental conditions: column: (A) 15 m \times 0.32 mm ID Chiraldex® B-TA (trifluoroacetyl- β -cyclodextrin (Astec)); (B) 15 m \times 0.32 mm ID Chiraldex® G-TA (trifluoroacetyl- γ -cyclodextrin (Astec)); carrier gas: helium (linear velocity 25 cm s⁻¹); temperatures: column 150–200°C (2°C min⁻¹), injector 210°C, detector 210°C; detection: FID; injection: 1 μ L split (split ratio 1/100).

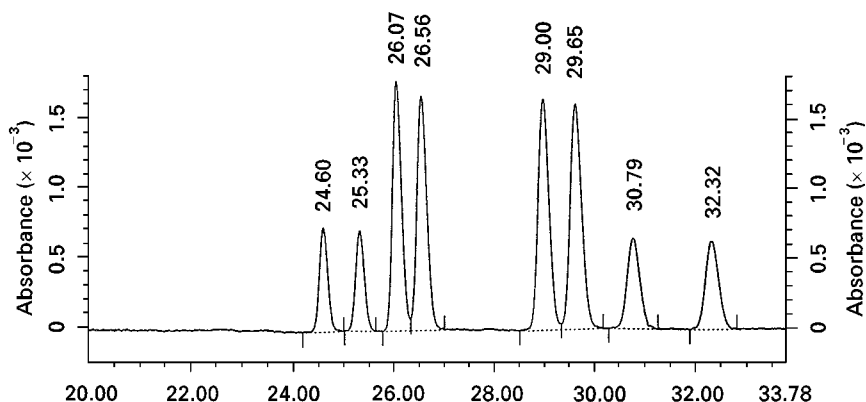


Figure 14 Capillary electrophoresis using a derivatized cyclodextrin as electrolyte additive. Experimental conditions: equipment: P/Ace system 5500 (Beckman); capillary: 50 μm ID uncoated fused silica; total length: 57 cm; length to detector: 50 cm; electrolyte: 20 mM Heptakis (2,3,6-tri-*O*-methyl) β -cyclodextrin 10 mM disodium hydrogen phosphate solution adjusted to pH 2.2 with phosphoric acid; analysis: temperature 25°C, voltage + 20 kV, inject sample 2 s, detection UV (220 nm).

The usefulness of cyclodextrins as an electrolyte additive is illustrated in the following example. A substance containing three optical centres, which means eight possible isomers, had to be separated. HPLC experiments on different types of chiral stationary phases did not succeed in a complete resolution of the mixture. The result of a capillary electrophoresis experiment using Heptakis (2,3,6-tri-*O*-methyl) β -cyclodextrin as electrolyte additive is illustrated in Figure 14.

Compared with HPLC, in capillary electrophoresis many more parameters can be varied to improve separation. Therefore, most of the methods developed on one of the commonly used chiral stationary phases can be replaced by a capillary electrophoresis methods, using cyclodextrins or another chiral auxiliary as electrolyte additive.

See also: II/Chromatography: Liquid: Ion Pair Liquid Chromatography; Mechanisms: Chiral; III/Chiral Separations: Amino Acids and Derivatives; Capillary Electrophoresis; Cellulose and Cellulose Derived Phases; Chiral Derivatization; Gas Chromatography; Ion-Pair Chromatography; Ligand Exchange Chromatography; Liquid Chromatography; Molecular Imprints as Stationary Phases; Protein Stationary Phases; Synthetic Multiple

Interaction ('Pirkle') Stationary Phases; Thin-Layer (Planar) Chromatography.

Further Reading

- Allenmark S (1991) *Chromatographic Enantioseparations, Methods and Applications*. London: Ellis Horwood.
- Beesley TE and Scott RPW (1998) *Chiral Chromatography*. Chichester: Wiley.
- Bender ML and Komiyama M (1978) *Cyclodextrin Chemistry*. Berlin: Springer.
- Chiraldex GC Handbook*, 5th edn (1996) Whippany, NJ: Advanced Separation Technologies.
- Coventry L (1989) Cyclodextrin inclusion complexation. In Lough WJ (ed.) *Chiral Liquid Chromatography*. Glasgow: Blackie.
- Cyclobond Handbook* (1996) Whippany, NJ: Advanced Separation Technologies.
- Han SM and Armstrong DW (1989) Separation of enantiomers and other isomers with cyclodextrin-bonded phases: rules for chiral recognition. In Krstulović (ed.) *Chiral Separations by HPLC, Applications to Pharmaceutical Compounds*, pp. 208–286. Chichester: Ellis Horwood.
- Hinze WL (1981) In: van Oss CJ (ed.) *Separation and Purification Methods*, vol. 10, p. 159.
- Kaiser R (1965) *Chromatographie in der Gasphase I*. Mannheim: Bibliographisches Institut.

Gas Chromatography

V. Schurig, University of Tübingen, Germany

Copyright © 2000 Academic Press

Introduction

The separation of enantiomers (optical isomers) by capillary gas chromatography on a chiral stationary

phase (CSP) was discovered by Gil-Av and co-workers at the Weizmann Institute of Science, Israel, in 1966. At the outset of this work, according to Gil-Av,

this topic was in a 'state of frustration'. Nobody believed it could be done. In fact, people were

convinced that there could not possibly be a large enough difference in the interaction between the D- and L-solute with an asymmetric solvent. This was the feeling people had, even those known as unorthodox thinkers. This view had also some experimental basis, because a number of communications had been published, in which it was claimed that such resolutions could be effected, but nobody was able to reproduce these results, and some of them were shown to be definitely wrong.

Today, almost a reversal of this situation exists. According to the *GC Chirbase data bank*, for most volatile racemic compounds of a variety of different chemical classes, ranging from apolar to polar, an appropriate CSP is available and 22 200 chiral separations by gas chromatography (GC) of 7637 analytes on 684 CSPs (120 are commercialized) have been reported up to the end of 1997.

Three principal CSPs are currently employed; these undergo hydrogen bonding, coordination and inclusion. Modified α -, β - and γ -cyclodextrins have proved to be the most versatile and universal CSPs in GC. Anchoring the CSPs to a polysiloxane backbone leads to Chirasil-type stationary phases with improved temperature stability, efficiency and robustness. Immobilization of Chirasil-type stationary phases on the inner column wall furnishes chemically bonded CSPs. Because of the high efficiency, sensitivity and speed, chiral separation by high resolution capillary GC represents a versatile and attractive method for enantiomer analysis. However the prerequisites of the method, i.e. volatility, thermal stability and resolvability of the chiral analytes, restrict its universal use.

The main application of chiral separations by GC is concerned with the precise determination of enantiomeric compositions of chiral research chemicals, intermediates, auxiliaries, metabolites, precursors, drugs, pesticides, fungicides, herbicides, pheromones, flavours and fragrances. As the insight into chirality-activity relationships steadily improves and, as a consequence, legislation on chiral compounds becomes more stringent, the development of reliable methods for the determination of the enantiomeric excess up to 99.9% is of great importance (% enantiomeric excess = $100(R - S)/(R + S)$, where R is the major enantiomer and S the minor enantiomer). This goal is readily met by enantioselective GC.

Methodology

The separation of enantiomers by GC can be performed in two modes.

1. *Indirect method.* Enantiomers are converted off-column into diastereomeric derivatives by chem-

ical reaction with an enantiomerically pure resolving agent and subsequent gas chromatographic separation of the diastereomers is achieved using a conventional achiral stationary phase.

2. *Direct method.* Gas chromatographic separation of the enantiomers is achieved using a chiral stationary phase (CSP) containing a resolving agent of high (but not necessarily 100%) enantiomeric purity.

While the first method entails the formation of diastereomers before separation, the second involves the rapid and reversible diastereomeric association between the CSP (selector) and the racemic, or non-racemic, analyte (selectand). Since diastereomers display different physical properties, discrimination by incomplete recovery, decomposition and losses may occur during work-up, isolation and sample handling in method (1). Also the detector response can be, in principle, different for diastereomers. Because an achiral detection device does not discriminate between enantiomers, the comparison of relative peak areas employing method (2) provides a direct measure of the enantiomeric composition, provided the detector response is linear over a wide concentration range. Consequently, method (2) is preferred for the determination of enantiomeric excess. This approach requires an efficient selector-selectand system displaying chiral recognition.

Enantioselectivity is governed by the biased diastereomeric association between the enantiomers of the selectand and the chiral selector. Fortunately, by employing capillary columns, efficiency is mostly high enough to resolve racemates having a difference of the Gibbs free energy of diastereomeric association as little as $-\Delta_{R,S}(\Delta G) = 0.025 \text{ kJ mol}^{-1}$ (at 25°C), corresponding to a separation factor, α , of 1.01 ($\alpha = k_R/k_S$, with k = the retention factor and the subscript R referring to the second eluted enantiomer and S to the first eluted enantiomer). The measured enantiomeric composition of the analyte determined by method (2) is independent of the enantiomeric purity of the CSP. Lowering the enantiomeric purity of the CSP, however, results in a decrease of α and it is unity when the chiral selector in the stationary phase is racemic. Method (2) is especially useful for the determination of enantiomeric excess when no sample derivatization is required. Owing to the enormous separation power of capillary GC, contaminants and impurities are usually separated from the enantiomers and the simultaneous analysis of the enantiomers of different compounds (e.g. all proteinogenic amino acids) is feasible in one analytical run (cf. Figure 1).

Temperature programming and established ancillary techniques such as multidimensional chromatography

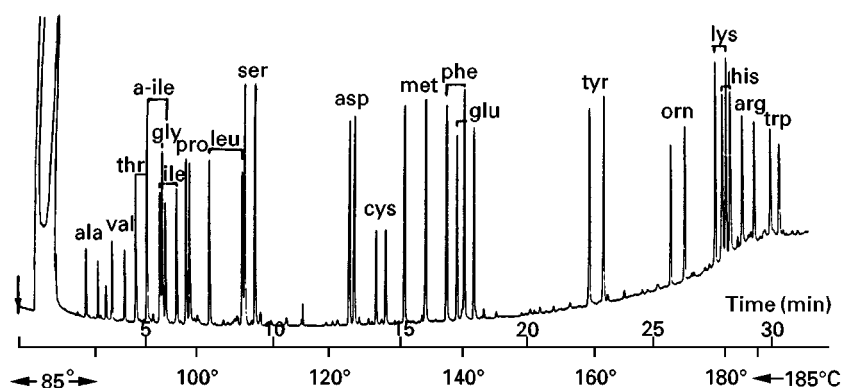


Figure 1 Simultaneous enantiomer separation of 20 proteinogenic amino acids as *N*, *O*, *S*-pentafluoropropanoate-isopropylester (histidine as *N*^m-ethoxycarbonyl) derivatives by GC on Chirasil-Val [IV] between 85 and 185°C at 0.35 bar (gauge) hydrogen. Column, 50 m × 0.27 mm (i.d.) glass capillary. D-Enantiomers are eluted before L-enantiomers. (From Bayer E (1983) Chiral recognition of natural products on optically active polysiloxanes. *Zeitschrift für Naturforschung* 38b: 1281–1291.)

and the use of interfacing and coupling methods can readily be adapted to chiral separations. Sensitivity can be extended to the picogram level by electron capture detection or by the combination of gas chromatography with mass spectrometry (GC-MS). GC-MS-selected ion monitoring (SIM) can detect trace amounts of enantiomers in complex matrices.

When the racemate is highly volatile and the chiral separation factor is large ($\alpha > 1.3$), preparative enantiomer separation by GC with packed columns is possible. The development of simulated moving bed (SMB) approaches can be expected in the future. Semipreparative separations can already be carried out at low α values. Recovery from the gaseous carrier is straightforward and pure enantiomers can be obtained even on enantiomerically impure CSPs. For analytical purposes it may be important to differentiate a separation of a chiral compound into enantiomers from the common separation of two achiral analytes. A racemate, when resolved, should produce an exact 1 : 1 peak ratio of the enantiomers. Clearly, only one peak (peak coalescence, $\alpha = 1$) is expected when the racemic CSP is employed. When two CSPs of opposite configurations are applied in different columns, peak inversion (peak switching) can be observed for a chiral analyte in which one enantiomer is in excess.

Classification of Chiral Stationary Phases

Enantiomer separation by GC is mainly performed on three types of CSPs:

- chiral amino acid derivatives via hydrogen bonding;

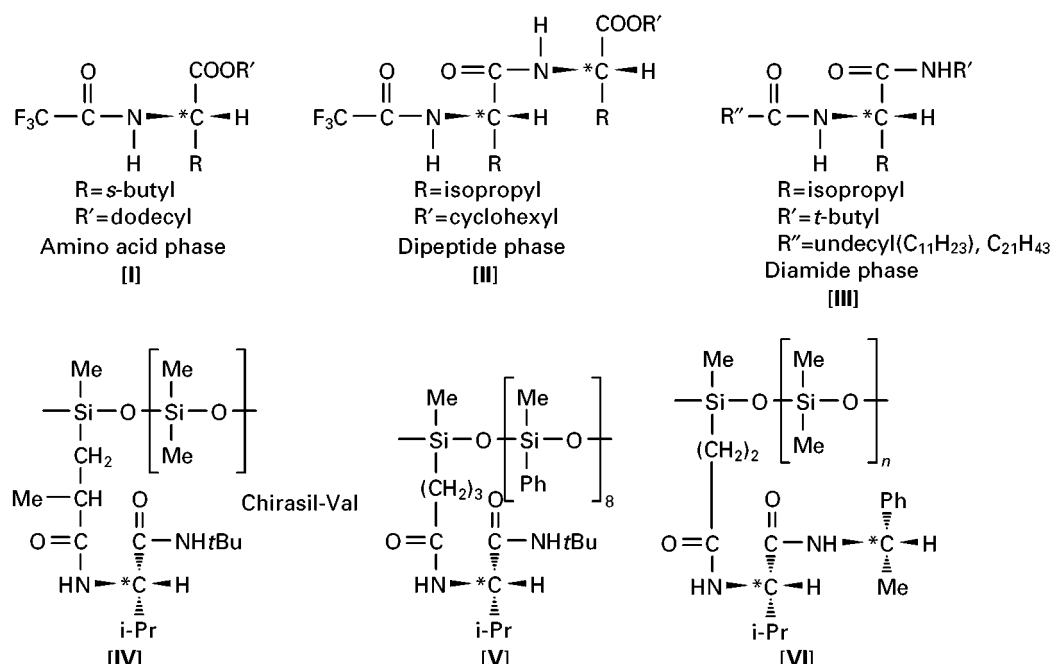
- chiral metal chelates via coordination (complexation GC);
- cyclodextrin derivatives via inclusion.

Initially, the chiral selectors were used as involatile neat liquids or as solutions in squalane or polysiloxanes, respectively. Subsequently, a number of chiral selectors have been chemically linked to polysiloxanes (Chirasil-type stationary phases).

Chiral Stationary Phases Based on Hydrogen Bonding

The first successful separation of racemic *N*-trifluoroacetyl amino acid alkyl esters on glass capillary columns coated with involatile *N*-trifluoroacetyl-L-isoleucine lauryl ester [I] (cf. **Scheme 1**) was achieved by Gil-Av and co-workers in 1966 and a semipreparative version of this method was reported later. Since then the great potential of this fundamental approach has stimulated continuing research on enantiomer separation not only by GC, but also by other chromatographic techniques such as HPLC.

It was recognized that in the dipeptide phase [II] (cf. **Scheme 1**) the C-terminal amino acid was not essential to chiral recognition while the additional amide function was important for additional hydrogen bonding. The second chiral centre was therefore sacrificed by preparing the diamide [III], e.g. derived from valine. This chiral selector was subsequently coupled via the amino function to a statistical copolymer of dimethylsiloxane and (2-carboxypropyl)methylsiloxane. The resulting polymeric CSP, Chirasil-Val [IV], combining enantioselectivity and efficiency of silicones, exhibits excellent GC properties for the enantiomer separation of chiral compounds undergoing hydrogen bonding. Chirasil-Val [IV] is commercially available in both enantiomeric



Scheme 1 Hydrogen-bonding-type chiral stationary phases.

forms. The temperature-programmed simultaneous enantiomer separation of all proteinogenic amino acids in less than 25 min is illustrated in Figure 1. A straightforward approach to polymeric CSPs is based on the modification of cyanoalkyl-substituted polysiloxanes (XE-60, OV-225). For instance the diamide **[III]** was chemically linked to the polysiloxane to give (L)-**[V]**. The diastereomeric selectors (L, R, and L, S)-**[VI]** contain two chiral centres that enhance enantioselectivity (matched case) or compensate enantioselectivity (mismatched case).

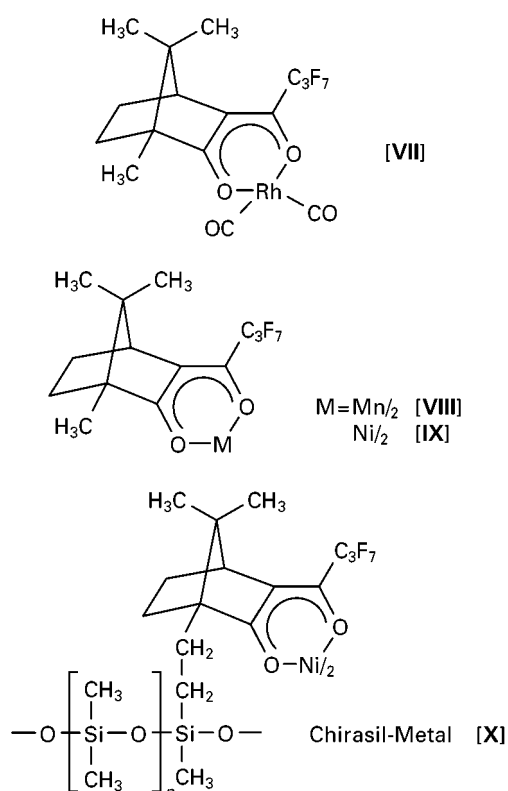
Enantiomer separation by hydrogen-bonding CSPs generally requires derivatization of the analyte in order to increase volatility and/or to introduce suitable functions for additional hydrogen-bonding association.

Chiral Stationary Phases Based on Coordination

The chiral metal coordination compound dicarbonyl-rhodium(I)-3-trifluoroacetyl-(1*R*)-camphorate **[VII]** (cf. **Scheme 2**) was used for the enantiomeric separation of the chiral olefin 3-methylcyclopentene by complexation GC in 1977. The scope of enantiomer separation by complexation GC was later extended to oxygen-, nitrogen- and sulfur-functionalized compounds using chiral ketoenolate-*bis*-chelates of, among others, manganese(II) and nickel(II) ions derived from terpene ketones such as camphor **[VIII, IX]**, menthone, carvone, pulegone, and others after perfluoroacylation.

Figure 2 illustrates the enantiomer separation by complexation GC of simple aliphatic oxiranes,

belonging to the smallest chiral molecules. A limiting factor of coordination-type CSPs **[VIII, IX]** is the low temperature range of operation (25–120°C). The thermal stability has been increased by the



Scheme 2 Coordination-type chiral stationary phases.

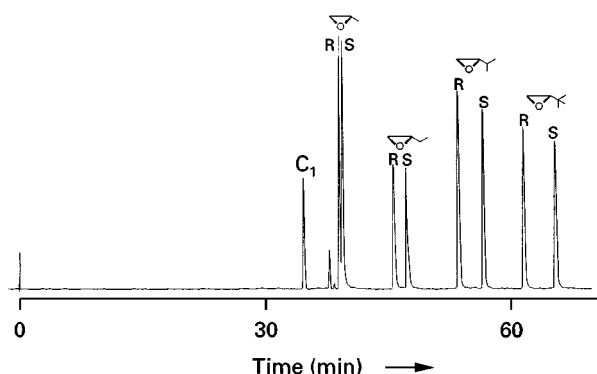


Figure 2 Enantiomer separation of monoalkyl-substituted oxiranes by complexation GC on manganese (II) bis[3-(heptafluorobutanoyl)-(1*R*)-camphorate] [IX] (0.05 molal in squalane) at 60°C. C_1 = Methane. Column, 160 m \times 0.4 mm (i.d.) stainless steel capillary. (From Schurig V and Weber R (1981) *Journal of Chromatography* 217: 51–70.)

preparation of immobilized polymeric CSPs (Chirasil-Metal; [X] in Scheme 2). In Figure 3 the GC enantiomer separation of homofuran at 95°C on Chirasil-Nickel [X] is shown.

Chiral Stationary Phases Based on Inclusion

The first enantiomer separation using an inclusion-type CSP in GC was reported in 1983 for α - and β -pinene and *cis*- and *trans*-pinane on packed columns containing native α -cyclodextrin in formamide. Later it was recognized that alkylated cyclodextrins

(CDs) can be employed in high resolution capillary columns for enantiomer analysis. Thus, neat permethylated β -cyclodextrin, [XI] (cf. Scheme 3), was used above its melting point and in a supercooled state. Per-*n*-pentylated and 3-acyl-2,6-*n*-pentylated CDs are liquids at room temperature. The CD derivatives, [XIII]–[XVII], have been used in the undiluted form for the separation of enantiomers of many classes of compounds on deactivated Pyrex glass capillary columns. The more polar CD derivatives, [XX]–[XXIII], have been coated on fused silica capillary columns.

To combine the enantioselectivity of CDs with the excellent coating properties and efficiency of polysiloxanes, alkylated CDs have been preferentially dissolved in moderately polar polysiloxanes (silicones) such as OV-1701. Thus, the CD derivatives can be employed for GC enantiomer separation irrespective of their melting point and phase transitions. The simultaneous separation of a test mixture of enantiomers of different classes of compounds is depicted in Figure 4.

The presence of three hydroxyl groups that can be regioselectively alkylated and acylated offers an enormous number of possible α -, β - and γ -cyclodextrin derivatives, which are not always readily accessible and may require tedious purification steps. Occasionally, CD derivatives such as octakis(3-*O*-butanoyl-2,6-di-*O*-*n*-pentyl)- γ -cyclodextrin [XVII] are highly enantioselective for the GC enantiomer

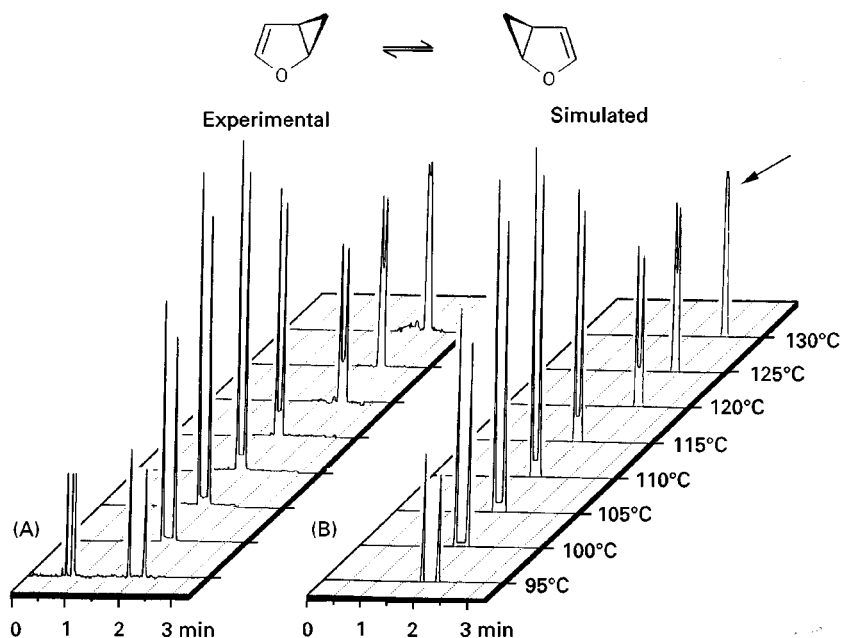


Figure 3 Enantiomer separation of homofuran at 95°C and transient elution profiles at higher temperatures on Chirasil-Nickel [X]. (A) Experimental gas chromatograms (column 10 m \times 0.1 mm (i.d.) fused silica capillary; film thickness, 0.25 μ m). (B) Simulated chromatograms. (From Schurig V, Jung M, Schleimer M and Klärner F-G (1992) *Chem. Ber.* 125: 1301–1303.)

Heptakis(2,3,6-tri- <i>O</i> -methyl)- β -cyclodextrin	[XI]
Heptakis(2,6-di- <i>O</i> -methyl-3- <i>O</i> -trifluoroacetyl)- β -cyclodextrin	[XII]
Hexakis(2,3,6-tri- <i>O</i> - <i>n</i> -pentyl)- α -cyclodextrin (Lipodex A)	[XIII]
Hexakis(3- <i>O</i> -acetyl-2,6-di- <i>O</i> - <i>n</i> -pentyl)- α -cyclodextrin (Lipodex B)	[XIV]
Heptakis(2,3,6-tri- <i>O</i> - <i>n</i> -pentyl)- β -cyclodextrin (Lipodex C)	[XV]
Heptakis(3- <i>O</i> -acetyl-2,6-di- <i>O</i> - <i>n</i> -pentyl)- β -cyclodextrin (Lipodex D)	[XVI]
Octakis(3- <i>O</i> -butanoyl-2,6-di- <i>O</i> - <i>n</i> -pentyl)- γ -cyclodextrin (Lipodex E)	[XVII]
Hepatakis(2,3-di- <i>O</i> -acetyl-6- <i>O</i> - <i>t</i> -butyldimethylsilyl)- β -cyclodextrin	[XVIII]
Hepatakis(6- <i>O</i> - <i>t</i> -butyldimethylsilyl-2,3-di- <i>O</i> -methyl)- β -cyclodextrin	[XIX]
Heptakis(<i>O</i> -(<i>S</i> -2-hydroxypropyl)-per- <i>O</i> -methyl)- β -cyclodextrin (PMHP- β -CD, mixture)	[XX]
Hexakis(2,6-di- <i>O</i> - <i>n</i> -pentyl)- α -cyclodextrin (Dipentyl- α -CD)	[XXI]
Heptakis(2,6-di- <i>O</i> - <i>n</i> -pentyl)- β -cyclodextrin (Dipentyl- β -CD)	[XXII]
Heptakis(3- <i>O</i> -trifluoroacetyl-2,6-di- <i>O</i> - <i>n</i> -pentyl)- β -cyclodextrin (DPTFA- β -CD)	[XXIII]

Scheme 3 Cyclodextrin-type chiral stationary phases.

separation of certain racemates (cf. Figure 5). Also derivatives containing the bulky butyldimethylsilyl substituent at the lower rim of the CD ([XVIII] and [XIX]) represent useful complementary CSPs.

A superior class of CSP has been obtained by chemically linking the CD derivatives to the polysiloxane backbone furnishing Chirasil-Dex [XXIV] (cf. Scheme 4).

Fused silica columns coated with Chirasil-Dex have advantages such as:

- use of a nonpolar polysiloxane matrix (in which CD derivatives cannot be physically diluted) resulting in low elution temperatures for polar analytes;
- high degree of inertness allowing analysis of polar compounds without prior derivatization;
- higher CD concentration resulting in increased separation factors;

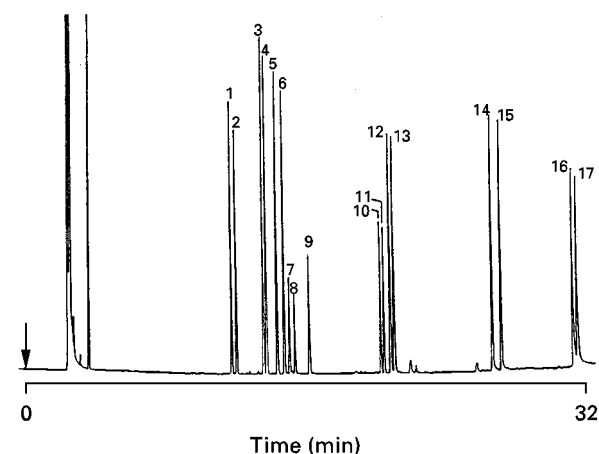


Figure 4 Enantiomer separation of the test mixture α -pinene (1, 2), *trans*-pinane (3, 4), *cis*-pinane (5, 6), 2,3-butanediol (rac) (7, 8), 2,3-butanediol (*meso*) (9), γ -valerolactone (10, 11), 1-phenylethylamine (12, 13), 1-phenylethanol (14, 15) and 2-ethylhexanoic acid (16, 17) by GC on heptakis(2,3,6-tri-*O*-methyl)- β -cyclodextrin [XI] (10% (w/w) in OV-1701) at 50°C and 0.7 bar (gauge) helium. Column, 50 m \times 0.25 mm (i.d.) fused silica capillary; film thickness, 0.25 μ m. (Courtesy Chrompack International, Middelburg, The Netherlands.)

- long-term stability with absence of droplet formation leading to loss of efficiency;
- immobilization by crosslinking and/or surface bonding;
- compatibility with all injection techniques.

The rationalization of chiral recognition involving CD derivatives is difficult since almost all classes of chiral compounds, ranging from apolar to highly polar, are susceptible to enantiomer separation on a certain CD-derived CSP, often with no logical dependence on molecular shape, size and functionalities of the selectand and the selector (α , β , γ). Clearly, multimodal recognition processes are important which

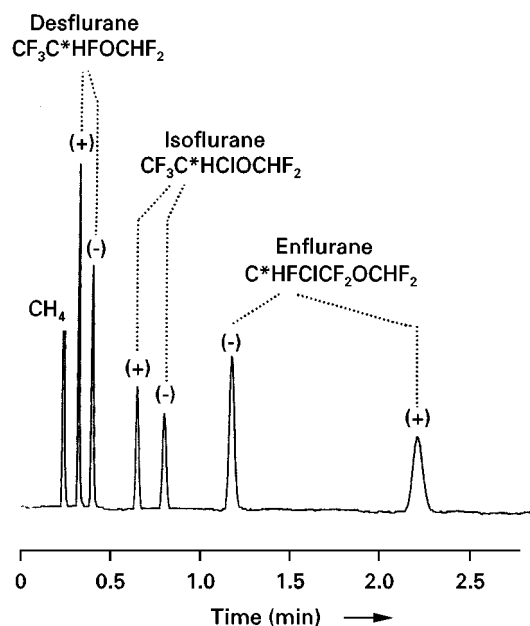
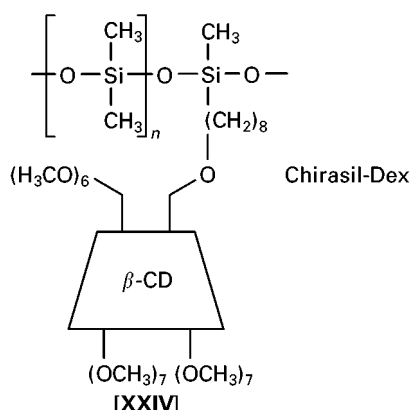


Figure 5 Enantiomer separation of the inhalation anaesthetics desflurane, isoflurane and enflurane by GC on immobilized polysiloxane-bonded octakis(3-*O*-butanoyl-2,6-di-*O*-*n*-pentyl)- γ -cyclodextrin [XVIII] at 28°C. Column, 10 m \times 0.25 mm (i.d.) fused silica capillary; film thickness, 0.18 μ m. (From Grosenick H and Schurig V (1997) *Journal of Chromatography A* 761: 181–193.)



Scheme 4 Chirasil-Dex-type chiral stationary phase.

may involve inclusion, hydrogen bonding, dipole-dipole interactions and dispersion forces. Since enantiomer separations have also been observed with per-*n*-pentylated amylose, inclusion may not be a prerequisite for chiral recognition using CDs. Mechanistic investigations, some of which include molecular modelling studies, have been carried out although no clear-cut rationale for chiral recognition has emerged thus far.

Thermodynamics of Enantiomer Separation

Enantiomer separation by GC is brought about by the difference in the Gibbs free energy $-\Delta_{R,S}(\Delta G)$ of the diastereomeric association equilibria between the enantiomers (selectand) and the CSP (selector). An important prerequisite is a fast and reversible association equilibrium (fast kinetics). The chemical association equilibria in the stationary phase are described by K_R and K_S , with R referring to the second eluted enantiomer and S to the first eluted enantiomer. For enantiomer separation, the Gibbs-Helmholtz equation [1] applies, where R is the universal gas constant, T is the temperature (K), H is the enthalpy and S is the entropy.

$$-\Delta_{R,S}(\Delta G) = RT \ln \frac{K_R}{K_S} = -\Delta_{R,S}(\Delta H) + T \Delta_{R,S}(\Delta S) \quad [1]$$

For a 1:1 molecular association, the quantities $\Delta_{R,S}(\Delta S)$ and $\Delta_{R,S}(\Delta H)$ display an opposing effect on $-\Delta_{R,S}(\Delta G)$. At the isoenantioselective temperature T_{iso} , given by eqn [2], peak coalescence (second kind) occurs ($\Delta_{R,S}(\Delta G) = 0$, $K_R = K_S$; no enantiomer separation).

$$T_{iso} = \frac{\Delta_{R,S}(\Delta H)}{\Delta_{R,S}(\Delta S)} \quad [2]$$

Above T_{iso} the sign of enantioselectivity changes, leading to peak inversion (second kind). Below the coalescence temperature, the sign of enantioselectivity $\Delta_{R,S}(\Delta G)$ is governed by $-\Delta_{R,S}(\Delta H)$ and above it, by $\Delta_{R,S}(\Delta S)$. A rare example of the temperature-dependent reversal of enantioselectivity in GC enantiomer separation on a single CSP is demonstrated in Figure 6. Usually, even at high temperatures, enantioselectivity is dominated by enthalpy control and separation factors increase with decreasing temperature. Therefore, it is recommended that the lowest possible temperature is used for enantiomer separation by GC.

For undiluted CSPs the quantity $-\Delta_{R,S}(\Delta G)$ can easily be obtained from the separation factor α_{undil} ,

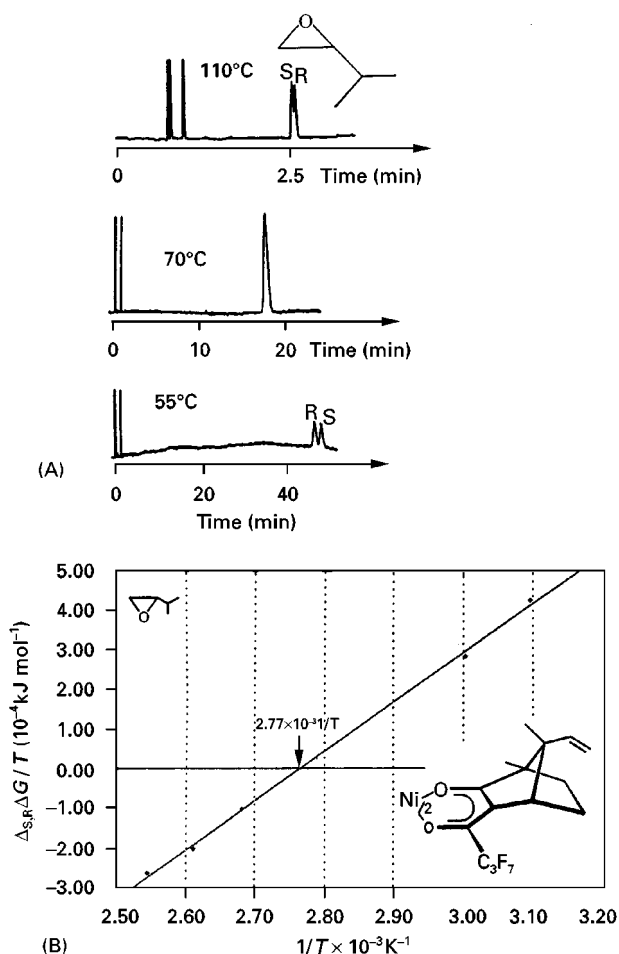


Figure 6 (A) Temperature-dependent peak inversion (second kind) at 55 and 110°C and peak coalescence (second kind) at 70°C during GC enantiomer separation of isopropylloxirane on nickel (II) bis[3-(heptafluorobutanoyl)-(1*R*)-8-methylene-camphorate] (a derivative of [IX]) (0.126 molal in OV-101). Column, 22 m × 0.25 mm (i.d.) glass capillary. (B) Linear van't Hoff plot and determination of T_{iso} . (From Schurig V (1997) In: Jinno K (ed.) *Chromatographic Separations Based on Molecular Recognition*, ch. 7, pp. 371–418. New York: Wiley-VCH.)

according to eqn [3].

$$-\Delta_{R,S}(\Delta G) = RT \ln \alpha_{\text{undil}} \quad [3]$$

Although it is occasionally used, eqn [3] is not valid for diluted CSPs because α_{dil} is concentration dependent.

Enantiomerization

The configurational integrity of the enantiomers during the GC process of separation is essential for a correct enantiomer analysis. When enantiomers invert the configuration (or conformation) during separation, transient elution profiles are obtained that are characterized by plateau formation between the terminal peaks of the enantiomers. The barrier of enantiomerization (ΔG^\ddagger) can be determined by dynamic GC via peak form analysis of interconversion profiles and the comparison of experimental and simulated chromatograms (cf. Figure 2). Only minute amounts of the easily available racemic compound are required. If enantiomerization is fast within the chromatographic timescale, peak coalescence (third kind) occurs (cf. Figure 2 at 130°C).

Another on-column method for determining interconversion kinetics is based on the 'stopped-flow' technique. In the first part of the column enantiomers are quantitatively separated. Afterwards, the flow is stopped and the column is heated, whereby enantiomerization in the separated fractions commences. After cooling, the flow is restored and the enantiomerized fractions are separated in the second part of the column. From the reaction time and enantiomeric compositions the rate constant can be calculated. Using a combination of three columns, i.e. a separation column, an empty reactor column and another separation column, connected via switching valves for peak-cutting, enantiomerization can be carried out in the gas phase and in the absence of the CSP in the reactor column (enantioselective multidimensional stopped-flow GC).

Assignment of Absolute Configurations by Enantioselective GC

The determination of absolute configurations of chiral analytes is an important task in enantiomer analysis. Absolute configurations of minute amounts of chiral samples may be determined directly, and free of chiroptical evidence, by GC via co-injection of reference compounds with known stereochemistry. Absolute configurations may also be predicted indirectly by empirical rules that correlate the absolute

configuration and the order of elution for enantiomers belonging to homologous series of compounds. Although consistent relationships between the order of elution and absolute configuration of congeners have been observed in many instances, remarkable inconsistencies are also known. As a rule, such comparisons, if any, should be restricted to measurements at the same temperature since peak inversion (second kind) may occur at different temperatures as the result of enthalpy versus entropy compensation or multimodal chiral recognition mechanisms. Therefore, the assignment of absolute configurations by GC can be ambiguous.

Method of Enantiomer Labelling

Enantiomers can be quantified in complex matrices when a known amount of the pure enantiomer is added as an internal standard. The pure enantiomer is an ideal internal standard as the enantiomeric excess is not influenced by sample manipulations in diluted systems (achiral derivatization, dilution, injection, detection, chemical and physical losses). The method of enantiomer labelling presupposes the precise knowledge of the enantiomeric excess of the sample and the standards.

Simultaneous enantiomer and isotopic labelling in enantiomer analysis can also be carried in the GC-MS-SIM mode.

Precision and Sources of Error

The precision of enantiomeric excess determined by GC is high over the whole range from 0 (racemic) to 99.9% (nearly enantiomerically pure). At a high enantiomeric excess, the minor enantiomer should preferentially elute as the first peak in order to facilitate correct integration.

Despite the great success of GC for determining enantiomeric excess, potential sources of error should be considered:

- decomposition of the sample during chromatography (the enantiomer which spends a longer time in the column will be lost preferentially, causing an error in enantiomeric excess);
- coelution of impurities accidentally increasing peak areas;
- enantiomerization causing peak distortions (plateau formation);
- peak distortions caused by inadequate instrumentation;
- nonlinear detector response.

In general, the error in enantiomeric excess due to decomposition of the analyte can be reduced if the

difference of the residence time in the column is minimized for both enantiomers. This goal may be realized by using short columns, high pressure drops, elevated temperatures and CSPs exhibiting only small separation factors α . A rather frequent cause for the deviation from the expected 1:1 ratio for the racemic mixture consists of the coelution of impurities. This interference can be recognized by determining the enantiomeric excess on two columns coated with CSPs of opposite chirality. The verification of the ideal 1:1 ratio of a racemic mixture is always recommended in enantiomer analysis by chromatography. It may also be used to test integration devices.

Practical Considerations

The merit of GC enantiomer separation is the great range of resolvable classes of compounds. With a few exceptions, enantiomer separation by GC is characterized by low separation factors α , and, as a (beneficial) consequence, reduced separation times. The use of highly efficient capillary columns is recommended. Chirasil-Val [IV], Chirasil-Dex [XXIV], and most cyclodextrin derivatives, [XI]–[XXIII], coated onto fused silica capillary columns, are commercially available. Factors such as availability, price, performance and reproducibility should guide the analyst when selecting chiral stationary phases for GC. Immobilized chiral stationary phases, such as Chirasil-Dex [XXIV], have the advantage of solvent compatibility, resistance to temperature shock and longevity. Enantiomer separation on Chirasil-type stationary phases can be performed in the usual temperature range 25–220°C. For special applications it is also possible to use cryogenic temperatures down to –20°C.

The dimensions of commercial columns are typically 10–25 m \times 0.25 mm (i.d.) and the film thickness of the chiral stationary phase is 0.25 μ m. Column miniaturization has important merits. Since enantiomer separation represents a binary separation system, the whole elution window required for multi-component mixtures need not be exploited unless enantiomers are detected in complex matrices. With shorter columns, the elution temperature can be decreased, so that the chiral separation factor α is increased in the common enthalpy-controlled region of enantioselectivity. The loss of efficiency is compensated by the gain of selectivity leading to comparable resolution factors R_s . The shorter analysis times increase the sharpness of peaks and hence the detectability of the enantiomers. Recommended are 2 m \times 0.25 mm (i.d.) columns with a film thickness of 0.25 μ m. Further miniaturization via reduction of the

internal diameter of the columns to 0.1 and 0.05 mm (i.d.) requires thinner films of the stationary phase in order to keep the phase ratio constant. The reduced amount of stationary phase decreases the sample capacity. The reduced signal-to-noise ratio may become critical in regard to the precision of the enantiomeric excess determination.

Unfortunately, there is no universal CSP available and column selection is a matter of trial and error. Chirasil-Val [IV], Chirasil-Dex [XXIV] and permethylated β -cyclodextrin dissolved in polysiloxane [XI] represent the most popular CSPs. On a given enantioselective column, the parameters column length, temperature, film thickness, concentration of CSP, mobile phase velocity and their influences on the resolution factor R_s (which is governed by the retention factor k , separation factor α and efficiency N) have to be carefully balanced. Some variables cannot be freely selected when commercial columns are used.

While Chirasil-Val [IV] and Chirasil-Metal [X] are available in both enantiomeric forms, Chirasil-Dex [XXIV] and other modified cyclodextrins, [XI]–[XXIII], occur only in the D form. The strategy of peak inversion (first kind), employed to elute the minor enantiomer as the first peak, is precluded with carbohydrate-based CSPs.

See also: II/Chromatography: Gas: Derivatization. III/Chiral Separations: Chiral Derivatization; Cyclodextrins and Other Inclusion Complexation Approaches; Ion-Pair Chromatography; Ligand Exchange Chromatography; Liquid Chromatography; Supercritical Fluid Chromatography; Synthetic Multiple Interaction ('Pirkle') Stationary Phase.

Further Reading

- Gil-Av E (1975) Present status of enantiomeric analysis by gas chromatography. *Journal of Molecular Evolution* 6: 131–144.
- Helmchen G, Hoffmann RW, Mulzer J and Schaumann E (eds) (1995) *Houben-Weyl*, vol E 21a *Stereoselective Synthesis*, Schurig V *Gas Chromatography*, Stuttgart: Thieme, 168–187.
- König WA (1987) *The Practice of Enantiomer Separation by Capillary Gas Chromatography*. Heidelberg: Hüthig.
- König WA (1992) *Enantioselective Gas Chromatography with Modified Cyclodextrins*. Heidelberg: Hüthig.
- König WA (1993) Enantioselective gas chromatography. *Trends in Analytical Chemistry* 12: 130–137.
- Koppenhoefer B, Epperlein U and Schwierskott M (1997) *Fresenius Journal of Analytical Chemistry* 359: 107–114.
- Schreier P, Bernreuther A and Huffer M (1995) *Analysis of Chiral Organic Molecules—Methodology and Applications*, Ch 3.5, pp. 132–233. Berlin: Walter de Gruyter.

- Schurig V (1984) Gas chromatographic separation of enantiomers on optically active stationary phases. *Angewandte Chemie International Edition English* 23: 747–765.
- Schurig V (1994) Enantiomer separation by gas chromatography on chiral stationary phases. *Journal of Chromatography* 666: 111–129.
- Schurig V and Nowotny H-P (1990) Gas chromatographic separation of enantiomers on cyclodextrin derivatives.

Angewandte Chemie International Edition English 29: 939–957.

- Snopek J, Smolková-Keulemansová E, Cserháti T, Gahm K and Stalcup A (1996) Cyclodextrins in analytical separation methods. In: Atwood JL, Davies JED, MacNicol DD and Vögtle F (eds) *Comprehensive Supramolecular Chemistry*, vol. 3, ch. 18, pp. 515–571. Oxford: Pergamon.

Ion-Pair Chromatography

E. Hedin, Uppsala University, Uppsala, Sweden

Copyright © 2000 Academic Press

Introduction

In ion pair chromatography, the solute ion is distributed between the mobile and the stationary phase together with an ion of opposite charge (a so-called counterion). The technique is often used in reversed-phase chromatography as a convenient method to control the retention of solutes. The principle may, for example, be applied to direct chiral separations using either chiral or achiral counterions. When using an achiral counterion, the chromatographic system has to contain a chiral selector, e.g., a chiral stationary phase. The purpose of an achiral counterion then is to control the retention of the solute. However, the counterion may also influence the stereoselectivity by interactions with the chiral selector molecules. A chiral counterion may, on the other hand, be used with non-chiral stationary phases to promote chiral separation.

Ion Pairs: Principles

In order to distribute the solute molecules in a nonpolar environment, it has to be uncharged. However, if an ion of opposite charge is present in enough concentration the two ions may be distributed as a pair in the same way. An ion being double charged may be distributed together with two ions of single charge or one double charged, the only prerequisite being electroneutrality of the pair (Figure 1).

The equilibrium for a simple 1:1 ion pair may be given as:



and is characterized by an extraction constant:

$$K_{\text{ex}} = \frac{[\text{HBC}]_{\text{org}}}{[\text{HB}^+]_{\text{aq}} \times [\text{C}^-]_{\text{aq}}} \quad [1]$$

The nonpolar environment may be a liquid (mobile or stationary), a surface or a micelle in the liquid. For simplicity the principle for a liquid–liquid chromatographic system with aqueous mobile phase will be presented. Here the retention factor for the solute, k_{HB^+} , is equal to:

$$k_{\text{HB}^+} = D_{\text{HB}^+} \times (V_s/V_m) \quad [2]$$

where D_{HB^+} is the distribution coefficient of the solute between the aqueous mobile phase and the organic stationary phase and V_s and V_m are the volumes of the two phases.

The distribution coefficient is defined as:

$$D = \frac{C_{\text{org}}}{C_{\text{aq}}} \quad [3]$$

i.e., the ratio of the total concentration of solute in organic phase over the total concentration in aqueous phase. For the ion pair, D_{HB^+} may be expressed as:

$$D_{\text{HB}^+} = \frac{[\text{HBC}]_{\text{org}}}{[\text{HB}^+]_{\text{aq}}} = K_{\text{ex}} \times [\text{C}^-]_{\text{aq}} \quad [4]$$

Thus, the retention factor will depend on the extraction constant of the ion pair and the concentration of counterion in the aqueous mobile phase. The magnitude of the extraction constants depends on the hydrophobicity of the solute and the counterion, the

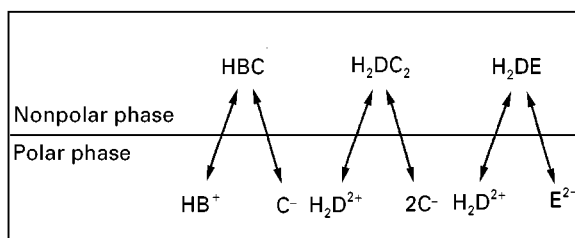


Figure 1 Distribution of charged compounds to a nonpolar phase together with a counterion.

kind of interaction forces between the two ions, and the physiochemical properties of the organic phase.

For protolytic solutes, the retention will also depend on the pH of the aqueous phase, as the charge of the solute is pH dependent. At a pH where an amine is uncharged, its distribution coefficient is:

$$D_B = \frac{[B]_{\text{org}}}{[B]_{\text{aq}}} = K_{D(B)} \quad [5]$$

where $K_{D(B)}$ is the distribution constant of B.

Considering a more general expression for the distribution coefficient for a basic compound over the entire pH range in the presence of a counterion, the equation is as follows:

$$D = \frac{C_{\text{org}}}{C_{\text{aq}}} = \frac{[B]_{\text{org}} + [\text{HBC}]_{\text{org}}}{[B]_{\text{aq}} + [\text{HB}^+]_{\text{aq}}} \\ = \frac{K_{D(B)}K'_{(\text{HB}^+)}}{K'_{(\text{HB}^+)} + a_{\text{H}^+}} + \frac{K_{\text{ex}(\text{HBX})}[\text{C}^-]_{\text{aq}}a_{\text{H}^+}}{K'_{(\text{HB}^+)} + a_{\text{H}^+}} \quad [6]$$

Uncharged form Ion pair

where $K'_{(\text{HB}^+)}$ is the acid dissociation constant of HB^+ defined as:

$$K'_{[\text{HB}^+]} = \frac{[\text{B}] \cdot a_{\text{H}^+}}{[\text{HB}^+]} \quad [7]$$

Equation [6] means that the retention of a solute may be made up of two parts: the retention as an ion pair and the retention in an uncharged form:

$$k = k_{\text{uncharged}} + k_{\text{ion pair}} \quad [8]$$

In chromatographic systems with solid stationary phases, the retention involves distribution with a solid surface. The limited capacity of the surface and the possibility to have competition for the limited adsorption sites have to be considered in the equation

but the models otherwise resemble each other to a large extent.

Principles of Chiral Separation Using Achiral Counterions

The achiral counterion itself does not provide stereochemical interactions and thus it is expected to only influence the retention and not the separation of an enantiomeric pair. Different counterions have been added to the aqueous mobile phase in a liquid-liquid chromatographic system with a nonpolar chiral stationary phase (a tartaric acid ester). The enantioselectivity was about the same for all counterions studied and, as expected, the type of ion and its concentration could be used to control the retention (Table 1).

Several of the chiral selectors used are, however, complex biomolecules, e.g., proteins which cannot be treated as simple organic phases. The addition of charged (and uncharged) compounds to the mobile phase, when a protein is used as the stationary phase, may change both the retention and the enantioselectivity. The changes in enantioselectivity may be dramatic; the two enantiomers in a pair may even elute in an opposite order.

Principles of Chiral Separation Using Chiral Counterions

The chiral counterion may be the only chiral compound needed for separation of enantiomers in a chromatographic system. The solute enantiomers form diastereomeric ion pairs with the chiral counterion, also called the selector (Figure 2). In order to achieve enantioselectivity, the ion pairs formed should have different stabilities and/or different distribution properties with the stationary phase. If the difference in distribution properties with the stationary phase is responsible for the stereoselectivity, it is important that the retention as a diastereomeric ion pair (k_{chiral}) is more pronounced than the retention of

Table 1 Influence of counterion structure on retention and enantioselectivity

Solute	—		ClO_4^- (45 mM)		PF_6^- (45 mM)		Heptane SO_3^- (45 mM)		Hexane SO_3^- (45 mM)		Hexane SO_3^- (90 mM)	
	α	k	α	k	α	k	α	k	α	k	α	k
N-methylephedrine	1.14	1.1	1.13	2.2	1.13	4.6	1.11	7.3	1.12	3.4	1.10	6.2
Ephedrine	1.15	1.1	1.15	2.2	1.15	4.0	1.13	7.7	1.41	3.4	1.13	6.9
Norephedrine	1.16	1.2	1.16	2.5	1.16	4.2	1.14	9.6	1.15	4.1	1.14	8.6

Solid phase: Novapak Phenyl (4 μm -particles); liquid stationary phase, (2*R*,3*R*)-di-*n*-butyltartrate; mobile phase, counterion in phosphate buffer pH 2.8 (ionic strength 0.1). PF_6^- = hexafluorophosphate, Heptane SO_3^- = heptanesulfonate, Hexane SO_3^- = hexanesulfonate.

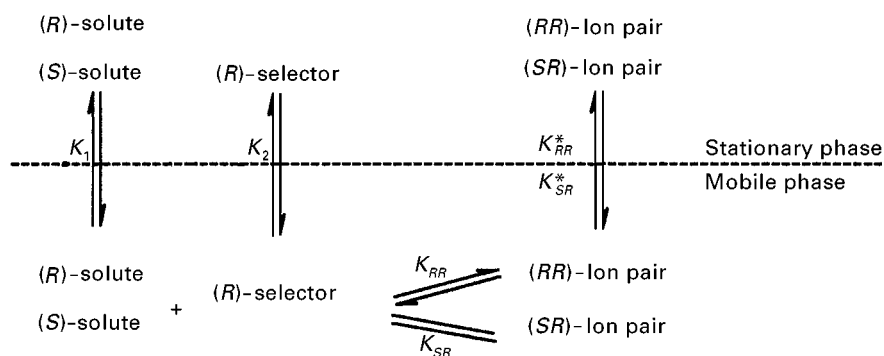


Figure 2 Ion pair formation in mobile phase and possible distribution to stationary phase.

the solute alone (k_{achiral}) (Figures 2 and 3). Referring to eqn [8] the retention factor may be described as:

$$k = k_{\text{achiral}} + k_{\text{chiral}} \quad [9]$$

and the observed α value ($\alpha_{R/S}$) compared to the maximal α (only chiral retention) as:

$$\alpha_{R/S} = \frac{k_R}{k_S} = \frac{\alpha_{\text{max}} + (k_{\text{achiral}}/k_{S(\text{chiral})})}{1 + (k_{\text{achiral}}/k_{S(\text{chiral})})} \quad [10]$$

where the *S*-form is eluted first. Therefore, the concentration of selector has to reach a certain level to assure maximal stereoselectivities (α values).

In order to promote the formation of an ion pair in the mobile phase, solvents of low polarity have often been used, e.g., hexane and dichloromethane. The retention and stereoselectivity is controlled by the temperature, the mobile phase composition (i.e. type and concentration of counterion, competing substances and polar modifiers) as well as the choice of stationary phase.

The chiral counterion and its concentration influences the equilibria outlined in Figure 2. Equation [11] expresses the stereoselectivity when varying the counterion concentration. From eqn [11] it is obvious that the influence of selector concentration on enantioselectivity is difficult to predict. The effect of a changed selector concentration will depend on the relative magnitudes of ion pair formation constants in the mobile phase and stereoselective distribution to the stationary phase:

$$\alpha_{S/R} = \frac{(K_1 + K_1 K_{RR} [(R)\text{-Selector}]_{\text{mob}} + K_{SR} K_{SR}^* [(R)\text{-Selector}]_{\text{mob}} + K_{SR} K_{RR} K_{SR}^* [(R)\text{-Selector}]_{\text{mob}}^2)}{(K_1 + K_1 K_{SR} [(R)\text{-Selector}]_{\text{mob}} + K_{RR} K_{RR}^* [(R)\text{-Selector}]_{\text{mob}} + K_{SR} K_{RR} K_{RR}^* [(R)\text{-Selector}]_{\text{mob}}^2)} \quad [11]$$

K_1 = adsorption constant for achiral adsorption of solute.

K_{RR} = formation constant of (R)-Solute : (R)-Selector in mobile phase.

K_{SR} = formation constant of (S)-Solute : (R)-Selector in mobile phase.

K_{RR}^* = adsorption constant of the diastereomeric ion pair (R)-Solute : (R)-Selector.

K_{SR}^* = adsorption constant of the diastereomeric ion pair (S)-Solute : (R)-Selector.

$[(R)\text{-Selector}]_{\text{mob}}$ = concentration of chiral selector in the mobile phase.

The chiral selector does not have to be optically pure, as the interactions are noncovalent. An enantiomerically impure selector will affect the stereoselectivity but only an impurity of exactly 50% may ruin it completely. The expected stereoselectivity, $\alpha_{S/R}^*$ when using enantiomerically impure selectors in the mobile phase may be calculated from the following expression:

$$\begin{aligned} \alpha_{S/R}^* &= \frac{\alpha_{S/R} [(R)\text{-Selector}]_{\text{mob}} + [(S)\text{-Selector}]_{\text{mob}}}{[(R)\text{-Selector}]_{\text{mob}} + \alpha_{S/R} [(S)\text{-Selector}]_{\text{mob}}} \\ &= \frac{\alpha_{S/R} P + [100 - P]_{\text{mob}}}{P + \alpha_{S/R} [100 - P]_{\text{mob}}} \end{aligned} \quad [12]$$

where $\alpha_{S/R}$ is the stereoselectivity obtained when the selector is present in one pure enantiomeric form (here the *R*-form) and *P* is the fraction of selector present in the *R*-form. Experiments have shown good agreement with theory (Table 2).

Chiral Counterions Used

In order to obtain chiral discrimination of the solutes, the counterion and solute ions have to establish

multipoint interactions where the stability of the interactions differ between the enantiomers. For the stability of the diastereomeric ion pair, it is advantageous if the molecules involved have a rigid structure, and most of the chiral counterions used are rigid. At least three points of interaction for one of the

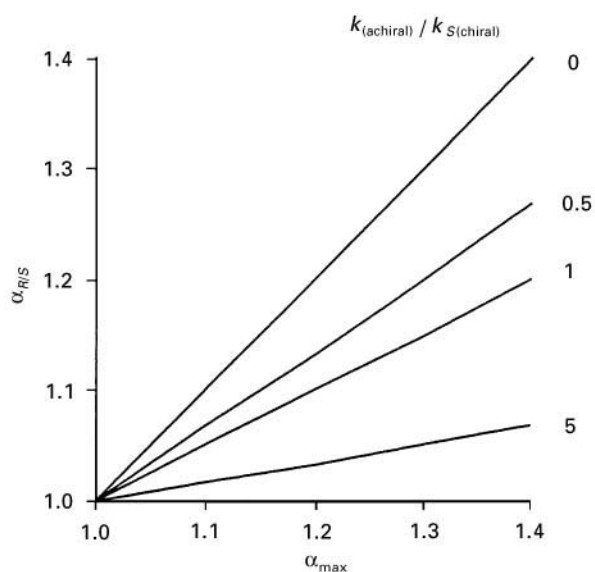


Figure 3 Influence of achiral retention on the separation factor for the enantiomers. (Reprinted from Heldin E. (1991) Tartaric acid derivatives as chiral selectors in liquid chromatography. *Comprehensive Summaries of Uppsala Dissertations from the Faculty of Pharmacy* 74: 1–37, with permission from Acta Universitatis Upsaliensis.)

enantiomers are necessary for recognition of the three-dimensional structure. All these points do not, however, have to be only between selector and solute but may also involve solvent molecules and the achiral packing material.

Most of the early studies with chiral ion-pairing selectors in the mobile phase were performed with a silica-based DIOL stationary phase. The DIOL functionality was chosen after comparing several phases (nitrile, nitro, C2, silica) as it gave the most

Table 2 Influence of enantiomeric purity of counterion on stereoselectivity

D-form of counterion (%)	$\alpha_{S/R}^*$	
	Calculated	Found
0	–	1.38
5	1.34	1.33
10	1.29	1.28
15	1.23	1.26
50	1.00	1.01
100	0.72 ^a	0.72 ^a

^a $\alpha_{R/S}^* = 1.38$. Solid phase: LiChrosorb DIOL. Mobile phase: 2.5 mM mixtures of benzoxycarbonylglycyl-L- and D-proline and 0.25 mM triethylamine in dichloromethane (80 ppm water). $\alpha_{S/R}^* = k'$ for (S)-propranolol/ k' for (R)-propranolol. Results reproduced from Pettersson C, Karlsson A and Gioeli C (1987). Influence of enantiomeric purity of a chiral selector on stereoselectivity. *Journal of Chromatography* 407: 217–229, with permission from Elsevier Science.

symmetrical peaks. Uncoated silica has in some cases been used for the purpose of retaining hydrophilic compounds. As the solid phase, i.e., the particle surface, plays an important role in the chiral recognition process it should be considered in the optimization process. The introduction of porous graphitic carbon (PGC) as packing material thus opened new possibilities and has broadened the use of chiral mobile phase additives. PGC is a very hydrophobic material whose unique three-dimensional structure is suitable for the recognition of isomers. Another advantage is that it may be used with more polar mobile phases, e.g., methanol–water mixtures. The use of polar mobile phases has several advantages in the separation process, among them the possibility of direct injection of biological fluids.

(+)-10-Camphorsulfonic Acid and Analogues

(+)-10-Camphorsulfonic acid [I] has been used to separate the enantiomers of amino alcohols, mainly β -blocking agents (derivatives of 1-aryl-2-amino alcohols). These solutes have an aromatic part to which a side chain is connected. The selectivity has been found to be dependent on the distance between the hydroxyl and the amine groups, implying that both these structural features play an important role in chiral recognition. (+)-10-Camphorsulfonic acid is an aprotic acid and it also contains an oxo group which may take part in hydrogen bonding. A model for the interaction between (+)-10-camphorsulfonic acid and β -blocking agents has been suggested and is shown in **Figure 4**. Several chiral separations have been performed using (+)-10-camphorsulfonic acid in dichloromethane: 1-pentanol (199:1) as mobile phase and a DIOL stationary phase. When using a DIOL functionalized packing material and sulfonic acid in the mobile phase, it is of vital importance to choose a solvent with a low content of polar components as the mobile phase in order to promote ion pair

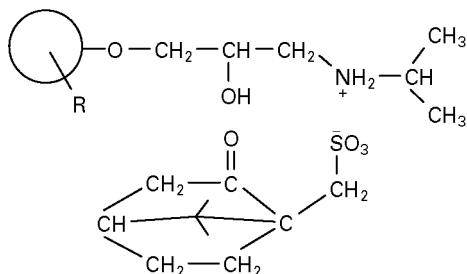
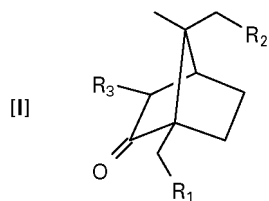


Figure 4 Model for interaction between the (+)-10-camphorsulfonic acid and amino alcohols. (Reprinted from Pettersson C and Schill G (1986) Separation of enantiomers in ion-pair chromatographic systems. *Journal of Liquid Chromatography* 9: 269–290, by courtesy of Marcel Dekker, Inc.)

formation. Attempts to use Br-3-(+)-10-camphorsulfonic acid in a system with a DIOL stationary phase, in order to separate β -blocking agents, have not been successful. With these solutes and in that particular system, the Br group was believed to sterically prevent the three-point contact between the selector and the solute. Moving the sulfonate group away from the oxy group to position 8 (Br-3-(+)-8-camphorsulfonic acid) restored the stereoselectivity to some extent.



	R ₁	R ₂	R ₃
(+)-10-Camphorsulfonic acid	SO ₃ H	H	H
(+)-3-Br-10-Camphorsulfonic acid	SO ₃ H	H	Br
(+)-3-Br-8-Camphorsulfonic acid	H	SO ₃ H	Br

The selector has been used in a system with porous graphitic carbon (PGC) as support in order to separate some dihydropyridines. The enantiomers of amlodipine and an analogue, UK52.829, were separated

with a mobile phase consisting of 5×10^{-3} M (+)-10-camphorsulfonic acid in dichloromethane : methanol (25 : 75) (Figure 5). As stated above, PGC may be used together with polar mobile phases. A fairly high content of dichloromethane is needed in order to elute the dihydropyridines from the highly retentive surface of PGC. Exchanging (+)-10-camphorsulfonic acid for Br-3-(+)-10-camphorsulfonic acid still separated the enantiomers although with somewhat lower selectivities.

Cinchona Alkaloids

The cinchona alkaloids are rigid molecules containing four chiral carbons [II] and their use as chiral selectors have been studied. Quinine has the absolute configuration 3(*R*),4(*S*),8(*S*),9(*R*) while quinidine has 3(*R*),4(*S*),8(*R*),9(*S*). It is at the positions 8 and 9 that the chiral recognition is believed to take place due to hydrogen bonding groups, and the exchange of quinine for quinidine reverses the retention order of some enantiomers, e.g., 10-camphorsulfonic acid and O-methylmandelic acid (Table 3). The mechanism of chiral recognition is, however, not simple as the effect of an exchange of the hydroxyl for an ethylcarbonate group at position 9 reduces the enantioselectivities but not to the same extent for all solutes. Furthermore, the exchange of an ethoxy group for hydrogen at the aromatic moiety (cinchonidine) also had an influence on the stereoselectivity. The results in

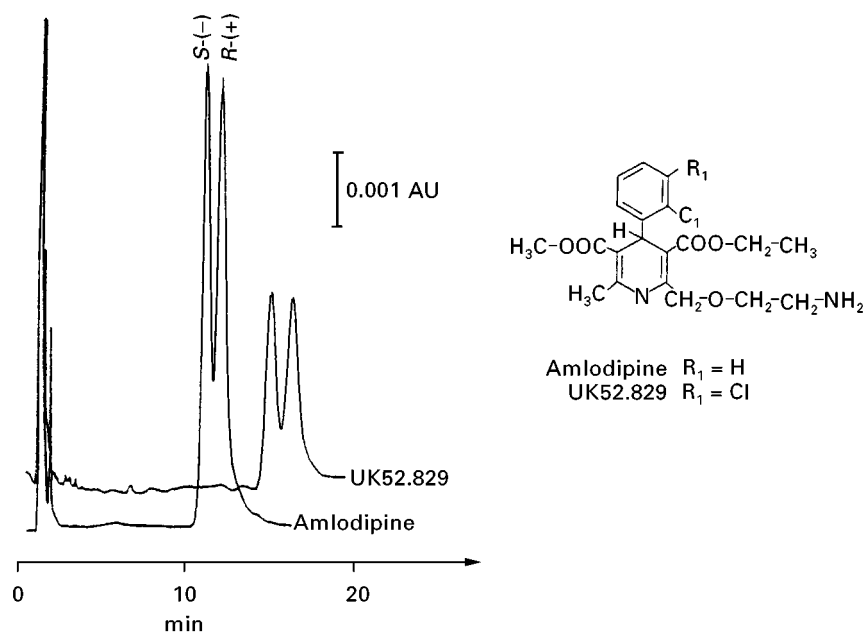


Figure 5 Separation of racemic amlodipine and UK52.829 on Hypercarb-S™. Column temperature: 30°C. Mobile phase: 5 mM (1*S*)-(+)-10-camphorsulfonic acid in dichloromethane–ethanol (25 : 75, v/v). Flow-rate: 1.5 mL min⁻¹. (Reprinted from Josefsson M, Carlsson B and Norlander B (1994) Chiral ion-pair chromatographic separation of two dihydropyridines with camphorsulfonic acids on porous graphitic carbon. *Journal of Chromatography* 684: 23–27, with permission from Elsevier Science.)

Table 3 Influence of counterion structure on retention and enantioselectivity

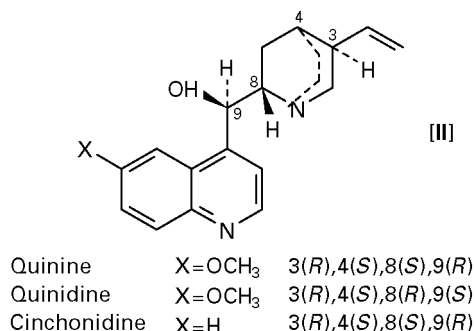
Solutes	Quinine ethyl carbonate		Quinine		Quinidine		Cinchonidine	
	α	k_1	α	k_1	α	k_1	α	k_1
10-Camphorsulfonic acid	1.28	1.7(+)	1.47	5.2(−)	1.30	3.0(+)	1.24	6.7(−)
<i>N</i> -(1-Phenylethyl)phthalamic acid	1.01	12.9 ^a	1.14	6.7(+)	1.15	4.2(−)	1.18	9.6(+)
O-methylmandelic acid			1.12	7.8(−)	1.18	3.8(+)	1.02	8.7 ^b
α -Methoxy- α -trifluoromethylphenylacetic acid	1.09	1.7 ^a	1.16	2.4(−)	1.10	1.1(+)	1.0	2.6

Solid phase: LiChrosorb DIOL. Mobile phase: 0.35 mM chiral amine and 0.35 mM acetic acid in dichloromethane (dry) : 1-pentanol (99 : 1). $\alpha = k'_2/k'_1$.

^aMobile phase consisted of 0.35 mM quinine ethyl carbonate and 0.35 mM acetic acid in dichloromethane (dry) : n-hexane : 1-pentanol (49 : 50 : 1). Results from Pettersson C and No K (1983) *Journal of Chromatography* 282: 671–684 and Pettersson C (1984) *Journal of Chromatography* 316: 553–567 with permission from Elsevier Science.

^bRetention order uncertain.

Table 3 come from two different mobile phases. Stereoselectivities should be comparable, as n-hexane does not have a significant effect on enantioselectivity. A high content of n-hexane is needed to retain hydrophilic compounds.



The complexity of the systems is high as the solutes may form ion pairs in the mobile phase, as well as be distributed to the stationary phase both as ion pairs and as uncharged compounds (see Figure 2). In addition, the selectors may be distributed to the stationary phase alone or together with mobile phase ions. In the cinchona systems, the mobile phase often contains an acid to control the retention and the stereoselectivity of the acidic solutes. It is not possible to provide a simple guideline to know which acid to use as the effect on enantioselectivity differs between the solutes studied. The distribution to the packing material is important and influences both the retention and the enantioselectivity.

When optimizing chiral ion pair separations it is therefore important to carefully consider both the mobile phase and the packing material. Enantiomers of *N*-blocked amino acids, sulfonic acids and carboxylic acids have been separated with the cinchona alkaloids as mobile phase additives. An example of

the resolution of D- and L-dansyl-valine is shown in Figure 6.

Peptides

The first peptide used for a chiral separation was L-leucine-L-leucine-L-leucine, a zwitterionic compound. Some amino acids, including, D,L-tryptophan and glycyl-D,L-phenylalanine, have been partially resolved by reversed-phase chromatography. The *N*-protected dipeptide *N*-benzyloxycarbonyl-glycyl-L-proline (L-ZGP), shown in Table 4, has been used successfully as a counterion in the separation of enantiomers of amines. When bare silica or modified silicas are used as packing material, an enantiomeric pair generally has to be a β -amino alcohol in order to be separable. In order to separate the enantiomers of amines (which lack a strong hydrogen-bonding group in the vicinity of the asymmetric carbon atom) or rather hydrophilic amino alcohols, PGC is a good choice of stationary phase. Most recent separations have been performed on PGC material and a large number of different enantiomers have been shown to be separable, of which some examples are given in Table 5. The influence of the structure of the chiral selector on the enantioselectivity of alprenolol has been studied using both DIOL functionalized particles and PGC as packing material. In the DIOL system, one analogue of ZGP with an esterified acid function (L-ZGP methyl ester) and one lacking the glycyl group (Z-L-proline) have been tested. It was found that the acidic function is needed and that this function, together with the keto group in the benzyloxycarbonyl group, was enough for enantioselectivity. Exchanging the glycyl in L-ZGP for L-alanyl will, however, completely ruin the stereoselectivity and the methyl group in alanyl is believed to block the hydrogen-accepting

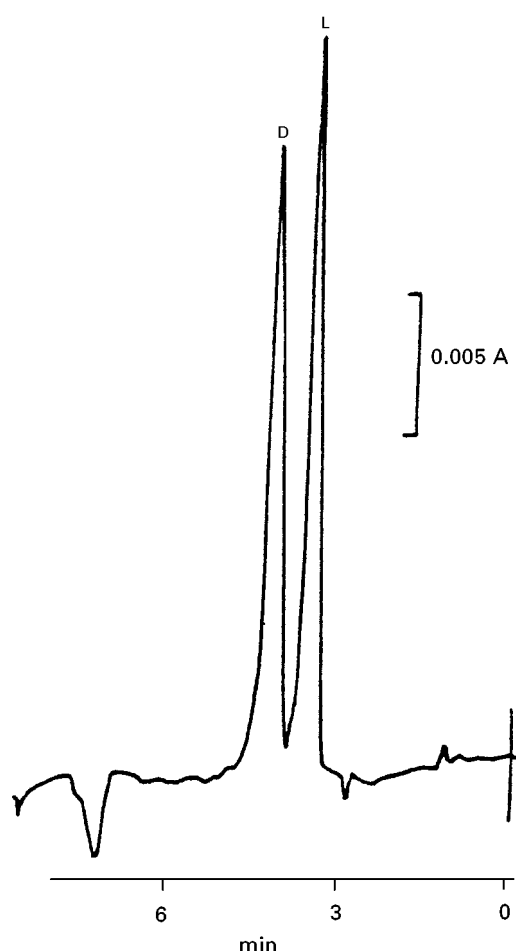


Figure 6 Resolution of D,L-dansyl-valine. Solid phase: LiChrosorb DIOL. Mobile phase: Quinine and acetic acid 0.35 mM in dichloromethane (dry) + 1-pentanol (99 + 1). (Reprinted from Pettersson C (1984) Chromatographic separation of enantiomers of acids with quinine as chiral counterion. *Journal of Chromatography* 316: 553–567, with permission from Elsevier Science.)

keto group. Reversing the positions of alanine and proline restores the selectivity to some extent (Table 4).

The aromatic function in L-ZGP provided by the *N*-blocking benzyloxycarbonyl group seems not to be a prerequisite for chiral recognition as a low enantioselectivity has been observed for some solutes using *N*-cyclopentylpropionyl-L-proline as chiral selector. Thus, when using a DIOL stationary phase, chiral recognition is believed to involve an electrostatic attraction to the acidic function in L-proline and hydrogen bonding to the carbonyl group.

Several selectors structurally related to L-ZGP have been studied in systems with PGC as support. In Table 6, the results from one of these studies is presented. L-ZGP, *N*-benzyloxycarbonyl-glycylglycyl-L-proline (L-ZGGP) and 1-[(2*S*)-3-mercapto-2-methylpropionyl]-L-proline (captopril) may be re-

garded as three supplementary selectors. Although all three show enantioselectivity for metoprolol, L-ZGP is not 'usable' for metoprolol analogues having a distance larger than two carbons between the hydroxyl and amine function. In order to match the increase in the distance between possible points of interaction, introduction of a hydrogen-bonding group further apart in the selector promotes the enantioselectivity.

Recently, two new *N*-derivatized dipeptides, *N*-benzyloxycarbonyl-L-glutamyl-L-proline (Z-L-Glu-L-Pro) and *N*-benzyloxycarbonyl-L-glutamyl-D-proline (Z-L-Glu-D-Pro), have been reported. Only one of the dipeptides, Z-L-Glu-L-Pro, shows enantioselectivity for the amino alcohols studied (metoprolol and analogues), although ion pairing occurred with both peptides. The possibility of using Z-L-Glu-L-Pro at temperatures above ambient has been investigated. In contrast to using L-ZGP, the enantioselectivity is, however, only slightly affected when increasing the temperature. Although the retention is decreasing at elevated temperatures, the enantiomers of, for example, metoprolol, may be separated within a wide temperature range, 10 to 45°C. An enantiomeric separation of metoprolol is given in Figure 7. It may also be worth noting that the elution order of the enantiomers were opposite using Z-L-Glu-L-Pro and L-ZGP as selectors, even though in both cases the terminal peptide was L-proline. The relative retention order of the studied amino alcohols was independent of the selector used, L-ZGP or Z-L-Glu-L-Pro.

(–)-2,3:4,6-Di-O-isopropylidene-2-keto-L-gulonic Acid ((–)DIKGA)

(–)-DIKGA [III], has been used to resolve enantiomers by fractional crystallization and has also been

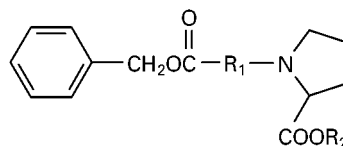
Table 4 Counterion structure and stereoselectivity

Counterion	R_1	R_2	k_R^b	$\alpha_{S/R}$
Z-glycyl-L-proline (L-ZGP)	HNCH ₂ CO	H	4.4	1.24
Z-L-proline	–	H	3.2	1.15
Z-L-proline methylester ^a	–	CH ₃	1.9	1.00
Z-L-alanyl-L-proline	HNCH(CH ₃)CO	H	2.6	1.00
Z-L-prolyl-L-alanine			6.4	1.10

Solid phase: LiChrosorb DIOL. Mobile phase: 2.5 mM counterion and 1.0 mM triethylamine in dichloromethane (80 p.p.m. H₂O).

^aTriethylamine 4.0×10^{-5} M in mobile phase. Reprinted from Pettersson C and Josefsson M (1986) *Chromatographia* 21: 321 with permission from the authors.

^bSolute: *R*- and *S*-alprenol.



used as chiral selector in liquid chromatography. Several compounds including β -blocking agents, local anaesthetics and neuroleptics are resolved into their enantiomers when (–)-DIKGA is present in a polar mobile and PGC is used as support. An example is given in Figure 8. The enantiomers of *p*-hydro-

Table 5 Examples of different solutes separated in systems with L-ZGP as chiral counterion

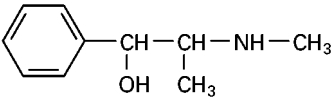
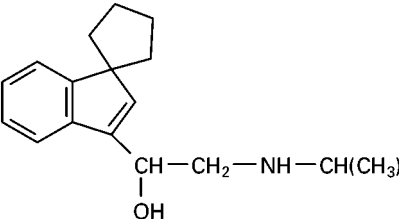
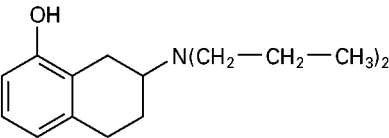
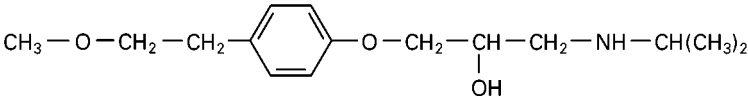
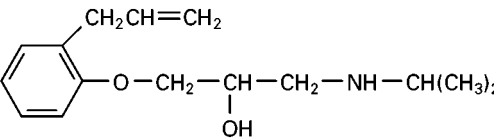
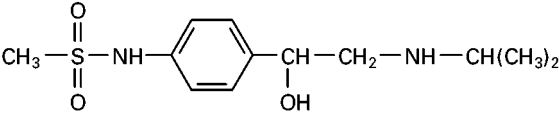
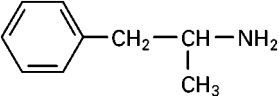
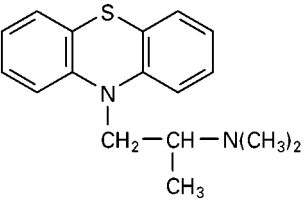
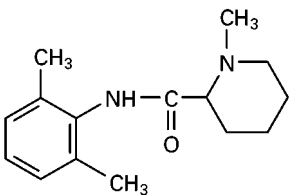
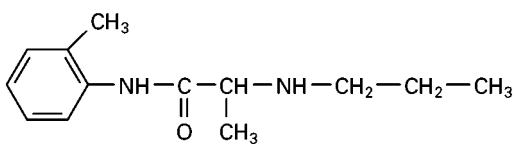
Solute	Structure	k_1	α
Ephedrine		7.06 ^a	1.34
<i>N</i> -Isopropyl-2-hydroxy-2-(spirocyclopentane-1,1'-inden)-3'-ylethylamine		1.63 ^a	1.57
8-Hydroxy-2-(di- <i>n</i> -propyl-amino) tetraline		2.24 ^a (3.5 ^c)	1.12 (2.04 ^c)
Metoprolol		18 ^b (2.4 ^c)	1.09 (1.25 ^c)
Alprenolol		22 ^b	1.17
Sotalol		9.8 ^b	1.13
1-Phenyl-2-aminopropane		3.8 ^c	1.15
Promethazine		1.0 ^c	1.15

Table 5 Continued

Solute	Structure	k_1	α
Mepivacaine		9.6 ^d	1.35
Prilocaine		0.91 ^c	1.12

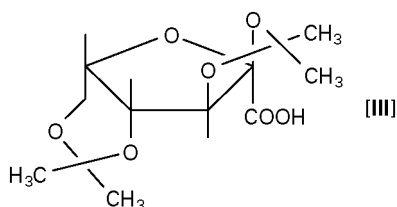
^aSolid phase: Nucleosil CN. Mobile phase: 2.5 mM L-ZGP and 0.25 mM triethylamine in dichloromethane (80 ppm water). Results from Pettersson C, Karlsson A and Gioeli C (1987) *Journal of Chromatography* 407: 217–229 with permission from Elsevier Science.

^bSolid phase: PGC. Mobile phase: 5 mM L-ZGP and 4.5 mM NaOH in methanol. Results from Huynh NG, Karlsson A and Pettersson C (1995) *Journal of Chromatography* 705: 275–287 with permission from Elsevier Science.

^cSolid phase: PGC. Mobile phase: 10 mM L-ZGP in dichloromethane (80 ppm water). Results from Karlsson A and Pettersson C (1991) *Journal of Chromatography* 543: 287–297 with permission from Elsevier Science and Karlsson A, Luthman K, Pettersson A and Hacksell U (1993) *Acta Chemica Scandinavica* 47: 469–481.

^dSolid phase: PGC. Mobile phase: 5 mM L-ZGP in dichloromethane : hexane (1 : 1). Results from Karlsson A and Pettersson C (1992) *Chirality* 4: 323–332, reprinted by permission Wiley–Liss, Inc., a subsidiary of John Wiley and Sons, Inc.

xyephedrine are separated within 4 min.



General Mobile Phase Considerations

Beside the counterion and its concentration, the composition of the mobile phase will depend on the column packing material used and the type of solutes to analyse. Uncharged or charged modifiers may be needed in the mobile phase in order to elute the solutes in a reasonable time and also to resolve them into their enantiomers.

Mobile Phase Composition when using DIOL Functionalized Silica as Stationary Phase

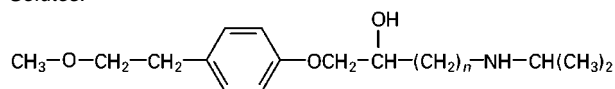
When DIOL functionalized silica particles are used as stationary phase, the mobile phase has to be a non-polar solvent. The water concentration in the non-polar solvent may then be of vital importance for the success of the separation and should, together with some of the chiral counterions, quinine and camphor-

sulfonic acid, be as low as possible in order to promote the chiral separations. The equilibration time needed to obtain a stable system with dry solvent is, however, very long and therefore it is convenient to work with higher water contents although not a water-saturated mobile phase. The water content does not influence the enantioselectivity when L-ZGP is used as counterion. Longer retention times are, however, obtained when more water is present in the solvent. Water-saturated injection solutions can be injected into the system without influence on either retention or stereoselectivity.

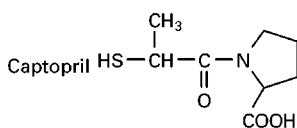
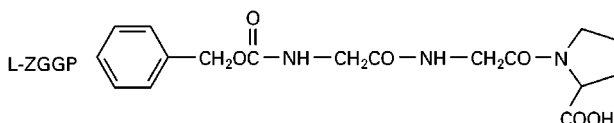
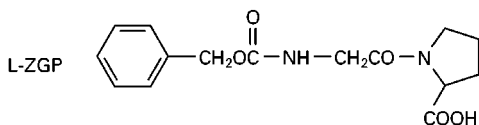
As the polarity of the mobile phase controls the retention of the solutes, modifiers like alcohols, acetonitrile or tetrahydrofuran have sometimes to be used in order to elute solutes in a reasonable time. Several of these modifiers also have an effect on the enantioselectivities of these systems. Some modifiers have been studied in a system with (+)-10-camphor-sulfonate in dichloromethane as mobile phase. (In these cases the mobile phases were prepared from dry dichloromethane.) It was found that the stereoselectivity was lower with hydrogen donating modifiers than with hydrogen accepting ones (Table 7). One hypothesis is that the modifiers may interact with the hydrogen-bonding groups in the selectors. It should be noted that 1-pentanol is preferred as a modifier since the peaks obtained are more symmetrical than

Table 6 Counterion structure and enantioselective retention

Solutes:



Counterions:



Solute (n)	Counterion					
	L-ZGP		L-ZGGP		Captopril	
	k_1	α	k_1	α	k_1	α
1	1.8	1.32	4.9	1.05	9.0	1.07
2	2.2	1.0	3.9	1.09	7.0	1.0
3	1.2	1.06	4.0	1.44	—	—

Solid phase: PGC. Mobile phase: 7.2 mM of counterion in dichloromethane (80 ppm H_2O). Reprinted from Karlsson A and Pettersson C (1992) *Chirality* 4: 323 with permission from Wiley-Liss, Inc., a subsidiary of John Wiley and Sons, Inc.

when using, for example, tetrahydrofuran. The improved peak shape is believed to be due to deactivation of strong adsorption sites on the silica surface.

Peak shapes may also be improved by adding to the mobile phase a compound with the same protolytic character as the solute enantiomers. Thus, for the separation of amines, triethylamine is often used to improve peak symmetry. Acidic compounds to be analysed with, for example, quinine, may need addition of acid to the mobile phase in order to effect elution. The added acid is believed to compete for adsorption to the solid phase and for ion pair formation with quinine.

Mobile Phase Composition when using PGC as Stationary Phase

When PGC is used as stationary phase, both nonpolar and polar mobile phases may be used. The nonpolar

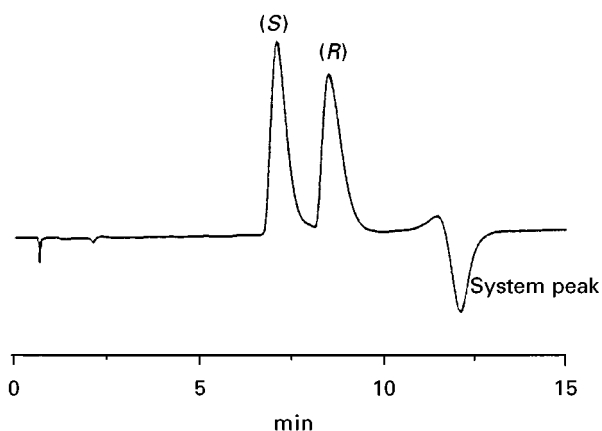


Figure 7 Separation of (R)- and (S)-metoprolol. Solid phase: Hypercarb. Mobile phase: 3.4 mM Z-L-Glu-L-Pro and 5.5 mM NaOH in methanol. Column temperature: 35°C. (Reprinted from Karlsson A and Karlsson O (1997) Enantiomeric separation of amino alcohols using Z-L-Glu-L-Pro or Z-L-Glu-D-Pro as chiral counterions and Hypercarb as the solid phase. *Chirality* 9: 650–655, with permission from Wiley-Liss, Inc., a subsidiary of John Wiley & Sons, Inc.)

phases resemble those used with the DIOL stationary phase. The addition of a nonchiral hydrophobic acid may, however, be needed in order to elute some of the hydrophobic acids from the PGC. Naproxen was found to be too strongly retained using a mobile phase consisting of quinine in dichloromethane and hexane. When adding β -naphthalenecarboxylic acid to the mobile phase, naproxen was eluted within a reasonable time and the enantiomers were separated (Figure 9). The effect of addition of an acid to the mobile phase is not easy to predict as the added acid may compete for both the distribution to limited adsorption sites on the support and also for ion pair formation with the chiral selector. Furthermore, if the counterion added to the polar mobile phase is expected to remain in an uncharged form, an acid or base has to be added in order to obtain a charged counterion. L-ZGP has a pK_a of 7–9 in methanol. The amount of base added (e.g., sodium hydroxide) will determine the degree of protolysis of the L-ZGP. However, an excess of base will result in an alkaline solution where the solutes may be uncharged. The added base may thereby influence the retention and the stereoselectivity, in other words influence both k and the ratio $k_{\text{achiral}}/k_{\text{chiral}}$ (Figure 3).

Conclusions

The addition of a counterion to the mobile phase is a technique often used to control the retention of solutes. If the added counterion is chiral, chiral separations may be achieved provided that appropriate

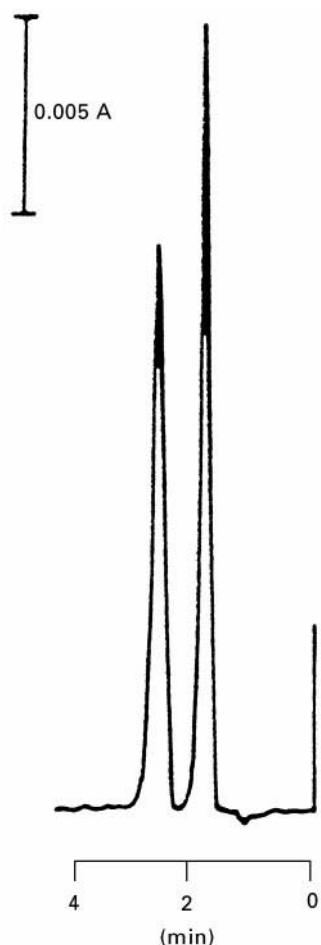


Figure 8 Separation of rac-*p*-hydroxyephedrine. Solid phase: Hypercarb. Mobile phase: 20 mM (–)-DIKGA and 15 mM NaOH in isopropanol: acetonitrile (9 : 1). Flow rate: 1.0 mL min^{–1}. (Reprinted from Pettersson C and Gioeli C (1993) Chiral separation of amines using reversed-phased ion-pair chromatography. *Chirality* 5: 241–245, with permission from Wiley-Liss, Inc., a subsidiary of John Wiley & Sons, Inc.)

solvents and solid supports are chosen. Using mobile phase additives is an easy way to screen for new chiral selectors. Furthermore, if the chiral counterion is

Table 7 Influence of polar components in the mobile phase

Polar solvent	Content (%)	k_1	$\alpha_{+/-}$	Asf ^a
Pentanol	0.5	20.3	1.08	1.5
	1	10.8	1.06	1.1
	5	2.02	1.02	1.1
Isopropanol	0.5	13.5	1.07	2.6
Acetonitrile	1	25.1	1.09	2.2
Tetrahydrofuran	1	11.9	1.10	3.7
Ethyl acetate	1	29.0	1.10	3.6

Sample: Alprenolol (+ and – forms). Mobile phase: (+)-10-camporsulfonate, 2.1 mM in dichloromethane–polar solvent. ^aAsf = asymmetry factor measured at baseline. Back part of peak/front part of peak. Results from Pettersson C and Schill G (1981) *Journal of Chromatography* 204: 179–183, with permission from Elsevier Science.

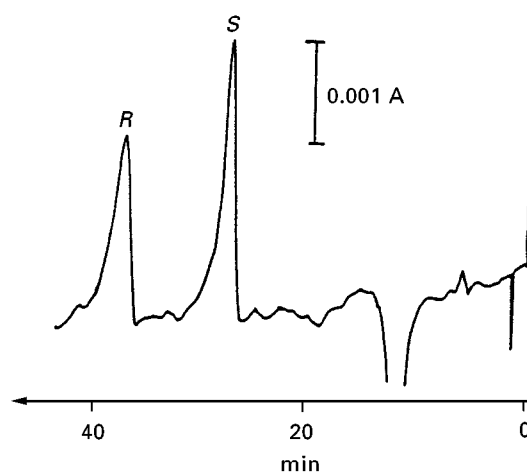


Figure 9 Resolution of (*R,S*)-naproxene. Solid phase: PGC. Mobile phase: 0.35 mM quinine and 0.10 mM β -dinaphthalenecarboxylic acid in dichloromethane: hexane (1 : 1) (Reprinted from Karlsson A and Pettersson C (1992) Separation of enantiomeric amines and acids using chiral ion-pair chromatography on porous graphitic carbon. *Chirality* 5: 323–332, with permission from Wiley-Liss, Inc., a subsidiary of John Wiley and Sons, Inc.)

available in both its enantiomeric forms, the retention order of a pair of enantiomers may be controlled. In contrast to derivatization with chiral reagents, there is no need for optically pure counterions or counterions with exactly known purities. An optically impure selector will, in chiral ion pair chromatography, still give enantiomerically pure peaks, although eluting closer to each other than they would if an optically pure selector were used.

See also: II/Chromatography: Liquid: Ion Pair Liquid Chromatography. Chromatography: Thin-Layer (Planar): Ion Pair Thin-Layer (Planar) Chromatography. III/Chiral Separations: Capillary Electrophoresis; Chiral Derivatization; Cyclodextrins and Other Inclusion Complexation Approaches; Ligand Exchange Chromatography; Liquid Chromatography; Molecular Imprints as Stationary Phases; Protein Stationary Phases; Synthetic Multiple Interaction ('Pinkle') Stationary Phases.

Further Reading

- Davankov VA, Meyer VR and Rais MA (1990) Vivid model illustrating chiral recognition induced by achiral structures. *Chirality* 2: 208–210.
- Huynh NG, Karlsson A and Pettersson C (1995) Enantiomeric separation of basic drugs using *N*-benzyloxycarbonylglycyl-L-proline as counter ion in methanol. *Journal of Chromatography* 705: 275–287.
- Josefsson M, Carlsson B and Norlander B (1994) Chiral ion-pair chromatographic separation of two dihydropyridines with camphorsulfonic acids on porous graphitic carbon. *Journal of Chromatography* 684: 23–27.

- Karlsson A and Karlsson O (1997) Enantiomeric separation of amino alcohols using Z-L-Glu-L-Pro or Z-L-Glu-D-Pro as chiral counter ions and Hypercarb as the solid phase. *Chirality* 9: 650–655.
- Knox JH and Jurand J (1982) Separation of optical isomers by zwitterion pair chromatography. *Journal of Chromatography* 234: 222–224.
- Knox JH and Ross P (1997) Carbon-based packing materials for liquid chromatography. *Advances in Chromatography*, 74–162.
- Petterson C and Heldin E (1994) A practical approach to chiral separations by liquid chromatography. In: Subramanian G (ed.) *Ion-Pair Chromatography in Enantiomer Separations*, pp. 279–310. Weinheim: VCH.
- Schill G, Wainer IW and Barkan SA (1986) Chiral separation of cationic drugs on an α_1 -acid glycoprotein bonded stationary phase (Enantiopac®). *Journal of Chromatography* 365: 73–78.

Ligand Exchange Chromatography

V. A. Davankov, Nesmeyanov-Institute of Organo-Element Compounds, Russian Academy of Sciences, Moscow, Russia

Copyright © 2000 Academic Press

Introduction

Ligand exchange chromatography (LEC) was first introduced by Helfferich in 1961 as a general chromatographic technique to separate compounds which are able to form labile complexes with transition metal cations. The basic idea was to immobilize such ions as Cu(II) or Ni(II) on a stationary phase, in particular, a cation exchanger with sulfonic or carboxylic functional groups, and then let the ions form labile coordination compounds with analytes which possess electron-donating functional groups and can enter the coordination sphere of the metal ion, thus acting as ligands. Those analytes that form stronger complexes with the central ion, are retained longer on such a metal ion-incorporating stationary phase.

Starting with the idea that, in the densely packed coordination sphere, ligands enter multipoint interactions with each other and should therefore mutually recognize the spatial configuration of neighbours, Davankov and Rogozhin (1968–71) synthesized chiral complex-forming resins and further developed LEC into a powerful chiral chromatographic method. This technique, for the first time in liquid chromatography, resulted in a complete and reliable resolution of a racemate into constituent enantiomers. Typical analytes for enantioselective LEC are members of such important classes of chiral compounds as amino acids, hydroxy acids and amino alcohols. Having soon become one of the most extensively investigated methods for the direct resolution of enantiomers, LEC maintained for a long period of

time its leading positions in developing novel chiral chromatographic systems and evaluating mechanisms of chiral recognition and discrimination. This technique contributed much to the successful development of chiral silica-bonded stationary phases, both monomeric and polymeric, chiral coatings on column-packing materials and chiral mobile phase additives. In this last technique, it transpired that the central metal ion does not need to reside in the stationary phase, but, instead, can be a part of a chiral complex that is doped into the mobile phase to interact there with the analytes. This widens significantly the definition of LEC to a chromatographic process in which the formation and breaking of labile coordinate bonds to a central metal cation are responsible for the separation of complex forming analytes.

Ligand exchange has been realized in all known modes of enantioselective chromatography, including liquid chromatography, thin layer chromatography, gas chromatography, capillary electrophoresis and countercurrent liquid chromatography. In gas chromatography the principle of ligand exchange is more commonly known under the name ‘complexation chromatography’.

Theoretical Aspects of Chiral Discrimination in LEC

Being built of protons, neutrons and electrons, which basically are chiral elementary species, all atoms possess inherent chirality. Therefore, two enantiomeric molecules resulting from a mirror-symmetric arrangement of a certain ensemble of atoms in space, can differ in their thermodynamic stability. However, this difference may only amount to about 10^{-14} J mol⁻¹, which practically makes the enantiomers energetically identical and indistinguishable in any achiral environment. Using any chromatographic technique, two enantiomers can be recognized and

discriminated by the action of a chiral selector only. The latter has to be involved in interaction with the enantiomers, resulting in the formation of adducts which, being diastereomeric species, may differ in their stability. These adducts in LEC are ternary complexes composed of the molecule of the chiral selector, the complexing metal ion, and the enantiomer to be recognized. Thermodynamic enantioselectivity of the system, i.e. the difference in stability of the above two diastereomeric ternary complexes which incorporate (*R*) or (*S*) enantiomers of the analyte, represents the sole source of chiral discrimination of the enantiomers in LEC. For an analytical scale resolution of enantiomers, the enantioselectivity does not need to be high, since, in principle, enantioselectivity of $\delta\Delta G^0 = 25 \text{ J mol}^{-1}$ would correspond to a separation factor $\alpha = 1.01$, which is fully sufficient for two peaks to be resolved in a gas chromatographic capillary column generating about 10^5 theoretical plates. For a preparative scale liquid chromatography, one would prefer to deal with a separation factor of at least $\alpha = 1.5$, which would correspond to enantioselectivity of about 1 kJ mol^{-1} . Ligand exchange often generates a discrimination effect of this order of magnitude. With the $\delta\Delta G^0$ increasing further, the column selectivity, α , rises exponentially, according to the general relation $\delta\Delta G^0 = RT \ln \alpha$. In LEC systems with polydentate ligands, separation selectivities of up to $\alpha = 10$ are known.

As a matter of principle, a chiral selector has to enter into at least a three-point interaction with the enantiomers, in order to be able to recognize the difference in the spatial structure of the latter. This requirement is easily met with tridentate ligands forming ternary complexes with metal ions which have a coordination number of six. Among practically important classes of organic compounds, however, are molecules with two electron-donating heteroatoms, N and/or O, situated in a chain of carbon atoms in positions 1,2 or 1,3, e.g. in 1,2- and 1,3-diamines, 1,2- and 1,3-amino alcohols, α - and β -amino acids and α - and β -hydroxy acids. When forming complexes with metal ions, these compounds usually function as bidentate ligands with both heteroatoms coordinated to the same metal ion in the form of a five- or six-membered chelate ring.

It is very important that formation and dissociation of the bonds in the coordination sphere of the metal ion be fast. Otherwise, a slow rate of ligand exchange would degrade the efficiency of the chromatographic system. Therefore, only metals forming kinetically labile complexes can be employed in LEC, preferably Cu(II), Ni(II) and Zn(II). Even with the above metal ions, it has been repeatedly reported that the efficiency of ligand exchanging systems can be enhanced by

raising the column temperature to about 50°C , which speeds up the ligand exchange. Ions of Cr(III), Co(III), Pd(II) and the like, form kinetically inert, stable complexes unsuitable for LEC. However, the second coordination sphere of these complexes, which actually is their solvation shell, is well organized, too, and it does exchange its ligands readily, so that an enantioselective chromatography process can also be based on outer coordination sphere ligand exchange.

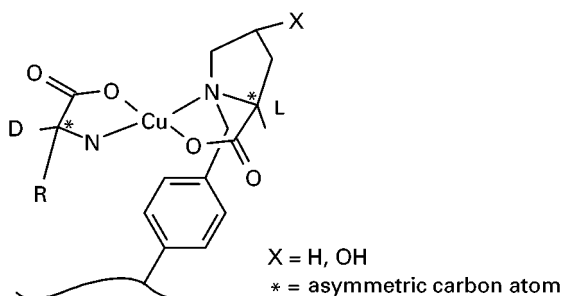
Zn(II) would usually coordinate four heteroatoms with lone electron pairs in the form of a tetrahedron. The coordination number of the Ni(II) ion is six and its ligands are usually arranged in an octahedron. Copper binds four ligands in its main coordination square, but offers two additional, more remote axial positions, so that a complex with the coordination number six adopts a distorted octahedral structure.

It is worth noting, that the optical purity of a complex-forming chiral selector employed in an LEC system does not need to be necessarily 100%. It is a distinguishing feature of all direct chromatographic separations of enantiomers that even a selector contaminated by its enantiomeric form can provide a complete resolution of racemic analytes. Enantiomeric impurities in the chiral selector do not diminish column efficiency but merely result in the two sharp enantiomeric peaks of the analyte approaching each other and completely coalescing into one sharp peak when the enantiomeric excess (e.e.) of the selector falls to zero. This phenomenon (which is not an issue, at all, with proteins or natural carbohydrates as the chiral selectors, since these selectors are available in only one enantiomeric form) has been repeatedly proven experimentally in chiral exchanging systems involving amino acids of known e.e. as the selector.

Chiral-Bonded Ligand Exchanging Stationary Phases

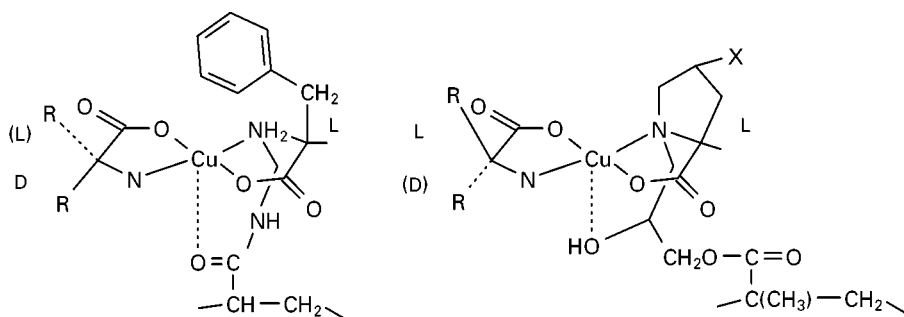
The first chiral ligand exchanging polystyrene-type stationary phases were synthesized and tested by Rogozhin and Davankov as early as 1968, while analogous silica-bonded phases emerged a decade later. Even nowadays, cross-linked polystyrene resins remain popular in preparative chromatography, mainly due to their excellent chemical durability and high loading capacity. To prepare such chiral packings, spherical particles of styrene-divinylbenzene copolymers are usually subjected to chloromethylation and the active chlorine atoms are then replaced by amino groups of chiral natural α -L-amino acids, in particular (*S*)-proline and (*S*)-hydroxyproline.

(According to modern stereochemical nomenclature, L- and D- α -amino acids belong to R and S configuration series, respectively, with a few exceptions, however.) The structure of a chiral selector immobilized in this way as well as its complex with a Cu(II) ion and an amino acid analyte, both of which bind to the selector during the process of LEC, can be represented by the following scheme:



tate amino acid-type ligands, like histidine or alloxypyrroline, the opposite elution order of the enantiomers is observed, thus giving α values smaller than 1. Many other types of chiral selectors have been similarly immobilized on chloromethylated cross-linked polystyrene beads, with the result that cyclic amino acids as well as benzyl-substituted chiral propan-1,2-diamine display the highest selectivity and largest application range. Typical examples for resolving racemates of common α -amino acids on these phases are presented in Table 1.

Two additional polymeric matrixes, cross linked polyacrylamide and poly(glycidylmethacrylate), have also been shown to be useful for immobilizing chiral amino acid selectors. The mode of functionalizing of these resins, when they incorporate (S)-phenylalanine and (S)-proline as typical chiral selectors, can be represented by the following structures:



Here, the most important features of the ternary mixed-ligand bis(amino acidato)copper complex are:

- the formation of two five-membered chelate rings;
- the occupation of the four positions of the Cu(II) ion main coordination square by four electron-donating atoms of the ligands;
- the *trans*-arrangement of the two negatively charged carboxyl groups and the bi-substituted nitrogen atoms, respectively, which minimizes both the electrostatic and sterical repulsion of the ligands in the complex.

The resins incorporating (S)-proline and (S)-hydroxyproline, when loaded with Cu(II) ions and eluted with ammonia solution, are usually found to retain α -amino acids of the opposite, (R)-configuration more effectively. In this case, the enantioselectivity of the system, when expressed as the ratio of retention factors of the (R)- and (S)-enantiomers of the analyte, $\alpha = k_R/k_S$, is larger than 1. With triden-

The first resin demonstrates higher affinity to (R)-isomers of all amino acids, without any exception, resolving all racemates with a selectivity of at least $\alpha = 1.3$.

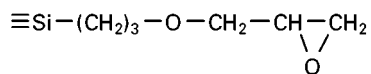
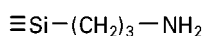
All the above polymeric ligand exchangers have been used successfully for both analytical and preparative resolution, e.g. for obtaining highly radioactive tritium-labelled optically active amino acids. In order to remove trace copper ions from enantiomers resolved in preparative experiments, the fractions of interest can be gravity filtered through a small additional column packed with silica, any chelating resin or even the same chiral resin, with a blue band of Cu(II) gradually forming at the top of the subsidiary column.

Silica-bonded chiral ligand exchangers were expected to demonstrate in analytical-scale separations still better column efficiency than polymer gels. Three types of bonded phases were suggested independently and simultaneously in 1979 by the groups of Foucault, Davankov and Guebitz, based on three different ways of activating the initial macroporous

Table 1 Enantioselectivity, $\alpha = k_D/k_L$, of resolution of racemic amino acids on the Cu(II) forms of polystyrene resins which incorporate residues of L-proline, L-hydroxyproline, L-allo-hydroxyproline, L-azetidine carboxylic acid and *N*-benzyl-(*R*)-propane-1,2-diamine. Mobile phases: aqueous ammonia solutions. Ambient temperature

Racemic amino acid	RPro	RHyp	RaHyp	RAzCA	RBzpn
Alanine	1.08	1.04	1.04	1.06	0.70
Aminobutyric acid	1.17	1.22	1.18	1.29	0.49
Norvaline	1.34	1.65	1.42	1.24	0.48
Norleucine	1.54	2.20	1.46	1.40	0.49
Valine	1.29	1.61	1.58	1.76	0.31
Isovaline	–	1.25	–	–	–
Leucine	1.27	1.70	1.54	1.24	0.49
Isoleucine	1.50	1.89	1.74	1.68	0.62
Serine	1.09	1.29	1.24	2.15	0.62
Threonine	1.38	1.52	1.48	0.78	0.44
Allothreonine	1.55	1.45	–	–	–
Homoserine	–	1.25	–	–	–
Methionine	1.04	1.22	1.52	1.29	0.60
Asparagine	1.18	1.17	1.20	1.44	0.70
Glutamine	1.20	1.50	1.40	1.25	–
Phenylglycine	1.67	2.22	1.78	1.38	0.49
Phenylalanine	1.61	2.89	3.10	1.86	0.52
α -Phenyl α -alanine	–	1.07	–	–	0.38
Tyrosine	2.46	2.23	2.36	1.78	–
Phenylserine	–	1.82	–	–	–
Proline	4.05	3.95	1.84	2.48	0.47
Hydroxyproline	3.85	3.17	1.63	2.25	–
Allo-hydroxyproline	0.43	0.61	1.48	1.46	–
Azetidine carboxylic acid	–	2.25	–	–	–
Ornithine	1.0	1.0	1.20	1.0	1.0
Lysine	1.10	1.22	1.33	1.06	1.0
Histidine	0.37	0.36	1.32	0.56	0.85
Tryptophan	1.40	1.77	1.10	1.13	–
Aspartic acid	0.91	1.0	0.81	0.88	1.0
Glutamic acid	0.62	0.82	0.69	0.77	–

microparticulate silica gel, namely, by first grafting silica with aminopropyl, chloroalkyl, and 3-glycidoxypentyl groups, respectively:



Whereas the aminopropyl spacer binds a chiral amino acid-type selector via the carboxyl group, the other two functions easily react with the amino group of the selector. The epoxy-activated and L-proline incorporating silica was the first chiral-bonded stationary phase on the market (Chiral ProCu, Serva, Heidelberg, Germany). Silica-bonded ligand exchangers have been used successfully to resolve racemates of numerous amino acids, hydroxy acids, *N*-dansyl- and *N*-alkyl-amino acids, α -trifluoromethyl- α -amino

acids, dipeptides, some β -amino acids, etc. Amino alcohols do not form stable chelates with Cu(II) ions, but are easily resolved after conversion into Schiff bases or, better still, after reaction with bromoacetic acid, which converts the amino group into a chelating glycine moiety.

The silica-bonded phases, however, still require elevated temperatures (usually 50°C) to generate sufficient column plate numbers. In addition only neutral or weakly acidic aqueous-organic eluents, in particular, in the pH range between 6.0 and 4.0 can be applied. Therefore, a much more hydrolytically stable packing was introduced by multiple-point binding of chloromethylated polystyrene chains to the silica matrix, followed by substituting the active chlorine atoms of the polymer for chiral selectors. This type of polymer-bonded phase can safely be used at elevated temperatures, and display high resolving power towards numerous racemates, as exemplified in Figure 1. In LEC, the elevated temperature does not noticeably affect the enantioselectivity of the column.

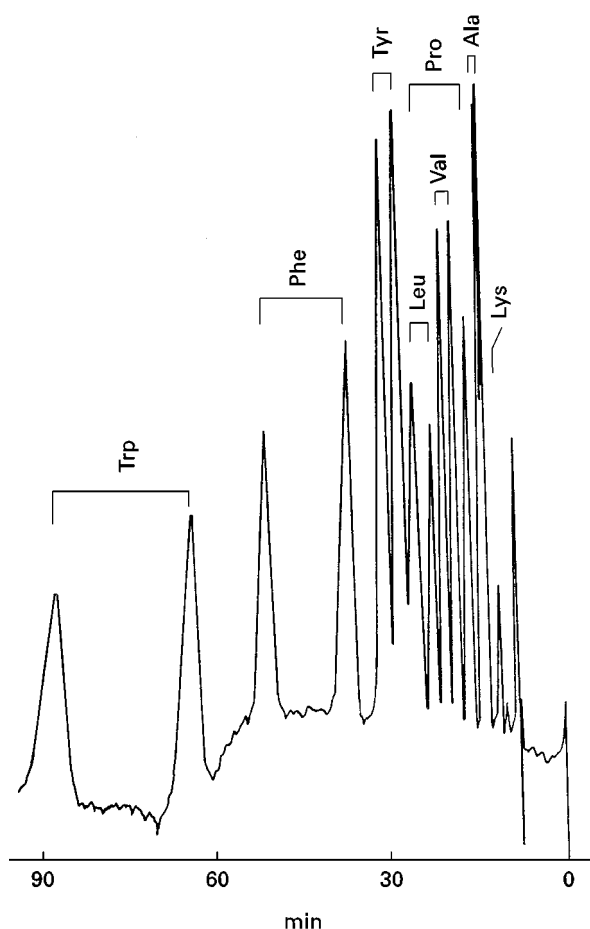


Figure 1 Enantiomeric resolution of a mixture of eight DL-amino acids with a chiral stationary phase, polystyrene grafted on silica gel and substituted with L-Hydro. Conditions: column, 250 × 4 mm i.d., dp 5 µm; eluent, 0.5 mM copper acetate, 10 mM ammonium acetate, pH 4.5, acetonitrile 30%; flow rate, 0.7 mL min⁻¹; temperature, 75°C; UV 254 nm. (Reprinted with permission from Davankov VA (1989) Chapter 15, Figure 5, p. 464. In: Krstulovic AM (ed.) *Chiral Separations by HPLC. Applications to Pharmaceutical Compounds*, pp. 446–475. Chichester, England: Ellis Horwood.)

When dealing with complicated analyte matrixes, it is often useful to combine in sequence a chiral column with a conventional achiral one, in order to supplement the resolution of enantiomeric pairs in the chiral column with the selectivity towards different analytes of the second column. Thus, chiral ligand exchanging bonded phases are easily compatible with achiral reversed phase columns, since both columns can be operated in a gradient mode with aqueous-organic eluents which contain about 0.1 mM copper acetate and about 0.25 M ammonium acetate.

Several silica-bonded and polymeric chiral ligand exchangers are commercially available, e.g. Chiral-Si 100 L-ProCu, Chiral-Si 100 L-ValCu, Chiral-Si 100 L-HyProCu (Serva, Heidelberg, Germany), Nucleosil Chiral-1 (Macherey-Nagel, Dueren, Germany),

Chiralpak WH and WM (Daicel, Japan), TSK gel Enantio L1 (Toso, Japan), MCI gel CRS 10W (Japan), Chirosolve L-proline, Chirosolve L-valine (JPS Chimie, Switzerland). Any scientific evaluation of results obtained by using these phases is, however, complicated, since the exact structure of immobilized chiral ligands on many commercially available chiral stationary phases is not specified by the manufacturers.

Chiral Dynamically Coated Stationary Phases

Ligand exchanging columns of an exceptional efficiency and enantioselectivity can be easily prepared from commercially available reversed-phase columns by dynamically coating the column with a hydrophobic chiral selector. According to the technique suggested by Davankov and Unger in 1980, percolating a solution of *N*-alkyl-L-hydroxyproline in aqueous methanol through the column results in depositing the chiral selector on the bonded alkyl stationary phase. After a subsequent saturation of the retained ligand with copper ions, the column is ready for racemate resolutions in water-rich eluents which do not desorb the chiral selector. Depending on the length of the *N*-alkyl group (heptyl, decyl or hexadecyl) and conditions of coating, the amount of the chiral selector deposited can be easily regulated over a very broad range. Such columns (also commercially available from Regis Technologies, USA, as 'Davankov columns') display a high resolving power toward numerous amino acids (Figure 2) and their derivatives, racemic glycyl-di- and tripeptides, 3-amino-ε-caprolactam, as well as norephedrine and its analogous amino alcohols. Interestingly, the *N*-alkyl-L-hydroxyproline-coated columns, under severe overloading conditions, show a peculiar distortion of elution profiles of the enantiomers in that the first peak has no tail whereas the second peak shows a very sharp front, which enormously increased the column loadability, implying high preparative potential of the system.

Coating reversed-phase columns with *N,N*-dioctyl-L-alanine has proved especially efficient in resolving racemic α-hydroxy acids. Chiral coatings prepared with *N*²-decyl-L-histidine, *N*¹⁰-decyl-L-histidine, *N*²-octyl-(L)-phenylalaninamide, *N,S*-dioctyl-*N*-methyl-(D)-penicillamine, hydrophobic Schiff bases of chiral amino alcohols and *N*-dodecyl-*N*-carboxymethyl-(1*S*,2*R*)-norephedrine show high efficiency and selectivity. Reversed-phases coated with *N,S*-dioctyl-(D)-penicillamine and (*R,R*)-tartaric acid mono-(*R*)-1-(α-naphthyl)ethylamide are commercially available under the name Sumichiral OA-5000 and 6000 (Sumica Chemical Analysis Service, Japan).

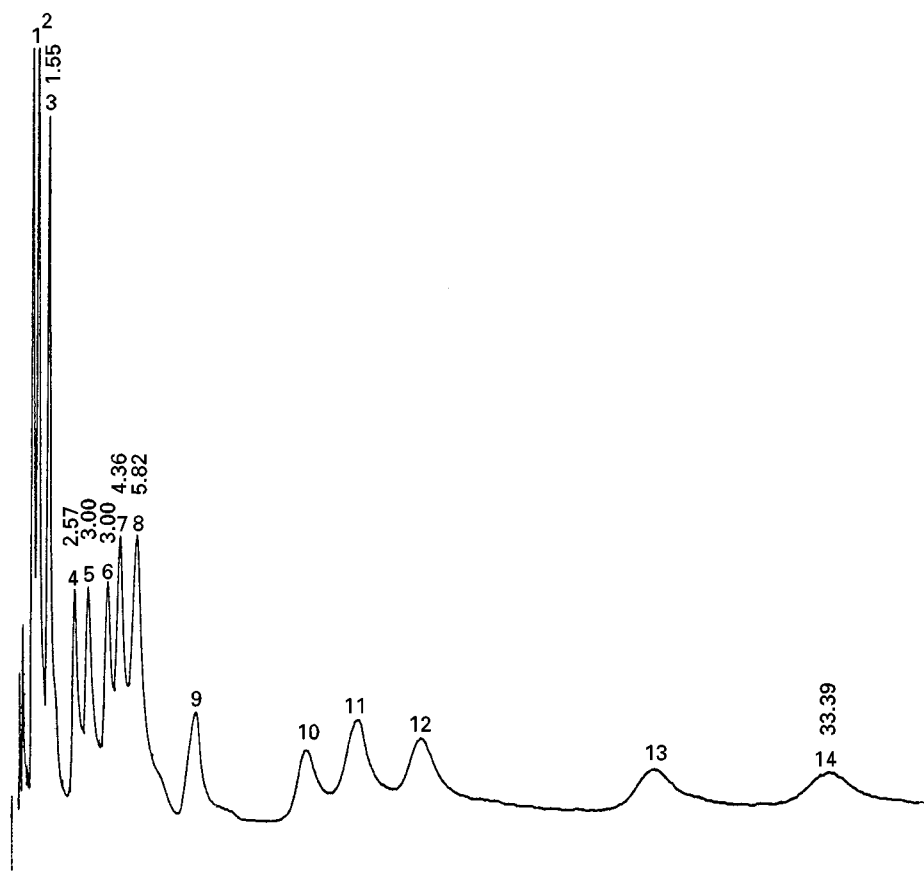


Figure 2 Enantiomeric resolution of a mixture of seven DL-amino acids with a chiral coating of *N*-decyl-L-Hypro on reverse phase material. Conditions: column, 100 × 4.2 mm, LiChrosorb RP 18, dp 5 μm; eluent, methanol-water (15 : 85), 0.1 mM Cu(II) acetate, pH 5.0; flow rate 2 mL min⁻¹; temperature 20°C, UV 254 nm; elution sequence; 1, L-Ala; 2, D-Ala; 3, L-Val; 4, L-Arg; 5, D-Arg; 6, L-Leu; 7, L-Nleu; 8, D-Val; 9, L-Phe; 10, D-Leu; 11, L-Trp; 12, D-Nleu; 13, D-Phe; 14, D-Trp. (From Davankov VA, Bochkov AS, Kurganov AA, Roumeliotis P and Unger KK (1980) Separation of unmodified α-amino acid enantiomers by reverse phase HPLC. *Chromatographia* 13: 677–685, Figure 2, p. 680.)

Whereas long *N*-alkyl substituents of the above chiral selectors are best suitable to bring about the intercalation of the latter between the surface alkyl groups of the reversed phase support, porous graphite offers a flat and rigid surface for the chiral selector to stick to. In this case, polyaromatic substituents show better retention and resolving power of the coated chiral selector, as is the case with *N*-naphthylmethyl-L-proline or *N*-(2-naphthalenesulfonyl)phenylalanine (see Figure 3).

Similarly, hydroxylated macroporous silica gel can be coated with hydrophilic chiral selectors such as silver(I)-*d*-camphor-10-sulfonate or (+)-cobalt(III)-tris-ethylenediamine trichloride. In non-aqueous media, these phases easily resolve racemates of some chiral diene and cyclopentadienylrhodium(I)-norbornadiene complexes. Since in the latter case ethylenediamine ligands of the inert cobalt complex are not exchanged for any new ligands, the separation

should be ascribed to ligand exchange in the outer, solvation shell of this complex.

Finally, polymeric chains of polyacrylamide grafted with L-proline can also be permanently adsorbed onto the surface of silica gel, to give a chiral ligand exchanger which resolves amino acids in polar media.

The ease of preparation of chiral-coated ligand exchanging phases, their exceptional efficiency, durability, wide application range and the opportunity of regulating the elution order of the enantiomers of interest by simply changing the configuration of the selector applied, make the technique increasingly popular.

Chiral Ligand Exchanging Mobile Phases

In the technique described in the previous section, the chiral selector permanently resides on the surface of

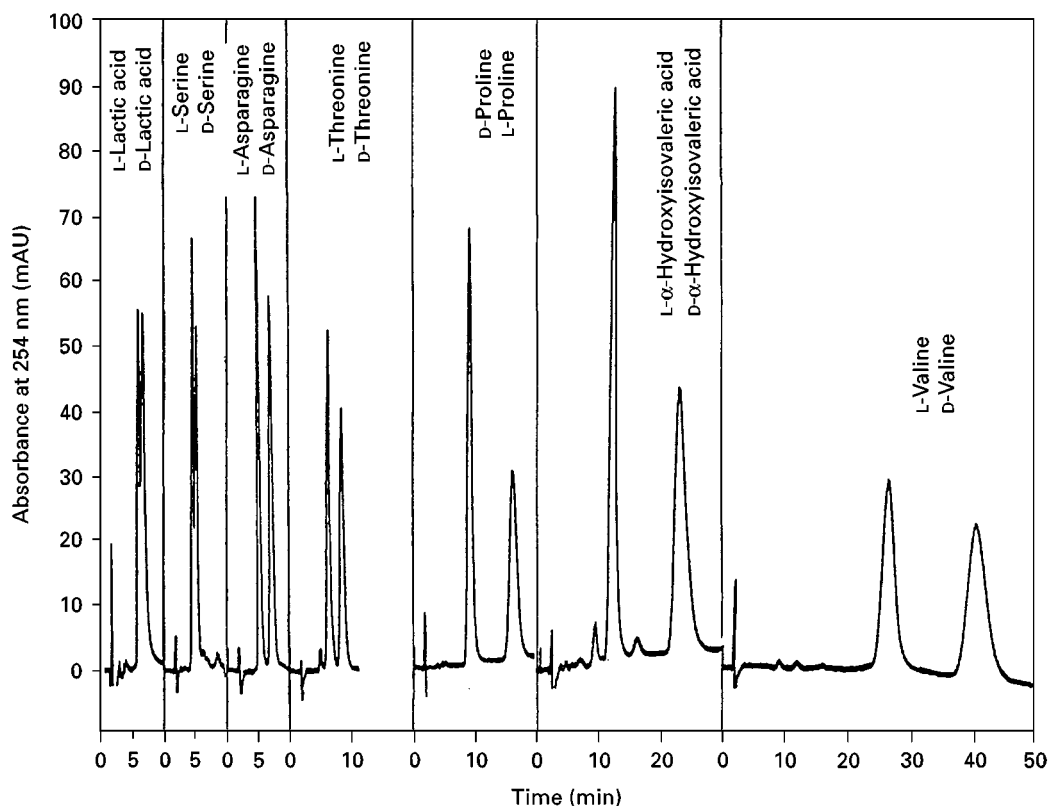


Figure 3 Enantiomeric separation of racemic amino acids and hydroxy acids with a chiral coating of *N*-(2-naphthalenesulfonyl)-L-phenylalanine on porous graphite. Conditions: column PGC 94F (5 μ m, 50 \times 4.6 mm), eluent 2.0 mM Cu(CH₃COO)₂, pH 5.6, flow rate 0.5 mL min⁻¹, UV 254 nm, temperature 30°C. (Reprinted with permission from Knox JH and Wan Q-H (1995) *Chromatographia* 40: 9–14.)

the column packing. The coating is deposited prior to the chromatographic experiments and no eluents should be used which cause a leakage of the selector. A different approach, which was independently suggested in 1979 by the groups of Karger and Lindner and Hare and Gil-Av, consists in using chiral selectors which predominantly reside in the mobile phase. In this case, the selector complex has to be continuously introduced into the column. Analytes to be resolved in such a chiral eluant form mixed-ligand complexes with the selector, which are diastereomeric in their structure, and, therefore, may be differently retained through the interaction with the column packing. A great advantage of this technique is that many different chiral selectors can be easily tested with respect to the analyte to be resolved. Another advantage is that smaller ligands are usually applied as the eluent dopants, which results in enhanced rates of ligand exchange and better efficiency of the columns. A disadvantage is the loss of the chiral selector and problems of separating the selector from the enantiomers resolved in the case of preparative experiments. It should be emphasized also that the two enantiomers separated in the achiral column enter the de-

tector cell with the chiral eluent in the form of ternary complexes. These complexes are diastereomeric and can significantly differ in molar extinction. Indeed, a case of enantioselective fluorescence quenching of dansylamino acids by a chiral Cu(II) complex of L-phenylalanylamide in aqueous solutions has been reported, thus requiring two calibration curves for a quantitative determination of the two enantiomers.

In combination with Cu(II), Zn(II), Ni(II) and some other transition metal ions, many chiral selectors have been shown to function successfully in reversed phase systems as chiral dopants. They mainly belong to the following classes of chelating compounds:

- unsubstituted L- α -amino acids (proline, phenylalanine, isoleucine, histidine, etc.);
- N-alkyl-L-amino acids (N-benzyl-proline, N,N-di-propyl-alanine, N,N-dimethyl-valine);
- L- α -amino acid amides (valine amide, phenylalanine amide, prolyloctylamide, aspartyl-alkylamide);
- esters of L- α -amino acids (histidine methyl ester);
- peptides (prolyl-valine, aspartylphenylalanine methyl ester or aspartame);

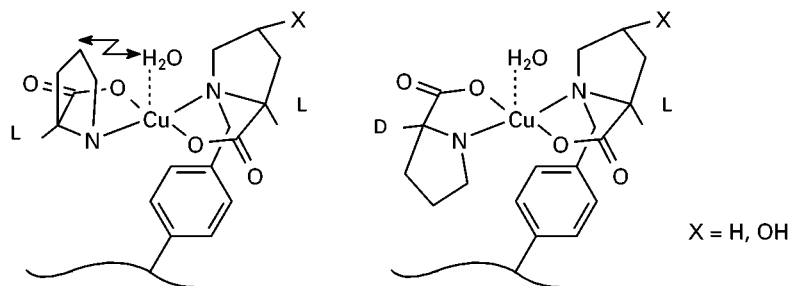
- chiral diamine (*N,N,N',N'*-tetramethyl-(*R*)-propanediamine-1,2-(*L*)-alkyl-4-octyl-diethylene-triamine);
- mandelic acid;
- derivatives of (*R,R*)-tartaric acid (tartaric acid mono-*n*-octylamide);
- nucleotides (adenosine diphosphate, β -nicotinamide, adenine dinucleotide and, in particular, flavine adenine dinucleotide).

Mainly racemic α -amino acids and their numerous derivatives, α -hydroxy acids and amino alcohols are successfully resolved. Less common, but nevertheless successful, are resolution of substituted pterins, phenylhydantoins and ornithine analogues.

Depending on the hydrophobicity of the analyte and chiral selector applied, the content of the organic modifier in the chiral mobile phase has to be adjusted in such a manner that the retention of enantiomers remains in the desired time window. In addition to this parameter, retention (and enantioselectivity) in LEC would slightly decrease with the rise in the ionic strength of the eluent and temperature of the column. Conversely, rising pH and concentration of the chiral additive in the mobile phase cause a clear increase in retention and a less marked increase in enantiomeric resolution.

Under normal phase conditions, with bare silica gel as the packing, copper complexes of *N,N,N',N'*-tetramethyl-(*R*)-propane-1,2-diamine can be used to resolve amino acids and mandelic acid. Bis(*L*-prolinato)copper is efficient even in combination with sulfonated polystyrene cation exchangers, which additionally demonstrates the versatility of the chiral mobile phase approach.

The high efficiency of the method is exemplified by Figure 4.



It is easy to imagine that, by using a mobile phase with a chiral selector of the opposite configuration, we reverse the elution order of the resolved enantio-

mers. This approach is useful in analysing enantiomeric impurities in chiral compounds, where it is always advisable to have the trace component eluting before the major enantiomer.

Finally, it is worth mentioning that the chiral mobile phase mode of LEC is very convenient to prove the reciprocity relations in chiral recognition, where the selector is exchanged for the analyte and vice versa. The enantioselectivity of the system should remain the same, unless some additional factors interfere with the essential interactions within the diastereomeric sorption complexes.

Mechanisms of Chiral Discrimination in LEC

Of many enantioselective chromatographic systems developed thus far, ligand exchanging systems are the most examined. Understanding of the mechanism of chiral discrimination is greatly facilitated here by the fact that, of the three interactions needed for the chiral selector to recognize the solute enantiomers, two are well defined as the *trans*-coordination bonds of pairs of carboxylic and amino groups in the main coordination square of the Cu(II) ion. The third interaction should be looked for in the out-of-plane sterical interactions or coordination in remote axial positions of the coordination sphere. Thus with *L*-proline or *L*-hydroxyproline incorporating polystyrene-type resins, retention of *L*-isomers of amino acids is diminished by sterical interactions with the water molecule coordinated in one of the axial positions. On the other hand, the binding of *D*-isomers is facilitated by favourable hydrophobic interaction between the solute α -substituent and the polystyrene matrix, as shown below:

Tridentate amino acids, *L*-His, *L*-Asp, *L*-Glu, *L*-aHyp, manage to replace the water molecule from the axial position and form one additional coordination

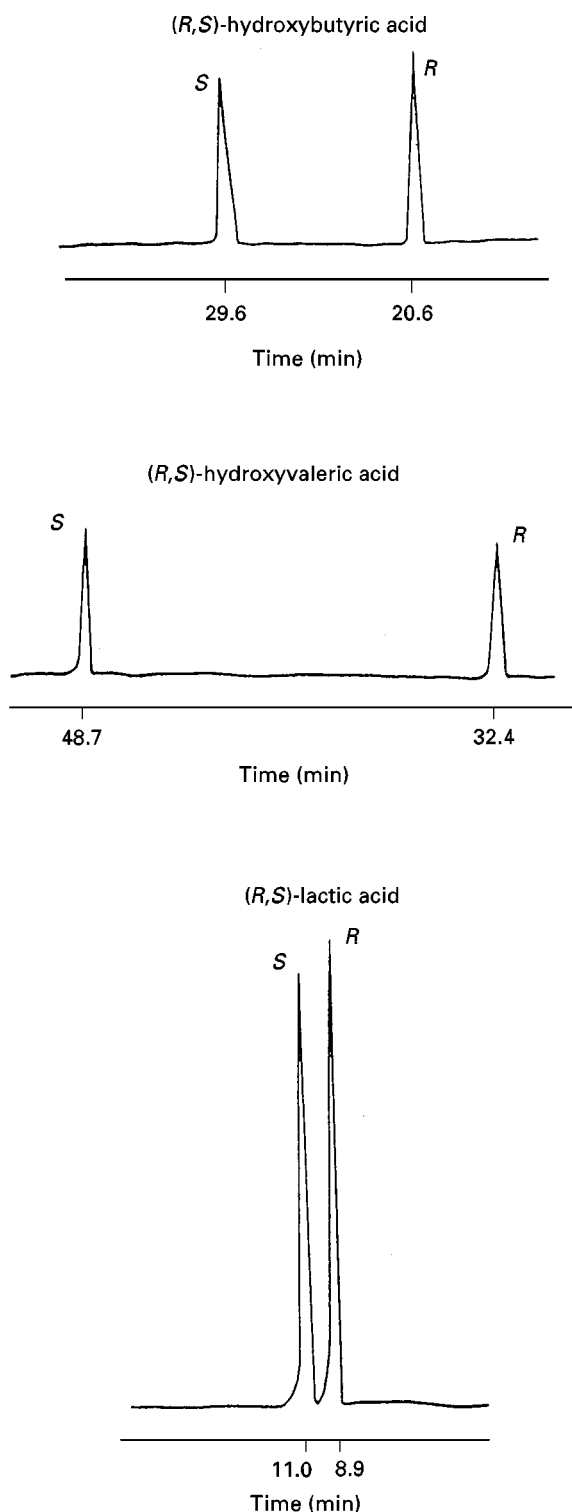


Figure 4 Enantiomeric separation of *R,S*-hydroxy acids with a chiral mobile phase. Conditions: 8 mM L-PheNH₂, 4 mM Cu(CH₃COO)₂, pH 6.0, ambient temperature, column Spherisorb 3 ODS-2 (3 μ m, 150 \times 4.6 mm), flow rate 1 mL min⁻¹, postcolumn derivatization with Fe(ClO₄)₃, UV 436 nm. (Reprinted with permission from Galaverna G, Panto F, Dossena A, Marchelli R and Bigi F (1995) *Chirality* 7: 331–336. Wiley-Liss, Inc., a subsidiary of John Wiley & Sons, Inc.)

Other Chromatographic and Related Techniques of Resolving Enantiomers in Ligand Exchanging Systems

In gas chromatography, ligand exchange has acquired great importance since Schurig introduced metal complexes of chiral terpeneketonate (acylated camphor, carvone, pulegone, menthone) as additives to stationary phase in capillary GC in 1977. Ni(II), Mn(II), Cu(II), Zn(II), and Rh(I) proved especially useful in this 'complexation' chromatography. The resolution mechanism is ascribed in terms of the interaction between the above sterically or electronically unsaturated metal chelates with volatile ligands which offer lone electron pairs to form a labile mixed-ligand sorption complex. Enantioselectivity of this process is small, but, due to the extremely high plate numbers attainable with capillary GC columns, excellent resolution is achieved for many classes of alkenes, alcohols, ethers, oxirane, sulfur-containing compounds, aziridine, etc. It is important that even compounds containing one single electron-donating atom (O, N, S) are successfully resolved by GC, contrary to LC, where the presence of two donors to form a chelate with the central metal ion is highly desirable.

Similar bonded chiral selectors, e.g. polysiloxane-anchored Ni(II)-bis-[(3-heptafluorobutanoyl)-(1*R*)-camphorate], Chirasil-Nickel, can also be used in the supercritical fluid chromatography (SFC) mode. Although SFC cannot compete with GC with regard to efficiency, a significant increase in selectivity, due to a substantially lower temperature of the column, can compensate for the loss in plate number. Because of the high solvation strength of supercritical carbon dioxide, a number of low-volatility racemic alcohols, diols and esters have been resolved by ligand exchange SFC at temperatures as low as 40–70°C.

In capillary electrophoresis (CE) and other electromigration techniques, chiral ligand exchange can be involved in several ways. Cu(L-His)₂ has just been added to the ammonium acetate electrolyte to induce chiral resolution of dansylated amino acids. Analyte enantiomers which are strongly involved in the formation of positively charged mixed complexes with Cu(L-His) move toward the cathode at a higher rate than the uncomplexed ligands. Since the enantioselectivity of the ligand exchange reaction in the bulk solution is small, the resolution of enantiomers is also small. It is only slightly better with copper-aspartame as chiral additive. A significant improvement in selectivity can be obtained by adding tetradecyl sulfate, as a micelle-forming surfactant. Obviously, the enantioselectivity increases through the interaction of the diastereomeric ternary complexes

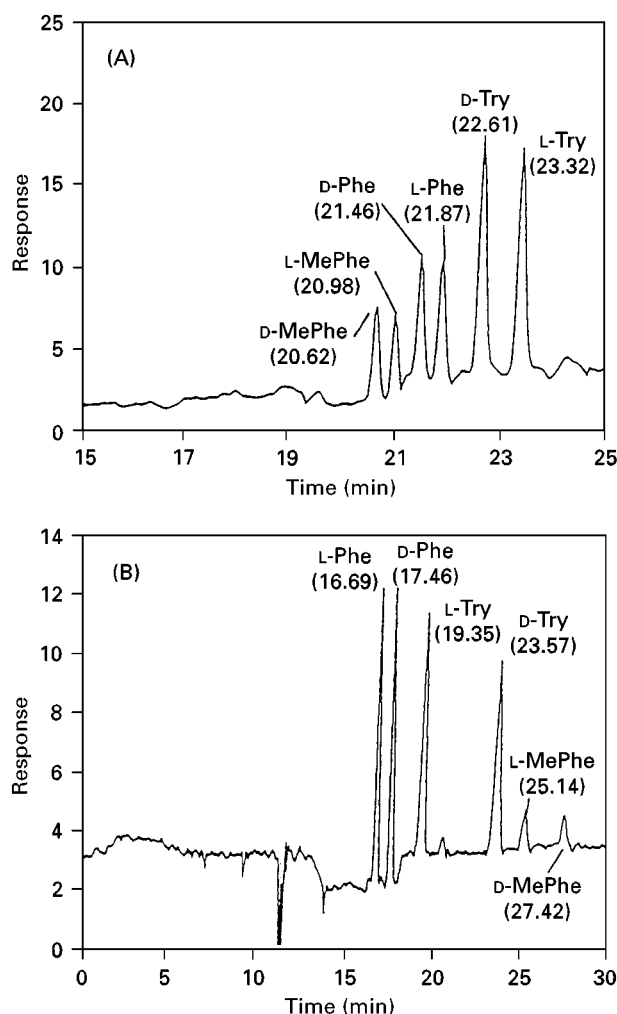


Figure 5 Electrophoregram of the enantiomer separation of DL-Phe, DL-Trp and DL-MeTrp with and without SDS. Conditions: (a) 80 mM L-Hyp, 40 mM Cu(II) sulfate, pH 4.0; (b) 50 mM L-Hyp, 25 mM Cu(II) sulfate, 15 mM SDS, 3 M urea, pH 4.0. Capillary: fused silica, 75 cm \times 75 μ m i.d. (effective length, 66 cm) $U = 27$ kV, UV 208 nm, ambient temperature. (Reproduced with permission from Schmid MG and Guebitz G (1996) *Enantiomer* 1: 23–27. Gordon and Breach Publishers.)

with the surface of the pseudo-stationary micelle phase. Good resolution for dansyl (DNS) amino acids has been obtained with mixed-micelle solutions containing sodium dodecyl sulfate (SDS) and copper complexes of *N,N*-didecyl-L-alanine. Figure 5 shows an example of CE resolution of underivatized racemic amino acids with Cu(L-Hyp)₂ in the support electrolyte, which is facilitated by SDS micelles. Note the inversion of the elution order of the enantiomers and solutes on transition from the homogeneous support electrolyte solution to the pseudo-heterogeneous micellar system.

In addition to paper chromatography which represents the oldest chiral planar chromatography tech-

nique, ligand exchange opened enormous possibilities for chiral thin-layer chromatography. Macherey-Nagel in cooperation with Degussa (Germany) developed reversed-phase plates coated with copper complexes of *N*-(2-hydroxydodecyl)-L-hydroxyproline in the manner described earlier by Davankov for chiral coating of RP-columns. The Chiralplate® has proved to be extremely versatile in the resolution of racemic α -amino acids, their *N*-methyl-, *N*-formyl-, α -alkyl-, and halogenated amino acids, dipeptides, α -hydroxy acids, thiazolidine derivatives, anomers of several nucleobases, etc. Copper complexes of *N,N*-dialkyl amino acids have also been tested as chiral coatings of plates, but so far have not found broad application.

Finally, enantiomeric separation of phenylalanine and lactic acid by diffusion through a liquid membrane was studied, using a solution of *N*-decyl-L-hydroxyproline copper complexes in hexanol-decane mixtures as the membrane. The rate of migration of the D-Phe was found to be about 2.4 times faster as compared to those of the L-isomer. Though the productivity potential of the technique is high, the above value of the kinetic enantioselectivity is still insufficient for practical use.

Applications

Two principal advantages of chiral LEC should be mentioned with respect to practical application of the method. Firstly, the detection of compounds which do not absorb in the near UV region is greatly facilitated by the fact that they partially elute from the LEC column in the form of metal complexes. Even having no strong chromophore in the molecule, they strongly absorb at 254 nm in the complexed form. When complexed to Fe(III), hydroxy acids can be selectively detected at 420 nm. The second great advantage of ligand exchange is that enantioselectivity of the separation is largely unaffected by the temperature of the column and the presence of buffer salts and organic modifier in the eluent. This makes the method easily compatible with numerous other separation techniques, including multidimensional and multicolumn chromatography.

In general, the efficiency and easiness of the direct resolution of amino acids and hydroxy acids, without any prior derivatization of the analyte, make LEC a technique of choice for serial determinations of enantiomeric compositions. This is the case, for example in fossil dating where, depending on the rate of racemization of the amino acid under investigation, the dating can be performed in the time range from several hundred years to one million years. Another application area of this kind is the

determination of D-amino acids in food products caused by partial racemization through heat or microwave treatment, and to fermentation processes. Occurrence of D-amino acids in biological fluids (e.g. serum, cerebrospinal fluid, urine), bone and tissues is also of great importance from a diagnostic point of view. Rapid enantiomeric analysis techniques are needed when asymmetric synthesis or chemical or enzymic racemate resolution processes are being developed. Examination of the enantiomeric composition of hydroxy acids, in particular malic acid, helps to investigate adulteration of apple juice and other soft drinks. Rapid preparation of enantiomers of compounds labeled with highly radioactive atoms, where only dilute solutions can be handled, is another excellent application area for chiral LEC.

Three decades of the existence and intensive development of enantioselective LEC have shown this technique to be an extremely versatile and productive general approach to resolving racemates of compounds that form complexes with metal ions. Other types of molecular interactions have been later found to provide alternative successful ways of organizing the formation of labile diastereomeric adducts with appropriate chiral selectors, e.g. formation of inclusion complexes of analytes with cyclodextrins and cyclic antibiotics or formation of charge-transfer complexes between electron-donating and electron-deficient aromatic groups in Pirkle-type chiral stationary phases. Designing novel chiral selectors which simultaneously offer to the analyte several different modes of interactions could probably result in developing chiral chromatographic systems with wider application areas or higher enantioselectivity with respect to particular important racemates. Thus first attempts of providing cyclodextrins with a copper complexed residue moiety have recently been reported in the literature. Another practically unexplored field for further development could be ligand exchange in nonaqueous and even nonpolar media. With the solvent molecules not competing for the coordination positions of the metal ion, much weaker electron donors than carboxylic or amino functional group of the analyte, should suffice for the complex formation. Ether, sulfide and carbon-carbon double bonds should thus be suitable for complexation. Achievements of complexing gas chromatography and 'argentation' thin-layer chromatography corroborate the feasibility of this development of

ligand exchanging enantioselective column liquid chromatography.

See also: II/Chromatography: Liquid: Chiral Separations in Liquid Chromatography: Mechanisms. II/Chromatography: Thin-Layer (Planar): Ion Pair Thin-Layer (Planar) Chromatography. III/Amino Acids and Derivatives: Chiral Separations. Chiral Separations: Capillary Electrophoresis; Cellulose and Cellulose Derived Phases; Chiral Derivatization; Cyclodextrins and Other Inclusion Complexation Approaches; Ion-Pair Chromatography; Liquid Chromatography; Molecular Imprints as Stationary Phases; Protein Stationary Phases; Synthetic Multiple Interaction ('Pirkle') Stationary Phases; Thin-Layer (Planar) Chromatography.

Further Reading

- Davankov VA (1980) Resolution of racemates by ligand-exchange chromatography. *Advances in Chromatography* 18: 139-195.
- Davankov V (1989) Ligand exchange phases. In: Krstulovic AM (ed.) *Chiral Separations by HPLC. Applications to Pharmaceutical Compounds*, pp. 446-475. Chichester, England: Ellis Horwood.
- Davankov VA (1992) Ligand-exchange chromatography of chiral compounds. In: Cagniant D (ed.) *Complexation Chromatography*, pp. 197-245. New York: Marcel Dekker.
- Davankov VA (1994) Chiral selectors with chelating properties in liquid chromatography: fundamental reflections and selective review of recent developments. *Journal of Chromatography A* 666: 55-76.
- Davankov VA and Kurganov AA (1983) The role of achiral sorbent matrix in chiral recognition of amino acid enantiomers in ligand-exchange chromatography. *Chromatographia* 17: 686-690.
- Davankov VA, Kurganov AA and Bochkov AS (1983) Resolution of racemates by high-performance liquid chromatography. *Advances in Chromatography* 22: 71-166.
- Davankov VA, Navratil JD and Walton HF (1988) *Ligand Exchange Chromatography*. Boca Raton, Florida: CRC Press.
- Gil-Av E, Tishbee A and Hare PE (1980) Resolution of underivatized amino acids by reversed phase chromatography. *Journal of the American Chemical Society* 102: 5115-5117.
- Guenther K (1988) Thin-layer chromatographic enantiomeric resolution via ligand exchange. *Journal of Chromatography* 448: 11-30.
- Schurig V (1988) Enantiomer analysis by complexation gas chromatography: scope, merits and limitations. *Journal of Chromatography* 441: 135-153.

Liquid Chromatography

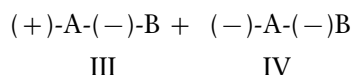
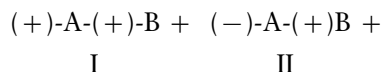
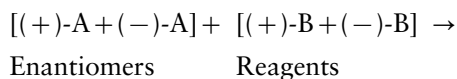
J. Haginaka, Mukogawa Women's University,
Nishinomiya, Japan

Copyright © 2000 Academic Press

A pair of enantiomers only differ in their optical rotation, but their physical properties such as melting point, boiling point, refractive index and solubility are identical. On the other hand, the physical and chemical properties of a pair of diastereomers are different. For the separation of enantiomers by liquid chromatography, it is essential to form a diastereomeric complex in the mobile phase or in the stationary phase or to convert to diastereomers. The former is called the direct method, and is based on the addition of chiral additives to the eluent or the use of chiral stationary phases, resulting in the formation of a diastereomeric complex in the mobile or stationary phase. The second indirect method is based on the reaction of the enantiomers with a homochiral reagent, resulting in the formation of a pair of diastereomers. This article deals with both the indirect and direct methods using liquid chromatography.

Purity of Chiral Derivatization Reagent or Chiral Selector

For the chiral derivatization method, there is one point which necessitates careful interpretations of the results. When the enantiomeric mixture of (+)-A and (–)-A are derivatized with the chiral derivatizing reagent of (+)-B, it often includes (–)-B as a chiral impurity. If the reagent B is 100% optically pure, two diastereomers (+)-A-(+)-B (I) and (–)-A-(+)-B (II) are formed. If reagent B is not optically pure, additional diastereomers (+)-A-(–)-B (III) and (–)-A-(–)-B (IV) are formed.



Reaction products

The enantiomers of A to be separated and determined as their diastereomeric derivatives (I and II) can be resolved as the respective peaks on an achiral stationary phase. However, the peaks of the products

III and IV produced with (–)-B overlap with the peaks of II and I, respectively, on achiral stationary phases, because II and III, and I and IV are enantiomeric pairs. Therefore, if the optical purity of the derivatization reagent is not known or not taken into consideration, the optical purity of the target compound will not be determined accurately. Further, this is the case when the separation of enantiomers is carried out by the use of chiral additives to the eluent on achiral stationary phases.

In contrast, direct resolution of enantiomers using chiral stationary phases does not have the drawbacks described above. We can easily determine 0.1% or 0.05% of the antipode using chiral stationary phases.

Indirect Methods

The indirect method, involving reaction with a homochiral reagent, is an efficient technique for the separation of many enantiomers. It is essential that the chiral derivatization proceeds completely in both enantiomers, and that racemization does not occur. The indirect methods are unsuitable for analysis of enantiomers in a standard sample and pharmaceutical preparations, because the low amount of the antipode level should be determined, and are unsuitable for preparative purposes. However, they are suitable for trace analysis of enantiomers in complex matrices such as biological samples and environmental samples because of the introduction of highly sensitive tags. These include UV-visible, fluorescent and electrochemical tags. Fluorescence derivatization is the most effective to determine the target compound in complex matrices in terms of sensitivity and/or selectivity. **Table 1** shows the fluorescence derivatization reagents (**Figures 1** and **2**) used for the separation of enantiomers bearing amino, keto, hydroxyl and carboxyl groups.

Direct Methods

Direct methods using chiral mobile-phase additives can separate many enantiomers by addition of chiral selectors to an eluent on achiral stationary phases. However, for preparative applications, the additives must be removed. Separations on chiral stationary phases can be used for both analytical and preparative purposes. At the present time, the trend is to use chiral stationary phases for the separation of enantiomers by liquid chromatography whenever possible.

Table 1 Fluorescence derivatizing reagents used for the separation of enantiomers

Reagent	Enantiomer	Separation mode
OPA + N-protected L-cystein	Amino acids, amino alcohols, baclofen, tranlycypromine	Reversed-phase
FLEC	Amino acids, methamphetamine, ephedrine, atenolol	Reversed-phase
DANE	Amino acids, ibuprofen, indoprofen, naproxen, loxoprofen	Normal-phase
NEIC	Propranolol, nadolol, prenylamine, betaxolol, acebutolol	Reversed-phase and normal-phase
Methyl-BNCC	Hydroxyls, β -hydroxy acids, propranolol, penbutolol	Normal-phase
NBD-Apy	N-acetyl amino acids, antiinflammatory drugs	Reversed-phase
NBD-Pro-COCl	Alcohols, amine	Reversed-phase
NBD-ProCZ	Ketones	Reversed-phase
NBD-PyNCS	Amines, β -blockers, amino acids, peptides	Reversed-phase
FLOPA	Ibuprofen, α -phenylcyclopentyl acid	Reversed-phase and normal-phase
FLOP-Cl	Amino acids, peptides	Reversed-phase and normal-phase
MNE-OTf	α -Methoxyphenylacetic acid, propranolol	Reversed-phase

See Figures 1 and 2 for definitions of abbreviations.

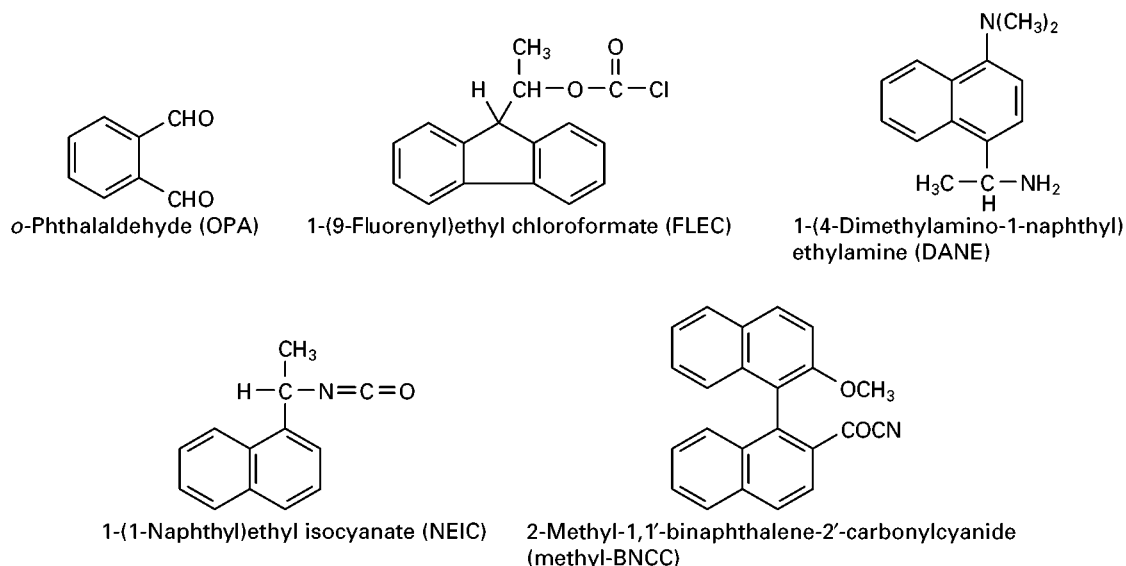
Chiral Stationary Phases

Many chiral selectors are adsorbed or immobilized covalently on to liquid chromatography supports. The chiral stationary phases obtained are classified into two types with respect to their general structure. One type is based on synthetic or natural polymers, which are totally or intrinsically chiral; the other type is based on a chiral selector of low molecular weight. Chiral stationary phases can be further classified into five types based on the solute and chiral stationary-phase interactions:

- Type I: the diastereomeric complexes of the solute and chiral stationary phase are formed by attractive interactions such as hydrogen-bonding, π - π , dipole stacking, etc., between the solute and chiral stationary phase.

- Type II: the primary mechanism for the formation of the solute and chiral stationary phase complex is through attractive interactions, but inclusion complexes also play an important role.
- Type III: the solute enters into chiral cavities within the chiral stationary phase to form inclusion complexes.
- Type IV: the solute is a part of a diastereomeric metal complex; this is called chiral ligand exchange chromatography.
- Type V: the chiral stationary phase is a protein and the solute and chiral stationary phase complexes are based on combinations of hydrophobic, electrostatic and hydrogen-bonding interactions.

Table 2 shows commercially available chiral stationary phases which are classified into these five types.

**Figure 1** Structure of reagents (see Table 1).

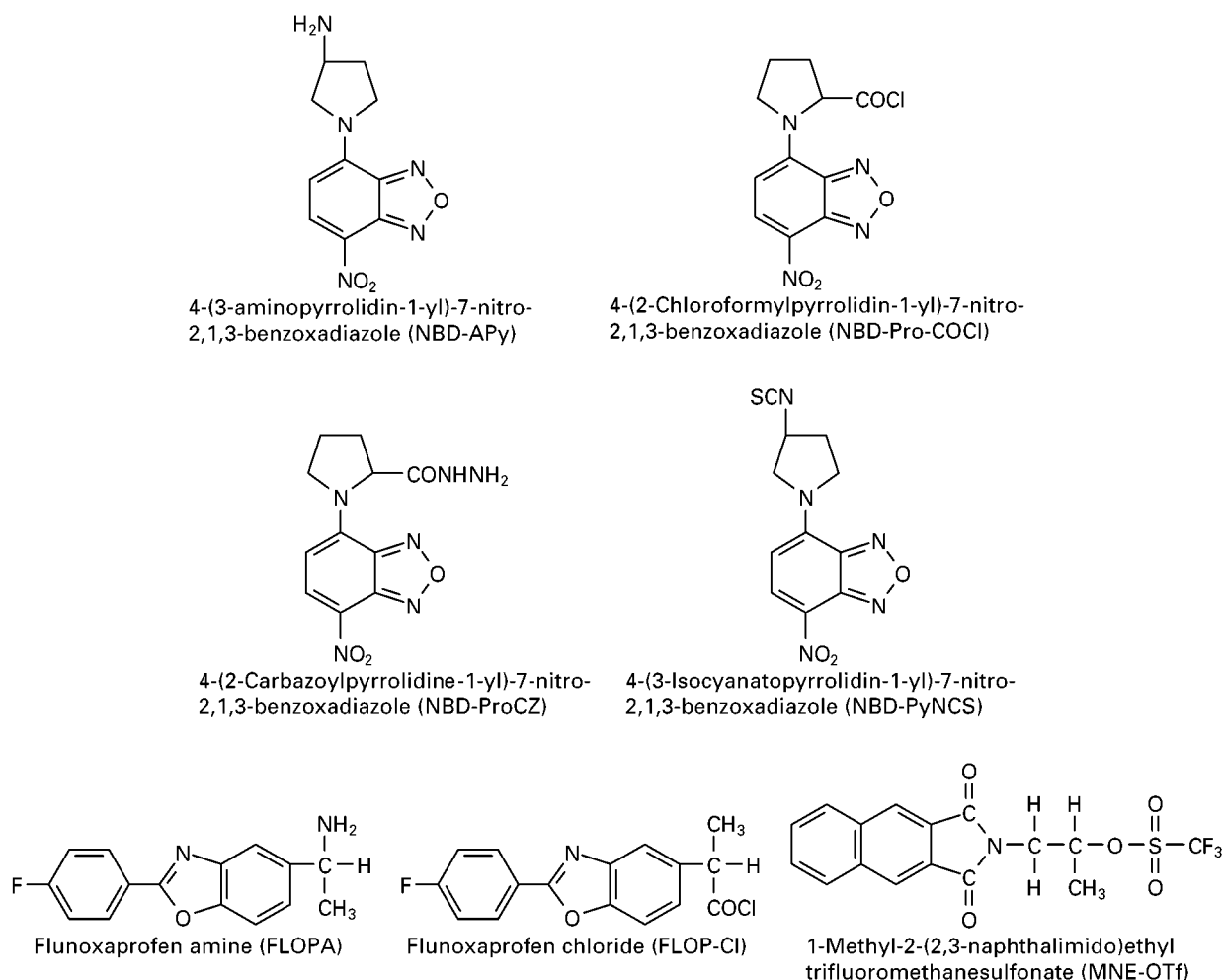


Figure 2 Structure of reagents (see Table 1).

Type I Chiral Stationary Phases

These stationary phases were based on aromatic π -acid (3,5-dinitrobenzene) and π -base (a naphthalene moiety) derivatives. In addition to π - π interaction sites, they have hydrogen-bonding and dipole-dipole interaction sites provided by an amide, urea or ester moiety. By nuclear magnetic resonance measurements in solution, three interactions are proposed to occur in the more favoured diastereomeric complex between an *N*-(3,5-dinitrobenzoyl)- α -amino amide and an *N*-(2-naphthyl)- α -amino ester: a π -donor-acceptor interaction and two hydrogen-bonding interactions, as shown in **Figure 3**. In the development of these stationary phases, the reciprocity concept was introduced as follows: if optically active A resolves the enantiomers B, then optically active B resolves the enantiomers of A. As a result, π -acid and π -base compounds have been separated using chiral stationary phases based on π -base and π -acid derivatives. Since a combination of simultaneous π - π and hydro-

gen-bonding interactions in the nonpolar solvent used as the mobile phase play an important role in chiral recognition, as described above, these stationary phases are mainly used in the normal-phase mode, although it is possible to separate some enantiomers in the reversed-phase mode.

Recently, chiral stationary phases based on the macrocyclic antibiotics, vancomycin and teicoplanin, have been developed. These stationary phases can separate many enantiomers in both normal- and reversed-phase modes.

Type II Chiral Stationary Phases

Underivatized saccharides such as cellulose and starch have been used as chiral stationary phases. Cellulose, which contains *c.* 200 glucose units (micro-crystalline cellulose), has been extensively used for the chiral resolution of highly polar compounds such as amino acids, amino acid derivatives and diaminodicarboxylic acids. The chiral recognition ability

Table 2 Chiral stationary phases for liquid chromatography

Type	Ligand	Trade name
Type I	<i>N</i> -(3,5-Dinitrobenzoyl)-D-, <i>N</i> -(3,5-Dinitrobenzoyl)-L-phenylglycine	D-,L-Phenylglycine
	<i>N</i> -(3,5-Dinitrobenzoyl)-D-, <i>N</i> -(3,5-Dinitrobenzoyl)-L-leucine	D-,L-Leucine
	Naphthyl-D-, naphthyl-L-alanine	D-, L-Naphthylalanine
	Naphthyl-D-, naphthyl-L-leucine	D-,L-Naphthylleucine
	<i>N</i> -(3,5-Dinitrobenzoyl)-(R)-1-naphthylglycine	Sumichiral OA-2500
	<i>N</i> -(3,5-Dinitrobenzoyl)-aminocarbonyl-L-valine	Sumichiral OA-3100
	<i>N</i> -[(S)-(1-Naphthyl) ethylaminocarbonyl]-L-valine	Sumichiral OA-4000
	(R)-, (S)-1-Naphthylethylamine	LC-(R)-, LC-(S)-Naphthyl urea
	Teicoplanin	Chirobiotic T
	Vancomycin	Chirobiotic V
Type II	Microcrystalline cellulose triacetate	Chiralcel CA-1
		Cellulose triacetate
	Cellulose <i>tris</i> (4-methylbenzoate)	Chiralcel OJ, OJ-R
	Cellulose tribenzoate	Chiralcel OB, OB-H
	Cellulose triacetate	Chiralcel OA
	Cellulose tricinnamate	Chiralcel OK
	Cellulose <i>tris</i> (3,5-dimethylphenylcarbamate)	Chiralcel OD, OD-H, OD-R
	Cellulose <i>tris</i> -phenylcarbamate	Chiralcel OC
	Cellulose <i>tris</i> (4-methylphenylcarbamate)	Chiralcel OG
	Cellulose <i>tris</i> (4-chlorophenylcarbamate)	Chiralcel OF
	Amylose <i>tris</i> (3,5-dimethylphenylcarbamate)	Chiralpak AD
	Amylose <i>tris</i> [(S)-1-phenylethylcarbamate]	Chiralpak AS
	Poly- <i>N</i> -acryloyl-(S)-phenylalanine ethylester	ChiraSpher
	(+)-Poly(triphenylmethyl methacrylate)	Chiralpak OT(+)
	(+)-Poly(diphenyl-2-pyridylmethyl methacrylate)	Chiralpak OP(+)
Type III	2,2'-Diphenyl-1,1'-binaphthol derivatives of 18-crown-6	Crownpak CR(+)
		Crownpak CR(-)
	α -, β -, γ -Cyclodextrin	Cyclobond III, I, II
	β -, γ -Cyclodextrin	ChiraDex, ChiraDex Gamma
	β -Cyclodextrin derivatives	Cyclobond I Ac, SP, RSP, SN, RN, DMP, PT ^a ; Ultron ES-PhCD ^b ; Nucleosil β -PM ^c
	α -, γ -Cyclodextrin derivatives	Cyclobond III Ac, II Ac
Type IV	L-Hydroxyproline	Nucleosil Chiral-1
	2-Amino-1,2-diphenylethanol	Chiralpak WE
	<i>N,S</i> -Dioctyl-D-penicillamine	Sumichiral OA-5000
Type V	Bovine serum albumin	Resolvosil BSA-7, BSA-7PX
		Ultron ES-BSA
		Chiral-BSA
	Human serum albumin	Chiral-HSA
		Chiral-HSA
	α_1 -Acid glycoprotein	Chiral-AGP
	Ovomucoid	Ultron ES-OVM
	Avidin	Bioptric AV-1
	Cellulase	Chiral-CBH
	Pepsin	Ultron ES-Pepsin

^a Ac, Acetate; SP, (S)-2-hydroxypropyl ether; RSP, racemic 2-hydroxypropyl ether; SN, (S)-naphthylethylcarbamate; RN, (R)-naphthylethylcarbamate; DMP, 2,6-dimethylphenylcarbamate; PT, *para*-toluoyl ester.

^b PhCD, Phenylcarbamate.

^c β -PM, Permethylate.

of the cellulose is based on the microcrystallinity because, when treated with dilute alkali, cellulose loses its chiral recognition ability, resulting in a stable amorphous form.

It was found that microcrystalline cellulose triacetate preserved microcrystallinity and had excellent chiral recognition ability. In contrast, microcrystalline cellulose triacetate precipitated from a solution

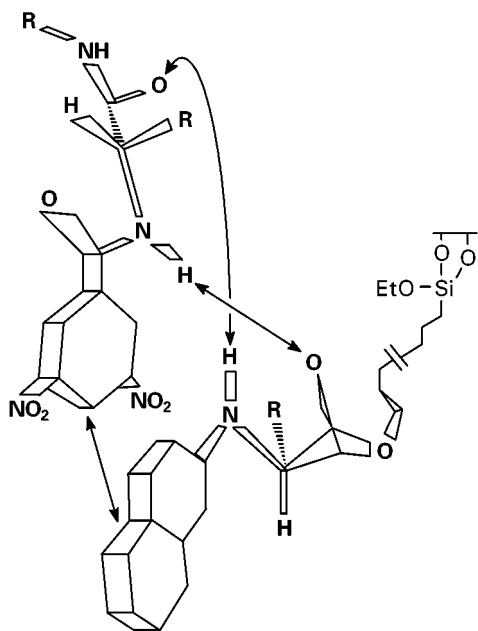


Figure 3 The more favoured diastereomeric complex between an *N*-(3,5-dinitrobenzoyl)- α -amino amide and an *N*-(2-naphthyl)- α -amino ester. A π -donor-acceptor interaction and two hydrogen-bonding interactions are indicated by arrows. (Reproduced with permission from Pirkle WH and Pochapsky TC (1987) *Advances in Chromatography*, vol. 27, p. 116. New York: Marcel Dekker.)

has another morphology, and different chiral recognition properties, compared with microcrystalline cellulose triacetate. The chiral stationary phases based on the cellulose triacetate precipitated from a solution are prepared by coating the polymer on a silica gel matrix. Many chiral stationary phases prepared by this technique are commercially available as triacetate, tribenzoate, trisphenylcarbamate, tribenzyl ether and tricinnamate derivatives of cellulose.

Chiral stationary phases based on cellulose and amylose derivatives could separate 78% of racemates examined. However, the disadvantage of stationary phases based on the cellulose and amylose derivatives coated on silica gels is the restriction of the eluents used; the coated polymer is soluble in some eluents and removed. Polysaccharide derivatives chemically bound to silica gel overcome this problem. The coated and the chemically bound polymers showed different chiral recognition properties.

With regard to the chiral recognition mechanism, the interaction of the solute and the chiral stationary phase based on cellulose phenylcarbamate derivatives has been investigated by computational chemistry and nuclear magnetic resonance measurements of the complex. It was found that π - π and hydrogen-bonding interactions play an important role in chiral recognition of the solute.

Type III Chiral Stationary Phases

Type III chiral stationary phases include cyclodextrin (CD), polymethacrylate and crown ether stationary phases. The solute enters into chiral cavities to form inclusion complexes and the relative stability constants of the resulting diastereomeric complexes are different. The cavities of CD and polymethacrylate are hydrophobic, while those of crown ethers are hydrophilic.

α -, β - and γ -CD are cyclic oligosaccharides containing 6, 7 and 8 β -1, 4-D-glucoside units, respectively. Because an aromatic portion of a molecule can enter into the chiral cavity, solutes having an aromatic moiety at, or adjacent to, the chiral centre are well resolved. Acetyl, hydroxypropyl, naphthylethyl carbamate and phenyl carbamate derivatives of CDs have been prepared and used for chiral resolution of many solutes which cannot be separated using native CDs. Chiral stationary phases based on CDs and derivatized CDs have been predominantly used in reversed-phase mode.

Chiral stationary phases based on polymethacrylate have been prepared using a chiral monomer such as (*S*)-acryloylphenylalanine, and achiral monomers such as triphenylmethyl methacrylate and diphenyl-2-pyridylmethyl methacrylate together with chiral cation catalysts. In normal-phase mode, chiral stationary phases based on these polymers can separate many racemic solutes that are difficult to resolve by other methods because of a lack of functionality.

Crown ethers, which are synthetic macrocyclic polyethers, can form selective complexes with various cations. Chiral crown ethers covalently bound or adsorbed on to silica supports can separate enantiomeric ammonium compounds such as amino acid esters, amines and amino alcohols. The multiple hydrogen-bonding interactions between the ammonium group and the ether oxygens play an important role in the chiral recognition.

Type IV Chiral Stationary Phases

Chiral ligand exchange chromatography is based on the formation of diastereomeric ternary complexes that involve a transition metal ion (M), chiral ligand (L), and the enantiomers of the racemic solute (R and S). Of all the transition metals examined [Cu(II), Ni(II), Zn(II), Hg(II), Co(III), Fe(III), etc.], Cu(II) forms the most stable complexes, and cyclic amino acids such as L-proline and L-hydroxyproline are the best chiral selectors, when bound to a polymer or silica support. The diastereomeric mixed chelate complexes formed in this system are represented by the formulas L-M-R and L-M-S. When these

complexes have different stabilities, the less stable complex is eluted first, and the enantiomeric solutes are separated. The enantiomers resolved include amino acids, amino acid derivatives, 2-amino alcohols, barbiturates and hydantoins.

Type V Chiral Stationary Phases

Chiral stationary phases based on a protein are of special interest because of their unique properties of stereoselectivity and because they are suited for separating a wide range of enantiomeric mixtures. Protein-based stationary phases so far developed have included albumins such as bovine and human serum albumin, enzymes such as trypsin, α -chymotrypsin, lysozyme and pepsin, and glycoproteins such as α_1 -acid glycoprotein from human or bovine serum, cellobiohydrolase I from the fungus *Trichoderma reesei*, ovomucoid (in fact, ovoglycoprotein), avidin

and ovotransferrin from egg whites, and flavoprotein (riboflavin-binding protein) from egg whites and yolks. The advantages of protein-based stationary phases generally include the use in reversed-phase mode, enantioselectivity for a wide range of compounds and direct analysis without derivatization. The disadvantages are low capacity, lack of column ruggedness and limited understanding of the chiral recognition mechanism. These stationary phases are mainly used for analytical purposes.

With regard to the chiral recognition mechanism, hydrophobic, electrostatic and hydrogen-bonding interactions take place between the chiral stationary phase and the solute.

Chiral Mobile Phase Additives

There are no fundamental differences between the techniques using chiral stationary phases and chiral

Table 3 Chiral selectors used as mobile-phase additives

Chiral selector	Enantiomers	Stationary phase
Metal complex		
L- or D-Proline + Cu(II), L-Phenylalanine + Cu(II), N-Methyl-L-phenylalanine + Cu(II), N,N-Dimethyl-L-phenylalanine + Cu(II), (R, R)-Tartaric acid mono-1-octylamide + Cu(II)	Amino acids	Cation exchanger, ODS, OS
L-Propyl-n-octylamide + Ni(II), L-Proline + Cu(II), L-Arginine + Cu(II), L-Histidine + Cu(II)	Dansyl amino acids	ODS, OS
(R, R)-Tartaric acid mono-1-octylamide + Cu(II)	β -Amino alcohols	ODS
Uncharged additives		
1,1'-Binaphthyl derivatives of 18-crown-6	Amino acids	ODS
Cyclodextrins		
α -Cyclodextrin	α -, β -Pinene	ES
β -Cyclodextrin	Propranolol, pseudoephedrine, salsolinol, thalidomide, dansyl amino acids	Porous graphite carbon, CN, ODS
γ -Cyclodextrin	Norgesterol	ODS, CN
TM- β -Cyclodextrin	Benzoin, ethyl mandelate 5-Butyl-1-methyl-5-phenylbarbituric acid, Dansyl phenylalanine	Si ODS
CM-, CE- β -Cyclodextrin	Aminoethylbenzodioxane derivatives, hexobarbital	BS
Chiral acid		
10-Caphorsulfonic acid	Amino alcohols	Diol
Z-Glycyl-L-proline	Amino alcohols, N-alkylated-2-aminotetralines	Diol
Chiral amine		
Alprenolol, quinine, quinidine, cinchonidine	10-Caphorsulfonic acid, N-(1-phenylethyl) phthalamic acid, O-methylmandelic acid, O-methoxy- α -trifluoromethyl-phenylacetic acid, 2-phenylacetic acid, naproxen	Diol

ODS, octadecylsilyl; OS, octylsilyl; ES, ethylsilyl; CN, cyanopropylsilyl; TM, heptakis(2,3,6-tri-O-methyl); Si, silica gels; CM, carboxymethyl; CE, carboxyethyl; BS, butylsilyl; Z, N-benzoxycarbonyl.

mobile phase additives. This means that all chiral selectors covalently bound to supports can be used for the separation of enantiomers by addition to the mobile phase. With chiral mobile phase additive techniques, there are at least two possible mechanisms; one is that the chiral mobile phase additive and the enantiomers may form diastereomers in the mobile phase. Another is that the stationary phase may be coated with the chiral mobile phase additive, resulting in diastereomeric interactions with the enantiomeric pairs during chromatography. It is thought that both mechanisms occur depending on both the stationary and mobile phases used.

The techniques using chiral mobile phase additives can be divided into three categories: metal complexation used in chiral ligand exchange chromatography, the use of various uncharged additives, and the ion-pairing techniques used for charged analytes. **Table 3** shows chiral selectors used as mobile phase additives.

See also: **II/Chromatography: Liquid:** Derivatization; Mechanisms: Chiral; **III/Chiral Separations:** Cellulose and Cellulose Derived Phases; Chiral Derivatization; Cyclodextrins and Other Inclusion Complexation Approaches; Ligand Exchange Chromatography; Ion-Pair Chromatography; Protein Stationary Phases; Synthetic Multiple Interaction ('Pirkle') Stationary Phases. **Inclusion Complexation: Liquid Chromatography.**

Further Reading

- Allenmark S (1991) *Chromatographic Enantioseparation: Methods and Applications*, 2nd edn. Chichester: Ellis Horwood.
- Krstulovic AM (ed.) (1989) *Chiral Separations by HPLC: Applications to Pharmaceutical Compounds*. Chichester: Ellis Horwood.
- Lipkowitz KB (1995) Theoretical studies of type II-V chiral stationary phases. *Journal of Chromatography A*, 694: 15-37.
- Lough WJ (ed.) (1989) *Chiral Liquid Chromatography*. London: Blackie.
- Pirkle WH and Pochapsky TC (1987) Chiral stationary phases for direct LC separation of enantiomers. *Advances in Chromatography* 27: 73-127.
- Stevenson D and Wilson ID (eds) (1988) *Chiral Separations*. New York: Plenum Press.
- Taylor DR and Maher K (1992) Chiral separations by high-performance liquid chromatography. *Journal of Chromatographic Science*, 30: 67-85.
- Toyo'oka T (1996) Recent progress in liquid chromatographic enantioseparation based upon diastereomer formation with fluorescent chiral derivatization reagents. *Biomedical Chromatography*, 10: 265.
- Wainer IW (1993) *Drug Stereochemistry: Analytical Methods and Pharmacology*, 2nd edn. New York: Marcel Dekker.
- Zief M and Crane LJ (eds) (1988) *Chromatographic Chiral Separations*. New York: Marcel Dekker.

Molecular Imprints as Stationary Phases

M. Kempe, Lund University, Lund, Sweden

Copyright © 2000 Academic Press

In 1949, Frank Dickey published what can be considered the first paper on a molecularly imprinted synthetic material. The work was inspired by the theories of Dickey's mentor Linus Pauling, who had suggested that the primary structures of all polypeptides constituting the antibodies are the same and that the diversity originates from folding directed by physical contact with the antigens. Even if Pauling's hypothesis on antibodies later turned out to be incorrect, his ideas laid the foundation for the concept of molecular imprinting. Consistent with these early studies, molecular imprinting can be defined as a method in which the selectivity of a material for a chosen molecule is induced by the presence of the molecule during the preparation, assembling or rearrangement of the material.

Dickey's studies were followed by several other investigations in the same direction, but it was not

until the 1970s that the field of molecular imprinting started to mature to its present form. Wulff introduced a new approach that allowed the introduction of functional groups at defined positions in synthetic network polymers. This approach is often referred to as covalent molecular imprinting, to distinguish it from the noncovalent approach developed by Mosbach and his co-workers in the early 1980s.

The field of molecular imprinting is growing rapidly. Molecularly imprinted polymers (MIPs) have found application as stationary phases for chiral separations and solid-phase extractions, as synthetic antibodies in competitive ligand-binding assays, as recognition elements in sensors and as catalysts of chemical reactions. The concepts of molecular imprinting will be described briefly here. For a more detailed description of the imprinting principle and the preparation of molecularly imprinted polymers, see 'Affinity Separation: Imprint Polymers' in this encyclopedia. The remainder of this paper focuses on the use of molecularly imprinted polymers as chiral stationary phases (CSPs).

The Concepts of Molecular Imprinting

Molecular imprinting, sometimes referred to as template polymerization, is a technique for preparing synthetic polymers of predetermined selectivity. Receptor-like binding sites are tailor-made *in situ* by the copolymerization of cross-linkers and functional monomers, which are interacting covalently or noncovalently with print molecules (or templates). After polymerization, the print molecules are removed from the polymer, either by extraction or by chemical cleavage, leaving recognition sites complementary to the print molecules in the shape and positioning of functional groups. The polymer is subsequently able to rebind the print molecules. The noncovalent approach of molecular imprinting is exemplified in Figure 1.

The association/dissociation kinetics of noncovalent MIPs is in general faster than is observed with polymers prepared by the covalent approach. For this reason, the former polymers are more attract-

ive as stationary phases for chromatography. Even if several examples of covalently imprinted stationary phases have been reported, it was not until the development of the noncovalent approach that the technique became competitive for the preparation of CSPs. This review will therefore focus on noncovalent molecular imprinting. The covalent approach has been covered in several excellent reviews by Wulff.

Even if the general understanding has been that the selectivity of MIPs is due to the formation of specific recognition sites complementary to the print molecules, early critics of the technique argued that the recognition could come from binding to print molecules entrapped in the highly cross-linked polymers. A small percentage of the print molecules are inaccessible and remain in the polymer network after extraction (normally less than 1%). However, this was ruled out as the cause of the selectivity by experiments showing that a polymer containing covalently bound print molecules did not exhibit any selective binding of the print molecule.

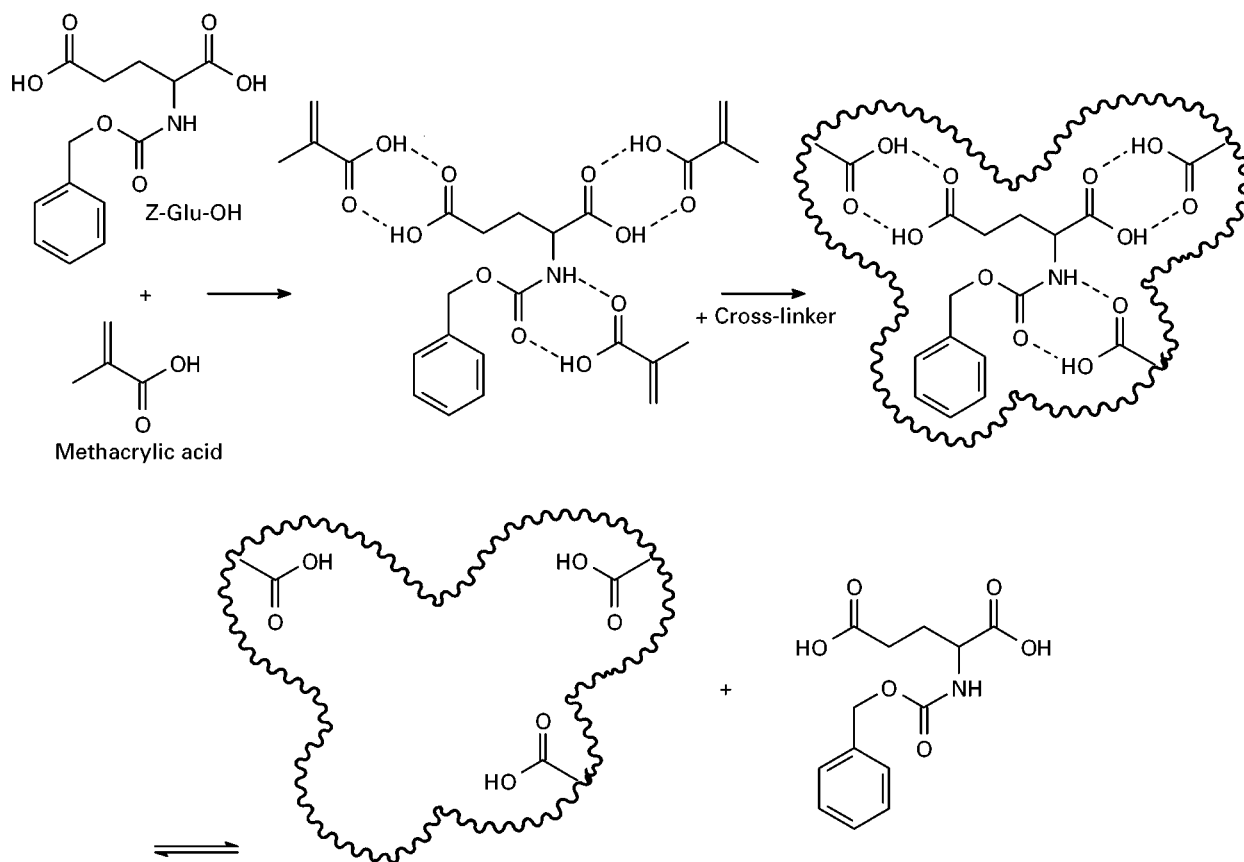


Figure 1 Schematic representation of the concept of noncovalent molecular imprinting. Functional monomers, in this case methacrylic acid, interact with the print molecule, Z-Glu-OH. Cross-linker is added and the polymerization is initiated. The interactions are maintained in the resulting polymer. The print molecule is removed from the polymer by extraction, leaving a specific recognition site complementary to the print molecule in shape and positioning of the functional groups. The polymer has attained a memory of the print molecule and is able selectively to rebind it.

Molecular imprinting produce recognition sites with a distribution of binding strengths; the sites are heterogeneous. Some sites have a highly selective affinity for the template, whereas others are less selective. When used for chromatographic applications, the heterogeneity is reflected in band broadening and asymmetric peaks.

Chiral Separations

Initial studies on noncovalent MIPs focused mainly on the preparation of materials selective for amino acid derivatives. The polymers possessed not only a selectivity for the amino acid used as the print molecule, but were also found to be enantioselective; the enantiomer present during the polymerization was preferentially bound. These findings, together with observations that the polymers were mechanically and chemically stable, made them attractive as CSPs and spurred further research.

The imprinting effects of MIPs prepared with optically active compounds as the print molecules are readily demonstrated by chromatographic evaluation. For example, when the L-enantiomer of an amino acid derivative is used as the print species, a column packed with the resulting polymer will retain the L-enantiomer longer than the D-enantiomer, and vice versa when the D-enantiomer is used as the print molecule. Reference polymers prepared with the racemate or without print molecule will not be able to resolve the racemate. A stereoselective memory is hence induced in the polymers by the print molecules.

Molecularly imprinted CSPs have been prepared for applications in high performance liquid chromatography (HPLC), thin-layer chromatography (TLC), capillary electrophoresis (CE) and capillary electrochromatography (CEC). CSPs for HPLC are by far the most studied.

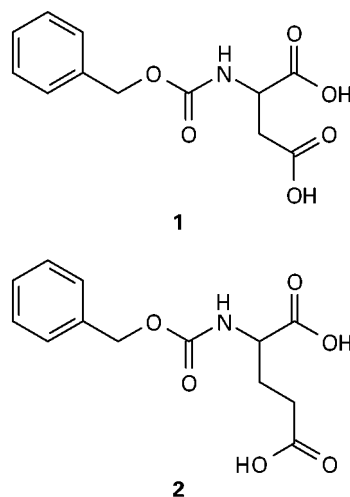
HPLC

A large number of chiral amino acids and peptides have been imprinted. Several MIPs selective for pharmaceuticals have also been described. The most widely used method has been bulk polymerization followed by grinding, sieving and packing into HPLC columns. Alternatively, the polymers can be prepared by any of the methods discussed in 'Affinity Separation: Imprint Polymers' in this encyclopedia. Some examples of MIP CSPs are shown in Table 1.

The selectivities are in many cases comparable to those of commercially available CSPs. For example, a separation factor (α) of 17.8 was found for the separation of the two enantiomers of a dipeptide on *poly*(methacrylic acid-*co*-EDMA) (EDMA = ethy-

lene glycol dimethacrylate) imprinted with one of the enantiomers (Figure 2).

The specificity and selectivity of MIPs can be fine-tuned by careful choice of monomers and solvent, and by optimizing the molar ratios of the components in the polymerization mixture. The recognition relies on multiple interaction points. The more functionalized the print molecule is, the more interactions are possible. An example of a highly selective polymer is *poly*(4-vinylpyridine-*co*-EDMA) imprinted with Z-L-aspartic acid (1). The chromatogram in Figure 3A shows the separation of racemic Z-aspartic acid on this CSP. Aspartic acid and glutamic acid differ by only one methylene unit, but despite this small difference, the Z-aspartic acid-imprinted CSP was not able to resolve racemic Z-glutamic acid (2) (Figure 3B). The side chain of Z-L-glutamic acid cannot be accommodated into the recognition site in a way that allows specific interaction between the carboxy functionality and the positioned pyridine group of the polymer. The same type of polymer, imprinted with Z-L-glutamic acid, was able to resolve racemic Z-glutamic acid, but not racemic Z-aspartic acid. Similar observations have been done on *poly*(methacrylic acid-*co*-EDMA) imprinted with these print molecules.



Polymers imprinted with Z-L-phenylalanine (3a) were able to separate racemic Z-phenylalanine efficiently (Table 2). Racemic Z-alanine (3b) could also be separated on these CSPs, even if lower separation factors were observed. When the amino-group of the racemate was protected with *tert*-butoxycarbonyl (Boc) (3c) or 9-fluorenylmethoxycarbonyl (Fmoc) (3d), the separations were poorer than with the racemate of the print molecule, which was protected with benzyloxycarbonyl (Z). In contrast to the CSPs described above, which were unable to separate the racemate of a molecule which only differed from the

Table 1 A selection of molecularly imprinted CSPs for HPLC^a

Print molecule	Polymer ^b	α^c	R_s^d	f/g^e
Amino acids				
H-L-Phe-OH ^f	<i>poly</i> (CuVBIDA- <i>co</i> -EDMA)	1.45	n.d.	n.d.
H-L-Phe-NHPh ^g	<i>poly</i> (MAA- <i>co</i> -EDMA)	13	n.d.	n.d.
H-D- <i>p</i> -NH ₂ Phe-NHPh ^h	<i>poly</i> (MAA- <i>co</i> -EDMA)	15	n.d.	n.d.
Ac-D-Trp-OMe ⁱ	<i>poly</i> (MAA- <i>co</i> -EDMA)	3.92	2.2	1.0
Ac-L-Trp-OH ^j	<i>poly</i> (AA- <i>co</i> -EDMA)	3.24	2.02	n.d.
Boc-L-Trp-OH ^j	<i>poly</i> (MAA- <i>co</i> -2VPy- <i>co</i> -EDMA)	4.35	1.9	1.0
Fmoc-L-Phe-OH ^k	<i>poly</i> (MAA- <i>co</i> -EDMA)	1.36	n.d.	n.d.
Z-L-Asp-OH ^l	<i>poly</i> (4VPy- <i>co</i> -EDMA)	2.81	1.22	0.81
Z-L-Phe-OH ^m	<i>poly</i> (MAA- <i>co</i> -TRIM)	2.29	3.14	1.00
Z-L-Tyr-OH ^m	<i>poly</i> (MAA- <i>co</i> -PETRA)	2.86	5.47	1.00
Dansyl-L-Phe-OH ⁱ	<i>poly</i> (MAA- <i>co</i> -2VPy- <i>co</i> -EDMA)	3.15	1.6	0.96
Small peptides				
H-L-Phe-Gly-NHPh ⁿ	<i>poly</i> (MAA- <i>co</i> -EDMA)	5.1	n.d.	n.d.
Boc-L-Phe-Gly-OEt ^m	<i>poly</i> (MAA- <i>co</i> -TRIM)	3.04	3.44	1.00
Z-L-Ala-L-Ala-OMe ^m	<i>poly</i> (MAA- <i>co</i> -TRIM)	3.19	4.50	1.00
Ac-L-Phe-L-Trp-OMe ^o	<i>poly</i> (MAA- <i>co</i> -EDMA)	17.8	n.d.	1.00
Z-L-Ala-Gly-L-Phe-OMe ^m	<i>poly</i> (MAA- <i>co</i> -TRIM)	3.60	4.15	1.00
Pharmaceuticals				
(S)-Timolol ^p	<i>poly</i> (MAA- <i>co</i> -EDMA)	2.9	2.0	n.d.
(S)-Naproxen ^q	<i>poly</i> (4VPy- <i>co</i> -EDMA)	1.65	n.d.	n.d.
(S,R)-Ephedrine ^r	<i>poly</i> (MAA- <i>co</i> -TRIM)	3.42	1.6	n.d.
(S,S)-Pseudoephedrine ^r	<i>poly</i> (MAA- <i>co</i> -TRIM)	3.19	1.8	n.d.

^aThe print molecules and their optical antipodes were separated.

^bAA, Acrylamide; CuVBIDA, Cu(II)[N-(4-vinylbenzyl)]iminodiacetate; EDMA, ethylene glycol dimethacrylate; Ita, itaconic acid; MAA, methacrylic acid; PETRA, pentaerythritol triacrylate; TRIM, trimethylolpropane trimethacrylate; 2VPy, 2-vinylpyridine; 4VPy, 4-vinylpyridine.

^cThe separation factor were calculated as $\alpha = k'_{\text{print molecule}}/k'_{\text{optical antipode}}$; $k' = (t - t_0)/t_0$; t is the retention time of the analyte and t_0 is the retention time of unretained compound (the void).

^dThe resolution factors (R_s) were calculated according to Wulff G, Poll HG and Minárik M (1986) Enzyme-analogue built polymers. XIX. Racemic resolution on polymers containing chiral cavities. *Journal of Liquid Chromatography* 9: 385–405.

^eThe resolution factors (f/g) were calculated according to Meyer VR (1987) Some aspects of the preparative separation of enantiomers on chiral stationary phases. *Chromatographia* 24: 639–645.

^fData from Vidyasankar S, Ru M and Arnold FH (1997) Molecularly imprinted ligand-exchange adsorbents for the chiral separation of underivatized amino acids. *Journal of Chromatography A* 775: 51–63.

^gData from Sellergren B and Shea KJ (1993) Chiral ion-exchange chromatography. Correlation between solute retention and a theoretical ion-exchange model using imprinted polymers. *Journal of Chromatography A* 654: 17–28.

^hData from Sellergren B and Nilsson KGI (1989) Molecular imprinting by multiple noncovalent host-guest interactions: Synthetic polymers with induced specificity. *Methods in Molecular and Cellular Biology* 1: 59–62.

ⁱData from Ramström O, Andersson LI and Mosbach K (1993) Recognition sites incorporating both pyridinyl and carboxy functionalities prepared by molecular imprinting. *Journal of Organic Chemistry* 58: 7562–7564.

^jData from Yu C and Mosbach K (1997) Molecular imprinting utilizing an amide functional group for hydrogen bonding leading to highly efficient polymers. *Journal of Organic Chemistry* 62: 4057–4064.

^kData from Kempe M and Mosbach K (1994) Chiral recognition of N^z-protected amino acids and derivatives in non-covalently molecularly imprinted polymers. *International Journal of Peptide and Protein Research* 44: 603–606.

^lData from Kempe M, Fischer L and Mosbach K (1993) Chiral separation using molecularly imprinted heteroaromatic polymers. *Journal of Molecular Recognition* 6: 25–29.

^mData from Kempe M (1996) Antibody-mimicking polymers as chiral stationary phases in HPLC. *Analytical Chemistry* 68: 1948–1953.

ⁿData from Andersson LI, O'Shannessy DJ and Mosbach K (1990) Molecular recognition in synthetic polymers: preparation of chiral stationary phases by molecular imprinting of amino acid amides. *Journal of Chromatography* 513: 167–179.

^oData from Ramström O, Nicholls IA and Mosbach K (1994) Synthetic peptide receptor mimics: Highly stereoselective recognition in non-covalent molecularly imprinted polymers. *Tetrahedron: Asymmetry* 5: 649–656.

^pData from Fischer L, Müller R, Ekberg B and Mosbach K (1991) Direct enantioseparation of β -adrenergic blockers using a chiral stationary phase prepared by molecular imprinting. *Journal of the American Chemistry Society* 113: 9358–9360.

^qData from Kempe M and Mosbach K (1994) Direct resolution of naproxen on a non-covalently molecularly imprinted chiral stationary phase. *Journal of Chromatography A* 664: 276–279.

^rData from Ramström O, Yu C and Mosbach K (1996) Chiral recognition in adrenergic receptor binding mimics prepared by molecular imprinting. *Journal of Molecular Recognition* 9: 691–696.

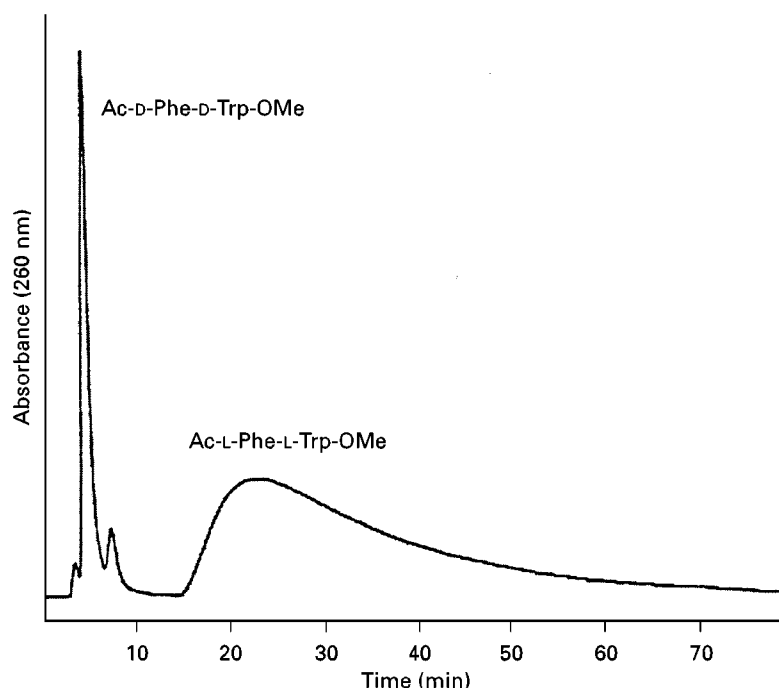


Figure 2 Separation of 10 μg of a mixture of Ac-L-Phe-L-Trp-OMe and Ac-D-Phe-D-Trp-OMe on a *poly*(methacrylic acid-*co*-EDMA) CSP (4.6×200 mm column) imprinted with Ac-L-Phe-L-Trp-OMe. Isocratic elution at 1 mL min^{-1} with CHCl_3 -HOAc (99 : 1). Attenuation was increased 10-fold at 10 min. (Adapted from Ramström O, Nicholls IA and Mosbach K (1994) *Tetrahedron: Asymmetry* 5: 649–656, © 1994, with permission from Elsevier Science, UK.)

print molecule by one methylene unit, these polymers were able to separate all of the tested structurally related racemates, even if the separations were not as good as with the print molecule and its optical antipode. This shows that the polymer recognizes both

the amino-protecting group and the side chain, but that an exact fit is not necessary for enantioseparation in these cases.

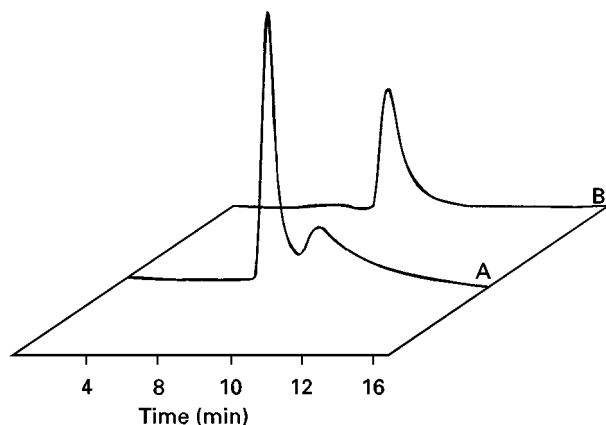
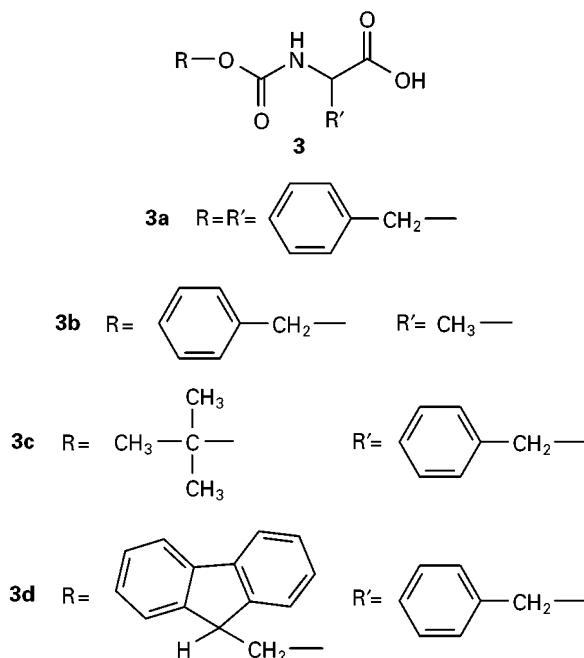


Figure 3 *Poly*(4-vinylpyridine-*co*-EDMA) CSP (4.6×200 mm column) imprinted with Z-L-aspartic acid. (A) 20 μg of racemic Z-aspartic acid was applied. Isocratic elution at 0.5 mL min^{-1} with tetrahydrofuran-HOAc (24 : 1) and detection at 260 nm. (B) 20 μg of racemic Z-glumatic acid was applied. Isocratic elution at 0.5 mL min^{-1} with tetrahydrofuran-HOAc (199 : 1) and detection at 260 nm. (Adapted from Kempe M, Fischer L and Mosbach K (1993) *Journal of Molecular Recognition* 6: 25–29, © 1993, with permission from John Wiley & Sons, UK.)



In a study on β -adrenergic blockers, (*S*)-timolol was imprinted in EDMA-based polymers. When the functional monomer was methacrylic acid, the

Table 2 Separation of racemic amino acid derivatives on Z-L-Phe-OH-imprinted CSPs

Racemate	poly(MAA-co-EDMA) ^{a,b,c} α	poly(MAA-co-TRIM) ^{a,b,d} α
Z-Phe-OH	1.84	2.49
Boc-Phe-OH	1.31	1.78
Fmoc-Phe-OH	1.21	1.66
Z-Ala-OH	1.28	1.59

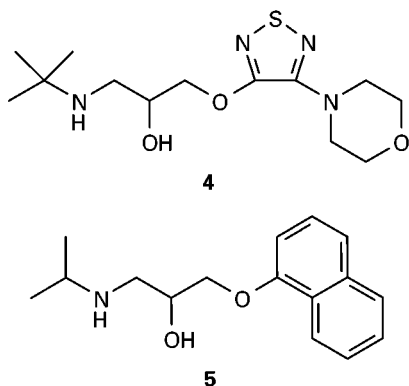
^aEDMA, Ethylene glycol dimethacrylate; MAA, methacrylic acid; TRIM, trimethylolpropane trimethacrylate.

^bThe separation factors were calculated as $\alpha = k_L/k_D$; $k = (t - t_0)/t_0$; t is the retention time of the analyte and t_0 is the retention time of unretained compound (the void).

^cData from Kempe M and Mosbach K (1994) Chiral recognition of N²-protected amino acids and derivatives in non-covalently molecularly imprinted polymers. *International Journal of Peptide and Protein Research* 44: 603–606.

^dData from Kempe M (1996) Antibody-mimicking polymers as chiral stationary phases in HPLC. *Analytical Chemistry* 68: 1948–1953.

polymer was able to resolve not only racemic timolol (4), but also racemic propanolol (5). In contrast to this, a timolol-imprinted polymer prepared with itaconic acid as the functional monomer instead of methacrylic acid could only resolve racemic timolol out of a number of racemates of structurally related β -blockers (Figure 4). This clearly demonstrates that the selectivity of MIPs can be highly dependent on the functional monomer used.



A comparison of six different CSPs, all imprinted with the same print molecule (Z-L-phenylalanine), confirms that the choice of monomers is important for the selectivity of the resulting polymers (Table 3). The selectivity of EDMA-based polymers was higher when vinylpyridines were used, either alone or together with methacrylic acid, than when methacrylic acid was used alone. Methacrylic acid interacts with the print molecule through hydrogen bonds. The beneficial effect of vinylpyridine is attributed to strong ionic interactions between the carboxy groups of the print molecule and the pyridinyl groups. The polymer prepared with acrylamide also showed a higher selectivity than the one prepared with methacrylic acid. Acrylamide forms strong hydrogen bonds even in a polar solvent such as acetonitrile.

It is noteworthy that the load capacity and the resolving capability increased when the trifunctional cross-linker pentaerythritol triacrylate (PETRA) was used instead of EDMA. The same features have been seen with polymers prepared with trimethylolpropane trimethacrylate (TRIM), another trifunctional cross-linker. *Poly(methacrylic acid-co-TRIM)* imprinted with a dipeptide was able to resolve 1 mg of the racemate with almost baseline separation (analytical column: 4.6×250 mm) (Figure 5).

(S)-Naproxen (6), a nonsteroidal anti-inflammatory drug, has been imprinted in *poly(4-vinylpyridine-co-EDMA)* by two different approaches. Bulk polymerization followed by grinding and sieving resulted in highly irregular particles and a two-step swelling and polymerization method gave uniformly sized beads. Both materials, used in the chromatographic mode, were able to separate naproxen from the related ibuprofen (7) and ketoprofen (8). The polymers were also able to resolve racemic naproxen, but not the racemates of ibuprofen and ketoprofen (Figure 6). Even

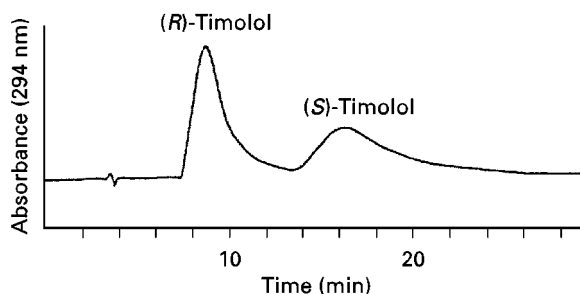


Figure 4 Separation of 20 μ g of racemic timolol on a *poly(itaconic acid-co-EDMA)* CSP (4.6×200 mm column) imprinted with (S)-timolol. Isocratic elution at 1 mL min^{-1} with EtOH-tetrahydrofuran-HOAc (5 : 4 : 1). (Adapted from Fischer L, Müller R, Ekberg B and Mosbach K (1991) *Journal of the American Chemical Society* 113: 9358–9360, © 1991, with permission from the American Chemical Society, USA.)

Table 3 Chiral separation of racemic Z-Tyr-OH on molecularly imprinted CSPs

Polymer ^a	Separated amount (μg)	α^b	R_s^c	f/g ^d
poly(AA-co-EDMA) ^e	40	3.62	2.52	n.d.
poly(MAA-co-EDMA) ^f	10	1.82	n.d.	0.50
poly(4VPy-co-EDMA) ^g	20	4.00	1.53	0.94
poly(2VPy-co-EDMA) ^f	10	3.81	1.90	0.95
poly(MAA-co-2VPy-co-EDMA) ^f	10	4.32	1.90	0.97
poly(MAA-co-PETRA) ^h	100	2.86	5.47	1.00
poly(MAA-co-PETRA) ^h	1000	2.06	n.d.	0.93

^aAA, Acrylamide; EDMA, ethylene glycol dimethacrylate; MAA, methacrylic acid; 2VPy, 2-vinylpyridine; 4VPy, 4-vinylpyridine; PETRA, pentaerythritol triacrylate.

^bThe separation factors were calculated as $\alpha = k'_1/k'_2$; $k' = (t - t_0)/t_0$; t is the retention time of the analyte and t_0 is the retention time of unretained compound (the void).

^cThe resolution factors (R_s) were calculated according to Wulff G, Poll HG and Minárik M (1986) Enzyme-analogue built polymers. XIX. Racemic resolution on polymers containing chiral cavities. *Journal of Liquid Chromatography* 9: 385–405.

^dThe resolution factors (f/g) were calculated according to Meyer VR (1987) Some aspects of the preparative separation of enantiomers on chiral stationary phases. *Chromatographia* 24: 639–645.

^eData from Yu C and Mosbach K (1997) Molecular imprinting utilizing an amide functional group for hydrogen bonding leading to highly efficient polymers. *Journal of Organic Chemistry* 62: 4057–4064.

^fData from Ramström O, Andersson LI and Mosbach K (1993) Recognition sites incorporating both pyridinyl and carboxy functionalities prepared by molecular imprinting. *Journal of Organic Chemistry* 58: 7562–7564.

^gData from Kempe M, Fischer L and Mosbach K (1993) Chiral separation using molecularly imprinted heteroaromatic polymers. *Journal of Molecular Recognition* 6: 25–29.

^hData from Kempe M (1996) Antibody-mimicking polymers as chiral stationary phases in HPLC. *Analytical Chemistry* 68: 1948–1953.

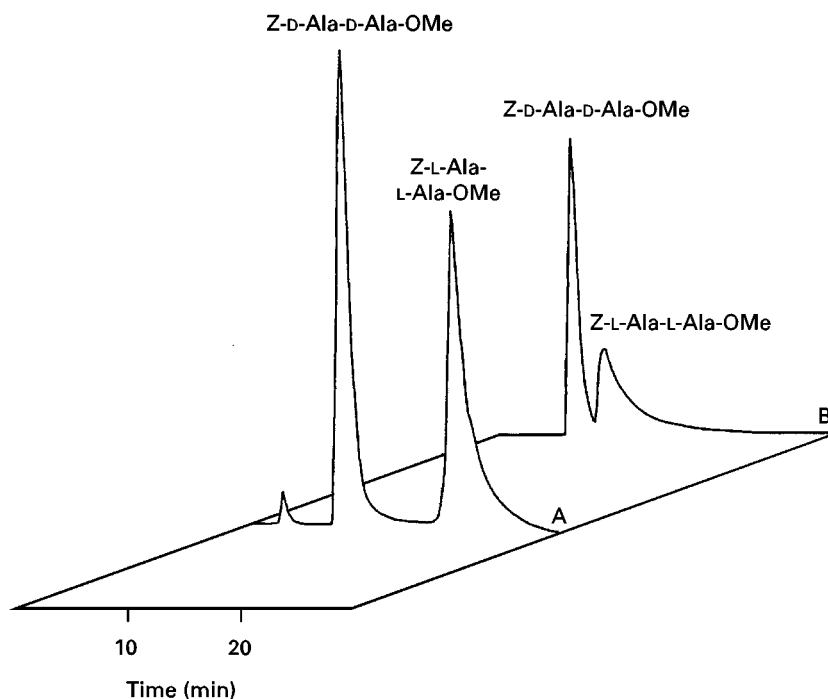


Figure 5 Separation of mixtures of Z-L-Ala-L-Ala-OMe and Z-D-Ala-D-Ala-OMe on a poly(methacrylic acid-co-TRIM) CSP (4.6 × 250 mm column) imprinted with Z-L-Ala-L-Ala-OMe. (A) 100 μg was applied. Gradient elution at 1 mL min⁻¹ with CHCl₃-HOAc (99.75 : 0.25) and CHCl₃-HOAc (4 : 1) (= B). Gradient: 0–10 min, 0% B; 10–18 min, 0–5% B; 18–22 min, 5% B; 22–24 min 5–0% B. Detection at 260 nm. (B) 1 mg was applied. Isocratic elution at 1 mL min⁻¹ with CHCl₃-HOAc (99.75 : 0.25). Detection at 260 nm. (Adapted from Kempe M (1996) *Analytical Chemistry* 68: 1948–1953, © 1996, with permission from the American Chemical Society, USA.)

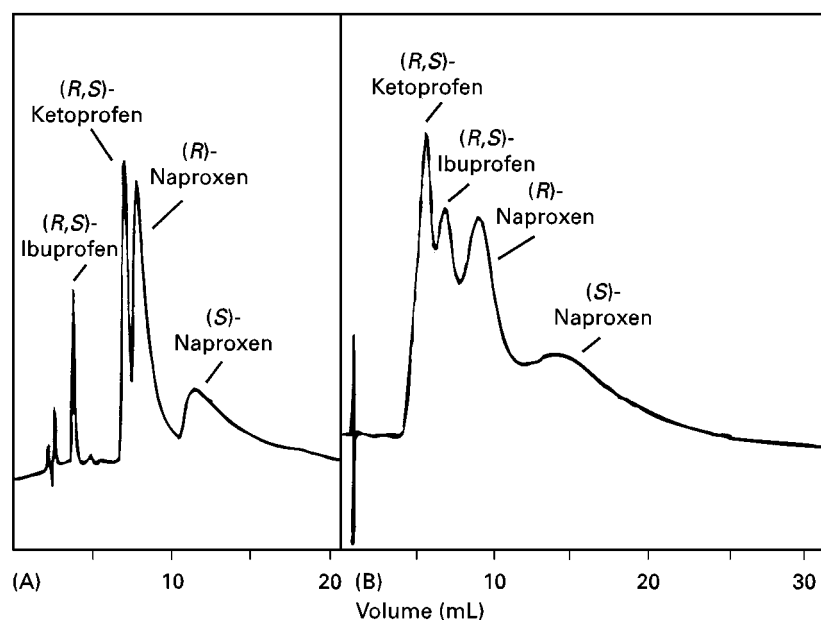
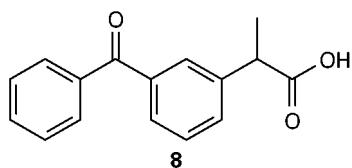
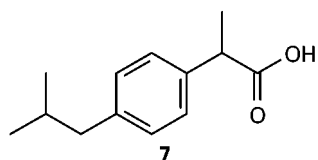
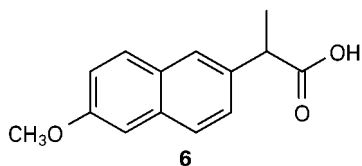


Figure 6 Separation of racemic mixtures of naproxen, ibuprofen and ketoprofen on *poly*(4-vinylpyridine-*co*-EDMA) CSPs (4.6×100 mm columns) imprinted with (*S*)-naproxen. (A) The column was packed with particles prepared by grinding and sieving a bulk polymer. Isocratic elution at 0.1 mL min^{-1} with tetrahydrofuran–heptane–HOAc (250 : 250 : 1) and detection at 260 nm. (Adapted from Kempe M and Mosbach K (1994) *Journal of Chromatography A* 664: 276–279, © 1994, with permission from Elsevier Science, UK.) (B) The column was packed with beads prepared by a two-step swelling and polymerization method. Isocratic elution at 1.0 mL min^{-1} with CH_3CN –phosphate buffer (20 mmol L^{-1} , pH 4.0) (1 : 1) and detection at 254 nm. (Adapted from Haginaka J, Takehira H, Hosoya K and Tanaka N (1997) *Chemistry Letters*, 555–556, © 1997, with permission from the Chemical Society of Japan.)

if comparisons of the two chromatograms cannot be done because of differing flow rates, it is not obvious that the chromatographic efficiency was better with the uniformly sized beads (Figure 6B) than with the irregular particles (Figure 6A). This may be due to impairment on the selectivity by water interfering with the monomer–print molecule complex, since water was used as the suspension medium in the two-step swelling and polymerization method.



In general, the polymerizations in noncovalent molecular imprinting have to be done in nonaqueous solutions to prevent water molecules from interfering with the interactions between the monomers and the templates, as previously discussed. Several reports, however, show that the chromatography can be performed efficiently with buffered aqueous eluents.

An approach has been developed which allows both the imprinting and the chiral separation of free amino acids to be carried out in aqueous solutions. The recognition was based on metal coordination–chelation interactions using *N*-(4-vinylbenzyl)imino-diacetic acid as the functional monomer. The method worked best for aromatic amino acids (Figure 7).

TLC

MIPs selective for phenylalanine anilide have been evaluated as stationary phases in TLC. Glass backing plates were coated with mixtures of finely ground MIP particles and binders. The plates showed preferential retardation of the enantiomer used as the print molecule (Figure 8). The R_F values of both enantiomers on nonimprinted polymers were higher than those observed on the imprinted polymers. The separations suffered from spot broadening, which was attributed to the heterogeneity of the recognition sites.

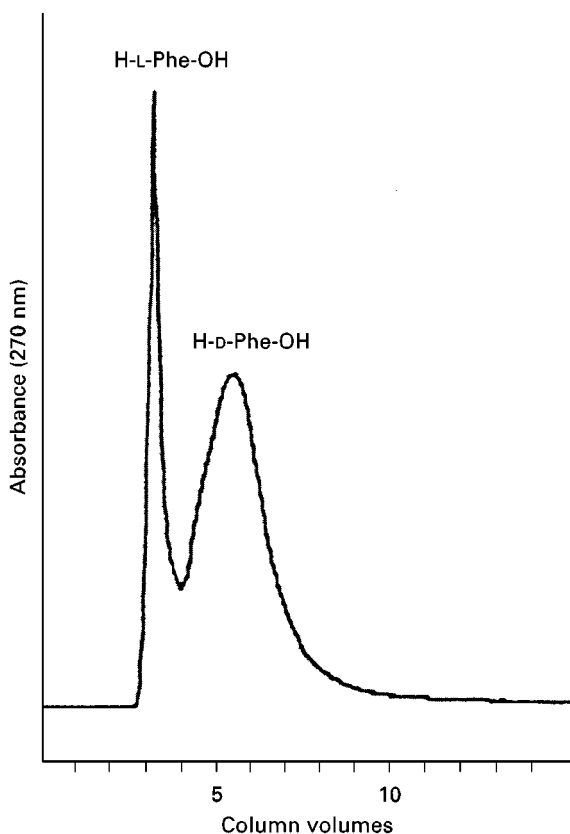


Figure 7 Separation of 17 μg of racemic phenylalanine on $\text{poly}(\text{Cu}(\text{II})[N-(4\text{-vinylbenzyl})]\text{iminodiacetate-co-EDMA})$ grafted to silica particles (4.6 \times 50 mm column). The polymer was imprinted with D-phenylalanine. Isocratic elution at 1 mL min^{-1} , 50°C with 1.5 mmol L^{-1} glycine in water. (Adapted from Vidyasankar S, Ru M and Arnold FH (1997) *Journal of Chromatography A* 775: 51–63, © 1997, with permission from Elsevier Science, UK.)

The technique is attractive because it is simple, fast and allows multiple analyses in the same run.

CE and CEC

Chiral separation by CE and CEC is achieved using a chiral selector which is either free in the mobile phase or immobilized to the stationary phase. MIPs can be used as the selector in both approaches. Molecularly imprinted capillary columns have been prepared by various approaches:

1. packing performed MIP particles into the capillaries
2. dispersion polymerization *in situ* in the capillaries
3. incorporating preformed MIP particles into polyacrylamide gels
4. *in situ* polymerization on the inner walls of the capillaries
5. filling the capillaries with a monolithic polymer with continuous pores by *in situ* polymerization.

Figure 9A shows the separation of racemic propanolol by CEC on a capillary column filled with $\text{poly}(\text{methacrylic acid-co-TRIM})$, polymerized *in situ* using (*R*)-propanolol as the print molecule. Several attractive features make this system look promising for the future: very low consumption of the print molecule (in this case only 10 μg), fast preparation of the capillaries (3 h) and fast separation (less than 2 min). In Figure 9B, MIP particles selective for (*S*)-propanolol were added to the mobile phase in a CE separation.

Future Developments

Molecular imprinting is a technique which has great potential. MIPs have found many applications, and many more are likely to be developed. One of the first applications investigated was CSPs, the subject of this chapter. A number of polymer systems have been developed and these have been used to imprint different classes of compounds.

To be able to attribute the binding of an MIP to an imprinting effect it is of the utmost importance to show that specific recognition sites were formed due to the presence of the print molecules during the polymerization. This is done by comparison with appropriate reference polymers. Polymers prepared without print molecules are not always the best choice, since the physical properties (surface area,

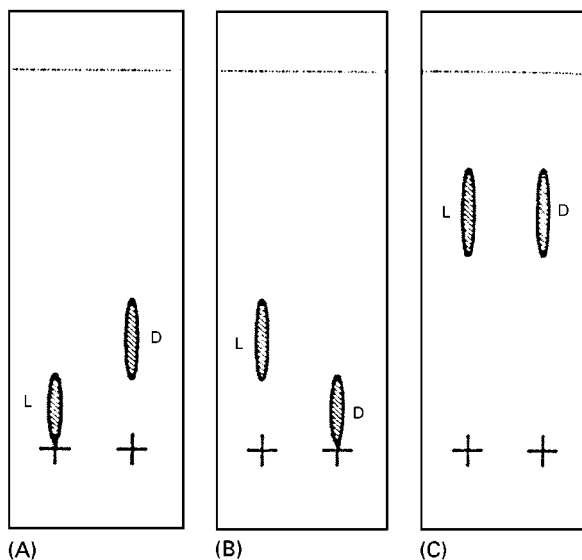


Figure 8 Separation of L- and D-phenylalanine anilide on TLC plates covered with $\text{poly}(\text{methacrylic acid-co-EDMA})$ imprinted with (A) L-phenylalanine anilide; (B) D-phenylalanine anilide and (C) no print molecule. Elution with $\text{CH}_3\text{CN-HOAc}$ (99 : 5). (Adapted from Kriz D, Berggren Kriz C, Andersson LI and Mosbach K (1994) *Analytical Chemistry* 66: 2636–2639, © 1994, with permission from the American Chemical Society, USA.)

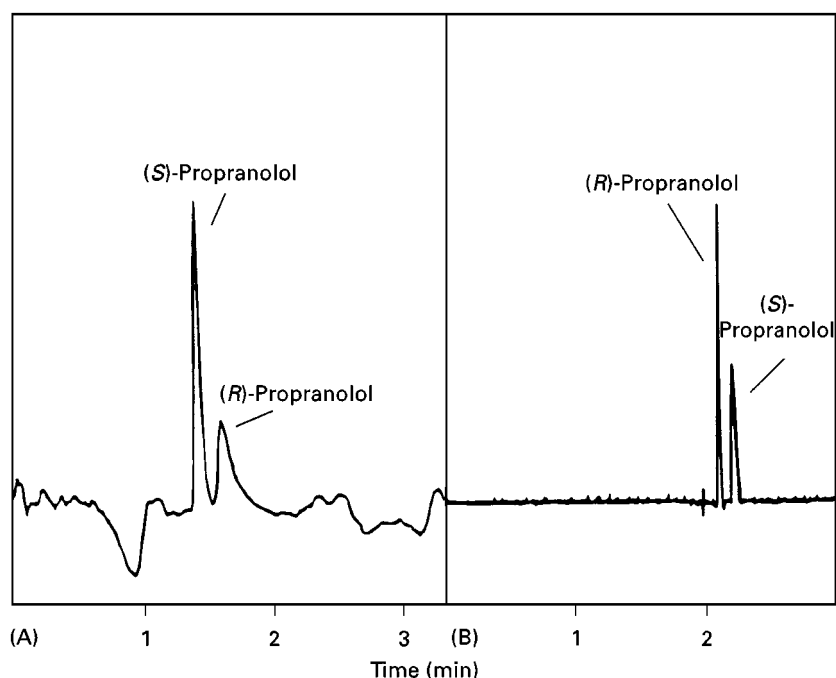


Figure 9 (A) Capillary electrochromatography (CEC). Separation of racemic propranolol on a *poly*(methacrylic acid-*co*-TRIM) CSP ($75\ \mu\text{m} \times 350\ \text{mm}$ capillary column) imprinted with (*R*)-propranolol. The sample was injected electrokinetically (5 kV, 3 s) and was separated at a constant voltage of 30 kV. The electrolyte was CH_3CN -acetate buffer ($4\ \text{mol L}^{-1}$, pH 3.0) (8 : 2). Detection at 214 nm. The capillary was thermostated to 60°C and an overpressure of 7 bar was applied. (Adapted from Schweitz L, Andersson LI and Nilsson S (1997) *Analytical Chemistry* 69: 1179–1183, © 1997, with permission from the American Chemical Society, USA.) (B) Capillary electrophoresis (CE). Separation of racemic propranolol using 0.05% (w/v) *poly*(*N*-acryloylalanine-*co*-EDMA) particles imprinted with (*S*)-propranolol as a chiral additive in the background electrolyte ($100\ \mu\text{m} \times 470\ \text{mm}$ capillary column). The sample was injected by a 3 s pressure injection and was separated at a constant voltage of 15 kV. The electrolyte was $5\ \text{mmol L}^{-1}$ phosphate buffer, pH 7.0. Detection at 210 nm. Temperature: 25°C . (Adapted from Walshe M, Garcia E, Howarth J, Smyth MR and Kelly MT (1997) *Analytical Communications* 34: 119–122, © 1997, with permission from the Royal Society of Chemistry, UK.)

porosity, etc.) of these polymers are often different from those of imprinted polymers. Reference polymers prepared with the optical antipode or a racemic mixture as the print species are preferred. The selectivity will be reversed when using the optical antipode, and a racemic mixture will give a polymer incapable of separating the two enantiomers (unless the monomers are chiral).

The goal of an endeavour involving chromatographic separation is to achieve the best possible performance with respect to selectivity, resolution, load capacity and analysis time. Much research effort on MIPs has therefore focused on improving the chromatographic performance. The use of monodisperse spherical beads instead of irregular particles improves the efficiency and investigations in this direction with MIPs have already given promising results. Another issue that needs to be investigated further is the heterogeneity of the binding sites. A more homogeneous population of sites would improve the chromatographic performance. The load capacity of MIPs has been shown to be improved by the use of trifunctional cross-linkers such as TRIM

and PETRA instead of the bifunctional EDMA. These findings look promising for future developments of MIPs for semipreparative and preparative purifications.

Molecular imprinting is an expanding area attracting an increasing number of scientists, in both industry and academia. This is evidenced by the fact that three-quarters of all papers on molecular imprinting were published during the last decade and one-third during 1996–1997. The rapid development of this technique is likely to result in many breakthroughs within the next few years.

See also: II/Affinity Separation: Imprint Polymers.

Further Reading

- Ansell RJ and Mosbach K (1996) Molecularly imprinted polymers: new tools for biomedical science. *Pharmaceutical News* 3: 16–20.
- Dickey FH (1949) The preparation of specific adsorbents. *Proceedings of the National Academy of Science of USA* 35: 227–229. (seminal paper)

- Kempe M and Mosbach K (1995) Separation of amino acids, peptides and proteins on molecularly imprinted stationary phases. *Journal of Chromatography A* 691: 317–323.
- Kempe M and Mosbach K (1995) Molecular imprinting used for chiral separations. *Journal of Chromatography A* 694: 3–13.
- Mayes A and Mosbach K (1997) Molecularly imprinted polymers: useful materials for analytical chemistry. *Trends in Analytical Chemistry* 16: 321–331.
- Mosbach K and Ramström O (1996) The emerging technique of molecular imprinting and its future impact on biotechnology. *BioTechnology* 14: 163–169.
- Sellergren B (1994) Enantiomer separation using tailor-made phases prepared by molecular imprinting. In: Subramanian G (ed.) *A Practical Approach to Chiral Separations by Liquid Chromatography*, pp. 69–93. Weinheim: VCH.
- Vidyasankar S and Arnold FH (1995) Molecular imprinting: selective materials for separations, sensors and catalysis. *Current Opinions in Biotechnology* 6: 218–224.
- Wulff G (1986) Molecular recognition in polymers prepared by imprinting with templates. In: Ford WT (ed.) *Polymeric Reagents and Catalysts*, pp. 186–230. Washington, DC: American Chemical Society.
- Wulff G (1995) Molecular imprinting in cross-linked materials with the aid of molecular templates – a way toward artificial antibodies. *Angewandte Chemie International Edition English* 34: 1812–1832.

Protein Stationary Phases

J. Haginaka, Mukogawa Women's University,
Nishinomiya, Japan

Copyright © 2000 Academic Press

In the early 1950s, it was reported that the binding of the enantiomers of an anionic azo-dye to bovine serum albumin (BSA) or human serum albumin (HSA) was different. Further, it was reported that L-tryptophan was bound to serum albumin (bovine mercaptoalbumin) more strongly than the D-form. These studies clearly indicated the possibility of enantioselective binding of ligands to proteins. In 1973, BSA-Sepharose was used for the separation of tryptophan enantiomers; this is the first report on the use of a protein stationary phase for chiral resolution purposes. With this stationary phase, D- and L-tryptophan were clearly resolved, and the D-form was eluted first, as shown in the previous binding studies in solution. In the following years, high performance liquid chromatography (HPLC) chiral stationary phases based on a protein were developed and used to separate a variety of enantiomers. HPLC chiral stationary phases based on a protein are of special interest because of their unique properties of stereoselectivity and because they are suited for separating a wide range of enantiomeric mixtures. Protein-based stationary phases developed so far have included albumins such as BSA and HSA, enzymes such as trypsin, α -chymotrypsin, lysozyme and pepsin, and glycoproteins such as α_1 -acid glycoprotein (AGP) from human or bovine serum, cellobiohydrolase I (CBH I), ovomucoid (in fact, ovoglycoprotein), avidin, ovotransferrin and flavoprotein (riboflavin-binding protein). The physical properties of these proteins are shown in Table 1. Chiral stationary

phases based on BSA, HSA, pepsin, AGP, CBH I, ovomucoid and avidin are now commercially available. Among those, AGP and ovomucoid-based stationary phases can separate a wide range of weakly acidic, weakly basic and neutral racemates.

The advantages of protein-based stationary phases generally include the use of an aqueous mobile phase, enantioselectivity for a wide range of compounds and direct analysis without derivatization. The disadvantages included low capacity, lack of ruggedness and limited understanding of the chiral recognition mechanism. Thus, the protein-based stationary phases are useful for analytical purposes, but are not generally applicable to preparative isolation. To stabilize the protein-based stationary phases, chemical modification of the side chains of the amino acids in the protein has been tried. Further, chiral stationary phases based on a protein fragment or protein domain have been prepared. These can be of higher capacity because only the active protein mass is used. Also, it is possible to understand the chiral recognition sites of protein-based stationary phases by investigating whether or not independent chiral binding sites exist on each fragment or domain.

This article deals with the preparation of HPLC chiral stationary phases based on a protein, their chiral recognition properties and the chiral recognition mechanisms of these stationary phases.

Preparation of HPLC Chiral Stationary Phases Based on a Protein

Generally, a protein is bound to derivatized silica gels. The disadvantage of silica-based stationary

Table 1 Physical properties of proteins

Protein	Molecular mass (kDa)	Carbohydrate composition (%)	Isoelectric point	Origin
<i>Albumins</i>				
BSA	66		4.7	Bovine serum
HSA	66		4.7	Human serum
<i>Enzymes</i>				
Trypsin	24		10.1	Bovine pancreas
α -Chymotrypsin	25		8.1–8.6	Bovine pancreas
Pepsin	34		< 1	Porcine stomach
Lysozyme	14		10.5–11.0	Egg white
<i>Glycoproteins</i>				
α_1 -Acid glycoprotein	44	45	2.7	Human or bovine serum
Cellobiohydrolase I	60	6	3.6	Fungus
Ovoglycoprotein	30	25	4.1	Egg white
Avidin	68	7	10.0	Egg white
Ovotransferrin	77	2.6	6.1	Egg white
Flavoprotein	32–36	14	4	Egg white or yolk

phases is that the eluent pH is limited to the ranges 2–8. However, in a strong acidic or alkaline solution, a protein sometimes suffers from denaturation. The separation of enantiomers on a protein-based stationary phase is generally attained using an eluent whose pH is between 3 and 8. Thus, the limitation of eluent pH ranges originated from silica-based materials is no problem for the use of protein-based stationary phases. **Figure 1** shows the typical preparation method for protein-based HPLC chiral stationary phases; in part A the method includes activation of porous aminopropylsilica gels by *N,N'*-disuccinimidylcarbonate (DSC), binding of a protein and blocking of the activated amino groups. In this case, a side chain amino group(s) of a protein such as lysine and arginine and/or an *N*-terminal amino group could be used for binding the protein to the activated gel. On the other hand, using water-soluble carbodiimide and *N*-hydroxysulfosuccinimide (HSSI), the carboxyl group of a protein can be bound to aminopropylsilica gels, as shown in **Figure 1B**.

Further, proteins can be bound to aminopropylsilica gels using glutaraldehyde as a cross-linker, resulting in cross-linking by Schiff-base formation. The resulted imino functions are reduced by using sodium cyanoborohydride. Glycerylpropylsilica gels activated with 1,1'-carbonyldiimidazole have been used for the preparation of chiral stationary phases. According to the two methods described above, an amino group of a protein is used to bind to the derivatized silica gels. In addition, a protein can be physically adsorbed on to porous silica gels. The disadvantage of the adsorption method is that the

adsorbed protein can be eluted, and it is better to bind a protein covalently to the base materials in order to avoid losses. The chiral recognition properties of a bound or adsorbed protein may be different from those of the protein in solution because of blocking of functional groups and/or conformational changes. The bound protein is often more stable to the changes of eluent pH and eluent composition compared to the protein in solution.

Retention and Enantioselectivity of Solutes on Protein-based Stationary Phases, and Optimization of Resolution

Table 2 shows the influence of eluent pH on the retention and enantioselectivity of various solutes on AGP-based chiral stationary phases. The retention factor of a basic solute, metoprolol, increased with an increase in the eluent pH. The decrease in the retention factor of an acidic solute, 2-phenoxypropionic acid, is ascribable to ion exclusion in addition to ionic repulsion between the carboxyl group of the 2-phenoxypropionic acid and the negatively charged AGP with an increase in eluent pH. The retention of basic solutes should be due to electrostatic interactions with the positively charged solutes and the negatively charged protein, in addition to hydrophobic interactions. Although the retention factor of an uncharged solute (ethotoin, hexobarbital) shows almost no pH dependence, a slight increase is observed with increasing eluent pH. This increase might be

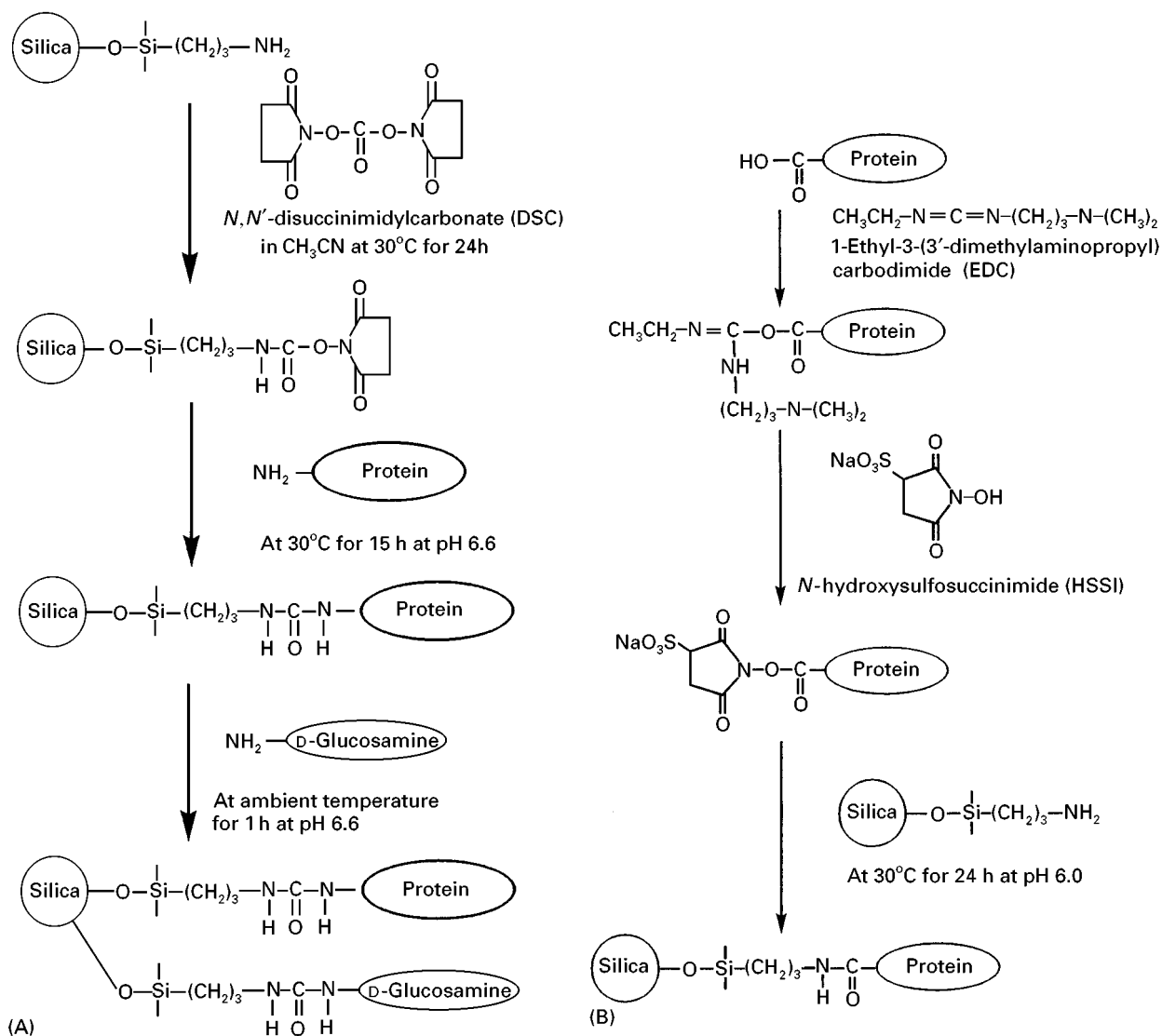


Figure 1 Synthesis scheme for the preparation of protein-based stationary phases: (A) via an amino group of a protein; (B) via a carboxyl group of a protein.

due to changes in the binding properties of the protein resulting from conformational changes. Table 3 shows the influence of the 2-propanol content on

retention and enantioselectivity of various solutes on AGP-based chiral stationary phases. With an increase in the 2-propanol content, the retention and

Table 2 Influence of eluent pH on retention of enantioselectivity of various solutes on AGP-based chiral stationary phase

Solute	pH 4.5		pH 5.5		pH 6.5		pH 7.5	
	<i>k</i> ₁	α	<i>k</i> ₁	α	<i>k</i> ₁	α	<i>k</i> ₁	α
2-Phenoxypropionic acid	8.55	1.59	1.77	1.57	0.32	1.48		
Ethotoin	4.06	3.82	3.87	4.19	3.82	4.59	4.13	5.06
Metoprolol	0.40	1.25	2.20	1.29	9.23	1.42	22.5	1.48
Hexobarbital	9.39	1.44	9.47	1.47	10.3	1.66	11.6	2.10

Mobile phase, 0.01 mol L⁻¹ phosphate buffer; *k*₁ is the retention factor of the first eluted enantiomer; α is enantio separation factor = *k*₂/*k*₁, where *k*₂ is the retention factor of the second eluted enantiomer. (Reproduced with permission from Hermansson J (1989) Enantiomeric separation of drugs and related compounds based on their interaction with α_1 -acid glycoprotein. *Trends in Analytical Chemistry* 8: 251.)

Table 3 Influence of 2-propanol on the retentivity and enantioselectivity of various solutes on AGP-based chiral stationary phase

Solute	2-PrOH (%)									
	1		2		4		6		8	
	k_1	α	k_1	α	k_1	α	k_1	α	k_1	α
Disopyramide					8.51	3.70	3.62	3.37	1.77	3.20
Chlorpheniramine	11.2	2.34	7.35	1.71	4.59	1.38				
Mepensolate			6.35	1.54	2.65	1.40	1.42	1.38	1.00	1.21
Mepivacaine	26.0	1.36	10.7	1.31	4.42	1.33	2.48	1.36	1.58	1.35
Bupivacaine					18.6	1.70	8.84	1.72	5.01	1.74

Mobile phase, 2-propanol in phosphate buffer, pH 7.2; k_1 , retention factor of the first eluted enantiomer; α , enantioselectivity factor = k_2/k_1 , where k_2 is the retention factor of the second eluted enantiomer. (Reproduced with permission from Hermansson J (1989) Enantiomeric separation of drugs and related compounds based on their interaction with α_1 -acid glycoprotein. *Trends in Analytical Chemistry* 8: 251.)

enantioselectivity of solutes are decreased. These results suggest that hydrophobic and electrostatic interactions play an important role in the retention and enantioselectivity of racemic solutes on AGP-based columns. Further, the hydrogen bonding properties of the organic modifier influence enantioselectivity to a large extent. As shown in **Figure 2**, verapamil enantiomers are not resolved on the AGP-based column using 1-propanol as an organic modifier, but are resolved using acetonitrile.

Similar retentive and enantioselective properties are observed with other protein-based stationary

phases. As described above, hydrophobic, electrostatic and hydrogen bonding interactions play an important role in chiral recognition of solutes on these phases. Thus, enantioseparations of solutes can be optimized by changing eluent pH, and the type and content of the uncharged organic modifier. Sometimes, charged modifiers such as *N,N*-dimethyloctylamine and octanoic acid are used for the enantioseparation of a charged solute. **Figure 3** shows a scheme for the optimization procedure for ovomucoid-based stationary phases.

Albumin-based Stationary Phases

BSA and HSA are closely related proteins and, consequently, the chromatographic properties of the chiral stationary phases based on these proteins are similar. Sometimes the elution order is reversed between chiral stationary phases based on these proteins; on the HSA-based phases (*S*)-warfarin elutes before (*R*)-warfarin, whereas on the BSA-based phases the opposite elution order is observed.

A variety of weakly acidic and neutral compounds are resolved on chiral stationary phases based on BSA and HSA. 2-Arylpropionic acid derivatives such as naproxen, flurbiprofen, ibuprofen, ketoprofen and fenoprofen, reduced folates such as leucovorin and 5-methyltetrahydrofolate, and benzodiazepines such as oxazepam, lorazepam and temazepam are separated. **Figure 4** shows enantioseparations of leucovorin, lorazepam hemisuccinate and *N*-benzoyl-phenylalanine on an HSA-based column. However, cationic compounds are not resolved on BSA and HSA phases. The structure-binding relationship for benzodiazepines using HSA stationary phases reveals that the binding of benzodiazepines occurs at a site that contains both a hydrophobic pocket and an area

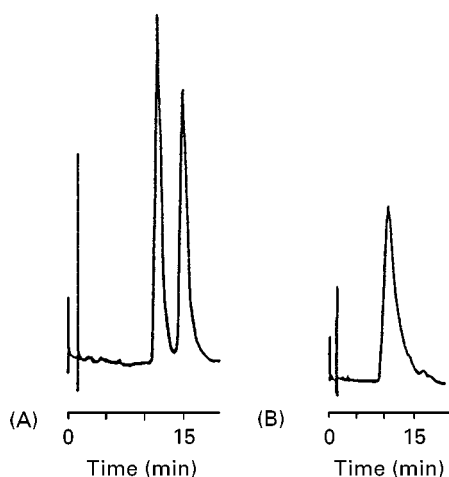


Figure 2 Influence of the nature of the organic modifier on the enantioselectivity of verapamil on an AGP-based column. HPLC conditions: column, Chiral-AGP (4.0 mm i.d. \times 100 mm); eluent: (A) 10% acetonitrile in 0.01 mol L⁻¹ phosphate buffer, pH 7.0; (B) 4% 1-propanol in 0.01 mol L⁻¹ phosphate buffer, pH 7.0. (Reproduced with permission from Hermansson J (1989) Enantiomeric separation of drugs and related compounds based on their interaction with α_1 -acid glycoprotein. *Trends in Analytical Chemistry* 8: 251.)

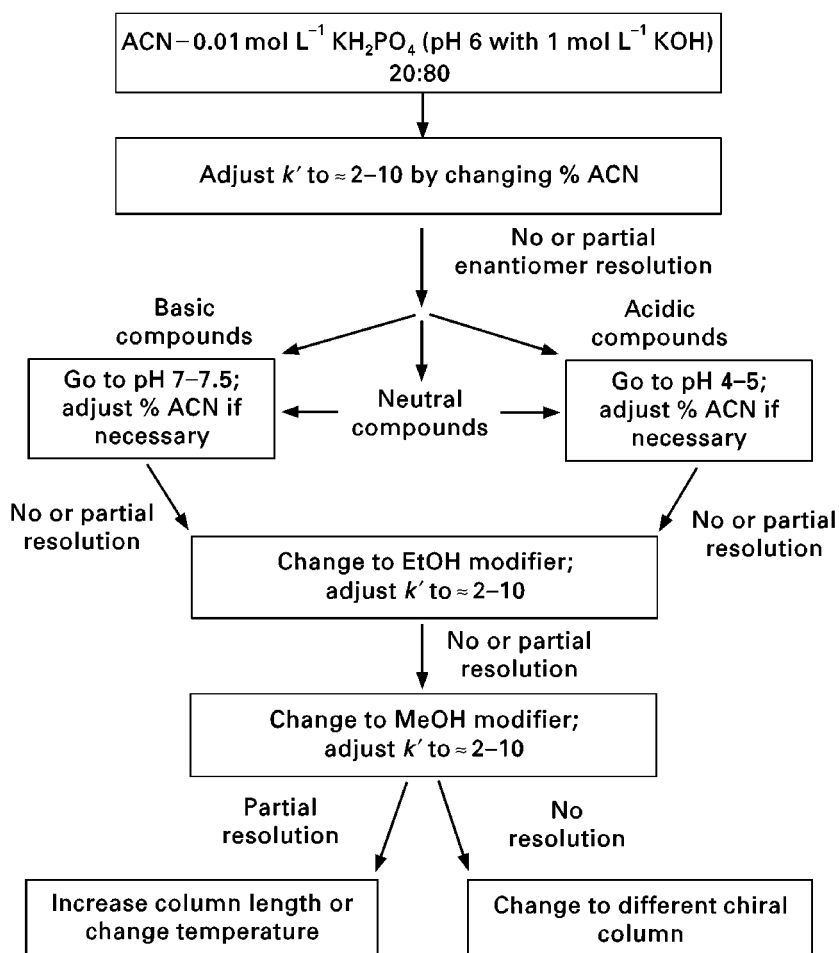


Figure 3 Scheme for the optimization procedure for ovomucoid-based stationary phases. ACN, acetonitrile. (Reproduced with permission from Kirkland KM and McCombs DA (1994) Changes in chiral selectivity with temperature with an ovomucoid protein-based column. *Journal of Chromatography A* 666: 211.)

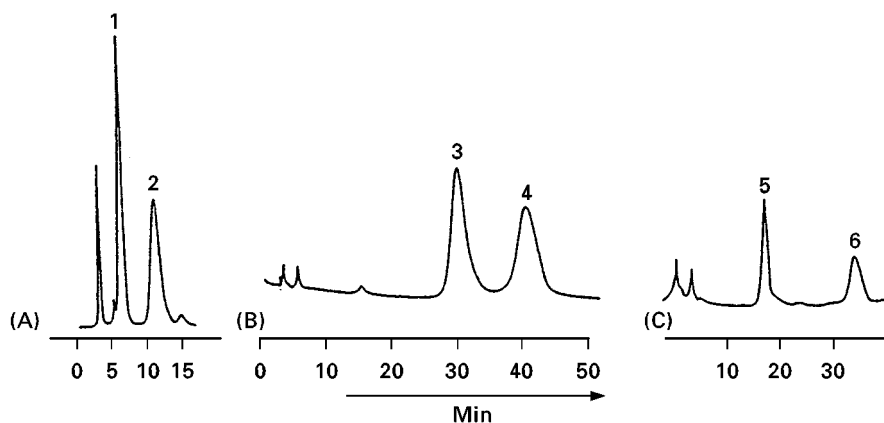


Figure 4 Enantioseparations of (A) leucovorin, (B) lorazepam hemisuccinate and (C) *N*-benzoyl-phenylalanine on an HSA-based column. HPLC conditions: column, 4.6 mm i.d. \times 150 mm; eluent, 50 mmol L⁻¹ phosphate buffer (pH 7.0): 1-propanol (94 : 6, v/v); flow rate, 0.8 mL min⁻¹. Peaks: 1, (6*S*)-leucovorin; 2, (6*R*)-leucovorin; 3, (-)-(*R*)-lorazepam hemisuccinate; 4, (+)-(*S*)-lorazepam hemisuccinate; 5, *N*-benzoyl-D-phenylalanine; 6, *N*-benzoyl-L-phenylalanine. (Reproduced with permission from Domenici E, Bertucci C, Salvadori P *et al.* (1990) Synthesis and chromatographic properties of an HPLC chiral stationary phase based upon human serum albumin. *Chromatographia* 29: 170.)

of cationic charge, and that the chiral recognition occurs in this binding site.

Enantioselectivity of stationary phases based on BSA produced with isolated protein fragments has been investigated. The BSA fragment following peptic digest of BSA has molecular weights of about 35 kDa which is an N-terminal half of amino acid residues 1–307. The BSA fragment phases give longer retentions for benzoin and benzodiazepines, and higher enantioselectivity for lorazepam, benzoin and fenoprofen because of a higher density of chiral recognition site(s), compared with native BSA phases. Figure 5 shows chromatograms of lorazepam enantiomers on BSA and BSA fragment-based columns. However, it is plausible that the conformation of the BSA fragment might be different from that of the native BSA.

Enzyme-based Stationary Phase

Trypsin and α -chymotrypsin are a family of serine proteases. Trypsin-based stationary phases can resolve O-, N,O-derivatized amino acids which are substrates of the enzyme. This means that chiral separations are due to the activity of the enzyme, and that the chiral recognition site is on the enzyme activity site. α -Chymotrypsin stationary phases can resolve amino acids and amino acid derivatives.

When the eluent of pH 7 is continuously delivered, the pepsin-based stationary phases lose their chiral recognition properties. This result reveals that the immobilized pepsin is irreversibly denatured above pH 7. Thus, the use of an eluent with pH less than 6 is

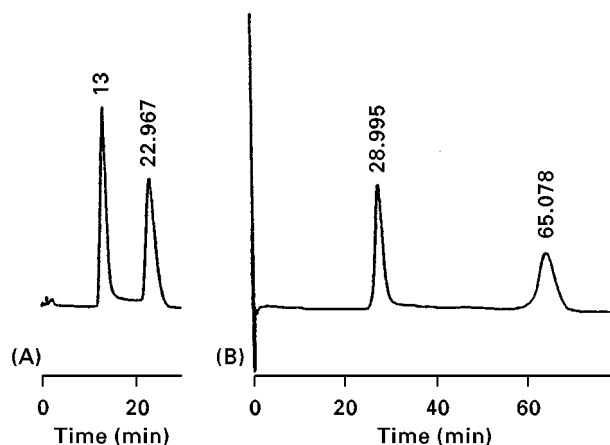


Figure 5 Chromatograms of lorazepam enantiomers on (A) BSA-based and (B) BSA-fragment-based columns. HPLC conditions: column, 2.1 mm i.d. \times 100 mm; eluent, 50 mmol L⁻¹ phosphate buffer (pH 7.5) containing 4% 1-propanol; flow rate, 0.2 mL min⁻¹. (Reproduced with permission from Haginaka J and Kanasugi K (1995) Enantioselectivity of bovine serum albumin-bonded columns produced with isolated protein fragments. *Journal of Chromatography A* 694: 71.)

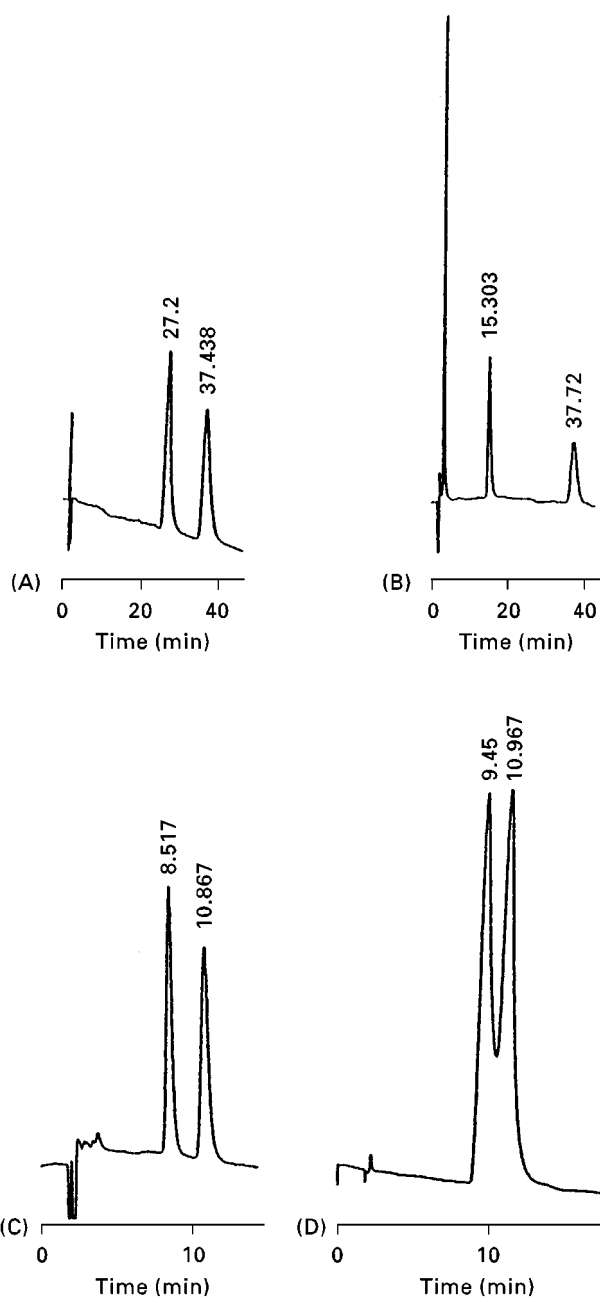


Figure 6 Enantioseparations of (A) homochlorcyclizine, (B) verapamil, (C) alprenolol and (D) oxazepam on a pepsin-based column. HPLC conditions: column, 4.6 mm i.d. \times 100 mm; eluent, 20 mmol L⁻¹ phosphate buffer (pH 5.1) containing (A) 5 and (B) 10% acetonitrile and (C) and (D) 5% ethanol; flow rate, 0.8 mL min⁻¹. (Reproduced with permission from Haginaka J, Miyano Y, Saizen Y *et al.* (1995) Separation of enantiomers on a pepsin-bonded column. *Journal of Chromatography A* 708: 161.)

recommended. By using a mixture of phosphate buffer and organic modifier as an eluent, cationic (especially β -blocking agents) and neutral enantiomers are resolved, while no resolution of acidic enantiomers is observed. Figure 6 shows enantioseparations of

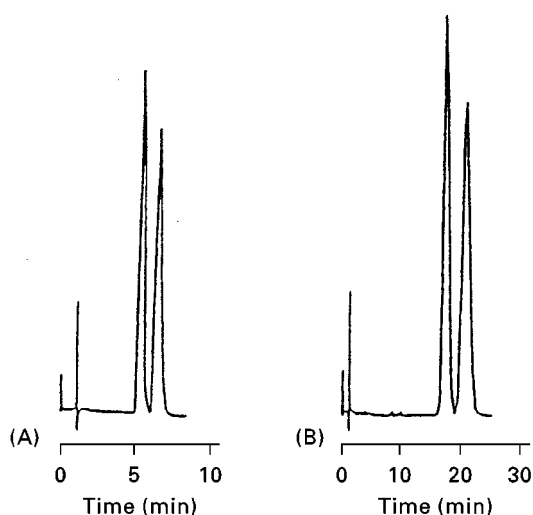


Figure 7 Enantioseparations of (A) metoprolol and (B) pindolol on an AGP-based column. HPLC conditions: column, Chiral-AGP (4.0 mm i.d. \times 100 mm); eluent (A) 3.8% ethanol in 0.01 mol L⁻¹ phosphate buffer, pH 7.0; (B) 15% methanol in 0.01 mol L⁻¹ phosphate buffer, pH 7.0. (Reproduced with permission from Hermansson J (1989) Enantiomeric separation of drugs and related compounds based on their interaction with α_1 -acid glycoprotein. *Trends in Analytical Chemistry* 8: 251.)

homochlorcyclizine, verapamil, alprenolol and oxazepam on a pepsin-based column. Also, lysozyme-based stationary phases showed chiral recognition ability to cationic and neutral solutes but no resolution of anionic solutes.

α_1 -Acid Glycoprotein-based Stationary Phase

AGP is the major plasma protein responsible for the protein binding of basic drugs. A variety of cationic, anionic and uncharged compounds can be resolved using this stationary phase. Cationic compounds resolved include β -blockers such as alprenolol, oxprenolol, propranolol, metoprolol and pindolol and histamine antagonists such as chlorpheniramine and dimethindene. **Figure 7** shows enantioseparations of metoprolol and pindolol on an AGP-based column. Anionic compounds resolved include 2-arylpropionic acid derivatives such as fenoprofen, ibuprofen and naproxen. As described above, separation of enantiomers is optimized by changing eluent pH, and the type and content of the uncharged organic modifier. However, cationic modifiers such as *N,N*-dimethyloctylamine and tetrabutylammonium bromide and anionic modifiers such as octanoic acid and butyric acid can be used effectively with AGP-based materials. An ion-pairing modifier, *N,N*-dimethyloctylamine, in the eluent gives a large increase in enantioselectivity of racemic acid, naproxen, on an AGP-

based stationary phase, where the retention factor of the second-eluted enantiomer is increased drastically. This is due to an allosteric interaction in which the affinity of the protein for the enantiomer is increased by the addition of the modifier.

AGP consists of a protein domain and sugar moieties, both of which have chiral components. It was thought that drug binding to AGP occurred at a single hydrophobic pocket or cleft within the protein domain of the molecule. However, the role of sugar moieties on enantioselective binding by AGP has not been investigated. It has been reported that sialic acid residues influence the enantioselective binding of basic drugs in different ways. They are not involved in the enantioselective verapamil-AGP binding. On the other hand, they participate in the binding of (*S*)-propranolol but not of (*R*)-propranolol. Further studies are required to clarify the role of sugar moieties in chiral recognition and the chiral recognition mechanism of AGP.

Cellobiohydrolase-based Stationary Phases

Chiral stationary phases based on CBH I can resolve acidic and basic racemates into their enantiomers. Higher enantioselectivity is especially obtained for the separation of β -blocking agents such as propranolol, oxprenolol and metoprolol. **Figure 8** shows a chromatogram of propranolol enantiomers on a CBH I-based column.

CBH I has a structural organization with a terminal, 36 residue-long binding domain connected to the rest of the enzyme (i.e. the core) through a flexible arm. The interconnecting region is rich in serine, threonine and proline residues and is highly glycosylated. The core is enzymatically active. CBH I is enzymatically degraded into two fragments, core

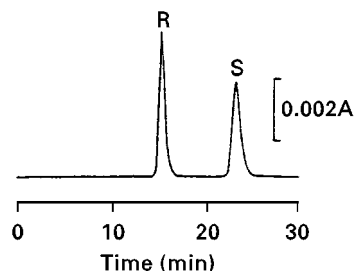


Figure 8 Chromatogram of propranolol enantiomers on a CBH I-based column. HPLC conditions: column, 5.0 mm i.d. \times 250 mm; eluent, sodium-acetate buffer pH 4.7, I = 0.01, containing 0.5% 2-propanol; flow rate, 0.3 mL min⁻¹; detection, 254 nm. (Reproduced with permission from Erlandsson P, Marle I, Hansson L *et al.* (1990) Immobilized cellulase (CBH I) as a chiral stationary phase for direct resolution of enantiomers. *Journal of the American Chemical Society* 112: 4573.)

and binding domain. Each fragment has been shown to contain at least one enantioselective site for propranolol. The dominating enantioselective site for propranolol and other solutes is located on the core, the main part of the enzyme. The three-dimensional structure of the active site of CBH I has been elucidated by X-ray crystallography, and it has been shown that the binding site is a tunnel with the dimensions $0.4 \times 0.7 \times 4$ nm. There are seven acidic amino acid residues, four tryptophan residues and also, tyrosine, serine, threonine, arginine and histidine lining the tunnel. This gives the prerequisite for obtaining stereoselective binding of a broad range of chiral solutes.

Ovogloboprotein-based Stationary Phases

Chiral stationary phases based on chicken ovomucoid (OMCHI) from egg whites have been prepared, which show chiral recognition abilities for a wide range of cationic, anionic and uncharged compounds, similar to AGP phases. However, the chiral recognition ability of OMCHI comes from other glycoproteins, as described below.

Ovomucoid from turkey egg whites (OMTKY) and OMCHI, which exist as three tandem, independent domains, have been isolated, purified and characterized, and columns based on OMTKY and OMCHI domains have been made to test their chiral recognition properties. The third domain of OMTKY and OMCHI consists of glycosylated (OMTKY3S and OMCHI3S) and unglycosylated domains (OMTKY3 and OMCHI3). The OMTKY3 and OMTKY3S, and OMCHI3 and OMCHI3S are enantioselective to at least two classes of compounds, benzodiazepines and 2-arylpropionic acid derivatives. Glycosylation of the third domain does not affect chiral recognition. The chiral recognition mechanism of the OMTKY3 has been elucidated using nuclear magnetic resonance measurements, molecular modelling and computational chemistry. The selected binding model for each of the (*R*)- and (*S*)-enantiomers of U-80 413 (whose structure is illustrated in Figure 9), a 2-arylpropionic acid derivative, with OMTKY3 shows similarities and differences in orientation and intermolecular interactions between the (*R*)- and (*S*)-enantiomers. The carboxyl groups of each enantiomer engage in electrostatic interactions with the positive charge on arginine-21. The carbonyl group on U-80 413's central ring shares a hydrogen bond with the NH_3^+ group of lysine-34. The distinguishing difference between the enantiomers is the proximity of the phenyl group of the (*R*)-enantiomer and phenylalanine-53. However, neither the first nor the second domain of the OMTKY and a

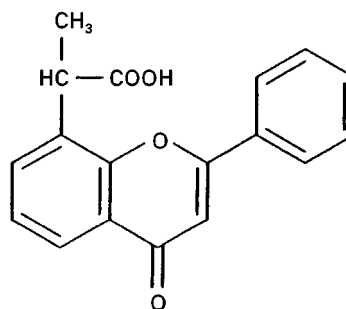


Figure 9 Structure of U-80 413.

combination of the first and second domains, or the second domain of the OMCHI gives chiral recognition ability.

These results suggest that three domains may be needed to work in concert for chiral recognition of various solutes, because columns made with the whole, intact OMTKY and OMCHI can resolve a wide range of weakly acidic, weakly basic and neutral racemates. Recently, a new protein from chicken egg whites has been isolated and characterized. It is termed ovogloboprotein (OGCHI, which means ovogloboprotein from chicken egg whites). It is found that 10% of OGCHI is included in crude OMCHI preparations. OMCHI and OGCHI columns made from isolated pure proteins have been compared with regard to their chiral recognition abilities. It is found that the pure OMCHI gives no chiral recognition abilities, and that the pure OGCHI gives better chiral recognition than those of the impure OMCHI reported previously, as shown in Table 4.

Table 4 Comparison of retention factor (k_1), enantioselectivity (α) and resolution (R_s) of various solutes on columns made with crude OMCHI and isolated OGCHI

Compound	Column					
	Crude OMCHI			OGCHI		
	k_1	α	R_s	k_1	α	R_s
Benzoin	2.50	2.71	6.06	11.4	3.18	10.1
Hexobarbital	0.35	1.00		1.52	1.29	0.83
Alprenolol	2.53	1.12	0.31	15.9	1.13	0.84
Propranolol	7.49	1.12	0.44	42.6	1.18	0.78
Chlorpheniramine	1.03	2.05	3.00	5.42	2.27	5.89
Ibuprofen	4.05	1.18	0.88	9.03	1.39	2.58
Ketoprofen	7.69	1.11	0.82	23.5	1.20	1.97

All values were averages of three replicates. HPLC conditions: column, 2.0 mm i.d. \times 100 mm; eluent, 20 mmol L^{-1} phosphate buffer (pH 5.1)-ethanol 90 : 10 (v/v); column temperature, 25°C; flow rate, 0.2 mL min^{-1} ; detection, 220 nm. (Reproduced with permission from Haginaka J, Seyama C and Kanasugi N (1995) The absence of chiral recognition ability in ovomucoid: ovogloboprotein-bonded HPLC stationary phases for chiral recognition. *Analytical Chemistry* 67: 2539.)

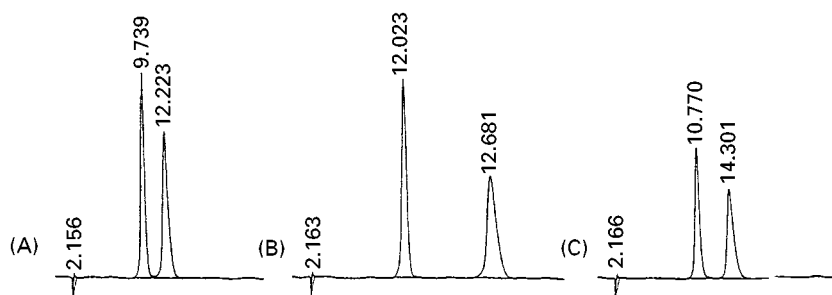


Figure 10 Enantioseparations of (A) ibuprofen, (B) ketoprofen and (C) flurbiprofen on an avidin-based column. HPLC conditions: column, 4.6 mm i.d. \times 150 mm; eluent, 20 mmol L⁻¹ potassium phosphate (pH 6.5) containing 6% ethanol; flow rate, 1.2 mL min⁻¹. (Reproduced with permission from Miwa T, Miyakawa T and Miyake Y (1988) Characteristics of an avidin-conjugated column in direct liquid chromatographic resolution of racemic compounds. *Journal of Chromatography* 457: 227.)

Though only 10% OGCHI was included in the impure OMCHI, the impure OMCHI-based column gave moderate chiral recognition (Table 4). This is due to the fact that OGCHI is preferentially bound to DSC-activated aminopropyl-silica gels compared with OMCHI, despite similarity in their average molecular masses (30 and 27 kDa, respectively).

Other Protein-based Stationary Phases

A number of further minor protein-based stationary phases for HPLC, based on avidin, ovotransferrin and flavoprotein, have been described. Avidin, a basic protein, strongly binds biotin with an association constant of 10^{15} mol L⁻¹. Avidin-based stationary phase shows excellent chiral recognition ability for 2-arylpropionic acid derivatives such as ibuprofen, ketoprofen, flurbiprofen, pranoprofen and fenoprofen. Figure 10 shows enantioseparations of ibuprofen, ketoprofen and flurbiprofen on an avidin-based column. A biotin-bound avidin stationary phase does not exhibit chiral recognition ability, because the biotin modifies the structure of the avidin.

Ovotransferrin is labile to heat and acid, but it seems that it is stable to heat when combined with metal ions such as iron, copper, manganese and zinc. Ovotransferrin is further stabilized by conjugation to silica gel as a chiral stationary phase, and ovo-transferrin-based stationary phases have been used for the separation of a basic compound, azelastine.

Flavoprotein, the riboflavin-binding protein, in egg whites and yolks has been introduced as a chiral stationary phase for HPLC. Egg white and yolk flavoproteins appear to be the product of the same gene but to have undergone different post-translational modifications. The amino acid sequence is the same but the yolk flavoprotein is between 11 and 13

amino acids shorter. There are differences in the carbohydrate links between flavoproteins from egg yolks and whites. Chiral stationary phases based on flavoproteins from egg whites and yolks exhibit chiral recognition abilities for uncharged, anionic and cationic compounds. There is no evidence whether the drugs interact with the riboflavin-binding site or not.

Future Trends

Chiral recognition sites of protein-based stationary phases will be located and their chiral recognition mechanisms will be elucidated using X-ray crystallography, ¹H-nuclear magnetic resonance spectroscopy and computational chemistry. Based on these findings, a protein, protein fragment or protein domain having chiral recognition abilities or a point-mutated protein can be overexpressed by genetic technologies. In the future, we could make protein-based stationary phases, which have better chiral recognition abilities and higher loadability, and are more stable than those so far prepared.

See also: III/Chiral Separations: Cellulose and Cellulose Derived Phases; Cyclodextrins and Other Inclusion Complexation Approaches; Ion-Pair Chromatography; Liquid Chromatography; Liquid Exchange Chromatography; Molecular Imprints as Stationary Phases.

Further Reading

- Allenmark S (1991) *Chromatographic Enantioseparation: Methods and Applications*, 2nd edn. Chichester: Ellis Horwood.
- Allenmark SG and Andersson S (1994) Proteins and peptides as chiral selectors in liquid chromatography. *Journal of Chromatography A* 666: 167.
- Haginaka J (1997) HPLC chiral stationary phases based on a glycoprotein. *Trends in Glycoscience and Glycotechnology* 9: 399.

- Krstulovic AM (ed.) (1989) *Chiral Separations by HPLC: Applications to Pharmaceutical Compounds*. Chichester: Ellis Horwood.
- Lough WJ (ed.) (1989) *Chiral Liquid Chromatography*. London: Blackie.
- Narayanan SR (1992) Immobilized proteins as chromatographic supports for chiral resolution. *Journal of Pharmaceutical and Biomedical Analysis* 10: 251.
- Stevenson D and Wilson ID (eds) (1988) *Chiral Separations*. New York: Plenum Press.
- Wainer IW (1993) *Drug Stereochemistry: Analytical Methods and Pharmacology*, 2nd edn. New York: Marcel Dekker.
- Zief M and Crane LJ (eds) (1988) *Chromatographic Chiral Separations*. New York: Marcel Dekker.

Supercritical Fluid Chromatography

N. Bargmann-Leyder and M. Caude, Laboratoire de Chimie Analytique (unité de recherche associée au CNRS) de l'Ecole Supérieure de Physique et Chimie Industrielles de Paris, Paris, France

A. Tambuté, Centre d'Etudes du Bouchet, Le Bouchet, France

Copyright © 2000 Academic Press

Introduction

Great emphasis is currently placed on differences in biological activities, potencies and toxicities of enantiomeric pharmaceutical compounds. The US Food and Drug Administration (FDA) has recently implemented regulations for the enantiomeric purity of enantiomeric drugs and chemicals. This has led to the development of chromatographic methods for the enantiomeric resolution of racemates including gas chromatography, liquid chromatography, and more recently supercritical fluid chromatography (SFC).

The physicochemical properties of enantiomers are the same except when they are placed in an asymmetric environment. This can be obtained before the chromatographic column or within the column by using a chiral derivatizing agent in the mobile phase or by using a chiral stationary phase.

Formation of Diastereomers by Using a Pre-Column Derivatization

In this method, the racemate is reacted with an optically pure compound leading to formation of diastereomers. Owing to their different physicochemical properties, diastereomers can be resolved by using classical achiral mobile and stationary phases. This method can only be applied to molecules bearing reactive functions such as amines, acids and alcohols. For preparative purposes, partial racemization can occur when recovering the initial enantiomer. This

problem represents the major limitation of this method. Moreover, this method has some disadvantages: (1) the chiral reagent must be optically pure, or its optical purity has to be well known (otherwise, poor accuracy will be achieved); (2) the derivatizing reaction must be quick and quantitative; and (3) the chromatographic behaviour of the derived diastereomers should be suitable (easy separation, good stability under the chromatographic conditions, ease of recovery with absence of racemization during the step leading to the initial enantiomers).

This was the method of choice before the development of chiral stationary phases (CSPs). It is still applied, but usually in order to improve detection limits. The method is not commonly used with SFC although (*S*)-trolox methyl ether has been used to derivatize chiral alcohols for attempted separation by GC and SFC with achiral systems. Using this derivatizing method, several compounds were successfully resolved by SFC but GC failed because of thermal decomposition of the ester derivatives.

Formation of Labile Diastereomers in the Mobile Phase

This method generally consumes chiral reagent. Moreover, the major limitation concerns detection, which must be compatible with the nature of the chiral reagent contained in the mobile phase. In the case of preparative applications the limitation is related to the recovery of the sample, which must be separated from the chiral reagent. Although, the optical purity of the reagent has no effect on the accuracy of the results, it decreases the selectivity of the method. One example of the use of SFC in this way is the chiral separation of amino alcohols using chiral ion pairing (**Figure 1**). In this case SFC analysis time was significantly less than that for high performance liquid chromatography (HPLC) separation.

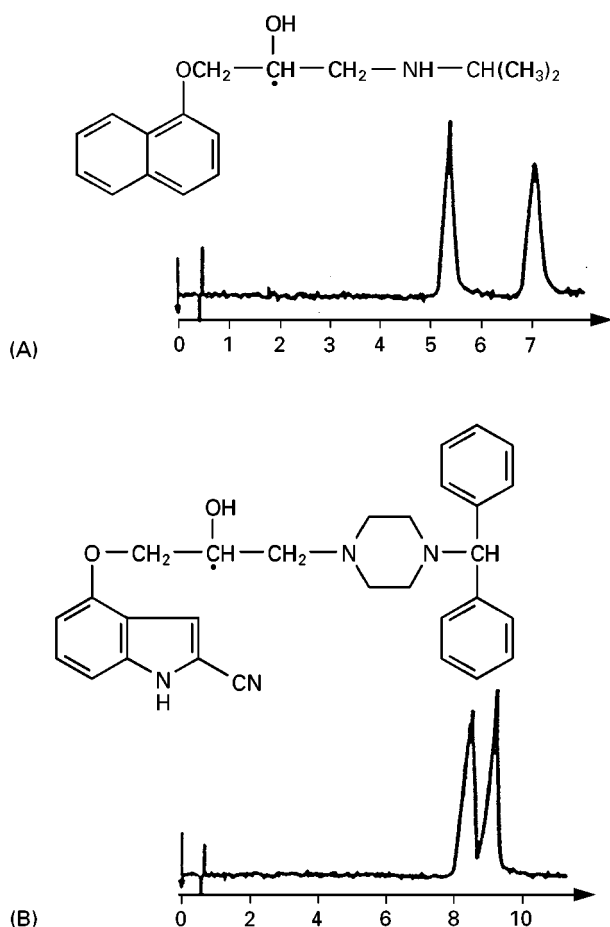


Figure 1 Chiral separation of propranolol (A) and DPI 101-106 (B) using ion pair SFC. Operating conditions: 100×4.6 mm i.d. column packed with $5 \mu\text{m}$ cyanopropyl-grafted silica (Brownlee GS-GU); mobile phase: carbon dioxide/acetonitrile (80 : 20, v/v) containing $5 \times 10^{-3} \text{ mol L}^{-1}$ of triethylamine and $3.5 \times 10^{-2} \text{ mol L}^{-1}$ of *N*-benzoxycarbonylglycyl-1-proline; pressure 250 bar; temperature: 21°C . (Reproduced from Steuer W, Schindler M, Schill G and Erni F (1988) *Supercritical fluid chromatography with ion-pairing modifiers. Separation of enantiomeric 1,2-aminoalcohols as diastereomeric ion pairs. Journal of Chromatography* 447: 287-296, with permission from Elsevier Science.)

Use of Chiral Stationary Phases

As in HPLC, SFC with chiral stationary phases, which was described for the first time by Mourier and colleagues, is the most powerful technique for the separation of enantiomers.

Capillary Columns

The coupling of SFC-CSPs can be performed either with capillary or packed columns. However, few applications have been described using capillary columns since the number of commercially available GC-CSPs is low and setting up the back-pressure regu-

lator is somewhat difficult to adjust precisely with a capillary column. Packed columns provide greater scope for applications, mainly due to the greater number of chiral stationary phases commercially available and their ease of use. Consequently only SFC on chiral packed columns will be described here.

Packed Columns

CSPs designed for HPLC are widely used in SFC. This is because separations are performed at room temperature so that there is greater interaction energy between CSP-racemate (and therefore higher selectivities) with fewer racemization problems. Packed-column SFC has the same advantages and this is why, since 1985, this technique has been successfully applied to chiral separations. However, the lack of commercial equipment for packed-column SFC has long been a major problem in the development of the technique; this handicap is now being overcome. The advantages of SFC over HPLC include: faster analysis, faster column equilibration, faster method development and also reduced generation of hazardous waste. It must also be underlined that SFC sometime exhibits thermodynamic advantages over HPLC by providing greater selectivity values (particularly with natural polymer CSPs).

Chiral Stationary Phases

The first commercial LC-CSP was described in 1981 and more than 100 CSPs are now commercially available (Table 1). These CSPs can be divided into four groups, depending on their chemical structure and the chiral recognition mechanisms involved.

Group I Group I CSPs are divided into two subgroups. Brush-type CSPs (Pirkle-type and analogues, constitute the first subgroup (IA in Table 1). They are the most amenable to scientific investigation because they work as independent CSPs, since each chiral graft operates independently in distinguishing the solute enantiomers.

Ligand-exchange CSPs (subgroup IB in Table 1) cannot be used in SFC because the formation of the ternary complex, chiral selector- Cu^{II} -solute, takes place almost exclusively in an aqueous medium.

Group II This group contains cyclodextrin CSPs and crown ether CSPs. Only the cyclodextrins have been applied in SFC (Table 1).

Group III The chiral selector is here a polymer, natural (as with amylose and cellulose) or synthetic (as with polyacrylamide) bearing a lot of stereogenic centres and asymmetric cavities. The formation of the

Table 1 Commercially available CSPs

<i>Chiral selector</i>	<i>Commercial name</i>	<i>Supplier</i>
<i>Type IA</i>		
(<i>R</i>)- or (<i>S</i>)-(3,5-Dinitrobenzoyl)phenylglycine	DNBPG	B, R
	ChiralDNBPG-C	Ser
	Sumichiral OA-2000	Sum
	Sumichiral OA-2000S	Sum
(<i>R</i>)- or (<i>S</i>)- <i>N</i> -(3,5-Dinitrobenzoyl)tyrosine <i>n</i> -butylamide	ChyRoSine-A	Sed
(<i>S</i>)-(<i>S</i>)- <i>N</i> -(3,5-dinitrobenzoyl)tyrosine [1-(1-naphthyl)-ethyl]amide	ChyRoSine-AD	Sed
(<i>S</i>)-(3,5-Dinitrobenzoyl)leucine	DNBLeu	B, R
	ChiralDNBL-C	Ser
(<i>S</i>)-(3,5-Dinitro-benzoyl)phenylalanine	Chiraline	SFCC
(<i>R</i>)- α -Methylbenzyl urea	Supelcosil-LC-(<i>R</i>)-urea	Sup
(<i>R</i>)- or (<i>S</i>)- <i>N</i> -(2-Naphthyl)alanine		R
(<i>S</i>)- α -(1-Naphthyl)ethylamine	Sumichiral OA-1000	Sum
(<i>R</i>)-Phenylglycine amide derivative and (<i>S</i>)-(4-(4-Chlorophenyl) isovaleric acid derivative	Sumichiral OA-2100	Sum
(<i>R</i>)-Phenylglycine amide derivative		
(1 <i>R</i> ,3 <i>R</i>)-Chrysanthemic acid derivative	Sumichiral OA-2200	Sum
(<i>R</i>)- or (<i>S</i>)-1-(3,5-Dinitrobenzoyl)naphthyl glycine	Sumichiral OA-2500	Sum
	Sumichiral OA-2500S	Sum
(<i>S</i>)-Valine <i>t</i> -butyl urea	Sumichiral OA-3000	Sum
(<i>S</i>)-(3,5-Dinitrobenzylurea)valine	Sumichiral OA-3100	Sum
(<i>S</i>)-(3,5-Dinitrobenzylurea) <i>tert</i> -leucine	Sumichiral OA-3200	Sum
(<i>S</i>)-Valine-(<i>S</i>)-[1-(1-naphthyl)ethyl]urea	Sumichiral OA-4000	Sum
(<i>S</i>)-Valine-(<i>R</i>)-[1-(1-naphthyl)ethyl]urea	Sumichiral OA-4100	Sum
(<i>R</i>)-Phenylglycine-(<i>R</i>)-[1-(1-naphthyl)ethyl]urea	Sumichiral OA-4200	Sum
(<i>R</i>)-Phenylglycine-(<i>S</i>)-[1-(1-naphthyl)ethyl]urea	Sumichiral OA-4300	Sum
(<i>S</i>)-Proline-(<i>S</i>)-[1-(1-naphthyl)ethyl]urea	Sumichiral OA-4400	Sum
(<i>S</i>)-Proline-(<i>R</i>)-[1-(1-naphthyl)ethyl]urea	Sumichiral OA-4500	Sum
(<i>S</i>)- <i>t</i> -Leucine-(<i>S</i>)-[1-(1-naphthyl)ethyl]urea	Sumichiral OA-4600	Sum
(<i>S</i>)- <i>t</i> -Leucine-(<i>R</i>)-[1-(1-naphthyl)ethyl]urea	Sumichiral OA-4700	Sum
Tartric acid and 3,5-dinitrobenzylphenylethylamine	Nucleosil Chiral-2	MN
Dimethyl <i>N</i> -3,5-dinitrobenzoyl- α -amino-2,2-dimethyl-4-pentyl phosphonate	(<i>R</i>)- α -Burke 1	B, R
(<i>S</i> , <i>S</i>)- or (<i>R</i> , <i>R</i>)-1-[(3,5-Dinitrobenzoyl)amino] 2-allyl-1,2,3,4-tetrahydrophenanthrene	(<i>S</i> , <i>S</i>) or (<i>R</i> , <i>R</i>) Whelk-O 1	B, R
<i>N</i> -3,5-Dinitrobenzoyl-3-amino-3 phenyl-2-(1,1-dimethylethyl)propanoate	β -GEM 1	B, R
<i>Type IB</i>		
Silica-grafted amino acids (proline, valine, hydroxyproline)	Chiral hydroxyCu	Ser
	Chiral proCu	Ser
	Chiral valCu	Ser
	Nucleosil Chiral-1	MN
	Chiralgel L-prolinamide	MN
	Chiralgel L-valinamide	MN
	Chiralgel L-phenylalaninamide	MN
	Chiralpak WM/WE	D
	Chiralpak MA (+)	D
	Accusphere	JW
1,2-(2-Carboxymethylamino)-diphenyl ethanol	Chiralpak WE	D
<i>Type IIA</i>		
α -Cyclodextrin	Cyclobond III	A
β -Cyclodextrin	Cyclobond I	A
	Chiradex	M
	Chiral β -dex	Ser
γ -Cyclodextrin	Cyclobond II	A
Acetylated α -cyclodextrin	Cyclobond III Ac	A
Acetylated β -cyclodextrin	Cyclobond I Ac	A
β -Cyclodextrin derived (<i>S</i>)-2-hydroxy-propyl	Cyclobond I SP	A
β -Cyclodextrin derived 2-hydroxy-propyl (racemic)	Cyclobond I RSP	A
β -Cyclodextrin derived (<i>S</i>)-[1-(1-naphthyl)ethyl]carbamate	Cyclobond I SN	A
β -Cyclodextrin derived (<i>R</i>)-[1-(1-naphthyl)ethyl]carbamate	Cyclobond I RN	A
β -Cyclodextrin derived [1-(1-naphthyl)ethyl]carbamate (rac)	Cyclobond I RSN	A
β -Cyclodextrin derived 3,5-dimethylphenylcarbamate	Cyclobond I DMP	A
β -Cyclodextrin derived 4-methylphenylcarbamate	Cyclobond I PT	A

Table 1 *Continued*

<i>Chiral selector</i>	<i>Commercial name</i>	<i>Supplier</i>
<i>Type IIB</i>		
Grafted silica crown ether	Crownpak CR(+)	D
<i>Type IIIA</i>		
Triacetylated microcrystalline cellulose (raw polymer)	Cellulose triacetate	M
	Chiral triacel	MN
	Chiralcel CA-1	D
Cellulose triacetate	Chiralcel OA	D
Tribenzoate cellulose	Chiralcel OB; OB-H	D
Triphenylcarbamate cellulose	Chiralcel OC	D
Tri(3,5-dimethylphenyl)carbamate cellulose	Chiralcel OD; OD-H	D
	Chiralcel OD-R	D
	(reversed-phase)	
<i>Type IIIB</i>		
Tri(4-chlorophenyl)carbamate cellulose	Chiralcel OF	D
Tri(4-methylphenyl)carbamate cellulose	Chiralcel OG	D
Tri(4-methylbenzoate)cellulose	Chiralcel OJ	D
Tricinamate cellulose	Chiralcel OK	D
Tri(3,5-dimethylphenyl)carbamate amylose	Chiralpak AD	D
Tri-(<i>R</i>)-(1-phenylethyl)]carbamate amylose	Chiralpak AS	D
<i>Type IIIB</i>		
Poly(<i>N</i> -1-acryloylphenylalanine ethylester)	Chiraspher	M
Poly(triphenylmethylmethacrylate)	Chiralpak OT(+)	D
Poly(2-pyridyl-diphenylmethylmethacrylate)	Chiralpak OP(+)	D
<i>Type IV</i>		
Bovine serum albumin	Resolvosil-BSA-7	MN
α_1 -Glycoproteic acid	Enantiopac	LKB
	Chiral-AGP	CT
Human serum albumin	Chiral protein 2	SFCC
Ovomucoide	Ultron ES-OVM	MM
Vancomycin	Chirobiotic V	A
Teicoplanin (macrocyclic antibiotics)	Chirobiotic T	A
Cellobiohydrolase (stable enzyme)	Chiral CBH	A

Suppliers: A, Astec; B, Baker; CT, ChromTech AB; D, Daicel; JW, J&W Scientific; LKB, Merck; MM, MAC-MOD Analytical; MN, Macherey-Nagel; R, Regis; Sed, SEDERE; Ser, Serva; Sum, Sumitomo; Sup, Supelco.

solute-CSP complex involves inclusion of the solute in the chiral cavities acting cooperatively. Group III CSPs (Table 1) can be applied in SFC.

Group IV Group IV contains protein and antibiotic-grafted silica. As for the phases in sub-group Ib, these CSPs cannot be used in SFC.

Applications

The most interesting applications of SFC concern the type IA and III CSPs, and to a lesser extent type II CSPs.

Group IA

As a general rule, most applications concern the brush-type CSPs having a π -electron acceptor charac-

ter. This is because many compounds of pharmaceutical interest contain a π -donor group.

CSPs derived from *N*-(3,5-dinitrobenzoyl)amino acids are among the most widely used for enantiomeric separations of numerous compounds. The early commercialization of the well-known (*R*)-*N*-(3,5-dinitrobenzoyl)phenylglycine-derived CSP ((*R*)-DNBPG), designed by Pirkle and co-workers in 1980, and the easy and inexpensive preparation of this type of CSP, has prompted many researchers to design new π -acid CSPs. Although the scope of applications of these CSPs does not vary very much, all workers agree that small structural changes in the phases can have significant effects on the chromatographic behaviour. Our laboratories have been involved in the development of CSPs derived from tyrosine. Among them, a 'broad-spectrum' CSP has been marketed under the

registered name ChyRoSine-A and an improved version of this has been described. Their enantiomer-recognition abilities have been evaluated both by LC and SFC and the scope of applications including numerous racemates such as benzodiazepines, sulfoxides, phosphine oxides, lactams and β -blockers demonstrated.

An anthrylamine derivative adsorbed onto porous graphitic carbon has been used to separate two commercial anti-inflammatory agents (ibuprofen and flurbiprofen) and a series of racemic tropic acid derivatives. The enantioselective properties of this material were compared with the corresponding silica-based CSP and it was concluded that the former was more efficient.

π -Basic CSPs, deriving from tyrosine and bearing two stereogenic centres, were designed and successfully applied to the enantioseparation of pharmaceutical compounds using SFC. Warfarin and ICI 176334 (a potential nonsteroidal antiandrogen used in the treatment of prostate cancer) were baseline-resolved on these phases without any prior derivatization step into 3,5-dinitrobenzoyl derivatives. Several π -donor CSPs, with (*R*)-*N*-pivaloylnaphthylethylamide as the chiral selector group, have been applied to SFC.

Valine-diamide phases have been used in SFC for the enantioseparation of racemic *N*-4-nitrobenzoylamino acid isopropyl esters. The enantioselectivity in SFC was comparable to that in LC using the mixture 2-propanol/*n*-hexane as mobile phase but the time required for analysis was less than 5 min by SFC.

As a general rule, the use of SFC does not improve enantioselectivity for type I CSPs. The selectivities obtained in LC and SFC are identical, showing that the chiral recognition mechanisms are the same for hexane and carbon dioxide. In this case, the advantage of SFC over LC is of a kinetic nature, giving higher efficiency per unit time and therefore faster analysis. **Figure 2** illustrates the kinetic advantage of SFC over LC by showing the separation of the enantiomers of Oxazepam on ChyRoSine-A in both LC and SFC. At constant resolution, the analysis time by SFC is 6 min, and 24 min by LC. However, it must be emphasized that in some cases different selectivities between LC and SFC are encountered.

The first of these cases concerns the nonconventional separation of π -acceptor solutes on π -acceptor CSPs. In such a case, π - π charge transfer interactions cannot take place during the chiral

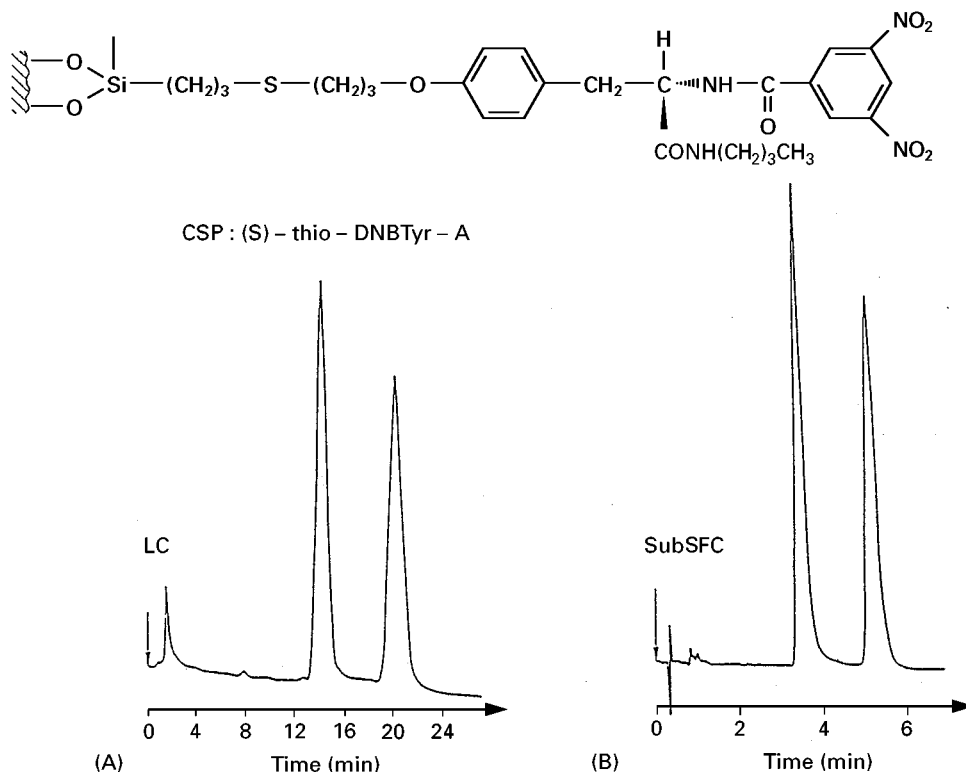


Figure 2 LC (A) and SFC (B) separations of the enantiomers of oxazepam using a ChyRoSine-A CSP: a comparison of analysis time at constant resolution ($R_s = 3.5$). Operating conditions: 150×4.6 mm i.d. column packed with $5 \mu\text{m}$ ChyRoSine-A CSP. LC: mobile phase, hexane/ethanol (90 : 10); flow rate, 2 mL min^{-1} . SubSFC: mobile phase, carbon dioxide/ethanol (92 : 8); flow rate, 4.5 mL min^{-1} at 0°C ; outlet pressure 200 bar. Temperature, 25°C ; UV detection at 229 nm. (Reproduced from Bargmann-Leyder N, Tambuté A and Caude M (1992) Chiralité et chromatographie en phase supercritique. A review. *Analysis* 20: 189–200.)

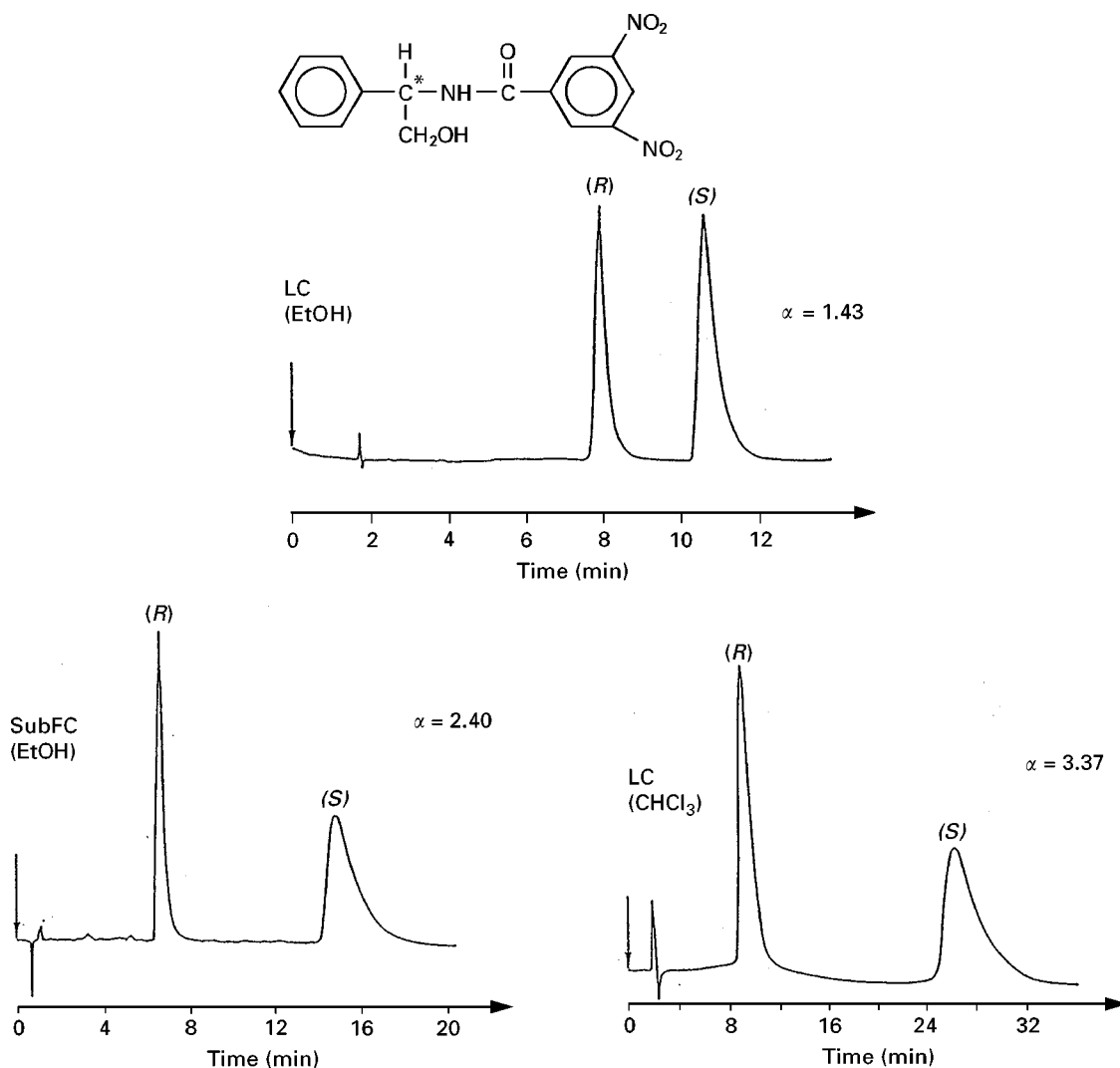


Figure 3 Influence of the nature of the mobile phase on the resolution of *N*-(3,5-dinitrobenzoyl)phenylglycinol on (R)-DNBPG. LC conditions: mobile phase, hexane/ethanol (85:15, v/v) ($k'(r) = 3.9$, $k'(s) = 5.6$) or hexane/chloroform (10:90, v/v) ($k'(r) = 4.3$, $k'(s) = 16.3$); flow rate 2 mL min^{-1} ; temperature, 25°C ; UV detection at 254 nm. SubSFC conditions: mobile phase, carbon dioxide/ethanol (93:7, w/w); flow rate 4.5 mL min^{-1} at 0°C ; average column pressure, 200 bar; temperature, 25°C ; UV detection at 254 nm. (Reproduced from Maccaudière P, Lienne M, Caude M, Rosset R and Tambuté A (1989) Resolution of π -acid racemates on π -acid chiral stationary phases in normal-phase liquid and subcritical fluid chromatographic modes. A unique reversal of elution order on changing the nature of the achiral modifier. *Journal of Chromatography* 467:357–372, with permission from Elsevier Science.)

recognition mechanism. This is why the main mechanism may vary depending on the mobile phase composition, sometimes resulting in a reversal of the elution order. As shown in **Figure 3**, important discrepancies in the selectivity values are noted between hexane/ethanol in LC and the supercritical mobile phase carbon dioxide/ethanol. The chromatographic behaviour observed in SFC is somewhat similar to that observed in LC with hexane/methylene chloride/chloroform mobile phases.

The second major exception concerns the separation of β -blockers using ChyRoSine-A as CSP. Surprisingly, the direct separation of a series of β -

blockers was achieved on commercially available ChyRoSine-A CSP and on its improved version, whereas these solutes appear to be unresolved or poorly resolved by normal-phase liquid chromatography (**Figure 4**; **Table 2**). The chromatographic behaviour (both in SFC and LC) of various propranolol analogues has been thoroughly studied and further spectroscopic investigations carried out. Starting from these data, detailed chiral recognition mechanisms have been proposed, based on molecular modelling. The solute conformations are selected by taking into account the information provided by the ^1H NMR spectra and it appears that the solvating

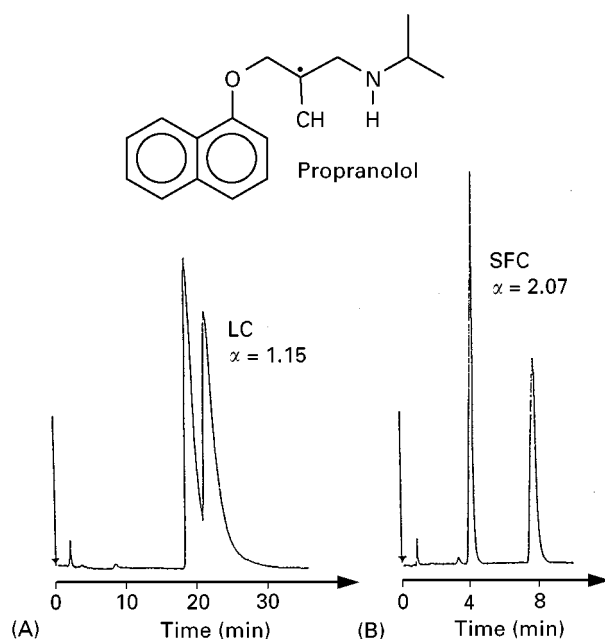


Figure 4 Comparative chromatograms of the resolution of propranolol on ChyRoSine-A CSP by LC (A) and SFC (B). Operating conditions: 150×4.6 mm i.d. column packed with $5 \mu\text{m}$ ChyRoSine-A CSP. LC: mobile phase/hexane/ethanol containing 1% v/v of *n*-propylamine (95 : 5, v/v); flow rate 1 mL min^{-1} . SFC: mobile phase, carbon dioxide/ethanol containing 1% v/v of *n*-propylamine (90 : 10); flow rate, 4 mL min^{-1} at 0°C , outlet pressure 200 bar. Room temperature; UV detection at 224 nm. (Reproduced with permission from Siret L, Bargmann N, Tambuté A and Caude M (1992) Direct enantiomeric separation of β -blockers on ChyRoSine-A by supercritical fluid chromatography: supercritical carbon dioxide as transient *in situ* derivatizing agent. *Chirality* 4: 252–262.)

effect of carbon dioxide induces a change in conformation of propranolol (Figure 5). This change occurs in the presence of carbon dioxide but only if the solute bears both an amino proton and an ether function separated by three carbon atoms. Without carbon dioxide, (*R*)- and (*S*)-propranolol conformers have geometrical structures such that the chiral recognition process is poor: the chiral centre of the solute cannot develop stereoselective interactions with the CSP and the interactions involved are the same for both enantiomers (Figure 6). On the other hand, the conformation of propranolol in the presence of carbon dioxide is geometrically favourable to the chiral discrimination. The conformations of the chiral stationary phase, (*R*)-solute, (*S*)-solute and their respective associations are shown in Figure 7. In this case, the (*R*)-propranolol conformer involves higher energy interactions with (*S*)-CSP than the (*S*) conformer.

High speed chiral separations (analysis duration < 1.5 min) of β -blockers have been achieved using

a short packed column and a high mobile phase flow rate. The use of high speed chiral separations allows a decrease in solvent consumption (CO_2 and polar modifier), and by minimizing band broadening in the column gives better detectability. As an example, Figure 8 shows the enantioseparation of propranolol and pindolol. These results again demonstrate the kinetic superiority of the SFC over LC. Moreover, in the case of β -blockers, the better kinetics of SFC is combined with enhanced thermodynamics owing to the favoured chiral recognition provided by the conformation of the molecules in the presence of carbon dioxide.

Finally, it should be noted that type I CSPs have been successfully applied to preparative SFC.

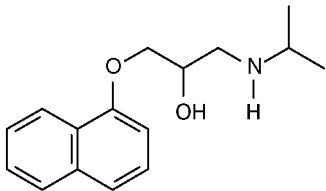
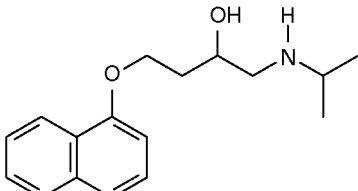
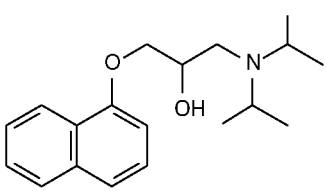
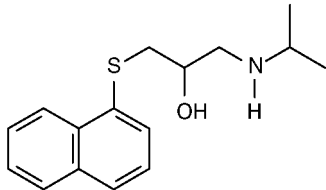
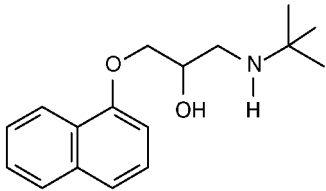
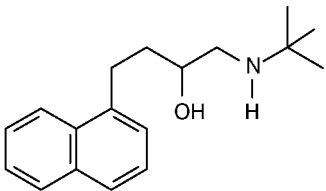
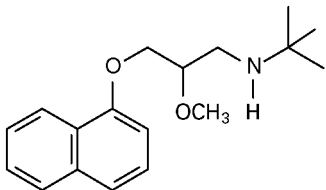
Group II

The scope of applications of a given cyclodextrin is determined by the goodness of the fit between the chiral cavity and the size of the solute to be resolved. If the cavity is too large compared with the solute, there is no preferred orientation (and therefore no selectivity); on the other hand, if the cavity is too small, there is no solute inclusion. Most separations are therefore achieved using β -cyclodextrin for which the internal diameter of the cavity (0.78 nm) is well suited to naphthyl, biphenyl, benzoyl or cyclohexyl moieties present in numerous molecules of pharmaceutical interest. γ -Cyclodextrin is well adapted to molecules bearing large substituents (such as phenobarbital); α -cyclodextrin is preferentially used for smaller molecules bearing a single aromatic group or a small aliphatic chain.

Cyclodextrin CSPs have been used for SFC, although they are, *a priori*, better adapted to the separation of enantiomers in reversed-phase LC. In fact, in normal-phase liquid chromatography, the hydrophobic solvent, e.g. hexane, chloroform, etc., occupies the cyclodextrin cavity and cannot easily be displaced by solutes. The average behaviour of the column is then somewhat similar to that of a diol column (almost no chiral resolution has been obtained using cyclodextrin phases in normal-phase liquid chromatography). The small size of the carbon dioxide molecule means that it can be displaced more easily than other apolar solvents such as hexane from the cyclodextrin cavities. Moreover, the carbon dioxide molecule exhibits an induced dipole moment, giving it a higher polarity than hexane.

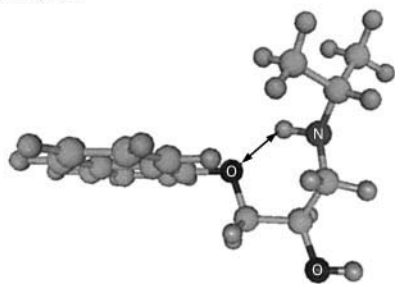
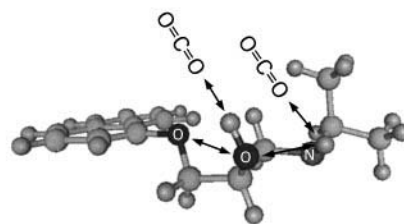
The use of polar modifiers induces a decrease in retention (polar modifier competes with the solute and increases the solubility of the solute). In terms of selectivity, all the polar modifiers that have been used (methanol, ethanol, 1-butanol, 2-butanol,

Table 2 Chromatographic data for the resolution of propranolol and some analogues on ChyRoSine-A CSP by LC and SFC

Compounds	LC			SFC		
	% polar modifier	k_2	α	% polar modifier	k_2	α
1 	5	11.7	1.14	12	19.8	2.07
2 	5	15.5	1	12	12.8	1.07
3 	5	13.2	1	12	11.3	1
4 	2.5	10.7	1	12	10.9	1.07
5 	5	9.72	1.32	12	24.7	2.27
6 	5	9.2	1	12	13.2	1.08
7 	5 2.5	1.7 2.3	1.01 1.03	12	13.9	1.47

Operating conditions: column 150×4.6 mm i.d., UV detection 224 nm. LC: mobile phase hexane/ethanol containing 1% (v/v) of *n*-propylamine, the percentage (v/v) of polar modifier in hexane is indicated in the table; room temperature; flow rate 2 mL min^{-1} . SFC: mobile phase carbon dioxide/methanol containing 1% (v/v) of *n*-propylamine, the percentage (v/v) of polar modifier in CO_2 is indicated in the table; temperature 25°C ; average column pressure 180 bar; flow rate at 0°C 4 mL min^{-1} .

(R)-Propranolol

(R)-Propranolol, $n\text{CO}_2$ 

(S)-Propranolol

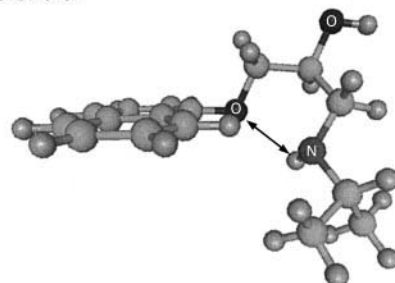
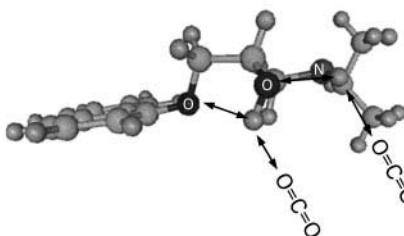
(S)-Propranolol, $n\text{CO}_2$ 

Figure 5 Change of the propranolol conformation induced by carbon dioxide. (A) Optimized structures of (R)- and (S)-propranolol without CO_2 . The intramolecular hydrogen bonding is by an arrow. (B) Optimized structures of (R)- and (S)-propranolol with CO_2 . In order to simplify the figure, only two molecules of carbon dioxide are illustrated. (Reproduced with permission from Bargmann-Leyder N, Sella C, Bauer D, Tambuté A and Caude M (1995) Separation of β -blockers using supercritical fluid chromatography: investigation of the chiral recognition mechanism using molecular modelling. *Analytical Chemistry* 67: 952–958.)

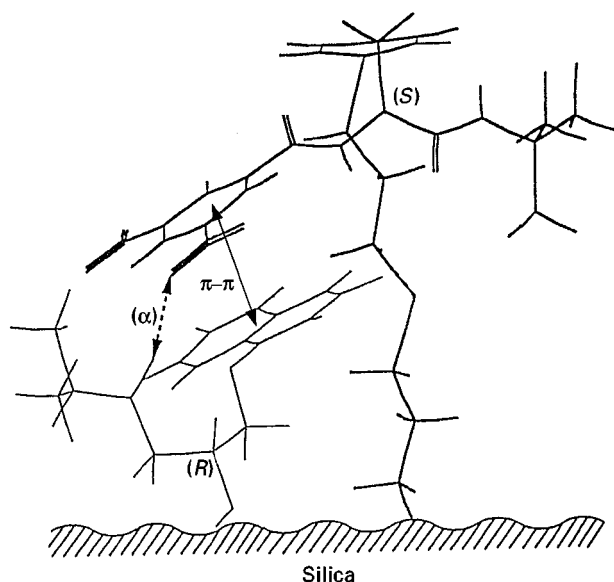


Figure 6 Optimized association between the optimized structures of (R)-propranolol (without carbon dioxide) and ChyRoSine-A CSP. (Reproduced with permission from Bargmann-Leyder N, Sella C, Bauer D, Tambuté, A and Caude M (1995) Separation of β -blockers using supercritical fluid chromatography: investigation of the chiral recognition mechanism using molecular modelling. *Analytical Chemistry* 67: 952–958.)

2-propanol) are almost equivalent. Water should not be used since it decreases selectivity significantly.

As reported by Macaudière and co-workers, the use of cyclodextrin CSPs in SFC allows particular selectivities to be obtained. A comparison between solute behaviour in reversed-phase and in normal-phase liquid chromatography clearly demonstrated that SFC and reversed-phase liquid chromatography are two complementary techniques; this result has widened the range of cyclodextrin phase applications. **Figure 9** shows the comparison of the separation of the 2-naphthyl and *o*-anisyl phosphine oxides on Cyclobond I in normal-phase LC and SFC. No or very weak enantiomeric resolution is achieved using normal-phase LC.

Enantiomeric separation of a variety of drugs and related compounds (ancymidol, coumachlor, ibuprofen, mephénytoin, tropicamide, verapamil, etc.) on an (S)-naphthylethylcarbamoylated- β -cyclodextrin phase using sub- and supercritical fluid chromatography has been accomplished by Williams and co-workers. Compounds previously resolved on native or derivatized cyclodextrin CSPs in LC using reversed-phase or polar organic mobile phases could be resolved in SFC using a simple carbon dioxide/methanol eluent. Resolution of cromakalim was

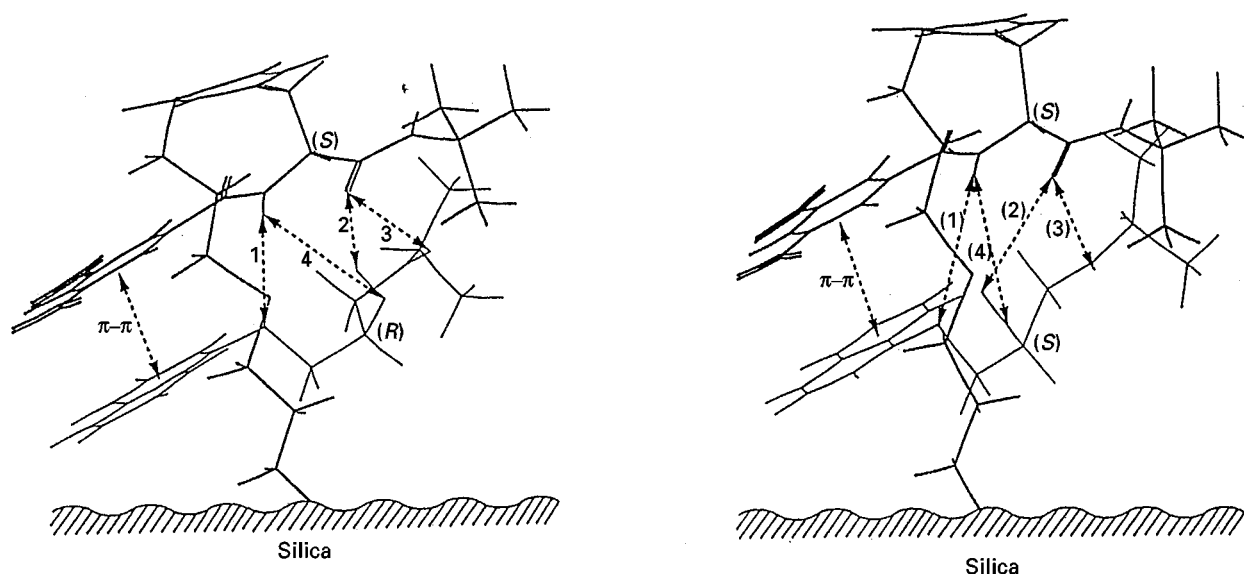


Figure 7 Optimized associations between the optimized structures of (*R*)- and (*S*)-propranolol (with carbon dioxide) and ChyRoSine-A CSP. (Reproduced with permission from Bargmann-Leyder N, Sella C, Bauer D, Tambuté A and Caude M (1995) Separation of β -blockers using supercritical fluid chromatography: investigation of the chiral recognition mechanism using molecular modelling. *Analytical Chemistry* 67: 952–958.)

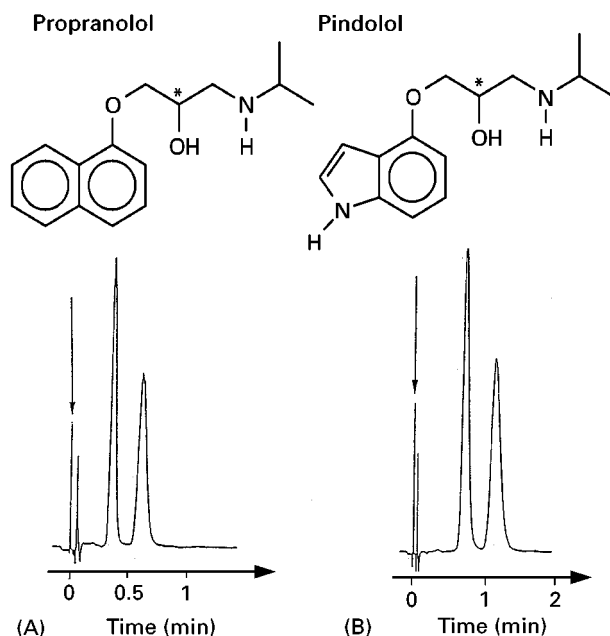


Figure 8 High-speed enantiomeric separation of (A) propranolol and (B) pindolol on ChyRoSine-A CSP. Operating conditions: column, 50×3.2 mm i.d.; mobile phase, carbon dioxide/(ethanol containing 1% (v/v) of *n*-propylamine) (80:20, (v/v)); flow rate 7.5 mL min^{-1} at 0°C ; temperature, 27°C ; pressure, 220 bar; UV detection at 224 nm. (Reproduced with permission from Bargmann-Leyder N, Thiebaut D and Vergne F *et al.* (1995) High speed chiral separation of β -blockers by supercritical fluid chromatography on ChyRoSine-A. *Chromatographia* 39: 673–681.)

not obtained on the (*S*)-naphthylethylcarbamoylated- β -cyclodextrin CSP using LC, but was readily accomplished using SFC (Figure 10). The separation of the enantiomers of *N*-(3,5-dinitrobenzoyl)valine methyl ester, ancymidol and proglumide was also obtained in a single run using carbon dioxide/methanol eluent, whereas the same separations in LC required three different mobile phases.

Group III

Chiralcel-OD CSP tris(3,5-dimethylphenyl carbamate cellulose) has been used successfully for the SFC enantioseparation of β -blockers, potassium channel activator analogues and other compounds. A Chiralpak-AD column, tris(3,5-dimethylphenyl carbamate amylose), has been used to resolve enantiomeric mixtures of nonsteroidal anti-inflammatories.

Other CSPs derived from cellulose have been successfully applied to the SFC enantioseparation of compounds of pharmaceutical interest. For example, an intermediate in the synthesis of a drug targeted for cardiac arrhythmia was separated on Chiralcel-OB; the four optical isomers of a new calcium channel blocker, LF 2.0254, were resolved on Chiralcel-OJ; and some CSPs have been applied to the SFC separation of various frequently used drug racemates such as profens and barbiturate derivatives, benzodiazepines, etc.

A Chiralcel-OD-H column and an achiral aminopropyl column have been employed for the analysis of products formed in rat liver microsomal metabolism

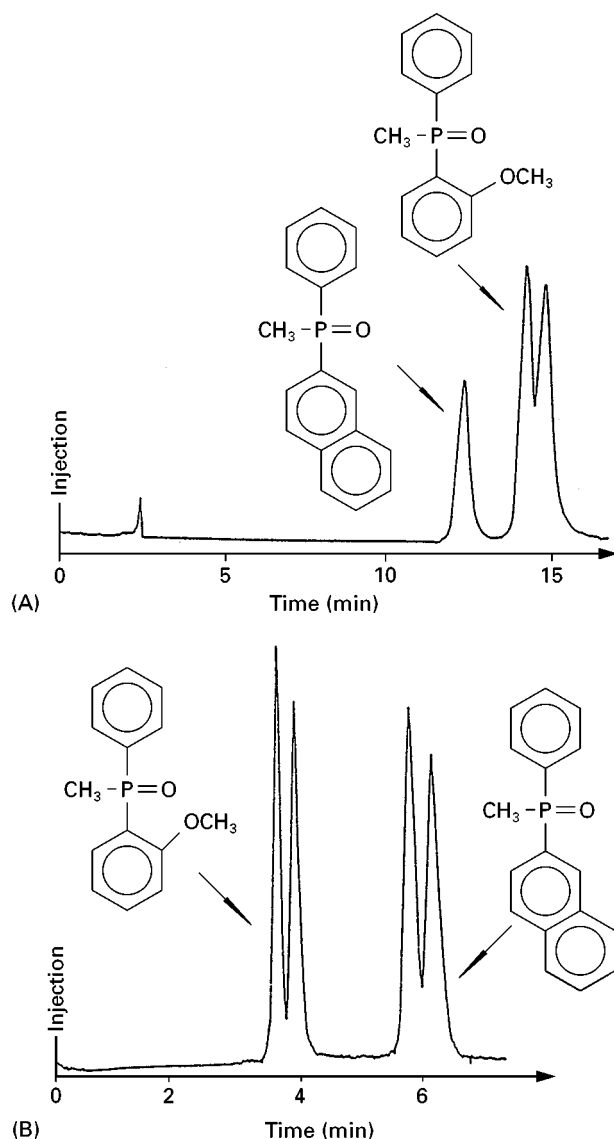


Figure 9 Comparison of the separation of the 2-naphthyl and *o*-anisyl phosphine oxides on Cyclobond I using LC and SFC. LC conditions: mobile phase, hexane/ethanol (85 : 15, v/v); flow rate, 1 mL min⁻¹; UV detection at 234 nm. SFC conditions: mobile phase, carbon dioxide/methanol (94 : 6, w/w); flow rate, 4.5 mL min⁻¹; temperature 25°C; pressure, 150 bar; UV detection at 234 nm. (Reproduced from Macaudière P, Caude M, Rosset R and Tambuté A (1987) Resolution of racemic amides and phosphine oxides on a β -cyclodextrin-bonded stationary phase by subcritical fluid chromatography. *Journal of Chromatography* 405:135–143, with permission from Elsevier Science.)

of racemic camazepam (a hypnotic/anxiolytic drug in clinical use) and the fast chiral separation of different compounds (oxprenolol, pindolol, warfarin) has been achieved by microbore SFC using a Chiralcel-OD type stationary phase.

Kot and co-workers proposed the serial coupling of different CSP columns (Chiralpak-AD, Chiralcel-OD and Chirex 3022 (brush-type with π -donor

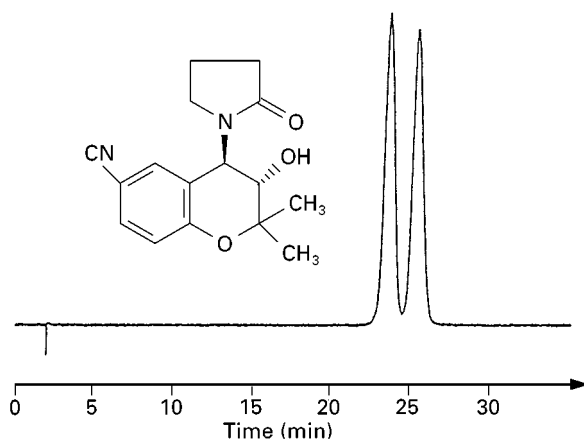


Figure 10 SFC separation of the cromakalim enantiomers on the (*S*)-naphthylethylcarbamoylated- β -cyclodextrin CSP. Operating conditions: mobile phase, carbon dioxide/methanol (96 : 4); flow rate, 2 mL min⁻¹; temperature 30°C; pressure, 15 MPa; UV detection at 254 nm. (Reproduced from Williams KL, Sander LC, and Wise SA (1996) Comparison of liquid and supercritical fluid chromatography using naphthylethylcarbamoylated- β -cyclodextrin chiral stationary phases. *Journal of Chromatography A* 746: 91–101, with permission from Elsevier Science.)

characteristics)). This coupling allowed the authors to achieve baseline separations with all solutes investigated, basic (β -blockers, benzodiazepines)

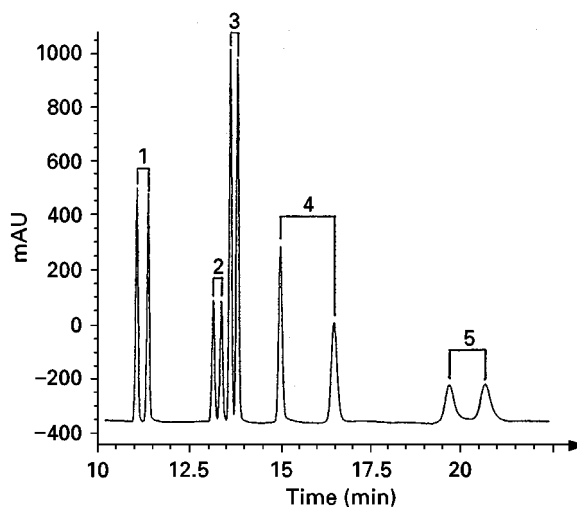


Figure 11 SFC separation of ibuprofen (1), fenoprofen (2), clenbuterol (3), propranolol (4) and lorazepam (5) using the serial coupling of different CSP columns. Operating conditions: columns, Chiralpak AD-Chiralcel OD-Chirex 3022; mobile phase, carbon dioxide/methanol (0.5% triethylamine + 0.5% trifluoroacetic acid) with methanol programmed from 4% (5 min) to 30% at 5% min⁻¹; flow rate 2 mL min⁻¹; temperature, 25°C; pressure, 200 bar. (Reproduced with permission from Kot A, Sandra P and Venema A (1994) Sub- and supercritical fluid chromatography on packed columns a versatile tool for the enantioselective separation of basic and acidic drugs. *Journal of Chromatographic Science* 32: 423–448.)

and acidic (nonsteroidal anti-inflammatory drugs, β -agonists). As an example, **Figure 11** shows the separation of ibuprofen, fenoprofen, clenbuterol, propranolol and lorazepam in a modifier-programmed run.

Systematic comparison of the chiral recognition mechanisms in LC and SFC for type III CSPs has been

performed. It appears that, contrary to what occurs for type I CSPs, important discrepancies in selectivity values may exist between LC and SFC. The systematic comparison of LC and SFC for Chiralcel-OD and Chiralpak-AD CSPs demonstrates clearly that the presence of polar functional groups such as primary or secondary hydroxyl or amine functions may cause

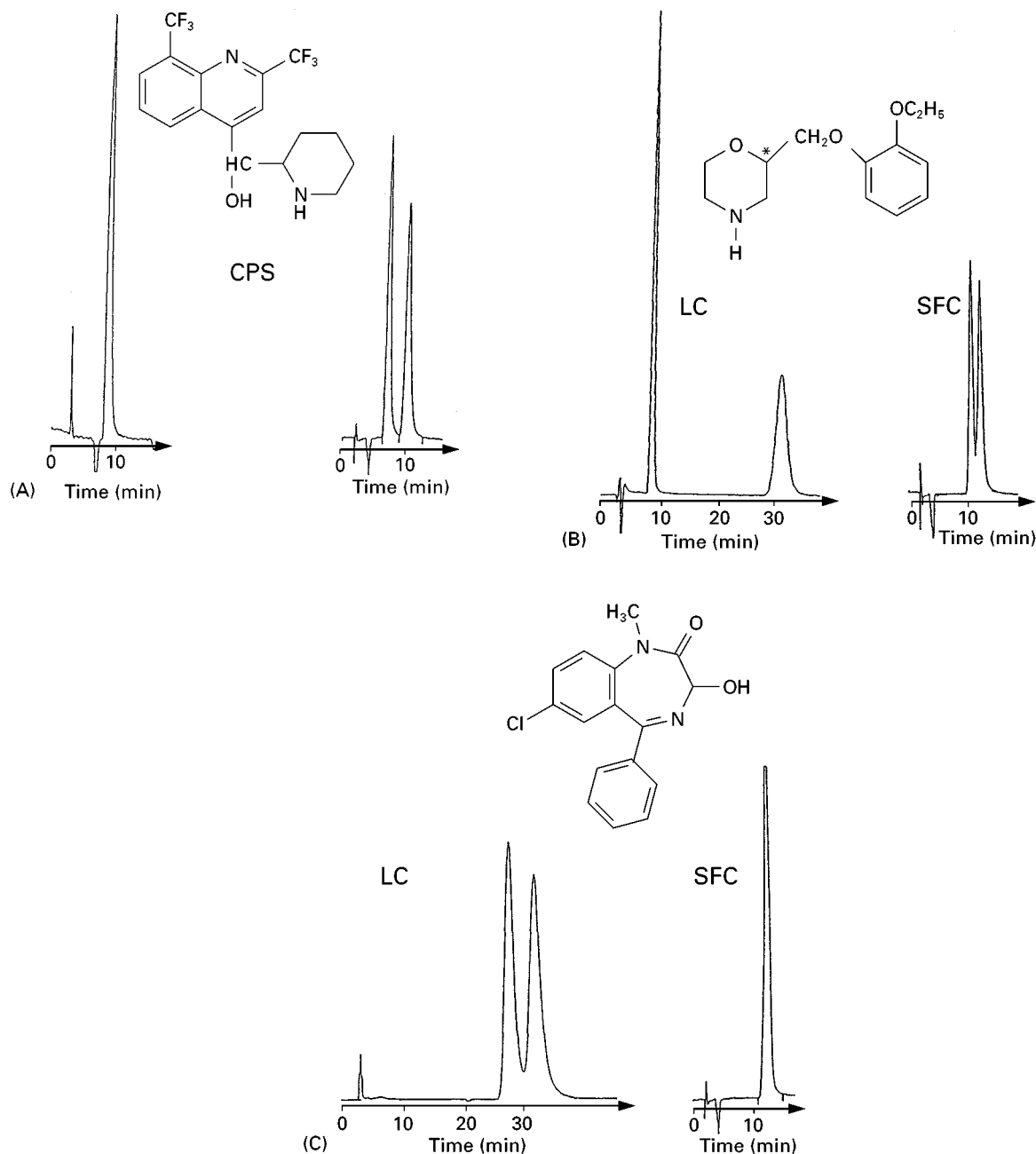


Figure 12 Comparison of LC and SFC for the separation of mefloquine (A), viloxazine (B) and temazepam (C) using Chiralcel OD CSP. Operating conditions: column, Chiralcel OD. LC, mobile phase hexane/ethanol containing 1% (v/v) of *n*-propylamine (90 : 10, v/v) for (A) and (C), 50 : 50 (v/v) for (B); flow rate 1 mL min⁻¹; room temperature. SFC: mobile phase, carbon dioxide/ethanol containing 1% (v/v) of *n*-propylamine 90 : 10 (v/v) for (A) and (B) 95 : 5 (v/v) for (C); flow rate, 2 mL min⁻¹; temperature, 25°C; pressure: 200 bar. UV detection. Separations are optimized for selectivity. (Reproduced with permission from Bargmann-Leyder N, Tambuté A and Caude M (1995) A comparison LC-SFC for cellulose and amylose-derived chiral stationary phases. *Chirality* 7: 311–325.)

large discrepancies in selectivity between LC and SFC. This result is peculiar to cellulose and amylose-derived CSPs, for which the interactions involved in chiral recognition are not always well balanced. Therefore, in the case of chiral resolution of polar solutes, the analyst should try both LC and SFC so that the more stereoselective one can be chosen. Figure 12A–C show some examples of the different selectivities that may exist between LC and SFC for polymer-type CSPs.

Other polymer-type CSPs have been used in SFC, such as those based on polymethacrylates of helical conformation and a polysiloxane CSP (polyWhelk-O), the 'polymeric version' of the commercially available brush-type CSP, Whelk-O 1. For the latter, the comparison was performed between the polymeric CSPs and its brush-type analogue, and it appeared that the polyWhelk-O CSP affords greater enantioselectivity and shorter retention under the same conditions.

Conclusion

Chiral separation is one of the fields where SFC is recognized to have better characteristics than HPLC, both from a kinetic and sometimes thermodynamic point of view.

In general, SFC offers faster separations than LC and often better selectivity values (particularly with cellulosic and amylosic polymer-type chiral stationary phases, and also with brush-type CSPs in particular cases). Consequently, SFC should be considered as a powerful analytical tool for the separation of basic and acidic drugs.

Capillary columns should be chosen for the analysis of chiral compounds having a low or medium polarity. On the other hand, packed columns are preferred for analytes of high polarity for which a polar modifier must be added to the supercritical carbon dioxide mobile phase.

Currently, to meet the requirements of quality control laboratories, most analyses are performed with packed columns. This is mainly due to the progress in

SFC instrumentation (full control over many chromatographic parameters and particularly full control of the pressure). Analysts are looking for the chiral column that is best able to achieve racemate separation easily and in a single run. This objective will probably never be achieved, but we can expect that the serial coupling of chiral columns (two or three) will allow some progress in this direction owing to the kinetic advantage exhibited by SFC over LC.

Further Reading

- Ariëns EJ (1989) Racemates – an impediment in the use of drugs and agrochemicals. In: AM Krstulovic (ed.) *Chiral Separations by HPLC: Applications to Pharmaceutical Compounds*. Chichester: Ellis Horwood. pp. 31–68.
- Kot A, Sandra P and Venema A (1994) Sub- and supercritical fluid chromatography on packed columns a versatile tool for the enantioselective separation of basic and acidic drugs. *Journal of Chromatographic Science* 32: 423–448.
- Mourier P, Eliot E, Caude M, Rosset R and Tambuté A (1985) Supercritical and subcritical fluid chromatography on a chiral stationary phase for the resolution of phosphine oxide enantiomers. *Analytical Chemistry* 57: 2819–2823.
- Pirkle WH, House DW and Finn JM (1980) Broad spectrum resolution of optical isomers using chiral high-performance liquid chromatographic bonded phases. *Journal of Chromatography* 192: 143–158.
- Siret L, Tambuté A, Caude M and Rosset R (1991) Chiral recognition mechanisms on chiral stationary phases derived from tyrosine – Specific influence of the nature of the asymmetric centre vicinal functional group. *Journal of Chromatography* 540: 129–143.
- Wainer IW and Drayer DE (eds) (1988) *Drug Stereochemistry: Analytical Methods and Pharmacology*. New York: Marcel Dekker.
- Williams KL, Sander LC and Wise SA (1996) Use of naphthylethylcarbamoylated- β -cyclodextrin chiral stationary phase for the separation of drug enantiomers and related compounds by sub- and supercritical fluid chromatography. *Chirality* 8: 325–331.

Synthetic Multiple Interaction ('Pirkle') Stationary Phases

C. J. Welch, Merck & Co. Inc., Rahway, NJ, USA

Copyright © 2000 Academic Press

Introduction

Among the many types of chiral stationary phases (CSPs) that have been developed, synthetic multiple

interaction (Pirkle-type, or brush-type) CSPs have proven to be among the most useful for many liquid chromatographic enantiomer separations. These CSPs consist of an enantioenriched small molecule selector immobilized on an inert chromatographic support, typically silica gel. Separation is achieved when the two enantiomers of the analyte are differentially adsorbed by the CSP (Figure 1). A combination

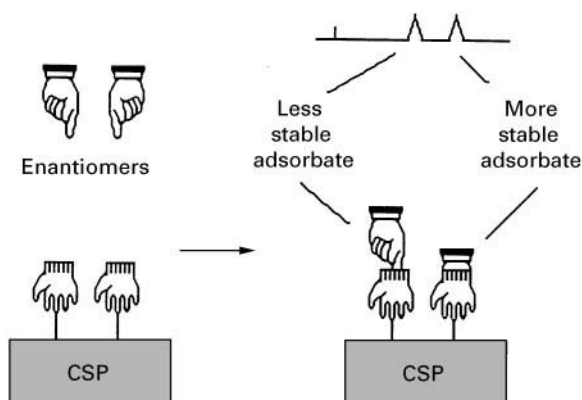


Figure 1 Enantiomer separation on CSPs is made possible by formation of transient diastereomeric adsorbates with differing free energies. In this illustration, the analyte enantiomers are depicted as right and left hands, and the CSP is depicted as immobilized right-handed gloves.

of simultaneous, geometrically constrained, intermolecular interactions utilizing forces such as hydrogen bonding, π - π attraction, ionic interactions, and steric repulsion can result in diastereomeric adsorbates with differing free energies, the prerequisite for enantioseparation.

Brush-type CSPs are just one of the several types of CSPs that have been developed to date. Other types include CSPs based on natural polymers such as polysaccharides or proteins, artificial polymers, and 'imprinted' polymers. Exactly what constitutes a brush-type CSP is a matter of some debate. In the broadest definition, CSPs based on immobilized cyclodextrins, antibiotics, etc. should perhaps be included in this category. However, this article will deal primarily with the synthetic CSPs developed by Professor William H Pirkle.

Background

Although Pirkle's name is strongly associated with the development of synthetic multiple interaction CSPs, several important materials of this type were developed by earlier researchers. Landmark events from the 1960s include the development of TAPA CSPs and chiral GC stationary phases. The 1970s brought a number of further advances, including Davankov's development of ligand exchange CSPs, Baczuk's pioneering development of a synthetic CSP designed specifically for the chromatographic separation of the enantiomers of a particular analyte molecule (DOPA), and Cram's development of chiral crown ether CSPs. During this same decade, Pirkle's investigations into the development of ^1H NMR chiral solvating agents led to the development of several useful brush-type CSPs.

Advantages of Brush-Type CSPs

In general, brush-type CSPs possess a number of advantages; since the selector is a small molecule, which is often completely synthetic, a structure which contains no labile or reactive components can usually be developed and the mode of attachment of the selector to the chromatographic support can be chosen for durability. Brush-type CSPs are typically covalently attached to the chromatographic support. Thus, most brush-type phases are chemically robust and are generally quite long-lived. Longevity is desirable for an analytical CSP, but truly essential for a preparative CSP, where continuous operation for several years may be required. The chemical robustness of brush-type CSPs results in the ability of these materials to be used with a wide variety of mobile phases, which provides greater flexibility in method development, especially when poorly soluble analytes are being investigated. The ability to utilize a variety of mobile phases is of even greater importance in preparative chromatography, where compound solubility can drastically limit enantioseparation productivity.

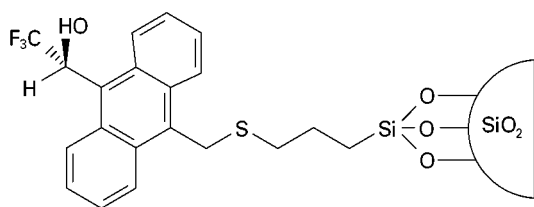
An additional advantage of brush-type phases stems from the fact that the selectors which are used are typically small molecules with molecular mass of less than 11000 Da. Consequently, the selectors can be very densely arrayed on the chromatographic surface, resulting in a phase which is highly resistant to sample overload and which has a very high preparative capacity.

Finally, most synthetic CSPs are available in either enantiomeric form. Consequently, either elution order (+ before - , or - before +) can be chosen. Elution of the minor enantiomer before the major is generally preferred in analysis, while elution of the desired component before the undesired can greatly increase productivity in preparative HPLC.

Survey of Some Important Pirkle-Type CSPs

The Beginnings: A Carbinol CSP

The Work on CSPs in the Pirkle laboratories grew out of studies on ^1H NMR chiral solvating agents. Immobilization of an analogue of the enantiopure chiral resolving reagent, trifluoromethyl-9-anthryl carbinol, afforded a CSP capable of separating the enantiomers of electron-deficient aromatic sulfoxides and many other racemates. Further studies showed that 3,5-dinitrobenzamide (DNB) derivatives of the enantiomers of a variety of amines, amino alcohols, amino acids and related compounds were separated with the following CSP structure [I].

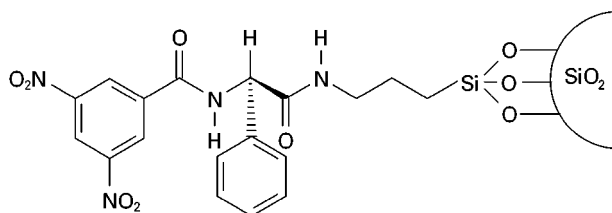


Structure [I]

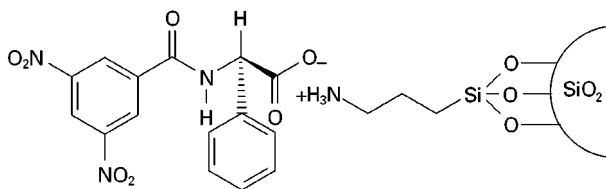
Principle of Reciprocity, and its Importance in CSP Development: Development of DNB Amino Acid CSPs

The observation that the enantiomers of some DNB derivatives are well resolved on CSP structure [I] prompted an investigation of the reciprocal situation. As a general rule, if a CSP is useful for separating the two enantiomers of an analyte, then a second CSP derived from one of the enantiomers of that analyte should be useful for separating the enantiomers of compounds which are structurally related to the chiral selector of the original CSP. This concept is known as the 'principle of reciprocity', and has been of great use in the development of new CSPs by Pirkle and his co-workers. The principle holds true generally, although the manner in which the chiral selector is tethered to the silica surface can influence chiral recognition in either a beneficial or detrimental fashion. After finding that several DNB phenylglycine-derived analytes were particularly well resolved on CSP structure [I], Pirkle and co-workers prepared and evaluated several phases derived from DNB phenylglycine and related compounds. The ready availability of enantiopure (*R*)-phenylglycine, which is utilized in the commercial production of an antibiotic, suggested that phenylglycine-derived CSPs might provide an economical and convenient method for resolving the enantiomers of the highly useful chiral solvating agent, trifluoromethyl-9-anthryl carbinol, and perhaps other alcohols as well.

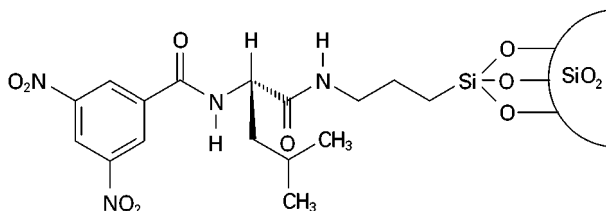
As expected, CSP structure [II] afforded resolution of the enantiomers of the trifluoromethyl-9-anthryl carbinol chiral solvating reagent as well as some related compounds. The related ionically bonded amino acid-derived CSPs structures [III] and [V] were



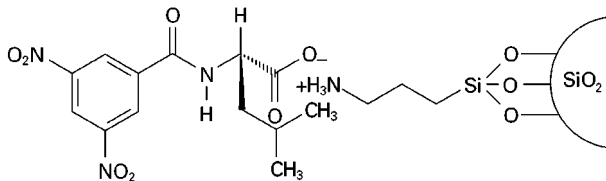
Structure [II] (DNB PG)



Structure [III] (DNB PG-Ionic)



Structure [IV] (DNB Leu)



Structure [V] (DNB Leu-Ionic)

subsequently prepared and also found to be useful for the resolution of the enantiomers of a variety of arylalkylcarbinols, with the phenylglycine-derived CSP structure [III] generally performing better than the leucine-derived CSP structure [IV]. CSP structure [III] was found to be widely useful for the separation of the enantiomers of racemates from a variety of functional group classes, and was shown to be useful for the gram-scale preparative resolution of racemates using automated preparative chromatography. The general ability of CSP structure [III] to resolve the enantiomers of a variety of analytes led to its introduction as the Pirkle 1A CSP by Regis Chemical Company in 1980 – the first commercially available HPLC chiral stationary phase. Somewhat later, CSP structures [II], [IV] and [V] were also made commercially available, and today a wide variety of CSPs incorporating the highly useful DNB moiety have been developed. Commercialization of these early Pirkle phases provided researchers in a number of fields with tools for separating the enantiomers of structurally diverse racemates. Surprisingly, the ionically tethered DNB amino acid CSP structures [III] and [V], are quite long lived when used with relatively non-polar mobile phases, although they are readily degraded when highly polar eluents such as methanol or water are used.

CSPs based on DNB derivatives of the amino acid, tyrosine, were subsequently developed by a team of French researchers including Caude, Rosset, and Tambuté, and a CSP based on DNB naphthylglycine was developed by Ôi and co-workers in Japan. The 3,5-dinitrobenzamide group has proven useful in the development of a number of additional phases, as will be described later.

Second Generation Pirkle CSPs with Electron Rich Aromatic Groups

Studies in the Pirkle laboratories and elsewhere showed that the DNB amino acid-derived CSPs were capable of separating the enantiomers of a wide variety of analytes possessing electron-rich aromatic groups. At this point, it was only natural to again turn to the principle of reciprocity and prepare and evaluate 'reciprocal' materials based on some of these structures. A number of reciprocal phases were prepared and evaluated, although they lacked the requisite generality required of a commercial CSP. Nevertheless, these studies revealed many important design features that would prove useful later.

The enantiomers of aryl hydantoin are well resolved on DNB amino acid-derived CSPs, and several hydantoin-based CSPs were prepared to study the mechanisms for chiral recognition of these types of analytes and to probe the ability of this type of phase to afford separation of various racemates.

Separation of the enantiomers of a number of aryl-substituted phthalides was studied using DNB amino acid-derived CSPs such as CSP structures [III] and [V], and a detailed study of the effect of analyte structure on chromatographic performance led to some optimized structures for chiral recognition. One such compound was used to prepare a reciprocal aryl phthalide CSP which, as expected, showed a general ability to resolve a number of racemates containing electron-deficient aromatic systems.

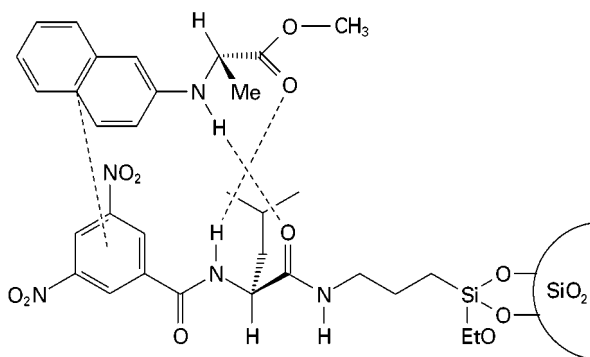
Another class of compounds which are well resolved on the DNB amino acid-derived CSPs are general amide structures bearing at least one aromatic ring. In an extensive series of studies, Pirkle, Hyun and co-workers prepared and evaluated more than 10 CSPs derived from various analogues of (1-naphthyl)ethylamine (α -NEA) in which a variety of different tether geometries and substituent patterns were explored. Study of this group revealed a number of interesting and useful principles of CSP design. However, the CSPs themselves were somewhat limited in that they were useful primarily for separation of the enantiomers of analytes bearing electron-deficient aromatic groups. Similar CSPs were prepared and studied by Ôi and co-workers.

N-Aryl Amino Acid-Derived CSPs

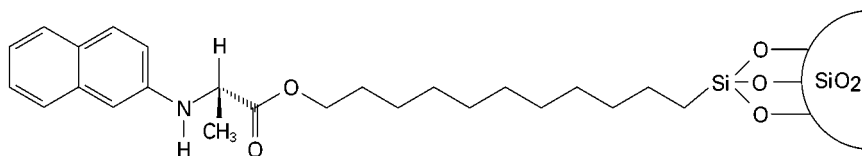
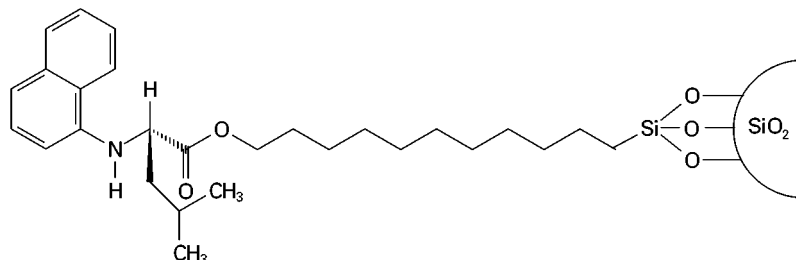
The development of second generation Pirkle phases with electron-rich aromatic groups reached its zenith with the investigations by Pirkle and Pochapsky of compounds derived from the enantiomers of the readily prepared electron-rich *N*-aryl amino acid derivatives. This is perhaps the best understood chiral recognition system yet studied. In some preliminary studies, it was shown that *N*-aryl amino acid derivatives were well resolved using the DNB Leu-Ionic CSP structure [V]. Subsequently, the structural requirements for chiral recognition were defined, and a chiral recognition rationale was proposed. The high degree of enantioselectivity observed in this system ($\alpha > 10$ in some cases) can be attributed to the intimate association of the two components of the more stable diastereomeric adsorbate as illustrated later. This chiral recognition system has been studied at great length using spectroscopic as well as chromatographic techniques. An X-ray structure of a 1:1 complex of soluble analogues of the compounds shows essentially the same adsorbate structure as that initially proposed based upon chromatographic and spectroscopic studies (structure [VI]):

A reciprocal *N*-(2-naphthyl)valine-derived stationary phase was prepared and shown to provide unprecedented levels of resolution for a variety of racemates containing electron-deficient aromatic groups. The related alanine-derived CSP structure [VII] was subsequently reported, and commercialized, and has proven to be a valuable and widely used research tool:

Subsequent structural refinements led to the preparation and commercialization of the leucine-derived CSP structure [VIII], which generally affords significantly greater enantioselectivity in the separation of DNB-containing enantiomers than does CSP structure [VI]. The predominant effect seems to be a greatly diminished retention of the initially eluted enantiomer, presumably owing to the ability of the more



Structure [VI]

Structure [VII] (N_2N -Ala CSP)Structure [VIII] (N_1N -Leu CSP)

bulky leucine sidechain to inhibit approach of the least retained enantiomer from the undesired face of the aromatic ring of the CSP.

These phases have proven to be widely useful for separating the enantiomers of chiral amines, amino alcohols, amino acids, etc., and are sometimes also useful for separating the enantiomers of chiral alcohols, thiols, etc. However, analysis with these phases generally requires that the analyte be derivatized so as to incorporate an electron-deficient aromatic group. Typically, derivatization reagents such as 3,5-dinitrobenzoyl chloride or 3,5-dinitrophenylisocyanate are used. Despite this somewhat bothersome need to make derivatives, these CSPs remain quite useful and show a tremendous generality.

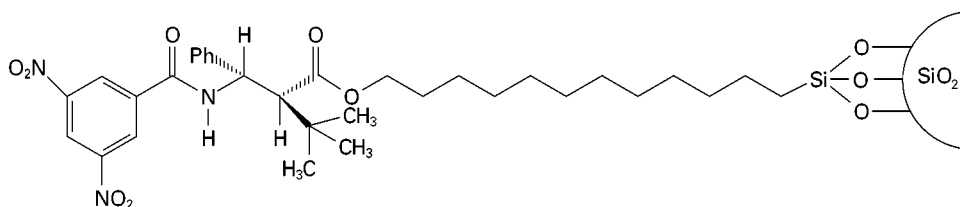
Recently, a group of CSPs based on proline anilides have been developed in the Pirkle laboratories. These exhibit remarkable enantioselectivities for some DNB derivatives.

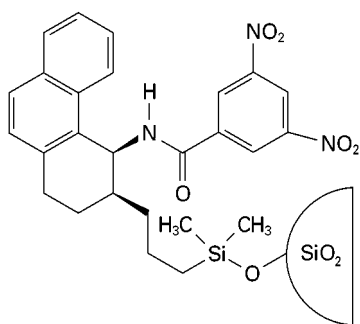
Improved DNB CSPs

The design of CSPs is an evolutionary process so that continuing refinements and improvements in both the understanding of chiral recognition and the design of such phases are constantly being made. Several CSPs,

representing improvements upon the widely used DNB phenylglycine-derived CSP structure [II] have been developed in the Pirkle laboratories and subsequently commercialized. The first of these, the β GEM 1 CSP (CSP structure [IX]), grew out of studies of the enantiopurity analysis of some chiral β -lactams. The finding that some DNB β -amino acid derivatives were well resolved led to the preparation and evaluation of the DNB β -amino acid-derived structure [IX]. An X-ray crystal structure of the selector used in CSP structure [IX] shows the *t*-butyl and phenyl substituents projecting from opposite faces of the stationary phase. The bulky *t*-butyl substituent at the 2-position is thought to play a major role in controlling the conformation of this phase, preventing intramolecular hydrogen bonding, and restricting access to one face. The β GEM CSP is useful for the separation of the enantiomers of anilide derivatives of aromatic carboxylic acids and *N*-protected amino acids.

As will be related later, the most general CSP yet developed in the Pirkle laboratories, the Whelk-O 1 (CSP structure [X]), was actually designed to separate the enantiomers of one particular compound, naproxen. In addition to resolving the enantiomers of

Structure [IX] (β -GEM I CSP)



Structure [X] (Whelk-O 1 CSP)

naproxen and nearly all related nonsteroidal anti-inflammatory drugs (NSAIDs) this CSP is useful for resolving the enantiomers of analytes from a host of functional group classes.

A very useful DNB-containing CSP based upon diphenylethylenediamine has been prepared and investigated by Uray, Lindner and Maier. This CSP, commercialized as the ULMO CSP (structure [XI]), shows a general ability to separate the enantiomers of a number of analytes containing electron-rich aromatic groups. In addition, it shows an ability to separate the enantiomers of aryl carbinols which is unsurpassed among Pirkle-type CSPs.

Another improved DNB-containing CSP based on the relatively inexpensive *trans* 1,2-diaminocyclohexane (DACH) was developed by the research team of Gasparrini, Misiti, Villani, and co-workers; this phase has never been commercialized, but has been studied extensively.

β -Blocker-Specific CSPs

In the mid-1980s, some of the principles of CSP design were becoming fairly well understood in the Pirkle laboratories, and attempts were made to design selectors for particular target racemates of significant scientific and economic importance.

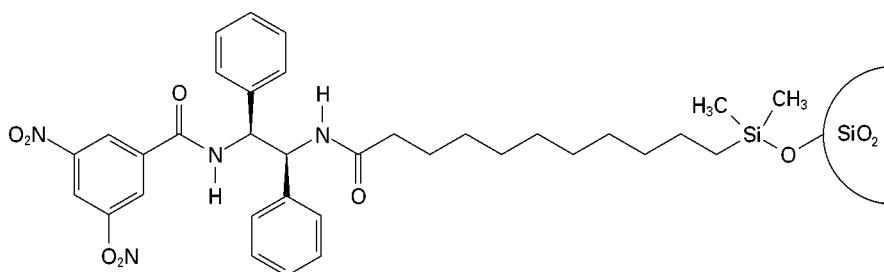
For example, the enantiomers of the β -blocker drug propranolol had been shown to be marginally resolved on the DNB phenylglycine-derived CSP structure [II] as any of a variety of *N*-acylated derivatives.

A research programme directed at developing a phase capable of separating the enantiomers of underivatized propranolol enantiomers was undertaken. A group of three CSPs were designed, prepared, evaluated, and shown to separate the enantiomers of propranolol with the elution order predicted by the chiral recognition model. Several other β -blockers were similarly resolved, however, the poor chromatographic efficiency of these materials limited their practical utility.

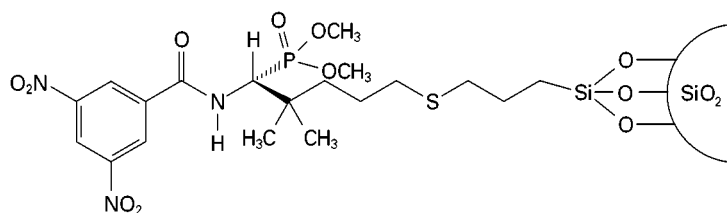
In an effort to overcome this obstacle, a group of amino phosphonic acid-derived CSPs were prepared and shown to provide improved resolution of propranolol. Consequently, CSP structure [XII] was prepared, evaluated, and found to provide very good resolution for the enantiomers of propranolol and a number of related β -blockers. This stationary phase was commercialized as the α -Burke I CSP. Subsequent minor improvements in the tethering chemistry led to an improved version commercialized as the α -Burke II CSP (structure [XII]).

Naproxen-Specific CSPs Using the Immobilized Guest Method

As mentioned earlier, one of the most general Pirkle-type CSPs resulted from a study aimed at developing something which would be useful for separating the enantiomers of the drug, naproxen. At the time of the inception of this project, separation of the enantiomers of naproxen and related NSAIDs with Pirkle-type CSPs generally required formation of derivatives. The finding that underivatized naproxen enantiomers could be marginally resolved on the β -GEM 1 CSP prompted an investigation into the development of improved separations. Drawing on the familiar principle of reciprocity, a new approach termed the 'immobilized guest method' was utilized in this study. Two CSPs were prepared from enantiopure naproxen, and these were used to investigate the enantioseparation of a variety of different chiral analytes. This study led to an understanding of the structural requirements for enantioselective naproxen recognition, and a new chiral selector incorporating



Structure [XI] (ULMO CSP)

Structure [XII] (α -Burke I CSP)

many of these key structural features was proposed. This new selector was synthesized and found to be well separated on the immobilized guest naproxen CSPs. Larger scale synthesis, resolution, and immobilization of the selector afforded a CSP which resolved naproxen enantiomers with a very high degree of enantioselectivity ($\alpha = 2.25$). In addition, structurally related NSAIDs such as ibuprofen, ketoprofen, flurbiprofen, etc. are also resolved. Subsequent mechanism-based structural modifications led to the development and commercialization of the Whelk-O 1 CSP (CSP structure [X]) which affords improved resolution of NSAID enantiomers. In addition to resolving the enantiomers of NSAIDs, the Whelk-O 1 CSP has proven to be the most general CSP developed to date in the Pirkle laboratories, as it is capable of resolving the enantiomers of racemates from a host of functional group classes.

A number of variations on the Whelk-O structure have been developed in the Pirkle laboratories and at Regis Technologies. For example, the same selector immobilized via a trifunctional silane linkage has been commercialized as the Whelk-O II CSP (structure [XIV]). This CSP is more resistant to selector cleavage under harsh mobile phase conditions.

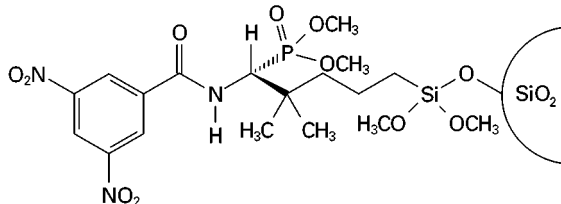
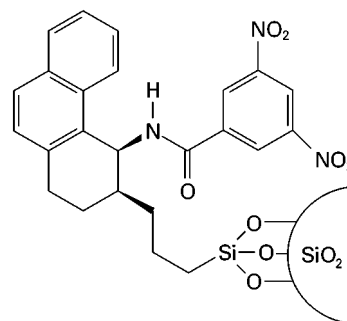
Another analogue of the Whelk-O CSP has proven useful for separations utilizing supercritical or subcritical carbon dioxide as an eluent. This phase, commercialized as the PolyWhelk-O CSP, is prepared by first immobilizing the Whelk-O chiral selector onto a polysiloxane polymer, then covalently bonding the resulting polymer to silica gel. The resulting material often shows improved efficiency and enantioselectivity when operated in the SFC mode.

New Trends in Design and Development of Pirkle-Type CSPs

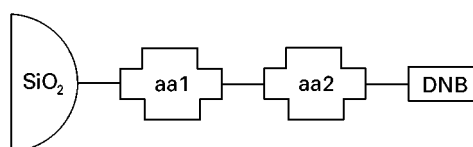
The design and development of new CSPs continues at an active pace in the Pirkle laboratories, with an emphasis on using an array of analytical tools to develop a mechanistic understanding of CSP behaviour. Developing CSPs which will be useful in the preparative chromatographic separation of pharmaceutical enantiomers is another major research area.

A new method for microscale synthesis and evaluation of libraries of Pirkle-type phases has recently

been developed at Regis Technologies. In this technique, libraries of CSPs are prepared on a 50 milligram scale by solid phase synthesis on silica particles. The resulting libraries are then rapidly evaluated using a process which does not require packing into a column. This technique provides a useful tool for rapidly determining which CSP from a library of many hundreds shows the greatest enantioselectivity for a particular analyte. In addition, some of the necessary structural requirements for chiral recognition can be determined by comparing the relative performance of various CSPs in the library. This information can, in turn, suggest further CSP libraries, which can be prepared and evaluated. Ultimately, the process can lead to discovering CSPs which display preparatively useful enantioselectivity for given target racemates.

Structure [XIII] (α -Burke II CSP)

Structure [XIV] (Whelk-O II CSP)



Structure [XV]

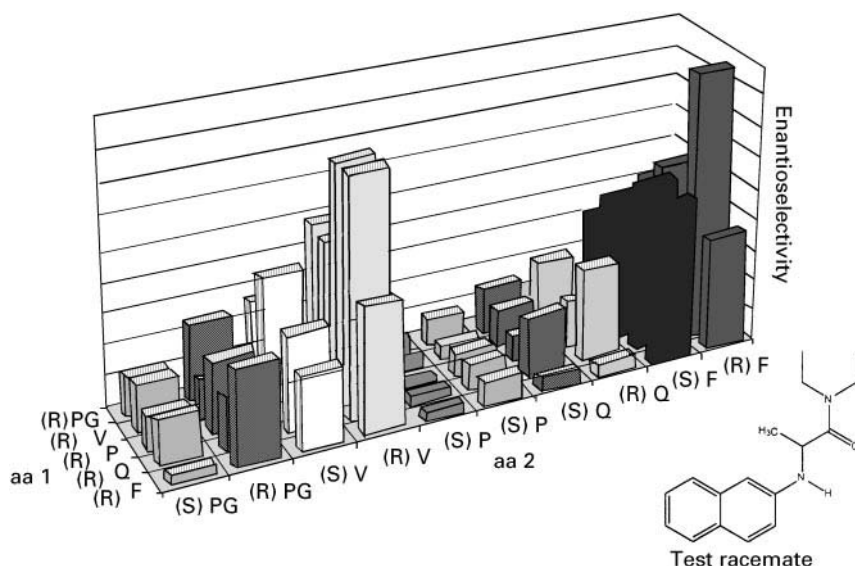


Figure 2 Relative enantioselectivity seen by a library of 50 dipeptide DNB CSPs for the enantiomers of a test racemate.

For example, preparation of a library of 50 dipeptide DNB CSPs and screening for the ability to separate the enantiomers of the test analyte shown (structure [XV]) afforded the results presented in Figure 2, which suggest that bulky groups in the aa 2 position and hydrogen bonding groups in the aa 1 position are advantageous.

Subsequent preparation and evaluation of such a 'focused' library revealed a number of new CSPs with very high enantioselectivity for the target analyte. One of the better performing members of this library was prepared on a larger scale, packed into a column, and shown to be able to afford exceptionally high productivity for the preparative separation of the enantiomers of the racemic test analyte. This new approach to CSP development promises to be very useful for large-scale preparative chromatographic enantioseparation, and a variety of structurally diverse CSP libraries are now being investigated by a number of different research groups.

Conclusion

A number of Pirkle-type CSPs are of great use in the chromatographic separation of enantiomers. Several of these materials are commercially available and widely used in diverse research disciplines. An ever-increasing understanding of the requirements for chiral recognition and the design of useful CSPs is evident from a survey of Pirkle's work over the past two decades. The entry of other research groups into the area of CSP design suggests that there will be continued developments in this area in coming years.

See also: III/Chiral Separations: Amino Acids and Derivatives; Capillary Electrophoresis; Cellulose and Cellulose Derived Phases; Chiral Derivatization; Countercurrent Chromatography; Crystallization; Gas Chromatography; Ion-Pair Chromatography; Ligand Exchange Chromatography; Liquid Chromatography; Molecular Imprints as Stationary Phases; Protein Stationary Phases; Supercritical Fluid Chromatography; Thin-Layer (Planar) Chromatography.

Further Reading

- Allenmark S (1991) *Chromatographic Enantioseparation: Methods and Applications*, 2nd edn, New York: Ellis Horwood.
- Pirkle WH and Pochapsky TC (1986) A new, easily accessible reciprocal chiral stationary phase for the chromatographic separation of enantiomers. *Journal of the American Chemistry Society* 108: 352–354.
- Pirkle WH, Finn JM, Hamper BC and Schreiner JL (1982) *American Chemistry Society Symposium Series No. 185*. Eliel and Otsuba (eds) ch. 18, 245.
- Pirkle WH, Welch CJ, Burke JA and Lamm B (1992) *Analytical Proceedings* 29: 225.
- Pirkle WH, Welch CJ and Lamm B (1992) Design, synthesis and evaluation of an improved enantioselective naproxen selector. *Journal of Organic Chemistry* 57: 3854–3860.
- Welch CJ (1994) Evolution of chiral stationary phase design in the Pirkle laboratories. *Journal of Chromatography* 666: 3–26.
- Welch CJ, Bhat GA and Protopopova MN, *Enantiomer* 3: 463.
- Welch CJ, Protopopova MN and Bhat GA, *Enantiomer*, 3, 471.

Thin-Layer (Planar) Chromatography

L. Lepri and M. Del Bubba, University of Florence, Florence, France

Copyright © 2000 Academic Press

Introduction

In chiral chromatography, two diastereomeric adducts with different physicochemical properties are formed during elution. The adducts differ in their stability (in chiral stationary phases, CSPs, or chiral coated phases, CCPs) and/or in their interphase distribution ratio (in chiral mobile phases, CMPs).

According to Dalglish, three active positions of the selector must interact simultaneously with the active positions of the enantiomer to reveal differences between optical antipodes. This is a sufficient condition for resolution to occur but it is not essential. Chiral discrimination may happen as a result of hydrogen bonding and steric interactions, making only one attractive force necessary in this type of chromatography. Moreover, the creation of specific chiral cavities in a polymer network (as in 'molecular imprinting' techniques) could make it possible to base enantiomeric separations entirely on steric fit.

Chiral Stationary Phases and Chiral Coated Phases

Few chiral phases are used in TLC; one of the main reasons for this is that chiral stationary phases with very high UV background can only be used only with fluorescent or coloured solutes. For example, amino-modified ready-to-use layers bonded or coated with Pirkle-type selectors, such as *N*-(3,5-dinitrobenzoyl)-L-leucine or *R*(-)- α -phenylglycine, are pale yellow and strongly adsorb UV light. Another reason is the high price of most CSPs.

The most widely used CSPs or CCPs are polysaccharides and their derivatives and silanized silica gel impregnated with an optically active copper (II) complex of derivatized hydroxyproline. The use of silica gel impregnated with chiral polar selectors, such as D-galacturonic acid, (+)-tartaric acid, (-)-brucine, L-aspartic acid or a complex of copper (II) with L-proline, should also be mentioned.

In CSPs, owing to the nature of the polymeric structure, the simultaneous participation of several chiral sites or several polymeric chains is conceivable. In CCPs, the chiral sites are distributed at the surface or in the network of the achiral matrix relatively far

away from each other and only a bimolecular interaction is generally possible with the optical antipodes to be separated.

Cellulose

The linear polysaccharide cellulose is composed of (+)-D-glucose units and its relative molecular mass ranges from 2.5×10^5 to 1×10^6 or more. The long chains are arranged on a partially crystalline fibre structure and held together by numerous hydrogen bonds between the hydroxyl groups. The hydrolysis of cellulose with 2.5 mol L^{-1} hydrochloric acid at *c.* 100°C removes amorphous material and yields a more crystalline polymer called 'microcrystalline cellulose' and marketed as Avicel by several companies.

The mechanism of chiral recognition is not yet completely clarified even though a significant role is attributed to the cellulose structure and to the hydroxyl groups, the protection of which with BrCN resulted in the loss of chiral recognition. The optical antipodes resolved are highly polar, such as amino acids, with multiple sites for hydrogen bond formation.

Cellulose Derivatives

Among derivatized polysaccharides, cellulose triacetate (CTA) is the most used stationary phase for the resolution of racemic compounds by TLC.

The different fit of the two enantiomers into the laminae of the polymer leads to separation of the optical antipodes which is mainly governed by the shape of the solutes (flat molecules showing a better permeation into the cavities) and only to a minor extent by electrostatic interactions involving the functional groups of the molecules. Hence the name 'inclusion chromatography'. In addition, the chiral recognition of CTA depends strongly on its structure and the type of eluent and increases as the crystallinity of the polysaccharide is increased. Microcrystalline cellulose triacetate (MCTA) can be prepared from microcrystalline cellulose with almost complete preservation of microcrystallinity. Usually, the type of eluent and its composition are important for chiral recognition because these produce different swelling of MCTA, which in turns enables the separation of solutes of different sizes and characteristics.

The use of *n*-hexane-isopropanol mixtures resulted in unsatisfactory separations since extremely elongated spots are generally obtained. Aqueous-alcoholic solutions have the opposite effect, giving rise to round and compact spots.

This CSP is able to resolve a broad range of structurally different racemates. In general, more polar molecules require a higher percentage of water than hydrophobic compounds.

Hydrophobic Silica Gel Impregnated with Copper (II) Complex of (2*S*,4*R*,2'*RS*)-*N*-(2'-hydroxydodecyl)-4-hydroxyproline

The structure of the selector is shown in Figure 1. Chiralplate and HPTLC-CHIR are the only precoated plates built up from such material. The chiral layer on the latter plates is combined with a so-called 'concentrating zone'. The sample to be separated is applied to this small band and is transported with the solvent front, forming a narrow band at the interface of the two sections; consequently, a higher efficiency of the separation process is obtained.

Many racemates have been resolved on both layers by ligand-exchange chromatography (LEC). The separated enantiomers are those capable of forming diastereomeric complexes of different stability with the metal ion and the chiral selector. The requirement of sufficient stability of the ternary complex involves five-membered ring formation and compounds such as α -amino and α -hydroxy acids are the most suitable.

Chiral Mobile Phases

CMPs permit the use of conventional stationary phases and show fewer detection problems than CSPs or CCPs. However, high cost chiral selectors (i.e. γ -cyclodextrin) are certainly not advisable for TLC.

Enantiomer separations have been achieved using chiral mobile phases in both normal and reversed-phase chromatography. The first technique employs silica gel and, mostly, Diol F₂₅₄ HPTLC plates (Merck) and, as chiral selectors, D-galacturonic acid, *N*-carbobenzoxy(CBZ)-L-amino acids or peptides, 1*R*-(-)-ammonium-10-camphorsulfonate and 2-*O*-[(*R*)-2-hydroxypropyl]- β -cyclodextrin.

Most separations have been obtained by reversed-phase chromatography on hydrophobic silica gel with β -cyclodextrin (β -CD) and its derivatives, bovine

serum albumin (BSA) and the macrocyclic antibiotic vancomycin as chiral agents.

Unmodified and Modified β -Cyclodextrins as Mobile-Phase Additives

Among the three cyclodextrins (α , β , γ), only β -CD and its derivatives have been used for successful resolution of various racemates by TLC. In an aqueous solution β -CD is represented as a truncated cone with different sized mouths (0.60–0.65 nm); the height of the cavity is 0.78 nm. The 2- and 3-hydroxyl groups are oriented towards the outside and are responsible for the aqueous solubility properties of this oligosaccharide. The hydrogen atoms and glycosidic oxygen groups are located inside the molecule, forming the relatively hydrophobic cavity that interacts with organic optical isomers to form diastereomeric inclusion complexes. Under reversed-phase conditions, the combination of hydrophobic and steric interactions with hydrogen bonding between the chiral solutes and the 2- and/or 3-hydroxyl groups may be the cause of enantioselectivity.

Aqueous-organic solutions (i.e. methanol-water or acetonitrile-water mixtures) are usually used as eluents. β -CD is enantioselective in TLC only at the high concentrations reached by adding large amounts of urea, which increases the aqueous solubility of β -CD more than ten-fold. However, urea tends to compete with solutes for the preferred location in the hydrophobic cavity, thus decreasing the separation factor. Chemical modification with hydroxypropyl, hydroxyethyl or methyl groups has been used to increase the solubility of β -CD and its complexes in water, eliminating the need to use urea. Optimization of the enantioselectivity can be achieved by modifying the concentration and nature of organic solvent, pH and buffer concentration of the eluent.

Bovine Serum Albumin as Mobile-Phase Modifier

BSA is a protein of relative molecular mass 66 210, consisting of 581 amino acids in a single chain. It is a relatively acidic protein (isoelectric point 4.7), highly soluble in water, but precipitates from high salt solutions. At pH 7.0 its net charge is -18 . Hydrophobic interactions strongly contribute to the affinity of organic solutes for BSA; simultaneous contributions exist from electrostatic interactions, steric effects, hydrogen bonding and charge-transfer processes.

Mobile phases containing this chiral selector have been employed for the resolution of a broad variety of racemic compounds on silanized silica plates. Eluents were prepared by dissolving BSA (Serva, Heidelberg,

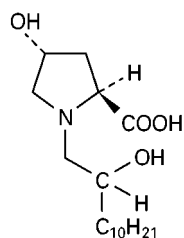


Figure 1 Structure of (2*S*,4*R*,2'*RS*)-*N*-(2'-hydroxydodecyl)-4-hydroxyproline.

FRG), fraction V, pH 5.2 or 7.0, in different buffer systems and then adding the desired amount of 2-propanol. The results suggest the use of acidic eluents to separate *N*-derivatized amino acids on wettable RP-18W/UV₂₅₄ (Macherey-Nagel) or RP-18W/F₂₅₄ (Merck) plates. On the other hand, the resolution of free amino acids increases with increasing eluent pH; in particular, the useful pH range on SIL C₁₈-50/UV₂₅₄ layers (Macherey-Nagel) is 9–10.

A prerequisite for optical discrimination is the presence of aromatic as well as polar groups in the solute. The existence of stereospecific binding sites on albumin is well known (i.e. tryptophan and warfarin) and it is believed that this binding occurs at a number of relatively defined regions. Two independent non-cooperative types of sites (chiral and achiral) coexist on the protein; the retention mechanism is partially in accord with that proposed on columns packed with immobilized BSA since in TLC albumin is used as a mobile-phase additive.

Retention and Resolution Data

In this article the contribution of chiral TLC to enantiomeric separations is surveyed, emphasizing the versatility of the method but without discussing the chiral recognition mechanism; this aspect has been examined elsewhere and in other parts of this Encyclopedia.

Amino Acids and Their Derivatives

A broad variety of racemic amino acids has already been resolved by chiral TLC. Table 1 summarizes the analytical separations achieved in this field on 20 cm × 20 cm Chiralplates (Cat. No. 811058, Macherey-Nagel; thickness 0.25 mm). The separations can be easily transferred to the 10 cm × 10 cm HPTLC-CHIR plates with concentrating zone since they are precoated with the same chiral selector.

With eluents A, B and C, 2 µL of a 1% solution of the racemates in methanol or methanol–water and with eluent D, 2 µL of a 0.5% solution of the racemates in 0.1 mol L⁻¹ hydrochloric acid–methanol 1 : 1 were applied to the plates. Migration time increases from 0.5 h (eluent A) to 1.5 h (eluent C). Detection was performed by dipping the plates for 3 s in a 0.3% ninhydrin solution in acetone and then heating at 110°C for *c.* 5 min. Red spots appear on a white background.

The amount of solute applied to the plates (10–20 µg) is an order of magnitude greater than that generally employed in TLC; the use of HPTLC-CHIR layers improves the sensitivity of the method.

Thus far, 84 proteinogenic and nonproteinogenic amino acids have been separated without derivatization using mostly methanol–water–acetonitrile (50 : 50 : 200, v/v/v) as eluent. Usually the *D* enantiomer is the more retained. Racemic serine shows low resolution, while threonine and basic amino acids have not been resolved as yet.

The separations of enantiomeric amino acids reported in Table 2 using a variety of chiral selectors are very interesting since they also include the unresolved compounds mentioned above. Round, compact spots are generally obtained on silica gel plates eluted with 2-*O*-[(*R*)-2-hydroxypropyl]- β -cyclodextrin solutions as deduced from *R_s* values which are equal to or higher than the α value for all the amino acids with the only exception of *DL*-citrulline (*R_s* = 0.94). Visualization is performed by spraying the plates with a salicylaldehyde solution (1.5 g) in 100 mL toluene and then heating at 50°C for 10 min (yellow spots).

Table 3 gives the performance of cellulose plates, which are very effective in resolving racemates of aromatic and basic amino acids. Home-made layers of microcrystalline cellulose powder (commercially available from Merck, and Fluka) can be obtained with optimal homogeneity by spreading an aqueous suspension with about 25% chiral material. The plates are dried at room temperature and do not require activation before use. Polar mixtures (i.e. ethanol–pyridine–water) are the best eluents since they separate enantiomers as efficiently as an aqueous solvent (i.e. 0.1 mol L⁻¹ NaCl) but give rise to more compact spots.

Chiralplates were very effective in resolving racemates of *N*-alkyl, *N*-carbamyl and *N*-formyl amino acids and of several dipeptides (Table 4). It is worth noting that the dipeptide with the C-terminal *L*-configuration always has a higher retention than the one with the C-terminal *D*-configuration. Some racemic dipeptides were also resolved on microcrystalline cellulose with pyridine–water (2 : 1 or 4 : 1) and on SIL C₁₈-50/UV₂₅₄ plates using BSA as chiral mobile phase additive.

Derivatization of amino acids may be used to improve chiral recognition, detectability and sensitivity of the method and to label amino acids residues of peptides and proteins, especially the *N*-terminal amino acid. Dimethylaminonaphthalenesulfonyl (dansyl) amino acids form when primary and secondary amino acids react with dansyl chloride, generating strongly fluorescent compounds. The best chromatographic conditions for their separation are reported in Table 5. The most complete study, performed on KC18 F plates (Whatman) using β -CD as chiral agent, concerns the racemates of 26

Table 1 Enantiomeric separation of proteinogenic and nonproteinogenic amino acids on Chiralplates^a

<i>Racemate</i>	<i>hR_{F1}</i> ^b	<i>hR_{F2}</i>	α^c	Eluent ^d
Ala	69(D)	73	1.22	D
Ser	73(D)	76	1.17	D
Abu	48	52	1.17	A
Val	54(D)	62	1.39	A
Nva	49(D)	56	1.32	A
Leu	53(D)	63	1.51	C
Ile	47(D)	58	1.55	A
Nle	53(D)	62	1.44	A
allo-Ile	51(D)	61	1.50	A
<i>t</i> -Leucine	40(D)	51	1.56	A
Met	54(D)	59	1.23	A
Eth	52(D)	59	1.32	A
Pro	41(D)	47	1.27	A
cis-Hyp ^e	41(L)	59	2.08	A
allo-Hyp	41(L)	59	2.08	A
Pipecolic acid	51	58	1.32	D
Phe	49(D)	59	1.49	A
Homophenylalanine	49(D)	58	1.43	A
Tyr	58(D)	66	1.40	A
Dopa	47(L)	58	1.55	B
Trp	51(D)	61	1.50	A
Asp	50(D)	55	1.22	A
Glu	54(D)	59	1.22	A
Gln	41(L)	55	1.76	A
Thyroxine	38(D)	49	1.56	A
PhenylGly	57(D)	67	1.53	A
CyclopentylGly	43	50	1.32	A
(1-Methylcyclopropyl)-Gly	49	57	1.38	A
(2-Thienyl)-Gly	55	66	1.58	A
3-Cyclopentyl-Ala	46	56	1.49	A
3-(1-Naphthyl)-Ala	49(D)	56	1.32	A
3-(2-Naphthyl)-Ala	44(D)	59	1.82	A
Met(O ₂) ^f	62(D)	66	1.18	A
Eth(O ₂)	55	59	1.18	A
Seleno-Met	53(D)	61	1.38	A
S-Methylthio-Cys	47(D)	55	1.38	A
S-Methylthio-HomoCys	44	52	1.38	A
S-(2-Chlorobenzyl)-Cys	45	58	1.68	A
S-(3-Thiobutyl)-Cys	53	64	1.58	A
S-(2-Thiopropyl)-Cys	53	64	1.58	A
O-Benzyl-Ser	54(D)	65	1.58	A
O-Benzyl-Tyr	48(D)	64	1.92	A
3,3-Dimethyl-Nva	40(D)	56	1.91	A
4-Methyl-Trp	50	58	1.38	A
5-Methyl-Trp	52	63	1.57	A
6-Methyl-Trp	52	64	1.64	A
7-Methyl-Trp	51	64	1.70	A
4-Methoxy-Phe	52	64	1.64	A
5-Methoxy-Trp	55	66	1.58	A
3-Chloro-Ala	57	64	1.34	A
4-Amino-Phe	33	47	1.80	A
4-Bromo-Phe	44	58	1.75	A
4-Chloro-Phe	46	59	1.68	A
2-Fluoro-Phe	55	61	1.28	A
4-Iodo-Phe	45(D)	61	1.91	A
4-Nitro-Phe	52	61	1.44	A
3-Fluoro-Tyr	64	71	1.37	A
5-Bromo-Trp	46	58	1.61	A
α -Methyl-Ser	56(L)	67	1.59	B
α -Methyl-Abu	50	60	1.50	A
α -Methyl-Val	51	56	1.22	A

Table 1 Continued

Racemate	hR_{F1}^b	hR_{F2}	α^c	Eluent ^d
α -Methyl-Leu	48	59	1.55	A
α -Methyl-Met	56(D)	64	1.39	A
α -Methyl-Phe	53(L)	66	1.72	A
α -Methyl-Tyr	63(D)	70	1.37	A
α -Methyl-Dopa	46(L)	66	2.27	B
α -Methyl-Trp	54	65	1.58	A
α -Methyl-Asp	52(D)	56	1.17	A
α -Methyl-Glu	58(L)	62	1.18	A
α -Ethyl-Ala	55	61	1.28	A
α -Propyl-Ala	55	63	1.39	A
α -Butyl-Ala	51	63	1.63	A
α -Difluoromethyl-Phe	63	70	1.37	A
α -Propenyl-Phe	57	63	1.28	A
2'-Methyl-Phe	43(D)	54	1.55	A
β -Methyl-Phe	36(R, R)	56(S, S)	2.26	A
2'-Methyl- β -methyl-Phe	48(S, R)	55(R, S)	1.32	A
2'-6'-Dimethyl-Phe	38(D)	52	1.76	A
β -Methyl-p-nitro-Phe	43(R, R)	62(S, S)	2.16	A
	52(S, R)	60(R, S)	1.38	A
2',5'-Dimethyl-4-methoxy-Phe	45(D)	57	1.61	A
β -Hydroxy-Phe	49(R, R)	63(S, S)	1.77	A
β -Methyl-Tyr	52(R, R)	67(S, S)	1.87	A
	55(S, R)	67(R, S)	1.66	A
2'-Methyl-Tyr	54(D)	62	1.39	A
2',5'-Dimethyl-Tyr	56(D)	67	1.59	A

^a Migration distance 13 cm; chamber saturation.^b $hR_F = R_F \times 100$.^c $\alpha = (1 \div R_{F1} - 1)/(1 \div R_{F2} - 1)$.^d A = methanol-water-acetonitrile 50 : 50 : 200 (v/v/v); B = methanol-water-acetonitrile 50 : 50 : 30 (v/v/v); C = methanol-water 10 : 80 (v/v); D = acetone-methanol-water 10 : 2 : 2 (v/v/v).^e Hyp = hydroxyproline.^f Met(O₂) = methionine sulfone.

common and uncommon dansyl (Dns) amino acids. Similar results can be obtained on 10 cm \times 10 cm SIL C₁₈-50/UV₂₅₄ layers with the same eluents but with lower migration times. Some enantiomeric Dns-amino acids such as Lys, Met, Nva, Pro and aromatic compounds show low selectivity coefficients with β -CD. Therefore, it can be useful to resolve these racemates on RP-18W/UV₂₅₄ plates with eluents containing BSA since very high α values have been achieved.

Other *N*- and *C*-terminal substituents studied by chiral TLC include 2,4-dinitrophenyl (DNP), 3,5-dinitro-2-pyridyl (DNPy), 3,5-dinitrobenzoyl (DNB), *o*-nitrophenylsulfenyl (*o*-NPS), 9-fluorenylmethoxycarbonyl (FMOC), methylthiohydanthoin (MTH), phenylthiohydanthoin (PTH), *t*-butoxycarbonyl (*t*-BOC), carbobenzoxy (CBZ), phthalyl, acetyl, *p*-nitroanilide (pNA) and β -naphthylamide (β NA) (Table 6).

The maximum ΔR_F for the enantiomers of FMOC amino acids was obtained at different concentrations of 2-propanol. It is worth noting that this is the first

time optical isomers have been separated with eluents containing BSA in the presence of very high levels (12–36%) of organic modifier. The resulting spots have the shape of a reversed triangle. FMOC-DL-Asn and FMOC-DL-Gln are not resolved. The order of retention of the *D* and *L* forms of the different compounds is variable. The *D* forms of FMOC-Pro, FMOC-Trp and FMOC-Met are more retained than the *L* forms, whereas the opposite is noted for the other amino acids. This behaviour is also shown from DNP-amino acids and other *N*-derivatives.

Most DNP, DNPy and DNB-DL-amino acids are resolved on RP-18W/UV₂₅₄ plates with 0.1 mol L⁻¹ acetate buffer solutions containing 2% isopropanol and different BSA concentrations (2–6%) but few of them show chiral separation with phosphate buffer (0.05 mol L⁻¹ potassium dihydrogen phosphate + 0.05 mol L⁻¹ disodium hydrogen phosphate), an eluent of higher pH (6.86) than that previously used. Enantiomeric DNPy-Ala, DNPy-Nva and DNP-Eth(O₂) are completely separated at low

Table 2 Resolution of racemic amino acids by chiral TLC

Racemate	hR_{F1}^a	hR_{F2}	α^b	Separation technique
Ala	18(D)	53	5.13	Slurry of silica gel (Merck) and (–)-brucine brought to pH 7.1 with 0.1 mol L ⁻¹ NaOH and spread on 20 cm × 20 cm plates. Eluent: butanol–acetic acid–water 3 : 1 : 4 (v/v/v). Migration distance, 10 cm; development time 0.5 h. Visualization: ninhydrin.
Ser	12(D)	50	7.33	
Thr	16(D)	29	2.15	
Ile	16(D)	35	2.82	
Met	18(D)	29	1.86	
Phe	27(D)	40	1.80	
Tyr	22(D)	29	1.45	
Trp	17(D)	31	2.19	
Trp	59(D)	72	1.77	SIL C ₁₈ -50/UV ₂₅₄ plates (Cat. No. 711308, MN) 10 cm × 10 cm, thickness 0.20 mm. Eluent: 0.05 mol L ⁻¹ NaHCO ₃ + 0.05 mol L ⁻¹ Na ₂ CO ₃ containing 6% BSA and 6% isopropanol (pH 9.8); for the resolution of 7-methylTrp, 5-methoxyTrp and Kynurenine, 0.05 mol L ⁻¹ sodium tetraborate was used. Migration distance, 8 cm; development time 1 h 50 min. Visualization: <i>p</i> -dimethylaminobenzaldehyde.
Trp-NH ₂ ^c	31(L)	40	1.48	
4-Methyl-Trp	42	65	2.56	
5-Methyl-Trp	37	61	2.53	
6-Methyl-Trp	66	78	1.82	
7-Methyl-Trp	41	50	1.43	
5-Methoxy-Trp	42	49	1.32	
4-Fluoro-Trp	51	66	1.86	
5-Fluoro-Trp	43	63	2.23	
6-Fluoro-Trp	42	54	1.62	
Kynurenine	69(D)	80	1.80	
3-(1-Naphthyl)-Ala	34(D)	40	1.29	
Val	62(D)	68	1.30	DC plastikfolien, Kieselgel 60 F ₂₅₄ (Merck), 20 cm × 20 cm, thickness 0.2 mm. Eluent: acetonitrile–water 1 : 2.5 for Arg, His and Lys and 1.5 : 2 for the others; the water containing 6.5 · 10 ⁻³ mol L ⁻¹ 2- <i>O</i> -[(<i>R</i>)-2-hydroxypropyl]- β -CD. Migration distance, 18 cm at 19°C.
Gln	59(D)	66	1.35	
Arg	50(D)	59	1.44	
Cit	65(D)	69	1.20	
His	46(D)	55	1.43	
Lys	49(D)	60	1.56	

^a $hR_F = R_F \times 100$.^b $\alpha = (1 \div R_{F1} - 1)/(1 \div R_{F2} - 1)$.^cTryptophanamide.

temperature (10°C) and pH values (0.5 mol L⁻¹ acetic acid) where their retention by the layer is sufficient. The unresolved racemates include DNP γ -Ser, DNP-Asp, DNP-Glu and DNP γ -Trp. The first three amino acids are markedly polar and are only slightly retained by silanized silica gel plates, even when eluted with acidic solution; this may be the reason for their not being resolved. In general, planar chromatography clearly separates the enantiomers of *N*-derivatized hydrophobic amino acids.

The complete resolution of DNP γ -DL-Trp is obtained on layers of SIL C₁₈-50/UV₂₅₄ with β -CD as chiral agent.

The optical isomers of PTH-amino acids are sensitive to light and readily racemize. Racemization of these optical active derivatives is observed on silanized silica gel plates with acidic eluents. MCTA plates may be useful since they are able to separate enantiomeric MTH-Phe, MTH-Tyr, MTH-Pro and PTH-Pro with neutral aqueous–alcoholic eluents.

Among C-terminal substituents, the enantiomeric β NA derivatives of amino acids were well separated on silanized silica gel plates with β -CD as

mobile phase modifier while pNA derivatives show discordant results. In fact, DL-Leu-pNA is fully resolved but DL-Ala-pNA failed since the latter optical antipodes do not form inclusion complexes of sufficient stability with β -CD. In addition, BSA seems efficient in the enantioseparation of pNA derivatives.

α -Hydroxycarboxylic Acids

Table 7 reports the separation and resolution data for aliphatic and aromatic DL- α -hydroxycarboxylic acids on HPTLC-CHIR plates with concentrating zone where the selectivity coefficients appear to be higher than those obtained on Chiralplates using the same eluent (dichloromethane–methanol, 45 : 5 v/v). Vanadium pentoxide may be used for detection of aromatic and aliphatic compounds. The oxide (1.82 g) is dissolved in 30 mL of 1 mol L⁻¹ sodium carbonate by ultrasonic bath and, after cooling, 46 mL of 2.5 mol L⁻¹ sulfuric acid and acetonitrile to 100 mL are added. Plates dipped in this solution and allowed to stand at room temperature give blue spots on a yellow background. All racemates studied were

Table 3 Retention and resolution data for racemic amino acids on home-made and precoated cellulose plates

<i>Racemate</i>	hR_{F1}^a	hR_{F2}	α^b	<i>Eluent</i>	<i>Remarks</i>
Trp	50(D)	53	1.12	A	Home-made microcrystalline cellulose plates (Avicel SF, Funakoshi, Japan) 20 cm × 20 cm. Development time 2.3 h; visualization: UV ₃₆₅ . A = methanol–butanol–benzene–water 2 : 1 : 1 : 1 (v/v/v/v).
5-HydroxyTrp	25(D)	31	1.35	A	
Kynurenine	54(D)	61	1.33	A	
3-Hydroxykynurenine	47(D)	53	1.27	A	
5-Hydroxykynurenine	20(D)	26	1.40	A	
3-Methoxykynurenine	55(D)	62	1.33	A	
<i>N</i> - α -acetylkynurenine	74(D)	82	1.60	A	
Diaminoadipic acid	23(D, D)	28	1.30	B	Cellulose plates (Merck); B = methanol–water–acetic acid 40 : 10 : 2 (v/v/v).
Diaminopimelic acid	25(D, D)	37	1.76	B	
Trp	46(L)	52	1.27	C	DC-Alufolien Cellulose F ₂₅₄ plates (Merck) (20 cm × 20 cm × 0.1 mm). Development time 1.8–4.5 h; migration distance 15 cm; visualization: ninhydrin. Eluents: methanol–water 3 : 1 (D), 7 : 3 (F), 3 : 2 (C); <i>n</i> -butanol–acetic acid–water 1 : 1 : 1 (E). Layers heated at 110°C for 5 min before use.
5-HydroxyTrp	34(L)	41	1.34	C	
Kynurenine	38(D)	47	1.44	C	
4-AminoPhe	40(L)	45	1.22	D	
Phe-4-sulfonic acid	70(L)	73	1.15	E ^c	
<i>o</i> -Tyr	57	61	1.17	F	
<i>m</i> -Tyr	55	59	1.17	F	
<i>p</i> -Tyr	81(L)	83	1.14	F ^c	
<i>p</i> -Tyr-3-sulfonic acid	30(L)	40	1.55	E	
Dopa	53(L)	57	1.17	C	
Trp	40(L)	49	1.44	G	Avicel SF plates 20 cm × 20 cm, Lot 8390, Funakoshi, Japan. Development time 11.5 h at 0°C. Visualization: ninhydrin. G = ethanol–pyridine–water 2 : 3 : 1 (v/v/v) or 1 : 1 : 1 (v/v/v).
His	11(D)	13	1.20	G	
Phe	55(L)	59	1.17	G	
Tyr	53(L)	60	1.33	G	
Dopa	43(L)	50	1.32	G	
Cys	6(D)	8	1.35	G	
Thr	51(D)	56	1.22	G	
Tyr	75(L)	81	1.42	H	DC-Plastikfolien Cellulose plates (Merck, Cat. No. 5577), 20 cm × 20 cm × 0.1 mm. Migration distance 10 cm. Visualization: iodine vapour. Eluents: 0.1 mol L ⁻¹ NaCl (H); ethanol–pyridine–water 1 : 1 : 1 (I).
Trp	57(L)	62	1.23	H	
4-MethylTrp	29(L)	36	1.37	H	
	42(L)	52	1.50	I	
5-MethylTrp	37(L)	46	1.45	H	
	48(L)	54	1.27	I	
6-MethylTrp	32(L)	39	1.35	H	
	47(L)	55	1.37	I	
7-MethylTrp	34(L)	41	1.34	H	
4-FluoroTrp	38(L)	44	1.28	H	
	53(L)	60	1.33	I	
5-FluoroTrp	39(L)	45	1.27	H	
	59(L)	64	1.23	I	
6-FluoroTrp	41(L)	46	1.22	H	
	61(L)	65	1.18	I	
5-HydroxyTrp	31(L)	36	1.25	H	
	41(L)	48	1.33	I	
Kynurenine	48(L)	55	1.32	H	
	43(L)	51	1.38	I	

^a $hR_F = R_F \times 100$.^b $\alpha = (1 \div R_{F1} - 1)/(1 \div R_{F2} - 1)$.^cTwo successive developments with the same eluent.

completely resolved, the D forms being the most retained.

Acidic and Basic Drugs

The enantiomers of basic β -blocking drugs can be separated on HPTLC DIOL F₂₅₄ plates (Merck) with *N*-CBZ-Gly-L-Pro (or similar chiral agents) in the mobile phase, while the separation of the same drugs, derivatized with (R)-(-)-1-(1-naphthyl)ethyl

isocyanate in dichloromethane, has been performed on HPTLC-NH₂ F₂₅₄ plates chemically bonded with *N*-(3,5-dinitrobenzoyl)-*R*-(–)- α -phenylglycine (DNBPg) and eluted with different mixtures of *n*-hexane/isopropanol.

Interesting separations of racemates with a β -aminoalcohol structure (i.e. ephedrine and norephedrine, and β -blockers) can be achieved on MCTA plates after their cyclization with phosgene to form 5-substituted oxazolidinones.

Table 4 Enantiomeric separation of *N*-alkyl, *N*-carbamyl and *N*-formyl amino acids and of dipeptides on Chiralplates

Racemate	hR_{F1}^a	hR_{F2}	Eluent	Remarks
<i>N</i> -Formyl- <i>t</i> -Leu	48(+)	61(-)	A	A = methanol–water–acetic acid 50 : 50 : 200 (v/v/v).
<i>N</i> -Methyl-Abu	65	73	D	B = methanol–water–acetic acid 50 : 50 : 30 (v/v/v).
<i>N</i> -Ethyl-Abu	69	72	D	D = acetone–methanol–water 10 : 2 : 2 (v/v/v).
<i>N</i> -Methyl-Ala	64	70	D	M = 1 mmol L ⁻¹ copper (II) acetate, 5% methanol (pH 5.8).
<i>N</i> -Methyl-Asp	58(L)	67(D)	B	Migration distance 13 cm; chamber saturation.
<i>N</i> -Methyl-Leu	49(L)	57(D)	A	Visualization; Ehrlich's reagent for <i>N</i> -carbamylTrp, iodine for
<i>N</i> -Methyl-Nle	68	77	D	<i>N,N</i> -dimethyl-Phe, and ninhydrin for the others.
<i>N</i> -Methyl-Nva	67	76	D	
<i>N</i> -Ethyl-Nva	70	74	D	
<i>N</i> -Methyl-Phe	50(D)	61(L)	A	
<i>N,N</i> -Dimethyl-Phe	55(D)	61(L)	B	
<i>N</i> -Methyl- <i>m</i> -Tyr	36	52	B	
<i>N</i> -Methyl-Val	65(L)	70(D)	B	
<i>N</i> -Carbamyl-Trp	44(L)	55(D)	M	
Gly-Phe	57(L)	63(D)	B	
Gly-Leu	53(L)	60(D)	B	
Gly-Ile	54(L)	61(D)	B	
Gly-Val	58(L)	62(D)	B	
Gly-Trp	48(L)	55(D)	B	
Leu-Leu	19(D, L)	26(L, D)	A	
	48(D, L)	57(L, D)	B	
Ala-Phe	21(D, L)	26(L, D)	A	
	59(D, L)	65(L, D)	B	
Met-Met	29(D, L)	33(L, D)	A	
	64(D, L)	71(L, D)	B	
Asp-Phe-OCH ₃	50(L, L)	62(D, D)	A	
	50(L, D)	62(D, L)	A	

$$^a hR_F = R_F \times 100.$$

Many acidic drugs (Figure 2) are resolved as 3,5-dinitroanilyl (DNAn) derivatives on precoated HPTLC-NH₂ F₂₅₄ plates derivatized with *R*-(–)-1-(1-naphthyl)ethyl isocyanate (Table 8). Although the naphthylethyl chromophore has a high UV adsorptivity, the detection problems found on plates bonded with DNBPg were not observed.

High selectivity coefficients are obtained for un-derivatized acidic drugs on MCTA and diphenyl-F plates eluted with aqueous–organic solutions containing, in the latter case, a chiral macrocyclic antibiotic (vancomycin).

Other pharmaceuticals resolved include bendroflumethiazide, coumachlor, mephentoin, oxindanac benzyl ester, warfarin, chlorowarfarin, hexobarbital, oxazepam, lorazepam, norphenylephedrine, hyoscyamine and colchicine.

Flavanones

Flavanones occur in nature and have been isolated in an optically active form. They contain only hydroxyl and methoxy groups and differ from one another in the number and/or position of such substituents (Table 9).

With the exception of glycosides, 5-methoxy-, 7-hydroxy- and 5-hydroxy-7-methoxyflavanone, the

enantiomers of the tested compounds can be separated by at least one of the chiral phases reported in Table 10.

In the series of flavanones no chiral discrimination was observed on MCTA plates for racemic 2'-hydroxy-, 4'-hydroxy- and 4'-methoxyflavanone in contrast to polysubstituted compounds. Partial resolution was obtained for flavanone, 6-methoxy- and 6-hydroxyflavanone. Two successive developments with the same eluent (ethanol–water, 80 : 20 v/v) effectively improves the separation of these racemates on MCTA layers.

The addition of β -CD to the mobile phase permits separation of enantiomeric flavanone and its 2'-hydroxy-, 4'-hydroxy- and 4'-methoxy derivatives.

Albumin is able to resolve racemic polysubstituted flavanones and 2'-hydroxyflavanone. Alkaline mobile phases must be used for their separation.

Miscellaneous Compounds

The chiral NMR solvating agent 1-(9-anthryl)-2,2,2-trifluoroethanol (TFAE) has been separated by a variety of chromatographic techniques and has become a reference compound for testing new optically active selectors. For example, α values of 2.02 and 2.34

Table 5 Enantioseparation of racemic Dns-amino acids with chiral mobile phases

<i>Dns-Amino acid</i>	hR_{F1}^a	hR_{F2}	α^b	<i>Eluent</i>	<i>Remarks</i>
Abu	42(L)	47	1.22	C	Reversed-phase plates: 5 cm \times 20 cm and 20 cm \times 20 cm, KC18F, Whatman, USA. Development time 6–8 h. Eluents: acetonitrile–0.133 mol L ⁻¹ β -CD, 25 : 75 (A); methanol–0.163 mol L ⁻¹ β -CD, 35 : 65 (B); acetonitrile–0.151 mol L ⁻¹ β -CD, 30 : 70 (C); acetonitrile–0.133 mol L ⁻¹ β -CD, 20 : 80 (D); methanol–0.151 mol L ⁻¹ β -CD, 30 : 70 (E); acetonitrile–0.231 mol L ⁻¹ β -CD, 35 : 65 (F); methanol–0.2 mol L ⁻¹ β -CD, 35 : 65 (G); acetonitrile–0.2 mol L ⁻¹ β -CD, 20 : 80 (H); methanol–0.2 mol L ⁻¹ β -CD, 55 : 45 (I); acetonitrile–0.2 mol L ⁻¹ β -CD, 32 : 68 (L); methanol-saturated β -CD, 60 : 40 (M); methanol–0.2 mol L ⁻¹ β -CD, 50 : 50 (N). Aqueous solutions of β -CD also contain urea (saturated solution) and 3.5% sodium chloride. Visualization: UV ₂₅₄ .
Ala	40(L)	47	1.33	G	
Arg	55(L)	65	1.52	H	
Asn	60(L)	69	1.48	H	
Asp	64(L)	70	1.31	A	
Cit	54(L)	63	1.45	H	
Cys	37(L)	42	1.23	I	
Gln	57(L)	66	1.46	H	
Glu	65(L)	72	1.38	B	
His	58(L)	64	1.28	H	
Ile	33(L)	40	1.35	L	
allo-Ile	30(L)	38	1.43	L	
Leu	30(L)	35	1.25	C	
Lys	35(L)	39	1.18	M	
Met	34(L)	38	1.19	C	
Nle	24(L)	28	1.23	C	
Nva	32(L)	34	1.09	C	
Orn	35(L)	40	1.23	M	
Phe	35(L)	39	1.18	C	
Pro	39(L)	41	1.08	N	
Ser	41(L)	47	1.27	D	
Thr	42(L)	51	1.43	E	
Trp	43(L)	45	1.08	F	
Tyr	23(L)	26	1.17	M	
Val	36(L)	43	1.34	C	
<i>N</i> -Methyl-Val	24(L)	28	1.23	N	
Abu	34(L)	56	2.47	O	RP-18W/UV ₂₅₄ plates (Art. 811075, Macherey-Nagel). Migration distance 7 cm. Eluents: 5% BSA in 0.1 mol L ⁻¹ acetate buffer (O); 5% BSA and 1% NaCl in 0.5 mol L ⁻¹ acetic acid (P); 6% BSA in 0.1 mol L ⁻¹ acetate buffer (Q); 7% BSA in 0.5 mol L ⁻¹ acetic acid (R). Eluents also contain 2% isopropanol. Visualization: UV ₂₅₄ .
Asp	68(D)	79	1.77	O	
Glu	45(D)	65	2.27	O	
Leu	6(D)	15	2.76	P	
Met	32(L)	50	2.12	Q	
Nle	38	50	1.63	Q	
Nva	25(L)	73	8.13	O	
Phe	24(L)	45	2.59	Q	
Ser	39(D)	46	1.33	R	
Thr	34(L)	43	1.46	Q	
	25(D)	32	1.41	R	
Trp	37(D)	62	2.77	O	
Val	20(L)	33	1.97	O	

^a $hR_F = R_F \times 100$.^b $\alpha = (1 \div R_{F1} - 1)/(1 \div R_{F2} - 1)$.

were obtained, respectively, on OPTI-TAC F₂₅₄ (Antec) plates eluted with ethanol–water 80 : 20 (v/v) and on SIL C₁₈-50/UV₂₅₄ layers using 6% BSA in 0.05 mol L⁻¹ sodium tetraborate containing 20% isopropanol (pH 9.75) as mobile phase.

(\pm)-1-(9-Fluorenyl)ethanol an analogue of TFAE, was also resolved on home-made MCTA plates eluting with 2-propanol–water 80 : 20 (v/v) (α = 2.24).

The separation of chiral compounds with restricted rotation, as in the case of binaphthyl type of substances, can be effected both on CSPs and with CMPs. The first technique requires the use of MCTA plates to resolve (\pm)-1,1'-binaphthyl-2,2'-diamine (α = 1.99) while the latter involves chiral mobile

phases containing BSA for the separation of (\pm)-1,1'-bi-2-naphthol (α = 2.15) and (\pm)-binaphthyl-2,2'-diyl-hydrogen phosphate (α = 4.65).

The enantiomeric separations of synthetic pyrethroids, such as alfamethrin and fenpropathrin, on home-made MCTA plates with ethanol–water 80 : 20 (α = 1.37 and 1.20, respectively) should be noted since their optical antipodes have different rates of degradation and biological activity towards animals and plants.

The resolution of racemic fenoxaprop-ethyl on the above-mentioned CSP (α = 1.52, isopropanol–water 80 : 20) is interesting since chlorophenoxyalkyl carboxylic acids and esters are widely used herbicides.

Table 6 Enantioseparation of derivatized amino acids by chiral TLC

Derivative	hR_{F1}^a	hR_{F2}	α^b	R_s^c	Plate	Eluent ^e
Fmoc-Ala	89(L)	37	1.43	1.1	SIL C ₁₈ -50/UV ₂₅₄	A
Fmoc-Cha ^d	17(L)	30	2.09	2.3	SIL C ₁₈ -50/UV ₂₅₄	B
Fmoc-Leu	29(L)	36	1.37	1.3	SIL C ₁₈ -50/UV ₂₅₄	C
Fmoc-Met	20(D)	28	1.55	1.1	SIL C ₁₈ -50/UV ₂₅₄	D
Fmoc-Nle	18(L)	27	1.68	1.4	SIL C ₁₈ -50/UV ₂₅₄	B
Fmoc-Nva	19(L)	27	1.57	1.6	SIL C ₁₈ -50/UV ₂₅₄	B
Fmoc-Phe	41(L)	50	1.43	1.2	SIL C ₁₈ -50/UV ₂₅₄	C
Fmoc-Pro	47(D)	77	3.78	1.6	SIL C ₁₈ -50/UV ₂₅₄	B
	34(D)	40	1.29	2.0	MCTA	E
Fmoc-Trp	20(D)	41	2.79	2.7	SIL C ₁₈ -50/UV ₂₅₄	D
Fmoc-Val	36(L)	43	1.35	2.3	SIL C ₁₈ -50/UV ₂₅₄	C
DNP-Abu	59	89	5.75	4.0	RP-18W/UV ₂₅₄	F
DNP-Cit	34	41	1.35	1.7	RP-18W/UV ₂₅₄	G
DNP-Eth	45	61	1.94	2.0	RP-18W/UV ₂₅₄	G
DNP-Eth(O ₂)	26	35	1.53	2.0	RP-18W/UV ₂₅₄	H
DNP-Leu	28(L)	54	3.02	3.6	RP-18W/UV ₂₅₄	I
	24(D)	31	1.42	1.8	SIL C ₁₈ -50/UV ₂₅₄	L
DNP-Met	28	61	4.02	3.3	RP-18W/UV ₂₅₄	M
DNP-Met(O ₂)	44(D)	50	1.27	2.0	RP-18W/UV ₂₅₄	N
DNP-Met(O)	27	34	1.39	2.3	RP-18W/UV ₂₅₄	N
DNP-Nle	31	63	3.78	5.1	RP-18W/UV ₂₅₄	I
DNP-Nva	40	89	12.19	5.0	RP-18W/UV ₂₅₄	O
DNP-Pip	45	56	1.56	1.3	RP-18W/UV ₂₅₄	F
DNPy-Ala	47	53	1.27	1.6	RP-18W/UV ₂₅₄	H
DNPy-Leu	45	70	2.85	4.0	RP-18W/UV ₂₅₄	N
	38	43	1.23	1.5	SIL C ₁₈ -50/UV ₂₅₄	L
	23	31	1.50	2.5	SIL C ₁₈ -50/UV ₂₅₄	P
DNPy-Met	31	56	2.61	4.2	RP-18W/UV ₂₅₄	Q
DNPy-Nle	25	63	5.11	5.7	RP-18W/UV ₂₅₄	N
DNPy-Nva	21	31	1.69	2.3	RP-18W/UV ₂₅₄	H
DNPy-Phe	28	61	4.02	5.0	RP-18W/UV ₂₅₄	Q
	47	51	1.17	1.2	SIL C ₁₈ -50/UV ₂₅₄	L
	18	26	1.60	2.0	SIL C ₁₈ -50/UV ₂₅₄	P
DNPy-Trp	30	49	2.24	5.0	SIL C ₁₈ -50/UV ₂₅₄	L
DNB-Leu	34(L)	51	2.02	3.0	RP-18W/UV ₂₅₄	N
DNB-PhenylGly	30(L)	67	4.75	7.3	RP-18W/F _{254S}	N
MTH-Pro	12	16	1.39	1.3	RP-18W/UV ₂₅₄	R
	33	37	1.19	1.0	MCTA	E
MTH-Phe	43	49	1.27	1.7	MCTA	S
MTH-Tyr	42	45	1.13	1.0	MCTA	E
PTH-Pro	13	25	2.23	2.5	MCTA	E
N-[1-(1-Naphthyl)ethyl]phthalamic acid	54(R)	58	1.17	1.6	MCTA	T
N-Benzylproline ethyl ester	19(D)	22	1.20	1.0	MCTA	U
Amethopterin	9(L)	19	2.34	2.3	RP-18W/UV ₂₅₄	V
N-Acetyl-5-methyl-Trp	33	76	6.44	3.0	RP-18W/UV ₂₅₄	M
N-CBZ-Trp	44(D)	88	9.33	3.0	RP-18W/UV ₂₅₄	Z
N-t-BOC-Trp	16(L)	23	1.57	1.2	RP-18W/UV ₂₅₄	V
N-t-BOC-p-nitro-Phe	20(D)	30	1.71	2.3	SIL C ₁₈ -50/UV ₂₅₄	W
Ala-β-NA	68(L)	76	1.49	1.5	SIL C ₁₈ -50/UV ₂₅₄	Y
	59	66	1.35	–	KC18F	J
Leu-β-NA	54(L)	64	1.50	2.0	SIL C ₁₈ -50/UV ₂₅₄	L
Met-β-NA	45(L)	55	1.50	2.3	SIL C ₁₈ -50/UV ₂₅₄	L
Ala-p-NA	12(L)	14	1.19	0.4	RP-18W/UV ₂₅₄	K
Leu-p-NA	4(L)	7	1.81	1.2	RP-18W/UV ₂₅₄	K ₁
	19(L)	23	1.27	1.0	SIL C ₁₈ -50/UV ₂₅₄	K ₂
	56(L)	63	1.33	1.7	SIL C ₁₈ -50/UV ₂₅₄	L

^a $hR_F = R_F \times 100$.^b $\alpha = (1 \div R_{F1} - 1) / (1 \div R_{F2} - 1)$.^c $R_s = 2 \times (\text{distance between the centres of two adjacent spots}) / (\text{sum of the width of the two spots in the direction of development})$.^dCha = β-Cyclohexylalanine.

^eEluents: A = 6% BSA, 23% 2-propanol, 0.1 mol L⁻¹ acetate buffer; B = 5% BSA, 23% 2-propanol, 0.1 mol L⁻¹ acetate buffer; C = 5% BSA, 36% 2-propanol, 0.1 mol L⁻¹ acetate buffer; D = 6% BSA, 12% 2-propanol, 0.1 mol L⁻¹ acetate buffer; E = 2-propanol/water 60 : 40 (v/v); F = 4% BSA, 2% 2-propanol, 0.1 mol L⁻¹ acetate buffer (10°C); G = 6% BSA, 2% 2-propanol, 0.1 mol L⁻¹ acetate buffer; H = 4% BSA, 1% NaCl, 2% 2-propanol, 0.5 mol L⁻¹ acetic acid (10°C); I = 4% BSA, 2% 2-propanol, 0.05 mol L⁻¹ phosphate buffer; L = 0.15 mol L⁻¹ β-CD in a water-acetonitrile solution (80 : 20, v/v) containing 26% urea and 3% NaCl; M = 3% BSA, 2% 2-propanol, 0.05 mol L⁻¹ phosphate buffer; N = 5% BSA, 2% 2-propanol, 0.1 mol L⁻¹ acetate buffer; O = 4% BSA, 2% 2-propanol, 0.1 mol L⁻¹ acetate buffer; P = Hydroxypropyl-β-CD (13.8 g) in water-acetonitrile-acetic acid (45 : 4 : 1, v/v/v, 100 mL); Q = 2% BSA, 2% 2-propanol, 0.1 mol L⁻¹ acetate buffer; R = 9% BSA, 2% 2-propanol, 0.1 mol L⁻¹ acetate buffer; S = 2-propanol-water 80 : 20 (v/v); T = ethanol-water 70 : 30 (v/v); U = 2-propanol-water 40 : 60 (v/v); V = 8% BSA, 2% 2-propanol, 0.5 mol L⁻¹ acetic acid; Z = 5% BSA, 2% 2-propanol, 0.5 mol L⁻¹ acetic acid; W = 6% BSA, 6% 2-propanol, 0.05 mol L⁻¹ NaHCO₃ + 0.05 mol L⁻¹ Na₂CO₃; Y = 0.1 mol L⁻¹ β-CD in a water-acetonitrile solution (80 : 20, v/v) containing 20% urea and 3% NaCl; J = 0.163 mol L⁻¹ β-CD in a water-methanol solution (65 : 35, v/v) containing 3.5% NaCl and saturated with urea; K = 8% BSA, 3% 2-propanol, 0.1 mol L⁻¹ acetate buffer; K₁ = 6% BSA, 8% 2-propanol, 0.1 mol L⁻¹ acetate buffer; K₂ = 8% BSA, 20% 2-propanol, 0.1 mol L⁻¹ acetate buffer.

Table 7 Separation of enantiomeric α -hydroxycarboxylic acids on HPTLC-CHIR plates^a

Racemate	hR_{F1}^b	hR_{F2}^b	α^c	Eluent ^d
Mandelic acid	36	48	1.64	A
4-Bromo-mandelic acid	33	44	1.59	B
4-Chloro-mandelic acid	35	42	1.34	B
3-Hydroxy-mandelic acid	47	59	1.62	B
4-Hydroxy-mandelic acid	45	57	1.61	C
3,4-Dihydroxy-mandelic acid	33	44	1.59	C
4-Hydroxy-3-methoxy-mandelic acid	24	33	1.55	A
2-Hydroxy-2-phenyl-propanoic acid	38	47	1.44	A
2-Hydroxy-3-phenyl-propanoic acid	39	51	1.62	A
Lactic acid	70(D)	76(L)	1.38	D
2-Hydroxy-butanoic acid	27	37	1.58	A
2-Hydroxy-3-methoxy-butanoic acid	33	46	1.73	A
2-Hydroxy-4-methylthio-butanoic acid	33	45	1.66	A
2-Hydroxy-pentanoic acid	25	39	1.91	A
2-Hydroxy-3-methyl-pentanoic acid	34	49	1.86	A
2-Hydroxy-4-methyl-pentanoic acid	35	47	1.64	A
2-Hydroxy-hexanoic acid	62(D)	69(L)	1.36	D
2-Hydroxy-octanoic acid	36	50	1.78	A
2-Hydroxy-tetradecanoic acid	34	49	1.86	A
2-Hydroxy-hexadecanoic acid	39	56	1.99	A
2-Hydroxy-docosahexanoic acid	39	56	1.99	A

^aMigration distance, measured from concentrating zone, 13 cm; visualization: (a) the plates were dipped in MnCl_2 -sulfuric acid heating up to 120°C for 30 min for aromatic α -hydroxycarboxylic acids; (b) the plates were dipped for 2 s in vanadium (V)-sulfuric acid solution and dried at room temperature for c. 45 min for aromatic and aliphatic α -hydroxycarboxylic acids.

^b $hR_F = R_F \times 100$.

^c $\alpha = (1 \div R_{F1} - 1)/(1 \div R_{F2} - 1)$.

^dEluents: A = dichloromethane/methanol 45 : 5 (v/v); B = 0.05 mol L⁻¹ KH_2PO_4 in a methanol-acetonitrile-water 50 : 50 : 200 (v/v/v) mixture; C = 0.1 mol L⁻¹ LiCl in a dichloromethane-ethanol 85 : 15 (v/v) mixture; D = acetonitrile-water 3 : 2 (v/v).

The use of mobile phases containing β -CD seems to be particularly appropriate for the resolution of racemic *S*-(1-ferrocenyl-2-methylpropyl)thioethanol and *S*-(1-ferrocenylethyl)thioethanol ($\alpha = 1.43$ and 1.18, respectively).

Many noncharged solutes with a carbonyl group close to the stereogenic centre can be resolved on MCTA plates (benzoin, benzoin methyl ether, 2-phenylbutyrophenone, 2- and 3-methylindanone, 2-phenylcyclohexanone, 2-phenylcycloheptanone and 2-oxazolidone derivatives).

Quantitative Analysis of TLC-Separated Enantiomers

TLC is generally coupled with spectrophotometric methods for quantitative analysis. Quantification can be achieved by *in situ* densitometry or after extraction of solutes from the scraped layer. The evaluation of detection limits for separated enantiomers is essential because precise determinations of trace levels of D- or L-enantiomer in an excess of the other is becoming more and more important.

On Chiralplates and HPTLC-CHIR layers, densitometry can be performed after postchromatographic derivatization of compounds with ninhydrin or vanadium pentoxide. Successful separation of amino acids on Chiralplates depends on the hydrochloric acid content of the applied solution (usually a methanol-0.1 mol L⁻¹ HCl 1 : 1 (v/v) mixture).

Remission-location curves of DL- α -hydroxycarboxylic acids, achieved in reflectance mode with a Shimadzu CS930 scanner or a Desaga CD60 densitometer, show that only enantiomers with high ΔR_F values (≥ 0.10) can be baseline resolved on 10 cm \times 10 cm HPTLC-CHIR plates (Figure 3). On such plates, L-2-hydroxy-3-phenylpropionic acid spiked with 1% D enantiomer ($\Delta R_F = 0.12$) gives rise to partially resolved peaks but the D isomer is still visible. With respect to small particle size HPTLC-CHIR layers, higher R_F values have been obtained on 20 cm \times 20 cm Chiralplates owing to migration distances being twice as long (α values being equal).

The remission-location curves of Figure 4 and the calibration line for L-phenylalanine (Figure 5) demonstrate that quantitative determinations of L-isomer in D-phenylalanine on Chiralplates ($\Delta R_F = 0.10$) are possible in a working range of 0.04–0.4 $\mu\text{g/spot}$, that is 0.1–1%. Further determinations include 0.1% D-*t*-Leu in L-*t*-Leu ($\Delta R_F = 0.11$), 0.1% L-5,5-dimethylthiazolidine-4-carboxylic acid in the D-enantiomer ($\Delta R_F = 0.14$) and 1% D-hydroxyphenylalanine in the L-enantiomer.

The peak of 1% Dns-D-Glu in L-enantiomer is visible on 20 cm \times 20 cm RP-18 plates (Merck) impregnated with a solution of 8 mol L⁻¹ N,N-di-*n*-propyl-L-alanine and 4 mmol L⁻¹ cupric acetate.

On 10 cm \times 20 cm cellulose plates L-tryptophan spiked with 5% D-enantiomer gives rise to partially resolved peaks owing to the small ΔR_F value (0.06).

The use of MCTA allows the determination of enantiomeric mixtures in the ratios 100 : 1 and 200 : 1. (*S*)-2,2,2-Trifluoro-1-(9-anthryl)ethanol can be detected at 1% level in (*R*) enantiomer on OPTI-TAC F₂₅₄ plates eluted with ethanol-water 80 : 20 ($\Delta R_F = 0.17$; length of run 10 cm). Baseline-resolved

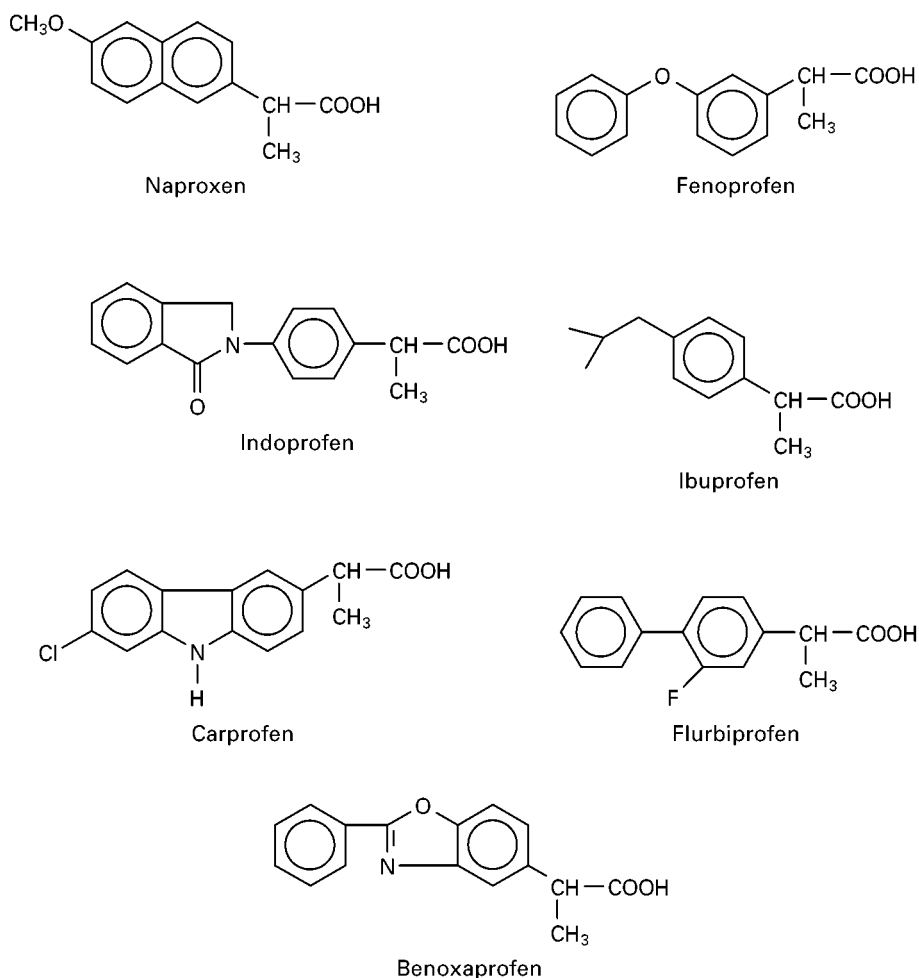


Figure 2 Structure of acidic drugs.

peaks ($\Delta R_F = 0.10$) were obtained for the two atropisomers of 1,1'-binaphthyl-2,2'-diamine on 20 cm \times 20 cm home-made MCTA plates at 100 : 1 ratio. Partial resolution only was observed at a ratio of 200 : 1, but the *S* isomer is still visible (Figure 6).

Conclusions

Chiral TLC plays a significant role both in economical routine analyses and in determination of optical purity of individual antipodes. Detection limits of $\geq 0.1\%$ D- or L-isomer can be currently achieved.

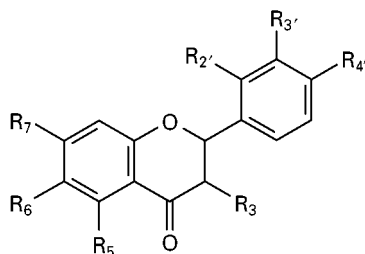
Table 8 Retention and resolution data for derivatized and free acidic drugs by chiral TLC

Drug	hR_{F1}^a	hR_{F2}	α^b	Eluent ^c	Plates and remarks
DNAn-ibuprofen	28 (S)	45 (R)	2.10	A	Precoated 10 cm \times 10 cm HPTLC-NH ₂ F ₂₅₄ s plates (Altech, Deerfield, IL, USA), derivatized with (<i>R</i>)-(-)-1-(1-naphthyl)ethyl isocyanate. Visualization: UV ₂₅₄ and UV ₃₆₀ .
DNAn-naproxen	15 (S)	24 (R)	1.79	A	
DNAn-fenopropfen	23	33	1.65	A	
DNAn-flurbiprofen	23	33	1.65	A	
DNAn-benoxapropfen	20	30	1.71	A	MCTA plates. Visualization: UV. 5 cm \times 20 cm chemically-bonded diphenyl-F plates.
Flurbiprofen	18	24	1.44	B	
Carprofen	36	41	1.23	C	
Indopropfen	58	63	1.22	D	

^a $hR_F = R_F \times 100$.

^b $\alpha = (1 \div R_{F1} - 1) / (1 \div R_{F2} - 1)$.

^cEluents: A = *n*-hexane-isopropanol-acetonitrile 20 : 8 : 1 (v/v/v); B = ethanol-water 40 : 60 (v/v); C = isopropanol-water 60 : 40 (v/v); D = acetonitrile-0.6 mol L⁻¹ NaCl-1% triethylammonium acetate buffer (pH 4.1) containing vancomycin.

Table 9 The structure of racemic flavanones

R_3	R_5	R_6	R_7	$R_{2'}$	$R_{3'}$	$R_{4'}$	Name
H	H	H	H	H	H	H	Flavanone
H	OCH ₃	H	H	H	H	H	5-Methoxyflavanone
H	H	OH	H	H	H	H	6-Hydroxyflavanone
H	H	OCH ₃	H	H	H	H	6-Methoxyflavanone
H	H	H	OH	H	H	H	7-Hydroxyflavanone
H	H	H	H	OH	H	H	2'-Hydroxyflavanone
H	H	H	H	H	H	OH	4'-Hydroxyflavanone
H	H	H	H	H	H	OCH ₃	4'-Methoxyflavanone
H	OH	H	OH	H	H	H	Pinocembrin
H	OH	H	OCH ₃	H	H	H	Pinocembrin-7-methylether
H	OH	H	OH	H	H	OH	Naringenin
H	OH	H	OH	H	H	OCH ₃	Isosakuranetin
H	OH	H	OCH ₃	H	H	OH	Sakuranetin
H	OH	H	Gl ^a	H	H	OH	Naringenin-7-glucoside
H	OH	H	Rh-Gl ^b	H	H	OH	Naringin
H	OH	H	OH	H	OH	OH	Eriodictyol
H	OH	H	OH	H	OCH ₃	OH	Homoeriodictyol
H	OH	H	OH	H	OH	OCH ₃	Hesperetin
OH	OH	H	OH	H	OH	OH	Taxifolin

^aGl = Glucoside.^bRh-Gl = Rhamnosidoglucoside.**Table 10** Retention and resolution data for racemic flavanones by chiral TLC

Racemate	hR_{F1}^a	hR_{F2}	α^b	R_s^c	Plate	Eluent ^d
Flavanone (F)	16	20	1.31	1.6	SIL C ₁₈ -50/UV ₂₅₄	A
	22	24	1.12	0.4	MCTA	B
6-Hydroxy-F	36	39	1.14	0.8	MCTA	B
6-Methoxy-F	24	27	1.17	0.8	MCTA	B
2'-Hydroxy-F	10	16	1.71	2.0	SIL C ₁₈ -50/UV ₂₅₄	C
	19	24	1.35	1.6	SIL C ₁₈ -50/UV ₂₅₄	A
4'-Hydroxy-F	38	42	1.18	1.2	SIL C ₁₈ -50/UV ₂₅₄	A
4'-Methoxy-F	13	19	1.57	2.0	SIL C ₁₈ -50/UV ₂₅₄	A
5,7-Dihydroxy-F	54	60	1.27	1.8	MCTA	D
4',5,7-Trihydroxy-F	23	28	1.30	1.6	MCTA	E
5,7-Dihydroxy-4'-methoxy-F	18	21	1.21	1.3	MCTA	E
4',5-Dihydroxy-7-methoxy-F	43	48	1.22	1.2	MCTA	D
3',4',5,7-Tetrahydroxy-F	26	30	1.21	1.5	MCTA	E
4',5,7-Trihydroxy-3'-methoxy-F	23	26	1.17	0.8	MCTA	E
3',5,7-Trihydroxy-4'-methoxy-F	23	27	1.24	1.5	MCTA	E
3,3',4',5,7-Pentahydroxy-F	44	48	1.17	1.3	MCTA	E

^a $hR_F = R_F \times 100$.^b $\alpha = (1 \div R_{F1} - 1)/(1 \div R_{F2} - 1)$.^c $R_s = 2 \times (\text{distance between the centres of two adjacent spots})/(\text{sum of the width of the two spots in the direction of development})$.^dEluents: A = 0.15 mol L⁻¹ β -CD aqueous solution with urea (32%) and NaCl (2%)-acetonitrile 80 : 20 (v/v), migration distance 8.5 cm; B = ethanol-water 80 : 20 (v/v), migration distance 12 cm; C = 0.05 mol L⁻¹ sodium bicarbonate + 0.05 mol L⁻¹ sodium carbonate solution containing 6% BSA and 12% isopropanol, migration distance 8 cm; D = ethanol-water 70 : 30 (v/v), migration distance 14 cm; E = methanol-water 80 : 20 (v/v), migration distance 16 cm.

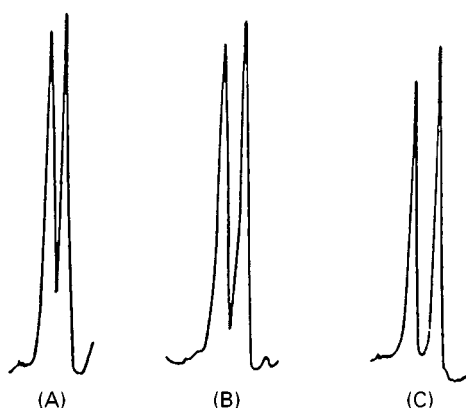


Figure 3 Remission-location curves recorded on 10 cm \times 10 cm HPTLC-CHIR plates. (A) D,L-Lactic acid ($\Delta R_F = 0.05$); (B) D,L-2-hydroxybutanoic acid ($\Delta R_F = 0.10$); (C) D,L-2-hydroxyoctanoic acid ($\Delta R_F = 0.14$).



Figure 4 Remission-location curves recorded on 20 cm \times 20 cm Chiralplates. (A) D-Phe spiked with 0.1% L-Phe; (B) 0.1% L-Phe.

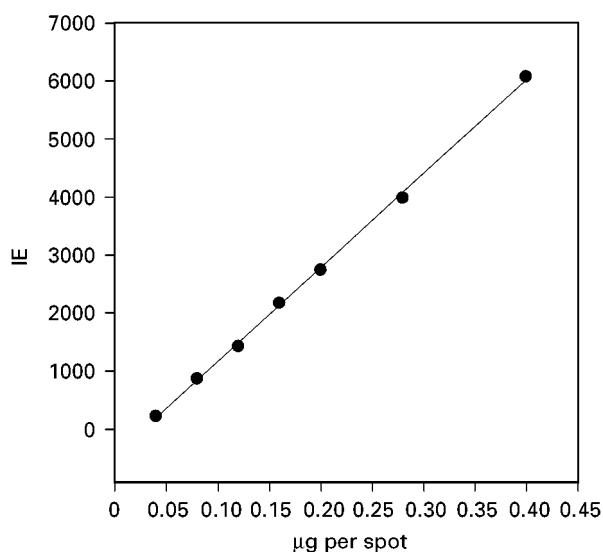


Figure 5 Calibration line for L-phenylalanine. IE, integration units; $y = -463 + 16349x$; $r = 0.9992$; $S_{x_0} = 0.0038 \mu\text{g per spot}$; $\lambda = 540 \text{ nm}$.

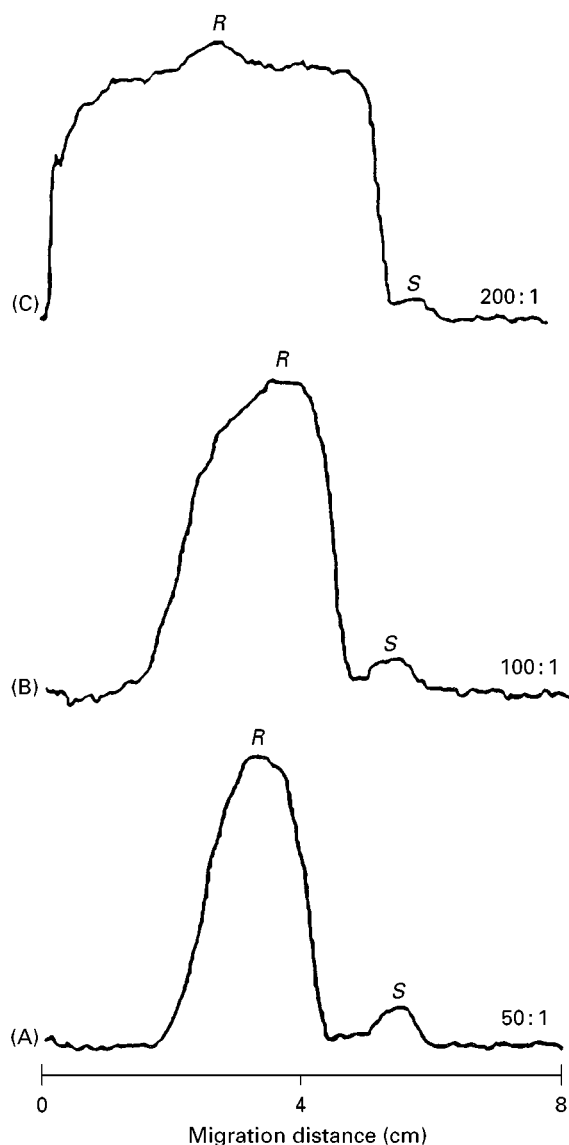


Figure 6 Densitograms of (*R*) and (*S*) - 1,1'-binaphthyl-2,2'-diamine mixtures in the ratios 50 : 1, 100 : 1 and 200 : 1 on MCTA layers, eluted with ethanol-water 80 : 20 (v/v). Migration distance 17 cm. (A) (*R*) = 10 μg , (*S*) = 0.2 μg ; (B) (*R*) = 20 μg ; (*S*) = 0.2 μg ; (C) (*R*) = 40 μg ; (*S*) = 0.2 μg .

Less work is being carried out on chiral TLC than on column chromatography, even though the two techniques may give complementary results and TLC has advantages such as low cost and easy evaluation of the tests.

Future possibilities of chiral TLC include:

1. the synthesis of enantiomeric derivatives that are easier to resolve and more sensitively detected than those so far investigated;
2. the availability of layers prepared from new cellulose derivatives and, in addition, the availability of more versatile MCTA plates using highly crystalline and homogeneously sized material;

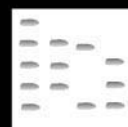
3. more extensive application of normal-phase chromatography with a chiral mobile phase additive (DIOL plates are particularly advisable);
4. the use of eluents containing new chiral selectors in reversed-phase systems, which is the technique most widely used for enantioseparations.

See also: **II/Chromatography: Thin-Layer (Planar):** Densitometry and Image Analysis; Layers; Spray Reagents. **III/Amino Acids and Derivatives: Chiral Separations: Chiral Separations:** Capillary Electrophoresis; Cellulose and Cellulose Derived Phases; Chiral Derivatization; Cyclodextrins and Other Inclusion Complexation Approaches; Ion-Pair Chromatography; Ligand Exchange Chromatography; Liquid Chromatography; Molecular Imprints as Stationary Phases; Protein Stationary Phases; Supercritical Fluid Chromatography; Synthetic Multiple Interaction ('Pirkle') Stationary Phases.

Further Reading

- Armstrong DW, He FY and Han SM (1988) Planar chromatographic separation of enantiomers and diastereomers with cyclodextrin mobile phase additives. *Journal of Chromatography* 448: 345–354.
- Dalglish CE (1952) The optical resolution of aromatic amino acids on paper chromatograms. *Journal of the Chemical Society* III: 3940–3942.
- Gunther R and Möller K (1996) Enantiomer separations. In: Sherma J and Fried B (eds) *Handbook of Thin Layer Chromatography*, pp. 621–682. New York: Marcel Dekker.
- Lepri L (1997) Enantiomer separation by TLC. *Journal of Planar Chromatography, Modern TLC* 10: 320–331.
- Lepri L, Coas V and Desideri PG (1992) Planar chromatography of optical isomers with bovine serum albumin in the mobile phase. *Journal of Planar Chromatography, Modern TLC* 5: 175–178.

CITRUS OILS: LIQUID CHROMATOGRAPHY



P. Dugo, Università di Messina, Messina, Italy
L. Mondello and G. Dugo, Facoltà di Farmacia,
Messina, Italy

Copyright © 2000 Academic Press

Citrus essential oils are very complex matrices which contain numerous compounds of different chemical classes. These compounds are generally divided into two fractions: the volatile fraction, which is the most representative, and ranges between 85 and 99% in the different cold-pressed citrus oils, and the non-volatile residue, which ranges between 1 and 15%.

The development of new instrumental analytical techniques, mainly chromatographic, has allowed the characterization of citrus essential oils to become more precise.

Gas chromatography is an essential tool for the study of the volatile fraction, while liquid chromatography (thin-layer chromatography (TLC) and high-performance liquid chromatography (HPLC) combined with spectral absorption and fluorescence measurements) is widely used for the study of the composition of the non-volatile residue. This fraction consists largely of oxygen heterocyclic compounds (coumarins, psoralens (furanocoumarins) and polymethoxylated flavones) that exhibit strong absorption in the ultraviolet region (λ_{max} about 315 nm).

The presence of coumarin compounds is widespread in plants of the *Rutaceae* family to which the citrus species belong. Their presence is qualitatively and quantitatively different in the different citrus oils, so knowledge of the oxygen heterocyclic fraction may be useful to assess authenticity, the geographical origin and the possible adulteration of the oils.

Figure 1 shows the basic structures of the oxygen heterocyclic compounds present in citrus oils. In the numbered position, coumarins and psoralens may contain hydroxyl, methoxyl, isopentenyl, isopentenyl, geranyloxy groups; polymethoxylated flavones contain methoxyl groups. Table 1 lists the oxygen heterocyclic compounds identified in citrus oils.

TLC Separations

The literature from the 1930s to the end of 1970s reports numerous TLC separations of non-volatile residue of citrus oils with the aim of isolating the

components. Often these components were not identified before and were responsible for ultraviolet (UV) absorption. Knowledge of the chromatographic characteristics and the chemical structures of these compounds was considered very important in order to determine the authenticity of the oils. In fact, valuable cold-pressed oils may be adulterated with less valuable cold-pressed or distilled oils. In these cases the presence and/or the content of some oxygen heterocyclic compounds may be useful to determine the kind and also the degree of adulteration.

Many methods developed for the TLC analysis of oxygen heterocyclic compounds of citrus oils used silica gel as a stationary phase, and mixtures of hexane or cyclohexane with variable amounts of ethyl acetate as mobile phases. For example, a paper of 1965 reports the separation of coumarins of many citrus oils by TLC, obtained on silica gel plates, using mixtures of hexane with variable amounts (25–70%) of ethyl acetate, according to the different polarity of the components. The spots were detected by UV absorbance at 254 and 366 nm. The components were also isolated from the plates, extracted from silica gel and analysed by UV spectroscopy. Table 2 provides chromatographic and spectroscopic data for the oxygen heterocyclic compounds of lemon, bergamot, mandarin, sweet orange and bitter orange. Identification was carried out by comparison of R_f values and spectroscopic data with those of standard compounds.

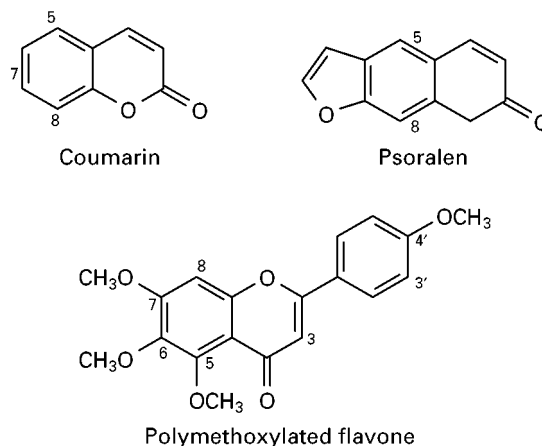


Figure 1 Structures of oxygen heterocyclic compounds present in citrus oil.

Table 1 Oxygen heterocyclic compounds identified in citrus essential oils

	<i>Bitter orange</i>	<i>Sweet orange</i>	<i>Lemon</i>	<i>Lime</i>	<i>Bergamot</i>	<i>Mandarin</i>	<i>Grape fruit</i>
Aurapten (7-geranyloxy coumarin)	X		X				X
Auraptenol (7-(2'-hydroxy-isopent-3'-enyloxy) coumarin)	X						
Marmin (7-(6',7'-dihydroxygeranyloxy) coumarin)							X
Umbelliferone (7-hydroxycoumarin)	X						
Herniarin (7-methoxycoumarin)			X	X			
Epoxyaurapten (7-(6',7'-epoxygeranyloxy) coumarin)							X
7-Isopentenyl oxy coumarin			X				
Meranzin (7-methoxy-8(2',3'-epoxy) isopentenyl coumarin)	X						X
Osthol (7-methoxy-8-isopentenyl coumarin)	X						X
Meranzin hydrate (7-methoxy-8(2',3'-dihydroxy) isopentyl oxy- coumarin)	X						X
Isomeranzin (7-methoxy-8-(2'-one-isopentyl) coumarin)	X						X
7-(Methoxy-8(2'-formyl-2'-methylpropyl) coumarin)							X
Citropten (5,7-dimethoxycoumarin)	X	X	X	X	X		X
5-Isopentenyl oxy-7-methoxycoumarin			X	X	X		
5-(2',3'-Epoxy-isopentyl oxy)-7-methoxycoumarin			X				
5-Geranyloxy-7-methoxycoumarin			X	X	X		
5-(2',3'-Dihydroxy-isopentyl oxy)-7-methoxycoumarin)			X				
Bergapten (5-methoxypsoralen)	X	X		X	X		X
Epoxybergamottin (5-(6',7'-epoxy-geranyloxy) psoralen)	X						X
Epoxybergamottin hydrate (5-(6',7'-dihydroxy-geranyloxy) psoralen)	X						X
Bergamottin (5-geranyloxy psoralen)			X	X	X		X
Bergaptol (5-hydroxypsoralen)	X	X	X		X		X
Oxypeucedanin (5-(2',3'-epoxy-isopentyl oxy) psoralen)			X	X	X		
Oxypeucedanin hydrate (5-(2',3'-dihydroxy-isopentyl oxy) psoralen)			X	X	X		
Pabulenol/Gosferol (5-(2'-hydroxy-3'-methylbut-3'-enyloxy) psoralen)			X				
Isoimperatorin (5-isopentenyl oxy psoralen)			X	X			
8-Geranyloxy psoralen			X	X			
Heraclenin (8-(2',3'-epoxy-isopentyl oxy) psoralen)			X	X			
Heraclenol (8-(2',3'-dihydroxy isopentyl oxy) psoralen)			X				
Imperatorin (8-isopentenyl oxy psoralen)			X	X			
8-(6',7'-Epoxygeranyloxy) psoralen			X				
5-Methoxy-8(2',3'-epoxy-isopentyl oxy) psoralen			X				
5-Geranyloxy-8-methoxypsoralen			X	X			
Byakangelicin (8-(2',3'-dihydroxy-isopentyl oxy)-5-methoxypsoralen)			X		X		
Isobyakangelicol (5-methoxy-8-(2'-one-isopentyl) psoralen)				X			
5-Isopent-2'-enyloxy-8-(2',3'-epoxy-isopentyl oxy) psoralen)			X				
Phellopterin (5-methoxy-8-isopentenyl oxy psoralen)			X				
Byakangelicol (5-methoxy-8-(2',3'-epoxy-isopentyl oxy) psoralen)			X	X	X		
Isopimpinellin (5,8-dimethoxypsoralen)				X			
Cnidilin (5-Isopentenyl oxy-8-methoxypsoralen)				X			
Neobyakangelicol (5-methoxy-8-(2'-hydroxy-3'-methylbut-3'- enyloxy) psoralen)			X				
5-Isopentenyl oxy-8-(2',3'-dihydroxy-isopentyl oxy) psoralen			X				
Cnidicin (5,8-diisopentenyl oxy) psoralen			X				
5-Methoxy-8-geranyloxy psoralen			X				
3,6,7,8,4'-pentamethoxyflavone	X						
Tangeretin (4',5,6,7,8-pentamethoxyflavone)	X	X				X	X
Nobiletin (3',4',5,6,7,8-hexamethoxyflavone)	X	X				X	X
3,3',4',5,6,7,8-Heptamethoxyflavone	X	X				X	X
Sinensetin (3',4',5,6,7-pentamethoxyflavone)		X			X	X	
3,3',4',5,6,7-Hexamethoxyflavone		X					
Tetra-O-methylscutellarein (4',5,6,7-tetramethoxyflavone)	X	X			X	X	

Isopentenyl oxy = 3'-methylbut-2'-enyloxy; Geranyloxy = 3'7'-dimethyloct-2',6'-enyloxy.

Figure 2 shows another example of a TLC separation of coumarins of a cold-pressed lemon oil, obtained using butyl acetate instead of ethyl acetate, in particular, hexane-butyl acetate 65 : 35 (A) and

75 : 25 (B). Detection was by UV absorbance at 254 nm. As can be seen, 21 components have been separated, but only the main components were identified: (1) bergamottin; (3) 5-geranyloxy-7-methoxy-

Table 2 Chromatographic and spectroscopic data of the oxygen heterocyclic compounds of lemon, bergamot, mandarin, sweet orange and bitter orange oils

Fluorescence	<i>Rf</i> ₂₅ [*]	<i>Rf</i> ₃₀ [*]	<i>Rf</i> ₄₀ [*]	<i>Rf</i> ₅₀ [*]	<i>Rf</i> ₆₀ [*]	<i>Rf</i> ₇₀ [*]	<i>λ</i> max	<i>λ</i> min	<i>λ</i> shoulder
<i>Lemon oil</i>									
1. yellow	0	0	0				315	280	–
2. yellow (bergaptol)	0.02	0.04	0.05				265, 310	260, 280	250
3. violet	–	0.08	0.15				315	280	230, 245, 255
4. red (byakangelicin)	0.14	0.16	0.20				240, 265, 310	235, 255, 285	250
5. yellow (5, 8 -... psoralen)	0.20	0.26	0.27				250, 307	235, 275	260
6. blue (citropten)	0.33	0.36	0.38				245, 325	240, 265	255
7. yellow (8-geranyloxypsoralen)									
8. blue	0.39	0.41	0.49				315	280	245, 270
9. blue (5-geranyloxy-7-methoxycoumarin)	0.44	0.46	0.55				323	277	245, 270
10. yellow (bergamottin)	0.50	0.52	0.59				250, 310	240, 278	270
<i>Bergamot oil</i>									
1. Yellow	0	0	0	0	0	0	–	–	–
2. Red	0	0	0	0	0	0.02	–	–	–
3. Blue	0	0	0	0.03	0.03	0.04	–	–	–
4. Blue	0	0	0	0.03	0.06	0.12	–	–	–
5. Violet	0.01	0.02	0.04	0.06	0.12	0.17	325	285	270
6. Yellow/red	–	0.03	0.09	0.14	0.20	0.26	270, 320	285	270
7. Blue	–	0.08	0.16	0.25	0.29	0.32	–	–	265
8. Green	–	0.08	0.22	0.29	0.40	0.44	270, 325	260, 305	–
9. Blue	0.14	0.17	0.28	0.32	–	–	324	275	270
10. Yellow (bergapten)	0.20	0.22	0.29	0.37	0.50	0.55	250, 260, 310	235, 255, 280	–
11. Blue (citropten)	0.33	0.36	0.38	0.42	0.53	0.59	245, 255, 270, 325	240, 250, 265, 275	–
12. Blue (5-geranyloxy-7-methoxycoumarin)	0.44	0.46	0.52	0.56	0.67	0.68	323	278	250, 270
13. Yellow (bergamottin)	0.50	0.52	0.59	0.60	0.67	0.68	240, 310	235, 280	270
14. Red	–	–	0.62	0.64	0.72	0.73	–	–	–
<i>Mandarin oil</i>									
1. Yellow			0	0	0	0	325	–	–
2. Blue			0	0	0.05	0.07	–	–	–
3. Blue			0.03	0.06	0.12	0.16	325	285	270
4. Yellow/green (nobiletin)			0.06	0.10	0.19	0.22	270, 333	260, 290	245
5. Yellow (tangeretin)			0.09	0.15	0.27	0.32	270, 325	245, 290	–
6. Red (a polymethoxyflavone)			0.13	0.18	0.32	0.34	270, 325	245, 290	–
7. Yellow/green (a flavanone)			0.18	0.26	0.35	0.38	275, 322	260, 300	–
8. Brown (a flavanone)			0.23	0.29	0.38	0.47	275, 332	265, 310	–
9. Red (a flavanone)			0.30	0.31	0.46	0.51	265, 275	260, 270	–
10. Blue (citropten)			0.37	0.41	0.54	0.56	–	–	–
11. Pale blue			0.53	–	–	–	–	–	–
12. Blue (methyl anthranilate)			0.56	0.61	0.63	0.66	–	–	–
13. Blue (N-methyl methylanthranilate)			0.64	0.65	0.70	0.70	253, 355	240, 290	–
<i>Sweet orange oil</i>									
1. Yellow			0	0	0	0	–	–	–
2. Blue			0	0.03	0.05	0.07	–	–	–
3. Blue			0.03	0.06	0.12	0.16	265, 325	260, 295	–
4. Yellow/green (nobiletin)			0.05	0.10	0.19	0.22	250, 270, 333	240, 260, 290	–
5. Yellow/red (tangeretin)			0.10	0.17	0.26	0.33	270, 324	250, 285	–
6. Green (5,8-dihydroxy-3,7,3',4'-tetramethoxyflavone)			0.18	0.27	0.37	0.48	255, 270, 330	245, 260, 290	–
7. Blue (citropten)			0.38	0.44	0.53	0.59	–	–	–
8. Blue (methyl anthranilate)			0.56	0.61	0.63	0.66	–	–	–
9. Yellow			0.67	0.70	0.74	0.87	–	–	–

Table 2 continued

Fluorescence	$R_{f_{25}}^*$	$R_{f_{30}}^*$	$R_{f_{40}}^*$	$R_{f_{50}}^*$	$R_{f_{60}}^*$	$R_{f_{70}}^*$	λ max	λ min	λ shoulder
<i>Bitter Orange oil</i>									
1. Yellow	0	0	0	0	0	0	—	—	—
2. Blue	0	0.02	0.03	0.05	0.07	0.18	320	268	260
3. Blue/yellow	0	0.04	0.06	0.13	0.18	0.22	313	280	270
4. Yellow/green (nobiletin)	0.02	0.05	0.11	0.18	0.22	0.27	270, 329	265, 285	250
5. Yellow/red (tangeretin)	0.03	0.10	0.17	0.26	0.33	0.49	270, 324	250, 290	—
6. Blue (aurapten)	0.10	0.18	0.25	0.34	0.44	0.55	255, 322	250, 265	—
7. Violet (umbelliferone)	0.14	0.20	0.29	0.38	0.49	0.59	245, 255, 325	240, 250, 265	320
8. Blue	0.16	0.24	0.33	0.43	0.50	0.59	320	265	255
9. Yellow (bergapten)	0.23	0.29	0.38	0.48	0.55	0.59	250, 260, 310	245, 255, 280	235, 250
10. Blue (citropten)	0.23	0.35	0.48	0.51	0.59	—	—	—	—
11. Yellow (isoimperatorin)	0.29	0.39	0.47	—	—	—	250, 310	245, 280	240
12. Blue	0.29	0.39	0.47	—	—	—	260, 270, 320	245, 265, 275	—
13. Violet	0.32	0.39	0.47	—	—	—	258, 320	240, 270	—
14. Blue (methyl anthranilate)	0.42	0.48	—	—	—	—	—	—	—
15. Blue	0.49	0.48	—	—	—	—	235	—	—
16. Yellow	0.54	0.59	0.62	0.70	0.73	—	—	—	230, 310
17. Blue	0.66	—	—	—	—	—	270	265	—

*The subscript number represents the % amount of ethyl acetate in the eluent mixture. (Reproduced with permission from D'Amore G and Calapaj R (1965) *Rassegna Chimica* 6: 264–269.)

psoralen; (7) 8-geranyloxypsoralen; (9) citropten; (12) oxypeucedanin; (14) byakangelicol. These main components were isolated by preparative column chromatography, crystallized and analysed by spectroscopic methods [infrared (IR), UV, nuclear magnetic resonance (NMR)].

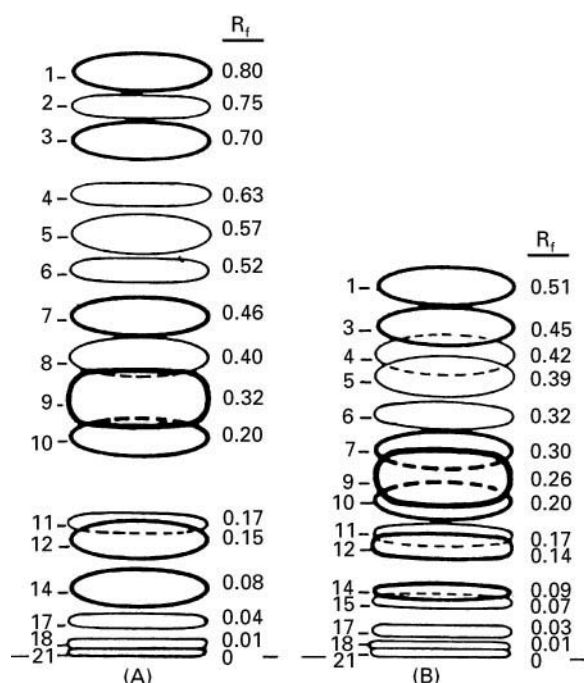


Figure 2 TLC separation of coumarins and psoralens of lemon oil. Eluent: hexane–butyl acetate, 65 : 35 (A) and 75 : 25 (B). (Reproduced with permission from Glandian R, Corneteau H, Drouet S and Rouzet M (1978) *Plantes, Medicinales et Phytoterapie*, 12 (2), 112–122.)

TLC separation of citrus oils has also been coupled with detection by *in situ* fluorimetry. This method shows the advantages of both the techniques, and a good selectivity and sensibility. As an example, the quantitative determination of 5-geranyloxy-7-methoxycoumarin and 5,7-dimethoxycoumarin (citropten) present in bergamot, lime and lemon oils, and the qualitative profile of citrus oils have been obtained by measuring the fluorescence and the fluorescence quenching profiles directly on the TLC plates. Emission monochromator wavelength settings of 403, 440 and 490 nm were used to obtain the various fluorescence emission profiles. An excitation wavelength of 272 nm and an emission wavelength of 520 nm were used to obtain the fluorescence quenching profile. These values correspond to the maximum of excitation and emission of the fluorescent indicator in the adsorbent layer.

Analytical and preparative TLC of coumarins and psoralens have been widely used. Some of the advantages of this technique are its simplicity and low cost. Disadvantages may be the difficulty of controlling the flow rate, the low resolution, the low reproducibility and the long time required for development. In recent years various modern planar chromatographic methods have been reported for the analysis of coumarins. Some of these methods use a new forced-flow TLC technique, developed by Tyiháck and co-workers between 1979 and 1981, called OPLC (overpressured layer chromatography). This new planar technique combines the advantages of classical TLC and HPLC: shorter analysis times, lower solvent consumption, simultaneous analysis of a large number of

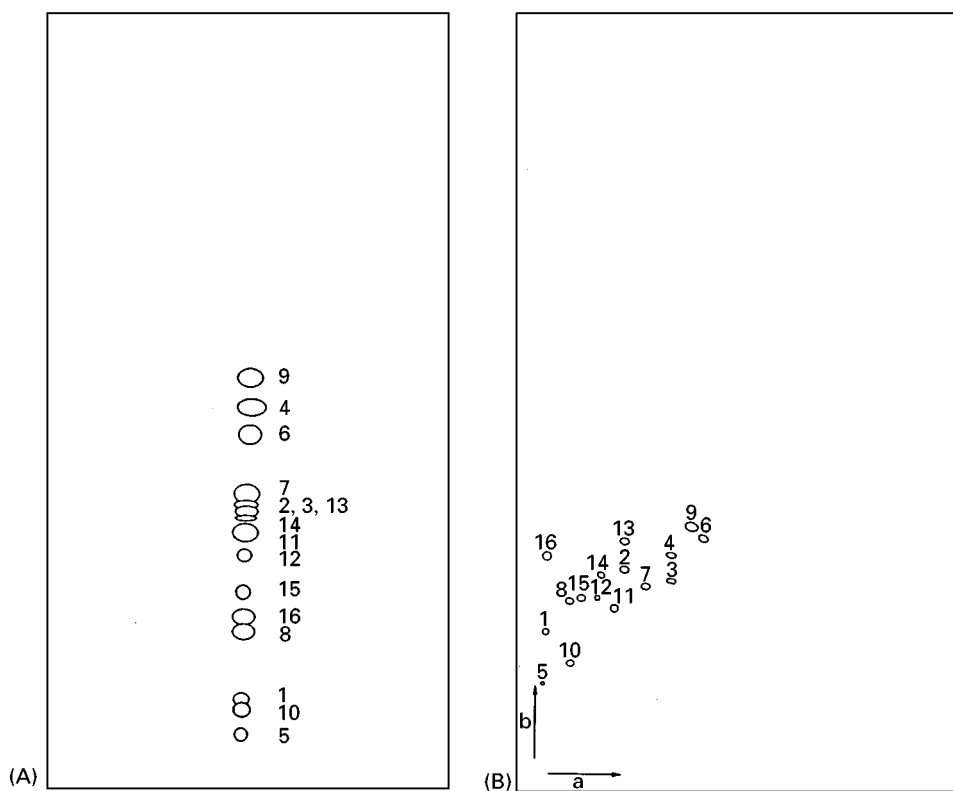


Figure 3 (A) One-dimensional OPLC development and (B) two-dimensional OPLC development of 16 closely related coumarins. (1) Umbelliferone; (2) herniarin; (3) psoralen; (4) osthol; (5) apterin; (6) angelicin; (7) bergapten; (8) oxypeucedanin; (9) isobergapten; (10) scopoletin; (11) sphondin; (12) xanthotoxin; (13) imperatorin; (14) pimpinellin; (15) isopimpinellin; (16) new archangelicin derivative. (Reproduced with permission from Harmala P, Botz L, Sticher O and Hiltunen R (1990) *Journal of Planar Chromatography* 3: 515–520.)

samples, the possibility of performing isocratic or gradient elution, control of the flow rate and higher efficiency. The literature reports some examples of the applications of OPLC technique to the analysis of coumarins and psoralens.

As shown by Härmälä *et al.* in 1990, TLC separation methods can be improved by use of two-

dimensional high performance TLC (2D TLC). **Figure 3** shows the one-dimensional (A) and the two-dimensional (B) OPLC development of 16 coumarins.

Another way to increase the efficiency of TLC separation is by using the stepwise gradient technique. By increasing the strength of the mobile phase, the separation of compounds with similar R_f values is

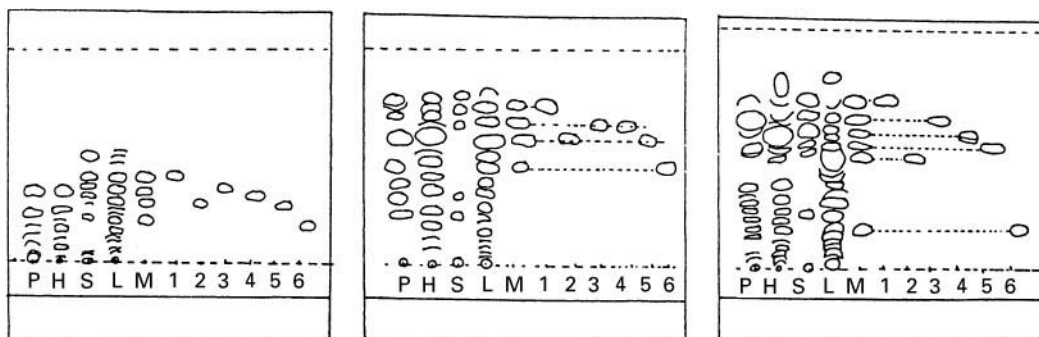


Figure 4 Chromatograms of plant extracts and references coumarins corresponding to the following stepwise gradient programs: (A) 10–50% methyl ethyl ketone in n-heptane; (B) 30–70% methyl ethyl ketone in n-heptane; (C) 2.5–15% ethyl acetate in chloroform. P = *Pastinaca sativa*; H = *Heracleum sphondylium*; S = *Sium sisarum*; L = *Libanotis intermedia*. (1) Osthol; (2) isopimpinellin; (3) imperatorin; (4) bergapten; (5) xanthotoxin; (6) umbelliferone. (Reproduced with permission from Glowinski K, Matysik G, Bieganski M and Soczewinski E (1986) *Chromatographia* 22: 307–310.)

Table 3 R_f values obtained using chloroform–*n*-butyl acetate–hexane, 9 : 1 : 15 as eluent

Compound	Fluorescence at 366 nm	Sweet orange	Bitter orange	Mandarin	Grape- fruit	Lemon	Bergamot	Mexican lime
Bergamottin	Y				0.52	0.52	0.52	0.52
Aurapten	V				0.41			
5-Geranyloxy-7-methoxycoumarin	B					0.39	0.38	0.38
8-Geranyloxypsoralen	Y					0.34		
Osthol	V		0.38		0.38			
Bergapten + Epoxybergamottin	Y		0.30		0.30			
Bergapten	Y						0.30	0.30
Citropten	B					0.26	0.25	0.25
Meranzin + Isomeranzin	V		0.25		0.25			
Herniarin	B							0.23
Epoxyaurapten	V				0.18			
?	B					0.18		
?	P							0.17
Oxypeucedanin	Y					0.10		0.11
Epoxybergamottin hydrate	Y		0.10		0.10			
Meranzin hydrate	V		0.08		0.08			
Byakangelicol	Y					0.04		0.04
Polymethoxylated flavones	Y	0.04	0.04	0.04	0.04			
Polymethoxylated flavones	B	0.03	0.03	0.03	0.03			

B: Blue; Y: Yellow; V: Violet; P: Pink. (Reproduced with permission from Dugo P, Mondello L, Lamonica G and Dugo G (1996) *Journal of Planar Chromatography* 9: 120–125.)

Table 4 R_f values obtained using *n*-butyl acetate–hexane, 80 : 20 as eluent

Compound	Fluorescence at 366 nm	Sweet orange	Bitter orange	Mandarin	Grape- fruit	Lemon	Bergamot	Mexican lime
Bergamottin	Y				0.96			
Bergamottin + 5-Geranyloxy-7-methoxycoumarin	Y + B					0.97	0.97	0.97
8-Geranyloxypsoralen	Y					0.92		0.92
Aurapten	V				0.90			
?	B				0.82			
?	B							0.82
Osthol	V		0.74		0.74			
Citropten	B					0.71	0.71	0.71
?	B				0.71			
Epoxybergamottin	Y		0.70		0.68			
Bergapten	Y		0.65				0.65	0.66
Bergapten + epoxyaurapten	Y + V				0.65			
Herniarin	V							0.62
Oxypeucedanin	Y					0.61		0.60
?	Y				0.60			
?	B				0.56			
Byakangelicol	Y					0.49		0.49
Isomeranzin	V		0.49		0.49			
Meranzin	V		0.45		0.45			
?	B		0.41		0.40			
Tangeretin	P	0.25	0.25	0.25	0.25			
Heptamethoxyflavone	Y	0.21	0.21	0.21	0.21			
Tetra-O-methylscutellarein	P	0.20		0.20				
Hexamethoxyflavone	SB	0.16						
Nobiletin	Y	0.14	0.14	0.14	0.14			
Sinensetin	SB	0.10		0.10				
Epoxybergamottin hydrate	Y		0.10		0.10			
Meranzin hydrate	V		0.04		0.04			

B: Blue; SB: Sky-blue; Y: Yellow; V: Violet; P: Pink. (Reproduced with permission from Dugo P, Mondello L, Lamonica G and Dugo G (1996) *Journal of Planar Chromatography* 9: 120–125.)

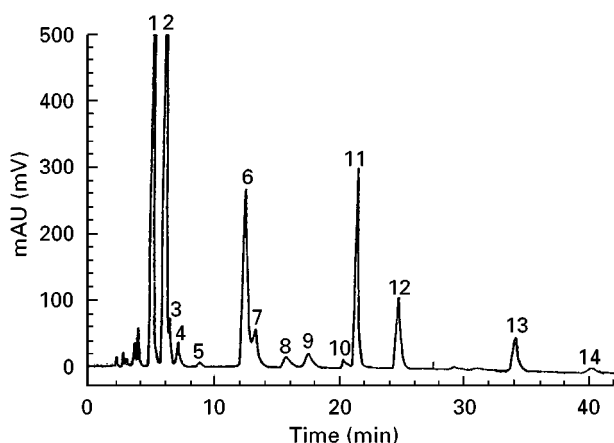


Figure 5 HPLC chromatogram of oxygen heterocyclic components of genuine cold-pressed lemon oil. Column 25 cm \times 4.6 mm internal diameter Zorbax 6 μ m spherical silica; gradient elution, solvent A hexane–ethyl acetate (9 : 1), solvent B hexane–ethyl alcohol (9 : 1), 2–95% B over 25 min; flow rate, 1.5 mL min⁻¹; sample volume 20 μ L (20% solution of lemon oil in dichloromethane); detection UV absorbance at 315 nm. For peak assignment, see Table 5. (Reproduced with permission from McHale D and Sheridan JB (1988) *Flavour Fragrance Journal* 3: 127–133.)

improved. **Figure 4** shows an example of gradient TLC of coumarins and psoralens of some plant extracts.

Tables 3 and 4 provide results obtained for the OPLC analysis applied to seven citrus oils, using silica gel 60 F254 HPTLC plates with impregnated edges (flow rate: 0.7 mL min⁻¹). Detection was by UV at 366 nm; time of analysis: 10 min. Because of its advantages, this method has been proposed as a rapid, preliminary check to evaluate the authenticity of citrus oils.

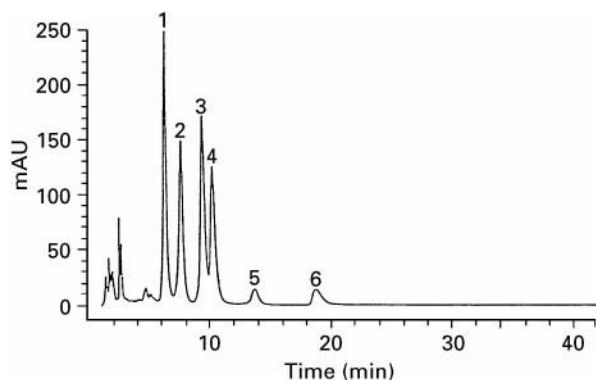


Figure 6 HPLC chromatogram of oxygen heterocyclic components of cold-pressed sweet orange oil. (1) Tangeretin; (2) heptamethoxyflavone; (3) nobilletin; (4) tetra-*O*-methylscutellarein; (5) 3,3',4',5,6,7-hexamethoxyflavone; (6) sinensetin. (Reproduced with permission from McHale D and Sheridan JB (1989) *Journal of Essential Oil Research* 1: 139–149.)

HPLC Separations

As well as TLC methods the literature reports numerous qualitative and quantitative methods for the analysis of coumarins and related compounds by both normal- and reversed-phase HPLC. Detection is commonly performed by UV absorbance, but methods which use the highly selective and sensible fluorescence detector are also reported.

Two important papers are those of McHale and Sheridan of 1988 and 1989 in which the authors developed normal-phase HPLC methods for the analysis of the most common citrus oils, making huge progress in the identification and in the quantitative determination of oxygen heterocyclic compounds. The first paper refers on the composition of

Table 5 Composition of oxygen heterocyclic fraction of cold-pressed Sicilian lemon oil reported by McHale and Sheridan (1988)

Peak no.	Component	Concentration mg L ⁻¹ (ppm)
1	Bergamottin	2200
2	5-Geranyloxy-7-methoxycoumarin	1600
3	Isoimperatorin	180
4	5-Isopentenylxy-7-methoxycoumarin	80
5	Unidentified (UV 7-substituted coumarin)	10
6	Citropten	650
7	8-Geranyloxypsoralen	750
8	Phellopterin + Imperatorin	90 + 60
9	5-Isopentenylxy-8-epoxyisopentenylxyoxypsoralen	220
10	Unidentified (UV ill-defined)	–
11	Oxypeucedanin	1100
12	Byakangelicol	450
13	Oxypeucedanin hydrate	260
14	Byakangelicin	70

(Reproduced with permission from McHale D and Sheridan JB (1988) *Flavour Fragrance Journal* 3: 127–133.)

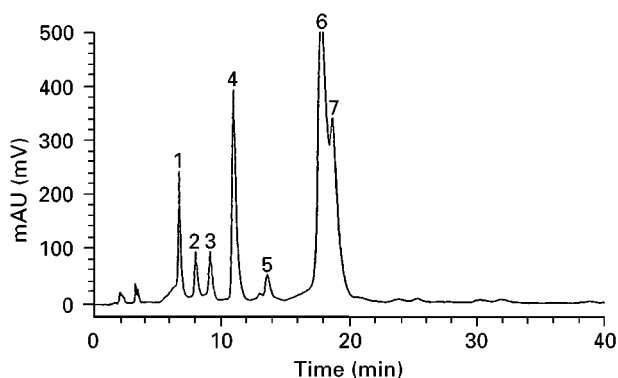


Figure 7 HPLC chromatogram of oxygen heterocyclic components of cold-pressed bitter orange oil. (1) Osthol; (2) epoxybergamottin; (3) bergapten; (4) tangeretin; (5) heptamethoxyflavone; (6) meranzin; (7) isomeranzin + nobiletin. (Reproduced with permission from McHale D and Sheridan JB (1989) *Journal of Essential Oil Research* 1: 139–149.)

cold-pressed lemon oil. **Figure 5** shows the HPLC chromatogram in which 14 components were detected and quantitatively determined. The experimental conditions are shown in the figure legend. **Table 5** reports the quantitative results.

These workers identified and quantified not only the main components, but also those present in lower amounts. Moreover, they analysed commercial samples of lemon oils, and demonstrated the validity of the method to detect some adulterations practised to increase the UV absorbance of oils previously diluted with distilled ones. The method allows for the detection of *p*-dimethylaminobenzoate, grapefruit oil and/or lime oil, that are the most common substances used to increase UV absorbance. The paper of 1989 shows normal-phase HPLC chromatograms of ber-

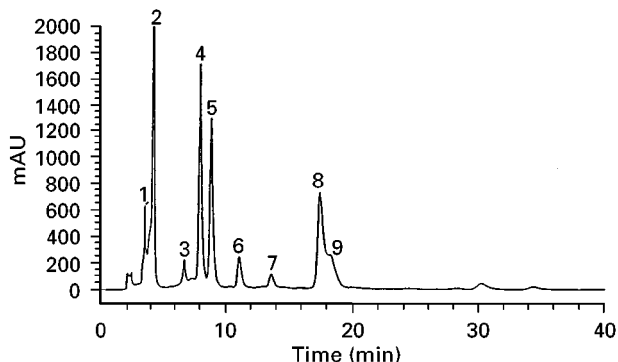


Figure 8 HPLC chromatogram of oxygen heterocyclic components of cold-pressed grapefruit oil. (1) Bergamottin; (2) aurapten; (3) osthol; (4) epoxybergamottin; (5) epoxyaurapten; (6) tangeretin; (7) heptamethoxyflavone; (8) meranzin; (9) isomeranzin + nobiletin. (Reproduced with permission from McHale D and Sheridan JB (1989) *Journal of Essential Oil Research* 1: 139–149.)

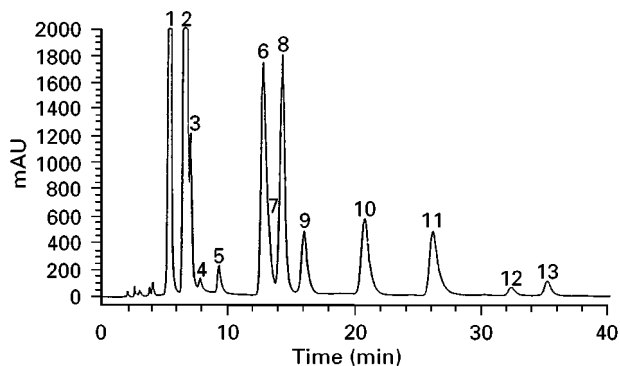


Figure 9 HPLC chromatogram of oxygen heterocyclic components of cold-pressed lime oil. (1) Bergamottin; (2) 5-geranyloxy-7-methoxycoumarin; (3) 5-geranyloxy-8-methoxyypsoralen; (4) 5-isopentenyl-7-methoxycoumarin; (5) 5-isopentenyl-8-methoxyypsoralen; (6) citropten; (7) 8-geranyloxyypsoralen; (8) herniarin; (9) bergapten; (10) isopimpinellin; (11) oxypeucedanin; (12) isobyakangelicol; (13) byakangelicol + heraclenin. (Reproduced with permission from McHale D and Sheridan JB (1989) *Journal of Essential Oil Research* 1: 139–149.)

gamot, sweet orange, bitter orange, grapefruit and lime oils, as illustrated in **Figures 6–9**.

Table 6 reports the experimental conditions used for these analyses. The paper reported quantitative data for all the oils analysed, according to their geographical origin.

Figure 10 shows a reversed-phase HPLC chromatogram obtained in 1992 by Ziegler and Spiteller for a lemon oil under the following experimental conditions: column, Spherisorb ODS2 (C_{18} – particle size 5 μ m), 250 \times 4.6 mm internal diameter; flow, 1 mL min⁻¹; solvents: A, methanol–water–acetonitrile (1 : 1.35 : 0.5) B, acetonitrile. Program: 10% B to

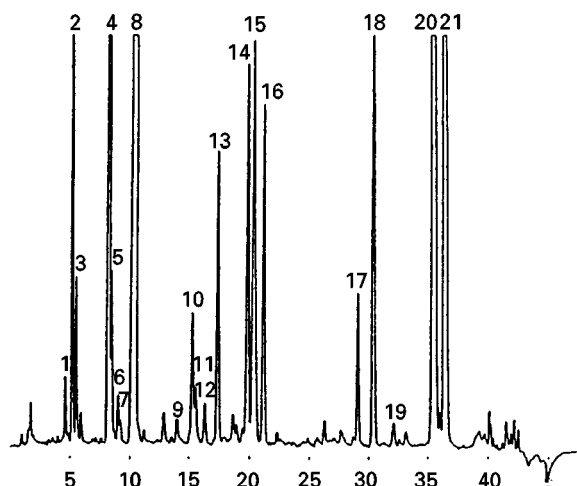


Figure 10 Reversed phase HPLC chromatogram of oxygen heterocyclic components of cold-pressed lemon oil. For peak assignment, see **Table 7**. (Reproduced with permission from Ziegler H and Spiteller G (1992) *Flavour Fragrance Journal* 7: 129–139.)

Table 6 HPLC conditions reported by McHale and Sheridan (1989) for the analysis of oxygen heterocyclic compounds of citrus oils

	<i>Lemon</i>	<i>Lime</i>	<i>Mandarin</i>	<i>Grape fruit</i>	<i>Bitter orange</i>	<i>Sweet orange</i>
Eluent	(A) hexane–ethyl acetate, 9 : 1 (B) hexane–ethyl alcohol, 9 : 1			Hexane–ethyl alcohol, 19 : 1		Hexane–ethyl alcohol, 9 : 1
Programme	From 98 A : 2 B to 5 A : 95 B over 25 min			Isocratic		Isocratic
Column	6 µm Zorbax SIL spherical, 25 cm × 4.6 mm internal diameter					
Injection volume	20 µL of a 20% solution of oil in dichloromethane					
Detection	UV absorbance at 315 nm					
Flow rate	1.5 mL min ^{−1}					

40% B in 20 min; 40% B to 70% B in 15 min; 70% B to 90% B in 2 min. Injection: 100 μ L of a 0.2% solution of original lemon oil in 10% B and 90% A. Detection: UV at 220 and 310 nm.

Table 7 lists the 25 components identified by HPLC, MS, GC–MS and NMR, 11 of which identified for the first time in a cold-pressed lemon oil as trace constituents. It is noteworthy that on the basis of the spectroscopic data obtained, bergapten does not result to be present in genuine lemon oil, in contrast with data previously reported in literature.

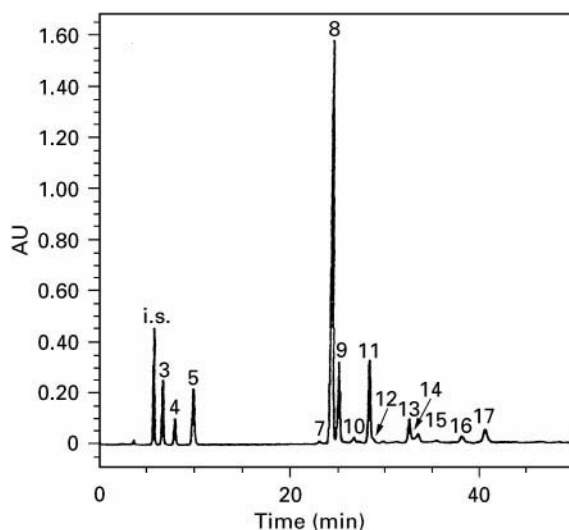
Table 7 Components identified in the oxygen heterocyclic fraction of cold-pressed Sicilian lemon oil by Ziegler and Spiteller

Peak no. in HPLC run	Components
1	5-(2',3'-Dihydroxyisopentyloxy)-7-methoxycoumarin* Heraclenol*
2	Oxypeucedanin hydrate
3	Byakangelicin
4	Citropten
5	Heraclenin
6	Pabulenol/Gosferenol*
7	Neobyakangelicol*
8	Oxypeucedanin Byakangelicol 5-(2',3'-Epoxyisopentyloxy)-7-methoxycoumarin*
9	5-Isopentenylloxy-8-(2',3'-dihydroxyisopentyloxy)psoralen*
10	Imperatorin
11	7-Isopentenylloxycoumarin*
12	8-(6',7'-Epoxygeranyloxy)psoralen*
13	Phellopterin
14	Isoimperatorin
15	5-Isopentenylloxy-7-methoxycoumarin
16	5-Isopentenylloxy-8-(2',3'-epoxyisopentyloxy)psoralen
17	Cnidicin*
18	8-Geranyloxypsoralen
19	Aurapten*
20	5-Methoxy-8-geranyloxypsoralen*
21	Bergamottin 5-Geranyloxy-7-methoxycoumarin

*Compounds previously unknown in cold-pressed lemon oil.

Citrus oils that show a quite complex composition of the oxygen heterocyclic fraction are difficult to analyse either by normal- or reversed-phase HPLC with a single column. In these cases the 'column switching' technique can be useful to improve the separation of those critical peaks. This technique has been applied successfully to the analysis of bitter orange and grapefruit oils, which show a very similar composition, to separate 17 components and, in particular, to the couple meranzin–isomeranzin. **Figures 11** and **12** show the results obtained, together with the experimental conditions and peak identification.

Most of the data found in the literature refer to the characterization of bergamot oil, and in particular to the determination of 5-methoxypsoralen (bergapten), which is known to have a higher phototoxic action than other psoralens found in citrus oils. Bergamot oil is widely used in the cosmetic and pharmaceutical

**Figure 11** HPLC chromatogram of oxygen heterocyclic components of cold-pressed bitter orange oil. For peak assignment and experimental conditions see Figure 12. (Reproduced with permission from Dugo P, Mondello L, Stagno d'Alcontres I, Cavazza A and Dugo G (1997) *Perfumer and Flavorist* 22: 25–30.)

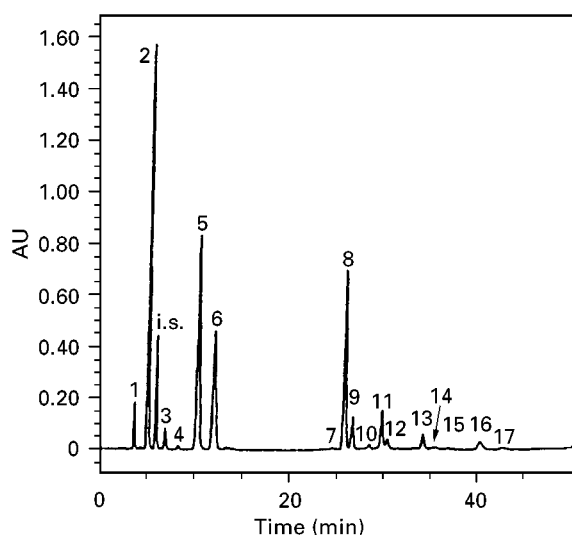


Figure 12 HPLC chromatogram of oxygen heterocyclic components of cold-pressed grapefruit oil obtained in the following conditions: μ -porasil column 30 cm \times 3.9 mm internal diameter (10 μ m) for the first 12 min, then the flow was switched to a second column, Zorbax silica 25 cm \times 4.6 mm internal diameter (7 μ m). Eluent A, hexane-ethyl acetate, 9 : 1; eluent B, hexane-ethyl alcohol, 9 : 1. 2–95% B over 23 min (2–25 min) with a concave gradient, then 20 min isocratic 95% B, flow rate 1.6 mL min⁻¹; sample volume 20 μ L (5% solution of oil in hexane-ethyl acetate, 75 : 25); detection by UV absorbance at 315 nm. Peak assignment: (1) bergamottin; (2) auranpten; (3) osthol; (4) bergapten; (5) epoxybergamottin; (6) epoxyaurapten; (7) unknown coumarin; (8) meranzin; (9) isomeranzin; (10) unknown coumarin 2; (11) tangeretin; (12) 3,3',4',5,6,7,8-heptamethoxyflavone; (13) nobiletin; (14) tetra-*O*-methylscutellarein; (15) unknown coumarin; (16) epoxybergamottin hydrate; (17) meranzin hydrate; (i.s.) internal standard, coumarin. (Reproduced with permission from Dugo P, Mondello L, Stagno d'Alcontres I, Cavazza A and Dugo G (1997) *Perfumer and Flavorist* 22: 25–30.)

industries. Usually, genuine cold-pressed bergamot oil contains about 2000–3000 ppm of bergapten, but many industrial processes have been developed with the aim to reduce its concentration to values of only a few parts per million. The oils so obtained are known as 'bergapten-free' oils. Table 8 summarizes some of the TLC and HPLC methods proposed for the quantitative determination of bergapten in bergamot oil.

HPLC–MS

To obtain more information on the nature and the structure of the components analysed by HPLC, an MS detector can be coupled on-line to the HPLC system. An innovative interface for the HPLC–MS coupling is the API (atmospheric pressure ionization), that differs from the traditional interfaces because the ionization takes place at atmospheric pressure.

The API technique can use two different interfaces, the electrospray (ES) or the atmospheric pressure chemical ionization (APCI), and can give different information than those obtained with conventional LC–MS interfaces. Both the techniques are classified as 'soft' ionization methods. By varying the voltage of the sample cone it is possible to obtain different degrees of fragmentation.

The HPLC–MS technique with the APCI interface has been applied to the analysis of coumarins of citrus oils to confirm the identification of some components or to obtain more information for those not identified yet. As an example, Figure 13 shows the HPLC–UV chromatogram of a cold-pressed bergamot oil, compared to the full scan HPLC–MS chromatogram acquired at different cone voltage values.

Figure 14 shows the MS spectra obtained at different cone voltage values for one of the components of bergamot oil (bergamottin). As can be seen, at the lower cone voltage value the $(M + H)^+$ ion is visible, while at higher values additional fragmentation occurs.

The HPLC–MS technique allowed the confirmation of the presence of oxygen heterocyclic compounds previously not identified in bergamot oil, such as tetra-*O*-methylscutellarein and sinensetin. Figure 15 shows the HPLC–UV chromatogram at cone voltage value of 20 V, and the extracted chromatogram at m/z 243 and 273, corresponding to the $(M + H)^+$ ions of tetra-*O*-methylscutellarein and sinensetin.

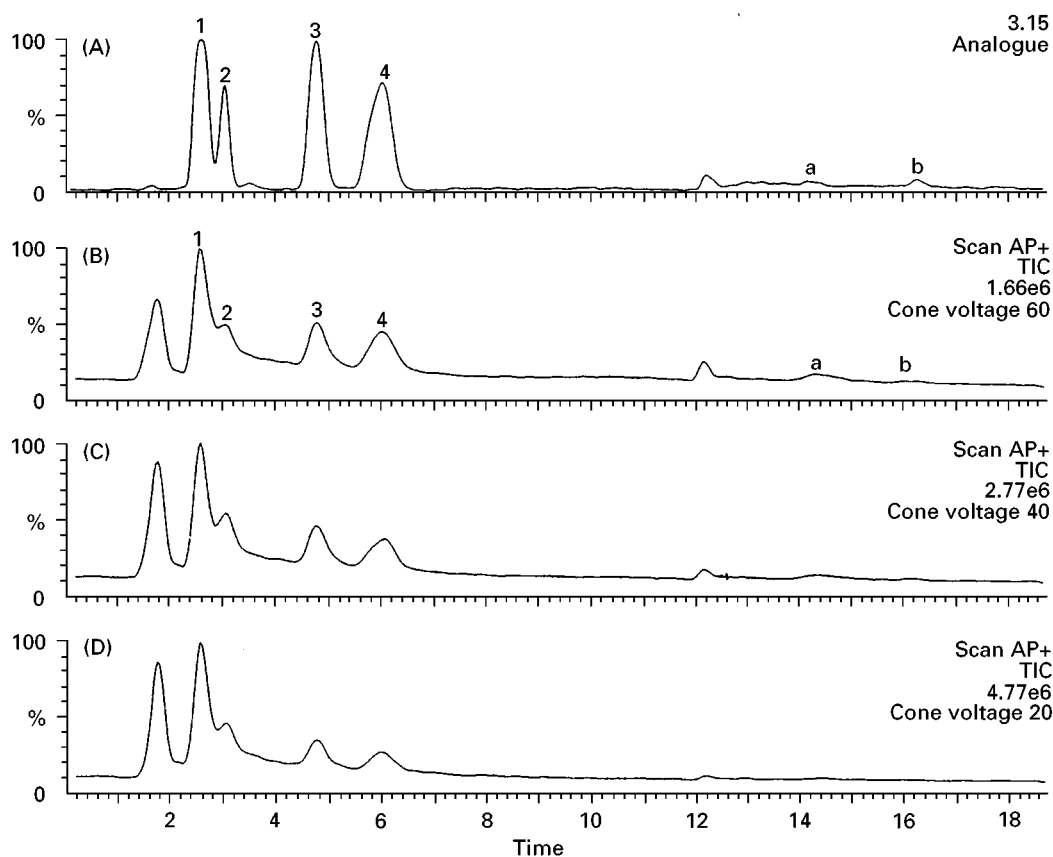
Supercritical Fluid Chromatography (SFC)

A few applications of supercritical fluid chromatography (SFC) to the analysis of citrus coumarins have been reported. Even though this technique is less popular in the analysis of citrus coumarins, it is interesting to compare the results obtained by SFC to those obtained by HPLC. Figure 16 shows a normal phase HPLC chromatogram of the polymethoxylated flavones of sweet orange oil (A), compared to the packed SFC chromatogram obtained for the same oil (B).

Table 9 provides the chromatographic conditions under which the two analyses have been carried out. Both the analyses allowed a complete separation of the six polymethoxylated flavones (PMFs) known to be present in sweet orange oil. The SFC analysis was completed in less than 6 min, while the HPLC analysis took more than 25 min. This represents a reduction in the analysis time by a factor of four. Quantitative results obtained with the SFC method compared well with those obtained with the HPLC method.

Table 8 TLC and HPLC methods for the analysis of bergapten in bergamot oil.

Technique	Stationary phase	Mobile phase	Detection method	Flow rate	Sample
HPLC	2 cm × 2.3 mm internal diameter stainless steel tubing packed with 37-50 Corasil II	Hexane–chloroform, 75 : 25	UV abs. at 254 nm	0.25 mL min ⁻¹ <i>P</i> = 100 psi	10 µL of a solution of 0.05 g of oil in 10 mL of CHCl ₃
TLC	Silica gel plates F-254	Isoctane–ethyl acetate, 83 : 17	UV abs. at 254 nm		Oil diluted 1 : 10 in CHCl ₃
TLC	Silica gel plates F-254 (20 µm)	Cyclohexane–ethyl acetate–acetic acid, 80 : 20 : 2	UV abs. at 254 and 366 nm		
TLC	10 × 10 cm Silica gel HPTLC plates 60 F-254 (5 µm)	Petroleum ether or benzene followed by cyclohexane–ethyl acetate, 75 : 25	Densitometer at 254 or 308 nm or Fluorescence (λ_{exc} 330 nm, λ_{em} 450 nm)		
TLC	10 × 10 cm RP 18 TLC plates (7 µm)	Methanol–water, 80 : 20	Densitometer at 254 or 308 nm		Oil diluted in methanol
HPLC	Lichrosorb Si 60 (5 µm) 23 cm × 4.35 mm internal diameter	Heptane–isopropanol, 93 : 7	UV abs at 254 nm	0.85 mL min ⁻¹ , <i>P</i> = 23 bar	
HPLC	Lichrosorb RP 18 (5 µm) 17 cm × 4.35 mm internal diameter	Methanol–water, 9 : 1	UV abs at 254 nm	1.1 mL min ⁻¹ , <i>P</i> = 24 bar	
HPLC	Lichrosorb Si 60 (5 µm) 25 cm × 4.6 mm internal diameter	Hexane–ethyl acetate–propan-2-ol, 88 : 10 : 2 (isocratic)	UV absorbance at 305 nm	1 mL min ⁻¹	Undiluted for oil with less than 40 mg L ⁻¹ of bergapten, or diluted in the range 20–40 mg L ⁻¹ with CHCl ₃ · 20 µL inj

**Figure 13** (A) HPLC–UV chromatogram and (B), (C) and (D) total ion current (TIC) HPLC chromatograms acquired at cone voltage values of 60, 40 and 20 V, respectively, of coumarin fraction of a genuine bergamot essential oil. (1) Bergamottin; (2) 5-geranyloxy-7-methoxycoumarin; (3) citropten; (4) bergapten; (a) tetra-*O*-methylscutellarein; (b) sinensetin; (i.s.) internal standard.

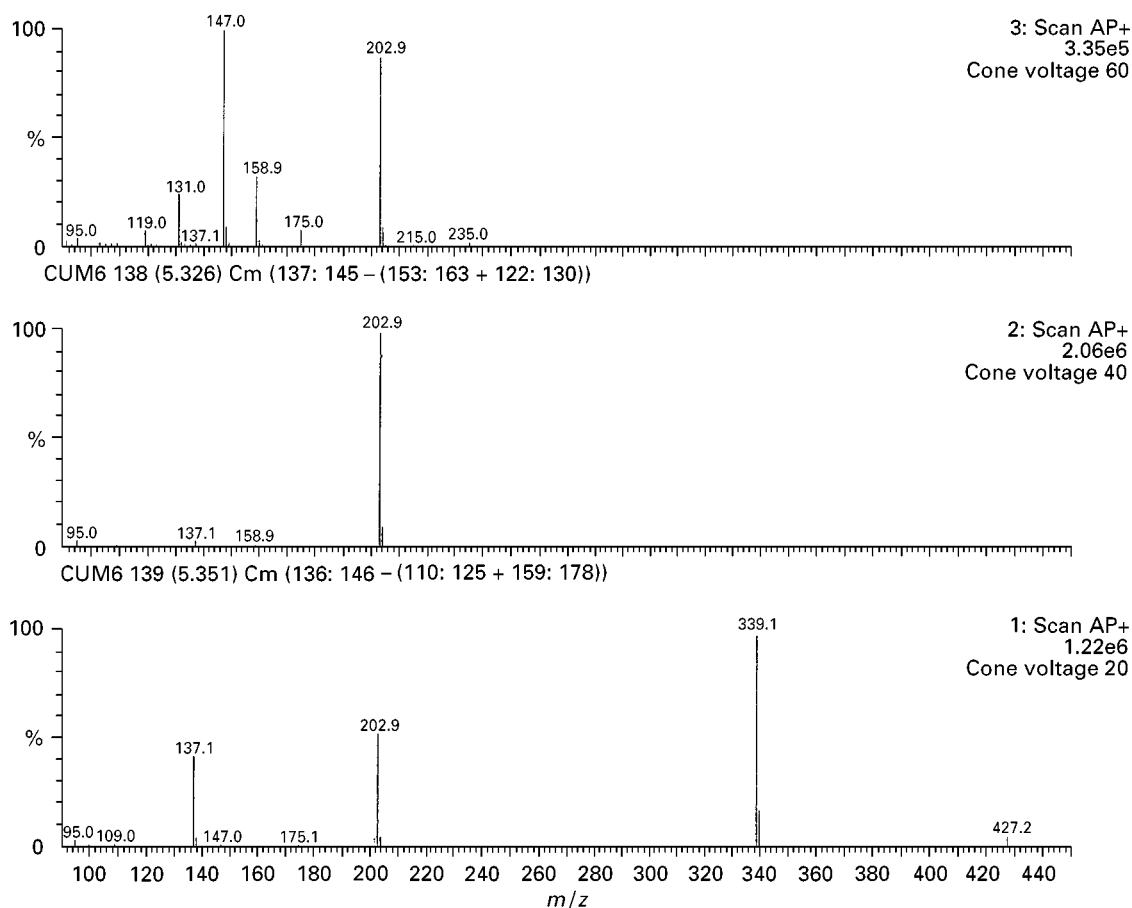


Figure 14 Cone voltage fragmentation of bergamottin using APCI ionization.

Conclusion

Citrus essential oils show a characteristic composition of their oxygen heterocyclic fraction. These components make it possible to differentiate the individual oils and to detect mixtures or mutual contamination. Quantitative analysis is often necessary to assess authenticity or geographical origin of an oil. Sometimes, quantitative analysis has to be preceded by isolation of single components for structure elucidation and also to obtain pure standard compounds to be used for preparation of standard solutions, since they are not always commercially available. Moreover, these components possess numerous pharmacological activities, so isolation may be necessary for testing specific biological activities.

Both analytical and preparative analyses can be carried out with planar and column liquid chromatographic methods (TLC, OPLC, HPLC). Usually, the preparative separations, that may be long and laborious, are followed by further purification steps and by spectroscopic analyses for identification.

Working with natural products, efficient detection and rapid characterization are often essential. Fur-

thermore, the achievement of structural information on unknown constituents of a complex mixture is a strategic element for guiding an efficient and selective isolation procedure.

A big advantage can be achieved by using hyphenated techniques. In the last few years, LC-MS is becoming more and more popular, because of the introduction of API (atmospheric pressure ionization) techniques as a means for mass spectrometric sample introduction. This interface permits a highly selective and sensitive detection method, to be obtained and use of HPLC-MS in routine analysis. Recently, LC-NMR has been introduced as another powerful complementary technique for on-line structural identification, even though it is much less sensitive than LC-MS. Application of planar chromatography coupled with mass spectrometric (MS) or Fourier transformed infrared (FT-IR) have also been developed.

Looking to the future, it is reasonable to expect a much wider use of hyphenated techniques that will allow the rapid structural determination of constituents of complex matrices requiring only a small amount of samples, and the use of shorter HPLC columns packed with smaller particles that will

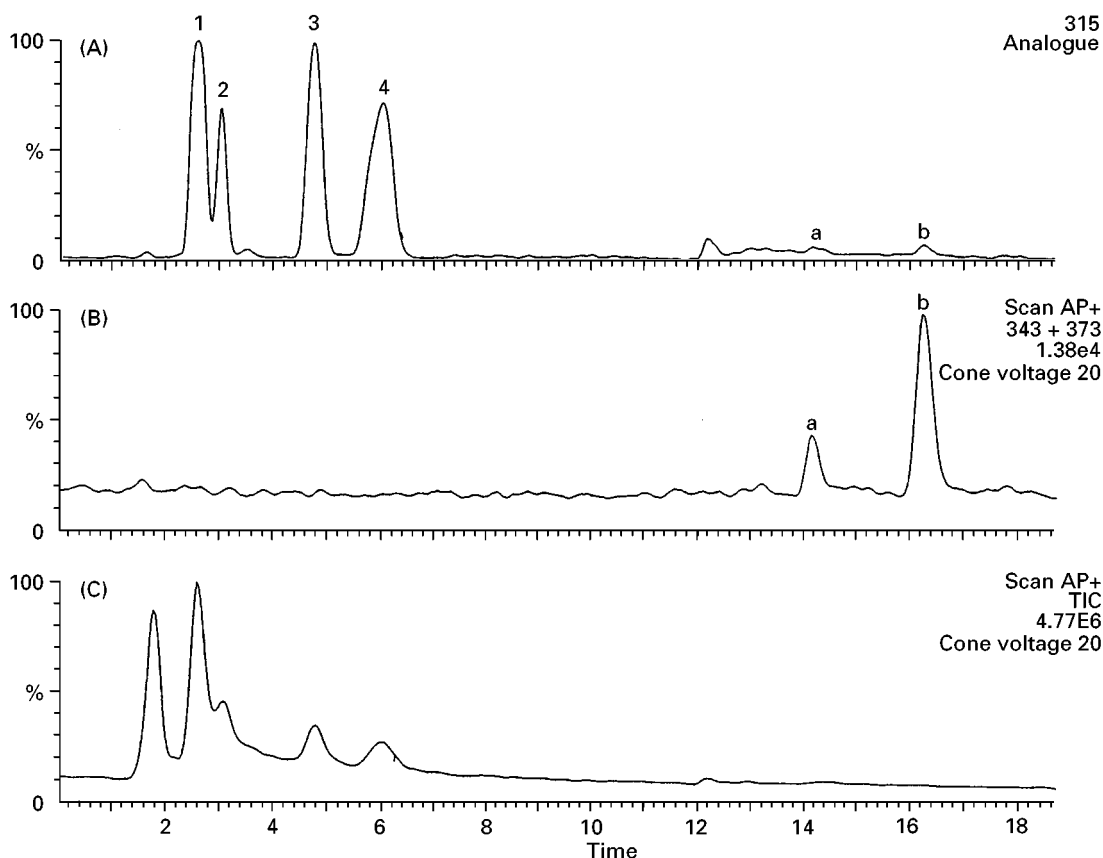


Figure 15 (A) HPLC-UV chromatogram, (C) TIC HPLC chromatogram acquired at cone voltage of 20 V and (B) TIC HPLC chromatogram extracted at m/z 343 + 373, of coumarin fraction of a genuine bergamot oil.

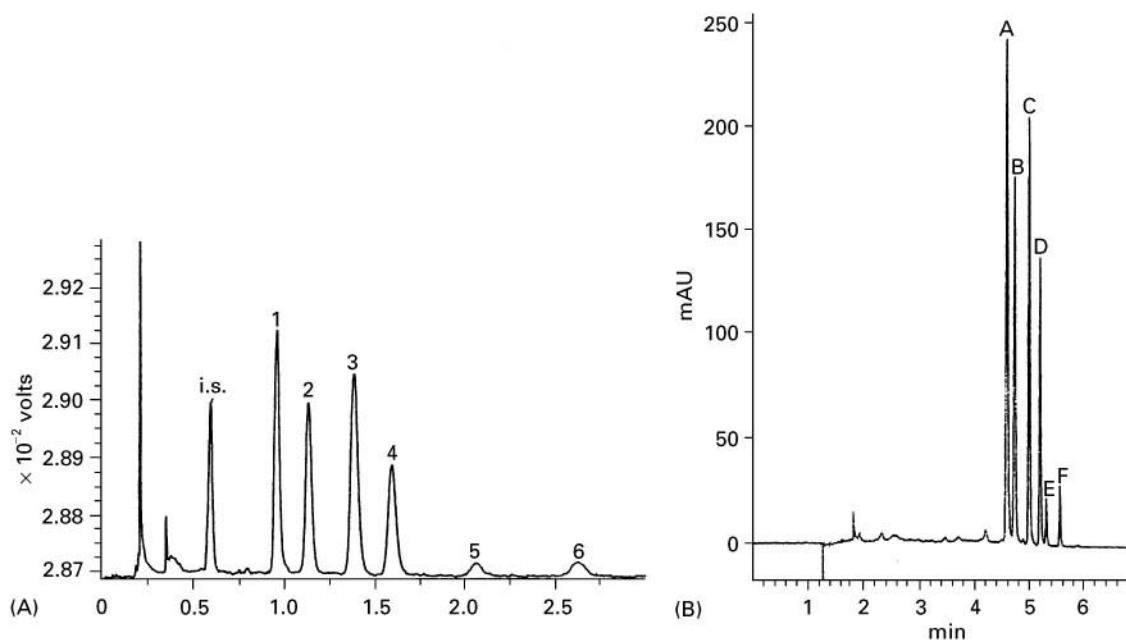


Figure 16 (A) HPLC chromatogram and (B) packed SFC chromatogram of polymethoxylated flavones of sweet orange oil. 1 = (A) tangeretin; 2 = (B) heptamethoxyflavone; 3 = (C) nobiletin; 4 = (D) tetra-*O*-methylscutellarein; 5 = (E) 3,3',4',5,6,7-hexamethoxyflavone; 6 = (F) sinensetin. ((A) Reproduced with permission from Dugo P, Mondello L, Cogliandro E, Stagno d'Alcontres I and Controneo A (1994) *Flavour and Fragrance Journal* 9: 105-111 and (B) reproduced with permission from Dugo P, Mondello L, Dugo G, et al. (1996) *Journal of Agricultural and Food Chemistry* 44: 3900-3905.)

Table 9 Experimental conditions of the HPLC and of the SFC analyses of polymethoxylated flavones of sweet orange oil

	HPLC	SFC
Column	Zorbax silica, 25 cm × 4.6 mm internal diameter (7 µm)	S5W uncoated silica, 25 cm × 4.6 mm internal diameter (5 µm)
Eluent	Hexane–ethyl acetate, 95 : 5	CO ₂ modified with small amounts of methanol
Flow rate	1.6 mL min ⁻¹	2 mL min ⁻¹ for 4 min, then gradient of 2 up to 5 mL min ⁻¹ thereafter held constant
Programme	Isocratic	$P = 100$ atm, $T = 40^{\circ}\text{C}$; modifier, 1.5% min ⁻¹ from 10% to 30% thereafter held constant
Injected amount	20 µL of a 5% solution of oil in ethyl acetate	100 µL of a solution obtained by diluting 0.71 g of oil to 20 mL of ethyl acetate
Detection	UV absorbance at 315 nm	UV absorbance at 315 nm

provide faster separations with the same resolution as that observed in longer columns packed with particles of larger diameter.

See also: II/Chromatography: Liquid: Detectors: Mass Spectrometry. Chromatography: Thin-Layer (Planar): Densitometry and Image Analysis; Modes of Development: Forced Flow, Over Pressured Layer Chromatography and Centrifugal; Preparative Thin-Layer (Planar) Chromatography. III/Essential Oils: Gas Chromatography; Thin-Layer (Planar) Chromatography; Distillation.

Further Reading

Di Giacomo A and Calvarano M (1978) Il Contenuto di Bergaptene nell'Essenza di Bergamotto Estratta a Freddo. *Essenze Derivati Agrumari* 48: 51–83.

Di Giacomo A and Mincione B (1994) *Gli Olii Essenziali Agrumari in Italia*. Reggio Calabria: La Ruffa.

Dugo P, Mondello L, Stagno d'Alcontres I, Cavazza A and Dugo G (1997) Oxygen heterocyclic compounds of citrus essential oils. *Perfumer and Flavorist* 22: 25–30.

McHale D and Sheridan JB (1988) Detection of adulteration of cold-pressed lemon oil. *Flavour and Fragrance Journal* 3: 127–133.

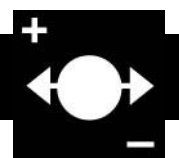
McHale D and Sheridan JB (1989) The oxygen heterocyclic compounds of citrus peel oils. *Journal of Essential Oil Research* 1: 139–149.

Murray RDH, Mendez J and Brown SA (1982) *The Natural Coumarins, Occurrence, Chemistry and Biochemistry*. Chichester: John Wiley.

Proceedings of the Symposium *Cumarine: Ricerca ed Applicazioni*, Padova, Italy 20–22 September 1990. Padova, Italy: Imprimitur.

Sherma J and Fried B (1996) *Handbook of Thin-Layer Chromatography*. New York: Marcel Dekker.

CLINICAL APPLICATIONS



Capillary Electrophoresis

P. G. Righetti, University of Verona, Verona, Italy
C. Gelfi, ITBA, CNR, Milan, Italy

Copyright © 2000 Academic Press

Introduction

The area of clinical applications of capillary electrophoresis (CZE) is such a rapidly growing field that it would be impossible here to cover it in detail. We thus offer a list of major reviews to which the reader is referred for a more comprehensive coverage of the

literature. Such reviews can be divided into:

1. Broad-coverage reviews, such as those of Lehmann *et al.* (1997), Perrett (1999; CZE in clinical chemistry) and Guzman *et al.* (1997; dedicated also to on-line analyte concentration and micro-reaction). Also of interest are special issues of the *Journal of Chromatography B* dedicated to CZE in the life sciences (Krstulovic 1997) and of *Electrophoresis* devoted to CZE in the clinical sciences (Landers 1997) and in forensic science (McCord, 1998).
2. Specialized reviews, such as those of Thormann *et al.* (1996, 1997; drug analysis in body fluids); Lurie (1996; analysis of seized drugs), Hong and Baldwin (1997; metabolite profiling in human urine), Righetti and Gelfi (1997a,b, 1998; CZE of

DNA for molecular diagnostics), Jellum *et al.* (1996, analysis of urinary diagnostic metabolites and serum proteins), Lazaruk *et al.* (1998; genotyping of forensic short tandem repeat systems).

CZE: Some Basic Concepts Related to Clinical Chemistry

An important aspect of CZE relevant to clinical chemistry is the paradox by which one of the noted advantages of CZE, namely the small volume of the capillary, also leads to a significant drawback, i.e. the minute amount (3–10 nL) of sample introduced, which results in poor concentration limits of detection, one to two orders of magnitude lower than in high-performance liquid chromatography (HPLC). Thus, preconcentration techniques are often required for compounds present in very low concentrations in biological fluids. These include transient isotachopheresis, analyte stacking, field-amplified sample injection (all on-capillary techniques) or off-column preconcentration techniques, such as liquid-liquid or liquid-solid extraction. Alternative on-column methods include miniaturized solid-phase extraction with cartridges containing reversed-phase HPLC packing materials or with impregnated membranes. When analysing small analytes or drugs in sera, it is often necessary to deproteinize the sample. This can be efficiently achieved by extracting sera with 60% acetonitrile, which accomplishes two tasks: protein precipitation and analyte stacking upon electrokinetic injection because of the very low con-

ductivity of such a solution. Some areas of interest where CZE offers unique resolution and sample quantification are discussed below.

Drug Analysis

With the more efficient therapeutic application of various drugs and the necessity for screening and confirmation of drugs in body fluids for diagnostic and research purposes, there has evolved a need for reliable analytical procedures. CZE is becoming the method of choice for drug monitoring in body fluids, including plasma, serum, saliva and urine. Some relevant data are given in Tables 1–3.

Profiling Clinically Important Metabolites in Urines

There are approximately 300 known metabolic disorders many of which, if not treated, have serious and sometimes life-threatening consequences. Generally, the diagnosis of these disorders is made or confirmed by identification and quantification of characteristic metabolite(s) occurring in body fluids as a result of the particular enzyme deficiency involved in each disease. In addition, once the diagnosis has been made, the effectiveness of subsequent therapy can also be evaluated by analogous monitoring of the levels of the same metabolic markers. Recently, CZE has become an attractive tool for monitoring clinically important metabolic markers, including alditols, carbohydrates and amino acids, which can be profiled directly in urine with electrochemical (EC) detection at a copper electrode. EC detection allows sensitivity down to the femtomolar level and can be performed

Table 1 Selected validated CZE/MEKC^a assays for drugs^b

Drug	Body fluid	Therapeutic range ($\mu\text{g mL}^{-1}$)	Calibration range ($\mu\text{g mL}^{-1}$)	CE method	Sample preparation/ detection ^c	Reference assay
Theophylline	Serum	8–20	2.0–28.3	MEKC	DSI/275	EMIT
Phenobarbital	Serum	15–40	5.3–52.6	MEKC	DSI/245	EMIT
Ethosuximide	Serum	40–100	19.8–99.2	MEKC	DSI/220	FPIA
Flucytosine	Serum	20–80	20–123	MEKC	DSI/210	Bioassay
Antipyrine	Plasma	—	1.0–40	MEKC	DSI/240	HPLC
Antipyrine	Saliva	—	1.9–66	MEKC	DSI/260	HPLC
Felbamate	Serum	15–135	5.0–160	MEKC	DSI/214	HPLC
Pentobarbital	Serum	—	10–100	CZE	PPI/253	HPLC
Thiopental	Serum	—	2.0–60	MEKC	EXI/290	HPLC
Bupivacaine	Drain	—	0.5–20	CZE	EXI/200	GC
Cicletanine	Plasma	—	0.01–1.0	MEKC	EXI/214	HPLC
Retinol	Serum	—	0.003–0.035	CZE	UF/LIF	HPLC

^aMEKC, micellar electrokinetic capillary chromatography; CZE, capillary zone electrophoresis; DSI, direct sample injection; EXI, extract injection; PPI, injection of supernatant after protein precipitation; EMIT, enzyme-multiplied immunoassay technique; FPIA, fluorescence polarization immunoassay; GC, gas chromatography; HPLC, high-performance liquid chromatography; UF, ultrafiltration; LIF, laser-induced fluorescence detection with 325 nm excitation and 465 nm emission.

^bReprinted from Thormann W, Zhang CX and Schmutz A (1996) *Therapeutic Drug Monitor* 18, 506–520, with permission.

^cThe number represents the detection wavelength.

Table 2 Selected CZE/MEKC^a screening confirmation assays for illicit, abused and banned drugs^b

Drugs, drug classes	Body fluid, tissue	CZE method	Sample preparation	Reference assay
Barbiturates	Urine, serum	MEKC	DSI, EXI	EMIT
Salicylate, paracetamol, antiepileptics	Urine, serum	MEKC, CZE	DSI, EXI	FPIA, EMIT, UF
11-Nor- Δ -tetrahydrocannabinol-9-carboxylic acid	Urine	MEKC	EXI	FPIA
Methadone and its primary metabolite	Urine	CZE	DSI, EXI	EMIT, GC-MS
Benzodiazepines	Urine	MEKC	EXI	EMIT, GC-MS
Benzoylcegonine, opioids, methaqualone, amphetamines	Urine	MEKC	EXI	EMIT
Cocaine and all above mentioned classes	Urine	MEKC, CZE	EXI	EMIT, FPIA, GC-MS
Cocaine, morphine	Hair	MEKC	EXI	HPLC
β -Blockers	Serum	MEKC	EXI	—
Diuretics	Urine, serum	CZE	EXI	GC-MS

^aFor abbreviations, see Table 1.^bReprinted from Thormann W, Zhang CX and Schmutz A (1996) *Therapeutic Drug Monitor* 18, 506–520, with permission.

directly on urine without extensive sample clean-up or analyte derivatization. Some examples are given in Table 4. Other interesting data on profiling the

Table 3 Retention of anabolic steroids relative to testosterone^a

Compound ^b	MEKC ^c	HPLC	GC
Fluoxymesterone	0.925	0.78	1.50
Boldenone	0.964	0.74	1.05
Nandrolone	0.979	0.84	0.91
Methandrostenolone	0.985	0.86	1.12
Testosterone	1.00	1.00	1.00
Methyltestosterone	1.02	1.17	1.05
Methandriol	1.06	1.25	0.89
Stanolone	1.07	1.25	0.89
Boldenone acetate	1.12	1.46	1.27
Stanozolol	1.16	1.69	1.68
Testosterone acetate	1.17	1.76	1.21
Nandrolone propionate	1.22	1.88	1.29
Danazol	1.23	1.52	—
Clostebol acetate	1.24	1.90	—
Testosterone propionate	1.26	2.01	1.43
Methandriol 3 acetate	1.26	2.13	1.10
Testosterone isobutyrate	1.35	2.17	1.54
Nandrolone phenylpropionate	1.44	2.25	2.28
Testosterone cypionate	1.64	2.63	2.19
Testosterone enanthate	1.69	2.60	1.92
Methandriol dipropionate	1.81	2.98	1.70
Nandrolone decanoate	2.06	2.87	2.26
Boldenone undecylenate	2.20	2.73	2.62
Testosterone undecanoate	2.36	3.18	2.56
Oxymetholone	—	—	1.28
Oxandrolone	—	—	1.17
Testosterone isocaproate	—	—	1.77
Testosterone decanoate	—	—	2.36

^aReprinted from Lurie IS (1996) *International Laboratory*, with permission.^bIn order of increasing retention times.^cFor abbreviations, see Table 1.

following metabolites: orotic acid, pyroglutamate, adenylosuccinate and propionic acid, for the following diseases: HHH-syndrome (hyperornithinemia-hyperammonemia-homocitrullinuria), glutathione deficiency, adenylosuccinase deficiency and propionyl CoA carboxylase deficiency, respectively, can be found in Jellum *et al.* (1997).

Profiling Proteins in Biological Matrices

Separation and quantification of distinct proteins from biological matrices is another goal now being accomplished by CZE. A list of some major proteins of importance for clinical diagnosis is given in Table 5. In some cases, immunosubtraction can be an efficient way of quantifying some protein families by CZE. A typical example is the quantification of specific immunoglobulin subclasses by sequential immunosubtraction. The sample is exposed to five different Sepharose supports, each containing an immunoglobulin-specific binder. Three of them are specific for the heavy chains IgG, IgA and IgM and two are specific for the light chains κ or λ . After incubation and sedimentation, the treated samples and an untreated control are separated by CZE. Six electropherograms are generated per sample. The class and type of monoclonal component can be determined by overlaying electropherograms from before and after immunosubtraction.

CZE Separations of Clinically Relevant Diagnostic DNA

A number of applications of CZE in sieving liquid polymers (notably linear polyacrylamides and

Table 4 Normal constituents of human urine and expected response for CZE at a Cu electrode^a

Compound	Related metabolic disorder	Normal concentrations (μM) ^b	Migration time in 0.1 N NaOH (min)	Detection limit (μM)
Alditols				
Erythritol	—	608	12.6	0.5
Inositol	Diabetes, renal failure	357	12.6	0.3
Ribitol	—	35	12.8	—
Xylitol	—	35	12.8	—
Arabitol	—	195	12.8	—
Glucitol	—	35	12.9	0.5
Mannitol	Diabetes	104	14.6	0.5
Carbohydrates				
Sucrose	—	43	16.9	1
Lactose	—	15	19.6	1
Fucose	—	97	19.6	—
Galactose	Galactosaemia	29	21.3	1
Glucose	Diabetes	262	22.4	1
Rhamnose	—	115	22.8	—
Arabinose	Pentosuria	89	23.4	—
Fructose	Fructosuria	72	23.4	1
Xylose	Pentosuria	53	25.4	—
Ribose	Pentosuria	31	26.2	1
Amino acids				
Lysine	Hyperlysinaemia	328	31.6	4
Threonine	Aminoaciduria	183	35.4	2
Histidine	Histidinaemia	860	43.1	1
Others				
Creatinine	Muscle and renal disease	8800	12.8	80
Uric acid	Gout	2093	> 60	1.6

^aReprinted from Hong J and Baldwin RP (1997) *Journal of Capillary Electrophoresis*, 4, 65–71, with permission.^bCalculated assuming that the average urine volume for a 24-h period is 1.5 L.

celluloses) for the analysis of polymerase chain reaction (PCR) products of clinically relevant, diagnostic DNA have been reported. **Table 6** lists some major

applications, divided into four classes: human genetics, quantitative gene dosage, microbiology/virology and forensic medicine.

Table 5 Survey of CZE separations of proteins in biological matrices^a

Proteins	Matrix	CZE ^b mode	Detection mode
Immunoglobulin G, transferrin, albumin, prealbumin, β -trace proteins	CSF	CZE	UV 185 nm
Apolipoprotein A-I, A-II, B100, B48, C-III and E	Serum	MECC	UV 190 nm
Lipoprotein subfractions (HDL, VLDL, IDL, LDL)	Serum	CITP	Vis 570 nm
Leucine aminopeptidase	Serum, urine	CZE	LIF
Cerebrospinal fluid proteins	CSF	CZE	UF 200 nm
Myoglobin	Urine, tissue	CZE	Vis 405 nm
Albumin, α 1-acidic glycoprotein, transferrin, β -microglobulin, immunoglobulin light chains	Urine	CZE	UV 200 nm
Monoclonal antibodies (anti-TNF, anti-CEA)	Serum containing culture medium	CZE, CIEF, CGE	UV 200 nm
Imidodipeptides (prolidase deficiency)	Urine	CZE	UV 269 nm
Cathepsin D	Breast tissue	CZE	UV 214 nm
Hemoglobin variants	Plasma	CZE, CIEF	UV 210 nm
36 low side M _r proteins, cut-off 30 and 5 kDa	Seminal, vaginal fluids, serum, saliva	CZE	UV 214 nm

^aReprinted from Lehmann R, Voelter W and Liebich HM (1997) *Journal of Chromatography B* 697, 37–66, with permission.^bAbbreviations: CIEF, capillary isoelectric focusing; CGE, capillary gel electrophoresis; CITP, capillary isotachopheresis; CSF, cerebrospinal fluid; CEA, carcino-embryonic antigen; TNF, tumour necrosis factor; HDL, high density lipoproteins; LDL, low density lipoproteins; VLDL, very low density lipoproteins.

Table 6 Survey of selected capillary gel electrophoretic separations of clinically relevant diagnostic DNA^a

<i>Disease</i>	<i>DNA amplification</i>	<i>Sieving polymers</i>	<i>Detection</i>
<i>Human genetics</i>			
Cystic fibrosis	Allele specific PCR and restriction digest of PCR products (deletion)	6% linear PAA ^b	UV 254 nm
Cystic fibrosis	PCR, $\Delta F508$	6% linear PAA	UV 254 nm
Cystic fibrosis	PCR/GATT microsatellites	6% linear PAA	UV 254 nm
Cystic fibrosis	Point mutants, TGCE	8% linear poly(AAEE)	UV 254 nm
Duchenne/Becker muscular dystrophy	PCR multiplex reaction	6–10% linear PAA	UV 260 nm
Dystrophin gene	RFLP	0.5% HPMC	UV 254 nm
Thalassaemia	Point mutants, TGCE	4% poly(AAP), 1.5% HEC	UV 254 nm
Congenital adrenal hyperplasia	PCR deletion	6% linear PAA	UV 254 nm
Androgen insensitivity syndrome	CAG triplet analysis	6% linear PAA	UV 254 nm
Kennedy's disease	CAG triplet expansion	8% poly(AAEE)	UV 254 nm
N-ras gene (human cancer)	Point mutants SSCP	8% PAA	UV 260 nm
ERBB2 oncogene	RFLP	0.5% HPMC	UV 260 nm
TX gene	PCR	3% PAA	LIF
P-53	SSCP	4% PAA	UV 260 nm
P-53	SSCP	2% PAA	LIF
Cancer (microsatellites instability)	PCR	Bio-Rad sieving polymer	UV 260 nm
Apolipoprotein B gene	PCR/VNTR	0.7% MC	UV 260 nm
Apolipoprotein E gene	PCR/RFLP	3% T PAA	UV 260 nm
Apolipoprotein E gene	PCR/RFLP	Beckman e/CAP	LIF
Medium chain AcylCoA dehydrogenase deficiency	PCR/allele specific	Polyacrylamide gel	LIF
von Willebrand Factor gene	PCR/VNTR	1% HEC	LIF
Fetal DNA (Y-chromosome)	PCR	Beckman dsDNA 1000 gel buffer	LIF
<i>Quantitative gene dosage</i>			
Down's Syndrome	Quantitative PCR	8% PAA	UV 254 nm
Rh D/d genotyping	Quantitative PCR	8% PAA	UV 254 nm
Follicular lymphomas	Competitive PCR	4% PAA	UV 260 nm
Basic fibroblast growth factor	Competitive RT-PCR	6% PAA	UV 254 nm
<i>Microbiology/virology</i>			
<i>Mycobacterium tuberculosis</i>	SSCP and ddF	1% HEC or 3% T, 0.5% C PAA gel	LIF
Hepatitis C virus	RT-PCR	1% HEC	LIF
Polio Virus	RT-PCR	3% T linear PAA	UV 254 nm
HIV-1	RT-PCR	3% linear PAA	LIF
Mitochondrial DNA	PCR	1% HEC	LIF
Mitochondrial DNA	PCR	0.5% MC	LIF
VNTRs at locus D1S80	PCR/VNTR	0.5% HEC	LIF
VNTRs at locus D1S80	PCR/VNTR	0.5% MC	LIF
VNTRs at locus HUMTH01	PCR/VNTR	1% HEC	LIF
VNTRs at locus HUMTH01	PCR/VNTR	3% T, 3% C gel	UV 260 nm
<i>Therapeutic DNA</i>			
Antisense oligonucleotides		18% PAA	MALDI-MS LIF
Antisense oligonucleotides		10% PAA, isoelectric His	UV 254 nm
Antisense oligonucleotides		10% T PAA, pH gradient	UV 254 nm

^aReprinted from Righetti PG and Gelfi C (1997), with permission.^bAbbreviations: PAA, polyacrylamide; VNTR, variable number of tandem repeats; HEC, hydroxyethyl cellulose; MC, methyl cellulose; SSCP, single strand chain polymorphism; RT, reverse transcription; HPMS, hydroxypropyl methyl cellulose; AAP, acryloyl amino propanol; AAEE, acryloyl amino ethoxy ethanol, TGCE, temperature gradient capillary electrophoresis; RFLP, restriction fragment length polymorphism; LIF, laser induced fluorescence.

Examples of Some Separations

It is quite difficult to compress in such a few pages the vast literature in the field of clinico-chemical applica-

tions of CZE. From our experience in DNA separations, we offer here a few examples pertaining to the screening for human genetic diseases. **Figure 1** displays the CZE analysis of a multiplex PCR for the

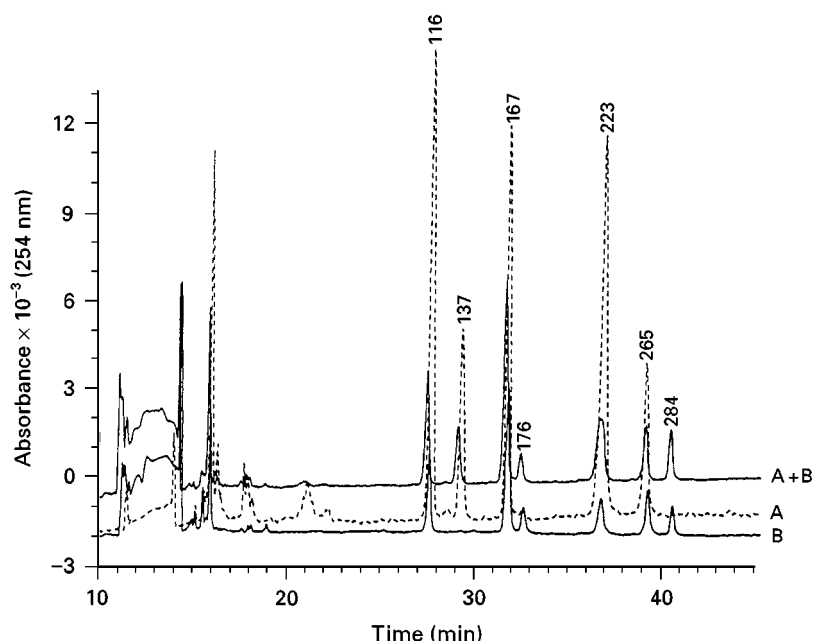


Figure 1 Simultaneous detection of $\Delta F508$, G542X, N1303K and 1717-1G \rightarrow A mutations in cystic fibrosis by CZE in polymer networks. Traces: A, patient carrying the mutations 1717-1G \rightarrow A and $\Delta F508$; B, patient affected by the G542X/N1303K mutations; A + B, artificial mixture of the amplified DNA fragments of patients A and B. Conditions: 100 μ m ID, 37 cm long capillary, filled with a viscous solution of linear 6% T polyacrylamide in 100 mmol L⁻¹ TBE (Tris-borate-EDTA) buffer, 10 μ mol L⁻¹ ethidium bromide, pH 8.3; Run at 165 V cm⁻¹ with detection at 254 nm; electrophoretic sample injection at 165 V cm⁻¹ for 8 s. Reprinted from Gelfi C, Righetti PG, Magnani C, Cremonesi L and Ferrari M (1994) *Clinica Chimica Acta* 229, 181–189, with permission from Elsevier Science.

simultaneous detection of four mutations, $\Delta F508$, G542X, N1303K and 1717-1G \rightarrow A in cystic fibrosis (CF). This is an interesting example, in that it offers a fast and reliable method for the simultaneous detection of mutations which are predominant in a given population. In Italy, a survey of 391 CF patients, originating from all geographical regions, revealed that $\Delta F508$ (53% of CF chromosomes), G542X (4%), 1717-1G \rightarrow A (4%) and N1303K (4%) are the most frequent mutations, accounting for 65% of all molecular defects pertaining to CF. **Figure 2** gives the CZE analysis for the Duchenne (DMD) and Becker (BMD) muscular dystrophies, which represent the two most common myopathies described to date. They are given the names of Chamberlain and Beggs since these two scientists proposed two PCR assays (each based on co-amplification of nine dystrophin gene exons) allowing for the detection of over 98% DMD/BMD deletions. Thus, a method attempting simultaneous analysis of DMD/BMD should offer unambiguous resolution and identification of 18 fragments ranging in size from *c.* 100–500 bp. This is in fact achieved in the lower trace of **Figure 2** (representing a healthy individual). The upper trace shows a patient affected by muscular dystrophy, in which four fragments (196, 202, 331 and 357 bp) are missing. We hope that these two examples, albeit limited,

provide an insight on the unique resolving power and capability of CZE as applied to problem solving in clinical chemistry.

Conclusions and Future Horizons

Compared with HPLC and gas chromatography, CZE has some distinct advantages, such as small sample size, minimal sample preparation, use of very small amounts of organic solvents and inexpensive chemicals, ease of buffer change and method development and low cost of capillary columns. Electrokinetic capillary assays are complementary to the widely employed immunoassays. For the widespread adoption of CE in routine laboratories, a number of improvements should be made. With the availability of instrumentation comprising multiple capillaries in parallel, sample throughputs comparable to those obtained in automated immunoassays should be possible. The same goal will be reached with the availability of chip-based instrumentation, i.e. CZE on a glass chip on which separation channels, a picolitre sample injector and solute detection are combined on an area of a few cm². In this approach, fluid flow is driven electrokinetically (thus via a plug, not a laminar flow) through a network of intersecting small channels fabricated on planar glass substrates

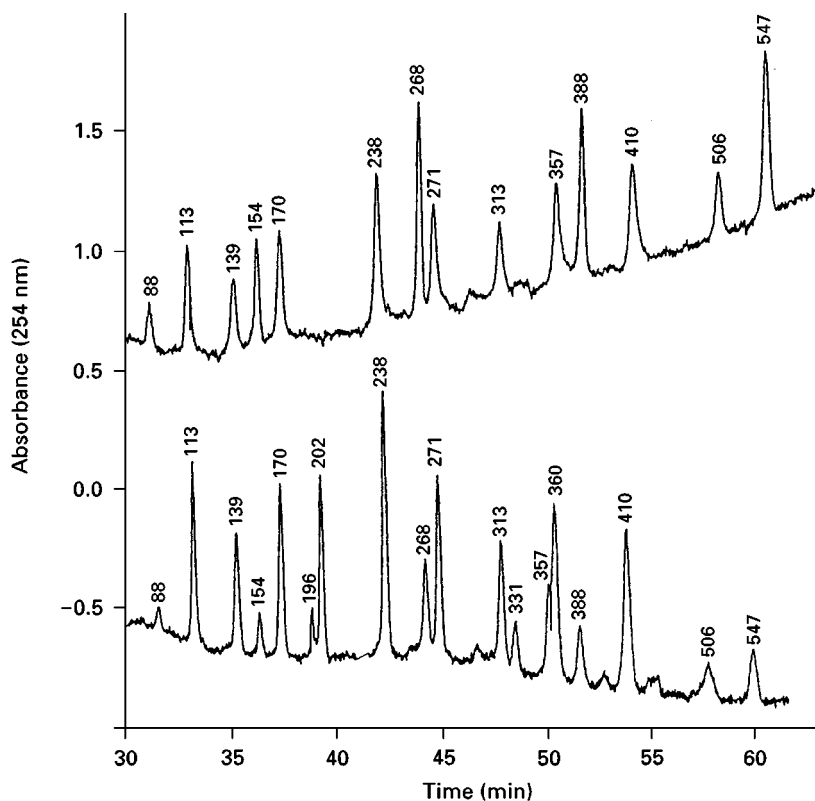


Figure 2 Screening for Duchenne (DMD) and Becker (BMD) muscular dystrophies by CZE in sieving liquid polymers. The upper trace represents the separation of 14 exons of modified deleted Chamberlains' and Beggs' mixed multiplex. The lower electropherogram shows the separation of 18 exons of modified nondeleted Chamberlains' and Beggs' multiplex. All runs were in a 32 cm long, 75 μm internal diameter capillary, filled with short-chain polyacrylamide, obtained by chain transfer at 70°C, in 89 mM TBE buffer, pH 8.3. Run: 165 V cm^{-1} with detection at 254 nm. Sample injection: 100 V cm^{-1} for 25 s. Reprinted from Gelfi C, Orsi A, Leoncini F, Righetti PG, Spiga I, Carrera P and Ferrari M (1995) *BioTechniques* 19, 254–263, with permission from Elsevier Science.

by photolithographic masking and chemical etching techniques and formed by bonding the etched substrate to a plain glass plate. Capillaries 30–70 μm wide, about 10 μm high and a few centimetres long have been shown to provide analytical runs in a few seconds.

Further Reading

- Guzman NA, Park SS, Schaufelberger D, Hernandez L, Paez X, Rada P, Tomlison AJ and Naylor S (1997) New approaches in clinical chemistry: on-line analyte concentration and microreaction capillary electrophoresis for determination of drugs, metabolic intermediates and biopolymers in biological fluids. *Journal of Chromatography B* 697: 37–66.
- Hong J and Baldwin RP (1997) Profiling clinically important metabolites in human urine by capillary electrophoresis and electrochemical detection. *Journal of Capillary Electrophoresis* 4: 65–71.
- Jellum E, Dollekamp H and Blessum C (1997) Capillary electrophoresis for clinical problem solving: analysis of urinary diagnostic metabolites and serum proteins. *Journal of Chromatography B* 683: 55–65.
- Krstulovic AM (guest ed.) (1997) Capillary electrophoresis in the clinical sciences. *Journal of Chromatography B* 697: 1–289.
- Landers JP (guest ed.) (1997) Capillary electrophoresis in the clinical sciences. *Electrophoresis* 18: 1707–1906.
- Lazaruk K, Walsh PS, Oaks F, Gilbert D, Rosenblum BB, Menchen S, Scheibler D, Wenz HM, Holt C and Wallin J (1998) Genotyping of forensic short tandem repeat (STR) systems based on sizing precision in a capillary electrophoresis instrument. *Electrophoresis* 19: 86–93.
- Lehmann R, Voelter W and Liebich HM (1997) Capillary zone electrophoresis in clinical chemistry. *Journal of Chromatography B* 697: 37–66.
- Lurie IS (1996) Applications of capillary zone electrophoresis to the analysis of seized drugs. *International Laboratory* 24: 21–29.
- McCord BR (1998) Capillary Electrophoresis in Forensic Science. *Electrophoresis* 19: 1–126.
- Perrett D (1999) Capillary zone electrophoresis in clinical chemistry. *Annals of Clinical Biochemistry* 36: 133–150.
- Righetti PG and Gelfi C (1997a) Capillary zone electrophoresis of DNA for molecular diagnostics. *Electrophoresis* 18: 1709–1714.

- Righetti PG and Gelfi C (1997b) Non-isocratic capillary electrophoresis for detection of DNA point mutations. *Journal of Chromatography B* 697: 195–205.
- Righetti PG and Gelfi C (1998) Analysis of clinically-relevant, diagnostic DNA by capillary zone and double-gradient gel slab electrophoresis. *Journal of Chromatography A* 806: 97–112.
- Thormann W (1997) Drug monitoring by capillary electrophoresis. In Wong SHY, Sunshine I (Eds) *Analytical Therapeutic Drug Monitoring*, pp. 1–19. Boca Raton: CRC Press.
- Thormann W, Zhang CX and Schmutz A (1996) Capillary zone electrophoresis for drug analysis in body fluids. *Therapeutic Drug Monitor* 18: 506–520.

Electrophoresis

J.-D. Tissot, A. Layer and P. Schneider,
Fondation CRS, Lausanne, Switzerland
H. Henry, Centre Hospitalier Universitaire Vaudois,
Lausanne, Switzerland

Copyright © 2000 Academic Press

Introduction

It is somewhat arbitrary to outline electrophoretic applications that are used in a routine clinical laboratory because they are highly dependent on the specificity of each application. Nowadays, a multitude of electrophoretic methods are routinely used in various clinical laboratories, according to the specific research being developed. More and more sophisticated methods are needed to resolve specific clinical problems, the reason why specialization of laboratories is mandatory in order to provide accurate results at the lowest possible cost. In addition, quality control is of major importance. Therefore, automation is progressively introduced in all the steps involved in the analytical process, and only a few manual methods will survive in the future. However, highly sophisticated electrophoretic techniques should be maintained and developed in a limited number of specialized laboratories, in order to resolve the different problems that are encountered in clinical medicine. Here, we present selected examples of electrophoretic techniques that are employed in the clinical laboratory.

Serum Protein Electrophoresis

Electrophoretic techniques for the separation of human serum proteins have been used for fifty years. Resolution has been improved by the use of support media such as paper, starch gel, cellulose acetate, agarose, and polyacrylamide gels, which have rendered electrophoretic methods very popular in the diagnostic area. However, many of those methods have remained labour intensive, being difficult to

automate. Serum protein electrophoresis is widely used in clinical laboratories, especially for the evaluation of changes in proteins associated with inflammation, liver or kidney diseases as well as for the detection and identification of paraproteins. Traditional clinical electrophoretic procedures are manual methods that use agarose gels or cellulose acetate membranes as the separation bed. Quantitation of the five major serum fractions is done by densitometric scanning of the gel or the membrane. Clinical interpretation is based on the alteration of the content of one or more of the five fractions. Agarose, as supporting medium for protein electrophoresis, has been reported to give better resolution as well as to allow better detection of paraproteins than is cellulose acetate. Semiautomated agarose electrophoresis and immunofixation can be performed with various commercially available systems. No differences between manual and semiautomated methods have been seen with respect to paraprotein identification.

Over the last few years, capillary zone electrophoresis (CZE) has emerged as a powerful new tool for rapid separation of various biopolymers, including proteins. Separation by this technique depends on the electrophoretic mobility of the analyte and the electroosmotic flow of the bulk solution, and can be easily automated. Direct quantitation of proteins via peptide bonds is possible using UV detection at 214 nm. Separation patterns obtained by CZE are similar to those obtained after densitometric scanning of cellulose acetate membrane electrophoresis or agarose gel electrophoresis. Recently, dedicated automated systems for the routine analysis of human serum proteins in clinical laboratories have become commercially available. High sample throughput is attained due to the presence of several fused-silica capillaries, which allow the simultaneous analysis of different samples. Several studies have clearly shown that the electrophoretic patterns and the clinical information obtained by CZE are comparable with the data obtained by classical methods. In addition, the method is also suited to detect monoclonal gammopathies. Multicapillary instruments have been

designed for automation of both routine serum protein electrophoresis and for monoclonal component typing by subtraction (immunofixation electrophoresis – immunosubtraction). In this latter technique, CZE is performed on the supernatant of serum samples that have reacted with Sepharose beads coated with an immunospecific binder (IgG, IgA, IgM, κ and λ). The low detection limit of the technique (0.5 g L^{-1} for IgG, 0.75 g L^{-1} for IgA and IgM) contributes to the ability of CZE to detect small monoclonal gammopathies.

Lipoprotein Analysis

The cardiac risk profile that is routinely measured in the clinical laboratory is an important indicator of susceptibility to the development of atherosclerosis. There is clearly a need to develop a more comprehensive cardiovascular risk profile that includes more factors than cholesterol and triglycerides. Triglycerides and cholesterol are transported in blood in association with lipoproteins, that can be separated by ultracentrifugation into four main classes according to their density: chylomicrons, very low-density lipoproteins (VLDL), low-density-lipoproteins (LDL), and high-density lipoproteins (HDL). The current lipid profile measured focuses on the lipid components of lipoproteins. Because proteins associated with lipoproteins, apoproteins, play a central role in lipid homeostasis, important research efforts have been directed to the study of apoproteins.

Free-flow isotachopheresis (ITP) and capillary ITP (cITP) has been utilized for many years to study plasma lipoproteins. The discriminating principle is based on the net charge of lipoproteins. cITP is a high-resolution electrophoretic technique, by which ionic sample components are separated according to their net electric charge and without molecular sieve effects. With cITP, lipoprotein analysis can be performed directly from whole serum and offers the potential of a reliable and automated quantitation of lipoprotein subpopulations. Sample pretreatment is negligible and only few nanolitres of sample are necessary for the analysis. LDL are a heterogeneous population of particles that varies in size, density, composition, and electric charge. One significant aspect of this variability, relevant to atherosclerosis, is the phenotypic pattern of LDL density and size distribution among individuals with and without coronary artery disease. Using nondenaturing gradient gel electrophoresis, various LDL subgroups have been identified on the basis of size. Individuals with lipoprotein profiles enriched in small dense LDL were found to be predisposed to coronary artery disease. Higher plasma levels of LDL have been found in patients

with acute myocardial infarction, unstable angina, and thrombogenic carotid atherosclerosis. The method of study of LDL, which uses ion exchange chromatography of LDL isolated by ultracentrifugation, requires particular care to avoid artefacts due to *in vitro* auto-oxidation of the LDL and is time consuming. HDL are a family of protein–lipid complexes that play a central role in cholesterol transport. HDL collectively contain apolipoproteins (apo) A-I and A-II as major protein components, together with apoC, E, and A-IV. Changes in HDL composition occur during normal metabolism, as the result of a particular genetic profile, or as a consequence of disease. The protein composition of lipoproteins can be analysed by chromatography, electrophoresis, or immunoassay. SDS-PAGE resolves proteins according to molecular size, while charge separation can be achieved by zone electrophoresis or isoelectric focusing. Quantification of protein bands after electrophoresis is achieved by immunoblotting or by staining with Coomassie Blue. However, due to differences in the chromogenicity of different apolipoproteins, these staining methods are only semiquantitative. Immunoassays offer good sensitivity and precision, but results can vary with different antisera. Furthermore, immunoassays do not distinguish between different apo isoforms. The availability of high performance capillary electrophoresis systems has created the possibility of applying this technology to lipoprotein analysis. Protein separation is performed at high field strengths in micropore capillaries, with direct monitoring by online UV detection. The separation is analogous to that achieved with slab gel systems, except that no support media are used, electrophoresis being carried out in a free solution, and results are obtained in minutes rather than hours. Separations based on differences in molecular size are performed in a SDS-containing UV transparent polymer network. This mode, usually termed ‘capillary SDS gel electrophoresis’ (though it actually uses a non-gel matrix), has been found to give similar results to those obtained with SDS slab gel electrophoresis.

Determination of Serum Protein Phenotypes and Microheterogeneities

The determination of the phenotype of particular serum proteins may have clinical relevance. Hereditary deficiencies of the proteinase inhibitor α_1 -antitrypsin, one of the most common inborn metabolic errors in Europeans, lead to pulmonary emphysema in young adults and to liver cirrhosis in children. Many distinct subtypes have been identified using isoelectric focusing, the most common normal phenotype being MM, whereas the major deficient

phenotypes are termed MS, MZ, SS, SZ and ZZ. The last form, ZZ, is associated with low concentration of the protein in plasma and with severe clinical manifestations. Isoelectric focusing in immobilized pH gradients represents a major improvement, and the method can be utilized for subtyping many different proteins with high reproducibility.

The microheterogeneity of serum glycoproteins in patients with chronic alcohol abuse as well as in patients with carbohydrate-deficient glycoprotein syndrome can be globally studied by two-dimensional electrophoresis, whereas SDS-PAGE and Western blotting allows detailed comparison and characterization of specific proteins.

Diagnosis of Haemoglobinopathies and Haemoglobin A1c

Disorders of haemoglobin synthesis such as sickle cell disease, β - and α -thalassaemias or haemoglobin variants – grouped under the term ‘haemoglobinopathies’ – are frequently observed, and up to 45% of the newborns from regions at risk present an abnormal haemoglobin. Therefore, it is of importance to have cost-effective methods to screen large populations. Isoelectric focusing has been used for many years, and when performed correctly, produces excellent haemoglobin separation, with very little band overlap when bands are measured to 0.1 mm against controls. It has been shown that high-power liquid chromatography also allows accurate diagnosis of the haemoglobinopathies, and that both approaches can be used for a universal screening. Another interesting approach to study haemoglobin variants is capillary isoelectric focusing. The technique allows high-efficiency separation and precise quantitation of haemoglobin variants over a wide range of concentrations.

Haemoglobin A1c (Hb A1c) is the analyte of choice for monitoring metabolic control in patient with diabetes mellitus. Hb A1c can be measured using capillary electrophoresis, without apparent interference by other haemoglobin variants such as Hb F, Hb S or Hb C.

Genotyping of Proteins

Many complex biological questions, encountered in all fields of medicine, have been solved using DNA-based technologies. It is now possible to make many different prenatal diagnoses using genetic testing with one technique or a combination of the three basic molecular testing techniques – nucleotide sequencing, restriction fragment length polymorphism mapping and molecular DNA analysis using the polymerase chain reaction (PCR) – routinely used to assess gene

mutations. Apolipoprotein E (apoE) is a secreted glycoprotein with a molecular mass of 35 kDa which is synthesized primarily in the liver and brain. ApoE plays a critical role in lipid metabolism through its function of redistributing lipids amongst the cells of various organs. It is a constituent of VLDL and of a subclass of HDL. The *APOE* gene is polymorphic and its three common alleles ϵ 2, ϵ 3, and ϵ 4 code for isoforms E2, E3 and E4, respectively. The isoforms E3 and E4 differ from E2 by single arginine (R) substitution at one or both cysteine (C) at position 130 and 176 of the apoE amino acid sequence (accession number P02649; SwissProt database). Compared with allele ϵ 3, reduced LDL cholesterol (LDL-c) and apoB levels frequently accompany the ϵ 2 allele, higher LDL-c levels occurring with the ϵ 4 allele, and both ϵ 2 and ϵ 4 alleles are associated with hypertriglyceridaemia. In addition to the dyslipidaemic tendency, the relative odds for prevalent coronary heart disease are found to be increased with the ϵ 4 allele. A compelling association between risk of Alzheimer’s disease in both late-onset familial Alzheimer’s disease and sporadic Alzheimer’s disease with the ϵ 4 allele has been also demonstrated. *APOE* genotyping is usually determined by a blood test using DNA isolated from leukocytes, embedded tissues, Guthrie spots, buccal epithelial cells and restriction isotyping. The method is based on the existence of a GCGC recognition site for the endonuclease *HhaI* overlapping the coding sequences present for amino acids 130 and 170 in the ϵ 4 allele, absent in position 130 in the ϵ 3 allele, and absent in both position 130 and 170 in the ϵ 2 allele. A 244-bp sequence including the two polymorphic sites is amplified by using PCR and is digested by *HhaI* (Figure 1). The resulting fragments are separated by electrophoresis on polyacrylamide gels. After electrophoresis, the gels are either treated with ethidium bromide or are silver stained. The method cannot detect rare *APOE* variants unless nucleotide substitution alter the *HhaI*-restriction sites within the PCR-amplified region. In that case the rare variants are identified only by using DNA sequencing. PCR and restriction isotyping for *APOE* genotyping must be preferred to isoelectric focusing (IEF). Because the post-translational modifications of apoE such as glycosylation or desialylation alter the electric charges of the isoforms, misclassification of genotypes currently occurs when using IEF.

Small Molecules (Drugs, Steroids) Monitoring

Drugs, licit or illicit, play a pivotal role in almost all aspects of life. Monitoring of drugs is of major importance for regulatory authorities, in clinical

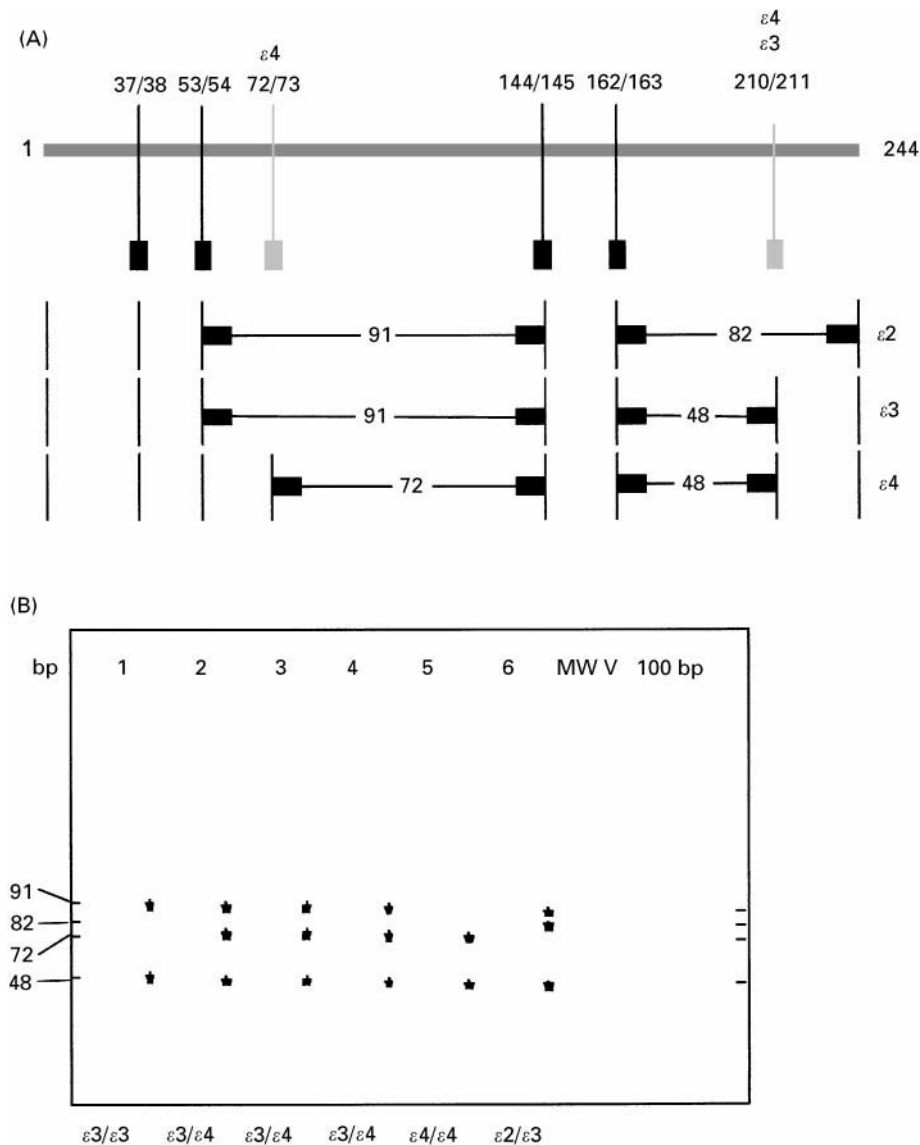


Figure 1 Application of PCR to the analysis of apolipoprotein E. (A) Map of the PCR-amplified region encoding common *APOE* isoforms and location of *HhaI* cleavage sites. The distance in basepairs between the *HhaI* sites that distinguish isoforms are shown for each genotype. (B) Silver-stained PAGE after the electrophoretic separation of *HhaI* fragments from different patients.

settings, in forensic science, for drug testing at the workplace, and in the pharmaceutical industry. With the advent of fused-silica capillary instrumentation, drug analysis by capillary electrophoresis has made important progress. Capillary electrophoresis of drugs, as well as their metabolites in almost all biological samples, has been shown to provide high-quality data that can be used for diagnostic drug monitoring. Corticosteroid hormones are usually analysed by immunological techniques or HPLC. Immunoassays are prone to interference from various compounds, a disadvantage not observed with HPLC. However, the latter technique is hampered by the large sample and eluent volumes needed. Corticosteroid hormones such as cortisone, cortisol, progesterone and oestro-

gen can be studied using mixed micellar electrokinetic capillary chromatography (MEKC), using borate buffer and SDS. The separation is rapid and quantitation is efficient.

Cerebrospinal Fluid Analysis

Analysis of cerebrospinal fluid (CSF) proteins using electrophoretic techniques is particularly useful in the diagnosis and management of neurological diseases particularly in the detection of immune response within the central nervous system (CNS). In healthy individuals, all CSF immunoglobulins are derived from plasma. However, in most of the inflammatory conditions within the CNS, activated B-lymphocytes

secrete their immunoglobulins directly into the brain extracellular space. This local immune response occurs typically in demyelinating disorders such as multiple sclerosis, in chronic CNS infections as well as in autoimmune disorders with neurological involvement. An intrathecal synthesis of immunoglobulins can be detected either by quantitative methods and the results are expressed using various indexes or by qualitative methods such as IEF and Western blotting. Because the locally synthesized immunoglobulins are the product of a limited number of clones, they currently produce an oligoclonal pattern superposed to the plasma pattern (Figure 2). IEF is now considered as a more sensitive test than the quantitative index for the detection of an intrathecal immune response. The diagnostic sensitivity and specificity of both quantitative and qualitative tests has

been evaluated in samples from 1007 patients with neurological diseases. It was found that IEF has a sensitivity of 95% for multiple sclerosis against 67% for the quantitative tests and a specificity with a false-positive rate of 0% versus 3.5% for the quantitative tests.

The diagnosis and the treatment of the discharge of CSF (liquorrhea) from the subarachnoid space into the nasal or aural mucosa (CSF rhinorrhea and otorrhea) is a critical clinical problem. The most common cause of liquorrhea is traumatic fracture; in a large series of pediatric patients with temporal bone fractures, liquorrhea was noted in 25% of the patients. Other causes are neurosurgical procedures, intra- and extracranial tumours, as well as primary CSF rhinorrhea through congenital bony dehiscences. The diagnosis of liquorrhea is important in view of developing a potentially fatal meningitis. The use of prophylactic antibiotics does not appear to be beneficial in reducing the incidence of post-traumatic meningitis. Surgical intervention is therefore necessary. Detection of β_2 -transferrin is now considered as the most reliable test in the identification of CSF rhinorrhea and otorrhea. β_2 -transferrin is a transferrin isoform which is locally synthesized in the central nervous system. This isoform is characterized by the presence of truncated N-glycans devoid of terminal galactose and sialic acid. The serum transferrin and β_2 -transferrin isoforms found in CSF are separated by native electrophoresis using agarose and detected by immunoblotting. Because there is no gold standard for the diagnosis of liquorrhea, the sensitivity and the specificity of the test are unknown.

Urine Analysis

Electrophoretic methods have been widely used for the clinical analysis of the proteins contained in urine (proteinuria). Normally, the renal glomeruli restrict filtration of plasma proteins, and only traces are present in the urine. In several renal diseases and particularly in patients with glomerulonephritis, nephrosis, glomerulosclerosis and IgA nephropathy, large amounts of proteins may be present in the urine. This is the reason why so many different electrophoretic techniques, including SDS-PAGE, isoelectric focusing, and high-resolution two-dimensional polyacrylamide gel electrophoresis have been applied over the years to study in detail the protein composition of the urine of patients with kidney diseases.

The Diagnosis of Infectious Diseases by Western Blotting

Despite the analytical power of gel electrophoresis, direct specific identification of separated components

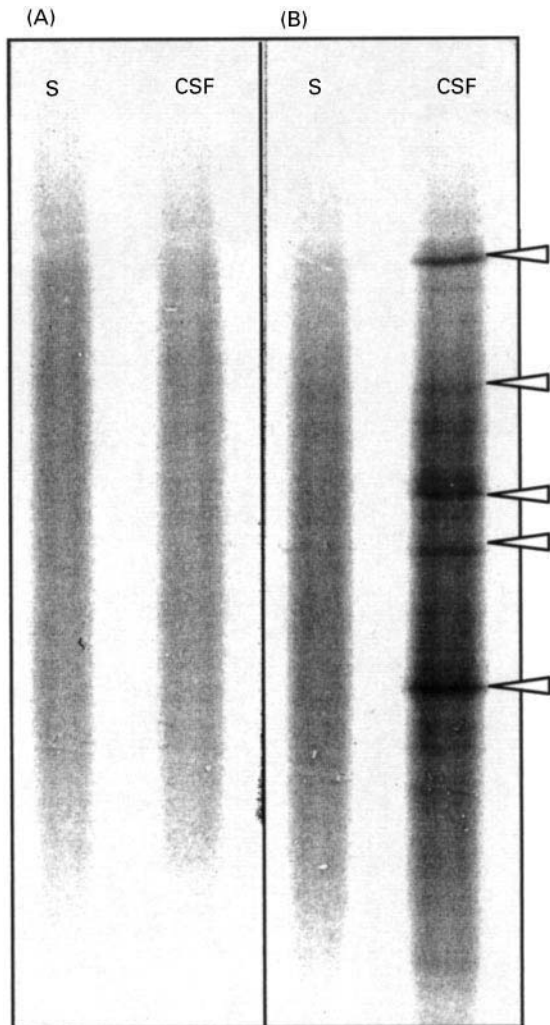


Figure 2 Analysis of the immunoglobulins of the cerebrospinal fluid. Typical IgG patterns of sera (S) and of cerebrospinal fluid (CSF) separated by isoelectric focusing and revealed by Western blot. (A) Normal control. (B) Patient with multiple sclerosis. The arrow heads indicate the oligoclonal bands found only in the CSF.

by ligands such as antibodies, lectin or enzymes was generally hindered by the pore size of the gel matrix. Thus the development of protein blotting techniques that enabled the separate components to be transferred from gels onto membranes where they were bound and available for participation in a range of reactions was of enormous practical significance. Basically, with these techniques, viral proteins, either from culture fluid or obtained by recombinant molecular technologies, are separated by SDS-PAGE, then blotted from the polyacrylamide gel matrix onto membranes by an electrophoretic transfer, and finally identified using enzyme immunoassay. The Western blot method has been used in key epidemiological studies that reported the unambiguous association of human immunodeficiency virus (HIV) with AIDS, and is still an essential tool for confirming the presence of antibodies to HIV. Western blot has been used as the 'gold standard' confirmatory test for specimens found to be reactive in screening assays. Protein blotting can be applied to a large variety of infectious diseases, to study allergens in patients with allergy as well as to identify autoantigens in patients suffering from autoimmune disorders.

The transmissible spongiform encephalopathies or prion diseases constitute a group of progressive and fatal neurodegenerative diseases that affect both human and animals. The diseases affecting humans include Creutzfeldt-Jakob disease (CJD) for which three main forms have been recognized: inherited, sporadic, and acquired (iatrogenic). Patients with CJD present a progressive dementia with myoclonus usually associated with the presence of sharp-wave complexes on their electroencephalogram. The gold standard for a definitive diagnosis of CJD require a histological examination of the brain and immunostaining for the protease-resistant prion protein (PrP^{res}). Several CSF proteins such as neurone-specific enolase, S-100b, CK-BB, ubiquitin and protein 14-3-3 have been proposed as potential pre-mortem markers for CJD. Amongst them, only protein 14-3-3 proved useful diagnostically. The differential expression of CSF proteins in patients with CJD has been evaluated by using two-dimensional electrophoresis, and two protein spots with CJD has been evaluated by using two-dimensional electrophoresis, and two protein spots (proteins 130 and 131) were identified. N-terminal sequencing of protein 130 matches the sequence of 14-3-3 β , a brain-specific protein of 28 kDa which is believed to have a regulatory function in monoamine biosynthesis. A Western blot assay has been developed, using a commercially available antibody directed against 14-3-3 β (Santa Cruz Biotechnology) which cross-reacts with protein 130 and 131 (Figure 3). It was

found that the 14-3-3 immunoassay had an overall sensitivity of 96% (68 true-positive results and 3 false-negative results) and an overall specificity of 88% (164 true-negative and 22 false-positive results). Interestingly, the specificity of the immunoassay amongst all patients with dementia was 96% (90 true-negative and 4 false-positive results). It was also observed that the immunoassay may become positive early in the course of CJD. However the immunoassay does not allow a quantitation of the 14-3-3 proteins and needs further validation with larger numbers of patients.

Identification of Microorganisms

Pulsed-field gel electrophoresis (PFGE) is a method widely used to separate fragments of DNA as long as several million bases by subjecting the gel to an electrical current alternately delivered from two angles in timed intervals, which minimizes diffusion of large molecules. PFGE has many important clinical applications, particularly in the field of infectious diseases. PFGE allows typing bacteria such as group A streptococci, *Staphylococcus aureus*, *Escherichia coli* or *Salmonella enterica*. PFGE can be particularly useful for assisting epidemiological investigations of illnesses caused by a common-source of pathogen such as *Escherichia coli* O157:H7 in food poisoning or to demonstrate that recurrent episodes of staphylococcal bacteraemia are primarily related to relapses rather than to new infections. The technique is commonly known as DNA fingerprinting.

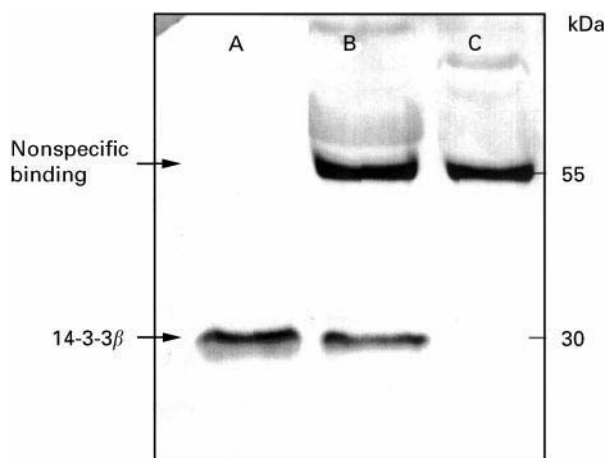


Figure 3 Application of Western blot to the diagnosis of Creutzfeldt-Jakob disease. Immunoblot by using anti-14-3-3 β after SDS-PAGE separation of (A) human brain proteins, (B) cerebrospinal fluid proteins from a patient with Creutzfeldt-Jakob disease and (C) normal control cerebrospinal fluid. Note that anti-14-3-3 β immunoglobulins bound nonspecifically to a cerebrospinal fluid protein with a molecular mass close to 55 kDa.

Summary

Electrophoretic techniques will certainly continue to be applied in the clinical laboratory for many years to come. However, only highly reproducible methods such as those based on capillary electrophoresis will survive on the condition that they can be applied to resolve heterogeneous clinical problems and that they can be fully automated with electronic handling of the data. The evolution of electrophoretic techniques achieved over the last few years has allowed a revolution in medical science. However, in terms of manual operations, the good old time of 'blue fingers' has probably finished.

See Colour Plate 68.

Further Reading

- Bienvenu J, Graziani MS, Arpin F, Bernon H, Blessum C, Marchetti C, Righetti G, Somenzini M, Verga G and Aguzzi F (1998) Multicenter evaluation of the Paragon CZETM 2000 capillary zone electrophoresis system for serum protein electrophoresis and monoclonal component typing. *Clinical Chemistry* 44: 599–605.
- Bossuyt X, Schiettekatte G, Bogaerts A and Blanckaert N (1998) Serum protein electrophoresis by CZE 2000 clinical capillary electrophoresis system. *Clinical Chemistry* 44: 749–759.
- Campbell M, Henthorn JS and Davies SC (1999) Evaluation of cation-exchange HPLC compared with isoelectric focusing for neonatal hemoglobinopathy screening. *Clinical Chemistry* 45: 969–975.
- Clark R, Katzmann JA, Kyle RA, Fleisher M and Landers JP (1988) Differential diagnosis of gammopathies by capillary electrophoresis and immunosubtraction: analysis of serum samples problematic by agarose gel electrophoresis. *Electrophoresis* 19: 2479–2484.
- Conti M, Gelfi C, Bosisio AB and Righetti PG (1996) Quantitation of glycated hemoglobins in human adult blood by capillary isoelectric focusing. *Electrophoresis* 17: 1590–1596.
- Doelman CJ, Siebelder CW, Nijhof WA, Weykamp CW, Janssens J and Penders TJ (1997) Capillary electrophoresis system for hemoglobin A1c determinations evaluated. *Clinical Chemistry* 43: 644–648.
- Fowler VG Jr, Kong LK, Corey GR, Gottlieb GS, McClelland RS, Sexton DJ, Gesty-Palmer D and Harrell LJ (1999) Recurrent *Staphylococcus aureus* bacteremia: pulsed-field gel electrophoresis findings in 29 patients. *Journal of Infectious Disease* 179: 1157–1161.
- Harrington MG, Merrill CR, Asher DM and Gajdusek DC (1986) Abnormal proteins in the cerebrospinal fluid of patients with Creutzfeldt–Jakob disease. *New England Journal of Medicine* 315: 279–283.
- Hempe JM, Granger JN and Craver (1997) Capillary isoelectric focusing of hemoglobin variants in the pediatric clinical laboratory. *Electrophoresis* 18: 1785–1795.
- Henry H, Froehlich F, Perret R, Tissot JD, Eilers-Messerli B, Lavanchy D, Dionisi-Vici C, Gonvers JJ and Bachmann C (1999) Microheterogeneity of serum glycoproteins in patients with chronic alcohol abuse compared to carbohydrate-deficient glycoprotein syndrome type I. *Clinical Chemistry* 45: 1408–1413.
- Hixson JE and Vernier DT (1990) Restriction isotyping of human apolipoprotein E by gene amplification and cleavage with *Hha*I. *Journal of Lipid Research* 31: 545–548.
- Hoffmann A, Nimtz M, Getzlaff R and Conradt HS (1995) 'Brain-type' N-glycosylation of asialotransferrin from human cerebrospinal fluid. *FEBS Letters* 359: 164–168.
- Hsieh G, Kenney K, Gibbs CJ, Lee KH and Harrington MG (1996) The 14-3-3 brain protein in cerebrospinal fluid as a marker for transmissible spongiform encephalopathies. *New England Journal of Medicine* 335: 924–930.
- James RW, Hochstrasser DF, Tissot JD, Funk M, Appel RD, Barja F, Pellegrini C, Muller AF and Pometta D (1988) Protein heterogeneity of lipoprotein particles containing apolipoprotein A-I without apolipoprotein A-II and apolipoprotein A-I with apolipoprotein A-II isolated from human plasma. *Journal of Lipid Research* 29: 1557–1571.
- Keir G, Zeman A, Brookes G, Porter M and Thompson EJ (1992) Immunoblotting of transferrin in the identification of cerebrospinal fluid otorrhoea and rhinorrhea. *Annals of Clinical Biochemistry* 29: 210–213.
- Marshall T and Williams KM (1998) Clinical analysis of human urinary proteins using high resolution electrophoretic methods. *Electrophoresis* 19: 1752–1770.
- Mayeux R, Saunders AM, Shea SS, Evans D, Roses AD, Hyman BT, Crain B, Tang MX and Phelps CH (1998) Utility of the apolipoprotein E genotype in the diagnosis of Alzheimer disease. *New England Journal of Medicine* 338: 506–511.
- McLean BN, Luxton RW and Thompson EJ (1990) A study of immunoglobulin G in the cerebrospinal fluid of 1007 patients with suspected neurological disease using isoelectric focusing and the log IgG-index. *Brain* 113: 1269–1289.
- Righetti PG and Bossi A (1997) Isoelectric focusing in immobilized pH gradients. *Journal of Chromatography B, Biomedical Sciences and Applications* 699: 77–89.
- Schmitz G, Möller C and Richter V (1997) Analytical capillary isotachopheresis of human serum lipoproteins. *Electrophoresis* 18: 1807–1813.
- Shihabi ZK and Frieberg MA (1997) Analysis of small molecules for clinical diagnosis by capillary electrophoresis. *Electrophoresis* 18: 1724–1732.
- Stocks J, Nazeem Nanjee M and Miller NE (1998). Analysis of high density lipoprotein apolipoproteins by capillary zone and capillary SDS gel electrophoresis. *Journal of Lipid Research* 39: 218–227.
- Wilson PW, Myers RH, Larson MG, Ordovas JM, Wolf PA and Schaefer EJ (1994) Apolipoprotein E alleles, dyslipidemia, and coronary heart disease. The Framingham offspring study. *Journal of the American Medical Association* 272: 1666–1671.
- Zerr I, Bodemer M and Weber T (1997) The 14-3-3 brain protein and transmissible spongiform encephalopathy. *New England Journal of Medicine* 336: 874.

Gel Electrophoresis

J.-D. Tissot, A. Layer and P. Schneider, Foundation CRS, Lausanne Switzerland

F. Forestier, Institut de Puériculture de Paris, Paris, France

H. Henry, Centre Hospitalier Universitaire Vaudois, Lausanne, Switzerland

Copyright © 2000 Academic Press

Introduction

The separation of polypeptides by electrophoresis allowed Arne Tiselius to describe protein fractions corresponding to albumin, α -, β -, and γ -globulins in serum with the first published diagram of human serum protein electrophoresis in 1939. The number of fractions slowly expanded into electrophoretic subfractions identified as α_1 , α_2 , β_1 , β_2 , γ_1 and γ_2 . The mobility characteristics of these fractions are still used to denote serum proteins such as α_1 -macroglobulin, α_2 -antiplasmin or β_2 -microglobulin. Sophisticated new electrophoretic techniques for identifying many proteins simultaneously and relating them to diseases have been developed over the years, many of them being described in other studies. Almost all body fluids have been studied by electrophoresis, serum, urine and cerebrospinal fluid being evaluated in great detail by different techniques. However, despite the major developments and progress achieved in protein separation, only a restricted number of methods are routinely used in the clinical laboratory. Nowadays, serum protein electrophoresis is mainly used to study major serum protein alterations such as those observed in patients with inflammatory, liver or kidney diseases, as well as in patients presenting lymphoproliferative disorders and alterations of immunoglobulin (Ig) production. Electrophoretic techniques, in association with ultracentrifugation, are also used to study lipoproteins and to classify hyperlipidaemic disorders.

Here, we provide selected clinical situations studied by electrophoretic methods, with a particular emphasis on 2D-PAGE, in order to illustrate how electrophoresis can be used to gain insight into particular clinical problems.

Monoclonal Immunoglobulins

The large diversity of antibodies in an individual results from highly complex mechanisms influencing B-cell development, expansion, and immunoglobulin (Ig) secretion. This diversity is so complex that elec-

trophoretic techniques applied to sera from healthy adults cannot separate individual clonal products. Immunoglobulin produced by an expanding B cell clone to a level permitting detection by electrophoretic techniques is known as 'monoclonal gammopathy' (MG), and has been observed in a wide variety of disease. MG can be also observed in humans without overt disease and is termed 'benign MG', or 'monoclonal gammopathy of undetermined significance'. The frequency of benign MG has been increasing in parallel with the refinement of the techniques. Identification of monoclonal immunoglobulins requires sensitive and rapid screening methods. Electrophoresis on cellulose acetate membrane is satisfactory for initial screening.

High-resolution agarose gel electrophoresis (HRE) is more sensitive for the detection of rare monoclonal proteins (**Figure 1**). Confirmation of the presence of an MG should be performed using methods such as immunoelectrophoresis (IEP) or immunofixation electrophoresis (IFE). IEP was described in 1953, and, until recently, was considered as the method of reference. As a routine procedure, it is time-consuming, and requires a high level of technical expertise. The consequence of the long diffusion process is that small amounts of protein become too dilute to be detected, resulting in low sensitivity. The most important drawback of IEP is the so-called 'umbrella effect'. Furthermore, the demonstration of κ and λ monoclonal light chains belonging to IgA or IgM isotypes is often masked by the presence of polyclonal IgG, that, because of faster diffusion, migrates ahead to an area situated between IgA and IgM. IFE, like IEP, includes two steps, but without the diffusion process. In the first step, protein fractions are separated by agarose gel electrophoresis; in the second step, they are revealed by overlaying of antiserum specific to the different immunoglobulin heavy and light chains. The technique is considered as the procedure of choice in the routine diagnosis of MG, because of its simplicity, speed, and sensitivity. Other advantages of the method are ease of interpretation and the absence of diffusion. Furthermore, the enhanced sensitivity of IFE also yields more frequent detection of low concentration MG and, what is more important, of multiple immunoglobulin bands or subtle bands of restricted heterogeneity. In such cases, further assessment of the clonality of immunoglobulins depends on additional techniques such as immunoblotting, immuno-isoelectric focusing or high-resolution two-dimensional polyacrylamide gel

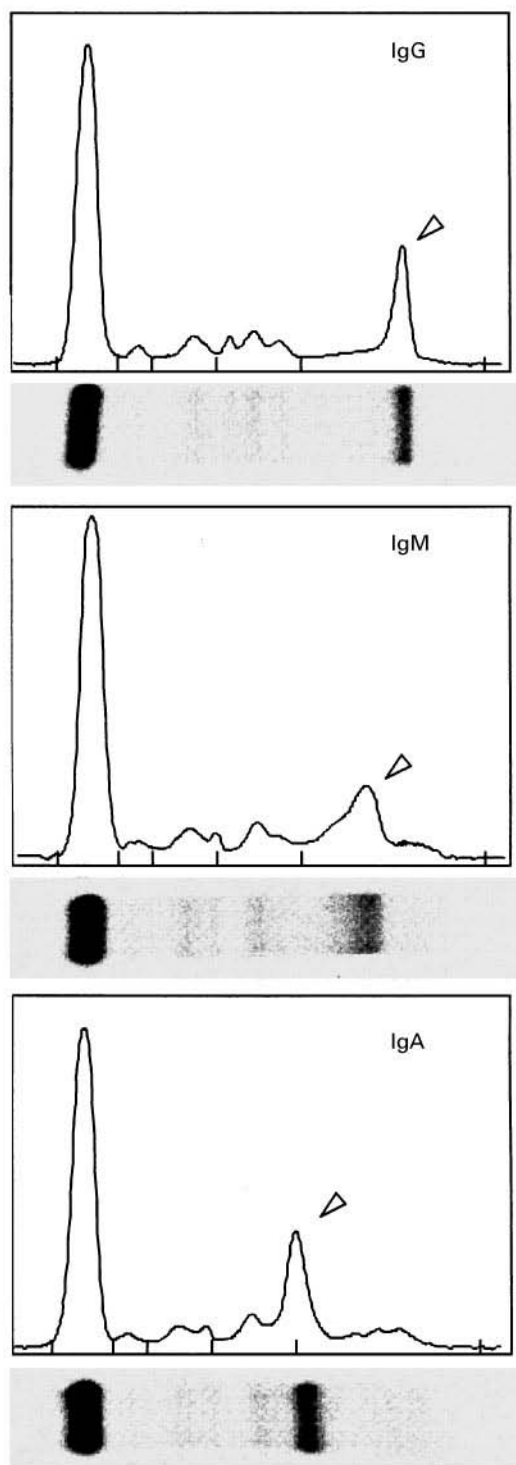


Figure 1 High resolution serum protein agarose electrophoresis profiles. Serum protein electrophoresis, and protein densitometry of serum samples from patients presenting monoclonal IgG- λ , IgM- λ and IgA- λ gammopathies were performed by using commercially available kits. The isotype of the monoclonal heavy chains as well as the type of the monoclonal light chains were identified using immunofixation electrophoresis. The protein peaks corresponding to the monoclonal components are shown by arrowheads.

electrophoresis (2D-PAGE). With 2D-PAGE, α , μ , γ and δ chains appear in nonoverlapping regions of protein maps (Figure 2). Monoclonal heavy chains are easily differentiated from polyclonal heavy chains, according to their different two-dimensional electrophoretic patterns. Polyclonal heavy chains are highly heterogeneous and are resolved as 'unspotted' diffuse zones whereas monoclonal heavy chains show charge and, to a lesser degree, size microheterogeneity.

Polyclonal light chains appear as clustered nondiscrete spots following 2D-PAGE, and form cloudy zones with unevenly distributed densities. In about two-thirds of patients with MG, monoclonal light chains are detected as a dominant and well-defined spot. In the remaining one-third of the patients, examined monoclonal light chains disseminate in more than one spot. In patients with monoclonal heavy chain disease, only fragments of monoclonal heavy chains are synthesized and released into the circulation by malignant lymphoplasmocytic cells. Such fragments are identified with immunofixation electrophoresis as proteins bands that only bind specific anti-heavy chain antibodies, but not specific anti- κ or anti- λ light chain antibodies (Figure 3).

However, the abnormal characteristics of such monoclonal heavy chains are best studied using 2D-PAGE of protein-G purified fractions, as demonstrated in Figure 4. A set of spots (γ') is observed at the basic side of the gel, in an area corresponding to pI from 5.8 to 6.8, and M_r of 32 to 38 kDa. Spots corresponding to polyclonal IgG γ chains and polyclonal immunoglobulin light κ and λ chains are also identified. No spot corresponding to a monoclonal immunoglobulin light chain is observed. The 32 to 38 kDa M_r of the monoclonal γ' chain indicates that it is a fragment of a normal γ chain, and the microheterogeneities of the pI suggest that it is glycosylated. Finally, the binding of the molecule to protein G implies that the Fc region of the immunoglobulin is intact. In contrast to what was seen in the serum of another patient presenting the same disease, abnormal monoclonal γ chains of higher M_r are not observed.

Cold Agglutinins and Cryoglobulins

Cold agglutinins (CAs) are immunoglobulins, most frequently IgM, that agglutinate erythrocytes at temperatures below 37°C. Immunohaemolytic anaemia related to CAs can be observed in a wide variety of diseases (Figure 5).

Monoclonal CAs, generally belonging to the IgM isotype, are observed in patients with lymphopro-

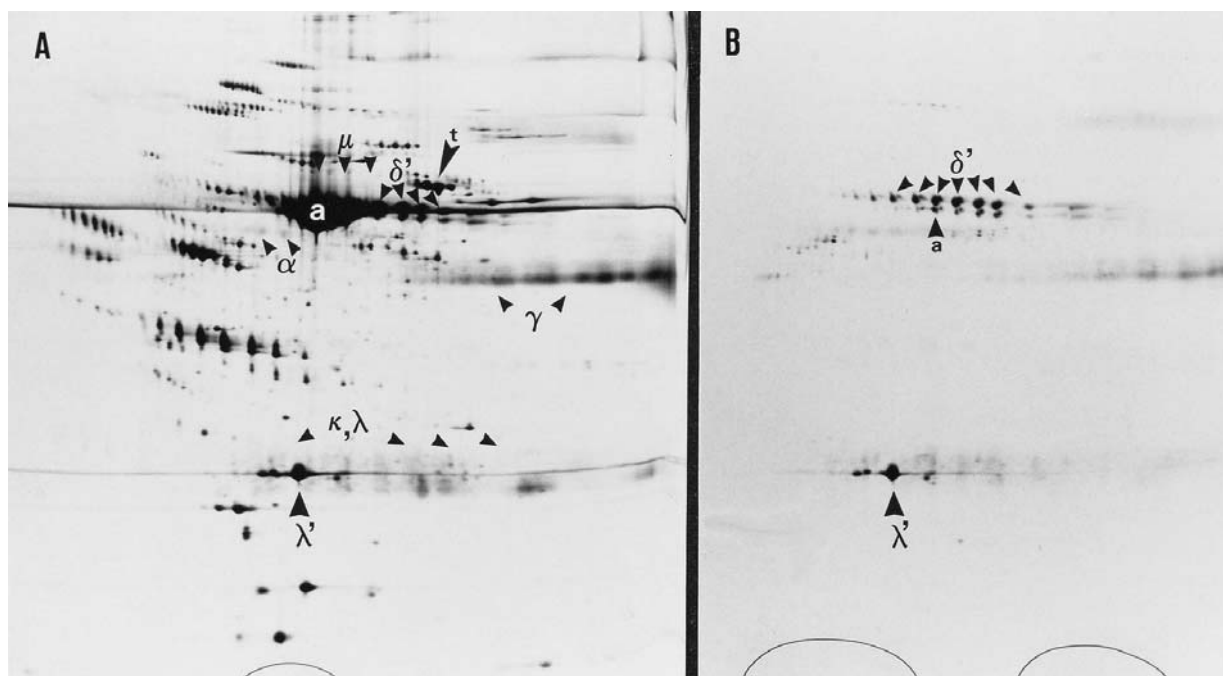


Figure 2 High-resolution two-dimensional polyacrylamide gel electrophoresis in a case of monoclonal IgD- λ . (A) Serum and (B) purified IgD (anti- λ Sepharose). a, albumin; μ , polyclonal heavy chains of IgM; α , polyclonal heavy chains of IgA; γ , polyclonal heavy chains of IgG; κ, λ , polyclonal immunoglobulin light chains; δ' , monoclonal δ -chain monoclonal; λ' , monoclonal λ chain; t, transferrin. The gels were silver stained, and presented with the higher molecular weights at the top, and the acidic side on the left. (Reproduced from Tissot JD, Schneider P, Hohlfield P *et al.* (1993) Two-dimensional electrophoresis as an aid in the analysis of the clonality of immunoglobulins. *Electrophoresis* 14: 1366, with permission from Wiley-VCH, Weinheim.)

liferative disorders or suffering from the 'idiopathic' chronic cold agglutinin disease, whereas polyclonal CAs, also belonging to the IgM isotype, may be found in patients with various infectious diseases, but more particularly in patients with Epstein-Barr virus or *Mycoplasma pneumoniae* infection. The evaluation of the clonality of CAs, that are frequently at very low

concentrations in serum, can be easily performed using 2D-PAGE. CAs are isolated from serum by cold absorption of immunoglobulins on red blood cells. After several cold washes, red blood cells coated with CAs are rewarmed to 37°C. After centrifugation, the supernatant is collected and studied with 2D-PAGE. As mentioned in the previous section, polyclonal IgM are quite easily differentiated from monoclonal IgM according to their different electrophoretic patterns (Figure 6).

Cryoproteins are defined as proteins precipitating at low temperature. Most frequently, the precipitate contains immunoglobulins, and are therefore called cryoglobulins. Three types of cryoglobulins have been described: type I contains a single monoclonal immunoglobulin, whereas type II is a mixture of a monoclonal immunoglobulin with polyclonal immunoglobulins, and type III is a mixture of polyclonal immunoglobulins of different isotypes, most frequently IgG and IgM (Figure 7). Type II and type III are also called mixed cryoglobulins. A new type II-III class of cryoglobulins, containing polyclonal IgG associated with a mixture of polyclonal and monoclonal IgM has been recently described through 2D-PAGE. In a series of 265 cryoglobulins studied with 2D-PAGE, we identified type I, II, II-III, and III in 3.4%, 26, 22.6 and 43.8% of the cases, respectively.

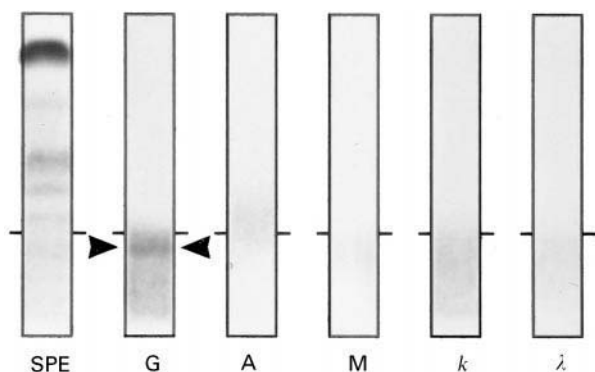


Figure 3 Immunofixation electrophoresis in a case of γ -chain disease. A serum sample from a 56-year-old patient was analysed by immunofixation electrophoresis. A protein band (arrowheads) was shown to react with anti-human immunoglobulin chain antiserum, but not with anti-human κ or λ light-chain antibodies. SPE, serum, protein electrophoresis; G, A, M, κ , λ , immunodetection of protein bands with corresponding antisera.

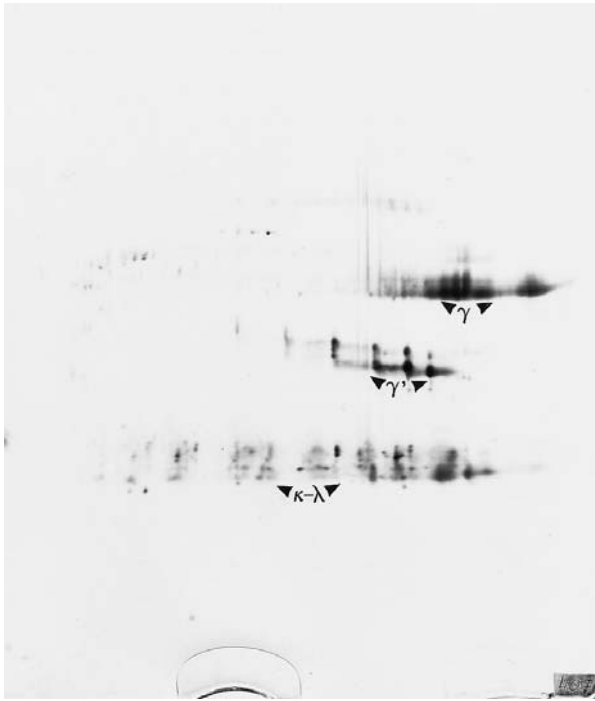


Figure 4 High resolution two-dimensional polyacrylamide gel electrophoresis in a case of γ -chain disease. Protein G purified protein fraction from a 56-year-old patients presenting γ -chain disease was analysed using 2D-PAGE. γ , polyclonal heavy chains of IgG; γ' , spots corresponding to monoclonal γ chain fragments; κ - λ , polyclonal immunoglobulin light chains. The gel was silver stained, and presented with the higher molecular weights at the top, and the acidic side on the left.

They were composed of oligoclonal immunoglobulins mixed with traces of polyclonal IgG in 4.2% of the cryoglobulins studied. These cryoproteins were tentatively named type II-III_{variant} cryoglobulins.

Fetal Proteins

Gene expression and regulation are dependent on highly sophisticated mechanisms. The genome-related modifications of protein synthesis and expression are most evident during fetal development.

The development of a safe and easy technique for fetal blood sampling has greatly improved our know-

ledge of normal fetal physiology, including some aspects of protein biology. However, the amount of pure fetal blood which can be derived for research purposes from samples obtained for prenatal diagnosis is obviously limited. Thus, electrophoretic techniques that allow studies of plasma and serum proteins contained in minute samples (usually less than 1 μ L) must be applied. Many proteins detected in the plasma and serum of adults are already present in the blood of normal embryos at a very early stage of gestation. Not all proteins are produced by the conceptus but many are the result of transfer from the mother across the placenta. Some proteins remain at a fraction of their adult levels throughout intrauterine life, others are progressively produced in increasing amounts when term approaches, and finally, others are present in higher concentrations during fetal life than after delivery. Modifications of plasma and serum protein concentrations during early extrauterine life have been well documented. The plasma concentration of a given protein is governed not only by fetal synthesis and degradation, but also by the result of the exchange between mother and fetus through the placenta. Materno-fetal transfer of proteins involves several different mechanisms such as a first-order process or active transport. The concentration of each fetal plasma protein results of a balance between opposing dynamic metabolic and physiological processes which proceed simultaneously. The relative impact of these factors contributing to a plasma protein concentration continuously shifts during development, and not always in the same manner. 2D-PAGE is an ideal tool to study such a dynamic process. Fetal protein maps reveal spots which are always absent in those of adults. A readily evident set of spots, located at the acid side of albumin is found in such fetal samples and corresponds to α -fetoprotein (Figure 8). This protein is less apparent as gestational age increases. A second 'fetal' polypeptide, characterized by an apparent M_r of 46 kD and a pI of 5.0 is observed as a small spot, located under those of α_1 -antitrypsin. N-terminal microsequencing (25-EDPQ) and immunoblotting using specific anti- α_1 -antitrypsin antibodies reveal that this spot most likely

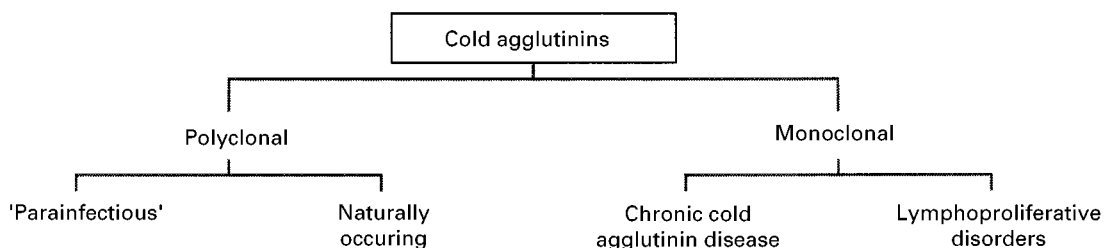


Figure 5 Classification of cold agglutinins.

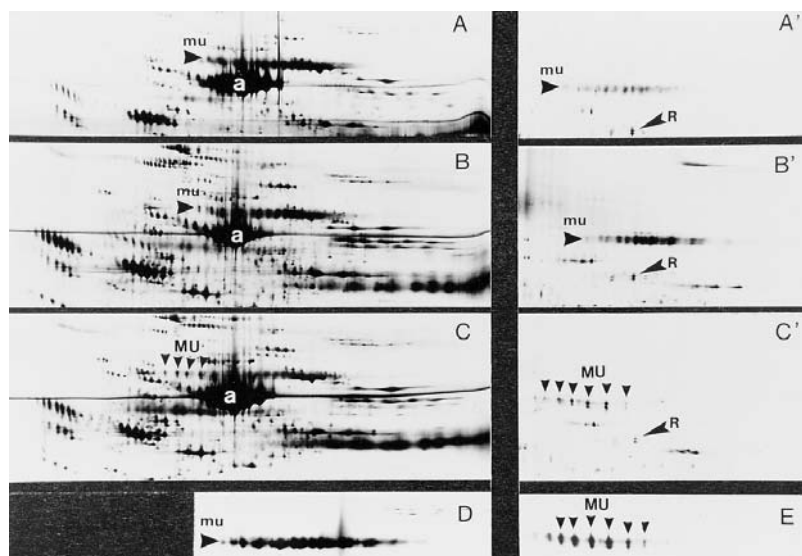


Figure 6 Characterization of cold agglutinins using high resolution two-dimensional polyacrylamide gel electrophoresis. Details of electrophoretograms of plasma/serum samples (A–C) and their purified cold agglutinins fractions (A'–C'). Purified polyclonal (D) and monoclonal (E) IgM heavy chains are shown as controls. A–A', serum and purified CAs from a patient with chronic virus C hepatitis; B–B', plasma and purified CAs from a patient with *Mycoplasma pneumoniae* infection; C–C', plasma and purified CA from a patient with chronic cold agglutinin disease. a, albumin; R, reference protein used to highlight the relatively acidic pI of the monoclonal μ -chain found in patient C; μ , polyclonal μ chain; MU, monoclonal μ chains. The charge microheterogeneity of monoclonal μ chains is highlighted by arrowheads. The gels were silver stained, and presented with the higher molecular weights at the top, and the acidic side on the left. (Reproduced from Tissot JD and Spertini F (1995) Analysis of immunoglobulin by two-dimensional gel electrophoresis. *Journal of Chromatography A* 698: 225–250, with permission from Elsevier Science.)

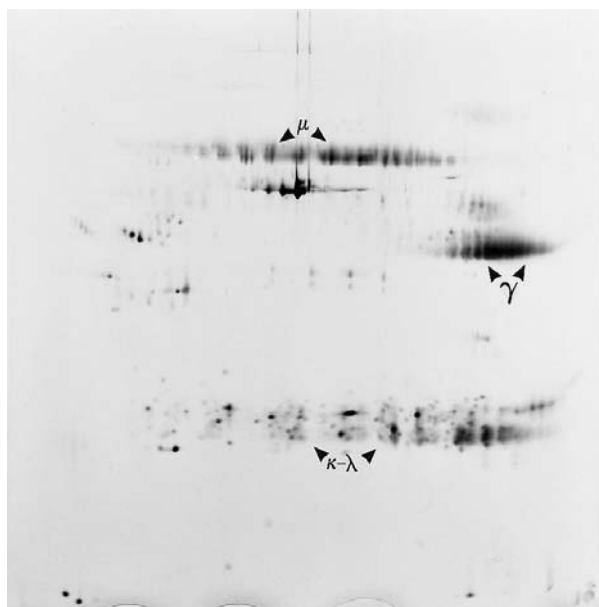


Figure 7 High-resolution two-dimensional polyacrylamide gel electrophoresis of mixed type III cryoglobulins. The cryoprecipitate is characterized by the presence of a mixture of polyclonal IgM and polyclonal IgG. μ , polyclonal IgM μ chains; γ , polyclonal IgG γ chains; κ - λ , immunoglobulin light chains. The gel was silver stained, and presented with the higher molecular weights at the top, and the acidic side on the left.

corresponds to a fetal-specific form of α_1 -antitrypsin, already identified in mouse plasma. This polypeptide is observed in all fetal samples and in all samples obtained from infants of under two years of age but is either undetectable or appears as a shaded spot in adults.

Genetic polymorphism of some serum proteins such as Gc-globulin, Apo A-IV, or Apo E (Figure 9) can be also studied using 2D-PAGE. As shown in Table 1, the technique allows determination of the frequency of the Apo-E phenotypes, as well as the calculation of the gene frequencies.

During fetal development, 2D-PAGE reveals a progressively more and more complex protein pattern and an increase in the size of many spots. Three major protein pattern modifications are observed on 2D gels of fetuses at different gestational ages: (a) the progressive appearance of the protease inhibitor α_1 -antichymotrypsin; (b) the progressive increase of polyclonal IgG, which is particularly evident during the last weeks of pregnancy; (c) the gradual diminution of α -fetoprotein which is undetectable on protein maps of term newborns. On the other hand, before the 38th week of gestation, polyclonal IgA or IgM heavy chains, as well as the two main proteins involved in free haemoglobin transport and catabolism — haptoglobin and hemopexin — are not detectable.

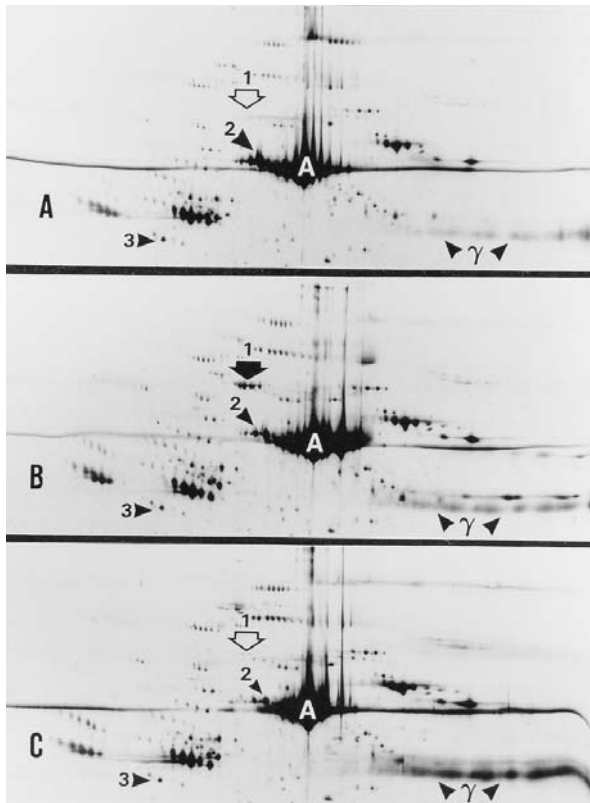


Figure 8 Fetal proteins. Details of electrophoretograms of plasma samples obtained from fetuses at 22 (A), 28 (B), and 32 weeks (C) of gestation. A, albumin; γ , immunoglobulin gamma chains; 1, dimers of fibrin (γ chains), only observed when small clots were present in the sample; 2, α -fetoprotein; 3, fetal form of α_1 -antitrypsin. The gel was silver stained, and presented with the higher molecular weights at the top, and the acidic side on the left.

Carbohydrate-deficient Glycoprotein Syndrome (CGDS)

Carbohydrate-deficient glycoprotein syndrome (CDGS) is a group of autosomal recessive disorders affecting multiple organ systems. All of the affected patients present moderate or severe brain disorders. In the first years of life, CDGS is characterized by hypotonia with failure to thrive, dysmorphism and coagulation abnormalities. These clinical manifestations are the direct embryologic and physiological consequences of an underglycosylation of protein. The alterations are related to a reduced number of entire *N*-glycans on glycoproteins and they have been described for serum transferrin, α_1 -antitrypsin, α_1 -acid glycoprotein, α_1 -antichymotrypsin, fetuin, ceruloplasmin and antithrombin III, C3a and C4a. In patients with CDGS type 1a and type 1b, the post-translational defect is due either to a deficiency of phosphomannomutase or a deficiency of phos-

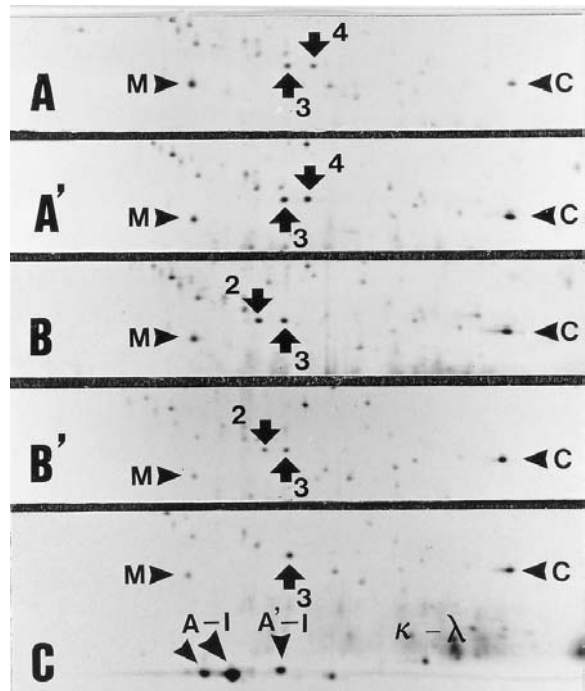


Figure 9 Genetic polymorphism of apolipoprotein E in fetuses. Phenotype E3/4 (A, fetus at the age of 22 weeks, A' fetus at the age of 30 weeks), phenotype E2/3 (B, fetus at the age of 22 weeks, B' fetus at the age of 30 weeks), phenotype E3/3 (C, fetus at the age of 22 weeks). M, α_1 -microglobulin; C, γ chain of complement factor C4; A-I, apolipoprotein A-I, A'-I, pre-apolipoprotein A-I; κ and λ , immunoglobulin light chains. The gel were silver stained, and presented with the higher weights at the top, and the acidic side on the left.

phomannose isomerase. Both these defects alter the metabolism of mannose in cells and result in a decrease of GDP-mannose for *N*-glycan synthesis. The diagnosis is usually made by isoelectric focusing of serum transferrin showing a different pattern of cathodal shift due to the loss of terminal sialic acids. Another way of diagnosis is to separate the transferrin isoforms lacking their *N*-glycans by using SDS-PAGE. Other more complex diagnostic methods have been

Table 1 Distribution of ApoE in fetuses and adults determined by 2D-PAGE

Phenotypes	Fetuses	Adults	Total ^a	Expected ^b
E2/2	0	2	2	1
E2/3	10	21	31	31
E2/4	1	1	2	4
E3/3	76	152	228	225
E3/4	18	32	50	57
E4/4	2	6	8	4
Total	107	214	321	322

^aAllele frequencies: Apo E*2: 0.058, Apo E*3: 0.836, Apo E*4: 0.106.

^bHardy-Weinberg equilibrium.

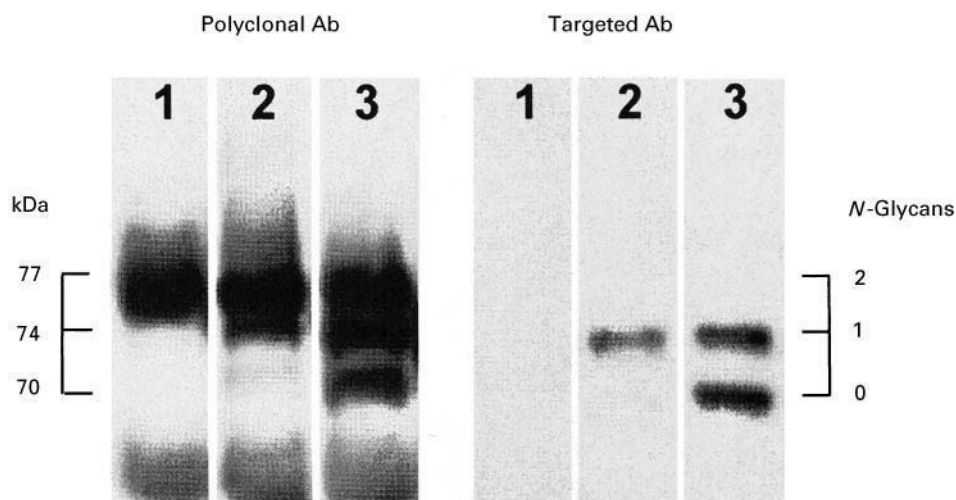


Figure 10 Comparison of the specificity of antibodies raised against transferrin. Transferrin isoforms identified by antibodies directed against multiple epitopes (polyclonal Ab) and transferrin isoforms that presented the *N*-432 transferrin epitope recognized by a targeted antibody (targeted Ab). Lane 1, normal serum control; lane 2, serum from a patient with alcoholism; lane 3, serum from a patient with type 1 carbohydrate-deficient glycoprotein syndrome (CDGS).

reported such as 2D-PAGE and matrix-assisted laser desorption ionization–time of flight (MALDI–TOF) mass spectrometry of serum transferrin.

We have described the characterization of a new antibody which is specifically directed against the *N*-glycan binding site localized on the asparagine-432 of transferrin and which allows immunodetection of transferrin devoid of *N*-glycan (Figure 10). This antibody has the potential to provide a new immunochemical tool for the CDGS diagnostic.

Conclusion

Numerous diseases can be diagnosed using electrophoretic analyses of body fluid proteins. However, many different electrophoretic techniques are available. Electrophoresis on cellulose acetate is employed to study many different enzymes such as serum amylase, pancreatic isolipase, and pyruvate kinase. Agarose gel electrophoresis is extensively used to gain insight into the understanding of lipoprotein biology. Isotachopheresis or ‘displacement’ electrophoresis allows the simultaneous concentration and effective separation of different charged substances, including biological macromolecules. Affinity electrophoresis is used to evaluate cross-reactivity of antihapten antibodies whereas lectin affinity electrophoresis is best used to characterize serum glycoproteins. Capillary electrophoresis offers the possibility of rapid and automated analysis of different kinds of molecules, with high reproducibility and improved quantification. Isoelectric focusing as well as SDS-PAGE are cornerstone techniques used to characterize polypeptides.

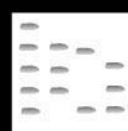
2D-PAGE is increasingly used as an important tool for biological research. However, despite the fact that these techniques are particularly useful for studying a clinical problem, routine clinical analysis is frequently incompatible with the use of such sophisticated techniques. As illustrated by several examples presented in this article, 2D-PAGE can be chosen as a complementary technique to gain insight into several specific clinical problems. The combination of different electrophoretic techniques can be very useful to resolve complex problems.

Further Reading

- Henry H, Tissot JD, Messerli B *et al.* (1997) Microheterogeneity of serum glycoproteins and their liver precursors in patients with carbohydrate-deficient glycoprotein syndrome type I: apparent deficiencies in apolipoprotein J and serum amyloid P. *Journal of Laboratory and Clinical Medicine* 129: 412–421.
- Keren DF (1999) Procedures for the evaluation of monoclonal immunoglobulins. *Archives of Pathology and Laboratory Medicine* 123: 126–132.
- Krasnewich D and Gahl WA (1997) Carbohydrate-deficient glycoprotein syndrome. *Advances in Pediatrics* 44: 109–140.
- Levinson SS and Keren DF (1994) Free light chains of immunoglobulins: clinical laboratory analysis. *Clinical Chemistry* 40: 1869–1878.
- Marshall T and Williams KM (1998) Clinical analysis of human urinary proteins using high resolution electrophoretic methods. *Electrophoresis* 19: 1752–1770.
- Nathoo SA and Finlay TA (1987) Fetal-specific forms of alpha 1-protease inhibitors in mouse plasma. *Pediatric Research* 22: 1–5.

- Tissot JD, Hohlfield P, Forestier F *et al.* (1993) Plasma/serum protein patterns in human fetuses and infants: a study by high-resolution two-dimensional polyacrylamide gel electrophoresis. *Applied and Theoretical Electrophoresis* 3: 183–190.
- Tissot JD and Spertini F (1995) Analysis of immunoglobulins by two-dimensional gel electrophoresis. *Journal of Chromatography A* 698: 225–250.
- Tissot JD, Invernizzi F, Schifferli J, Spertini F and Schneider P (1999) Two-dimensional electrophoretic analysis of cryoproteins: a report of 335 samples. *Electrophoresis* 20: 606–613.
- Young DS and Tracy RP (1995) Clinical applications of two-dimensional electrophoresis. *Journal of Chromatography A* 698: 163–179.

CLINICAL CHEMISTRY: THIN-LAYER (PLANAR) CHROMATOGRAPHY



J. Bładek, Military University of Technology,
Warsaw, Poland
A. Zdrojewski, Institute of Chemistry, Warsaw,
Poland

Copyright © 2000 Academic Press

Introduction

Clinical medicine is mainly based on the results of chemical analysis and these results are very important. It is estimated that more than 50% of diagnoses are based on laboratory data. The analyses are usually done using immunoassays, chromatographic and spectroscopic methods. The combined techniques, e.g. liquid chromatography–mass spectrometry (LC/MS) gas chromatography–tandem mass spectrometry (GC-MS-MS) are also applied. The development of sophisticated methods of analyses reduced interest in simple and rapid methods such as thin-layer chromatography (TLC). Starting from paper chromatography and improved over the years, TLC has become very useful also for clinical medicine. TLC has been used to solve analytical, and sometimes preparative, problems.

A large number of publications on the use of TLC for clinical medicine analysis can be found in the literature. An excellent compilation concerning different applications of analytical methods (including TLC) for isolation and identification of drugs in pharmaceutical, body fluids and post-mortem materials is the book edited by Moffat. This work, prepared in the Department of Pharmaceutical Sciences of the Pharmaceutical Society of Great Britain, is a comprehensive and clear account of clinical analytical chemistry up to 1986. An excellent supplement, covering the early 1990s, is the monograph of Jain. More recent works more commonly refer to applications of instrumental TLC.

General Principles of Clinical Medicine Analyses by TLC

TLC is a most economical and cost-effective technique and ideally suited for performing clinical analyses of biological samples, where the sample load is high. The method is characterized by high selectivity, enabling separation of the analyte from interfering substances. At least two basic groups of applications of TLC in clinical medicine analysis can be distinguished. The most important of them are where TLC has been applied for analytical and screening purposes where qualitative or semi-quantitative results are required. The second group concerns work, where TLC performs the function of a clean-up technique for initial sample preparation.

Clinical analysis presents a difficult analytical problem. The proteins, lipids, or carbohydrates, usually present in biological samples, may interfere with analytes. Analyses are also made difficult by the fact that many substances of interest are only slightly soluble in organic solvents.

Sample Preparation

There is a generally accepted view in laboratory practice, that the TLC stage of sample preparation is of little importance because it is merely a clean-up technique. This is incorrect, especially in the case of clinical medicine analysis where analytes are to be found in complex matrices such as plasma, serum or urine, whole blood, faeces, saliva, cerebrospinal fluid, gastric fluid or body tissues. These matrices are very complex multicomponent mixtures and therefore sample preparation prior to analysis cannot be omitted.

The process of separation from biological samples and purification of analytes is usually realized by protein precipitation, dialysis, hydrolysis, ultrafiltration, dilution, liquid–liquid or solid-phase extraction. Originally, the most common extraction method was

liquid-liquid extraction but in recent years solid-phase extraction has become an increasingly popular method for isolation of compounds from biological matrices. Lyophilization, saponification, microwave processing and supercritical fluid extraction are used less commonly.

Chromatogram Development Techniques

Chromatographic separation of clinical samples is carried out mainly in normal phase systems. High performance silica gel, aluminium oxide, polyamide and amino-bonded silica gel are commonly used as stationary phases for the separation of basic and acidic drugs and other polar substances such as amino acids. It is better to separate neutral drugs and other nonpolar compounds in reversed-phase (RP) systems. The commonest stationary phases for RP systems are silica gel with chemically bonded octyl and octadecyl groups. Numerous solvent systems consisting of mixtures of organic solvents such as hexane, methanol, chloroform, ethyl acetate or mixtures of polar solvents with water, organic acids or ammonia have been used. It is sometimes advantageous to introduce modifying agents to the mobile phase to improve selectivity.

One-dimensional ascending or horizontal techniques have usually been applied for the development of chromatograms in a closed chamber. For clinical medicine needs, there are standard TLC kits (Toxi-Prep type and Toxi-Lab). These are commercially available and have been used above all for extraction, concentration and analysis of the acidic, basic, and neutral drugs. Recently, multiple gradient development (AMD), two-dimensional techniques and over-pressure layer chromatography have been more often applied to the analyses listed in Table 1.

Visualization and Quantification

Identification of analytes is achieved by co-chromatography of reference standards with the unknown and comparison of R_F values. TLC retention indices are less reliable than for other chromatographic methods so that additional information from individual spots is needed. Post-chromatographic derivatization is the basic method of visualization especially when there exists a specific reaction that can confirm the presence of particular analytes in the spot or band. Physical methods such as fluorescence under ultraviolet light are also often applied. The possibility of confirmation of identity based on at least two criteria is the essential advantage of TLC. The colorimetric reactions of drugs, narcotics, and other substances of clinical interest with different visualiza-

tion reagents are listed in Table 2. Identification can also be made using spectroscopic techniques such as TLC/FABMS or FABMS-MS (fast atom bombardment mass spectrometry or tandem mass spectrometry).

Densitometric measurement of the *in situ* fluorescence or absorbance provides information about the quantity of an analyte in a chromatographic band. Such measurements are suitable for the quantification of drugs such as chlorpromazine, tricyclic antidepressant and anticonvulsant in blood serum and plasma. Quantitative analyses are also performed by combination of TLC with other analytical techniques, e.g. UV-densitometry.

Applications

In a view of the complexity of clinical analysis, it is not possible to cover all applications extensively. Therefore, only the most important applications of TLC in clinical medicine analyses are presented. The criteria of aims of analysis are: (1) the diagnosis and treatment of hard intoxication, (2) screening research, (3) monitoring of therapeutic drugs concentration, and (4) evaluation of the efficiency of new methods of therapy. In such applications, the drugs and their metabolites, carbohydrates, amino acids, bile acids, lipids, porphyrins and other compounds of clinical interest are analysed. The results of such work are collected in libraries (databases) that significantly facilitate diagnosis and therapy.

The Diagnosis and Hard Intoxication Treatment

The term hard intoxication is applied to the determination of harmful effects, arising in a short time after introducing a large dose of poison to the body. These effects are mainly observed after drugs or alcohol overdose or the introduction of organic solvents, pesticides, etc., into body. The symptoms of intoxication can be similar to those caused by disease so that diagnosis based only on clinic symptoms is insufficient; in such situations analytical data are very important. Only laboratory results, can determine the type and concentration of poison in a biological material or a functional disorder caused by overdose intoxication or poisoning. The biological samples, where poisons and/or their metabolites are found are mainly blood or urine. The most important features of such analyses are the necessity to determine the type of poison as quickly as possible. The basic requirement (especially in analysis followed by diagnosis) is for information about the poison, from simple, rapid and reliable qualitative or semiquantitative methods. The common use of TLC in clinical medicine analyses of hard intoxication is due to its ability to provide such data.

Table 1 The applications of thin-layer chromatography (TLC) in clinical medicine research. The representative examples of separations

No.	Matrix and analyte		Chromatographic system		Type of development
	Analyte	Body fluid	Stationary phase	Mobile phase	
1	Theophylline	Serum	Aminopropylsiloxane modified silica	Ethanol–5% aqueous diethylamine solution (95 : 5)	One-dimensional, isocratic
2	Tetrahydrocannabinol (THC) metabolites	Urine	HPTLC silica gel	SPE elution solution: ethyl acetate–concentrated ammonium hydroxide (98 : 2) Developing solution: heptane–ethyl acetate–glacial acetic acid (7 : 3 : 10)	Toxi-Prep system: incorporate SPE with direct spotting onto TLC plate, one-dimensional, isocratic elution
3	Bile acid	Bile	Silica gel	Chloroform–methanol–acetic acid (85 : 20 : 9)	One-dimensional, isocratic
4	Porphyrins	Urine, faeces	RP-HPTLC (C-18 bonded wettable phase)	Acetonitrile–ion-pair reagent (IPR)–acetate buffer pH4.1 (9 : 5 : 5) IPR = <i>N</i> -cetyl- <i>N,N,N</i> -trimethylammonium bromide	One-dimensional, isocratic
5	Amino acids	Urine	Cellulose	(I) Pyridine–acetone–aqueous ammonium hydroxide–water (13 : 8.5 : 2.5 : 6) (II) Isopropanol–formic acid–water (25 : 3 : 2)	Two-dimensional, isocratic
6	Amphetamine derivatives	Urine	Aminopropylsiloxane modified silica	(I) Ethanol–triethylamine–hexane (15 : 9 : 76) (II) Acetone–triethylamine–hexane (23 : 9 : 68)	Two-dimensional, isocratic
7	Lipids	Sebaceous gland	Silica gel with concentrating zone	Hexane–diethyl ether–acetic acid (80 : 20 : 1)	One-dimensional, isocratic
8	Prostaglandins	Serum	HPTLC silica gel	Ethyl acetate–diethyl ether–benzene–dioxane–hexane (45 : 12 : 5 : 8 : 30)	OPLC one-dimensional
9	Amino acid derivatives	Urine	Silica gel	Chloroform–methanol–ethyl acetate–acetic acid	AMD gradient elution
10	Barbiturate derivatives	Serum, urine	HPTLC silica gel	(I) Ethyl acetate–ethanol–hexane (2.5 : 2.5 : 95) (II) Pyridine–hexane (2 : 8)	OPLC two-dimensional
11	Tetrahydrocannabinol (THC)	Urine	HPTLC I-silica gel WRFs II-silica gel F	(I) Dichloromethane–hexane–methanol (7 : 2 : 1) (II) Dichloromethane–hexane–methanol (7 : 1 : 2)	One-dimensional, isocratic
12	Ecdysteroids	Plasma	RP-TLC (C-2, C-8, C-12, C-18, aminopropyl, cyanopropyl bonded phases)	Methanol–water (9 : 1)	One-dimensional, isocratic

The majority of this work is aimed at the determination of analytical parameters of xenobiotics and/or their metabolites. In diagnostic tests using

TLC, identification is based mainly on comparison of R_F values and on visualization with specific colour reactions. Tests for the identification of alkaloids,

Table 2 Examples of visualization and quantification

Analyte	Visualization method	Quantification	
		Yes	No
Amino acids			
Common protein amino acids	3-Phenyl-2-thiohydantoin (PTH) derivative, 270 nm absorption		X
Urinary amino acids (incl. proline and hydroxyproline)	Ninhydrin, isatin, isatin- <i>p</i> -dimethylaminobenzaldehyde		X
Bile acids	Manganese dichloride in a mixture of water, methanol and sulfuric acid and fluorescent measurement		X
Cholesterol and its esters	Aniline blue, bromophenol blue, helasol green and alkaline blue	X	
Drugs			
Antibiotics			
Doxycycline, oxytetracycline and tetracycline	Fluorescent measurement, 365 nm /> 440 nm	X	
Aminoglycoside streptomycin and neomycin	Dansylation and fluorescent measurement	X	
Baclofen	Dansylation and fluorescent measurement,	X	
Barbiturates	Mercuric chloride-diphenylcarbazone reagent; fluorescein solution; mercurous nitrate spray		X
Benzodiazepines	UV radiation 254/366 nm, dipped in concentrated sulfuric acid and observed under UV (366 nm); diazotization and coupling with 1-naphthol	X	
	or Bratton–Marshall reagent and next fluorescent measurement	X	
β -Blocking drugs			
Atenolol, celiprolol, metoprolol, propafenone, propranolol and talinolol	Brilliant Blue B, UV light absorption (254 nm)	X	
Halofantrine	UV light absorption (256 nm)	X	
Nonsteroidal anti-inflammatory drugs (e.g. ketoprofen, piroxicam, diclofenac, ibuprofen, paracetamol)	UV light absorption (254 nm)		X
Narcotics			
Amphetamine metabolites	UV light absorption (278, 283 nm) and by fluorescence after derivatization with fluorescamine 365 nm/ > 440 nm	X	
Heroin (diacetylmorphine)	HgCl ₂ –K ₃ Fe(CN) ₆ and light absorption (580 nm)		X
Δ^9 -Tetrahydrocannabinol (THC)	UV light absorption (210 nm)	X	
Tricyclic antidepressive drugs	Amelinka's reagent or tested by UV irradiation	X	
Fluoxetine, imipramine, doxepine, opipramol			
Phospholipids	Iodine vapour		X
Free porphyrins	Fluorescent measurement	X	
Prostaglandins	α -Bromo-2'-acetonaphthone (BAN) and fluorescent measurement	X	

barbituric acid derivatives, benzodiazepine derivatives and other drugs from other pharmacological groups have been known for many years.

Mathematical methods have recently been applied in the diagnosis of hard intoxication. The first step of these methods is to evaluate the R_F values in two, three and sometimes four chromatographic systems. These systems must be carefully selected to ensure an appropriate distribution of R_F values across the plates, the reproducibility of the measurement of these parameters and the correlation of chromatographic properties between systems. Next, the sets of correlated R_F values are determined (experimentally determined R_F values are converted into correlated

R_F values by a graphical standardization procedure) in a possibly large group of substances. In case of clinical analyses there are usually hundreds of drugs and their metabolites. A mathematical function (e.g. 'discriminating power' or 'principal component analysis') for calculation of analytical data is then chosen. The data set obtained allows for relatively rapid identification of investigated (unknown) xenobiotics. A full description of the application of such methods can be found in the work by de Zeeuw *et al.*

TLC as a Screening Method

Screening methods reduce the cost and time of analysis of numerous groups of samples. In clinical

medicine analysis, this term is referred to a set of biological samples (laboratory screening methods) or to a set of individuals endangered by contact with harmful substances (metabolic screening). In both cases, the aim of analysis is the exclusion of a particular sample (for an individual) from the set of samples (individuals), which should be examined with great care. Application of TLC to such aims is attractive as this technique enables simultaneous analysis of several samples.

Laboratory screening methods are similar to diagnostic analyses, but the object of investigation is usually known. During the screening other properties such as changes in the body under xenobiotics influence, e.g. changes in enzyme activity, creation of methemoglobine, increased porphyrin expulsion, etc. are measured. Because drugs or their metabolites are excreted and concentrated in urine, this is the matrix most commonly used for such examination. Especially useful for screening investigations are kits such as the Toxi-Prep (TP) kit, proposed by Steinberg and coworkers which can simultaneously extract up to

seven specimens. The method is based on TLC and involves five major steps: solid phase extraction, concentration, spotting, development of chromatograms and detection.

The kits have been found to be particularly useful for analysis of basic and neutral drugs. The comparison of the usability of three kits (TL-A, TL and TP) in the monitoring of basic drugs is presented in Table 3.

Another example of screening methods is the detection of an unknown, potentially toxic xenobiotic in the presence of a number of endogenous substances. Such defined screening methods are focused on limiting the number of expensive methods of analyses.

Metabolic screening is based on observation of changes in biochemical profile of patients within a relatively short time. The commonest analyses are for cholesterol and lipids or amino acids and porphyrins. An example of such an application of TLC is the work of Lai *et al.* They proposed a simple test for the determination of porphyrins (porphyrins play a crucial role in the biological processes of haem synthesis; in the case of defects in the biosynthetic

Table 3 Overall urine basic drug analysis^a

Drug	Occurrences on		
	Both TP and TL	TP only	TL-A only
Amitypyline and metabolites	5	4	2
Caffeine		0(1)	
Cimetidine		1(1)	
Clindamycin and metabolites	2		4
Codeine		1	
Cyclobenzaprine		1	
Desipramine and metabolites	1	1	
Diphenhydramine	5(3)	1(7)	
Doxepin		1	
High migrator	13	3	5(3 = cocaine; 2 = lidocaine)
Imipramine	1		
Low migrator		0(1)	
Meperidine and metabolites		1(1)	1
Methadone and metabolites	16(1)		5
Metoprolol			1
Morphine	0(1)	0(2)	6
Nicotine and metabolites	17	2	34
Nortriptyline and metabolites	16	10(2)	2
Oxycodone		1	
Phenothiazine	3		1
Quinidine/quinine	46	8(5)	
Ranitidine	2		
Sympathomimetic amines	2(2)	0(1)	
Trazodone metabolites	2(1)		
Verapamil	2	2	
Unidentified substance		1	3
Totals	141	59	64
(33 distinct drugs)	[133(8)] ^b	[38(21)] ^b	[64] ^b

^aReprinted from Steinberg DM *et al.* (1997) *Clinical Chemistry* 43(11): 2099–2105, with permission from the American Association of Clinical Chemistry.

^bNumber of times definitively identified (questionable identifications).

pathway of haem an increase of porphyrin excreted is observed). Numerous groups of people are occupationally exposed to the substances causing porphyrias, and these have to be periodically screened. The urinary porphyrin-free acids are separated on a RP-HPTLC plate coated with C_{18} bonded silica gel. The mobile phase is buffered (pH 4.1) with a ternary mixture (acetonitrile, ammonium acetate buffer, ion-pairing reagent). Porphyrins, separated by TLC, create spots with a characteristic profile (fingerprints), and these profiles (differing in the quantity of excreted porphyrins) are observed in porphyria (Figure 1). By observing chromatograms in UV light, the basic criteria of metabolic screening can be fulfilled.

TLC has the advantage over other methods in that it can screen for many drugs simultaneously, with a relatively high sensitivity, and can handle several samples per plate.

Drug Concentration Monitoring

The pharmacological action of many drugs depends not on the amount taken but on the concentration in the blood. Relations between these two values (dose and therapeutic concentration) depend on the drug and often have individual characteristics. It was found that after taking the same dose of phenytoin (drug in anticonvulsants) its concentration in patients blood differed more than twentyfold. Therefore, one of the tasks of clinical medicine analyses is to establish relationships between the concentration of the drug in blood and its dosage. Such analyses are called drug concentration monitoring. They are performed mainly on the dosage of drugs of little therapeutic value, combined therapy, etc. Drug concentration monitoring requires use of relatively simple, cheap

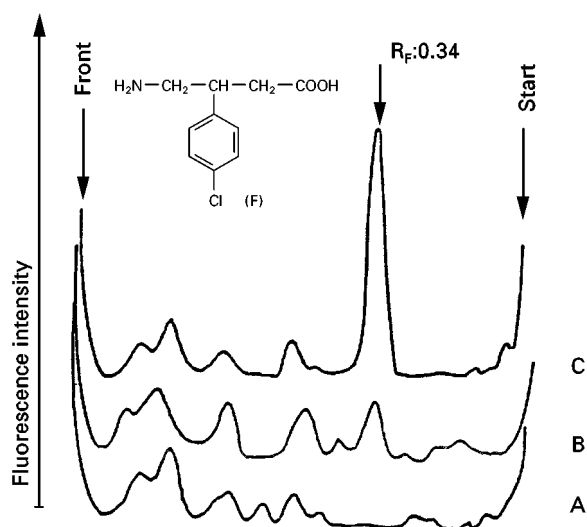


Figure 2 Representative TLC chromatograms of (A) a blank plasma sample, (B) derivatization product of baclofen after extraction from volunteer plasma ($70 \text{ ng baclofen mL}^{-1}$), (C) derivatization product of the fluoro analogue after extraction from volunteer plasma ($320 \text{ ng of the fluoro analogue mL}^{-1}$). Reprinted from Krauss D, Spahn H and Mutschler E (1988) *Arzneimittel Forschung Research* 38(II)(10): 1533–1536, with permission.

and rapid methods, which indicates the special suitability of TLC for such analysis. Drug concentration monitoring requires (in contrast to diagnostic and screening methods) quantitative analysis.

A good example of the application of TLC for drug concentration monitoring is the work by Krauss *et al.* on baclofen and its fluoro analogue (these are centrally acting muscle relaxants, which are used for the treatment of spastic disorders). Gas chromatography with electron-capture detection requires a time-

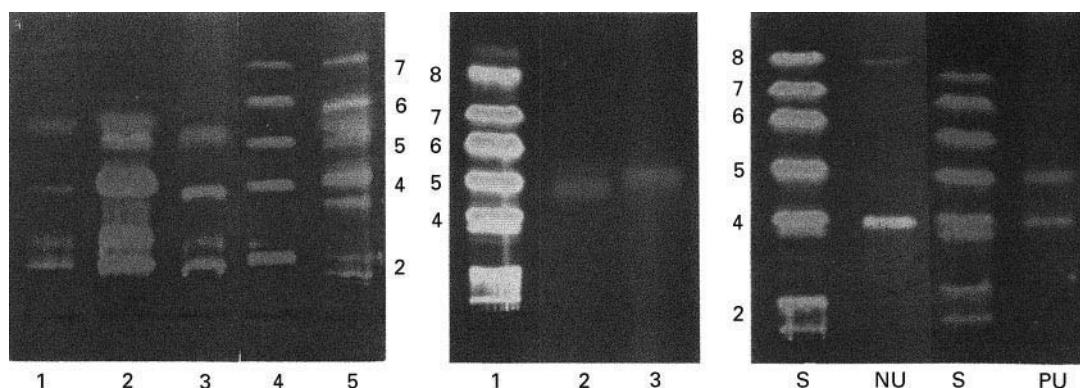


Figure 1 (See Colour Plate 69). RP-HPTLC chromatograms of fecal porphyrins of porphyria cutanea tarda (PCT) and variegate porphyria (VP) patients. Left panel: lane 1, VP feces of patient 1; lane 2, VP feces of patient 2; lane 3, external quality control sample of VP; lane 4, mixed calibrators of free porphyrins; lane 5, PCT feces; d, deuteroporphyrin. Middle panel: lane 1, mixed calibrators of free porphyrins; lane 2, i-urobilin standard; lane 3, stercobilin standard. Right panel: S, mixed calibrators of free porphyrins; NU, commercial urine control with a negative Urobilistix result; PU, urine obtained from a patient with hepatitis and a positive Urobilistix result; 8, uroporphyrin; 7, heptacarboxylic porphyrin; 6, hexacarboxylic porphyrin; 5, pentacarboxylic porphyrin; 4, coproporphyrin, 3, tricarboxylic porphyrin; 2, protoporphyrin. Reprinted from Lam C-W, Lai C-K and Chan Y-W (1998) *Clinical Chemistry* 44 (2): 345–346, with permission from the American Association of Clinical Chemistry.

consuming separation and derivatization step; HPLC does not require derivatization but the detection limit is insufficient for such studies. Several enantiospecific methods have also been developed but their applicability to biological material has not been shown. The method proposed by Krauss is based on fluorescent derivatization of the drug with benoxapropen chloride, TLC separation of the resulting amides and their quantification by direct measurement of the fluorescence. This method requires extensive purification of the samples (e.g. solid-phase extraction) in order to remove interfering endogenous amino acids. Chromatograms are obtained with a stationary phase of silica gel 60 without a fluorescence indicator (plates with concentrating zones) and a mobile phase of diisopropyl ether–2-propanol–tetrahydrofuran, 90 : 6 : 5, v/v. After development, both compounds

were separated from constituents of the biological material (Figure 2). The fluorescence intensity of the derivatization products is sufficient to determine plasma concentrations over a suitable period of time after single dose administration of both drugs. The detection limit (10 ng mL^{-1}), linearity (60 ng spot^{-1}) and method deviation have been estimated. The applicability of the method has been proved by investigating plasma (and urine) samples of two volunteers after oral administration of 20 mg baclofen as a single dose. Full suitability of the method for pharmacokinetic routine analyses was demonstrated.

Evaluation of the Efficiency of New Methods of Therapy

Evaluation of the efficiency of new methods of therapy mainly concerns drugs newly introduced into

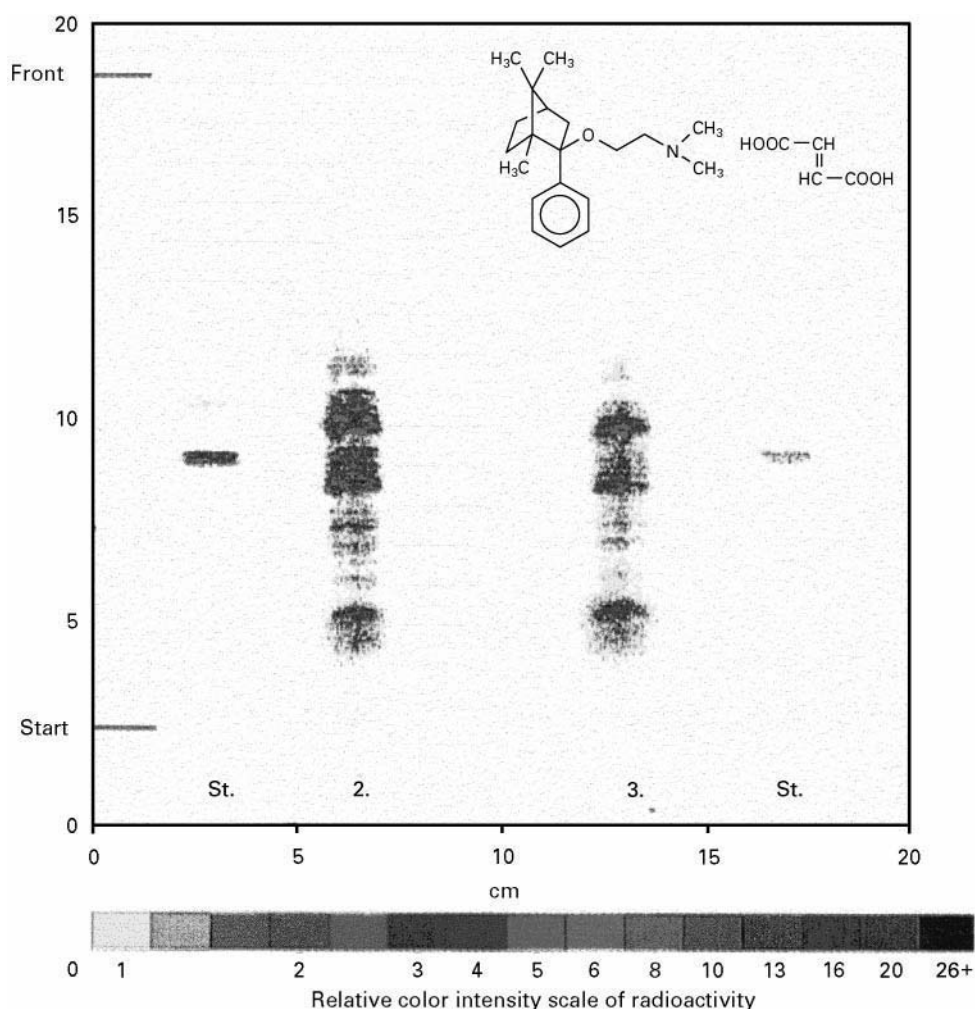


Figure 3 (See Colour Plate 70). OPLC–DAR profile of dog urine extracts. Sample, dog urine samples after 10 mg kg^{-1} oral dosing of ^{14}C -daramciclane. The first and fourth tracks are standards (St); tracks 2 and 3, 0–24-h and 24–48-h urine fractions, respectively. Single OPLC development eluent A; external pressure, 5.0 Mpa; flow rate, $250 \text{ } \mu\text{L min}^{-1}$, rapid volume, $250 \text{ } \mu\text{L}$; eluent volume, $4100 \text{ } \mu\text{L}$; time, 994 s; DAR run time, 60 min. Reprinted from Szűnyog J, Mincsovcics E, Hazai I and Klebovich I (1998) *Journal of Planar Chromatography-Modern TLC* 11 (1): 25–29, with permission.

clinical medicine. From an analytical point of view it is a more complicated process than drug concentration monitoring since the object of investigation is not only concentration of the drug in blood but also its assimilation and excretion, harmfulness, metabolism, etc. Such investigations are performed mainly on blood and urine samples.

An interesting example of abilities of TLC in the above applications is the work of Szűnyog *et al.* They applied a combination of overpressure-layer chromatography (OPLC) with the relatively high sensitive and rapidity of digital autoradiography (DAR). Biological samples were analysed after one- or two-dimensional separation. Using the example of deramciclane (a new anxiolytic compound) they demonstrated, that the proposed method could be successfully used for study of *in vivo* metabolism in different phases of studies. The main advantages of the method were the extremely rapid separation and purification by OPLC, the possibility of the quantitative evaluation of metabolites over a wide linear range, visual and numeric comparison of metabolite profiles in various biological matrices and cost-effective metabolism studies (Figure 3).

TLC as a Clean-up Technique

The basic method of applications of TLC as a clean-up technique consists of the preparative separation of analytes and removal from the TLC plate together with adsorbent and elution with an appropriate solvent. This technique is used mainly in pharmacological work. In clinical medical analyses the method is used to separate mixtures and then

introduce the fractions obtained to other analytical instruments. From the analytical point of view, in these methods TLC has the role of a clean-up technique.

In analytical practice two basic methods of TLC combined with other analytical methods are applied. The older method of off-line coupling is similar to preparative cleaning of the sample. Eluate obtained after chromatographic separation and sorbent separation is introduced into the analytical instrument. The technique should be used when the recovery of an analyte is of secondary importance. An advantage of off-line methods is the possibility of performing analysis with optional detectors. In on-line methods the TLC plate is introduced to the detector step-by-step. Analytes are removed from the adsorbent by cathode sputtering or laser desorption. An important advantage of such methods is the full quantitative analysis of practically all substances of clinical interest. Unfortunately, these techniques are expensive and require very specific injectors that are not usually commercially available.

Martin *et al.* applied TLC coupled with MS-MS to the analysis of antipyrine and its metabolites in extracts of human urine. The urine samples were obtained from a volunteer who had received a single oral dose of antipyrine. After 12 h, an aliquot was enzymatic hydrolysed to liberate the analytes from glucuronide conjugates. Next, analytes were extracted (LLE), concentrated and separated by TLC. A good separation (Figure 4) was obtained on silica gel HPTLC plates with a mobile phase of chloroform-methanol-trifluoro-acetic acid, 95 : 5 : 1, v/v.

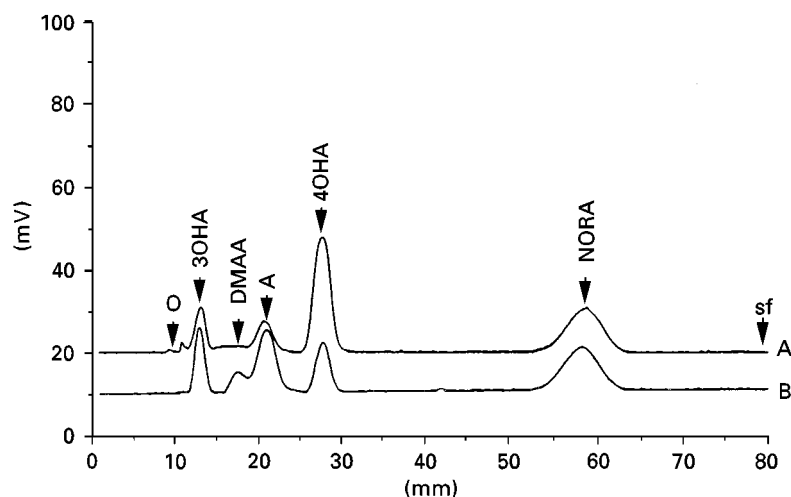


Figure 4 Chromatograms obtained from (A) a urine sample following enzymic hydrolysis and solvent extraction and (B) a standard mixture of the analytes and the internal standard: o, origin; sf, solvent front; 3OHA, 3-hydroxyantipyrine; DMAA, dimethylaminoantipyrine; A, antipyrine; 4OHA, 4-hydroxyantipyrine; NORA, norantipyrine. Reprinted from Martin P, Morden W, Wall P and Wilson I (1992) *Journal of Planar Chromatography-Modern TLC* 5(4): 255-258, with permission.

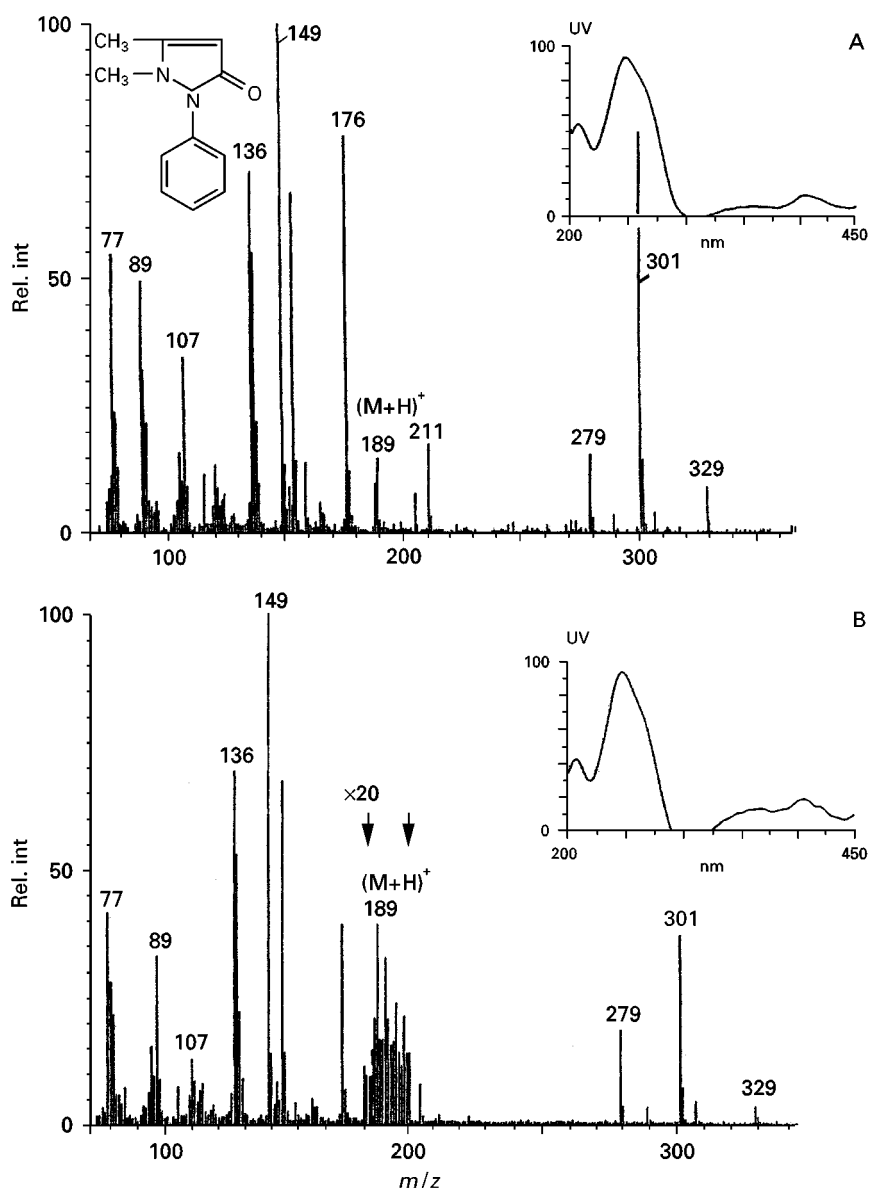


Figure 5 TLC-FABMS spectra obtained directly from the silica gel for (A) antipyrine and (B) material co-chromatographing with antipyrine from the urine extract (insets: structure and UV spectra). Reprinted from Martin P, Morden W, Wall P and Wilson I (1992) *Journal of Planar Chromatography-Modern TLC* 5(4): 255-258, with permission.

The appropriate areas of the plate were then removed for further analysis by FAB MS and FAB MS-MS. The authors demonstrated (Figure 5) that this relatively simple technique would appear to make TLC-FAB MS-MS eminently suitable for confirming the identity of drug metabolites in body fluids for the study of drug metabolism or the detection of drugs abuse, etc.

Conclusions

The analytical tasks connected with clinical needs are very large. It is estimated that the annual increase

in the number of such analyses is about 15-20% with systematic increases in the number of different clinical chemical parameters. However, not all clinical analyses can be performed using TLC. TLC is relatively simple, comes with low equipment cost, and has both a high efficiency and sensitivity. Some disadvantages of TLC include only fair specificity and the requirement of skill in accurately recognizing drug patterns by interpreting the coloured spots visualized with selective reagents, etc. It should also be emphasized that TLC is a comparative method; more complicated tasks in clinical medicine (investigation of metabolism and metabolite

structure) can be performed by this method but only in combination with other, mainly spectroscopic, analytical techniques.

See Colour Plates 69, 70.

See also: **II/Chromatography:** Paper Chromatography. **Chromatography: Gas:** Detectors: Selective; Gas Chromatography–Mass Spectrometry. **Chromatography: Liquid:** Detectors: Mass Spectrometry. **Chromatography: Thin-Layer (Planar):** Densitometry and Image Analysis; Layers; Mass Spectrometry; Modes of Development: Conventional; Modes of Development: Forced Flow, Over Pressured Layer Chromatography and Centrifugal; Spray Reagents. **Extraction:** Analytical Extractions; Solid-Phase Extraction; Solvent Based Separation; Supercritical Fluid Extraction. **III/Amino Acids:** Thin-Layer (Planar) Chromatography. **Bases: Thin-Layer (Planar) Chromatography.** **Bile Compounds: Thin Layer (Planar) Chromatography.** **Biomedical Applications:** Gas Chromatography–Mass Spectrometry; Thin-Layer (Planar) Chromatography. **Carbohydrates:** Thin-Layer (Planar) Chromatography. **In-Born Metabolic Disorders: Thin-layer (Planar) Chromatography.** **Lipids:** Thin-Layer (Planar) Chromatography. **Proteins:** Thin-Layer (Planar) Chromatography.

Further Reading

- Jain R (1996) Thin-layer chromatography in clinical chemistry. In: Fried B and Sherma J (eds) *Practical Thin-layer Chromatography. A Multidisciplinary Approach*, ch. 7, pp. 131–152. Boca Raton: CRC Press.
- Jork H, Funk W, Fischer W and Wimmer H (1994) *Thin-Layer Chromatography: Reagents and Detection Methods – Physical and Chemical Detection Methods; Fundamentals, Reagent I*, vol. 1a. Weinheim: VCH.

Jork H, Funk W, Fischer W and Wimmer H (1994) *Thin-Layer Chromatography: Reagents and Detection Methods – Physical and Chemical Detection Methods; Activation Reactions, Reagent Sequences, Reagents II*, vol. 1b. Weinheim: VCH.

Krauss D, Spahn H and Mutschler E (1988) Quantification of Baclofen and its fluoro analogue in plasma and urine after fluorescent derivatisation with Benoxaprofen chloride and thin-layer chromatographic separation. *Arzneim.-Forschung/Drug Res.* 38(II): 1533–1536.

Lai CK, Lam CW and Chan YW (1994) High-performance thin-layer chromatography of free porphyrins for diagnosis of porphyria. *Clinical Chemistry* 40: 2026–2029.

Martin P, Morden W, Wall P and Wilson I (1992) TLC combined with tandem mass spectrometry: application to the analysis of antipyrine and its metabolites in extracts of human urine. *Journal of Planar Chromatography – Modern TLC* 5: 255–258.

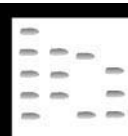
Moffat AC (ed.) (1986) *Clarke's Isolation and Identification of Drugs*. London: Pharmaceutical Press.

Steinberg DM, Sokoll LJ, Bowles KC, Nichols JH, Roberts R, Schultheis SK and O'Donnell CM (1997) Clinical evaluation of Toxi-Prep: a semi-automated solid-phase extraction system for screening of drugs in urine. *Clinical Chemistry* 43: 2099–2105.

Szűnyog J, Mincsovcics E, Hazai I and Klebovich I (1998) A new tool in planar chromatography: combination of OPLC and DAR for fast separation and detection of metabolites in biological samples. *Journal of Planar Chromatography – Modern TLC* 11: 25–29.

de Zeeuw RA, Franke JP, Degel F, Machbert G, Shütz H and Wijsbeck J (eds) (1992) *Thin Layer Chromatographic R_f Values of Toxicologically Relevant Substances on Standardized Systems*. Weinheim: VCH.

CLINICAL DIAGNOSIS: CHROMATOGRAPHY



I. D. Watson, University Hospital, Liverpool, UK

Copyright © 2000 Academic Press

Clinical laboratories within the UK are responsible for providing services for the diagnosis and monitoring of disease. There are several specialities within clinical laboratories or pathology: haematology – examining blood cells and factors relating to blood cell production; biochemistry – measurement of metabolites, hormones, drugs, proteins; histopathology – examination of tissues and cells, usually microscop-

ically; immunology – assessment of antibody status in disease; molecular biology and cytogenetics – specialist services looking at genetic disease. Of these departments, the clinical biochemistry repertoire is the most amenable to chromatography.

Clinical biochemistry laboratories in an average district general hospital perform over a million analyses per annum. The large volume of samples (average request/analysis ratio ~1:4) received each day, the clinical demand for rapid turnaround plus the need for analytical imprecision of less than 5% with acceptable relative accuracy means that high levels

Table 1 Analytes, methodology, volume and cost: Illustration of a 'typical' clinical biochemistry laboratory workload, ranked in order of cost

Analyte	Tests per day (approx)	Method	Cost/test ^a (approx)
Urea and electrolytes (Na ⁺ , K ⁺)	4000	Automated wet chemistries and ion-selective electrodes	£1.00 each, i.e. £4.00 profile
C-reactive protein	50	Automated nephelometry	£4.00
Thyroid function (thyroid stimulating hormone, thyroxine)	200	Automated non-isotopic immunoassay	£5.00
Bedside device for a single drug of abuse	1	Immunochromatography	£5.00
Serum proteins	30	Electrophoresis	£15.00
Drugs of abuse	30	Automated immunoassay and chromatography	£15.00
Haemoglobin A _{1c}	50	Automated chromatography	£10.00

^aCost includes consumables, reagents, labour overheads and equipment depreciation.

of automation are not only desirable but essential. Most chemistries used are either wet chemistry or dry-film technology. The nature of certain analytes may make them less amenable to the high volume chemistries or the volumes of the rarer analytes make the development of automated chemistries more expensive or time consuming. Chromatography fits this last scenario in clinical laboratories. An illustrative workload pattern is presented in **Table 1**.

Clearly chromatography is utilized for those tests that are low volume and for which, generally, rapid turnaround is not required. **Table 2** illustrates the analytes, the mode of chromatography and reasons for use.

Thin Layer Chromatography (TLC)

Of all chromatographic techniques this is the best for parallel analyses enabling cost-effective high

throughput, yet surprisingly this potential has never been utilized apart from a few aficionados. Traditional TLC lacked chromatographic efficiency with consequent loss of resolution and lack of sensitivity. Widely used in many formative studies over 30 years ago, having replaced paper chromatography, it is still used for analytes such as testing drugs of abuse. To ensure reproducibility from plate to plate, commercial plates are used, often with a fluorescent indicator to aid detection although final detection relies on location reagents.

Nearly 20 years ago two developments still in current use greatly improved the utility of TLC: the advent and provision of HPLC column packing materials led to their introduction in TLC giving the anticipated high performance, i.e. high performance thin-layer chromatography (HPTLC). The improved resolution and sensitivity when coupled to significant improvements in densitometers and location re-

Table 2 Common current clinical chromatographic applications

Analyte class	Chromatographic mode ^a	Reason for use
Haemoglobin A _{1c}	LC	Most specific, rapid
Haemoglobin variants	LC	Specific for certain variants
Metabolites associated with inborn errors of metabolism	LC/GCMS	Specificity/flexibility
	LC-MS-MS	Introduced to selected centres as cost-effective and high specificity
Drugs		
Therapeutic drug monitoring	LC/GC	Cost/flexibility
Drugs of abuse		
Screening	TLC/HPTLC/GC	Specificity/flexibility/cost
Confirmation	GC/GCMS/LC-MS	Specificity
Toxicology	TLC/GC/LC	Flexibility
Markers of bone turnover	LC	Specificity, being superseded by immunoassay
Near patient testing devices, e.g. drugs of abuse	Immunochromatography 'stick' tests	Convenience

^aLC, liquid chromatography; GC, gas chromatography; MS, linked mass spectrometer; TLC, thin layer chromatography; HPTLC, high performance thin layer chromatography.

agents, meant that for the first time quantitative TLC with performance equivalent to GC or LC was possible. While some laboratories, particularly in Germany, enthusiastically adopted this technique it gained very few adherents elsewhere, particularly in clinical laboratories where the demand and skill base were inadequate.

Since the mid-1980s there has been an increasing problem of drug abuse. The initial assays developed for screening in the late 1970s used enzyme-multiplied immunoassay technique (EMIT), followed a little later by fluorescence polarization immunoassay (FPIA). These techniques were good for screening large numbers of individuals for a range of substances or classes of substances, e.g. cannabis, cocaine, opiates, benzodiazepines, barbiturates. The test for opiates was designed to detect heroin abuse but in fact it detects other opiates, i.e. codeine and dihydrocodeine, which are legitimately available. Clearly, therefore, any positive for this assay system, and also for others, requires confirmation. Immunoassay-based methods inherently depend on the specificity of their antibody and may not detect subtle structural differences between compounds leading to false positives. This clearly has implications for the subject tested, whether for clinical, forensic or employment purposes. It is now a firmly established principle, regrettably not always adhered to, that before taking action confirmation with a non-correlated technique should be performed. Chromatography is the technique of choice.

In clinical testing, HPTLC with appropriate location reagents and visual inspection is adequate as a confirmation technique, although this would usually be supported by other chromatographic modes. HPTLC also enables screening for many of these compounds not detected by the immunoassay screens; consequently HPTLC is a dynamically utilized

method in clinical laboratories performing substance abuse testing (Figure 1).

However, the other development in TLC was the development of a cellulose-based commercial system with a stylized Marquis reaction with reference to R_F and sequential colour changes collected in a compendium. This system was developed for clinical toxicology work allowing it to be performed by the non-specialist. In overdoses it works well despite its lack of chromatographic efficiency. Unfortunately the system was inappropriately applied to drugs of abuse testing which has greater sensitivity and specificity requirements and external quality assurance data consistently demonstrate poor performance.

In clinical practice, knowledge of which drug has been taken as determined by laboratory studies is useful for only a very few drugs and the concept of screening, usually using chromatography, is no longer commonly performed in the UK; in difficult cases, however, this is the preferred method of investigation.

TLC has a further unique property in clinical investigation. The plate complete with separation can be sent from the original investigating laboratory to a reference centre which will be able to investigate directly (perhaps using TLC-MS-MS) (Figure 2) any difficulty to identify/confirm spots. Currently this type of approach is a neglected area.

Gas Chromatography (GC)

The heyday of GC in clinical laboratories was in the 1970s. Biological fluids contain proteins in high concentration ($\sim 75 \text{ g L}^{-1}$) in a complex mixture of endogenous and exogenous metabolites and the compound of interest may be nonvolatile and present in low concentrations. The trick therefore was to extract the compound of interest quantitatively, make it vol-

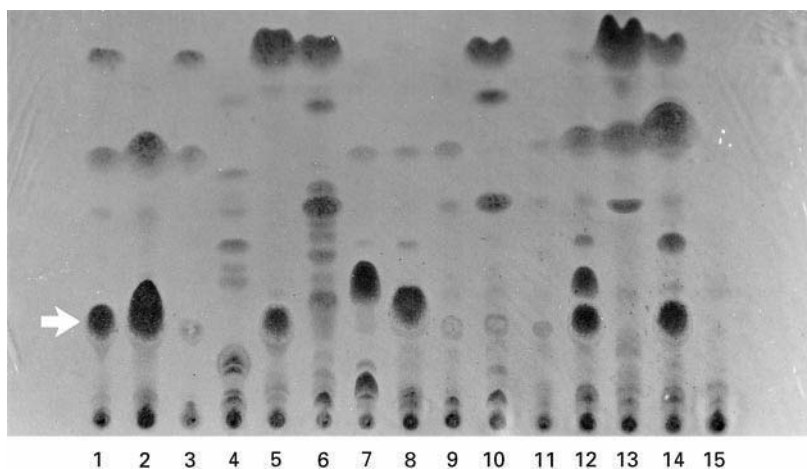


Figure 1 HPTLC of extracted urine from drug abusers. Morphine, the principal metabolite of heroin, is indicated with an arrow.

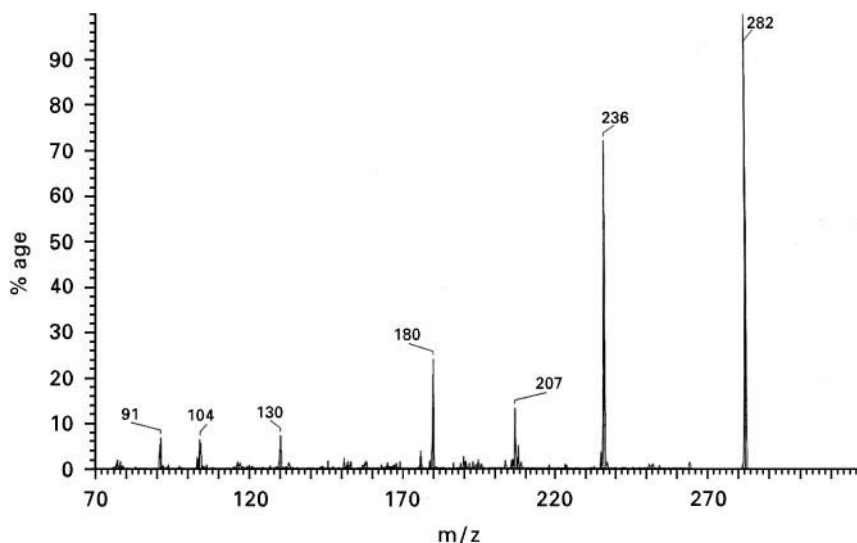


Figure 2 HPTLC – fast atom bombardment spectra of nitrazepam (100 ng on plate). Daughter on 282, delta of 46 (MW 236) characteristic of nitrazepam. (Reproduced with permission from Watson ID (1998) *Therapeutic Drug Monitoring* 20: 490–497.)

atile and chromatograph it. Method development could take many man-hours and while some automation pre- and post-chromatography could be performed, these were labour-intensive methods best suited to low molecular weight metabolites. In the 1980s with increasingly better LC systems, GC usage in clinical laboratories went into decline.

Continued use of GC is necessary for a few analytes, however. Methanol, ethylene glycol, propanol and ethanol poisoning present overlapping clinical pictures; knowledge of which alcohol has been taken and how much is vital. GC with flame ionization detection is the ideal method giving rapid, reliable results and can be utilized in an emergency situation (**Figure 3**). Some laboratories still use GC for drug analysis.

Capillary GC with flame ionization and/or nitrogen-phosphorus detectors offers high sensitivity and in the latter case good specificity for determining biological analytes. Applications cover substance abuse, therapeutic drug monitoring and intermediate endogenous metabolites. However, GC-MS as bench-top analysers, either ion-trap or quadrupole, are becoming more common, though they are still rare, in clinical laboratories. The main reasons for the poor uptake of this combination are cost, demand and staff skills required.

As noted in Table 2 intermediate metabolites found in inborn errors of metabolism which can lead to significant morbidity and mortality, are currently detected by capillary GC. Early detection is vital, and although family screening can now be performed by

molecular biology, many cases are sporadic mutations requiring resolution for the optimal care of that individual. Failure to achieve this results not only in incapacity for the individuals and their family, but also in significant costs to the health service.

Capillary GC is satisfactory for a clinical service for drugs of abuse although GC-MS is essential in any forensic or employment issues, in which some clinical laboratories are involved.

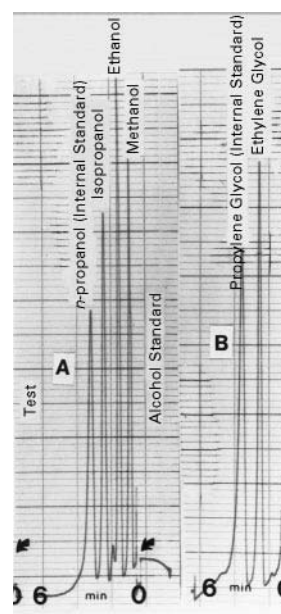


Figure 3 Gas chromatography of alcohols in blood. (Reproduced with permission from Tames F.)

Liquid Chromatography (LC)

Liquid chromatography, with its wide range of modes and better biocompatibility than other chromatographic methods, has been utilized in clinical laboratories. Classical column chromatography was used in sample preparation of many of the standard wet chemistry methods in the past. Protein isolation using affinity chromatography enabled isolation of antibodies and subsequent labelled antibodies to provide the first radioimmunoassays in the 1950s and 1960s. Moore and Stein in 1954 developed an amino acid analyser which was refined over the years. Although primitive by today's standards, it enabled the first reliable measurement of the common amino acids allowing investigation into their metabolism, role in nutrition and relevance in inborn errors of metabolism. Amino acid analysers were automated with post-column reaction for detection and to a limited extent specificity. Much of the basic knowledge learnt through this pioneering work formed the basis for subsequent biological applications of LC.

Ten to fifteen years ago LC was making a significant impact in research-orientated clinical laboratories. Initially work focused on reversed-phase materials with many publications on the separation of a wide variety of drugs, endogenous metabolites and steroid hormones. A major difficulty was sensitivity and there was no true universal detector, nonetheless therapeutic drug monitoring already expanding due to the availability of EMIT technology consolidated using LC procedures for previously difficult analytes. A classic example was the common anticonvulsant carbamazepine which suffered thermal degradation on GC leading to significant imprecision. This was resolved by using LC. Additionally, it became readily possible to measure several drugs simultaneously. While this had been done using temperature-programmed GC it was frequently necessary to derivatize compounds to obtain satisfactory volatility and polarity and this could affect the selectivity. LC enabled the same approach, initially using solvent gradient programming on underivatized samples, often with minimal sample preparation. This approach enabled separation of a full range of anticonvulsants: ethosuximide, primidone, phenytoin, phenobarbitone and carbamazepine and their metabolites (Figure 4).

This meant that efficient processing, all samples followed the same analytical track, reduced costs per analyte and the occasional detection of inappropriate medication. In this particular area the wide and increasing range of nonisotopic immunoassays compatible with automation has meant many clinical laboratories find it more organizationally efficient to perform these assays by automated immunoassay; a hard

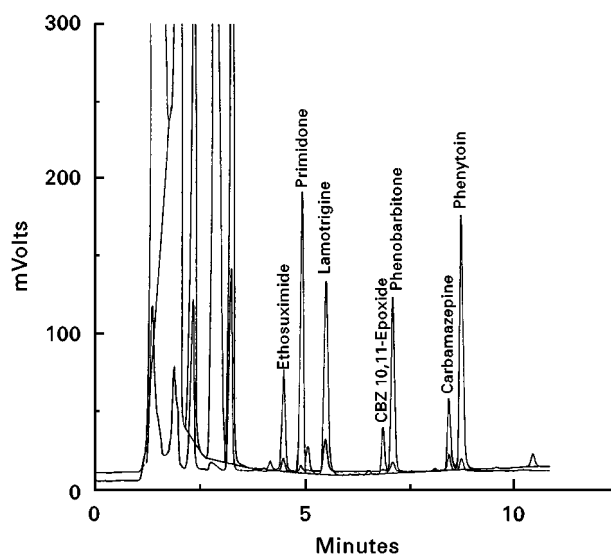


Figure 4 Isocratic liquid chromatography of anticonvulsants in serum. Analysed on Gilson ASTED system with sample pre-dialysis and trace enrichment prior to chromatography. (Reproduced with permission from O'Connell, D.)

core still use LC, though whenever possible using an automated system. Surveys through the UK National External Quality Assurance Programme have consistently shown LC methods to have the best accuracy with acceptable imprecision. The introduction of new anticonvulsants, e.g. lamotrigine, has led to a demand for analysis. This has meant development of LC assays demonstrating the role of chromatography in development of clinical investigations.

This is a common scenario in method development in that research or reference centres develop an LC assay for a new analyte to detect or monitor disease. As the utility of this determinand is demonstrated, demand rises, causing processing difficulties for the reference centre, parallel to an increasing demand from less specialist centres. Some will invest in an LC solution but the reagent manufacturers are alerted to the developing interest in the analyte. Knowing that clinical laboratories have a predilection for rapid, automated large single or multiple similar medium analysers, they develop wet chemistry or immunoassay methods. This approach will be reagent expensive but require minimal labour utilizing pre-existing equipment. Once this is marketed and adopted the LC procedure, albeit more accurate, declines and may be dropped altogether.

A further illustration of this is the measurement of bone turnover; the original analyte hydroxyproline was determined by a cumbersome, manual, wet chemistry assay. As interest grew in hormone replacement therapy effects in osteoporosis much effort was expended in developing a gold standard LC assay for pyridinoline and deoxypyridinoline. There were

particular problems, eventually resolved, with obtaining a satisfactory internal standard. This has become established as the reference method, but is now being supplanted by immunoassay measurement of deoxyproline.

Screening methods using LC have suffered from the lack of reproducibility between reversed phases. The REMEDI system for drug abuse screening is however an established screening technique linked to a linear diode array with spectral library and has been shown to provide satisfactory identifications on screening for drugs.

The detection of inborn errors of metabolism by reference paediatric biochemistry laboratories has hitherto relied heavily on GC-MS with all the inherent problems plus the need for separate assay condition for different compound classes, e.g. organic acids and amino acids. Recently the NHS Research and Development Programme – Health Technology Assessment – after an evidence-based medicine research exercise, has indicated that LC-MS-MS would deliver appreciably greater benefits than current systems for the detection of a variety of different forms of inborn error of metabolism. Hitherto, funding for such equipment had been stalled on the capital cost, but demonstration of the economies delivered by LC tandem MS argued in favour of the system which is now being introduced in selected centres. It is such economic analyses that may progress and sustain chromatographic methods in the face of a decreasing skill base and drive for consolidation in clinical laboratories.

An example of where the specificity of LC is valued and is allied to an improvement in efficiency is the analysis of haemoglobin A_{1c} (Hb A_{1c}). Hb A_{1c} is glycated haemoglobin A, and is a long-term measure of control in diabetes mellitus. Recent international advice has called for close control of Hb A_{1c} in diabetics and requires an accurate and precise method. Early studies on Hb A_{1c} used classical column chromatography on mini-columns, this was labour intensive and commercial 'kit' LC solutions began to be offered. Soon an automated wet chemistry analyser compatible methods were developed and embraced.

However, significant proportions of the population, depending on ethnic mix, do not have haemoglobin A as their sole haemoglobin and to assess glycaemic control one must look at the glycation of the variant haemoglobin; the wet chemistry method cannot do this. There has therefore been a resurgence of interest in the 'kit' LC solutions; popular ones use anion exchange chromatography which have run times of 4 min providing full sample automation for over 250 samples per day (Figure 5).

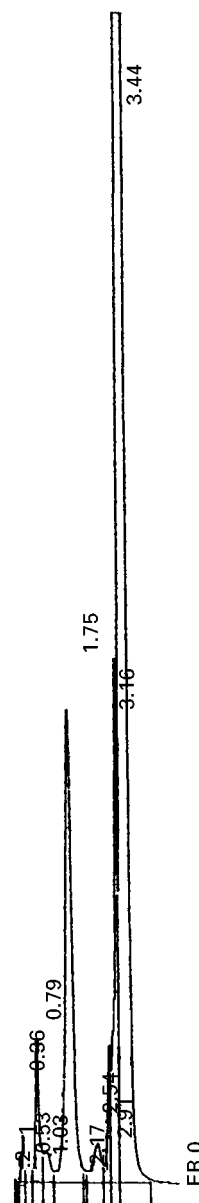


Figure 5 Ion exchange chromatography of haemoglobin A_{1c}, an indicator of glucose control in diabetics. Hb A_{1c} retention 1.75 min.

As diabetic assessment is performed regularly and many organ systems are examined, it is not uncommon for blood to be drawn from a patient and the Hb A_{1c} to be measured in the clinic using LC while they wait. This provides the clinician with the result when seeing the patient and improves the patient throughput.

Immunochromatography

Immunochromatography is the preserve of research laboratories as a laboratory technique. Near-patient testing, however, utilizes commercially produced

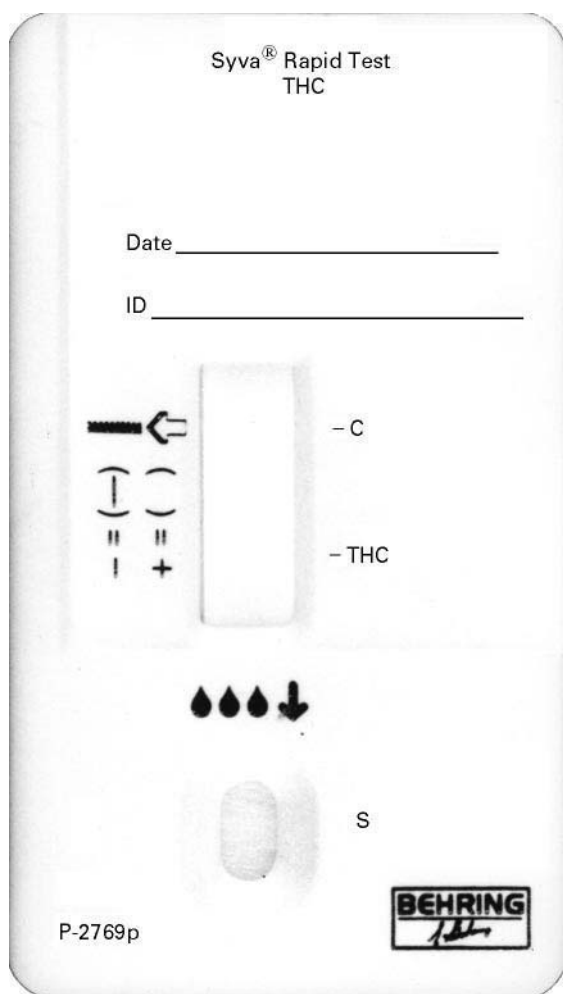


Figure 6 Immunochromatography slide for once-only use near the subject testing to detect abused drugs. C = control, THC = tetrahydrocannabinol, a metabolite of cannabis.

'sticks' which use immunochromatography. The principle is that the sample, e.g. urine, is applied to the stick which is then developed, e.g. by capillary attraction, the analyte of interest binding at a zone where there are antibodies. There are sometimes built-in

positive and negative controls. When the antigen and antibody combine they develop a visible colour spot or band which confirms the presence of the compound of interest (**Figure 6**). While these devices are expensive and inaccurate they have the benefit of immediacy which may be clinically acceptable provided they are used appropriately.

The Future

Chromatography has maintained its role in certain niches in clinical laboratories. Interest in manufacturer-supplied solutions for chromatography, particularly LC, exists and compensates for the lack of skill base. For difficult low throughput analyses this may be how developments will be consolidated. Capillary zone electrophoresis could impact on much current LC work but again skill and capital costs militate against this. If accuracy rather than imprecision becomes a major clinical laboratory issue, as it may, then the inherent accuracy of chromatography probably linked to mass spectrometry will provide a role for definitive methods and may provide a role for methods used in routine laboratories.

See also: II/Chromatography: Thin-Layer (Planar): Mass Spectrometry. III/Toxicological Analysis: Liquid Chromatography.

Further Reading

- Baselt RC (1987) *Analytical Procedures for Therapeutic Drug Monitoring and Emergency Toxicology*, 2nd edn. Massachusetts: PSG Publishing.
- Bowers LD, Ullman MD and Burtis CA (1994) Chromatography in: Burtis CA and Ashwood ER (eds) *Tietz Textbook of Clinical Chemistry*, 2nd edn. Philadelphia: WB Saunders.
- Kuenigsberger RU (1988) High performance liquid chromatography. In: Williams DL and Marks V (eds) *Principles of Clinical Biochemistry*, 2nd edn. London: Heinemann.

COAL: FLOTATION

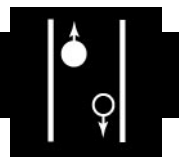
B.K. Parekh, University of Kentucky, Lexington, KY, USA

Copyright © 2000 Academic Press

Introduction

The process of froth flotation for upgrading the quality of coal by removing mineral matter (ash and

pyrite) has received increased attention since the 1960s. The froth flotation process is typically used for treating <0.5-mm size coal and is currently the only technique both effective and economical to clean coal on a commercial scale. In the USA, the majority of coal preparation plants discard the <0.5-mm coal owing to the high cost of processing of the fine coal.



Recovering fine coal offers important economic and environmental functions. In economy terms, the plant recovers an extra amount of clean coal that would have otherwise been discarded to the impoundment. Recovering the clean coal reduces the amount of fines to the ponds, and improves the quality of recycled water.

The basic coal flotation technology has been derived from ore flotation, where the technology has been extensively used. The first froth flotation plant for coal was established in the United Kingdom in 1920 and the first US plant was established in 1930. Froth flotation technology has made substantial progress over the last fifty years.

Coal is a solid combustible material and exists in the ground along with impurities. Coal, being composed of carbon elements, is hydrophobic in nature and thus is a good candidate for the froth flotation technique. The impurities present in coal basically consist of clays, quartz, calcite, dolomite, pyrite, chlorite, etc. which are hydrophilic in nature and thus, can be easily removed in an aqueous medium. Pyrite minerals present in coal have an ambivalent character and are sometimes difficult to remove by the flotation technique.

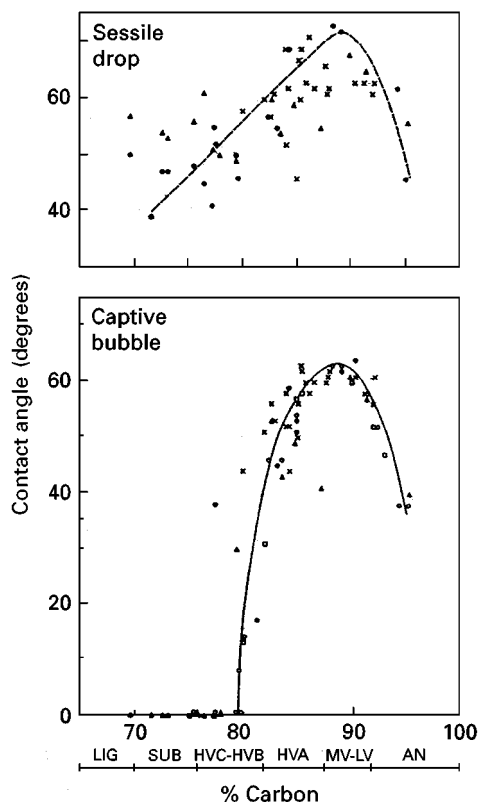


Figure 1 Hydrophobicity of various coals as a function of percentage carbon based on the contact angle technique. (Aplan (1989), courtesy of SME, Littleton, Colorado, USA.)

Hydrophobicity of Coal

The hydrophobicity of coal varies with the rank of the coal and oxygen functional group present in the coal. The high volatile bituminous coals are the most hydrophobic, whereas lignite is the least hydrophobic. One technique to quantify the hydrophobicity of coal is through measuring contact angles of water on coal surfaces. **Figure 1** shows the contact angle data of water on various coals. Note that the maximum contact angle or the hydrophobicity occurs at $\sim 88\%$ C, and the high-carbon content anthracite coals are less hydrophobic.

Zeta Potential of Coal

The zeta potential of various coals with respect to pH is shown in **Figure 2**. Note that the point of zero charge (PZC) is highly variable and depends on the source and type of coal. The sub-bituminous and lignite have a PZC of ~ 2 , whereas the high volatile (hva) bituminous and anthracite coals have a PZC of ~ 5 . In general, a reduction in the PZC value indicates a reduction in hydrophobicity.

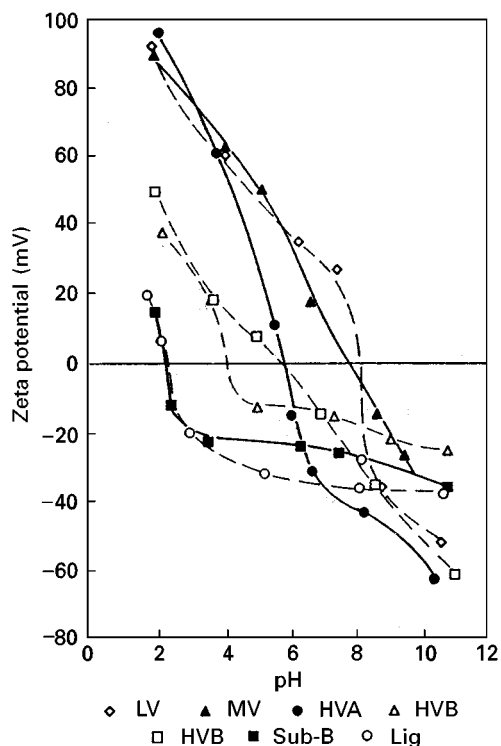


Figure 2 Zeta potential and point-of-zero charge (PZC) of coals of various ranks. (Aplan and Arnold (1991), courtesy of SME, Littleton, Colorado, USA.)

Reagents

The purpose of flotation reagents is to provide a strong hydrophobic surface and to create small relatively stable bubbles. For coal flotation, in general, only the collector and frother reagents are used.

Collectors

Theoretically speaking, the highly hydrophobic coals (containing 85–90% C) should not require any collector. In practice, a small amount of either No. 2 fuel oil or kerosene is used as collector. The amount of a collector required varies from a low ($0.11\text{--}0.2\text{ kg t}^{-1}$) for a high rank coal to a high ($1.0\text{--}2.0\text{ kg t}^{-1}$) for a low rank coal.

Frothers

The primary function of the frother is to produce a large quantity of fine size bubbles. The bubbles should be able to carry the coal to the surface without breaking, and once out of the flotation machine, it should break down. The most commonly used frothers for coal flotation are either pure alcohol, e.g. MIBC (methyl isobutyl carbinol) or a mixture of various alcohols and the polypropylene glycol-based frothers. The amount of frother required varies from 0.2 to 0.5 kg t^{-1} .

Depressant

The function of depressant is to suppress the flotation of one component of the mixture of solids by adding a specific chemical. In coal flotation, pyrite usually floats along with the coal. Many papers have been published on the subject; however, Chaudhari and Aplan, and Xu and Aplan, have conducted a detailed investigation of various reagents for depressing flotation of pyrite. They concluded that there is no universal reagent for depressing pyrite. In the coal industry, pyrite depression is not practised; however, in the future this might become an important step for the coal industry to survive.

There are some other variables for flotation, such as pH, dispersing reagents, percentage solids, particle size, etc. However, in the coal industry, very little or no attention is given to these factors. Readers interested should refer to Aplan's work.

Flotation Machines

The coal industry uses either mechanical or column cells.

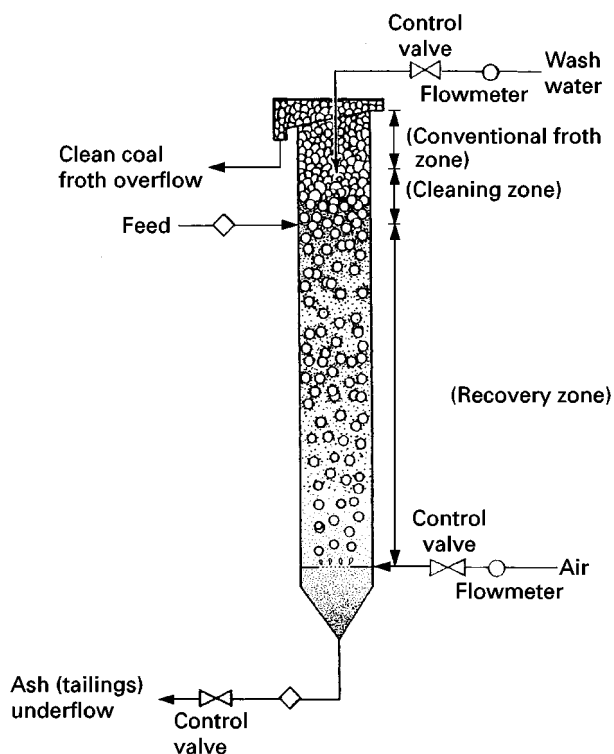


Figure 3 A line diagram of a column flotation cell.

Mechanical

The most commonly used flotation machine is one in which a mechanically driven impeller agitates in the pulp and disperses air into it. The major development in mechanical flotation cells has been in the design of

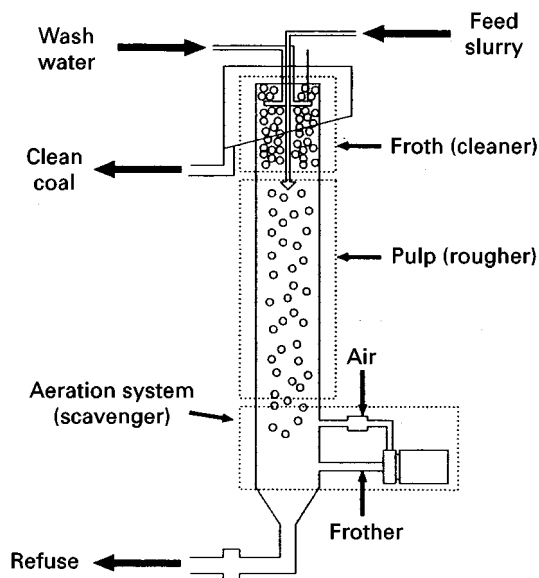


Figure 4 Schematic diagram of the Microcell™. (Yoon *et al.* (1992), courtesy of Gordon and Breach Science Publishers.)

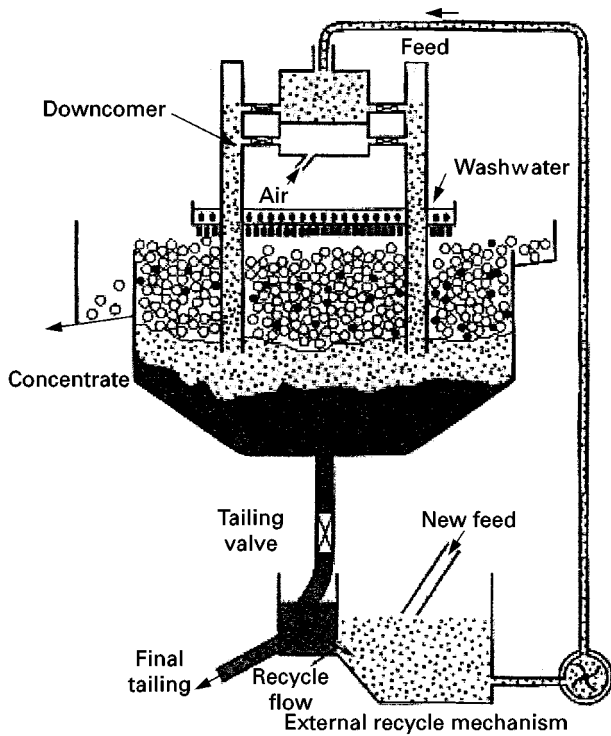


Figure 5 Schematic of Jameson cell. (Courtesy of Richwood Industry, Huntington, West Virginia, USA.)

larger volume machines (3000 ft³ or 84 m³). For coal flotation, mechanical cells are usually arranged in banks of four to six cells in an 'open-flow' arrangement.

Column

The column flotation cell which has achieved success in the mineral industry was introduced to the coal industry in the 1990s. The machine consists of a long (~6 m) vertical tube ranging from 2.4 to 3.0 m in

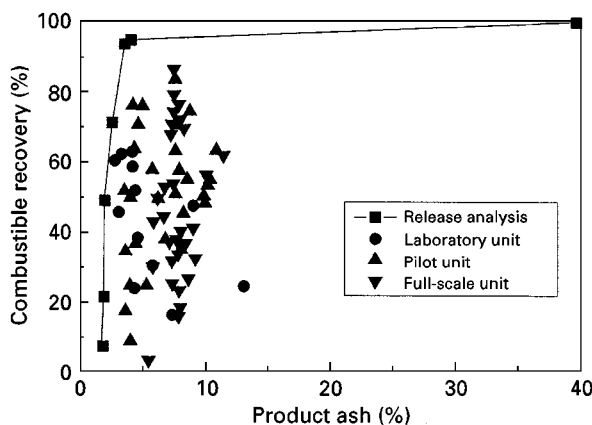
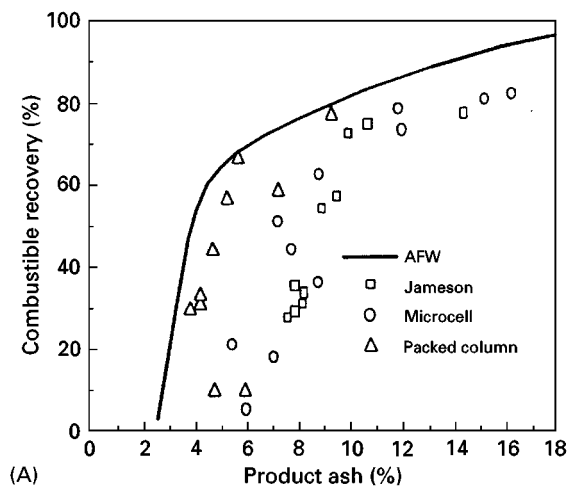
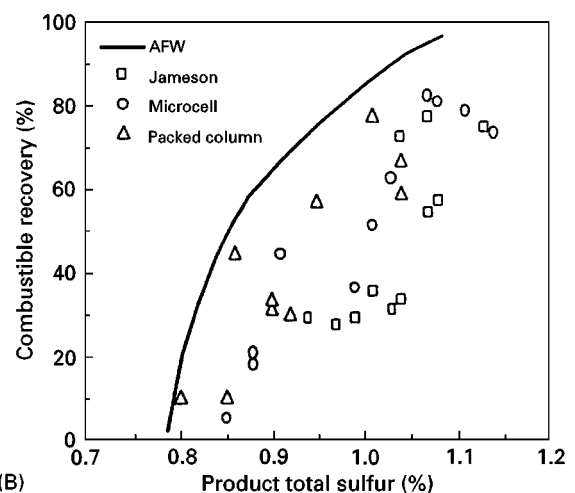


Figure 6 Performance data of the Jameson cell at the laboratory, pilot, and full scale. (Honaker *et al.* (1999), courtesy of SME, Littleton, Colorado, USA.)

diameter. Figure 3 shows a sketch of the column flotation machine. The feed (coal slurry containing flotation reagents) to the column is introduced at about the 5-m level. The froth height is maintained close to 1 m and wash water introduced into the froth layer to remove any entrapped and entrained impurities. The tailings containing the impurities (ash) are discharged at the bottom of the column. A variety of column flotation machines have been developed over the last few decades. The Ken-Flote column developed at the University of Kentucky Center for Applied Energy uses either a porous cylinder or a 'foam-jet' system to generate bubbles and provides a quiescent zone for attachment of coal particles to the air bubbles, which keeps ash entrainment to a minimum. In 1989, the first commercial Ken-Flote



(A)



(B)

Figure 7 Metallurgical performance achieved by the three column flotation technologies and the advanced flotation washability (AFW) analysis on the basis of (A) product ash and (B) total sulfur contents (feed ash: 42.6%; total sulfur: 0.86%). (Mohanty and Honaker (1999), courtesy of Elsevier Science.)

columns were installed in the USA at the Powell Mountain Coal Company, Virginia.

The 'Microcel' column flotation developed at the Virginia Polytechnique and State University uses an inline mixture to generate fine bubbles in the column. In this column, a part of the reject stream is passed through the inline mixture along with the frother and air to generate fine bubbles. **Figure 4** shows a diagram of the MicrocellTM column.

The Static Tube flotation system developed at the Michigan Technology University uses corrugated plates packed inside the column to break up large bubbles into a smaller size bubble. The machine does not utilize any special bubble-generating device.

The Jamison cell is a column cell that is much shorter than any of the columns described earlier. As shown in **Figure 5**, the Jamison cell utilizes a pressurized feed stream injected through a long tube called the downcomer to draw atmospheric air into the device. The resulting jet formed is discharged into a short column where coal floats to the surface and tailings are discharged at the bottom. Wash water is generally added through a tray located above the froth phase. Currently, quite a few Jamison cells are being used in Australia and a few coal preparation plants in the USA. **Figure 6** compares the separation performance as a function of ash content for a coal using the laboratory-, pilot- and full-scale Jamison cell units. The L-shape of the release curve indicates that the impurities in the coal are well liberated. The laboratory- and pilot-scale units were nearly able to produce the performance of the release

analysis. An ash content reduction of about 40–45% was achieved while recovering 77% of the combustible material, which equates to an ash rejection of about 95%.

Mohanty and Honaker published a comparative evaluation of the three leading column flotation technologies. According to them, the packed column produced the best separation performance owing to its ability to support a deep froth zone. However, because of the absence of an air-sparging system and consequently larger bubbles, the solids-carrying capacity of the froth was minimal. On the other hand, the solids-carrying capacity or solids throughput achieved with the Jameson cell, was found to be maximal. The MicrocellTM achieved maximum carrying capacity while providing a high energy recovery with a reasonably low amount of reagents. **Figure 7** shows the combustible recovery (amount of combustible material) as a function of product ash and total sulfur obtained for a coal using the three column technologies. The AFW (advanced flotation washability) is a limiting curve indicating the possible ash and sulfur that could be achieved using froth flotation technology. Note that the packed column provided both low ash and sulfur; however, the MicrocellTM and Jameson cell both provided high combustible recovery.

In all work on coal flotation, a high ash rejection has been reported using column flotation technology. However, removal of pyritic sulfur has been marginal. The main reason for this is attributed to the ambivalent nature of coal pyrite; some pyrites are

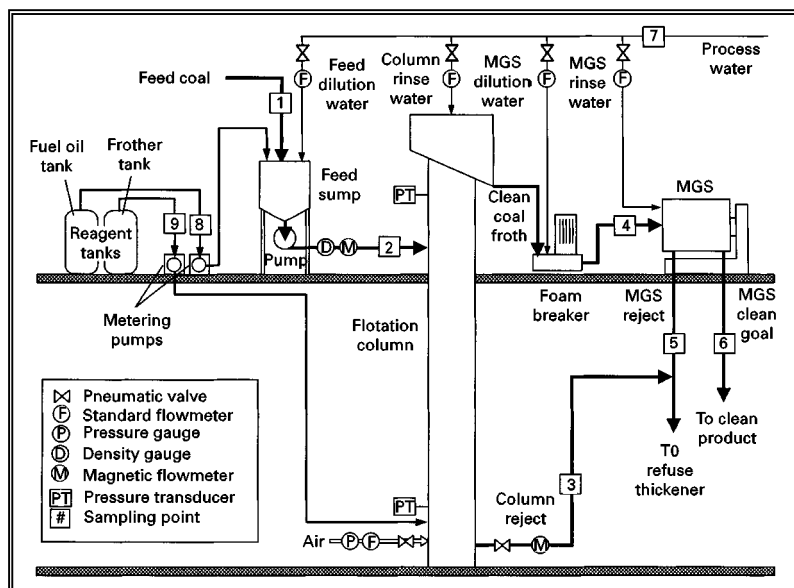


Figure 8 Schematic drawing of the combined advanced flotation/enhanced gravity separation circuit. (Luttrell *et al.* (1998), courtesy of Gordon and Breach Publishers.)

hydrophobic and some are hydrophilic in nature. In the case of coal, pyrite is always associated with some carbon which affords it hydrophobic and makes it float with coal. Luttrell *et al.* conducted studies on combining column flotation with an advanced gravity separation technology to remove pyrite from coal. The process flowsheet for the two-stage circuit is shown in Figure 8. A Microcell™ flotation column froth product after derating was sent to a multi-gravity separator (MGS) developed by the Mosley Ltd, UK. The MGS is similar to the shaking table, except that the particles in the flowing film are also subjected to centrifugal forces. Figure 9 compares the performance of the flotation column alone to that obtained using the combined flotation column/MGS circuit. The rejection of pyritic sulfur improved from 60.5% to 83.6% and ash rejection improved from 83.8% to 87.7% using the combined techniques. Using the MGS unit, the loss of coal (energy) was very low, in the order of 2–3% points.

Coal flotation is a manually operated process. Recently, process optimization has been achieved through more efficient circuit designs and innovative sensor development. Some new approaches have been developed in the sensor area, which help in designing a controlled reagent delivery system. The Consol Co. has developed an inexpensive optical-based system shown in Figure 10. The main components of the detector are a glass tube, a photoconductor, an opaque barrier, and a light-emitting diode (LED). The light from the LED is reflected from the slurry to the main photoconductor. The photoconductor changes resistance in proportion to the light reflected from the tailing stream. The higher the tailings slurry ash con-

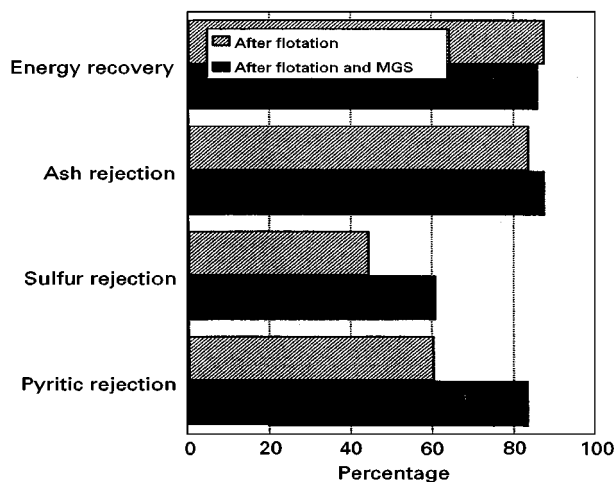


Figure 9 Separation performance obtained using the flotation column and combined flotation column/MGS circuit. (Luttrell *et al.* (1998), courtesy of Gordon and Breach Publishers.)

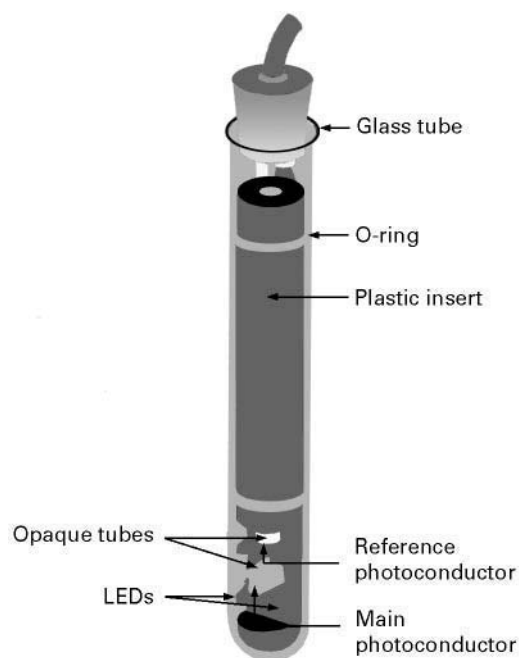


Figure 10 Optoelectronic tailings detector. (Meenan (1999), courtesy of SME, Littleton, Colorado, USA.)

tent, the more light reflected back to the photoconductor and the lower the resistance.

A machine-vision or 'video-based' analyser system has also been successfully tested by Virginia Polytechnic Institute and State University. The video-based system could detect changes in slurries over an operating range of 60–90% ash.

Conclusion

In summary, coal flotation, column flotation has shown significant advantages from the technical and economic points of view. A combination of column with advanced gravity separators provides a much cleaner coal with low ash and pyritic sulfur contents. In the future, all new coal preparation plants will utilize column technology along with process optimization and sensors for the economic recovery of ultra-fine coal particles.

Further Reading

- Adel GT, Luttrell GH, Cruz EB and Dunn PL (1997) In-plant testing of a video-based coal slurry ash analyzer. Presented at the 14th International Coal Preparation Conference, pp. 39–156.
- Aplan FF (1989) Coal flotation – the promise and the problems. In: Chander S and Klimpel RR (eds) *Advances in Coal and Mineral Processing Using Flotation*. pp. 95–104. Littleton, CO: Society of Mining, Metallurgy, and Exploration, Inc. (SME).

- Aplan FF and Arnold BJ (1991) Flotation. In: Leonard JW (ed.) *Coal Preparation*, pp. 450–485. Littleton, CO: Society of Mining, Metallurgy, and Exploration, Inc. (SME).
- Arnold BJ and Aplan FF. (1989) The hydrophobicity of coal macerals. *Fuel* 68: 651–658.
- Bury E. and Bicknell A (1921) Purification of coal by froth flotation. *Colliery Guardian* 21: 337.
- Bury E, Broadbridge W and Hutchinson A (1920) Froth flotation as applied to the washing of industrial coal. *Institute of Mining Engineers* 60: 243–253.
- Chaudhari V and Aplan FF (1992) Pyrite depression during coal flotation – Part I. Inorganic. *Mining and Mineral Processing Journal* 9: 51–56.
- Davis DH (1948) Froth flotation of minus 48 mesh bituminous coal slurries. *Transactions AIME* 177: 320–337.
- Gutierrez JA, Purcell RJ and Aplan FF (1984) Estimating the hydrophobicity of coals. *Colloids and Surfaces* 12: 1–25.
- Honaker RQ, Patwardhan A, Mohanty MK and Bhaskar K (1999) Fine coal cleaning using the Jamison cell: The North American Experience. In: Parekh BK and Miller JD (eds) *Advances in Flotation Technology*, pp. 331–341. Littleton, CO: Society of Mining, Metallurgy, and Exploration, Inc (SME).
- Horsley RM and Smith HG (1951) Principles of coal flotation. *Fuel* 30: 54–63.
- Luttrell GH, Venkatraman P and Yoon RH (1998) Removal of hazardous air pollutant precursors by advanced coal preparation. *Coal Preparation* 19: 2243–2255.
- Meenan, GF (1999) Modern coal flotation practices. In: Parekh BK and Miller JD (eds) *Advances in Flotation Technology*, pp. 309–319. Littleton, CO: Society of Mining, Metallurgy, and Exploration, Inc. (SME).
- Mohanty MK and Honaker RQ (1999) A comparative evaluation of the leading advanced flotation technologies. *Minerals Engineering* 12(1): 1–13.
- Parekh BK, Bland AE and Groppo JG (1990) A parametric study of column flotation. *Coal Preparation* 8: 49–60.
- Yang DC (1986) *Column froth flotation*. US Patent No. 4,592,834 (January 1986).
- Yoon RH, Luttrell GH, Adel GT and Mankosa MJ (1992) The application of microcell column to fine coal cleaning. *Coal Preparation* 10: 177–188.
- Xu DD and Aplan FF Joint use of metal ion hydroxy compounds and organic polymers to depress pyrite and ash during coal flotation.

COBALT ORES: FLOTATION

See III/NICKEL AND COBALT ORES: FLOTATION

COLLOIDS: FIELD FLOW FRACTIONATION



G. Karaiskakis, University of Patras, Patras, Greece

Copyright © 2000 Academic Press

Introduction

When dealing with colloidal materials, the parameters of size and size distributions are needed, because many physicochemical processes, like aggregation and deposition on solid surfaces, are influenced by the size and size distributions of these materials.

For the analysis of submicron or supramicron colloidal particles, a sedimentation process, either under gravity or with centrifugal force, is necessary to sort different diameter particles into classes, and then to obtain an average size and a size distribution. Among the successful techniques used for this purpose, are electrophoretic mobility and the methods of size exclusion chromatography,

hydrodynamic chromatography and field-flow fractionation (FFF).

FFF is a family of separation methods introduced by Giddings in 1966, but several groups all around the world have contributed significantly to the development. The various subtechniques of FFF are best suited to the separation and characterization of colloidal materials and macromolecules, including biological components ranging in size from proteins to living cells, environmental colloidal particles, as well as industrial polymers and colloids, powders, latexes and emulsions.

Principles of FFF

FFF is a flow elution method with retention achieved by using applied fields to drive the solutes into quiet flow regions. The applied fields are able to achieve

the task of separation more gently and with more accurate control than the two-phase distribution forces used in chromatography.

Just as its name suggests, fractionation in FFF is the combined effect of an applied cross-field and the laminar parabolic flow profile of the carrier mobile phase. The separation process in FFF is carried out in a thin, unobstructed, ribbon-like channel with a rectangular cross-section and elongated extremities connected to capillary tubes allowing the continuous flow of the carrier liquid (Figure 1). Flow velocity is highest at the middle of the channel and lowest near the two channel walls. As the carrier stream moves through the channel, an external force field or gradient is applied perpendicularly to the flow, which pushes the components of the sample into the slower moving streams near the outer wall, so that they form a thin, steady-state layer against that wall.

The mean thickness of the layer is different for each distinct chemical or particulate species, and depends on the strength of the interaction between the field and the species and on the diffusion coefficient corresponding to that species. Larger colloidal species and macromolecules are usually forced more vigorously toward the wall than are smaller ones. This is the basis for selective retention in normal FFF, which produces in general an elution spectrum in which small particles are eluted first and large particles last, until steric effects dominate. At this transition point a foldback in elution order occurs, and the larger particles elute from the system before the smaller ones – a trend opposite to that observed in normal FFF. Steric FFF (StFFF) predominates when the particle radius exceeds the mean layer thickness of the solute,

such that the protrusion of the particle out of the flow system is determined by the particle's size rather than by its Brownian motion.

Sub-techniques of FFF

Among the various fields and gradients used to drive species to the channel wall, four specific kinds have been most developed, yielding a different subtechnique of FFF. Among those used are centrifugal or gravitational forces (sedimentation FFF = SdFFF), thermal gradients (thermal FFF = ThFFF), cross-flow (flow FFF = FIFFF) and electrical fields (electrical FFF = ElFFF). All these subtechniques can be worked under the normal mode of operation, in which the concentration distribution along the axis which is perpendicular to the carrier flow is exponential as a consequence of the balance between field-induced displacements and diffusion, or under the steric mode of operation in which the elution order is inverted relative to that observed for normal FFF. They can also be used in the hyperlayer and potential barrier modes of operation, which will be described in detail later.

Retention Theory

The peak retention in FFF can be expressed by the retention ratio, R , defined as the ratio of the void volume, V_o , to the component retention volume, V_R :

$$R = \frac{V_o}{V_R} \quad [1]$$

The retention ratio R in normal FFF is related to the dimensionless retention parameter λ ($\lambda = l/w$, where l is the mean layer thickness and w is the channel thickness) by the equation:

$$R = 6\lambda[\coth(1/2\lambda) - 2\lambda] \approx 6\lambda \quad [2]$$

The last approximation is valid for highly retained components. Eqn [2] is general for all FFF subtechniques, but as the parameter λ varies with the applied external field or gradient, the experimental parameter R is related to different physicochemical quantities of the sample under study, thus leading to the sample's separation depending on its interactions with the external field:

$$R = \frac{6kN_A T \rho_s}{MG\Delta\rho} = \frac{36kT}{d^3\pi w G \Delta\rho} \quad (\text{SdFFF}) \quad [3]$$

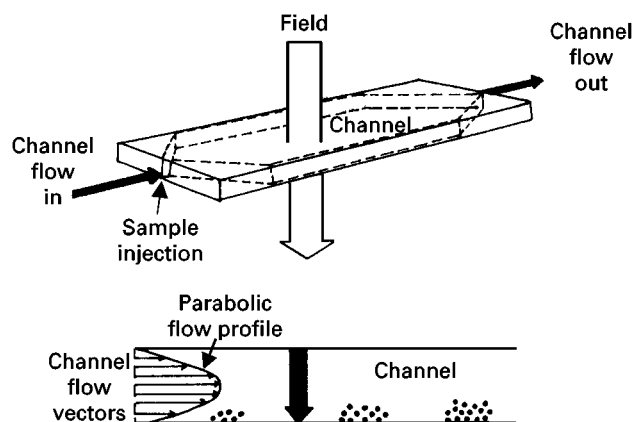


Figure 1 Schematic representation of the FFF channel with the parabolic flow profile in detail. Reproduced with permission from Giddings JC (1979) Field-flow fractionation of polymers: one-phase chromatography. *Pure and Applied Chemistry* 51: 1459.

$$R = \frac{6T}{aw(dT/dx)} = \frac{6D}{D_T w(dT/dx)} \quad (\text{ThFFF}) \quad [4]$$

$$R = \frac{6DV_o}{\dot{V}_c w^2} \quad (\text{FIFFF}) \quad [5]$$

$$R = \frac{6D}{\mu E w} \quad (\text{ElFFF}) \quad [6]$$

$$R = \frac{3\gamma d}{w} \quad (\text{StFFF}) \quad [7]$$

where M is the solute molecular weight, d is the Stokes diameter, $\Delta\rho = |\rho_s - \rho|$ is the density difference between the particle (ρ_s) and the carrier liquid (ρ), G is the field strength expressed in acceleration, T is the absolute temperature, k the Boltzmann's constant, N_A Avogadro's number, D is the solute-solvent diffusion coefficient, D_T the coefficient of thermal diffusion, a the dimensionless thermal diffusion factor, dT/dx is the temperature gradient applied at right angles to flow, \dot{V}_c is the volumetric cross-flow rate, μ is the particle's electrophoretic mobility, E is the electrical field strength, and γ is a dimensionless factor that accounts for the drag-induced reduction in velocity, and for the increase in velocity due to the activity of lift forces.

The above equations show that the solute parameters controlling retention, and thus characterized by retention, are M , d and ρ_s in SdFFF, D_T and a in ThFFF, D and d in FIFFF, μ and D in ElFFF, and d , γ in StFFF. As in all FFF techniques, the retention ratio is related to the particle size and the fractionation is based on particle size differences or on the D and D_T coefficients.

We note that all R values in the normal FFF mode are inversely proportional to the strength of the field or gradient employed: G , dT/dx , \dot{V}_c and E – therefore making possible the manipulation of the retention ratios by changes in field strength. This makes FFF applicable to many different sample types over a wide particle size distribution range. A wide variety of components can be handled within a run by applying field programming methodologies in which the field strength is gradually reduced during the separation.

In the present work, we focus on sedimentation FFF (centrifugal and gravitational) and flow FFF, which are the most usable and accurate for the separation and characterization of colloidal materials.

Instrumentation

Sedimentation FFF

The apparatus of SdFFF consists of a channel with highly polished walls and rectangular cross-section which is fitted to the inside of a centrifuge basket. Solvent is pumped into and out of the system with the aid of special low volume rotor seal and subsequently to a UV detector. The associated parts of the system (e.g. pumps, detectors, recorders, sample injectors) are readily available liquid chromatography components. At present, the SdFFF rotor can be operated at a maximum speed of 32 000 rpm, which corresponds to an applied field of approximately 85 000 g for the common rotors used. With such a rotor, colloidal particles as small as 0.005 μm can be retained and analysed, when their density is between 1.5 and 3.0 g cm⁻³. The upper limit of particle size is reached when the mean layer thickness becomes equal to or less than the particle radius, and steric factors determine the retention ratio.

In gravitational FFF (GrFFF) the earth's gravitational field is used and the apparatus consists of a channel formed between two glass plates separated by a Mylar spacer.

Flow FFF

In flow FFF the external field is simply the flow of a second solute stream perpendicular to the carrier stream. The walls of the FFF channel are constructed of semipermeable membranes, so as to accommodate the cross-flow and, at the same time, to retain solute particles in the channel. The semipermeable membrane material is the limiting factor in the performance of the flow FFF system.

Applications

SdFFF and FIFFF can be applied to the separation and characterization of spherical or irregular, monodisperse or polydisperse colloidal particles. The particle size analysis of colloids can be carried out successfully by working in the four modes of FFF.

Normal SdFFF

Normal SdFFF has been applied to many systems involving polymers, biological macromolecules (such as DNAs, virus particles and protein aggregates), subcellular particles, emulsions and a great variety of natural and industrial colloids. An example of SdFFF is shown in **Figure 2**, which illustrates the separation of colloidal polystyrene latex microspheres. No other method can yield comparable resolution for submic-

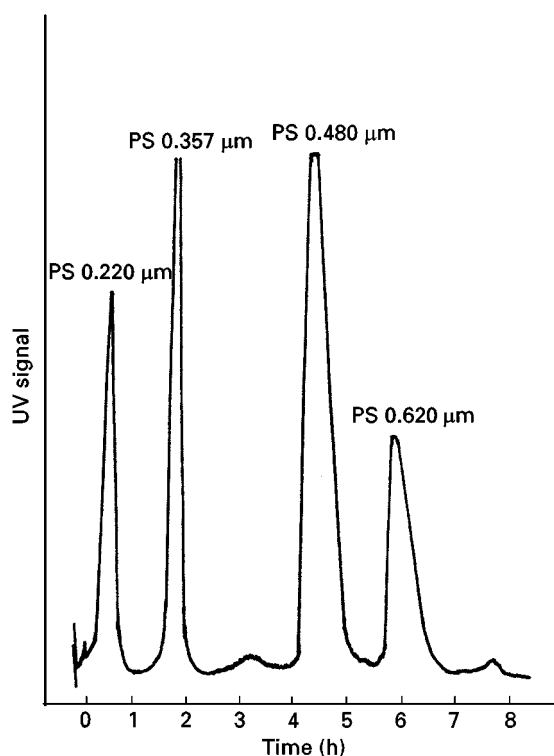


Figure 2 Separation by SdFFF of four polystyrene (PS) latex beads with the diameters indicated in the scheme. The experimental conditions were as follows: field strength 193.7 g; flow rate $12 \text{ cm}^3 \text{ h}^{-1}$; void volume of the channel 2.0 cm^3 . Reproduced from Giddings JC, Myers MN, Caldwell KD and Fisher SR (1980) Analysis of biological macromolecules and particles by field-flow fractionation. *Methods of Biochemical Analysis* 26: 79, with permission from Wiley and Sons, Inc.

ron particles. One of the advantages of SdFFF in characterizing colloids is the fact that they are separated into sharp fractions and that certain properties of each fraction can be deduced by the measurement of the fraction's retention time. Accurate characterization is possible without calibration because of the simplicity and theoretical tractability of the SdFFF system (cf. eqn [3]), when interactions between the particles and the channel wall are absent. Particle parameters subject to characterization include mass, density, polydispersity, diffusivity and various particle dimensions (number and weight average diameters, differential and cumulative size distributions).

A series of papers relating to colloid characterization by SdFFF has been published by Giddings. The first paper showed that relatively monodisperse colloidal populations can be characterized with respect to particle mass, diameter, density and polydispersity. Subsequent papers described methods for obtaining particle size distributions for polydis-

perse colloids and emulsions, and the separation and characterization of narrow populations or subsets within a polydisperse population of colloidal particles.

A wide variety of inorganic colloids of industrial importance, including ceramics, carbon black, quartz, clay silica, alumina, titania, haematite and hydroxyapatite, have been separated and characterized by SdFFF with high resolution in less than 15 min, under optimum conditions. SdFFF also permits analytical separations of submilligram quantities, and the separated components are easily collected for subsequent work. SdFFF can be used on a larger scale to separate quantities of the order of a gram of purified components. Fractionation and characterization by SdFFF of the submicron colloidal particles contained in natural waters have also been carried out. With the aid of an on-channel concentration procedure, SdFFF has been shown to be applicable to an area of analysis where the particle system in natural water is complex and the particles are present in much lower concentrations than in samples which can be analysed without the preconcentration procedure. Although particle diameter can be obtained by SdFFF only if the particle density is known, this apparent weakness can be converted into a major strength. By changing the density of the suspending medium, the difference between it and the density of the solute particles can be changed by known increments, and it becomes simple to split up the d parameter and $\Delta\rho$ terms of eqn [3]. Therefore, both particle size and density can be found by SdFFF.

Particle size distribution analyses have been carried out on a wide variety of suspended organic and inorganic particulates (such as polychloroprene and polymethyl methacrylate lattices, water-based titania and carbon black dispersions, phthalocyanine blue dyes) using the methodology of time-delayed exponential force-field sedimentation field-flow fractionation (TDE-SdFFF). Particle retention time in TDE-SdFFF correlates simply and accurately with the logarithm of particle size (diameter or mass). Relative to constant-field SdFFF, the TDE-SdFFF method provides the advantages of decreased analysis time and improved detection sensitivity, while maintaining adequate resolution for accurate differential and cumulative particle size distributions.

SdFFF has been also used for the kinetic study of aggregation of various inorganic colloids, including hydroxyapatite and sulfide samples. From the variation of the number average diameter obtained by SdFFF with time, rate constants for the bimolecular process of aggregation and stability factors of the colloids have been determined.

Normal FIFFF

FIFFF has been applied to a variety of species including silica gel, latex and virus particles, as well as proteins, protein clusters and water-soluble polymers. FIFFF has also been applied to humic materials, pushing the lower molecular weight limit to a few hundred. An asymmetric version of FIFFF has been introduced in which only one wall, the accumulation wall, is permeable to the liquid, whereas the other wall is solid. Thus, the cross-flow is generated by the fraction of the inlet flow that exists through the membrane. With this asymmetric system, various biological macromolecules and water-soluble polymers have been successfully analysed.

Steric FFF

StFFF represents the upper limit of the field strength applied. Although any effective field may be applied to the StFFF mode, the gravitational field represents the most practical means of utilizing the principle of StFFF to the analysis of particles in the diameter range 1–100 μm . The first experimental evidence for the applicability of StFFF was presented in 1978 by Giddings for the fractionation of glass beads having diameters 10–32 μm . Later the technique was applied to the separation of a mixture of spherical silica beads in the diameter range 5–14 μm , to the separation of a number of large particle samples, including chromatographic support materials and fine-ground coals, as well as to useful applications in biochemistry and biology (yeast cells, whole blood).

Recently, the StFFF technique has been applied to particle size analysis (number and weight average particle diameters, as well as differential and cumulative particle size distributions) of polydisperse supramicron particles of strengite ($\text{FePO}_4 \cdot 2\text{H}_2\text{O}$ with number average diameter of 3.5 μm), which is of great significance in natural waters, and mixed sulfides ($\text{Cu}_x\text{Zn}_{(1-x)}\text{S}$, $0 < x < 1$, with number average diameter in the range 5.7–7.6 μm), which are of paramount importance in industrial chemistry. The particle size distributions, which correspond to the longest axis of the needle-shaped $\text{FePO}_4 \cdot 2\text{H}_2\text{O}$ particles, found under various experimental conditions by StFFF, are in good agreement with those obtained by transmission electron microscopy (TEM). This confirms the feasibility of the StFFF technique for characterizing polydisperse, irregular, inorganic colloids, and verifies the general features of the theory.

From the variation of the number and weight average diameter of the $\text{Cu}_x\text{Zn}_{(1-x)}\text{S}$ particles deter-

mined by GrFFF with various parameters, such as solution pH and ionic strength, kind of detergent and time, in combination with microelectrophoresis measurements, useful conclusions about the stability and consequently the aggregation and deposition phenomena of these sulfides can be deduced.

In the normal mode of SdFFF operation the relationship between V_R and d can be established using eqn [3], without empirical calibration. In the steric mode of SdFFF (Sd/StFFF), calibration must be established empirically, as the steric correction factor in eqn [7] is unknown, increasing with the flow velocity and decreasing with the increase of field strength. As retention is based on particle density as well as size, a purely size-based calibration is not generally valid. By examining the balance between driving and lift forces, it is observed that an equal retention ratio is obtained for equal size particles subject to equal driving forces independently of the particle density. Thus, by adjusting the field strength G to compensate exactly for the density difference $\Delta\rho$, so that the product $G\Delta\rho$ in eqn [3] is the same for the sample and the standard polystyrene latexes, linear calibration plots of $\log(\text{retention time})$ versus $\log(\text{diameter})$ for the latexes can be used to characterize the sample under study. This calibration procedure for Sd/StFFF has been successfully applied to the rapid size separation and measurement of particle size distribution of various starch granules.

Hyperlayer FFF (HyFFF)

The sedimentation hyperlayer field-flow fractionation (SdHyFFF) technique differs from conventional FFF methods in that the solute zone is focused into a thin layer by the opposing forces of centrifugal acceleration and buoyancy in a density gradient, which is formed while the carrier is flowing through the channel. So an equilibrium distribution is established by the time the fluid reaches the downstream injection size. Solutes with low molecular weights require impractically high field strengths to form substantial gradients, whereas particulate density modifiers establish the gradient both rapidly and effectively. Ideally each particle type in SdHyFFF is focused into a very thin layer at its own characteristic elevation. Here it occupies a thin fluid layer flowing at a fixed velocity. The difference of SdHyFFF from the normal SdFFF is that it is the only FFF methodology for which each distinct species is narrowly confined to its own unique velocity state.

The applications of SdHyFFF include the fractionation of polystyrene latex and biological particles

(human and animal cells). With the introduction of denser particles its effective density range has been extended to silica, thus making the technique applicable to environmental particles. Another application of SdHyFFF technique is the fractionation of coal and limestone particles.

In general, the SdHyFFF method is applicable to larger particles than SdFFF, where (wall-induced) steric effects become important for particle sizes around 1 μm . The focusing of sample zones at locations removed from the wall in SdHyFFF has the advantage of eliminating interface-related nonidealities, such as sample adhesion and zone broadening caused by surface roughness.

Important developments include the so-called hyperlayer flow FFF, which has extended the applications to particles larger than 1 μm in diameter. Also, the introduction of various programming procedures has been of importance. A number of reports of the combined use of FIFFF and multi-angle laser light scattering (MALLS) instruments have also been published, illustrating the usefulness of this hyphenated technique in characterizing colloidal particles.

Potential Barrier FFF (PBFFF)

Potential barrier field-flow fractionation (PBFFF), developed by Karaiskakis, is a combination of potential barrier chromatography and FFF. Potential barrier chromatography can be applied to separate particles based on differences in size or in any of the physicochemical parameters involved in the potential energy of interaction between the particles and the packing of the chromatographic column. The particle size analysis of colloidal materials by PBFFF is based either on particle size differences or on Hamaker constant, surface potential and Debye-Huckel reciprocal differences. The method, which is based on the existence of a surmountable potential barrier between the colloidal particles and the FFF channel wall, is classified as an FFF method rather than a chromatographic method, because the selective interaction is experienced in one phase. Thus, by combining potential barrier chromatography with normal or steric FFF one could separate according to two mechanisms, one governed by the depth of the potential energy well for the different particles and the other determined by the interactive force between the particles and the external field. In its simplest form the

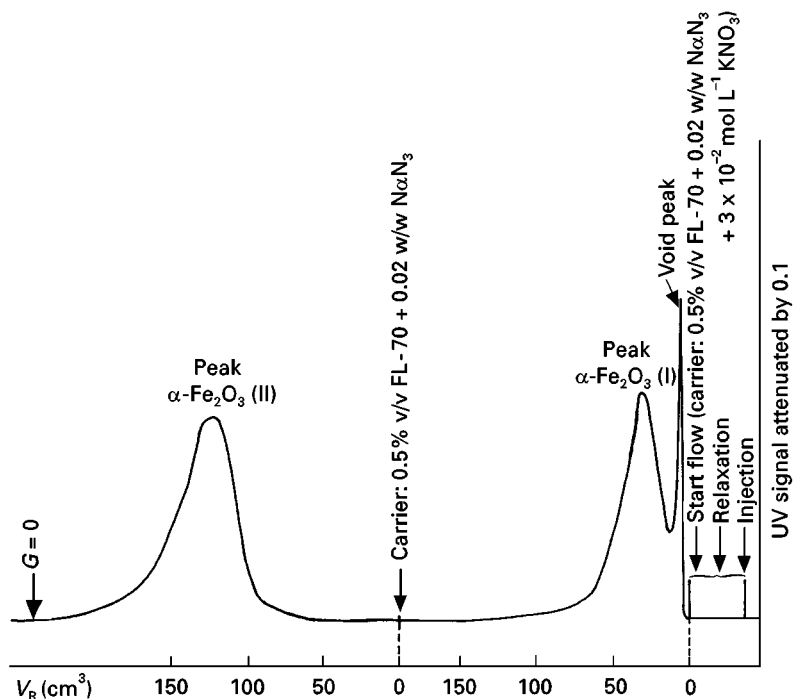


Figure 3 Fractionation of haematite-I ($\alpha\text{-Fe}_2\text{O}_3(\text{I})$) with nominal diameter 0.148 μm and haematite-II ($\alpha\text{-Fe}_2\text{O}_3(\text{II})$) with nominal diameter 0.248 μm) colloidal particles by the potential barrier SdFFF technique. The experimental conditions, except for those given in the scheme, were as follows: field strength 15.5 g ; flow rate 150 $\text{cm}^3 \text{h}^{-1}$; void volume of the channel 2.06 cm^3 . Reproduced from Koliadima A and Karaiskakis G (1990) Potential-barrier field-flow fractionation, a versatile new separation method. *Journal of Chromatography* 517: 345, with permission from Elsevier Science.

technique consists of changing the ionic strength of the carrier solution from a high value, where only one of the colloidal materials of the binary mixture to be separated totally adheres at the beginning of the FFF channel wall, to a lower value, where all the adhered particles are released.

Figure 3 shows the fractionation of two haematite samples (α -Fe₂O₃(I) with nominal particle diameter 0.148 μ m and α -Fe₂O₃(II) with nominal particle diameter 0.248 μ m) with monodisperse spherical particles, by the PBSdFFF technique. The mixture was introduced into the channel with a carrier solution containing 0.5% v/v detergent FL-70, 0.02% w/w NaN₃ and 3×10^{-2} mol L⁻¹ KNO₃. At this high electrolyte concentration all of the α -Fe₂O₃(II) particles adhered at the beginning of the SdFFF Hastelloy-C channel wall, whereas all of the α -Fe₂O₃(I) particles were eluted from the channel. The average diameter of the eluted α -Fe₂O₃(I) particles was found from eqn [3] to be 0.151 μ m, in good agreement with that obtained by normal SdFFF (0.145 μ m) or determined by TEM (0.148 μ m). Variation of the carrier solution to one containing only 0.5% v/v detergent FL-70 and 0.02% w/w NaN₃ without any KNO₃ released all the adhered α -Fe₂O₃(II) particles and gave a particle diameter (0.244 μ m) in good agreement with that found by normal SdFFF (0.237 μ m) or obtained by TEM (0.248 μ m).

A general methodology for the analysis of a colloidal mixture by PB SdFFF consists of injecting into the column the mixture with a carrier solution in which the ionic strength is too high to ensure total adhesion of all the components of the mixture, except for one with the lower attractive force with the channel wall. Then a programmed variation (decrease) of the ionic strength of the carrier solution is applied to release, in time, the adherent particles according to their size and/or surface characteristics. As the PBSdFFF technique is based on particle-wall interactions, its applications can be extended by using different materials, such as stainless steel, Teflon and polyimide. PBSdFFF is also a convenient and accurate method for the concentration and analysis of dilute colloidal samples. This makes PBSdFFF a highly attractive technique for the characterization of samples where even particles of the same size but of different chemical composition are present in low concentration.

Future Developments

From the detailed description of the FFF techniques presented above, it is concluded that the most usable FFF methods for particle size analysis of colloids are SdFFF and FIFFF. Looking to the future, it

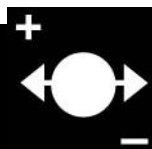
is reasonable to expect serious efforts by the companies producing FFF equipments, to improve their resolution and expand the particle size range to lower limits of analysis. As far as FFF applications are concerned, it is believed that future efforts will be focused on the size separation and characterization of polydisperse, irregular colloidal particles, as well as on the aggregation and deposition phenomena of colloids on solid surfaces.

See also: II/Particle Size Separation: Field Flow fractionation: Electric Fields; Field Flow Fractionation: Thermal; Theory and Instrumentation of Field Flow Fractionation. III/Cells and Cell Organelles: Field Flow Fractionation. Colloids: Field Flow Fractionation. Polymers: Fixed Flow Fractionation. Proteins: Field Flow Fractionation.

Further Reading

- Beckett R and Hart BT (1993) Use of field-flow fractionation techniques to characterize aquatic particles, colloids and macromolecules. In: Buffle J and van Leeuwen HP (eds) *Environmental Particles*, vol. 2, pp. 165–205. Boca Raton, FL: Lewis Publishers.
- Dondi F and Guiochon G (eds) (1992) *Theoretical Advancements in Chromatography and Related Separation Techniques*, vol. 383. NATO ASI series. Dordrecht: Kluwer Academic.
- Giddings JC (1966) A new separation concept based on a coupling of concentration and flow nonuniformities. *Separation Science* 1: 123–125.
- Giddings JC (1991) *Unified Separation Science*. New York: Wiley.
- Giddings JC, Martin MN, Moon MH and Barman BN (1991) Particles separation and size characterization by sedimentation field-flow fractionation. In: Provder J (ed.) *Particle Size Distribution II: Assessment and Characterization*, American Chemical Society, Series no. 472, Ch. 13, pp. 198–216. Washington, DC: ACS Symposium.
- Hiemenz PC (1977) *Principles of Colloid and Surface Chemistry*. New York: Marcel Dekker.
- Janca J (1988) *Field-Flow Fractionation: Analysis of Macromolecules and Particles*. New York: Marcel Dekker.
- Karaiskakis G and Cazes J (eds) (1997) *Journal of Liquid Chromatography & Related Technologies, Special Issue on Field-Flow Fractionation* (Vol. 20, Nos 16 & 17). New York: Marcel Dekker.
- Lloyd PJ (ed.) (1987) *Particle Size Analysis 1985*. New York: Wiley.
- Martin M and Williams PS (1992) Theoretical basis of field-flow fractionation. In: Dondi F and Guiochon G (eds) *Theoretical Advancement in Chromatography and Related Separation Techniques*, vol. 383. NATO ASI series, pp. 513–580. Dordrecht: Kluwer Academic.

COMPUTER DATABASES FOR TWO-DIMENSIONAL ELECTROPHORESIS



T. Toda, Tokyo Metropolitan Institute of Gerontology,
Tokyo, Japan

Copyright © 2000 Academic Press

Two-dimensional (2-D) electrophoresis is an unrivalled technique of the highest capacity to separate many thousands of proteins in complex specimens such as a crude extract of cells. The development of computer systems for 2-D gel image analysis has promoted the construction of comprehensive databases for 2-D electrophoresis. The recent advance in the Internet computer network has allowed us to share useful pieces of information located in many 2-D electrophoresis databases on the worldwide web (WWW) via the Internet. And a new field of research named proteomics has been growing based on 2-D electrophoresis databases.

2-D Electrophoresis

2-D electrophoresis, established by O'Farrell in 1975, is a combined technique of isoelectric focusing (IEF) and sodium dodecyl sulfate (SDS)-polyacrylamide gel electrophoresis (PAGE) for achieving the finest resolution of proteins in crude specimens. Protein molecules of different isoelectric points (pI) are separated at the first stage of IEF, and components of different molecular masses are resolved in the second-dimensional SDS-PAGE.

The IEF in a mobile pH gradient, which is automatically generated by lining up carrier ampholytes in the order of pI, is performed in the original protocol of O'Farrell's 2-D electrophoresis. However, there is still a problem with the conventional IEF method in the drift of the pH gradient toward the cathode. Righetti and colleagues have devised an improved method of IEF which runs on an immobilized pH gradient (IPG) to prevent cathodic drift. The IPG-IEF is adopted in most current protocols of 2-D electrophoresis for constructing computer databases.

Protein Detection

Proteins separated on a gel plate are detected by autoradiography if they are labelled with a radioisotope. Nonradioactive proteins are visualized by silver or dye staining depending on the protein amount on

the gel. The protein profile on the 2-D gel reports useful information about qualitative and quantitative states of proteins in the specimen. Most computer databases for 2-D electrophoresis have generally been constructed on such visualized 2-D gel images.

2-D Gel Image Analysis

Computer analysis of the 2-D gel images was developed after O'Farrell's paper because 2-D gel images were too complicated to be analysed manually. Lipkin and Lemkin of the National Institutes of Health in the USA made their GELLAB system on a DEC minicomputer in 1980, and independently of this, Anderson *et al.* constructed their original TYCHO system in 1981. Garrels and Franza prepared a prototype software for 2-D gel image analysis on a compact Hewlett Packard desktop computer in 1979, and then developed it into the QUEST system for an UNIX-based minicomputer in 1983. The PDQUEST, which is a commercially available software package for SUN UNIX workstations, was a revision of the QUEST system. Many other software packages, such as Melanie II and GELLAB II, have been made commercially available. Those Macintosh- and Windows-based software packages have allowed 2-D gel image analysis to be performed easily for database construction.

Western Blotting

Western blotting is an immunochemical technique for detecting specific proteins. Protein spots separated by 2-D electrophoresis are transferred on to a nitrocellulose or polyvinylidene difluoride (PVDF) membrane by electrotransfer blotting. After blocking, the membranes are treated with a specific antibody and followed by a second enzyme-linked antibody. Localization of specific protein on the membrane is visualized by an enzyme reaction. The results of spot protein identification by Western blotting are also included in 2-D electrophoresis databases.

Microsequencing

The N-terminal peptide sequences of proteins are directly determined with an automatic peptide sequencer after electrotransfer blotting on to a PVDF membrane, if the N-terminal α -amino group is free.

Proteins that are blocked at the N-terminus are often cleaved with endopeptidase. The digests are separated by reversed-phase high performance liquid chromatography (HPLC) and then subjected to sequencing. Protein databases on the Internet may answer a query on the homology of the amino acid sequence for identification of the protein if the database includes an entry of the protein itself or family gene products. The sequence data and the results of homology search are both valuable information for constructing 2-D electrophoresis databases.

Mass Spectrometry

Mass spectrometry is another powerful technique for identification of proteins separated by 2-D electrophoresis. The peptide mass fingerprinting of endopeptidase digests is extensively used for primary assignment of the protein. The ExPASy Molecular Biology server (<http://www.expasy.ch/>) offers useful proteomic tools such as PeptIdent, which helps us in peptide mass fingerprinting works for protein identification (Figure 1).

Peptide Mass Fingerprinting

Name of the unknown protein: new

Database: new

Note: For proteins from TrEMBL, peptides with masses >10000 Da have not been indexed.

pI: within pI range:

Mw: within Mw range (in percent):

Species to be searched:

Note: As of SWISS-PROT release 37, OC (Organism Classification) lines contain the classification terms proposed by the NCBI.

Enter a list of peptide masses (separated by spaces or newlines) that correspond to the unknown protein:

Or upload a file in .pkm format from your computer (only works if you see a 'browse' button next to the text entry field, e.g. for Netscape browsers resp. Internet Explorer 4). The peptide masses will be extracted automatically from this file:

All peptide masses are

- ☒ [M+H]⁺ or ☐ [M], and
- ☒ monoisotopic or ☐ average.

The peptide masses are with cysteines treated with:

- ☐ with acrylamide adducts on cysteines
- ☐ with methionines oxidized.

Mass tolerance:

Enzyme:

Allow for missed cleavage sites (MC).

Report only proteins with at least peptide hits.

Display a maximum of matching proteins.

Figure 1 Proteomic analysis tool PeptIdent in the ExPASy Molecular Biology server. The URL is <http://www.expasy.ch/tools/peptident.html>.

History of 2-D Electrophoresis Databases

The 2-D electrophoresis database, reported by Lipkin and Lemkin in 1980, was only for multiple 2-D gel image analyses on a stand-alone minicomputer. In their GELLAB system, a composite gel (CGEL) database was made by extracting spot data from multiple gels and merging them into a representative gel. The primary database consisted of the lists of corresponding spots, their associated properties and interrelations. The human serum protein 2-D electrophoresis database for clinical use, reported by

Anderson and his co-workers in 1981, was also only for personal use on an offline computer. Human keratinocyte 2-D electrophoresis databases, made by Celis *et al.* on a UNIX workstation with PDQUEST software, were offered to many research groups commercially, but not made accessible on the Internet.

Appel and his co-workers constructed their SWISS-2DPAGE database (Figure 2) on the ExPASy molecular biology server of the Swiss Geneva University Hospital in 1993. It was the first regular 2-D electrophoresis database on the WWW, and it has been accessible on the Internet.

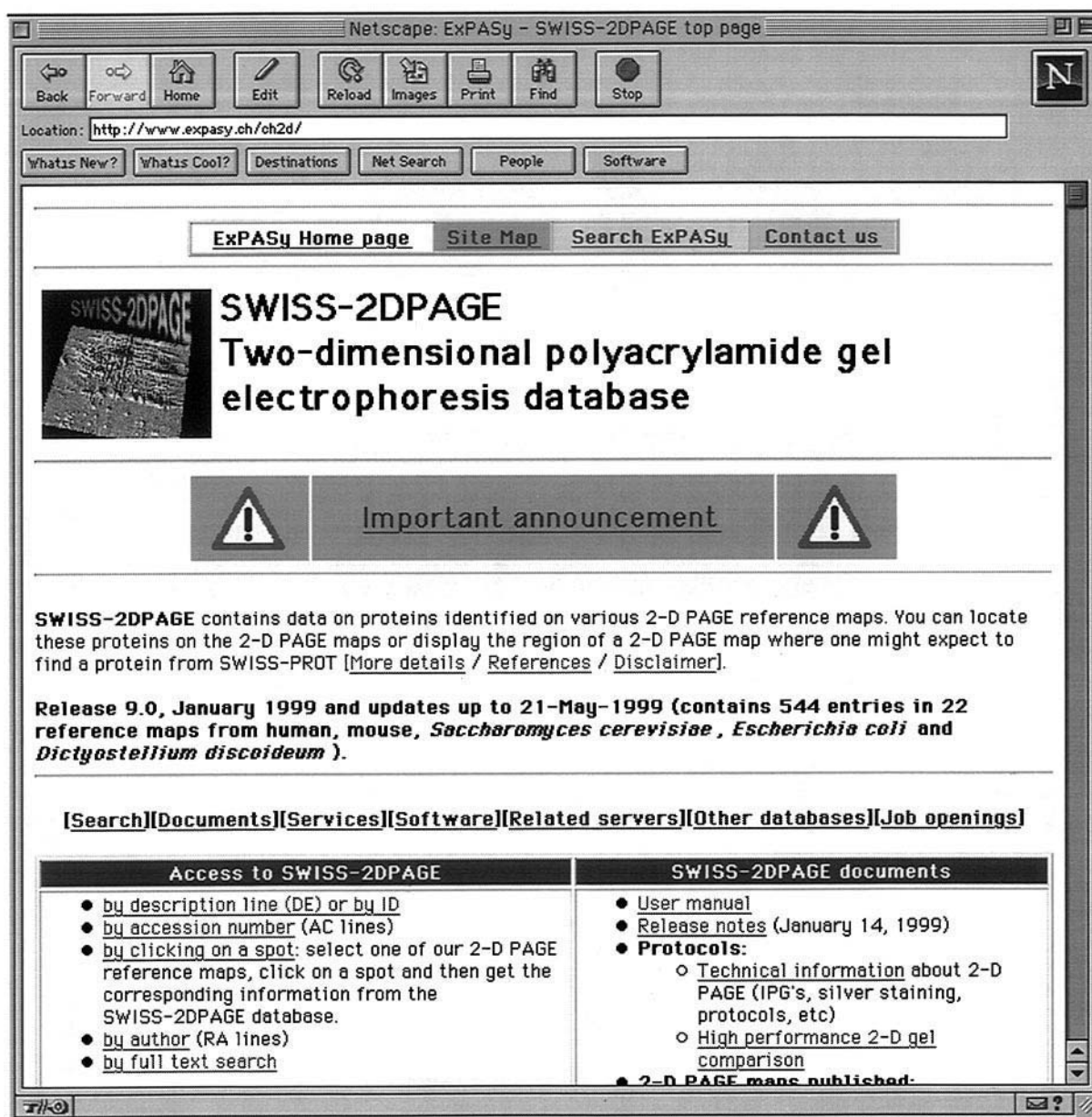


Figure 2 The SWISS-2DPAGE top page in the ExPASy Molecular Biology server of the Swiss Geneva University Hospital. The URL is <http://www.expasy.ch/ch2d/>.

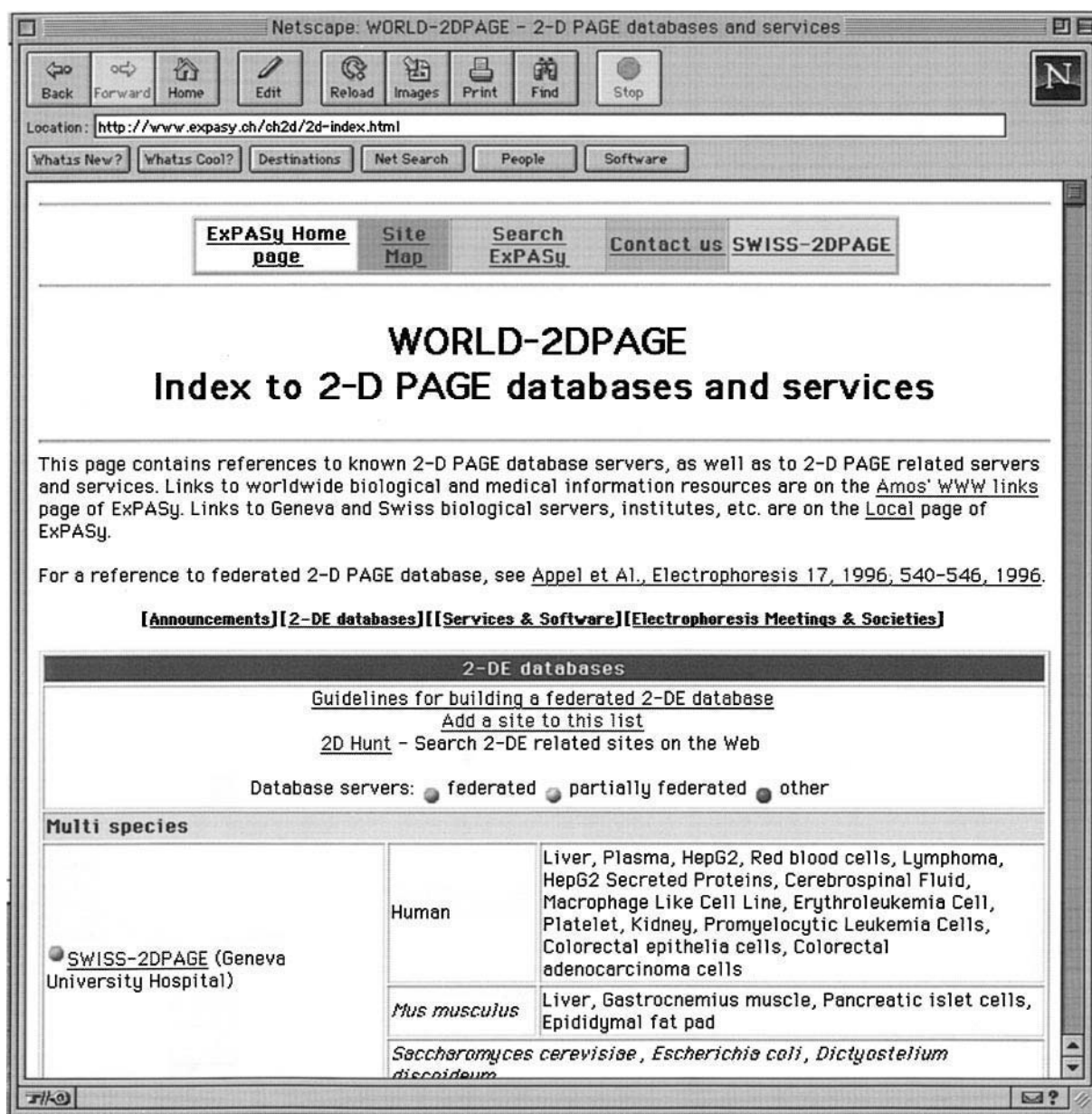


Figure 3 The WORLD-2DPAGE home page for indexing to 2-D PAGE databases and services throughout the world. The URL is <http://www.expasy.ch/ch2d/2d-index.html>.

WORLD-2DPAGE home page (Figure 3) presented at <http://www.expasy.ch/ch2d/2d-index.html> in the ExPASy server offers a convenient link to many 2-DE databases in the world.

The databases listed in Table 1 were indexed in the WORLD-2DPAGE page for link as of 15 June, 1999.

Some of the databases have been built following the guidelines for the federated 2-D electrophoresis database recommended by Appel *et al.* Rules for the database federation are summarized in Table 2.

World-Wide Web for 2-D Electrophoresis Database

The WWW is a database server system which was initiated in the European Centre for Nuclear Research on the basis of Internet protocol technology. The WWW allows browsers on a computer to access information stored on remote servers through the Internet. One of the main features of WWW documents is the hypertext structure; another significant feature is the function of a clickable image map.

Table 1 A partial list of 2-D electrophoresis databases indexed in the WORLD-2DPAGE home page

SWISS-2DPAGE (Geneva University Hospital)	http://www.expasy.ch/ch2d/
SIENA-2DPAGE: 2D-PAGE database at Department of Molecular Biology, University of Siena, Italy	http://www.bio-mol.unisi.it/2d/2d.html
2-DE maps at LSB Corp	http://WWW.LSBC.COM/2dmaps/patterns.htm
Human and mouse 2-D PAGE databases:	
Danish Centre for Human Genome Research	http://biobase.dk/cgi-bin/celis
RAT HEART-2DPAGE (German Heart Institute, Berlin)	http://gelmatching.inf.fu-berlin.de/~pleiss/2d/
HEART-2DPAGE (German Heart Institute, Berlin)	http://userpage.chemie.fu-berlin.de/~pleiss/dhzb.html
HSC-2DPAGE (Heart Science Centre, Harefield Hospital)	http://www.harefield.nthames.nhs.uk/nhli/protein/
PDD: Protein Disease Database (NIMH-NCI)	http://www-lecb.ncifcrf.gov/PDD/
PPDB: PhosphoProtein DataBase	http://www-lecb.ncifcrf.gov/phosphoDB/
Molecular Anatomy Laboratory at Indiana University, Columbus	http://iupucbio1.iupui.edu/frankw/molan.htm
Human Colon Carcinoma Protein Database at JPSL, Ludwig Institute for Cancer Research, Melbourne, Australia	http://www.ludwig.edu.au/jpsl/jpslhome.html
TMIG-2DPAGE: Age-related Protein Database at Tokyo Metropolitan Institute of Gerontology	http://proteome.tmig.or.jp/2D/
UCSF 2D PAGE (A375 cell line)	http://rafael.ucsf.edu/2DPAGE/home.html

NIMH-NCI, National Institute of Mental Health and National Cancer Institute.

Hypertext Cross-Reference

Links from the 2-D electrophoresis database to related databases, such as GenBank DNA database in NCBI Entrez, SWISS-PROT protein database or SWISS-3DIMAGE three-dimensional structure databases, through hypertext cross-references is a common function of most databases for 2-D electrophoresis. The function is achieved with anchor tags in hypertext mark-up language (HTML) and executive scripts for common gateway interface (CGI). For example, in TMIG-2DPAGE, the data entry for human nm-23 carries the following hypertext cross-reference to the corresponding SWISS-PROT (P15531) and NCBI GenBank (X75598) entries respectively.

SWISS-PROT

```
<A HREF = "http://www.expasy.ch/cgi-bin/
sprot-search-ac?P15531" TARGET = "_blank">
P15531 </A>
```

Table 2 Guidelines for building a federated 2-DE database

1. Individual entries in the database must be accessible from remote by keyword search
2. The database must be linked to other databases through active hypertext cross-references
3. A main index has to be supplied that provides a means of querying all databases through one unique entry point
4. Individual protein entries must be accessible through clickable images
5. 2-DE analysis software, been designed for use with federated 2-DE database, must be able to access directly individual entries in any federated 2-DE database

For full details, see Appel RD *et al.* (1996) in *Electrophoresis* 17: 540–546.

GenBank

```
<A HREF = "http://www3.ncbi.nlm.nih.gov/
htbin-post/Entrez/ query?db = n&form =
6&dopt = g&uid = X75598" TARGET =
"_blank"> X75598 </A>
```

Clickable Image Map

Clickable image map is a function of CGI installed in the WWW server software for achieving an active link from a location on an image to a corresponding file. All federated 2-D electrophoresis databases on the WWW have 2-D gel images for the clickable image map. The content of each protein data entry is displayed on the monitor screen when the mouse button is clicked on the corresponding spot on the 2-D gel image.

Setting up a 2-D Electrophoresis Database on the WWW

To set up a 2-D electrophoresis database, software for WWW server, such as Apache httpd, must be working on a UNIX or LINUX server computer connected to the Internet. The function of clickable image map is included in the Apache modules if they are properly installed. To set up a new 2-D electrophoresis database, prepare the following four types of files first, according to the *Apache Reference Manual*, which is available in the Apache directory.

1. A hypertext file for the image map top page (*.html).
2. A 2-D gel image file in the GIF format for the clickable image map (*.gif).

3. A map file for directing the jumping destination (***.map).
4. Text files of protein data entries as destinations for links (***.html).

When these files are placed in the appropriate directories in the WWW server, the basal activity of the 2-D electrophoresis database starts running.

2-D Electrophoresis Databases on the WWW

SWISS-2DPAGE

The SWISS-2DPAGE is a fully implemented 2-DE federated database. The ExPASy WWW server is

home to five locally maintained databases (SWISS-PROT, SWISS-2DPAGE, PROSITE, SWISS-3DIMAGE and ENZYME). Besides the database service, the server offers special tools for proteomic analysis, such as PeptIdent for peptide mass fingerprinting. SWISS-PROT serves as a searchable main index, prepared according to rule 3, and has cross-references to the other four databases. SWISS-2DPAGE contains data on protein identified on various 2-D PAGE reference maps. The hypertext cross-references as of 15 June 1999 include links to SWISS-PROT, YPD database of yeast *Saccharomyces* and the ECO2DBASE *E. coli* database. The X-ray crystallography Protein Data Bank (PDB), the Mendelian Inheritance in Man data bank (OMIM), the G-protein-coupled receptor database (GCRDb) and the

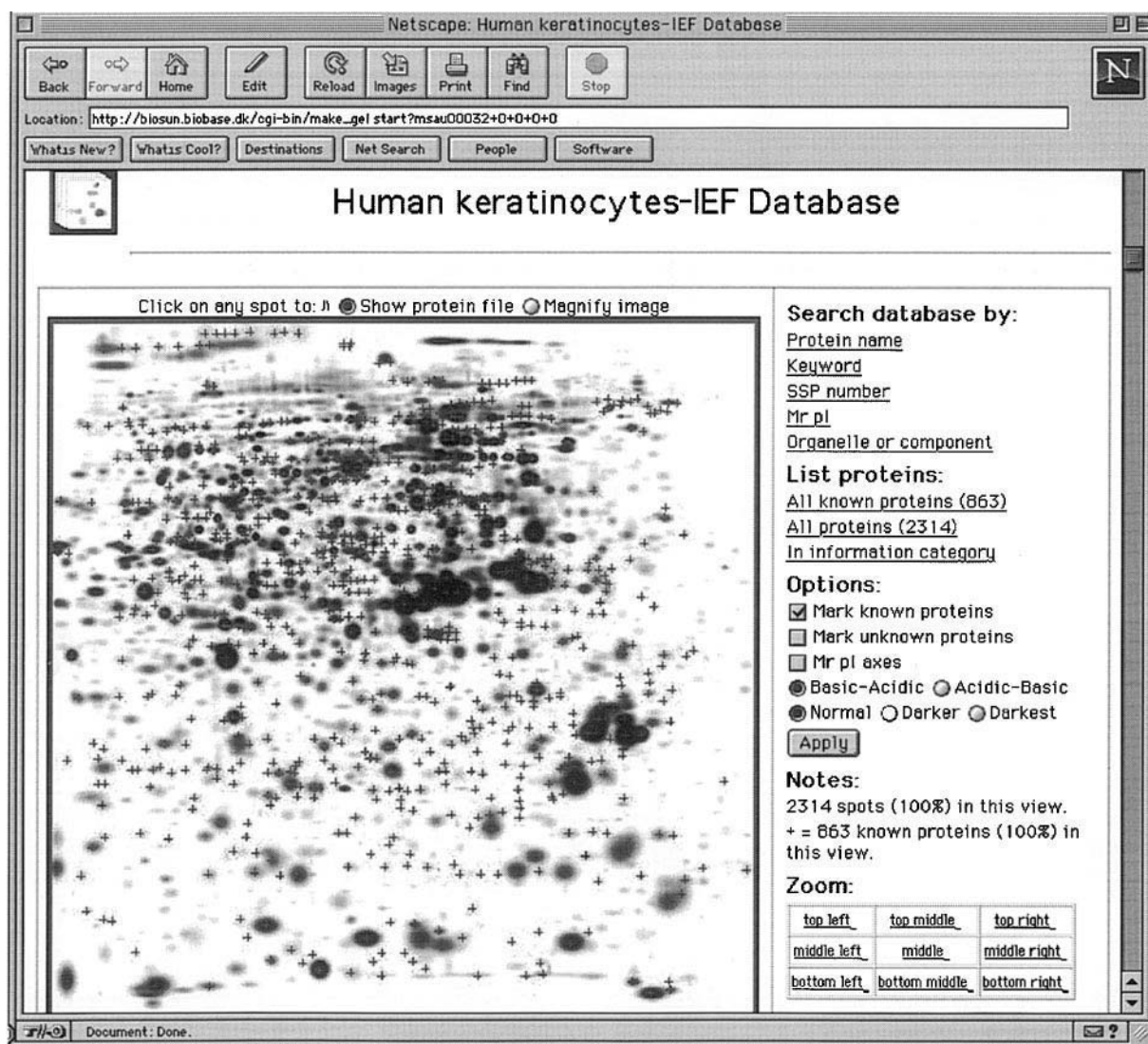


Figure 4 Human keratinocytes 2-D PAGE database in the Danish Centre for Human Genome Research. The URL is http://biosun.biobase.dk/cgi-bin/make_gel.start?msau00032+0+0+0+0.

database of yeast (*Saccharomyces cerevisiae*) genes coding for proteins (LISTA) are also linked through SWISS-PROT.

Human 2-D PAGE Databases of the Danish Centre For Human Genome Research

The human 2-D PAGE databases at the University of Aarhus, which were developed for functional genome analysis in health and disease, contain data on pro-

teins identified on various reference maps. Databases of human keratinocytes (Figure 4) are served for the study of skin biology, and those of transitional cell carcinomas are for the study of bladder cancer.

Heart-2DPAGE

The Heart-2DPAGE at the German Heart Institute in Berlin is a human myocardial 2-D protein database that implements the first four rules of the

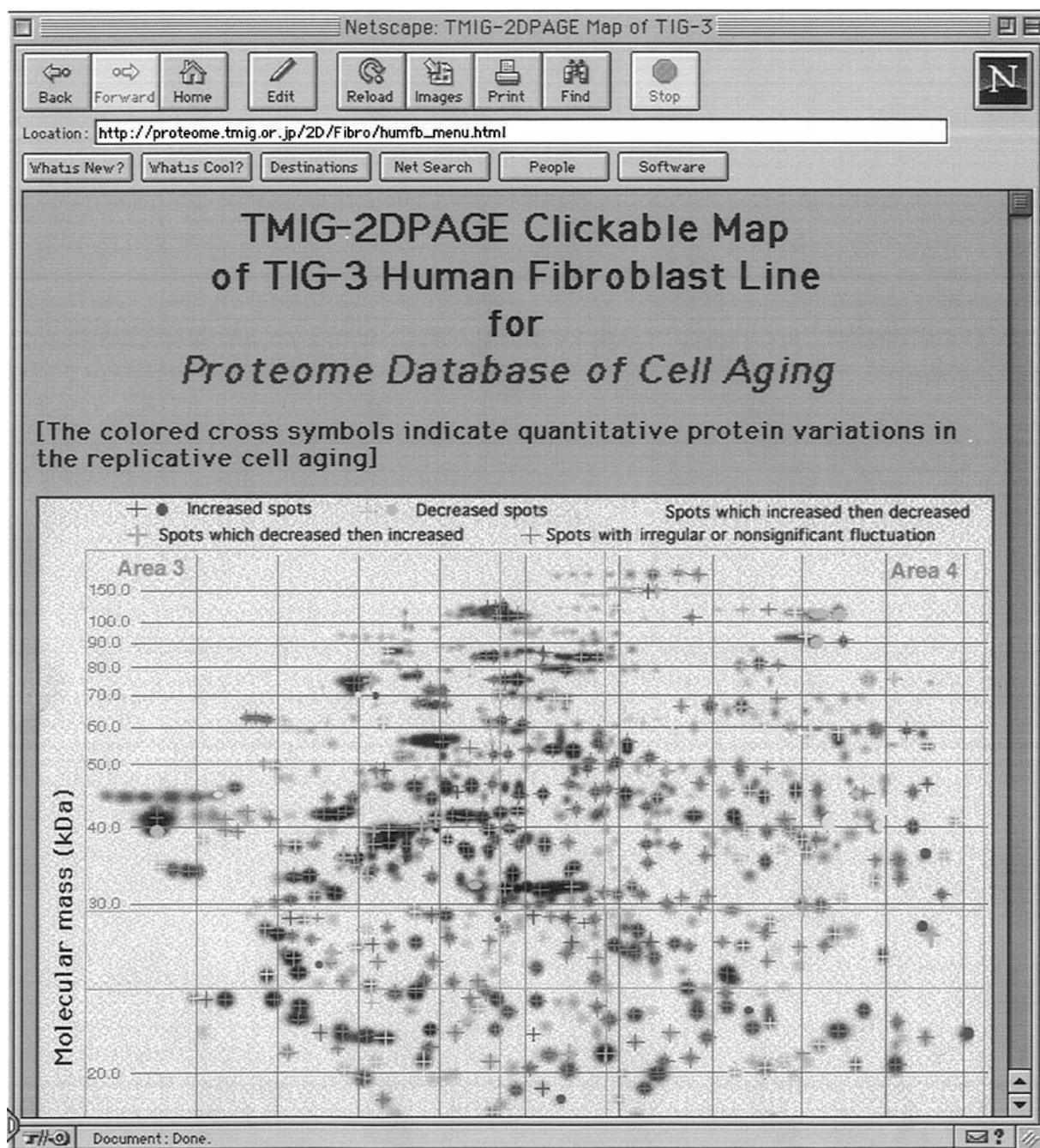


Figure 5 TMIG-2DPAGE clickable map of TIG-3 human fibroblast line. The URL is http://proteome.tmig.or.jp/2D/Fibro/humfb_menu.html.

federated 2-D database. It contains data on the human heart ventricle and atrium. The data are accessible both by keyword search on the protein name and by mouse-clicking on two images of 2-D. Entries provide data related to the isoelectric point, the molecular mass and the amino acid sequence of each spot protein.

PDD Protein Disease Database

The PDD Protein Disease Database on the WWW server is a part of the National Institute of Mental Health and National Cancer Institute (NIMH-NCI) Protein-Disease Database Project for correlating diseases with proteins observed in serum, cerebrospinal fluid, urine and other common human body fluids based on biomedical literature. The PDD database includes the data of quantitative and qualitative protein variations with disease states, answering questions on protein patterns found in common body fluids with respect to disease conditions in the literature.

TMIG-2DPAGE

TMIG-2DPAGE is a database of human proteins involved in the mechanisms of cell ageing. It includes two clickable image maps for data entries of proteins in normal cell ageing, and for those in the disease state of Werner's syndrome patients. On the TMIG-2DPAGE clickable map of TIG-3 human fibroblast line, quantitative variations of proteins observed in the process of replicative cell ageing are demonstrated with coloured crosses (Figure 5).

As a mouse button is clicked on a protein spot, the corresponding data entry is displayed on the browser. Each data entry contains information on age-related protein variation, physicochemical properties, references and active links to both SWISS-PROT and NCBI Entrez nucleotide sequence databases.

Keyword Search of 2-D Electrophoresis Databases

The 2DHunt on the ExPASy server (<http://www.expasy.ch/ch2d/2DHunt/>) is a convenient search engine for WWW sites of 2-D electrophoresis databases. The site list for 2DHunt search is periodically created by the site retrieval robot supplied from the Marvin

(Multi-Agent Retrieval Vagabond on Information Networks). Although some irrelevant sites may sometimes be hit, the search engine is helpful for many researchers to find specific 2-D electrophoresis databases of their own interests.

Further Reading

- Anderson NL, Taylor J, Scandore A *et al.* (1981) The TYCHO system for computer analysis of two-dimensional gel electrophoresis patterns. *Clinical Chemistry* 27(11): 1807-1820.
- Appel RD, Hoogland C, Bairoch A and Hochstrasser DF (1999) Constructing a 2-D database for the World Wide Web. *Methods in Molecular Biology* 112: 411-416.
- Celis JE, Gromov P, Stergaard M *et al.* (1996) Human 2-D PAGE databases for proteome analysis in health and disease: <http://biobase.dk/cgi-bin/celis>. *FEBS Letters* 398(2-3): 129-134.
- Garrels JI and Franza Jr BRF (1989) The REF52 protein database. *Journal of Biological Chemistry* 264(9): 5283-5298.
- Hoogland C, Sanchez JC, Tonella L *et al.* (1998) Current status of the SWISS-2DPAGE database. *Nucleic Acids Research* 26(1): 332-333.
- Lemkin PF (1997) The 2DWG meta-database of two-dimensional electrophoretic gel images on the Internet. *Electrophoresis* 18(15): 2759-2773.
- Lipkin LE and Lemkin PF (1980) Data-base techniques for multiple two-dimensional polyacrylamide gel electrophoresis analyses. *Clinical Chemistry* 26(10): 1403-1412.
- O'Farrell PH (1975) High resolution two-dimensional electrophoresis of proteins. *Journal of Biological Chemistry* 250(10): 4007-4021.
- Righetti PG, Gianazza E and Bjellqvist B (1983) Modern aspects of isoelectric focusing: two-dimensional maps and immobilized pH gradients. *Biochemical and Biophysical Methods* 8(2): 89-108.
- Toda T and Kimura N (1998) TMIG-2DPAGE: a new concept of two-dimensional gel protein database for research on aging. *Electrophoresis* 18(2): 344-348.
- Toda T and Ohashi M (1995) Review: Current status and perspectives of computer-aided two-dimensional densitometry. *Journal of Chromatography A* 698(1): 41-54.
- Vesterberg O and Svensson H (1966) Isoelectric fractionation, analysis, and characterization of ampholytes in natural pH gradients. IV. Further studies on the resolving power in connection with separation of myoglobins. *Acta Chemica Scandinavica* 20(3): 820-834.

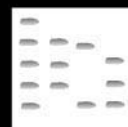
CONTINUOUS ION EXCHANGE USING POWDERED RESINS

See III/POWDERED RESINS: CONTINUOUS ION EXCHANGE

COPRECIPITATION: TRACE ELEMENTS: EXTRACTION

See III/TRACE ELEMENTS BY COPRECIPITATION: EXTRACTION

COSMETICS AND TOILETRIES: CHROMATOGRAPHY



M. Carini and R. M. Facino, Istituto Chimico Farmaceutico Tossicologico, University of Milan, Italy

This article is reproduced from *Encyclopedia of Analytical Science*, Copyright © 1995 Academic Press

Toiletries, used by millions of consumers for the daily care and hygiene of the body, include several products (mainly rinse products) with different formulae: soaps, shampoos, bath foams, toothpastes, deodorants.

Since surfactants are the basic materials used in toiletries (in soaps and shampoos they increase the washing properties of water; in shaving products they act as wetting and foaming agents; in bath oils they make the perfume water-soluble; in hair products they are used as conditioners), this article will deal with the techniques used for the analysis of these important constituents.

Leaving aside the rough, but still used, organoleptic testing (odour, colour, clarity, opalescence), analytical procedures for quality control may range from physical evaluations (specific gravity, refractive index, optical rotation, viscosity) to chemical analysis by standard volumetric and gravimetric methods, and instrumental analysis by chromatographic techniques (thin-layer, gas and liquid chromatography) and spectroscopic techniques (ultraviolet, infrared and nuclear magnetic resonance spectroscopy and mass spectrometry). Chromatographic and spectroscopic methods now find wide application, since toiletries and raw materials are complex mixtures, and there is a constant need to distinguish subtle structural differences in composition and determine impurities even if present in trace amounts.

The term surfactant (a contraction for surface-active agent) is used to describe organic chemicals that, when added to a liquid, change the interfacial properties of that liquid. Chemically surfactants can be divided into two major classes: nonionic

(uncharged substances) which do not dissociate in aqueous solution, and ionic (charged substances) which dissociate and form ions, one of which becomes the actual surface-active agent. Ionic surfactants are classified by the nature of their charges in solution: anionic (negatively charged), cationic (positively charged), amphoteric (both positively and negatively charged).

Anionic Surfactants

Anionic surfactants constitute about 65% of all surfactants manufactured and it is not surprising that the bulk of literature on surfactants deals with the analysis of these compounds. **Table 1** reports the main types of anionic surfactants used in toiletries.

The quality control of anionics in raw materials and in finished products is mainly quantitative and several methods that give a total estimate of active ingredients have been developed. The two-phase mixed indicator titration and other titrimetric analyses, such as direct colorimetric titration and precipitation titration are the simplest procedures, since they are sufficiently reliable, require little and inexpensive equipment, and can be used for both product development and quality control applications. The two-phase mixed indicator titration is based on the extraction of an anionic-indicator or cationic-indicator complex into a nonaqueous solvent (usually chloroform) in equilibrium with an aqueous solution of the unknown anionic surfactant or the titrating cationic surfactant. The method is not quantitative for compounds containing fewer than 12 carbon atoms when chloroform is the organic phase (in this case a mixed organic phase of 2:3 (v/v) chloroform-1-nitropropane must be used). Sodium, magnesium or sulfate ions at concentrations up to 0.4 mol L^{-1} do not interfere, while chloride interferes above $5 \times 10^{-3} \text{ mol L}^{-1}$.

All the spectrophotometric procedures are based on the formation of a solvent-extractable compound

Table 1 Anionic surfactants

Type	General structure
Alkyl carboxylates (soaps)	$R-COO^-X^+$ C_8-C_{18} fatty acids; salts with NaOH, KOH, NH_4OH , monoethanolamine (MEA), diethanolamine (DEA), triethanolamine (TEA)
Alkylethoxylated carboxylates	$R-(OCH_2CH_2)_nOCH_2COO^-X^+$ $R = C_8-C_{18}$ fatty alcohols $X = Na, K, NH_4, MEA, DEA, TEA$
Alkyl sulfates	$R-O-SO_3^-X^+$ $R = C_8-C_{18}$ fatty alcohols $X = Na, K, Mg, NH_4, MEA, DEA, TEA$
Alkylethoxylated sulfates (AES)	$R-(OCH_2CH_2)_n-O-SO_3^-X^+$ $R = C_8-C_{18}$ fatty alcohols $X = Na, K, Mg, NH_4, MEA, DEA, TEA$
Alkylarylsulfonates	$R-C_6H_5-SO_3^-X^+$ $R = C_{10}-C_{12}$
α -Olefin sulfonates	$R-SO_3^-Na^+$ $R = C_{14}-C_{16}$
Isethionates	$R-CO-O-CH_2CH_2-SO_3^-Na^+$ $R-CO = C_{12}-C_{18}$ fatty acids

between the anionic surfactant and a coloured cationic species: Methylene blue, Methyl green, Toluidine blue, Rosaniline, Brilliant green and Methyl violet being the most widely used. These cationic compounds are not extractable as such by organic solvents, but in the presence of anionic species they form a stable, stoichiometric ion-association complex that is poorly soluble in water, because it has no nett charge. The complex is extracted into the organic solvent and the absorbance gives a direct measure of the surfactant present.

These techniques are not suited for establishing the qualitative composition of these surfactants, e.g. for differentiating homologues and oligomers, for characterization of single components of a surfactant mixture, or for detection and quantification of impurities (unreacted materials, by-products), and when such determinations are required for finished detergent formulations.

Hence, more specific and sensitive chromatographic techniques such as thin-layer chromatography (TLC), gas chromatography (GC) and liquid chromatography (LC) have been developed and are now widely accepted in the surfactant industry. Mass spectrometry (MS) and tandem mass spectrometry (MS-MS), although considered the techniques of choice for rapid characterization of surfactant mixtures, have not yet gained general acceptance as routine analytical techniques.

TLC, because of its rapidity and low cost, is particularly useful. Anionics (sulfates, sulfonates, soaps) can easily be separated under the following conditions (all ratios given are volume ratios).

One-dimensional chromatography

Alumina 60 F254 with isopropanol.

Silica gel 60 with propanol-chloroform-methanol-10 mol L⁻¹ ammonia (10:10:5:2); ethylacetate-acetic acid-methanol-10 mol L⁻¹ ammonia (45:5:2.5); ethanol-acetic acid (9:1).

Silica gel G containing 10% ammonium sulfate with chloroform-methanol-0.05 mol L⁻¹ sulfuric acid (80:19:1).

Two-dimensional chromatography

Silica gel with acetone-tetrahydrofuran (9:1) followed by propanol-chloroform-methanol-10 mol L⁻¹ ammonia (10:10:5:2).

Several spray reagents are used for detection and identification: Pinakryptol Yellow, Dragendorff, ninhydrin, leucomalachite green and iodine vapour.

This method can be applied to all classes of tensides as it distinguishes anionics from nonionics (fatty diethanolamides and ethoxylates) in shampoos, bath foams and soaps. The aqueous samples can be freeze-dried and extracted with a suitable solvent (ethanol-water) to minimize foaming.

Basically, anionics are analysed by reversed-phase LC using an ion-pairing agent and an organic solvent (acetonitrile, methanol, tetrahydrofuran)-water gradient. In reversed-phase ion pair chromatography, the addition of an appropriate ion-pairing reagent (tetrabutylammonium hydrogensulfate) to the mobile phase suppresses the ionic nature of the sample while introducing some charge to the nonpolar surface of the stationary phase. The retention of the resulting

ion pair is then controlled by pH, counterion concentration and mobile phase polarity. Linear and branched-chain (C_4 – C_{18}) alkylbenzenesulfonates are separated by this method according to the length and structure of the alkyl chain, using as the mobile phase 0.1 mol L^{-1} tetrabutylammonium hydrogensulfate (pH 5)–water–acetonitrile (gradient elution). At pH 5, the sulfonates and pairing reagent are completely ionized, as are the carboxylated surfactants, whose pK_a values are somewhat higher ($pK_a \sim 4$). The structure and concentration of the pairing agent also influences the retention behaviour: increasing the lipophilicity increases the retention of the surfactant ion pair by enhancing its affinity for the nonpolar stationary phase. The increase in the concentration of the pairing agent will lead to greater coverage of the stationary phase surface and consequently to longer sample retention.

A limitation is that only the chromophoric components of such mixtures can be monitored by ultraviolet (UV) absorption detection. Nonchromophoric anionic surfactants such as alkyl sulfates or their corresponding alcohols and acids can be determined by LC after derivatization to 3,5-dinitrobenzoate esters or *p*-(methylthio)benzoate esters. The acidic forms of α -olefin sulfonates, alkyl sulfates, alkyl-ethoxylated sulfates and alkyl phosphates react with 4-diazomethyl-*N,N*-dimethylbenzenesulfonamide to produce UV-absorbing derivatives that can be separated by reversed-phase LC. Direct detection (no derivatization) can be achieved by the use of a spectrofluorimetric detector operating at 225 nm (excitation) and 295 nm (emission) (reversed-phase C_{18} (RP-18) column; mobile phase: 0.1 mol L^{-1} sodium perchlorate in 80:20 methanol–water) or by a differential refractometer (refractive index) detector. Long-chain alkane sulfonates (C_{12} – C_{20}) are separated by this method using a phenyl column with a 75% methanol–25% 0.1 mol L^{-1} sodium nitrate mobile phase.

An alternative approach to separating and detecting aliphatic anionic surfactants is ion interaction chromatography (reversed-phase column) with an aromatic ion-pairing agent also acting as chromophore for UV detection at 254 nm (cetylpyridinium chloride, phenethylammonium ion).

Anion exchange chromatography with indirect detection is not a common approach for aliphatic sulfonates, although it is simpler than ion pair chromatography. Using hydrogenphthalate, sulfosalicylic acid or *m*-sulfo benzoic acid in 60:40 acetonitrile–water as mobile phase, C_2 – C_8 sulfonates can be separated on a strong cation exchange column with indirect UV absorbance detection at 297, 320 and 298 nm, respectively. C_6 – C_{12} aliphatic sulfonates

and sulfates can also be analysed using sodium naphthalenedisulfonate–acetonitrile as the mobile phase on a polymeric fluorocarbon–amine cross-linked weak anion exchange silica column with either indirect conductivity or photometric detection modes.

The solid-phase reagent (SPR) procedure has been introduced recently as a new method of postcolumn conductivity detection of alkylsulfates and alkyl-sulfonates. SPR, an aqueous suspension of sub-micrometre particles of a polymeric cation exchange material in the hydrogen form, is pumped into the eluent stream coming from the column (silica-based reversed-phase). The postcolumn reaction transforms the tetrabutylammonium alkyl sulfate or sulfonate into the corresponding free acid. This changes the analytes into more conductive species and tetrabutylammonium borate eluent to the low conductivity boric acid. The conductivity detection method with SPR makes it possible to employ gradient elution for separation of complex mixtures.

GC and GC-MS cannot be applied directly to the analysis of anionic surfactants since these compounds are too polar and nonvolatile to be amenable either to GC or to conventional electron-impact MS (desulfonation with acids, alkali fusion sulfochlorination, methylation, pyrolysis-GC are well known methods of prederivatization for GC analysis). The use of soft ionization techniques such as field desorption (FD) and fast atom bombardment (FAB) is highly suited for characterization of these polar compounds by MS.

FAB-MS (in positive or negative ion mode) can be used to analyse complex anionic mixtures without prior separation of the components, since it gives abundant deprotonated (negative) or cationized (positive) molecular ions, and no fragmentation. As is shown in the case of a mixture of ethoxylated alcohol (C_{12}/C_{14}) sulfates (Figure 1), the technique not only gives the complete pattern of oligomer distribution (length of the alkyl and/or of the ethoxylate chain), but also information about the purity of the raw material (the c and d series in Figure 1B are the cationized molecular ions of unreacted materials, the unsulfated ethoxylated fatty alcohols). Ethoxylated alcohol sulfates are easily detected by this technique in finished detergent formulations, even in the presence of other surfactant types (i.e. amphoteric tensides), as has been demonstrated for shampoos.

Nonionic Surfactants

Nonionic surfactants constitute the second most important class of tensides: although their foaming properties are low in respect to those of anionics, they

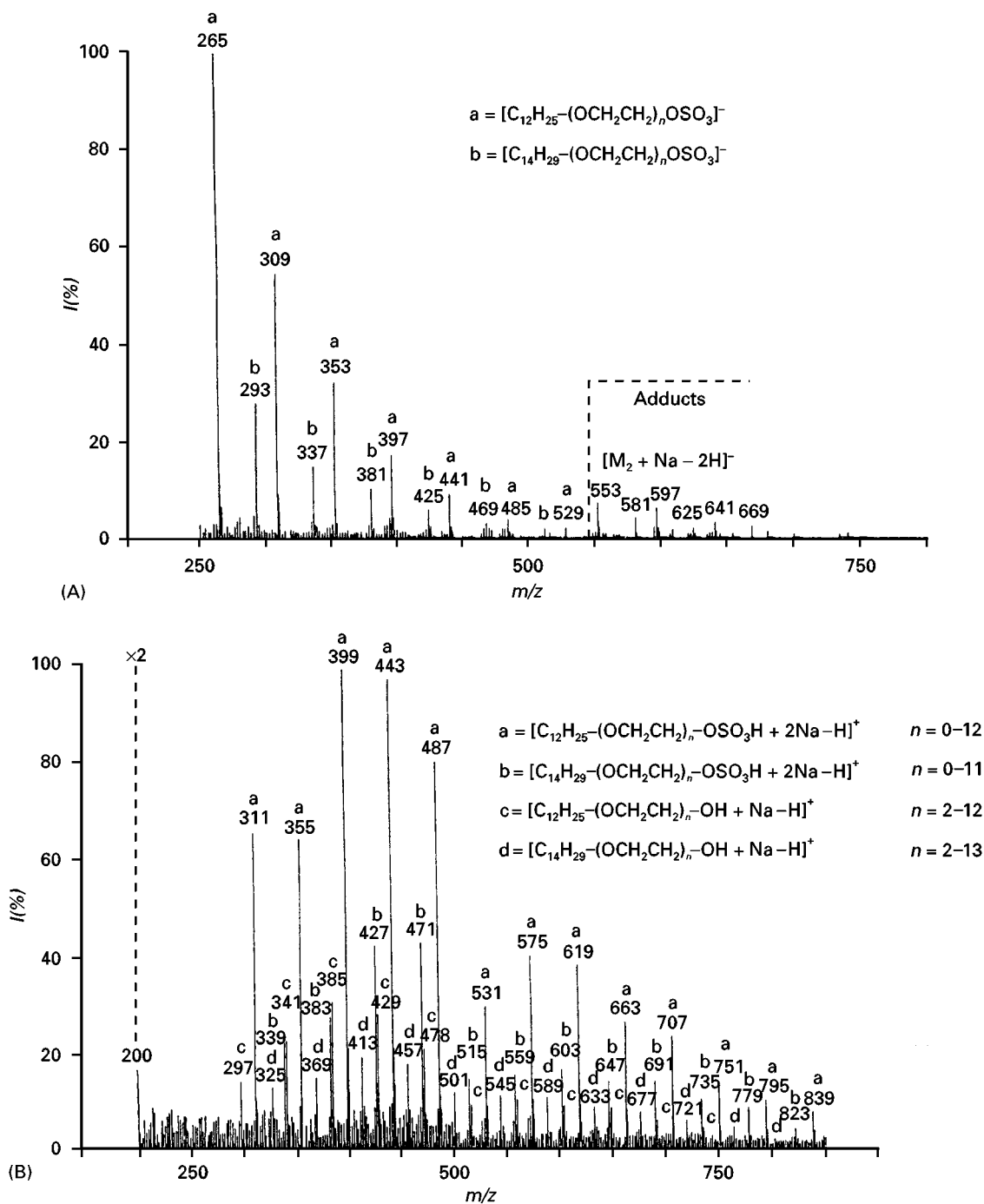


Figure 1 (A) Negative-ion and (B) positive-ion FAB mass spectra of ethoxylated alcohol sulfates (anionic surfactants). (From Maffei Facino *et al.*, 1989.)

are widely used in detergent formulations (especially in bath foams) to increase viscosity and as foam boosters. Table 2 reports the chemical classification of the most important nonionic surfactants.

Spectrophotometric methods for the quantitative analysis of nonionic surfactants are popular: they are based on complex formation with tungstophosphoric

acid, molybdophosphoric acid, picric acid, Malachite green, potassium tetracyanatozincate and ammonium tetrathiocyanatocobaltate (III). This last reagent gives better results than tungstophosphoric acid and than the potentiometric method with Dragendorff's reagent. It can be applied for determination of ethoxylate compounds in detergent solutions: the sur-

Table 2 Nonionic surfactants

Type	General structure
Ethoxylated alcohols	$R-O(CH_2CH_2O)_nH$ Reaction product between ethylene oxide and fatty alcohols
Ethoxylated alkylphenols	$R-C_6H_4-O(CH_2CH_2O)_nH$ Reaction product between ethylene oxide and alkylphenol ($R = C_8/C_9$)
Alkanolamides	$R-CO-N-(CH_2CH_2OH)_n$ $n = 1, 2$ Reaction product of fatty acids ($C_{10}-C_{18}$) with mono- or diethanolamine
Alkylglycosides (glucose ethers)	$R-O-(Gluc)_n$ Reaction product between glucose and fatty alcohols ($R = C_8-C_{14}$)

factant is extracted from the aqueous solution with chloroform and the extract is treated with the reagent to form a blue complex that is then analysed spectrophotometrically. The absorbance is not affected by temperature, electrolytes or dilution.

Several electrochemical and potentiometric techniques are also available for quantitative analysis of nonionic tensides: for example, using a barium ion selective electrode it is possible directly to quantitate the surfactant in the range of 2×10^{-5} to 1×10^{-3} mol L⁻¹. A typical potentiometric titration is based on formation of insoluble complexes with molybdophosphoric acid: the sample dissolved in aqueous ethanol containing barium chloride is treated with an excess of the complexant and the unreacted molybdophosphoric acid is titrated potentiometrically with diantipyrylmethane, using a platinum indicator cathode.

In the quality control of ethoxylated compounds, it is important to determine their composition, since they are manufactured as mixtures of homologous compounds that differ in the length of the ethoxylate and/or the alkyl chain. Several spectroscopic nuclear magnetic resonance (NMR) and infrared (IR) and chromatographic techniques (TLC, GC, LC) and supercritical fluid chromatography (SFC) are available to determine the degree of ethoxylation and the distribution of homologues in nonionic surfactant mixtures.

Both IR spectroscopy and NMR spectroscopy may be used for the determination of the average molecular mass (M_r), the average degree of condensation (x), and the hydrophilic/lipophilic balance (HLB) of nonylphenol ethylene oxide condensates. The IR method is based on the regression between the logarithm of the surfactant properties and the logarithm of the ratio of the heights of the bands at 840 and 960 cm⁻¹, corresponding to aromatic C-H vibrations: the first band is greater than the second for compounds of smaller degree of condensation, but this relationship becomes inverted as the degree of polymerization increases.

The NMR approach involves the calculation of absolute integrals of three types of hydrogen atoms: from these integration values it is possible to calculate the degree of condensation and the alkyl residue composition, as each surfactant molecule contains four aromatic hydrogen atoms that can be used as an internal reference to determine the number of hydrogen atoms corresponding to the remainder of the peaks.

TLC with a flame ionization detector (FID) has been applied for the separation and quantitative determination of nonionic surfactants containing an average number of oxyethylene units not higher than 8.0. The oligomers are separated on Chromarod S-II (silica gel-coated rods) with double development; (a) benzene-ethyl acetate (6:4) for 10 cm from the start; (b) ethyl acetate-acetic acid-water (8:1:1) up to a distance of 8 cm. After development, the rods are passed through a FID operating with hydrogen (160 mL min⁻¹) and air (2 L min⁻¹). The major advantage of LC in the analysis of nonionic surfactants lies in its ability to separate and quantitate alcohol or alkylphenol ethoxylate oligomers that differ in the length of the ethoxylate chain. While alkylphenol ethoxylates can readily be identified by UV detection, aliphatic compounds, since they do not possess significant UV absorption, must be derivatized prior to LC (for example by esterification with 3,5-dinitrobenzoyl chloride). Reversed-phase LC with refractive index detection has been proposed to establish the retention behaviour of a wide range of ethoxylated and/or propoxylated adducts: there is a linear relationship between the logarithm of the capacity factor and the degree of polymerization of the ethoxylated and/or propoxylated C₁₂, C₁₆, C₁₈ alcohols, ethylene oxide-propylene oxide copolymers, poly(ethylene glycol)s and poly(propylene glycol)s. This can be used not only for the prediction of chromatographic separation, but also for the estimation of the degree of polymerization and of the length of the alkyl chain.

Recently, the evaporative light-scattering (ELS) detector, also known as the mass detector, was

introduced as a universal detector for separation and quantification of all surfactant species. The detector measures light refracted by the nonvolatile particles after the effluent from the LC is nebulized and the carrier solvent is evaporated. The detector gives an equal and linear response factor for each class of surfactant that is independent of molecular mass (the amount of refracted light is proportional to the concentration of the analyte species).

Alcohol ethoxylates have been characterized by GC as acetate derivatives on a packed column or as silylated derivatives using a fused silica capillary column. However GC gives only a partial fingerprint, since only low molecular mass components can be detected (the free alcohols and short-chain ethoxylated homologues, up to approximately 12 ethylene oxide oligomers).

High temperature capillary gas chromatography and SFC are new alternative procedures for the analysis of these compounds that are thermally unstable or have low volatility. The alcohol and ethoxylate distributions, mean molecular mass and average number of moles of ethylene oxide can be calculated rapidly with both the methods (polyglycols with average molecular masses of 2000–2500 Da have been successfully analysed by SFC). Advantages and limitations of the SFC and high temperature capillary GC procedures can be summarized as follows: (1) for routine quality control analyses of known alcohol ethoxylates, both techniques appear to be equally suited; (2) SFC is time-saving because derivatization is not required, although for complex mixtures derivatization improves resolution (acetylation by means of acetic anhydride and pyridine or silylation with bis(trimethylsilyl)trifluoroacetamide and pyridine); (3) the GC technique is able to resolve C_{12} – C_{18} alcohol ethoxylate oligomers, thus avoiding ambiguous identification of components. Figure 2 shows the chromatographic profiles of a C_{12}/C_{13} alcohol ethoxylate with an average of 6.6 moles of ethylene oxide obtained by SFC and by high temperature capillary GC after silylation.

Among the mass spectrometric methods, the use of conventional GC-MS electron impact (EI) ionization is limited to nonionic surfactants with a low degree of ethoxylation. Compounds with a high degree of ethoxylation (20–25 units) can be identified directly in raw materials and in finished detergent formulations by soft ionization techniques such as direct chemical ionization (DCI), FD and FAB. This last, in positive ion mode, furnishes the complete pattern of oligomer distribution of ethoxylated compounds, since it gives a series of ions at 44-Da intervals (protonated and/or cationized molecular ions only, with no fragmentation). In addition FAB-MS (in positive or

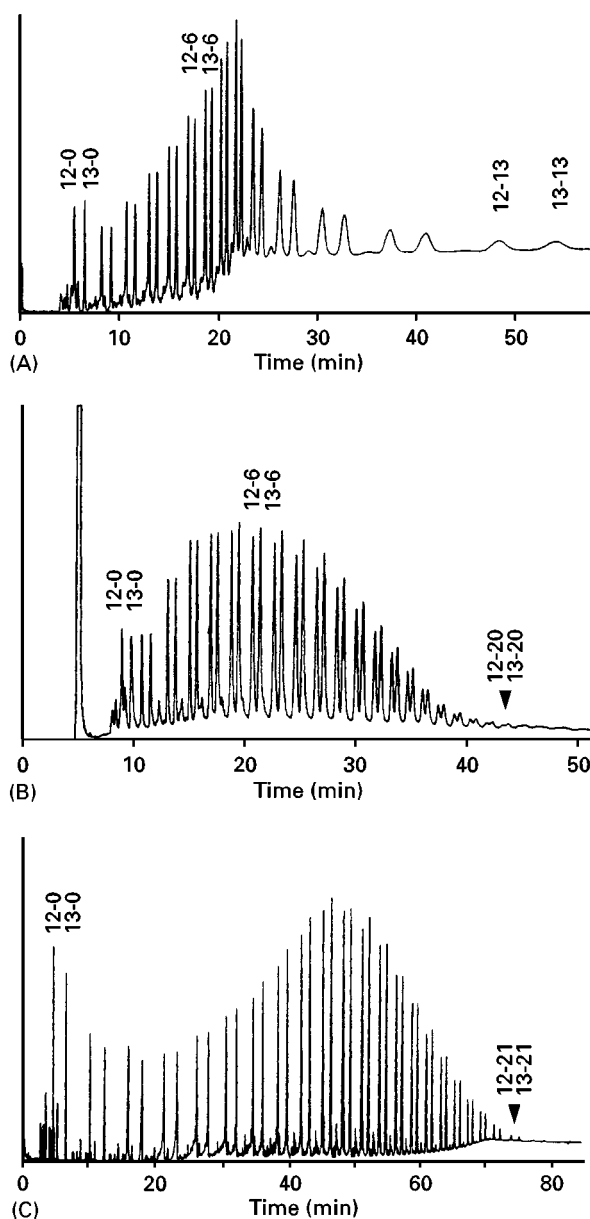


Figure 2 Analysis of ethoxylated alcohols (nonionic surfactants) by GC, high temperature GC and SFC. (A) Capillary GC of a silylated C_{12}/C_{13} alcohol ethoxylate with an average of 6.6 moles of ethylene oxide. (B) Capillary SFC of the same mixture (un-derivatized). (C) Capillary high temperature GC of the same mixture (after silylation). (From Silver AH and Kalinoski HT (1992) *Journal of the American Oil Chemist's Society* 67: 599–608.)

negative ion mode) gives direct characterization of alkylpolyglycosides, a new generation of highly polar nonionic tensides not amenable to analysis by conventional chromatographic methods. The method, which is based on unambiguous molecular mass determination of the single components (protonated or deprotonated molecular ions), allows the definition of length of both the alkyl and the glucosidic chains (up to 10 glucose units).

Free poly(ethylene glycol)s (PEGs) are the main contaminants of ethoxylated derivatives and are frequently found in the products obtained from them, because they can be formed as side-products in the reaction of ethylene oxide with the hydrophobic component (in which case they are present as a mixture of homologous polymeric derivatives with a molecular mass distribution that depends on the reaction conditions); they can be added intentionally to obtain specific performances of the final product; and they can arise from the decomposition of adducts in the synthetic reaction or during the processing. Hence determination of free PEGs is important not only from the viewpoint of routine quality control of the manufacturing process, but also for the determination of the suitability of surfactants for specific purposes. Among the procedures used for the separation of PEGs from adducts and the unreacted starting material, a simple method involves extraction of an ethyl acetate solution of surfactants with 5 mol L⁻¹ sodium chloride, followed by extraction of the aqueous phase with chloroform, evaporation of the solvent and gravimetric determination of PEGs (accurate temperature control is required).

Column LC is faster and more reproducible for the separation of free PEGs from the other components of the mixture. Silica, hydrophobized with dichlorodimethylsilane, with chlorobenzene as the stationary phase, separates PEGs from their adducts using acetone–water–acetic acid as the mobile phase. Utilizing reversed-phase chromatography on silanized silica gel, and 30% aqueous isopropanol as mobile phase, PEGs are eluted, while adducts are desorbed with 96% ethanol. Partition chromatography, with ethyl acetate as the mobile phase and cellulose as support for the stationary phase (30% sodium chloride solution), is used for the determination of PEGs in adducts of fatty alcohols, alkylphenols, fatty acids and alkanolamides.

By applying hexane–isopropanol–water mobile phases of controlled composition (different ratios of hexane to isopropanol), either ethylene oxide adduct (EOA) or PEG oligomers can be separated on a bonded diol phase, and their distributions evaluated (refractive index detection). The PEG or EOA oligomers can easily be separated up to the 30-mer even without gradient elution, and ethoxylated surfactants (fatty alcohols, fatty acids, fatty acid monoethanolamides and alkylphenols) up to an ethoxylation degree of 20.

Another important contaminant of ethoxylated derivatives (both anionic and nonionic) is 1,4-dioxane: according to the European Economic Community Directive on Cosmetics, commercial products must be free from this compound, since it is carcinogenic in

rats and mice. 1,4-Dioxane is formed by dimerization of ethylene oxide during the process of alcohol/phenol ethoxylation and might be found in the final detergent formulations via the use of ethoxylated fatty alcohol sulfates as cleansing agents.

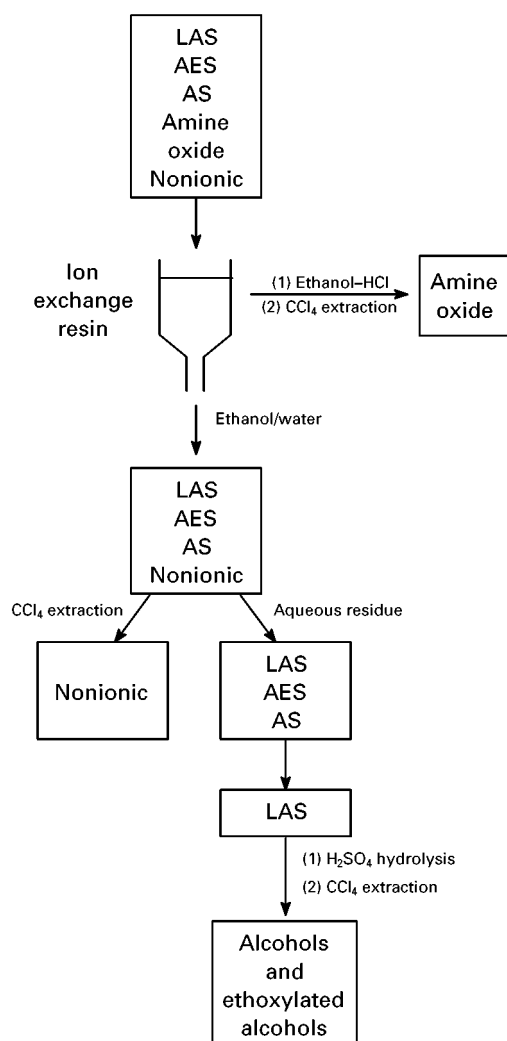
1,4-Dioxane is commonly determined by GC. A simple method applied to shampoos, requiring minimal sample preparation (dilution with water containing the internal standard isobutanol and direct injection), is carried out with packed column (15% OV-1 on 100/120 Chromosorb WHP) and FID (injection temperature 185°C; detector temperature 325°C; temperature programme 85°C (2 min), 5°C min⁻¹ to 95°C, followed by clean-up step). Linearity is in the concentration range 1–250 mg kg⁻¹; limit of detection 1 mg kg⁻¹.

An alternative technique than can be applied to different cosmetic matrices is GC-MS with selected ion monitoring (SIM); prior to analysis, rapid and efficient purification from the interfering materials of the cosmetic products is achieved by use of combined silica/octadecylsilica cartridges (limit of detection 3 mg kg⁻¹).

Scheme 1 shows a procedure useful for separation and quantitation of a hypothetical detergent product (liquid or powdered) formulated with different types of active ingredients: amine oxide, ethoxylated alcohols (nonionic), alcohol sulfate (AS), ethoxylated alcohol sulfates (AES) and linear alkyl sulfonates (LAS). Under basic and neutral conditions, amine oxide behaves as a nonionic material, while under acidic conditions it acts as a cationic agent.

A sample (~5 g) of liquid detergent or of the alcohol-soluble material (1–2 g) from a powdered detergent is dissolved in a minimum volume of ethanol–water (1:1) and passed through a strong cationic ion exchange column (Dowex 50WX4, 200–400 mesh, sulfonic acid form). Elution with ethanol–water (1:1) separates anionic and nonionic surfactants from amine oxide selectively absorbed on the resin. The amine oxide is eluted from the column with 1 mol L⁻¹ ethanolic hydrochloric acid and the eluate, after neutralization, is extracted with carbon tetrachloride. The isolated amine oxide fraction can be further characterized by NMR, IR or GC and quantified by a titration method: under acidic conditions amine oxides are determined as quaternaries with a standard alkylbenzene sulfonate and methylene blue indicator (see Cationic Surfactants). This method does not distinguish amine oxides from their precursor alkyl dimethylamines: the latter can be analysed by gas liquid chromatography (GLC).

If the amine oxide distribution and average molecular mass are unknown, they can be determined by packed column (Apiezon L on 60/80 Chromosorb W.



Scheme 1 Separation of different types of surfactants. AS = alcohol sulfates; AES = ethoxylated alcohol sulfates; LAS = linear alkyl sulfonates.

HMDS) GC: these compounds pyrolyse to 1-olefins (column temperature 280°C; injection temperature 240°C; detector temperature 330°C) and pyrolysis is essentially complete over the range of C₁₂ to C₁₈ alkyl chains. Alkyldimethylamines do not decompose in these conditions and their peaks are well separated from olefins: therefore determination of the precursors should be possible by the use of a suitable internal standard.

The aqueous alcohol phase containing free nonionic ethoxylated alcohols, sulfated anionic and sulfonated anionic material is extracted with carbon tetrachloride to separate nonionic surfactants, which can then be analysed according to one of the methods mentioned previously. The aqueous alcohol residue containing only sulfated and sulfonated anionic materials is concentrated *in vacuo* to remove the alcohol

and then hydrolysed with 1 mol L⁻¹ sulfuric acid. Hydrolysis converts all the sulfated anionic material to ethoxylated alcohols or fatty alcohols (the sulfonated anionic fraction is not affected by acid hydrolysis), which, after neutralization, can be recovered by carbon tetrachloride extraction.

The remaining ethanol-water phase containing sulfonated species is evaporated and the sulfonate is recovered and weighed by a salting out procedure; alternatively, it can be qualitatively and quantitatively analysed by the methods previously described.

Cationic Surfactants

Cationic surfactants are devoid of detergent or foaming properties, but are excellent hair conditioners: for these reasons their use in toiletries is limited to formulations of specific shampoos. Table 3 shows the main types of cationic surfactants used in cosmetics.

The ion pair extraction technique has proved suited for the determination of cationic surfactants by two-phase titrations and/or by spectrophotometry (the method is based on extraction of an ion pair between surfactant and dye, which is the basis of the well known Epton Methylene blue and The Cosmetic, Toiletry and Fragrance Association (CTFA) mixed indicator method). In the two-phase titration of cationics by lauryl sulfate in the presence of a suitable indicator dye (Methylene blue, Thymol blue, Bromophenol green, disulfine blue–dimidium bromide), the dye-surfactant ion pair is extracted almost completely by the organic solvent chloroform or methylene chloride.

When the titrant (an oppositely charged surfactant) is added, surfactant-surfactant ion pair formation takes place. The end point is indicated when enough titrant is added so that the small amount of the dye present is displaced from the dye-surfactant ion pair and returns to the aqueous phase. Alternatively, the dye-surfactant ion pair can be spectrophotometrically determined after chloroform extraction from the aqueous solution.

Using Bromophenol blue as dye indicator, it is possible to quantitate cationic surfactants and the corresponding amines when both are present in a detergent mixture. It has been shown that with long-chain quaternary ammonium compounds (cetyltrimethylammonium bromide), Bromophenol blue forms two different compounds: in alkaline solutions a blue di(cetyltrimethylammonium) salt, but in acid solution a yellow mono(cetyltrimethylammonium) salt.

Hence cationics can be estimated spectrophotometrically in two different ways, as the blue di-salt in

Table 3 Cationic surfactants

Type	General structure
Alkyltrimethylammonium halides	$\left[\begin{array}{c} \text{Me} \\ \\ \text{R}-\text{N}-\text{Me} \\ \\ \text{Me} \end{array} \right]^+ \text{X}^- \quad \text{R} = \text{C}_{12}-\text{C}_{18}$
Alkylethoxylated ammonium halides	$\left[\begin{array}{c} (\text{CH}_2\text{CH}_2\text{O})_n\text{H} \\ \\ \text{R}-\text{N}-\text{Me} \\ \\ (\text{CH}_2\text{CH}_2\text{O})_n\text{H} \end{array} \right]^+ \text{X}^- \quad \text{R} = \text{C}_{12}-\text{C}_{18}$
Dialkyldimethylammonium halides/saccharinates	$\left[\begin{array}{c} \text{Me} \\ \\ \text{R}-\text{N}-\text{R}' \\ \\ \text{Me} \end{array} \right]^+ \text{X}^- \quad \text{X} = \text{Saccharinate} \quad \text{R, R}' = \text{C}_8-\text{C}_{18}$
Alkylbenzyltrimethylammonium halides	$\left[\begin{array}{c} \text{Me} \\ \\ \text{R}-\text{N}-\text{CH}_2-\text{C}_6\text{H}_5 \\ \\ \text{Me} \end{array} \right]^+ \text{X}^- \quad \text{R} = \text{C}_{10}-\text{C}_{18}$
Alkylpyridinium halides	$\left[\text{R}-\text{N} \begin{array}{c} \diagup \diagdown \\ \text{C}_5\text{H}_5 \end{array} \right]^+ \text{X}^- \quad \text{R} = \text{C}_{12}-\text{C}_{18}$
Alkylisoquinolinium halides/saccharinates	$\left[\text{C}_8\text{H}_7\text{N}-\text{R} \right]^+ \text{X}^- \quad \text{R} = \text{C}_{10}-\text{C}_{18}$

alkaline solutions (absorbance maximum at 606 nm) and as the yellow mono-salt in acid solutions (absorbance maximum at 416 nm).

Separate estimations of the quaternaries (which do not hydrolyse) and the amine salts (which can hydrolyse easily in alkaline solutions) can be carried out working at different pH values: a higher pH will decrease the contribution of the amine even more because the higher the pH, the greater the hydrolysis of the amine salts into the amine and removal by the organic solvent. Determination of the amine salts in the presence of cationics can be carried out by estimating the total cationics in acid solution and the quaternaries only in alkaline solution: the amine content is obtained by difference. The spectrophotometric de-

termination of cationic surfactants with Orange II as dye indicator has the same kind of applications: dye salts are determined at 490 nm after chloroform extraction from aqueous solutions of surfactants and excess of Orange II dye: Orange II reacts with a 1 : 1 stoichiometry with cationic tensides and the molar absorptivity and the wavelength of maximum absorbance for the dye salts in chloroform are independent of the reacting surfactant. Isolation of dye salt in chloroform can be also used as a means of estimating average equivalent weights of commercial cationic surfactants.

By selective changing of the pH, the method might be applied for quantification of cationic precursors such as amines and amine oxides of amphoteric sur-

factants and of mixtures of amine and quaternary ammonium compounds.

The prerequisite for the extraction method is the formation of a lipophilic surfactant-dye ion pair which is then extracted into chloroform or methylene chloride. However, there are many cationic polymers used as hair conditioners that do not form lipophilic ion pairs, such as cationic polypeptides, and in addition many surfactants form an emulsion during extraction with lipophilic solvents, causing problems in determining the end point. In all these cases, quantitative analysis of cationic surfactants can be performed by a potentiometric method using a 'surfactant' electrode and sodium dodecyl sulfate as titrant.

Quaternary ammonium salts are not amenable as such to GC because of their low volatility and limited thermal stability. Long chain quaternary ammonium compounds undergo extensive but reproducible decomposition in a classical gas chromatographic system, to tertiary amines and alkyl halides. This chromatographic behaviour has led to the development of an analytical approach carried out with dedicated instruments such as a Curie point pyrolyser or a filament pyrolyser coupled to a GC-MS system, which has been applied both for structure elucidation (distribution of homologous compounds) and for quantitative determination of cationic surfactants in various matrices.

Long chain *N*-alkylpyridinium (alkyl = C₁₀-C₁₈) salts can be determined by GLC of the reduction products obtained by treatment with sodium tetrahydroborate and nickel(II) chloride. The procedure is useful for routine analysis of *N*-alkylpyridinium salts, as the reduction to perhydrogenated derivatives takes place quantitatively and cleanly in aqueous media at room temperature with easily handled reagents.

The most promising and convenient approach is LC, although its application is limited to UV-absorbing quaternaries (quantification of both UV- and non-UV-absorbing quaternaries can be achieved with a LC system coupled to a conductivity detector). Both normal-phase ion pair LC and reversed-phase LC have been used for analysis of cationics: reversed-phase chromatography is common but problematic, since these compounds mostly elute from octadecylsilica columns as badly tailing peaks.

The addition of ion-pairing agents and/or quaternary amines to the mobile phase generally does not eliminate this unwanted phenomenon. The substitution of an octadecylsilica by a polymeric polystyrene-divinylbenzene column was found to afford a considerable improvement in the peak shapes. For example, a homologous series of alkylbenzyl-

dimethylammonium and alkylpyridinium halides with C₁₀-C₁₈ alkyl groups can be separated by employing porous microspherical poly(styrene-divinylbenzene) gel as the stationary phase and 0.5 mol L⁻¹ perchloric acid in methanol as the mobile phase (the logarithm of the capacity factor for each homologous series is directly proportional to the alkyl chain length). Figure 3 shows the reversed-phase liquid chromatograms of a homologous series (C₁₂-C₁₈) of *n*-alkylbenzyltrimethylammonium chlorides obtained under different experimental conditions.

The mass spectrometric soft ionization techniques (FD, FAB) allow a rapid and unequivocal structure elucidation of the components of a mixture of cationic surfactants. FAB in the positive ion mode gives unambiguous spectra, with abundant molecular ions and no fragmentation, furnishing detailed information on the length of both the alkyl and the ethoxylate chains in polyethoxylated derivatives (these last compounds are frequently used as hair conditioners).

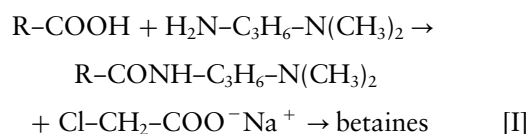
Amphoteric Surfactants

By definition, amphoteric surfactants are those that have anionic or cationic properties depending on the pH and that have an isoelectric point. Because of the highly nucleophilic character of oxygen, amine oxides also have salt formation potential, and for this reason their analysis is similar to that of amphoteric surfactants.

Table 4 shows the main amphoteric types produced today: alkylamido and alkyl betaines (and their respective amine oxides), alkylamido- and alkylsulfobetaines, amphoglycinates (formerly imidazolines).

Among the surfactants, amphoteric surfactants are those more prone to contamination from intermediates, since their synthesis involves several reaction steps.

Alkylamidobetaines are synthesized from the intermediate amidoamines, which in turn are obtained by reaction of fatty acids with amines (mainly dimethylaminopropylamine); the amidoamines react with sodium monochloroacetate in aqueous solution (alkaline medium) to give betaine derivatives (eqn [I]):



The corresponding amine oxides are prepared by oxidation of the intermediates amidoamines with hydrogen peroxide in aqueous solution.

In a similar way, alkylbetaines are prepared by carboxylation (with sodium chloroacetate) of the

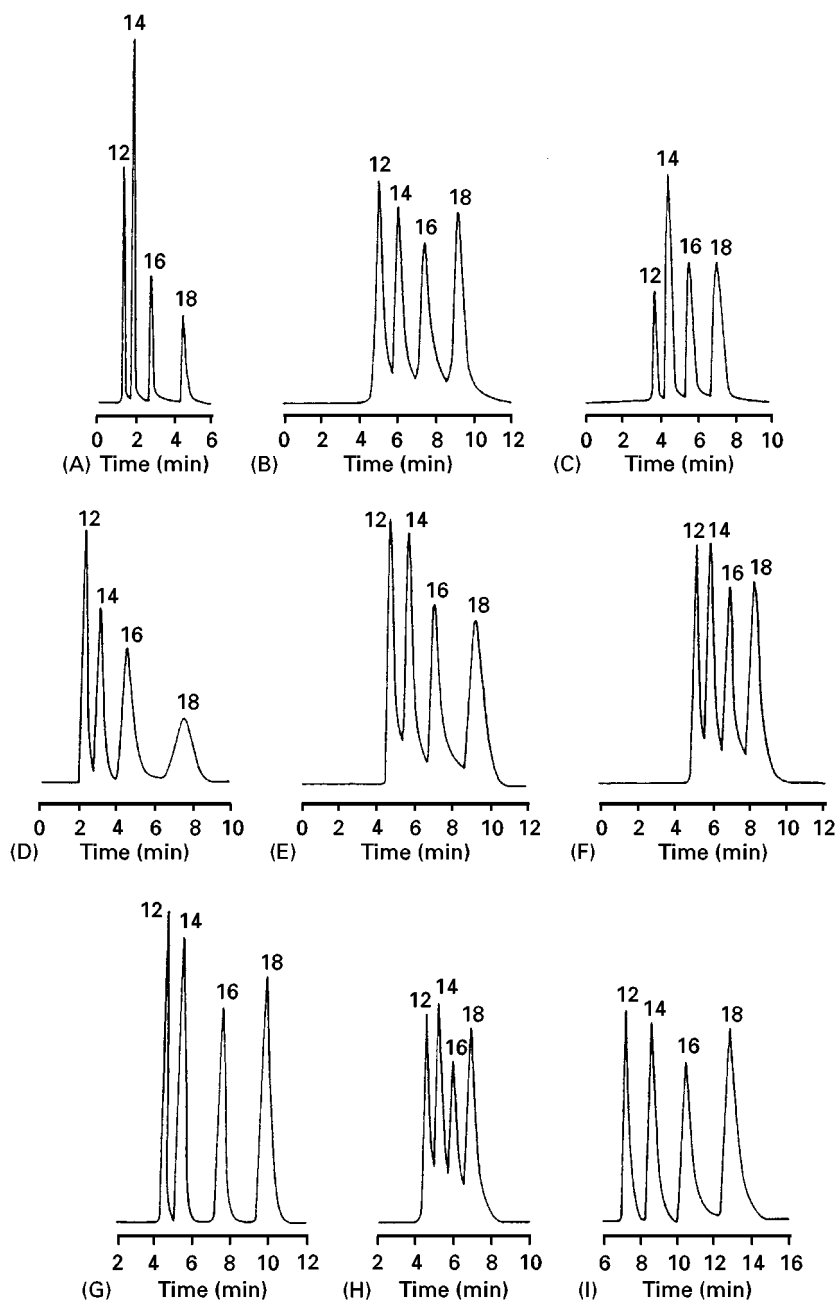
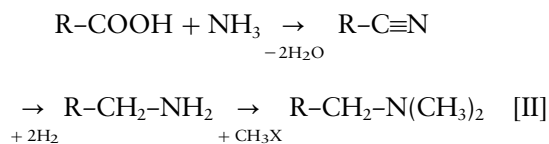


Figure 3 Reversed-phase LC peaks of a homologous series of *n*-alkylbenzyltrimethylammonium chlorides (cationic surfactants). LC conditions: all mobile phases contain 0.1 mol L^{-1} sodium perchlorate (pH 3); (A) acetonitrile–water (9 : 1); (B) acetonitrile–water (1 : 1); (C) acetonitrile–water (7 : 3); (D) methanol–water (9 : 1); (E) methanol–water (3 : 2); (F) methanol–water (17 : 3); (G) THF–water (3 : 2); (H) THF–water (1 : 1); (I) THF–water (3 : 2) (THF = tetrahydrofuran). Stationary phases: octadecylsilica (A, D, G); cyanopropylsilica (B, E, H); phenylpropylsilica (C, F, I). (From Abidi SL (1985) *Journal of Chromatography* 324: 209–230.)

alkyldimethylamines according to eqn [II]:



Sulfobetaines are synthesized according to eqn [III]:

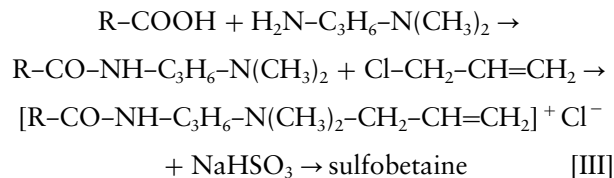


Table 4 Amphoteric surfactants

Type	General structure	
Alkylbetaines	$R-N^+(CH_3)_2-CH_2COO^-$	$R = C_{12}-C_{18}$
Alkylamine oxides	$R-N(CH_3)_2 \rightarrow O$	
Alkylamidobetaines	$R-CO-NH-(CH_2)_n-N^+(CH_3)_2-CH_2-COO^-$	$R-CO = \text{fatty acids}$
Alkylamidoamine oxides	$R-CO-NH-(CH_2)_n-N(CH_3)_2 \rightarrow O$	
Amphoglycinates	$R-CO-NH-CH_2-CH_2-N \begin{cases} CH_2-CH_2OH \\ CH_2-COOH \end{cases}$	$R-CO = \text{fatty acids}$
Sulfobetaines	$R-CO-NH-(CH_2)_n-N^+(CH_3)_2-C_3H_6-SO_3^-$	$R-CO = \text{fatty acids}$

The position of the sulfo group is not certain, and the resulting amphoteric surfactants are thought to be a mixture of the 2- and 3-sulfopropylated quaternary ammonium compounds.

Amphoglycinates are prepared by reaction of fatty acids with aminoethylethanolamine to give intermediate cyclic compounds, imidazolines (it is common knowledge that this first step does not produce the linear amides). By carboxylation with sodium chloroacetate in aqueous solution, ring opening occurs with formation of amphoglycinates that are not of uniform composition.

Isoelectric point determination is the first measure to identify amphoteric surfactants: this can be carried out by conductivity titration, potentiometric titration or electrophoresis (isoelectric focusing). By potentiometric titration, the following isoelectric points have been determined: alkylamidobetaines ~ 7.0 ; alkylbetaines ~ 6.0 ; alkylamidoamine oxides ~ 8.5 ; alkylamine oxides ~ 9.0 .

TLC on silica gel plates with chloroform-methanol-ammonia (30:50:2) or ethanol-chloroform-ammonia (45:40:15) as mobile phases rapidly distinguishes and identifies different amphoteric, even when present in detergent formulations; detection is with 0.1% Bromophenol blue followed by treatment with 0.1% sodium periodate in aqueous solution.

IR spectroscopy is an alternative method for identification of amphoteric: in the case of amino oxides, special precautions must be taken during preparation of the samples (freeze-drying and not drying at 105°C must be used to remove the water, otherwise the N-O bond will be broken). The typical N-O bands are at approximately 960 and 930 cm^{-1} for both alkylamido and alkylamine oxides; for the alkylamido derivatives, the secondary amide bands at $c. 3300$, 1640 and 1550 cm^{-1} are diagnostic; the characteristic bands of betaines are at 1605 , 1402 , 1340 cm^{-1} (carboxylate bands), 890 cm^{-1} (quaternary N band), and 3275 , 1633 and 1549 cm^{-1} (secondary amide bands, only present in alkylamidobetaines).

The alkyl distribution in alkylamidobetaines, amidoamine oxides and amphoglycinates can be evaluated by GC, while alkylbetaines, sulfobetaines or amine oxides are preferably analysed by LC. The determination of alkyl distribution in amide derivatives is carried out after hydrolysis (with concentrated hydrochloric acid) of the amide bonds: the free fatty acids are then converted into the corresponding methyl esters by derivatization with conventional methods (such as methanol-sulfuric acid).

Reversed-phase LC (RP-18 column) is successfully used for characterization of all amphoteric, both in raw materials and in cosmetic formulations, using methanol-water (80:20) (Figure 4) or methanol-aqueous sodium hypochlorite as mobile phase. Alkylamido products (including alkylamidoamine oxides) can be detected by absorbance at 215 nm , while for alkyl distribution in alkylamine compounds a refractive index detector is recommended.

Direct analysis of amphoteric (sulfobetaines) in combination with coconut and tallow soaps can be carried out by reversed-phase LC (detection by differential refractometry) using methanol-water (85:15) as the mobile phase containing 0.2% (v/v) acetic acid ($\text{pH} \sim 4$). At this pH value, tallow and coconut soap mixtures are analysed as fatty acids and are easily separated from the sulfobetaine components.

Ionic and amphoteric surfactants can also be separated on reversed-phase columns with 2-naphthalene-sulfonic acid as counterion in the mobile phase (aqueous methanol) and detected by UV absorbance and differential refractometry. The simultaneous use of both UV and refractive index detectors allows ion pairing (ionic) and nonpairing (amphoteric) components in a mixture to be distinguished.

In the case of sulfobetaines, it is possible to separate the final product from reagents and intermediates: neither amphoteric nor long-chain fatty acids form ion pairs with the counterion in the mobile phase and they are detected by differential refractometry only. The intermediates amidoamine and long chain allyl

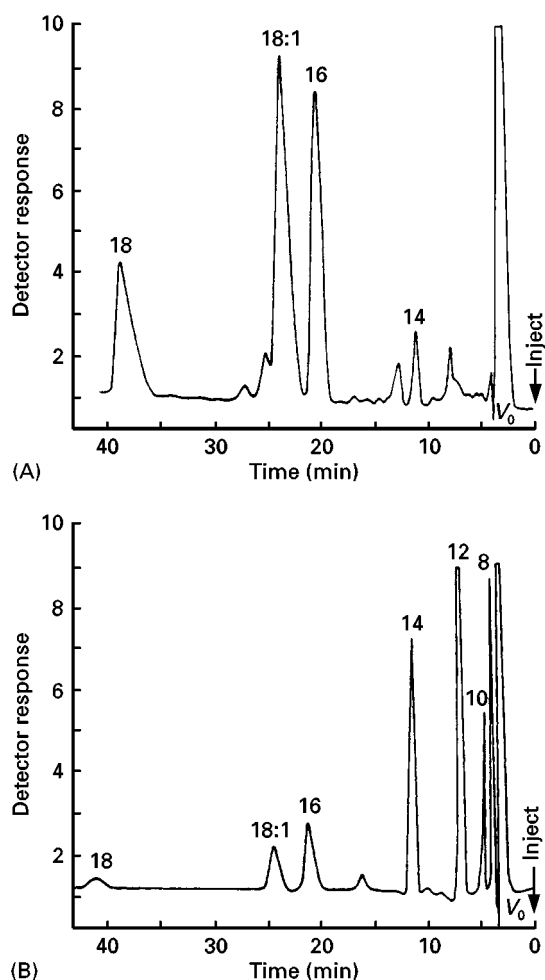


Figure 4 Reversed-phase LC peaks of (A) tallow-derived sulfobetaines and (B) coconut oil-derived sulfobetaines (mobile phase methanol–water, 80:20; refractive index detection). (From: Parris N *et al.* (1977) *Analytical Chemistry* 49: 2228–2231.)

quaternary ammonium chloride are detected as ion pairs by both UV absorbance and refractive index detection. Detection of ionizable surfactants as UV-absorbing ion pairs improves detection limits 100-fold over those obtained by differential refractometry.

Amphoterics are frequently contaminated with various by-products: free fatty acids; free amines (long chain amines and long chain amidoamines); and free chloroacetic acid. The determination of free fatty acids is limited to amide products, and especially to alkylamidobetaines (in this case the presence of residual amounts of free fatty acids is not a drawback, since these compounds positively affect the viscosity characteristics of the alkylamidobetaine in combination with anionics). Fatty acids can be determined as methyl esters by GC after extraction with diethyl ether of the dried product.

Unlike alkyl dimethylamines, whose presence in alkylbetaines and alkylamino oxides is undesirable, residual levels of long chain amidoamines in alkylamidobetaines are ‘cosmetically’ acceptable (they increase viscosity and have foam booster properties).

Titration methods for the determination of amine residues are primarily used for alkylbetaines or alkylamine oxides. In the method of Metcalfe, the total amine content is determined by titration (in isopropanol as solvent) with hydrochloric acid in isopropanol. After quaternarization of the residual tertiary amines with methyl iodide at 50°C, and repeated titration with acid, the total amine oxide content is determined; the tertiary amine content can be determined by subtraction (limit of detection approximately 0.5%).

LC furnishes a more selective and sensitive determination of these amine residues in all classes of amphoteric. The separation is carried out on a reversed-phase column (C_{18}) with hexane–isopropanol (60:40) as mobile phase containing 2 mmol L⁻¹ octanosulfonic acid (for the ionic pairing of the amines); detection is by UV absorbance at 215 nm for amidoamines and refractive index for alkylamines.

Alternatively, postcolumn detection can be employed for primary, secondary and tertiary amines, but not for quaternaries: the compounds separated by the LC column are first converted into the corresponding *N*-chloramines with hypochlorite; the *N*-chloramines are then treated with iodide to form triiodide, which can be monitored by its absorbance at 355 nm.

Chloroacetic acid residues can be evaluated by titration or by chromatographic methods. In the titration method, the first step involves estimation of total chlorine content by silver nitrate, after sodium hydroxide hydrolysis of the sample (2 h under reflux: under these conditions chloroacetic acid is hydrolysed to glycolic acid and chloride). The titration of an unsaponified sample gives the chloride content. The amount of ‘organic chloride’ corresponding to chloroacetic acid is obtained by subtracting the chloride content from the total chlorine. The detection limit of the method lies at 0.03% organic chloride, equivalent to 0.08% (800 mg kg⁻¹) chloroacetic acid. Using ion chromatography with a conductivity detector (amino exchange column with a hydroxide gradient elution), the limit of detection reduces to approximately 20 mg kg⁻¹.

The low volatility of alkylbetaines hampers the use of conventional EI and chemical ionization (CI) MS for structure determination. The pyrolytic behaviour of this class of compounds has been studied under EI conditions: the most important pyrolytic process

is the intermolecular isomerization to tertiary aminoesters $(\text{CH}_3)_2\text{N}-\text{CH}_2-\text{COOCH}_3$. Although pyrolysis EI spectra are useful for structure confirmation of pure compounds, they have limited or no utility for the analysis of mixtures of constituents of unknown chain length, since the spectra are dominated by the ions generated by C-N cleavage and the intensities of the molecular ions of the esters are low.

An alternative approach to structure determination is FD-MS, which gives as prominent ions the protonated species $[\text{M} + \text{H}]^+$; intermolecular alkyl transfer also occurs during field desorption, resulting in mass spectra containing structurally diagnostic adduct ions (methyl, ethyl, propyl groups linked to nitrogen readily undergo intermolecular transfer to give $[\text{M} + \text{CH}_3]^+$, $[\text{M} + \text{C}_2\text{H}_5]^+$ and $[\text{M} + \text{C}_3\text{H}_7]^+$). The presence in the mass spectra of several other

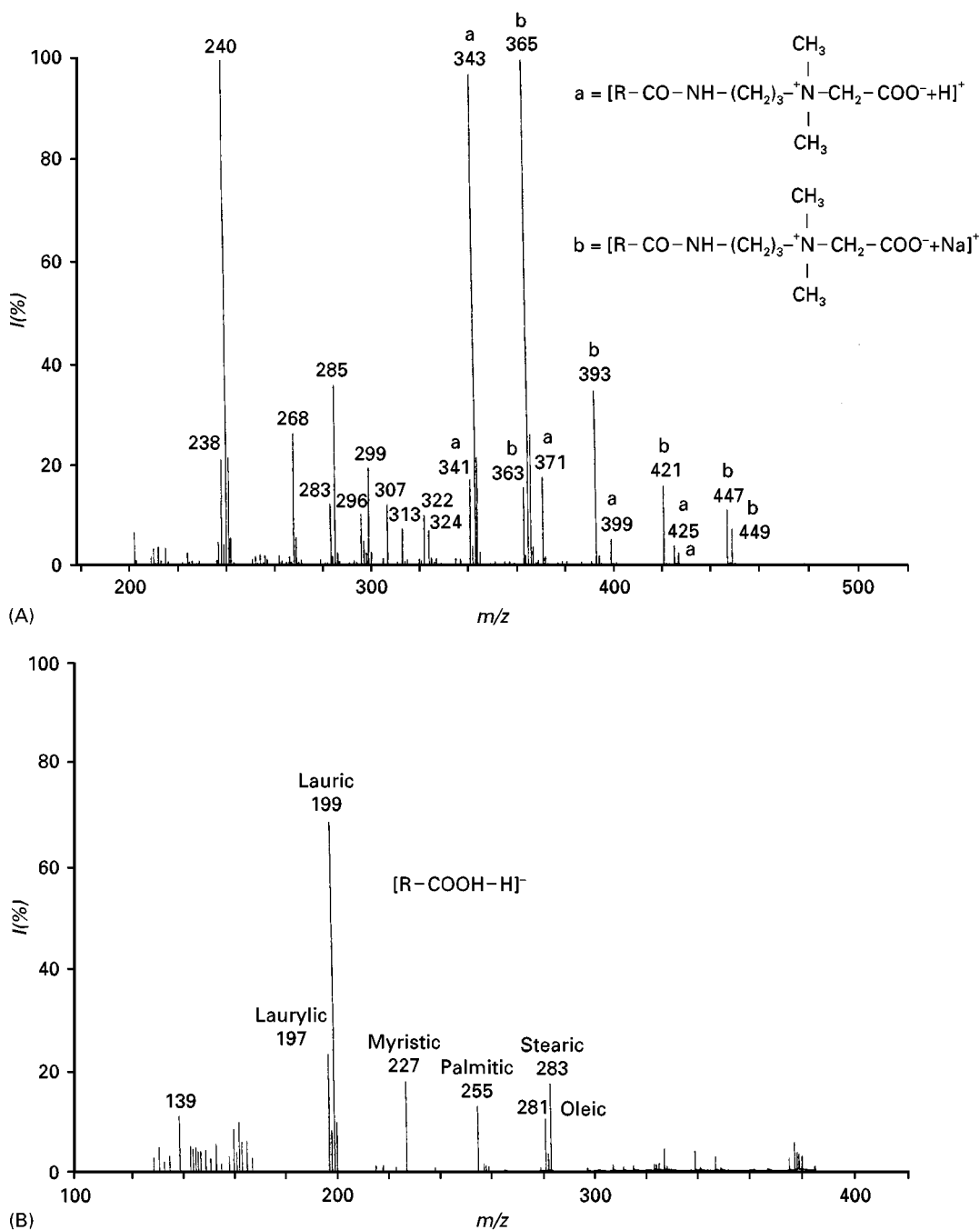


Figure 5 (A) Positive ion and (B) negative ion FAB mass spectra of cocamidopropylbetaine (amphoteric surfactants). (From Maffei Facino *et al.*, 1989.)

adduct and fragment ions (whose relative intensities strictly depend on emitter current) complicates the analysis of complex mixtures by this technique.

FAB-MS in the positive or negative ion mode is more promising, since gives not only an immediate fingerprint of the alkyl distribution in a mixture of amphoteric surfactants, but also direct information on the presence of contaminants.

As is shown with a commercial sample of cocamidopropylbetaine, in the positive ion mode (Figure 5A) the protonated (a series) and cationized (b series) molecular ions of the propylamidobetaine derivatives of coconut fatty acids (C_{12} – C_{18}) can easily be detected; the mass spectra also contain a few ions (at m/z 238, 240, 268, 296, 322, 324) that are due to fragmentation reactions (loss of a dimethylaminoacetic acid residue and loss of the carboxylic group) and some ions that, as determined by MS-MS (parent scan mode) correspond to the protonated molecular species of the dimethylaminopropylamide derivatives $[R-CO-NH-(CH_2)_3-N(CH_3)_2 + H]^+$ of fatty acids present in the mixture as unreacted materials (ions at m/z 283, 285, 313).

Negative FAB ionization cannot be used for identification of amphoteric surfactants because these compounds do not give $[M-H]^-$ ions, but it is an excellent tool for a rapid detection of unreacted fatty acids, which under these conditions give abundant deprotonated molecular ions $[M-H]^-$ (m/z 143 caprylic; m/z 171 capric; m/z 197 laurylic; m/z 199 lauric; m/z 227 myristic; m/z 255 palmitic; m/z 281 oleic; m/z 283 stearic acid) (Figure 5B). Where alkyl (C_{12} – C_{14}) betaines and cocamidopropylbetaine have been identified, this approach can also be successfully applied for the rapid detection of amphoteric surfactants in finished detergent formulations.

Recent Developments

The more recent developments in the field of surfactants analysis, in raw materials, in detergent formulations, or in environmental samples, are all based on the application of new mass spectrometric soft ionization techniques (thermospray and atmospheric pressure ionization (API)). These techniques are more rapid and versatile than conventional FAB-MS, which is dependent upon the surface activity of the sample in a given viscous liquid matrix and requires time-consuming screening of the matrix compounds to achieve maximal ionization response.

Thermospray mass spectrometry coupled to reversed-phase LC has been applied for the quantitative determination of linear primary alcohol ethoxylate (AE) surfactants in environmental samples at levels from 25 to 102 ppb (total AE), corresponding to

a range of individual AE concentration from 60 ppt to 2.17 ppb. The method is able to distinguish highly branched propylene-based alcohol ethoxylates from isomeric linear ethylene-based alcohol ethoxylates.

Positive ion atmospheric pressure chemical ionization mass spectrometry (APCI-MS) has been successfully applied to the determination of the oligomer distribution of alkylphenol polyethoxylates and fatty alcohol polyethoxylates. Positive ion and negative ion API-MS techniques have been used for quality control of the individual steps of the manufacturing process (intermediates and final products) of new classes of anionic surfactants, the alkylpolyglucoside esters of sulfosuccinic, citric and tartaric acid. With both techniques, the complex mixtures can be injected directly into the ion source without prior chromatographic separation, and the constituents are identified on the basis of quasi-molecular ions: cationized ions or solute-solute cluster ions in positive ion mode and deprotonated ions in negative ion mode.

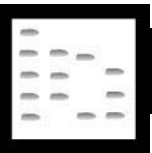
See also: II/Chromatography: Gas: Derivatization; Detectors: Mass Spectrometry. Chromatography: Liquid: Derivatization; Detectors: Refractive Index Detectors; Ion Pair Liquid Chromatography. Chromatography: Thin-Layer (Planar): Spray Reagents. Extraction: Solid-Phase Extraction. III/Fatty Acids: Gas Chromatography. Flame Ionization Detection: Thin Layer (Planar) Chromatography. Surfactants: Chromatography; Liquid Chromatography.

Further Reading

- Borè P (1985) *Cosmetic Analysis. Selective Methods and Techniques*, Cosmetic Science and Technology Series, vol. 4. New York: Marcel Dekker.
- Cross J (1977) *Anionic Surfactants – Chemical Analysis*, Surfactant Science Series, vol. 8. New York: Marcel Dekker.
- Cross J (1987) *Nonionic Surfactants – Chemical Analysis*, Surfactant Science Series, vol. 19. New York: Marcel Dekker.
- Evans KA, Dubey ST, Kravetz L, Dzidic I, Gumulka J, Mueller R and Stock JR (1994) Quantitative determination of linear primary alcohol ethoxylate surfactants in environmental samples by thermospray LC/MS. *Analytical Chemistry* 66: 699–705.
- Hummel DO (1996) *Analysis of Surfactants*. Munich: Hanser Publishers.
- Maffei Facino R, Carini M, Minghetti P, Moneti G, Arlandini E and Melis S (1989) Direct analysis of different classes of surfactants in raw materials and in finished detergent formulations by fast atom bombardment mass spectrometry. *Biomedical and Environmental Mass Spectrometry* 18: 673–689.

- Maffei Facino R, Carini M, Depta G, *et al.* (1995) Atmospheric pressure ionization mass spectrometric analysis of new anionic surfactants: the alkylpolyglucoside esters. *Journal of the American Oil Chemists' Society* 72: 1–9.
- Metcalf LD (1962) Potentiometric titration of long chain amine oxides using alkyl halide to remove tertiary amine interference. *Analytical Chemistry* 34: 1849.
- Milwidsky BM and Gabriel DM (1982) *Detergent Analysis*. New York: Halsted-Wiley.
- Porter RM (ed.) (1991) *Critical Reports on Applied Chemistry*, vol. 32: *Recent Developments in the Analysis of Surfactants*. London: Elsevier.
- Rieger MM (1997) *Surfactants in Cosmetics*. Surfactant Science Series, vol. 68. New York: Marcel Dekker.
- Rosen MJ and Goldsmith HA (1972) *Systematic Analysis of Surface Active Agents*. New York: Wiley-Interscience.
- Schmitt TM (1992) *Analysis of Surfactants*. Surfactant Science Series, vol. 40. New York: Marcel Dekker.

CRUDE OIL: LIQUID CHROMATOGRAPHY



B. N. Barman, Equilon Enterprises, LLC, Houston, TX, USA

Copyright © 2000 Academic Press

Introduction

Chromatographic methods that utilize liquid mobile phases include open-column liquid chromatography, high performance liquid chromatography (HPLC), size exclusion chromatography (SEC) and thin-layer chromatography (TLC). These techniques have been widely applied for the evaluation of crude oils (as well as their subfractions) for their quality, processability or hazards. This overview covers various approaches to the characterization of crude oils by these techniques. Specific applications, operational advantages and limitations of these methods are also highlighted.

The major applications of open-column liquid chromatography and HPLC to the characterization of crude oils and related materials including residua, topped crude oils, coal liquids or shale oils involve preparative fractionation for the determination of hydrocarbon types or class separation to be followed by the determination of important subgroups and individual components. There are also numerous reports where analytical HPLC with various detection schemes has been applied to the quantitative characterization of crude oils as well as other fossil fuels.

Crude oils are usually fractionated into several compound classes according to their molecular structures. A majority of class separations have dealt with the determination of saturates, aromatics, resins (or polars) and asphaltenes (SARA). Saturates consist of paraffinic and naphthenic compounds. If olefins are present in the sample, they are usually grouped with saturates. Aromatics range from alkylbenzenes

(and other monoaromatics) to polycyclic aromatic hydrocarbons (PAHs). The polars are usually aromatic in nature and consist of compounds that may contain nitrogen, sulfur and oxygen as heteroatoms. Asphaltenes are highly condensed aromatic structures.

Conventional TLC with silica and alumina adsorbents provides separation of components from crude oils based on their polarity. TLC with flame ionization detection (TLC-FID) has been applied for the determination of hydrocarbon types. SEC has been particularly useful for the characterization of heavy crude oil fractions.

Open-Column Liquid Chromatography

Crude oils have been fractionated into saturates, aromatics, resins and asphaltenes using open-column liquid chromatography. Asphaltenes are *n*-pentane, *n*-hexane- or *n*-heptane-insolubles depending on the *n*-alkane used. The *n*-alkane-soluble materials, termed maltenes, are usually fractionated on a silica or alumina column using appropriate solvents. In general, saturates are extracted with an *n*-alkane (such as *n*-hexane) followed by elution of aromatic and polar fractions with solvents or solvent mixtures of higher eluotropic strengths. Quantitative data are obtained by the gravimetric determination of each fraction after evaporation of solvent or solvent mixture. Rotary evaporation under mild vacuum is a common practice for the concentration of the collected fractions.

A crude oil separation scheme is shown in **Figure 1**. Maltenes are obtained by precipitation of asphaltenes from the crude oil using *n*-heptane. Using column liquid chromatography on alumina, and solvents or solvent mixtures as indicated in Figure 1, fractions enriched with saturates, aromatics I and II and polars can be obtained. The aromatics I fraction contains

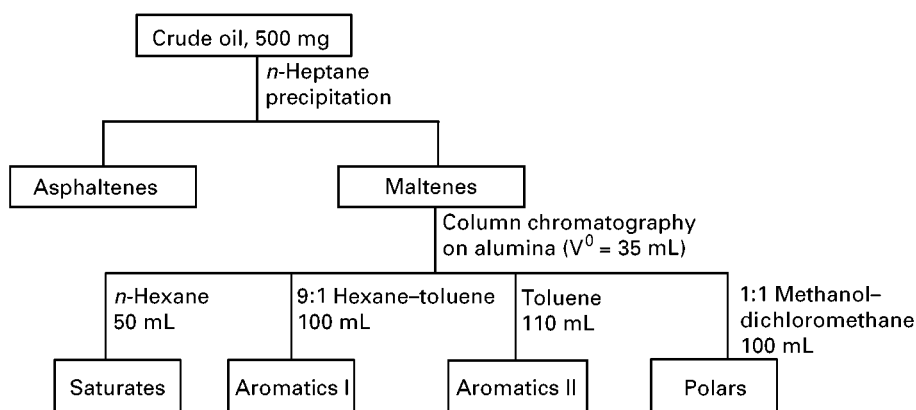


Figure 1 Fractionation of crude oil by open-column liquid chromatography. Column void volume $V^0 = 35$ mL.

monoaromatics, and aromatics II fraction is composed of diaromatics and polycyclic aromatic compounds.

Many special separation schemes have been applied to obtain fractions enriched with specific types of compounds by tailoring the adsorbents as well as the eluting solvents. Beside enrichment and type separation of hydrocarbons, the following have been typical separation schemes for the characterization of crude oil.

1. Solubility fractionation of crude oil with solvents of increasing eluotropic strength, for example, in the order of *n*-pentane, cyclohexane, toluene and methylene chloride.
2. Crude oil fractionation of sulfur and nitrogen compounds for their characterization or identification by other methods.
3. Fractionation of PAHs for their determination, ring number distribution and degree of alkylation.
4. Fractionation of saturates into *n*-alkanes and cyclic plus iso-alkanes using a 0.5 nm molecular sieve column.
5. Fractionation of acidic and basic materials from crude oil using anion exchange and cation exchange resins, respectively.

ASTM D2007 clay-gel method (approved by the American Society for Testing and Materials for the determination of characteristic groups in rubber extender and processing oils and other petroleum-derived oils) has been applied to hydrocarbon-type determination of crude oils. In this method, two glass percolation columns are connected in series with the upper column containing clay and the lower one having clay at the top and silica gel at the bottom. The sample solution in pentane is added at the top of the upper column. *n*-Pentane is then used to elute saturates from clay and silica, leaving polars on the clay

and aromatics on the silica. After removing residual aromatics from the clay adsorbent by washing with *n*-pentane, polars are desorbed with a 1:1 toluene-acetone mixture. Saturates and polars are determined gravimetrically by complete evaporation of solvents from the *n*-pentane and toluene-acetone fractions, respectively. The amount of aromatics is calculated by difference or, if desired, aromatics can be recovered by Soxhlet extraction using toluene.

Both small (mg or less) and large (multigram) scale fractionations of crude oil can be carried out by open-column solid-liquid chromatography to obtain fractions for further evaluation. These fractions are analysed by a host of analytical techniques such as gas chromatography (GC), pyrolysis GC, HPLC, infrared (IR) spectroscopy, and nuclear magnetic resonance (NMR) spectroscopy. Elemental compositions for C, H, N, S, O, V and Ni can also be determined.

Class separation by open-column liquid chromatography is labour-intensive and often suffers from inaccuracies due primarily to overloading effects that result in cross-contamination of hydrocarbon types. Moreover, there is possible loss of light components during evaporation of solvent from a collected fraction that can add significant uncertainties in the quantitative data. There can also be recovery problems arising from irreversible adsorption of some compounds on the adsorbents.

High Performance Liquid Chromatography

Modern HPLC provides both preparative and analytical scale separation of hydrocarbon types from crude oils. Preparative separation is carried out primarily for gravimetric determination of hydrocarbon types after the removal of solvents from the collected fractions. HPLC offers flexibility to allow separation

of different compound types based on their polarity and affinity using various solvents and adsorbents. An HPLC system can also be automated. Since rapid fractionation of materials for collection is possible by HPLC, the method offers a much desired alternative to lengthy and multistep open-column liquid chromatography.

Crude oils are complex materials consisting of hundreds of individual compounds of different sizes and molecular structures. The resolution level obtained during initial separation of crude oil for compound classes by HPLC is often marginal. Therefore, when determination of individual compounds or functionalities is involved, fractions from the initial HPLC separation are subjected to offline or online analysis by high resolution chromatographic or spectroscopic techniques.

Columns and Solvents

Both analytical and preparative scale separations of hydrocarbon types by HPLC have been carried out on commercially available silica, aminopropylsiloxane-bonded silica, 2,4-dinitroanilinopropylsiloxane-bonded silica or cyanopropylsiloxane-bonded silica columns. Amino- and cyanopropylsiloxane columns have been used extensively in the class separation of crude oils and other fossil fuels.

n-Hexane and *n*-heptane have been the most commonly used mobile phases for the separation of saturates from other hydrocarbon classes. Mobile-phase modifiers such as methylene chloride, chloroform, tetrahydrofuran, methanol or 2-propanol have also been used to facilitate the elution of aromatics and polars.

Preparative columns can be much larger in size (with typical column dimensions 80×0.6 cm compared to 25×0.46 cm or less for the analytical column) to allow the separation of a few tenths of a gram or more of sample in each run. The particle size of the porous packing materials can also be much larger than that for the analytical column (50–100 versus 5–10 μm). Typical flow rates for preparative separations are 20 mL min^{-1} or higher, compared to 2 mL min^{-1} or less for analytical separations. Separation times in both cases can be 30 min or less.

Detectors

The choice of detectors for the quantitative determination of various compound classes has been a major concern in HPLC. Conventional diode-array UV detector and differential refractive index (RI) detector are commonly used with HPLC. A UV detector is not suitable for saturates as they do not have chromophores. The response from a UV de-

tector at a specific wavelength varies with the number of aromatic rings, or with the isomeric compounds having the same number of aromatic rings. The very small difference in the RI of *n*-hexane (or *n*-heptane) and saturates is a serious limitation of an RI detector to be highly effective for the determination of saturates. The RI responses from aromatics and polar compounds are much lower compared to those from UV detection. The response factors of different hydrocarbon types, defined as peak area per unit concentration for both RI and UV detectors, show variations with many factors, including the crude oil, column type, column dimensions and mobile phase. Therefore, experimental response factors are often determined by preparative separation and collection of different hydrocarbon groups followed by analytical separation and detection of the collected fractions. For hydrocarbon-type analysis, each calibration is only valid for samples of the same source of crude oil.

Some special HPLC detectors, including FID, mass spectrometric detector (MSD) and evaporative light-scattering detector (ELSD) have been used in conjunction with HPLC separation of crude oils or their high boiling residua. These detectors have some attractive features. FID and ELSD are more sensitive than RI detectors and provide reasonably uniform response factors for different hydrocarbon types. MSD provides detection of materials with high sensitivity and specificity, and affords valuable information on molecular weight, structure and functionality of the molecules.

Although both FID and MSD have been successful as universal detectors in gas chromatography, the use of these detectors with HPLC has been limited, primarily because of the lack of effective interfaces to remove the mobile phase and to transport the sample to the detection system. A rotating disc FID has been demonstrated with samples boiling above 340°C to obtain hydrocarbon-type data covering a wide range of compositions. HPLC-MSD with thermospray or moving belt interface has been applied to the characterization of heavy hydrocarbons.

The ELSD has been applied to the hydrocarbon-type determination of fossil fuels boiling above 315°C (600°F). With the ELSD, mobile phase containing the analyte is nebulized with an inert gas (such as nitrogen) and sprayed into a heated drift tube where the mobile phase is vaporized, leaving behind a fine mist of dry micrometre-sized droplets in solvent vapour. As the sample particles pass through a flow cell, they scatter light from a laser beam to produce a signal. The mass versus signal from ELSD is usually non-linear. However, the signal can be linearized using a power-law model $c = ms^b$, where c and s are mass

and signal, and m and b refer to the proportionality constant and power-law exponent, respectively.

Element-specific detectors such as graphite furnace atomic absorption (GFAA) detector and inductively coupled plasma-atomic emission spectrometry (ICP-AES) detector have been interfaced with HPLC for the speciation of metal-containing compounds, including metal porphyrins. Electrochemical detectors have been applied to the detection of electroactive compounds such as phenols.

Separation Schemes

There have been a few efforts to optimize separation between hydrocarbon groups or subgroups. Most involve trials with the separation and detection of model compounds expected to be present in the sample. In almost all previous HPLC studies of crude oils and related materials, instruments have been automated for separation, detection and collection of fractions.

A simple HPLC separation scheme (scheme A) is shown in **Figure 2** where a single six-port valve and a single column (or a series of columns) have been used. Usually, deasphalted crude oil solution in hexane is injected for analysis by HPLC. The saturates and neutral aromatics (monoaromatics, diaromatics, triaromatics and tetraaromatics) are separated first with the forward flow of hexane. After this, the valve-switching causes a reversal of mobile-phase flow through the column, allowing the backflushing of the column for the elution of polar compounds. The cut point between saturates and aromatics is determined by an RI detector while cut points between aromatic ring subfractions as well as polar compounds are determined by a UV detector.

Both resolution and selectivity of hydrocarbon type separations can be enhanced using different column types and multiple mobile phases during a single run. A solvent with higher eluotropic strength than an n -alkane or a multisolvent step gradient has been found to be more effective for total recovery of aromatic and polar compounds.

A separation scheme B (reported by Pearson and Gharfeh, 1986) utilizes two pumps, two six-port valves, one cyanopropyl silica column and two aminopropyl and cyanopropyl silica columns. Using n -hexane from the first pump, the sample is allowed to pass through the cyanopropyl silica column where polar compounds are strongly retained. The saturates and aromatics pass on to the two aminopropyl and cyanopropyl silica columns. The cyanopropyl silica column is then isolated using the first switching valve. As soon as the saturates elute, the second valve is used to backflush the aminopropyl and cyanopropyl silica columns for the elution of aromatics. The polar compounds are then eluted by back flushing the cyanopropyl silica column with methyl *tert*-butyl ether from the second pump. **Figure 3** shows a chromatogram of a crude oil residue obtained by the separation scheme B using FID for detection. Since a crude oil residue meets the boiling point requirements for an ELSD to be quantitative, ELSD can also be applied to detect and determine its components separated by HPLC.

Special HPLC Applications

Both preparative HPLC and analytical HPLC have been utilized for sample clean-up and separation of specific groups of compounds for online or offline characterization by capillary GC, GC-mass spectrometry (MS) or GC-element-specific detection. Column-liquid chromatography or semipreparative

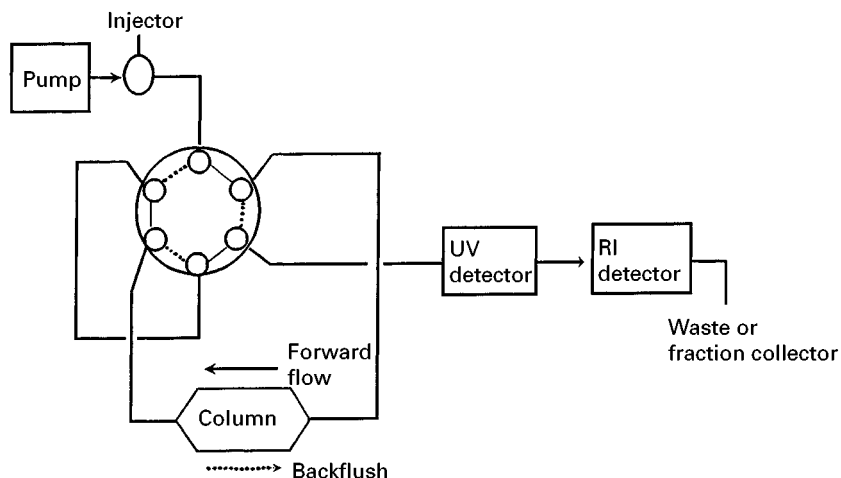


Figure 2 A scheme for hydrocarbon-type separation from crude oil by HPLC.

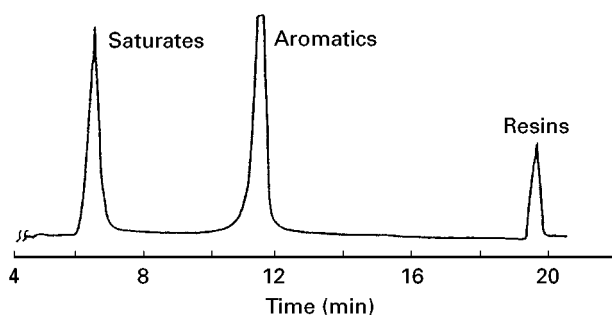


Figure 3 HPLC chromatogram of a crude oil residue. (Modified with permission from Pearson and Gharfeh, 1986. Copyright 1986 American Chemical Society.)

HPLC fractionation followed by analytical HPLC have also been very effective for the determination of certain compound types, including PAHs, petroporphyrins, sulfur heterocycles, phenols and nitrogen bases such as azarenes.

Size Exclusion Chromatography

SEC is usually applied to the analysis of high molecular weight materials. Unless there are specific interactions between the column packing and the sample components, the elution of molecules in SEC is bounded by limits representing total exclusion and total permeation through macroporous particles packed into a column. In this method, the high molecular weight materials elute first, followed by smaller molecules, which is the basis for the determination of molecular weight distribution by SEC.

Typical crude oils contain compounds having low (<100 Da) to high molecular weights (>2000 Da). The average molecular weight can be around 1000–1500 Da. Since 30% or more of the materials in the crude oil may have molecular weights similar to that of the mobile phase and therefore, falling close to the total permeation limit of typical SEC columns, SEC is more suitable for the determination of molecular weights of heavy petroleum fractions derived from crude oil. Atmospheric or vacuum residua and polars and asphaltene fractions from crude oil have been analysed by SEC to monitor changes during their processing or to fractionate them into narrower cuts for further analysis. SEC can also be used as a sample clean-up technique to remove small molecules from high molecular weight materials or vice versa.

The analysis of crude oil or its fractions by SEC is carried out using a series of small pore size (usually ≤ 100 nm) poly(styrene-divinylbenzene) columns and mobile phases of tetrahydrofuran, toluene, chloroform, *N*-methyl-2-pyrrolidone or pyridine. The sample size can be 5 mg or less. Almost all detectors used with HPLC can be coupled with SEC. The most

common detectors are RI, ELSD and UV. Typical separation times are 40 min or less.

Usually molecular weight distributions of fossil samples are determined relative to narrow polystyrene standards. Although both RI and ELSD provide mass versus molecular weight distribution of the sample, a UV detector can be used for similar distribution for specific compound type, using a compound-specific wavelength. For example, distribution of petroporphyrins in polar fractions can be obtained by monitoring sample elution with a UV detector at around 400 nm. Petroporphyrin distributions have also been obtained by SEC-GFAA and SEC-ICP-AES detections.

Thin-Layer Chromatography

TLC using silica or alumina plates and appropriate solvents can provide quick class separation of a crude oil primarily for collection of its fractions. The detection methods for the separated components include visual examination of coloured spots, observation by irradiation with UV light, UV-fluorescence scanning and spraying of chromogenic or fluorogenic reagents.

Rapid and direct determination of hydrocarbon types of a crude oil can be achieved by TLC coupled with FID. In TLC-FID (which is also known as Iatroscan), thin reusable quartz rods (Chromarods) sintered with micrometre-sized silica or alumina particles are used as the stationary phase. After spotting a few micrograms of the sample, the Chromarods are developed sequentially with several solvents or their mixtures of decreasing eluotropic strengths to achieve desired separation. For example, the Chromarods can be developed first with toluene for 5 min to separate saturates plus aromatics from polar compounds. After this, they can again be developed with an *n*-alkane (such as *n*-heptane) for 30 min, for the separation of saturates from aromatics. During the second step, the position of polar compounds remains unchanged, and aromatics are distributed broadly according to their polarity or the number of aromatic rings. As an option, polar compounds can also be subdivided into two resin types by developing the Chromarods with a 9:1 chloroform-methanol mixture for 3.5 min. The Chromarods are dried in an oven after each development. Finally, each Chromarod is scanned by passing it through an oxygen-hydrogen flame for the detection of separated components.

Due to limitations in the design of the commercially available instruments, the TLC-FID method is only quantitative for samples boiling above 300°C. The low boiling materials present in the whole crude oil evaporate during development and drying. Such

evaporation may also occur when Chromarods are exposed to the flame during scanning of the adjacent rod. Therefore, TLC-FID is more suitable for high boiling residua or fractions derived from crude oils than for whole crude oils.

The three TLC-FID chromatograms in **Figure 4** have been obtained by developing Chromarods with toluene for 5 min followed by *n*-heptane for 30 min. Figure 4A demonstrates the capability of TLC-FID for the resolution of saturates and aromatics, and of the ring-based separation of aromatic compounds. Peaks 1–5 in this chromatogram are for Nujol, *n*-heptadecylbenzene, 2,3-dimethylnaphthalene, 9-methylanthracene and 9,10-dimethyl-1,2-benzanthracene, respectively. The unidentified peaks (right-hand side of Figure 4A) are for polar impurities.

A cursory examination of chromatograms of a topped crude oil in Figure 4B and of a vacuum residue in Figure 4C suggests a marked compositional difference between these two samples. Note that the vacuum residue was derived from the topped crude oil as vacuum tower bottoms after vacuum distillation. The vacuum residue contains much more polar and large ring aromatic compounds than the topped crude oil. Specifically, the amounts of saturates, aromatics and polars are 28.6, 56.8 and 14.6% (w/w) in the topped crude oil compared to 9.0, 58.5 and 32.5% (w/w), respectively, in the vacuum residue.

Unlike model aromatic compounds in Figure 4A, aromatics in both topped crude oils and vacuum residua do not show distinct peaks for different ring types. This is primarily due to chromatographic over-

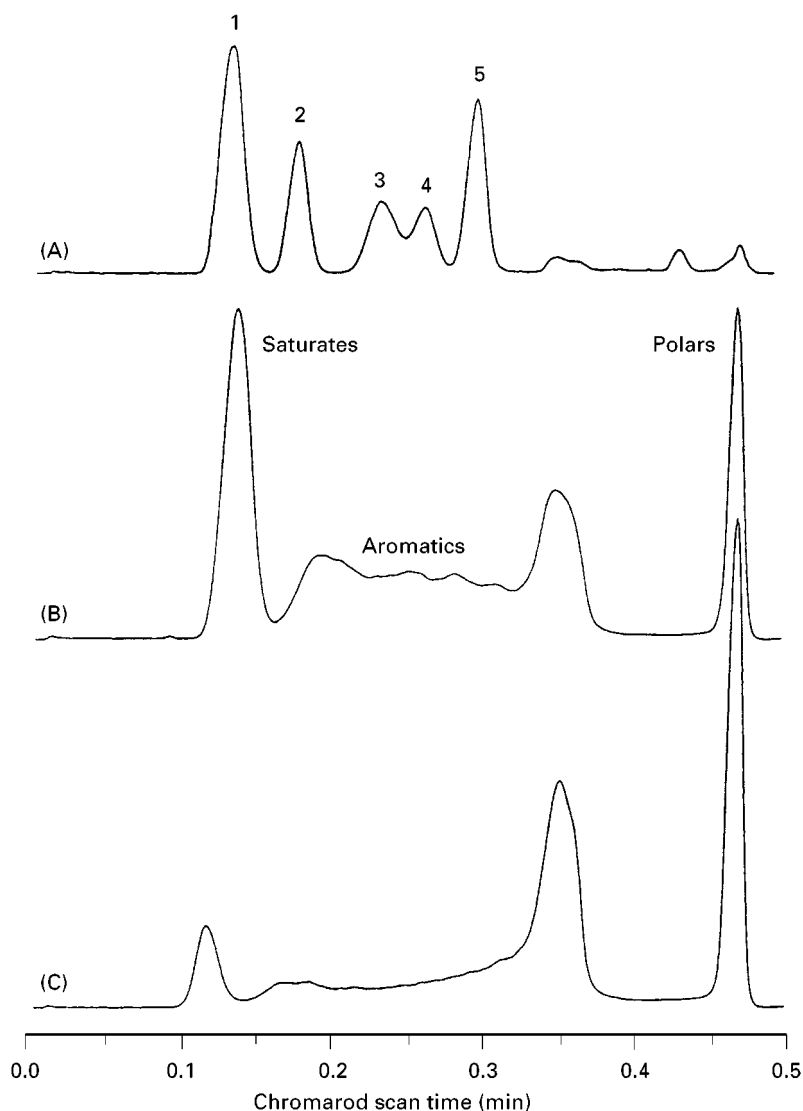


Figure 4 TLC-FID chromatograms. (A) Separation of hydrocarbons by class and number of aromatic rings using a model mixture described in the text; (B) topped crude oil; (C) vacuum residue.

lap arising from degree of substitution as well as substituents of diverse chemical structures attached to the monoaromatic as well as polycyclic aromatic compounds.

Future Possibilities

At present, relevant analytical data on crude oil composition are very useful in crude oil processing as petroleum refiners are increasingly using blended feeds instead of limiting the plant operation to a single type of crude oil. The compositional data will be more important as the depletion of light and sweet crude oils continues and refineries process more heavy and sour crude oils. For process control, product quality, catalyst performance and environmental compliance, faster and better analytical approaches to crude oil characterization will become a vital part of the refinery operation. As far as liquid chromatographic methods are concerned, multistep column-liquid chromatography will be less attractive due to limitations such as lengthy turnaround times, high level of uncertainties in the compositional data, excessive solvent consumption and costs involved in their disposal. Modern HPLC, SEC and TLC-FID methods will continue to provide valuable information on crude oils. Most likely, faster and better results will be achieved through major developments in system automation for coupling these techniques with other chromatographic and spectroscopic methods. Such hyphenated techniques are already being pursued to find better approaches to the characterization of fossil fuels, including crude oils.

See Colour Plate 71.

See also: II/Chromatography: Liquid: Detectors: Ultra-violet and Visible Detection; Mechanisms: Size Exclusion Chromatography. III/Flame Ionization Detection: Thin-Layer (Planar) Chromatography. Flash Chromatography.

Further Reading

- Ali MA and Nofal WA (1994) Application of high performance liquid chromatography for hydrocarbon group type analysis of crude oils. *Fuel Science and Technology International* 12: 21–33.
- Altgelt KH and Gouw TH (eds) (1979) *Chromatography in Petroleum Analysis. Chromatographic Science*, vol. 11. New York: Marcel Dekker.
- Barman BN (1996) Hydrocarbon type analysis of base oils and other heavy distillates by thin-layer chromatography with flame-ionization detection. *Journal of Chromatographic Science* 34: 219–225.
- Grizzle PL and Sablotny DM (1986) Automated liquid chromatographic compound class group-type separation of crude oils and bitumens using chemically bonded aminosilane. *Analytical Chemistry* 58: 2389–2396.
- Hsu CS and Qian K (1993) High boiling aromatic hydrocarbons characterized by liquid chromatography–thermospray–mass spectrometry. *Energy & Fuels* 7: 268–272.
- Neal AC (1995) HPLC and column liquid chromatography. In: Adlard ER (ed.) *Chromatography in the Petroleum Industry*, Ch. 12, pp. 247–394. Amsterdam: Elsevier.
- Padlo DM, Subramanian RB and Kugler EL (1996) Hydrocarbon class analysis of coal-derived liquids using high performance liquid chromatography. *Fuel Processing Technology* 49: 247–258.
- Pearson CD and Gharfeh SG (1986) Automated high-performance liquid chromatography determination of hydrocarbon types in crude oil residues using a flame ionization detector. *Analytical Chemistry* 58: 307–311.
- Sinninghe Dansté JS, Rijpstra WIC, de Leeuw JW and Lijmbach GWM (1994) Molecular characterization of organically-bound sulfur in crude oils. *Journal of High Resolution Chromatography* 17: 489–500.
- Willsch H, Clegg H, Horsfield B *et al.* (1997) Liquid chromatographic separation of sediment, rock and coal extracts and crude oil into compound classes. *Analytical Chemistry* 69: 4203–4209.
- Xu H and Lesage S (1992) Separation of vanadyl and nickel petroporphyrins on an aminopropyl column by high-performance liquid chromatography. *Journal of Chromatography* 607: 139–144.

DECANTER CENTRIFUGES IN PHARMACEUTICAL APPLICATIONS



J. V. McKenna, Alfa Laval, Warminster, PA, USA

Copyright © 2000 Academic Press

Centrifugation continues to perform a vital role in pharmaceutical process operations. In the 1990s new enhancements to the technology attracted many new

areas of application. Growing demands for higher yields and dryer cell cake, punctuated by the pursuit of lower cost solutions, continue to keep high performance centrifuges at centre stage in the quest for better separation procedures. In addition, tighter regulations and inspection procedures continue to act as catalysts for the development of fail-safe

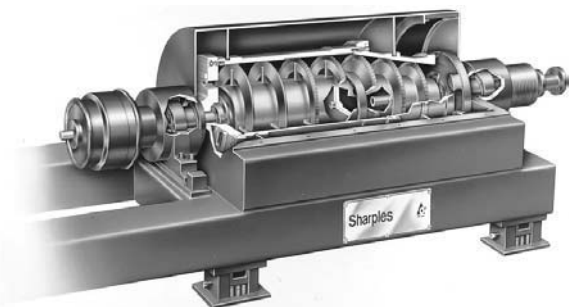


Figure 1 Basic decanter.

equipment for sterility and containment to meet more stringent user demands. Within this environment, a decanter (**Figure 1**), which is the most compact type of separation equipment available, is often the centrifuge of choice for producing pharmaceuticals such as erythromycin, insulin (human and animal) and many other large bulk products. These workhorse machines perform a wide range of separation duties, including liquid–solid, liquid–liquid, and liquid–liquid–solid separations and liquid–liquid extractions. Decaners have become most useful for many pharmaceutical operations including recovery and solids purity. These reliable and versatile machines are active in many of industry's typical process steps, e.g. cell harvesting, concentration and washing, cell debris removal, inclusion body recovery and purification, solvent extraction, dewatering and recovery.

Currently, the trend in solid–liquid separation is towards higher solids fractions in the fermentation process. This translates into greater productivity and lower capital costs per pound of product produced. Typical fermentation processes involve amino acids, antibiotics, bacteria, enzymes, ethanol, fungi, inorganic salts, organic acids, polypeptides, polysaccharides, steroids, vaccines, vitamins and yeasts. Decanter centrifuges are also used in extraction and fractionation processes for hormones, alkaloids, blood separation (animal) and natural product isolation.

General Operation

Normally decaners handle two- or three-phase separation of high-solids slurries (**Figure 2**). The slurry enters the centre of the bowl, and denser solid particles are sedimented against a rotating bowl wall. The less dense liquid forms a concentric inner layer. Centrifugal force compacts the solids as they are 'ploughed' out of the pond and up the conical 'beach' by a helical screw conveyor. Solids exit through dis-

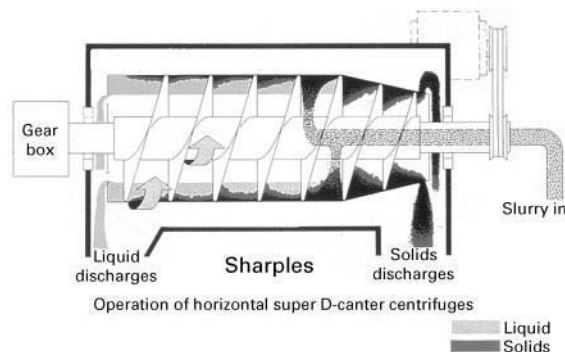


Figure 2 (See Colour Plate 72). General decanter operation.

charge ports, while clarified liquid or centrate overflows the plate dams situated at the opposite end of the bowl. While decaners can handle a wide range of particle sizes, dryer cake is always produced when particle size is maximized – preferably to 2–10 μm depending upon G-force. It is important to note that in biotech lysed *Escherichia coli* separations, cakes that are 30–40% dry have been achieved with particle sizes of 1 μm or less.

In practise, decanting centrifuges provide excellent performance levels when handling slurries with significant amounts of solids (generally > 10% by volume), and are often the only choice for solids concentrations above 40% by volume. With appropriate conveyor modifications they can also be used to separate two liquids from each other or from a solid phase. The scroll of the decanter provides a continuous discharge of solids. By interposing nozzles near the beach section it is possible to provide a washing step before the solids are discharged. This method can be used to wash various crystals. In contrast to basket or disc-stack centrifuges, where liquid flow is laminar and flow patterns are relatively simple and contained, the flow patterns and consequent design calculations are more complex for decaners. Separation performance is more subject to analysis by experience and pilot testing.

Vertical Units

Most decanter centrifuges are horizontal, but vertical orientations (**Figure 3**) are also available. The same centrifugal operating principles apply to both types, and process performance is not affected by whether the axis of rotation is vertical or horizontal. The main difference between the two types lies in the seal design. A vertical machine has only one high speed rotating seal plus one low speed (42–52 rpm) or static seal, while a horizontal unit has at least three high speed seals. For this reason, a vertical configuration is

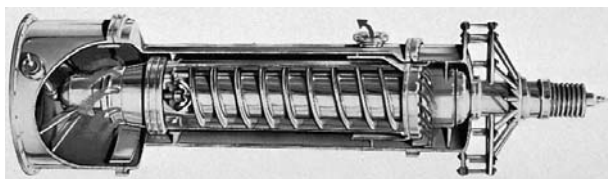


Figure 3 (See Colour Plate 73). Vertical decanter.

easier to seal. With only one sealing surface this unit is often the preferred choice when handling hazardous materials or toxic materials. Vertical centrifuges are often used in high temperature, high pressure applications for handling pressures from vacuum up to 10 bar with process temperatures from -10 to 700°F .

If floor space is a concern, vertical decanters offer distinct advantages over horizontal machines as they require 60–80% less floor area. They also provide more production per square foot with less investment in piping, foundations and real estate.

Factors of Acceptance

For small batch fermentations (100 L or less) membrane technology and mechanical filtration remain the prevalent technologies for processing diverse stream arrays. However, for large volume runs requiring environmental measures and control, decanters are normally specified for several reasons. First, the enclosed seal design of this type of centrifuge type offers inherent advantages. Decanters can be sealed hermetically for the protection of operating personnel, and offer clean-in-place operation and sterilization. Second, the efficient operation of a decanter can produce a dry continually discharged solids phase without contamination of either the product stream or the centrate. Also advancing work on new metallic finishes continues to offer promise for new sterility solutions and safeguards.

Additional factors also work in favour of these machines. Possibly foremost is the growing need to produce dryer cake. As expected, when there is less water solids require less energy for drying. Depending upon the application, decanters can produce dry solids as high as 30–95% for dry solids. The high G-force capabilities of the units can separate out even the finest particles, resulting in cleaner centrate.

The ability to operate at higher G-forces remains a goal. Indeed, high G-force separation continues to expand. Five years ago decanter centrifuges could only generate forces up to 5000 G. During that period

disc-stack centrifuges were primarily used for applications, from pilot to full production. Today decanters are capable of 10 000 G operation, making the machines competitive with disc-stack centrifuges for specific pharmaceutical applications.

Continuous operation is another reason why the industry often opts for decanters. The feed and discharge operations (solids and liquids) never cease. There is less downtime and maintenance is substantially lower than with other separation alternatives. At the same time decanters are less affected by feed variations, such as varying particle size, than filter systems which require changing media mesh sizes. The centrifuges also more efficiently separate adhesive, slimy, high viscosity or fluffy materials, which often blind or impair filters. They also provide dryer cake results for these materials than do filters.

Minimal liquid loss is also associated with decanters. Permeable filters lose liquid through absorption as well as losing fluids via filter disposals. This loss becomes critical if a high value is attached to the liquid phase. Also, filters usually separate only two phases simultaneously, requiring another pass for a third separation, while centrifuges are capable of one-step, three-phase liquid–liquid–solid separations (e.g. oil, water, solids).

Improvements to Decanters

Several changes to decanter technology have affected the performance of the machines in the last 10 years.

Settling Vanes

New conveyors have been fitted with unique incline vanes to enhance the collection area of the disc unit. Settling vanes (**Figure 4**) reduce turbulence and stratify feed flow in the clarification zone to promote settling and prevent re-entrainment of solids. This

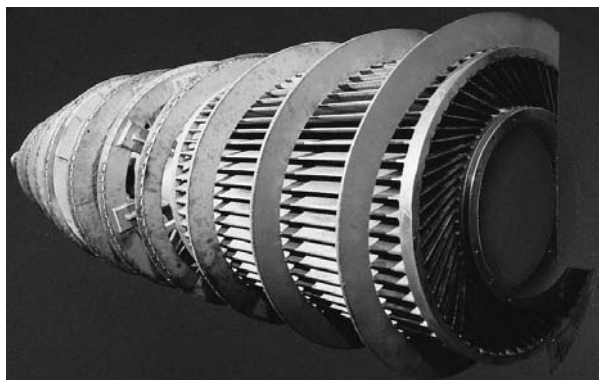


Figure 4 Conveyor with settling vanes.

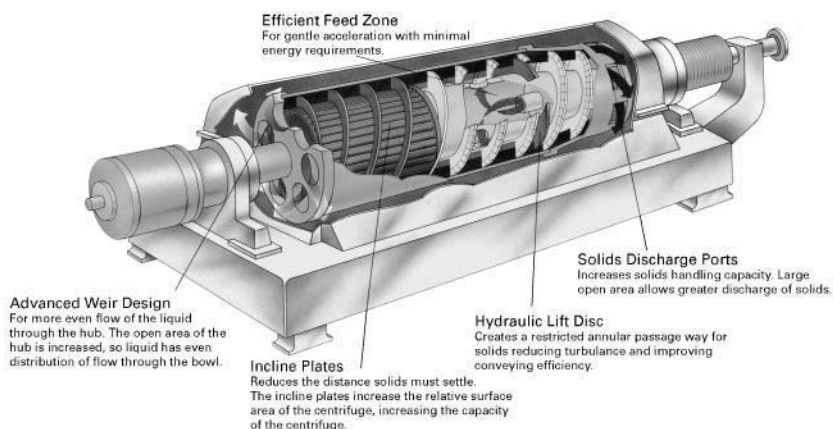


Figure 5 (See Colour Plate 74). Performance-enhancing features of a decanter centrifuge.

results in more efficient solids recovery and a 50% improvement in centrate clarity.

Hydraulic Disc (Baffle Disc)

This feature shown in Figure 5 enhances the separation of soft, gelatinous materials such as proteins, enzymes, and fermented products. The disc is used to increase the separation efficiency on hard-to-scroll materials (materials that tend to slip on the conical section of a decanter). Acting like a dam, solids build up around the disc, holding in the liquid centrate to provide ultra-deep pond settlings above the level of the solids discharge. The resulting hydrodynamic pressure compacts solids, assists scrolling, and extrudes the compacted solids past the disc and out of the centrifuge.

Dryer Cake: Plough Tile/Conveyor Innovations

New designs now provide purer and dryer cake. Recent innovations permit the centrifugal retention of solids for longer periods of time under maximum G-force. A new conveyor handling compressible solids, such as fibrous materials, has been able to produce up to 35% dryer solids in vitamin, gluten, and cornstarch processing applications.

A newly developed plough tile conveyor (Figure 6) uses scoop-shaped tiles to reduce the torque produced by the solids moving through the centrifuge. By lifting and turning the solids from the bowl wall these tiles reduce the torque, produce dryer cake, and increase capacity. The addition of this innovation enables the conveyor to achieve up to twice the throughput of standard conveyors.

Another additional improvement is the 'Kiwi conveyor' (Figure 7), a patented flightless conveyor that achieves dryer cake to improve clarity. This unique

innovation acts as a catalyst to force newer solids to move old solids out of the bowl.

Efficient Feed Zone

Redesign of the feed zone as shown in Figure 5 has helped to reduce the shear forces on the feed material as much as possible. Shear forces on the liquid stream can cause problems, especially when liquid goes from rest to bowl speed. Upgrade designs now allow for gentle acceleration and entrance into the bowl by means of a low-shear feed zone. This improvement has eliminated the need for acceleration blades.

Variable Speed and Differential Control

Programmable Logic Controller (PDC) and digital controllers are now used to control the large speed swings of a decanter's backdrive motor that are associated with differential control. These systems provide the necessary control features to monitor and stabilize a decanter's eddy current brakes, direct current motor, and alternating current variable

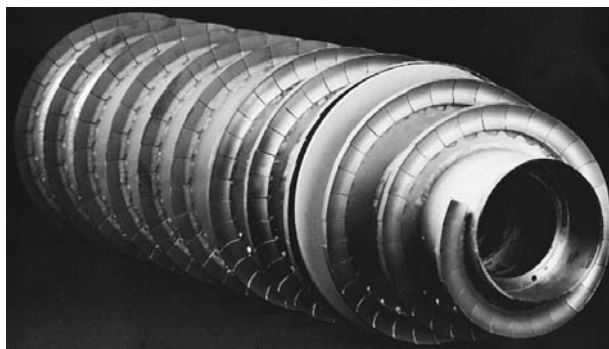


Figure 6 Plough tile conveyor.



Figure 7 'Kiwi' conveyor.

frequency drives to within 0.1 rpm of the desired set points. By maintaining lower differential controls, users achieve dry cake.

Centripetal Pumps and Containment

Optional centripetal pumps can be added to minimize foaming and aerosols, and gently discharge delicate pharmaceuticals without the risk of oxidation or contamination to the product stream. Such pumps help control liquid creasing and the separation efficiency of the unit.

Vapour Sealant

For applications requiring biohazard-safe, vapour-sealed operation, casing seals are available to contain pressure up to 14.4 kPa inches of water. Lip seals, labyrinth seals, and gas-purged mechanical seals are typically used. If required, decanters can be equipped with steam sterilization for aseptic steam processing.

Clean-In-Place Operation

Self-cleaning units are also available for faster and safer pharmaceutical processing. Built-in motor controls safely reduce rotation to 1 G and automatically clean the decanter's bowl and casing. This eliminates the need to tear down or dismantle the centrifuge.

Conditioning Monitoring

Together with the decanter improvements, the capability to maintain product integrity has been further enhanced by conditioning monitoring programs

available from some manufacturers. New software eliminates second guessing and enables users to analyse machines on a continuous basis, e.g. monthly, weekly, etc., by checking for new vibrational patterns due to changes in unit load, balance, or the hydraulic dynamics of the bearing. Conditioning monitoring provides real-time information about the working operation of the centrifuge. Accompanying instrumentation and probes also analyse critical areas such as bearing patterns to note changes, predict failure and prevent unexpected costly shutdowns. Data acquired and stored in the program can also be used to determine what spare parts to keep in stock.

Conclusion

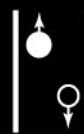
The development of pharmaceutical products requires separation equipment that delivers high recoveries and high solids purity. During the 1990s decanter centrifuges closed the gap on or, depending upon the application, even surpassed the advantages once held by alternative separation devices. In centrifugation, operating costs are notably lower than with filtration devices with capital investment of hardware as the only significant cost. Decanters also require less auxiliary equipment such as secondary pumps, tanks, and extra ventilation machines. Thus large-scale pharmaceutical operations rely on continuous centrifuges to produce maximum possible amounts of dry cake and decanters are well suited to this task.

See Colour Plates 72, 73, 74.

Further Reading

- Alfa Laval (1984) *Complete Range of Centrifuges for the Fermentation Industry*. Technical Brochure IB 41045E. Tumba, Sweden: Alfa Laval.
- Amber CM (1961) Centrifugation equipment theory. *Industrial Engineering Chemistry* 53: 430–433.
- Arkinson B and Mavituna F (1983) *Biochemical Engineering and Biotechnology Handbook*. New York: Nature Press.
- Axelsson HAC (1998) *Centrifugation*. Technical Brochure. Tumba, Sweden: Alfa Laval.
- Davies E (1965) Selection of equipment for solid-liquid separation. *Transactions of the Institution of Chemical Engineers* 43: T256–T259.

DE-INKING OF WASTE PAPER: FLOTATION



C. Jiang and J. Ma, Enzymatic Deinking Technologies,
Norcross, GA, USA

Copyright © 2000 Academic Press

Introduction

The earliest work on utilization of froth flotation for de-inking of wastepapers dates back to the 1930s. The first flotation de-inking patent was filed by Hines in 1933. However, it was not until 1952 that the first commercial flotation de-inking system was installed at a paper mill in the USA, and the first European installation was at a tissue mill in Greece in 1959. Up to 1970, the growth of flotation de-inking technology was relatively slow. However, in the past 20 years, the market has grown extremely rapidly. The world-wide flotation capacity for de-inking of wastepapers has increased from 0.2 million tons in 1965 to about 25 million tons in 1995.

De-inking is a separation process to remove inks and other nonfibrous contaminants from wastepapers. Different types of units are required to separate inks from fibres, and this mainly includes washing, flotation, cleaning and screening. The selection and operation of these units are based on the types of wastepapers and the requirements of the finished de-inked pulp. Wastepaper is commonly grouped into five categories, which include mixed paper, old newspapers, old corrugated containers, pulp substitutes and high grade de-inked. **Table 1** shows a typical wastepaper classification and the finished products obtained from different kinds of wastepapers.

De-inking is a two-stage process which involves dislodging the ink and nonfibrous contaminants from

the fibre surface and removing them by washing, flotation, cleaning and screening. Common contaminants include ink, staples, paper clips, sand, plastics and stickies. The most important and widely used de-inking process to date is the froth flotation process. This process removes the widest range of ink particles from wastepapers. Flotation alone or in combination with other processes can remove almost all types of ink particles and other contaminants from the slurry of wastepaper.

Flotation Process and Equipment

Flotation Process

Pulping The first step in de-inking wastepaper is pulping. Because of the nature of the chemicals and equipment used to pulp wastepaper, the pulping process is analogous to sulfite 'cooking'. Chemicals, together with heat and mechanical energy, are used to detach the ink particles and other contaminants from the fibres in a pulper. Pulping can be either a batch or continuous process. Newsprint mills typically use continuous pulping at a consistency of 4–8%. Other mills usually use batch pulping at a higher consistency of 8–18%.

Flotation Flotation de-inking is a selective separation process that utilizes the difference of surface physicochemical properties between the ink and fibre. Flotation chemicals are fed to the wastepaper slurry to render the ink particles selectively more hydrophobic and hence to increase the floatability. When the air bubbles are sparged into the flotation cell containing the wastepaper slurry, the ink particles get at-

Table 1 Typical wastepapers and their classification

<i>Category</i>	<i>Compositions and abbreviations</i>	<i>Finished products</i>
Old newspapers	Old newspapers (ONP), white blank newspapers	Newsprint, boxboard, tissue, paper towels
Old corrugated containers	Old corrugated containers (OCC), double linerboard kraft corrugated clippings (DLK)	Linerboard, boxboard, corrugating medium, kraft towels
Mixed paper	Mixed office waste (MOW), old magazines (OMG), sorted ledgers, computer printout (CPO), manifold white ledger (MWL), sorted office waste (SOW)	Printing and writing paper, paperboard, tissue, paper towels, magazine newsprint
Pulp substitutes	Unprinted paper and board, boxboard cuttings, printer trims, envelope cuttings	Fine paper, tissue, envelopes
High grade de-inked		Fine paper, tissue, printing and writing papers

tached to the air bubbles due to their relatively high hydrophobicity and are floated to the surface of suspension, and the hydrophilic fibres remain in the water phase.

Flotation De-Inking System

Flotation is traditionally the standard European de-inking system for old newspapers. The stocks or wastepaper slurry after pulping generally go through a soaking stage in a dump chest to swell the fibres and to improve ink detachment from the fibre.

The stock is subsequently aerated at 0.7–1.5% consistency in a series of flotation cells. Typically, six to 10 flotation cells in series (primary flotation) are required for efficient ink removal. The froth from primary flotation is subsequently cleaned in a secondary or recovery stage (usually two cells) to further recover food fibres and to decrease fibre loss. A typical and representative example of a flotation system is illustrated in Figure 1.

Most technical advances made during the past 10 years involved utilization of a combination of flotation and washing stages to remove inks from the more complex wastepaper. The concept of the post-flotation system is to add a disperger or kneader between two standard flotation stages. The dispersion or kneading stage further helps the detachment and size reduction of ink and other nonfibrous particles, and hence improves the overall flotation performance.

Evolution of Flotation Cells

Froth flotation is the most widely used separation process in modern paper mills. During the last 10 years, the development of flotation de-inking cells has been pursued more aggressively than the technologies of any other segment of the pulp and paper industry.

Initially, Denver flotation cells used in the mineral industry were installed in paper mills. These cells are open, rectangular vats, with mechanical removal of flotation froth by a rotating paddle and mechanical mixing of air and pulp suspension at the bottom. However, these cells are not currently in use.

Although the development of flotation cells for de-inking was less dramatic in the early years, there have been many changes in cell design in the last two decades. Table 2 lists the historical development of flotation de-inking cells.

The major driving forces of the evolution of modern flotation cells are the reduction in energy and water consumption, lower footprint space and an increase in efficiency and capacity. Although many changes in flotation cell design have been made, the improvements in flotation de-inking performance are not always obvious. More recently, because of the great advances in printing, coating and modification of paper by converters to impart special properties, flotation de-inking has evolved from removing ink particles only to removing an ever-increasing variety

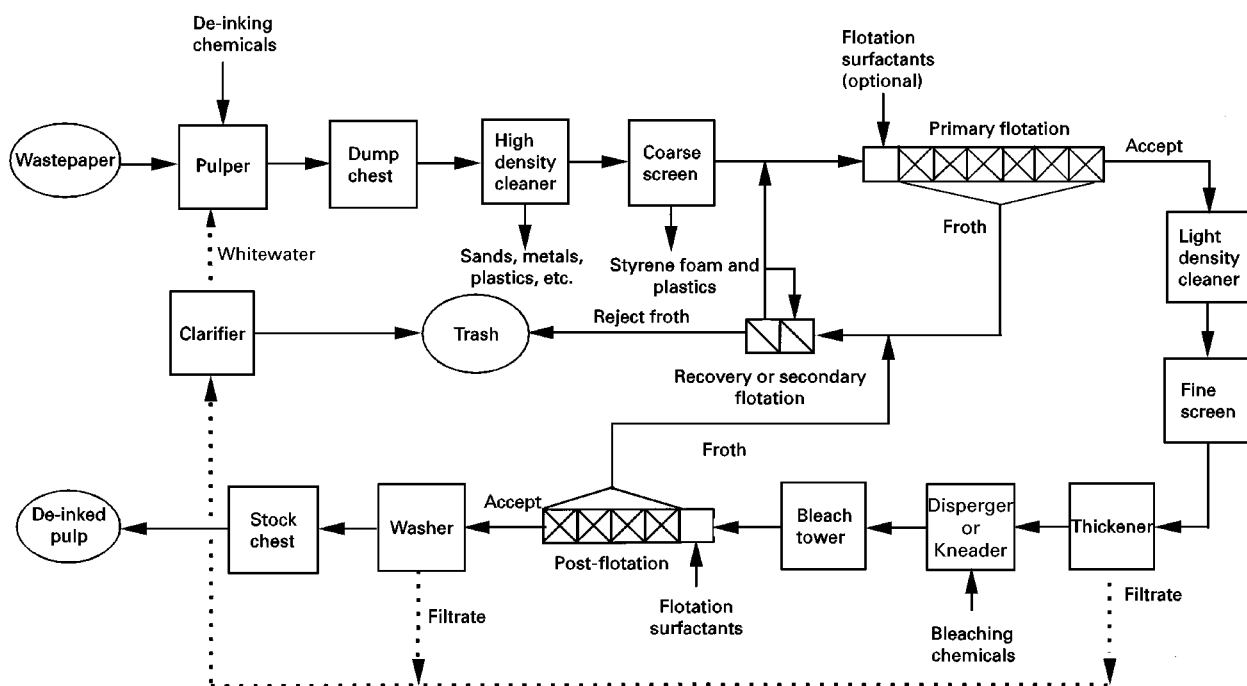


Figure 1 Flow diagram of a typical flotation de-inking mill for mixed paper.

Table 2 Historical evolution of flotation de-inking cells

<i>Year</i>	<i>Flotation cell name</i>	<i>Comments</i>	<i>Year</i>	<i>Flotation cell name</i>	<i>Comments</i>
1952	Denver cell	First commercial de-inking flotation cell	1986	Lamort DA Verticel	Double aeration
1959	Voith paddle cell	First cell designed specifically for de-inking with improved air mixing	1987	Beloit PDM cell	First cell to use pressure to improve efficiency and pressurized rejects removal
1972	Escher Wyss FZ-1 cell	First cell to use compressed air	1990	Voith elliptical cell	First cell totally sealed Tubular shape compressed from cylindrical to elliptical to promote faster air removal
1975	Swemac Hellberg cell	First cell without agitator and with controlled air bubble sizes First cylindrical cell	1990	Eshcer Wyss CFS cell	Designed for speck removal
1976	Escher Wyess FZ-U cell	No agitator compressed air enters bottom of cell	1991	Black Clawson IHI/BC cell	Turbine acts as an agitator and distributes air through cell
1978	Lamort Verticel	First cell with vacuum to remove rejects First cell with multi-feed and aeration stages with no agitator	1991	Kamyr gas-sparged cyclone	Cyclone body with porous media
1981	Black Clawson ULTRACELL	First cell with gravity feed between stages	1992	Eshcer Wyss CFC cell	Stacked cell units
1981	Voith tubular injector cell	First tubular cell with air drawn through injectors	1993	Comer Spidercel	First cell with agitation provided by reactor blades
1981	Shinham HIFLO FLOTATORS	Hydrocyclone body	1994	Thermo/Black Clawson Verticel Mac cell	Similar to Lamort Verticel with multiple aeration closed
1983	Beloit Lineacell	First cell with separate aeration, mixing and separation stages	1995	Voith Sulzer EcoCell	Similar to Voith elliptical cell with Escher CF cell air injector
1984	Esher Wyss CF	Step diffuser improves mixing	1996	Kvaerner Hymac column flotation cell	First cell to use two types of air spargers to provide different size air bubbles

of objectionable, noncellulosic materials. However, in terms of ink removal efficiency, older flotation cells perform satisfactorily.

Factors Affecting Pulping and Flotation

The performance of flotation de-inking is affected by many factors such as pH, consistency, temperature, ink/fibre particle size, chemical types, water hardness and air bubble size. Properly controlling these factors ensures the efficient removal of ink.

pH pH significantly affects both the pulping and flotation processes by altering the physical and chemical properties of fibres and inks. High pH helps swelling of fibres and promotes the detachment of inks from fibre. However, if the pH is too high (e.g. > 10), it may cause yellowing or darkening of lignin-containing pulps. The conventional fatty acids

and soaps used as ink collectors are only effective at alkaline pHs. Neutral pH flotation de-inking requires the use of more effective and selective nonionic surfactants.

Temperature Pulping and flotation temperatures are typically maintained at 40–55°C and 35–45°C, respectively. In general, elevated temperatures are used to improve the defibrization of special waste-paper such as wet strength paper. Lower temperature is beneficial to high stickies-containing wastepaper, such as magazines.

Consistency Consistency or dry fibre per cent weight in water has a direct impact on the ink particle size distribution. Depending on the types of waste-paper, different pulping consistencies are used. In newsprint mills, low-consistency (4–8%) pulping is generally used. However, in office paper de-inking

mills, medium (8–12%) or high consistency (12–18%) pulping is widely applied. In general, the higher the pulping consistency and the longer the pulping time, the smaller the ink particles liberated. Typical fibre consistency in flotation operation is 0.7–1.2%.

Particle size Flotation is most effective for removing ink particles ranging from 10 to 150 μm . In general, particles smaller than 10 μm and larger than 150 μm cannot be efficiently removed by flotation process.

Water hardness In newsprint flotation, fatty acids or soaps are used as ink collectors, and a moderate amount of calcium ions (100–300 p.p.m.) is required to make the ink floatable. No additional hardness or calcium ions are added when nonionic surfactants are used.

Ash or filler content There is a strong relationship between the amount of clay or fillers in the wastepaper and the ink removed in a flotation stage. Flotation de-inking becomes much more effective when the wastepaper has significant ash content. An 8–10% ash is considered a minimum requirement, and 12–14% is preferable.

Evaluation of Flotation Performance

Three major parameters are widely used in the paper industry to characterize the flotation deinking efficiency: brightness, ink removal and reject rate.

Brightness is the percentage of reflectance measurement of pulp or paper products at a wavelength of 457 nm. It is originally developed to evaluate bleaching efficiency. In general, pulp brightness increases as ink is removed. The brightness increase is usually in the order of 10–15 units for newsprint de-inking and of 5–10 units for white grades.

Reject rate is defined as the mass rate of reject to total stock fed into flotation. A main objective of flotation de-inking is to obtain the maximum ink removal at a minimum reject rate. For mixed office wastepaper (MOW), reject rate is commonly 10% and for ONP/OMG, it is about 15%.

Ink removal is calculated based on the ink concentration of the pulp before and after flotation. Image analysis techniques are used to measure ink particle size ($> 3 \mu\text{m}$), total counts and the total surface area. Effective residual ink concentration (ERIC) measurement was developed to determine the visual effect of residual inks on the de-inked pulp. The visual effect is primarily dependent on the presence of small size ink particles ($< 3 \mu\text{m}$) rather than the total ink content of the paper.

To evaluate the de-inking efficiency, both the ink removal of different size particles and brightness should be reported together with reject rate. For newsprint mills, brightness and ERIC measurements are usually employed and, for white grades, ink count measurement is very common.

De-inking Chemicals and Recipes

The use of chemicals is involved in almost every aspect of the key processes in de-inking. Chemistry is of great importance in flotation de-inking in terms of fibre swelling, ink detachment, dispersion, anti-redeposition, ink agglomeration, ink collection and removal. Most of the chemicals used for de-inking are fairly standard commodity products, such as sodium hydroxide and sodium silicate. On the other hand, some other chemicals are relatively complex and have multiple functions. In general, most de-inking chemicals are added in the pulper. Commonly used de-inking chemicals in pulping and flotation, their functions and addition points are listed in Table 3.

Pulper Chemicals

The chemicals used in the pulper depend strongly on the types of wastepaper processed. The principal chemicals used for pulping and flotation are sodium hydroxide, sodium silicate, chelating agents, hydrogen peroxide, surfactants and solvents. The roles of these major de-inking chemicals are briefly discussed below.

Sodium hydroxide Sodium hydroxide is used to promote fibre swelling and to saponify or hydrolyse the ink resins by increasing pH and alkalinity. The type and amount of alkali required in the pulper depend on the type of mechanical treatment, temperature and pulping time. However, the addition of excessive caustic soda to ground wood-containing furnishes will cause the pulp to yellow or darken. This is termed as 'alkali darkening or yellowing'. Sodium carbonate is rarely used in modern de-inking mills.

Sodium silicate Sodium silicate or water glass is frequently used in conjunction with sodium hydroxide, especially in the de-inking of groundwood papers. It not only serves as an alkali to swell fibre and as a dispersant of ink particles, but also buffers the pulp to a pH range which is favourable to the action of hydrogen peroxide.

Hydrogen peroxide Hydrogen peroxide is one of the most commonly used pulping chemicals in the

Table 3 Chemicals used in flotation de-inking and their functions

<i>Chemical</i>	<i>Structure/formula</i>	<i>Function</i>	<i>Furnish type</i>	<i>Dosage (% of fibre)</i>	<i>Addition point</i>
Sodium hydroxide	NaOH	Fibre swelling – ink break-up Saponification	All grades	0–5	Pulper
Sodium silicate	Na ₂ SiO ₃	Ink dispersion Wetting	Groundwood grades	0.5–5	Pulper
Sodium carbonate	Na ₂ CO ₃	Ink dispersion Peroxide stabilization Alkalinity and buffering	Lightly inked ledger		
		Alkalinity Buffering Water softening	Groundwood grades Lightly inked ledger	0.25–5	Pulper
Hydrogen peroxide	H ₂ O ₂	Prevention of fibre yellowing	Groundwood grades Coloured ledgers	0.5–2.5	Pulper
Sodium hydrosulfite	Na ₂ S ₂ O ₄	Bleach, colour stripping	Groundwood grades Coloured ledgers	0.5–1.5	Pulper Pulp storage
Sodium or potassium phosphate	Hexametaphosphate Tripolyphosphate	Metal ion sequestrant Ink dispersion Alkalinity and buffering	All grades	0.2–1	Pulper
Chelating agents	EDTA DTPA	Detergency Metal ion chelation	All grades	0–0.5	Pulper
Calcium ions	CaCl ₂	Peroxide stabilizer Fatty acid/soap collector aid	Groundwood grades	90–300 p.p.m.	Flotation Pulper
Hydrophilic polymers	Polyacrylate Carboxymethylcellulose	Ink anti-redeposition Anti-redeposition	All grades	0.1–0.5	Pulper
Nonionic surfactants	Ethoxylated alcohol Ethoxylated alkyl phenols	Ink collector Flotation frother Wetting Emulsification	All grades	0.1–2	Pulper Flotation
Fatty acids or soaps	Stearic acid Oleic acid Fatty acid mixtures	Ink collector Flotation frother	All grades	0.5–3	Pulper Flotation
Solvents	C ₁ –C ₁₄ aliphatic saturated hydrocarbons	Ink softening Solvation of wax	Wood-free grades	0.5–2	Pulper

recycling of groundwood wastepaper. It is also widely used as a bleaching chemical. The addition of hydrogen peroxide in the pulper is to offset the formation of chromophores created by high alkaline pH.

Sodium hydrosulfite Hydrosulfite is mainly used as a reductive bleaching agent to bleach recycled pulp and to decolourize the coloured fibres.

Chelating/sequestering agent Chelating compounds are commonly added in the pulper to form complexes with multivalent metal ions to prevent peroxide decomposition. Diethylenetriaminepentaacetic acid (DTPA) and ethylenediaminetetraacetic acid (EDTA) are the most common chelates used in the

paper recycling industry. Compounds like DTPA and EDTA have been banned in some countries, for example, Sweden and Norway.

Dispersants Sodium tripolyphosphate and tetrasodium pyrophosphate are sometimes added to the pulper to provide multiple functions such as ink dispersion and metal chelating. Use of laundering anti-redeposition agents such as carboxymethylcellulose and sodium polyacrylate can also help disperse the ink particles, prevent redeposition of ink on the fibre, and increase de-inked pulp brightness.

Solvents Organic solvents were once widely used to dissolve waxes and varnishes, but environmental

concern has curtailed the use of these chemicals. Solvents used in wastepaper deinking include C_{12} – C_{14} hydrocarbons and glycol ethers.

Flotation Chemicals

Surfactants are probably the most important chemicals in flotation de-inking. They consist of two principal components – a hydrophilic component and a hydrophobic component. It is assumed that the hydrophilic end of the molecule attaches to the ink particle, leaving the treated surface state hydrophobic. Most surfactants used in flotation de-inking play two important roles. Firstly, they function as ink collectors that selectively render the ink particle surface more hydrophobic and facilitate ink particle–air bubble attachment. Secondly, they serve as flotation frothers that generate moderate foaming. Surfactants used in flotation de-inking can be cationic, anionic, nonionic or amphoteric, and are added either at the pulper or just before the flotation cells.

The most frequently used surfactants are fatty acids and their soaps, as well as nonionic surfactants. Cationic surfactants are not currently used in flotation cells. Commonly used flotation de-inking surfactants and their formulas are shown in **Table 4**.

Fatty acids and soaps Fatty acids and their soaps are early flotation de-inking surfactants, and are commonly used in Europe than in North America. Mixtures of fatty acids with carbon chain lengths of 16–18, such as stearic, oleic, palmitic and linoleic acids, are commonly used as ink collectors. Saturated fatty acid soaps usually have better ink collection while unsaturated fatty acid soaps have higher foam-

ing. To function effectively as ink collectors, fatty acids require the presence of moderate concentration of calcium ions such as at least 12 degree German hardness (dH) or approximately 200 p.p.m. as calcium carbonate. The calcium ions can be sourced from the paper fillers such as calcium carbonate, or from the addition of calcium chloride or oxide. To maximize the function of any source of calcium ions, it is important to maintain the flotation in alkaline conditions (>8 – 8.5), otherwise fatty acids precipitate. However, the presence of excess calcium ions in the system may cause fibre loss.

Nonionic surfactants Nonionic surfactants encompass a large number of synthetic chemicals of varied types and structures. Major types of nonionic surfactants include fatty ethoxylate, alkyl phenol ethoxylate and fatty acid alkoxyate. Cloud point and hydrophilic/lipophilic balance (HLB) value are two important terms used to describe a given nonionic surfactant. Cloud point is the temperature at which nonionic surfactants become separated from the solution. Below the cloud point, surfactant has higher foaming and above the cloud point, the foaming of surfactants decreases dramatically. HLB value is the ratio of weight percentages of hydrophilic to hydrophobic groups in the structure. Generally, for the same surfactant, the higher the HLB value, the higher the foaming ability, and the lower the ink collection ability. An effective nonionic flotation surfactant usually possesses the properties of good ink collection and adequate foaming.

Some of the most common nonionic surfactants used in flotation deinking are EO/PO copolymers, in

Table 4 Typical flotation de-inking surfactants

<i>Types</i>	<i>Name</i>	<i>Formula and structure</i>
Anionic	Fatty acid and emulsion	$CH_3(CH_2)_nCOOH$
	Fatty acid soap (stearic/palmitic/oleic acid and soap)	$CH_3(CH_2)_nCOONa$ $CH_3(CH_2)_nCOONa$
	Alkylbenzene sulfonate	$R-(C_6H_4)-SO_3Na$
	Fatty alcohol sulfate	$R-OSO_3Na$
	Fatty alcohol ether sulfate	$R-O-(CH_2CH_2O)_nSO_3Na$
Cationic	Dodecyltrimethylammonium bromide	$CH_3(CH_2)_{12}NH_4Br$
Amphoteric	Sulfobetaine	$RN^+(CH_3)_2(CH_2)_xSO_3^-$
Nonionic	Fatty alcohol ethoxylate	$R-O-(CH_2CH_2O)_xH$
	Ethoxylated alkyl phenol	$R-(C_6H_4)-O-(CH_2CH_2O)_xH$, $n = 8-9$
	EO/PO copolymers	$HO-(EO)_x-(PO)_y-(EO)_z-H$
	Fatty acid alkoxyate	$RCOO-(CH_2CH_2O)_xH$
	Alkyl phosphate ester	$(RO(CH_2CH_2O)_n)_2POONa$
	Fuel oil	$CH_3(CH_2)_nCH_3$
	Fatty oil alkyleneoxide derivative	

EO, Ethylene oxide; PO, propylene oxide.

which the hydrophilic part is EO (ethylene oxide) and the hydrophobic part is PO (propylene oxide). Alkoxylates of fatty alcohols or fatty acids containing both EO and PO units have been used as flotation surfactants.

As environmental regulations become tougher, de-inking mills tend to prefer to use surfactants that are easily biodegradable. Because of the difficulty of breaking down alkyl phenols in wastewaters, they are gradually being replaced by readily biodegradable products such as alcohol ethoxylates.

Flotation Recipes

The selection of optimal flotation chemistry recipes depends strongly on both ink properties and types of wastepaper. The flotation recipes that are commonly employed are summarized in Table 5.

Old newspapers Newsprint (100%) is often de-inked by washing. However, flotation can also be effective to remove newsprint inks with fatty acid/calcium ion chemistry. In the absence of calcium ions, the ink particles do not float using fatty acid collectors. The addition of calcium is indispensable for a fatty acid or a soap to function properly as a collector. Positively charged calcium ions are bonded to the fatty acid and to the negatively charged ink particles, and thereby promote ink flotation. Calcium ions (often as calcium chloride) should be added to the pulp simultaneously or before the fatty acid at a level of above 100–150 p.p.m. as calcium carbonate.

ONP/OMG mixture Ash plays a very important role in the flotation de-inking of newsprint. It is a common practice to include a certain per cent of old magazines (OMG) in old newsprint (ONP) for better flotation de-inking efficacy. Since OMG and mixed office waste (MOW) contain fillers such as calcium carbonate, the presence of these fillers in the wastepaper promotes ink flotation. This is because the fillers can provide the calcium ions needed by the fatty acids. Traditionally, the mixtures of ONP and OMG, usually in the ratios of 70 : 30 and 50 : 50, are de-inked by flotation at an alkaline pH using fatty acids or soaps. A significant improvement in ink removal of newsprint can also be achieved by adding clay to the pulper.

Mixed paper Most of the early plants used alkaline conditions to de-ink mixed wastepaper. However, there is a trend for modern de-inking mills to switch to neutral conditions. Fatty acids are commonly used in Europe and Asia and nonionic surfactants alone are commonly used in North America for de-inking mixed paper. However, fatty acids in combination with nonionic surfactants are found to be the most effective in removing both large and small ink particles.

Flexographic inks Flexographic inks are water-based inks and are difficult to de-ink using flotation due to the hydrophilic nature and very small size ($< 5 \mu\text{m}$) of the ink particles. Flexographic inks tend

Table 5 Typical flotation recipes of waste paper de-inking

Medium	Pulping			Flotation	
	Alkali and bleaching agent	Chelate or dispersant	pH	Collector and frother	Furnishes suitable for the flotation chemistry
Alkaline de-inking	NaOH Na ₂ SiO ₃ H ₂ O ₂	EDTA DTPA Phosphate	8.5–11.5	Fatty acids or soaps with calcium ions	100% ONP, 100% flexographic ONP/OMG
				Fatty acids or soaps	ONP/OMG, ONP/SOW, OMG trimming/MOW
				Fatty acids or soaps and nonionic surfactants	ONP/OMG, ONP/SOW, OMG trimming/MOW
				Nonionic surfactants	Sorted ledger, MOW, CPO
Neutral de-inking	NaOH (optional)	EDTA DTPA (optional)	5.5–8.0	Fuel oil and nonionic surfactants	100% flexographic ONP and OMG
				Fatty acids or soaps	
				Fatty acids or soaps and nonionic surfactants	MOW, sorted ledger, OMG trimming/MOW
				Nonionic surfactants	MOW, sorted ledger, OMG/MOW, CPO, manifold
				Fuel oil and nonionic surfactants	MOW, sorted ledger, OMG/MOW, toners
					Flexographic ONP/OMG

For abbreviations, see Table 1.

to redeposit on the fibres and may cause a dramatic brightness drop of the pulp. Similar to 100% newsprint, fatty acid soaps and calcium ions are found to be effective in removing flexographic inks.

Toner inks Xerographic paper and laser computer printout (LCPO) are frequently found in government publications and general office waste. The inks in these papers are thermoplastic powders or toners, and are firmly bonded to the fibres with a heat fusion printing process. The toner ink particles are hydrophobic, but their removal efficiency by flotation is poor compared with conventional inks since the toner inks are large in size and cannot be sufficiently detached from fibres in the pulper. Effective removal of toner inks can be realized using high consistency mechanical dispersion of the pulp with kneader and disperger followed by flotation using nonionic surfactants. Kneader and disperger assist flotation by improving toner-fibre detachment and by reducing the ink size distribution to a more floatable range.

Future Trends

Flotation de-inking is a complex separation process of inks and other contaminants from fibres. Due to economical reasons and strict environmental regulations, new materials used by paper manufacturers and new printing technologies, paper mills require environmentally benign de-inking technologies which can easily fit into the current de-inking system without extra capital investment.

In recent years, great progress has been made in flotation de-inking technologies with respect to flotation cell design, utilization of new surfactants and the understanding of de-inking chemistry. However, the rapid advances in printing, coating and other modifications of paper make de-inking more difficult. More effort is needed to understand the flotation behaviour of new types of wastepapers.

Flotation chemistry plays the most important role in determining the ink removal efficiency. Neutral flotation de-inking has become increasingly popular in the last 10 years. This is mainly because neutral de-inking has great potential to lower chemical usage and cost, to reduce water treatment cost, to improve product quality and paper machine runnability. Mills will benefit from switching from alkaline to neutral flotation de-inking. Since no caustic or silicate is added in the pulper, fibres are not yellowed or darkened. As a result, bleaching chemicals such as peroxide may not be required.

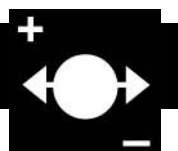
Enzymatic de-inking represents a new approach to modern paper-recycling mills. Extensive research has

been conducted to use enzymes to improve de-inking efficiency. The enzymes used included primarily cellulases, hemicellulases, amylase, lipase or resinase. Commercial application of enzymes to the flotation de-inking of wastepapers showed enhanced ink removal efficiency. Neutral pH de-inking further benefits the use of enzymes since it can improve ink detachment from the fibres and repulping efficiency. Since most enzymes work at acidic pH and lower temperature, enzyme manufacturers have to develop thermophilic and alkaline-stable enzymes to lower usage and enhance their effectiveness.

Further Reading

- Borchardt JK (1997) An introduction to deinking chemistry. In: Doshi MR and Dyer JM (eds) *Paper Recycling Challenge*, vol. II. *Deinking and Bleaching*, pp. 18–30. Appleton, Wisconsin: Doshi.
- Borchardt JK and Ferguson LD (1998) Deinking chemistry. In: Doshi RM and Dyer JM (eds) *Paper Recycling Challenge*, vol. III. *Process Technology*, pp. 71–81. Appleton, Wisconsin: Doshi.
- Ferguson LD (1992) Deinking chemistry: part 1. *Tappi Journal* 75(7): 75–83.
- Ferguson LD (1992) Deinking chemistry: part 2. *Tappi Journal* 75(8): 49–58.
- Hines PR (1933) US patent no. 2,005,742.
- Jelks JW (1954) Development in flotation deinking of waste paper. *Tappi Journal* 37(10): 176A–180A.
- Larsson A, Stenius P and Ödberg L (1984) Surface chemistry in flotation deinking, part 2. The importance of ink particle size. *Svensk Papperstidning* 87(18): R165–R169.
- McCool M (1993) Flotation deinking. In: Spangenberg RJ (ed.) *Secondary Fiber Recycling*, pp. 141–162. Atlanta, Georgia: TAPPI Press.
- McKinney R (1998) Flotation deinking overview. In: Doshi RM and Dyer JM (eds), *Paper Recycling Challenge*, vol. III. *Process Technology*, pp. 99–114. Appleton, Wisconsin: Doshi.
- Shrinath A, Szewczak JT and Bowen IJ (1991) A review of ink-removal techniques in current deinking technology. *Tappi Journal* 74(7): 85–93.
- Smook GA (1994) *Handbook for Pulp and Paper Technologists*, 2nd edn. Vancouver: Angus Wilde.
- Somasundaran P and Zhang L (1998) Fundamentals of flotation deinking. In: Doshi RM and Dyer JM (eds), *Paper Recycling Challenge*, vol. III. *Process Technology*, pp. 83–98. Appleton, Wisconsin: Doshi.
- Welt T and Dinus RJ (1997) Enzymatic deinking. In: Doshi MR and Dyer JM (eds), *Paper Recycling Challenge*, vol. II. *Deinking and Bleaching*, pp. 235–246. Appleton, Wisconsin: Doshi.
- Woodward TM (1986) Appropriate chemical additives are key to improved deinking operations. *Pulp Paper* 60(11): 59.

DEOXYRIBONUCLEIC ACID PROFILING



Overview

R. Coquoz, Institut de Police Scientifique et de Criminologie, Lausanne, Switzerland

This article is reproduced from *Encyclopedia of Analytical Science*, Copyright © 1995 Academic Press

Introduction

The forensic biologist has traditionally used a large set of markers including blood group antigens and serum proteins to establish links between evidence and comparison samples. These markers are polymorphic and genetically determined. In 1985, a new technique was introduced which opened the door to the forensic use of deoxyribonucleic acid (DNA) technology: its inventor coined the term 'DNA fingerprinting'. Since then, DNA typing in this and many other forms has flourished and the forensic biologist now has access to a large variety of powerful techniques.

DNA and its Polymorphism

DNA is an extremely large linear molecule which stores genetic information in the form of a sequence of its constituent elements: the nucleotides. The DNA molecule is made up of two complementary chains or strands of nucleotides (Figure 1). There are four different nucleotides (symbolized by the letters A, C, T, G) whose chemical affinity determines the complementarity of the nucleotide sequences of the two strands of the DNA molecule. Nucleotides A and T, and G and C always face each other; as a consequence, the length of DNA fragments is usually expressed in 'base pair' (bp) units. This chemical affinity allows single strands of complementary DNA to hybridize to each other. Nucleotide chains are oriented, having so called 5' and 3' ends, and the two strands of DNA have an opposite orientation. The DNA synthesis occurs in the direction 5' → 3'.

The polymorphism within DNA resides partly in the existence of minor nucleotide sequence variations among different individuals at various locations (loci) in the DNA molecule, which has its counterpart in the polymorphism of the amino acid sequence of the proteins. The gene variants (the alleles) differ

in their sequence. However, a more extensive and DNA-specific polymorphism exists in the noncoding DNA: the tandemly repeated sequences. These polymorphic loci are DNA fragments, made up of a nucleotide sequence (the repeat unit), tandemly repeated like a series of identical beads on a necklace (Figure 1). The repeat unit can be from two to more than 100 nucleotides long. The polymorphism comes from the extreme variation in the number of repeats. The alleles differ then by their size (length polymorphism). This kind of repetitive sequence has been called minisatellites or also variable number tandem repeat (VNTR). There is a huge reservoir of polymorphism in these sequences and it is their potential use which has stimulated the development of the various DNA typing procedures.

DNA Typing Procedures

Any biological material containing DNA may be useful, including blood, sperm, saliva, hair, autopsy tissue, bone. All DNA typing procedures involve a DNA isolation step, which allows the elimination of substances such as proteins which can interfere in the sometimes delicate enzymatic steps involved in any DNA typing method.

The traditional way to prepare samples is to dissolve them in a sodium dodecylsulfate (SDS) proteinase K solution which lyses the cells and digests the proteins. The samples are then extracted with a phenol/chloroform mixture and the DNA is finally ethanol-precipitated and dissolved in the adequate buffer. Polymerase chain reaction (PCR) analysis requires minimal amounts of DNA so that it is possible to start with samples so small that they are unlikely to contain substantial amounts of interfering molecules. Simple boiling of the samples in the presence of a heavy-metal chelator (Chelex resin) is then usually sufficient as a preparation method.

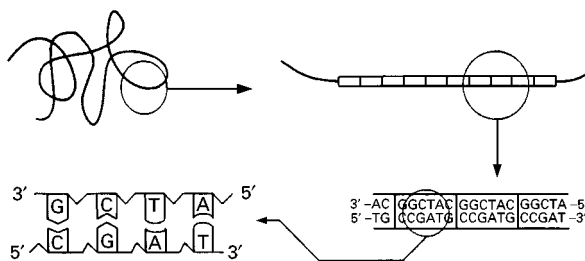


Figure 1 Schematic description at four increasing levels of magnification for DNA and VNTRs.

Restriction Fragment Length Polymorphism (RFLP) Typing

The isolated DNA is reproducibly cut into fragments by the action of a sequence specific DNA cutting enzyme, a restriction enzyme (hence RFLP). The fragments, which can be more than 20 000 bp long, are then separated according to their sizes by electrophoresis on agarose gel. The DNA fragments are transferred to a nylon membrane to which they will remain attached but are still accessible for hybridization with a probe. This membrane will provide a replica of the electrophoresis product. Labelled pieces of DNA having a sequence complementary to the repetitive sequence to be detected (the probe) are added to the nylon membrane and hybridize to the appropriate DNA fragments. These can finally be detected by autoradiography with a film sensitive to the labelled probe (**Figure 2**). The DNA fragments to be detected will appear on the film as dark bands (**Figures 2** and **3**). Their position will be a measure of their size, which is itself proportional to the number of repetitive elements in the VNTR. A comparison with DNA fragments of known sizes allows an accurate size determination. This first probe can be stripped from the membrane allowing for reprobing with a second probe, etc. There is a large choice of VNTRs available for RFLP typing (**Table 1**). It is the same for restriction enzymes: but a few have found wider use because of their robustness and their ability to cut DNA into small fragments. These enzymes are *Hae* III, *Hinf* I, *Pst* I, *Alu* I and *Pvu* II, the first two being the most used. The labelling of the probe is traditionally done through the use of ^{32}P -labelled nucleotides. However, probes coupled to enzymes catalysing the production of a chemiluminescent substance allow detection limits as low as those obtained by radioactive means.

The probe can be designed so as to detect a single VNTR locus; it is then a single locus probe (SLP). If the individual has inherited DNA from his parents with a different number of repeats at the analysed VNTR, the result is in the form of two bands (heterozygote); otherwise, there will be a single band (homozygote). But since the repeat units of different VNTRs often have sequence similarities to each other, it is possible to detect a whole family of VNTRs at the same time provided a probe is used under conditions allowing hybridization with partially complementary DNA fragments. In this case we speak of a multilocus probe (MLP) and the result appears in the form of a set of bands with a very individual pattern similar to a bar code.

Polymerase Chain Reaction (PCR)

The advent of the PCR has dramatically enlarged the spectrum of methods available for DNA typing. The PCR is a DNA amplification method which cyclically reproduces the natural DNA replication. Each cycle consists of (1) a denaturation step where the two DNA strands are separated by heating, (2) an annealing step where, after cooling, short synthetic DNA strands (the primers) are hybridized on both sides of the DNA fragment to be amplified, and (3) an elongation step where a DNA polymerase adds nucleotides to the primers to synthesize the DNA strands complementary to the template DNA. The result of many cycles is millions of copies of DNA fragment delimited by the primers. The use of a heat-stable polymerase has rendered the whole process very easy and allowed it to be automated. The nature of a PCR makes it naturally extremely sensitive, with a theoretical detection threshold of one molecule. The primers allow the amplification to be highly specific and the amplification product can then frequently be detected using a simple nonspecific detection method, which

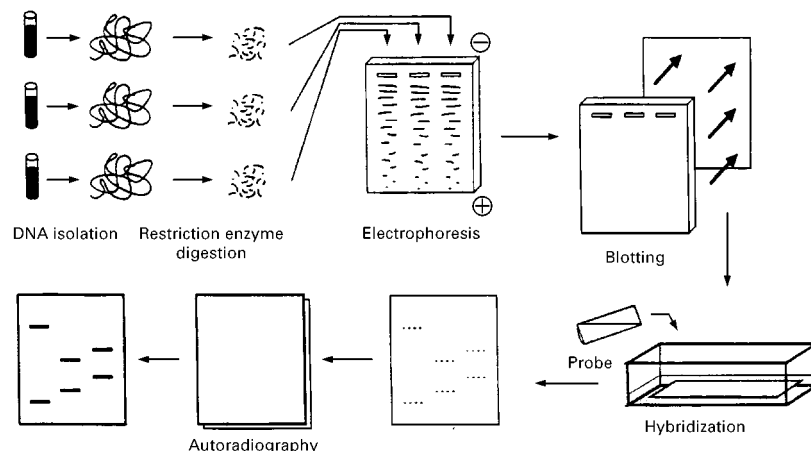


Figure 2 Schematic description of the main steps in RFLP typing.

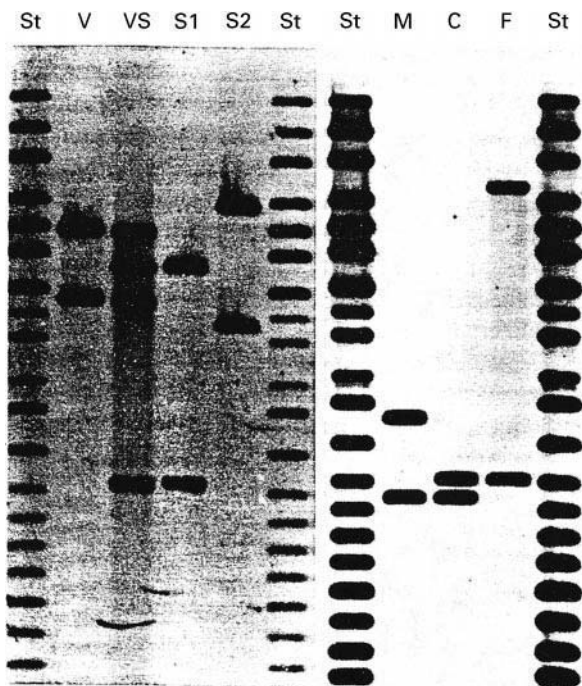


Figure 3 Typical examples of RFLP typing of forensic cases. On the left: sexual assault case; St, size markers, V, victim, VS, vaginal swab (containing material from the victim and her assailant), S1, suspect 1, S2, suspect 2. On the right: paternity test with M, mother, C, child, F, putative father.

makes the whole analytical process convenient and rapid.

PCR and Dot-Blot Analysis

Many methodologies have been designed which make use of the main principle of a PCR. In forensic science, PCR was first used to analyse sequence polymorphisms such as the polymorphism of the *HLA-DQ α* locus. In that case, the alleles, which differ only by a few nucleotide changes, are identified after use of a PCR through hybridization with allele-specific

probes, using a reverse dot-blot format (Figure 4): the various probes are attached to a membrane strip, arranged as a series of invisible dots to which the amplification products can hybridize depending upon their sequence. Through the use of labelled nucleotides during the PCR, the genotype of the sample can be read through the appearance or not of coloured dots on the strip, at the position of each probe (Figure 4). In a way, the format is not very different from that of the strips for urine analysis so widely used in clinical medicine.

Amplification Fragment Length Polymorphism (AMP-FLP) Typing

Another use of a PCR has been the amplification of VNTRs to analyse their length polymorphism. However, the quite poor performance of PCRs in the amplification of large DNA fragments, such as those of the VNTR loci analysed through RFLP typing, has led to the search for smaller VNTRs (Table 1). By designing primers located on each side of a VNTR, it can be amplified by a PCR and the amplified fragments can be analysed by electrophoresis on agarose or polyacrylamide gels and compared to standards (Figure 4). While RFLP typing required the use of probes to detect specific VNTR-DNA fragments among thousands of other fragments, the amplification process here allows the use of nonspecific detection methods (ethidium bromide staining, silver staining) to make the bands visible. This kind of PCR-analysed VNTR polymorphism has been called amplification fragment length polymorphism (AMP-FLP).

Short Tandem Repeats (STR) Typing

The particularly high efficiency of PCR in the amplification of very small fragments has attracted attention toward a class of VNTRs made of very small repeats (di-, tri-, tetranucleotide repeats) (Table 1). They are sometimes called microsatellites

Table 1 Selection of some of the main DNA loci analysed by the various DNA typing methods

Locus	Corresponding probe	Chromosome location	Repeat unit length (bp)	Typing method used	Heterozygosity ^b (%)
—	33.6	1 ^a	37 ^a	multilocus RFLP	—
<i>D1S7</i>	<i>MS1</i>	1	9	monolocus RFLP	> 99
<i>D7S21</i>	<i>MS31</i>	7	20	monolocus RFLP	98
<i>D2S44</i>	<i>YNH24</i>	2	31	monolocus RFLP	94
<i>D10S28</i>	<i>TBQ7</i>	10	33	monolocus RFLP	97
<i>HLA-DQα</i>	—	6	—	PCR + dot blotting	79
<i>D1S80</i>	<i>MCT118</i>	1	16	AMP-FLP	80
<i>D17S5</i>	<i>YNZ22</i>	17	70	AMP-FLP	82
<i>APOC2</i>	<i>Mdf 5</i>	19	2	STR	80
<i>HUMTH01</i>	—	11	4	STR	80

^aThese characteristics refer to the VNTR used as the multilocus probe.

^bHeterozygosity is calculated here as the percentage of apparent heterozygotes in the population (Caucasian in this case).

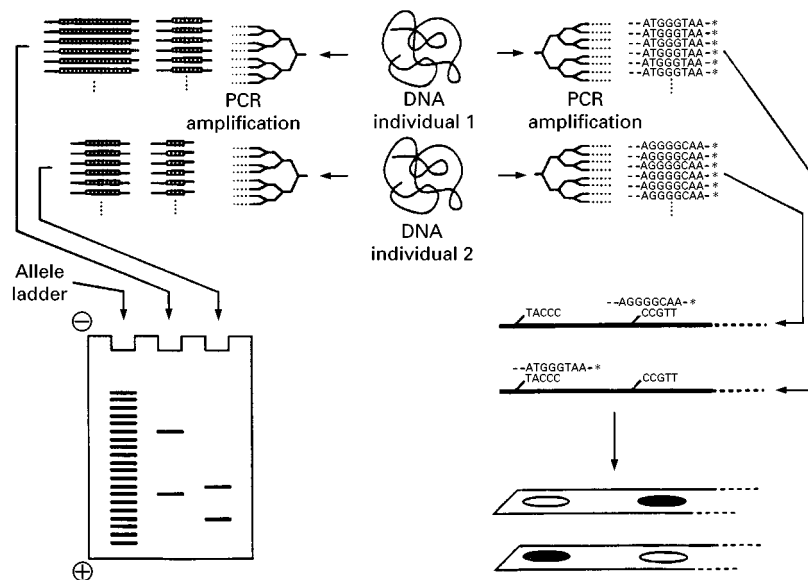


Figure 4 A PCR amplification for AMP-FLP typing (left) and reverse dot-blot analysis (right).

or short tandem repeats (STRs) and they are probably the richest class of polymorphic loci available. Their amplification conditions are simple and the size range of their alleles is usually narrow. They are then well suited to multiplexing; it is indeed easy to choose microsatellite loci and adequate primers so as to obtain amplified DNA fragments situated in well separated size ranges for each locus. Consequently a whole group of STRs can be amplified at the same time and analysed on the same gel. The small size of their repeat unit, however, is also a disadvantage. The various alleles only differ in length by two, three or four nucleotides. Such a separation power is only possible through the more complex technology of sequencing gel electrophoresis. However, the sequencing technology is undergoing constant improvement due to the challenge of the human genome sequencing project, and STR typing has benefited from the developments in that field such as fluorescent labelling and automatic sequencing.

Minisatellite Variant Repeat (MVR)-PCR

The polymerase chain reaction has made possible yet another powerful DNA typing method: MVR-PCR. This has been designed to reveal a polymorphism consisting of variations in the sequence of the repeat unit within some VNTRs. Instead of being a pure repetition of one repeat unit, some VNTRs are composed of combinations of two or more almost identical repeat units. It is easy to calculate that even with only two repeat variants a and b, the number of possible combinations of repeats is huge. The sequence of repeats is revealed through a process somewhat similar to the Sanger DNA sequencing method

(Figure 5). The PCR is carried out in parallel in two tubes in a mixture containing a primer complementary to a DNA sequence outside the VNTR and a low concentration of primer complementary to the repeat unit variant a. This set of two primers allows the multiplication of an array of all the possible fragment going from one end of the VNTR to every repeat a. In the second tube, the use of a primer complementary to the repeat unit variant b allows the multiplication of another array of all the possible fragments going from one end of the VNTR to every repeat b. An unequal amplification of the short versus long fragments is avoided through the use of a tag attached to the two alternative primers. This tag is a short strand of DNA. A fourth primer complementary to this tag is then used to allow the further amplification of the arrays of fragments. The content of the two tubes is then loaded on two adjacent lanes of an agarose gel. After electrophoresis, Southern blotting, hybridization with a probe for the VNTR and autoradiography, the result appears in the form of two parallel ladders of bands with fainter or missing rungs. For an individual, the result is indeed the sum of the results given by two VNTR fragments, those inherited from the mother and the father: at each repeat position in the VNTR the subject can have variant a twice, variant b twice, or a once and b once. These three possibilities can easily be coded by the numbers 1, 2, 3, allowing a simple digitization of the result (Figure 5). It is clear that the existence of more than two repeat variants makes the coding more complex and the system more informative but the principle remains the same. With MVR-PCR, there is no need to have carefully standardized electrophoretic conditions. Each

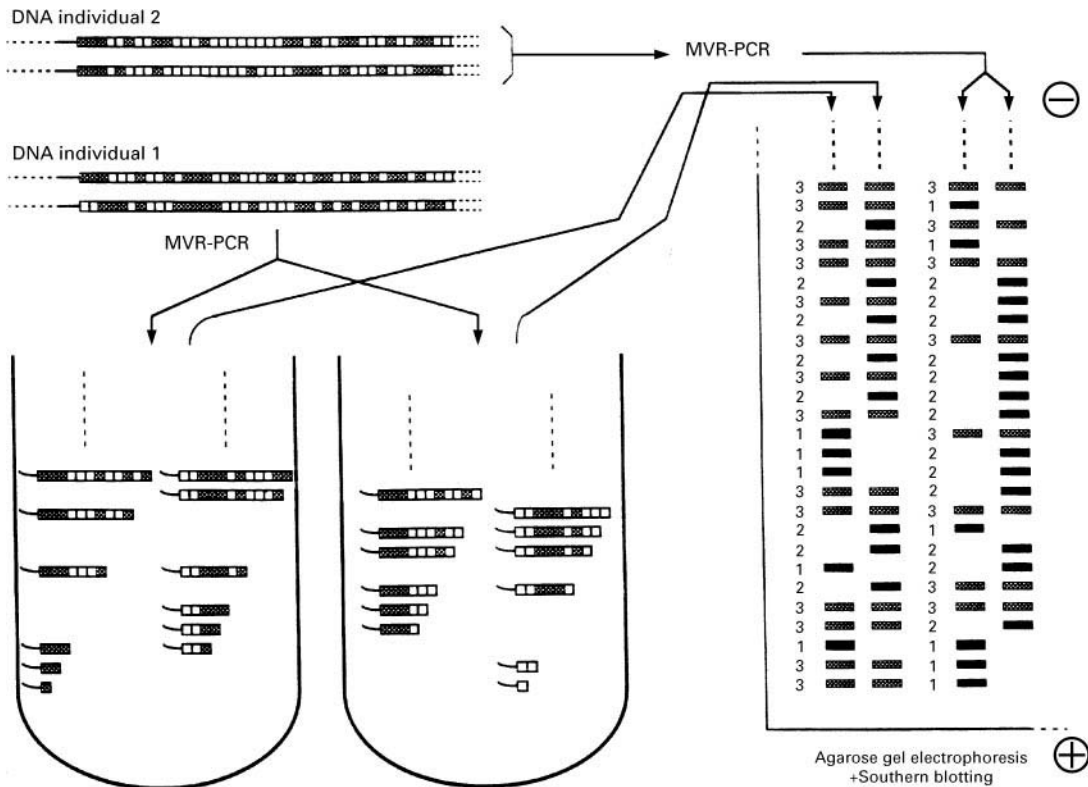


Figure 5 Schematic description of MVR-PCR.

result is literally read by itself, and different samples are simply compared at the level of their codes.

Other Methods

Other DNA typing methods have been developed or proposed, and still others are yet to appear. Two methods are worth mentioning. One is mitochondrial DNA (mtDNA) sequence analysis. A DNA sequence analysis after PCR amplification is a natural way to examine DNA polymorphism. However, because it is unable to reveal more than a few hundred base pairs at a time, and because of its complexity, it is not as attractive as the above-mentioned methods. However, it has been a precious tool in the analysis of mitochondrial DNA, which is a small piece of DNA, maternally inherited, present in all mitochondria. Part of it (the D-loop) contains a highly polymorphic sequence and its sequence determination is therefore very informative. Owing to the presence of more than 1000 copies in each cell, mtDNA analysis is very sensitive. Moreover, hair shafts, which do not contain nuclear DNA, are rich in mtDNA and are therefore amenable to genetic analysis.

The second method is polymorphic sequence-tagged sites (pSTS) analysis. This is a method designed to reveal single base pair changes. After a PCR amplification of the DNA fragment containing the

polymorphic base pair, a ligation assay is performed using an antigen-labelled primer and one of two biotin-labelled primers each being specific for one of the two possible alleles. In the presence of the corresponding sample allele, the biotin-labelled primer is ligated to the antigen-labelled primer. After capture of the product in microtitre plates coated with streptavidin (a binding protein for biotin), the presence of the antigen can be detected using a traditional immunoenzymatic method (ELISA procedure). The combined analysis of more than 15 such two-allele sites can reveal genotypes with frequencies below 10^{-6} . The most interesting features of this method are its technical simplicity and its straightforward interpretation (positive or negative readout) which make it particularly amenable to automation. It could reach its highest performance if all the loci could be analysed simultaneously within the same tube.

Applications

Deoxyribonucleic acid typing gained prominence from the start because of its identification power. It is the most powerful identification technique after fingerprint examination. It represents a big jump from the traditional protein polymorphism analysis where powerful identification could only be reached by the

sequential analysis of more than 20 polymorphic systems, each requiring its own analytical process. The improvement is particularly evident in semen analysis where the number of available polymorphic systems was extremely low. In RFLP typing, the analysed VNTR loci are so polymorphic that most of the possible genotypes have frequencies below 1%. It is then easy to calculate that the combined analysis of four such loci reveals genotypes with frequencies of the order of 10^{-8} . Both AMP-FLP typing and STR typing use smaller, less polymorphic and therefore less informative VNTRs, but a similarly high information yield can be reached by increasing the number of loci analysed.

Interpretation

Forensic identification is achieved through the demonstration of matching biological characteristics between evidence and comparison material. The matching is straightforward when discrete and well-identifiable alleles are analysed such as in the various methods derived from a PCR. However, in RFLP typing, a match is not always easy to establish. First there is the intrinsic difficulty of having to deal with alleles which cannot each be differentiated by electrophoresis. Indeed, because of the size range of the DNA fragments, the separation power of electrophoresis is insufficient to separate alleles differing in length by only one repeat unit. Two samples having bands at an identical position may in fact possess different alleles. Secondly, there is the possibility that a DNA sample originating from the same person as the comparison sample contains interfering molecules, leading to a different electrophoretic behaviour and shifted band positions. This bandshifting can only be demonstrated and evaluated through the use of proper controls (internal standards).

The next step in the interpretation is the evaluation of the power of the evidence. It is usually expressed as a ratio of the probability of the evidence under the hypothesis that the evidential material has the same source as the comparison sample and the probability of the evidence under the hypothesis that somebody else is the source of the evidence material. This ratio is normally inversely proportional to the frequency of the genetic characteristics detected in the adequate reference population. The determination of these frequencies is a difficult task. The extreme variability of the VNTR loci makes the gathering of genotype frequency data unrealistic. Statistically trustworthy frequencies would require the analysis of a huge number of individuals. It is thus necessary to rely on allele frequencies to calculate the genotype frequencies by multiplication. The frequency of genotype A_1A_2 at locus A is the product $2a_1a_2$ (with a_1 and a_2 being the

respective allele frequencies). The frequency of the combined genotypes at four loci is then $2a_1a_2 \times 2b_1b_2 \times 2c_1c_2 \times 2d_1d_2$. However, these multiplications can only be done under the assumption of statistical independence of the multiplied factors. This translates into certain assumptions related to the genetic independence of the analysed VNTR loci and to the genetic structure of the populations (Hardy-Weinberg equilibrium).

Controversy has arisen over the possibility of the existence of genetic substructuring within the populations. Some geneticists expressed concern that the frequency of a genotype A_1A_2 might have an apparent value using the general population database, but that the true frequency might be much higher owing to the high frequency of these specific alleles in a genetically distinct population subgroup. At the extreme, if alleles A_1A_2 only appear in this subpopulation where they have a frequency of 50% each, the detection of allele A_1 in a sample would make the detection of allele A_2 almost certain. Because of such effects, combined genotype frequencies could be underestimated by several orders of magnitude. The accumulating data suggest, however, that there is not much reason to worry about such effects. The VNTR loci are extremely polymorphic in every population studied and, for any given genotype constellation, there is an extremely low probability of having substantial frequency differences when calculating with one population data or another. Moreover, within the major races, the frequency distributions are very similar between different populations. And finally, forensic laboratories use very conservative approaches which always favour the accused at each interpretation step.

Paternity Testing

The identification power of DNA typing has naturally been used in paternity testing (Figure 3). But here the question relates to the transmission of genetic material from one generation to the other. Mutations which can cause apparent exclusions of true fathers then have to be taken into account. The polymorphism of the VNTRs is linked to an exceptionally high mutation rate. This mutation rate can be below 10^{-4} to more than 0.05 mutations, per meiosis for the most polymorphic loci such as *D1S7*. This has to be compared to the mutation rate of coding DNA sequences which is estimated to be around 10^{-5} for a 1000 bp gene. The calculation of probability of paternity has to integrate these mutation rates. But it remains true that the increased power of DNA typing has made paternity testing much easier and has allowed the solution of complex situations, such as the unavailability of the putative father, which sometimes remained unsolved with traditional typing.

Practical Use

In the real world of forensic science, there are practical contingencies which can be the source of difficulties or even interpretation errors. An important contingency is the quantity of the evidential material. Any living cell contains about 6 pg of DNA, and the main forensic DNA sources contain about 30 ng μL^{-1} (blood), 400 ng μL^{-1} (semen), 2 ng μL^{-1} (saliva) and 0–250 ng per hair root. As indicated in Table 2. RFLP typing would require at least a few microlitres of blood and the various PCR methods require about 0.05 μL . The theoretical PCR sensitivity of one molecule would suggest that less than 1 nL of blood should be sufficient. However, this does not take into account the potential loss during DNA isolation, or, more importantly, that one of the alleles may be absent or underrepresented in small samples containing only a few molecules, for simple stochastic reasons. As a consequence, it will not appear at the end of the process: a heterozygote will appear as a homozygote. In other words, there may be an allele drop-out.

Another important factor is the quality of the material. Although DNA is a robust molecule and usable DNA fragments have been recovered from thousand year old mummified bodies, it can very quickly be degraded into smaller fragments when exposed to humidity, heat or sunlight. With such degraded samples, DNA typing methods like STR typing, which analyse very short DNA fragments, may still be applied successfully. However, RFLP typing may be no longer possible. Or even worse, a DNA sample possessing a large and a small allele at a VNTR locus may have larger fragments which are too degraded to be detected while the smaller ones will have survived enough to give a detectable band. Here again, the result is an allele drop-out. That is why, in the usual procedure, a small portion of the sample is loaded on

a minielectrophoresis gel followed by nonspecific DNA staining. The examination of the intensity of the staining and the average size of the DNA fragments allows both quantitative and qualitative evaluation of the available DNA. The quality of the material can also affect RFLP typing through the inhibition of the restriction enzyme. One of the expected DNA fragments may appear at a position corresponding to a larger size than it should, because the enzyme has failed to cut the restriction site closest to the VNTR efficiently.

The experienced analyst usually has no problems avoiding interpretation errors arising from the above-mentioned situations or others (extra bands due to unsufficiently stringent hybridization, incomplete stripping, internal restriction site or bacterial contamination, missing bands due to blotting problems, etc.). However, without extensive controls, it may be difficult to prove the tentative explanation. And the limited amount of evidence material usually precludes repeating an analysis.

With PCR-derived methods, there are a few specific potential sources of error worth mentioning. The first is contamination. A PCR is so sensitive that inadvertent transfer of DNA from one sample to another, from laboratory personnel to the samples, etc., can happen and be unnoticed. The large-scale use of negative controls should reveal any such contamination. Moreover, the establishment of adequate laboratory design and use of pertinent working guidelines and decontamination procedures should prevent the occurrence of such damaging episodes. The second source of error is differential amplification. The trustful amplification of a heterozygote requires that the two alleles are amplified with the same efficiency, otherwise the result is an allele drop-out. Consequently, the conditions which lead to such differential amplification have to be established and the proper precautions must be taken.

Table 2 Main characteristics of the various techniques available for DNA typing

	<i>Amount of genomic DNA required</i>	<i>Ability to use damaged DNA</i>	<i>Probability of matching per locus analysed^a</i>	<i>Degree of automation possible</i>
RFLP typing with single locus probes	> 20 ng	—	< 1%	—
RFLP typing with multilocus probes	> 500 ng	—	< 10 ^{-7b}	—
PCR + dot-blot analysis (<i>HLA-DQα</i> typing)	< 1 ng	+	7%	+
AMP-FLP typing	< 1 ng	+	5–10%	+
STR typing	< 1 ng	+	2–10%	+
MVR-PCR	> 1 ng	+	< 10 ^{-6c}	+
mtDNA sequencing	≤ 1 ng	+	10 ^{-4c}	+
pSTS analysis	< 1 ng	+	40%	+

^aThe probability of matching (P_m) is the probability that two individuals taken at random have the same genotype. $P_m = \sum_{i=1}^n P_i^2$ where P_i is the frequency of the genotype for the analysed locus.

^b P_m is that for the whole set of loci detected by this probe.

^cThese numbers are estimates based on limited population samples.

The potent identification power of DNA typing makes the establishment of databases for the storage of DNA profiles possible and desirable. New profiles can be compared with stored profiles to identify criminals, link unsolved cases, etc. This necessitates a high level of standardization among the laboratories participating in the information exchange networks. They must at least analyse the same polymorphic loci and, for RFLP typing, they must use the same enzymes and similar analytical protocols. Because of the large choice of polymorphic loci and analytical methods, the minimum degree of coherence is not at all warranted unless a strong effort is made between the laboratories to reach a consensus. And a consensus is difficult to reach in a fast moving field where new technologies are constantly being developed.

There is no doubt that DNA typing is the 'safest' identification technique ever used in forensic biology. But, because of its power and its consequent impact in a courtroom, it is and will remain under intense scrutiny by the forensic and legal communities. Consequently, a lot of attention has been paid to quality control and proficiency testing. There is certainly the opportunity for future improvements and developments in this field.

See Colour Plate 75.

See also: II/Electrophoresis: Blotting; Deoxyribonucleic Acid, Theory of Techniques for Separation; One-dimensional Polyacrylamide Gel Electrophoresis; One-dimensional Sodium Dodecyl Sulphate Polyacrylamide Gel Electrophoresis.

Further Reading

- Ballantyne J, Sensabaugh G and Witkowski J (1989) *DNA Technology and Forensic Science*, Banbury report 32. Cold Spring Harbor: Cold Spring Harbor Laboratory Press.
- Burke T, Dolf G, Jeffreys AJ and Wolff R (eds) (1991) *DNA Fingerprinting: Approaches and Applications*. Basel: Birkhauser Verlag.
- DNA Fingerprinting (1991) Symposium paper. *Electrophoresis* 12: 101–232.
- Farley MA and Harrington JJ (1991) *Forensic DNA Technology*. Chelsea, MI: Lewis Publishers.
- Kirby LT (1990) *DNA Fingerprinting: An Introduction*. New York: Stockholm Press.
- Proceedings of the Second International Symposium on Human Identification* (1991) Madison, WI: Promega Corporation.
- Rittner C and Schneider PM (eds) (1992) *Advances in Forensic Haemogenetics*, vol. 4. Berlin, Heidelberg: Springer-Verlag.

Capillary Electrophoresis

M. Chiari and L. Ceriotti, Institute of Biocatalysis and Molecular Recognition, CNR, Milan, Italy

Copyright © 2000 Academic Press

Introduction

One of the earliest reports on DNA capillary electrophoresis (CE) was by Cohen *et al.* who demonstrated the high resolution of nucleosides and oligonucleotides, in the absence of a sieving gel, by simply trapping the analyte into sodium dodecyl sulfate (SDS) micelles. One year later, in 1988, the same author discussed the separation of DNA restriction fragments in a gel-free environment. The first reports on the use of polyacrylamide gel capillary columns to separate DNA with remarkable efficiency and resolution were presented the same year by Guttman *et al.* and Cohen *et al.* By 1989, gel-filled CE was already a well-established technique. These preliminary reports were then followed by a flurry of articles describing applications of capillary gel electrophoresis (CGE) to the separation of DNA restriction fragments. In spite of the high resolving power and efficiency offered by CGE in the analysis of nucleic acids (15–30 million plates per metre and a single-

base resolution for fragments ranging from 15 to more than 500 bases were reported), the difficulties of producing adequate gel-filled capillaries hindered their greater application. Heiger *et al.* proposed, as early as 1990, the use of polyacrylamide cross-linked with a very low or zero concentration of *N,N*-methylenebisacrylamide. Strangely enough, the revolution brought about by the use of polymer solutions as sieving matrices was only evident in 1991 as a result of the work of Guttman and Cooke and Grossman and Soane. Since then, hundreds of reports have demonstrated the advantages of performing DNA separations in a narrow fused silica capillary. Due to its high resolving power and quantitative capability, CE has been successfully applied to different kinds of DNA analysis, including the following: DNA sequencing, separation of restriction fragments, polymerase chain reaction (PCR) products and synthetic oligonucleotides.

Advantages of Capillary over Slab Gel Electrophoresis

For many years electrophoretic separations of DNA were carried out in slab gels. One of the main

Table 1 Typical field strengths applied in different DNA electrophoretic systems and analysis time

Separation system	Typical field strength ($V\text{ cm}^{-1}$)	Time
Agarose slab gel	5	Hours
Conventional polyacrylamide slab gel	8	Hours
Sequencing in thin polyacrylamide DNA slab gel	40	Hours
Capillary electrophoresis	300–700	Minutes or seconds

problems in electrophoresis is the dissipation of Joule heat created by the passage of current through the gel and the buffer solution. When the gel is not sufficiently and uniformly cooled, significant Joule heating occurs and temperature gradients are formed in the gel. The existence of a thermal gradient within the gel can cause band broadening and, eventually, DNA denaturation. An efficient way to overcome this problem is to carry out the separation in a fused silica capillary. At present, a typical capillary used for DNA electrophoresis has a 50–100 μm internal diameter (i.d.), a fused silica wall about 150 μm thick and a thin exterior coating (10 μm) of polyimide to provide flexibility. The high surface-to-volume ratio of the capillary leads to an efficient dissipation of Joule heat, which eliminates thermal and gravitational convection and allows the use of electric fields up to 700 $V\text{ cm}^{-1}$. **Table 1** shows typical values of field strengths applied in slab gel and CE and analysis times required by the different systems. As a result of the high field strengths typically used in CE, DNA separation 25 times faster than in slab gel electrophoresis is easily achieved.

Besides high speeds, another great advantage of CE is that DNA samples can be automatically loaded and the separated zones can be detected online by fluorescence or UV absorbance. Furthermore, the ease of online detection renders CE suitable for automation. The amount of samples typically loaded in CE is about three orders of magnitude lower (2–100 nL) than that used in slab gel electrophoresis, making the technique useful as a tool for the analysis of molecular biology products, which are often available only in minute amounts. Two types of online injection modes are performed in CE: electrokinetic injection and hydrodynamic injection. Electrokinetic injection is accomplished by placing one end of the capillary in the sample vial (which may contain as little as 2 μL of sample) along with a platinum wire electrode. The application of an electric field for a short time forces charged analytes to enter into the capillary through electrophoretic migration. DNA molecules, being negatively charged, are injected at the cathode end of

the capillary with the detector located at the anode end. In hydrodynamic injection, the capillary is placed in the sample vial and a sample plug is forced to enter into the capillary by applying, for a given amount of time, a differential pressure across the capillary. Both injection systems present advantages and disadvantages. Hydrodynamic injection avoids bias in the amount of the sample injected with the faster analytes injected in greater quantities and is more suitable for quantitation.

DNA Sieving Matrices

At neutral pH, DNA molecules being negatively charged migrate towards the anode when placed in a potential field. Their electrophoretic mobility is given by this simple expression:

$$\mu_e = \frac{q}{f} \quad [1]$$

where q is the net charge on the molecule and f is the molecular friction coefficient. DNA molecules in free solution adopt an open, extended conformation that allows solvent molecules to stream around each segment of the biopolymer equally. This implies that electrophoretic mobility of double-stranded DNA in free solution is independent of molecular size as both the net charge on the DNA molecule and its frictional coefficient increase linearly with the number of base pairs. A size-dependent separation of DNA requires the addition of a sieving medium to the running buffer. In slab gel electrophoresis, cross-linked polyacrylamide and agarose became commonly adopted in DNA work as support matrices due to their ability to reduce thermal and gravitational convection which would suppress the resolution. In addition, porous gels allow the passage of analytes providing the size-based separation of free-draining polyelectrolytes with nearly equal free solution electrophoretic mobility.

In a fused silica capillary the anticonvective role and the DNA-separating role of the electrophoresis matrix can be decoupled. In CE, even in the absence of a dense gel matrix, only very minimal thermal convection and diffusion of analyte molecules occur during electrophoresis due to the high electrical resistance of fused silica, resulting in low current generation. This feature allows the replacement of the gel with a solution of a linear neutral polymer. Most of the problems resulting from difficulties in the production of good quality gel-filled columns and with their limited lifetime have simply been overcome with the introduction of polymer solutions. Capillaries filled with linear polymers are relatively easy to prepare and use. Due to their low viscosity, solutions of polymers can be automatically pumped into the

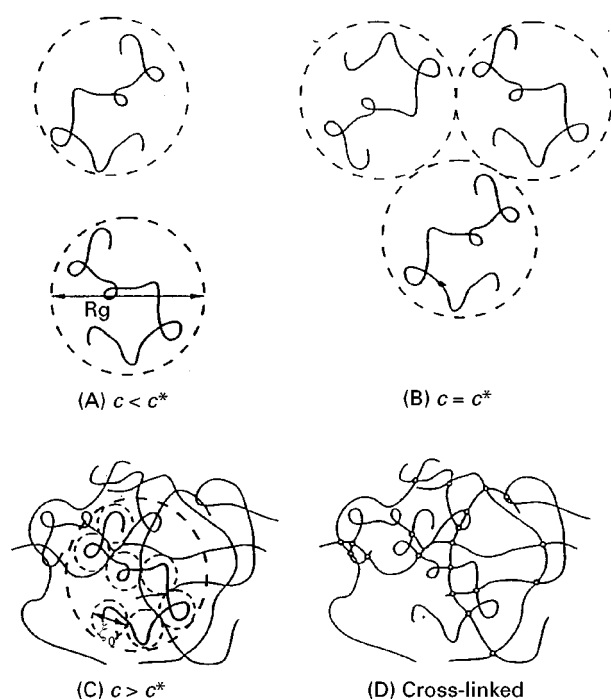


Figure 1 Schematic representation of flexible polymer in solution. (A) dilute solution; (B) $c = c^*$; (C) semidiluted solution; (D) cross-linked chains. (Reproduced with permission from Heller C (1997) *Analysis of Nucleic Acids by Capillary Electrophoresis*. Wiesbaden: Vieweg.)

capillary before each run and removed at the end of the separation. The automatic replacement of the sieving matrix increases the capillary lifetime dramatically while reducing the need for sample clean-up.

Polymer Solutions as DNA Sieving Matrices

A number of polymers with different properties (such as molecular weight, hydrophilicity, chain stiffness) have been tested for their ability to sieve DNA molecules. Cellulose derivatives (hydroxyethyl, hydroxypropyl and hydroxypropylmethyl cellulose), uncross-linked polyacrylamide and polyacrylamide derivatives, dextran, polyvinyl alcohol, polyethylene oxide and polyethylene glycol represent some examples of sieving matrices used in CE with varying degrees of success.

According to Grossman and Soane, as size-dependent DNA electrophoretic separation requires the use of an entangled polymer solution. Coils of linear polymers, above a critical concentration, c^* , defined as the entanglement threshold concentration, begin to interact physically and form a physical gel with transient pores (Figure 1). The c^* concentration, characteristic for each polymer, can be experimentally estimated by measuring viscosity at different polymer

concentrations and finding the point of deviation from linearity on the viscosity vs. concentration plot. In an entangled polymer solution the DNA migration mechanism is similar to that observed in chemical gels (cross-linked gels), complicated by the dynamic nature of the DNA-polymer and polymer-polymer interactions. A high resolution can only be achieved in a rather narrow DNA size range (from 100 to 2000 bp).

When a polymer solution is far below the entanglement threshold concentration, polymer chains remain isolated in solution and, even if they transiently interact with DNA molecules, they do not form a porous network. However, DNA molecules larger than 2 kbp can be separated in ultradilute hydroxyethyl cellulose (HEC) solutions, although with a lower resolution. A new separation mechanism, transient entanglement coupling mechanism, was proposed to explain why the separation occurs in the absence of a sieving effect. When DNA and isolated polymer chains encounter each other, they become transiently entangled. DNA molecules, more stiff and extended in solution than polymer chains, drag the latter until they escape, slowing down their electrophoretic mobility. Large DNA fragments experience stronger entanglement interactions, therefore the time required to escape is size-dependent and DNA mobility becomes size-dependent. Below c^* , high molecular weight polymer chains provide a high speed separation of large molecules with a moderate resolution.

A polymer, in order to be a good sieving matrix for DNA in capillary electrophoresis, should meet the following requirements:

1. high water solubility;
2. low viscosity when used above its entanglement threshold concentration;
3. high chemical stability;
4. good sieving capacity;
5. UV transparency.

Most studies have demonstrated that the molecular mass of the polymer dissolved in the electrophoresis buffer influences the resolution and the interval of DNA sizes which can be separated. Polyacrylamide has, for a long time, been the matrix of choice for DNA sequencing and for dsDNA fragments up to 600 bp. Recently, several authors have replaced polyacrylamide with polymers obtained by radical polymerization of *N*-mono and di-substituted acrylamido derivatives. These polymers offer the advantage of being more resistant to alkaline hydrolysis than polyacrylamide. One of the most promising derivatives of polyacrylamide that has found application in CE is the *N,N*-dimethylacrylamide (DMA). Short chain poly(DMA) is produced by carrying out polymerization in organic solvents such as dioxane and *t*-

butanol or in the presence of a chain transfer agent. Besides optimal sieving capacity, this polymer possesses the unique feature of suppressing electroosmotic flow (EOF) even at 0.001% w/v concentration, allowing DNA separation to be carried out in uncoated capillaries. For large DNA (600 bp to 23 kbp) cellulose ethers, hydroxyethyl, hydroxypropyl, hydroxypropylmethyl (HPMC) and methyl cellulose (MC) have been used as separation media. Chemically modified cellulose derivatives are typically used to separate DNA fragments at concentrations of 0.2–1% w/v. Due to the fact that stiff and extended chains become entangled more easily than flexible random coil polymers, the operative concentration of cellulosic polymers is considerably lower than that used with polyacrylamides.

Influence of Electroosmotic Flow on DNA Separation

The most important characteristic of CZE capillary columns is associated with the chemical structure of the fused silica. The presence of several types of silanol groups (SiOH) on the inner surface of the capillary column which are weakly acid in character dramatically influences the CZE separation mechanism by inducing an electroosmotic component to the transport of ions during the analysis. Negative immobile charges on the wall surface generate an electric double layer at the silica–buffer interface consisting of an immobile layer of positive ions strongly adsorbed on to the surface and a diffuse layer extending into the liquid, which is made up of hydrated ions loosely and aspecifically bonded to the surface. When an electric field is applied tangentially to the surface, electrical forces acting on the mobile part of the diffuse double layer cause the movement of ions toward the oppositely charged electrode. The migration of these ions drags the surrounding solvent molecules; this overall movement of solution is known as EOF.

The control of the EOF and the suppression of wall adsorption is a key aspect in the achievement of successful DNA separations for two reasons: firstly, EOF can cause the extrusion of the sieving matrix during electrophoresis and secondly, immobile charges on the wall can electrostatically interact with ions which are oppositely charged. DNA molecules, being negatively charged under typical separation conditions, e.g. pH 8.0, 100 mmol L⁻¹ Tris–borate or acetate–EDTA buffer, are generally repelled by the wall. However, DNA sample contaminants and cationic intercalating dyes adsorb onto the wall, causing peak broadening and a reduction in efficiency.

There are a number of approaches to eliminate EOF and wall adsorption that act on the composition

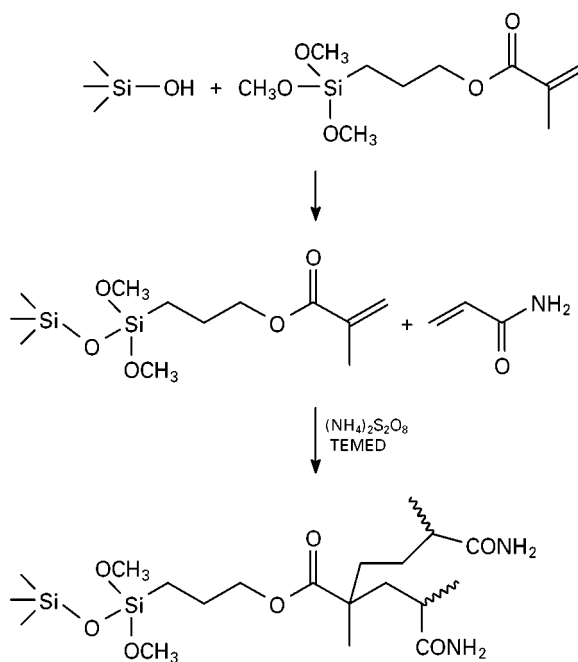


Figure 2 Synthetic scheme for a polyacrylamide coating.

of the conducting medium. Most of these methods cannot be used for DNA since the operative pH and buffer ionic strengths that are typically used in the separation are chosen to maintain DNA molecules in their native, double-stranded helical conformation. Therefore there are severe limitations in the choice of buffer composition.

An effective way to suppress EOF which is fully compatible with DNA separation conditions is by coating the capillary inner surface with a neutral polymer. This can be accomplished in several ways:

1. by dynamic adsorption of water-soluble neutral polymers. These modifiers, generally contained in the running buffer, are strongly adsorbed to the wall by hydrogen bonding or hydrophobic interactions. Methylcellulose and poly(vinyl alcohol), for instance, have been used to produce a layer of high viscosity on the capillary wall which suppresses EOF.
2. permanent coating with small or large molecules chemically bonded to the surface silanols or immobilized as films of various thicknesses on the capillary wall. The simplest way to prepare these coatings is by bonding an organosilane bearing a reactive group that can be used, in a second step, to incorporate the organosilane into the polymer (Figure 2). Polyacrylamide, polyvinylpyrrolidone, and epoxy polymer coatings have been successfully prepared in this way.

Independently of the type of neutral polymer and of the mechanism which the polymer uses to bond to the wall, the viscosity in the thick layer of the double layer appears to govern EOF suppression. However, the nature of the interaction with the wall and the structure of the polymer play an important role on the coating stability.

Detection

One of the major advantages of CE is that the separated zones can be detected online. A short stretch (1–2 mm) of the polyimide coating is removed from the outside of the capillary and the UV transparent (UV cut-off of 170 nm) fused silica 'window' is directly placed inside the detector. Online detection prevents diffusion of separated zones resulting from flowing through the connections required by an off-column detection system. Nucleic acids are detected by UV absorbance at 260 nm or fluorescence. UV absorbance is simple and inexpensive; furthermore, this detection system allows the detection of nucleic acids based on their intrinsic UV absorbance without any need for intercalating dyes that can alter DNA electrophoretic mobility. The main drawback of UV absorbance detection in CE is its limited sensitivity resulting from the short path length available across the 50 μm capillaries typically used for DNA separation. Because of this limitation, laser-induced fluorescence (LIF) is currently employed for applications that require a higher sensitivity. An example is DNA sequencing where separated zones contain 1–10 attomoles of material.

Although an LIF detection system is more expensive and complicated to build than a UV absorbance

detector, its remarkable sensitivity renders this system the most popular method for DNA detection. The use of efficient fluorophores and laser excitation gives sensitivities up to six orders of magnitude greater than that typically achieved with UV absorbance. It has been demonstrated that bands containing 1 pg of DNA can be detected using ethidium bromide as fluorescent label. Several different labels with distinct spectral properties are available (FAM, JOE, TAMRA and ROX are four fluorophores used for DNA sequencing which has relatively widely spaced absorbance and emission spectra). These fluorophores are excited by the 488 nm and 514 nm lines of a common argon laser. Their $\lambda_{\text{ex,max}}$ varies from 550 to 610 nm whereas their $\lambda_{\text{em,max}}$ are between 520 and 605 nm.

Most of the efforts in developing LIF detection were carried out in the area of DNA sequencing by CE. The availability of good labelling strategies is at the heart of LIF detection development. Recently, energy transfer primers have been developed to increase sensitivity. These primers contain a common donor dye at the 5' end and an acceptor dye about 8–10 nucleotides away. The presence of a common donor allows the use of a single laser at 488 nm to excite all four fluorophore pairs efficiently.

Applications

The advantages of DNA CE over slab gel are such that an increasing number of molecular biologists around the world are beginning to apply this rapid and efficient technique to DNA mapping and sizing separations of medical and genetic interest.

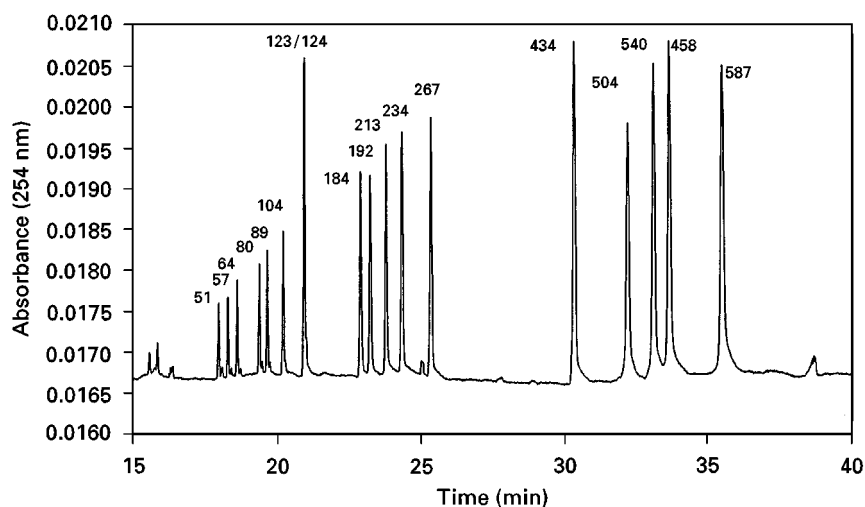


Figure 3 Electropherogram demonstrating the efficient separation of a DNA molecular mass marker containing a mixture of fragments from cleavage of plasmid pBR322 with restriction endonuclease HAE III. Buffer 100 mmol L⁻¹ Tris-borate, 2 mmol L⁻¹ EDTA, pH 8.2. Temperature: 25°C; injection: 5 s at 1 kV; separation 200 V cm⁻¹.

Restriction Endonucleases and DNA Digests

Most work in CE literature has involved separating DNA restriction digests. The discovery of enzymes capable of recognizing and cutting a particular short sequence of base pairs (usually 4–8 bp long) in a double-stranded DNA molecule has been of fundamental importance in molecular biology. Restriction enzymes are used to compare near-similar DNA molecules by cutting them into smaller fragments which differ in length or sequence. Restriction digests such as Φ 174-HaeI-II, pBR322 HaeIII and pBR322 MspI, containing fragments in the size range from 50 to 1550 bp, have been separated by CE. Larger DNA fragments, from 125 to 23 130 bp, are usually generated with λ -HindIII. These restriction digests are relatively inexpensive, can be obtained at high concentration in a purified form and contain fragments of known size. They are often used in CE to test the separation efficiency of a given separation system (Figure 3).

Polymerase Chain Reaction

Polymerase chain reaction (PCR) is a molecular copying process that allows the amplification of the quantity of DNA available for a given test. Using a three-step temperature cycle, PCR allows specific regions of DNA to be amplified to a detectable level. The analysis of PCR products requires the ability to separate the target sequence from nonspecific prod-

ucts that may result from the use of nonoptimized conditions or from overamplification. CE has been successfully used for quantification and sizing of amplified products. Given its small sample requirements, CE can detect PCR products at a low cycle number using LIF, providing an efficient tool to evaluate PCR reaction parameters. Many of the separations which can be carried out on a slab gel have been successfully performed in CE. Some of the most significant papers on separation of PCR products by CE are reported in Table 2.

Capillary Sequencing

The first separations of DNA sequencing fragments by CE were reported in 1990 by groups at DuPont, Utah, Wisconsin, Northeastern and Alberta. DNA sequencing involves the separation of a set of single-stranded fragments differing by one nucleotide in length which share a common starting point and terminate randomly at a particular base. Since 1977, two methods have been developed and refined to sequence DNA fragments up to 500 bp. They are based on nucleotide-specific chemical cleavage or on the use of chain-terminating inhibitors of DNA polymerases (dideoxynucleotides -ddNTP-). Almost all DNA sequencing reactions nowadays are carried out according to the enzymatic protocol of Sanger. DNA sequencing provides the ultimate tool in the detection of DNA sequence variation. However, for measuring variations in large DNA regions it is necessary first to

Table 2 Application of PCR product analysis by CE

Type	System examined	PCR product size (bp) (resolution needed)
Diagnostic	Androgen insensitivity syndrome	136, 139, 160 (3 bp)
Diagnostic	Congenital adrenal hyperplasia	127, 135 (8 bp)
Diagnostic	Cystic fibrosis Δ F508	95, 98 (3 bp)
Diagnostic	Cystic fibrosis, GATT microsatellites (for linkage)	111, 115 (4 bp)
Diagnostic	Down's syndrome, D21S11	220, 224 (4 bp)
Diagnostic	Duchenne and Becker muscular dystrophy (18) exon	88, 547 (3 bp)
Diagnostic	Dystrophin: DXS 164 locus	740 bp \rightarrow 220, 520 bp
Diagnostic	ERBB2 oncogene	1.1 kb bp \rightarrow 500, 520 bp
Diagnostic	Factor V mutation	115, 138, 202
Diagnostic	Hepatitis C virus	380, 187, 289
Diagnostic	HIV-1 virus (<i>gag</i> gene)	115
	<i>gag</i> , <i>pol</i> and <i>env</i> genes	142, 394, 442
Diagnostic	Kennedy's disease	480, 540
Diagnostic	Medium-chain acyl-coenzyme A dehydrogenase deficiency	175, 202
Diagnostic (SSCP)	p53 gene mutation clusters A and B	372
Diagnostic	Polio virus	53, 71, 97, 163
Diagnostic	VNTR: <i>aboB</i> locus	600–1000 (16 bp)
Diagnostic	ZFY gene, Y-chromosome	307
Forensic	HLA-DQa	242
Forensic	Mitochondrial DNA	402, 437, 1021
Forensic	STR: HUMTH01 locus	179–203 (4 bp)
Forensic	VNTR: D1S80	401–801 (16 bp)
Genotyping	Soybean plant simple sequence repeats (SSRs)	401–801 (16 bp)

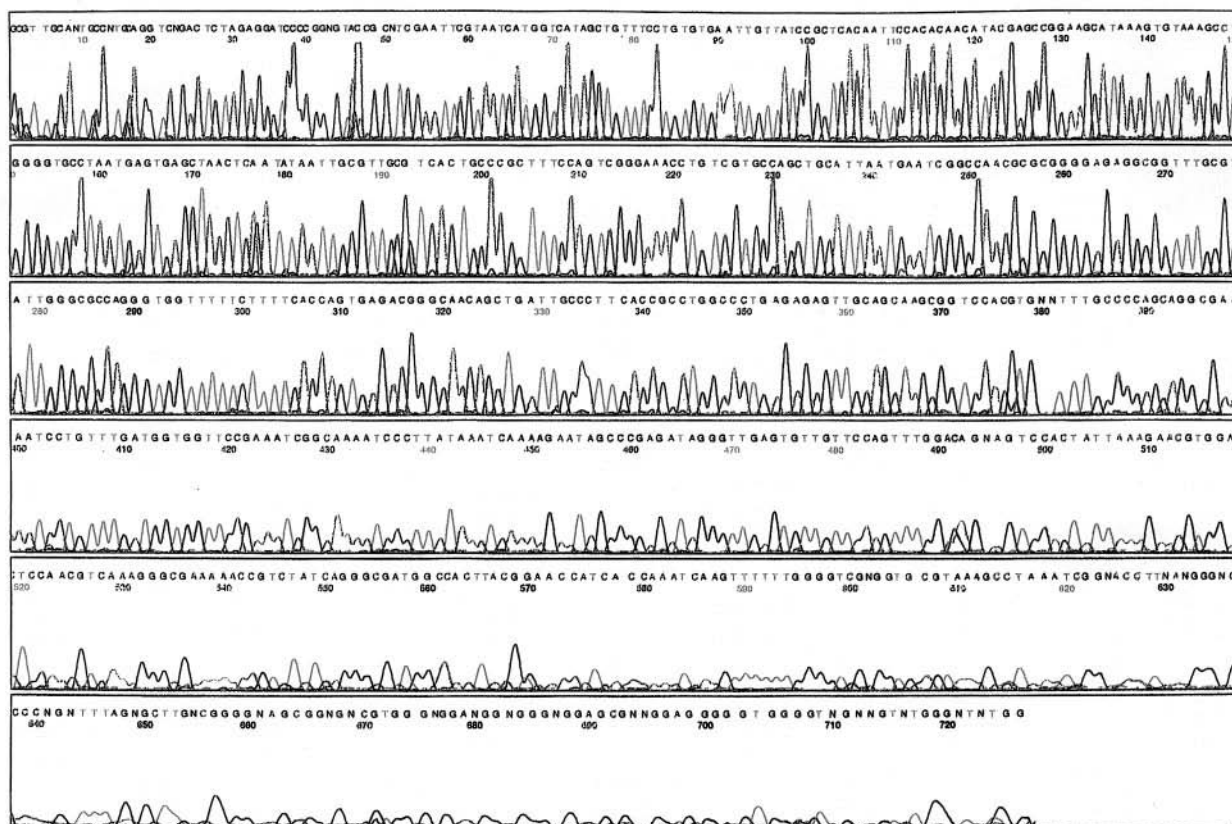


Figure 4 (See Colour Plate 76). Four-colour M13mp18 sequencing separation at 42°C. The separation of DNA sequencing fragments was performed in a 6.5% poly(dimethylacrylamide) (98 kDa) solution (75 cP) in 100 mmol L⁻¹ TAPS buffer (pH 8.0) containing 8 mol L⁻¹ urea. A 50 µm i.d. bare silica capillary, 51 cm long (40 cm to the window) was used. DNA was electrokinetically injected for 20 s at 60 V cm⁻¹, and the fragments were separated for 125 min at 160 V cm⁻¹. Reproduced from Madabhushi (1998), *Electrophoresis* 19: 224–230, with permission Wiley–VCH.

subdivide the region into smaller sections of about 400 bp. Hence, large numbers of sequencing reactions must be performed in each sample. To become applicable for screening purposes, DNA sequencing requires dramatic improvements in speed. CE provides a tool to increase sequencing rates significantly; at present, over 700 bases of sequence are routinely generated in a 2 h separation, and occasionally runs of 1,000 in 135 min have been generated. **Figure 4** shows a four-colour M13mp18 DNA sequencing separation.

Unlike in slab gel, where the four sets of A, C, G and T terminated fragments run in parallel in four different lines, in CE it is more convenient to run the four sets of fragments in the same capillary because this eliminates capillary-to-capillary variation in the migration velocity of different fragments. Different strategies have been developed to accomplish this goal, making use of four different labels with distinct spectral properties. Several labels, such as FAM, JOE, TAMRA and ROX, are available for sequencing. Some authors have reported the use of primers marked with different fluorophores whereas others

have suggested the association of a particular dye to a specific ddNTP chain terminator. In one approach, fluorescence was excited with two lasers, collected with a single microscope objective and discriminated with a filter wheel. Alternatively, a single laser-excited fluorescence and a two-channel directly reading fluorescence detector were used to discriminate fluorescence between the dyes.

A number of capillary array electrophoresis instruments with UF detection have recently become commercially available. These instruments have great potential for all those involved in the human genome project. In capillary array electrophoresis, many capillaries (typically six arrays of 16 capillaries) are set in parallel allowing parallel separations to be run as in slab gel but offering the advantages of analysis speed and automation typical of capillary electrophoresis.

Mutational Analysis

Detection and localization of single-base differences in specific regions of genomic DNA are of primary importance in the analysis of mutations associated

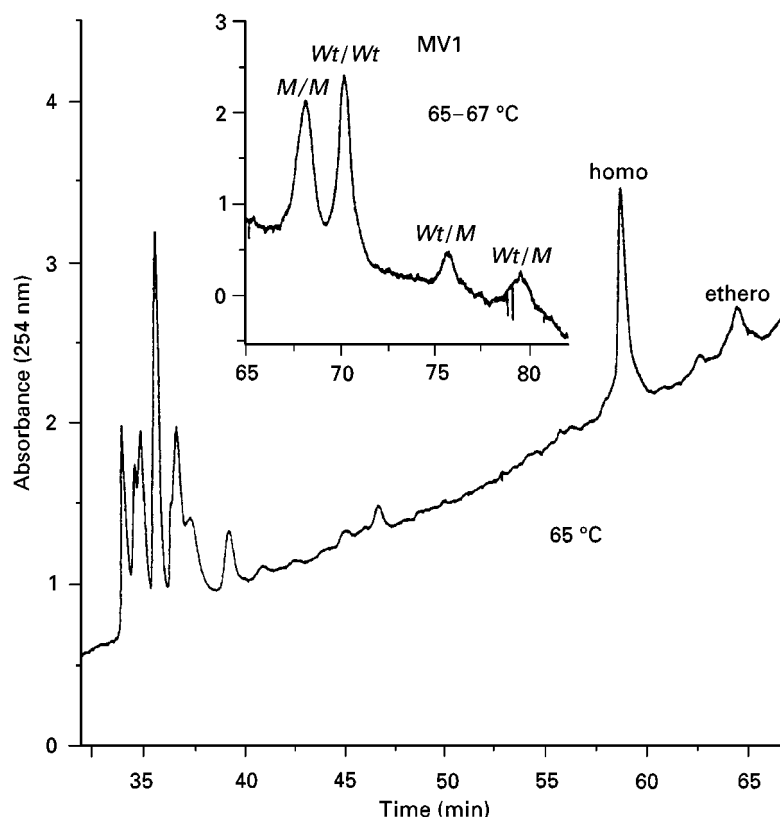


Figure 5 CZE analysis of mutant MV1 in exon 1 of the CFTR gene. The panel shows a run at a constant temperature plateau of 65 °C. Inset: run in a 65–67 °C temperature gradient, with a slope of 0.1 °C min. Sample injection: electrokinetic, 3 s at 4 kV. Reproduced with permission from Heller (1997) *Analysis of Nucleic Acids by Capillary Electrophoresis*. Viesbaden: Vieweg.)

with human disease. The methods used to detect point mutations exploit sequence-dependent variations in base-pairing which cause differences in conformation and lead to altered electrophoretic mobilities. Differences in melting behaviour of duplex molecules are the bases for separation of DNA sequence variants by electrophoresis. By running the separation under a temperature-programmed gradient (TGCE or thermal gradient capillary electrophoresis), a local loss of interstrand base pairing is induced, generating DNA molecules with a conformation very different from the normal worm-like rods. This allows the separation of molecules according to their melting characteristics and the detection of deviations from a wild-type sequence (Figure 5). In CE, the denaturing temperature gradients can be generated internally via ohmic heat produced by voltage ramps. The temperature increase linked to voltage ramps inside the capillary can be predicted as it depends on capillary diameter, its total length, the electric current values linked to a given applied voltage, the buffer electric conductivity and its coefficient of thermal conductivity. With the help of appropriate software, given these input parameters it is easy to assess dependence of

temperature on voltage ramps. A voltage gradient is then generated during the run, taking into account the melting profiles of the amplified fragments that can be predicted by the dedicated software of Lerman and Silverstein.

Future Developments

Looking to the future, we can expect new developments in instrumentation and technology. Another promising area is micromachining technology which has found widespread use in electronic and mechanic engineering, and is now increasingly applied to analytical chemistry and biotechnology. Photolithography and chemical etching techniques have been combined to create the field of micromachining in which three-dimensional microstructures have been fabricated on a micrometer scale. Electrophoresis on a chip has been successfully used for the separation of oligonucleotides, DNA restriction fragments and PCR products. In these microchip systems, fluid flow and reagent mixing are achieved using electrokinetic transport phenomena. Future developments can also be expected in this last area.

See Colour Plate 76.

See also: II/Electrophoresis: Capillary Electrophoresis; Capillary Electrophoresis–Mass Spectrometry; Capillary Electrophoresis–Nuclear Magnetic Resonance. III/Deoxyribonucleic Acid Profiling: Overview.

Further Reading

Andrews AT (ed.) (1986) *Electrophoresis: Theory, Techniques and Biochemical Clinical Applications*. Oxford: Clarendon Press.

Barron AE and Blanch HW (1995) DNA separations by slab gel and capillary electrophoresis: theory and practice. *Separation and Purification Methods* 24: 1–118.

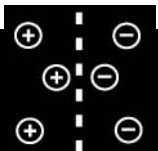
De Gennes (ed.) (1979) *Scaling Concepts in Polymer Physics*. Ithaca, NY: Cornell University Press.

Dovich NJ (1997) DNA sequencing by capillary electrophoresis. *Electrophoresis* 18: 2393–2399.

Heller C (ed.) (1997) *Analysis of Nucleic Acids by Capillary Electrophoresis*. Viesbaden: Vieweg.

Righetti PG (ed.) (1995) *Capillary Electrophoresis in Analytical Biotechnology*. Boca Raton: CRC.

DETERGENT FORMULATIONS: ION EXCHANGE



S. P. Chopade and K. Nagarajan,
Michigan State University, East Lansing, MI, USA

Copyright © 2000 Academic Press

Introduction

The primary ingredients of a detergent are the surfactants, whereas *builders* provide the necessary backbone. The maximum efficiency of surfactants is achieved when the hardness in water is removed. Builders provide this essential function of water softening, primarily by means of ion exchange. Although the performance of surfactants is directly dependent on the efficacy of the builder, the consumer rarely notices the importance of the latter. The development in detergent technology during the last decade has been to improve the property of ion exchange that can lead to enhanced washing power of the detergent, while considering other factors such as environmental concerns and cost. This has been largely due to the development of ion exchange materials and molecular sieve type materials that have been used in detergent formulations as builders. Laundry detergents have a yearly \$4.4 billion market alone in the United States, shared equally by the liquid and powder detergents. A typical detergent composition is shown in **Table 1**. In today's detergents, builders constitute about 6–25 wt% of liquid detergents and about 20–55 wt% of powder detergent formulations. Thus builders play a significant role in the detergents market.

Until the early twentieth century, cleaning products were essentially soaps, i.e. sodium salts of natural fatty acids. The surfactants in the first synthetic detergents were short chain alkyl naphthalenesulfonates, which were followed by long chain alkyl benzenesulfonates (ABS). ABS were prepared by alkylation of benzene with propylene tetramer followed by

sulfonation. Although ABS had very good cleaning properties, they were non-biodegradable and their accumulation in the environment caused foaming in sewage treatment plants and rivers. Hence ABS were replaced by their straight chain analogues, linear alkylarylsulfonates (LAS) in 1965. Surfactants can be broadly classified as anionic, cationic and non-ionic. Today's detergent formulations contain mainly the anionic surfactants and a lesser amount of non-ionic surfactants. Cationic surfactants have very small market share compared to the anionic and non-ionic materials. The use of non-ionics is increasing in liquid detergents as they offer greater stability and formulation flexibility. Whereas the main function of builders is to provide water softening capability and alkalinity, they also serve other important functions as dispersants, antiredeposition agents, and anticorrosion, bleach stabilization and processing aid. **Figure 1** illustrates the various important functions played by zeolites in the washing process. Hard water, if not

Table 1 Typical detergent composition

<i>Ingredient</i>	<i>Powder detergent</i>	<i>Heavy-duty liquid detergent</i>
Surfactants		
Anionic	15–20	10–40
Non-ionic	0–3	0–10
Builders		
Zeolite	20–30	0–25
Citrate	0–5	0–10
Polycarboxylates	0–3	–
Carbonate	8–12	0–25
Sodium silicates	1–3	–
Sodium sulfate	20–25	–
Enzymes	0–2	0–1.5
Perborate bleach	0–5	0–10
Polymer stabilizer	–	0–1
Enzyme stabilizer	–	0–5

See Colour Plate 76.

See also: II/Electrophoresis: Capillary Electrophoresis; Capillary Electrophoresis–Mass Spectrometry; Capillary Electrophoresis–Nuclear Magnetic Resonance. III/Deoxyribonucleic Acid Profiling: Overview.

Further Reading

Andrews AT (ed.) (1986) *Electrophoresis: Theory, Techniques and Biochemical Clinical Applications*. Oxford: Clarendon Press.

Barron AE and Blanch HW (1995) DNA separations by slab gel and capillary electrophoresis: theory and practice. *Separation and Purification Methods* 24: 1–118.

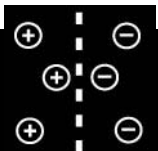
De Gennes (ed.) (1979) *Scaling Concepts in Polymer Physics*. Ithaca, NY: Cornell University Press.

Dovich NJ (1997) DNA sequencing by capillary electrophoresis. *Electrophoresis* 18: 2393–2399.

Heller C (ed.) (1997) *Analysis of Nucleic Acids by Capillary Electrophoresis*. Viesbaden: Vieweg.

Righetti PG (ed.) (1995) *Capillary Electrophoresis in Analytical Biotechnology*. Boca Raton: CRC.

DETERGENT FORMULATIONS: ION EXCHANGE



S. P. Chopade and K. Nagarajan,
Michigan State University, East Lansing, MI, USA

Copyright © 2000 Academic Press

Introduction

The primary ingredients of a detergent are the surfactants, whereas *builders* provide the necessary backbone. The maximum efficiency of surfactants is achieved when the hardness in water is removed. Builders provide this essential function of water softening, primarily by means of ion exchange. Although the performance of surfactants is directly dependent on the efficacy of the builder, the consumer rarely notices the importance of the latter. The development in detergent technology during the last decade has been to improve the property of ion exchange that can lead to enhanced washing power of the detergent, while considering other factors such as environmental concerns and cost. This has been largely due to the development of ion exchange materials and molecular sieve type materials that have been used in detergent formulations as builders. Laundry detergents have a yearly \$4.4 billion market alone in the United States, shared equally by the liquid and powder detergents. A typical detergent composition is shown in **Table 1**. In today's detergents, builders constitute about 6–25 wt% of liquid detergents and about 20–55 wt% of powder detergent formulations. Thus builders play a significant role in the detergents market.

Until the early twentieth century, cleaning products were essentially soaps, i.e. sodium salts of natural fatty acids. The surfactants in the first synthetic detergents were short chain alkyl naphthalenesulfonates, which were followed by long chain alkyl benzenesulfonates (ABS). ABS were prepared by alkylation of benzene with propylene tetramer followed by

sulfonation. Although ABS had very good cleaning properties, they were non-biodegradable and their accumulation in the environment caused foaming in sewage treatment plants and rivers. Hence ABS were replaced by their straight chain analogues, linear alkylarylsulfonates (LAS) in 1965. Surfactants can be broadly classified as anionic, cationic and non-ionic. Today's detergent formulations contain mainly the anionic surfactants and a lesser amount of non-ionic surfactants. Cationic surfactants have very small market share compared to the anionic and non-ionic materials. The use of non-ionics is increasing in liquid detergents as they offer greater stability and formulation flexibility. Whereas the main function of builders is to provide water softening capability and alkalinity, they also serve other important functions as dispersants, antiredeposition agents, and anticorrosion, bleach stabilization and processing aid. **Figure 1** illustrates the various important functions played by zeolites in the washing process. Hard water, if not

Table 1 Typical detergent composition

<i>Ingredient</i>	<i>Powder detergent</i>	<i>Heavy-duty liquid detergent</i>
Surfactants		
Anionic	15–20	10–40
Non-ionic	0–3	0–10
Builders		
Zeolite	20–30	0–25
Citrate	0–5	0–10
Polycarboxylates	0–3	–
Carbonate	8–12	0–25
Sodium silicates	1–3	–
Sodium sulfate	20–25	–
Enzymes	0–2	0–1.5
Perborate bleach	0–5	0–10
Polymer stabilizer	–	0–1
Enzyme stabilizer	–	0–5

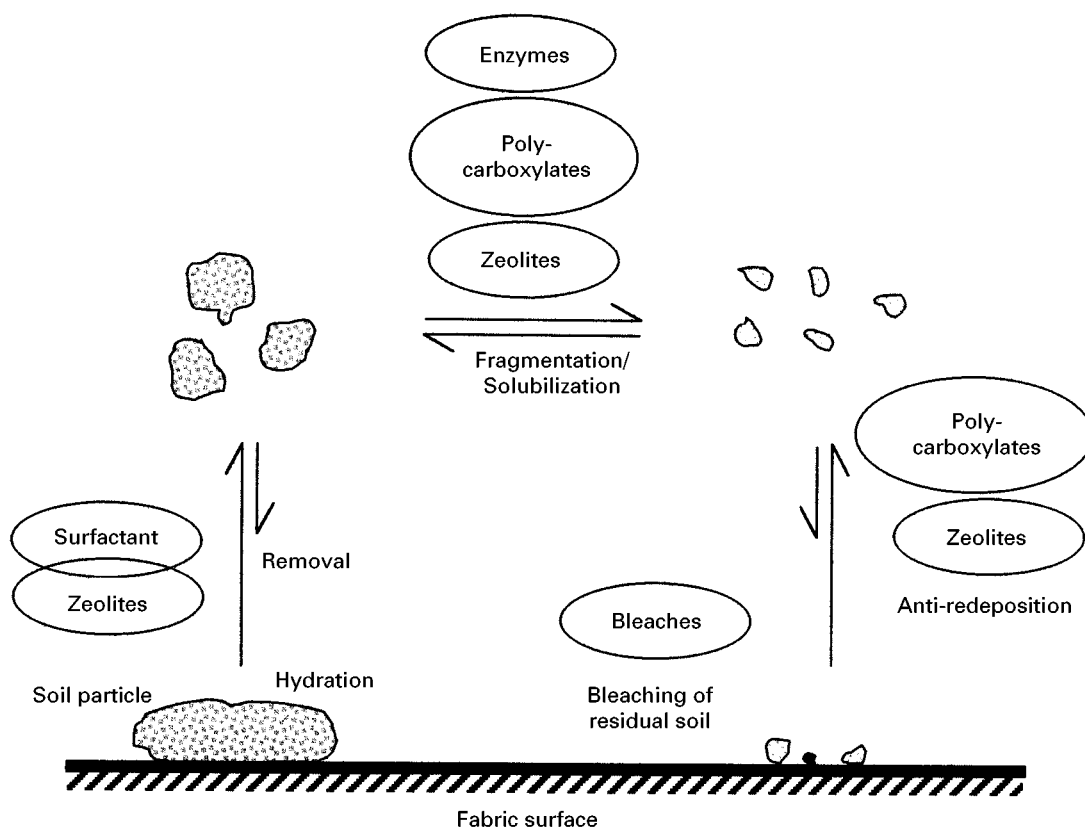


Figure 1 Function of various detergent ingredients in the washing process.

softened by builders, would react with the anionic surfactants and make them insoluble, thereby rendering them inefficient.

Development of Today's Builders

The earliest builders consisted of sodium carbonate and sodium silicate. Although inexpensive, the disadvantage of using these as water softeners is that they form sparingly soluble precipitates that deposit on fabrics and cause incrustation. In the 1950s, these builders were replaced by a complexing agent, sodium diphosphate. However, it was found that diphosphates also had similar shortcomings of forming precipitates. These drawbacks were overcome by introduction of sodium triphosphate (STP) and sodium tripolyphosphate (STPP) in the early 1960s. STP and STPP act as sequestering agents, which trap calcium and magnesium ions in the water very efficiently, forming water-soluble complexes. They also provide other functions like loosening the bond between soil and fabrics and buffering capacity. However, due to their nutrient value, the phosphates caused excessive fertilization and growth of algae in lakes and slow-flowing rivers, a phenomenon more commonly known as eutrophication. Nitrilotriacetic

acid was introduced in some countries as an STPP substitute, but was withdrawn after concern about its toxicological properties. In the 1970s, the aluminosilicate zeolite A, was introduced. The aluminosilicates differ from the STPP builders in that they are water insoluble and the mechanism of removal of the calcium and magnesium ions from the water is ion exchange instead of complexation. Usually they are used in conjunction with sodium

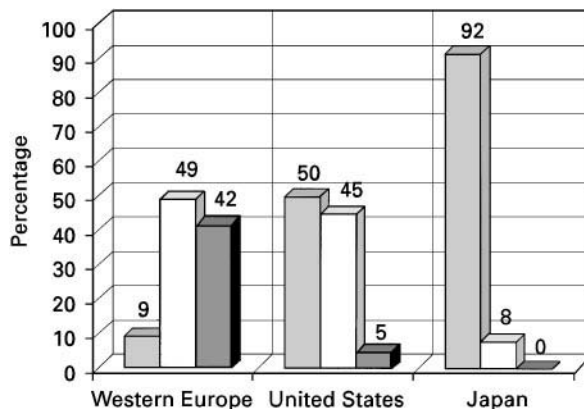


Figure 2 Water hardness distributions. CaCO_3 (ppm): \square , < 90; \square , 90-270; \blacksquare , > 270. (After Showell, with permission from Marcel Dekker.)

carbonate and polycarboxylates or citrates. Today in countries like the United States, Japan and some Central European countries, zeolites have almost completely replaced phosphates in detergents.

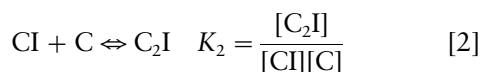
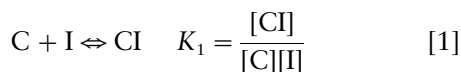
Builders for Water Softening

The percentage of builders in detergents depends on factors like water hardness, wash temperature and wash time. The dissolved inorganic salts of calcium and magnesium impart hardness to water. For the washing process to proceed effectively, it is important to remove the hardness ions in the water and replace them with sodium ions, rendering softness to the water. Thus the builder must exhibit high capacity for selective removal of these ions from water. The hardness level of water is different in different countries, leading to slight differences in detergent formulations. For example, water in Japan has relatively low hardness, typically less than 90 ppm CaCO_3 , whereas in the United States it is of low-to-intermediate hardness. The water in Western Europe has very high hardness (greater than 270 ppm CaCO_3 in 42% of the region) (Figure 2).

Phosphates ruled the detergent world until the introduction of inorganic builders. They are still widely used in a significant part of the world, e.g. Eastern Europe, Southern Asia, Africa, Australia and Latin America. We will discuss the phosphates briefly before going into detail on zeolites as detergent builders. We will also include some other inorganic silicate builders that may have impact on the detergent industry of the future. The main focus will be on the ion exchange properties of the materials, particularly zeolites.

Phosphates

Phosphates are excellent chelating agents and work by a sequestering mechanism, i.e. as previously mentioned, by trapping the calcium and magnesium ions and forming water-soluble complexes. A chelating agent possesses multiple sites with lone-pair electrons that are available to interact with corresponding electron-deficient coordination sites on metal ions like Ca^{2+} and Mg^{2+} ions. The chelation is reversible and the strength of chelation is indicated by the equilibrium constant, also known as a stability constant. The chelation proceeds in a stepwise manner between metal ions, I, and chelating agent, C. For a divalent cation it is a two step process given as:



The overall stability constant, K , is the product of the stability constants for each step ($K_1 \cdot K_2$). The log K values for stability constants of polyphosphates for binding of Ca^{2+} and Mg^{2+} ions are fairly high (5.2 and 5.7, respectively) at $> \text{pH } 9$. Hence, under normal washing conditions, STPP shows excellent sequestering capacity for both calcium and magnesium ions in solution. The binding capacity of STPP is fairly high, 158 mg CaO g^{-1} at 20°C and 113 mg CaO g^{-1} at 90°C . As the phosphates and the calcium and magnesium chelates formed are water soluble, the removal is very fast. In addition to water softening, after removal of the soil, they offer the function of suspending soil by electrostatic repulsion. They do not provide as high buffering capacity/alkalinity as sodium carbonate or sodium silicate. The low capacity of STPP to absorb non-ionic surfactants limits its use in the new compact detergents where considerable amounts of the latter are used. Efficiency and low cost are the biggest advantages of STPP. In many countries, where phosphates are not banned for environmental reasons, STPP is still the major player in the detergent builder market.

Zeolite A

The need for a substitute for STPP led to development of zeolites as detergent builders. Among the aluminosilicates, zeolite A is most preferred because of its high ion exchange capacity (170 mg CaO g^{-1}) and low cost of manufacturing. As opposed to chelation by STPP, zeolite A removes hardness of water by means of ion exchange, a process we will discuss in more detail in further sections. Another important difference that zeolite A exhibits from STPP is the selectivity for removal of divalent ions. STPP simply chelates both the Ca^{2+} and Mg^{2+} ions non-selectively from water. Zeolite A being a molecular sieve, shows higher selectivity toward Ca^{2+} ions over Mg^{2+} ions due to high hydration of Mg^{2+} ions. This is advantageous, as studies have indicated that the presence of a certain level of Mg^{2+} ions in fact improves the detergent performance. The ion exchange kinetics are strongly dependent on the wash temperature, and hence zeolites tend to be more effective at higher wash temperatures.

In addition to these properties, zeolite A offers other functionality to the detergents. It shows adsorption characteristics that are pH dependent. At pH 10, which is the pH during a normal wash, there is minimal adsorption of anionic or cationic surfactants, leaving them available for the soil removal. As the pH drops during the rinse cycle, the adsorption tendency of zeolites increases, leading to adsorption of colloiddally dispersed soil particles by heterocoagulation. Thus zeolites act as anti-redeposition

agents, minimizing fabric incrustation. In a mixed wash of coloured and white clothes, zeolite A suppresses the dye transfer from coloured to whites prohibiting staining. Zeolite A will ion-exchange trace metal ions such as Cu^{2+} , Zn^{2+} , etc. as well as remove them by the surface deposition of basic salts. As these metal ions are often responsible for decomposition of bleaches, use of zeolite A leads to an increase in the bleach performance. The only major shortcoming of zeolite A over STPP is the slower rate of ion exchange at low temperatures. This is often overcome by use of a soluble complexation agent, like citrate or a polycarboxylate. The complexation agent acts catalytically. The soluble complexation agent binds reversibly with the Ca^{2+} ions of the precipitate (either by ion exchange or by chelation), making them soluble. These solubilized Ca^{2+} ions are then readily exchanged by zeolite, making the complexation agent free for more transport. Usually about 2–8% of polycarboxylates are used as co-builders to enhance the performance of zeolite A.

Zeolite MAP

Other than zeolite A, zeolite P and in a few cases zeolite X are the only important zeolites that have been considered for detergent applications. Zeolite MAP, the maximum aluminium P which is a synthetic gismondine, is an improved version of zeolite P. In addition to the high binding capacity ($\sim 160 \text{ mg CaO g}^{-1}$), zeolite MAP has several distinct advantages over zeolite A. First, it enhances the stability of the sensitive and environment friendly bleaching agent, sodium percarbonate. Sodium percarbonate is sensitive to moisture present in the detergent formulation. The low mobility of water in the zeolite MAP structure imparts more stability to the water-sensitive bleach. Secondly, it exchanges calcium ions more rapidly and more selectively. Especially at low temperatures, the ion exchange kinetics are considerably faster than those of zeolite A. Finally, zeolite P exhibits higher liquid carrying capacity, e.g. for carrying non-ionic liquid surfactants, allowing free-flowing powder at higher liquid loading. With all these advantages, zeolite MAP is replacing zeolite A in more and more detergent formulations.

δ -Disilicate

Amorphous sodium silicates were among the earliest compounds that were used as builders. These compounds remove the water hardness by sequestering Ca^{2+} and Mg^{2+} ions, but form insoluble precipitates. Therefore amorphous silicates are used only in small proportions (0–3 wt%) mostly as a co-builder in the zeolite A builder systems. Here they provide a source of alkalinity and show selectivity towards Mg^{2+} ions. In contrast with amorphous silicates, layered silicates are crystalline and work by an ion exchange mechanism. These are polymeric crystalline materials, which have a layered structure. The monovalent metal ions (Na^+) in the interstices can be easily exchanged with divalent ions in solution and are responsible for the ion exchange capacity of the material. δ -Disilicate, which has the empirical formula $\text{Na}_2\text{Si}_2\text{O}_5$, is an anhydrous alkali silicate that is most important for its ion exchange properties. The formation of δ -disilicate is not thermodynamically favoured over the corresponding α - and β -phases; hence production requires a specialized high-temperature crystallization process. The δ -disilicate has a very regular structure (Figure 3) as opposed to the amorphous silicates.

The δ -disilicate does not have a thermodynamically stable structure in aqueous media. It disintegrates slowly into monomeric sodium silicate, commonly known as water glass solution but this process is much slower than the ion exchange kinetics. The hardness ions of water replace the sodium ions in the δ -disilicate interstices and give stability to the framework. During the wash cycle, the pH of the solution is generally maintained at a high level, and the ion-exchanged disilicate is stable. As the pH drops in the rinsing cycle, the Ca^{2+} and Mg^{2+} ions are released as silicates and the disilicate disintegrates into the wash water. The size of these insoluble calcium and magnesium silicates formed is small and does not cause incrustation.

The δ -disilicate is characterized further by its multi-functionality in detergent building. It is a very good source of alkalinity and has the high buffering capacity required for the washing process. It exhibits high adsorption capacity for the non-ionic surfactants. Its mild desiccant properties and ability to combine with heavy metal ions make it compatible with unstable bleaches like sodium percarbonate. This imparts good storage stability to the detergent formulation and allows the use of environmentally friendly bleaches. Once again, due to cost considerations, δ -disilicate cannot completely replace zeolite A at this point, but it certainly has great potential to act as a supplement to the zeolite A systems.

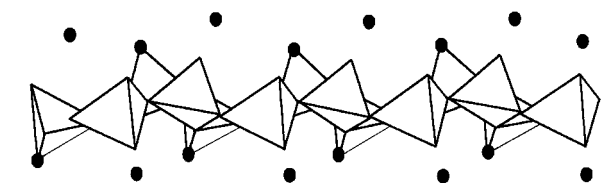


Figure 3 Polymeric structure of δ -disilicate. ●, sodium; ▴, SiO_4 tetrahedra.

Zeolites: Synthesis, Structure and Ion Exchange

Aluminosilicates are denoted by the general formula $M_{x/n}[(AlO_2)_x \cdot (SiO_2)_y] \cdot wH_2O$ where M is the cation of valence n , w is the number of water molecules and y/x usually has values of 1–5 depending upon the structure. The sum $(x + y)$ represents the total number of tetrahedra in a unit cell and the formula within parentheses represents the framework composition. The cation M , which functions as a charge balance in various solids, can be exchanged depending upon the equilibrium constant and this property finds use in several applications including catalysis, wastewater treatment, treatment of radioactive waste and in our context, detergents.

There are around 80 species of natural zeolitic minerals and about 150 types of synthetic zeolites. Of these, only a few have practical significance and a very few among them have importance in detergents. The synthetic zeolites, mainly zeolite A, and to some extent zeolite P and zeolite X are used in detergent formulations, mainly as ion exchangers.

Synthesis of Zeolites

Zeolites are normally synthesized in the sodium form. Most of the crystalline sodium zeolite is produced by crystallization from sodium aluminosilicate gels at a temperature below 150°C. The properties of the product zeolite depend greatly on the gel preparation and it is therefore a key step in zeolite preparation.

In a typical process for the synthesis of zeolite A, sodium silicate and sodium aluminate solutions are first mixed together. The resulting aluminosilicate is precipitated and crystallized hydrothermally to obtain the zeolite. Seed crystals of zeolite A are often used to obtain crystalline zeolite A in high selectivity. The crystallized zeolite is then washed, filtered and dried. The usual gel preparation temperature is 50–80°C and the temperature during crystallization is slightly higher 80–90°C. The time required for gel preparation may vary from 0.5 to 1.5 h, whereas 1–2 h is necessary for the crystallization. Optimizing the following variables controls the product quality: mixing sequence, speed of agitation, seed crystals, aging time and temperature. The desired properties for optimum detergent application are small particle size (typically < 10 µm), narrow particle size range, poor adhesive capacity (achieved by having crystalline material), high calcium binding power and good wettability.

Structure of Zeolite A

The structure of the crystallized zeolite A is quite unique. It is classified as a type 3 zeolite, for the

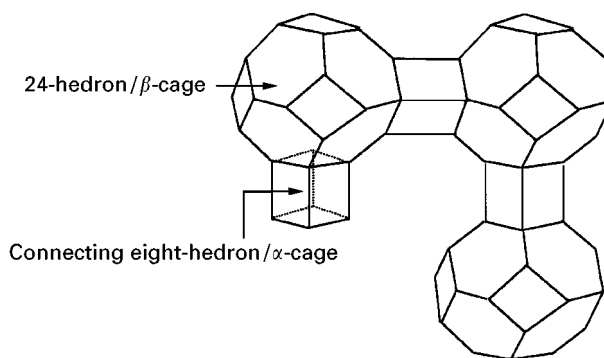


Figure 4 Structure of zeolite A.

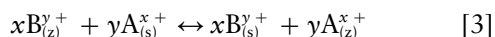
interconnecting system is a double four-ring or an octahedron. The structure can be described in terms of two types of polyhedra; one is a simple cubic arrangement of octahedron or α -cage and the other is a truncated octahedron of 24-hedron or β -cage as shown in **Figure 4**. The cubic α -cages ($Al_4Si_4O_{16}$) are placed in the centres of the edges of a cube in the truncated octahedra. These α -cages connect the β -cages, creating a three-dimensional structure having pores of size 4.2 Å. Each corner of the cube (α -cage) is occupied by the truncated octahedra (β -cage) enclosing a cavity with a free diameter of 6.6 Å. The centre of the unit cell is a large cavity, which has a free diameter of 11.4 Å. A unit cell of zeolite A contains 24 tetrahedra; 12 each of AlO_4 and SiO_4 . A fully hydrated zeolite A contains 27 water molecules per unit cell. The theoretical Si/Al ratio in zeolite A is 1 but in many preparations the Si/Al ratio is slightly less than 1.

Structure of Zeolite MAP (Synthetic Gismondine)

Zeolite MAP is a type 1 zeolite, meaning that the interconnecting units are single four-ring units (also known as S4R). The eight-membered rings are interconnected by S4R units as shown in **Figure 5**. The interconnecting chains run parallel to both X- and Y-axes, creating a three-dimensional channel system. The mean free openings of the pores are 3.1×4.5 Å and 2.8×4.8 Å. The structure is somewhat flexible, as the connecting S4R units are two-dimensional. Due to this flexibility, slight structural differences are observed by dehydration of the zeolite. MAP has a Si/Al ratio of 1. This high aluminium content leads to a higher negative charge in the crystal lattice and therefore it has the highest theoretical ion exchange capacity.

Theory of Ion Exchange in Zeolites

The ion exchange process may be represented by the following equation:



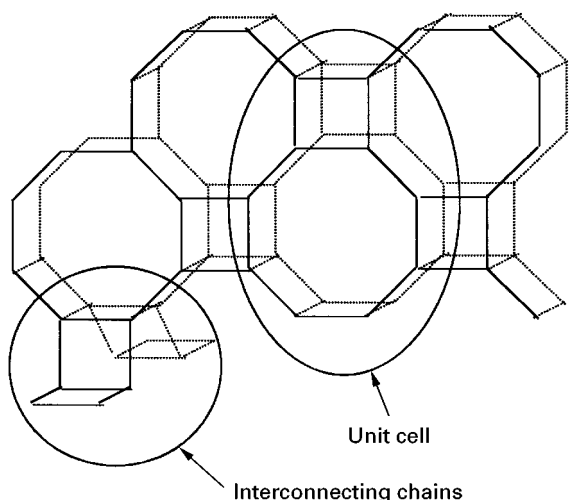


Figure 5 Structure of zeolite MAP (synthetic gismondine).

where x and y are the charges of cations A and B and the subscripts z and s refer to the zeolite and solution, respectively. The equivalent fractions of the exchanging cation in the solution and zeolite are defined by:

$$A_s = \frac{xm_s^A}{xm_s^A + ym_s^B} \quad [4]$$

$$A_z = \frac{\text{number equivalent of exchanging cation A}}{\text{total equivalent of cations in the zeolite}} \quad [5]$$

where m_s^A and m_s^B are the molalities of the ions A and B respectively, in the equilibrium solution; also $(A_z + B_z) = 1$ and $(A_s + B_s) = 1$. The ion exchange isotherm is a plot of A_z as a function of A_s at a given total concentration in the equilibrium solution and at constant temperature. The preference of a zeolite for one of the two ions is expressed by the separation factor, α_B^A , defined by:

$$\alpha_B^A = \frac{A_z B_s}{B_z A_s} \quad [6]$$

If ion A is preferred, then α_B^A is greater than unity. The separation factor depends on the total concentration of the solution, the temperature and A_s . It is not affected by the choice of the concentration units.

If $\alpha_B^A = 1$, the exchange is ideal and obeys the Law of Mass Action. However, ideal behaviour is seldom observed and preference for one of the two ions is usually shown. The rational selectivity coefficient is:

$$K_B^A = \frac{A_z^x B_s^x}{B_z^y A_s^y} \quad [7]$$

If the ions are equal valence ($x = y$) then:

$$K_B^A = \alpha_B^A \quad [8]$$

If $x \neq y$, then:

$$[\alpha_B^A]^x = K_B^A \left[\frac{A_z}{A_s} \right]^{x-y} \quad [9]$$

The corrected selectivity coefficient $K_B'^A$ includes a correction for the activity coefficient of the ions in the equilibrium:

$$K_B'^A = \frac{A_z^x B_s^x \gamma_B^x}{B_z^y A_s^y \gamma_A^y} \quad [10]$$

where γ_A and γ_B are mean ionic activity coefficients of the ions in solution.

Ion Exchange by Zeolites

The cation exchange properties of zeolites were observed some one hundred years ago. It was this property and the ease with which it was happening that led to an early interest in ion exchange materials for use as water-softening agents. The cation exchange behaviour of zeolites depends upon the following:

- Si/Al ratio;
- nature of the cation species, cation size (both anhydrous and hydrated) and cation charge;
- temperature;
- concentration of the cation species in solution;
- anion species associated with the cation in solution;
- solvent (most of the exchange is carried out in aqueous solution although some work has been done in organic solvents); and the
- structural characteristic of the particular zeolite.

The cations that contribute towards the hardness of water are calcium and magnesium ions. It is therefore evident that the property of zeolite should be such that it has a large ion exchange capacity and should be selective towards the exchange of these ions. Zeolite A, zeolite MAP, and to a certain extent zeolite X, have been shown to exhibit this property and consequently are the favourable candidates of choice towards being incorporated in the detergent formulation.

Ion exchange in zeolite A seems to be possible only with univalent and divalent counterions. Exchange of higher valence ions fails with zeolite A. The order of decreasing selectivity for univalent ions in zeolite A is as follows: $\text{Ag} > \text{Ti} > \text{Na} > \text{K} > \text{NH}_4 > \text{Rb} > \text{Li} > \text{Cs}$. For divalent ions, the order of decreasing selectivity is: $\text{Zn} > \text{Sr} > \text{Ba} > \text{Ca} > \text{Co} > \text{Ni} > \text{Cd} > \text{Hg} > \text{Mg}$.

The ion exchange kinetics depends on the zeolite structure and cation properties. As zeolite A has

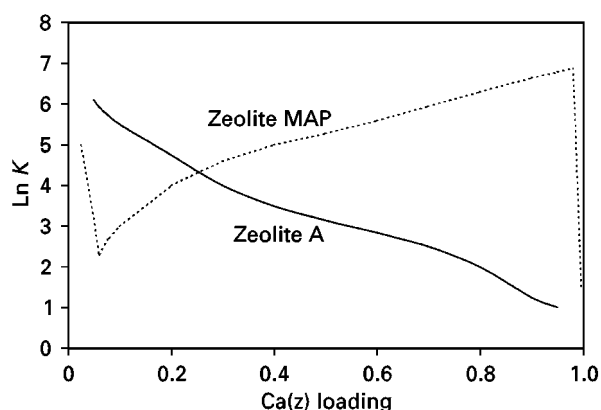


Figure 6 Kielland plots for zeolite MAP and zeolite A calcium-sodium exchange, 25°C, 0.1 mol L⁻¹ solution.

a small pore diameter of 4.1 Å, the exchange of ions like Mg²⁺ is slow due to its high hydration at low temperatures. At higher temperatures, the hydration shell is reduced, making the effective ion size smaller. Thus the diffusion kinetics and in effect, exchange kinetics of Mg²⁺, are enhanced at higher temperature. Ions like Ca²⁺ diffuse easily at room temperatures as they exhibit smaller hydration. This sieving action is responsible for the selectivity of zeolite A towards Ca²⁺ ions as compared to Mg²⁺ ions.

Zeolite MAP is more selective than zeolite A towards calcium exchange. The plot of calcium selectivity constant log *K* versus the calcium loading (Kielland plot, **Figure 6**) shows peculiar behaviour for zeolite MAP. For zeolite A, as expected, the selectivity constant decreases with increase in calcium loading. In case of zeolite MAP, the opposite behaviour is observed, which indicates a cooperative exchange process. The insertion of some calcium ions in the structure causes a structural change in zeolite MAP, predisposing the framework to accept further calcium ions more readily. Its flexible structure, which was explained earlier, allows this phenomenon.

The ultimate base exchange capacity of a zeolite depends on the Si/Al ratio; it increases as the Si/Al ratio approaches unity (**Table 2**). This is the primary

reason for the dominance of zeolite A among other zeolites as far as builder applications are concerned. The table indicates that the exchange capacity of zeolite MAP approaches that of zeolite A as the Si/Al ratio approaches unity. The exchange kinetics and total exchange capacity are also dependent on the Si/Al ratio. **Table 2** shows comparison of time required to reduce concentration of 2 mmol L⁻¹ Ca²⁺ ions in a solution to the level specified. Although zeolite MAP with a Si/Al ratio approaching unity shows high capacity and faster kinetics, it becomes increasingly difficult to prepare an aluminosilicate material with a zeolite MAP structure at lower Si/Al ratios. In many cases the measured exchange capacities deviate from theoretical values due to impurities or variation in chemical composition. The specific exchange capacity also varies with the exchange cation.

Environmental Aspects of Detergent Building

STPP is a very efficient and cost-effective builder. As it is water soluble, and the hardness removal is by chelation, the process is very fast even at low temperatures. Irrespective of these advantages, many countries have stopped using STPP in detergents as it causes environmental problems. Phosphates, being essential nutrients, cause excessive fertilization in stagnant waters and slow-flowing rivers, which leads to excessive growth of algae. These problems can be avoided by employing a wastewater treatment system that removes the phosphorus. However, as aluminosilicates made an entry, it was preferred to limit the use of phosphorus compounds in detergents. Aluminosilicates are environment friendly materials. Aluminosilicates are produced by combining silica and alumina (from bauxite ore). After use in detergents, they are returned to the environment, where they decompose back to silica and alumina. The only concern about the aluminosilicates arises from their insoluble nature. There are some reports of zeolites leading to enhanced sludge in the wastewater. As long as the particles are larger than 1 µm, they can be

Table 2 Ion exchange capacity and rate of removal of Ca²⁺ from aqueous solutions by zeolites

Zeolite	Si/Al	Effective ion exchange capacity (mg CaO g ⁻¹ zeolite)	^a Time required to achieve 0.5 mmol L ⁻¹ Ca ²⁺ (s)	^a Time required to achieve 0.01 mmol L ⁻¹ (s)
Zeolite MAP	1.46	123	1	Ineffective
	1.21	146	1	5
	1.12	155	1	4
	1.005	159	2	11.5
Zeolite A	1.0	152	14	95

^aInitial Ca²⁺ concentration 2 mmol L⁻¹, 1.48 g dm⁻³ zeolite, 25°C.

easily removed by sedimentation. The δ -disilicate, though insoluble during the wash process, dissolves when the solution becomes dilute during the rinse cycle.

Future Trends

The builder development for detergents is now more and more driven by environmental issues. Zeolite A was a major breakthrough over the conventional phosphates. An ideal builder would be one combining the efficacy of STPP and the environment friendly nature of (alumino) silicates. At this point, combination of builders and co-builders is the way detergents are being formulated. The new materials zeolite MAP and δ -disilicate, are the future; though more efficient, they still have to cross the cost barrier to become major players in the detergent industry. As efforts are constantly underway to come up with more and more

efficient builder and detergent formulations, the challenge is to achieve compatibility, environment friendliness, and low production cost, all at the same time.

See also: II/Ion Exchange: Inorganic Ion Exchangers; Novel Layered Materials: Phosphates; Novel Layered Materials: Non-Phosphates.

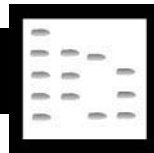
Further Reading

- Adams CJ, Araya A, Carr SW *et al.* (1997) Zeolite MAP: The new detergent zeolite. *Studies in Surface Science and Catalysis* 105: 1667.
- Breck DW (1974) *Zeolite Molecular Sieves: Structure, Chemistry and Use*. New York: John Wiley.
- Cutler WG and Kissa E (eds) (1987) *Detergency Theory and Technology*. New York: Marcel Dekker.
- Showell MS (ed.) (1998) *Powdered Detergents*. New York: Marcel Dekker.

DNA

See III/DEOXYRIBONUCLEIC ACID PROFILING: Overview; Capillary Electrophoresis

DRUGS AND METABOLITES



Liquid Chromatography–Mass Spectrometry

R. P. W. Scott, Avon, CT, USA

Copyright © 2000 Academic Press

The tandem analytical instrument, comprising a liquid chromatograph and a mass spectrometer is ideally suited for identifying drug metabolites and for following their metabolic pathways. The segregation of each drug metabolite from the sample matrix, and its subsequent identification, firstly requires a very efficient separation technique. As the metabolites are often chemically very similar to the parent drug, this exigency is adroitly furnished by the liquid chromatography (LC) column (usually microbore) packed with very small particles. Secondly, the materials of interest are inevitably present in the biological system in very small quantities and thus, despite the use of sample concentrating techniques, a very sensitive detection technique is essential. The required

high sensitivity is effectively supplied by the ion multiplier of the mass spectrometer sensor. Thirdly, in order to identify the individual metabolites, structural information is required which must be highly specific and contain adequate detail at high resolution. Such data is readily provided by the mass spectrum of each eluted solute, which can either be compared with standard spectra or identified by using well-established interpretation procedures. In some cases, the liquid chromatograph can be coupled to a MS/MS instrument that will provide mass spectra of each fragment ion, from each eluted solute, should more detailed information be needed.

For the effective use of LC/MS, special sample preparation techniques are necessary and suitable LC/MS interfaces should be employed. Both these subjects are discussed in detail in other parts of the Encyclopedia, and it will be sufficient here to give the sample preparation details of each typical application that is discussed. In addition, the general interface systems that are used, such as thermospray, electrospray, atmospheric pressure chemical ionization devices, transport interfaces etc., are also described in

detail under LC interface devices and can be referred to when appropriate. Drug and drug metabolites find their way to many parts of the body in a variety of ways: via the alimentary canal, via the blood stream, or through the lymph system, and sometimes by direct diffusion through specific tissues. In animal tests, drug and drug metabolites can be found, extracted and assayed in many specialized tissues such as the liver, kidneys, heart muscle, brain, etc. and are usually extracted using standard procedures after homogenizing the tissue. In human tests, the drug and drug metabolites are usually measured in biological fluids, such as whole blood, blood plasma, gastric fluids, urine, saliva, etc., although occasionally samples of tissue from biopsies are also examined. In simple cases of drug monitoring, the concentration of a particular drug and its metabolites may be monitored during treatment merely to ensure that the drug level is kept at an optimum for prime response. In more complicated procedures, the drug and its metabolites may be monitored in a number of different fluids and tissues to determine not only the metabolic pathway, but also those tissues and sites where specific types of metabolism or drug breakdown occur.

The unique advantages of the various techniques and procedures used in LC/MS for monitoring drugs and their metabolites are best illustrated by means of a number of carefully selected applications. There is a wide range of LC/MS applications available for drug and drug metabolite analysis and the following have been chosen as typical examples of the use of the technique in pharmacology. Furazolidone (*N*-(5-nitro-3-furfurylidene-3-amino)-2-oxazolodinone) is a 5-nitrofuran antibiotic that is added to animal feeds to help prevent such infections as *Escherichia coli* and *Salmonella* in cattle, pigs and poultry. It follows that it would be important to know the amount of residues (if any) remaining after slaughter in any meat used for human consumption. In Europe, for example, the maximum amount of furazolidone that is tolerated is $5 \mu\text{g kg}^{-1}$ of animal foodstuff. Furazolidone is light sensitive and so operations must be carried out under artificial yellow light. An example of the measurement of furazolidone in some pharmacokinetic studies is afforded by the work of McCracken *et al.* who used thermospray ionization LC/MS for its determination. The procedure that was used is as follows. 2-g samples of liver and muscle tissue were homogenized with 40 mL of a mixture of McLlvaine buffer and methanol (7:3) and then centrifuged for 15 min. The supernatant liquid was then removed and evaporated down to 15 mL at 40°C . 25 mL of dichloromethane was then added and the mixture shaken for about 1 min. The upper aque-

ous layer was discarded and the solvent extract carefully evaporated to dryness and then dissolved in a mixture of 2 mL of dichloromethane and 6 mL of hexane. The solution was then extracted by passing it through a prepared Bond-Elut NH_2 extraction cartridge, which was then washed with 5 mL of a hexane/dichloromethane mixture (1:1) and 2 mL of a hexane/chloroform mixture (1:1). The cartridge was then extracted with 5 mL of a mixture of chloroform and methanol (7:3) and the extract evaporated to dryness. The residue was then redissolved in 100 μL of mobile phase, which consisted of 0.1 mol L^{-1} ammonium acetate/acetonitrile (3:1). The sample was injected onto a reversed phase column, 12.5 cm long and 4 mm i.d., containing RP18 stationary phase bonded to 5- μm particles. Chromatograms showing the elution of the Furazolidone by single ion monitoring are shown in Figure 1. It is seen that as a result of the use of single ion monitoring, the procedure can be made highly selective. The recovery of the drug ranged between 65 and 70%. The minimum detectable level of contamination was about $1 \mu\text{g kg}^{-1}$ of tissue, which was quite adequate to confirm that a sample did not contain the drug in excess of the tolerance level.

Another example of the use of the thermospray interface for monitoring drugs in cellular matter from animals is given in the work of Cannavan *et al.* who developed a technique for measuring levamisole in pig and sheep tissue. Levamisole L-(–)-2,3,5,6-tetrahydro-6-phenylimidazole(1,1-b)thiazole, the laevorotatory isomer of tetramisole, is an anthelmintic drug used to control gastrointestinal parasites in cattle, pigs and sheep. In a similar way to that used in the assay of furazolidone, a somewhat complicated sample preparation procedure was necessary. 3 g of the tissue sample was mixed with 2 g of anhydrous sodium sulfate, 9 mL of ethyl acetate and 0.5 mL of 50% (w/v) potassium hydroxide solution, and the mixture homogenized. The mixture was then centrifuged and 6 mL of *n*-hexane was added to 6 mL of the supernatant liquid, and then passed through a Baker Bond CN cartridge column. The column was washed with 5 mL of chloroform/*n*-hexane mixture (1:1) and air-dried. The levamisole was eluted with two 5-mL aliquots of methanol, evaporated to dryness, and the residue taken up in 200 μL of the mobile phase consisting of acetonitrile–tetrahydrofuran–triethylamine–water (350:50:2:598 v/v) containing ammonium acetate (0.1 mol L^{-1}). This solution was then used for the LC/MS analysis. 50- μL samples were placed on a Li-Chrospher 60RP-select B column (12.5 cm long, 4 mm i.d), packed with 5- μm particles. Then mass spectrometer was the Hewlett-Packard 5989A MS engine with thermospray. Single ion

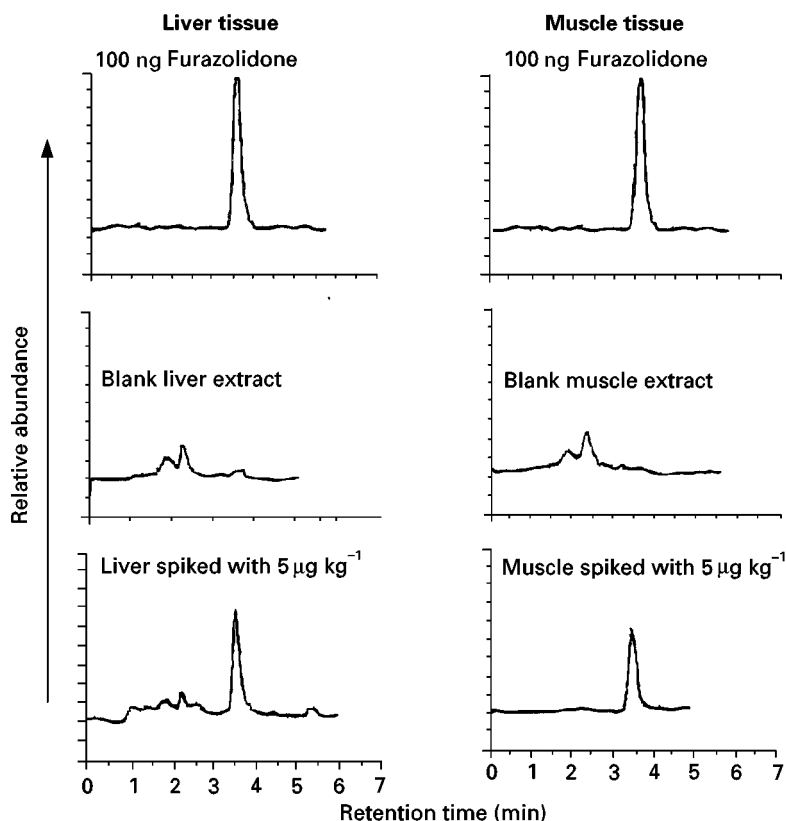


Figure 1 Single ion chromatograms ($m/z = 243$) of furazolidone demonstrating the sensitivity levels obtainable. (Reproduced with permission from McCracken *et al.*, 1995.)

chromatograms obtained from the analysis are shown in **Figure 2**. They again emphasize the advantages of single ion monitoring; the peak of interest is selected from a complex mixture of peaks with only one other appearing in the chromatogram. The limit of detection was found to be about 5 ng g^{-1} of tissue and the calculated mean recovery for liver, kidney and muscle tissue was found to be 93, 85 and 79%, respectively.

Many penicillins, particularly penicillin G, are extensively used in veterinary medicine. It follows that to prevent antibiotic residues from entering the human food chain, their levels in animal products that have been prepared for human consumption need to be carefully monitored. Blanchflower *et al.* developed a procedure for simultaneously monitoring five penicillins, including oxacillin, cloxacillin and dicloxacillin in both muscle and kidney tissue and also in milk. Blanchflower *et al.* employed an LC/MS tandem instrument fitted with an electrospray interface, and utilized single ion monitoring to selectively locate and measure each antibiotic. The extraction process was exceedingly complicated. An appropriate tissue sample was pulverized, spiked with an appropriate standard and homogenized. Acetonitrile was then ad-

ded to the homogenate, which was sonicated and finally centrifuged. A portion of the supernatant liquid was then treated with phosphoric acid mixed with dichloromethane and again centrifuged. Acetonitrile and *n*-hexane were added, the mixture shaken and again centrifuged. The lower layer was separated and then washed with water. The solvent mixture was then extracted with phosphate buffer, centrifuged once again and the lower layer treated with tetrabutylammonium hydrogen sulfate. The solution was then extracted with dichloromethane, the extract evaporated to dryness and dissolved in an acetonitrile water mixture. Separations were performed on an Intersil ODS-2 reversed-phase column (15 cm long and 4.6 mm i.d). The outlet from the column was coupled to a Megabore probe of a VG Platform ES-MS, which was operated in the negative ion mode. The source was maintained at 120°C and the flow rate of the drying and nebulizing gas was 10 L h^{-1} . The extraction and focus voltages were about 17 and 24 V, respectively. It was found that the fragmentation pattern was significantly changed by adjusting the voltage on the extraction cone. As the voltage was increased, the degree of fragmentation increased. The effect of extraction cone voltage is

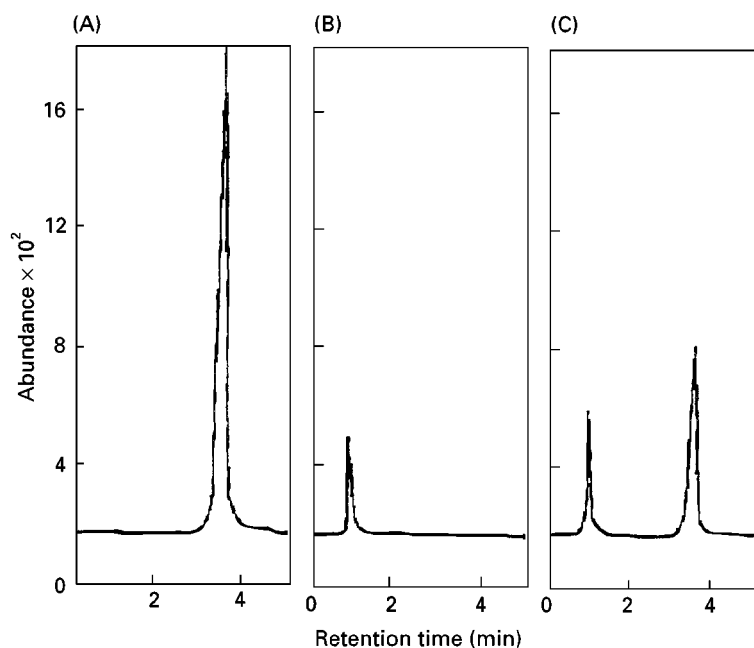


Figure 2 Single ion chromatograms of levamisole extracted from liver tissue. (A) Levamisole standard ($1 \mu\text{m mL}^{-1}$), (B) negative liver sample, and (C) liver samples + levamisole (34.8 ng g^{-1}). (Reproduced with permission from Cannavan *et al.*, 1995.)

demonstrated in Figure 3. It would appear that a potential of 5 V on the extraction cone produced just two ions above an m/z value of 160, i.e. $m/z = 434$ and 436. Increasing the potential to 10 V produced another peak at an m/z value of 293. At a potential of

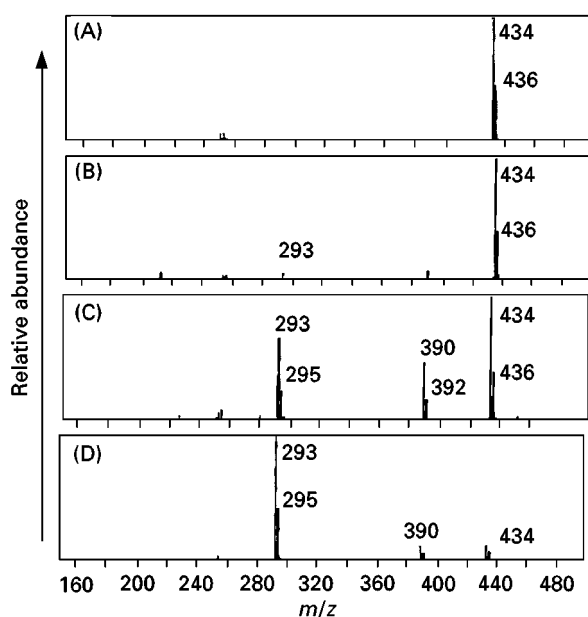


Figure 3 The effect of changing the extraction voltage on the fragmentation pattern. Extraction potential 5 V (A), 10 V (B), 15 V (C) and 20 V (D). (Reproduced with permission from Blanchflower *et al.*, 1994.)

20 V, the peak at an m/z value of 293 has markedly increased and has been joined by a significant peak at $m/z = 295$. At the same time, the original major peak at $m/z = 434$ had shrunk to a minor peak and peak at $m/z = 436$ was barely visible. It is obvious that the operating conditions of the interface can be critical in order to achieve the desired selectivity and sensitivity. This effect is typical for electrospray interfaces. In the antibiotic assays, the extraction potential was maintained between 15 and 17 V. Examples of the chromatograms obtained for cloxacillin and penicillin G contained in muscle tissue and obtained by single ion monitoring at different m/z values are shown in Figure 4. It shows that monitoring at m/z values of 293, 390 and 434 selects the cloxacillin from the accompanying unresolved substances almost exclusively. It would also appear that the best signal-to-noise ratio was achieved employing m/z values of 293 and 434. The apparent magnitude of the signal-to-noise ratio indicates that the assay could detect levels of cloxacillin as low as 40 ng g^{-1} . The optimum extraction voltage for assaying penicillin G in milk appears to be far more critical, the best selectivity being obtained at a m/z value of 333. The lower limit of detection, however, is much smaller and it would appear that an antibiotic level of 1 ng g^{-1} might be detectable.

Although the technique of LC/MS is ideal for the detection and identification of drugs and their metabolites in samples of biological origin, it is often

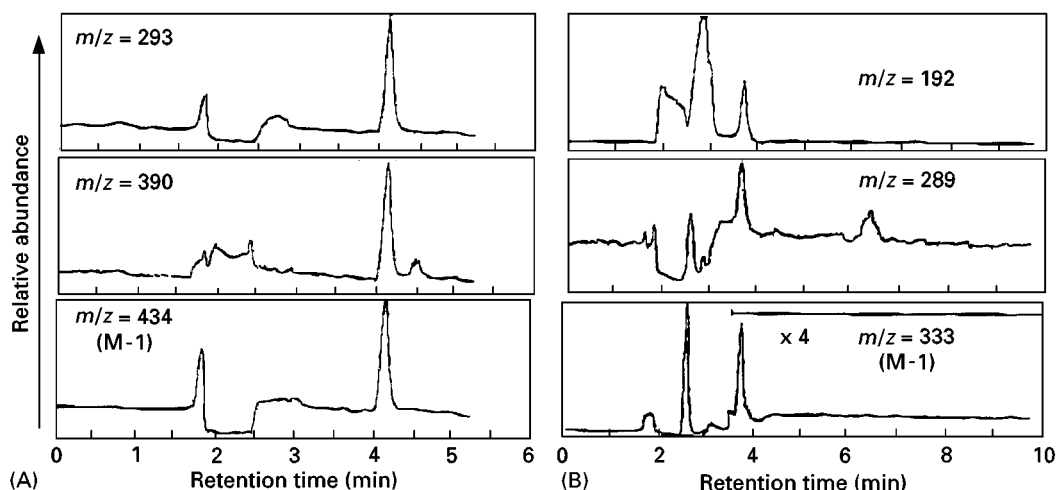


Figure 4 Chromatogram from the assay of cloxacillin and penicillin G monitored at different m/z values. (A) Muscle spiked with 200 ng g^{-1} cloxacillin, (B) milk spiked with 4 ng g^{-1} penicillin G. (Reproduced with permission from Blanchflower *et al.*, 1994.)

necessary to use quite complicated sampling procedures. For example, Cai and Henion developed an intricate combination of sampling techniques to determine LSD and its analogues in urine. The urine sample was first subjected to affinity chromatography, which selectively removed the LSD and its metabolites from the urine. The materials isolated on the affinity column were then displaced and collected in a special trap, from which the materials of interest

were then again displaced onto the LC column for separation. The column eluent was then passed through an atmospheric pressure chemical ionization interface to the mass spectrometer. A diagram of their apparatus is shown in Figure 5. The analytical procedure was quite complicated. The immuno-affinity column that was employed was an HiPac protein G column ($3.3 \text{ mm} \times 2.1 \text{ mm}$) packed with $30\text{-}\mu\text{m}$ particles. Prior to use, the column was equilibrated

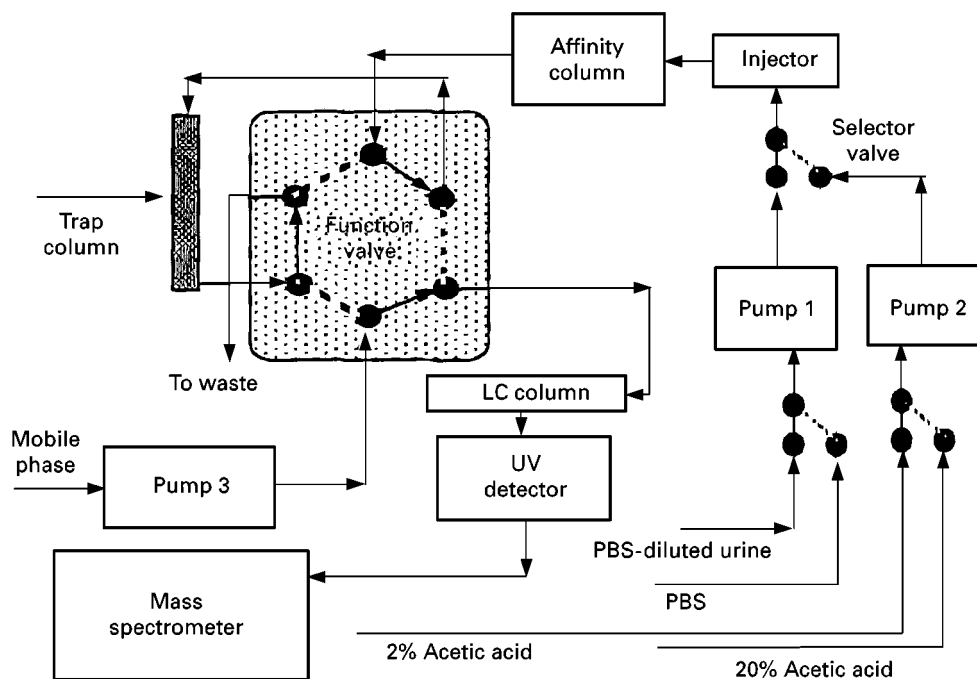


Figure 5 Diagram of the sampling arrangement for the analysis of LSD in urine by an LC/MS. (Reproduced with permission from Cai and Henion, 1996.)

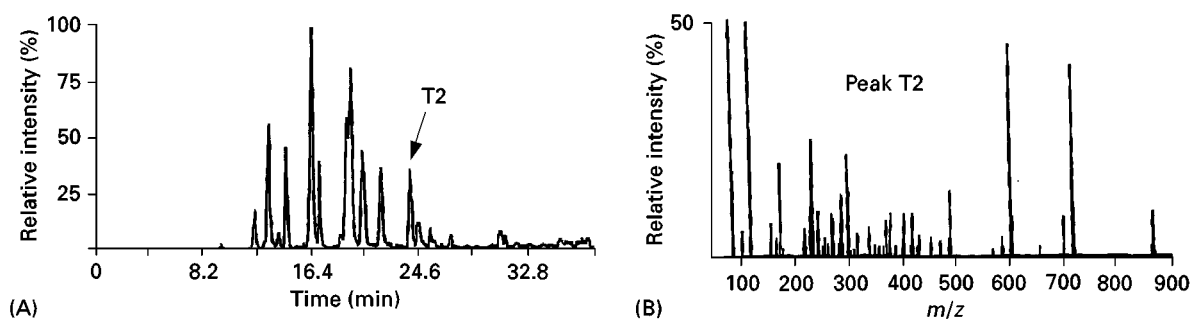


Figure 6 (A) Total ion current chromatogram of a tryptic digest sample of human growth hormone. (B) Spectrum of a product from the tryptic digest of human growth hormone obtained from low dead volume atmospheric ionization interface.

with phosphate buffered saline (PBS). 30 μL of PBS-diluted antibody solution (10% antibody/90% PBS) was then injected onto the column. Then, the sample of human urine, diluted with PBS (50% urine/50% PBS), was pumped through the protein G column and immediately flushed with PBS to remove the weakly bound impurities. While this process was taking place, the trapping column (1.5 cm long, 1 mm i.d.; packed with 5- μm C_{18} particles) and the LC column (15 cm long, 0.3 mm i.d.; packed with 3- μm C_{18} particles) were equilibrated with the mobile phase. The PBS was then pumped through the affinity column and the trap, desorbing the materials from the affinity column and re-adsorbing them on the trap. The trap was then back-flushed and the desorbed materials eluted through the LC column into an API interface and thence into the mass spectrometer. Four metabolic products in addition to the unchanged LSD itself were separated and identified from their mass spectra. The concentration of LSD in the original urine sample was 0.9 ng mL^{-1} . The results of Cai and Henion demonstrate how, by utilizing the selective extraction that is provided by affinity chromatography, very high sensitivities can be obtained.

Recently Thomson *et al.* described a modification of the atmospheric pressure chemical ionization technique involving a special low dead volume interface. Thomson *et al.* employed packed microbore columns (170, 320 and 500 μm i.d., with lengths ranging from 5 to 15 cm) in conjunction with a low-volume, wall-coated capillary column as an interface. The total ion current chromatogram of the tryptic digest sample from about 1 pmol of human growth hormone is shown in Figure 6A. The column was packed with an octadecyl bonded-phase having a mean pore size of 300 \AA and a particle diameter of 7 μm . The separation was developed by employing a gradient of from 20% solvent (0.1% TFA in water, Figure 6A) to 80% solvent (75% of 0.1% TFA and 25% acetonitrile, Figure 6B) over a period of 1 h. Flow

rates of about 80 to 100 $\mu\text{L min}^{-1}$ were used, and about 3 $\mu\text{L min}^{-1}$ of the flow was split from the mainstream and passed to the capillary column *via* the capillary interface. It can be seen from Figure 6 that an excellent separation is obtained and apparently little resolution is lost in the capillary interface. The mass spectrum of the peak marked T2 in the chromatogram is shown in Figure 6B. It is clear that good quality spectra can be obtained for ion masses of up to at least 900. Such a combination of techniques can be invaluable for the structural elucidation of compounds generated in biochemical research.

See also: II/Chromatography: Liquid: Detectors: Mass Spectrometry. **Extraction:** Solid-Phase Extraction.

Further Reading

- Blanchflower WJ, Hewitt SA and Kennedy DG (1994) Confirmatory assay for the simultaneous detection of five penicillins in muscle, kidney and milk using liquid chromatography–electrospray mass spectrometry. *Analyst* 119: 2595–2601.
- Cai J and Henion J (1996) On-line immunoaffinity extraction-coupled column capillary liquid chromatography/tandem mass spectrometry: trace analysis of LSD analogs and metabolites in human urine. *Analytical Chemistry* 68(1): 72–78.
- Cannavan A, Blanchflower WJ and Kennedy DG (1995) Determination of levamisole in animal tissues using liquid chromatography–thermospray mass spectrometry. *Analyst* 120: 331–333.
- McCracken RJ, Blanchflower WJ, Rowen C, McCoy MA and Kennedy DG (1995) The determination of furazolidone in porcine tissue using thermospray liquid chromatography–mass spectrometry and study of the pharmacokinetics and stability of its residues. *Analyst* 120: 2347–2351.
- Thomson B, Covey T, Shushanm B, Allen M and Sakuma T (private communication) A low dead volume atmospheric ionization interface, Perkin Elmer Corporation.

Liquid Chromatography–Nuclear Magnetic Resonance–Mass Spectrometry

R. Plumb, G. Dear, I. Ismail and B. Sweatman,
Glaxo Wellcome Research and Development,
Ware, UK

Copyright © 2000 Academic Press

Introduction

As part of the development process of any new chemical entity as a drug substance, evidence is required that its metabolism in humans is similar to its metabolism in the animal species selected for toxicological evaluation. In order to obtain this information a number of studies are carried out using both radiolabelled and unlabelled material. Xenobiotics are generally metabolized to generate more polar compounds that are then more readily eliminated from the body. The metabolism of drugs commonly occurs in two main phases: phase I, functionalization type reactions such as oxidation, reduction and hydrolysis and phase II where metabolism reactions are generally conjugative reactions such as glucuronidation, sulfation, methylation, and acetylation whereby an endogenous group is attached to the molecule.

Historically drug metabolite identification has usually been based on the comparison of UV detected high-performance liquid chromatography (HPLC) retention times of isolated 'unknown' metabolites with authentic standards. This method of detecting drug metabolites, and subsequently characterizing, is not only a time-consuming process, and hence expensive, but yields no or very limited structural information.

The application and use of mass spectrometry in drug metabolism studies has contributed significantly to the improved structural characterization of novel drug metabolites. More recently, tandem mass spectrometry (MS/MS) has been increasingly used in both the characterization and quantitation of metabolites in microsomal incubates, urine, plasma and faecal extracts derived from both *in vitro* and *in vivo* sources.

Even though mass spectrometry is an exquisitely sensitive and specific detector capable of providing drug metabolite information from complex biological matrices, it does not always provide unequivocal structural identification, and in these instances NMR spectroscopy is often needed to provide conclusive site specific structural characterization. Increasingly the complementary information provided by MS and NMR is used in conjunction with HPLC separation techniques and indeed reports exist where all three techniques have been linked to generate on-line LC/NMR/MS.

A Systematic Approach to Drug Metabolite Identification

This section describes an approach to drug metabolite identification which utilizes semi-preparative HPLC, LC/MSⁿ, NMR and HPLC/NMR. The potential of coupling NMR and tandem mass spectrometry (MSⁿ) in the form of an ion trap mass spectrometer is also highlighted. The advantage of using an ion trap mass spectrometer over a quadrupole instrument is primarily the ability to generate MSⁿ spectra by repetitively isolating and fragmenting stored ions, and thereby producing second, third and subsequent generation product ions. This enables advantage to be taken of both structural and molecular weight information generated by the MS to complement the NMR data. The power of the use of these techniques in combination with each other is illustrated, using the example of novel non-nucleoside reverse transcriptase inhibitor, GW420867 (see **Figure 1**) which serves to demonstrate the approach currently taken to drug metabolite characterization in our laboratory.

Sample Fractionation

Urine samples collected following oral administration of GW420867 to animal species and man were pooled to provide 100 mL of sample in each case. The pooled urine samples were separately freeze-dried and then reconstituted in distilled water to give a final volume equal to one tenth of the initial volume. The resulting concentrated urine samples were centrifuged and the supernatants removed and stored at 0–8°C prior to isolation by preparative HPLC. Injections of the concentrated urine samples (10 mL) were made onto a preparative HPLC column, and analytes separated with reversed-phase gradient elution. The column eluent was collected into 96 well microtitre plates at 15 s fraction intervals. The microtitre plates were transferred to a 96 well dry down station

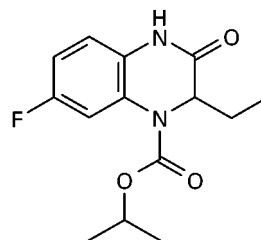


Figure 1 Structure of GW420867.

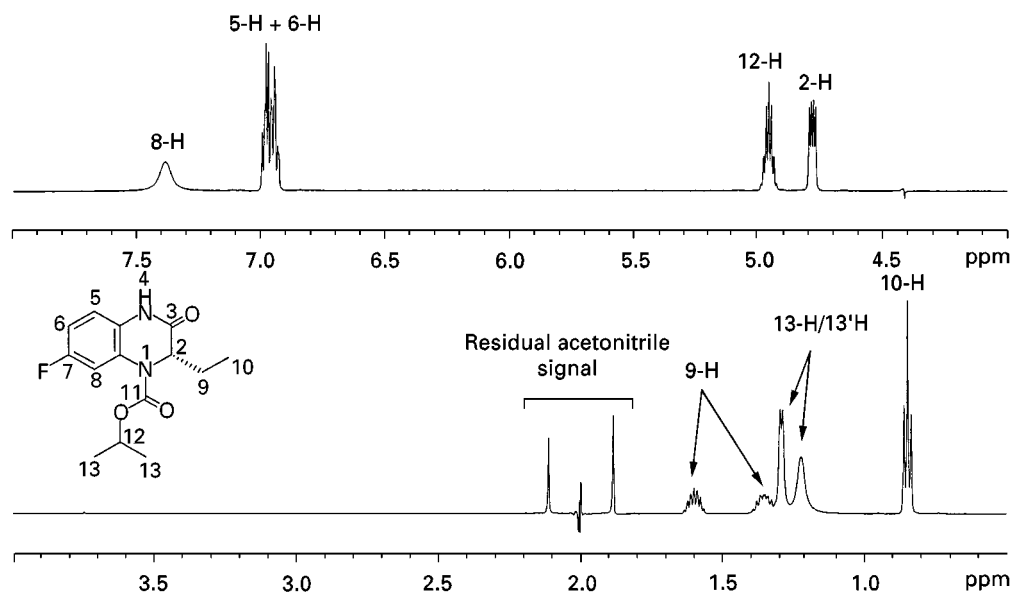


Figure 2 ^1H -NMR spectrum of a 1 mg mL^{-1} solution of authentic GW420867X in 50:50 acetonitrile – deuterium oxide, obtained on a Bruker DRX-600 spectrometer over 256 scans with dual solvent suppression.

and evaporated to dryness under a constant flow of nitrogen at 25°C . The dried fractions were re-dissolved in 50:50 acetonitrile – deuterium oxide. The microtitre plates were sonicated for 10 min in an ultrasonic bath to aid the resolution process and the resulting dissolved fractions transferred individually to 5 mm NMR tubes for analysis by ^1H and ^{19}F NMR spectroscopy for the presence of drug-related material.

Fraction Screening by ^1H and ^{19}F NMR

In this particular example the ^{19}F NMR spectra may be used to ascertain the distribution of drug-related material in the processed fractions as the drug

molecule contained a fluorine atom and there are little or no endogenous fluorinated background signals in urine. However comparison of the ^1H NMR spectra obtained for the isolated fractions with that acquired for the authentic parent compound may also be used for this purpose. The ^1H NMR spectrum of the parent drug is shown in **Figure 2**. The aromatic protons at 6.78 and 6.94 ppm and the aliphatic protons at 0.85 and 1.29 ppm were used to identify possible drug metabolites and also to indicate structural changes where appropriate. By contrast the ^{19}F NMR spectra only provides limited structural information on changes in the immediate vicinity of the fluorine atom.

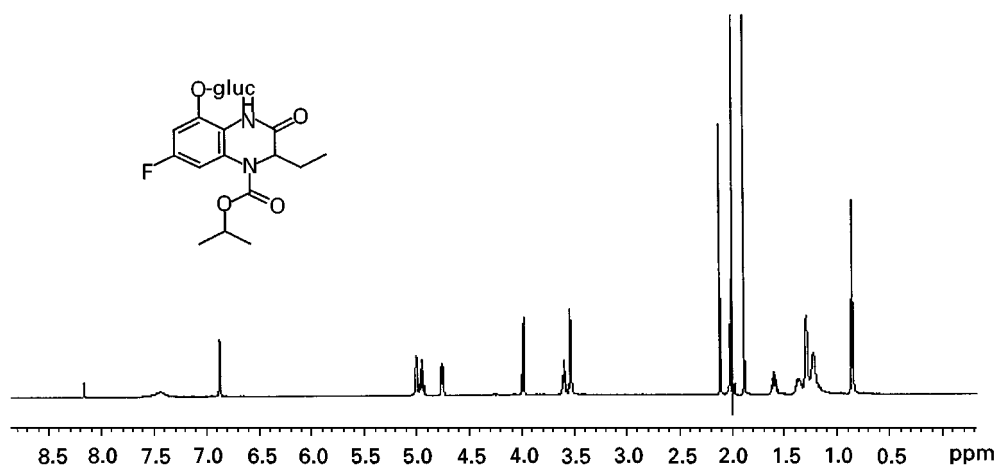


Figure 3 ^1H -NMR spectrum of the H-5 hydroxyl glucuronide metabolite of GW420867X in-acetonitrile – deuterium oxide (1:1) obtained on a Bruker DRX-600 spectrometer over 64 scans with dual solvent suppression, following isolation from rabbit urine.

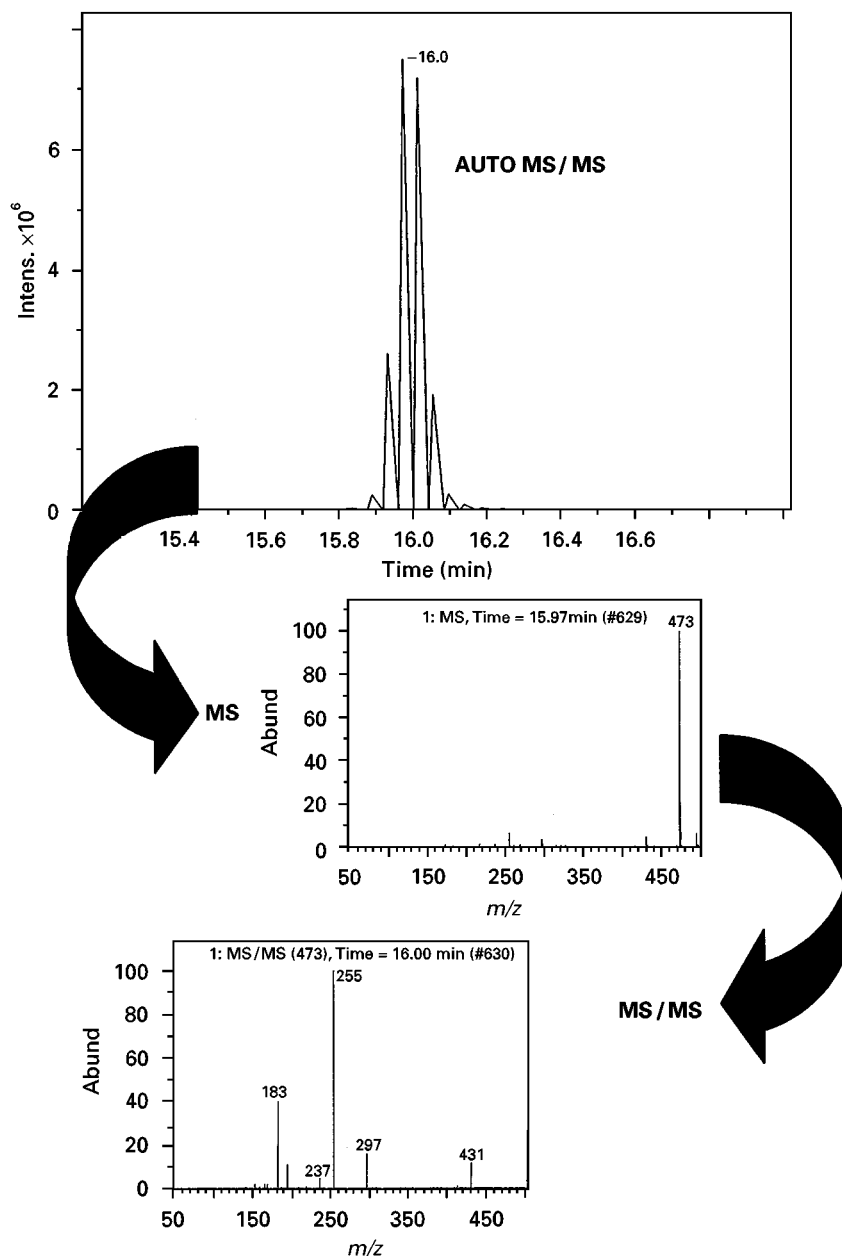


Figure 4 LC/MS/MS analysis of the H-5 hydroxyl glucuronide metabolite of GW420867X following injection of a rabbit urine fraction on to a 250×4.6 mm Zorbax RX-C8 $5 \mu\text{m}$ column. Analytes were eluted with a 0–100% aqueous 0.1% formic acid/acetonitrile gradient over 30 min at 1 mL min^{-1} . The column eluent was monitored using the Esquire ion trap operating in positive ion electrospray ‘auto’ MS/MS, with a resonance fragmentation amplitude of 1.2 V.

A ^1H NMR spectrum from an isolated rabbit urine fraction acquired using only 64 scans, is given in Figure 3 and illustrates that metabolites can potentially be isolated with high degree of purity. Inspection of the ^1H NMR spectrum readily enabled the metabolite to be identified as a glucuronic acid conjugate of the 5-hydroxylated species (as shown in Figure 3); the anomeric H1 (5.1 ppm) and H2–H5 (3.4–3.6 ppm) glucuronyl protons being clearly visible.

Analysis of Metabolite Containing Fraction by Mass Spectrometry

Fractions highlighted using ^{19}F and ^1H NMR spectroscopy as containing drug-related material were further investigated using electrospray LC/MS/MS operating in data dependent MS/MS mode. Small injections enabled discernible MH^+ or $[\text{M} - \text{H}]^-$ ions for all metabolites to be obtained to provide complemen-

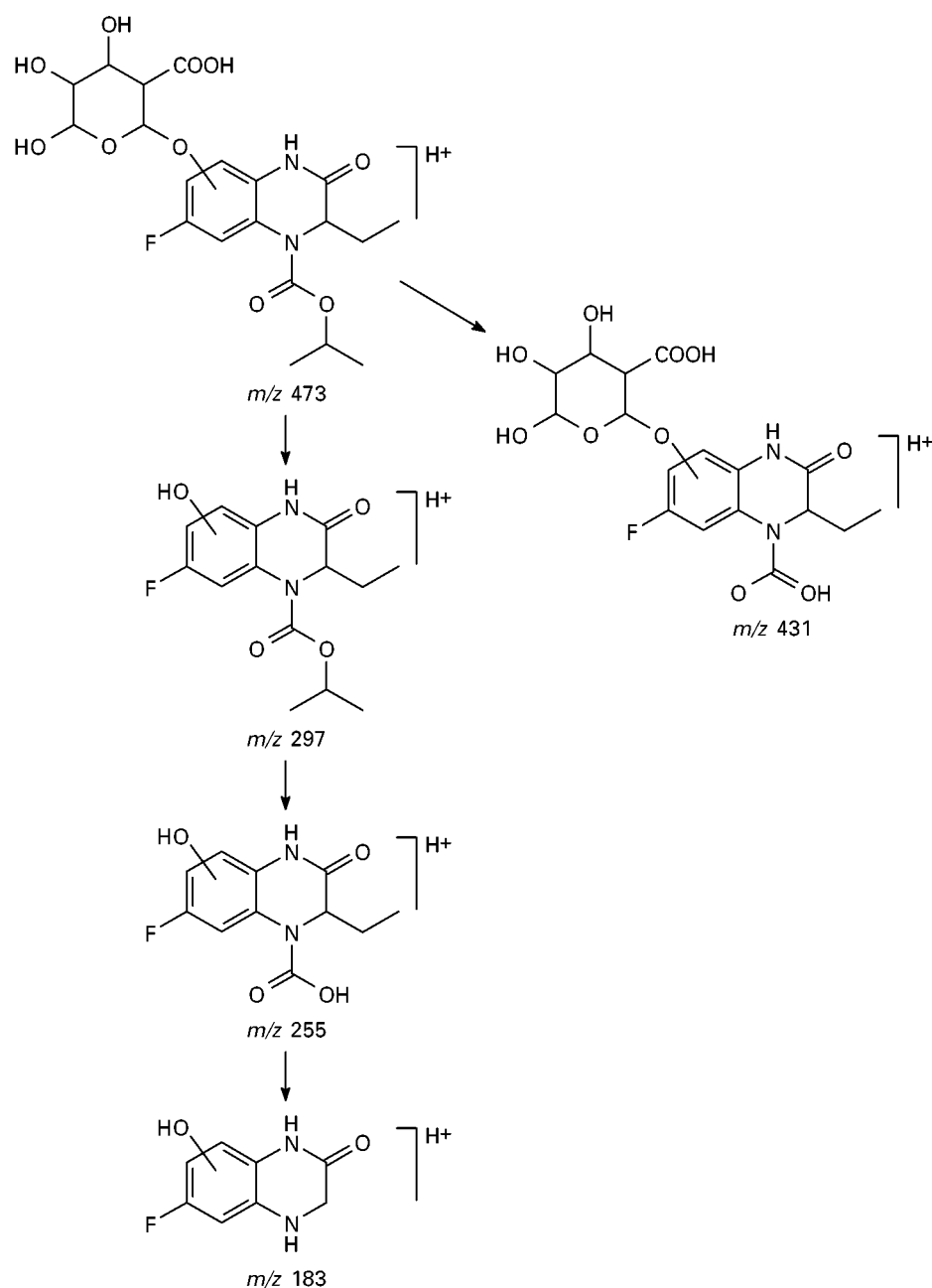


Figure 5 Rationalization of the product ions resulting from MS/MS of the isolated H-5 hydroxyl glucuronide of GW420867.

tary molecular weight and structural information to supplement. LC/MS/MS chromatograms and spectra corresponding to the NMR spectrum in Figure 3 are given in Figure 4. This metabolite could be rationalized as a hydroxyl glucuronide (see Figure 5), and therefore complemented the NMR data already acquired. In common with many glucuronide conjugates, the loss of the glucuronyl moiety in the MS/MS spectrum (-176 amu) is clearly observed. MS/MS data interpretation of all spectra was assisted by comparison with the MS/MS spectrum of an authentic standard.

The example cited above is an extremely common and representative example where the precise position of aromatic protons are established unequivocally through the use of ^1H NMR spectroscopy. The MS data provided added confidence by providing both molecular weight and some structural information. Thus by combining the NMR and MS data full structural elucidation is more effectively and rapidly achieved. Thus for GW4208657 using NMR and MS as described above, a total of 17 metabolites were unequivocally identified following extraction from various matrices.

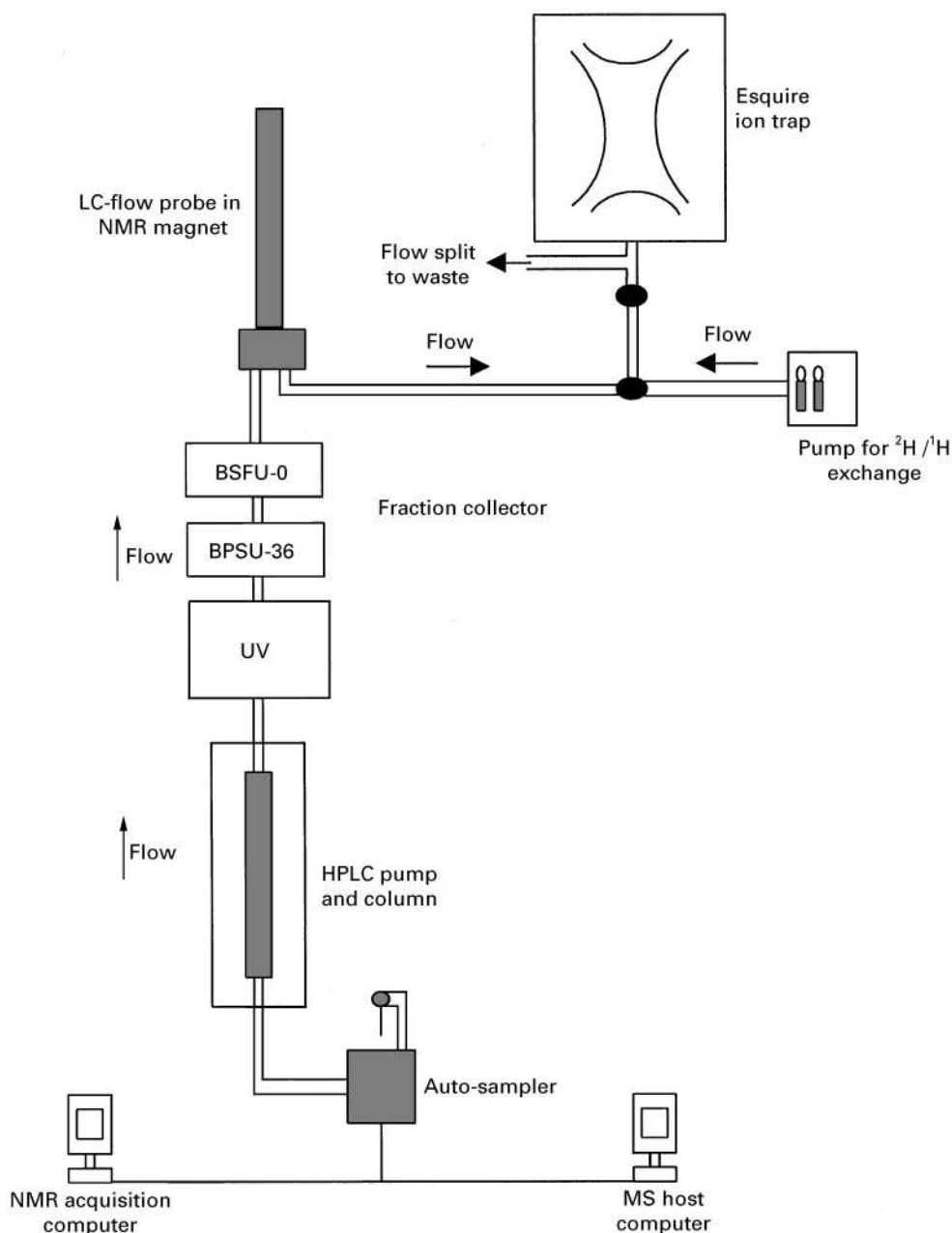


Figure 6 The LC/NMR/MSⁿ system was configured as depicted by connecting the Bruker DRX-600 NMR spectrometer and the Bruker–Esquire mass spectrometer in series. In this configuration the mass spectrometer was operated just outside the 5 Gauss line of the NMR magnet.

Further Analysis Using Directly Coupled LC/NMR/MSⁿ

In most cases metabolites isolated directly from the preparative HPLC fractions alone gave satisfactory ¹H NMR and MS spectra and could therefore be readily characterized without further investigation. However some fractions which had either a low concentration of metabolite or which were

impure mixtures of metabolites required further separation and/or longer data acquisition using LC/NMR/MSⁿ.

LC/NMR probes are generally more sensitive than standard NMR probes as the sample is concentrated into a smaller volume by the chromatographic process and the superior filling factors (this is the proximity of the NMR RF coils to the sample) obtained in LC/NMR probes.

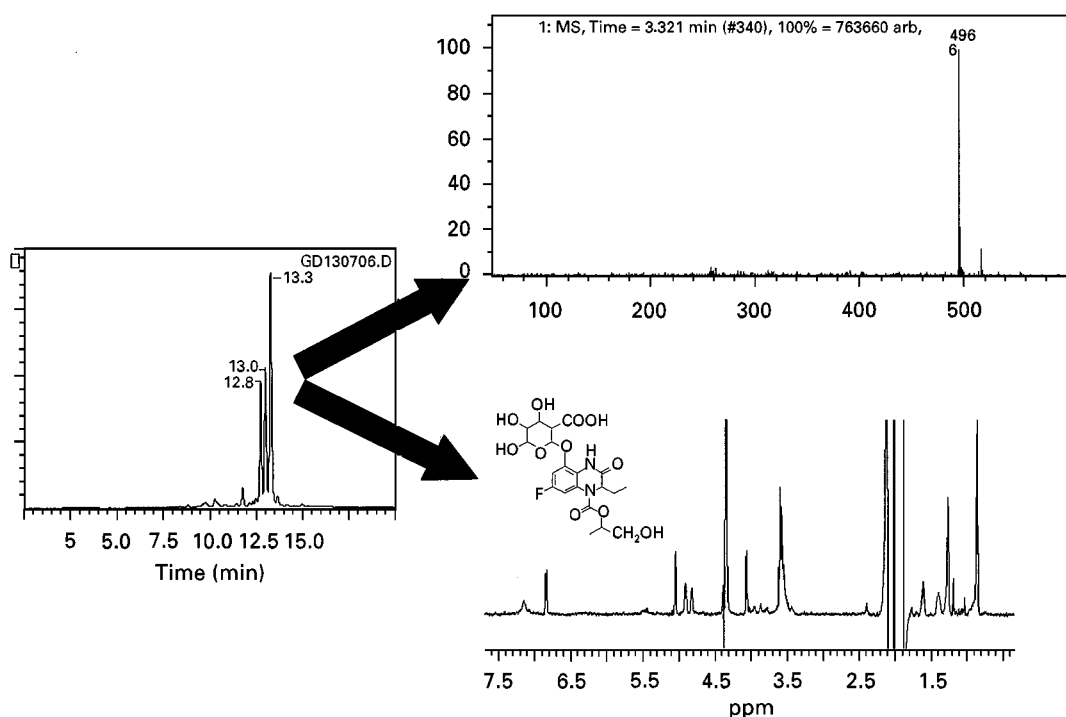


Figure 7 Chromatogram, mass spectrum and ¹H NMR spectrum acquired following the injection of a human urine fraction onto the LC/NMR/MSⁿ system illustrated in Figure 6. The peak at 13.3 min was trapped in the NMR flow probe, and a ¹H NMR spectrum acquired over 256 scans. The peak was then pumped into the ion trap through the electrospray source and the subsequent mass spectrum acquired in positive ion mode using deuterated solvents. Chromatography was performed on a 250 × 3.2 mm Phenomenex Magellen C18 column, eluted with a 0–80% aqueous 0.1% formic acid/acetonitrile gradient, over 35 min.

Additionally the combination of LC/NMR/MS allows an impure fraction to become further purified through the use of an analytical chromatographic system step following the initial semipreparative isolation. An example of the use of LC/NMR/MS for the identification of a novel human urine metabolite of GW420867 is given below.

For the application of LC/NMR/MS the instruments are configured in series as shown in Figure 6. This arrangement allows easy operation of peak storage followed by transfer to the NMR spectrometer and stop flow analysis, and it avoids difficulties with synchronization of the NMR and MS data capture; NMR data acquisition occurs first.

Following acquisition of the ¹H-NMR spectrum, the metabolite was transferred from the NMR probe to the ion trap mass spectrometer, where MS and MSⁿ spectra were obtained. The system was operated in one of two ways; in one approach, the flow from the NMR probe was split directly into the electrospray interface. In this mode, the presence of deuterium oxide in the mobile phase produced MD⁺ ions in which all labile hydrogens had been exchanged with deuterium. In the second mode, an aqueous make up flow was employed to effect

deuterium ‘back exchange’, resulting in undeuterated MH⁺ ions.

An UV chromatogram acquired from an on-line LC/NMR/MSⁿ analytical run from a human urine fraction is shown in Figure 7 and indicates the presence of three main peaks. The ¹H NMR spectrum and the resulting MS spectrum acquired for peak III, eluting at 13.3 min is also shown in Figure 7. Inspection of the ¹H NMR spectrum indicates that aromatic substitution has occurred in the position meta to the fluorine-bearing carbon, resulting in the loss of an aromatic proton. The remaining 2 aromatic protons at 6.84 ppm (doublet of doublets, *J* = 10.6 Hz and 1.47 Hz) and 7.15 ppm (broad due to restricted rotation at the amide bond) are consistent with substitution in the 5-hydroxy position.

The presence of glucuronic acid anomeric H1 proton at 5.04 ppm suggests the presence of a glucuronide. Calculation of the signal integrals in the aliphatic region at 1.26 ppm indicated the loss of one of the isopropyl methyl groups. Hydroxylation at the isopropyl group would generate a CH₂OH group whose protons will be evident in the NMR spectrum in the region of 3.5 ppm. Although these signals could not be clearly observed, as the signals from the H2–H4 of

the glucuronic acid were obscuring this region, the sum total of integral values of all the protons in this region indicated the presence of five protons. This was in support of the hypothesis of hydroxylation at the isopropyl methyl.

The MS spectrum shown in Figure 7 was acquired by directly coupling the LC/NMR probe outlet to the MS. As NMR spectra are acquired in a mixture of D₂O/ACN the resulting ion at m/z 496 from this directly coupled arrangement is in a deuterated form (MD^+). In order to simplify matters an MS spectrum of the same peak was acquired, using the 'back exchange' configuration, which allows all the deuterium atoms to be exchanged with hydrogens. This is given in Figure 8. In this spectrum the MH^+ ion can be observed at m/z 489, which indicates that there are six exchangeable hydrogens on the original metabolite. Subsequent MS^4 experiments on m/z 489 were conducted as the peak eluted into the ion trap and these MS/MS spectra are also given in Figure 8. MS^n spectra enhance the interpretation of the original MS/MS spectrum and can be used to assist the elu-

cination of the structure and fragmentation pathway, as shown in the case of this novel human urinary metabolite. In this example, comparison of the product ions at m/z 183 and 255 to their equivalents formed from parent drug (m/z 167 and 239 respectively, data not shown), indicates aromatic hydroxylation the position of which was confirmed by the 1H NMR spectrum. Loss of the isopropyl group to generate m/z 255 from m/z 313 suggested that the site of secondary hydroxylation was the isopropyl group, and this is supported by the NMR data. The use of an ion trap mass spectrometer providing molecular weight and structural fragmentation information, from MS and MS^n experiments respectively, when combined with NMR provides an extremely powerful structure elucidation tool.

Conclusions

The importance of combining data from different analytical techniques has been demonstrated. NMR and MS^n have been coupled with preparative and

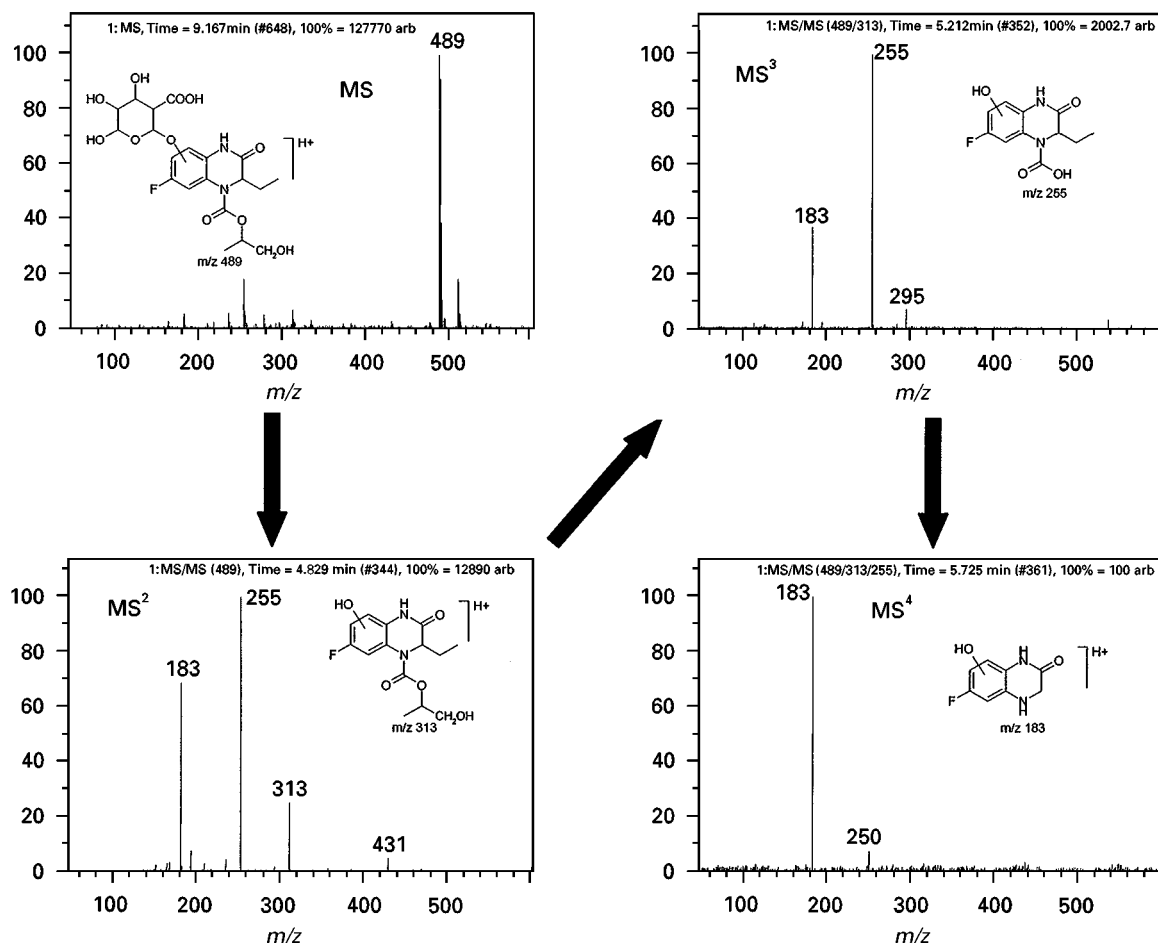


Figure 8 MS and MS^n spectra acquired following the injection of human urine fraction onto the LC/NMR/ MS^n system operating in 'back-exchange' mode. Fragmentation was induced using a resonant excitation amplitude of 1.2 V, following mass isolation.

analytical HPLC to allow rapid and effective identification of metabolites in urine, following the oral administration of GW420867. The combination of these techniques enables structural and molecular weight information to be interpreted with greater efficiency and accuracy.

Future Prospects

The advantages of capillary HPLC and nanospray MS, both 'miniaturized' versions of their predecessors, HPLC and electrospray, are well documented and there is also a move towards miniaturization in most other modern analytical techniques. The enhanced sensitivity obtained by capillary LC using a capillary UV flow cell may be extended to NMR, with the development of capillary NMR flow cells. The higher efficiency separations and reduced band broadening that result from capillary LC has the effect of producing a more concentrated sample eluting from the column and therefore a higher sample concentration into the NMR flow cell. This potentially leads to a better signal to noise ratio at lower analyte concentrations in the acquisition of NMR data. A further advantage of capillary LC is the reduced solvent consumption associated with this

technique, which can lead to particularly significant cost-savings when dealing with the expensive deuterated solvents used in NMR spectroscopy. Residual protonated solvent suppression in the NMR spectrum then becomes an easier task.

Capillary LC and capillary electrochromatography (CEC) coupled to mass spectrometry are already in widespread use within the pharmaceutical industry and therefore the connection of capillary LC or CEC to both NMR and MS would be a natural progression.

See also: II/Chromatography: Liquid: Detectors: Mass Spectrometry; Large-Scale Liquid Chromatography; Nuclear Magnetic Resonance Detectors.

Further Reading

- Chervet JP, Ursen M and Salzmann JP (1996) *Anal. Chem.* 68: 1507.
 Olson DL, Lacey ME and Sweedler JV (1998) *Anal. Chemistry News and Features*, April.
 Vanhoutte K, Van Dongen W and Esmans L (1998) *Rapid Commun. Mass Spectrom.*, 12: 15.
 Vanhoutte K, Van Dongen W, Hoes I *et al.* (1997) *Anal. Chem.* 69: 3161.

DRUGS OF ABUSE: SOLID-PHASE EXTRACTION



F. Musshoff, Institute of Legal Medicine, Bonn, Germany

Copyright © 2000 Academic Press

Introduction

In toxicological analysis, two basic approaches can be distinguished: first, a directed search, geared to a limited number of substances, such as in workplace testing or the analysis of alcohol or special drugs in traffic offences; and second, an undirected search, also called systematic toxicological analysis (STA). STA can be defined as an undirected search for potentially harmful substances whose presence are uncertain and whose identities are unknown. STA is required if little or no information is available in so-called general unknown cases. However, if one toxicant is known, the analyst is required to establish whether other compounds of toxicological relevance are present.

The drug screening process can generally be divided into two stages, sample preparation and analysis of the drugs. Some forms of sample work-up – isolation and concentration – are required for most analytical techniques, such as thin-layer chromatography (TLC), high performance liquid chromatography (HPLC) and gas chromatography (GC) coupled to various detector systems. The samples available for analysis are complex biological matrices, in which toxicologically relevant substances are present in trace amounts compared to the endogenous compounds present. Therefore, work-up procedures should retain all relevant substances, at the same time removing all irrelevant substances and interferences.

Liquid-liquid extraction (LLE), often combined with sample pretreatment procedures such as conjugate hydrolysis, digestion or protein removal, was the standard method in the past. Although LLE proved to be suitable in a great number of cases, there are many disadvantages of this technique, e.g. matrix interferences, emulsion formation or the use of large

Table 1 Various solid-phase extraction adsorption phases and solvents

Solubility of the sample	Water-soluble					Water-insoluble		
	Nonionic Aqueous			Ionic Aqueous		Aqueous	Organic	Organic
Solvent								
Polarity of the sample	Nonpolar	Middle polar	Polar	Cationic	Anionic	Nonpolar	Middle polar	Polar
Recommendable adsorption phase	C ₁₈ ec C ₁₈ C ₈ C ₄ C ₂ Phenyl CN	SiOH NH ₂	CN OH PA DMA NH ₂	SA	SB NH ₂ DMA	C ₁₈ ec C ₁₈ C ₈ C ₄ C ₂ Phenyl CN	SiOH NH ₂	CN OH PA DMA NH ₂
Selection of recommendable elution solvents	Hexane CH ₂ Cl ₂ Acetonitrile Alcohols	CHCl ₃ CH ₂ Cl ₂ Ethyl acetate Alcohols Water	CHCl ₃ CH ₂ Cl ₂ Ethyl acetate Alcohols Water	Acids Salt solutions Buffers	Bases Salt solutions Buffers	Hexane CH ₂ Cl ₂ Acetonitrile Alcohols	CHCl ₃ CH ₂ Cl ₂ Ethyl acetate Alcohols	CHCl ₃ CH ₂ Cl ₂ Ethyl acetate Alcohols

volumes of organic solvents. In recent years, sample preparation by solid-phase extraction (SPE) has received widespread interest and today many types of SPE materials are commercially available (Table 1). Most publications have been geared towards the isolation of one compound or a limited number of substances, i.e. directed analysis. However, in STA (undirected analysis), a compromise between acceptable recovery of many substances and adequate removal of matrix compounds should be reached. In order to develop a SPE method, each step of the procedure should be evaluated very carefully, including the selection of a suitable sorbent, the pH of the sample and the extraction system, the clean-up step, the properties and the volume of the eluent, the flow rate of the sample and the eluent passed through column.

Pretreatment of Biological Fluids and Tissues

The main purposes of sample pretreatment are first, release of drugs from the biological matrix; second, removal of proteins and other compounds which could interfere with further analysis; and third, adjustment of the pH, ionic strength and concentration of the sample to allow optimum extraction.

For the analysis of plasma/serum samples, buffer solutions are widely used for dilution. Protein precipitation is a common method to obtain deproteinized samples. Proteins can be precipitated by organic solvents, inorganic salts, metallic ions or acids (Table 2). However, it must be emphasized that co-precipitation often results in losses of the relevant drugs. Urine

Table 2 Relative efficiencies of various protein precipitants towards removing proteins

Precipitant	pH of supernatant	Volume of precipitant (mL) to precipitate > 98% protein in 0.5 mL plasma
Trichloroacetic acid, 10% (w/v)	1.4–2.0	0.2
Perchloric acid, 6% (w/v)	< 1.5	0.4
Tungstic acid	2.2–3.9	0.6
Metaphosphoric acid, 5%	1.6–2.7	0.6
Copper sulfate–sodium tungstate	5.7–7.3	1.5
Zinc sulfate–sodium hydroxide	6.5–7.5	2.0
Zinc sulfate–barium hydroxide	6.6–8.3	2.0
Ammonium sulfate (saturated)	7.0–7.7	2.0
Acetonitrile	8.5–9.5	1.5
Acetone	9.0–10.0	1.5
Ethanol	9.0–10.0	2.0
Methanol	8.5–9.5	2.0

Reprinted from Blanchard J (1981) Evaluation of the relative efficacy of various techniques for deproteinizing plasma samples prior to high-performance liquid chromatographic analysis. *Journal of Chromatography* 226: 455, with permission from Elsevier Science.

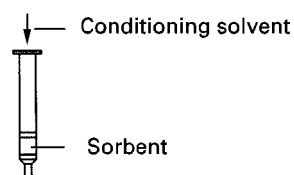
samples can usually be diluted like plasma/serum samples. However, since many relevant substances or metabolites will be excreted in a conjugated form, a deconjugation step prior to SPE is recommended. Because of the highly variable salt content, the urine samples should be diluted with at least an equal volume of water or buffer before applying the sample on to the SPE column. This is particularly important when ion exchange is the preferred extraction mode; otherwise counterions may compete with the relevant drugs during sample application and result in losses of the latter. Sonication combined with buffer dilution is a useful technique for the pretreatment of whole blood samples. For pretreating tissue samples, homogenization followed by enzyme digestion (i.e. papain, subtilisin-A, neutrase, collagenase or trypsin) and/or protein precipitation and centrifugation of samples such as liver, kidney or intestine prior to application on to SPE cartridges are useful. Brain tissue with a high content of lipids can be used after incubation with lipase prior to extraction. High flow SPE columns are available for use with more viscous fluids.

As in LLE, pH is an important factor in SPE. The optimal pH values of the sample and the extraction system depend on the properties of the relevant drugs and the sorbent and the interaction between the drugs and the functional groups of the sorbent. When a nonpolar sorbent, for example, octadecyl-bonded silica (C_{18}), is used, the main interactions are van der Waals forces/hydrogen bonding. Therefore, the pH of both sample and the column should be adjusted to a value so that the relevant drugs are in their uncharged forms. With ion exchange as the underlying principle, the pH of the sample must be adjusted to such a value that most of the drugs are charged, so that they can be retained on the column by the opposite charge of the functional groups of the sorbent. Additionally, total ionic strength of the sample is important in ion exchange SPE. A low ionic strength, often obtained by diluting the sample with water or a low ionic strength buffer solution ($< 0.1 \text{ mol L}^{-1}$) is preferred, because any species that can act as counterions reduces the retention of ionic drugs.

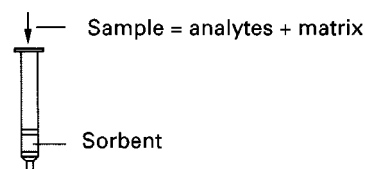
The Principles of Solid-phase Extraction

SPE is a physical extraction process that involves a solid phase and a liquid phase. It is based on the principle of liquid chromatography, but with different purposes. The aims of SPE are to isolate the relevant compounds from a sample matrix and to concentrate them, while those of liquid chromatogra-

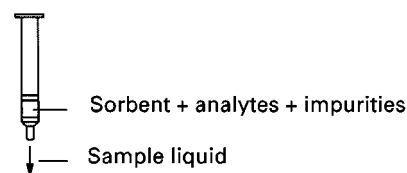
1. Condition column with appropriate solvent



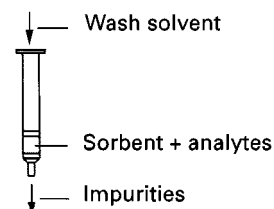
2. Apply sample on to column



3. Aspirate/force sample through column



4. Remove impurities with wash solvent



5. Elute analytes with elution solvent

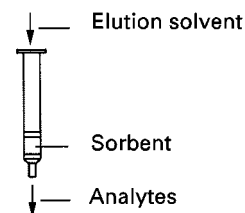


Figure 1 Solid-phase extraction process.

phy are to separate each compound with a good peak shape and with relatively short retention times. Today, various sorbent materials are commercially available. **Figure 1** illustrates the steps of SPE. The column is first conditioned with an appropriate solvent to solvate the functional groups of the sorbent. After the solvent is further conditioned with the sample matrix buffer, the pretreated sample is forced

through the sorbent by aspiration or positive pressure. The column containing retained analytes is subsequently washed with an appropriate solvent that selectively elutes the impurities but leaves the analytes on the column. The purified analytes are finally eluted with a solvent strong enough to displace the analytes from the sorbent.

Basic Types of Solid Phases

Diatomaceous Earth (Extrelut®, Chemelut®)

The principle of SPE using diatomaceous earth is closely related to conventional LLE. The aqueous phase is absorbed on to the diatomaceous earth, a porous material which acts as support for the aqueous phase. This provides a large surface area for partition into an elution solvent, which flows through the immobilized specimen on the column under gravity. The elution is a continuous process and may give superior recoveries in a shorter time compared to LLE. Other advantages are the elimination of centrifugation, aspiration and filtration steps and the prevention of emulsion formation. However, relatively large volumes of organic solvents are still required. For screening purposes this type of SPE must be carried out with at least two columns: one for acidic and neutral substances and one for basic and neutral compounds. A typical procedure with this type of material is as follows: the biological sample is diluted with an appropriate buffer and poured on to the column. The bed mass of the column and the sample volume must be in agreement with each other. After a 10–15 min equilibration period, twice the volume of the diluted aqueous sample is used for elution from an organic solvent, which is waterimmiscible.

Styrene-divinylbenzene Resin (SDB)

Polystyrene-divinylbenzene copolymer (e.g. XAD-2) is a hydrophobic resin that can absorb many water-soluble organic compounds, principally by van der Waals forces and additionally by hydrophobic bonding and dipole–dipole interactions. For binding to the resin the substances must be in a hydrophobic state. Therefore, usually two columns are needed: one for acidic and neutral substances and one for basic and neutral compounds. Generally the extracts are clean enough to allow GC or TLC determinations at therapeutic and toxic concentrations. SDB resin is especially interesting for analysing urine samples since glucuronide and sulfate conjugates can be isolated. However, the extraction yields of drugs isolated from different biological samples may vary considerably. The resin has to be

cleaned very carefully, otherwise interfering substances originating from the resin will appear in the extracts. SDB extractions in columns have now been largely replaced by SPE using silica-based columns. Recently, new SDB-based SPE columns (e.g. Bond Elut ENV, Varian) have become available, with which the drawbacks may be overcome. A typical procedure with this type of material is as follows: the biological sample is diluted and the pH is adjusted to the desired value. The resin is washed with four column volumes of acetone, three column volumes of methanol and three times with three column volumes of distilled water. The diluted sample is passed through the column where the analytes are absorbed. After the resin is washed with water, the analytes are eluted with an organic solvent (e.g. methanol, ethyl acetate, methanol–chloroform, acetone–diethyl ether, etc.).

Octadecyl-bonded Silica

Octadecyl-bonded silica absorption phases (e.g. C₁₈-end-capped) are often used for the directed search to a limited number of substances, such as in testing for special drugs of abuse in traffic incidents. The nonpolar phase retains, at a suitable pH, substances by hydrophobic interactions with the alkyl chains. For example, the simultaneous analysis of tetrahydrocannabinol (THC) and its metabolites, 11-hydroxy-THC (11-OH-THC) and 11-nor- Δ^9 -THC carboxylic acid (THC-COOH) in serum samples is possible as follows: the biological sample is diluted with 0.01 mol L⁻¹ acetic acid and the pH is adjusted to 4. An organic solvent (methanol) is used to solvate the bonded functional groups and to remove organic residues from the sorbent. Buffer is added afterwards to exchange the organic solvent with an aqueous solution. The diluted sample is passed through the column where analytes absorb. After the column is washed with water followed by a solution of 40% acetonitrile in water, the analytes are eluted with acetonitrile (Figure 2).

Mixed-mode Bonded Silica

The most widely used SPE materials are bonded silica gels, in which end silanol groups have been derivatized with organic moieties consisting of alkyl chains with and without a variety of functional groups, such as –OH, –C₆H₅, –NH₂, –CN, –SO₃H and –COOH. Based on the modes of the interaction mechanisms between the functional groups of the SPE materials and the relevant compounds, the extraction can be divided into three types: nonpolar, polar and ion exchange. However, there is no bonded silica SPE column which only contains one type of functional

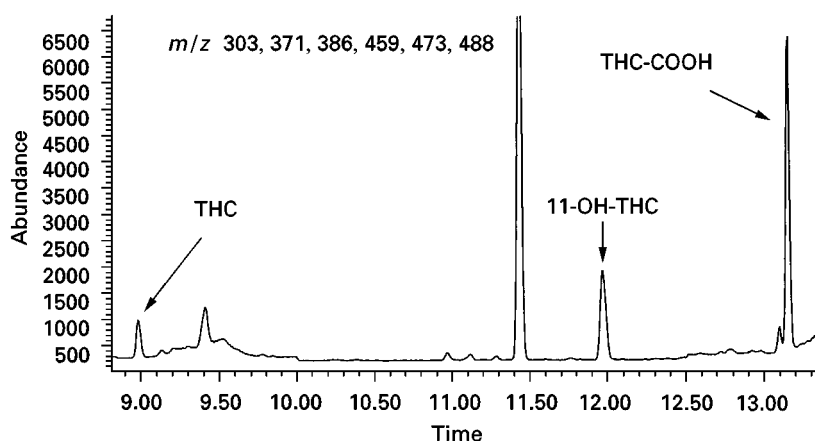


Figure 2 GC-MS chromatogram recorded in the selected ion monitoring (SIM) mode. The serum sample was worked up using a C_{18} -end-capped extraction column and after derivatization of the dried extract using MSTFA after cannabinoids had been determined: THC (5.2 ng mL^{-1}), 11-hydroxy-THC (4.5 ng mL^{-1}) and THC-COOH (105.6 ng mL^{-1}).

group. Multiple modes of interactions will happen during the extraction process and the influence of secondary interactions should be kept in mind. Additionally, in so-called mixed-mode silica-bonded SPE columns, the silanol groups are partially derivatized with medium length alkyl chains and partially with cation exchange substituents, which can exert at least two types of interactions. Screening procedures using this type of SPE material have been of increasing interest and SPE columns with mixed-mode phases are available from a number of manufacturers, e.g. Bond Elut Certify (Varian Sample Preparation Products), Clean Screen DAU (Worldwide Monitoring Corp.), Isolute HCX (International Sorbent Technology) and TSC (Merck). Mixed-mode bonded silica can retain, at a suitable pH, acidic and neutral substances by hydrophobic interactions with the alkyl chains and the basic substances by interactions with the cation exchange groups. Differential elution can take place by a suitable adjustment of the pH and the choice of solvents.

A typical extraction procedure is described here in more detail.

Sample pretreatment Dilution with a 0.1 mol L^{-1} phosphate buffer at pH 6.0 is most widely used. At this pH the weakly basic, the neutral and the weakly acidic compounds, such as barbiturates, are in the nonionized form and retained by the octadecyl substituent of the sorbent. However, strongly acidic compounds like many nonsteroidal anti-inflammatory drugs are deprotonated, ionized and therefore not retained. When blood samples are brought to lower pH values coagulation of proteins occurs, resulting in difficulties in the sample applica-

tion step. When a serum or plasma sample is added to 0.1 mol L^{-1} phosphoric acid, this coagulation can be avoided.

Column preconditioning The dried sorbents in SPE columns are not in a state to interact with analytes and appropriate conditioning is required prior to sample application. For nonpolar and multiple-interaction phases (mixed-mode), the sorbent must be preconditioned with suitable solvents, for example methanol, followed by water or a buffer wash. The organic solvent used is to solvate the bonded functional groups and to remove organic residues from the sorbent. Water or buffer, of which the pH, ionic strength and polarity have been adjusted, is added afterwards to remove the organic solvent with an aqueous solution to prepare the SPE column to receive an aqueous sample. For a polar phase, for example aminopropylsiloxane-bonded silica, the column needs to be treated with a nonpolar solvent, such as hexane, to activate the surface.

Sample application After column preconditioning, the pretreated sample is transferred onto the SPE column and is drawn through it by applying a light vacuum. Normally the flow rate of sample passing through the SPE cartridge should be kept to $1\text{--}2 \text{ mL min}^{-1}$.

Column wash and pH adjustment Usually the column is washed with $1\text{--}2 \text{ mL}$ deionized water or an appropriate solvent (20% methanol in water) selectively to remove the impurities which may interfere with the analysis. To find a wash solvent which is

able to clean the column effectively without losses of the drugs, the analyst must compromise between acceptable recoveries of a great number of different substances and adequate removal of matrix compounds. In many cases, pH adjustment is introduced into this stage to bring the pH of the column to a given value for selective, pH-dependent elution of the drugs. In order to get a reproducible differential elution using mixed-mode bonded silica, the pH of the column has to be adjusted to about pH 3. At higher pH values a large number of basic compounds will elute in the first fraction (acidic and neutral substances). Lower pH values can cause deterioration of the extraction column. To adjust pH, 0.5–1.0 mL diluted acetic acid is sufficient.

Column drying Drying of the columns is necessary when no water is allowed in the analysing step (GC). Drying is carried out by applying vacuum to the column for about 5 min or centrifugation of the column. Further drying can be carried out by applying a small volume of methanol (50 μ L) or a larger volume of hexane (1 mL) followed by vacuum. A dry column is easily obtained, but there is a risk of partially eluting hydrophobic substances such as benzodiazepines in this wash process.

Elution of relevant drugs For drug elution, the eluent should be strong enough so that the drugs can be eluted completely with a reasonably small eluent vol-

ume. Furthermore, the eluent should be selective, so that interfering compounds will not be eluted together with the relevant drugs. Theoretically, eluent selection may be achieved by considering the polarity index (P'), the solvent selectivity and the eluotropic strength (ε^0) of the solution solvents. The strength of a solvent is its ability preferentially to dissolve compounds according to polarity, while the selectivity is its ability selectively to dissolve one compound as opposed to another. Solvents have been classified into eight selectivity groups according to their proton donor, proton acceptor and dipole interaction characteristics. Figure 3 represents the properties of various solvent groups with different selectivities. For example, solvents in group I are strong proton acceptors/weak donors with intermediate dipole moments and solvents in group VIII are relatively strong donors/weak proton acceptors with virtually no dipole interactions.

The P' values and the selectivities of common solvents used in SPE are listed in Table 3. The desired P' value can be obtained by using a binary mixture and can be calculated by the following equation:

$$P' = \phi_a P_a + \phi_b P_b \quad [1]$$

where ϕ_a and ϕ_b are the volume fractions of solvents A and B in the mixture; P_a and P_b are the P' values of the pure solvents A and B. In practice, both P' and selectivity of the solvents should be considered when selecting the best eluent system to elute drugs but not the impurities. Data shown in Table 3 indicate that the P' values of 2-propanol, chloroform and ethyl acetate are very similar, yet they belong to different selectivity groups.

The eluotropic strength ε^0 , which defines solvent strength quantitatively for a given adsorbent, is another helpful parameter for choosing a suitable eluent. The eluotropic strength is the adsorption energy per unit area of the solvent and Table 3 lists the ε^0 values of some common solvents and binary mixtures. This knowledge can be helpful in the development of a new SPE method. If a certain eluent system gives high recoveries of test drugs but also elutes many impurities, the use of another eluent mixture with a similar ε^0 value could be helpful.

The volume of a selected eluent is another important factor in the development of an extraction procedure. Generally, the volume of the eluent should be as small as possible. Increasing volumes will prolong the extraction period, may elute more impurities and may lose more volatile drugs (such as amphetamines) when an evaporation step is required after column extraction. The flow rate of the eluent passing through the column should allow adequate interac-

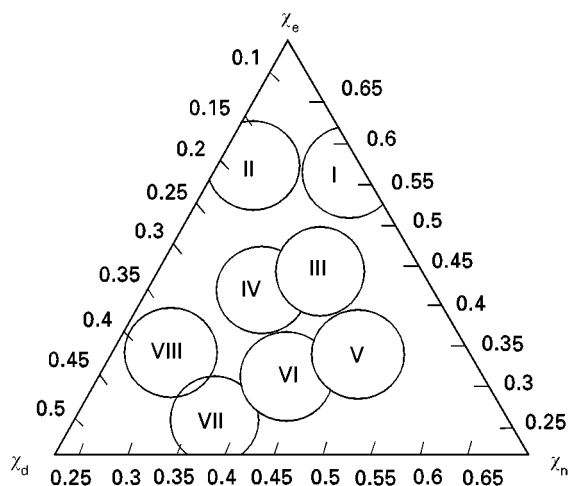


Figure 3 Classification of solvent selectivities (the Roman numbers represent various groups of solvent selectivities). χ_e , χ_d and χ_n represent the fraction of P' contributed by interactions associated with ethanol (acceptor), dioxane (donor) and nitromethane (polar). Modified with permission from Snyder LR (1974) *Journal of Chromatography* 92: 223.

Table 3 Solvent eluotropic strength on silica (ϵ^0), polarity indices (P') (measure of solvent's ability to interact as proton donor, proton acceptor or dipole) and selectivities of some common solvents

<i>Solvent</i>	<i>Eluotropic strength (ϵ^0)</i>	<i>Polarity (P')</i>	<i>Selectivity group</i>
Water	> 0.73	10.20	VIII
Acetic acid	> 0.73	6.20	IV
Methanol	> 0.73	6.60	II
Methanol–acetonitrile (40 : 60)	0.67		
Methanol–diethyl ether (20 : 80)	0.65		
2-Propanol	0.63	4.30	II
Methanol–methylene chloride (20 : 80)	0.63		
Pyridine	0.55	5.30	III
Isobutyl alcohol	0.54	3.00	
Acetonitrile	0.50	6.20	VI
Diethyl ether–acetonitrile (80 : 20)	0.45		
Ethyl acetate	0.45	4.30	VI
Acetone	0.43	5.40	VI
Methyl ethyl ketone	0.39	4.50	VI
Tetrahydrofuran	0.35	4.20	III
Methylene chloride	0.32	3.40	V
Chloroform	0.31	4.40	VIII
Diethyl ether	0.29	2.90	I
Benzene	0.27	3.00	VI
Toluene	0.22	2.40	VI
Pentane–diethyl ether (80 : 20)	0.20		
Cyclohexane	0.03	0.00	
Pentane	0.00	0.00	
<i>n</i> -Hexane	0.00	0.06	
<i>n</i> -Heptane	0.00	0.20	

tion. When ion exchange is the main interaction, the flow rate should be $<2 \text{ mL min}^{-1}$ since ion exchange interactions occur at a slower rate than polar and nonpolar interactions.

Using mixed-mode bonded silica extraction columns in the first fraction, fraction *A*, the analytes retained by the hydrophobic groups of the sorbent are eluted using a moderately polar solvent like dichloromethane or combinations, e.g. acetone–chloroform (1 : 1), hexane–diethyl ether (40 : 60), hexane–ethyl acetate (75 : 25). To avoid dirty extracts in the second fraction, fraction *B* (basic compounds), an in-between polar washing step, for instance with methanol, may be needed.

The basic substances retained by the cation exchange groups of the sorbent in their protonated form are eluted by an organic solvent mixture, usually with 2% ammonia. Ammoniated ethyl acetate or ammoniated dichloromethane–2-propanol (80 : 20) for the elution of more polar substances is widely used. Table 4 gives an overview of extraction methods using mixed-mode SPE phases for drug screening. Amphetamines and other relatively volatile substances often show lower recoveries, probably caused by evaporation in the final step of the SPE procedure. Polar drugs like acids and acetaminophenes are scarcely retained under the condition used and

may be washed away. Therefore, an additional LLE on the sample coming from the column and column wash could be introduced in a general screening procedure.

Conclusions and Further Developments

The use of SPE for the toxicological analysis of drugs of abuse in biological samples has increased rapidly. Due to the different properties of the drugs of interest, mixed-mode SPE columns are better suited for screening purposes than single-mode columns. However, although the same type of SPE material can be obtained from different manufacturers, the results using different materials, and even results obtained from different batches from the same manufacturer, may show significant differences in behaviour, i.e. in particle size distribution and flow velocities. Today, chemically modified silica and SDB sorbents are also available in extraction discs. These materials are very promising, since samples can be processed faster using smaller volumes of organic solvents while still allowing relatively large sample volumes. Furthermore, extractions can be performed outside working hours by automation of manual SPE methods with the addi-

Table 4 Overview of mixed-mode SPE methods for drug screening

Sample type	SPE column type	Sample volume	Drug conc. ($\mu\text{g mL}^{-1}$ or $\mu\text{g g}^{-1}$)	Elution method (fraction A and fraction B)	Detection yield (%)	Extraction (%)	Relative standard deviation
Urine (U)	CS DAU	A: 4 mL U	0.5–2	A: 10 mL DCM	TLC		
Plasma (P)		B: 5 mL U		B: DCM–2PrOH–25% NH_3 (147 : 49 : 4)	GC-MS	61–88 ^a	< 9
	BEC	2 mL U/P	10	A: 4 mL Clf–Ac (1 : 1)	GC-FID	97–104	< 6
	BEC	1 mL U	0.05	B: 2 mL EtAc–33% NH_3 (98 : 2)	GC-MS		
				A: 1 mL Hex–ETAC (8 : 2)			
				B: 2 mL DCM–2PrOH–25% NH_3 (80 : 20 : 2)			
	1: BEC	5 mL U	0.4–1	A: 3 mL Hex–EtAc (75 : 25)	GC-MS	1: 60–88 ^b	1: < 10
	2: Isolute			B: 3 mL EtAc–28% NH_3 (98 : 2)		2: 48–88 ^b	2: < 8
	BEC	1 mL U/P	0.1–0.2	A: 4 mL Clf–Ac (1 : 1)	GC-NPD	U: 82–105	U: < 8
				B: 2 mL EtAc–33% NH_3 (98 : 2)		P: 77–103	P: < 7
Whole blood	BEC	1 mL	0.05–5	A: 4 mL DCM	GC-FID	25–104 ^c	< 14
				B: 4 mL EtAc–25% NH_3 (98 : 2)			
	BEC	1 mL	2	A: 4 mL Clf–Ac (1 : 1)	GC-FID	81–103	< 8
				B: 2 mL EtAc–33% NH_3 (98 : 2)			
	BEC	1 mL	0.2–4	A: 2 mL 60% acetone ^d	GC-NPD	50–100	< 8
				B: 2 mL DCM–2PrOH–25% NH_3 (80 : 20 : 2)			
	1: BEC	1 mL	1	A: 3 mL Hex–EtAc (1 : 1)	GC-NPD	1: 73–112	1: 9.7 ^e
	2: CS DAU			B: 3 mL DCM–2PrOH–28% NH_3 (78 : 20 : 2)		2: 59–115	2: 7.8
	BEC	1 mL	0.5	A: 4 mL Clf–Ac (1 : 1)	GC-MS ^f		
				B: 2 mL EtAc–25% NH_3 (98 : 2)			
				C: 2 mL DCM–2PrOH–25% NH_3 (80 : 20 : 2)			
	BEC	1 mL	0.05–0.5	A: 2 mL Clf–Ac (1 : 1)	GC-NPD	58–107 ^d	< 11
				B: 3 mL EtAc–33% NH_3 (98 : 2)	GC-MS ^f	26–117	< 16
Tissue	XTRACT	1.25 g		A: 2 mL DCM; 2 mL Hex–Eth (4 : 6)	GC-MS		
				B: 4 mL DCM–2PrOH–25% NH_3 (80 : 20 : 2); 4 mL EtAc			
	BEC	0.1 g	20	4 mL Clf–Ac (1 : 1)	GC-NPD	45–101	< 9
				B: 2 mL EtAc, 33% NH_3 (98 : 2)	GC-FID		

SPE column materials: CS DAU: Clean screen DAU, Worldwide Monitoring, Horsham, PA.

BEC: Bond Elut Certify, Varian Sample Preparation Products, Harbor City, CA.

Isolute: Isolute HXC, International Sorbent Technology, Hengoed Mid Glamorgan, UK.

XTRACT: Worldwide Monitoring, Horsham, PA.

Abbreviations AC, acetone; Clf, chloroform; DCM, dichloromethane; EtAc, ethyl acetate; Eth, diethyl ether; Hex, hexane; NH_3 , concentrated ammonia; 2PrOH, 2-propyl alcohol.

^aOne SPE column is used for acidic and neutral drugs and one for basic drugs.

^bLow recoveries for barbital and ephedrine.

^cMorphine and amphetamine are hardly recovered.

^dBasic fractions of SPE were cleaned up by liquid–liquid extraction with butyl acetate; recovery of paracetamol is low.

^eMean values.

^fTMS derivatization.

^gExtraction yields at a spiked concentration of respectively 0.1 and 0.25 $\mu\text{g mL}^{-1}$.

Reproduced from Franke and de Zeeuw (1998) with permission.

tional intention of improving the reproducibility, offering high throughput, and reducing labour costs. Various automated SPE systems are commercially available.

See also: II/Extraction: Solid-Phase Extractions. III/Solid-Phase Extraction with Cartridges. Sorbent Selection for Solid-Phase Extraction.

Further Reading

Chen XH, Franke JP and de Zeeuw RA (1992) Solid-phase extraction for systematic toxicological analysis. *Forensic Science Review* 4: 147.

Chen XH, Wijsbeek J, Franke JP and de Zeeuw RA (1992) A single-column procedure on Bond Elut Certify for systematic toxicological analysis of drugs in plasma and urine. *Journal of Forensic Sciences* 37: 61.

Ferrara SD, Tedeschi L, Frison G and Castagna F (1992) Solid-phase extraction and HPLC-UV confirmation of drugs of abuse in urine. *Journal of Analytical Toxicology* 16: 217.

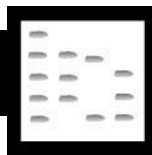
Franke JP and de Zeeuw RA (1998) Solid-phase extraction procedures in systematic toxicological analysis (review). *Journal of Chromatography* 713: 51.

Scheurer J and Moore CM (1992) Solid-phase extraction of drugs from biological tissues – a review. *Journal of Analytical Toxicology* 16: 264.

Van Horne KC (1985) *Sorbent Extraction Technology*. Harbor City, CA: Analytichem International.

Zief M and Kiser R (1988) *Solid Phase Extraction for Sample Preparation*. Phillipsburg, NJ: JT Baker.

DYES



High-Speed Countercurrent Chromatography

A. Weisz, Food and Drug Administration, Washington DC, USA

Y. Ito, National Institutes of Health, Bethesda, MD, USA

Copyright © 2000 Academic Press

Countercurrent chromatography is one of the liquid-liquid partition chromatographic techniques that do not use a solid support. High-speed countercurrent chromatography (HSCCC) uses centrifugal force to retain one of the liquid phases in an lto multilayered coil column while the second liquid phase is pumped through the column. The principles of this technique have been discussed by Ito.

HSCCC in its two forms, conventional and pH-zone-refining CCC, is relatively new among the preparative techniques used for the separation of dyes. Conventional HSCCC has been applied to this purpose since the mid-1980s when Fales *et al.* separated various components present in a sample of the triphenylmethane biological stain, Methyl Violet 2B, and when Freeman and co-workers purified azo textile and ink dyes (i.e. acid, direct and disperse azo-dyes). This technique was subsequently used for the separation and purification of components from other colours, such as D&C Red No. 28 (Phloxine B, CI 45410), Sulforhodamine B (CI 45100) and Gardenia Yellow. It was also effectively implemented as a complement to preparative high performance liquid chromatography (HPLC) for the separation of a complex synthetic mixture of brominated tetrachlorofluorescein dyes. Conventional HSCCC was applied to the separation of quantities of dyes of up to several hundred milligrams when the common 1.6 mm i.d./325 mL volume column was used. By contrast, the more recently developed (1993) pH-zone-refining

CCC was applied from the outset to the separation of multi-gram quantities of dye mixtures such as xanthene and fluoran dyes used as colour additives in food, drugs or cosmetics and as biological stains.

Using a modified procedure, the applications of this technique have been extended to the separation of gram quantities of the highly polar mono-, di- and trisulfonated components of D&C Yellow No. 10 and Yellow No. 203 (both Quinoline Yellow, CI 47005) and of other sulfonated dyes such as FD&C Yellow No. 6 (Sunset Yellow, CI 15985) and D&C Green No. 8 (Pyranine Concentrated, CI 59040). A general approach to the separation of dyes by HSCCC is presented in Figure 1.

Instrumentation

For the separation of dyes, both by conventional and pH-zone-refining CCC, commercially available high speed CCC centrifuges are used. Such instruments are described in the HSCCC entry in this volume. The separations described below were performed with HSCCC systems from PC, Potomac, MD, USA and Pharma-Tech Research, Baltimore, MD, USA. A schematic diagram of a HSCCC system used for separation of dyes is shown in Figure 2.

Conventional HSCCC

Conventional HSCCC may be applied only to the separation of relatively small amounts (up to several hundred milligrams when the common 325 mL volume column is used) of dye mixtures. In contrast to pH-zone-refining CCC, conventional HSCCC also permits separation of nonionic components. Analytical size separations (less than 10–20 mg of an ionic or nonionic component of interest) should be performed by conventional HSCCC.

Selection of the Solvent System

The solvent system used for a conventional HSCCC separation is selected according to the hydrophobicity

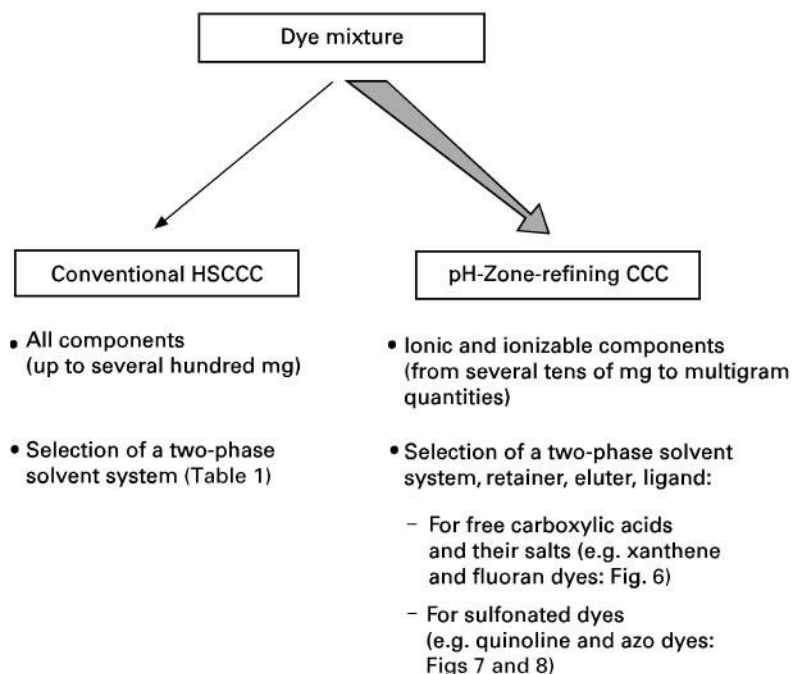


Figure 1 General approach to the preparative separation of dyes by HSCCC.

of the targeted components so that the respective partition coefficients (K) of these components are close to 1. **Table 1** summarizes the solvent systems used for specific dye separations. Also listed in **Table 1** are the general requirements for the selection of a solvent system. The procedures for a systematic search for a suitable solvent system have been discussed previously.

Separation Procedure

The separation is initiated by filling the column with the stationary phase (usually the upper organic phase of the biphasic solvent system) using the liquid

chromatography pump (Figure 2). The sample to be separated, dissolved in a minimum volume of the solvent system (equal volumes of each phase), is then loaded into the column through the sample injection valve (which facilitates the elimination of air bubbles) by syringe or with pressurized nitrogen (60 psi). The mobile phase is then pumped into the column while the column is rotated (usually at 3 mL min^{-1} and 800 rpm). The effluent is passed through a UV-visible detector, and fractions of 3 or 6 mL per test tube are collected with the aid of a fraction collector. The fractions obtained from the HSCCC separation are then further analysed (e.g. by HPLC).

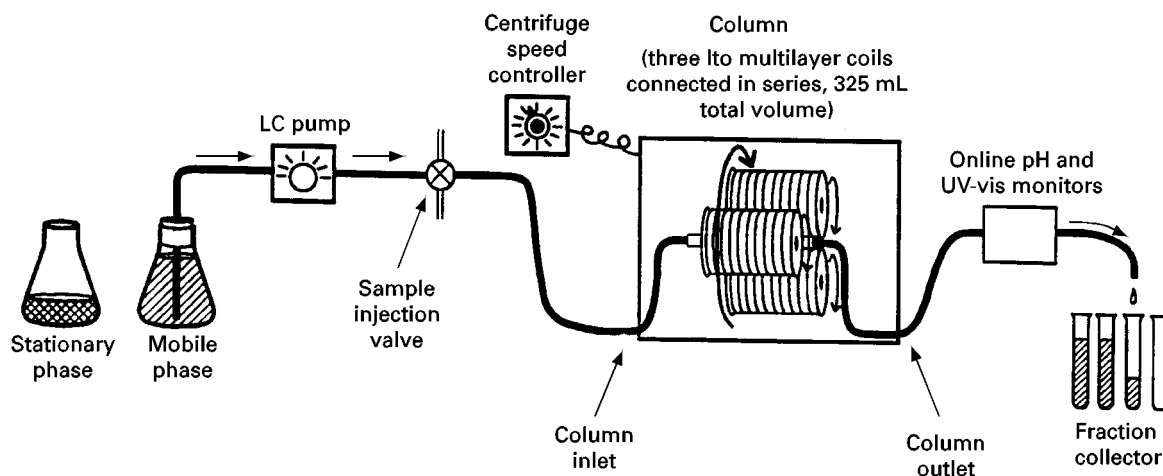


Figure 2 Schematic presentation of a HSCCC system.

Table 1 Selection of a two-phase solvent system for conventional HSCCC of dyes*Reported solvent systems*

Methyl Violet 2B (CHCl_3 -AcOH-0.1 mol L⁻¹ HCl (2 : 2 : 1))
 Sulforhodamine B (*n*-BuOH-0.01 mol L⁻¹ aq trifluoroacetic acid (1 : 1))
 Gardenia Yellow (EtOAc-*n*-BuOH-H₂O (2 : 3 : 5))
 Azo-dyes (acid, direct and disperse azo-dyes)
 Phloxine B (CI 45410) (EtOAc-*n*-BuOH-0.01 mol L⁻¹ aq NH₄OAc (1 : 1 : 2))
 Brominated tetrachlorofluoresceins (EtOAc-*n*-BuOH-0.01 mol L⁻¹ aq NH₄OAc (1 : 1 : 2))

New solvent systems: general requirements

Settling time shorter than 30 s
 Partition coefficient (*K*) close to 1 and should be different for each component of the dye mixture
 Solvent system should provide nearly equal volumes of upper and lower phases

Applications

Table 1 summarizes the applications of conventional HSCCC to the separation of components from synthetic and natural dye mixtures. Figures 3 and 4 show two examples in which this technique was successfully applied to the separation of dye mixtures.

Oka *et al.* employed conventional HSCCC to separate the main components from the gardenia fruit extract (*Gardenia jasminoides* Ellis) used extensively in Japan as a food colour additive under the name Gardenia Yellow (Figure 3). The solvent system used for the separation, ethyl acetate-*n*-butanol-water (2 : 3 : 5), was chosen based on the partition coefficient (*K*) of each of the 14 components, as determined by HPLC. Figure 3A shows the HPLC analysis of the original mixture. The chromatogram obtained for the separation of the three main components (geniposide, *trans*-crocin and 13-*cis*-crocin) from a 25 mg portion of Gardenia Yellow by conventional HSCCC, using the upper organic layer as the stationary phase, is shown in Figure 3B.

Figure 4 shows the chromatogram obtained by Fales *et al.* for the HSCCC separation of the components of a 6 mg portion of the triphenylmethane dye Methyl Violet 2B, composed of a mixture of *N*-methylated forms of pararosaniline. The solvent system used in this case, CHCl_3 -acetic acid-0.1 mol L⁻¹ HCl (2 : 2 : 1), succeeded in separating the various methylated homologues and several contaminants. For this separation, the aqueous layer was used as the stationary phase. The proposed structures of the separated components and of one of the isolated contaminants (mol.wt 491; Figure 4) are based on their ²⁵²Cf plasma desorption mass spectra.

pH-Zone-Refining CCC

pH-zone-refining CCC can only be applied to the separation of ionic or ionizable components. The

principles of this technique are discussed in this volume. Ideally, the sample components should be stable over a wide pH range, from 1 to 10 for dyes containing a carboxylic acid group and from 0.5 to 13.5 for sulfonated dyes. The quantity of each targeted component in the sample mixture must be at least 0.1 mmol and preferably over 1 mmol. Depending on the solubility of the sample mixture in the solvent system, multi-gram quantities of dyes can be separated in one experiment using a typical preparative column of approximately 325 mL capacity. A general approach to the separation of dyes by pH-zone-refining CCC is presented in Figure 5. This method is applied to the separation of dyes containing carboxylic acid groups (e.g. xanthene dyes or their lactone analogues, fluoran dyes) by using an organic acid (e.g. trifluoroacetic acid, TFA) as a retainer in the organic stationary phase and a base (e.g. ammonia) as an eluter in the aqueous mobile phase. Compounds containing one or more amine groups (e.g. Methyl Violet 2B) may also be separated by pH-zone-refining CCC by using an organic base as a retainer (e.g. triethylamine) and an inorganic acid as an eluter (e.g. HCl), as described elsewhere in the present volume.

The more polar sulfonated dyes can be separated by affinity-ligand pH-zone-refining CCC (right column in Figure 5), in which case a ligand is added to enhance the partitioning of the dye components into the organic stationary phase.

Selection of the Solvent System

The process of selecting a solvent system for pH-zone-refining CCC separations is very different from that conducted when selecting a solvent system for conventional HSCCC separations. For most pH-zone-refining CCC separations, a suitable solvent system can be found by testing various volume ratios of ether (diethyl or methyl-*tert*-butyl, MTBE)-acetonitrile (CH_3CN)-water. To the chosen system, an or-

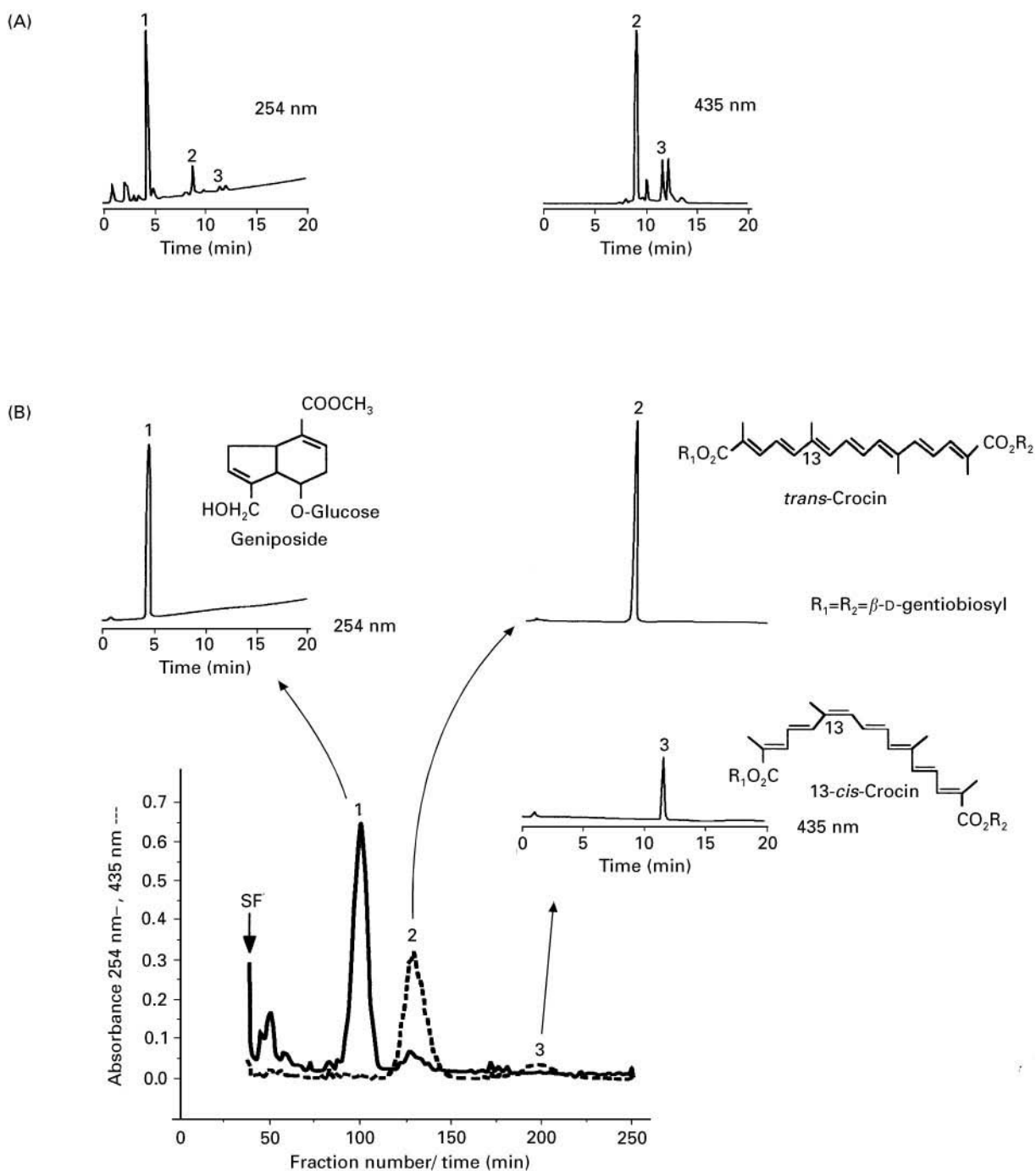


Figure 3 Separation by conventional HSCCC of components from a sample of the Japanese food colour additive Gardenia Yellow. (A) High performance liquid chromatograms at 254 nm and 435 nm of the original sample. (B) Conventional HSCCC for the separation of a 25 mg portion of the sample and the HPLC chromatograms of the separated components. Experimental conditions: solvent system: ethyl acetate-*n*-butanol-water (2:3:5 by volume). The aqueous phase was used as mobile phase. Sample: 25 mg Gardenia Yellow dissolved in 2 mL solvent (1 mL of each phase). Flow rate: 2 mL min⁻¹ in the head-to-tail elution mode. Detection: 254 (continuous line) and 435 nm (dashed line). Speed of revolution: 800 rpm. Stationary-phase retention: 65.8%. SF, Solvent front. (Oka *et al.*, 1995 with modifications.)

ganic acid (TFA) is added to the organic layer as a retainer and an inorganic base such as ammonia is added to the aqueous layer as an eluter if dyes containing carboxylic acid groups are to be separated.

For the separation of dyes containing amino groups, an organic base (such as triethylamine) is added to the organic stationary phase as a retainer and an inorganic acid (HCl) is added to the aqueous

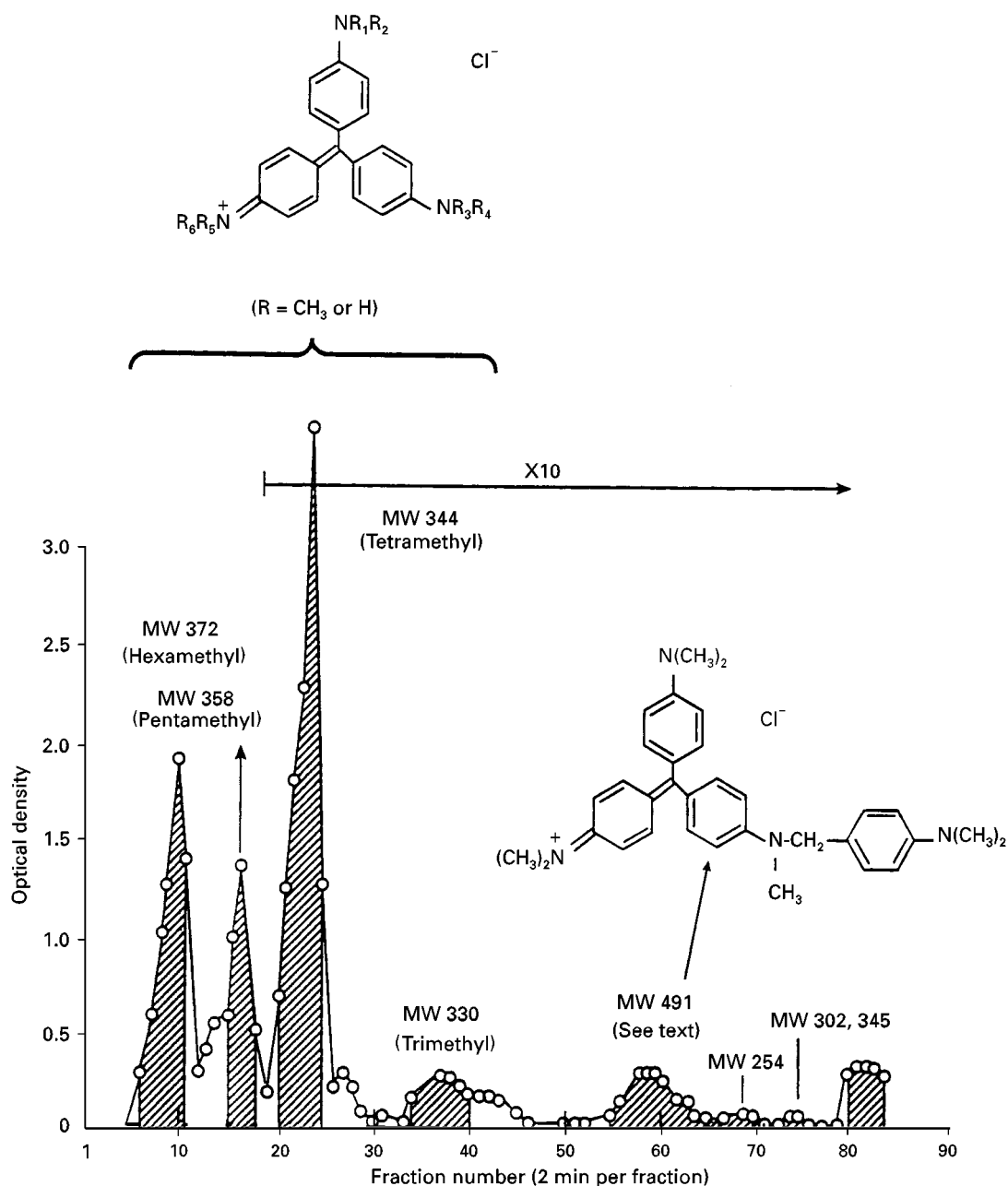


Figure 4 Separation by conventional HSCCC of components from a sample of Methyl Violet 2B. Experimental conditions: Solvent system: chloroform–acetic acid–0.1 mol L⁻¹ HCl (2 : 2 : 1 by volume). The organic phase was used as mobile phase. Sample: 6 mg Methyl Violet 2B dissolved in 5 mL organic phase. Flow rate: 4 mL min⁻¹ in the head-to-tail elution mode. Speed of revolution: 800 rpm. (Fales *et al.*, 1985 with modifications.)

mobile phase as an eluter. For affinity-ligand pH-zone-refining CCC separations (for sulfonated dyes), a ligand is added to the stationary phase to retain the sulfonated dyes in the column by enhancing their partitioning into the organic stationary phase.

Standard pH-zone-refining CCC The following steps are recommended for the selection of an appro-

priate two-phase solvent system for the separation by standard pH-zone-refining CCC of a dye containing a carboxylic acid group (summarized in **Figure 6**):

1. Prepare a two-phase solvent system by thoroughly equilibrating water and either MTBE or diethyl ether in a separatory funnel at room temperature.

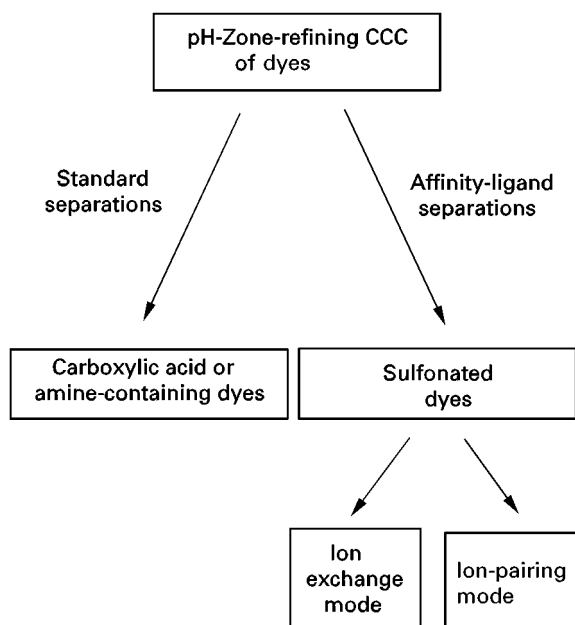


Figure 5 General approach to the separation of dyes by pH-zone-refining CCC. (Reproduced from Fales *et al.*, 1985 with permission from the American Chemical Society.)

2. Deliver a 2 mL aliquot of the upper (U) and of the lower (L) phase into a test tube. Add a very small amount of dye and agitate to equilibrate the contents.
3. Add a small amount of aqueous ammonia ($\approx 28\%$; eluter) to the mixture (to give a base concentration of approximately 12 mmol L^{-1} , pH 10) and equilibrate the mixture. If almost all the colour visibly partitions into the lower aqueous phase, then the partition coefficient $K_{\text{base}}(\text{U/L}) \ll 1$. If visual assessment is unclear, K_{base} may be determined by spectrophotometry. Dilute an aliquot from each phase with solvent

(e.g. methanol) and measure the absorbance at an appropriate wavelength using a spectrophotometer. Obtain the partition coefficient, $K_{\text{base}}(\text{U/L})$, by dividing the absorbance of the dye in the upper phase by that in the lower phase.

4. If $K_{\text{base}} \geq 0.5$, the above test should be repeated with a less polar (more hydrophobic) solvent system such as *n*-hexane–ethyl acetate–methanol–water (1:1:1:1).
5. If $K_{\text{base}} \ll 1$, add retainer acid TFA (approximately 20 mmol L^{-1}) to the mixture to bring the pH to approximately 2, and re-equilibrate the mixture by agitation. Using procedure 3, obtain K_{acid} . If $K_{\text{acid}} \gg 1$, the solvent system can be effectively used to separate the sample components.
6. If $K_{\text{acid}} \leq 2$, the above tests should be repeated with a more polar (more hydrophilic) solvent system such as *n*-butanol–water.

For amine-containing dyes, substitute HCl for ammonia in step 3 above to obtain $K_{\text{acid}} \ll 1$ and substitute triethylamine for TFA in step 5 above to obtain $K_{\text{base}} \gg 1$.

Affinity-ligand separations Sulfonated dyes are much more polar (hydrophilic) compounds than the carboxylic acid dyes. They tend to distribute predominantly in the aqueous phase of a conventional two-phase solvent system, even if the aqueous phase is highly acidic. For the separation of sulfonated dyes by pH-zone-refining CCC, the addition of a hydrophobic ligand is necessary in order to retain the dyes in the organic stationary phase. Two kinds of ligands were used successfully for the separation of sulfonated dyes: ion exchange reagents (e.g. dodecylamine, tridodecylamine), which are always retained in the organic stationary phase, and

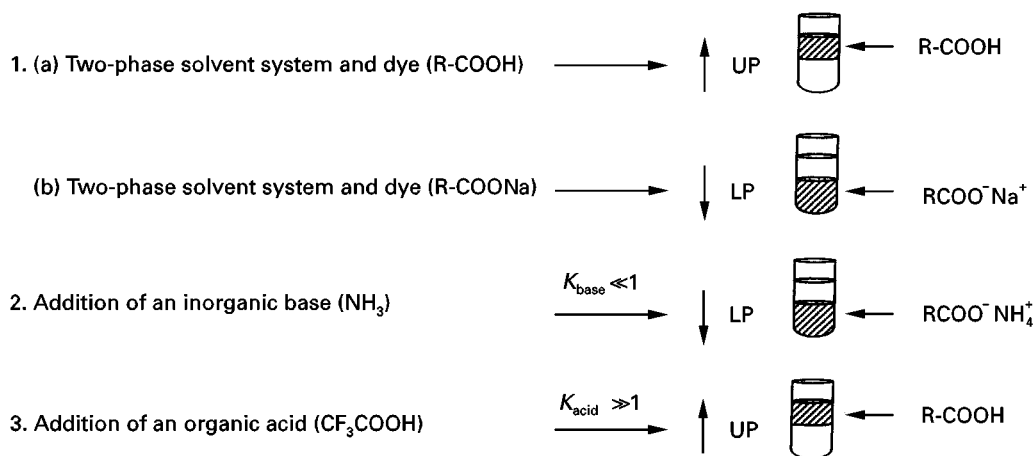


Figure 6 Conditions required for the separation of dyes containing carboxylic acid groups by pH-zone-refining CCC. For conditions required for the separation of dyes containing amino groups, see text.

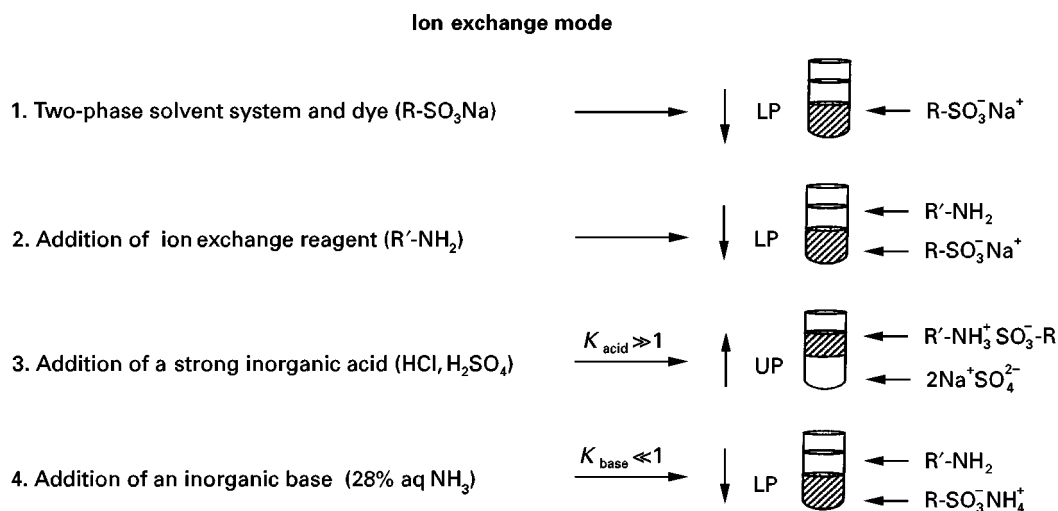


Figure 7 Conditions required for the separation of sulfonated dyes by affinity-ligand pH-zone-refining CCC in the ion exchange mode.

ion-pairing reagents (e.g. tetrabutylammonium hydroxide), which partition into either phase. These ligands are dissolved in the organic phase (stationary phase and/or sample solution) at a concentration determined in preliminary experiments.

Ion exchange mode separations (Figure 7) The following steps are recommended for the selection of an appropriate two-phase solvent system for the separation of sulfonated dyes by affinity-ligand pH-zone-refining CCC in the ion exchange mode:

1. Prepare a two-phase solvent system composed of either MTBE- CH_3CN -water at a volume ratio of 2:2:3 (used for the separation of the main component from FD&C Yellow No. 6, Sunset Yellow, CI 15985) or iso-amyl alcohol (iAA)-MTBE- CH_3CN -water at volume ratios from 3:1:1:5 to 3:5:1:7 (used for the separation of mono-, di- and trisulfonated components of Quinoline Yellow, CI 47005).
2. Deliver a 2 mL aliquot of the upper (U) and of the lower (L) phase into a test tube. Add a small amount of dye and agitate to equilibrate the contents.
3. Add a small amount of ion exchange reagent (e.g. dodecylamine, tridodecylamine at 5–20% concentration) and equilibrate the mixture by agitation.
4. Add a small amount of a strong inorganic acid (e.g. HCl , H_2SO_4 at 3–4%, pH 0.8). Measure the K_{acid} as above.
5. If $K_{\text{acid}} \leq 5$, add more acid and retest.
6. If $K_{\text{acid}} \gg 1$, add eluter NH_3 (28% aq NH_3) to the mixture to give a base concentration of approximately 110 mmol L^{-1} and a pH of 11. Re-equilibrate

the contents. Measure the K_{base} as above. If $K_{\text{base}} \ll 1$, the solvent composition is adequate for separation.

7. If $K_{\text{base}} \geq 0.2$, add more base and retest.

A concentration of 5% ligand (dodecylamine) in the stationary phase was used for the separation of the monosulfonated components of D&C Yellow No. 10, while a higher concentration (up to 20%) of ligand was required for the separation of the di- and trisulfonated components from Quinoline Yellow (including Yellow No. 203).

Ion-pairing mode separations (Figure 8) The following steps are recommended for the selection of an appropriate two-phase solvent system for the separation of sulfonated dyes by affinity-ligand pH-zone-refining CCC in the ion-pairing mode:

1. Follow steps 1 and 2 as described above for the ion exchange mode separations.
2. Add a small amount of ion-pairing reagent (tetrabutylammonium hydroxide, TBAOH, 40% weight solution in water, 0.4 mmol) to give a concentration of approximately 100 mmol L^{-1} and a pH of 12.8. Equilibrate the mixture by agitation. Measure the partition coefficient K_{base} as described above.
3. If $K_{\text{base}} \leq 5$, add more ion-pairing reagent and retest.
4. If $K_{\text{base}} \gg 1$, add an organic acid, TFA (eluter), to give an acid concentration of approximately 80 mmol L^{-1} and a pH of 1.6. Re-equilibrate the mixture by agitation. Measure the partition coefficient K as above. If $K_{\text{acid}} \ll 1$, the solvent composition is adequate for separation.

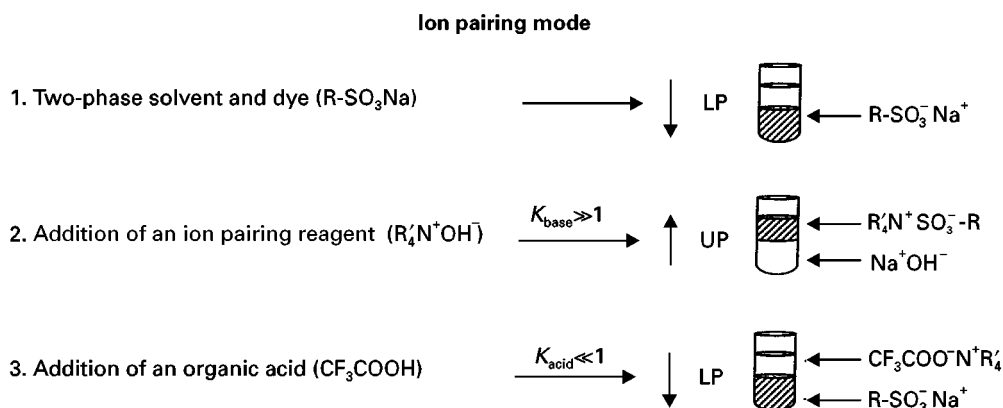


Figure 8 Conditions required for the separation of sulfonated dyes by affinity-ligand pH-zone-refining CCC in the ion-pairing mode.

5. If K_{acid} is not small enough (greater than 0.2), add more TFA and retest.

Separation Procedure

Standard pH-zone-refining CCC A standard separation is initiated by completely filling the column with the acidified (or basified) organic stationary phase using the liquid chromatography pump (Figure 2). Then the sample solution is loaded into the column through the sample injection valve by syringe or with pressurized nitrogen (60–80 psi). When dyes that contain a carboxylic group are separated, the sample solution is prepared as follows: the sample is dissolved in the organic stationary phase containing the retainer (TFA) and a smaller amount of aqueous lower phase (free of eluter). The sample solution should have a low pH, thus ensuring that the target dye is distributed into the upper (stationary) phase of the sample solution. It is desirable that the sample be completely dissolved in the sample solution. If the sample does not dissolve completely in the sample solution, it can be loaded into the column if it can be homogenized into a fine suspension by sonication for a short time. Ideally, the volume of the sample solution should not exceed 100–140 mL for a preparative separation column of 325 mL capacity. After the sample solution is loaded into the column, the mobile phase containing the eluter (basified aqueous phase) is then pumped (usually at 3 mL min^{-1}) into the column while the column is rotated (800–1000 rpm). The effluent is passed through a UV-visible detector flow cell that is further connected to a pH flow cell (for continuous pH monitoring; alternatively, the pH of each collected fraction is manually recorded with a pH meter) and fractions – usually 3 mL per test tube – are collected with a fraction collector.

Affinity-ligand pH-zone-refining CCC Ion exchange mode A separation is initiated by completely filling the column with ligand-free stationary phase (upper organic phase) by using the liquid chromatography pump. Approximately 100 mL of ligand-containing stationary phase is pumped into the column, thereby displacing part of the column contents. Then the sample solution is loaded into the column through the sample injection valve by syringe or with pressurized nitrogen (60–80 psi). The sample solution is prepared as follows: the sample is dissolved in lower aqueous phase (e.g. 60 mL for 5 g of Quinoline Yellow) and mixed with stationary phase (60 mL) containing the ligand. The sulfonated dyes are brought into the upper phase of the sample solution by the cautious addition of H_2SO_4 (95–98%, 2.2 mL), at which point the pH of the sample solution is approximately 0.8.

After the sample solution is loaded into the column, the aqueous mobile phase containing the basic eluter is pumped through the rotating column as described above for performing standard pH-zone-refining CCC. If carryover of the stationary phase occurs, the elution is stopped (after approximately 60 mL of stationary phase has been eluted) while the rotation of the column is continued. After 3–4 h of rotation, the elution of the mobile phase is restarted, and usually no more carryover of the stationary phase is observed.

Ion-pairing mode A separation is initiated by completely filling the column with ligand-free stationary phase (upper organic phase) by using the liquid chromatography pump. The sample solution is then loaded into the column through the sample injection valve by syringe or with pressurized nitrogen (60–80 psi). The sample solution is prepared as follows: the sample is dissolved in lower aqueous phase.

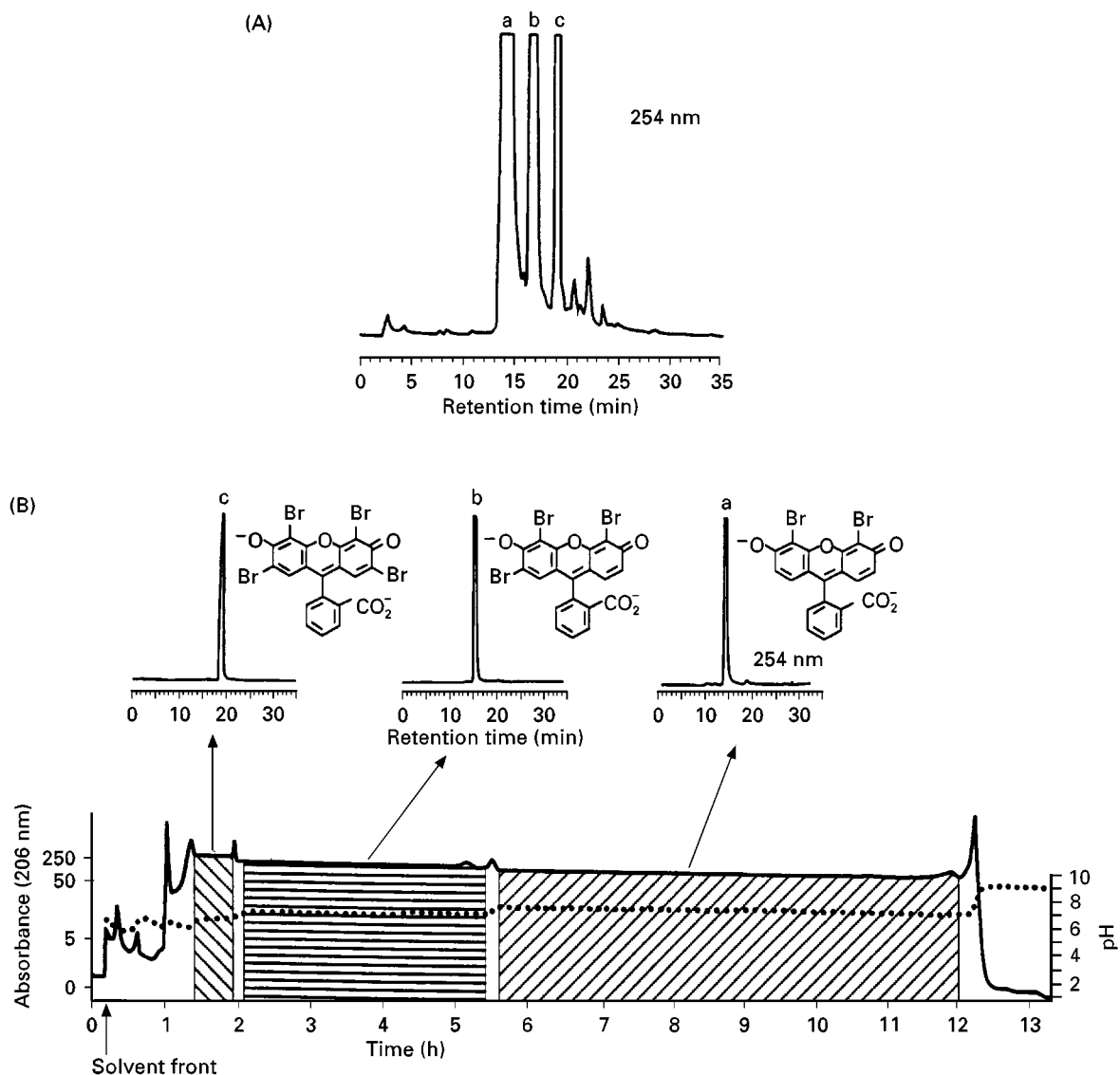


Figure 9 Separation by standard pH-zone-refining CCC of components from the colour additive D&C Orange No. 5 (CI 45370: 1). (A) HPLC analysis of the original sample. (B) pH-zone-refining CCC of the separation and the HPLC chromatograms of the separated components. Continuous line, absorbance (206 nm); dotted line, pH. Experimental conditions: solvent system: diethyl ether–acetonitrile–0.01 mol L⁻¹ aqueous ammonium acetate adjusted to pH 9 with aqueous NH₃ (4 : 1 : 5 by volume). The aqueous phase was used as mobile phase. Sample: 5 g D&C Orange No. 5 suspended in 80 mL solvent system (40 mL each of the upper and lower phases). TFA 200 µL was added to the sample solution as a retainer. Flow rate: 3 mL min⁻¹ in the head-to-tail elution mode. Speed of revolution: 800 rpm. Detection: 206 nm. (Weisz *et al.*, 1994 with modifications.)

To this solution an equal volume of upper phase that contains approximately 100 mmol L⁻¹ of the ion-pairing reagent (TBAOH) is added. The pH of the sample solution is approximately 12.8, and the dye partitions mostly into the upper phase. After the sample solution is loaded into the column, the mobile phase, consisting of the aqueous lower phase and 80 mmol L⁻¹ TFA as an acid eluter, is pumped through the rotating column as described above for standard pH-zone-refining CCC. The pH of the mobile phase is approximately 1.6. If carryover of the

stationary phase occurs, follow the directions given above for the ion exchange mode separation.

Applications

Figures 9–13 show successful applications of pH-zone-refining CCC to the preparative separation of components of fluorescein and sulfonated dyes.

Standard pH-zone-refining CCC separations Figure 9 shows the separation of the three brominated homologues contained in the colour additive D&C

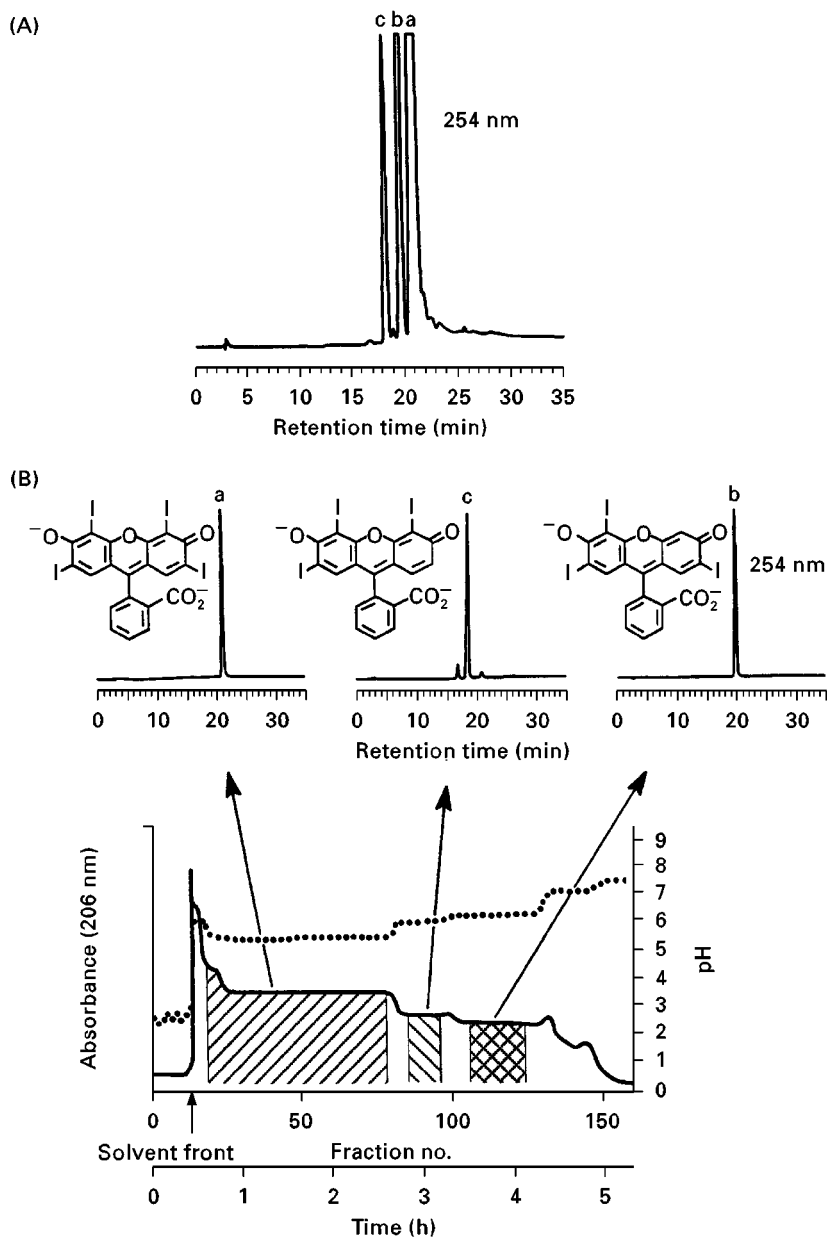


Figure 10 Separation by standard pH-zone-refining CCC of components from the colour additive FD&C Red No. 3 (erythrosine, CI 45430). (A) HPLC analysis of the original sample. (B) pH-zone-refining CCC of the separation and HPLC analyses of the separated components. Continuous line, absorbance (206 nm); dotted line, pH. Experimental conditions: solvent system: diethyl ether–acetonitrile–0.01 mol L⁻¹ aqueous ammonium acetate (4 : 1 : 5 by volume). The aqueous phase, adjusted to pH 7.53 with aqueous NH₃, was used as mobile phase. The organic phase (500 mL), to which was added TFA (400 μ L) as a retainer, was used as stationary phase. Sample: 3 g FD&C Red No. 3 suspended in 40 mL solvent system (20 mL of the lower phase and 20 mL of the unacidified upper phase). Flow rate: 3 mL min⁻¹ in the head-to-tail elution mode. Speed of revolution: 800 rpm. Detection: 206 nm. (Weisz, 1996 with modifications.)

Orange No. 5 (CI 45370:1) by standard pH-zone-refining CCC. The HPLC chromatogram of the original sample is shown in Figure 9A. The pH-zone-refining CCC chromatogram of a suspension containing 5 g of this mixture is shown in Figure 9B. The three broad absorbance plateaux (solid line) correspond to the three pH plateaux. Each plateau represents

elution of a pure component of the mixture, as illustrated by the associated HPLC chromatograms of aliquots of the combined fractions from the three hatched regions. The recoveries of the three dye components were good (a: 82%; b: 90.3%; c: 77%).

Figure 10 shows the use of standard pH-zone-refining CCC for the separation of iodinated homologues

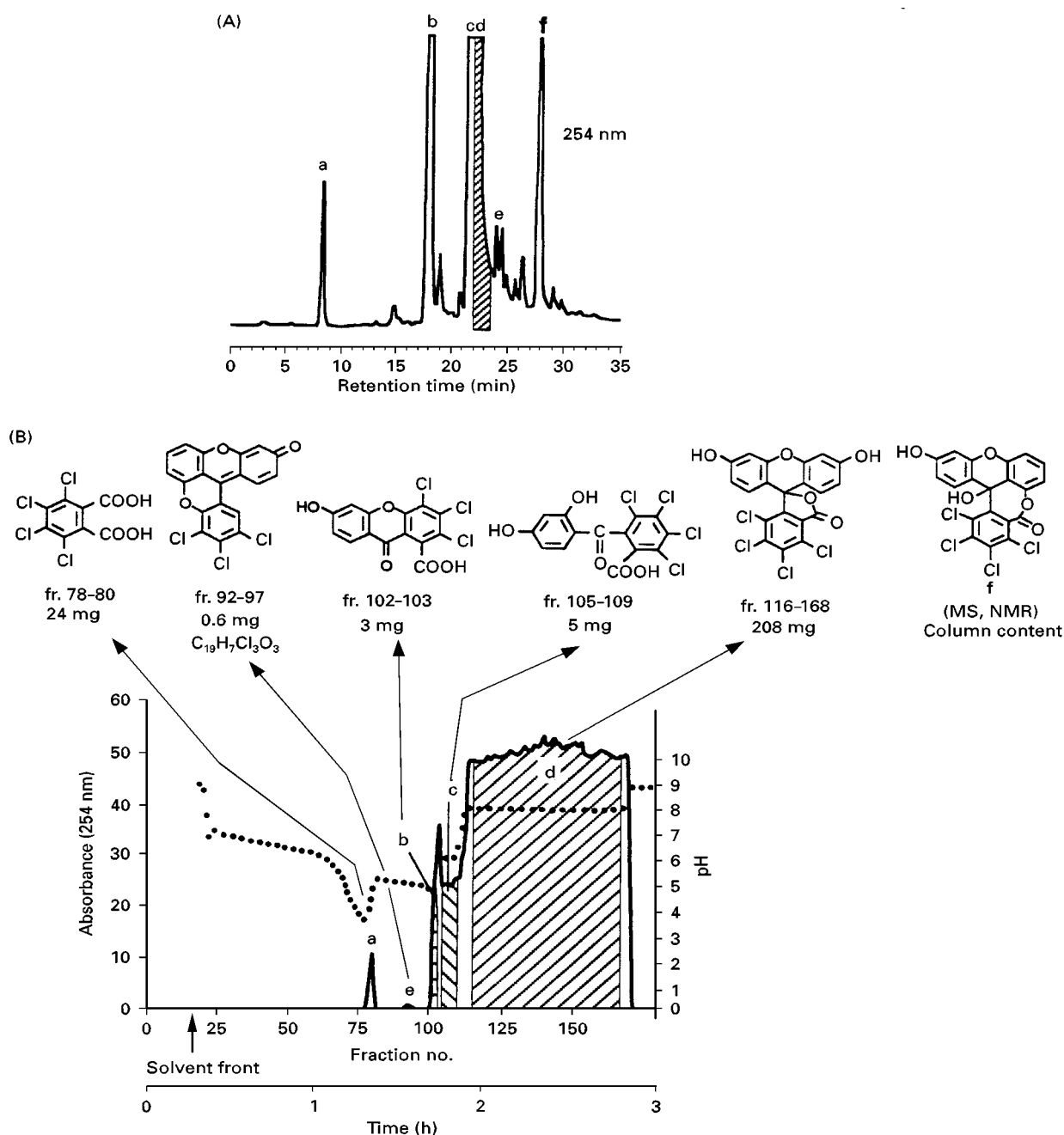


Figure 11 Separation by standard pH-zone-refining CCC of components from a sample of tetrachlorofluorescein (TCF). (A) HPLC analysis of the original mixture. (B) pH-zone-refining CCC of the separation and the assigned structures of the isolated components. Continuous line, absorbance (206 nm); dotted line, pH. Experimental conditions: solvent system: diethyl ether-acetonitrile-0.01 mol L⁻¹ aqueous ammonium acetate (4:1:5 by volume). The aqueous phase adjusted to pH 9.06 with aqueous NH₃ (0.1%, c. 14 mmol L⁻¹) was used as mobile phase. The organic phase was used as stationary phase. Sample: 350 mg TCF suspended in 5.5 mL of each of upper and lower phases. TFA (200 µL) was added as a retainer in the sample solution. Flow rate: 3 mL min⁻¹ in the head-to-tail elution mode. Speed of revolution: 800 rpm. Detection: 254 nm. Retention of the stationary phase: 74.8%. (Weisz *et al.*, 1995 with modifications.)

and positional isomers from a 3 g sample of the colour additive FD&C Red No. 3 (erythrosine, CI 45430). All three components were well-separated with small mixing zones between them.

Figure 11 illustrates the separation of the main component and five contaminants from a sample of 350 mg of commercial tetrachlorofluorescein (TCF). TCF is an important intermediate in the preparation

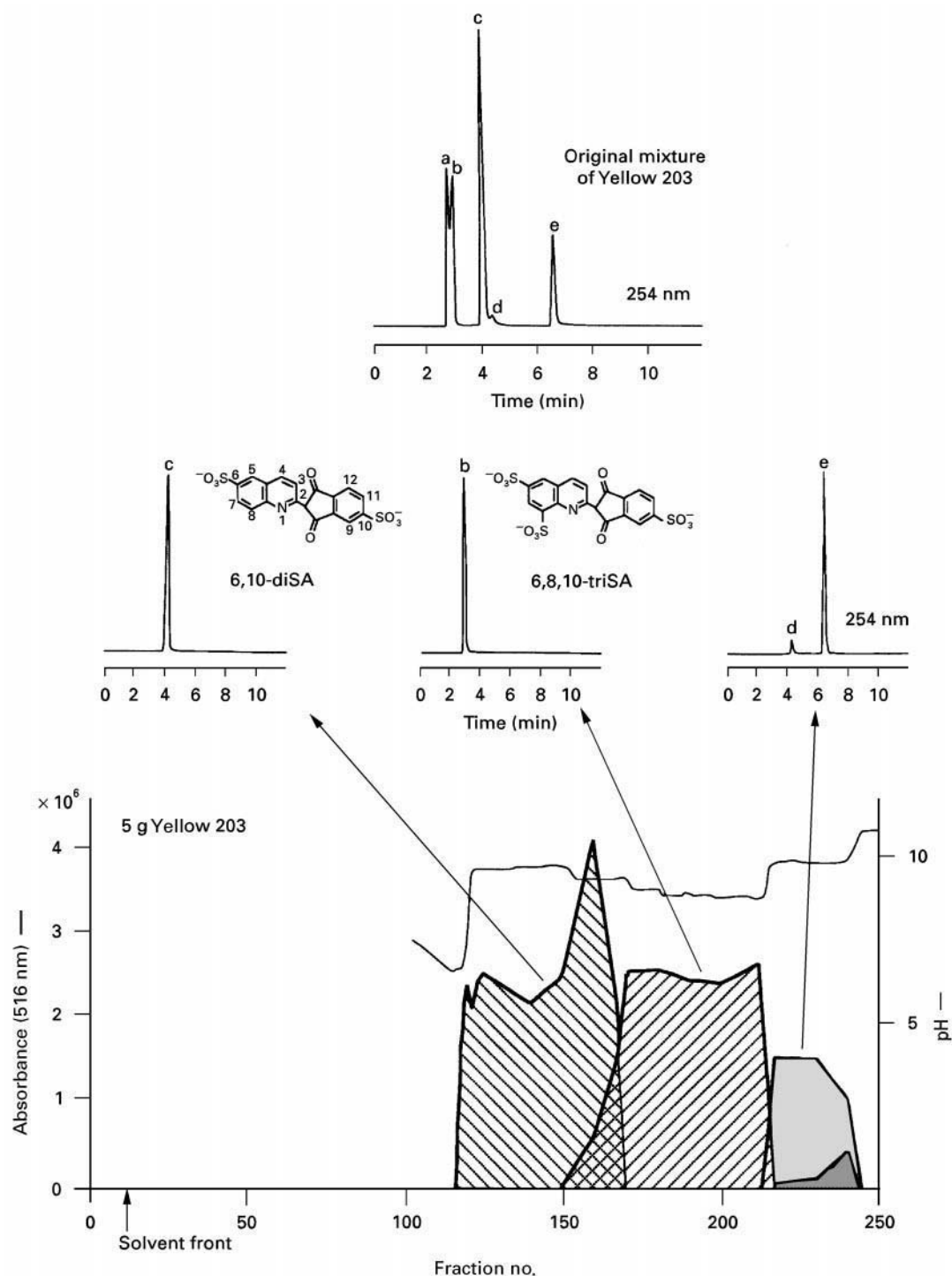


Figure 12 Separation by affinity-ligand pH-zone-refining CCC in the ion exchange mode of components from a sample of the Japanese colour additive Yellow No. 203 (Quinoline Yellow, CI 47005). Top: HPLC analysis of the original mixture. Bottom: reconstructed pH-zone-refining CCC elution profile (a constant amount from each CCC collected fraction was analysed by HPLC and the area of the peak obtained at 516 nm was plotted). Experimental conditions: solvent system: iso-amyl alcohol-methyl-*tert*-butyl ether-acetonitrile-water (3 : 5 : 1 : 7 by volume). Stationary phase: 100 mL upper phase, to which was added 20% dodecylamine as a retainer (pH 11.7) and 220 mL of ligand-free upper phase (see text). Mobile phase: lower phase, to which was added aqueous NH_3 (163 mmol L^{-1} , pH 11.7). Sample solution: 5 g of Yellow No. 203 dissolved in 60 mL each of lower phase and ligand-containing upper phase. To this mixture was added conc. H_2SO_4 (40 mmol). The pH of the sample solution (light line, top) became 0.8 and the dye partitioned mostly in the upper phase. Flow rate: 3 mL min^{-1} (see text). Speed of revolution: 800 rpm. Detection: 516 nm (bold line). Retention of the stationary phase: 36.1%. Time of the separation: equilibration 12 h; actual separation time: 5 h. For more details, see text. Reproduced from Weisz *et al.* (1995) with permission from the American Chemical Society.

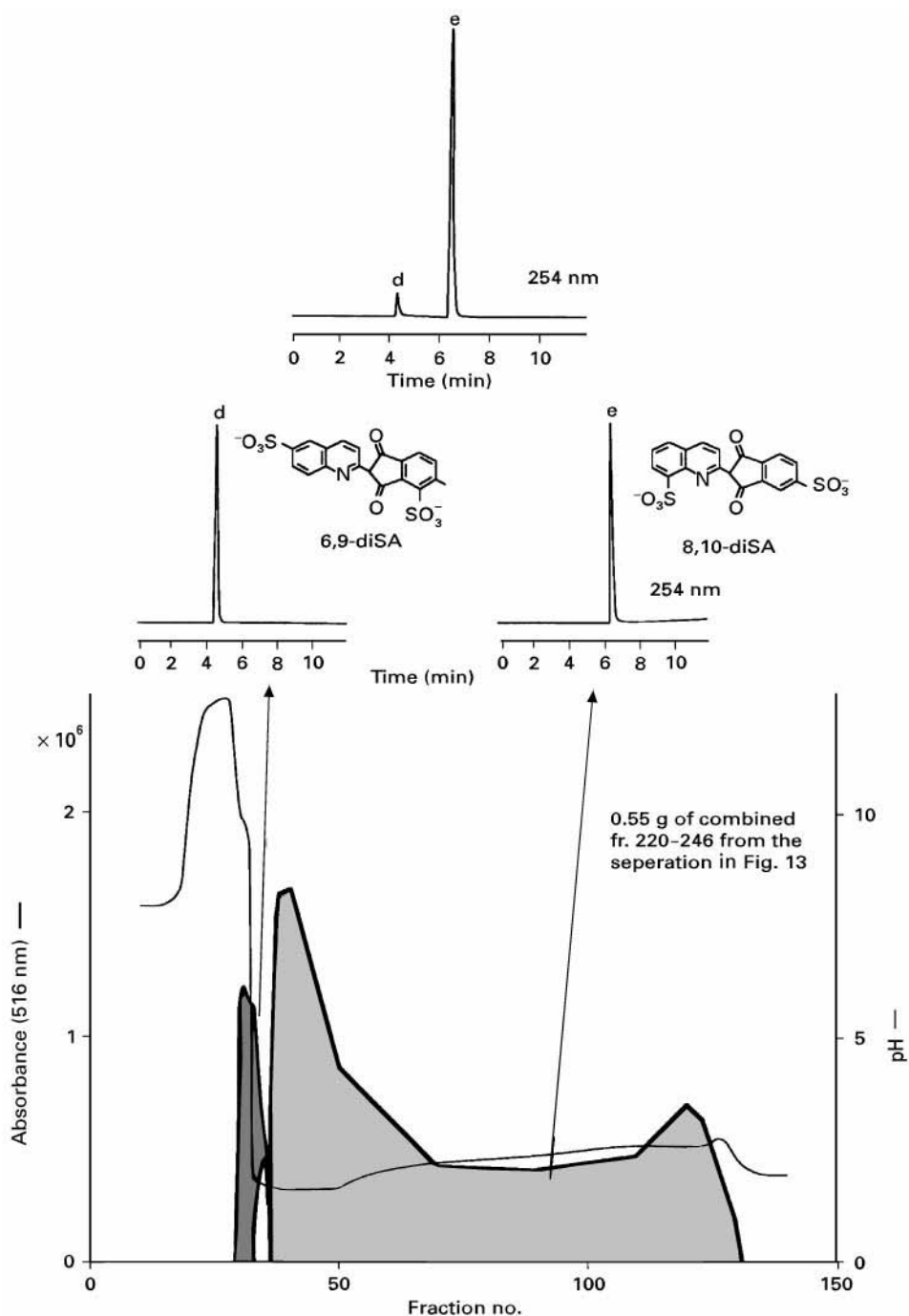


Figure 13 Separation by affinity-ligand pH-zone-refining CCC in the ion-pairing mode of the two components of Yellow No. 203 that elute together in the separation shown in Figure 12. Top: HPLC analysis of the combined fractions 220–246 from the separation in Figure 12. Bottom: reconstructed pH-zone-refining CCC of the separation and HPLC analyses of the separated components. Experimental conditions: solvent system: iso-amyl alcohol-methyl-*tert*-butyl ether-acetonitrile-water (3:4:1:7 by volume). Stationary phase: upper phase. Mobile phase: lower phase to which was added TFA (80.7 mmol L⁻¹, pH 1.6). Sample solution: 0.55 g of residue from combined fractions 220–246 from the separation in Figure 12 dissolved in 30 mL of solvent system (15 mL each of lower and upper phases), to which was added tetrabutylammonium hydroxide (100 mmol L⁻¹). The pH of the sample solution (light line, top) became 12.8 and the dye partitioned mostly in the upper phase. Flow rate: 3 mL min⁻¹. Speed of revolution: 825 rpm. Detection: 516 nm (bold line). Retention of the stationary phase: 75%. Time of the separation: 2.5 h.

of higher halogenated dyes (e.g. Phloxine B, Rose Bengal), and its contaminants can be carried over during the manufacturing process. Two of the isolated contaminants (e and f) had not been reported previously.

Affinity-ligand pH-zone-refining CCC separations
Ion exchange mode Figure 12 shows the separation of a 5 g portion of the Japanese colour additive Yellow No. 203 (Quinoline Yellow, CI 47005) with the ion exchange reagent dodecylamine as the retainer in the stationary phase at a concentration of 20%. To retain the stationary phase in the column, at the point in the separation when the column contains approximately 50% of the mobile and 50% of the stationary phase, reduce the flow rate of the mobile phase to one-fifth of the original flow rate (i.e. 0.6 mL min^{-1} instead of 3 mL min^{-1}) for several hours, and then the flow rate is increased to its original value. This procedure results in a satisfactory retention of the stationary phase of 36.1% (measured at the end of the separation). A good separation was obtained for two major components, c and b. The first few fractions containing c were contaminated with component a (not shown in Figure 12). Two other components (d and e) eluted together, as shown by the associated HPLC chromatograms in Figure 12.

Ion-pairing mode By using an ion-pairing reagent (TBAOH) as the retainer in the sample solution containing the two components of Yellow No. 203 (0.55 g) that eluted together in Figure 12, d and e were well-separated, as shown in Figure 13. Compound d is a newly identified disulfonated positional isomer of Quinoline Yellow. The results presented in Figures 12 and 13 for the separation of the components of Yellow No. 203 demonstrate that the ion exchange and ion-pairing modes can complement each other.

Conclusion

HSCCC has been used to accomplish the difficult task of separating and/or purifying multi-gram amounts of dyes containing either sulfonic or carboxylic acid groups. No other preparative-scale chromatographic separation of multi-gram quantities of these dyes has been previously reported. It is envisioned that HSCCC could be scaled up to separate kilogram quantities of dyes through modifications of the instrumentation. The availability of large quantities of highly purified dyes will have many benefits, such as enabling standardization of biological stains and lowering the cost of the ultra-pure laser-quality dyes.

See also: II/Chromatography: Countercurrent Chromatography and High-Speed Countercurrent Chromatography Instrumentation. III/Dyes: High-Speed Countercurrent Chromatography.

Further Reading

- Fales HM, Pannell LK, Sokoloski EA and Carmeci, P. (1985) Separation of methyl violet 2B by high-speed countercurrent chromatography and identification by Californium-252 plasma desorption mass spectrometry. *Analytical Chemistry* 57: 376–378.
- Freeman HS and Williard CS (1986) Purification procedures for synthetic dyes: 2. Countercurrent chromatography. *Dyes and Pigments* 7: 407–417.
- Freeman HS, Hao Z, McIntosh SA and Mills KP (1988) Purification of some water soluble azo dyes by high-speed countercurrent chromatography. *Journal of Liquid Chromatography* 11: 251–266.
- Ito Y and Weisz A (1994) pH-Zone-Refining Countercurrent Chromatography. *US Patent Number* 5,332, 504.
- Ito Y (1996) Principle, apparatus, and methodology of high-speed countercurrent chromatography. In: Ito Y and Conway WD (eds) *High-speed Countercurrent Chromatography*, pp. 3–44. New York: John Wiley.
- Ito Y and Ma Y (1996) Review: pH-Zone-refining countercurrent chromatography. *Journal of Chromatography A* 753: 1–36.
- Lyon HO, De Leenheer AP, Horobin RW *et al.* (1994) Standardization of reagents and methods used in cytological and histological practice with emphasis on dyes, stains and chromogenic reagents. *Histochemical Journal* 26: 533–544.
- Oka H, Ikai Y and Kawamura N *et al.* (1991) Purification of food color red no. 106 (Acid Red) using high-speed counter-current chromatography. *Journal of Chromatography* 538: 149–156.
- Oka H, Ikai Y and Yamada S *et al.* (1995) Separation of Gardenia Yellow components by high-speed countercurrent chromatography. In: Conway WD and Petroski RJ (eds) *Modern Countercurrent Chromatography*. ACS Symposium Series, vol. 593, pp. 92–106. Washington, DC: American Chemical Society.
- Weisz A (1996) Separation and purification of dyes by conventional high-speed countercurrent chromatography and pH-zone-refining countercurrent chromatography. In: Ito Y and Conway WD (eds) *High-speed Countercurrent Chromatography*, pp. 337–384. New York: John Wiley.
- Weisz A, Langowski AL, Meyers MB, Thieken MA and Ito Y (1991) Preparative purification of tetrabromotetrachlorofluorescein and Phloxine B by centrifugal countercurrent chromatography. *Journal of Chromatography* 538: 157–164.
- Weisz A, Scher AL, Andrzejewski D, Shibusawa Y and Ito Y (1992) Complementary use of counter-current chromatography and preparative reversed-phase high-performance liquid chromatography in the separation of a synthetic mixture of brominated tetrachlorofluoresceins. *Journal of Chromatography* 607: 47–53.

- Weisz A, Scher AL, Shinomiya K, *et al.* (1994) A new preparative-scale purification technique: pH-zone-refining countercurrent chromatography. *Journal of the American Chemical Society* 116: 704–708.
- Weisz A, Andrzejewski D, Shinomiya K and Ito Y (1995) Preparative separation of components of commercial 4,5,6,7-tetrachlorofluorescein by pH-zone-refining countercurrent chromatography. In: Conway WD and Petroski RJ (eds) *Modern Countercurrent Chromatography*. ACS Symposium Series no. 593, pp. 203–217. Washington, DC: American Chemical Society.
- Weisz A, Andrzejewski D, Highet RJ and Ito Y (1998) Separation of a newly-identified contaminant from commercial 4,5,6,7-tetrachlorofluorescein by pH-zone-refining countercurrent chromatography. *Journal of Liquid Chromatography & Related Technologies* 21: 183–193.
- Weisz A, Mazzola EP, Matusik JE and Ito Y (1999) Separation of components of the color additive D&C Yellow No. 10 (Quinoline Yellow) by pH-zone-refining countercurrent chromatography. *Journal of Chromatography* (in press).

Liquid Chromatography

W. Nowik, Laboratoire de Recherche des Monuments Historiques, Champs-sur-Marne, France

Copyright © 2000 Academic Press

Introduction

Natural dyes are organic matter made up of coloured compounds originating from natural living sources such as plants and animals. These compounds can be found either directly in the extracts or become coloured by hydrolysis, oxidation, condensation, etc., from extracted colourless precursors. Some of them change colour following such reactions or by complexation with certain metallic cations.

These dyestuffs are generally employed for dyeing fibres and fabrics (usually protein and cellulosic), staining several organic and mineral materials (histological preparations, wood, hair, feathers, Easter egg shells), producing organic pigments (painting, printing) and colouring of food, beverages, cosmetics and pharmaceutical products. They are used in analytical chemistry as well as acid–base indicators or complexation agents. A large number of naturally occurring coloured substances are chemically labile. This excludes their direct use principally because of poor light-fastness. Some dyestuffs, in addition to their colouring qualities, have therapeutic properties like regulation of metabolism, anti-inflammatory treatment and anti-cancer prevention among others.

Used frequently around the world in traditional societies, starting probably from the Stone Age, natural dyes were rapidly replaced by synthetic dyes from the second half of the nineteenth century onwards. Nowadays, natural dyes have a growing importance in our lives since almost all of them are hypoallergenic and nontoxic for humans, which is a significant advantage over many synthetic dyes.

Chemical classification of dyestuffs follows the general arrangement of organic compounds and

depends on the generic, basic structure. There are over 20 family structures which many hundreds of compounds belong to. Examples of the most frequently encountered structures are shown in **Table 1**.

The most important application of dyes, from a historical point of view, is textile dyeing. For this reason, the most common classification of dyestuffs is determined by their dyeing properties and dyeing technology. According to their dyeing properties, natural dyes belong to four principal groups: direct dyes (e.g. curcumin, a diaryloylmethane from *Curcuma longa*), mordant dyes (e.g. alizarin and other anthraquinones from various madders), reactive dyes (e.g. depsides and depsidones from lichens) and vat dyes (e.g. indigotine from indigo, woad, dyer's knotweed and others).

Membership to one of the dye families is determined by the type of 'connection' between colorant and support. However, many dyestuffs may show more than one dyeing mechanism, simultaneously or according to applied dyeing conditions. The type of connection determines the method of liberation of dyestuff prior to analysis. Identification of type and origin of dyestuffs requires an understanding of composition.

Extraction

Direct Raw Material Extraction

Many natural dyestuffs or their precursors (e.g. indican and isatan B for indigotine) are water-soluble. Their extraction from raw plant or animal material can be achieved by water, sometimes heated to facilitate penetration into the cells. This process, along with possible cell destruction, can also be accelerated by the use of an ultrasound bath. In several cases, the addition of water-miscible solvents (e.g. methanol, ethanol or acetonitrile) improves the recovery of relatively hydrophobic compounds, such as curcumin, certain anthraquinones, etc. Moderately polar solvents

Table 1 Some important chemical families of dyestuffs

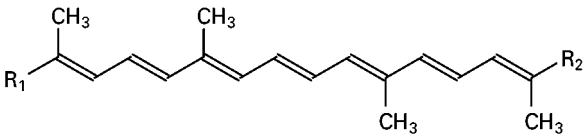
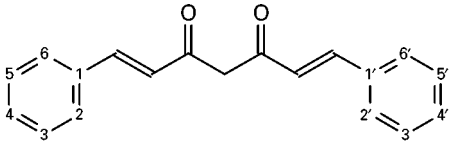
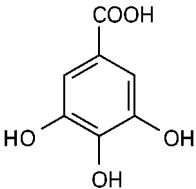
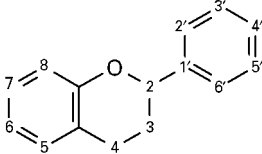
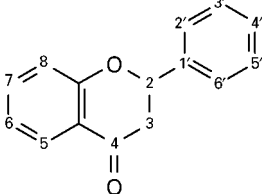
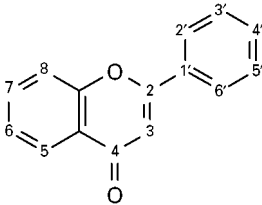
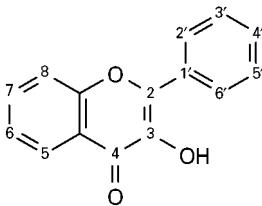
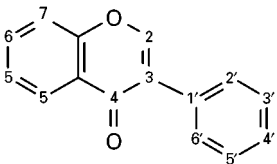
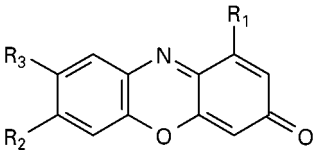
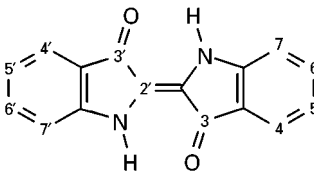
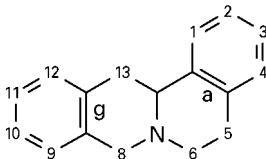
Generic name	Generic structure	Example	
		Name	Usual name
Carotenoid		Carotenoid-dicarboxylic acid ($R_1, R_2 = \text{COOH}$)	Crocin
Diarylmethane		Diferuoylmethane (4,4' = -OH, 5,5' = -OMe)	Curcumine
Gallotannin		Digaloylhamamelose	Hamamelitannin
Flavane		3,3',4',5,7-Pentahydroxyflavane	Catechin
Flavanone		3,3',4',7-Tetrahydroxyflavanone	Fustin
Flavone		4',5,7-Trihydroxyflavone	Apigenin
Flavonol		3,4',5,7-Tetrahydroxyflavone	Kaempferol
Isoflavone		3',4',5-Trihydroxy-7-methoxyisoflavone	Santal

Table 1 *Continued*

Generic name	Generic structure	Example	
		Name	Usual name
Homoisoflavone		3,4',5',7-Tetrahydrohomoisoflavone	Sappanon A
Chalcone		3,4,4',5,6'-Pentahydroxychalcone	Robtein
Aurone		3',4',6-Trihydroxyaurone-6-glucoside	Sulfurein
Benzoquinone		3,6-Dihydroxy-2,5-di(p-hydroxyphenyl) benzoquinone	Atromentine
Naphthoquinone		2-Hydroxynaphtoquinone	Lawsone
Coumarin		7,8-Dihydroxycoumarin-7-β-D-glucoside	Daphnin
Anthraquinone		1,3-Hydroxy-2-carboxyanthraquinone	Munjistin
Xanthone		1,7-Dihydroxy-9H-xanthen-9-on-7-D-glucuronide	Euxanthic acid

Table 1 Continued

Generic name	Generic structure	Example	
		Name	Usual name
Phenoxazone		α -Aminoorcein ($R_1 = \text{Me}$, $R_2 = \text{NH}_2$, $R_3 = \text{orcinol}$)	Orcein ^a
Indole		6,6'-Dibromoindigotine	Purple ^a
Berberine		5,6-Dihydro-3-hydroxy-2,9,10-trimethoxy dibenzo[a,g]quinolizinium hydroxide	Berberine

^aThe name of a natural mixture of related compounds. It's applied here when the particular usual name of the compound does not exist.

such as ethyl acetate have been proposed for general extraction purposes. The choice of extraction solvent and conditions affects the quantitative aspects of dyestuff analysis.

Even the use of water, and especially warm water – traditionally used for the recovery of colouring matter – may also introduce composition changes. Many natural dyestuffs are heterosides (gluco-, rhamno-, primeverosides and other) and can become aglycone forms through the action of enzymes (e.g. glucosidases) present in living organisms. Their activity can be inhibited either by excessive heating (boiling) or by the addition of denaturation factors (alcohols, strong electrolytes).

For quantification purposes, especially in pharmaceutical and cosmetic laboratories, extracts are analysed after acid hydrolysis. The hydrolysis of heterosides transforms them into related aglycones (e.g. ruberythric acid to alizarin). This treatment simplifies the chromatogram, because one aglycone can be obtained from several monosaccharide or disaccharide derivatives and the number of chromatographic peaks decreases (Figure 1).

Coloured Matter Samples Extraction

Acid hydrolysis has remained a quasi-universal method of natural dyestuff extraction from dyed and stained supports. The extraction medium is usually composed of an aqueous mineral acid solution (e.g. HCl or H₂SO₄), sometimes with the addition of meth-

anol to prevent possible precipitation of some compounds. This hydrolysis destroys chemical ionic and coordination links between dye molecules and support or mordant complexes. Fixed extraction conditions are the goal of repetitive results, because of possible partial structural change or destruction of several compounds. In applied acid solutions a depolymerization of oligomeric and polymeric molecules (e.g. gallotanins to gallic acid, lacmus to orceines) can be observed. The amount of acid usually employed in the extraction medium is also enough to catalyse the oxidation of homoisoflavonoids (e.g. haematein to haematoxylin). The major transformation remains, nevertheless, the aglyconeization of the heterosides. Decomplexation with ligands stronger than the dyestuffs has been proposed to improve the recovery of complex dyes by avoiding hydrolysis of heterosides.

In the special case of a non-soluble matrix, as for organic pigments in drying oil layers from paintings, the direct derivatization with *m*-(trifluoromethyl) phenyltrimethylammonium hydroxide (TMTFTH), followed by methylation of paint medium with boron trifluoride/methanol (BF₃/MeOH) is employed. This method provides good recovery of dyestuffs, principally anthraquinoids. Its main inconvenience is the formation of multiple methylated derivatives for some compounds.

Vat dye constituents are very sparingly soluble in aqueous solutions. Some indigoids are soluble in

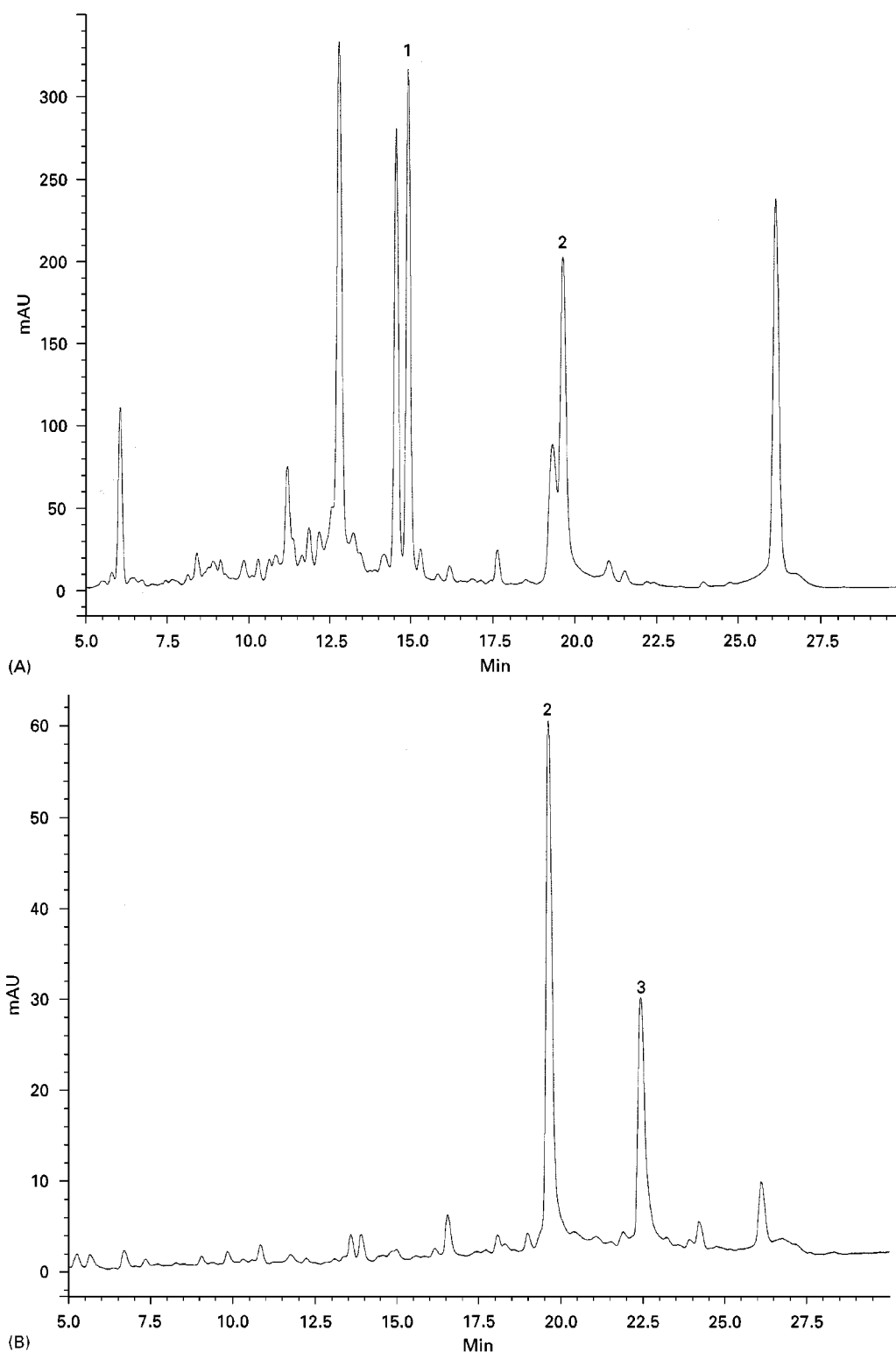


Figure 1 Influence of hydrolysis on composition of dyestuff extracted from root of Madder (*Rubia tinctorum* L.). (A) Chromatogram of fresh aqueous extract; (B) the same extract after acid hydrolysis. Compounds: 1 ruberythric acid (β -2-alizarin primeveroside), 2 alizarin, 3 purpurin.

chloroform, but one of them – 6,6'-dibromoindigotine from so called 'true' or 'Tyrian' purple – is well known as a 'soluble-in-nothing' compound. In fact,

for a satisfactory extraction of all compounds from vat dyes, heated pyridine, dimethylformamide (DMF) or dimethyl sulfoxide (DMSO) is necessary. Pyridine

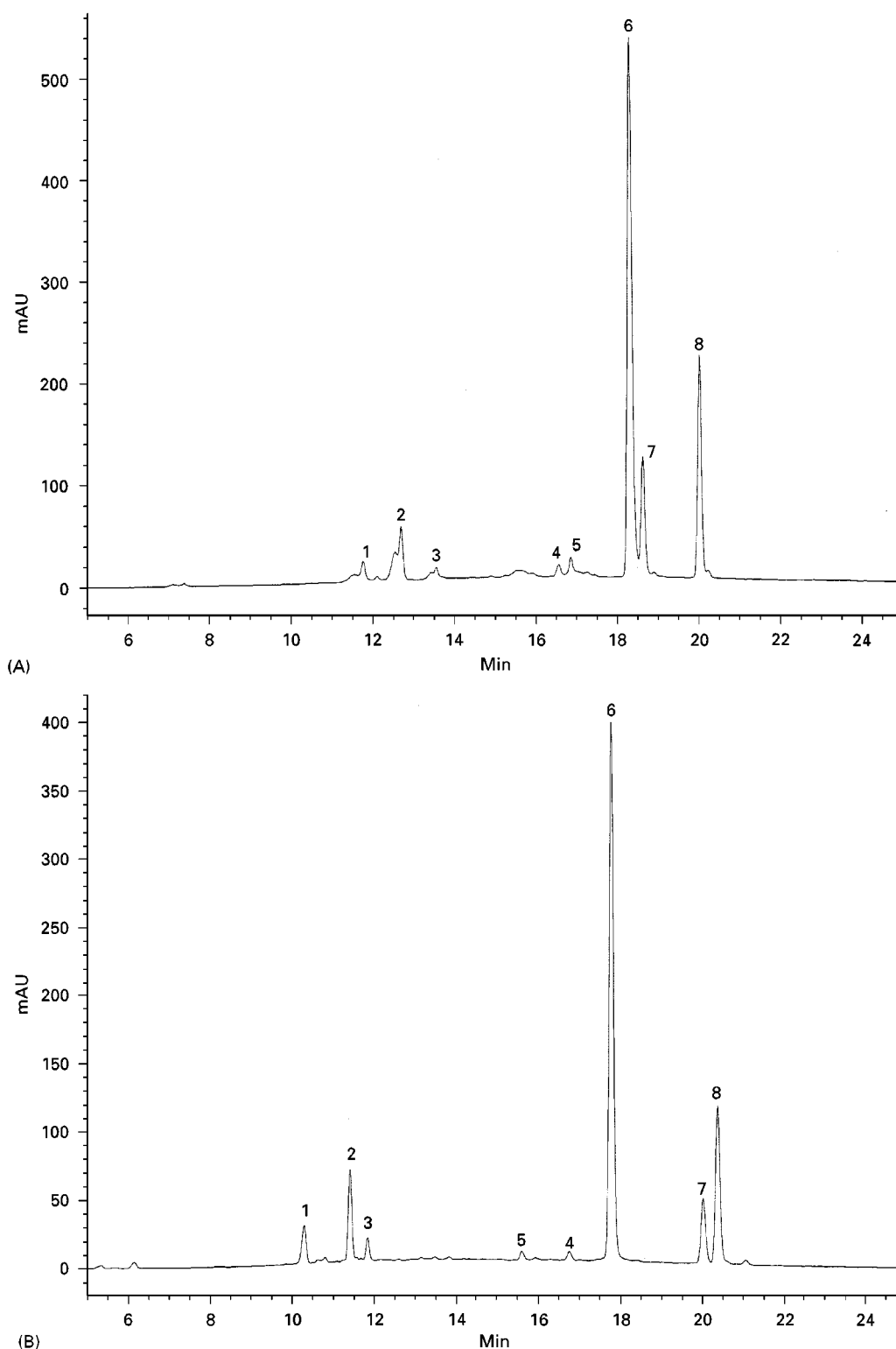


Figure 2 Influence of aqueous mobile phase composition and RP-18 stationary phase brand on separation of dyestuff from Dyer's Broom (*Genista tinctoria* L.). (A) Hypersil BDS, 3 μ m, 100 \times 4.6 mm; 80% H₂O–10% MeOH–10% of 0.5% H₃PO₄, from 1 to 40 mn gradient MeOH 90%. (B) Hypersil BDS, 3 μ m, 100 \times 4.6 mm, 85% H₂O–5% MeCN–10% of 1% MSA, from 1 to 40 mn gradient MeCN 50%. (C) Adsorbosphere HS, 3 μ m, 100 \times 4.6 mm; 85% H₂O–5% MeCN–10% of 1% MSA, from 1 to 40 mn gradient MeCN 50%. Compounds: 1–5 nonidentified, 6 luteolin, 7 genistein, 8 apigenin.

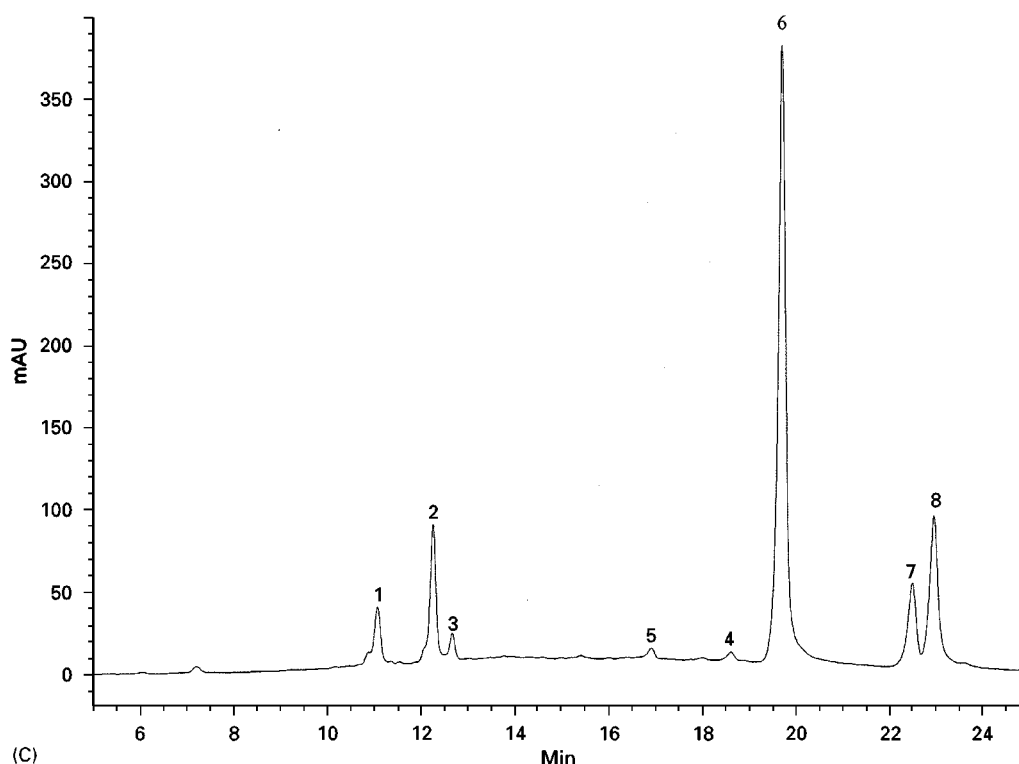


Figure 2 Continued

is quite toxic and apparently destroys alkyl-bonded silica stationary phase when extracts are separated. The indigotins in DMF solutions isomerize to related indirubins with the help of ultraviolet light. DMSO is very viscous and displays mixing problems (known as 'viscous fingering') when the aqueous mobile phase is employed and affects stationary phase efficiency (ranging from poor peak shape to multiple peaks). It appears that DMF is the best medium, under conditions of time- and temperature-controlled extraction, even if its viscosity makes large volume injections difficult.

Chromatography

Mobile Phases

The solubility of natural dyestuffs covers practically the entire range of solvent polarities, from water to *n*-hexane. Still, many of them are soluble in both moderately polar organic solvents (e.g. chloroform) and water. These properties are linked to the compounds' structures. In addition to their generic, low polar, aromatic or isoprene structures, they usually contain polar groups, especially proton-releasing ones such as hydroxyl and carboxyl. Practice shows that the use of water with some organic water-miscible solvents solubilizes almost all classes of dyestuffs.

Such behaviour of natural dyes determines the type of chromatographic system used. Apart from the tentative applications of a normal phase (silica) and a nonpolar eluent, reversed-phase conditions are most often applied.

The solvent system is commonly composed of water, an organic modifier and an ion suppressor or counterion.

Many ion suppression reagents are used to control pH. At pH around 2.5 most dyestuffs are unionized but some basic compounds become ionized (e.g. berberine, which is fortunately rather rarely encountered). The most popular acids are *o*-phosphoric (H_3PO_4) and acetic (CH_3COOH , AcH), but in the case of mass spectrometry (MS) on-line detection they should be replaced by volatile trifluoroacetic acid (TFA). To avoid the formation of poorly soluble salts of basic compounds and/or to improve peak shapes, methanesulfonic acid (MSA) has been proposed (Figure 2, compare A and B).

The use of counterions is less habitual owing to the considerable equilibrium stabilization time needed for the stationary phase in gradient analysis.

Analysis time in both isocratic and gradient elution is usually between 15 to 45 min, depending on the type and the number of compounds requiring separation.

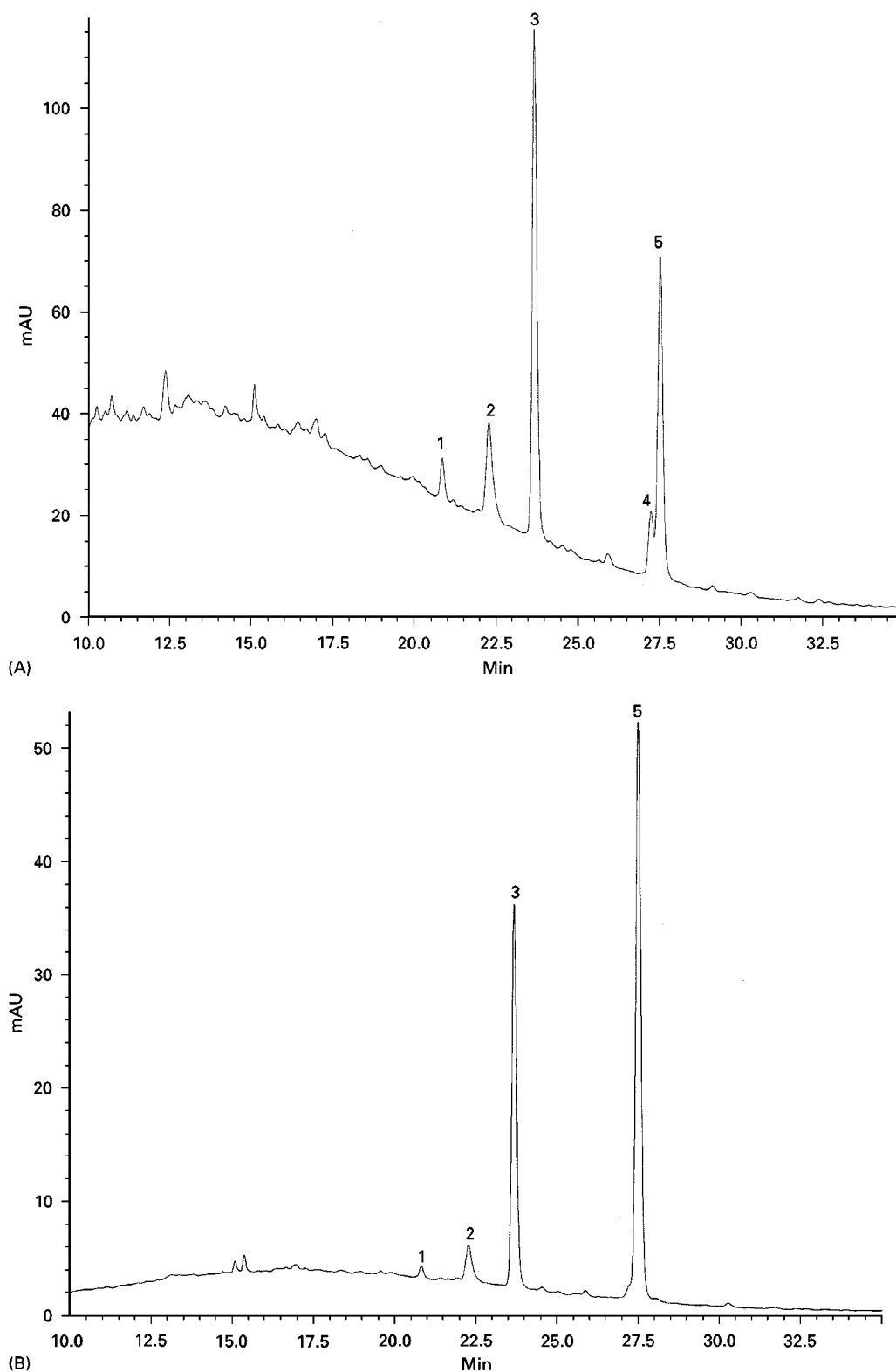


Figure 3 General and selective UV-vis channel detection of violet dyed wool sample (Coptic textile, 6th century). (A) General detection at 285 nm; (B) specific detection of red components corresponding to Madder at 450 nm; (C) specific detection of indigo blue at 615 nm. Compounds: 1 anthragallol, 2 pseudopurpurin, 3 alizarin, 4 indigotin, 5 purpurin.

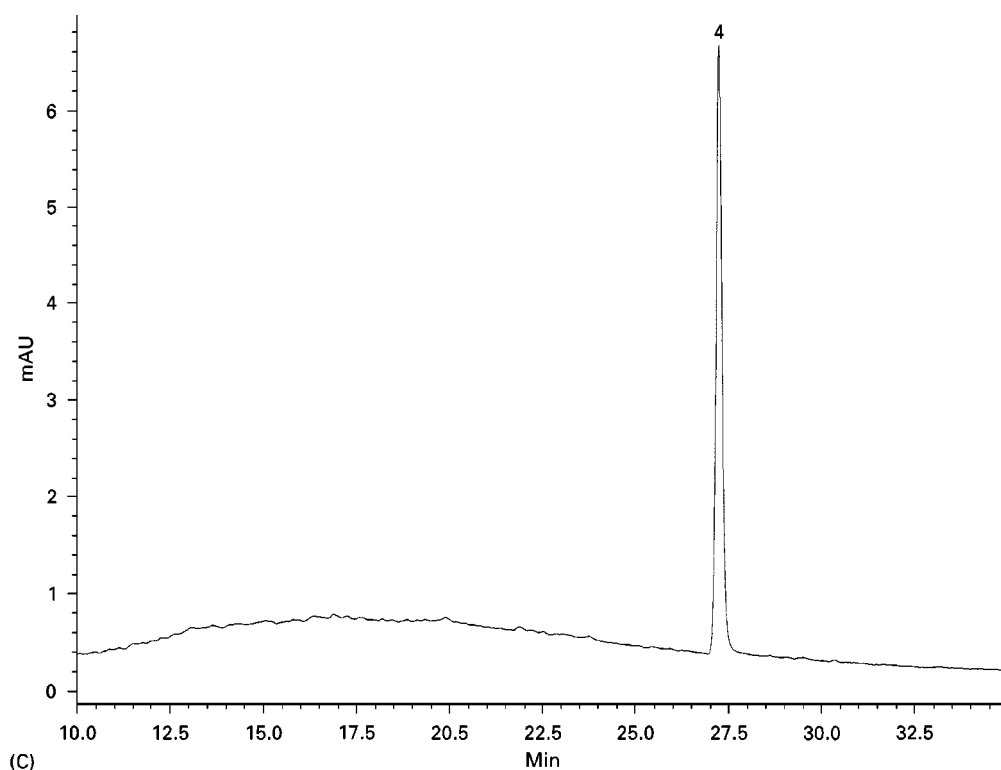


Figure 3 Continued

Stationary Phases

Among the stationary phases used in natural dye-stuffs analysis, the major part of applications is achieved on octadecyl (called RP 18, or C 18) bonded silica. This type of phase is the most versatile; however, different brands bring about important differences in separation characteristics (Figure 2, compare B and C). The octyl (RP 8) and phenyl (Ph) phases have some specific applications and can offer other, sometimes more satisfactory separations than RP 18 in specific cases.

Advances in natural dyes chromatography follow general trends: a growing efficiency of separations and reduced separation time as well as increased sensitivity of detection. This is the reason for the constant testing of the types of stationary phases, and of the rising use of smaller and more uniform particles and also of shorter and narrower columns.

Detection and Identification

Detectors

Dyestuff components show strong selective absorption in the UV-vis spectrum. This effect is responsible for their coloration and makes absorption detection simple. In the case of single or multichannel detectors, the recognition of compounds is based on retention

time and, if possible, on absorption at characteristic wavelengths, usually in the visible (e.g. 360 nm for yellows, 485 nm for reds, 650 nm for blues, etc., with a suitably large bandwidth) (Figure 3). The photodiode array (PDA) gives the possibility of confirmation of compound identity by the corresponding peak spectra (Figure 4).

The principal inconvenience of UV-vis detection is the recognition of only those substances entered as references in the database. Even the PDA gives only partial structure recognition because of limited UV-vis information contained in the spectra and their possible alteration in different mobile phase compositions. New compounds have to be collected at the detector exit and analysed by other, usually spectrometric, methods. This problem can be avoided by application of on-line mass spectrometry, giving more precise information about the molecular structure. An interesting approach to detection can be in-line tandem of PDA and a mass-selective detector (MSD) permitting pre-selection of coloured compounds and thus their detailed analysis.

Sources Recognition Criteria

High-performance liquid chromatography analysis of natural dyes gives an identification of compounds. From this information, as a first step, a chemical class or dyeing group can be deduced. Moreover, the

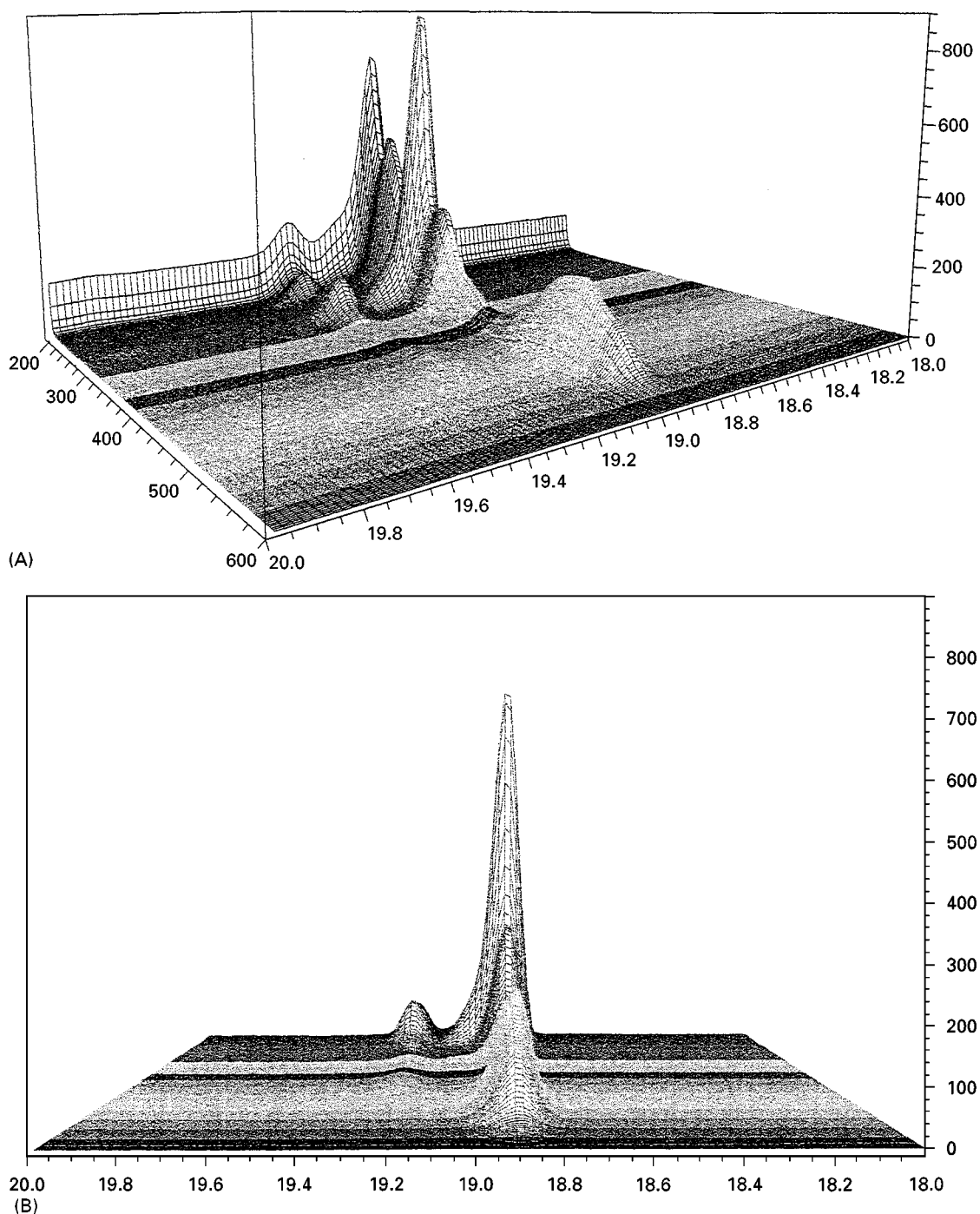


Figure 4 Representation of a fragment of data collected from PAD during the analysis of extract from females of Kermes (*Kermes vermilio* PLANCH). Kermesic acid (higher absorption) and flavokermesic acid (lower absorption). (A) General view (axes: x = time, y = wavelength, z = absorption); (B) Chromatograms cut display (x , z). (C) Spectra cut display (y , z).

qualitative and quantitative information about the compounds detected in a chromatogram can help in dyestuff source recognition. This is the aim of chemotaxonomy, employed for many purposes: in biology, in the history of civilizations, in forensic sciences, etc. In general, analysis of colorants from plant and animal material give a few major and a lot

of minor peaks on chromatograms recorded at the colour-characteristic wavelengths. The corresponding characteristic compounds are adequate for the identification of botanical or zoological phylum, family, subfamily, group or genus, but can also be common for several, quite different species (Figure 5). Species identification is based on the relative

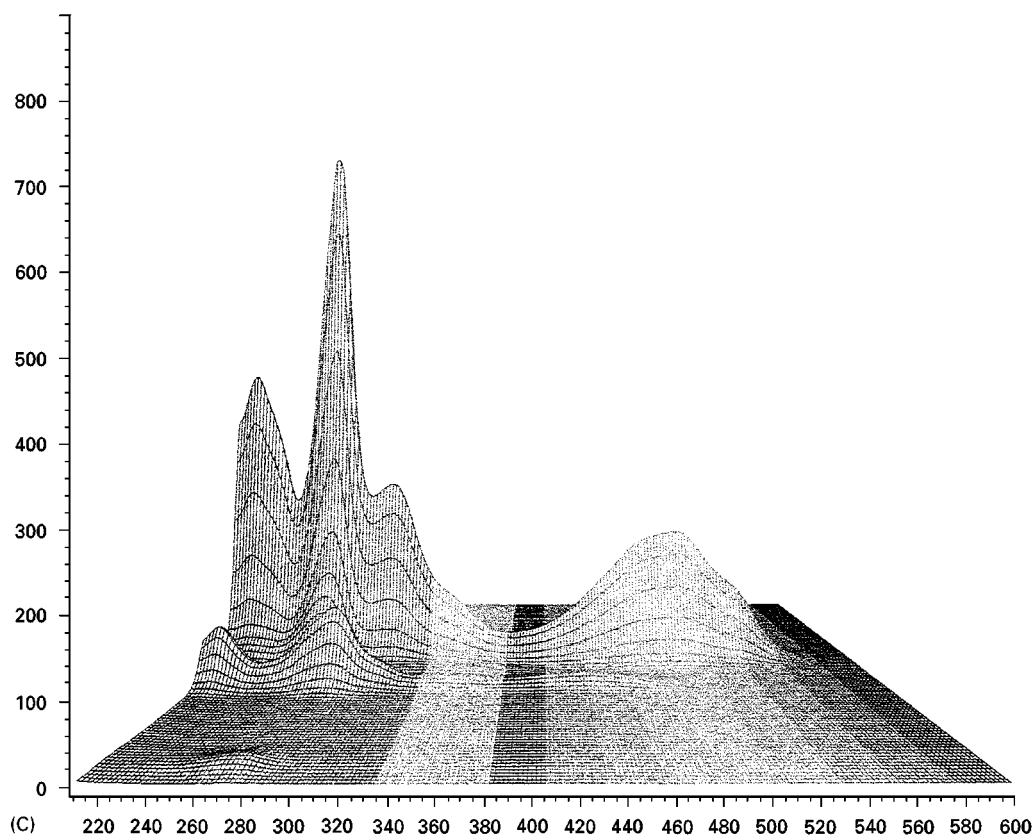


Figure 4 *Continued*

quantity and identity of marker compounds. Their presence or absence is characteristic for only one species. Given the complexity of colorants originating from natural sources, as is the case for other natural substances, sometimes it should be satisfactory to obtain and to compare just their fingerprints.

The chromatographic fingerprints appearance depends on sample preparation, separation conditions and detection principles. That is why the constitution of one's own database containing the results of analysis of reference samples according to established, invariable and repeatable procedure is required.

Extra-Analysis Factors Affecting Dyes Composition

The analytical results obtained from real, coloured objects sometimes show important differences in dye composition in comparison with reference samples from one's own database or published data. These differences limit a clear interpretation and source identification. Such a situation is a result of one or more factors, of which the most important are quantity of sample, method of dyestuff preparation and ageing of the dye.

The quantity of coloured sample necessary for analysis depends on the total contents of the dyestuff

in the sample. In the first approach this can be evaluated as a function of colour intensity. Of course, precise evaluation is more complex and should consider the substrate (or matrix) material properties such as surface-to-mass ratio, parameters of penetration of dyestuff in mass of matrix and others. Substrate physicochemical behaviour can influence the sample preparation method prior to analysis and extraction efficiency. Preparatory treatment may modify dyestuff component proportions.

By diminishing sample size, the analytical information about dyestuff composition is progressively lost, starting with 'disappearance' from chromatograms of trace substances and continuing through the vague appearance of minor components until the identification of principal compounds is finally uncertain. As a result source recognition precision declines and becomes more difficult to perform. Still, this effect does not affect the relative quantity of dyestuff components. The lower limit of detection depends on performances of the chromatographic system and detector used.

Another modifying factor, dyestuff preparation, affects many stages, from raw material extraction to deposition on substrate. For each step, a multitude of recipes were invented using diverse plant parts and

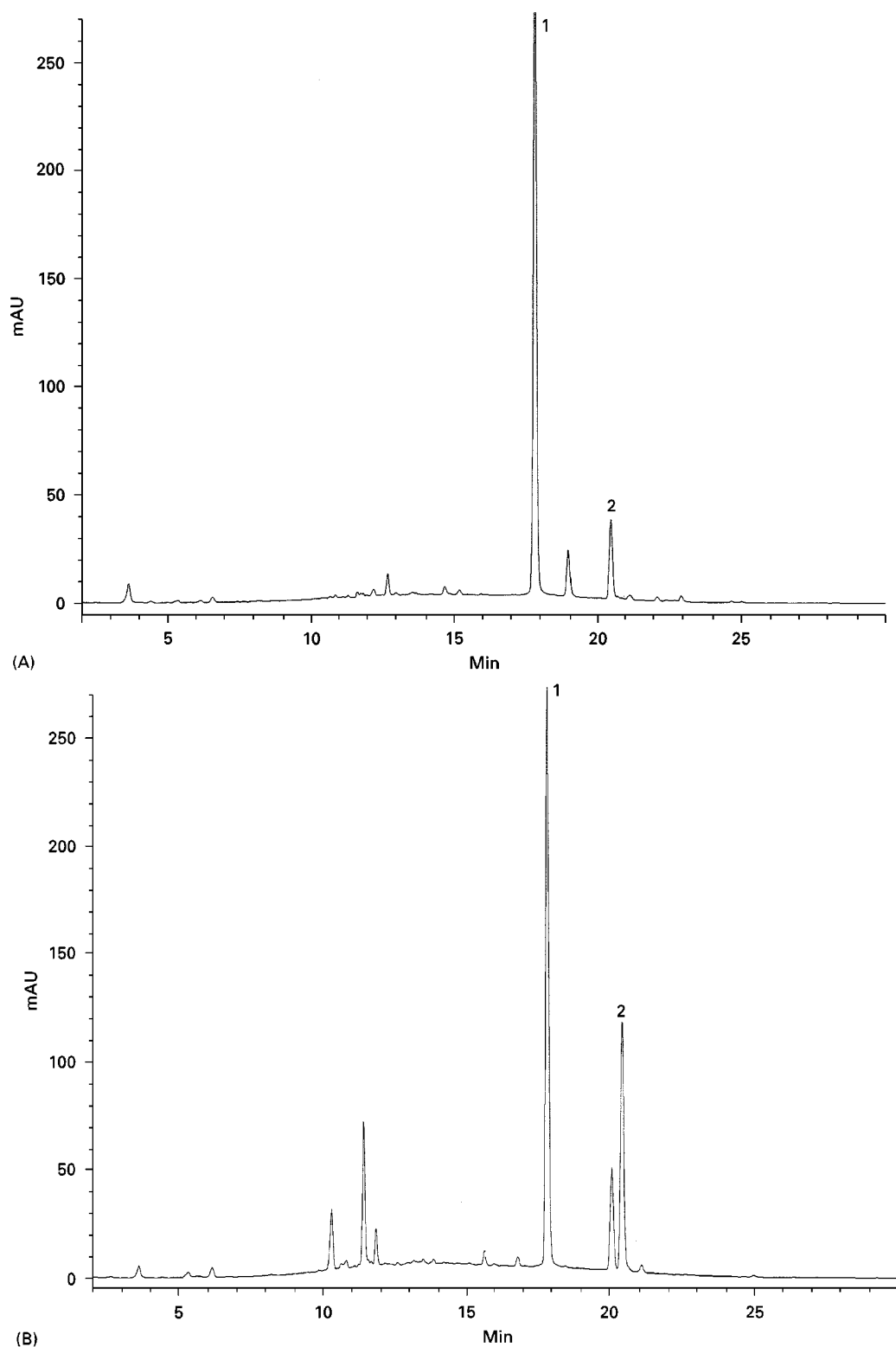
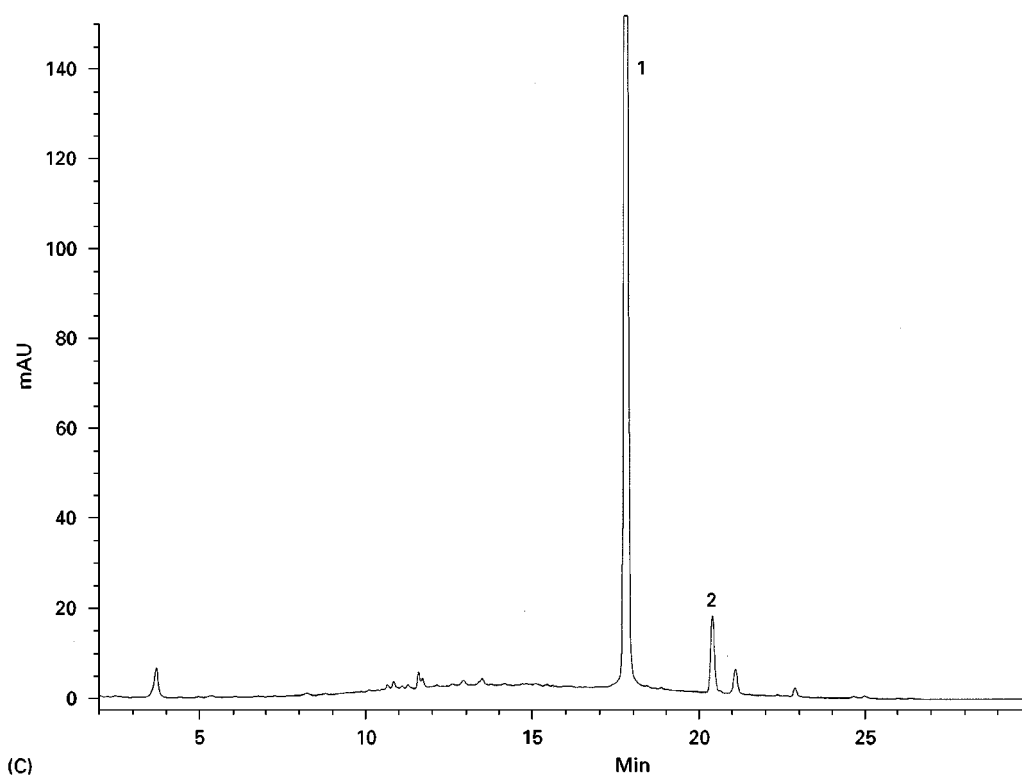
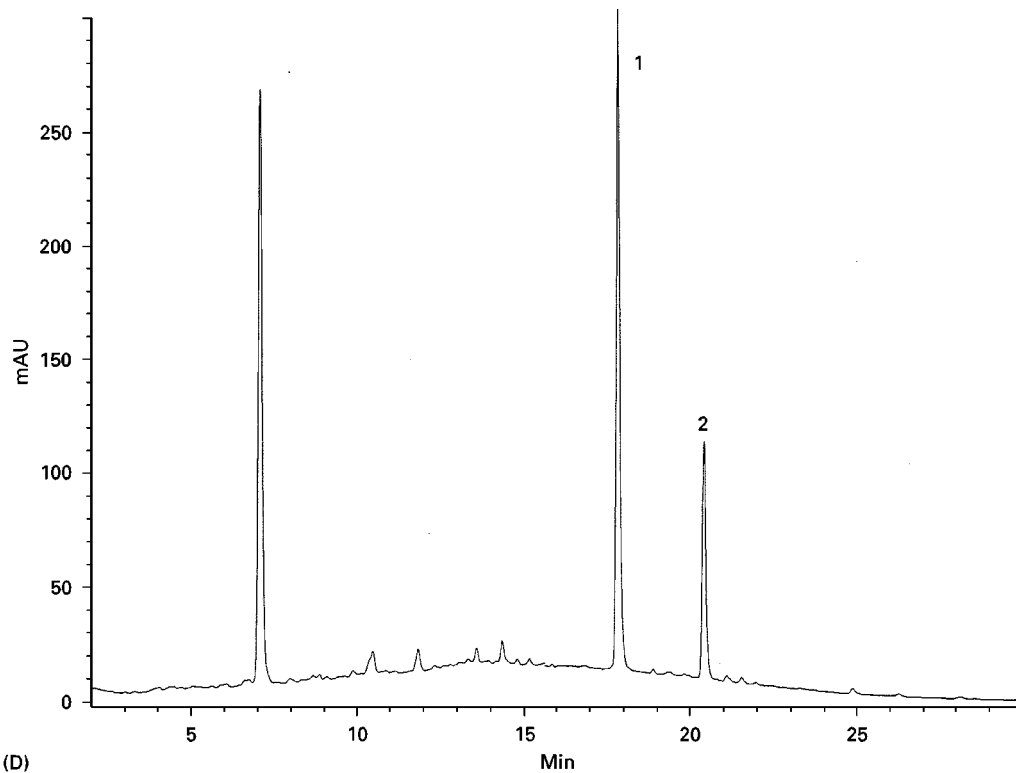


Figure 5 Some reference samples dyed with European plant extracts containing both luteolin (1) and apigenin (2) (detection at 345 nm). (A) Saw-wort (*Serratula tinctoria* L.); (B) Dyer's Broom (*Genista tinctoria* L.); (C) Weld (*Reseda luteola* L.); (D) *Daphne gnidium* L.



(C)



(D)

Figure 5 *Continued*

varying operation procedures, as well as the addition of different organic and mineral substances to the dyestuffs extracts and dyebaths (Figure 6). Lack of

recent systematic study of the influence of different operations and additives on dye composition restricts interpretation.

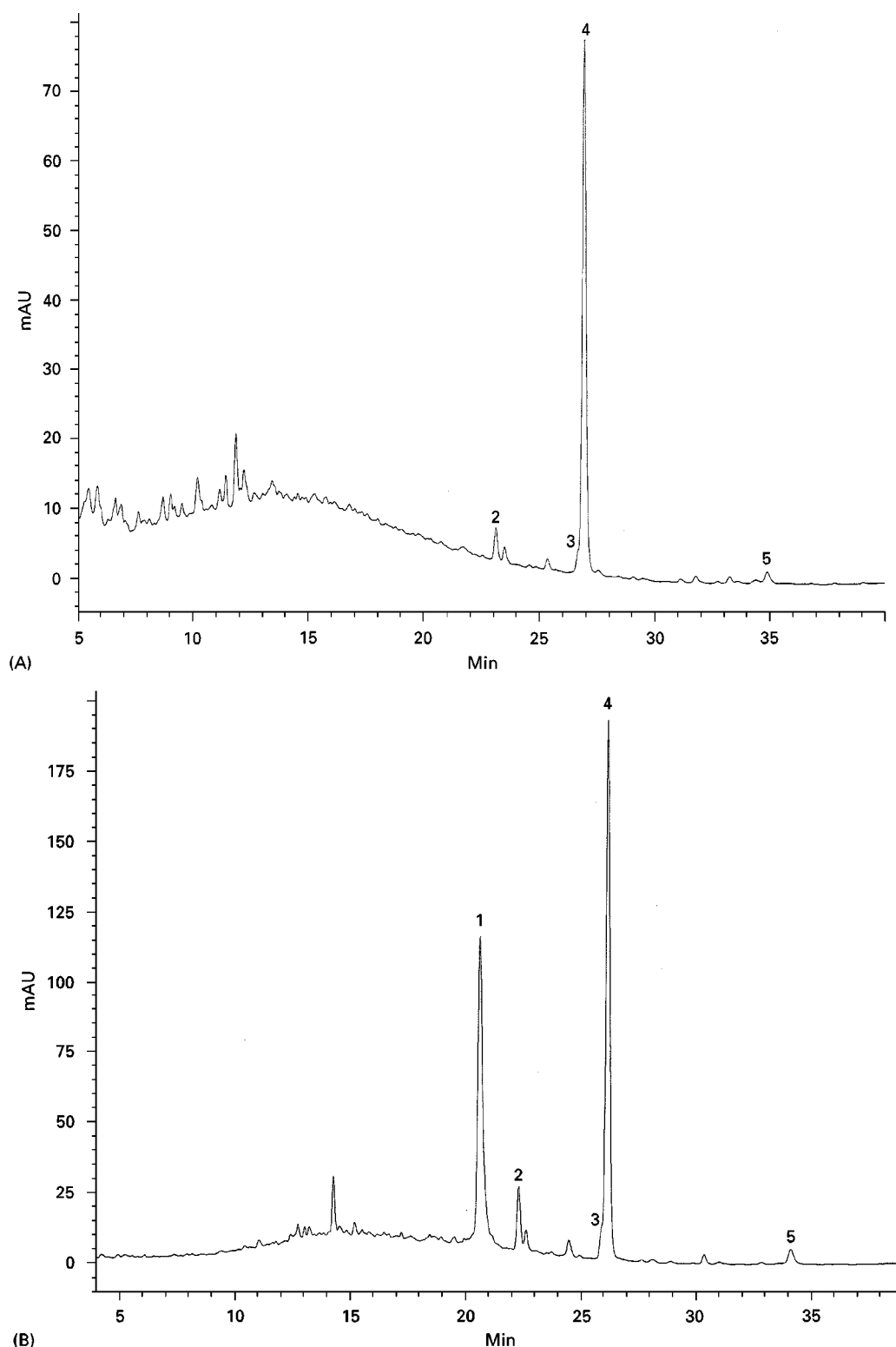
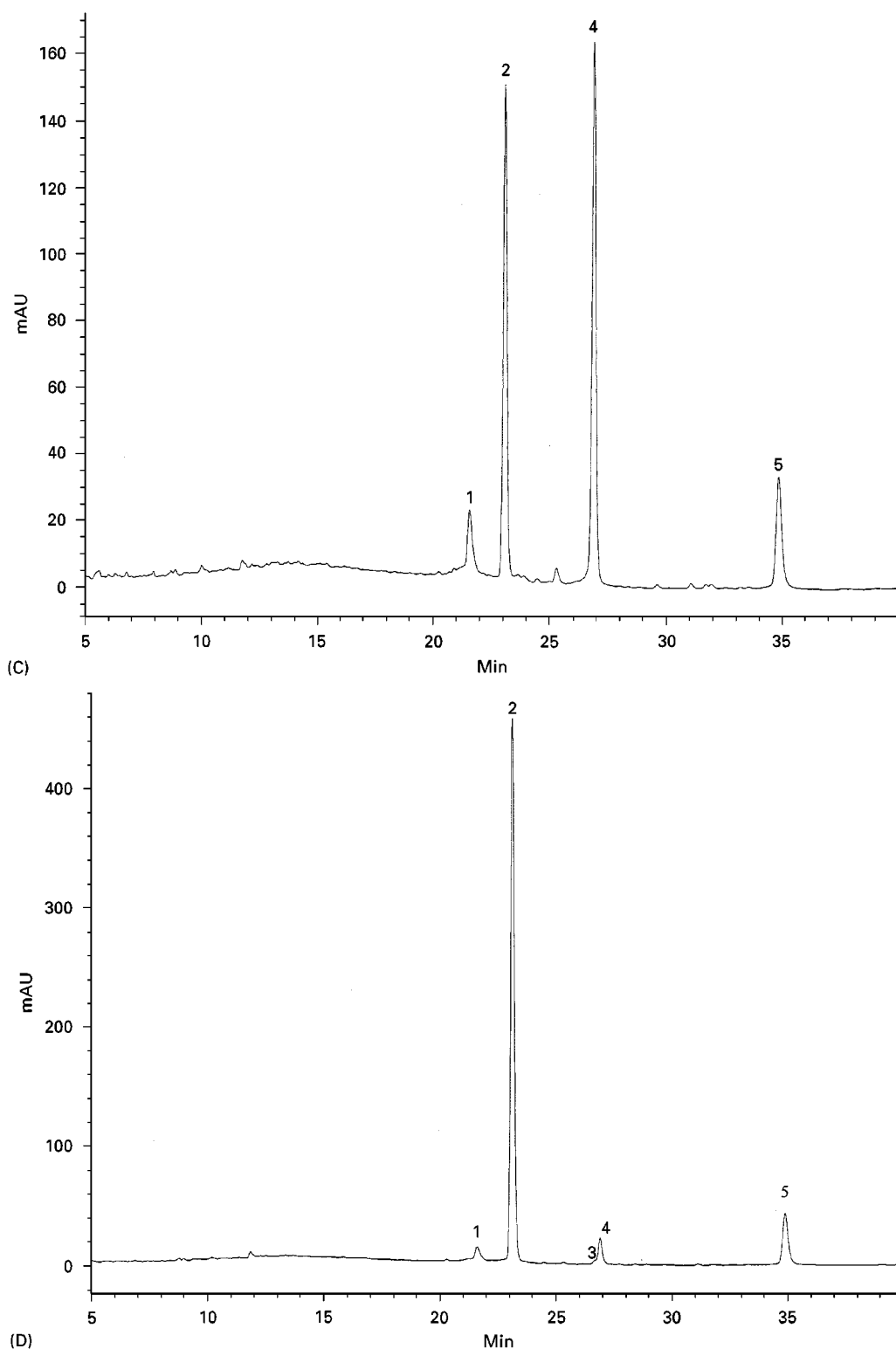


Figure 6 Four contemporary reference samples of wool dyed with Madder (*Rubia tinctorium* L.) obtained from different dyers (detection at 254 nm). Compounds: 1 pseudopurpurin, 2 alizarin, 3 xanthopurpurin, 4 purpurin, 5 unidentified anthraquinone.

A third possible dyestuff composition change determinant, which is very important in historical samples, is ageing (Figure 7). The generic name ‘ageing’ en-

folds the conjugated impacts of many physical and chemical factors. Light is considered as the most important of them in dyestuffs degradation. In

**Figure 6** *Continued*

comparison with other colouring matter (e.g. mineral pigments), the stability of dyes' molecular structures under visible light, and especially ultraviolet excita-

tion is poor. Other important factors are water (even as air humidity), air constituents (e.g. ozone), air pollutants (above all sulfur and nitrogen oxides) and,

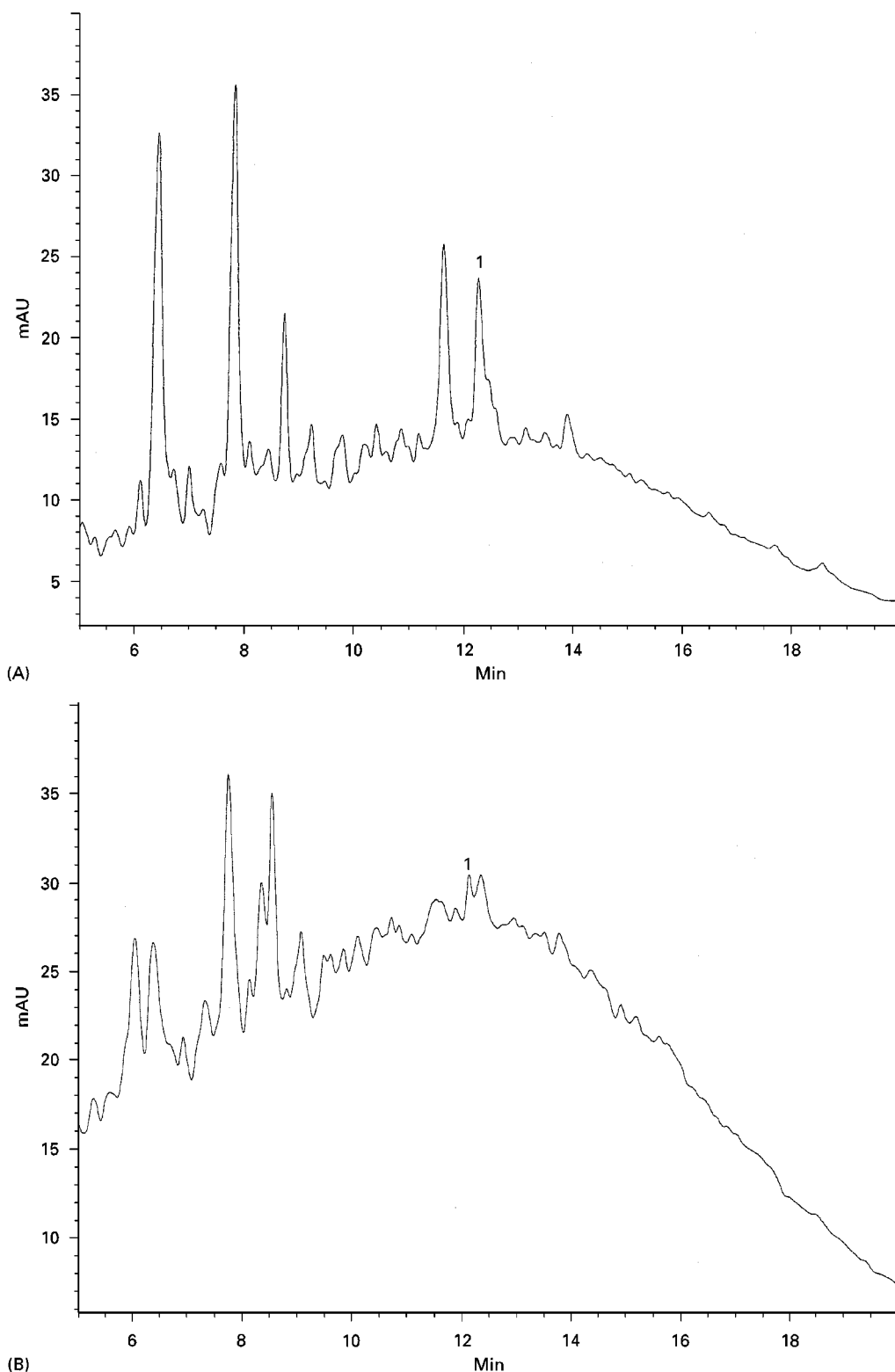


Figure 7 Accelerated ageing of dyestuff extracted from Brazil (*Caesalpinia sappan* L.) (detection at 285 nm) (A) Freshly dyed wool; (B) Sample after standardized accelerated ageing. Compound 1: brazilein derivative formed during acid hydrolysis.

for archaeological excavated objects, mineral salts solutions giving dangerous pH values. Each of the ageing elements presented represents just a part of the

global process. Determination of their particular roles is possible but does not allow exact modelling or reproduction because of probable synergy between

them. In any case, the methods of 'artificial' ageing (also called 'accelerated' ageing) give a good approximation, sufficient for comparative colour fastness testing.

For textile fabrics it is important to mention the influence of washing and solvent cleaning on the presence of dyestuffs. Their resistance to wet cleaning methods (wash-fastness) is principally related to the dyeing group and washing conditions. Some dyestuffs or their components are sensitive to washing. Such textile handling also belongs to 'ageing', but the adjective 'natural' is in this case probably less adequate.

During ageing two effects are generally observed: hue change and fading. Change of hue is a result of partial dyestuff fading, because of different degradation rates of dye components. Chromatograms obtained from such samples show qualitative and quantitative differences from the original dyestuff. Real sample composition can be ambiguous and similar to several sources, especially if the markers are absent: *in extremis* it can be so far from any known reference that the question of a 'new', not yet identified source can appear. This kind of hypothesis always merits scrupulous verification.

Fading usually signifies transformation of coloured compounds into colourless products. Recent developments in HPLC-MS provides a way to identify original dyestuffs in discoloured samples from their degradation products, even in small amounts. This approach corresponds to expectations of specialists in various domains and will certainly be developed in the future.

Conclusion

In spite of many historic and recent scientific works concerning the chemistry and analysis of natural dyestuffs, our knowledge of this subject still seems to be far from exhaustive. The contribution of HPLC in advances of chemotaxonomy of dyestuffs of plant and animal origin has attracted growing interest in recent years. This technique is relatively easy to perform and does not need any complex sample preparation. Its performances are sufficient for good separation of many dyestuff components in a reasonable time. The HPLC technique provides the possibility of both qualitative and quantitative analysis of separated compounds by employing detectors considered as standard in liquid chromatography (UV, UV-Vis, PDA) or recently adapted, powerful techniques of detection (MSD).

Problems still remaining are directly linked to the biosynthesis of natural dyes (possible pathway vari-

ation) and to their properties (stability, transformation and degradation). They are the principal phenomena affecting chromatogram interpretation. Many of the compounds separated have not yet been identified. Their identification will thus certainly be the objective of future works.

See also: II/Chromatography: Liquid: Detectors: Ultra-violet and Visible Detection. **Extraction:** Solvent Based Separation.

Further Reading

- Dzido TH, Soczewinski E and Gudej J (1991) Computer-aided optimization of high performance liquid chromatographic analysis of flavonoids from some species of the genus *Althea*. *Journal of chromatography* 550: 71.
- Evans KP and Truslove NJ (1993) Advances in chromatography for dyestuffs. *Review of Progress in Coloration* 23: 36.
- Fischer Ch-H, Bischof M and Rabe JG (1990) Identification of natural and early synthetic textile dyes with HPLC and UV/Vis spectroscopy by diode array detection. *Journal of Liquid Chromatography* 13(2): 319.
- Halpine SM (1995) An improved dye and lake pigment analysis method for high-performance liquid chromatography and diode-array detector. *Studies in Conservation* 41: 76.
- Justensen U, Knutsen P and Leth T (1998) Quantitative analysis of flavonols, flavones, and flavanones in fruits, vegetables and beverages by high-performance liquid chromatography with photo-diode and mass spectrometric detection. *Journal of Chromatography A* 799: 101.
- Kirby J and White (1996) The identification of red lake pigment dyestuffs and a discussion of their use. *National Gallery Technical Bulletin* 17: 56.
- Koren ZC (1994) HPLC analysis of the natural scale insect, madder and indigoid dyes. *Journal of the Society of Dyers and Colourists* 110: 237.
- Nogata Y, Ohta H, Yoza K-I, Berhow M and Hasegawa S (1994) High performance liquid chromatographic determination of naturally occurring flavonoids in *Citrus* with a photodiode-array detector. *Journal of Chromatography A* 667: 59.
- Schweppe H (1992) *Hanbuch der Naturfarbstoffe*. Landsberg am Lech: Ecomed.
- Wouters J (1998) Qualitative and quantitative analysis of tannins extracted from new and aged leathers, by high performance liquid chromatography. *Bulletin de l'Institut Royal du Patrimoine Artistique* 26: 199.
- Wouters J and Verhecken A (1989) The coccid insect dyes: HPLC and computerized diode-array analysis of dyed yarns. *Studies in Conservation* 34: 189.
- Wouters J and Verhecken A (1991) High-performance liquid chromatography of blue and purple indigoid natural dyes. *Journal of the Society of Dyers and Colourists* 107: 266.

Thin-Layer (Planar) Chromatography

P. E. Wall, Merck Limited, Poole, Dorset, UK

Copyright © 2000 Academic Press

Introduction

Synthetic dyes comprise a large group of organic, organic salt and organometallic compounds which number in the thousands. Most individual dyes are assigned colour index (CI) numbers which helps to identify structure and properties as well as identity where a series of names have been used by the manufacturers for the same dye. Pigments are also listed and can be either organic or inorganic in nature. The value of planar chromatography in the identification of dyes and separation of impurities and their quantification is the main subject of this article. Synthetic dyes will be split into nine groups, the first three being the major ones. For all these groups, the development of modern thin-layer chromatographic (TLC) methods will be compared where possible with older TLC procedures.

Use of TLC for the Separation of Dyes

Synthetic dyes and pigments are used in a wide range of industries. They are the colours of printing inks, textile dyes, cosmetics, plastics, histological and cytological stains, and some are permitted as food and drink colorants. In some of these applications purity is important, in others it is the presence or absence of certain impurities or intermediates, and in still others it is the identification and uniformity that is important. In all these instances planar chromatography has proved to be the ideal solution with the separation power and spot/zone capacity necessary to resolve closely related dyes and intermediates. This has been made possible by the wide selection of stationary phases and the almost unlimited variations possible with mobile-phase mixtures, sometimes composed of quite aggressive solvents that would not be used in column liquid chromatography. The only limiting criteria for the solvent mixtures are adverse effects on the adsorbent binder, reaction with the bonded phases and high viscosity and surface tension of the solvents.

There are a number of other advantages to the use of TLC for the analysis of dyes compared with other chromatographic techniques. The most obvious is

that dyes are easily visualized on a chromatographic layer by their colour. Often slight differences in hue are more clearly seen on the layer than in solution and hence are easily distinguishable. It is therefore rarely necessary to employ detection reagents unless the area of interest is dye intermediates which may lack the conjugation needed in their molecular structure to be coloured in visible light. Of course, there are a large number of dyes which either exhibit fluorescence quenching in short wavelength ultraviolet (UV) light (254 nm) or naturally fluoresce by excitation in long wavelength UV light (usually 366 nm). Where separated dyes on the chromatographic layer do fluoresce, the limit of sensitivity of detection is often in the low nanogram or high picogram level. In the commercial environment, as dye quality can vary from batch to batch and colour can be matched by using different dyes, the planar chromatographic technique allows the analysis of many samples against references or certified standards on the same layer under the same conditions in one development run. Hence the analysis time and the cost per sample are substantially lower when compared with liquid chromatography.

In most forms of chromatography, as in many spectroscopic analyses, the extraction of the dye from whatever matrix is being considered and the subsequent sample pretreatment are often time-consuming, but usually necessary as impure dyes notoriously contain many impurities that are easily and firmly retained on the chromatographic adsorbents. Liquid chromatographic columns and pre-columns quickly become 'poisoned' and then either have to be discarded or require extensive solvent clean-up before re-use. In TLC only minimal clean-up or extraction is required as most polar impurities will remain at or near the origin of application and more nonpolar ones will migrate with the solvent front (normal-phase separation). As the thin-layer plate is not re-used, the unseparated material at the origin or at the solvent front is of no consequence. However, the chromatograms obtained are a source of extensive data about the dye separation. Not only can the chromatographic tracks be scanned spectrodensitometrically, but individual UV/visible spectra of the separated chromatographic zones can be recorded, and a number of other spectroscopic techniques such as mass spectrometry (MS), nuclear magnetic resonance (NMR), Fourier transform infrared (FTIR) and Raman spectra can be applied.

For use in histology, many reference standards are available, as tested and approved by the Biological Stains Commission. Such dyes and stains are labelled accordingly, usually giving the dye content for the batch as numbered. Most such dyes are single components, but where it is known to be composed of two or more components (e.g. methylene violet (3)), azure A or C (up to 6), methyl violet (4), aniline blue (3) and fast green FCF (3)), the dye content will be based on the named dye (usually the major component). The testing of dyes suitable for histology and cytology has always relied on a number of wet chemistry tests, UV/visible spectral analysis, TLC analysis and the actual performance as a stain. The wet chemistry tests include titanous chloride assay, sulfated ash and moisture content. The total dye content has been determined by titration with standard titanous chloride solution and measurement of absorbance (UV). High performance TLC (HPTLC) not only can be used to determine accurately the total dye content, but also the concentration of the individual components if, as so often happens, the sample is either a mixture of dyes or there are impurities present that are closely related structurally to the parent dye (e.g. determination of crystal violet (hexamethyl-pararosanilin) in methyl violet 2B, 3B, 6B or 10B (a mixture of various proportions of hexamethyl-, pentamethyl-, tetramethyl-, and trimethyl-pararosanilin)).

In most industrial uses of dyes (textiles, printing and plastics) and in forensic work, TLC is used for identification and on some occasions to quantify these results. In the commercial environment textile dyes are not normally marketed in the pure state. Both the end user and the manufacturer of the dyes are mainly interested in a dye of standard reproducible quality in their application rather than chemical purity. For this reason the TLC analysis of the dyes for textile, cosmetic or printing purposes presents different problems to that for staining purposes in histology. A commercial dye will often contain impurities composed of by-products of the dye synthesis and starting materials. Inorganic salts are usually present: these have been used to 'salt out' or precipitate the dye during manufacture or they may have been added as extenders, so that different batches have the same dyeing potential. Variations in colour hue are sometimes adjusted by the addition of another dye.

In histology and cytology, although the identity of the dye is important, the purity plays an important part. It has also been realized that other dye impurities need to be present to give a superior quality stain. Both Giemsa and Leishman's stain are classic examples of this. In food and drinks, TLC of dyes can

Table 1 Individual permitted food dyes (depending on country)

<i>Permitted dye</i>	<i>E number</i>	<i>CI number</i>
Amaranth	E123	16185
Brilliant black (black PN)	E151	28440
Brilliant blue FCF	E133	42090
Carmoisine (azorubine)	E122	14720
Erythrosine	E127	45430
Ponceau 4R	E124	16255
Indigo carmine	E132	73015
Quinoline yellow	E104	47005
Red 2G	E128	18050
Sunset yellow FCF	E110	15985
Tartrazine	E102	19140
Yellow 2G (food yellow 5)	E107	

also be a useful technique, as only a limited number of dyes are permitted for food use (Tables 1–4). These are indicated on the label of the food or drink product and can easily be identified by TLC. The presence and identification of nonpermitted food dyes is one of the strengths of TLC.

Many of the early planar chromatography methods for dye analysis in the 1960s used paper or cellulose thin layers. Later, more methods, some still currently used, were based on silica gel G and aluminium oxide thin layers. In more recent times, commercially available pre-coated silica gel and cellulose layers with better reproducibility have become the preferred adsorbents for dye separations. This has become particularly the case where quantitative determinations are required for dye content on HPTLC plates.

Table 2 Recommended solvents/solvent mixture for the separation of lipophilic solvent (fat) dyes on silica gel 60 pre-coated TLC plates

<i>Solvent dye</i>	<i>CI numbers</i>	<i>Solvents for separation^a</i>
Sudan black B	26150	Dichloromethane
Fat red 7B	26050	Toluene
Sudan I	12055	Heptane–ethyl acetate (80 + 10 v/v)
Sudan II	12140	Cyclohexane–ethyl acetate (90 + 10 v/v)
Sudan III	26100	
Sudan IV	26105	
Butter yellow	11020	
Sudan red G	12150	
Indophenol blue	49700	
Diethyl yellow	11021	
Oil blue APS	61551	
Waxoline green G-FW	61565	
Waxoline red MP-FW	60505	
Waxoline yellow E	47000	
Oil red O	26125	

^aThese recommended solvents and solvent mixtures apply to all the solvent dyes.

Table 3 R_F values for a number of solvent (fat) dyes developed on silica gel 60 pre-coated plates

Solvent dye	R_F values (dichloromethane)	R_F values (n-hexane-ethylacetate (90 + 10 v/v))
Diethyl yellow	0.72	
Oil blue APS	0.34	
Waxoline green G-FW	0.64	
Waxoline red MP-FW	0.54	
Waxoline yellow E	0.12	
Sudan black B	0.10 (f), 0.18 (f), 0.22 (m), 0.61 (m), 0.85 (f)	
Waxoline blue	0.43 (m), 0.13, 0.79	
Sudan I		0.68
Sudan II		0.2
Sudan III		0.56
Sudan IV		0.56
Sudan orange G		0.14
Sudan R		0.18

f, Faint zone; m, main zone.

For the purposes of planar chromatography, separations of synthetic dyes can be split into a number of groups depending on the ionic nature and molecular structure of the dye. These are:

1. Solvent (fat) dyes.
2. Basic dyes.
3. Acid dyes.
4. Reactive dyes.
5. Disperse dyes.
6. Metal complex dyes.
7. Direct dyes.
8. Organic pigments.
9. Food colorants.

As mixtures of dyes generally fall into these respective groups and it is rare, if ever, that a dye from one of the major structural groups is found mixed with another, the TLC will be examined in detail for each group in turn. This is important as the polarity

of solvents employed for the TLC separations of dyes within each group is similar and notably different from those used for other groups.

Solvent (Fat) Dyes

As their name suggests, solvent dyes are dyes soluble in nonpolar solvents (mostly water-immiscible), and are used to colour mineral oils, waxes, fats and plastics. They are lipophilic in nature and do not form organic salts. Structurally the dyes are characterized by the azo, quinone-imine (indophenol dyes), or anthraquinone (waxoline dyes) groups they contain. By far the largest group is the azo dyes. These are mainly monoazo (sudan dyes) and a few disazo dyes (e.g. Sudan red B (CI 26110), oil red O (CI 26125; Figure 1).

Although TLC separations of solvent dyes have been reported on alumina layers, silica gel is by far the preferred adsorbent. Separation of solvent dyes

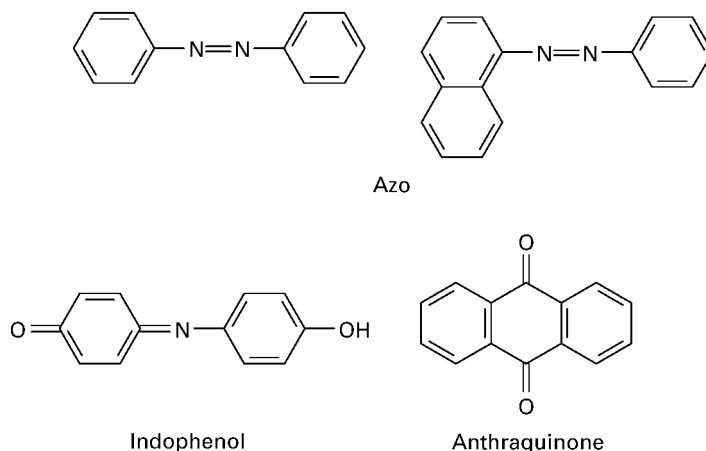
**Figure 1** Solvent dyes. Structures of characteristic groups.

Table 4 R_F values for Sudan III and IV on silica gel 60 RP8 HPTLC pre-coated plates. Plate developed in a saturated chamber

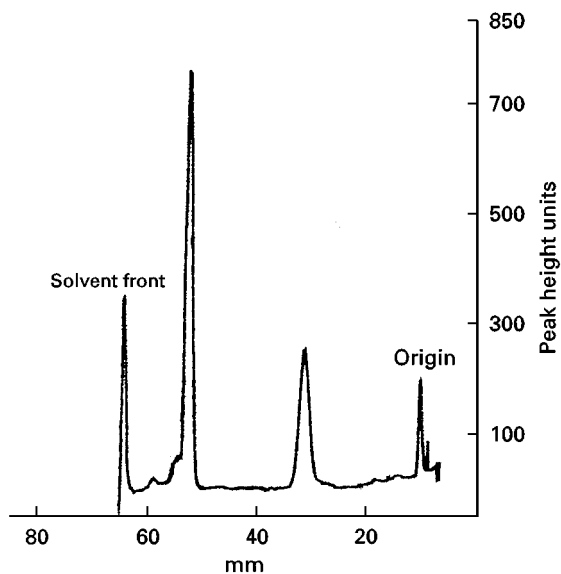
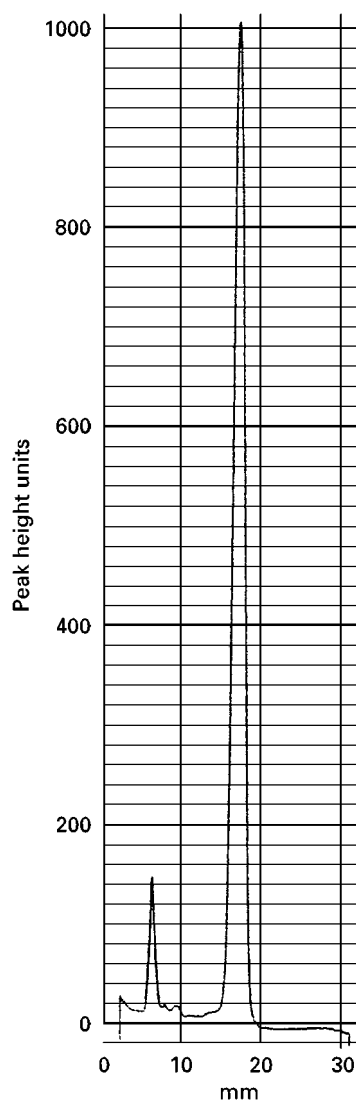
Solvent dye	R_F value	Developing solvent
Sudan III	0.32	Methanol-acetic acid-water
Sudan IV	0.22	(90 + 5 + 5 v/v)

on standardized silica gel G layers was reported in the early 1960s by Stahl. This was one of the first recorded separations on silica gel and described the resolution of butter yellow (CI 11020), Sudan R (CI 12150) and indophenol (CI 49700) using a mobile phase of pure benzene. In the years that followed, a variety of similar-polarity solvents were reported as suitable with silica gel G. Chloroform and benzene and mixtures of petroleum spirits, and single aliphatic hydrocarbons with ethyl acetate, diethyl ether, acetone and methanol were used to separate butter yellow, Sudan orange R (CI 12055), Sudan III (CI 26100) and Sudan red BB (CI 26105). The anthraquinone series of dyes have been separated with toluene-cyclohexane (50 + 50% v/v) on silica gel G. This readily resolves solvent blue 36, waxoline purple A (CI 60725) and waxoline green G (CI 61565). Dimethylaminoazobenzene and related dyes are separated using the solvent chloroform-methanol (95 + 5% v/v) on the same stationary phase.

Most solvent dyes will readily migrate and separate from each other on commercially pre-coated silica gel 60 TLC layers using the same or similar polarity

solvents to those used on silica gel G. However, the separated chromatographic zones on pre-coated plates are much sharper, noticeably less diffuse and misshapen, leading to good overall resolution (Figures 2 and 3). This should be expected as the silica gel will have a much narrower particle size distribution over the particle size range, and a mean particle size (10–12 μm) less than that of a 'home-made' plate.

The resolution can be further improved for Sudan dyes by using a reversed-phase adsorbent. In fact, the resolution is so good that results can be quantified on an HPTLC silica gel 60 RP8 plate (Merck) by scanning the developed plate at 540 nm (Figure 4). In this example, samples were applied as spots of 100 nL with a manual nanoapplicator (CAMAG). The relative standard deviation was 4.5%.

**Figure 2** Separation of two main components of Sudan black B on silica gel 60 pre-coated TLC plates. Developed in a saturated tank with dichloromethane as solvent. Scanned with a spectrodensitometer at 540 nm.**Figure 3** Separation of fat red 7B from one main impurity on silica gel 60 pre-coated TLC plates.

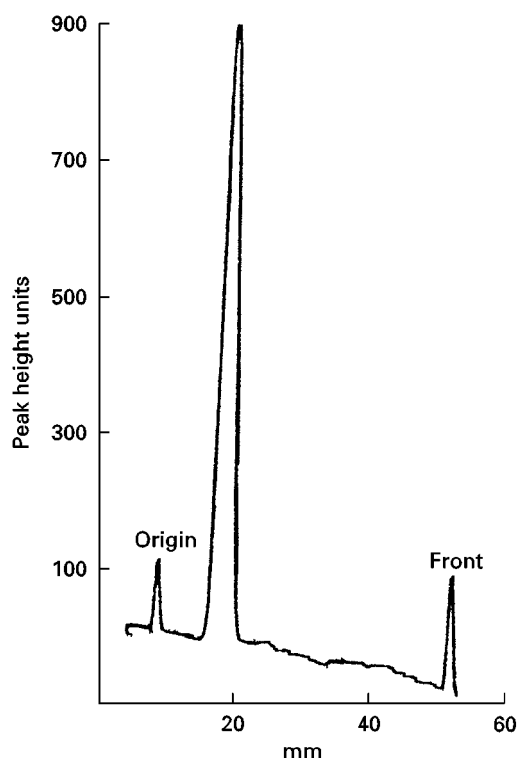


Figure 4 Pure Sudan IV resolved on silica gel 60 TLC plates using *n*-hexane–ethyl acetate (90 + 10 v/v) as mobile phase in a saturated tank.

Basic Dyes

Basic dyes form one of the larger areas of interest when it comes to TLC. As their name suggests, they are bases which can form salts which are soluble in water. Their applications vary widely in industry, including colouring paper, some textiles and plastics, and are used as the basis of many biological stains.

Basic dyes include the following structural groups: triarylmethanes (mostly triphenylmethanes), quinon-eimines, azo, acridine and xanthene compounds (**Figure 5**). These can be further split: the triarylmethanes into amino and hydroxy derivatives and the quinone-imines into indamins, azins, thiazins and oxazines. **Table 5** shows some of the commonly named dyes which fit into these groups.

As with solvent dyes, much of the early separation work was performed on silica gel G. **Table 6** lists a number of solvent mixtures which have proved useful in the separation of the general classes of basic dyes. With the advent of commercial TLC and HPTLC pre-coated silica gel 60 and bonded phases, the separation methods have improved, allowing resolution of dyes with closely related structures, and the determination of concentrations of individual dyes by *in situ* scanning using a spectrodensitometer (**Table 7**). Hence thiazin dyes are now easily resolved, including

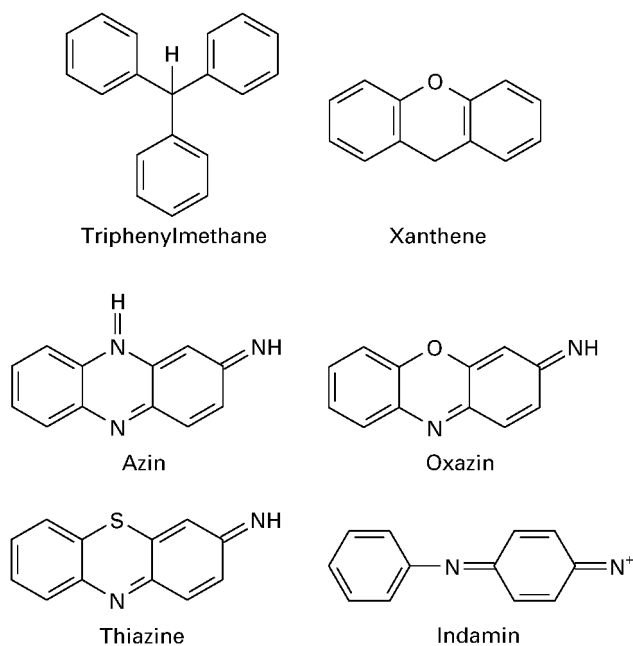


Figure 5 Acid and basic dyes. Structures of characteristic groups.

Table 5 Commonly named basic dyes according to their structural groups

Basic dye groups	Commonly named dyes
Triaminotriarylmethane	Pararosanilin New fuchsin Rosanilin
Diaminotriarylmethane	Malachite green Brilliant green Victoria blue
Monoaminotriarylmethane	Methyl violet Crystal violet Ethyl violet
Acridine	Acridine red Acridine orange
Xanthene	Pyronin B Pyronin G Rhodamine B Rhodamine 6G Safranin O
Azin	Brilliant cresyl blue
Oxazine	Orcein Resazurin Gallocyanine Cresyl fast violet Nile blue Cellestine blue Azure A, B, C Methylene blue Toluidine blue New methylene blue Thionine Methylene violet
Thiazin	Janus green Chrysoidin Bismarck brown R and Y
Azo	

Table 6 Solvent systems recommended for the separation of basic dyes on silica gel 60 pre-coated TLC plates and sheets

<i>Basic dyes</i>	<i>Solvent mixtures</i>
Malachite green, methyl violet	Butan-1-ol-ethanol-water (90 + 10 + 10 v/v)
Basic fuchsin, rhodamine B, rhodamine 6G	Butan-1-ol-acetic acid-water (40 + 10 + 50 v/v)
Methylene blue, victoria blue B, crystal violet, malachite green, rhodamine B	Butanone-acetic acid-propan-2-ol (40 + 40 + 20 v/v)
Pyronine G, acridine red, rhodamine B	Propan-1-ol-formic acid (80 + 20 v/v)
Methylene blue, malachite green	Ethyl acetate-acetic acid-water (30 + 10 + 20 v/v)
Crystal violet, methylene blue, malachite green, basic fuchsin	Butan-1-ol-acetic acid-water (20 + 5 + 10 v/v)

thionine, azure A, B, C and methylene blue on HPTLC silica gel 60 using a mobile phase of butan-1-ol-butanone-acetic acid-water (30 + 20 + 10 + 10 v/v). Methylene blue can easily be distinguished from new methylene blue even though their visible/UV spectra are almost identical (Figure 6).

Many of these dyes are the basis of the biological Romanowski stains (Giemsa, Leishman, Wright, Jenner and May-Grunwald). An assessment of the dye quality of the stain and its individual dye components can be made by the above chromatographic methods. Usually the 'ripened' or oxidized versions of these stains produce the better histological staining properties. Oxidation produces more azures and thionine, all of which can be determined, if required, by HPTLC procedures. The complete resolution of methylene blue and its oxidation products including azures and thionine presents a difficult problem even for HPTLC as these dyes are all closely structurally related. A typical example of such a separation is

shown in Figure 7 (separation of the blue dye components of Wright's stain) on a normal-phase pre-coated silica gel 60 plate (Merck).

For most basic dyes, TLC and HPTLC silica gel 60 layers normally give sufficient resolution and have proved in some cases to be suitable even for the separation of dyes from closely related impurities (Figure 8). In special cases, either reversed-phase layers or other bonded layers have solved particularly difficult separation problems. One of these has been the separation of pararosanilin from rosanilin, new fuchsin and magenta II. Pure pararosanilin is used in the preparation of Feulgen and Schiff's reagent for aldehyde and ketone detection and in biological staining. All four compounds are triaminotriphenylmethane dyes, differing consecutively by one methyl group. Although silica gel 60 RP8 HPTLC layers are able to resolve just the four components, tailing problems make it difficult to scan the zones quantitatively. However, by introducing the ion-pairing reagent

Table 7 Solvent systems for individual basic dyes on silica gel 60 TLC and HPTLC pre-coated plates. R_F values obtained and recommended scanning wavelength for detection

<i>Basic dye</i>	<i>Solvent mixture</i>	<i>R_F value</i>	<i>Detection wavelength</i>
Brilliant cresyl blue	Ethyl acetate-methanol-ammonia (0.88)-water (35 + 11 + 5 + 5 v/v)	0.56	605 nm
Crystal violet	Butan-1-ol-acetic acid-water (50 + 5 + 10 v/v)	0.39	620 nm
Ethyl violet		0.58	585 nm
Acridine orange	Ethyl acetate-methanol-ammonia (0.88)-water (33 + 11 + 5 + 5 v/v)	0.64	360 nm (fluorescence)
Azure B	Butan-1-ol-acetic acid-water (50 + 5 + 10 v/v)	0.12 (m), 0.19 (m), 0.29 (m), 0.33, 0.40	620 nm
Brilliant green		0.46	620 nm
Malachite green		0.36	620 nm
Methyl violet 6B		0.39 (m), 0.46, 0.51	620 nm
Methylene blue	Butan-1-ol-acetic acid-water (50 + 10 + 20 v/v)	0.29 (m), 0.34	620 nm
New methylene blue	Butan-1-ol-acetic acid-water (50 + 5 + 10 v/v)	0.32	610 nm
Nile blue		0.48	620 nm
Orcein	Ethyl acetate-methanol-ammonia (0.88)-water (35 + 11 + 5 + 5 v/v)	0.44 (m), origin, 0.19, 0.26, 0.37, 0.39, 0.41, 0.42, 0.47, 0.48, 0.49, 0.54	Visual
Pyronin G		0.27	360 nm (fluorescence)
Rhodamine B	Butan-1-ol-acetic acid-water (50 + 5 + 10 v/v)	0.48	540 nm
Safranin O		0.45 (m), 0.53	540 nm
Thionine	Butan-1-ol-acetic acid-water (50 + 10 + 20 v/v)	0.50	620 nm

m, Main zone.

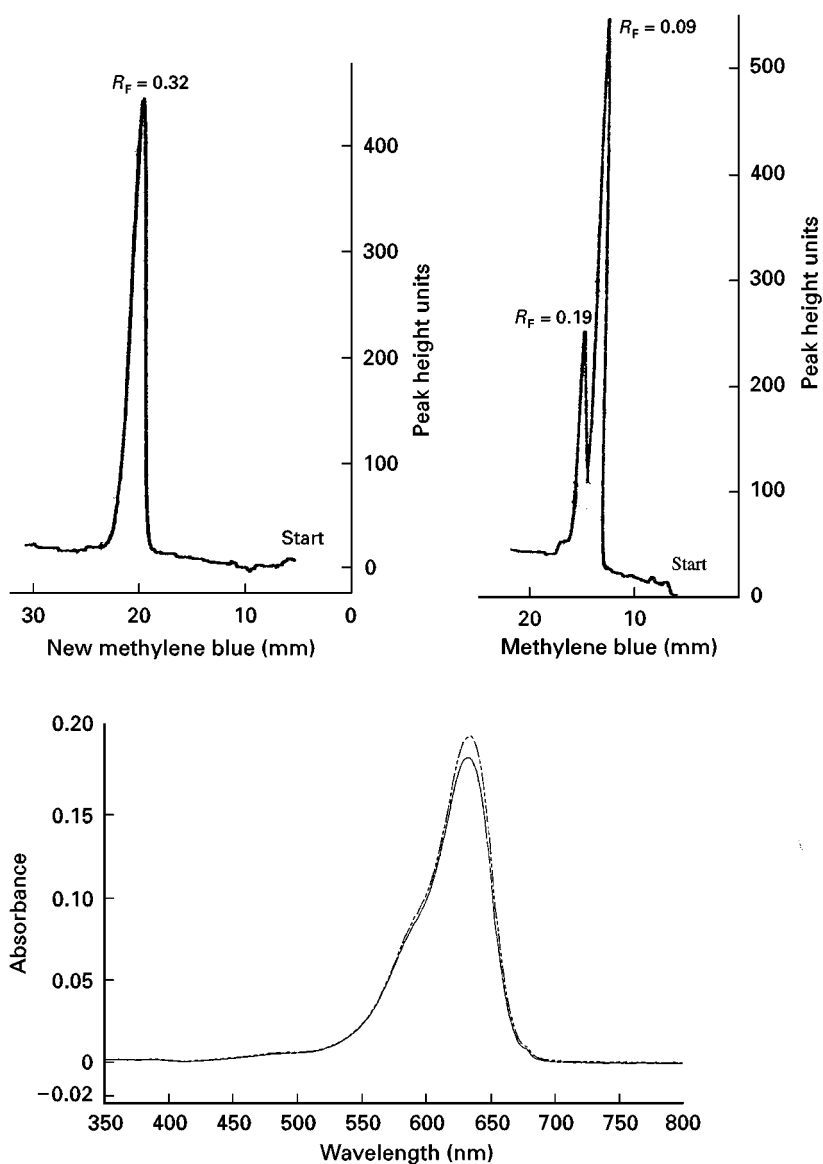


Figure 6 Comparison of methylene blue separation with new methylene blue. Both separated on silica gel 60 pre-coated TLC plates with butan-1-ol–acetic acid–water (50 + 5 + 10 v/v) as mobile phase. Overlaid spectra also shown.

pentanesulfonic acid sodium salt (2%) into the developing solvent mixture (methanol–water–formic acid: 75 + 20 + 5 v/v), the effect of tailing is dramatically reduced, allowing quantitative determination of all four dyes. Another difficult separation problem arises with Bismarck brown Y and R. Resolving the dyes from their impurities is not easily achieved. In this instance silica gel 60 NH_2 -bonded HPTLC layers have proved successful (Figure 9).

Acid Dyes

Like basic dyes, acid dyes are used widely throughout industry. They are the basis of inks and biological

stains and are used for colouring wool, polymer fibres, leather and paper. They are mostly sulfonic and carboxylic acid compounds, often prepared as their sodium salts to enable good water solubility. They can be split into a range of structural groups: azo, triarylmethane, xanthene, anthraquinone and quinone-imine. The separation of these groups on silica gel G and cellulose using a variety of solvent mixtures for development is given in a number of the older TLC books found in the Further Reading list.

Commercial pre-coated silica gel 60 TLC and HPTLC plates, where the adsorbent has a carefully controlled pore size and particle size, give improved resolution of acid dyes compared with that obtained

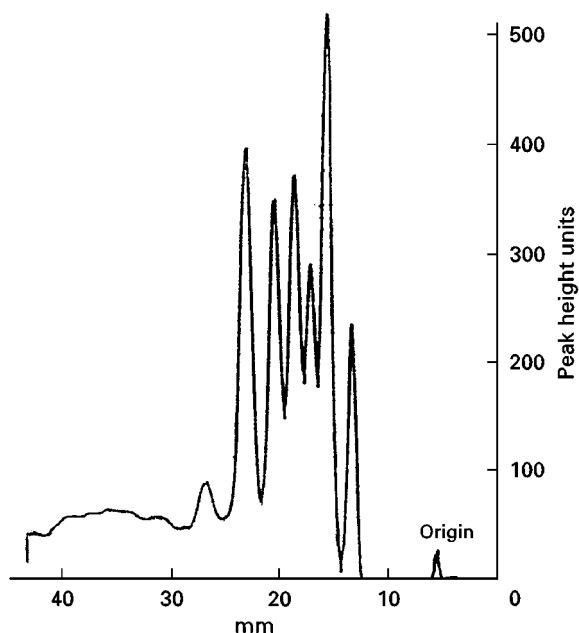


Figure 7 Separation of blue components of Wright's stain. Stationary phase is silica gel 60 pre-coated TLC plate. Mobile phase is ethyl acetate-methanol-ammonia solution (0.88)-water (35 + 11 + 5 + 5 v/v). Mixture of methylene blue, azures A, B and C, and thionine and other oxidation products.

for example with silica gel G. It has been possible to quantify results by spectrodensitometric scanning in a comparable way to basic dyes (**Figure 10**). Purity can be determined with a high degree of accuracy as is shown with the commercial samples of light green (**Figure 11**). Typically, five standards of certified dye are developed on the same plate alongside the samples. Peak measurements are made by reflectance and an x-power curve plotted against concentration. Unknowns are determined with about $\pm 1\%$ standard

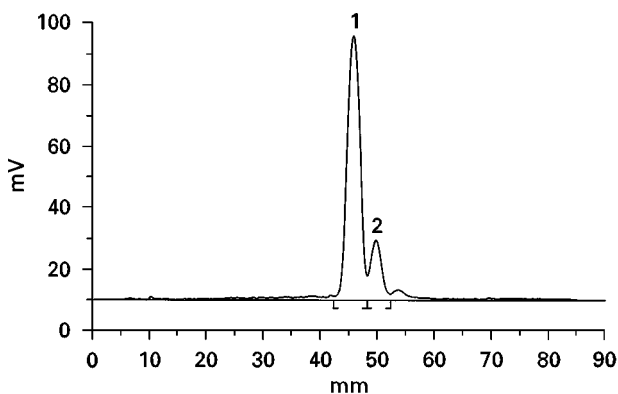


Figure 8 Separation of crystal violet from other closely related less methylated pararosanilins. Stationary phase: silica gel 60 pre-coated HPTLC plates. Mobile phase: butan-1-ol-acetic acid-water (50 + 5 + 10 v/v). Peak 1: hexamethylpararosanilin (crystal violet), peak 2: pentamethylpararosanilin.

deviation. It is also possible to determine where rogue dyes have been used to try and replace the genuine dye. Examples of Congo red and brilliant cresyl blue are shown in **Plates 1** and **2**.

More recently, reversed-phase silica gel layers have proved useful for acid dyes where separation has not been possible on normal-phase silica gel. An example of this is eosin bluish shade, where reversed-phase plates have proved satisfactory, as shown in **Table 8**.

Reactive Dyes

Reactive dyes attach themselves to cellulose fibres in wool and cotton. They are structurally defined into the groups azo, anthraquinone and phthalocyanine derivatives. One well-known commercial group is the procion dyes which can be separated on silica gel G with solvent mixtures – butan-1-ol-propan-1-ol-ethyl acetate-water (20 + 40 + 10 + 30 v/v) and dioxane-acetone (50 + 50 v/v).

Hydrolysis products of reactive dyes have also been examined by TLC on silica gel using the solvent mixture butan-1-ol-pyridine-water-ammonia (0.88 solution: 15 + 5 + 3 + 2 v/v), and with solvent mixture chloroform-methanol-acetone (18 + 3 + 2 v/v) with detection at 310 and 614 nm using a spectrodensitometer. The TLC of the reaction product and hydrolytic by-products of terminal ring isomers of reactive blue 2 (an anthraquinone dye) have been studied on silica gel using butan-1-ol-propan-2-ol-ethyl acetate-water (20 + 40 + 10 + 30) as developing solvent.

Disperse Dyes

Similar in structure to fat-soluble dyes, disperse dyes are mainly used to colour cellulose acetate and polymer fibres (principally polyester). They exhibit low solubility in water, but are soluble in organic solvents. Disperse dyes are types of nitrodiphenylamine, azo and anthraquinone dyes, but not those associated with either sulfonic or carboxylic acid groups. Commercially they belong to the Celliton group of dyes which can be separated by TLC on silica gel G adsorbent using chloroform-methanol (95 + 5 v/v) as mobile phase. Better separations of amino derivatives of anthraquinones have been obtained using chloroform-acetone (90 + 10 v/v). Mixtures of chloroform-ethyl acetate (50 + 50 v/v) or various dilutions of toluene with acetone can be employed on pre-coated silica gel 60 layers. When analysis of the dyes is required in natural and synthetic polymers, dichloromethane, acetone or dimethylformamide can be used to extract them ready for application to the TLC plate.

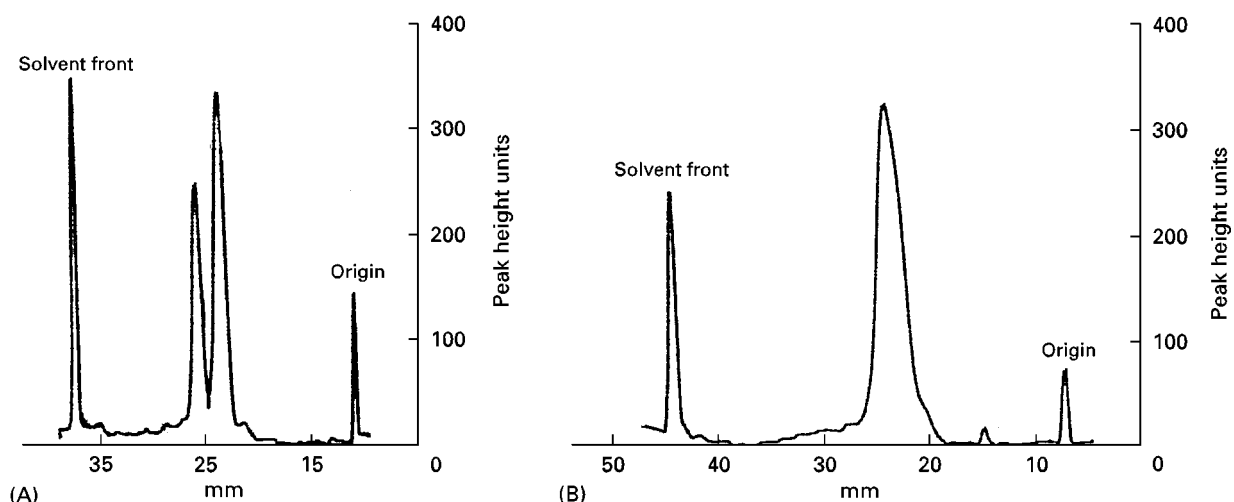


Figure 9 Separation of Bismarck brown Y and R on silica gel 60 NH_2 pre-coated HPTLC plates. Mobile phase: industrial methylated spirit. (A) The two components of Bismarck brown Y; (B) Bismarck brown R.

Metal Complex Dyes

These are acid dyes, mostly belonging to the azo group. They can be divided into two distinct types: 1 : 1 and 1 : 2 complexes.

1 : 1 Complexes

These are water-soluble dyes of sulfonic acid type which can be separated by TLC on silica gel using the solvent systems described under the section on acid dyes. For the most part they are chromium complex dyes.

1 : 2 Complexes

These are water-insoluble, but solvent-soluble dyes. They are metal complexes of chromium and cobalt. The best adsorbent for separation on thin layers is polyamide using a solvent mixture of methanol–water–ammonia (0.88 solution: 80 + 16 + 4 v/v).

Direct Dyes

Direct dyes are used for dyeing cotton fibres and leather. They are mainly polyazo dyes which can be

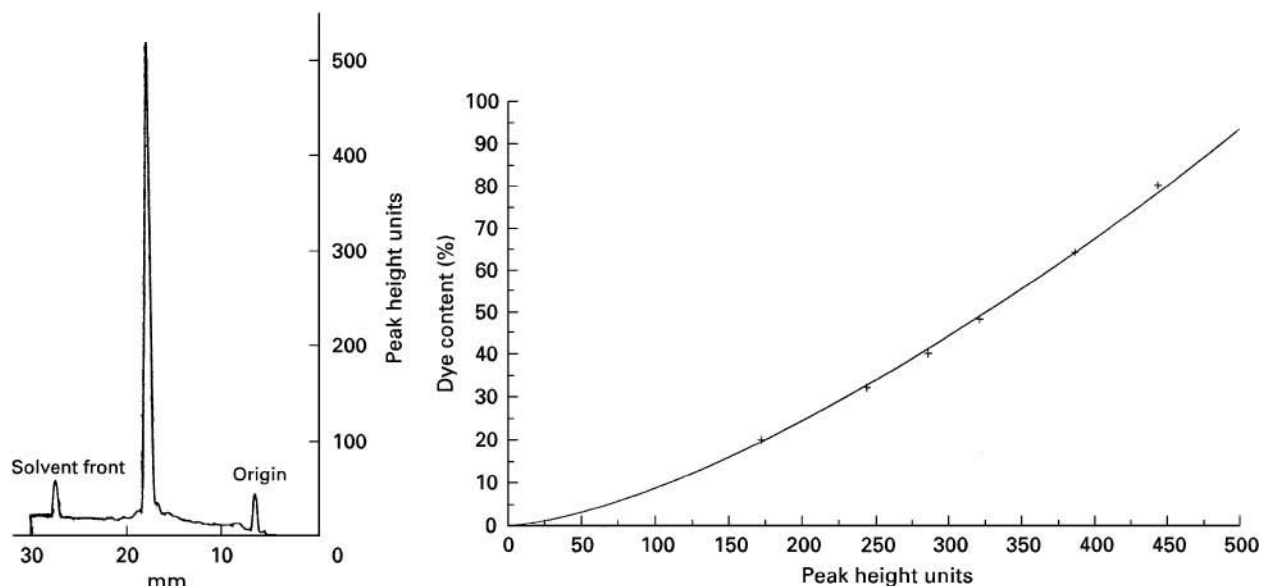


Figure 10 Quantification of Congo red dye. Single component dye. Typical x-power fit for reflectance data against concentration for a batch of certified dye. Stationary phase: silica gel 60 pre-coated HPTLC plates. Mobile phase: ethyl acetate–methanol–ammonia solution (0.88)–water (35 + 11 + 5 + 5 v/v).

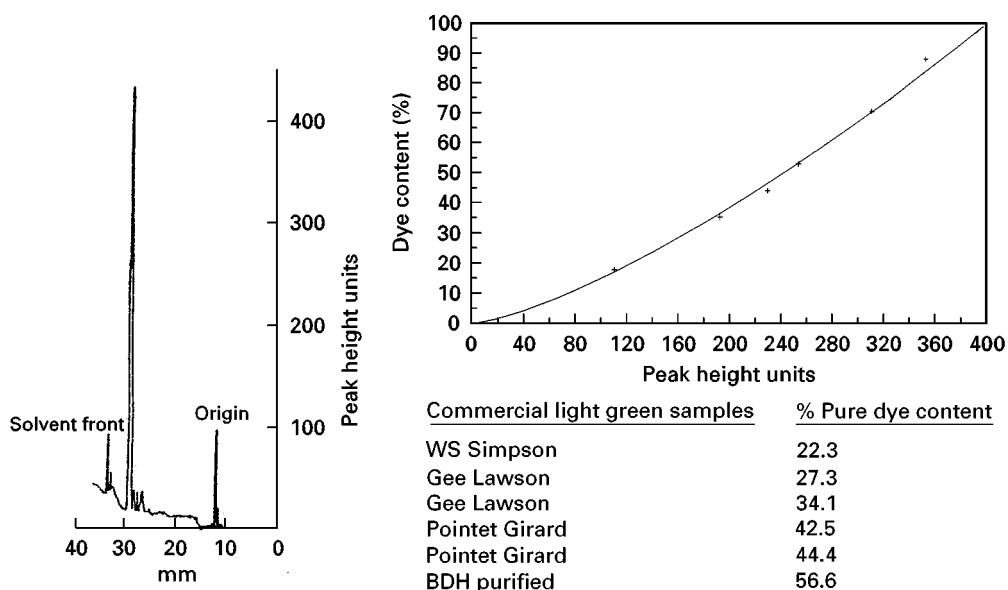


Figure 11 Quantification of light green on silica gel 60 pre-coated HPTLC plates. Six standards applied as spots of nL loadings using a certified light green dye. The pure dye content of a number of commercial light green batches are listed as determined using this chromatographic procedure.

well separated on silica gel layers. Some, like Congo red, Evan's blue and trypan blue, have already been discussed under the acid dye section, but others can be resolved using the same solvent mixtures as recommended for the above dyes in Table 9. Slight modifications to the ratio of the solvents can often further optimize the solvent mixture for the specific dye.

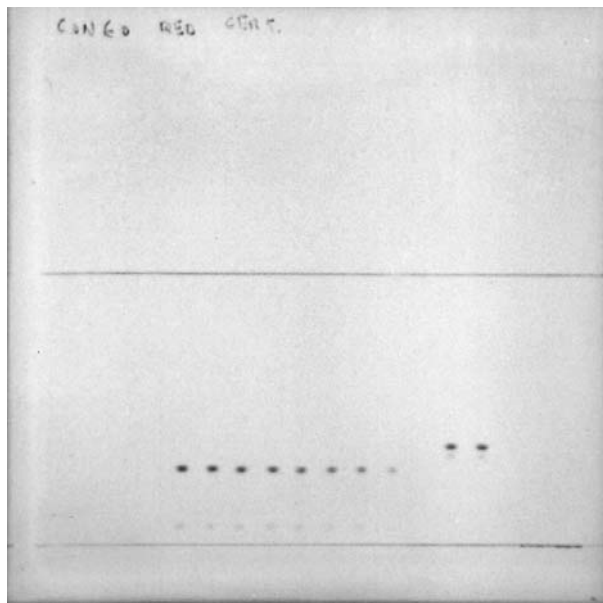


Figure 12 (See Colour Plate 78). Set of certified Congo red standards developed on a silica gel 60 HPTLC layer. Mobile phase: ethyl acetate-methanol-ammonia solution (0.88)-water (35 + 11 + 5 + 5 v/v). A minor impurity is visible at R_f value 0.07. The two dye substances alongside these are of a dye that was claimed to be Congo red.

Organic Pigments

These are the colours of artist's paints which are also used for pigmenting rubbers and plastics. Included

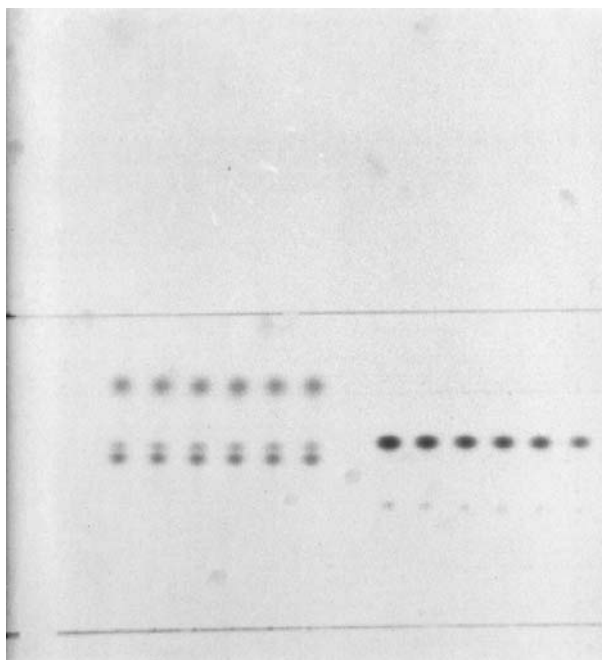


Figure 13 (See Colour Plate 79). Separation of brilliant cresyl blue on silica gel 60 HPTLC plate. Mobile phase: ethyl acetate-methanol-ammonia solution (0.88)-water (35 + 11 + 5 + 5 v/v), saturated tank. Six standards applied at increasing concentration (from 50 ng) on the right side of the plate. The six samples developed on the left, all of equal concentration, were claimed to be brilliant cresyl blue, but in fact were a mixture of toluidine blue and Nile blue sulfate.

Table 8 Commonly named acid dyes according to their structural groups

<i>Acid dye groups</i>	<i>Commonly named dyes</i>	<i>Colour index numbers</i>
Azo	Methyl red	13020
	Methyl orange	13025
	Tropaeolin O	14270
	Orange II	15510
	Ponceau 2R	16150
	Orange G	16230
	Chromotrope 2R	16570
	Tartrazine	19140
	Congo red	22120
	Trypan blue	23850
	Evans blue	23860
	Ponceau S	27195
Triarylmethane	Acid fuchsin	42685
	Fast green FCF	42053
	Light green SF	42095
	Alkali blue 5B	42750
	Aniline blue	42755
	Xylene cyanol FF	43535
	Sulfonphthaleins	
Xanthene	Fluorescein	45350
	Eosin Y	45380
	Phloxine	45405
	Erythrosine B	45430
	Rose bengal	45440
Quinone-imine	Azocarmine G	50085
	Azocarmine B	50090
Anthraquinone	Alizarin red S	58005
	Indigo carmine	73015

here are the phthalocyanine dyes along with some azo, vat and anthraquinone dyes. They are for the most part insoluble in both organic solvents and water. Hence chromatographic separations have proved difficult. However, some chromatographic work has been described. Some pigments will dissolve in hot dimethylformamide. They can then be applied as such to silica gel layers. Thorough drying is recommended before development with benzene or benzene modified with chloroform. The use of paper chromatography has also been described with propan-1-ol-ammonia (0.88 solution: 20 + 10 v/v) as mobile phase.

Food Colorants

Acid dyes are used as colorants in food and drink. In the past, the recommended stationary phase for food dye separations was either cellulose or modified celluloses (diethylaminoethyl (DEAE), PAB). However, as in other areas of modern TLC, silica gel 60 has taken over as the preferred stationary phase. The optimum chromatographic conditions have therefore to a large extent already been described in the acid dye section. However, for completeness the optimum resolution

of many of these dyes is listed in Table 10. These dyes are all water-soluble and separate readily on thin layers of silica gel 60. As they are ionic in nature, it is important that either acid or base modifiers are used in the solvent mixture (e.g. acetic or formic acids or ammonia solution). This reduces 'tailing' or 'streaking' of chromatographic zones by either suppressing ionization or totally ionizing the components of the sample.

Commercial dyes for food use are often blends of permitted acid dyes, e.g. green food dye is usually a mixture of brilliant blue FCF (E133) and tartrazine (E102); red food dye can be a mixture of red 2G (E128) and tartrazine (E102). The TLC methods must therefore have the ability not only to separate impurities, but also to resolve the parent dyes.

Most food dyes are prepared for use in a glycerine base. Although little pre-chromatographic preparation of samples is required, it is important where this base is used to solubilize these dyes further with water-methanol (50 : 50 v/v) so that when the sample is applied to the plate, the sample solution will properly 'wet' the layer. Solutions can be filtered if required. As the dyes are so readily soluble in water, their extraction from the food matrix does not usually present a problem. For colours in drink, the sample normally only requires dilution with methanol before application as a spot or band to the chromatographic layer.

Future prospects

Future prospects of dye analysis using TLC/HPTLC are likely to be closely linked with the use of video imaging techniques (charged coupled devices). Usually dye analysis involves many samples in a commercial environment. Hence a technique that has the ability to take a video image of an entire developed plate which could contain many chromatograms, and has the software capabilities to determine concentrations with some degree of accuracy from the image density of the chromatographic zones, has a real benefit to the analyst. Hard-copy pictures of the chromatograms can be produced for entry into analytical reports. The speed of such analysis will undoubtedly improve as the speed of computation becomes ever faster and further software improvements are made.

The identification and possible quantification of minor dye impurities will also become more feasible as hyphenated techniques such as FTIR, MS and Raman spectroscopy are linked to HPTLC and become more widely used. Manufacturers of pre-coated plates are now commercially producing smaller particle size adsorbents (3–5 µm), some based on spheri-

Table 9 Solvent systems for individual acid dyes on silica gel 60 TLC and HPTLC pre-coated plates. R_F values obtained and recommended scanning wavelength for detection

<i>Acid dye</i>	<i>Solvent mixture</i>	<i>R_F values</i>	<i>Detection wavelength</i>
Alizarin red S	Butan-1-ol–acetic acid–water (50 + 10 + 20 v/v)	0.29 (m), 0.22, 0.46	Visual
Aniline blue		0.22 (m), 0.39 (m), 0.08, 0.27, 0.32, 0.49, 0.64	620 nm
Fast green FCF		0.31	620 nm
Light green SF		0.19	620 nm
Orange G	Ethyl acetate–methanol–ammonia (0.88)–water (35 + 11 + 5 + 5 v/v)	0.28	470 nm
Alkali blue 5B, 6B		0.28, 0.35, 0.41, 0.47, 0.52, 0.55, 0.87, 0.91	540 nm
Congo red		0.47	470 nm
Crystal ponceau		0.45	470 nm
Ponceau S	Butan-1-ol–IMS–water–ammonia (0.88) (50 + 25 + 25 + 10 v/v)	0.37	470 nm
Indigo carmine		0.53	620 nm
Acid fuchsin		0.46 (m), 0.33, 0.42	540 nm
Eosin Y		0.42 (m), 0.38	470 nm
Erythrosin B	Ethyl acetate–methanol–ammonia (0.88)–water (33 + 11 + 5 + 5 v/v)	0.43	540 nm
Naphthol yellow S		0.33 (m), 0.44 (f)	400 nm
Evans blue		0.16 (m), 0.42 (f)	620 nm
Fast garnet GBC salt		0.82 (m), 0.48 (f)	400 nm
Trypan blue	Ethyl acetate–methanol–ammonia (0.88)–water (35 + 11 + 5 + 6 v/v)	0.11 (m), 0.32, 0.42	620 nm
Azocarmine G		0.28	540 nm
Phloxine		0.38	540 nm

m, Main zone; f, faint zone.

cal shaped particles. These will have the advantage of better flow characteristics for the migrating solvent, although slower flow rates and, most importantly for dye impurity analysis, improvement in sensitivity. The smaller average particle size and spherical shape will mean that such minor components on the layer

will be more concentrated with less diffusion than that presently seen on an HPTLC plate.

See Colour Plates 77, 78, 79.

See also: II/Chromatography: Thin-Layer (Planar): Densitometry and Image Analysis; Mass Spectrometry. III/Thin-Layer Chromatography-Vibration Spectroscopy. Dyes: High-Speed Countercurrent Chromatography; Liquid Chromatography.

Table 10 Solvent systems and R_F values for food dyes separated on silica gel 60 pre-coated TLC plates

<i>Food dye</i>	<i>Solvent system</i>	<i>R_F value</i>
Erythrosin	Ethyl acetate–methanol–ammonia (0.88 solution)–water (33 + 11 + 5 + 5 v/v)	0.43
Sunset yellow		0.33
Tartrazine		0.11
Indigo carmine	Butan-1-ol–IMS–water–ammonia (0.88 solution: 50 + 25 + 25 + 10 v/v)	0.53
Red 2G		
Brilliant blue FCF	Ethyl acetate–methanol–water–ammonia (0.88 solution: 30 + 15 + 5 + 10 v/v)	

IMS, industrial methylated spirits.

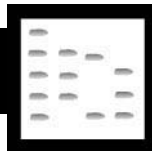
Further Reading

- The Colour Index*, 3rd edn (1982) Bradford, UK: Society of Dyers and Colourists.
- Gupta VK (1990) Synthetic dyes. In: Sherma J and Fried B (eds), *Handbook of Thin-layer Chromatography*, pp. 939–969. New York: Marcel Dekker.
- Liedekerke BM, Leenheer AP and De Spiegeleer BM (1991) High-performance thin-layer chromatographic analysis of thiazine dyes on silica, cyano, and reversed-phase C_{18} layers. *Journal of Chromatographic Science* 29: 49–53.
- Loach KW (1971) Thin-layer chromatographic separation of methylene blue and related thiazine dyes. *Journal of Chromatography* 60: 119–126.

- Marshall PN and Lewis SM (1974) A rapid thin-layer chromatographic system for Romanowsky blood stains. *Stain Technology* 49: 235–240.
- Randerath K (1963) *Thin-Layer Chromatography*, pp. 211–214. London: Academic Press.
- Stahl E (ed) (1969) *Thin-Layer Chromatography: A Laboratory Handbook*. Berlin: Springer-Verlag.
- Wall PE (1988) Separation and quantification of Fuchsin Basic using reversed-phase thin-layer chromatography. In: Dallas FAA, Read H, Ruane RJ and Wilson ID (eds)

- Recent Advances in Thin-Layer Chromatography*, pp. 207–210. New York: Plenum Press.
- Wall PE (1989) HPTLC as a quantitative method for the determination of the purity of dyes of histological importance. *Journal of Planar Chromatography* 2: 246–247.
- Wall PE (1991) Thin layer chromatographic separation of thiazins: problems and solutions. *Journal of Planar Chromatography* 4: 365–369.
- Wall PE (1993) The value of planar chromatography for the analysis of triphenylmethane dyes. *Journal of Planar Chromatography* 6: 394–403.

ECDYSTEROIDS: CHROMATOGRAPHY



R. Lafont and C. Blais, Ecole Normale Supérieure et Université Pierre et Marie Curie, Paris, France

J. Harmatha, Academy of Sciences of the Czech Republic, Prague, Czech Republic

I. D. Wilson, AstraZeneca Pharmaceuticals Ltd, Macclesfield, Cheshire, UK

Copyright © 2000 Academic Press

Introduction

Ecdysteroids are present both in animals (mainly Arthropods) and plants and comprise about 300 different molecules related to ecdysone (**Figure 1**). Structural variation in the number of carbons on the side-chain and of substituents at various positions (**Table 1**) results in the presence of compounds displaying very different polarities. Most available chromatographic techniques have been applied to the isolation and analysis of ecdysteroids. Paper chromatography is now obsolete and no longer used. Gas chromatography (GC) is of limited use, as the derivatization procedures necessary to make volatile derivatives require careful control. Currently, the most widely used techniques are high performance liquid chromatography (HPLC) and thin-layer chromatography (TLC), with the former providing the major analytical methods.

Liquid-Liquid Partitions

The simplest separation method concerns partitioning between two non-miscible solvents, and it is currently used for clean-up of biological samples. On this basis, several procedures have been designed, which allow the preparation of almost pure compounds in the gram scale.

Solvent Partitioning

Partition between n-butanol and water can be used to remove polar contaminants, whereas partition between aqueous methanol and hexane removes non-polar materials. Lipids can also be removed from aqueous extracts with hexane-methanol (7 : 3, v/v), light petroleum or n-propanol-hexane (3 : 1, v/v). The nature of the contaminants to be removed and that of the ecdysteroids to be isolated govern the choice for a given partition system. The number of free -OH groups significantly affects partition coefficients (**Table 2**).

The combination of two successive partition steps allows the elimination of both polar and apolar contaminants. It is thus possible to combine (1) chloroform/water and (2) water/butanol. This results in a butanol-containing fraction that is significantly enriched. It is possible to select a narrower range of polarity by replacing chloroform with a more polar organic solvent, e.g. isobutyl acetate, that nevertheless allows ecdysteroids to remain in the water phase.

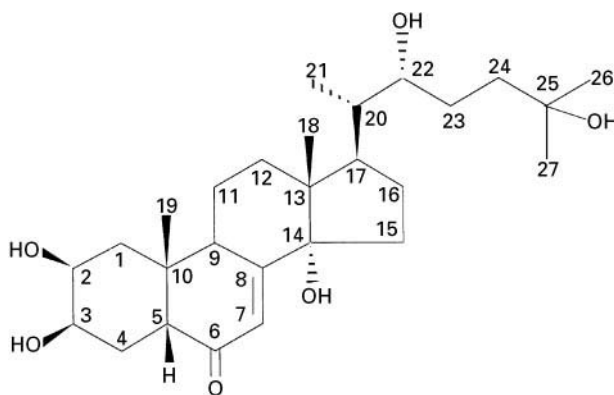


Figure 1 The structure of ecdysone, the first ecdysteroid isolated from *Bombyx mori* pupae.

Table 1 Variations on the 20-hydroxyecdysone molecule

Type	Positions on the molecule
Hydroxyl groups	
Additional -OH	1, 5, 11, 16, 18, 19, 23, 24, 26
Missing -OH	2, 20, 22, 25
Oxidation	
(>CHOH → >C = O)	3, 22
(-CH ₂ OH → -COOH)	26
(→ epoxide)	22-23
Epimerization	3 α /3 β , 5 α /5 β
Alkyl substitution	24 (methyl, methylene, ethyl, etc.)
Esterification	
Acetates	2, 3, 22, 25
Fatty acyls	22
Benzoates	20, 22, 25
Cinnamates	2
Coumarates	3
Phosphates	2, 22, 26
Sulfates	22
Lactone ring formation	Concerns mainly C-28 or C-29 ecdysteroids
Etherification	
Intramolecular	Between C-22 and C-25
Methoxy ether	25
Ketal/acetal formation	
Acetonides	2-3, 20-22
Benzylidene acetals	20-22
Glycosylation	
Galactosides	3, 22
Glucosides	3, 22, 25, 26
Dehydration	9(11), 14(15), 24(25), 25(26)
Side-chain cleavage	C-20/C-22, C-17/C-20

Counter-current Distribution

Counter-current distribution (CCD) is a multi-tube extension of the above partition procedure. Butenandt and Karlson (1954) purified the first ecdysteroid (ecdysone) from *Bombyx* pupae by CCD with butanol-cyclohexane-water (4 : 6 : 1). This technique is presently of limited use, and it has been replaced by the more convenient droplet counter-current chromatography technique described below.

Droplet Counter-current Chromatography

Droplet counter-current chromatography (DCCC) allows an efficient purification of crude samples up to the gram range (Table 3). DCCC enables the preparation of reasonably, although not absolutely, pure compounds (a subsequent HPLC step may be required to get pure ecdysteroids). One DCCC separation usually lasts several days: exchanges between

Table 2 Partition coefficients (*K*) of ecdysteroids (data from Lafont *et al.*, 1994b)

Ecdysteroid	<i>K</i>
<i>Cyclohexane-n-butanol-water</i> (5 : 5 : 10)	
Ecdysone	3.54
Makisterone A	1.27
20-Hydroxyecdysone	0.52
3-Epi-20-hydroxyecdysone	0.52
26-Hydroxyecdysone	0.39
20,26-Dihydroxyecdysone	0.06
<i>Chloroform-methanol-water</i> (2 : 1 : 1)	
2,22-Dideoxyecdysone	13.0
2-Deoxyecdysone	2.7
Ecdysone	0.4
20-Hydroxyecdysone	0.1

$$K = \frac{\text{concentration in the non-polar phase}}{\text{concentration in the polar phase}}$$

mobile droplets and the stationary phase is the rate-limiting process. High-speed counter-current chromatography (HSCCC) overcomes this drawback and separations are performed within a few hours. This technique has so far only been applied to the ecdysteroids in a small number of cases.

Thin-Layer Chromatography (TLC)

Normal-phase (absorption) chromatography on silica gel has been used extensively in the isolation of ecdysteroids and for metabolic work. Despite the advent of HPLC, the low expense, simplicity and speed of TLC ensures a continuing role for this technique in ecdysone research.

Chromatographic Procedures

Normal-phase systems Many solvent systems have been used for TLC of ecdysone and related compounds, and these are summarized in Table 4. A wide range of *R_F* values on silica gel have been reported.

Table 3 Solvent systems for droplet counter-current chromatography (DCCC)

Solvent system	Mode
CHCl ₃ /MeOH/H ₂ O (13 : 7 : 4)	Ascending
CHCl ₃ /C ₆ H ₆ /EtOAc/MeOH/H ₂ O (45 : 2 : 3 : 60 : 40)	Descending
C ₆ H ₆ /CHCl ₃ /MeOH/H ₂ O (5 : 5 : 7 : 2)	Descending
CHCl ₃ /MeOH/H ₂ O (65 : 20 : 20)	Descending

CHCl₃, chloroform; MeOH, methanol; C₆H₆, benzene; EtOAc, ethyl acetate.

Table 4 Some representative solvent systems for TLC of ecdysteroids on silica gel

Solvent system	Composition	$[R_F]$	
		E	20E
CHCl ₃ /95% EtOH	7 : 3	0.39	0.34
CHCl ₃ /MeOH	9 : 1	0.10	0.07
CHCl ₃ /Pr-1-OH	9 : 5	0.21	0.12
CH ₂ Cl ₂ /Me ₂ CO/MeOH	2 : 1 : 1	0.69	0.62
CH ₂ Cl ₂ /Me ₂ CO/EtOH	16 : 4 : 5	0.32	0.10
CH ₂ Cl ₂ /MeOH/H ₂ O	79 : 15 : 1	0.32	0.19
CH ₂ Cl ₂ /MeOH/ 25% NH ₃ -H ₂ O/H ₂ O	77 : 20 : 2 : 1	0.47	0.40
EtOAc/EtOH	4 : 1	0.49	0.46

E, ecdysone; 20E, 20-hydroxyecdysone. CHCl₃, chloroform; EtOH, ethanol; MeOH, methanol; Pr-1-OH, n-propanol; CH₂Cl₂, dichloromethane; Me₂CO, acetone; EtOAc, ethyl acetate.

For consistent results, plates should be heated at 120°C for 1 hr, then deactivated to constant activity over saturated saline. An example of the type of separation that can be achieved in metabolic studies in insects is shown in Figure 2.

Reversed-phase systems An alternative to normal-phase TLC (NP-TLC) is reversed-phase TLC (RP-TLC) on silica bound to alkyl chains (2 to 18 carbons). Methanol-water, ethanol-water, isopropanol-water, acetonitrile-water and acetone-water systems have been used as mobile phases, with methanol-water solvents providing the most general solvent system. The order of migration in RP-TLC is roughly opposite of that seen using NP-TLC (Table 5). Results vary significantly with plate manufacturers. Changing the proportion of methanol in the sol-

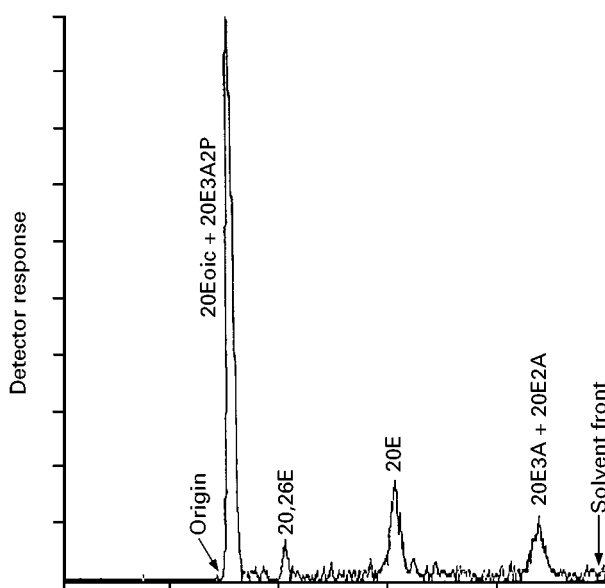


Figure 2 Normal-phase TLC on a silica gel high-performance TLC plate using chloroform-ethanol (4 : 1) to separate 20-hydroxyecdysone (20E) metabolites formed in an insect. 20E3A2P, 20-hydroxyecdysone 3-acetate 2-phosphate; 20Eic, 20-hydroxyecdysoneic acid; 20,26E, 20,26-dihydroxyecdysone; 20E2A, 20-hydroxyecdysone 2-acetate; 20E3A, 20-hydroxyecdysone 3-acetate. After Wilson ID and Lafont R (1986). Thin-layer chromatography and high-performance thin-layer chromatography of [³H] metabolites of 20-hydroxyecdysone. *Insect Biochemistry* 16: 33–40, reprinted with permission.

vent over the range 0 to 100% increases the R_F values of ecdysone and 20-hydroxyecdysone, and this shows a quite linear relationship between the percentage of methanol in the solvent and R_F (Figure 3).

Table 5 R_F for representative ecdysteroids in TLC

Compound	System 1	System 2	System 3
Calonysterone	0.42	0.20	0.37
Cyasterone	0.33	0.40	0.51
2-Deoxy-20-hydroxyecdysone	0.31	0.21	0.29
2-Deoxyecdysone	0.38	0.15	0.17
Ecdysone	0.21	0.29	0.28
20-Hydroxyecdysone	0.15	0.44	0.38
20-Hydroxyecdysone 2-cinnamate	0.53	0.04	0.03
Inokosterone	0.17	0.44	0.37
Kaladasterone	0.49	0.17	0.30
Makisterone A	0.20	0.31	0.40
Muristerone A	0.27	0.32	0.31
Polypodine B	0.22	0.42	0.44
Ponasterone A	0.42	0.16	0.18
Ponasterone C	0.38	0.29	0.37
Ponasterone C 2-cinnamate	0.65	0	0
Poststerone	0.32	0.37	0.38

System 1, silicagel plates, solvent CHCl₃-MeOH (4 : 1); System 2, Merck C₁₈-bonded plates, solvent MeOH-H₂O (1 : 1); System 3, Whatman C₁₈-bonded plates, solvent MeOH-H₂O (1 : 1).

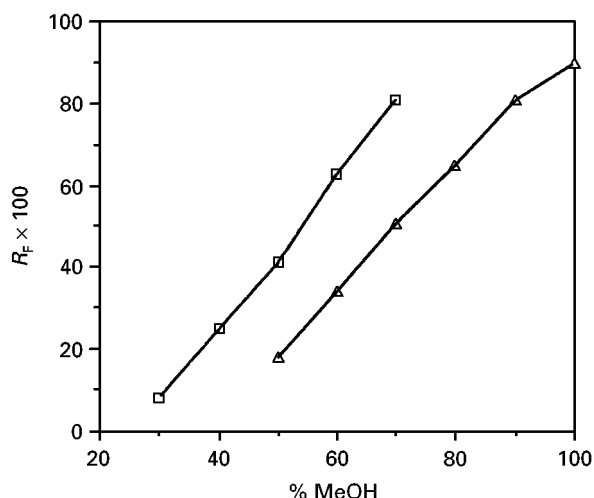


Figure 3 Influence of the solvent composition (MeOH-water) on the R_F of ecdysone and 20-hydroxyecdysone analysed by RP-TLC on C_{18} -bonded plates. \square , 20-hydroxyecdysone; Δ , ecdysone.

Detection of Ecdysteroids after TLC

Detection of ecdysteroids on the TLC plate can be accomplished using a set of techniques of varying specificities (Table 6). Non-specific techniques include iodine vapour, heating in the presence of ammonium carbonate (which produces fluorescent spots), or fluorescence quenching if a fluorescing agent is incorporated into the silica. More specific reagents such as the vanillin-sulfuric acid spray can be used to give spots of characteristic colour. Sulfuric

acid or ammonia give fluorescent reactions, with the former being slightly more specific.

Evolved TLC Techniques

Automatic multiple development (AMD) In AMD, the plate is repeatedly developed with the same solvent, which migrates more and more with each development. This method allows a reconcentration of ecdysteroids at each run, in particular by suppressing tailing, and this finally results in sharper bands and improved resolution.

Over-pressure layer chromatography (OPLC) In OPLC, the solvent is forced through the layer by an HPLC pump and the plate can be developed within minutes. The use of high-performance TLC plates rather than conventional TLC plates is recommended for optimal results. Developing the plates under these conditions will minimize diffusion, while allowing mass transfer to proceed.

Neither AMD nor OPLC have been used to any significant extent for the separation of ecdysteroids, although where they have been employed for these compounds good results have been obtained.

Low-Pressure Column Chromatography

Preparative Columns

These systems are used for the isolation and purification of ecdysteroids from crude extracts. Columns are

Table 6 Various methods for the visualization of ecdysteroids after TLC

Method	Operating mode
UV absorbance	Direct visualization under UV light: poorly sensitive method Use of a scanner and obtention of UV spectra
¹ Fluorescence quenching	Use of silica plates containing a luminescent agent (ZnSe)
Non-specific colour reactions	I ₂ vapours Phosphotungstic acid gives blue colour Anisaldehyde
Fluorescence induction	H ₂ SO ₄ (NH ₄) ₂ CO ₃
¹ Vanillin spray reagent	Spray with vanillin/95% EtOH/H ₂ SO ₄ (5 : 70 : 25, w/v/v), then heat at 100–120°C for 10 min
Reactions for 3-oxoecdysteroids	Folin-Ciocalteu gives blue colour 2,4-Diphenylhydrazine gives yellow colour (+ K ₃ Fe(CN) ₆ gives orange colour) Triphenyltetrazolium chloride gives red colour
Radioactivity	Scanner or autoradiography (metabolic studies)
Mass spectrometry	Direct introduction of the plate, or FAB-MS on scraped silica

¹Classical methods.

Table 7 Some low pressure chromatographic systems for medium- or large-scale purification of ecdysteroids

Stationary phase	Solvent system
<i>Normal phases</i>	
Silica (silica gel, silicic acid or celite)	CHCl ₃ /MeOH (100 : 3; 95 : 5; 80 : 20; or SG ¹) CHCl ₃ /EtOH (19 : 1) CH ₂ Cl ₂ /EtOH (SG) EtOAc/MeOH (SG)
Alumina	CHCl ₃ /MeOH (2 : 1; or SG) CHCl ₃ /EtOH (SG) CH ₂ Cl ₂ /EtOH (9 : 1; or SG) EtOAc/MeOH (1 : 1) EtOAc/EtOH (2 : 1; 1 : 1; or SG) Me ₂ CO/CH ₂ Cl ₂ /H ₂ O (62.5 : 15 : 10)
Sephadex LH20	CHCl ₃ /EtOH (88 : 12) CH ₂ Cl ₂ /MeOH (SG) CH ₂ Cl ₂ /Me ₂ CO
<i>Reversed-phases</i>	
Amberlite XAD-2	H ₂ O/MeOH (SG) H ₂ O, then EtOH
Amberlite XAD-16	H ₂ O, then EtOH
Sephadex LH20	EtOH/H ₂ O (7 : 3) MeOH
Polyamide	H ₂ O
<i>Ion-exchange</i>	
DEAE-Sephadex	Step-gradient of NaCl in H ₂ O

¹SG, step-gradient.CHCl₃, chloroform; MeOH, methanol; EtOH, ethanol; CH₂Cl₂, dichloromethane; EtOAc, ethyl acetate; Me₂CO, acetone.

filled with either normal (polar) phases (silica or alumina) eluted with organic solvents, or non-polar phases (Amberlite XAD-2, polyamide or Sephadex LH20) eluted with aqueous mixtures (Table 7). Ion-exchange phases (e.g. DEAE-Sephadex) eluted with buffers can be used for polar anionic ecdysteroids (Figure 4). The size of the column has to be adapted to that of the sample, with a sorbent-to-sample ratio higher than 50 (w : w), and these methods can be used with very large samples. They represent a rather cheap and reasonably efficient procedure for getting fractions from which ecdysteroids can be crystallized (if present in large amounts) or further purified by HPLC (see below). Step-gradient elution with solvents of increasing strength allows the separation of ecdysteroids over a wide range of polarity.

Disposable Cartridges

Small solid phase extraction (SPE) cartridges containing 0.2–1 g of non-polar HPLC phase allow the clean-up of small samples with a good recovery (Figure 5). They can also be used to adsorb ecdysteroids from aqueous media, thus allowing an easy and quantitative recovery of ecdysteroids from organ/cell culture media or from HPLC fractions when a non-

volatile buffer is used. Normal-phase SPE cartridges have also been used for the fractionation of biological extracts.

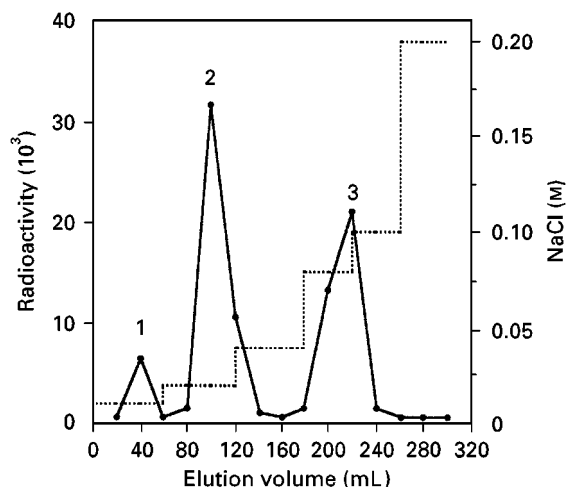


Figure 4 Separation of acidic ecdysteroids from *Manduca sexta* using a DEAE-Sephadex column (6.5 cm long, 2 cm i.d.). Elution was performed with a step-gradient of NaCl. Peak 2 contains ecdysonic acids, peak 3 contains phosphate conjugates. Redrawn with permission from Lozano R, Thompson MJ, Svoboda JA and Lusby WR (1988) Isolation of acidic and conjugated ecdysteroid fractions from *Manduca sexta* pupae. *Insect Biochemistry* 18: 163–168.

High Performance Liquid Chromatography

High performance liquid chromatography (HPLC) offers a wide range of techniques for analytical and preparative purposes. Co-migration of a compound with a reference ecdysteroid in one (or several) solvent system(s) represents the usual way for identification of the compound. Some common HPLC systems are listed in Table 8.

Chromatographic Procedures

Ecdysteroid detection

UV detectors are well-suited to the detection of ecdysteroids, as most ecdysteroids possess a conjugated 7-en-6-one moiety which provides a strongly absorbing chromophore (λ_{\max} 242 nm, $\log \epsilon$ ca. 4). This allows the easy detection of less than 10 pmol amounts.

Diode-array detectors provide information about the absorbance spectrum of all eluted peaks. It can thus be directly checked whether a compound co-migrating with a reference ecdysteroid has a suitable UV spectrum. Good spectra can be obtained with very small amounts (less than 100 ng) of ecdysteroids and such data provide an additional criterion to assess the identity of UV-absorbing peaks.

Fluorescence detectors require the preparation of fluorescent derivatives of ecdysteroids, which may increase the sensitivity of detection by two orders of magnitude when compared with UV. Phenanthrene boronic acid, a reagent specific for α -diols (here the 20,22-diol), and 1-anthroyl nitrile, which reacts with alcohols (here the 2-OH of ecdysteroids), have been used. These reactions, however, are not specific enough for ecdysteroids and they have not been widely adopted.

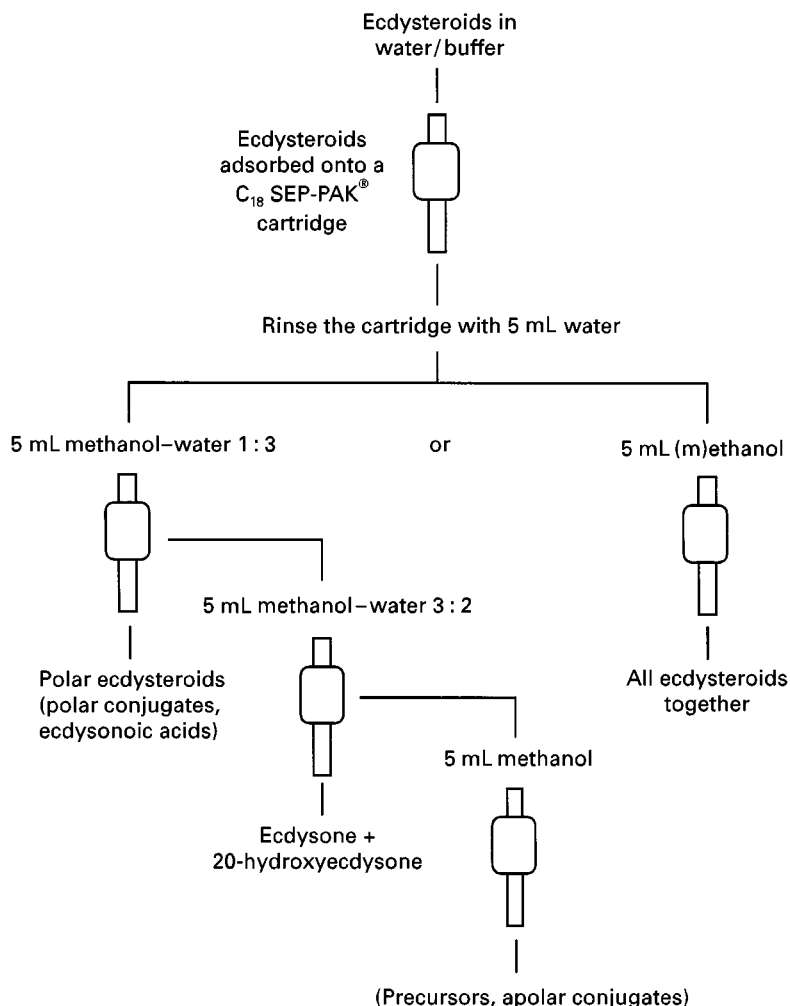


Figure 5 Utilization of reversed-phase cartridges for ecdysteroid purification. The cartridge must be rinsed with 5 mL MeOH then 5 mL water prior to use. Redrawn from Lafont R, Morgan ED and Wilson ID (1994) Chromatographic procedures for phytoecdysteroids. *Journal of Chromatography* 658: 31–53, with permission from Elsevier Science.

Table 8 Chromatographic systems commonly used for the HPLC analysis of ecdysteroids

Mode of chromatography	Polar		Medium	Apolar
	Ionic	Nonionic		
Normal-phase (silica, diol, APS, TMS)				
Chloroform/95% ethanol	—		+	+
Chloroform/methanol	—		+	+
Cyclohexane/isopropanol/water	—	—	+	+
Dichloroethane/isopropanol/water	—		+	+
Dichloromethane/tetrahydrofuran/methanol	—		+	+
Dichloromethane/ethanol/water	—		+	+
Dichloromethane/isopropanol/methanol	—		+	+
Dichloromethane/isopropanol/water	—	+	+	+
Dichloromethane/methanol	—		+	+
Dichloromethane/methanol/water/acetic acid	—		+	+
Hexane/ethanol/methanol/acetonitrile	—	—	+	+
Isooctane/isopropanol/water	—	—	+	+
Reverse-phase (C ₁₈ , C ₈ , phenyl, etc.)				
Acetonitrile/isopropanol				+
Acetonitrile/isopropanol/water	+	+	+	
Acetonitrile/water	+	+	+	
Acetonitrile/Tris-HClO ₄ , Tris-HCl, Na citrate, TFA 0.1%	+	+	+	
Isopropanol/water	+	+	+	
Methanol/water, Na acetate, Na phosphate	+	+	+	
Methanol				+
Ion-pair				
Acetonitrile/cetrimide-phosphate	+			
Methanol/tetrabutylammonium	+			
Ion-exchange				
Ammonium acetate	+	—	—	—

—, does not apply. APS, aminopropyl silane; TFA, trifluoroacetic acid; TMS, trimethylsilane.

Radioactivity monitoring provides a direct comparison with UV absorbance, and this easily allows one to make correspondence between the radioactive peaks and unlabelled reference compounds added in the sample before injection. They are currently used for metabolic studies.

Mass spectrometry (MS) gives important structural information. The interfacing problems between HPLC and MS have been overcome in recent years and this technique will undoubtedly develop in the future. An example of HPLC-MS applied to an ecdysteroid-containing plant extract is given in **Figure 6**.

Nuclear magnetic resonance spectrometry can also be used on-line to identify ecdysteroids. This requires rather expensive deuterated HPLC solvents and the method is only suitable for plant extracts where ecdysteroid concentrations are high enough. An example of the use of this emerging technology in a plant extract is shown in **Figure 7**.

Off-line procedures may be used to improve the sensitivity and/or selectivity of ecdysteroid detection (or to identify ecdysteroids after preparative HPLC purification). These analytical methods include chiefly immunoassays (RIA, EIA) and also several recently designed *in vitro* bioassays.

Normal-phase systems Normal-phase HPLC systems generally use silica columns (sometimes polar-bonded columns) and, for example, dichloromethane-isopropanol-water mixtures. Non-polar ecdysteroids (such as esters or precursors) can be separated with a 125 : 15 : 1 (v/v/v) mixture, medium-polarity compounds (such as ecdysone and 20-hydroxyecdysone) with a 125 : 30 : 2 mixture, and more polar (but non-ionic) ecdysteroids (such as 26-hydroxyecdysteroids and glucosides) with 125 : 40 : 3 or 100 : 40 : 3 mixtures.

Dichloromethane-based solvents strongly absorb UV and do not allow UV spectra to be obtained with diode-array detectors, nor are they well suited to in-line radioactivity monitoring (due to their quenching properties). These problems do not exist with

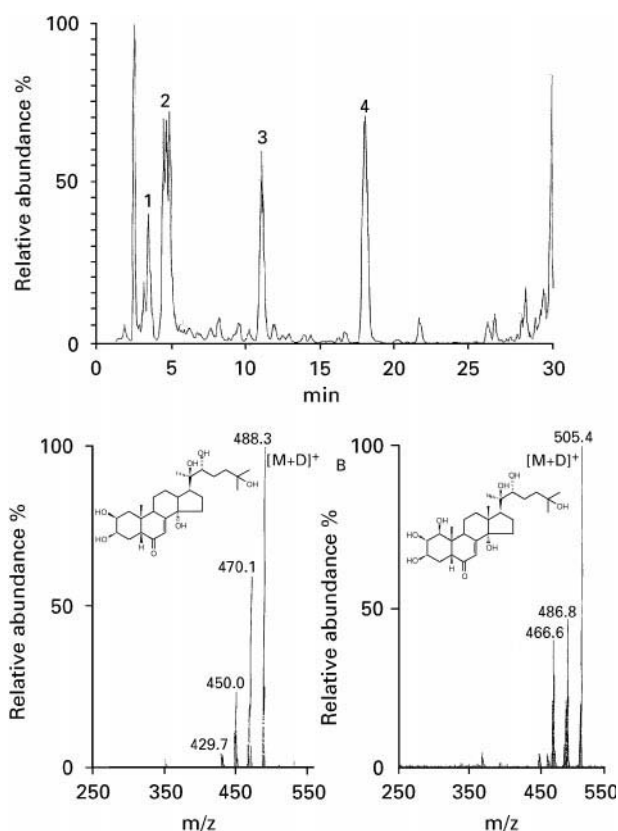


Figure 6 Reversed-phase HPLC-MS total ion current trace (upper) of an extract of *Silene otites*. Peak 1, integristerone A; 2, 20-hydroxyecdysone; 3, 2-deoxy-20-hydroxyecdysone; 4, 2-deoxyecdysone. The mass spectra (lower) are of 20-hydroxyecdysone (left) and integristerone A (right). Structures in insets to mass spectra. After Wilson ID, Lafont R, Shockcor JP *et al.* (1999) High-performance liquid chromatography coupled to nuclear magnetic resonance spectroscopy and mass spectrometry applied to plant products: Identification of ecdysteroids from *Silene otites*. *Chromatographia* 49: 374–378, reprinted with permission.

cyclohexane-based mixtures, however, the poor solubility of ecdysteroids in these mixtures causes some problems for the analysis of polar ecdysteroids and also for preparative purposes.

Polar-bonded columns (e.g. -diol, -polyol or -aminopropylsilane, APS) can also be used. Diol-bonded columns used with extracts of the phasmid *Carausius morosus* allowed the separation of a wide array of polar and non-polar metabolites, whereas the APS phase has provided efficient separations of mixtures containing 3 α -OH, 3 β -OH and 3-oxo ecdysteroids. One major interest in such polar-bonded columns is that solvent gradients can be used, whereas lengthy re-equilibration times would be the case with silica columns.

Reversed-phase systems Reversed-phase HPLC on C₁₈-bonded columns eluted with methanol–water

mixtures provides the most widely used system. Acetonitrile–water (acetonitrile–buffer) mixtures are more efficient, especially when polar conjugates and/or ecdysonic acids are present. Adequate systems have been designed for polar and apolar metabolites, which may both be present within the same sample. Surprisingly, apolar fatty acyl esters of ecdysteroids are not eluted with pure acetonitrile, whereas they are with methanol, despite the fact it is a more polar solvent (the same is true for cholesterol).

In the case of polar (ionizable) metabolites, it may be of interest to use different pHs, which will result in modified retention times, while uncharged ecdysteroids will retain the same elution time. Moreover, this gives an easy access to the pK_a value of ionizable groups, which is of interest for the characterization of conjugates.

Ion-exchange chromatography Anion-exchange columns are used for the purification of polar conjugates. They represent an efficient method, complementary to reversed-phase HPLC. However, using two different pHs (e.g. pH 7.5, then 2.5) with HPLC, provides an equivalent opportunity for obtaining pure ionizable conjugates, e.g. phosphate esters.

Various Aims of HPLC

Analytical and preparative HPLC Columns of different sizes with the same packing are available, therefore it is very easy to scale up any chromatographic separation. Maximum sample load is related to the amount of stationary phase in the column. In

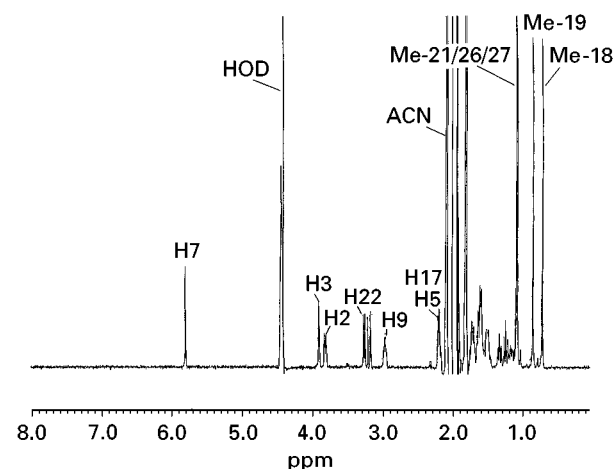


Figure 7 Stopped-flow HPLC-NMR spectrum of 20-hydroxyecdysone following reversed-phase HPLC on a C₁₈-bonded column with D₂O acetonitrile as mobile phase. (Reproduced with permission from Wilson ID, Morgan ED, Lafont R and Wright B (1998) High-performance liquid chromatography coupled to nuclear magnetic resonance spectroscopy. Applications to the ecdysteroids of *Silene otites*. *Journal of Chromatography A* 799: 333–336).

favourable cases, samples up to the milligram range can be run on analytical columns. Larger amounts, of course, require wide-bore columns. It may happen that some compounds that are baseline resolved when loading is low, are not well separated with a larger load. This is, for instance, observed with the inokosterone/20-hydroxyecdysone pair run on a semi-preparative column (Zorbax®-SIL, 9.6 mm i.d.), even when less than 0.5 mg is injected.

Quantitative analyses HPLC has been used for the direct quantification of individual ecdysteroids in biological samples. For animal extracts, this requires a high sensitivity because of the low concentrations

present and adequate sample clean-up. The most reliable quantification is obtained if an internal standard is added before sample purification. Many phytoecdysteroids can be used as internal standards. The choice must be made after a preliminary run of a representative sample in order to select a compound that does not co-migrate with major impurities and of course differs from the ecdysteroids present in the biological extract.

Selectivity in HPLC

Both isocratic reversed-phase and normal-phase systems can separate rather complex ecdysteroid mixtures, and the use of solvent gradients increases the

Table 9 HPLC data on a set of ecdysteroids using several chromatographic systems

Compound	DIW	CIW	AW	MW	IW
2-Deoxy-20-hydroxyecdysone	13.9	11.7	12.5	11.8	14.8
2-Deoxyecdysone	9.5	8.9	31.9	22.6	44.1
3-Dehydro-20-hydroxyecdysone	9.2	16.2	6.5	5.8	
3-Epi-20-hydroxyecdysone	25.7	19.6	5.6	5.4	
5 α -2-Deoxy-20-hydroxyecdysone	13.6	13.6	11.6	10.7	13.0
5 α -2-Deoxyecdysone	9.2	10.0	30.2	21.7	38.3
5 α -20-hydroxyecdysone	24.9	24.1	4.9	4.8	5.0
5 α -Ecdysone	15.0	16.2	9.3	7.3	9.9
20-Hydroxyecdysone	28.9	21.3	5.2	5.4	6.0
20-Hydroxyecdysone 2-acetate	10.7	13.8	14.6	11.3	
20-Hydroxyecdysone 3-acetate	11.3	14.9	10.4	7.7	
20-Hydroxyecdysone 22-acetate	17.3	17.3	12.0	7.6	
20-Hydroxyecdysone 25-acetate	8.7	11.5	18.0	9.5	
20,26-Dihydroxyecdysone	89.9	47.1	3.7	3.7	4.3
22-Deoxy-20-hydroxyecdysone	21.7	15.3	13.5	11.7	18.5
22-Epi-20-hydroxyecdysone	50.0	25.8	4.6	4.7	
22-Oxo-20-hydroxyecdysone	16.8	15.1	12.4	9.8	
24-Epi-makisterone A	16.8	15.5	7.8	6.9	
25-Deoxyecdysone	6.1	6.4	102.9	32.7	
Abutasterone	35.5	27.1	4.4	4.8	5.0
Ajugalactone	7.2	20.2	14.5	7.5	
Cyasterone	9.9	14.5	8.1	5.8	
Ecdysone	18.8	15.1	9.7	8.4	13.0
Gerardiasterone	40.6	27.9	5.5	6.0	
Integristerone A	38.7	28.8	4.2	4.4	5.0
Makisterone A	20.5	17.7	7.0	6.9	
Makisterone C	11.3	11.3	16.8	12.9	
Polypodine B	18.8	21.5	5.4	5.4	5.5
Ponasterone A	6.6	7.9	32.8	17.5	48.8
Poststerone	9.0	13.3	9.3	6.4	
Rubrosterone	8.7	13.3	5.6	4.3	
Sidisterone	9.6	26.0	12.2	6.3	
Stachysterone C	7.2	8.1	22.7	13.2	
Turkesterone	89.9	36.4	4.4	4.1	3.7
$\Delta^{24,25}$ -25-Deoxyecdysone	6.4	6.8		24.3	
$\Delta^{24,28}$ -Makisterone A	13.6	13.6	8.0	7.5	
$\Delta^{25,26}$ -25-Deoxyecdysone	6.4	6.8		21.1	
$\Delta^{9,11}$ -20-Hydroxyecdysone	7.2	7.7		14.1	
$\Delta^{9,11}$ -Ecdysone	22.5	16.8		7.2	

Analytical columns were either a Zorbax-Sil column (DuPont), 25 cm \times 4.6 mm i.d., eluted with DIW (dichloromethane-isopropanol-water, 125 : 30 : 2) or CIW (cyclohexane-isopropanol-water, 100 : 40 : 3) or a Spherisorb 5ODS2 (Biochrom), 25 cm \times 4.6 mm i.d., eluted with water + 1% (final concentration) trifluoroacetic acid and either 23% acetonitrile (AW), 50% methanol (MW), or 18% isopropanol (IW). Flow rate was 1 mL min⁻¹ in every case.

power of these systems. In order to draw up general rules, it is necessary to analyse the HPLC behaviour of numerous ecdysteroids differing by single or multiple modifications, and to use a set of different HPLC systems. A set of such data are given in Table 9, and the corresponding conclusions are given in Table 10.

Selectivity in NP-HPLC

Columns NP-HPLC columns are packed with either silica or polar-bonded silica. The use of diol-bonded material instead of silica does not introduce large changes; retention times vary, but the elution order

Table 10 Effects of individual changes (with reference to the 20E molecule) on the chromatographic behaviour of ecdysteroids as analysed using various chromatographic systems

Change	Effect on capacity factor (k')			
	Normal-phase		Reversed-phase	
	DIW	CIW	MW	AW
Change of the number of -OH groups				
+ 1, 11, 24, 26	++ (1 < 24 < 11 = 26)	+(24 < 1 < 11 < 26)	-(26 < 11 < 1 < 24) -	-(26 < 1 < 11 = 24)
+ 5	-	=	(-)	(+)
- 2, 20, 22, 25	-(25 < 2 < 20 < 22)	-(25 < 2 < 20 = 22)	+(20 < 2 = 22 < 25)	+(20 < 2 < 22 < 25)
Change of stereochemistry at C-5 (5 β \rightarrow 5 α)				
If 2-OH present	-	+	(+)	(-)
If 2-OH absent	=	+	=	(-)
Change of stereochemistry at C-22	++	+	-	-
Change at C-3				
3 β -OH \rightarrow 3-oxo	--	-	(+)	+
3 β -OH \rightarrow 3 α -OH	-	-	=	(+)
Presence of substituents at C-24				
24-Me	-	-	+	+
24-Et	--	--	++	++
Conjugation of 20E				
Monoacetates	-- (25 < 2 = 3 < 22)	-(25 < 2 < 3 < 22)	+(22 = 3 < 25 < 2)	++ (3 < 22 < 2 < 25)
Monoglucosides	++ (22 < 25 < 2 = 3)	Not tested	+(22 < 25 < 2 = 3)	-(22 < 25 < 2 = 3)
Presence of double bonds				
9, 11	(+)	(+)	-	-
25, 26	+	-	-	-
24, 25	+	+	-	-
Presence of a lactone on the side-chain (cyasterone vs. 20E)	--	(-)		
Side-chain cleavage products				
Poststerone (C ₂₁)	--	--	+	+
Rubrosterone (C ₁₉)	--	--	-	-

Changes of the k' value are described as follows: --, strong reduction; -, reduction; (-), weak reduction; =, almost no change; (+), weak increase; +, increase; ++, large increase. Numbers in parentheses refer to the positions concerned, and the molecules are classified according to increasing k' values. DIW, dichloromethane-isopropanol-water; CIW, cyclohexane-isopropanol-water; MW, methanol-water; AW, acetonitrile-water.

usually remains the same. Aminopropyl (APS) columns may interact specifically with 3-oxoecdysteroids and therefore introduce a different selectivity. C_2 -bonded phases behave like weakly active silicas and give very symmetrical peaks; they may be of interest for very polar non-ionic ecdysteroids.

The retention times obtained with silica columns may decrease upon prolonged use, because water-containing solvents slowly deactivate the column. A reactivation cycle with anhydrous solvents: alcohol, dichloromethane, hexane, dichloromethane (50–100 mL each) allows an almost complete recovery of initial retention times.

Solvents UV monitoring of the HPLC effluent precludes the use of solvents such as ethyl acetate, benzene or acetone (such limitations were not encountered with TLC). The solvent is usually based on a chlorinated hydrocarbon (dichloro(m)ethane, chloroform) modified with an alcohol (methanol, ethanol or isopropanol). Water added just below saturation reduces peak tailing.

Dichloromethane- and cyclohexane-based mixtures display a different selectivity, as shown in **Figure 8**. Selectivity changes are particularly impressive when considering the pair $5\alpha/5\beta$, or compounds bearing a lactone ring on the side-chain. As cyclohexane-based mixtures are highly viscous, the working pressures may exceed 100 bar with analytical columns run at a flow-rate of 1 mL min^{-1} . Increasing temperatures to 50°C overcomes this drawback and results in about a 40% decrease of working pressure without affecting the separation.

NP-HPLC is rather inefficient for the separation of compounds with or without extra double bonds, whereas RP-HPLC allows their easy resolution.

Selectivity in RP-HPLC

Columns Many different types of column are available, which differ by the type (C_6 , C_8 , C_{18} , C_{22} , phenyl, CN, etc.) and extent (percentage of the carbon load) of bonding, and also by the porosity (6–30 nm) of the silica used. All these parameters influence the selectivity of the column, thus, ensuring reproduction of a separation described in the literature requires the same type of column. C_{18} (or ODS) bonded silicas are the most widely used column packings.

Solvents The most common RP-HPLC solvents contain water and either methanol or acetonitrile, although other organic modifiers (ethanol, isopropanol, butanol, etc.) can be used. Using a buffer instead of water, or adding 0.1% (v/v) trifluoroacetic acid often results in much improved separations, especially when ionizable ecdysteroids are present.

The relative retention of ecdysteroids differing by a single -OH group varies with the organic solvent of the mobile phase. Extra -OH groups generally increase the polarity; their effect depends both on their position in the molecule (**Figure 9**) and on the solvent system used.

Isopropanol–water mixtures provide the best separations for $5\alpha/5\beta$ pairs. Methanol is particularly efficient towards extra double bonds and gives a base-

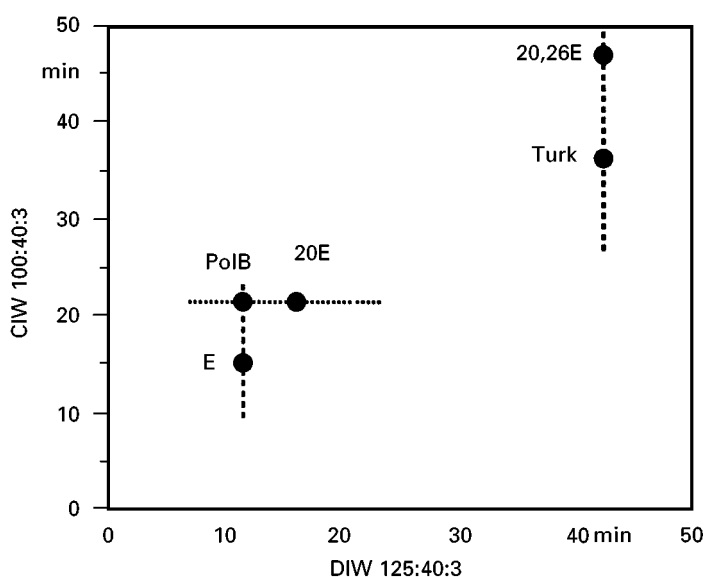


Figure 8 An example of selectivity in NP-HPLC. E, ecdysone; 20E, 20-hydroxyecdysone; 20,26E, 20,26-dihydroxyecdysone; PoIB, polypodine B; Turk, turkesterone. CIW, cyclohexane–isopropanol–water; DIW, dichloromethane–isopropanol–water.

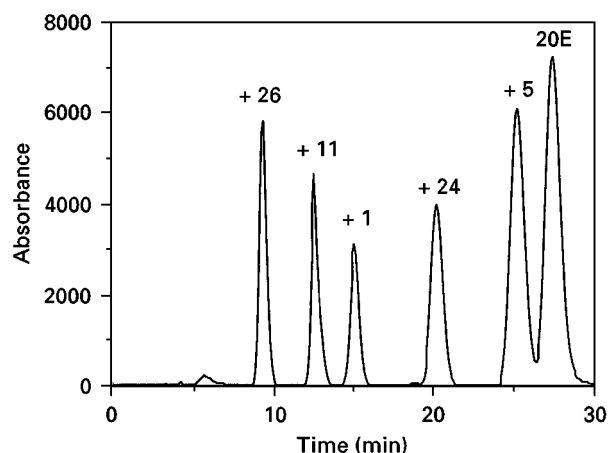


Figure 9 Separation of reference ecdysteroids by RP-HPLC (column Spherisorb 5ODS2, 250 mm \times 4.6 mm, solvent 35% methanol in water, isocratic, flow-rate 1 mL min⁻¹). The numbers indicate the position of the additional -OH group by reference to 20-hydroxyecdysone (20E).

line separation of 24,25-ene and 25,26-ene pairs. Higher temperatures increase efficiency, decrease pressure and result in a reduction of k with only limited effects on selectivity.

Supercritical Fluid Chromatography (SFC)

Supercritical carbon dioxide is a non-polar fluid and therefore SFC is more or less equivalent to normal-phase HPLC. The eluting power is increased by adding methanol to the fluid. Various types of packed columns can be used (Table 11), including silica or bonded silica; bonded silica is less retentive as is observed with NP-HPLC. Alternatively, fused silica capillary columns can be used.

A major advantage of SFC over HPLC is shorter retention times. The compounds elute as very sharp peaks and the sensitivity of detection is increased accordingly. A second advantage is the high transparency of carbon dioxide in the infrared (IR), which allows the use of FT-IR detectors. Furthermore, SFC is compatible with both flame ionization detec-

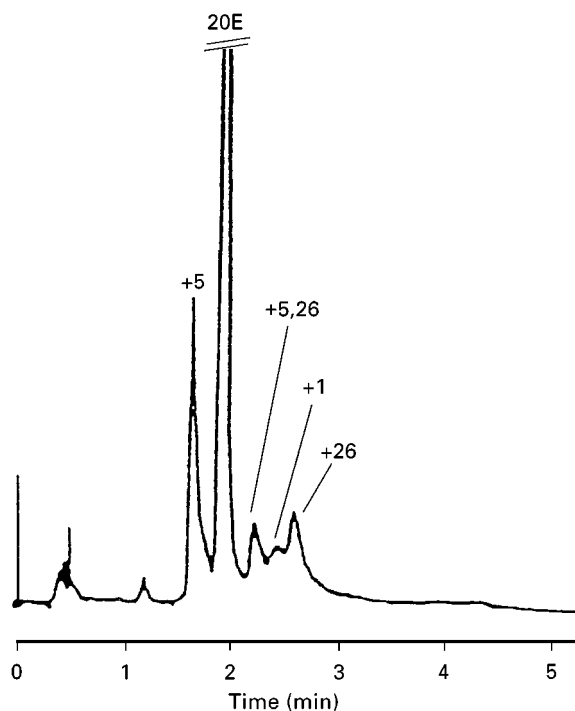


Figure 10 SFC of ecdysteroids on 5 μ m-cyanopropyl-bonded silica gel with carbon dioxide-methanol (9 : 1) as mobile phase at 3 mL min⁻¹, 60°C and 290 bar (sample from *Silene otites*). (Reproduced from Raynor MW, Kithinji JP, Bartle K *et al.* (1989) Packed column supercritical-fluid chromatography and linked supercritical-fluid chromatography-mass spectrometry for the analysis of phytoecdysteroids from *Silene nutans* and *Silene otites*. *Journal of Chromatography* 467: 292-298, with permission from Elsevier Science.)

tion (the universal detection used with GC) and mass spectrometry (interfacing causes far fewer problems than with HPLC). No derivatization is required, and this represents an important advantage over GC. SFC appears, therefore, to be an interesting compromise, but its use has been up to now limited to plant extracts containing particularly high concentrations of ecdysteroids. The easy removal of carbon dioxide after fraction collection represents an advantage for preparative uses. An example of the separation of ecdysteroids by SFC is given in Figure 10.

Table 11 Some SFC systems used for ecdysteroid analysis

Column	Solvent system
Normal phase (silica)	
Hypersil 5 μ m (10 cm \times 4.6 mm i.d.)	CO ₂ -MeOH (4 : 1) 300 bar, 80°C, 4 mL min ⁻¹
Bonded phases	
Spherisorb-CN 5 μ m	CO ₂ or CO ₂ -MeOH (9 : 1)
Spherisorb-ODS2 5 μ m	CO ₂ or CO ₂ -MeOH (9 : 1)

See Lafont *et al.* (1994b) for more details.

Gas Chromatography

Gas chromatography (GC) was first developed for ecdysteroids during the early 1970s. Despite the advantages of GC (especially in combination with the electron capture detector), concerning sensitivity and specificity compared with other techniques, its use for ecdysteroids has been limited. As a majority of bio-synthetic intermediates of the ecdysteroids are involatile, it is necessary to convert them into volatile trimethylsilyl ether derivatives. Derivatization is usually performed with either trimethylsilylimidazole (TMSI) or *N,O*-bis-trimethylsilyltrifluoroacetamide, although other more specialized derivatives have been used. Complete derivatization is not always obtained and a single ecdysteroid can give rise to several chromatographic peaks.

Not all ecdysteroids are suitable for GC even after silylation. Silylation of compounds such as cyasterone (which contains a lactone in the side-chain) can result in a variety of derivatives characterized either by long retention times or poor peak shapes. Some ecdysteroid conjugates such as coumarate esters, appear to break down to the free ecdysteroid during the silylation procedure.

Chromatographic Systems

Chromatography was first performed with packed columns (1–3 m long, 2 mm i.d.) containing non-polar stationary phases such as OV-1 and OV-101 coated on Gas Chrom Q and Gas Chrom P. Fused-silica columns (10–25 m long, 0.22 mm i.d.) now provide much better separations. A typical operation temperature for the columns is 280°C.

Flame ionization detectors (FID) allow detection limits in the nanogram range. Electron-capture detection (ECD) provides the best available sensitivity among chromatographic methods (5 pg), and GC coupled with MS gives structural information with as few as 0.1 ng of ecdysteroids (particularly important with animal extracts). However, the need for derivatization is such a drawback that this powerful method is seldom used for ecdysteroids nowadays.

Conclusion

HPLC is the most widely used method for the separation of ecdysteroids. At the present time, hyphenated techniques (HPLC-MS and HPLC-NMR) are developing and will provide particularly powerful tools for the analysis of ecdysteroid-rich (plant) samples in the future.

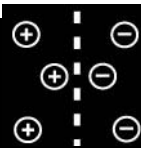
See Colour Plate 80.

See also: II/Chromatography: **Gas:** Derivatization; Detectors: Selective. **Chromatography: Liquid:** Counter-current Liquid Chromatography; Derivatization; Detectors: Mass Spectrometry; Detectors: Ultraviolet and Visible Detection; Fluorescence Detectors in Liquid Chromatography; Nuclear Magnetic Resonance Detectors. **Chromatography: Thin-Layer (Planar):** Densitometry and Image Analysis; Layers; Mass Spectrometry; Modes of Development: Conventional; Modes of Development: Forced Flow Over Pressured Layer Chromatography and Centrifugal; Spray Reagents. **Extraction:** Analytical Extractions; Multistage Countercurrent Distribution. III/Im-mobilised Boronic Acids: **Extraction. Natural Products:** Liquid Chromatography – Nuclear Magnetic Resonance. **Steroids:** Liquid Chromatography and Thin-Layer (Planar) Chromatography; Gas Chromatography; Super-critical Fluid Chromatography.

Further Reading

- Horn DHS and Bergamasco R (1985) Chemistry of ecdysteroids. In: Kerkut GA and Gilbert LI (eds) *Comprehensive Insect Physiology, Biochemistry and Pharmacology*, vol. 7, pp. 185–248. Oxford: Pergamon Press.
- Lafont R (1988) HPLC analysis of ecdysteroids in plants and animals. In: Kalasz H and Ettre S (eds) *Chromatography '87*, pp. 1–15. Budapest: Akademiai Kiado.
- Lafont R and Beydon P (1990) Methods for ecdysteroid analysis. In: Gupta AP (ed.) *Morphogenetic Hormones of Arthropods. Discoveries, Syntheses, Metabolism, Evolution, Mode of Action and Techniques*, vol.1, pp. 485–512. New Brunswick: Rutgers University Press.
- Lafont R and Wilson ID (1996) *The Ecdysone Handbook*, 2nd edn. Nottingham: The Chromatographic Society Press.
- Lafont R, Kaouadji N, Morgan ED and Wilson ID (1994) Selectivity in the HPLC analysis of ecdysteroids. *Journal of Chromatography* 658: 55–67.
- Lafont R, Morgan ED and Wilson ID (1994) Chromatographic procedures for phytoecdysteroids. *Journal of Chromatography* 658: 31–53.
- McCaffery AR and Wilson ID (eds) (1990) *Chromatography and Isolation of Insect Hormones and Pheromones*. London: Plenum Press.
- Morgan ED and Marco MP (1990) Advances in techniques for ecdysteroid analysis. *Invertebrate Reproduction and Development* 18: 55–66.
- Koolman J (ed.) (1989) *Ecdysone, From Chemistry to Mode of Action*. Stuttgart: Georg Thieme Verlag.
- Thompson MJ, Svoboda JA and Feldlaufer MF (1989) Analysis of free and conjugated ecdysteroids and polar metabolites of insects. In: Nes WD and Parish EJ (eds) *Analysis of Sterols and Other Biologically Significant Steroids*, pp. 81–105. San Diego: Academic Press.

ECOLOGICALLY SAFE ION EXCHANGE TECHNOLOGIES



D. Muraviev, Autonomous University of Barcelona, Barcelona, Spain

Copyright © 2000 Academic Press

The industrial application of ion exchange (IE) is growing. In many instances IE can successfully replace existing large scale industrial processes which do not satisfy modern ecological standards. To be competitive, IE technology should be highly efficient and ecologically safe. The general scheme of standard IE processes comprises several auxiliary operations (besides IE treatment), listed in Table 1. Several approaches have been applied to eliminate some of these auxiliary operations and to improve the efficiency and ecological safety of the process through significant savings of chemicals and energy and reduction of waste.

One of these approaches is based on the application of dual-temperature IE processes which exploit the different affinities of the resin towards ions to be separated at different temperatures. The main advantage of dual-temperature IE comes from avoiding the use of auxiliary reagents which are conventionally required to displace (strip) the ions to be separated from the resin phase and to regenerate the ion exchanger. This last stage is known to be the main source of waste in IE technology (Table 1). In dual-temperature IE, both stages can be combined in one through the use of a thermo-stripping procedure. This allows the exclusion of auxiliary operations 4 and 5. Hence, essentially reagentless and wasteless separation processes can be designed.

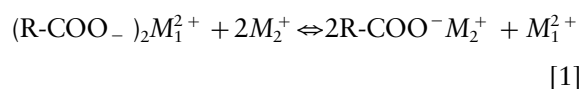
Another route to avoid auxiliary operations (e.g. numbers 2 and 3; Table 1) is based on a combination of IE conversion and the product concentration processes into one stage. Frontal IE chromatography and reverse frontal separation can be applied for this purpose. In certain instances, both of these IE separation techniques allow the concentration of the target substance to a level exceeding its solubility at a given temperature. Moreover, this supersaturated solution (SS) remains stable for a long period, while after leaving the column it crystallizes spontaneously. This allows the design of a nearly ideal process where a crystalline product is obtained directly after the IE treatment. The tailored application of this phenomenon (discovered by Muraviev and known as ion

exchange isothermal supersaturation or IXISS) allows, in certain instances, for additional elimination of operations 4 and 5. Several examples of the tailored application of dual-temperature IE and IXISS effects to design ecologically safe IE technologies are given below.

IXISS-based IE Processes¹

The tailored application of IXISS to design highly efficient IE technologies is based on the use of the IXISS-active stripping agents, which must meet the following requirements:

1. The IXISS-active eluent must on the one hand bear the desired counterion to combine the desorption of the product with the regeneration of the ion exchanger. On the other hand, it must also contain an appropriate co-ion to provide the formation of a stable SS of a low solubility compound (the product) and to shift the IE equilibrium in the system to the desired direction. For example, the IE reaction of displacement of a divalent metal ion, M_1^{2+} (e.g. Mg^{2+} or Ca^{2+}), by a monovalent one, M_2^+ (e.g. Na^+), from a carboxylic cation exchanger can be written as follows:



The equilibrium in reaction 1 is characterized by the equilibrium coefficient, $K_{M_2}^{M_1}$:

$$K_{M_2}^{M_1} = \frac{Q_{M_2}(C_{M_1})^{1/2}}{(Q_{M_1})^{1/2}C_{M_2}} \quad [2]$$

where C and Q are the concentrations of ions in the solution and resin phases, respectively. For chloride media, $K_{M_2}^{M_1}$ is usually $\ll 1$. If reaction 1 proceeds in a carbonate medium, for example, when the resin in the M_1 form is treated with

¹ Adapted with permission from Muraviev D, Khamizov R, Tikhonov N *et al.* (1998). Clean ion-exchange technologies. I. Synthesis of chlorine-free potassium fertilizers by an ion-exchange isothermal supersaturation technique. *Industrial Engineering and Chemistry Research* 37: 1950–1955.

Table 1 Basic auxiliary operations of standard ion exchange process

No.	Operation	Consumption of		Wastes (approx. % of total)
		Energy	Chemicals	
1	Preparation of stock solution	Low	Low	Up to 5
2	Concentration of solution after IE treatment (e.g. by evaporation)	High	Low	
3	Recovery of purified product (e.g. by crystallization)	Medium	Low	Up to 5
4	Regeneration of ion exchanger and auxiliary chemicals for reuse	Low/medium	High	Up to 80
5	Neutralization of waste before their disposal	Low	High/medium	Up to 10

M_2 carbonate solution (C_o , mol dm⁻³), it is coupled with the formation of M_1 carbonate, which can be described by the solubility product of M_1CO_3 ($L_{M_1CO_3}$), where:

$$L_{M_1CO_3} = C_{M_1^{2+}} C_{CO_3^{2-}} \quad [3]$$

If M_1CO_3 forms a stable SS, where it exists in an associated (molecular) form at a concentration C_M mol dm⁻³ exceeding γ times its solubility, C_s , at a given temperature, eqn [3] takes the following form:

$$L_{M_1CO_3} = C_{M_1^{2+}} (C_o - C_M) \quad [4]$$

By introducing $C_M = \gamma C_s$, and after substitution of $C_{M_1^{2+}}$ from [4] into [2], one obtains:

$$K_{M_2}^{M_1} = \frac{Q_{M_2}(L_{M_1CO_3})^{1/2}}{(Q_{M_1})^{1/2} C_o (C_o - \gamma C_s)} \quad [5]$$

As follows from eqn [5], at constant C_o , C_s and $L_{M_1CO_3}$, $K_{M_2}^{M_1}$ increases with γ and may reach sufficiently high value ($\gg 1$), as $\gamma \rightarrow C_o/C_s$. Equation [5] can be rewritten in a more general form for the displacement of the divalent metal ion from the resin with an IXISS-active stripping agent bearing a monovalent counterion as follows:

$$K_{Sss}^{Dis} = \frac{Q_{Dis} L_{Sss}^{1/2}}{(Q_{Sss})^{1/2} C_o (C_o - \gamma C_s)} \quad [6]$$

Here 'Dis' and 'Sss' superscript and subscript denote the displacer and the substance under supersaturation (the product), respectively; C_o is the concentration of the displacer solution, L is the solubility product of the target compound, C_s is the solubility of the product at a given temperature, and γ is the degree of supersaturation for the product solution. Relationship [6] is the fundamental equation describing the shift of IE equilibrium in IXISS systems of different types.

- The successful application of the IXISS effect requires, on the one hand, maximum stability of the

SS in the interstitial space of the column during the IE treatment cycle and, on the other hand, fast decomposition (crystallization) of this solution after its removal from the column. In the case of inorganic substances a unified interpretation of the IXISS phenomenon must be based on general principles of the aggregative stability of dispersion systems, adapted to the particular IE system.

- The following main factors may influence the stability of dispersions of precrystalline molecular aggregates in the interstitial space of a column: firstly, an effective charge of the polymolecular aggregate (micelle), which is due to the sorption of either counter- or co-ions on the particle surface; and secondly, the ionic strength of the medium, which may strongly influence the coagulation (crystallization) conditions. If, for example, an excess of co-ions exists in the interstitial space, the charge of the micelles will be the same as that of the functional groups of the ion exchanger. In this case, the sorption of the micelles on the surface of the ion exchanger beads becomes impossible and a stabilizing action of the resin bed towards SS can be expected. In contrast, in the presence of an excess of counterions, the charge sign of the precrystalline aggregates will be opposite to that of the functional groups and fast decomposition of SS must be observed due to the sorption of micelles on the surface of the ion exchanger, followed by crystallization of the component under supersaturation.

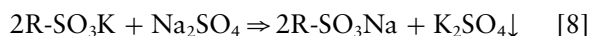
Manufacture of Chlorine-free Potassium Fertilizers²

The production of chlorine-free potassium salts (with minimum Cl⁻ admixture) such as K₂SO₄, and others, is of particular interest since it deals with the problem

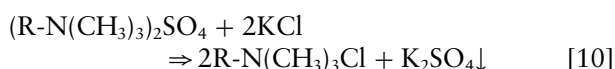
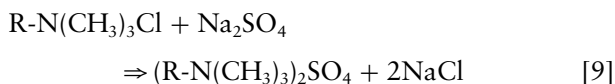
² Adapted with permission from Muraviev D, Khamizov R, Tikhonov N *et al.* (1998). Clean ion-exchange technologies. I. Synthesis of chlorine-free potassium fertilizers by an ion-exchange isothermal supersaturation technique. *Industrial Engineering and Chemistry Research* 37: 1950–1955.

of effectively cultivating some chlorophobic plants (e.g. citruses, vegetables and herbs) which are adversely affected by high Cl^- concentration. Potassium sulfate is produced in substantial quantities in Europe by the Mannheim process from K_2CO_3 and H_2SO_4 or by reaction of H_2SO_4 with KCl . Both versions of the Mannheim process are complicated by problems of utilizing gaseous wastes (CO_2 and HCl). In the USA and some other countries, K_2SO_4 is manufactured by exchange reactions between potassium, sodium and magnesium salts by their dissolution and fractional crystallization. This latter process requires utilization of large volumes of liquid waste. The IE synthesis of K_2SO_4 from KCl and $\text{Na}_2\text{SO}_4 \cdot 10\text{H}_2\text{O}$ is based either on cation or anion exchange reactions:

Cation exchange synthesis



Anion exchange synthesis



In the first process, a sulfonate cation exchanger is first converted from the Na^+ into the K^+ form with dilute KCl solution (0.1 mol dm^{-3}), followed by desorption (stripping) of the product (K_2SO_4) with concentrated Na_2SO_4 solution (2 mol dm^{-3}). The second process starts with the conversion of a strong base anion exchanger from the Cl^- into the SO_4^{2-} form with dilute Na_2SO_4 solution ($\sim 0.25 \text{ mol dm}^{-3}$). K_2SO_4 is then produced during the stripping of sulfate ions with concentrated KCl solution ($\sim 3\text{--}4 \text{ mol dm}^{-3}$). The stripping of K_2SO_4 from the resins in both cases leads to the formation of an SS of K_2SO_4 with a degree of supersaturation, γ , of approximately 2. Nevertheless, K_2SO_4 does not precipitate in the column and remains as a stable SS at least for a period of several hours. At the same time, this SS crystallizes spontaneously following its removal from the column. The maximum efficiency of the first process (see eqns [7] and [8]) is achieved when the stripping of the product is carried out at 308 K, followed by crystallization of K_2SO_4 at 293 K to provide the highest difference in sodium and potassium sulfate solubilities inside the column. The second process (see

eqns [9] and [10]) appears to be more efficient when carried out at 282 K to minimize the solubility of K_2SO_4 in the solution collected.

The IE equilibrium in both systems is shifted to the right when using dilute KCl and Na_2SO_4 solutions at the first stages of both processes. Application of IXISS effect in the flowsheets of both processes allows the product formation stage to be improved due to the shift of IE equilibrium in reactions 8 and 10 to the right. This clearly follows from eqn [5], which can be rewritten for, e.g. $\text{SO}_4^{2-}\text{--Cl}^-$ exchange (see reaction [9]), in terms of the equilibrium separation factor α (usually written using either equivalent or equivalent fraction concentration scales):

$$\alpha_{\text{SO}_4}^{\text{Cl}} = \frac{q_{\text{Cl}}}{q_{\text{SO}_4}} \frac{K_D \gamma C_S}{C_o(C_o - \gamma C_S)} \quad [11]$$

Here K_D is the dissociation constant of K_2SO_4 . The same reasoning is applicable to interpret the selectivity reversal in the cation exchange system.

Another advantage of the IXISS-based synthesis of K_2SO_4 deals with the possibility of reusing the supernatants obtained after crystallization of K_2SO_4 as a displacer in the subsequent stripping cycles. For example, after separation of K_2SO_4 crystals, the supernatant obtained in the first process is fortified with Na_2SO_4 up to the desired concentration of sulfate ions (2 mol dm^{-3}) and is then directed to the next stripping cycle. A diagram of the cation exchange version of the process for the synthesis of chlorine-free potassium sulfate is given in **Figure 1**. The unit comprises two ion exchange columns operating intermittently in a loading (see eqn [7]) or displacement (see eqn [8]) mode of operation. The second stage (displacement) is carried out using an Na_2SO_4 (or a $\text{Na}_2\text{SO}_4\text{--K}_2\text{SO}_4$ mixture) solution at 308 K. The rinsing water produced after each stage is returned to the process and is used to dissolve either KCl (rinsing after loading) or Na_2SO_4 (rinsing after displacement). The NaCl effluent obtained after the loading stage is directed into the reverse osmosis unit, which produces desalinated water and NaCl concentrate, used to manufacture crystalline NaCl . The desalinated water obtained is returned to the process. Hence, the process is essentially wasteless and ecologically clean.

Decalcination of Mineralized Waters

A number of modern technologies include water treatment processes, which in many instances involve a calcium removal stage. IE methods are widely applied to solve this problem for low mineralized surface waters. The problem of processing highly

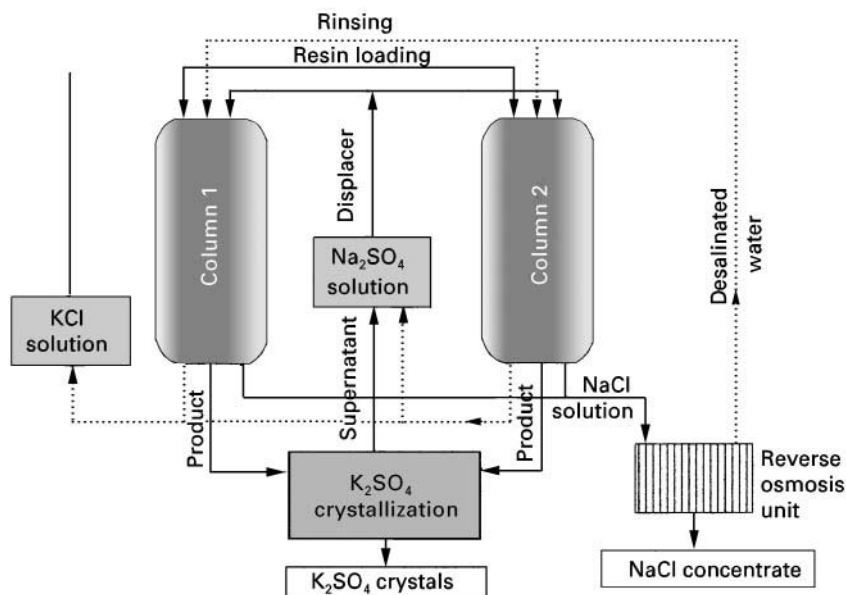
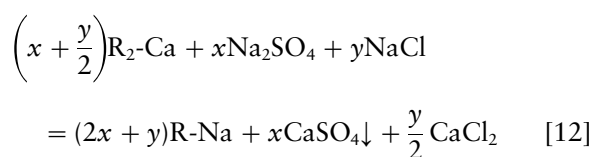


Figure 1 Flowsheet of process for cation exchange synthesis of chlorine-free potassium sulfate. (Reproduced from Muraviev D, Khamizov R, Tikhonov N *et al.* (1998). Clean ion-exchange technologies. I. Synthesis of chlorine-free potassium fertilizers by an ion-exchange isothermal supersaturation technique. *Ind. Eng. Chem. Res.* 37: 1950–1955, with permission from the American Chemical Society.

mineralized waters is far more complicated. For example, preliminary treatment of seawater prior to its further desalination requires extensive decalcination to solve the problem of gypsum formation on heater surfaces of distillers and clogging of membranes in reverse osmosis or electrodialysis units. Modern seawater-processing technologies, such as IE recovery of magnesium, also require preliminary removal of calcium.

The problem of calcium removal from seawater (and highly mineralized waters and brines) can be successfully solved by using an IXISS-based process on specially modified conventional (low cost) sorbents with enhanced selectivity for Ca^{2+} . The first requirement is dictated by the necessity for the efficient use of the sorbent capacity towards Ca^{2+} at \sim five-fold magnesium over calcium excess in the seawater under treatment. The second arises from the need to process 1000 m^3 of seawater to produce 1 ton of magnesium. For example, several successive treatments of zeolites (e.g. of A type) with seawater and a concentrated NaCl solution result in their stable modification due to irreversible sorption of Mg^{2+} . An average $\alpha_{\text{Mg}}^{\text{Ca}}$ value for the modified zeolite (from seawater) rises to ~ 27 in comparison with 4.5 for the unmodified sorbent. The sorbent removes virtually no Mg^{2+} from seawater, whereas Ca^{2+} uptake appears to be nearly equal to its capacity ($\sim 4 \text{ mmol kg}^{-1}$). At the same time, $\alpha_{\text{Na}}^{\text{Ca}}$ for the modified zeolite remains at a sufficiently low level (~ 3.6) to simplify its regeneration with sodium salt solutions

after the loading with Ca^{2+} . The most efficient desorption of Ca^{2+} from zeolite is achieved by using an NaCl– Na_2SO_4 mixture. The reaction of Ca^{2+} – Na^+ exchange is coupled in this case with the reaction of CaSO_4 formation and, as a result, the equilibrium in the system is shifted to the right. The overall desorption process is described by the following equation:



The optimal molar ratio of Na_2SO_4 to NaCl (x/y in eqn [12]) in the regenerating solution is 0.2. In this case the regeneration of zeolite requires a close to stoichiometric amount of the regenerating agent. The eluate obtained during the stripping stage (Figure 2) is supersaturated ($\gamma \approx 5$). Nevertheless, it coexists with the granulated sorbent phase for a long period ($\sim 24 \text{ h}$ at 293 K) as a stable SS. This solution spontaneously crystallizes following removal from the column with the formation of gypsum, which is the only waste product in the process. After removal of the CaSO_4 precipitate by filtration, the supernatant can be fortified with the desired amount of NaCl– Na_2SO_4 mixture and returned to the process for reuse. The process is carried out in a two-fixed bed column set-up. The columns operate intermittently in a calcium removal and regeneration mode.

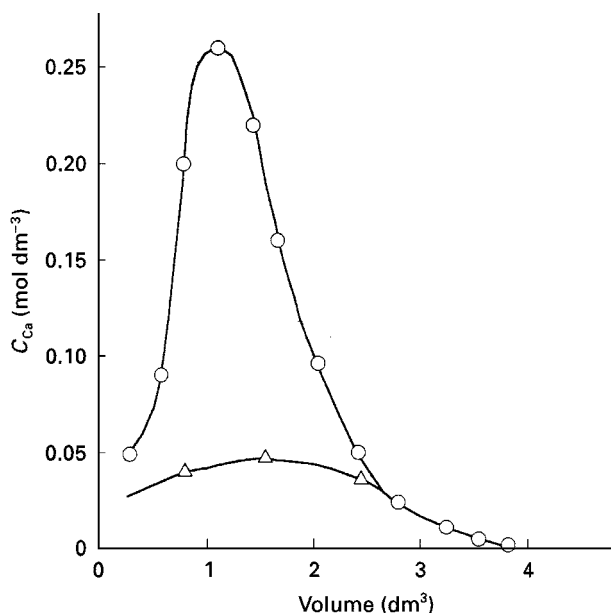


Figure 2 Desorption of Ca^{2+} from modified zeolite A with $1.25 \text{ mol L}^{-1} \text{ NaCl} + 0.25 \text{ mol L}^{-1} \text{ Na}_2\text{SO}_4$ mixture (circles). Triangles, calcium concentration in supernatant after crystallization of supersaturated solution samples. (Modified with permission from Muraviev *et al.*, 1998).

Recovery of High Purity Magnesium Compounds from Seawater³

The traditional magnesium-from-seawater technology includes mixing the raw seawater with 'milk of lime' filtration of $\text{Mg}(\text{OH})_2$ slurry, followed by its treatment with HCl , evaporation, drying and electrolysis. The process does not allow for producing sufficiently pure Mg . The possibility of designing an alternative IXISS-based process for recovery of high purity Mg compounds from seawater has appeared from the discovery of IXISS of MgCO_3 in the resin bed. The IXISS effect is observed during elution of Mg^{2+} from carboxylic resin pre-loaded with decalcinated seawater with a solution of Na_2CO_3 – NaHCO_3 mixture. Magnesium carbonate does not precipitate in the column and remains as a stable SS (with $\gamma \approx 5$) at least over a period of 72 h. After removal of this solution from the column (Figure 3), the desorbed magnesium spontaneously crystallizes in the form of well-shaped nesquegonite ($\text{MgCO}_3 \cdot 3\text{H}_2\text{O}$) crystals. The purity of magnesium compound obtained appears to be $> 99.9\%$ since, unlike magnesite

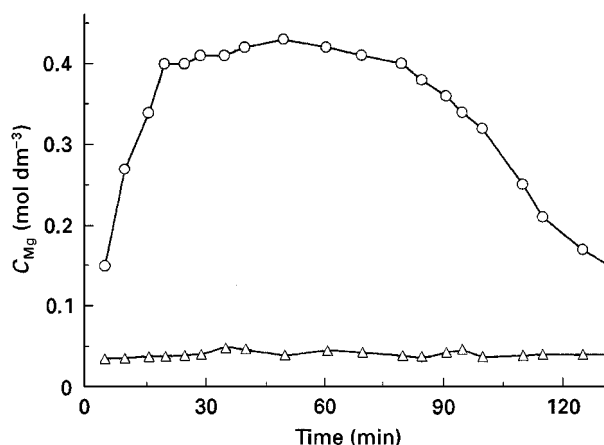


Figure 3 Concentration-time history of desorption of Mg^{2+} with $1.5 \text{ mol L}^{-1} \text{ Na}_2\text{CO}_3 + 0.60 \text{ mol L}^{-1} \text{ NaHCO}_3$ (circles) from carboxylic resin pre-loaded with decalcinated natural seawater at 293 K. Triangles, Mg^{2+} concentration in supernatant after short-term heating (during 10 min from 290 to 310 K) followed by crystallization of supersaturated solution samples. (Reproduced from Khamizov R, Muraviev D, Tikhonov N *et al.* (1998). Clean ion-exchange technologies. II. Recovery of high-purity magnesium compounds from seawater by an ion-exchange, isothermal supersaturation technique. *Ind. Eng. Chem. Res.* 37: 2496–2501, with permission from the American Chemical Society.

(MgCO_3), nesquegonite crystals are calcium-free. The yield of $\text{MgCO}_3 \cdot 3\text{H}_2\text{O}$ depends on the conditions of crystallization of the SS collected. Thus, crystallization at ambient temperature over several hours gives $\sim 70\%$ yield of the product in one desorption cycle. A rapid increase of temperature in the crystallizer from $\sim 290 \text{ K}$ to $\sim 310 \text{ K}$ over 10 min) allows for a substantial increase in the rate of crystallization, which results in the rise of the product yield to $> 90\%$.

The block scheme of the pilot unit for recovery of high purity MgCO_3 from seawater is shown in Figure 4. Ca-free seawater (see previous section) passes from the top to the bottom through two of the three columns C_1 – C_3 , loaded with carboxylic resin in the Na form. At the same time the third column is working in the regeneration (magnesium-stripping) mode of operation. After conversion of resin in the Mg form the columns are treated from the bottom to the top with a stripping solution of $1.5 \text{ mol L}^{-1} \text{ Na}_2\text{CO}_3 + 0.6 \text{ mol L}^{-1} \text{ NaHCO}_3$ mixture (also containing a residual MgCO_3 from the recycled stripping solution). Ca-free seawater, displaced from the columns, is directed to tank T_1 until the appearance of supersaturated eluate which, in turn, is directed to tanks T_2 and T_3 (crystallizers supplied with heating and filtration facilities to collect the crystalline product) by reswitching the automatic valve V_1 . After crystallization and removal of magnesium carbonate,

³ Adapted with permission from Muraviev D, Khamizov R, Tikhonov N *et al.* (1998). Clean ion-exchange technologies. II. Recovery of high-purity magnesium compounds from seawater by an ion-exchange isothermal supersaturation technique. *Industrial Engineering and Chemistry Research* 37: 2496–2501.

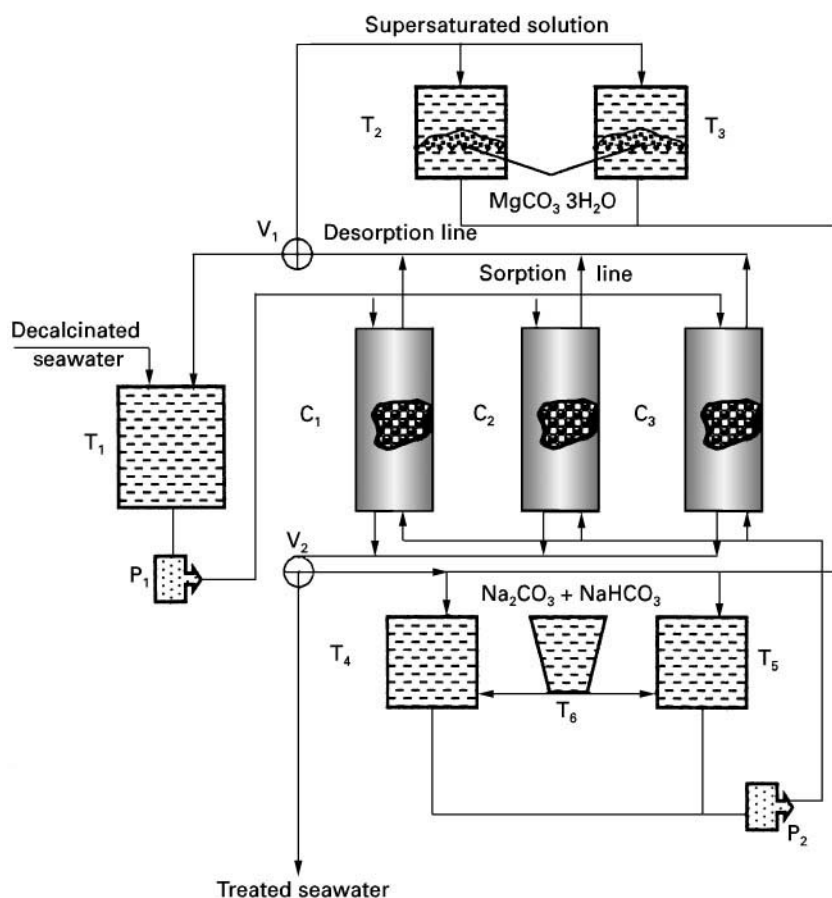


Figure 4 Schematic diagram of experimental pilot unit for recovery of high purity magnesium compounds from seawater: ion exchange columns C_1 – C_3 ; solution tanks T_1 – T_6 ; solution pumps P_1 and P_2 ; automatic valves V_1 and V_2 . (Reproduced from Khamizov R, Muraviev D, Tikhonov N *et al.* (1998). Clean ion-exchange technologies. II. Recovery of high-purity magnesium compounds from seawater by an ion-exchange isothermal supersaturation technique. *Ind. Eng. Chem. Res.* 37: 2496–2501, with permission from the American Chemical Society.

the stripping solution is returned to tanks T_4 and T_5 for fortification with the desired amount of the Na_2CO_3 – NaHCO_3 mixture from T_6 and reuse. Then the sorption cycle is repeated. The stripping solution displaced from the columns is also returned to T_4 and T_5 until the appearance of treated seawater in the line that is controlled by the automatic valve V_2 . Hence, the process shown in Figure 4 is totally free of waste.

Dual-temperature IE Processes

The efficiency of the dual-temperature IE process is primarily determined by the temperature sensitivity of the IE system which, in turn, depends on the value of the heat effect of a given IE reaction. The thermodynamics of a reversible IE reaction in the system including, for example, counterions A^{z_A+} and B^{z_B+} , a co-ion X^{z_X-} and a cation exchanger R bearing univalent functional groups can be described by the

Gibbs–Helmholtz equation:

$$\Delta G = \Delta H + T \left(\frac{\partial \Delta G}{\partial T} \right)_P \quad [13]$$

and the isotherm of an IE reaction by:

$$\Delta G_{P,T} = \Delta G_T^\circ + RT \ln \left(\frac{a_{AR}^{-1/z_A} a_{BX}^{1/z_B z_X}}{a_{BR}^{-1/z_B} a_{AX}^{1/z_A z_X}} \right) \quad [14]$$

where $\Delta G^\circ = -RT \ln K$, and K is the thermodynamic equilibrium constant of the IE reaction corresponding to the condition $\Delta G_{P,T} = 0$.

Eqns [13] and [14] lead to the van't Hoff equation:

$$\left(\frac{\partial \ln K}{\partial T} \right)_P = \frac{\Delta H}{RT^2} \quad [15]$$

Under standard conditions (when K depends only on temperature), eqn [15] can be rewritten in conventional derivatives and then integrated from T_1 to T_2 .

In the simplest case, when ΔH is independent of temperature, one obtains:

$$\ln \frac{K_{T_2}}{K_{T_1}} = -\frac{\Delta H}{R} \left(\frac{1}{T_1} - \frac{1}{T_2} \right) \quad [16]$$

The resulting relationship [16] is widely used to describe dual-temperature IE processes.

Concentration of Magnesium and Bromine from Seawater

At present, around 25% of overall world production of magnesium and 70% of that of bromine is provided from the sea and other hydromineral resources. Traditional methods for producing Mg (see previous section) and Br (air-stripping technique) by processing seawater, despite their profitability, do not satisfy increasingly stringent ecological standards. Consequently, new alternative ecologically clean technologies, based on IE separation methods, have to be developed. The dual-temperature IE concentration of Mg and Br from seawater is based on the strong temperature dependence of the separation coefficients α_{Na}^{Mg} and α_{Cl}^{Br} of weak acid (for Mg) and strong base (for Br) IE resins, respectively. For example, the α_{Cl}^{Br} value decreases by a factor of ~ 2 , while α_{Na}^{Mg} value increases by a factor of ~ 1.2 when the temperature of seawater rises from 283 to 363 K. The principle of the dual-temperature concentration of Mg and Br by using a cascade of fixed-bed columns is shown in Figure 5. The first column is intermittently treated with hot and cold seawater depending on the mode of

operation, e.g. thermosorption or thermostripping. Respective concentration–volume histories are shown in Figure 6 for the Mg concentration process. The resulting eluate is either collected in tank Conc. 1 (Mg or Br concentrate after thermostripping) or returned to the sea (after thermosorption). The concentrate obtained after the first column is subjected to the same sequence of operations on the second column to produce the second concentrate, and so forth.

In a subsequent treatment of cold and hot seawater in a fixed-bed IE column, the concentration of Br^- in the hot stripping solution increases by a factor of 2, while the concentration of Cl^- and SO_4^{2-} decreases. The multistage process (using AV-17 anion exchange resin, Reakhim, Moscow, Russia, Russian analogue of strong base anion exchangers such as, e.g. Dowex-1, Amberlite IRA 400, Purolite A 400 and Lewatit M 500) enriches Br^- concentration in the final concentrate up to an acceptable level for further processing ($> 5 \text{ g L}^{-1}$). Four dual-temperature sorption-stripping cycles (using Lewatit R 250 K resin, Bayer, Germany) allow for concentrating Mg up to $\sim 0.4 \text{ mol dm}^{-3}$ (versus 0.11 mol dm^{-3} in the initial seawater), as shown in Figure 7. The final concentrate can be decalcinated and used for producing high purity magnesium (see above). The resins used in both processes do not require any regeneration. Hence, the processes are completely free of waste products.

Reduction in energy expenditure for heating the seawater can be successfully solved by using conventional, or concentrated, sunlight (in areas with a high level of solar radiation) as the principle and

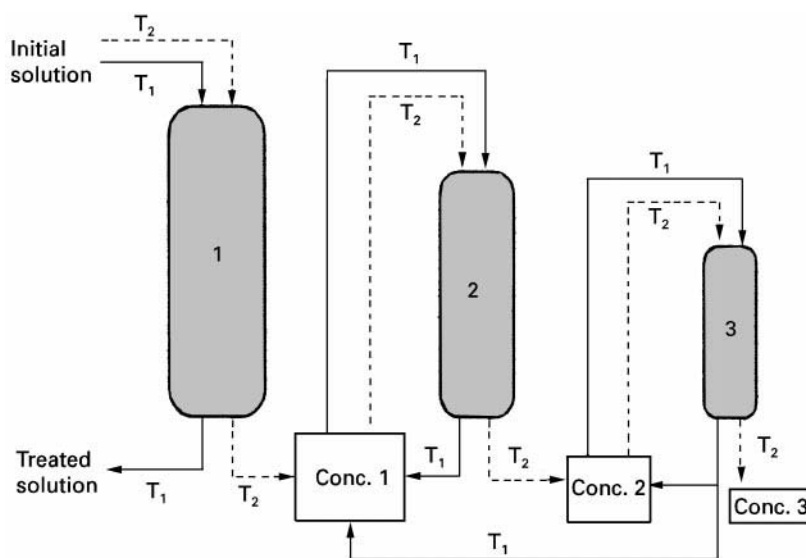
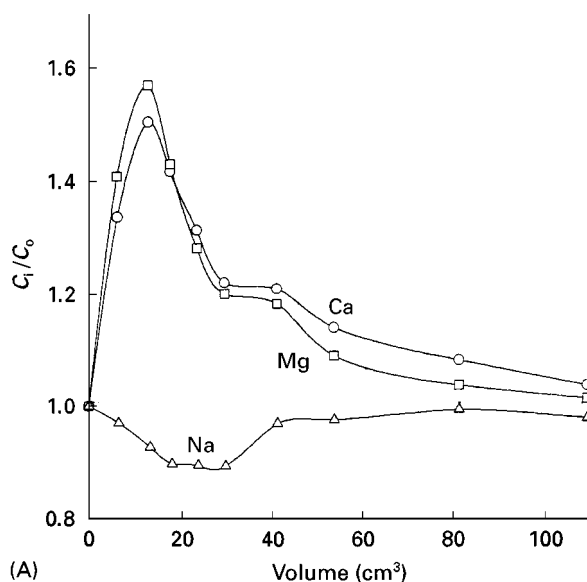
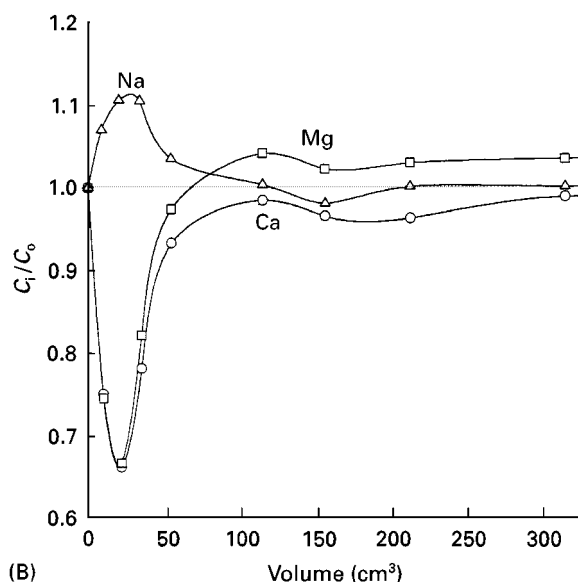


Figure 5 Flowsheet of reagentless dual-temperature ion exchange processing of seawater. (Reproduced from Muraviev D, Noguero J and Valiente M (1997) Seawater as auxiliary reagent in dual-temperature ion-exchange processing of acidic mine waters. *Environ. Sci. Technol.* 31: 379–383, with permission from the American Chemical Society.



(A)



(B)

Figure 6 (A) Thermostripping ($T = 263\text{ K}$) and (B) thermosorption ($T = 353\text{ K}$) breakthrough curves obtained from natural seawater (Mediterranean sea) on polyacrylic Lewatit R 250-K resin. Circles, calcium; squares, magnesium; triangles, sodium. (Reproduced from Muraviev D, Noguero J and Valiente M (1996). Separation and concentration of calcium and magnesium from seawater by carboxylic resins with temperature-induced selectivity. *Reactive and Functional Polymers* 28: 111–126, with permission from Elsevier Science.

ecologically clean energy source (sun-boiler systems). An alternative solution can be the use of seawater in the cooling cycles of steam power stations. The amount of seawater pumped through the cooling cycles of these stations is approximately $20\,000\text{--}30\,000\text{ m}^3\text{ h}^{-1}$. This hot seawater is currently pumped back into the sea, which means that billions of joules of heat are wasted. This seawater could be used

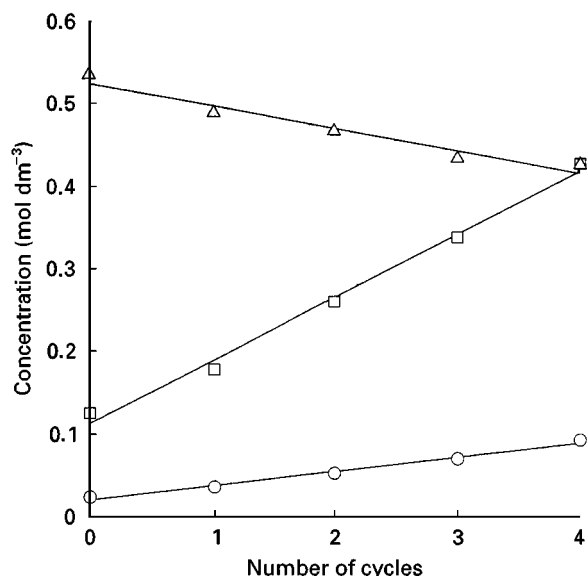


Figure 7 Concentration of Ca^{2+} (circles), Mg^{2+} (squares) and Na^+ (triangles) obtained in consecutive thermostripping-sorption cycles vs number of cycles. (Reproduced from Muraviev D, Noguero J and Valiente M (1996) Separation and concentration of calcium and magnesium from seawater by carboxylic resins with temperature-induced selectivity. *Reactive and Functional Polymers* 28: 111–126, with permission from Elsevier Science.

for recovering minerals (e.g. Mg and Br). In this way, the power costs in heating seawater and moving it through the mineral recovery process (which substantially exceeds 50% of the overall expenditures for electricity) could be written off.

Concentration of Copper from Acidic Mine Waters⁴

The treatment of acidic mine waters (AMW), representing natural effluents from pyritic ore deposits, is of great economic and ecological importance. The AMW are characterized by low pH (~ 2) and relatively high concentrations of metal ions such as Fe^{3+} , Zn^{2+} and Cu^{2+} (Table 2). The initial AMW requires pre-conditioning by selective removal of iron prior to IE treatment. This conditioning is carried out by adjusting the pH to 3.4–3.5 with alkali followed by either conventional or biooxidation of Fe(II) to Fe(III). The final removal of the $\text{Fe}(\text{OH})_3$ precipitate is carried out by filtration.

Two commercial IE resins, namely a polyacrylic (e.g. Lewatit R 250-K) and an iminodiacetic (e.g.

⁴ Adapted with permission from Muraviev D, Noguero J and Valiente M (1997). Application of the reagentless dual-temperature ion-exchange technique to a selective separation and concentration of copper versus aluminium from acidic mine waters. *Hydrometallurgy* 44: 331–346.

Table 2 Composition of initial and conditioned samples of native acidic mine waters (AMW) from Rio Tinto area (Huelva, Spain)^a

AMW sample	Concentration (mg L ⁻¹)								pH
	SO ₄ ²⁻	Fe	Cu	Zn	Al	Mn	Mg	Ca	
1 (initial)	16 450	5050	239	912	399	75	751	326	1.9
1 (conditioned)	16 300	3	235	890	386	73	735	319	3.5
2 (conditioned)	17 350	0.3	115	1275	530	90	950	475	3.5

^aThe AMW samples have been collected from the natural generic metal-bearing effluents originated from the pyritic ore deposits typical for the southern provinces of Spain and Portugal.

Lewatit TP-207) can be used for the dual-temperature IE concentration of copper from AMW. Acrylic resin is selective for Al³⁺ (over other AMW metal ions) and iminodiacetic resin manifests high selectivity towards Cu²⁺. The uptake of Al³⁺ increases remarkably while that of Cu²⁺ decreases with temperature for both resins and that for the rest of the metals depends weakly on temperature. This effect gives the possibility for the dual-temperature IE concentration of copper from AMW by using the same set-up and the mode of operation as shown in Figure 5. The resins are first equilibrated with cold AMW (at 293 K). Then a selective thermostripping of Cu²⁺ is carried out using hot AMW (at 353 K), leading to an increase in Cu²⁺ concentration in the eluate by a factor of 1.3 (for acrylic resin) or 1.2 (for iminodiacetic resin). The concentration of Al³⁺ in the same eluate drops to 50% in the first case and to 70% in the second. The efficiency of both thermosorption and thermostripping processes (at constant solution flow rates and resin bed heights) depends on the interval of working temperatures (see eqn [11] and is higher the greater this interval (Figure 8).

The concentration of Cu²⁺ achieved after the fourth thermosorption–thermostripping cycle increases (in comparison with the initial AMW) by a factor of ~3, while that of Al³⁺ decreases by one order of magnitude (Figure 9). The substantial increase in the efficiency of the process (higher degree of concentration) can be achieved using either higher fixed resin bed columns (see Figure 5) or a cascade of countercurrent columns, as shown in Figure 10. The unit comprises several two-section countercurrent columns which are operated at different temperatures to provide thermosorption/ thermostripping conditions in the sections. The first column is fed by the native AMW and produces the first concentrate, which is collected from the boundary between sections and then directed to the bottom section of the second column and so on. The resin in all columns circulates in a closed cycle and does not require regeneration. The unit shown in Figure 10 can also be used for the dual-temperature IE processing of seawater to

produce magnesium or bromine concentrates in a continuous mode of operation.

Concluding Remarks

The number of large scale industrial applications of both dual-temperature IE and IXISS-based IE processes is still very limited. For example, the dual-temperature partial demineralization of surface waters using specially synthesized polyampholyte resins (so-called Sirotherm process) so far remains the only industrial application of dual-temperature IE. At present, a large scale pilot plant using the counter-current version of an IXISS-based process for the recovery of more than 300 tons of high purity magnesium carbonate from seawater per year has started operation in the Vladivostok region of Russia. The unit shown in Figure 4 adequately imitates the basic flowsheet of Vladivostok plant in the fixed-bed mode of operation.

The prospects for wider implementations of ecologically clean IE processes in different fields of industry are primarily determined by their obvious advantages and relative simplicity. For example, the use of IXISS effect in the design of highly efficient and ecologically safe IE technology does not require any specific IE equipment and can be easily realized using standard IE columns. At the same time, a deeper insight into the IXISS phenomenon can substantially widen the area of practical application of this effect. In this regard, the solution of the following problems seems to be of particular importance:

1. Identification of chemical compounds (both organic and inorganic) exhibiting IXISS effect (IXISS-active compounds)
2. Evaluation of stabilizing efficiency of commercially available IE materials towards SS of IXISS-active compounds of different types (electrolytes, nonelectrolytes, polyampholytes and zwitterlytes)
3. Development of theoretical fundamentals of IXISS effect and some others

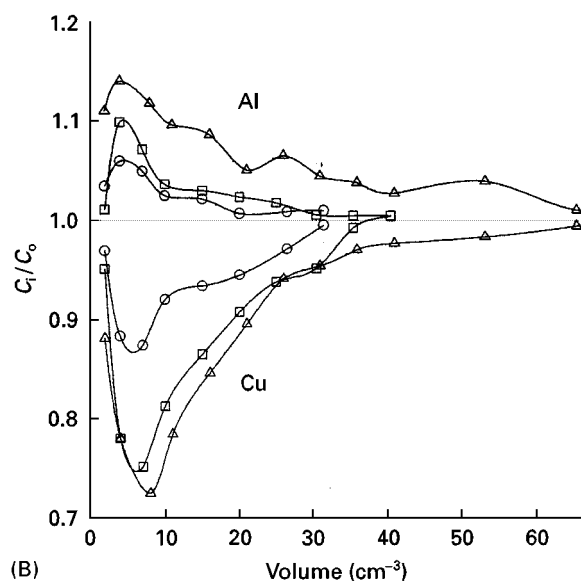
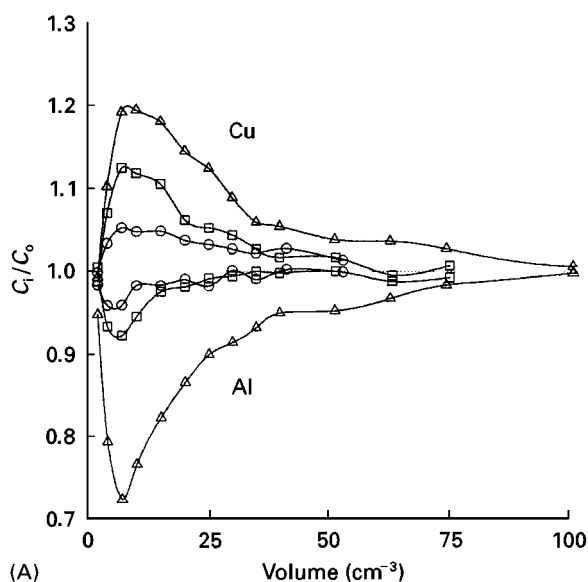


Figure 8 (A) Thermostripping and (B) thermosorption break-through curves for Cu^{2+} and Al^{3+} obtained from native AMW (see Table 2) on iminodiacetic Lewatit TP-207 resin at various thermostripping temperatures: 313 K (circles); 333 K (squares); 353 K (triangles). Thermostripping is carried out at indicated temperature after loading of resin at 293 K. Thermosorption is carried out at 293 K after finishing the thermostripping cycle at the indicated temperature. (Reproduced from Muraviev D, Noguerol J and Valiente M (1997) Application of the reagentless dual-temperature ion-exchange technique to a selective separation and concentration of copper versus aluminium from acidic mine waters. *Hydrometallurgy* 44: 331–346, with permission from Elsevier Science.

Several recent publications and reviews by the author are recommended to those interested in this subject.

Unlike IXISS-based IE processes, large scale industrial applications of dual-temperature IE requires in

certain instances the design of special IE equipment such as, for example, two-sectional jacketed IE columns providing the dual-temperature mode of operation. At the same time, it seems useful to emphasize that the shift of chemical equilibrium to the desired direction due to the modulation of temperature in the system represents one of the basic physicochemical concepts which are widely used in different fields of chemical technology. From this viewpoint the dual-temperature IE cannot be considered as a somewhat exotic separation method as in many instances the experience (both theoretical and experimental) accumulated in other areas of chemical science and engineering can be successfully applied for the further development of this fractionation technique. On the other hand, it seems useful to distinguish the following problems, the solution of which can help to widen the application of dual-temperature IE in industry:

1. the evaluation of temperature sensitivity of commercially available ion exchangers towards different ionic systems of practical interest to estimate their potential use in dual-temperature IE processes
2. the tailored design and synthesis of temperature-responsive IE resins tuned for the dual-temperature IE fractionation of certain ion mixtures. Ion exchangers of this type are not so far commercially

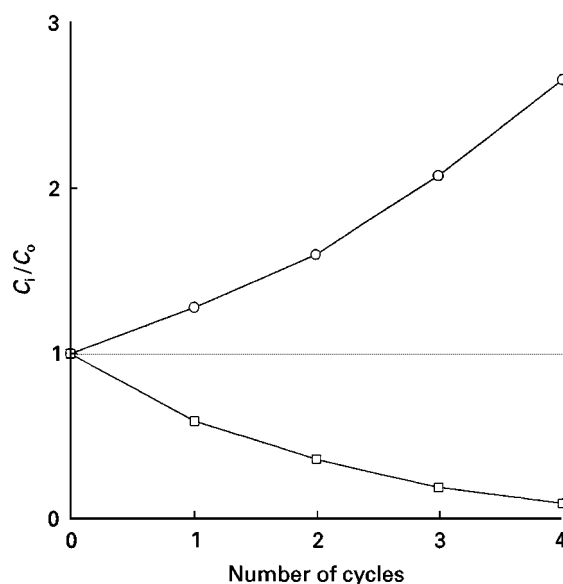


Figure 9 Concentrations of Cu (circles) and Al (squares) obtained in consecutive thermosorption–stripping cycles from AMW on iminodiacetic Lewatit TP-207 resin vs number of cycles. (Reproduced from Muraviev D, Noguerol J and Valiente M (1997) Application of the reagentless dual-temperature ion-exchange technique to a selective separation and concentration of copper versus aluminium from acidic mine waters. *Hydrometallurgy* 44: 331–346, with permission from Elsevier Science.

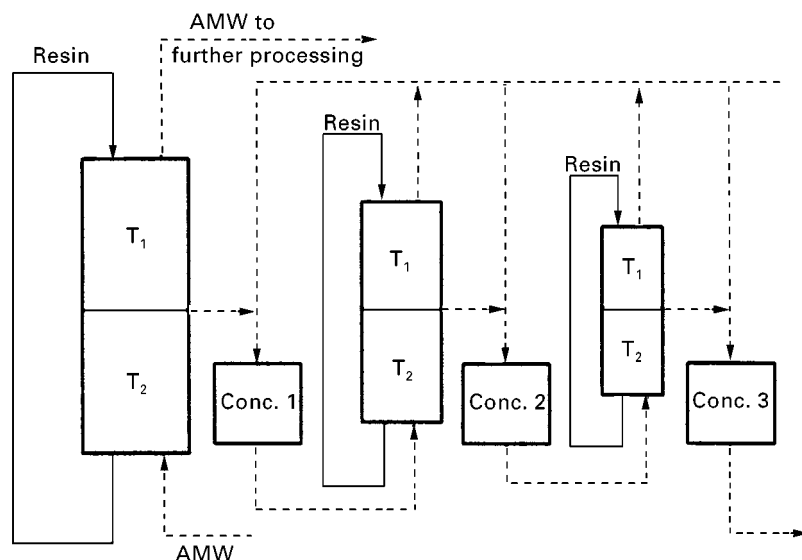


Figure 10 Flowsheet of continuous process for dual-temperature ion exchange treatment of acidic mine waters. (Reproduced from Muraviev D, Noguerol J and Valiente M (1997) Application of the reagentless dual-temperature ion-exchange technique to a selective separation and concentration of copper versus aluminium from acidic mine waters. *Hydrometallurgy* 44: 331–346, with permission from Elsevier Science.

available. Their appearance can dramatically stimulate the further development and wider application of dual-temperature IE techniques

3. the combination of dual-temperature-based and conventional IE processes within one technological flowsheet will increase the efficiency of the whole process

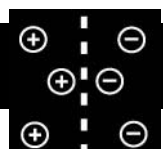
Interested readers can find more detail on the subject in the recent review by Muraviev *et al.*

See also: II/Ion Exchange: Organic Ion Exchangers; Historical Development; Theory of Ion Exchange.

Further Reading

- Arkhangelsky LK and Belinskaya FA (1982) *Ion Exchange in Chemical Technology* (in Russian). Leningrad: Khimiya.
- Bobleter O and Bonn G (1991) Ion exchange chromatography. In: Dorfner K (ed.) *Ion Exchangers*, pp. 1187–1242. Berlin: Walter de Gruyter.
- Gorshkov VI (1995) Ion exchange in countercurrent columns. In: Marinsky A and Marcus Y (eds) *Ion Exchange and Solvent Extraction*, vol. 12, pp. 29–92. New York: Marcel Dekker.
- Gorshkov VI and Ivanov VA (1999) Reagent-free ion-exchange separation. *Solvent Extraction and Ion Exchange* 17: 695–766.
- Gorshkov VI, Muraviev D and Warshawsky A (1998) Ion-exchange methods for ultra purification of inorganic, organic, and biological substances. *Solvent Extraction and Ion Exchange* 16: 1–74.
- Grevillot G (1986) Principles of parametric pumping. In: Cheremisinoff NP (ed.) *Handbook of Heat and Mass Transfer*, vol. 2, *Mass Transfer and Reactor Design*, pp. 1429–1474. Houston: Gulf Publishers.
- Khamizov RKh, Muraviev D and Warshawsky A (1995) Recovery of valuable mineral components from sea-water by ion exchange and sorption methods. In: Marinsky A and Marcus Y (eds) *Ion Exchange and Solvent Extraction*, vol. 12, pp. 93–148. New York: Marcel Dekker.
- Muraviev D, Khamizov RKh and Tikhonov NA (1998) Ion-exchange isothermal supersaturation. *Solvent Extraction and Ion Exchange* 16: 151–222.
- Muraviev D, Noguerol J and Valiente M (1999) Dual-temperature ion-exchange fractionation. *Solvent Extraction and Ion Exchange* 17: 767–850.
- Streat M (1991) General ion exchange technology. In: Dorfner K (ed.) *Ion Exchangers*, pp. 685–716. Berlin: Walter de Gruyter.
- Tondeur D and Grevillot G (1986) Parametric ion exchange processes (parametric pumping and allied techniques). In: Rodrigues AE (ed.) *Ion Exchange Science and Technology*. NATO ACI Series, vol. 107, pp. 369–399. Dordrecht: Martinus Nijhoff.
- Wankat PC (1981) Cyclic separation techniques. In: Rodrigues AE and Tondeur D (eds) *Percolation Processes. Theory and Applications*, pp. 443–515. Rockville: Sijthoff and Noordhoff.

ELECTROCHEMICAL ION EXCHANGE



J. P. H. Sukanto, S. D. Rassat, R. J. Orth and
M. A. Lilga, Pacific Northwest National
Laboratory, Richland, WA, USA

Copyright © 2000 Academic Press

Introduction

Electrochemical ion exchange (EIX) is a process where electrochemistry and ion exchange (IX) are combined to effect the separation of ions more efficiently than the use of either technique alone, especially in minimizing secondary waste generation. The varieties of EIX, beginning with those using electrochemically inactive IX materials and proceeding to those using electrochemically active ion exchange (EaIX) materials, are discussed here.

EIX Processes Using Electrochemically Inactive Ion Exchange Materials

Some materials used in the EIX process are not active electrochemically, that is, they do not contain functional groups that can be reduced or oxidized. Examples of commonly used separation techniques of this type include *electrodialysis* and *electrophoresis/electrochromatography*. In electrodialysis, the permselectivity of IX membranes is used in combination with an electric field to separate anions and cations. In a variation of conventional electrodialysis called *electrodialysis polishing*, IX materials are packed between the IX membranes; the IX material serves as an immobile electrolyte. The schematic of the process shown in **Figure 1** shows that the water is processed through the IX materials. Due to the high concentration of ionic sites in the IX material, fairly resistive (up to 15 MΩ) water can be produced at the outlet. In electrophoresis/electrochromatography where IX packing materials are used, IX interactions between the analyte and the column material enhance the separation capability over that available if differences in electrophoretic mobilities alone were used.

Another process in this category, a process termed *EIX* by the original researchers (Allen *et al.*), uses an assembly consisting of an electrochemically inactive IX material attached to an electrode as the separation agent. This approach, for the separation of cations, is shown in **Figure 2**. (It should be noted that the term

'EIX' is used more broadly here to denote a set of separation techniques that use electrochemistry and IX, not just the process shown in **Figure 2**.) Here, a cathodic potential is applied to the electrode material assembly for the uptake of cations. The applied potential serves to generate an electric field that increases the transport rate of cations toward the electrode material assembly and to electrolyse water to produce hydroxyl ions that activate the IX material. To elute the sorbed cations, an anodic potential is applied to the electrode/cationic ion exchange material assembly. This results in the local

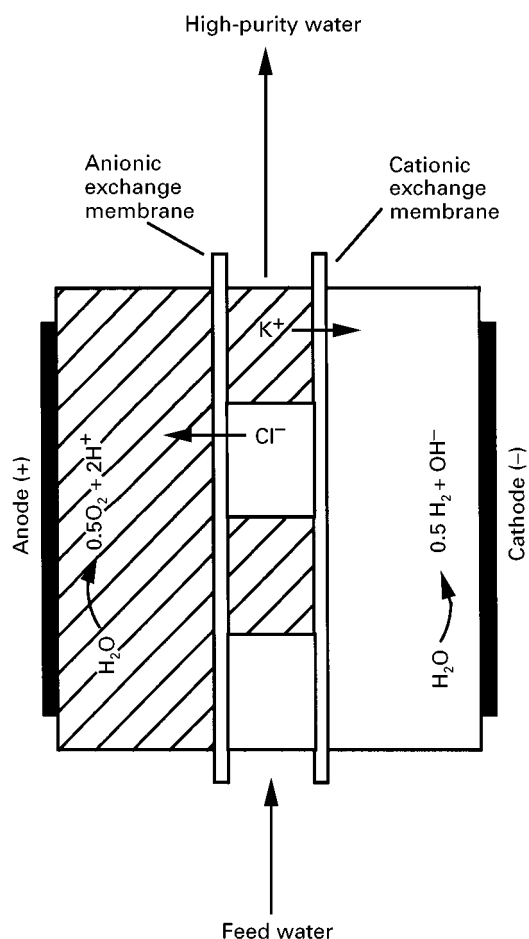


Figure 1 Cationic and anionic IX resins are depicted as hatched and open areas, respectively. Only cations are mobile in the cationic IX material, and only anions are mobile in the anionic IX material. Cations in the feed water are expelled from the water while flowing through the cationic IX material. Similarly, anions are expelled from the feed water while flowing through the anionic IX material.

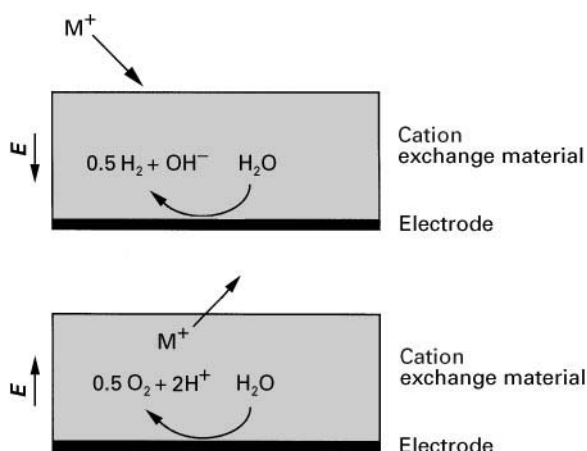


Figure 2 Cation uptake (top) and elution (bottom) at the EIX electrodes. Water reduction leads to production of hydroxyl ions resulting in the de-protonation of sites in the cationic IX resin. In turn, the IX resin will uptake cations to maintain electroneutrality. The electric field, E , present during the water-reduction process, serves to enhance cation transport to/within the cationic IX resin. The reverse reactions occur during cation elution.

production of hydrogen ions from the splitting of water, which in turn displaces the sorbed cations as in conventional IX processes. In addition, an electric field is generated which accelerates the transport rate

of cations. For anions, anionic IX materials are used; an anodic potential is applied to the assembly during uptake and a cathodic potential is applied during elution. The advantages of this approach over conventional IX processes are increased uptake rate due to the applied electric field and more efficient use of hydrogen or hydroxyl ions for both uptake and elution. Although the thermodynamics of the elution process have not changed as compared to conventional IX, the close proximity of the generated hydrogen or hydroxyl ions to the exchange sites increases the overall process rate by reducing the time required for uptake and elution. In addition, fewer excess hydrogen or hydroxyl ions are required.

EIX Processes Using Electroactive Ion Exchange Materials

Figures 3(A) to (D) show conceptually the electroactive ion exchange (EaIX) approach, a subset of EIX techniques. Here, EIX processes, where EaIX materials are used, will be denoted as EIX/EaIX. Figure 3(A) and (B) illustrate cation separation. The reduction of a generic EaIX material, X , results in a net negative charge that has to be compensated by a cation (see Figure 3A). Provided that X is selective

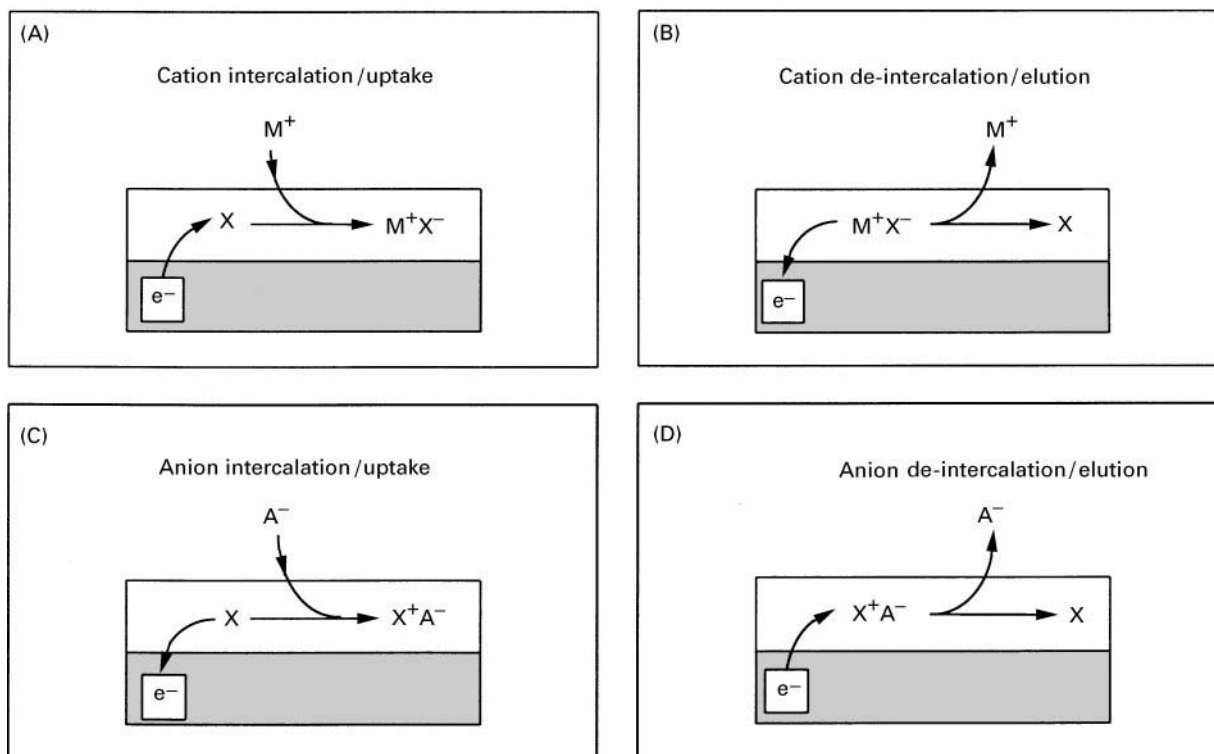


Figure 3 (A) Cation intercalation/uptake during film reduction. (B) Cation de-intercalation/elution during film oxidation. (C) Anion intercalation/uptake during film oxidation. (D) Anion de-intercalation/elution during film reduction.

for a specific cation, then the cation uptake shown in **Figure 3(A)** results in the selective separation of a cation, M_1^+ , from, say M_2^+ . Elution of M_1^+ is simply achieved by oxidizing X^- back to X , which is necessarily accompanied by the expulsion of M_1^+ (see **Figure 3B**). The analogous uptake and elution of anions are shown in **Figure 3(C)** and **(D)**, respectively. For anions, uptake occurs during oxidation, and elution accompanies reduction. It should be noted that the same sequence of oxidation and reduction is used for the EIX/EaIX approach and the process shown in **Figure 2**. More importantly, however, the two approaches are very different with respect to the specific electrochemical reactions that take place during oxidation and reduction. In the process shown in **Figure 2**, both oxidation and reduction reactions are water-splitting. The reductive water-splitting results in hydrogen gas and hydroxyl ion production, whereas the oxidative water-splitting results in oxygen gas and hydrogen ion production. While this approach results in relatively efficient use of the protons and hydroxyls, the exchange ratio is not one to one. That is, more than one equivalent of protons is required to displace one equivalent of cations (or uptake one equivalent of anions). In addition, in the processing of radioactive materials, hydrogen gas generation is undesirable because of safety issues. On the other hand, with the use of EaIX materials (as shown in **Figure 3A** to **D**), only one equivalent of electrons is needed to elute one equivalent of ions. Therefore, using EaIX materials further reduces the amount of secondary waste generated. The electric field generated within EaIX materials has two functions: firstly to increase the transport rate of ions through the EaIX material and secondly to attract (or expel) the ions to the binding sites since the electric field is strongest near an oxidized or reduced site. The last point is particularly noteworthy since it implies that highly selective materials can be used. Although the requirements of high selectivity and ease of elution are typically in conflict, the two requirements are not mutually exclusive if the elution is purely electrostatic in nature.

EaIX materials have been applied for analytical-scale separation in a process called *electrochemical chromatography*. This process is very similar to conventional liquid chromatography except that the stationary phase is electroactive. As in conventional chromatographic processes, the retention times for different ions are largely controlled by interactions with the stationary phase. However, the redox state of the stationary phase allows additional control of the interactions between the analytes and the stationary phase. For example, anions can be easily separated from cations by applying a positive or anodic potential to the stationary phase. Separation of the different an-

ions, however, still relies on the specific interactions between the stationary phase and the ions.

EaIX materials may also be used for preparative-scale separations. Two modes of operation are possible: packed bed and membrane. The sequence of operational events in the packed bed mode in EIX/EaIX is a combination of the sequences used in electrochemical chromatography and conventional IX processes: firstly, analyte is sorbed into the EaIX material during the uptake cycle (with or without the application of a potential) and secondly the sorbed ions are eluted from the EaIX material by the application of a potential (see **Figure 4**). It should be noted that EaIX materials can be used as conventional IX materials during the sorption cycle; the distinguishing feature of the EaIX material is the ability to elute sorbed ions by simply applying the appropriate potential (**Figure 3B** and **D**). In the second mode of operation, the EaIX materials are made as membranes (see **Figure 5**). This mode of operation is superior to the packed-bed approach since solution switching is not required. This in turn implies that continuous operation is possible and that neither the process nor waste stream will be diluted, which necessarily occurs when solution switching takes place in the packed-bed mode. On the other hand, the packed-bed mode is more advantageous in treating very

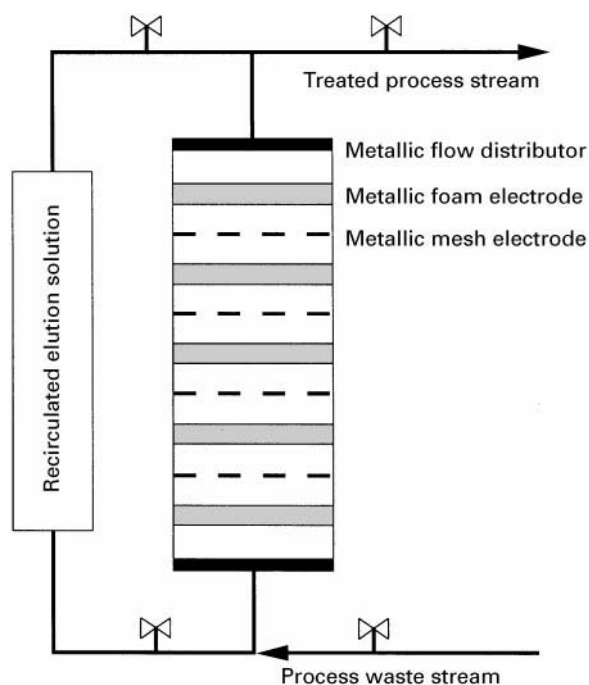


Figure 4 EIX/EaIX columns consist of the EaIX electrodes and counterelectrodes. Connections to the elution solutions are closed during sorption of target ions from the process waste stream. Sorption can be with or without an applied potential (see eqns [2] and [3] in the text). Elution is achieved by applying a potential (see **Figure 3B** and **D**) and flowing the elution solution.

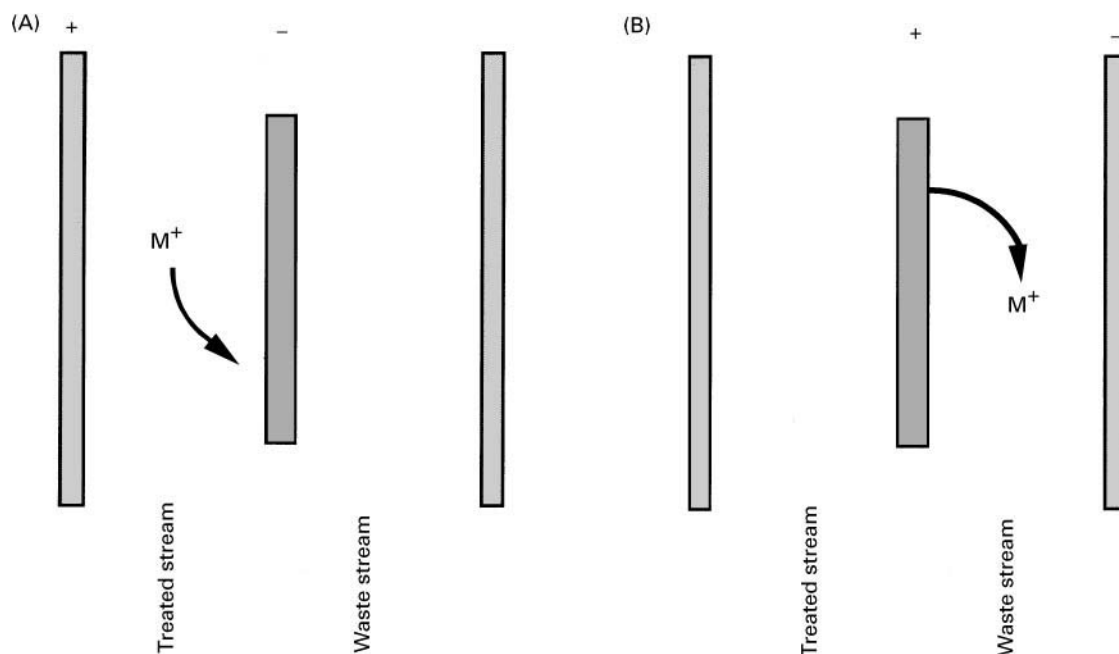


Figure 5 The EalX membrane is always an electrode when used in the membrane mode. (A) Reduction of EalX membrane (negative electrode) results in uptake of cations from the treated stream. (B) Oxidation of EalX membrane (positive electrode) results in elution of cations to the waste stream. The treated and waste streams never come in contact.

dilute streams since more intimate contact between the process stream and the EalX materials is possible. In addition, there are possibly more difficulties associated with preparing EalX materials as membranes than as packed-bed materials.

Characterization of EalX Materials

In the development and testing of an EIX/EalX process, the ion-loading capacity and specific ion selectivity of the EalX materials are of particular interest. Selectivity is defined in terms of a separation factor α_1^2 , which describes the selectivity for species '2' over species '1':

$$\alpha_1^2 = \frac{x_2'/x_1'}{x_2/x_1} \quad [1]$$

The numerator is the ratio of ion mole fractions within the EalX material, and the denominator is the mole fraction (or concentration) ratio in the bulk binary solution contacting the EalX material. The separation factor is especially useful for estimating process performance. For example, Figure 6 shows the fraction of Na^+ recovered as a function of K^+ removed for various values of α_{Na}^K . The plots show that if a minimum of 90% Na^+ recovery is required while expelling $>70\%$ of the K^+ , then an α_{Na}^K of approximately 30 is needed.

Electrochemical Methods

In addition to standard bulk contact methods typically used to characterize IX materials, electrochemical methods are well suited for evaluating EalX materials, especially for evaluating their expected performance when an applied potential is used in the uptake cycle. Two conventional electrochemical methods – *cyclic voltammetry* and *chronoamperometry* – are particularly useful in evaluating the ion-loading capacity of EalX materials. Cyclic voltammetry is best suited for a planar geometry since

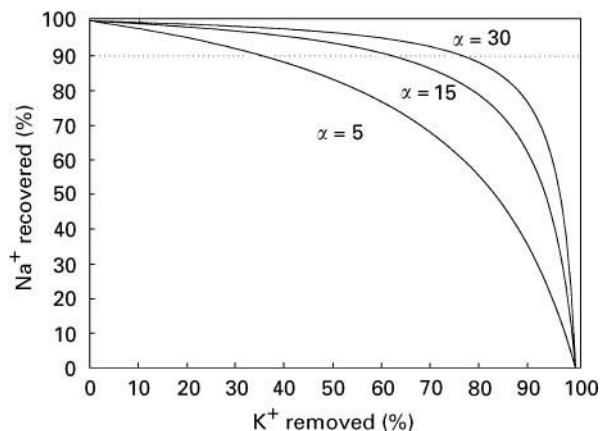


Figure 6 Fraction of Na^+ recovered as a function of K^+ removed for various separation factor, α_K^{Na} .

the slowly ramped applied potential is less intrusive on the samples. Chronoamperometry, on the other hand, is more suitable for determining the capacity of EaIX materials deposited on a high-surface area electrode because mass transfer limitations affect measured cyclic voltammograms (CVs).

A CV is obtained by measuring the current passed at the electrode as the applied potential is swept linearly at a fixed scan rate between two potential limits. When a suitable potential window is selected, cations (anions) are loaded into the EaIX material during the cathodic (anodic) sweep and the ions are eluted during the reverse sweep. The total charge passes in a load or unload cycle, as determined by integrating the current over any linear sweep, is a direct measure of the ion-loading capacity when the charge transfer is only a result of a known electrochemical reaction (see eqn [2] below). In chronoamperometry, the potential is stepped from one potential limit to the other. The current is measured while the potential is held at a limit for a fixed period of time, and again, the integrated charge passed is a measure of the ions loaded into or eluted from an EaIX electrode assembly.

Electrochemical and Gravimetric Methods

The two electrochemical methods described above yield only the ion-loading capacity. In order to determine the separation factor, an additional independent measurement is required. This is accomplished by combining the electrochemical measurements with gravimetric measurements. A common term for this combined method is electrochemical quartz crystal microgravimetry (EQCM). As the name suggests, mass accumulation within the EaIX material is monitored in addition to the total charge passed. Typically, quartz crystals are coated with an electrode on which a layer of an EaIX material is deposited. The fundamental frequency of the crystal is very sensitive to the mass loaded in the EaIX material; monitoring this fundamental frequency, the mass loaded during uptake and elution can be determined. For a crystal oscillating at 5.9 MHz, a 1 Hz decrease in the frequency corresponds to a mass increase of $\sim 4.0 \times 10^{-9}$ g. In EQCM, the oscillation frequency is monitored at the same time that the potential is swept to obtain a CV. This combination of measurements gives simultaneous information on electrochemical (ion) capacity and mass changes during load and elution cycles. Since mass change differs according to the molecular weight of the ions transported in and out of the EaIX film, the selectivity of the EaIX material for an ion in a binary mixture of known composition can be determined using EQCM. The

analysis is complicated, but not prohibitively, by the simultaneous transport of solvent (e.g., hydration water) and other species with the ions of interest.

Flow Cell Methods

Flow cell methods for EIX/EaIX characterization differ from conventional IX methodologies only in the material preparation. To achieve high volumetric ion-loading capacity, EaIX materials are typically coated on high surface-area electrodes (e.g., porous metal foam or mesh). These EaIX electrodes can be used in any of the modes represented in eqns [2] and [3]. To create an EaIX bed, multiple porous electrodes are used in series (see Figure 7A and B). When used in the conventional mode in the uptake cycle, the process stream simply flows through the electrodes. The effluent solution composition is analysed and breakthrough curves are obtained.

Properties of EaIX Materials

Functional requirements of EaIX materials are electronic conductivity, ionic conductivity, selectivity for the ion of interest, and reasonable stability (physical and chemical). Of the numerous inorganic and organic materials that fulfil all or some of the listed requirements, discussions will be limited to nickel hexacyanoferrate (NiHCF) as an example of a cationic EaIX material and polyvinylferrocene (PVF) as an example for an anionic EaIX material.

Hexacyanoferrate materials (including NiHCF) are known to be selective for alkali metals and, in

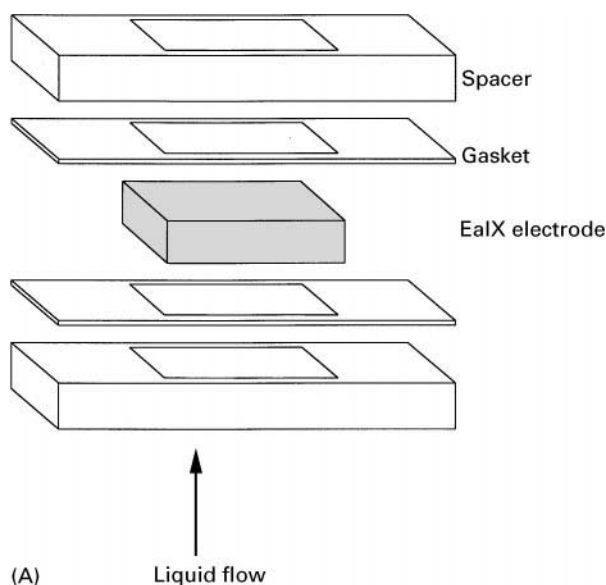


Figure 7 (A) Single electrode with the associated spacers and gaskets. (B) Eight-stack cell used for flow-through studies.

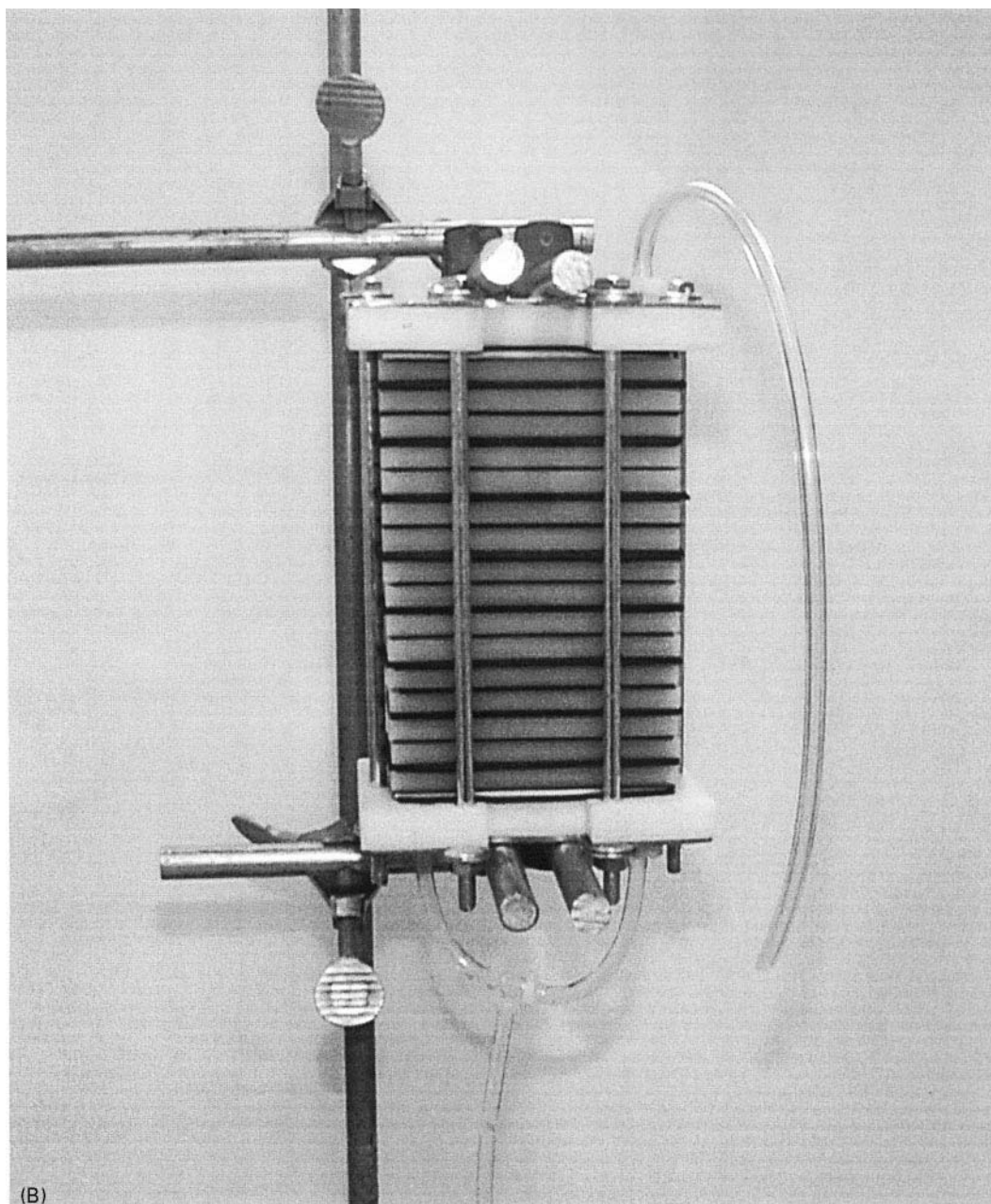


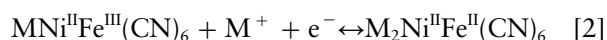
Figure 7 Continued

particular, are extremely selective for cesium (Cs^+) over sodium (Na^+) and potassium (K^+). More recently, the preference of polyvinylferrocene for perchlorate (nonradioactive chemical analogue of pertechnetate) anions over nitrate anions has been demonstrated.

Nickel Hexacyanoferrate

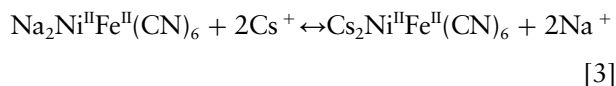
Nickel hexacyanoferrate $[\text{Ni}^{\text{II}}\text{Fe}^{\text{II/III}}(\text{CN})_6]^{2-/-}$ (NiHCF), an electroactive material, is known to complex reversibly with the alkali metal cations such as Na^+ , K^+ , and Cs^+ . Upon reduction of the iron (Fe^{III})

centre in NiHCF, an alkali cation associates with the ferrocyanide moiety to maintain charge neutrality through the following reaction, where M^+ is an alkali metal cation:



The reverse reaction, upon oxidation of the Fe^{II} centre, results in the dissociation of a single alkali metal cation per molecule of hexacyanoferrate. Oxidation of NiHCF film deposited on a substrate electrode, therefore, leads to the expulsion or

deintercalation of alkali cations from the film into a contacting solution, while the reduction of deposited NiHCF film leads to the uptake or intercalation of alkali cations from solution into the film (see Figure 3B and A, respectively). The selectivity for alkali cations M^+ by NiHCF increases with molecular weights, $Cs^+ \gg K^+ > Na^+$. Therefore, K^+ or/and Na^+ is readily exchanged for Cs^+ ; for example:



Equation [3] shows that the EaIX material can be used in conventional IX. The Cs^+ is bound so strongly that elution is only possible through oxidation of the Fe centre from II to III. Chemical oxidation has been demonstrated with NiHCF as well as for the copper and zinc analogues. Approximately five column volumes of 8 mol L^{-1} nitric acid are required for effective elution of all the sorbed Cs^+ . The cost and hazard associated with this eluent are significant. Use of the EIX/EaIX approach, therefore, provides an attractive alternative since the oxidation can be done more efficiently via the electrochemical approach.

It is imperative for the EIX/EaIX process that there is intimate contact between the EaIX material and the electronically conducting substrate. NiHCF can be conveniently deposited onto a conducting substrate electrochemically. A nickel surface corroded in a solution containing hexacyanoferrate ions results in the precipitation/deposition of NiHCF on the surface. The electrochemical route is particularly advantageous over other methods (e.g., precipitation and sol-gel) since deposition within the pores of a porous electrode can be carried out readily.

Applications The selectivity of NiHCF for alkali cations with an affinity order $Cs^+ \gg K^+ > Na^+$ is attributed to the relative sizes of the ions, both hydrated and not, and the NiHCF cubic lattice structure that the ions must penetrate and then occupy. Because NiHCF is both electronically and ion conducting, is readily deposited as a film on conductive electrode substrates, and is alkali cation-specific, it is an ideal EaIX material for K^+ and Cs^+ separation applications.

Potassium separation The forest products industry requires selective removal of K^+ and recovery of Na^+ . As the plots in Figure 6 show, the separation factor is critical in determining the extent to which Na^+ can be recovered for a required removal of K^+ . Therefore, quantification of α_{Na}^K is essential for scale-up purposes and capital cost estimation. Because

equipment capital costs scale roughly with the electrode costs, it is necessary to minimize electrode area to make the EaIX process financially attractive. The larger the separation factor α_{Na}^K , the smaller the EaIX electrode area necessary to remove a given amount of K^+ . Electrode area is also reduced if the ion capacity of the EaIX material per unit electrode area is increased.

The selectivity of NiHCF for K^+ in preference to Na^+ was quantified by EQCM and by bulk-contact experiments. Separation factors α_{Na}^K ranged from about 5 using EQCM to a maximum of 24 in bulk-contact tests; these differences will be discussed further below. Figure 8(A) and (B) show the results of EQCM experiments for a NiHCF-coated quartz crystal in contact with potassium and sodium sulfate solutions and mixtures. The CVs in Figure 8(A) show

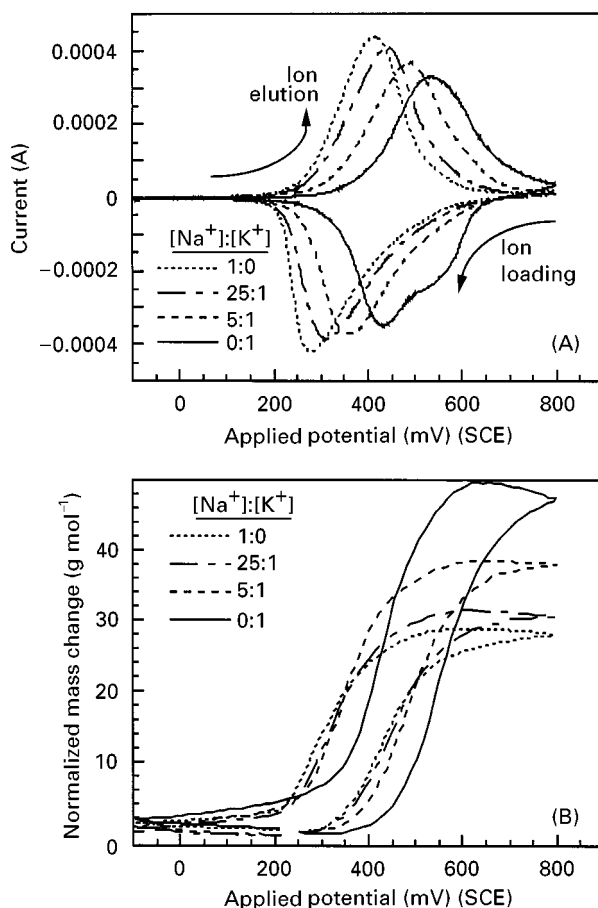


Figure 8 EQCM results for a series of $0.5 \text{ mol L}^{-1} \text{ Na}_2\text{SO}_4$ and $0.5 \text{ mol L}^{-1} \text{ K}_2\text{SO}_4$ solution mixtures demonstrating selectivity of a NiHCF film for K^+ over Na^+ : (A) Cyclic voltammograms indicate sensitivity to K^+ in solutions > 25 times more concentrated in Na^+ ; and (B) QCM mass data, normalized by the ion-loading capacity and converted to units of apparent molar weight, indicate greater mass changes as solutions become more concentrated in K^+ and relatively more K^+ is loaded into the film. (Adapted, with permission from Rassat *et al.* (1999), Elsevier Science.)

Table 1 Apparent molar masses and separation factors in mixtures of 0.5 mol L⁻¹ sodium and potassium sulfate solutions. (Adapted, with permission from Rassat *et al.* (1999), Elsevier Science)

Solution $x_{\text{Na}} : x_{\text{K}}$	Experiment 1		Experiment 2		Experiment 3	
	M' (g mol ⁻¹)	$\alpha_{\text{Na}}^{\text{K}}$	M' (g mol ⁻¹)	$\alpha_{\text{Na}}^{\text{K}}$	M' (g mol ⁻¹)	$\alpha_{\text{Na}}^{\text{K}}$
1 : 0	29.0 ± 0.5		25.3 ± 0.4		22.8 ± 0.4	
25 : 1	31.7 ± 0.5	3.8 ± 1.1	30.2 ± 0.6	5.3 ± 0.8	28.4 ± 0.4	5.9 ± 0.7
10 : 1	35.4 ± 0.5	4.6 ± 0.6	35.2 ± 0.6	5.6 ± 0.5	32.7 ± 0.5	5.1 ± 0.4
5 : 1	39.2 ± 0.6	5.0 ± 0.7	39.4 ± 0.6	5.2 ± 0.5	36.9 ± 0.6	4.6 ± 0.4
0 : 1	49.4 ± 0.9		53.0 ± 0.9		52.3 ± 0.8	

the reversibility of the cation uptake (negative currents) and elution (positive currents). In addition, the area between the abscissa and either the negative or positive currents is proportional to the net ionic loading. Combined with the apparent molar weights shown in Figure 8(B), separation factors ranging from 3.8 to 5.9 were calculated (see Table 1). In addition to providing quantitative estimates of the separation factors, Figure 8(A) and (B) qualitatively show the preference of K⁺ over Na⁺. As the mixtures become more concentrated in K⁺, the peaks shift to higher potential, more in line with that of pure K₂SO₄ solution. Even in solutions five times more concentrated in Na⁺, the peaks shift substantially toward those for pure K₂SO₄ solution, indicating the relative selectivity of NiHCF for K⁺. The shift towards higher apparent molecular weights in the mixtures also indicates the preference for K⁺.

Bulk-contact tests of NiHCF, a more direct measure of selectivity, resulted in separation factors ranging from 14 to 24. Representative experimental details and results are shown in Table 2. In all the tests shown in Table 2, the Na⁺ : K⁺ molar concentration ratio was ~12, which is the approximate ratio of the ions in pulp mill application. The amount of K⁺ taken up by the NiHCF without any applied potential (IX mode, eqn [3]) was determined from the total solution volume and the difference in K⁺ concentration before and after contact. The sep-

aration factor, $\alpha_{\text{Na}}^{\text{K}}$, determined by this bulk-contact method, is very sensitive to the total capacity value. Since there are more uncertainties in determining the total capacity for the foam electrodes (in comparison to the small planar EQCM electrodes), the variability and uncertainty of bulk-contact separation factors obtained are greater. Despite the uncertainties associated with the total capacity, the batch-contact tests are in agreement with the EQCM results in that NiHCF materials are selective for K⁺ over Na⁺. The reason for the difference in the magnitude of the separation factors determined by the two techniques is presently unclear. Three possibilities are (1) differences in NiHCF film preparations resulting from differences in the electrode substrate on which they were deposited, (2) differences in solution ionic strengths (~1 mol L⁻¹ alkali for EQCM and < 0.1 mol L⁻¹ alkali for bulk contacting), and (3) the potential was applied to NiHCF in the EQCM experiments but not in the bulk-contact tests.

Cesium separation The radioactive isotope ¹³⁷Cs, a fission product of nuclear fuel processing and corrosion of fuel rods in commercial nuclear reactors, is a trace component of several process and waste streams in the nuclear industry. Because of the strong affinity of NiHCF for Cs⁺, separation of this ion by EIX/EaIX is ideal. Figure 9(A) and (B) show the EQCM results for dilute Cs⁺ in competition with excess Na⁺. The experiments are analogous to those described for K⁺ separation above, but the shifts toward pure Cs⁺ solutions observed in the mixtures are more pronounced.

Table 3 summarizes the apparent molar masses and separation factors $\alpha_{\text{Na}}^{\text{Cs}}$ for a series of Na⁺ : Cs⁺ mixtures. The separation factors range from 178 to 593, clearly demonstrating the enhanced selectivity of NiHCF for Cs⁺ relative to Na⁺ and K⁺ (compare to Table 1). Neglecting the results for the 81 Na⁺ : 1 Cs⁺ mixture, which had a higher estimated uncertainty, there appears to be a trend of increasing Cs⁺ selectivity with decreasing Cs⁺ concentration.

Table 2 NiHCF bulk-contact separation factors and experimental conditions. (NiHCF-coated circular disc electrodes ~5-cm diameter by ~0.6-cm thick, 80 pores inch⁻¹ porosity, and ~60 cm² cm⁻³ specific volume contacted with 18 mL of mixed ion solution)

Test	[K ⁺] (mM)		[Na ⁺] (mM)		Capacity (C)	$\alpha_{\text{Na}}^{\text{K}}$
	Initial	Final	Initial	Final		
1	2.19	1.30	28.0	29.1	2.06	14
2	0.97	0.30	13.0	13.7	2.31	15
3	4.81	3.44	56.8	54.1	1.97	24

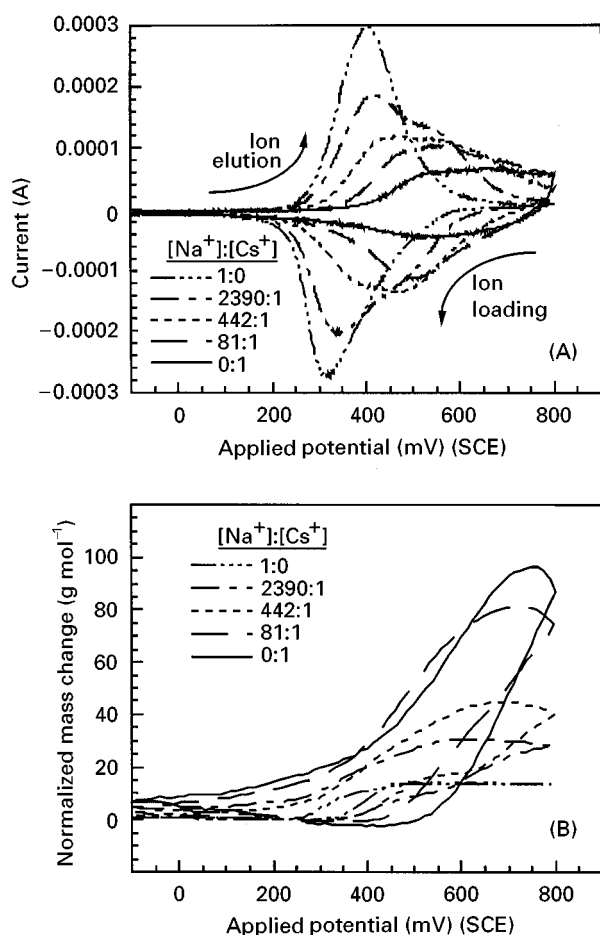


Figure 9 EQCM results for a series of 1.0 mol L⁻¹ NaNO₃ and 1.0 mol L⁻¹ CsNO₃ solution mixtures demonstrating selectivity of NiHCF film for Cs⁺ over Na⁺: (A) cyclic voltammograms indicate sensitivity to Cs⁺ in solutions ~2400 times more concentrated in Na⁺; and (B) QCM mass data, normalized by the ion-loading capacity and converted to units of apparent molar weight, indicate greater mass changes as solutions become more concentrated in Cs⁺ and relatively more Cs⁺ is loaded into the film. (Adapted, with permission from Rassat *et al.* (1999), Elsevier Science.)

In the limited range of K⁺ and Na⁺ mixtures tested, such a trend was not detected.

Flow-through EIX/EaIX experiments demonstrate the regenerability of the EaIX material without the use of highly oxidizing solutions. Breakthrough curves for a 0.2-ppm Cs⁺ feed stream are shown in Figure 10. Here, the EIX/EaIX system was operated in the conventional IX mode in the uptake cycle. The breakthrough curve for the first flow test shows that the breakthrough point (where the concentration of Cs⁺ in the effluent stream is one-half the feed concentration) occurs after ~110 bed volumes were passed in the first flow test. In subsequent flow tests, each following regeneration of the NiHCF electrodes, the breakthrough capacity was reduced to ~40 bed volumes and the breakthrough profiles were consistent.

Table 3 Apparent molar masses and separation factors in mixtures of 1.0 mol L⁻¹ sodium and cesium nitrate solutions. Rassat *et al.* (1999), courtesy of Elsevier Scientific.

Solution $x_{\text{Na}} : x_{\text{Cs}}$	$M' \text{ (g mol}^{-1}\text{)}$	$\alpha_{\text{Na}}^{\text{Cs}}$
1 : 0	14.4 ± 0.2	
*2390 : 1	31.1 ± 0.9	593 ± 40
*910 : 1	37.3 ± 2.1	341 ± 36
442 : 1	46.1 ± 1.0	268 ± 15
155 : 1	59.3 ± 1.0	178 ± 12
81 : 1	83.0 ± 1.3	361 ± 60
0 : 1	98.4 ± 2.2	

*Gravimetric and/or electrochemical measurements not at steady state.

Regeneration cycles were carried out by potential cycling in a solution of sodium nitrate. The reasons for the diminished breakthrough volume after the first cycle are presently unclear. It is speculated that this is a 'plugging' issue. One hypothesis is that because of the great affinity of NiHCF for Cs⁺ and strong binding in the cubic lattice, migration of Cs⁺ to all sites within the film is hindered, and therefore, some Cs⁺ are permanently bound in the NiHCF. The most noteworthy point is that regeneration of the EaIX material is reversible (starting with the second cycle) without the need for strong oxidiz-

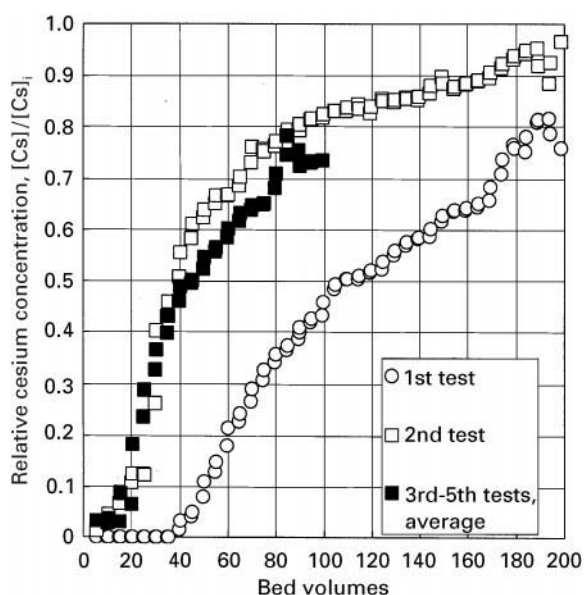


Figure 10 Breakthrough curves for a feed stream of 0.2-ppm Cs in an EaIX bed consisting of eight NiHCF-coated porous nickel foam electrodes operated in IX mode. The electrodes were regenerated electrochemically in concentrated NaNO₃ solution between each test. Experimental conditions: 80 pores inch⁻¹ or ~60 cm² cm⁻³ nickel foam; CsNO₃ solution flowed at 24 mL min⁻¹; bed volume of ~39 mL; and maximum ion capacity ~2.0 C.

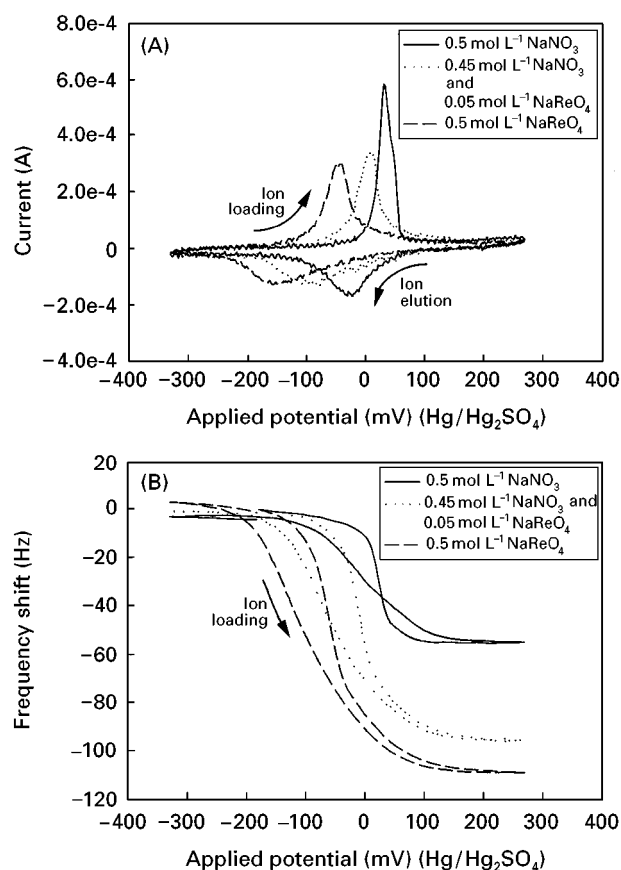


Figure 11 EQCM results for a series of 0.5 mol L⁻¹ NaNO₃ and 0.5 mol L⁻¹ NaReO₄ solution mixtures demonstrating selectivity of a PVF film for ReO₄⁻ over NO₃⁻: (A) cyclic voltammograms indicate sensitivity to ReO₄⁻ in solutions nine times more concentrated in NO₃⁻; and (B) QCM frequency shifts indicate greater mass changes as solutions become more concentrated in ReO₄⁻ and relatively more ReO₄⁻ is loaded into the film.

ing solutions (i.e., 8 mol L⁻¹ nitric acid used by previous researchers).

Polyvinylferrocene

Polyvinylferrocene $[-(\text{Fe}^{\text{II/III}}(\text{C}_5\text{H}_5)(\text{C}_5\text{H}_4\text{CH}_2\text{CH}_2)^{1+/0})-]$, or PVF, is a well-studied organometallic polymer. In contrast to NiHCF, oxidation of PVF to the 1+ state requires the uptake of anions to maintain electroneutrality (see Figure 3C), making PVF a suitable anionic EaIX material candidate. Recently, the preference of PVF for perrhenate (ReO₄⁻) over nitrate (NO₃⁻) was demonstrated. The uptake and elution reactions are analogues to that shown in eqn [2]. As with NiHCF, PVF can also be used as conventional IX materials. Specifically, the NO₃⁻ in (PVF⁺)(NO₃⁻) is readily exchanged for ReO₄⁻. Other possible applications for PVF include the extraction of arsenates and chromates.

PVF has been prepared through chemical, electrochemical, and plasma polymerization. Both plasma

and electrochemical polymerizations should be suitable for depositing PVF within porous substrate.

Applications The preference of polyvinylferrocene for perrhenate (nonradioactive chemical analogue of pertechnetate) anions over nitrate anions has been demonstrated. Nitrates are the main competing anions for separation of pertechnetate in radioactive tank wastes. The current and the frequency responses of a PVF-coated EQCM as a function of a cyclic potential scan are shown in Figure 11(A) and (B). (The frequency response is shown rather than the normalized mass change because of complications due to the less rigid PVF films compared to the NiHCF films.) The more negative (cathodic) potential peaks observed in the pure ReO₄⁻ solution and in the mixture, compared to a pure NO₃⁻ solution, indicate the preference of ReO₄⁻ over NO₃⁻. In addition, the frequency responses shown in Figure 11(B) indicate a substantial mass gained in the PVF film upon oxidation in a solution containing both NO₃⁻ and ReO₄⁻, more mass than can be attributed to NO₃⁻ alone. This supports the contention that ReO₄⁻ ions (which are heavier than NO₃⁻) are preferentially taken up by the PVF. The data shown in Figure 11(A) and (B) correspond to a separation factor of 30.

Future Developments

EIX processes (using EaIX and nonelectroactive IX materials) are very promising methods for ion separation due to the potential savings resulting from minimization of secondary waste generation. Better understanding of system performance through large-scale (e.g., pilot-scale) studies still needs to be carried out as well as the development of new materials. For example, EaIX materials selective for strontium (Sr²⁺) are of interest to the nuclear industry. Calcium (Ca²⁺) selective materials are valuable for preventing scale formation in many industries. Finally, effective removal of NO₃⁻ and arsenate anions is critical for safe drinking water.

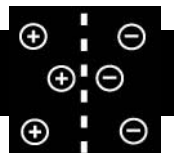
See also: II/Ion Exchange: Historical Development; Inorganic Ion Exchangers; Organic Ion Exchangers; Theory of Ion Exchange.

Further Reading

- Genders D and Weinberg NL (eds) (1992) *Electrochemistry for a Cleaner Environment*. East Amherst, NY: The Electrosynthesis Company Inc.
- Krishnan R and Ibanez J (1997) *Environmental Electrochemistry. Fundamentals and Applications in Pollution Abatement*. San Diego: Academic Press.

- Lewis TM, Wallace GG and Smyth MR (1999) Electrofunctional polymers: their role in the development of new analytical systems. *Analyst* 124: 213.
- Rassat SD, Sukanto JH, Orth RJ, Lilga MA and Hallen RT (1999) Development of an electrically switched ion exchange process for selective ion separations. *Separation and Purification Technology* 15: 207.
- Rose TL, Rudd E, Murphy O and Conway BE (eds) (1994) *Proceedings of the Symposium on Water Purification by Photocatalytic, Photoelectrochemical, and Electrochemical Processes*. Pennington, NJ: The Electrochemical Society.
- Tsuda T (ed.) (1995) *Electric Field Applications in Chromatography, Industrial and Chemical Processes*. Weinheim: VCH.

ELECTRODIALYSIS: ION EXCHANGE



G. Pourcelly, Laboratory of Materials and Membrane Processes, Montpellier, France

Copyright © 2000 Academic Press

Introduction

Separations with synthetic membranes have become increasingly important; today membrane processes are used in a wide range of applications and their number will certainly increase.

A membrane is a permselective polymer, inorganic or metal phase which restricts the motion of certain species. By controlling the relative rates of transport of various species it gives one product depleted in certain components and a second product concentrated in these components. Membrane performance is characterized by two terms: flux and selectivity. Flux (or permeation rate) is the volumetric mass flow of fluid passing through the membrane per unit area of membrane and unit mass time. Selectivity is a measure of the relative permeation rates of different components through the membrane.

Processes may be classified according to the driving force used: (1) a pressure differential leads to micro-, ultra- and nanofiltration and reverse osmosis; (2) a concentration difference across the membrane leads to diffusion of a species between two solutions (dialysis); (3) a potential field applied to an ion exchange membrane leads to migration of ions through the membrane (electrodialysis, membrane electrolysis and electrochemical devices). This last category and more specifically electrodialysis is the subject of this section. This electrically driven process uses ion exchange membranes, a description of which follows.

Ion Exchange Membranes

Electrodialysis (ED) uses membranes containing fixed charged groups attached to the polymer backbone of its membrane. Two kinds of ion exchange membranes (IEMs) are used in ED: *homopolar membranes*

bearing fixed charges of the same sign and *bipolar membranes* bearing positive and negative fixed charges located on each side of the membrane.

IEMs are sheet-shaped materials through which a selective ion transport can be established under a driving force, generally an electric field and/or a concentration gradient.

Most of them are of a polymeric nature. They are constituted of reticulated macromolecular chains forming a tridimensional structure. In this network, ionizable functionalized groups are attached to the polymeric matrix and are at the origin of the membrane selectivity. For example cation exchange membranes (CEMs) contain fixed negative charges and mobile cations which can be exchanged with other cations present in an external phase in contact with the membrane. The ions balancing the fixed exchange sites are called counterions. The concentration of counterions is relatively high and therefore counterions carry most of the electric current through the membrane. The fixed charges attached to the polymer matrix repel ions of the same charges (co-ions). This exclusion, which is a result of electrostatic repulsion, is called Donnan exclusion, named after F. G. Donnan, who first reported the phenomenon in 1910. However, as the membrane selectivity is never ideal, the membrane material can be penetrated by a non-negligible amount of electrolyte. A schematic structure of such a homopolar CEM is depicted in Figure 1. Under an applied electric field, the CEM bearing sulfonic exchange groups ($-\text{SO}_3^-$) mainly allows the transport of counterions.

A bipolar membrane (BPM) is composed of two layers of ion exchangers joined by a hydrophilic junction. The diffusion of water from both sides of the BPM allows it to dissociate under the electrical field to generate protons and hydroxyl ions, which further migrate from the junction layer through the cation exchange and anion exchange layers of the bipolar membrane. Generally, the cation exchange groups are sulfonic and the anions are trimethyl quaternary

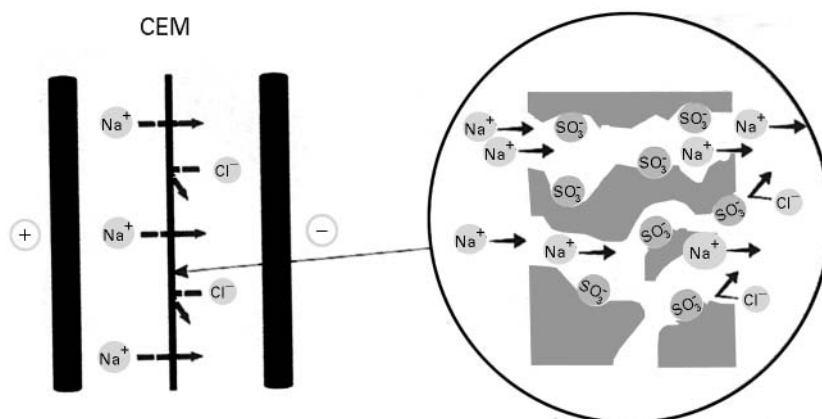


Figure 1 Schematic process of transport of counterion (Na^+) through a cation exchange membrane (CEM, bearing sulfonic sites).

ammonium groups ($-\text{N}(\text{CH}_3)_3^+$). The principle of this water-splitting phenomenon is depicted in **Figure 2**.

The requirements for suitability of homopolar IEMs for industrial applications are the following:

1. high ionic conductivity with a concentration of fixed charges as high as possible;
2. high ionic permselectivity combining simultaneously a high conductivity and a moderate water uptake;
3. chemical stability of the fixed ions and a good mechanical resistance;
4. reasonable price.

Bipolar membranes must have all of these requirements and, in addition, must have an experimental potential to achieve a water-splitting capability as close as possible to the theoretical one, equal to 0.83 V at 25°C.

Nowadays, superior styrene-divinylbenzene copolymer membranes can be easily purchased; perfluorinated membranes with great chemical stability

are now being marketed and BPMs with an industrial-scale lifetime are becoming available.

Principles of Electrodialysis

Electrodialysis with Homopolar Ion Exchange Membranes

IEMs can be organized into two-, three- or four-compartment electrodialysis cells.

Two compartment electrodialysis The principle of ED is depicted in **Figure 3**. Electrically charged membranes are used to remove ions from an aqueous solution. A number of anion exchange membranes (AEMs) and CEMs are placed in an alternative pattern between a cathode and an anode. When an ionic feed solution (for example, a sodium chloride solution) flows through the channels of the electrodialyser, the positively charged sodium ions migrate to the cathode and the negatively charged chloride ions migrate to the anode. As the chloride ions

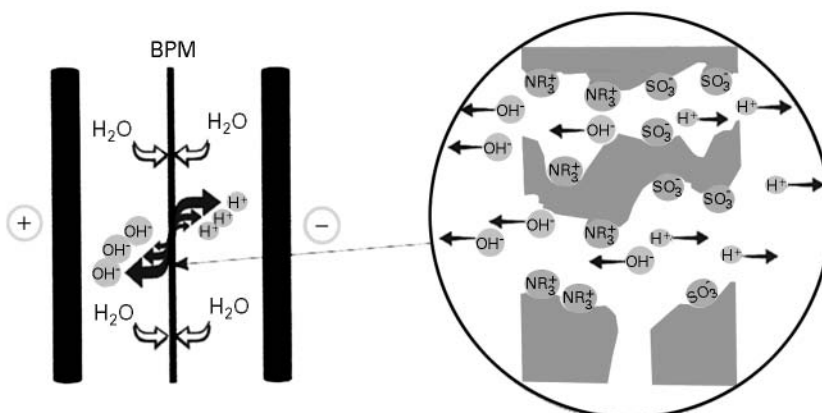


Figure 2 Schematic principle of water dissociation by a bipolar membrane (BPM).

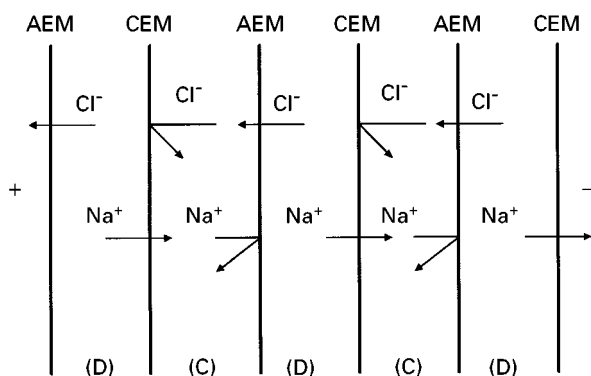
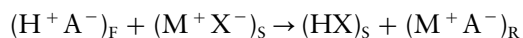


Figure 3 Schematic of two-compartment electrodialysis. AEM and CEM, anion and cation exchange membranes; (D), dilute; (C), concentrate.

cannot pass the CEM and the sodium ions cannot pass the AEM, the overall effect is a simultaneous ionic concentration increase in alternating compartments and an ionic concentration decrease in the other compartments. Consequently, alternate dilute and concentrated solutions are formed. A set of two compartments (dilute (D) and concentrated (C)) forms a cell pair. In commercial applications several hundreds of cell pairs are assembled in a stack.

Three compartment electrodialysis A three-compartment ED process is depicted in Figure 4 and concerns the transformation of an electrolyte M^+X^- into its acid HX , which is weakly dissociated, according to the reaction:



The strong acid H^+A^- (HCl or H_2SO_4) is introduced into the feed compartment (F). Protons migrate to the substitution compartment (S) to transform the salt $(M^+X^-)_S$ into the weak acid $(HX)_S$. Simultaneously,

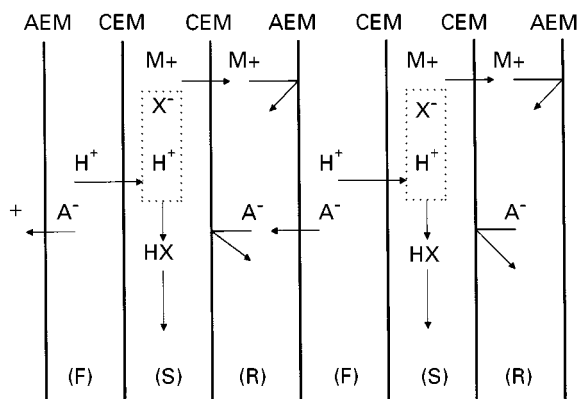


Figure 4 Schematic of three-compartment electrodialysis for the conversion of a salt M^+X^- into its weak acid HX .

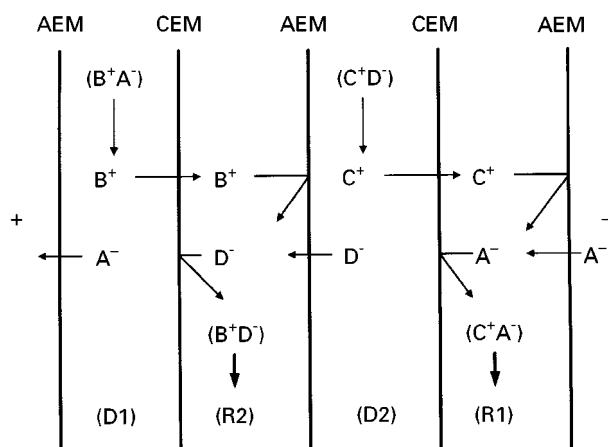
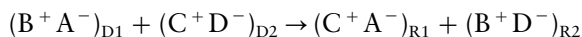


Figure 5 Schematic of four-compartment electrodialysis for the double substitution reaction.

M^+ ions migrate to the recovery compartment (R) to form the salt $(M^+A^-)_R$.

Four-compartment electrodialysis A complex four-compartment ED process is depicted in Figure 5. The elementary cell is composed of four compartments and allows the reaction of double substitution according to



The electrolytes to be substituted, (B^+A^-) and (C^+D^-) , feed the dilutes D1 and D2. In the first recovery compartment R1, A^- combines with C^+ to give C^+A^- , while simultaneously B^+ combines with D^- to give B^+D^- in the second recovery compartment.

Process parameters and limiting phenomena in electrodialysis The amount of ions transported through the membrane is directly proportional to the electric current (i) or current density, which is given by

$$i = \frac{ZFQ\Delta c}{\eta}$$

where z is the valency, F the Faraday constant, Q the flow rate, Δc the concentration difference between the feed and the permeate (dilute) and η the current efficiency. Theoretically, 1 faraday of current (96 500 coulombs) will transfer 1 mol of sodium ions to the cathode and 1 mol of chloride ions to the anode. Practically, the permeation of water through the ion exchange membranes and the fact that the membranes are not completely selective slightly reduces the current efficiency to an average of 0.90–0.95.

Electric current is related to electrical potential E by Ohm's law:

$$E = Ri$$

where R is the resistance of the total membrane stack. Increasing the current density leads to an increase in the number of ions transferred. However, current density cannot be increased by an unlimited amount. In the steady state, the flux of a species through a membrane can never exceed the flux of that species to the surface of the membrane. Concentration polarization is a well-known phenomenon arising at the interface between an IEM and an electrolyte solution when current passes through it. It is due to the difference in transport numbers of the counterion between the membrane and the solution. Gradients of concentration arise in the diffusion layer as depicted in **Figure 6**, and when the concentration of the counterions becomes negligible at the depleted solution-membrane interface a limiting current appears.

This limiting current density j_L is the current density when the flux of ions through the boundary layers has reached its maximum value and no further increase in ion flux (or current) is possible. It is given by the relation.

$$j_L = \frac{zDFC}{\delta(t_m - t_s)}$$

where D is the diffusion coefficient of the counterion in the solution, C the concentration of the bulk solution, δ the thickness of the diffusion layer (also named the Nernst layer or unstirred boundary layer), and t_m and t_s are the transport number in the membrane and the solution, respectively. If the current density is allowed to exceed j_L , then the current crossing the membrane must be carried by another ion and dissociation of water occurs at higher current density. The limitations of the rate of ion transport through a membrane can be seen from a current density versus voltage plot for the membrane as depicted in **Figure 7**. This current-voltage plot is composed of three regions: a first, ohmic one in which current is carried

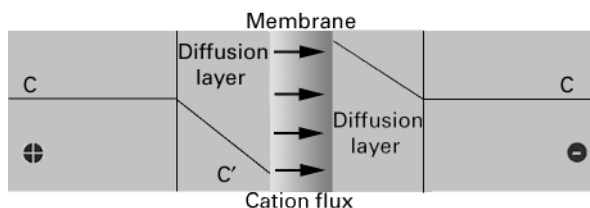


Figure 6 Concentration profile in diffusion layers: depleted and concentrated regions (for a cation exchange membrane).

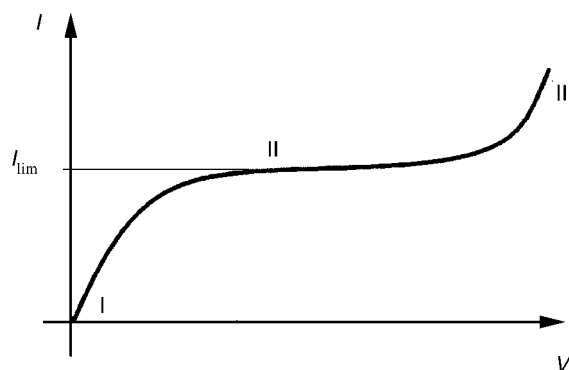


Figure 7 Current-voltage curve for an ion exchange membrane; limiting current.

by the ions of the electrolyte, a second plateau-shaped one corresponding to the limiting current, and a third region in which water splitting occurs. Because D/δ is equal to k , the mass transfer coefficient, j_L is strongly determined by the hydrodynamics of the system (cross-flow velocity, geometry of the cell). Moreover, the distance between membranes has to be very thin to reduce the ohmic drop due to the electrolyte thickness. Practically, separators of 0.8–1.5 mm thick acting as turbulent promoters are introduced alternately into membranes.

Electrodialysis with Bipolar Membranes

The conventional method for generating H^+ and OH^- ions from water utilizes electrolysis. Electrolysis also generates O_2 and H_2 , and the overvoltage for this generation consumes about half of the electrical energy of the process. Nowadays, special ion exchange membranes are available for splitting water directly into H^+ and OH^- ions without generating gases. Membrane water-splitting technology is a general-purpose unit operation for converting water-soluble salts to their corresponding acids and bases. The process uses BPMs in conjunction with conventional CEMs and/or AEMs, respectively). The separation and rearrangement of ions is effected by a direct current driving force. BPM electrodialysis (EDBM) is therefore an alternative method of electrolysis for the generation of H^+ and OH^- ions which can be used to generate acid and base from salts, without the production of oxygen and hydrogen gases.

The principle of water splitting by a BPM is illustrated in **Figure 8**. The diffusion of water from both sides of the BPM allows its dissociation under the electrical field to generate protons and hydroxyl ions, which further migrate from the junction layer through the cation exchange and anion exchange layers of the BPM.

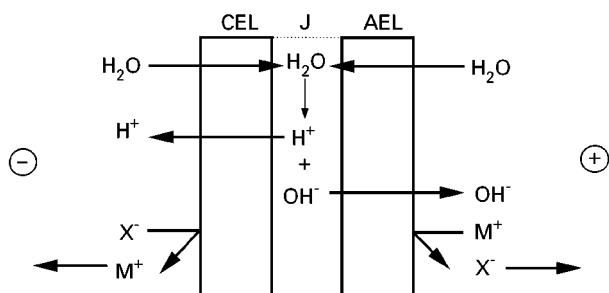


Figure 8 Diffusion and dissociation of water in a bipolar membrane. AEL and CEL, anion and cation exchange layers.

The application of BPM reduces the energy costs associated with electrode polarization in the more conventional electrolytic approach.

The theoretical potential to achieve the water-splitting capability is 0.83 V at 25°C. The actual potential drop across a BPM is quite close to this, being in the range of 0.9–1.1 V for current densities between 500 and 1500 A m⁻², which is the general region of practical interest. The value of the membrane potential drops equate to theoretical energy consumptions of the order of 600–700 kWh per ton of NaOH. Of course, the actual energy consumptions are significantly higher because of the ohmic resistances in the other cell stack components, in practical operating units.

The configuration of the EDBM process depends on the application. Typical use of BPM is in the treatment of concentrated salt solutions such as Na₂SO₄ from the chemical industry to produce H₂SO₄ and NaOH. A cell system consists of an AEM, a BPM and a CEM as a repeating unit. In this case the configuration is a *three-compartment EDBM*, illustrated in **Figure 9**. This elementary cell is repeated

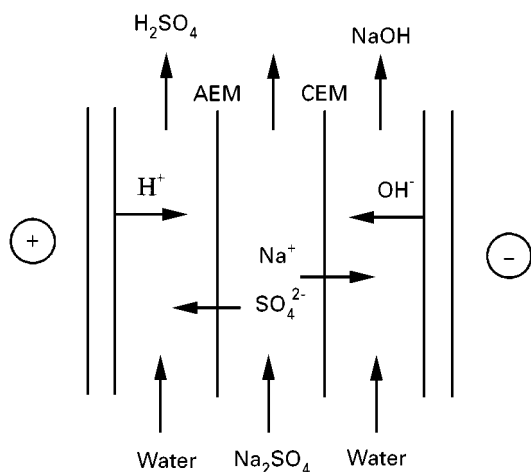


Figure 9 Generation of H₂SO₄ and NaOH from Na₂SO₄ solution (three-compartment cell).

and placed between two electrodes. The Na₂SO₄ solution flows between the CEM and the AEM. When direct current is applied, water will dissociate in the BPM to form the equivalent amounts of H⁺ and OH⁻ ions. The H⁺ ions permeate through the cation exchange side of the BPM and form H₂SO₄ with the sulfate ions provided by the Na₂SO₄ solution from the adjacent cell. The OH⁻ ions permeate the anion exchange side of the BPM and form NaOH with the sodium ions permeating into the cell from the Na₂SO₄ solution through the adjacent CEM. The final result is the production of NaOH and H₂SO₄ from Na₂SO₄ at a significantly lower cost than by other methods.

There are applications where it is not possible to obtain high purity of both acid and base, or may even generate problems during the process. For example, in the splitting of a salt from a weak acid (sodium acetate), the pure acid is weakly dissociated, so its conductivity is low. It would not therefore be practical to achieve the splitting of sodium acetate in a three-compartment cell. Instead, a two-compartment cell with the acetate solution flowing between a BPM and a CEM is recommended (**Figure 10A**). When the conversion of the salt stream reaches 95%, the conductivity becomes very low. Therefore it is not possible to pursue the EDBM more deeply. The EDBM is then stopped and the residual Na⁺ ions are removed using cation exchange resins. In a similar way, an ammonium or amine salt can be treated in a two-compartment cell with an AEM instead of a CEM (**Figure 10B**).

BPM can thus also be used in an alternative two-compartment cell configuration, regenerating only one base or acid. The cation/BPM two-compartment cell is useful for the processing of the salts of weak acids (or organic acids) to give a relatively pure base stream and a mixed acid/salt stream (**Figure 10A**), while the anion/BPM configuration is useful for converting salts of weak bases (e.g. ammonium nitrate) to a salt/base mixture and a relatively pure acid (**Figure 10B**).

Applications of Electrodialysis

Electrodialysis with Homopolar Membranes

Separation electromembrane processes such as ED are being applied to bioindustries and to the treatment of industry of wastewater. ED is a method which is used both for the removal of salts (e.g. to produce drinking water from brackish sources, to remove salts from foodstuffs) and for the concentration of salt solutions (e.g. for the manufacture of table salt from seawater, the concentration of process

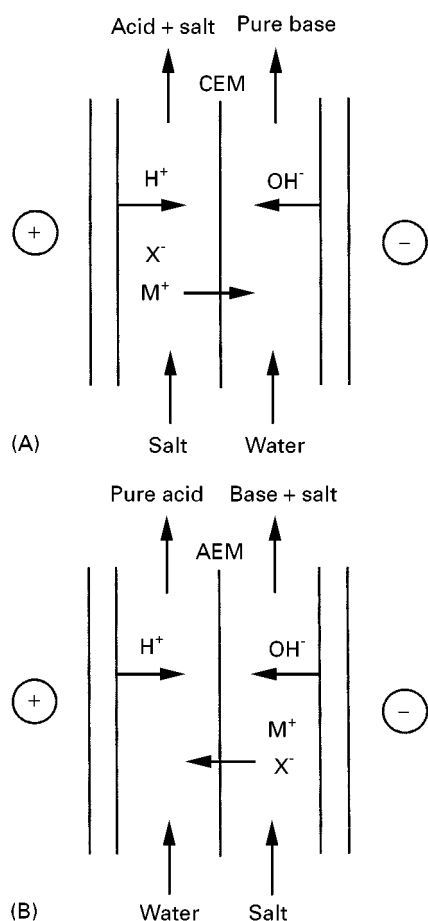


Figure 10 Two-compartment bipolar membrane electrodialysis to produce only pure acid or base.

streams and the recovery of salts from effluents). An example of conventional two-compartment ED is depicted in **Figure 11** and some of the many applications of ED are listed in **Table 1**.

The main application of ED is the production of potable water from brackish water whose salt content is close to 5 g L^{-1} . Beyond this value the reverse osmosis technique is more suitable. A new application of desalination is the reduction of nitrate content in drinking water. AEMs tend to selectively transfer nitrate in preference to other anions common in drinking water. Nowadays, electrodialysis plants produce several hundreds of cubic metres of potable water per day (reduction of nitrates to 5 mg L^{-1} and NaCl to 200 mg L^{-1}).

Another potential increasing area for ED is in the rough desalting of water that will be subjected to subsequent purification for use as boiler feed or rinse water in the electronics industry. Ion exchange has commonly been used for preparing waters with a very low salinity. However, the cost for regenerating and the magnitude of the waste disposal problem are proportional to the salinity of the feed water. A variant of ED which has achieved commercial success is electrodeionization. The depleted compartment is filled with an ion exchange material, generally an ion exchange resin. This material, providing high conductive paths for the ions, prevents the occurrence of the concentration polarization and a drastic increase of the electrical resistance. **Figure 12** illustrates the electrodeionization process with ion exchange resins. It allows the production of high resistivity water ($10\text{--}15 \text{ M}\Omega \text{ cm}^{-1}$) from water treated by reverse osmosis ($50\text{--}100 \text{ k}\Omega \text{ cm}^{-1}$). Ion exchange resins can be replaced by ion exchange textiles, which present a higher porosity and allow operation at high flow rates. Moreover, due to their sheet form, ion exchange textiles maintain their shape and dismantling of ED stacks for clearing or repair is easier.

The second historical application of ED is the concentration of recovered salts to high levels. That capa-

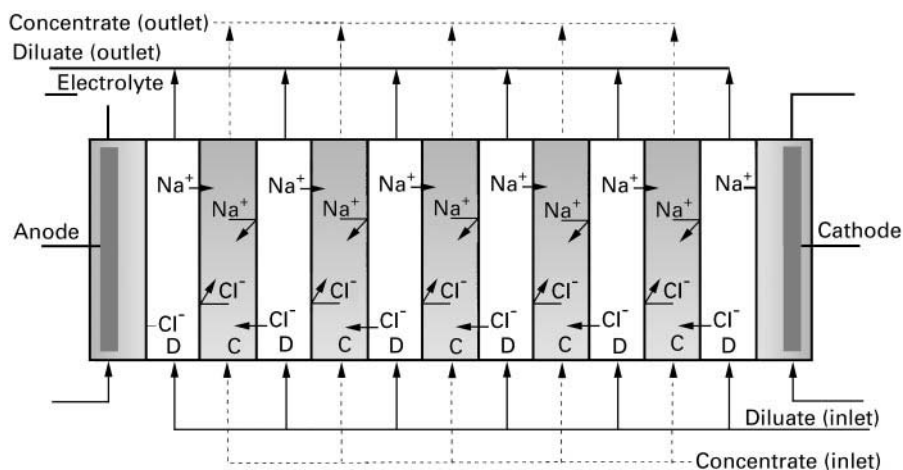


Figure 11 Schematic of a conventional two-compartment electrodialysis applied to the reconcentration/diffusion of NaCl solutions. C and D, concentrate and diluate.

Table 1 Applications of electrodialysis with homopolar membranes

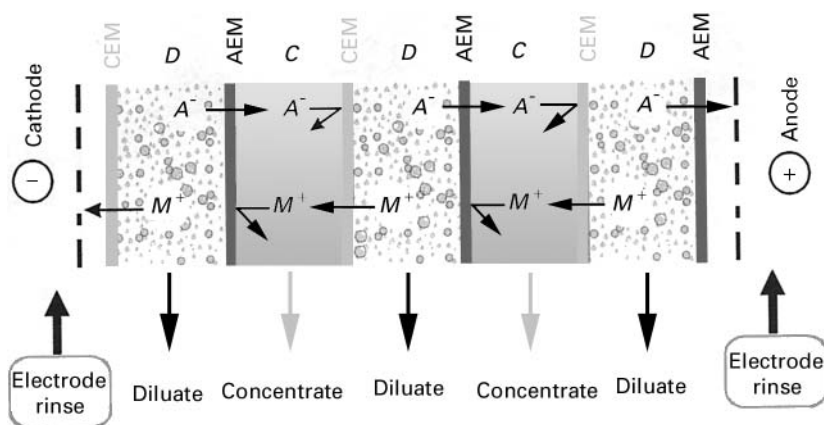
<i>Reduction of electrolyte content</i>	<i>Recovery of electrolytes</i>
Potable from brackish water	Pure NaCl from seawater
Food products, milk whey, fruit juice	Ag(I) salts from photographic waste
Nitrate from drinking water	Ni(II) from electroplating rinse water
Rinse water for electronics	Zn(II) from galvanizing rinse water
Effluent streams	Salts of organic acids from fermentation broths
Electroless plating baths	Acids from metal pickling baths and rinse
Protein hydrolysates	Amino acids from protein hydrolysates
Sugar and molasses	HCl from cellulose
Potassium tartrate from wine	
Chloride purge in kraft paper process	<i>Miscellaneous</i>
Photographic developer regeneration	Ion substitution

bility has been used for the recovery of crystalline NaCl from seawater. There are several ED plants in Japan with 100 000 m² of ED membranes being used for NaCl recovery from seawater. Another important field of ED application has been in whey desalting. Whey is a by-product from cheese making containing useful quantities of proteins, lactose and lactic acid. However, the high mineral content makes it unacceptable for human consumption and of marginal value for animal feed. In terms of membrane area installed, this application is the third largest ED process. ED also has important applications in the pharmaceutical and biochemical industries, where gentle processing conditions are required for materials such as human blood plasma. The production of essential amino acids will require various demineralization steps. Certain waste streams in biochemical and pharmaceutical operations contain ammonium sulfate, urea and guanidine hydrochloride which can be recovered by ED. There are several other applications of ED for salt removal which include the production of protein fractions and the separation of amino acids into acidic, basic and neutral groups. Concerning this

latter example, amino acids are mainly produced from protein hydrolysates. The solutions obtained contain both natural amino acids and inorganic salts and therefore necessitate a demineralization step. **Figure 13** shows the two-compartment ED configuration for this operation. The hydrolysates to be treated are generally mixtures containing 2–3 mol L⁻¹ of amino acids and 2.5 M NaCl at pH 5–6.

The diluate containing hydrolysate is demineralized from 2.5 M to 0.2 M without significant loss of amino acids. Such a process is running on an industrial scale in Europe. The second step is the obtention of fractions of amino acids. This operation is achieved by a four-compartment ED as depicted in **Figure 14**. Charged amino acid forms are less mobile than the ions of the salts. During this operation pure anionic and cationic amino acid fractions are obtained in the concentrate compartments (C1 and C2, respectively), while the zwitterionic forms remain in the diluate D1. The zwitterionic fraction will then be purified using a BPM.

ED is also applied to the treatment of inorganic media. The metal-finishing industry offers numerous

**Figure 12** Schematic of the electrodeionization process. The ion exchange material (resin or textile) fills the diluate compartment.

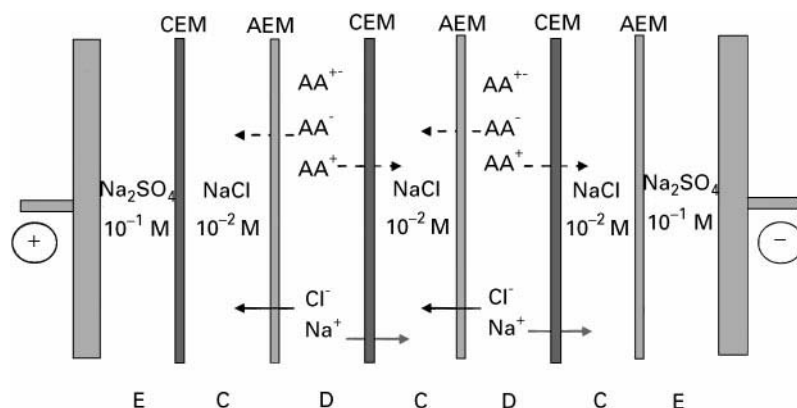


Figure 13 Schematic of the demineralization of protein hydrolysates by electrodialysis. (Reproduced from Sandeaux *et al.*, 1998, with permission from John Wiley & Sons Limited.)

applications for ED in pollution control and material recovery. The rinse streams from such processes pose pollution problems. They are usually too dilute for direct metal recovery and too concentrated for disposal. For example, ED processing of a rinse stream from a nickel electroplating system allows the production of a dilute stream to be recycled in the rinse tank and a concentrated stream which can be recirculated in the electrodialysis to build up its metal content to a level that is useful for further recovery or direct return to the plating bath. Other similar applications concern the removal of phosphite from an electroless nickel bath or the recovery of HF and HNO₃ used to clean stainless steel.

Industrial countries are increasingly concerned with environment protection issues. The treatment of spent acids containing divalent metallic salts is a problem in several industries where these acids are used in pickling and surface treatment of metals. ED is an attractive technique for treating these waste acids because purified and reconcentrated acids can be obtained and reused. The advantage of this process

is not only the possibility of recycling acids but also the production of lower amounts of salt effluents or sludges. For example, the recovery of sulfuric acid from effluents containing metallic salts (Mg, Zn, Mn, 50 g L⁻¹) in an H₂SO₄ solution (200 g L⁻¹) from zinc hydrometallurgy is achieved in a two-compartment ED cell with modified CEMs having high selectivity protons/multivalent cations, and AEMs having a low proton leakage (Figure 15). A solution of 150 g L⁻¹ H₂SO₄ containing less than 0.5 g L⁻¹ of metals was so obtained.

Electrodialysis with Bipolar Membranes

A large number of applications have been identified. The applications have been classified under the broad categories of pollution control/resource recovery and chemical processing in Table 2.

The oldest industrial application of EDBM in pollution/control resource recovery is the recovery of HF and HNO₃ from a stream containing KF and KNO₃ generated from pickling baths in the steel plant.

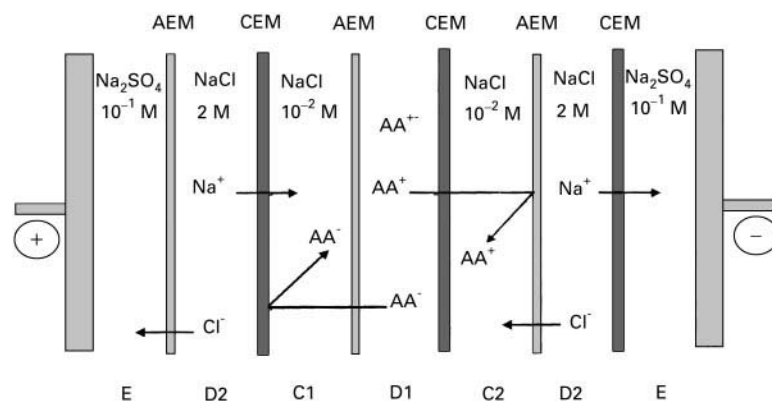


Figure 14 Schematic of four-compartment electrodialysis for obtaining anionic forms (in C1), cationic forms (in C2), and zwitterionic amino acids (remaining in D1). (Reproduced from Sandeaux *et al.*, 1998, with permission from John Wiley & Sons Limited.)

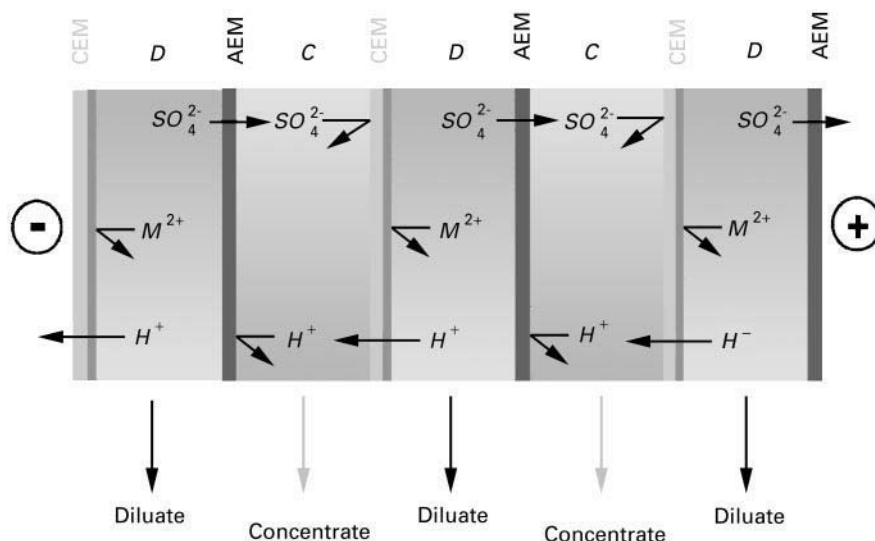


Figure 15 Schematic of the recovery of an acid by electrodialysis. Diluate: H_2SO_4 and MSO_4 . Pure H_2SO_4 is obtained in the concentrate.

This first commercial use of BPM began operation in 1987 at Washington Steel in Pennsylvania. **Figure 16** illustrates the process. Spent pickling acid is neutralized with KOH to precipitate the heavy metals, which are then removed by filtration. The remaining neutral solution of $\text{KF} + \text{KNO}_3$ is then treated in a three-compartment EDBM cell in which the salts are split to form KOH, which is directed to the neutralization tank, and the mixed acids ($\text{HF} + \text{HNO}_3$),

which are directed to the pickling operation. The dilute salt solution from the salt compartment of the EDBM process is then reconcentrated by conventional ED and is then returned to the bipolar stack, while the diluate is used to rinse the filter cake.

The main application of EDBM in chemical processing is the recovery of organic acids which can be recovered from fermentation. The performance of fermentation is better when the pH is slightly higher

Table 2 Some technology applications of water splitting on BPM

<i>Pollution control/resource recovery</i>	
HF/mixed acid recovery	Stainless steel pickle liquor recovery HF/NaOH recovery from spent aluminium potlinings Fluorosilicic acid conversion to HF, SiO_2 Fluoride emission control in chemical processing
Sulfate recovery	Battery acid recovery Waste sodium sulfate conversion Sodium sulfate conversion in rayon manufacture
Nitrate recovery	Ammonium nitrate conversion from uranium processing KNO_3 conversion Recovery of catalyst used to cure epoxy resins in Al coating moulds
Amine recovery	Sodium alkali recycling in pulping and bleaching operations
Pulp and papers	Soxal® process SO_2 recovery
Flue gas desulfurization	Dry sodium scrubbing alkali recovery
<i>Chemical processing</i>	
Organic acid production recovery	Acetic, formic, acetylsalicylic and organic acids Amino acids
Ion exchanger regeneration	Production of highly generated ion exchange resins
Potassium and sodium mineral processing	KCl conversion Solution mining of trona and subsequent sodium alkali production
Sodium methoxide production	Sodium alkali production from natural brines and solid trona
Methanesulfonic acid production	EDBM in methanolic solutions
High purity water production	EDBM of sodium methanesulfonate Continuous electrodeionization

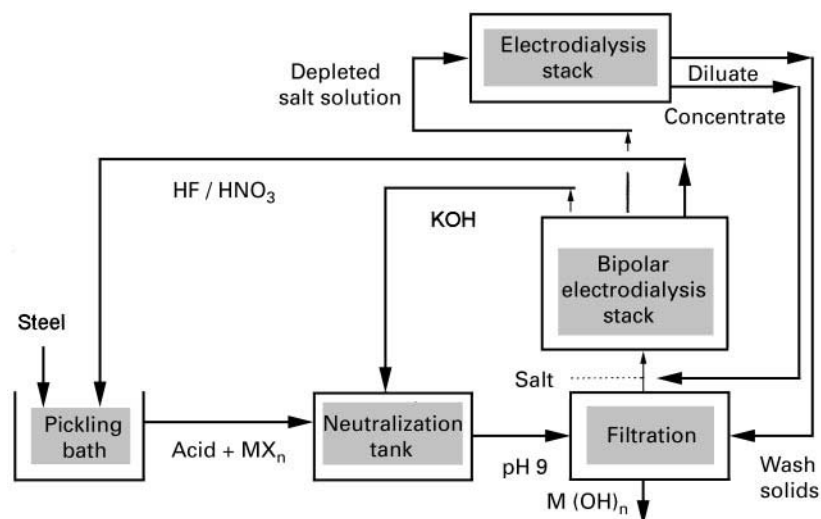


Figure 16 Process for recycling of HF/HNO₃ steel pickling solution using bipolar membrane electrodesialysis. (Reproduced with permission from Davies *et al.*, 1997.)

than the pK_a of the organic acid to be produced. This condition requires addition of a base to maintain this elevated pH. Thus, the product of the fermentation is a dilute salt of the organic acid. For example, in the case of lactic acid production, the conventional process requires many different ion exchange steps, resulting in a high volume of wastewater and organic solvents that have to be recovered. In addition, possible losses of product and a potential contamination

of the product have to be taken into account. The recovery of lactic acid from fermentation broth can also be performed by the use of two ED steps. In the first, the dilute sodium lactate solution is concentrated by a conventional two-compartment ED. This step also purifies the product because only the ionized components of the broth are transported by the current through IEMs. The other components of the broth are redirected to the fermentation reactor. In

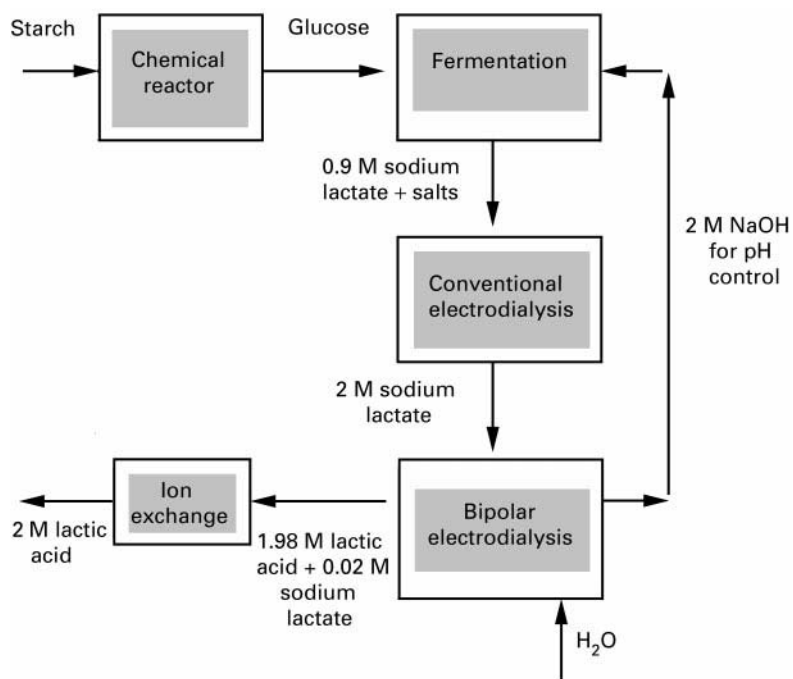


Figure 17 Schematic of the production of lactic acid from fermentation broth using both conventional electrodesialysis and bipolar membrane electrodesialysis. (Reproduced with permission from Davies *et al.*, 1997.)

the second step, the concentrated sodium lactate is split in a two-compartment bipolar ED with a CEM (configuration of **Figure 10A**) to generate lactic acid and NaOH. The acid stream, still containing Na^+ ions, is then purified by a cation exchange resin, while caustic soda is recycled to the fermenter for pH control. For economical reasons in the bipolar ED step, the conversion rate of sodium lactate is kept at 95%, but almost 100% could be easily achieved. A simplified schema of this process is reported in **Figure 17**.

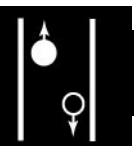
Conclusion

ED with homopolar membranes was first developed several years ago, essentially for desalting brackish waters and reconcentrating brine for seawater. Conventional ED is also widely used on a large industrial scale in the dairy industry for demineralization of whey. The technical feasibility of applying ED with BPMs to a variety of commercially interesting processes has been demonstrated. ED techniques are very promising because they can be applied to environmental protection (depollution and recycling of chemicals) and to bioindustries (food, pharmaceuticals and biotechnology). For all these kinds of applications, special membranes have been elaborated showing adapted selectivity in ion transport under an electric driving force. For improvement of most of the other applications of ion exchange membranes, research is mainly focused on the membrane processes themselves rather than on the synthesis of new membranes.

Further Reading

- Daufin G, René F and Aimar P (eds) (1998) *Les Séparations par Membrane dans les Procédés de l'Industrie Alimentaire*, Collection: Sciences et Techniques Alimentaires. Paris: Lavoisier.
- Davies TA, Genders JD and Pletcher D (1997) *Ion Permeable Membranes*. Alresford, UK: Electrochemical Consultancy/Alresford Press.
- Gavach C, Bribes JL, Chapotot A *et al.* (1994) Improvements of the selectivity of ionic transport through electrodialysis membranes in relation with the performances of separation electromembrane processes. *Journal de Physique IV, Colloque C1 4*: 233.
- Mani KN (1991) Electrodialysis water splitting technology. *Journal of Membrane Science* 58: 117–138.
- Mani KN, Chandla FP and Byszewski CH (1988) Aquatech membrane technology for recovery of acid/base values from salt stream. *Desalination* 68: 149.
- Mulder M (1991) *Basic Principles of Membrane Technology*. Dordrecht: Kluwer.
- Sandeaux J, Sandeaux R, Gavach C *et al.* (1998) Extraction of amino acids from protein hydrolysates by electrodialysis. *Journal of Chemical Technology and Biotechnology* 71: 267.
- Scott K (1995) *Handbook of Industrial Membranes*, 1st edn. Oxford: Elsevier.
- Sistat P, Huguet P, Resbeut S *et al.* (1999) Polymeric ion-exchange membranes: material, characterization, transport analysis, applications. In *Recent Research Developments in Electroanalytical Chemistry*. India: Transworld Research Network.
- Strathmann H (1996) *Electromembrane Processes*, Membrane and Science Technology Series. Oxford: Elsevier.

ENVIRONMENTAL APPLICATIONS



Flotation

M. A. Burstein, NPACI Edcenter on Computational Science and Engineering, San Diego State University, San Diego, CA, USA

I. M. Flint, CPTI, Vancouver, BC, Canada

Copyright © 2000 Academic Press

Introduction

Flotation is the selective separation of solid particles, liquid droplets, chemicals or ions, or biological entities from a bulk liquid, based on their surface properties. In the process two actions occur: the collision

between rising bubbles and matter suspended in the liquid, followed by adhesion of the particle to the bubble surface and separation of the resulting bubble-particle aggregate from that liquid. Environmental application of this technology includes the selective separation of specific solids or liquids from solid suspensions, liquids from liquid suspensions or certain dissolved species from solutions.

Separations which are based essentially on the adsorption from solution include colloidal suspensions of solid or liquid products, and the separation of certain dissolved substances and ions. In order to make a separation, there must be a drop in free energy for the removed substance when it attaches to the bubble. For selective separations this drop must significantly exceed those of the competing ions or colloids. In general, this results when the substance to

be removed is hydrophobic (if it is separate phase) or surface-active (if it is dissolved) and the substances to remain with the carrying liquid are hydrophilic.

There are many variations of flotation vessel that attempt to perform these actions, including induced air machines like flotation columns, agitated tanks and turbulent contact vessels; dissolved air flotation units; or electroflotation units where electrolytic bubbles are the carrier. The principal factor which influences the design is the ability of the unit to generate bubbles of a size that will maximize the likelihood of attachment of the dispersed particles and removal of bubble-particle aggregate from suspension.

Hydrocarbon Removal from Water

Flotation itself is not restricted by the concentration of the input contaminates, but the equipment used may be limited in its fractional removal and the purity of its products. Liquid hydrocarbons are generally highly hydrophobic and form very stable bubble aggregates. However, low density differences between the hydrocarbon and water mean that the droplet velocity relative to carrying water flow is low. As the relative velocity between the rising bubble and the settling droplet in a still suspension is low, flotation columns, with their quiescent collection environment are generally used to separate larger droplets, whereas mechanical cells can operate on smaller sizes and high intensity contact devices on yet smaller sized droplets. However, the high turbulence devices produce a large population of very small bubbles which, because of their low rise velocity, cannot easily be separated from the transport water. Depending on the droplet size distribution, with conventional units the residual hydrocarbon concentration in the water will be limited to purity levels between 10 and 30 p.p.m.

Recent designs specifically engineered to overcome the small bubble problem have produced aqueous underflow with less than 6 p.p.m. hydrocarbon content. This improvement trend is expected to continue as the principles behind fine bubble separation are better understood.

Some products that can be separated from water using this technology are diesel, motor oils and other automotive products, crude oil and tar sands products, creosote, polyaromatic hydrocarbon and polyaromatic phenol groups, chlorinated hydrocarbons, plant and animal oils, waxes, and many paints and organic solvents.

Usually, flotation is used after settling tanks for oil-water separation and prior to granular media filters. Typical applications are offshore platforms, oil refineries, large garages and vehicle service sta-

tions, and also at machinery plants where oil testing of production is used. On offshore platforms, natural gas is supplied instead of air to float hydrocarbon droplets and remove them to an oil pad.

Typically, for oil-water separation, a froth layer is not formed and oil is removed in a form of oil pad continuously or in batch mode by rising liquid level in the vessel.

Rendering By-Product Recovery

In the food industry, the processing of fish, fowl, wool or slaughterhouses produces a stream of liquid that carries animal oils and/or suspended solids. These streams have a high oxygen demand and often cause odour problems. The organic contaminants can be removed by flotation. This can be done by first screening and/or settling the process stream to remove larger products. The remainder is floated in a quiescent vessel to remove the larger products, followed by more intense flotation contactors to remove remnant oils. A properly designed circuit should recover all but approximately 10 p.p.m. of the organic wastes.

Reprocessing of Existing Mineral Waste Dumps

Flotation is used in the processing of secondary materials in mining industry. As high grade mineral deposits are exhausted, reprocessing of old tailings dams and ponds, stockpiles of low grade and oxidized ores as well as metallurgical slags becomes economically feasible with technical improvements in processing. It will also extend the lifetime cycle of mines and concentrators. Although this reprocessing of waste dumps and tailings dams will in turn produce new dumps and dams, they will be of a lower metal content so that acid damage will be reduced. In many cases, the grade of waste material from 50–100-year-old mines is higher than that of ores mined today, for example, copper content in old tailings dams is often over 0.8%, whereas its typical content in run-of-mine porphyry ores is 0.4–0.6%. Reprocessing of mine tailings usually does not require substantial expense because the particle size has already been reduced to the point that different mineral crystals are liberated from each other.

Site Run-off Treatment and Soil Decontamination

Many sites, such as pole treatment yards, truck and bus-washing facilities, and others which are still in use may be producing surface run-off or underground

plumes of contaminants. Most of these steams contain contaminants that are floatable. Also, flotation is becoming widely used for soil treatment at industrial and military sites, where soil contains substantial concentrations of oil or other chemical poisonous products.

Run-off water is collected by ditching and the contaminated feed is pumped to a processing facility. The first stage of separation is usually a gravity mixer settler, in which the resident liquid contains about 50% of organic matter, which effectively coalesces the finer organic droplets. The residence time of the suspension in the settling unit has to be sufficient to ensure that the coalesced droplets report to the organic-rich product stream. The required residence time is dependent on the hydrocarbons to be removed. The organic-rich stream is bled off and may be burned or shipped off site after passing through a further aqueous coalescing device. The aqueous stream, or underflow of the gravity separator, then passes through a hydrocyclone (high capacity streams only) followed by a flotation cell. The organic products of both the hydrocyclone and flotation device are recycled to the mixer settler for further processing. The aqueous stream, or underflow of the flotation device, is the final product to be returned to the environment.

The system for processing plume water is the same as run-off water, with the exception that a series of wells must be made to lower the water table locally, thus preventing water from leaving the contaminated site. This well water is then processed with the site run-off water.

Flotation systems can have very high capacities and produce a high purity final aqueous stream. However, they are more expensive than gravity units at low throughputs.

Possible Effluent Treatments

Ion flotation is widely used to extract ions from aqueous solutions. Bubbles can be stabilized by surfactants of various types. The bubble surface charge can thus be tailored to affect the preferential removal of a specific ion or ionic complex. Normally, some reagent (collector) is added to improve ion sorption at the gas-liquid interface. As ion flotation is a mass transfer process of dissolved substances, its rate is proportional to a specific bubble surface area. Therefore, minimizing the average bubble size is critically important; dissolved air, electroflotation, cavitation, or high turbulence are used to generate microbubbles. It includes saturation of feed stream with dissolved air at high pressure, and then releasing the pressure to atmospheric and discharging into a clarifier-type

vessel. Similarly, microbubble dispersions can be used to float colloidal solids, although it is usual to add coagulants to increase the size of the colloidal aggregates.

Flotation systems can operate under externally supplied electrical potentials which, by altering the surface charge of the particles in the field, will optimize bubble-particle attachment. As bacteria and other microorganisms such as microalgae, are normally hydrophobic, they potentially can be removed from water by microbubble flotation.

Flotation is used as the main method for de-inking of recycled paper. The aim of the process is to remove only the ink from wastepaper fibres suspended in a slurry. Under current practice using conventional mineral-processing mechanical cells, it is not possible to get a fibre-free ink-rich overflow product. The disposal of this as landfill is both expensive and environmentally objectionable. For these reasons, and because the partially de-linked product only has a limited use in low quality products, there is a need for the replacement of the existing cells by units specifically designed for this application.

Conclusions

The number of environmental applications of the flotation process has increased dramatically over the last 10 years. This trend will continue in the foreseeable future, as increased environmental concerns are manifested with respect to the treatment of liquid effluents and solid waste materials.

The treatment of these effluents will lead to the development of unconventional devices and methods for flotation of ultra-fine particles, ions and aggressive media.

The relatively low capital and operational costs of flotation make it attractive for industrial use as an integral part of the flow sheet.

See also: I/Flotation. II/Flotation: Cyclones for Oil/Water Separations; Historical Development; Oil and water Separation. III/De Inking of Waste Paper: Flotation.

Further Reading

- Clift R, Grace JR and Weber ME (1987) *Bubbles: Drops and Particles*. New York: Academic Press.
- Finch JA and Dobby GS (1990) *Column Flotation*. New York: Pergamon.
- Levenspiel O (1972) *Chemical Reaction Engineering*, 2nd edn. New York: Wiley.
- Lynch AJ, Johnson NW, Manlapig EV and Thorne CG (1981) *Mineral and Coal Flotation Circuits, Their Simulation and Control*. New York: Elsevier.

- Pinfold TA (1972) Chapter 4: Ion flotation. Chapter 5: Precipitate flotation. In: Lemlich R and Arod J (eds) *Adsorptive Bubble Separation Techniques*, pp. 53–90. New York: Academic Press.
- Rubinstein JB (1995) *Column Flotation, Processes, Designs and Practices*. Basel, Switzerland: Gordon and Breach.
- Seba F (1962) *Ion Flotation*. New York: American Elsevier.
- Zhou ZA, Xu Z and Finch JA (1994) On the role of cavitation in particle collection during flotation – a critical review. *Mineral Engineering* 7: 1073–1084.

Gas Chromatography–Mass Spectrometry

N. Scott and G. Gutnikov, California State Polytechnic University, Pomona, CA, USA

Copyright © 2000 Academic Press

Introduction

Increasing public concern over environmental pollution reflects the heightened awareness of the toxicity of a large number of chemicals that find extensive application in wide-ranging fields. The consequent impetus to reduce chemical contamination of the environment has generated a growing body of legislation and mechanisms for enforcement via specific regulatory agencies. For example, following the discovery of trihalomethanes in chlorinated drinking water in the 1970s the Safe Drinking Water Act (SDWA) was passed that directed the United States Environmental Protection Agency (US EPA) to undertake a comprehensive study of the contaminants present in drinking water. The pre-eminent technique employed in these investigations was gas chromatography with mass spectrometric detection (GC-MS). The distinctiveness of the mass spectra of the target analytes and their volatility were two vital characteristics required for GC-MS. As the studies initiated by the SWDA yielded results, GC-MS has been recommended for analysis of many environmental contaminants.

Since many pollutants occurring at trace levels in complex matrices are either volatile or amenable to derivatization to volatile products, GC-MS has proved to be an effective means for verification of compliance with environmental regulations. GC and MS play complementary roles in the analysis of mixtures. Volatile constituents of complex mixtures may be conveniently separated by GC but not identified unambiguously with conventional detectors. MS provides much more definitive structural information that permits identification. The sample sizes necessary for GC and MS are also comparable and sample volatility is necessary for both.

The utility of GC-MS for environmental analysis has been further enhanced by the development of relatively inexpensive table-top instruments that has

brought the technique within the reach of most laboratories. Computer-assisted operation of these instruments, including automated sample injection, data acquisition, online searches of mass spectral libraries and quantification by selected ion monitoring (SIM) has led to rapid, efficient and convenient analytical systems. These advances have made compact, rugged, portable GC-MS instruments available for field applications, thereby rendering GC-MS a vital technique in environmental analysis.

Sample Pre-Treatment

The low concentrations of pollutants and the complex matrices in which they frequently occur generally preclude direct injection of environmental samples into a chromatograph. Sample pretreatment is then necessary to remove components that would interfere in the analysis and to concentrate target analytes that are present at extremely low levels. Pretreatment varies considerably with the nature of the sample and the information sought. Pollutants are dispersed in air, water and soil.

Atmospheric samples may contain numerous species ranging from gaseous to nonvolatile substances adsorbed on particles. They are usually collected in highly polished SUMMA[®] canisters and Tedlar[®] bags or on sorbents or in an impinger solution. Specifically, the EPA Compendium Method TO-14 mandates SUMMA passivated canister sampling. Particles are commonly retained on membrane filters or impactors. Gaseous components and volatile organic compounds (VOCs) are collected by trapping, either cryogenically for the most volatile or on sorbents of increasing retentivity for the less volatile.

The constituents of particulates are separated into approximately organic and inorganic substances by Soxhlet extraction or ultrasonication with an appropriate organic solvent (methanol, dichloromethane, cyclohexane, etc.) or by supercritical fluid extraction (SFE) with CO₂. SFE is becoming increasingly accepted for the extraction of analytes because it is

more rapid, reliable and efficient for a variety of matrices than the older techniques and is environmentally friendly in reducing the need for organic solvents.

The soluble fraction comprises a complex mixture of various organic compounds that may require further fractionation prior to GC-MS analysis. This has entailed separation into fractions of different polarities by such techniques as liquid–liquid extraction or column chromatography following preliminary removal of the acidic and basic components. Solid-phase extraction (SPE) has become a popular alternative because of its simplicity, speed, improved sample clean-up, easy automation and the capacity to handle multiple samples simultaneously. More recently filter discs have been introduced to perform the same functions more conveniently.

VOCs are generally preconcentrated on adsorbent traps. Different traps are often necessary as no single sorbent performs satisfactorily over the entire range of organic volatilities and polarities encountered. Two (or more) sorbents are used in tandem, first

a weak one to adsorb the heavier organics, followed by strong one to retain all the remaining. The analytes are desorbed by flash-heating from weak adsorbents (primarily graphitized carbon black and Tenax); by solvent extraction from strong ones (activated charcoals), using carbon disulfide, dichloromethane, etc. (Figure 1).

For aqueous samples preconcentration and clean-up are often achieved concurrently. In the purge-and-trap (dynamic headspace sampling) technique, the volatile species that are present in water are swept out of solution by a stream of nitrogen or helium into a sorbent trap consisting of activated carbon, Tenax or silica gel. The analytes are desorbed thermally and transferred along with the carrier gas to the GC-MS instrument. If the number of volatile compounds is few, analysis of the headspace gases is possible directly but with the drawback that water vapour is likely to be injected into the instrument.

Semi-volatile species present in water must be first extracted into a suitable organic solvent or retained

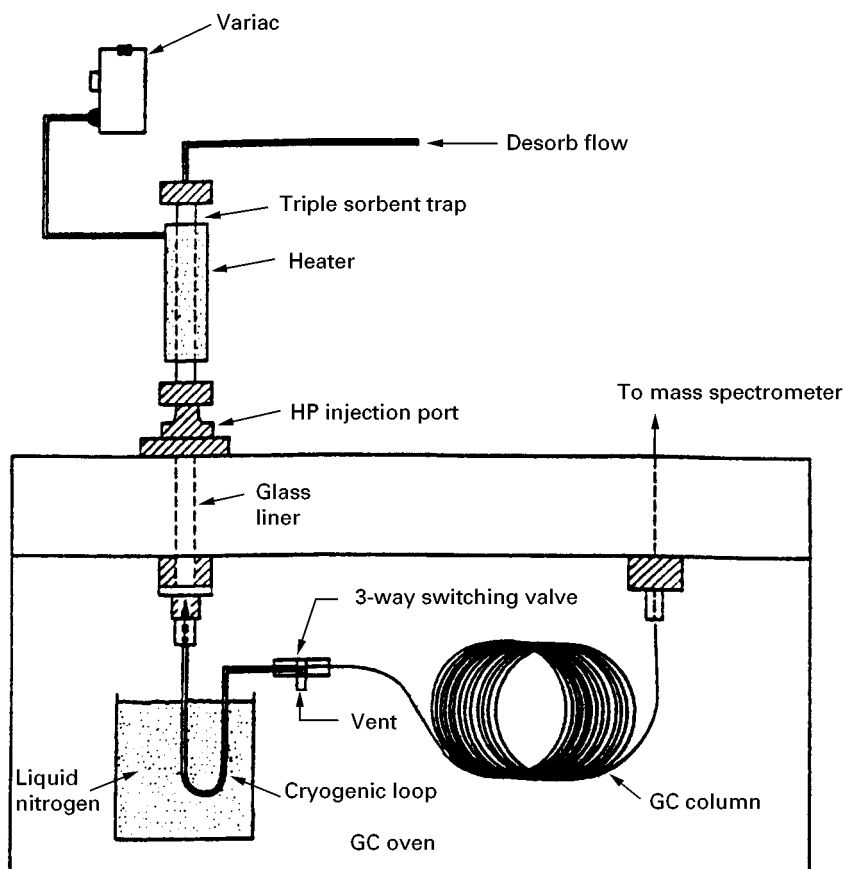


Figure 1 Schematic diagram for thermal desorption–gas chromatography–mass spectrometry system. (Reproduced from Ma C (1997) Performance evaluation of a thermal desorption/gas chromatographic/mass spectrometric method for the characterization of waste tank headspace samples. *Environmental Science and Technology* 31(3): 853–859, with permission from the American Chemical Society.)

on an SPE cartridge and then eluted for injection. The polarity of the organic stationary phase, which is bonded to a silica support, determines the retention selectivity.

For solid samples, VOCs are first extracted into methanol, which is then added to water for purge-and-trap. For extraction of semivolatiles from solid samples SCF is particularly advantageous. The extracted analytes collect in an appropriate solvent on reducing the pressure to atmospheric level.

Sample pretreatment is beset with a serious problem – the potential loss of analytes – which necessitates monitoring solute recovery by employing internal standards with similar properties. Also accumulation of water during preconcentration can affect the GC-MS instrument, especially the pumps necessary to maintain the vacuum. A remedy that has been attempted is the use of Nafion diffusion dryers, but this may cause the loss of small, polar organic compounds.

Instrumentation

Capillary columns (0.32 mm i.d.) of appropriate polarity are routinely used in view of their greater efficiency. However, for relatively high concentrations megabore capillary columns (0.53 mm i.d.) are preferred with connection to the mass spectrometer ion source being achieved via a glass jet separator for whose optimum functioning a stream of make-up gas is provided. This approach has been widely used for the analysis of ambient air samples; waste and solid samples; purge-and-trap analysis; as well as thermal desorption analysis of sorbent tubes.

The mass spectrometer of a GC-MS system must be capable of rapid response to monitor the solutes that are eluted from the chromatographic column in quick succession. Hence ion trap and quadrupole instruments are the most widely used mass analysers. The compact ion trap detector (ITD) also enhances the portability of GC-MS instruments for field analysis.

Calibration of a mass spectrometer is usually based on the diagnostic ions of either perfluorotributylamine (PFTBA) or perfluorokerosene (PFK). However the US EPA has introduced m/z abundance calibration for checking the performance of the entire GC-MS system, not merely of the mass spectrometer. Two compounds mandated for this purpose are bromofluorobenzene (BFB) for volatile analytes and decafluorotriphenylphosphine (DFTPP) for semivolatiles.

Electron impact (EI) ionization is the most widely used mode of ionization mainly because the databases available for mass spectral library searches (such as those provided by the National Institute of Science

and Technology and John Wiley & Sons) are compilations of EI-mass spectra. However, negative chemical ionization mass spectrometry (NCIMS) is used sometimes, e.g. for the analysis of positional isomers of nitropolycyclic aromatic hydrocarbons via high resolution mass spectrometry (HRMS). Organophosphates can be analysed by either EI or CI.

Quantification of very low concentrations necessitates operating in the SIM mode. SIM involves acquiring ion currents only at a few specified m/z values that are characteristic of the analyte(s). Data acquisition in this mode avoids sampling the barren regions of a full scan spectrum, thereby improving the ion counting and the sensitivity of detection. Internal standards are usually isotopically labelled compounds that may be purchased individually or as mixtures from agencies such as the National Institute of Science and Technology (NIST) or the EPA.

Despite enhanced sensitivity, SIM limits the detectable analytes to those producing ions of the specified m/z values. Hence, for identification, scanning the entire mass spectrum of each compound may be necessary. But this compromises the detection sensitivity. Therefore one strategy is to use GC with a multi-detector system (GC/MD) in conjunction with GC-MS. The multidetector system enables sensitive quantification while the mass spectrometer operated in the full-scan mode enables identification of some of the unknown pollutants. The primary quantification system is thus the GC/MD system that comprises conventional GC detectors such as FID, PID (photoionization detector) and ECD (electron-capture detector).

Applications

Environmental analysis serves different objectives, including routine monitoring, quality assurance, litigation and research. The list of target pollutants and the desired detection limits undergo continual revision in light of toxicological research. For the determination of a particular pollutant at the desired level of sensitivity, the same analytical technique is not adopted by all environmental agencies. GC-MS is sometimes mandated, sometimes suggested as an alternative method. Hence some examples that are presented in this article may not (yet) be approved by regulatory agencies but are nevertheless acceptable to environmental chemists as representing the wide applicability of GC-MS in this field.

The US EPA classifies organic pollutants into two classes: volatiles (compounds that exist as gases at room temperature and are easily removed from the sample matrix); and semivolatiles (compounds that can also exist as gases but need some form of extraction to be removed from the matrix). Both

classes of compounds occur in outdoor, indoor and workplace atmospheres as well as in soil and water, and their concentrations may range from 100 ppm in the vicinity of emission points to a few parts per trillion (ppt) in pristine environments. The components of a particular mixture are likely to occur at different concentrations, with the more toxic target compounds being at times at much lower levels than the less hazardous ones.

VOCs for which US EPA approved GC-MS methods of analysis exist cover a broad range of compounds, including highly volatile organics (carbon tetrachloride, chloroform, acrylonitrile, allyl chloride, etc.); semivolatile organics (benzene, nitrobenzene, chlorobenzenes, toluene, trichloroethane, etc.); *N*-nitrosodimethylamines; polychlorinated dibenzo-*p*-dioxins (PCDDs) and polychlorinated biphenyls (PCBs); and a variety of miscellaneous compounds including chlorinated compounds and aromatics.

A major fraction of VOCs are hydrocarbons, especially by roadsides where traffic is heavy. For example, in West Los Angeles, petroleum residues are the main solvent-soluble organic fraction of carbonaceous aerosols. For analysis, these particles are collected on quartz filters and extracted by ultrasonication first with hexane and then with benzene/isopropanol. The extracted constituents are determined by high resolution gas chromatography-MS. A bonded OV-1701 (86% dimethyl/14% cyanopropylphenyl polysiloxane) column and a quadrupole mass spectrometer operated in the EI mode have been employed in such studies.

Hydrocarbon contamination of ground water and soil often occurs through leaking fuel tanks. In the California Leaking Underground Fuel Tank (LUFT) method GC-MS is preferred to GC-FID for monitoring such leakage without interference by other semivolatile species. The most abundant ions in the mass spectra result from the fragmentation of C_{10} – C_{23} *n*-alkanes and occur at m/z values of 43 and 57. They correspond to $C_3H_7^+$ and $C_4H_9^+$, respectively, and are regarded as qualifier and target ions for monitoring purposes.

GC-MS is an invaluable technique for chemical fingerprinting of crude oil spills in land or marine environments. Initial screening by fluorescence spectroscopy and GC is followed by GC-MS identification of specific compounds such as steranes, triterpanes, phytanes, pristanes, etc., that are most resistant to weathering. Similar analysis of tarballs, which are formed by highly weathered oils, may enable identification of the petroleum source (Figure 2). When considerably more components are monitored, multivariate and pattern recognition statistical analysis methods become necessary for data interpretation.

In order to avoid the cumbersome process of determining individual compounds, more convenient methods have been accepted as regulatory benchmarks. These include the GC-MS or GC-FID analysis of total petroleum hydrocarbons (TPH) or mixtures of benzene, toluene, ethylbenzene and xylene isomers (BTEX). In the TPH method the total area of unresolved and resolved chromatographic peaks is measured.

Interest in monitoring the indoor environment has been prompted by the well-known 'sick building syndrome'. The environment indoors can be worse than that outdoors because of the accumulation of volatile pollutants owing to poor air circulation. These pollutants not only enter from the air outdoors but are also released from building materials and furnishings, cleaners, air fresheners, gas-burning stoves, etc. GC-MS has been invaluable for their analysis following preconcentration on Tenax and thermal desorption. Separation has been achieved on a bonded SE-54 capillary column with temperature programming (Figure 3).

Polycyclic aromatic hydrocarbons (PAHs) are ubiquitous environmental contaminants with carcinogenic properties and present an analytical challenge because of the complexity of the mixtures in which they exist as many different isomers of the parent compounds. Hence a separation step is indispensable but volatility requirements restrict the applicability of GC to compounds of low and moderate molecular mass, the heavier ones being analysed by HPLC with fluorescence detection. PAHs are isolated from airborne samples by a combination of a Teflon filter and polyurethane foam sampling; from solid matrices either by extraction with SCF employing carbon dioxide, or by microwave-assisted extraction (MAE) into an organic solvent. For concentration and sample clean-up SPE with combined C_{18} amino (NH_2) or cyano (CN) solid phases can be employed with subsequent elution being carried out with CH_2Cl_2 . Deuterated PAHs are available from US EPA to serve as internal standards. More than 60 compounds encompassing parent PAHs, their alkylated derivatives and heterocyclic analogues have been analysed at 5–100 ppb levels with a DB-5 capillary column employing both the scanning and SIM modes. Of even greater toxicological interest are the nitro-PAHs that have been ranked by the International Agency for Research on Cancer (IARC) as probable human carcinogens. Their analysis is even more difficult because of the much lower concentrations and the presence of many positional isomers. Moreover, unlike the parent PAHs, nitro-PAHs are not fluorescent, thereby limiting the sensitivity attainable by HPLC. Hence GC-NCI-MS is the technique of choice for the

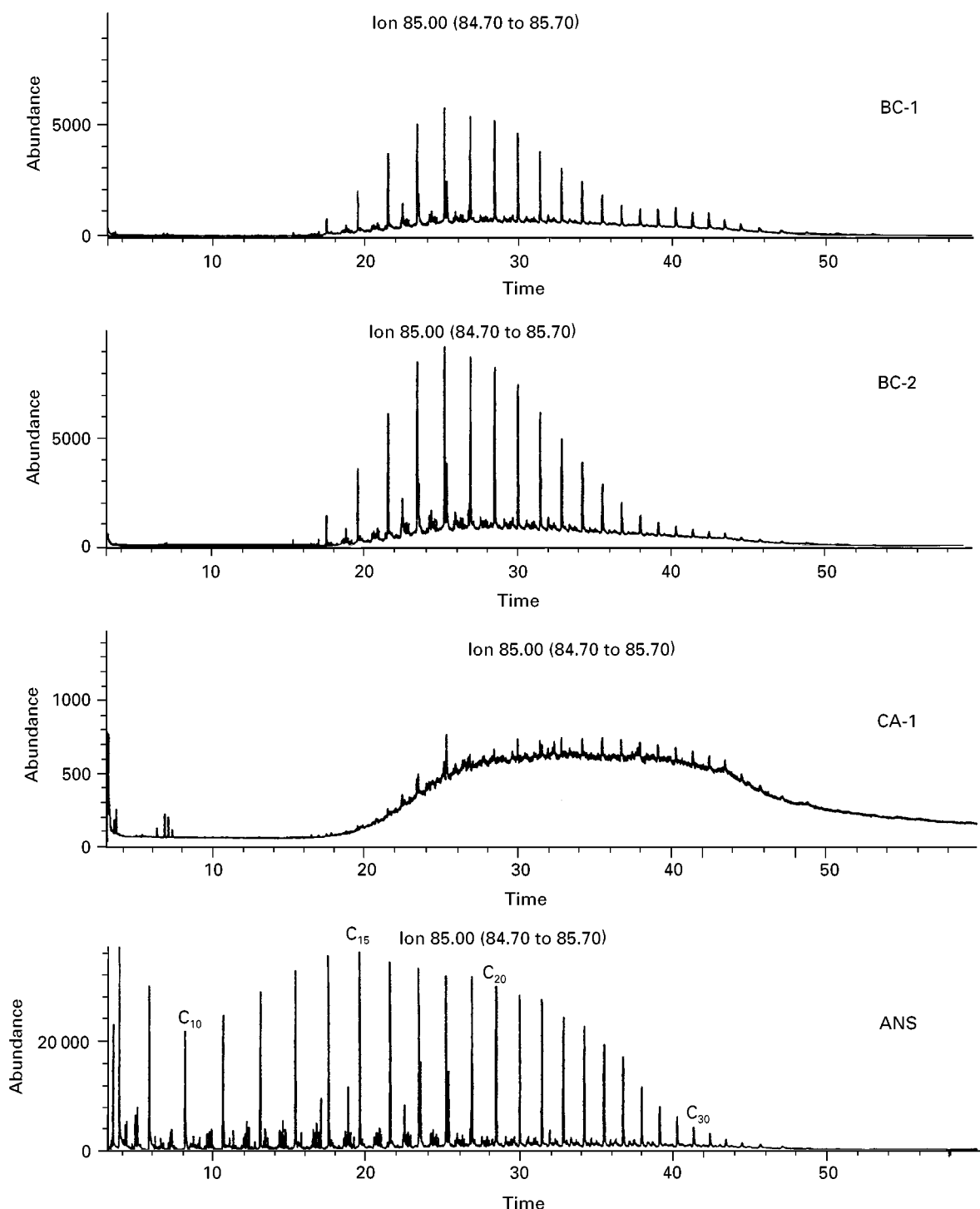


Figure 2 GC-MS *n*-alkane distribution patterns (m/z 85) for tarball samples BC-1, BC-2, CA-1 and ANS reference oil. (Reproduced from Wang Z *et al.*, 1998, with permission from Wiley–VCH.)

determination of nitro-PAHs. Polar or moderately polar capillary columns have been utilized for their separation with d_9 -1-nitopyrene or d_5 -dinitropyrene serving as internal standards for quantification.

Organochloro and organophosphate pesticides constitute another major category of toxic pollutants.

Chlorinated herbicides and pesticides are routinely analysed by capillary GC with MS or ECD. In view of the volatility of organophosphates GC is the technique of choice for analysis via phosphorus-specific detectors. However, MS detectors operated in the SIM mode are gaining popularity, especially with

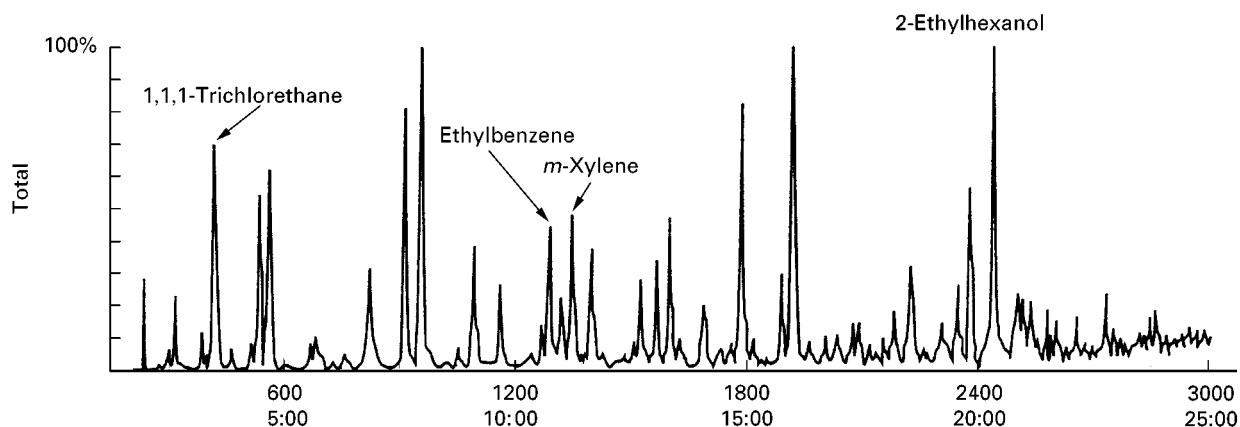


Figure 3 Indoor air at a Swedish preschool. (Reproduced from Subramanian, 1995, with permission from Wiley–VCH.)

electron impact (EI) or chemical (CI) ionization for detection at low ppb. For characterization, CI is preferred because when CH_2Cl_2 is used as reagent gas the $(\text{M} + \text{Cl})^-$ ion is formed that gives a peak at a higher m/z value, thereby enhancing selectivity.

Insecticidal carbamates readily undergo thermal degradation and hence must be derivatized with heptafluorobutyric anhydride (HFBA) prior to GC-MS analysis. Ethylenethiourea, an environmental metabolite of carbamate fungicides and an accelerator used in synthetic rubber production, has been classified by the IARC as a potential human carcinogen. Its high polarity and water solubility require derivatization to a volatile compound and extraction into an organic solvent. This has been achieved by conversion to an *S*-alkyl derivative with *m*-trifluoromethylbenzyl chloride or 3,5-bis(trifluoromethyl)benzyl bromide. GC-NCI-MS on a D-1701 capillary column and the SIM mode has permitted sub-ppb detection limits to be realized.

Other organochloro compounds of great interest include the highly toxic, and environmentally persistent, polychloro-dibenzo-*p*-dioxins (PCDDs), -furans (PCDFs) and -biphenyls (PCBs), which are generated mainly during various combustion and manufacturing processes. They usually occur as very complex mixtures of a large number of compounds. For example, there are 22 isomers of tetrachlorodibenzo-*p*-dioxin (TCDD) alone, the 2,3,7,8-isomer being the most toxic. The very similar masses of these compounds demand high mass spectrometric resolving powers for peak separation. Hence much attention has been focused on simplifying the composition of the mixtures by appropriate sample extraction and clean-up prior to GC-MS. They are extracted from solids such as soil, sediments, dust, etc., into an organic solvent and the extracts are cleaned up via column chromatography on silica gel or alumina. Analysis is invariably carried out by GC-MS. A non-

polar column such as DB-5 enables determination of homologous groups of the dioxins but a polar column such as SP-2331 is necessary for separation of most of the 2,3,7,8-congeners. EI is the usual method of ionization and ^{13}C -2,3,7,8-TCDD is widely used as an internal standard in quantification. A mass spectrometer resolving power of even 10 000 is insufficient to separate a TCDD ($m/z = 321.8936$) that is coeluted with heptachlorobiphenyl ($m/z = 321.8678$). This difficulty underscores the importance of high resolution GC-high resolution MS. Despite this difficulty, by the mid-1980s GC-MS analytical methods had been developed for the separation of all TCDD isomers and quantification at the 10^{-15} level (Figure 4).

PCBs and polychloroterphenyls, which number over 200, are stable compounds that can cause serious toxicity through bioaccumulation. PCBs have been used in transformers, hydraulic fluids, etc. The method of choice for their analysis is GC-MS. In the EI mode, a PCB molecule can lose an ortho-chlorine atom giving a $(\text{M} - 35)^+$ ion, which facilitates distinguishing between two coeluted PCBs one of which lacks an ortho-chlorine atom. NCI, with methane as reagent gas, has improved detection sensitivities 10 to 100-fold not only for PCBs, but also for other organochlorine compounds such as toxaphene, chlordane, etc. In NCI, the base peak is usually either M^- or $(\text{M} - \text{H})^-$.

Large volume (100 μL) on-column injection capillary GC-MS has been applied to the determination of aliphatic and aromatic organochlorine compounds present in process water at low ppt levels. In the extraction of these solutes into hexane, the tedium of manual operation has been obviated by an automated procedure involving a laboratory robot. This has led to significant savings in extracting solvent, sample size, labour and time of analysis.

In recent years concern over the possible use of chemical warfare agents has generated interest in

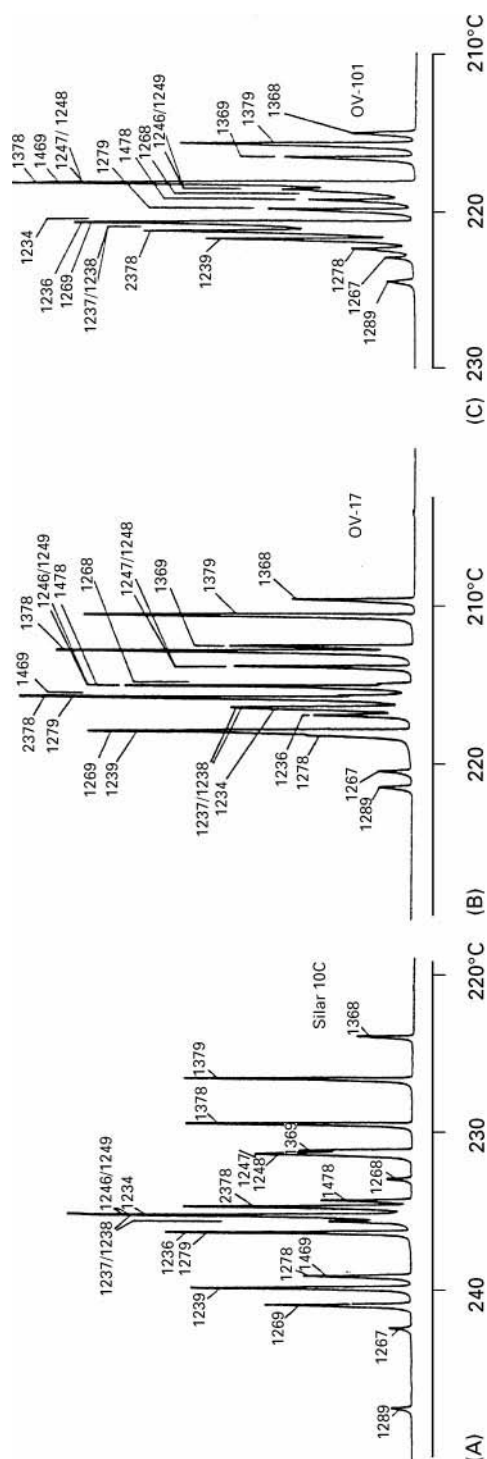


Figure 4 Mass fragmentogram (m/z 320) of a composite sampling showing elution of all 22 TCDD isomers on (A) 55 m Silar 10C, (B) 50 m OV-17, and (C) 50 m OV-101 HRGC columns. (Reproduced from Buser HR (1980) High resolution gas chromatography of the 22 tetrachlorodibenzo-p-dioxin isomers. *Analytical Chemistry* 52: 2257–2262, with permission from the American Chemical Society.)

their sensitive and reliable determination. The most common include 1,1-thiobis(2-chloroethane) (sulfur mustard gas); O-ethyl-N,N-dimethylphosphorodiamidate (tabun); isopropylmethylphosphonofluoridate (sarin) and pinacolyl methylphosphonofluoridate (soman). Their degradation products include methylphosphoric acid (MPA); iP MPA; pinacolyl MPA; cyclohexyl MPA and dithioglycol (DTG). GC-MS is advantageous for their analysis since their mass spectra are well known and available for comparison. From samples such as clothing, soil, exhumed skeletons, etc., the parent compounds are extracted into CH_2Cl_2 ; the degradation products are extracted into water and converted to *t*-butyldimethylsilyl (TBDMS) derivatives. After preliminary screening by low resolution EI GC-MS, confirmatory evidence is obtained by one of two methods: (1) GC-MS with EI or CI with NH_3 as reagent gas or (2) GC-tandem mass spectrometry (GC-MS/MS), where a precursor ion further fragments in a collisional deactivation chamber. For confirming the presence of sarin at low ppb to ppm level, GC-MS/MS using both EI and NH_3 CI has been carried out, employing two columns of different polarity (Figure 5).

GC-MS has been extended to the analysis of highly polar compounds such as aliphatic glycols that are used as antifreeze in automobiles and in aircraft de-icing. Interest in their determination stems from the

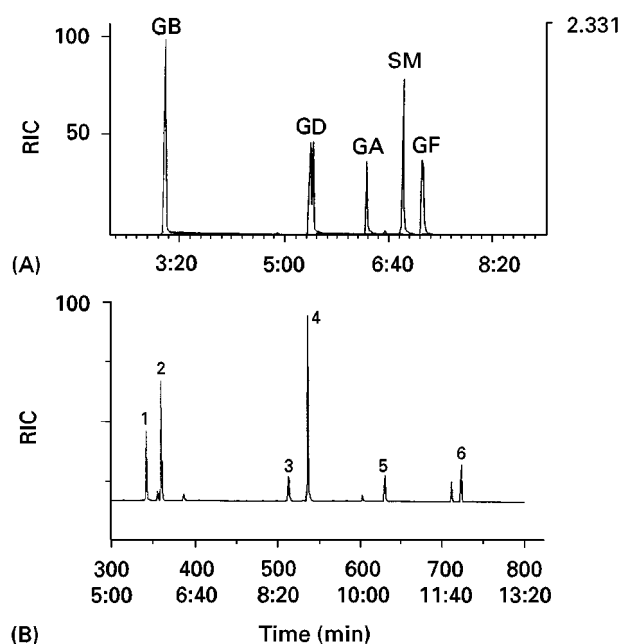


Figure 5 Reconstructed ion chromatograms for (A) nerve agents GA, GB, GD, GF and sulfur mustard (SM) (1 ng injected) and (B) TBDMS derivatives of: 1, ethyl MPA; 2, iPMPA; 3, pinacolyl MPA; 4, cyclohexyl MPA; 5, 5-cyclohexyl MPA; and 6, DTG (500 pg injected). (Reproduced from Black *et al.*, 1994, with permission from Elsevier Science.)

acute toxicity of their metabolic products. Glycols form volatile *n*-butylboronate derivatives with the characteristic $^{10}\text{B} : ^{11}\text{B}$ isotopic ratio (1 : 4) assisting in identification. Employing a DB-1 column and an ion trap detector operated in the SIM mode, sub-ppm detection limits have been attained. Haloacids that are formed during disinfection of drinking water constitute another group of polar compounds that have been analysed by GC-MS. These acids are readily derivatized to their methyl esters with diazomethane.

GC-MS interfaced to inductively coupled plasma-mass spectrometry (ICP-MS) enables speciation of elements at trace levels and has been applied, in conjunction with isotope dilution, to the analysis of some environmentally significant inorganic species.

A knowledge of the total content of an element is of limited toxicological value since the toxicity is species dependent. Organometallic compounds of lead and tin have been reduced to their hydrides and sorbed on the GC column of a GC-ICP-MS unit and detection limits of $0.3\text{--}2\text{ ng mL}^{-1}$ for tin have been attained. Developing a convenient method for the analysis of mixtures of arsenic(III), arsenic(V), monomethylarsonic and dimethylarsinic acids continues to be a formidable analytical challenge. In a recent low resolution EI GC-MS method, which has employed hexachlorobenzene as internal standard, ppb detection limits have been attained following derivatization to methyl thioglycolates. However, arsenic(III) and arsenic(V) have been left unresolved (Figure 6).

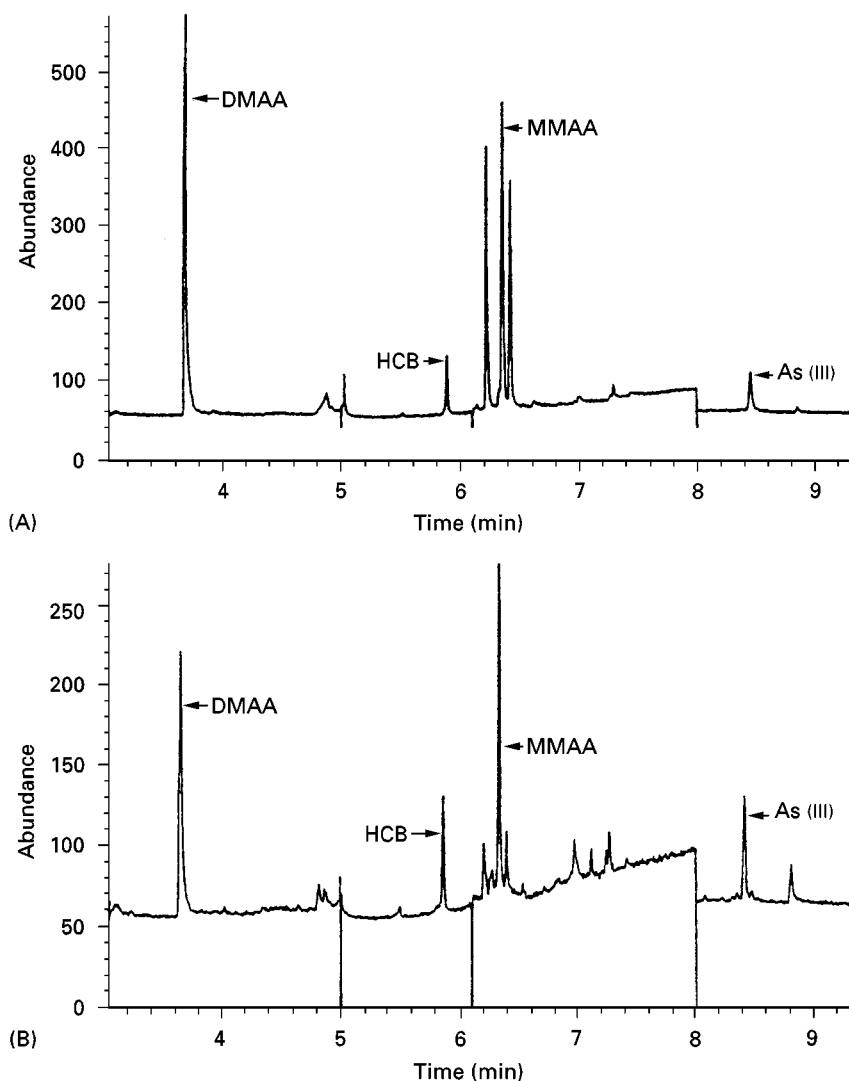


Figure 6 Representative chromatograms of HCB and the TGM derivatives of DMAA, MMAA and As(III). (A) Calibration standard containing 10 ppb DMAA and MMAA and 20 ppb As(III). (B) River water spiked with 5 ppb DMAA and MMAA and 40 ppb total inorganic arsenic (As(III) and As(V)). SIM program: m/z 195 from 3.0 to 5.0 min, m/z 282 from 5.0 to 6.1 min, m/z 195 from 6.1 to 8.0 min, and m/z 285 from 8.0 to 9.3 min. (Reproduced from Claussen, 1997, with permission from Elsevier Science.)

Conclusion

Future developments of GC-MS in environmental analysis will encompass both sampling and instrumentation. Environmentally friendly extraction methods such as SFE and MAE that reduce or eliminate the need for organic solvents are likely to gain greater acceptance. A striking development in this trend is the solventless extraction technique of solid-phase microextraction (SPME), which concentrates the analytes on a stationary phase that is bonded or coated onto a fused silica fibre. Subsequent thermal desorption introduces the analytes into the injection port of the GC-MS unit. This method has been applied to the analysis of volatile organic solvents, organochlorine and organophosphate compounds and sub-ppb to ppt detection levels have been attained with ion trap mass spectrometry.

There is tremendous interest in developing miniaturized, field-portable GC-MS units to facilitate on-site, real-time monitoring. For unattended operation and reduced labour, the sampling, extraction and injection steps should be carried out by a robot, the

entire system being under computer control. A paramount consideration is the ability of the system to withstand shocks and vibrations during transport to and from the site(s). The greater speed, sensitivity and resolution needed for analysis of toxic pollutants produced in fast processes such as fires are continually the focus of developments in HRGC/HRMS. For faster analysis, short (1 m) capillary columns called 'transfer lines' and supersonic molecular beams for sampling and ionization have been employed. The low sample capacity associated with very short columns has been overcome via multicapillary columns. For monitoring solutes that are rapidly eluted from columns, mass spectrometer scan speeds must be increased significantly without compromising resolution. Alternatively, all masses must be scanned at the same time as is done in Fourier transform-MS (FTMS) and ITD. However, both these techniques operate in the pulse mode, making sample utilization inefficient. Hence other modes of array detection have been attempted, an interesting example being the development of an electro-optical ion detector (EOID) for microbore capillary column chromatography. In

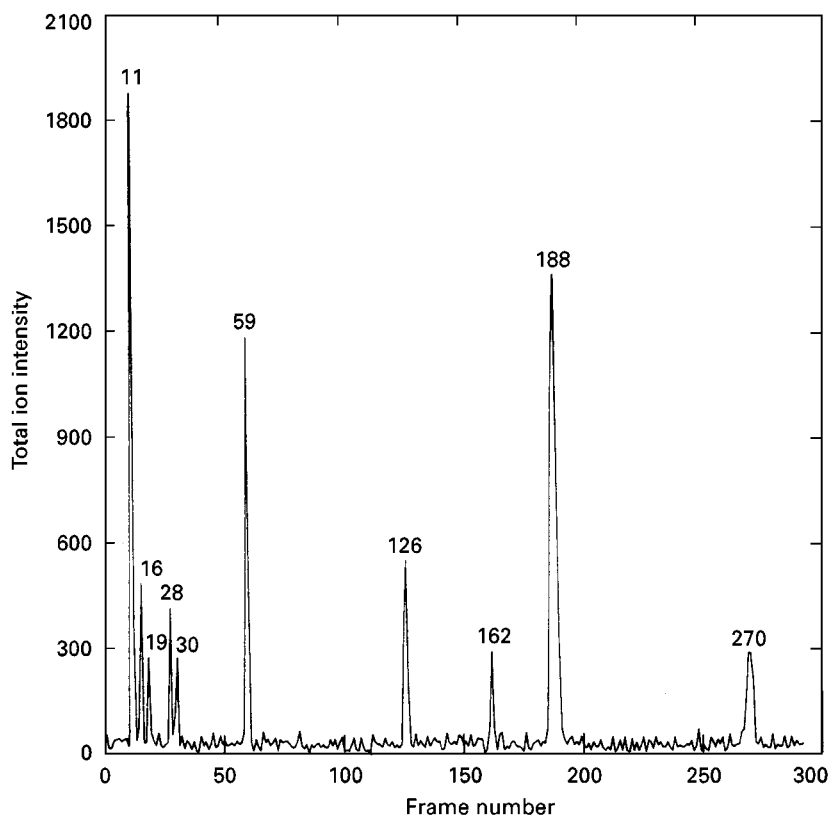


Figure 7 Total ion chromatogram obtained from a mixture of compounds consisting of air (11), dichlorofluoromethane (16), chloromethane (19), bromoethane (28), chloroethane (30), dichloromethane (59), 1,1,1-trichloroethane (126), chloroform (162), benzene (188), and trichloroethylene (270). Each compound in the mixture has a concentration of 1 ppmv. A sample volume of 0.5 μ L was injected, and a signal integration time of 250 ms was used for each frame. (Reproduced from Gutnikov G. (1991) Development of a miniaturized gas chromatograph-mass spectrometer with a microbore column and an array detector. *Analytical Chemistry* 63(18): 2012–2016, with permission from the American Chemical Society.)

EOID the electrons generated by a microchannel electron multiplier array are converted to photons by a phosphor screen and detected via an array of photodiodes (Figure 7). Very high sensitivities have been reported, with benzene being detected at 7.5×10^{-14} g levels.

Multidimensional gas chromatography (MDGC) is another technique that seeks to overcome the problems involved in the analysis of multicomponent mixtures of volatile constituents. It is based on the separation of the constituents via one column and isolating the coeluted species in one or more cryotrap to be separated by a second column of different selectivity. MDGC is usually coupled with detectors such as IR and MS for increased specificity.

GC-MS has emerged as one of the premier methods for the rapid, convenient and sensitive analysis of pollutants. This development is partly a result of the public concern and legislative pressure for reliable monitoring of environmental quality. The commercial availability of relatively inexpensive, computer-interfaced, bench-top instruments has rendered the technique almost routine for cost-effective analysis. Even greater speeds and resolving powers of the future generations of instruments will augment the significance of GC-MS in the environmental field.

See also: II/Chromatography: Gas: Detectors: Mass Spectrometry. Extraction: Solid-Phase Extraction. III/Fungicides: Gas Chromatography. Herbicides: Gas Chromatography. Pesticides: Gas Chromatography. Polychlorinated Biphenyls: Gas Chromatography. Polycyclic Aromatic Hydrocarbons: Gas Chromatography.

Further Reading

- Berezkin VG and Drugov YS (1991) *Gas Chromatography in Air Pollution Analysis*. Amsterdam: Elsevier.
- Black RM, Clarke RJ, Read RW and Reid TJ (1994) Application of gas chromatography-mass spectrometry and gas chromatography-tandem mass spectrometry

to the analysis of chemical warfare samples, found to contain residues of the nerve agent sarin, sulphur mustard and their degradation products. *Journal of Chromatography A* 662: 301-321.

- Bruner F (1993) *Gas Chromatographic Environmental Analysis*. New York: VCH Publishers.
- Claussen FA (1997) Arsenic speciation of aqueous environmental samples by derivatization with thioglycolic acid methyl ester and capillary gas-liquid chromatography-mass spectrometry. *Journal of Chromatographic Science* 35: 568-572.
- Jones FE (1994) *Toxic Organic Vapors in the Workplace*. Boca Raton, FL: Lewis Publishers.
- Karasek FW, Hutzinger O and Safe S (eds.) (1985) *Mass Spectrometry in the Environmental Sciences*. New York: Plenum Press.
- Keith LH (ed.) (1992) *Compilation of E.P.A.'s Sampling and Analysis Methods*. Grand Rapids, MI: Lewis Publishers.
- Sinha MP and Gutnikov G (1991) Development of a Miniaturized Gas Chromatograph-Mass Spectrometer with a Microbore Capillary Column and an Array Detector. *Analytical Chemistry* 63, 2012-2016.
- Subramanian G (ed.) (1995) *Quality Assurance in Environmental Monitoring, Instrumental Methods*. Weinheim: VCH Publishers.
- Tamilarasan R, Morabito PL, Lamparski L, Hazelwood P and Butt A (1994) Determination of neutral chlorinated extractable organic compounds in water samples using large volume on-column injection capillary gas chromatography-mass spectrometry. *Journal of High Resolution Chromatography* 17: 689-694.
- Wang Z, Fingas M, Landriault M *et al.* (1998) Identification and linkage of tarballs from the coasts of Vancouver Island and Northern California using GC/MS and isotopic techniques. *Journal of High Resolution Chromatography* 21(7): 383-395.
- Wilkins CL (1994) Multidimensional GC for qualitative IR and MS of mixtures. *Analytical Chemistry* 66(5): 295A-301A.
- Winegar ED and Keith LH (eds.) (1993) *Sampling and Analysis of Airborne Pollutants*. Boca Raton, FL: Lewis Publishers.

Pressurized Fluid Extraction

S. R. Sumpter, DuPont Agricultural Products, Wilmington, DE, USA

Copyright © 2000 Academic Press

Introduction

Pressurized fluid extraction (PFE) is used to extract a wide variety of compounds from solid and semi-solid environmental samples. Soil is the predominant environmental solid extracted. Sediment samples are

also frequently extracted. Sludge, chimney brick, fly ash and urban dust comprise other materials that are extracted using PFE. There are several reasons to use pressurized fluid extraction for environmental samples. PFE methods are:

- automated
- easy to transfer
- environmentally friendly, consuming little solvent
- relatively fast

- simple, requiring little expertise
- acceptable to regulatory agencies.

Several PFE methods have been developed to extract compounds from environmental samples. These are listed in **Table 1**. These methods are summarized in the sections that follow. One promulgated method in particular has extensive applicability. This method is United States Environmental Protection Agency (EPA) Method 3545. It is suitable for the extraction of several compound classes from environmental solid and semisolid samples. Compound classes listed in Table 1 that are extracted using EPA Method 3545 are noted.

The authors of EPA Method 3545 found the PFE method gives recoveries comparable to those obtained by rigorous Soxhlet extraction and other techniques, such as shaking, supercritical fluid and sonication extraction methods. Compared to these techniques, PFE takes less time (< 30 min) and consumes less solvent (15–30 mL). Using PFE, the method is applicable to the extraction of polychlorinated biphenyls (PCBs), semi-volatile base/neutral/acids (BNAs), organophosphorous pesticides (OPPs) organochlorine pesticides (OCPs), polycyclic aromatic hydrocarbons (PAHs) and chlorinated herbicides from soil. Of all of the extraction conditions, only the extraction solvent is changed when extracting different compound classes. For example, acetone–hexane is used to extract a sample when analysing for OCPs and PCBs, methylene chloride–acetone is used to extract a sample when analysing BNAs and OPPs, and acetone–methylene chloride acidified with phosphoric acid is used to extract a sample when analysing for chlorinated herbicides. Extraction conditions for Method 3545 are shown in **Table 2**.

Relative recoveries of the PFE method (Method 3545) compared to other methods such as shaking or sonication extraction are summarized in **Table 3**. In this work, relative recoveries are the quotient of PFE recoveries divided by shaking, sonication, or Soxhlet extraction recoveries.

The following sections summarize details of critical sample preparation steps that are necessary before PFE, as well as the conditions used to extract the compounds listed in **Table 1**.

Applications

Aliphatic Hydrocarbons

Aliphatic hydrocarbons are readily extracted by PFE using aqueous and organic extraction solvents. Using organic extraction solvent, pentane, nonane, decane,

Table 1 Compound classes of environmental importance extracted using pressurized fluid extraction

<i>Compound class</i>
Aliphatic hydrocarbons
Alkylphenols
BTEX
^a Chlorinated herbicides
Chlorinated hydrocarbons
Ethoxylates
Explosives (HMX, RDX, TNT, DNT)
Gasoline
Linear alkylbenzenesulfonates (LASs)
^a Organochlorine pesticides (OCPs)
^a Organophosphorus pesticides (OPPs)
Phenoxyacid herbicides
^a Polychlorinated bipheyls (PCBs)
Polychlorinated dibenzofurans (PCDFs)
Polychlorinated dibenzo- <i>p</i> -dioxins (PCDDs)
^a Polycyclic aromatic hydrocarbons (PAHs)
^a Semi-volatile base/neutral/acid (BNAs)
Acids
Alcohols
Amides
Aromatic amines
Aromatic chloroethers
Azobenzenes
Benzidines
Chloroanilines
Chlorobenzenes
Chlorophenols
Methylphenols
Nitroanilines'
Nitrobenzenes
Nitrophenols
Nitrosamines
Phenyl hydrazines
Phthalates
Toluidines
Total petroleum hydrocarbons (TPHs)

^aCompounds extracted using U.S. EPA Method 3545.

undecane, tetradecane, and pentadecane are efficiently extracted using the conditions listed in **Table 4**. Due to its volatility, pentane recoveries are the lowest of these analytes. Pentane boils at 36°C, so special precautions are required to keep it from evaporating from the extraction cell before the extraction is performed. To prevent loss of pentane, extraction cells are cooled and aluminium retention discs are added into the tops of the extraction cells.

Water in the form of super-heated steam may also be used to extract aliphatic hydrocarbons. Dodecane, pentadecane, octadecane, heneicosane, tetracosane, heptacosane, triacontane, and tritriacontane are efficiently extracted from solid and semi-solid environmental samples using the conditions listed in **Table 5**.

Table 2 Summary of sample preparation and extraction conditions used in EPA Method 3454 to extract PCBs, semi-volatile BNAs, OPPs, OCPs and chlorinated herbicides from solid and semisolid environmental samples

<i>Extraction conditions</i>	<i>Extraction analysis conditions</i>
Sample preparation	Grind sample to 100–200 mesh (150–75 µm particle size)
Dispersing or drying agent	Mix sample with anhydrous sodium sulfate or diatomaceous earth
Sample size	Up to 30 g if a dispersing agent is not used
Extraction cell volume	11, 22, or 33 mL cell, depending on sample size
Extraction solvent	OCPs and PCBs: 1 : 1 acetone : hexane BNAs and OPPs: 1 : 1 methylene chloride : acetone Chlorinated herbicides: 2 : 1 acetone : methylene chloride acidified with phosphoric acid
Temperature	100°C
Heat step	5 min
Static time	5 min
Flow type	Static, dynamic, or mix of both
Number of cycles	1–5
Extraction pressure	2000 psi
Flush volume	60% of cell volume
Purge time	60 s

Extraction conditions from USEPA SW-846, 3rd edn., Update III (July 1995) Test methods for evaluating solid waste, Method 3545, Accelerated solvent extraction. U.S. GPO: Washington, DC.

Alkylphenols

Alkylphenols are metabolites of alkylphenol ethoxylates: a class of non-ionic surfactants that were used as cleaning agents and still find use today. Alkylphenols are monitored in the environment as they pose potential risk to animals. Time, and the amount of organic solvent, are saved in the pressurized fluid extraction of alkylphenols from sediment. For the extraction, CO₂ extraction solvent is modified with organic solvent. Either methanol, ethanol, 1-butanol, 2-propanol, acetone, or dioxane may be used. Sediment spiked with heptylphenol and nonylphenol is extracted with 100% recovery after 15 min extraction times. Longer times are required to extract 100% nonylphenol from the sediment. A dynamic extraction time of 60 min with 27.5% methanol does not completely extract aged nonylphenol from soil. Table 6 shows a summary of sample preparation and extraction conditions for alkylphenols.

If the extractor does not allow the use of CO₂, 100% methanol, ethanol, 1-butanol, 2-propanol,

acetone, or dioxane may be used as the extraction solvent. Since the solvent is typically evaporated before analysis, the most volatile solvent should be used.

BTEX (Benzene, Toluene, Ethylbenzene, and Xylene)

BTEX (benzene, toluene, ethylbenzene, and xylene) mixtures are efficiently extracted from solid and semisolid environmental samples by PFE using organic and aqueous solvents. BTEX mixtures are extracted from sand spiked with BTEX by PFE using organic solvent and standard conditions described in Table 4. BTEX mixtures are also quantitatively extracted by subcritical water using the conditions listed in Table 5.

Ethoxylates

Alkylphenol ethoxylates are non-ionic surfactants used for cleaning that are monitored in the environment. Ethoxylates are extracted from sediment by

Table 3 Summary of pressurized fluid extraction validation data for EPA Method 3545. Reported relative recoveries for the various compounds are the results of the PFE method used divided by the U.S. EPA reference methods listed

<i>Compound class</i>	<i>U.S. EPA reference method</i>	<i>% Relative recovery</i>
Chlorinated herbicides	8150A (shake method)	113
Organochlorine pesticides	3541 (automated Soxhlet)	97
Organophosphorous pesticides	3540 (Soxhlet)	99
Polychlorinated biphenyls	3540 (Soxhlet)	98
Polycyclic aromatic hydrocarbons	3540 (Soxhlet)	105
Semivolatile base/neutral/acids	3541 (automated Soxhlet)	99

Data compiled from the following sources: Ezzell (1998) *American Environmental Laboratory* January/February 24; Ezzell *et al.* (1995) *LC.GC* 13: 390; and Richter *et al.* (1995) *American Laboratory* February, 24.

Table 4 Summary of standard sample preparation and extraction conditions used to extract aliphatic hydrocarbons, BTEX, gasoline and TPH from soil

Extraction conditions	Extraction/analysis conditions
Dispersing or drying agent	None used
Sample size	10 g
Extraction cell volume	11 mL
Extraction solvent	Methylene chloride for aliphatic hydrocarbons and BTEX
Temperature	100°C
Heat step	5 min
Static time	5 min
Flow type	Mix of both static and dynamic extraction
Number of cycles	1
Extraction pressure	1500 psi

Extraction conditions from Ezzell JL and Richter BE (1996) *American Environmental Laboratory* February, 16.

PFE. Extraction conditions for octylphenol-9,5-ethoxylate, nonylphenol-13-ethoxylate and decylphenol monoethoxylate are the same as those for alkylphenols (see Table 6). Using the modified CO₂ as the extraction solvent with dynamic extraction, 60 min longer are required.

Explosives

Explosives are another important class of compounds that are monitored in the environment. They are monitored in military site or decommissioned site soil

Table 5 Summary of sample preparation and extraction conditions used to extract aliphatic hydrocarbons, BTEX, PCBs, and PAHs from soil, sediment, sludge, and urban dust using water as the extraction solvent

Extraction conditions	Extraction analysis conditions
Sample preparation	Soil is homogenized
Dispersing or drying agent	None used
Sample size	0.2–0.5 g, cell void volume filled with sand
Extraction cell volume	0.5–0.8 mL (4.6 mm i.d. × 30 mm stainless steel HPLC column or 4.6 mm i.d. × 50 mm stainless steel SFE cell)
Extraction solvent	HPLC grade water purged two hours with nitrogen to remove dissolved oxygen
Temperature	250°C
Extraction time	15 min
Flow type	Dynamic, 1 mL ⁻¹ min ⁻¹
Number of cycles	1
Extraction pressure	73.5 psi for aliphatic hydrocarbons and 735 psi for BTEX, PCBs, and PAHs

Extraction conditions from Yang *et al.* (1997) *Environmental Science and Technology* 31: 430. Reproduced with permission from the American Chemical Society.

Table 6 Summary of sample preparation and extraction conditions used to extract alkylphenols, ethoxylates, and linear alkylbenzene sulfonates from environmental solid and semi-solid samples

Extraction conditions	Extraction analysis conditions
Sample preparation	Water was separated from sediment by centrifugation. Sediment was dried at ambient temperature and ground to a particle size of less than 10 µm and water content was adjusted to 10% (w/w). After filling the cells, empty space in the extraction cell was filled with 3 mm diameter glass beads. Any remaining space, 2 mL was filled with modifier solvent.
Dispersing or drying agent	None used
Sample size	1 g
Extraction cell volume	5 mL
Extraction solvent	CO ₂ , modified with methanol, ethanol, 1-butanol, 2-propanol, acetone, or dioxane.
Temperature	100°C
Heat step	None
Static time	10 min
Flow type	Mix of static (10 min) and dynamic (5–60 min) extraction
Number of cycles	1
Extraction pressure	2200 and 2940 psi

Kreißelmeier and Durbeck (1996) *Fresenius Journal of Analytical Chemistry* 354: 921.

since the explosives can potentially contaminate water supplies. PFE extracts HMX (octahydro-1,3,5,7-tetranitro-1,3,5,7-tetrazocine), RDX (hexahydro-1,3,5-trinitro-1,3,5-triazine), TNT (2,4,6-trinitrotoluene), and DNT (2,4-dinitrotoluene) using the conditions shown in Table 7.

The extraction solvent used depends on the analytical technique preferred. Acetone is the best choice for GC and methanol is the best solvent for LC analysis. For the results shown in Figure 1, methanol was used as the extraction solvent. The extraction step takes 12 min per sample, resulting in 45 mL of extract.

Gasoline

Gasoline is extracted from spiked sand using the standard PFE conditions listed in Table 4. The average recovery of gasoline using these conditions is 94.4%, as determined by IR detection.

Linear Alkylbenzenesulfonates

Anionic surfactants are widely used for industrial as well as household cleaning and for pesticide formulations. Of the anionic surfactants, biodegradable

Table 7 Summary of sample preparation and extraction conditions used to extract explosives from soil

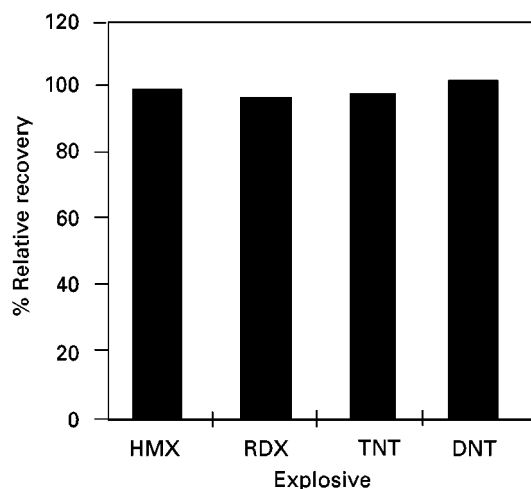
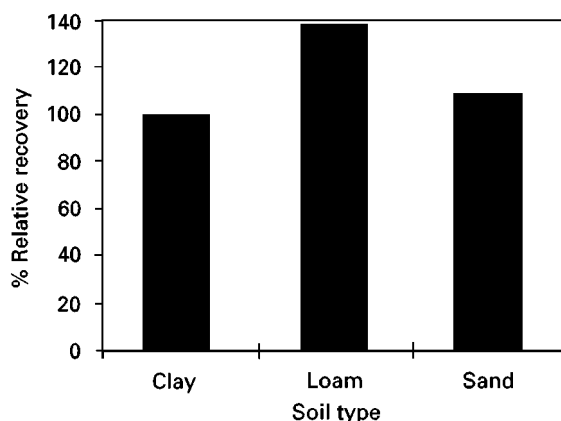
Extraction conditions	Extraction analysis conditions
Sample preparation	Soil is homogenized
Dispersing or drying agent	None used
Sample size	30 g
Extraction cell volume	33 mL
Extraction solvent	Methanol or acetone
Temperature	100°C
Heat step	5 min
Static time	5 min
Flow type	Mix of both static and dynamic
Number of cycles	1
Extraction pressure	1500 psi
Flush volume	60% of cell volume
Purge time	90 s

Extraction conditions from Ezzell (1998) *American Environmental Laboratory* January/February 24.

linear alkylbenzenesulfonates (LAS) are the most common and can be found in waste water systems and river water. From these water sources, anionic surfactants partition to sediment. LAS are selectively extracted from sediment by PFE allowing simple quantitation by high performance liquid chromatography. Extraction conditions for linear LAS [linear decyl- up to tridecylbenzenesulfonate (LAS-10 to LAS-13)] are the same as those for alkylphenols listed in Table 6. Methanol is the best CO₂ modifier (at 2200 psi) for these compounds.

Pesticides

Pesticides including herbicides, insecticides and fungicides are broadly applied throughout the world to

**Figure 1** Average percent relative recovery data of explosives extracted from soil spiked at 3 mg kg⁻¹ level. (Reprinted from Ezzell 1998. Copyright 1998 by International Scientific Communications, Inc.)**Figure 2** Average percent relative recovery data of herbicides extracted from three soil types. Soils were fortified with 50–500 and 500–5000 µg kg⁻¹. (Data from Ezzell *et al.* 1995.)

generate greater harvests and to protect food supplies. As pesticides are present in soil, sediment and water, they are an important class of environmental compounds. Pesticides are extracted by PFE using organic and aqueous solvents.

Sample preparation and extraction conditions for chlorinated herbicides, OCPs, OPPs in soil using EPA Method 3545 are shown in Table 2. The method (Method 3545) specifies the use of mixtures of organic solvents to extract a wide variety of organochlorine and organophosphate pesticides and chlorinated herbicides.

At least eight chlorinated herbicides (2,4-D; 2,4-DB; 2,4,5-T; 2,4,5-TP; dalapon, dicamba, dichloroprop and dinoseb) are extracted using this method. Extraction takes 12 min per sample, generating 15 mL of extract. Average relative recoveries for the

Table 8 Summary of sample preparation and extraction conditions used to extract pyriithiobac sodium from soil

Extraction conditions	Extraction analysis conditions
Sample preparation	Remove sticks and rocks and break up clumps of soil
Dispersing or drying agent	Mix 10 g soil with 7 g of silica gel
Sample size	10 g
Extraction cell volume	22 mL cell
Extraction solvent	Water
Temperature	100°C
Heat step	5 min
Static time	5 min
Flow type	Mix of both static and dynamic extraction
Number of cycles	1
Extraction pressure	200 psi
Flush volume	60% of cell volume
Purge time	60 s

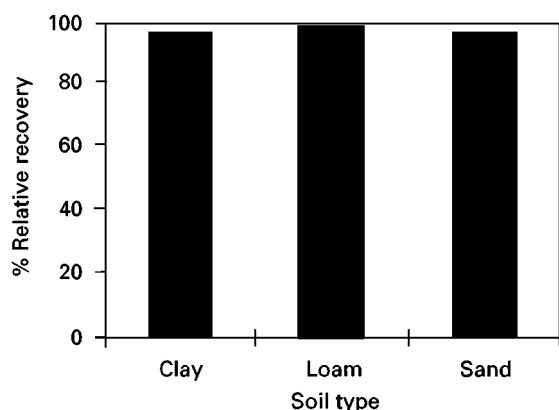


Figure 3 Average percent relative recovery data of organochlorine pesticides extracted from three soil types. Soils were fortified at 5, 50 and 250 $\mu\text{g kg}^{-1}$. (Data from Richter *et al.*, 1995. Copyright 1995 by International Scientific Communications, Inc.)

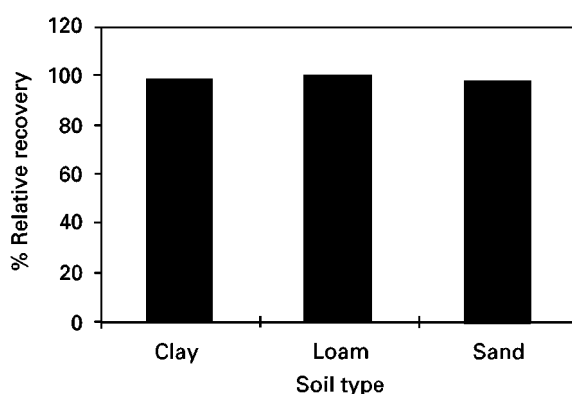


Figure 4 Average percent relative recovery data of organophosphorous pesticides spiked at low and high levels on three soil types and then extracted using EPA Method 3545. Soils were fortified with 250 and 2500 $\mu\text{g kg}^{-1}$. (Data from Ezzell *et al.*, 1995.)

eight chlorinated herbicides are shown in Figure 2. Relative recoveries are the quotient of PFE recoveries divided by shaker extraction recoveries.

Organic acids are extracted using organic solvents and by subcritical water. The advantages of using aqueous extraction solvent are (1) purchase and disposal costs are low and (2) it is environmentally friendly. Conditions used to selectively extract pyriithobac sodium (the active ingredient in Staple® herbicide, used to control broadleaf weeds in cotton) are listed in Table 8.

Organochlorine pesticides (OCPs) are extracted using the conditions listed in Table 2. Average relative recoveries for the 20 OCPs are shown in Figure 3. Relative recoveries are the quotient of PFE recoveries divided by automated Soxhlet extraction recoveries.

Organophosphate pesticides (OPPs) listed in Table 9 are extracted from soil using the conditions listed in Table 2. Average relative recoveries for the 24 OPPs are shown in Figure 4. Relative recoveries are the quotient of PFE recoveries divided by Soxhlet extraction recoveries.

Table 9 Twenty-four organophosphate pesticides extracted by EPA Method 3545

Azinphos methyl	Mevinphos
Chlorpyrifos	Monocrotophos
Coumaphos	Naled
Demeton-O,S	Parathion ethyl
Diazinon	Parathion methyl
Dichlorovos	Phorate
Dimethoate	Ronnel
Disulfoton	Sulfotepp
EPN	Sulprofos
Ethoprop	TEPP
Fensulfothion	Tetrachlorvinphos
Fenthion	Tokuthion

Polychlorinated Biphenyls

Polychlorinated biphenyls (PCBs) are significant environmental pollutants that are routinely monitored in soil, sediment and sludge. PCBs are extracted from these matrices using organic and aqueous extraction solvents. PFE conditions using organic solvents are listed in Table 2; PFE conditions used for aqueous solvents are listed in Table 5. Although not listed in Table 2, acetonitrile and methylene chloride also provide adequate extraction of PAHs in environmental solid and semi-solid samples. Concentrations of PCBs extracted from soil, sediment, urban dust and sludge using PFE and exhaustive Soxhlet extraction are similar. This is true for both organic and aqueous extraction solvents in PFE.

Table 10 Summary of sample preparation and extraction conditions used to extract dioxins and furans from chimney brick, urban dust, fly ash and sediments

Extraction conditions	Extraction analysis conditions
Sample preparation	Grind soil to 100–200 mesh (150–75 μm particle size)
Dispersing or drying agent	Mix with anhydrous sodium sulfate or Hydromatrix™
Sample size	4–10 g
Extraction cell volume	11, 22 or 33 mL cell, depending on sample size
Extraction solvent	Toluene, 15 mL
Temperature	180°C
Heat step	9 min
Static time	5 min
Flow type	Static, dynamic, or mix of both
Number of cycles	1–2
Extraction pressure	2000 psi

Extraction condition reproduced from Richter *et al.* (1997) *Chemosphere* 34: 975, with permission from Elsevier Science.

Polychlorinated Dioxins and Furans

Polychlorinated dibenzo-p-dioxins (PCDDs) and polychlorinated dibenzofurans (PCDFs) are environmental pollutants that are extracted from chimney brick, urban dust, fly ash, soil and sediment using PFE. Conditions for the extraction of PCDDs and PCDFs are listed in Table 10.

PFE and Soxhlet extraction results of PCDDs and PCDFs levels found are essentially equivalent for the matrices tested. PFE required less time and solvent than Soxhlet extraction.

Polycyclic Aromatic Hydrocarbons

Polycyclic aromatic hydrocarbons (PAHs) are important environmental compounds being carcinogenic and mutagenic. They are extracted by organic solvents and by subcritical water. Using organic solvents, PAHs are extracted from urban dust, sediment and soil using the PFE conditions listed in Table 2. Subcritical water extraction requires the conditions listed in Table 5. Results from certified reference ma-

terials indicate that PFE efficiently extracts PAHs from these matrices. Figure 5 shows a comparison of the amounts of PAHs found in PFE extracts and certified values.

The following organic solvents also provide adequate extraction of PAHs in environmental samples: toluene/methanol 1 : 1 (v : v), toluene, methylene chloride, acetonitrile, hexane/acetone 1 : 1 (v : v) and water. Figure 6 shows the amounts of PAHs found in urban dust (SRM 1649) extracts comparing various organic and aqueous extraction solvents.

Semi-Volatile Base/Neutral/Acid Compounds

Semi-volatile base/neutral/acid compounds (BNAs) are extracted from solid and semi-solid environmental samples using the conditions listed in Table 2. Average relative recoveries for the 56 US EPA priority pollutants list (PPL) and target compound list (TCL) are shown in Figure 7. Relative recoveries are the quotients of PFE recoveries divided by Soxhlet extraction recoveries.

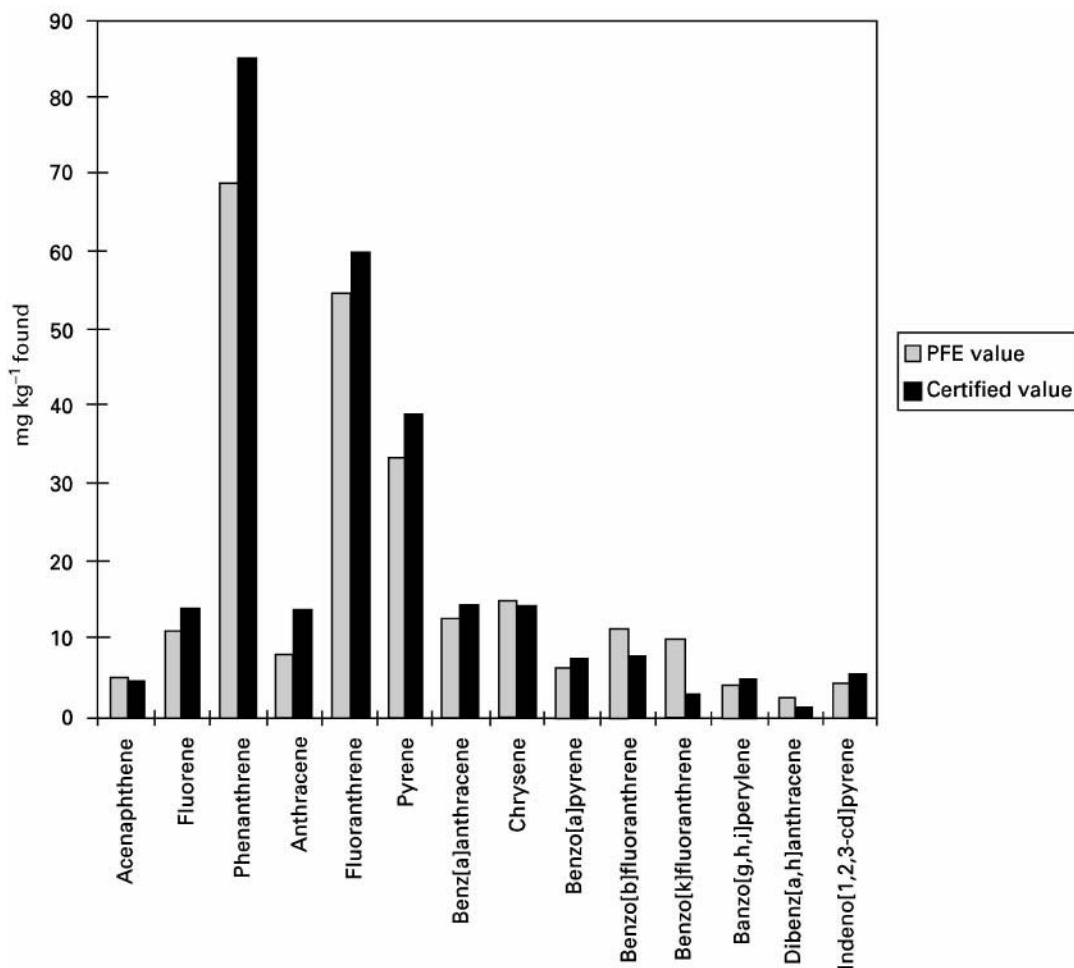


Figure 5 Comparison of amounts of PAHs found in PFE extracts and certified values. (Data from Richter, Jones, Ezzell *et al.* 1996.)

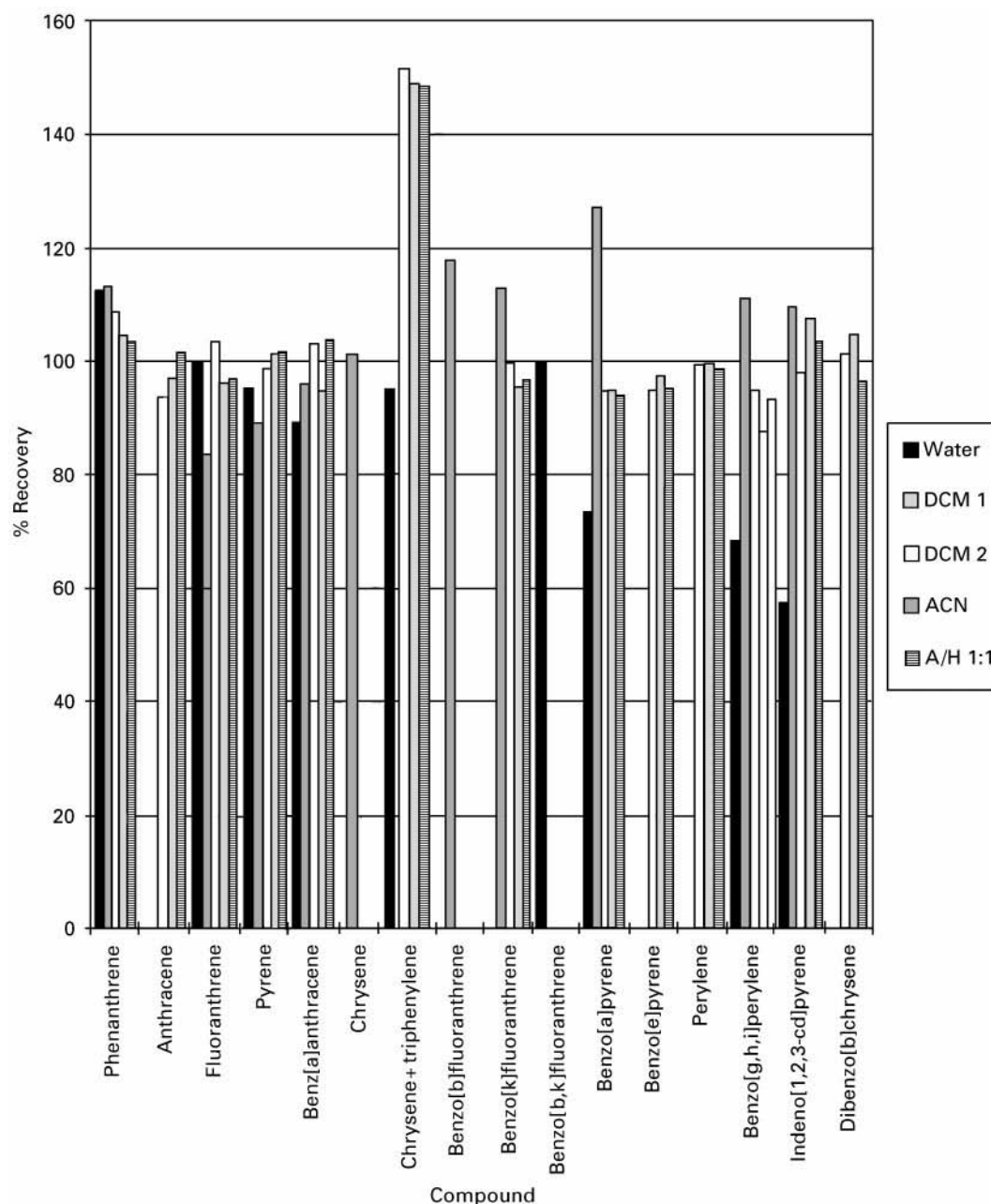


Figure 6 Recovery of PAHs from urban dust (certified reference NIST SRM 1649) extracted by PFE. Extraction solvents were water (250°C, 725 psi) and methylene chloride/acetone 1 : 1. (Data for water extraction from Hawthorne *et al.*, 1994.) Data for methylene chloride extraction (DCM 1) from Richter *et al.*, 1995. Data for methylene chloride extraction (DCM 2) from Schantz *et al.*, 1997.)

Total Petroleum Hydrocarbons

Total petroleum hydrocarbons (TPHs) are extracted from soil samples using the standard PFE conditions listed in Table 4. Levels of TPHs extracted by PFE and Soxhlet extraction are typically similar.

Future Applications

There are several reasons why analysts use PFE to extract analytes of interest from solid and semisolid

environmental samples. In comparing PFE to Soxhlet, sonication and shaking extraction methods, researchers find that the amounts of analyte extracted from solid and semi-solid samples are similar, but PFE requires less extraction time and less extraction solvent. PFE methods are easy to develop and to transfer. PFE provides automated sample extraction, allowing increased productivity of laboratory personnel. Finally, PFE methods are being accepted by regulatory agencies. Given these advantages, researchers

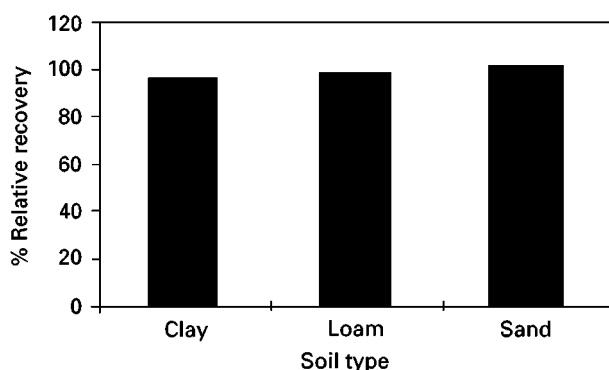


Figure 7 Average percent relative recovery data of 56 semi-volatile base/neutral/acid components extracted from three soil types using PFE. Soils were fortified at 250, 2500, and 12 500 $\mu\text{g kg}^{-1}$. (Data from Richter *et al.* (1995) reproduced with permission from International Scientific Communications Inc.)

will continue to use PFE to develop many more environmental sample applications.

See also: II/Extraction: Supercritical Fluid Extraction. III/Environmental Applications: Supercritical Fluid Extraction; Soxhlet Extraction. Superheated Water Mobile Phases: Liquid Chromatography.

Further Reading

- Ezzell J (1998) The Use of SW-846 Method 3545 for automated extraction of environmental samples. *American Environmental Laboratory*. 10: 24–25.
- Ezzell JL and Richter BE (1996) Automated sample preparation for environmental laboratories using accelerated solvent extraction. *American Environmental Laboratory*. 16–18.
- Ezzell J, Richter BE, Felix WD, Black SR and Meikle JE (1995) A comparison of accelerated solvent extraction

- with conventional solvent extraction for organophosphorus pesticides and herbicides. *LC/GC* 13: 390–398.
- Hawthorne SB, Yang Y and Miller DJ (1994) Extraction of organic pollutants from environmental solids with sub- and supercritical water. *Analytical Chemistry*. 66: 2912–2920.
- Kreibelmeier A and Durbeck H-W (1996) Determination of alkylphenols and linear alkylbenzene sulfonates in sediments applying accelerated solvent extraction (ASE). *Fresenius Journal of Analytical Chemistry*. 354: 921–924.
- Richter BE, Ezzell JL, Felix D, Roberts KA and Later DW (1995) An accelerated solvent extraction system for the rapid preparation of environmental organic compounds in soil. *American Laboratory* 27: 24–28.
- Richter BE, Jones BA, Ezzell JL, Porter NL, Avdalovic N and Pohl C (1996) Accelerated solvent extraction: a technique for sample preparation. *Analytical Chemistry* 68: 1033–1039.
- Richter BE, Ezzell JL, Knowles DE, Hoefler F, Mattulat AKR, Scheutwinkel M, Waddell DS, Gobran T and Khurana V (1997) *Chemosphere* 34: 975–978.
- Schantz MM, Nichols JJ and Wise SA (1997) Evaluation of pressurised fluid extraction for the extraction of environmental matrix reference materials. *Analytical Chemistry* 69: 4210–4219.
- USEPA SW-846, 3rd Edn., Update III (July 1995) *Test Methods for Evaluating Solid Waste, Method 3545, Accelerated Solvent Extraction*. Washington. U.S. GPO.
- Yang Y, Bowadt S, Hawthorn SB and Miller DJ (1995) Subcritical water extraction of polychlorinated biphenyls from soil and sediment. *Analytical Chemistry*. 67: 4571–4576.
- Yang Y, Hawthorne SB and Miller DJ (1997) Class-selective extraction of polar, moderately polar, and nonpolar organics from hydrocarbon wastes using subcritical water. *Environmental Science and Technology*. 31: 430–437.

Solid-Phase Microextraction

T. Nilsson, Technical University of Denmark, Lyngby, Denmark

Copyright © 2000 Academic Press

Solid-phase microextraction (SPME) is a technique for the extraction of organic compounds from gaseous, aqueous and solid matrices such as many environmental samples. It is rapid and simple, which makes it ideal for automation and *in situ* measurements, and no harmful solvents are used. The principle of SPME is equilibration of the analytes between an organic polymeric phase coated on to a fused-silica fibre and the sample matrix. The parameters of importance for the equilibration process are described below and

various environmental applications are discussed. Traditionally, SPME has been combined with analysis by gas chromatography (GC), and mainly aqueous samples have been analysed. This combination has proved to be sensitive, accurate and precise for the quantitative analysis of volatile organic compounds and different classes of pesticides. Solid samples can also be analysed by SPME in spite of the stronger matrix effects, and recently SPME has been coupled with liquid chromatography (LC) for the analysis of polar pesticides.

Principle

The principle of SPME is that a fused-silica fibre is coated with an organic polymer and exposed to the

sample. The fibre is mounted inside a steel syringe needle for protection in order to be able to penetrate the septum of the sample vial and the GC injector without damaging the fibre. Subsequently, the fibre can be pushed out of the needle for exposure to the sample. The analytes will then diffuse into the fibre coating until equilibrium has been established.

Extraction Efficiency

Basically, the extraction efficiency is determined by the extraction time, the sample concentration and the distribution constant of the analyte between the fibre coating and the sample. The classical situation is extraction with the fibre immersed in a water sample.

The amount of analyte extracted by the fibre coating equilibrium n_1^∞ is determined by the expression:

$$n_1^\infty = \frac{KV_1V_2C_2^0}{KV_1 + V_2} \quad [1]$$

where K is the distribution constant, V_1 is the volume of the fibre coating, V_2 is the sample volume, and C_2^0 is the initial sample concentration.

Another SPME approach is sampling from a headspace above the sample in the vial. In this case, the amount of analyte adsorbed after infinite time n_1^∞ is given by the equation:

$$n_1^\infty = \frac{C_2^0V_1V_2k}{kV_1 + k'V_3 + V_2} \quad [2]$$

where V_3 is the volume of the headspace, k is the fibre coating–gas distribution constant, and k' is the gas–water distribution constant of the analyte. k' is directly proportional to Henry's constant and is usually relatively low for the compounds analysed by SPME. Thus, only if V_3 is considerable compared to V_2 , a lower sensitivity will be observed with headspace–SPME (HS–SPME). The advantage of HS–SPME is that equilibration times will be much shorter due to the fact that the diffusion is several orders of magnitude faster in the gas phase than in liquids. Another advantage of HS–SPME is that it can be applied for the analysis of solid and dirty samples. However, such applications are not so amenable to

a theoretical treatment because of unpredictable matrix effects.

Adsorption Kinetics

Basically, the kinetics of adsorption are governed by diffusion. A number of models have been reported for different situations, but they provide only approximate descriptions under ideal conditions. In practice, a number of factors will cause deviations from these conditions, thus a simple, empirical model has been described for practical purposes:

$$n_1 = n_1^\infty [1 - \exp(-t/\tau)] \quad [3]$$

where τ is a measure of the equilibration velocity, and n_1 is the amount adsorbed on the fibre coating at the time t .

Extraction

The extraction conditions are optimized in order to obtain a rapid and sensitive analysis. It is important to remember that SPME depends on diffusion and distribution. Thus, the required extraction time can be reduced by increasing the diffusion rates, and the extraction efficiency can be improved by increasing the distribution constant.

Choice of Fibre Coating

Various SPME fibres are commercially available (Table 1). The polydimethylsiloxane (PDMS) coating is recommended for the extraction of nonpolar compounds. Three different PDMS fibres exist with a coating thickness of 7, 30 and 100 μm , respectively. Usually, 100 μm coating is used due to its higher extraction capacity. However, for higher boiling compounds with high distribution constants and long equilibration times, the thinner coatings should be used. The 7 μm coating has the advantage that it is chemically bonded and can be used at temperatures up to 340°C.

Extraction Parameters

Reliable quantitative analysis can be performed under nonequilibrium conditions, but the sensitivity will be

Table 1 SPME fibres and their recommended use

<i>Fibre coating material</i>	<i>Abbreviation</i>	<i>Recommended use</i>
Polydimethylsiloxane	PDMS	Nonpolar compounds
Carboxen/polydimethylsiloxane	Carboxen/PDMS	Very volatile compounds
Polyacrylate	PA	General
Polydimethylsiloxane/divinylbenzene	PDMS/DVB	General
Carbowax/divinylbenzene	CW/DVB	Polar compounds
Carbowax/templated resin	CW/TPR	Polar compounds

better when the extraction time is sufficient to reach near-equilibrium. The equilibration time can be shortened by agitation or heating of the sample which increase the diffusion rates. Normally, an extraction time comparable to the time of the chromatographic analysis is chosen in order to maximize sample throughput. Rapid stirring using a magnetic bar is efficient, but may not always be very reproducible; vibration of the fibre is a valid alternative for small samples. At higher temperatures the equilibration will proceed faster due to the higher diffusion rates; however, the amount adsorbed at equilibrium will be lower.

An internally cooled SPME device has been developed for the purpose of maintaining favourable distribution constants while extracting from a heated sample. Sample heating may be necessary to release analytes that are adsorbed on solid matrices. Addition of a salt normally has a positive influence on the extraction efficiency due to the increased ionic strength of the solution. When acidic compounds are analysed, the pH should be below the lowest pK_a value, because ionic compounds are not extracted but the lifetime of the fibre is reduced at low pH values. A methanol content of less than 1% in spiked samples does not affect the SPME process significantly. It must always be borne in mind that relatively large amounts of other compounds in a complex matrix may have a significant effect on the distribution constant.

Desorption

In case of analysis by GC, thermal desorption is performed in the injector. For analysis by LC, the injection loop is replaced by a special SPME desorption chamber and the desorption is performed in the mobile phase or a solvent mixture. It is important to

optimize the desorption parameters in order to guarantee that the fibre can be used for subsequent analysis without intermediate cleaning. This is essential for automation purposes and for trace analysis. For GC analysis, desorption should be as rapid as possible. The best injection is obtained when the desorption temperature is sufficiently high to ensure an almost complete desorption within 1 min or less. However, a longer desorption time is often required to avoid carry-over, in which case cryogenic focusing may be necessary. For LC analysis, desorption using the mobile phase is the best solution and can even be performed in the flowing mobile phase (dynamic mode) if the desorption is rapid. However, a higher content of an organic solvent is often needed to obtain a satisfactory desorption. In this case, the desorption chamber is filled with the appropriate solvent mixture and desorption takes place (static mode) before the injection is performed by switching the valve. A high content of organic solvent may adversely affect the chromatography if the initial mobile phase is much weaker. Furthermore, the SPME fibres are not very resistant to organic solvents, so the coupling of SPME with LC is still at the experimental stage.

Analysis of Aqueous Samples

Numerous successful applications of SPME for the analysis of aqueous samples have been reported. The analytical conditions are summarized in Table 2, and the results for the different classes of compounds are discussed below. In most of the studies, only spiked samples have been analysed; however, considering the limited effect of suspended solids and humic substances at levels typical for lake, river and groundwater, such environmental samples can also be analysed. In more complex sample matrices, SPME can be used to measure the freely dissolved

Table 2 Applications of SPME for the analysis of aqueous samples

<i>Compound</i>	<i>Fibre coating</i>	<i>Analysis (alternative detector for some compounds)</i>
Volatile organic hydrocarbons	PDMS	GC-MS (FID)
Halogenated volatile organic compounds	PDMS	GC-MS (ECD)
Polychlorinated biphenyls, polyaromatic hydrocarbons and heteroaromatic compounds	PDMS or PA	GC-MS (ECD, FID)
Phenols and nitro-compounds	PA or more polar	GC-MS (ECD)
Organochlorine, organonitrogen and organophosphorus pesticides	PA or more polar	GC-MS (ECD, AED, NPD)
Fatty acids, phenoxy acid herbicides and amines	PA or PDMS/DVB	Derivatization/GC-MS (ECD, FID)
Organometallics and inorganic metal ions	PDMS	Derivatization/GC-MS
Phenoxy acid, sulfonyleurea, phenylurea, carbamate and other polar herbicides	CW/TPR	LC-ESI/APCI-MS (UV, DAD)

Abbreviations: MS, mass spectrometry; FID, flame ionization detection; ECD, electron capture detection; AED, atomic emission detection; NPD, nitrogen and phosphorus detection; ESI, electrospray ionization; APCI, atmospheric pressure chemical ionization; UV, ultraviolet absorption; DAD, diode array detection.

compounds. While the traditional techniques extract the total amount, only a small amount is extracted by SPME, so the equilibrium with the matrix is not perturbed. By addition of an internal standard, e.g. a deuterated surrogate, the total concentration and the distribution of the analytes can be determined. Unless an isotope-labelled analogue of the analyte is used, the benefit of an internal standard in SPME analyses is very limited because even similar compounds may behave differently in the SPME process.

Volatile Organic Hydrocarbons

The analysis of benzene, toluene, ethylbenzene and *m*-, *o*- and *p*-xylene (BTEX compounds) by SPME has been studied extensively. Many other gasoline and fuel-related hydrocarbons have also been analysed. Generally, the standard deviation of replicates is around 5% and detection limits are in the low $\mu\text{g L}^{-1}$ range for the lightest compounds down to low ng L^{-1} level for the higher boiling analytes with the PDMS fibre coating.

Halogenated Volatile Organic Compounds

Numerous applications of SPME for the analysis of halogenated volatile organic compounds have been reported. The PDMS fibre coating performs well for these compounds. The precision and sensitivity are similar to those reported for the volatile organic hydrocarbons.

Polychlorinated Biphenyls, Polycyclic Aromatic Hydrocarbons and Hetero-Aromatic Compounds

Polychlorinated biphenyls (PCBs) and polycyclic aromatic hydrocarbons (PAHs) have been analysed in spiked water samples and in groundwater. The equilibration times were approximately 60 min with the PDMS fibre coating. However, detection limits in the low ng L^{-1} range can be obtained with an extraction time of only 10 min. The relative standard deviations of these analyses are around 20% for the PCBs and 10% for the PAHs. Possibly, better precision could be achieved by increasing the extraction time in order to approach equilibrium. Pyrazines and several other heteroaromatic compounds have been analysed successfully with detection limits from low $\mu\text{g L}^{-1}$ levels for the volatile analytes down to low ng L^{-1} levels for the semivolatile analytes. The precision is in the range from 3 to 14% relative standard deviation. The extraction efficiency is strongly enhanced by salt addition.

Phenols and Nitro-Compounds

Usually, salt addition has a positive effect on the extraction of phenols and nitrophenols, and for analytes with pK_a values below 7 the extraction effi-

ciency is higher at low pH values. Typically, detection limits are in the low $\mu\text{g L}^{-1}$ range and the relative standard deviations are from 5 to 12%. The sensitivity and chromatography can be improved for most of the phenols by aqueous-phase acetylation prior to extraction. Nitrotoluenes, nitroanilines and nitrobenzenes have also been analysed successfully by SPME.

Organochlorine, Organonitrogen and Organophosphorus Pesticides

In several studies, the analysis of organochlorine pesticides has been examined. Generally, equilibration times range from 30 to 90 min, detection limits are in the low ng L^{-1} range with electron-capture detection (ECD) and mass spectrometry (MS), and standard deviations vary from 5 to 20%. For the organonitrogen and organophosphorus pesticides, similar precision and equilibration times have been observed, and the detection limits are at very low ng L^{-1} level with MS and nitrogen and phosphorus detectors.

Fatty Acids, Phenoxy Acid Herbicides and Amines

Fatty acids can be analysed directly from aqueous samples by SPME. However, for short chain fatty acids the detection limits are in the high $\mu\text{g L}^{-1}$ range with the polyacrylate fibre coating and worse with other fibre coatings. However, the sensitivity can be considerably improved by derivatization. Different derivatization procedures have been examined and detection limits below $\mu\text{g L}^{-1}$ can be obtained in the best cases. Similar detection limits are obtained for phenoxy acid herbicides and amines by derivatization-SPME.

Organometallics and Inorganic Metal Ions

SPME has mainly been applied for organic trace analysis. However, a few applications for inorganic metal ions and organometallics have been reported: bismuth was extracted using an experimental SPME fibre coated with a liquid ion exchanger; aqueous-phase derivatization with tetraethylborate followed by SPME has been applied to analyse methylmercury and labile Hg^{2+} in river water, and the same derivatization approach can be used for the analysis of tin and lead. The detection limits are in the low ng L^{-1} range.

Phenoxy Acid, Sulfonylurea, Phenylurea, Carbamate and Other Polar Herbicides

SPME coupled with LC-electron spray ionization (ESI)/atmospheric pressure chemical ionization (APCI)-MS has been applied for the trace analysis of polar pesticides in spiked water samples and lake

water. Acidic, as well as neutral, priority pesticides representing all major pesticide classes can be analysed successfully with single ion monitoring (SIM) detection limits in the ng L^{-1} range. Detection limits in the low $\mu\text{g L}^{-1}$ range and standard deviations below 10% were reported when UV detection was used. Finally, SPME-flow injection-MS-MS has been developed for the purpose of rapid, target-oriented screening analysis.

Validation of Standard Methods for Routine Analysis

In order for SPME to be applied for routine analysis, two issues are very important: automation and quality assurance. Thus, an autosampler has been developed for SPME-GC analysis, and three interlaboratory studies have been performed to validate the quantitative performance of SPME. One study addressed the analysis of 12 organochlorine, organonitrogen and organophosphate pesticides at low $\mu\text{g L}^{-1}$ level in aqueous samples. In the other two studies, standard methods for the analysis of volatile organic compounds and triazine herbicides in aqueous samples were validated at low $\mu\text{g L}^{-1}$ levels and around the European limit of $0.1 \mu\text{g L}^{-1}$ for individual pesticides in drinking water. Subsequently, both methods were presented by the Italian Standardization Organization, Unichim. The validations were performed in accordance with the International Standardization standard method 5725-1994 concerning interlaboratory statistics. The results regarding accuracy and precision are given in Table 3. The 95% confidence interval of the gross average of the reported results always included the true concentration of the test sample, i.e. the accuracy of the methods was very good. The precision obtained would meet the requirements for most routine analyses.

In Situ Measurements

Many well-established extraction techniques have been applied for the analysis of groundwater samples

from wells. These methods require pumping of the groundwater to the surface, sampling into appropriate containers, and transport to the analytical laboratory. Sample loss and sample composition variation may occur during these steps. Thus, a number of downhole sampling devices have been developed. However, each has limitations with respect to flexibility of sample type and sample size, maximum operating pressures and depth, portability and adaptability to difficult field conditions. The characteristics of SPME make it ideal for field sampling, i.e. it is simple, robust, portable, independent of sample volume and instrument configuration, and it is impossible to plug the fibre with particulate matter. Thus, SPME sampling probes have been developed for use in monitoring wells (Figure 1) and for fitting to the head of a cone penetrometer. They were tested in a mobile laboratory for on-site measurements of volatile organic compounds in groundwater and soil gas. Comparison of results obtained by *in situ* SPME and SPME after traditional sampling from the same groundwater wells confirmed the feasibility of the *in situ* sampling approach. Slightly lower results were obtained in most cases after traditional sampling.

Solid Samples

The major complication in the analysis of soil samples is the strong sorption of the analytes to the matrix. A nearly complete exhaustive extraction could be achieved for the BTEX compounds from sand and clay matrices by heating the sample and using an internally cooled SPME fibre for the extraction. However, in the case of less volatile and more polar analytes, the sorption is stronger and the recovery is very dependent on the organic carbon content of the soil. Thus, calibration using a model matrix would only be acceptable for screening purposes, while calibration by standard addition is needed for reliable quantitative analysis. Addition of water to the sample helps to release the analytes from the sample matrix and improves the recoveries drastically. A nearly complete extraction of polyaromatic

Table 3 Interlaboratory validation of SPME for quantitative analysis

Analytes	Number of participating laboratories	Concentration of the test sample ($\mu\text{g L}^{-1}$)	Accuracy	Average repeatability (%)	Average reproducibility (%)
Volatile organic compounds	12	3	True values within confidence intervals	9.3	28.7
Organochlorine, organonitrogen and organophosphorus pesticides	11	2–25	True values within confidence intervals	11.5	28.3
Triazine herbicides	8	0.05–0.12	True values within confidence intervals	9.6	13.6

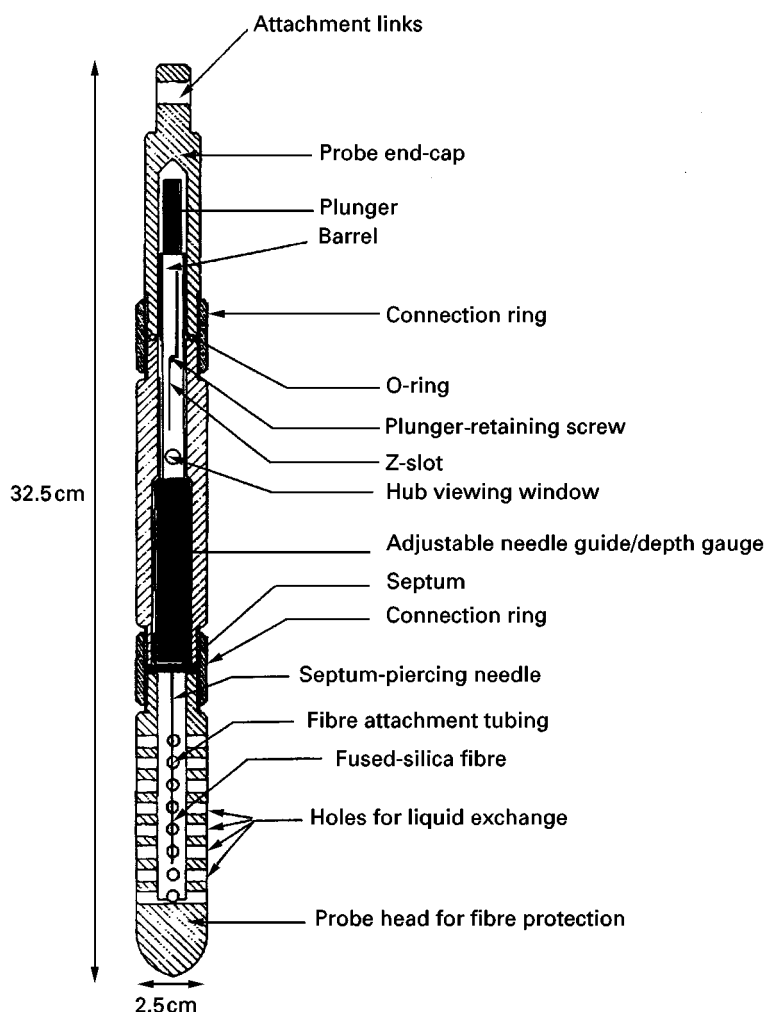


Figure 1 SPME probe for *in situ* groundwater sampling from wells. (Reproduced with permission from Nilsson *et al.*, 1998.)

hydrocarbons from different soils has been achieved by high temperature or subcritical water extraction. Finally, the leachability of pesticides from soils has been studied by SPME.

Conclusion

SPME has successfully been applied for the quantitative analysis of most of the organic, environmental priority compounds, which can be analysed by GC, in aqueous samples. In more complex sample matrices, such as wastewater and soils samples, quantitative analysis by SPME may be difficult because matrix effects influence the distribution constants significantly. Standard methods have been developed and validated regarding sensitivity, precision and accuracy for the trace analysis of volatile organic compounds and several classes of pesticides in aqueous samples. Derivatization/SPME-GC and SPME-LC have been applied for the analysis of more polar

organic compounds. However, further development of these methods is needed before they can be applied for routine analysis. Especially, further research on the coupling of SPME and LC-MS may allow many new environmental applications. Inorganic metal ions and organometallics have been analysed as well, and the use of an ion exchange fibre coating may allow more applications in this field. The small volume and the noninterfering character of SPME are important factors for numerous applications. Finally, the easy handling and simple design make SPME a good choice for in-field analytical work.

See also: II/Extraction: Solid-Phase Microextraction.

Further Reading

Ai J (1997) Solid phase microextraction for quantitative analysis in nonequilibrium situations. *Analytical Chemistry* 69: 1230.

- Chen J and Pawliszyn JB (1995) Solid-phase microextraction coupled to high-performance liquid chromatography. *Analytical Chemistry* 67: 2530.
- Daimon H and Pawliszyn J (1996) High temperature water extraction combined with solid phase microextraction. *Analytical Communications* 33: 421.
- Eisert R and Levsen K (1996) Solid-phase microextraction coupled to gas chromatography: a new method for the analysis of organics in water. *Journal of Chromatography A* 733: 143.
- Eisert R and Pawliszyn J (1997) New trends in solid-phase microextraction. *Critical Reviews in Analytical Chemistry* 27: 103.
- Fromberg A, Nilsson T, Larsen BR *et al.* (1996) Analysis of chloro- and nitroanilines and -benzenes in soils by headspace solid-phase microextraction. *Journal of Chromatography A* 746: 71.
- Hageman KJ, Mazeas L, Grabanski CB *et al.* (1996) Coupled subcritical water extraction with solid-phase microextraction for determining semivolatile organics in environmental solids. *Analytical Chemistry* 68: 3892.
- Louch D, Motlagh S and Pawliszyn J (1992) Dynamics of organic compounds extraction from water using liquid-coated fused silica fibres. *Analytical Chemistry* 64: 1187.
- Nilsson T, Pelusio F, Montanarella L *et al.* (1995) An evaluation of solid-phase microextraction for analysis of volatile organic compounds in drinking water. *Journal of High Resolution Chromatography* 18: 617.
- Nilsson T, Ferrari R and Facchetti S (1997) Inter-laboratory studies for the validation of solid-phase microextraction for the quantitative analysis of volatile organic compounds in aqueous samples. *Analytica Chimica Acta* 356: 113.
- Nilsson T, Montanarella L, Baglio D *et al.* (1998) Analysis of volatile organic compounds in environmental water samples and soil gas by solid-phase microextraction. *International Journal of Environmental Analytical Chemistry* 69: 217.
- Pawliszyn J (1997) *Solid Phase Microextraction, Theory and Practice*. New York: Wiley-VCH.
- Pawliszyn J (ed.) (1999) *Applications of Solid Phase Microextraction*. Cambridge: Chromatography Monographs Series, Royal Society of Chemistry.
- Zhang Z and Pawliszyn J (1993) Headspace solid-phase microextraction. *Analytical Chemistry* 65: 1843.
- Zhang Z, Yang MJ and Pawliszyn J (1994) Solid-phase microextraction, a solvent-free alternative for sample preparation. *Analytical Chemistry* 66: 844A.

Soxhlet Extraction

M. D. Luque de Castro and L. E. García Ayuso,
University of Córdoba, Córdoba, Spain

Copyright © 2000 Academic Press

The health of our environment is now a matter of great concern. This has stimulated an intensive search for an understanding of both the ways in which the natural environment works and the anthropogenic actions that bring about environmental changes. A large number of studies have been, or are in the process of being, developed in order to increase our knowledge of the processes causing environmental pollution and to propose clean analytical methods for monitoring and subsequent control. Thus, a high percentage of the studies developed so far fall within the field of analytical chemistry. There are a number of stages involved in any analytical method: definition of the aim, selection and establishment of an appropriate method, sampling plan, sample collection, sample handling and pretreatment, final measurements (detection/determination), method validation, assessment and interpretation of the results and, finally, safety.

In spite of the evolution of analytical techniques involved in some of the above mentioned stages (particularly detection/determination), the development

of some of these has not been as great as desirable. These steps constitute 'critical points' of an analytical method and, consequently, the main source of errors. The pretreatment step (including separation techniques) can be considered as a 'critical step'. Conventional Soxhlet extraction is currently one of the most frequently used pretreatment techniques, not only in environmental analysis, but also in many other fields. Its principles, performance, environmental applications and improvements are considered in more detail below.

Principles of Conventional Soxhlet Extraction

Soxhlet extraction is a very useful tool for preparative purposes in which the analyte is concentrated from the matrix as a whole or separated from particular interfering substances. Sample preparation of environmental samples has been developed for decades using a wide variety of techniques. Solvent extraction of solid samples, which is commonly known as solid-liquid extraction (also referred to as leaching or Lixiviation in a more correct use of the physicochemical terminology), is one of the oldest methods for solid sample pretreatment. Conventional Soxhlet extraction remains as one of the most

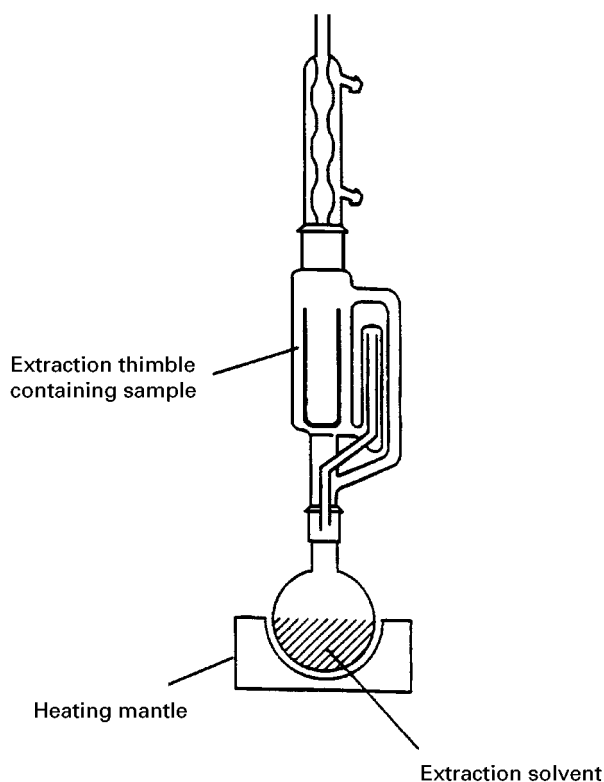


Figure 1 Soxhlet extraction apparatus. (Reproduced from Reeves RN (1994) *Environmental Analysis*. New York: John Wiley.)

relevant techniques in the environmental extraction field. This assertion is supported by the double use of conventional Soxhlet: (1) as an extraction step in a given method, and/or (2) as a well-established model for comparison of new extraction alternatives.

In conventional Soxhlet, the sample is placed in a thimble-holder and during operation is gradually filled with condensed fresh solvent from a distillation flask. When the liquid reaches an overflow level, a siphon aspirates the whole contents of the thimble-holder and unloads it back into the distillation flask, carrying the extracted analytes in the bulk liquid. This operation is repeated until complete extraction is achieved. This performance makes Soxhlet a hybrid continuous-discontinuous technique. Inasmuch as the solvent acts stepwise, the assembly can be considered as a batch system; however, since the solvent is recirculated through the sample, the system also bears a continuous character. **Figure 1** shows a scheme of a conventional Soxhlet device. As can be seen, Soxhlet extraction is a very simple technique. This simplicity makes the procedures for different samples very similar. For this reason, an overview of its extensive application in the environmental field during the last two decades is presented here, which cover the kind of samples, analytes, solvents, etc. used

and the role of Soxhlet extraction in the overall analytical process.

Table 1 summarizes the main characteristics of Soxhlet extraction, clean up and detection/determination for each group of pollutants discussed below.

Use of Conventional Soxhlet Extraction for Leaching of Organic Pollutants

Organic pollutants present in solid environmental samples from natural or man-made sources are most of the time properly extracted with organic solvents in a Soxhlet device. The following sections show how conventional Soxhlet extraction is used as a technique for separation of the analytes from the solid matrix. The pollutants are classified into three groups depending on the matrices in which they are present: air, solid and liquid samples. It is worth noting that, in spite of the solid character of particulates, the samples are classified as a function of the medium in which they are present. Thus, airborne and water particulates are classified as air and liquid samples, respectively.

Organic Pollutants in Air

Organic pollutants are in the gas phase of the atmosphere and are associated with airborne particulate matter. Sampling of organic pollutants is usually carried out by filters through which a large volume of air is circulated. After filtration, the filter is extracted with an appropriate solvent and the target analytes are removed in the extract. When the extract is not suitable for direct individual separation/determination a prior clean-up stage must be applied. These and other aspects are discussed below.

Polycyclic aromatic hydrocarbons Polycyclic aromatic hydrocarbons (PAHs) and their derivatives are among the most studied environmental pollutants. This is due to both their continuous emissions from combustion and their biological activities, such as toxicity, mutagenicity and carcinogenicity. Determination of PAHs from air requires a suitable sampling device, including an aspiration pump, which retains the air particulates on glass or quartz fibre, cellulose or paper filters. However, the filter is not the sole collection medium for PAH-containing small-size aerosols. Chemicals such as Tenax GC, PUFs (see **Table 2** for abbreviations) or Amberlite XAD-2 resins should provide a back up to these filters by retaining PAHs not trapped by the filter. A layer of activated charcoal between two filters is used for collection of gaseous components.

Table 1 Selection of the most representative characteristics of methods for determination of organic pollutants with Soxhlet extraction as pretreatment step

Compound	Matrix	Sampling	Soxhlet features		Clean up	Detect/Determ.
			Solvent	Time		
PAHs	Solid samples (soil, sediment, sludge, biological tissue, etc.)	Homogenization (mix, ground and sieve)	<i>Polar species</i> Dimethyl formamide	From 8 to 48 h depending on the matrix, analyte and solvent	* <i>Sorbents</i> Alumina (non-polar analytes with polar interferences) Silica gel (strongly polar species) Florisil (aromatic and aliphatic interferences) Activated carbon (non-polar analytes from aqueous samples)	<i>Techniques</i> GC HPLC TLC SFC Spectroscopy <i>Detectors</i> FID (hydrocarbons) NPD (nitrogen and phosphorous) FPD (sulfur and phosphorus) ECD (halogenated) UV/VIS and DAD MS (universal) Flourescence
PCDDs/PCDFs		Moisture control	Tetrahydrofuran Acetonitrile Acetone Methanol Ethanol			
PCBs/OCPs			<i>Non-polar species</i> Hexane Iso-octane			
Phenols			Ethers Light petroleum			
Benzidines		Filters (glass or quartz fibre) and PUFs, XAD resins, Tenax GC, etc.	<i>Aromatics</i> Benzene Toluene			
Nitrosamines	Particulates, vapour, smoke, liquid samples		<i>General use</i> Dichloromethane Ethyl acetate Isopropyl alcohol Chloroform	* <i>Solid phase extraction</i> -(non-polar species) C ₁₈ C ₈ Cyclohexyl Phenyl Cyano -(polar species) Amino Diol *Chromatography *Distillation *LLE		
Phthalate esters						
Etc.						

Table 2 Abbreviations

ASE	Accelerated solvent extraction
CE	Capillary electrophoresis
CIMS	Chemical ionization mass spectrometry
ECD	Electron capture detector
EIMS	Electron impact mass spectrometry
EPA	Environmental protection agency
FID	Flame ionization detector
FMASE	Focused microwave-assisted Soxhlet extraction
GC	Gas chromatography
HPLC	High performance liquid chromatography
HPS	High pressure Soxhlet extraction
LC	Liquid chromatography
LLE	Liquid-liquid extraction
MAE	Microwave assisted extraction
MS	Mass spectrometry
NPD	Nitrogen phosphorus selective detector
OCPs	Organochlorine pesticides
PAHs	Polycyclic aromatic hydrocarbons
PCBs	Polychlorinated biphenyls
PCDDs	Polychlorinated dibenzo-dioxins
PCDFs	Polychlorinated dibenzo-furans
PUFs	Polyurethane foam plugs
SEC	Size-exclusion chromatography
SFC	Supercritical fluid chromatography
SFE	Supercritical fluid extraction
SIM	Selected ion monitoring
TLC	Thin-layer chromatography
UV	Ultraviolet
VOCs	Volatile organic compounds

The adsorbed compounds are extracted by Soxhlet into different organic solvents such as toluene, benzene, cyclohexane, tetrahydrofuran, dichloromethane and liquid CO₂. Clean-up extract procedures are mainly performed by the use of silica gel (SFC, LLE and LC are also used), and the individual separation/determination stage involves HPLC-UV and GC-MS. A less common technique for PAH determination is TLC-UV.

Polychlorinated dibenzo-dioxins (PCDDs) and polychlorinated dibenzo-furans (PCDFs) Analysis of dioxins has become an issue of major importance because of their carcinogenic nature. The main source of dioxin emission is combustion (in waste incineration and the steel industry). In comparison with the wide variety of methods used for the determination of PAHs from air, the method for determination of PCDDs and PCDFs is well established and only some minor modifications are found in the literature. These compounds are sampled by splitting the air into two phases. The split involves glass fibre filters, which retain airborne particulates, and PUF solid sorbents, which retain vapours. The PUF sorbents are fortified with a range of ¹³C-labelled PCDDs and PCDFs before sampling (sometimes spiking precedes the sampling step). The same spiked procedure is applied to

particulate phases before extraction. The filter and foam are then extracted by Soxhlet with toluene (benzene/ethanol and dichloromethane have also been used but less frequently than toluene), followed by an acid-base clean-up step, then drawing of the extract through micro-columns of silica gel, alumina and carbon (sometimes a chromatographic clean up is applied before). Individual separation of the analytes and determination are performed by high-resolution GC-EIMS-SIM.

Polychlorinated biphenyls (PCBs) and other chlorinated compounds A wide variety of pollutants other than PCDDs and PCDFs contain chlorine. This makes them very harmful due to their activity in the atmosphere. PCBs and other compounds (chlorinated solvents, halogenated methoxybenzenes (halogenated anisoles), polychlorinated naphthalenes, etc.) are the most representative chlorinated compounds in addition to OCPs (alpha and gamma hexachlorocyclohexane (HCHs), chlorothalonil, dichlofluanid, toxaphene, chlorpyrifos, alachlor, etc.).

Sampling of these compounds is similar to that described in the previous two sections and either the adsorbent used or the extraction solvent and post-extraction procedures applied are widely documented in the literature. Thus, the performance of different sorbents, such as Chromosorb 102, Porapak R, Supelpak-2, Amberlite XAD-2, Amberlite XAD-4, Carbonaceous Ambersorb XE-340 and polyurethane foam, has been evaluated with use of atmospheres containing known concentrations of OCPs. The most efficient trap for HCH and PCBs was found to be two cartridges containing PUFs-Tenax-GC sandwich traps, connected in series. Halogenated anisoles and hexachlorobenzene (HCB) have been sampled from air using a high volume sampling technique in which air was pumped through two layers of solid sorbent: the upper sorbent layer was a mixture of silica gel 60/ENVI-Carb or ANGI-Sorb 5B/ANGI-Sorb 10B and the lower sorbent layer was silica gel 60/ENVI-Carb or ANGI-Sorb 2.5B. These solid sorbents are Soxhlet extracted with organic solvents, mainly dichloromethane (but also with others such as petroleum ether, ethyl ether, hexane, acetone and mixtures) and, after the appropriate clean up, the detection/determination step is developed mainly by GC-ECD.

Other pollutants usually determined in air In addition to PAHs and chlorinated pollutants from the atmosphere, there are some other families of pollutants that have a significant effect on the environment. Thus, alcohols and phenols, organophosphorous compounds, anilines and benzidines, aliphatic hydrocarbons, etc., can be included in this

classification. The procedures for determination and the general characteristics of the chemicals and instruments used (solid sorbents, extractant, extraction time, clean up and detection/determination) are similar to those discussed in previous sections.

Organic pollutants in solid samples Organic pollutants are present in a wide range of environmental solid samples. Thus, soil, sediment, sewage sludge and ash are the most commonly studied matrices in the environmental field. All these matrices can be leached by conventional Soxhlet extraction. There are two criteria that solid samples must meet before extraction: (1) they must be finely divided (in order to improve the sample-solvent contact), and (2) sample moisture must be carefully controlled. After the extraction step by an organic solvent, a clean-up procedure is necessary due to the co-extraction of both fat residues and other interferent substances. The usual procedures for analytical processing of the most representative organic pollutants are as outlined below.

Polycyclic aromatic hydrocarbons Soil or sediment samples are dried to constant weight, ground, sieved and mixed with anhydrous Na_2SO_4 . Soxhlet extraction is performed with dichloromethane (chlorobenzene, benzene, cyclohexane and hexane/acetone are less common for this purpose) and the extract is reduced in a Kuderna-Danish concentrator, a rotary-evaporator or under a N_2 stream. Clean up (if needed) involves: (1) passing the extract through one or more microcolumns containing silica gel, alumina, C_{18} , Florisil, Amberlite XAD-2, etc., and/or (2) fractionation by semi-preparative normal-phase LC. The PAHs are determined either by HPLC (with UV, MS or fluorimetric detection) or GC (with FID or MS detection).

Fly ash is Soxhlet extracted with toluene (or benzene) and the extract is cleaned up by TLC on a plate coated with silica gel. Detection/determination involves the same techniques as those used in soil.

Sewage sludge is Soxhlet extracted with toluene. The extract is evaporated and then, liquid-liquid partitioned between cyclohexane, dichloromethane and H_2O . The cyclohexane extract is purified on a silica column. Separation of neutral and polar PAHs is performed by HPLC-UV with individual separation/determination by GC-FID.

Polychlorinated dibenzo-dioxins and polychlorinated dibenzo-furans As could be seen in the previous section, the extraction of PCDDs and PCDFs is usually performed in a single step. The special character-

istics of these compounds makes it mandatory to study them apart from the rest of the chlorinated pollutants. Despite the existence of papers on determination of dioxins and furans from solid matrices such as soil or sediment, the main source of emission in the literature is combustion processes. Here, the most important solid matrix is fly ash from incinerators. However, the procedure followed for fly ash could be applied to other matrices with minor changes of the sample preparation step. Fly ash samples are collected at the bottom of the electrostatic precipitators of the incinerator (this is why they are considered as solid pollutants; however, when ashes are in the atmosphere they are considered as air pollutants). The fly ash is treated with 1 N HCl, filtered, washed with H_2O and air-dried at room temperature. After addition of ^{13}C -labelled PCDD and PCDF internal standards, the sample is Soxhlet-extracted with toluene (benzene and hexane/acetone have also been used) and the extract is concentrated, then subjected to clean up involving partitioning with concentrated H_2SO_4 and sequential LC on multi-layered silica gel (containing acid-modified, base-modified, AgNO_3 -modified and neutral forms of silica gel), acid alumina and Celite/Carbopack stationary phases as described in US EPA Method 8280A. A portion of the resulting solution is analysed by high resolution GC-EIMS-SIM.

Polychlorinated biphenyls and other chlorinated compounds The large number of chlorinated pollutants in solid samples present in the environment makes their classification and study very difficult. However, it has been clearly demonstrated that there are three groups (PCBs, OCPs and polychlorinated phenols), which are the subject of most of the papers found in the literature. Despite that the following paragraphs are devoted to these groups of organic pollutants, the procedures described are also applicable to the rest of the chlorinated compounds (particularly with regard to Soxhlet extraction).

The first step of the analysis of chlorinated phenolic compounds in polluted soils is wetting of the sample with H_2SO_4 , followed by Soxhlet extraction with hexane/acetone or diethyl ether/petroleum ether. Different techniques can be used for subsequent treatment of the extract, the most representative being acetylation and LLE. After evaporation, the acetates are cleaned up on a deactivated silica gel column and subjected to GC (with ECD or MS detection). The chlorophenols are also individually separated/determined by LC-atmospheric-pressure-CIMS.

PCBs are among the most studied pollutants in solid samples in recent years. Their properties (resistance to oxidation, acids, bases, and other chemicals,

high thermal stability, dielectric behaviour, etc.) make them the most frequently used organic compounds and, consequently, the greatest environmental pollutant.

As the overall procedures followed for the determination of PCBs and OCPs are similar, both groups are usually determined together. Solid sample preparation is similar to that shown for the determination of pollutants from solid samples (see PAHs from soils). Soxhlet extraction is performed with either a single solvent (toluene or dichloromethane) or a mixture of solvents such as, hexane/acetone, pentane/dichloromethane, etc. Clean up usually involves sulfur removal by reaction with Cu or tetrabutylammonium sulfite and the use of silica gel, Florisil and fractionation by SEC if required. The most usual way for individual separation/determination of PCBs and OCPs is GC-ECD.

Other pollutants in solid samples There are some other pollutants that are frequently determined in solid samples. These compounds (in general, the same as those covered in Organic Pollutants in Air) are usually in trace amounts in the environment. Thus, organic pollutants such as aliphatic hydrocarbons, aldehydes, non-chlorinated phenols, cresols, anilines and benzidines, VOCs (mainly organic solvents), phthalates, amines, non-chlorinated pesticides, etc., are also determined due to their importance in the environment. Soxhlet extraction has shown its suitability as a technique for separation of these pollutants from solid environmental matrices.

Organic Pollutants in Water

Water is the most important liquid in the environment. A wide range of human activities, such as mining, coal and fuel combustion, industrial and agricultural processes, domestic sewage, etc, contribute to the pollution of the aquatic environment. However, the key contribution to water pollution is the solubilization of pollutants. Thus, the study of pollutants in water can be divided into pollutants that are solubilized in water (mainly inorganic pollutants) and those present as the solid phases of the aquatic medium, such as sludge, sediment, particulates and biological species (organic and inorganic pollutants).

The way in which sludge and sediment are Soxhlet extracted in order to isolate the analytes from the solid matrix has been discussed in previous sections. This section is therefore devoted to the analysis of organic pollutants (mainly PCBs and pesticides) from water and associated particulates. In spite of the fact that biological samples are also a part of the environment, they are considered to be a matter concerning

biochemistry and toxicology and, therefore, beyond the scope of this article.

It is obvious that Soxhlet extraction is not a suitable method for direct separation of analytes from liquid sample, but that it must be used after a previous filtration step. This procedure is very similar to that followed for air samples. The two phases existing in water within suspension matter samples (liquid and particulate) are split by filters (paper, glass-fibre or quartz-fibre) and solid sorbents (PUFs, granular activated carbon, Aquapak 440A, Separon SE, ODS gel and Amberlite XAD-2, -4 or -7 resins). The solid sorbents and the particulate matter constitute the solid sample to be subsequently extracted by Soxhlet. Collection of the solid matter by centrifugation is an alternative to filtration. Some of the procedures found in the literature are discussed below.

PCBs and OCPs are Soxhlet extracted from solid particulate matter with dichloromethane. After silica gel or Florisil clean up in the presence of activated Cu, analyses are developed by GC-ECD (or GC-MS). The determination of organophosphorus and organonitrogen pesticides in solid particulate matter from surface water is developed by dichloromethane Soxhlet extraction and GC-NPD. The determination of PAHs from water samples requires hexane/acetone Soxhlet extraction, cleanup on both an Al_2O_3 - Na_2SO_3 column and silica column, and finally, individual separation by HPLC and fluorimetric detection.

Many aquatic organisms accumulate pollutants inside their tissues by bioaccumulation. This behaviour is used in pollution surveillance programmes, due to the following advantages it provides: (1) the analyses of soil, air, water, etc. yield levels of pollutants present at the time the samples were taken, whereas those observed in bioaccumulator species reflect the level over a period of time; and (2) pollutants concentrate in biological species at high levels, and can therefore be monitored by analytical techniques with relatively high detection limits.

The most relevant field in which biological samples are used is in the analysis of the aquatic environment. Fish, mussels and a number of other species are studied in order to evaluate pollution levels in the surrounding environment. The pollutants studied are the same as in previous sections, and Soxhlet extraction has great relevance as a pretreatment technique due to the solid character of the matrix. In spite of this, one of the most relevant drawbacks in Soxhlet extraction of these samples is their high water content (the presence of water in samples subjected to Soxhlet extraction constitutes a shortcoming whose importance is a function of the amount of water). Thus, it is necessary to macerate the sample initially with anhydrous Na_2SO_4 . After this, a conventional Soxhlet

extraction of the mixture with an organic solvent (depending on the nature of the analytes) is performed.

Use of Conventional Soxhlet Extraction for the Leaching of Inorganic Pollutants

The application of conventional Soxhlet extraction in the field of inorganic pollutants has been developed to a much less extent than that of organic pollutants. There are in the literature only a few applications of Soxhlet extraction to inorganic compounds. Soxhlet extraction is used mainly as a clean up step prior to the determination of inorganic pollutants with the aim of removing organic substances in the extract. As an exception to this, metals have been determined in the extract after a Soxhlet step. This is possible either when metals are forming organometal compounds or are concentrated by sorption on PUFs impregnated with an organic substance. However, the suitability of Soxhlet extraction for the isolation of inorganic pollutants is poor and some other techniques such as hydrolysis, digestion, distillation, etc. are recommended for this purpose.

Improvements in Soxhlet Extraction

Soxhlet extraction has been the most frequently used technique for isolation of organic pollutants from environmental samples for the last twenty years. However, the use of new extraction techniques that overcome the drawbacks associated with Soxhlet is, today, one of the most promising research lines in the field of solid sample treatment.

The most significant drawbacks of Soxhlet extraction are the long time required for the extraction and the large amount of organic solvent wasted, which is not only expensive to dispose of but which can cause environmental pollution itself. Moreover, the conventional device is not easily automated. There are two different ways in which to circumvent the drawbacks of conventional Soxhlet extraction, namely: (1) the use of one of the new alternatives (such as SFE, MAE, ASE, etc.); and (2) the improvement of conventional Soxhlet. As this article is devoted to Soxhlet extraction, the following sections discuss only the latter way, that is, improving the shortcomings of the conventional device while keeping its positive characteristics.

High-pressure Soxhlet extraction

High pressure in Soxhlet devices is achieved by placing the extractor in a cylindrical stainless-steel

autoclave or by the use of either commercial or laboratory-made supercritical fluid-Soxhlet extractors. Thus, PAHs and PCBs can be removed from environmental samples using HPS with liquid CO₂ in working conditions close to those corresponding to the supercritical state of the extractant. The main drawback of this alternative is the change from supercritical to liquid state of the extractant, which affects Soxhlet performance.

Automated Soxhlet (Soxtec HT and Büchi B811)

Commercial automated Soxhlet devices perform the extraction with similar precision to conventional Soxhlet but with a significant saving of time and extractant. The most relevant characteristic of a Soxtec system is the possibility of developing three different steps, namely, boiling, rinsing and recovery of the solvent, by switching a lever. The B811 extractor is able to perform the same steps as a Soxtec device but it can also work as a conventional Soxhlet. The overall performance of the B811 extractor is computer controlled. The analysis of organic pollutants from soil and sediments is an example of the methods developed for use with this device.

Focused microwave-assisted Soxhlet extraction (Soxwave and FMASE)

The Soxwave is a commercial system with an operational performance similar to that of Soxtec HT. The system performs the same three steps but with two significant differences: (1) a different heating source (microwave instead of electricity) is used; and (2) the sample is also irradiated with microwave energy, making it easier to rupture the analyte-matrix bonds. The main drawback of Soxwave is its dependence on the extractant dielectric constant. Thus, efficient extractions are only obtained with polar solvents (due to the characteristics of microwave irradiation) and, consequently, this device is not as universal as a conventional Soxhlet is. Moreover, the energy the analytes receive is at least as high as that necessary to reach the boiling point of the solvent, which can cause degradation of thermolabile analytes. Some applications of Soxwave have been developed in the environmental field and, due to its suitability for water-based extractions, quantitative extractions have been achieved in the isolation of metals from solid samples such as coal or soils.

FMASE is the last of the improvements carried out on the conventional Soxhlet extractor. In fact, the FMASE device works as a conventional Soxhlet, but the cartridge zone, where the extractant and sample are in contact, is placed in the microwave cavity of a specially designed focused microwave oven.

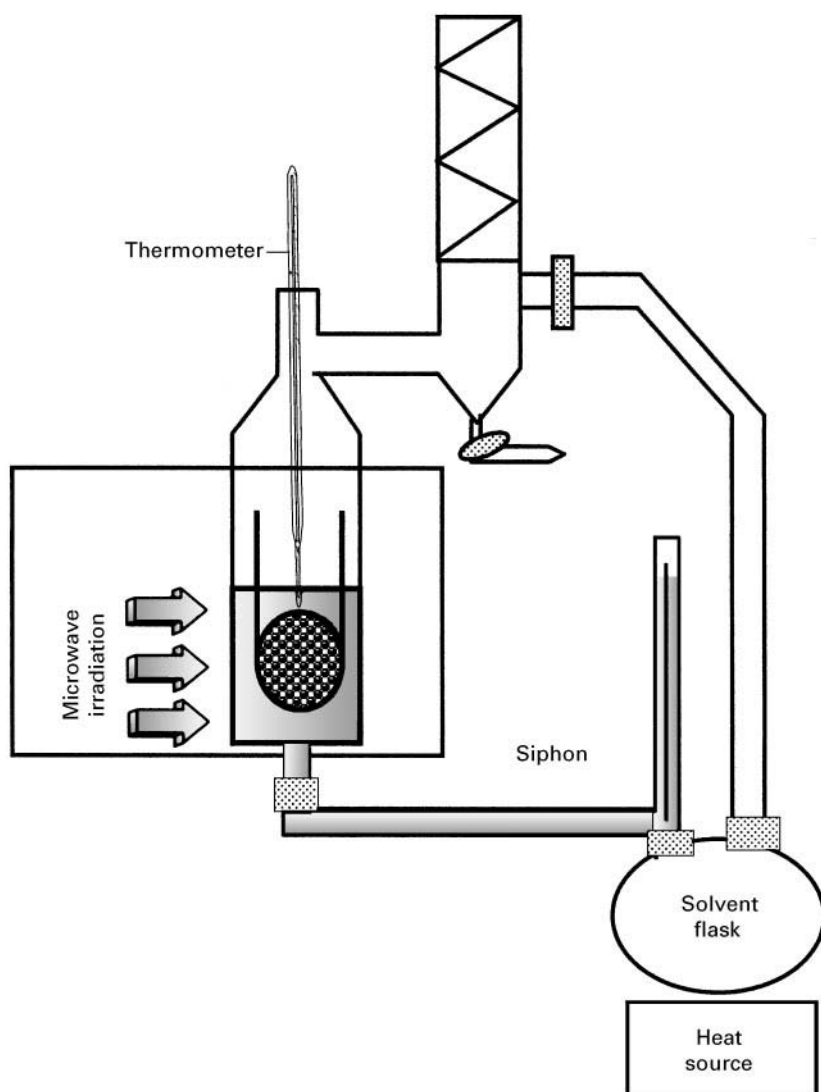


Figure 2 Scheme of the FMASE device. (Reproduced with permission from García-Ayuso LE and Luque de Castro MD (1999) *Analytica Chimica Acta* 382: 309.)

Figure 2 shows a scheme of the FMASE device. The similar performance with respect to its conventional counterpart makes FMASE a suitable alternative for almost all the applications developed in a conventional Soxhlet, that can be developed without changes, except in the time required for quantitative extraction.

FMASE maintains the advantages of conventional Soxhlet extraction while overcoming the limitations, such as the long extraction time, non-quantitative extraction of strongly retained analytes and unsuitability for automation. Solvent distillation in FMASE is achieved by electrical heating, which is independent of the extractant polarity, and recycling saves 75–85% of the total extractant volume. The main drawback in FMASE is the difficulty of using water as

extractant due to its design, as both thermal insulation and shortening of the present distillation device is mandatory for reception of water vapour on the sample-cartridge vessel, condensation there and dropping on the sample. A comparison between conventional Soxhlet and FMASE for leaching of PAHs, herbicides and n-alkanes from soil shows the advantages of the latter when compared with the conventional design. FMASE provides efficiencies similar to those obtained by conventional Soxhlet with extraction times at least eight times shorter.

Further Reading

Anderson R (1987) *Sample Pre-treatment and Separation*. New York: John Wiley.

- Ballschmeyer K (1993) Sample treatment techniques for organic trace analysis. *Pure Applied Chemistry* 55: 1943.
- Fifield FW and Haines PJ (1995) *Environmental Analytical Chemistry*. London: Chapman and Hall.
- Luque de Castro MD and Da Silva MP (1997) Strategies for solid sample pretreatment. *Trends in Analytical Chemistry* 16: 16.
- Luque de Castro MD and Garcia-Ayuso LE (1998) Soxhlet extraction of solid materials: an outdated technique with a promising innovative future. *Analytica Chimica Acta* 369: 1.
- Poole CF and Poole SK (1996) Trends in extraction of semivolatile compounds from solids for environmental analysis. *Analytical Communications* 33: 11H.
- Poole SK, Dean TA, Oudsema JW and Poole CF (1990) Sample preparation for chromatographic separations: an overview. *Analytica Chimica Acta* 236: 3.
- Prichard E, MacKay GM and Points J (1996) *Trace Analysis: A Structured Approach to Obtaining Reliable Results*. Cambridge: The Royal Society of Chemistry.
- Warner PO (1976) *Analysis of Air Pollutants*. New York: John Wiley.

Supercritical Fluid Extraction

V. Camel, Institut National Agronomique
Paris-Grignon, Paris, France

Copyright © 2000 Academic Press

There has been growing interest in supercritical fluid extraction (SFE) in the past few years due to its numerous advantages over liquid extraction (rapidity, low solvent volumes, nontoxicity of carbon dioxide, great selectivity by modifying the fluid density, low dilution of the extracts, possibility of online coupling with chromatographic techniques and automation).

Analytical applications of SFE began in the late 1980s, with particular focus on environmental samples. While early reports were on spiked matrices and/or highly contaminated samples, recent applications deal with samples containing low levels of incurred contaminants. It was soon found that extraction conditions are strongly dependent on both the solutes and the matrix, so that parameters need to be adjusted for every new application.

This article will focus on the main pollutants extracted, showing the important parameters that influence extraction recoveries, and illustrating the great potential of this technique together with its limitations.

Sample Preparation Prior to Extraction

To ensure better desorption of analytes from the matrix, several sample treatments can be performed, either physical (e.g. grinding) or chemical (e.g. addition of derivatization reagents).

Pretreatment of the Sample

This step is of prime importance, as it may greatly enhance the extraction efficiency.

Solids The moderate water solubility in supercritical CO₂ may lead to restrictor plugging; in addition,

water can be detrimental to the extraction of nonpolar compounds. Consequently, matrices with a high water content (typically 75%) require the addition of a drying agent to the sample (e.g. hydromatrix, a pelletized diatomaceous earth, magnesium or sodium sulfate). This also enlarges the surface area of the sample. However, the presence of residual water usually favours the extraction of polar compounds.

Grinding the sample should also enhance the extraction but, excessive grinding may lead to a pressure drop within the extraction cell, thereby decreasing the solubility of the analyte at the bottom of the cell. The pressure drop problem may be overcome by mixing the finely ground sample with a coarse dispersing agent.

Finally, the presence of sulfur in some matrices (e.g. sediments or sewage sludges) can cause lack of reproducibility and restrictor blockages. To overcome these problems, it is suggested to mix the sample with copper prior to extraction to act as sulfur scavenger.

Liquids A few studies have been performed on the direct SFE of aqueous matrices using a special extraction vessel. However, such analytes are mainly preconcentrated on to a solid-phase extraction (SPE) disk or cartridge, before being eluted with the supercritical fluid. This SPE-SFE combination offers a greater selectivity compared to elution with an organic solvent (e.g. CO₂ at low density selectively extracts organochlorine pesticides from C₁₈ disks, while extraction at a higher density in the presence of methanol is required to elute organophosphorus pesticides).

Derivatization Reactions

Extraction of highly polar compounds may be improved by coupling derivatization reactions with SFE, to convert polar functions into less polar groups for better solubility in the fluid. This procedure affords extracted compounds that are readily amenable to

gas chromatography. Besides, the derivatizing agent may react with active sites of the matrix, leading to better desorption of solutes.

The three main reactions are alkylation (with acidic methanol, alkyl halides, tetraalkylammonium salts or Grignard reagents), acylation (mostly with acetic anhydride, in the presence of organic bases such as pyridine) and silylation (with hexamethyldisilazane and trimethylchlorosilane). As the latter requires relatively anhydrous conditions, matrices with moisture contents greater than 0.4% may reduce derivatization efficiency.

Derivatization may be performed prior to extraction or under supercritical fluid conditions (*in situ* derivatization). The latter approach is most common as it reduces sample handling. Pre-extraction derivatization is used for particular applications (e.g. alkylation with Grignard reagents due to their low solubility in CO₂). As complex environmental matrices contain many potential interferences that can be derivatized, excess quantities of reagent should be used.

Ion Pairing

SFE of ionic compounds may be possible by formation of an ion pair, which is soluble in the fluid. The ion-pairing reagent may also react with the matrix active sites, thus favouring the desorption of solute molecules.

Common Pollutants Extracted by SFE

SFE has been successfully applied to the determination of several pollutants from different matrices. The strong solute-matrix interactions usually impose proper modifier selection and elevated temperature. Typical extraction conditions for the main pollutants are given in Table 1.

Polynuclear Aromatic Hydrocarbons

Polynuclear aromatic hydrocarbons (PAHs) have commonly been extracted from environmental matrices, and SFE has recently been adopted as an official method (US Environmental Protection Agency method 3561).

These analytes are relatively nonpolar and should be extracted with neat CO₂. However, the delocalized π -electron system of PAHs can cause strong interactions with the active sites of the matrix surface, hindering their extraction. Extraction of high molecular weight PAHs from real samples therefore requires high pressure and temperature, as illustrated in Figure 1 for urban dust particulates. Elevated temperature are suspected to favour analyte desorption from the active sites of the matrix.

PAH solubility in supercritical CO₂ decreases with increasing number of fused aromatic rings, so addition of a modifier is recommended to achieve acceptable recoveries. Methanol is the most common modifier, but satisfactory results can be obtained with other modifiers. For example, toluene-modified CO₂ is efficient in extracting two to six fused aromatic ring PAHs from soil with high carbon content (50%); addition of toluene to the sample also improves the extraction of nitro-PAHs from diesel and air particulates. A combination of toluene, trifluoroacetic acid and triethylamine is an even better modifier for PAHs and nitro-PAHs; the additives are thought to block the matrix active sites, thus preventing possible read-sorption of solute molecules. Extraction of PAHs from air particulate matter is also improved in the presence of diethylamine or acetonitrile, as illustrated in Figure 2.

The efficacy of the modifier is highly dependent on matrix characteristics. For example, the addition of methylene chloride as a static modifier allowed the quantitative extraction of PAHs from soil with CO₂; this modifier solubilizes the soil aggregates, thus increasing the contact between soil particles and supercritical CO₂.

The effect of increasing the temperature is always advantageous at constant density. Modifier and temperature effects are additive, so that extraction using CO₂ with modifiers at high temperature is usually the most rigorous SFE method for the extraction of particularly difficult samples such as urban air particulates, as shown in Figure 3.

Another approach has been the use of *in situ* chemical derivatization to determine PAHs from a harbour sediment. The derivatizing agent (Tri-Sil, a 2:1 (v/v) mixture of hexamethyldisilazane and trimethylchlorosilane) was added to the extraction vessel prior to the extraction step. As shown in Figure 4, results were improved compared with extraction with CO₂ or 10% methanol-modified CO₂. As PAHs cannot be derivatized, the effect of the reagent was to help displacement of the analytes from the matrix.

Although nitrous oxide modified with 5% methanol may be considered to be the most efficient fluid for extracting PAHs, its use should be avoided due to the possibility of explosion with this combination. Difluorochloromethane is also efficient but environmental concern discourages its common use. Subcritical water (250°C, 50 bar) seems a more viable alternative to CO₂ for the SFE of organic compounds with a wide range of polarities. The dielectric constant of water decreases as the temperature increases so that at moderate temperatures (50–100°C) polar compounds are extracted (e.g. phenols, amines), while nonpolar to moderately polar organics (including

Table 1 Typical applications of SFE to solid environmental matrices

Compounds		Matrices	Reagent added to the matrix	Fluid	Observations
Polyaromatic hydrocarbons		Soils, sediments, urban dust, fly ash	None	CO ₂ -CH ₃ OH (10%) CO ₂ -toluene (10%) CO ₂ -diethylamine (10%) Subcritical H ₂ O	Strong interactions with the matrix High temperatures recommended, as well as with addition of modifier
			CH ₂ Cl ₂	CO ₂	Solubilization of soil aggregates by CH ₂ Cl ₂
			Tri-Sil	CO ₂	Tri-Sil displaces the solutes from the matrix
Polychlorinated biphenyls		Soils, sediments, sewage sludge	None	CO ₂ CO ₂ -CH ₃ OH (1-2%) CO ₂ -diethylamine Subcritical H ₂ O	Moderate temperatures (70-100°C)
Dioxins		Fly ash, sediments	None	CO ₂ -CH ₃ OH (2%)	Strong interactions with the matrix Better recoveries with a dry matrix
Phenols		Soils, house dust	Strong acid	CO ₂	Destruction of the matrix by the acid
			None	CO ₂ -CH ₃ OH (2-20%) CO ₂ -CH ₃ OH (32%)-H ₂ O (8%)	High temperatures recommended
Pesticides	Organochlorine	Soils, sediments	Acetic anhydride and pyridine	CO ₂	<i>In situ</i> acetylation of phenols
	None		CO ₂ -toluene	Toluene disrupts solute-matrix interactions	
	Organophosphorus Triazines		None None	CO ₂ -CH ₃ OH (5%) CO ₂ -CH ₃ OH (10-30%) CO ₂ -[CH ₃ OH + 2%H ₂ O] (10%)	Matrix moisture enhances the extraction
Surfactants	Phenoxyacetic acids	Soils, sediments, sewage sludges	None	CO ₂ -CH ₃ OH (20%)	
			TMPA	CO ₂	Ion pairing and methylation
	Nonionic		BF ₃ /CH ₃ OH	CO ₂	Methylation
			None	CO ₂ -CH ₃ OH (27.5%)	
	Anionic		None	CO ₂	CO ₂ -CH ₃ OH (40%)
Metallic species	Cationic Organometallics	Sediments	TAA salts	CO ₂	Ion pairing
			Methylation reagent	CO ₂	Methylation
			None	CO ₂ -CH ₃ OH (30%)	
	Metal ions	Sediments	None	CO ₂ -CH ₃ OH (10-20%)	
			Organic ligand ^a Derivatization reagent ^b	CO ₂ -CH ₃ OH (5%)	
			Organic ligand ^c	CO ₂ -CH ₃ OH (5%)	Formation of a metal chelate Methanol increases the chelate solubility

TMPA, trimethylphenylammonium hydroxide; TAA, tetraalkylammonium.

^aOrganic ligands: dithiocarbamates (mainly sodium diethyldithiocarbamate and diethylammonium diethyldithiocarbamate).^bDerivatization reagents: hexylmagnesium bromide, thioglycolic acid methylester.^cOrganic ligands: dithiocarbamates, β -diketones, crown ethers, organophosphorus compounds.

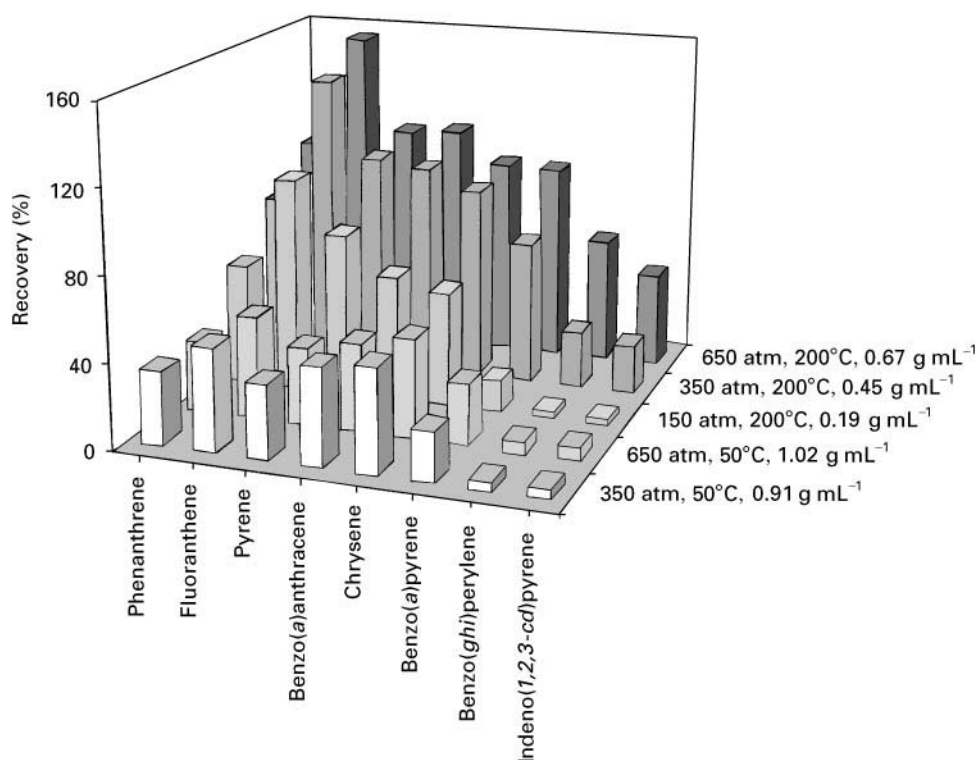


Figure 1 Recoveries of PAHs from urban air particulates (standard reference material SRM 1649) using supercritical CO_2^a extraction at different pressures and temperatures. ^a40-min extractions. (From Langenfeld JJ, Hawthorne SB, Miller DJ and Pawliszyn J (1993) Effects of temperature and pressure on supercritical fluid extraction efficiencies of polycyclic aromatic hydrocarbons and polychlorinated biphenyls. *Analytical Chemistry* 65: 338–344. Copyright 1993 American Chemical Society.)

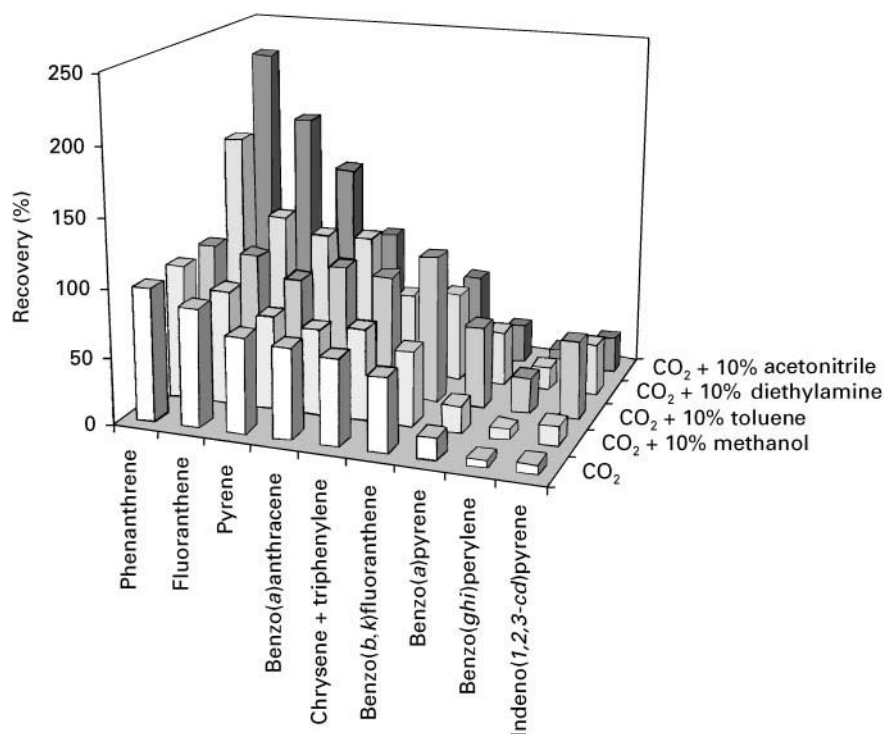


Figure 2 Influence of the presence of a modifier in supercritical CO_2 on the recoveries of PAHs from air particulate matter (standard reference material SRM 1649)^a. ^a400 bar, 80°C, 250 μL (10% v/v) modifier added to the sample, 5 min static/10 min dynamic. (From Langenfeld JJ, Hawthorne SB, Miller DJ and Pawliszyn J (1994) Role of modifiers for analytical-scale supercritical fluid extraction of environmental samples. *Analytical Chemistry* 66: 909–916. Copyright 1994 American Chemical Society.)

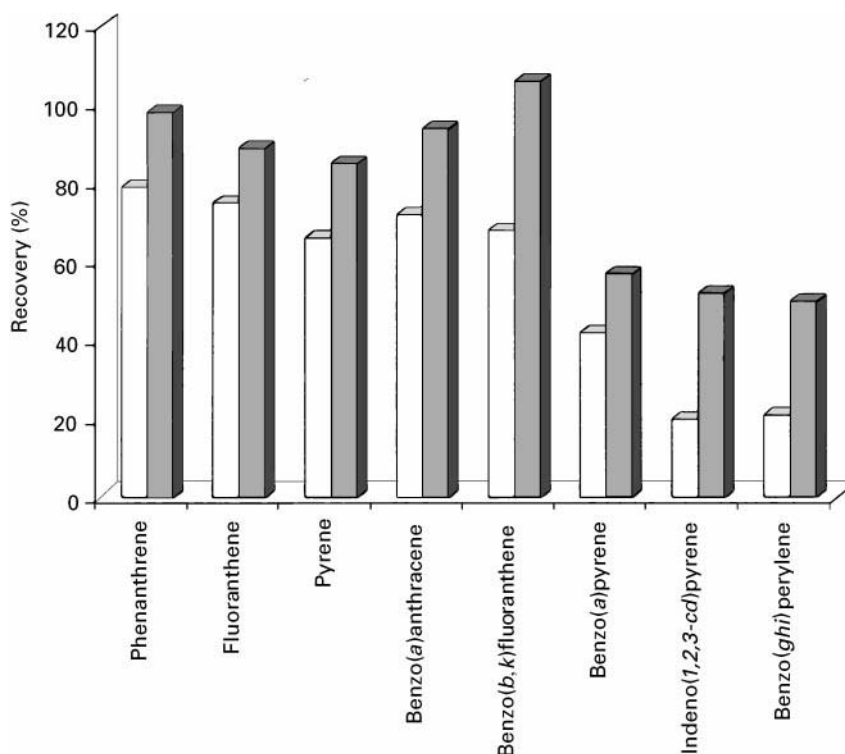


Figure 3 Temperature effect on the recoveries of PAHs from air particulate matter (standard reference material SRM 1649) using methanol modified CO_2 . ^a400 bar, 80 μL (10% v/v) methanol added to the sample, 15 min static/15 min dynamic. (From Yang Y, Gharaibeh A, Hawthorne SB and Miller DJ (1995) Combined temperature/modifier effects on supercritical CO_2 extraction efficiencies of polycyclic aromatic hydrocarbons from environmental samples. *Analytical Chemistry* 67: 641–646. Copyright 1995 American Chemical Society.)

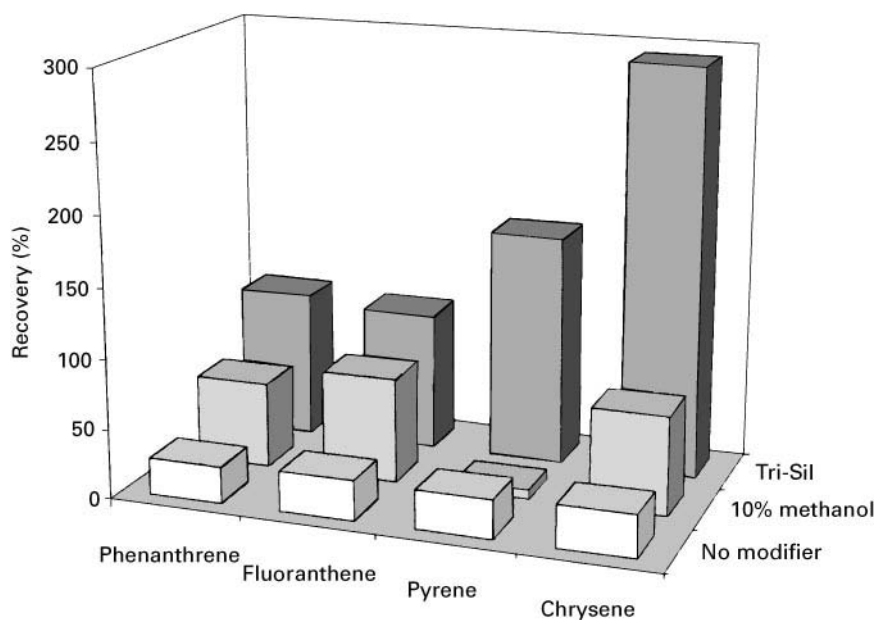


Figure 4 Recoveries of PAHs from a harbour sediment (HS-3) using either supercritical CO_2 , 10% methanol modified CO_2 , or *in situ* derivatization with Tri-Sil^a followed by CO_2 extraction. Three sequential extractions were conducted (each at 350 bar and 60°C, 15 min static/15 min dynamic). ^aTri-Sil is a mixture of hexamethyldisilane and trimethylchlorosilane 2 : 1 (v/v); 0.5 mL of this reagent was added to the cell prior to the extraction. The derivatizing agent was added just prior to each static step. (From Hills JW and Hill HH (1993) Carbon dioxide supercritical fluid extraction with a reactive solvent modifier for the determination of polycyclic aromatic hydrocarbons. *Journal of Chromatographic Science* 31: 6–12. With permission of Preston Publications, a Division of Preston Industries Inc.)

PAHs) are extracted at higher temperatures (200–250°C), as illustrated in Figure 5.

PAHs have also been determined in water samples after their preconcentration on to C₁₈ disks and their further elution with supercritical CO₂.

Polychlorinated Biphenyls

Polychlorinated biphenyls (PCBs) are lipophilic and thereby highly soluble in CO₂. Hence, CO₂ alone or modified with a small amount of methanol (typically 1–2%) is efficient for their extraction. Figure 6 illustrates the effects of both pressure and temperature on the recovery of PCBs from river sediment using neat CO₂. Best recoveries are obtained at high temperature, whatever the pressure. Surprisingly, high molecular weight PCBs are more efficiently extracted, despite their expected reduced solubilities; in fact, this is in agreement with the tighter binding of low molecular weight PCBs to the sediment matrix.

Recovery rates may be improved by addition of modifiers, especially methanol, as illustrated in Figure 7. Thus, methanol-modified CO₂ allowed the SFE of PCBs and organochlorine pesticides at the part-per-trillion level in marine sediments. Water under subcritical conditions is also an effective extractant for PCBs.

Recently, a single SFE method for field extraction of PCBs and PAHs in soils has been developed with neat CO₂ (150°C, 400 bar) to avoid co-extraction of matrix material, allowing direct gas chromatography. The simultaneous extraction and clean-up of mussel samples can be achieved by adding Florisil on top of the sample, enabling the direct determination of 11 PCBs (as well as 15 organochlorine pesticides).

Dioxins

Dioxins (polychlorinated dibenzo-*p*-dioxins (PCDDs) and polychlorinated dibenzofurans (PCDFs)) are of great environmental concern owing to their acute toxicity. Like PCBs, they are readily amenable to extraction by SFE. As these pollutants have been mainly detected in emissions from municipal incinerators, their extraction from fly ash matrices has been investigated. SFE gave satisfactory results, as compared to Soxhlet extraction. Despite the high solubility of these compounds in pure CO₂, it gave almost no extraction due to the strong matrix adsorption of the dioxins. Upon addition of 2% methanol to the CO₂, 2,3,7,8-tetrachlorodibenzo-*p*-dioxin was efficiently extracted from a dry sediment; the presence of water in the matrix hindered its extraction. The suitability of nitrous oxide for the SFE of PCDDs and PCDFs

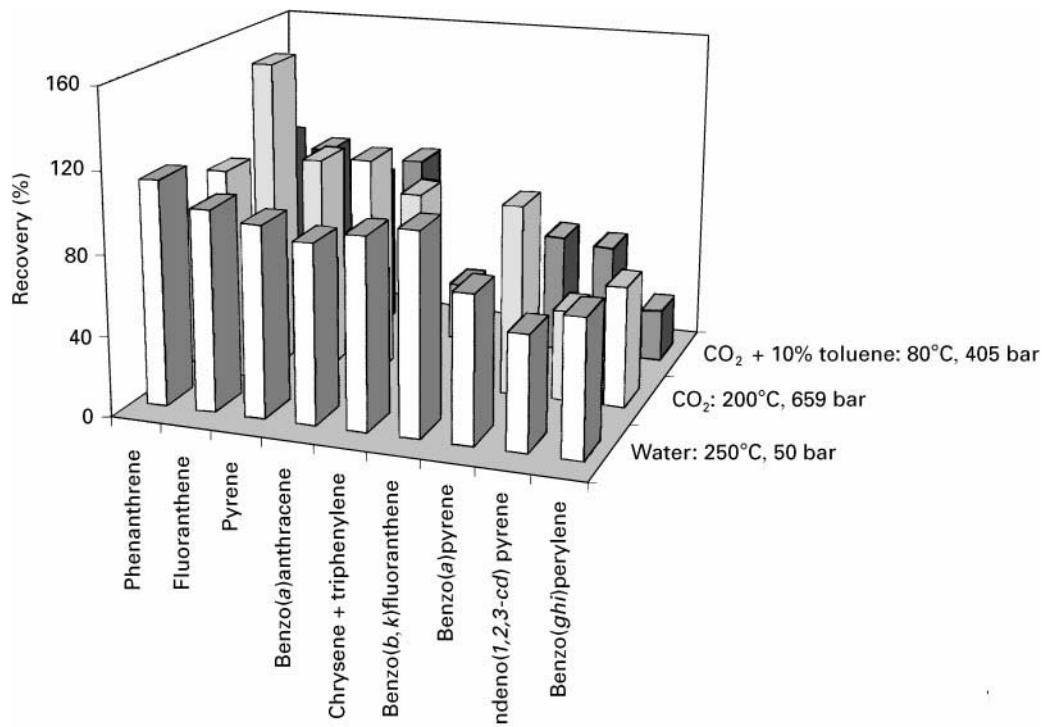


Figure 5 Recoveries of PAHs from urban air particulate (National Institute for Standards and Technology NIST 1649) using either supercritical CO₂^a (200°C, 659 bar), 10% toluene modified CO₂^b (80°C, 405 bar) or subcritical water (250°C, 50 bar). ^a40-min extractions. ^b20-min extractions (10 min static/10 min dynamic). (From Hawthorne SB, Yang Y and Miller DJ (1994) Extraction of organic pollutants from environmental solids with sub- and supercritical water. *Analytical Chemistry* 66: 2912–2920. Copyright 1994 American Chemical Society.)

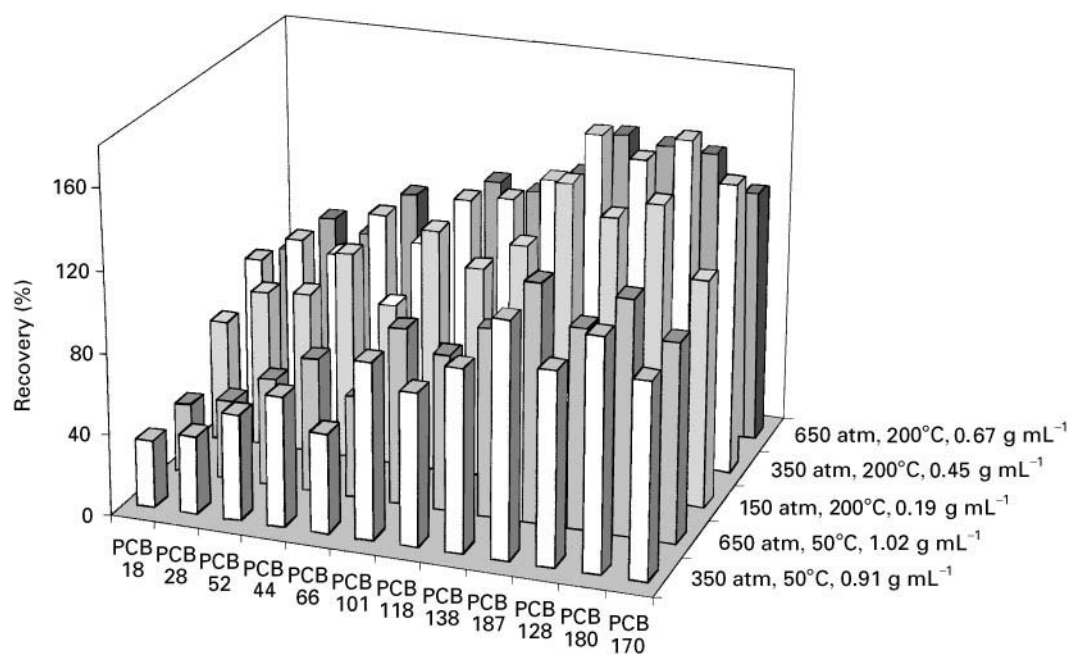


Figure 6 Recoveries of PCBs from river sediment (standard reference material SRM 1939, containing 3% water and 10% organic matter) using supercritical CO₂^a extraction at different pressures and temperatures. ^a40-min extractions. (From Langenfeld JJ, Hawthorne SB, Miller DJ and Pawliszyn J (1993) Effects of temperature and pressure on supercritical fluid extraction efficiencies of polycyclic aromatic hydrocarbons and polychlorinated biphenyls. *Analytical Chemistry* 65: 338–344. Copyright 1993 American Chemical Society.)

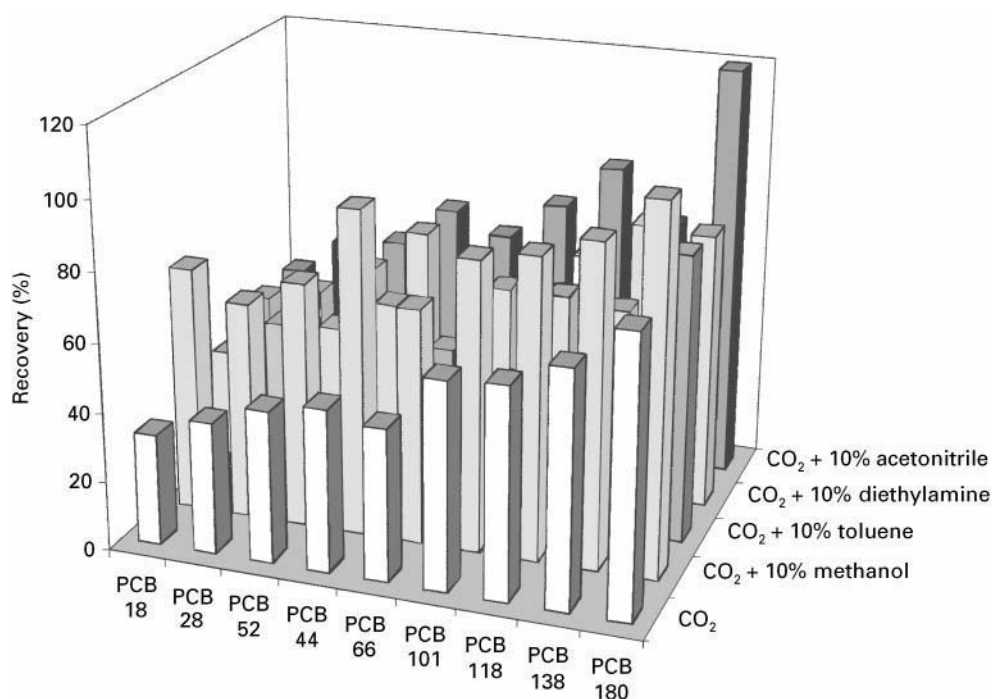


Figure 7 Influence of the presence of a modifier in supercritical CO₂ on the recoveries of PCBs from river sediment (standard reference material SRM 1941)^a. ^a400 bar, 80°C, 250 μ L (10% v/v) modifier added to the sample, 5 min static/10 min dynamic. (From Langenfeld JJ, Hawthorne SB, Miller DJ and Pawliszyn J (1994) Role of modifiers for analytical-scale supercritical fluid extraction of environmental samples. *Analytical Chemistry* 66: 909–916. Copyright 1994 American Chemical Society.)

has also been described. Alternatively, the matrix may be destroyed by exposure to a strong acid, and further extracted with neat CO₂.

Phenols

Phenols are moderate to highly polar compounds. Thus, several approaches have been used for their SFE: direct addition of a polar modifier (e.g. water, acetonitrile, methanol) to the matrix, dynamic addition of the modifier to the CO₂, or *in situ* acetylation.

For example, addition of 2% methanol improved their extraction from soil. Enhanced-fluidity liquid extraction (CO₂ with 20% methanol) improved the recovery of phenols from house dust. Further improvements could be achieved using a methanol–water–CO₂ mixture (32.1/7.9/60 mol %), as water is supposed to swell the matrix material, allowing more efficient penetration and interruption of matrix–analyte interactions. Similar results have been obtained with sediments.

As illustrated in Figure 8, phenols are efficiently acetylated during SFE by means of direct reaction with acetic anhydride. Even though recoveries of phenols decrease as the activated charcoal content of

the soil increases due to stronger solute–matrix interactions, improvement upon derivatization is evident. In addition, extracts are cleaner because of milder extraction conditions.

Similarly, the SFE of pentachlorophenol and related compounds from soil samples can be achieved using *in situ* acetylation (with acetic anhydride and triethylamine at 80°C) followed by CO₂ extraction. Increasing the extraction temperature from 50 to 200°C resulted in higher recoveries of chlorophenols from an industrial soil.

Pesticides

Pesticides have a broad range of physical properties and chemical structures. Their solubility in pure CO₂ may be evaluated from their octanol–water partition coefficients. Organochlorine pesticides are highly soluble in pure CO₂, while organophosphorous compounds require a modifier; addition of a polar modifier becomes crucial for triazines. In the case of phenoxyacetic acids, an ion-pairing or derivatization reagent needs to be added.

Another useful parameter is the soil–water partition coefficient, as it is indicative of the pesticide's soil adsorption; recoveries have been shown to decrease

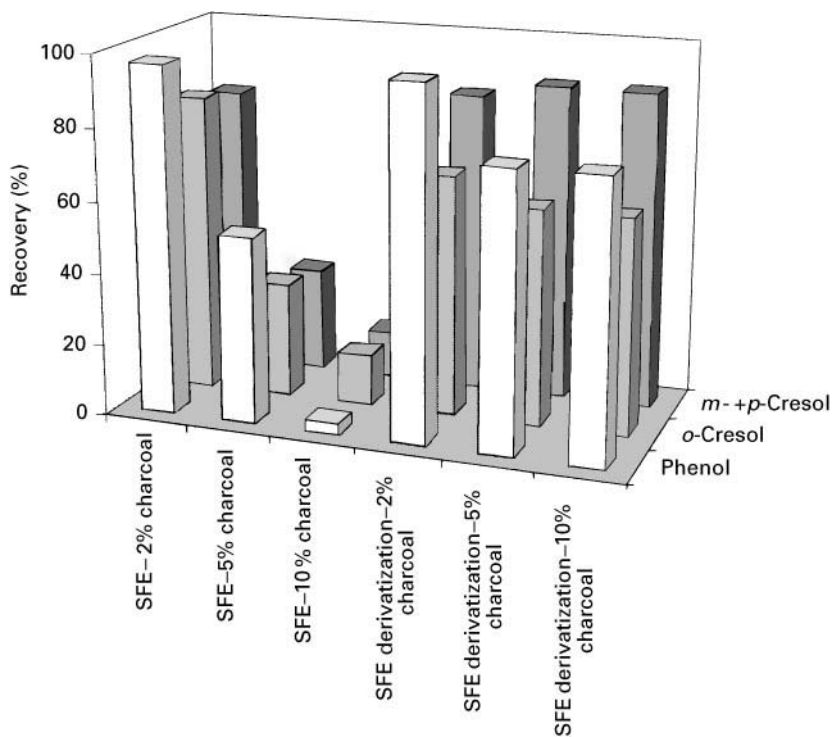


Figure 8 Recoveries of phenolic compounds from three garden soils with 2, 5 and 10% activated charcoal content, using SFE alone^a or SFE-derivatization^b. ^aCO₂, 90°C, 382 bar, 0.77 g mL⁻¹, addition of 100 µL methanol to the sample, 10 min static/15 min dynamic. ^bCO₂, 115°C, 0.4 g mL⁻¹, addition of 20 µL pyridine and 115 µL acetic anhydride to the sample, 5 min static/15 min dynamic. (From Llompart MP, Lorenzo RA, Cela R, Li K, Belanger JMR and Pare JRJ (1997) Evaluation of supercritical fluid extraction, microwave-assisted extraction and sonication in the determination of some phenolic compounds from various soil matrices. *Journal of Chromatography A* 774:243–251. With permission from Elsevier Science.)

as the soil organic content is increased, due to strong analyte–matrix interactions.

Nonpolar pesticides Despite their high solubility in CO_2 , the solute–matrix interactions may yield lower recoveries than expected from solubility alone. Thus, extractions of organochlorine pesticides from spiked soils were unsatisfactory, especially for soils with a high organic content. Modifiers have been tested to enhance the SFE of organochlorine pesticides from different matrices. For example, toluene added to a contaminated soil improved the extraction with CO_2 of hexachlorocyclohexane isomers.

Several organochlorine pesticides were also efficiently extracted from aqueous matrices using a combination of SPE (on to C_{18} disks and cartridges) and pure CO_2 SFE.

Moderately polar and polar pesticides Methanol-modified (5%) CO_2 is a common extractant for organophosphorus pesticides. The polar triazine herbicides require a higher percentage of methanol (10%) in CO_2 to increase their solubility and disrupt solute–matrix interactions. Methanol (10%) containing 2% water may also be used. The ternary mixture acetone–water–triethylamine (90/10/1.5 v/v/v) is also efficient. Water is suspected of increasing the surface area of clay containing soils by swelling. Thus, a direct correlation between diuron extraction from montmorillonite clay and the percentage swelling of the matrix (due to the modifier) was observed at different pressures and temperatures. In contrast, triethylamine should compete with solute molecules on to the active sites of the soil. Also, soil moisture has been reported to enhance triazine extraction, as well as addition of a surfactant (Triton X-100), which probably leads to the matrix swelling and the formation of nonionic reverse micelles.

Extraction of bound pesticide residues in soils may require more severe conditions (for example, extraction of triazine from a mineral soil entailed 30% methanol, 350 bar and 125°C).

Ionic pesticides Specific SFE conditions are required to improve their solubility and/or to overcome strong solute–matrix interactions. Addition of 20% methanol to CO_2 allowed the extraction of four herbicides (dicamba, 2,4-dichlorophenoxyacetic acid (2,4-D), 2-(2,4,5-trichlorophenoxy)propionic acid (2,4,5-TP) and 2,4,5-trichlorophenoxyacetic acid (2,4,5-T)) from house dust (440 bar and 100 or 150°C). Pre-extraction of extraneous matrix material was achieved with CO_2 after hexane was added to the sample. The mixture acetone–water–triethylamine (90/10/1.5 v/v/v) also enhanced extraction of 2,4-D from soil.

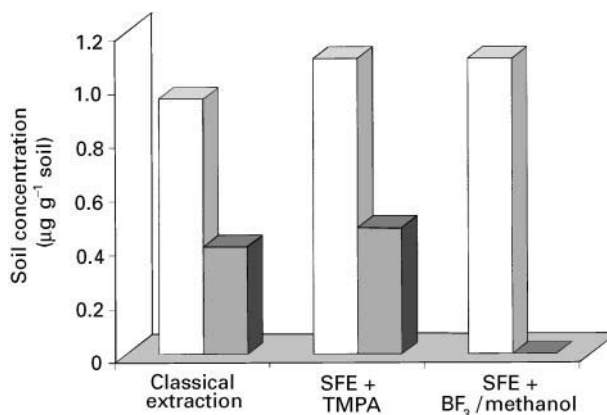


Figure 9 Extraction of native pesticides from an agricultural soil using either classical extraction (two sequential extractions with 0.5 mol L^{-1} KOH in 10% KCl/water) or SFE (with TMPA (three sequential extractions (each 15 min static/15 min dynamic), CO_2 , 400 bar, 80°C) or BF_3 –methanol (a single extraction (15 min static/15 min dynamic), CO_2 , 400 bar, 80°C) as derivatization reagents). Open bars, 2,4-D; filled bars, dicamba. (Reproduced with permission from Hawthorne *et al.*, 1992. Copyright 1992 American Chemical Society.)

The ion-pairing methylating reagent TMPA facilitated the CO_2 extraction of 2,4-D and dicamba from sediments. The presence of methyl iodide improved the recoveries of 2,4-D and 2,4,5-T from soil. Alkylation with methanol and BF_3 as a catalyst is also promising for the preferential extraction of 2,4-D over dicamba, as illustrated in Figure 9.

Surfactants

Nonionic surfactants (e.g. alkylphenoethoxylates) have been extracted from sediments with 27.5% methanol-modified CO_2 (450 bar and 100°C). Water-modified CO_2 (350 bar and 80°C) was also efficient in extracting nonylphenol polyethoxylates from dried sewage sludge, yielding recoveries higher than traditional techniques.

Quantitative extraction of anionic surfactants (linear alkylbenzenesulfonates) from soil, sediment and sludge can be obtained using 40% methanol-modified CO_2 (380 bar and 125°C). Also, TAA salts have been used as ion-pairing reagents to extract linear alkylbenzenesulfonates and linear alkylsulfonates from sewage sludge. Finally, derivatization of anionic surfactants into their methyl esters may also be performed to enhance their extraction.

The ditallowdimethylammonium cation was extracted from anaerobically stabilized sewage sludge and marine sediment using 30% methanol-modified CO_2 (380 bar, 100°C). No improvement could be obtained in the presence of ion pair reagents. Due to the ionic character of this surfactant, it was assumed that high concentrations of anionic surfactants ini-

tially present in the matrix allowed the formation of ion pairs with the cationic surfactant, thereby enabling its extraction.

Surfactants (e.g. alcohol phenol ethoxylate) were also extracted from aqueous samples with either direct SFE (by means of a modified extraction cell) or SPE-SFE. In the latter case, methanol-modified CO₂ was required for efficient elution from the C₁₈ discs.

Metallic Compounds

Metals exist in the environment as organometallic compounds, ionic species or inorganic compounds. Organometallic compounds are usually soluble in supercritical fluids and may be extracted directly. On the other hand, ionic species require the addition of a ligand to be extracted. Consequently, speciation can be achieved by SFE using sequential extractions (with proper selection of ligands). As an example, methylmercuric chloride and dimethylmercury could be extracted with neat CO₂ and 100 bar (50°C) from solid materials; a dithiocarbamate reagent was further introduced into the matrix to extract Hg²⁺ ions.

Organometallic compounds Several studies have investigated the use of SFE for extracting organometallic compounds from environmental samples. Thus, tributyltin has been successfully extracted from sediments using methanol (20% v/v)-modified supercritical CO₂. Methanol as a modifier provided the most favourable recovery of trimethyllead, triethyllead and diethyllead from sediment and urban dust, as compared to water and acetone (446 bar and 80°C, 10% modifier).

Other approaches have been tested: binding to an organic ligand, formation of an ion pair and *in situ* derivatization. Thus, with the addition of diethylammonium diethyldithiocarbamate as a ligand, di-, tri- and tetra-substituted organotin species could be extracted from soils and sediments using 5% methanol-modified CO₂ (while recoveries of monoalkyltins remained low). Monobutyltin was efficiently extracted from a reference sediment on addition of sodium diethyldithiocarbamate in the extraction vessel (Figure 10); increased extraction efficiencies of trimethyllead, trimethyltin, dibutyltin and tributyltin were also observed in this way.

Hexylmagnesium bromide as a derivatizing agent assisted the CO₂ extraction of monophenyltin, diphenyltin and triphenyltin from sediment. Dimethylarsenic acid and monomethylarsenic acid could be extracted from a solid sample by supercritical CO₂ after *in situ* derivatization with thioglycolic acid methyl ester.

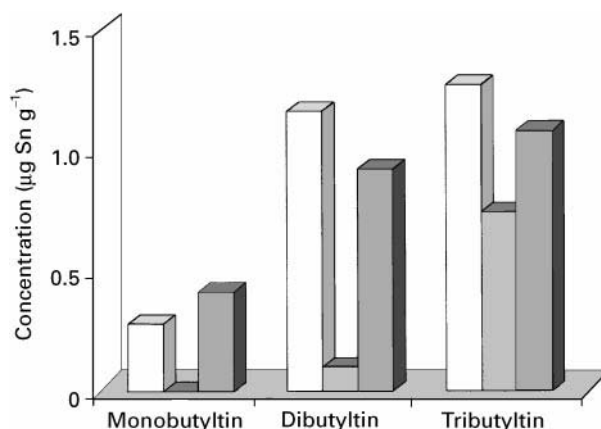


Figure 10 Comparison of extraction efficiencies of organotin compounds from a reference sediment (PACS-1) using SFE with or without the addition of sodium diethyldithiocarbamate (NaDCC). Open bars, certified value; grey bars, no NaDCC; black bars, with NaDCC. (Reproduced with permission from Chau *et al.*, 1995, and with permission from Elsevier Science.)

Organotins in aqueous matrices were ethylated with sodium tetraethylborate, enriched on C₁₈ disks and further extracted with acid-modified supercritical CO₂. Alternatively, aqueous matrices containing butyl-, phenyl- and cyclohexyltin compounds were collected on a C₁₈ disk, before being derivatized via Grignard ethylation and extracted using supercritical CO₂.

Metal ions Extraction of free metal ions by supercritical CO₂ requires charge neutralization. This can be achieved by binding the metal ion to organic ligands, thereby resulting in neutral stable complexes that are soluble in CO₂. Obviously, rapid complexation kinetics and a high stability constant for the neutral complex will enhance the extraction process. A key factor is the solubility of the complex in the supercritical fluid.

Different organic ligands (dithiocarbamates, β -diketones, crown ethers and organophosphorus reagents) have been tested for their ability to extract heavy metals, lanthanides and actinides from several matrices. In particular, fluorinated ligands yield metal complexes with higher solubility in supercritical CO₂, making them more effective for the extraction of metal ions. In addition, alkyl substitutions in ligands may enhance the solubility of metal complexes in CO₂. As an example, diethyldithiocarbamates and fluorinated β -diketones are effective chelating agents for extracting transition metal ions from solid matrices, as shown in Figure 11 for Cd²⁺. Recoveries are improved with methanol (5%)-modified CO₂, as the solubility of the metal chelate is enhanced. As dithiocarbamates tend to decompose in supercritical

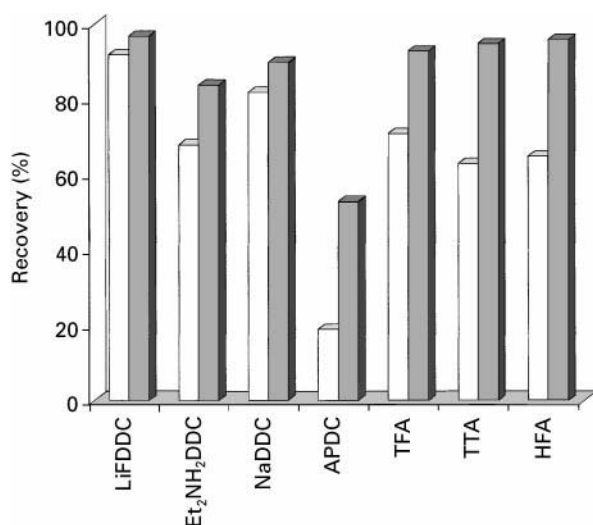


Figure 11 Recoveries of Cd^{2+} from spiked sand samples using SFE with dithiocarbamates or β -diketones as chelating agents. Open bars, CO_2 ; filled bars, 5% methanol-modified CO_2 ; 45°C, 250 bar; 15 min static/15 min dynamic. LiFDDC; bis(trifluoroethyl)dithiocarbamate; $\text{Et}_2\text{NH}_2\text{DDC}$; diethylammonium diethyldithiocarbamate; NaDDC; sodium diethyldithiocarbamate; APDC, ammonium pyrrolidinedithiocarbamate; TFA, trifluoroacetylacetone; TTA, thenoyltrifluoroacetone; HFA, hexafluoroacetylacetone. (Reproduced with permission from Wai *et al.*, 1996, and with permission from Elsevier Science.)

CO_2 in the presence of water, an excess of reagent is recommended to achieve good metal extraction efficiencies.

Addition of a proton-ionizable crown ether (*tert*-butyl-substituted dibenzobistriazolocrown ether) in methanol (5%)-modified CO_2 allowed the selective extraction of Hg^{2+} from sand if a small amount of water was present in the matrix (200 bar and 60°C). Other divalent metal ions (Cd^{2+} , Pb^{2+} , Co^{2+} , Mn^{2+} , Ni^{2+}) remained in the sand under these conditions.

Very recently, fluorinated hydroxamic acids have been used for the SFE of Fe(III) with unmodified CO_2 . Toxic metals (As, Cd, Cr, Cu, Pb) have been extracted from real contaminated soil and wood samples using the Cyanex reagent (*bis*(2,4,4-trimethylpentyl)-monothiophosphinic acid) as an extractant in supercritical CO_2 modified with 5% methanol.

Up to the present, most of the experiments conducted have focused on spiked samples and future studies need to be conducted with real environmental samples. In such samples, the active sites and natural ligands present may bind strongly to certain metal ions, thereby hindering their complexation with added ligands. Native metals can also be in highly insoluble forms (such as oxides and sulfides), leading to a fraction of the metals that may not be extractable by SFE. It seems that SFE may be used to evaluate the amounts of leachable metals in solid matrices.

Metal ions have also been directly extracted from aqueous samples. First, the supercritical CO_2 is passed through a vessel filled with the ligand. Next, the fluid saturated with the ligand passes through the aqueous phase. For example, CO_2 containing thenoyltrifluoroacetone and tributyl phosphate

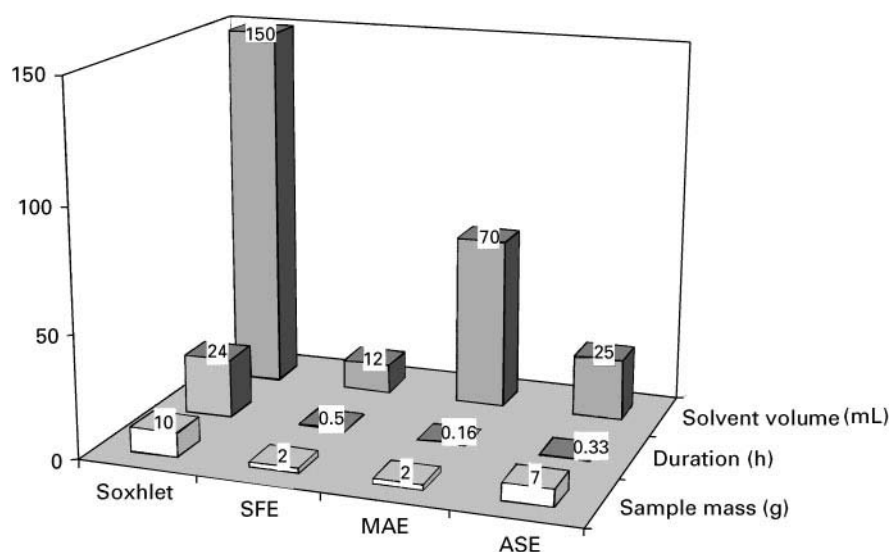


Figure 12 Comparison of extraction techniques for the determination of PAHs from contaminated soil: Soxhlet extraction (10 g sample mixed with 10 g anhydrous sodium sulfate; 150 mL dichloromethane; heating 24 h), SFE (2 g sample; 20% methanol-modified CO_2 ; 70°C, 250 kg cm^{-2} , 30 min), atmospheric microwave-assisted extraction (MAE) (2 g sample; 70 mL dichloromethane; heat 297 W; 20 min) and accelerated solvent extraction (ASE) (7 g sample; dichloromethane–acetone 1:1 (v/v); 100°C, 2000 psi; 10 min). (Reproduced with permission from Saim *et al.*, 1997, and with permission of Elsevier Science.)

extracted lanthanides (La^{3+} , Eu^{3+} and Lu^{3+}) from a buffered acetate solution.

Future Trends

Despite rapid growth in the past few years, SFE is still rarely used for routine applications. This is mainly because of the large number of parameters to control, as well as the influence of the matrix. The strong matrix-analyte interactions that may occur in environmental matrices frequently make the development of quantitative extraction conditions based solely on solubility considerations and spike recoveries invalid for real samples. In addition, its development is also limited by the high capital cost required.

Yet SFE has several advantages over other techniques (especially rapidity and low solvent volumes, as shown in **Figure 12**). It is successful in extracting a broad range of pollutants from numerous matrices. In particular, polar compounds and ionic species can be extracted through addition of a polar modifier, a derivatization reagent, an ion-pairing reagent or a ligand. These recent applications will be more thoroughly studied in the next few years, especially the possible speciation, due to selective extraction, of metallic compounds.

Subcritical water appears to be a very promising fluid, as it offers the opportunity to extract polar to nonpolar compounds by simply increasing the temperature. No doubt this fluid will be more common in future SFE applications.

Finally, extraction conditions will be optimized for numerous real environmental samples, including certified reference materials, thereby leading to wider use of this technique.

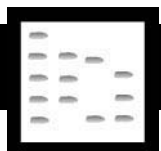
See also: II/Chromatography: Gas: Derivatization. Chromatography: Liquid: Ion Pair Liquid Chromatography; Mechanisms: Ion Chromatography. Extraction: Solid-Phase Extraction; Solvent Based Separation. III/Metal Complexes: Ion Chromatography.

Further Reading

- Chau YK, Yang F and Brown M (1995) Supercritical fluid extraction of butyltin compounds from sediment. *Analytica Chimica Acta* 304: 85–89.
- Hawthorne SB, Miller DJ, Nivens DE and White DC (1992) Supercritical fluid extraction of polar analytes using *in situ* chemical derivatization. *Analytical Chemistry* 64: 405–412.

- Hawthorne SB, Yang Y and Miller DJ (1994) Extraction of organic pollutants from environmental solids with sub- and supercritical water. *Analytical Chemistry* 66: 2912–2920.
- Hills JW and Hill HH (1993) Carbon dioxide supercritical fluid extraction with a reactive solvent modifier for the determination of polycyclic aromatic hydrocarbons. *Journal of Chromatographic Science* 31: 6–12.
- Langenfeld JJ, Hawthorne SB, Miller DJ and Pawliszyn J (1993) Effects of temperature and pressure on supercritical fluid extraction efficiencies of polycyclic aromatic hydrocarbons and polychlorinated biphenyls. *Analytical Chemistry* 65: 338–344.
- Langenfeld JJ, Hawthorne SB, Miller DJ and Pawliszyn J (1994) Role of modifiers for analytical-scale supercritical fluid extraction of environmental samples. *Analytical Chemistry* 66: 909–916.
- Lee ML and Markides KE (eds) (1990) *Analytical Supercritical Fluid Chromatography and Extraction*. Provo, UT: Chromatography Conferences.
- Llompard MP, Lorenzo RA, Cela R *et al.* (1997) Evaluation of supercritical fluid extraction, microwave-assisted extraction and sonication in the determination of some phenolic compounds from various soil matrices. *Journal of Chromatography A* 774: 243–251.
- Luque de Castro MD, Valcarcel M and Tena MT (1994) *Analytical Supercritical Fluid Extraction*. New York, Springer-Verlag.
- McHugh M and Krukoni V (1994) *Supercritical Fluid Extraction*, 2nd edn. Boston, MA: Butterworths.
- Saim N, Dean JR, Abdullah MDP and Zakaria Z (1997) Extraction of polycyclic aromatic hydrocarbons from contaminated soil using Soxhlet extraction, pressurised and atmospheric microwave-assisted extraction, supercritical fluid extraction and accelerated solvent extraction. *Journal of Chromatography A* 791: 361–366.
- Taylor LT (1996) *Supercritical Fluid Extraction*. New York: Wiley-Interscience.
- Wai CM, Wang S, Liu Y, Lopez-Avila V and Beckert WF (1996) Evaluation of dithiocarbamates and β -diketones as chelating agents in supercritical fluid extraction of Cd, Pb, and Hg from solid samples. *Talanta* 43: 2083–2091.
- Westwood SA (ed.) (1992) *Supercritical Fluid Extraction and its use in Chromatographic Sample Preparation*. Glasgow: Blackie Academic and Professional.
- Yang Y, Gharaibeh A, Hawthorne SB and Miller DJ (1995) Combined temperature/modifier effects on supercritical CO_2 extraction efficiencies of polycyclic aromatic hydrocarbons from environmental samples. *Analytical Chemistry* 67: 641–646.

ENZYMES



Chromatography

S. Nilsson and S. Santesson,
University of Lund, Lund, Sweden

This article is reproduced from *Encyclopedia of Analytical Science*, Copyright © 1995 Academic Press

Separation and Determination in Physiological Samples

The determination of an absolute enzyme concentration in a physiological sample is principally straightforward; the main problem is the need for a purified sample to use as a standard.

Enzymes are proteins found in nature in complex mixtures, usually in cells which perhaps contain several hundreds of different enzymes. In order to understand and interpret enzyme data from complex biological systems in, for instance, a subcellular organelle (such as a mitochondrion), a cell or whole organism, we must try to understand its properties in as simple a system as possible. From studies of an isolated enzyme we can learn about its specificity for certain substrates, the kinetic parameters for the reaction and the possible means of regulation. All these parameters are useful for understanding the role of the enzyme in more complex systems. The ready availability of isolated enzymes has been of considerable value in a number of medical and industrial applications.

To study a given enzyme properly in physiological samples it must be purified. Maintenance of biological activity is the goal throughout the whole purification scheme. Extracellular enzymes usually withstand the variety of stresses they are exposed to during the purification. In contrast, when released from their natural protective environment, intracellular enzymes are very sensitive to various steps in the purification scheme. Integral membrane enzymes are especially vulnerable during solubilization.

Specific examples, together with trends in enzyme determination in physiological samples, will be discussed in this article.

Preparation of Enzymes with Biological Activity from Physiological Samples

Enzyme Activity Measurement Process

To elucidate enzymatic activity from physiological samples certain steps have to be performed.

1. Preparation of reaction mixture and enzyme, where the reaction mixture usually consists of a controlled substrate solution with the correct temperature, pH and any cofactors needed for catalysis. Enzymes often demand a more complex preparation methodology than substrates and the reaction mixture. This will be discussed later.
2. Initiation and incubation, which are usually started by adding the proper enzyme preparation to the reaction mixture or vice versa. All subsequent time measurements are related to this initial time.
3. Termination, which can be achieved in various ways. Normally, this means inactivation of the catalytic activity of the enzyme.
4. Separation of the enzyme products from the enzyme and its substrates.
5. Detection and identification of the enzymatically formed product(s) during specific incubation intervals.
6. Under certain conditions enzyme activity can be followed dynamically, i.e. by rate measurement ($\Delta f/\Delta t$, where f is temperature, absorbance, fluorescence, etc., and t is time).
7. Interpretation of the produced data.

Handling of Specimens and Samples (the Preanalytical Phase)

For all biological material (tissue, urine, cerebrospinal fluid, cell cultures, etc.) the same basic sequence of procedures applies.

1. Preparation of subject to be investigated.
2. Collection of specimen.
3. Separation of sample from specimen.
4. Transport of specimen and/or sample.
5. Storage of specimen and/or sample.
6. Pretreatment of samples for enzymatic analysis.

The specimen is defined as that part of the subject which is taken as representative for the analysis. The sample is the material that is actually analysed. The sample can be derived from, prepared from or be a part of the specimen which is homogenized for measurement of enzyme activities. Consequently the aliquot of homogenate that is analysed is the sample. Only under certain conditions is the sample identical to the specimen.

Sample Preparation Strategy

Two factors should be considered during preparation of enzymes with biological activity from physiological samples. The first factor for consideration is the selection of the biological sample that is to be used as the starting material for the purification. The samples can be subdivided into three groups, depending on their complexity (see Figure 1).

The first group (I) includes samples containing different cell types and extracellular compartments, e.g. samples containing organs, tissue, biological fluids, microbial cells, and unicellular organisms from a culture medium or fermentation broth. Initially cellular compartments have to be separated from noncellular compartments. The second group (II) consists of

different cell types within the cellular compartments being separated from each other. Group II samples are thus homogeneous populations of each type of cell. This becomes the starting material for samples where cell-surface activities can be directly assayed or the cells can be lysed (broken up), thus providing access to the activities in intracellular organelles and on cytoplasmic fragments.

The third group (III) consists of subcellular fragments liberated by lysis of group II samples. These fragments include organelles such as mitochondria as well as those operationally defined as the membrane fraction or a fraction containing soluble components. The initial steps within this group will be separation of different organelles and separation of soluble from insoluble material. This is followed by solubilization

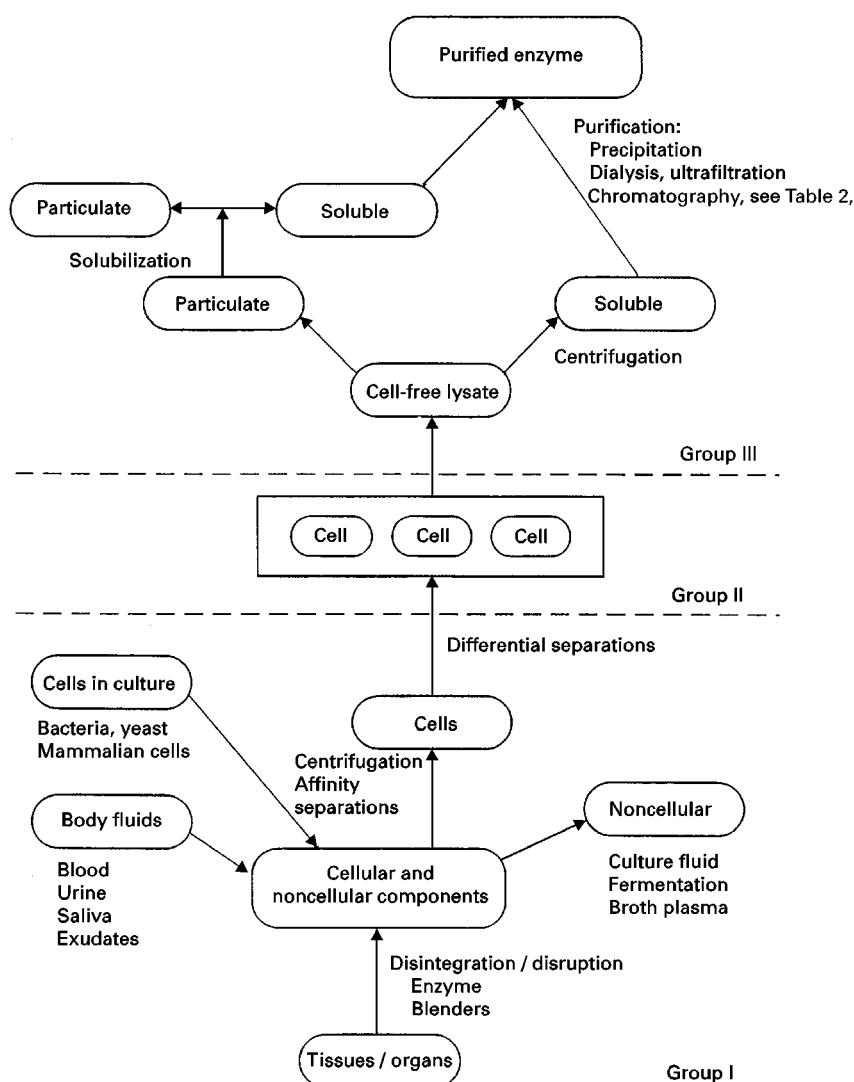


Figure 1 Enzyme purification scheme. Samples can be divided into three groups, I, II and III, depending on their complexity. Samples in the different groups enter and leave the purification process at different points. The samples in group I are the most complex, consisting of both extracellular and cellular enzyme-containing material which must first be separated. Group II samples contain different types of cells, one of which contains the enzyme of interest. In group III the enzyme source is from only one type of cell, from which the 'right' subcellular fraction gives the 'right' enzyme. (Adapted from Rossomando, 1987.)

of membrane fractions and finally separation of molecular species from each other.

The second factor for consideration during the preparation of biologically active enzymes concerns to what extent the sample should be purified. The traditional end point of any purification scheme would be a homogeneous protein. The main goal should be to assay a single enzymatic activity without interference from other activities. However, for some studies it is advantageous or even necessary to assay the activity of interest in the presence of other activities.

Sample Obtained from Tissue or Organ

Tissues and organs (e.g. skin, liver) can be divided into at least two compartments, the cellular compartment and the extracellular compartment. The activity of interest could be localized in either of the compartments. Cell-sorting techniques should be used where whole undamaged cells are separated from the stable fibrillar matrix. Some cell damage is unavoidable with the harsh methods often used for disrupting the matrix, e.g. cutting or dicing with scissors, shearing in a blender, or grinding. Specific disruption of the matrix can be performed using purified enzymes, e.g. collagenase for mammalian tissues. Trypsin and other proteolytic enzymes have also been used with success. Such procedures result in a mixture of cells extracellular compartments including some insoluble fragments, and added enzymes (including reagents).

Samples Obtained from Tissue or Organ Culture

Cultured samples are usually treated in the manner described previously. Precautions must be taken to avoid errors due to the additional extracellular compartments and the culture medium, which may contain enzymatic activities originating from the medium itself or produced during sample growth.

Samples Obtained from Biological Fluids

Body fluids such as blood, cerebrospinal fluid and saliva contain cells as a normal component. However, in other fluids cells are a contamination. Cells in urine may indicate a disease process. The study of enzymes in such fluids also requires separation of the two compartments (cells from biological fluid). Because biological fluids do not contain fibrillar matrix material, the separation will, for instance, be a simple centrifugation step (5000 g for 15 min) which will produce a pellet containing most of the cellular material. The supernatant produced by centrifugation can be assayed for enzymatically active proteins.

Samples Obtained from Cell Culture

For cells grown in liquid culture, including mammalian cells, fungi, protozoa and bacteria, noncellular compounds should be separated from the cells before analysis takes place. Even here, a low-speed centrifugation is sufficient for separation of cells from culture media. The supernatant should be assayed for enzymatic activity and the cell-pellet material could be set aside for later assay or lysis.

Enzyme Activity Determination

Extracellular Enzymes

The extracellular fluid around tissues or the growth medium around mammalian cells, bacteria, yeast or fungi cells often contains the enzyme activity of interest. Several factors have to be considered before activity measurements can be started. Proteolytic enzymes must be inhibited early in the determination process, because otherwise they will degrade and destroy the enzymatic activity of interest. Another factor for consideration is the interference of small molecules, which could be erroneously measured as enzyme substrate or product. A special case is inhibitors which diminish enzyme activity. If a serum-free medium is not used during mammalian cell propagation, special care concerning serum enzymatic activity measurements and purification has to be taken.

Within the Cellular Compartment

After sample preparation, cells are separated from noncellular material in different manners depending on the complexity of the original sample (i.e. from which organ the sample originates). Because a number of different types of cells could remain, an assay of any complex sample should begin with the preparation of only one cell type.

Many separation methods utilizing different properties of the cells have been used. In sucrose gradient centrifugation, density differences between cell types are used and each cell type finds its equilibrium position in the sucrose gradient. Field flow fractionation can also be used for separating cells according to their size and shape. Adipose tissue cells will separate without centrifugation; they just float. Antibodies raised against any special marker on the cell surface could be explored for selection of that special cell type with various techniques. For example, using metallic iron coupled to antibodies a strong neodymium permanent magnet could be used for selecting a specific cell type. Selective chemical lysis of cell types that are not of interest followed by mild centrifugation will provide the cells containing the enzyme of interest. Even

homogeneous mammalian cells can differ in enzymatic activity if the age or nutritional status of the animals is not identical.

Intact Cells

When a reaction mixture consists only of one type of cell any assay of enzymes on the cell surface will only be straightforward if the cells are not disrupted during determination, because the presence of intracellular components could give rise to false results. For example, if cell-surface adenosine triphosphatase (ATPase) activity is to be measured it is suitable to monitor the product ADP (adenosine diphosphate). However, if the cells are lysed, intracellular ADP will affect the enzyme activity determination.

Subcellular Samples

Depending on the localization of the enzyme of interest, different strategies for the cell lysis have to be considered. A subcellular fractionation could be quite rewarding later in the enzyme purification route. Methods such as sonication, use of a French press, blending or homogenization are useful for the lysis of different types of cells.

For example, a French press is needed for the lysis of bacterial cells with rigid cell walls. The use of a Potter-Elvehjem homogenizer (PTFE (poly(tetra fluoroethylene)) pestle in a glass mortar) for the homogenization of cells with fragile cell membranes is a procedure that will merely break the outer cell membrane, leaving most of the cell organelles intact.

Table 1 Marker enzymes for different subcellular fractions

<i>Subcellular fraction</i>	<i>Enzyme</i>
Nuclei	DNA nucleotidyltransferase
Nuclei	Nicotinamide-nucleotide adenyltransferase
Mitochondria	Succinate dehydrogenase
Mitochondria	Cytochrome <i>c</i> oxidase
Endoplasmic reticulum	Glucose-6-phosphatase
Lysosomes	Acid phosphatase
Lysosomes	Ribonuclease
Peroxisomes	Catalase
Peroxisomes	Urate oxidase
Plasma membrane	5'-Nucleotidase
Cytosol	Glucose 6-phosphate dehydrogenase
Cytosol	Lactate dehydrogenase
Cytosol	6-Phosphofructokinase

From Price and Stevens (1989), p. 369.

A subcellular fractionation scheme based on centrifugation for mammalian cells is outlined in **Figure 2**.

The enzymatic activity of interest can be followed, together with the activity of marker enzymes, through the subcellular scheme (**Table 1**). The subcellular localization is then predicted and further purification can be performed.

Enzyme Purification Methods

Maintenance of Biological Activity

Soluble proteins, either cytoplasmic or inside organelles, are present in highly concentrated soups

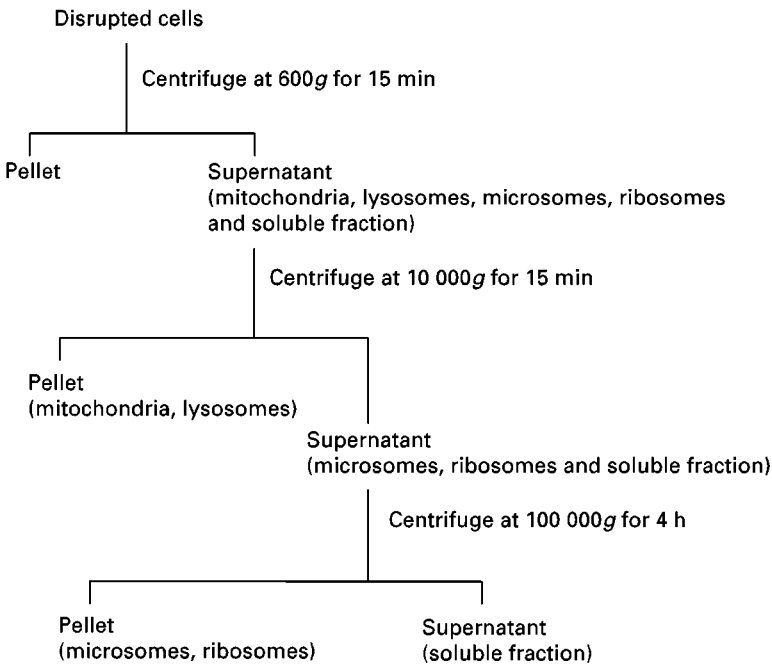


Figure 2 A subcellular fractionation scheme for mammalian cells by differential centrifugation. (From Price and Stevens (1989), p. 368.)

of proteins, with concentrations ranging from 100 mg mL^{-1} to as high as 400 mg mL^{-1} inside the mitochondrial matrix. Oxygen tension is low and different natural reducing compounds such as glutathione are present to maintain a high reducing potential. Other stabilizing agents are also present, such as different substrates and products. When the tissue is disrupted during purification proteins are released from their protective environment and proteolytic enzymes which are held in separate compartments are also released. As a consequence the enzyme of interest has to be protected from oxidation, proteolytic degradation and irreversible unfolding of their tertiary structure. This can be achieved in many different ways and should be tailor-made for each purification scheme and enzyme.

Denaturation during purification can be minimized if precautions are taken according to extremes of pH, temperature and organic solvents. The natural pH inside a cell is normally in the range 6–8. Using buffers within this pH range at appropriate ionic strength should protect against pH denaturation. Reducing the temperature by $15\text{--}25^\circ\text{C}$ decreases many degradation processes three- to five-fold. Reducing the temperature also slows down the processes involved in the separation method, for instance in size exclusion chromatography.

Enzymes in dilute preparations may denature due to adsorption onto the wall of the container or onto the chromatography matrix used. Enzymes with quarternary structure will dissociate and the activity of interest will be lost.

Adsorption and denaturation of dilute enzyme samples can be circumvented by using a carrier protein such as bovine serum albumin (BSA), or even better a commercial synthetic carrier protein with a simple and known structure at a concentration as high as 1 mg mL^{-1} . Care must be taken to avoid interaction between the carrier protein and the enzymes of interest. The molecular size of the carrier protein should also differ by at least a factor of two from the enzyme of interest, for easy removal by size exclusion chromatography if the pure enzyme protein is needed, for instance in amino acid sequencing.

Catalytic site inactivation by specific reactions is hard to avoid. Loss of cofactors can be prevented by including them in the purification buffer. Covalent modification of the active site which contains reactive amino acid residues responsible for the catalysis is common. The most troublesome amino acid is cysteine, which is very susceptible to modification. Sulfhydryl residues at the active site may be in the ionized form, which is prone to oxidation and can form disulfide bonds, or may be partially oxidized to

the sulfinic acid or irreversibly oxidized to the sulfonic acid.

These reactions can be suppressed by using different additives such as ethylenediaminetetraacetic acid (EDTA), which masks by complexation cations that would otherwise catalyse the formation of disulfide bonds with cysteine residues at the catalytic site. Other commonly used reducing agents are sulfhydryl-containing reagents such as β -mercaptoethanol, 2,3-dimercaptopropanol, thioglycolate, glutathione, cysteine and the dithio-analogues of the reduced C_4 sugars, threitol and erythritol (DTT, DTE). EDTA and other complexing agents often cannot be used for enzymes that have an essential metal ion in the active site.

Proteinases or proteolytic enzymes are contained inside living cells. In mammalian cells they are packed in lysosomes. In microorganisms they are often found between the plasma membrane and the cell wall. During preparation of an enzyme extract by cell homogenization, release of proteolytic enzymes will occur and their activity has to be inhibited. Depending on the wide scale of different proteinases present in the cell homogenate, many types of inhibitors have to be used.

Diisopropyl fluorophosphate (DFP) inhibits serine proteases. Note that DFP is dangerous to handle because it is volatile and attacks human acetylcholinesterase, vital in nerve conduction. Phenylmethylsulfonyl fluoride (PMSF) is a nonvolatile serine protease inhibitor and does not attack acetylcholinesterase. It inhibits some thiolproteases and some carboxypeptidases, but it has to be dissolved in acetone or isopropanol.

Pepstatin, leupeptin and antipain are peptide-based inhibitors that are very potent against acid proteases such as pepsin, cathepsin D and yeast protease A. Normal concentrations of inhibitors used in freshly prepared extracts are 5 mmol L^{-1} EDTA, 1 mmol L^{-1} PMSF, $10 \mu\text{mol L}^{-1}$ pepstatin, $10 \mu\text{mol L}^{-1}$ leupeptin and $10 \mu\text{mol L}^{-1}$ antipain.

Other stabilizing factors during enzyme purification are some nonaqueous hydrophilic molecules. Owing to the high nonaqueous content in cell cytoplasm ($10\text{--}15\%$ w/v), the water around the protein molecules is not freely mobile and thus stabilizes the protein structure. To mimic this situation in prepared enzyme extracts glycerol is added at $10\text{--}50\%$ (w/v). Below 30% the viscosity is not harmful for most methods used during enzyme purification except for ultrafiltration and centrifugation and in some 'salting-out' experiments because hydrogen bonding and hydrophobic forces decrease. Sugar or sugar alcohol solutions such as glucose, fructose, lactose and sorbitol and be used instead of glycerol. The mechanism of protection is similar.

Separation Methods Based on Size, Shape, Mass, Charge, Hydrophobicity, Solubility and Biological Recognition

The different physicochemical properties of the enzyme that should be utilized during a purification scheme include size, shape, charge, hydrophobicity, solubility and biological recognition. The salient points of various separation methods are listed in Table 2.

After each step in a purification scheme, a proper enzyme activity assay should be carried out and the amount of protein determined. If correctly done the specific activity (in units per milligram) (1 U is the

amount of enzyme that converts 1 μmol of substrate per min under defined reaction conditions) can be followed through the purification scheme – it should rise and then reach a plateau. Crude extracts should be concentrated by fractional precipitation with ammonium sulfate or poly(ethylene glycol) (PEG) or adsorbed and desorbed from a chromatographic matrix as soon as possible. Precipitated proteins, after dissolution in a small volume, are more stable because they are more concentrated. Centrifugation with field strength from 5000 to 50 000 g is widely used for subcellular fractionation and for ammonium sulfate and PEG-precipitated enzymes.

Table 2 Enzyme separation methods

<i>Physicochemical property</i>	<i>Method</i>	<i>Characteristic</i>	<i>Scale</i>	<i>Use</i>	<i>Enzyme activity recovery</i>
Size, shape or mass	Centrifugation	Moderate resolution; slow	Large or small	Partial fractionation	Good
	Gel filtration	Moderate resolution; slow	Small	Desalting, size determination, fractionation	Good
	Field flow fractionation	Good resolution; fast	Small	Size determination, fractionation	Good
	Ultrafiltration	Bad resolution; slow/medium	Large or small	Desalting, concentration	Good
	Dialysis	Bad resolution; slow	Large or small	Desalting, concentration	Good
Polarity (a) Charge	Ion exchange chromatography	High resolution; fast	Large or small	Fractionation, concentration	Good
	Chromatofocusing	Excellent resolution; fast	Medium	Fractionation, concentration	Poor
	Electrophoresis	High resolution; medium/fast	Small/medium	Fractionation, visualization	Medium/poor
	Isoelectric focusing	Excellent resolution; medium	Small/medium	Fractionation, visualization	Poor
	Capillary electrophoresis	Excellent resolution; fast	Extremely small	Fractionation, size determination possible	Good
(b) Hydrophobic character	Hydrophobic interaction chromatography	Good resolution; fast	Large or small	Fractionation, concentration	Good
	Reversed-phase chromatography	Excellent resolution; fast	Large or small	Fractionation, concentration	Poor
Solubility	Change in pH	Medium resolution; fast	Large or small	Concentration, fractionation	Medium
	Change in ionic strength	Medium resolution; fast	Large or small	Concentration, fractionation	Medium/good
	Decrease in dielectric constant	Medium resolution; fast	Large or small	Concentration, fractionation	Medium
	Two-phase separation	Medium/good resolution; medium	Large or small	Fractionation, concentration	Good
Biological activity	Affinity chromatography	Excellent resolution	Generally small	Fractionation, concentration	Medium/good
Specific binding or structure features	Dye–ligand chromatography	Good resolution; fast	Large or small	Fractionation, concentration	Medium/good
	Immuno-chromatography	Excellent resolution; fast	Generally small	Fractionation	Medium/good
	Covalent chromatography	Medium/good resolution; fast	Medium/small	Fractionation	Medium

Field flow fractionation Field flow fractionation (FFF) is a chromatography-like separation technique which is designed for fractionation of macromolecules, colloids and particles. The principle is simple. A laminar flow of carrier liquid between two walls, separated by *c.* 0.1 mm, creates a parabolic velocity profile. The sample is injected into the carrier stream at the inlet of the channel and exits through the outlet end which is connected to a detector.

Sample retention is achieved when molecules are pushed to the accumulation wall (an ultrafiltration membrane) by an external field force (a cross-flow), so that they obtain different average distances from the wall and are placed at different heights in the parabolic flow profile. The different sample molecules are consequently transported down the channel at different velocities. Thus separation can be achieved.

The size range embraced by FFF is from small proteins (*c.* 10 kDa), up to organelles and cells with a diameter of several micrometers. FFF does not rely on a stationary phase, which makes it very useful for separation of labile enzyme molecules. Separation times are very short (3–10 min) and selectivity according to size is better than for gel filtration. Loadability is so far limited to *c.* 200 µg per separation run.

Examples of Enzyme Determination in Physiological Samples

Hormone-Sensitive Lipase from Adipose Tissue

Hormone-sensitive lipase (HSL, EC 3.1.1.3) is an amphiphilic enzyme and the key control of energy substrate flow in mammals. Its activity in adipose tissue determines the rate of hydrolysis of stored triacylglycerols and thereby the production of fatty acids for release as free fatty acids (FFAs) into the circulation.

The following parameters were considered during purification.

1. Development of a suitable assay procedure
2. Selection of the best source from which the molecule could be purified.
3. Solubilization of the desired molecule.
4. Development of a series of isolation and concentration procedures which includes stabilizing the molecule at each stage.

Lipase activity was measured against emulsified [³H]-oleic acid-labelled monooleoylglycerol (a diacylglycerol ether analogue). An enzyme activity of 1 U corresponds to the release of 1 µmol of fatty acids per minute at 37°C. The assay was performed between each purification step. The enzyme source was rat adipose tissue (epididymal fat pads).

A summary of the steps taken in the purification of HSL from rat epididymal adipose tissue is given in **Figure 3**.

Step 1. Fat pads frozen in 0.25 mol L⁻¹ sucrose, 1 mmol L⁻¹ EDTA, 1 mmol L⁻¹ DTE and 10 µmol L⁻¹ of leupeptin and antipain in liquid nitrogen were homogenized (Potter–Elvehjem homogenizer) in 30% (w/v) 0.25 mol L⁻¹ sucrose and partially delipidated by removing the fat floating after centrifugation at 5000 g for 10 min at 4°C.

Step 2. The supernatant was further delipidated and separated from the pelleted material by centrifuging at 100 000 g for 45 min (referred to as the '100 000 g supernatant').

Step 3. The pH was lowered to 5.2 with acetic acid. HSL was precipitated over 30 min on ice and the pellet collected after 30 min of 10 000 g centrifugation. The pellet was resuspended in 20 mmol L⁻¹ Tris-HCl (2-amino-2-hydroxymethylpropane-1,3-diol hydrochloride), pH 7.0, containing sucrose as before (this fraction is referred to as 'the pH 5.2 ppt fraction'). This fraction contains practically all the HSL and about 25% of the contaminating proteins. The preparation is stable for several months at –80°C.

Step 4. Further solubilization of the pH 5.2 ppt fraction was by sonication at 10°C in the nonionic detergent C₁₃E₁₂ (heterogeneous alkyl polyoxyethylene glycol type). The solubilized HSL was fractionated by gradient sievortptive chromatography on quaternary aminoethyl (QAE)-Sephadex, for a separation time of 12 h at 10°C. 70% of the recovered enzyme was pooled and concentrated 15-fold by ultrafiltration and referred to as the QAE-Sephadex fraction.

Step 5. This fraction was dialysed and concentrated three-fold further against 20 mmol L⁻¹ Tris-acetic acid, pH 7.50, containing 20% (w/v) glycerol, 15% PEG, 1 mmol L⁻¹ DTE, 0.2% C₁₃E₁₂ and 10 µmol L⁻¹ leupeptin for 8 h at 4°C, immediately followed by chromatography on a Mono Q column (polymer-based strong anion exchanger for liquid chromatography from Pharmacia) as described in detail in **Figure 4**. The enzyme peak fractions collected were immediately brought to pH 7.0 by addition of a potassium phosphate buffer to give a final concentration of 30 mmol L⁻¹ and the fractions were stored at –80°C in 50% (w/v) glycerol. This enzyme preparation is referred to as the 'Mono Q enzyme'.

Step 6. The last step of the purification scheme consisted of Mono S chromatography (polymer-based strong cation exchanger for liquid chromatography from pharmacia). Before chromatography the Mono Q enzyme was dialysed and concentrated three-fold for 3 h against 10 mmol L⁻¹ potassium

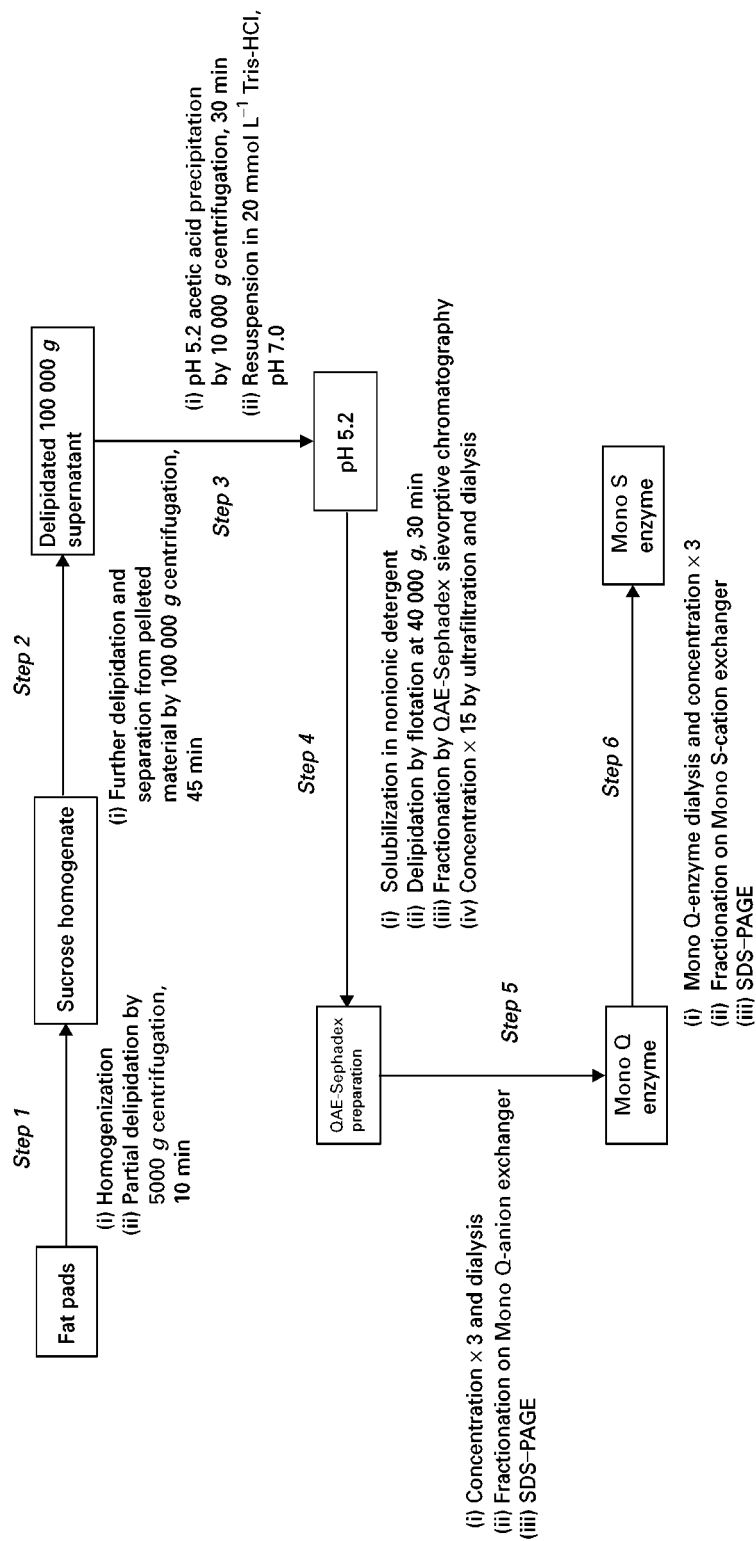


Figure 3 Purification scheme for HSL from rat epididymal adipose tissue. Enzyme activity was monitored at each step. (Reproduced with permission from Nilsson and Belfrage (1986).)

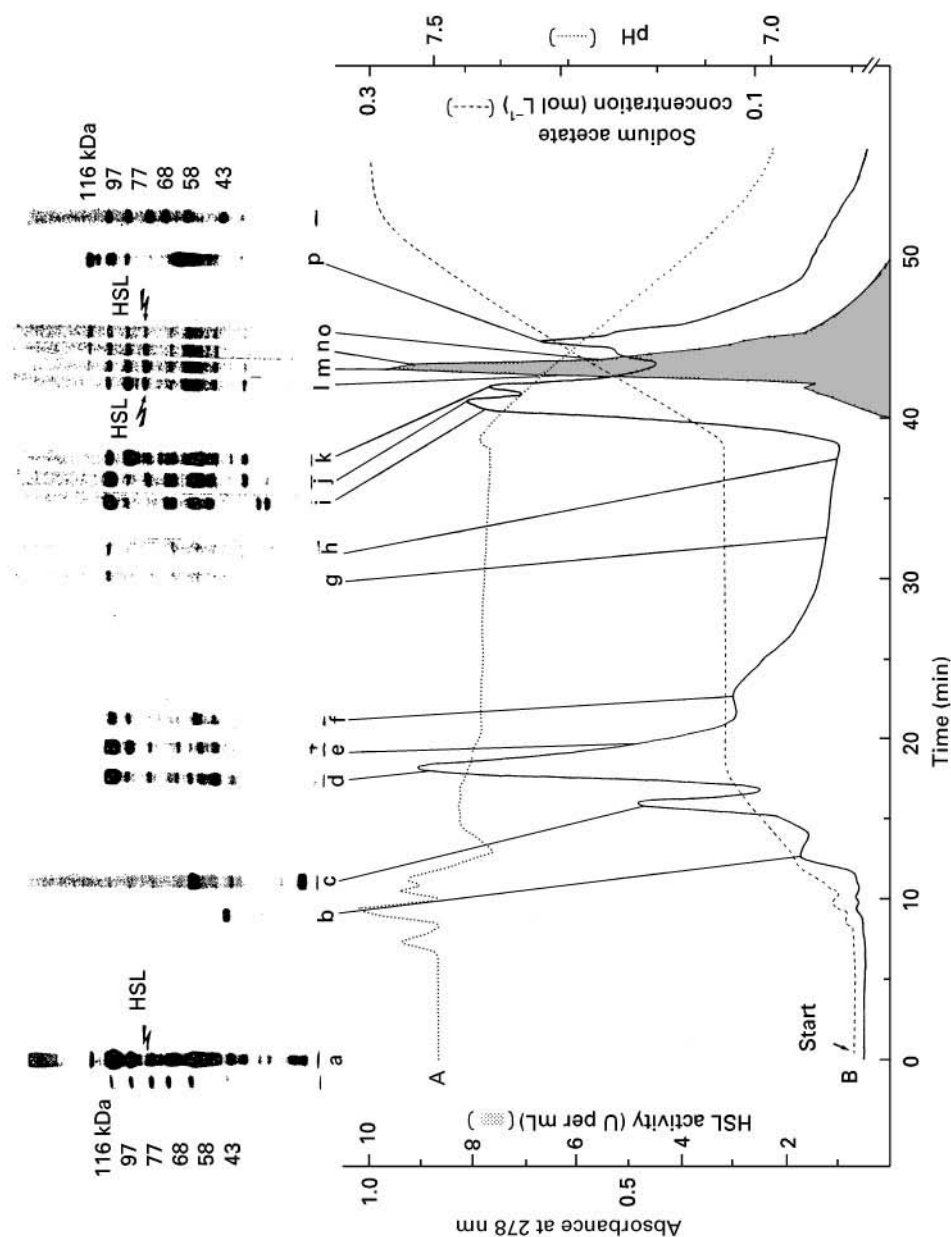


Figure 4 Fractionation of partially purified HSL by high-performance Mono Q anion exchange chromatography. (A) The sample, 7.5 mL of concentrated QAE-Sephadex enzyme (about 17 mg of protein), representing half of the preparation from adipose tissue of 500 rats, was applied to an 8 mL Mono Q column (fitted with a precolumn, flow rate 1.0 mL min^{-1} at a back-pressure of about 1.5 MPa) pre-equilibrated in 50 mmol L^{-1} Tris-acetate, pH 7.5, containing 1 mmol L^{-1} DTE, 20% (w/v) glycerol and 0.2% (w/v) of the nonionic detergent $\text{C}_{13}\text{E}_{12}$. (B) After adsorption the lipase was eluted (4.0 mL min^{-1} at a back-pressure of about 4.2 MPa) by the increasing salt and decreasing pH gradient obtained by addition of 0.3 mol L^{-1} sodium acetate, pH 7.0, as indicated by the conductivity and pH profile in the figure. HSL activity (shaded area) was measured towards an emulsified lipid substrate. One unit (U) of enzyme activity corresponds to $1 \mu\text{mol}$ of fatty acid released per minute at 37°C . The protein composition of the QAE-Sephadex enzyme sample applied to the column (lane a), and the indicated column fractions (lanes b-o), analysed by SDS-PAGE and Coomassie blue staining. Lanes to the extreme left and right are reference proteins; values are in kilodaltons. Arrow labelled HSL signifies the HSL $M_r = 84\,000$ subunit. Enzyme peak fractions corresponding to 70% of the total enzyme eluted were pooled for the next step. (Reproduced with permission from Nilsson and Belfrage (1986).)

Table 3 Purification of HSL from rat adipose tissue^a

Purification step	Volume (mL)	Protein (mg)	Enzyme activity (μ mol fatty acids per min)	Specific activity (μ mol fatty acids per min per mg protein)	Purification (-fold)	Yield (%)
100 000 g supernatant	790	4900	314	0.06	1	100
pH 5.2 ppt	50	1204	289	0.24	4	92
QAE-Sephadex	46	33	112	3.40	57	36
Mon Q LC ^b	16	2.1	58	27	450	18
Mono S LC ^b	8	0.2	34	154	2567	11

^aEnzyme was purified from about 600 g of epididymal fat pads from 500 rats. Enzyme activity was measured with monoacylalkyl-glycerol substrate at 37°C.

^bCombined enzyme from two identical chromatographic treatments of half the initial batch.

Reproduced with permission from Nilsson and Belfrage (1986).

phosphate buffer, pH 7.0, followed by 3 h against the same buffer, pH 6.5, both containing the same concentration of glycerol, PEG, C₁₃E₁₂, DTE and leupeptin as used for the Mono Q chromatography. The enzyme peak fractions (70% of the enzyme activity recovered) were brought to pH 7.0 and glycerol was added to 50% (w/v). The results of the purification are illustrated in Table 3.

The obstacles encountered in the determination of enzymes in biological samples are well illustrated in this purification scheme for the enzyme HSL, which has been notoriously recalcitrant to purification because of its low tissue abundance, amphiphilicity and general lability. What are the necessary precautions that have to be fulfilled during the process? After every solubilization, fractionation or concentration step, the biological activity has to be estimated to detect any inhibition, destruction or loss of the enzyme of interest. To obtain optimum enzyme activity, certain precautions have to be taken in between every step as discussed previously, by adding reducing agents or stabilizers, lowering the temperature or speeding up the separations where possible. To elucidate the effectiveness of different fractionation steps used, protein purity must also be examined with a nonchromatographic method such as sodium dodecyl sulfate-polyacrylamide gel electrophoresis (SDS-PAGE) or capillary electrophoresis. Another, not easy, problem of importance is the identification of the protein band on SDS-PAGE that corresponds to the enzymatic activity.

In the case of HSL, it was possible to carry out the identification in rather crude preparations because the enzyme was activated through covalent modification, i.e. phosphorylation. Then it was possible to 'tag' HSL with ³²P and identify the SDS-PAGE band by autoradiography. After the Mono Q purification step there was only one phosphorylated band.

A single band on SDS-PAGE with Coomassie blue, or even silver staining together with maximum enzyme activity, are not conclusive evidence for identification.

Plasminogen Activator in Gingival Crevicular Fluid

There is a correlation between plasminogen activator (PA) concentration in gingival crevicular fluid (GCF), which is an extracellular exudate occurring in the gingival crevice, and gingival inflammation. The concentration of plasminogen activator inhibitor (PAI) in GCF also plays an important role. The fibrinolytic system is activated by PAs, which are serine proteases that catalyse the conversion of the inactive proenzyme plasminogen to the active enzyme plasmin which then activates collagenase and thereby participates in the tissue destruction seen at inflammatory lesions.

Sampling of GCF was performed by placing small discs (Millipore GWVP-filter 0.22 μ m, calibrated in size to absorb a determined volume) in the gingival crevice.

PA determination is performed by two different methods.

1. Enzyme-linked immunosorbent assay (ELISA), where the amount of protein is determined by placing the small discs in the wells of the microtitre plates used for ELISA (further details of ELISA are given elsewhere). This can be done providing monoclonal or polyclonal antibodies that have been raised against the enzyme, which in turn demands a relatively pure enzyme for immunization.
2. Gel lysis can be used for the determination of enzymatic activity of PA. The filter discs are placed on plasminogen-rich fibrin plates and incubated for 18 h. PA activity can then be derived from the size of the gel lysis.

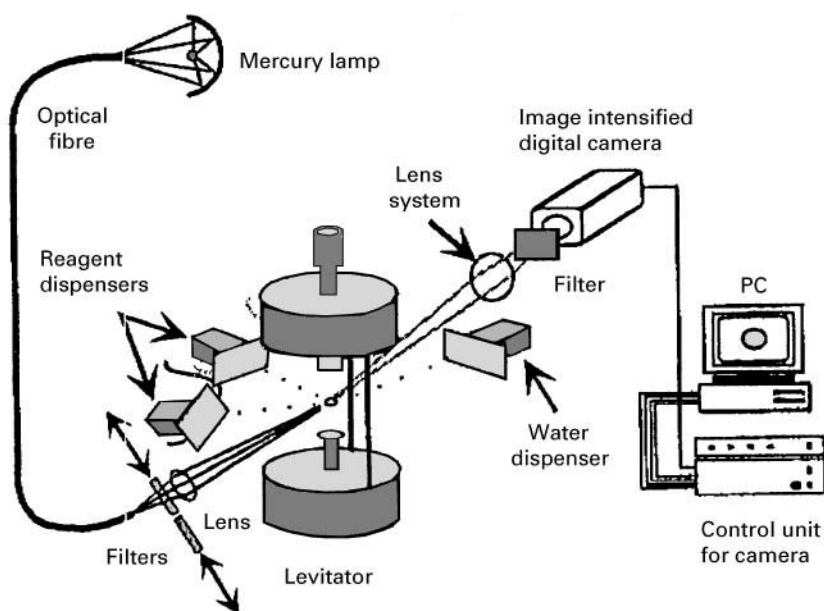


Figure 5 Instrumental set-up for levitation single cell analysis.

Single Cell Analysis

The key step in future enzyme determination is miniaturization, combined with highly selective separation and detection methods. Separation and determination should be done simultaneously. The goal is to be able to study the molecular processes of life at the level of a single cell and its subcellular compartments, if possible without destroying the cell's integrity, and analysing for a specific enzyme. Capillary liquid chromatography and capillary electrophoresis are good candidates for single-cell analysis. In fact, small molecules such as catecholamines, dipeptides and proteins have already been determined in single viable cells. This can be achieved either by sucking a single cell into the capillary and causing cell lysis by use of a high ionic strength buffer, or penetrating the outer cell membrane with an ultrathin capillary (2 μm i.d.) and sucking in some of the cell contents.

By introducing a substrate for a specific enzyme during the separation, it is possible to follow its activity directly after cell lysis by studying the decrease of the substrate and increase of the product concentrations. In some cases the enzyme itself can be monitored during the separation if the amount is high enough. Detection techniques sensitive enough to detect substrates, products and enzymes at the concentration levels derived from a single cell experiment are laser-induced fluorescence or amperometric detection.

Single cell analysis can also be achieved using other miniaturized analysis systems. A very suitable method for studying living cells and biochemical reactions is acoustically levitated microdroplets. Cell studies have

for example been performed on freshly prepared, intact and living primary adipocytes. The instrumental set-up is shown in **Figure 5**. A single adipose cell in a 500 nL droplet is acoustically levitated. Stimulation of adipocytes with β -adrenergic agonists results in activation of adenylate cyclase, production of cAMP and activation of cAMP dependent protein kinase (PKA). PKA phosphorylates HSL, leading to activation of enzyme activity and increased lipolysis, resulting in FFA release and a consequent pH decrease in the surrounding buffer droplet. Addition of insulin antagonizes this effect and hence also the decrease in pH. The change in pH, i.e. the cell response in the droplet, is followed by a pH-dependent fluorophore continuously monitored by fluorescence imaging detection. Additions to the levitated droplet are achieved using continuous flow-through droplet dispensers. To counteract droplet evaporation, which affects the fluorescence intensities, a dispenser is used to continually add water, thus keeping the droplet volume constant. An image analysis computer program is employed to calculate droplet fluorescence intensities during experiments. The method is particularly useful for studying of dynamic events in natural cellular environments at the single cell level, e.g. for the screening of new drug candidates or for studying side effects and reactions between cells.

Subcellular fractionation at the single-cell level using a two-phase levitated droplet system is under development at the author's laboratory.

See also: I/Affinity Separation. II/Affinity Separation: Theory and Development of Affinity Chromatography.

Centrifugation: Analytical Centrifugation. **Chromatography:** Protein Separation. **III/Enzymes:** Liquid Chromatography. **Proteins:** Capillary Electrophoresis; Centrifugation; Crystallization; Electrophoresis; Glycoproteins: Liquid Chromatography; High-Speed Countercurrent Chromatography; Ion Exchange; Metalloproteins: Chromatography. **Appendix 1/Essential Guides for Isolation/Purification of Enzymes and Proteins.**

Further Reading

Bergmeyer HU, Bergmeyer J and Grass M (1986) *Methods of Enzymatic Analysis*, 3rd edn, vols. I–XII. Weinheim: VCH.

Nilsson S and Belfrage P (1986) Purification of hormone-sensitive lipase by high-performance ion exchange chromatography. *Analytical Biochemistry* 158: 399–407.

Prince NC and Stevens L (1989) *Fundamentals of Enzymology*, 2nd edn. Oxford: Oxford University Press.

Rossomando FE (1987) *High Performance Liquid Chromatography in Enzymatic Analysis*. New York: Wiley-Interscience.

Scopes KR (1987) In: Cantor RC (ed.) *Protein Purification Principles and Practice*, 2nd edn. New York: Springer-Verlag.

Suelter HC (1985) *A Practical Guide to Enzymology and Biochemistry*. New York: John Wiley & Sons.

Liquid Chromatography

D. Shekhawat and N. Kirthivasan, Michigan State University, East Lansing, MI, USA

Copyright © 2000 Academic Press

Introduction

Enzymes find applications in food, pharmaceutical and biochemical industries. They are found in combination with other macromolecules or various small molecules. Their uses require identification and purification of the enzymes. The nature, quality, and quantity of the desired enzyme are determined by its intended use. For example, the food industry needs enzymes in large quantities and the pharmaceutical industry requires ultra pure enzymes. High-performance liquid chromatography (HPLC) is widely used for the separation or purification of enzymes on a preparative or analytical scale. It is also used for the analysis of the enzymatic activity.

Properties of Proteins and Practical Implications

All enzymes are proteins. All proteins are macromolecules with molecular weights ranging from hundreds to several thousands. The sequence of amino acid in a protein is specific and this gives each protein unique properties. A protein with just amino acids as a building block is a simple protein; those that contain additional units, such as a nucleic acid, a lipid or a metal etc., are called conjugated proteins.

There are 20 naturally occurring amino acids found in proteins that vary in structure; thus, it is the amino acid sequence and composition that determine the properties of enzymes. Two distinct properties are the size and polarity of the protein, which are impor-

tant factors for understanding their separation. The size of a protein depends upon the number of amino acid units in the protein, whereas the polarity depends on the hydrophilic and hydrophobic units present.

A protein molecule contains one of the three groups: uncharged polar, potentially positively charged (basic side chain) or a potentially negatively charged (acidic side chain). These side chains are normally ionizable and this leads to proteins having characteristic isoelectric points. Since there are other issues governing the protein molecule, such as size, shape and nature of the solution (pH), the overall net charge and polarity depends upon the combination of these factors. In general, the chromatographic processes associated with the properties of enzymes can be summed up as indicated in Table 1.

High-Performance Liquid Chromatographic Techniques

Size-Exclusion Chromatography

Size-exclusive chromatography (SEC) is primarily used as a first step in purification when molecules

Table 1 Chromatographic processes associated with enzyme properties

Enzyme property	Chromatographic method
Net charge	Ion-exchange chromatography
Size	Size-exclusion chromatography
Substrate affinity and conformation	Affinity chromatography
Polarity	Reversed-phase chromatography and hydrophobic-interaction chromatography

differ significantly in size. This technique is used extensively in biochemistry for fractionation and molecular weight determination of proteins and enzymes. The basis of separation in SEC, as the name suggests, is the size of the molecules to be separated. Spherical beads made of a cross-linked gel of a polymer such as silica, agarose, or polyacrylamide are used as column packings. Small molecules can enter all pores and elute with a characteristic volume equivalent to the column hold-up volume. Large molecules are excluded from those pores with a smaller cross-section than the solute and elute in a smaller volume than the small molecules. Consequently, molecules passing through the column separate on the basis of their size and elute in order of decreasing molecular weight.

The resolution depends on gel bead size, pore size, column size, sample size, and flow rate of the mobile phase. Low flow rates of the mobile phase, long and narrow columns, and small gel bead sizes give the highest resolution. The pore size of gel beads is designed according to the size of the molecules of interest.

The nature of the mobile phase in SEC is very important in enzymatic separation as the protein (enzyme) conformation can be changed due to solvent polarity, pH, ionic strength, and salt concentration. Conformational change can change the whole chromatographic behaviour of an enzyme. In SEC, solute-stationary phase interaction is completely prohibited for better separation. However, the mobile phase may produce (ionic or hydrophobic or both) solute-stationary phase interactions. It is necessary to design an ideal mobile phase for chromatography to avoid the above problems. Most enzymes are stable in the pH range of 5–8. The desired pH of mobile phase in SEC is obtained by using buffers suitable for both the enzyme to be analysed and the stationary phase. Tris(hydroxymethyl)aminomethane salt solution or phosphate buffers are widely used for enzymes. Denaturing solvents are sometimes also employed for the chromatographic separation of enzymes. Protein denaturants, detergents in mobile phase, change the original proteins to random coil conformations.

Organic solvents such as acetonitrile can be used for SEC of enzymes. Using acetonitrile is very advantageous because it can be evaporated after elution to concentrate the enzyme solution. Acetonitrile is an ideal organic solvent if a UV detection method is used. However, the solubility of enzymes in acetonitrile solution limits its use in the mobile phase.

A prepacked column of cross-linked methacrylate gel (Ultrasphere from Waters) was used for preliminary isolation of fractions of peptidoglutaminase

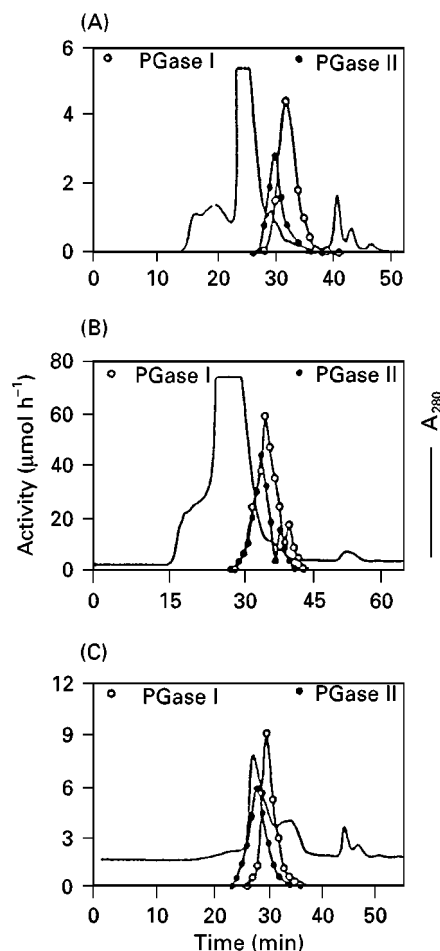


Figure 1 Gel permeation of *Bacillus circulans* proteins on acrylate gel (300 × 7.8 mm) at flow-rate of 0.5 mL min⁻¹ using 2 mg (A) and 20 mg (B) of cell extract proteins. Pooled active peaks (0.1 mg) from (B) were reinjected (C). Reproduced from Hamada JS (1995) *Journal of Chromatography A* 702, 163–172, with permission from Elsevier Science.

(PGase) from *Bacillus circulans* cell extract (1). PGase sample loading was 2–30 mg in 0.05 M sodium phosphate buffer (pH 8.0) and the eluent was 0.05 M sodium phosphate at flow rate of 0.3 mL min⁻¹ (Figure 1). The pooled PGase peak from multiple injections was then further purified by anion-exchange chromatography.

Ion Exchange Chromatography

Ion exchange chromatography (IEC) is a widely used technique for enzyme purification because of the net charge characteristics of enzymes. In IEC, the charged functional groups are covalently bound to the solid surface of the matrix. Cellulose, silica or styrene-divinylbenzene is used as a matrix. Cation exchanger resins contain immobilized negatively charged functional groups (i.e. RSO₃⁻, RCO₂⁻, RPO₄⁻ and RO⁻) and anion exchangers contain immobilized positively

charged functional groups (i.e. quaternary ammonium groups). Resins containing sulfonyl and quaternary ammonium groups are strong ion exchangers and ionize at any pH, whereas weak ion exchangers containing functional groups like carboxyl and secondary or primary amines ionize within a certain range of pHs. When an ionized solute passes through an ion exchange column, the sample ions adsorb and displace counter ions on the surface. The adsorption process is reversible and adsorbed ions are eluted by a salt solution. Using a suitable mobile phase regenerates the resins.

The choice of the appropriate ion exchange resin for a particular enzyme separation depends on the isoelectric point of the enzyme to be separated. The isoelectric point of any molecule is the pH value at which the molecule has no net charge, i.e. an equal number of negative and positive charges. Enzymes are acidic at a pH above the isoelectric point and anion-exchange resins are used for separation of such enzymes. Similarly, cation-exchange resins are used for basic enzymes.

Column packing material, particle size and pore diameter of the support, column length, mobile phase, and temperature are some important parameters which affect separation of enzymes in IEC. In a column with smaller packing particle sizes, large enzyme molecules diffuse at a slower rate and this results in enhanced resolution and lower elution time. Most of the surface area of a support is confined within the pores and the diameter of pores affects the penetration of enzyme molecules into the column matrix and hence the mass transfer and loading capacity. Pore diameters of $\approx 300 \text{ \AA}$ are ideal for most enzymes with molecular weight up to 100 000, providing loading capacity and good resolution. Larger pore diameters are needed for higher molecular weight enzymes. The column length is not an important factor in the resolution of enzymes in IEC. Using short columns has many advantages, e.g. concentrated eluents, lower pressure and lower column cost. Lower loading capacity is a disadvantage of using a short column.

The pH, ionic strength and salt composition of mobile phase are also important factors in IEC separation of enzymes. Aqueous organic solvents are used as mobile phases. The amount of organic solvent in the mobile phase is determined by trial and error and depends completely on the nature of the molecules to be separated. Excessive organic solvent should be avoided because it can destroy the stability of enzyme molecules. The isoelectric point (pI) of enzymes determines the type of column used for separation (discussed earlier) as well as the pH of the mobile phase. The net charge on enzyme molecules depends on the

pH of the solvent. Ionization of ammonium groups occurs at any pH below the isoelectric point (pI) and contributes a positive charge on the enzyme. Similarly, a negative charge on the enzyme is obtained by a pH above its pI. The retention on ion exchange columns therefore depends on the net charge carried by the enzyme molecule to be separated and the pH of the mobile phase is chosen accordingly. The pH of the mobile phase should be slightly above the pI of the enzymes to be separated for anion-exchange columns and vice versa for cation-exchange columns. The nature of displacing counterion in the salt used also affects the enzyme retention on the column. Higher valent ions are stronger displacers than lower valent ions and thus give lower retention. The smaller size of ions also favours lower retention if the charge on the counterion is the same. Gradient elution based on ionic strength variation or pH changes is used in IEC. Chromatographic separation of most enzymes is carried out at a low temperature to preserve enzyme stability.

The quaternary methylamine resin from Waters (Accel Plus QMA) has been used for the separation of peptidoglutaminase from *B. circulam* cell extract. Enzyme load was 1.0 mg in 20 μL of 0.02 M phosphate buffer (pH 8.0) and the eluent used was 0.05 M sodium phosphate buffer and 0.1–0.8 M KCl at a flow rate of 0.5 mL min^{-1} for analytical separation and 1.5–10.0 mL min^{-1} for preparative separation (Figure 2).

Reversed-Phase Chromatography

Reverse-phase chromatography (RPC) is the most popular chromatographic method for the purification, separation, and analysis of the biological molecules because of its high resolution and ease of handling. Column packings are usually prepared from silica particles and hydrophobic long-chain alkylsilyl ligands. n-Butyl (C4), n-octyl (C8), n-octadecyl (C18), and alkylphenyl groups are used for separating enzymes. The nonhydrophobic molecules in the sample do not strongly interact with the hydrophobic stationary phase of the column and elute earlier, while hydrophobic molecules in the sample interact with the hydrophobic stationary phase of the column and elute later.

The column packing material, particle size and pore diameter of support, column dimension, mobile phase, and length of hydrophobic ligands, determine the effectiveness of an RPC procedure. Silica is the most widely used support because of its mechanical stability, efficiency, and ability to be bonded with hydrophobic ligands. However, silica supports are not stable under basic conditions (pH > 8). Small

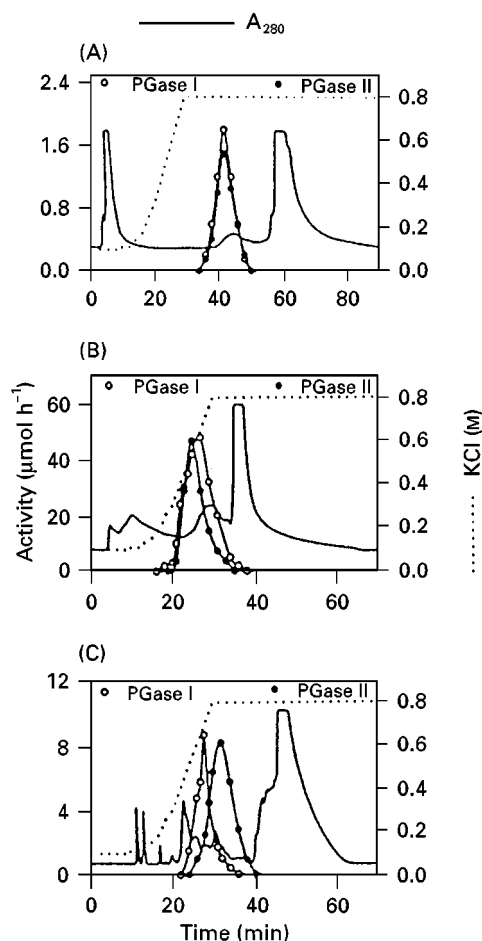


Figure 2 Anion-exchange separation of *Bacillus circulans* proteins using (A) QM anion exchange (150 × 3.9 mm) column at 1.0 mg load and 0.5 mL min⁻¹ flow rate, (B) 150 × 19 mm QM anion exchange column at 30 mg load and 5.0 mL min⁻¹ flow rate, and (C) DEAE anion exchange (150 × 21.5 mm) column at 5 mg load and 5 mL min⁻¹ flow rate. Reproduced from Hamada JS (1995) *Journal of Chromatography A* 702, 163–172, with permission from Elsevier Science.

support particles favour higher resolution, but high column backpressures and the large size of enzyme molecules to be separated do not favour the smaller particle sizes. A particle size of $\approx 20 \mu\text{m}$ is optimal for RPC column for enzymatic HPLC. A pore size of 300 Å is the most commonly available size in commercial RPC columns. For large enzyme molecules use of a large pore size (≈ 1000 or greater) is suggested to avoid any diffusional problems.

The hydrophobicity of n-alkyl group attached to the silica decreases with decreasing chain length of n-alkyl group (C18 > C8 > C4 > C2). Smaller n-alkyl group chains are favoured for highly hydrophobic samples and vice versa. More hydrophobic columns (e.g. C18) require a stronger mobile phase (higher amount of organic solvent). Organic solvents such as acetonitrile, methanol or isopropanol and ion-pairing

agents or buffers are added to the mobile phase to achieve reasonable retention times. The effectiveness of these organic modifiers depends on solvent polarity and increases with decrease in polarity. Isopropanol is a very good solvent for highly hydrophobic enzymes and methanol is better for hydrophilic enzymes. Acetonitrile is the most suitable organic modifier because it has intermediate polarity, low viscosity, and low UV adsorption. It is volatile and can be easily removed from the eluent. The function of added solvents is to decrease the interaction between the stationary phase and highly hydrophobic molecules and thus reduce the retention time. Ion-pairing agents or buffers set the eluent pH and interact with the enzyme to enhance the separation. Trifluoroacetic acid (TFA) is widely used as an ion pairing agent. Buffers such as phosphate or hydrochloric acid are also used. The mobile phase for RPC typically consists of water, organic solvent, and trifluoroacetic acid (0.1%) or phosphoric acid.

Capillary columns packed with nonporous (pellicular) supports have been used for fast separation of enzymes or proteins at high temperatures and at high flow rates. Packed capillary RP-HPLC columns have several advantages over conventional columns – fast separation, reduction in solvent usage and the ability to work with small samples. The mass transfer between the stationary phase and the mobile phase is fast with pellicular packings because the diffusional distances in the stationary phase are short owing to limited chromatographic interaction at the outer surface. Capillary columns are stable at higher temperatures and at higher pressures because of the solid, fluid-impervious core of the micropellicular packing. Rapid mass transfer resulting from the pellicular configuration and higher temperature is mainly responsible for the fast separation of enzymes. Higher temperatures may not be appropriate for the stability of some enzymes.

Fast separation of a mixture of four proteins was performed in 6 s at 120°C on a 3 cm column packed with 2 μm pellicular ODS-silica (Figure 3).

The biological activity of enzymes is sometimes lost due to high backpressures, mobile phase (low pH and organic modifiers) and a strong hydrophobic stationary phase. Hydrophobic interaction chromatography (HIC) has less harsh chromatographic conditions than RPC and can be used to preserve the biological activity of enzymes.

Hydrophobic Interaction Chromatography

The basis of separation in hydrophobic interaction chromatography (HIC) is the same as for RPC. These methods differ in the properties of the mobile and stationary phases. HIC is carried out with an aqueous

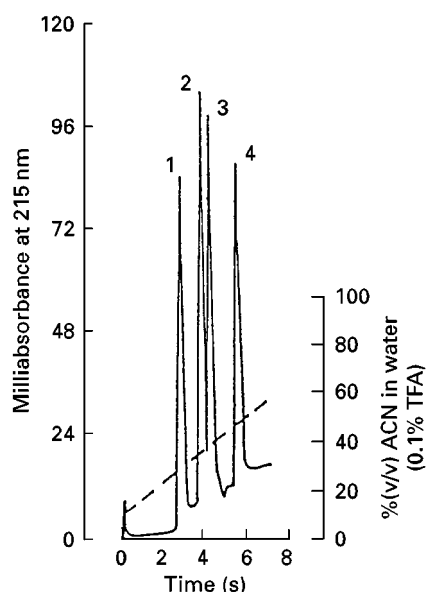


Figure 3 Fast separation of standard mixture of proteins: 1 = ribonuclease A; 2 = cytochrome *c*; 3 = lysozyme; 4 = lactoglobulin B. Column (30 × 4.6 mm) packed with 2 μm pellicular ODS-silica; 12 s linear gradient from 10 to 90% (v/v) acetonitrile (ACN) in water containing 0.1% trifluoroacetic acid (TFA), temperature = 120°C, flow rate = 5 mL min⁻¹ and column inlet pressure = 240 bar. Reproduced from Chen H and Horvath CS (1995) *Journal of Chromatography A*, 705, 3–20, with permission from Elsevier Science.

solution of higher salt concentration at neutral conditions and uses a weak hydrophobic stationary phase. The higher concentration of salt in the mobile phase

enhances the binding between enzymes and weakens the hydrophobic stationary phase.

Most separation variables in HIC behave in the same way as in RPC but the nature of the mobile phases and stationary phases differs in these two HPLC methods. The HIC performs separation under nondenaturing conditions whereas RPC denatures enzymes during separation because of the mobile phase conditions (organic solvent and highly acidic) and the highly hydrophobic stationary phase. The mobile phase in HIC is neutral and nonorganic and protects enzymes from denaturation. Salts such as sodium or potassium phosphate are added into the mobile phase to buffer it at pH ≈ 7. The bonded phase in HPHIC is an aryl or smaller alkyl ($n < 5$) group, weak hydrophobic ligands, attached to silica support.

The purification of *Chromobacterium viscosum* lipase has been studied using hydrophobic interaction chromatography. The stationary phase was prepared by covalent immobilization of polyethylene glycol on Sepharose gel (Sepharose CL-6B, Pharmacia). The extent of lipase was affected by the salt used and increases with increasing ionic strength in the eluent buffer and with higher pH value. The best recovery of lipase was observed when potassium phosphate was used as a salt compared to NaCl, Na₂SO₄ and (NH₄)₂SO₄ (Figure 4).

Affinity Chromatography

The basis of affinity chromatography (AC) is the selective adsorption of the molecule to be separated

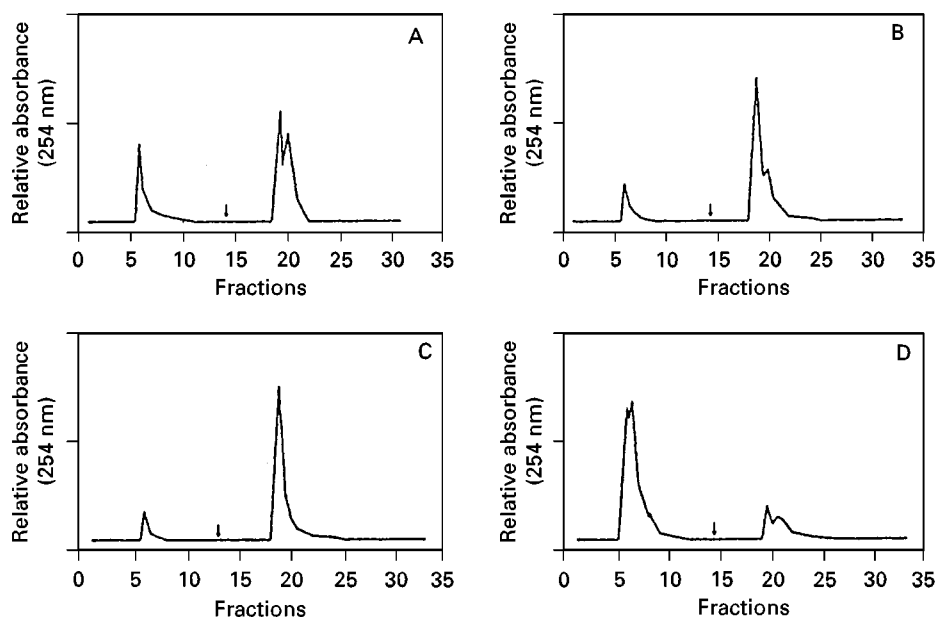


Figure 4 HIC on PEG 10 000-Sepharose CL-6B column. Buffer: (A) 15% (w/w) K₃PO₄; (B) 20% (w/v) (NH₄)₂SO₄; (C) 15% (w/v) Na₂SO₄; (D) 4 M NaCl in 10 mM phosphate (pH 7). Desorption with 10 mM phosphate buffer (pH 7). From Queiroz JA, Garcia FAP and Cabral JMS (1996) *Journal of Chromatography A* 734, 213–219, with permission.

from mixture on the matrix of the column. A specific ligand for a specific biological molecule is chosen and it is covalently bound to the matrix of the column. For example, a ligand such as adenosine will bind only enzyme adenosine deaminase and not any other molecules. When a mixture is applied to the affinity chromatography column then the molecule that has specific affinity for the ligand will stay in the column and all other unbound molecules will migrate through the column. The interaction between adsorbed molecule and ligand is reversible. Changing the pH or other conditions of the mobile phase can desorb the bound molecule. A molecule that has more affinity for the ligand than the bound molecule can be included in the mobile phase to elute the desired bound molecule. This chromatographic method is carried out under nondenaturing conditions during the separation of enzymes or proteins.

The type of ligand and its support, state of mobile phase at each stage of separation and flow rate determine the resolution in AC. Ligands can be specific for a molecule or a group of molecules. The desired ligand must be highly specific for enzyme molecule(s) to be separated, be stable under applied conditions, have reversible binding with applied sample and possess an appropriate functional group to couple with the support. Cross-linked agarose or other pressure-stable polymer is used as a support for the ligand.

Buffers at each step of separation must be non-denaturing to maintain specificity of ligand and eluting enzyme(s). Low pH buffers are employed in the desorption step to break the solute-ligand interaction. Specific desorbing agents, which compete with adsorbed solute molecule(s) for the same binding site, are sometimes also used. The flow rate of mobile phase also affects the retention time and peak shape.

Alhama *et al.* have applied AC technique for the purification of glutathione reductase and glucose-6-phosphate dehydrogenase from cell-free extract of baker's yeast, fish liver, and rabbit hemolysates with high recovery. They used an epoxy-activated silica column derivatized with the ligand 8-[(6-aminoethyl)amino]-2'-phosphoadenosine-5'-diphosphoribose. The bound ligand concentration was $11.4 \mu\text{mol g}^{-1}$ of dry silica and the loading capacity was 2–3 mg of glutathione reductase.

Hydroxyapatite High-Performance Liquid Chromatography

Hydroxyapatite, $\text{Ca}_{10}(\text{PO}_4)_6(\text{OH})_2$, is a form of calcium phosphate which has been used, in particular, as a packing material for enzymes and proteins separations. The basis of separation is ionic interactions

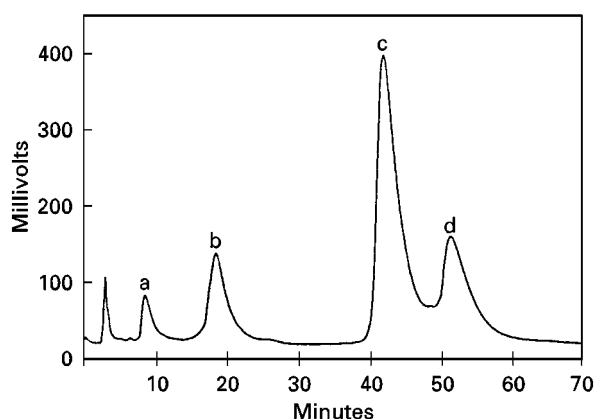


Figure 5 Separation of a protein mixture: a = transferrin, b = myoglobin, c = lysozyme, and d = cytochrome *c*. Packing: Nucleosil 1000-5 DIOL CaP-HA 2.5% (100 × 6 mm). Linear gradient of sodium phosphate (pH 6.8), 1–350 mM (60 min); flow rate = 1 mL min^{-1} , temperature = 25°C . Reproduced from Bruno G, Gasparrini F, Misiti D, Arrigonimartelli E, and Bronzetti M (1990) *Journal of Chromatography A* 504, 319–333, with permission from Elsevier Science.

between amine groups of the enzymes and phosphate groups on the surface of the hydroxyapatite and, also, calcium coordination complex formation between calcium groups in the hydroxyapatite and carboxyl groups in enzymes. Low concentration phosphate buffers are used to elute acidic and neutral enzymes and high concentration buffers are used to elute basic enzymes.

A protein mixture containing transferrin, myoglobin, lysozyme, and cytochrome *c* was separated using hydroxyapatite as a support. Protein solution ($10\text{--}50 \mu\text{L}$; $1 \mu\text{g } \mu\text{L}^{-1}$ protein) was loaded onto the column and eluted with a linear gradient of sodium phosphate buffer (pH 6.8) (Figure 5).

Perfusion Chromatography

Perfusion chromatography is a new chromatographic technique, introduced by Afeyan and coworkers in 1989–1991, for reducing resistance to stagnant mobile phase mass transfer in liquid chromatography. It may be used for both rapid analysis and preparative chromatography of large molecules such as enzymes. A new chromatographic packing material (POROS, Perseptive Biosystems) which contains two sets of interconnecting bimodal pores has been employed in perfusion chromatography. The members of one pore set having a mean diameter in the range $6000\text{--}8000 \text{ \AA}$ are called throughpores. The high surface area needed for adequate sample capacity is achieved by the smaller diffusive pores ($d_{\text{pore}} \approx 1000 \text{ \AA}$). The mobile phase flows through the through-pores. In this manner, solutes enter the interior of the particles convectively by the through-pores and then diffuse into the diffusive pores.

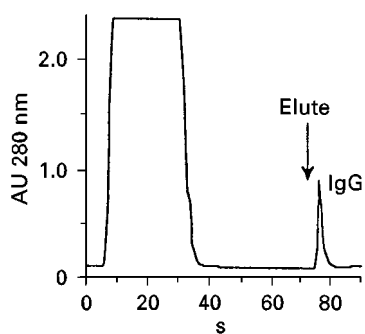


Figure 6 Separations of hybridoma cell cultural supernatant on protein A POROS M. 0.5 mL injection; 30×2.1 mm column; 10 mM phosphate pH 7.4, 0.15 M NaCl; elution with 0.3 M acetic acid (2%, v/v), 0.3 M MgCl_2 ; 2 mL min^{-1} flow-rate. Reproduced from Afeyan NB, Fulton SP and Regnier FE (1991) *Journal of Chromatography A* 544, 267–279, with permission from Elsevier Science.

POROS-based chromatographic packing material can be used in any chromatographic mode such as ion exchange, reversed-phase, hydrophobic interaction, and affinity chromatography. These supports separate proteins rapidly compared with conventional HPLC using higher mobile phase velocities.

The separation of immunoglobulin G (IgG) from hybridoma cell culture supernatant has been completed in 80 s using a POROS protein A (aldehyde-coupled) column. The sample was loaded in a 0.1 M phosphate buffer pH 7.4 with 0.15 M NaCl and eluted with 0.3 M acetic acid (2%, v/v) with 0.3 M MgCl_2 . The column was loaded with 0.5 mL of hybridoma cell culture supernatant with the flow rate of 2 mL min^{-1} (Figure 6).

Assay of Enzymatic Activity

An important aspect of the separation of enzymes by HPLC is the assay of enzyme activity. Enzyme-catalysed reactions can be monitored spectrophotometrically and many of the substrates or products absorb visible or UV light. It allows determination of the progress of a reaction by direct and continuous monitoring. While other methods of discontinuous assay focus on monitoring one of the compounds of the reaction, the HPLC technique offers the simultaneous determination of several substrates of the reaction. This method is probably the best as it offers a complete mass balance of the reaction being analysed.

Detectors for Enzyme Analysis

Ultraviolet-visible (UV-vis) detectors are the most commonly encountered detectors in enzyme analysis because enzymes are UV-active and UV detectors are

simple to use and relatively inexpensive. The analysis is also nondestructive and hence suitable for preparative work. Furthermore the solvents best suited for liquid chromatography are transparent to UV-vis. Refractive index detectors are nondestructive, concentration sensitive and universal in that they respond to virtually all compounds with the proper choice of mobile phase but are of low sensitivity. The specificity of analysis of enzymes by fluorescence detection arises because many parameters related to the fluorescence intensity can be exploited. However, this technique requires the use of very selective reagents that react with specific functional groups of the analyte to produce fluorescent derivatives.

Future Trends

HPLC will continue to be the important tool for separation of enzymes. The new capillary columns packed with nonporous support and microsporous support in perfusion chromatography will be helpful in fast analysis of enzymes or proteins. Separation is faster and more selective when HPLC is carried out at higher temperatures. A heat exchanger, which can bring the eluent rapidly to column temperature, will increase separation reliability at higher temperatures. Conventionally, HPLC is used for the analytical separation as well as for preparative separation of enzymes. Discontinuity of the HPLC process and the dilution of the products after elution are two major disadvantages. The simulated moving bed (SMB) technique can make HPLC a continuous process. A column packing material should be designed for a higher sample loading and for fast HPLC. Thus, a large-scale separation should be fully automated and continuously operating, loading samples, collecting fractions, regenerating the column and with various fail-safe devices to protect the column and product.

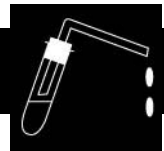
See also: II/Affinity Separation: Theory and Development of Affinity Chromatography. **Chromatography:** Liquid: Mechanisms: Ion Chromatography; Mechanisms: Reversed Phases; Mechanisms: Size Exclusion Chromatography. III/Peptides and Proteins: Liquid Chromatography.

Further Reading

- Afeyan NB, Fulton SP, and Regnier FE (1991) *Journal of Chromatography A* 544: 267–279.
 Alhama J, Lopezbarea J and Toribio F (1991) *Journal of Chromatography A* 586: 51–59.
 Bruno G, Gasparrini F, Misiti D, Arrigonimartelli E and Bronzetti M (1990) *Journal of Chromatography A* 504: 319–333.

- Chen H and Horvath CS (1995) *Journal of Chromatography A* 705: 3–20.
- Hamada JS (1995) *Journal of Chromatography A* 702: 163–172.
- Mant CT and Hodges RS (eds) (1991) *High-Performance Liquid Chromatography of Peptides and Proteins: Separation, Analysis and Conformation*. Boca Raton: CRC Press, Inc.
- Queiroz JA, Garcia FAP, and Cabral JMS (1996) *Journal of Chromatography A* 734: 213–219.
- Rossomando EF (1991) *High Performance Liquid Chromatography in Enzymatic Analysis*. John Wiley and Sons, Inc., New York.
- Wiseman A (ed.) (1985) *Handbook of Enzyme Biotechnology*. New York: John Wiley and Sons, Inc.

ESSENTIAL OILS



Distillation

E. Hernandez, Texas A&M University,
College Station, TX, USA

Copyright © 2000 Academic Press

Introduction

Essential oils are generally understood to be volatile compounds which are freely soluble in alcohol, ether and vegetable and mineral oils and are usually assumed to be the result of distillation or a steam-stripping process. The use and processing of essential oils began in the East more than 2500 years ago. The process of distillation, which is the technical basis of the essential oil industry, was also conceived and first employed in the Orient, especially in Egypt, Persia and India. Turpentine and camphor appear to be the first documented essential oils prepared by distillation in Greece by Herodotus (484–425 BC).

The use of essential oils in ancient times consisted of preparing ointments by mixing oils from flowers with fatty oils; this was done by placing flowers and roots with the oil in glass bottles which were then allowed to sit for periods of time. Sometimes the flowers or roots were macerated with wine before the fatty oil was added, and the product obtained by digestion filtered and boiled down to a thicker consistency.

Medieval alchemists laboured for many years to extract from materials found in nature what they called the *quinta essentia* or the fifth essence. They believed that a combination of earth, air, fire and water existed in some form or other from which quintessential materials could be extracted from some plants. These quintessential extracts derived from plants were believed to be remedies for a wide variety of diseases.

The production and use of essential oils did not become widespread until the second half of the 16th

century. In 1507, Hieronymus Brunschwig's book on distillation, *Liber De Arte Distillandi*, described distillation techniques for four essential oils, namely, turpentine (known since antiquity), juniper wood, rosemary and spike.

Before the ninth century it was still widely believed that most essential oils had strong curative properties. Therefore it was chiefly pharmacists who developed and improved methods of distillation for the recovery and purification of natural essential oils.

Eventually, with the development of the fields of medicine and pharmacology and the dispelling of some medicinal myths, the use of essential oils in pharmaceutical products lost importance and their use became restricted to perfumes, beverages and foodstuffs.

Applications of Essential Oils

Attractive aromas which leave a pleasant memory association are used as marketing devices to sell edible and cosmetic products, including unlikely materials such as detergents. The producer is counting on the consumer preferring a product that left a pleasant aromatic memory.

Current specific uses of essential oils are to add flavour to foodstuffs and beverages and to scent perfumes, lotions, soaps, detergents and household cleaners. For example, *d*-limonene from citrus peel is a very strong solvent and it is used in a wide variety of cleaning products. Essential oils are a major part of carbonated beverage flavourings; the most common flavours include lemon, lime, orange, cassia, cinnamon and nutmeg. Essential oils are also used to flavour many foods such as sweets and candies, cookies, snacks and chewing gum.

The field of aromatherapy constitutes a small part of the essential oils industry but it is a fast-growing area and requires a wide variety of essences. Not much scientific work has been done in this area to support any of the medicinal and psychosomatic

claims. Practitioners suggest that aromatherapy goes beyond the effect of simply imparting an agreeable sensation and psychological state of well-being. Some speculate that inhaling certain essential aromas can affect the limbic system, producing a measurable physiological response. More research is certainly needed to document the benefits of this application.

Other properties of essential oils with commercial potential include antimicrobial effects. The inhibition of 25 different bacteria using an essential oil of marjoram has been reported. Similar effects are noted for other volatiles and essences derived from plant materials. It was found that the short chain volatiles such as 5–8 carbon aldehydes and ketones resulting from the distillation of vegetable oils had antimicrobial properties against bacteria such as *Staphylococcus aureus* and *Escherichia coli*. In fact, this antimicrobial effect is believed to be a defence mechanism in plants against microbial pathogens. Another function of essential oils in plants is reported to be as an attractant of insects, enabling plants to use the insects as pollen carriers for plant reproduction.

The production of essential oils on a larger scale was started in the USA in the earlier 19th century. Three indigenous plants, sassafras, American wormseed, and wintergreen, as well as turpentine, were the first oils to be produced in the USA in large amounts for export worldwide.

Many aromatic plants for essential oils grow wild or are cultivated in small scale family-oriented businesses. Today only a few essential oils are produced by modern or centralized methods. An example of these is the cultivation and harvesting of aromatic flowers in the Grasse region of southern France, where essential oil distillation units are placed near the fields to extract and recover the essential oils on site. In the case of citrus oils, for example, much larger scale distillation systems are set in place at juice-processing plants. These aroma distillation units are set up next to the evaporators where the concentration of juices is taking place. These systems are common in the USA as well as in other large citrus-producing countries such as Brazil and China. It should be noted that these aroma distillation units are used not only in citrus-processing plants but in any plant that concentrates fruit juices by evaporation.

In addition to improving production and purification processes for the recovery of essential oils, the essential oil industry has been active in developing synthetic aromas. Essential oils are some of the most studied chemical compounds as regards their composition and physical and chemical properties. Advances in organic chemistry have allowed for the establishment of techniques to define the component

Table 1 Classification of components in essential oils

Component	Examples
Hydrocarbons	<i>d</i> -Limonene in lemon oil
Alcohols	Borneol in camphor
Esters	Methyl salicylate in oil of wintergreen
Aldehydes	Benzaldehyde, decanals
Ketones	Menthone in oil of peppermint
Lactones	Coumarin from Tonka beans

profiles of many aromas and fragrances which permit the establishment of composition standards for trade regulations and for the synthesis of aromas using less costly starting raw materials.

Essential oils are commonly grouped into six classes according to their chemical nature. Tables 1 and 2 list some of the most commonly utilized essential oils worldwide.

The most common essential oil used as a food aroma and flavour is orange essence (Table 2). Over 50% of the commercial essential oils and natural extracts are obtained from cultivated plants. Examples of these include mint aroma and flower essences such as rose, geranium, mints, coriander, lavender and jasmine.

Citrus oils such as orange, lemon and grapefruit aromas are considered by-products of juice extraction and concentration. Orange oil, for example, is marketed both as a flavour and as a material for use in cleaning products. In this case the distinction has to be made that orange oil and citrus oils in general are recovered in two ways; one way is as *d*-limonene, in which the oil resulting from the peel of the fruit as the

Table 2 Main essential oils produced in the world

Essential oil	Main components
Orange	Limonene, terpeniols
Mint	Linalool, linalil acetate
Eucalyptus	Cineole, pinene, limonene
Citronella	Geraniol, citronellal, citronelol
Clove	Eugenol, caryophyllene
Lime	Limonene, terpeniols
Spearmint	Mentheol, menthone, pulegone
Lavender	Pinene, lemonene, caphene, octanone
Marjoram	Tojuene, pinene, sabinene
Camphor	Bisabolol, cadinol cubenol
Coriander	Terpinene, <i>p</i> -cymene, pinene
Patchouli	Patchoulol, sesquiterpenes
Rose	Citronellol, geraniol, linalool
Cinnamon	Fenchene, cinnamaldehyde, pinene
Sandalwood	Santalene, curcumen
Lemongrass	Citral, linalool, geraniol
Jasmin	Benzyl acetate, linalool, benzyl benzoate
Ginger	Terpenio, neral, geraneal
Anis	<i>Trans</i> anethol, chavicol

juice is extracted. This has a lower value and is sold as flavouring and also as a cleaning agent. The true volatiles from citrus are what results from volatilization during the evaporation of the juice and this is a product that commands a higher value and has a wider range of aroma components such as aldehydes, ketones and terpenes. Other oils such as clove or pepper oil may come from spices, or as oils, oleoresins, extracts or flavours.

Other raw materials for essential oil production are harvested in the wild. Wild thyme and rosemary, for example, are common in Spain and grow back abundantly following harvest. Sumatran cinnamon trees are similarly self-rejuvenating. However, due to high demand, some countries have resorted to overharvesting plants for essential oil production from the wild. This has created local problems of forest destruction and the sustainability of the industry has become a serious concern for some underdeveloped countries. As a result, some countries, such as Brazil, have implemented harvest moratoriums or banned the harvesting of some species in order to avoid wiping out some species of aromatic plants. These conservation efforts and replanting programmes have meant that some oils are now available again commercially.

Recovery of Essential Oils

The aroma and fragrance industry has been estimated at approximately \$2 billion per year, with a growth rate of 3.5% per year. Orange oil is both the largest volume oil and, as a by-product of the orange juice industry, relatively inexpensive, ranging from \$0.75 to \$1.40 a pound. Although the US production of citrus oil is declining, with South America and China growing in importance as a major producer, the USA continues to be a major producer of mint and cedar oils. The mint oils as a group – peppermint, spearmint (both grown in the USA) and cornmint (produced in India and China and as a by-product of menthol production) – are the highest value oils, with peppermint selling for about \$12–15 a pound.

Distilled essential oils are generally recovered by three methods, classified according to the way heat is applied to materials: boiling water, steam distillation or a combination of both. Conditions of temperature, pressure or vacuum, and processing time will depend on the characteristics of the essential oil, particularly as regards susceptibility to oxidation and heat decomposition.

The basic process consists of macerating or comminuting the plant materials to rupture the oil sacs. This allows the essential oil to be exposed and carried by the steam or water used. Common materials used

in the recovery of essential oils are flowers, roots, seeds, leaves and twigs of aromatic plants.

Once the plant materials have been prepared, the method for removing the essential oil depends on the type of product being handled. For example, a combination of boiling water and steam injection is used with flower petals in order to avoid agglutination of the materials in the distillation unit. **Figure 1** illustrates this simple method of distilling essential oils. This type of distillation is commonly set up in the fields where the raw materials are being harvested in order to prevent spoilage and deterioration of aromas during transportation or storage.

A simple distillation apparatus consists of a retort or still, a condenser and a receiver. This system is commonly used in the fields for processing lavender. Typical conditions for this method are to heat a mixture of raw material with water to boiling point (100°C) while injecting steam. The resulting vapours are then condensed and recovered. This usually results in two phases: a heavy phase, mostly composed of water, and a light phase, which contains the essential oil.

A variation of this method is to apply vacuum (10–25 in Hg) to the system to allow boiling to take place at a lower temperature and thus prevent the thermal decomposition of the essential oil.

Some aroma systems involve the use of only steam in order to obtain a more concentrated essential oil in the condenser. This system is applicable where there is no agglomeration or agglutination of raw materials. When the raw material is liquid, such as fruit juice or macerated materials in water, the fresh liquid flows in countercurrent with vapour. Vapour–liquid-contacting devices such as a sieve plate column or a packed column are sometimes used. Under ideal conditions, it is advisable to have a rectification column next to the distillation unit in order to obtain a more concentrated and pure essential oil. This is the most efficient way from the standpoint of steam consumption as well. Such a scheme is illustrated in **Figure 2**, with distillation/rectification as the concentration step.

As mentioned above, essential aromas from citrus are recovered as a by-product from the production of citrus juice concentrates. These juices are usually concentrated by multiple effect evaporation. There are four or more effects where the first effect is usually heated by live steam and then subsequent effects are heated by the steam generated in the preceding effect. The vapours generated in the first effect are the richest in the essential oils and the essence is condensed and recovered in a distillation column. This is the most important source of essential oils with regard to volume, estimated worldwide at 25 000 metric tons and more than 60 million US dollars.

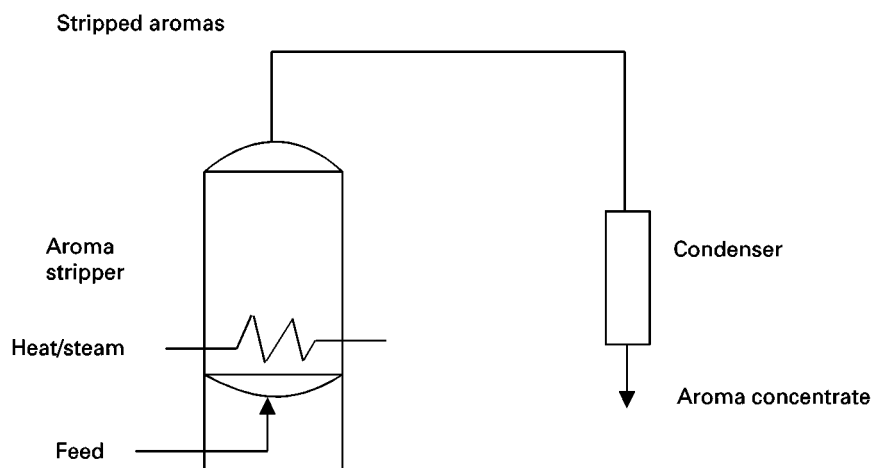


Figure 1 Aroma recovery unit by hydrodistillation.

There is another method of distillation used by very specialized flavour companies called molecular distillation. In this evaporation system the liquid introduced is spread on the walls of a heated vertical cylinder under high vacuum (less than 50 mmHg) by wiper blades forming a thin layer. This produces highly efficient mixing and heat transfer of the fluid, reducing the residence time to a minimum. Variable temperature allows for the fractionation of aroma components according to their molecular weight. Heat-sensitive aromas and specialized aromas such as dairy flavours are manufactured by the industry using this type of distillation system.

Other methods for recovering aromas and fragrances are solvent extraction (hexane, alcohols) and supercritical CO₂ extraction. Strictly speaking, the resulting oils from these extraction methods are not essential oils since no evaporation or distillation takes place. However, recovery of high priced aromas and fragrances by supercritical extraction is growing worldwide and extraction of some low price essential oils is also done using hexane or alcohol. Supercritical extraction has the advantage that it does not involve the application of high heat and addition of steam or water. Also, the extractability properties of CO₂, namely affinity for hydrophobic or hydrophilic com-

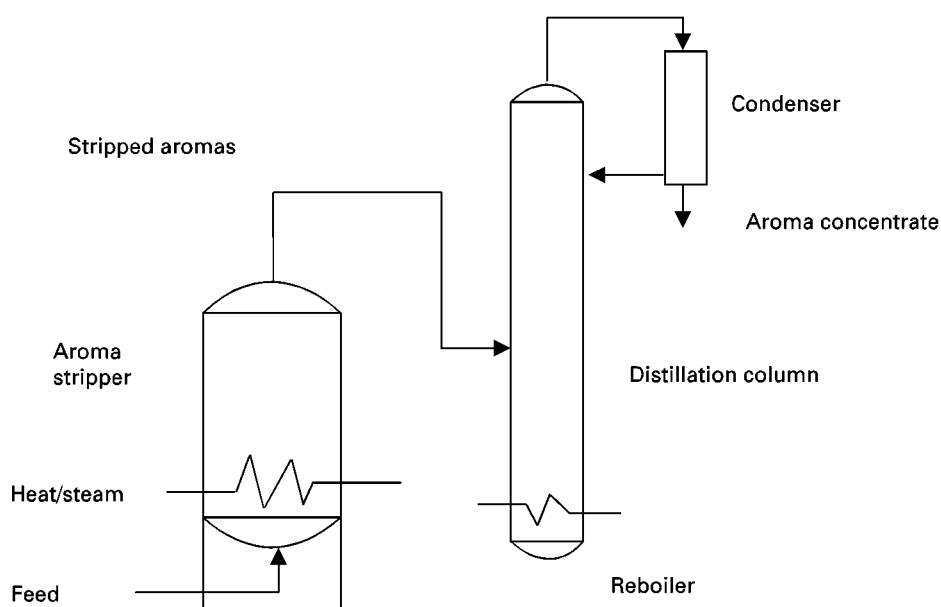


Figure 2 Aroma recovery unit with distillation column.

pounds, can be manipulated with pressure and temperature. Extraction methods by steam distillation, solvent extraction and supercritical CO₂ usually produce different results with regards to yield and composition profiles of the extracted materials. Steam distillation usually gives the lowest yield of recovered aroma but produces a concentrate that is a true essential oil. Solvent extraction with hexane or alcohols produces the highest yield but there is always the possibility that unwanted involatile materials might end up in the final product. Also, solvent extraction uses high temperatures. Supercritical CO₂ extraction produces a lower yield than conventional solvent extraction but higher than steam distillation and it also has the advantage of using little or no heat and no steam or moisture in the process. However, this method has the disadvantage of being expensive since it involves high pressure and sophisticated equipment and controls. In some cases the quality of the aroma extracts from CO₂ extraction is superior to aromas recovered by steam distillation.

Industry Standards and Trends

With the exception of large companies that have access to sophisticated analytical means, the assessment of quality of essential oils is difficult. However, the composition of many essential oils is well known and the industry can adopt standards that can be applied to essential oils. Oils used in medical applications, for example, camphor oil, must meet the standards set forth in the US pharmacopeia. Oils used in food products must meet the Food Chemical Codex standards and the Fragrance Manufacturers Association (formerly the Essential Oil Association, or EOA) is in the process of updating a specifications book.

It is common practice for large producers of essential oils to process their oils further following pressing or distillation, either to produce a standard product year after year, or to change the characteristics of the oil. For example, peppermint oil is commonly redistilled to remove some of the front-end components that give the oil an unwanted flavour or aroma note.

Another common practice is folding of oils, or concentrating them by removing certain components. It is common practice to redistil citrus essential oils, in some cases removing up to 90% of the original volume in order to remove most of the unwanted terpenes. This is known as terpeneless citrus oils, which carry a higher price in the essence markets. These folded oils are more stable, have a better fla-

vour, are more water-soluble and are easier to blend in beverages and foodstuffs.

Well-known profiles of components of essential oils are instrumental in setting standards for the assessment of quality and prevention of adulteration. Knowing the chemistry of essential oils has allowed the successful manufacture of synthetic essential oils; however, some essential oils are so complex that the odour and flavour characteristics just cannot be duplicated.

See Colour Plates 81, 82.

See also: II/Chromatography: Gas: Headspace Gas Chromatography. **Distillation:** Extractive Distillation. **Extraction:** Solvent Based Separation. **III/Citrus Oils:** Liquid Chromatography.

Further Reading

- Abdallah MA, Foda YH, Saleh M, Saki MSA and Mostafa MM (1975) Identification of the volatile constituents of the Egyptian lemongrass oil. I. Gas chromatographic analysis *Nahrung* 19: 195–200.
- Azzouz MA, Reineccius and Moshonas MG (1976) Comparison between cold-pressed and distilled lime oils through the application of gas chromatography and mass spectrometry. *Journal of Food Science* 41: 324–328.
- Bednarczyk AA and Kramer A (1975) Identification and evaluation of the flavour-significant components of ginger essential oil. *Chemical Senses Flavour* 1: 377–386.
- Deans SG and Svoda KP (1990) The antimicrobial properties of marjoram (*Origanum majorana* L.). *Journal of Flavour and Fragrances* 5: 187.
- Garnero J, Guichard G and Buil J (1976) L'huile essentielle et le concrete de rose de Turquie *Parfumes, Cosmetiques et Savons* 8: 33.
- Gill LS, Lawrance BM and Morton JK (1973) Variation in *Mentha arvensis* L. (Labiatae). The North American Populations. *Botanical Journal of the Linnean Society* 67: 213–232.
- Gunther E (1972) *The Essential Oils*. Huntington, NY: RE Krieger Publ. Co.
- Hernandez E and Rathbone SJ (1998) Properties of odorizer distillate byproducts recovered in a molecular still. *Annual Report-Food Protein R&D Center*. College Station, Texas: Texas A&M University.
- Ikeda RM, Stanley WI, Vaniere SH and Spittler EM (1962) Monoterpene hydrocarbons of some essential oils. *Journal of Food Science* 27: 455–458.
- Moyler DA (1996) Commercial extraction of flavours and perfumes. *Journal of Chemical Technology and Biotechnology* 65: 296.
- Penfold AR and Willis JL (1961) *The Eucalyptus*. London: Leonard Harris Ed.
- Saravacos GD and Moyer JC (1968) Volatility of some aroma compounds during vacuum-drying of fruit juices. *Food Technology* 22: 623–628.

- Shaw P and Coleman RL (1975) Compositions and flavour evaluation of a volatile fraction from cold pressed valencia orange oil. *International Flavours Food Additives* 6: 190–193.
- Steltenkamp RJ and Cazzasa WT (1967) Composition of the essential oil of lavandin. *Journal of Agriculture and Food Chemistry* 15: 1063–1069.
- Tabacchi R, Garnero J and Buil P (1974) Contribution a l'etude de la composition de l'huile de fruits d'anise de Turque. *Revista Italiana* 56: 683.
- Takaoka D, Takaoka A, Ohshita T and Hiroi M (1976) Sesquiterpene alcohols in camphor oil. *Phytochemistry* 15: 425–426.
- Taskinen J (1974) Composition of the essential oil of sweet marjoram obtained by distillation with steam and by extraction and distillation with alcohol-water mixture. *Acta Chemica Scandinavica* B28: 1221–1228.
- Teisseire P, Maupetit P and Corbier B (1974) Contribution to the knowledge of Patchouli oil. *Reserches* 19: 8–35.
- Thijssen HAC (1970) Concentration processes for liquid food containing volatile flavors and aromas. *Journal of Food Technology* 5: 211–229.
- Urdang G (1943) Pharmacy in Ancient Greece and Rome. *Amercian Journal of Pharmaceutical Education* 7: 169.
- Van der Gen A (1972) Corps olfactifs a l'odeau de jasmin. *Parfumes, Cosmetiques et Savon* 2: 356–370.
- Virmani OP and Datta SC (1971) Essential oil of *Cymbopogon winteranius* (Oil of Citronella, Java). *Flavour Industry* 3: 595–602.
- Walker GT (1968) Sandalwood oil. The chemistry of oil of sandalwood. *Perfumes and Essential Oil Research* 59: 778–785.

Gas Chromatography

C. Bicchi, University of Turin, Turin, Italy

Copyright © 2000 Academic Press

An essential oil is internationally defined as the product obtained by steam distillation, hydrodistillation or expression (for citrus fruits) of a plant or of a part of it. This definition is now less strictly applied, and the fractions resulting from several other techniques that sample the volatile fraction of a plant are now erroneously classified as essential oils. In general it would be more correct to call them volatile fractions of a vegetable matrix, and to use the term essential oil more specifically for samples obtained by distillation or expression. In addition to distillation or expression, the volatile fraction of a vegetable matrix can be obtained through static or dynamic headspace gas chromatography (HS-GC), solid-phase microextraction (SPME-GC), simultaneous distillation–extraction (SDE), solvent extraction or supercritical fluid extraction (SFE).

Components of an essential oil are generally medium-to-highly volatile with medium-to-low polarity, and as a consequence GC is the technique of choice for their analysis. Figure 1 shows the structure of some typical essential oil components. These characteristics also facilitate their identification, which in general can be achieved by combining chromatographic (retention indices) data with mass spectrometry (GC-MS) and Fourier transform infrared spectroscopy (GC-FTIR).

This article aims to cover the main aspects related to the analysis of essential oils, in particular with sample preparation techniques related to GC; GC

separation of enantiomers; multidimensional GC; identification of essential oil components through GC and/or combined techniques (GC-MS, GC-FTIR); GC-Isotope ratio mass spectrometry and authenticity of an essential oil; GC-sniffing for sensory evaluation; and statistical analysis applied to GC profiles.

Sample Preparation

Steam Distillation and Hydrodistillation

An essential oil is classically obtained by steam or hydrodistillation via equipment based on the circulatory distillation apparatus introduced by Clevenger in 1928. Apparatus and operation modes are now well established. Several pharmacopoeias give diagrams and instructions of how to obtain essential oils. Figure 2 is taken from the *European Pharmacopoeia*.

On the other hand, sampling techniques for the volatile material are under constant evolution. The most used techniques are static or dynamic HS-GC, SPME/GC, SDE and SFE.

Headspace Sampling (HS-GC)

Static HS-GC, dynamic HS-GC HS is a sampling technique applied to the determination of volatiles in the gaseous phase in equilibrium with the matrix to be sampled.

HS-GC sampling is generally classified as static or dynamic HS. In static HS-GC, the analyte is sampled from a hermetically sealed vial after the matrix has reached equilibrium with its vapour at a pre-determined temperature. Figure 3A shows the static HS-GC pattern of a sage sample. The sample was

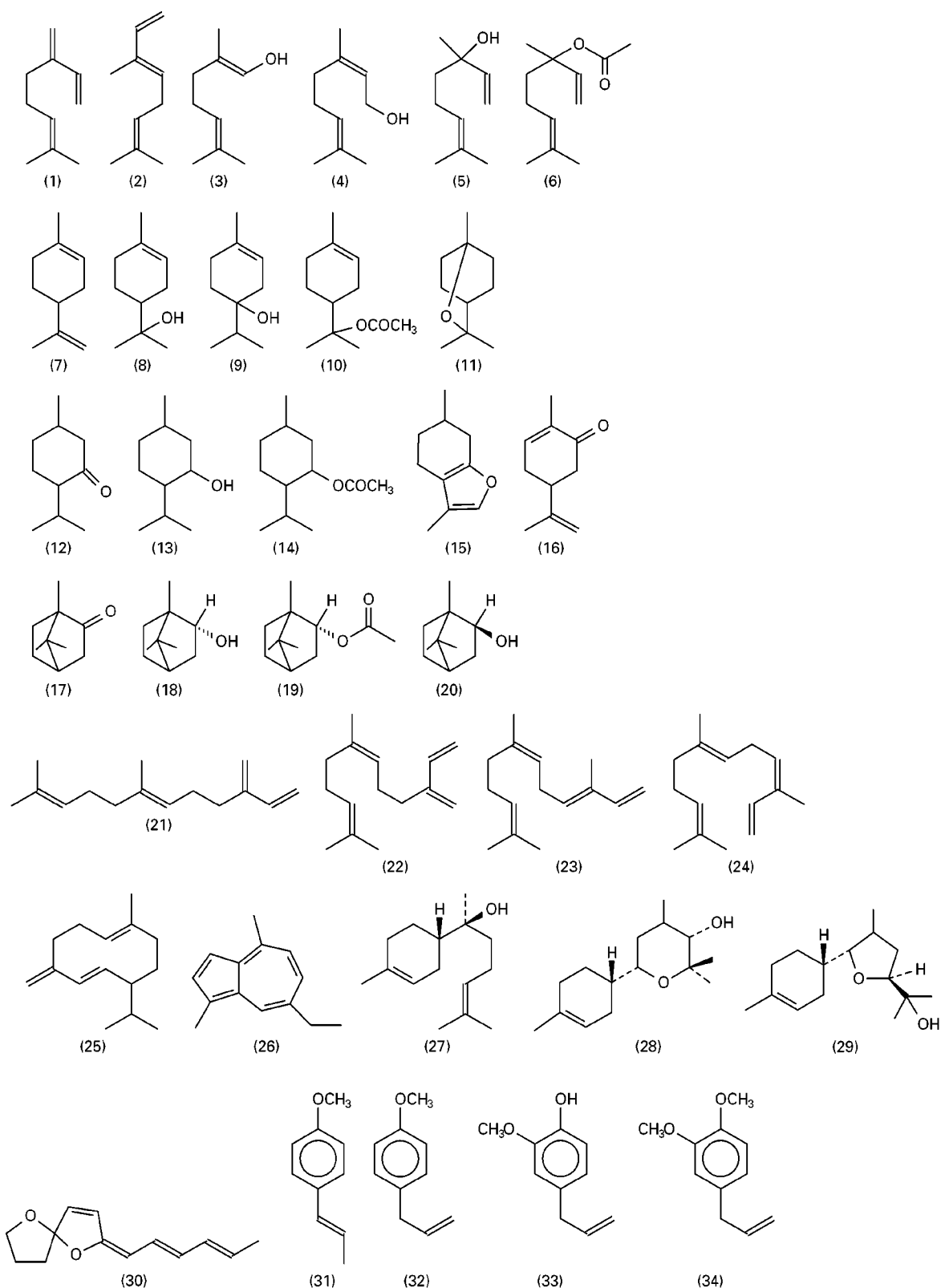


Figure 1 Structure of some typical essential oil components. 1, Myrcene; 2, *t*-ocimene; 3, geraniol; 4, nerol; 5, linalol; 6, linalyl acetate; 7, limonene; 8, α -terpineol; 9, terpinen-4-ol; 10, terpinyl acetate; 11, 1,8-cineole; 12, menthone; 13, menthol; 14, menthyl acetate; 15, menthofuran; 16, carvone; 17, camphor; 18, borneol; 19, bornyl acetate; 20, *i*-borneol; 21, *t*- β -farnesene; 22, (*Z,Z*)- α -farnesene; 23, (*Z,E*)- α -farnesene; 24, (*E,Z*)- α -farnesene; 25, germacrene D; 26, chamazulene; 27, (–)- α -bisabolol; 28, bisabolol oxide A; 29, bisabolol oxide B; 30, spiroether; 31, anethole; 32, estragole; 33, eugenol; 34, methyl eugenol.

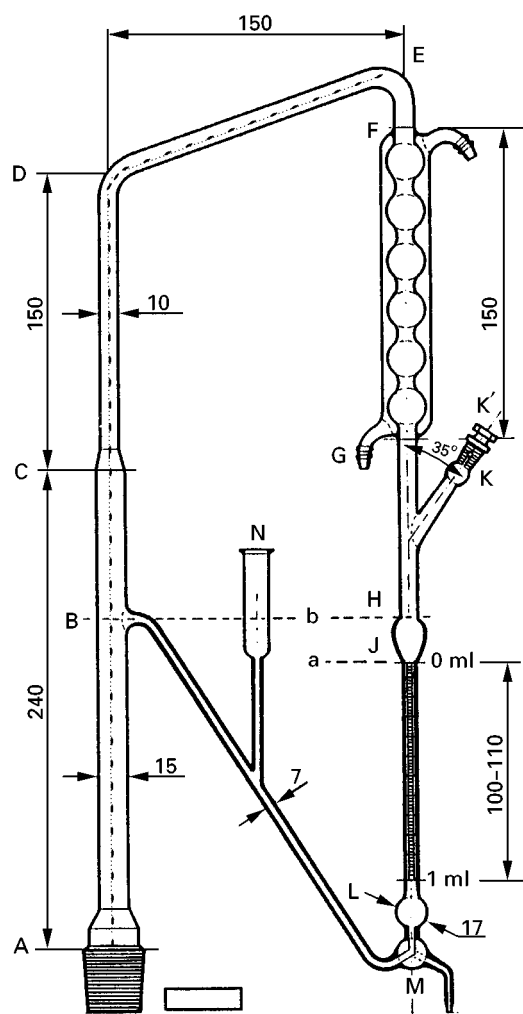


Figure 2 Apparatus for the determination of essential oils in vegetable drugs (*European Pharmacopoeia* (2000) 3rd edn, Copyright Council of Europe). Plant material suspended in water is heated to boiling; the resulting vapour, consisting of a homogeneous mixture of essential oil and steam, is then condensed in the refrigerator (F,G) and recovered in the collecting bubble (J); two layers are formed, the upper with the essential oil and the lower with the aqueous phase, the latter being continuously circulated through the (M-B) tubing.

equilibrated for 1 h at 60°C and 1 mL of the gas phase in equilibrium with the vegetable matrix was automatically injected and analysed by GC.

In dynamic HS-GC, the sample is obtained by capturing the volatiles in a gaseous effluent passed through or over the matrix on to a suitable trapping system, such as cryotrap, solid adsorbents, liquid stationary phases or selective reagents for a given class (or classes) of compounds, coated on a solid support. The trapped volatiles are then recovered through heat or solvent elution either on-line or off-line to the gas chromatograph. **Figure 3B** shows the GC pattern of the same sage sample as in **Figure 3A**. The volatile fraction was transferred to a 50 mg Ten-

ax TA cartridge through a nitrogen flowstream of 30 mL min⁻¹ for 2 min.

Solid-phase microextraction SPME is a sampling technique based on absorption developed by Arthur and Pawliszyn. With SPME, the analytes are absorbed from the liquid or gaseous sample on to an absorbent coated fused silica fibre, which is part of the syringe needle, for a fixed time. The fibre is then inserted directly into a GC injection port for thermal desorption. SPME is a solvent-free technique which is sensitive because of the concentration factor achieved by the fibre, and selective because of the different coating materials which can be used. One of the advantages of SPME is the possibility to sample directly the vapour phase in equilibrium with the matrix (headspace (HS)-SPME), or the matrix extract or solution (liquid sampling-SPME) directly, provided that suitable fibres are used. **Figure 3C** shows the SPME-GC pattern of the same sage sample already analysed. The dried sage leaves are equilibrated as for static headspace sampling for 1 hour with a 100 µm polymethylsiloxane-coated fibre.

All these headspace techniques are easy to automate and to standardize. This is particularly true for static HS-GC and SPME-GC which can be used for fully automatic routine analysis. Static HS-GC is highly reliable for quantitative analysis, when associated with the multiple headspace extraction method developed by Kolb. Dynamic HS-GC is also quite easy to standardize, now that automatic purge-and-trap systems are commercially available. However, reproducible dynamic HS sampling is conditioned by a large number of parameters (volume to be sampled, volume of the headspace system, sampling time and speed, carrier flow rate, trapping material, including batch and producer, kinetics of component release in different matrices) that make it quite difficult to compare results from different laboratories.

The different HS sampling techniques are normally used for different applications: in general, static HS-GC is suitable for the analysis of highly volatile fractions, HS SPME-GC is suitable for the analysis of medium-volatile fractions, while dynamic HS-GC is used for trace analysis or for very diluted headspace.

Supercritical Fluid Extraction

The high selectivity of supercritical fluids, together with the low polarity and molecular weight of most of the volatile fraction components, permits low extraction pressure and temperature to be used, thus limiting the classes of the extracted components to those that characterize an essential oil (mono- and sesqui-terpenoids, phenylpropanoids and aliphatic oxygenated compounds). This often makes the com-

position of SFE extracts quite similar to that of the corresponding essential oil obtained through hydro- or steam distillation. In addition, several organoleptically important components that are water-soluble and which are generally lost in the water phase during the steam distillation are quantitatively recovered by SFE. Typical is the case of phenylethanol, which is the main component in a rose SFE extract, while it is a minor component in the corresponding essential oil.

GC Analysis

Classical GC Analysis

Essential oils are generally analysed by capillary GC. The most popular stationary phases used for essential oil analysis are methylpolysiloxanes (SE-30, OV-1, OV-101, DB-1, PS-347.5) and methylphenylpolysiloxanes (SE-52, SE-54, PS-086, DB-5) as apolar stationary phases; and polyethylene glycol

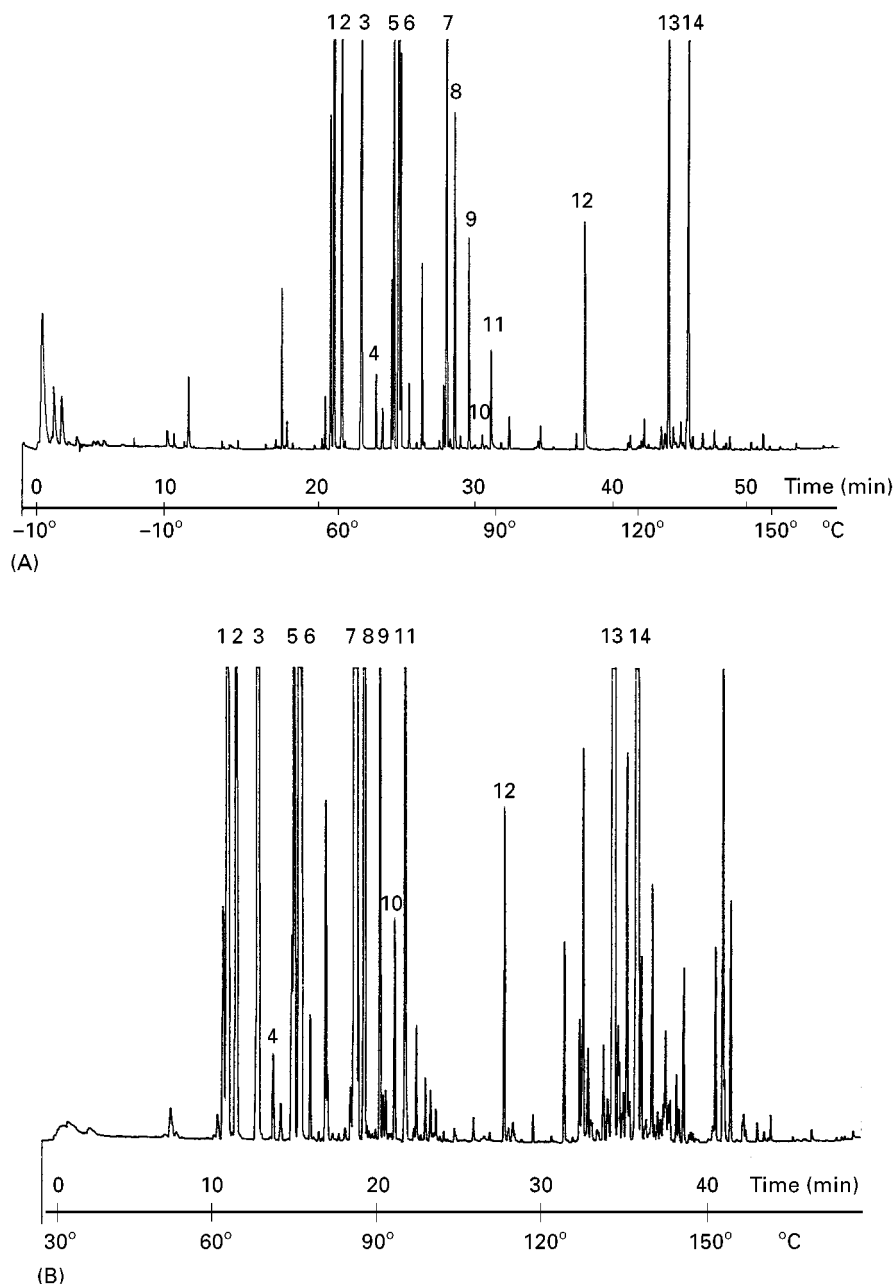


Figure 3 Capillary GC patterns of (A) the static HS-GC; (B) dynamic HS-GC and (C) HS SPME-GC of a sample of dried sage leaves. Analysis conditions: column 15 m, 0.25 mm i.d. OV-1, df: 0.3 μ m; temperature programme: (A) from -10°C (10 min) to 30°C at $30^{\circ}\text{C min}^{-1}$ then to 150°C at $3^{\circ}\text{C min}^{-1}$ and to 200°C at $5^{\circ}\text{C min}^{-1}$; (B) and (C) from 30°C to 150°C at $3^{\circ}\text{C min}^{-1}$ and to 200°C at $5^{\circ}\text{C min}^{-1}$. Peak identification: 1, α -pinene; 2, camphene; 3, β -pinene; 4, myrcene; 5, limonene; 6, 1,8-cineole; 7, α -thujone; 8, β -thujone; 9, camphor; 10, *iso*-borneol; 11, borneol; 12, bornyl acetate; 13, β -caryophyllene; 14, α -humulene.

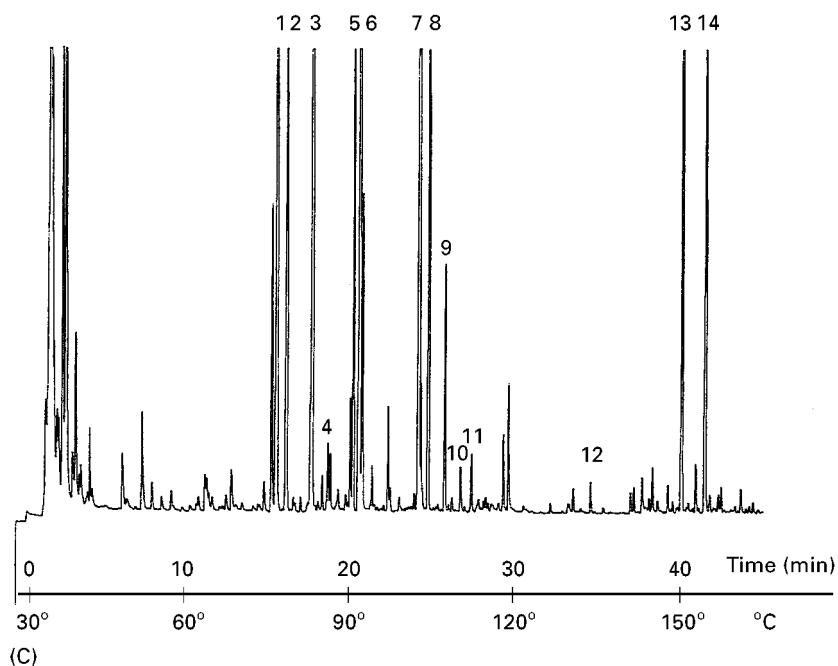


Figure 3 Continued

(Carbowax 20M) as a polar stationary phase. GC data are also very useful to identify most of the components in an essential oil: an effective approach is to combine the retention data from two different-polarity stationary phases (see below).

Enantiomer GC Analysis

One of the most important successes of the last 10 years has been enantioselective GC recognition of chiral essential oil components with cyclodextrin derivatives (CDs). The importance of enantiomer separation and of determining enantiomer excess is well known. Biosynthetic and geographical origins, as well as technological treatments and/or authenticity of most of the essential oils, can now also be evaluated through the enantiomeric composition of their underivatized optically active components. This is also important because optical isomers can have different sensory properties, such as the well-known cases of the different smells of both carvone and limonene enantiomers. The first GC separations of enantiomers through CDs were obtained by Koscielski and Sibilska in 1983; they separated α - and β -pinene, the corresponding pinanes and Δ -3-carene with a column packed with underivatized α -CDs. The first capillary column applications were in 1987 with the almost contemporary work of Juvancz and Schurig. CDs are generally carried in apolar to moderately polar polysiloxanes, as first proposed by Schurig. The chief reasons for this are the wider range of operating temperatures; the inertness and efficien-

cy of columns prepared by high temperature silylation; the possibilities of tuning column polarity by using different diluting phases; the small CD amounts necessary to prepare columns; shorter analysis times; and the possibility of measuring the thermodynamic parameters involved in enantiomer discrimination.

Almost all the essential oil components can now be separated on CD stationary phases without derivatization. This is particularly true for the so-called second-generation CDs, developed especially for GC, which show high enantioselectivity, and afford highly reliable column performance. The most successful CDs are symmetrically and asymmetrically alkylated CDs, acylated CDs and CDs asymmetrically substituted in position 6 with the groups *tert*-butyldimethylsilyl or hexyldimethylsilyl, and in positions 2 and 3 with methyl, ethyl or acetyl groups. In general, the most popular matrices for the CDs are polyphenylcyanopropylsiloxes (including various OV-1701 types), polyphenylsiloxanes (including SE-52 or PS-086) and methyl polysiloxanes (including SE-30, OV-1 and PS-347.5). The latest generation of CDs makes it possible to characterize an essential oil by determining the enantiomer abundances of several of its optically active components simultaneously, very often in a single GC run. Figure 4 shows the simultaneous enantiomer separation of optically active components characterizing lavender oil: linalyl oxides, linalol, linalyl acetate, camphor, borneol, bornyl acetate, α -terpineol and *cis*- and *trans*-nerolidols are successfully and simultaneously

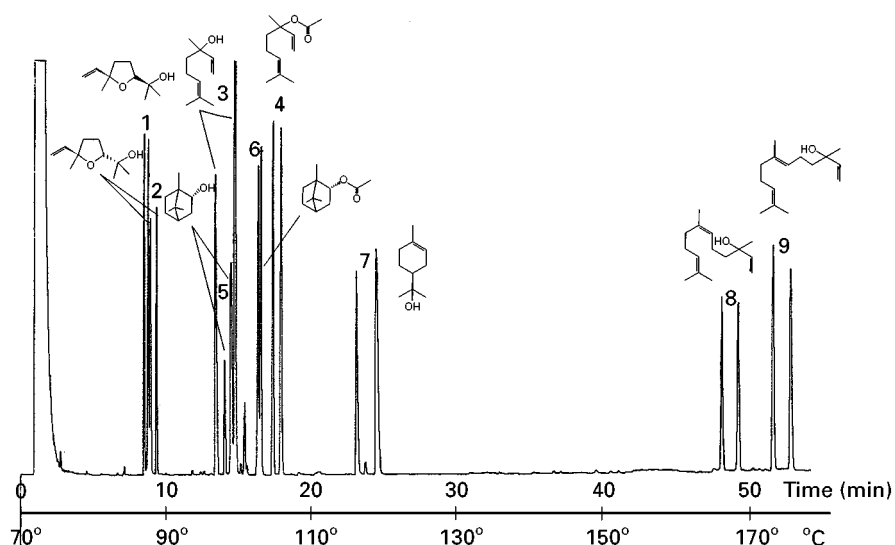


Figure 4 Simultaneous enantiomer GC separation of optically active components characterizing lavender oil: 1, *cis*-linalyl oxide; 2, *trans*-linalyl oxide; 3, linalol; 4, linalyl acetate; 5, borneol; 6, bornyl acetate; 7, α -terpineol; 8, *cis*-nerolidol; 9, *trans*-nerolidol. Column: 25 m, 0.25 mm 30% 2,3-diethyl-6-*t*-butyl-dimethylsilyl- β -CD/PS-086, film thickness 0.15 μ m. Analysis conditions: from 70°C (1 min) to 190°C (10 min) at 2°C min⁻¹.

separated with a 30% 2,3-diethyl-6-*t*-butyl-dimethylsilyl- β -CD in PS-086.

Koenig and Joulain have made a very important contribution to this field: they have identified and structurally characterized about 330 sesquiterpene hydrocarbons, including the enantiomer recognition of the optically active ones. **Figure 5** shows the enantioselective GC pattern of a group of sesquiterpene hydrocarbons (δ -elemene, α -copaene, *ar*-curcumene, β -bisabolene and (*E*)- α -bisabolene) separated on a 20% 2,6-di-*O*-methyl-3-*O*-pentyl- β -CD/OV-1701 column.

Multidimensional GC

Multidimensional GC (MDGC) is a very useful technique to analyse a complex mixture such as an essential oil. In MDGC, groups of components not separated on the first column can automatically be transferred on-line to a second column coated with a different stationary phase. The possibilities of MDGC are still not fully appreciated: it is true that early systems were difficult to tune, inflexible and above all very expensive; however, most of the present systems

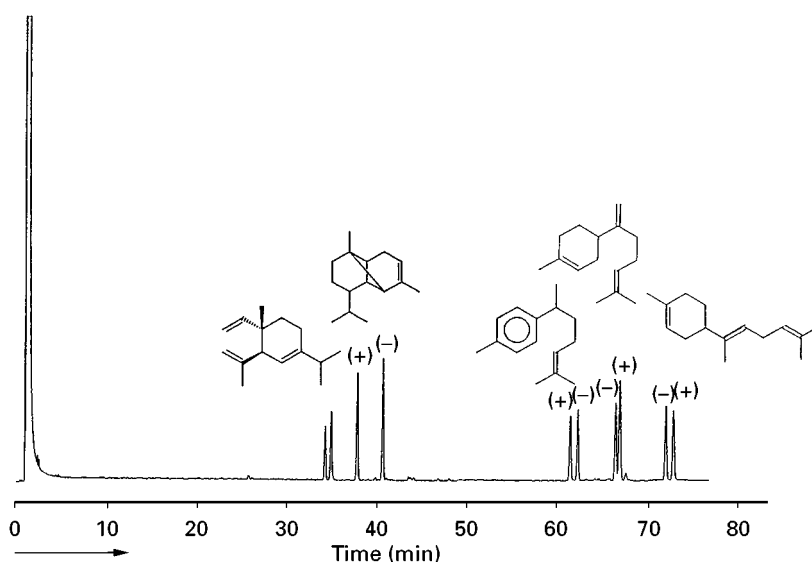


Figure 5 Enantioselective GC pattern of a δ -elemene, α -copaene, *ar*-curcumene, β -bisabolene and (*E*)- α -bisabolene separated on a 20% 2,6-di-*O*-methyl-3-*O*-pentyl- β -CD/OV-1701 column. Analysis conditions: from 60°C (1 min) to 190°C (10 min) at 0.6°C min⁻¹. (Courtesy of Professor W. Koenig, University of Hamburg.)

are fully automatic and not too expensive. Above all, they consist of two independent GC units connected through a transfer interface, which can be used independently when MDGC is not necessary.

MDGC is particularly useful with enantiomer GC analysis, which may double the number of peaks of the optically active components, making the chromatogram resulting from the analysis of an essential oil even more complex, and increasing the probability of peak overlap, thus interfering with a correct determination of enantiomeric ratios. In these cases MDGC operates a sort of clean-up on the first column, so that only selected peaks are transferred to the chiral column.

Identification

Essential oil components are generally identified through GC or GC-MS or, better, through their combination. The safest way to identify an essential oil component, and in particular a sesquiterpene, is to combine dual-column GC data and mass spectrometry (MS) data with IR data, because of the high structure-related specificity of infrared spectroscopy (IR) signals. It is important to remember that identification and structure elucidation are totally different things: identification can only be by comparison with reference data. It is risky to propose a new structure or, worse, a new skeleton, from results obtained only by combined techniques (GC, GC-MS, GC-FTIR) without parallel isolation and spectroscopic investigation (in particular, nuclear magnetic resonance) of the new compound.

As in all fields of analytical chemistry, the introduction of data systems has revolutionized the approach to identification. Operators can now build their own personal libraries with retention indices and mass spectra obtained with their own instruments, and combine the GC and GC-MS data for crossed identification of essential oil components.

Identification through Chromatographic Data

Since essential oils are generally very complex mixtures, reliable GC location and identification of their components can only be through retention indices, calculated by the Kováts method or with the van den Dool algorithm; these make retention values independent of GC conditions. Identification through retention indices is in general only considered significant when two successful matches are obtained from different-polarity stationary phases. When a suitable reference database is available, the percentage of correct identifications obtained through retention data is generally around 65% with one column, 80% with two different-polarity columns, and above 90% with

three columns. The last two percentages are close to that obtainable with MS, which is generally around 90%. Since a GC system affording simultaneous injection into two columns is simple to assemble, and today's processing systems can easily handle two detector signals, a manual or automatic crossed-identification procedure is not difficult to set up. This is particularly true with the latest-generation instruments: the development of GC instruments with electronic pressure control of the mobile phase and of GC ovens in which the temperature is strictly controlled and evenly distributed, has overcome several problems with instrumentation. These give rigorous control of mobile-phase parameters (flow rate, pressure and average linear velocity) and of temperature parameters over the whole GC run. Thus the chromatographic process, and hence retention, becomes highly reproducible: as an example, under fixed conditions a retention index precision of 1 unit was maintained over 1 month for some of the most significant essential oil components of both *Matricaria chamomilla* (OV-1 column) and *Tagetes lucida* (CW-20M column; Table 1).

Retention indices are fundamental in making retention a reliable identification tool for GC, although many problems still exist; in particular, the variation of stationary-phase polarity and mobile-phase characteristics as a function of temperature in programmed analysis. As a consequence, a comparison of data from different laboratories can only be made with analyses run under carefully controlled operating conditions.

Identification by GC-MS

Mass spectral data are often – and perhaps to some extent erroneously – considered the key for component identification. Many people give too much priority to mass spectrometry (MS) data over chromatographic data, and seldom give due weight to the complementarity of GC and MS data. This is probably because many manufacturers and operators do not yet consider GC-MS as a technique in its own right, but a simple coupling between GC and MS.

Nowadays, identification is generally made through commercially available mass spectra libraries (NBS, NIST, Wiley, TNO); these are nonspecialized collections of spectra mainly taken from the literature. As a consequence, the identification of a component must be carefully confirmed, since the mass spectra are from different origins and have been recorded under different operative conditions. A classical example is the differences in the spectra produced by different mass analysers: ion trap, quadrupole or magnetic sector instruments. Most operators overcome this problem by building dedicated libraries

Table 1 Reproducibility over time of reference index of *Matricaria chamomilla* L. essential oil component (OV-1) and of *Tagetes lucida* Cav. essential oil components (CW-20M)

Matricaria chamomilla L				Tagetes lucida Cav			
	Compound	RI ^a	RI ^b		Compound	RI ^a	RI ^b
1	<i>Trans</i> - β -farnesene	1442	1441	1	Myrcene	1159	1157
2	Bisabolol oxide B	1619	1618	2	<i>Trans</i> - β -ocimene	1247	1246
3	α -Bisabolone oxide A	1637	1637	3	Linalol	1553	1553
4	α -Bisabolol	1649	1649	4	Estragole	1656	1656
5	Chamazulene	1674	1674	5	Anethole	1807	1805
6	Bisabolol oxide A	1702	1701	6	Methyl eugenol	2006	2005
7	Spiroether	1805	1805	7	β -Caryophyllene	1566	1566
				8	Germacrene D	1675	1673

RI^a Reference initial index; RI^b Reference index calculated 1 month later under the same conditions. GC analysis: columns: 25 m, 0.25 mm i.d. OV-1 column, df: 0.3 μ m; 25 m, 0.25 mm i.d. CW-20 m column, df: 0.25 μ m. Analysis conditions: injection: split, split ratio 1 : 20, temperature 230°C; detector: FID, temperature 250°C; temperature programme: from 50°C (1 min) to 220°C (10 min) at 3°C min⁻¹; carrier gas: hydrogen, constant flow: 1.5 mL min⁻¹.

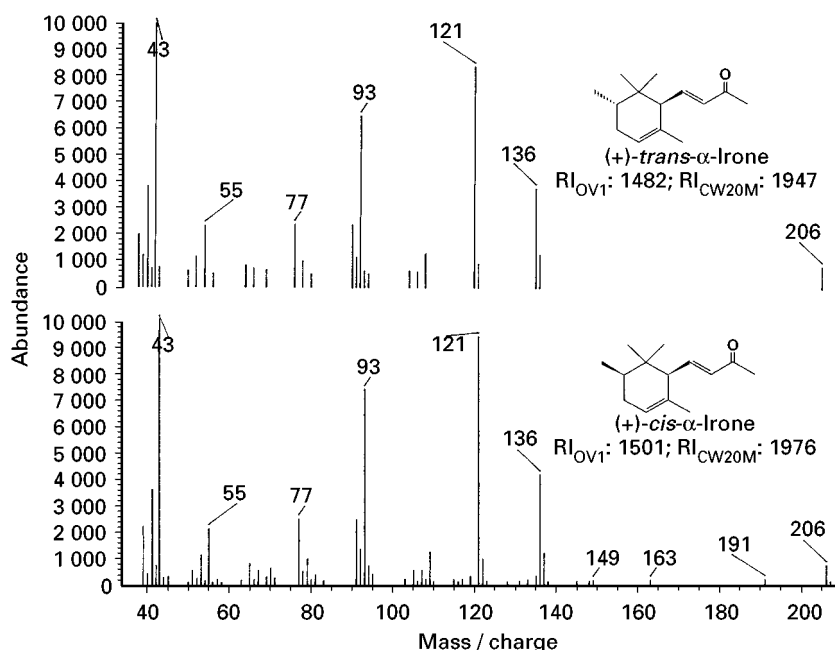
consisting of spectra recorded with their own GC-MS systems. Libraries dedicated to the essential oil field are also available, as is the case of Adams library for ion trap mass spectra, or the Joulain and Koenig collection of sesquiterpene hydrocarbon spectral data.

Chromatographic data used either actively or passively in a library search can play a fundamental role in the successful identification of essential oil components. Several compounds, in particular sesquiterpenoids, have low resolution mass spectra that are almost indistinguishable. In this case, mass spectra can mainly be used to locate the spectra in the total chromatogram; retention indices (better if from two

different polarity columns) are then used to identify each component. **Figure 6** shows retention indices and mass spectra of *cis* and *trans*- α -irones.

The use of retention indices, as a further active identification key in combination with mass spectra or within the classical library search procedure, can be extremely useful. The ideal procedure should include simultaneous and/or sequential searches with retention indices from two different stationary phases, and mass spectra in which flexible and selectable priorities can be actuated.

Unfortunately, identification by retention indices associated with mass spectra is not absolutely risk-

**Figure 6** Retention indices on OV-1 and CW-20M and mass spectra of *cis* and *trans*- α -irones.

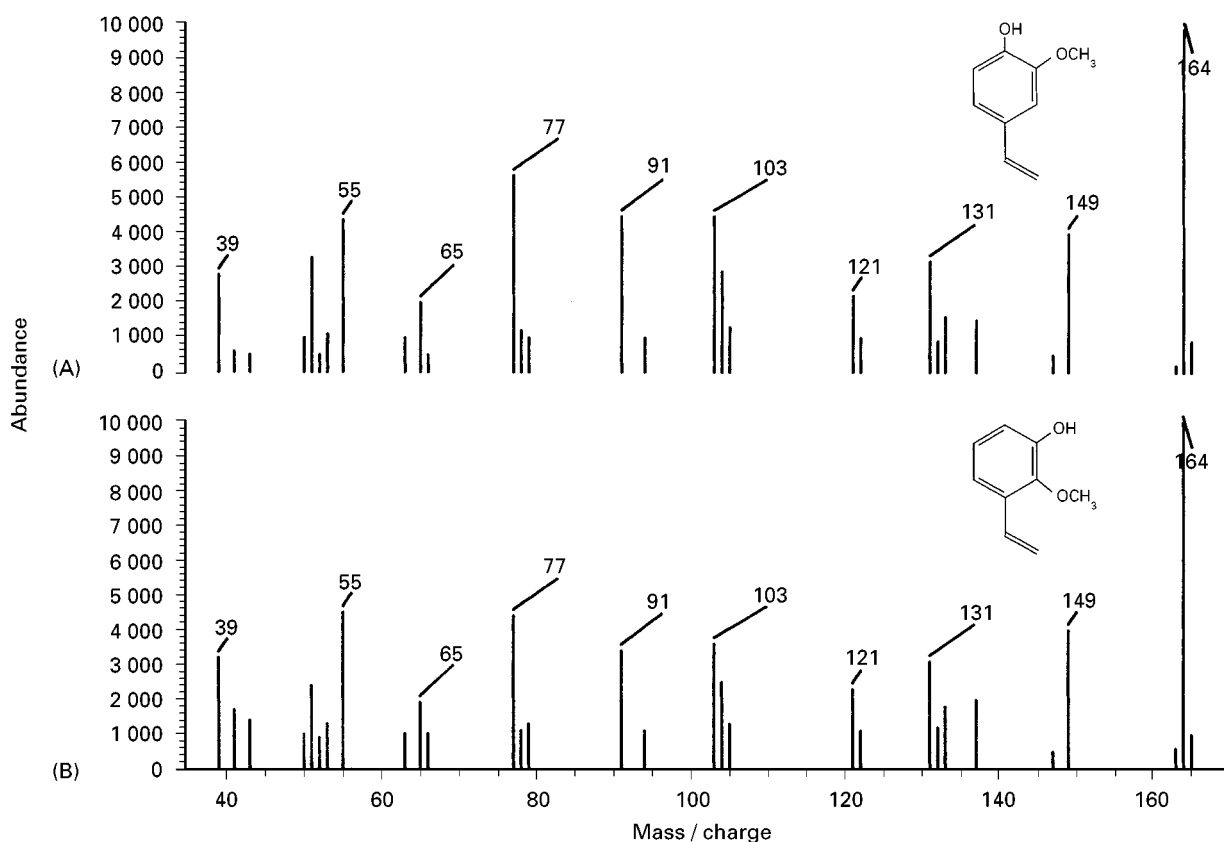


Figure 7 Retention indices on OV-101 and DB-Wax and mass spectra of (A) eugenol (RI(OV-101): 1323; RI(DB-Wax): 2158) and (B) 2-methoxy-3-hydroxy-allylbenzene (RI(OV-101): 1325; RI(DB-Wax): 2160). (Courtesy of Professor K.-H. Kubeczka, University of Hamburg.)

free: there are some rare exceptions in which pairs of compounds have almost identical mass spectra, and also have retention indices which fall within the instrumental and analytical limit on two different stationary phases. This is the case of mass spectra and retention indices of 2-methoxy-3-hydroxy-allylbenzene and eugenol on OV-101 and DB-Wax (Figure 7).

A last approach, no less important, is GC/single ion monitoring (SIM)-MS, which is very selective and as a consequence the most reliable procedure for quantitative analysis. In particular, GC-SIM-MS can be an alternative to MDGC for direct determination of enantiomeric ratios of optically active components in the essential oil. A suitable choice of specific diagnostic ions can overcome the interferences to a correct determination of enantiomeric ratio due to peaks coeluting with the two (or more) enantiomers.

Identification by GC-FTIR

Although MS is the preeminent technique to identify a component in a complex mixture analysed by GC, it has some drawbacks, e.g. in the differentiation of structural isomers giving identical mass spectra.

Fourier transform infrared spectroscopy (FTIR) combined with GC has emerged as a powerful technique and as the ideal complement to MS for component identification in complex mixtures, thanks to its ability to distinguish geometric and positional isomers and to characterize organic functions; moreover, the identification of a compound through its FTIR spectrum is very reliable. To exploit in full the complementarity between FTIR and MS data, systems combining online GC, FTIR and MS or FID have also been assembled. In spite of this, FTIR, as a detector for GC, is not as popular as MS, because of the lack of sensitivity for many compounds when compared to GC or GC-MS systems. Another reason is the lack of extensive libraries. The cheapest and most widely adopted GC-FTIR system is based on the so-called light-pipe interface, which produces vapour-phase spectra: this makes existing collections of spectra useless for automatic identification, because they are mainly recorded in the liquid or solid phase. Some relatively small collections of vapour-phase spectra of compounds in the essential oils and flavour fields are now commercially available.

GC-Isotope Ratio Mass Spectrometry

The stable isotope ratio is an important parameter in biochemistry, nutrition and drug research, and in origin assignment and authenticity control of essential oils. This ratio has gained in importance with the introduction of on-line coupled GC-isotope ratio MS systems, where the analytes eluting from the GC column are combusted to carbon dioxide in an oven and analysed in an isotope ratio mass spectrometer, adjusted for the simultaneous determination of mass 44 ($^{12}\text{C}^{16}\text{O}_2$), 45 ($^{13}\text{C}^{16}\text{O}_2$, $^{12}\text{C}^{16}\text{O}^{17}\text{O}$) and 46 ($^{12}\text{C}^{16}\text{O}^{18}\text{O}$) in the nmol range and with high precision ($\leq 0.3\text{‰}$). The actual ratio is obtained from the ratio of the areas of two isotope peaks; this value is then compared to a standard value by applying the following expression:

$$\delta = (R_{\text{sa}}/R_{\text{st}} - 1) \times 1000$$

where R_{sa} is the isotope ratio of the sample and R_{st} that of the standard; $\delta\text{-C}^{13}$ is given in parts per thousand.

The $\delta\text{-C}^{13}$ value is particularly effective when combined with enantiomeric recognition of the chiral component(s) characterizing an essential oil. Enantiomer GC analysis may fail in authenticity determination when recemates of natural origin are present, or when racemization occurs during processing or storage of natural products, and chiral essential oil components are blended with the corresponding synthetic chiral compounds.

Enantiomeric GC separation combined with isotope ratio MS is a very effective method of evaluating the authenticity of an essential oil since the mass spectrometer detects enantiomers of the same natural source which have identical $\delta\text{-C}^{13}$ values. As a consequence, identical $\delta\text{-C}^{13}$ ratios are expected for enantiomers from genuine compounds, even if the chiral molecules to be analysed are partially racemized: it seems improbable that racemic compounds would be synthesized through different biochemical pathways in the same organism. Enantiomer GC-isotope ratio MS or, even better, multidimensional GC-isotope ratio MS of enantiomers can therefore detect blends of optically pure chiral essential oil components with synthetic racemates.

Sensory Analysis (GC-Sniffing Detection)

The GC profile of an essential oil does not necessarily reflect the sensory properties of its components. Some of the components, present in large quantities, are not

relevant to the overall smell while others, present in trace amounts but with low detection thresholds, are not revealed by FID, nitrogen-phosphorous detector (NPD) or flame photometric detector (FPD) but are detected by GC-sniffing. Sensory methods are therefore needed to detect trace components responsible for the smell of an essential oil. A sniffing device is very simple and inexpensive to assemble. Several have been described: in a typical one, the flow of the gas eluting from the analytical column is split through a T piece on one side to an FID and on the other to the sniffing port, which consists of a shaped glass funnel. A stream of air (or nitrogen) saturated with water is sent coaxially with the mobile phase to the sniffing port to avoid dehydration of the nasal tissues. The results of olfactory measurements can be qualitative, giving a description of the odour of each peak corresponding to an odour-active component; on the basis of these qualitative results, a semiquantitative evaluation is also possible. Several approaches have been developed for semiquantitative sensory evaluation: the best known are Charm analysis developed by Accree and AEDA (aroma extract dilution analysis), developed by Grosch. Charm analysis is based on sniffing a series of decreasing dilutions of the components eluting in the GC odour-active zones characterized with a specific sensorial descriptor. The beginning and end of each particular odour perception are fixed. Charm values are calculated through the formula $c = d^{n-1}$, where n is the number of coincident responses and d is the dilution factor. AEDA is similar but it uses a dilution factor equal to the last dilution in which an odour-active component is detected.

GC Profile Analysis

Identification and quantitation of the characterizing components are not always sufficient to discriminate between essential oils from a single species, or to classify them, evaluate their quality or origin, or detect adulterations. On the other hand, although sensory analysis (sniffing) is of prime importance in overall evaluation, it is also sometimes insufficient and, above all, it is generally considered insufficiently objective. This is particularly true when series of samples of different origins have to be evaluated at the same time. In these cases, the overall GC profiles of the essential oils under investigation (or the profile of the volatile fraction obtained through related sampling techniques) can be a successful marker to characterize and/or discriminate between them objectively. However, essential oil profiles are so complex that multivariate statistics is needed to obtain an exhaustive evaluation. Several statistical approaches have

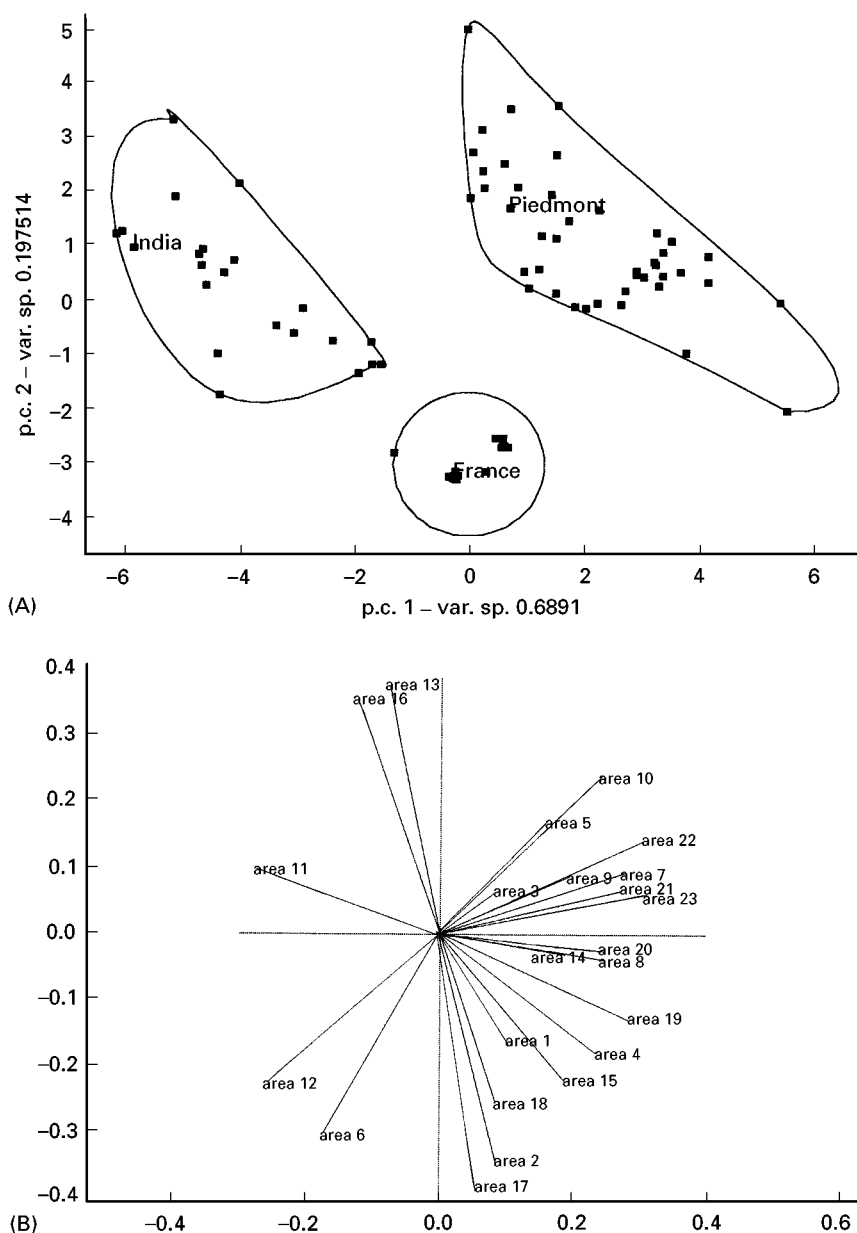


Figure 8 (A) Scatterplot of principal components and (B) distribution of the loadings considered for PCA of a set of peppermint essential oils of different origins (Piedmont (Italy), France and India.)

been proposed (cluster analysis, fuzzy clustering, linear discrimination analysis, neural network, principal component analysis (PCA), and principal component similarity analysis). PCA is successful in analysing multivariate data, since it can investigate relationships between large numbers of variables, and it is useful for reducing the numbers of variables in a data set by finding linear combinations of those variables that explain most of the variability. These characteristics make PCA successful in comparing and discriminating groups of essential oils, for instance versus a series of reference samples,

in particular for routine purposes. The success of PCA is strictly related to a correct selection of variables (the peak areas corresponding to specific essential oil components, generally chosen among those whose peak areas are detectable and reproducibly measurable in all samples under investigation). Figure 8 shows the distribution of the loadings considered for PCA and the scatterplot of principal components of a set of peppermint essential oils of different origins (Piedmont (Italy), France and India): PCA clearly distinguishes the origins of the samples.

Conclusions

Although essential oil analysis is now a well-established field, further work is needed, not only to improve sample preparation and analysis techniques, but also to deal with one of the main aims of this research field: to isolate and elucidate the structure of new odorous compounds. These studies evolve along two main lines. The first and classical one combines isolation and spectroscopic techniques and mainly concerns new mono- and sesquiterpenoids. The second mainly involves the so-called supervolatile fraction and perfumed trace compounds, two fractions that play a fundamental role in odour impact. For the supervolatile fraction, some topics requiring further study are HS combined with effective cryotrapping techniques, systems for direct GC injection of large volumes of gas samples and GC columns with a high retention capacity. For compounds present in the essential oil at the p.p.m. level (e.g. pyridine derivatives in peppermint and orange oils), a number of points would benefit from further investigation. These include increased selectivity of sample preparation techniques and increased sensitivity and selectivity of analysis techniques.

See also: II/Chromatography: Gas: Column Technology; Detectors: Mass Spectrometry; Detectors: Selective; Headspace Gas Chromatography; Sampling Systems; III/Essentials Oils: Distillation. Terpenoids: Liquid Chromatography.

Further Reading

- Accree T (1997) GC/Olfactometry with a sense of smell. *Analytical Chemistry* 69: 170–175A.
- Accree T and Teranishi R (1993) Sensible principle and techniques. In *Flavor Science*. Washington, DC: American Chemical Society.
- Adams RP (1989) *Identification of Essential Oils by Ion Trap Mass Spectroscopy*. New York: Academic Press.
- Bicchi C and Joulain D (1990) Headspace-gas chromatographic analysis of medicinal and aromatic plants

- and flowers. *Flavour and Fragrance Journal* 5: 131–145.
- Bicchi C, Manzin V, D'Amato A and Rubiolo P (1995) Cyclodextrin derivatives in GC separation of enantiomers of essential oil, aroma and flavour compounds. *Flavour and Fragrance Journal* 10: 127–137.
- Bicchi C, D'Amato A and Rubiolo P (1999) Cyclodextrin derivatives as chiral selector for direct gas chromatographic separations of enantiomers. *Journal of Chromatography A* 843: 99–121.
- Blank I (1996) Gas chromatography-olfactometry in food aroma analysis. In: Marsili R (ed.) *Techniques for Analysing Food Aroma*. New York: Dekker.
- Grosch W (1993) Detection of potent odorants in foods by aroma extract dilution analysis. *Trends in Food Science Technology* 4: 68–73.
- Ishibara M, Tsumeya T, Shiga M *et al.* (1992) New pyridine derivatives and basic components in spearmint oil (*Mentha gentilis* f. *cardiaca*) and peppermint oil (*Mentha piperita*). *Journal of Agricultural and Food Chemistry* 40: 1647–1655.
- Joulain D and Koenig W (1998) *The Atlas of Spectral Data of Sesquiterpene Hydrocarbons*. Hamburg: E.B. Verlag.
- Kolb B and Ettre L (1997) *Static Headspace-Gas Chromatography*. New York: Wiley-VCH.
- Mosandl A (1995) Enantioselective capillary gas chromatography and stable isotope ratio mass spectrometry in the authenticity of flavours and essential oils. *Food Review International* 7: 597–664.
- Pawliszyn J (1997) *Solid Phase Microextraction: Theory and Practice*. New York: Wiley-VCH.
- Sandra P and Bicchi C (eds) (1987) *Capillary Gas Chromatography in Essential Oil Analysis*. Heidelberg: Huethig.
- Schurig V and Novotny H-P (1990) Gas chromatographic separation of enantiomers on cyclodextrin derivatives. *Angewandte Chemie, International Edition English* 29: 939–957.
- Tarján G Nyiredy Sc, Györ M *et al.* (1989) Thirtieth anniversary of the retention index according to Kovatz in gas-liquid chromatography. *Journal of Chromatography* 472: 1–92.
- Thomas AF and Bassols F (1992) Occurrence of pyridines and other bases in orange oil. *Journal of Agricultural and Food Chemistry* 40: 2236–2243.

Thin-Layer (Planar) Chromatography

P. Dugo, L. Mondello and G. Dugo,
Università di Messina, Messina, Italy

Copyright © 2000 Academic Press

Introduction

Essential oils are mixtures of mainly volatile components belonging to different chemical classes. They

are characterized by a pleasant smell and are generally obtained by steam distillation of aromatic plants, with the exception of citrus peel essential oils, which are produced by cold-pressing the peel of the fruits. This process involves the abrasion of peel and the removal of the oil in an aqueous emulsion that is subsequently separated in a centrifuge. Other methods may be water distillation or extraction with sub- or supercritical fluids. Essential oils are not soluble in water, but are quite soluble in alcohol.

Resins can be either natural or prepared: natural resins are exudations from trees or plants, and are formed in nature by the oxidation of terpenes; prepared resins are oleoresins from which the essential oils have been removed. Resins are mixtures of many components; they are solid, amorphous, more or less coloured, nonvolatile, with a characteristic smell, insoluble in water, but soluble in alcohol or other organic solvents.

Balsams are natural raw materials exuded from a tree or a plant; they have a high content of benzoic acid, benzoates or cinnamates.

The main constituents of essential oils, balsams and resins are terpene or aromatic hydrocarbons, and their oxygenated derivatives (alcohols, aldehydes, esters, ketones, oxides, etc.).

The physiological role of oils and resins in plants and trees is not well understood. It is likely that they play a role as lures for insects. They may also serve to protect plants from parasites, increase the rate of transpiration and act as a seal for wounds. They are largely used in perfumery, food or pharmaceutical industries, as flavouring agents or because of their different pharmacological actions.

Characterization of Essential Oils, Balsams and Resins

Essential oils may be characterized by the determination of physicochemical properties such as boiling point, freezing point, solubility, density, optical rotation, refractive index, etc. These parameters can also help in the detection of adulteration. For the study of the qualitative and quantitative composition of essential oils and resins, chromatographic methods are the techniques of choice. Since the main part of the oil consists of volatile components, gas chromatography (GC) equipped with FID (flame ionization) or MS (mass spectrometer) detectors is the most used technique.

High performance liquid chromatography (HPLC) is also widely used for separation of semi-volatile or nonvolatile components, for preparative purposes, or for the analysis of thermally labile components. The limitation of HPLC is detection, because many com-

ponents of essential oils do not absorb in the UV-visible region, and UV detectors are the most popular in HPLC. Thin-layer chromatography (TLC) is a very widely used chromatographic technique, and modern HPTLC can be advantageously used instead of HPLC or GC in many analytical situations.

Some of the advantages of TLC are its simplicity, economy in materials, simultaneous analysis of a large number of samples and the use of complementary post-chromatographic universal and selective detection methods. Some disadvantages of TLC, such as the long times required for development or the difficulties in controlling the speed of solvent migration, may be overcome by OPLC (overpressured layer chromatography). OPLC, developed by Tyihak and co-workers at the end of the 1970s, is a planar liquid chromatographic technique with advantages over classical TLC and HPLC: the stationary phase is covered completely by a flexible membrane under external pressure and, because the eluent is introduced to the layer by means of a pump, the solvent flow rate may be controlled. Improved separation efficiency, shorter time requirement, better resolution, and lower solvent consumption than classical TLC or HPLC can thus be obtained. Moreover, OPLC can be used for analytical or preparative purposes and maintains all the advantages already mentioned for classical TLC.

Another advance in the development of TLC is chromatography on permanent rod-shaped layers (Chromarods), whose mechanical and chemical properties permit detection of the separated components in an ionization detector; this technique was developed in the late 1960s and can be successfully used for quantitative separations of substances that cannot be analysed by GC because of their low volatility.

There are many papers on planar chromatography that well illustrate the most recent developments of this technique: the use of multidimensional development, the coupling with particular detectors such as MS or FT-IR detectors, or the use of fully computerized image processing instruments. All these developments are accompanied by improvements in the performance and in the reproducibility of pre-coated layers for planar chromatography.

The literature reports some applications of planar chromatography to the analysis of essential oils, balsams and resins, to obtain different information. Methods have been developed that use both conventional TLC, HPTLC and OPLC for analytical and/or preparative separations. Only a few papers have been published on the separation of terpenes and related substances on Chromarods. One of the reasons for this is probably the volatility of terpenes of low

relative molecules mass, leading to low, irreproducible FID response. Resins have been separated from arnica (benzene/chloroform, 67:33) and Tolu balsam (benzene/chloroform/formic acid, 69:29:2), but the results obtained were not satisfactory. The number of applications is limited, if compared with the applications of GC or HPLC to the analysis of essential oils and plant extracts. However, often TLC is essential as a simple analytical and preparative technique. A recent review summarized the chromatographic methods reported by the *European Pharmacopoeia* (2nd edn) for the analysis of products from medicinal plants, including essential oils, balsams and resins. Over half of the methods reported for medicinal plant products are chromatographic methods, of which TLC represents 82%.

Preparative TLC

Essential oils and resins are complex mixtures containing numerous components that belong to different chemical classes present in different concentration. Often it is necessary to fractionate the mixture into single chemical classes or to isolate single components, particularly useful for the determination of properties such as authenticity, geographical origin or pharmacological activity.

This fractionation can be carried out by preparative TLC. For example, for detecting illegal adulteration of pharmacognostic mint (*Mentha arvensis*) or peppermint (*M. piperita*) oils with racemic menthyl acetate, samples were separated by TLC (polygram SIL G/UV plates, CH_2Cl_2 as mobile phase) and the zone of menthyl acetate extracted from the plate and analysed by chiral capillary GC. Since natural mint oils contain 100% of the (–)-isomer of menthyl acetate, the presence of the (+)-isomer can be used to quantify this kind of adulteration. In this case, pre-separation is necessary to obtain a reliable stereodifferentiation without problems of peak overlap in a direct GC analysis.

TLC has been used as preparative tool to obtain pure components to be used for further characterization. For example, components of the sesquiterpene fraction of camomile oil were separated by semipreparative TLC. The components so obtained – *trans*-farnesene, chamazulene, *cis*-en-in-dicycloether, *trans*-en-in-dicycloether, (–)- α -bisabolol, (–)- α -bisabolol oxide A, and (–)- α -bisabolol oxide B – were analysed by GC-MS, and the MS spectra were used to build a database since mass spectra of these components are not included in some commercial MS libraries. **Figure 1** shows the TLC separation obtained using silica gel TLC plates. **Table 1** reports the R_F values and identification of components.

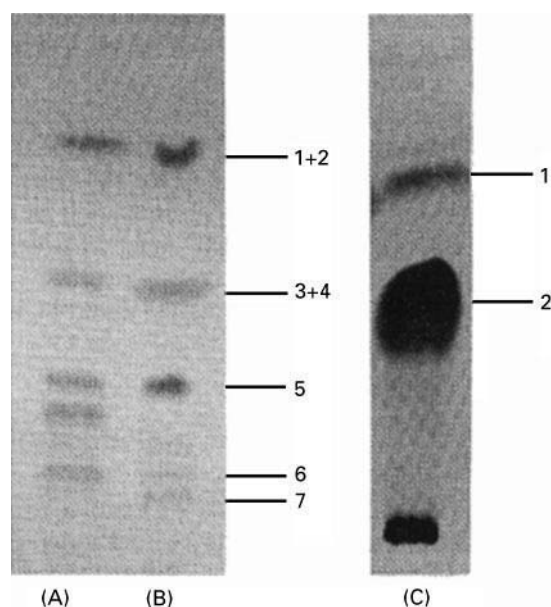


Figure 1 TLC chromatograms of tetraploid camomile (CFH) essential oil obtained by steam distillation (A), compounds isolated from CFH oil (B) and separation of *trans*-farnesene and chamazulene (C). Mobile phase: (A) and (B) dichloromethane/toluene/ethyl acetate (70:28:2, v/v/v); (C) cyclohexane. Detection by spraying the plates with 1% vanillin solution. (Reproduced with permission from Zekovic Z, Pekii B, Lepojevic Z and Petrovic L (1994) *Chromatographia*, 39: 587–590.)

Preparative separations have also been carried out by OPLC to isolate antifungal compounds of the essential oil obtained by water distillation of the fresh bark of *Ocotea usambarensis* from Rwanda. The strategy followed for characterization of essential oil constituents is illustrated in **Figure 2**. This scheme shows how a combination of chromatographic techniques, including TLC, can be useful to characterize bioactive constituents of medicinal plants.

Quantitative Analysis by TLC

Some methods have been developed for the quantitative analysis of the main volatile components of essential oils by TLC as a rapid and easy alternative to other chromatographic determinations, in particular GC and HPLC which are more expensive and time-consuming.

It is difficult to find applications of TLC densitometry to problems in the field of essential oils, e.g. for the quantification of individual components, probably because of the volatility of the various components. One example is the quantitative determination of linalool, linalyl acetate and terpinen-4-ol in lavender oil. The first two compounds are the main components of the oil.

Table 1 hR_F values of camomile oil components separated in Figure 1

N	Compounds	hR_F (%)		Colour
		A, B	C	
1	<i>Trans</i> -farnesene	93.22	64.61	Dark green
2	Chamazulene		46.15	Dark red
3	<i>Cis</i> -en-in-dicycloether	63.13	–	Light brown
4	<i>Trans</i> -en-in-dicycloether		–	
5	(–)- α -Bisabolol	41.53	–	Violet
6	(–)- α -Bisabolol oxide A	20.76	–	Yellow
7	(–)- α -Bisabolol oxide B	16.94	–	Yellow

A,B, mobile phase dichloromethane/toluol/ethyl acetate (70 : 28 : 2, v/v/v). C, mobile phase cyclohexane. (Reproduced with permission from (1994) *Chromatographia*, 39: 587–590.)

Figure 3 shows the TLC and GC analysis of a lavender oil. The quantitative results obtained with the two techniques are comparable. This result shows that TLC densitometry is a good technique for both

qualitative and quantitative analysis of the main components of essential oils. It can be useful in the identification of an oil, and can simultaneously also detect less volatile components.

Other examples are the quantitative determination of citral in citrus oils and 1,8-cineole in eucalyptus oils. The determination of citral (a mixture of two terpene aldehydes, neral and geranial) is of particular importance for citrus oils, mainly for lemon oils. TLC determination of citral has been carried out on silica gel plates, developed with hexane/chloroform (70 : 30) and measured at 250 nm with a TLC scanner. The results were compared with those obtained by GC, and the ratio between TLC and GC values was constant at 0.8.

Eucalyptus essential oil contains a high amount of 1,8-cineole, an oxygenated monoterpene. In recent years, interest in developing new uses for cineole-rich eucalyptus oils has been renewed. The determination of 1,8-cineole by TLC has been carried out using silica gel plates and a mixture of light petroleum/chloroform (70 : 30) as mobile phase. Visualization is with 4-dimethylaminobenzaldehyde-S reagent (4-DMAB) and quantitation is with a scanner. Quantitative results compared with GC-MS data were found to be essentially identical.

TLC for Detection of Authenticity and Botanical Origin

TLC can be used for screening samples to establish their authenticity and botanical origin. An example is the determination of the quality of cinnamon by TLC densitometry. Cinnamon is one of the oldest known spices; the cinnamons of commerce are derived from the dried inner bark of several species of *Cinnamomum*. Cinnamon oil derived from the inner bark of *Cinnamomum zeylanicum* Nees is generally

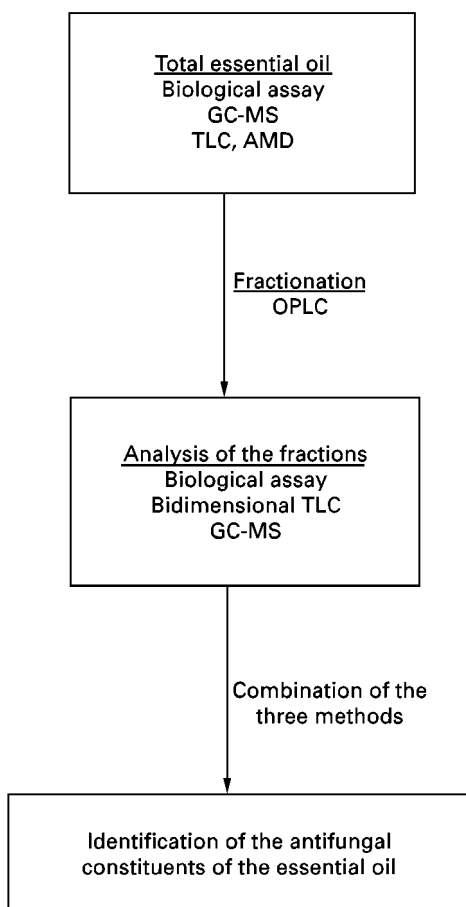


Figure 2 Strategy for the characterization of essential oil constituents from the bark of *Ocotea usambarensis* (Laureaceae). (Reproduced with permission from Hostettmann K., Terreaux, C, Marston, A and Petterat O, (1997) *Journal of Planar Chromatography*, 10: 251–257.

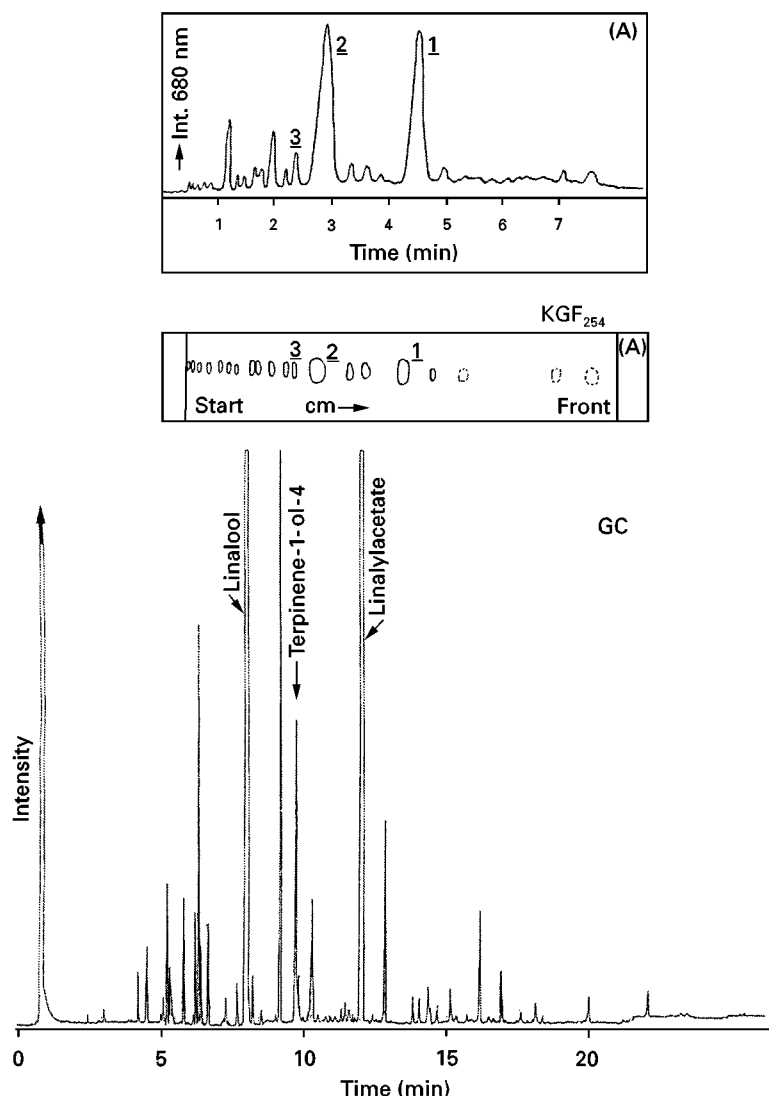


Figure 3 TLC (middle), densitometry (upper) and GC (lower) of lavender oil. TLC conditions: 20 × 20 cm plates, coated with 0.25 mm silica gel 60. Mobile phase: dichloromethane/methanol, 10 : 1.

Detection: anisaldehyde/sulfuric acid ($\lambda = 680$ nm); copper-acetate/phosphoric acid (white light); copper-sulfate/phosphoric acid followed by sulfuric acid spray (white light).

Sample volume: 15 mL of a 5% dichloromethane solution of oil or pure standard components. GC conditions: 25 m × 0.32 mm i.d. HP-5 fused silica capillary column (0.17 μ m film thickness); carrier gas: H₂; detector (FID) and injector (split) at 250°C. Temperature program: 60–240°C, 6°C min⁻¹. (Reproduced from (1989) *Mikrochim. Acta (Wien)*, 3: 1–6, with permission from Springer-Verlag, Wien.)

considered to have a better flavour, and commands the highest price.

This oil can be adulterated with cinnamon leaf or root bark oils, that have a different composition from inner bark oil and are less valuable. Moreover, some countries consider oil obtained from *C. cassia* Blume as cassia oil, and it is unlawful to present cassia as cinnamon, or to prepare mixtures of the two and present the result as cinnamon.

Figure 4 shows the TLC densitometry separation of polar aromatic semivolatile compounds of cinna-

mon and cassia. As can be seen, cinnamon and cassia oils can be easily distinguished because of the presence of higher amount of coumarin and the absence of eugenol in cassia oil.

Another example is the method developed to discover the poisonous Japanese star anise or shikimi fruits (*Illicium anisatum*), when they are mixed with those of the Chinese anise or star anise (*I. verum*). Miristicin only occurs in the essential oil of shikimi, albeit in small amounts, but it is absent in star anise. TLC allows the detection of an admixture of only 5% shikimi, as shown in Figure 5.

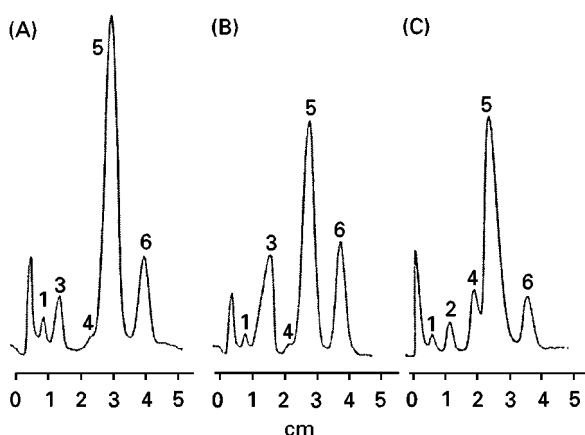


Figure 4 Separation of cinnamon and cassia oils by silica gel HPTLC plates. (A) Authentic sample of essential oil from the inner bark of *Cinnamomum zeylanicum* Nees; (B) cinnamon oil adulterated with leaf oil; (C) authentic sample of cassia oil from *C. cassia* Blume. Peaks: 1, cinnamyl alcohol; 2, coumarin; 3, eugenol; 4, 2-methoxy-cinnamaldehyde; 5, *trans*-cinnamaldehyde; 6, cinnamyl acetate. TLC conditions: TLC plates predeveloped in hexane/triethylamine (46 + 4, v/v) and separation in unsaturated chamber with hexane/chloroform/triethylamine (90 + 6 + 4, v/v/v). The separation was scanned at $\lambda = 255$ nm. (Reproduced with permission from Poole SK, Kiridena W, Miller KG and Poole CF (1995) *Journal of Planar Chromatography*, 8: 257–268.

Determination of the Antioxidant Activity of Essential Oils

The versatility of TLC is also illustrated in the following example, where the composition and the antioxidant activity of essential oils from oregano plants

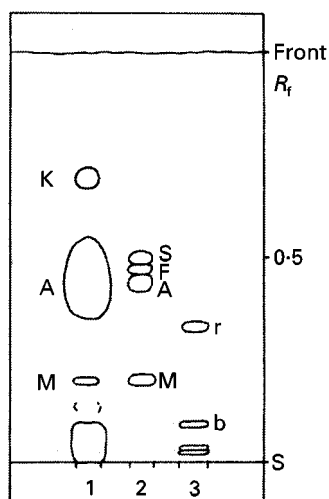


Figure 5 TLC chromatogram of (1) mixture of shikimi fruit and star anise fruit oils; (2) mixture of standard compounds; and (3) reference mixture. Key: A, anethole; F, foeniculin; M, myristicin; S, safrol; r, red; b, blue. (Reproduced from (1990) *Deutsche Apotheker Zeitung*, 130: 1194–1201, with permission from Deutscher Apotheker, Verlag.)

grown wild in Greece is studied. The composition has been studied by GC-MS (ITD) and carvacrol found to be the main components. A variety of oregano, *O. vulgare* subsp. *hirtum*, has a high thymol content, while the other plant species contain less than 1% of thymol. The antioxidant activity of essential oils, pure carvacrol, thymol and butylated hydroxytoluene (BHT) was tested on silica gel TLC plates. The plates were sprayed with a solution of β -carotene and linoleic acid and then exposed to daylight until the background colour disappeared. Spots of components having antioxidant activity remained yellow for a longer period.

TLC for the Analysis of Phenolic Compounds

TLC has been used to analyse less volatile components such as flavonoids, phenolic acids or coumarins. These classes of components are very important for the characterization of plant materials, and can have specific pharmacological activities. For example, the spasmolytic activity of camomile is mainly due to the presence of flavonoids apigenin, apigenin-7-*O*- β -glucoside and its acetylated derivatives. Figure 6 show the HPTLC chromatogram of camomile flavonoids. HPTLC is the fastest chromatographic method for qualitative identification of apigenin and its glucosides in camomile. Quantitative

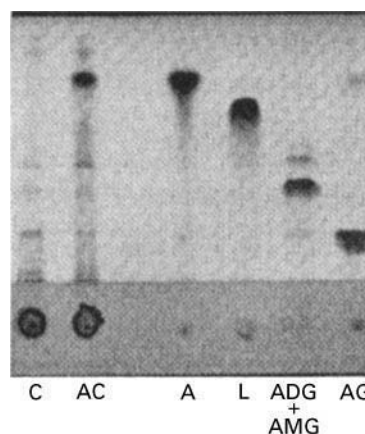


Figure 6 TLC chromatogram of camomile flavonoids. Key: C, dry extract of camomile ligulate flowers (CLF); AC, dry extract of autofermented CLF; A, apigenin; L, luteolin; ADG + AMG, mixture of apigenin-7-*O*- β -diacetylglucoside and apigenin-7-*O*- β -monoacetylglucoside; AG, apigenin-7-*O*- β -glucoside. Experimental details: silica gel 60 F254 HPTLC plates precoated with concentrating zone; eluent: benzol/ethylmethylketone/methanol (5 : 5.3 : 1.5); detection, $\lambda = 254$ nm. Yellow spots of separated flavonoids appear after spraying the plate with 96% sulfuric acid and heating briefly to 120°C. (Reproduced with permission from (1994) *Chromatography*, 39: 587–590.

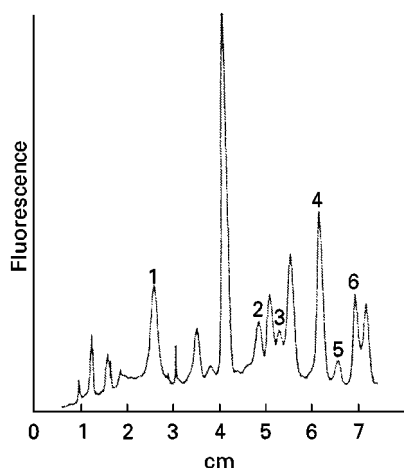


Figure 7 Densitogram of a camomile sample. Peaks: 1, apigenin-7-*O*-glucoside; 2, caffeic acid; 3, apigenin; 4, umbelliferone; 5, ferulic acid; 6, herniarin. (Reproduced from Menziani E, Tosi, B, Bonora A, Reschiglian, P and Lodi G (1990) *Journal of Chromatography*, 511: 396–401, with permission from Elsevier Science.)

determination is possible using appropriate instruments.

With the development of the automated multiple development (AMD) technique, planar chromatography may be applied successfully to the analysis of complex matrices. AMD-HPTLC gives the opportunity to carry out separation processes using a gradient development mode. An optimized AMD-HPTLC procedure has been applied to the separation of phenolic compounds (flavonoids, coumarin, phenylcarboxylic acids) of *Chamomilla recutita* flower extracts. **Figure 7** shows the densitogram obtained under optimized conditions: HPTLC plates and stepwise gradient development in an enclosed chamber. Fifteen steps were used, with drying times 6 min for the first four steps, then 4 min for the next 13 steps, and 10 min for the last step. As preconditioning, nitrogen was bubbled through water; the preconditioning time was 15 s for each step.

Cold-pressed citrus essential oils contain about 90–99% of volatile components, with a nonvolatile residue that ranges from approximately 1 to 10% in the different oils and consists, in large part, of many oxygen containing heterocyclic compounds, mainly the coumarins, psoralens and polymethoxylated flavones. The qualitative and quantitative composition of the nonvolatile residue characterizes the different citrus oils, and play an important role in identification, quality control and authenticity. The literature reports numerous TLC methods for the analysis or preparative isolation of oxygen heterocyclic

compounds in citrus oils. An OPLC method has been developed to separate these components in seven citrus oils: sweet orange, bitter orange, mandarin, grapefruit, lemon, bergamot and Mexican lime. The OPLC separation is fast (10 min) and allows the differentiation of the various oils and the determination of possible contamination or sophistication of the oils.

In particular, many methods for the determination of bergapten (5-methoxypsoralen) have been reported, because of the problems linked with its phototoxicity. The *European Pharmacopoeia* (3rd edn) reports a TLC method to detect the presence of bergapten in bitter orange flower oil. Bergapten shows a greenish-yellow fluorescence at 365 nm. The presence of this psoralen may be an indication of the presence of bitter orange peel oil.

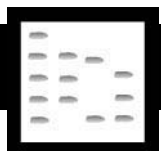
Conclusion

The examples described above show that both analytical and preparative, planar chromatography can be used successfully in a very wide range of applications to essential oils, balsams and resins. Thin-layer chromatography has the ability to separate mixtures of substances of similar structure and the flexibility of a variety of methods of detection. It also has the advantages of being cheap and easy to perform. As recently stated by J. Sherma in a review that appeared in *Analytical Chemistry* in 1996, 'fully instrumental planar chromatography, performed properly is the most economic, powerful, and accurate quantitative analytical method for mixtures of soluble substances of low vapour pressure'.

Further Reading

- European Pharmacopoeia* (3rd edn) (1997–1999). Strasbourg: Council of Europe.
- Poole CF and Poole SK (1995) Multidimensionality in planar chromatography. *Journal of Chromatography A* 703: 573–612.
- Ranny M (1987) *Thin Layer Chromatography with Flame Ionisation Detection*. Dordrecht Holland D. Reidel Publishing Company.
- Sherma J (1996) Planar chromatography. *Analytical Chemistry* 68: 1R–19R.
- Sherma J and Fried B (1996) *Handbook of Thin-Layer Chromatography*. New York: Marcel Dekker.
- Somsen GW, Morden W and Wilson ID (1995) Planar Chromatography coupled with spectroscopic techniques. *Journal of Chromatography A* 703: 613–665.
- Touchstone JC (1993) Column watch. *LC-GC* 11: 404–411.

EXPLOSIVES



Gas Chromatography

J. Yinon, Weizmann Institute of Science,
Rehovot, Israel

Copyright © 2000 Academic Press

Introduction

Although some explosives are thermally labile and others are not volatile enough, gas chromatography (GC), with a variety of detectors, has been found to be a good method for separation and analysis of a certain number of organic explosives. This can be achieved when using the GC under controlled experimental conditions, such as the temperature of the column, injector and detector, type and length of the column, special injection techniques and the use of selective detectors.

In this article we will describe some of the GC methods used for the analysis of explosives – the preferred columns, the injection techniques and the preferred detectors. In order to be able to evaluate GC as a method for the analysis of explosives, it is necessary to present a short overview of the main organic explosives (Figure 1). These explosives can be divided into the three following groups:

1. Nitroaromatic compounds
2. Nitrate esters
3. Nitramines

The most widely used nitroaromatic explosive is 2,4,6-trinitrotoluene (TNT). Nitrate esters include ethylene glycol dinitrate (EGDN), glycerol trinitrate (nitroglycerin, NG) and pentaerythritol tetranitrate (PETN). Nitramine explosives include 1,3,5-trinitro-1,3,5-triazacyclohexane (RDX), 1,3,5,7-tetranitro-1,3,5,7-tetrazacyclooctane (HMX) and 2,4,6-*N*-tetra-nitro-*N*-methylaniline (teteryl).

Additional nitroaromatic compounds encountered are 2-, 3- and 4-nitrotoluene, 2,4- and 2,6-dinitrotoluene (DNT) and degradation products of TNT such as 2-amino-4,6-dinitrotoluene and 4-amino-2,6-dinitrotoluene.

Extraction Procedures

Various extraction procedures can be used. Several of them are described as follows.

Extraction of Explosives from Water

1. Liquid-liquid extraction is carried out with a separation funnel using 1 L of water (containing TNT and other nitroaromatic compounds) and shaking three times with 30 mL of methylene chloride. The combined organic phases are dried over anhydrous sodium sulfate and reduced in volume to 1 mL in a rotary evaporator at 40°C, after the exchange of the methylene chloride with methanol. Other solvents can be used, such as benzene or toluene for nitroaromatic compounds, or isoamyl acetate for nitramines. Extraction can also be carried out using 100 mL of water. In that case only about 6 mL solvent are required.
2. Solid-phase extraction is carried out using Amberlite XAD-2, XAD-4, XAD-8 resins (1 : 1 : 1), C18 phases, phenyl phases and cyano phases, 2.5 g of XAD resin is placed in a 15 × 1 cm i.d. glass column plugged with silanized glass wool and flushed with methanol and water. 1 L of water, containing the explosives, is forced through the column at a flow rate of 30 mL min⁻¹, using nitrogen pressure. The column is then dried with a stream of nitrogen and eluted twice with 15 mL of methylene chloride. Drying, concentration and solvent exchange are carried out as in the liquid-liquid extraction method. Recovery for TNT is 95%.

Extraction of Explosives from Soil

1. 10 g of undried, homogenized soil is extracted with 25 mL acetone in an ultrasonic bath for 30 min. The extract, after passing through filter paper, is ready for analysis. Recovery for RDX is 95%.
2. Supercritical fluid extraction (SFE) can be used for the extraction of explosives from soil. Extraction is made with supercritical CO₂ at 5000 psi and 50°C. The dynamic SFE mode is being used, where fresh supercritical fluid is flushed continuously through the sample matrix and then passes through a trap in which the analytes of interest are collected. This mode of operation gives a better recovery than the static mode.

Capillary Columns

Low polarity columns are used, because the polar interaction of the nitro groups can produce irreversible adsorption on the stationary phase or decomposition of the explosives at higher temperatures.

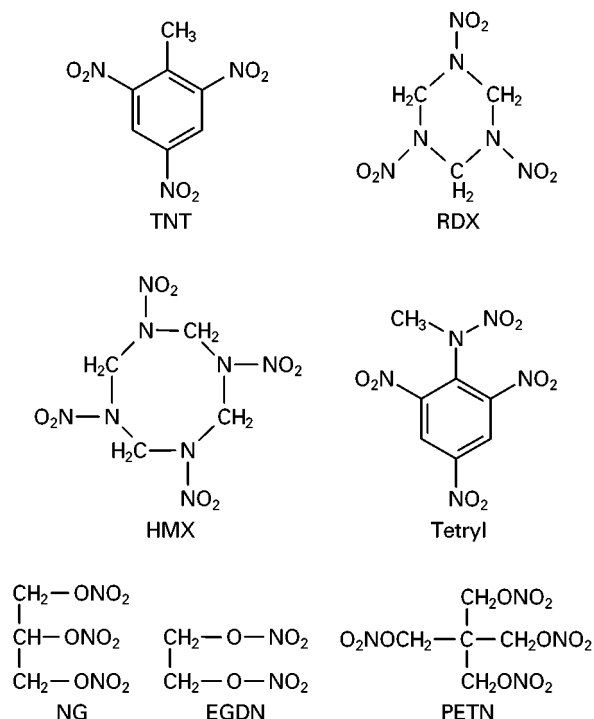


Figure 1 Structure of commonly used explosives (see text for abbreviations used).

Columns commonly used for the separation and analysis of explosives include DB-1 (BP-1 or CP-Sil 5CB) (100% dimethylpolysiloxane) and DB-5 (5% phenylmethylpolysiloxane). Other columns, such as DB-17 (50% phenylmethylpolysiloxane) and OV-225 (50% cyanopropylphenylmethylpolysiloxane) have also been used, but only for separation of nitroaromatic compounds.

Another important factor is the column length. Compounds which evaporate at higher temperatures, such as RDX and PETN, should be eluted from the column as fast as possible in order to minimize their decomposition. This can be done by either increasing the flow rate of the carrier gas or decreasing the length of the column. Columns as short as 1.5 m have been used although short columns will, of course, have a poorer separation capability.

Table 1 shows a summary of GC columns and conditions which have been used for the separation of a variety of explosives.

Injectors

Injectors used include split-splitless injectors at temperatures ranging from 170°C to 250°C, a flash vaporizing injector at 270°C and a temperature-programmable injector (cooled with liquid CO₂),

programmed from -5°C to 250°C at a rate of 200°C min⁻¹. A temperature-programmed injector is much better suited for GC analysis of thermally labile compounds, as it will minimize decomposition in the injector.

Detectors

Electron-Capture Detector (ECD)

An electron-capture detector is an ionization chamber in which electrons are produced from a radioactive source (usually tritium or nickel-63). These electrons are injected into a stream of inert carrier gas (helium or nitrogen), where they reach thermal energy equilibrium through collisions with the carrier gas. The thermal electrons are collected at an anode, thus producing a standing current. When an electron-capturing compound (the sample), such as a halogen- or a nitro-containing compound, is introduced into the carrier gas, the standing current is reduced. The reduction in current is proportional to the concentration of the sample. Electron-capture detectors have a fast response and are highly sensitive for most electron-capturing compounds. However, their specificity for explosives is low. Detection limits are in the 5–50 pg range for the various explosives.

An example is presented in **Figure 2**, which shows the GC-ECD chromatogram of a soil sample taken from a former explosives storage bunker. The column used was a 30 m, DB-5 capillary column, held at 180°C isothermal. The dinitrotoluenes were by-products of TNT, while the aminodinitrotoluenes were microbial degradation products of TNT.

Thermal Energy Analyser (TEA) Detector

The TEA detector, also known as a chemiluminescence detector, is a nitrogen-specific detector. In the TEA detector, nitro compounds are pyrolysed to form NO[•] radicals, which pass into a reaction chamber where they are oxidized by ozone to form electronically excited nitrogen dioxide (NO₂^{*}). The excited nitrogen dioxide decays back to its ground state with emission of chemiluminescent light in the near-infrared region ($\lambda \approx 0.6\text{--}2.8 \mu\text{m}$). The intensity of the emitted light is proportional to the NO concentration and hence to the nitro compound concentration. The TEA detector, although more specific for explosives than the ECD, is less sensitive by one to two orders of magnitude. An example is presented in **Figure 3**, which shows the GC-TEA chromatograms of pure PETN and of a sample taken from the debris of a bombing, containing traces of PETN.

Table 1 GC columns used for separation of explosives

Column type	Column dimensions	Temperature programme	Carrier gas	Detector/s used	Explosives analysed
DB-1	30 m × 0.32 mm i.d. 0.25 µm film	70–250°C at 3°C min ⁻¹	He	MS	DNT, TNT
DB-1	5 m × 0.20 mm i.d. 0.33 µm film	75–225°C at 20°C min ⁻¹	He	ECD, MS	Semtex ^a , PETN, RDX
DB-1	15 × 0.25 mm i.d. 0.25 µm film	80–250°C at 25°C min ⁻¹	He	MS	TNT, Tetryl, RDX, HMX, PETN
BP-1	12.5 m × 0.22 mm i.d. 0.25 µm film	60–240°C at 40°C min ⁻¹	He	TEA	NG, TNT, RDX
BP-1	12 m × 0.25 mm i.d. 0.25 µm film	60–250°C at 40°C min ⁻¹	He	ECD	EGDN, NG, PETN, DNT, TNT, RDX
DB-5	10 m × 0.32 mm i.d. 0.25 µm film	50–250°C at 10°C min ⁻¹	He	TEA	EGDN, NG, PETN, DNT, TNT
DB-5	15 m × 0.25 mm i.d. 0.25 µm film	50–260°C at 25°C min ⁻¹	He	MS	DNT isomers
DB-5	1.5 m × 0.25 mm i.d. 0.25 µm film	60–220°C at 20°C min ⁻¹	He	MS	NG, PETN
CP-Sil 5CB	20 m × 0.25 mm i.d. 0.25 µm film	50–90°C at 5°C min ⁻¹ 90–250°C at 3.5°C min ⁻¹	H ₂	ECD	DNT, TNT
DB-17	30 m × 0.32 mm i.d. 0.25 µm film	70–250°C at 3°C min ⁻¹	He	ECD, TEA	DNT, TNT
OV-225	30 m × 0.32 mm i.d. 0.25 µm film	70–250°C at 3°C min ⁻¹	He	ECD, TEA	DNT, TNT
OV-101	25 m × 0.25 mm i.d. 0.1 µm film	50–240°C at 40°C min ⁻¹	He	ECD	EGDN, NG, PETN, DNT, TNT, RDX, HMX, Tetryl
DB-1301	4.5 m wide bore 1.0 µm film	128–225°C at 30°C min ⁻¹	He or H ₂	ECD	DNT, TNT, RDX, HMX

^aSemtex is a plastic explosive containing RDX and PETN.

The chromatograms were recorded at two different injection temperatures: 170°C and 250°C. At 250°C PETN decomposes, therefore a decomposition peak appears in the chromatogram. The column used was a 10 m, DB-5 capillary. Injections at 170°C and

250°C were done with a split–splitless injector, in the splitless mode.

Gas Chromatography–Mass Spectrometry (GC-MS)

The good separation capability of capillary column GC, together with the high sensitivity and identification capability of the mass spectrometer, have made GC-MS a powerful method in analytical chemistry. The use of GC-MS for the analysis of explosives is limited by the thermal decomposition characteristics of some of the explosives. Precautions to be taken when analysing explosives by GC-MS are similar to those taken when using GC with any other detector.

GC-MS for the analysis of explosives has been used in three different ionization modes: electron ionization (EI), chemical ionization (CI) and negative-ion chemical ionization (NCI). The produced ions are mass separated by a mass analyser (magnetic sector, quadrupole or ion trap), detected by an electron multiplier, recorded by a data system and stored in the computer as a mass spectrum. There are different ways to display the results: (i) as a total ion

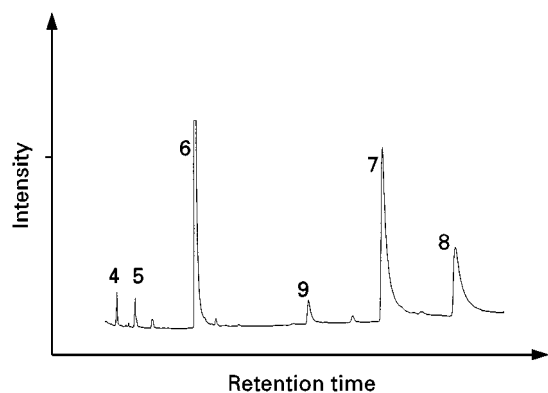


Figure 2 GC-ECD chromatogram of a sample taken from a former explosives storage bunker. Peak identity: 4: 2,6-dinitrotoluene; 5: 2,4-dinitrotoluene; 6: TNT; 7: 4-amino-2,6-dinitrotoluene; 8: 2-amino-4,6-dinitrotoluene; 9: RDX. (Reproduced from Haas R. *et al.* (1990) *Fresenius Journal of Analytical Chemistry* 338: 41–45, by permission of Springer-Verlag.)

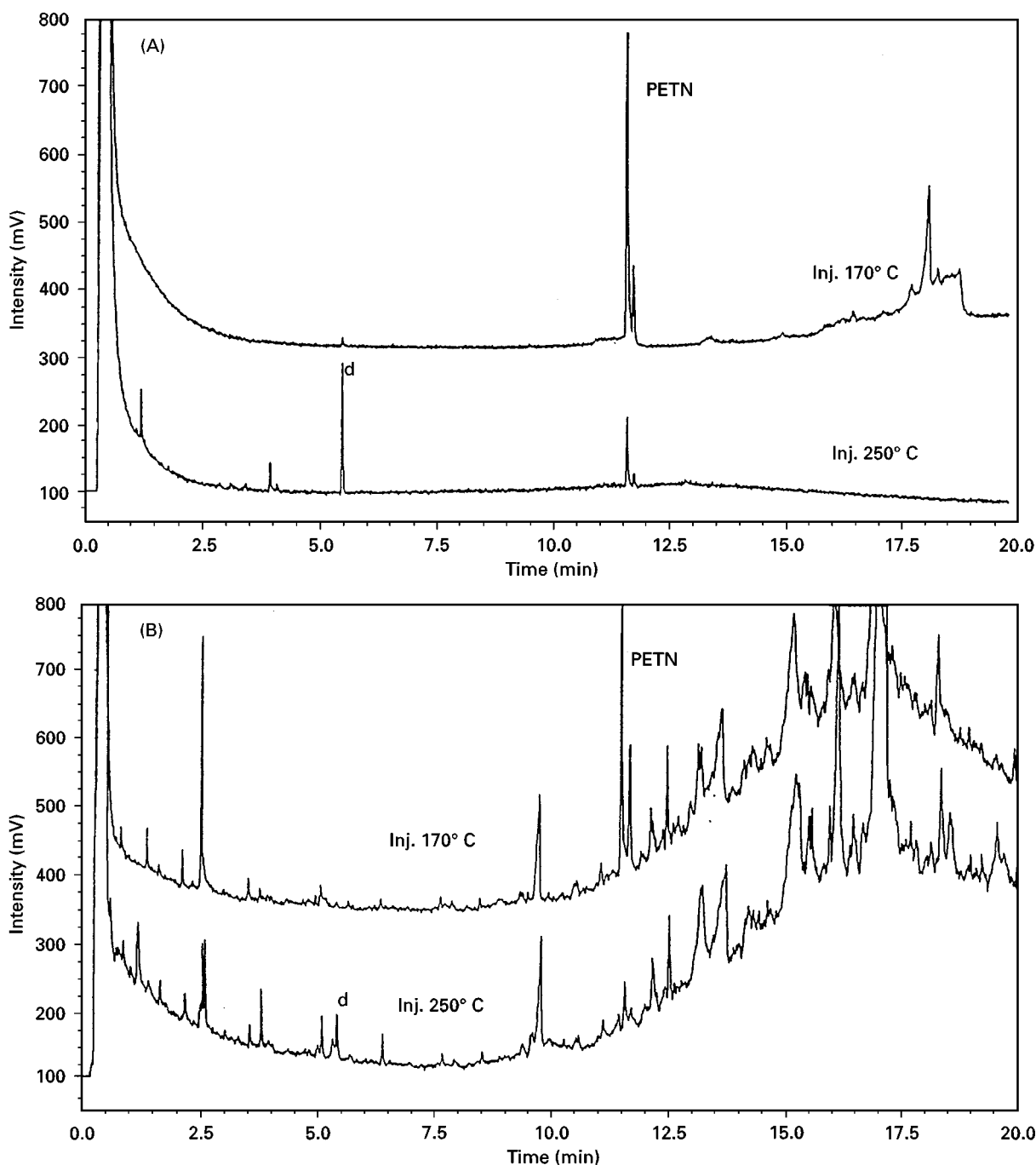


Figure 3 GC-TEA chromatograms. (A) Pure PETN. (B) A sample from a bombing scene, containing PETN. Chromatograms were run at injection temperatures of 170°C and 250°C. Peak d is a decomposition product of PETN. (Reproduced from Kolla P (1994) *Journal of Chromatography A* 674: 309–318, by permission of Elsevier Science Publishers.)

chromatogram (TIC) or reconstructed ion chromatogram (RIC), which is equivalent to a GC chromatogram – a mass spectrum of each one of the GC peaks can be displayed; (ii) as mass chromatograms, which are GC chromatograms including only preselected masses. Each one of the GC separated compounds can be represented by one or several masses which are characteristic of the full mass spectrum.

Electron Ionization (EI)

The basic form of ionization in mass spectrometry is electron ionization (EI), where an electron beam, usually at an energy of 70 eV, collides with the molecules of the sample to transform them into positively charged ions. In addition, extensive fragmentation of the ions occurs, resulting in a mass spectrum which

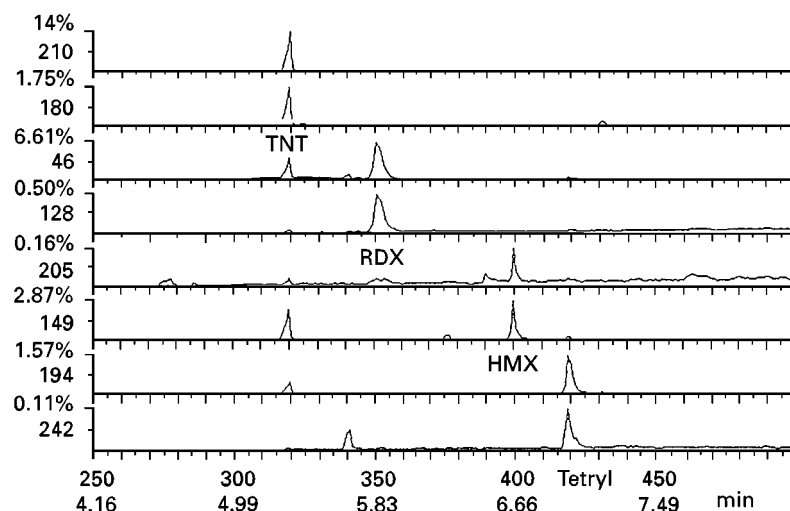


Figure 4 GC-MS EI mass chromatograms of a mixture of explosives (10 ppb each), extracted from water by liquid-liquid extraction. (Reproduced from Yinon J (1996) *Journal of Chromatography A* 742: 205–209, by permission of Elsevier Science Publishers.)

does not always contain a molecular ion. The fragmentation patterns thus obtained can be correlated with specific functional groups, enabling recognition of many structural features in the analysed molecule. An EI mass spectrum of a molecule can, therefore, be considered a 'fingerprint' of that molecule and can be used as an identification tool.

An example is presented in **Figure 4** which shows the GC-MS EI mass chromatograms of a mixture of explosives (10 ppb each), extracted from water by liquid-liquid extraction with methylene chloride. Each of the explosives could be identified by at least one characteristic ion (in most compounds a fragment ion). The column used was a 15 m \times 0.255 mm i.d. DB-1 capillary column. Column temperature programme was 80°C to 250°C at 25°C min⁻¹. Injector temperature was programmed from -5°C to 250°C at 200°C min⁻¹. The mass spectrometer was an ion trap operated in the EI mode.

Chemical Ionization (CI)

In chemical ionization (CI) ions are formed by reaction of the sample molecules with a known pre-selected set of reagent ions. These reagent ions are produced by ion-molecule reactions in a reagent gas introduced in the ion source of the mass spectrometer at a pressure of 0.1 to 1.0 Torr. Common reagent gases are methane and isobutane.

CI mass spectra contain usually an MH⁺ ion and little fragment ions. It is, therefore, suitable for molecular weight identification. In many cases, in the CI mass spectrum of an explosive an MH⁺ ion might be observed, while in the EI mass spectrum of the same compound there is no molecular ion. For example, the EI mass spectra of NG and PETN are similar,

containing abundant ions at m/z 30 (NO⁺), m/z 46 (NO₂⁺) and m/z 76 (CH₂ONO₂⁺). However, they have different GC retention times, but this means that their identification is based on chromatographic properties. In the CI mass spectra of NG and PETN, MH⁺ ions are observed, at m/z 228 and m/z 317, respectively.

Negative-ion Chemical Ionization (NCI)

In negative-ion chemical ionization (NCI) a reagent gas at 0.1 to 1.0 Torr is introduced in the ion source of the mass spectrometer. This reagent gas acts primarily as a moderator in producing high concentrations of low energy electrons. Negative ions are formed in the analysed sample by electron capture. These ions are either molecular ions or (M-H)⁻ ions. Fragment ions are also formed by dissociation of part of the molecular ions. Special reagents can be introduced into the ion source causing ion-molecule reactions, thus forming characteristic adduct ions. For example, the NCI mass spectrum of TNT will contain abundant anions at m/z 227, M⁻, m/z 210, (M-OH)⁻, m/z 197, (M-NO)⁻ and m/z 181, (M-NO₂)⁻. The detection limit of explosives in the NCI mode is, in general, lower by one order of magnitude than in the positive CI mode.

Conclusions

While GC is a chromatographic method and needs comparison of retention times with standards, mass spectrometry is an identification method and provides a 'fingerprint' of the investigated compound. The combination of GC with MS incorporates both

separation and identification capabilities, and is therefore superior to GC alone.

Both GC and GC-MS, although being suitable techniques for the separation and analysis of explosives, have a limitation in that the injector and column have to be heated. This fact necessitates taking special precautions when dealing with the more thermally labile compounds. Liquid chromatography-mass spectrometry (LC-MS), where the injector and column are at room temperature, does not have these limitations, and is therefore a better choice when analysing the more thermally labile explosives. However, GC-MS is readily available in most analytical laboratories, while LC-MS is not. This situation is expected to change in the next 5 to 10 years, which will place LC-MS as the method of choice for the separation and analysis of explosives.

In both GC-MS and LC-MS, the addition of tandem mass spectrometry (MS-MS) provides an extra dimension for improved selectivity and therefore improved identification.

See Colour Plate 83.

See also: II/Chromatography: **Gas:** Detectors: Mass Spectrometry; Detectors: Selective. **Extraction:** Analytical Extractions; Solid-Phase Extraction; Solid-Phase Microextraction. **Explosives:** Liquid Chromatography; Thin-Layer (Planar) Chromatography.

Further Reading

- Douse JMF (1987) Improved method for the trace analysis of explosives by silica capillary column gas chromatography with thermal energy analysis detection. *Journal of Chromatography* 410: 181–189.
- Douse JMF and Smith RN (1986) Trace analysis of explosives and firearm discharge residues in the Metropolitan Police Forensic Science Laboratory. *Journal of Energetic Materials* 4: 169–186.
- Feltes J, Levsen K, Volmer D and Spiekermann M (1990) Gas chromatographic and mass spectrometric deter-

- mination of nitroaromatics in water. *Journal of Chromatography* 518: 21–40.
- Francis ES, Wu M, Farnsworth PB and Lee ML (1995) Supercritical fluid extraction/gas chromatography with thermal desorption modulator interface and nitro-specific detection for the analysis of explosives. *Journal of Microcolumn Separations* 7: 23–28.
- Haas R, Schreiber I, v. Low E and Stork G (1990) Conception for the investigation of contaminated munition plants. 2. Investigation of former RDX-plants and filling stations. *Fresenius Journal of Analytical Chemistry* 338: 41–45.
- Hable M, Stern C, Asowata C and Williams K (1991) The determination of nitroaromatics and nitramines in ground and drinking water by wide-bore capillary gas chromatography. *Journal of Chromatographic Science* 29: 131–135.
- Kolla P (1994) Gas chromatography, liquid chromatography and ion chromatography adapted to the trace analysis of explosives. *Journal of Chromatography A* 674: 309–318.
- Slack GC, McNair HM and Wasserzug L (1992) Characterization of Semtex by supercritical fluid extraction and off-line GC-ECD and GC-MS. *Journal of High Resolution Chromatography* 15: 102–104.
- Tamiri T, Zitrin S, Abramovich-Bar S, Bamberger Y and Sterling J (1992) GC/MS Analysis of PETN and NG in Post-Explosion Residues. In: Yinon J (ed.) *Advances in Analysis and Detection of Explosives*, pp. 323–334. Dordrecht: Kluwer Academic Publishers.
- Welsch T and Block H (1997) Separation and enrichment of traces of explosives and their by-products from water by multiple micro liquid extraction for their determination by capillary gas chromatography. *Fresenius Journal of Analytical Chemistry* 357: 904–908.
- Yinon J (1996) Trace analysis of explosives in water by gas chromatography-mass spectrometry with a temperature-programmed injector. *Journal of Chromatography A* 742: 205–209.
- Yinon J and Zitrin S (1993) *Modern Methods and Applications in Analysis of Explosives*. Chichester: John Wiley.

Liquid Chromatography

**U. Lewin-Kretzschmar, J. Efer and
W. Engewald**, University of Leipzig, Leipzig,
Germany

Copyright © 2000 Academic Press

Introduction

Explosive analysis is important in different areas: explosive manufacture (quality and wastewater control),

forensic science and toxicology (investigation of explosions or of criminal actions) and environmental monitoring (water and soil analysis at sites intensively used for military purposes). **Figure 1** shows some of the more common explosives.

In the literature various methods and procedures have been described for analysing these compounds. In the last few years, the investigation of explosives in the water and soil around former ammunition plants,

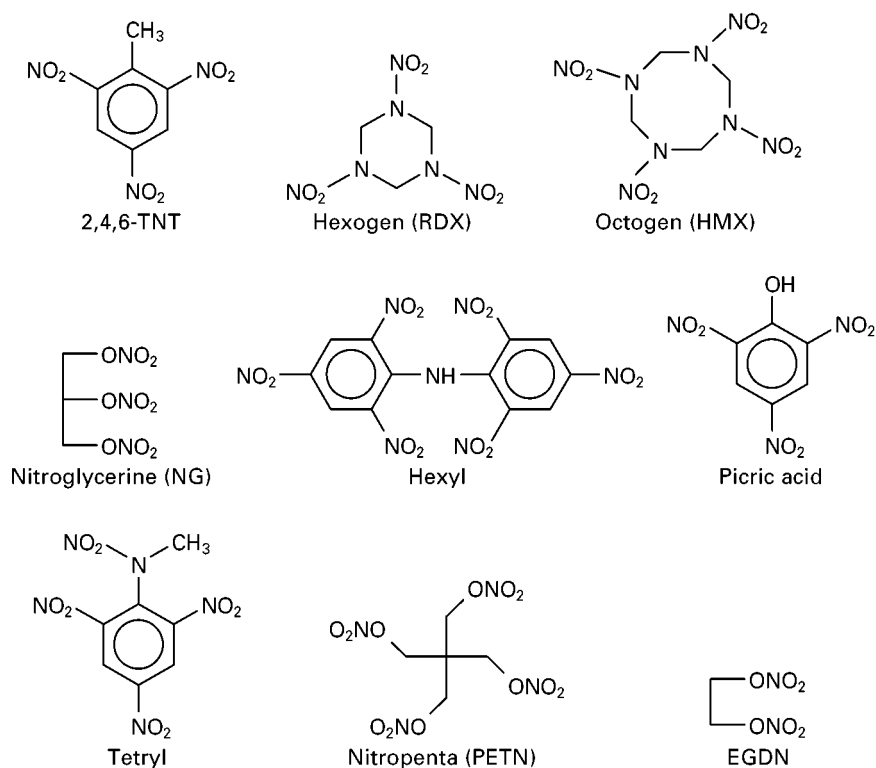


Figure 1 Structures of common explosives.

munition depots or dumps dating back to World War II has become increasingly important. In these samples there are not only explosives but also their by-products and metabolites. For example, water samples from around the former ammunition plant at Elsnig (Saxony, Germany) contained many explosive-related compounds of various classes (Table 1).

These constituents, which range in concentrations from ng L^{-1} to mg L^{-1} , make it difficult to analyse such samples. However, to assess the toxic potential, reliable analysis of all the compounds down to the trace amounts (about $0.1 \mu\text{g L}^{-1}$) is necessary, as some are highly toxic, carcinogenic or mutagenic.

Capillary gas chromatography offers advantages of separation efficiency and favourable detection limits; however, because of the thermal instability and high polarity of some compounds, high performance liquid chromatography (HPLC) determination is often the method of choice. This requires thorough optimization of HPLC conditions (stationary and mobile-phase) as well as selective and sensitive detection systems and, in some cases, selective sample preparation or pre-separation of the sample into different fractions.

The aim of this article is to provide an overview of the possibilities given by HPLC methods to determine

explosive-related compounds in complex samples, including separation, detection and sample preparation, focusing in particular on compounds occurring in samples around former ammunition plants (Table 1).

Sample Preparation

Water Samples

Brown glass bottles should be filled up to the brim with water samples and the bottles made gas-tight, for example, using Teflon packings, and stored at 4°C . To prevent adsorption losses or degradation at the glass surfaces, the addition of methanol or acetonitrile or the use of silanized glass vessels is recommended. To prevent bacterial degradation, sodium azide (about 0.5 g L^{-1}) can be added to the samples.

In principle, for extraction and enrichment, various methods such as liquid–liquid extraction (LLE), solid-phase extraction (SPE) or solid-phase microextraction (SPME) can be used.

Neutral compounds An effective and reproducible liquid–liquid extraction of neutral explosive compounds such as the nitroaromatics can take place with various solvents such as dichloromethane, ethyl

Table 1 Compounds in water samples in the neighbourhood of the former ammunition plant in Elsnig

Compounds	Abbreviations
<i>Nitroaromatics and nitramines</i>	
2,4,6-Trinitrotoluene	2,4,6-TNT
Hexahydro-1,3,5-trinitro-1,3,5-triazine	RDX/Hexogen
2,2',4,4',6,6'-Hexanitrodiphenylamine	Hexyl
1,3-Dinitrobenzene	1,3-DNB
2,4-Dinitrotoluene	2,4-DNT
2,6-Dinitrotoluene	2,6-DNT
3,4-Dinitrotoluene	3,4-DNT
Nitrobenzene	NB
2-Nitrotoluene	2-NT
3-Nitrotoluene	3-NT
4-Nitrotoluene	4-NT
Octahydro-1,3,5,7-tetranitro-1,3,5,7-tetrazocine	Octogen/HMX
1,3,5-Trinitrobenzene	1,3,5-TNB
<i>Chloroaromatics</i>	
Chlorobenzene	CIB
1-Chloro-2,4-dinitrobenzene	1-CI-2,4-DNB
1-Chloro-4-nitrobenzene	1-CI-4-NB
1,2-Dichlorobenzene	1,2-DCIB
1,4-Dichlorobenzene	1,4-DCIB
2,3-Dichloronitrobenzene	2,3-DCINB
2,5-Dichloronitrobenzene	2,5-DCINB
1,2,4-Trichlorobenzene	1,2,4-TCIB
<i>Amino- and aminonitroaromatics</i>	
2-Amino-4,6-dinitrotoluene	2-A-4,6-DNT
4-Amino-2,6-dinitrotoluene	4-A-2,6-DNT
2-Amino-4-nitrotoluene	2-A-4-NT
2-Amino-6-nitrotoluene	2-A-6-NT
4-Amino-2-nitrotoluene	4-A-2-NT
2,6-Diamino-4-nitrotoluene	2,6-DA-4-NT
2,3-Diaminotoluene	2,3-DAT
2,4-Diaminotoluene	2,4-DAT
2,6-Diaminotoluene	2,6-DAT
3,5-Dinitroaniline	3,5-DNA
<i>Nitrophenols</i>	
2,4-Dinitrophenol	2,4-DNP
3,4-Dinitrophenol	3,4-DNP
3,5-Dinitrophenol	3,5-DNP
2-Methyl-4,6-dinitrophenol	2-M-4,6-DNP
4-Methyl-2,6-dinitrophenol	4-M-2,6-DNP
3-Methyl-2-nitrophenol	3-M-2-NP
3-Methyl-4-nitrophenol	3-M-4-NP
4-Methyl-2-nitrophenol	4-M-2-NP
5-Methyl-2-nitrophenol	5-M-2-NP
3-Nitrophenol	3-NP
4-Nitrophenol	4-NP
2,4,6-Trinitrophenol	Picric acid/PA
<i>Nitrobenzoic acids</i>	
2-Amino-4-nitrobenzoic acid	2-A-4-NBA
2,4-Dinitrobenzoic acid	2,4-DNBA
2-Nitrobenzoic acid	2-NBA
3-Nitrobenzoic acid	3-NBA
4-Nitrobenzoic acid	4-NBA

acetate, methyl isobutylketone and methyl tert-butyl ether at different pH values. As a rule, recovery of >70% can be achieved with triple extraction

(stirring or shaking in an Erlenmeyer flask). In order to obtain good recovery for the relatively highly volatile mononitrated aromatics and chloroaromatics, great care should be taken when concentrating or redissolving extracts. To extract polar compounds like hexogen, octogen or nitroguanidine, continuous LLE in rotary perforators is more effective (Figure 2).

Good results are also obtained with SPE. For neutral nitroaromatics recoveries of between 70 and 100% are reached with octadecylsiloxane-bonded silica materials (RP-18). Increasingly, the highly porous (specific surface >1200 m² g⁻¹) and high purity adsorbents based on styrene-divinylbenzene (SDVB) copolymer are used and these are particularly suitable for the more water soluble compounds such as nitramines.

The US Environmental Protection Agency (EPA) method makes use of salting-out-effects in the extraction. This enables nitramines, nitroaromatics and nitrate esters to be extracted with solvents freely miscible with water, such as acetonitrile. Here, good recoveries are obtained, but reproducibility is not as good as with the methods mentioned above.

Acidic compounds The extraction of acidic compounds such as nitrophenols and nitrobenzoic acids should take place at low pH in order to ensure the presence of these compounds in their nondissociated form. For this purpose a pH value of 2 has proved successful.

Also, continuous extraction in a rotary extractor leads to a higher yield than is the case in discontinuous extraction (Figure 3). Suitable solvents are dichloromethane and ethyl acetate.

In general, lower recoveries will be obtained for the volatile ortho-substituted nitrophenols if a concentration step is necessary after the extraction.

High recoveries are obtained on SDVB copolymers. In SPE with RP-18 materials, recoveries >70% for the mononitrophenols are only reached if large amounts of salt (300 g NaCl L⁻¹) are added.

An efficient enrichment of acidic compounds is also possible after ion pair formation with tetrabutylammonium chloride in a neutral to basic medium or by extractive derivatization by means of acetic anhydride or pentafluorobenzoyl chloride in the presence of a phase transfer catalyst with dichloromethane as solvent.

Basic compounds An efficient enrichment of aminoaromatics and especially of diaminoaromatics can be reached at pH 12 with continuous LLE with dichloromethane or SPE on SDVB copolymer materials (Figure 4). Discontinuous extraction with

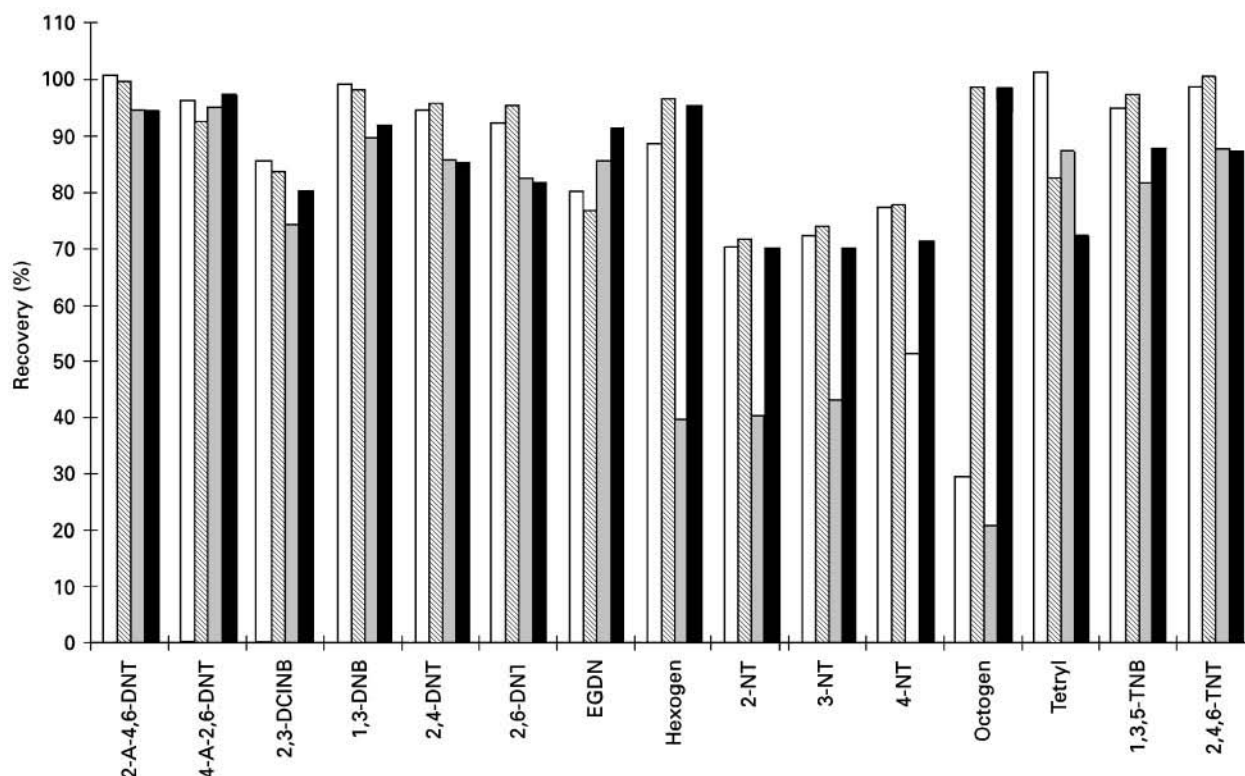


Figure 2 Comparison of various extraction techniques for neutral compounds. Samples of 0.5 L (water spiked with $2 \mu\text{g L}^{-1}$ for each component and adjusted to pH 9 with 0.1 mol L^{-1} sodium hydroxide) were enriched as follows: (A) discontinuous LLE (open columns): stirring three times with 25 mL dichloromethane for 30 min in an Erlenmeyer flask; (B) continuous LLE (hatched columns): 0.5 L extraction with 150 mL dichloromethane in a heavy-phase rotary perforator (Normag); (C) SPE-RP-18 (dotted columns): enriched on 2 g PolarPlus (Baker), conditioned with 3 mL acetone, methanol and water, and eluted with 6 mL methanol; (D) SPE-SDVB (filled columns): enriched on 200 mg LiChrolut EN (Merck), conditioned with 3 mL acetonitrile, methanol and 9 mL water, and eluted with 2 mL methanol acetonitrile mixture (1 : 1).

dichloromethane is not effective. The use of RP-18 materials or ethyl acetate as a solvent is out of the question because of the high pH.

Fractionation Where there are very complex samples, for example, the water samples from Elsnig, precise qualitative and quantitative analysis is only possible after pre-separation of the components. A suitable method is class fractionation based on LLE (Figure 5) at various pH values.

Here, by means of the discontinuous dichloromethane extraction at pH 9, the nitro and mono-aminoaromatics – which in most cases are the main contaminants – can be almost completely separated from the acidic and basic compounds. Only the more polar nitramines are not completely extracted and are partially included in the other two fractions. Using a more efficient extraction technique in the first extraction step (for example, continuous extraction or SPE on SDVB), selective pre-separation is not possible since acidic and basic compounds would also be partially extracted.

Soil Samples

The basic condition for reliable analysis of soil samples is representative sampling and good homogenization of the samples.

The method most frequently used to prepare the soil samples to analyse explosives is extraction in an ultrasonic bath. Compared with Soxhlet extraction it has several advantages: careful treatment of thermolabile compounds, easy handling, minimum apparatus expenditure and low consumption of solvents.

Suitable solvents are, in principle, acetone, methanol and acetonitrile. However, with a view to the subsequent HPLC determination, methanol and acetonitrile should rank first.

Nitroaromatics are quantitatively extracted by both solvents. But for the more polar compounds like octogen, hexogen and hexyl, acetonitrile is preferred (Table 2).

Ultrasonic extraction is described in detail in US-EPA-8330. In this case, 2 g of soil is extracted

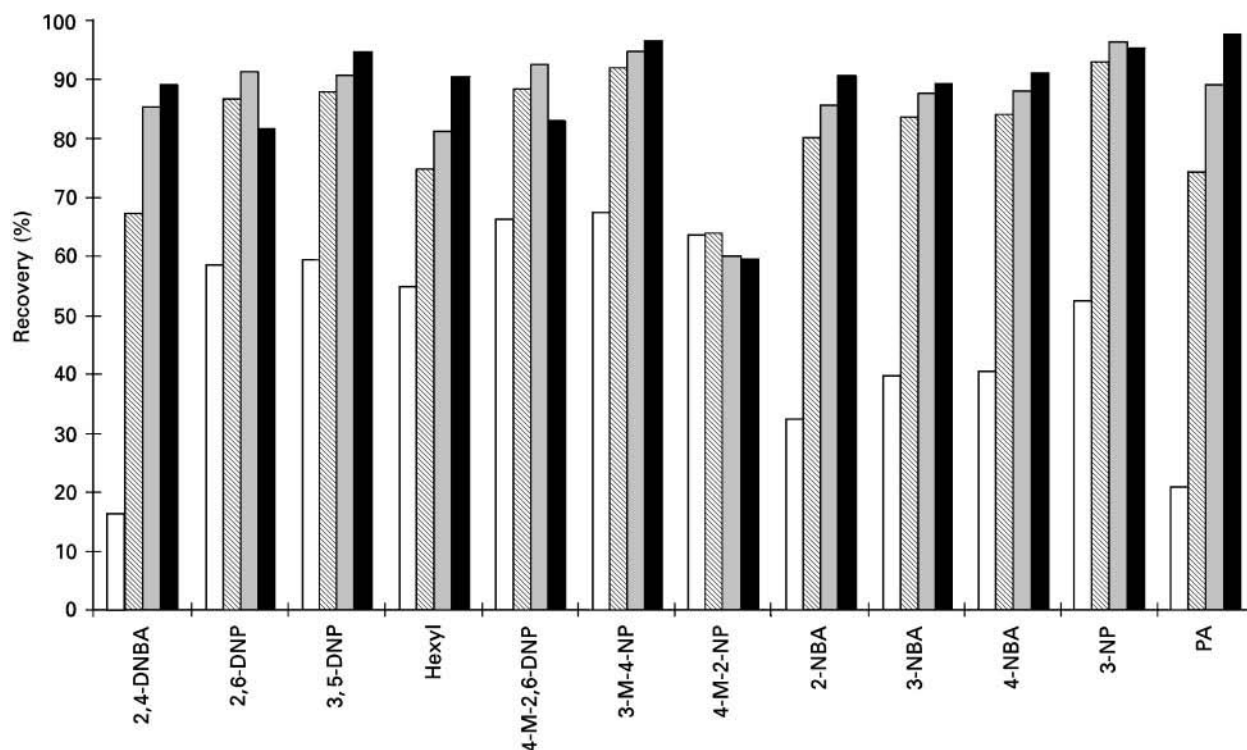


Figure 3 Optimization of extraction for acidic compounds. Samples of 0.5 L (water spiked with $2 \mu\text{g L}^{-1}$ for each component and adjusted to pH 2 with 0.1 mol L^{-1} hydrochloric acid) were extracted with 150 mL dichloromethane in a heavy-phase rotary perforator or with 200 mL ethyl acetate in a light-phase rotary perforator, respectively. Open columns, MeCl 3 \times 30 min; hatched columns, MeCl 4 h; dotted columns, MeCl 10 h; filled columns, Etac 4 h.

with 10 mL acetonitrile over 18 h at room temperature.

A new efficient method for extraction of soil samples is accelerated solvent extraction (ASE), which has proved suitable for nitroaromatics.

HPLC Separation Systems

In general, RP-18 materials are used to separate explosive-related compounds. According to sample composition and detector selection, the composition of the mobile phase (type and amount of organic modifier, buffer additives) varies considerably. The most common mobile phases are buffered or unbuffered methanol–water and acetonitrile–water mixtures in isocratic or gradient operation.

Ethanol, *n*-propanol and dioxane as modifiers or ternary solvent mixtures such as water–methanol–acetonitrile or water–methanol–tetrahydrofuran are of little practical importance and result in too small a selectivity change compared with binary mobile phases.

Because of the generally limited separation performance of HPLC, complete separation of all explosive-related compounds cannot be achieved on any one column in one chromatographic run, not even under

carefully optimized separation conditions. Therefore, before separation in the case of complex samples, pre-separation of the components into different fractions by HPLC is useful.

Neutral Compounds

RP-18 phases are very suitable for separation of complex mixtures of nitro- and nitroaminoaromatics, nitramines and nitrate esters with methanol–water or methanol–buffer mobile phases.

In general, at a methanol–water ratio of about 1:1, the retention of compounds on RP-18 phases will increase as follows: nitroguanidine < octogen < hexogen < EGDN < DEGN < 1,3-DNB < 2,4,6-TNT < 4-A-2,6-DNT < 2-A-4,6-DNT < 2,6-DNT < 2,4-DNT < 2-NT < 4-NT < 3-NT < PETN < diphenylamine (Figure 6).

For some compounds, however, various RP-18 columns show different selectivities, which result in co-elution and retention reversal of various pairs of substances, as shown in Table 3. Two columns of complementary selectivity can be used to verify the separation results or to reduce peak overlapping.

If chlorinated aromatics additionally occur in real samples (Table 1) these can be determined under the same conditions as the nitroaromatics. However, for

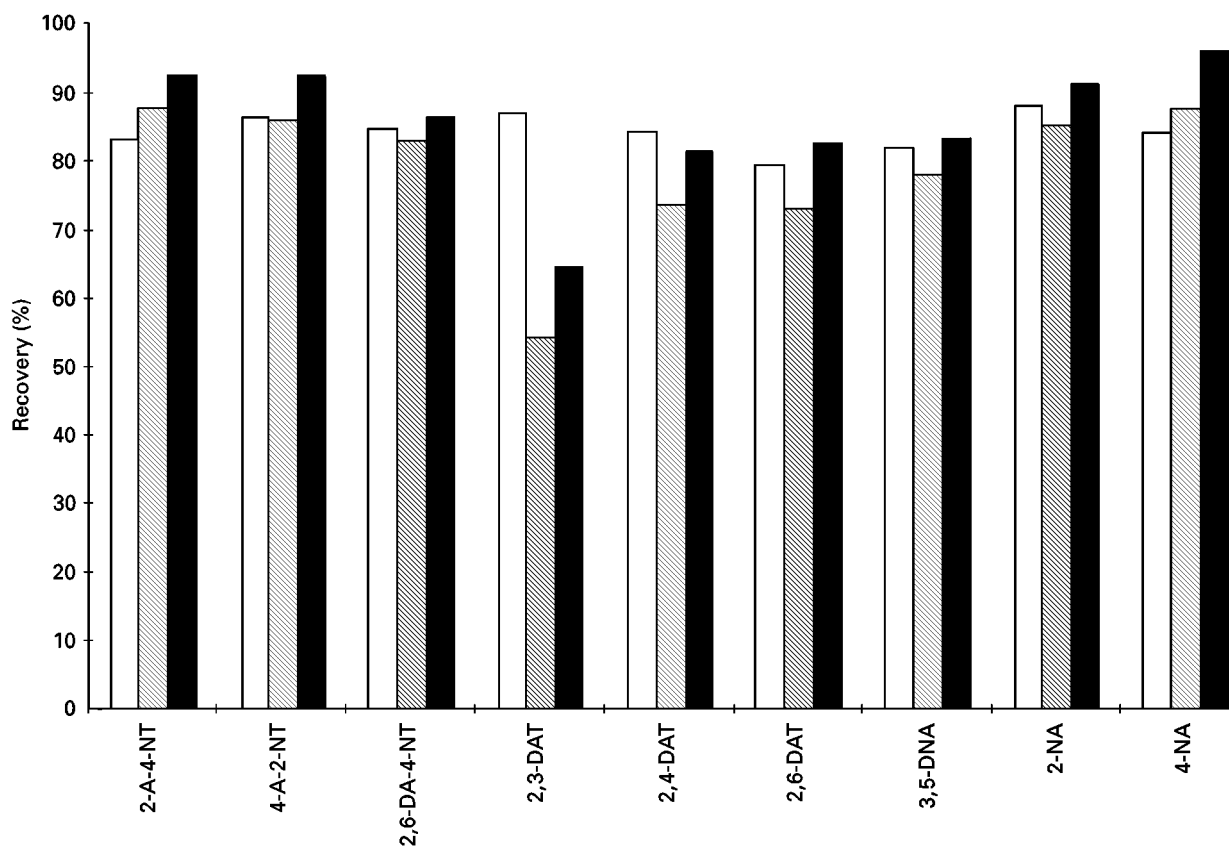


Figure 4 Extraction of basic compounds. Samples of 0.5 L (water spiked with $2 \mu\text{g L}^{-1}$ for each component and adjusted to pH 12 with 1 mol L^{-1} sodium hydroxide) enriched (A) by continuous LLE with 150 mL dichloromethane and (B) by SPE on 500 mg LiChrolut EN (Merck), conditioned with 3 mL acetonitrile, methanol and 9 mL water, and eluted with a 2 mL methanol/acetonitrile mixture (1:1). Open columns, LLE 4 h; hatched columns, LLE 10 h; filled columns, SPE-SVDB.

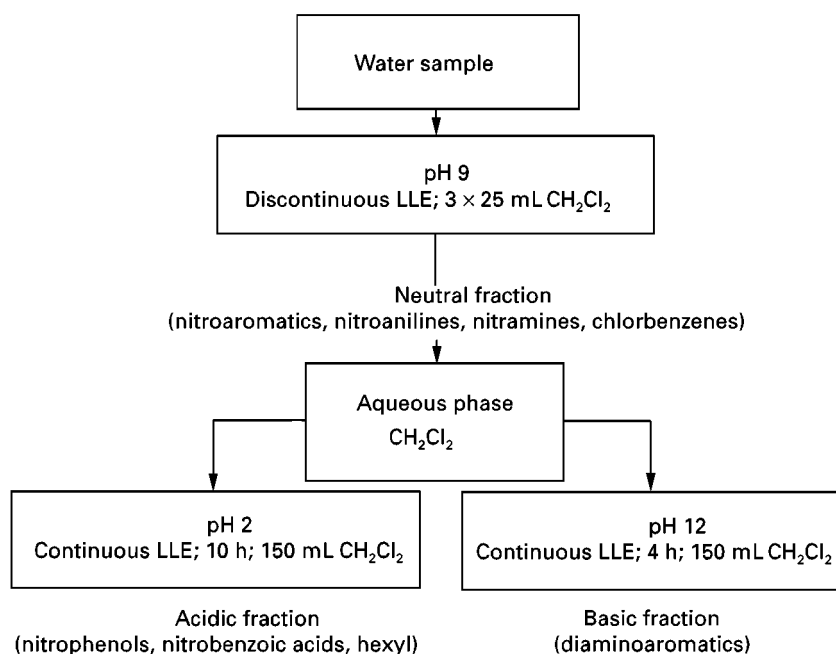


Figure 5 Optimized fractionated extraction procedure. For description of the extraction steps see Figures 2–4. (Reproduced with permission from Lewin U *et al.* (1997) *Chromatographia* 45: 91.)

Table 2 Extraction of spiked soil samples with different solvents

Compound	Acetonitrile		Methanol	
	Recovery (%)	RSD (%)	Recovery (%)	RSD (%)
Hexogen	97	2.5	82	2.4
Hexyl	86	2.2	73	1.5
Octogen	95	3.4	69	4.3
2,4,6-TNT	98	2.1	98	2.1

2 g soil spiked with 10 mg kg⁻¹ for each component, extracted with 10 ml solvent for 15 min in an ultrasonic bath. RSD, relative standard deviation ($n = 3$).

the more retained dichlorocompounds, gradient elution is recommended.

To clarify peak overlapping, other phases in addition to RP-18 phases have proven their value. US-EPA, for example, recommends a cyanopropyl column as a second column showing a clearly different selectivity: nitroguanidine < NB < toluol < 2-NT < 4-N....T < 3-NT < EGDN < 1,3-DNB < 2,6-DNT < 2,4-DNT < TNT < 4-A-2,6-DNT < 2-A-4,6-DNT < hexogen < tetryl < diphenylamine < octogen < PETN.

Similar retention orders are also observed under normal-phase conditions on silica gel, cyanopropyl-

siloxane and aminopropylsiloxane-bonded silica sorbents. As the normal-phase mode has considerable disadvantages (disturbance by traces of water, no gradient elution), these separation systems are used only rarely and in most cases only with detectors which are incompatible with aqueous mobile phases, such as the thermal energy analyser (TEA) and the electron-capture detector (ECD).

Large selectivity differences in RP-18 phases are also obtained on nitrophenyl-modified silica gel and on porous graphitic carbon (PGC) (Table 4).

Thus, retention on these phases will increase with the growing number of nitro groups. Furthermore, in contrast to the RP-18 columns, large retention differences are observed for the isomeric dinitro and aminodinitro compounds. In addition, the PGC phase, due to its high hydrophobicity, shows generally higher retentions, which require a higher methanol content (> 85%) and the separation performance is not satisfactory, due to the low efficiency of such columns.

In addition to the commercially obtainable columns, special materials such as the charge transfer phases like arylpropylether, *N*-propylaniline and safrol phases or a two-dimensional coupling of RP-18 phases with these columns for increasing the selectivity have been tested but offer no great advantage over the common materials.

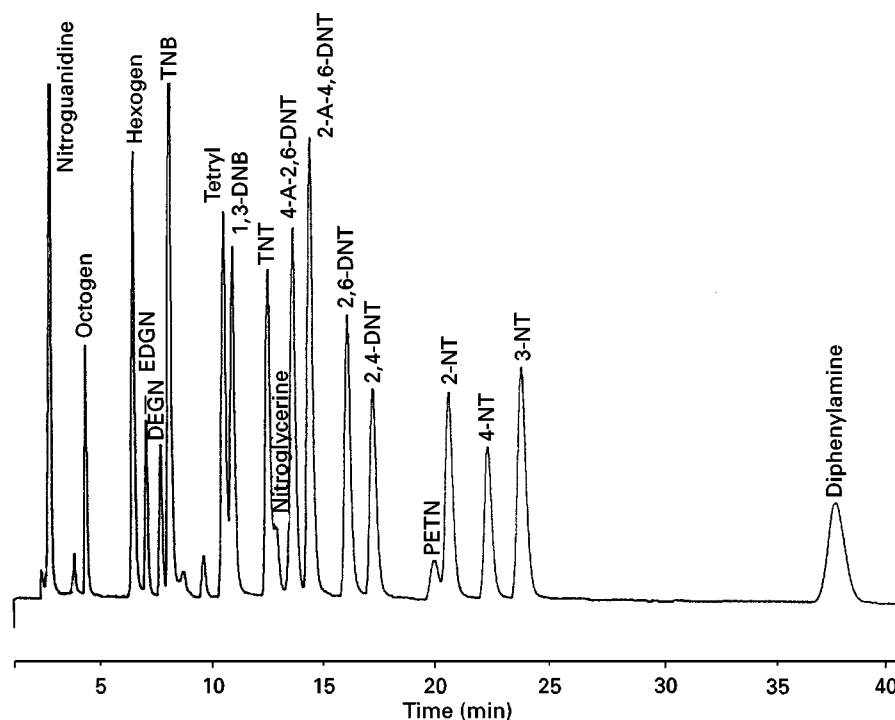


Figure 6 Chromatogram of a standard mixture of explosive-related compounds. 51% methanol–49% water (v/v); Spherisorb ODS 2 column, 5 μ m, 250 \times 4 mm (HP); 1 mL min⁻¹; 25°C; UV 254 nm.

Table 3 Retention behaviour of neutral explosive-related compounds on different RP-18 columns

Column	Spherisorb ODS 2 (HP)		Eurospher 100 C18 (Knauer)		UltraSep Es EX (Sepserv)	
Compound	Peak order	k^a	Peak order	k^b	Peak order	k^c
NG	1	0.22	1	0.14	1	0.07
Octogen	2	0.60	2	0.63	2	0.51
Hexogen	3	1.55	3	1.67	3	1.82
1,3,5-TNB	4	2.21	5	2.26	4	2.51
2-A-6-NT	5	2.23	4	2.00	5	2.71
2-A-4-NT	6	2.74	6	2.59	6	3.03
Tetryl	7	3.03	8	3.84	7	3.61
1,3-DNB	8	3.48	7	3.47	8	4.37
2,4,6-TNT	9	3.90	11	4.98	10	4.56
NB	10	4.00	9	4.14	8	4.14
4-A-2,6-DNT	11	4.36	12	5.63	11	5.36
3,4-DNT	12	4.68	10	4.36	12	5.41
2-A-4,6-DNT	13	4.72	13	5.85	13	6.18
2,6-DNT	14	5.55	14	6.09	14	6.67
2,4-DNT	15	6.06	15	6.28	15	7.63
2-NT	16	7.67	16	7.60	16	8.48
4-NT	17	8.36	17	8.32	17	9.46
3-NT	18	9.05	18	8.98	18	10.16

Dimension of each column: 250 × 4 mm; 5 µm; ^ahold-up time 1.57 min; ^bhold-up time 1.70 min; ^chold-up time 1.18 min. 51% methanol–49% water (v/v); 1 ml min⁻¹; 27°C; 10 µg mL⁻¹ per component.

Acidic Compounds

The separation of the acidic explosives hexyl and picric acid and the metabolites nitrophenols and nitrobenzoic acids is, in principle, possible on RP-materials under the following conditions: at acidic pH value; with the addition of ion pair reagents like hexadecyltrimethylammonium chloride at neutral or basic pH values; and after methylation.

The separation of the underivatized compounds at acidic pH between approximately pH 2 and 4 is relatively simple. For acidification of the mobile phase, many acids and buffers can be used. For example, to separate nitrophenols, in addition to octogen and hexogen, a 0.01 mol L⁻¹ sodium dihydrogen phosphate/phosphoric acid buffer (pH 3) on RP-18-columns is suitable (Table 5).

Table 4 Retention behaviour of neutral explosive-related compounds on different RP phases

Column	RP-18 phase ^a (Eurospher 100; Knauer)		Nitrophenyl phase ^b (Cosmosil 5 NPE)		PGC phase ^c (Hypercarb; Shandon)	
Mobile phase	51% MeOH/49% H ₂ O		62% MeOH/38% H ₂ O		95% MeOH/5% H ₂ O	
Compound	Peak order	k	Peak order	k	Peak order	k
Octogen	1	0.63	13	18.94	3	3.18
Hexogen	2	1.67	7	8.21	1	1.22
1,3,5-TNB	3	2.26	5	6.95	12	41.23
Tetryl	4	3.84	8	8.28	4	4.39
1,3-DNB	5	3.47	4	6.23	9	18.39
2,4,6-TNT	6	4.98	11	13.93	10	28.22
4-A-2,6-DNT	7	5.63	9	9.95	8	17.26
2-A-4,6-DNT	8	5.85	12	17.83	13	41.40
2,6-DNT	9	6.09	6	7.31	5	5.19
2,4-DNT	10	6.28	10	13.35	11	28.47
2-NT	11	7.60	1	4.64	2	3.00
4-NT	12	8.32	2	5.42	7	6.71
3-NT	13	8.98	3	5.62	6	5.24

^aColumn: 250 × 4 mm; 5 µm, hold-up time 1.73 min. ^bColumn: 150 × 4.6 mm; 5 µm, hold-up time 1.09 min. ^cColumn: 100 × 4.6 mm; 7 µm, hold-up time 1.18 min. 1 mL min⁻¹; 27°C; 10 µg mL⁻¹ per component.

Table 5 Retention of nitrophenols and nitramines on RP-18 columns at pH 3

Column		<i>Eurospher 100 C₁₈</i>		<i>Spherisorb-ODS 2</i>	
Compound	Peak order	<i>k^a</i>	Peak order	<i>k^b</i>	
Octogen	1	0.60	1	0.53	
2,6-DNP	2	1.39	2	0.66	
Hexogen	3	1.67	3	0.98	
PA	4	2.06	4	1.07	
2,4-DNP	5	2.31	5	1.13	
4-NP	6	2.46	6	1.84	
3-NP	7	2.76	7	2.03	
2,5-DNP	8	3.22	8	2.30	
3,4-DNP	9	3.25	10	2.96	
4-M-2,6-DNP	10	3.38	9	2.27	
3-M-2-NP	11	3.56	11	2.98	
2-NP	12	3.73	12	3.10	
3-M-4-NP	13	3.83	13	3.78	
2-M-4,6-DNP	14	6.20	15	5.45	
3,5-DNP	15	6.78	14	4.58	
4-M-2-NP	16	8.37	16	7.79	
5-M-2-NP	16	8.37	16	7.79	

Dimension of both columns: 250 × 4 mm; 5 µm; ^ahold-up time 1.73 min; ^bhold-up time 1.59 min. 51% methanol–49% 0.01 mol L⁻¹ sodium dihydrogen phosphate–phosphoric acid. buffer pH 3(v/v); 1 mL min⁻¹; 27°C; 10 µg mL⁻¹ per component.

To separate nitrobenzoic acids a further decrease in pH is necessary. Good separation of these compounds in the presence of nitrophenols and nitramines can be obtained at pH 2 (addition of 0.005 mol L⁻¹ sulfuric acid) and a methanol content of 47% (Figure 7).

Under these conditions for the determination of hexyl a gradient after 20 min to 85% methanol within 20 min is used.

Basic Compounds

The RP-18 phases based on silica are, in principle, also suitable for the determination of the metabolites diaminotoluenes, diaminonitrotoluenes and nitroanilines. For this, however, particularly inert materials with a low silanol group activity are necessary because otherwise the peaks show marked tailing and large peak widths. For example, a Eurospher column showed good properties in this respect (Figure 8).

We have not been able to observe an increase in separation performance with falling pH improving peak shapes, as is often described in the literature. On the other hand there is, as expected a reduction in the retention under these conditions. An increase in retention by restraining the protonation of the basic compounds at pH values > 10 is not to be recommended because of the instability of the phases used.

Alternatives to the separation of the diamino compounds, which on RP-18 phases are insignificantly

retained or only poorly separated should be separated on porous polymer or PGC phases, because these phases have relatively homogeneous nonpolar surfaces and high stability over the full pH range.

Even using various mobile phases and buffer systems, these columns do not show any satisfactory separation of the compounds of interest; this is due to the low efficiency of commercial columns.

Detection

UV Detection

To detect explosive-related compounds, UV is mainly used. Aromatic nitrocompounds are UV-absorbing and can, as a rule, be sensitively detected at 254 nm (Figure 9). At this wavelength it is also possible to detect nitramines and aminoaromatics. In addition to sensitive detection, selectivity against matrix components and eluent impurities is reached at this wavelength, as most interferents absorb at lower wavelengths.

As a rule, nitrate esters and chlorobenzenes do not show a maximum at wavelengths higher than 200 nm. Therefore, these compounds should be detected at the lowest possible wavelength. For methanol-containing eluents the minimum practicable wavelength is around 210 nm.

The UV detector shows a high linearity for the explosive-related compounds in the concentration range of about 0.01 to 100 µg mL⁻¹.

For aromatic nitro-compounds, limits of detection (LODs) reach 5–50 ng mL⁻¹ (0.1–1 ng absolutely for an injection volume of 20 µL) in the sample solution. For nitrate esters and nonnitrated chlorobenzenes the LODs are around 100–250 ng mL⁻¹ (or 2–5 ng absolutely).

Using variable wavelength detectors, multichannel wavelength detectors or photodiode array detectors, it is possible to optimize the selectivities and LODs for certain purposes, by measuring at the absorption maximum or at several wavelengths in one chromatographic run. For example, hexyl can be selectively detected at high and sensitively at 420 nm.

Additionally, the photodiode array detector enables compounds to be identified with marked absorption maxima and minima (e.g. nitrophenols, nitrobenzoic acids and nitroaromatics) by means of the simultaneously recordable spectra.

Electrochemical Detection

In principle, all the nitrocompounds can be determined by means of the electrochemical detector in the reduction mode. Phenols and amino compounds can be detected in the oxidation mode.

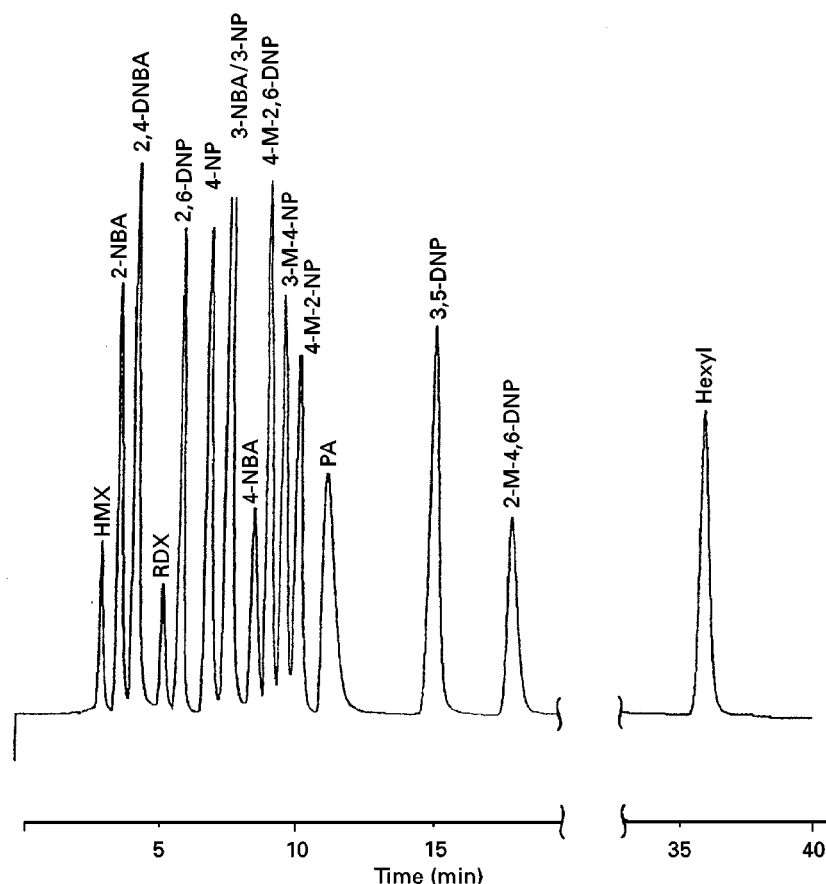


Figure 7 Chromatogram of a standard mixture of nitrophenols, nitro benzoic acids, nitramines and hexyl. Eurospher 100 RP 18 column, 5 μm , 250 \times 4 mm; 47% methanol–53% 0.01 mol L⁻¹ sulfuric acid (pH 2) (v/v), after 20 min linear gradient to 85% methanol within 20 min, 1.0 mL min⁻¹, 27°C; UV 254 nm. (Reproduced with permission from Lewin U *et al.* (1997) *Chromatographia* 45: 91.)

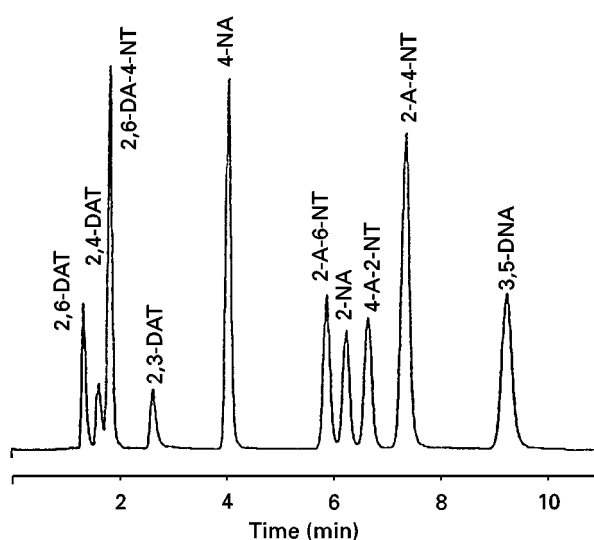


Figure 8 Chromatogram of a standard mixture of amino and diaminoaromatics Eurospher 100 RP 18 column, 5 μm , 250 \times 4 mm (Knauer); 40% methanol–60% 0.01 mol L⁻¹ water (v/v), 1.0 mL min⁻¹, 27°C; UV 254 nm.

The method mainly used in HPLC for electrochemical detection is amperometry: a constant optimized potential difference (working potential) is applied between the working and reference electrode, which has previously been determined from cyclovoltammograms or hydrodynamic voltammograms.

In commercially available electrochemical detectors, solid electrodes are used as they are easier to handle, although nitroaromatics can be detected sensitively with liquid mercury electrodes and in particular with the hanging mercury drop electrode.

To determine explosive-related compounds, the standard electrode material, glassy carbon, has proved its value, because it can be used over a wide potential range of about -1.3 to about $+1.3$ V. In addition, amalgamated gold electrodes or mercury film electrodes have been used for reductive detection.

The selectivity of detection can be influenced by the choice of working potential. In general, substances

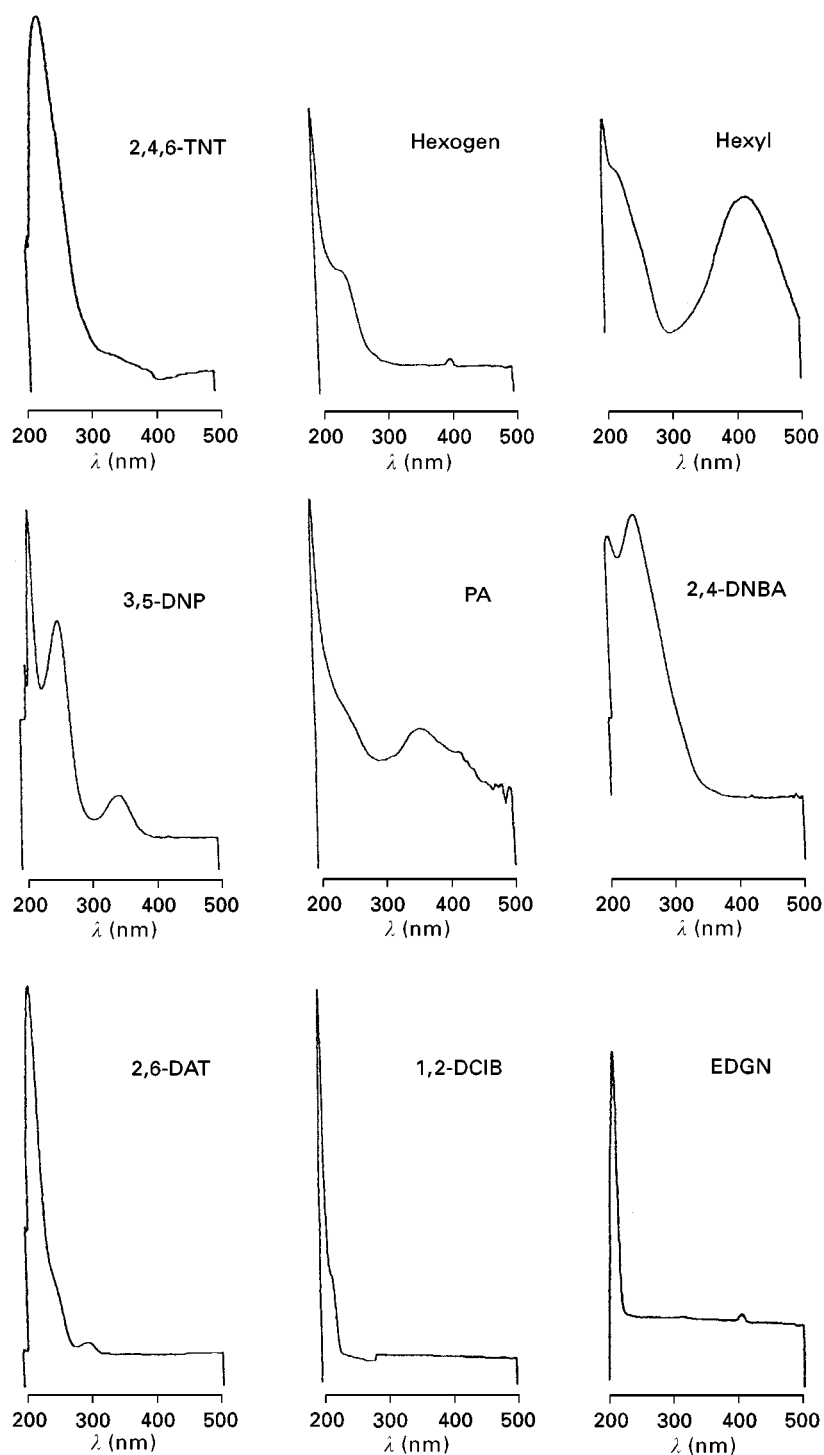


Figure 9 Spectra of explosive-related compounds. Detected with HP 1050 variable wavelength detector in the scanning mode with 51% methanol–49% water or 0.01 mol L⁻¹ phosphate buffer (pH 3) (v/v) for the acidic compounds, respectively.

whose half-wave potential is at least 150 mV larger than the working potential are not detected.

Dual cells or electrode arrays may result in an increase in the informational content of a chromatographic run or in a reduction in the limit of detection

by measuring simultaneously at various potentials or at each optimal potential of the compounds.

Reduction mode Nitro compounds have very different half-wave potentials. They depend on the type,

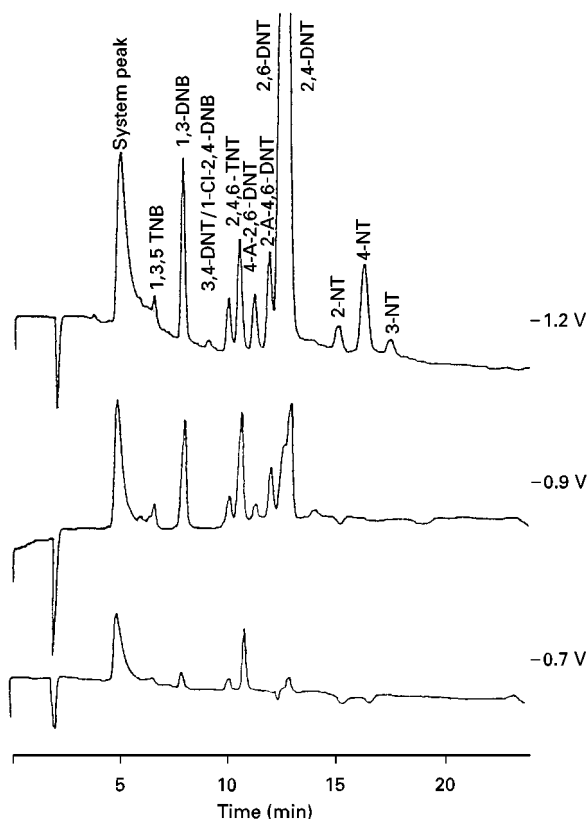
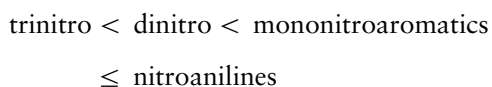


Figure 10 Electrochemical detector chromatograms of the neutral fraction of a groundwater sample from Elsnig at different potentials. Eurospher 100 RP 18 column, 5 μm , 250 \times 4 mm (Knauer); 51% methanol–49% 0.01 mol L⁻¹ phosphate buffer (pH 3) (v/v). (Reproduced from Lewin U *et al.* (1996) *Journal of Chromatography A* 730: 161, with permission from Elsevier Science.)

number and position of the substituents and rise, for example in the following way:



In this way a limited selective detection of certain compounds is possible (Figure 10). The optimum potential for the detection of all components is in perchlorate eluent (pH 5.5) at around -1.2 V.

General problems in reductive detection are caused by the difficulty of complete removal of oxygen dissolved in the mobile phase or in the sample, which is reduced at potentials of about -0.5 V and leads to greater disturbances by system peaks and high residual currents. In most cases it is not possible to reach much lower LODs than with UV detection.

Oxidation mode A great advantage of oxidative detection is that, unlike the reductive mode, oxygen has no negative influence on the detection. Like reductive

detection, the aminoaromatics and nitrophenols have very different half-wave potentials, depending on the type, number and position of the substituents (Table 6).

For example, nitro groups will increase half-wave potentials, whereas they are reduced by amino and methyl groups, which can be utilized for selective detection.

However, the greatest selectivity advantages of anodic detection in analysing explosive-related compounds is that aminoaromatics become selective in the presence of nitroaromatics and nitramines (Figure 11).

Likewise, phenols and hexyl can be detected selectively, in addition to nitrobenzoic acids and nitramines (Figure 12).

In this way, the electrochemical detector, especially coupled with the UV detector, which is almost universal for explosive-related compounds, leads to a valuable gain in information in real samples.

Furthermore, for most nitrophenols and aminoaromatics, lower LODs are reached by anodic detection compared with UV detection. In particular, the detection limits for diamino compounds are lower by a factor of up to 100 (up to 0.05 ng mL⁻¹ or 1 pg absolute) without enrichment.

Table 6 Half-wave and optimal working potentials for oxidative detection

Compound	$E_{1,2}$ (V)	$E_{opt.}$ (V)
2-A-4,6-DNT	1.05	> 1.20
4-A-2,6-DNT	1.05	> 1.20
2-A-3-NT	0.95	1.20
2-A-4-NT	0.95	1.20
2-A-6-NT	0.95	1.20
4-A-2-NT	0.90	1.10
2,3-DAT	0.08	0.30
2,4-DAT	0.25	0.50
2,6-DAT	0.28	0.50
2-M-4,6-DNP	1.05	1.20
4-M-2,6-DNP	1.00	1.20
2,6-DA-4-NT	0.60	0.75
2-M-3-NP	0.65	0.80
3-M-2-NP	0.65	0.80
3-M-4-NP	0.90	1.25
4-M-2-NP	0.85	1.15
4-M-3-NP	0.65	0.80
5-M-2-NP	0.85	1.15
2-NA	1.15	> 1.20
4-NA	1.05	1.20
2-NP	0.90	1.20
3-NP	0.80	1.00
4-NP	0.95	1.20
PA	> 1.20	> 1.20

Conditions: ELCD HP 1049 A with glassy carbon thin-layer working electrode and Ag/AgCl reference electrode; 51% methanol–49% 0.01 mol L⁻¹ sodium dihydrogen phosphate–phosphoric acid buffer pH 3 (v/v) or sodium perchlorate solution (pH 5.5) for diaminoaromatics, respectively; 1 mL min⁻¹; 27°C.

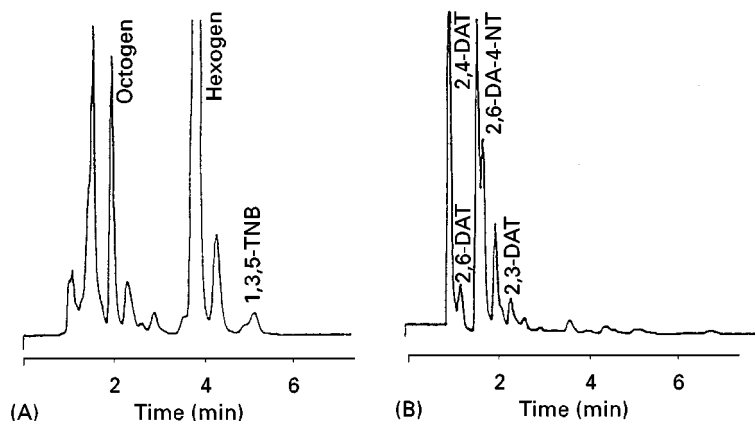


Figure 11 Chromatograms of the basic fraction of a groundwater sample from Elsng (upper level). (A) UV (254 nm); (B) electrochemical detector (+ 0.7 V). Eurospher 100 RP 18 column, 5 μm , 250 \times 4 mm; 40% methanol–60% 0.01 mol L⁻¹ sodium perchlorate solution (v/v), 1.0 mL min⁻¹, 27°C. (Reproduced with permission from Lewin U *et al.* (1997) *Chromatographia* 45: 91.)

The electrochemical detector shows high linearity over a concentration range of 10^4 but, compared with UV detection, reproducibility is somewhat lower. Furthermore, there is often a decrease in the response over a long measuring period: this can be attributed to passivation of the electrode surface and requires its regeneration.

Determination of the nitroaromatics in the easier oxidation mode takes place after photolysis in a post-column reactor via the nitrite produced, which is

oxidized on a glassy carbon electrode. For this, LODs of 120–250 pg have been found. The expense of the apparatus, however, is relatively high and the yield of the photolysis is very different for the various compounds.

Mass Spectrometric Detection

In the last few years the development of mass selective detectors for coupling with HPLC has made good progress. In addition to thermospray ionization (TSI),

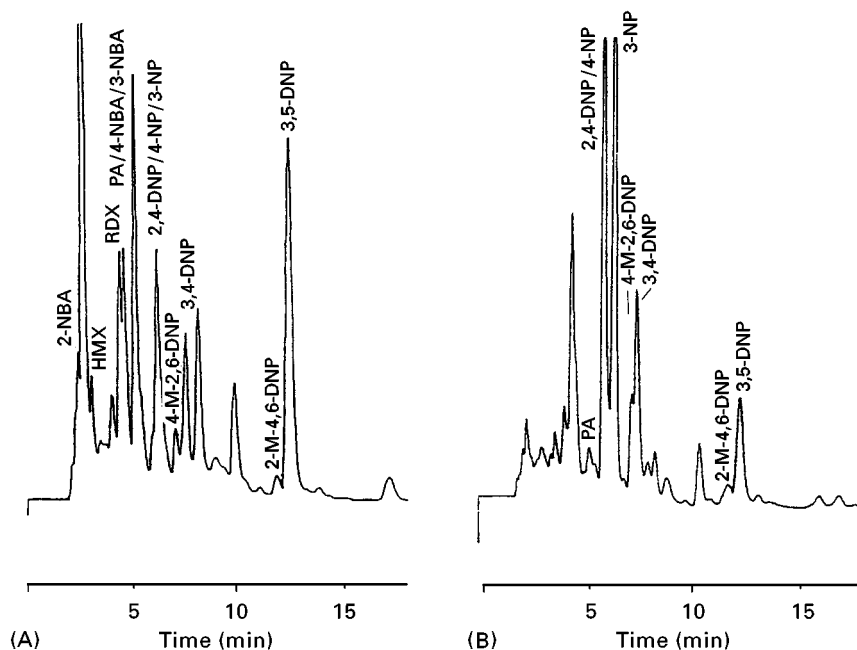


Figure 12 Chromatograms of the acidic fraction of a groundwater sample from Elsng (lower level). (A) UV (254 nm); (B) electrochemical detector (+ 1.2 V). Eurospher 100 RP 18 column, 5 μm , 250 \times 4 mm (Knauer, Berlin); 51% methanol–49% 0.01 mol L⁻¹ phosphate buffer (pH 3) (v/v), after 20 min linear gradient to 80% methanol within 20 min, 1.0 mL min⁻¹ (Reproduced with permission from Lewin U *et al.* (1997) *Chromatographia* 45: 91.)

the atmospheric pressure ionization (API) techniques, electrospray ionization (ESI) and atmospheric pressure chemical ionization (APCI) are increasingly gaining in importance.

Explosives can be detected with TSI as negative ions (mostly $[M + \text{CH}_3\text{COO}]^-$ or $[M - \text{H}]^-$). Nitramines and amino compounds can be registered as positive ions (mostly $[M + \text{NH}_4]^+$). With negative ionization in the full-scan mode, LODs are in the ng mL^{-1} range. With selected ion monitoring in the filament-on negative ion mode, the LODs are a factor of 100 lower.

As a result of the electron-withdrawing effect of the nitro groups, nitroaromatics can be detected with API as negative ions $[M - \text{H}]^-$ (Figure 13).

The sensitivity of detection depends on the type, number and position of the substituents. It increases with the number of nitro groups and is considerably higher for nitrophenols and nitrobenzoic acids than for the corresponding neutral nitrobenzenes and nitrotoluenes.

Furthermore, sensitivity depends on the composition of the mobile phase such as the type and quantity of the organic modifier, buffer additives and pH value.

As with TSI, hexogen and octogen form clusters with acetate ions $[M + \text{CH}_3\text{COO}]^-$. A cluster formation of these compounds with ammonium ions $[M + \text{NH}_4]^+$ should, in principle, also be possible in the positive mode.

In addition to the molecular ions and molecular cluster ions, fragment ions are also formed, and elimination of oxygen or reductions and rearrangements of the nitro group are observed. Nitrophenols fragment with the loss of the hydroxyl and the nitro group. This can be used to obtain structural information. However, the assignment of position isomers is difficult, so that to investigate complex samples, carefully optimized HPLC conditions are needed and the additional use of a UV detector is an advantage.

The LODs largely depend on the particular compound and are between 0.1 and $10 \mu\text{g mL}^{-1}$ for the neutral nitroaromatics and nitramines and around $10\text{--}100 \text{ ng mL}^{-1}$ for the nitrophenols. Reproducibility is acceptable (about 2–5%).

Nuclear Magnetic Resonance Spectroscopy

Proton nuclear magnetic resonance spectroscopy ($^1\text{H-NMR}$) is well suited for the determination of explosives because these analytes are small aromatic molecules which offer good manageable spectra; their aromatic protons appear over a relatively wide frequency range (approximately 3 ppm) because of the various substituents (nitro, carboxyl, methyl, hy-

droxyl and amino groups). Thus, reliable identification in very complex samples is possible by the HPLC-NMR coupling which has been developed over the last few years.

In the continuous flow mode at low flow rates ($< 0.02 \text{ mL min}^{-1}$) and large injection volumes (approximately $400 \mu\text{L}$), determination of explosives in the lower microgram range is possible. The reproducibility of about 2% in the upper microgram range is acceptable.

Further Detection Techniques

Fluorescence detection is not suitable for the determination of nitro compounds, as nitro groups will diminish fluorescence intensity. However amino compounds can be determined very selectively and sensitively.

As nitro compounds form nitrogen monoxide by pyrolysis, they can also be detected by a thermal energy analyser. The sensitivity depends on the substance class and is lower for nitroaromatics than for nitramines and nitrate esters. An advantage of the detector is its specificity for compounds carrying oxynitrogen functional groups. Because of the complex apparatus and the restriction to the normal-phase separation mode, the detector has not achieved wide usage.

Occasionally, reports have been published on further pre-column and post-column derivatization techniques. For example, for the amino compounds the diazotization and coupling with *N*-(1-naphthyl)-ethylenediammonium chloride into azo dyes is suitable. This reaction is also suitable for the determination of nitroaromatics after conversion with titanium(III) chloride into the amines or after photolysis and diazotization of the nitrite formed with sulfanilamide.

The electron-capture detector, widely used in gas chromatography, was not successful in practice because of incompatibility with polar mobile phases.

Conclusions

To determine the thermally unstable explosive-related compounds, the method of choice is HPLC. However, because of the limited separation performance, where there are very complex samples, HPLC determination is only possible after optimization of the method and pre-separation of the samples into different fractions.

RP-18 phases have proved their value as standard columns. In special separation problems the use of a second column is useful.

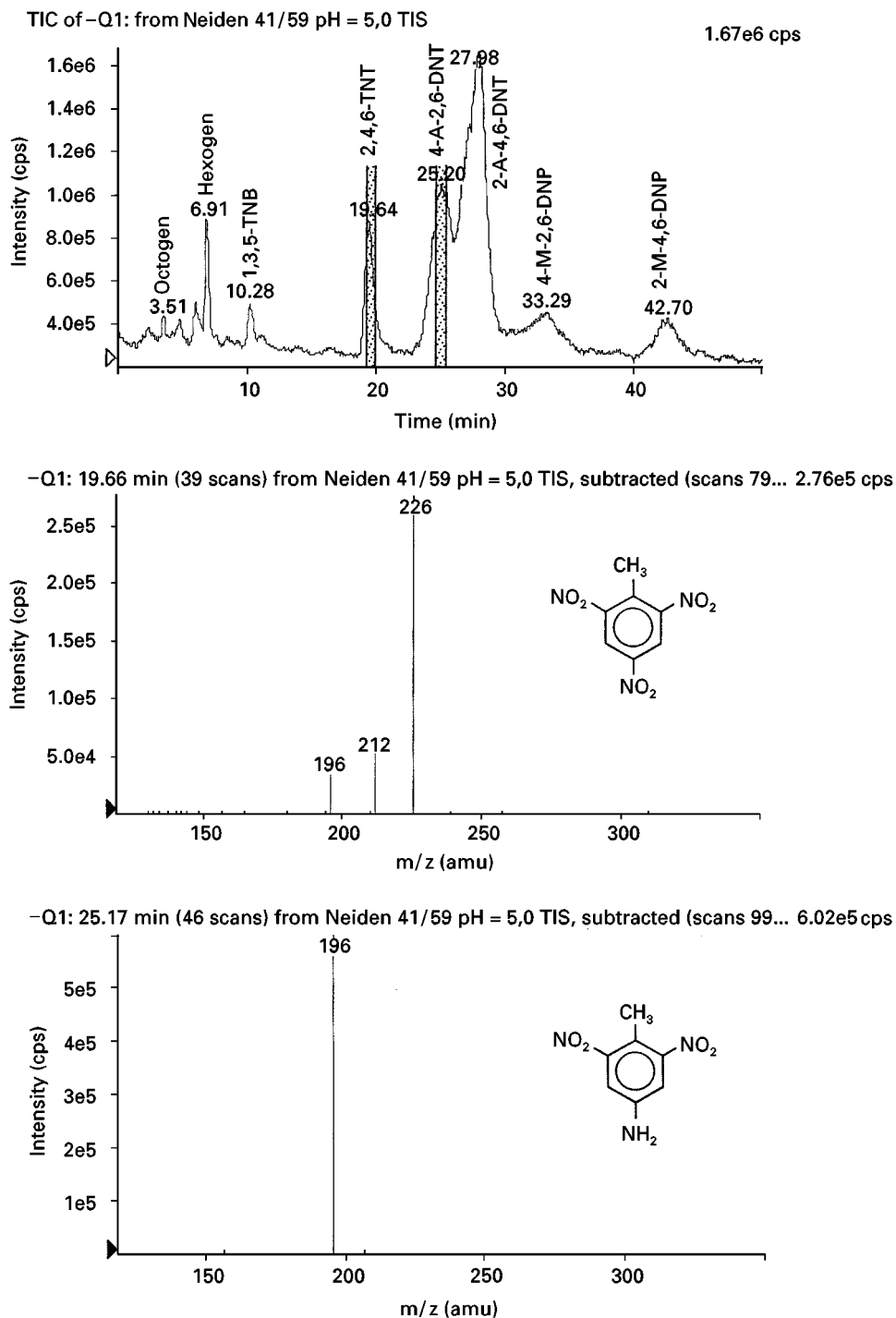


Figure 13 TIC and several mass spectra of an extract of drainage water from contaminated soil. PE-SCIEX API 100 LC/MS-System; Heated Nebulizer™ (PE), Ultrasep ES RP 18 column, 5 μ m, 250 \times 4 mm (Sepsev, Berlin); 41% methanol–59% water (v/v) adjusted to pH 5.0 by means of acetic acid, 20°C.

In most cases, UV detection, which is almost universal for explosive-related compounds, is used. Because of the complexity of samples, to clarify signal overlapping, and last but not least for identification, the use of selective detectors such as the electrochemical and mass spectrometric detector as well as HPLC-

NMR coupling, which has been recently commercially introduced, are of great advantage.

In general, the available techniques (including sample preparation) enable explosives, their by-products and metabolites to be determined down to a range of 0.1 μ g L⁻¹.

See also: II/Chromatography: Liquid: Detectors: Mass Spectrometry; Detectors: Ultraviolet and Visible Detection; Nuclear Magnetic Resonance Detectors. **Extraction:** Solid-Phase Extraction; Solvent Based Separation; Ultrasound Extractions. III/Solid Phase Extraction with Cartridges.

Further Reading

- Berberich DW, Yost RA and Fetterolf DD (1988) Analysis of explosives by liquid chromatography/thermospray/mass spectrometry. *Journal of Forensic Science* 33: 946.
- Bratin K, Kissinger PT, Briner RC and Bruntlett CS (1981) Determination of nitro aromatic, nitramine and nitrate ester explosive compounds in explosive mixtures and gunshot residue by liquid chromatography and reductive electrochemical detection. *Analytical Chimica Acta* 130: 295.
- Fedoroff BT (ed.) (1960–83) *Encyclopedia of Explosives and Related Items*, vols 1–10. Dover: Picatinny Arsenal.
- Hubball J (1992) The use of chromatography in forensic science. *Advances in Chromatography* 32: 154–172.
- Jenkins TF, Leggett DC, Grant CL and Bauer CF (1986) Reverse-phase high-performance liquid chromatographic determination of nitroorganics in munitions wastewater. *Analytical Chemistry* 58: 170.
- Levsen K, Preiss A and Feltes J (1995) Analysenmethoden für Explosivstoffe. In: Rippen G (ed.) *Handbuch der Umweltchemikalien* vol. 3, 31st edn, pp. 36–75. Landsberg: Ecomod.
- Lewin U, Wennrich L, Efer J and Engewald W (1997) Determination of highly polar compounds in water samples around former ammunition plants. *Chromatographia* 45: 91.
- Lloyd JBF (1992) HPLC of explosive materials. *Advances in Chromatography* 32: 173–261.
- US Environmental Protection Agency (1992) *Method 8330, revision 1*. Washington, DC: EPA.
- Yinon J and Zitrin S (1993) *Modern Methods and Applications in Analysis of Explosives*. New York: Wiley.

Thin-Layer (Planar) Chromatography

J. Bladdek, Military University of Technology, Warsaw, Poland

Copyright © 2000 Academic Press

Introduction

The term explosive has two meanings. It is used for individual chemical compounds among which trinitrotoluene (TNT), 1,3,4-trinitro-1,3,5-triazacyclohexane (hexogen-RDX), 1,3,5,7-tetranitro-1,3,5,7-tetrazacyclooctane (octagen-HMX), pentaerythritol tetranitrate (pentrik-PETN) nitroglycerine (NG) and nitrocellulose (NC) are commonly known. This term is also used for mixtures of the above individual compounds and their mixtures with other, non-explosive substances; the type and amount of components in a mixture determines its properties (brisance, melting, plasticity and the like). Explosives have been classified in many ways according to different criteria. Most important is the kind of addition, the NO₂ group and type, and the velocity of the reaction involved. The first are divided into the following groups; nitro compounds containing the C-NO₂ group, nitrate esters with C-O-NO₂ group and nitramines with C-N-NO₂ group. The second criterion divides explosives into high and low explosives (HEs and LEs respectively).

The identification and quantification of the HEs or LEs are very valid and also present difficult analytical problems. These problems become evident especially

during: (i) testing of environmental pollutants, (ii) forensic investigations, and (iii) checking technological processes and service conditions of munitions manufacture. From an analytical point of view, at least three groups of TLC applications in explosive investigations can be distinguished. The first of them, most often represented in the research literature, concerns qualitative (including screening methods) and quantitative analysis of explosives. The second is where TLC is applied as a clean-up technique. In this case analysis is completed by other analytical techniques. The last group of applications mainly covers the evaluation of LE stability.

Although, recently, more sophisticated methods such as thermal analyses and gas or liquid chromatography are commonly used in many laboratories, TLC is still in use. Starting from paper chromatography and improved over many years, TLC has become very effective in the analysis of explosives. Apart from high performance adsorbents, and the ability to perform separations in both normal and reversed-phase systems, the real advances are due to the development of densitometry and the spray-on technique of sampling.

Analyses of Explosives

Early TLC analysis was performed on home-made chromatographic plates and involved the separation of classical HEs such as TNT, RDX,

Table 1 Examples of TLC separation of explosives

Analyses	Chromatographic system		Type of elution
	Stationary phase	Moblie phase	
TNT, RDX, PETN, tetryl, NC, NG	Silica gel	Trichloroethylene–acetone (4 : 1)	One-dimensional, isocratic
TNT, RDX, HMX, PETN, tetryl	Silica gel HPTLC F ₂₅₄	Carbon tetrachloride–aceto-nitrile (8 : 1)	One-dimensional, isocratic
HMX, RDX, 2,4-DNT, TNT, NG, PETN, tetryl	Silica gel HPTLC F ₂₅₄	I petrol ether – acetone (3 : 1) II petrol ether – ethyl acetate (8 : 1)	Two-dimensional, isocratic
Trinitrobenzene, 2,4-DNT, TNT tetryl, NG, PETN, RDX	Silica gel HPTLC F ₂₅₄	Benzene - petrol ether–methanol (8 : 6 : 1)	One-dimensional, isocratic
TNT m-dinitrobenzene, trinitrobenzene, tetryl, 2,4-dinitrochlorobenzene, picramide, heksyl	Silica gel G-magnesium silicate (1 : 1)	Xylene	One-dimensional, isocratic
2,3,4-TNT, 2,4,6-TNT: 1,2-DNB: RDX	Silica gel HF ₂₅₄	Benzene–hexane–pentane (5 : 4 : 1)	One-dimensional, isocratic
RDX, HMX, tetryl, PETN, TNT, 2,4-DNT, 2,6-DNT	Silica gel with chemical bonded octadecyl, RP-C-18		AMD, gradient elution
Hexyl, picric acid, RDX, HMX, 2,4,6-N-tetranitro-N-methylaniline, 2,4- and 2,6-dinitrotoluenes, TNT, 1,3-dinitrobenzene, 2-amino-4,6-dinitrotoluene, 4-amino-2,6-dinitrotoluene	Silica gel HPTLC		AMD, gradient elution

HMX and PETN (see Yinon and Zitrin in Further Reading).

One-dimensional ascending or horizontal techniques have usually been applied for the development of chromatograms in a closed chamber (Table 1). Multiple and two-dimensional development techniques have seldom been used but automated multiple development (AMD) and gradient development are becoming more frequently used.

In TLC much attention is paid to the methods of analyte visualization, especially to search for specific reactions which can confirm the presence of an analyte in a spot or band. Confirmation of the identity of an analyte is thus based on at least two criteria,

R_F and colour reaction. The majority of more or less specific explosive visualization schemes have been worked out long ago (Table 2). Exhaustive reviews of those methods can be found in the publication by Yinon and Zitrin, mentioned above, and in York *et al.* (see Further Reading).

Most investigations on the analysis of explosives by TLC have been confined to environmental protection. In such research, classical TLC has been applied mainly as a screening method and has served to provide essentially qualitative analysis; instrumental TLC provides both qualitative (screening) and quantitative determination. Environmental analysis of explosives is justified by the fact that nitrotoluenes and

Table 2 Examples of visualization of explosives

Visualization method	Analyte	Quantification	
		Yes	No
UV absorption	2,3,4-TNT, 2,4,6-TNT, 1,2-DNB, RDX	x	
NaOH in methanol acetone (1 : 1)	Nitroaromatic compounds		x
π complex formation with <i>o</i> -toluidine, N,N-dimethylaniline, m-chloroaniline or anthracene	m-DNB, TNB, TNT, tetryl, 2,4-dinitrochlorobenzene, picramide, heksyl		x
Griess reagent	RDX, HMX	x	
UV followed by 5% DPA in methanol acidified by H ₂ SO ₄	RDX and nitrates		x
5% DPA in methanol	Nitroaromatic compounds		x
NaOH/ Griess reagent	NG, NC	x	
0.2% Würster's salt in methanol	NC, NG, PETN		x

especially trinitrotoluenes are highly toxic compounds. The aromatic amines formed by their biodegradation are suspected to be carcinogenic. Due to careless handling during the manufacture, loading, and packing etc., of explosives, groundwater, surface water and soil may be contaminated with these compounds. Occasional plant accidents, and residues from World War II are also sources of pollution.

Screening methods, which most often use colorimetric visualization reactions, serve to lower the cost and are less time-consuming for the analysis of a large number of samples. An excellent example which illustrates the advantages of TLC for such applications is provided by Haas and Stork. The most interesting information in this work lies in the method of sample preparation (liquid-liquid extraction) and the technique of separation of large numbers of analytes. Water samples taken from waste-heaps, containing post-production residues of TNT, were extracted with isopropyl ether under a range of pHs. At pH 4 aromatic amines were retained in the aqueous phase and phenols and nitro compounds were extracted into the organic phase (ether extract A). To enable extraction of amines into the organic phase, the pH was adjusted to 8 (ether extract B). Phenols were isolated from extract A by treating with 1M NaOH (nitrotoluenes remained in the extract). The aqueous phase, of extract A was then re-adjusted to pH 4 and re-extracted to transfer phenols to the organic phase (extract C). After drying and concentration, the three extracts are analysed by normal phase chromatography using two-dimensional isocratic elution. Analytes are identified by the quenching of fluorescence or by colour reactions. In extract A (nitrotoluenes) 25 compounds were found and 2,4-, 2,6-dinitrotoluene and TNT were identified. In extract B (nitroamines) 26 compounds were found. In extract C, containing phenols, 28 compounds were found and 2,4-dinitro-6-methylphenol and 2,6-dinitro-4-methylphenol were identified. Confirmation of TLC results and quantification were performed using spectrophotometry and gas chromatography.

On-site TLC screening methods for explosives in soil have been reviewed by Nam who suggested that the results obtained using two colorimetric-based methods (TNT and RDX-methods), commonly used for on-site analysis of explosives in the USA, are not perfect. The first of the methods, is based on the reaction of an acetone soil extract of TNT with base, to produce reddish coloured Jankowsky ions. For the RDX method, the soil extract is first acidified and reacted with zinc to reduce the RDX to nitrous acid; the solution obtained is reacted with Griess reagent to produce a reddish coloured azo dye. Unfortunately,

these are not specific reactions and require other techniques for confirmation. The work describes the separation techniques for nitroaromatics, nitroamines and nitrate esters, classical, colour visualization methods and also the costs of analysis. Laboratory analytical methods for the most commonly found components of explosives, and environmental transformation of these substances in a soil matrix, have been developed in the work of Jenkins *et al.*

More recently gradient automated multiple development (AMD) HPTLC using a normal phase system has been applied to the determination of explosives and their biodegradation products in contaminated soil and water. The subjects of examination were hexyl, picric acid, RDX, HMX, 2,4,6-N-tetranitro-N-methylaniline, 2,4- and 2,6-dinitrotoluenes, TNT, and other by-products such as 1,3-dinitrobenzene, 2-amino-4,6-dinitrotoluene, and 4-amino-2,6-dinitrotoluene found in former ammunition site waste in Germany. The use of optimized gradient elution and an AMD system allowed the separation of analytes from environmental samples and quantification at the 5–20 ng level; humic substances presented in water samples do not interfere. In the case of samples of soil with a high concentration of humic substances, a clean-up technique is necessary. The superiority of TLC is displayed by the fact that similar analyses using GC or HPLC require (even for water samples) very careful sample clean-up or the application of size exclusion chromatography.

Modern TLC equipment has also been applied to the quantitative determination of HE residues in soil and water using a reversed-phase system with automated multiple development gradient elution after liquid-liquid and solid-phase extraction. Quantification was carried out by UV or visible absorption light measurement *in situ*. The work demonstrated that the application of AMD was effective for the isolation and separation of relative complex HE mixtures in one analytical process (Figure 1). Most of the examined HEs absorb UV light, which allows their quantification by densitometry (Table 3).

During the measurement of PETN, Wurster's salts were applied (organic nitrate esters oxidize Wurster's salts yielding the so-called 'Wurster's cations' which are intensely coloured). It has been proved that this reaction can also be used for quantitative analysis. The extraction of HEs from water samples, using solid-phase extraction (SPE) cartridges filled with SDB-1 phase (recoveries $\approx 90\%$), was shown to be more effective than liquid-liquid extraction. Slightly lower values of recoveries during extraction from soil (77.0–84.4%) were obtained but these result from the more complex procedure for their preparation for analysis (necessity of purification).

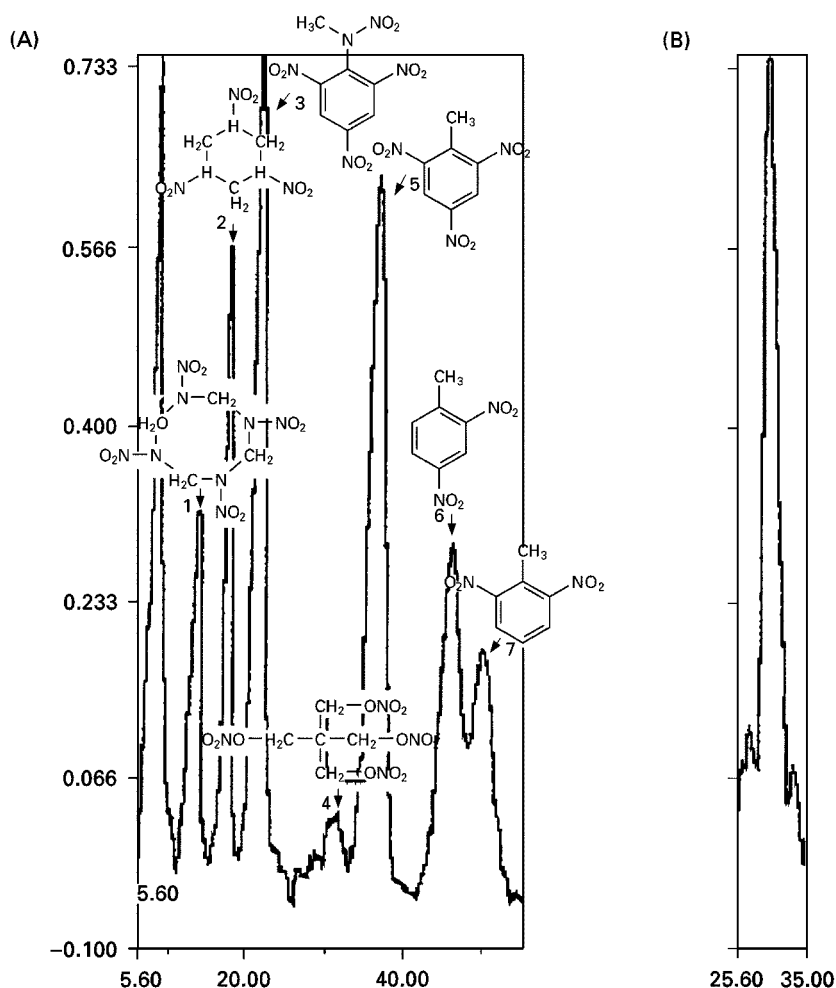


Figure 1 Chromatogram of high explosives: 1 = octagen, 2 = hexogen, 3 = tetryl, 4 = pentrit, 5 = trotyl, 6 = 2,4-DNT, 7 = 2,6-DNT: (A) scanning at wavelength 220 nm, (B) pentrit, scanning at 600 nm. Abscissa – absorbance, ordinate – range of the spots in mm. (Reproduced with permission from Bładek J *et al.* 1998.)

The proposed technique for the elimination of the majority of non-polar impurities from soil extracts using SPE is very effective for the identification and quantification of the analytes examined (Figure 2).

Post-blast analyses, or identification of explosive residues in forensic investigations, are directly associated with combat, and criminal or terrorist activity. Results of such analyses may give information about the type, and sometimes also about the source of

Table 3 Parameters of quantification

High explosive	λ_{max} nm	Calibration curve			Detection limits, ng
		$A \cdot 10^{-3} =$	Correlation coefficient	Max, range of linearity, ng	
Octagen	215	$8.8c - 0.1$	0.9861	1600	200
Hexogen	220	$10.7c + 0.6$	0.9858	1600	200
Tetryl	220	$28.5c + 3.1$	0.9989	1000	50
Pentrit	600	$30.9c + 0.3$	0.9899	1600	200
TNT	220	$12.5c + 50.5c - 0.6$	0.9989	-	50
2,4-DNT	240	$29.7c - 1.0$	0.9378	1000	100
2,6-DNT	220	$10.7c - 0.7$	0.9728	2000	200

*A, densitometric peak area; c, amount of the pesticide in the band.

(Reproduced with permission from Bładek J *et al.* 1998.)

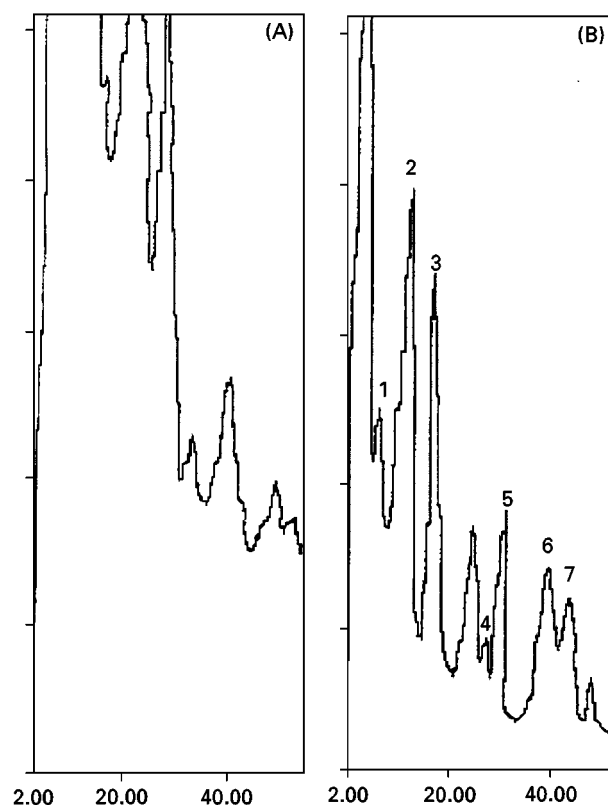


Figure 2 Chromatograms of soil sample: (A) before purification, (B) after purification by SPE. Notation as in Figure 1. (Reproduced with permission from Bładek J *et al.* 1998.)

explosives or about possible contact with explosives. From an analytical point of view, these methods are similar to investigations of explosives in environmental matrices; the difference concerns isolation from the matrix (debris, bodies and surfaces). These matrices are usually extracted in two ways: by water and by organic solvent. The water extract is then analysed for inorganic ions and the organic extract for the explosives. Yinon and Zitrin have described the complexity of such analysis (see Further Reading).

TLC as a Clean-up Method

Forensic and environmental analyses are usually performed in several stages, one of the most important being sample preparation. This stage covers the isolation, concentration, and purification of analytes for further analysis. Three basic methods of purification of analytes may be distinguished: liquid–liquid extraction, solid-phase extraction and preparative thin layer chromatography. For preparative TLC, the analytes are spotted as a long band on the start line. After developing chromatograms the plates are dried, and cut, if plastic or aluminium, or scored, if glass, so that they contain the standard lanes and part of the sample. Classic, preparative TLC has been rarely used for the purification of explosives. Easy access and a variety of stationary phases for SPE make it more useful than preparative TLC in this application.

Table 4 Examples of TLC separation and visualization of stabilizers

Stabilizer	Chromatographic system		Type of elution	Visualization
	Stationary phase	Mobile phase		
DPA and its derivatives	Silica gel HPTLC	1 step: petrol ether–benzene (1 : 1) 2 step: benzene 1 dimension: benzene-1,2-dichloroethane– carbon tetrachloride (10 : 5 : 6)	One-dimensional, two-steps, isocratic	UV or VIS absorption
DPA and its derivatives	Silica gel	2 dimension: ethyl acetate–petrol ether (2 : 8)	Two-dimensional, isocratic	UV or VIS absorption
EC and its derivatives	Silica gel	1 dimension: benzene 2 dimension: benzene–diisopropyl ether (3 : 1)	Two-dimensional, isocratic	UV or VIS absorption
DPA and its derivatives	Silica gel with zinc powder	1 dimension: petrol ether–benzene– acetone (99 : 99 : 2) 2 dimension: petrol ether–ethyl acetate (4 : 1)	Two-dimensional, isocratic	0.25% ethanol solution of <i>p</i> -diethylaminebenzaldehyde in 0.25 M HCl
EC and its derivatives	Silica gel with zinc powder	1 dimension: 1,2-dichloroethane 2 dimension: petrol ether–ethyl acetate (4 : 1)	Two-dimensional, isocratic	EC: 0.003% dichlorofluoresceine in ethanol followed by UV; derivatives: 0.25% ethanol solution of <i>p</i> -diethylaminebenzaldehyde in 0.25 M HCl

TLC in Research

This work mainly concerns LEs (propellants). Nitrate ester-based propellant compositions decompose under normal storage conditions producing nitrogen dioxide as a primary decomposition product. This NO_2 is the source of further, autocatalytic decomposition of propellants, limiting their safe storage life. In order to reduce the rate of deterioration of propellants, stabilizers (usually diphenylamine – DPA) or centralite I-(N,N'-diethyl-N,N'-diphenylurea) –EC, which react with the primary decomposition products, are usually incorporated, to inhibit degradation. The amount of stabilizers added varies, but is typically less than 1% (in the case of DPA) and 3% (in the case of centralite). The stabilizers react with nitrogen oxides forming different degradation products and whilst some of these products also act as stabi-

lizers others contribute to stabilizer depletion. Examples of the application of TLC to stabilizer measurement are presented in Table 4.

One example of the application of TLC for propellant stability research uses three chromatographic systems for the isolation of stabilizers (Figure 3) from single-base, free emulsion double base and emulsion propellants (Table 5). Samples are divided into 2 parts. One is heated for 1 h at 120°C in an open vessel and the other left unheated. All samples are then dissolved in acetone (this procedure is more effective than the extraction of stabilizers) and analysed to observe the differences between the state of chemical change of the stabilizer and its reaction products before and after ageing. Analyses are performed using a liquid-crystal detector, and confirmation was done using densitometry.

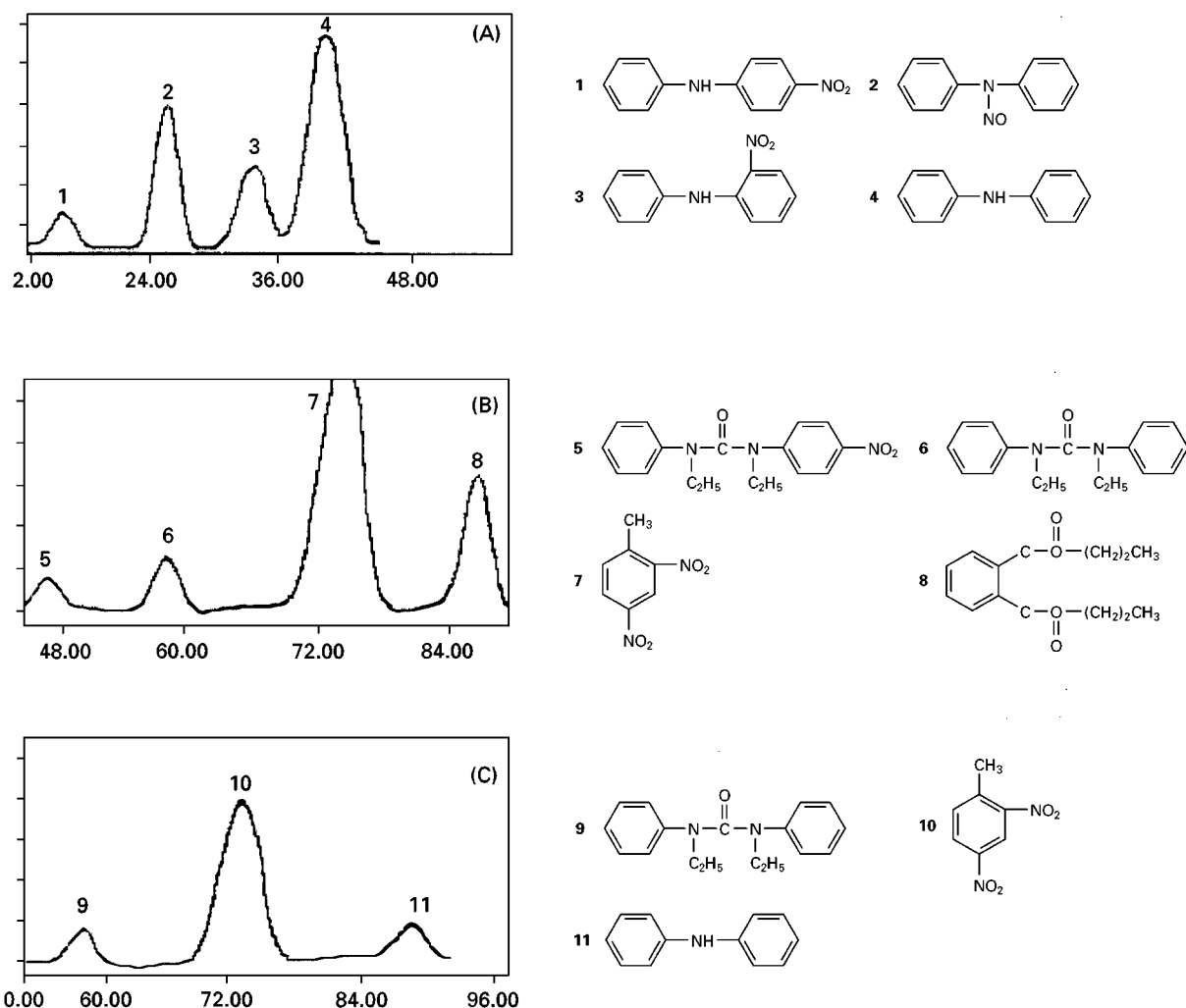


Figure 3 Fragments of propellant chromatograms: (A) single-base, (B) double base, (C) emulsion propellant. Abscissa – absorbance, ordinate – range of the spots in mm. Peaks notation: 1 = 4-nitrodiphenylamine, 2 = N-NO-diphenylamine, 3 = 2-nitrodiphenylamine, 4 = diphenylamine, 5 = 4-nitro centralite, 6 = centralite, 7 = 2,4-dinitrotoluene, 8 = dibutylphthalate, (c) 9 = centralite, 10 = 2,4-dinitrotoluene, 11 = diphenylamine. (Reproduced with permission from Bładek J *et al.* 1993.)

Table 5 Characteristic compositions of propellant samples

Propellant	Concentration [%]						
	NC	EC	NG	DPA	DNT	DBP	Others
Single-base	96–99		0.7–2.0				0.0–1.8
Emulsion-free double-base	56–66	20–45		0.7–3.0	7–12	0.0–5.0	0.0–1.5
Emulsion	56–70	10–20	0.5–1.0	3–4	10–15		0.0–1.5

(Reproduced with permission from Błażek J *et al.* 1993.)

In three lots of single-base propellants, stored for 48, 47 and 41 years consumption of DPA in the range 75–100% was determined (before heating). The main products of chemical change are N-NO-DPA, 4-NO₂-DPA, 2-NO₂-DPA and also traces of dinitro-DPA. The most often observed differences in the concentrations of DPA before and after heating were in the range 0.2–0.6% (m/m). In most stable double-base propellants during storage of up to 50 years, a small decrease of 5–10% EC content was observed. Rarely, traces of 4-NO₂-EC were found. This work also found that in some unstable double-base propellants (stored for 40 years) and mortar propellants (stored for 38 and 23 years), 90–100% of the EC had changed into its reaction products mostly into mono-nitro-EC. Studying chemical changes of EC stable propellants before and after heating, there were determined differences in EC concentrations in the range 0.2–0.8% (m/m). As in single-base propellants, the dynamics of stabilizer changes in double-base propellants, both under natural and accelerated ageing varies up to ten times under the same conditions of ageing. It means, that the quality, especially of basic components of the propellants, has greater influence on their decomposition than the 'age'. The use of TLC methods to determine the stabilizers and their reaction products in the propellants seems to be suitable and reliable.

Conclusions

There are a large set of analytical needs connected with the analysis of explosives. The importance of this problem can be appreciated by looking at the statistics on recent bombings in the world. Besides the tasks mentioned above, there is a need for vehicles or mail screening, bomb search, protection of special infrastructure features, and so on. Of course, not all analysis can be performed using TLC.

In the history of TLC for analysis of explosives the 1960s and 1970s was a time of very intensive use. The development of modern analytical methods has caused a decrease in interest in TLC. An increase of interest in TLC, as applied to the analysis of explosives,

can be observed in the 1990s and is connected with the intensive development of the method.

TLC, like all other chromatographic techniques, is a comparative method. It is impossible to obtain information about the structure or identification of unknown compounds or mixtures. In such cases there exists the possibility of combining TLC with other, mainly spectroscopic, analytical techniques (e.g. TLC-MS). Such combinations will probably start widening the application of TLC in the analysis of explosives.

See also: II/Chromatography: Thin-layer (Planar): Densitometry and Image Analysis; Instrumentation; Layers; Mass Spectrometry; Modes of Development: Conventional; Preparative Thin-layer (Planar) Chromatography; Spray Reagents; **Extraction:** Solvent Based Separation; Solid-Phase Extraction. III/Explosives: Gas Chromatography; Liquid Chromatography. **Humic Substances:** Liquid Chromatography.

Further Reading

- Błażek J, Miszczak M and Śliwakowski M (1993) Application of liquid-crystalline detectors to the quantitation of propellant's stabilizers by thin layer chromatography. *Chemical Analysis*, 38: 339.
- Błażek J, Papliński A, Neffe S, and Rostkowski A (1998) Application of TLC for Determination of High Explosive Residues in Water and Soil Samples. *Chemical Analysis*, 43:711.
- Crockett AB, Jenkins TF, Craig HD and Sisk WE (1998) *Overview of On-Site Analytical Methods for Explosives in Soil*. US Army Corps of Engineers. Cold Regions Research and Engineering Laboratory. Special Report 98: 4.
- Hass R and Stork G (1989) Konzept zur Untersuchung von Rüstungsaltslasten. 1. Untersuchung chemaliger TNT-Fabriken und Füllstellen. *Fresenius Z. Analytical Chemistry* 335: 839.
- Kirchner JG (1978) *Thin Layer Chromatography*. Chichester: John Wiley & Sons.
- Nam SI (1997) *On-Site Analysis of Explosives in Soil: Evaluation of Thin Layer Chromatography for Confirmation of Analyte Identity*. US Army Corps of Engineers. Cold Regions Research and Engineering Laboratory. Special Report 97: 21.

- Steuckart C, Berger-Preiss E and Levsen K (1994) Determination of explosives and their biodegradation products in contaminated soil and water from former ammunition plants by automated multiple development high-performance thin-layer chromatography. *Analytical Chemistry* 66: 2570.
- Yinon J and Zitrin S (1981). *The Analysis of Explosives*. Oxford: Pergamon Press.
- Yinon J and Zitrin S (1993). *Modern Methods and Applications in Analysis of Explosives*. Chichester: John Wiley & Sons.
- York H, Funk W, Fischer W and Wimmer H (1994) *Thin Layer Chromatography: Reagents and Detection Methods – Physical and Chemical Detection Methods: Fundamentals. Reagent 1*. Volume 1a. Weinheim: VCH.
- York H, Funk W, Fischer W and Wimmer H (1994) *Thin Layer Chromatography: Reagents and Detection Methods – Physical and Chemical Detection Methods: Activation Reactions, Reagent Sequences, Reagents II*. Volume 1b. Weinheim: VCH.

EXTRACTION: PRESSURIZED FLUID EXTRACTION

See **III / ENVIRONMENTAL APPLICATIONS: Pressurized Fluid Extraction;**
PRESSURIZED FLUID EXTRACTION: NON-ENVIRONMENTAL APPLICATIONS

FATS



Crystallization

K. Sato, Hiroshima University, Higashi-Hiroshima, Japan

Copyright © 2000 Academic Press

Introduction

Fats, as mostly represented by triacylglycerols, are employed in foods, cosmetics, pharmaceuticals, etc. as the main bodies of end products, or as the matrices in which fine chemicals are dispersed. The crystallization behaviour of fats has two major industrial implications: (a) processing of the end products made of fat crystals, such as chocolate, margarine and shortening, whipping cream, etc. and (b) separation of specific fats and lipids materials from natural resources, mostly from vegetable or animal fats and oils, which contain various molecular species having different chemical and physical properties. As for the separation technology of crude fat resources, such as palm oil, milk fats, hydrogenated vegetable oils, etc. it may be worth noting that current market demands raise a great necessity to develop the fractionation of high-melting and low-melting fats and lipids through dry fractionation. The main causes for this are the replacement of hydrogenation by dry fractionation, a new regulation of usage of fat materials for confectionery fats, better functionality of physically refined

vegetable oils compared to conventional materials, etc. This review highlights the basic information on recent research on the crystallization of fats, with a specific emphasis on the separation phenomena.

The specific characteristics of the crystallization of fats are, on the one hand, polymorphism, and molecular interactions on the other. No long-chain compound without polymorphic modifications is present, and this property is more enhanced in triacylglycerol (TAG) crystals. The molecular interactions in TAG crystals are operative mostly through van der Waals forces between hydrophobic aliphatic chains, in which geometrical and steric hindrance is critical between the glycerol groups.

Polymorphism in Fats

Polymorphism is defined as the ability for a chemical compound to form different crystalline or mesophase (liquid crystalline) structures. The melting and crystallization behaviour differs from one polymorph to others, since the different crystal structures correspond to different Gibbs energies.

Polymorphic crystallization is primarily determined by the rate of nucleation, as determined by thermodynamic and kinetic factors. If the first crystallizing form is less stable, it converts to more stable polymorphs through the solid matrix or liquid mediation. As a consequence, morphology of fat crystals is a function of the crystal structure itself, and the thermal processes of the crystallization and sub-

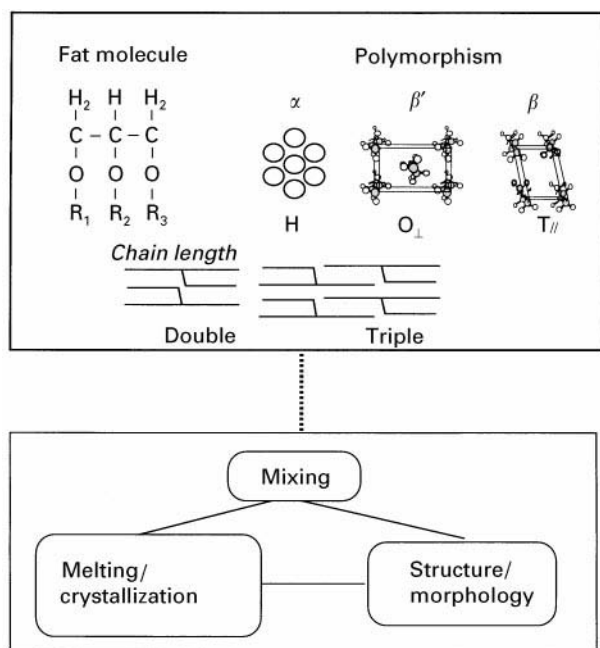


Figure 1 Relationship of molecular properties of fat crystals and macroscopic physical properties of fats.

sequent transformation. The interrelationships among fat molecule structures, polymorphic crystal-line structures, phase behaviour of the mixing of different fats and other ingredients, melting and solidification, and transformation and crystal morphology are illustrated in Figure 1.

Molecule Structures and Polymorphism of Fats

This section briefly describes the molecular structural properties of fat polymorphs.

Typically, three polymorphs, α , β' and β , are usually observed in TAG crystals. However, two or even three more forms are present in TAGs if their fatty acid structures are rather complicated, in the sense that the three fatty acid moieties (R_1 , R_2 and R_3 in Figure 1) differ in their chemical structures (length, saturated/unsaturated, even-chain or odd-chain, etc.). The three forms are basically characterized by the lateral chain packing mode, expressed in subcell structures: hexagonal (H) packing for α , orthorhombic perpendicular (O_{\perp}) packing for β' , and triclinic parallel (T_{\parallel}) packing for β . Since the lateral packing mostly determines the crystalline density, it follows that α is the least dense packing, β' intermediate and β the densest packing. As for the chain length structure, the double chain length is revealed in the TAGs containing similar types of three fatty acid moieties, and, by contrast, the triple chain length structures are revealed in the TAGs where one or two of the fatty acid moieties are largely different in their shapes from the others.

Polymorphism and Macroscopic Physical Properties

The microscopic properties of the fat polymorphs eventually result in complex macroscopic physical properties of mixing, melting/crystallization and the structure/morphology of the crystallized materials. In particular, the rate of crystallization and the crystal morphology are directly influenced by polymorphism.

Mixing of fats The mixing properties of different TAG materials, is highly relevant in fat materials, because many fats present in real systems are multi-component in two ways: (a) a fat phase containing many different types of TAGs and (b) each TAG molecule involving different types of fatty acid moieties, namely mixed-acid TAGs. Three typical phases occur in binary solid mixtures, when the two components are miscible in all proportions in a liquid state: solid solution phase, eutectic phase, and compound formation. The general tendency in the relationship between the molecular interactions and the phase behaviour may be summarized as follows: structural affinity results in solid solutions, poor interactions form eutectic phases and specific interactions give rise to molecular compounds.

In addition, polymorphism makes the mixing behaviour more complicated. For example, in the mixture of mono-saturated acid TAGs, a eutectic phase with a limited region of solid solution is the stable form when the chain length difference is no larger than two carbon atoms. However, metastable forms of α and β' exhibit solid solution phases. Furthermore, the chain length structure also affects the mixing behaviour, even if the polymorphic properties are similar between the component TAGs: for example, the double chain length and triple chain length structures are not miscible with each other.

As for the formation of compound systems, compound formation occurs in particular sets of TAG mixtures, in such mixtures as SOS/SSO (1,2-distearoyl-3-oleoylglycerol) and POP/OPO (P = palmitoyl), where the compound is formed at a concentration ratio around 1 : 1. The mixing behaviour and the crystallization properties in binary fat mixtures will be discussed in a later section.

Melting behaviour The melting behaviour in relation to fatty acid composition of TAGs is straightforward: the longer the fatty acid chain, the higher the melting point, and saturated-acid TAGs have higher melting points than unsaturated fatty acid TAGs. The next concern is the effects of polymorphism of fats (which are mostly of a monotropic nature) on the melting and crystallization behaviour. As an example, we take three polymorphic forms of

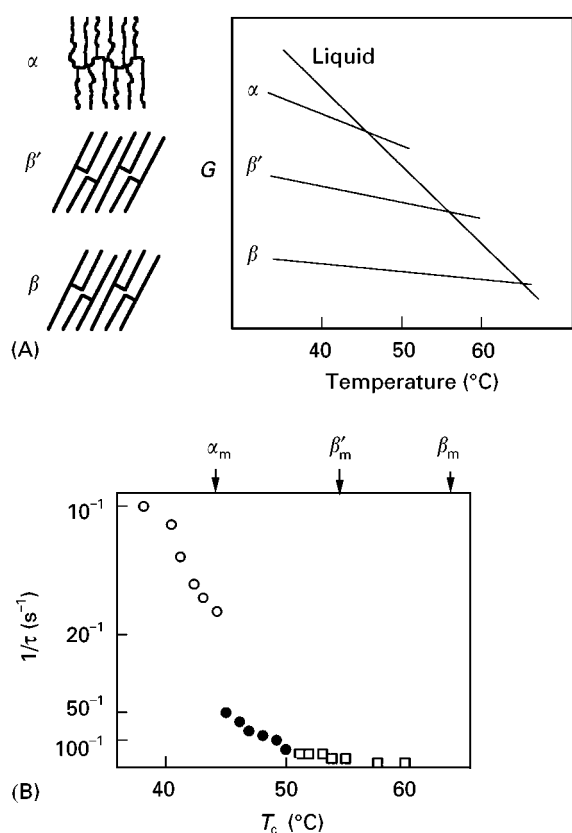


Figure 2 (A) Structure models and Gibbs energy (G)-temperature (T) relationship of three polymorphs of PPP, and (B) rate of nucleation of PPP polymorphs. \circ , α form; \bullet , β' form; \square , β form. T_c , crystallization temperature.

tripalmitoylglycerol (PPP), whose structural and crystallization properties have been well elucidated, as illustrated in Figure 2.

Figure 2(A) shows α , β' and β forms of PPP. Molecular structures of the three forms are briefly specified by the following: disordered conformation in α , intermediate packing in β' and most dense packing in β . Therefore, the Gibbs free energy (G) values are highest in α , intermediate in β' and lowest in β , resulting in the lowest melting temperature for α , etc. As a result of the combined effects of the molecular structures and the rate of crystallization, the crystal morphology is of amorphous irregularity for α , tiny bulky shape for β' and needle shape for β .

The polymorphic properties of PPP are basically common to those in the other fats. However, more complexity is revealed when the fatty acid compositions of the three moieties become heterogeneous, in particular for TAGs involving saturated and unsaturated fatty acid moieties as present in many vegetable fats.

Structure and morphology The crystal structures as determined by X-ray analysis using single crystals, are

unique for the specific polymorph of a specific TAG. The morphology of crystals, however, is a result of combined interactions of the crystal structure itself, and rate of crystal growth of the specific crystalline faces which are influenced by the growth conditions. For simplicity, however, it may safely be referred to the polymorph-dependent crystal morphology; α reveals irregular shaped tiny crystals, β' bulky-shaped tiny crystals, and β lozenge-shaped needle crystals.

Polymorphic Crystallization

Polymorphic crystallization is primarily determined by the rate of nucleation, being governed by thermodynamic and kinetic factors. A primary concern is the polymorphic nucleation, in which the so-called Ostwald step rule is of great interest. This predicts that a phase change may occur step by step by way of successively more stable phases. Thus, the metastable forms nucleate first, prior to the most stable form, when nucleation is induced under large kinetic factors, e.g. supercooling or supersaturation. When the kinetic factors are minimized, the step rule is broken, and the more stable forms are nucleated at very reduced rates.

This tendency was confirmed in the crystallization of three forms of PPP. For PPP, induction time (τ), the time until the occurrence of the first-appearing crystals are detectable, is shortest for α , intermediate for β' and longest for β as shown in Figure 2(B) for the case of simple cooling of the liquid. However, when the temperature of cooling fluctuates around the melting points of α or β' , the nucleation of more stable forms is markedly accelerated, because of melt-mediated crystallization.

Melt-mediated nucleation is ascribed to the monotropic nature of polymorphism, as revealed in the following processes: (a) melting of the less stable form, (b) nucleation and growth of more stable forms, and (c) mass transfer in the liquid formed by melting of the less stable form. It often occurs that the rate of melt-mediated transformation is considerably higher than the rates of crystallization of the stable polymorph without passage through metastable forms. Dynamic X-ray diffraction studied using synchrotron radiation (SR-XRD) has enabled *in situ* observation of the melt-mediated transformation over a time scale of tens of seconds.

In regard to the SR-XRD studies, deeper insights of the polymorphic crystallization have been unveiled by the time-resolved analyses of the crystallization from neat liquid. The result has shown that: (a) the formation of lamella ordering, both for double or triple chain length structures occurs more rapidly

than that of the subcell packing; (b) the rate of the α - β' melt-mediated transformation is remarkably high when the lamella structures of the pre-existing form (α) remains. So-called 'melt-memory effect', meaning the effect of solid structures present in the liquid phase, may be clarified by the time-resolved SR-XRD under temperature variation.

The control of the polymorphic crystallization may be affected by the addition of crystal seeding and the application of shear stresses. As to the former effect, it was found that specific molecular interactions between the crystal seed materials and the polymorphic forms of specific fats are a prerequisite for the seeding effect, in polymorphic correspondence, structural similarity and thermal stability. As a typical demonstration, a quite interesting seeding effect has been observed in cocoa butter crystallization, which has been applied to solidification control of chocolate production processes.

Cocoa butter has six polymorphs of form I through to VI, in which form V is the most desirable. For optimally obtaining form V in the solidification process, a tempering process is applied using the following temperature profile: first cooling the molten chocolate to 26–27°C, reheating to around 30°C, and subsequent cooling for bulk solidification. During the first cooling process, rapid crystallization causes the formation of unstable polymorphic forms of cocoa butter crystals due to Ostwald's Law of stages. The occurrence of the unstable forms are not favourable, because they cause poor moulding and induce fat bloom. Therefore, the first-cooled chocolate is heated to around 30°C, so that the unstable forms melt and quickly change to form V by the melt-mediated transition. After the tempering, chocolate is poured into a mould, and cooled for complete solidification.

The seed crystallization technique aims at achieving two major advantages, compared to the tempering technique: (a) it accelerates the crystallization of form V of cocoa butter, and (b) it does not use the cooling/heating process of tempering. For this purpose, a technique using BOB (1,3-dibehenoyl-2-*sn*-oleoylglycerol) β_2 polymorph has been developed.

Figure 3 shows the relative crystallization time (t_r) of seeded dark chocolate examined at 30°C. The crystallization time was measured with a rotational viscometer and t_r is defined as the ratio of the crystallization times with and without seeding. Figure 3 clearly shows that the stable form β_1 of SOS, which is a major component TAG in cocoa butter, is most effective, stable form β_2 of BOB is in-between and β of SSS is least effective. From this result, one may argue that there are three factors in the crystal seeding effect: (a) similarity in the crystal structure between the seed crystal and form V of cocoa butter, (b)

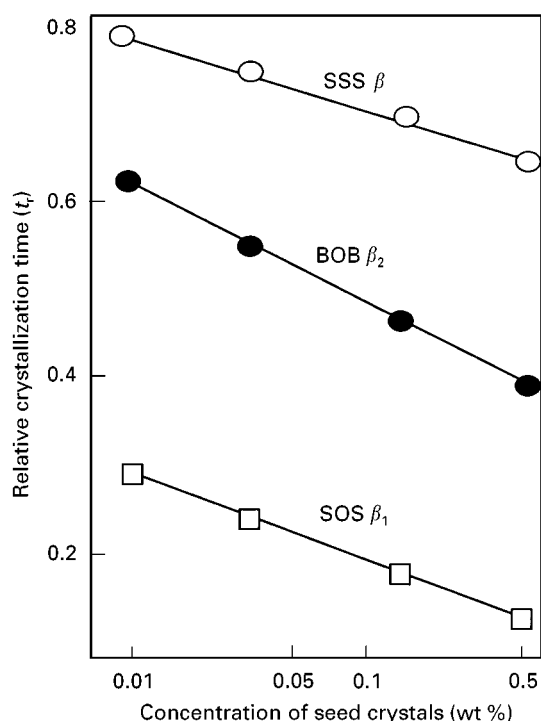


Figure 3 Relative crystallization time (t_r) of cocoa butter with the addition of three crystal seeding materials (SSS, tristearoylglycerol).

thermodynamic stability of the seed crystal, which is related to its solubility in the molten cocoa butter, and (c) the relationship of the acyl chain length of TAG between the seed material and cocoa butter. As to (a), it was shown that the β_2 of BOB or SOS and form V show identical structural properties to each other. However, the melting point of SOS β form, around 43°C, is too low for it to be put into molten cocoa butter at 30°C, and thereby no effect of crystal seeding is operative. As to the β form of SSS (tristearoyl-glycerol), its melting point, 70°C, is optimal as far as the thermodynamic stability is concerned. However, the molecular structural affinity between the β of SSS and β_2 of BOB is poorest, because of the difference in the chain length structure: double chain length for β of SSS and triple chain length for β_2 of BOB. Therefore, a final solution of the finest seeding material is the β_2 of BOB.

As to the shear effect, the newest finding of the shear stress application on cocoa butter crystallization indicates a by-passing effect to crystallize β -type polymorph (form V), which otherwise does not crystallize directly from the quenched liquid. A time-resolved SR-XRD spectra revealed the transformation from β' -type to β -type polymorphs during the initial stages of crystallization under shear stresses. The molecular mechanism for this conversion is not fully understood.

Phase Behaviour and Crystallization Kinetics in Binary Fat Mixtures

Fats present in natural sources are mixtures of different types of TAGs. Therefore, the complicated behaviour of melting, crystallization and transformation, morphology, etc. of real fat systems is partly due to the physical properties of the component TAGs, and partly or more importantly due to the phase behaviour of the mixtures. To resolve these complexities in mixed systems, a fundamental study has been made on binary and ternary mixtures of specific TAG components. Recent studies carried out on the phase behaviour and crystallization kinetics of the binary mixtures of principal TAGs, are given below.

In general, three typical phases may occur in binary solid mixtures, when the two components are miscible in all proportions in a liquid state: a solid solution phase, a eutectic phase and compound formation. For TAG mixtures, two factors are concurrently dominating: polymorphism and chain-chain interactions.

The polymorphic influence is clearly seen for the PPP-SSS mixture system, where the carbon numbers (n_c) of the fatty acid moieties of the two TAGs differ by two. Solid solutions are formed in the α and β' forms, yet the eutectic phase was formed in the most stable β form. This contrast is ascribed to the less condensed molecular packing in α and β' and to the most dense packing for β . It is reported, however, that the formation of the solid solution in the metastable forms is hindered when the difference in n_c between the component TAGs exceeds four, and that eutectic phases become predominant.

It has recently been found that the phenomena observed in the PPP-SSS mixture above does not simply apply to the mixtures of saturated-unsaturated mixed-acid TAGs such as POP-OPO, POP-PPO and many other similar mixtures, where O is oleic acid moiety, and PPO, for example, is a stereoisomer of POP where the fatty acids are connected to different glycerol carbon atoms. Despite the quite diversified phase behaviour exhibited in these combinations, one may make two important points: (a) steric hindrance between the saturated acid and oleic acid moieties induces the formation of eutectic phases for the α , β' and β polymorphs for the mixture of POP-PPP, and (b) attractive interactions through the saturated and oleic acid moieties cause the formation of molecular compound at a 50 : 50 concentration ratio of the two components. Quite interestingly, the chain length structure of the molecular compound is largely deformed from those of the component molecules, e.g. a triple chain length structure in POP and PPO, but a double chain length structure in the molecular compound of POP-PPO.

Therefore, the eutectic phase is revealed in the component and compound materials.

The formation of the molecular compound has two implications for the fat separation problems: firstly, no easy separation is possible by dry fractionation for the molecular-compound mixtures, and secondly polymorphic transformation is affected by the presence of the molecular compounds. More interestingly, the rate of nucleation of the molecular compound is much higher than those of the component TAGs.

The diverse properties in fat mixing behaviour, as illustrated above for a typical model substance, might also be revealed in natural fats having high melting fractions, such as palm oil, shea fats, etc. Therefore, for the purpose of the separation of the high-melting and low-melting fractions, it is pertinent to examine physical analyses of the mixing behaviour of the principal TAG components, as basic research on the one hand, and to extend the main results to more multi-component systems tightly mimicking real systems.

See Colour Plate 84.

See also: II/Crystallization: Melt Crystallization; Polymorphism; Control of Crystallizers and Dynamic Behaviour.

Further Reading

- Hachiya I, Koyano T and Sato K (1989) Seeding effects on solidification behavior of cocoa butter and dark chocolate. I. Kinetics of solidification. *Journal of the American Oil Chemists' Society* 66: 1757-1762.
- Hagemann JW (1988) Thermal behaviour and polymorphism of acylglycerols. In Garti N and Sato K (eds) *Crystallization and Polymorphism of Fats and Fatty Acids*, pp. 9-95. New York: Marcel Dekker.
- Hui YH (ed.) (1996) *Bailey's Industrial Oil and Fat Products*, Vol. 3, 5th edn. New York: John Wiley.
- Kellens M, Meeussen W, Riekel C and Reynaers H (1990) Time resolved X-ray diffraction studies of the polymorphic behaviour of tripalmitin using synchrotron radiation. *Chemistry and Physics of Lipids* 52: 79-98.
- Padley FD (1997) Chocolate and confectionery fats. In Gunstone FD and Padley FB (eds) *Lipid Technologies and Applications*, pp. 391-432. New York: Marcel Dekker.
- Sato K (1986) Polymorphism of pure triacylglycerols and natural fats. In Padley FD (ed.) *Advances in Applied Lipid Research*, pp. 213-268. London: Jai Press.
- Sato K and Kuroda T (1987) Kinetics of melt crystallization and transformation of tripalmitin polymorphs. *Journal of the American Oil Chemists' Society* 64: 124-127.
- Sato K, Ueno S and Yano J (1999) Molecular interactions and kinetic properties of fats. *Progress in Lipid Research* 38: 91-116.
- Ueno S, Minato A, Seto H, Amemiya Y and Sato K (1997) Synchrotron radiation X-ray diffraction study of liquid crystal formation and polymorphic crystallization of SOS (*sn*-1,3-distearoyl-2-oleoyl glycerol). *The Journal of Physical Chemistry B* 101: 6847-6854.

Extraction by Solvent Based Methods

E. J. Birch, University of Otago, Dunedin, New Zealand

Copyright © 2000 Academic Press

Along with proteins and carbohydrates, fats and oils make up the major classes of food components. Edible fat and oil usage falls into four major product categories: cooking and salad oils, shortenings, margarines and specialty products. Tissues from animals liberate oils on being boiled and oils can be pressed from fruits, vegetables and seeds, such as olives, soybean and sesame. Solvent extraction is a viable alternative to pressing and can recover nearly all the oil from the seeds. Figures for world production of fats and oils have only been kept since 1942 and, although growth in the use of fats and oils since then has outstripped population increases, there has been a significant shift from animal to vegetable fats. Table 1 shows the relative changes in world production figures for selected major fats and oils since 1935.

Traditional methods employing liquid extraction rely on the use of simple processing equipment and low pressure applications. They fall into two main categories of water flotation and traditional pestle and mortar extraction procedures. The water flotation method involves heating in water followed by size reduction (pestle and mortar-type equipment) and skimming off of the oil followed by heating to remove the moisture. Coconut and palm oil extraction efficiencies range from 40 to 60%, though free fatty acid contents are high. The Ghani mill (typically powered by animals) has been used in India for 3000 years and at the beginning of this century approximately 97% of oilseeds were processed this way, utilizing over half a million ghanis. This figure has dropped to 4% in modern times, owing to the introduction of screw and hydraulic presses, and solvent extraction.

The hydraulic press was invented by Joseph Bramah in 1795 and continued to be used in the American oilseed crushing industry until the 1940s. By then, new options were replacing the labour-intensive batch-processing presses, with expellers (continuous screw presses) and direct solvent extraction with the two unit operations often occurring together as a two-stage process. Mechanical expression can only reduce oilseed oil content to 2–3% whereas solvent extraction will reduce this figure to about 0.5%. Low temperatures during solvent extraction can produce a higher quality oil than higher temperature screw pressing but may also extract nontriglyceride material, making the oil inferior to pressed oil.

Solvent extraction of fats and oils from seeds became possible from the middle of the 19th century. In 1948 the first commercial solvent extraction plant was built. Since then, over 200 extractors have been supplied worldwide for capacities up to 6000 tons per day. Solvent processes found favour in the vegetable oilseed refining industry, with continuous miscella (solvent plus pressed cake) refining and continuous solvent fractionation (e.g. winterization) becoming commercial reality in the early 1950s.

Solvent Extraction Methodology

Extraction Theory

Solvent extraction is usually used to recover a component from either a solid or liquid. The sample is contacted with a solvent that will dissolve the solutes of interest. Solvent extraction is of major commercial importance to the chemical and biochemical industries, as it is often the most efficient method of separation of valuable products from complex feedstocks or reaction products. Some extraction techniques involve partition between two immiscible liquids; others involve either continuous extractions or batch extraction of solid. Because of environmental concerns, many common liquid-liquid processes have been modified either to utilize benign solvents, or replaced by processes such as solid-phase extraction. The solvent can be a vapour, supercritical fluid or liquid, and the sample can be a gas, liquid or solid.

Table 1 World production of commercially important edible fats and oils

Fat/oil source	World production (MMT)			
	1935	1955	1975	1995
Soybean	0.5	2	8.5	16
Palm	0.5	1	2	14.5
Rapeseed (canola)	1.3	1.5	2	9.5
Butter	4	3.5	5.3	8
Sunflower	0.4	1.5	3.5	7.5
Tallow	1.7	3	5.5	7
Lard	3	3.5	4.2	5.5
Cottonseed	1.5	1.8	2.8	4.8
Peanut	1.8	2	3.2	3.9
Coconut	1.7	2	2.5	3.3
Sesame	0.8	1	1.7	1.9
Fish	0.5	0.5	1.2	1.5
Olive	0.6	0.6	0.7	0.8
Total	18.3	23.9	43.1	84.2

MMT, million metric tons.

Fats and oils are hydrophobic and hence insoluble in polar solvents. Use is made of their affinity for nonpolar media in oil extraction, separation of oil from bleaching earths and oil-refining technology. Fatty acids accompanying oil extraction are also soluble in polar solvents and use can be made of this in refining methods to separate the two groups. However, difficulty is experienced in that fatty acids and other liquids may be more soluble in the oils themselves than in the selected separation solvent. Solubility covers a wide range and is influenced by a rise in temperature (which increases solubility) and an increase in chain length (lower solubility) of fatty acids making up the triglycerides.

Choice of Solvent

The ideal solvent for oil extraction must possess several features that are impossible to find in any one solvent. These properties include the ability to solubilize the oil at low temperatures, selectivity towards triglycerides, chemical inertness, immiscibility with water, nonflammable, low viscosity and surface tension, nonexplosive, noncaustic, low boiling point, nonirritant and nonpoisonous.

Hexane is the almost exclusively chosen solvent due to its solvent power, volatility, low and nontoxic residue levels and immiscibility with water. However, care in handling is required due to high flammability. Before hexane, carbon disulfide and trichloroethylene were used; however, the former has since been banned and the latter declared undesirable for preparing animal feeds. The greater solvency and nonflammability of trichloromethane renders it of use for extraction of tallow from meat and bone but, due to desolventizing problems, it is not used with oilseeds. Replacement with dichloromethane is an option but not favoured due to the risk of hydrochloric acid formation and the use of ethanol, either as a solvent or as an azeotrope with hexane, has been studied but not commercialized.

Recovery of solvent from the extraction of fats is a major consideration in solvent choice. The acceptable recovery standard is 99.92%, which can be represented by a loss of 1.135 litres of hexane per processed tonne of soya. Losses may occur from desolventizing the meal, from stripping the final oil product and from air and water discharges to waste. In the US the Environmental Protection Agency is charged with controlling emission levels with respect to hexane, although required levels are still to be set under the Federal Clean Air Act. A likely example for soybean processing is 0.2–0.25 kg for every 100 kg of beans processed. To date, the industry relies on self-regulation, required because of the high cost of lost solvent.

Supercritical fluids have been investigated since the last century, with the strongest commercial interest initially focusing on the use of supercritical toluene in petroleum and shale oil refining during the 1970s and latterly supercritical carbon dioxide for fats and oils. Carbon dioxide cannot be used as a simple substitute for organic solvents, however. Phosphatides (e.g. lecithin) are selected against compared with hexane when extracting vegetable and fish oils, for example. As a solvent, dense carbon dioxide tends to be selective for lower molecular weight lipophilic compounds. This can be utilized for partial fractionation of free fatty acids from triglycerides, decreasing cholesterol levels and increasing β -carotene content by selective control of solvent temperature and pressure to exploit differences in solubility, vapour pressure and molecular weight.

General Processes

The main disadvantage of solvent extraction is the high equipment cost and plants tend to be large, processing hundreds to thousands of tons per day. The extracted miscella (solution of solvent plus oil) contains fines, which need to be separated and well washed. Solvent and oil will also be held up in the solids (marc).

Pretreatment Before oil can be extracted from fruits and vegetables, the seeds must be prepared. Seed preparation for extraction involves cleaning, dehulling, cooking to denature proteins, adjusting moisture content to the right level and then crushing or rolling into particles or flakes of uniform size and thickness.

For solvent extraction, the optimum moisture level allows flaking of the seeds whilst minimizing crumbling. Ready penetration of the solvent is enhanced without blocking the extractor so that the miscella which forms can be easily separated from the cake.

Improving pretreatment of press-cakes allows a reduction in solvent-to-solids ratios and a reduction in solvent hold-up in the desolventization process. The French Enhanser Press is an extruder used to pelletize oil-bearing seeds or pre-press cake to provide an ideal medium for solvent extraction. As pellets discharge from the die plate of the Enhanser Press, they expand and flash off moisture. This creates dense pellets with a vast matrix of open-structured, internal solvent passages. These pellets yield much better extraction results than flakes or pre-press cake. This results in savings in distillation energy (steam required).

Extraction The extraction operation typically follows a countercurrent flow process where the solids move in the opposite direction to the solvent-oil

miscella, which meets the oil-rich flakes at high oil concentration. The flakes are sequentially extracted with solvent of lesser oil content through the different stages until the almost entirely extracted meal is finally met with pure solvent to complete the extraction efficiently. The first miscella wash leaves the system for distillation and oil recovery while the final extracted flakes go to a desolventizing process.

Batch extractors. The process involves sequential washing of oil-bearing material with progressively leaner miscellas until the final wash is with solvent alone. The vessels are loaded one at a time and are no longer used for any other than specialty runs.

Total immersion extractors. The material to be processed travels through a pool of solvent. These are early designs (1930–1950s) and suffered from excess fines carried along in the solvent.

Percolation extractors. These may be either batch or continuous and differ from the immersion extractor in that the solvent passes through the solids, dissolving out the oil. Five main types are in use: basket, rotary, perforated belt, sliding-bed and rectangular loop extractors.

Combined plants. Percolation and immersion extraction may be combined sequentially to advantage (e.g. C.M.B. Percolimm). Flaked seed, which has been percolation-extracted, is immersion-extracted and then desolventized. The immersion miscella is used as a solvent in the percolation extractor for the original seed flakes. The extractors are of two main types: deep- or shallow-bed. The deep-bed-type (or rotary extractor) is semi-continuous with a number of baskets supported on a drainage screen, designed to allow the miscella to pass. The screens can be rotating or fixed, as can the baskets and washing manifolds. The extractor moves slowly and miscella drains through the screen until the basket reaches the final position when the solids are released, the screen reclosed and a fresh load of solids deposited. The shallow-bed-type

works similarly for drainage of miscella and operates in continuous mode where the flakes meet solvent in a countercurrent direction in different zones of the extractor. The percolation extractor employs solvent being pumped over and percolating down through a bed of flakes or a cake and leaving via a perforated plate at the bottom. Immersion extractors are claimed to allow better extraction from fine cake particles, which may block the bed of a percolation extractor. Examples of immersion and percolation extractors are shown in Figures 1 and 2.

Desolventizing The extracted flake material may contain 25–35% residual solvent. In the desolventizer/toaster, steam is used to evaporate the volatile solvent countercurrently. The vapour phase is condensed and collected. The meal is toasted in steam-jacketed trays, then dried and cooled. For edible flour, the process may be replaced with a flash desolventizing system.

Solvent stripping of the extracted oil is carried out by evaporation. Removal of flavour components is likely at this stage also. The miscella is normally separated into oil and vapour through a series of falling film evaporators and stills with the miscella on the tube side and the vapours on the shell side. The first-effect evaporator uses steam and solvent vapour from the desolventizer/toaster to concentrate the miscella to about 80% oil content. The second stage operates atmospherically or under vacuum to bring the concentration up to 95–98% oil, and the remaining volatiles are stripped in the still operating under vacuum. Refinements to the process are used depending on the oil being extracted. For cottonseed oil, caustic may be added during the first- and second-effect evaporators and the mix centrifuged to remove colour bodies before they set during distillation.

Recovery of the solvent from immersion extractors traditionally took place in a series of interconnected cylindrical vessels where the marc progressed by dropping from one vessel to the next in a zigzag fashion. These early models were often named schneckens (winding staircase) desolventizers. With

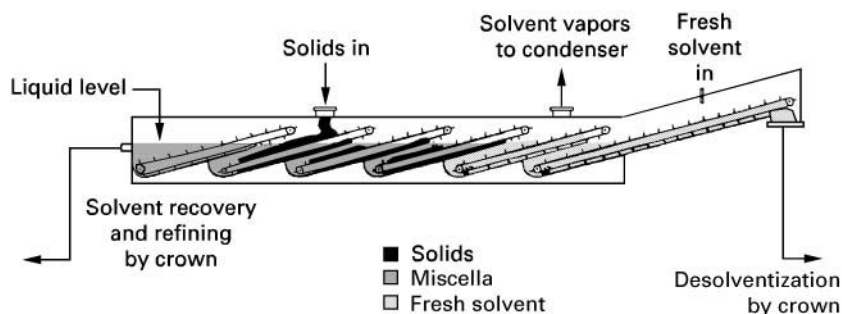


Figure 1 Oil solvent extraction apparatus (immersion type). Courtesy of Europa Crown Ltd., Hessle, UK.

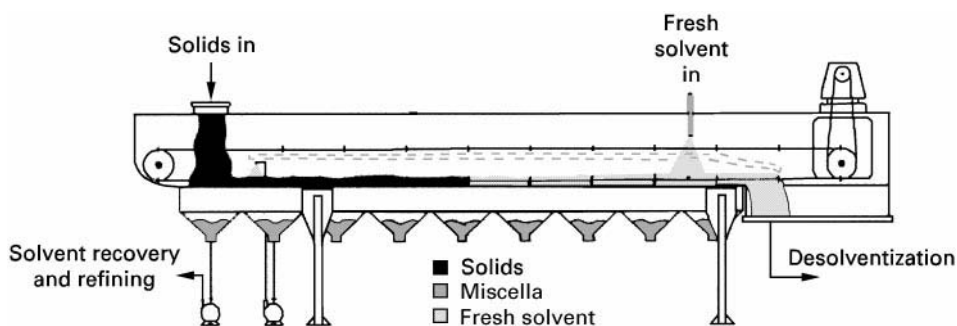


Figure 2 Oil solvent extraction apparatus (percolation type). Courtesy of Europa Crown Ltd., Hesse, UK.

the advent of percolation extractors, the desolventizer/toaster appeared in the 1950s. This consists of an upright cylinder divided into horizontal sections or trays. Material is agitated via a sweep arm which also opens a door, allowing product to fall to the tray below. Heat is supplied to vaporize the solvent, which is flashed off the topmost trays with sparge steam, which also partially cooks (toasts) the solids. The sparge steam can be absorbed by the solids on condensing, which prevents carry-over of dust to the condenser. A variation to the basic models allows flash desolventizing, where recirculating steam under high velocity strips the solvent at low temperature to avoid denaturing the protein. Another variation is countercurrent desolventizer/toasters, where the steam is introduced at the bottom and travels through to the top to a steam-jacketed desolventizing tray, where indirect steam flashes off surface solvent. Flash desolventizers are used to prepare high nitrogen soy protein for meat analogues and the desolventizer/toasters recover solids as animal feed. In the solvent extraction industry, the term DTDC stands for desolventizing–toasting–drying–cooling. These four operations can be performed in a single DTDC machine, or split between two separate DT and DC machines. Both types of configurations have specific advantages which may make one or the other preferable in certain applications. **Figure 3** shows a DTDC system.

Solvent refining of fats and oils Fractionation using solvents involves forming a miscella of oil in the solvent, which is then cooled to produce crystallization. Filtration of the stearin fraction follows and both fractions are then heated to recover the solvent. The Bernardini process uses hexane as solvent and produces two stearin and one olein fractions. Acetone and 2-nitropropane have also been utilized as solvents. The process for palm oil involves cooling an equal mixture of oil and hexane to 30–33°C and pumping to the chiller where the mixture is held at 20°C, when crystallization begins. The cooled mass is

passed to a second vessel and the temperature reduced to 10°C. Filtration using rotary drums separates out the first stearin fraction and the oil plus solvent is carried through a further series of cooling steps at 7°C, 4°C and 2°C respectively. The second stearin fraction is then removed through drum filters. All three fractions are freed from solvent by distillation.

Beef tallow and hydrogenated vegetable oils can also be similarly doubly fractionated. The first stearin fraction can be used for shortenings, the second for confectionery butters and the third (or olein fraction) as a frying oil which is liquid at room temperature. Without solvent, the conventional dry fractionation yields a stearin fraction which contains too much entrained oil to be of use as a confectioner's hard butter.

Winterization is beneficial for rice bran oil where the oil is frequently cloudy at room temperature. Solvent winterization separates the high and low melting triglycerides. Solvents used include hexane, acetone and isopropyl acetate. Although fractional crystallization from miscella has had limited acceptance, it is potentially less labour-intensive than the conventional batch winterizing process with faster throughput and yields greater quantities of winterized oil. In addition, manufacturers could produce modified fats without the formation of *trans* isomers by fractionally crystallizing mixtures of vegetable and animal oils from miscella. Other options involve adaptation of the technology for continuous miscella hydrogenation and miscella bleaching employing silica gel to remove colour.

Solvent extraction of oils from used bleaching earths is a logical method of recovery but only for large volumes to make it economical. Enclosed filters allow hexane to extract the oil from the earth in several stages before recovery of oil by evaporation of the miscella. Chlorinated solvents are also effective solvents depending on the end use of the recovered oil. Supercritical fluids are being researched as a cheaper alternative.

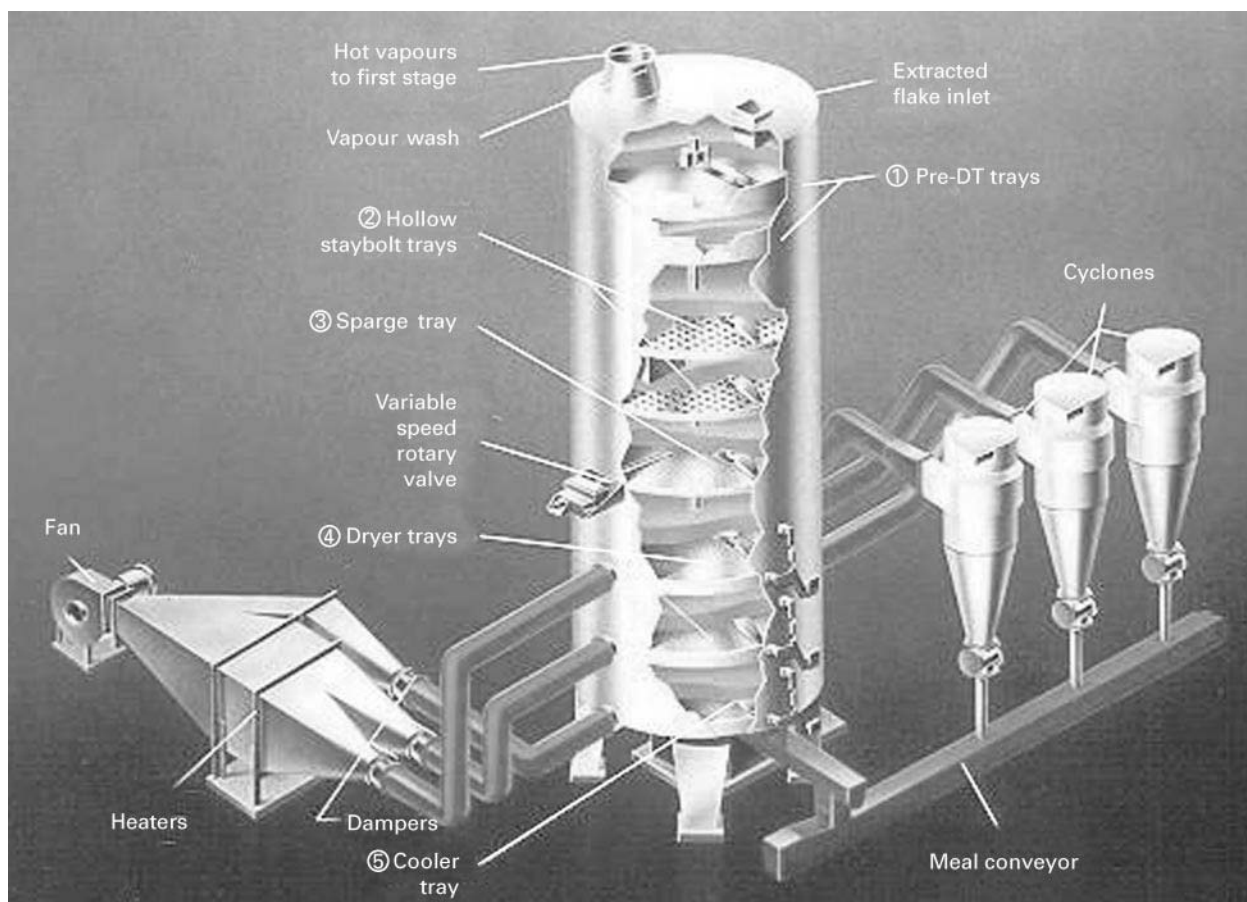


Figure 3 A desolventizing–toasting–drying–cooling system. Courtesy of Europa Crown Ltd., Hesse, UK.

Selected Applications in the Fats and Oils Processing Industry

Table 2 shows a range of applications arising from patents during the 1970s. Other examples include separation of fat-free protein and oil from peanuts, rice bran and soybean (hexane), cottonseed (hexane plus acetic acid), starch plus oil from corn grits, germ, hulls and gluten (hexane or isopropyl alcohol) and separation of beef tallow into five fractions with distinctive thermal characteristics by multistep crystallization. Direct solvent extraction is used for low content (<20%) oilseeds such as soya, rice bran and milled corn germ. Pre-pressing followed by solvent extraction is utilized with high oil content seeds, although some manufacturers claim high efficiency with direct methods.

Using water as a solvent for oil extraction has commercial applications for palm, olive and coconut oils but not for oilseeds due to high residual oil in the extracted meal and extra energy needed in the separation and drying steps. Adding enzymes to the aqueous medium to digest cell walls can be advantageous,

as in the development of processes to extract olive, canola and coconut oils. Hexane may also be added to aid the separation.

Isopropanol and ethanol were used to extract cottonseed oil since the combination made it possible to extract the gossypol and render the solids more suitable as animal feed. However the oil needs more refining due to phosphatides and carbohydrates which are also extracted.

Two-phase extraction employing polar and non-polar solvents has been successfully used in rapemeal processing. An extraction with methanol followed by washing with hexane and phase separation lowers the glucosinate content.

Soybeans

Soybean oil had very rapid growth to become the dominant edible oil in the world, partly due to the versatility of the oil which enables it to be used in a wide variety of products and applications.

Solvent extraction is the preferential method for soybeans, the others being hydraulic pressing and expeller pressing. Soybeans form stable flakes,

Table 2 Patents issued for solvent extraction applications from 1973 to 1977

<i>Solvent system</i>	<i>Oil source</i>	<i>Equipment</i>	<i>Patent</i>
Hexane-ethanol (2-30%)	Soybean, cottonseed, safflower, sunflower, peanut, sesame	Countercurrent extraction, centrifugation, steam stripping	AE Staley
2-Propanol-H ₂ O ₂ (0.1-1.0%)	Oats	Soxhlet, centrifugation, evaporation	Du Pont
Hexane	Yeast powder	Continuous solvent extraction (Rotocel)	Simon-Rosedowns
Water (1 part) plus 2 parts acetone or ethyl alcohol-ethyl acetate-acetone (1 : 1 : 1) or ethyl alcohol-ethyl acetate-isopropyl ether (4 : 2 : 1)	Palm fruit, olives	Multistage countercurrent disintegrator-extractor basket centrifuge Buchner filter vacuum stripping	RA Gouche
Heptane, ethylene dichloride, trichlorethylene, perchlorethylene, hexane	Animals, fish, vegetables	Upward fluidized bed exchange, azeo-extraction	French Oil

unlike cottonseed, peanut and other high oil-bearing seeds, where meals need to be processed through slotted wall extruders before being solvent-extracted.

Palm

For extraction of palm oil it is common practice to use screw presses and not employ wet methods. Similarly, solvent fractionation processes are available for fractionation but the comparative operational cost of miscella crystallization and filtration restricts the process to production of 2-oleodipalmitin-rich fractions for use in cocoa butter substitutes. Yield of olein from the miscella is about 80%.

Canola (Rapeseed) and Sunflower

Canola and sunflower are high oil content seeds and are generally processed by a pre-press solvent extraction. This removes the oil from the seed in two steps, which maximizes oil yields while minimizing residual oil in the meal. The canola presscake, which yields approximately 60% oil, may be mechanically extruded to improve the solvent extraction process. The industry increasingly relies on DTDC equipment for desolventizing.

Animal Fats

Screw presses are the method of choice for most renderers, although some animal fats are solvent-extracted. Use of solvents such as acetone to remove unwanted components such as cholesterol from milk fat has proven effective. The potential for solvent residues in the product does not meet with regulatory or consumer approval, however, hence the solvent

extraction process is only applied for technical purposes.

Using an immersion system (e.g. Kurd), raw material from animal processing is first heated and broken into small pieces before being mixed with the solvent (usually perchlorethylene) in an autoclave. The miscella is drained and may be used again for a second extraction, when the solvent is evaporated and the solids returned to the extractor for desolventizing with steam. The solids, free of solvent, contain 40-60% water and are then dried and milled for meal. Continuous percolation plants may also be utilized (De Smet extractors). The raw material is broken up in a cooking step and excess tallow drips through a perforated plate, leaving the residue with 30-35% fat. This is ground and extracted (usually with hexane) in a similar fashion to the system described for immersion extractors earlier and the solvent separated from the miscella by evaporation. The solids are toasted to desolventize them.

Solvent extraction may be combined with press extraction, either by using solvent techniques for further oil recovery after pressing or by pressing miscella out of the solid residue rather than recovery by decantation. These options reduce the amount of solvent that has to be removed, lowering cost and saving energy.

Fish Oils

Conventional fish oil extraction requires relatively high temperatures and solvent extraction can provide a low temperature alternative, but solvent choice is limited to food grade-approved cases. The use of alcohol, an approved solvent, has proven uneconomical due to poor extraction efficiencies. Supercritical

carbon dioxide extraction is considered safe but, although the product is of good quality, possible removal of antioxidants, such as tocopherols and phospholipids, and the retention of residual trace components is of concern.

Cottonseed

Cottonseeds contain about 30% oil. Screw pressing is commonly used for cottonseed oil pressing, but direct solvent (hexane) extraction yields 11.5% more oil, leaving less than 1% in the meal. Pre-pressing followed by solvent extraction is the most economical alternative due to the cost of solvent. Refining is necessary to remove the gossypol and related pigments.

Safflower

Oil extraction in the safflower industry has shifted from a largely screw press expeller base to less costly expander-extruders which are capable of extracting two-thirds of the oil and preparing collets ideal for solvent extraction. Solvent is able to move naturally through the fibre channels and the bed acts as a natural filter medium.

Coconut

Copra is processed using a dry process comprising crushing or expelling and optional further solvent extraction to recover the residual oil. This contrasts with the wet method for the fresh kernel which separates oil from the coconut milk by centrifugation.

Olives

Solvent recovery of oil from olives is limited to pomace processing. Superior olive oil is produced by pressing. The solvent extracts minor components at higher levels than physical methods and requires refining before use.

Cocoa Butter

Cocoa beans possess a chocolate aroma which develops during roasting of the beans. However, this aroma is lost if solvent extraction is employed during processing. The yield of cocoa butter is higher but the value may be less if the odour is desired.

The major triglyceride found in cocoa butter is 2-oleopalmitostearin. Cocoa butter substitutes can be manufactured using solvent systems based on methanol and hexane to prepare this triglyceride via isolation of saturated 1,3-diglycerides from the reaction of palm oil (hydrogenated soybean or cottonseed oils have also been employed) and glycerine using sodium methoxide catalysts. The isolated diglycerides are

then reacted with oleic anhydride to give the 2-oleo-disaturated product.

Recent Developments

Advances in solvent extraction technology have involved the areas of energy conservation, influences of increasing size of extraction plants, adaptation of conventional extraction plants to produce edible meals, percolation versus immersion extractors and direct solvent extraction versus pre-pressing followed by solvent extraction.

Commercial developments are attractive for alternative or specialty oils compared with traditional oil products and for overcoming the costs and constraints of traditional solvent extraction systems for minimizing industrial wastes. Utilization of vapour contactors to conserve heat during processing and dual-stage stripping columns in removing the last traces of solvent from the oil also contribute to efficiency.

The biggest interest in the last decade has been the applications of supercritical carbon dioxide, because it has a near-ambient critical temperature (31°C), thus biological materials can be processed at temperatures around 35°C. The density of the supercritical CO₂ at around 200 bar pressure is close to that of hexane, and the solvation characteristics are also similar to hexane, thus it acts as a nonpolar solvent. Around the supercritical region, CO₂ can dissolve triglycerides at concentrations up to 1% mass. The major advantage is that a small reduction in temperature, or a slightly larger reduction in pressure, will result in almost all of the solute precipitating out as the supercritical conditions are changed or made subcritical. Supercritical fluids can produce a product with no solvent residues. A wide range of fats and oils have been extracted employing supercritical fluid extraction from sources including fish, vegetable oils, nuts, cereals, citrus peel, egg yolk, wormwood and yeast extract. Examples of pilot and production-scale products include decaffeinated coffee, cholesterol-free butter, low fat meat, evening primrose oil and squalene from shark liver oil.

Processes for the selective extraction of fats and oils employing propane and a mixture of propane with up to 50% carbon dioxide in the subcritical state have been described (European patents 0-591-981, 1993 and 0-721-980, 1995) for the extraction of fats and oils from vegetable, animal and microbial materials. The low pressures involved allow milder extraction conditions than conventional processing, providing a good yield of high grade products.

See also: **II/Extraction:** Supercritical Fluid Extraction. **III/Food Technology:** Supercritical Fluid Extraction.

Further Reading

- Achaya KT (1994) Ghani: a traditional method of oil processing in India. *Food, Nutrition and Agriculture* 4(11): 23.
- Bockisch M (1998) *Fats and Oils Handbook*. Illinois: AOCS Press.
- Cavanagh GC (1997) Looking back: AOCS and vegetable oil processing. *Inform* 8(7): 762.
- Davie J and Vincent L (1980) Extraction of vegetable oils and fats. In: Hamilton RJ and Bhati A (eds) *Fats and Oils: Chemistry and Technology*, p. 217. London: Applied Science Publishers.
- Gunstone FD (ed.) (1987) *Palm Oil. Critical Reports in Applied Chemistry*, vol. 15. New York: Society of Chemical Industry/Wiley.
- Gutcho M (ed.) (1979) *Edible Oils and Fats: Recent Developments. Food Technology Review* No. 49. New Jersey: Noyes Data Corporation.
- Head S and Sweeten T (1999) Traditional methods for processing oilseeds. *Inform* 10(2): 151.
- Keeper TG (1996) Minimising solvent loss. *Grasas-y-Aceites* 6(24): 373.
- Palmer MV and Ting SST (1995) Applications for supercritical fluid technology in food processing. *Food Chemistry* 52: 345.
- Uh YH (ed.) (1996) *Bailey's Industrial Oil and Fat Products*, 5th edn, vols 1–5. New York: Wiley.
- Weiss TJ (ed.) (1983) *Food Oils and their Uses*, 2nd edn. Westport, CT: AVI.

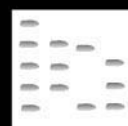
SUPERCritical FLUID CHROMATOGRAPHY

See III / OILS, FATS AND WAXES: SUPERCRITICAL FLUID CHROMATOGRAPHY

FATTY ACIDS: GAS CHROMATOGRAPHY

See III / LIPIDS: Gas Chromatography

FLAME IONIZATION DETECTION: THIN-LAYER (PLANAR) CHROMATOGRAPHY



R. G. Ackman, Canadian Institute of Fisheries,
Halifax, Nova Scotia, Canada

Copyright © 2000 Academic Press

The Iatroscan is a British invention brought to fruition in Japan by Iatron Laboratories of Tokyo, which is basically a hospital equipment company. It has become unexpectedly popular in such diverse analytical areas as marine lipids and heavy petroleum fractions. The combination of the resolving power of thin-layer chromatography (TLC), itself only somewhat more than 40 years old, with the simplicity and sensitivity of the hydrogen flame ionization detector (FID), developed about that time as a superb detector for gas-liquid chromatography (GC), was a happy marriage, usually summarized as TLC-FID. The basic separation technology of the Chromarod-SIII is conducted on a quartz rod 0.9 mm in diameter and 152 mm in length, coated with 75 μ m thickness of

silica gel (10 μ m particles) held in place by a soft glass frit. Ten Chromarods are conveniently held in a stainless steel rack for application of samples and subsequent development in a covered solvent tank, exactly as for planar TLC. The removal of solvent takes only a few minutes and the rack can then be dropped into a holding frame in the Iatroscan proper for scanning. This process can be controlled for maximum sensitivity but usually takes less than 10 min.

A virtue of the 10 Chromarods is that 10 different samples can be quickly compared or any combination can be replicated or compared to calibration standards run at the same time. The basic mechanism for passing the rod through the flame is fully automated. In the popular Mark III Iatroscan, the frame holding the development rack of up to 10 Chromarods was inclined. This has been replaced in the Mark V unit (Figure 1) with a horizontal frame. In the Mark IV Iatroscan the TLC-FID principles remained the same



Figure 1 Top view of Mark V Iatroscan with horizontal rack holding 10 Chromarods in position for automatic scanning in the FID. The flame jet on the right is visible below the ion collector. The Chromarods pass between the two FID parts as the frame holding the development rack cycles for scanning. After each scan the frame moves sideways and returns between the Chromarods, bypassing the FID and moving sideways to start the next Chromarod. The right-hand rod is reflected in part of the ion collector.

but some improvements in quantitation of lipids were found in a new detector design, and that development led to an improved FID arrangement installed in the Mark V. It has not yet been rigorously evaluated for quantitation, for example in conjunction with hydrogenation of complex lipid extracts, but should be an improvement over the robust Mark III as regards quantitation.

General Considerations

GC and high performance liquid chromatography may frequently require an hour for each analysis. With several sets of Chromarods at hand, an analyst can conduct several types or sets of analyses per hour, since the development times (40–50 min) and scan times (~10 min) can overlap. Tanks with different solvent systems can be ready to participate in this

process. Generally, the Iatroscan has not found wide application in the food industry. The response of carbohydrates in the FID is low because of the high oxygen content of the molecules.

The first problem in taking up TLC-FID is that those familiar with planar TLC often think in mg, and must adapt to μg – usually not more than 20 μg total per Chromarod. The second is that the application of a few micrograms of nonvolatile material in 1 μl of solvent can be automated or manual, but always results in some band spreading at the point of application. Solvent focusing has been found to overcome this usually minor problem and to narrow the sample band mixtures prior to actual development. Usually the choice is of a poor solvent for the materials in question, and for focusing, a development of the solvent front of less than 1 cm is adequate. An example is presented in Figure 2.

It is rare to find any unburnt organic material after analysis but it is good practice to clean the silica gel Chromarods regularly overnight in strong sulfuric acid, rinsing thoroughly in water, and passing through the scan cycle prior to use. If the previous samples generate any residue problems, such as from the calcium, magnesium and zinc of phytic acid, it will show up in this conditioning scan.

Early Chromarods showed variations in thickness and polarity that were mostly overcome with the introduction of the machine-produced silica gel Chromarods S-III. Alumina rods are also available but the literature does not indicate their wide use. Although there is a tendency to regard many solids and liquids as nonvolatile, this can be a tricky subject. Polar groups such as those of fatty acids and esters



Figure 2 (A) Caffeine deposited on a Chromarod S-III from an aqueous solution and then developed and scanned. (B) Benefit of solvent focusing with methanol prior to development. (Reproduced with permission from Ackman RG and Heras H (1997) Recent applications of Iatroscan TLC-FID methodology. In McDonald RE and Mossoba MM (eds) *New Techniques and Applications in Lipid Analysis*, pp. 325–340. Champaign, IL: AOCS Press.

adhere to the silica gel quite well. Sterols are polar (R-OH) molecules of reasonably high molecular weight (387 for cholesterol), but the planar molecule may make hydrogen bonding difficult, and erratic calibration factors have been reported. It is assumed that the radiant heating of the approaching flame can sometimes vaporize part of the sterol band before it can be combusted to form ions. Squalene (molecular weight 411) had practically no binding capability and can lose half its apparent mass for similar reasons, but we have found that it is easily made less volatile and gives a full response if the Chromarod is exposed to iodine vapour for a few minutes prior to scanning.

The Chromarod-Iatroscan technology for analysis of nonvolatile materials is especially useful for high-molecular-weight polymeric oxygenated materials such as are found in oxidized oils. These are usually not easy to move along the Chromarod with developing solvents, whereas simple dimeric and trimeric triacylglycerols can be resolved by development. With the use of a nitrogen-specific attachment, the FID has greatly augmented sensitivity in the N-sensitive mode. This thermionic detector mode has long been available in GC, and is notoriously temperamental. It can extend TLC-FID into the selective analysis of many shellfish toxins, many of which contain a few atoms of nitrogen in very large molecules (e.g. mol. wt 301, $7 \times N$, for saxitoxin).

For brevity this review will focus on two materials, marine lipids and heavy hydrocarbon fractions, but the possibilities for analysing reasonably large molecules are almost unlimited.

Marine Lipids

The first installation of an Iatroscan in North America was in 1976 in a marine lipids laboratory. The resulting publications on analyses of various complex materials attracted much attention among lipid chemists and biochemists, leading to a special issue of the journal *Lipids* in August 1985. Lipids of individual small marine organisms could be analysed for the first time and the sensitivity enabled extraction of water-soluble lipids to be modified to collect and extract less sample, and thus conserve on solvent use. The Iatroscan was quickly adopted in many countries with marine research programmes.

It is not often recognized that many human body lipids, especially those of muscle, liver and the blood, have fatty acid compositions spanning the same range as are found in fish oils and lipids. The latter include all varieties of lipids found in ourselves and other animals, and can be good materials to train with. Some will be featured in the few following examples of separations as demonstrations. In fish muscle lipids the fatty acid extremes in all lipid classes are the relatively short chain myristic acid (14:0) and palmitic acid (16:0) on the one hand, and the long chain, highly unsaturated eicosapentaenoic acid (20:5n-3) and docosahexaenoic acid (22:6n-3) on the other hand. A superefficient separation is shown in **Figure 3**. In the A and B chromatograms the free fatty acids and sterol esters are split into two respective subclasses, one with 14:0 and 16:0 as the principal fatty acids and the other with 20:5 + 22:6 as the dominant fatty acids. After hydrogenation,

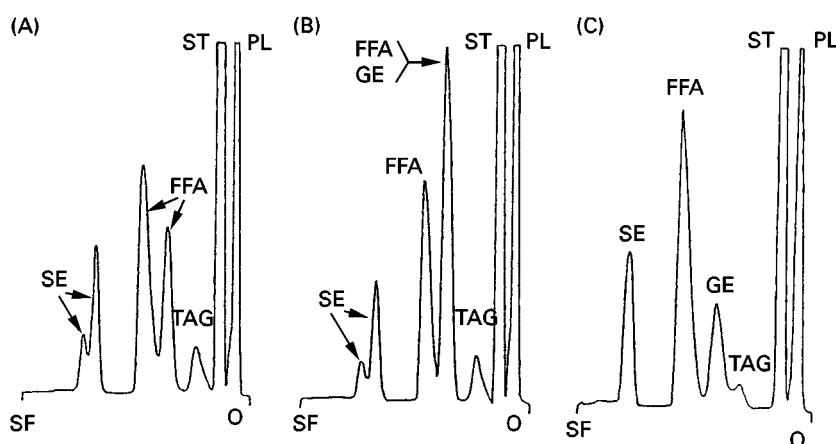


Figure 3 Iatroscan TLC-FID chromatograms of a fraction enriched with neutral lipids isolated from cod flesh lipids. (A) Neutral lipid (NL) fraction from cod flesh stored on ice for 3 days after being caught; (B) NL spiked with authentic 1-O-palmitoyl glyceryl ether dipalmitate (GE) coinciding with highly unsaturated free fatty acid; (C) Hydrogenated NL spiked with GE. Solvent system hexane:diethyl ether:formic acid; 97:3:1. FFA, Free fatty acid; PL, phospholipids; SE, steryl ester; SF, solvent front; ST, free sterol; TAG, triacylglycerol. (Reproduced with permission from Ohshima T, Ratnayake WMN and Ackman RG (1987) Cod lipids, solvent systems and the effect of fatty acid chain length and unsaturation on lipid class analysis by Iatroscan TLC-FID. *Journal of American Oil Chemists' Society* 64: 219–223.)

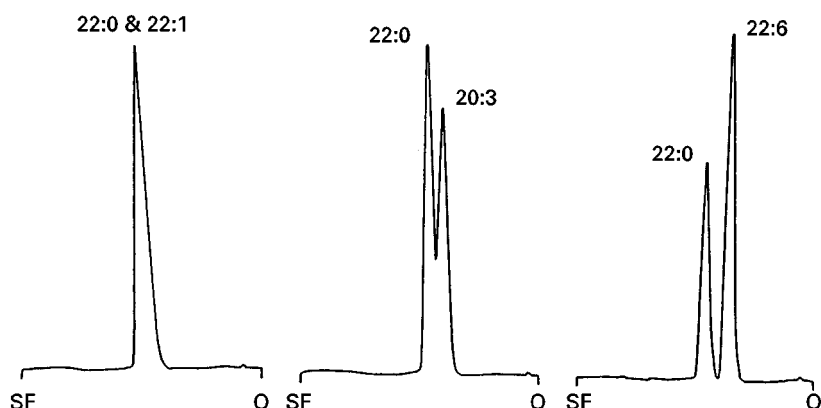


Figure 4 Iatroscan TLC-FID showing the effect of the degree of unsaturation on the separation of C_{22} free fatty acid standards on Chromarods-SII. Experimental conditions are development in hexane:diethyl ether:formic acid (97:3:1, v:v:v) for 40 min. O, Origin; SF, solvent front. Shorthand gives chain length and number of methylene interrupted ethylenic bonds.

chromatogram C shows that the pairs have collapsed into single peaks as the Chromarod behaviours of the resulting 14:0, 16:0, 20:0 and 22:0 are not very different. This is shown by the behaviours of selected sets of fatty acids and triacylglycerols (Figures 4 and 5).

Hydrogenation is not possible with many classes of organic compounds: it is not only feasible in analyses of lipid classes, but it has a unique advantage. The hydrogenated lipid fatty acids, unlike the natural highly unsaturated fatty acids, are stable to oxidation and can be studied and analysed at leisure, or with different solvent systems. Peaks are also sharper, improving sensitivity limits slightly.

For most simple lipid classes such as are found in vegetable oil products and mixtures, separation by lipid classes is facilitated by the fact that the common fatty acids are palmitic (16:0), stearic (18:0), oleic (18:1), linoleic (18:2n-6) and α -linolenic (18:3n-6). Except for palmitic acid, these are all identical in chain length (C_{18}), and the unsaturated acids differ

only in having the 1, 2 or 3 ethylenic bonds. Chromarods dipped in silver nitrate can resolve such mixtures as well as handle some types of *cis-trans* separations, but these simple vegetable lipid cases are usually best handled by GC.

It is possible to develop one or more classes of lipids along the Chromarod, while 'parking' the rest at or near the point of application, scanning partway down the Chromarod to determine the most mobile class, then redeveloping the balance of the material applied to whatever extent is desired into the clean space thus presented by the first scan. This means that multiple scans are always of the same original sample and conducted on the same Chromarod.

A good example of multiple development is provided by a lipid class analysis of the total lipids of the muscle of the fish silver hake (Figure 6). The actual separation of the lipid classes was conducted with a development sequence of three different solvent systems. The extracted lipids were dissolved in

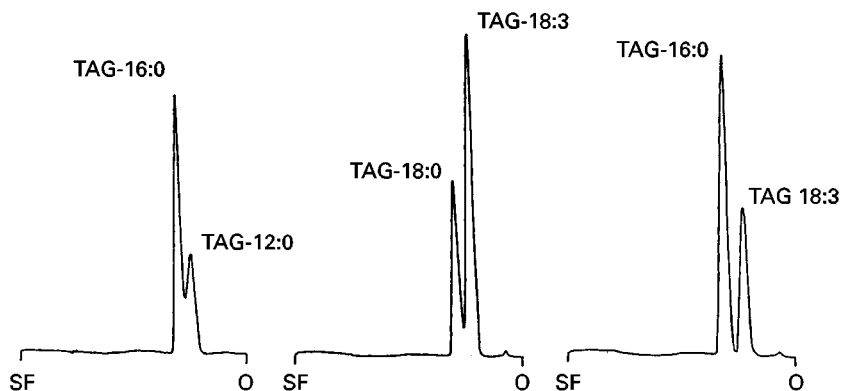


Figure 5 Iatroscan TLC-FID showing the effect of the degree of unsaturation and chain length on the separation of triacylglycerol standards on Chromarods-SII. Experimental conditions and abbreviations are the same as in Figure 4. TAG-16:0, tripalmitin; TAG-12:0, trilaurin; TAG-18:0, tristearin; TAG-18:3, trilinolenin. (Reproduced with permission from Ohshima T and Ackman RG (1991) New developments in Chromarod/Iatroscan TLC-FID: analysis of lipid class composition. *Journal of Planar Chromatography* 4: 27-34.)

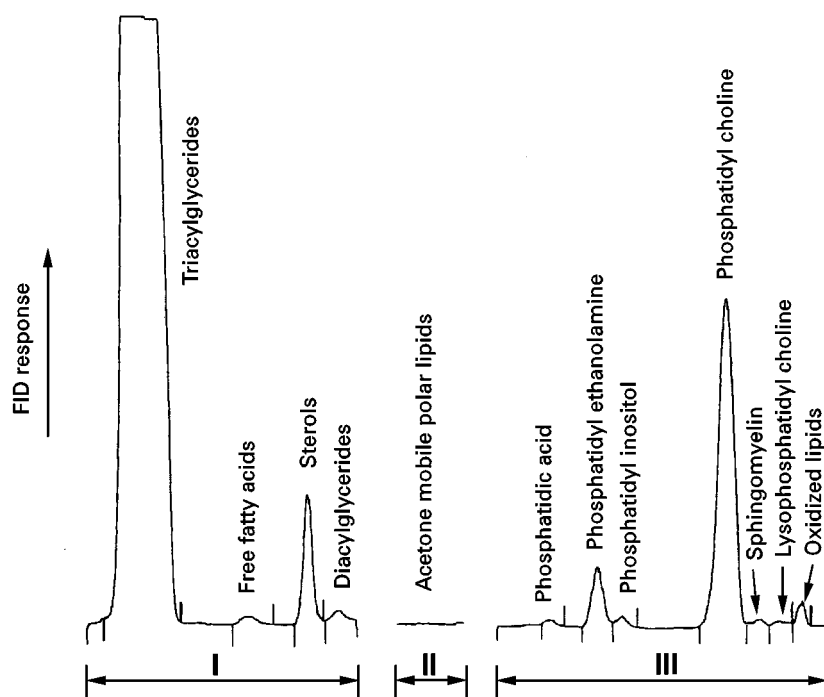


Figure 6 Sequential TLC-FID profiles of partial chromatograms of the lipid classes extracted from silver hake muscle tissue. I, II, and III represent the three-stage development sequence to separate total lipids on a silica gel Chromarod-SIII as described in the text. (Reproduced with permission from Zhou S and Ackman RG (1996) Interference of polar lipids with the alkali metric determination of free fatty acids in fish lipids. *Journal of the American Oil Chemists' Society* 73: 1019–1023.)

chloroform at an appropriate concentration, and this solution was then spotted on to Chromarods-SIII in 1 μ L volumes from glass Microcap 1 μ L disposable pipettes. The Chromarods were then conditioned in a constant humidity chamber for 5 min. The first development was carried out for 55 min in hexane:chloroform:propan-2-ol:formic acid; 80:14:1:0.2, by vol. The Chromarods were then dried at 100°C for 1.5 min and partially scanned from the top to a point just below the diacylglycerol peak (Figure 6I). The Chromarods were then redeveloped in acetone for 15 min, dried at 100°C for 1.5 min and partially scanned to below the acetone-mobile polar lipid position (Figure 6II). Finally, the Chromarods were again developed in chloroform:methanol:water (70:30:3, by volume) for 60 min, dried at 100°C for 3 min and completely scanned to reveal different phospholipids (Figure 6III).

In this example the free fatty acids are clearly separated from triacylglycerols. This is sometimes difficult to achieve in a single development of a mixture of animal lipids with one of the common lipid class solvent systems such as hexane:diethyl ether:formic acid 85:9:1 (by volume). The problem can be clarified by considering the free fatty acids as having a key position on the silica gel of the Chromarod, and adjusting the solvent polarity to

achieve relative movement of the rest of the neutral lipids, which usually develop in the order wax/sterol esters, triacylglycerols, cholesterol, and di- and monoacylglycerols, to positions where there is no conflict with the free fatty acids.

Solving such problems with TLC-FID may be compared with GC with only one column, and changes in temperature programming may be the only variable possible. With the Chromarod an unlimited choice of solvent systems is available and, when combined with scan and redevelopment, almost any lipid class separation is possible.

Figure 7 is of a commercial animal lipid mixture. The A chromatogram appears to show that the dominant triacylglycerol is accompanied by two peaks matching exactly 1,3-diacylglycerols and 1,2-diacylglycerols. This was considered to be an unusual composition. To verify it, hydrogenation of 10 mg of the sample (a simple process carried out by stirring in methanol:hexane : : 3:2 under hydrogen for 1 h, with a few mg of PtO₂), gave the materials of the B chromatogram. The triacylglycerol peak is sharper and the supposed 1,2-diacylglycerol is now added to the original 1,3-diacylglycerol peak. Clearly, the supposed 1,2-diacylglycerol component consisted of two highly unsaturated fatty acids, probably a mixture of arachidonic acid (20:4n-6) and docosahexaenoic acid

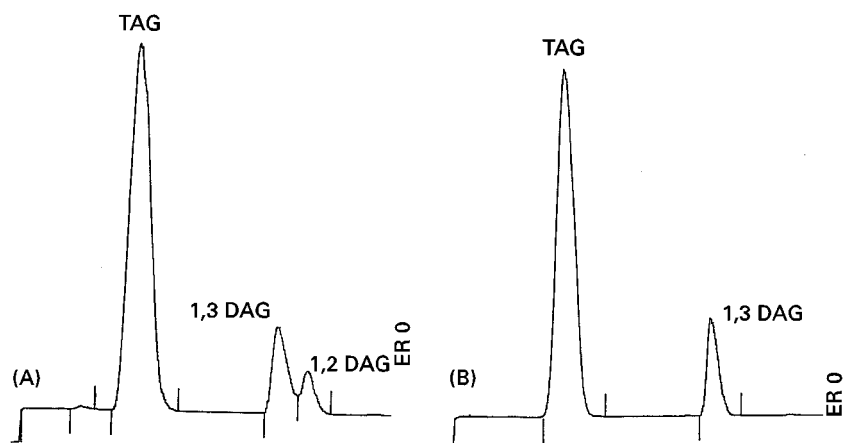


Figure 7 A commercial lipid product developed (A) in a solvent mixture of hexane:ethyl acetate:formic acid; 94:6:1 (v:v:v) hydrogenated, and (B) reanalysed. The smaller peaks, ostensibly 1,3-diacylglycerols (1,3 DAG) and 1,2-diacylglycerols (1,2 DAG), were shown to be two types of 1,3-diacylglycerol. TAG, Triacylglycerol.

(22:6n-3), materials currently of interest in infant nutrition.

Heavy Hydrocarbon Fractions

At one time coal provided a variety of liquid and semisolid materials, the latter usually referred to as pitch. The high-molecular-weight materials consisted of polycyclic aromatic hydrocarbons that could be individually defined with some difficulty, and more complex materials that were defined, mostly by solubility, as maltenes, asphaltenes and pre-asphaltenes. The use of TLC-FID in their analysis has been investigated for more than a decade and it promises to reduce solvent use and speed up analysis time enormously. The trend to coal liquification to produce fuel fractions competing with petroleum fractions makes new analytical technology even more useful to that industry, and at the same time the petroleum industry is turning to heavy crude oils and raw materials recovered from tar sands.

The products recovered from crude petroleum range all the way from hydrocarbon gases to alkanes of chain lengths up to C_{100} , polycyclic aromatics ranging from naphthalene upward, and other very complex high-molecular-weight materials, often incorporating nitrogen or sulfur. In the petroleum industry, standard methods tend to be time-consuming and complex. To make the life of the petroleum analyst even more difficult, 'cracking' to produce more valuable volatile fractions leaves residues of heavy materials such as asphaltenes. The application of TLC-FID to the latter has shown superiority to conventional methods, and has gradually been accepted, as shown by numerous publications.

The problem in crude petroleum analyses was basically the lack of natural standards, so that the quantitation of the FID response would reflect the mass of the particular complex fraction and pure chemicals representative of a fraction were unsatisfactory reference materials. For North Sea crude oils this difficulty has been overcome by preparation of appropriate standard fractions from typical crude oils, so that TLC-FID can provide data reliable for interlaboratory comparisons. In the petroleum laboratory particular difficulty is found with methods for heavy aromatic fractions and the more polar classes of materials. The latter often contain sulfur and nitrogen molecules and this makes some reporting technologies of little use, but the impact on TLC-FID response is not very significant.

One reason for industry laboratory problems is the obsolescence of standard methods, a problem not limited to the petroleum industry alone. When very large volumes of commodities are bought and sold there must be standards (and applicable methods) agreed on by all parties. Many have been around for decades with no changes. Meanwhile the internal combustion engine has been progressively fine-tuned to conserve energy, and even the robust diesel engine needs higher standards for volatile distillates. Complex refining and cracking steps produce even more heavy residues which must be investigated and utilized. The TLC-FID, introduced in about 1976, was immediately seized on by the petroleum industry and offers distinct advantages. The example given in **Figure 8** is taken from a recent paper on the subject. The Chromarod scans illustrate the weaknesses of the ASTM method D2007-91, based on rather lengthy and cumbersome open column chromatography on clay and silica gel columns in series.

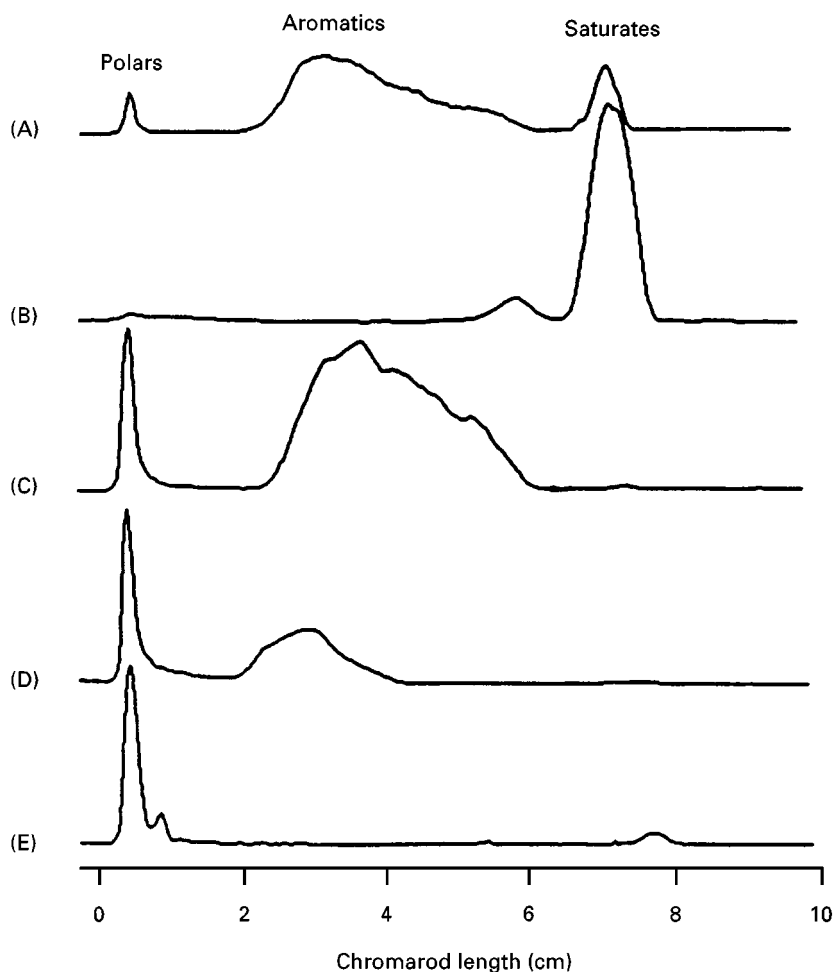


Figure 8 Superiority of Iatroscan TLC-FID over ASTM D2007 method in hydrocarbon analyses as exemplified with an aromatic petroleum extract and its fractions from the ASTM method. Chromatograms are for (A) TLC-FID of aromatic extract; (B) saturates by ASTM D2007, (C) aromatics by ASTM D2007, (D) polars by ASTM D2007; (E) residual polars from clay. Two-step Chromarod development of *n*-heptane for 30 min, followed by development with toluene for 5 min. (Reproduced with permission from Barman BN (1996) Hydrocarbon-type analysis of base oils and other heavy distillates by thin-layer chromatography with flame ionization detection and by the clay-gel method. *Journal of Chromatography Science* 34: 219–225.)

Conclusion

A recent paper on supercritical fluid chromatography suggested that often attempts to replace older and proven GC and HPLC methods with novel technology can be disappointing. That the TLC-FID system has been popular in only a few analytical fields may be due to the need for close interaction between the analyst and the method – almost a lost art in the face of contemporary automated equipment.

One exception to this is the TLC-FID of the Chromarod-Iatroscan combination, mostly used in research laboratories. As long as researchers have relatively nonvolatile organic materials to analyse, their resolution and determination by TLC is often a challenge for which the flexibility of the Iatroscan is ideally suited. Their chemical nature may have been

defined by decades of patient work by others, but the adaptation to rapid analysis by thin-layer silica gel chromatography on a microgram scale may require a combination of imagination, knowledge and perseverance. The TLC-FID is a system that offers the challenge that makes science enjoyable!

See also: III/Geochemical Analysis: Gas Chromatography. Lipids: Gas Chromatography; Liquid Chromatography; Thin-Layer (Planar) Chromatography. Oils, Fats and Waxes: Supercritical Fluid Chromatography. Petroleum Products: Thin-Layer (Planar) Chromatography.

Further Reading

Lipids

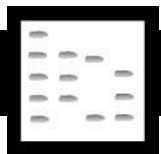
Ackman RG and Heras H (1997) Recent applications of Iatroscan TLC-FID methodology. In: MacDonald RE

- and Mossaba MM (eds) *New Techniques and Applications in Lipid Analysis*, pp. 325–340. Champaign: AOCS Press.
- Hara K, Cho S-Y and Fujimoto K (1989) Measurement of polymer and polar material content for assessment of the deterioration of soybean oil due to heat cooking. *Journal of the Japan Oil Chemists' Society* 38: 463–470.
- Kaitaranta JK and Ke PJ (1981) TLC-FID assessment of lipid oxidation as applied to fish lipids rich in triglycerides. *Journal of the American Oil Chemists' Society* 58: 710–713.
- Ohshima T and Ackman RG (1991) New developments in Chromarod/Iatroscan TLC-FID: analysis of lipid class composition. *Journal of Planar Chromatography* 4: 27–34.
- Ohshima T, Ratnayake WMN and Ackman RG (1987) Cod lipids, solvent systems and the effect of fatty acid chain length and unsaturation on lipid class analysis by Iatroscan TLC-FID. *Journal of the American Oil Chemists' Society* 64: 219–223.
- Parrish CC (1987) Separation of aquatic lipid classes by Chromarod thin-layer chromatography with measurement by Iatroscan flame ionization detection. *Canadian Journal of Fisheries and Aquatic Science* 44: 722–731.
- Sebedio J-L, Farquharson TE and Ackman RG (1985) Quantitative analyses of methyl esters of fatty acid geometrical isomers, and of triglycerides differing in unsaturation, by the Iatroscan TLC-FID technique using AgNO₃ impregnated rods. *Lipids* 20: 555–560.
- Shantha NC and Ackman RG (1990) Advantages of total lipid hydrogenation prior to lipid class determination on Chromarods S-III. *Lipids* 25: 570–574.

Hydrocarbons

- Barman BN (1996) Hydrocarbon-type analysis of base oils and other heavy distillates by thin-layer chromatography with flame ionization detection and by the clay-gel method. *Journal of Chromatographic Science* 34: 219–225.
- Bharati S, Patience R, Mills N and Hanesand T (1997) A new North Sea oil-based standard for Iatroscan analysis. *Organic Geochemistry* 26: 49–57.
- Poirier MA, Rahimi P and Ahmed SM (1984) Quantitative analysis of coal-derived liquids residues by TLC with flame ionization detection. *Journal of Chromatographic Science* 22: 116–119.

FLASH CHROMATOGRAPHY



C. F. Poole, Wayne State University, Detroit, MI, USA

Copyright © 2000 Academic Press

Flash chromatography and related techniques are widely used for laboratory-scale fractionation of mixtures from organic synthesis or for analysis when only a modest increase in resolution over conventional column liquid chromatography is required. These techniques employ short columns packed with particles of an intermediate size (typically 40–60 µm) combined with accelerated solvent flow achieved through modest pressure or suction. Compared to conventional column liquid chromatography, separations are obtained in less time; isolated compounds are often purer because resolution between bands is increased and band tailing is reduced; and compounds that are degraded or altered during chromatography are recovered in higher purity because of the shorter contact time with the chromatographic system.

The main applications of flash chromatography are purification of synthetic products, isolation of target compounds from natural products, the simplification of mixtures prior to high resolution preparative (usually) liquid chromatography and the fractionation of

complex mixtures into simpler groups for analysis. Its primary virtue is low cost, since virtually no special equipment is required, and the stationary and mobile phases are inexpensive enough to be discarded after a single use, or can be recycled. Resolution is less than that obtained by medium and high pressure liquid chromatography but the operational costs and equipment needs are greater for these techniques. Flash chromatography is often employed as a pre-separation technique to remove particulate matter and sample components that are either weakly or strongly retained on the separation column in medium and high pressure liquid chromatography. This allows higher sample loads to be separated under more selective separation conditions and avoids column contamination and regeneration problems. The production costs of the isolated products are thus rendered more favourable.

Dry-column Chromatography

Dry-column chromatography (**Figure 1**) is a variant of preparative thin-layer chromatography with similar resolution but a higher sample loading capacity. A glass column or nylon tube is packed with thin-layer chromatographic grade sorbent, usually silica gel, to a height of 10–15 cm. Sample is added as

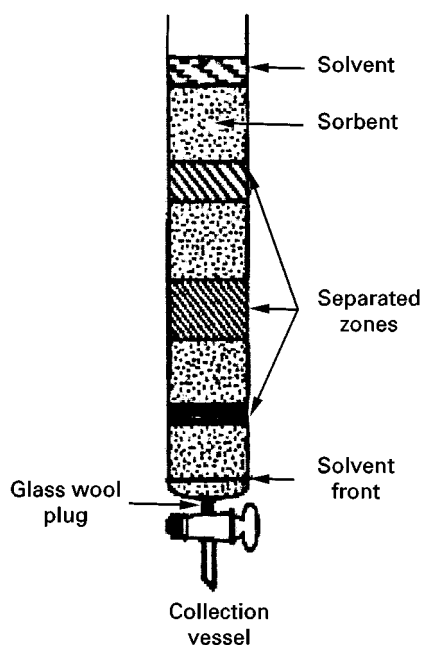


Figure 1 Apparatus for dry-column chromatography.

a concentrated solution or preadsorbed on to a small amount of sorbent. Separation is achieved by developing with a suitable volume of solvent to reach the lower end of the bed. Suction at the bottom of the column and/or slight overpressure at the top may be required to supplement capillary forces in moving the mobile phase down the column. Separated bands are removed by extrusion, slicing (if a nylon column is used) or by digging out, and the products freed from the sorbent by solvent extraction. The separation is fast, requires very little solvent and provides higher resolution than classical column techniques due to the use of sorbents with a smaller average particle size. It is suitable for the recovery of small quantities of material since the loading capacity is only about 0.2–1.0% w/w of the sorbent used, depending on the difficulty of separating the bands of interest.

Thin-layer chromatography provides a suitable technique for method development in most cases, although significant differences in separations can arise for mixed solvents, particularly when the solvent components differ in polarity and/or volatility. These differences result from the absence of pre-equilibrium with a vapour phase in the dry-column technique. Nylon columns can be more difficult to pack than glass columns, particularly when longer lengths are used, but nylon columns are easier to section and allow colourless bands to be observed with a UV lamp. Glass columns built up of segments connected by ground-glass joints can be useful for simplifying the extrusion process.

Dry-column chromatography is not a widely used technique. Preparative thin-layer chromatography or flash chromatography has generally been preferred. Although separations are fast, the recovery of separated zones is slow and labour-intensive compared to elution methods.

Vacuum Chromatography

Vacuum chromatography can be taken to mean the operation of a short column under suction to accelerate solvent migration. Either a short column or a Büchner filter funnel fitted with a glass frit is dry-packed with sorbent. The sorbent bed is consolidated initially by tapping the side of the column during filling and pressing the top layer of the sorbent bed with a flat object, such as a stopper, while suction is applied at the other end. Consolidation is completed by releasing the vacuum and pouring a solvent of low polarity over the surface of the sorbent bed followed by restitution of the vacuum. If the column is packed correctly the solvent front will descend the column in a horizontal line; otherwise the column should be sucked dry, repacked and tested again. When all the solvent has passed through the column, residual solvent trapped between particles is removed by suction. A solution of the sample in a suitable (weak) solvent or preadsorbed on to a small amount of sorbent or inert material, such as Celite, is applied to the top of the column (Figure 2). The sample solvent, if used, is sucked gently into the column packing. A piece of filter paper with the same diameter as the inside diameter of the column or funnel is placed on top of the sorbent bed to prevent disruption of the bed during addition of solvent. The column is then eluted with appropriate solvent mixtures of gradually increasing solvent strength. Between solvent applications the column is sucked dry and the eluent collected in test tubes or round-bottom flasks. Using a multiport manifold (similar to a pig adapter for distillation) or a separatory funnel allows sequential fraction collection without having to disassemble the apparatus after each fraction is collected.

Vacuum chromatography is simple, rapid and convenient. Optimum sample loads are similar to flash chromatography. However, it is not unusual to use sample overload conditions to separate simple mixtures by stepwise gradient elution or to simplify mixtures for further separation. Under these conditions the sample loads may reach 10% (w/w), or even higher, of the bed mass. Compared to flash chromatography, solvent changes are easy because the head of the column is at atmospheric pressure.

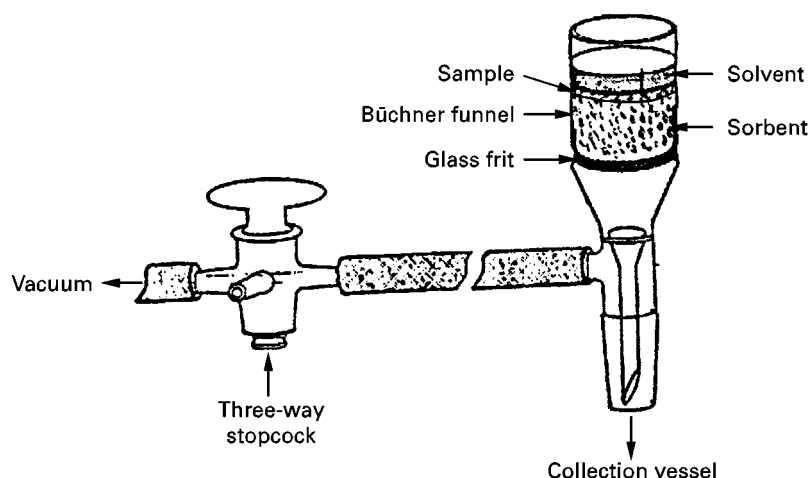


Figure 2 Apparatus for vacuum chromatography. (Reproduced from Pelletier SW, Chokshi HP and Desai HK (1986) Separation of diterpenoid alkaloid mixtures using vacuum liquid chromatography. *Journal of Natural Products* 49: 892, with permission from the American Chemical Society.)

Flash Chromatography

A glass column of a suitable length containing a small glass-wool plug and a layer of acid-washed sand or glass frit at its base is partially filled with sorbent using the dry-packing or slurry-packing technique. Incremental addition of the sorbent followed by tapping of the column with a hard object generally gives better results for dry packing than bulk filling of the column. After packing, the column is freed from trapped air and further consolidated by forcing several column volumes of a weak solvent through the sorbent bed until no further air bubbles are seen exiting the column and the bed is stable. It is difficult to pack wide-diameter columns (> 5 cm) by dry-packing procedures and in this case slurry packing is nearly always used. In this case, the column is partially filled with a small volume of weak solvent and a dilute suspension of the sorbent in the same solvent is added slowly in increments, with excess solvent intermittently drained away. Periodic pressurization of the sorbent bed is used to aid consolidation. Tapping the sides of the column is not normally employed. The sample is added to the column in a small volume of solvent or adsorbed to a small amount of packing material.

Finally, a thin layer of glass beads, acid-washed sand or other inert material is added to the top of the column to prevent disturbance of the column bed by solvent added for elution. The amount of free space above the sorbent bed must be sufficient to hold the volume of solvent equivalent to the fraction size collected, or a solvent reservoir must be inserted between the column and the pressure regulation valve. The flow rate is adjusted to about 5 cm min^{-1} by application of gas pressure and controlled by the regulation

valve. Pressures employed are typically less than 1–2 atm, with the various parts of the apparatus (Figure 3) held in place by springs, clamps or screw-thread connectors. It is a wise precaution to use plastic-coated glass columns or a safety shield to minimize the possibility of accidents. The column should not be allowed to run dry during the elution sequence.

Flash chromatography is simple to perform and is widely used in many laboratories. The main disadvantage is that the apparatus requires constant disassembly and reassembly of the air pressure inlet adapter in order to introduce new solvent into the column. Potter described an apparatus with a lateral solvent reservoir to overcome this problem. The essential feature of this apparatus is that a solvent reservoir with tap at the reservoir-to-column inlet is attached to the side of the column with the inlet situated above the height of the sorbent bed. A second tap at the top of the column allows air pressures to be equalized for rapid solvent addition to the column, without having to disassemble the apparatus. Radial compression columns have also been used with some commercial flash chromatography apparatus.

Stationary Phases

Silica, and to a lesser extent alumina, are the most common stationary phases used for the separation of low molecular weight organic compounds. Chemically bonded silica sorbents are used for the separation of polar organic compounds in the normal and reversed-phase modes. Wide-pore, chemically bonded phases are used for the separation of biopolymers. There is no technical reason why any

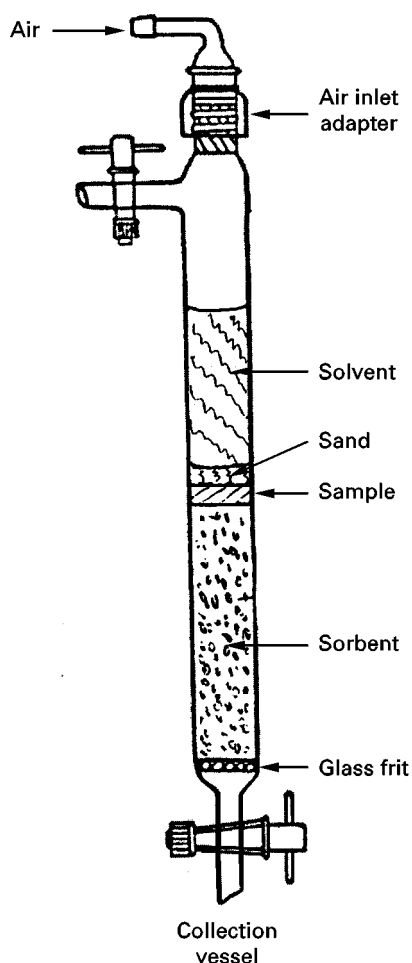


Figure 3 Apparatus for flash chromatography.

moderately rigid chromatographic sorbent, stable to solvent changes and available in the required particle size range, could not be used. In practice, the cost of the sorbent has to be set against the value of the product isolated, since the sorbent is often used for a single sample application and regeneration may be impossible, or tedious, costly and uncertain. Chemically bonded phases are more expensive than silica, or have to be synthesized from silica prior to use, and for this reason are less popular. For low molecular weight neutral organic compounds, small-pore silicas with a high surface area and high loading capacity are preferred, in particle size ranges of 20–40 or 40–63 μm . The smaller particle size materials provide higher resolution per unit length but generate greater back-pressure. Since longer columns can be used for the larger particle size sorbent, differences in resolution are often not great. Because of the limited operating pressure, columns are rarely longer than 30 cm, and 10–15 cm is recommended, unless longer columns are required to provide additional resolution. The optimum mobile-phase velocity for these particle

sizes is about 5 cm min^{-1} . At this velocity well-packed columns are expected to provide about 5–20 theoretical plates per centimetre of bed height, depending on the column packing density and the quality of the sorbent material.

Some separations demand specially prepared stationary phases. A method has been described for impregnating silica with silver nitrate for the isolation of compounds with unsaturated groups capable of forming charge transfer complexes with silver. Silica was impregnated with phosphoric acid and the calcium salt of ethylenediaminetetraacetic acid to isolate microtoxins that were either unstable or produced tailing bands on normal silica gel. Thin-layer chromatography is generally a suitable technique to identify suitable additives for improving chromatographic properties in flash chromatography. Silica and chemically bonded phases coated with cellulose *tris*(3,5-dimethylphenyl carbamate) were used to isolate 10–100 mg amounts of pure enantiomers from racemic mixtures. The selection of mobile phases for this application is conveniently optimized using high pressure liquid chromatography.

Sample Loading

The sample is usually added to the column in a small volume of a weak solvent and the solution forced into the sorbent bed, forming a narrow sample application zone. For samples of low solubility in weak solvents, the sample is taken up in a strong solvent and added to a small amount of column packing material or other inert support. The solvent is then stripped from the slurry under vacuum to produce a dry free-flowing powder that can be added to the top of the column. Sorbent (1–2 g) may be required for each gram of sample. It is important that the sample is completely dry (high vacuum is used to remove the last traces of solvent) and free of lumps to obtain symmetrical separated zones. If the sample layer is relatively long compared to the column bed length, then a stepwise solvent gradient must be used for elution to minimize zone broadening.

There are no simple relationships between the sample amount that can be separated, the dimensions of the sorbent bed and the volume and number of collected fractions. The loading capacity depends on the ease of separation of neighbouring zones, the sorption capacity of the sorbent and the method of sample elution. It can be increased by using wider columns and sorbents with a larger specific surface area. A rough empirical guide is presented in **Table 1**. For stepwise gradient elution it has been assumed that the sample can be separated into fractions of different polarity when estimating the typical sample load.

Even for difficult samples it is often more productive to use column overload conditions, combining fractions containing pure materials, and recycle those containing mixtures. Flash chromatography may lack the resolving power needed to separate the components of interest. In this case a higher resolution technique, such as medium or high pressure liquid chromatography, would be a better choice, perhaps using flash chromatography to isolate fractions containing the components of interest from other sample components.

Method Development

Thin-layer chromatography is widely used to optimize the separation conditions for silica gel flash chromatography. For isocratic separations a mobile phase which provides an R_F of about 0.35 for the zone of interest is chosen. If several zones are to be separated, then the solvent strength is adjusted such that the centre zone has an R_F of 0.35. If all zones of interest are well separated from each other and from impurities ($\Delta R_F \geq 0.2$), then the solvent strength can be adjusted so that the most retained zone of interest has a $R_F \approx 0.35$. For fractionation and large sample loads it is critical that the most selective solvent composition for the separation is used. This can be quickly identified using the PRISMA model, a guided trial-and-error procedure using thin-layer chromatography and parallel separations with different solvents. The same process can be used to identify the composition of solvents suitable for the recovery of individual sample zones in order of increasing polarity by stepwise gradient elution.

For samples of wide polarity a useful gradient is to start from a weak solvent, such as hexane, and add to this various volume increments of a strong dipolar solvent (such as ethyl acetate, dichloromethane, chloroform or acetone), terminating with the strong dipolar solvent. Then continue adding volume increments of a strong hydrogen-bond solvent (methanol, ethanol, 2-propanol) to the strong dipolar solvent, terminating with the strong hydrogen-bond solvent. Monitoring the separation by thin-layer chromatography allows the solvent gradient to be trimmed and optimized to suit the requirements for individual separations. Predicting the number of fractions required at each step remains quite arbitrary and is best conducted by monitoring the composition of each fraction as it is collected. When adding a strong solvent in a binary mobile phase for a silica gel sorbent, it is important to note that the solvent strength for the mixture has a steep curved profile. For compositions containing low volume fractions of strong solvent, the volume fraction of strong solvent should be incremented by small changes, resulting in relatively large changes in retention, for example, 1%, 3%, 5%, 10% (v/v). At higher volume fractions of strong solvent, the changes in volume fraction should be larger to produce a significant change in retention, for example, 30%, 40%, 60%, 80%, 100% (v/v).

Silica gel (or alumina) is the most suitable sorbent for the separation of low molecular weight organic compounds soluble in organic solvents and for separations of geometric isomers and diastereomers. For compounds at the extreme end of the general adsorption scale (Figure 4), separations are difficult because

Table 1 Approximate sample-loading conditions for flash chromatography (density of silica $\approx 0.45 \text{ g mL}^{-1}$)

Column diameter (cm)	Amount of silica gel (g)	Sample loading for a particular TLC resolution (g)		Sample loading (g)	Typical fraction volume (ml)
		$\Delta R_F \geq 0.2$	$\Delta R_F \geq 0.1$		
Isocratic elution (bed height=15 cm)					
1	5	0.1	0.04		5
2	20	0.4	0.16		10
3	45	0.9	0.36		20
4	80	1.6	0.6		30
5	130	2.5	1.0		50
Stepwise gradient elution (bed height=10 cm)					
3	30			1–3	50–100
4	55			3–8	100–200
6	125			8–35	200–300
8	250			35–60	200–300
10	350			60–80	300–500
14	700			80–150	300–500

Difficult to separate because solvent strength is too high	Alkanes	Weak ↓ Strong
	Aromatics	
	Halogenated compounds	
	Ethers	
	Nitro compounds	
	Nitriles	
	Carbonyl compounds	
	Alcohols	
	Phenols	
	Amines	
	Amides	
	Carboxylic acids	
Difficult to separate because solvent selectivity is too low	Sulfonic acids	

Figure 4 General adsorption scale for silica gel chromatography.

of inadequate selectivity. Water-soluble compounds, including biopolymers and easily ionized compounds, are generally better handled by reversed-phase chromatography. Compounds of low polarity that are weakly retained on silica gel with hexane as a solvent can be separated on chemically bonded phases in the normal or reversed-phase modes. For reversed-phase separations, chemically bonded phases with water as the weak solvent are used, and the solvent strength and selectivity of the eluting solvent changed by adding different volumes of water-miscible organic solvents, such as acetone, methanol, acetonitrile, tetrahydrofuran, etc. Optimization of solvent composition by thin-layer chromatography is possible but predictions may be unreliable due to differences in sorption properties between the column and layers. A better solution is to pack a short (10 cm) metal column with the sorbent for flash chromatography and use high pressure liquid chromatography to optimize separation conditions. Ideally, for isocratic elution a solvent composition should be chosen that provides a retention factor of 2–3 for the component of interest or those components of a mixture that are the most difficult to separate. For mixtures of wide polarity, stepwise solvent gradients are easily constructed and optimized by the same approach.

Detection

Monitoring separations by flash chromatography can be online and continuous using standard liquid chromatographic detectors (e.g. UV-visible, refractive index, or evaporative light scattering) but is more commonly done offline by collecting fractions that are subsequently combined, based on the similarity of their composition. Suitable monitoring techniques are thin-layer, gas or liquid chromatography, electrophoresis, bioassays, immunoassays and spectroscopy (e.g. infrared and nuclear magnetic resonance).

For neutral organic compounds, thin-layer chromatography is widely used. Microscope slide-sized plates are suitable to screen individual fractions as they are obtained and larger plates for the grouping of multiple fractions. A wide range of selective and universal visualizing reagents are available to meet most detection requirements. Compounds with UV absorption can be visualized by fluorescence diminution using layers containing an inorganic fluorescent indicator. But most of all, thin-layer chromatography is used because it is quick, portable, inexpensive and generally adequate for the task.

Future Developments

Flash chromatography and related laboratory-scale techniques are already widely used for preparative chromatography when only modest resolution is required. The virtues of these techniques are favourable cost considerations and minimal instrumentation requirements. They are not a substitute for high resolution, preparative-scale techniques but a complement to them. Consequently, radical changes in how flash chromatography is carried out are not expected. The most likely future development is the wider use of sorbents other than silica gel in generally optimized separation schemes, made possible by the declining cost of chemically modified and other selective sorbents.

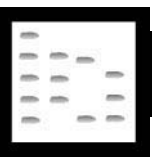
See also: II/Chromatography: Thin-Layer (Planar): Modes of Development: Conventional; Spray Reagents.

Further Reading

- Chappell I and Baines PE (1991) Bio-flash chromatography. Rapid, low-cost, purification of peptides. *Biochromatography* 10: 236–238.
- Claeson P, Tuchinda F and Reutrakul V (1993) Some empirical aspects on the practical use of flash chromatography and medium pressure liquid chromatography for the isolation of biologically active compounds from plants. *Journal of the Scientific Society of Thailand* 19: 73–86.
- Conway WD, Bachert EL, Sarlo AM and Chan CW (1998) Comparison of countercurrent chromatography with flash chromatography. *Journal of Liquid Chromatography & Related Technologies* 21: 53–63.
- Edwards C, Lawton LA, Coyle SM and Ross P (1996) Laboratory-scale purification of microcystins using flash chromatography and reversed-phase liquid chromatography. *Journal of Chromatography A* 734: 163–173.
- Gogou AI, Apostolaki M and Stephanou EG (1998) Determination of organic molecular markers in marine aerosols and sediments: one-step flash chromatography compound class fractionation and capillary gas chromatographic analysis. *Journal of Chromatography A* 799: 215–231.

- Grieb SJ, Matlin SA and Belenguer AM (1996) Flash chromatography with cellulose tris(3,5-dimethylphenylcarbamate)-coated phases. Improved resolution of basic analytes. *Journal of Chromatography A* 728: 195–199.
- Hostettmann K, Marston A and Hostettmann M (1997) *Preparative Chromatography Techniques. Applications in Natural Product Isolation*. Berlin: Springer.
- Li T-S, Li J-T and Li H-Z (1995) Modified and convenient preparation of silica impregnated with silver nitrate and its application to the separation of steroids and triterpenes. *Journal of Chromatography A* 715: 372–375.
- Milat M-L and Blein J-P (1995) *Cercospora beticola* toxins III. Purification and thin-layer and high-pressure liquid chromatographic analyses. *Journal of Chromatography A* 699: 277–283.
- Poole CF and Poole SK (1991) *Chromatography Today*. Amsterdam: Elsevier.
- Potter GA (1994) New lateral reservoir flash chromatography system for the expeditious preparative purification of organic compounds. *Journal of Chromatography A* 675: 237–239.
- Still WC, Kahn M and Mitra A (1978) Rapid chromatographic technique for preparative separations with moderate resolution. *Journal of Organic Chemistry* 43: 2923–2926.

FLAVOURS: GAS CHROMATOGRAPHY



F. P. Scanlan, Quest International, Naarden,
The Netherlands

Copyright © 2000 Academic Press

Flavours are composed from a wide variety of materials such as essential oils, extracts of natural products, individual aroma chemicals and many other materials having an organoleptic impact producing a desired effect. Flavour analysis by gas chromatography (GC) is only associated with volatile and semi-volatile compounds. From an early stage in the development of GC, the analysis of flavours has played an important part. Up until the 1980s, the emphasis was on using GC to identify individual flavour molecules at trace levels (parts per million (ppm) to parts per trillion (ppt) range and sometimes less). This is still an important part of the job for flavour analysts, although today there is a greater tendency to correlate molecular structures with sensory attributes. GC methods that have been developed for flavour analysis include temperature-programmed capillary GC and GC combined with mass spectrometry (MS). Likewise, a technique such as GC-Olfactometry (GC-O), which was once the realm of the flavour and fragrance industry, is currently enjoying applications in the food and beverage, cosmetics, packaging, plastics, and pharmaceuticals industries.

This article provides a comprehensive review of the most important GC applications in flavour analysis. The Further Reading section lists some important literature sources that provide a useful overview of GC as applied to flavour analysis. In addition there is the Food Science & Technology Series from Elsevier Science Ltd. This series contains the proceedings from the International Flavor Conferences and the

Weurman Flavour Research Symposia. Many GC methods have been used for a variety of purposes, including flavour and raw material quality control, flavour stability, identification of off-flavours and taints, studies of flavour biogenesis and metabolic pathways of plant volatiles, identification of new flavour molecules, consumer product development, and process optimization. The flavour analysis techniques covered here are: headspace GC including solid-phase microextraction (SPME) combined with GC thermal desorption techniques, pyrolysis-GC-MS, multidimensional GC, GC-MS and GC with selective detectors, chiral separations, GC-O and the recently developed fast GC process. Of course the quality of an analysis depends on the extraction techniques and sample preparation procedures. These areas are covered in other chapters in this encyclopedia. Headspace analysis and pyrolysis are also considered to be sampling techniques, but they are included here as they can be used in a coupled mode.

Headspace Gas Chromatography and Thermal Desorption Techniques

Since the early application of headspace GC analysis to flavours the technique has undergone a considerable degree of automation. Now it is possible to perform high throughput analysis, and reduce variability by automating the sampling and injection process. Basically there are two forms of headspace analysis: static and dynamic. In both forms volatiles that could be a source of interferences for the GC separation are removed from a complex sample matrix. It is important to note that the headspace contains the part of the flavour that one perceives first. Static

headspace analysis is performed in a closed vessel in which the volatiles reach an equilibrium between two phases. The results depend on the partition coefficients of the individual molecules between these phases. In dynamic systems an inert carrier gas is swept over the sample and the volatiles are trapped onto a support. Static headspace analysis has been automated in combination with cryofocusing devices. Dynamic headspace analysis can handle higher sample throughputs using automated thermal desorption devices in combination with cryofocusing to treat a series of sampling tubes containing the trapped volatiles. A variety of adsorbent phases are used for trapping volatiles according to their polarity. In recent years the solid phase micro-extraction (SPME) technique has been developed for sampling volatiles. It is based on the principle of using a stationary phase coated onto a fibre that traps the volatiles in contact with the surface. The fibre can be placed in the headspace above the sample or indeed can be plunged into a liquid sample. After a predetermined time, the fibre is removed and inserted directly into the GC injection port. Commonly used phases are polydimethylsiloxane (PDMS) and polyacrylate (PA) as well as the more conventional octadecylsilyl C18. The simplicity and cost effectiveness of this technique has led to its widespread application for flavour analysis. It is also possible to use this technique with some GC autosamplers. The GC chromatograms in Figures 1 and 2 allow a comparison of results obtained from solvent extraction and SPME, respectively. The sample was a lemon flavour. For SPME extraction, a PDMS fibre was placed over the sample in a closed conical flask

for 15 min at room temperature. A 50 : 50 v/v (100 mL) mixture of pentane and ether was used for the solvent extraction. To obtain a representative extract, a combination of polar and apolar solvents is often used in flavour analysis. GC analysis was run on a 50 m \times 0.32 mm i.d. \times 1 μ m HP-5 apolar phase column. The first observation to be made is that the solvent peaks at the beginning of Figure 1 are absent on Figure 2. Also absent in Figure 2 is the very broad peak at 39–45 min. This peak is benzoic acid, which unfortunately also creates interferences with other compounds eluting over the same time period. As expected, solvent extraction also shows some smaller broad peaks belonging to the polar acids eluting before 24 min. The absence of these peaks with SPME is expected as PDMS is an apolar material. This absence can also be an advantage in that interferences can be reduced. Relative concentrations of extracted compounds can be lower with SPME as compared with solvent extraction. This is because of the limited surface area available for adsorption on the SPME fibre. Quantitative results are difficult to compare, but qualitatively both techniques reveal nearly all the same apolar flavour compounds. The most abundant apolar compound after just 31 min is limonene. Another difference between the two techniques is the molecular weight range extracted. Solvent extraction allows the largest molecular weight range to be extracted. While there are limitations to SPME, this can be advantageous for some applications in which it is necessary to avoid interfering compounds and produce a 'cleaner' extract. Thermal desorption techniques involve the extraction of volatiles from

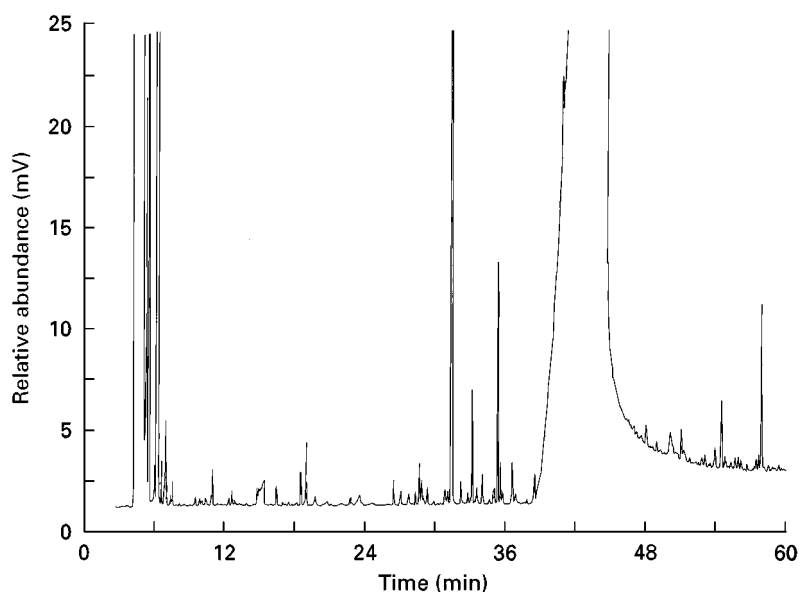


Figure 1 GC trace obtained after solvent extraction of a lemon flavour.

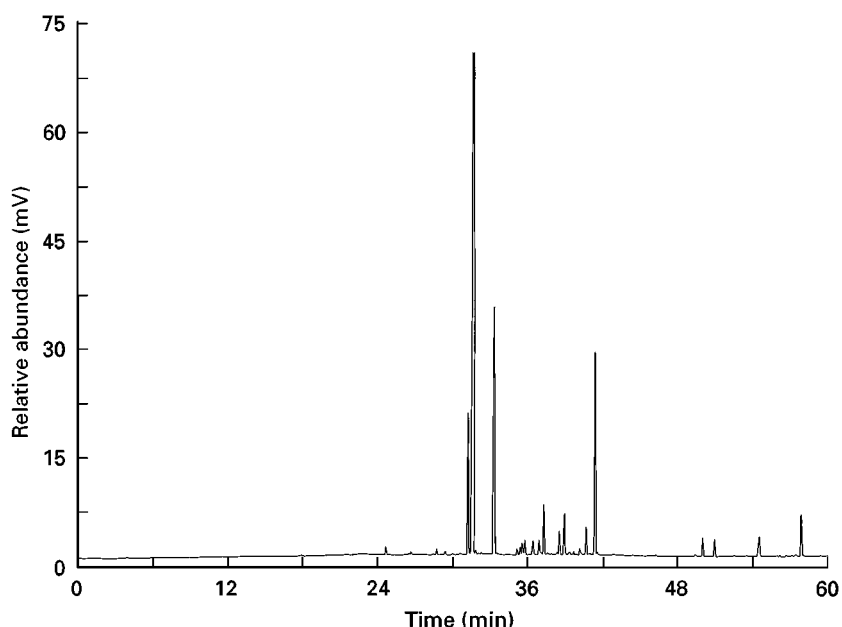


Figure 2 GC trace obtained after SPME of a lemon flavour for 15 min.

a sample contained in a glass tube, or as mentioned previously from a trapping material, directly into a GC injection port. A form of cryofocusing or cooled injection is required for reliable quantitative analysis.

Multidimensional Gas Chromatography (MDGC)

Flavours and especially natural flavour extracts can be extremely complex, containing hundreds of compounds that are not always completely resolved. The problems of separating overlapping peaks can be overcome by the use of very high resolution columns and also by using two columns instead of one to improve the peak capacity. The use of a switching mechanism between the columns makes it possible to select a segment of the chromatogram obtained with the first column and transfer it to a second column for further separation (heart-cutting). The second column may be of another polarity or performance or indeed may be a chiral column. Such a system can also be used in connection with a collection device to recover the isolated component. The collection device may be a cryogenic system or glass tubes filled with a suitable trapping materials. An elegant possibility exists whereby the glass collection tubes fit into the injection port of a GC column fitted with a septum-less cooled injection system, facilitating the transfer of the isolated volatiles into a GC-MS or GC-O usually fitted with a pre-column. Equally, using a simple accessory the isolated volatiles can be transferred to a suitable support for nuclear magnetic resonance

(NMR) or infrared (IR) analysis. Another variation on the single oven is the dual-oven system. This has the advantage of controlling the temperature of both columns. Multidimensional systems can be used for performing semipreparative GC isolations. They have also been used with a isotope ratio mass spectrometer for authenticity analysis. Multidimensional systems are very flexible and are extremely useful in the flavour laboratory for ultratrace analysis.

Gas Chromatography–Mass Spectrometry and Gas Chromatography–Selective Detection

Gas Chromatography–Mass Spectrometry (GC-MS)

GC analysis benefited from the advances in more stable and higher resolution columns and became more powerful when used with a mass spectrometer. Without underestimating other analytical techniques, GC-MS is probably by far the technique that has contributed the most to the analysis of flavours over the last 30 years. The literature is plentiful on GC-MS applications to flavour analysis. The combination of the separation power of the gas chromatograph with the selectivity of the mass spectrometer has been the major analytical tool for revealing components of essential oils and natural products as well as all volatile flavouring materials. GC-MS applications enabled the VCF (volatile compounds in food) list of known flavour molecules to grow from about 500 in the early 1960s to nearly 7000 today.

Gas Chromatography–Atomic Emission Detection (GC-AED)

The atomic emission detector is a multi-elemental detector based on the principle of scanning the atomic emission bands of several elements as compounds elute from the GC and enter a microwave plasma. For the selected element, AED is generally more sensitive than the flame ionization detector (FID) (at low parts per million (ppm) levels) and there is the possibility of acquiring data for several elemental wavelengths simultaneously. AED can be used as a low-level screening tool for organohalogens, organosulfur, organometallics and also some isotopes useful for isotopic labelling studies. With respect to essential oils and flavours, this technique has been used for the detection of trace contaminants such as pesticides. One of the advantages of AED is that complex matrices such as a citrus oil may be injected neat or as a simple dilute solution to avoid the need for tedious extraction techniques. GC-AED is a useful complementary technique to benchtop GC-MS.

Gas Chromatography–Sulfur Detection

It was only in the 1980s that attention was given to the relevance of sulfur volatiles and semi-volatiles to the character of flavours. Previously, sulfur molecules were not considered very important and were more often associated with off-odours and contaminations. Studies carried out on products such as cheese, truffles and fresh strawberries have revealed the importance and flavour impact of sulfur compounds. Both sulfur chemiluminescence detection (SCD) and flame photometric detection (FPD) are used for selective sulfur detection. These techniques have also been used in combination with sniffing port detection and headspace analyses. Generally, the identification of sulfur compounds has been difficult because their olfactory detection threshold is extremely low. Thus, they may be detected by the nose but the analyst must carry out several extractions and concentrations of the product to obtain a sample large enough to cause a peak to appear on the chromatogram.

Gas Chromatography–Nitrogen Detection

Nitrogen–phosphorus detection (NPD) has been applied to the analysis of nitrogenous compounds in cheese, meat and yeast extracts for flavouring specialities. Amino compounds and breakdown products of proteins are often associated with bitterness and are important when considering the taste of a flavouring.

Gas Chromatography–Electron-Capture Detection (GC-ECD)

The analysis of some classes of flavour compounds, such as the highly volatile aldehydes or volatile fatty acids, is facilitated by employing derivatization techniques using halogen-containing reagents, e.g. pentafluorobenzylhydroxylamine (PFBOA). The high sensitivity of the ECD technique is therefore advantageous for detecting trace-level derivatized carbonyl compounds. This approach has also been applied in flavour studies of lipid oxidation compounds.

Chiral Separations

Many flavour molecules have one or more chiral carbons and can exist as enantiomers. The separation of enantiomers by GC can be used as a method for studying their individual odours or for the purposes of authenticity analysis. Most natural biosynthetic pathways produce flavour molecules with one predominant enantiomer. This can be exploited for the control of food and beverage adulteration. The chiral GC chromatograms shown in **Figures 3** and **4** are analyses of flavour extracts made from strawberry fruit preparations. The chiral column was 25 m long and contained a diacetyl tert-butyltrimethylsilyl β -cyclodextrin stationary phase. Figure 3 shows the separation of both the (*R*)- and (*S*)-enantiomers of ethyl-2-methylbutyrate at 9 min while only the (*S*)-enantiomer is present in Figure 4. Both enantiomers in Figure 3 are present in almost equal abundance which is indicative of the addition of a ‘nature identical’ ester. The development of chiral stationary phases (mainly modified β -cyclodextrin phases) has allowed the resolution of many enantiomers. When enantiomer separations have been combined with CG-O to differentiate the odour of each enantiomer they have revealed three main classes of enantiomers: enantiomers of equal odour; enantiomers having the same odour but different intensities or secondary notes; and enantiomers with quite different odours. Examples of enantiomers with different odours are (+)-nootkatone, which has the aroma of grape-fruit peel, and (–)-nootkatone, which has stronger woody, spicy notes and only minor grapefruit peel character. Also, (+)-(*S*)-carvone has a typical caraway oil smell while (–)-(*R*)-carvone has a minty odour. An interesting compound is 5 α -androsterone, where the (–) enantiomer is odourless and the (+) enantiomer is characterized as either musk-like or urine-like. Human genetics throws in a further complication with this molecule, in that a third of the population perceive it as odour-

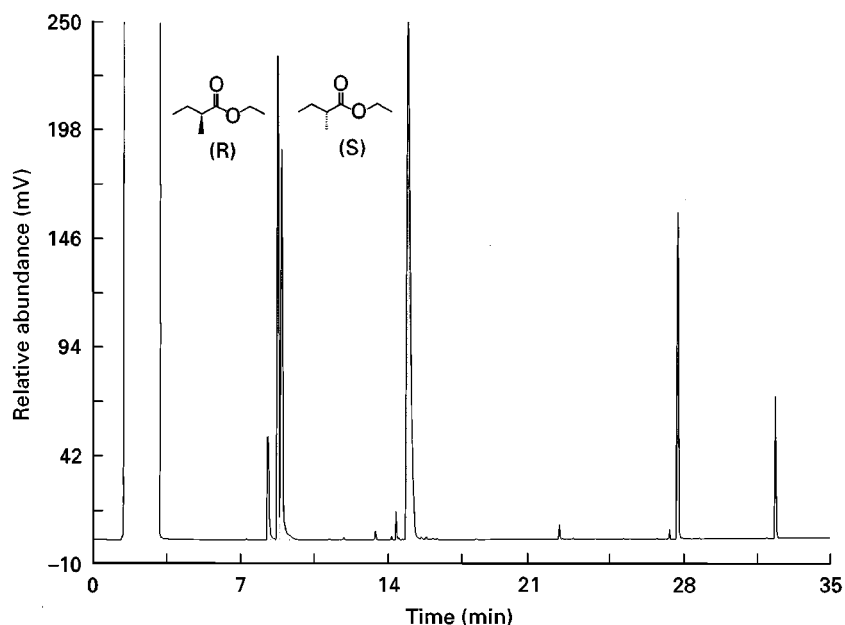


Figure 3 Separation of (*R*)- and (*S*)-enantiomers of ethyl-2-methylbutyrate at 9 min.

less, another third as musk-like and the remaining third as urine-like.

Gas Chromatography–Olfactometry (GC-O)

The most valuable detector in flavour analysis is the human nose. GC-O is the technique in the flavour

analyst's arsenal that correlates analytical and sensory data. The use of a sniffing port as well as a physical detector to sniff GC effluents dates back to the early 1960s. The technique has since improved, because of technological advances in GC instrumentation, sniffing port design and the use of computer tools for data processing. The strength of GC-O lies in the fact that the odorous compounds in a product's

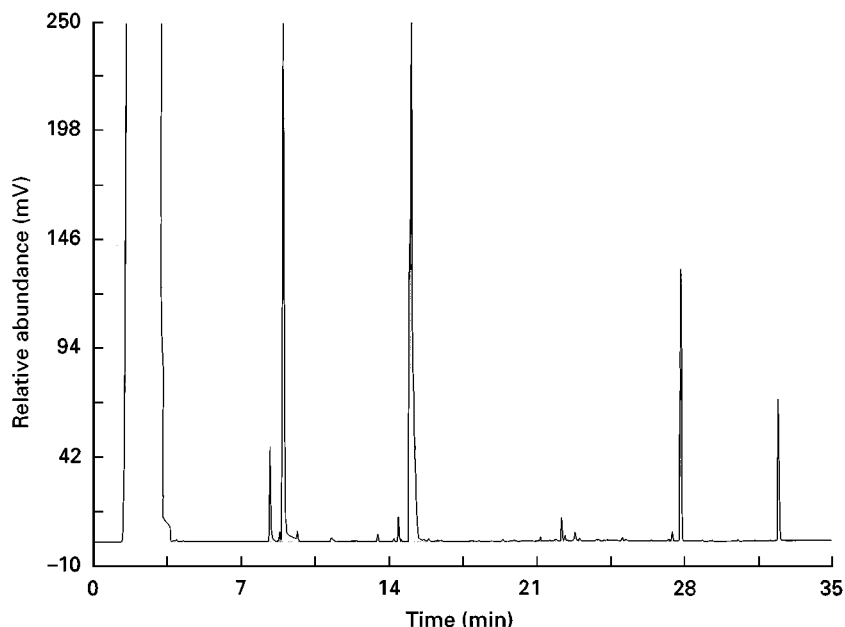


Figure 4 Separation of the (*S*)-enantiomer of ethyl-2-methylbutyrate.

extract can be detected from among all the other non-odorous compounds in the sample. GC-O involves measuring the perceived odour and its retention time. The odour of a molecule can be described in terms of its aromatic quality, intensity and potency. Intensity pertains to the perception one has at a given concentration, whereas potency refers to a comparison of concentration amounts with respect to other molecules at the same intensity level. As for all GC analysis, identification is helped by using compilations and databases of relative retention times. There are a few variations of the GC-O technique: Charm (combined hedonistic response method), AEDA (aroma extract dilution analysis) and OSME (Greek for smell). Charm and AEDA are techniques for measuring potency and OSME quantifies intensity. In its simplest form the nose sniffs effluents from the GC column and the retention times of interesting compounds can be noted along with an odour descriptor. A sniffing port can be mounted on top of the GC or in the GC oven door, or can be connected via a heated transfer line as is the case with the recently commercialized flexible sniffing port. By making it possible to use an electronic push-button device or joystick an electronic signal can be generated that represents the nose response, see **Figure 5**. Overlaying the signals for the nose and for a physical GC detector (often an FID device) results in a chromatogram displaying the retention times of the odorous molecules on top of the normal FID peaks of the mixture. This result can be termed an 'aromagram' and an example is displayed by **Figure 6**. This is an example of head-

space analysis carried out on a commercial American roast coffee purchased in a supermarket. Coffee aroma is very complex, containing over 800 volatile compounds. To facilitate explanation, the example shown is the 30–39 min segment of the chromatogram. The FID signal is in blue and the electronic push-button signal generated while sniffing is overlaid in red. Flavour descriptors as stated by the observer are shown. The retention indices for the odorous peaks are indicated at the baseline of the red signal. It is interesting to note that many peaks do not necessarily have an odour and many odorous molecules are too low in concentration to have a detector response. Sulfur-containing molecules (e.g. the peak at retention index 1236) often have extremely low odour thresholds and never show up on a chromatogram unless the sample has undergone some pretreatment. In these cases, GC-O in combination with a retention index database can be very useful. As the nose is generally more sensitive than any physical detector, the retention times of odorous molecules often correspond with the absence of any chromatographic peak. To resolve this, more sample work-up, column liquid chromatography and/or MDGC are possible solutions. There are some limitations to the technique. Unfortunately, human noses are not standardized and some suffer from anosmia, the inability to perceive a certain odour, and also sensitivities are different. Some people are more sensitive to particular odours than others. Another difficulty is in attributing a meaningful and consistent flavour descriptor. To overcome this, subjects can be tested for anosmia and

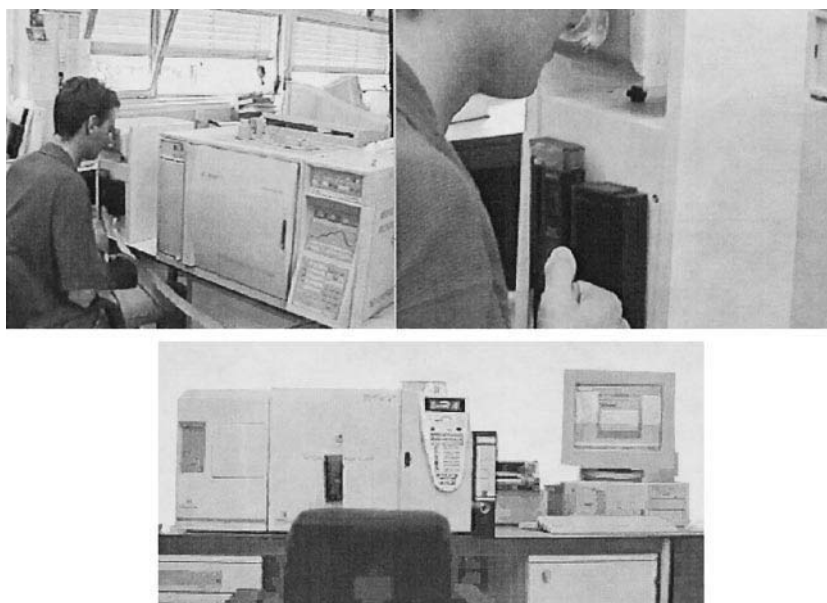


Figure 5 GC-O instrumentation.

trained in flavour language. Also, it is known that some molecules exert a synergistic effect when in the flavour but do not show this when eluted separately on the column. Thus, the odour impact can be different. Finally, a subject must be very experienced to be able to relate the sniffing of individual compounds back to the organoleptic impact of the entire flavour mixture. What is important is that the subject's perception is reproducible. The most potent odour molecules contributing to a flavour can be determined by performing GC-O with successive dilutions of the injected sample. GC-O can be made more powerful for routine flavour analysis by combining it directly with MS detection. Thus retention indices, mass spectra and flavour descriptors can be obtained. The combination of retention indices with mass spectra are especially useful when identifying some terpenes that have very similar mass spectra.

Pyrolysis–Gas Chromatography–Mass Spectrometry

Pyrolysis-GC-MS has found some limited applications in flavour analysis, primarily in the study of process or reaction flavours. In fact, the very first use of a glass capillary column was on the pyrolysis products of tobacco, to study cigarette aroma and filtration. The area of most interest has been the study of flavour volatiles formed from Maillard reactions between amino acids and reducing sugars. The Maillard reaction is responsible for the brown colour and the taste of bread crusts and meat and is essential in most savoury flavour systems. The applications studied by pyrolysis generally involve a great variety

of flavour compounds, and the use of a pyrolysis probe mounted on a GC column that is coupled to a mass spectrometer is a pre-requisite for their identification. For Maillard studies, the pyrolysis chamber is used as a reactor. A limiting parameter of commercial pyrolysis devices is the small sample capacity (generally milligrams). Thus the concentrations of volatiles generated are equally low and can limit the analysis to the study of the major compounds formed. However, this may yield useful information. Another way to exploit this technique is by using model mixtures of flavour components to investigate the reactions that control or favour the development of flavours from their thermal precursors.

Fast Gas Chromatography

Recent advances in GC instrumentation, notably in electronic pressure control of column and split flows, faster ovens and the use of narrow bore columns, have made it possible to increase the speed of analysis without loss of resolution. Generally, GC runs of more than 2–3 h are common for determining the quality of an essential oil. It has recently been shown that analyses of nutmeg and lemon essential oils that once took 80 min can now be achieved in less than 20 min. Fast GC has reduced run times considerably and is consequently very advantageous for routine quality control laboratories under pressure to achieve a greater sample throughput per shift. Figures 7 and 8 illustrate the fast GC analysis of a lemon oil. The 80 min chromatogram (Figure 7) was obtained on a standard 60 m \times 0.32 mm i.d. \times 1.2 μ m RSL-200 column (apolar phase). The 8 min chromatogram

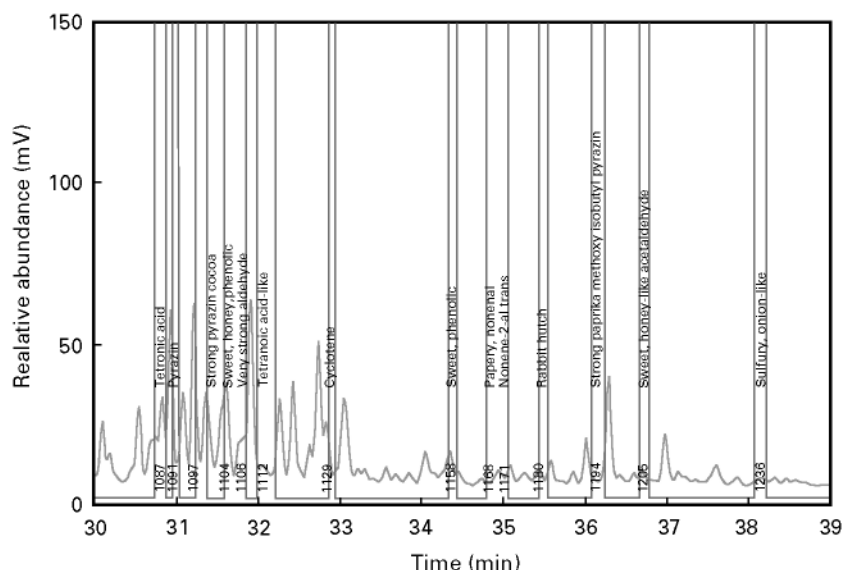


Figure 6 An example of an aromagram of an American toast coffee.

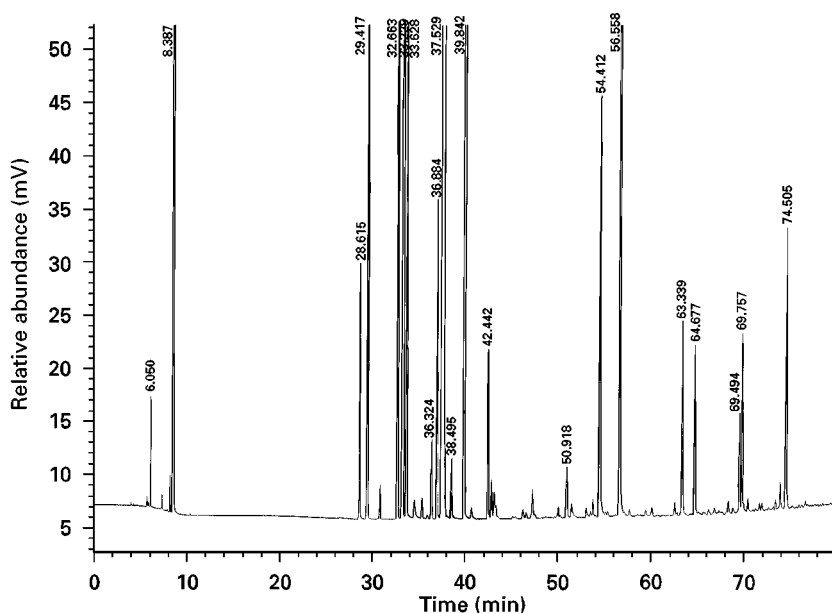


Figure 7 Fast GC analysis of a lemon oil (80 min chromatogram).

(Figure 8) was obtained with a column of the same phase but with the dimensions $15\text{ m} \times 0.1\text{ mm i.d.} \times 0.25\text{ }\mu\text{m}$. The analyses were performed in constant pressure mode. The hydrogen carrier gas velocity was changed from 27 cm s^{-1} to 46 cm s^{-1} . Pressures were 48 kPa and 227 kPa respectively. Likewise the split ratio was modified from 1/25 to 1/1000. In both cases the injection volume was $1\text{ }\mu\text{L}$. The oven temperature programme was also modified

to obtain similar resolutions. As shown, peak elution order was not changed and relative abundances are satisfactory in spite of a ten-fold reduction in analysis time.

Future Developments

Advances in GC instrumentation, column technology and application of computer tools will have positive

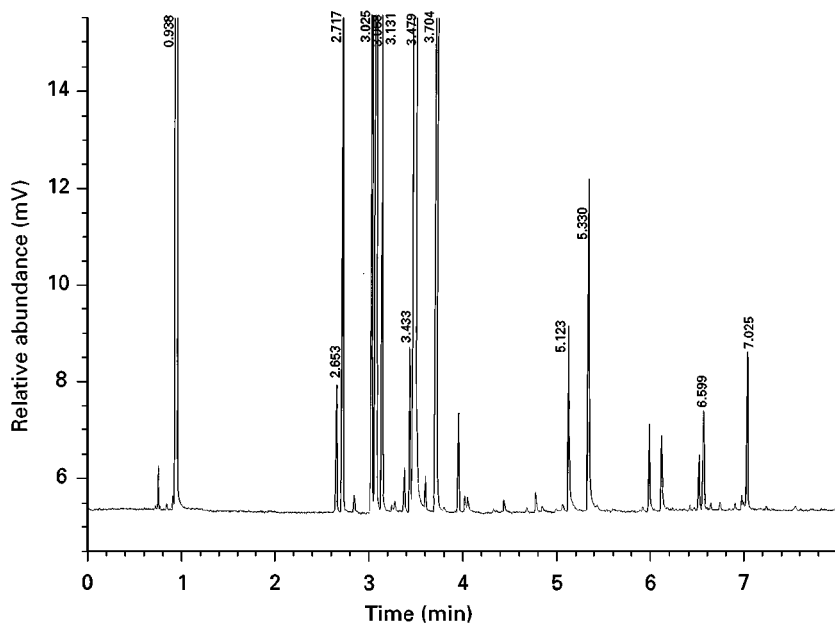


Figure 8 Fast GC analysis of a lemon oil (8 min chromatogram).

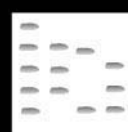
consequences for flavour analysis. There will most likely be a development of larger capacity sampling devices using adsorbant tubes and SPME fibres for headspace analysis. The desire to analyse unstable volatiles will lead the analyst to develop derivatization techniques. GC-O will become better known and will not be used only for flavour and fragrance analysis. The evolution of this technique may see the development of expert systems, such as voice recognition software to automatically annotate aromagrams and software to help with interpretation against known chemical data and correlation with sensory data. The development of flavour databases that combine chromatographic and spectroscopic data will continue. Increasing the speed of analysis will see fast GC develop for flavour quality control analysis. An interesting development in the task of comparing data from different instruments with different detectors is retention-time (RT) locking. This has already been successfully applied and will be aided by the development of specific RT lock flavour and fragrance libraries.

See also: II/Chromatography: **Gas:** Derivatization; Detectors: General (Flame Ionization Detectors and Thermal Conductivity Detectors); Detectors: Mass Spectrometry; Detectors: Selective; Headspace Gas Chromatography; Large-Scale Gas Chromatography; Multidimensional Gas Chromatography; **Extraction:** Solid-Phase Microextraction. III/Allergens in Perfumes: **Gas Chromatography-Mass Spectrometry.** Chiral Separations: Gas Chromatography. **Fragrances: Gas Chromatography.** **Pheromones:** Gas Chromatography. **Solid-Phase Micro-Extraction:** Overview.

Further Reading

- Charalambous G, ed. (1978) *Analysis of Foods and Beverages – Headspace Techniques*. New York: Academic Press.
- David F, Gere GR, Scanlan F and Sandra P (1999) Instrumentation and applications of fast high-resolution capillary gas chromatography. *Journal of Chromatography A* 842: 309–319.
- König WA (1987) *The Practice of Enantiomer Separation by Capillary Gas Chromatography*. Heidelberg: Huethig.
- Kondjoyan N and Berdagué J-L (1996) *A Compilation of Relative Retention Indices for the Analysis of Aromatic Compounds*. Saint Genes Chapanelle: Laboratoire Flaveur INRA.
- Marsili R, ed. (1997) *Techniques for Analyzing Food Aroma*. Food Science & Technology Series 79. New York: Marcel Dekker.
- Mussinan CJ and Morello MJ, eds (1998) *Flavor Analysis – Developments in Isolation and Characterization*. ACS Symposium Series 705. Washington: American Chemical Society.
- Nijssen LM, Visscher CA, Maarse H, Willemsens LC and Boelens MH, eds (1996) *Volatile Compounds in Food, Qualitative and Quantitative Data*. 7th edn (including supplement 1, 1997). Zeist: TNO Nutrition and Food Research Institute.
- Pawliszyn J (1997) *Solid Phase Microextraction – Theory and Practice*. New York: Wiley-VCH.
- Sandra P and Bicchi C (1987) *Capillary Gas Chromatography in Essential Oil Analysis*. Heidelberg: Huethig.
- Schreier P, ed. (1984) *Analysis of Volatiles-Methods-Applications*. Berlin: W. de Gruyter & Co.
- Werkhoff P, Brennecke S, Bretschneider W, et al. Chiro-specific analysis in essential oil, fragrance and flavour research. *Zeitschrift für Lebensmittel Untersuchung und Forschung* 196: 307–328.

FOAM COUNTERCURRENT CHROMATOGRAPHY



H. Oka, Aichi Prefectural Institute of Public Health, Nagoya, Japan

Y. Ito, National Institute of Health, Bethesda, MD, USA

Copyright © 2000 Academic Press

Introduction

Foam separation methods have long been used for the separation of various samples ranging from metal ions to mineral particles. The separation is based on a unique parameter of foaming capacity or foam

affinity of samples in aqueous solution and it has a great potential for application to biological samples. However, the use of this method in research laboratories has been extremely limited, mainly due to a lack of efficient instruments. Foam separation instruments generally consist of a single tubular column where the foam is generated by introducing the gas phase at the bottom of the column (Figure 1). Under the gravitational field, the foam moves upwards towards the top of the column to collect foam-active materials. Although various mixing devices such as baffles, solid beads and rotary mixers are used to improve contact, the use of a short column under

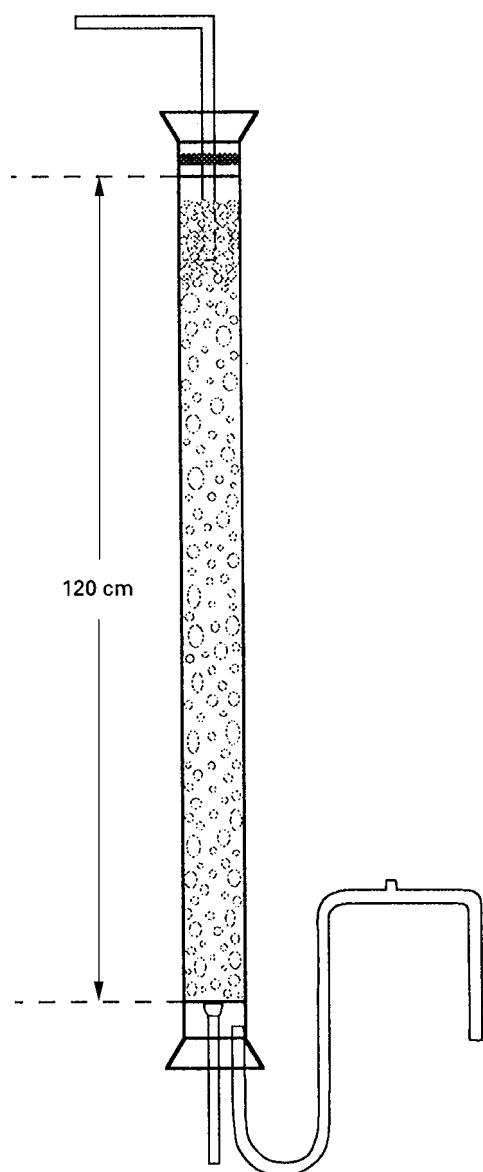


Figure 1 Conventional foam separation column.

a gravitational field limits the efficiency of these systems and consequently, the separation is inefficient.

In 1976, foam countercurrent chromatography (CCC) was developed to improve the foam separation technology. In this foam CCC method, foam and liquid undergo countercurrent movement through a long, fine, Teflon tube (10 m \times 2.6 mm i.d.) under a strong centrifugal force field as illustrated in Figure 2. This article describes the foam CCC technology and its application to a variety of samples.

Apparatus of Foam CCC

Figure 3 illustrates the design of the foam countercurrent chromatograph. The motor drives the rotary

frame around the central axis of the centrifuge. The rotary frame holds a coiled separation column and a counterweight symmetrically at a distance of 20 cm from the central axis of the centrifuge. A set of gears and pulleys produces synchronous planetary motion of the coiled column. This planetary motion induces a countercurrent movement between foam and the mother liquid through a long, narrow, coiled tube. Introduction of a sample mixture into the coil results in the separation of sample components. Foam-active components are quickly carried with the foaming stream and are collected from one end of the coil while the rest move with the liquid stream in the opposite direction and are collected from the other end of the coil (Figure 2).

The column design for foam CCC is shown in Figure 4. The coil consists of a 10 m long, 2.6 mm i.d. Teflon tube with a 50 mL capacity. The column is equipped with five flow channels. The liquid is fed from the liquid feed line at the tail and collected from the liquid collection line at the head. Nitrogen gas is fed from the gas feed line at the head and discharged through the foam collection line at the tail while the sample solution is introduced through the sample feed line at the middle of the coil. The head-tail relationship of the rotating coil is conventionally defined by an Archimedeian screw force where all objects of different density are driven towards the head. Liquid feed rate and sample injection rate are each separately regulated using needle valves while the foam collection line is left open to the air.

Application

Foam CCC can be applied to a variety of samples having foam affinity. Foam affinity can be classified into two categories: (i) the affinity to the foam-producing carrier; and (ii) the direct affinity to the gas-liquid interface. Samples which lack direct affinity to the gas-liquid interface can be indirectly absorbed to the foam if they have an affinity to the foam-producing agents such as a surfactant. Samples, such as detergents and other foam-producing substances, can be separated without special treatment because they have affinity to the gas-liquid interface.

Foam Separation Using Surfactants

This technique is applied to the sample having affinity to the foam-producing carrier. Sodium dodecyl sulfate (SDS) and cetyl pyridinium chloride (CPC) were used as carriers to study the effects of electric charges on the foam affinity of various compounds. Figure 5

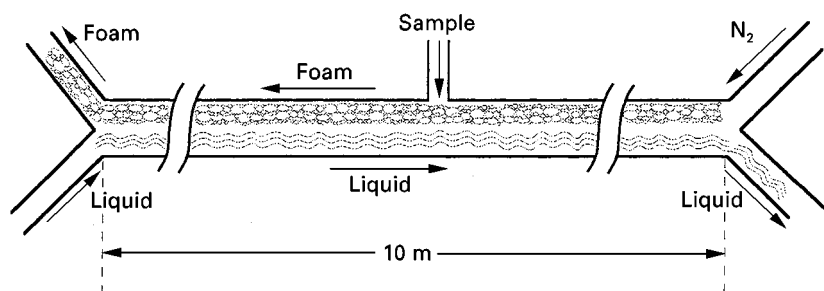


Figure 2 Foam CCC scheme.

illustrates two sets of foam chromatograms obtained from a mixture of methylene blue and DNP-leucine mixture using SDS (top) and CPC (bottom) as carrier reagents. In each chromatogram, the ordinate indicates absorbance values measured at two wavelengths, 430 nm for DNP-leucine and 620 nm

for methylene blue. When the sample mixture was introduced with the anionic SDS surfactant, the positively charged methylene blue was adsorbed on to the foam and quickly eluted through the foam collection line (top, right) while the negatively charged DNP-leucine was carried with the liquid stream in

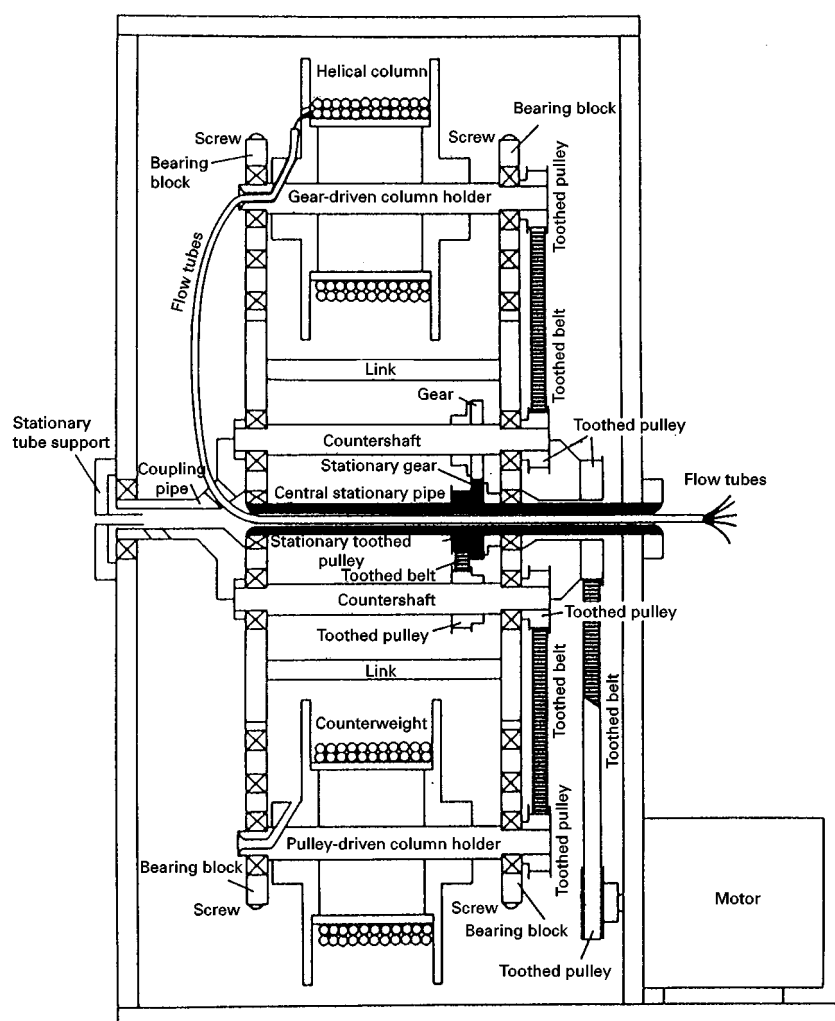


Figure 3 Design of foam CCC centrifuge. (Reproduced from Ito (1985) with permission from Marcel Dekker Inc.)

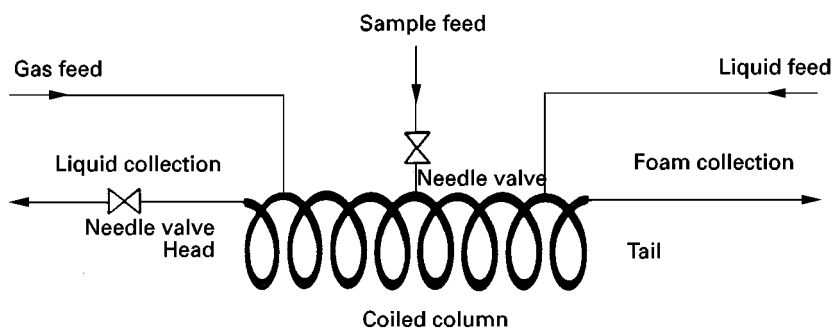


Figure 4 Column design for foam CCC.

the opposite direction and eluted through the liquid collection line (top, left). Similarly, when the same sample mixture was eluted with the cationic CPC surfactant, the negatively charged DNP-leucine

was totally eluted through the foam collection line (bottom, right) and positively charged methylene blue through the liquid collection line (bottom, left).

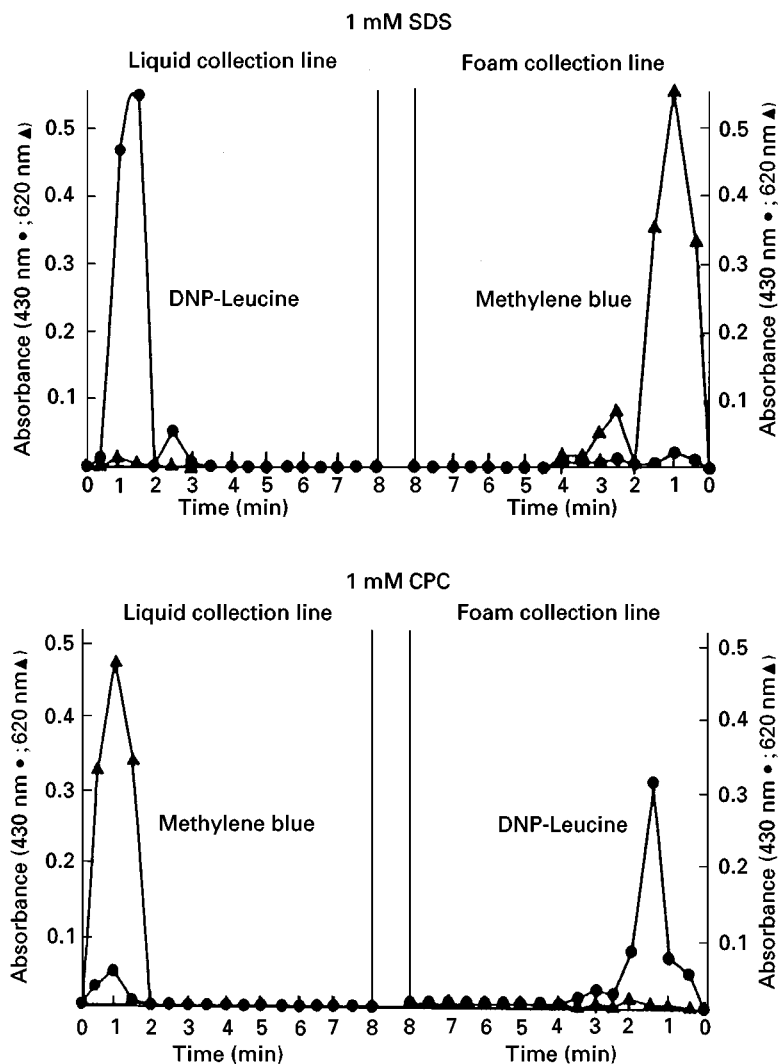


Figure 5 Separation of methylene blue and DNP-leucine by foam CCC. (Reproduced from Bhatnagar and Ito (1988) with permission from Marcel Dekker Inc.)

Foam Separation Without Surfactants

Using ionic surfactant as carriers, the samples which lack direct affinity to the gas-liquid phase interface can be separated if they have opposite electric charges. However, in this case complicated procedures are required to remove the surfactants after fractionation. On the other hand, many natural products have foaming capacity, and therefore foam CCC may be performed without such surfactants.

In order to demonstrate this possibility, bacitracin complex (BC) was selected as a test sample, because it has a strong foaming capacity. Foam CCC for separation and enrichment of BC components has been conducted using nitrogen gas and distilled water entirely free of surfactant or other additives. The following sections describe chromatographic fractionation of BC with batch sample loading and enrichment of foam-active compounds from a bulk liquid on continuous sample feeding.

Batch sample loading BC is a basic cyclic peptide antibiotic commonly used as a feed additive for livestock worldwide. It consists of more than 20 components, but chemical structures of these components are still unknown except for BCs-A and -F.

Foam separation of BC components was initiated by simultaneous introduction of distilled water from the tail and nitrogen gas from the head into the rotating column while the needle valve at the liquid collection line was fully opened. After a steady-state hydrodynamic equilibrium was reached, the pump was stopped and the sample solution was injected through the sample port. After the desired standing time, the needle valve opening was adjusted to the desired level and pumping was started again. Effluents from both outlets were collected at 15 second intervals.

Figure 6 shows the elution curve of BC components from the foam outlet. The vertical axis indicates the absorbance at 234 nm and the horizontal line, the fraction number. This elution curve shows three major peaks as indicated by arrows. The fractions corresponding to these peaks were subjected to HPLC analysis.

HPLC chromatograms of BC components in the foam fractions are shown in Figure 7. Under reversed-phase HPLC conditions, BC was separated into more than fifteen peaks. Generally, hydrophilic compounds elute earlier than hydrophobic compounds under these conditions. In this study, the HPLC elution time is used to indicate the polarity of the BC components. Thus, BC-A which elutes earlier in HPLC is more hydrophilic than BC-F. The most hydrophobic compounds (peaks 14 and 15) with the



Figure 6 Elution curve of bacitracin components from foam line. Foam CCC conditions: liquid flow rate, 3.2 mL min^{-1} ; needle valve, 0.8 turn open; standing time after sample injection, 5 min; N_2 gas pressure, 80 psi; revolution speed, 500 rpm; sample size, 5 mg per 0.5 mL in H_2O ; fractionation, 15 s per tube.

longest retention time in HPLC analysis were collected in the first foam fraction with a small amount of less hydrophobic compounds (peaks 11 and 13). Peak 15 is hardly visible in the HPLC chromatogram of the original sample due to its low concentration, but the same peak is clearly observed in the chromatogram of the first foam fraction. BC-A was almost completely isolated in peak 11 from other components eluted in the tenth fraction. In the twentieth fraction, peak 7 appeared in the HPLC chromatogram. Components with lower hydrophobicity than peak 7 did not appear in the foam fractions. These results clearly indicate that the bacitracin components are separated in the order of hydrophobicity of the molecule in the foam fractions with the most hydrophobic compounds being eluted first.

As described above, BC components were separated according to their hydrophobicity using foam CCC without surfactant. This method can also be applied to continuous sample feeding as described below.

Continuous sample feeding On the basis of the preliminary experimental results, the following foam CCC conditions were chosen for large scale sample feeding. The conditions were as follows: needle valve, 2.0 turns open; sample concentration, 50 p.p.m.; sample size, 2.5 L; sample feed rate, 1.5 mL min^{-1} at 40 psi; ni-

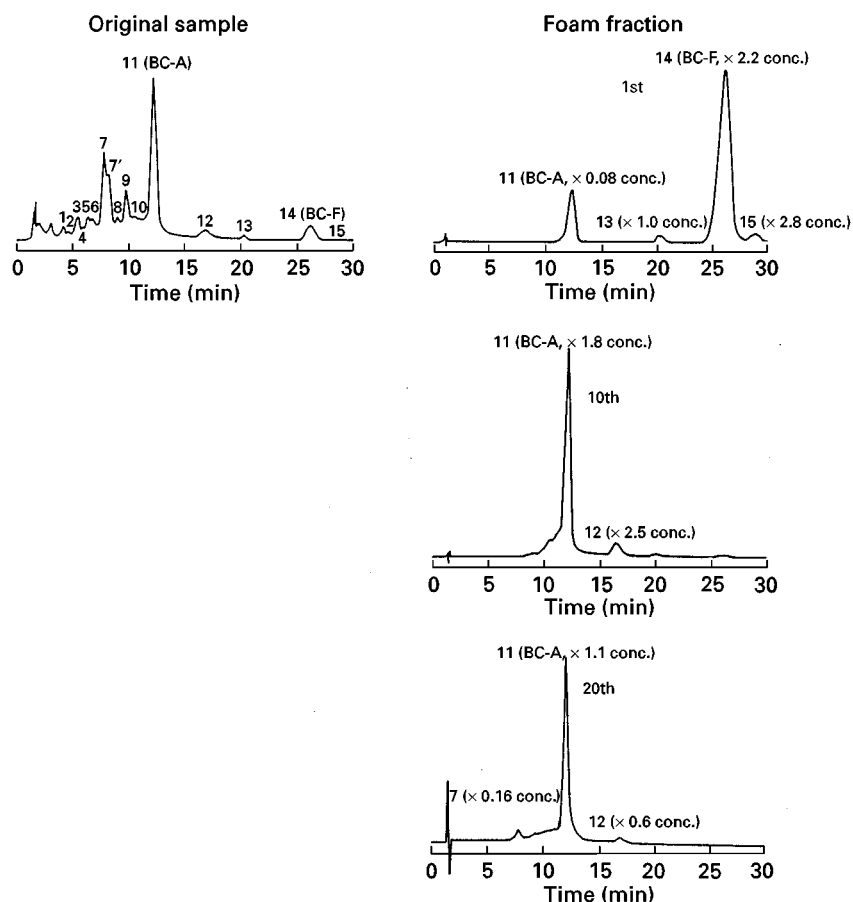


Figure 7 High performance liquid chromatographic analyses of bacitracin components in foam fractions. HPLC conditions: column, Capcell Pak C18 (5 μ m, 150 \times 4.6 mm, i.d.); mobile phase, CH₃OH/0.04 M Na₂HPO₄ (62/38); flow rate: 1 mL min⁻¹; detection, 234 nm.

trogen gas feed pressure, 80 psi; liquid flow rate, 0; sample collection, pooling the foam and the liquid effluents separately; and revolution speed, 500 rpm.

Figure 8 shows the results of HPLC analyses of bacitracin in the foam and liquid fractions obtained by large scale continuous foam CCC. The concentration in the foam fraction increases with the hydrophobicity of the components. Peak 3 was enriched 22 times; peak 7, 31 times; peak 11, 1400 times; peak 12, 1070 times; peak 13, 1380 times; and peak 14, 2260 times. In the liquid fraction, peaks 3 and 7 were barely detected. Thus, continuous enrichment and concentration in foam CCC is quite effective for the detection and isolation of a small amount of natural product with a foaming capacity.

Estimation of applicability of the sample to foam CCC In order to apply the foam CCC technique to various natural products, it is necessary to establish a set of physicochemical parameters which reliably indicate their suitability for foam CCC. In foam CCC the sample solution is introduced from the sample inlet at the middle of the coiled column where it is

immediately mixed with the N₂ stream and the generated foam moves towards the foam outlet at the tail. Since the coiled column consists of a 10-m-long tube, the foam must travel through a 5-m-long narrow coiled path before it reaches the foam outlet. As the foam travels through the decreasing pressure gradient along the coil, every bubble is expanded while the excess fluid is removed by the centrifugal force. Therefore, we assume that the foam must be subjected to a repetitive process of coalescence, eruption and regeneration before reaching the foam outlet at the tail. Consequently, successful foam CCC using nitrogen gas and distilled water free of surfactant requires strong foam-producing capability and foam stability of analytes. A lack of either property would result in its failure.

For this purpose, two parameters were selected, i.e. 'foaming power' and 'foam stability', which can be determined by one simple test. In each test, the sample solution (20 mL) is delivered into a 100 mL graduated cylinder with a ground stopper and the cylinder vigorously shaken for 10 s. The foaming power is expressed by the volume ratio of the result-

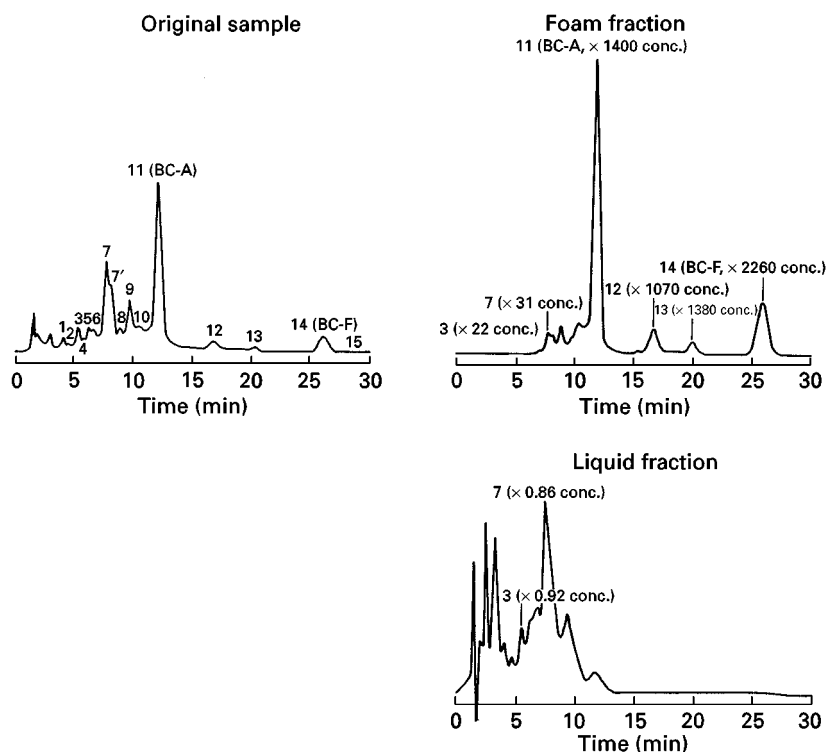


Figure 8 High performance liquid chromatographic analyses of bacitracin components in foam and liquid fractions. HPLC conditions: column, Capcell Pak C18 (5 μ m, 150 \times 4.6 mm, i.d.); mobile phase, CH₃OH/0.04 M Na₂HPO₄ (62/38); flow rate, 1 mL min⁻¹; detection, 234 nm.

ing foam to the remaining solution, and the foam stability by the duration of the foam.

In order to correlate the foaming parameters measured by this simple test method to the productivity in foam CCC, the following five samples were selected because of their strong foaming capacities: bacitracin, gardenia yellow, rose bengal, phloxine B, and senega methanol extract. The results of our studies indicated that a sample having a foaming power greater than 1.0 and a foam stability over 250 min could be effectively

enriched by foam CCC. These minimum requirements of foaming parameters tentatively determined by the bacitracin experiment were found to be consistent with those obtained from the other four samples.

The above simple test has been applied to enrichment of microcystins, hepatotoxic cyclic peptides produced by cyanobacteria. Microcystins was extracted from the bloom sample 917S with distilled water to obtain two extracts with different foaming capacities. The first extract had foaming power of 1.88 and

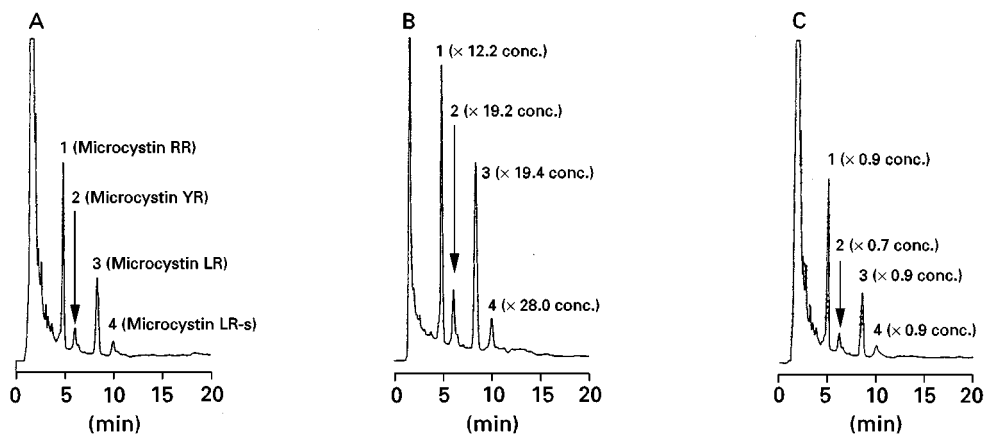


Figure 9 High performance liquid chromatographic analyses of bloom sample 917S extract that satisfies the foaming parameters: A, original sample; B, foam fraction; C, liquid fraction.

foam stability of 93 min which satisfied only the former requirement. The second extract had a foaming power of 1.32 and the foam stability of 720 min which satisfied both requirements for foam CCC. Then, both samples were subjected to foam CCC.

Figure 9A shows a typical HPLC chromatogram of an extract from cyanobacteria bloom sample 917S containing microcystins. As indicated in the chromatogram, peaks 1 (microcystin RR), 2 (microcystin YR), 3 (microcystin LR), and 4 (microcystin LR-s) were chosen to evaluate their foam enrichment. In the first extract, the enriched concentrations of the components are only 3–4 times and polar components with retention times shorter than that of microcystin RR were still present in the foam fraction. The HPLC analysis of foam fraction and liquid fraction of the second extract is shown in Figures 9B and C. The enrichment reached 10–30 times and polar components are eliminated from the foam fraction indicating that the target compounds are selectively enriched. The HPLC analysis of liquid fraction of both extracts showed similar profiles. These results indicate that these foaming parameters can be effectively applied to a crude mixture containing a large amount of impurities.

Conclusions

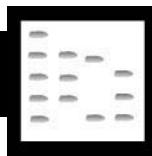
Foam CCC can be successfully applied to a variety of samples having foam affinity with or without surfactants. The present method offers important advantages over the conventional foam separation methods by allowing efficient chromatographic separation of sample in both batch loading and continuous feeding. We believe that the foam CCC technique has a great potential in enrichment, stripping and isolation of foam-active components from various natural and synthetic products in both research laboratories and industrial plants.

See also: II/Chromatography: Liquid: Countercurrent Liquid Chromatography. III/Antibiotics: High-Speed Countercurrent Chromatography; Liquid Chromatography; Supercritical Fluid Chromatography.

Further Reading

- Bhatnagar M and Ito Y (1988) Foam countercurrent chromatography on various test samples and the effects of additives on foam affinity. *Journal of Liquid Chromatography* 11: 21.
- Ito Y (1976) Foam countercurrent chromatography: New foam separation technique with flow-through coil planet centrifuge. *Separation Science* 11: 201.
- Ito Y (1985) Foam countercurrent chromatography based on dual countercurrent system. *Journal of Liquid Chromatography* 8: 2131.
- Ito Y (1987) Foam countercurrent chromatography with the cross-axis synchronous flow-through coil planet centrifuge. *Journal of Chromatography* 403: 77.
- Oka H (1996) Foam countercurrent chromatography of bacitracin complex. In Ito Y and Conway WD (eds) *High-Speed Countercurrent Chromatography*, pp. 107–120. New York: Wiley.
- Oka H, Harada K-I, Suzuki M, Nakazawa H and Ito Y (1989) Foam countercurrent chromatography of bacitracin with nitrogen and additive-free water. *Analytical Chemistry* 61: 1998.
- Oka H, Harada K-I, Suzuki M, Nakazawa H and Ito Y (1989) Foam countercurrent chromatography of bacitracin I. Batch separation with nitrogen and water free of additives. *Journal of Chromatography* 482: 197.
- Oka H, Harada K-I, Suzuki M, Nakazawa H and Ito Y (1991) Foam countercurrent chromatography of bacitracin II. Continuous removal and concentration of hydrophobic components with nitrogen gas and distilled water free of surfactants or other additives. *Journal of Chromatography* 538: 213.
- Oka H, Iwaya M, Harada K-I, Muarata H, Suzuki M, Ikai Y, Hayakawa J and Ito Y (1997) Effect of foaming power and foam stability on continuous concentration with foam countercurrent chromatography. *Journal of Chromatography A* 791: 53.

FOOD ADDITIVES



Liquid Chromatography

V. D. Sattigeri, L. R. Gowda and
P. R. Ramasarma, Central Food Technological
Research Institute, Mysore, India
Copyright © 2000 Academic Press

Introduction

Food is a complex heterogeneous mixture of a wide range of chemical constituents such as moisture, carbohydrates, proteins, fibres, vitamins, etc. Besides these, processed foods contain a wide array of additives and contaminants. Analysis of product composition is a prerequisite for ascertaining product quality,

implementing regulatory enforcements, checking compliance with national and international food standards, contracting specifications and nutrient labelling requirements and providing quality assurance for use of the product for the supplementation of other foods.

Food preservatives form an important class of food additives. They are primarily used to prevent microbial growth, to improve or maintain the nutritional value of food, to maintain palatability and wholesomeness and to enhance flavour and colour. Other food additives used include colours, colour modifiers, flavours, flavour enhancers, humectants, non-nutritive sweeteners, pH control agents, thickeners, stabilizers and emulsifiers. Food additives are regulated and specified by law in most countries to ensure safety for the consumer and prevent deception and fraudulent practices. Labelling regulations require that information be provided on the kind of food, its processing and the additives contained in it.

The complex heterogeneous nature of foods demands effective separation techniques such as High Performance Liquid Chromatography (HPLC) with its wide array of column materials, and detectors. Food additives are usually present in small quantities in processed food items. Their separation from food constituents therefore requires a thorough understanding of the chemistry and physics of the food constituents and additives in order to select the best analytical procedures. Increased automation has gained universal acceptance for the effective separation and analysis of nearly all food components and food additives.

Typical HPLC Analytical Systems

In HPLC analysis of food additives, a single solvent (or solvent mixture) is often not sufficient to carry out the separation under isocratic conditions. Hence, solvent systems of varying proportions are generally used for gradient elution. Abundant literature is available on convenient, versatile and precise liquid chromatography (LC) separations of complex food constituents and additives. Problem areas such as band tailing, trace analysis, preparative separations and so on have received considerable attention and these particular problems can now be tackled in relatively systematic and simple ways.

LC is ideally suited for the separation of macromolecules and ionic species, heat-labile natural products and high molecular weight or less stable compounds such as proteins, nucleic acids, amino acids, dyes, synthetic polymers and food additives.

HPLC is well suited for the quantitative determination of food additives in one step and it has largely replaced other analytical methods.

On account of the wide range of different classes of chemical compounds and matrices encountered, it is not possible to give a universally applicable analytical scheme for food additives. **Figure 1** illustrates the various steps involved in the analysis of antioxidants in potato chips by HPLC as a typical example.

Preservatives

Preservatives are chemicals added to food products to prevent or inhibit the growth of microbes. Benzoic acid, sorbic acid, propionic acid and methyl-, ethyl- and propyl-esters of *p*-hydroxybenzoic acid (parabens) are the most commonly used preservatives.

Preliminary extraction from the food matrix before analysis is required. Steam distillation, solvent and solid phase extractions are the most commonly used methods. Hild and Gertz have reviewed the analytical methods available for the quantitative determination of preservatives in food.

For the HPLC determination of benzoates and sorbates, many methods have been reported using either isocratic or gradient techniques with RP-columns and UV detection at ambient temperatures. LC has been used to separate the homologous esters of *p*-hydroxybenzoic acid (parabens) including methyl- and propyl-hydroxybenzoates. This is of specific importance as the homologous esters of *p*-hydroxybenzoic acid (parabens) are a group of similar compounds having closely related properties. The method described can efficiently determine parabens along with BHA, TBHQ, PG, NDGA and Ionox-100 on reverse phase systems with electrochemical detection. The typical linear range extends from 10^{-11} to 10^{-6} mole of injected analyte. Recovery of parabens is about 80%. Detector potential for parabens is +1.10 V and the electrochemical detector provides low limits of detectability.

Normal as well as reversed phase methods have been used to determine the esters of *p*-hydroxybenzoic acid by extraction with acetonitrile. For normal phase HPLC, the use of LiChrosorb Si 60 columns with a mobile phase of iso-octane + diethyl ether + acetonitrile (500 + 35 + 0.3) and for RP HPLC, RP-18 columns with methanol-water (80 : 20) and UV detection have been suggested. Recoveries are 95–104% with 1–2% RSD. A method for the analysis of parabens in meat products has been developed in which the samples are extracted with acetonitrile, filtered and analysed on a C18 column. The peaks are detected and quantitated using UV detector at 254 nm. Average recoveries are 92% for methyl paraben and 94% for propyl paraben.

HPLC has been used to determine sorbic acid, benzoic acid and *p*-hydroxybenzoic acid (PHB) esters

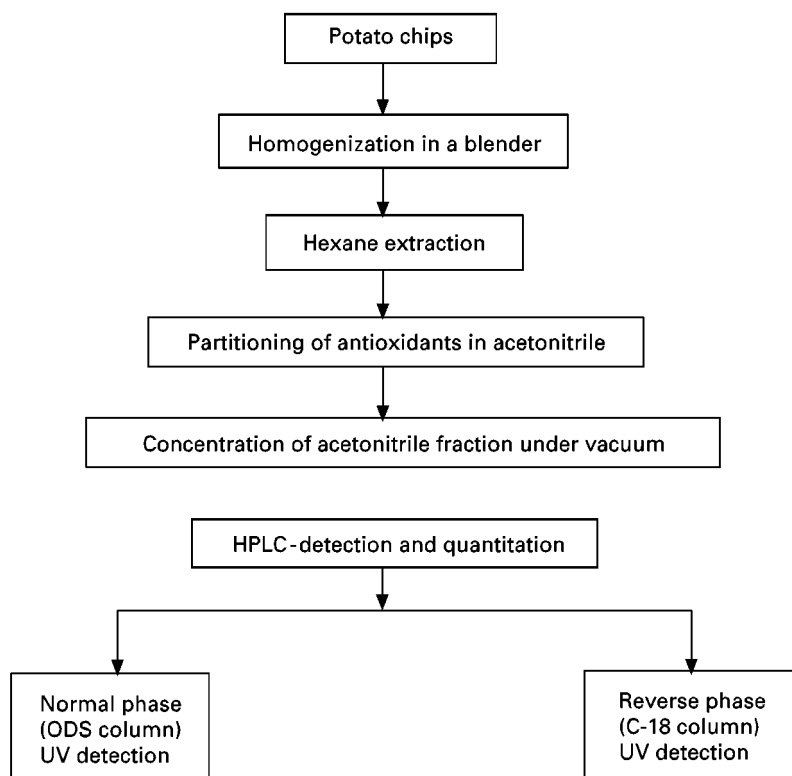


Figure 1 Stages of typical HPLC analysis of antioxidants in potato chips.

in foods. A mixture of acetonitrile, 2-propanol, ethanol and oxalic acid was used for extraction. After refrigerating and separating the interfering materials by centrifugation, the extract was analysed without further cleanup, using Spherisorb ODS II (3 μ m) and methanol–water–phosphoric acid–tetrahydrofuran as eluant and detection at 230 nm and 245 nm. The detection limits were 0.5 mg/kg, 2 mg/kg and 10 ng/kg for sorbic acid, benzoic acid and esters of p-hydroxybenzoic acid, respectively.

Using C-18 silica with methanol and phosphate buffer (1:9, v/v) a lower limit of detections ranging from 5 mg/kg to 1 mg/kg can be obtained for benzoic and sorbic esters of PHB.

The sorbate content of commercial yoghurt sample following ion-pair extraction of sorbic acid and benzoic acid in tri-n-octylamine has been reported. It uses a RP-18 column with methanol–phosphate buffer (40:60, pH 4.5, ionic strength 0.1). Mean recoveries are 70–88% with a precision of 1.1 to 3.3% RSD. Isocratic HPLC is suitable for the determination of the benzoic and sorbic acid in beer. Steam distillation and direct extraction as sample pretreatment methods for analysis of benzoic acid and sorbic acids in salad dressing mayonnaise have been compared. Benzoic acid in chilli sauce can be determined by using RP-HPLC with detection at 254 nm.

Gradient elution methods have been compared for the simultaneous determination of benzoic acid, sorbic acid and parabens in ground beef, non-meat products and pork sausages. These preservatives were extracted with 70% ethanol and analysed on a Novapak C-18 column with a linear gradient mobile phase consisting of 10–70% methanol in 1.5% aqueous ammonium acetate and 1.5% aqueous acetic acid over 10 minutes, with 10 minute hold. Recoveries of benzoic acid, sorbic acid, methyl-, ethyl-, and propyl parabens range from 99–103%. Seven preservatives have been simultaneously measured in 28 food samples. Better selectivity and sensitivity for HPLC compared to other procedures have been reported.

A method applicable to many liquid and solid foods has been described. A C-18 column is used with methanol–phosphate buffer (5:95, v/v) as a mobile phase. This work was carried out to check the specificity of the isocratic-LC method for common food additives such as L-ascorbic acid, caffeine, artificial sweeteners, antioxidants and synthetic colours. The method is applicable for determining benzoic acid and sorbic acid in a wide variety of foods such as beverages, fruits, seafoods, vegetables, sauces, dairy products, bakery products and confectionery products. 4-Hydroxyacetanilide is used as internal standard and detection is at 227 nm. Mean recoveries of

90–105% with a precision of 1–6% and detection limit of 20 mg/kg have been achieved. RP-HPLC for quantitative and simultaneous determination of benzoic acid, sorbic acid, PHB, salicylic acid, 5-nitro-furylacrylic acid, *p*-chlorobenzoic acid and PHB esters in wines and beverages has also been reported.

Sulfites and sulfiting agents permitted in the food industry include sodium sulfite, sodium hydrogen sulfite, sodium metabisulfite, potassium metabisulfite, calcium sulfite and potassium hydrogen sulfite. In the 1980s, an ion-pair method was introduced for the determination of sulfites in fruit juices, dried bread, salad dressing, ground beef, liquid caramel, fruit cake, apple pie, raisin, apple juice, apple sauce, dried onions and white wine using high pressure ion-exchange (I-E) polystyrene with $-\text{NH}_3^+$ and $-\text{NR}_3^+$ groups as stationary phase and 0.0024 M Na_2CO_3 and 0.003 M Na_2HCO_3 as mobile phase with conductivity detector. It has a very good detection limit of 1 ppm and an analysis time of 25 minutes. The results were not affected by the presence of volatile acids or even organic sulfur compounds. Average recoveries of 98.3% with standard deviation of 1.88 were reported with a detection limit of 1 p.p.m.

Electrochemical detectors are now preferred for sulfite analysis due to their better sensitivity. Sulfites have been analysed in lemon juice, beer, mashed potato and white wines using anion exchange

stationary phase and 6 mM H_2SO_4 as mobile phase with electrochemical detectors. Average recoveries were 81–103% with standard deviation of 4.6%. Other food products analysed by different workers by this method include apple, avocado mix, broccoli, cabbage, ketchup, grape juice, mushrooms, onions and raisins.

Table 1 gives details of some methods for the analysis of preservatives in foods and food products.

Antioxidants

During storage, oils and fats undergo various reactions that reduce their nutritive value and also produce volatile compounds, to give unpleasant smells and tastes; the phenomenon is referred to as rancidity. In many cases the presence of antioxidants can inhibit the onset of rancidity.

Synthetic antioxidants permitted to be added to food are:

BHA – 1(or 3)-(*t*-butyl)-4-hydroxy anisole

PG – Propyl gallate

TBHQ – *t*-Butyl hydroquinone

NDGA – Nor dihydroguaiaretic acid

OG – Octyl gallate

DG – Dodecyl gallate

(BHT – Butylated hydroxytoluene is allowed in a few countries)

Table 1 Details of some methods for the analysis of preservatives in food and food products

Food Products	Preservative analysed	Analytical details		
		Stationary phase/ column	Mobile phase	Detection system
Meat samples	Parabens	μ -Bondapak C-18	45% acetonitrile in water	UV at 254 nm
Yoghurt	Sorbic acid, benzoic acid	RP-18	Methanol-phosphate buffer (pH 4.5, ionic strength 0.1) (40 : 60)	UV at 254 nm
Fruit ready to serve, beverages, jams, jellies, meat products	Benzoic acid, sorbic acid, parabens	Novapak C-18	Gradient elution of 10–79% methanol in 1.5% aqueous ammonium acetate and 1.5% aqueous acetic acid over 10 min	UV at 254 nm
Beverages, fruits, seafoods, vegetables, sauces, dairy, bakery and confectionery products	Benzoic acid, sorbic acid	C-18	Methanol : phosphate buffer (0.03 M, pH 6.5) (5 + 95)	UV at 227 nm
Salad dressing, caramel, fruit cake, apple pie, raisins, onions, sauce, white wine, fruit cocktail	Sulfites (free and total)	I-E polystyrene column	0.003 M NaHCO_3 , 0.024 M, Na_2CO_3 , in pure water	Dionex conductivity detector

Satisfactory and complete extraction of antioxidants from a food matrix into various organic solvents is not always easy because of co-extraction of interfering substances. Antioxidants such as BHA, BHT, TBHQ and Ionox-100 are susceptible to losses due to evaporation and utmost care needs to be exercised during concentration under vacuum. NDGA, PG, OG and DG are relatively polar nonvolatile compounds and their recovery is usually satisfactory. HPLC produces good separation between chemically similar compounds in mixtures to be analysed and enables the determination of up to 15 different antioxidants in one single run.

The general analysis protocols for antioxidants in foods comprise extraction in solvents and determination by reversed phase HPLC. The best solvents for extracting antioxidants from fats are acetonitrile and water-alcohol mixtures. The fat is usually dissolved in hexane or petroleum ether and the antioxidant is then extracted into the polar solvent. The literature indicates the use of a variety of chromatographic procedures with UV detection at 280 nm as most commonly used. Mobile phases are acetonitrile, acetic acid, methanol and water.

A HPLC method for the simultaneous determination of phenolic antioxidants in vegetable oils, lard and shortening has been reported. It was concluded that nine antioxidants, viz, BHA, TBHQ, IONOX-100 and THBP, PG, OG, DH and NDGA in vegetable oils, lards and shortening could be separated by gradient elution with water-acetonitrile plus 5% acetic acid as mobile phase. The recoveries ranged from 96 to 103%. A rapid and specific HPLC method for analysis of TBHQ in vegetable oils is also documented. A HPLC method was investigated with amperometric detection to analyse BHA, BHT and TBHQ in edible oils. The antioxidants were well separated, identified and quantified with high sensitivity. Recoveries ranged from 98 to 101%.

The use of RP-HPLC to quantitatively determine five antioxidants—BHA, BHT, PG, OG and DG—in fats has been described. HPLC enables the determination of the full range of antioxidants from polar compounds to the non-polar substances in a single chromatogram using gradient elution. Sensitive detection wavelengths are at 280 nm for UV and at 315 nm for fluorescence emission measurements.

Amperometric detection, which is both sensitive and specific has been used. Determination of BHA and BHT in chewing gums after extraction in hexane and with a second extraction into dimethyl sulfoxide has been reported. The resulting extract was acidified with hydrochloric acid and separated on a μ -Bon-

dapak C-18 column with a mobile phase of acetonitrile–water (55 : 45, v/v). Antioxidants and antimicrobials (Parabens) have been analysed in a variety of commercial products, such as cereals, snacks and shortenings using amperometric detection. The typical linear range is from 10^{-11} to 10^{-6} mole of injected analyte.

Seven antioxidants have been determined using a linear gradient from 30% solution B (acetonitrile–acetic acid 95 : 5, v/v) in solution A (water–acetic acid 95 : 5, v/v) to 100% solution B over 10 minutes with detection at 280 nm. Fifteen antioxidants have been measured in dried foods as well as fats and oils. The antioxidants were separated by isocratic elution with fluorescence and UV detection. Recoveries ranged from 80–106.7%.

The antioxidants diphenylamine and ethoxyquin were estimated using methanol–0.01 M ammonium acetate (60 : 30, v/v) with fluorescence and UV detection. This method has been used successfully for the separation of fungicide residues and antioxidants in fresh fruits. BHA, BHT, PG, OG, DG and TBHQ in corn oil, cottonseed oil and beef fat have been determined. A procedure for the determination of antioxidants in vegetable oils without prior extraction did not resolve BHT from neutral lipids and suffered from interference due to co-eluting materials. PG, trihydroxybutyrophene, TBHQ, BHA, BHT, NDGA and 3,5-di-tert-butyl-4-hydroxy-methylphenol have been determined in fats, oils and dry foods. Antioxidants in dried foods such as potato flakes, dry coffee, whiteners and dessert topping mixes were isolated after rehydration and extraction in acetonitrile and subsequent separation on a C-18 column. The overall recoveries ranged from 64.3 to 103.6%. The method is highly accurate and hence was adopted as an official method (AOAC).

Tocopherols in vegetable oils have been separated by both reversed-phase and normal-phase LC. A method using a Radial PAK cartridge has been used for analysing individual tocopherols in eleven samples of lupine oil. The results showed the presence of γ -tocopherol (42–69 mg/100 g oil), and δ -tocopherol in traces (0.1–0.7 mg/100 g oil). This method is superior to GC in which up to 30% tocopherol losses occur during pretreatment of the sample. The simultaneous determination of α -tocopheryl acetate, tocopherols and tocotrienols in food involving extraction in hexane, separation on Lichrosorb Si-60 with hexane–di-isopropyl ether (93 : 3) as mobile phase and fluorescence detection at 290 nm, 330 nm, has been reported. Recoveries are 95–100% with a detection limit of ≤ 20 ng.

Most methods for the analysis of antioxidants use C₁₈ columns with detection at 280 nm. However,

electrochemical or fluorimetric detection or simultaneous detection by two or more techniques has also been used. Mobile phases are usually composed of aqueous acid (acetic/phosphoric acid), buffers or salts together with methanol or acetonitrile. In many cases results are improved by gradient elution.

A method using a C-18 column for α -tocopheryl acetate and tocopherols has been described which allows separation of nine synthetic phenolic antioxidants along with natural antioxidants. Gradient elution is with water-acetonitrile-methanol-isopropanol. This method not only allows simultaneous detection of antioxidants and triglycerides but is also useful in studying inhibition effects of antioxidants in oil.

BHA, BHT, TBHQ, NDGA and gallates have been resolved and quantitatively determined on a Lichrosorb RP-18 column with gradient elution using acetonitrile–water–phosphoric acid and detection at 280 nm. Fluorimetric detection can also be used. The analysis of BHA, BHT, TBHQ and gallates in carrot juice, powdered milk, appetizers and cake using electrochemical detection has also been reported. It was suggested that as many as twelve antioxidants could be detected by a single isocratic HPLC analysis. The quantitation of BHA, BHT, TBHQ, NDGA, gallates and other antioxidants in foods using Supelcosil LC-

18 column with acetic acid–water–acetonitrile as mobile phase and UV detector at 280 nm has also been documented.

Murakita (1992) and Klein & Leubolt (1993) have reviewed the analysis of various antioxidants by HPLC.

Table 2 shows details of major liquid chromatographic methods for the analysis of antioxidants in foods and food products.

Non-Nutritive Sweeteners

Saccharin, cyclamates, aspartame, acesulfame-K are some of the widely used non-nutritive sweeteners.

Soft drinks containing saccharin are readily analysed with minimal sample treatment. For juice, sweets, jams or desserts, an additional extraction step has to be performed. A method for the separation and detection of saccharin, sodium benzoate and caffeine has been reported involving the use of 5% acetic acid as mobile phase and UV detection at 254 nm. The resolution factor was > 2.0 between saccharin and sodium benzoate and between benzoate and caffeine. The detection limits were 0.14, 0.05 and 0.024 μg for saccharin, benzoate and caffeine respectively. Analysis of non-artificially sweetened soft drinks gave no interfering peaks with these additives. This method has been adopted by the AOAC because of its accu-

Table 2 Liquid chromatographic methods for the analysis of antioxidants in foods and food products

Food products	Antioxidant analysed	Analytical details		
		Stationary phase/ column	Mobile phase	Detection system
Potato flakes	BHA, BHT	C-18	Reversed phase gradient elution by acetonitrile with 5% acetic acid and 5% acetic acid in water	UV, 280 nm
Coffee whiteners	TBHQ, BHA	C-18	Reversed phase gradient elution by acetonitrile with 5% acetic acid and 5% acetic acid in water	UV, 280 nm
Dessert topping PG, DG, OG mixes		C-18	Reversed phase gradient elution by acetonitrile with 5% acetic acid and 5% acetic acid in water	UV, 280 nm
Cheese, snacks, cake mix	BHA, BHT, TBHQ, PG, OD, DG	C-18	Reversed phase gradient elution by acetonitrile with 5% acetic acid and 5% acetic acid in water	UV, 280 nm
Oils, lards, shortenings	BHA, BHT, TBHQ, THBP, Ionox-100, NDGA	C-18	Reversed phase gradient elution. Water-acetonitrile with 5% acetic acid	UV, 280 nm
Instant cereals, snacks, gelatin desserts, hydrogenated fats	BHA, TBHQ, PG, NDGA and Parabens	μ -Bondapak C-18	Methanol–0.1 M ammonium acetate (or 0.01 M phosphate) buffer (1 : 1, v/v)	Amperometric detection

racy. An isocratic HPLC method using a cation exchange column, a 0.1 M ammonium dihydrogenphosphate mobile phase and UV detection at 214 nm has been reported for the detection of saccharin, aspartame, benzoic acid and caffeine in soft drinks. Base-line separations of these four additives were achieved. Changing the wavelength of detection from 254 nm to 214 nm led to an increase in the detection response of aspartame. At all levels of addition the recovery for aspartame was 100%. Analysis time could be reduced by increasing the flow rates without sacrificing resolution.

A gradient method for the separation of saccharin, aspartame, benzoic acid and some colours in soft drinks using a detection wavelength of 214 nm has been reported. The mobile phase was methanol (10% increasing to 60%) with 50 mM phosphate buffer at pH 3.6. For aspartame, either isocratic or gradient elution was used. A method for the determination of aspartame, cyclamate, dulcin and saccharin using an ion-pair separation with indirect photometric detection has also been reported. A method for determining acesulfame-K using UV detection at 237 nm and a mobile phase of water-methanol (9 : 1, v/v) containing 10 mM tetrabutylammonium hydrogensulfate has been reported. The absence of appreciable absorption above 200 nm by cyclamate has led to the advent of special methods for its detection. Post-column ion-pairing of cyclamate with either methyl violet or crystal violet renders it easily detectable. Pre-column derivatization agents used are sodium hypochlorite or *o*-phthalaldehyde. An ion pair HPLC method with indirect photometric detection of cyclamate has been used for thick yoghurt samples and solid foods such as biscuits.

A method has been described for the detection of acesulfame-K, saccharin, dulcin, benzoic acid, caffeine and vanillin in ready-to-serve beverages, dry beverage mix samples and other food products. The separation was carried out on a μ -Bondapak C-18 column using methanol-acetic acid-water (35 : 5 : 60, v/v/v) as mobile phase and with UV detection at 254 nm. This method is advantageous because all the additives can be detected in a single step, which renders it useful in routine food analysis. Biemer analysed acesulfame-K in candy gum using an anion exchange column, sodium carbonate (300 mg/L) as mobile phase and conductometric detection.

A method for the determination of aspartame, saccharin, benzoic acid, sorbic acid and caffeine in cola drinks, table-top sweeteners, soft drinks and complex foods on a LiChrosorb C-18, column using acetonitrile-0.1 M sodium dihydrogenphosphate (15 : 85, v/v) at pH 4.5 and UV detection at 215 nm has been

reported. Analysis of acesulfame-K, alitame, aspartame, caffeine, sorbic acid, theobromine, theophylline and vanillin in table-top sweeteners, candy, liquid beverages and other foods using a μ -Bondapak C-18, column and a mobile phase of acetonitrile-0.0125 M potassium dihydrogen phosphate (10 : 90, v/v) at pH 3.5 and UV detection at 220 nm has been advocated. This method allows for the simultaneous determination of theobromine, theophylline, caffeine, vanillin, dulcin, sorbic acid, saccharin, alitame, aspartame and their degradation products in a single run of 60 min duration. Table-top sweetener, candy, soft drink, fruit juice, fruit nectar, yoghurt, cream, custard, chocolate and biscuits have been analysed by simple extraction or by just dilution using this method.

Some of the simpler LC methods for sweetener analysis are given in Table 3.

Food Colours

Colour is a prime sensory quality by which foods are judged and food quality and flavour are closely associated with colour. Consumers are conditioned to expect foods of certain colours and to reject any deviation from these expectations. Colourants also play a significant role in enhancing the aesthetic appeal of food. Colourants are very important ingredients in many convenience foods such as confectionery products, desserts, snacks and beverages.

The regulatory status of colourants used in different countries throughout the world is in a constant state of flux due to the toxicological considerations. An extensive review of genotoxicity of food, drug and cosmetic colours and other azo triphenylmethane and xanthan dyes has been published by Combes and Haveland-Smith (1982).

Synthetic colours can be classified by their chemical structure as azo (mono, di and tris), indol, triphenylmethane and methin dyes. They are mostly acidic or anionic and acidic groups like sulfuric acid, carboxylic acid or hydroxy groups form a negatively charged coloured ion. Basic or cationic dyes contain substituted amino groups.

The dyes have to be first extracted from the complex food matrix; adsorbents like wool fibres, powdered polyamide, cellulose ion exchange resins or RP cartridges (Sep-Pak C18) are frequently used. Ion-pair chromatography has been used for the quantitative analysis of twelve primary food colours in grape beverages with a mobile phase of 45 : 55 methanol-water, the useful detection wavelengths were 610 nm for blues and greens and 480 nm for reds, oranges

Table 3 Simpler methods for the analysis of food products for non-nutritive sweeteners

Food products	Sweetener analysed	Analytical details		
		Stationary phase/ column	Mobile phase	Detection system
Coffee, carbonated cola, lemon beverages	Sucralose	RadialPak C-18	Water-methanol 70 : 30	RI
Fruit drinks, cherry nectar, mayonnaise, chocolate	Cyclamate	Nucleosil C-18	Methanol-water 80 : 20	UV, 313 nm
Fruit juice, yoghurt, Cola	Acesulfam-K	Lichrosorb RP-18	Methanol-water 9 : 1 with 1 mM tetra butyl ammonium hydrogen sulfate	UV, 237 nm
Cola, pudding, chocolate	Saccharin, cyclamate, Alitame	μ Bondapak C-18 or Supelcosil LC-18	Phosphate buffer 20 mM (pH 3.5) : acetonitrile 97 : 3	RI, UV 200 nm
Ready-to-drink and dry mixes of beverages, tomato sauce	Saccharin, Acesulfam-K	μ Bondapak C-18	Methanol-acetic acid-water, 35 : 5 : 60	UV, 254 nm
Candy, chewing gum	Saccharin, Acesulfam-K	AS4A, anion exchange resin	Sodium carbonate (140 mg/L)	Conductivity
Candy, beverages, pickles, soy sauce	Rebausides A and C, Stevioside	Lichrosorb NH ₂	Acetonitrile-water	UV, 210 nm
Diet cola	Saccharin, Acesulfam-K	Hypersil ODS	Phosphate buffer (pH 3.5)-acetonitrile 85 : 15	UV, 216 nm
Soft drinks, candy, pickle	Rebausides A, Stevioside	Finepak SIL NH ₂	Acetonitrile-water 80 : 18 with tetrabutyl-ammonium phosphate	UV, 210 nm
Fruit yoghurts	Aspartame	μ Bondapak C-18	Phosphate buffer 125 mM (pH 3.5)-acetonitrile 90 : 10	UV, array 400
Soft drinks, table-top sweeteners	Acesulfam-K, Sucralose, Saccharin, cyclamate	Supelcosil LC-18	Acetonitrile (20 mM) : phosphate buffer (pH 3.5)-gradient of 97 : 3 to 85 : 15	Vis 585 nm (after post column ion-pairing)
Candy, soft drinks, yoghurt, custard, fruit juice, nectar, biscuit, chocolate	Aspartame and its decomposition products, Saccharin, Alitame, Acesulfam-K	μ Bondapak C-18	Phosphate buffer 125 mM (pH 3.5)-acetonitrile 90 : 10, 85 : 15, 98 : 2	UV, 220 nm
Table-top sweeteners	Acesulfam-K	Lichrosorb RP-18	Potassium phosphate buffer	UV, 227 nm
Shrimp	Saccharin	IonPac AS-5	Sodium carbonate (7.7 mM) acetonitrile, sodium hydroxide (33 mM) Cyanophenol	Conductivity

and yellow. Ponceau, Fast red-E, Benzyl violet 4B, erythrosine and some non-permitted synthetic colours were separated. The procedure has been reported to be a viable and quicker alternative to TLC-spectrophotometric techniques. A method for the determination of L-orange, Sunset Yellow FCF and Ponceau 4R by means of ion-pair chromatography has also been described. It has been used for analysis of food dyes E 110, E 111 and E 12 in fish samples

using Nucleosil, C-18 or Lichrosorb RP-8 columns and detection at 505 nm. The mobile phase consisted of water-acetone mixtures (80 : 20) with tetrabutylammonium chloride added as ion-pair agent (0.2 g/L).

Carotenoids in red bell peppers were separated without saponification using a C₁₈ column and methanol-ethyl acetate as mobile phase with detection at 475 nm.

Table 4 Simpler methods for the analysis of colours in food and food products

Food products	Colour analysed	Analytical details		
		Stationary phase/ column	Mobile phase	Detection system
Fruit juices, grape beverages, confectionery	Ponceau, Fastred E, benzyl violet 4B, erythrosine	Ion-pair HPLC	Methanol–water	480 nm, 610 nm
Fish, bakery, meat products, miscellaneous products	E-110-orange II E-III-orange I and E-124 Ponceau 4R	Lichrosorb RP-8	Water – acetonitrile (80 : 20)	505 nm
Olive oil	Chlorophylls, carotenoids	C-18	Methanol – acetone	410 nm
Red bell pepper	Carotenoids	ODS	Methanol – ethylacetates (1 : 1)	410 nm
Strawberry	Anthocyanins	ODS	10–30% aq. acetonitrile with 0.5% TFA	Photodiode array detector

A rapid method has been reported for quantitation of chlorophylls and carotenoids in virgin olive oil, by solid phase extraction on a C-18 column. The fat free pigments were separated and concentrated. A total of 17 pigments were separated and quantitated with a C-18 column and gradient elution of water–ionic pairing reagent–methanol and methanol–acetone (1 : 1). Detection was at 410 nm and 430 nm. β -Carotene and other hydrocarbon carotenoids have been determined in red grape fruit cultivars with non-aqueous eluents using a C-18 column and isocratic mobile phase consisting of acetonitrile, methylene chloride and methanol (65 : 25 : 1, v/v/v).

Anthocyanins have been extracted from cultured cells of strawberry plants using a 35% solution of acetic acid–acetonitrile–water (20 : 25 : 55), containing 0.1% trifluoroacetic acid; using a C-18 column, and using 10 to 30% aqueous acetonitrile containing 0.5% of trifluoroacetic acid as eluent in 30 min at 40°C with photodiode array detection. The method yielded higher concentration of anthocyanin than other methods.

Table 4 gives details of methods for the analysis of colours in foods and food products.

Emulsifiers and Wetting Agents

Food emulsifiers assist the stabilization and formation of emulsions by reducing surface tension at the oil–water interface. Common food emulsifiers used are:

- lecithin and lecithin derivatives
- glycerol fatty acid esters
- hydroxycarboxylic acid and fatty acid esters
- lactylate fatty acid esters
- polyglycerol fatty acid esters

- ethylene or propylene glycol fatty acid esters
- ethoxylated derivatives of monoglycerides.

Quantitative analysis of emulsifiers is difficult as most of them are similar in structure, their commercial sources are quite heterogeneous and their extraction from starchy foods is very difficult. A key problem is the quantitative extraction of emulsifiers and the exclusion of interfering substances. This problem is further complicated by the presence of food ingredients such as proteins, and the innate heterogeneity of most of the emulsifiers as well as the wide variation in their composition. The schemes of analysis for lecithin, monoglycerides, TEMS, acetylated monoglycerides, partial polyglycerol esters, propylene glycol esters, polysorbates, lactic acid esters, ethoxylated monoglycerides and sugar esters have been discussed. Baur has recommended solvents for extraction of emulsifiers.

A method for the separation of monoglyceride (E 471), sodium stearoyllactylate (E 481), calcium stearoyllactylate (E 482), diacetyltartaric acid esters of mono- and diglycerides (E 472e) and mixed acetic and tartaric acid esters of mono- and diglycerides (E 472f) on a semi-preparative column has been described. Various emulsifiers were identified by off-line high resolution mass spectrometer. Analysis of sodium or calcium stearoyllactylate showed that the major components were 2-stearoyl and 2-palmitoyl lactic acid and their salts.

Sodium dioctylsulfosuccinate, a wetting agent, has been permitted in a variety of food products including dry beverage bases. A post-column ion-pair extraction method was employed using methylene blue as counterion. Then the compound was extracted into chloroform from the aqueous phase

For analysis, a CN column was used with acetone–0.01 M KH_2PO_4 (1 : 5, v/v) as a mobile phase.

See also: II/Chromatography: Liquid: Mechanisms: Reversed Phases. III/Food Additives: Thin-Layer (Planar) Chromatography.

Further Reading

- Baur FJ (1973) *J. Am. Oil. Chem. Soc.* 50: 85.
 Combes RD and Haveland-Smith RB (1982) *Mutat. Res.* 98: 101.
 Grendy TH (1991) Intense Sweeteners for Food Industry: An Overview. *Trends in Food Sci. Tech.*, 2: 1.
 Klein H and Leubolt R (1993) *J. Chromatogr.* 640: 259.
 Kurihara Y and Nirasawa S (1994) Sweet, antisweet and sweetness-inducing substances. *Trends in Food Sci. Tech.* 5: 37.

- Macrae R (1982) *HPLC in Food Analysis*. London: Academic Press.
 Malissek R and Wittkowski R (1993) *High Performance Liquid Chromatography in Food Control and Research*. Lancaster: Technomic.
 Nollet LM (ed.) (1992) *Food Analysis by HPLC*. New York: Marcel Dekker.
 Nollet LM (1996) *Handbook of Food Analysis*. New York: Marcel Dekker.
 O'Brien Nabors L and Gelardi RC (1992) *Alternative Sweeteners*. New York: Marcel Dekker.
 Prodoliet J and Bruehart M (1993) Determination of Acesulfam-K in foods. *J. AOAC International*, 76: 268.
 Sardesai VM and Waldsham TH (1991) Natural and Synthetic Sweeteners. *J. Nutr. Biochem.* 2: 236.
 Walters DE, Orthoefer FT and Dubois GE (1991) *Sweeteners: Discovery, Molecular Design and Chemoreception*, ACS Symposium Series 450. Washington: American Chemical Society.

Thin-Layer (Planar) Chromatography

M. Vega, Faculty of Pharmacy, University of Concepción, Concepción, Chile

Copyright © 2000 Academic Press

Introduction

Thin-layer chromatography (TLC) is a relatively old technique among the other chromatographic separation methods. In food additive analysis, this simple technique is the tool of choice, mainly because the high throughput of samples that it can manage in parallel and the wide range of compounds that can be analysed simultaneously.

Food Additives

Anything added to food is not necessarily a food additive. Generally, a food additive is a substance or a mixture of substances different to the bulk of the food and present as a result of any aspect of production, processing or packing. This definition does not include hazardous contaminants.

The Codex Alimentarius Commission for Food Additives defines these as follows:

Food additive means any substance not normally consumed as a food by itself and normally used as a typical ingredient of the food, whether or not it has nutritive value, the intentional addition of which to food for a technological (including

organoleptic) purpose in the manufacture, processing, preparation, treatment, packing, packaging, transport or holding of such foods, results or may reasonably expect to result (directly or indirectly), in it or its by-products becoming a component of or otherwise affecting the characteristics of such foods. The term does not include 'contaminant' or substances added to the food for maintaining or improving nutritional qualities.

Others definitions include:

Substance with non-nutritive properties, known chemical composition, intentionally added to food; generally in small amounts, with the aim of improving presentation (appearance, flavour, texture) and conservation properties of foods.

In other countries, such as Spain, additives are all substances that can be added intentionally to food and drink, without the purpose of changing the nutritive value, to modify processing and conservation characteristics, as well as to improve their adaptation to the use for which it is produced.

Classification of Food Additives

Many methods have been used to classify food additives. The majority imply functional grouping.

Chemical-type grouping is convenient because it puts together moieties of similar structures and chemical properties in comparative categories. Toxicological and metabolic studies can also be correlated with chemical grouping. However, compounds belonging to the same chemical family have different functions in the food industry. In spite of the fact that a compound can have two or more different functional groups, this classification is more practical in the food industry. **Table 1** shows a typical classification of food additives.

Table 1 shows the diversity of compounds included in the different classes generated. Grouping by functional group type can include chemical substances both naturally and structurally quite different. This is an additional problem for the analysis of substances considered, classified or included in lists of food additives.

In modern quality control, analysis is required at every step and not just in the final product. This is to prevent possible defects directly at the critical points but it produces a significant increase in the number of samples and the number of analyses to be carried out.

On the other hand, it is important to consider that additives can be applied exclusively to those foods where regulation points out specifically that they must be used and normally they must be declared on labels attached to the food.

In spite of tolerance limits for some additives, the amount added should not exceed the amount adequate to attain the objective, using the appropriate manufacturing procedure. This justifies the necessity to detect and quantify food additives. Today there are many analytical procedures applied to these substances. Obviously the method used will depend on the analytes, and their characteristic and/or physico-chemical properties.

Table 1 Permitted classes of food additives in Australia

<i>Class of additive</i>	<i>Property of food influenced</i>
Preservatives	Shelf-life
Colourings	Appearance
Flavouring and flavour enhancers	Flavour
Antioxidants	Shelf-life
Artificial sweetening substances	Flavour, energy value
Vitamins and minerals	Nutritive value
Modifying agents	
Vegetable gums	Texture, appearance
Mineral salts	Texture, appearance
Food acids	Shelf-life, flavour, texture
Emulsifiers	Texture, appearance
Humectants	Texture, shelf-life
Thickeners	Texture

It is necessary to extract the additive compound from the food matrix and to apply additional purification procedures where necessary. Chromatographic methods, which involve a separation process, allow the isolation of the compound(s) to be analysed. High performance liquid chromatography (HPLC), gas chromatography (GC) and TLC have all been used extensively for the final analysis.

For large numbers of samples, the comparative advantage of TLC is that it is a completely instrumental technique that can deal with many samples simultaneously, and with samples of a diverse nature.

In the past few years, many reviews have been published with the aim of featuring the relevant characteristics of instrumental planar chromatography, or high performance thin-layer chromatography (HPTLC).

In the first place, it is necessary to describe the advances obtained in the preparation of sorbents for stationary phases.

Silica still represents the most frequently used material for the stationary phase. Approximately 90% of separations by TLC are still carried out using silica. Modern sorbents are characterized by smaller and more uniform particle size, implying a reduction of equivalent plate height. This results in a higher number of theoretical plates for a given run length compared with traditional phases and, in turn, this allows separations in shorter distances with corresponding time savings and reduction of diffusion problems that appear when the mobile phase is retarded excessively.

Stationary phases of polarity from intermediate to reversed phase, have been developed. Most of them are obtained by chemical modification of silica gel (**Table 2**).

Recently, sorbents with spherical particles such as Lichrospher Si 60 F254s have appeared. They offer shorter analysis times, improved separation

Table 2 HPTLC stationary phases used in food additives analysis

<i>Stationary phase</i>	<i>Food additives</i>
3-Aminopropyl	Sugars, carboxylic acids, preservatives
Reversed-phase, C18	Preservatives, antioxidants
Aluminium oxide	Lipophilic food dyes
Silica normal	Antioxidants, sweeteners, surfactants, dyes
Cellulose	Artificial sweeteners, carboxylic acids
Cellulose MN 300	Food dyes

efficiency, more compact spots, higher spot capacity and lower detection limits. All these new plates are applicable to the analysis of many analytes including those used as food additives.

Advances in instrumentation in the whole chromatographic process, ranging from application devices through automatic developing chambers, and automated multiple development (AMD) chambers with computer control, all deserve special consideration. Computer-controlled AMD using polarity gradients increases efficiency in separation to limits comparable to HPLC, and retains the high throughput of samples to be analysed in the same chromatographic run.

Major developments in densitometers have meant improvements in the quantitative analytical ability of planar chromatography. These, coupled to software, allow quantitative analysis of substances at very low concentrations thanks to the high sensitivity of detectors that allow measurements over the whole UV-visible spectrum as well as fluorescence.

Another important aspect of HPTLC in food additive analysis, is that there are some compounds with difficult detection characteristics. The variety of reagents available, overcomes this difficulty and they can be used as pre- or postchromatographic derivatizing agents.

Finally, video scanning not only allows information to be saved digitally but also gives quantitative results from image integration.

Unlike HPLC, TLC needs very little sample purification and can be used with raw or dirty materials, thereby saving time and additional expense.

Applications of HPTLC in Food Additive Analysis

TLC has been used for many years in the analysis of food additives, such as food dyes, preservatives (Table 3), antioxidants and sweeteners.

Food colourants are in many cases fundamental food additives because consumers judge product quality by its colour. On the other hand, before a dye (natural or synthetic) is permitted for use on food it has to be shown that it is nontoxic and noncarcinogenic. The current list in western European countries comprises about 30 natural or artificial substances permitted as food dyes, and is very small compared to the vast number of known dyes. This makes it necessary to have easy and fast methods to detect forbidden or unapproved food dyes (Table 4).

Because the importance of colourings in foods, a variety of separation procedures are still being examined with the aim of improving performance.

Table 3 Analysis of preservatives by HPTLC

<i>Preservatives</i>	<i>Layer</i>	<i>Eluent</i>	<i>Detection</i>	<i>Reference</i>
p-Hydroxybenzoates n-propyl, ethyl, methyl	Silanized silica C18	Methanol–water (7 + 3, 6 + 4, 5 + 5, 4 + 6 v/v)	UV λ = 270 nm	Volkman D (1980) <i>HRC and CC</i> , 3: 189
8 different preservatives	Mixed layers of silica and cellulose, F254	Petroleum ether–CCl ₄ – CHCl ₃ –formic acid– glacial acetic acid (50 + 40 + 20 + 8 + 2 v/v)	UV λ = 254 nm	Gosselé JAW (1971) <i>Journal of Chromatography</i> 63: 433
Propyl, ethyl, methyl, hydroxybenzoates, 4- hydroxybenzoic acid	RP18 W/F254	Acetone–water (40 + 60 v/v)	UV λ = 254 nm	Machery-Nagel (1990) TLC department
Parabens (hydroxybenzoic acid esters)	Silicagel 60, F254	1) pentane– dichloromethane–acetic acid (25 + 25 + 3 v/v) 2) petroleum ether–diethyl ketone–acetic acid (88 + 5 + 12, v/v)	UV λ = 255 and 310 nm	Zimmermann A <i>8th Symposium of German Association of Scientific and Applied Cosmetics</i> , Hamburg, November 1989
Benzoic acid, sorbic acid and parabens	Polyamide/cellulose	Toluene–petroleum ether– CHCl ₃ –acetic acid (30 + 15 + 10 + 1 v/v)	UV λ = 230 benzoic acid λ = 260 others	Duden R, Frikers R, Calverley KH, Park, Rios VM, Lebensm Z (1973) <i>Unters, und Forsch</i> 151: 23

Table 4 HPTLC systems for food dye analysis

<i>Food dye</i>	<i>Layer</i>	<i>Eluent</i>	<i>Detection</i>	<i>Reference</i>
Seven dyes: erythrosine, brilliant black NN, fast red E, naphthol red, yellow orange S, ponceau 4R, tartrazine	Cellulose MN300	Sodium citrate 2.5%–25% ammonia–methanol (20 + 5 + 3, v/v/v)	Coloured substances	Machery-Nagel (1990) TLC Department
Tartrazine, Amaranth Indigo Carmine, New coccine, Sunset yellow FCF, Allura Red Ac, Fast green FCF, Brilliant blue FCF, R-106, R-103, R-3, R-105, and R-104	Silica-RP18	(A) methanol–acetonitrile–5% sodium sulfate (3 + 3 + 10, v/v/v) (B) methanol–MEK–5% sodium sulfate (1 + 1 + 1, v/v/v)	Scanning at different wavelengths	Oka H <i>et al.</i> (1987) <i>Journal of Chromatography</i> 411: 437–444
Sulfonated dyes ponceau, tartrazine, azorubin etc.	RP18; ion pair optimization	(A) Methanol–water (8 + 2, v/v) (B) Methanol–water + 20 mM solution of tetrabutylammonium bromide	Visual comparison	Korner A (1993) <i>Journal of Planar Chromatography</i> 8: 138–143
Unlawful food dyes detection	Silica-RP18	(A) methanol–acetonitrile–5% sodium sulfate (3 + 3 + 10, v/v/v) (B) Methanol–MEK–5% sodium sulfate (1 + 1 + 1, v/v/v)	TLC–FAB–MS	Oka H <i>et al.</i> (1994) <i>Journal of Chromatography A</i> 674: 301–307
Quinoline Yellow, Sunset Yellow, Cochineal Red A, Indigo Carmine, Tartrazine, Amaranth, Erythroline	Silica 60, F254 OPLC	(A) NH ₃ –methanol–ethyl acetate (1 + 3 + 6, v/v/v) (B) NH ₃ –MEK–n-butanol (2 + 3 + 5, v/v/v)	Different wavelengths	Rózylo JK and Siembida KR (1997) <i>Proceedings of the 9th International Symposium on Instrumental Planar Chromatography</i>

The use of surfactants, (hexadecyltrimethylammonium bromide) incorporated in the mobile phase for the separation of acids and alkaline food colourings, new polymer coatings for plates and new adsorbents such as Scolecite (corresponding to a natural zeolite) are recent approaches. Some colourants such as indigo carmine, cochineal red, acid amaranth and tartrazine G, have been separated on thin magnesium oxide layers with mixtures of 15% sodium citrate and methanol. Reversed-phase plates, obtained by impregnation of silica plates with 10% liquid paraffin in petrol ether are used for separation of different food dyes with advantage.

For food preservatives like benzoic and sorbic acid, the use of methods such as solid phase extraction (SPE) allow a better separation of these food additives from natural ingredients present in beverages.

Overpressured thin layer chromatography (OPTLC) has been shown to be a good tool for the separation

of a variety of food additives, like antioxidants, natural food colourings, preservatives and water-soluble vitamins with silica plates. In this field, AMD has also been successful in the separation, identification and quantification of a diverse range of antioxidants.

Other food additives that requires adequate control are artificial sweeteners and antioxidants, because of the carcinogenic properties attributed to some of them. Analysis of these is frequently carried out by HPLC, but, HPTLC shows the comparative advantages formerly mentioned. **Table 5** summarizes some HPTLC systems for analysis of these food additives.

See also: II/Chromatography: Thin-Layer (Planar): Layers; Modes of Development: Forced Flow; Over Pressured Layer Chromatography and Centrifugal; Spray Reagents. **Dyes:** High-speed Countercurrent Chromatography; Liquid Chromatography; Thin-Layer (Planar)

Table 5 HPTLC systems for antioxidants and sweeteners

Additive	Layer	Eluent*	Detection	Reference
BHA, BHT, NDGA, Gallic acid esters	Silicagel 60, F254 OPLC	CHCl ₃ -HAc CHCl ₃ -Methanol-HAc Benzene-Methanol-acetone-HAc Methanol-acetone-water	Spraying with 0.5% solution of 2,6 dichloroquinone-4 chlorimide and heating to 105°C	Siembida R (1997) <i>Proceedings of the 9th International Symposium on Instrumental Planar Chromatography</i>
Gallic acid esters, BHA, BHT, DBH, TBH	Silicagel-G25 HR	Petroleum ether-benzene-HAc (2 + 2 + 1, v/v/v)	Spraying with 0.5% solution of 2,6 dichloroquinone-4 chlorimide and heating to 105°C	Machery-Nagel (1990) TLC Department
BHA and dodecylgallate	Silicagel	Xylene-CHCl ₃ -propanol-formic acid-HAc (45 + 45 + 10 + 1 + 1, v/v/v/v/v)	10% Phosphomolybdate or vainillin in sulfuric acid	Sherma J and Fried B (1991) <i>Handbook of Thin Layer Chromatography</i> . Marcel Dekker, Inc.: 702
Saccharin, cyclamate	Laboratory made mixed layers Cellulose MN300-polyamide; (3 + 2)	Xylene-HAc-n-propanol-formic acid (45 + 7 + 6 + 2 v/v)	Spray of developed plate with ethanolic dichlorofluorescein solution	Wooldich <i>et al.</i> (1969) <i>Z Lebenm. Unters. Forsch.</i> 139: 142
Aspartam, acesulfam, saccharin	Silicagel G-25, UV ₂₅₄	Xylene-HAc-n-propanol-formic acid (45 + 7 + 6 + 2 v/v)	Scanner dual wavelength 215/370 nm	Machery-Nagel (1990) TLC Department

* HAc = acetic acid

Chromatography. **Food Additives:** Liquid Chromatography. **Impregnation Techniques: Thin Layer (Planar) Chromatography. Pigments:** Liquid Chromatography; Thin-Layer (Planar) Chromatography.

Further Reading

- Cserháti T and Fogács E (1997) Trend in thin - layer chromatography. *Journal of Chromatography Science* 35: 383-391.
- Fried B and Sherma J (1994) In: Fried B and Sherma J, *Thin-Layer Chromatography: Techniques and Applications*, 3rd edn. New York: Marcel Dekker Inc.
- Furia TE (ed.) (1972) *Handbook of Food Additives*, 2nd edn. Boca Raton: CRC Press, Inc.
- Jork H, Funk W, Fisher W and Wimmer H (1994) *Thin Layer Chromatography: Reagents and Detection Methods*, vol. IB. Weinheim: VCH.
- Sherma J and Fried B (eds) (1990) *Handbook of Thin-Layer Chromatography*. New York: Marcel Dekker, Inc.
- Stahl E (ed.) (1969) *Thin-Layer Chromatography. A Laboratory Handbook*, 2nd edn. Heidelberg, New York: Springer-Verlag Berlin.
- Touchtone JC (ed.) (1992) *Practice of Thin Layer Chromatography*, 3rd edn. New York: John Wiley and Sons. Inc.

FOOD MICROORGANISMS: BUOYANT DENSITY CENTRIFUGATION



R. Lindqvist, National Food Administration,
Uppsala, Sweden

Copyright © 2000 Academic Press

Introduction

Density gradient centrifugation is an established technique for the separation and purification of eukaryotic and prokaryotic cells, viruses and subcellular components such as plasmids, mitochondria and nucleic acids. Using this technique, components may be separated based on their differences in density or size during centrifugation in a gradient medium. Gradient media that have been used include caesium chloride, sodium metrizoate, sucrose, Ficoll, Ludox®, Percoll® and BactXtractor™. One of the limitations with this technique has often been the properties of the gradient medium used. For instance, it is crucial that the gradient medium is at physiological ionic strength to avoid cell lysis or dehydration effects. Further, the gradient medium should be nontoxic and not affect the viability of the cells.

Density gradient centrifugation using different gradient media has been used to separate a wide range of microorganisms from various types of samples. For example, bacteria have been recovered from soil using sucrose gradients and different types of protozoa have been separated from river water, faeces, etc., using various gradient media. Further, gradient centrifugation in Percoll® has been used to distinguish subpopulations of pathogenic bacteria and to separate live from dead eukaryotic cells.

To some extent this technique has also been used to separate microorganisms from food, e.g. in the separation of bacteria from milk and natural yoghurt. The main benefits of using density centrifugation is its simplicity and speed in separating and concentrating intact organisms from foods while at the same time removing compounds that might interfere with or inhibit the detection method. The ability to remove inhibiting or interfering material present in food has been evaluated by subsequent detection of prepared microorganisms through methods of varying sensitivity such as traditional plate count procedures, the polymerase chain reaction (PCR), nucleic acid sequence based amplification (NASBA), and ATP measurements.

The present work describes how to use buoyant density centrifugation and gives an example of how

to design a procedure for the separation of microorganisms from a specific food. This approach has been successful for several food/microorganism combinations and it has been possible to separate and concentrate bacteria from food and to remove inhibitors sufficiently to allow detection of bacteria by both PCR and NASBA. However, in some cases, especially when the food contains denser components, there can be limitations which may be overcome by use of a two-layer technique also described here. The protocols presented are based on work described in Lindqvist *et al.* (1997), Lindqvist (1997) and Anonymous (1995) (see Further Reading).

General Theory and Methodology

Principles of Centrifugation

Equation [1] describes the sedimentation of a sphere in a centrifugal field:

$$v = [d^2(\rho - \rho_1)/18\eta] \times g \quad [1]$$

where v = sedimentation rate, d = diameter of the particle (hydrodynamically equivalent sphere), ρ = particle density, ρ_1 = liquid density, η = viscosity of the medium and g = centrifugal force.

From this relationship it can be seen that the sedimentation rate of a particle is proportional to its size and to the density difference between the particle and the medium. Also, the sedimentation rate is zero when the density of the particle is equal to the density of the surrounding medium. Further, the sedimentation rate decreases with increasing viscosity of the medium and increases with increasing centrifugal force applied. From this it also follows that separation depending on the conditions chosen may be carried out based on either the size (rate zonal centrifugation) or the density differences (isopycnic centrifugation) between particles. In the latter case, each particle will sediment to an equilibrium position in the gradient where the gradient density is equal to the density of the particle. In the present work, the isopycnic technique is discussed.

The specific cell density, i.e. cell weight/cell volume when measured by buoyancy in a given medium capable of forming density gradients, is referred to as the buoyant density. Consequently, anything that affects the size of the microorganism, e.g. osmotic

conditions and growth phase, may also affect their buoyant densities and, thus, separation. This stresses the importance of the properties of the gradient medium and of using standardized conditions when developing and using the separation protocol.

Gradient Media

Two gradient media with favourable properties for work with microorganisms are Percoll® and BactXtractor™. The composition and properties of these gradient media are similar (see below). The most important difference is that BactXtractor may be autoclaved after NaCl and peptone have been added to prepare a standard isotonic medium (SIM). Percoll and BactXtractor are nontoxic, have a low osmotic pressure and viscosity. These media consist of colloidal silica particles of 15–30 nm diameter coated with polyvinylpyrrolidone (PVP). They can form self-generated gradients in the range of 1.0–1.3 g mL⁻¹, which correspond to the cell densities of many microorganisms. When a solution of Percoll® (or BactXtractor™) is centrifuged at > 10 000 × *g* in an angle-head rotor, the coated and hydrated silica particles will sediment resulting in an uneven distribution of particles and the formation of a self-generated density gradient. The gradient is formed isometrically around the initial density of the gradient medium and becomes steeper with centrifugation time. The shape of the gradient can be visualized by the use of coloured density marker beads and is related approxim-

ately linearly to the *g* force and time of the centrifugation. Rotor geometry and the size of the tubes also have a marked effect on gradient shape. In contrast to the self-generated continuous gradient, for some applications a uniform density centrifugation using one (cushion) or several layers (step gradient) of the gradient medium is preferred. The latter approaches are discussed here for the separation of bacteria from food.

Overview of Methodology

When designing a separation protocol, the same procedure may be followed independent of the subsequent detection method. This procedure includes the following steps (Figure 1): (1) determination of the buoyant density of the microorganism; (2) determination of the buoyant density of the food; (3) selection of the concentration of the gradient medium to be used in the separation of the microorganism from food; (4) evaluation of the separation protocol with the desired detection method; and (5) optimization of the protocol if necessary.

Preparation of the Gradient Medium

The gradient media, Percoll® (Pharmacia Biotech, Sweden) or BactXtractor™ (QRAB, Uppsala, Sweden) have a density of around 1.130 g mL⁻¹. Before use, the medium is made isotonic with physiological saline by aseptically adding 8.5 g L⁻¹ NaCl, and

Step	Method
1. Determination of buoyant density of microorganism	Self-generated gradient centrifugation
2. Determination of buoyant density of food	Self-generated gradient centrifugation
3. Selection of gradient medium concentration	Based on results in steps 1 and 2, and from Figure 2. Test separation by visual inspection of centrifuge tube after centrifugation of food and microorganisms
4. Evaluation of separation protocol	Inoculate homogenate, prepare samples by centrifugation using the selected SIM concentration, analyse with the desired detection method
5. Optimize protocol (if necessary)	Vary homogenization and / or centrifugation conditions, sample retrieval, etc.

Figure 1 Schematic overview of the sequential steps involved in designing a protocol for separation of microorganisms from food.

its suitability for maintaining microorganisms is improved by addition of 1.0 g L^{-1} peptone. This stock solution is termed 100% standard isotonic medium (100% SIM) and may be autoclaved if prepared with BactXtractor™. The solution of 100% SIM is diluted to the required concentration with the appropriate volume of peptone-water (8.5 g NaCl and 1.0 g peptone in 1 litre of Millipore water).

The density of the 100% SIM solution described above is calculated by the following formula:

$$\begin{aligned}\rho_s &= [V_g \times \rho_g + m_{\text{NaCl}} + m_p]/V_g \\ &= [100 \times 1.130 + 0.85 + 0.1]/100 = 1.1395 \quad [2]\end{aligned}$$

where ρ_s = the density of 100% SIM (g mL^{-1}), V_g = the volume of gradient medium to be prepared (mL), assumed here to be 100 mL (the volume change by addition of solutes is negligible), ρ_g = the actual density of the gradient medium, assumed here to be 1.130 g mL^{-1} , m_{NaCl} = the amount of NaCl added (g), assumed here to be 0.85 g and m_p = the amount of peptone added (g), assumed here to be 0.1 g.

By using eqn [2], the density of 100% SIM was calculated to be 1.1395 g mL^{-1} , assuming that 100 mL of gradient medium with a density of 1.130 g mL^{-1} was mixed with NaCl and peptone. The relationship between density and concentration of SIM can be determined by plotting the calculated density of a 100% solution and the density of a 0% solution, i.e. the density of the diluent, as a function of percent SIM concentration and then determining the equation for the straight line between these two

points:

$$\begin{aligned}\rho_{\text{sy}} &= [(\rho_g - \rho_p)/(100)] \times C_s + \rho_p \\ &= [(1.1395 - 1.0095)/100]C_s + 1.0095 \\ &= 0.0013 \times C_s + 1.0095 \quad [3]\end{aligned}$$

where ρ_{sy} = the density of SIM of concentration C_s (g mL^{-1}), ρ_p = density of peptone water, estimated here to be 1.0095 g mL^{-1} , C_s = concentration of SIM (%) and ρ_g = the actual density of the gradient medium, assumed here to be 1.130 g mL^{-1} .

The line described by eqn [3] and shown in Figure 2 is valid only for the properties of the gradient medium and diluent assumed in this work but similar graphs can easily be constructed for other experimental conditions. The graph can then be used to determine what concentration of SIM is required to produce a gradient medium of a particular density.

Determination of the Buoyant Densities of Microorganisms

Since the buoyant densities of microorganisms may be affected by a number of factors, it is important that they are handled and separated from food under standardized conditions. For instance, the buoyant densities of bacteria in Percoll® gradients have been shown to vary with growth rate and during the cell cycle for some bacteria but not for others. Further, efforts to inactivate bacteria by, for instance, boiling, heating, and low pH treatment have shown that,

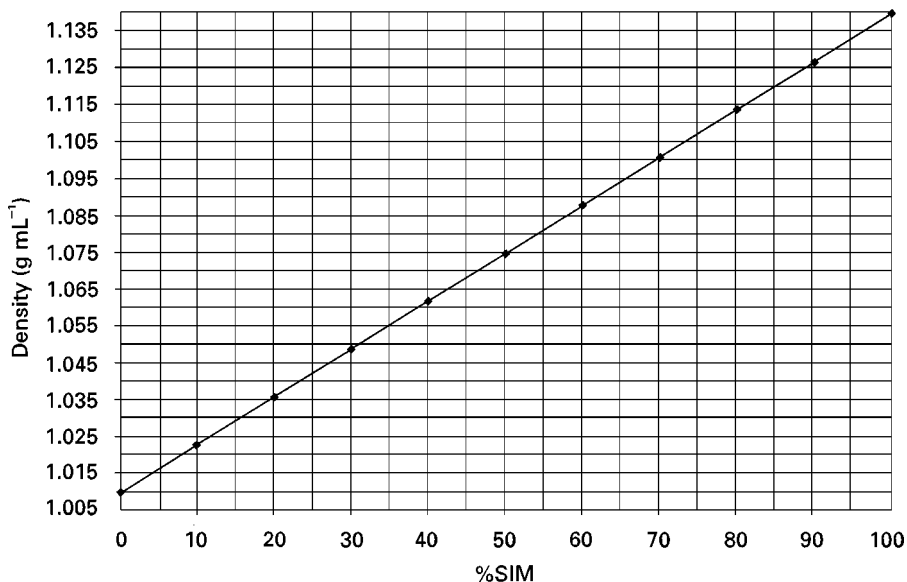


Figure 2 The relationship between density and concentration of the standard isotonic medium (SIM). The relationship described by this line is only an example and was calculated based on the conditions described in this work. The exact relationship must be calculated based on the density of the gradient medium and the diluent used.

depending on the treatment and the strain used, this may or may not affect their buoyant densities. Some variation in buoyant densities of a given strain may be expected depending on the culture media used, storage time after growth, etc., but ideally this is in a density range where separation is not affected. However, the presence of different subpopulations in the sample, e.g. log-phase and stationary cells, may result in a wide continuous distribution, or even separate bands, of microorganisms within the centrifuge tube.

Preparation of Microorganisms

A sufficient number of strains are cultured and treated under relevant conditions to collect data on the buoyant density of the microorganism and its variation. The number of cells loaded on to the gradient must be large enough to form a visible band in the centrifuge tube after centrifugation. In most cases a solution containing 10^8 – 10^9 cfu mL⁻¹ is sufficient. The solution is prepared by centrifuging an appropriate volume of culture, washing, and resuspending in physiological saline or peptone-water. The washing and resuspension of cells in fresh physiological saline solution serves to suppress variations in osmotic pressure introduced by the presence of metabolites, etc.

Sampling Loading

The appropriate volume of the microorganism suspension or solution containing the density marker beads is carefully layered on the standard isotonic medium. There are no definite rules on how much sample it is possible to load on to the gradient and

this must be tested empirically. The best SIM concentration to use depends of course on the microorganisms. In our work, concentrations between 50% and 80% and between 40% and 70% have been used with microorganisms and food, respectively. However, in addition to buoyant density, specific requirements on the amount of sample and the shape of the gradient may influence the scale of the experiment, i.e. rotor geometry and size of the tubes. **Figure 3** shows examples of a large scale and a small scale protocol.

Generation and Reading of the Gradient

The gradient is generated by centrifugation and is visualized by substituting the sample volume with a solution of colour-coded density marker beads (Pharmacia Biotech, Sweden) on top of the gradient medium. A volume of marker solution equivalent to the sample volume is prepared by adding approximately 5–10 µL of each marker bead to a physiological saline solution. During centrifugation, the density beads equilibrate at positions in the gradient corresponding to their densities. The distance of the differently coloured density beads from the bottom of the tube is recorded and the densities of the beads are plotted versus the position to generate a calibration curve (**Figure 4**). Similarly, the position of the microorganisms in the centrifuge tube is recorded and the corresponding buoyant density is read from the calibration curves. The best resolution is obtained in the steep part of the curves where a large distance in the centrifuge tubes corresponds to a small difference in density (**Figure 4**). By comparing the shapes and locations of the three gradients in **Figure 4** it can be seen that the resolution in the 60% SIM gradient is

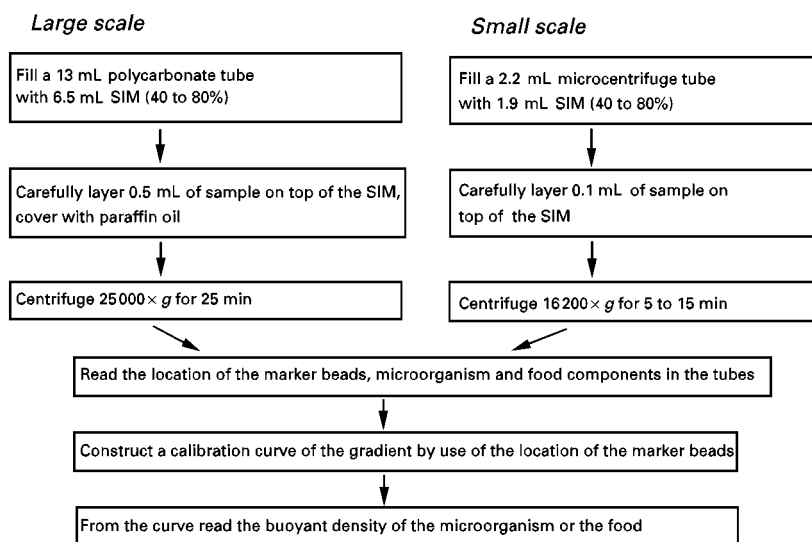


Figure 3 Example of two protocols for the determination of the buoyant density of microorganisms and food.

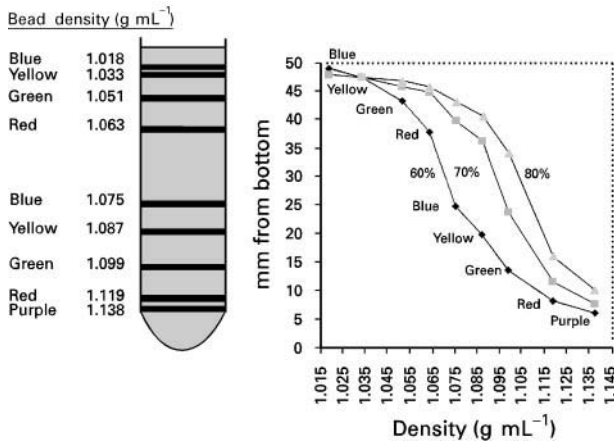


Figure 4 Illustration of how to construct calibration curves for the determination of the buoyant densities of microorganisms and food. The gradients were generated by layering 0.5 mL of density marker beads on 6.5 mL of 60%, 70% or 80% SIM and centrifuging at $25000 \times g$ for 25 min. Left: the positions of the different bands of colour-coded density marker beads in 60% SIM. Right: the curves were constructed by plotting the position and the density of the density marker beads in the diagram. The best resolution is obtained in the steep part of the curves, i.e. large difference in position corresponds to a small difference in density.

better at lower densities and vice versa for the 80% SIM. However, in addition to the selection of the SIM concentration, it is sometimes useful to vary the centrifugation time and speed when optimizing the gradient for a specific microorganism or food. In a given gradient, the width of the more or less well-defined band of microorganisms following centrifugation depends on the number of microorganisms and the range of buoyant densities present in the population under study.

Determination of the Buoyant Densities of Food

The food homogenate to be loaded on the gradient medium must be sufficiently concentrated to be visible in the centrifuge tube. Thus, a more concentrated homogenate is often used for this step than will be used in the final separation protocol. Typically a 1:1 to 1:10 (w/v) homogenate is suitable. The determination of the buoyant density of food is then carried out by centrifugation in a self-generated density gradient as described above for the microorganism.

Selecting the Concentration of the Gradient Medium

The simplest technique to separate microorganisms from food is to centrifuge the sample on a single layer

of gradient medium of a uniform density (cushion centrifugation). During the previous steps the buoyant densities of the microorganism and of the food have been determined under the relevant conditions which will indicate if separation is possible, i.e. if there is a difference in buoyant densities that may be exploited. The food is generally less dense than the microorganisms and the density of the gradient medium is chosen so that it lies between the densities of the food and the microorganism. Thus, the microorganisms will be found in the bottom of the tube after centrifugation. The optimum concentration of SIM to use to obtain the cutoff density between food and microorganisms can be determined from the relationship between density and SIM concentration described in eqn [3] and Figure 2.

Separation by a Uniform Density Centrifugation

A quick way to test if the correct concentration of SIM has been selected is to run a uniform density centrifugation (see below) of a cell suspension and food homogenate, respectively. After centrifugation, food should remain on top of the gradient medium and cells should be visible in the lower part of the tube. Based on the exact position of microorganisms, the volume of sample that needs to be retrieved is determined. The sample volume is the amount of medium contained in the centrifuge tube from the upper band limit to the bottom of the tube.

In order to run a uniform density centrifugation, gradient formation during centrifugation should be avoided. This may be achieved either by centrifugation in a swing-out rotor or, if using an angle-head rotor, by centrifuging under conditions where gradient formation is negligible (e.g. low g forces or short centrifugation times).

Evaluation of Protocol

To evaluate the separation procedure, inoculated food homogenates are analysed with the desired method of detection, e.g. plate counts or PCR. The size of the centrifuge tubes to use depends on the amount of sample needed for detection as well as the number of samples to be analysed in a given time.

In Figure 5, examples of a large scale (larger sample capacity) and a small scale (larger sample throughput) protocol for separation of microorganisms from food are offered to assist in the selection of which centrifugation conditions to be used. Similar, or identical, protocols have been used to separate microorganisms, e.g. *Shigella* spp., *E. coli* O157:H7, *Yersinia enterocolitica*, *Campylobacter* spp. and

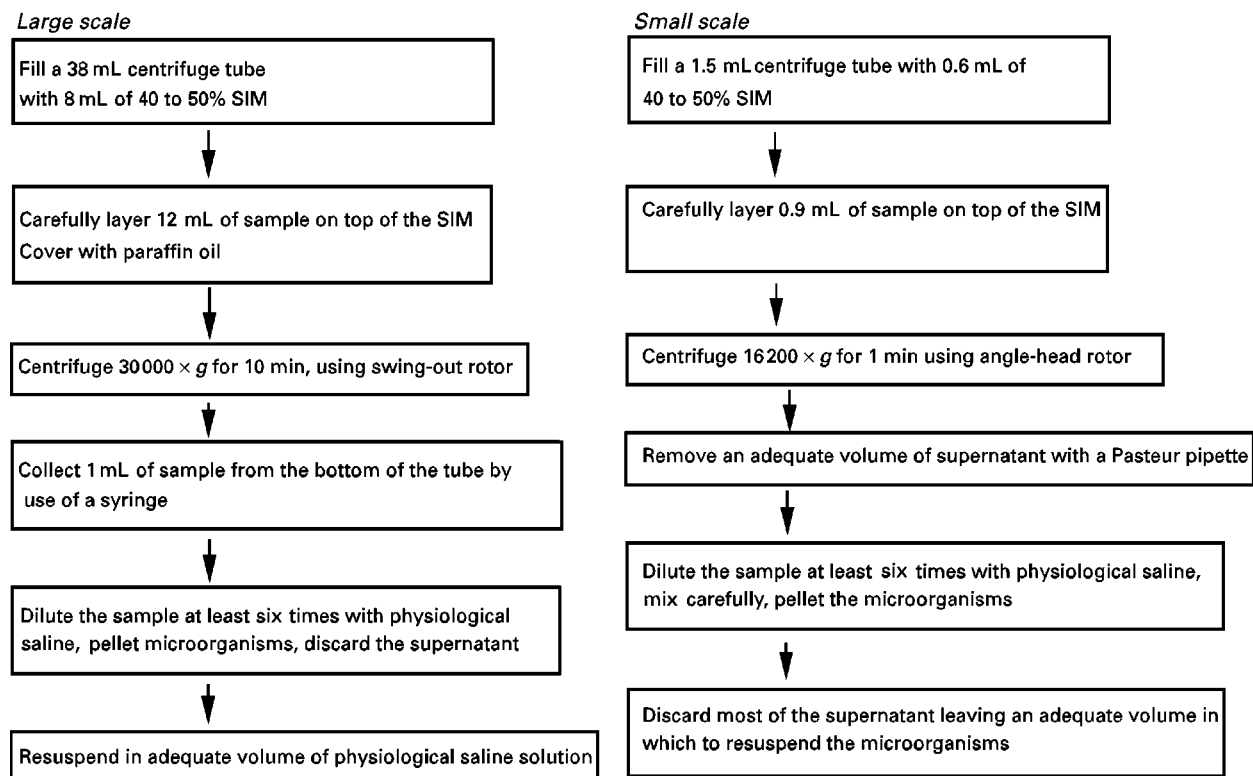


Figure 5 Example of two protocols for the separation of microorganisms from food by a uniform density centrifugation.

Zygosaccharomyces rouxii from different foods, e.g. raw beef, ground beef, different vegetables, shrimps, chicken, blackcurrant syrup, and milk, prior to detection by methods such as PCR, NASBA and plate count procedures.

Optimization of Protocol

If, due to incomplete separation, the detection limit is not satisfactory there are some key separation parameters that can be changed. Initially it can be helpful to add density marker beads corresponding to densities similar to those of the microorganisms during the uniform density centrifugation. The location of the beads will indicate where in the tube the microorganisms will be found and if the optimal SIM concentration has been used. The beads may also indicate if a gradient has formed during centrifugation.

Instead of sampling from above, as suggested in Figure 5, microorganisms can be retrieved by insertion of a syringe through the bottom of the centrifuge tube to avoid the mixing of inhibitory compounds or particles from the supernatant during cell removal.

If particles from the food end up in the treated sample, one can try to decrease the particle content in the sample volume prior to centrifugation by diluting

the homogenate and/or preparing the homogenate in a stomacher bag with a filter bag. If this does not help, or if the food contains particles denser than the microorganism, it is possible to use two layers of gradient medium of different but uniform concentrations (step gradient). The density of the second layer is chosen to lie between that of the microorganisms of interest and the denser components of the food. This technique has been used to separate pathogenic bacteria in a blue cheese from the lighter cheese particles and from denser fungal mycelia. The sample is retrieved at the interface between the gradient layers and this position can be identified by centrifugation of an identical tube where the sample is replaced with density marker beads.

Another possibility, if the exact buoyant density of the microorganism is known such as in a well-defined and constant experimental system, is to perform the separation step using a continuous gradient centrifugation.

Future Developments

Buoyant density centrifugation is a general method which recovers nonattached microorganisms over a specific buoyant density. This suggests two possible areas for development and improvement. The first

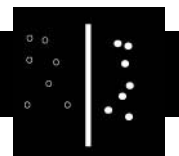
would be to increase the fraction of nonattached cells by optimization of the homogenization or stomaching process. The second area is the exciting possibility of developing a separation protocol specific for single types of microorganisms, or a systematic or metabolic group of microorganisms. This may be achieved by manipulating the buoyant density of an organism through a selective uptake of a specific compound. Further, since it is possible to perform the separation on a micro scale, it may be feasible to design automated systems for sample preparation and analysis with a high sample capacity.

See also: II/Centrifugation: Theory of Centrifugation.

Further Reading

- Anonymous (1992) *Percoll® Reference List*, 2nd edn. Sweden: Pharmacia P-L Biochemicals Inc.
- Anonymous (1995) *Percoll® Methodology and Applications*, 2nd edn. Sweden: Pharmacia Biotech Inc.
- Basel RM, Richter ER and Banwart GJ (1983) Monitoring microbial numbers in food by density centrifugation. *Applied and Environmental Microbiology* 45: 1156–1159.
- Guerrero R, Mas J and Pedros-Alio C (1984) Buoyant density changes due to intracellular content of sulphur in *Chromatium warmingii* and *Chromatium vinosum*. *Archives in Microbiology* 137: 350–356.
- Guerrero R, Pedros-Alio C, Schmidt TM and Mas J (1985) A survey of buoyant density of microorganisms in pure cultures and natural samples. *Microbiologia* 1: 53–65.
- Kubitschek HE (1987) Buoyant density variation during the cell cycle in microorganisms. *Critical Reviews in Microbiology* 14: 73–97.
- Lindqvist R (1997) Preparation of PCR samples from food by a rapid and simple centrifugation technique evaluated by detection of *Escherichia coli* O157:H7. *International Journal of Food Microbiology* 37: 73–82.
- Lindqvist R, Norling B and Thisted Lambert S (1997) A rapid sample preparation method for PCR detection of food pathogens based on buoyant density centrifugation. *Letters in Applied Microbiology* 24: 306–310.
- Payne MJ and Kroll RG (1991) Methods for the separation and concentration of bacteria from foods. *Trends in Food Science & Technology* 5: 384–389.
- Pertoft H and Laurent TC (1968) The use of gradients of colloidal silica for the separation of cells and subcellular particles. In: Gerritsen T (ed.) *Modern Separation Methods of Macromolecules and Particles*, vol. 2, pp. 71–90. New York: Wiley Interscience.
- Scherer P (1983) Separation of bacteria from a methanogenic wastewater population by utilizing a self-generating percoll gradient. *Journal of Applied Bacteriology* 55: 481–486.

FOOD TECHNOLOGY



Membrane Separations

M. Cheryan, University of Illinois, Urbana, Illinois, USA

Copyright © 2000 Academic Press

One of the earliest successful industrial applications of membrane technology was in the food industry. In 1972, a dairy plant in New York began processing cheese whey by reverse osmosis. Membrane separations are now ubiquitous in the food industry, as shown in Table 1. The main use of reverse osmosis is the concentration of liquid foods, to complement or replace evaporation. Nanofiltration is used for desalting and de-acidification with partial concentration, while ultrafiltration is used for fractionation, concentration and purification of food streams. Microfiltration is used for clarification and removal of suspended matter to replace centrifuges and filter presses. It is also used for pasteurizing and sterilizing liquids instead of using heat. Electrodialysis is finding use for demineralization and de-acidification, as a possible

partial replacement for ion exchange. To date, pervaporation applications are few in the food industry, although it could be used for purification of volatile aroma compounds partially to replace distillation. This article focuses on selected food products with varying physical properties and chemical composition and will illustrate the general applicability of membrane technology in the food industry.

Dairy Industry

Milk

The dairy industry probably accounts for the largest share of installed membrane capacity among food-processing applications. Figure 1 is a general schematic of possible applications of membranes in the processing of milk. Reverse osmosis (RO) is mostly used to preconcentrate milk prior to evaporation (although there are RO techniques that could concentrate skim milk up to 45% solids, as with the Fresh-note process, described later). This not only saves sufficient energy to justify the technology, but it also

Table 1 Food industry applications of membrane technology*Dairy*

RO: Preconcentration of milk and whey prior to evaporation; bulk transport; specialty fluid milk products

NF: Partial demineralization and concentration of whey

UF: Fractionation of milk for cheese manufacture; fractionation of whey for whey protein concentrates; specialty fluid milk products

MF: Clarification of cheese whey; defatting and reducing microbial load of milk

ED: Demineralization of milk and whey

Fruits and vegetables

Juices: apple (UF, RO), apricot, citrus (MF, UF, RO, ED), cranberry, grape (UF, RO), kiwi, peach (UF, RO), pear, pineapple (MF, UF, RO), tomato (RO)

Pigments: anthocyanins, betanins (UF, RO)

Wastewater: apple, pineapple, potato (UF, RO)

Animal products

Gelatin: concentration and de-ashing (UF)

Eggs: concentration and reduction of glucose (UF, RO)

Animal by-products: blood, wastewater treatment (UF)

Beverages

MF, UF: Wine, beer, vinegar – clarification

RO: Low-alcohol beer

Sugar refining

Beet and cane extracts, maple syrup, candy wastewaters – clarification (MF, UF), desalting (ED), preconcentration (RO)

Oilseeds, cereals, legumes

Soybean processing: Protein concentrates and isolates (UF); protein hydrolysates (CMR); oil degumming and refining (UF, NF); recovery of soy whey proteins (UF, RO); wastewater treatment (MF, UF, NF, RO)

Corn refining: Steepwater clarification and concentration (MF, UF, RO); light-middlings treatment: water recycle (RO); saccharification of liquefied starch (CMR); purification of dextrose streams (MF, UF); fermentation of glucose to ethanol (CMR); downstream processing of fermentation broths (MF, UF, NF, RO, ED, PV); wastewater treatment (MF, UF, NF, RO)

RO, reverse osmosis; NF, nanofiltration; UF, ultrafiltration; MF, microfiltration; ED, electrodialysis; CMR, continuous membrane reactor; PV, pervaporation.

exposes milk to less heat during the concentration process, which minimizes protein denaturation and development of the 'cooked' flavour and other heat-damaging effects on the constituents of milk.

Perhaps the greatest potential for RO and/or ultrafiltration (UF) in the dairy industry is in bulk milk transport, especially in those countries which have large distances between producing and consumption areas. Considering that milk is more than 85% water, preconcentration of the milk prior to shipment to central dairies should result in considerable savings in transportation costs, as well as reducing chilling and storage costs. RO milk products, when reconstituted with good-quality water, are indistinguishable from unconcentrated milks in flavour and other quality attributes. On-farm ultrafiltration of milk is technically feasible for large dairy herds if the concentrated milk is used for the manufacture of cheese. Stability of ultrafiltered milk is satisfactory with proper pretreatment such as thermalization at 65–70°C for 10–20 s to minimize lipase activity, and if health and safety requirements are met on the farm.

Ultrafiltration of milk RO milk could be used in the manufacture of several other products, such as cultured milk products and cheese. However, UF seems

to be the preferred technique in these applications. UF allows the passage of the lactose and soluble salts while retaining the protein and fat and some of the insoluble or bound salts. There is considerable potential in the manufacture of specialty milk-based beverages such as lactose-reduced and calcium-enhanced fluid milk products. Total milk protein isolates are usually manufactured by co-precipitation using a combination of heat, acid and/or calcium salts. This generally results in low protein solubility, which restricts its use as a functional food ingredient. UF of milk in combination with diafiltration can produce 90% protein isolates from milk with lactose concentrations of less than 0.1%.

The principal use of milk UF in the dairy industry today is the manufacture of cheese. From a membrane technologist's point of view, cheese can be defined as a fractionation process whereby protein (casein) and fat are concentrated in the curd, while lactose, soluble proteins, minerals and other minor components are lost in the whey. In the UF cheese-making process, milk is first concentrated to a 'pre-cheese' which will have the same protein, fat and/or solid levels normally found in cheese. This pre-cheese is then converted to cheese by conventional or modified cheese-making methods. Some of the benefits of

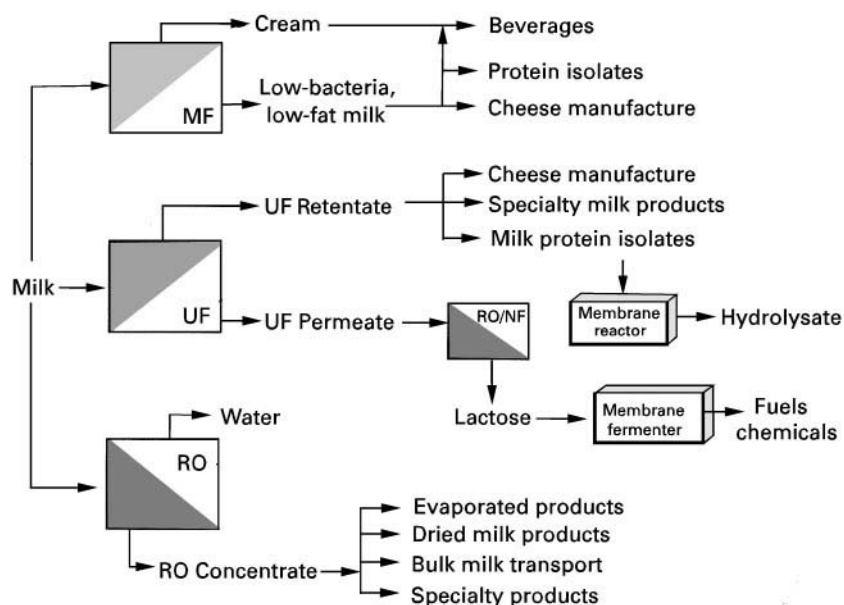


Figure 1 Membrane processing of milk. (Reprinted with permission from Cheryan and Alvarez (1995).)

using UF in cheese-making are:

- There is an increase in yield of 10–30% with soft and semi-soft cheeses due to the inclusion of the whey proteins
- The amount of enzyme (rennet) required is sometimes lower
- There is a reduced volume of milk to handle
- Fewer cheese-making vats are required
- Plant space is used better
- There is little or no whey production because most of the water and lactose has already been removed

Considerable research has been conducted with a variety of cheeses such as feta, quarg, white cheeses from Turkey, Egypt (domiati, kariesh), Greece (teleme) and South America (queso fresco), goat's milk cheese, Camembert, ricotta, mozzarella, cheddar and processed cheese.

Microfiltration of milk The main applications of microfiltration (MF) in milk processing are fat separation and bacterial removal. This concept has been put into commercial practice as the uniform transmembrane pressure (UTP) or co-current permeate flow (CPF) process. Tubular ceramic membranes with 1.4 μm pores are operated in a double-loop constant-pressure operation. Because of the uniform and low pressure profiles in the membrane module, fouling is low and flux is very high (700–1000 $\text{L m}^{-2} \text{h}^{-1}$ at 10-fold concentration of skim milk). Bacterial retention is 99% and the microbial load usually found in milk and fat is also substantially rejected. On the

other hand, there is no significant change in the concentration of other components, so the permeate is essentially bacteria-free skim milk.

This process became commercial in 1989 to produce more stable pasteurized and refrigerated milk products. It could also be useful in subtropical and tropical countries, where inadequate refrigeration and transportation facilities result in high microbial loads in the milk coming into dairy plants. Such a membrane system in the bulk-milk holding station or on the receiving dock of the milk-processing plant could lower the microbial load significantly and improve the quality of milk products in these countries.

Enriched casein fractions (i.e. separated from whey proteins and other soluble milk components without isoelectric precipitation) can be produced using MF membranes. In addition, β -casein can be isolated from casein micelles if the temperature is lowered to less than 5°C, which causes β -casein to dissociate from the micelle and be removed in the permeate (a loose UF membrane of 100 000 (molecular weight cut-off) can also be used to isolate β -casein from milk). This protein has biological activity potential in pharmotherapeutic applications.

Cheese Whey

Whey is a by-product of the cheese industry. During the manufacture of cheese, most of the milk protein (the casein) and fat is concentrated in the curd, which eventually becomes the cheese, while other constituents go into the water phase and become the whey. Every 100 kg of milk will give about 10–20 kg of

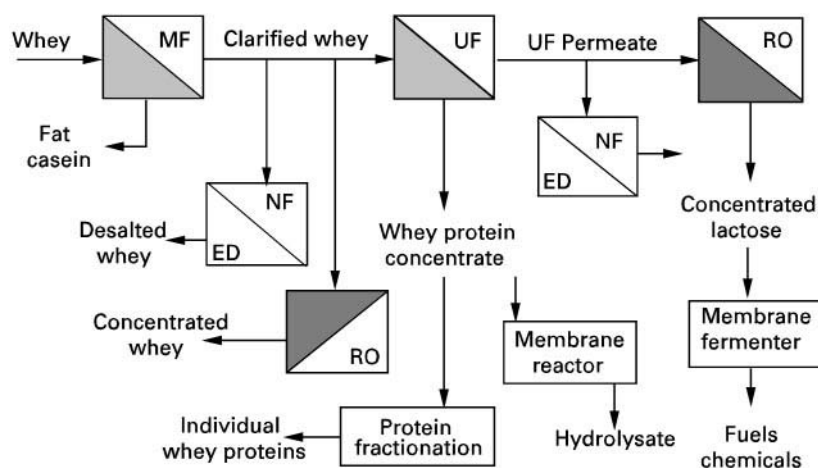


Figure 2 Membrane processing of cheese whey. (Reprinted with permission from Cheryan (1998).)

cheese depending on the variety, and about 80–90 kg of liquid whey. The disposal of whey is a problem: its biological oxygen demand (BOD) is 32 000–60 000 p.p.m. It has low solid content and a very unfavourable ratio of lactose to protein, which makes it difficult to utilize in food products without changing its composition. Prior to membrane technology, as much as 60–70% of the whey produced was disposed as sewage, with the rest being used primarily for animal feed or human food. World production in 1996 was estimated at 80–130 million tons per year: the USA produced about 30 million tons per year.

Membrane technology, and UF in particular, has provided a valuable means of upgrading cheese whey and increasing its utilization as a human food. The appropriate membrane can simultaneously fractionate, purify and concentrate whey components (Figure 2), enhancing their market value and reducing the pollution problem. Today, whey protein concentrates (WPC) produced by UF are well established in the food and dairy industries. Owing to the relatively mild process conditions of temperature and pH, the functionality of the whey proteins remains good, giving rise to a wide range of applications. The initial protein content of 10–12% (dry basis) can be increased by UF, to result in 35, 50 or 80% protein products, with a concomitant decrease in lactose and some salts. WPC can be further fractionated into β -lactoglobulin and α -lactalbumin fractions as shown, or be used for the manufacture of caseinomacropепptide, a compound which may have a pharmaceutical value.

Fruit Juices

Next to the dairy industry, fruit and vegetable juices have benefited the most from membrane technology.

There are three primary areas where membranes can be applied in this application: firstly, clarification, e.g. in the production of sparkling clear beverages using microfiltration or ultrafiltration; secondly, concentration, e.g. using reverse osmosis to produce fruit juice concentrates of greater than 42° Brix (a measure of sugar concentration); and thirdly, de-acidification, e.g. electrodialysis or nanofiltration to reduce the acidity in citrus juices.

Clarification of Fruit Juice

Fruit juices are prepared by extraction followed by a series of filtration and clarification steps to yield clear single-strength juices (Figure 3). These operations are usually labour- and time-consuming. Membrane filtration can replace the holding, filtration and decantation steps. The properties of the membrane, especially its pore size distribution, affect flux and capacity, as well as juice properties such as clarity, browning compounds and total phenolics in the finished product.

Membrane filtration has several advantages over traditional methods. It eliminates fining agents (bentonite, gelatin, etc.), most enzymes (pectinase, amylase), centrifugation and diatomaceous earth filtration. Process times are reduced from 12–36 to 2–4 h. Juice yields are higher, by 2–15%, and product quality is better. The largest application is apple juice, but the following have also received considerable attention: apricot, carrot, cherry, cranberry (which was one of the earliest applications of ceramic membranes), blackcurrant, grape, guava, kiwi, lemon, lime, maple sap, melon, orange, passion fruit, peach, pear, pineapple, plum, raspberry, strawberry and tomato.

Citrus juices (grapefruit, orange, lemon, lime) are being upgraded by combining UF and adsorbent resin

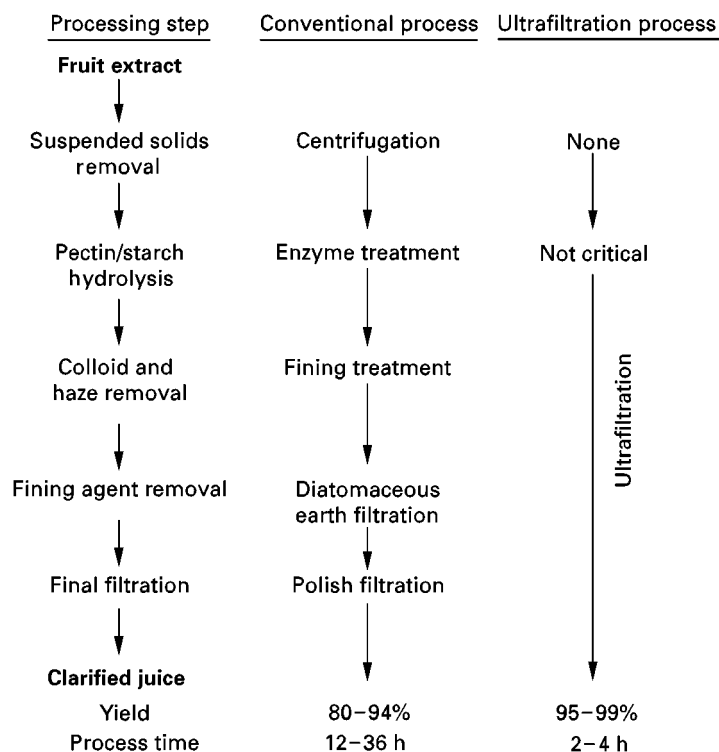


Figure 3 Processing fruit juices by conventional and membrane technology. (Reprinted with permission from Cheryan (1998).)

technology to remove bitter compounds such as limonin, naringin, hesperidin, polyphenols and many other off-flavour compounds. These compounds are in the aqueous phase of the juice. Fresh or reconstituted citrus juice which has been de-oiled and pasteurized is first ultrafiltered to separate the pulp. The clarified permeate containing the sugars and bitter compounds enters the absorption column which contains an adsorbent resin specifically designed to remove these compounds. The debittered juice is then recombined with the pulp (the UF retentate) to give a product with less than 5 p.p.m. limonin, which is its apparent taste threshold (400–500 p.p.m. for naringin).

In recent years, several fruit juice installations have incorporated ceramic membranes. The higher cost has been justified by the higher flux, much longer life and their resistance to aggressive processing and cleaning conditions. The ability to backflush to unblock feed channels and back-pulsing during operation are other advantages.

Concentration of Fruit Juice

Orange and other citrus juice concentrates are mostly produced by conventional multi-stage evaporation. RO with the appropriate polyamide composite membrane can concentrate juice without a significant loss of aroma, sugar or acids. The low temperatures avoid thermal damage of delicate aroma components.

However, conventional RO is limited by osmotic pressure and viscosity considerations to less than 30° Brix. Therefore, RO can be used as a preconcentration step, with thermal evaporation completing the required concentration to 42–45° Brix. Adding RO ahead of the evaporators can increase evaporator capacity and reduce thermal treatment.

A significant development in the 1980s was the development of the FreshNote process by Du Pont and FMC. It allowed the production of highly concentrated (42–70° Brix) fruit juices using a combination of high and low retention RO membranes. UF is first used to separate the pulpy solids from the serum. The UF retentate, about 1/10th–1/20th the feed volume, is subjected to a pasteurization treatment that destroys spoilage microorganisms and improves stability of the finished product when blended back with the concentrated UF permeate. The serum (UF permeate), which amounts to about 90–95% of the feed volume, is concentrated by RO using hollow fine fibres made of aromatic polyamide. Pressures are typically 1000–2000 psi. A multistage system is used with high rejection membranes in the early stages and low rejection membranes in later stages. Permeates with significant sugar or flavour compounds are returned to stages containing high rejection membranes. Fruit juice concentrates of 45–55° Brix have been obtained commercially, and up to 70° Brix has been obtained in pilot trials. Careful control of

operating conditions is necessary. For example, the freshly extracted juice is blanketed with nitrogen and its temperature is controlled below 10°C throughout the remainder of the process. The flavour compounds in the serum are not subjected to any heat during processing, which also explains the high flavour scores for this product. Flavour and cost comparisons indicate very good market potential for this process. Commercial installations to date include tangerine juice and apple juice concentrates.

Concentration of tomato juice presents a difficult problem, because it has a high pulp content (25% fibre) and a high viscosity (which behaves in a non-Newtonian manner). Because of this, tubular modules are probably best. The colour of the final tomato concentrate is very good, and shows none of the browning normally associated with evaporation.

The interest in RO of maple syrup grew in the 1970s in response to increasing energy prices. RO is able to remove about 60% of water from the maple sap, resulting in a decrease of 33% in the processing cost compared to the all-thermal process. The concentrate is then boiled in a conventional open-pan evaporator to develop the characteristic colour and flavour.

Sugar Refining

The most appropriate application of membranes in this industry is for clarification and purification of the extraction juices. If UF or MF were used at the mill to remove the colloidal and macromolecular impurities, a clear decolorized thin juice would be obtained with little or no need for addition of lime, carbon dioxide or sulfite. If ion exchange is done immediately after UF, lime could be eliminated completely. An added benefit of membrane technology is that, with no macromolecules and reduced lime levels, fouling and scaling of the evaporator is reduced, which in turn reduces down time and cleaning costs. Higher yield of sugar and better crystallization are also possible: near-white sugar could be made in a single crystalliza-

tion step. The MF or UF pretreatment is well suited for subsequent ion exchange softening and chromatographic purification. Another advantage is that a high quality soft cane molasses is obtained and this can go directly to chromatographic separation to recover sucrose and fructose, or to MF to remove some of the monovalent salts.

Another place in the sugar industry for UF or MF is to clarify thick juice (after evaporation), reducing bacterial counts and storage losses. Treating thick juice has the advantage of handling lower volumes, but this is partially compensated for by higher viscosity and lower flux.

Vegetable Proteins

Most of the work in this area has been done with soya beans. Once the oil has been removed from soya beans, the resulting meal is mostly used for animal feed, with perhaps only about 3–5% being used directly as human food. UF has been successfully used to upgrade the quality of the soy protein by selectively removing undesirable components such as oligosaccharides (implicated in gastrointestinal stress when consuming soya beans) and phytic acid (which forms insoluble chelates with minerals and can form complexes with proteins that reduce their bioavailability). To produce soy protein concentrates, the raw material is defatted soy flour which is extracted with dilute alkali. The extract is then ultrafiltered. The final composition will approximate to a soy protein concentrate of 70% protein, dry basis. To produce isolates (90% protein), the fibre and insoluble carbohydrate are removed by centrifugation or filtration prior to UF. The UF technique usually results in higher yields because of the inclusion of soy whey proteins that are normally lost in conventional manufacturing methods. These whey proteins could also be contributing to the superior functional properties of the UF soy products, in addition to the benefits of the nonthermal and nonchemical nature of the UF process.

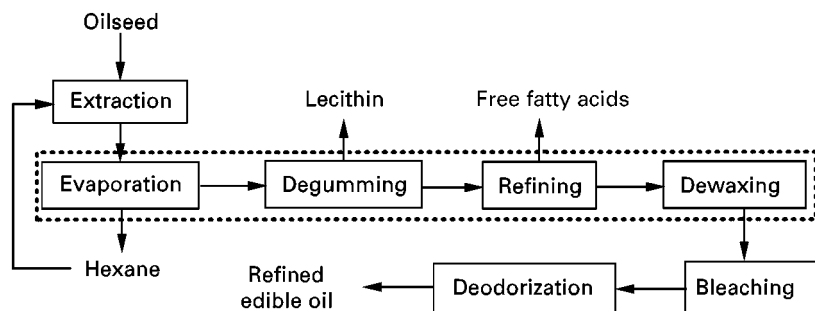


Figure 4 Edible oil processing. Membrane technology can be used in the four unit operations within the enclosed box.

Vegetable Oils

The basic unit operations in vegetable oil processing are shown in Figure 4. Oil is extracted from plant material (oilseeds) using a solvent, usually hexane. Published research indicates that about 50–70% of the hexane can be recovered and recycled using nanofiltration membranes instead of the evaporators used today, thus reducing energy consumption substantially. The extracted crude oil is mostly triglycerides, but it also contains small amounts of free fatty acids, phosphatides (lecithins/gums) and waxes, among other impurities. In place of physical or chemical refining, it is possible to use UF membranes for the degumming step, thereby producing a substantially oil-free lecithin.

In membrane refining, the crude oil is treated with a solvent such as methanol to extract the free fatty acids. After phase separation, the methanol layer is subjected to nanofiltration to recycle the methanol while producing a free fatty acid concentrate. This avoids the traditional alkali-refining process which results in soapstock formation and oil losses. Dewaxing with microfiltration membranes can also be done. In this process, the oil is cooled to a temperature below the wax crystallization temperature before being microfiltered to produce a stable edible oil. The application of membrane technology in the edible oil industry is expected to reduce energy consumption, reduce losses of oil, reduce the usage of chemicals and water and reduce the discharge of contaminated effluents.

Conclusions

The food industry is one of the largest users of membrane technology. With new developments in low-fouling membranes and modules, and membranes

stable in organic solvents, the applicability of this technology will widen considerably in the industry, especially in the production of 'neutraceuticals' (minor compounds in plants that are thought to have considerable health benefits) and grain processing (e.g., corn, soyabeans, wheat).

Further Reading

- Bhave RR (ed.) (1991) *Inorganic Membranes. Synthesis, Characteristics and Applications*. New York: Van Nostrand Reinhold.
- Cheryan M (1992) Concentration of liquid foods by reverse osmosis. In: Lund DB and Heldman DR (eds) *Handbook of Food Engineering*, p. 393. New York: Marcel Dekker.
- Cheryan M (1998) *Ultrafiltration and Microfiltration Handbook*. Lancaster, PA: Technomic.
- Cheryan M and Alvarez J (1995) Membranes in food processing. In: Noble RD and Stern SA (eds) *Membrane Separations. Technology, Principles and Applications*, p. 415. Amsterdam: Elsevier.
- Cheryan M and Nicholas DJ (1992) Modelling of membrane processes. In: Thorne S (ed.) *Mathematical Modelling of Food Processes*, p. 49. London: Elsevier.
- Ho WSW and Sirkar KK (eds) (1992) *Membrane Handbook*. New York: Chapman and Hall.
- Lloyd DR (ed.) (1985) *Materials Science of Synthetic Membranes*. Washington, DC: American Chemical Society.
- Matsuura T (1994) *Synthetic Membranes and Membrane Separation Processes*. Boca Raton, FL: CRC Press.
- Raman LP, Cheryan M and Rajagopalan N (1994) Consider nanofiltration for membrane separations. *Chemical Engineering Progress* 90: 68.
- Renner E and El-Salam MH (1991) *Application of Ultrafiltration in the Dairy Industry*. New York: Elsevier.
- Singh N and Cheryan M (1997) Membrane applications in corn wet milling. *Cereal Foods World* 42: 520.

Supercritical Fluid Chromatography

J. W. King, National Center for Agricultural Utilization Research, Agricultural Research Service/USDA, Peoria, IL, USA

The role of supercritical fluid chromatography (SFC) in the analysis of foods and agriculturally derived products has been somewhat moderated by uncertainties in the availability of required instrumentation for the past 15 years. In addition, SFC competes for the same analytical opportunities as gas (GC) and

high performance liquid chromatography (HPLC) and hence is often ignored or relegated to a minor role by food analysts. Despite these difficulties, SFC has been applied to a variety of applications for the detection and quantification of analytes, that are at least soluble to even a minor extent in supercritical carbon dioxide (SC-CO₂) – by far the most popular mobile phase utilized in the technique.

The application of SFC to food matrices came naturally due in part to the early application of SC-CO₂ extraction in the food industry, i.e. for the

extraction of coffee, hops and similar food items used routinely by the consuming public. SFC is particularly applicable to the analysis of lipid-containing materials, due to relative high solubilities exhibited by these solutes (analytes) in SC-CO₂. Analysis and detection of ultra-trace components in foodstuffs, e.g. pesticides or drugs, has not been generally successful because of the problems in routinely interfacing and using sensitive detectors, such as the electron-capture detector (ECD) with SFC, due to the change in mobile-phase characteristics with respect to time during the analysis. However, the ability routinely to use the flame ionization detector (FID) with SFC has provided the analyst with a useful technique to detect an array of components, or a specific moiety, in complex food matrices.

With respect to the chromatographic technique utilized, it is capillary SFC which has been cited more often than packed-column SFC in the analysis of foods. This is somewhat unfortunate since the packed-column mode also offers interesting possibilities, particularly when interfaced with a ultraviolet (UV) detector or evaporative light-scattering detector (ELSD). The recent use of this technique for the analysis of chiral compounds may also create some opportunities in food analysis, where the knowledge of the chirality of certain compounds (e.g. flavour esters) is of importance. In general, the coupling of analytical supercritical fluid extraction (SFE) with SFC has not been adopted to any considerable extent

by food analysts, due to the lack of an interface that permits routine coupling and use of the SFE/SFC mode. However, preparative and even production scale SFC has been utilized for specialized applications in the food production industries, and probably will see increased application due to the current interest in producing high value nutraceutical components, in a natural and environmentally benign manner.

Since SFC is perceived as a niche technique in the food industry, it is important to recognize when and where it can be used to advantage relative to what can be achieved using GC and HPLC. Some of these opportunities are as follows:

1. Reduction of the use of organic solvents relative to HPLC;
2. Direct analysis of samples avoiding sample preparation steps;
3. Deformulation of commercial food products;
4. Detection of product adulteration or deterioration;
5. Support of food engineering extraction/reaction process development.

With respect to nonpolar solutes, pressure-or density-programmed SFC provides the capability to analyse compounds having molecular weights approaching 1200 amu in one chromatographic analysis. Separation of these compounds is a function of their

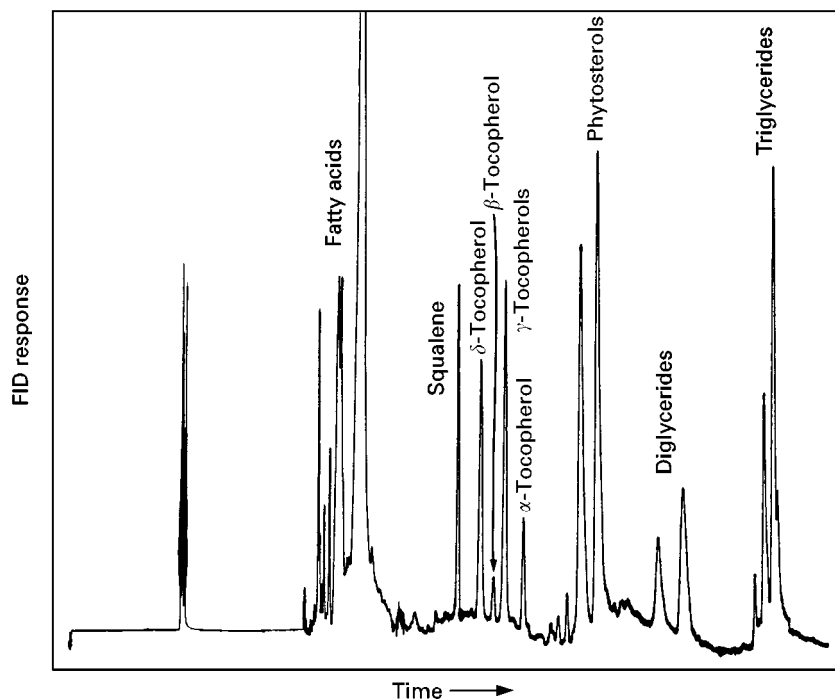


Figure 1 Supercritical fluid chromatography analysis of deodorizer distillate with an SB-octyl-50 column using flame ionization detection (FID).

solubility in the mobile phase, their respective vapour pressures and miscibility of the solute in the fluid phase. For example, in **Figure 1**, a number of components have been separated using a capillary SFC method that traditionally would have required the use of both GC and HPLC, and derivatization of some of the analytes. Utilizing SFC allows the analyst to avoid the above approaches, and to analyse directly the sample, obtaining a snapshot of the entire molecular composition. These characteristic elution patterns produced by SFC can be used to identify the presence or absence of a particular molecular constituent in a food sample, thereby providing valuable information for the food product formulator, to match or alter in developing new and competitive products.

Increasing concerns about minimizing or eliminating the use of hazardous organic solvents in the laboratory also bodes well for the application of SFC. Incorporating SFC for the separation and detection of food-related solutes, eliminates not only most of the traditional solvent needs associated with HPLC, but any solvents utilized in the extraction or sample work-up steps prior to analysis. In this regard, SFC is an excellent tool for monitoring the end-result of an extraction or reaction of a food component using supercritical fluid media. Also, by using SFC, food-related analytes that are thermally labile or susceptible to degradation via oxidation are not exposed to the harsh conditions that often accompany their analysis by GC or HPLC. This advantage can be attributed to the protective action of CO₂ which excludes oxygen, and the low temperatures used when separating components via SFC.

Selecting and Optimizing Separation Conditions for Food Components

For the SFC analysis of food-related samples, the analyst will undoubtedly want to start with a general fluid-programming sequence to interrogate the sample matrix as to its components. These programmes are executed for an extended time to ensure optimum resolution and detection of the unknown or target analyte(s). Run times of 90 min in length are not unusual in this initial stage of method development. After the target analytes have been identified by retention time-matching with standards, or via an independent method such as mass spectrometry (MS), the original programme can be modified to reduce the analysis time or improve the resolution within the chromatogram. However, changes in the mobile-phase programme will usually be done to hasten the elution of early or late eluting components that are of no importance in the analysis. In the

analysis of food components, both changes in the rate of increase of the fluid pressure or density with respect to time, or in some cases changeover to an exponentially-based fluid programme, will suffice to optimize the SFC run.

Because of the molecular complexity exhibited by many food ingredients and compositions, it is not unusual to have a temperature gradient with respect to time superimposed on the mobile-phase pressure programme during the SFC run. For example, separation of the like-carbon number triglycerides in soybean oil is not possible by pressure or density programming alone, but by superimposing a temperature gradient during the analysis, these oil components can be well separated. SFC analysis under isobaric conditions is limited in application when analysing foods; however, it should not be overlooked since it can often yield the most precise and accurate results.

The FID is the most commonly used detector for SFC. FID sensitivity to food components is lower than that obtained with GC since expansion of the mobile phase dilutes the detector signal substantially. However, the FID signal can be amplified to permit analysis down to the p.p.m. level, provided any shift in the baseline can be compensated for. Analytes with chromaphoric properties are amenable to UV detection in conjunction with SFC. The absorption maxima of components shift as a function of fluid density or pressure, but most detector units constructed for operation at these elevated pressures allows for stop flow or *in situ*, on-the-fly scanning of peaks to determine absorbance maxima shifts. For example, bathochromic shifts of 15–20 nm have been recorded for carotenoids over a 250 atm pressure interval in SC-CO₂. The mating of the ELSD detector with SFC has been reported by several investigators; however, day-to-day stability is inferior to that experienced with HPLC-ELSD couplings when applied to food analysis. Hetero-element-specific detectors, such as ECD or flame photometric detector, have mostly been utilized in research studies using SFC and have not seen serious adoption for routine analysis. Again, detector sensitivity and stability under SFC conditions limit their sensitivity at best to parts per million range. The use of SFC with mass spectroscopy has remained mainly an academic art, and commercial instrumentation development has been limited to date.

Most of the promising applications of capillary SFC have utilized nonpolar bonded phases such as methyl, octyl, phenyl and biphenyl silicas. The weak elutropic strength of neat SC-CO₂ has favoured the use of short chain length; monomeric silane-modified columns have C₁, C₄, C₁₈, phenyl, amino and diol

phases for packed-column SFC. The choice of these phases is not so much related to their selective interaction with food-related solutes, but to their surface-modifying properties which reduce peak tailing and solute interaction with the silica matrix. Resin columns have also been utilized, but they are susceptible to voiding unless specifically packed for use under supercritical fluid conditions.

Types of Food Components Analysed by SFC

A myriad of food-related components and matrices have been analysed by SFC, as indicated by the partial listing in Table 1. These include naturally occurring ingredients such as fats/oils, spices, etc.; minor unwanted constituents like pesticides, antibiotic drugs and mycotoxins; and specific food components, including nutraceuticals and flavouring aids. Inspection of Table 1 indicates a preponderance of applications in the lipid analysis area. Indeed, SFC is tailor-made for lipid analysis, although somewhat lacking in the high resolution capabilities demonstrated by high temperature GC. The retention pattern for lipid solutes in SFC, as shown in Figure 1, follows a distinct pattern governed approximately by the solute's molecular weight/volatility characteristics. Elution of the following classes of lipids is in the order: fatty acid methyl esters, free fatty acids, hydrocarbons, vitamins, sterols, wax esters, mono- followed by diglycerides, and then triglycerides/steryl esters. Although there is some overlap between individual classes of the above solutes, due to the overlapping molecular weights ranges (e.g. triglycerides and steryl esters), this separation pattern has proven very useful in tracking conversion of lipid species undergoing

reaction as well as in the quality control of food raw products and ingredients.

Triglyceride-based oils/fats are also readily amenable to analysis by SFC. Separation of the individual components is once again governed by molecular weight considerations, thereby allowing SFC to facilitate the separation of the major triglyceride species, i.e. T_{50} , T_{52} , T_{54} , etc. For some oils, such as coconut oil, well-resolved chromatograms result, while for other oils, e.g. soybean oil, there is overlap between the saturated and unsaturated triglyceride species, making superimposition of temperature gradient along with the pressure gradient programme for the mobile phase necessary to achieve adequate resolution. However, even without ideal resolution, the rapid analysis afforded by SFC can be used to considerable advantage for quality control, where speed, rather than optimal separation, is often desired.

Detection of minor components in foods is limited by the detector stability problems noted previously; however, those components which can be detected by using FID, UV or ELSD are often analysed more rapidly by SFC, due to the time savings afforded by avoiding elaborate preparation of the sample prior to analysis. SFC analysis provides a more detailed profile of the entire sample in addition to detecting the target analyte. This allows a more accurate assessment of the total contribution of the minor constituent to the entire ingredient profile, e.g. the presence of sterol esters in sawtooth palmetto berry extracts, where fatty acids and triglycerides are the major constituents.

Other food sample types that are readily analysed by SFC are the fat-soluble vitamins, essential and flavour oil ingredients, spice materials, hop compo-

Table 1 Food components separated and analysed by SFC

Carbohydrates	Derivatized corn syrups, mannose glycans
Chiral compounds	Monoterpenes, pyrazines, clenbuterol
Drugs/antibiotics	Caffeine, erythromycin, polycyclic ether antibiotics, sulfonamides, assorted steroids
Hydrocarbons	Sesquiterpenes, squalene, waxes and wax esters
Lipids	Fatty acids, fatty acid esters, monoglycerides, diglycerides, triglycerides, sterol esters, sterols (cholesterol), fat-soluble vitamins, tocopherols, phospholipids (lecithin), lipid hydroperoxides, glycolipids
Nutraceuticals	Valeriana, ginkgolides, sawtooth palmetto berry
Oils/fats	Celery oil, coconut, fish, soybean, wheat germ, palm oil, rice oil, milk/cheese triglycerides
Packaging/film components	Polypropylene oligomers, polyvinyl chloride, phenolic antioxidants, low molecular weight polystyrene
Pesticides	Halogenated, organophosphorus, carbamate, pyrethrins, acidic phenoxy herbicides, sulfonyl ureas
Pigments	Carotenoids, xanthophylls
Speciality ingredients	Hops components
Spices/flavours	Capsicum, cardoman, coumarin, curry, garlic components, majoran, rosemary, vanillin
Terpenes/essential and fruit oils	Grapefruit oil, limonenes, mint, lemon
Other toxicants	Mycotoxins, nitrosamines, polycyclic aromatic hydrocarbons

nents and nutraceutical formulations. Some SFC-based separations require the use of a co-solvent (usually 5–20 vol%) in addition to the SC-CO₂ for the mobile phase. For example, phospholipids are only sparingly soluble in neat SC-CO₂, but these polar lipid compounds can be chromatographed successfully on packed silica columns by incorporating ethanol and/or water as a modifier into the mobile phase. Likewise, carbohydrate moieties, which exhibit limited or no solubility in SC-CO₂ or SC-CO₂/co-solvent mobile phases, can be derivatized to allow their analysis by SFC.

Selected Applications of SFC in Food Analysis

In this section, several brief examples will be given to illustrate the utility and potential of SFC in food analysis. **Figure 2** illustrates the SFC separation and detection of α -tocopherol and cholesterol in a fish oil capsule. This was achieved on a capillary SB-methyl column at 120°C using the density programme noted on the horizontal axis. Although this analysis took over 90 min to perform, it illustrates some of the benefits that can be achieved using SFC. For example, the chromatogram in **Figure 2** was achieved with no sample preparation other than to dilute the oil in a small quantity of solvent and to inject it into the chromatograph. In addition, no derivatization of the sample was required and adequate resolution be-

tween the α -tocopherol and cholesterol was achieved using the lengthy density programme. However, it is perhaps more important that, by adjusting the elution conditions, the background components (fish oil triglycerides) that were of no interest in this analysis can be programmed off the column without resorting to a pre-fractionation of the sample prior to SFC analysis or derivatization of the sample matrix.

Not all applications of SFC require the above conditions for high resolution separations. For example, packed-column SFC (5 μ m, C₈ Deltabond) has been used to clean up samples prior to other types of chromatographic analysis (GC). In this case, organochlorine and organophosphorus pesticides were extracted by SFE with SC-CO₂ from a meat sample, and the pesticides separated from the co-extracted fat moieties using the packed SFC column. Hence, by 'heart-cutting' the appropriate elution fraction, a lipid-free, pesticide-containing fraction was provided for GC residue analysis.

SFC is an excellent technique to monitor reaction chemistry between lipid species, since it avoids the need to employ more than one analytical technique or sample derivatization. Further, it permits the successful chromatography of all of the relevant reactants and products in one chromatographic analysis. Examples where SFC has been applied are in the esterification or transesterification of lipids, glycerolysis reactions and randomization of fats/oils. **Table 2** shows the analysis of the glyceride content of

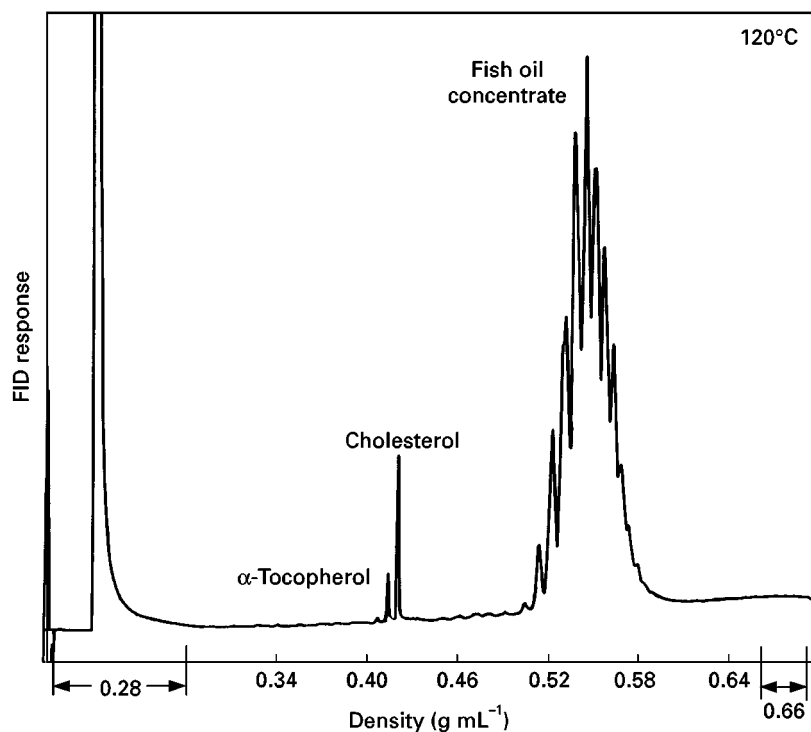


Figure 2 Determination of cholesterol and α -tocopherol in a fish oil capsule by capillary SFC.

Table 2 Analysis of glycerides in a randomized fat sample

Methods of analysis	MG	DG	TG	Time of analysis
SFC-FID	0.2	9.6	90.1	25 min
GC-FID	0.1	6.9	92.9	30 min
HPLC-FID		13.5	86.5	1 h
HPLC-ELSD		8.0	92.0	30 min
LC-silica column	1.0	7.7	93.1	2 h
TLC	2.0	11.0	87.0	30 min

MG, Monoglyceride; DG, diglyceride; TG, triglyceride.

a randomized fat sample using six different analysis methods. The results given in Table 2 suggest that SFC-FID analysis yields comparable data for an equivalent analysis time to that obtained using the GC-FID and HPLC-ELSD methods. However, the SFC method does not require the time and effort for sample preparation associated with the alternative techniques and, in addition, saves on the cost of solvents and chemical reagents. A further illustration of the cost- and time-saving advantages of SFC is noted by its ability to monitor free and methylated fatty acids, thereby providing a reasonably quick and accurate assay for these compounds in foodstuffs to support nutritional analysis claims and the detection of frying oil deterioration as a function on time.

Preparative or production scale SFC is now being used as a separation technique in the food industry. Fractionation and isolation of higher value food components, such as tocopherols and phospholipids, or the ω -fatty acids/esters from fish oils, have been cited in the literature. Recently, a production plant for the separation of fish oil ethyl esters has been constructed in Spain to produce $\geq 95\%$ pure polyunsaturated fatty acids for the nutraceutical market. The basic separation design of this production scale plant is

based on chromatographic fractionations initially developed using analytical scale packed SFC columns.

Further Reading

- Anton C and Berger C (eds) (1997) *Supercritical Fluid Chromatography with Packed Columns*. New York: Marcel Dekker.
- Caude M and Thiebaut D (eds) (1999) *Practical Supercritical Fluid Chromatography and Extraction*. Amsterdam: Harwood Academic.
- Dean JR (ed.) (1993) *Applications of Supercritical Fluids in Industrial Analysis*. Boca Raton, Florida: CRC Press.
- King JW (1990) Applications of capillary supercritical fluid chromatography – supercritical fluid extraction to natural products. *Journal of Chromatographic Science* 28: 9.
- King JW (ed.) (1996) Supercritical fluid extraction and chromatography. *Seminars in Food Analysis* 1: 101–116, 133–144, 163–165.
- King JW and List GR (eds) (1996) *Supercritical Fluid Technology in Oil and Lipid Chemistry*. Champaign, Illinois: AOCS Press.
- Lee ML and Markides KE (eds) (1990) *Analytical Supercritical Fluid Chromatography and Extraction*. Provo, Utah: Chromatography Conferences.
- McDonald RE and Mossoba MM (eds) (1997) *New Techniques and Applications in Lipid Analysis*. Champaign, Illinois: AOCS Press.
- Nam KS and King JW (1994) Coupled SFE/SFC/GC for the trace analysis of pesticide residues in food samples. *Journal of High Resolution Chromatography* 17: 577.
- Saito M, Yamauchi Y and Okuyama T (eds) (1994) *Fractionation by Packed Column SFC and SFE*. New York: VCH.
- Smith RM (ed) (1988) *Supercritical Fluid Chromatography*. London: Royal Society of Chemistry.
- Wenclawiak B (ed.) (1992) *Analysis with Supercritical Fluids: Extraction and Chromatography*. Berlin: Springer-Verlag.

Supercritical Fluid Extraction

S. S. H. Rizvi, Institute of Food Science,
Cornell University, Ithaca, New York, NY, USA

Copyright © 2000 Academic Press

In the food industry, supercritical fluid extraction (SFE) is currently being used in a number of areas, shown in Table 1. The most attractive features of SFE in food processing is the fact that separation can be carried out at relatively low temperatures (40–60°C) using benign solvents. The solvent most widely used thus far is carbon dioxide, which is inexpensive, nontoxic, nonflammable, easily recoverable, and

nonpolluting. The solubility and selectivity properties of SC-CO₂ has been compared with hexane. While both are nonpolar solvents, the selectivity of SC-CO₂ is enhanced in the presence of modifiers (entrainers). For example, in the absence of such polar modifiers as water and ethanol, SC-CO₂ alone is a poor solvent for extraction of caffeine from coffee beans or nicotine from tobacco. While the selectivity of SC-CO₂ and the mechanism of modifier action are not completely understood, studies in the area of supercritical fluid chromatography (SFC) have indicated that Lewis acid–base pairing, induced-dipole interactions

Table 1 Selected applications of supercritical fluid extraction in food processing

Process	Commercial manufacturers	Literature source
Coffee decaffeination	KaffeHAG AG, Germany; General Foods, Texas USA; SKW-Trotsberg, Pozzillo, Italy	Zosel (1978) Williams (1981)
Hops and spices extraction	SKW-Trotsburg, Munchmuenstar, Germany; Paul and White Beigat, UK; Pfizer, Sydney, Nerbraska; J.I. Hass, Yakima, Washington	Hubert and Vitzthum (1978) Vollbrecht (1982)
Flavours and fragrances	Flavax GmbH, Rehlingen Germany; Canilli Albert and Louis, Grasse, France	Calame and Steiner (1982) Caragay and Little (1981)
Vegetable oils and fatty acids	Mohi Oil Mills, Japan; Marbert GmbH, Dusseldorf, Germany	Stahl <i>et al.</i> (1980) Friedreich (1984)

and hydrogen bonding play an important role in determining the selectivity of SC-CO₂.

The principal disadvantage of SFE is that relatively high pressures (typically 50–100 atm or more) are required. Even though the energy savings make SFE attractive, the initial capital cost of high-pressure equipment overrides these considerations, especially at current energy prices. While the overall cost of SFE is dictated by such other factors as volume, price and the continuous or batch nature of the process, economic considerations have slowed its commercialization. Generally, SFE is best suited for difficult separations, not attainable by conventional processes. In situations where SFE can produce a new product or when environmental or regulatory concerns make its use more attractive, the application may more than justify the cost. The hazards of high pressure and the use of flammable solvents are also perceived unfavourably by many not experienced in these areas. While common in the petroleum industry, the food industry also uses a number of processes like homogenization, extrusion and compression routinely and thus should be able to deal with moderate pressures.

Another frequently overlooked problem associated with SFE is patent infringement. There are over one

hundred patents on SFE of biomaterials in the United States alone. A potential user of these processes is likely to be faced with the involved task of determining if patent infringements exist or identify sources of legitimate licensing agreements. While SFE developments are growing globally, further research is needed both in terms of fundamental studies and applications.

The feasibility of extraction of a number of food materials using supercritical fluids has been investigated over the past two decades. In particular, much activity has focussed on extracting and refining fats, oils and their derivatives. The equilibrium solubility values of some of these are shown in Table 2. A number of advantages have been cited for the use of SFE in the processing of food-grade fats and oils from both animal and plant sources. These include:

- Low temperature processing reduces degradation of temperature and oxygen-sensitive components.
- Both extract and raffinate are free of solvent and can be used in food.
- Extraction and fractionation into various cuts of different physicochemical properties can be performed simultaneously.

Table 2 Solubilities of selected food materials in supercritical fluids

Food material	SC solvent	Solubility (%wt/wt)	Extraction (°C)	Conditions (bar)	Co-solvent	Reference
Beta-carotene	Ethylene	{ 0.17 0.23	50 70	374 374	–	Chang and Randolph (1989)
Cholesterol	CO ₂	{ 0.33 0.37	60 60	270 270	– MeOH	Wong and Johnston (1986)
Coumarin	CO ₂	0.7	40	100	–	King and Friedrich (1990)
Butterfat	CO ₂	{ 2.2 1.1*	40 75	248 300	–	Yu <i>et al.</i> (1992) Brunner (1994)
Palm oil triglycerides	Ethylene	2.2*	70	300	–	
Soybean triglycerides	CO ₂	{ 0.6* 3.0*	50 50	300 600	–	Friedrich (1984)
Hop extract	CO ₂	9.4	80	400	–	Stahl <i>et al.</i> (1987)
Evening primrose oil	CO ₂	8.0	40	300	–	Lee <i>et al.</i> (1994)

*Estimated from graphs.

- A continuous and large-scale process can be economically competitive to hexane-based operations.

Exploiting the commonality of high pressure between supercritical fluid and extrusion processing operations, a hybrid unit operation called supercritical fluid extrusion (SCFX) has been recently developed. This new process permits generation of microcellular structure at low temperature by using SC-CO₂ as a blowing agent instead of steam to puff the extrudate, thus decoupling the conventional dual role of water, which otherwise serves both as a blowing agent as well as a plasticizer. The use of supercritical fluid also permits deposition of solute into the extrudate matrix.

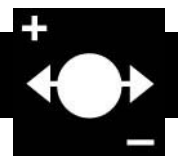
Significant progress has also been made in the analysis of food and related materials using SFE with SFC. Sample preparation for analysis often requires orders of magnitude more time than the analysis itself and the use of supercritical fluids obviates the need for hazardous organic solvents with no additional treatment prior to identification of the analyte by other techniques such as GC, GC-MS, FTIR, etc. The solubility of lipid-like materials in SC-CO₂ ranges from 1 to 30 wt%, depending on the density of the fluid used, and therefore, SFE has become a method of choice for rapid extraction of fats and oils from a variety of food matrices such as animal, vegetable, grain and seafood products. Other successful applications include extraction of fat-soluble vitamins, pesticides, sterols, and fatty acids. As an analytical tool, SFC has also made significant progress over the past decades but has yet to prove its superiority over the more conventional techniques.

See also: II/Extraction: Supercritical Fluid Extraction. III/Food Technology: Supercritical Fluid Chromatography. On-Line Sample Preparation: Supercritical Fluid Extraction.

Further Reading

- Brunner G (1994) *Gas Extraction*. New York: Springer.
- Chang AD and Randolph AD (1989) Precipitation of microsize organic particles from supercritical fluids. *AIChE Journal* 35: 1876–1882.
- Charpentier BA and Sevenantes MR (eds) (1988) *Techniques and Applications. Supercritical Fluid Extraction and Chromatography*. ACS Symposium Series 366. Washington DC: American Chemical Society.
- Friedrich, JP (1984) Supercritical CO₂ extraction of lipids from lipids containing materials. U.S. Patent 4,466,923.
- Lee BC, Kim JD, Hwang KY and Lee YY (1994) In: Rizvi SSH (ed.) *Supercritical Fluid Processing of Food and Biomaterials*. New York: Chapman and Hall.
- King JW and Friedrich JP (1990) Quantitative correlations between solute molecular structure and solubility in supercritical fluids. *Journal of Chromatography* 517: 449–458.
- McHugh M and Krukonis VA (1994) *Supercritical Fluid Extraction*. Boston: Butterworth-Heinemann.
- Rizvi SSH, Mulvaney SJ and Sokey AS (1995) The combined application of supercritical fluid and extrusion technology. *Trends in Food Science Technology* 6(7): 232–240.
- Rizvi SSH (ed.) (1984) *Supercritical Fluid Processing of Biomaterial*. New York: Blackie Academic and Professional.
- Stahl E, Quirin KW and Gerard D (1987) *Dense Gases for Extraction and Refining*. New York: Springer-Verlag.
- Taylor LT (1996) *Supercritical Fluid Extraction*. New York: John Wiley.
- Williams DF (1981) Extraction with supercritical gases. *Chemical Engineering Science* 36(11): 1769.
- Wong JM and Johnston KP (1986) Solubilization of biomolecules in carbon dioxide based supercritical fluids. *Biotechnology Progress* 2: 29–39.
- Yu ZR, Rizvi SSH and Zollweg JA (1992) Extraction of oil from evening primrose seed with supercritical carbon dioxide. *Journal of Supercritical Fluids* 5: 114.
- Zosel K (1978) Separation with supercritical gases: practical applications. *Angewandte Chemie International Edition English* 17: 702.

FORENSIC SCIENCES



Capillary Electrophoresis

J. Sadecka, Slovak Technical University,
Bratislava, Slovak Republic

Copyright © 2000 Academic Press

Several slab electrophoretic techniques have frequently been used to discriminate between red cell

enzyme markers as a means of identification in criminal cases over many years. In 1991 capillary electrophoresis (CE) was introduced to forensic analysis. The separation of bulk heroin, heroin impurities and degradation products using micellar electrokinetic capillary chromatography (MEKC), the determination of drugs of abuse in urine and also the determination of benzodiazepines and sulfonamides in urine by CE-mass spectrometry were described in the same

year. Today, forensic applications of CE include analysis of drugs of abuse, gunshot residues, explosives, pen inks and toxins as well as polymerase chain reaction (PCR) amplified DNA.

Drugs of Abuse

One of the major tasks for forensic laboratories is the analysis of illicit and controlled drugs, in both the seizure and biological samples.

Seizure Samples

Seizure samples are analysed in order to identify the major compounds. In addition, the determination of trace compounds permits the samples to be allocated to the source and production procedures. Seizure samples may consist of a mixture of acidic, neutral and basic compounds that may be nonpolar and/or polar. At least two independent analytical parameters should be used to establish the identity of the drug, and infrared spectroscopy and thin-layer chromatography (TLC) are widely used for this purpose. Quantitation is usually carried out by gas chromatography (GC) and high performance liquid chromatography (HPLC). GC is a high resolution technique, but problems can arise for thermally degradable, polar and nonvolatile substances. HPLC is less suited to drug profiling, because it is a relatively low resolution technique compared with GC.

CE is a relatively new technique in forensic drug analysis. The three main separation mechanisms have been used for seizure samples: (i) low pH to analyse basic compounds; (ii) high pH to analyse acidic com-

pounds; and (iii) MEKC to analyse neutral and/or charged compounds.

Most abused drugs are bases which are generally water-soluble and ionized as cations at low pH. The use of simple electrolyte solutions such as phosphate, citrate and formate at pH values of 2–3 gives a useful initial separation. Basic drugs can be analysed by TLC and HPLC, but interactions with the stationary phases can lead to peak tailing. This problem does not occur so frequently in CE. In addition, these simple electrolytes have low background UV absorbance and can be operated at low wavelengths of 190–200 nm, where many drugs have significantly enhanced UV absorbance coefficient. CE at low pH can be used to detect by-products in purified codeine, to investigate amphetamine derivatives in Ecstasy tablets, and for assay for various pharmaceutical formulations which contain 1,4-benzodiazepines and phenothiazines.

At high pH the migration direction of acidic compounds is against the electroosmotic flow, which maximizes mobility differences. Operation with simple electrolytes such as phosphate pH 7 or borate pH 9.5 often leads to useful initial separation for acidic compounds.

MEKC can be used when dealing with uncharged solutes or mixtures of charged and neutral species. This approach may also be considered when simple mobility differences prove insufficient in capillary zone electrophoresis (CZE). Both anionic and cationic surfactants have been used as micelle modifiers, which, furthermore, are complementary approaches. MEKC has been applied to a wide range of controlled substances, including heroin, cocaine, opium alkaloids, amphetamines, hallucinogens,

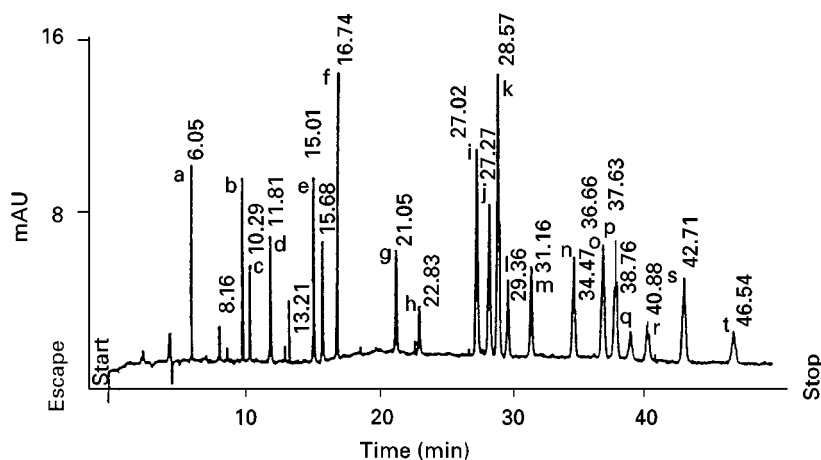


Figure 1 Typical example of a MEKC separation of the components of a drug mixture. Buffer: 25 mmol L⁻¹ borate (pH 9.24)–20% methanol–100 mmol L⁻¹ SDS. Capillary: bare fused silica, i.d. 50 μ m, total length 55 cm (35 cm to detector). Potential 20 kV. UV detection at 200 nm. Peak identification: a, caffeine; b, barbital; c, pentobarbitone; d, morphine; e, narceine; f, 6-monoacetylmorphine; g, codeine; h, nalorphine; i, lidocaine; j, procaine; k, heroin; l, flunitrazepam; m, acetylcodeine; n, thebaine; o, papaverine; p, amphetamine; q, narcotine; r, cocaine; s, diazepam; t, tetracaine. (Reprinted with kind permission of Elsevier Science from Tagliaro F *et al.* (1996) *Journal of Chromatography A* 735: 227–235.)

barbiturates, benzodiazepines and cannabinoids. An electropherogram of a complex mixture of 20 drugs (acidic, neutral and basic) is shown in **Figure 1**.

It is clear that MEKC represents an excellent technique for drug screening. In addition, photodiode-array UV, laser-induced fluorescence (LIF) and mass spectrometry (MS) detection can greatly increase specificity of the analysis. Greater specificity of screening could be obtained by using two complementary separation techniques, e.g. MEKC with either GC or HPLC. The complementary nature of MEKC and CZE for the identification of 17 illicit drugs and related compounds ionized at pH 2.35 has also been demonstrated. MEKC with sodium dodecyl sulfate (SDS) at pH 9.2 gave a highly noncorrelated separation compared to that obtained on a CZE system at pH 2.35. MEKC was found to be significantly, but inversely, correlated with a CZE system at pH 9.2. The reproducibility of migration times or relative migration times in MEKC is most important for screening applications. Migration time precision of 1% relative standard deviation (RSD) for repeated injection has been shown; this is essential to allow confirmation of the identity of each individual compounds present. Relative migration times generally give better repeatability, with RSD values of less than 1%.

The results generated by MEKC are often compared with those of HPLC and/or GC. GC affords higher resolution than MEKC; however, derivatizations are commonly required. MEKC offers significantly greater efficiency, selectivity, peak symmetry and speed compared to HPLC. In addition, the drugs that are poorly chromatographed by HPLC or not at all by GC exhibit good electrophoretic behaviour using MEKC. A recognized deficiency of MEKC is sensitivity, which is below that for HPLC-UV.

Biological Samples

The analysis scheme of drugs of abuse in biological samples involves screening using an immunoassay test. This does not enable positive identification to be made, but permits negative samples to be detected and discarded. Subsequently, the results must be confirmed by a more specific method. Without doubt, GC-MS is the reference method to confirm positive screening tests. At present, blood and urine represent most samples analysed for abused drugs and toxicants in most laboratories. If analyte concentrations are high enough, biological fluids, even those containing high concentrations of ions and proteins, can be directly injected on to a CE system, after simple filtration/centrifugation of the sample. Urine analysis can be very fast and simple, while SDS additive must be used with plasma to solubilize protein.

The important problem faced by CE in the field of biological sample analysis is still its relatively low concentration sensitivity. Increased sensitivity can be obtained both instrumentally and by processing the sample before analysis. Liquid-liquid extraction (LLE) and solid-phase extraction (SPE) methods have been used as sample pretreatment for CE. After LLE and SPE, extracted mixtures can be dried and resolved with a small volume of solvent, thus achieving detection limits of about 10 ng mL^{-1} . The sensitivity can be gained from employing more sensitive fluorescence detection. When LIF can be applied, the sensitivity limit of CE can be improved by a factor of about 1000 or more over UV absorbance detection. Unfortunately, the choice of wavelength emitted by laser is limited and this is the main limitation of LIF application to drug analysis. Concentrating the sample on the capillary – ‘stacking’ – is a simple technique that overcomes the poor detection limits of CE. Three general stacking methods are used in CE: (i) low ionic strength buffer in the sample; (ii) stacking by including acetonitrile in the sample; and (iii) isotachopheresis (ITP).

For forensic purposes it is often more appropriate to identify the metabolite rather than the parent drug, since additional information yielded by the full metabolic profile of a drug may be important in ascertaining the route of administration. Drug metabolites are most often studied by HPLC; however, phase II metabolites, e.g. glucuronide and sulfate conjugates, are acidic and highly polar and elute with little resolution in reversed-phase HPLC systems. Phase II metabolites are ideal for direct analysis by CE without the need for previous derivatization or hydrolysis. MEKC with diode array detection has been used for the determination of morphine, morphine-3-glucuronide, morphine-6-glucuronide, normorphine, meclofenamic acid and its metabolites in equine urine. SPE procedures were developed to concentrate and purify the analytes from post-administration urines. The low concentration sensitivity of MEKC in comparison with HPLC and GC-MS can be overcome by using a suitable sample preparation procedure, in particular offline SPE.

Hair analysis is a tool to prove drug abuse in questions of drug-related fatalities, revocation and restoration of driver licences, criminal responsibility, prenatal drug exposure and offences of narcotics law. The concentration of drugs in the hair are in the ng mL^{-1} range, at least in cases of chronic abuse. CE applications in hair analysis are still in an early stage of development. The few reports published until now come from Tagliaro's group. The use of CE with UV detection, at 238 nm for cocaine and 214 nm for morphine, has permitted the achievement of

moderate sensitivity 0.2 ng mL^{-1} for both analytes. Later, stacking techniques were developed in order to increase sensitivity (about five times). MEKC has also been applied to hair analysis. The sensitivity was slightly worse – 0.4 ng mL^{-1} – than with CZE, but selectivity was much higher. Good resolution and efficiency were obtained with both methods. The same-day RSDs of migration time were $< 1\%$ in CZE and $< 2\%$ in MEKC. Same-day precision RSD was 3–5%.

Among banned pharmaceutical substances, those which are of greatest relevance to sport medicine are anabolic agents, stimulants, diuretics, narcotics and β -blockers. In addition to several methods for screening (immunoassays, GC and HPLC), confirmation by MS, if needed, is used. Also, CE is a useful technique for the simultaneous screening of different types of drugs, e.g. β -blockers, anabolic steroids, diuretics and narcotics. LIF detection provides ultimate sensitivity while maintaining the extreme separation efficiency of CE. Both CE and MEKC have been applied. The main advantage of MEKC over CZE is that neutral and charged compounds as well as compounds which are insoluble in water can be separated in a single run.

Chiral Separations

The chiral resolution of drugs is of forensic significance for legal and intelligence purpose. In many instances, only one enantiomer is controlled under legal status, and proper identification is therefore critical. For example, only the (+)-enantiomer of nerpseudoephedrine and the (–)-enantiomer of propoxyphene are controlled. In addition, the enantiomeric composition of seized samples can provide information on the possible different synthetic routes. The enantiomeric purity of drug detected in urine or other biological samples may exclude the possibility that the subject has taken that drug in a racemic preparation.

CE is a technique that has been shown to be ideally suited for chiral separations. When compared to other techniques, such as liquid chromatography, CE has the advantages of efficiency, resolution, selectivity, speed and direct chiral separation. Therefore, CE has become a method of choice in the chiral analysis of therapeutic drugs, but the attention paid to controlled or illicit drugs is still low. As for chromatography, it is possible to separate enantiomers directly or after a pre-derivatization step.

In the separation of amphetamine analogues, 2,3,4,4-tetra-*O*-acetyl- β -D-glucopyranosyl isothiocyanate as a derivatization reagent was used and enantiomers were separated using MEKC. However, more applications are conducted by CE with β -cyc-

lodextrin (β -CD) as a chiral selector. Different β -CD derivatives have been used with success to separate ephedrine and analogous compounds, amphetamines, methamphetamine and methylenedioxy-derivatives of amphetamines.

The versatility of modified uncharged and charged β -CDs in the direct resolution of β -agonists, β -antagonists, phenylethylamines, alcohol stimulants and thalidomide and its metabolites by CE was shown. A total of 42 compounds were optically resolved using hydroxypropyl- β -CD and 20 with sodium sulfobutyl ether- β -CD. The preliminary analysis of ephedrine, amphetamine, methamphetamine and methylenedioxy-derivatives of amphetamine in urine (Figure 2) and hair (Figure 3) showed that after a liquid–liquid extraction, urine samples could be analysed with a sensitivity below 500 ng mL^{-1} . For hair analysis, it is necessary to increase sensitivity (0.1 ng mL^{-1}) by applying a stacking procedure.

Forensic DNA Samples

DNA polymorphism analysis has recently been recognized as a source of identification for individuals in criminal cases and unidentified human remains. The conventional technique for DNA typing based on restriction fragment length polymorphism (RFLP) has been replaced by more accurate, sensitive and faster PCR procedures. In contrast to RFLP, the PCR procedures require less DNA and can be used on DNA which is degraded. There are several PCR-based procedures under development; however, short tandem repeat (STR) sequences are currently of major importance in the field of identification of individuals in forensic cases. STRs are DNA segments, typically found in noncoding regions, which are composed of repeating units of 2–5 base pairs (bp). Co-amplification of two or more of these loci in one PCR provides an efficient mechanism for typing multiple genetic loci simultaneously. The detection of STRs is based on the variation in the length of STR-containing PCR products. These PCR-amplified STRs must be separated to determine the size, quantity and/or sequence of each fragment.

DNA restriction fragments and PCR products have traditionally been separated by slab gel electrophoresis.

Recently, CE has emerged as a novel, high performance DNA analysis tool. Early work on DNA separation was done on cross-linked polyacrylamide gel-filled capillaries. However, gel-filled capillaries are difficult to prepare and have a short life time. The utility of CE has been greatly enhanced by using noncross-linked polymer networks instead of rigid gel media. These polymer solutions offer low-to-medium

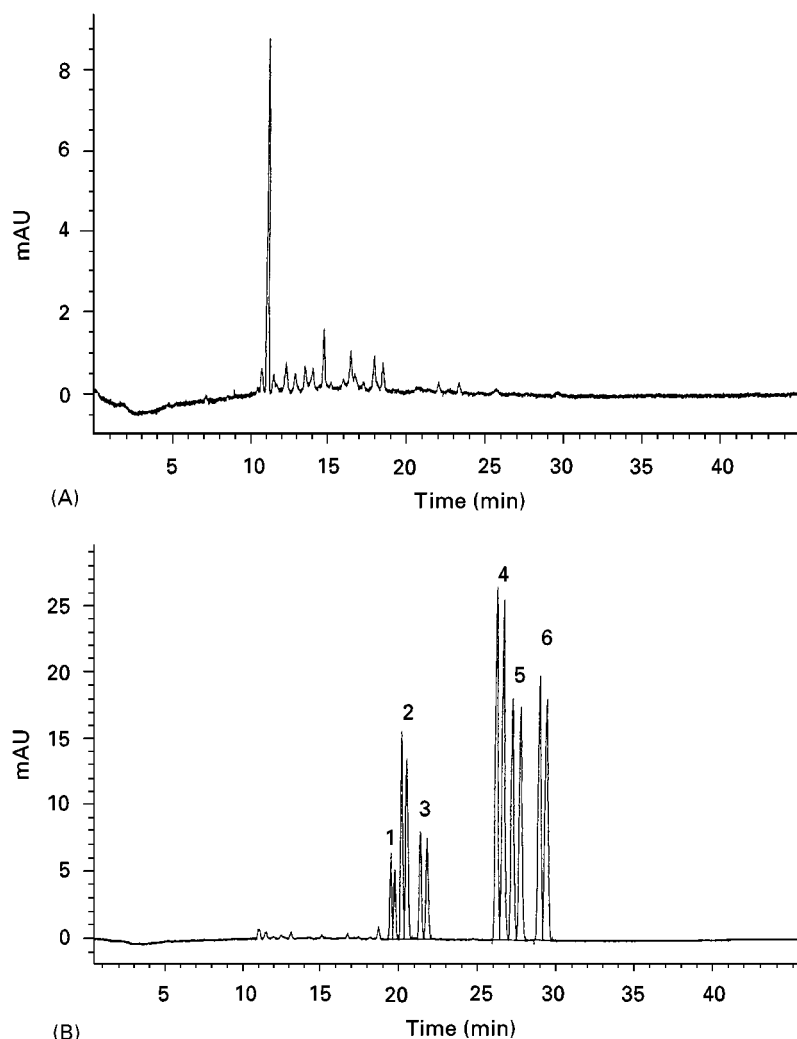


Figure 2 Typical electropherograms of: (A) blank human urine extract; (B) extract from blank human urine spiked with: 1, racemic ephedrine; 2, amphetamine; 3, methamphetamine; 4, 3,4-methylenedioxyamphetamine; 5, 3,4-methylenedioxymethamphetamine; 6, 3,4-methylenedioxyethylamphetamine, at concentrations of $1 \mu\text{g mL}^{-1}$ for every racemic analyte. Conditions: buffer, 100 mmol L^{-1} phosphate, pH 2.5, containing 10 mmol L^{-1} β -cyclodextrin. Capillary, uncoated fused silica, $45 \text{ cm} \times 50 \mu\text{m}$ i.d. Potential, 10 kV. Detection, UV absorbance at 200 nm. (Reprinted with kind permission of Wiley-VCH from Tagliaro F *et al.* (1998) *Electrophoresis* 19: 42–50.)

viscosity, which makes replacement of separation medium possible after each electrophoresis run. The polymer solution also has a broader effective DNA size range due to its flexible and larger effective pore size structure.

The CE system produced results which were comparable to those obtained on slab gel electrophoresis, with a level of precision of $\pm 0.1\%$ bp (between instruments). This comparison is very important if a comparison is to be made of results obtained by different laboratories and to standardize available procedures.

DNA fragments cannot normally be separated in free solution. However, the first clinical experimental results demonstrated that adding an uncharged mol-

ecule at the end(s) of the DNA fragments could lead to efficient separation of relatively large DNA fragments (100–900 bp) in free solution. Contrary to current electrophoretic methods, this method requires no sieving matrix, provides better results at high voltage and leads to shorter preparation time and faster separations.

Detection of PCR products has been achieved in three ways: (i) UV absorbance by the DNA fragment; (ii) LIF using intercalating dyes; and (iii) fluorescence of primers tagged with fluorescence dyes.

In automated fluorescence analysis the alleles from an STR locus are PCR-amplified from human genomic DNA using an unlabelled primer and one primer labelled at the 5'-end with a fluorescent dye.

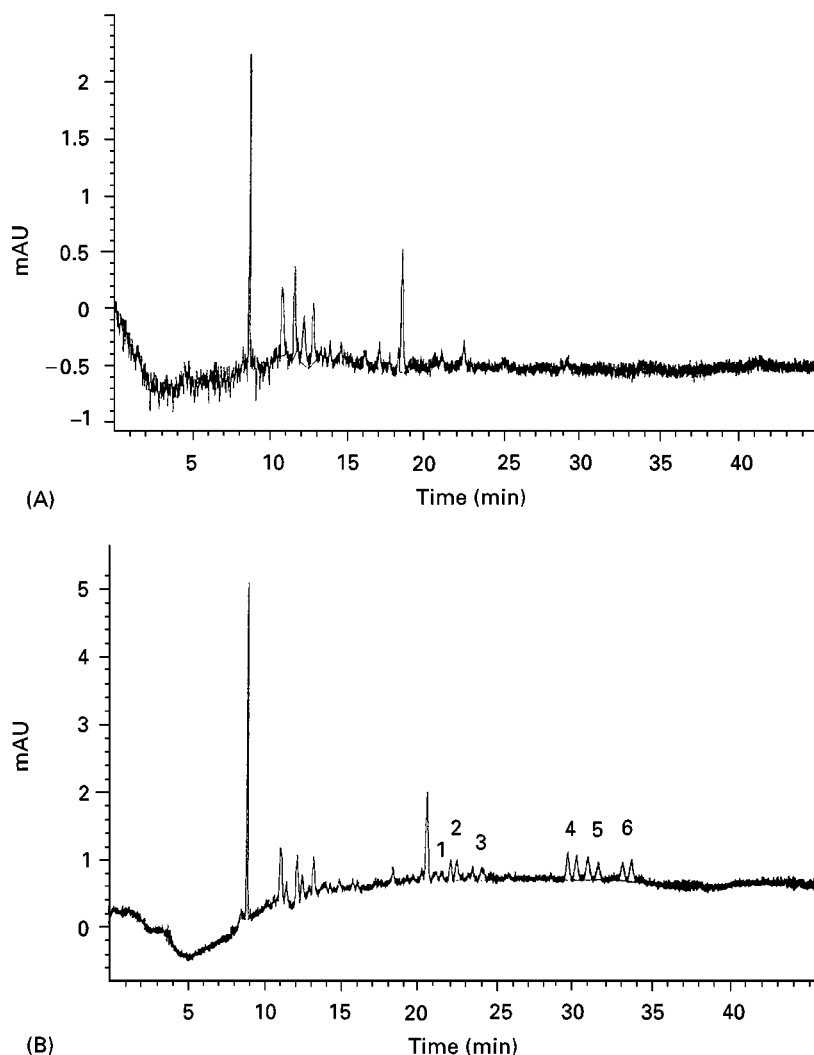


Figure 3 Typical electropherograms of: (A) blank human hair extract; (B) extract from blank human hair spiked with: 1, racemic ephedrine; 2, amphetamine; 3, methamphetamine; 4, 3,4-methylenedioxyamphetamine; 5, 3,4-methylenedioxymethamphetamine; 6, 3,4-methylenedioxyethylamphetamine, at concentrations of 1 ng mg^{-1} for every racemic analyte. Conditions: Buffer, 100 mmol L^{-1} phosphate, pH 2.5, containing 15 mmol L^{-1} β -cyclodextrin. Capillary, uncoated fused silica, $45 \text{ cm} \times 50 \text{ }\mu\text{m}$ i.d. Potential, 10 kV. Detection, UV absorbance at 200 nm. (Reprinted with kind permission of Wiley-VCH from Tagliaro F *et al.* (1998) *Electrophoresis* 19: 42–50.)

Denatured PCR products are then analysed by CE with in-lane size standard (DNA-fragments of known size labelled in a different colour dye) on slab gel or CE capable of real-time multicolour fluorescence detection. The collected data are then analysed by software which automatically determine allele size based on a standard curve for the in-line size standard. STR loci which overlap in size can be distinguished using different dyes that fluoresce at different wavelengths. Results have indicated that the sizes obtained for STR alleles can differ depending on the gel and electrophoresis conditions and depending on the instrument used, however, high precision can be obtained in multiplex PCR analysis by using an in-line internal standard (< 0.16 nucleotide SD).

Recently, a new CE instrument capable of simultaneous multicolour detection and high resolution of DNA fragments was developed. This instrument, the ABI Prism 310 Genetic Analyser, is highly automated. Multiplex STR products are sequentially injected into a single capillary and detected by LIF. LIF is detected on a charged coupled device camera, which simultaneously detects all wavelengths from 525 to 680 nm. Ninety-six samples in a single tray can be analysed by the instrument. The polymer used on the instrument has many performance features that are critical to the success of STR analysis in forensic work: alleles differing in size by a single base (up to 250 bp in length) can be detected; sizing precision (between alleles of the same length) of less than 0.15 nucleotide SD is

possible; analysis time per sample is less than 30 min; capillary life is at least 100 injections; and the run temperature is set at 60°C to provide a highly denaturing environment for the DNA samples.

The disadvantage of CE is that it is a serial technique, making its total throughput no better than the long run times and parallel separations in conventional slab gel electrophoresis. Several attempts to obtain faster and higher throughput separations have been reported. These include capillary array electrophoresis in ultra thin slab gels. These two techniques are limited by difficulty in assembling the separation system and in carrying out sample introduction. The use of CE to provide continuous automated loading of PCR products on to ultra thin slab gels shows new potential for increasing sample throughput in STR analysis, although separation resolution still needs to be improved.

Over the years CE has become widely used as a power tool in post-PCR analysis. However, it is difficult to introduce PCR to routine laboratories, because of the possibility of false-positive results. These false positives may be caused by sample-to-sample contamination or by the carry-over of previously amplified PCR product. The online coupling of fused silica capillary as the microreactor for PCR

and CE for separation and detection can be recommended in order to avoid false-positive results.

Other

The analysis of inks as part of the detection of fraudulent documents is a small but important part in the operation of a forensic laboratory. TLC and HPLC have been extensively used to separate and distinguish inks during the last decades. In comparison, CE has been applied only rarely. UV-Vis, fluorescence and particle-induced X-ray emission (PIXE) detection of electrophoretically separated diluted original inks and ink extracts (**Figure 4**) from substrate material provide sufficient information for the comparison of different inks (**Table 1**). The possibility of comparison of 50 forensic inks by MEKC has also been investigated. The separation patterns of individual dyes were compared with those obtained by HPLC and TLC, showing a much higher separation efficiency for MEKC. Some inks, which cannot be discriminated by applying the HPLC and TLC method, can definitely be distinguished using MEKC.

Nicotine, nornicotine and anabasine, the active principal components in all tobacco products, have been separated by CE and the potential for CE to

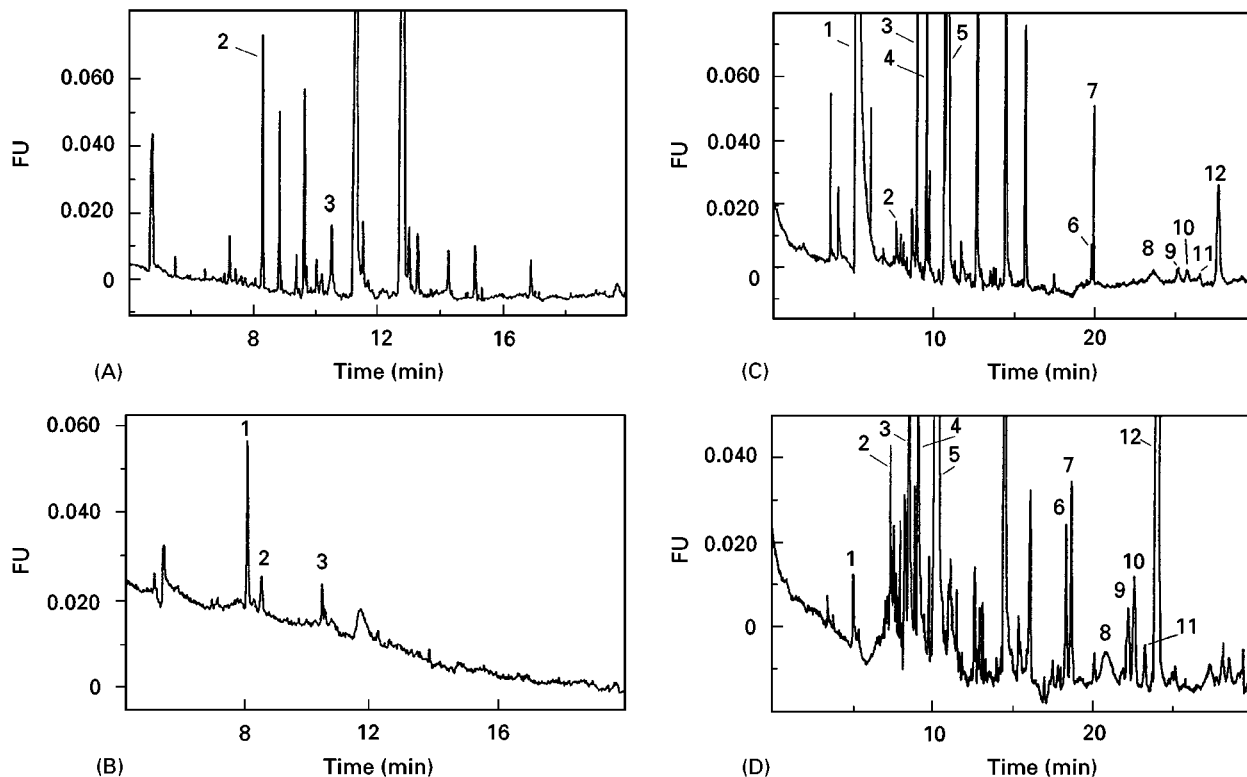


Figure 4 Electropherograms of extracts from dried blue and black inks see (see **Table 1**) and original inks diluted 100-fold in 5 mmol L⁻¹ borate buffer, pH 8.25. Capillary, fused silica 45 cm × 50 μm i.d. Potential, 25 kV. Detection, laser-induced fluorescence at λ_{exc/em} = 320/436 nm. (A) Extract ink 1; (B) original ink 1 (diluted 1 : 100); (C) extract ink 2; (D) original ink 2 (diluted 1 : 100).

Table 1 Listing of fountain pen inks investigated

<i>Ink number</i>	<i>Colour</i>	<i>Manufacturer</i>	<i>Country of origin</i>
1	Blue	Cross	USA
2	Black	Cross	USA
3	Royal blue	Pelikan	Germany
4	Brilliant black	Pelikan	Germany
5	Blue	Pilot	Japan
6	Black	Pilot	Japan
7	Blue	Lamy	Germany
8	Black	Lamy	Germany
9	Royal blue	Geha	Germany
10	Brilliant black	Geha	Germany
11	Blue-black	Parker	USA
12	Washable blue	Parker	USA
13	Permanent black	Parker	USA
14	Royal blue washable	Parker	France
15	Permanent blue	Parker	France
16	Black	Waterman	France
17	Royal blue	Mont Blanc	Germany

(Reprinted with kind permission of Wiley-VCH from Rohde *et al.* (1998) *Electrophoresis* 19: 31–41.)

characterize tobacco products on their alkaloid profiles for classification purposes has also been demonstrated.

Marine phytotoxins present a major public health problem because they can contaminate seafood. CE and MEKC enable okadaic acid, microcystins and maitotoxin to be detected in the picogram range.

Since any case of mushroom intoxication may have legal consequences, the accurate determination of mushroom toxins is of primary importance for forensic pathologists and toxicologists. The analysis of amatoxins by CE instead of radioimmunoassay has several advantages: analysis is faster, less costly and it requires smaller amounts of sample. Rapid and sensitive CE method for the separation and determination of the psilocybin and baeocystin in hallucinogenic mushrooms has also been reported.

Many types of explosives consisting of inorganic and organic components have been used in criminal cases. It has been demonstrated that the original composition of some explosive devices can be derived from the components of the post-blast residue. In short, CE offers a powerful tool which is suitable for both high and low explosive and gunshot residue analysis. CE is suitable for the determination of both inorganic and organic components, showing greater versatility than the traditional methods such as atomic absorption spectrometry and PIXE.

Conclusion

CE is a new technique in the forensic laboratory for the separation and quantitation of a wide variety of

molecules based not only on charge, but also on size, hydrophobicity and stereospecificity. CE offers certain advantages for forensic analysis:

1. higher theoretical plate number than HPLC;
2. in many instances CE is faster than GC and HPLC;
3. with regard to sample preparation, CE is easier than GC and HPLC. In many instances the sample can be injected directly with little or no preparation;
4. lower cost per analysis;
5. full automation;
6. CE is complementary to GC and HPLC;
7. two complementary techniques such as CE and MECC can be carried out with the same instrument.

Despite these features, the technique has not yet been widely accepted in the forensic community. This may be in part due to the legal system. Different countries have different standards to achieve legal defensibility of analytical results in court and forensic laboratories rely to a large extent on commercial instruments which are specially built and approved by a governmental agency for specific analysis. Even so, the US Drug Enforcement Agency is now using CE for general drug screening to quantitate heroin samples.

Two drawbacks of CE are often stated: low reproducibility and low sensitivity. However, due to several recently presented results (e.g. detection limits in the region of ng mL^{-1} , the precision of migration times $< 1\%$ RSD, same-day and day-to-day repeatability characterized by RSD values in the range of 1–4%, when peak area ratios were used), these drawbacks seem not to be so critical.

As stated by Kuffner *et al.*: ‘The legal criteria of Daubert, as long as they are met by the scientific community, will allow CE into evidence as acceptable expert testimony’.

See also: II/**Electrophoresis:** Capillary Electrophoresis; Capillary Electrophoresis-Mass Spectrometry; Capillary Electrophoresis-Nuclear Magnetic Resonance. III/**Clinical Chemistry:** Thin-Layer (Planar) Chromatography. **Forensic Sciences:** Liquid Chromatography.

Further Reading

- Kuffner CA Jr, Marchi E, Morgado JM and Rubio CR (1996) Capillary electrophoresis and Daubert: time for admission. *Analytical Chemistry* 68 (7): 241A.
- Lurie IS (1997) Application of micellar electrokinetic capillary chromatography to the analysis of illicit drug seizures. *Journal of Chromatography A* 780: 265.

- McCord BR (ed.) (1998) Volume symposium capillary electrophoresis in forensic science. *Electrophoresis* 19(1): 11.
- Tagliaro F and Smith FP (1996) Forensic capillary electrophoresis. *Trends in Analytical Chemistry* 15 (10): 513.
- Tagliaro F, Turrina S and Smith FP (1996) Capillary electrophoresis: principles and applications in illicit drug analysis. *Forensic Science International* 77: 211.
- Tagliaro F, Smith FP, Turrina S *et al.* (1996) Complementary use of capillary zone electrophoresis and micellar electrokinetic capillary chromatography for mutual confirmation of results in forensic drug analysis. *Journal of Chromatography A* 735: 227.
- Tagliaro F, Turrina S, Pisi P *et al.* (1998) Determination of illicit and/or abused drugs and compounds of forensic interest in biosamples by capillary electrophoretic/electrokinetic methods. *Journal of Chromatography B* 713: 27.
- Thormann W, Molteni S, Caslavská J and Schmutz A (1994) Clinical and forensic applications of capillary electrophoresis. *Electrophoresis* 15: 3.
- von Heeren F and Thormann W (1997) Capillary electrophoresis in clinical and forensic analysis. *Electrophoresis* 18: 2415.

Liquid Chromatography

L. A. Kaine, C. L. Flurer and K. A. Wolnik,
Forensic Chemistry Center, US Food and
Drug Administration, Cincinnati,
OH, USA

Copyright © 2000 Academic Press

Forensic science is the application of the sciences to the court of law. Consequently, forensic science and the legal system are intimately intertwined. Results obtained from the examination and analysis of forensic samples and the forensic samples themselves comprise evidence of a crime. It is the individualization of the sample, i.e. the singular association between the samples(s) and an illegal act, that is unique to forensic science. Because of the legal consequences, results require a high degree of certainty and the techniques used must be admissible in court. The Daubert rule, a 1993 decision upheld by the US Supreme Court, assigns to the judge the role of determining admissibility of scientific evidence. Among the factors considered by the judge are: (i) whether the technique has been tested and subjected to peer review; (ii) whether error rates have been defined; (iii) whether standards controlling the operation of a technique exist; and (iv) whether the technique has been widely accepted in the scientific community. Techniques used in a forensic laboratory may be applied to the investigation of a wide variety of crimes. Some examples are illegal drug use, counterfeiting, arson, tampering, fraud, poisoning, terrorism and environmental crimes. It is this diversity of cases, variety of sample matrices and the staggering number of potential analytes that necessitate a continuous evaluation of the testing that is needed to constitute proof in each situation.

Analytical requests in a forensics laboratory may be classified into four categories: (i) screen for the

presence or absence of known compounds or class of compounds; (ii) screen for unspecified analytes; (iii) perform a comparative analysis; and (iv) verify and/or quantify substances in a sample. Many qualitative tests are used in forensic laboratories for their speed and ability to identify unknowns. In some cases qualitative results (identity) suffice, while in others quantification is important. Like gas chromatography (GC), high performance liquid chromatography (HPLC) can be used for both qualitative and quantitative analyses. However, 80–85% of all known compounds are not amenable to GC. The stationary and mobile-phase combinations available and the many detection modes possible make HPLC a universal separation scheme. Unlike GC, it is not limited by the volatility or thermal stability of an analyte. HPLC can analyse solutes encompassing a wide molecular weight range, from monatomic species to proteins. A range of solute hydrophobicities and polarities can be accommodated, from acidic and basic species that incorporate many drugs of abuse, pharmaceuticals, dyes and food colourings, to neutral and/or hydrophobic molecules such as pesticides and herbicides, hydrocarbons in petroleum products and carotenoids in foods. In situations where GC can determine certain compounds more readily with greater selectivity, resolution and sensitivity, HPLC offers a secondary, confirmatory method. In other cases, the use of HPLC avoids sample derivatization required by GC, and eliminates steps that could contribute to sample loss and increase analysis time. Another advance in HPLC in recent years involves the introduction of narrow-bore (2.1 mm inner diameter) and microbore (1 mm inner diameter) columns. These smaller columns decrease the sample size required for injection and increase mass detection sensitivity versus the typical 4.6 mm inner diameter analytical columns.

Thin-layer chromatography (TLC) is also utilized in forensic chemistry, particularly for sample screening. Although TLC permits analysis of many samples at one time, facilitating the side-by-side comparison of suspect and authentic samples, it can suffer from a lack of resolution and from difficulties in both quantification and isolation of an individual component. Immunoassays are generally more sensitive; however, they may provide class-only determinations, may be prone to interferences and may not be available for classes such as neuroleptics and β -blockers. HPLC is useful for sample screening, comparison and quantification, and fraction collection for further analysis is more straightforward.

The UV-visible detector, and more recently the diode array detector (DAD), are the most commonly used detectors for HPLC analyses. As an alternative, one may utilize more specific devices such as fluorescence, electrochemical, chiral or mass spectrometric detectors. Because these detectors take advantage of specific molecular characteristics of the analyte(s) of interest, they are less susceptible to background interferences from sample matrix, and tend to be more sensitive. The choice of a particular detector and method depends upon the requirements of the case in hand – whether the sample is being screened for unknowns, analysed for a particular compound, compared against another sample, or quantified.

Sample Preparation

Each manipulation of the forensic sample may irreversibly alter the evidence and introduces the possibility of incomplete analyte recovery and inadvertent contamination. Therefore, sample preparation requires careful consideration and always follows a preliminary visual, and perhaps microscopic, examination. Sample preparation steps may also affect the form of the analyte, which is problematic for speciation work and subsequent toxicological evaluation. Additional complications in forensic work are the variety of sample matrices (drugs, body fluids, food, soils, etc.) and limited sample sizes (arson residues, traces of blood in a syringe, a spot on blotter paper, etc.) frequently encountered. Ideally, a portion of the sample should be reserved in case of trial to allow independent analysis. If appropriate, the sample can be homogenized. However, portions may need to be analysed separately to characterize the sample accurately. Individual samplings may also be advisable when there are visual differences within portions of a sample. Sampling in the vicinity of a visual contaminant reduces dilution with the matrix and improves detection limits.

Analytes must be in solution for determination by HPLC. Sample preparation is necessary to remove compounds such as proteins that might damage an HPLC column, as well as compounds that interfere with an analysis. Liquid-liquid extractions (LLE) are commonly used, and can be manipulated by choice of solvent, addition of salts (salting-out effect) and control of pH. For biological matrices, extractions using chloroform/2-propanol/*n*-heptane under alkaline conditions provide clean extracts with good recoveries of basic and neutral compounds. However, acidic compounds such as barbiturates and salicylates are poorly recovered (20–50%). LLE is not easily automated and can require large volumes of solvent. Solid-phase extraction (SPE) cartridges are now widely used in toxicology screens, mainly for low viscosity samples such as urine or serum. SPE has the advantages of higher efficiencies and selectivity, lower solvent volume requirements, absence of emulsions, and automation options. However, the packing materials can be irreproducible, even within batches of the same brand, resulting in variable recoveries and poor analytical reproducibility. The use of an internal standard is highly recommended for quantitative results. SPE cartridges should not be re-used due to decreased extraction performance and increased possibility of the introduction of contaminants.

General Unknowns

Screening for unknowns is a very challenging task due to the vast number of potential contaminants. Screening methods in a forensic laboratory are designed to detect the most relevant drugs and potentially hazardous chemicals. Often, screens are performed in response to a crisis such as an acute poisoning and as such require rapid response. While immunoassay techniques and TLC remain invaluable for initial screening, these methods must be supplemented by HPLC-DAD for those analytes for which the initial screen does not offer sufficient selectivity or sensitivity. Identification of a compound by HPLC-DAD is based on retention time match and spectral match, as shown in Figure 1.

Additionally, plotting the ratios of absorbance measurements obtained during a chromatographic analysis, taken at well-separated and characteristic wavelengths, permits evaluation of interferences and a more confident identification. For example, variation in the ratio across a peak indicates co-elution, as seen in Figure 2.

Since forensic screens for unknowns are often performed in biological matrices, which are inherently variable, the analysis of blanks is an additional safeguard against false positives that could be caused by

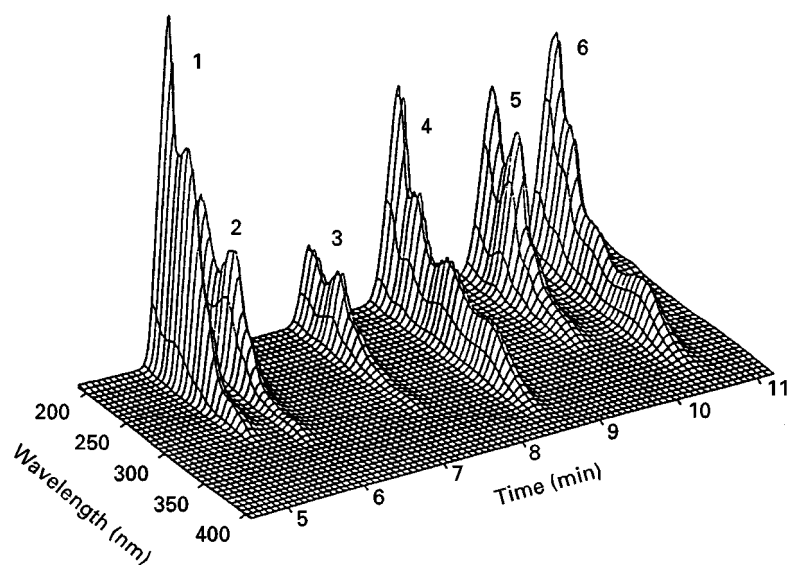


Figure 1 Spectrochromatogram showing spectral and chromatographic data for the separation of six benzodiazepines. Solutes: 1, midazolam; 2, flurazepam; 3, oxazepam; 4, nitrazepam; 5, alprazolam; 6, clonazepam. Column, 25 cm Lichrosorb RP-8; mobile phase, 35% CH_3CN in $0.05 \text{ mol L}^{-1} \text{ KH}_2\text{PO}_4\text{-H}_3\text{PO}_4$ buffer, pH 3; flow rate, 1.5 mL min^{-1} ; spectra collected between 190 and 400 nm. Reproduced from Logan (1994), with permission from Elsevier Science.

the effect of poisons on the matrix or due to putrefaction processes. Blanks should include reagents, and matrix that is contaminant-free. Screening methods also need to detect indirect indicators of the compound of interest. A screen of biological fluids should include major drug/poison metabolites such as benzoylecgonine, the primary indicator of cocaine use, which is found in urine. The addition of bleach to carbonated beverages leads to the formation of chlorate, chloride and sometimes chloroform.

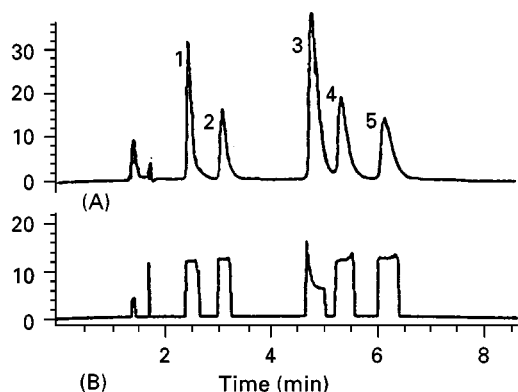


Figure 2 Use of wavelength ratioing to indicate peak impurity in the analysis of tricyclic antidepressants and metabolites by LC-photodiode array detection. (A) Chromatogram at 252 nm; (B) ratiogram 252 nm/230 nm. Asymmetric ratio of peak 3 indicates inhomogeneity and co-elution. Solutes: 1, 10-hydroxynortriptyline; 2, 10-hydroxyamitriptyline; 3, protriptyline/imipramine (co-elution); 4, nortriptyline; 5, amitriptyline. Column, 25 cm Lichrospher RP-8 (CH100); mobile phase, 40% CH_3CN in 0.05 mol L^{-1} phosphate buffer, pH 3; flow rate, 2.0 mL min^{-1} . Reproduced from Logan (1994), with permission from Elsevier Science.

Statistical toxicological analysis (STA), a general screening method for toxins in biological matrices as described by Tracqui *et al.*, often utilizes HPLC-DAD. Many laboratories have had success in creating their own databases and/or using multicomponent analysis for the identification of hundreds of substances from several classes in one run. Widespread use of HPLC-DAD for STA requires libraries that can be shared among laboratories. Unfortunately, libraries are not as common for HPLC as they are in GC work. Because the mobile phase in HPLC interacts much more strongly with analytes than the carrier gas in GC, small deviations in chromatographic conditions such as column type and batch, mobile-phase composition and pH, temperature and flow rate may affect retention time. The use of retention indices is necessary to minimize interlaboratory differences. Bogusz *et al.* proposed the use of a 1-nitroalkane index scale for toxicological screens since the C_1 to C_6 homologues are commercially available and have high UV absorbance between 200 and 220 nm. The retention times of 1-nitroalkanes are not affected by pH changes between 3.2 and 8.5, but are affected by changes in acetonitrile concentration. Because compounds are affected differently by changes in chromatographic conditions, the use of selected drugs as retention markers to correct retention indices improves accuracy and precision. One toxicological screening library that includes 900 substances is available commercially. To improve the possibility of obtaining a match, it is important to use the same chromatographic conditions as the library.

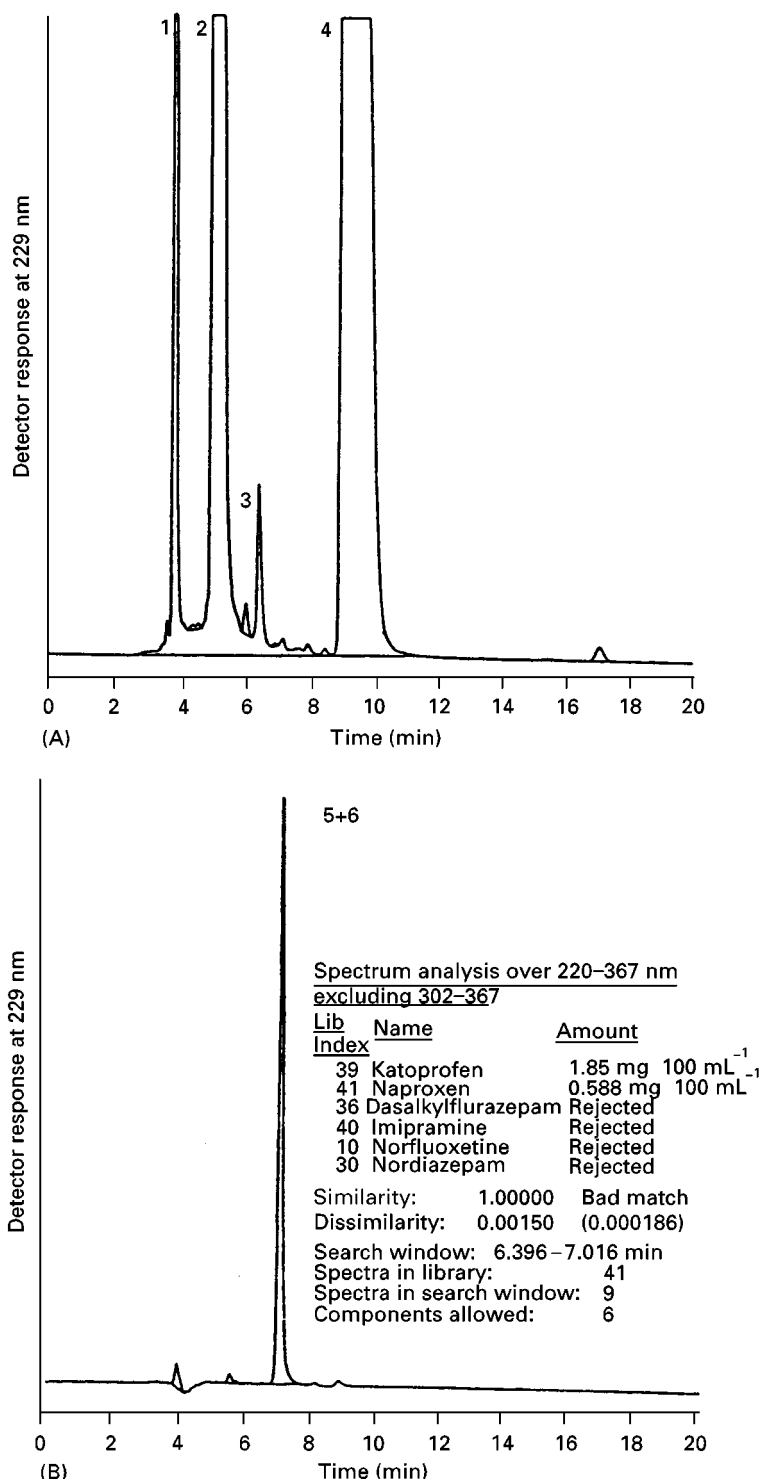


Figure 3 Chromatograms obtained from extracts of two gastric contents (A and B). Solutes; 1, zopiclone, 2, mesoridazine; 3, perphenazine; 4, thioridazine; 5 and 6, co-elution of ketoprofen and naproxen. The spectral library was developed over the wavelength range of 210–367 nm. Solute identification utilized a retention time window of $\pm 5\%$ and a peak purity parameter of ± 1 nm. Columns: 250×4.6 mm i.d. Supelcosil LC-DP (diphenyl) and 250×4.0 mm. i.d. LiChrospher 100 RP-8; mobile phase, isocratic CH_3CN –0.025% (v/v) H_3PO_4 –TEA buffer, pH 3.4; flow rate, 0.6 mL min^{-1} ; detection, 229 nm. Reproduced from Koves (1995) with permission from Elsevier Science.

Figure 3 is an illustration of the process used to identify substances found in gastric contents. The search window needs to be set wide (20%), and peak purity should be considered. Consequently, a library search may yield as many as 10 possible matches. Spectra should be compared between a sample and

a standard run in-house for a positive identification. Even in the absence of a positive identification, the diode array spectrum can give class indications. The analysis can then be pursued by modifying the HPLC conditions or by utilizing another technique.

Analysis for a Known Analyte or Analyte Class

In contrast to screening for unknowns, sample preparation and separations can be optimized for the analysis of a known analyte or class of analytes. In order to avoid interferences and to maximize analyte recovery from the sample matrix, experimental conditions can be tailored for the class of compounds of interest. It is often necessary to determine components such as diluents, excipients, metabolites and synthesis or degradation products. **Table 1** lists examples of compounds that are analysed by HPLC in forensic laboratories. HPLC may not be the primary method for all of these analytes but may instead be the confirmatory technique.

Analysis of drugs of abuse constitutes a major portion of forensic work. While UV may lack the necessary sensitivity, electrochemical detection offers sensitivity and selectivity for compounds such as morphine, benzodiazepines, cannabinoids, hallucinogens, fentanyl and some cyclic antidepressants. Additional compounds can be analysed using post-column photolytic derivatization followed by electrochemical detection. Sample preparation may be minimized de-

pending on detector selection. For example, morphine can be analysed directly in poppy seed extract with electrochemical detection because it is easily oxidized at low potentials, unlike most opium alkaloids from natural products. **Figure 4** compares the sensitivity and selectivity obtained with UV, fluorescence and electrochemical detection of various alkaloids.

HPLC separations can resolve lysergic acid diethylamide (LSD) from ergot alkaloids. Because LSD is typically ingested in small amounts, fluorescence detection is commonly used for its sensitivity and selectivity. Analysis of opium alkaloids by HPLC must also separate caffeine, quinine and strychnine – common additives or diluents.

Although there are more than 2000 known steroids, only a portion are controlled substances. Analysis of steroids is required in a variety of matrices, including dosage forms, oils, body fluids and tissues. Spot tests are useful for the rapid initial verification of the presence of steroids. A more specific identification is possible by either GC or HPLC with similar resolving power but different co-eluting pairs. HPLC-DAD adds the potential of distinguishing between some steroids based on differences in UV spectra.

In drug abuse cases, creatinine is analysed using ion pair reversed-phase separation and UV detection at 220 nm to determine if urine samples have been diluted. The HPLC method suffers from fewer interferences than other methods. HPLC reversed-phase or ion exchange separations of proteins for blood grouping or species identification are rapid and efficient.

Pesticides, herbicides and rodenticides may be determined by HPLC in poisoning cases. Warfarin and its metabolites have been identified in matrices such as urine and food. Carbamates are more readily analysed by HPLC with post-column derivatization than by GC because they are thermally labile.

Explosives are difficult to analyse by GC due to their thermal instability. HPLC is used for the analysis of nitroglycerin, propellants, stabilizers, plasticizers and weapon discharge residues. Inorganic explosives and explosive residues can be determined with ion chromatography. Explosives such as ammonium nitrate and residues such as chloride, chlorate, sulfide and sulfate can be determined by anion exchange with UV or conductivity detection, as illustrated in **Figure 5**.

Separations in ion chromatography (IC) are based on ion exchange, ion exclusion and reversed-phase adsorption. The use of a suppressor column to reduce the mobile-phase background chemically and increase the analyte signal permits conductivity detection of inorganic ions. There are also methods known

Table 1 Types of analytes determined by HPLC in forensic laboratories

Analgesics
Anticonvulsants
Antidiabetic drugs
Creatinine
Digitalis glycosides
Drugs of abuse (barbiturates, benzodiazepines, cannabinoids, cocaine and related compounds, LSD, opium alkaloids)
Dyes and colourings (natural and synthetic)
Ergot alkaloids
Explosives, propellants, stabilizers
Hydrocarbons (petroleum distillates, engine oils, greases)
Inks
Inorganic and organic anions (fluoride, chloride, phosphate, sulfate, azide, citrate)
Inorganic cations (sodium, potassium, calcium, ammonium)
Pesticides, herbicides, rodenticides
Pharmaceuticals
Phenothiazines
Plastics, plasticizers, polymers
Proteins
Sugars
Tricyclic antidepressants

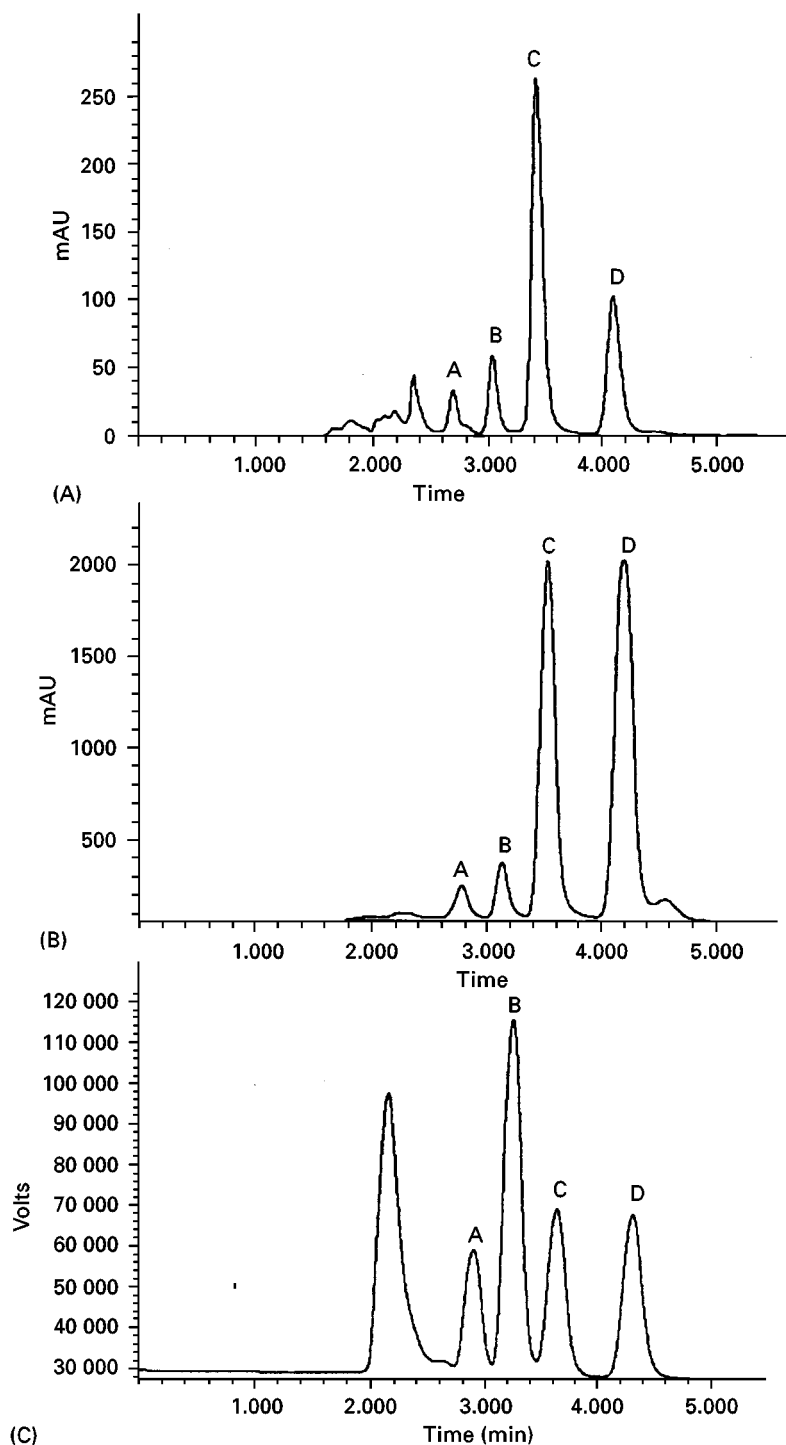


Figure 4 Comparison of detector signals. (A) UV; (B) fluorescence; (C) electrochemical. Chromatograms of orange juice samples spiked with: A, morphine; B, codeine; C, eserine; D, apomorphine. Column, 250 \times 4.6 mm i.d. Interaction chemicals C_{18} ; mobile phase, 55% methanol, 15 mmol L^{-1} KH_2PO_4 , 3.75 mmol L^{-1} 1-octanesulfonic acid, 7.5 mmol L^{-1} KCl, adjusted to pH 4.00 with 10% H_3PO_4 ; flow rate, 1.0 mL min^{-1} ; 30°C. Detection: UV, 254 nm; fluorescence, $\lambda_{ex} = 254$ nm, $\lambda_{em} = 408$ nm; electrochemical, 1.2 V vs. Ag/AgCl reference electrode with a glassy carbon working electrode. Reproduced from Lin (1993) with permission from Elsevier Science.

as single column which do not utilize a suppressor, but instead utilize low capacity columns and low ionic strength, low conductance mobile phases.

Although conductivity detectors are the most commonly used, a variety of other detectors are available: UV-visible (direct or following post-column

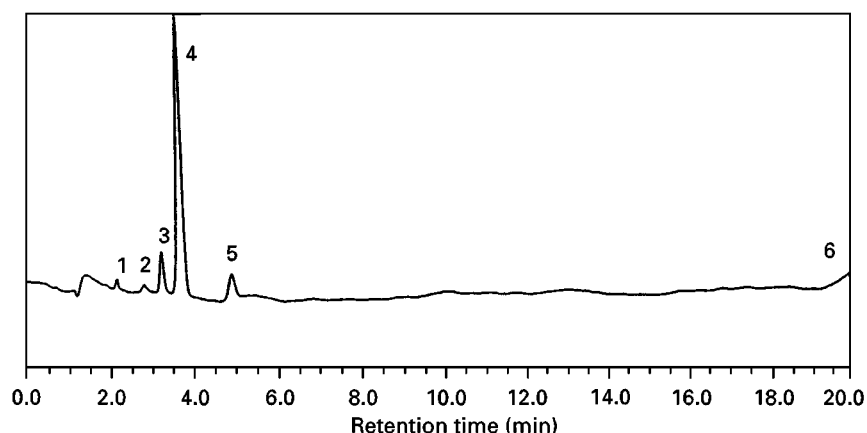


Figure 5 Analysis of residue taken from a black powder pipe bomb using ion chromatography. Solutes: 1, chloride; 2, nitrite; 3, nitrate; 4, sulfate; 5, sulfide; 6, hydrogen carbonate. Column, Vydac 302IC4.6; mobile phase 0.75 g isophthalic acid in 3 L H_2O , adjusted to pH 4.6 with 2 mol L^{-1} KOH; flow rate, 2.5 mL min^{-1} ; detection, 280 nm. Adapted from Hargadon and McCord (1992) with permission from Elsevier Science.

reactions), amperometry, fluorescence and atomic spectroscopy. IC analysis of strong acids and alkalis can be important in poisoning cases. Speciation by IC of compounds such as arsenic may be important due to the higher toxicity of inorganic anions compared to the methylated forms. IC can also be used to determine counterions of drugs, as well as cleaning products and their components.

Comparison of Samples

HPLC analysis may be required to compare samples, either to differentiate one from another or to trace the source of a sample. Although retention times can be used for tentative identification of specific compounds, it is not always necessary to identify every component in the sample. Often, pattern recognition will suffice when comparing the content of a class of compounds from one sample to the next. IC has been used in the analysis of sugars present in suspect infant formulas, as seen in Figure 6. HPLC with refractive

index detection can be used to analyse the types and amounts of sugars found as diluents in illicit street drugs, possibly linking seized evidence from several cases. Figure 7 demonstrates an excellent separation of cannabinoids and their metabolites. Comparative analysis of cannabinoids in cannabis samples by HPLC has been shown to connect suppliers with customers.

Through the knowledge of peak area ratios among carotenoids that occur naturally in orange juice, a suspect orange juice can be analysed to determine whether carotenoids have been added to enhance the colour. Dyes extracted from fibres gathered at a crime scene and from fibres from a suspect could be profiled and compared. The profile of the subunits of haemoglobin present in a blood drop permits its source identification as human adult, human neonatal or animal.

When comparing chromatograms, the presence of extra peaks in a profile may suggest the deliberate addition of a foreign substance, or simply sample

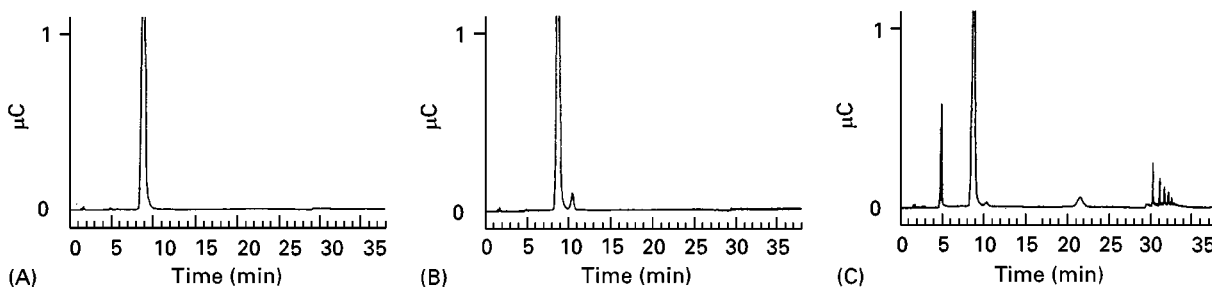


Figure 6 Comparison of sugar profiles using IC; (A) a known formula and (B,C) suspect infant formulas labelled as the known. Column, 4 × 250 mm Dionex Carbopac PA-1; mobile phase, 150 mmol L^{-1} NaOH in 0–600 mmol L^{-1} sodium acetate; flow rate, 1.0 mL min^{-1} ; detection, pulsed electrochemical detection with a gold working electrode and a pH/Ag/AgCl reference electrode. Adapted from Kaine and Wolnik (1998) with permission from Elsevier Science.

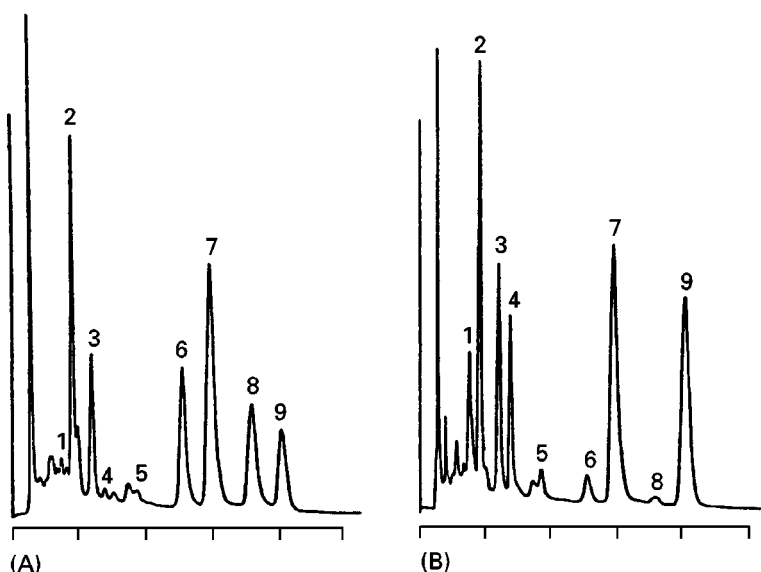


Figure 7 HPLC of cannabis resin at (A) 254 nm and 26°C, (B) 220 nm and 26°C. Solutes: 1, cannabidiol and cannabigerol (shoulder); 2, cannabidiolic acid; 3, cannabinol and cannabigerolic acid; 4, tetrahydrocannabinol; 5, cannabichromene; 6, cannabinolic acid; 7, tetrahydrocannabinolic acid; 8, cannabichromenic acid; 9, di-*n*-octyl phthalate (internal standard). Chromatographic conditions: 100 mg resin extracted with 1 mL chloroform–methanol (1:9) containing 8 g L^{-1} di-*n*-octyl phthalate; 2 μL extract injected. Column, $250 \times 4.9 \text{ mm}$ Partisil 5 C_{18} ; mobile phase, 80% methanol–20% 0.02 mol L^{-1} H_2SO_4 ; flow rate, 2 mL min^{-1} . Reproduced from Smith and Vaughan (1976) with permission from Elsevier Science.

degradation. The lack of expected peaks may suggest that the sample is not what it claims to be. However, because many species absorb at lower wavelengths, the mobile-phase composition may affect the outcome of an analysis. The molar absorptivity of a compound may change with small changes in the mobile-phase composition, affecting quantification. A high background absorbance from the mobile phase may obscure species that are present in the sample at low concentrations. This could lead to the erroneous conclusion that there are no apparent differences between suspect and authentic samples.

Whenever the analysis of samples requires a long period of time, e.g. for a large number of samples, the variation of retention times due to chromatographic factors must be considered. An internal standard may be added to samples, or a control sample may be analysed with each set of suspect samples. For comparative analysis, there is added importance to representative sampling and replicate analyses. It is easier to state that samples are different, rather than identical. Results of comparative analyses indicating two samples appear the same might be worded as ‘the samples were analytically indistinguishable using techniques x, y, z ’. In some cases, the individualization of a sample can be quantified. For example, a statistical probability of a blood sample matching a specific person can be based upon the

analysis of blood group and Rh antigens if the distribution of these factors among the population is known.

Verification of Analyte Identity

A high degree of certainty is required for the identification of solutes in forensic cases in order to defend the work in court. An orthogonal technique may be used for confirmation, and the use of selective detectors aids in the certainty of identification. In HPLC, diode array detectors add the ability to match spectra, while fluorescence and electrochemical detectors are more specific. Both the excitation and emission wavelengths can be selected for fluorescence detection. The oxidation potential can be adjusted to reduce interferences of some analytes determined electrochemically.

GC-mass spectrometry (GC-MS) and GC-MS-MS are widely used in forensic analysis to verify analyte identification, particularly in cases concerning illegal drugs and drugs of abuse. The retention time identifies an analyte, and the mass spectrum serves as confirmation. Until recently, the argument against the use of HPLC as the primary method in forensic analysis was the difficulty of solute confirmation. Tremendous improvements in instrumentation and interface designs have made the coupling of HPLC to a mass spectrometer straightforward, particularly with the

recent introduction of relatively inexpensive bench-top models.

The ionization methods that are available permit the analysis of a wide variety of compounds. Particle beam is effective for moderately polar compounds (certain steroids and rodenticides), operates more efficiently with narrow-bore columns, and causes fragmentation during the ionization process. Both atmospheric pressure chemical ionization (APCI) and electrospray ionization (ESI) are amenable to gradient elution methods, thereby permitting their use in the analysis of a group of compounds. APCI is compatible with conventional columns and is used primarily to determine moderately polar analytes that are not thermally labile (clenbuterol, basic pharmaceuticals). Polar (conjugated oestrogens, proteins, peptides) and/or thermally fragile molecules (glucuronide metabolites of morphine and codeine) are analysed more effectively by ESI. ESI requires narrow- and microbore columns. In any of these methods, quantification can be performed in either the full scan mode or in the selected ion monitoring (SIM) mode. SIM offers greater sensitivity (10–100×), comparable to that obtained with GC-MS.

The utilization of MS-MS provides even greater specificity, further decreasing the chance of the incorrect identification of an analyte. Even if two compounds co-elute and have the same $[M + H]^+$ ion exiting the first quadrupole, it is unlikely that they would produce the same fragmentation pattern in the third quadrupole. The technique called selected reaction monitoring utilizes the known losses that occur during fragmentation of an analyte or a particular group of analytes. The method is useful when co-elution of two or more compounds is suspected. Another benefit to this method is that its sensitivity is typically 10–100 times greater than that obtained in the full scan mode.

Conclusions

Numerous aspects of separation science are applicable to forensic science. Because HPLC is so versatile and can be used to determine so many different compounds, the technique is particularly well suited to the demands of a forensic laboratory. Both qualitative and quantitative information can be obtained, often with minimal sample preparation. Because only small volumes are needed for analysis, sample consumption can be minimized. Eluting fractions can be collected for further analysis – an important consideration when dealing with trace evidence. HPLC offers a cost-effective technique with the ruggedness and reliability necessary for forensic testing and

consequently is widely used in forensic laboratories today.

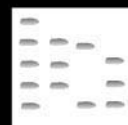
See also: III/Carbamate Insecticides in Foodstuff: Chromatography & Immunoassay. Clinical Diagnosis: Chromatography. Explosives: Gas Chromatography; Liquid Chromatography; Thin-Layer (Planar) Chromatography. Forensic Toxicology: Thin-Layer (Planar) Chromatography. Heroin: Liquid Chromatography and Capillary Electrophoresis. Toxicological Analysis: Liquid Chromatography. Steroids: Gas Chromatography; Liquid Chromatography and Thin-Layer (Planar) Chromatography.

Further Reading

- Bogusz M, Franke JP, de Zeeuw RA and Erkens M (1993) An overview on the standardization of chromatographic methods for screening analysis in toxicology by means of retention indices and secondary standards. *Fresenius Journal of Analytical Chemistry* 347: 73–81.
- Bohan TL and Heels EJ (1995) The case against Daubert: the new scientific evidence “standard” and the standards of the several states. *Journal of Forensic Sciences* 40: 1030–1044.
- Busch KL, Glish GK and McLuckey SA (1988) *Mass Spectrometry/Mass Spectrometry: Techniques and Applications of Tandem Mass Spectrometry*. New York: VCH.
- DeForest P, Gaensslen RE and Lee HC (1983) *Forensic Science: An Introduction to Criminalistics*. New York: McGraw Hill.
- Hargadon KA and McCord BR (1992) Explosive residue analysis by capillary electrophoresis and ion chromatography. *Journal of Chromatography* 602: 241–247.
- Kaine LA and Wolnik KA (1998) Detection of counterfeit and relabeled infant formulas using high pH anion exchange chromatography-pulsed amperometric detection for the determination of sugar profiles. *Journal of Chromatography A* 804: 279–298.
- Koves EM (1995) Use of high-performance liquid chromatography-diode array detection in forensic toxicology. *Journal of Chromatography A* 692: 103–119.
- Lin LA (1993) Detection of alkaloids in foods with multi-detector high-performance liquid chromatographic system. *Journal of Chromatography* 632: 69–78.
- Logan BK (1994) Liquid chromatography with photodiode array spectrophotometric detection in the forensic sciences. *Analytical Chimica Acta* 288: 111–122.
- Lurie IS, Sperling AR and Meyers RP (1994) The determination of anabolic steroids by MECC, gradient HPLC, and capillary GC. *Journal of Forensic Sciences* 39: 74–85.
- Selevka CM and Krull IS (1987) The forensic determination of drugs of abuse using liquid chromatography with electrochemical detection: a review. *Journal of Liquid Chromatography* 10: 345–375.

- Smith RN (1982) Forensic applications of high-performance liquid chromatography. In: Saferstein R. (ed.) *Forensic Science Handbook*. New Jersey: Prentice Hall.
- Smith RN and Vaughan CG (1976) High-pressure liquid chromatography of cannabis. Quantitative analysis of acidic and neutral cannabinoids. *Journal of Chromatography* 129: 347–354.
- Tracqui A, Kintz P and Mangin P (1995) Systematic toxicological analysis using HPLC/DAD. *Journal of Forensic Sciences* 40: 254–262.
- Weiss J (1995) *Ion Chromatography*, 2nd edn. New York: VCH.
- White P (1998) *Crime Scene to Court. The Essentials of Forensic Science*. Cambridge: Royal Society of Chemistry.

FORENSIC TOXICOLOGY: THIN-LAYER (PLANAR) CHROMATOGRAPHY



I. Ojanperä, University of Helsinki, Helsinki, Finland

Copyright © 2000 Academic Press

The selection of appropriate analytical methodology for forensic toxicological investigations depends on the scope of the laboratory. Postmortem forensic toxicology investigates the cause of death, and consequently a very broad-range screening is needed to detect all potential poisons. In traffic toxicology, only such substances are relevant which may impair the driver's ability to control the vehicle. Doping control focuses on those substances that have been banned by the International Olympic Committee. Prisoners and rehabilitation clinic patients are tested for psychotropic drugs, whereas the US Mandatory Guidelines for Federal Workplace Drug Testing Programs are limited to the major drugs of abuse, cannabis, cocaine, amphetamine, opiates and phen-cyclidine.

Thin-layer chromatography (TLC) has found extensive use in forensic toxicology since the early 1960s when the famous book of Stahl made the technique well known. The first edition of the classic laboratory manual by AS Curry, *Poison Detection in Human Organs* from 1963 (Charles C. Thomas, Springfield, IL), still relies on paper chromatography but the second edition in 1969 utilizes TLC as a major technique for drugs. Gas chromatography (GC) and gas chromatography-mass spectrometry (GC-MS) in the 1970s, and especially high performance liquid chromatography (HPLC) in the 1980s gradually began to replace TLC but today the planar technique is having a renaissance due to the progress in instrumentation and software. From 1990 to 1996, 26% of published TLC applications were in the field of medical, clinical and biological analysis, which also includes forensic toxicology.

The commonly recognized advantages of classical manual TLC are high throughput, low cost, easy sample preparation and versatile visual detection possibilities. Instrumental TLC extends the scope to reproducible quantitative analysis and allows the utilization of *in situ* UV spectral information for identification. The main disadvantage of TLC is low chromatographic resolution, which can be partly overcome by instrumental techniques. Another disadvantage is that quantitative calibration curves are not reproducible enough to be stored, making it necessary to co-analyse several standards along with samples on each TLC plate. Most of the substances frequently encountered in forensic toxicology can be readily analysed by TLC. These include therapeutic drugs, drugs of abuse, pesticides and naturally occurring alkaloids, which are all relatively small molecular weight organic compounds with functional groups amenable to visualization by colour reactions.

It is practical to divide the discussion of TLC in forensic toxicology into two categories, the broad-scale screening analysis and target analysis. The former approach is related to the concepts of systematic toxicological analysis or general unknown, i.e. the search for a rational qualitative analysis strategy for hundreds of potential poisons. TLC drug screening is often performed in urine or liver, where the drug concentrations are higher than in the blood. In target analysis, the aim is specifically to detect and often also to quantify a substance or a limited number of substances.

Broad-scale Screening Analysis

Chromatographic Systems

Evaluation of systems The rational selection of TLC systems for screening analysis differs from the optimization of the separation of a few-component

mixture. In screening systems, the most important features are the distribution of R_F values across the plate, the reproducibility of the measurement of those values, and the correlation of chromatographic properties between systems. The computational methods capable of taking into account these features include discriminating power, mean list length (MLL), in-

formation content, quotient of distribution equality and principal component analysis. The (MLL) method has found widespread use, and it can also be used in computerized substance identification. The MLL approach is not related to the separation number (SN), i.e. the number of spots that can be separated by a system with a certain resolution. **Table 1**

Table 1 TLC systems for broad-scale toxicological screening analysis

<i>Mobile phase</i>	<i>Stationary phase</i>	<i>Correction standards</i>	<i>hR_F^c</i>	<i>Application</i>
1 Chloroform–acetone 80 + 20	Silica gel	Paracetamol Clonazepam Secobarbital Methylphenobarbital	15 35 55 70	Acidic and neutral drugs
2 Ethyl acetate	Silica gel	Sulfathiazole Phenacetin Salicylamide Secobarbital	20 38 55 68	Acidic and neutral drugs
3 Ethyl acetate–methanol– conc. ammonia 85 + 10 + 5	Silica gel	Hydrochlorothiazide Sulfafurazole Phenacetin Prazepam	11 33 52 72	Acidic and neutral drugs
4 Methanol–water 65 + 35	Silica gel RP 18	Diazepam Secobarbital Phenobarbital Paracetamol	16 35 54 74	Acidic and neutral drugs
5 Methanol–water– conc. hydrochloric acid 50 + 50 + 1	Silica gel RP 18	Hydroxyzine Lignocaine Codeine Morphine	20 46 66 81	Basic, amphoteric and quaternary drugs
6 Toluene–acetone–ethanol– conc. ammonia 45 + 45 + 7 + 3	Silica gel	Codeine Promazine Clomipramine Cocaine	16 36 49 66	Basic and neutral drugs
7 Ethyl acetate–methanol– ammonia 85 + 10 + 5	Silica gel	Morphine Codeine Hydroxyzine Trimipramine	20 35 53 80	Basic and neutral drugs
8 Methanol	Silica gel	Codeine Trimipramine Hydroxyzine Diazepam	20 36 56 82	Basic and neutral drugs
9 Methanol–ammonia 100 + 1.5	Silica gel ^a	Atropine Codeine Chlorprothixene Diazepam	18 33 56 75	Basic and neutral drugs
10 Cyclohexane–toluene– diethylamine 75 + 15 + 10	Silica gel ^a	Codeine Desipramine Prazepam Trimipramine	6 20 36 62	Basic and neutral drugs

^aImpregnated with 0.1 mol L⁻¹ KOH and dried.

shows TLC systems for broad-scale toxicological screening analysis, chosen partly on grounds of the MLL method, while the corresponding R_F libraries can be found from the books of de Zeeuw *et al.* and Fried and Sherma. For acidic and neutral drugs, recommended combinations of systems which possess low mutual correlation are 2 and 3, and 1 and 3, for basic drugs 5 and 6, and 8 and 10.

R_F correction In screening analysis, where R_F libraries of hundreds of compounds are utilized, the reproducibility of the values is an essential factor. TLC is an open technique, and the R_F values, and consequently the separation, are affected by environmental factors, such as humidity, layer activity and temperature. In contrast to column chromatography, the use of a single R_F standard for compensating the variation, corresponding to the relative retention time, may produce erroneous results. The method, which uses three to five correction standards that are structurally close to the analytes and linear interpolation between the standards, is now generally accepted to obtain corrected R_F values (hR_F^c). Table 1 indicates the correction standards chosen for the screening systems listed.

Identification

Migration distance By carefully adjusting the chromatographic and environmental conditions it is possible to obtain reproducible results with precoated plates. Reversed-phase (RP) layers show more batch-to-batch variation than silica gel but RP separations,

using aqueous mobile phases, are less dependent on humidity. The R_F and hR_F^c values can be determined manually or by using a scanning densitometer. The correction of R_F values makes it possible to obtain reproducible values in varying conditions and allows the use of the large hR_F^c libraries even in interlaboratory use.

Commercial software are available that utilizes the concept of hR_F^c for identification. Chrom TOX (Merck Tox Screening System, Merck, Darmstadt, Germany) is statistical search software that utilizes the MLL method for identification by R_F values and digitally coded colour reactions, giving a hit list of candidates with probability values. The software is also capable of adding information from other analytical techniques, such as retention indices from GC, molecular weights from MS and UV spectra from HPLC. A drawback is that the TLC data have to be fed manually. CATS software (Camag, Muttens, Switzerland) combines instrumental densitometric evaluation of chromatographic plates with substance identification by hR_F^c values and *in situ* UV spectra (see below).

Visualization reagents The possibility of using visualization reagents for the detection and identification of fractions is a unique feature of TLC. Post-chromatography derivatization by spraying or dipping has been used more extensively than pre-chromatography derivatization. The limits of detection by colour reactions generally range from 0.1 to 1 µg per fraction and by fluorescence reactions,

Table 2 Visualization reagents for broad-scale screening analysis

Reagent	Application
Bratton-Marshall reagent (diazotization and coupling)	Benzophenones (from benzodiazepines), sulfonamides
7-Chloro-4-nitrobenzo-2-oxa-1,3-diazole (NBD-Cl)	Amphetamines, amino acids
2,6-Dibromoquinone-4-chlorimide (Gibbs reagent)	Pesticides
2,6-Dichlorophenol-indophenol (Tillmann's reagent)	Organic acids
<i>p</i> -Dimethylaminobenzaldehyde (Van Urk's reagent)	Drugs, sulfonamides, pesticides
Dragendorff's reagent	Drugs and alkaloids
Fast Black K salt	Amphetamines, adrenergic β -blocking drugs, nor-metabolites
Fast Blue B salt, Fast Blue BB salt	Cannabinoids
Fluorescamine	Amphetamines, amino acids, sulfonamides
Forrest reagent	Phenothiazines, antidepressants
FPN reagent	Phenothiazines, dibenzazepines
Furfuraldehyde	Carbamates, phenothiazines
Iodoplatinate, acidic	Alkaloids, drugs, quaternary ammonium compounds
Mandelin's reagent	Drugs
Marquis reagent	Drugs
Mercuric chloride-diphenylcarbazone	Barbiturates
Mercurous nitrate	Barbiturates
Ninhydrin	Amphetamines, amino acids
4-(4-Nitrobenzyl)pyridine-tetraethylenepentamine	Pesticides
Salkowski reagent ($\text{FeCl}_3 + \text{H}_2\text{SO}_4$)	Phenothiazines, thioxanthenes
3,3',5,5'-Tetramethylbenzidine, <i>o</i> -tolidine, after Cl_2	Pesticides, acidic and neutral drugs

especially using pre-chromatography derivatization, 20–100 ng per fraction. The visualization reactions can be divided into class and substance selective. In visualization sequences, several reagents can be oversprayed one after another to amplify the amount of information obtained from a single plate. An example of such sequence for basic drugs is ninhydrin, FPN ($\text{FeCl}_3 + \text{HClO}_4 + \text{HNO}_3$) reagent, Dragendorff's reagent and acidified iodoplatinate. Table 2 lists reagents that are commonly used in forensic toxicology.

In situ spectra Earlier it was common to scrape off a separated fraction from the TLC plate and submit it to a further spectrometric or spot test analysis. Today it is possible to measure the *in situ* UV spectrum of a fraction and compare this with stored spectrum libraries for identification. Representative spectra can generally be obtained from well-separated fractions with substance amounts over 0.5 μg on standard TLC plates and over 0.1 μg on high performance thin-layer chromatography (HPTLC) plates, although these limits depend on the shape of the fraction and on the absorption characteristics of the compound in question. The upper limit is not a problem as the reflectance saturates after certain level and the spectra remain practically the same. The CATS software from Camag allows the complete sequence of instrumental screening analysis, including R_F correction, spectrum measurement, automated search against hR_F^c /UV libraries and reporting (Figure 1).

Other spectrometric techniques than UV have been tested for the measurement of TLC fractions. *In situ* diffuse reflectance Fourier transform infrared (FTIR) measurements have proved to be feasible for the identification of drugs using a spectral region where silica gel has no strong absorption, and a commercial TLC-FTIR interface is available.

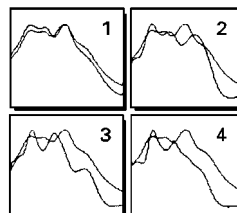
Proprietary Drug Screening Schemes

Particularly in North America, a TLC scheme called Toxi-Lab (Ansys, Irvine, CA, USA) has gained popularity in analytical toxicology. This product comprises the extraction, development, visualization and interpretation steps of analysis. The Toxi-Lab A detects basic and neutral substances and the Toxi-Lab B detects acidic and neutral substances. The plates consist of silica, impregnated with a vanadium salt for detection purposes, in a glass fibre matrix. The Toxi-Gram C8 are octylsilica bonded phase plates for the confirmation of basic and neutral drugs. All the plates have holes at the origin for the inoculation of factory-made standard substance discs and discs containing the evaporated sample residues. Detection is carried out by using a standardized four-stage

Method: C:\CAMAG\DATA_SC3\KRIMSPEC.PAM
Raw data: C:\CAMAG\DATA_SC3\KY140798.DFS
Library: C:\CAMAG\KRIM1.SCL

Track 15, Analysis n: 2561

Peak #5, Measured hR_F^c : 34, Area: 9682.6



No.	Substance name	Diff	Correlation
1	Clozapine	2	0.984415
2	Thiothixene	−9	0.948759
3	Norchlorprothixene	0	0.915627
4	Flupenthixol	−1	0.902411
5	Olanzapine	−1	0.891046
6	Norlevomepromazine	−3	0.877048

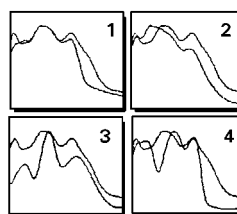
Confirmation: ☐ necessary ☐ not necessary

Hit # _____ confirmed by A: _____ B: _____

Method: C:\CAMAG\DATA_SC3\RPSPEC.PAM
Raw data: C:\CAMAG\DATA_SC3\RY140798.DFS
Library: C:\CAMAG\RP1.SCL

Track 15, Analysis n: 2561

Peak #2, Measured hR_F^c : 46, Area: 13178.0



No.	Substance name	Diff	Correlation
1	Clozapine	3	0.940416
2	Clothiapine	−9	0.937639
3	Molindone	−9	0.893862
4	Brucine	−4	0.868569
5	Apomorphine	2	0.857298
6	Metoclopramide	−6	0.855726

Confirmation: ☐ necessary ☐ not necessary

Hit # _____ confirmed by A: _____ B: _____

Figure 1 Identification hit lists produced by CATS software (Camag) for an analyte fraction on two TLC systems in broad-scale screening analysis for drugs in liver. The reports were obtained by comparing the hR_F^c values (window ± 9 units) and *in situ* UV spectrum correlation against a library of 325 drug substances on each system.

visualization sequence, and the interpretation of the colour patterns is performed with a help of the Toxi-Lab Drug Compendium showing indexed colour photograms for hundreds of compounds. The sequence consists of formaldehyde vapour + Mandelin's reagent, water, fluorescence under 366 nm UV light and modified Dragendorff's reagent. There are also procedures and tests available for specific substances and classes of substances, such as opiates and cannabis. There is ample literature available on the applications of Toxi-Lab to clinical and forensic toxicology.

Another TLC screening scheme, Spot Chek (Analytical Bio-Chemistries, PA, USA), relies on a single mobile phase, a set of visualization reactions, and computerized interpretation of the patterns. Acidic/neutral and basic drugs are developed on separate plates, and on each plate the sample is divided into two or three equal portions that are developed in parallel to facilitate the use of visualization reactions. The migration distance is divided into five R_F zones with reference compounds. The computer program database is based on nine colour reaction responses and the plate zone locations for 243 drug substances but requires entry of only one TLC property to generate a matching list.

Automated Multiple Development

There are currently two alternative instrumental means to improve the Separation number (SN) in TLC: automated multiple development (AMD) and overpressured layer chromatography (OPLC). In AMD, the plate is developed repeatedly in the same direction, and each partial run goes over a longer solvent migration distance than the previous one. Each partial run uses a solvent of lower elution strength than the previous one and in this way a step-wise gradient is formed. SN values of up to 40–50 can be obtained by AMD but a disadvantage is the time

required for the analysis, which may be several hours. There are no strictly forensic toxicological applications of AMD in the literature but the technique has an established position in the broad-scale screening for pesticides in the environment and has great potential in toxicology.

Overpressured Layer Chromatography

OPLC is based on the forced flow of the mobile phase against an external pressure, which results in short development times and decreased diffusion of the analyte fractions, making it possible to take advantage of longer developing distances. Silica gel plates are exclusively used in OPLC as reversed-phase chromatography has become complicated. Method development may be laborious due to disturbing adsorption zones, often obtained with multicomponent mobile phases. A commercial OPLC instrument is available from OPLC-NIT (Budapest, Hungary). OPLC has found use in the separation of closely related compounds in a particular pharmacological category or compounds originating from a particular botanical source. Two complementary OPLC systems have been developed for broad-scale screening for basic and neutral drugs with SN values close to 30, which is more than twice the values obtained typically with ordinary TLC: trichloroethylene-methylethylketone-*n*-butanol-acetic acid-water 17 + 8 + 25 + 6 + 4, and butyl acetate-ethanol-triethylamine-water 85 + 9.25 + 5 + 0.75, with layer pre-saturation.

Target Analysis

Drugs of Abuse

Amphetamines and related stimulants, especially amphetamine, methamphetamine and 3,4-methylenedioxymethamphetamine (MDMA, an Ecstasy

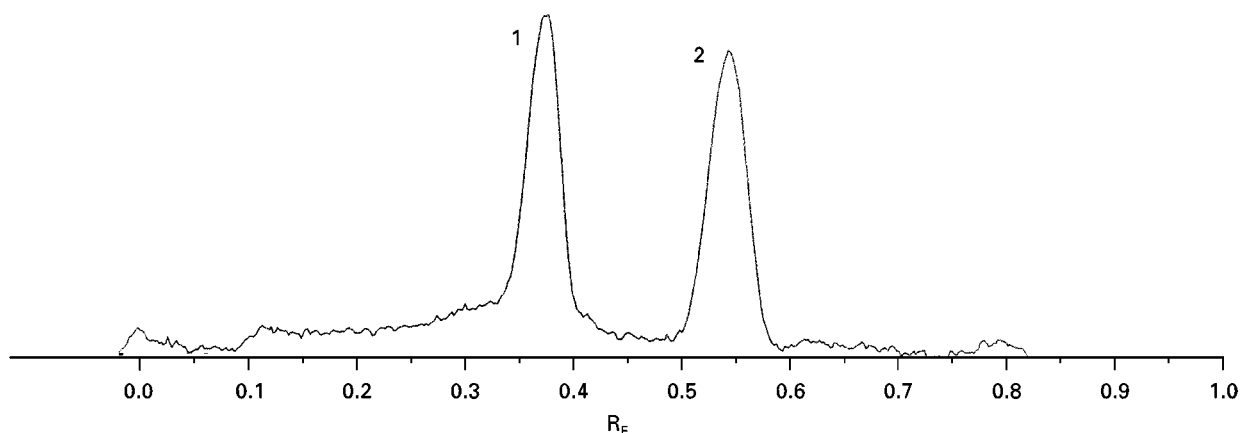


Figure 2 Separation of (1) methamphetamine and (2) amphetamine on the TLC system 6 of Table 1.

component), can be separated by a variety of TLC systems, such as those in Table 1 (Figure 2), and sensitively detected as fluorescent derivatives of, for example, fluorescamine or NBD-Cl (4-chloro-7-nitro-2,1,3-benzoxadiazole). Ninhydrin is a traditional reagent for amphetamines. Fast Black K salt reagent is capable of differentiating aliphatic primary and secondary amines, giving violet and orange-red colours, respectively, while tertiary amines do not react. Thus amphetamine and methamphetamine, or MDMA and 3,4-methylenedioxyamphetamine, are readily separated. Amphetamines possess poor UV characteristics, so they cannot be analysed by UV densitometric methods at low levels without derivatization. However, the methylenedioxy-derivatives can be easily recognized by their UV spectra (Figure 3). Despite the low limits of detection obtained with pure amphetamine-like substances, the limits of detection in urine are of the order of $250\text{--}500\text{ ng mL}^{-1}$ which is close to the standard immunoassay cutoff value (300 ng mL^{-1}).

The analysis of the main urinary cannabinoid, 11-nor- Δ^9 -tetrahydrocannabinol-9-carboxylic acid (THCA), is usually carried out with dedicated TLC systems, such as ethyl acetate-methanol-water-conc. ammonia $12 + 5 + 0.5 + 1$. The detection of THCA is performed with various diazonium salts, such as Fast Blue B salt, Fast Blue BB salt and Fast Blue RR salt. Detection limits of $2\text{--}10\text{ ng mL}^{-1}$ can be obtained for THCA, and these concentrations compare favourably with the standard immunoassay cutoff level of 20 ng mL^{-1} .

Screening for cocaine is usually based on the detection of its metabolite benzoylecgonine (BE) in urine. The combination of the following two mobile phases can be applied to the separation: methanol-chloroform-ammonia $60 + 60 + 1$, and ethyl acetate-methanol-water-ammonia $85 + 13.5 + 1 + 0.5$. The detection of BE is performed with Dragendorff's reagent or Ludy Tenger reagent, followed by sulfuric acid, with the limit of detection of 200 ng mL^{-1} in urine. The standard immunoassay cutoff level is 300 ng mL^{-1} .

The opiates of interest in drug abuse testing programmes include the heroin metabolites, 6-mono-acetylmorphine and morphine, and codeine. The combination of the following two mobile phases can be applied to the separation: ethyl acetate-isopropyl alcohol-methanol-ammonia $80 + 15 + 3 + 8$, and 1,2-dichloroethane-isopropyl alcohol-methanol-ammonia $20 + 20 + 20 + 7$. The limit of detection for opiates with iodoplatinate ranges from 100 to 500 ng mL^{-1} in urine, depending on the compound, while the standard immunoassay cutoff level is 300 ng mL^{-1} .

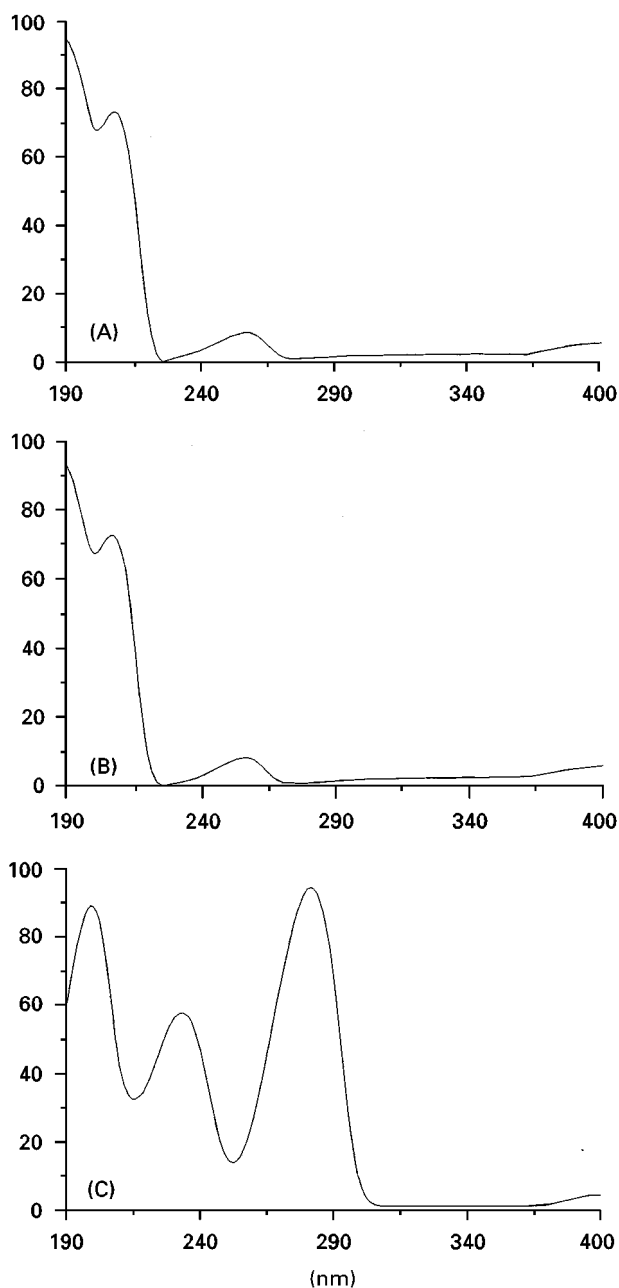


Figure 3 The *in situ* UV spectra of (A) amphetamine, (B) methamphetamine and (C) methylenedioxymethamphetamine (MDMA). Amphetamine and methamphetamine have similar spectra but they can be differentiated, e.g. by using the Fast Black K reagent.

Other Substances

Toxicological Analysis by Müller lists 1453 published TLC systems for potentially toxic compounds. A TLC bibliography is available from Camag on CD-ROM, listing 5500 abstracts of papers from 1982 to 1996. The biennial TLC reviews by Sherma in *Analytical Chemistry* provide a wealth of information on systems for individual substances in forensic toxicology.

Status of TLC in Forensic Toxicology Laboratory

In forensic toxicology, the unique features of TLC are best utilized in the broad-scale screening analysis for drugs and poisons in urine or liver samples. For this application, there are equipment, dedicated software and reference libraries available from several manufacturers. Compared to HPLC or capillary electrophoresis, TLC allows the detection of even poorly UV-absorbing compounds using selective visualization reactions. Compared to GC or GC-MS, TLC allows the chromatography of polar compounds without prior derivatization. Another important application of TLC is the screening or confirmation of drugs of abuse, although the supremacy of the combination of immunoassay and GC-MS in this area has hindered the development of modern dedicated TLC methods. Immunoassay screening, however, is vulnerable to sample adulteration and high background noise. In larger, broad-service laboratories, the various techniques available today, including TLC, are considered complementary rather than exclusive.

See also: II/Chromatography: Thin-Layer (Planar): Modes of Development: Conventional; Modes of Development: Forced Flow, Over Pressured Layer Chromatography and Centrifugal; Spray Reagents. III/Alcohol and Biological Markers of Alcohol Abuse: Gas Chromatography. Clinical Chemistry: Thin-Layer (Planar) Chromatography. Clinical Diagnosis: Chromatography. Forensic Sciences: Capillary Electrophoresis.

Further Reading

Adamovics JA (ed.) (1995) *Analysis of Addictive and Misused Drugs*. New York: Marcel Dekker.

De Zeeuw RA, Franke JP, Degel F *et al.* (eds) (1992) *Thin-layer Chromatographic R_F Values of Toxicologically Relevant Substances on Standardized Systems*, 2nd edn. Weinheim: DFG/TIAFT, VCH.

Fried B and Sherma J (eds) (1996) *Practical Thin-layer Chromatography*. Boca Raton: CRC Press.

Gough TA (ed.) (1991) *The Analysis of Drugs of Abuse*. Chichester: John Wiley.

Jork H, Funk W, and Wimmer H (1990) *Thin-layer Chromatography, Reagents and Detection Methods*, vol. Ia. Weinheim: VCH.

Jork H, Funk W, Fischer W and Wimmer H (1994) *Thin-layer Chromatography, Reagents and Detection Methods*, vol. Ib. Weinheim: VCH.

Moffat AC (ed.) (1986) *Clarke's Isolation and Identification of Drugs*, 2nd edn. London: Pharmaceutical Press.

Müller RK (ed.) (1995) *Toxicological Analysis*. Leipzig: Edition Molina Press.

Ojanperä I and Jänchen P (1994) The application of instrumental qualitative thin-layer chromatography to drug screening. *LC-GC International* 7: 164.

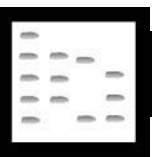
Ojanperä I, Goebel K and Vuori E (1999) Toxicological drug screening by overpressured layer chromatography. *Journal of Liquid Chromatography & Related Technologies* 22: 161.

Siek TJ, Stradling CW, McCain MW and Mehary TC (1997) Computer-aided identifications of thin-layer chromatographic patterns in broad spectrum drug screening. *Clinical Chemistry* 43: 619.

Stahl E (1967) *Dünnschicht-Chromatographie*, 2nd edn. Berlin: Springer-Verlag.

Stead AH, Gill R, Wright T, Gibbs JP and Moffat AC (1982) Standardised thin-layer chromatographic systems for the identification of drugs and poisons. *Analyst* 107: 1106.

FRAGRANCES: GAS CHROMATOGRAPHY



E. R. Adlard, Delryn Burton, Wirral, UK
M. Cooke, Royal Holloway University of London,
 Egham, Surrey, UK

Copyright © 2000 Academic Press

Introduction

It is difficult to distinguish between aromas, flavours, taints and perfumes, because to a large extent these are artificial categories that overlap. An aroma may be defined as the smell emanating naturally (possibly in the process of cooking or other method of prepara-

tion) of a foodstuff or beverage. The aroma from coffee beans on roasting is a prime example but there are many others. The main criterion is that the aroma material is essentially all in the vapour phase and the nose is responsible for sensing the aroma. A flavour is intimately related to an aroma but may contain involatile compounds that give rise to the sensation of taste but in practice it is common to have a flavour with an associated aroma. A tainted foodstuff or beverage is often unsatisfactory for consumption because there are compounds present that have an unpleasant smell or taste. Taints may arise from natural

chemical reactions such as the oxidation of the acids in an oil or fat to turn it rancid or the production of amines in fish. Other taints may occur because of leaching of material from packaging such as phenolic compounds from paper wrapping and solvents from the ink used in printing labels. Perfumes are natural or synthetic mixtures that have a pleasant smell to most people, although some of the constituents may have an unpleasant odour, a different odour or no odour when present in bulk. For example, coumarin in low concentrations has the smell of new-mown hay but this is not apparent at high concentrations. Although this article is specifically about aromas most, if not all of the techniques described are equally applicable to perfume studies. The only significant difference is that perfumes, in their final commercial form, normally exist as a solution (usually in ethanol) so that in this form they may be analysed as conventional liquid samples.

Another group of compounds that have much in common with aromas are pheromones, which cause specific behavioural effects in animals and insects. Indeed, it could be claimed that aromas and perfumes are the equivalent materials in humans (although there are true human pheromones, they are of small importance compared to those in the insect world).

Aromas frequently occur as complex, multicomponent mixtures with many of the important components (from an olfactory point of view) in very low concentrations – often at the ppm level or less.

Aroma Compounds

Since, by definition, aromas are volatile mixtures that produce an olfactory response, it follows that they should be amenable to analysis by gas chromatography (GC). This was appreciated quite early in the development of GC and Teranishi *et al.* did a considerable amount of work in the 1960s on strawberry aroma. The work was hampered by the use of packed columns and detectors of relatively low sensitivity and poor qualitative diagnostic information, but these investigations still go on today with modern equipment (see Further Reading).

Aromas contain many different types of compounds. Among the commonest are aliphatic, olefinic and aromatic hydrocarbons. A number of essential oils fall into this category but many aroma compounds have hetero-elements such as oxygen, nitrogen and sulfur in the molecule as well as a variety of functional groups such as alcohol, aldehyde, acid, phenol, ester and ether moieties. The smell of cheeses such as Camembert is due to the presence of fatty acids such as butyric acid. The smell of garlic is due to a fairly simple mixture of sulfur compounds including

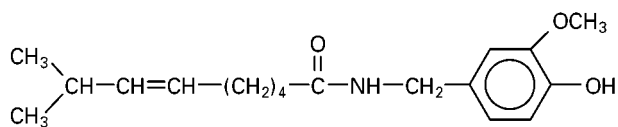


Figure 1 Structure of capsaicin, the hot agent of peppers.

diallyl disulfide, $\text{CH}_2=\text{CH}.\text{CH}_2.\text{S}.\text{S}.\text{CH}_2.\text{CH}=\text{CH}_2$, and lager owes its distinctive aroma to the presence of p.p.m. concentrations of lower mercaptans. As can be imagined, the actual amount is a vital part of quality control.

Figure 1 shows the structure of capsaicin, the hot agent in peppers. It contains a nitrogen-containing amido group, a phenolic group and an ether group as well as olefinic double bonds. Aroma compounds frequently exist as *cis* and *trans* isomers arising from such double bonds and there is also a possibility of the presence of chiral compounds.

Identification of geometrical and optical isomers is of great importance since the isomers often exhibit a very large variation in physiological properties, including smell. An example of this is carvone (**Figure 2**) where the D isomer has an odour of dill, whereas the L isomer has a spearmint smell. In **Figure 2** it can be seen that the centre of asymmetry is at the carbon atom at which the isopropenyl group is attached to the cyclohexene ring. The situation is also complicated by the reverse situation, i.e. it is possible to have two compounds of quite different chemical structure that smell the same. The best known examples of the latter are benzaldehyde and hydrogen cyanide, both of which have a smell of bitter almonds and both give rise to this smell in natural products.

Sampling

Since the sample is gaseous but is in contact with a liquid or a solid, all the methods of gas sampling may be used as appropriate but the most important are static and dynamic headspace sampling. Dynamic headspace sampling results in greater sensitivity since all the volatile material from a given sample is removed from the headspace but it has to be retained in a trap packed with a sorbent such as Tenax. It is difficult to adjust the purge gas conditions so that all

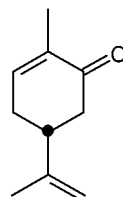


Figure 2 Structure of carvone showing the position of the chiral centre.

the compounds of low volatility are removed without losing those of high volatility in the trap and vice versa. Whilst this may not be a problem if the volatility range of the compounds is small, it may make accurate quantitative analysis in one run impossible if the range of volatility is large. One way to circumvent this problem is by closed-loop stripping but this is at the expense of considerable extra experimental complications. Quantitative analysis is much easier by static headspace sampling but this technique has a poorer lower limit of detection, especially for compounds of low volatility. When using the term volatility, it must be remembered that many samples are in an essentially aqueous medium and a nonpolar compound will have a large activity coefficient in an aqueous system and a much higher volatility than might be expected from the boiling point of the pure compound.

Transfer of the aroma sample from the sorbent trap to the GC is by thermal or solvent desorption. Both have advantages and disadvantages. Thermal desorption is a one-shot method and may cause decomposition of some of the components of the sample. It has the complication of the need for a secondary trap that can be heated very rapidly so that the sample enters the column with a plug profile. The presence of water from aqueous samples may also cause problems if steps are not taken to remove most of it. Solvent desorption has the disadvantage that the solvent may give a large peak early in the chromatogram that masks some of the volatile components of the sample. The use of CS₂ minimizes the problem if a flame ionization detector (FID) is used as the detector since this compound has a small FID response but it is toxic and highly flammable.

A more recent method of sampling is the use of solid-phase microextraction (SPME) where a quartz fibre coated with a film of stationary phase is exposed to a liquid or gaseous sample followed by thermal or solvent desorption. Although it is very convenient to use, the limit of detection is not likely to be as good with SPME as with dynamic headspace sampling since SPME is essentially the same as static headspace sampling and the mass of the sorbent film on the quartz fibre is much smaller than in a conventional headspace trap. Discrimination is also possible if the correct choice of fibre coating is not made. To find a polymeric stationary-phase material that is equally selective for a broad range of compounds of different polarity is difficult and there may be memory problems with the fibre and low recoveries. In spite of this problem, SPME is becoming more popular and many recent publications use this technique with excellent results.

The concentration of the important compounds in an aroma sample may be extremely small and it may

be necessary to carry out a large scale GC separation or some other enrichment procedure before GC analysis. One way of effecting preconcentration is by using supercritical fluid extraction (SFE) with CO₂ containing small amounts (\approx 5–10%) of a more polar solvent such as methanol. The great virtues of SFE are that it is conducted at around ambient temperature and that it is very easy to remove the solvent (CO₂).

GC Separation Conditions

Columns

All analysis of aroma samples is now carried out on open tubular columns except if small scale preparative GC is carried out for prior enrichment.

Aroma samples consist of compounds ranging from nonpolar hydrocarbons to polar aldehydes, alcohols and acids but since they are in the gas phase under ambient conditions they will be of relatively low boiling point. These two conditions point to the use of polyglycol (CarbowaxTM) phases which can be operated up to about 230°C. Wax columns are particularly favoured for the analysis of fatty acid methyl esters because of their ability to separate *cis/trans* isomers (Figure 3).

Other phases such as phenyl, trifluoromethyl, cyano and hydroxy silicones have also been used. For chiral separations silicone phases containing β -cyclodextrins dissolved in the silicone have been employed. Figure 4 shows the chiral separation of + / - 1-octen-3-ol and + / - carvone and Figure 5 shows the separation of the chiral components of rosemary oil.

The columns should be capable of handling as large a sample as possible since some of the important aroma constituents may be present at p.p.m. level or less. In order to have a large sample capacity, the stationary-phase film should be relatively thick and films up to 5 μ m have been used in large bore columns (0.53 mm i.d.). Thick films cause a significant reduction in resolution so a compromise is a film of 1 μ m thickness. For higher resolution and with mass spectrometric detection, standard 0.25 mm and 0.32 mm i.d. columns are used with a film thickness of 0.25 μ m or less. Most applications now standardize on columns 30 m long, with some samples requiring 60 m length; columns longer than this are now seldom employed in the aroma field since they carry the penalty of longer analysis time and a greater possibility of decomposition.

Carrier Gas

The carrier gas is not of great importance on aroma analysis; nitrogen gives the highest resolution but the

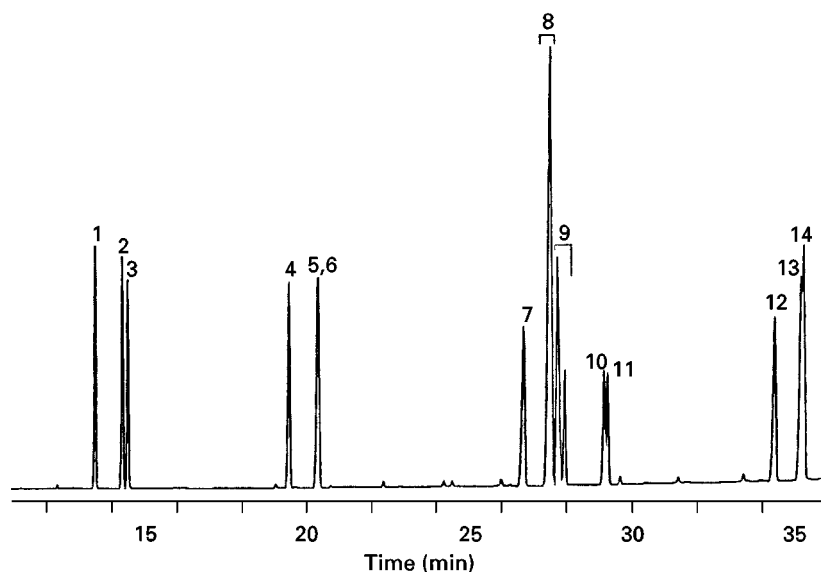


Figure 3 Separation of *cis* and *trans* isomers of fatty acids. 60 m, 0.25 mm i.d., 0.25 μ m Rtx-Wax; on-column concentration 40–75 ng. Oven temperature 165–250°C at 2°C min⁻¹. Injection/detection temperature 220/250°C; carrier gas, helium. Linear velocity 20 cm s⁻¹ set at 165°C; split ratio 50 : 1. Peak identification 1, C₁₄ : 0; 2, C₁₄ : 1 n5*cis*; 3, C₁₄ : 1 n5*trans*; 4, C₁₆ : 0; 5, C₁₆ : 1 n7*cis*; 6, C₁₆ : 1 n7*trans*; 7, C₁₈ : 0; 8, C₁₈ : 1 *cis* isomers (n12, n9, n7); 9, C₁₈ : 1 *trans* isomers (n12, n9, n7); 10, C₁₈ : 2 n6*cis*; 11, C₁₈ : 2 n6*trans*; 12, C₂₀ : 0; 13, C₂₀ : 1 n9*cis*; 14, C₂₀ : 1 n9*trans*. Reproduced by permission of Restek Corp.

slowest analysis, as may be seen from van Deemter curves for hydrogen, helium and nitrogen. Helium is the most commonly used carrier gas.

Detection

The FID is the workhorse detector for aroma analysis. It has many advantages but lacks the sensitivity of some of the selective detectors which may exhibit up to 10³ times better lower limit of detection as well as giving qualitative information. **Figure 6** gives two headspace chromatograms of coffee aroma, one obtained with an FID and the other with a helium

ionization detector with less than half the gas volume (40 μ L as opposed to 100 μ L for the FID) which shows the much bigger response of the latter; the tailing in the helium detector chromatogram is due to the response to a water peak. In this instance,

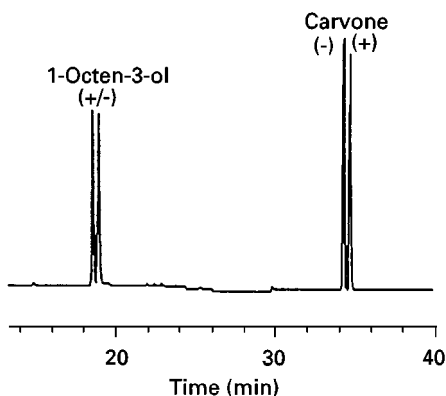


Figure 4 Chiral separation of +/– octen-3-ol and +/– carvone. 30 mm, 0.32 mm i.d., 0.25 μ m, Rt- β DEXsa. Oven temperature: 40°C (hold 1 min) to 230°C at 2°C min⁻¹ (hold 3 min). Carrier gas: hydrogen 80 cm s⁻¹ set at 40°C. Detector: FID set at 220°C. Reproduced by permission of Restek Corp.

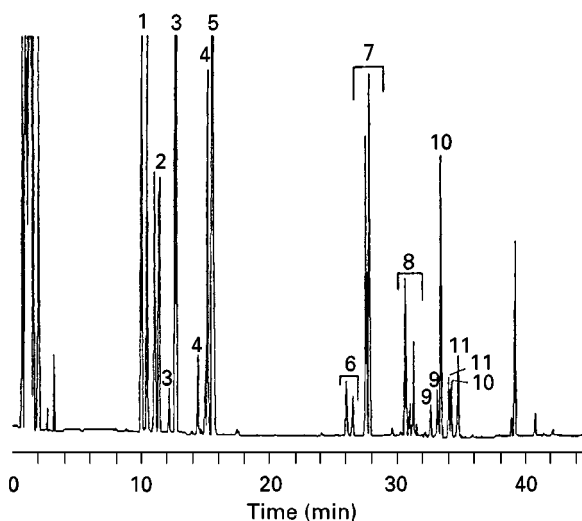


Figure 5 Chiral separation of the components of rosemary oil. 30 m, 0.32 mm i.d., 0.25 μ m Rt- β DEXsm. Oven temperature 40°C (hold 1 min) to 200°C at 2°C min⁻¹ (hold 3 min). Carrier gas: hydrogen 80 cm s⁻¹. Detector: FID set at 220°C. Peak identification: 1, (–/+) α -pinene; 2, (+/–) camphene; 3, (+/–) β -pinene; 4, (–/+) limonene; 5, eucalyptol (1,8-cineole); 6, (–/+) linalool; 7, (+/–) camphor; 8, (–/+) teripinen-4-ol; 9, (+/–) isoborneol; 10, (+/–) borneol; 11, (+/–) α -terpineol. Reproduced by permission of Restek Corp.

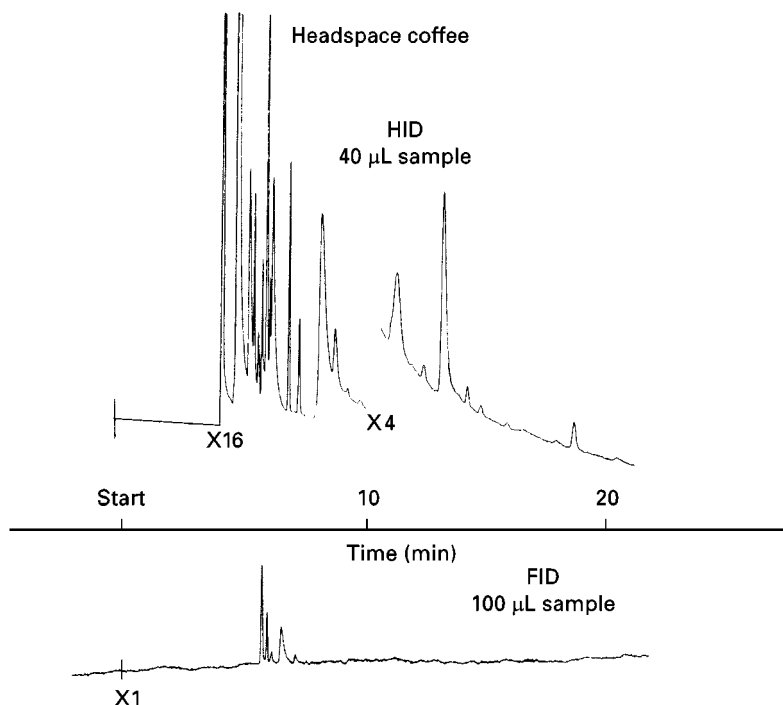


Figure 6 Helium ionization detector and FID chromatograms of coffee aroma. Column: 100 m \times 0.5 mm i.d. stainless steel coated with Witconol LA-23. Column temperature 60°C isothermal. Sample introduced via a gas sampling valve. (Reproduced from Andrawes FF and Gibson EK *Journal of High Resolution Chromatography* (1982), with permission from Wiley-VCH.)

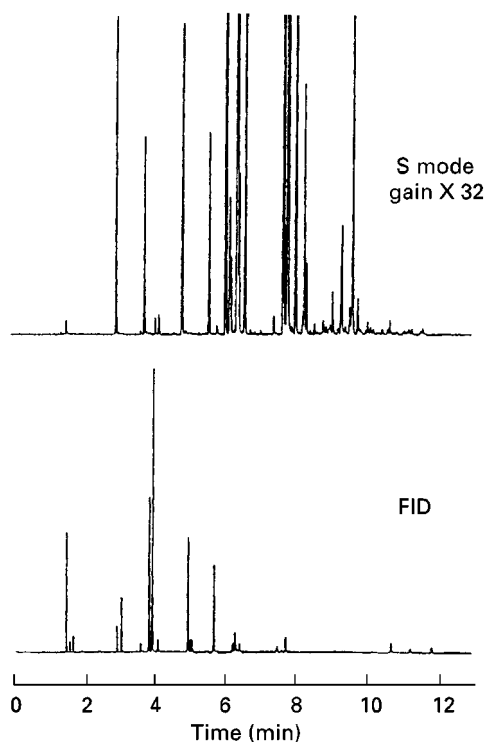


Figure 7 Pulsed flame photometric detector (in S mode) and FID chromatograms of coffee aroma. (From Varian publication 03-914625-00, 1998. By courtesy of Varian Associates.)

the helium detector clearly has great advantages over the FID.

As pointed out earlier, many aroma compounds contain hetero-elements and **Figure 7** shows headspace chromatograms of coffee aroma obtained with an FID and the pulsed flame photometric detector in the sulfur mode, which shows the presence of a large number of sulfur compounds. This detector can also be used in a nitrogen-selective mode to reveal the presence of pyrroles, pyrazines and caffeine in the coffee aroma.

The Fourier transform infrared detector (FTIR) should be extremely useful in aroma analysis because of its ability to give a response to specific functional groups in a molecule. This detector is gradually coming into use for this type of work (see Further Reading) but the sensitivity to different functional groups varies considerably and the capital cost is quite large. The mass spectrometer in the selective ion monitoring mode probably gives the best all-round sensitivity. Full scan mass spectra can give sensitivities in the pg range under favourable circumstances. **Figure 8** shows a mass chromatogram and a Gram-Schmidt FTIR chromatogram of a dynamic headspace sample of the vapour above a particular variety of strawberries. The identity of the peaks is given in **Table 1**. Although there is a general similarity between the two chromatograms, there is a considerable difference in detailed quantitative response, with

Table 1 Compounds in strawberry aroma identified by GC-MS and GC-FTIR

Peak no. ^a	Compound	RRT (%SD, <i>n</i> = 3)	<i>m/z</i>	λ_{max} (cm ⁻¹)
1	Acetic acid	0.141 (5.4%)	43 (100%), 60 (M ⁺ , 83%)	No data
2	Methyl acetate	0.156 (5.2%)	43 (100%), 74 (M ⁺ , 15%)	2966, 1777, 1757, 1448 1372, 1240, 1048
3	Ethyl acetate	0.255 (3.6%)	43 (100%), 61 (5%), 88 (M ⁺ , 19%)	2992, 1769, 1755, 1373, 1238, 1093, 1052
4	Isopropyl acetate	0.310 (2.6%)	43 (100%), 59 (6%), 61 (26%), 87 (2%), 102 (M ⁺ , 9%)	2985, 2904, 1755, 1383, 1239, 1138, 1021
5	Ethyl propionate	0.393 (1.7%)	57 (100%), 74 (12%), 102 (M ⁺ , 33%)	2992, 2958, 1753, 1185
6	Methyl butyrate	0.415 (3.4%)	43 (100%), 55 (11%), 59 (13%), 71 (28%), 74 (33%), 87 (8%), 102 (M ⁺ , 12%)	2968, 1760, 1444, 1359, 1297, 1256, 1184, 1103
7	4-Methyl- 2-pentanone	0.440 (1.8%)	43 (100%), 58 (13%), 85 (40%), 100 (M ⁺ , 26%)	2960, 2881, 1729, 1373, 1285, 1240, 1176
8	Ethyl isobutyrate	0.499 (1.5%)	43 (100%), 71 (29%), 88 (14%), 116 (M ⁺ , 22%)	2973, 2895, 1755, 1461, 1442, 1390, 1365, 1249, 1234, 1188, 1154, 1096 1083, 1021
9	Methyl 2-methylbutyrate	0.518 (1.7%)	41 (55%), 43 (100%), 55 (20%), 57 (58%), 59 (25%), 69 (12%), 74 (12%), 85 (20%), 88 (52%), 101 (13%), 116 (M ⁺ , 4%)	2966, 2889, 1759, 1440, 1363, 1292, 1242, 1186, 1112, 1017
10	Methyl isobutyrate	0.518 (1.5%)	41 (40%), 43 (100%), 57 (17%), 59 (17%), 74 (22%), 85 (9%), 101 (5%), 116 (M ⁺ , 6%)	2969, 2896, 1757, 1466, 1445, 1378, 1363, 1299, 1257, 1187, 1161, 1112, 1099, 1018
11	<i>n</i> -Hexanal	0.567 (1.1%)	41 (100%), 44 (45%), 56 (30%), 72 (7%), 82 (16%), 99 (7%), 100 (M ⁺ , 4%)	2940, 2885, 2811, 2714, 1744
12	Ethyl butyrate	0.567 (1.4%)	43 (100%), 60 (10%), 70 (4%), 71 (45%), 88 (19%), 89 (15%), 101 (4%), 116 (M ⁺ , 14%)	2983, 1754, 1255, 1181
13	Isobutyl acetate	0.587 (1.1%)	41 (18%), 43 (100%), 56 (14%), 61 (21%), 69 (8%), 71 (8%), 116 (M ⁺ , 10%)	2969, 2886, 1764, 1485, 1372, 1234, 1064, 1032
14	Isopropyl isobutyrate	0.637 (1.2%)	41 (43%), 43 (100%), 71 (40%), 89 (35%), 130 (M ⁺ , 2%)	2981, 2944, 2890, 1750, 1468, 1376, 1238, 1184, 1152, 1091, 1030
15	Ethyl 2-methylbutyrate	0.674 (0.7%)	41 (100%), 43 (50%), 57 (67%), 69 (21%), 74 (12%), 85 (11%), 115 (5%), 130 (M ⁺ , 12%)	2979, 2948, 2891, 1750, 1466, 1377, 1248, 1182, 1149, 1088, 1033

Table 1 Continued

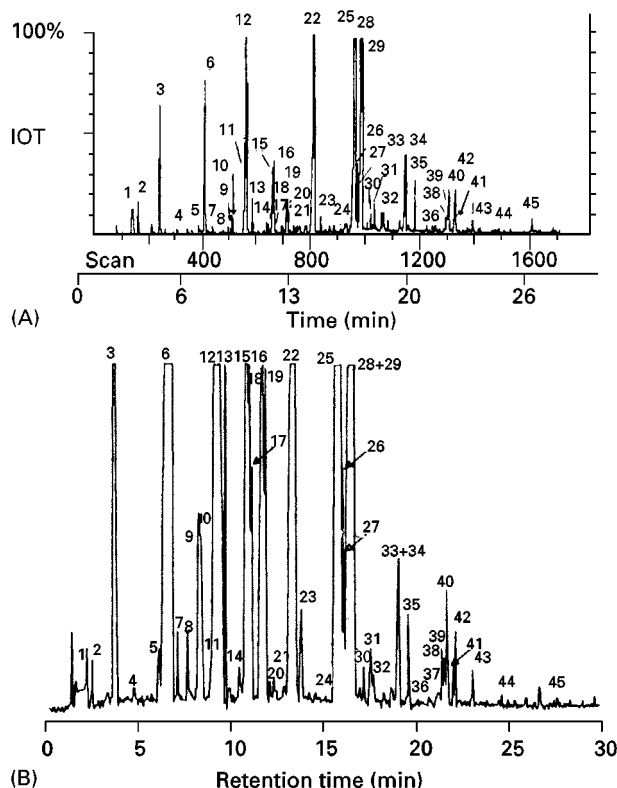
Peak no. ^a	Compound	RRT (%SD, n = 3)	m/z	λ_{max} (cm ⁻¹)
16	Ethyl isovalerate	0.678 (0.8%)	43 (100%), 57, (59%) 69 (10%), 87 (20%), 130 (M ⁺ , 10%)	2971, 2884, 1753, 1468, 1374, 1295, 1250, 1184, 1115, 1039
17	Hex-2(Z)-enal	0.681 (0.9%)	41 (100%), 55 (41%), 69 (18%), 83 (11%), 98 (M ⁺ , 14%)	2972, 2949, 2885, 2814, 2727, 1715, 1634, 1151, 1091, 1037, 981
18	Isoamyl acetate	0.712 (1.5%)	43 (100%), 55 (24%), 61 (7%), 70 (17%), 87 (4%), 130 (M ⁺ , 4%)	2969, 2887, 1761, 1468 1371, 1234, 1038
19	2-Methylbutyl acetate	0.72 (1.6%)	43 (100%), 55 (13%), 61 (6%), 70 (12%), 87 (1%)	2972, 2899, 1762, 1468 1373, 1233, 1039
20	3-Methyl- 2-heptanol ^b	0.747 (0.6%)	45 (100%), 55 (26%), 57 (23%), 69 (8%), 83 (7%), 92 (7%), 112 (1%)	No data
21	Amyl acetate	0.798 (0.3%)	43 (100%), 55 (13%), 61 (25%), 70 (11%), 130 (M ⁺ , 2%)	2963, 2944, 1767, 1361, 1234, 1143, 1048
22	Methyl caproate	0.816 (0.5%)	43 (100%), 55 (24%), 59 (21%), 69 (13%), 74 (40%), 87 (13%), 99 (11%), 130 (M ⁺ , 13%)	2963, 2879, 1760, 1440, 1241, 1215, 1173, 1110
23	Ethyl 3-methyl- 2-butenate	0.849 (1.5%)	43 (20%), 55 (100%), 83 (40%), 100 (13%), 113 (27%), 128 (M ⁺ , 5%)	2987, 2948, 2936, 2904, 1731, 1652, 1268, 1138, 1081, 1053
24	2,5-Dimethyl- 4-methoxy- 3(2H)-furanone	0.933 (0.8%)	43 (100%), 55 (30%), 69 (10%), 85 (13%), 101 (5%), 127 (4%), 142 (M ⁺ , 2%)	No data
25	Ethyl caproate	0.966 (1.6%)	43 (100%), 55 (27%), 60 (72%), 73 (40%), 88 (42%), 99 (37%), 101 (18%), 115 (10%), 144 (M ⁺ , 8%)	2969, 2943, 2882, 1754, 1464, 1375, 1241, 1172, 1109, 1041
26	2,5-Dimethyl- 3-hydroxy- 4-methoxy- 2,3-dihydrofuran ^a	0.990 (0.1%)	43 (70%), 67 (45%), 83 (100%), 112 (6%), 129 (2%), 128 (3%), 144 (M ⁺ , 6%)	No data
27	Hexyl acetate	0.994 (0.1%)	43 (100%), 55 (13%), 56 (22%), 61 (14%), 69 (7%), 84 (5%), 144 (4%)	2966, 2942, 2871, 1762, 1369, 1234, 1060, 1030
28	Hex-2-(E)-enyl acetate	0.997 (0.1%)	43 (100%), 55 (17%), 67 (48%), 82 (31%), 142 (M ⁺ , 3%)	2969, 2942, 2883, 1762 1675, 1455, 1358, 1230 1081 1024, 968
29	Cyclohexyl acetate	1	43 (100%), 55 (13%), 67 (19%), 82 (35%), 83 (44%), 142 (M ⁺ , 4%)	3018, 2970, 2947, 2908, 2886, 1752, 1465, 1375, 1233, 1042

Table 1 *Continued*

Peak no. ^a	Compound	RRT (%SD, <i>n</i> = 3)	<i>m/z</i>	λ_{max} (cm ⁻¹)
30	2-Ethyl hexenoate (isomer)	1.028 (1.1%)	41 (55%), 55 (100%), 68 (18%), 69 (18%), 73 (22%), 97 (31%), 142 (M ⁺ , 16%)	2975, 2939, 1743, 1650, 1528, 1312, 1252, 1176, 1047, 991
31	Amyl butyrate	1.054 (0.5%)	43 (100%), 55 (29%), 60 (6%), 70 (27%), 71 (52%), 89 (10%), 158 (M ⁺ , 3%)	2969, 2908, 2887, 1752, 1460, 1353, 1238, 1177, 1096
32	Unidentified unsaturated aldehyde	1.073 (0.6%)	41 (100%), 55 (78%), 69 (42%), 83 (32%), 93 (7%), 109 (57%), 128 (48%), 144 (50%),	2966, 2934, 2882, 2817, 2738, 1787, 1716, 1623
33	Nona-2,4-dienal (isomer)	1.155 (0.9%)	43 (39%), 81 (100%), 95 (19%), 138 (M ⁺ , 9%)	2749, 1745, 1673
34	Non-2-en-1-ol (isomer)	1.175 (0.8%)	57 (100%), 67 (36%), 68 (18%), 69 (67%) 70 (34%), 81 (39%), 83 (36%), 95 (13%) 96 (10%), 124 (7%), 142 (M ⁺ , 2%)	No data
35	Methyl caprylate	1.194 (0.9%)	43 (100%), 55 (40%), 69 (11%), 74 (65%), 87 (25%), 101 (9%), 115 (8%), 127 (11%), 158 (M ⁺ , 7%)	2937, 2867, 1758, 1443, 1353, 1238, 1191, 1113, 1045
36	Benzyl acetate	1.244 (1.3%)	43 (100%), 51 (9%), 69 (9%), 77 (14%), 79 (29%), 91 (87%), 108 (54%), 150 (M ⁺ , 4%)	No data
37	Ethyl benzoate	1.267 (1.2%)	43 (33%), 51 (15%), 69 (10%), 77 (53%), 105 (100%), 122 (19%) 150 (M ⁺ , 10%)	No data
38	<i>n</i> -Hexyl butyrate	1.316 (1.2%)	43 (100%), 56 (30%), 71 (54%), 84 (7%), 89 (52%), 117 (16%), 172 (M ⁺ , 15%)	2943, 2895, 2877, 1754, 1263, 1176, 1097
39	Hexyl isobutyrate	1.319 (1.1%)	43 (97%), 55 (48%), 71 (89%), 84 (100%), 89 (16%), 101 (9%), 172 (M ⁺ , 26%)	2971, 2943, 1754, 1265, 1173, 1095, 1053, 976
40	Ethyl caprylate	1.322 (1.2%)	43 (100%), 57 (35%), 60 (29%), 61 (20%), 69 (28%), 81 (17%), 88 (26%), 101 (13%), 115 (5%), 127 (8%), 172 (M ⁺ , 10%)	2967, 2938, 2678, 1753, 1465, 1366, 1342, 1263, 1188, 1167, 1107, 1042
41	Decanal	1.339 (1.2%)	43 (100%), 57 (78%), 69 (37%), 70 (28%), 83 (75%), 95 (28%), 109 (9%), 156 (M ⁺ , 2%)	2934, 2865, 2780, 2765, 1746

Table 1 Continued

Peak no. ^a	Compound	RRT (%SD, n = 3)	m/z	λ_{\max} (cm ⁻¹)
42	Octyl acetate	1.354 (0.1%)	43 (100%), 55 (30%), 83 (12%), 56 (17%), 57 (30%), 61 (37%), 69 (28%), 70 (15%), 71 (42%), 112 (23%), 172 (M ⁺ , 12%)	2937, 2866, 1760, 1462, 1369, 1233, 1038, 1018
43	Amyl caproate	1.427 (1.5%)	43 (100%), 55 (32%), 60 (8%), 70 (30%), 71 (31%), 99 (8%), 117 (16%), 186 (M ⁺ , 1%)	2967, 2907, 2880, 1753, 1466, 1369, 1239, 1194 1163, 1113
44	Nonyl acetate	1.511 (1.6%)	43 (100%), 55 (31%), 61 (13%), 69 (22%), 83 (11%), 97 (9%), 186 (M ⁺ , 1%)	No data
45	n-Decyl acetate	1.657 (4.4%)	43 (100%), 55 (31%), 69 (28%), 83 (40%), 97 (16%), 200 (M ⁺ , 2%)	2936, 2982, 2865, 2846, 1755, 1456, 1272, 1175 1094
46	Hex-3(Z)-en-1-ol	^c	41 (100%), 55 (19%), 67 (38%), 69 (8%), 81 (11%), 82 (15%), 100 (M ⁺ , 3%)	No data

^aNumbering 1–45 from **Figure 1**.^bTentative identification.^cReproduced with permission from Marco *et al.*, *Journal of High Resolution Chromatography* (1997), 20: 276–278.**Figure 8** (A) Mass chromatogram of a headspace sample above strawberries; (B) FTIR chromatogram of the same sample. For peak identities see **Table 1**. (By courtesy of the *Journal of High Resolution Chromatography* (1997), 20: 279.)

some minor peaks in the mass chromatogram giving a large FTIR response.

One detector specific to aroma/perfumery studies is the human nose. The effluent from the GC is split between a conventional detector such as the FID and a sniffing port which is purged with humidified nitrogen. Because the ability to recognize the presence of an odour varies considerably from one individual to another it is necessary to select a panel from people who have been shown to possess a keen sense of smell and to train them to recognize the odour of particular compounds. Although it is always stated how insensitive the human nose is compared to those of animals, nevertheless it is still a highly sensitive organ. It is possible, apparently, for trained panellists to indicate the emergence of an odoriferous compound from a GC column in parts of the chromatogram where no signal is obtained from conventional detectors. Under these circumstances the procedure is to use small scale preparative GC and to collect fractions at the points indicated by the panel; these fractions are then re-run under analytical GC conditions.

Conclusion

The study of aromas is intimately connected to the study of flavours, taints and perfumes in that they all make extensive use of GC with a variety of detectors,

of which the mass spectrometer is the most important. Advances in this type of work will depend on advances in the instrumentation, particularly in the sensitivity of the mass spectrometer and on general advances in knowledge of food components under various circumstances.

See also: II/Chromatography: Gas: Detectors: Mass Spectrometry; Detectors: Selective. III/Natural Products: Liquid Chromatography. Solid Phase Micro-Extraction: Environmental Applications; Food Technology Applications. Tobacco Volatiles: Gas Chromatography.

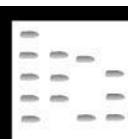
Further Reading

There do not seem to be any modern texts which deal specifically with aroma analysis but the literature contains numerous references. The following is a partial list of papers published from 1997 to 1999 showing the wide variety of foodstuffs and drinks covered, ranging from wine, yogurt and tomato juice to strawberries and alligator meat. Although mass spectrometry is the main method of detection, other techniques are covered, together with a variety of methods for extraction prior to analysis.

- Ahn DU, Jo C and Olson DG (1999) Volatility profiles of raw and cooked turkey thigh as affected by purge temperature and holding time before purge. *Journal of Food Science* 64(2): 230–233.
- Baek HH and Cadwallader KR (1997) Aroma volatiles in cooked alligator meat. *Journal of Food Science* 62(2): 321–325.
- Clarke RJ and Macrae R (1985) *Coffee*, Vol. 1 Chemistry. Amsterdam: Elsevier.
- De la Calle-Garcia, Reichenbacher D, Danzer M *et al.* (1997) Investigations on wine bouquet components by solid-phase micro-extraction-capillary gas chromatography (SPME-CGC) using different fibres. *Journal of High Resolution Chromatography* 20(12): 665–668.

- De la Calle-Garcia, Reichenbacher D, Danzer M *et al.* (1998) Analysis of wine bouquet components using headspace solid phase micro-extraction-capillary gas chromatography. *Journal of High Resolution Chromatography* 21(7): 373–377.
- Gomes da Silva MDR and Chaves das Neves HJ (1997) Differentiation of strawberry varieties through purge-and-trap HRGC-MS, HRGC-FTIR and principal components analysis. *Journal of High Resolution Chromatography* 20(5): 275–283.
- Guadayol JM, Caixach J, Ribe J *et al.* (1997) Extraction and identification of volatile organic compounds from paprika oleoresin (Spanish type). *Journal of Agriculture and Food Chemistry* 45(5): 1868–1872.
- Kralj Cigic I and Zupancic-Krajc L (1999) Changes in odour of Bartlett pear brandy influenced by sunlight irradiation. *Chemosphere* 38(6): 1299–1303.
- Morales, MT Berry AJ, McIntyre PS and Aparicio R (1998) Tentative analysis of virgin olive oil aroma by supercritical fluid extraction–high resolution gas chromatography–mass spectrometry. *Journal of Chromatography A* 819(1–2): 267–275.
- Ott A, Fay LB and Chaintreau A (1997) Determination and origin of the aroma impact compounds of yogurt flavour. *Journal of Agriculture and Food Chemistry* 45(3): 850–858.
- Pinnel V and Vandegans J (1997) Study of the aroma profile of gherkin by purge-and-trap followed by GC-MS. *Journal of High Resolution Chromatography* 20(6): 343–346.
- Rapier S, Breheret S, Talou T and Bessiere J-M (1997) Volatile flavour constituents of fresh *Marasmius alleaceus* (garlic *Marasmius*). *Journal of Agricultural and Food Chemistry* 45(3): 820–825.
- Sucan MK and Russell GF (1997) A novel system for purge and trap with thermal desorption: optimization using tomato juice volatile compounds. *Journal of High Resolution Chromatography* 20(6): 310–314.
- Tarantilis PA and Polissiou MG (1997) Isolation and identification of the aroma components from saffron (*Crocus sativus*). *Journal of Agricultural and Food Chemistry* 45(2): 459–462.

FUELS AND LUBRICANTS: SUPERCRITICAL FLUID CHROMATOGRAPHY



M. M. Robson, University of Leeds, Leeds, UK

Copyright © 2000 Academic Press

Supercritical fluid chromatography (SFC) has a number of advantages over gas chromatography (GC) and high performance liquid chromatography (HPLC) for mixtures such as polyaromatic hydrocarbons

(PAH). SFC operates with diffusivities that are more gas-like, viscosities that are lower than liquids, and densities that are more liquid-like. The resulting mass transfer coefficients lead to more rapid analysis in SFC than in HPLC. The diffusion and viscosity range available in SFC allows GC-like separations on capillary columns but at much lower temperatures.

SFC on Packed Columns

During the initial development of SFC, commercial HPLC columns were used. The length and internal diameter of SFC packed columns are constrained by the large pressure drop as compared to open tubular columns and high mass flow rates, making interfacing to GC detectors more difficult. Therefore, narrow-bore packed columns with diameters of 1–2 mm were frequently used because they can be installed in a capillary SFC instrument and are compatible with many GC detectors. Packed fused silica columns have significant advantages, allowing the use of a large variety of liquid chromatography (LC) stationary phases with GC-based detectors.

The separation of PAH standards has been used throughout the development of SFC to determine chromatographic efficiency and performance of the system. Various-size stationary-phase particles have been used (10, 5 and 3 μm particle diameter) and it has been shown that the particle size influences the efficiency of the columns and that SFC reduced analysis times considerably in comparison with HPLC.

The elution order of PAH in SFC can be varied by changing the operating temperature and/or the pressure. Also, the mobile-phase modifier used in SFC can significantly affect the retention behaviour of PAH; dramatic changes in retention together with different selectivities have been demonstrated. The addition of

a modifier to the CO_2 mobile phase substantially reduces the retention times of the PAH. This effect is due to the intermolecular attraction between the modifier and the solute molecules and the subsequent increased solvating power. The successful separation of the 16 Environmental Protection Agency (EPA) target list of PAH using a single (15 cm \times 4.6 mm) column packed with specially bonded C_{18} silica has been achieved in 6 min (Figure 1).

The analysis of PAH and their derivatives from particulate matter has been of recent interest due to possible human exposure of the highly toxic nitro-PAH compounds. Sandra *et al.* provides an interesting approach to the analysis of PAHs using semipreparative SFC to separate the PAHs initially into the required types to analyse the peaks of interest, including nitro-PAH (Figure 2). A large amount of work has been carried out using supercritical fluid extraction (SFE) of particulates to extract the organic material followed by GC to characterize the extract.

Open Tubular Columns

The use of open tubular capillary columns in SFC for petroleum-derived mixtures was initiated by Lee *et al.* Capillary column SFC is mainly preferred because it provides the highest resolution. SFC can be carried out on capillary columns to achieve unique separations, especially for complex hydrocarbon mixtures

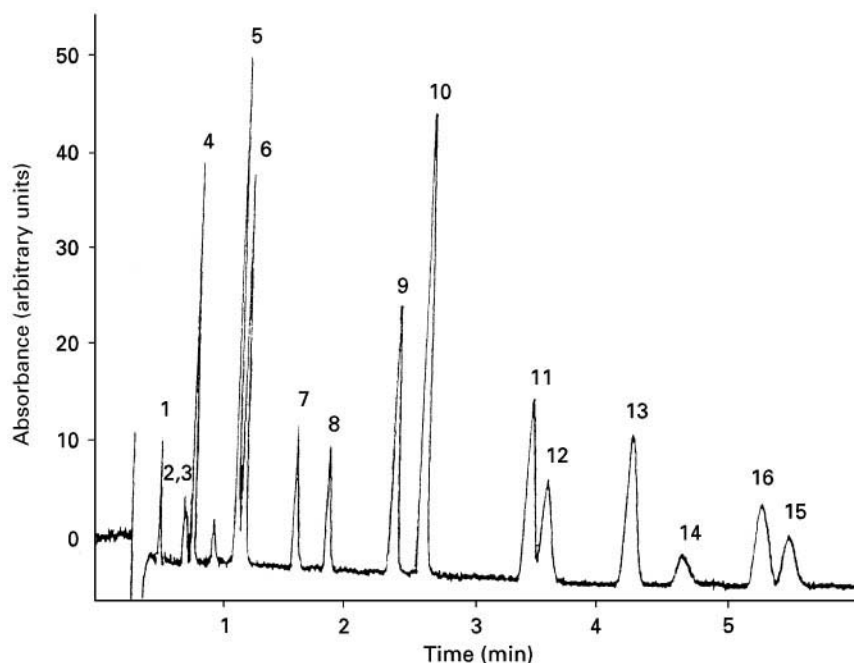


Figure 1 SFC of the EPA 16 priority PAH using 5 μm Waters Spherisorb PAH. Peak identification: 1, naphthalene; 2, acenaphthene; 3, acenaphthylene; 4, fluorene; 5, phenanthrene; 6, anthracene; 7, fluoranthene; 8, pyrene; 9, benzo[a]anthracene; 10, chrysene; 11, benzo[b]fluoranthene; 12, benzo[k]fluoranthene; 13, benzo[a]pyrene; 14, dibenzo[a,h]anthracene; 15, benzo[ghi]perylene; 16, indeno [1,2,3-*cd*]pyrene. (Courtesy of the University of Leeds.)

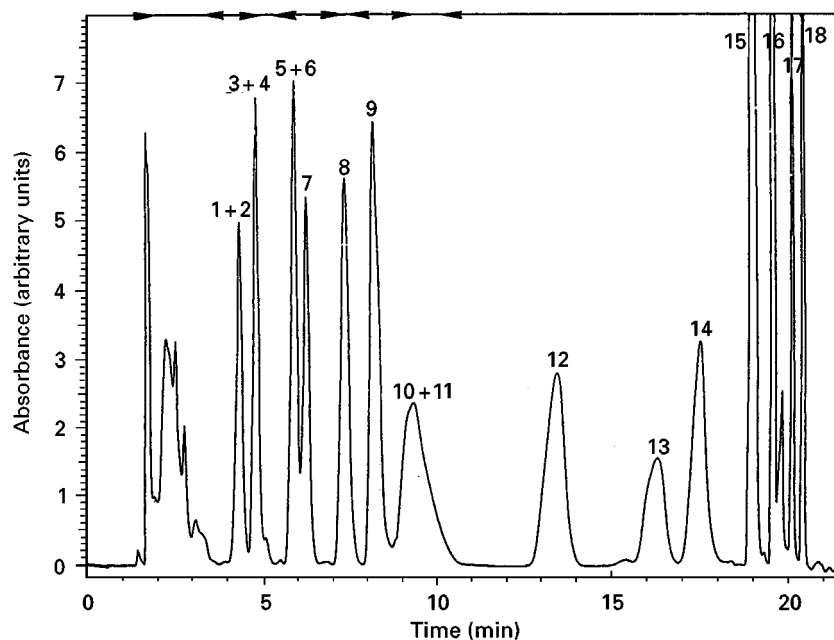


Figure 2 Semipreparative SFC separation of PAHs from particulate matter. Using a 25 cm \times 4.6 mm i.d. silica column at 50°C and 200 bar, supercritical fluid flow rate 2 mL min⁻¹, a 1 : 1 methanol : acetonitrile modifier was used and programmed from 1% (up to 5 min) to 2.5% at 0.15% min⁻¹, and then 27.5% and 5% min⁻¹. With ultraviolet detection: 1.5–3.7 min 2–3-ring PAH; 4.4–5.8 min 4-ring PAH; 7.0–8.3 5-ring PAH; 9.0–10.9 6 ring PAH. (Reprinted with permission of Sandra *et al.* (1998) *J. Microcol. Sep.*, 10: 89.)

such as PAH. Capillary columns provide selectivity and high efficiency. Essentially, the same range of stationary phases that have been used for analysis in capillary GC have also been used in capillary SFC. These stationary phases include 100% methyl, 100% phenyl, 5% phenyl, 5% biphenyl and cyanopropyl siloxanes. An *n*-octylpolysiloxane coated stationary phase has been used to perform SFC on petroleum-derived vacuum residues. The increased alkyl content of the *n*-octyl phase over methyl phases provides an increase in van der Waals interactions of the stationary phase with solutes.

SFC separations on liquid crystal phases are based on the length-to-breadth (L/B) ratio and the planarity of the PAH, and they interact with the ordered rod-like structure of the liquid crystal phase. In addition, interactions such as dispersion, dipole and induced dipole interactions contribute to a good separation. Kithinji *et al.* optimized chromatographic conditions (pressure and temperature) to achieve better SFC separations of high-molecular-weight PAH on a capillary column coated with a smectic mesomorphic crystalline phase with simultaneous temperature and density programming. The separation of PAH isomers on a liquid crystalline polysiloxane stationary phase is shown in Figure 3. Many of these isomers cannot be resolved on any other stationary phase.

Raynor *et al.* used dual capillary column SFC with phases of different polarity and selectivity to perform

simultaneous separation of a mixture of PAH isomers. The method not only reduces the development time by 50% but also provides two sets of retention data for identification of unknowns. The simultaneous separation of a mixture of three-, four-, five-ring, PAH isomers on biphenyl and smectic columns is shown in Figure 4.

However, unless column diameters are greatly reduced, open tubular column SFC cannot compete with conventional packed column SFC in terms of analysis time. Comparison of Figures 1 and 3 shows that separation of high-molecular-weight PAH can be achieved in less than 6 min with a conventional packed column, while more than an hour is required for an open tubular column.

Hydrocarbon Group-type Separations

Hydrocarbon group-type separations refer to the separation of alkanes, alkenes and aromatic compounds in petroleum feedstocks and products. LC is commonly used for this purpose but suffers from a lack of resolution, lack of a universal detector and long analysis time. GC has also been used but is limited to the analysis of light distillates due to the column temperatures required. Packed column SFC with CO₂ as the mobile phase has been used for the determination of saturates, olefins and aromatics in petroleum products boiling below 350°C. Separation is achieved

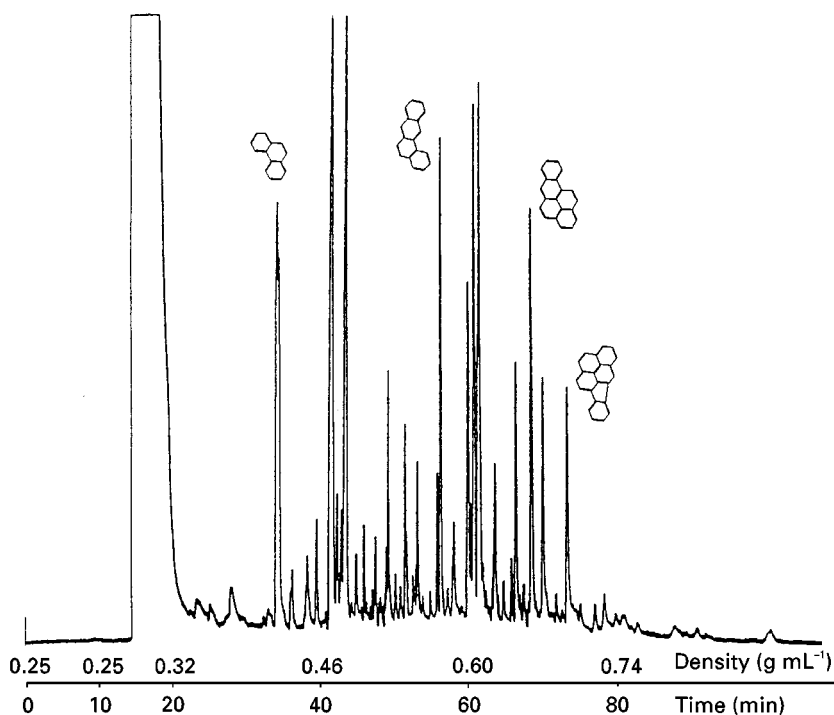


Figure 3 Chromatogram of total coal tar PAH obtained with linear density programming at a constant temperature of 110°C, 10 m × 50 μ m, SB-smectic column. (Courtesy of the University of Leeds.)

using two different columns connected in series – a silica and a silver nitrate-impregnated silica column – the analysis takes only 4 min per sample. The effect of temperature, pressure and column stationary phase on the separation has also been studied. At a low temperature (35°C), the saturates are better separated from the monoaromatics.

Another advantage of using a low column temperature is the shorter retention times and hence shorter analysis time per sample. An increase in pressure also results in improved separation between saturates and aromatics. Separations using a combination of silica and cyano or amino columns or the combination of silica and 20% silver nitrate column are not as good as the separation obtained with a single 5 μ m silica column at the same temperature.

The separation of aromatic types in middle distillates according to ring number has been studied. Two packed columns, a silica and an amino-modified silica, were used with a switching valve. The saturates are separated as a group from the aromatics on the silica column. The aromatics are then switched to the amino column where further separation into mono-, di- and polyaromatic types can be performed.

It has generally been found that the separation of saturates from olefins is incomplete when CO₂ is used as the mobile phase. This observation was thought to be due to the polarizability of CO₂ compared to the

hydrocarbons used as solvents in LC. Another approach uses supercritical sulfur hexafluoride (SF₆) as the mobile phase. SF₆ provided less peak tailing and a shorter analysis time. Although SF₆ is reasonably compatible with the flame ionization detector (FID), the detector has to be protected against the decomposition product hydrogen fluoride, either by being gold-plated or by having a platinum jet and upper electrode.

A more accurate, reproducible and rapid SFC method to separate hydrocarbon mixtures by chemical class for samples ranging from C₄ to C₄₀ uses a column-switching technique which allows interchange between a microbore (1 mm i.d.) silica gel column and a silver-ion loaded strong cation exchange silica gel microbore column, with 10% CO₂ in SF₆ as mobile phase. The silver-loaded cation exchange column gives the saturate and olefin separation, while temperature programming is used to elute the aromatic peaks. The only problem encountered with the use of silver-modified columns is that certain types of compounds can react with the silver ions, causing column instability.

The three-column system with column switching and backflushing can be used to separate saturates, aromatics and polar compounds in high-boiling residues. A multicolumn system for quantitative determination of crude oil and high-boiling fraction class separation has been developed. Three different col-

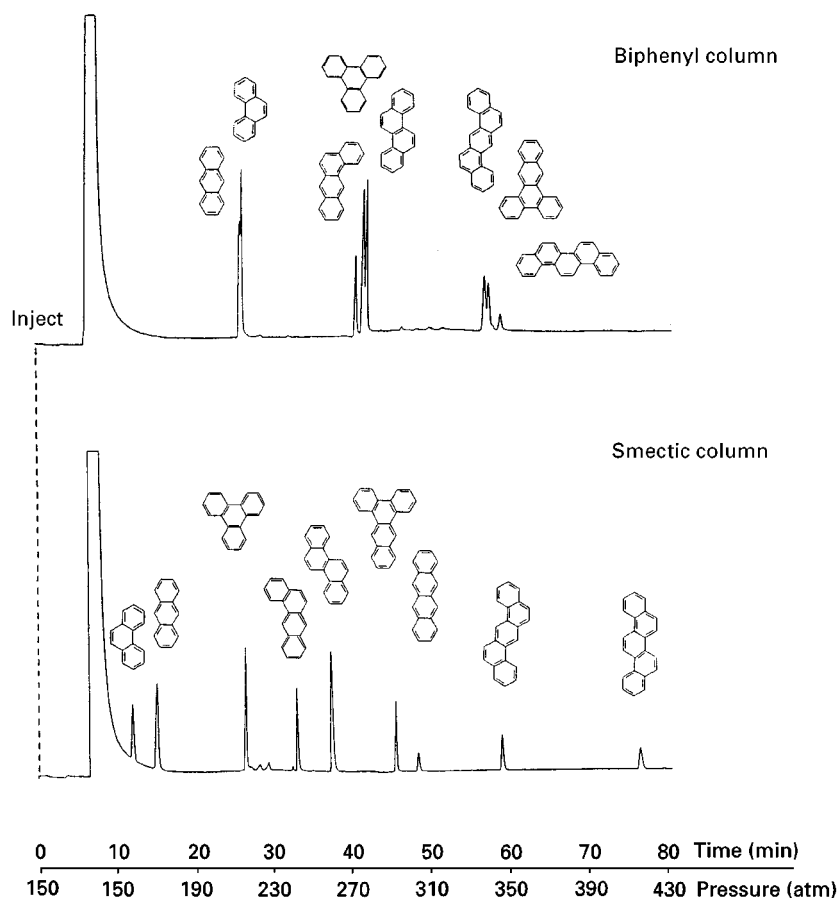


Figure 4 Simultaneous separation of three-, four- and five- ring PAH isomers on biphenyl and liquid crystalline columns. Conditions: CO_2 at 120°C ; programmed from 150 bar (10 min) to 450 bar at 4 bar min^{-1} . (Courtesy of the University of Leeds.)

umns are used – cyano, silica and silver-loaded silica – in order to separate saturate, aromatics and resins. The replacement of the silver-loaded silica column with a silver-loaded cation exchange column results in a more stable system. Similar effects have been observed when the silica column is replaced with a cyano column. The silica column prevents the aromatic components with strong π -interactions from entering the silver-loaded silica column and thus allows the aromatics to be backflushed from the silica column as a narrow band. The cyano column is used to trap the resins. Both carbon dioxide (CO_2) and nitrous oxide (N_2O) can be used as mobile phases; the latter provides better solubility of the resins and less tailing of the peaks.

A quantitative study of the determination of aromatics in jet and diesel fuels by SFC with FID used a single column ($25 \text{ cm} \times 2.0 \text{ mm i.d.}$ column packed with $5 \mu\text{m}$ Chromegasphere SI-60 silica), a CO_2 mobile phase under constant density and no temperature programming. It was found that the nonlinear response of the detector can be significantly improved

by the addition of air as make-up gas (approximately 15 mL min^{-1}).

The use of a specially treated silica-based packed column to separate saturate and aromatic compounds in diesel fuels by SFC has been reported. Separations are achieved in less than 8 min, with good resolution (greater than 9) being achieved in the separation of one-, two- and three-ring aromatics.

In 1991, SFC was approved for the separation of saturate and aromatic hydrocarbons in diesel fuels. The American Society of Testing Materials (ASTM) method D5186 requires that temperatures in the range of 30 – 40°C be used for this separation. At these low temperatures, the separation of saturates and monoaromatics is easily achieved. However, low temperatures are not adequate for separation between the mono- and polyaromatics.

A packed capillary column has also been used with the same methodology, and showed that good separation can still be achieved at temperatures as high as 85°C . A further increase in pressure and temperature also results in apparently higher efficiencies for the

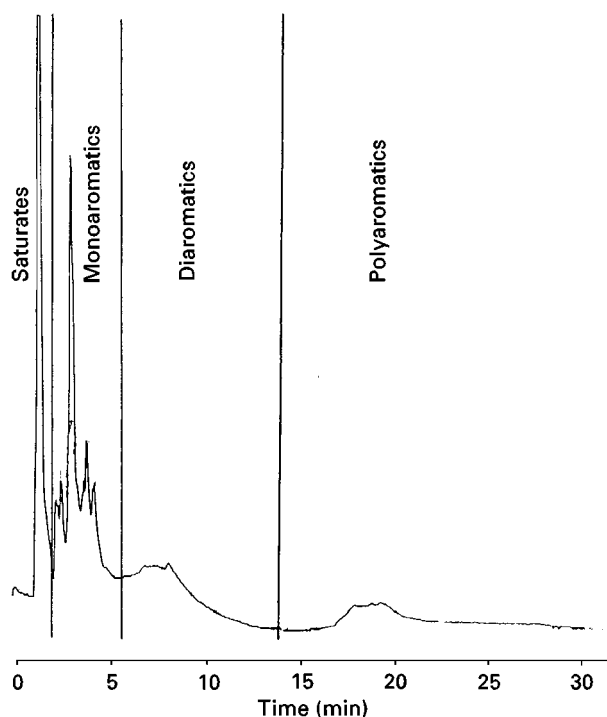


Figure 5 Chromatogram of base oil mixture containing 57.8% aromatic content. Operating conditions: column $1.3 \times 250 \mu\text{m}$ i.d. packed with Waters Spherisorb S5W. (Courtesy of the University of Leeds.)

heavier aromatic peaks with reduced analysis time. However, the ASTM method requires a minimum resolution of 4 between the saturates and aromatics peaks. As the temperature is raised, the separation between the saturates and aromatics decreases. For highly complex mixtures, such as coal liquefaction recycle solvents, an optimized group-type separation procedure involves SFC on a $250 \mu\text{m}$ i.d. \times 1.3 m long silica column operated at 80°C and 300 bar (Figure 5).

The separation of petroleum distillate into aliphatic and aromatic fractions has been achieved using a two-dimensional SFC-SFC system with a flow-switching interface. The columns used were a liquid crystal polysiloxane capillary column and a SB-Biphenyl-30 capillary. The use of a liquid crystal column in the second dimension to provide shape selectivity allows separation of various isomers, including chrysene, triphenylene, benz[*a*]anthracene and the benzo[*a*]fluoranthenes.

Simulated Distillation of Petroleum Compounds and Crude Oils

Distillation is the primary separation process in the petroleum used to characterize petroleum products before processing. Distillation data can be obtained

by using true distillation techniques or analytical techniques which simulate the distillation process. Simulated distillation (SD) is a technique which is inexpensive and rapid compared to distillation techniques but does not yield fractions for further characterization. GC simulated distillation techniques require the use of special high-temperature columns, and the high temperatures (up to 400°C) may compromise the integrity of the sample. SFC uses much milder conditions (typically below 150°C) than those necessary for simulated distillation by GC and can be used for the characterization of heavy crude components, with boiling points up to 760°C . The effect of temperature and pressure on resolution and retention have been studied, and generally analysis is conducted by pressure programming while keeping the temperature constant, although simultaneous temperature and pressure programming has been successfully used. A relatively nonpolar, 5% phenyl-95% dimethylpolysiloxane (DB5) phase is used. Such columns are very stable at SFC temperatures and, with the use of an integral restrictor installed at the end of the column, good results are obtained.

Linear density programming of the supercritical mobile phase provides a more nearly linear relationship between the elution pressure and homologous series boiling point. The use of open tubular columns eliminates the pressure drop effects which are common in packed columns. If an *n*-octylpolysiloxane stationary phase is used, the discrimination between aliphatic versus aromatic boiling points is minimized.

While SFC with open tubular columns seem to be well suited to SD, low sample capacity and loadability pose difficulties for complex mixtures. Recently, the analysis of hydrocarbon mixtures up to *n*- C_{130} has been achieved using a $300 \times 0.3 \text{ mm}$ i.d. column packed with $5 \mu\text{m}$ C_{18} bonded silica. The true boiling points and retention times of *n*-alkanes, alkylbenzenes, PAH and thiophenes have been correlated and it has been found that the retention time differences do not exceed 1 min for chemically different solutes with similar boiling points.

The effect of C_1 to C_{18} alkyl groups bonded to silica has been investigated and the oligomer peak resolution obtained with packed capillary columns approaches that obtained with open tubular columns. Figure 6 shows the SFC chromatogram of the SD calibration standard on a packed capillary hexylsilyl (C_6) column. The SD data from SFC correlated well with those obtained by GC. Higher-molecular-weight hydrocarbons can easily be eluted at operating pressures below 415 bar (density of CO_2 mobile phase approximately 0.71 g L^{-1}). At this maximum pressure a column packed with hexyl (C_6) bonded silica elutes hydrocarbons boiling at more than 756°C ,

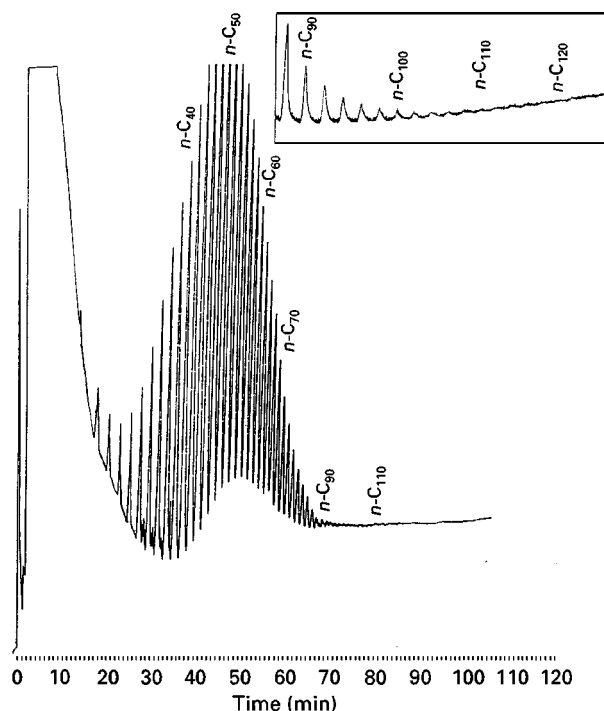


Figure 6 Simulated distillation chromatogram of Polywax 655 on a $0.25\text{ m} \times 250\text{ }\mu\text{m}$ i.d. column packed with Waters Spherisorb S5W C_6 . Conditions: linear pressure programming from 100 to 415 bar (hold for 60 min) at 3.5 bar min^{-1} , FID detection. (Courtesy of the University of Leeds.)

whereas a column packed with octadecyl silanol (ODS-2) (C_{18} ; **Figure 7**) is more retentive and only elutes hydrocarbons boiling up to 686°C . Hydrocarbons of even higher boiling points can be eluted if the column length is changed. The significant deviation

between the retention times of aromatics and straight chain alkanes of apparently similar boiling points which occurs when SD is performed by GC may be reduced using open tubular SFC and further minimized when packed capillary columns are used, especially for aromatic compounds with three or more rings. However, comparisons may not be valid in view of the discrepancies between published values of PAH boiling points.

Analysis of Zinc Dialkyldithiophosphate in Lubricating Oil

Zinc dialkyldithiophosphates (ZDDPs) are used in lubricating oils as extreme-pressure anti-wear additives. It is possible to analyse ZDDPs using SFC; if the sample is in a lubricating oil matrix then it is essential that a phosphorus-specific detector is used, i.e. nitrogen phosphorous detector (NPD) (**Figure 8**). This removes the interference from the base oil which is obtained if FID detection is used. **Figure 8** also shows that it is possible to determine other lubricating oil additives e.g. Irgafos 168.

Conclusions

The analysis of high-boiling hydrocarbon mixtures has historically been difficult due to their complex nature. Because of the favourable properties of supercritical fluids – low viscosity, low density and high diffusivity – SFC has found many applications in this area. The technique is becoming increasingly popular in the petroleum industry, especially for group-type separation and for simulated distillation. The main

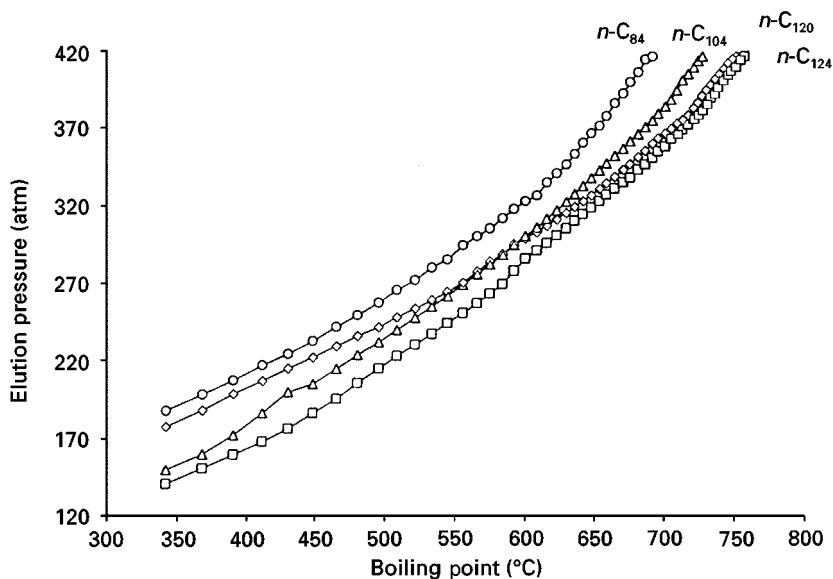


Figure 7 Graph of elution pressure versus the boiling point for packed columns. Diamonds, methyl (C_1); squares, hexyl (C_6); triangles, octyl (C_8); circles, ODS2 (C_{18}). (Courtesy of the University of Leeds.)

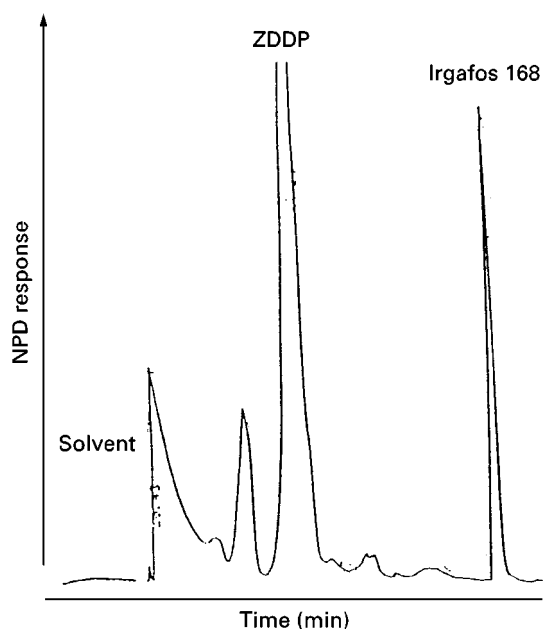


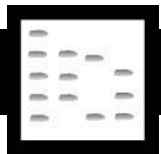
Figure 8 Chromatogram of used lubricating oil. Conditions: Diol packed column, temperature 50°C; ramp rate of 3 bar min⁻¹, NPD detection. (Courtesy of the University of Leeds.)

advantages of SFC are its speed of analysis and improved column efficiency when compared to liquid chromatography. The lower column temperature than needed for GC allows the analysis of higher-molecular-weight mixtures with carbon numbers up to C₁₂₀ and beyond.

Further Reading

- ASTM Method D5186 (1992) In: *Annual Book of ASTM Standards*, vol. 05.03, p. 855. Philadelphia, PA: American Society for Testing and Materials.
- Kithinji JP, Raynor MW, Egia B *et al.* (1990) Analysis of coal-tar polycyclic aromatic hydrocarbon LC-fractions by capillary SFC on a liquid-crystalline stationary phase. *Journal of High Resolution Chromatography* 13: 27–33.
- Lee ML and Markides KE (eds) (1990) *Analytical Supercritical Fluid Chromatography and Extraction*. Provo, UT: Chromatography Conferences Inc.
- Medvedovici A, David F, Desmet G and Sandra P (1998) Fractionation of nitro and hydroxy polynuclear aromatic hydrocarbons from extracts of air particulates by supercritical fluid chromatography. *Journal of Microcolumn Separations* 10: 89–97.
- Raynor MW, Moulder R, Davies IL *et al.* (1990) Dual capillary column supercritical fluid chromatography. *Journal of High Resolution Chromatography* 13: 22–26.
- Roberts I (1995) Supercritical fluid chromatography. In: Adlard ER (ed.) *Chromatography in the Petroleum Industry*. Journal of Chromatography Series, vol. 56, pp. 305–346. Oxford: Elsevier Science.
- Shariff SM, Robson MM, Myers P *et al.* (1998) Hydrocarbon group-type separations for high aromatic fuels by supercritical fluid chromatography on packed capillary columns. *Fuel* 77: 927–931.
- Westwood SA (ed.) (1993) *Supercritical Fluid Extraction and its Use in Chromatographic Sample Preparation*. London: Blackie Academic & Professional.

FULLERENES: LIQUID CHROMATOGRAPHY



V. L. Cebolla, L. Membrado and J. Vela,
Instituto de Carboquímica, CSIC, Zaragoza, Spain
Copyright © 2000 Academic Press

Introduction

Since the first separation in 1990 of C₆₀ and C₇₀ using column liquid chromatography (LC), this technique has played a very important role in fullerene chemistry. LC has allowed macroscopic quantities of fullerenes (particularly C₆₀) to be isolated and purified from the processing products. Obtaining sufficient amounts of pure fullerenes has been crucial both for determining physical and chemical properties in order to investigate practical applications of this new variety of carbon, and for developing a chemistry of these spherical and polyfunctional carbon molecules. A very rich chemistry has been developed in less than

a decade based mainly on C₆₀, and to a lesser extent on higher fullerenes. The starting reactives for this chemistry have been the compounds previously isolated by LC. It is now possible to bind covalently many types of compounds to the fullerene molecule.

LC is currently the method of choice for the separation, isolation and purification of fullerenes. Progress in fullerene chemistry therefore depends on the development of improved chromatographic methods, i.e. those with the highest efficacy and best resolution between the different components of fullerene mixtures, at both analytical and preparative scales, and at the lowest cost.

Contribution of LC in the Field of Fullerene Production

In early 1990, the design of LC methods was mostly geared towards isolating the most abundant

fullerenes obtained from the different production methods (e.g. laser vaporization of graphite, electric arc discharge, hydrocarbon flame combustion process, pyrolysis of carbon material). Each of these methods has its own specificity, with its advantages and drawbacks. In general, the objective of these methods was to obtain C_{60} and, to a lesser extent, C_{70} . On occasions, endohedral metallofullerenes (i.e. $M@C_{60}$) were also isolated. Therefore, chromatographic methods developed for this purpose should be (semi-) preparative. Likewise, the presence 'as impurities' of higher fullerenes and metallofullerenes (in low or very low concentration), polyaromatic compounds (PACs, created during production), residual solvents, solvates (due to strong interactions between fullerenes and some solvents), fullerene adducts (mostly with oxygen), and other artefacts produced during the production must be taken into account when designing an analytical procedure.

In this case, an extraction step for pre-purification is required. The origin of the soots, which is determined by the starting carbon material and the production method, influences the extraction yields and the nature of the fullerenes extracted.

LC in the Field of Organic and Organometallic Chemistry of Fullerenes

At the same time that C_{60} and C_{70} became available in significant amounts, the organic chemistry of fullerenes started to be developed. New reactions were performed and plentiful data about C_{60} reactivity were obtained. C_{60} was initially considered to be a polycyclic aromatic hydrocarbon (PAH), and the chromatographic methods that were developed were based on previous knowledge accumulated on PAHs. Further research, to which LC contributed significantly, demonstrated that the reactivity of C_{60} is more like that of a localized polyolefin. The LC contribution to this chemistry includes separation, identification and isolation of products. LC is also used to monitor the reactions typical of fullerenes: nucleophilic additions, cycloadditions, hydrogenation reactions, and oxidation and reactions with electrophiles. In addition, different isomers, diastereomers and enantiomers have been separated (Figure 1). Different examples of these separations are shown in Table 1.

The analytical designs required to separate fullerene derivatives from organic reactions differ considerably from those used to isolate fullerenes from their production methods. Several points must be considered. First, the structural similarities of these fullerene derivatives are often an obstacle in fullerene separations. Furthermore, the matrices and relative

percentages of compounds to be separated are different. Finally, some addends on the fullerene core have a dramatic influence on the solubility properties and the retention behaviour.

Separations Using Normal and Reversed Stationary Phases

In general, the poor solubility of fullerenes in most organic solvents limits the choice of mobile and stationary phases that can be used. Conventional stationary phases used for normal- and reversed-phase elution may exhibit reasonable fullerene selectivity, but only when using mobile phases in which the fullerenes are poorly soluble (e.g. *n*-hexane, dichloromethane, acetonitrile). These phases usually provide weak interactions with fullerenes when using eluents in which fullerenes are most soluble (e.g. *o*-dichlorobenzene, CS_2), which produce elution without adequate separation. Detection of fullerenes is not a problem: conventional or diode-array UV are used in the range 230 to 600 nm, depending on the cutoff of the solvent used.

Normal-Phase Elution

Open-column and low-pressure liquid chromatographic techniques, rather than HPLC, have been used for separations based on adsorption chromatography and performed with conventional normal-phase stationary phases (e.g. silica gel or alumina). In this subsection, we summarize the application of these methods, including the use of charcoal columns, to fullerene separations.

C_{60} was first separated from C_{70} using open-column LC on alumina as stationary phase, and *n*-hexane or *n*-hexane/toluene (95 : 5) as mobile phase. This method presents several disadvantages: as *n*-hexane is not a good solvent for fullerenes, a high consumption of both mobile and stationary phases is required; it is time-consuming, because several sequential separations are necessary in order to obtain sufficient amounts of C_{70} and other higher fullerenes, owing to peak tailing; and on-column degradation of C_{70} and higher fullerenes occurs (this phenomenon had been already described for PAHs). The preadsorption of fullerenes on alumina did not solve these problems.

A modification was introduced to overcome these deficiencies: the combination of Soxhlet extraction and LC on alumina, in which hot solvent was continuously recycled, allowed solvent consumption and labour to be reduced. However, the most inexpensive and efficient method for rapid separation of C_{60} and C_{70} involves an activated charcoal (Norit A) and silica gel mixture (1 : 2) as the stationary phase. As carbon

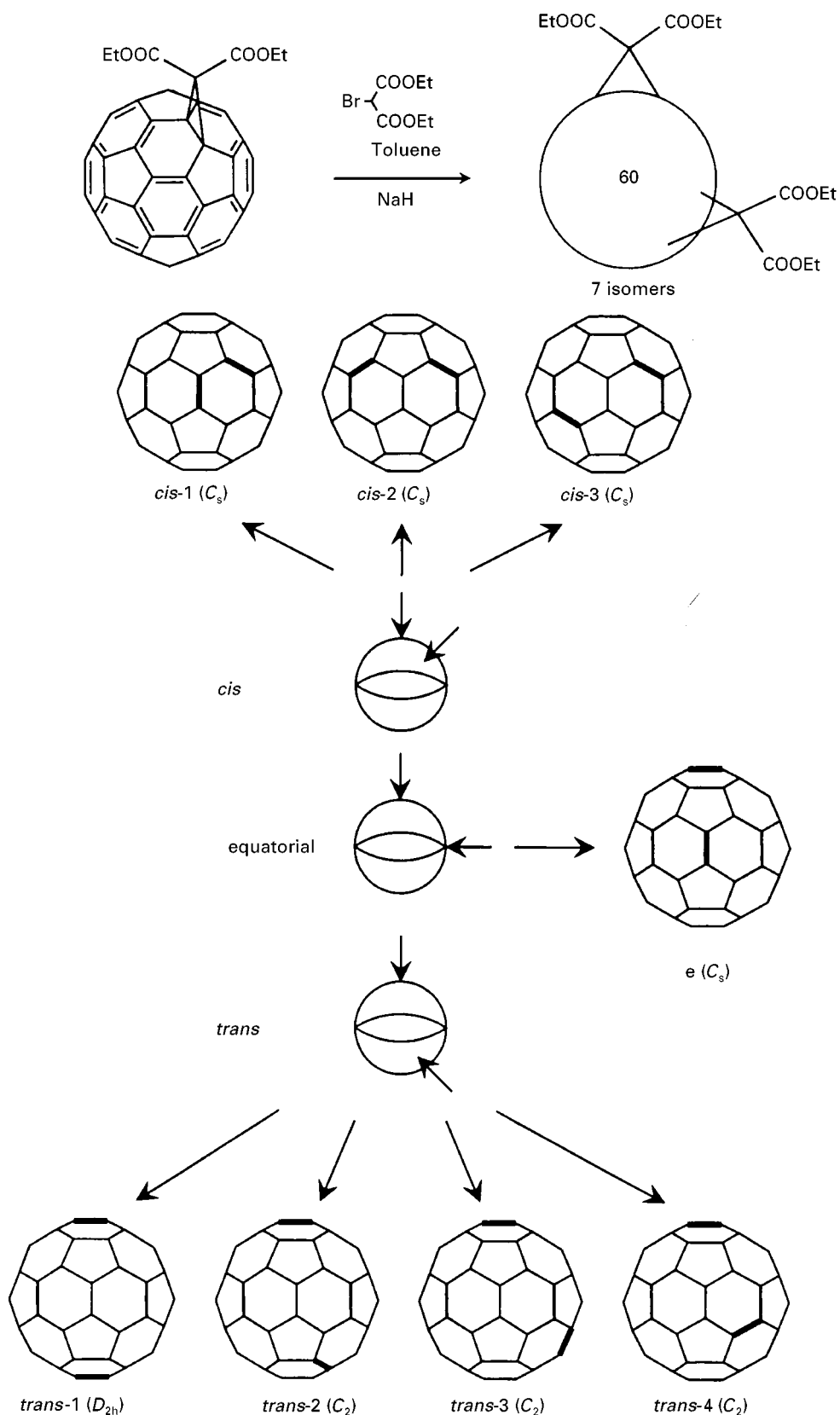


Figure 1 Positions of the ligand-carrying bonds in the eight possible regioisomers of C_{60} with symmetrical additions to 6-6 bonds and symmetry of the corresponding isomers. (Reprinted from Hirsch A (1994) *The Chemistry of the Fullerenes*, pp. 68 and 69, with permission from Thieme.)

Table 1 Some examples of LC contribution to organic and organometallic chemistry of fullerenes

<i>Reaction mechanism category</i>	<i>Reaction</i>	<i>LC contribution</i>
Nucleophilic additions	Hydroalkylation and hydroarylation of C ₆₀ and C ₇₀	Monitoring of products formation; consumption of C ₆₀ followed from HPLC peak areas
	C ₆₀ + RLi → C ₆₀ R [−] → C ₆₀ HR (protonation)	Purification of 1,2-organodihydrofullerenes (preparative C ₁₈ , chloroform/acetonitrile, 60/40)
	Synthesis of [6,6]-methanofullerenes from stabilized sulfonium ylides with C ₆₀ or C ₇₀	Monitoring of the reactions by HPLC Pure monoadducts obtained after column chromatography on silica gel Resolution of a racemic derived-amide on a chiral (S,S)-Whelk-O HPLC column
	Cyclopropanation of C ₆₀ and C ₇₀ and higher adducts (stabilization by intramolecular S _{Ni})	Isolation of seven stable regioisomeric bisadducts of C ₆₂ (COOEt) ₄ of the eight possible ones (see Figure 1). Identified by NMR and HPLC elution order Isolation of chiral trisadducts of C ₆₀ and di-(ethoxycarbonyl) methylene Purification using GPC columns and toluene
[4 + 2] Cycloadditions	Cycloadducts from C ₆₀ with: –cyclopentadiene –anthracene	Separation of products by GPC columns and chloroform, or toluene
	Cycloadducts from C ₆₀ -4 (4-fluoro-3-nitro benzoyl) benzo-cyclobutene with: –4,13-diaza[18]-crown-6 –1,6-bis (aminomethyl) hexane –4-amino-azobenzene	
	Cycloadducts from C ₆₀ with: –2-trimethyl-silyloxy-1,3-butadiene	
	Synthesis of fullerene-bound dendrimers	
[3 + 2] Cycloadditions	Methano-bridged cycloadducts from C ₆₀ with diazoamides (biological importance)	Isolation by GPC Isolation on silicagel using toluene
[2 + 2] Cycloadditions	Photochemical cycloaddition of enones to C ₆₀	Analysis of products using HPLC-Buckyclutcher® The corresponding enantiomers of each diastereomer for a methyl substituent of the enone have been resolved and isolated by HPLC using chiral stationary phases
Hydrogenation	Synthesis of C ₆₀ H ₂ via hydroboration and hydrazination, and also by Zn/acid reduction	The only regioisomer formed can be isolated from the reaction mixture by HPLC
	Polyhydrofullerenes from Birch–Hückel reduction	C ₆₀ H ₃₆ , C ₆₀ H ₁₈ obtained from the mixture using LC on silica gel in CH ₂ Cl ₂ /hexane
Oxidation and reactions with electrophiles	Oxygenation of C ₆₀ and C ₇₀	C ₆₀ O, C ₇₀ O and others isolated from fullerene extracts by preparative HPLC (neutral alumina)
	Thermal treatment of fullerene systems	Isolation of C ₁₂₀ O, C ₁₂₀ O ₂ , C ₁₈₀ O ₂ using Cosmosil Buckyrep® and PBB® in several steps, with <i>o</i> -dichlorobenzene, and toluene
	Bisosmylation of C ₆₀	Isolation of five regioisomers of C ₆₀ [OsO ₄ (t-bupy) ₂] ₂
	Asymmetrical osmylation of chiral C ₇₆ using chiral ligands (L*)	HPLC analysis of C ₇₆ [OsO ₄ L*] shows that two regioisomers are predominantly formed upon osmylation

compounds can adsorb fullerenes in a similar manner to alumina, silica gel is added to mitigate this effect. This system readily elutes C₆₀ (using toluene, at low pressure or even slight vacuum). By adding *o*-dichlorobenzene to the solvent system, gram quantities of both C₆₀ and C₇₀ can be purified and a fraction enriched in higher fullerenes collected, all in a single column pass.

Silica gel, in contrast, is not able to separate parent fullerenes on its own. However, column chromatog-

raphy on silica gel has occasionally been able to isolate pure C₆₀ and C₇₀ derived adducts from organic reactions (see Table 1). Likewise, silica gel has been used to separate PAHs cosynthesized during fullerene production.

Normal Elution Using Nonconventional Phases

γ-Cyclodextrin bound to silica gel, in HPLC mode, is mostly used for enantiomer separations. However, in the field of fullerenes, it has been used for separating

C₆₀ from C₇₀. γ -Cyclodextrin is a cyclic oligosaccharide that forms complexes with fullerenes. The interaction of C₇₀ with cyclodextrin is stronger than that with C₆₀, and both molecules can be separated, at analytical scale, even using *n*-hexane or *n*-hexane/toluene (70 : 30). However, the problem of fullerene solubility in these solvents has hampered further research on this stationary phase.

Bonded-Phase Sorbents

Octadecylsiloxane-bonded silica phases (C₁₈) have been used in HPLC mode for analytical-scale separations of fullerenes. Although *n*-hexane or *n*-heptane have been used as mobile phases, toluene has been mostly used, together with a counter solvent (e.g. acetonitrile, methanol) in variable proportions. Although the solubility of parent fullerenes is low in these solvent compositions in general, the use of toluene/acetonitrile provides adequate separation between C₆₀ and C₇₀ with selectivities (expressed as $\alpha_{C_{70}/C_{60}}$) near 2 for a 50 : 50 mixture. The use of toluene/methanol, in turn, shortens the analysis time in comparison with toluene/acetonitrile mixtures. Other profile phases, such as CHCl₃/acetonitrile on CH₂Cl₂/acetonitrile, have also proven suitable for separation of C₆₀ and C₇₀.

Monomeric and polymeric C₁₈ phases have also been used. They provide differences in retention for fullerenes. A 'topological' recognition ability of the polymeric phase has been invoked to explain these differences. Therefore, fullerenes would be separated as a function of their spherical diameters or their geometries in general.

Separations Using Charge-Transfer Stationary Phases

Considerable research has been carried out in developing supports that can provide strong interactions with fullerenes when using eluents that solubilize fullerenes. Charge-transfer chromatography is based on the donation or acceptance of electrons between the stationary phase and, in this case, the fullerene derivatives. The migration of fullerenes through the column is selectively retarded to a degree depending on the strength of the charge-transfer complex formed. Based on research on separation of PAHs, phases such as dinitroanilinopropyl silica (DNAP) or tetrachlorophthalimidopropyl silica (TCPP) were studied in the early 1990s. The latter presented adequate selectivity for C₆₀ and C₇₀ ($\alpha = 2.75$ in the best case).

Many of these phases, called Pirkle-type, have been synthesized and tested. In general, they are based on electron-deficient aromatic rings capable of simultaneous interaction with the spherical, electron-rich,

fullerene molecules. These phases afford greater interaction with fullerenes, thus allowing the use of toluene-based mobile phases.

In the second-half of the 1990s, several of these stationary phases became commercially available and are used now in many different types of fullerenes separations, at both analytical, semipreparative or preparative scale. Figure 2 shows, among other phases described in this work, the chemical structures of Buckyclutcher® (tri-(dinitrophenyl)-silica), Cosmosil PBB® (pentabromobenzyl-silica) and Cosmosil Buckyrep® (2-[(1-pyrenyl)ethyl]-silica). The Buckyclutcher column, developed by Pirkle, can be used in both normal and reversed phase mode. The capacity of this phase to separate fullerenes seems to be due, in addition to electron donor-acceptor interaction, to a steric effect created by a cone-shaped arrangement of dinitrophenyl groups.

High-capacity stationary phases containing condensed aromatic systems (e.g. Buckyrep®, 5-corononylpentyl-silica, COP) or heavy heteroatoms such as sulfur, chlorine or bromine (e.g. Cosmosil PBB®) showed high retentivity with excellent efficiency for separation of fullerenes, particularly Cosmosil PBB®. This phase allows the use of solvents providing high fullerene solubilities, such as CS₂ or 1,2,4-trichlorobenzene, for gram-scale separations with ordinary HPLC equipment. These solvents exceed toluene in solubility of fullerenes.

Although large aromatic systems were expected to show high fullerene retentivity according to electron donating-accepting the positive effect of heavy atoms is not correlated with the electron-withdrawing or donating properties and more research is needed on this point.

The use of the above-mentioned commercially available columns usually involves two or three steps in the process of separation, isolation and purification of fullerene derivatives. As an example, a typical scheme of proceeding may be a first step using an analytical Cosmosil PBB column® (with CS₂, *o*-dichlorobenzene or 1,2,4-trichlorobenzene as eluents) and a second step using a preparative Buckyrep® or Buckyclutcher® column (e.g. with toluene). HPLC with these columns has allowed the identification, separation and/or isolation of endohedral metallofullerenes (e.g. M@C₇₄, M@C₆₀, M@C₇₀), fullerenes higher than C₆₀ (e.g. C₈₆, C₉₂, C₉₄, C₁₂₀), odd-numbered clusters (e.g. C₁₁₉), products derived from fullerene oxidation (e.g. C₁₂₀O, C₁₂₀O₂, C₁₈₀O₂), and the separation of isomers (e.g. C₆₀H₄).

Tetraphenylporphyrin (TPP)-silica based stationary phase is another promising family for fullerene separation at both analytical and preparative scale. Figure 2 shows chemical structures of

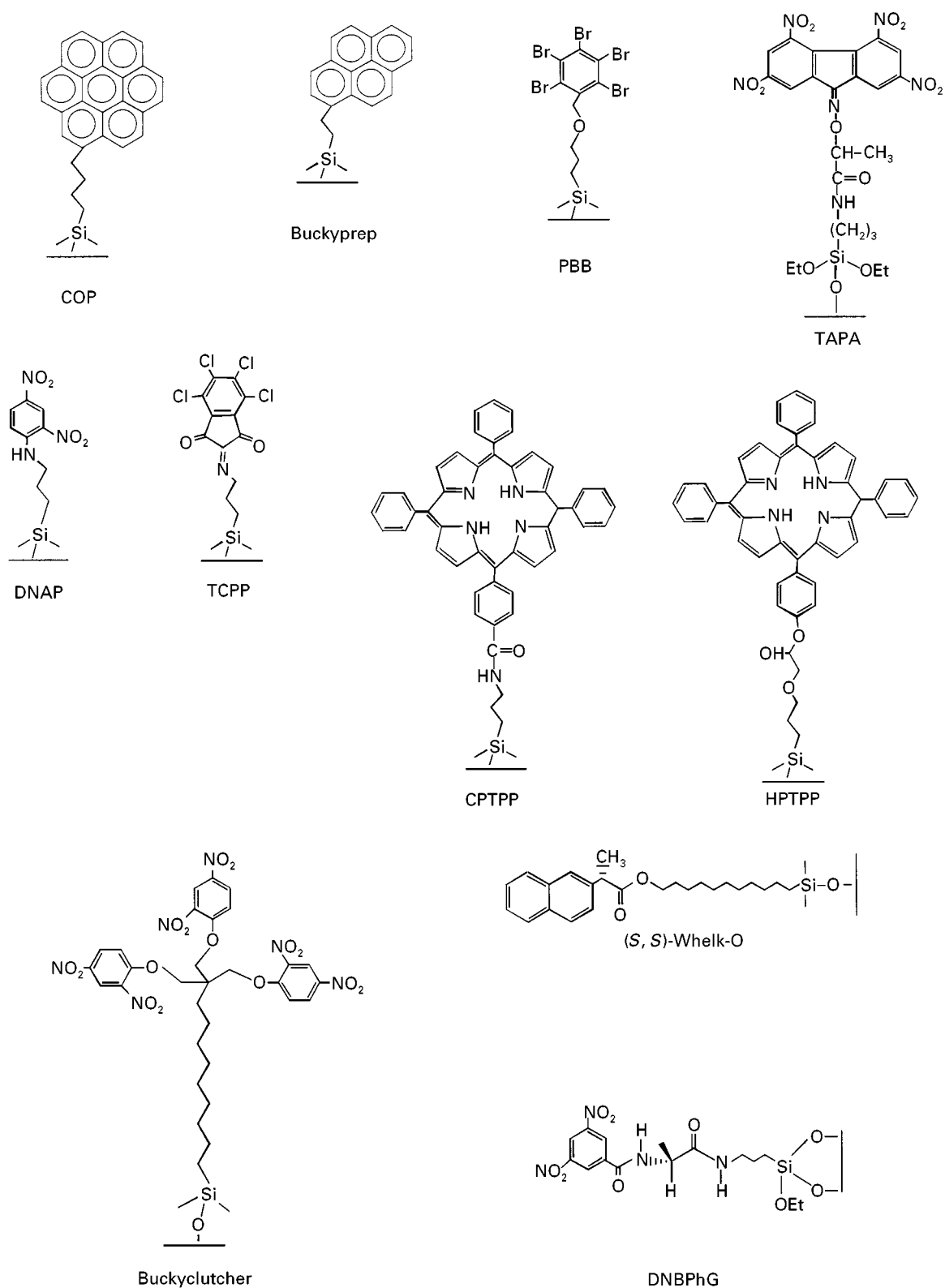


Figure 2 Some charge-transfer stationary phase used for fullerene separation (for abbreviations, see text).

[5-(*p*-hydroxyphenyl)-10,15,20-triphenyl]porphyrin-silica (HPTPP) and [5-(*p*-carboxyphenyl)-10,15,20-triphenyl]porphyrin-silica (CPTPP).

These phases have demonstrated strong retention and unmatched selectivity in the separation of C_{60} and C_{70} using strong mobile phases such as

Table 2 Fullerene selectivity, expressed as $\alpha_{C70/C60}$, of different stationary phases, using toluene as the mobile phase, under similar conditions

Stationary phase	$\alpha_{C70/C60}$
Buckyclutcher	1.5
PBB	2.5
Buckyprep	1.8
CPTPP	5.7
HPTPP	7.0

1,2-dichlorobenzene or CS_2 . Table 2 gives a rough picture of the influence under similar conditions of different stationary phases on fullerene selectivity, expressed as $\alpha_{C70/C60}$, using toluene as the mobile phase. Selectivity using toluene is the highest for all phases with regard to stronger eluents: $\alpha_{tol} > \alpha_{CS_2} > \alpha_{dichlorobenzene}$. Another important point for TPP-silica stationary phases is their potential for preparative-scale separations. This includes higher fullerenes. Owing to the usually low percentage of these kinds of fullerenes in the parent mixtures, their efficient separation using conventional or commercial phases becomes difficult and usually involves several reinjections, which are both solvent- and time-consuming. Currently, TPP phases present a good resolution in the separation of higher fullerene isomers in a single column pass, using strong eluents such as 1,2-dichlorobenzene, as shown in Figure 3.

Enantiomer Separation

Some charge-transfer stationary phases, such as (*R*)-*N*-(3,5-dinitrobenzoyl)phenylglycine or *R*-(–)[2-

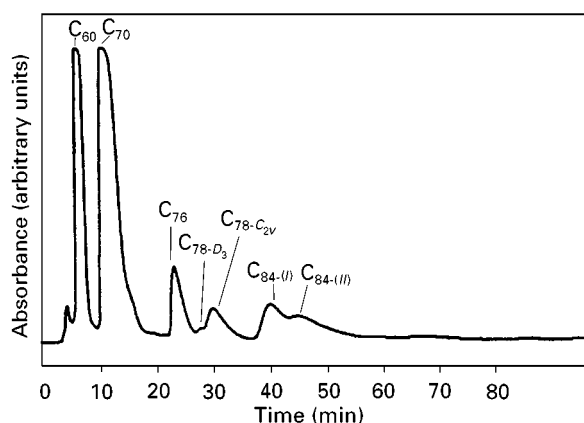


Figure 3 Separation of higher molecular mass fullerenes on a 250 mm \times 4.6 mm column packed with HPTPP(4)-silica. Injection of 12 mg of fullerene soot; mobile phase = 100% 1,2-dichlorobenzene; flow rate = 0.85 mL min⁻¹; detection wavelength = 410 nm; ambient column temperature. (Reprinted from Coutant DE, Clarke SA, Francis AH and Meyerhoff ME (1998) Selective separation of fullerenes on hydroxyphenyl-triphenylporphyrin-silica stationary phases. *Journal of Chromatography A* 824: 147–157, with permission from Elsevier Science.)

(2,4,5,7-tetranitro-9-fluorenylideneaminoxy)propionic acid] (TAPA) bound to silica gel (see Figure 2), have been used for the separation of enantiomeric fullerene derivatives.

Taking advantage of the fact that (*R*)-*N*-(3,5-dinitrobenzoyl)phenylglycine (DNBPhG) was able to separate fullerenes, other chiral stationary phases were designed. A stationary phase derived from *S*-naproxen (Whelk-O columns; see Figure 2) has provided successful separation of chiral fullerene derivatives (Table 1).

A strong charge-transfer interaction is necessary but on its own it is not a sufficient requirement for chiral discrimination. Both π -donor–acceptor interactions and one stereochemically significant interaction via hydrogen bonds are required.

TAPA-bounded silica gel has also been used for nonchiral separations (e.g. separation between C_{60} and C_{70}).

Size Exclusion Chromatography (SEC)

SEC is a molecular sieving technique that separates molecules according to their selective permeation into the gel pores on the basis of differences in their size in solution. Solute permeation into the gel increases with decreasing molecular size, resulting in later elution. By virtue of these particular characteristics of SEC, the total time of the chromatographic runs is previously known. This technique is also named GPC (gel permeation chromatography) when carried out using organic solvents.

SEC stationary phases consist of a gel, typically a three-dimensional network of cross-linked polymeric chains of controlled porosity. Compatibility between solvent and stationary phase is of prime importance. If the mobile phase is not suitable, gels can swell or shrink, often damaging the packing bed; this changes the pore distribution and hence the exclusion volume. SEC is therefore confined to isocratic elution using a limited range of pure solvents.

The differences in size between the fullerenes are sufficient to allow SEC separation. Because pure toluene can be used as the mobile phase (allowing fewer constraints for solvent recycling) and these columns have a greater lifetime than other LC columns (owing to the theoretical absence of interaction between the fullerenes and SEC stationary phase) it is possible to use SEC at preparative scale.

Polystyrene-divinylbenzene-based columns, from 10 to 100 nm pore size, have been used for fullerene separations. In spite of their low selectivity ($\alpha_{C70/C60} = 1.1$), the possibility of using automated systems with reinjection/sample collection and solvent recycling has allowed the separation of 10 g of

an extract (from production) a day, yielding C_{60} with high purity. The relatively short time of SEC runs allows the frequency of injections to be increased with respect to other LC techniques.

This kind of automated system has also been used to separate and isolate metallofullerenes from empty cage fullerenes in sufficient amounts, despite their low concentration in the production mixtures (e.g. 200 mg of metallofullerenes isolated in 16 h).

However, the fact the C_{60} is eluted before C_{70} and other higher fullerenes, regardless of the mobile phase used (e.g. toluene, $CHCl_3$), means that solutes are not separated according to their size. Non-size effects (due to adsorptions and other types of interactions) have been described in the case of other relatively small molecules (e.g. PACs) with relative molecular masses lower than 1000.

Further Trends

Research is now focused on finding more selective stationary phases (mainly based on charge-transfer chromatography) to improve fullerene separation. An efficient method for separating individual fullerenes on a large (preparative) scale is still required. Most of the separation methods reported here are limited to gram scale. This has hampered the study of higher molecular mass fullerenes.

Further Reading

Ajje H, Alvarez MM, Anz SJ *et al.* (1990) Characterization of the soluble all-carbon molecules C_{60} and C_{70} . *Journal of Physical Chemistry* 94: 8630–8633.

Coutant DE, Clarke SA, Francis AH and Meyerhoff ME (1998) Selective separation of fullerenes on hydroxyphenyl-triphenylporphyrin-silica stationary phases. *Journal of Chromatography A* 824: 147–157.

Gross B, Schurig V, Lamparth I and Hirsch A (1997) Enantiomer separation of [60]fullerene derivatives by micro-column high-performance liquid chromatography using (R)-(-)-2-(2,4,5,7-tetranitro-9-fluorenylidene-aminoxy) propionic acid as chiral stationary phase. *Journal of Chromatography A* 791: 65–69.

Hirsch A (1994) *The Chemistry of the Fullerenes*. Stuttgart: Georg Thieme-Verlag.

Kimata K, Hirose T, Moriuchi K *et al.* (1995) High-capacity stationary phases containing heavy atoms for HPLC separation of fullerenes. *Analytical Chemistry* 67: 2556–2561.

Pirkle WH and Welch CJ (1991) An unusual effect of temperature on the chromatographic behavior of buckminsterfullerene. *Journal of Organic Chemistry* 56: 6973–6974.

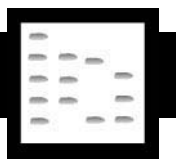
Scrivens WA, Cassell AM, North BL and Tour JM (1994) Single column purification of gram quantities of C_{70} . *Journal of the American Chemical Society* 116: 6939–6940.

Taylor R, Hare JP, Abdul-Sada AK and Kroto HW (1990) Isolation, separation and characterisation of the fullerenes C_{60} and C_{70} : the third form of carbon. *Journal of Chemical Society, Chemical Communications* 20: 1423–1425.

Theobald J, Perrut M, Weber JV, Millon E and Muller JF (1995) Extraction and purification of fullerenes: a comprehensive review. *Separation Science and Technology* 30: 2783–2819.

Welch CJ and Pirkle WH (1992) Progress in the design of selector for buckminsterfullerene. *Journal of Chromatography* 609: 89–101.

FUNGICIDES



Gas Chromatography

José L. Bernal, Department of Analytical Chemistry, Faculty of Sciences, University of Valladolid, Valladolid, Spain

Copyright © 2000 Academic Press

Fungicides, a class of pesticides, are toxic substances that are used to prevent or kill the growth of fungi which are hazardous for plants, animals and human beings. Most fungicides for agricultural use are fumigated or sprayed over seeds, leaves or fruits to control and avoid a variety of economically important fungal

diseases. The first fungicide of proven efficiency was the Bordeaux mixture, developed in 1882. This is a mixture of lime and copper(II) sulfate that has been used for a long time; nowadays a wide variety of compounds are used in a more selective way to fight specific fungi in specific plants. It is necessary to pay attention to their environmental impact (on water, the atmosphere, soil and food) and also to their presence in vegetables which are intended for direct human consumption. Among the important fungicides are those which are applied in greenhouses and in wine production.

There are two options for fungicide analysis: the determination of the composition of formulations, where the concentrations are relatively high, and the

evaluation of residues which appear after their use. Theoretically, it is assumed that the correct use of fungicides does not imply problems with residue because they should always be applied at nonhazardous levels. New pesticides are being developed with the aim of greater efficiency and lower environmental risk.

In formulation analysis there are not many analytical problems. In most cases high performance liquid chromatography (HPLC) is successfully applied. In some cases UV-Vis spectrophotometry or gas chromatography (GC) is used. In contrast, residue determination presents serious problems not only because it is focused on trace levels but also because the compound is usually found with other compounds or degradation products, and in a matrix that can present problems. This implies that the analyst must pay attention to all the steps in the analytical method from sampling to the interpretation of results. According to the problem the analyst will choose the best technique. This choice will affect other steps, especially which sample treatment is selected to achieve the lowest quantity of possible interference, good reproducibility and high recoveries. Sensitivity and selectivity always appear as opposed criteria, so it is necessary to balance the chance of a better signal-to-noise ratio against the risk of incompletely determining all the residues present.

There are three types of required analyses: the global determination of a group of compounds, e.g. ethylenbis(dithiocarbamate) (EBDCs); individual determinations; and, separation and quantification of chiral compounds. The method of analysis will vary according to the objective.

Table 1 summarizes common fungicides. The trend is to use several compounds of the same or a different chemical family, with the aim of achieving several modes of action over the development of the fungi. Because of this, a number of methods are devoted to the determination of several compounds in the same sample. Not all fungicides are shown in the table: inorganic materials such as sulfur, borax, mercury salts, arsenic and copper salts have been omitted. Recently developed compounds whose efficacy has not yet been proved or which are not registered in many countries, or whose mode of action is still unknown, are also omitted. As can be observed, there are a number of chemical families, the most important being phthalimides, benzimidazoles, dicarboximides, carbamates, sulfamides, anilinopyrimidines and phenylpyrrols. The nitrogen atom is common to all of them. In several cases there is a halogen atom and in fewer cases, sulfur or phosphorus atoms are included.

Technique Selection

Chromatographic techniques are the common choice for determining pesticide residues, and among them GC is useful for analysing organochlorine and organophosphorus residues because they have good thermal stability, they are volatile and they have a strong hydrophobic character. That this is valid for a great number of fungicides can be appreciated by the entries in the last column in **Table 1**. Nevertheless the thermal instability of some groups – EBDCs and benzimidazoles particularly – make the use of HPLC more appropriate, although it is also possible to produce derivatives that allow their determination by GC.

Column

Due to the large range of polarities of fungicides, it is difficult to select just one specific column, but many compounds can be separated using the mid-polarity columns. In several official methods for fungicide, glass columns (185 cm × 4 mm i.d.) packed with OV-101 or similar, on Chromosorb WHP (80–100 mesh) are still recommended, although nowadays fused silica open tubular capillary columns (FSOT) are preferred with lengths up to 60 m, inner diameter 0.2–0.7 mm and film thickness between 0.15 and 0.5 µm (DB-35, DB-1301, DB-1701 or similar). In commercial catalogues or application notes, many examples of fungicide separations are shown, together with the main chromatographic conditions and the equivalence between the different manufacturers.

Detectors

From the molecular formulae shown in **Table 1**, it is clear that the use of a nitrogen–phosphorus detector (NPD) is advantageous, although it is not as stable as the flame ionization detector (FID) and because of that it must be calibrated frequently. The electron-capture detector (ECD) is useful for many compounds, but in several cases, the co-extracted compounds can interfere with its response. As there are fungicides that have S and/or P atoms, the flame photometric detector (FPD) is also useful. Confirmation of identity can be obtained using two columns, one a 5% phenyl 95% methylsilicone bonded-phase column coupled to ECD and NPD and the other a 50% phenyl 50% methylsilicone column coupled to ECD and FPD. Such a system is very versatile and sensitive, allowing easy identification of the eluted compounds. Nevertheless, the best option to confirm compound identity is the use of coupled techniques such as gas chromatography–mass spectrometry (GC–MS); the specificity of GC–MS provides low

Table 1 Chemical group, molecular formula and recommended method of residue analysis of the most common fungicides

<i>Fungicide</i>	<i>Chemical group</i>	<i>Molecular formula</i>	<i>Method for residues</i>
Anilazine	Triazine	C ₉ H ₅ Cl ₃ N ₄	GC, HPLC
Benalaxyl	Acyalanine	C ₂₀ H ₂₃ NO ₃	HPLC, GC
Benomyl	Benzimidazole	C ₁₄ H ₁₈ N ₄ O ₃	HPLC
Bitertanol	Azole	C ₂₀ H ₂₃ N ₃ O ₂	GC
Bromuconazole	Azole	C ₁₃ H ₁₂ BrCl ₂ N ₃ O	GC
Bupyrimate	Pyrimidine	C ₁₃ H ₂₄ N ₄ O ₃ S	GC, HPLC
Captafol	Phthalimide	C ₁₀ H ₆ Cl ₄ NO ₂ S	GC
Captan	Phthalimide	C ₉ H ₈ Cl ₃ NO ₂ S	GC
Carbendazim	Benzimidazole	C ₉ H ₉ N ₃ O ₂	HPLC
Carboxin	Phenylamide	C ₁₂ H ₁₃ NO ₂ S	GC
Chlorothalonil	Methoxybenzene	C ₈ Cl ₄ N ₂	GC
Chlozolate	Phthalimide	C ₁₃ H ₁₁ Cl ₂ NO ₅	GC
Cymoxanil	Acetamide	C ₇ H ₁₀ N ₄ O ₃	GC
Cyproconazole	Azole	C ₁₅ H ₁₈ ClN ₃ O	GC
Cyprodinil	Pyrimidine	C ₁₄ H ₁₅ N ₃	HPLC
Dichlofuanid	Sulfamide	C ₉ H ₁₁ Cl ₂ FN ₂ O ₂ S ₂	GC
Diclomezine	Pyridazinone	C ₁₁ H ₈ Cl ₂ N ₂ O	GC
Dicloran	Nitrobenzamine	C ₈ H ₄ Cl ₂ N ₂ O ₂	GC
Diethofencarb	Carbamate	C ₁₄ H ₂₁ NO ₄	GC
Difenoconazole	Azole	C ₁₉ H ₁₇ Cl ₂ N ₃ O ₃	GC
Dimetomorph	Morpholine	C ₂₁ H ₂₂ ClNO ₄	GC, HPLC
Diniconazole	Azole	C ₁₅ H ₁₇ Cl ₂ N ₃ O	GC
Dinocap	Dinitrophenol	C ₁₈ H ₂₄ N ₂ O	GC
Diphenylamine	Amine	C ₁₂ H ₁₁ N	GC
Dodemorph	Morpholine	C ₁₈ H ₃₅ NO	GC
Edifenphos	Organophosphorus	C ₁₄ H ₁₅ O ₂ PS ₂	GC
Ethirimol	Pyrimidine	C ₁₁ H ₁₉ N ₃ O	HPLC/GC
Etridiazole	Azole	C ₅ H ₅ Cl ₃ N ₂ OS	GC
Fenarimol	Pyrimidine	C ₁₇ H ₁₂ Cl ₂ N ₂ O	GC
Fenfuran	Carboxamide	C ₁₂ H ₁₁ NO ₂	GC
Fenpiclonil	Pyrrole	C ₁₁ H ₆ Cl ₂ N ₂	HPLC
Fenpropidin	Morpholine	C ₁₉ H ₃₁ N	GC, HPLC
Fenpropimorph	Morpholine	C ₂₀ H ₃₃ NO	GC, HPLC
Ferbam	Dithiocarbamate	C ₉ H ₁₈ FeN ₃ S ₆	HPLC
Fludioxonil	Phenylpyrrole	C ₁₂ H ₆ F ₂ N ₂ O ₂	GC
Fluoroimide	Phenylpyrrole	C ₁₀ H ₄ Cl ₂ FNO ₂	GC
Flusilazole	Azole	C ₁₆ H ₁₅ F ₂ N ₃ Si	GC, HPLC
Flutolanil	Phenylamide	C ₁₇ H ₁₆ F ₃ NO ₂	GC
Flutriafol	Azole	C ₁₆ H ₁₃ F ₂ N ₃ O	GC
Folpet	Phthalimide	C ₉ H ₄ Cl ₃ NO ₂ S	GC
Fosetyl	Organophosphorus	C ₆ H ₁₈ AlO ₉ P ₃	GC
Hexaconazole	Azole	C ₁₄ H ₁₇ Cl ₂ N ₃ O	GC
Hymexazol	Azole	C ₄ H ₅ NO ₂	GC
Iprodione	Phthalimide	C ₁₃ H ₁₃ Cl ₂ N ₃ O ₃	HPLC, GC
Imazalil	Azole	C ₁₄ H ₁₄ Cl ₂ N ₂ O	GC
Mancozeb	Dithiocarbamate	(MnZnSCNH) _x	HPLC
Maneb	Dithiocarbamate	C ₄ H ₆ MnN ₂ S ₄	HPLC
Mepanypirim	Pyrimidine	C ₁₄ H ₁₃ N ₃	GC
Mepronil	Carboxamide	C ₁₇ H ₁₉ NO ₂	GC
Methalaxyl	Phenylamide	C ₁₅ H ₂₁ NO ₄	GC
Metiram	Dithiocarbamate	(C ₁₆ H ₃₃ N ₁₁ S ₁₆ Zn ₃) _x	HPLC
Myclobutanil	Azole	C ₁₅ H ₁₇ ClN ₄	GC
Nabam	Dithiocarbamate	C ₄ H ₆ N ₂ Na ₂ S ₄	HPLC
Nuarimol	Pyrimidine	C ₁₇ H ₁₂ ClFN ₂ O	GC
Ofurace	Phenylamide	C ₁₄ H ₁₆ ClNO ₃	GC
Oxadixyl	Phenylamide	C ₁₄ H ₁₈ N ₂ O ₄	GC
Oxycarboxin	Carboxamide	C ₁₂ H ₁₃ NO ₄ S	GC
Penconazole	Azole	C ₁₃ H ₁₅ Cl ₂ N ₃	GC
Phthalide	Benzofuranone	C ₈ H ₂ Cl ₄ O ₂	GC
Prochloraz	Azole	C ₁₅ H ₁₆ Cl ₃ N ₃ O ₂	GC
Procymidone	Carboximide	C ₁₃ H ₁₁ Cl ₂ NO ₂	GC
Propamocarb.HCl	Carbamate	C ₉ H ₂₁ Cl N ₂ O ₂	GC

Table 1 Continued

Fungicide	Chemical group	Molecular formula	Method for residues
Propiconazole	Azole	$C_{15}H_{17}Cl_2N_3O_2$	GC
Propineb	Dithiocarbamate	$(C_5H_8N_2S_4Zn)_x$	HPLC
Pyrazophos	Organophosphorus	$C_{14}H_{20}N_3O_5PS$	GC
Pyrifeno	Oxime	$C_{14}H_{12}Cl_2N_2O$	GC, HPLC
Pyrimethanil	Pyrimidine	$C_{12}H_{13}N_3$	HPLC
Tebuconazole	Azole	$C_{16}H_{22}ClN_3O$	GC
Tetraconazole	Azole	$C_{13}H_{11}Cl_2F_4N_3O$	GC, HPLC
Thiabendazole	Benzimidazole	$C_{10}H_7N_3S$	HPLC
Thiophanate methyl	Benzimidazole	$C_{12}H_{14}N_4O_4S_2$	GC, HPLC
Thiram	Thiocarbamate	$C_6H_{12}N_4S_4$	HPLC
Triadimefon	Azole	$C_{14}H_{16}ClN_3O_2$	GC
Triadimenol	Azole	$C_{14}H_{18}ClN_3O_2$	GC
Tricyclazole	Azole	$C_9H_7N_3S$	GC
Tridemorph	Morpholine	$C_{19}H_{39}NO$	GC
Triflumizole	Azole	$C_{15}H_{15}ClF_3N_3O$	HPLC
Vinclozolin	Phthalimide	$C_{12}H_9Cl_2NO_3$	GC
Zineb	Dithiocarbamate	$C_4H_6N_2S_4Zn$	HPLC
Ziram	Thiocarbamate	$C_6H_{12}N_2S_4Zn$	HPLC

Fungicides which appear in **bold** are those which are used most widely. (Reproduced from Jiménez JJ, Bernal JL, del Nozal MJ, Toribio L and Martín MT (1998) *Journal of Chromatography A* 823: 381–387, with permission from Elsevier Science.)

detection limits and unambiguous spectral confirmation in complex matrices.

Taking into account that the presence of heteroatoms is common, it is also possible to use the atomic emission detector (AED) to monitor characteristic wavelengths. Monitoring the emission lines for elements such as nitrogen, chlorine, phosphorus and sulfur ensures specific chromatograms for those elements, increasing the selectivity, which is especially desirable when dealing with environmental and food samples.

Multiresidue Methods

Multiresidue methods are desirable for the determination of specific components in samples of unknown origin or those which have been subjected to unknown pretreatments. Unfortunately, nitrogen-containing pesticides have been poorly investigated in comparison to the halogen- or phosphorus-containing pesticides as regards their possible combination in multiresidue methods. Nevertheless, there are several methods in which the behaviour of some fungicides is considered; some include up to 20 different fungicides. This type of research commonly relies on the use of more than one type of capillary column for the separation of broad groups of pesticides; usually the main column has a low polarity stationary phase, employing another one of mid or high polarity as a confirmatory column. The detection can be made directly or after derivatization, and using either a single or several detectors (ECD, NPD, FPD, AED, MS).

The use of the AED for multiresidue analysis partially overcomes some of the problems derived from

poor resolution between compounds, as does GC-MS. However, many laboratories cannot afford GC-AED or GC-MS because they are more expensive than other options.

Practical Considerations

According to the aim, a technique will be selected, as mentioned before and this will determine the prior steps in the method. There are always some general recommendations, such as the need to employ standards and surrogates, whose addition (spiking) gives recoveries (which should be higher than 80%). The use of solvents of adequate purity is necessary; each batch must be tested for a potential source of interference; at the same time all glassware must be adequately cleaned. Apart from these general precautions, it is necessary to be aware of the importance of other aspects that have a notable influence in the analysis of fungicide residues. Some are summarized here.

Standards

One of the first and most important steps in fungicide residue evaluation in food and environmental samples is the correct preparation of standard solutions, preferably from solid reagents of certified purity, because of their low stability in solution. For example, Imazalil solutions are sensitive to light; Fosetyl residues decompose during storage at -18°C . It is very common for derivatives to not last more than 24 h in a refrigerator; the stability should be checked for longer storage times. It has also been demonstrated

that the amount of fungicide residue in food is influenced by storage, handling and processing.

Sample Treatment

The sample may be simple or very complex; this will clearly have a great influence on the sample treatment. Isolation of the compounds using an extraction technique frequently needs a further clean-up step before determination. There are a great variety of possible approaches, from classic liquid-liquid extraction (LLE) to the use of supercritical fluids (SFE), and offline or online procedures.

Liquid-Liquid Extraction

There are many methods based on the use of a separating funnel, drying over anhydrous sodium sulfate and clean-up; Soxhlet extraction is also employed.

The commonly used solvents are ethyl acetate, acetonitrile, methanol, dichloromethane, acetone and *n*-hexane. Frequently, phase separation is hindered by emulsion formation in the separatory funnel, in which case filtration through a loose glass wool plug may be appropriate or another extraction procedure may be more suitable.

It is usual to find anomalous results for Vinclozolin, Captan, Folpet and Iprodione when LLE is used.

Solid-phase Extraction (SPE)

The laborious liquid-liquid partitioning clean-up procedures described in the literature have been re-

placed by fast SPE clean-up, with the additional advantage of a high enrichment factor.

The most recommended phase is octadecylsilane, although for some groups, the diol or cationic exchange phases may be better; graphitized carbon black is also a possibility nowadays. Florisil is frequently used to remove co-extractive interferences. When this is not sufficient, further clean-up can be achieved by gel permeation chromatography.

Solvent selection for recovery of fungicides from cartridges is very important. The results vary for individual compounds. **Figure 1** provides an example of the recovery of different fungicides and acaricides from the analysis of must samples.

In all cases it is necessary to optimize the type of sorbent, sorbent mass, flow rate, sample volume, pH, ionic strength, drying time and soaking time. Sometimes the complete elution of the compounds from the disposable extraction column requires several portions of eluting mixture instead of only one. It is well known that, for conazole fungicides and Captan, low recoveries are obtained because the sample volume and flow rate of extraction seriously affect the recoveries.

In the analysis of modern fungicides, extraction with methanol, partitioning with chloroform, purification of the extract by column chromatography on sodium sulfate/Florisil/celite/charcoal is often recommended.

In the multiresidue methods acetonitrile is usually preferred, with SPE offline using C_{18} or polymeric cartridges, followed by GC-MS. This gives better

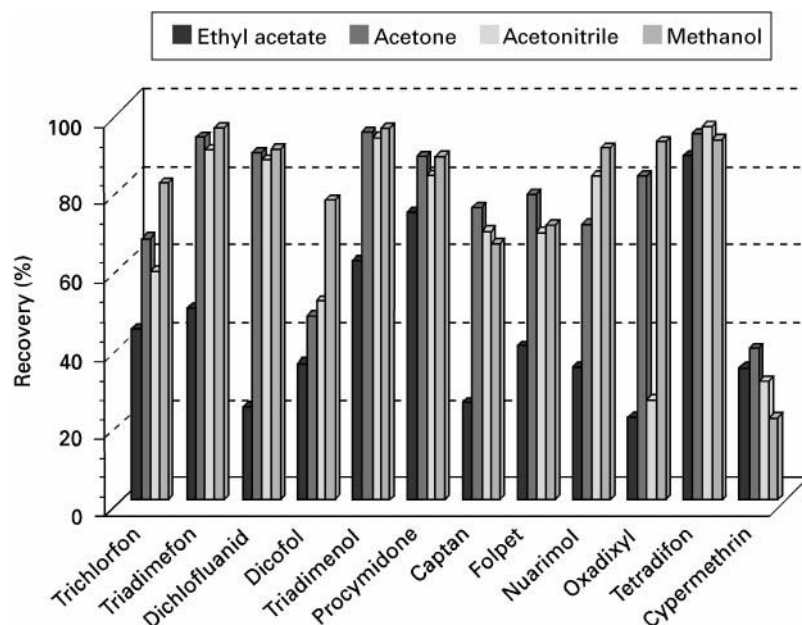


Figure 1 Recovery of pesticides from 500 mL of synthetic sample spiked with $4 \mu\text{g L}^{-1}$ by octadecylsilica cartridges eluted with 2 mL of solvent. (Reproduced from Bernal JL, del Nozal MJ, Jiménez JJ, and Rivera JM (1997) *Journal of Chromatography A* 778: 111–117, with permission from Elsevier Science.)

results than online HPLC-diode array detection (DAD) which has drawbacks for trace level determination as a result of many interferences.

In water analysis, SPE on disc (C_{18} Empore) gives good results and it has been successfully applied to the determination of fungicide residues, but in Vinclozoline determination errors are obtained, with the major losses occurring when the fungicide was collected from the surface of the disc.

Solid-phase microextraction is also useful for the analysis of fungicide residues in water samples, although in complex matrices it gives low reproducibility, which suggests that it is only useful for semiquantitative purposes. In addition, the duration of the process in relation to other extraction procedures can seriously limit its application to large numbers of samples. The extraction conditions – stationary phase, time, temperature, type and concentration of compound and matrix – must be taken into account. In Vinclozolin and Captan residue analysis on semi-solid spiked samples, lower recoveries are obtained when the amount added increases.

To prevent degradation or hydrolysis of certain fungicides (e.g. benzimidazoles), sometimes other extraction techniques such as those based on the use of pressurized hot water or supercritical CO_2 are recommended; even a cloud point preconcentration has been used, nevertheless, these procedures are not common as yet. The importance of sample preparation on the final chromatogram is seen from

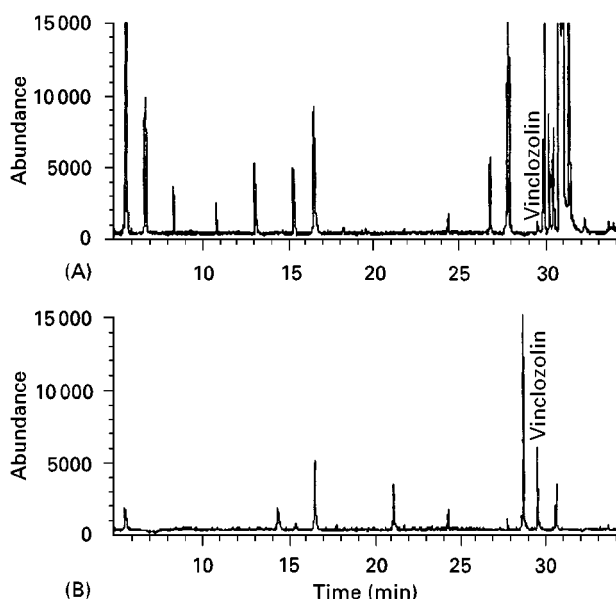


Figure 2 Chromatograms by EI-MSS (scan mode) for Vinclozolin residues in a larvae extract. (A) Hexane-acetone (70 : 30, v/v); (B) SPE. (Reproduced from Bernal JL, del Nozal MJ, Rivera JM, Jiménez JJ, and Atienza J (1996) *Journal of Chromatography A* 754: 507-513 with permission from Elsevier Science.)

Figure 2; it can be observed that SPE gives the simplest chromatograms.

Matrix Effects

GC analysis for fungicides frequently presents considerable errors due to the so-called matrix effect which has been described in the analysis of diverse compounds in wine, grape juice, honey, milk, butter, fruits and vegetables. This effect is explained by a higher transference of analytes from the injection port to the chromatographic column either as a result of the presence in the extract of associated carrier substances from the matrix or of a protective effect in the injection port performed by these substances.

The matrix effect is usually greater for lower quantities of analyte, as can be seen in **Table 2**, where some data for common fungicides are shown. The recovery can also be influenced by the total amount of sample (**Table 3**). From both tables it can be deduced that serious errors can arise when the effect is not considered.

Once the sample preparation has been checked, attention must be paid to calibration. To reduce quantitative errors from the matrix effects, a standard addition method or an external standard calibration with standards dissolved in an unspiked sample extract can be used. The use of two or more certified reference materials to establish a calibration curve can help recognize matrix effects. If the measurement shows the same slope with the regression, it can be concluded that the matrix has no dominant influence.

In general, an analyte addition method (AAM), a sample variation AAM (varying the test sample mass and keeping the added analyte amount constant) or, better, a sample and analyte variation AAM must be used for calibration.

The Analysis of Various Fungicide Groups

Phthalimides

Captan, Captafol, Folpet There are several methods devoted to the analysis of residues of these compounds. Usually an extraction with *n*-hexane-acetone mixtures is carried out; after drying with sodium sulfate and evaporating the solvent, *n*-hexane is added. This is followed by clean-up on a Florisil cartridge, eluting it with an *n*-hexane-acetone mixture, evaporating and dissolving the residue in toluene and injecting an aliquot of the solution into the GC.

To prevent hydrolysis, cloud-point preconcentration employing the nonionic surfactant Triton X-114 has been proposed.

Table 2 Recovery (%) of some fungicides from honey samples, after conventional solvent extraction, spiked at different levels (average seven determinations)

Fungicide	0.025 mg kg ⁻¹	0.125 mg kg ⁻¹	0.25 mg kg ⁻¹	1.0 mg kg ⁻¹	2.5 mg kg ⁻¹
Captan	1028	329	165	99	99
Folpet	2380	321	164	108	107
Iprodione	948	405	350	259	174
Vinclozolin	647	335	250	209	171

Captan and Captafol tend to decompose on columns that have been in use for some time. To avoid decomposition removal of the glass wool from the inlet of the GC column is recommended.

Benzimidazoles

Benomyl, Carbendazim, Thiabendazole, Thiophanate methyl This group is usually analysed by HPLC; nevertheless there are GC-MS methods using acid hydrolysis, re-extracting the amine and forming the *tert*-butyldimethylsilyl derivatives.

Carbendazim is a fungicide and the main metabolite for Benomyl, both of which are widely used on vegetables intended for direct human consumption. Methods usually provide residual levels in terms of Carbendazim because Benomyl degrades rapidly. To analyse Carbendazim by GC, the compound is usually extracted with ethyl acetate and derivatized with pentafluorobenzylbromide. After clean-up on a silica column, the product is determined by GC-ECD or GC-NPD.

Dicarboximides

Chlozolate, Iprodione, Procymidone, Vinclozolin

These compounds are frequently included in multi-residue methods and in many applications a significant influence of the spiking levels on recovery is observed. The most used techniques are GC-FID, GC-ECD and ion trap GC-MS in multiple ion-monitoring

Table 3 Recovery of Vinclozolin from honey and larvae samples, spiked with 25 mg kg⁻¹, by solvent extraction with hexane-acetone at different proportions and octadecylsilica clean-up (*n* = 5) (Reproduced from Bernal JL, del Nozal MJ, Rivera JM, Jiménez JJ, and Atienza J (1996) *Journal of Chromatography A* 754: 507–513, with permission from Elsevier Science.)

	Honey		Larvae	
Sample amount	1 g	5 g	1 g	
Extractant solvent (%)	Recovery		Recovery	
Hexane (100)	45	42	48	
Hexane-acetone (90 : 10, v/v)	64	63	67	
Hexane-acetone (80 : 20, v/v)	81	82	78	
Hexane-acetone (70 : 30, v/v)	99	98	95	
Hexane-acetone (60 : 40, v/v)	99	98	96	
Acetone (100)	99	98	95	

mode, with detection limits in the range of p.p.b.–p.p.t.

These fungicides are frequently investigated in wine analysis where it is known that the recovery not only depends on the concentration level but also on the variety of wine; attention must be paid to their metabolites, mainly those belonging to the 3,5-dichloroaniline group.

Triazole

Bitertanol, Triadimefon, Triadimenol, Tricyclazole Usually they are analysed by GC-NPD and GC-MS in the selected ion monitoring mode. Triadimefon is easily reduced to Triadimenol, so both appear together.

Bitertanol and Triadimenol have diastereoisomers that cannot easily be separated; depending on their relative proportion they frequently produce peaks with shoulders.

Dithiocarbamate fungicides

These are habitually classified into three families of compounds depending upon their structure:

1. Dimethyldithiocarbamates (Ferbam, Ziram, Thiram)
2. Ethylenebisdithiocarbamates (Mancozeb, Maneb, Zineb, Nabam)
3. Propylenedithiocarbamates (Propineb)

It is very difficult to isolate and determine specifically the fungicides which belong to the same family due to the fact they possess the same organic moiety. Thus, the typical determination of these compounds is carried out as a group, performing an acid hydrolysis to carbon disulfide which is then quantified by techniques such as headspace GC-ECD.

When an FPD is used to detect CS₂, *n*-hexane must be avoided because it may co-elute, resulting in the quenching of the S emission in the detector.

EBDCs differ chemically from dithiocarbamates because they have reactive hydrogen on the nitrogen atom, which reduces their stability and results in different biological behaviour. One of the most characteristic decomposition products is ethylenethiourea (ETU). GC determination of ETU can only be achieved after derivatization, forming

trifluoroacetylated S-benzyl or butyl ETU derivatives that can be analysed by GC-NPD, GC-ECD or GC-MS. In real samples EBDCs and ETU content decrease with storage time. To prevent this, the addition of cysteine hydrochloride has been recommended.

See also: **II/Chromatography: Gas:** Detectors: Selective; Detectors: Mass Spectrometry. **Extraction:** Solid-Phase Extraction; Supercritical Fluid Extraction. **III/Pesticides:** Gas Chromatography. **Herbicides:** Gas Chromatography; Solid-Phase Extraction.

Further Reading

- Barceló D (1993) *Environmental Analysis. Techniques, Applications and Quality Assurance*. Amsterdam: Elsevier.
- Barceló D and Hennion MC (1997) *Trace Determination of Pesticides and their Degradation Products in Water*. Amsterdam: Elsevier.
- Inspectorate for Health Protection (1996) *The Dutch Manual of Analytical Methods for Pesticide Residues in Foodstuffs*, 6th edn. Alkmaar, The Netherlands: Ministry of Public Health, Welfare and Sport.

- Kidd H and James DR (eds) (1993) *The Agrochemicals Handbook*, 3rd edn. London: Royal Society of Chemistry.
- Middleditch BS (1989) *Analytical Artifacts*. Amsterdam: Elsevier.
- Milne GWA (1995) *CRC Handbook of Pesticides*. Boca Raton, FL: CRC Press.
- Nielsen SS (1998) *Food Analysis*, 2nd edn. Gaithersburg, MA: Chapman and Hall.
- Pleger K, Manner HH and Weber A (1992) *Mass Spectral and GC Data of Drugs, Poisons, Pesticides, Pollutants and their Metabolites*. Parts I, II and III. Weinheim: VCH.
- Robinson J (1982) *Analysis of Pesticides in Water*. Vol. III. *Nitrogen-containing Pesticides*. Boca Raton: CRC Press.
- Thier HP and Kirchoff J (eds) (1992) *Manual of Pesticide Residue Analysis*, vols I and II. Weinheim: VCH.
- Tomlin CDS (ed.) (1997) *The Pesticide Manual*, 11th edn. Farnham, Surrey: British Crop Protection Council.
- US Environmental Protection Agency (1990) *Methods for Determination of Organic Compounds in Drinking Water*. Springfield, VA: National Technical Information Service.

Liquid Chromatography

M. Jesús del Nozal Nalda, University of Valladolid, Valladolid, Spain

Copyright © 2000 Academic Press

Introduction

There are some groups of fungicides of wide use (benzimidazoles, ethylenebisdithiocarbamates) whose thermal instability, high polarity and low volatility make them difficult to determine by gas chromatography (GC) unless derivatization methods are employed. This usually makes the process longer and introduces new errors. These compounds are easily measured by high performance liquid chromatography (HPLC) as are many pesticides that were typically analysed by GC in the past. Integrated systems of solid-phase extraction sample cleanup and on line HPLC allows multiple options, not only by including fungicides of very different polarity in the same analysis but also by achieving very high concentration factors and, at the same time, analysing a large number of samples. The use of pre- or post-column derivatization reactions allows the analysis of compounds that are very difficult to determine or have a low sensitivity.

Given these advantages HPLC not only complements GC in fungicide residue analysis but is

tending to displace it for many applications. Some considerations related to the use of HPLC are summarized below, with more attention being paid to the groups of fungicides most frequently determined by this technique.

Technique Selection

Most applications are based on the use of reversed-phase HPLC, nevertheless for some fungicides ion-pair HPLC (ethylenebisdithiocarbamates) (EBDC), micellar HPLC (Thiram) or chiral HPLC (Metalaxyl) are used. Normal phase HPLC, with amino-bonded stationary phases, is sometimes recommended, mainly for the benzimidazole group.

Chiral HPLC is very important for the determination of enantiomeric purity, mainly for large-scale synthesis. Resolution of C-chiral enantiomers seems to be easier than that of axial-chiral enantiomers (atropoisomers).

Columns

The most widely used stationary phases for fungicide residue analysis are the n-octyl and n-octadecylsilica because they allow the separation of compounds with a wide range of polarity. Some fungicides, mainly EBDCs, are easily ionized and because of this some

methods propose the use of ion-exchange phases. It may, however, be better to use C_{18} in the ion-pairing mode, adding a counter ion to the mobile phase. When it is necessary to separate enantiomers, then chiral columns are preferred although there is also the possibility of using the C_{18} with a chiral mobile phase.

Usually columns with a diameter of 4.6 mm, packed with 5 μ m material are employed, but nowadays it is possible to use shorter columns or even narrow bore, microbore or packed capillary columns. These later make the coupling to an MS detector easier. In both cases the lower mobile phase flow rate provides a big reduction in reagent consumption.

Several manufacturer's offer equivalent columns. Attention must always be paid to batch-to-batch reproducibility. The use of a pre-column helps to preserve the life of the column, and, if it is possible to work at room temperature, the column will last longer than when used with higher temperatures.

Mobile Phase

The selection of the stationary phase and the mode of detection is determined by the characteristics of the analytes to be separated; both, also, control the selection of the mobile phase. As C_{18} is usually employed, the mobile phase is frequently composed of a mixture of water with an organic solvent, mainly methanol or acetonitrile. To improve the peak shape or to separate compounds with acidic or basic character the addition of acid or buffer to vary the pH can be very useful. Also the temperature at which the separation is made, must be established when looking for the best resolution. The reagents used to prepare the mobile phase must be compatible with the detection mode. It is very important when a UV detector is used, because not all commercial methanol or acetonitrile are transparent enough in the low UV region. Attention must be paid to the transmission spectrum of the solvents and to the changes in batch or manufacturer. When there is a great difference between the polarity of the (aqueous) mobile phase, and the organic solvent used to inject the sample, it is possible that the first peaks will be distorted and in this case it is better to reconstitute or dilute the sample in the mobile phase.

Detection

Most of the fungicides that are analysed by HPLC can be detected in the UV region. In multiresidue methods it is more convenient to employ a diode array detector (DAD) which allows multiple wavelengths to be employed and peak purity to be checked.

The fluorescence detector gives higher sensitivity and selectivity, so it is preferred for residue analysis (e.g. benzimidazoles, bitertanol). It is also possible to programme the excitation and emission wavelengths to optimize the signal for all eluted compounds.

Occasionally the use of an electrochemical detector is recommended (Phthalimides, Thiram, Disulfiram, etc.); although it gives great sensitivity, it is more difficult to operate, and frequently the electrodes are contaminated; sometimes, for example for EBDC determination, it is coupled on-line after the UV detector.

Nowadays there is an increasing trend to MS detection but some difficulties are still encountered when coupling it to HPLC. It is advisable to use micro-HPLC and avoid, if possible, the presence of salts in the mobile phase. This, in addition to its high cost, means that only a few applications of its use to fungicides have been published.

Derivatization

A very useful option, in HPLC, is derivatization made pre- or post-column, which facilitates compound detection. A great number of derivatizing reagents lead the formation of products with a high absorbance or fluorescence, and in fungicide analysis they are often used in post-column reactions but care is needed to minimize band broadening, particularly for slow reactions. The present use of solid phase reactors has several advantages such as the simplicity in the instrumentation and compatibility with most mobile phases. A clear example is the monitoring of the carbamate pesticides.

As pre-column derivatization can be carried out with an automatic injector and post-column derivatization can be automated with modern devices, this facilitates improved precision.

Sample Treatment

Many applications of fungicide determination require a preliminary sample extraction using an organic solvents such as ethyl acetate followed by clean up by liquid-liquid partitioning. Obviously, the matrix has a great influence on the method. The heavy pigment content in many crops and vegetables has made the popular UV detector almost unusable; even when analysing fungicides in, for example, citrus, celery heart, mint and coriander. A large amount of fluorescent coextractives can appear, causing inference in detection. In these cases the sample treatment must be optimized, including for example a clean up with Florisil or changing the mobile phase polarity, so the coextracted interference elutes together with the solvent front. If the sample preparation step can be

carried out using solid-phase extraction, this favours direct coupling to HPLC and overall automation, facilitating routine multiresidue analysis.

Analysis of some specific fungicide groups

Phthalimides (Captan, Captafol, Folpet)

For formulation analysis extracting the compound with diethylphthalate in methylene chloride and chromatography on silica gel using degassed CH_2Cl_2 as mobile phase is recommended while for residue analysis GC is usually preferred. Nevertheless, recently an isocratic HPLC method using electrochemical detection with single and dual glassy-carbon electrodes has been evaluated, showing good recoveries and precision and with detection limits of about $4 \mu\text{g L}^{-1}$.

Benzimidazoles (Benomyl, Carbendazime, Thiabendazole, Methyl Thiophanate)

The high use of these post harvest fungicides means that many methods have been proposed for the determination of their residues.

It is possible to evaluate the total content (benomyl, carbendazime, methyl thiophanate) by transforming them into carbendazime, by refluxing at $\text{pH} = 6.8$. Multiresidue methods have been proposed, extracting the sample with HCl and analysing on LiChrosorb Si 60. Recently a clean up on strong cation exchange cartridges and analysis on C_{18} with UV and water-acetonitrile as mobile phase has been proposed, although ion-pairing HPLC coupled to UV or fluorescence detection can be used. Normal phase HPLC for carbendazime can be employed after extraction with methanol, partitioning in n-hexane-dichloromethane and fluorescence detection at 285/315 nm. Nevertheless, the majority of the proposed methods are devoted to the study of the pair benomyl-carbendazime, using reversed-phase HPLC.

This pair of compounds is normally analysed by monitoring carbendazime, although using light petroleum ether and a special drying step it is possible to analyse benomyl without conversion to carbendazime. The analysis involves an extraction with an organic solvent (methanol, ethyl acetate or acetone) followed by partitioning with n-hexane or an alkaline solution, using C_{18} columns and UV detection at 224 nm or better by fluorescence at 285/317 nm. The type of matrix, even quite similar ones, strongly conditions the sample preparation. In Figure 1 some schemes for the determination of carbendazime in apian samples are shown. In the case of pollen an additional partition with n-hexane is required be-

cause of the intense colour of the extracts. As is shown, pollen or beeswax are better extracted with methanol because ethyl acetate extraction gives an emulsion that makes the separation difficult. Another problem that must be taken into account is the influence of the fortification level on the carbendazime-benomyl recoveries. Thus when analysing vegetable samples, higher fungicide concentrations added to the samples results in lower recoveries, even for smaller samples. With samples bigger than 2 g, problems also appear because the pigments are extracted, giving a greenish-yellow colour and therefore the determination of carbendazime is hindered. Some relevant data are shown in Table 1.

Thiabendazole has also received special attention. Several HPLC methods have been proposed for its determination, usually employing ethyl acetate as extractant and C_{18} columns and acetonitrile-water or methanol/aqueous buffer mixtures as mobile phases. A mixture of n-hexane/ethanol/0.2 N HCl, with cation exchange columns or ion pairing HPLC has also been used. Detection can be made by UV (298 nm) although usually fluorescent detection is preferred. Changes in the extractant or of the chromatographic parameters require selection of the wavelength to achieve the best sensitivity. The use of several wave-lengths, mainly the couples 285/350 nm and 305/345 nm have been proposed. In some cases, the metabolite 5-hydroxythiabendazole has also been determined.

Dicarboximides (Iprodione, Vinclozolin)

There are not many HPLC methods to determine residues of these fungicides. Vinclozolin is perhaps the most frequently used compound and so, some methods have been proposed for its analysis, and of its metabolite (3,5-dichloroaniline) using reversed-phase HPLC with UV detection. In complex mixtures analysis it has also been proved that SPE cartridges are more selective than extraction with organic solvents and they provide simpler chromatograms.

Triazoles (Bitertanol, Triadimefon, Triadimenol, Tricyclazole)

Residues of Triadimefon and its metabolite Triadimenol are seldom determined by HPLC, but they can be analysed by reversed-phase HPLC on C_{18} columns with UV detection. The same stationary phase is recommended for Bitertanol, with acetonitrile-water as mobile phase and fluorescent detection at 254/322 nm. The selection of the extracting solvent (acetone/water, acetone, methanol) is very important in order to achieve high recoveries. If a cleanup is required, SPE on C_{18} cartridges eluted with cyclohexane-ethyl acetate seems to be the most adequate.

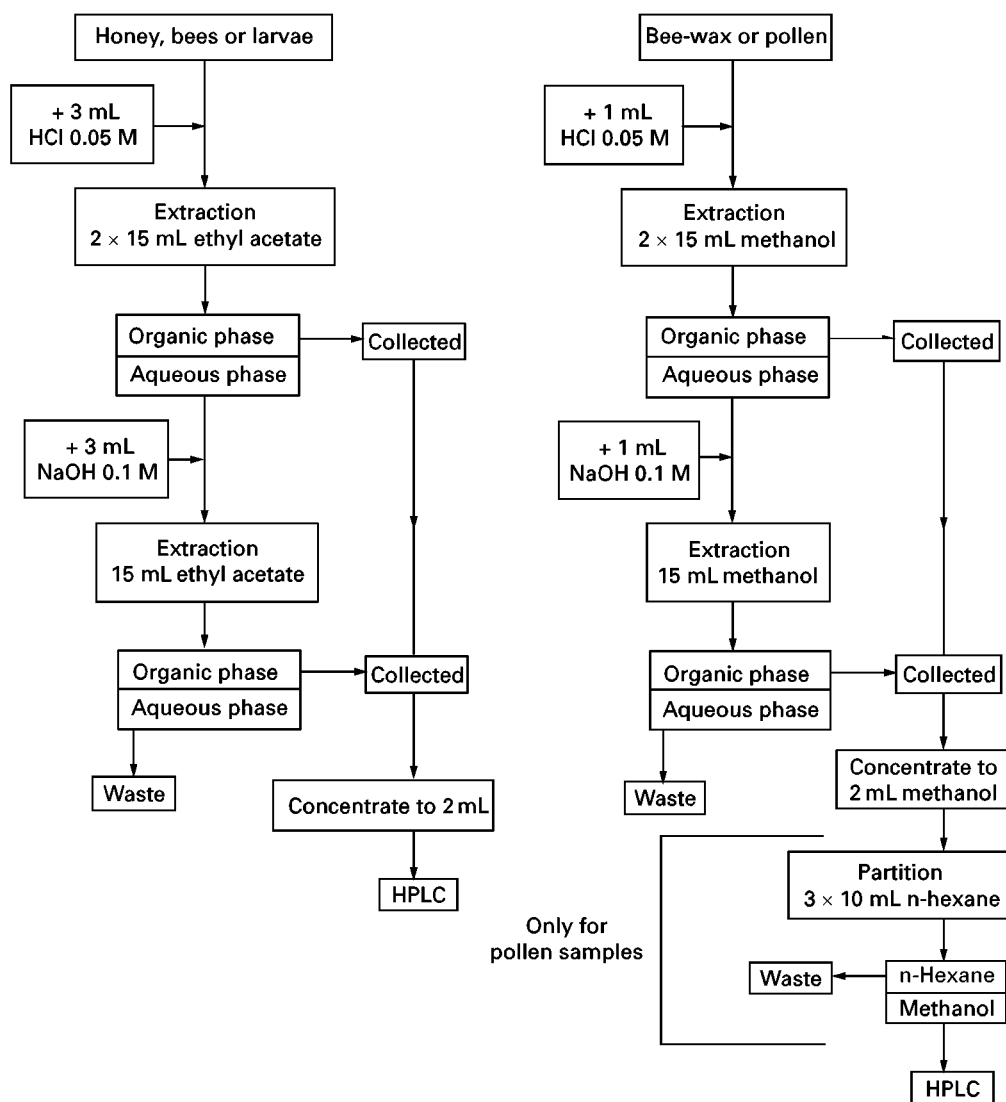


Figure 1 Flow charts showing the sample preparation procedures used in the analysis of carbendazime in apiarian products. (Reproduced from Bernal JL, del Nozal MJ, Toribio L, Jiménez JJ and Atienza J (1997) *Journal of Chromatography A* 787: 129–136, with permission from Elsevier Science.)

Dithiocarbamate fungicides

The US Food and Drug Administration (FDA) has recommended the evaluation of new uniresidue methods for the analysis of dithiocarbamates in vegetables, because of problems which have arisen from the application of the carbon disulfide method. This lacks specificity because naturally occurring carbon disulfide and degradation products of the EBDCs, such as dialkylthiocarbamate and thiuram disulfide, can give serious interference.

EBDCs have little or no solubility in water and, because of this, in many methods the compounds are converted into their soluble sodium salt by means of EDTA and subsequently hydrolysed to form carbon disulfide, but if the hydrolysis is not carried out the

final product is the fungicide Nabam. This is water soluble so some methods are based on this transformation. On the other hand, ethylene thiourea (ETU), ethylene urea and 2-imidazoline are decomposition products of the EBDCs. The parent compounds have a relatively low toxicity but ETU has been demonstrated to be goiterogenic, carcinogenic and teratogenic, so there is a great interest in determining this compound.

To analyse ETU by HPLC an extraction with methanol, a clean up on a mixture of sorbents and a mobile phase of ethanol–isooctane has been frequently used. The detection can be electrochemical or by HPLC/MS, with similar detection limits. Extraction of ETU from vegetables is preferred with methanol and analysis on a CN column, with a mobile phase of

Table 1 Recovery of carbendazime obtained by using an SFE-hplc procedure on spiked lettuce samples ($n = 5$). (Reproduced from Jiménez JJ, Atienza J, Bernal JL and Toribio L (1994) *Chromatographia* 38: 395–405, with permission from Vieweg-Publishing.)

Sample amount (g)	Fortification level (mg kg ⁻¹)	Recovery (%)	σ_{n-1}
0.20	1.0	98.4	3.0
0.20	6.0	98.3	2.9
0.20	12.0	96.4	3.3
0.50	0.3	98.3	3.2
0.50	6.0	98.0	3.4
0.50	12.0	83.3	3.5
1.00	0.3	98.2	3.3
1.00	0.6	98.0	3.3
1.00	12.0	72.4	3.9
2.00	0.3	88.3	3.7
2.00	0.6	68.4	5.5
2.00	12.0	53.7	7.0

methanol in chloroform/cyclohexane and detection at 240 nm. Another possibility is to extract ETU and react it with dihaloquinones to produce a yellow derivative that can easily be detected at 385 nm.

There is always a problem with fungicide determination because they are very similar in chemical structure and behaviour. Ferbam and Ziram have the same organic moiety and the difference is in the metallic ion. Nabam, Maneb, Zineb, Mancozeb and Propineb, frequently used in agriculture, have in com-

mon the ethylenebisdithiocarbamate group and therefore it is very difficult to separate them from their mixtures. So in some situations it is easier to determine the residue of only one fungicide. Another approach is to try to separate mixtures of three fungicides belonging to different chemical groups and the third and most difficult one is to try to separate all of them.

Some methods attempt to distinguish between compounds using both HPLC and atomic absorption methods. This can cause problems because in EBDC manufacture there is always an excess of the metallic ion that has not been incorporated into the compound, so if the extraction of the compound is not specific, the extract will contain not only the metal belonging to the fungicide but also the remaining metal coextracted. As a consequence, atomic absorption data are usually very much higher compared with those from HPLC.

To analyse individual fungicides, transition metal salts are frequently employed as ion-pairing reagents for reversed-phase HPLC with detection in the UV region. According to the complex used the wavelength selected is obviously different, so for Ziram, Maneb and Zineb forming as 1:1 Cu(II)-dithioligand the wavelengths are in the 260–287 nm range, with detection limits at the nM level.

Sometimes the problem arises of the presence of Thiram and Disulfiram which could interfere with the dithiocarbamate determination. This situation is usu-

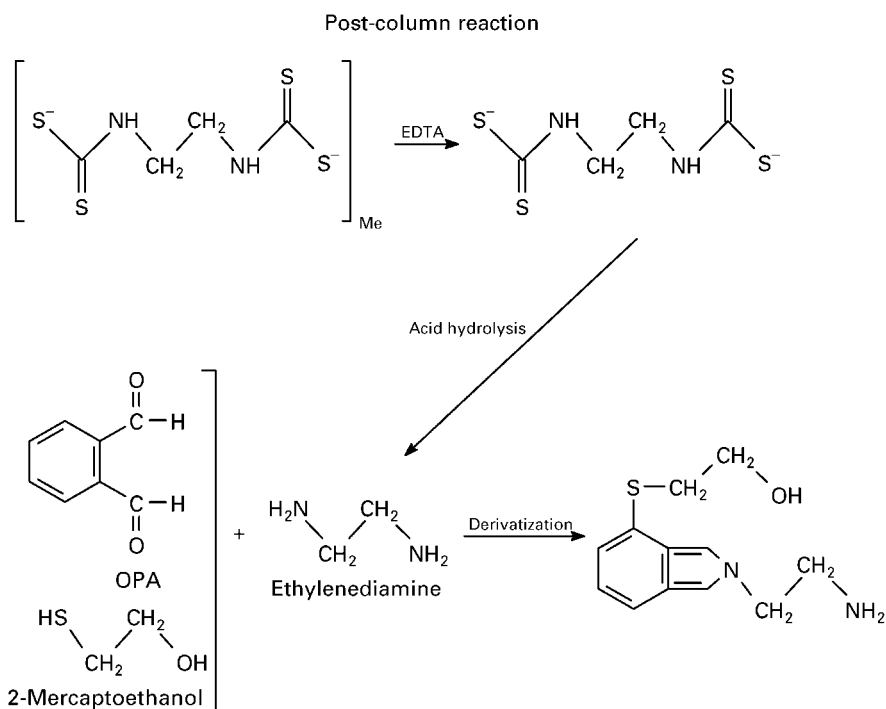


Figure 2 Post-column derivatization reaction for EBDCs.

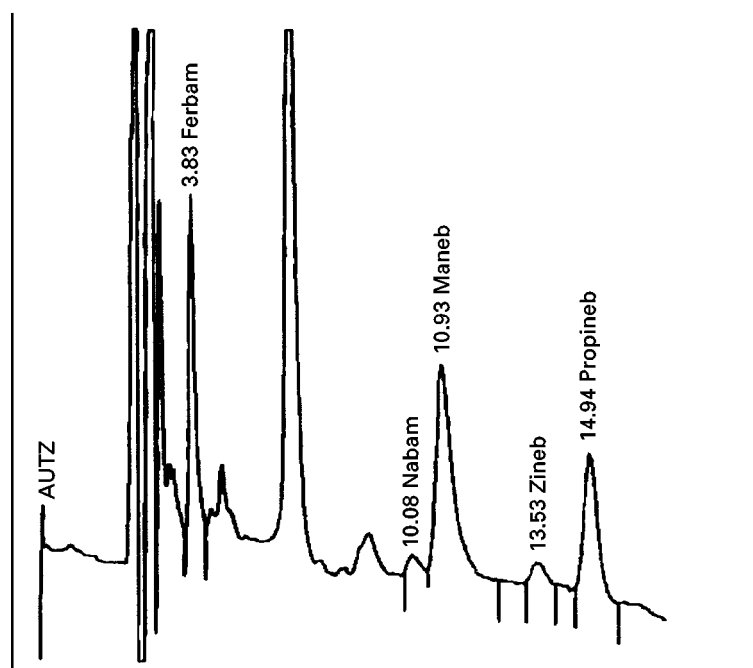


Figure 3 Chromatogram of a mixture of EBDCs. $1 \mu\text{g L}^{-1}$ each. Detection of 254 nm. Mobile phase: EDTA/MeOH/AcCN (60 : 13 : 27, v/v).

ally solved by using HPLC on a C_{18} column with electrochemical detection or by determining Thiram using micelles of CTAB in the mobile phase, so Nabam, Ziram and Ferbam do not interfere.

Nabam determination is of interest because EBDC fungicides can be converted into this fungicide and so they can be indirectly determined. In this case there is a method, very similar to one devoted to carbamate residues determination, based on a post-column reaction through an acid hydrolysis to form ethylenediamine that is afterwards fluorogenically labelled with *o*-phthalaldehyde-mercaptoethanol and detected at 356/450 nm. The scheme of the post-column reaction is shown in **Figure 2**.

Attention must be paid to carrying out the separation at the lowest possible temperature. The hydrolysis temperature must be considered because when the temperature is near 100°C the possibility of more by-products and background noise increases, and OPA degrades easily at higher temperatures. Separation of Nabam is carried out by micellar HPLC with a mobile phase of cetylpyridinium (CPC) phosphate buffer/acetonitrile.

The real problem is the difficulty to convert quantitatively EBDCs into Nabam and recoveries lower than 30% are usually obtained although if EDTA is used, the conversion is favoured. Thus a simpler method has been proposed based on the transformation into Nabam by means of an aqueous EDTA solution, followed by reverse-phase chromatography on an NH_2 column with acetonitrile-methanol and

detection at 272 nm. However, the lifetime of the column is only about 15 analyses.

A good separation between compounds of the three families (EBDC, PBDC and DMDC) can be obtained using reverse-phase HPLC on a C_{18} column, with a mobile phase of EDTA 0.05 M, pH = 7.7, and detection in series (UV at 280 nm and amperometric at 400 mV), but it is not possible to distinguish between compounds of the same group.

A method that allows the separation of five compounds (see **Figure 3**) uses ion-pair HPLC with tetrabutylammonium bromide as counterion on C_{18} columns, with a mobile phase of EDTA/methanol/acetonitrile and detection at 254 nm. However, there are still some problems because the separation is strongly dependent on the analyte concentration, achieving only the overall separation for very low concentrations.

As a conclusion, it can be said that the analysis of these fungicides is very difficult when there are several of them in the sample and that further work is necessary.

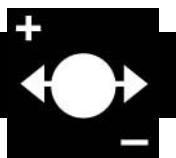
See also: II/Chromatography: Liquid: Derivatization. III/Fungicides: gas chromatography.

Further Reading

- Aizawa H (1982) *Metabolic Map of Pesticides*. Orlando: Academic Press.
- Frei RW and Lawrence JF (1982) *Chemical Derivatization in Analytical Chemistry*, Volumes 1 and 2. New York: Plenum Press.

- Helrich K (1995) *Official Methods of Analysis*, 16th edn, Vol. I. Arlington, VA: Association of Official Analytical Chemists.
- Krull IS (1986) *Reaction Detection in Liquid Chromatography*. New York: Marcel Dekker.
- Lawrence JF (1982) *High Performance Liquid Chromatography of Pesticides*. New York: Academic Press.
- Lingeman H and Underberg WJM (1990) *Detection-Oriented Derivatization Techniques in Liquid Chromatography*. New York: Marcel Dekker.
- Milne GWA (1995) *CRC Handbook of Pesticides*. Boca Raton: CRC Press.
- Moye HA (1980) *Analysis of Pesticide Residues*. New York: John Wiley & Sons.
- Pawliszyn J (1997) *Solid-phase Microextraction. Theory and Practice*. New York: Wiley-VCH.
- Thurman EM and Mills MS (1998) *Solid Phase Extraction. Principles and Practice*. New York: John Wiley & Sons.

FUSED SALTS: ELECTROPHORESIS



M. Lederer, Université de Lausanne, Lausanne, Switzerland

This article is reproduced from *Encyclopedia of Analytical Science*, Copyright © 1995 Academic Press

The interest in this technique is mainly centred around the solution chemistry of molten salts, which had its renaissance in the nuclear field and in the study of nonhydrated ions for the purpose of separating isotopes.

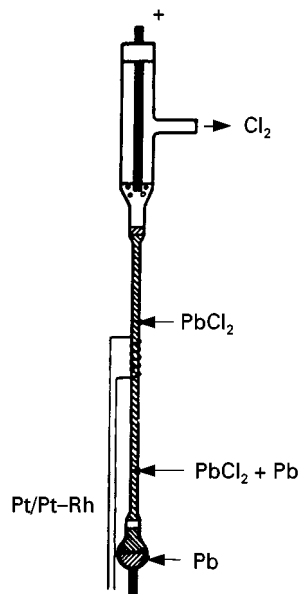


Figure 1 Cell for the determination of mobilities by observation of migrating boundaries. Reproduced with permission from Herzog and Kelmm (1961).

Techniques

Moving Boundary Method

Migrating boundaries can be observed using a cell like that shown in Figure 1.

Flat Bed Methods

Electromigration in a support to eliminate convection is carried out much as in normal electrophoresis,

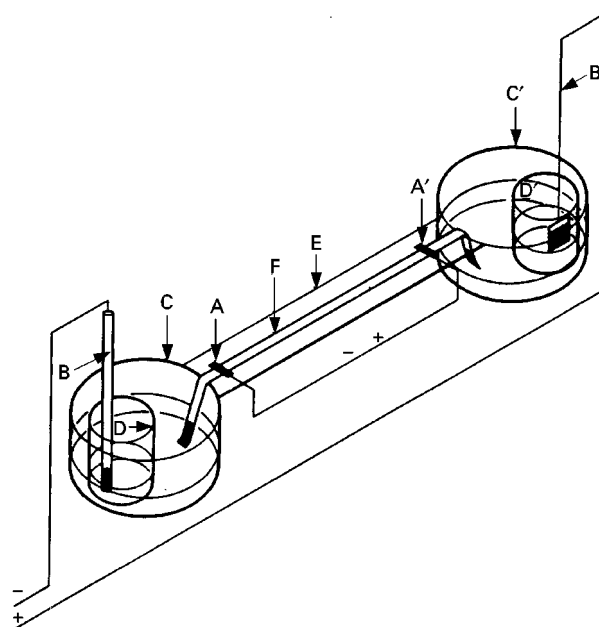


Figure 2 Apparatus for zone electrophoresis in molten salts. A and A', platinum wires for measurement of potential difference; B and B', electrodes; C and C', reservoirs; D and D', electrode compartments provided with sintered discs at the bottom; E, supporting glass plate; F, electrophoretic strip. Reproduced with permission from Alberti *et al.* (1964).

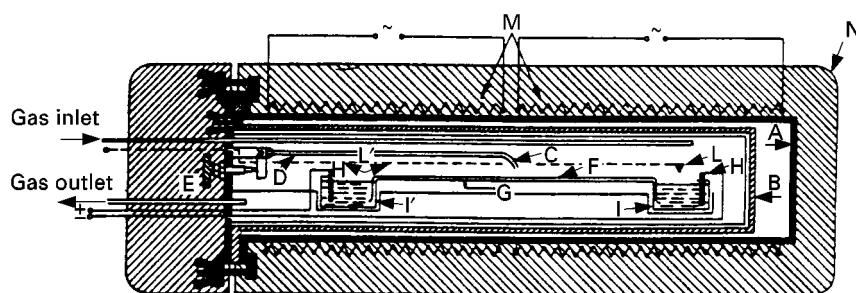


Figure 3 Cross-sectional view of an electrophoretic apparatus. A, furnace; B, electrophoresis chamber; C, capillary; D, tube supporting the capillary; E, screw to raise or lower tube D; F, glass fibre paper; G, heat-resistant glass plate; H and H', graphite electrodes; I and I', heat-resistant glass vessels; L and L6, thermocouples; M, Ni-Cr heating wire; N, insulating jacket. Reproduced with permission from Albert *et al.* (1964).

except that here evaporation is negligible and high temperatures are used to keep the molten salt liquid. **Figure 2** shows a typical apparatus. It can be made of glass or fused silica. Glass fibre paper is mainly used as the support material with this apparatus, but it lends itself equally well to electrophoresis on asbestos sheets. This kind of apparatus is best housed in an oven, as shown in **Figure 3**. Here provision is also made to circulate a gas to remove gaseous electrolysis products such as chlorine.

Supports

Asbestos paper and asbestos sheets were initially employed as supports; then glass fibre papers became available (e.g. from Whatman). These papers must be washed to removed impurities and are rather

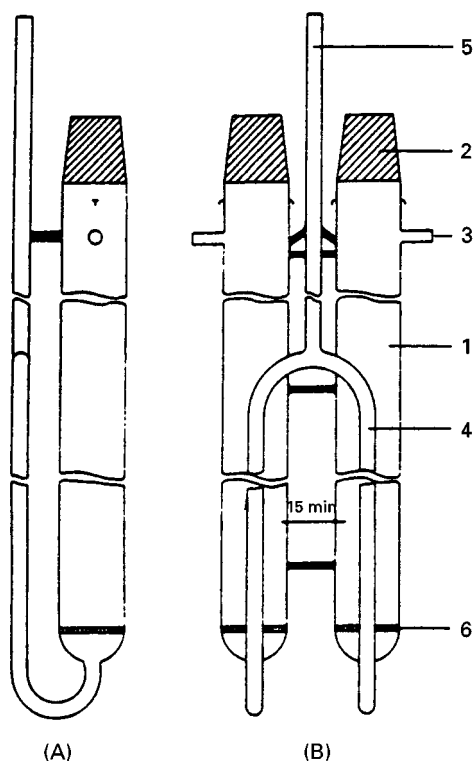


Figure 4 Apparatus for column electrophoresis. (A) Front view; (B) side view. 1, electrode space; 2, ground glass joint; 3, tube for gas evacuation; 4, separation column; 5, tube for admitting the salts to be separated; 6, sintered glass plate. Reproduced with permission from Kühnl and Khan (1966).

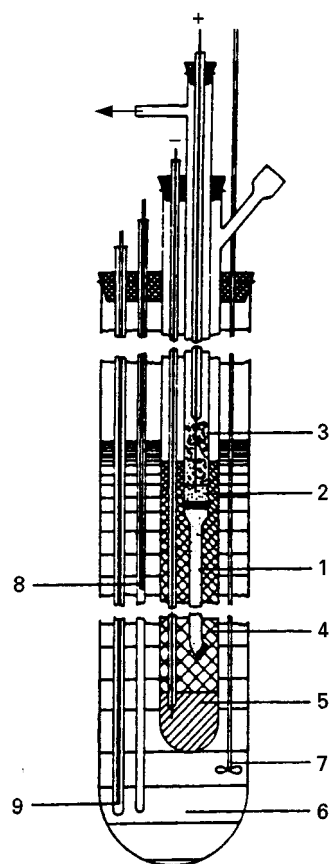


Figure 5 Apparatus for column electrophoresis. 1, separation column; 2, anode compartment; 3, foam at platinum anode; 4, cathode compartment; 5, molten zinc cathode; 6, molten salt bath; 7, stirrer; 8, thermocouple in fixed position; 9, movable thermocouple for measuring vertical temperature distribution. Reproduced with permission from Ljubimov and Lundén (1996).

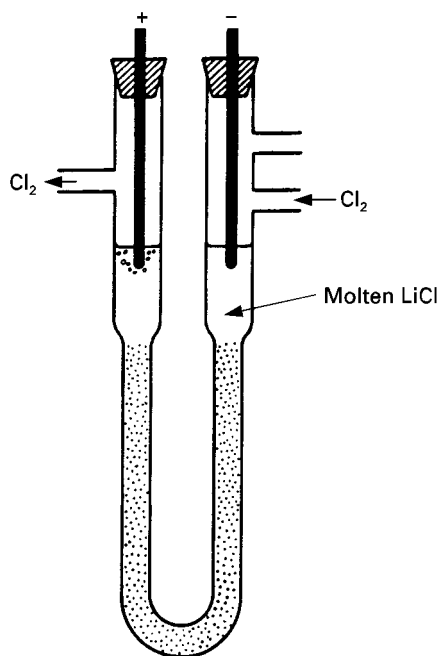


Figure 6 Apparatus used by Klemm for the separation of lithium isotopes. Chlorine is admitted at the cathode to prevent the deposit of metallic lithium. Reproduced from Klemm *et al.* (1947).

fragile, requiring careful handling. Some authors recommend converting the surface silanol groups to salt forms, e.g. by dipping into 4–6 mol L⁻¹ KNO₃ at pH 8–9, otherwise the melt does not wet the glass fibre paper.

Powdered thin layers for electrophoresis are made by spraying aqueous suspensions of ceramic oxides onto sintered ceramic strips.

Column electrophoresis is carried out in columns of glass powder, Al₂O₃ splinters, or quartz powder.

Electrodes

Platinum is generally used for the anode, and other materials such as tungsten, nickel, copper or graphite

Table 1 Effect of mass in electromigration of metals

Isotopes of	Fused medium	Effect of mass
Li	LiCl	0.14
Li	LiBr	0.26
Li	LiNO ₃	0.05
Zn	ZnCl ₂	0.078
Zn	ZnBr ₂	0.11
K	KNO ₃	0.037
Cu	CuCl	0.080
Ag	AgCl	0.064
Cd	CdCl ₂	0.067
Tl	TlCl	0.040
Pb	PbCl ₂	0.024

From Chemla (1959).

Table 2 Effect of mass in electromigration of halogens

Isotopes	Fused medium	Effect of mass
Cl	ZnCl ₂	0.043
Cl	TlCl	0.086
Cl	PbCl ₂	0.052
Br	PbBr ₂	0.042

From Chemla (1959).

as the cathode. Platinum may be attacked by the alkali metals formed on the cathode during electrophoresis.

Column Electrophoresis

Figures 4 and 5 show two arrangements that can be used for column electrophoresis.

Fused Salts Used as Electrolytes

Numerous electrophoretic mobilities of cations and anions have been published. Most work has been done at relatively low temperatures, i.e. between 150 and 300°C. A lithium nitrate–potassium nitrate eutectic (43 : 57) can be used at 160°C, a sodium nitrate–potassium nitrate eutectic (50 : 50) or lithium chlorate–potassium chlorate eutectic (76 : 24) at 250°C and 300°C, respectively, and potassium nitrate or sodium nitrate at 350°C.

Isotope Separations

The separation of isotopes performed in aqueous solutions is generally poorer than expected from mass

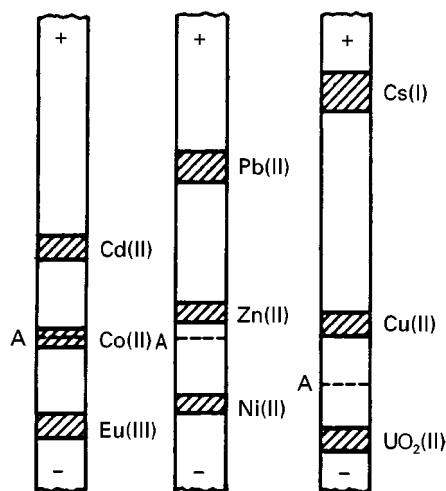


Figure 7 Some representative separations of inorganic ions by zone electrophoresis in molten LiNO₃–KNO₃ eutectic–10% NH₄NO₃ at 160°C. A, application point. Reproduced from Alberti *et al.* (1962).

Table 3 Movement of metal ions in fused salts

	Distance moved in 4 h (cm)	KCl–LiCl eutectic ($T = 450^{\circ}\text{C}$; 2 V cm^{-1})	KNO_3 – LiNO_3 eutectic ($T = 160^{\circ}\text{C}$; 5 V cm^{-1})
Anionic	0.5–3	Zn(II), Co(II)	
Isoelectric	0.5–3	Th(IV) ^a	Th(IV) ^a
	3–5.5	Ce(III)	Cd(II)
	5.5–8	Pb(II), Cd(II)	Pb(II)
Cationic	8–10.5	Cu(II)	Sr(II), Ba(II), Cs(I), Rb(I)
	10.5–13	Cs(I), Rb(I)	
		Na(I), Ag(I)	

^aInsoluble precipitate formed. From Alberti *et al.* (1962).

differences, since smaller ions are more hydrated than larger ones and thus mass differences are diminished with fully hydrated ions. This is not the case in molten salts and hence the ionic mobility differences of isotopes are nearer to those expected.

Countercurrent electrophoresis has been used for isotope separation of molten salts. In the system shown in Figure 6 molten lithium chloride is subjected to electrophoresis and the lithium metal formed on the cathode is reoxidized with a stream of chlorine. At 650°C and a current of 0.5 A, using granular quartz medium to decrease convection, rather high enrichments were reported (from 7.3 to

16.1% ^6Li in 4 days). This work served as the basis for a commercial separation of lithium isotopes.

Mass effects depend on the temperature as well as on the anion(s) in the melts. Typical data are shown in Tables 1 and 2.

Analytical Separations of Inorganic Ions

Table 3 gives some data on the movement of metal ions in fused salts and some representative separations by electrophoresis on glass fibre paper are shown in Figure 7.

A number of binary metal mixtures have been separated, as shown in Figure 8.

The main interest in molten salt separations seems, however, to reside in isotope separations and in the study of ionic mobilities in molten salts. It is worthy of note (see Table 3) that Ag^+ travels as a cation in a KCl–LiCl eutectic, while it readily forms an anionic complex AgCl_2^- in aqueous concentrated HCl solution.

See also: II/Electrophoresis: Theory of Electrophoresis.
III/Isotope Separations: Gas Centrifugation.

Further Reading

- Alberti G and Allulli S (1968) Chromatography and electrophoresis of inorganic ions in fused salts. *Chromatographic Reviews* 10: 99.
- Alberti G, Grassini G and Trucco R (1962) Separation of inorganic ions in fused salts by electrophoresis on glass fiber paper. *Journal of Electroanalytical Chemistry* 3: 283.
- Alberti G, Allulli A and Modugno G (1964) Separation of inorganic ions in fused salts by means of chromatography and electrophoresis on glass fiber paper. III. Effect of water, oxygen and support on the migration of inorganic ions dissolved in the LiCl–KCl eutectic at 450° . *Journal of Chromatography* 15: 420.

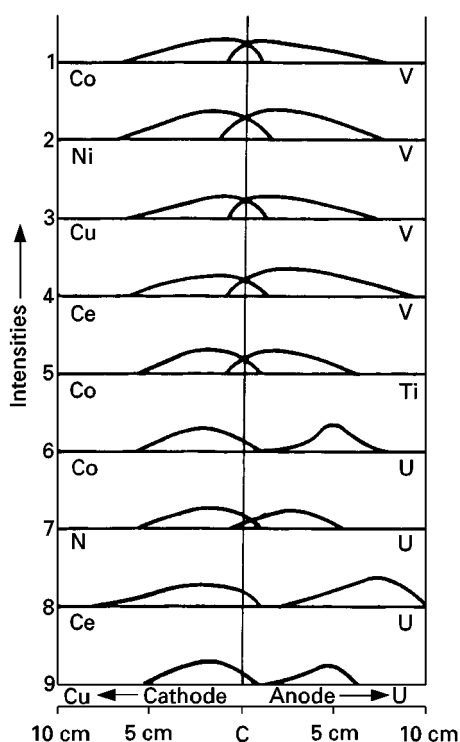
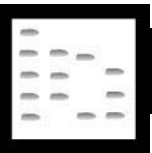


Figure 8 Separations of inorganic ions by column electrophoresis in molten KHSO_4 – $\text{K}_2\text{S}_2\text{O}_7$ eutectic. Reproduced with permission from Kühnl and Khan (1966).

- Chemla M (1959) Séparation d'isotopes par chromatographie et par électrophorèse. *Chromatography Reviews* 1: 246.
- Forcheri S and Berlin A (1967) The determination of transport quantities in molten salts with thin layer electrophoresis and diffusion on fitted ceramic oxides. *Journal of Chromatography* 15: 420.
- Herzog W and Klemm A (1961) Elektronenleitung in geschmolzenem PbCl_2 -Pb. *Zeitschrift für Naturforschung* 16a: 523.
- Klemm A, Hintenberger H and Hoernes P (1947) Anreicherung der schweren Isotope von Li und K durch elektrolytische Wanderung in geschmolzenen Chloriden. *Zeitschrift für Naturforschung* 2a: 245.
- Kühl H and Khan MA (1966) *Journal of Chromatography* 23: 149.
- Ljubimov V and Lundén A (1966) Electromigration in molten and solid binary sulfate mixtures: Relative cation mobilities and transport numbers. *Zeitschrift für Naturforschung* 21a: 1592.

GAS ANALYSIS: GAS CHROMATOGRAPHY



C. J. Cowper, GQ Tech, Walton on Thames, Surrey, UK
Copyright © 2000 Academic Press

Introduction

If gases are defined so as to be distinguished from vapours, which is to say only those gases whose critical temperatures are below ambient, and hence cannot be liquefied by pressure at ambient temperature, then the task of gas analysis appears to be a simple one. Applying the criterion of a critical temperature below, say 15°C , produces a very small list of elements and compounds, ranging from helium to ethene. It is, of course, more appropriate to define gases as those which are handled in the gas phase at ambient conditions. Widening the criterion to allow components with boiling points below 15°C produces a rather larger list, ranging from xenon to cyclobutane.

Any gas mixture will be based on one or more of these components, but can in addition contain higher boiling compounds whose low concentration allows them to be present without condensing out from the mixture. As an example, natural gas is treated before it is distributed so that it remains stable in the gas phase over a wide range of temperatures and pressures. It consists predominantly of methane, but contains a large number of other hydrocarbons, up to and including decane, at concentrations which are amenable to direct analysis by gas chromatography.

Analysis for decane and similar components in liquid hydrocarbon mixtures is well established, and similar analytical procedures can be applied to its measurement in natural gas. The main difference is in sample handling and introduction. This will generally be true for other low concentration components of gas mixtures which would normally be liquids or solids. Where techniques exist for analysis of such

materials as liquid or solid samples, they can be modified to handle those components in a gas mixture.

This article is not intended to give details of how to analyse all the chlorofluorocarbons or the hydrides of germanium, but aims to show the characteristic differences in equipment and procedures used for gas analysis.

Equipment and Procedures

A chromatograph which is configured for gas analysis will differ in a number of respects from one designed for liquids' analysis. Sample injection will almost invariably be by valve, and other valves may be used to alter the relative positions of different columns during the analysis. Some columns are specifically used for gas analysis, and others may be used in a different way from that for other applications. Carrier gas must be chosen with some care, as it may be a component of the sample, or have properties which do not favour the measurement of sample components. The thermal conductivity detector (TCD) is likely to play a major role; the flame ionization detector (FID) may be regarded as a selective detector in this context.

Sample Handling and Injection

A packed column will handle sample sizes typically in the region of 0.1 to 10 mg. For samples which are liquid, or solids dissolved in a solvent, this means volumes of 0.1 to 10 μL , which are conveniently measured and injected using microsyringes. For gas samples, this mass range approximates to volumes of 0.1 to 10 mL at ambient conditions.

Gas-tight syringes will easily cope with such sample sizes, but the main drawback with using them is poor repeatability, due to injection of a

compressible sample into an already compressed carrier gas. Most chromatographs equipped for gas analysis will be fitted with a gas sampling valve, sometimes referred to as a bypass injector. **Figure 1** shows a typical design of a six port valve. It consists of a base through which six holes or ports are drilled, equally spaced around the circumference of a circle, and a rotor, which rotates around the axis of the same circle. The rotor has three grooves machined into it, which connect adjacent pairs of ports. Rotation of the rotor through 60° alters the internal plumbing by connecting different pairs of ports. The ports are connected into the chromatograph by small bore tubing.

In **Figure 1**, the carrier gas inlet is connected to port 1, and port 2 goes to the column. Sample gas enters and exits through ports 5 and 4 respectively. A sample loop is connected between ports 3 and 6. The sample loop, usually a length of 2 mm i.d. tubing, defines the size of sample injected. **Figure 1A** shows the sample loading position, with the carrier gas going directly to the column, and **Figure 1B** shows the inject position. Here, the carrier gas sweeps the entire contents of the sample loop on to the column. Provided that the temperature and pressure of the

sample gas in the loop are constant just before injection, the technique is capable of excellent sample size precision, and hence very good quantitative behaviour.

Gas sampling valves can use other configurations – the motion can be linear rather than rotary, but the principle of isolating the sample in a defined volume and then purging it on to the column with carrier gas remains unchanged. Valves with more ports can also be used, to combine gas sampling with other switching operations which may be required.

Capillary columns need much smaller sample sizes for efficient operation, and hence the proliferation of techniques for liquid samples, ranging from sample splitting to solvent effects and retention gaps. It is possible to minimize the dead volume in a gas sampling valve to allow direct injection, but this becomes more difficult as the column i.d. is reduced. If a gas sample is stable when introduced into the chromatograph, it is most likely that splitting the carrier gas flow downstream of the valve will give a representative sample on to the column. In most instances this would be the preferred option.

Columns

Gas chromatographic separations are mainly influenced by the volatility of the components of the mixture. By using selective stationary phases, groups of components of higher polarity can be retained in the column for longer than components of lower polarity. Within similar groups, however, the order of elution will be dictated by boiling point. It is also the case that an isothermal analysis would use a column temperature of somewhere around the middle of the boiling range of the sample, and a temperature programme would very approximately mimic the distillation characteristics.

Permanent gases in particular do not have boiling points which would suggest a convenient choice of column temperature, and polarity differences do not appear to be strong enough to be helpful. Although columns have been operated at liquid nitrogen temperature for the separation of hydrogen isotopes, in general subambient operation is unattractive. Gas analysis, therefore, requires different separation mechanisms to allow use of more or less standard equipment at normal temperatures. The principle difference is the use of adsorption onto stationary phases with active surfaces as the means of separation, rather than partition into a dispersed liquid phase. Such adsorption phases separate, at least in part, by molecular size or shape. As a consequence, some have relatively limited applicability, and are used as part of a range of columns required for a complete analysis.

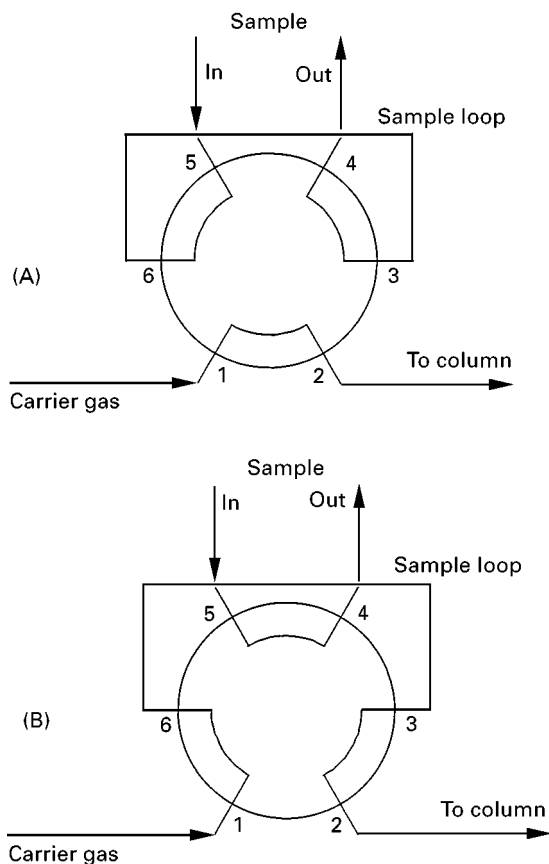


Figure 1 Gas sampling valve. (A) Sample loading. (B) Sample injection.

Molecular sieve The term is general, but in the context of gas analysis it refers to aluminosilicates of the alkali and alkaline earth metals. The most commonly used are type 5A, based on calcium, and 13X, based on sodium. They have average pore diameters of 0.5 and 1 nm respectively. Molecular sieves are the only materials available which can separate oxygen and nitrogen at normal chromatographic temperatures (35–100°C). On the other hand, they retain carbon dioxide under the same conditions for so long that it is sometimes regarded as being permanently absorbed. They also strongly adsorb water, and are widely used as drying agents.

Molecular sieves must be activated before use, to drive off water and other strongly adsorbed materials and to make the pores available to sample components. This can be done *in situ*, by heating the column to around 300°C for several hours with dry carrier gas flowing. During use, a column will slowly lose separating power due to adsorption of moisture from samples or carrier gas, and will eventually need to be conditioned again. With reasonable precautions, a column should continue to give good separations for a year or longer.

5A and 13X sieves have broadly similar behaviour, with some detail differences which may cause one to be preferred over the other for particular applications. When each is packed into a typical 2 m column, 5A sieve will give longer retention times, most evidently for carbon monoxide. **Figure 2** shows a chromatogram, from a 5A molecular sieve column, of helium, hydrogen, oxygen, nitrogen, methane and carbon monoxide, using argon carrier gas at 50°C. Under these conditions, rare gases can also be analysed, with neon eluting just after hydrogen, argon co-eluting with oxygen, krypton just before nitrogen, and xenon after carbon monoxide. Component relative retention times are influenced by the temperature and time of activation, and so in the unlikely event of rare gases being significantly present in a mixture such as that in **Figure 2**, it should be possible to find an activation procedure which will allow all to be separated.

Argon is the most abundant rare gas (0.93% v/v in air), and so its co-elution with oxygen can create a problem. It can be resolved before oxygen by using, for example, a 2 m column at –50°C, or a 5 m column at 0°C. The obvious drawback is the excessive retention times for other components. An alternative way of measuring oxygen without interference from argon is to use argon as carrier gas, as in **Figure 2**.

Capillary columns containing 5A sieve are available. The finely divided material is dispersed as a layer on the wall of the capillary. This is known as

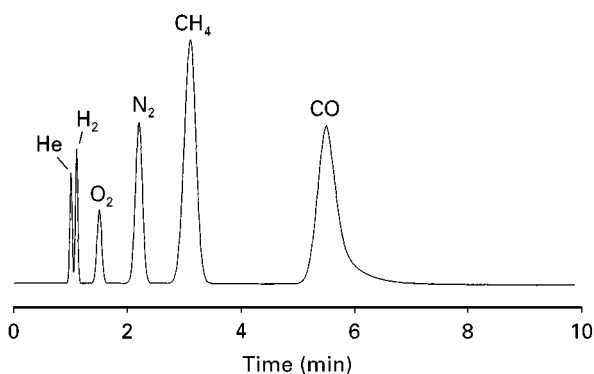


Figure 2 Molecular sieve 5A.

a porous-layer open-tubular or PLOT column. The combination of high efficiency and high carrier gas linear velocity means that argon and oxygen can be separated within an overall analysis time comparable to that of a 2 m packed column.

5A molecular sieve is also capable of exclusion chromatography, based on molecular shape. Ethane, propane and n-butane have increasingly longer retention times, so as to be unmeasurable, under the conditions of **Figure 2**. However, isobutane (2-methylpropane) elutes as a tailing peak just before methane; **Figure 3** shows this effect. Similar behaviour is found for neopentane (2,2-dimethylpropane), although it is less of a problem, since neopentane is likely to be at much lower concentration than isobutane. A further example is sulfur hexafluoride, which elutes before oxygen. This can be used where SF₆ is measured as an atmospheric tracer by electron-capture detector; oxygen is mildly electron-capturing, but does represent 21% of the atmosphere, and so having the trace of SF₆ eluting first makes detection easier.

Under the same conditions, 13X molecular sieve gives more uniform separation of components, with rather shorter retention times, as shown in **Figure 4**. 13X sieve does not display the exclusion mode of

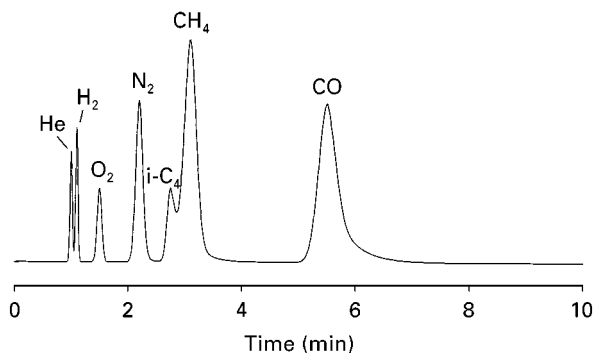


Figure 3 Molecular sieve 5A.

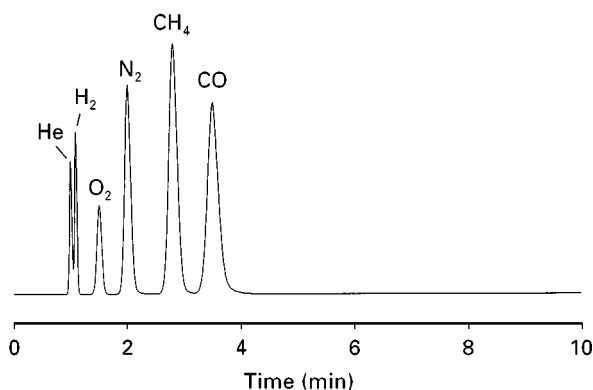


Figure 4 Molecular sieve 13X.

behaviour shown by 5A. Another difference is that the order of elution of methane and carbon monoxide can be reversed. If the temperature of activation is limited to 150°C, then a chromatogram similar to that in Figure 5 is produced. With this reduced level of activation, the long-term stability of the column is excellent. With the higher activation temperature required for Figure 4, the column performance, as with 5A sieve, slowly deteriorates. 13X sieve must have at least two types of pores, from one of which water is removed at relatively low temperature, giving the chromatogram in Figure 5; the other requiring higher temperatures to give the performance in Figure 4. Obviously, at some intermediate activation temperature, methane and carbon monoxide will co-elute.

Porous polymer beads Porous polymer beads are based on polyaromatic cross-linked resins. They have a regular pore size and form beads of uniform diameter, making a good packing material. They are available in a range of polarities, according to the method of preparation, which allow differences in elution order. They are not hygroscopic and hence need no activation before use, although treatment

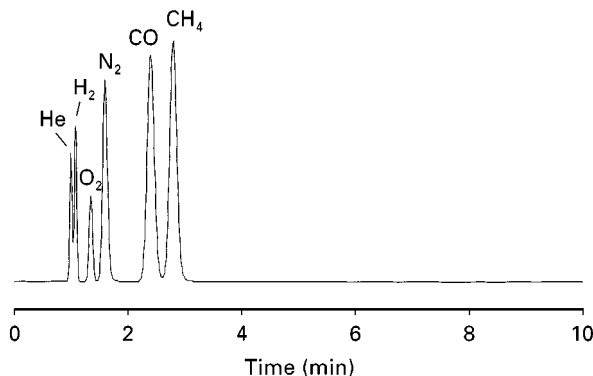


Figure 5 Molecular sieve 13X - partially activated.

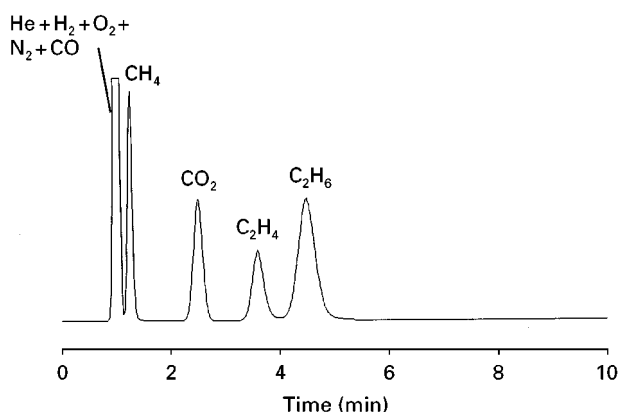


Figure 6 Porous polymer beads as packing material.

overnight near the maximum operating temperature will remove residual low relative molecular mass material and give more stable baselines. With operating temperatures from subambient to around 250°C, the range of samples to which they can be applied is large. Since there is no change in activity due to adsorbed moisture, porous polymers are frequently used in temperate-programmed applications, which considerably increases their flexibility.

A 2 m column packed with nonpolar material at 50°C does not separate oxygen, nitrogen and carbon monoxide, which elute at the beginning of the chromatogram, closely followed by methane. It does separate carbon dioxide, ethene and ethane in that order, which makes it a natural complementary column to molecular sieve for light gas analysis (Figure 6). Propene elutes just before propane, but C₄ saturated and unsaturated hydrocarbons are mixed together. At higher temperatures, porous polymers can analyse hydrocarbons to C₈. They are also good for sulfur-containing gases, separating H₂S, COS and SO₂ in that order. With temperature programming, organic thiols and sulfides can be included.

Alumina Activated alumina has a high polarity which is suitable for mixtures of saturated and unsaturated hydrocarbons. To avoid tailing peaks for unsaturated components, some controlled surface deactivation is necessary. Originally this was done with water, or a mixture of water and silicone oil to obtain the desired polarity. The water would slowly be stripped off by the dry carrier gas, increasing polarity and the tendency to tailing peaks. Alumina PLOT columns are now available, deactivated with inorganic salts, and these offer the optimum solution for this type of analysis. Figure 7 shows a chromatogram of C₁ to C₄ saturated and unsaturated hydrocarbons. This was produced using an FID, so the lack of

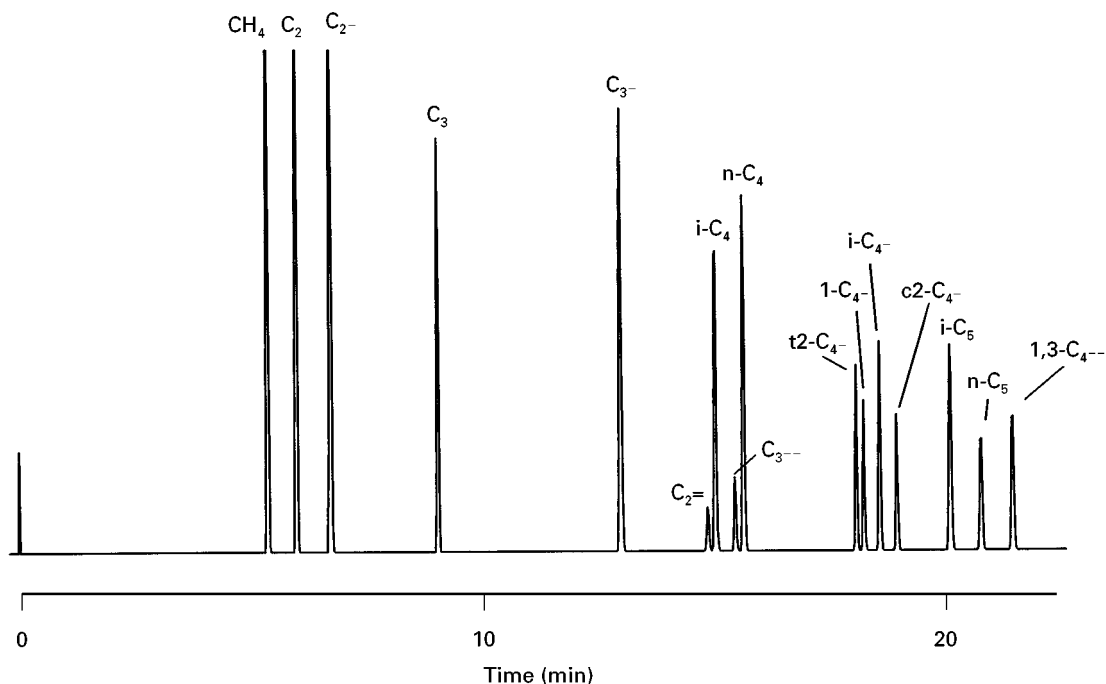


Figure 7 Porous-layer open-tubular (PLOT) alumina column.

separation between methane and inorganic gases is not a problem.

Carbon Active carbon has been used as a packing since the introduction of gas analysis by chromatography. Modern packings are based on graphitized carbon black or on carbon molecular sieve. Both have similar retention characteristics to porous polymers, but carbon molecular sieve, with a high surface area, requires higher temperatures. Another characteristic of carbon molecular sieve is its very low retention for water, typically eluting before CO₂. Either type of packing is used for samples containing adsorptive components, in which case the inert nature of all the

materials in the sample path, not just the packing material, must be considered.

Column Switching

Most gas analyses require the use of more than one column, given the restricted applicability of each. Rather than use the columns individually in separate chromatographs, they can be combined in a single unit by means of switching valves. Such valves are similar to the gas sampling valve described earlier, but configured for different uses.

Figure 8 shows a configuration suitable for the common combination of molecular sieve and porous polymer columns. V1 is the gas sampling valve and

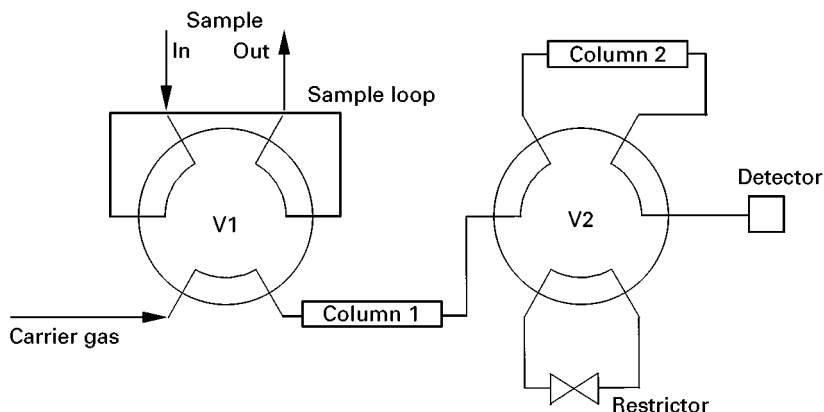


Figure 8 Column isolation.

V2 the column switching valve. Column 1 is porous polymer and column 2 molecular sieve. The restrictor on V2 is adjusted so that the carrier flow to the detector is the same for both positions of V2. Those components for which molecular sieve is appropriate (O_2 , N_2 , CH_4 and CO) are rapidly eluted from the porous polymer column with little or no separation. With V2 in the position shown, they pass into the molecular sieve column. Before CO_2 and other components have reached the end of the porous polymer column, valve V2 is switched, allowing them to bypass the molecular sieve and pass directly to the detector. Switching V2 also isolates the light components in the molecular sieve column, with no carrier gas flow. After the components directly eluted from the porous polymer column have been detected, V2 is switched back, and the light gases are measured. Figure 9 shows a chromatogram.

Another procedure is possible. If the gap on the porous polymer column between the initial unresolved components and CO_2 is sufficiently large, then the flow can continue through the molecular sieve to allow the light components to be measured before CO_2 reaches V2. V2 is then switched, allowing CO_2 and the other components to be measured.

Combined use For certain applications, one 10-port valve can be used in place of two 6-port valves. Figure 10 shows the configuration which would allow the second procedure described above to be achieved with one valve. With the valve in the first position, sample is being purged through the loop, and the carrier gas is following the sequence column 2 \rightarrow column 1 \rightarrow detector. Switching the valve injects the sample on to column 1 (porous polymer). After the light gases from column 2 have been measured, the valve is returned to the sample load position for measurement of CO_2 and other components.

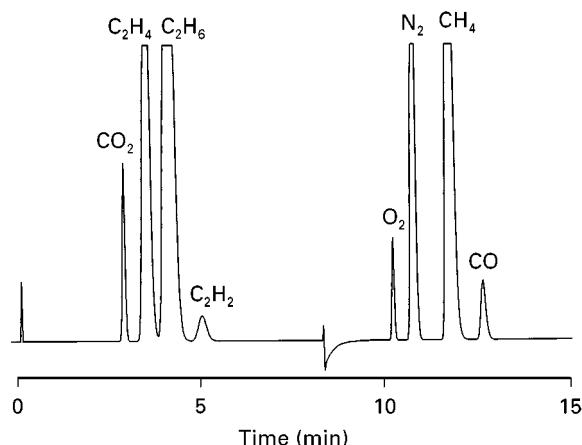


Figure 9 Combined column chromatogram.

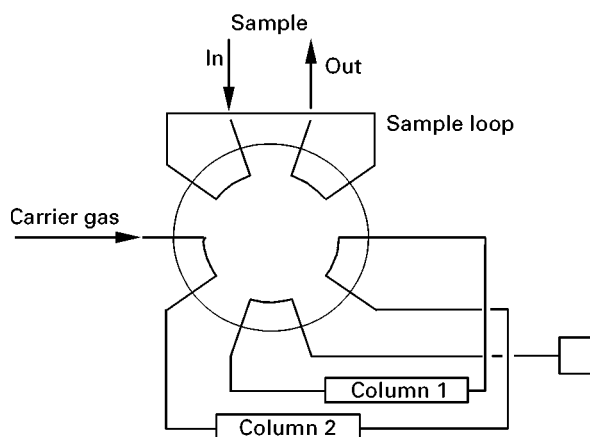


Figure 10 Combined injection and switching.

Multiple systems Natural gas and refinery gas are two examples of complex mixtures which require more elaborate systems than those described above. Although neither mixture should contain oxygen, a molecular sieve column is recommended because air contamination of the sample is always possible; measurement of the oxygen concentration allows the air content to be calculated and allowed for. A porous polymer column allows optimum separation of carbon dioxide, ethane and, if present, ethene. C_3 , C_4 and C_5 hydrocarbons can be dealt with by an appropriate liquid-phase column, and in a common implementation all heavier hydrocarbons are measured as a backflushed C_6+ group.

Figure 11 shows the configuration. Column 1 is divided into two sections, the longer 1B, on which C_3 , C_4 and C_5 hydrocarbons are separated, and the shorter 1A, from which C_6+ is backflushed. Valve V1 injects the sample and also alters the sequence of columns 1A and 1B. Valve V2 isolates and reconnects the porous polymer (column 2) and molecular sieve (column 3), and V3 does the same for column 3 alone.

After sample injection, V1 is left in that position until the C_5 components have passed on to column 1B, while the C_6 and heavier are still on column 1A. This time is found by trial and error. At this point, V1 is returned to the sample load position, which also reverses the flow through column 1A and places it directly before the detector. All heavier components are rapidly measured as a recombined C_6+ peak. After the light gases have been eluted from column 1B, rotation of V2 isolates them in columns 2 and 3. The timings and column lengths are chosen so that each group of light gases is isolated on the appropriate column. C_3 , C_4 and C_5 hydrocarbons elute from column 1B, pass through column 1A for the second time, and are detected. After that, valves V2 and V3

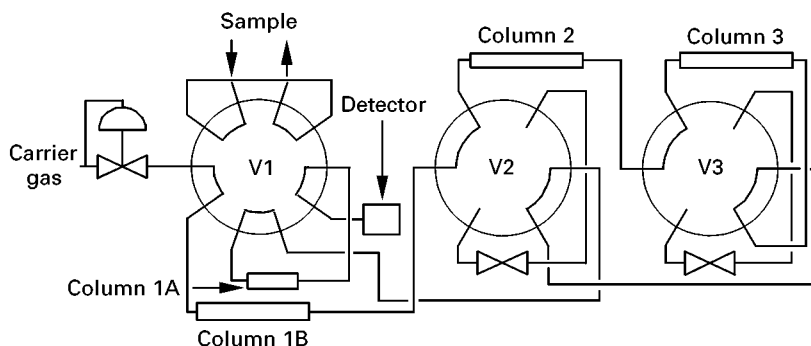


Figure 11 Multiple column analysers.

are rotated to reconnect column 2, and CO_2 and C_2 hydrocarbons are measured. Finally, V3 reconnects column 3, and the components from the molecular sieve column are measured. Figure 12 shows a chromatogram of natural gas.

Carrier Gas

Since the TCD is normally used for the major components of gas mixtures, the thermal conductivity of the carrier gas is one of its most important properties. Helium and hydrogen have similar high thermal conductivities, and allow other components to be detected with good sensitivity. All other things being equal, helium would be preferred for its inertness. Unfortunately, the thermal conductivities of helium/hydrogen mixtures have a significantly nonlinear relationship to concentration, which makes quantitative measurement of hydrogen in helium carrier gas difficult. Argon or nitrogen is suitable for the measurement of hydrogen and/or helium. As described above under 'Molecular sieve', argon can be used to measure oxygen without interference, and nitrogen may be the

best choice for measurement of other trace components in air.

When other detectors, such as the FID, are used, the choice of carrier gas is less critical. Maximum sensitivity from the FID is obtained with nitrogen or argon, but this is rarely the most important need. Helium allows higher carrier gas linear velocities without loss of efficiency, and is also preferred in cases where both TCD and FID are used in series.

Detectors

For specific applications, most types of detector are used or have been used. Electron capture, helium ionization, ultrasonic and flame photometric detectors are applicable where the properties or very low concentrations of sample components require them. For the majority of applications, however, the TCD is the most popular, followed by the FID. TCDs use either filaments or thermistors as sensing elements. Thermistors give greater sensitivity at lower detector temperatures, but are less good if the application demands a high detector temperature. When

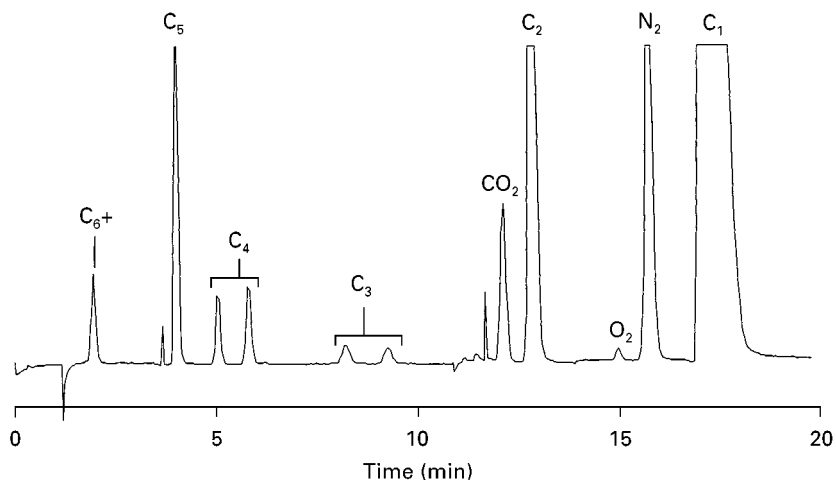


Figure 12 Natural gas chromatogram.

using adsorption columns, it is not always necessary to maintain a detector temperature higher than that of the column oven, and thermistors may still be preferred. The higher temperatures of filaments can cause sample components to react with them. As an example, a sample containing both oxygen and hydrogen sulfide can cause step baseline changes in opposite directions as each component in turn passes through the detector.

Quantitative Analysis

The importance of calibration is as great for analysis of gases as it is for liquid samples. In some respects it is even greater, since the TCD, which is used for the major components of gas samples, does not share the 'carbon counter' characteristic of the FID. If, for example C_3 to C_5 hydrocarbons in a gas are analysed using an FID, it would be possible to calibrate using a standard gas containing C_3 alone, and then quantify the other components by means of relative response factors. This is not the case when using TCD; while the relative response for a particular detector will be stable, they are not predictable as for the FID, and there is not a sufficient basis of knowledge to allow them to be transferred to other models of TCD from other suppliers.

Calibration gas mixtures of the highest accuracy can be prepared in cylinders gravimetrically. Although the mass of the cylinder is very much greater than the masses of the added components, the discrimination and accuracy of weighing are such that the uncertainties of the composition are very small. Such mixtures are, of course, expensive, and for regular use certified calibration mixtures, which have been analysed against a gravimetric mixture, are normal. If components are likely to react with or adsorb on to cylinder walls, then calibration mixtures can be prepared dynamically, at the time and place of use. Permeation tubes, where a component diffuses

through a membrane into a measured diluent gas flow under controlled conditions, are widely used for trace analysis.

If only a few specific components are to be measured, then the individual response factors calculated from the calibration gas are critical. It is necessary to calibrate with sufficient frequency that uncontrollable effects, such as that of barometric pressure on TCD response, do not degrade the result. Consistency of sample size between calibration and analysis is also important. A gas sampling valve (see above under 'Sample handling and injection') allows this, but the operator must ensure that the temperature and pressure of the calibration gas and sample are uniform.

If the analysis is comprehensive, as in the natural gas example shown in Figure 12, then the resulting composition will be normalized to 100%. This procedure effectively converts the individual response factors to relative ones. Since relative response factors for a single detector remain stable over long periods, consistency of sample size is less critical. Regular calibration is still important, but is used as much as a quality control test as for calibration in the traditional sense.

Further Reading

- Cowper CJ (1995) The analysis of hydrocarbon gases. In: Adlard ER (ed.) *Chromatography in the Petroleum Industry*. Amsterdam: Elsevier.
- Cowper CJ and DeRose AJ (1983) *The Analysis of Gases by Chromatography*. Oxford: Pergamon Press.
- Jeffery PG and Kipping PJ (1972) *Gas Analysis by Gas Chromatography*. Oxford: Pergamon Press.
- Leibbrand RJ (1967) Atlas of gas analysis by gas chromatography, *Journal of Gas Chromatography* 5: 518–524.
- Mindrup R (1978) The analysis of gases and light hydrocarbons by gas chromatography. *Journal of Chromatographic Science* 16: 380–389.
- Thompson, B. (1977) *Fundamentals of Gas Analysis by Gas Chromatography*. California: Varian Associates.

GAS CENTRIFUGE: ISOTOPES SEPARATION

See III/ISOTOPE SEPARATIONS: Gas Centrifugation

GAS CHROMATOGRAPHY-MASS SPECTROMETRY IN MEDICINE

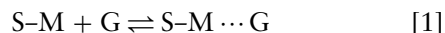
See III/BIOMEDICAL APPLICATIONS: Gas Chromatography–Mass Spectrometry

GAS SEPARATION BY METAL COMPLEXES: MEMBRANE SEPARATIONS

N. Toshima and S. Hara, Science University of Tokyo
in Yamaguchi, Yamaguchi, Japan

Copyright © 2000 Academic Press

temperature or pressure:



Introduction

Gases are separated on a very large scale by cryogenic distillation, membrane or sorption methods. For instance, the production of pure oxygen from air by cryogenic distillation is one of the most important separation processes. However, the membrane method is preferable when O₂-enriched air is required for medical use or effective combustion, and the sorption method is best for removal of O₂ from packaging. The fundamental mechanism of cryogenic distillation is due to a difference in boiling points of the various gases. In the case of the membrane method, a difference in solubility and diffusion of gases is essential for nonporous membranes, while molecular mass or size of gases is a decisive factor for porous membranes where Knudsen diffusion or molecular sieving occurs. The sorption method involves physical sorption and chemisorption, which are characterized by binding energies of about 5–50 kJ mol⁻¹ and about 150–500 kJ mol⁻¹.

Unlike most physical sorbents, gas adsorbents containing metal complexes adsorb gas molecules by chemical coordination of the molecules to a central metal atom. Some metal complex adsorbents, because of their strong chemical adsorption, can completely adsorb gas molecules, even at low gas concentrations. The equilibrium between the metal complex (S-M) and the gas (G) is shown in eqn [1]. When this equilibrium shifts to the right, the adsorbent adsorbs gas molecules. When the equilibrium shifts to the left, the adsorbent releases the adsorbed molecules. The equilibrium can be controlled by changing

Figure 1 shows a schematic illustration of carbon monoxide separation from a carbon monoxide–nitrogen gas mixture by a solid copper complex. Only carbon monoxide can coordinate to copper to form a complex when the adsorbent is exposed to the gas mixture. The adsorbed gas is released when the adsorbent is subjected to high temperature or reduced pressure.

The characteristics of metal complex adsorbents are as follows:

1. Various combination of metal–ligand systems are available for the development of appropriate adsorbents.
2. Even a very dilute gas component in a mixture can be removed due to strong coordinative binding between the central metal and gas molecules.
3. Selective adsorption can be achieved using suitable functional groups of ligands.
4. Such a selective adsorption can possibly be used as a sensor or an indicator by showing colour change of adsorbents.
5. The amount of adsorbed gas molecules per unit mass of the adsorbents is limited because only one or two molecules can coordinate to a central metal atom.
6. The metal complex adsorption system cannot separate gases by their molecular size.
7. In general, the metal complex adsorbent is less stable than other types of adsorbents, such as active carbon and zeolite.

Metal complexes can be used as free-standing adsorbents, but preferably should be spread on to an inert support, such as activated carbon, porous

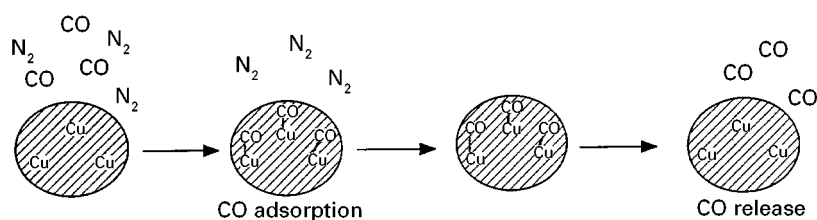


Figure 1 A schematic illustration of the separation of carbon monoxide from a carbon monoxide–nitrogen mixture by a supported copper complex.

carbon fibres, zeolite or porous polymer beads. These supports should have a large surface area to increase the adsorption capacity. Also the adsorbent support should be mechanically strong so as not to break up in use.

Polymeric supports have several advantages. Firstly, polymers can be processed into many shapes, such as thin membranes, hollow fibres or porous beads. Secondly, the wide variety of available polymers means that the structure and surface chemistry of the polymer are easily changed. Thirdly, the metal complex can be easily inserted into a hydrophobic domain, which cannot be achieved with inorganic materials. This offers some protection to water-sensitive metal complexes. Finally, composite materials can be easily formed.

Polymer-supported metal complexes or polymer-metal complexes are quite often more stable, more effective, and more easily handled than metal complexes without support for the following reasons:

1. *Diluting effect*: polymers can immobilize the metal complex separately so that aggregation of the metal complex is difficult.
2. *Concentrating effect*: metal complexes fixed in a polymeric support give a reaction field with a higher concentration of active centres than in a solution of the corresponding metal complex.
3. *Field effect*: polymeric supports form a specific reaction field to promote the reaction or to inhibit undesirable side reactions.
4. *Steric effect*: polymeric supports sterically control the approach of molecules to the metal complex.

The polymer-metal complexes can be used for gas separation in the form of adsorbents and membranes. In both cases, the coordination of gas molecules to the metal complex is much stronger than physical adsorption or solubilization into polymers, resulting in higher selectivity for gas separation than metal complexes supported on inorganic materials where the inorganic support itself may adsorb a considerable amount of gas molecules.

The following are industrially important applications of metal complexes for gas separation. However, most have been investigated on just a small laboratory scale. Only the separation of oxygen from air has been the subject of practical research for industrial application on a large scale.

Separation of Carbon Monoxide

Carbon monoxide, one of the most important starting materials for synthesizing organic chemicals, is usually obtained as a gas mixture containing methane, ethane, nitrogen, carbon dioxide and water vapour, by steam reforming of hydrocarbons, partial oxidation processes or gasification of coal. Thus, separation of carbon monoxide from gas mixtures is a significant target for investigation. Although the cryogenic separation process is widely used for carbon dioxide separation, it is difficult to separate carbon monoxide from gas mixtures containing N_2 because their boiling points are close ($CO = -191.5^\circ C$, $N_2 = -195.8^\circ C$). For this reason adsorption of carbon monoxide onto metal complexes is still of use. One process is adsorption of carbon monoxide by a copper liquor process using copper(I) ammonium solution, but dry systems have also been proposed. Some adsorbents investigated are listed in Table 1.

Introduction of copper(II) ion into Y-type zeolite by cation exchange, followed by reduction under 150 mmHg (1 mmHg \approx 133.3 Pa) of carbon monoxide at $400^\circ C$, gives a Y-type zeolite-supported Cu(I) adsorbent which adsorbs 1.65 mmol of carbon monoxide per g-adsorbent at $25^\circ C$, 99 mmHg. The amount of CO adsorbed is almost equal to the moles of attached Cu(I) ion, suggesting that a 1:1 Cu(I)-carbon monoxide complex is formed. A similar adsorbent can be made by replacing Y-type zeolite by ZSM-5. The disadvantages of the Cu(I) zeolite-type adsorbents are as follows:

1. Cu(I) is oxidized to Cu(II) by oxygen in the presence of water vapour or ammonia, losing the ability to adsorb carbon monoxide.

Table 1 Adsorption and release of CO by various adsorbents containing Cu

Adsorbent	Capacity of adsorption (cm^3 g adsorbent $^{-1}$)	Adsorption conditions	Release conditions
Cu/Y-type zeolite	30–40	100 Torr, $< 100^\circ C$	$> 300^\circ C$, vacuum
Cu/ZSM-5	16	200 Torr, $< 50^\circ C$	$> 300^\circ C$, vacuum
Cu(I)/active carbon	24	0.9 atm, $20^\circ C$	$120^\circ C$, 1 atm or $20^\circ C$, vacuum
Cu(I)/PS-NH $_2$	20	0.9 atm, $20^\circ C$	$80^\circ C$, vacuum
AlCuCl $_4$ /active carbon	28	0.9 atm, $20^\circ C$	$180^\circ C$, vacuum
AlCuCl $_4$ /PS	70	1.0 atm, $20^\circ C$	$90^\circ C$, vacuum

2. Release of carbon monoxide requires a temperature of 300–400°C under vacuum because of the strong carbon monoxide coordination of Cu(I). These severe conditions are unsuitable for good carbon monoxide recovery.

Although active carbon is capable of adsorbing gases, it cannot be used as a selective carbon monoxide adsorbent because of the general physical adsorption involved. However, activated carbon, having a very large surface area, can be used as a support. An adsorbent can be made holding 14.1 mmol of CuCl (94%), with a surface area of 744 m² g⁻¹, about 70% of that of the activated carbon (1044 m² g⁻¹) used. The activated carbon-supported CuCl adsorbs 88% carbon monoxide per Cu(I) (24 cm³ STP per g-adsorbent) under a CO-N₂ (9:1) mixture at 20°C. The adsorbent totally releases the adsorbed carbon monoxide at 120°C under 1 atm or 20°C under 0.4 mmHg, and can be used repeatedly. The high capacity of carbon monoxide adsorption results from the highly dispersed CuCl₂⁻ on active carbon prepared from CuCl in hydrochloric acid solution. Carbon-supported CuCl prepared in ethanol or water does not show high carbon monoxide adsorption. Carbon-supported CuCl prepared from CuCl in 20% ammonia solution exhibits 83% carbon monoxide adsorption to the Cu(I) content under the same conditions mentioned above. A similar carbon monoxide adsorbent, prepared from CuCl₂ instead of CuCl, adsorbs 67% carbon monoxide to the CuCl₂ added. The active site is however found to be Cu(I) by X-ray photoelectron spectroscopy (XPS), presumably because the Cu(II) is reduced by the activated carbon during the preparation.

Macroreticular (MR) polystyrene (PS) resin with primary and secondary amino groups can be used as a support for CuCl. The polymeric adsorbent adsorbs 15.9% carbon monoxide per Cu(I) (21 cm³ STP per g-adsorbent) under the same conditions described above. The adsorbent partially releases carbon monoxide in 10 min at 80°C under 1 atm, and repeatedly adsorbs 9.1% carbon monoxide per Cu(I). The other ion exchange resins show poor capacity of carbon monoxide adsorption (Table 2), showing that the coordination of the amino groups to Cu(I) is essential. The adsorbent does not adsorb methane, hydrogen or nitrogen, but does adsorb some carbon dioxide (3.7 cm³ per g-adsorbent). The capacity is however much smaller than that of carbon monoxide (21 cm³) because most of the amino groups of the resin coordinate to CuCl, and few free amino groups remain.

Polystyrene-supported CuCl shows very poor capacity for carbon monoxide adsorption (Table 2). Copper(I) chloride is known to make a double

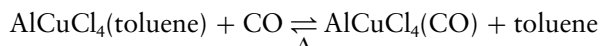
Table 2 Capacity of CO adsorption for various ion exchange resin-supported CuCl^a

<i>Ion exchange resin</i>	<i>Functional group</i>	<i>Adsorbed CO^b</i>
Anion exchange resin	-NH ₂ , -NH-	15.9
Weak cation exchange resin	-COOH	1.2
Strong cation exchange resin	-SO ₃ H	0.8
Polystyrene resin	None	2.2

^a The adsorbents were prepared from 10.0 g of resin and 9.9 g (100 mmol) of CuCl in 80 cm³ acetonitrile.

^b Adsorbed CO under 1 atm of CO-N₂ (9:1) mixture at 20°C.

salt with aluminium chloride, and the double salt forms a π -complex with aromatic hydrocarbons such as toluene, giving a stable carbon monoxide absorbent even in the presence of oxygen or carbon dioxide:



This absorbent (AlCuCl₄ toluene solution, so-called COSORB solution) is very unstable in water, however, decreasing irreversibly the capacity of carbon monoxide absorption. Therefore, the water content of gas mixtures must be reduced to less than 1 p.p.m. prior to using this solution. Addition of linear PS to an AlCuCl₄-toluene solution dramatically increases the stability to water, presumably because PS coordinates AlCuCl₄, forming a hydrophobic domain around the water-sensitive AlCuCl₄ molecule, thereby protecting it from water.

MR cross-linked PS resin (Bio-Beads SM-2, divinylbenzene content: 20%, surface area: 300 m² g⁻¹) is an excellent support for AlCuCl₄, providing a water-resistant solid carbon monoxide adsorbent. The adsorbent adsorbs an equimolar amount of carbon monoxide in 10 min under 1 atm of carbon monoxide at 20°C, and partially releases the carbon monoxide under 7 mmHg at 20°C. After 10 min desorption of CO, the adsorbent still adsorbs 54% carbon monoxide per Cu(I) the second time, and this is a reversible capacity for carbon monoxide adsorption under the conditions mentioned above. The capacity of reversible carbon monoxide adsorption increases by applying higher vacuum or higher temperatures during the desorption part of the cycle. The water-resistivity of the adsorbent strongly depends on the solvent used for preparation. Carbon disulfide gives a water-resistant adsorbent, while toluene gives a water-sensitive material. The water-resistant adsorbent has a uniform distribution of AlCuCl₄ in PS resin, whereas the water-sensitive adsorbent possesses a lot of crystalline

deposits, consisting mainly of CuCl_2 , in the beads and much salt, mainly AlCl_3 , on the surface.

Gel-type PS (divinylbenzene content: 1%)-supported AlCuCl_4 adsorbs carbon monoxide much more slowly than the MR-type adsorbent, and it takes about a day to attain equilibrium. In consequence, the MR-type resin, which possesses macropores even in a dry state, is essential for the preparation of solid gas adsorbents.

Separation of Nitrogen Monoxide (NO)

Nitrogen oxides and sulfur oxides are major air pollutants. Unlike sulfur oxides which have been decreasing in the atmosphere, nitrogen oxides, particularly nitrogen monoxide (NO) in combustion and exhaust gases, still cause difficulties. For removal of nitrogen monoxide, in general, catalytic processes using ammonia, carbon monoxide or hydrocarbons as a reducing agent are applied.

Another possibility of removing nitrogen monoxide from gas mixtures might be the use of metal complex adsorbents at lower temperatures. The nitrogen monoxide adsorbents are expected to adsorb nitrogen monoxide completely, even at very low concentrations of nitrogen monoxide, and to be stable to water vapour, SO_2 , dust, etc., which are often contained in combustion and exhaust gases.

Natural jarosite, $\text{KFe}_3(\text{SO}_4)_2(\text{OH})_6$, possesses a layer structure in the crystal. Jarosite synthesized from $\text{Fe}(\text{SO}_4)_2$ and K_2SO_4 (3 : 1) adsorbs 5.3×10^{-4} mmol of nitrogen monoxide per g-adsorbent (surface area: $7.3 \text{ m}^2 \text{ g}^{-1}$). The other synthetic jarosites, $\text{MFe}_3(\text{SO}_4)_2(\text{OH})_6$ (M = Na, Rb), show no difference in nitrogen monoxide adsorption.

α - FeOOH crystals can be prepared from $\text{Fe}_2(\text{SO}_4)_3$ and Na_2CO_3 by heat treatment. Powdery crystal α - FeOOH , whose surface area is $60 \text{ m}^2 \text{ g}^{-1}$, adsorbs 0.4 mmol of nitrogen monoxide per g-adsorbent at 30°C under 600 mmHg of nitrogen monoxide partial pressure, whereas α - FeOOH supported on activated carbon fibre (surface area: $870 \text{ m}^2 \text{ g}^{-1}$) adsorbs 4.67 mmol of nitrogen monoxide under the same condition (a 12 times higher capacity than that without activated carbon fibre as a support). This adsorbent adsorbs 0.043 mmol per g-adsorbent even under 300 p.p.m. of nitrogen monoxide at 100°C , but little more than 10% of the nitrogen monoxide adsorbed can be released under vacuum due to its strong adsorption.

Active carbon-supported FeCl_2 completely adsorbs nitrogen monoxide in 25 min from a 6 dm^3 NO- N_2 mixture (NO: 1000 p.p.m.) when the gas mixture is circulated at $1.6 \text{ dm}^3 \text{ min}^{-1}$. The adsorbent releases 28% adsorbed nitrogen monoxide in 15 min at

Table 3 Effects of the washing solvent on the ability for NO adsorption and the surface area for chelate resin-supported Fe(II)

Solvent	Adsorption rate ^a ($10^{-2} \text{ mmol min}^{-1}$)	Adsorbed NO ^b	Surface area ^c ($\text{m}^2 \text{ g}^{-1}$)
Chloroform	0.36	0.789	2.3
Water	0.30	> 0.425	3.2
Acetone	1.04	0.933	17.2
2-Propanol			31.7
Ethanol	1.54	0.997	31.1
Methanol	1.54	0.997	43.1

^a Amount of adsorbed NO in 15 min.

^b Equilibrium NO adsorbed against NO introduced.

^c Measured by a Brunauer-Emmett-Teller (BET) method.

120°C . The apparent equilibrium constant of the adsorbent is around 1500 atm^{-1} .

Iron(II) ethylenediaminetetraacetic acid (EDTA) solution is a well-known nitrogen monoxide absorbent, adsorbing 0.5 mol of nitrogen monoxide per mole of Fe from NO- N_2 mixtures (NO: 1000 p.p.m.) at 55°C . However, the absorbent is easily oxidized by oxygen due to the unstable Fe(II) ion. To overcome this problem, a chelate resin, cross-linked PS with iminodiacetic acid moieties, has been used as a polymeric support. The Fe(II) supported on chelate resin adsorbs almost all the nitrogen monoxide in 15–20 min from a 6 dm^3 of NO- N_2 mixture (NO: 1000 p.p.m.) when the gas mixture is circulated at $1.6 \text{ dm}^3 \text{ min}^{-1}$. The adsorbent releases all the adsorbed nitrogen monoxide under 3 mmHg at 100°C , and can be reused repeatedly. The capacity of nitrogen monoxide adsorption for the chelate resin-supported Fe(II) is dependent on the washing solvent. This is because the porosity or the surface area increases (Table 3) when the water-swollen resin-supported Fe(II) is dried after washing with water-miscible organic solvents. Coexistence of a high valent cation such as Fe(III) further increases the surface area to achieve more effective nitrogen monoxide adsorption.

Separation of Ethylene (C_2H_4)

Ethylene is one of the most important raw materials in the petrochemical industry and is also an accelerator for ripening fruit. Ethylene is produced on a large scale by the thermal cracking of naphtha and natural gas, and obtained in mixtures with methane, ethane, propane, propylene, hydrogen, carbon dioxide, nitrogen and water. In this case, a large quantity of gas mixture has to be treated to obtain pure ethylene. On the other hand, a small amount of ethylene must be thoroughly removed from fruit packaging so that fruit does not ripen too quickly.

In industry ethylene is purified mostly by large scale distillation, and sometimes by using membrane separation. For removal of ethylene from fruit packaging, no good adsorbent has yet been developed. The solid metal complex adsorbent mentioned here may provide a new material for both purposes.

Y-type zeolite-supported Cu(I) adsorbs 3.10 mmol of ethylene per g-adsorbent (1.9 mmol of ethylene per mole of Cu(I)) under 250 mmHg of ethylene at 25°C and releases 73% of the adsorbed gas in 60 min. Y-type zeolite-supported Ag(I) adsorbs 3.28 mmol of ethylene per g-adsorbent and releases 54% of the gas under the same conditions.

MR-type PS resin with primary and secondary amino groups, which is used as a support for CuCl as described above for carbon monoxide adsorption, also works as an ethylene adsorbent. An adsorbent prepared from 10 g of resin and 15.0 g (152 mmol) of CuCl in water-acetonitrile (1 : 1) reversibly adsorbs 15 mmol of ethylene and 1.9 mmol of ethane, while the resin itself (10 g) adsorbs 5.0 mmol of ethylene and 6.5 mmol of ethane at 20°C under 1 atm. The coverage of CuCl over the surface of the resin is supposed to restrict physical adsorption and increases chemisorption or coordination.

MR-type PS-supported AlCuCl₄ adsorbs ethylene very rapidly, and the equilibrium ratio of the adsorbed ethylene to the CuCl added is 1.40 mol-C₂H₄/mol-Cu (89 cm³ STP of ethylene per g-adsorbent). The adsorbent releases a part of the adsorbed gas under 8 mmHg at 20°C for 10 min, and adsorbs 0.29 of mol-ethylene per mol-Cu in the second and later passes. When an ethylene-adsorbed adsorbent is cycled at 90°C under 1 atm and at 142°C under 8 mmHg to release ethylene, the adsorbent removes 0.47 and 0.87 of mol-ethylene per mol-Cu, respectively, in the second adsorption cycle. Although the PS-supported AlCuCl₄ adsorbs both ethylene and carbon monoxide, the coordination of ethylene to Cu(I) is stronger than that of carbon monoxide. Thus, the equilibrium molar ratio of adsorbed ethylene-carbon monoxide is 5 : 1 when the adsorbent is exposed to a 1 : 1 ethylene-carbon monoxide mixture.

A similar adsorbent, MR-type PS-supported AgAlCl₄, adsorbs an equimolar amount of ethylene per Ag under 1 atm at 20°C and releases almost all the ethylene under 8 mmHg at 20°C. The adsorbent does not adsorb carbon monoxide at all under 1 atm at 20°C, and therefore can be used as a selective ethylene adsorbent. The adsorbent is water-resistant, although AgAlCl₄ is water-sensitive, as is AlCuCl₄. The stability of the adsorbent is attributable to the location of AgAlCl₄ at the hydrophobic sites of the PS resin surrounded by several aromatic rings.

Separation of Oxygen

Oxygen, which can be prepared by separation from air, is one of the most important industrial chemical products and is produced on the largest scale by weight in the world. Thus, separation of oxygen from air is an important process in industry, and is mainly performed by low temperature distillation. It is also important to increase (or decrease) oxygen concentration for medical use and effective combustion (or inhibition of nitrogen monoxide production).

Haemoglobin and nyoglobin are typical examples of metal complexes which can reversibly bind an oxygen molecule in nature. So, the separation of oxygen from air with solid metal complexes has received considerable attention in the search for alternative procedures to low temperature distillation. Cobalt(II) Schiff's base complexes, such as a complex of cobalt(II) with bis(salicylidene)diaminoethane (Co(salen)), were objects of initial research in the 1940s on reversible oxygen absorbents and were later developed for on-board oxygen support systems for the US Air Force. Oxygen binds preferentially to cobalt by exposing the complex to air at room temperature to form cobalt(III) superoxide. Heating (thermal swing adsorption: TSA) or reducing pressure (pressure swing adsorption: PSA) facilitates release of oxygen from the complex. Up to 3000 oxygenation/deoxygenation cycles have been carried out with the same sample. After 3000 cycles the remaining activity was still 50%. Chemical engineering research was carried out using the system involving Co(salen)-type adsorbents. The US Air Force studied the cobalt(II) complex of bis(3-fluorosalicylidene)diaminoethane or fluomine for potential use in providing breathing oxygen for crews of military aircraft. This compound gives the best performance among all oxygen adsorbents so far with its fast and reversible binding of oxygen, as well as good stability, but could not be applied in practice due to the high cost.

Several other transition metals, such as manganese, iron, chromium, nickel, copper, titanium, and so on, have been used to synthesize various kinds of oxygen adsorbents by complexing with various types of ligands. They show reversible oxygen binding and release, but none has achieved commercial success for separation of oxygen from air.

Cobalt(II) Schiff's base complex has been tried, fixed in a polymer matrix. A poly(4-vinylpyridine)-attached cobalt(II) Schiff's base complex can be used for gas chromatography because oxygen comes out later than the other gases, such as nitrogen. Cobalt bis(salicylideneamino)propylamine-attached polystyrene and polyoctylmethacrylatecobalt dialicylidenediethylenediamine films have been found to

be useful for concentrating oxygen. Membranes of this latter material concentrate 8.3% oxygen in 5 h and 13.1% in 42 h from air. The permeability coefficient and the separation factor (O_2/N_2) under 10 mmHg of feed gas are 10^{-9} and 15, respectively, for this membrane containing 12 wt% of the complex. The experimental results were analysed using the dual-mode sorption model. Although several interesting studies have been reported on facilitated oxygen transport membranes employing the transition metal-oxygen complexes, they have a number of inherent limitations from a practical viewpoint, for example, the lifetime of membranes, the relationship between quality and quantity of the separation, and so on.

Conclusion

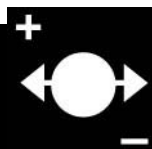
Metal complex adsorbents used for carbon monoxide, nitrogen monoxide, ethylene and oxygen separation have been described in this article. Few examples of adsorbents for other gases are known, but theoretically any gas capable of coordinating to metal complexes can be separated in this way. A variety of metal complexes can be synthesized by changing metal and ligand, and therefore supported metal complexes are promising materials for gas separation.

However, from a practical viewpoint, there are many limitations, for example, lifetime of the materials and the cost of the separation. Since the greatest advantage of systems using solid metal complexes is complete separation, the adsorbents of solid metal complexes may be used for the purpose of the complete removal of small amount of gaseous molecules from closed systems in the future.

Further Reading

- Endo T, Toshima N and Yamamoto T (1998) *Chemistry of Functional Polymeric Materials*. Tokyo: Asakura.
- Giddings JC (1991) *Unified Separation Science*. New York: John Wiley.
- Li GE and Govind R (1994) Separation of oxygen from air using coordination complexes: A review. *Ind. Eng. Chem. Res.* 33: 755–783.
- Senoo M, Takagi M, Takeda K *et al.* (eds) (1993) *Handbook of Separation Science*. Tokyo: Kyoritsu.
- Toshima N (ed.) (1992) *Polymers for Gas Separation*. New York: VCH.
- Toshima N, Kaneko M and Sekine M (1990) *Macromolecular Complexes*. Tokyo: Kyoritsu.
- Tsuchide E (ed.) (1991) *Macromolecular Complexes. Dynamic Interactions and Electronic Processes*. New York: VCH.

GENE TYPING: TWO-DIMENSIONAL ELECTROPHORESIS



N. J. van Orsouw, S. B. McGrath and J. Vijg,
Institute for Drug Development, Cancer Therapy and
Research Center, San Antonio, TX, USA
R. K. Dhandu, Mosaic Technologies, Boston, MA, USA
C. B. Scott, CBS Scientific Company, Del Mar, CA, USA

Copyright © 2000 Academic Press

Introduction

With the human genome program drawing to a close, attention is now rapidly shifting from obtaining consensus sequences of all human genes to the detection of individual DNA sequence variations. Based on complete sequence information for all human genes, it is theoretically possible to generate a catalogue of all gene mutations and polymorphisms in the human genome and test them directly for association to relevant phenotypes, e.g. of health and disease. Unfortunately, current methods for detecting DNA sequence variants are not optimized for generating data on multiple genes in large numbers of individuals, e.g. in population-based studies or in the clinical setting. The most reliable system for comprehensive gene sequence analysis is still nucleotide sequencing itself, which is not compatible with cost-effective large scale population-based genetic screening.

Recently, various systems have been proposed to analyse gene-coding and regulatory sequences more effectively for all possible variations. Here we review the development and application of one such system, two-dimensional gene scanning (TDGS). This method is based on the two-dimensional separation of polymerase chain reaction (PCR)-amplified gene fragments on the basis of both size and base pair sequence in polyacrylamide gels. Attention will be focused on most recent developments in automation and miniaturization of the two-dimensional electrophoresis procedure. Future developments towards a dedicated fully automated high-throughput system for gene analysis will be discussed.

Two-Dimensional Gene Scanning: Background and Principles

Denaturing Gradient Gel Electrophoresis

TDGS is based on denaturing gradient gel electrophoresis (DGGE) as the mutation detection

principle, in combination with PCR amplification to prepare the target sequences. In DGGE, DNA fragments are subjected to electrophoresis in a polyacrylamide gel against a gradient of ever higher temperature or chemical denaturants (i.e. a mixture of urea and formamide). Unlike nucleotide sequencing, DGGE detects mutations, including base pair substitutions and small insertions and deletions, on the basis of differences in the melting temperature of the target fragments. A given DNA fragment comprises one or more domains, each representing a stretch of between 50 and 300 base pairs with equal melting temperature (the temperature at which each base pair has a 50% probability of being in either the helical or the denatured state). Since the stability of each domain depends on its sequence, mutational differences among different fragments are revealed as migrational differences in the gel (Figure 1A).

In order to obtain virtually 100% accuracy in mutation detection, fragments to be subjected to DGGE can be clamped to a GC-rich sequence (a stretch of 30–50 G and C bases). A convenient way of attaching a GC-clamp to the target fragment is by making it part of one of the primers in a PCR. Without GC-clamping, a DNA fragment consisting of one melting domain will become completely single-stranded upon denaturation and run off the gel. By adding a GC-clamp, a single high-melting domain is artificially created at one end of the target fragment. As the GC-clamped target fragment migrates through the gradient of denaturants, melting of the target domain causes partial branching and halting of the fragment in the gel (Figure 1B). Thus, one function of the GC-clamp is to ensure branch formation after melting of the target fragment. However, when the target DNA fragment consists of multiple melting domains (Figure 1C), only mutations in the lowest melting domain are readily detected. To facilitate detection of all possible mutations, it is imperative that the target fragment represents only one melting domain. Fortunately, since the addition of a GC-clamp allows for stacking interactions with neighbouring bases, the entire fragment will often behave as one melting domain (Figure 1C). However, this is not always the case, and in practice, the target fragment needs to be designed, e.g. through the strategic positioning of PCR primers to achieve the ideal single

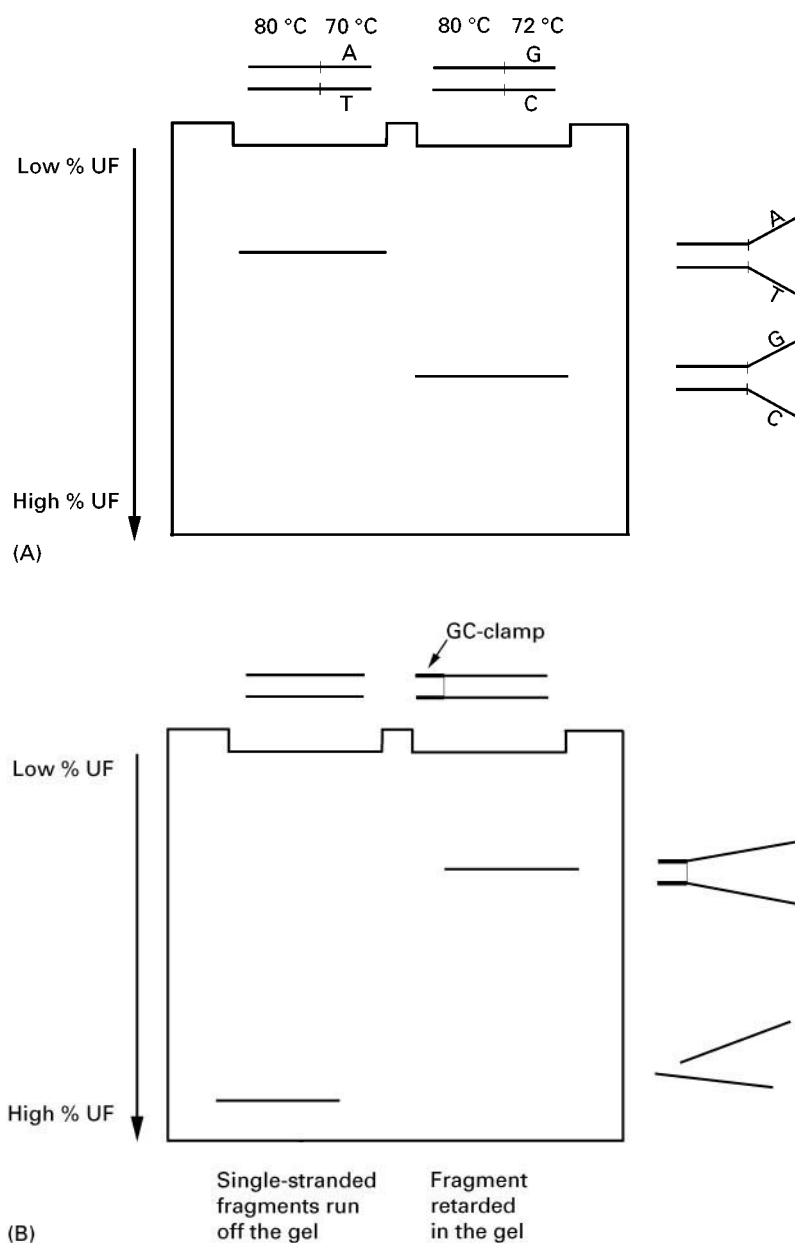


Figure 1 Principles of denaturing gradient gel electrophoresis. (A) Single base changes affect the melting temperature of a fragment, which results in a gel shift. (B) After complete denaturation, single-stranded fragments will run off the gel; the addition of a GC-clamp to the target fragment prevents complete denaturation and therefore fragments will be retarded in the gel. (C) The addition of a GC-clamp to a multiple-domain fragment can make the fragment behave as a single-domain fragment. Continuous line: target fragment without a GC-clamp. Dashed line: target fragment, including a 40 bp GC-clamp. (D) The introduction of a heteroduplex cycle at the end of PCR amplification of target fragments facilitates detection of heterozygous mutations as four molecules: two homoduplexes and two (early-melting) heteroduplexes.

melting domain. In general, target fragments in DGGE have an average size of 275 bp, including a GC-clamp and PCR primer sequences.

The sensitivity of DGGE for detecting variants is further enhanced by the introduction of a heteroduplexing step using one round of denaturation/renaturation, usually at the end of PCR amplification of the target fragment. In this manner, a heterozygous

mutation is revealed as four different double-stranded fragments: two homoduplex molecules (one wild-type homoduplex and one mutant homoduplex) and two heteroduplex molecules (each comprising one wild-type and one mutant strand). Since the stability of heteroduplexes is so much lower, they always melt earlier than the homoduplex molecules (Figure 1D).

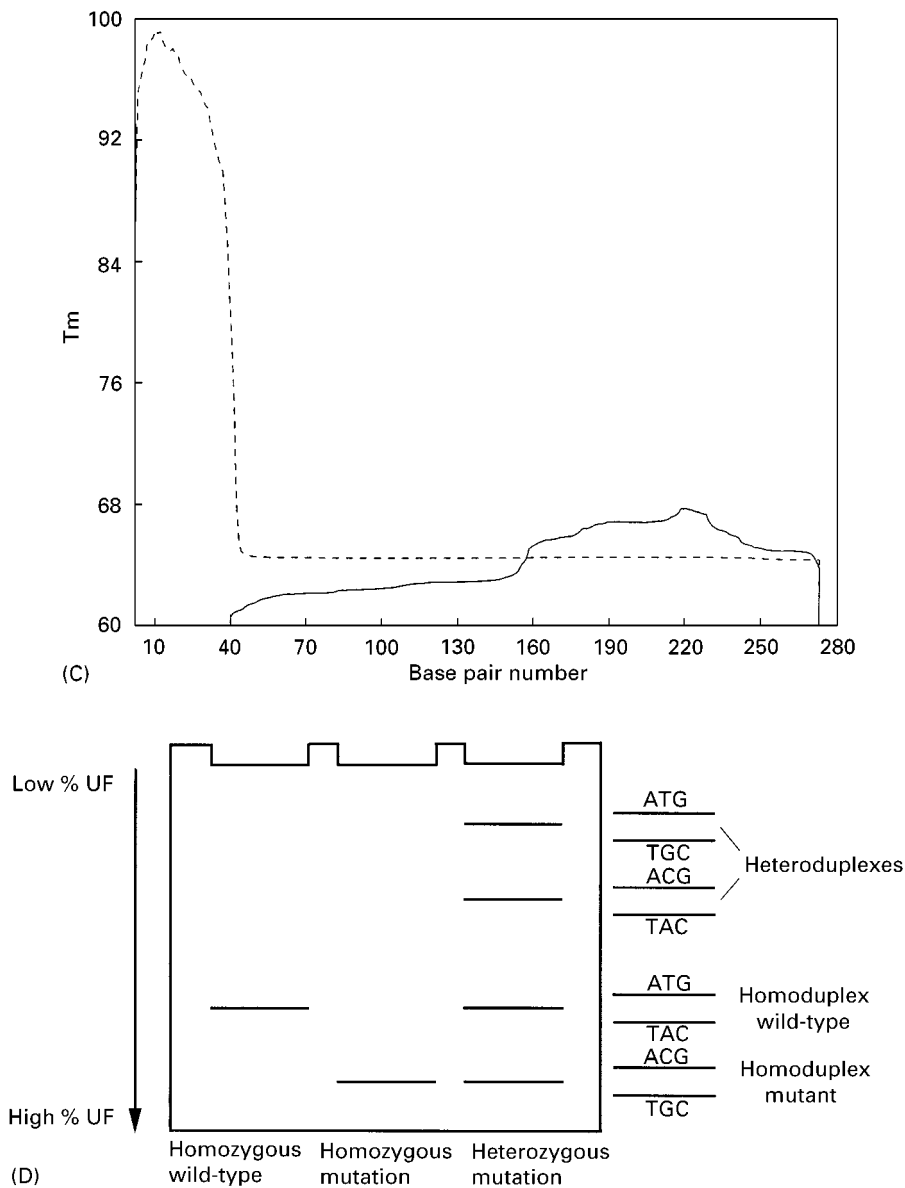


Figure 1 Continued

Although DGGE has the crucial advantage of having virtually 100% sensitivity in detecting mutations, it has typically been applied in a serial fashion, e.g. on a fragment-by-fragment basis. For analysing large genes or multiple genes this is not practical. A solution for this problem, which we adopted, is to apply the DGGE principle in the format as it was originally described, i.e. a two-dimensional system of separation by size followed by DGGE. Successful implementation of such a two-dimensional DNA electrophoresis system in mutation scanning of large genes requires an efficient multiplex PCR protocol. Indeed, without the possibility to PCR-amplify multiple target fragments (i.e. typically 10 or more) in one single reaction, the application of a parallel

analysis system offers only a limited advantage. Multiplex PCR systems for genes and genetic markers are now becoming available and it has been demonstrated that as many as 26 fragments can be co-amplified in one single tube under the same reaction conditions.

Two-Dimensional DNA Electrophoresis

The major advantage of two-dimensional electrophoresis is that it provides a high resolution system to screen multiple fragments under the same conditions. It has been demonstrated that DGGE provides virtually 100% mutation detection sensitivity even when applied with a broad range gradient of

denaturants. This opens up the possibility to analyse multiple fragments for all possible mutations under the same set of experimental conditions. The total number of target fragments that can be analysed simultaneously depends on the resolution of the gel system used. Although high resolution can be obtained by using one-dimensional denaturing gradient gels, two-dimensional separation allows characterization of each fragment on the basis of two independent criteria, size and melting temperature. In practice, a fragment mixture corresponding to all exons of a gene is electrophoresed in a nondenaturing size gel. Fragments are further sorted out in a denaturing gradient gel as the second dimension (Figure 2). By using the two-dimensional system, it is possible to visualize completely all fragments corresponding to

an entire gene for a particular DNA sample and immediately recognize each exon and variants therein. This has been demonstrated for several large human disease genes, including *CFTR*, *RB1*, *MLH1*, *TP53*, *TSC1*, *BRCA1*, as well as for a part of the mitochondrial genome.

Design Software and Instrumentation for TDGS Tests

Computer-Automated Design of Target Fragments for PCR and DGGE

A potential hindrance to the widespread application of TDGS to multiple novel genes involves the difficulties in the design of PCR primers generating

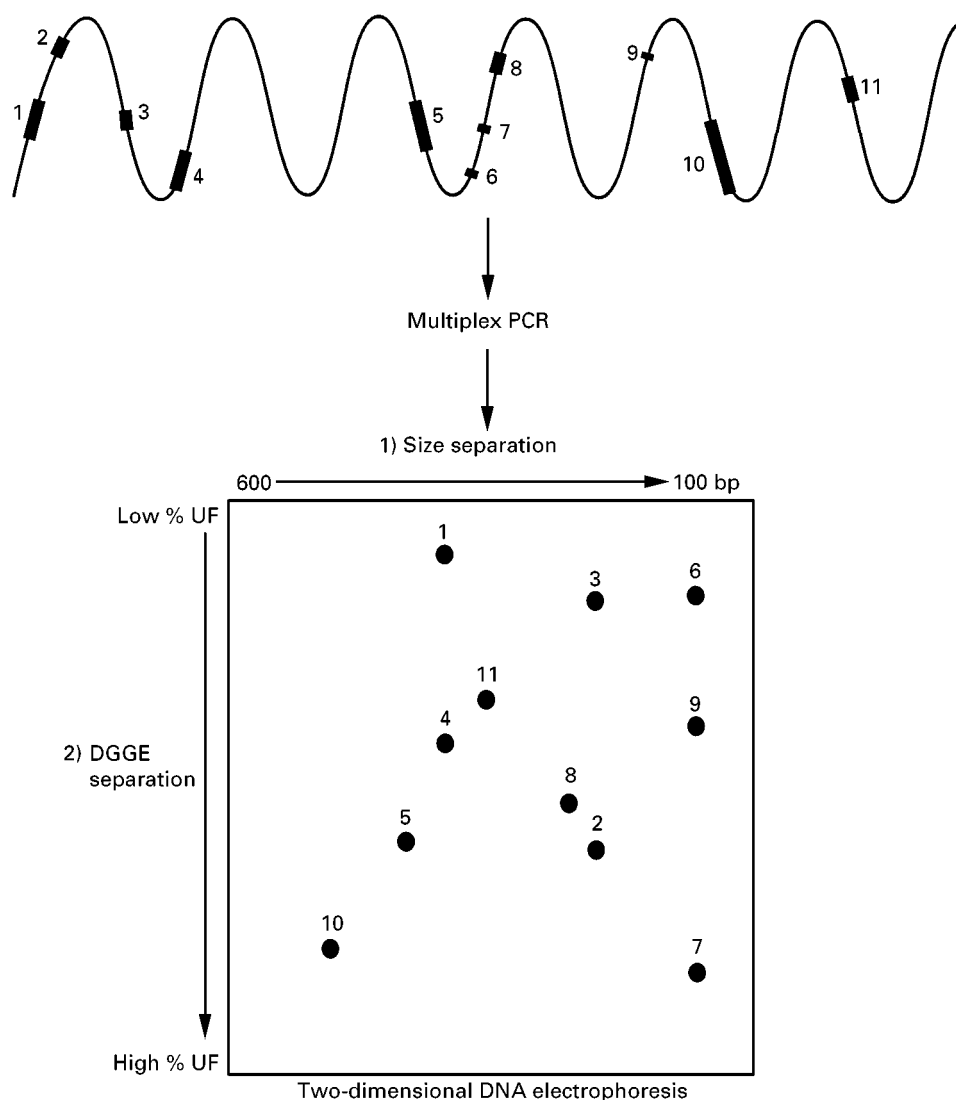


Figure 2 Schematic depiction of a TDGS test. All exons are amplified in an extensive multiplex reaction, and the fragments are resolved by size separation, followed by separation in a gradient of denaturants. Heterozygous mutations would show up as four spots instead of one.

single-domain fragments which can be resolved under one set of electrophoretic conditions. To design complete gene tests for mutational analysis by TDGS, an automated generally applicable computer program was developed, which was based on a commercially available primer design program (Primer Designer 3; Scientific and Educational Software, State Line, PA), the melting routine MELT87 and a newly generated spot distribution routine. After entering a gene's coding sequence as exons with their flanking intronic sequences, a rank of suitable PCR primers for each exon is designed by the PCR design subroutine. Next, the best primer pair is used in the melt subroutine to check for a one-domain target fragment. The program uses different GC-clamps at either the 5' or 3' end of the target fragment and, if necessary, additional small GC- or AT-clamps at either side of the target fragment. If it is impossible to design a one-domain fragment, the next optimal primer pair is tested, and so on. If a primer pair suitable to create a one-domain fragment cannot be found, the exon is split.

As soon as primers fulfil PCR and melting criteria, the fragment is positioned according to its size (x) and melting (y) coordinates. The spot distribution routine then checks for possible overlap. The output file of the program is a complete list of primers to be used in TDGS. (Questions regarding the use of the TDGS software should be directed to Accelerated Genomics, Concord, NH, <http://www.acceleratedgenomics.com> Tel.: (210) 616-5910; fax: (210) 692-7502.)

Electrophoresis

For two-dimensional DNA electrophoresis, originally two different gels were used for the first-dimen-

sion (separation according to size) and the subsequent second-dimension separation of these fragments by DGGE on the basis of their melting temperature. The first-dimension separation was carried out in polyacrylamide slab gels, which required staining of the gel to visualize the one-dimension separation pattern before this could be excised and transferred to the second-dimension denaturing gradient gel. Alternatively, tube gels have been employed for size separation, which obviated the need for gel staining and lane excision. However, routine application of TDGS requires standardization and automation, which is incompatible with the labour-intensive step of manual interference between the first- and second-dimension separation.

Recently, we developed a simple automated two-dimension instrument, which is based on an existing vertical electrophoresis system with an isolated horizontal unit on top (Figure 3). This top unit consists of two outer chambers and one middle chamber. The necessary contacts between the outer buffer chambers and the gel are provided by two strategically located openings in the inner glass plate.

In this system only one gel (a denaturing gradient gel) is used with the top part nondenaturing. This nondenaturing part functions as the lane for the first-dimension size separation. A slot former is placed in the top left part (Figure 4). In the current configuration, a gel is attached to each side of a gel holder, which can be placed in a buffer tank. Buffer tanks can hold multiple units so that multiple gels can be run simultaneously (Figure 5). The sample is electrophoresed on the basis of size horizontally in the nondenaturing top gel, and the second-dimension

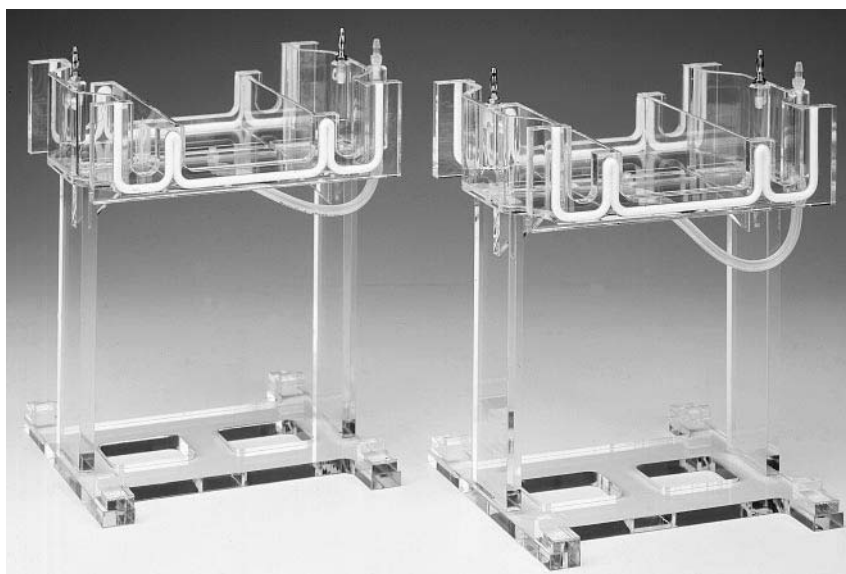


Figure 3 Two automatic dual-gel TDGS systems.

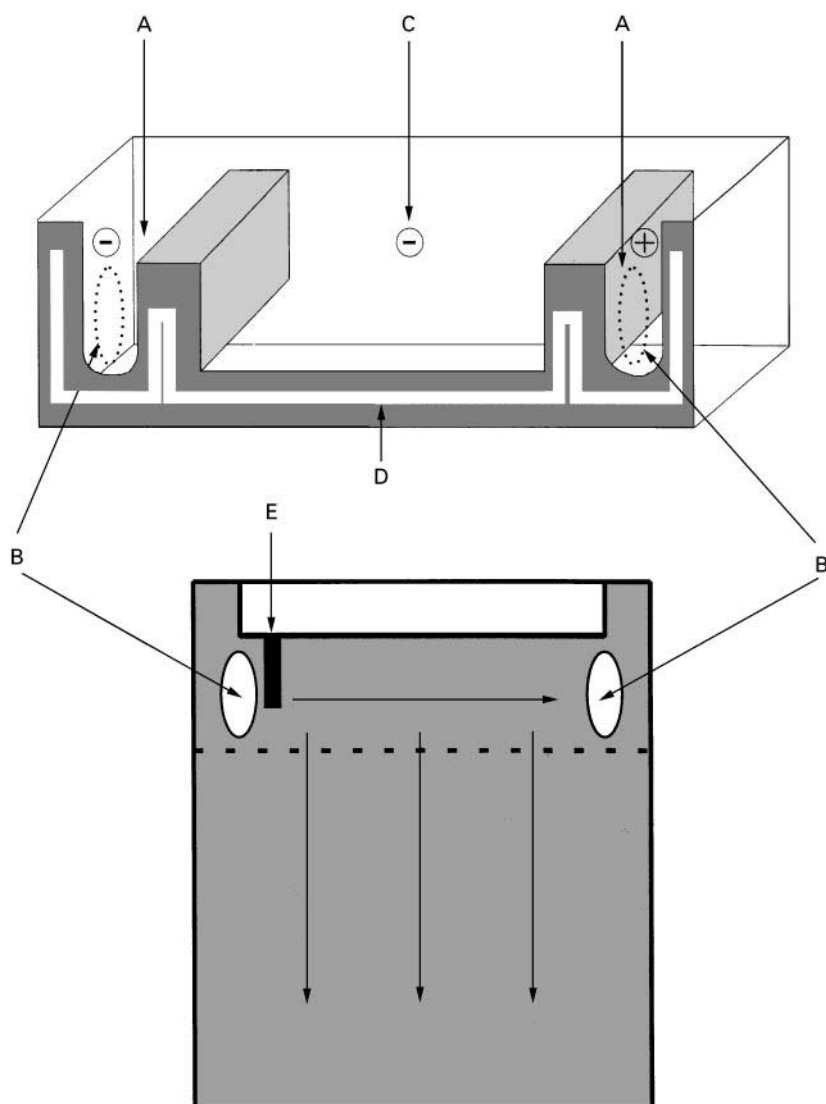


Figure 4 Schematic depiction of the automated two-dimensional electrophoresis unit. Buffer chambers for the first-dimension separation (A) are connected with the gel through openings in the (inner) glass plate (B). During the first-dimension electrophoresis, the middle buffer chamber (C) is isolated from the outer chambers. For the second-dimension run, buffer chamber C is flooded with buffer and the upper electrode is turned on in conjunction with a positive electrode in the lower reservoir (not shown in this figure). The gel cassette is sealed to the top unit with a serpentine silicone gasket (D), and sample is loaded in the single slot (E). The dashed line indicates the beginning of the gradient of urea/formamide.

electrophoresis is carried out vertically in the denaturing gradient gel. All components of the automatic TDGS electrophoresis system are depicted in Figure 6.

Gradient gels can be poured, up to nine at a time, using a simple linear gradient maker in combination with a multiple gel caster. The exact gradient that is to be applied is dependent on the GC-content of the gene(s) of interest and is determined by the TDGS primer designer software.

Miniaturization

Miniaturization of gene analysis systems, such as the TDGS system described here, offers two major advantages: increased speed and lower cost.

Speed The duration of electrophoresis depends on the voltage applied. For example, the optimal electrophoresis conditions for the retinoblastoma susceptibility gene *RB1* using standard 1.0 mm thick gels,



Figure 5 The entire automatic TDGS system. In this version of the system, four gels can be run simultaneously submerged in a buffer tank, which is equipped with a heater/stirrer to provide for a constant temperature. For more information, see <http://www.cbssci.com>

are 100 V, 5 h for the size separation and 100 V, 16 h for the second-dimension separation. Increasing the voltage increases the heat production, which negatively affects gel resolution. An obvious strategy is the use of thinner gels, which facilitate rapid heat dissipation into the surrounding buffer and thereby allow increasing the voltage while maintaining a good resolution. Currently, gels as thin as 0.35 mm are now run at 500 V, 0.8 h for the size separation and 500 V, 3.5 h for the second-dimension separation.

Cost The cost factor is of major importance for the large scale implementation of genetic testing. Since this is determined to a major extent by reagent and material cost, as well as space, miniaturization of analytical systems is of crucial importance. Miniaturization of TDGS results in thinner and smaller gels, which require less sample (smaller PCR volumes can now be applied) and lower gel and buffer amounts. Moreover, they take up less space. Instead of the current 17×22 cm format, two-dimensional patterns have already been produced on 10×10 cm mini-gels, and it is not unreasonable to expect that ultimately electrophoresis will be carried out on glass slides.

Detection of TDGS Patterns

After electrophoresis, the two-dimensional DNA fragment patterns can be visualized by incubating the gels with DNA staining dyes. Examples are ethidium bromide or the more sensitive dye Sybr-green. Patterns are photographed under UV light and evaluated

for the occurrence of variations (in the form of four spot patterns; see Figure 1D). An example of a TDGS pattern is shown in Figure 7, depicting the *RB1* gene, containing a mutation in exon 2.

However, for large scale application of TDGS, dye primer technology for the in-gel detection of two-dimensional spot patterns is an obvious strategy. Test results indicate similar two-dimensional patterns and sensitivity for fluorescein-labelled primers compared to Sybr-green-stained gels.

Introduction of fluorescent detection offers two advantages over gel staining. First, the reduction in labour is considerable and loss of gels due to breakage is prevented. Second, since there is no need to release the gel from between the glass plates it has become possible to use thinner gels, which will allow shorter electrophoresis times (see above). To increase the efficiency even further it is possible to label different samples with different fluorophores. Current fluorescence imagers have the option to analyse multiples fluorophores in the same gel.

Future Developments

Routine application of TDGS requires standardization and further streamlining of the procedure. Ultimately, one could envisage a fully automated system of PCR amplification, sample loading, electrophoresis, scanning of gels by a fluorescent imager, followed by online interpretation of gels by image analysis systems.

Much of the labour that is involved in PCR amplification, as well as the error rate, can be greatly

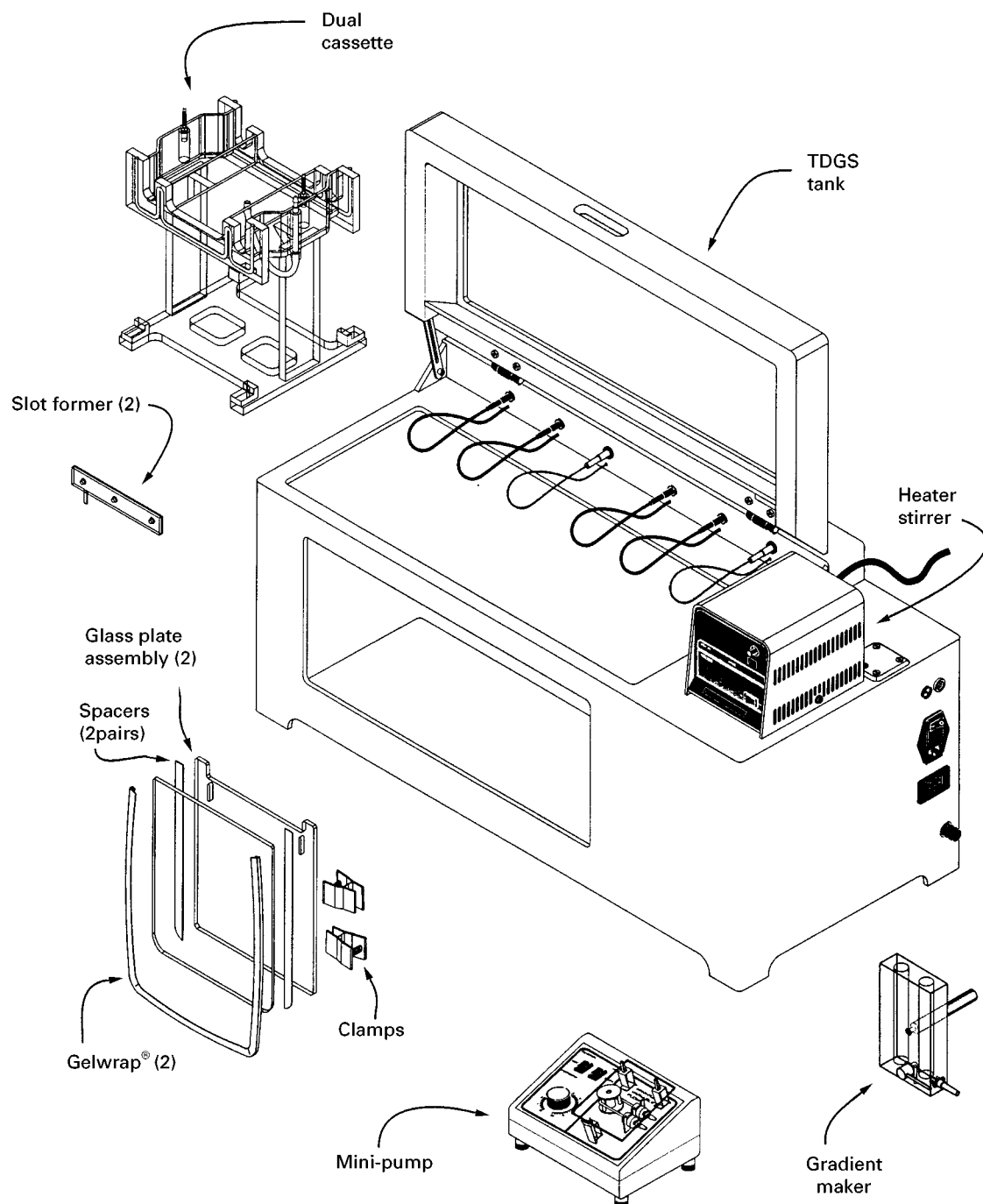


Figure 6 Line drawing of all the components of a 4-gel automatic TDGS system.

diminished by PCR robotics. Such instruments have now become widely available and, in combination with an ongoing effort to increase multiplex groups, are expected to increase greatly the front-end throughput of genetic testing. Multiple two-dimensional gels can be stacked for simultaneous electrophoresis of manifold samples. A simple robot arm could load the gel sandwiches into the fluorescent imager for quick gel scanning. Finally, while the ac-

tual interpretation of spot patterns is currently most conveniently done by eye, automated image analysis software is commercially available. The use of such software may, for example, facilitate the detection of subtle positional changes in the context of other spot variations. In this respect, one could envisage a programme with information on all possible spot positional variants to identify quickly recurrent mutations and polymorphisms on the basis of their unique

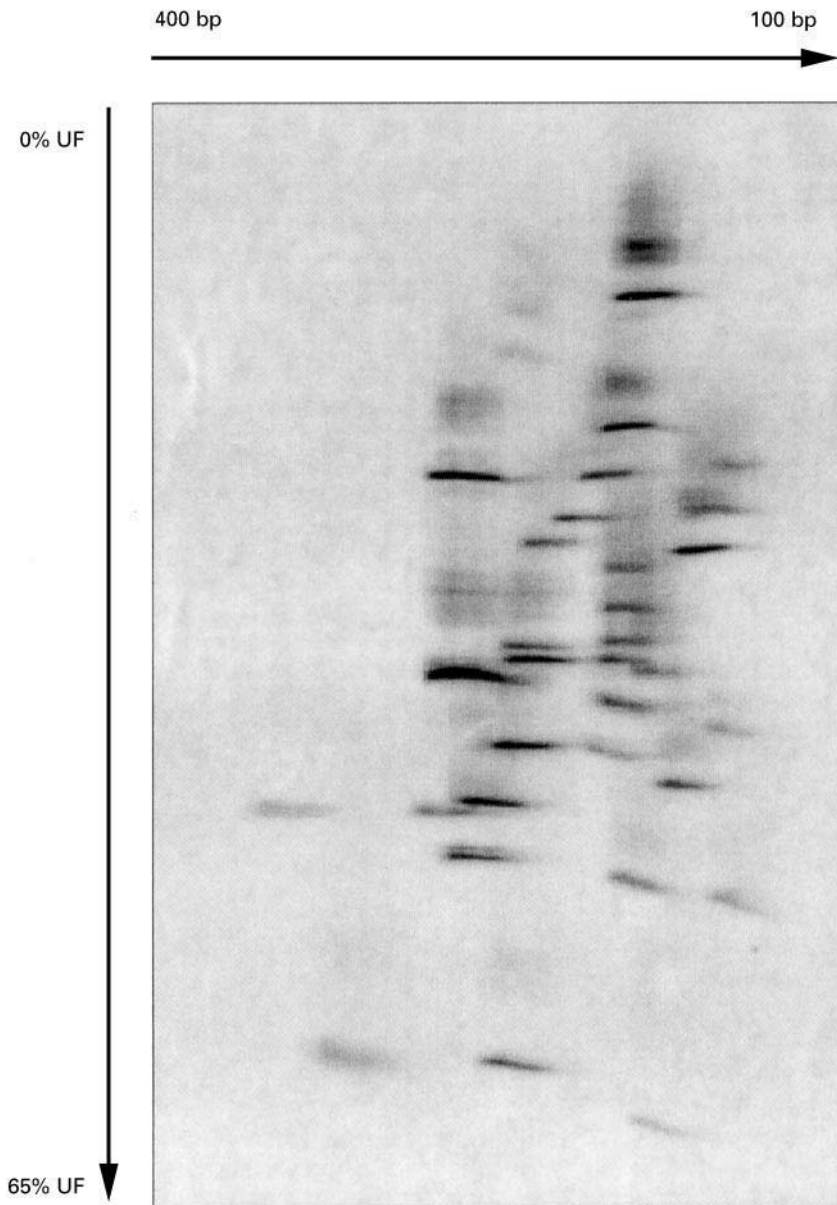


Figure 7 Empirical TDGS pattern of the retinoblastoma susceptibility gene *RB1*, containing a mutation in exon 2.

configuration. Such software should also be capable of storing two-dimensional patterns and link subsets of them in particular experiments requiring comparisons of large numbers of individuals. It could also provide for a sample tracking system.

Further Reading

- Cotton RGH (1997) *Mutation Detection*. Oxford: Oxford University Press.
- Dhanda RK, Smith WM, Scott CB *et al.* (1998) A simple system for automated two-dimensional electrophoresis: applications to genetic testing. *Genetic Testing* 2: 67–70.
- Eng C and Vijg J (1997) Genetic testing: the problems and the promise. *Nature Biotechnology* 15: 422–426.
- Fischer SG and Lerman LS (1979) Length-independent separation of DNA restriction fragments in two-dimensional gel electrophoresis. *Cell* 16: 191–200.
- Lerman LS and Silverstein K (1987) Computational simulation of DNA melting and its application to denaturing gradient gel electrophoresis. *Methods in Enzymology* 155: 501–527.
- Sheffield VC, Cox DR, Lerman LS and Myers RM (1989) Attachment of a 40-base pair G + C rich sequence (GC-clamp) to genomic DNA fragments by the polymerase chain reaction results in improved detection of single-base changes. *Proceedings of the National Academy of Science of the USA* 86: 232–236.

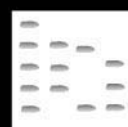
van Orsouw NJ, Li D, van der Vlies P *et al.* (1996) Mutational scanning of large genes by extensive PCR multiplexing and two-dimensional electrophoresis: application to the RB1 gene. *Human Molecular Genetics* 5: 755–761.

van Orsouw NJ, Dhanda RK, Rines DR *et al.* (1998) Rapid design of denaturing gradient-based two-dimensional

electrophoretic gene mutational scanning tests. *Nucleic Acids Research* 10: 2398–2406.

Vijg J and van Orsouw NJ (1999) Two-dimensional gene scanning: exploring human genetic variability. *Electrophoresis* 20: 1239–1249.

GEOCHEMICAL ANALYSIS: GAS CHROMATOGRAPHY AND GC-MS



R. P. Philp, University of Oklahoma, Norman, OK, USA

Copyright © 2000 Academic Press

Introduction

Geochemical analysis, and more specifically chromatography, is concerned with samples derived from two different sources: those of relatively recent origin, related to environmental problems; and those of a much greater geological age, related to fossil fuel exploration and exploitation. The chromatographic techniques utilized to analyse and characterize such samples are virtually identical regardless of the age and origin of the sample. The extracts from geochemical samples, whether they are rocks, soils, crude oil spills, contaminated wildlife or spills of refined products, are very complex mixtures of a wide variety of organic compounds. Compounds derived from fossil fuels typically will be complex mixtures of hydrocarbons, and the environmental samples from more recent sediments probably will contain a variety of other compounds such as chlorinated compounds, pesticides or herbicides. In view of the similarities of the techniques used for analysing the samples from these different sources, the majority of examples used in this article to illustrate the techniques will be based on the characterization of fossil fuel samples.

The major goal of any geochemical analysis is to take a sample and, through a variety of fractionations and analytical techniques, reach a point where either the presence or absence of specific target compounds can be determined, or fingerprints for specific classes of compounds can be obtained and used for correlation purposes. Applications related to petroleum exploration might use such fingerprints for oil–source rock or oil–oil correlation studies, whereas in environ-

mental studies one is more concerned with correlating a spilled product with its original source material or trying to evaluate the extent of removal during clean-up procedures.

Geochemical samples are extremely complex mixtures of a wide variety of compound classes. The analytical techniques commonly used to characterize such mixtures involve some form of chromatography, such as gas chromatography (GC), gas chromatography–mass spectrometry (GC-MS), gas chromatography–mass spectrometry/mass spectrometry (GC-MS/MS), and more recently gas chromatography–isotope ratio mass spectrometry (GC-IRMS). Liquid chromatography (LC) and combined liquid chromatography–mass spectrometry (LC-MS) are also used in certain applications, but not to the same extent as GC and GC-MS. In addition to the analytical chromatographic separations, most geochemical analyses require some sort of fractionation into compounds classes prior to the actual analysis. There are certain cases where total sediment extracts or whole crude oils are analysed directly but generally the mixtures are so complex that an initial fractionation(s) is required to simplify the extracts for subsequent analyses. For example gas chromatograms of many crude oils (Figure 1) are dominated by *n*-alkanes but, for the most part, compounds that are of much greater geochemical importance are not readily observable in these chromatograms but are hidden in the baseline of the chromatogram. It should be noted that there are also many naphthenic crudes not dominated by *n*-alkanes, e.g. Venezuelan and Russian crudes. Most of these naphthenic crudes are either severely biodegraded or have been generated at relatively low levels of maturity from sulfur-rich kerogens. A fractionation step involving thin-layer chromatography, column chromatography or liquid chromatography, all of which involve partitioning of components between a liquid and solid phase, leads to the separation of

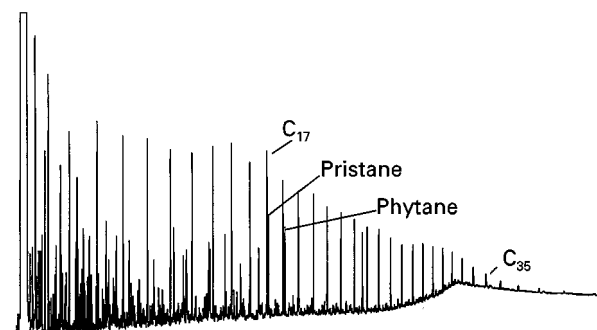


Figure 1 Gas chromatograms of crude oils, rock extracts, or refined petroleum products are typically dominated by *n*-alkanes and isoprenoids. While GC alone does not permit their identification, the fact that the isoprenoids pristane and phytane have very similar elution times to the C_{17} and C_{18} *n*-alkanes, respectively, generally make it relatively easy to identify the other members of the homologous series with a reasonably high degree of confidence.

compounds on the basis of factors such as polarity, shape and size. For hydrocarbon-containing samples, the fractionation step typically involves separation into three fractions – saturate and aromatic hydrocarbons and a polar fraction containing nitrogen, sulfur and oxygen compounds. In general it is the saturate and aromatic fractions that receive most attention in terms of additional analyses. Although the nitrogen, sulfur and oxygen fractions contain many compounds that possess useful information, the complexity of these fractions has precluded their detailed analyses. It is not proposed to go into the experimental details of such chromatographic fractionations since these are very basic techniques and descriptions of specific methods for particular classes of compounds are readily available in the literature.

Fractionation of the crude oil used for Figure 1 into various fractions produces saturate and aromatic fractions as shown in Figure 2. It should be noted when comparing Figures 1 and 2 that the result of the fractionation and evaporation of the solvents used in the fractionation process will lead to the loss of some of the more volatile compounds in the C_1 – C_{15} range of the saturate and aromatic fractions. GC analyses of the saturate fraction produces a chromatogram dominated by *n*-alkanes, typically in the carbon number range from C_{15} to around C_{40} when the analyses are performed using conventional GC. The isoprenoids pristane (Pr) and phytane (Ph) can also be clearly discerned on these chromatograms. Once again, it should be emphasized that although the *n*-alkanes are the predominant compounds in the chromatograms, there are many more minor compounds in the fraction that generally provide a great deal more information than the *n*-alkanes. These

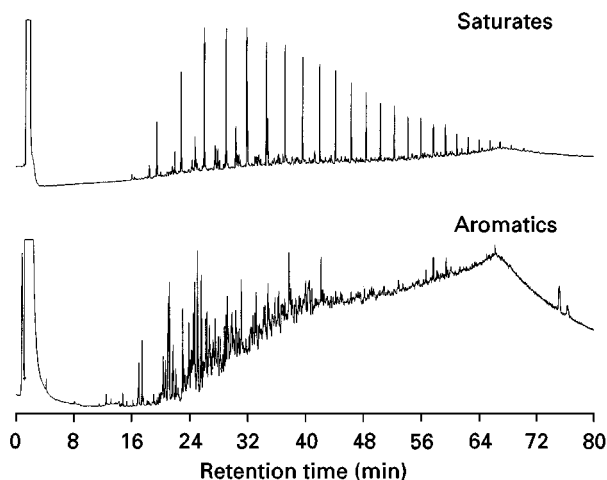


Figure 2 The whole oil chromatogram shown in Figure 1 does not give a true impression of the complexity of the mixture of compounds in a crude oil. While the *n*-alkanes are the dominant components in the chromatogram, a vast array of branched, cyclic, aromatic and polar compounds are also present. This figure shows the chromatograms for a saturate and aromatic fraction separated from a crude oil by thin-layer chromatography.

compounds can be further concentrated by such processes as molecular sieving or urea adduction, both of which will separate the *n*-alkanes from the branched and cyclic alkanes as shown in Figure 3. At this point fractionation and sieving of the original extract or crude oil will have produced a fraction that is readily

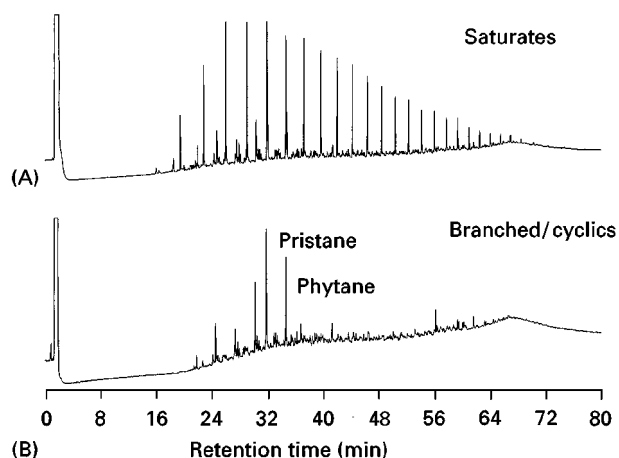


Figure 3 The saturate fraction shown in Figure 2 is again dominated by *n*-alkanes, which tend to mask the presence of a very complex mixture of branched and cyclic compounds also present in this fraction. The *n*-alkanes can be separated from these branched and cyclic compounds by processes such as molecular sieving or urea adduction to produce the branched and cyclic fraction shown in the bottom chromatogram of this figure. The top chromatogram (A), shown for comparison purposes, is the total saturate fraction from which the branched and cyclic compounds were isolated.

amenable to analysis by the techniques mentioned above, such as GC, GC-MS, GC-MS/MS or GC-IRMS. In the following sections a brief description of each technique and typical applications will be given. Again it should be reiterated that for the most part this article uses hydrocarbons for illustration purposes, but the majority of the techniques are equally applicable to the analysis of other samples of geochemical interest such as environmental samples, possibly with some slight modifications in the operating conditions.

Gas Chromatography

As can be seen from the chromatograms used in the Introduction, GC provides a great deal of information on the composition of geochemical samples. With the inclusion of an internal standard, this information can be both quantitative and qualitative in nature. However, it is important to remember that, for the most part, GC does not provide any information on the identification of individual components. In the saturate hydrocarbon fractions, individual compounds such as *n*-alkanes in the chromatograms can be readily recognized and their identification confirmed either by the use of co-injected standards or analysis of the sample by GC-MS as described below. In other cases where it may be necessary to detect certain classes of chlorinated compounds, or organosulfur compounds, additional information on the presence or absence of these compounds can be obtained by using detectors that are specific for these classes of compounds, such as electron capture, flame photometric or Hall detectors. It should also be noted that a number of recent studies have shown that atomic emission detection (AED) is a particularly sensitive and specific method of detection for sulfur-containing compounds. Although the flame photometric detector (FPD) is probably the most widely used detector for sulfur-containing compounds, it has some drawbacks including nonlinear compound-dependent response, and the quenching of sulfur signals by co-eluting hydrocarbons. The AED has a linear response and is compound-independent, permitting easy calibration using any sulfur-containing compounds. This feature is unique because other detectors require the construction of curves using target analytes as standards, which becomes a very time-consuming exercise.

GC has been utilized widely in geochemistry since the 1950s. As column technology and instrumentation have improved, so has the quality of the analytical data. There are many similarities between the gas chromatographs of today and the systems that were developed in the 1950s and 1960s. Detectors and

injectors have improved and temperature control of the ovens has improved, but probably the greatest advances have occurred in the field of column technology. Early columns were short, large-diameter packed columns made of stainless steel or copper. Over the years narrow-bore capillary columns were developed, initially made of stainless steel, then glass and more recently fused silica. At the same time as the evolution of capillary columns, the variety of liquid phases for different applications has also greatly improved. The most recent advance, and one that is quite significant for petroleum exploration and production, has been the development of high temperature GC phases. Traditionally most crude oil analyses have characterized hydrocarbons in the C_1 – C_{40} range but the advent of high temperature GC (HTGC) significantly changed the way in which we look at hydrocarbon distributions of crude oils. The use of HTGC has demonstrated that many crude oils contain a wide range of hydrocarbons significantly above C_{40} , extending to as far as C_{100} and possibly higher. This in turn has also led to changes in one of the very basic premises of geochemistry – that oils with a high wax content were thought to be derived only from higher plant sources. It is now clear that such oils may also be derived from lacustrine and marine source rocks as a result of analysing a number of samples from such source rocks using HTGC. Figure 4 provides an excellent illustration of the additional information obtained from the use of HTGC. The upper chromatogram shows the analysis of an ozocerite extract by conventional GC and the bottom chromatogram shows the same sample analysed by HTGC. Clearly the distribution of hydrocarbons is quite different in the lower chromatogram. The significance of this is related to the fact that the greater the concentration of the higher molecular weight alkanes, the greater the production problems associated with oils that contain such compounds. In other words, if the oils were only characterized by conventional GC, high molecular weight hydrocarbons would remain undetected. Once a production programme was initiated it would not be long before the wellhead facilities and pipelines would become blocked with paraffin deposits, which require costly measures to remove. While HTGC analyses do not eliminate the problem, production engineers would be aware of the potential for such a problem and steps could be introduced to minimize its occurrence.

With the availability of HTGC an increasing number of samples have been analysed using this approach and steps have been taken to develop methods that will quantitatively separate high molecular weight alkanes from the asphaltene fraction. Analyses

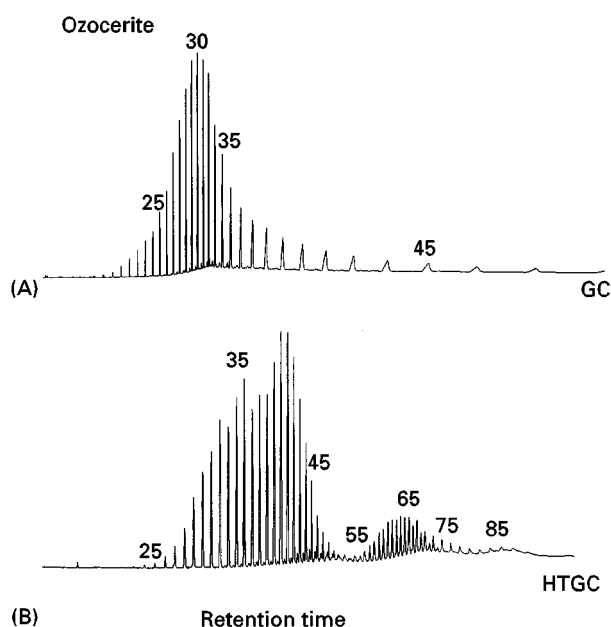


Figure 4 One of the most significant recent developments within GC has been the development of high temperature phases for the columns. Before this development it was generally only possible to analyse compounds with up to approximately 40 carbon atoms. The newer HTGC columns permit samples containing up to approximately 120 carbon atoms to be analysed. This figure illustrates the comparison between the analyses of the hydrocarbons in the fossil bitumen ozocerite by (A) conventional GC and (B) HTGC. The difference in distributions is very clear and also demonstrates how the composition of a fraction obtained by conventional GC may not necessarily reflect the true composition of the sample being investigated.

of a wide range of such samples have shown that, in addition to the *n*-alkanes, there is also a wide range of additional compounds in the higher molecular weight fraction including branched alkanes and alkylcyclohexanes. The distribution patterns for these compounds has provided an additional powerful tool for determination of the type of environment from which a sample has been generated. For example **Figure 5A** and **B** show the distributions of high molecular weight fractions from oils whose source materials were known to be deposited in lacustrine and marine depositional environments, respectively. Note the difference in the distributions of these monocyclic hydrocarbons, which are characteristic of the different environments. At present relatively little information is available concerning the origin of these compounds, although their widespread distribution suggests that they are probably related to an algal/phytoplanktonic source, possibly with additional contributions from higher plant waxes. It is known that many marine organisms contain abundant quantities of higher molecular weight esters, alcohols and fatty acids. Relatively simple transformations

could readily convert these compounds to the corresponding hydrocarbon and could easily represent a viable source for such hydrocarbons.

Another area of geochemistry that has become particularly important in the past few years is reservoir geochemistry, and GC has played an extremely important role in its development. Oil and gas reservoirs are very complex geological features with many compartments. A knowledge of the relative position of these compartments is extremely important for reservoir management, determination of where additional production wells should be drilled, and evaluating how a specific reservoir may have been filled. There are a number of ways in which the reservoir compartments may be delineated but one particularly interesting, innovative and relatively cheap method involves the utilization of high resolution GC. As indicated above, crude oils are very complex mixtures of hydrocarbons, but when the chromatograms are expanded the complexity of the mixtures becomes far more apparent and the presence of a large number of minor components is clearly visible. Reservoir geochemistry utilizes these minor components to assist in the delineation of the reservoir compartments. In brief it is first necessary to determine whether all of the oils in the reservoir are derived from the same source materials. Once this has been established, all of the oils need to be analysed by high resolution GC, the early eluting region of the chromatogram expanded and a number of pairs of minor peaks selected as shown in **Figure 6**. Ratios based on pairs of selected peaks are measured and subsequently plotted on a star or polar diagram. This process is then repeated for all the oils to be examined from the reservoir. It is important to ensure that the same pairs of peaks are selected for each oil, even if the identity of these peaks is unknown. Since the differences between the pairs of peaks in individual samples are often quite small it is extremely important to ensure that the GC analyses are highly reproducible for this particular application. However, once all of the oils have been analysed and the data plotted on the star diagram, it will be found that oils that are in the same compartment or in communication will appear virtually on top of each other, whereas those oils in different compartments will be slightly separated (**Figure 7**). These small difference may result from slight differences in oil-rock interactions, slight maturity differences or generation from slightly different sources.

Gas Chromatography–Mass Spectrometry

While GC can provide a great deal of information that is of interest and useful from a geochemical

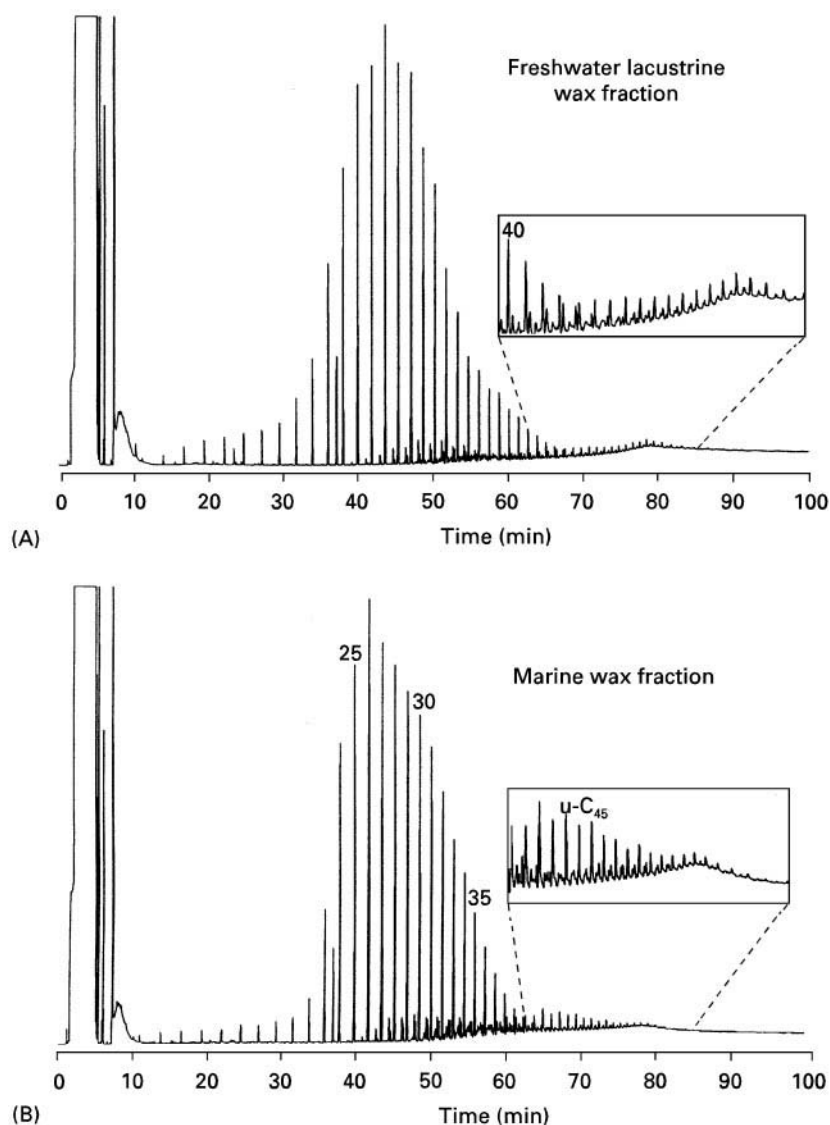


Figure 5 The availability of HTGC has led to the discovery of numerous new series of compounds present in oils and source rocks above C_{40} . Several of these series, and in particular a series of alkylcyclohexanes, have been shown to be useful in discriminating between oils derived from source materials deposited in lacustrine (A) versus marine settings (B). More subtle variations in these distributions allow the salinity levels of the depositional environments to be distinguished.

perspective, it should also be noted that in most cases GC only provides information on the distribution of the major components in the sample, and for the most part these are generally dominated by the n -alkanes. The more useful compounds are the more complex molecules, or biomarkers, which are typically present in relatively low concentrations and which require the use of GC-MS and more specifically single ion or multiple ion detection (MID) in order to determine their distributions. While there are many classes of biomarkers that are commonly used for correlation and other purposes, compounds such as the steranes and terpanes will typically provide the greatest

amounts of useful information for both an environmental and exploration context.

To illustrate the utility of the biomarker fingerprints, the gas chromatograms of three oils are shown in Figure 8. From the gas chromatograms alone it is virtually impossible to determine what relationship, if any, exists between these samples. In other words, are they from the same source rock or can they be correlated with each other? The effects of biodegradation are clearly evident in sample B since all of the n -alkanes have been removed, making it appear even more significantly different from the other two samples. Detailed analyses of the same samples by

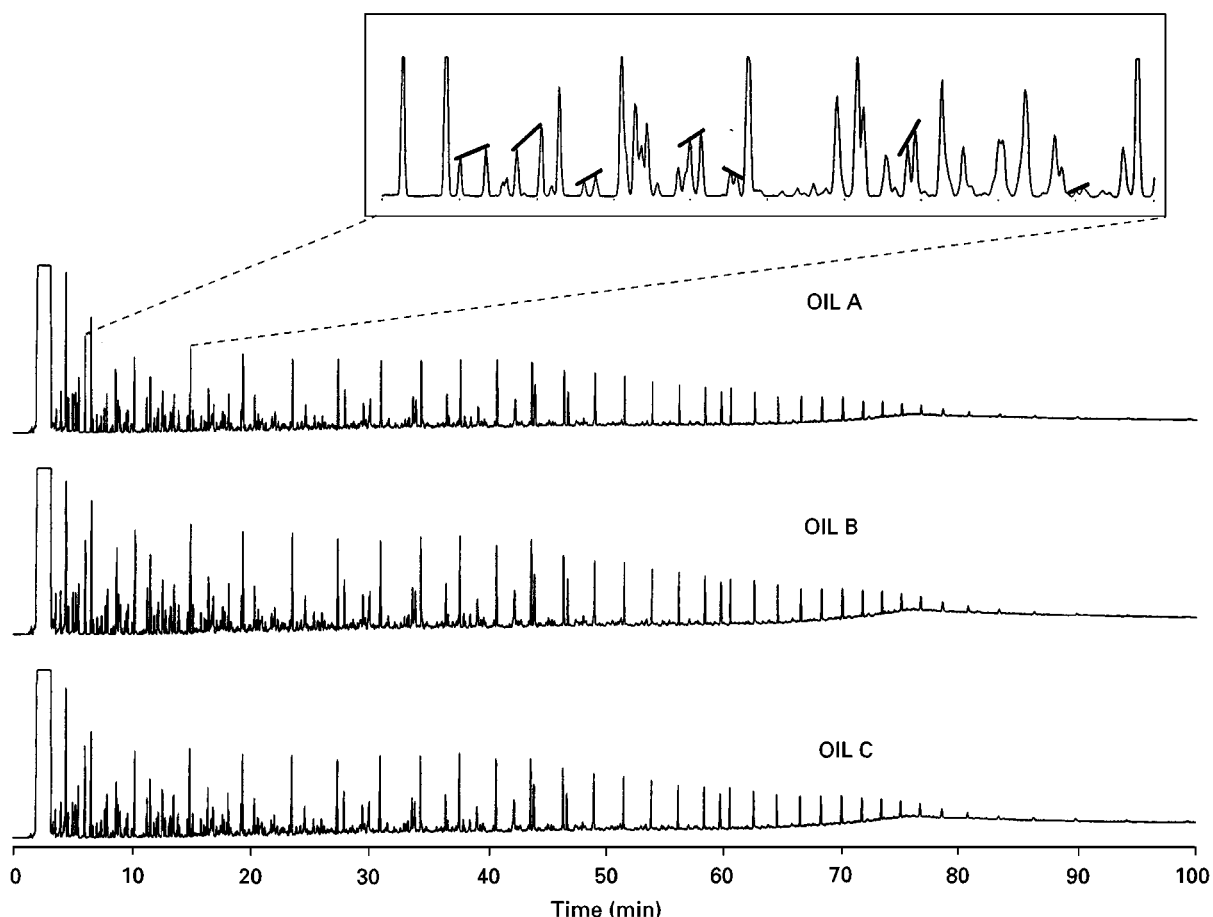


Figure 6 Reservoir geochemistry has provided an important means of determining continuity and communication within reservoir compartments. Once it has been established that the oil in a reservoir is from a common source, high resolution gas chromatograms are obtained for individual samples and ratios of various pairs of peaks are determined, as shown in the figure. The identity of the components does not have to be known; the important point is that the same pairs of peaks are used for all the samples examined in any particular study. Although the early studies typically used peaks in the early part of the chromatogram, it has been shown that the minor components in the higher regions of the chromatogram can also be used for the same purpose.

GC-MS and MID using the characteristic ions for the sterane and terpane biomarkers at m/z 217 and 191, respectively, produces the additional data shown in Figure 9. On the basis of the chromatograms shown in Figure 9, samples B and C are in all probability related to each other. It is not necessary to identify each component, rather one should think of the mass chromatograms as fingerprints. If two samples are derived from the same source, then their fingerprints should be the same, or at least very similar; samples from different sources will be different from each other. Hence when the fingerprint for sample A is compared with those for B and C in Figure 9, there are a number of significant differences between these samples that permit one to conclude that A is from a different source than B or C. The biomarker fingerprints obtained in this way are very

specific for a variety of applications, in addition to this type of correlation. The presence of individual compounds, for example oleanane and gammacerane, can provide information on the presence of specific types of source materials or the nature of the depositional environment.

To illustrate this type of application, Figure 10 shows the m/z 191 and 217 mass chromatograms of an oil that is derived from source material dominated by higher plant or terrestrial source material. This evidence is contained in the fact that the predominant component in the m/z 191 mass chromatogram is the terpane called 18 α (H)-oleanane. It has been established that this compound has its precursor in higher plant material and hence the presence of this compound in an oil will indicate that the sample is derived from such material. In support of such evidence is the

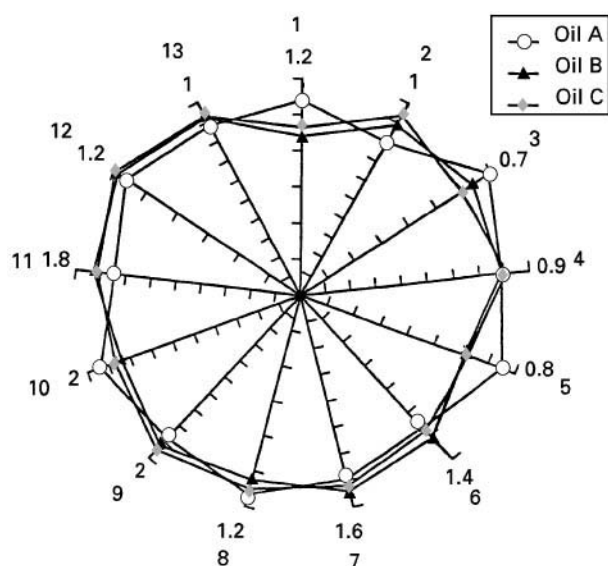


Figure 7 The ratios of the pairs of peaks measured in Figure 6 are plotted on a star or polar diagram. If two oils are in the same compartment, or in communication with each other, then on such a star plot the two oils will have identical plots (i.e. B and C). If they are not in communication with each other, then their plots will show some subtle differences (i.e. oil A).

fact that the sterane chromatogram is dominated by the C_{29} steranes. For oils of this nature it has been clearly established that the C_{29} steranes are also associated with higher plant source materials. In this

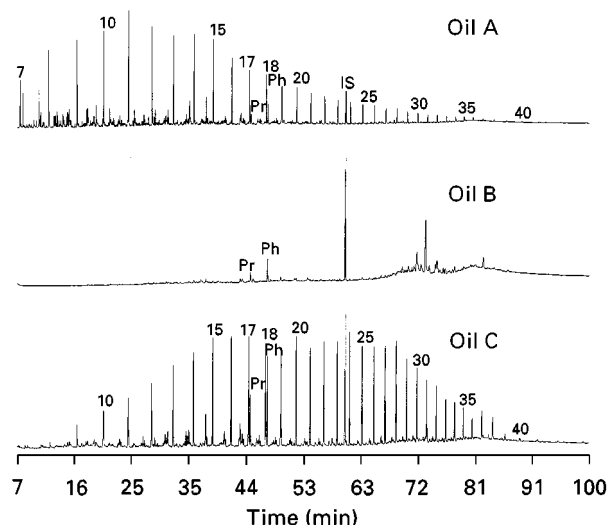


Figure 8 Gas chromatograms of three different oils provides limited information concerning the relationship between the samples. In this figure oil B clearly appears to be quite different from oils A and C, but all that can really be said is that oil B has been heavily biodegraded and the n -alkanes have been removed. It is impossible to say what, if any, similarities there may have been between the alkane distribution for this sample and the other two samples.

manner, pieces of evidence can be put together that in many cases will provide a very clear indication as to the origin of the material being analysed.

In the second example, shown in Figure 11, the presence of another very specific compound, gammacerane, can also be very clearly seen in the m/z 191 chromatogram. This compound is a very specific indicator of depositional environments of enhanced salinity. Recent attempts have been made to relate the presence of certain compounds, for example, dinosterane to the age of the source rock from which the sample was generated. Specific ratios of different sterane isomers or terpane isomers are also used extensively for determining the relative maturity of oils or source rocks.

The sterane and methylsterane distributions in crude oils are far more complex than the terpanes and no matter how good the GC resolution, it is impossible to obtain complete separation of all co-eluting isomers, epimers and homologues (Figure 12). In order to optimize this separation it is necessary to utilize GC combined with tandem mass spectrometry, or MS/MS, which provides an additional degree of separation based on the utilization of the MS/MS capability.

Gas Chromatography–Mass Spectrometry/Mass Spectrometry

To demonstrate the utility of the GC-MS/MS approach to the characterization and determination of biomarkers in geochemical samples, the resolution of a complex mixture of sterane isomers and homologues will be described. While this example utilizes the steranes, it should be borne in mind that the same approach can be used to resolve any very complex mixture of organic compounds from geochemical samples.

The mixture of steranes commonly analysed by MS/MS is in the C_{27} – C_{30} carbon number range and each homologue has a molecular mass at m/z 372, 386, 400 and 414, respectively. For each of the steranes the parent ions will undergo a collision-activated decomposition to produce a daughter ion at m/z 217. Hence a series of MS/MS parent–daughter experiments are performed utilizing these parent–daughter transitions in combination with the GC separation. The GC-MS analysis and single ion monitoring of m/z 217 produces the mass chromatogram shown in Figure 12 but with the GC-MS/MS analyses, the results shown in Figure 13 are obtained. It can be seen in Figure 13 that by using the C_{27} parent–daughter ion pair at m/z 372/217, respectively, the result of analysing the sample by MS/MS is to

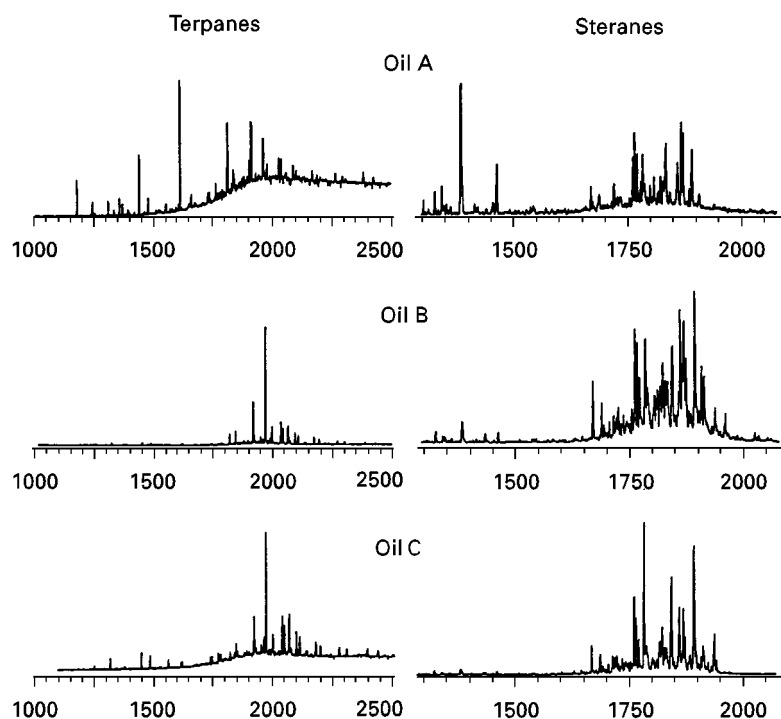


Figure 9 The terpene and sterane distributions for the same three oils as used in Figure 8 provide a more specific indication of the relationship between different samples. It is not necessary to know the identification of all the individual peaks but rather to think of the total chromatogram as a fingerprint. In this case it can be seen that oil A has quite a different set of fingerprints than oils B and C, suggesting it is not related to these other two samples. While the fingerprints of oils B and C may show some differences, these are actually due to small maturity differences in the samples.

totally resolve the C_{27} components from the rest of the complex mixture.

Similar results would be obtained if the parent–daughter pairs for the other members of the series were also illustrated. A similar approach could be applied to the methylsterane mixture using the parent ions and the daughter ion at mass 231 and a similar simplification of the mixture would be obtained. In this particular application the MS/MS serves to introduce an additional element of separation following the initial separation by GC.

Pyrolysis–Gas Chromatography–Mass Spectrometry

While a large proportion of the geochemical samples analysed are soluble in organic solvents and readily amenable to direct analysis by GC or GC-MS, there is another aspect to geochemical samples that is often overlooked. Samples of geochemical interest such as soils, source rocks or coals also have a significant insoluble organic component such as the humic fraction of soils or the kerogen fraction of a source rock. Characterization of these insoluble fractions requires

some type of degradation step prior to analysis. At present for geochemical purposes this degradation step typically consists of some type of pyrolysis reaction with the pyrolyser interfaced to the gas chromatograph or GC-MS system. There are also reports of the use of various NMR techniques to characterize this insoluble fraction, although this is a little less specific than the pyrolysis approach.

An example of the pyrolysis of the insoluble fraction of an organic-rich source rock is shown in Figure 14. This was produced by pyrolysing the sample at a temperature of 600°C for a short period of time and allowing the pyrolysis products to be transferred directly to the GC column. (There are of course a wide variety of pyrolysis conditions that could be used, but those cited here give a general idea of the typical conditions used.) The products of a sample pyrolysed in this manner produce a chromatogram dominated by alkane/alkene doublets plus a wide variety of minor components. From these distributions it is often possible to gain information about the nature of the source materials originally responsible for the formation of the kerogen plus the type of products it will subsequently produce if buried to

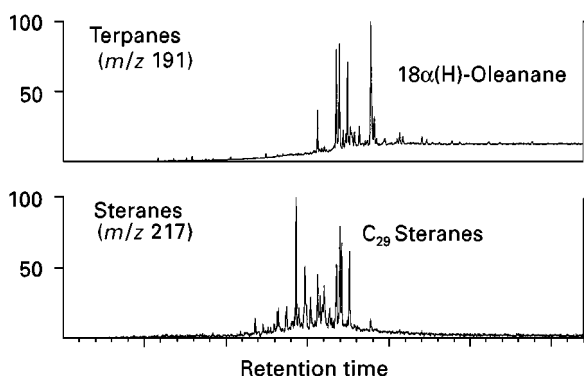


Figure 10 GC-MS analysis of crude oils reveals complex fingerprints of biomarkers. In many cases these compounds may be very specific indicators of particular types of source materials responsible for sourcing the oil. In this example the predominant component in the terpane chromatogram is $18\alpha(\text{H})$ -oleanane. Not only is this compound very specific in terms of being derived from higher plant source materials, but it is also more specifically related to the flowering plants or angiosperms that have only evolved since the Late Cretaceous–Early Tertiary periods. The presence of this compound can therefore be used to constrain the age of the source rock from which the oil was generated.

appropriate depths and subjected to thermal degradation.

Another useful application is the pyrolysis of asphaltenes, particularly those isolated from biodegraded crude oil samples. It is often difficult to determine the origin of a biodegraded oil sample. However, if there are a number of possible nondegraded samples with which it can be compared, then the asphaltenes can be isolated from all the samples

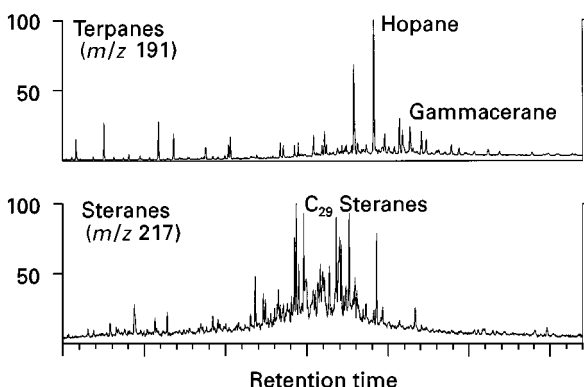


Figure 11 Gammacerane is another very specific biomarker that can be readily observed in the m/z 191 chromatogram. The relative concentration of this compound varies with the salinity of the original depositional environment. Hence samples deposited in a very saline lacustrine setting will generally have high gammacerane contents whereas those from freshwater lacustrine environments are generally depleted in gammacerane.

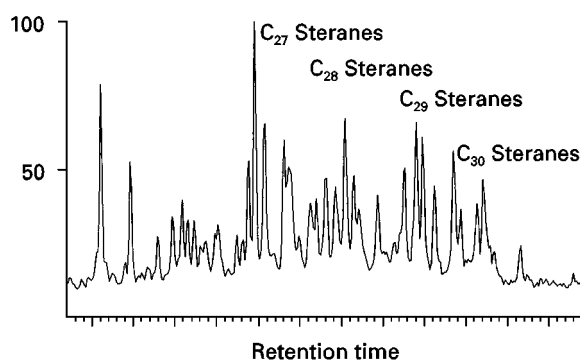


Figure 12 Sterane distributions in crude oils as typically determined by single ion monitoring of m/z 217 reflect the complex nature of the mixture of these components in a crude oil. It is virtually impossible to separate all of the co-eluting isomers, epimers and homologues by GC-MS, no matter how good the chromatography.

by pentane precipitation and pyrolysed. In this way it will be observed that the n -alkane/alkene fingerprints generated from the degraded and nondegraded samples will be virtually identical if the samples are derived from the same source, but quite different if the samples are unrelated.

Gas Chromatography–High Resolution Mass Spectrometry

The majority of geochemical analyses reported in the literature are concerned with the detection and identification of hydrocarbons. However, many

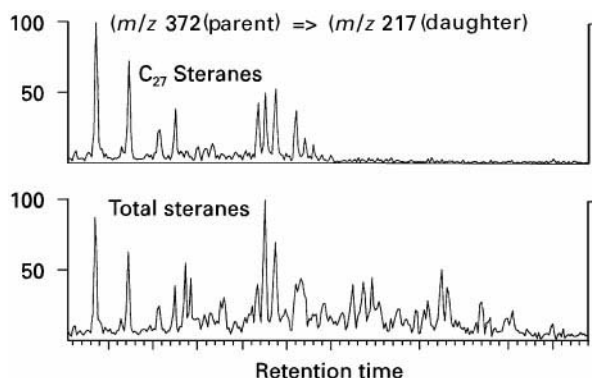


Figure 13 To simplify the sterane fingerprint to some degree GC-MS/MS becomes an important tool. In this diagram the same sterane mixture used for Figure 12 has been analysed in the GC-MS/MS mode. By filtering out the parent–daughter ions for the C_{27} steranes, the top chromatogram shows only the C_{27} compounds. Distributions for the C_{28} – C_{30} steranes could also be obtained using the appropriate parent–daughter ions.

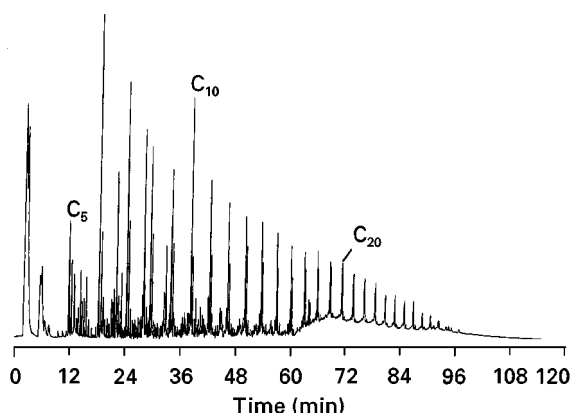


Figure 14 One of the most useful ways for characterizing the insoluble organic matter in a source rock, coal, shale or soil sample is by pyrolysis-GC. This figure illustrates the results obtained from pyrolysis-GC of Messel shale and shows that the major components obtained in the approach are a series of alkane/alkene doublets. Variations in these distributions can be used to characterize the organic matter in terms of whether it is algal or terrestrial as well as provide information on the relative maturity of the samples.

geochemical mixtures contain complex mixtures of compounds in which heteroatoms are mixed with the hydrocarbons in varying amounts. In certain applications knowledge of these components, particularly sulfur-containing compounds, may be extremely important. There are two approaches by which such distributions may be obtained. The first is by the use of element-selective GC detectors, such as the FPD, Hall detector, or one of the more recent types of AED that are selective for sulfur-containing compounds at the exclusion of non-sulfur-containing compounds. The second method combines GC with high resolution MS. Although this approach is not used routinely, it is a very powerful and specific technique for this type of application, as discussed by Tibbetts and Large in 1988. While the use of low resolution GC-MS and ancillary techniques such as single ion monitoring and multiple ion detection have been discussed elsewhere, it needs to be recognized that utilization of nominal masses in MID may lead to ambiguous results. As demonstrated by Tibbetts and Large, while the ion at nominal mass 184 may be used for the determination of dibenzothiophenes (DBT), it is also the nominal mass for the C_4 -substituted naphthalenes, leading to possible misinterpretation of the resulting chromatograms. However, use of the accurate mass at m/z 184.0347 permits detection of only the DBT and no substituted naphthalenes. Several examples have been given by Tibbetts and Large on the use of this approach for the correlation of crude oils or to distinguish oils from different sources or reservoirs.

Used in conjunction with the conventional detection of biomarkers, this method provides a very powerful and additional tool for geochemical analyses.

Gas Chromatography–Isotope Ratio Mass Spectrometry

Carbon naturally exists as a mixture of its two stable isotopes, ^{12}C and ^{13}C , in an approximate $^{12}\text{C}/^{13}\text{C}$ ratio of 99 : 1. The carbon isotopic composition of living organic matter in part depends on the species but is also determined by a number of environmental properties. For example, atmospheric carbon dioxide is assimilated by living plants during photosynthesis and the nature of the plants and whether they assimilate CO_2 via a C3 or C4 photosynthetic cycle will determine the extent of preferential assimilation of the lighter ^{12}C isotope. C3 plants are typically associated with warmer and more arid climates and in general have isotopic values in the -10 to -18‰ range. C4 plants are more typically associated with colder climates and have lighter isotopic values in the -22 to -30‰ range. To determine the ^{13}C composition, the sample is combusted to convert all of the carbon to CO_2 , which is analysed in a stable isotope ratio mass spectrometer and compared with the isotopic composition of a standard material (Pee Dee Belimnite, PDB), whose isotopic composition has been assigned a value of 0.

GC-IRMS and Isotopic Composition of Individual Components

GC-IRMS permits acquisition of $\delta^{13}\text{C}$ values for individual components in complex mixtures. The important part of the system is the interface between the GC and the isotope ratio mass spectrometer. This consists of a reactor tube, generally a narrow-bore ceramic tube, containing a bundle of wires, typically copper, nickel or platinum where complete combustion to CO_2 must occur. After combustion the water and CO_2 pass through a membrane separator to remove the water before the CO_2 enters the mass spectrometer, where the isotopic composition of the gas is determined relative to the standard. The isotopic values of individual components can be interpreted to obtain information on the diagenetic history of an individual component and the nature of the microbial community during deposition.

The isotopic composition of individual compounds is also of importance from an environmental viewpoint. For example, analysis of a whole oil, or the saturate fraction of a whole oil, allows the ready determination of $\delta^{13}\text{C}$ values of the n -alkanes and the

major isoprenoids, pristane and phytane. These values can be used for correlation purposes, to distinguish oils from different sources, to correlate oil spills with their suspected sources, or to determine the source of hydrocarbons that have contaminated wildlife. Examples of this approach are shown in **Figure 15**. Gas chromatograms of oil extracted from the feathers of birds that had been exposed to a crude oil spill and a suspected source are compared with each other and show certain differences, particularly at the lighter end of the chromatograms. Such differences could lead to a dispute as to whether or not this oil was actually the one that was responsible for contaminating the birds. The lower part of the figure shows the carbon isotope data for individual compounds in the two samples. It can be seen

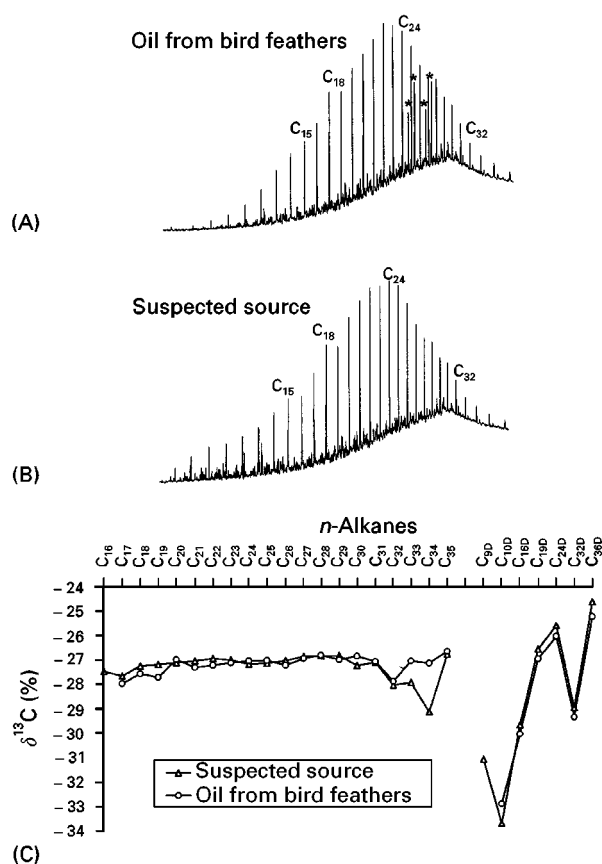


Figure 15 (A) Chromatogram of an extract from bird feathers contaminated by a crude oil; (B) shows the chromatogram for the suspected source of the contamination. The two chromatograms show some significant differences, particularly in the early part of the chromatogram, mainly as a result of weathering. However, in (C) we see that there is a strong relationship between the isotopic compositions for each individual n -alkane in the two samples. This isotopic information can be used in conjunction with the biomarker data and other parameters to establish a relationship between the two samples.

that, despite the loss of some of the light ends through evaporation, a good relationship between the two samples can be established. These data could also be used in support of the biomarker and other properties normally used to establish relationships between samples thought to be related. In an additional example, **Figure 16** shows the results from the GC-IRMS analyses of 20 oils from a region in SE Asia. It can be seen that on the basis of these analyses two distinct families of oils are present in the region. One family has isotopic values of around -20‰ for each compound whereas the other family has values around -28‰ . This information can be used in conjunction with the biomarker data to determine the significance of these differences.

While these are just two examples, we have also shown that GC-IRMS can be used in an environmental context to correlate weathered and unweathered oils and refined products and their weathered counterparts. If there are small amounts of the n -alkanes remaining it should be possible to obtain their isotopic composition and subsequently use these values to make the correlation. Alternatively if the samples have been so extensively biodegraded that all of the n -alkanes have been removed, it is possible to isolate the asphaltenes, pyrolyse them and analyse the pyrolysates by GC-IRMS. Correlations can then be made using these data. This is a particularly valuable approach for the correlation of refined products that only contain lower carbon number compounds and none of the more reliable biomarker compounds that are typically used for correlation purposes.

Summary

This article has attempted to illustrate the importance of GC to geochemical analyses. Geochemical samples from all sources, whether recent or ancient, oils or synthetic chemicals, refined or crude, are incredibly complex mixtures of organic compounds in most cases. To try and analyse such samples, whether simply for correlation purposes or to detect and identify unknown compounds, almost inevitably requires some level of chromatography to facilitate the analytical process. The most common forms of chromatography generally involve some form of liquid chromatography in the initial steps to simplify the mixture into compound classes, followed by GC to separate and resolve as many compounds as possible in the resulting fractions. Chromatography alone simply separates the components, hence it is very common in most geochemical analyses for the chromatographic step to be combined with an identification technique such as MS. The results of such

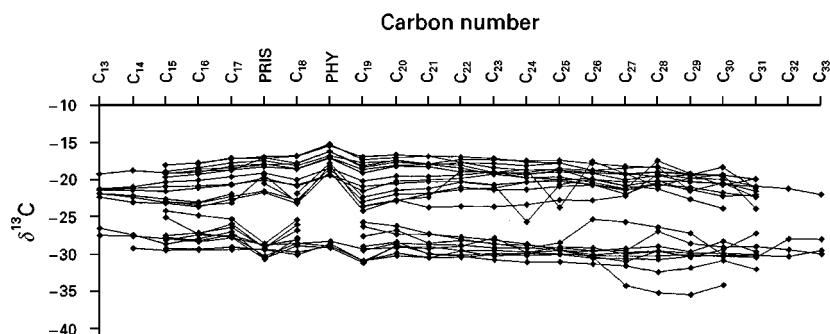


Figure 16 Analysis of 20 oils by GC-IRMS provides isotopic data for each major compound present in the oils. The oils plotted on this chart can be divided into isotopically heavy and isotopically light groups. Supporting evidence for these groupings can be obtained from the GC-MS data.

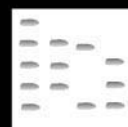
analyses generally provide the information necessary to determine the origin of a particular sample and, in the context of crude oil exploration, relate it to possible source rocks and such information as age, maturity, and migration pathways. For environmental samples the information obtained is generally for the purpose of determining the source of a spill and hence a great deal of use is made of these distributions in terms of their fingerprinting capability. As chromatographic and spectroscopic techniques continue to improve, clearly the degree of separation achievable for these complex mixtures will also greatly improve, but mixtures of even greater complexities will always be available to provide that next level of challenge.

See also: II/Chromatography: Gas: Column Technology; Detectors: General (Flame Ionization Detectors and Thermal Conductivity Detectors); Detectors: Mass Spectrometry; Detectors: Selective; Historical Development; Pyrolysis Gas Chromatography; Theory of Gas Chromatography.

Further Reading

- Baskin DK, Hwang RJ and Purdy RK (1995) Prediction of gas, oil, and water intervals in Niger Delta reservoirs using gas chromatography. *American Association of Petroleum Geologists Bulletin* 79: 337–350.
- Brooks J and Fleet AJ (eds) (1987) *Marine Petroleum Source Rocks*, Geological Society Special Publication, vol. 26, 444 pp. Oxford: Blackwell Scientific Publications.
- Carlson RMK, Teerman SC, Moldowan JM, Jacobson SR, Chan EI, Dorrough KS, Seetoo WC and Mertani B (1993) High temperature gas chromatography of high wax oils. In: *Proceedings of the 20th Annual Convention of the Indonesian Petroleum Association*, Jakarta, pp. 483–507.
- Connan J (1984) Biodegradation of crude oils in reservoirs. In: Brooks J and Welte DH (eds) *Advances in Petroleum Geochemistry*, vol. 1, pp. 299–335. London: Academic Press.
- England WA (1989) The organic geochemistry of petroleum reservoirs. *Organic Geochemistry* 16(1–3): 415–425.
- Hayes JM, Freeman KH, Popp BN and Hoham CH (1990) Compound-specific isotopic analyses: a novel tool for reconstruction of ancient biogeochemical processes. *Organic Geochemistry* 16 (1–3): 1115–1128.
- Johnson D, Quimby BD and Sullivan JJ (1995) An atomic emission detector for gas chromatography. *American Laboratory*, pp. 13–20.
- Killops SD and Readman JW (1985) HPLC fractionation and GC-MS determination of aromatic hydrocarbons from oils and sediments. *Organic Geochemistry* 8: 247–257.
- Levy JM (1994) Fossil fuel applications of SFC and SFE: a review. *Journal of High Resolution Chromatography* 17: 212–216.
- Peters KE and Moldowan JM (1992) *The Biomarker Guide: Interpreting Molecular Fossils in Petroleum and Ancient Sediments*. Englewood Cliffs, NJ: Prentice Hall.
- Philp RP and Oung J-N (1992) Biomarkers, occurrence, utility and detection. In: Vorell L (ed.) *Instrumentation in Analytical Chemistry*, 1988–1991, pp. 368–376. Washington, DC: American Chemical Society.
- Del Rio JC and Philp RP (1992) High molecular weight hydrocarbons: a new frontier in organic geochemistry. *Trends in Analytical Chemistry* 11 (15): 187–193.
- Tibbetts PJC and Large R (1988) Improvements in oil fingerprinting: GC/HRMS of sulphur heterocycles. In: Crump GB (ed.) *Petroanalysis* 87, pp. 45–57. London: John Wiley.

GLYCOPROTEINS: LIQUID CHROMATOGRAPHY



K. Miyazaki, Hokkaido University Hospital,
Hokkaido, Japan

Copyright © 2000 Academic Press

Introduction

Many proteins in cells and biological fluids are glycosylated, and these glycoproteins are present in animals, plants, microorganisms and viruses. The most commonly occurring monosaccharides found in oligosaccharide attachments to mammalian proteins are D-mannose (Man), D-galactose (Gal), D-glucose (Glu), L-fucose (Fuc), N-acetylglucosamine (GlcNAc), N-acetylgalactosamine (GalNAc), and N-acetylneuraminic acid (sialic acid or NeuAc).

The primary structure of glycoprotein glycans and their biological functions have been gradually unravelled by the improvements of methods for isolation and structure determination. High performance liquid chromatography (HPLC) is one of the most commonly used methods for the isolation and analysis of both glycoproteins and their derived carbohydrates, mainly due to the excellent resolution, ease of use, the generally high recoveries, the excellent reproducibility of repetitive separations, and the high productivity in terms of cost parameters.

Chemistry and Importance of the Glycan Chain of Glycoproteins

Basic Structure of Glycoprotein

In glycoproteins, glycans are conjugated to peptide chains by two types of primary covalent linkage, N-glycosyl and O-glycosyl. The former is called an N-linked sugar chain and contains a GlcNAc residue that is linked to the amide group of asparagine residues of a polypeptide. As shown in Figure 1, almost all N-linked glycoproteins have a common core of two GlcNAc and three Man residues. N-linked glycoproteins have three types of carbohydrate moieties: complex type (Figure 1), high mannose type and hybrid type. The hybrid type is a mixture of the complex and high mannose types. Complex type structures usually have from two to four branches attached to the two outer core Man residues. The branches are distributed over the two terminating core Man residues. The complex structures are termed diantennary, triantennary and tetraantennary, according to the

number of antennae. The basic branch structures are composed in most instances of one GlcNAc and one Gal residue (Figure 1).

O-Glycosyl glycoproteins contain at their reducing end a GalNAc residue that is linked to the hydroxyl group of either serine or threonine residues of a polypeptide. This linkage is called an O-linked or mucin-type sugar chain. In general, O-linked structures appear to be less complex than N-linkages in terms of the number of antennae and monosaccharides. However, they can be fucosylated and sialylated. Some glycoproteins have both the N-linked and O-linked forms in their molecules (N, O-glycoproteins).

The addition of carbohydrate to a peptide chain changes the shape and size of the protein structure. Several important discoveries have revealed the following biological roles of glycans: (i) protection of polypeptide chains against proteolytic enzymes; (ii) influence on heat stability, solubility, and many physicochemical properties; and (iii) interaction with other proteins or nonprotein components of the cell, including control of the lifetime of circulating glycoproteins and cells.

Microheterogeneity of Glycans

In addition to genetically determined variants expressed as variations in their polypeptide chains, almost all glycoproteins exhibit polymorphism associated with their glycan moieties. This type of diversity is termed microheterogeneity, and these different forms have recently been called glycoforms. These variants were first characterized in the α_1 -acid glycoprotein (AAG) from human serum using electrophoresis. As shown in the structure of major oligosaccharides of AAG (Figure 1), microheterogeneity was found to be due to the occurrence of di-, tri-, and tetraantennary glycans of the N-acetylglucosamine type at the five glycosylation sites.

This feature is widespread and has been observed in natural as well as in recombinant DNA glycoproteins. The existence of microheterogeneity gives rise to many interesting questions regarding the origin of this phenomenon and its relevance to the biological functioning of the glycoproteins that can be distinguished.

Recent interest has been shown in glycoproteins in the industrial field of genetic engineering of human glycoproteins of therapeutic interest. This gives rise to

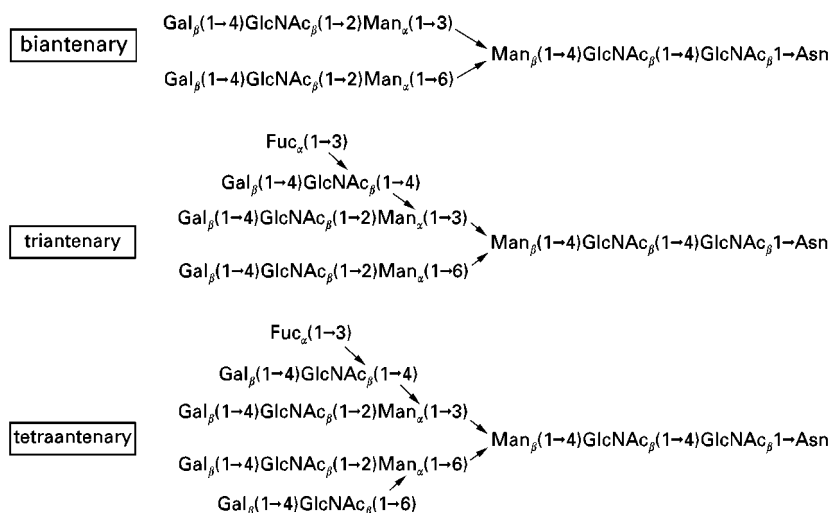


Figure 1 Structure of the major oligosaccharides of α_1 -acid glycoprotein (a complex type of the *N*-linked form). Several NeuAc are linked to Gal residues.

an enormous problem, because the production of recombinant human glycoproteins in nonhuman eukaryotic cells or in prokaryotic cells devoid of glycan biosynthesis machinery leads to the production of incorrectly glycosylated proteins. Incorrectly glycosylated glycoproteins may have an undesirable effect on therapeutic effectiveness and safety due to changes in the properties of the products, including a decrease in the stability against heat or protease, shortening of the *in vivo* life span of the molecules by an increase in clearance, a decrease in the affinity for specific receptors, and an increase in antigenicity.

Isolation and Quantitation of Glycoprotein Molecules and Analysis of Glycan Chains

Determination of the primary structure of glycoproteins necessitates analysis of the protein sequence, identification of the glycosylation sites, unravelling of the glycan structures and determination of the microheterogeneity of the glycans at each glycosylation. For these studies, it is essential that adequate starting materials are available.

For the isolation or purification of glycoproteins, a combination of several complementary separation methods such as gel permeation chromatography, affinity chromatography (lectin or others), anion- or cation-column chromatography, high performance capillary electrophoresis, and HPLC using several sorbents is generally used.

Determination of the carbohydrate composition, type and branching pattern is an important step for understanding the biological function of the native

glycoprotein molecules as well as for the development of a recombinant DNA-derived glycoprotein as a pharmaceutical agent. However, the composition, type and branching pattern of carbohydrates are complex due to the diversity of monosaccharides and the variety of possible linkages. Unlike amino acids, which are linked through an amido bond, monosaccharides are joined through a variety of hydroxyl groups present on the sugar to form glycosidic linkages. For example, two different amino acids can form only two dipeptides, while two different monosaccharides can lead to more than 60 disaccharides. However, the availability of improved and sophisticated methods for the isolation and characterization of glycoproteins and their derived glycans has paved the way for the analysis and characterization of the carbohydrate chains of glycoprotein. These analytical methods include mass spectrometry, enzymatic microsequencing, nuclear magnetic resonance (NMR), capillary electrophoresis, reversed-phase HPLC (RP-HPLC), and high pH anion exchange chromatography with pulsed amperometric detection (HPAEC-PAD), and generally a combination of several complementary analytical methods is needed to determine the carbohydrate structure.

In this section, we give an outline of the recently developed HPLC procedures for the purification, separation, and determination of glycoproteins and their glycoforms.

Examples of Isolation or Purification of Glycoproteins by Using HPLC

α_1 -Acid glycoprotein (AAG) AAG is a characteristic and dominant fraction of human serum sialoglycoproteins with a molecular mass approximately 44 000

Da, an unusually high carbohydrate content (45%) and a large number of sialyl residues. Although its exact biological function is still unknown, AAG is an acute-phase reactant that increases following cancer, myocardial infarction, and congestive heart failure and has also been reported to play an important role in immunoregulation.

Ion exchange chromatography and gel permeation chromatography previously used for purification are time-consuming and require a large volume of plasma or serum because of the low quantities recovered. These methods also lead to a strong possibility of denaturation and desialylation. Moreover, separation of AAG and α_1 -antitrypsin has been difficult, because the chromatographic behaviour of these compounds during anion exchange chromatography is similar. Recently, these problems have been overcome by the introduction of an HPLC system equipped with a hydroxyapatite column as the last step after the clean-up procedures with commercially available cartridge ion exchange columns.

Ceruloplasmin (CP) CP is a serum α_2 -glycoprotein that carries more than 95% of the copper present in plasma and is believed to have an active role in the regulation of copper and iron homeostasis. It has been pointed out that fragmentation of CP during purification and storage has hampered the study of its structure. The rapid degradation of purified CP reported by many laboratories may be largely due to the presence of one or more copurifying or contaminating proteases, at least one of which is a metalloproteinase.

Recently, a highly purified and nonlabile CP has been obtained from human plasma by combining the previously reported chromatographic steps with additional gel permeation and fast protein liquid chromatography (FPLC) steps. In the latter steps, further purification of CP by Sephadex G-50 chromatography and Mono Q FPLC were essential for the removal of plasma metalloproteinase, and this purification procedure yielded a protein that was completely stable even after incubation at 37°C for 4 weeks.

Erythropoietin (EPO) EPO, an acidic glycoprotein hormone, is synthesized in the kidney and circulates in the blood to stimulate red cell proliferation and differentiation in bone marrow. Native human EPO was first purified from the urine of patients suffering from severe aplastic anaemia. Since then, several methods for the purification of urinary human EPO (uHuEPO) have been developed. RP-HPLC has recently been used for the purification of uHuEPO with high *in vivo* activity. This purification

procedure involves two membrane filtration steps, Sephadex G-25, two DEAE-agarose steps, Sephadex G-75, wheat germ agglutinin (WGA)-agarose, and RP-HPLC. The final HPLC step is essential for the removal of nucleic acids.

Chromatographic Determination of AAG

There have been very few reports on chromatographic methods for determining concentrations of glycoproteins other than AAG in biological samples. Radial immunodiffusion (RID) utilizing the antibody against AAG has been widely used to determine AAG in serum because of its strong specificity. This method, however, is time-consuming and is not easily applicable to experimental animals. To overcome these problems, some simple and rapid HPLC methods have been developed.

After pretreatment of human serum with a chloroform/methanol mixture (2:1, v/v), 500 μ L of the upper phase was applied to the anion exchange FPLC system (Mono Q HR 5/5 column), and AAG was eluted with a pH/NaCl gradient elution programme. To measure the serum AAG content, the Mono Q HR column was calibrated with commercial AAG in the range 100–200 μ g/500 μ L of sample volume.

A rapid and sensitive determination method starting from the diluted human serum itself has also been reported. This procedure involves the anion exchange step for cleaning up serum (commercially available cartridge column, DEAE-M) and a hydroxyapatite HPLC system. A linear relationship between standard AAG concentration and peak height was observed over the concentration range 0.5–2.5 mg mL⁻¹ serum. The coefficient of variation at 0.5 mg mL⁻¹ AAG was 3.7% ($n = 8$). A good correlation was observed between this HPLC method (y) and the conventional RID (x) ($y = 1.009x + 0.004$, $r = 0.996$).

Determining the Carbohydrate Composition, Type and Branching Pattern

RP-HPLC has become a commonly used method for the analysis and purification of peptides, proteins and glycoproteins. The RP-HPLC experimental system usually comprises an n-alkylsilica-based sorbent. By using modern instrumentation and columns, complex mixtures of peptides and proteins can be separated and low picomolar amounts of resolved components can be collected. Separation can be easily performed by changing the gradient slope of solvents such as acetonitrile containing an ionic modifier (e.g. trifluoroacetic acid (TFA)); column temperature; or the organic solvent composition. The technique is equally applicable to the analysis of enzymatically derived

mixtures of peptides from proteins and glycoproteins. Separated fractions can be subsequently subjected to further analysis of carbohydrates and amino acids.

A new HPLC method, HPAEC-PAD, which bypasses the derivatization steps by using pulsed electrochemical detection on gold electrodes, has been developed. Monosaccharides and oligosaccharides can be directly resolved by anion exchange chromatography, because the hydroxyl groups of carbohydrates are weakly acidic and reveal anionic forms at pH values greater than pH 12. In addition to high sensitivity in the low picomole range of PAD, a major advantage of HPAEC-PAD is its usefulness in analysing both monosaccharides and all classes of oligosaccharides without derivatization. HPAEC-PAD has therefore been used successfully for resolving and quantitating the constituent monosaccharides released by acidic hydrolysis (e.g. TFA) of glycan chains and for resolving N-linked oligosaccharides separated by enzyme digestion (e.g. PNGase F).

Figure 2 shows the HPAEC-PAD chromatograms of fractions 23–27 from the RP-HPLC separation of a tryptic digest of recombinant tissue plasminogen activator (tPA). The peaks from RP-HPLC separation were collected manually, and aliquots of all 62 fractions were analysed for neutral and amino monosaccharides after acid hydrolysis. The chromatograms in

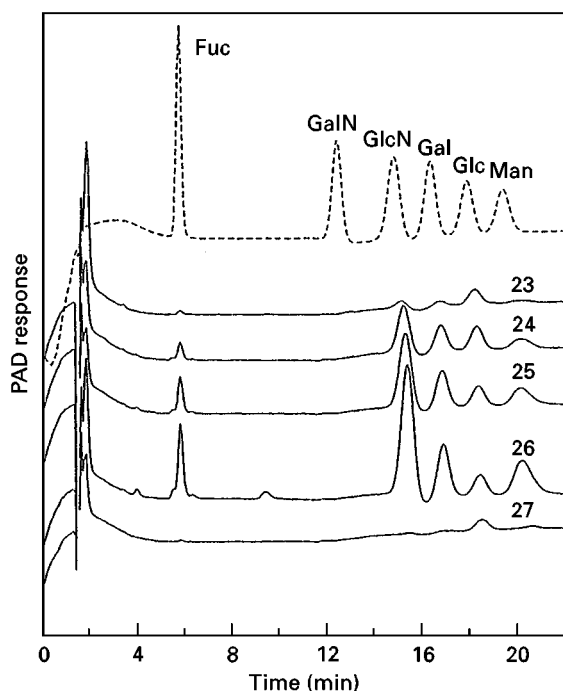


Figure 2 Monosaccharide analysis of fractions 23–27 from RP-HPLC separation of a tryptic digest of recombinant tissue plasminogen activator. Elution positions of monosaccharide standards are indicated on the upper trace. (Reproduced with permission from Townsend *et al.*, 1996.)

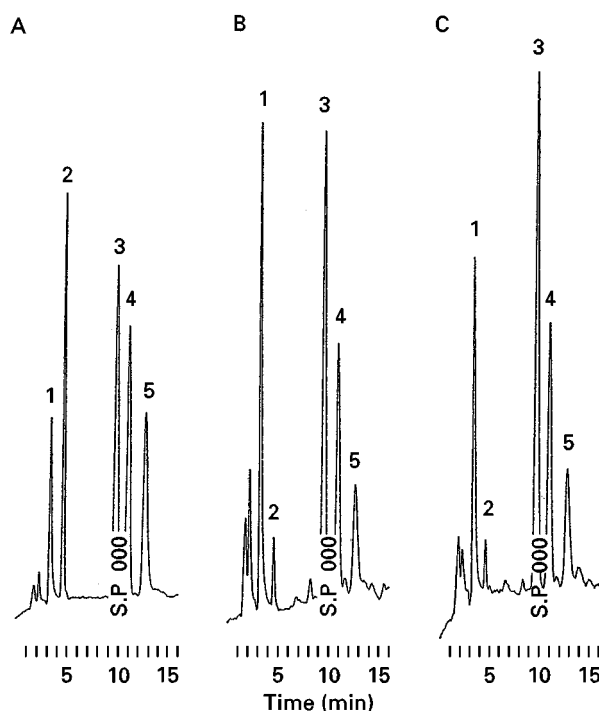


Figure 3 Representative chromatograms of monosaccharides after treatment of standard and plasma samples. (A) Standard sample containing $5.0 \mu\text{g mL}^{-1}$ of each monosaccharide; (B) healthy subject; (C) patient with renal insufficiency. Peaks: 1 = mannitol (internal standard); 2 = Fuc; 3 = GlcNAc; 4 = Gal; 5 = Man. (Reproduced with permission from Kishino *et al.*, 1995.)

Figure 2 indicate that fractions 24–26 contain glycopeptides, and the ratio of constituent monosaccharides suggests that their oligosaccharide structures are those of fucosylated N-acetylglucosamine-type oligosaccharides. Another N-acetylglucosamine-type chain and an oligomannose-type chain were identified similarly by the same analytical procedure.

The HPAEC-PAD method is also applicable to the quantitation of concentrations of monosaccharides after release by acid hydrolysis and following clean-up procedures with commercially available cartridge columns. Figure 3 shows the chromatograms of four monosaccharides in purified serum AAG from healthy subjects and from patients with renal insufficiency. The concentration of NeuAc can also be determined under different solvent conditions. This method enables composition analysis of the carbohydrate moiety of AAG with only 1.0 mL of plasma. Linear relations between the amount of NeuAc or monosaccharides and the peak-height ratio of NeuAc or monosaccharides to the internal standards are observed over the concentration range of 5.0 to $100 \mu\text{g mL}^{-1}$. N-Glycolylneuraminic acid and mannitol are used as the internal standard for NeuAc and the four monosaccharides, respectively.

Table 1 Analysis of NeuAc and monosaccharide levels in purified α_1 -acid glycoprotein (AAG) from plasma of healthy subjects, patients with renal insufficiency and patients with myocardial infarction

	Healthy subjects (n = 8)	Renal insufficiency (n = 6)	Myocardial infarction (n = 4)
Age (years)	65.8 \pm 12.5	60.2 \pm 7.2	69.7 \pm 11.7
AAG conc. (mg mL ⁻¹)	0.79 \pm 0.14	1.01 \pm 0.19 ^a	1.66 \pm 0.34 ^b
NeuAc (mg g ⁻¹ · AAG)	82.77 \pm 12.55	89.29 \pm 15.55	132.70 \pm 6.89 ^b
Fuc (mg g ⁻¹ · AAG)	9.84 \pm 3.08	12.79 \pm 3.37	10.40 \pm 3.42
GlcNAc (mg g ⁻¹ · AAG)	113.01 \pm 10.07	135.44 \pm 10.51 ^b	142.68 \pm 12.96 ^b
Gal (mg g ⁻¹ · AAG)	76.97 \pm 4.23	88.78 \pm 5.61 ^b	86.92 \pm 11.73 ^a
Man (mg g ⁻¹ · AAG)	49.14 \pm 2.57	57.26 \pm 3.80 ^b	50.16 \pm 1.67
GlcNAc/Man	2.18 \pm 0.37	2.50 \pm 0.35	2.84 \pm 0.21 ^a

Source: Kishino *et al.* (1995).

AAG concentration was determined by the HPLC method with a hydroxyapatite column.

NeuAc and each monosaccharide concentration were determined by HPAEC-PAD.

Values in the table are means \pm SD.

^aSignificantly different ($p < 0.05$) from healthy subjects.

^bSignificantly different ($p < 0.01$) from healthy subjects.

The resultant quantitation data (Table 1) for healthy subjects, patients with renal insufficiency and patients with myocardial infarction show that not only AAG levels but also the concentrations of several monosaccharides in patients increased significantly compared to those of healthy subjects, suggesting a change in the carbohydrate branching pattern in such pathologic conditions.

It is well known that the microheterogeneity of AAG is due to the occurrence of di-, tri-, and tetra-antennary glycans of the *N*-acetylglucosamine type at the five glycosylation sites. Moreover, the Man content is constant among the antennary glycans, and the number of branches increases with the addition of GlcNAc to Man residues. A highly branched glycan chain of AAG is constructed by the linkage of Gal to GlcNAc (Figure 1), which results in the formation of an antennary structure (*N*-acetylglucosamine). Therefore, in the case of AAG, determination of the concentration ratio of GlcNAc to Man (GlcNAc/Man) is important for estimating whether the carbohydrate moiety of glycoforms has a highly or less-branched glycan chain. The significantly higher GlcNAc/Man ratio in the patients with myocardial infarction suggests that a highly branched glycan chain was synthesized. Changes in the carbohydrate moiety in the glycoproteins have been reported in patients with various types of disease.

As shown in Figure 4, at least six fractions, which are possibly based on carbohydrate-mediated microheterogeneity, have been obtained from healthy human (Japanese) serum AAG by HPLC using a hydroxyapatite column under a gradient elution programme. From the determination of five monosac-

charides (NeuAc, Fuc, GlcNAc, Gal, Man) in each fraction by HPAEC-PAD, it was found that glycoforms rich in carbohydrates were eluted later (fractions 4, 5, 6) and that NeuAc was relatively abundant in these highly adsorbed glycoforms, especially in fraction 6. Furthermore, the ratio of GlcNAc/Man in fraction 2 was significantly higher than those in the other fractions, suggesting the presence of a highly branched glycan chain. Interestingly, it has been also shown that fractions 1 and 2, both relatively rich in highly branched glycan chains, showed a significantly lower binding capacity to disopyramide, a drug for the treatment of arrhythmia, than did the other fractions. This result suggests that the binding sites of AAG to disopyramide are hindered by relatively large carbohydrate moieties, such as a tetraantennary structure. These results are consistent with the findings that the binding capacity of purified AAG isolated from patients (with renal insufficiency or myocardial infarction) to disopyramide is significantly lower than that of healthy subjects and that the AAGs of these patients revealed a higher concentration ratio of GlcNAc/Man, an index of the abundance of highly branched glycan chains.

In conclusion, in order to gain further insight into the structure-function relations of the carbohydrate moiety, it is essential that sufficient quantities of glycoprotein variants are available. An effective combination of the sophisticated separation methods for glycoforms, such as the HPLC system using a hydroxyapatite column, and the qualitative and quantitative analytical methods for monosaccharides/oligosaccharides, such as HPAEC-PAD, must be established.

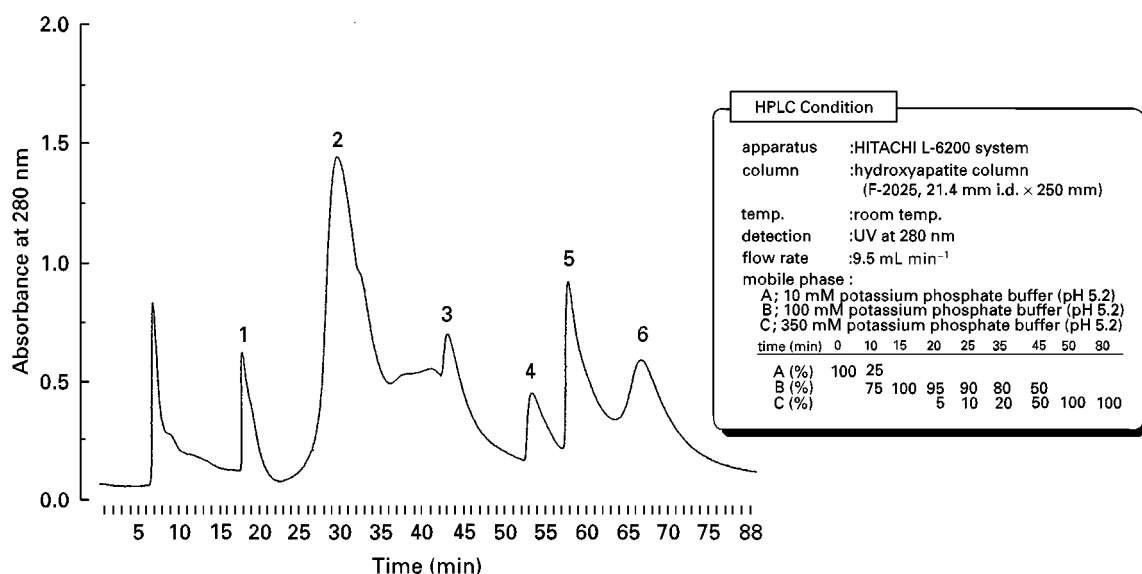


Figure 4 Typical chromatograms of the glycoforms of α_1 -acid glycoprotein (AAG) from the serum of healthy subjects by HPLC. Inlet is the gradient programme for the fractionation of the glycoforms of AAG. (Sampling time of each fraction: fraction 1, 17–22 min; 2, 27–36 min; 3, 43–50 min; 4, 53–57 min; 5, 58–62 min and 6, 65–72 min.) (Reproduced with permission from Kishino *et al.*, 1997.)

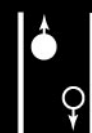
See also: **III/Carbohydrates:** Liquid Chromatography. **Peptides and Proteins:** Liquid Chromatography. **Poly-saccharides:** Liquid Chromatography.

Further Reading

- Clemetson KJ (1997) In: Montreuil J, Vliegthart JFG and Schachter H (eds) *Glycoproteins II*, pp. 173–201. Amsterdam: Elsevier.
- Hancock WS, Chakel AAJ, Souders C, M'Timkulu T, Pungor E Jr and Guzzetta AW (1996) In: Karger BL and Hancock WS (eds) *Methods in Enzymology*, vol. 271, pp. 403–427. San Diego: Academic Press.
- Hardy MR and Townsend RR (1994) In: Lennarz WJ and Hart GW (eds) *Methods in Enzymology*, vol. 230, pp. 208–225. San Diego: Academic Press.
- Kishino S, Nomura A, Sugawara M, Iseki K, Kakinoki S, Kitabatake A and Miyazaki K (1995) *Journal of Chromatography* 672: 199–205.

- Kishino S and Miyazaki K (1997) *Journal of Chromatography* 699: 371–381.
- Kishino S, Nomura A, Saitoh M, Sugawara M, Iseki K, Kitabatake A and Miyazaki K (1997) *Journal of Chromatography* 703: 1–6.
- Montreuil J (1995) In: Montreuil J, Schachter H and Vliegthart JFG (eds) *Glycoproteins*, pp. 1–12. Amsterdam: Elsevier.
- Schmid K (1989) In: Bauman P, Eap CB, Muler WE and Tillement J-P (eds) *Alpha₁-Acid Glycoprotein*, pp. 7–22. New York: Alan R. Liss.
- Townsend RR, Basa LJ and Spellman MW (1996) In: Karger BL and Hancock WS (eds) *Methods in Enzymology*, vol. 271, pp. 135–147. San Diego: Academic Press.
- Vliegthart JFG and Montreuil J (1995) In: Montreuil J, Schachter H and Vliegthart JFG (eds) *Glycoproteins*, pp. 13–28. Amsterdam: Elsevier.

GOLD RECOVERY: FLOTATION



S. Bulatovic and D. M. Wyslouzil, Lakefield Research, Lakefield, Ontario, Canada

Copyright © 2000 Academic Press

Introduction

The recovery of gold from gold-bearing ores depends largely on the nature of the deposit, the

mineralogy of the ore and the distribution of gold in the ore. The methods used for the recovery of gold consist of the following unit operations:

- The gravity preconcentration method, which is mainly used for recovery of gold from placer deposits that contain coarse native gold. Gravity is

often used in combination with flotation and/or cyanidation.

- Hydrometallurgical methods are normally employed for recovery of gold from oxidized deposits (heap leach), low grade sulfide ores (cyanidation, carbon-in-pulp (CIP), carbon-in-leach (CIL)) and refractory gold ores (autoclave, biological decomposition followed by cyanidation).
- A combination of pyrometallurgical (roasting) and hydrometallurgical route is used for highly refractory gold ores (carbonaceous sulfides, arsenical gold ores) and the ores that contain impurities that result in a high consumption of cyanide, which have to be removed before cyanidation.
- The flotation method is a widely used technique for the recovery of gold from gold-containing copper ores, base metal ores, copper–nickel ores, platinum group ores and many other ores where other processes are not applicable. Flotation is also used for the removal of interfering impurities before hydrometallurgical treatment (i.e. carbon prefloat), for upgrading of low sulfide and refractory ores for further treatment. Flotation is considered to be the most cost-effective method for concentrating gold.

Significant progress has been made over the past several decades in the recovery of gold using hydrometallurgical methods, including cyanidation (CIL, resin-in-pulp) and bio-oxidation. All of these processes are well documented in the literature and abundantly described. However, very little is known about the flotation properties of gold contained in various ores and the sulfides that carry gold. The sparse distribution of discrete gold minerals, as well as their exceedingly low concentrations in the ore, is one of the principal reasons for the lack of fundamental work on the flotation of gold-bearing ores.

In spite of the lack of basic research on flotation of gold-bearing ores, the flotation technique is used, not only for upgrading of low grade gold ore for further treatment, but also for beneficiation and separation of difficult-to-treat (refractory) gold ores. Flotation is also the best method for recovery of gold from base metal ores and gold-containing platinum group metals (PGM) ores. Excluding gravity preconcentration, flotation remains the most cost-effective beneficiation method.

Gold itself is a rare metal and the average grades for low grade deposits vary between 3 and 6 p.p.m. Gold occurs predominantly in its native form in silicate veins, alluvial and placer deposits or encapsulated in sulfides. Other common occurrences of gold are alloys with copper, tellurium, antimony, selenium, PGMs and silver. In massive sulfide ores,

gold may occur in several of the above forms, which affects flotation recovery.

During flotation of gold-bearing massive sulfide ores, the emphasis is generally placed on the production of base metal concentrates and gold recovery becomes a secondary consideration. In some cases, where significant quantities of gold are contained in base metal ores, the gold is floated from the base metal tailings.

The flotation of gold-bearing ores is classified according to ore type (i.e. gold ore, gold–copper ore, gold–antimony ores), because the flotation methods used for the recovery of gold from different ores is vastly different.

Geology and General Mineralogy of Gold-bearing Ores

The geology of the deposit and the mineralogy of the ore play a decisive role in the selection of the best treatment method for a particular gold ore. Geology of the gold deposits varies considerably, not only from deposit to deposit, but also within the deposit. Table 1 shows major genetic types of gold ores and their mineral composition. More than 50% of the total world gold production comes from clastic sedimentary deposits.

In many geological ore types, several subtypes can be found, including primary ores, secondary ores and

Table 1 Common genetic types of gold deposits

<i>Ore type</i>	<i>Description</i>
Magmatic	Gold occurs as an alloy with copper, nickel and platinum group metals Typically contains low amount of gold
Ores in clastic sedimentary rock	Placer deposits, in general conglomerates, which contain quartz, sericite, chlorite, tourmaline and sometimes rutile and graphite. Gold can be coarse. Some deposits contain up to 3% pyrite. Size of the gold contained in pyrite ranges from 0.01 to 0.07 μm
Hydrothermal	This type contains a variety of ores, including: Gold–pyrite ores Gold–copper ores Gold–polymetallic ores Gold–oxide ore, usually upper zone of sulfide zones The pyrite content of the ore varies from 3% to 90%. Other common waste minerals are quartz, aluminosilicates, dolomite
Metasomatic or scarn ores	Sometimes very complex and refractory gold ores. Normally the ores are composed of quartz, sericite, chlorites, calcite, magnetite. Sometimes the ore contains wolframite and sheelite

Table 2 Major gold minerals

<i>Group</i>	<i>Mineral</i>	<i>Chemical formula</i>	<i>Impurity content</i>
Native gold and its alloys	Native gold	Au	0–15% Ag
	Electrum	Au/Ag	15–50% Ag
	Cuproauride	Au/Cu	5–10% Cu
	Amalgam	Hg/Au	10–34% Au
	Bismuthauride	Au/Bi	2–4% Bi
Tellurides	Calaverite	AuTe ₂	
	Sylvanite	(Au, Ag)Te ₂	
	Petzite	(Au, Ag)Te	
	Magazite	Au(Pb, Sb, Fe)(S, Te _{II})	Unstable
Gold associated with platinum group metals	Krennerite	AuTe ₂ (Pt, Pl)	
	Platinum gold	AuPt	Up to 10% Pt
	Rhodite	AuRh	30–40% Rh
	Rhodian gold	AuRh	5–11% Rh
	Aurosmiride	Au, Ir, Os	5% Os + 5–7% Ir

oxide ores. Some of the secondary ores belong to a group of highly refractory ores, such as those from Nevada (USA), and El Indio (Chile). The number of gold minerals and their associations are relatively small and can be divided into the following three groups: native gold and its alloys, tellurides and gold associated with PGMs.

Table 2 lists major gold minerals and their associations.

Flotation Properties of Gold Minerals and Factors Affecting Floatability

Native gold and its alloys, which are free from surface contaminants, are readily floatable with xanthate collectors. Very often, however, gold surfaces are contaminated or covered with varieties of impurities. The impurities present on gold surfaces may be argentite, iron oxides, galena, arsenopyrite or copper oxides. The thickness of the layer may be in the order of 1–5 µm. Because of this, the flotation properties of native gold and its alloys vary widely. Gold covered with iron oxides or oxide copper is very difficult to float and requires special treatment to remove the contaminants.

Tellurides on the other hand are readily floatable in the presence of small quantities of collector, and it is believed that tellurides are naturally hydrophobic. Tellurides from Minnesota (USA) were floated using dithiophosphate collectors, with over 95% gold recovery.

Flotation behaviour of gold associated in the platinum group metals is apparently the same as that for the PGMs or other minerals associated with the PGMs (i.e. nickel, pyrrhotite, copper and pyrite). Therefore, the reagent scheme developed for PGMs

also recovers gold. Normally, for the flotation of PGMs and associated gold, a combination of xanthate and dithiophosphate is used, along with gangue depressants guar gum, dextrin or modified cellulose. In the South African PGM operations, gold recovery into the PGM concentrate ranges from 75% to 80%.

Perhaps the most difficult problem in flotation of native gold and its alloys is the tendency of gold to plate, vein, flake and assume many shapes during grinding. Particles with sharp edges tend to detach from the air bubbles, resulting in gold losses. This shape factor also affects gold recovery using a gravity method.

In flotation of gold-containing base metal ores, a number of modifiers normally used for selective flotation of copper–lead, lead–zinc and copper–lead–zinc have a negative effect on the floatability of gold. Such modifiers include $\text{ZnSO}_4 \times 7\text{H}_2\text{O}$, SO_2 , $\text{Na}_2\text{S}_2\text{O}_5$, and cyanide when added in excessive amounts.

The adsorption of collector on gold and its floatability are considerably improved by the presence of oxygen. Figure 1 shows the relationship between collector adsorption, oxygen concentration in the pulp and conditioning time. The type of modifier and the pH are also important parameters in flotation of gold.

Flotation of Low Sulfide-containing Gold Ores

The beneficiation of this ore type usually involves a combination of gravity concentration, cyanidation and flotation. For an ore with coarse gold, gold is often recovered by gravity and flotation, followed by cyanidation of the reground flotation concentrate. In some cases, flotation is also conducted on the cyanidation tailing. The reagent combination used in flotation depends on the nature of gangue present in the ore. The usual collectors are xanthates,

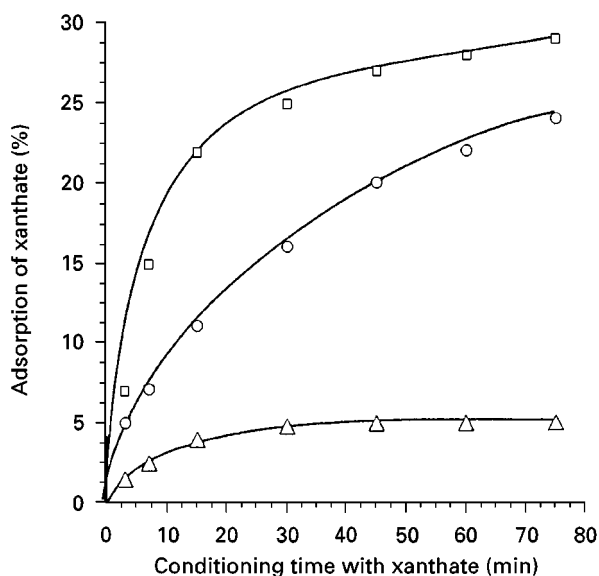


Figure 1 Relationship between adsorption of xanthate on gold and conditioning time in the presence of various concentrations of xanthate. Triangles, O_2 2 mg L⁻¹; circles; O_2 9 mg L⁻¹; squares, O_2 45 mg L⁻¹.

dithiophosphates and mercaptans. In the scavenging section of the flotation circuit, two types of collector are used as secondary collectors. In the case of a partially oxidized ore, auxiliary collectors, such as hydrocarbon oils with sulfidizer, often yield improved results. The preferred pH regulator is soda ash, which acts as a dispersant and also as a complexing reagent for some heavy metal cations that have a negative effect on gold flotation. Use of lime often results in the depression of native gold and gold-bearing sulfides. The optimum flotation pH ranges between 8.5 and 10.0. The type of frother also plays an important role in the flotation of native gold and gold-bearing sulfides. Glycol esters and cyclic alcohols (pine oil) can improve gold recovery significantly.

Amongst the modifying reagents (depressant), sodium silicate starch dextrans and low molecular weight polyacrylamides are often selected as gangue depressants. Fluorosilicic acid and its salts can also have a positive effect on the floatability of gold. The presence of soluble iron in a pulp is highly detrimental to gold flotation. The use of small quantities of iron-complexing agents, such as polyphosphates and organic acids, can eliminate the harmful effect of iron.

Flotation of Gold-containing Mercury/Antimony Ores

In general, these ores belong to a group of difficult-to-treat ores, where cyanidation usually produces poor extraction. Mercury is partially soluble in cyanide, which increases cyanide consumption and reduces extraction. A successful flotation method has been

developed using the flow sheet shown in Figure 2, where the best metallurgical results were obtained using a three-stage grinding and flotation approach. The metallurgical results obtained with different grinding configurations are shown in Table 3.

Flotation was carried out at an alkaline pH, controlled by lime. A xanthate collector with cyclic alcohol frother (pine oil, cresylic acid) was shown to be the most effective. The use of small quantities of a dithiophosphate-type collector, together with xanthate, was beneficial.

Flotation of Carbonaceous Clay-containing Gold Ores

These ores belong to a group of refractory gold ores, where flotation techniques can be used to remove interfering impurities before the hydrometallurgical treatment process of the ore for gold recovery and to preconcentrate the ore for further pyrometallurgical or hydrometallurgical treatment. There are several flotation methods used for beneficiation of this ore type. Some of the most important methods are described as follows:

- Preflotation of carbonaceous gangue and carbon. In this case, only carbonaceous gangue and carbon are recovered by flotation, in preparation for further hydrometallurgical treatment of the float tails for gold recovery. Carbonaceous gangue and carbon are naturally floatable using only a frother, or a combination of a frother and a light hydrocarbon oil (fuel oil, kerosene). When the ore contains clay, regulators for clay dispersion are used. Some of the more effective regulating reagents include sodium silicates and oxidized starch.
- Two-stage flotation method. In this case, carbonaceous gangue is prefloted using the method described above, followed by flotation of gold-containing sulfides using activator-collector combinations. In extensive studies conducted on carbonaceous gold-containing ores, it was established that primary amine-treated copper sulfate improved gold recovery considerably. Ammonium salts and sodium sulfide ($Na_2S \times 9H_2O$) also have a positive effect on gold-bearing sulfide flotation, at a pH between 7.5 and 9.0. The metallurgical results obtained with and without modified copper sulfate are shown in Table 4.
- Nitrogen atmosphere flotation method. This technique uses a nitrogen atmosphere in grinding and flotation to retard oxidation of reactive sulfides, and has been successfully applied on carbonaceous ores from Nevada (USA). The effectiveness of the method depends on the amount of carbonaceous gangue present in the ore, and the amount and type

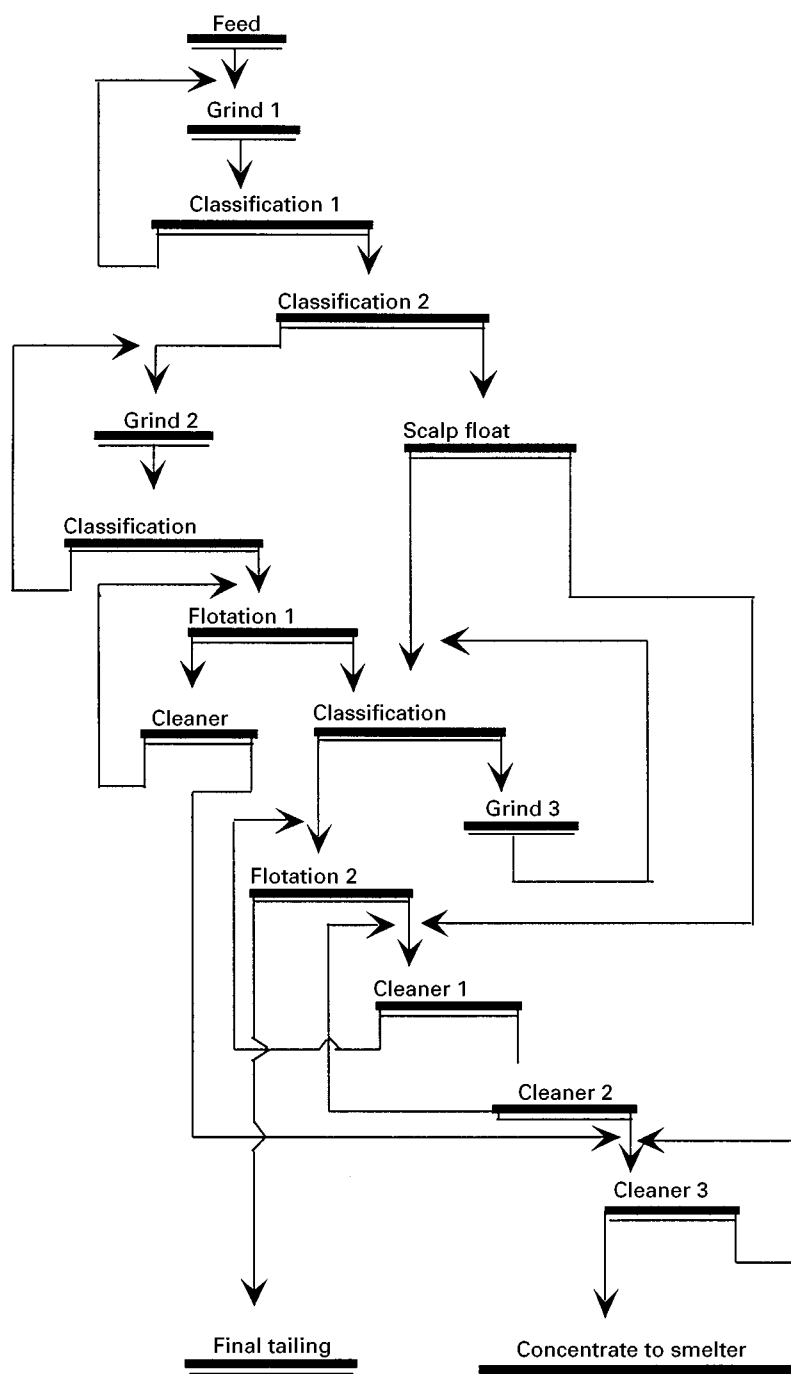


Figure 2 Flotation flow sheet developed for the treatment of gold-containing mercury-antimony ore.

of clay. Ores that are high in carbon or contain high clay content (or both) are not amenable for nitrogen atmosphere flotation.

Flotation of Gold-containing Copper Ores

The floatability of gold from gold-containing copper-gold ores depends on the nature and occurrence of gold in these ores, and its association with iron sulfides.

Gold in the porphyry copper ore may appear as native gold, electrum, cuproaurid and sulfosalts associated with silver. During the flotation of porphyry copper-gold ores, emphasis is usually placed on the production of a marketable copper-gold concentrate and optimization of gold recovery is usually constrained by the marketability of its concentrate.

Table 3 Gold recovery obtained using different flow sheets

Flow sheet	Recovery in concentrate (%)					Tailing Assays (% $g\ t^{-1}$)				
	Au	Ag	Sb	As	S	Au	Ag	Sb	As	S
Single-stage grind flotation	88.1	89.2	72.9	68.4	70.1	1.7	5.0	0.04	0.035	0.38
Two-stage grind flotation	92.2	91.8	93.4	78.7	81.2	1.0	4.1	0.015	0.022	0.27
Three-stage grind flotation	95.3	95.2	95.7	81.2	85.7	0.7	2.2	0.005	0.015	0.19

Reproduced from Sristinov (1964) with permission.

The minerals that influence gold recovery in these ores are iron sulfides (i.e. pyrite, marcasite), in which gold is usually associated as minute inclusions. Thus, the iron sulfide content of the ore determines gold recovery in the final concentrate. **Figure 3** shows the relationship between pyrite content of the ore and gold recovery in the copper concentrate for two different ore types. Most of the gold losses occur in the pyrite.

The reagent schemes used in commercial operations treating porphyry copper–gold ores vary considerably. Some operations, where pyrite rejection is a problem, use a dithiophosphate collector at an alkaline pH between 9.0 and 11.8 (e.g. OK Tedi, PNG Grasberg, Indonesia). When the pyrite content in the ore is low, xanthate and dithiophosphates are used in a lime or soda ash environment.

In more recent years, in the development of commercial processes for the recovery of gold from porphyry copper–gold ores, bulk flotation of all the sulfides has been emphasized, followed by regrinding of the bulk concentrate and sequential flotation of copper–gold from pyrite. Such a flow sheet (**Figure 4**) can also incorporate high intensity conditioning in the cleaner–scavenger stage. Comparison of metallurgical results using the standard sequential flotation flow sheet and the bulk flotation flow sheet is shown in **Table 5**. A considerable improvement in gold recovery was achieved using the bulk flotation flow sheet.

During beneficiation of clay-containing copper–gold ores, the use of small quantities of Na_2S (at natural pH) improves both copper and gold metallurgy considerably.

In the presence of soluble cations (e.g. Fe, Cu), additions of small quantities of organic acid (e.g. oxalic, tartaric) improve gold recovery in the copper concentrate.

Some porphyry copper ores contain naturally floatable gangue minerals, such as chlorites and aluminosilicates, as well as preactivated quartz. Sodium silicate, carboxymethylcellulose and dextrans are common depressants used to control gangue flotation.

Gold recovery from massive sulfide copper–gold ores is usually much lower than that of porphyry copper–gold ores, because very often a large portion of the gold is associated with pyrite. Normally, gold recovery from these ores does not exceed 60%. During the treatment of copper–gold ores containing pyrrhotite and marcasite, the use of $Na_2H_2PO_4$ at alkaline pHs depresses pyrrhotite and marcasite, and also improves copper and gold metallurgy.

Flotation of Oxide Copper–Gold Ores

Oxide copper–gold ores are usually accompanied by iron hydroxide slimes and various clay minerals. There are several deposits of this ore type around the world, some of which are located in Australia (Red Dome), Brazil (Igarape Bahia) and the Soviet Union (Kalima). Treatment of these ores is difficult, and even more complicated in the presence of clay minerals.

Recently, a new class of collectors, based on ester-modified xanthates, has been successfully used to treat gold-containing oxide copper ores, using a sulfidization method. **Table 6** compares the metallurgical results obtained on the Igarape Bahia ore using

Table 4 Effect of amine-modified $CuSO_4$ on gold-bearing sulfide flotation from carbonaceous refractory ore

Reagent used	Product	Weight (%)	Assays (% $g\ t^{-1}$)		Distribution (%)	
			Au	S	Au	S
$CuSO_4$ + xanthate	Gold sulfide conc.	30.11	9.63	4.50	69.1	79.7
	Gold sulfide tail	69.89	1.86	0.49	30.9	20.3
	Head	100.00	4.20	1.70	100.0	100.0
Amine modified $CuSO_4$ + xanthate	Gold sulfide conc.	26.30	13.2	5.80	84.7	90.8
	Gold sulfide tail	73.70	0.85	0.21	15.3	9.2
	Head	100.00	4.10	1.68	100.0	100.0

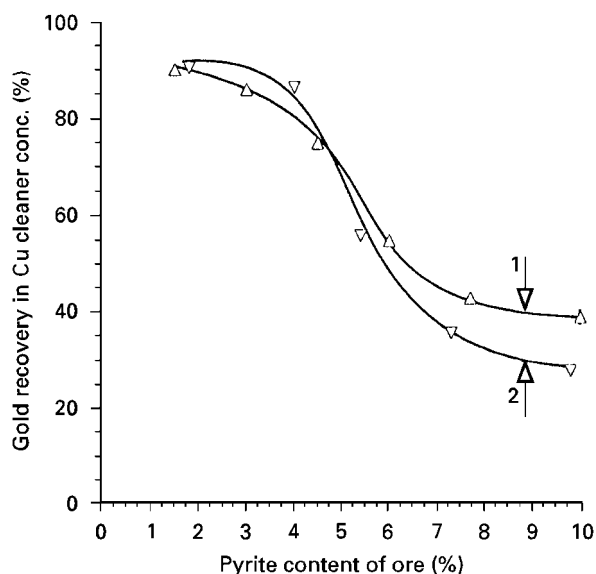


Figure 3 Effect of pyrite content of the ore on gold recovery in the copper-gold concentrate at 30% Cu concentrate grade. 1, Ore from Peru; 2, ore from Indonesia.

xanthate and a new collector (PM230, supplied by Senmin in South Africa).

The modifier used in the flotation of these ores included a mixture of sodium silicate and Calgon. Good selectivity was also achieved using boiled starch.

Flotation of Gold-Antimony Ores

Gold-antimony ores usually contain stibnite (1.5–4.0% Sb), pyrite, arsenopyrite gold (1.5–3.0 g t⁻¹) and silver (40–150 g t⁻¹). Several plants in the USA (Stibnite, Minnesota and Bradley) and Russia have been in operation for some time. There are two commercial processes available for treatment of these ores.

- Selective flotation of gold-containing sulfides followed by flotation of stibnite with pH change.

Stibnite floats well in neutral and weak acid pH, while in an alkaline pH (i.e. > 8), it is reduced. Utilizing this phenomenon, gold-bearing sulfides are floated with xanthate and alcohol frother in alkaline medium (pH > 9.3) followed by stibnite flotation at about pH 6.0, after activation with lead nitrate. Typical metallurgical results using this method are shown in Table 7.

- Bulk flotation followed by sequential flotation of gold-bearing sulfides, and depression of stibnite. This method was practised at the Bradley concentrator (USA) and consisted of the following steps: first, bulk flotation of stibnite and gold bearing sulfides at pH 6.5 using lead nitrate (Sb activator) and xanthate; second, the bulk concentrate is reground in the presence of NaOH (pH 10.5) and CuSO₄, and the gold-bearing sulfides are refloatated with additions of small quantities of xanthate; third, cleaning of the gold concentrate in the presence of NaOH and NaHS. The plant metallurgical results employing this method are shown in Table 8.

Recent studies conducted on ore from Kazakhstan have shown that sequential flotation using thionocarbamate collector gave better metallurgical results than those obtained with xanthate.

Flotation of Arsenical Gold Ores

There are two major groups of arsenical gold ores of economic value. These are the massive base metal sulfides with arsenical gold (e.g. the lead-zinc Olympias deposit, Greece) and arsenical gold ores without the presence of base metals. Massive, base metal arsenical gold ores are rare, and there are only a few deposits in the world. A typical arsenical gold ore contains arsenopyrite as the major arsenic mineral. However, some arsenical gold ores, such as those from Nevada in the USA (Getchel deposit), contain realgar and orpiment as the major arsenic-bearing

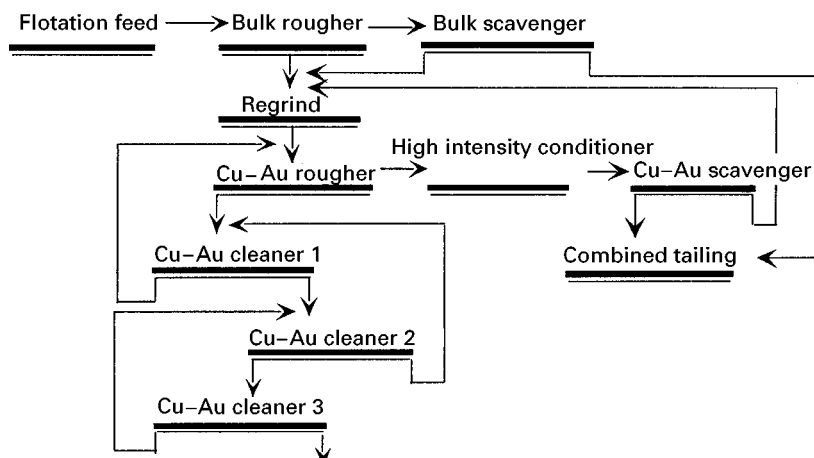


Figure 4 Bulk flow sheet used in the treatment of pyritic copper-gold ores. Reproduced with permission from Bulatovic (1997).

Table 5 Comparison of metallurgical results using conventional and bulk flotation flow sheets on ore from Peru

Flow sheet used	Product	Weight (%)	Assays (% $g\ t^{-1}$)		Distribution (%)	
			Cu	Au	Cu	Au
Conventional (sequential Cu/Au)	Cu/Au conc.	2.28	27.6	32.97	95.4	76.7
	Cu/Au tail	97.72	0.031	0.23	4.6	23.3
	Head	100.00	0.66	0.98	100.0	100.0
Bulk (Figure 4)	Cu/Au conc.	2.32	27.1	36.94	95.2	85.8
	Cu/Au tail	97.68	0.032	0.14	4.8	14.2
	Head	100.00	0.66	0.96	100.0	100.0

minerals. Pyrite, if present in an arsenical gold ore, may contain some gold as minute inclusions.

Flotation of arsenical gold ores associated with base metals is accomplished using a sequential flotation technique, with flotation of base metals followed by flotation of gold-containing pyrite–arsenopyrite. The pyrite–arsenopyrite is floated at a weakly acid pH with a xanthate collector.

Arsenical gold ores that do not contain significant base metals are treated using a bulk flotation method, where all the sulfides are first recovered into a bulk concentrate. In case the gold is contained either in pyrite or arsenopyrite, separation of pyrite and arsenopyrite is practised. There are two commercial methods available. The first method utilizes arsenopyrite depression and pyrite flotation, and consists of the following steps:

- Heat the bulk concentrate to 75°C at a pH of 4.5 (controlled by H_2SO_4) in the presence of small quantities of potassium permanganate or disodium phosphate. The temperature is maintained for about 10 min.
- Flotation of pyrite using either ethylxanthate or potassium butylxanthate as collector. Glycol frother is also usually employed in this separation.

This method is highly sensitive to temperature. Figure 5 shows the effect of temperature on pyrite–

arsenopyrite separation. In this particular case, most of the gold was associated with pyrite. Successful pyrite–arsenopyrite separation can also be achieved with the use of potassium peroxydisulfide as the arsenopyrite depressant.

The second method involves depression of pyrite and flotation of arsenopyrite. In this method, the bulk concentrate is treated with high dosages of lime ($pH > 12$), followed by a conditioning step with $CuSO_4$ to activate arsenopyrite. The arsenopyrite is then floated using a thionocarbamate collector.

Separation of arsenopyrite and pyrite is important from the point of view of reducing downstream processing costs. Normally, roasting or pressure oxidation followed by cyanidation is used to recover gold.

Flotation of Gold from Base Metal Sulfide Ores

Very often lead–zinc, copper–zinc, copper–lead–zinc and copper–nickel ores contain significant quantities of gold (i.e. between 1 and 9 g/t). The gold in these ore types is usually found as elemental gold. A large portion of the gold in these ores is finely disseminated in pyrite, which is considered nonrecoverable. Because of the importance of producing commercial-grade copper, lead and zinc concentrates, little or no consideration is given to improvement in gold recovery, although the possibility exists to optimize gold

Table 6 Effect of collector PM230 on copper–gold recovery from Igarape Bahia oxide copper–gold ore

Reagent used	Product	Weight (%)	Assays (% $g\ t^{-1}$)		Distribution (%)	
			Cu	Au	Cu	Au
$Na_2S = 2500\ g\ t^{-1}$ $PAX = 200\ g\ t^{-1}$	Copper Cl conc.	9.36	33.3	14.15	67.0	50.0
	Copper tail	90.64	1.61	1.46	33.0	50.0
	Feed	100.00	4.65	2.65	100.0	100.0
$Na_2S = 2500\ g\ t^{-1}$ $PAX/PM230$ (1 : 1) = 200 $g\ t^{-1}$	Copper Cl conc.	10.20	39.5	21.79	88.0	85.5
	Copper tail	89.80	0.61	0.42	12.0	14.5
	Feed	100.00	0.61	0.42	12.0	14.5

PAX, potassium amylxanthate.

Reproduced from Bulatovic (1997) with permission.

Table 7 Metallurgical results obtained using a sequential flotation method

Product	Weight (%)	Assays (% $g\ t^{-1}$)			Distribution (%)		
		Au	Ag	Sb	Au	Ag	Sb
Gold concentrate	2.34	42.3	269.3	20.0	53	13	15
Stibnite concentrate	4.04	6.2	559.8	51.0	13	51	64
Tailing	93.62	0.65	18.7	0.7	34	36	21
Feed	100.00	1.86	46.4	3.2	100	100	100

recovery in many cases. Normally, gold recovery from base metal ores ranges from 30 to 75%.

In the case of a copper–zinc and copper–lead–zinc ore, gold collects in the copper concentrate. During the treatment of lead–zinc ores, the gold tends to report to the lead concentrate. Information regarding gold recovery from base metal ores is sparse.

The most recent studies conducted on various base metal ores revealed some important features of flotation behaviour of gold from these ores. It has been demonstrated that gold recovery to the base metal concentrate can be substantially improved with the proper selection of reagent schemes. Some of these studies are discussed below.

Gold-containing lead–zinc ores Some of these ores contain significant quantities of gold, ranging from 0.9 to 6.0 $g\ t^{-1}$ (e.g. Grum, Yukon, Canada; Greens Creek, Alaska and Milpo, Peru). The gold recovery from these ores ranges from 35 to 75%. Laboratory studies have shown that the use of high dosages of zinc sulfate, which is a common zinc depressant used in lead flotation, reduces gold floatability significantly. The effect of $ZnSO_4 \times 7H_2O$ addition on gold recovery in the lead concentrate is illustrated in Figure 6.

In order to improve gold recovery in the lead concentrate, an alternative depressant to $ZnSO_4 \times 7H_2O$

can be used. Depressant combinations such as $Na_2S + NaCN$, or $Na_2SO_3 + NaCN$, may be used. The type of collector also plays an important role in gold flotation of lead–zinc ores. A phosphine-based collector, in combination with xanthate, gave better gold recovery than dithiophosphates.

Copper–zinc gold-containing ores Gold recovery from copper–zinc ores is usually higher than that obtained from either a lead–zinc or copper–lead–zinc ore. This is attributed to two main factors. When selecting a reagent scheme for treatment of copper–zinc ores, there are more choices than for the other ore types, which can lead to the selection of a reagent scheme which is more favourable for gold flotation. In addition, a noncyanide depressant system can be used for the treatment of these ores, which in turn results in improved gold recovery. This option is not available during treatment of lead–zinc ores. Table 9 shows the effect of different depressant combinations on gold recovery from a copper–zinc ore.

The use of a noncyanide depressant system resulted in a substantial improvement in gold recovery in the copper concentrate.

Gold-containing copper–lead–zinc ores Because of the complex nature of these ores, and the requirement for a relatively complex reagent scheme for treatment of this ore, the gold recovery is generally lower than that achieved from a lead–zinc or copper–zinc ore. One of the major problems associated with the flotation of gold from these ores is related to gold mineralogy. A large portion of the gold is usually contained in pyrite, at sub-micron size. If coarser elemental gold and electrum are present, the gold surfaces are often coated with iron or lead, which can result in a substantial reduction in floatability.

The type of collector and flow sheet configuration play an important role in gold recovery from these ores. With a flow sheet that uses bulk copper–lead flotation followed by copper–lead separation, the gold recovery is higher than that achieved with a

Table 8 Plant metallurgical results obtained using a bulk flotation method

Product	Weight (%)	Assays (% $g\ t^{-1}$)			Distribution (%)		
		Au	Ag	Sb	Au	Ag	Sb
Gold concentrate	1.80	91.1	248.8	1.5	61.0	31.3	2.0
Antimony concentrate	1.80	13.0	684.2	51.3	9.0	58.6	75.0
Middlings	0.50	46.6	248.8	20.0	8.6	6.0	8.0
Bulk concentrate	4.10	51.7	440.0	29.0	78.6	85.9	85.0
Tailing	95.90	0.6	3.1	0.2	21.4	14.1	15.0
Feed	100.00	2.7	21.0	1.3	100.0	100.0	100.0

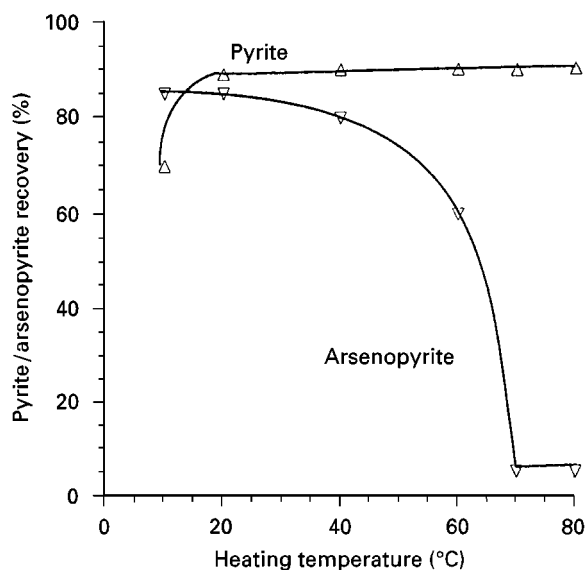


Figure 5 Effect of temperature on separation of pyrite and arsenopyrite from a bulk pyrite-arsenopyrite concentrate.

sequential copper-lead flotation flow sheet. In laboratory tests, an aerophine collector type, in combination with xanthate, had a positive effect on gold recovery as compared to either dithiophosphate or thionocarbamate collectors. Table 10 compares the metallurgical results obtained with an aerophine collector to those obtained with a dithiophosphate collector.

Because of the complex nature of gold-containing copper-lead-zinc ores, the reagent schemes used are also complex. Reagent modifiers such as ZnSO_4 , NaCN and lime have to be used, all of which have a negative effect on gold flotation.

Conclusions

- The flotation of gold-bearing ores, whether for production of bulk concentrates for further gold

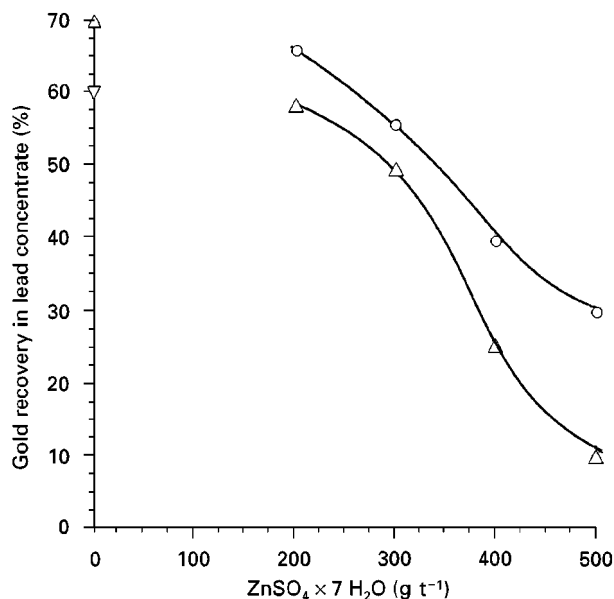


Figure 6 Effect of ZnSO_4 additions on gold recovery from lead-zinc ores. Circles, Greens Creek ore (Alaska); triangles, Grum ore Yukon (Canada).

recovery processes (i.e. pyrometallurgy, hydrometallurgy) or for recovery of gold to base metal concentrates, is a very important method for concentrating the gold and reducing downstream costs.

- The flotation of elemental gold, electrum and tellurides is usually very efficient, except when these minerals are floated from base metal massive sulfides.
- Flotation of gold-bearing sulfides from ores containing base metal sulfides presents many challenges and should be viewed as flotation of the particular mineral that contains gold (i.e. pyrite, arsenopyrite, copper), because gold is usually associated with these minerals at micron size.
- Selection of a flotation technique for gold preconcentration depends very much on the ore

Table 9 Effect of different depressant combinations on gold recovery to the copper concentrate from lower zone Kutcho Creek Ore

Depressant system	Product	Weight (%)	Assays (% g t^{-1})			Distribution (%)		
			Au	Cu	Zn	Au	Cu	Zn
ZnSO_4 , NaCN, CaO pH 8.5 Cu, 10.5 Zn	Cu concentrate	3.10	20.4	26.2	3.30	45.1	85.6	2.8
	Zn concentrate	5.34	1.20	0.61	55.4	4.6	3.4	82.2
	Tailings	91.56	0.77	0.11	0.58	50.3	11.0	15.0
	Feed	100.00	1.4	0.95	3.60	100.0	100.0	100.0
Na_2SO_3 , NaHS, CaO pH 8.5 Cu, 10.5 Zn	Cu concentrate	3.05	32.5	28.1	2.80	68.3	87.4	2.3
	Zn concentrate	5.65	1.20	0.55	54.8	4.7	3.2	84.6
	Tailings	91.30	0.43	0.10	0.52	27.0	9.4	13.1
	Feed	100.00	1.45	0.98	3.66	100.0	100.0	100.0

Table 10 Effect of collector type on Cu-Pb-Zn-Au metallurgical results from a high lead ore

Collector used	Product	Weight (%)	Assays (% $g\ t^{-1}$)				Distribution (%)			
			Au	Cu	Pb	Zn	Au	Cu	Pb	Zn
Xanthate = 30 g/t Dithiophosphate 3477 = 20 g/t	Cu concentrate	2.47	22.4	25.5	1.20	4.50	41.6	78.6	2.3	1.3
	Pb concentrate	1.80	2.50	0.80	51.5	8.30	3.4	1.8	71.3	1.7
	Zn concentrate	13.94	1.10	0.60	0.80	58.2	11.5	10.4	8.6	92.2
	Tailing	81.79	0.71	0.089	0.28	0.52	43.5	9.2	17.8	4.8
	Feed	100.00	1.33	0.80	1.30	8.80	100.0	100.0	100.0	100.0
Xanthate = 30 g/t Aerophine 3418A = 20 g/t	Cu concentrate	2.52	31.3	26.1	1.10	5.00	60.6	80.1	2.1	1.4
	Pb concentrate	1.92	2.80	0.90	51.1	9.20	4.1	2.1	72.5	2.0
	Zn concentrate	13.91	0.90	0.50	0.72	58.5	9.6	8.5	7.4	92.5
	Tailing	81.65	0.41	0.093	0.30	0.44	25.7	9.3	18.0	4.1
	Feed	100.00	1.30	0.82	1.35	8.80	100.0	100.0	100.0	100.0

mineralogy, gangue composition and gold particle size. There is no universal method for flotation of the gold-bearing minerals, and the process is tailored to the ore characteristics. A specific reagent scheme and flow sheet are required for each ore.

- There are opportunities on most operating plants for improving gold metallurgy. Most of these improvements come from selection of more effective reagent schemes, including collectors and modifiers.
- Perhaps the most difficult ores to treat are the clay-containing carbonaceous sulfides. Significant progress has been made in treatment options for these ores. New sulfide activators (e.g. amine-treated $CuSO_4$, ammonium salts) and nitrogen gas flotation are amongst the new methods available.

Further Reading

Baum W (1990) *Mineralogy as a Metallurgical Tool in Refractory Ore, Progress Selection and Optimization*. Squaw Valley, Salt Lake City: Randol Gold Forum.

Bulatovic SM (1993) Evaluation of new HD collectors in flotation of pyritic copper-gold ores from BC Canada. LR-029. Interim R&D report.

Bulatovic SM (1996) An investigation of gold flotation from base metal lead-zinc and copper-zinc ores. *Interim Report* LR-049.

Bulatovic SM (1997) An investigation of the recovery of copper and gold from Igarape Bahia oxide copper-gold ores. *Report of Investigation* LR-4533.

Bulatovic SM and Wyslouzil DM (1996) Flotation behaviour of gold during processing of porphyry copper-gold ores and refractory gold-bearing sulphides. *Second International Gold Symposium*. Lima, Peru.

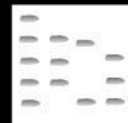
Fishman MA and Zelenov BI (1967) Practice in treatment of sulphides and precious metal ores. *Izdatelstro Nedra* (in Russian) 5: 22–101.

Kudryk V, Carigan DA and Liang WW (1982) *Precious Metals*. Mining Extraction and Processing, AIME.

Martins V, Dunne RC and Gelfi P (1991) *Treatment of Partially Refractory Gold Ores*. Perth, Australia: Randol Gold Forum.

Sristinov NB (1964) The effect of the use of stage grinding in processing of refractory clay-containing gold ore. *Kolima* 1: 34–40.

GRADIENT POLYMER CHROMATOGRAPHY: LIQUID CHROMATOGRAPHY



G. Glöckner, Dresden University of Technology,
Dresden, Germany

Copyright © 2000 Academic Press

Classical Precipitation Chromatography

Polymer Solubility and Precipitation

Solubility is governed by the general requirement that the change in Gibbs' free energy must be negative.

With low molecular weight substances this condition is easily fulfilled, because the entropy contribution is large owing to the large number of particles involved. But with polymer compounds, the entropy of dissolution is comparatively small and the enthalpy contribution gains in importance. The precept that '*similia similibus solventur*' becomes a stringent requirement; in terms of Hildebrand's solubility concept, this means that a polymer can dissolve only in fluids whose solubility parameters are very closely related

to those of the polymer. Therefore, most liquids are non-solvents and the number of solvents available for a given polymer is far fewer than the number of solvents available for a low molecular weight substance of comparable structure.

The solubility of polymers decreases with increasing molecular weight (MW) and can be measured easily by the controlled addition of a non-solvent to the solution of a polymer. The volume fraction ϕ_{NS} of non-solvent at the cloud point is related to the square root, $M^{0.5}$, of molecular weight by

$$100 \phi_{\text{NS}} = C_1 + C_2/M^{0.5}$$

where C_1 and C_2 are constants for the particular system.

This dependence can be used to separate polymers by either fractional precipitation or dissolution. The latter method can also be performed in packed columns by gradients whose solvent power increases in the course of the elution.

The solubility of polymers also depends on temperature. Usually, the temperature coefficient is positive, i.e. fractional dissolution can be carried out with a given solvent (or a non-solvent/solvent mixture at constant composition) by raising the temperature. This procedure can also be performed in columns.

Baker-Williams Fractionation

In 1956, Baker and Williams described 'a new chromatographic procedure and its application to high polymers'. This was column elution combining the effects of solvent strength and temperature. The important innovation was a temperature gradient along the column. The top of the column was heated to a temperature about 50 K higher than that of the cooled bottom. An aluminium jacket ensured a linear temperature profile. The polymer to be investigated was coated onto the part of the inert packing that subsequently was put into the uniformly heated uppermost section of the column. The temperature gradient enabled multistage separation to be performed. Any component dissolved from the sample bed was reprecipitated in a cooler zone of the column. Here it was redissolved later by a non-solvent/solvent mixture of higher solvent strength and transported to the next cooler zone for another reprecipitation. Thus, Baker-Williams fractionation was described as 'a chromatographic method based upon the equilibration of substances between a stationary precipitated phase and a moving solution'. Baker and Williams investigated polystyrene in a glass tube, 350 mm long and 24 mm wide, packed with glass beads of average

size 0.1 mm diameter. The sample size was 300 mg, the gradient ran from ethanol (non-solvent) to methyl ethyl ketone, and the temperature gradient spanned 10–60°C. The multistage mechanism ensured a high separation power, which was confirmed by both theory and experiment. The method became popular in polymer characterization; the second citation in the Bibliography provides a survey of application of the method to about 30 different polymers.

The development of size exclusion chromatography (SEC) made separation according to MW feasible and convenient. SEC allows the investigation of different polymers in a common eluent with very little preliminary work. Dissolved samples can be injected into a running eluent, e.g. tetrahydrofuran, which has sufficient solvent strength for a great many polymers. The elution curve can be monitored with a suitable detector and provides at least a first guess at the MW distribution (MWD). Using MW-sensitive detectors and sophisticated software, reliable MWD curves can be measured within minutes. Interest in the demanding Baker-Williams technique therefore faded away. Although this technique is no longer a competitor in analytical separations according to MW, it should still be considered a powerful tool for separations according to chemical differences and for preparative fractionation. The chemical composition distribution of copolymers, blends or modified polymers can be measured by SEC only in rare cases (if coupled with MWD in a known ratio). This was realized some years ago (see Bibliography).

High Performance Precipitation Liquid Chromatography (HPPLC)

Principle and Instrumentation

The renaissance of precipitation chromatography requires modern equipment, e.g. detectors and programmable gradient devices. The samples to be investigated should be applied in solution and injected into the eluent stream ahead of the column.

About 80% of all high performance liquid chromatography (HPLC) investigations are performed in the reversed-phase mode. Reversed-phase packing materials have a nonpolar surface. They usually consist of particles with a silica core and a bonded layer of alkane chains. Reversed-phase gradients run from a highly polar initial eluent to a final eluent of low polarity. The polar eluent forces nonpolar solutes to be retained by the stationary phase. Retention increases with decreasing polarity of the sample components. The mechanism is understood to be a solvophobic interaction that requires the

mobile phase to be an unfavourable environment for the solute.

The measures taken to force the polymer towards the stationary phase may easily reach or even transgress the limits of solubility. The latter effect has been observed occasionally in reversed-phase chromatography of low molecular weight compounds, but is almost the rule with polymers whose solubility is more restricted.

In normal-phase chromatography, the column is polar and gradient elution is performed with a non-polar starting component A and a polar component B is added during the run. Retention increases with increasing polarity of the sample constituents.

In order to achieve proper retention of a polymer, the starting eluent A must usually be a non-solvent. This means that sample solutions cannot be prepared in a portion of the starting eluent and that the polymer is precipitated at the top of the column. Since proper retention is required, the separation is by this step classified as precipitation chromatography. The precipitation at the top of the column yields preconcentration of the sample. Thus, HPPLC can cope with samples differing widely in concentration, e.g. SEC fractions. The column permeability is not affected. If the sample solvent is a portion of eluent B, the amount of solvent injected will not cause difficulties. The use of another solvent is not recommended because it could overload the column with an additional substance.

The mechanism of separation is, in general, a combination of precipitation and adsorption. The detector must be capable of measuring the eluting sample components without being affected by the solvent gradient. Suitable equipment became available in the late 1970s.

High Performance Precipitation Liquid Chromatography of Styrene-Acrylonitrile Copolymers

Styrene is a polymerizable substance of formula $\text{CH}_2=\text{CH}(\text{C}_6\text{H}_5)$, whose homopolymerization yields polystyrene (PS). It can be polymerized with numerous other monomers to yield copolymers. Styrene units have a strong UV absorption, which means that polystyrene and styrene-containing copolymers can be monitored by UV detectors. Copolymers of styrene and acrylonitrile are of commercial interest. Well-characterized samples graded in composition are available together with a considerable knowledge of styrene-acrylonitrile dissolution/precipitation behaviour. The polarity of acrylonitrile is higher than that of styrene units. Therefore a separation of styrene-acrylonitrile copolymers according to composition is also a separation into constituents dif-

fering in polarity, which is of basic interest in the framework of chromatography. Styrene-acrylonitrile copolymers therefore seemed to be well suited to early studies of high performance precipitation chromatography.

Preliminary studies published in 1982 showed that tetrahydrofuran (THF) has the capacity to separate a mixed styrene-acrylonitrile sample into its constituents, provided that the starting gradient component A enables proper retention of the injected samples. This was achieved by using at least 80% *n*-hexane in THF, i.e. with a non-solvent. The injected polymer was therefore precipitated at the top of the column. The elution characteristic (percentage THF in the eluent versus acrylonitrile content of the sample) was similar to the solubility borderline determined by turbidimetric titration. It was found that equivalent separations could be achieved on a silica column as well as on a nonpolar C_8 column. This surprising result was confirmed in systematic studies performed by Glöckner and van den Berg in 1987 using other polar and nonpolar columns including silica CN bonded phase, small-pore C_{18} , wide-pore C_{18} and μ -Bondagel E1000-10. Thus, the surface of the packings did not actively participate in the separation. It was found that the peak shapes obtained could not be improved further by a temperature gradient along the column (which had been so essential in Baker-Williams fractionation).

Multistage separation without the use of a temperature gradient or interaction with the surface can be achieved on porous packings where the polymer solute is excluded from the pores. The polymer solute then has a higher linear velocity than the eluent, which fills the interstitial volume as well as the pore volume of the column. The polymer bypasses the pores and thus overtakes the eluent which has sufficient solvent strength. The polymer is precipitated and retained until a more powerful eluent reaches its position.

In chromatographic terms, the gradient hexane \rightarrow THF is a normal-phase gradient, i.e. increasing in polarity. In combination with a polar column, e.g. silica or a CN bonded phase, it forms a standard normal-phase system, which should elute more polar sample constituents after less-polar ones. Thus, the observed efficiency of irregular combinations with nonpolar C_8 or C_{18} columns shows that the separation was not governed by the common polarity rules of chromatography. The separation of styrene-acrylonitrile copolymers was, under the conditions of these studies, dominated by a precipitation mechanism. Another example of precipitation mechanism in styrene-acrylonitrile gradient chromatography is given in the next section. However, it should be

firmly stated that styrene–acrylonitrile is an exception rather than the rule. In general, gradient chromatography of synthetic polymers is governed by the *combination of precipitation and adsorption*. Irregular phase combination will not often work, but they do with styrene–acrylonitrile.

Normal- and reversed-phase chromatography are like mirror images. It was a challenge to find out whether or not a given synthetic copolymer could be separated by both mechanisms. The first positive report appeared in 1987 when copolymers of styrene and ethyl methacrylate were measured by both modes of chromatography. All previous related work was by normal-phase separation. As expected, the elution order achieved by reversed-phase chromatography was the opposite of that in normal-phase chromatography. Since then, several polymer systems have been separated by normal-phase and reversed-phase chromatography with inversion of elution order, e.g. styrene–methyl methacrylate copolymers, styrene–methyl acrylate copolymers or methacrylate homopolymers graded in polarity of the ester group.

High Performance Precipitation Liquid Chromatography of Styrene–Acrylonitrile Copolymers with Inversion of Elution Order

The separation of styrene–acrylonitrile copolymers with an elution order as in reversed-phase chromatography was achieved on a column packed with polystyrene gel. Eluent A was methanol (MeOH), a polar non-solvent for styrene–acrylonitrile samples; the less polar eluent, B, was either THF or dichloromethane. In both cases, the gradient rate was 0–100% B in 25 min. Copolymers with acrylonitrile content between 2.3% and 27.3% were retained longer the less acrylonitrile they contained (see Figure 1). Although the phase system and the elution order conformed to the rules of reversed-phase chromatography, the solubility mechanism prevailed.

The samples were prepared by copolymerization to only about 5% conversion, but they still consisted of macromolecules differing in composition. The chemical composition distributions of the samples are essentially responsible for the shape of the elution curves. The chemical composition distributions of samples with, say, 8.6% or 17.6% average acrylonitrile content are obviously narrower than that of a sample with 12.5% acrylonitrile.

The shape of the elution curve for 36.2% acrylonitrile in Figure 1 looks rather odd. In addition, the position of its maximum is not where it might be expected. According to its high acrylonitrile content, the sample is the most polar of the series investigated. It should therefore be eluted before the copolymer

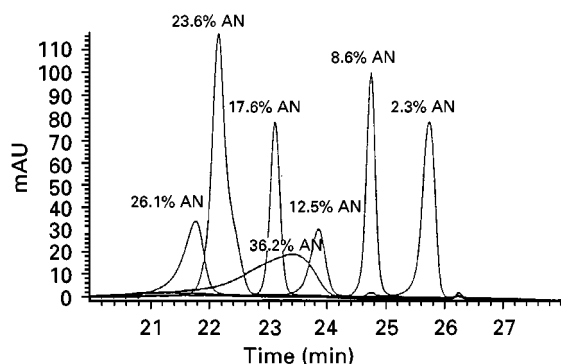


Figure 1 Merged plot of elution curves of seven styrene–acrylonitrile copolymers on a column (250 mm × 7.1 mm i.d.) packed with polystyrene gel. Gradient: methanol → tetrahydrofuran, 0–100% B in 25 min: UV signal detected at 254 nm. The acrylonitrile (AN) content of the samples is indicated on the curves; the amount of each injected was 30 µg. (Reproduced from Glöckner *et al.*, 1991, by courtesy of Vieweg-Verlag.)

labelled 26.1% acrylonitrile, but it was eluted between the samples 17.6% and 12.5% acrylonitrile. This puzzling observation can be understood with the help of the solubility diagram for styrene–acrylonitrile in THF/MeOH, which is shown in Figure 2. The solubility boundary has a maximum at 20–25% acrylonitrile content, where samples require only about 45 vol% THF in MeOH for dissolution, whereas copolymers with more or less acrylonitrile need up to 12% more THF.

Along the left-hand branch of the solubility boundary (0–20% acrylonitrile), both polarity and solubility decrease with decreasing acrylonitrile content. The sequence of the five late-eluting peaks in Figure 1 is supported by polarity and solubility. Beyond the point of inflection, polarity increases but solubility decreases with increasing acrylonitrile content. A sample with 36.2% acrylonitrile requires about 50% THF for dissolution but should, according to polarity, already be released from the column in a mixture of 35% THF in MeOH. The measured peak position between the peaks for 17.6% and 12.5% acrylonitrile is determined by solubility. This is another indication of precipitation prevailing in the chromatography of styrene–acrylonitrile copolymers.

Along the left-hand branch of the solubility boundary, polarity supports the effect of solubility but beyond the turning point the two effects counteract each other. This is the reason why the elution curve for 36.2% acrylonitrile is much broader than the others. With normal-phase gradients, the 36.2% sample yielded an elution curve of the usual narrow shape, even in irregular phase systems (see Figure 3).

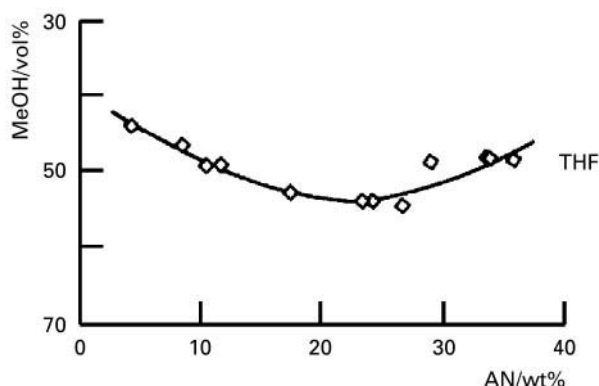


Figure 2 Solubility boundary for styrene-acrylonitrile copolymers in THF/MeOH as measured by turbidimetric titration at 20°C using THF as a sample solvent and methanol as the precipitating non-solvent. Phase separation (precipitation) occurs on crossing the curve from the upper part of the diagram (homogeneous solutions) to the lower part. (Reproduced from Glöckner *et al.*, 1991, by courtesy of Vieweg-Verlag.)

Sudden-Transition Gradient Chromatography of Synthetic Polymers

Interaction of Precipitation and Adsorption in Polymer Gradient Chromatography

Chromatographic retention and elution of synthetic polymers is generally governed by precipitation/dissolution and adsorption/desorption. The contribution of adsorption can be judged by comparing the solubility and elution characteristics of the sample

system. If solubility prevails (and both temperature and concentration are suitable), both curves coincide. Noticeable adsorption shifts the elution characteristic above the solubility boundary, i.e. a higher concentration of solvent B is necessary for *eluting* a given sample than for *dissolving* it. The least adsorption was observed in reversed-phase systems with polystyrene samples. The predominance of an adsorption mechanism causes a retention behaviour different from (or even opposite to) that observed with a precipitation mechanism (see Table 1).

Baker and Williams reported that classical precipitation chromatography can be performed with 'a column of inert material... providing that the polymer gel does not flow through the column'. This type of flow can also occur in high performance precipitation chromatography in which case an optical detector may register the strong signal characteristic of a turbid liquid. Such a signal is affected by many parameters including time and is therefore poorly reproducible. Gel breakthrough can be avoided if there is some contribution of adsorption to retention. Separation according to composition with the least superimposition of molecular weight effects requires adsorption to dominate, i.e. elution by changing polarity of the eluent rather than by solvent strength. On the other hand, the unfavourable effect of sample size owing to strong adsorption can be compensated by increasing the contribution of precipitation to retention.

Independent Control of Adsorption and Precipitation

In common binary gradients, the solvent power and polarity of the mobile phase change simultaneously in the course of the run. An optimum can be sought by using a variety of different eluents A and B and their combinations. However, this is a cumbersome procedure requiring an adequate supply of chemicals and a prolonged time. In addition, it may not be successful because thermodynamic reasons restrict the number of possible solvents for a given polymer, and several of these may be further ruled out by physical, physiological, or financial reasons. More promising and efficient is the use of ternary systems consisting of two non-solvents (A and B) and one solvent (C) for the polymers under investigation. A and B must be opposite in polarity, i.e. if A is a polar non-solvent, B is a nonpolar one. The polarity of solvent C is in between those of A and B. Solvent C must be miscible with A and B and must have sufficient strength to dissolve samples in the whole range of molecular weight and composition under investigation.

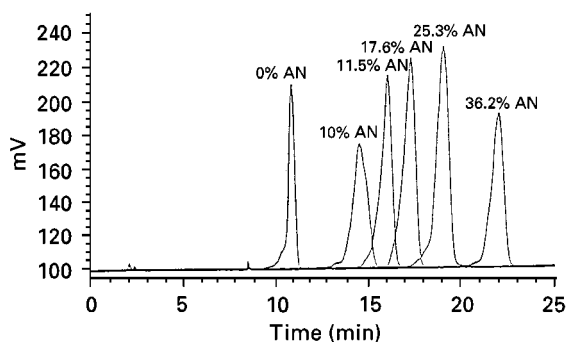


Figure 3 Merged plot of elution curves of six styrene-acrylonitrile copolymers on a reversed-phase column (250 mm \times 4.3 mm i.d.) packed with C_{18} bonded phase; in irregular combination with a normal-phase gradient *n*-heptane \rightarrow (THF + 20% methanol), 0–100% B in 25 min. Detection by signal from an evaporative light-scattering detector. The acrylonitrile (AN) content of the samples is indicated on the curves; the amount of each injected was 30 μ g. (Reproduced from Glöckner *et al.*, 1991, by courtesy of Vieweg-Verlag.)

Table 1 Features of polymer gradient chromatography with predominance of either precipitation/dissolution or adsorption/desorption

Dominating mechanism	Elution characteristic	Irregular phase combinations	Increasing temperature	Increasing sample size (overload)	Increasing molecular weight ^a
Precipitation	Coincident with the solubility boundary	Separating like standard ones	Decreases retention	Increases retention	Increases, retention, $C_2 = 2-4 \times 10^3$
Adsorption	Above the solubility boundary	Ineffective in separation	Increases the retention of polymers	Decreases retention	Increases retention slightly, $C_2 = 2-5 \times 10^2$

^aFor C_2 factors see the equation in the text. Values of C_2 are compiled in Glöckner G (1991) *Gradient HPLC of Copolymers and Chromatographic Cross-Fractionation*, p. 107. New York: Springer-Verlag.

Since with gradients of this kind the chromatographically significant process is the result of interactions between non-solvents there is, owing to the large variety of the latter, more freedom in adjusting optimum conditions than with binary non-solvent/solvent gradients.

The samples to be investigated are dissolved in solvent C and injected into a starting eluent (e.g. A), whose polarity and precipitating power ensure proper retention at the top of the column. Solvent C is then added to the eluent at a concentration that in itself does not suffice for elution. In order to achieve short chromatograms, the concentration of C is changed as rapidly as the apparatus allows. No unfavourable side effects of the shock caused by the sudden transition from injection to elution conditions have ever been observed. The disturbance is visible with the help of optical detectors. With cyanopropyl or C_{18} packings, it is swept through by the approximately three-fold volume of mobile phase in the column. The elution of the sample is then triggered by a gradient $A \rightarrow B$ at a constant level of solvent C.

The first results of gradient elution with sudden transition of solvent concentration were achieved in the normal-phase mode of chromatography. The column packing was polar (CN-modified silica), A was iso-octane (with addition of 2% MeOH to the starting eluent), B was MeOH and C was THF. The gradient $A \rightarrow B$ was performed at $5\% \text{ min}^{-1}$ and applied to copolymers of styrene and ethyl methacrylate (EMA), methyl methacrylate (MMA), or 2-methoxyethyl methacrylate.

Figure 4 is the merged plot of UV signals measured on the elution of a mixture of five styrene-EMA copolymers through a gradient iso-octane \rightarrow MeOH after sudden transition to 20, 25, 30 or 35% THF solvent. Both iso-octane and MeOH are non-solvents for styrene-EMA. The addition of 35% THF yielded too high a solubility: the sample with 4.7% EMA was swept through the column by the sample solvent. A proportion of 20 or 25% THF did not suffice

for baseline separation. The best result was obtained after addition of 30% THF.

The advantage of this technique in comparison with binary gradient elution is obvious (see Figure 5). The chromatogram in Figure 5 was obtained in the same laboratory as those of Figure 4 with the same instrument and identical solvents. The baseline shift in Figure 5 is due to the UV absorption of THF which, at 259 nm, is slightly higher than that of iso-octane. This causes the baseline rise with

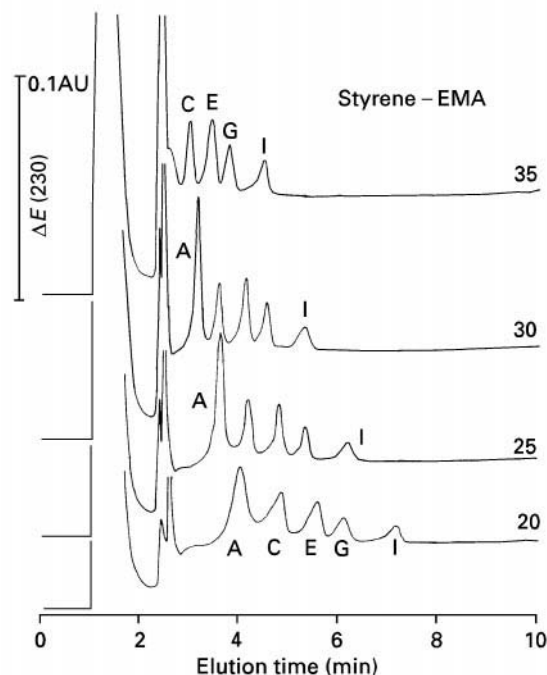


Figure 4 Separation of the mixture of five styrene-EMA copolymers at 50°C on a column (60 mm \times 4 mm i.d.) packed with cyanopropyl bonded phase. Gradient: iso-octane \rightarrow methanol ($5\% \text{ min}^{-1}$) after increase of THF concentration from zero to the percentage indicated at the curves; flow rate 0.5 mL min^{-1} . Sample: 1.8 μg copolymer A (4.7% EMA) + 1.2 μg C (32.2% EMA) + 2.0 μg E (54.6% EMA) + 1.2 μg G (68.0% EMA) + 2.0 μg I (92.5% EMA); UV signal detected at 230 nm. (Reproduced from Glöckner, 1991, by courtesy of Springer-Verlag.)

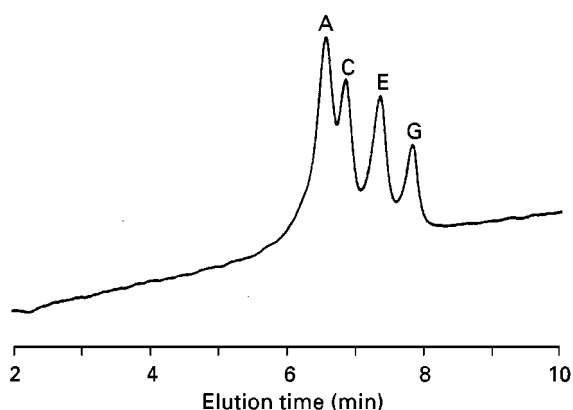


Figure 5 Separation of the mixture of four styrene-EMA copolymers at 50°C on a column (60 mm × 4 mm i.d.) packed with silica. Gradient: iso-octane → methanol (5% min⁻¹); flow rate 0.5 mL min⁻¹. Samples A to G as in Figure 4, 2.5 µg each; UV signal detected at 259 nm. (Reproduced from Glöckner, 1987a, by courtesy of Elsevier Science Publishers.)

increasing THF content of the eluent. The effect would be still more dramatic at a shorter wavelength, e.g. at 230 nm. Figure 4 presents horizontal baselines although the chromatograms were monitored at 230 nm. This is due to the constant concentration of THF throughout the elution, which disturbs the traces much less than a changing amount of THF does. The higher the THF addition, the higher the level of the baseline at the end of the chromatogram in comparison to the starting position in Figure 4.

The poor separation in Figure 5 is explained by the comparatively low molecular weight of these samples (50–80 × 10³) and the superimposition of separation by molecular weight and by composition. The peaks are indeed quite well separated when SEC fractions of the copolymer mixture are injected. Figure 4 indicates that the molecular weight effect in the investigation of the raw copolymers can be suppressed by the sudden-transition technique. **Table 2**

Table 2 Characteristics of polymer separation with separate control of solubility and adsorption^a

Factor	Details
Sample	20–100 µg polymer per injection, dissolved in about 50 µL solvent
Solvent	C, capable of dissolving samples of the system under investigation in the whole range of composition and molecular weight, used also for sample solutions (recommended: tetrahydrofuran, dichloromethane)
Non-solvents	A and B, opposite in polarity, both miscible with solvent C, e.g. A, acetonitrile, methanol; B, <i>n</i> -heptane. In general, the variety of non-solvents for a given polymer system is much broader than the list of suitable solvents
Interactions of eluents and detector	Eluents must not impede the monitoring of the eluting sample components, they must be transparent if optical detection is employed. This demand is more stringent for the gradient components A and B than for solvent C, whose concentration is not changed during the elution of sample components. For instance, separations at constant concentration of THF can be monitored at 230 nm or at constant DCM concentration with an evaporative light scattering detector without disturbance
Reversed-phase separation	Non-polar column, e.g. reversed-phase C ₁₈ bonded phase, injection into polar non-solvent A, gradient A → B after adjusting the solvent concentration to a suitable constant value
Normal-phase separation	Polar column, e.g. cyanopropyl bonded phase, injection into non-polar non-solvent B, gradient B → A after adjusting the solvent concentration to a suitable constant value
Reversed-phase and normal-phase separations	Can be performed with a common set of three eluents
Automated search for optimum separation method	Possible with programmable apparatus equipped with three storage bottles and a device for column switching
Balance between solubility and adsorption	Can be adjusted by the solvent concentration, which remains constant during the elution
Length of chromatograms	Can be optimized by sudden transition ^a of solvent concentration from zero to the selected level

^aInformation on how to perform sudden-transition gradients is available in Glöckner G, Wolf D and Engelhardt H (1994) *Chromatographia* 39: 557–563.

summarizes the characteristics of sudden-transition gradient elution.

Chromatography in Normal-Phase and Reversed-Phase Modes Using a Solvent and Two Non-Solvents

Independent control of adsorption and solubility enables normal-phase *and* reversed-phase separations to be performed with a common set of three liquids. This was first demonstrated with styrene-MMA copolymers in the system A (acetonitrile), B (*n*-heptane) and C (dichloromethane, DCM) on either CN or C₁₈ bonded phases.

Figure 6 shows chromatograms measured under reversed-phase and normal-phase conditions. Both modes yielded good separations. The elution order is inverted in the reversed-phase mode, as expected. The elution of styrene-MMA copolymers by the strong precipitant heptane (Figure 6A) is rather surprising.

Figure 7 shows the composition triangle of the eluent system used in Figure 6 with dichloromethane at the top, the polar non-solvent acetonitrile at the bottom left and the non-polar precipitant heptane at the bottom right. Acetonitrile and heptane have a miscibility gap that diminishes as dichloromethane is added. Eluent mixtures containing 25% or more dichloromethane are homogeneous. The elution characteristics of the styrene-MMA copolymers investigated in reversed-phase mode with 25–50% DCM or

in normal-phase mode with 25–40% dichloromethane are indicated. The characteristics of reversed-phase elutions form a group in the left-hand area of the triangle. The proportion of acetonitrile present means that eluent systems in this region have a higher polarity than those in the right-hand region. Reversed-phase chromatography starts with retention in a strongly polar medium. Sample components are released when the polarity of the eluent is no longer sufficient for retention. Thus, the characteristics of reversed-phase elution are to be expected on the polar side of the composition diagram. On the other hand, normal-phase elution characteristics are located in the right-hand part of the triangle. This can be understood by complementary reasoning because normal-phase chromatography starts with retention in a nonpolar medium.

The characteristics in Figure 7 are due to samples containing methyl methacrylate in the proportions (from left to right) 83.7%, 62.2%, 48.1%, 34.1%, 14.1% or 0% (polystyrene homopolymer). This sequence holds true with reversed-phase as well as with normal-phase elutions. In both modes, the copolymer with the highest content in polar methyl methacrylate units yields characteristics nearer to the polar (left) side of the diagram than the other samples. As expected, the least polar sample (polystyrene) marks the right border of the elution area in each mode.

All polymers considered here are soluble in the region beneath the solvent apex. The addition of

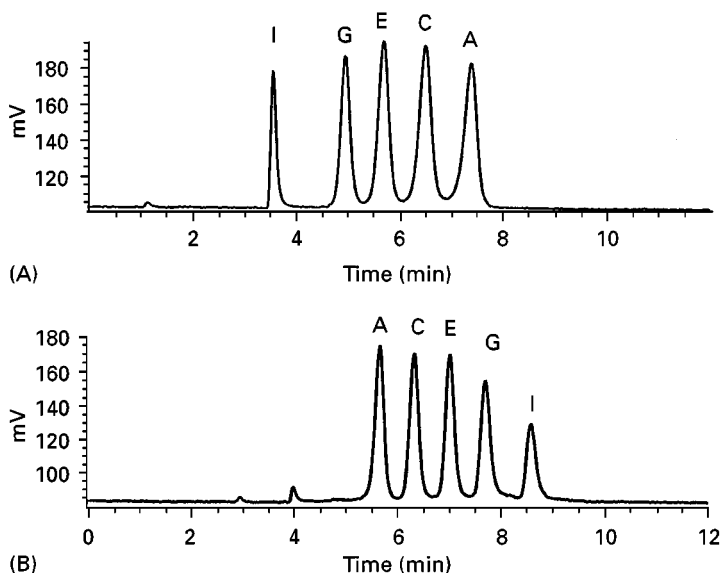


Figure 6 Separation of the mixture of five styrene-MMA copolymers at 35°C and flow rate 1 mL min⁻¹ by gradient elution in reversed-phase (A) or normal-phase mode (B) after a sudden increase of dichloromethane concentration from zero to 30%, monitored by an evaporative light-scattering detector. Sample in each mode: 6.76 µg copolymer A (14.1% MMA) + 5.54 µg C (34.1% MMA) + 5.28 µg E (48.1% MMA) + 5.48 µg G (62.2% MMA) + 5.02 µg I (83.7% MMA), dissolved in 10 µL DCM. (A) Column (250 mm × 4.1 mm i.d.) packed with reversed-phase C₁₈ bonded phase. Gradient: acetonitrile → *n*-heptane (4.99% min⁻¹). (B) Column (250 mm × 4.1 mm i.d.) packed with cyanopropyl bonded phase. Gradient: *n*-heptane → acetonitrile (4.99% min⁻¹). (Reproduced from Glöckner *et al.*, 1994, by courtesy of Vieweg-Verlag.)

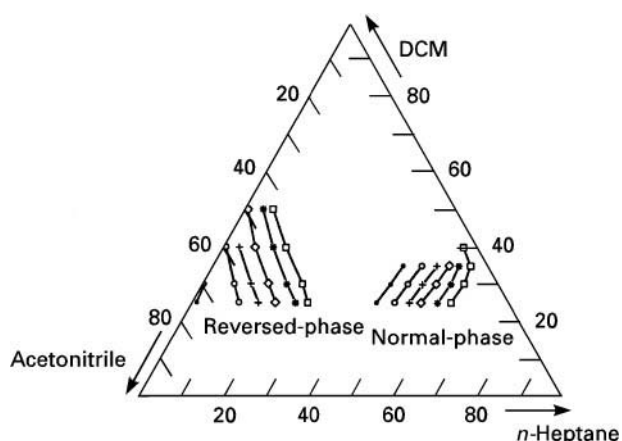


Figure 7 Composition triangle for acetonitrile/*n*-heptane/dichloromethane with elution characteristics of styrene-MMA copolymers in normal-phase and reversed-phase sudden-transition gradients. Samples: ●, 83.7% MMA; ○, 62.2% MMA; +, 48.1% MMA; ◇, 34.1% MMA; *, 14.1% MMA; □, polystyrene. (Reproduced from Glöckner, 1996, by courtesy of Gordon & Breach.)

small quantities of heptane or acetonitrile to dichloromethane will impair solubility but will not immediately cause precipitation. The polymers are still soluble in mixtures of dichloromethane with about 40% acetonitrile or 40% heptane. Thus, the upper sections of the solubility boundary follow the left and right sides of the eluent triangle. With increasing concentration of nonsolvent, a precipitation threshold is reached on each side. From these points, both branches of the solubility boundary bend towards each other. These sections may be determined experimentally by turbidimetric titration. For example, the elution characteristics of the copolymer containing 48.1% MMA run almost parallel to the corresponding sections of the solubility boundary. In both reversed-phase and normal-phase modes, the elution characteristics are shifted from the solubility boundary towards the centre of the solubility window. This shift indicates the contribution of adsorption to retention, which is well known in gradient HPLC of styrene-methyl methacrylate copolymers. Finally, both branches of the boundary will merge inside the triangle (above the miscibility gap). For details, see Glöckner G (1996).

Solubility windows of similar shape can be expected with many polymers in mixtures of a solvent with two non-solvents differing in polarity. Hence, HPLC separation generally should be possible in normal-phase as well as in reversed-phase mode with a suitable ternary eluent system. These separations should be achievable near the respective side of the solubility boundary. Thus, the use of ternary gradients consisting of a solvent and two non-sol-

vents and control of solubility by a sudden increase of solvent concentration to a constant level will not only offer the opportunity to improve separations with small additional effort, but will also contribute to a better understanding of the mechanisms of polymer chromatography.

See also: **II/Chromatography: Liquid:** Mechanisms: Normal Phase; Mechanisms: Reversed Phases; Mechanisms: Size Exclusion Chromatography. **III/Polyethers: Liquid Chromatography. Synthetic Polymers:** Liquid Chromatography.

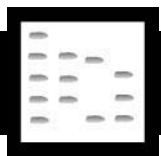
Further Reading

- Baker CA and Williams RJP (1956) A new chromatographic procedure and its application to high polymers. *Journal of Chemistry Society (London)* 1956: 2352-2362.
- Glöckner G (1987a) Normal- and reversed-phase separation of copolymers prepared from styrene and ethyl methacrylate. *Journal of Chromatography* 403: 280-284.
- Glöckner G (1987b) *Polymer Characterization by Liquid Chromatography*. Amsterdam: Elsevier Science Publishers.
- Glöckner G (1991) *Gradient HPLC of Copolymers and Chromatographic Cross-Fractionation*. New York: Heidelberg, Tokyo: Springer-Verlag.
- Glöckner G (1996) Solubility and chromatographic separation of styrene/methacrylate copolymers in ternary eluent systems. *International Journal of Polymer Analysis and Characterization* 2: 237-251.
- Glöckner G and van den Berg JHM (1987) Copolymer fractionation by gradient high-performance liquid chromatography. *Journal of Chromatography* 384: 135-144.
- Glöckner G, Wolf D and Engelhardt H (1991) Separation of copoly(styrene/acrylonitrile) samples according to composition under reversed phase conditions. *Chromatographia* 32: 107-112.
- Glöckner G, Wolf D and Engelhardt H (1994) Control of adsorption and solubility in gradient high performance liquid chromatography 5: separation of styrene/methyl methacrylate copolymers by sudden-transition gradients in normal-phase and reversed phase mode. *Chromatographia* 39: 557-563.
- Mourey TH and Schunk TC (1992) In E. Heftmann (ed.) *Chromatography - Fundamentals and Application of Chromatography and Related Differential Migration Methods*. Chapter 22. Amsterdam: Elsevier Science Publishers.
- Pasch H and Trathnigg B (1997) *HPLC of Polymers*. New York: Heidelberg, Tokyo: Springer-Verlag.
- Quarry MA, Stadalius MA, Mourey TH and Snyder LR (1986) General model for the separation of large molecules by gradient elution: sorption versus precipitation. *Journal of Chromatography* 358: 1-16.

Schultz R and Engelhardt H (1990) HPLC of synthetic polymers: characterization of polystyrenes by high performance precipitation liquid chromatography (HPPLC). *Chromatographia* 29: 205–213.

Schunk TC (1993) Chemical composition separation of synthetic polymers by reversed-phase liquid chromatography (review). *Journal of Chromatography A* 656: 591–615.

HERBICIDES



Gas Chromatography

J. L. Tadeo and C. Sanchez-Brunete, Department of Sustainable Use of Natural Resources, INIA, Madrid, Spain

Copyright © 2000 Academic Press

Herbicide Formulations

Weeds have been controlled by humans since the beginning of agriculture by means of mechanical tools or by hand. It was early in the 20th century that some inorganic compounds were first used with this aim. The discovery of the herbicidal properties of 2,4-D (2,4-dichlorophenoxyacetic acid) in 1945 can be considered the initiation of use of organic herbicides in agriculture. Since then, more than 130 different active compounds have been synthesized for their application as herbicides. These compounds can be grouped, according to their chemical structures, into different herbicide classes (Table 1).

Compounds belonging to the principal herbicide groups will be considered in this study. These compounds control weeds in a variety of ways, showing different modes of action, selectivity and application characteristics. Soil-applied herbicides are absorbed by roots or emerging shoots and foliage-applied herbicides are absorbed into the leaves, where they may be translocated to other parts of the plant.

The active ingredient of a herbicide is a compound, usually obtained by synthesis, which is formulated by a manufacturer in soil particles or liquid concentrates. These commercial formulations of herbicides are diluted with water before application in agriculture at the recommended doses. Herbicide formulations generally contain other materials to improve the efficiency of application.

Analysis of herbicide formulations was initially carried out by wet chemical procedures, such as determination of total chlorine, nitrogen or phosphorus, or by spectrometric procedures like ultraviolet absorption. The development of gas

chromatography (GC) allowed the analysis of these compounds in commercial formulations with high selectivity and sensitivity. The analytical procedure is commonly based on the dissolution of a known amount of the formulation in an organic solvent, which often contains an internal standard to improve the precision and accuracy of the determination. An aliquot of this solution is analysed by GC. Packed columns were used initially, but have now been replaced by capillary columns of low or medium polarity and flame ionization is the detection technique more widely used. When herbicides are not volatile or thermally stable, high performance liquid chromatography (HPLC) is the preferred technique for their determination in commercial formulations. Figure 1 shows the gas chromatographic separation of a mixture of phenoxy esters.

Herbicide Residue Analysis

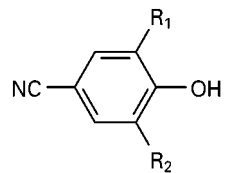
Residues of herbicides will persist in the plant or in the soil for a variable time, depending on their physicochemical properties and on the environmental conditions. Analysis of herbicide residues in these matrices is important, not only from the point of view of the efficacy of application, but also to know the distribution and persistence of these compounds in food and in the environment. Therefore, herbicides of a wide range of polarities have to be determined in complex environmental matrices at very low levels.

Initially, herbicide residues were analysed by colorimetric methods. These procedures were generally based on acidic or basic hydrolysis followed by formation of derivatives. These methods are time-consuming and do not usually distinguish between the parent herbicide and metabolites.

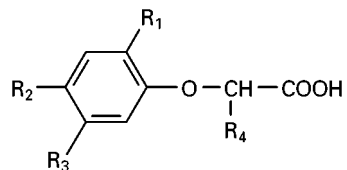
Since the development of GC, this technique has been widely used in the analysis of these compounds. Table 2 summarizes the preparation of different types of samples for residue determination. These samples are generally analysed by a procedure with the following main steps: sample extraction, clean-up of extracts, then GC determination and identification. Some compounds are not volatile or thermally stable

Table 1 Chemical structures of herbicides*Benzonitriles*

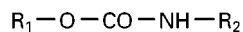
Bromoxynil; ioxynil

*Phenoxyacids*

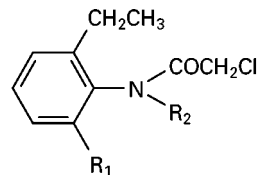
2,4-D; MCPA; MCPP; dichlorprop; diclofop; fenoxaprop

*Carbamates*

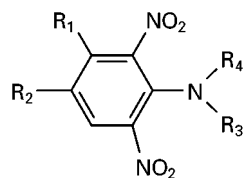
EPTC; triallate

*Chloroacetamides*

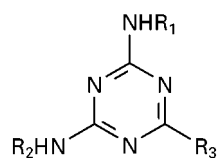
Alachlor; metolachlor

*Dinitroanilines*

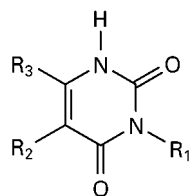
Butralin; ethalfluralin; pendimethalin; trifluralin

*Triazines*

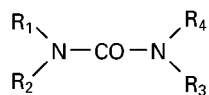
Ametryn; atrazine; cyanazine; simazine; terbutryn

*Uracils*

Bromacil; lenacil; terbacil

*Ureas*

Chlorotoluron; isoproturon; linuron; chlorsulfuron; metsulfuron; triasulfuron



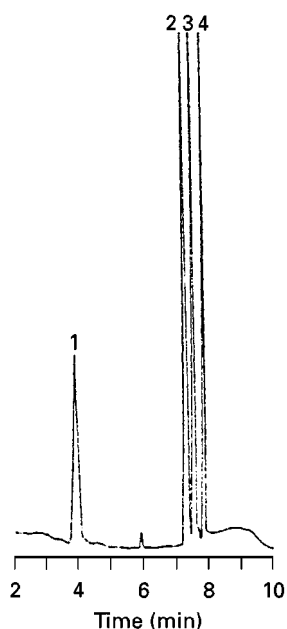


Figure 1 Analysis of a mixture of phenoxy esters by gas chromatography on a BP-5 fused silica column, 12 m \times 0.53 mm i.d., with helium as carrier gas at 10 mL min⁻¹ and flame ionization detection. Oven temperature was held at 180°C for 5 min, increased at 25°C min⁻¹ to 250°C and held for 10 min. 1, 2,4-D isobutyl ester; 2, MCPA 2-butoxyethyl ester, 3, 2,4-DP 2-butoxyethyl ester; 4, 2,4-D 2-butoxyethyl ester. Adapted from Sánchez-Brunete C, Pérez S and Tadeo JL (1991) Determination of phenoxy ester herbicides by gas and high-performance liquid chromatography. *Journal of Chromatography* 552: 235 with permission from Elsevier Science.

and need to be derivatized before being analysed by GC.

Currently capillary columns are most commonly used for residue analysis. Table 3 shows some representative examples of different packed and capillary columns used in the determination of herbicides.

In trace analysis, blank samples are commonly processed through the analytical method to identify the possibility of interferences in the herbicide determination from other sample or reagent components. In addition, recoveries of the analysed compound are also carried out through the extraction and clean-up procedures. The accepted normal range of these re-

coveries is 70–120%, with a standard deviation of 20%.

Several injection techniques are used in herbicide residue analysis. The techniques most often employed are splitless, on-column and programmed-temperature vaporizer injection and the volume normally injected is 1–2 μ L.

Various selective detectors are used in trace analysis of herbicides. The electron-capture detector (ECD) was first used for the determination of halogen-containing compounds or halogenated derivatives, due to its high sensitivity for these compounds. The nitrogen-phosphorus detector (NPD), also known as thermionic or alkali flame detector, is commonly used in the analysis of nitrogen-containing herbicides. Both detectors are highly sensitive and can detect herbicide concentrations lower than 1 pg. The flame photometric detector (FPD) has sometimes been used in the determination of sulfur-containing herbicides. The limit of detection (LOD) reflects the sensitivity of a detector for a given compound and it is defined as the amount producing a signal-to-noise ratio equal to 3. When this ratio is determined with extracts of real samples, processed through the whole analytical procedure, this parameter is known as the limit of quantification (LOQ), which depends on the efficacy of the extraction and clean-up procedures and on the selectivity and sensitivity of the detector. The coupling of mass spectrometry (MS) with GC allows the determination of herbicide residues with high selectivity and sensitivity and, in addition, the identification of residues by means of their mass spectra obtained at trace levels. The atomic emission detector allows monitoring characteristic wavelengths for carbon and hydrogen atoms, as well as the more specific emission lines for phosphorus, nitrogen and sulfur. Table 4 summarizes the detection techniques for herbicide residue determination by GC.

The analysis of herbicides, grouped into various chemical classes, is considered in more detail below.

Benzonitriles and Phenoxy Acids

Benzonitriles and phenoxy acids are widely applied as salts or esters, but they are hydrolysed to their

Table 2 Procedures used in sample preparation for herbicide residue determination

Matrix	Amount sampled	Sample preparation	Amount extracted	Extraction procedure
Soil	1 kg	Sieving (< 2 mm)	10–20 g	Shaking, Soxhlet, SFE
Water	1 L	Filtration	0.1–1 L	SPE, LLE
Plants	1 kg	Blending	20–50 g	Homogenization
Air	25–250 L	Adsorption or trapping		Thermal or solvent desorption

SFE, Supercritical fluid extraction; SPE, solid-phase extraction; LLE, liquid-liquid extraction.

Table 3 Chromatographic columns used in herbicide residue analysis

Column (length/diameter)	Stationary phase	Applications
Packed (1–3 m/2–4 mm)	Dimethylpolysiloxane (SE-30, DC-200)	Carbamates, ureas, dinitroanilines, triazines
	Phenylmethylpolysiloxane (OV-17, OV-25)	Benzonitriles, phenoxy acids
	Trifluoropropylpolysiloxane (QF-1, OV-210)	Carbamates, chloroacetamides, phenoxy acids
	Polyethyleneglycol (Carbowax)	Triazines
	Cyanoethylpolysiloxane (XE-60)	Triazines
	Cyanopropylpolysiloxane (OV-225)	Ureas
Capillary (10–30 m/0.2–0.5 mm)	Dimethylpolysiloxane	Nitrogen-containing herbicides
	Phenylmethylpolysiloxane	Triazines
	Polyethylene glycol	Triazines, phenoxy acids, benzonitriles
	Cyanopropylphenylmethylpolysiloxane	Multiresidue

respective phenols or acids in the matrix. Extraction of residues from soil and water is commonly performed at acidic pH with organic solvents of medium polarity. The extraction of these herbicides from vegetable matter is often done with aqueous solutions at basic pH, followed by extraction with organic solvents.

Purification of extracts is required in most cases and this step is accomplished by liquid–liquid partition at basic pH or by chromatography on silica columns.

Analysis of these compounds in air is carried out by trapping herbicides in ethylene glycol or in various adsorbents, like polyurethane or amberlite resins.

Derivatization of phenoxy acids, before GC determination, is necessary to make them volatile. Various alkyl, silyl or pentafluorobenzyl derivatives are obtained with this aim. Methyl esters have been commonly prepared for the determination of phenoxy acids and the reagents most often used are diazomethane and boron trifluoride–methanol. Benzo-

nitriles can be determined directly by GC, but the sensitivity and reproducibility achieved are poor. Various derivatives overcome these problems and diazomethane and heptafluorobutyric anhydride are the reagents most often used.

The determination of herbicides is widely carried out by GC with ECD, if the compound has halogen substituents or halogenated derivatives are obtained. MS detection has the advantage of being more selective and requiring less clean-up of extracts.

Carbamates

Carbamates are a wide group of pesticides and some of them have herbicide properties, like the thiocarbamates S-ethyl dipropylthiocarbamate (EPTC) and triallate. These compounds are extracted from soil with methanol or acetone and from water by means of hexane or dichloromethane. The extraction from plants is commonly accomplished with acetonitrile or by steam distillation. Clean-up of extracts is often

Table 4 Detection of herbicides in environmental samples

Herbicides	Detectors	LOD ($\mu\text{g g}^{-1}$)	Derivatives
Benzonitriles	ECD, MS	0.05–0.0003	Methyl ethers Heptafluorobutyryl
	MS	0.001	
Phenoxyacids	ECD, MS	0.05–0.001	Methyl esters
Carbamates	ECD, NPD, FPD, MS	0.1–0.001	
Chloroacetamides	NPD, MS	0.05–0.001	
Dinitroanilines	ECD, NPD, MS	0.05–0.0001	
Triazines	NPD, ECD, MS	0.01–0.0001	
Uracils	NPD, ECD, MS	0.04–0.001	
Ureas			
Phenylureas	NPD, MS	0.1–0.01	Methyl or ethyl Heptafluorobutyryl
	ECD	0.01–0.001	
Sulfonylureas	ECD	0.1–0.002	Methyl or PFB
Multiresidue	NPD, MS	0.02–0.001	

ECD, Electron capture detector; MS, mass spectrometry; NPD, nitrogen–phosphorus detector; FPD, flame photometric detector; PFB, pentafluorobenzyl.

done by chromatography on silica columns. Most carbamates are thermally unstable and are usually analysed by HPLC. Some carbamates, such as the thiocarbamates considered above, can be determined by GC and their residues are determined by this technique using different detectors, like ECD, NPD, FPD and MS.

Chloroacetamides

These compounds, also known as anilides, are very often used for weed control in maize, in combination with triazines. Chloroacetamides are extracted from soil by polar and medium polarity solvents and their determination is generally carried out without further purification. Extraction from water is performed by reversed-phase solid-phase extraction (SPE) or by liquid-liquid extraction with low polarity solvents and clean-up of extracts on silica columns is necessary in some cases.

Analysis of these herbicides in plants is done by extraction with polar solvents, followed by purification by liquid-liquid partition or column chromatography on silica or alumina adsorbents.

Analytical methods for the determination of these herbicides in air have been reported, using several adsorbents or an ethylene glycol phase for their extraction from air. NPD and MS are the detectors most widely used in the determination of chloroacetamides; the ECD is also sometimes used.

Dinitroanilines

Dinitroaniline herbicides are highly lipophilic with a low solubility in water and some compounds have a remarkable volatility. Extraction of these compounds from soil is carried out by polar as well as by low polarity solvents. Dinitroanilines are extracted from water by SPE or by liquid-liquid extraction with low polarity solvents, such as dichloromethane. Clean-up of water and soil extracts on silica columns is sometimes needed.

Extraction with polar solvents, like methanol, is the method often used for the determination of dinitroanilines in plants, followed by liquid-liquid partition or Florisil column clean-up of extracts.

Analysis of these herbicides in air is performed by means of several adsorbents or organic solvents as trapping phases to remove these compounds from air.

ECD is often used in the determination of these compounds due to the large response obtained, particularly with some halogen-containing dinitroanilines. NPD and MS are also used in the gas chromatographic analysis of these herbicides.

Triazines

These compounds form a wide group of herbicides often employed in fruit trees and cereals; in particular, simazine and atrazine are the most widely used triazines.

Triazine herbicides are extracted from soil by polar or medium polarity organic solvents, followed by liquid-liquid partition or column chromatography clean-up if necessary. Supercritical fluid extraction is also used in the analysis of triazines in soil.

These herbicides are extracted from water by reversed-phase SPE, by anion exchange columns or by liquid-liquid extraction with low polarity solvents, followed in some cases by Florisil column clean-up.

Analysis of these compounds in plants is performed by sample homogenization with polar organic solvents and column chromatography or liquid-liquid partition clean-up. Triazines are sometimes analysed in air and plugs of polyurethane foam have been used to extract these compounds from air.

The gas chromatographic determination of triazines is commonly performed with NPD, due to the high response obtained with this detector because of the number of nitrogen atoms in their molecules. ECD is also employed but its sensitivity and selectivity for these compounds are lower. GC-MS is used for confirmation of residues as well as for routine determination, due to the good sensitivity obtained with selected ion monitoring. **Figure 2** shows some chromatograms of the determination of various triazines, together with other herbicides, by GC with NPD and MS detection.

Uracils

These compounds, also named pyrimidines, are used to control weeds in some fruit trees, vegetables and sugar beet. Extraction of these herbicides from soil is carried out with polar organic solvents or with basic aqueous solutions. Extraction from water is performed by SPE or by liquid-liquid extraction with low polarity solvents. Uracils are extracted from plants by homogenization with basic aqueous solutions or with mixtures of polar solvents with water. Clean-up of extracts is commonly carried out by liquid-liquid partition at different pHs. The gas chromatographic determination of these herbicides is performed using ECD and NPD detectors, and also by MS and atomic emission detection.

Ureas

Substituted ureas constitute one important group of herbicides formed by two different classes of compounds: phenylureas, one of the first used herbicides, and sulfonylureas, introduced later and applied

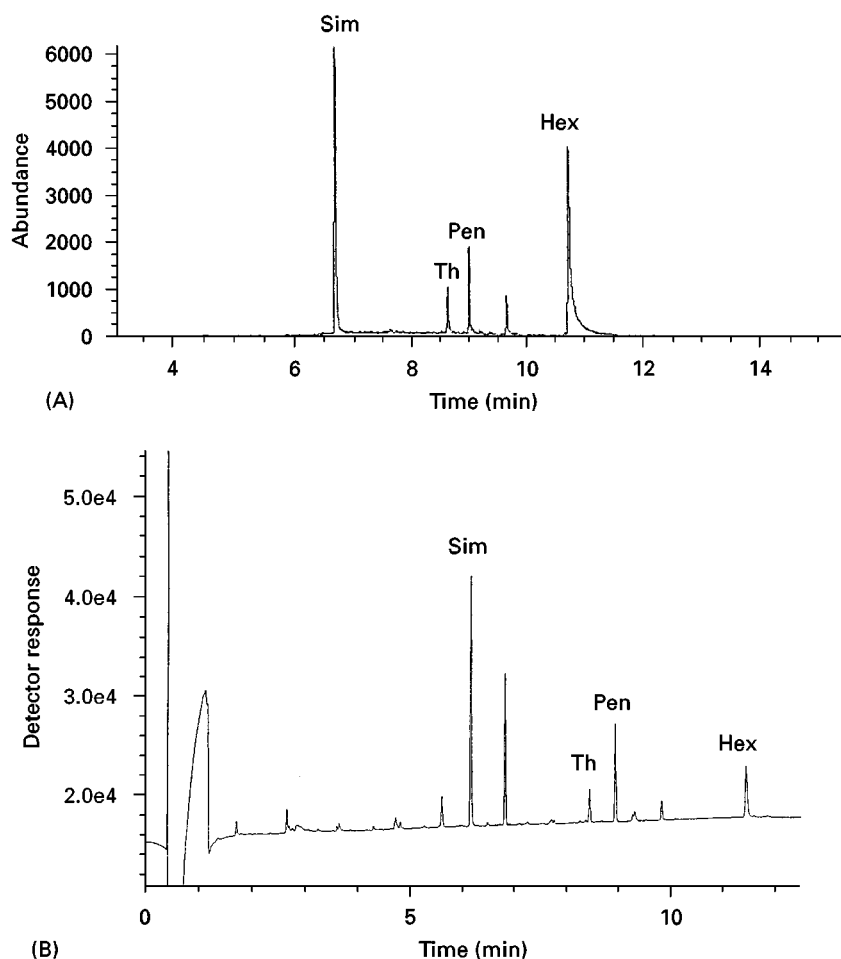


Figure 2 Gas chromatograms of herbicide residues in soil, fortified at $0.01 \mu\text{g g}^{-1}$, separated on an HP-1 capillary column, $12.5 \text{ m} \times 0.20 \text{ mm i.d.}$, with helium as carrier gas at 1 mL min^{-1} and detected (A) by GC-MS with selected ion monitoring or (B) by GC-NPD. Oven temperature was maintained at 100°C for 1 min, programmed at $15^\circ\text{C min}^{-1}$ to 250°C and held for 1 min. Sim, simazine; Th, thiazopyr; Pen, pendimethalin; Hex, hexazinone. Adapted with permission from Pérez RA, Sanchez-Brunet C, Miguel E and Tadeo JL (1998) Analytical methods for the determination in soil of herbicides used in forestry by GC-NPD and GC-MS. *Journal of Agriculture and Food Chemistry* 46: 1864.

at lower doses due to their high herbicidal activity. Both types of compounds suffer from thermal instability and their decomposition products, rather than the parent compounds, have been determined in some cases. To overcome this problem, various derivatives amenable to GC have been obtained, mainly their methyl, heptafluorobutyl or perfluorobenzyl derivatives.

Substituted ureas are extracted from soil by shaking with organic solvents of medium or high polarity, like methanol or acetone, sometimes followed by silica column or liquid-liquid partitioning clean-up. These herbicides are extracted from water by reversed-phase SPE or by liquid-liquid extraction with dichloromethane.

Urea herbicides are generally extracted from plants by homogenization with polar organic solvents. Supercritical fluid extraction of these compounds

from plants has also been reported. Clean-up of extracts through column chromatography or liquid-liquid partition is necessary before GC determination.

Detection of these herbicides is performed by NPD or by ECD, mainly when halogenated derivatives are obtained. MS is also used in the determination of substituted ureas in environmental matrices.

Multiresidue Analysis

The wide range of polarities and physico-chemical properties of herbicides does not allow the determination of the more than 130 available herbicides in one analytical method. Nevertheless, it is advisable to use analytical procedures that allow the determination of as many herbicides as possible in one method. These multiresidue methods permit reduction in time and cost of analysis as well as detection of the possible

presence of herbicide residues in samples with unknown origin or contamination. A multiresidue method is able to determine all the herbicides that can be extracted, cleaned up, separated and detected in the conditions used in the analytical procedure. In some cases, two detectors – generally ECD and NPD – are connected at the end of the same chromatographic column to allow the detection of a wider type of compounds. MS is used as a universal detector and also for residue identification purposes. Atomic emission detection is a more recent detection technique which is increasingly used in trace analysis.

Herbicide residues are extracted from soil and plants with medium or high polarity solvents, like

methanol, ethyl acetate and acetone. Vegetable samples are generally homogenized with organic solvent and soil samples are normally shaken and filtered. Matrix solid-phase dispersion (MSPD) is a technique which has recently been employed for pesticide residue determination in food samples: it performs sample extraction and purification at the same time. A simple multiresidue method, based on soil extraction in small columns, has been reported. **Figure 3** shows representative chromatograms of the analysis of various nitrogen-containing herbicides by this method.

Analysis of herbicides in water is generally based on liquid-liquid extraction with dichloromethane or on SPE using reversed phase columns, mainly C_{18} . Determination of herbicide residues in air is

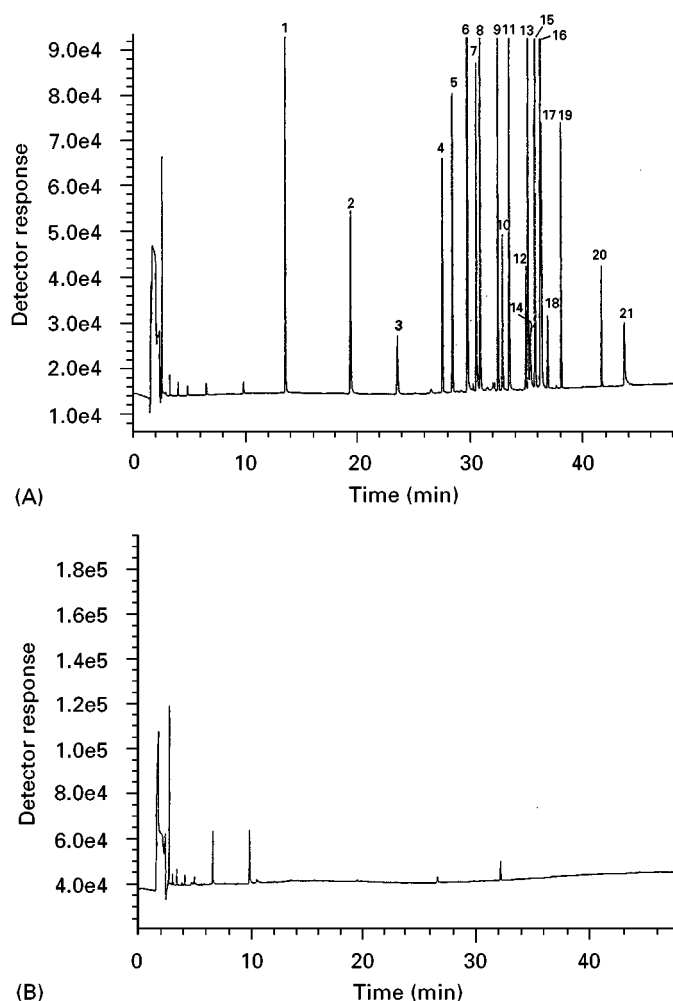


Figure 3 Multiresidue analysis of soil extracts separated on an HP-1 column, 30 m \times 0.25 mm i.d., with helium as carrier gas at 1 mL min⁻¹ and detected by GC-NPD. Oven temperature was kept at 80°C for 1 min, programmed at 5°C min⁻¹ to 140°C, held for 10 min and programmed at 5°C min⁻¹ to 250°C, held 15 min. (A) Soil fortified with nitrogen-containing herbicides at 0.5 μ g g⁻¹. (B) Blank soil. 1, EPTC; 2, molinate; 3, propachlor; 4, ethalfluralin; 5, trifluralin; 6, atrazine; 7, terbutometon; 8, terbutylazin; 9, dinitramine; 10, triallate; 11, prometryn; 12, alachlor; 13, metribuzin; 14, bromacil; 15, terbutryn; 16, cyanazine; 17, thiobencarb; 18, metolachlor; 19, butralin; 20, oxadiazon; 21, lenacil. Reproduced from Sánchez-Brunete C, Pérez RA, Miguel E and Tadeo JL (1998) Multiresidue herbicide analysis in soil samples by means of extraction in small columns and GC with NPD and MS detection. *Journal of Chromatography A* 823: 17, with permission from Elsevier Science.

accomplished by trapping these compounds on adsorbents, followed by extraction with organic solvents.

Future Developments

GC will continue to be the main chromatographic technique used in herbicide residue analysis in the near future, due to the high sensitivity and selectivity given by the detectors that can be coupled with this technique. In particular, the use of less expensive and more robust and sensitive GC-MS equipment will keep growing in the routine determination and confirmation of herbicide residues.

The time needed for sample processing is expected to be reduced as a consequence of the continuation in the development of automatic processes for sample preparation, extraction and clean-up. These processes will use less sample and lower volumes of organic solvents in the analytical procedure.

New improvements in the gas chromatographic equipment to allow higher injection volumes of less purified extracts can also be expected.

See Colour Plate 85.

See also: **II/Chromatography: Gas:** Detectors: Mass Spectrometry; Detectors: Selective. **Insecticides:** Gas Chromatography. **Pesticides:** Supercritical Fluid Chromatography; Gas Chromatography. **Solid-Phase Matrix Dispersion: Extraction. III/Sorbent Selection for Solid-Phase Extraction.**

Further Reading

- Barceló D and Henion MC (1997) *Trace Determination of Pesticides and their Degradation Products in Water*. Amsterdam: Elsevier.
- Blau K and King GS (eds) (1978) *Handbook of Derivatives for Chromatography*. London: Heyden.
- Dobrat W and Martijn A (eds) (1998) *CIPAC Handbook: Vol. H Analysis of Technical and Formulated Pesticides*. Cambridge: Black Bear Press.
- Hutson DH and Roberts TR (eds) (1987) *Progress in Pesticide Biochemistry and Toxicology*, vol. 6 *Herbicides*. New York: Wiley.
- Milne GWA (1995) *CRC Handbook of Pesticides*. Boca Raton: CRC Press.
- Nollet LML (ed.) (1996) *Handbook of Food Analysis*. New York: Marcel Dekker.
- Sherma J (ed.) (1989) *Analytical Methods for Pesticides and Plant Growth Regulators*: vol. XVII. *Advanced Analytical Techniques*. San Diego: Academic Press.
- Tadeo JL, Sánchez-Brunete C, García-Valcarcel AI *et al.* (1996) Review: determination of cereal herbicide residues in environmental samples by gas chromatography. *Journal of Chromatography A* 754: 347.
- Tekel' J and Kovačičová J (1993) Review: chromatographic methods in the determination of herbicide residues in crops, food and environmental samples. *Journal of Chromatography* 643: 291
- Zweig G (ed.) (1972) *Analytical Methods for Pesticides and Plant Growth Regulators*: vol. VI. *Gas Chromatographic Analysis*. New York: Academic Press.

Solid-Phase Extraction

Y. Picó, Universitat de València, València, Spain

Copyright © 2000 Academic Press

Solid-phase extraction (SPE) methods, using bonded-silicas, were first introduced in 1971 as an alternative to liquid partitioning. The method combines extraction and preconcentration of organic compounds in water by adsorption on proper solid material followed by desorption with a small quantity of an organic solvent. In comparison with liquid-liquid extraction, the following advantages are offered: the amount of solvent required for the clean up is greatly reduced, thus saving time for the evaporative concentration step and minimizing exposure of the analyst to the toxic solvent; the final eluate has less interfering material, and it could be analysed using any of a variety of detection, separation and identification techniques, including high performance

liquid chromatography (HPLC) or gas chromatography (GC); accuracy and precision are improved; and it is rapid and easily automated.

Another impressive feature of SPE is the commercial availability of sorbents in small and inexpensive cartridges. C₁₈-bonded silica cartridges, styrenedivinylbenzene Empore® extraction discs and Carbo-pack® cartridges have been extensively used for the extraction of organic molecules from water samples. Automated column switching systems and on-line SPE coupled to determination devices have also been often reported for determination of pollutants in drinking and surface water.

Because of the reasons given above, in recent years much analysis of herbicides in fruit, vegetable and water has been conducted using SPE. Phenoxy acids, phenylureas, aryloxyphenoxypionic acids, triazines, sulfonyleureas, imidazolinones, glyphosate, phenoxyacetic acids, bipyridinium compounds,

chloroacetamides, dinitroanilines and substituted phenols are examples of herbicides usually extracted and isolated by this technique.

It is undeniable that SPE is gaining in importance and, today, is a well-established and validated method, since the Environmental Protection Agency (EPA) in the United States currently offers one SPE procedure for the analysis of organic compounds (including neutral herbicides) and two for the analysis of acid herbicides.

Solid-Phase Extraction

Analyte Characteristics

The determination of herbicide residues is an intricate problem because of the large number of chemicals involved. As a general rule, to classify them into a wide variety of classes depending on their chemical structure results in a lot of groups that barely provide enough information in order to select the best SPE procedure.

In this way, the most practical approach is to organize the herbicides according to their acid/base character or other properties that condition the protocol following by SPE. Table 1 shows these characteristics for the major classes of herbicides and some examples of the structures included in each group.

Disposable Solid Phases

The modern SPE technique began in 1978 with the introduction of Sep-Pack cartridges, the first compact silica-based solid-phase extraction device for sample preparation on the market. Present-day, disposable prepacked columns or cartridges are available from more than 30 manufacturers, who offer phases such as C₁₈, C₈, cyano and amino. The containers are generally made of polypropylene. The sorbent bed varies from 100 to 1000 mg and is retained between two porous frits.

The use of Empore® discs are described in more recent studies. These devices include flat discs with large cross-sectional areas that provide advantages for preconcentration and clean-up methods with respect to the sorption, capacity, back pressure and stability after repeated use.

Reversed-phase silica-based sorbents, especially C₈ and C₁₈ bonded-silicas, are the most widely used packings for SPE. A typical SPE requires a previous sorbent activation step (wetting), usually with methanol, and removal of activation solvent excess (conditioning), usually with water.

Neutral herbicides can be extracted from 1 L samples with an average amount of sorbent (500 mg).

The sample is extracted under neutral or slightly alkaline conditions, and the pH is adjusted before the extraction to between 6 and 8. Under these conditions, salts of humic acids, which generally cause considerable interference in herbicide determination, are unlikely to be adsorbed during enrichment. As acid herbicides are highly polar, they are soluble in water and in aqueous solutions and are less soluble (in their dissociated form) in apolar sorbents. To overcome this difficulty, the aqueous phase has to be acidified before extraction to suppress the dissociation of this class of herbicides and to facilitate the transfer of the undissociated molecular species to the solid phase.

The recoveries and the relative standard deviation of the performance of different devices and solid phases are compared in Tables 2 and 3 for basic/neutral and acid/phenolic herbicides, respectively. The C₁₈ cartridges showed good recoveries with most of the basic/neutral and acidic/phenolic herbicides. Compounds having a small (deisopropylatrazine, tribensulfuron-methyl) or a very high (beta-cyfluthrine) affinity to the C₁₈ material gave the worst recoveries. In comparison with Empore® discs a lower breakthrough of polar metabolites of atrazine was reported, possibly due to the fact that Empore® discs contain only half the quantity of C₁₈ material. However, lower recoveries were achieved for medium polar and non-polar pesticides except trifluralin and triallate.

As reported in the literature on the subject, the bonded-silicas, in cartridge or in disc configuration, are the most commonly used supports, but they also have some limitations:

- For polar analytes, the retention is weak and often results in breakthrough during the loading step.
- Basic analytes interact strongly with the residual silanols, which in turn cause low recovery.
- The sorbent must remain wet prior to sample loading. (If one accidentally lets the cartridges run dry, the recovery is low and variable.)
- Poor stability in very acidic and basic media, which limits their use to the pH range of between 2 and 8.

These limitations have led to a search for new materials with improved characteristics. For example, the styrene-divinylbenzene resins have been extensively checked for their use in the extraction of pesticides. These polymers show higher retention of analytes and a wider pH range than C₁₈ silicas. The LC-grade polymers used as stationary phases have more commonly been used in precolumns (mainly PRP-1 and PLRP-S) for on-line purposes, because

Table 1 Chemical structure of major classes of herbicides according to the character that determines the SPE procedure used

Character	Class	Typical herbicide	Chemical structure
Basic/neutral	Triazine	Atrazine	
	Chloroacetamide	Metolachlor	
	Urea	Monuron	
	Carbamate	Desmedifam	
	Dinitroaniline	Pendimethalin	
Acid phenolic	Phenoxy acid	2,4,5-T	
	Substituted phenol	Bromoxynil	
	Aryloxyphenoxy propanoic acid	Fluazifop	
Cationics	Bipyridilium compound	Diquat	
Very soluble	Organophosphate	Glyphosate	

Table 2 Relative standard deviation (RSD), recoveries (Rec.) and determination limits (DL, P 95%) for the preconcentration of basic/neutral pesticides from 1000-mL Milli-Q-water

	Concentration range (ng L ⁻¹)	Preconcentration on											
		Bond Elut C ₁₈ cartridges				Empore® C ₁₈ discs				Empore® SDB discs			
		RSD (%)	Rec. (%)	DL (ng L ⁻¹)		RSD (%)	Rec. (%)	DL (ng L ⁻¹)		RSD (%)	Rec. (%)	DL (ng L ⁻¹)	
Desisopropylatrazine	54–270	9.9	33	133		10.6	21	143		15.9	16	221	
Desethylatrazine	50–248	8.7	82	113		8.8	49	110		3.6	72	46	
Metoxuron	108–538	1.9	95	58		3.4	106	95		4.8	94	134	
Hexazinon	107–535	8.1	96	224		6.9	102	186		6.7	104	182	
Simazine	49–245	1.5	102	20		4.5	102	57		5.2	100	66	
Metribuzin	94–470	4.7	94	120		4.0	104	99		4.1	109	99	
Cyanazine	57–285	7.9	81	119		5.0	110	73		6.3	93	91	
Carbofuran	179–895	6.4	92	309		4.4	107	211		6.8	95	311	
Methabenzthiazuron	100–498	5.2	89	138		5.0	98	127		3.9	103	101	
Chlortoluron	101–503	4.9	96	133		4.5	102	118		2.3	98	61	
Atrazine	50–250	5.6	96	75		5.6	100	72		3.6	93	47	
Monolinuron	149–745	4.0	96	166		13.7	105	473		5.7	114	221	
Diuron	102–510	7.3	89	194		5.1	101	134		4.9	94	130	
Isoproturon	109–543	6.7	90	191		5.7	102	158		7.3	95	199	
Metobromuron	102–508	13.4	88	334		9.2	93	230		4.5	96	119	
Metazachlor	123–165	7.3	85	235		6.5	106	204		2.2	100	72	
Sebutylatrazine	53–265	4.9	97	69		4.8	103	66		4.3	102	58	
Terbutylatrazine	53–263	6.3	104	87		6.6	104	89		5.7	98	77	
Linuron	102–508	2.3	101	66		3.6	96	97		3.2	106	87	
Napropamide	45–225	5.8	98	69		2.1	100	24		4.9	100	57	
Terbutonazol	164–820	6.5	90	282		2.1	101	98		5.2	101	224	
Metolachlor	127–633	3.3	103	115		6.3	100	204		7.1	104	226	
Propiconazol	225–1125	4.9	96	316		2.3	99	156		4.7	107	290	
Dinosebacetate	138–688	6.6	41	239		16.2	52	509		7.6	70	262	
Parathion-ethyl	148–740	4.6	90	189		8.0	101	294		7.1	97	264	
Pyrazophos	125–623	7.1	82	230		3.6	93	120		5.1	107	165	
Bifenox	67–333	3.9	98	70		3.5	93	61		8.8	92	147	
Prosulfocarb	140–698	4.8	91	182		11.6	94	385		5.5	72	198	
Pendimethalin	121–603	8.0	84	248		9.9	93	290		4.5	107	142	
Trifluralin	125–625	8.3	63	268		14.2	21	415		0.0	0	0	
Triallate	128–638	4.1	96	144		14.7	35	434		0.0	0	0	
Fluoroxypyrrester	81–403	3.2	86	71		5.1	89	105		6.0	98	123	
Beta-cyfluthrine	190–950	3.7	61	202		8.1	82	383		2.2	89	122	

(Reproduced with permission from Schülein J, Martens D, Spizauer P and Kertrup A (1995) Comparison of different solid phase extraction materials and techniques by application of multiresidue methods for the determination of pesticides in water. *Fresenius Journal of Analytical Chemistry* 352: 565–571.)

Table 3 Relative standard deviation (RSD), recoveries (Rec.) and determination limits (DL, P 95%) for the preconcentration of acidic phenolic pesticides from 1000-mL Milli-Q-water

Concentration range (ng L ⁻¹)	Preconcentration on											
	Bond Elut C ₁₈ cartridges				Empore® C ₁₈ discs				Empore-SDB discs			
	RSD (%)	Rec. (%)	DL (ng L ⁻¹)		RSD (%)	Rec. (%)	DL (ng L ⁻¹)		RSD (%)	Rec. (%)	DL (ng L ⁻¹)	
Trifluralin-methyl	5.3	38	71		7.4	93	99		5.2	68	67	
Metsulfuron-methyl	6.7	43	92		4.8	85	66		5.0	71	66	
Dicamba	3.9	63	96		3.8	46	93		4.9	115	116	
MCPA	8.5	98	208		6.5	99	164		12.8	59	300	
Bromoxynil	3.9	76	119		6.1	65	177		3.8	67	111	
Dichlorprop	4.1	99	118		4.2	94	119		3.0	83	84	
Ioxynil	6.6	100	151		4.7	95	110		6.3	76	140	
MCPB	8.7	88	202		5.0	94	121		9.9	106	220	
Bifenox acid	5.6	88	104		4.5	103	85		4.4	97	80	
Haloxifop	6.1	100	166		4.3	99	121		4.7	104	127	

(Reproduced with permission from Schülein J, Martens D, Spizauer P and Kertrup A (1995) Comparison of different solid phase extraction materials and techniques by application of multiresidue methods for the determination of pesticides in water. *Fresenius Journal of Analytical Chemistry* 352: 565-571.)

they are too expensive for use in disposable SPE cartridges. Empore® extraction discs have recently become available, with styrene divinylbenzene (SDB) copolymer sorbents enmeshed in the matrix.

Recoveries of acid herbicides from water samples have been compared by using C₁₈ and SDB discs; the results of this comparison are controversial. Some authors documented an improvement in the recoveries of phenoxy-carboxylic acid and phenols on SDB discs for the enrichment of samples down to 500 mL (see Table 4). The addition of salt considerably enhances the recovery and decreases the differences between the extraction efficiency of C₁₈ and resin discs. However, other authors reported that SDB discs showed worse recovery rates under acidic conditions, in comparison with C₁₈ when preconcentrations were carried out with 1-L samples (see Table 3). In any case, salting out the water sample enhances the retention of substances on both materials; this increases recovery rates for hydrophilic substances. However, salting out is avoided as it may introduce impurities into the samples. The addition of a small quantity of methanol or other organic solvent also enhances the recovery by the so-called 'dynamic solvation'. However, it is not recommended, as it produces a relatively early breakthrough of hydrophilic substances.

Graphitized carbon black (GCB) has been confirmed to be a valuable adsorbing material for SPE of pesticides in aqueous environmental samples. GCB cartridges proved to be more efficient than the more commonly used C₁₈ bonded-silica cartridges for the SPE of polar herbicides, whereas the extraction of non-polar compounds showed inferior results (see Table 3). Although GCB is known to behave as a natural reversed phase, it contains chemical heterogeneities on its surface, which are able to bind anions via electrostatic forces. GCB can behave as both a reversed-phase sorbent and an anion exchanger, retaining the acidic pesticides in their ionic form under acidic conditions. In this situation, the base-neutral/acid fractionation can be achieved by using solvent mixtures at different pHs.

Silica-based ion exchangers are found in disposable SPE cartridges. They are not widely used for the preconcentration of environmental samples owing to their low capacity. Strong anion exchanger discs have been used for the analysis of chlorinated acid and phenoxy acid herbicides. The main problem with these comes from the fact that environmental waters contain high amounts of inorganic ions, which overload the capacity of the sorbent.

Selective SPE from environmental waters has been accomplished by using different sorbents coupled in the same or in different cartridges.

Table 4 C_{18} and resin recoveries and effect of salting water

Analyte	Recoveries \pm RSD (%) $n = 3$			
	C_{18}^1	Resin ¹	C_{18}^2	Resin ²
Acifluorfen	77 \pm 20	82 \pm 5	104 \pm 5	121 \pm 1
Bentazon	0	ND	90 \pm 13	71 \pm 5
Chloramben	8 \pm 11	3 \pm 15	72 \pm 14	77 \pm 7
2,4-D	86 \pm 12	83 \pm 6	81 \pm 8	94 \pm 15
Dalapon	0	42 \pm 25	12 \pm 75	31 \pm 30
2,4-DB	81 \pm 13	80 \pm 14	118 \pm 10	130 \pm 8
Dacthal	53 \pm 17	99 \pm 8	67 \pm 16	97 \pm 5
Dicamba	73 \pm 13	71 \pm 14	83 \pm 3	94 \pm 15
3,5-Dichlorobenzoic acid	70 \pm 17	76 \pm 2	86 \pm 25	107 \pm 20
Dichloroprop	77 \pm 11	78 \pm 3	85 \pm 9	94 \pm 10
Dinoseb	72 \pm 16	75 \pm 5	92 \pm 26	85 \pm 6
Pentachlorophenol	69 \pm 14	70 \pm 2	65 \pm 15	73 \pm 8
Picloram	49 \pm 19	74 \pm 7	96 \pm 24	99 \pm 21
2,4,5-T	76 \pm 11	75 \pm 14	93 \pm 10	89 \pm 5
Silvex	73 \pm 14	74 \pm 14	82 \pm 9	80 \pm 5

¹Fortified, unsalted reagent water.²Fortified reagent water with 20% (w/w) Na_2SO_4 .

ND, no data.

(Reproduced with permission from Hodgeson J, Collins J and Bashe W (1994) Determination of acid herbicides in aqueous samples by liquid-solid disk extraction and capillary gas chromatography. *Journal of Chromatography A* 659: 395-401.)

One of the sorbents is non-specific, such as GCB, which traps the analytes of interest and many other compounds, while the other is more specific, such as a cation or anion exchanger, which retains and reconcentrates the analytes of interest. Table 5 shows the recoveries of nine phenoxy acid herbicides extracted by one miniaturized cartridge containing 50 mg of GCB at the top and 70 mg of a silica-based strong anion exchanger (SAX) at the bottom, compared with C_{18} and anion exchanger extraction. A large loss of dicamba and incomplete recovery of phenoxyacids were obtained by using the resin-based exchanger material.

Ammonium quaternary compounds and glyphosate constitute a special and complicated case. Their determination is very important because they are among the top herbicides used in the world. An important drawback in the preconcentration of such compounds from water is their high polarity. Several efforts have been made to analyse them in environmental samples.

SPE of ammonium quaternary herbicides has been mainly performed with silica, which is a well-known example of the solid phase using adsorption and ionic interaction mechanisms with the silanol groups. Recoveries are rather acceptable in the pH range 7.5-9. Taking into account that at pH values higher than 7 the silanol groups of the stationary phase are ionized, at these pH values the cation-exchange capacity of the solid-phase will be increased.

Glyphosate, due to its ionic form, can be preconcentrated using anionic and cationic resins. Derivatization of the analyte, prior to SPE of the water sample, seems to help the concentration from water samples.

Table 5 Recovery of herbicides from 200-mL groundwater samples by using one cartridge containing GCB and anion exchanger compared with that from two other extraction methods

	% Recovery ¹			
	C_{18}		Anion exchanger	GCB + anion exchanger
	pH 2	pH 7.9		
Dicamba	94.2	< 10	23.0	97.3
2,4-D	96.1	< 10	78.3	98.4
MCPA	96.4	< 10	77.7	97.6
2,4-DP	97.7	< 10	76.8	96.4
MCPP	94.4	< 10	82.0	97.3
2,4,5-T	93.5	< 10	81.4	95.4
2,4-DB	96.0	< 10	82.3	98.9
MCPB	95.8	< 10	81.5	96.5
2,4,5-T	93.1	< 10	77.3	95.2

¹Mean values were calculated for two determinations.(Reproduced with permission from Di Corcia A, Marchetti M and Sampieri R (1989) Extraction and isolation of phenoxyacid herbicides in environmental waters using two adsorbents in one mini-cartridge. *Analytical Chemistry* 61: 1363-1367.)

Table 6 Desorption efficiencies from the solid phase and overall recoveries of herbicides

Herbicide	Desorption efficiency (%)						Recovery from filtered river water (%) ⁵			
	Methanol			Ethyl acetate			Acetone		Acetone (6 mL)	
							3 mL + HX ³		Mean ¹	
	3 mL	6 mL	3 mL	6 mL	3 mL	6 mL	3 mL + HX ³	3 mL + DCM ⁴	Mean ¹	RSD ²
ACN	68.9	68.9	78.3	78.3	74.6	8.4	74.6	74.6	81.9	12
Alachlor	67.7	67.7	80.5	80.5	80.1	7.4	80.1	80.1	101	6.1
Benfluralin	48.1	48.1	73.4	73.4	55.0	13	69.6	70.3	67.9	1.8
Bifenox	< 5	< 5	78.3	78.3	69.2	9.1	69.2	79.0	92.9	8.2
Bromobutide	77.1	77.1	78.2	78.2	80.1	8.5	80.1	80.1	103	2.7
Bromobutide-debromo	76.4	76.4	76.6	76.6	79.5	7.8	79.5	79.5	92.7	7.8
Butachlor	50.6	64.0	79.6	79.6	73.4	9.3	83.5	83.1	100	5.2
Butamifos	73.9	73.9	81.4	81.4	81.2	9.2	81.2	81.2	96.5	3.9
Chlormethoxyfen	< 5	< 5	74.9	74.9	70.9	5.9	70.9	83.2	91.3	8.7
Chlornitrofen	< 5	< 5	77.8	77.8	63.2	13	70.6	80.5	71.9	3.2
Chlorprofam	57.5	57.5	81.1	81.1	68.2	5.1	68.2	79.1	95.7	5.4
Dimepiperate	< 5	42.2	80.1	80.1	71.7	7.8	84.0	85.8	104	8.9
Dimethametryn	64.5	64.5	83.1	83.1	79.4	6.9	79.4	79.4	96.4	3.2
Dithiopyr	73.5	73.5	79.5	79.5	74.4	6.6	74.4	82.4	84.1	8.6
Esprocarb	< 5	35.9	76.2	76.2	63.4	13	77.5	78.3	87.3	3.6
MCPA-ethyl	22.5	47.3	72.6	72.6	57.9	12	70.3	74.8	89.7	5.8
MCPA-thioethyl	< 5	< 5	76.6	76.6	57.9	14	74.8	82.6	98.1	4.0
Mefenacet	< 5	55.4	78.2	78.2	82.5	2.5	82.5	82.5	90.7	2.9
Molinate	25.8	45.9	76.8	76.8	64.1	9.7	75.9	80.5	90.8	7.0
Naproanilide	< 5	60.0	76.8	76.8	79.8	2.4	79.8	79.8	96.0	3.1
Oxadiazon	38.0	59.4	76.1	76.1	70.8	6.7	83.2	84.0	93.2	1.8
Pendimethalin	< 5	42.9	92.6	92.6	71.1	8.9	86.4	86.5	73.2	7.3
Piperophos	54.1	71.8	79.9	79.9	85.9	5.7	85.9	85.9	93.5	5.3
Pretlachlor	64.1	64.1	78.5	78.5	79.8	8.6	79.8	79.8	108	6.5
Prometryn	70.9	70.9	79.4	79.4	82.8	8.2	82.8	82.8	93.6	4.5
Simazine	84.6	84.6	78.1	78.1	78.9	11	78.9	78.9	102	9.6
Simetryn	78.8	78.8	77.9	77.9	80.4	9.2	80.4	80.4	93.5	9.4
Thiobencarb	< 5	30.7	80.3	80.3	64.4	13	77.6	80.6	97.6	5.1
Trifluralin	50.3	50.3	76.8	76.8	57.3	13	71.1	72.3	72.1	1.2

¹Percentage mean recovery ($n = 3$).²Percentage relative standard deviation.³A 3-mL volume of hexane.⁴A 3-mL volume of dichloromethane.⁵The herbicides were eluted with 6 mL of acetone.(Reproduced with permission from Tanabe A, Mitobe H, Kawata K and Sakai M (1996) Monitoring of herbicides in river water by gas chromatography-mass spectrometry and solid phase extraction. *Journal of Chromatography A* 754: 159-168.)

It can be concluded that C₁₈ material is inappropriate for some herbicides, especially more polar and very non-polar herbicides. In these cases, the SDB polymers and GCB offer a valuable alternative. The appropriate choice of solid phase for application to a separation problem will vary from case to case and must be adapted accordingly.

Elution of the Target Analytes

Desorption of the compounds from the concentration columns is mainly performed with a small volume of liquid. The partition coefficient in a given solid-phase eluent system should favour the shift of the studied herbicides. On the other hand, SPE is not a separate step, but it is part of a process that includes subsequent determination and so it should be taken into account that some determination systems, such as GC, are incompatible with the presence of water. In this way, the selection of the eluting solvent depends on the selected sorbent, the analytes and the detection method. Air-drying is often applied before analyte elution in order to remove residual water.

Methanol and acetonitrile are recommended solvents for the elution of herbicides adsorbed to C₈ or C₁₈ silicas. Dichloromethane and ethyl acetate have also been extensively used, especially when the presence of water is undesirable. Table 6 presents the

results obtained when herbicides were eluted from a cartridge using different solvents, such as methanol, ethyl acetate, acetone, hexane and dichloromethane following acetone.

Desorption of acid herbicides from the sorbents can also be performed using a solution adjusted to a pH where the analytes are in their ionic form (two units below or above the p*K*_a). The uniqueness of GCB is that acid compounds are retained in their ionic forms and neutral compounds are adsorbed by unspecific mechanisms. In this situation, base-neutral/acid fractionation can be easily achieved by first eluting base-neutral species with a neutral organic solvent mixture and then passing a basified or acidified solvent system to desorb acidic compounds. Table 7 reports the results obtained using base-neutral/acid fractionation in three kinds of GCB. In all cases, there was some carryover of 2,4-DB, which is the weakest compound included in this table.

With ion exchange sorbents, the analytes can be eluted from the SPE column by either adjusting the pH in order to neutralize the charge on the analyte or by using a buffer of high ionic strength.

Sample Requirements

Samples undergoing SPE need to be filtered to separate suspended matter. Filtration is especially necessary before extraction of surface water, but is also

Table 7 Base-neutral/acid fractionation by differential elution of selected compounds with cartridges containing three different types of GCB at two eluents

Compound	Sorbent material					
	Carbograph 1		Carbograph 4		Carbograph 5	
	Eluent A ¹	Eluent B ³	Eluent A	Eluent B	Eluent A	Eluent B
<i>Base/neutral</i>						
Atrazine	97	—	95	—	94	—
Linuron	99	—	98	—	95	—
Aldicarb	92	—	92	—	92	—
<i>Acidic</i>						
Dichlorprop (3.5) ³	—	95	—	97	30	73
2,4,5-T (2.2)	—	97	—	102	—	99
Ioxynil (3.9)	—	101	—	102	—	93
2,4-D (2.6)	—	99	—	100	—	93
2,4-DB (4.8)	40	63	18	81	50	49
Mecoprop (3.7)	—	99	—	99	—	96

Extraction from 1 L of Aldrich humic acid-spiked drinking water (spiked level, 10 µg L⁻¹). Mean recovery values obtained from three measurements.

¹Eluent phase: CH₂Cl₂-CH₃OH (80 : 20).

²Eluent phase: CH₂Cl₂-CH₃OH (80 : 20) + 10 mmol L⁻¹ tetrabutylammonium chloride (TBACl).

³Reported p*K*_a values of the acidic compounds are given in parentheses.

(Reproduced with permission from Crescenzi C, Di Corcia A, Passariello G, Samperi R and Turnes MI (1996) Evaluation of two new examples of graphitized carbon blacks for use in solid-phase extraction cartridges. *Journal of Chromatography A* 733: 41-55.)

often advisable for extraction of ground water to avoid blocking up the cartridge material. However, waters from different sources are very different in chemical composition. Matrix effects from the water itself can cause errors in quantitation and determination. The presence in waters of common contaminants (natural or xenobiotics), such as

humic acids, surfactants, inorganic salts, phenols, polycyclic aromatic hydrocarbons (PAH), other pesticides and related compounds, can negatively affect the analysis, significantly diminishing the recovery efficacy or interfering with the posterior determination. **Figure 1** shows that when natural samples are acidified, humic and fulvic acids are

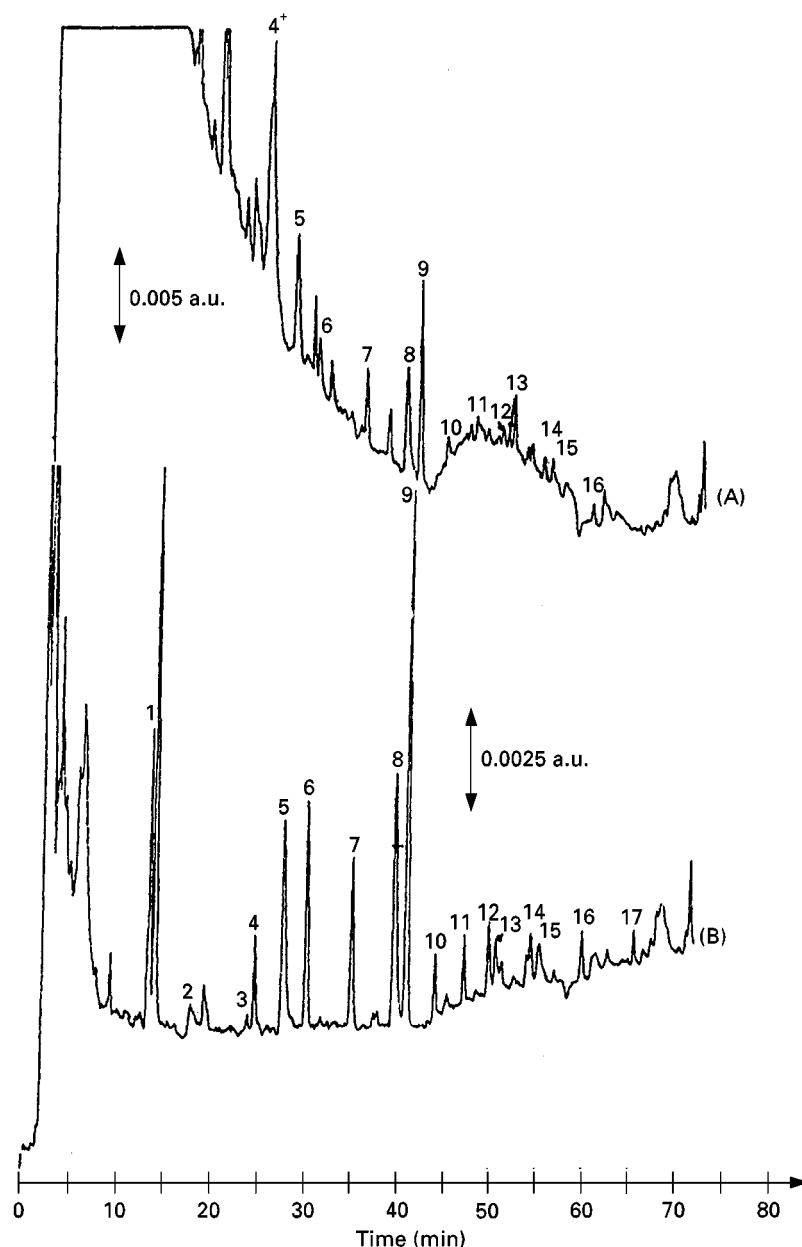


Figure 1 Effect of the pH of the sample on the preconcentration of 500 mL of drinking water spiked at $0.1 \mu\text{g L}^{-1}$. Sample (A) adjusted to pH 3 with perchloric acid and (B) not adjusted (pH 7). Analytical conditions: flow-rate, 1 mL min^{-1} , loop, $50 \mu\text{L}$; mobile phase, acetonitrile gradient with 0.005 M phosphate buffer acidified to pH 3 with HClO_4 , gradient from 10 to 30% acetonitrile from 0 to 10 min, and from 30 to 77% from 10 to 80 min; UV detection at 220 nm. Peaks: 1, chloridazon; 2, dicamba; 3, aldicarb; 4, methoxuron; 5, simazine; 6, cyanazine; 7, bentazone; 8, atrazine; 9, carbaryl; 10, isoproturon; 11, ioxynil; 12, MCPP; 13, difenoxuron; 14, 2,4-DB; 15, 2,4,5-T; 16, metolachlor; 17, dinoterb. (Reproduced with permission from Pichon V, Cau Dit Coumes C, Chen L, Guenu S and Henion MC (1996) Simple removal of humic and fulvic acid interferences using polymeric sorbents for the simultaneous solid-phase extraction of polar acidic, neutral and basic pesticides. *Journal of Chromatography A* 737: 25–33.)

Table 8 Recoveries of cationic herbicides ($4 \mu\text{g L}^{-1}$) from 0.25 L of water samples containing various concentrations of different surfactants

Surfactants	Concentration ($\mu\text{g L}^{-1}$)	Recovery (%) ¹		
		Diquat	Paraquat	Difenzoquat
Cetrimide	5	98	99	90
	50	93	92	92
	300	95	91	93
	3000	87	89	92
Benzalkonium chloride	5	114	114	94
	50	107	107	93
	300	102	102	95
	3000	105	105	103
Sodium tetradecyl sulfate	5	99	102	87
	50	98	95	93
	300	41	47	41
	3000	34	30	37
Lauryl sulfate	5	84	85	92
	50	109	100	93
	300	42	35	41
	3000	34	30	39
Laurylsulfobetaine	5	89	83	79
	50	91	94	84
	300	47	57	42
	3000	54	55	48
Brij-35	5	85	89	92
	50	83	101	91
	300	45	33	37
	3000	36	30	42
Triton X-100	5	86	89	92
	50	102	101	91
	300	45	33	37
	3000	36	30	42

¹Average recovery calculated from four determinations.

(Reproduced with permission from Ibáñez M, Picó Y and Mañes J (1996) Influence of organic matter and surfactants on solid-phase extraction of diqua, paraquat and difenzoquat from waters. *Journal of Chromatography A* 727: 245–252.)

co-extracted and co-eluted, which generates a large, unresolved peak in the chromatogram when HPLC with UV detection is used (chromatogram A). At pH 7, humic and fulvic acids are not co-extracted, as can be seen by the flat baseline from the beginning to the end of chromatogram (B).

Organic matter and anionic or non-ionic surfactants have demonstrated negative effect on the recovery of any class of herbicides. Although these undesirable effects are well known, only a few analytical studies have focused on ways in which to avoid them. The proposed methods for removing interferences are based on the use of chemical reagents, such as sulfite or cationic surfactants. In these cases, the recovery values after chemical treatment were similar to those when a Milli-Q-quality water standard was analysed. The recoveries reported in Table 8 show that the quantitative SPE of diquat, paraquat and difenzoquat is affected by the presence of anionic, zwitterionic and non-ionic surfactants when they are present in water at a level of up to $50 \mu\text{g L}^{-1}$.

Although some common contaminants of natural waters have a negative effect on the recoveries, SPE is useful for analysing herbicides in drinking and surface water because only in very extreme conditions does the concentration of these contaminants reach levels at which recoveries are significantly decreased.

The application of SPE to the isolation of herbicide residues from other matrices presents difficulties that must be overcome, which have, up to now, discouraged investigation into the use of other matrices. For liquid matrices (plasma, urine, blood or milk), acceptable recoveries have been obtained using protein precipitation prior to SPE but the impurities present can accumulate in the analytical columns and affect the chromatogram. The recoveries obtained by SPE for determining triazines from milk are compared with those obtained by liquid–liquid extraction (Hajšlova *et al.*) in Table 9. SPE was performed using a double trap: first, a non-specific adsorbent (GCB), and then a cation exchanger. The liquid–liquid extraction method, after an initial double protein precipitation using methanol in

Table 9 Recovery ($n = 6$) of triazines from fortified (50 ng mL^{-1}) skimmed milk using the proposed method and that of Hajšlová *et al.*

Compounds	Recovery % (mean \pm RSD)	
	SPE method	Hajšlová <i>et al.</i>
Simazine	89.7 \pm 4.1	86.1 \pm 5.2
Atrazine	89.3 \pm 3.9	84.3 \pm 4.7
Prometon	90.4 \pm 4.0	92.4 \pm 4.3
Ametryn	89.5 \pm 3.5	90.0 \pm 4.7
Propazine	93.4 \pm 3.6	88.6 \pm 4.2
Terbutylazine	91.6 \pm 3.4	87.3 \pm 4.2
Prometryn	87.2 \pm 3.8	85.5 \pm 4.0
Terbutryn	77.8 \pm 3.2	80.9 \pm 3.9

(Reproduced with permission from Lagana A, Marino A and Fago C (1995) Evaluation of double solid-phase extraction system for determining triazine herbicides in milk. *Chromatographia* 41: 178–182.)

basic and acid environments, used a partition with chloroform followed by a sample clean up using a silica cartridge. There were no significant differences in the triazine recovery using the two methods.

Solid matrices can also be extracted by SPE with cartridge or disc devices but require a separate homogenization step and other laborious processes. The reported recoveries are lower than those obtained with water, and the addition of methanol or acetonitrile as organic modifier is necessary. However, these recoveries are comparable to those obtained by other well known extraction methods for solid matrices. **Table 10** gives a comparison of the features of three extraction procedures for tribenuron methyl analysis in soil. Solid-phase and supercritical fluid extractions are the most adequate in terms of recovery percentage and precision, with acceptable detection limits; nevertheless, the recovery is affected by the amount of herbicide present in soil. SPE can also be performed by blending directly a homogenized sample with C_{18} sorbent, transferring the mixture to a glass chromatography column and eluting the analytes with appropriate solvent.

The SPE of matrices other than water requires further investigation.

On-line and Off-line Procedures

Nowadays, SPE methods using off-line procedures can be converted into on-line SPE methods by direct connection of the precolumn to the analytical column via switching valves. The concentrated analytes are then directly desorbed and transferred to the analytical system. Such systems often involve microprocessor control of the stages for sample switching and flushing of solvents and eluents through the concentration and chromatographic columns.

On-line procedures have gained popularity since European Union (EU) guidelines were introduced which limited the maximum amount allowed for a single pesticide in drinking water to $0.1 \mu\text{g L}^{-1}$ and for several pesticides to $0.5 \mu\text{g L}^{-1}$, including toxic transformation products. Very sensitive methods are required for monitoring herbicide residues in drinking water at such low concentrations. Furthermore the recent commercialization of automatic devices has certainly helped in the development of on-line trace enrichment methods in environmental analysis, because the sequence can be totally automated using systems such as the Prospect module (Spark Holland) or the OSP-2 system (Merck).

On-line SPE-LC is the most common procedure used because it is easily performed in any laboratory. The extracted compounds are eluted directly from the precolumn to the analytical column by a suitable mobile phase, which permits the separation of the trapped compounds. It is well established that on-line procedures enable lower concentrations of pesticides to be determined, and most compounds can be kept within EU limits. **Table 11** illustrates the improvement in detection limits obtained for triazine and phenylurea herbicides using on-line procedures when compared with off-line ones.

Breakthrough is the key parameter in on-line SPE because it indicates the sample volume and the amount of analyte that can be preconcentrated. Two factors can be responsible for breakthrough: insufficient retention of the analytes by the sorbent and overloading of the sorbent. One important factor of the concentration procedure is the selection of the

Table 10 Comparison of the extraction procedures for tribenuron methyl analysis

Extraction	Efficacy	Precision	Selectivity	Operation time	Affecting factors	Detection limit
Solvent	+	++	+++	++	No data	No data
Solid-phase	++	+++	+++	++	Concentration	+++
Supercritical fluid	++	+++	+++	+++	Concentration	+++

+, Bad; ++, regular; +++, good.

(Reproduced with permission from Berna JL, Jiménez JJ, Herguedas A and Atienza J (1997) Determination of chlorsulfuron and tribenuron-methyl residues in agricultural soils. *Journal of Chromatography A* 778: 119–125.)

Table 11 Range of linearity, r^2 and detection limit (LOD) for the on-line method

Pesticide	Off-line method			On-line method		
	Range of linearity ($\mu\text{g L}^{-1}$)	r^2	LOD ($\mu\text{g L}^{-1}$)	Range of linearity ($\mu\text{g L}^{-1}$)	r^2	LOD ($\mu\text{g L}^{-1}$)
Simazine	0.5–50	0.9985	0.1	0.1–8	0.9990	0.03
Cyanazine	0.5–50	0.9973	0.1	0.1–8	0.9987	0.03
Chlortoluron	0.5–50	0.9960	0.1	0.2–8	0.9956	0.05
Atrazine	0.5–50	0.9980	0.1	0.1–8	0.9999	0.03
Isoproturon	1.0–50	0.9990	0.1	0.2–8	0.9993	0.05
Ametryn	0.5–50	0.9985	0.05	0.1–8	0.9993	0.03
Prometryn	0.5–50	0.9989	0.05	0.1–8	0.9995	0.03
Terbutryn	0.5–50	0.9980	0.05	0.1–8	0.9985	0.03
Chlorpyrifos-methyl	2.0–50	0.9962	0.5	0.5–8	0.9980	0.20
Fenitrothion	2.0–50	0.9983	0.5	0.5–8	0.9993	0.20
Fenchlorphos	5.0–50	0.9950	1.0	1.0–8	0.9927	0.30
Parathion-ethyl	5.0–50	0.9944	1.0	1.0–8	0.9995	0.30

(Reproduced with permission from Aguilar C, Borrull F and Marcé RM (1996) On-line and off-line solid-phase extraction with styrene-divenylbenzene-membrane extraction disks for determining pesticides in water by reversed-phase liquid-chromatography-diode array detection. *Journal of Chromatography A* 754: 77–84)

sorbent, which must allow a convenient breakthrough of the analytes. **Table 12** shows a comparison of SPE sorbents for analysis of phenyl carbamate herbicides. The results were unsatisfactory with some herbicides. GCB is not used much in online SPE because it is not sufficiently pressureresistant.

Another factor in the procedure is to evaluate the maximum sample volume that can be preconcentrated without breakthrough of analytes, thus avoiding peak broadening. Generally, 50 mL was considered as optimum, but it could be increased for a particular kind of herbicide.

It should be taken into account that sorbents used in on-line SPE are not selective and numerous compounds from the matrix of natural samples are preconcentrated and can be eluted with the analytes of interest. Interferences depend on the nature of the water. They have an effect on both detection

limits and quantification. **Figure 2** shows some chromatograms obtained with different waters. In spite of the presence of interference peaks, it can be seen that making a good choice of preconcentration parameter and analytical conditions, allows low levels of many pesticides to be determined, even in highly contaminated surface waters.

In this way, the EPA in the United States currently offers an on-line SPE procedure followed by HPLC for the analysis of acidic herbicides in drinking water. The sample is first adjusted to pH 12 to hydrolyse esterified analytes, then it is acidified to a pH of 1 and a 20-mL aliquot is pumped through a reversed-phase concentration column. By use of a switching valve, the concentration column is then pumped in line with the analytical column and the sample constituents are then passed to the analytical column for separation and detection.

Table 12 Average recoveries and RSDs (%) of the analytes by the proposed on-line SPE-LC-DAD procedures in environmental water samples spiked at different levels

Compound	<i>C₁₈</i> pre-column				<i>PRP-1</i> pre-column			
	Drinking water		Surface water		Drinking water		Surface water	
	0.5 $\mu\text{g L}^{-1}$	4 $\mu\text{g L}^{-1}$	0.5 $\mu\text{g L}^{-1}$	4 $\mu\text{g L}^{-1}$	0.2 $\mu\text{g L}^{-1}$	1 $\mu\text{g L}^{-1}$	0.2 $\mu\text{g L}^{-1}$	1 $\mu\text{g L}^{-1}$
Carbetamide	—	105 (3)	—	105 (4)	84 (12)	101 (3)	102 (8)	101 (3)
Propham	101 (2)	98 (3)	99 (3)	97 (3)	90 (5)	102 (5)	97 (6)	102 (3)
Desmedipham	84 (9)	86 (8)	94 (7)	98 (7)	—	—	—	—
Phenmedipham	87 (2)	97 (6)	98 (10)	108 (7)	87 (3)	101 (2)	93 (6)	104 (3)
Chlorbufam	105 (5)	99 (2)	102 (4)	97 (1)	106 (7)	101 (3)	99 (5)	105 (2)
Chlorpropham	103 (2)	99 (1)	108 (3)	106 (2)	105 (5)	101 (4)	99 (5)	108 (2)

(Reproduced with permission from Hidalgo C, Sancho JV, López FJ, and Hernández F (1998) Automated determination of phenylcarbamate herbicides in environmental water by on-line trace enrichment and reversed-phase liquid chromatography-diode array detection. *Journal of Chromatography A* 823: 121–128.)

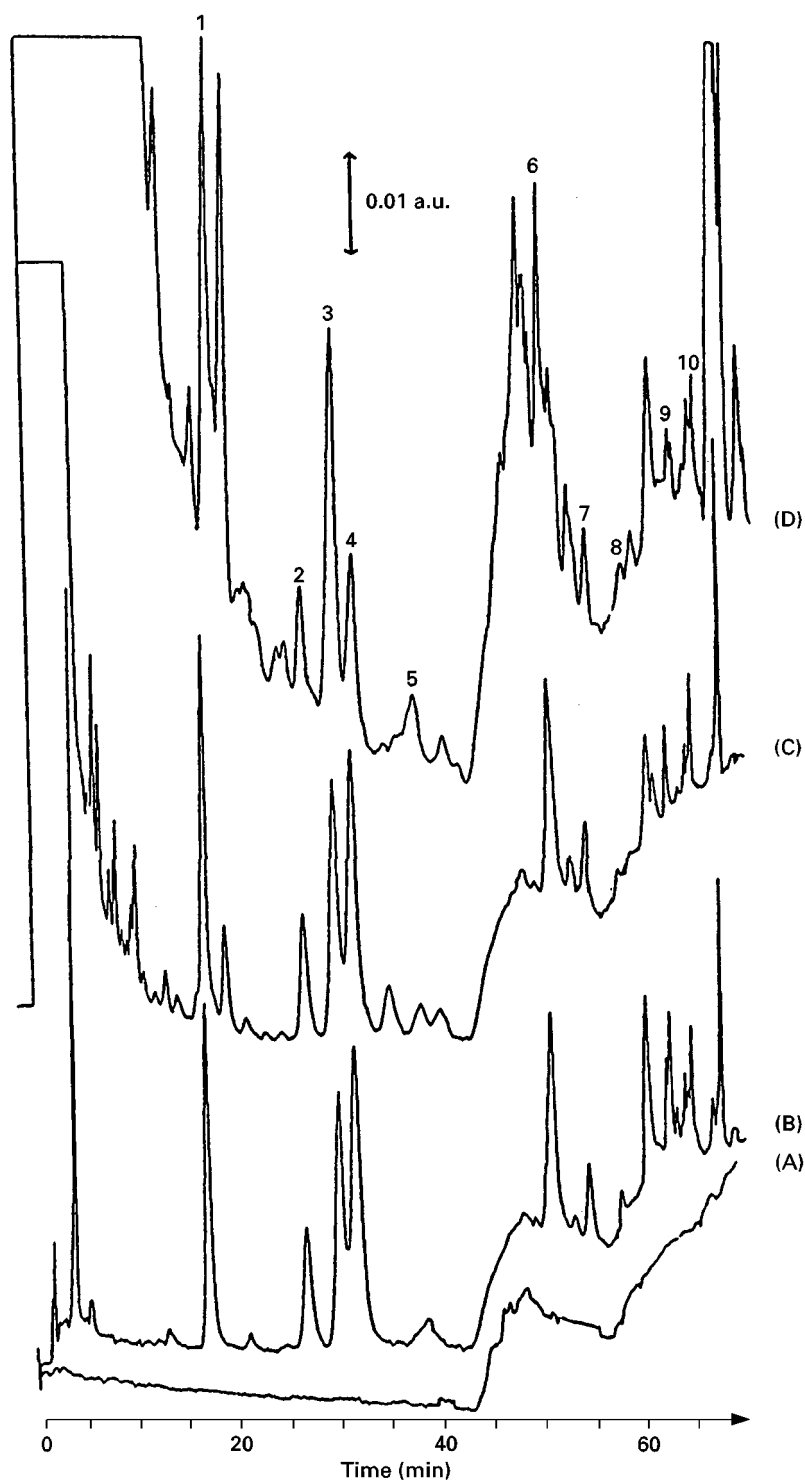


Figure 2 On-line analysis of 150 mL of different water samples spiked with $0.3 \mu\text{g L}^{-1}$ of (1) simazine, (2) methabenzthiazuron, (3) atrazine, (4) carbaryl, (5) isoproturon, (6) propanil, (7) linuron, (8) fenamiphos, (9) fenitrothion and (10) parathion. Precolumn, PRLP-S. (A) Blank gradient; (B) Milli-Q-purified water; (C) drinking water; (D) surface water from the Seine (28 June 1993). (Reproduced with permission from Pichon V and Henion MC (1994) Determination of pesticides in environmental water by automated on-line trace-enrichment and liquid chromatography. *Journal of Chromatography A* 665: 269–281.)

On-line SPE-GC is another interesting approach that has gained popularity over the last few years. The SPE-GC coupled techniques generally use an

uncoated, deactivated capillary precolumn, also known as a retention gap, which accommodates the liquid SPE eluent while it vaporizes, thereby providing

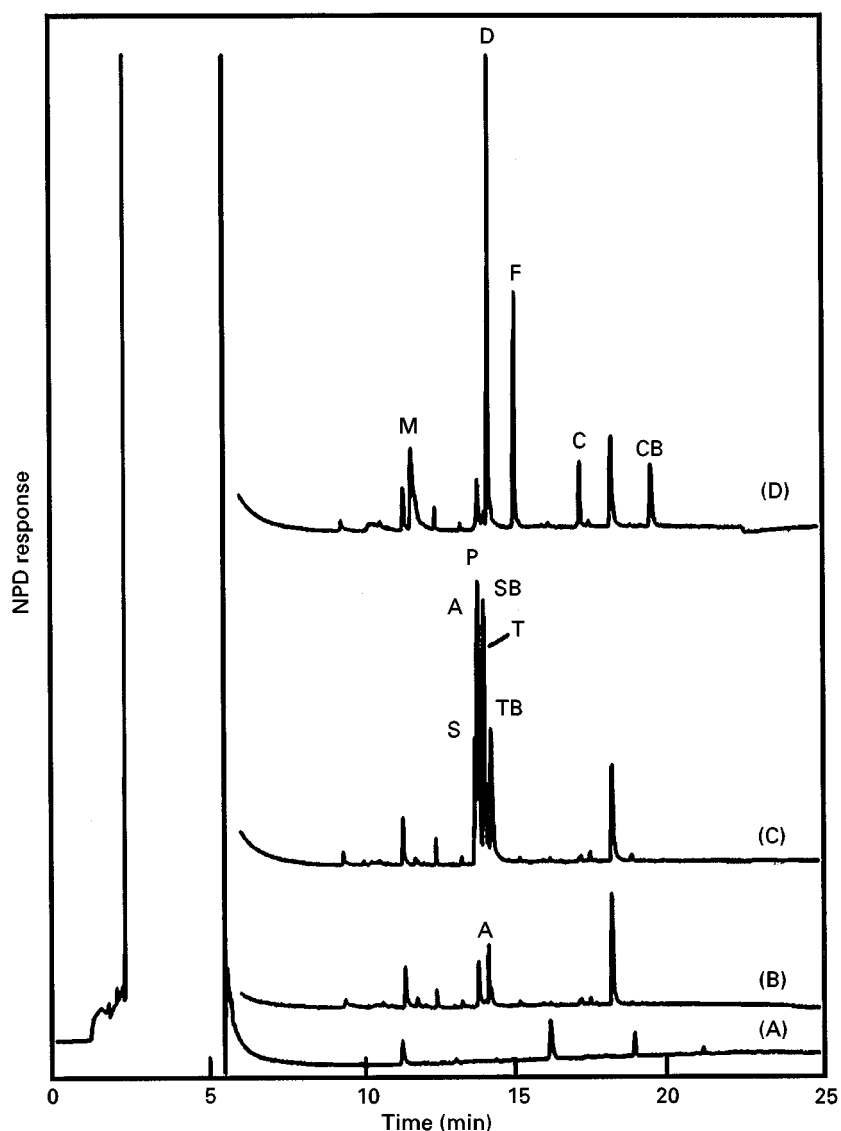


Figure 3 SPE-GC-NPD chromatograms obtained after preconcentration of 10 mL of (A) HPLC grade water, (B) Amsterdam drinking water, and drinking water spiked with (C) triazines ($0.1 \mu\text{g L}^{-1}$) and (D) OPPs ($0.03 \mu\text{g L}^{-1}$). Peak assignment for the herbicides: S, simazine; A, atrazine; P, propazine; SB, sebumeton; T, trietazine; and TB, terbutylazine. GC programme: 75°C during sample introduction, then to 300°C at $15^\circ\text{C min}^{-1}$; held at 300°C for 5 min. (Reproduced with permission from Picó Y, Louter AJH, Vreuls JJ and Brinkman UATH (1994) On-line trace-level enrichment gas chromatography of triazine herbicides, organophosphorus pesticides, and organosulfur compounds from drinking and surface waters. *Analyst* 119: 2025–2031.)

solute preconcentration. **Figure 3** shows typical results for the SPE-GC-nitrogen phosphorus detector (NPD) analysis of triazines. The most striking observation is the good baseline stability, because NPD is a very selective detector. The drawback of this technique is the high cost involved, which makes it unaffordable by most of the laboratories involved in herbicide analysis.

The analysis of herbicides, using an automated on-line solid-phase extraction device results in:

- a reduction in error
- a more efficient use of time

- savings in amount of solvent used
- an improved chromatographic separation
- a reduction of sample volume needed to achieve good results (up to 200 mL)
- a ten-fold improvement detection limit over that required by EPA and EU regulations (limit values)

The advantages cited for on-line procedures are convenient for some analysts, but many prefer the off-line approach, which gives a convenient extract in an organic solvent suitable for multiple analyses. Moreover, such an extract is generally much more stable than the aqueous sample from which it

was derived, and is therefore more suitable for long-term storage. Also, the off-line approach allows the processing of many samples at one time, an approach which is generally more productive in laboratories that are not fully automated.

Both off-line and on-line techniques are not mutually exclusive. The possibility of employing both methods gives the analyst more tools at his/her disposal for performing the analysis adequately.

Future Developments

Today, SPE has become generally accepted as the analytical method of choice for determination of all major herbicide groups in water. It is suitable for detecting approximately 300 pesticides and pesticide-related compounds and has undergone rigorous multi-laboratory calibration studies. SPE is also the backbone of residue analysis protocols for government agencies such as the EPA in the US. However, there is still much to be done. The development of new, more selective supports for SPE, its coupling with high separation power techniques, such as capillary electrophoresis (CE), and its application to extract herbicide residues from solid samples, may further reduce the detection limit and will represent an exciting challenge for researchers working in the area of herbicide residue analysis.

Looking to the future, it is interesting to note that new SPE sorbents involving antigen-antibody interaction, so-called immunosorbents, have been described. Due to their high affinity and high selectivity for these interactions, extraction and clean up of complex aqueous environmental samples is achieved in the same step. Their application to extracts from solid samples is solvent-free and simpler than any other clean-up procedure. Two class-selective immunosorbents have been optimized up to now that enable the trapping of two groups of widely used herbicides, phenyl urea and triazines.

Experiments have been recently designed to explore the possibility of recovering herbicide residues from food, soil, biological liquid and tissue samples by SPE. For liquid matrices, such as plasma, urine, fruit juice or milk, acceptable residue recovery may be obtained almost without clean up. Before SPE can be used with solid matrices (e.g. muscle, vegetables or soil) a separate homogenization step and often multiple filtration, sonication and centrifugation are required. Despite these drawbacks, SPE has been used a few times to extract residues of triazines, carbamates, ureas and other herbicides. More work is needed to further develop SPE for use with the many different types of matrices that may contain herbicide residues.

Capillary electrophoresis (CE) is very much suited for those analytes that are not amenable to GC or when existing LC methods do not offer sufficient separation power. Many impressive CE separations, including the separation of triazines and sulfonylureas, have been demonstrated in the last few years. The main disadvantages of these techniques are its inadequate detection limits and lack of selective detectors for the determination of residues in environmental matrices. As a result of coupling with SPE, use of CE has become competitive in trace analysis, and the door has been opened to environmental applications in real matrices. Thus, the potential of CE is very good indeed.

See also: II/Extraction: Solid-Phase Extraction. III/Immunoaffinity Extraction. Porous Graphitic Carbon: Liquid Chromatography. Solid-Phase Extraction with Cartridges. Sorbent Selection for Solid-Phase Extraction.

Further Reading

- Barceló D (ed) (1993) *Environmental Analysis. Techniques, Applications and Quality Assurance*. Amsterdam: Elsevier.
- Barceló D and Hennion MC (eds) (1997) *Trace Determination of Pesticides and Their Degradation Products in Water*. Amsterdam: Elsevier.
- Berrueta LA, Gallo B and Vicente F (1995) A review of solid-phase extraction: basic principles and new developments. *Chromatographia* 40: 474-483.
- Csárháti T and Forgács E (1998) Phenoxyacetic acids: separation and quantitative determination. *Journal of Chromatography A* 717: 157-178.
- Dean JR, Wade G and Barnabas IJ (1996) Determination of triazine herbicides in environmental samples. *Journal of Chromatography A* 733: 295-335.
- Font G, Mañes J, Moltó JC and Picó Y (1993) Solid phase extraction in multi-residue pesticide analysis of water. *Journal of Chromatography A* 642: 135-161.
- International Union of Pure and Applied Chemistry (1994) Analyte isolation by solid-phase extraction (SPE) on silica-bonded phases. Classification and recommended practices. *Pure and Applied Chemistry* 62: 277-304.
- Liska I, Kupcik J and Leclercq PA (1989) The use of solid sorbents for direct accumulation of organic compounds from water matrices. A review of solid-phase extraction techniques. *Journal of High Resolution Chromatography* 12: 577-590.
- Nollet LML (ed.) (1996) *Handbook of Food Analysis*. New York: Marcel Dekker.
- Pichon V (1998) Multiresidues solid-phase extraction for trace analysis of pesticides and their metabolites in environmental waters. *Analisis* 26: M91-M98.
- Picó Y, Moltó JC, Mañes J and Font G (1994) Solid phase techniques in the extraction of pesticides and related compounds from food and soils. *Journal of Microcolumn Separations* 6: 331-359.

Tekel, J and Kovačičová (1993) Chromatographic methods in the determination of herbicide residues in crops, food and environmental samples. *Journal of Chromatography A* 643: 291–303.

Zweig G and Sherma J (Eds) (1986) *Analytical Methods for Pesticides and Plant Growth Regulations*. New York: Academic Press.

Thin-Layer (Planar) Chromatography

V. Pacáková, Charles University, Prague, Czech Republic

Copyright © 2000 Academic Press

Introduction

Modern agricultural production in major agriculture countries depends heavily on the use of pesticides. Herbicides represent more than 50% of all pesticides used (in the USA and Germany the figure is about 60%) and are found in soil, ground and surface water and food. Triazines are the most common herbicides, and they represent *c.* 30% of all herbicides used. As they are relatively stable they are also the ones most commonly found in the environment. Triazine toxicity is low and they do not usually present a risk to humans. However, as they are extensively used, their presence in the environment and in food must be monitored (triazine residues, especially those of atrazine, can be found, in milk, butter and sugar). Phenylureas are replacing triazines as they are easily degraded, but this fact makes their analysis more difficult. Phenoxyacids are the oldest synthetic herbicides. Other herbicides include triazones, carbamates, uracils, pyridazines, substituted ureas and anilines (Figure 1).

Methods used to analyse herbicides and their residues are similar to those used for other pesticides. The methods applied should be able to determine multicomponent pesticide mixtures simultaneously, have a good reproducibility and a high recovery and a low limit of determination (the maximum permissible concentration in drinking water is as low as $0.1 \mu\text{g L}^{-1}$).

Principles of Thin Layer Chromatography and High Performance TLC (HPTLC)

Thin-layer chromatography (TLC) remains an important practical analytical method for the analysis of herbicides with well-developed standard procedures. Its main advantages for this type of analysis are simple equipment, the possibility of varying a large number of the experimental parameters, high throughput (up to 36 samples can be analysed simul-

taneously), fast analyses, economy and low solvent consumption. Sample clean-up is either simple or not required at all.

TLC thus provides a simple and inexpensive screening method for the analysis of herbicides.

In classical TLC the samples are applied to the thin layer and then the layer is developed by a mobile phase (a solvent or a solvent mixture). After the mobile phase is evaporated, the separated zones are evaluated. As capillary forces govern the migration of the solute through the stationary phase, the mobile-phase velocity is less than optimal. Higher velocity can be obtained by forced-flow development.

High performance TLC (HPTLC), which has developed from classical TLC, offers greater separation efficiency, greater sensitivity and reproducibility, accurate quantification and automation.

Modern instrumental HPTLC is thus a complementary technique to high performance liquid chromatography (HPLC) in the analysis of herbicides and is increasingly used in this application.

Chromatographic Systems

Silica gel is the most common stationary phase in TLC and HPTLC of herbicides but reversed-phases (silica gel modified with C_8 , C_{18} , e.g., RP-18 W, Nano-Sil C_{18} -100, silica gel impregnated with paraffin oil) can also be used. Silica gel impregnated with diethylene glycol is suitable for triazine herbicides. Good separation of herbicides can also be obtained on alumina. TLC layers covered with a transparent polymer film have been recommended to prevent evaporation of the mobile phase and volatile herbicide samples and to suppress the adsorption of environmental impurities.

Mobile phases frequently used in the TLC of herbicides in combination with silica gel include dichloromethane, hexane–acetone and hexane–butyl acetate mixtures. Methanol or acetonitrile with water is recommended when reversed-phase stationary phases are employed. Hexane–dioxane mixtures are used with alumina layers. The hydrophobicity of herbicides can be modified by the addition of cyclodextrins.

For the TLC systems commonly used in the analysis of herbicides, see Table 1.

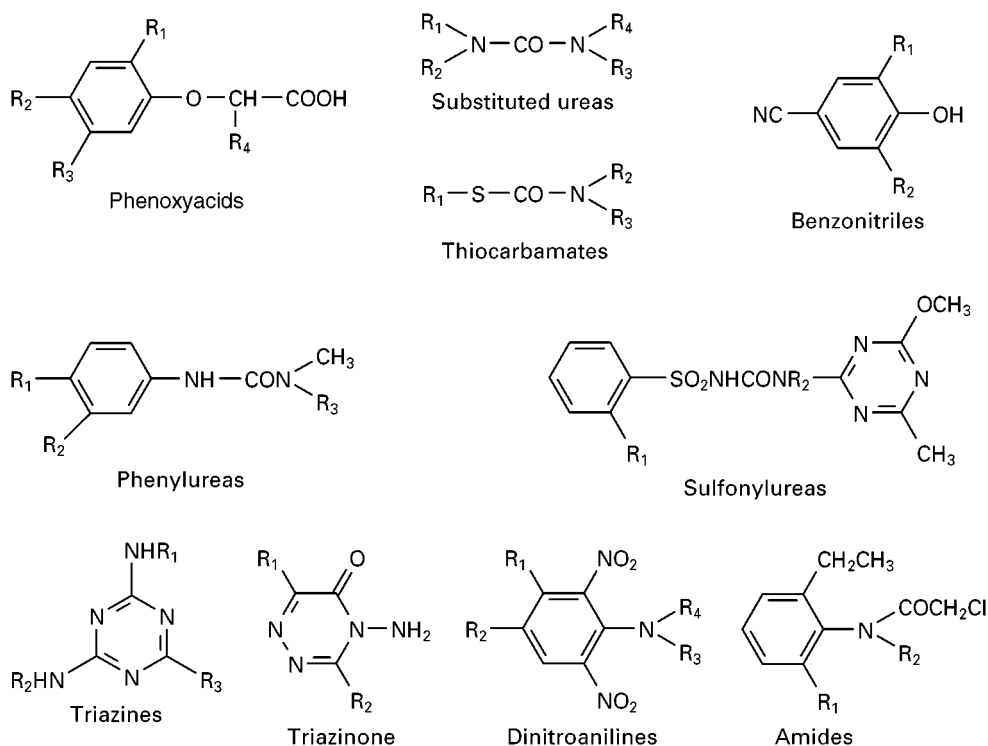


Figure 1 Structure of common herbicides.

Multiple Development

In multiple development the sample spots are re-concentrated whenever the solvent front contacts the chromatographic zone and the spots are re-focused to narrow bands. This results in increased separation efficiency and improved detection limits.

Automated multiple development (AMD) HPTLC has been applied to the screening of pesticides (including triazine, phenylurea, carbamate, phenoxy-carboxylic acids and other herbicides) in environmental samples. Herbicides from different classes can be resolved by a universal gradient, based on dichloromethane. Positive results are confirmed by a second analysis using special gradients optimized for indi-

vidual classes. Separated pesticides can be evaluated by densitometric detection and characterized by their UV spectra and migration distance. Most pesticides have detection limits in the range from 5 to 60 ng and their analysis does not require preconcentration methods. Only a few pesticides have higher detection limits and require preconcentration, e.g. by solid-phase extraction. An AMD-HPTLC method, DIN 38407, part 11, has been included in Germany's official methods for water analysis. An example of the AMD-HPTLC analysis of drinking water spiked with herbicides is shown in **Figure 2**; multi-wavelength detection was used. The optimized 20-step gradient for this separation is shown in **Figure 3**. Analysis takes 90 min (12 samples are analysed on one plate)

Table 1 Examples of TLC systems for the analysis of herbicides

Stationary phase	Mobile phase	Detection
Silica gel (60 or G)	Dichloromethane	Hill's reaction, sprayed with silver nitrate, <i>o</i> -toluidine 4,4'-tetramethyldiaminodiphenylmethane, 1% ferric chloride in butanol
	Ethyl acetate	
	Hexane-acetone (8 : 2)	
	Toluene-acetone (85 : 15)	
	Benzene-chloroform-methanol (9 : 3 : 2)	
	Chloroform-methanol (3 : 1)	
PR-18W, PR-18, Nano-Sil C ₁₈ -100	Methanol-water (7 : 3)	Sprayed with silver nitrate or <i>o</i> -toluidine
	Acetonitrile-water (7 : 3)	

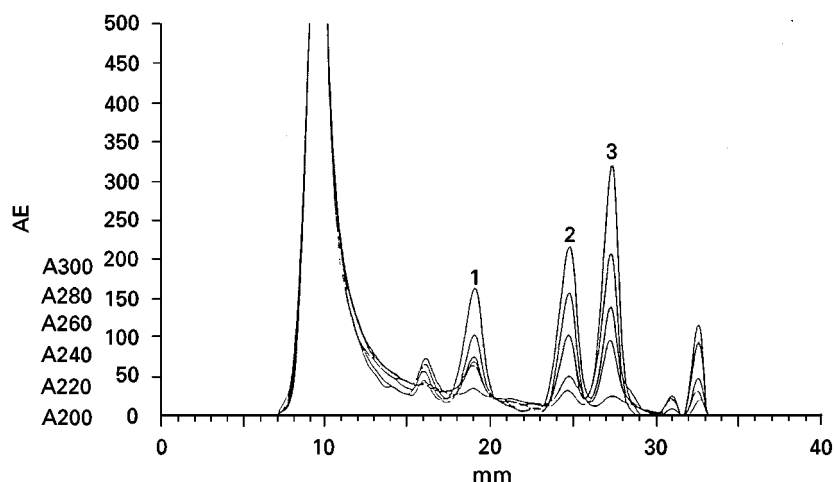


Figure 2 Multi-wavelength scan of drinking water spiked with 1, 2,4-dichlorophenoxyacetic acid; 2, mecoprop; 3, simazine. The optimized gradient is given in Figure 3. Reproduced with permission from Morlock (1996).

and peak capacity (separation number) is more than 40. This method was shown to be suitable for 283 pesticides, including herbicides.

Detection

Various agents have been used to visualize herbicide spots. They include silver nitrate, Gibbs reagent, diphenylamine and ninhydrin. The commonest detection method in TLC of herbicides is densitometry. Pre- and post-column derivatization can be carried out if the substances do not absorb visible or UV light. Simultaneous use of densitometry and fluorescence quenching is advantageous in the analysis of herbicides in multicomponent formulation, e.g. bromacil and diuron, chlortoluron and terbutryn.

Biochemical detection based on Hill's reaction is a very sensitive and selective method for herbicide residues that inhibit the enzyme system of isolated chloroplast. The concentration of the herbicide residues can also be determined from the lifetime of the spot. This method can be used for triazines, phenylureas, carbamates, uracils and pyridazone. Detection limits for herbicide residues in water, agriculture crops, foods and soil are in the range $1\text{--}10\ \mu\text{g kg}^{-1}$.

TLC with radioactive detection is useful in environmental studies, for example, in studies on the degradation of herbicides, formation of residues and their uptake and metabolism by plants.

Combination of TLC with mass spectrometry, recommended for the identification of herbicide metabolites, is less frequently used because of its high price.

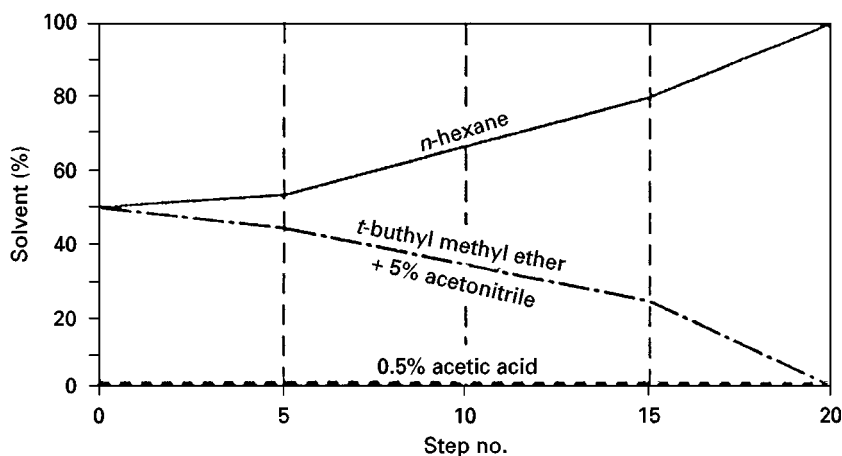


Figure 3 Optimized 20-step gradient for the determination of 2,4-dichlorophenoxyacetic acid, 4-chloro-2-methylphenoxyacetic acid (isooctyl ester) and atrazine. Reproduced with permission from Morlock (1996).

Selected Applications

TLC analysis of herbicides present in various matrices is usually preceded by isolation and/or preconcentration methods, e.g. solid-phase extraction (SPE) for water samples and supercritical fluid extraction (SFE) for solid samples, e.g. soils and plants; sample clean-up is usually not required. Some typical examples of the application of TLC in herbicide analysis are given below.

TLC can be used to determine triazine herbicides and their metabolites in drinking and surface water. Preconcentration by SPE is followed by chromatography on C_{18} plates with hexane–ethyl acetate–acetone (4 : 4 : 1 v/v) or silica gel with nitromethane–tetrachloromethane (1 : 1 v/v) and densitometric detection. The same chromatographic system can be used to determine triazine and triazone herbicides in soil after SFE. Detection limits range from 30 to 60 ng L⁻¹. A simple TLC method to determine atrazine in drinking and ground water is based on its extraction with chloroform, followed by separation on silica gel with toluene–acetone (85 : 15) as mobile phase and detection by spraying with 4,4'-tetramethyldiaminodiphenylmethane. The detection limit is 20 ng L⁻¹.

Phenoxyacetic acid herbicides can be analysed on silica gel with acidified mobile phases, e.g. ethyl acetate–acetic acid (49 : 1 v/v) or toluene–acetone–acetic acid (2 : 2 : 1 v/v) and detected by spraying with a solution of 3,5-dichloro-*p*-benzoquinonechlorimine.

Residue analysis of phenylurea herbicides in water, potatoes and soil is based on extraction with acetone or dichloromethane, clean-up on silica gel, hydrolysis to anilines and derivatization to fluorescent dansyl derivatives *in situ* on plate. This is followed by separation on silica gel with dichloromethane–methanol (99 : 1 v/v) as mobile phase and fluorescence detection. Detection limits of *ca.* 1, 20 and 200 mg kg⁻¹ can be attained for water, potato and soil samples.

Pre-coated silica gel plates impregnated either with a 20% solution of formamide (A) or diethylene glycol (B), with hexane–chloroform–diethyl ether (2 : 1 : 1 v/v) as a mobile phase for system A and hexane–benzene–acetone (1 : 1 : 1) for system B gave satisfactory separation of 12 substituted urea herbicides (Table 2).

The screening of drinking water (about 300 compounds, including herbicides) is based on SPE followed by AMD. Identification is by analysing the sample under different separation conditions, together with reference compounds, measurement of the UV spectra *in situ* and by the use of post-chromatographic detection with various reagents. Both SPE and HPTLC can be automated.

Table 2 R_F values of substituted urea herbicides

Herbicide	A	B
<i>N'</i> -(3-chloro-4-methoxyphenyl)- <i>N,N</i> -dimethylurea	0.16	0.36
<i>N'</i> -Phenyl- <i>N,N</i> -dimethylurea	0.20	0.40
<i>N'</i> -(4-Chlorophenyl)- <i>N,N</i> -dimethylurea	0.26	0.47
<i>N'</i> -(3,4-Dichlorophenyl)- <i>N,N</i> -dimethylurea	0.35	0.54
<i>N'</i> -(3-Chloro-4-methylphenyl)- <i>N,N</i> -dimethylurea	0.39	0.58
<i>N'</i> -[4-(4'-Chlorophenoxyphenyl)]- <i>N,N</i> -dimethylurea	0.45	0.62
<i>N'</i> -(4-Isopropylphenyl)- <i>N,N</i> -dimethylurea	0.46	0.64
<i>N'</i> -(4-Chlorophenyl)- <i>N,N</i> -methoxyphenylurea	0.70	0.77
<i>N'</i> -(4-Bromophenyl)- <i>N,N</i> -methoxyphenylurea	0.74	0.80
<i>N'</i> -(3,4-Dichlorophenyl)- <i>N,N</i> -methoxyphenylurea	0.78	0.83
<i>N'</i> -(4-Chlorophenyl)- <i>N,N</i> -methylisobutyl-2-urea	0.56	0.70
<i>N'</i> -(3,4-Dichlorophenyl)- <i>N,N</i> -methylbutylurea	0.72	0.79

Reproduced with permission from Ogierman L and Brysz G (1981) Partition thin-layer chromatography of some phenylurea herbicides. *Fresenius Zeitschrift für Analytische Chemie* 308: 464.

HPTLC can be used for the optimization of HPLC conditions where direct method development is more time-consuming and expensive. The herbicide migration data obtained in HPTLC on silica gel, RP-18, RP-8 and CN chemically bonded phases correlate well with HPLC.

Conclusions and Future Trends

TLC is useful in herbicide analysis when many samples have to be analysed. It requires minimal sample pretreatment and reduces the number of separation steps. The reason for using HPTLC for herbicide residue is that it can analyse samples in complex matrices with minimal matrix modification. The ability to separate a number of samples simultaneously is important in screening studies. HPLC should be applied in cases of complicated samples when TLC fails and when full automation is required.

It is expected that TLC will keep its place as a simple and rapid method for qualitative and semiquantitative analysis of herbicides. HPTLC will find increasing use in herbicide residue determinations due to its main advantages of increased separation efficiency, decreased detection limit, more accurate quantitative analysis and automation. There will be developments in mobile-phase optimization. Greater use of combined TLC-spectroscopic methods can be expected.

A growing demand for method validation can be expected.

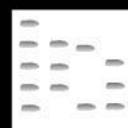
See also: II/Chromatography: Thin-Layer (Planar): Densitometry and Image Analysis; Layers; Modes of Development: Conventional; Modes of Development: Forced Flow, Over Pressured; Spray Reagents. **Extraction:** Analytical Extractions; Solid-Phase Extraction; III/Herbicides: Gas Chromatography; Solid-Phase Extraction. **Impregnation Techniques: Thin-Layer (Planar) Chromatography. Pesticides:** Gas Chromatography; Thin-Layer (Planar) Chromatography.

Further Reading

- Frey HP and Zieloff K (1992) *Qualitative und quantitative Dünnschicht-Chromatographie*. Weinheim: VCH.
- Fried B and Sherma J (eds) (1996) *Practical Thin Layer Chromatography: A Multidisciplinary Approach*. Boca Raton, FL: CRC Press.
- Jork H, Funk W, Fischer W and Wimmer H (1990) *Thin Layer Chromatography*, vol. 1a. *Physical and Chemical Detection Methods*. Weinheim: VCH.

- Jork H, Funk W, Fischer W and Wimmer H (1994) *Thin Layer Chromatography*, vol. 1b. *Reagents and Detection Methods*. Weinheim: VCH.
- Kaiser RE, Günther W, Gunz H and Wulf G (eds) (1996) *Thin Layer Chromatography*. Düsseldorf: InCom.
- Morlock GM (1996) Analysis of pesticide residues in drinking water by planar chromatography. *Journal of Chromatography A* 754: 423–430.
- Pacáková V, Štulík K and Jiskra J (1996) High performance separations in the determination of triazine herbicides and their residues. *Journal of Chromatography A* 754: 17–31.
- Rathore H-S and Begum T (1993) TLC methods for use in pesticide residue analysis. *Journal of Chromatography* 643: 271–290.
- Sherma J (1994) Determination of pesticides by thin-layer chromatography. *Journal of Planar Chromatography* 7: 265–272.
- Sherma J and Fried B (eds) (1996) *Handbook of Thin Layer Chromatography*, 2nd edn. New York: Marcel Dekker.
- Touchstone J (1992) *Practice of Thin Layer Chromatography*, 3rd edn. New York: Wiley.

HEROIN: LIQUID CHROMATOGRAPHY AND CAPILLARY ELECTROPHORESIS



R. B. Taylor, A. S. Low and R. G. Reid,
The Robert Gordon University, Aberdeen, UK

Copyright © 2000 Academic Press

Introduction

The separation and quantitative determination of opiates is required for a wide variety of purposes and applications. These include therapeutic drug monitoring, metabolism and pharmacokinetic studies and forensic investigations, as well as the detection and control of drug abuse. The determination of opiates in human urine is of considerable analytical interest, particularly in the context of detecting the consumption of heroin; it is in this context that the present article is written.

The first step in the establishment of such presumptive consumption of heroin is usually by enzyme immunoassay. This has the merit of low detection limit and large sample throughput, making it very suitable for large screening programmes. The immunoassay technique, however, is nonselective with respect to individual opiates and a positive result in such a screen for legal purposes must be followed by identification of individual opiates present. The purpose

of this is usually to confirm or refute the hypothesis that heroin has been consumed. The short metabolic half-life of heroin complicates its confirmation, so that its consumption is inferred by detection of its metabolites. One generally sought metabolite is morphine owing to its relatively long half-life. This approach has the disadvantage that morphine is also produced as a metabolite of codeine, so that heroin consumption is presumed or not on the basis of notional codeine-to-morphine ratios. The detection of the first metabolite of morphine, 6-monoacetylmorphine, is now taken as an unequivocal indicator of heroin consumption.

The detection of heroin consumption is further complicated by the quite general inclusion of legal opiates such as codeine, pholcodine and dihydrocodeine in commonly available medicines. This results in numbers of subjects being screened as positive for opiate consumption who are not confirmed by alternative methods as having consumed heroin or morphine.

To confirm the presence of individual opiates, techniques are required that are more selective than immunoassay. These are usually based on established chromatographic techniques. Several thin-layer systems have been used but in general these have

insufficiently low limits of detection to confirm adequately results obtained by immunoassay. This is a particular problem since immunoassay detects total opiates and, following separation, individual concentrations may be much lower. The most generally accepted confirmation is by combined gas chromatography-mass spectrometry (GC-MS), owing to the selectivity of the capillary gas chromatography separation coupled with the unequivocal identification by electron impact ionization mass spectrometry. The technique of high performance liquid chromatography (HPLC) has been extensively applied to heroin and some of its metabolites as well as individual related opiates for a variety of purposes associated with drug abuse. No liquid chromatography (LC) method has specifically addressed the problem of confirmation of results obtained from immunoassay. Work in this area has concentrated on developing LC methods capable of quantifying morphine and codeine individually since, as indicated above, the codeine-to-morphine ratio has been a major criterion in establishing heroin consumption. The emerging technique of capillary electrophoresis (CE) is potentially attractive as a separation technique because of its capability for high resolution and peak capacity. As yet little has appeared in the literature concerned with the capability of this technique to determine low concentrations of opiates in biological matrices.

The literature on the determination of drugs of abuse and screening procedures using GC-MS is extensive and will not be discussed here. The present article describes both normal and reversed phase LC systems for the separation and quantification of a set of opiates comprising heroin, 6-monoacetylmorphine, morphine, codeine, dihydrocodeine and pholcodine, and discusses their potential in acting as an intermediate test in determining opiate abuse. Such a test may eliminate so-called false positives arising from urine samples screened as containing opiate that is subsequently found not to originate from consumption of heroin. A method based on CE is also described and its potential in relation to the LC methods discussed. Heroin is rapidly metabolized and cannot be detected in urine. This drug is included in this set, however, as the separation with respect to legal opiates may be of relevance in forensic applications.

Reversed-Phase LC System

Several reversed-phase separations of selected groups of opiates have been reported in the literature using column switching, gradient elution and ion pairing techniques. From our experience in the analysis of

basic drugs in biological fluids, the most general approach to ion pairing is the use of mobile-phase additives. An anionic surfactant such as sodium dodecyl sulfate (SDS) or alkylsulfonic acid, which is adsorbed onto a C_{18} surface, is incorporated in the mobile phase to increase retention and thus separation. The inclusion, in addition, of a less hydrophobic species of similar charge to the analyte, such as a tetraalkylammonium bromide, has been found to reduce tailing of such basic compounds and also in some cases to alter selectivity. In using such systems the pH of the mobile phase is made acid, thus protonating the basic analytes.

For the opiates morphine, pholcodine, dihydrocodeine and codeine the best anionic mobile phase additive is pentanesulfonic acid used in conjunction with tetraethylammonium bromide. At concentrations of 1 mmol L^{-1} and 100 mmol L^{-1} , respectively, these additives in methanol/aqueous buffer (10:90 by vol.) containing disodium hydrogen phosphate at pH 2.5 give excellent separation of these four opiates in 15 min when dissolved in water. This system allows the inclusion of nalorphine as an internal standard, which elutes between pholcodine and dihydrocodeine. This optimum separation is shown in Figure 1. Both heroin and 6-monoacetylmorphine elute much later than codeine and therefore cannot be determined at sensitivities comparable with the other compounds. The separation of these four opiates is accompanied by excellent individual linearity of response of peak height ratios versus concentration over the range $1\text{--}5 \mu\text{g cm}^{-3}$ using UV detection at 285 nm.

A standard solid-phase extraction procedure was applied to urine spiked with the four opiates and the internal standard. Bond-Elut Certify extraction cartridges containing a mixed stationary phase of non-polar C8 and strong cation exchanger (SCX) were used. The extraction consisted of cartridge conditioning with methanol, water and acetate buffer followed by sample addition and washing with acetate buffer, water and methanol. After drying, the analytes were eluted with dichloromethane/isopropyl alcohol (80:20 by vol.) mixture containing 2% (v/v) ammonia. The resultant solution was dried at 40°C under nitrogen, reconstituted in 250 μL of ethyl acetate, and again dried under nitrogen. Immediately prior to injection, the sample was redissolved in 500 μL of mobile phase. This procedure gave percentage recoveries in excess of 80% for all the compounds other than morphine, for which the recovery was 71%, presumably as a result of its known propensity for being adsorbed onto glass surfaces.

This extraction procedure gives a large solvent peak in this reversed-phase solvent system. At the

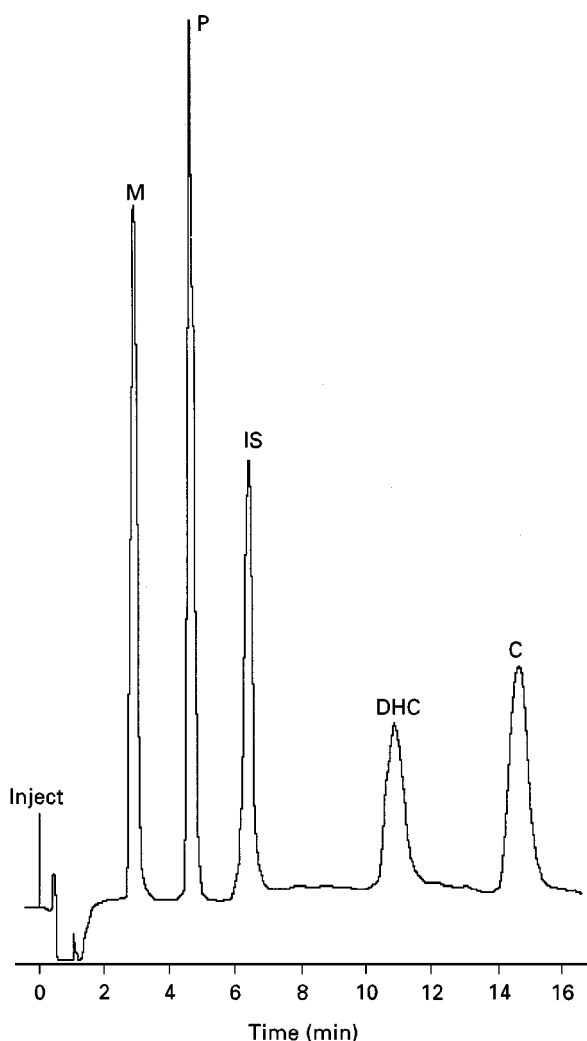


Figure 1 Representative reversed-phase separation of morphine (M), pholcodine (P), dihydrocodeine (DHC), codeine (C) and nalorphine (IS) using 10% methanol/90% water, containing 50 mmol L⁻¹ disodium hydrogen orthophosphate, 1 mmol L⁻¹ pentanesulfonic acid and 100 mmol L⁻¹ tetraethylammonium bromide as mobile phase at a flow rate of 0.4 mL min⁻¹, column 100 × 2 mm i.d. packed with 3 μm microporous octadecylsilica, detection by UV at 280 nm.

detector sensitivity required for 500 ng cm⁻³ opiate concentrations, it is not possible to quantify morphine or pholcodine since they are not separated from the solvent front. A specimen chromatogram of urine spiked (500 ng cm⁻³) with the four opiates and nalorphine is shown in Figure 2.

It appears that for such a set of opiates, which vary widely in hydrophobicity, the reversed-phase system is of minimal use for the purpose of detecting heroin consumption by urine analysis when coupled with UV detection. Neither heroin nor 6-monoacetylmorphine interfere with the quantification of the legal opiates. However, the retention time of the 6-monoacetyl metabolite is excessive for quantification and

the codeine-to-morphine ratio cannot be established because of the masking of the morphine peak at levels below 500 ng cm⁻³ by endogenous compounds in the solvent front when using UV detection. The inherent high resolution of reversed-phase chromatography is not helpful in the quantification of this widely differing range of analytes. The obvious choice of gradient elution, by analogy with GC, would result in compression of the timescale for elution of the complete range of compounds. However, the potential improvement in detection limits may not be wholly achievable owing to increased baseline noise. The use

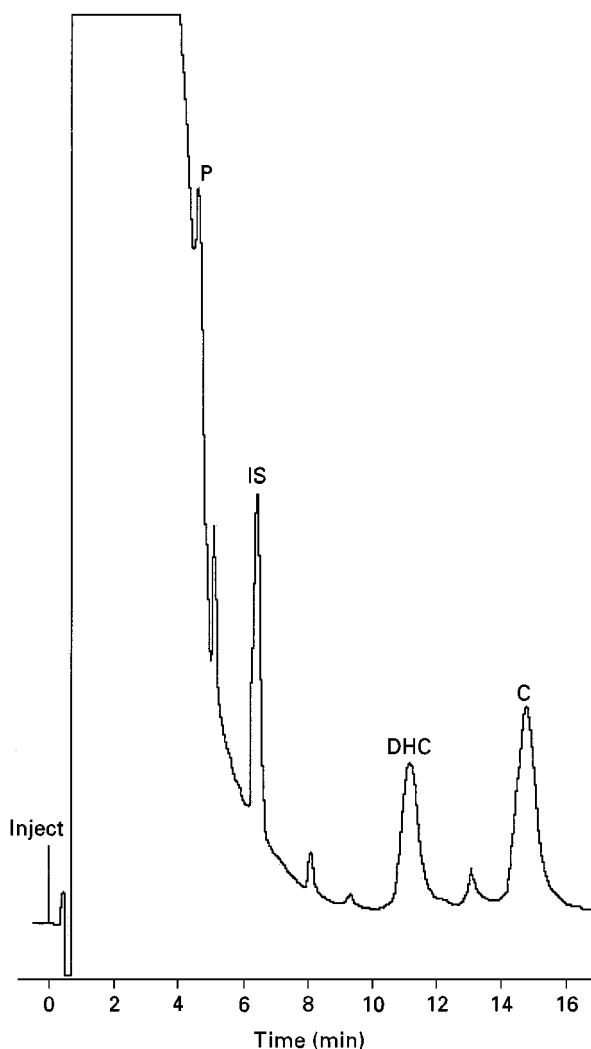


Figure 2 Representative chromatogram of a urine sample spiked with morphine (M), pholcodine (P), dihydrocodeine (DHC) and codeine (C) at a concentration of 500 ng cm⁻³ and incorporating nalorphine (IS) as internal standard after solid-phase extraction using 10% methanol/90% water containing 50 mmol L⁻¹ disodium hydrogen orthophosphate, 1 mmol L⁻¹ pentanesulfonic acid and 100 mmol L⁻¹ tetraethylammonium bromide as mobile phase at a flow rate of 0.4 mL min⁻¹, column 100 × 2 mm i.d. packed with 3 μm microporous octadecylsilica, detection by UV at 280 nm.

of electrochemical detection, while it has been shown to be highly sensitive in the detection of opiates, would not overcome the long retention time required to elute 6-monoacetylmorphine. Its characteristics were not examined using this separation system.

Normal-Phase LC System

In common with most drug separations by LC, reversed-phase methods predominate in the literature for the separation and quantification of opiates. Normal-phase solvent systems have been reported for the quantitative determination of selected groups of opiates. None of these, however, is suitable for the purpose of determining heroin consumption, either by identification of 6-monoacetylmorphine or by quantitative estimation of the concentration of morphine relation to other legal opiates present.

Using a 200 mm \times 2.1 mm column packed with 3 μ m Hypersil it has been found possible to resolve completely morphine, dihydrocodeine, pholcodine, codeine, 6-monoacetylmorphine, nalorphine (as internal standard) and heroin. The optimized mobile phase consists of dichloromethane/pentane/methanol (29.8:65:5.2 by vol.) containing 0.026% (v/v) diethylamine. **Figure 3** shows a representative chromatogram of this set of opiates. The resolutions between individual pairs of opiates are less than in the reversed-phase system, although still in excess of one. This system results in complete elution of all components of interest in approximately 16 min. This separation appears to be more advantageous for the detection of heroin consumption than the reversed-phase system in that the order of elution is reversed and heroin and 6-monoacetylmorphine are eluted fairly early in the chromatogram, thus allowing maximum sensitivity of detection of the latter.

When a solid-phase extraction procedure identical to that described above is used, it is found that the choice of solvent is critical to redissolve the dried analytes completely while preserving peak shape on injection. The final injection solvent consists of dichloromethane/pentane (10:90 by vol.). This ensures complete solution of the extracted analytes and allows injection in a solvent chromatographically weaker than the mobile phase, which maintains peak sharpness. **Figure 4** shows a chromatogram of the six opiates together with the internal standard, nalorphine, after extraction from a spiked urine sample. In contrast to the reversed-phase system, all the analytes of interest are completely resolved from the solvent front and can thus be readily quantified using UV absorption at 280 nm. The main quantitative characteristics of analysis for these six opiates are shown in **Table 1**. The separation is adequately rugged with

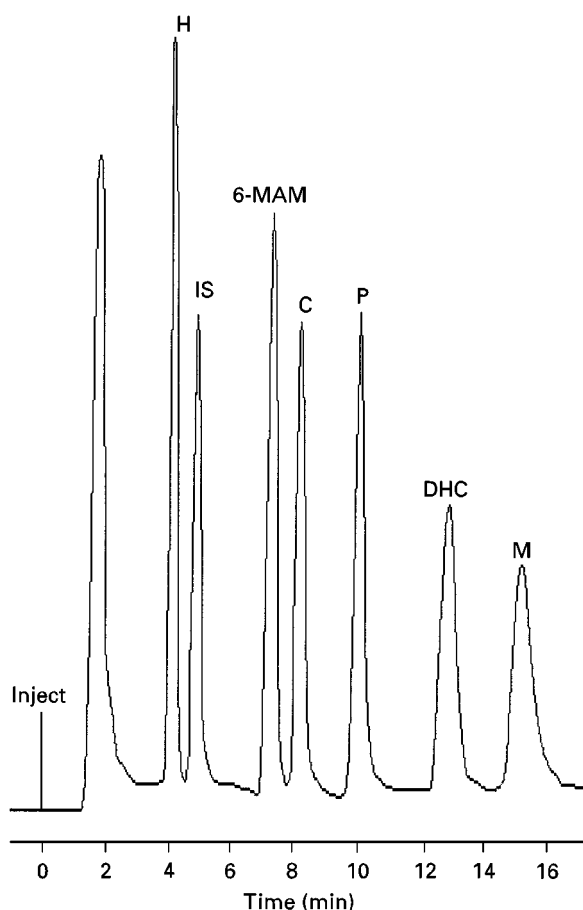


Figure 3 Representative chromatogram showing the separation of a pentane solution of morphine (M), dihydrocodeine (DHC), pholcodine (P), codeine (C), 6-monoacetylmorphine (6-MAM), nalorphine (IS) and heroin (H) (column 200 \times 2 mm i.d. packed with 3 μ m microporous silica mobile phase—dichloromethane/pentane/methanol 29.8:65:5.2 by volume containing 0.026% v/v diethylamine at a volumetric flow rate of 0.4 mL min⁻¹, detection by UV at 280 nm).

respect to the retention times as a result of the inclusion of nalorphine as an internal standard, even allowing for the relatively volatile solvents used in the mobile phase. The selectivity aspect of the separation is excellent with respect to both endogenous materials and the opiates of interest. The retention times of commonly ingested drugs, opiate metabolites and other compounds relative to nalorphine are listed in **Table 2**.

Table 2 shows that the selectivity with respect to the more commonly ingested drugs such as aspirin and caffeine, and also to several of the established opiate metabolites, is good in that retention times are appreciably different from the compounds of interest. Paracetamol, however, elutes between codeine and pholcodine and is incompletely resolved from the latter. At the wavelength of 280 nm used, the sensitivity for paracetamol is very low and

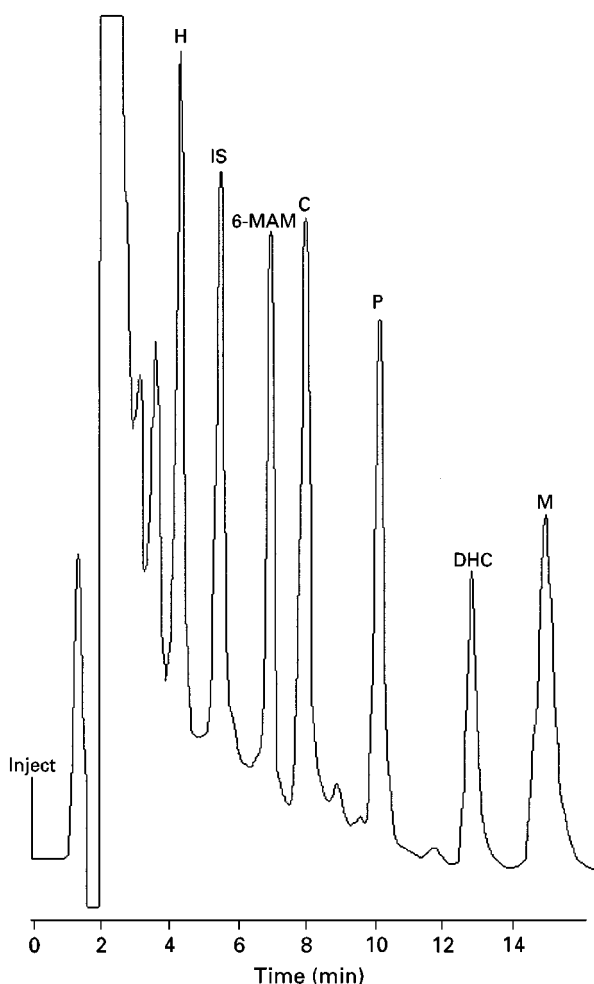


Figure 4 Representative chromatogram of a urine sample spiked with 500 ng cm⁻³ morphine (M), dihydrocodeine (DHC), pholcodine (P), codeine (C), 6-monoacetylmorphine (6-MAM), nalorphine (IS) and heroin (H) following solid-phase extraction on subsequent reconstitution in 10% dichloromethane/90% pentane and injected (column 200 × 2 mm i.d. packed with 3 μm microporous silica mobile phase dichloromethane/pentane/methanol 29.8:65:5.2 by volume containing 0.026% v/v diethylamine at a volumetric flow rate of 0.4 mL min⁻¹, detection by UV at 280 nm).

there would be minimal interference from paracetamol in the determination of any pholcodine present. The linearity and limits of quantification show that quantification after extraction and separation is adequate to confirm the presence of 6-monoacetylmorphine. The relative amounts of legal opiates as well as morphine detectable in urine are at levels corresponding to those that would result in the detection of opiate by immunoassay; the cutoff value generally used is 300 ng mL⁻¹.

An advantage of the normal-phase separation is the facility of coupling this with MS detection via an appropriate interface. The system described has been successfully linked via a particle beam interface with

some loss of resolution. Electron impact ionization allows unequivocal identification of all of the opiates.

Capillary Electrophoresis

Separation of charged analytes by utilizing their differential migration rates in an electric field has been achievable for many decades. The high theoretical plate numbers readily realized by using narrow capillaries, and the relatively recent (compared to LC) availability of reliable microprocessor-controlled equipment, have resulted in increased interest in the theory and application of this technique. The high efficiency can potentially be exploited to achieve resolution and also to accommodate higher peak capacity than is readily or conveniently achieved in LC. Both of these aspects are relevant to the identification and quantification of this group of opiates. However, because only a small sample volume can be injected onto a capillary and only a short pathlength is available when direct UV detection is used, the concentration sensitivity of capillary electrophoresis with UV detection suffers in comparison with LC methods when hydrodynamic injection is used. Within the extensive literature that now exists on CE methods, there are relatively few reports on applications concerning the determination of drugs in biological fluids such as plasma or urine, in which the analyte is generally at low concentration levels. Most applications in the literature reporting quantification of drugs at the ng mL⁻¹ concentration level in biological fluids have used sample pretreatment methods that involve a preconcentration step in order to reach the required limits of detection, and thus exploit the undoubted separational advantages of the technique.

Samples can also be introduced into the capillary electrokinetically, i.e. by application of a relatively low voltage with the capillary end immersed in the solution of analyte. It has been established both theoretically and practically that the amount of analyte of a particular charge introduced electrokinetically can be dramatically increased if the solution from which the sample is injected is of low ionic strength compared with that of the buffer used for the electrophoretic separation. While this injection method is subject to bias (not all analytes will be introduced into the capillary in this way), this can be a positive advantage when quantifying particular analytes in a given matrix.

An optimized separation of the six opiates and levallorphan (as internal standard) by CE is shown in **Figure 5**. The parameters affecting separation are buffer concentration and pH. As is general, increase of buffer ionic strength over the range 20 to 140 mmol L⁻¹ increases retention and resolu-

Table 1 Analytical characteristics of opiate determination in urine following normal-phase separation

	<i>Heroin</i>	<i>6-MAM</i>	<i>Codeine</i>	<i>Pholcodine</i>	<i>Dihydrocodeine</i>	<i>Morphine</i>
Relative retention drug/IS (%RSD)	0.785 (6.1)	1.25 (6.1)	1.51 (5.2)	1.99 (5.6)	2.57 (3.2)	3.04 (3.2)
Recovery (%)	89.1	82.7	82	88.4	79.7	79.3
Calibration correlation coefficient	0.9987	0.9901	0.9900	0.9980	0.9909	0.9964
Slope of calibration line $1 \times 10^3 (\pm \text{SD})$	12.6 (0.26)	9.5 (0.51)	3.8 (0.32)	3.1 (0.11)	2.2 (0.17)	7.8 (0.04)
Limit of quantification at $\text{S/N} = 4 (\text{ng cm}^{-3})$	3.0	5.4	4.2	6.3	6.0	15
Within day precision as %RSD at 200 ng cm^{-3}	5.03	4.45	4.34	6.38	4.29	5.85
Day to day precision as %RSD at 200 ng cm^{-3}	5.43	4.92	5.11	7.22	6.1	8.07

IS, internal standard; 6-MAM, 6-monoacetylmorphine; RSD, relative standard deviation; SD, standard deviation; S/N, signal-to-noise ratio. Reprinted in part from Low and Taylor (1995) with permission from Elsevier Scientific.

tion. Increase of buffer pH from 4 to 8 decreases the retention as a consequence of increased electro-osmotic flow. Figure 5 shows that all the opiates of interest are eluted in 12 min with resolution between individual pairs well in excess of that achieved by normal-phase LC. What is equally significant is that all seven compounds are eluted within a narrow time-scale of 9–12 min, so that there is much less disparity between the relative amounts of peak broadening than is the case in either of the LC methods described earlier.

A urine extraction procedure based on the method developed for LC has been developed in which a 0.5 cm^3 urine sample is extracted as previously but reconstituted in 1 cm^3 of a solvent consisting of water/methanol (9 : 1). The resultant electropherogram obtained from urine spiked at approximately 300 ng cm^{-3} subsequent to extraction and elec-

trokinetic injection is shown in Figure 6A. Figure 6B shows the corresponding electropherogram of a blank urine sample. In contrast to the LC methods there are very few endogenous compounds brought through the extraction and electrokinetic injection procedures. Only one of these is a potential interference as it elutes close to pholcodine.

The separational abilities of the CE method are clearly superior to those of either of the liquid LC methods, taking into account both the selectivity with respect to individual opiates and also the separation from endogenous urine components. The quantitative aspects of the CE method are also significant. It has been found that reconstitution of extracted and dried

Table 2 Retention times relative to nalorphine of some drugs that may interfere with normal-phase LC determination of opiates

<i>Drug</i>	<i>Relative retention time</i>
Chlodiaepoxide	< 0.39
Papaverine	0.43
Diazepam	0.48
Lignocaine	0.54
Methadone	0.58
Naloxone	0.62
Theophylline	0.65
Diphenylhydramine	0.74
Ephedrine	1.33
Hydrocodone	1.76
Paracetamol	1.84
Dextropropoxyphene	2.09
Quinine	2.28
Norcodeine	3.29
Caffeine	4.84
Normorphine	5.62
Acetylsalicylic acid	> 8
Procaine	> 8
Theobromine	> 8

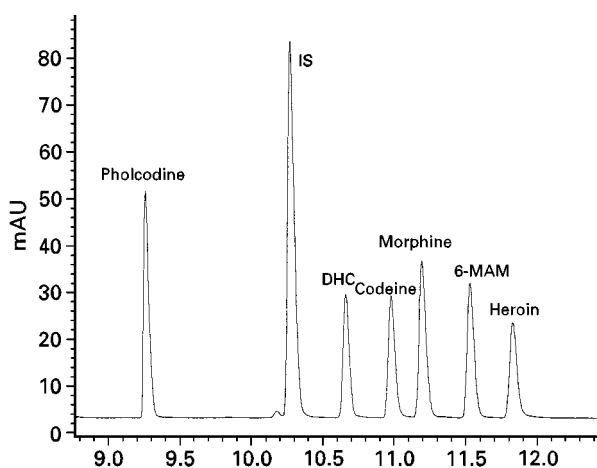


Figure 5 Representative separation of morphine, pholcodine, heroin, codeine, 6-monoacetylmorphine (6-MAM), dihydrocodeine (DHC) and levallorphan (IS) as internal standard in aqueous solutions using capillary electrophoresis (capillary $50 \mu\text{m}$ i.d. \times 500 mm effective length, running buffer 100 mmol L^{-1} disodium hydrogen phosphate at pH 6, applied voltage 20 kV, electrokinetic injection for 10 s at 5 kV, UV detection at 200 nm). (Reprinted in modified form from Taylor *et al.*, 1996, with permission from Elsevier Scientific.)

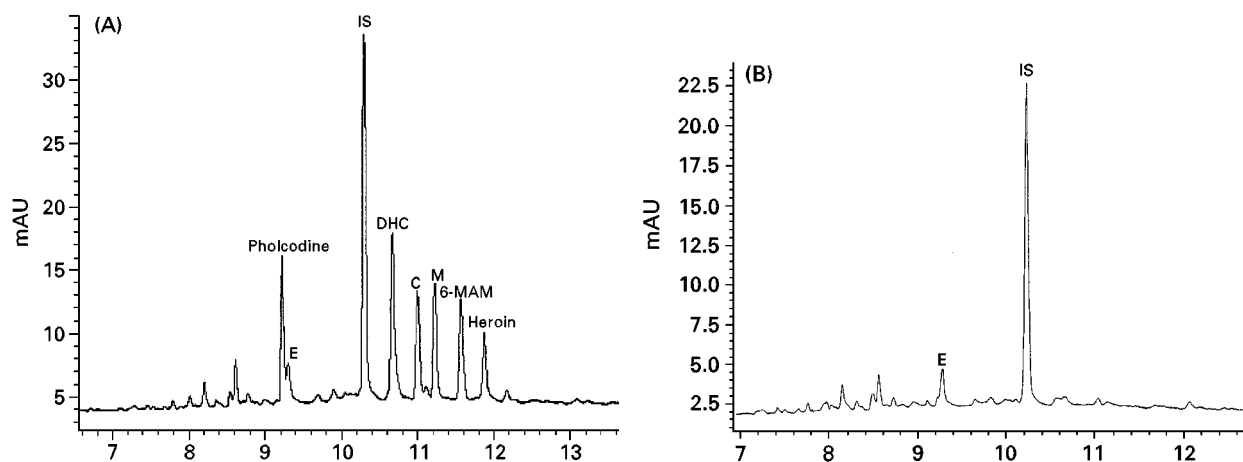


Figure 6 (A) Representative electropherogram of a urine sample spiked with 300.8 ng cm⁻³ pholcodine, 805 ng cm⁻³ levallorphan (IS), 241 ng cm⁻³ dihydrocodeine (DHC), 274 ng cm⁻³ codeine (C), 304.8 ng cm⁻³ morphine (M), 288.3 ng cm⁻³ 6-monoacetylmorphine (6-MAM) and 284.4 ng cm⁻³ heroin after solid-phase extraction. (E) designates an endogenous component in urine. (B) Representative electropherogram of a blank urine sample spiked with 805 ng cm⁻³ levallorphan after solid-phase extraction (capillary 50 μ m i.d. \times 500 mm effective length, running buffer 100 mmol L⁻¹ disodium hydrogen phosphate at pH6, applied voltage 20 kV, electrokinetic injection for 10 s at 5 kV, UV detection at 200 nm). (Reprinted in modified form from Taylor *et al.*, 1996, with permission from Elsevier Science.)

analytes in aqueous methanol allows the field-amplified sample injection technique to be applied extremely effectively. Indeed, in the method development it was found that the increase of peak areas when comparing electrokinetic injection from water with hydrodynamic injection ranged from 90 in the case of heroin to 160 for 6-monoacetylmorphine and pholcodine. This, coupled with the use of 200 nm as the wavelength of detection, allows limits of detection well below the cutoff level for immunoassay to be achieved. The electrokinetic injection technique for the enhancement of concentration sensitivity applied to this assay procedure is capable of overcoming the perceived limitation of CE as technique for determining these compounds in urine. Table 3 summarizes the main validation parameters of the assay of these drugs based on the CE procedure described.

The validation parameters in Table 3 show that the quantitative aspects are very comparable with those quoted for LC. The electrokinetic introduction of sample is in general more variable than hydrodynamic introduction but incorporation of an internal standard, which is required to accommodate variable extraction efficiencies, results in within day and day to day precision better than that achieved by normal-phase LC. The limits of quantification quoted are indicative only, since time of sampling could be considerably increased over the 10 s at 5 kV used. The significance is that there is more than adequate sensitivity to allow detection of these particular opiates at the required levels for elimination of common opiates that have resulted in so-called false positives during immunoassay screening. The elec-

trokinetic method of sample introduction, however, does require that the solution for injection into the capillary be of low ionic strength. Consideration must be given to the overall sample matrix pretreatment to ensure this. In addition, at very low concentrations, there is considerable sample depletion from the small sample volumes used and care has to be taken to limit the number of successive injections from a given sample vial.

Conclusions

There are many opiates for which a multitude of assays have been determined in a variety of matrices for often very widely different purposes. In screening for drugs of abuse, chromatographic methods are extensively used to increase the information gained by rapid immunoassay. The method of choice for unequivocal identification of particular opiates is likely to continue to be GC-MS on the basis of the mass spectral information obtainable. The present article indicates that, at least for the specified relevant group of opiates chosen, separations in the liquid phase are capable of achieving adequate separations and that these can be applied with variable success to the determination of the specified compounds in urine. The results quoted for the reversed-phase LC method show an inherent limitation of this approach when determining a number of compounds differing widely in hydrophobicity. Such methods, however, can usually be manipulated to allow good resolution and quantification for more restricted mixtures of compounds. The widely

Table 3 Analytical characteristics of opiate determination in urine by CE

	<i>Pholcodine</i>	<i>Levorphanol</i>	<i>Dihydrocodeine</i>	<i>Codeine</i>	<i>Morphine</i>	<i>6-MAM</i>	<i>Heroin</i>
Migration time (min)	9.18	10.18	10.68	10.99	11.21	11.55	11.87
(%RSD)	(1.1)	(0.80)	(0.71)	(0.77)	(0.79)	(0.79)	(0.74)
Resolution	13.4	4.7	3.7	2.3	3.9	3.4	
Peak efficiency $\times 10^{-5}$	2.5	2.7	2.8	2.6	2.2	2.2	2.8
Recovery (%)	94.8		90.7	92.4	88.5	91.8	96.4
Calibration correlation coefficient	0.9917		0.9924	0.9944	0.9966	0.9967	0.9980
Slope of calibration line $\times 10^3$	1.3		1.6	1.5	1.4	1.5	1.2
(%RSD)	(5.1)		(5.2)	(4.2)	(3.4)	(3.2)	(2.6)
Limit of quantification at S/N = 6 (ng cm ⁻³)	6.0		16	14	16	18	16
Within day precision as %RSD at 300 ng cm ⁻³	3.8		1.8	1.4	2.1	0.6	3.4
Day to day precision as %RSD at 300 ng cm ⁻³	2.9n		2.2	2.1	2.5	1.4	2.8

Reprinted in part from Taylor *et al.* (1996) with permission from Elsevier Scientific.

differing retention times for codeine and morphine tends to make reliable quantification of the ratio of these compounds difficult. The normal-phase method offers a viable alternative to GC as a separation procedure and is capable of quantifying the codeine-to-morphine ratio and of detecting 6-mono-acetylmorphine at useful concentration levels. More importantly, the normal-phase method is capable of detecting and quantifying the commonly ingested legal opiates that can obscure or delay the final results of an immunoassay opiate screen. The separation achieved by CE arguably offers the most realistic alternative to GC. Method development is rapid and the plate numbers are comparable with those achievable by capillary GC. The underlying difficulty of lack of concentration sensitivity can be overcome by electrokinetic injection techniques if suitable sample pretreatment methods are developed with appropriate sample solvent composition. The eventual linking of CE with MS on a commercial basis should result in a combined technique capable of challenging GC-MS in this area of drug analysis.

See Colour Plate 86.

See also: **III/Alkaloids:** Gas Chromatography; Liquid Chromatography. **Drugs of Abuse: Solid-Phase Extraction.**

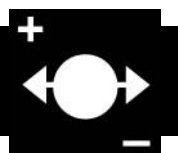
Further Reading

- Adamovics JA (ed.) (1994) *Analysis of Addictive and Misused Drugs*. New York: Marcel Dekker.
- Braithwaite RA, Jarvie DR, Minty PSB, Simpson D and Widdop B (1995) Screening for drugs of abuse. I: Opiates, amphetamines and cocaine. *Annals of Clinical Biochemistry* 32: 123–153.
- Gough TA (ed.) (1991) *The Analysis of Drugs of Abuse*. Chichester: John Wiley & Sons.
- Low AS and Taylor RB (1995) Analysis of common opiates and heroin metabolites in urine by HPLC. *Journal of Chromatography B* 663: 225–233.
- Tagliaro F, Turrina S and Smith FP (1996) Capillary electrophoresis: principles and applications in illicit drug analysis. *Forensic Science International* 77: 211–229.
- Taylor RB, Low AS and Reid RG (1996) Determination of opiates in urine by capillary electrophoresis. *Journal of Chromatography B* 675: 213–223.

HOT-PRESSURIZED WATER: EXTRACTION

See **III/SUPERCritical FLUID EXTRACTION-SUPERCritical FLUID CHROMATOGRAPHY**

HUMIC SUBSTANCES



Capillary Zone Electrophoresis

J. Havel, Masaryk University, Brno, Czech Republic

D. Fetsch, Surface Measurement Systems,
London, UK

Copyright © 2000 Academic Press

Humic substances (HS) which are widespread in the soil, present structural complexity and polyelectrolyte properties. Many techniques and methods have been used to obtain more information about them, as reviewed by Davies and Ghabbour in 1999. The characterization of HS has been the focus of intense research for many years because the organic matter in soil contributes to the quality of the soil more than the other constituents. Nowadays, one of the main goals is the separation of HS into fractions which can then be studied independently. The aim is to determine HS structure, which remains unknown, despite the enormous efforts and remarkable progress in this field. HS exhibit properties similar to weak acid polyelectrolytes, presenting a wide range in molecular weights, solubilities and acid strength. They are sparingly soluble in acid and slightly acidic solutions, but solubility increases with pH and they are only fully soluble alkaline solutions. Many general hypothetical models of HS structure have been proposed, and most of these have been discussed by Shevchenko and Bailey.

As HS play an important role in environmental chemistry, it is important to know their properties. HS are very important as regards the quality and productivity of a soil and in retention of metal ions and pollutants by the environment. Dissolved humic material has a tendency to interact with these compounds, complexing metal ions or pollutants, which may alter their fate and transfer in the soil. The mechanisms involved in the interaction of these compounds with HS are not clear and may vary depending on the physicochemical properties of the compounds, soil pH, redox status and the heterogeneous structure of HS. The effect of pH, for example, is related to the degree of humic R-COOH and R-OH dissociation; deprotonation increases the polarity of the humic material and altering its structure.

Electrophoretic methods have been applied for the purpose of HS studies since the 1960s. The first work on the separation of HS by a capillary technique was

performed in 1991 using capillary isotachopheresis. However, few really suitable methods for the separation of HS exist.

Nevertheless, to understand HS behaviour, it is useful to perform separation into fractions and determine the structure of each fraction. Capillary zone electrophoresis (CZE) has been applied by Rigol *et al.* in 1994 for this purpose.

HS Properties Studied by CZE

A short overview will be given here because the understanding of the properties of HS is the key to their successful separation.

Adsorption of HS

In the literature, most of authors have used high HS concentrations in order to reach or observe CZE separation patterns; however, no explanation was given (Table 1). In fact, it has been observed that when using a background electrolyte that did not interact with HS (rimantadine, for example), high adsorption of HS on bare fused silica capillary wall occurs. This explains why previous authors used rather high concentrations of HS solutions for analysis, because a considerable part of the HS was lost from the solution during the separation process. This observation is in agreement with the fact that HS are highly adsorbed on to silica rocks and silicates or induce interactions with metal ions on clay surface. Such adsorption processes of HS have already been studied on different silica-based materials with other methods. Adsorption on the surface of the silica capillary complicates CZE separation. It was demonstrated recently that the adsorption can be reduced using additives such as magnesium(II) ($>14 \text{ mmol L}^{-1}$) in the background electrolyte (BGE). In such magnesium-doped electrolytes, more fractions of HS can be observed, but also a secondary hump pattern. Via study of HS adsorption, a new method of CZE separation has been developed, which allows the concentration of HS in solution needed for CZE separation to be lowered to around $35\text{--}50 \text{ mg L}^{-1}$.

Oligomerization of HS

It has long been known that HS aggregate in solution. Various authors describe this property differently. Von Wandruszka *et al.* described the

Table 1 Review of background electrolytes used for HS separation by CZE, reported by Fetsch *et al.* in 1997 and references therein

Background electrolyte	Number of peaks	Hump	pH	[HS] (g L ⁻¹)	Reference
10–200 mmol L ⁻¹ tetraborate	1–4	+	8.3–10.0	0.01–1	All authors
6 mmol L ⁻¹ tetraborate–3 mmol L ⁻¹ dihydrogenphosphate	3–6	+	8.9	0.05–0.5	Pompe <i>et al.</i> Fetsch <i>et al.</i>
10 mmol L ⁻¹ tetraborate–5 mol L ⁻¹ urea	3–5	+	7.4	High	Dunkellog <i>et al.</i>
10 mmol L ⁻¹ tetraborate–10% v/v acetonitrile	1–2	+	9.0	1	Norden <i>et al.</i>
10 mmol L ⁻¹ tetraborate–10% v/v acetone	1	+	9.0	1	Norden <i>et al.</i>
10 mmol L ⁻¹ tetraborate–10% v/v isopropanol	2–3	+	9.0	0.01–0.1	Norden <i>et al.</i>
10 mmol L ⁻¹ tetraborate–10% v/v propanol	2–3	+	9.0	1	Norden <i>et al.</i>
10 mmol L ⁻¹ tetraborate–10% v/v 2-propanol–5 mmol L ⁻¹ urea	2–6	+	9.0	1	Norden <i>et al.</i>
10 mmol L ⁻¹ tetraborate–10% v/v tetrahydrofuran	2–3	+	9.0	1	Norden <i>et al.</i>
20 mmol L ⁻¹ tetraborate–5 mmol L ⁻¹ CDTA	2–4	+	8.6	0.01–0.1	Norden <i>et al.</i>
20 mmol L ⁻¹ tetraborate–100 mmol L ⁻¹ boric acid	2–5	+	8.45	0.1–0.25	Fetsch <i>et al.</i>
8 mmol L ⁻¹ L-Alanine	2–4	+	3.17	High	Dunkellog <i>et al.</i>
HCl–59.8 mmol L ⁻¹ L-Alanine	3	+	3.17	0.1	Rigol <i>et al.</i>
HCl–60 mmol L ⁻¹ DL-Alanine	3–4	+	3.2	0.1–0.25	Fetsch <i>et al.</i>
HCl–60 mmol L ⁻¹ DL-Alanine–10% v/v methanol	2–5	+	3.2	0.1–0.25	Fetsch <i>et al.</i>
HCl–60 mmol L ⁻¹ L-Alanine	3	+	3.2	0.1–0.5	Fetsch <i>et al.</i>
HCl–60 mmol L ⁻¹ D-Alanine	4	+	3.2	0.1–0.5	Fetsch <i>et al.</i>
HCl– β -Alanine	1–2	+	\approx 3	0.1	Fetsch <i>et al.</i>
HCl–60 mmol L ⁻¹ β -Alanine	1–2	+	3.2	0.1–0.25	Fetsch <i>et al.</i>
HCl–30 mmol L ⁻¹ β -Phenylalanine	1	+	3.2	0.1–0.25	Fetsch <i>et al.</i>
HCl–30 mmol L ⁻¹ L-Cystine	1–2	+	3.2	0.1–0.25	Fetsch <i>et al.</i>
HCl–L-Leucine	1–2	+	3.17	0.1	Rigol <i>et al.</i>
HCl–L-Lysine	1–2	+	\approx 3	0.1	Rigol <i>et al.</i>
HCl–L-Serine	1–2	+	3.17	0.1	Rigol <i>et al.</i>
HCl–10 mmol L ⁻¹ DL-Serine	1–2	+	3.2	0.1–0.25	Fetsch <i>et al.</i>
HCl–15 mmol L ⁻¹ DL-Proline	1–2	+	3.2	0.1–0.25	Fetsch <i>et al.</i>
HCl–L-Aspartic acid	1–2	+	\approx 3	0.1	Rigol <i>et al.</i>
HCl–60 mmol L ⁻¹ glycolic acid	1	+	3.2	0.1–0.25	Fetsch <i>et al.</i>
HCl–100 mmol L ⁻¹ boric acid	5–15	–	3.15	0.5	Fetsch <i>et al.</i>
HCl–350 mmol L ⁻¹ boric acid	10–30	–	3.15	0.25–0.5	Fetsch <i>et al.</i>
HCl–500 mmol L ⁻¹ boric acid	3–8	+	3.38	0.15	Fetsch <i>et al.</i>
25–50 mmol L ⁻¹ dihydrogenphosphate	5–15	–	9.2	0.01–0.5	Fetsch <i>et al.</i>
50–100 mmol L ⁻¹ phosphate	5–15	–	6.3–9.2	0.1–1	Garrison <i>et al.</i> Fetsch <i>et al.</i>
100 mmol L ⁻¹ dihydrogenphosphate–5 mmol L ⁻¹ phosphate– 250 mmol L ⁻¹ boric acid	3–8	+	3.3	0.15	Fetsch <i>et al.</i>
67 mmol L ⁻¹ dihydrogenphosphate–3.3 mmol L ⁻¹ phosphate– 167 mmol L ⁻¹ boric acid–3.3 mmol L ⁻¹ wolframate	3–8	+	5.0	0.15	Fetsch <i>et al.</i>
20 mmol L ⁻¹ rimantadine hydrochloride	1–3	+	3.40	0.01–0.5	Fetsch <i>et al.</i>
20 mmol L ⁻¹ rimantadine hydrochloride–2 to 50 mmol L ⁻¹ MgCl ₂	2–9	+	3.40	0.01–0.5	Fetsch <i>et al.</i>
50 mmol L ⁻¹ carbonate	1–4	+	9.0–11.4	\geq 0.05	Schmitt <i>et al.</i>
HCl–glycylglycine	1–2	+	\approx 3	0.1	Rigol <i>et al.</i>
HCl–glycine	1–2	+	3.17	0.1	Rigol <i>et al.</i>
Citric acid–citrate	1–2	+	\approx 3	0.1	Rigol <i>et al.</i>
HCl–imidazole	1–2	+	\approx 3	0.1	Rigol <i>et al.</i>
5 mmol L ⁻¹ imidazole–acetic acid–20 mmol L ⁻¹ boric acid	2–5	+	4.5	0.01–0.1	Norden <i>et al.</i>
50 mmol L ⁻¹ acetate	5–10	+	4.6–5.15	0.01–1	All authors
103 mmol L ⁻¹ urea	5–12	+	3.65–6.6	0.15	Fetsch <i>et al.</i>
20 mmol L ⁻¹ 2-(<i>N</i> -morpholino)ethanesulfonic acid (MES)	1–3	+	6.15	High	Dunkellog <i>et al.</i>
2-(<i>N</i> -morpholino)ethanesulfonic acid (MES)–NaOH	1–3	+	\approx 3	0.1	Rigol <i>et al.</i>
20 mmol L ⁻¹ tris(hydroxymethyl)aminomethane (TRIS)	1–3	+	8.30	High	Dunkellog <i>et al.</i>
HCl–tris(hydroxymethyl)aminomethane (TRIS)	1–3	+	\approx 3	0.1	Rigol <i>et al.</i>
20 mmol L ⁻¹ 3-(cyclohexylamino)-1-propanesulfonic acid (CAPS)	1–2	+	10.4	High	Dunkellog <i>et al.</i>
20 mmol L ⁻¹ 2-(<i>N</i> -cyclohexylamino)ethanesulfonic acid (CHES)	1–2	+	9.5	High	Dunkellog <i>et al.</i>

[HS], concentration of humic substances; + hump present; – no hump.

aggregates as pseudomicelles, whereas Wershaw and Chien *et al.* used humic membrane-micelle, Dachs *et al.* introduced the term fractal aggregates,

Shevchenko *et al.* used polymers and finally, the formation of oligomers was proposed by Havel *et al.* in 1997.

The most interesting theory from the last decade is that of Wershaw, who introduced a model for humic materials which provides a mean of understanding the interactions of hydrophobic compounds and HS. This model considers humic material to be constituted of a number of different oligomers and simple compounds. The resulting structures are similar to micelles or membranes in which the interiors are hydrophobic and exterior surfaces hydrophilic. Thus, the enhancement in the solubility of DDT was observed by Wershaw in concentrated HS solutions which implies the formation of HS micelles. According to Karckhoff *et al.* and Wang *et al.*, the adsorption of hydrophobic organic compounds by organic matter involves weak mechanisms of adsorption such as hydrogen bonding. Few papers concerning aggregation of HS have been published as yet. Schmitt *et al.*, using micellar electrokinetic chromatography (MECK), observed that some HS behave like ionic micelles and defined a humic initial micellar concentration (CMC) around 30 mg L⁻¹. The micellar properties of HS are due to both hydrophilic and hydrophobic sites which are responsible for the enhancement of the solubility of organic compounds in aqueous media or the lowering of the surface tension of water.

In 1998, the aggregation properties of HS were studied by CZE. Oligomerization of HS was observed during CZE when the effect of HS concentration on CZE separation patterns was studied. The phenomenon was described for several BGE: DL-alanine, phosphate and rimantadine systems. When either concentration or sample injection time were increased, significant changes in HS separation patterns were observed. The CMC of humic acid was estimated to be around 35 mg L⁻¹.

Interaction of HS with Metal Ions and Organic Compounds

Metal Ions

The interaction of metal ions with natural soil particles is complex, involving various mechanisms. Binding between trace metals and dissolved HS is important in controlling the chemical speciation, toxicity and bioavailability of trace metals. For example, it has been observed that, in the presence of HS dissolved in seawater, the accumulation rates of cadmium in organisms were faster in comparison to accumulation rates of cadmium from seawater without HS.

Different models of metal-HS interactions have been described. Due to the broad spectrum of binding sites reported by Ephraïm, HS can interact

with metal ions by adsorption, ion exchange, precipitation and/or surface complexation. Specific adsorption involves several heavy metal ions such as Cd²⁺, Ni²⁺, Co²⁺, Zn²⁺, Cu²⁺, Pb²⁺ and Hg²⁺. Coprecipitation of trace metals with carbonates is very important for semi-arid soils and in soils formed from limestone. Techniques like synchronous and time-resolved fluorescence, luminescence, anodic stripping voltammetry and modified carbon paste electrodes have been used in the study of the fate and distribution of inorganic pollutants in the environment. Many papers concerning the binding of metal ions to HS have been published.

In 1997, Nordén and Dabek-Zlotorzynska applied CZE to study Sr²⁺, Pb²⁺, Cu²⁺, Hg²⁺ and Al³⁺. Their interactions with HS were confirmed. Study of the influence of pH on the complexation showed that complexation can be better followed by direct rather than indirect detection. The following order of complexation was obtained by CZE: Al³⁺ > Hg²⁺ > Cu²⁺ > Pb²⁺ > Sr²⁺. This result is in agreement with other work on metal ion-HS interaction strengths. Furthermore, when pH is increased, complexes are more stable and, ageing of HS solutions showed an increase of more than 25% in the amount Hg²⁺ bound to HS after 5 months. This increase is supposed to be connected to the possible time dependence of the reduction process, and/or to be related to the macromolecule nature of HS. Changes in HS separation pattern were also observed when adding iron(III) to HS and forming Fe³⁺-HS complexes, when the study was performed at pH 12.

Radionuclides

The other important interactions which have been studied and are highly important with respect to environmental protection policies are those between HS and radionuclides like ⁶⁰Co, ⁸⁵Sr, ¹³⁷Cs, ²³⁷Np, ²⁴¹Am, etc. For example, it has been shown that samarium(III) (10⁻¹⁰ to 10⁻⁵ mol L⁻¹) and americium(III) (10⁻¹¹ mol L⁻¹) form 1 : 1 complexes with HS; their pH-independent complexation constants, log β, are respectively 7.1 ± 0.2 and 6.6 ± 0.2. Spiking actinide elements (Th, U, Np, Pu, Am) in HS fractions, it has been shown that these fractions vary greatly in their effectiveness and selectivity as ligands for early actinides.

Rigol *et al.* used CZE to study humic fractions in organic soil and their relationship with radiocaesium mobility. The quantification of the radiocaesium confirmed that there may be some organic matter-radionuclide interactions other than those originated by HS and which may govern radionuclides

retention in soils with a high content of organic matter.

Organic Compounds

It has been known for many years that organic compounds interact with HS. There have been studies on the interaction of pesticides (chlorodimeform and lindane) and herbicides (paraquat, 2,4-dichlorophenoxyacetic acid and atrazine) with HS. Later, the effect of HS was studied on solute transport in clays and it was suggested that humic and fulvic acids facilitate the transport of small organic molecules by encapsulation. Over the last 5 years, the effects of dissolved HS on the bioconcentration of xenobiotics have been studied by several authors. It was observed that dissolved HS can change the physicochemical properties of these pollutants in aqueous environments by modifying the hydrolysis kinetics, enhancing their water solubility or decreasing the toxicity of the organic chemicals. The binding of hydrophobic organic compounds to humic polymers has been studied, using a predictive thermodynamic HS–organic solute interaction model. A distributed reactivity model was studied for phenanthrene sorption and desorption equilibria by soils and sediments. Relationships were observed between the chemical and structural characteristics of associated organic matter and it was noted that hysteresis is important to the fate and transport of organic contaminants in environmental systems.

It was proposed to use the potential of dissolved HS to enhance the desorption of hydrophilic pollutants in remediation processes for soils and waters. Following this idea, some authors used a complexation–flocculation method to determine binding coefficients of phenanthrene, anthracene, pyrene and fluoranthene to dissolved HS. In some cases, pH dependence of the sorption was observed. While naphthalene binding to dissolved HS was not decreased at lower pH, dichlorodiphenyl trichloroethane (DDT) and polyaromatic hydrocarbons (PAHs) showed the opposite effect.

As reviewed in Table 1, the effect of organic solvents on the migration behaviour of HS in CZE

was also studied. Migration time values are usually shifted to longer values compared to aqueous BGE. This effect is attributed to either a decrease in electroosmotic flow (EOF) or an increase in the electrophoretic mobility of HS compounds, or even to both effects together. Furthermore, some additional fractions were distinguished when applying mixed solvents. They are attributed to the formation of supramolecules between the organic solvent and HS.

Paramagnetic studies have been carried out in the study of atrazine solubilized by humic micellar solutions. This work suggests that atrazine is preferably present in the hydrophobic interior of HS micelles. Other techniques, such as light and X-ray scattering also give evidence of molecular aggregation in humic solutions. Using ultraviolet-visible (UV/Vis), Fourier transform infrared and electron spin resonance spectroscopy, a group of authors studied the mechanism of atrazine sorption on HS and confirmed that hydrogen bonding is responsible for the interaction. Proton transfer and possibly also hydrophobic bonding are involved in the interactions between atrazines, and HS and CZE studies of the binding between S-triazines and HS confirmed that interactions between ionizable pesticides and HS occur: differences in the electropherograms were observed.

Capillary Electrophoretic Separation of HS

The major advances in the separation of HS are listed in Table 2.

CZE separations of HS have been performed using UV/Vis, diode array or laser-induced fluorescence detection. In Table 1, the BGE used for this purpose are listed; mainly borates, amines and amino acids have been applied. Nevertheless, even if a large variety of BGE were used, four main types of electropherogram separation patterns can be observed and the three most important types of HS separation are shown in Figure 1. The first type is obtained in a tetraborate BGE and represents separation patterns with one or more broad peaks, called usually the humic hump.

Table 2 Important advances in HS separation

1960–70	First applications of electrophoretic methods to HS
1980–90	Application of size exclusion chromatography to HS
1991	First HS separation by capillary technique (Kopáček <i>et al.</i>)
1994	First application of capillary zone electrophoresis (CZE) to HS separation (Rigol <i>et al.</i>)
1996–1997	CZE study of HS interactions with some metal ions and organic compounds
1998	First separation of HS on to 15–30 peaks or fractions (Fetsch and Havel)
	Study of HS properties by CZE as adsorption on capillary wall and oligomerization process (Fetsch <i>et al.</i>)
	Combination of ultrafiltration and CZE (Rigol <i>et al.</i>)

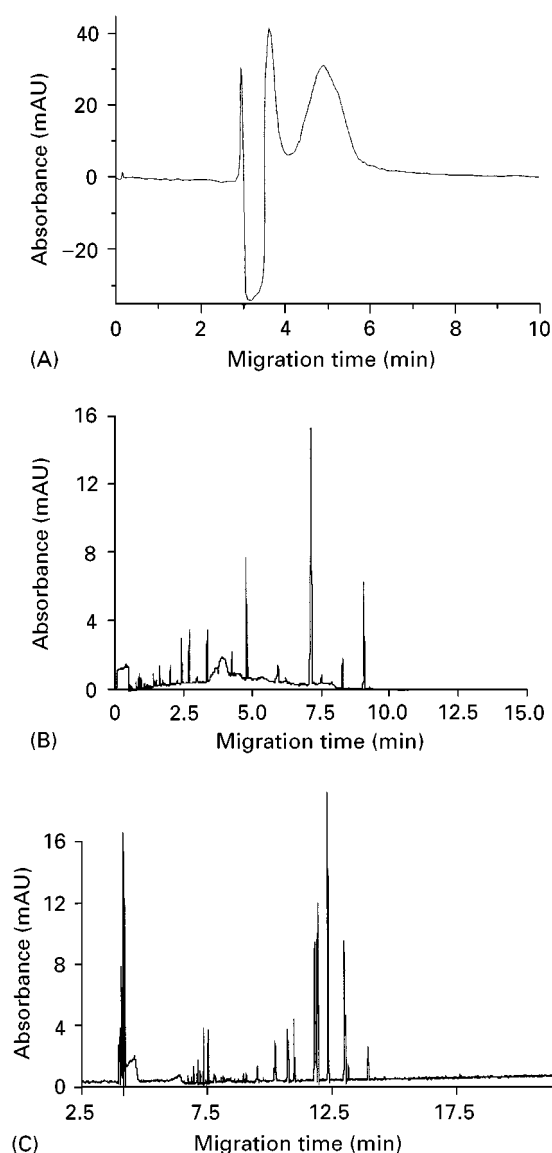


Figure 1 Three BGEs for coal-derived humic substances. Humic acid: Fluka no. 53680 (analysis number 38537/1 293) supplied by Fluka Chemika (Switzerland). Fused silica capillary: $L = 43.5$ cm ($l = 35.5$ cm) \times 75 μ m i.d. (A) BGE 1 and conditions: 60 mmol L^{-1} DL-alanine adjusted by HCl at pH 3.20; 15 kV, 20 s hydrodynamic injection, $40^{\circ}C$, 220 nm and $C_{HA} = 100$ mg L^{-1} . (B) BGE 2 and conditions: 50 mmol L^{-1} phosphate adjusted by NaOH at pH 9.20; 20 kV, 15 s hydrodynamic injection, $40^{\circ}C$, 220 nm and $C_{HA} = 100$ mg L^{-1} . (C) BGE 3 and conditions: 350 mmol L^{-1} boric acid adjusted by HCl at pH 3.20; 20 kV, 15 s hydrodynamic injection, $40^{\circ}C$, 220 nm and $C_{HA} = 530$ mg L^{-1} .

Sometimes, these humps do show shoulders and some resolution. It is usually suggested that the hump corresponds to the average electrophoretic mobility of the HS polymeric mixture.

The second type of electropherograms in L- or DL-alanine BGE consists of three fractions. These elec-

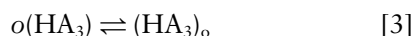
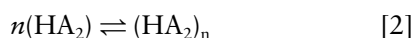
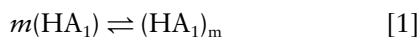
tropherograms can distinguish between HS of different origin via changes in migration times of the fractions and in the number of peaks. It was shown in these studies that temperature plays an important role in the patterns obtained. The best separation is obtained for temperatures in the range 30 – $40^{\circ}C$ and the highest peak area and peak height are obtained at $\approx 40^{\circ}C$. An example of separation under optimized conditions is shown in Figure 1A. Three main fractions were found and, for the wavelength lower than 220 nm, a negative peak was observed. Separation also depends on pH and buffer concentration. As the EOF changes with pH, the migration times of the separated components are directly affected and generally decrease as pH increases. In the pH range 5.0 – 9.5 , HS constituents are moving as anions. In the case of alanine-based BGE, it appears that one fraction is moving as a neutral molecule, while the others are moving as anions. Under the presence of HS, it is difficult to determine the EOF simultaneously with HS separation because common neutral markers used (mesityl oxide, methanol, acetone and water) interact with HS. Independent determination of the EOF is necessary.

In the case of borate BGE, when increasing BGE concentration, migration times increase but no important changes in separation patterns are observed.

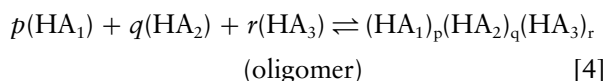
The next type of HS separation gives a humic hump with small peaks on it. This effect is generally observed with dihydrogen phosphate BGE (Figure 1C) or dihydrogenphosphate combined with borate BGE.

On the other hand, quite important changes in the separation patterns and number of peaks, were observed using slightly acid BGE, which consists of a high concentration of boric acid. This gives the best HS separation resolving from 10 to 30 peaks depending on the type of humic acid sample. In this case, highly concentrated (100 – 350 mmol L^{-1}) boric acid BGE is used as a complexing BGE (Figure 1C). The possible explanation for this excellent separation pattern is as follows: functional groups of hydroxycarboxylic acids, oxalic acid and oligoalcohols are present in the HS structure. Boric acid interacts with phenolic and carboxylic groups and therefore also reacts in a similar way with HS. This reaction was also proved by spectrophotometric and potentiometric studies. It was suggested that the large number of peaks observed in highly concentrated boric acid BGE is due to the breaking of HS oligomers into real fractions of humic substances (Figure 2). Humic substances contain a limited number of chemical entities (even as low as perhaps only 3 – 7). However, when the concentration of HS is increased, these species

do oligomerize. Complexation of boric acid with phenolic or carboxylic groups prevents the formation of oligomers and thus the individual chemical compounds can be separated by CZE. The species formed must be kinetically robust, which is the condition to observe separated peaks. If just three fractions, HA_1 , HA_2 and HA_3 , are considered, oligomerization might take place according to eqns [1–3]:



In addition, mixed oligomers can be formed according to the general reaction:



If reaction [4] is quantitative, instead of the peaks of HA_1 , HA_2 , HA_3 species, just one peak (one hump) of the oligomer will be observed.

This oligomer will be broken down by reaction with boric acid

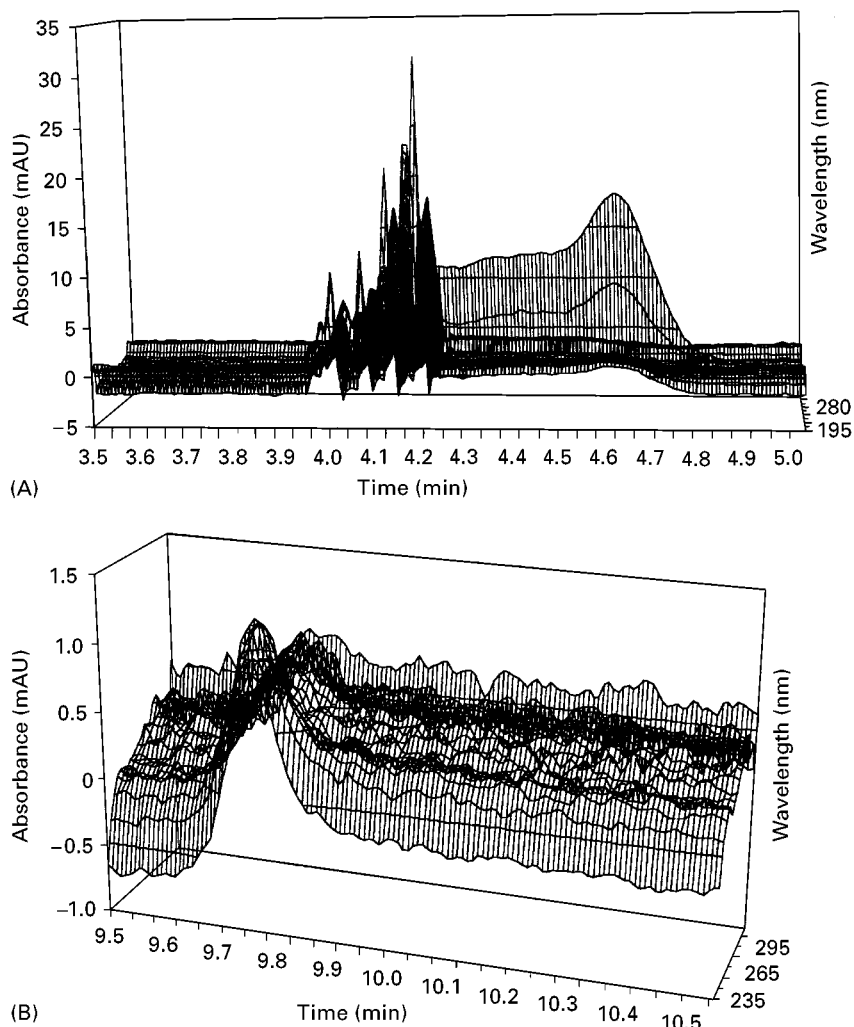
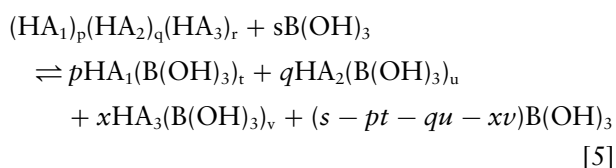


Figure 2 Fluka humic acid three-dimensional electropherogram at higher HS concentration in boric acid BGE. Humic acid: Fluka no. 53680 (analysis number 38537/1 594) supplied by Fluka Chemika (Switzerland). Fused silica capillary: $L = 43.5$ cm ($l = 35.5$ cm) $\times 75$ μ m i.d. BGE: 350 mmol L^{-1} H_3BO_3 adjusted by HCl at pH 3.15. Conditions. 20 kV, 40°C, 15 s hydrodynamic injection and $C_{HA} = 533$ mg L^{-1} . (A) HA Cathedrale; (B) HA Volcano; (C) HA Alpes; (D) HA Mt Everest (Reproduced with permission from Fetsch and Havel, 1998.)

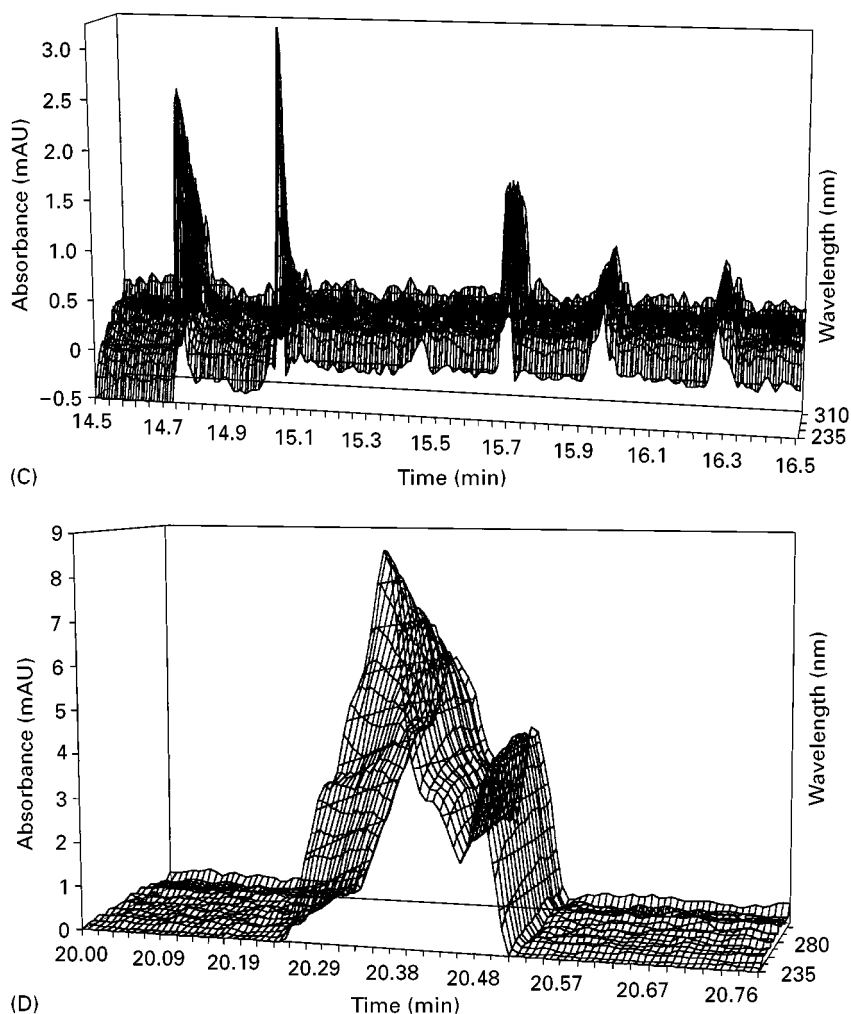


Figure 2 *Continued*

Oligomers are broken down and three monomers will be observed in this theoretical case. Thus, it seems that for the first time separation of HS into the real fractions, real chemical entities forming the humic substances mixture, has been achieved in highly concentrated boric acid BGE. Some other examples of fingerprints are presented in **Figure 3**, showing the separation of humic acids of peat, soil, oxyhumolite and tschernozem origin.

In conclusion, different CZE separations have been presented with very different results; the most interesting and efficient were the results of Fetsch and Havel in highly concentrated boric acid solution.

Future Developments

CZE has been shown to be the most powerful tool for the separation and characterization of HS due

to their ionic and/or polyelectrolyte properties. The CZE separation patterns of HS obtained may, in the future, find a direct application in forensic science.

Nevertheless, even if several different models of HS are proposed and various properties of HS intensively studied, the real structure of humic, fulvic, humin and hyatomelanic acids is still unknown. The latest results obtained by CZE showing separation into 10–30 fractions present an optimistic insight into the humic substances puzzle. On the basis of recent results, fraction collection in order to perform studies on individual fractions by gas chromatography–mass spectrometry, matrix assisted laser desorption–time of flight (MALDI-TOF) mass spectrometry and nuclear magnetic resonance is beginning to appear feasible. It is possible that the problem of HS structure is at last on the way to being resolved.

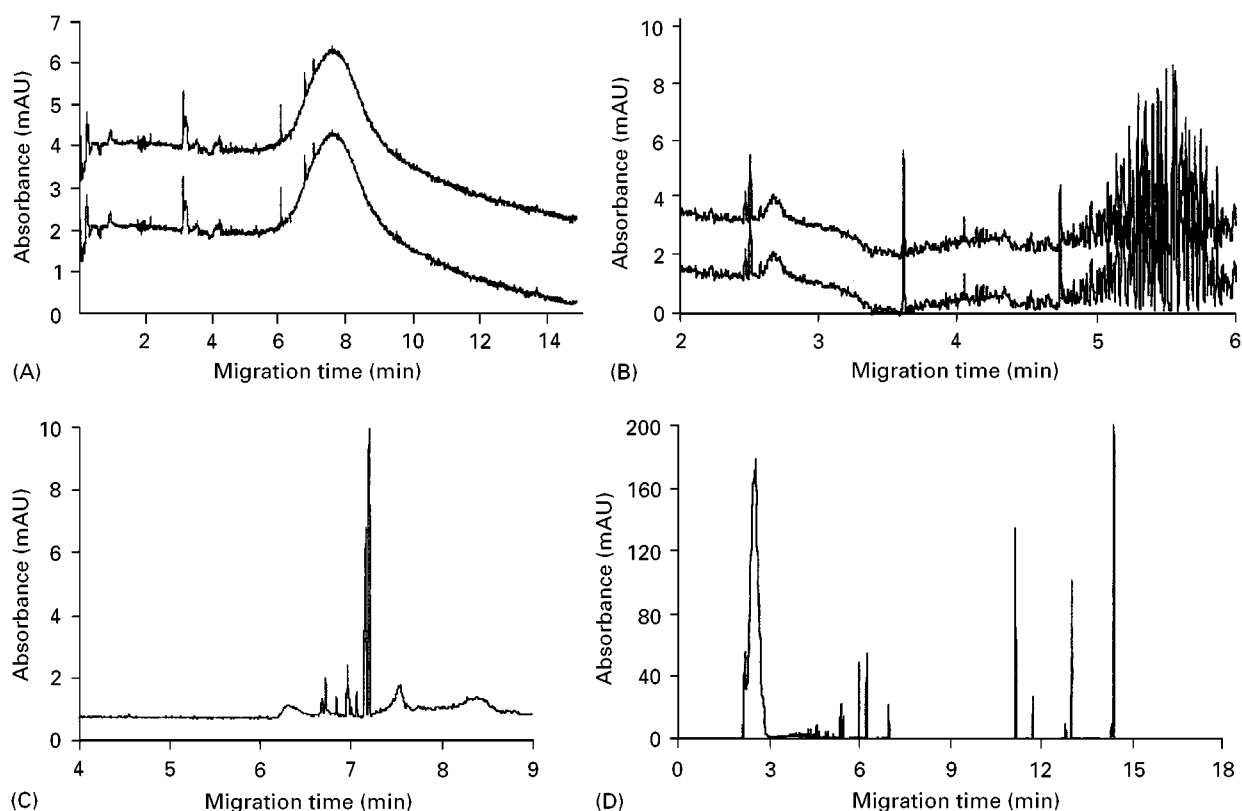


Figure 3 Electropherogram fingerprints of humic substances of different origin in boric acid BGE. (A) International humic substances society peat reference humic acid; (B) Desmonte soil humic acid, Argentina; (C) oxyhumolite-derived humic acid, Bilina, Czech Republic; (D) Tschemozem humic acid, Chotesov, Czech Republic. Fused silica capillary: $L = 43.4$ cm ($l = 35.4$ cm) \times 75 μ m i.d. BGE: 350 mmol L^{-1} H_3BO_3 adjusted by HCl at pH 3.20. Conditions: 20 kV, $40^\circ C$, 215 nm and 1 s hydrodynamic injection. Humic acid concentration: $C_{HA} \cong 600$ mg L^{-1} .

Further Reading

- Davies G and Ghabbour EA (1999) *Humic Substances: Structures, Properties and Uses*. Special publication no. 228. Letchworth, UK: Royal Society of Chemistry.
- Dunkellog R, Rüttinger H-H and Peisker K (1997) Comparative study for the separation of aquatic humic substances by electrophoresis. *Journal of Chromatography A* 777: 355.
- Fetsch D and Havel J (1998) Capillary zone electrophoresis for the separation and the characterization of humic acids. *Journal of Chromatography A* 802: 189.
- Fetsch D, Hradilová M, Peña Méndez EM and Havel J (1998) Capillary zone electrophoresis study of aggregation of humic substances. *Journal of Chromatography A* 817: 313.
- Kopáček P, Kaniánský D and Hejzlar J (1991) Characterization of humic substances by capillary isotachophoresis. *Journal of Chromatography A* 545: 461.
- Nordén M and Dabek-Zlotorzynska E (1997) Characterization of humic substances using capillary electrophoresis with photodiode array and laser-induced fluorescence detection. *Electrophoresis* 18: 292.
- Rigol A, Vidal M and Rauret G (1998) Ultrafiltration-capillary zone electrophoresis for the determination of humic acid fractions. *Journal of Chromatography A* 807: 275.
- Schmitt-Koplin Ph, Garisson AW, Perdue EM, Freitag D and Kettrup A (1998) Capillary electrophoresis in the analysis of humic substances facts and artifacts. *Journal of Chromatography A* 807: 101.
- Shevchenko SM and Bailey GW (1996) Life after death: lignin-humic relationships reexamined. *Critical Review of Environmental Science and Technology* 26: 95.
- Stevenson FJ (1982) *Humus Chemistry: Genesis, Composition, Reactions*. New York: Wiley-Interscience.

Gas Chromatography

J. Pöerschmann, Centre for Environmental Research, Leipzig, Germany

Copyright © 2000 Academic Press

The main mass of organic carbon in the aquatic environment and in soils/sediments is located in humic organic matter (HOM). A typical agricultural soil contains about 2–7% HOM in the upper level. Depending on the type of water (freshwater lake, marine origin, bog water, etc.), the content of aquatic HOM may range from 50 to almost 100% of the dissolved organic carbon. Terrestrial HOM acts mainly as a pollutant sink; aquatic HOM has a distinctive vehicle function. Thus, HOM influences fate, bioavailability and transport behaviour of organic and inorganic pollutants.

The detailed structural characterization of the ubiquitous HOM is an ambitious task because these polymers do not possess the uniform structure observed with other natural polymers. The extreme heterogeneity of both soil-derived and aquatic HOM in terms of chemical composition, monomer unit sequence, molar mass and functionality is associated with their genesis: for example, soil organic matter is composed of a variety of plant and animal residues in different stages of decomposition, of (radical) metabolites possessing mesomeric forms, and of products formed from these breakdown products. During the genesis, the chemical identity of the precursors is lost by abiotic and/or biotic condensation reactions.

The combined application of powerful analytical techniques may reveal some basic principles in HOM structure, but will probably never give a complete structure. Therefore, HOM analysis should not be targeted at the elucidation of discrete HOM structure but to recognizing substructures and functional groups (including their linkages), on the basis of which the fundamental interactions of HOM with environmental contaminants of organic and inorganic origin may be better understood. Nondestructive nuclear magnetic resonance (NMR) and Fourier transform infrared spectroscopy (FTIR) have proved to be very useful in providing information on functional groups and on the neighbourhood of substructures. Small scale analytical pyrolysis and controlled wet chemical degradation, in which the polymeric network is broken down to smaller subunits, constitute efficient supplements to non-destructive spectroscopic methods, in which an averaged structure is studied. Thermal and wet chemical degradation can give volatile products amenable

to gas chromatography (GC) analysis, including hyphenated techniques, such as gas chromatography–mass spectrometry (GC-MS) and gas chromatography–atomic emission detection (GC-AED). The combination of data obtained from the structure-related mass spectrum and the element-related atomic spectrum is especially useful for the detection of heterocyclic compounds as well as chlorinated structures in humic-like chlorolignins. The basic assumption in this strategy is to correlate the destructive products with original moieties present in the starting HOM network.

In addition to structure-related analytical investigations, destructive methods can also be applied for elucidation of the carbon cycle in soils and water, for solving geochemical problems (such as the diagenesis of HOM), in recognizing pathways of emissions from biomass combustion, in revealing pesticide contamination of soils, in studying humification processes taking place in landfills, in studying chlorinated aqueous HOM, in screening residues in bioremediated soils, and for other applications.

Conventional Analytical Pyrolysis

The traditional analytical pyrolysis, which can easily be performed using a flash pyrolyser or ferromagnetic wires with defined Curie temperatures, is useful in detecting certain building blocks, including polysaccharide-like substances, aromatic units, cyclopentenone units, *N*-containing units and aliphatic units in the HOM network, thus giving some evidence of the structure, origin, genesis, degree of decomposition and humification (condensation) of the polymer under study. As an example, pyrograms of marine samples are rich in protein products derived from phytoplankton, but are free from the lignin-derived guaiacyl (4-hydroxy-3-methoxyphenol) and syringyl (4-hydroxy-3,5-dimethoxyphenyl) compounds which are common in terrestrial and freshwater samples. Although there are many sources of typical fragments in the pyrolysate, it is generally accepted that furfural, levoglucosan (and other anhydrosugars), pyranones and acetic acid originate from carbohydrates, methoxyphenols from wood and lignin, ammonia, acetonitrile and pyrrole from proteins, while alkanes, alkylbenzenes (-naphthalenes, -phenanthrenes, etc.) and fatty acids originate from fossil fuels and biomass. Pyrograms of soil- and sediment-derived HOM are mainly characterized by the classical *n*-alkane/*n*-alk-1-ene/*n*- α,ω -alkadiene triplet series.

They may originate from esters, the saturated alkanes originating from decarboxylation of the fatty acid moiety, and the olefins from the alcohol moiety as a result of β -scission. Another source may be alkyl-benzenes with long side chains.

Generally, pyrograms are very complex, composed of several hundreds of compounds. **Figure 1** shows two extracted ion chromatograms used to trace thiophenes and benzenediols in the complex pyrogram. The (anthropogenic) fulvic acid under study was isolated from a coal wastewater pond, where it was formed spontaneously from coal wastewater components. High concentrations of phenols and benzenediols as well as of heterocyclic compounds are striking in comparison with pyrograms of HOM isolated from natural sources. The comparison between these patterns in the fulvic acid isolated from the coal wastewater, in the HOM of the associated sediment on the bottom of the pond, in the organic solvent extract of the sediment (obtained by means of accelerated solvent extraction or ASE) and the pollutant pattern in the wastewater allows conclusions to be drawn on the humification process and on the

pathways of contaminants present in the coal wastewater.

Reproducibility of the pyrograms is mainly determined by the steps in sample preparation, pyrolysis and pyrolysate transfer to the GC column rather than by the pyrolysate analysis by GC-MS (AED). Prior to pyrolysis, the HOM sample is usually subjected to an intense degreasing procedure, e.g. by Folch's chloroform-methanol (2 : 1) mixture to avoid ambiguous results with regard to the source of the pyrolysate. The extract from exhaustive solvent extraction contains the same compounds which are released during thermal desorption at subpyrolysis temperatures (e.g. 300°C). Both methods reveal contaminants attached to the HOM rather than covalently bound. To obtain a more homogeneous material and to simplify the pyrogram, a combination of pyrolysis and chemical modifications may be used: for example, acid hydrolysis removes carbohydrates and proteins/peptides, whereas the more resistant hydrocarbon fraction remains unchanged.

In general, pyrograms of HOM reveal overwhelmingly nonpolar hydrocarbons and less polar

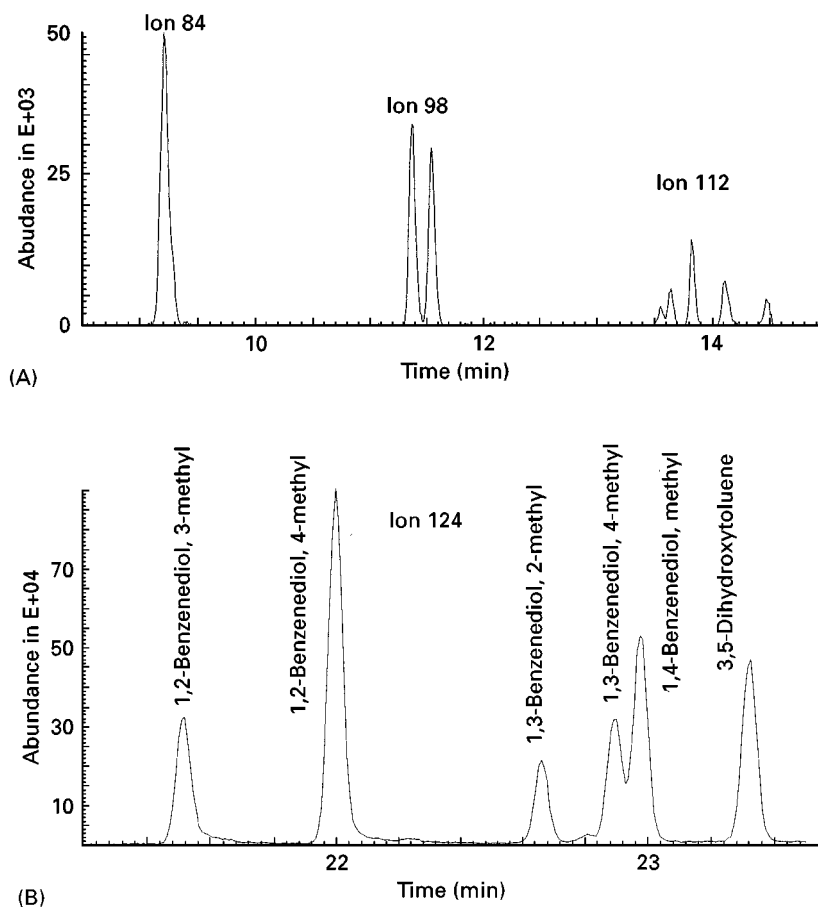


Figure 1 (A) Thiophene and (B) benzenediol pattern of an aquatic humic acid isolated from coal wastewater on an inert HP-5 capillary column.

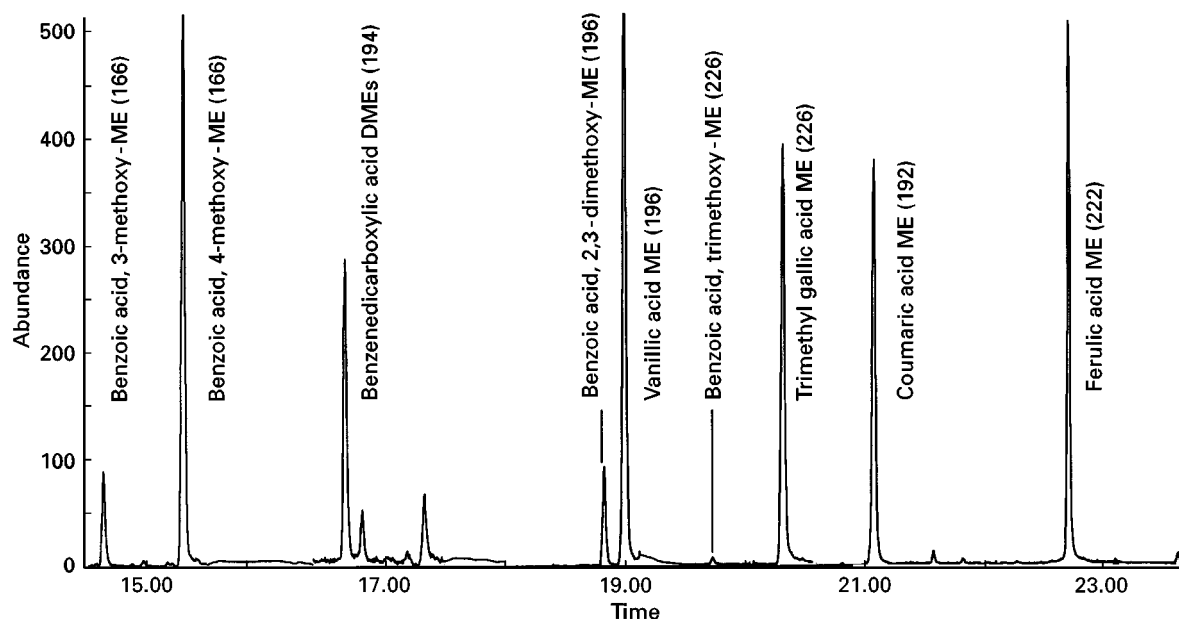


Figure 2 Aromatic methyl esters (ME) obtained in TMAH-assisted *in situ* methylation of a humic acid isolated from peat. Selected ion traces are given in parentheses.

heterocyclic compounds (e.g. benzofuranes, chinolines, benzothiophenes, etc.). Evidently, there are large discrepancies between NMR results and common titration results on the one hand, which indicate high carboxyl and hydroxyl group contents, and the basically nonpolar pyrolysates on the other hand. This finding is due to pitfalls occurring during pyrolysis, like the decarboxylation of fatty acids to give alkanes and the formation of polar, less volatile products inaccessible to GC (see below). Some efforts have been made to overcome these drawbacks. The coupling of pyrolysis with the 'soft' field ionization MS to give overwhelmingly molecular ions of thermal degradation products, including polar and higher molecular ones, turned out to be very useful in rapid profiling of HOM. The significance of this strategy can be further enhanced by using high resolution MS. The hyphenated technique thermogravimetry-MS, which allows running experiments in a time-resolved manner, can give further information on the binding state of the compounds released from the matrix. Another approach is to produce appropriate derivatives to preserve the analytical integrity of HOM in a better way.

Thermochemolysis with TMAH

Challinor was the first to introduce *in situ* methylation using a methanolic solution of tetramethylammonium hydroxide (TMAH) with biopolymers to convert polar carboxylic and hydroxyl groups to less polar and GC-accessible methyl derivatives so as

to avoid decarboxylation and dehydration. Methodological studies revealed that simultaneous pyrolysis/methylation (SPM) is not a pyrolysis but a thermally assisted chemolysis. This saponification/esterification reaction can be performed at subpyrolysis temperatures in both an online and offline (batch) approach, the latter including flushing of the thermochemolysis products into an organic solvent spiked with internal standards.

In contrast to conventional pyrolysis, some compound classes of diagnostic value can be detected by means of the SPM approach:

1. Aromatic acids, including mono-, di- and trimethoxybenzenecarboxylic acid methyl esters, benzenedicarboxylic acid dimethyl esters, mono- and dimethoxybenzenepropenoic acid methyl esters (Figure 2). The presence of trimethylgallic acid (3,4,5-trimethoxybenzoic acid) is of special diagnostic value, because it indicates the final step in the oxidation of side chains in lignin units¹. To verify the ambiguous origin of methoxy compounds (real methoxy moieties or resulting from originally free hydroxyls), deuterated TMAH can be used². Another approach is the application of

¹ The 3,4,5-trimethoxybenzoic acid methyl ester may also be derived from syringic acid (4-hydroxy-3,5-dimethoxybenzoic acid).

² Analogously, to investigate the role of methanolysis, the reagent TMAH/CD₃OH may be used.

tetrabutylammonium hydroxide, giving rise to *O*-butyl ethers only from phenolic groups, whereas aliphatic hydroxyls do not undergo a reaction with the weaker acidic reagent.

2. Long chain fatty acid methyl esters (FAMES). A pronounced even-over-odd discrimination constitutes a strong evidence of biogenic input, while uniform FAME patterns indicate anthropogenic origins. Iso- and anteiso FAMES (frequently C_{15} and C_{17}) are related to Gram-positive bacterial activities, whereas *cis*-vaccenic acid ($C_{18:1}$, double bond in $\Delta 11$ position) is related to Gram-negative bacteria.
3. The homologous series of α,ω -dicarboxylic acid methyl esters (DME). The α,ω -alkanedioic acids are of distinctive diagnostic value because they are thought to act as bridges in the HOM network and thus are considered to be markers for the cross-linking ratio. However, other pathways cannot be ruled out: the C_9 -DME is widely distributed in both aquatic and terrestrial HOM of natural origin. It may originate from fatty acids with double bonds in $\Delta 9$ position, e.g. oleic acid, which have undergone oxidation. Analogously, the C_{11} -DME is common in pyrolysates of bacteria, the lipids of which contain distinctive *cis*-vaccenic acid moieties.
4. The pristenes refer to chemically bound phytol and tocopherols.
5. 1-Methoxyalkanes formed by thermochemolysis represent mainly alkanols bound by ester groups.

SPM at 'mild' temperatures followed immediately by thermal treatment under more severe conditions can be used to estimate the share of ester, ether and C-C bonds in the HOM polymeric network. Pyrograms of HOM of both aquatic and terrestrial origin reveal a pronounced FAME pattern under mild conditions at 500°C, but do not reveal any alkanes. SPM at 750°C after the treatment at 500°C gives typical *n*-alkane patterns originating either from ether linkages or from alkylbenzenes. These findings may be attributed to the fact that ester bonds are cleaved at 500°C, whereas the more stable C-O-C and C-C bonds are resistant to decomposition at this 'mild' temperature.

Limitations of Pyrolysis in Structure Elucidation of HOM

Generally, pyrolysis work is aimed at obtaining a maximum yield of pyrolysis products to be analysed by means of GC and at ensuring that these volatile products reflect the structure of the polymer

from which they are generated as truly as possible³.

It was not until the mid 1990s that *Kopinke* carried out the first quantification experiments with HOM pyrolysis using a two-detector technique (MS to identify the pyrolysate, flame ionization detector (FID) to quantify organic carbon). Before that time, quantification was done in a semiquantitative way at best (+++ most abundant, ++ less abundant, etc.). Calibration can be done offline using on-column injection of calibration mixtures, or can be performed by vaporizing internal standards in the hot pyrolysis interface during equilibration just before the beginning of the pyrolysis process. Three fractions can be distinguished in the pyrolysate, the sum of which amounts to almost 100% of the original HOM organic carbon:

1. A solid residue, which consists almost exclusively of carbon, due to charring reactions resulting from the elimination of functional groups and additional cross-linking. This residue is about 30% of the original organic carbon content, largely independent of the kind of HOM studied. Thus, considering the fact that HOM consists of about 40–50% organic carbon, over 50% of the HOM's carbon, which is expected to carry substantial structural information, is lost on pyrolysis. Unfortunately, this residue cannot be significantly reduced by increasing the pyrolysis temperature, and it is also in the same order of magnitude when pyrolysing under in-source vacuum conditions. The latter finding indicates that the 'coke' formation is a solid-phase reaction rather than a transport-limited step. When pyrolysing soils, the tendency to form solid carbonaceous residue is correlated to organic carbon content.
2. Compounds in the pyrolysate with little structural significance. The remaining carbon is detected mainly as nonspecific light gases, including carbon dioxide, carbon monoxide and methane eluting at the beginning of the chromatogram. Although carbon dioxide is assumed to be a rough measure of decarboxylation and methane a rough measure of methyl substitution, etc., all these light gases are of minor diagnostic relevance to the HOM structure.
3. Compounds with supposed structural significance ($C > 4$, assumed arbitrarily), comprising about

³ Losses due to the limitations of the analytical system are outside this consideration. They may be circumvented by pyrolysis inside a GC precolumn; all volatile pyrolysates are completely transferred to the column.

6–10% of the organic carbon. A slight increase in the yield of structure-related compounds can be observed when turning from the conventional pyrolysis to SPM (15% at best).

However, the situation gets even worse when considering the real significance of the compounds in group 3 above. Whereas long aliphatic chains definitely originate from the HOM skeleton, aromatic and cyclic compounds may undergo unwanted thermal modifications, resulting in their misinterpretation, as already discussed above with alkanes/fatty acids. Further, the occurrence of furanes in the pyrolysate does not necessarily mean that furane moieties are present in the HOM backbone. It can also be related to thermal rearrangements and reactions originating from polysaccharide-related units (e.g. xylans, cellulose from terrestrial plants) or OH-substituted carbon chains with at least four carbons. Hence, if pyrolysis products are considered to be building blocks, cellulose should be made up of furans, pyranones, anhydrosugars, etc. Similar pitfalls occur with alkylbenzenes. They can be formed in the cracking of triglycerides and fatty acids (catalytically stimulated, e.g. by elemental sulfur). Most recent findings also indicate the formation of alkylbenzenes via a metal-catalysed alkylation of aromatic hydrocarbons, the cations being complexed in the HOM network. Therefore, structural models based on conventional pyrolysis studies are largely biased.

SPM is considered to be less error-prone. However, this approach has not been scrutinized as closely as conventional approach up until now. Saiz-Jimenez, who pioneered the SPM approach, found that model phenolic acids underwent decarboxylation reactions. Most recent results indicate that the occurrence of benzene carboxylic acids in the pyrogram does not necessarily indicate their presence in the HOM backbone: lignin models free of carboxylic groups may yield MEs of benzenecarboxylic acids during SPM. On the other hand, decarboxylation reactions and isomerization of unsaturated fatty acids have not been under intense study yet, but presumably they cannot be completely excluded. Hydroxyl- and carbonyl-containing resin acid MEs have been shown to undergo side reactions with the reagent, resulting in the formation of nitrogen-containing derivatives. Likewise, aldehydes have been recently shown to undergo a Cannizzaro-like reaction, in which the products are methylated to esters and ethers. In addition to that, the quantity of FAMES released in 500°C thermochemolysis surpasses by far the quantity of hydrocarbons (including alkanes, alkenes and alkylbenzenes) released in conventional pyrolysis, pointing to further aliphatic precursors. Moreover,

the FAME pattern does not necessarily coincide with the alkane pattern.

Apart from the ambiguous origin of markers in the pyrograms of HOM, these markers cannot be assigned to defined biological precursors by themselves. As an example, *n*-alkanes can be derived from anthropogenic sources (fuels), from direct input of biosynthesis (higher plants), from reduction of fatty alcohols (bacteria, higher plants), from decarboxylation of almost ubiquitous fatty acids and from depolymerization of aliphatic biopolymers. To assign these sources, isotope ratio GC-MS is very useful.

Controlled Wet Chemical Degradation

The ultimate aim of this approach (mostly conducted in an offline mode), elucidation of the HOM structure on the basis of degradation products, is similar to that of pyrolysis. As with HOM pyrolysis, large quantities of nondiscriminated building blocks are expected from an ideal chemical degradation method in a mechanistically predictable manner⁴. Common methods to obtain defined degradation products include mainly traditional approaches, such as:

1. Reductive degradation, e.g. using catalytic hydrogenation or alkali metals such as sodium or sodium amalgam in liquid ammonia, or lithium in liquid ethylamine. (The free or solvated electrons are provided in metallic reductions by the conversion of metal atoms to their cations.) In all cases, the carbon skeleton of aliphatic substructures is claimed to remain intact, whereas bonds between carbon and heteroatoms (in particular oxygen) are cleaved. A reagent with reactivity slightly higher than that in catalytic hydrogenolysis is iodotrimethylsilane, capable of cleaving ether and ester bonds. **Figure 3** shows the fatty acid pattern of a terrestrial HOM isolated from the sediment at the bottom of a coal wastewater pond after this treatment followed by methylation. The fatty acid pattern reflects both natural sources, expressed by the even-over-odd discrimination in the C₁₄–C₁₈ range, and the presence of bacterial iso- and anteiso-acids and anthropogenic sources, expressed by very long chain acids and a less pronounced even-over-odd discrimination at higher carbon numbers.
2. Oxidative and hydrolytic degradation. Common oxidative reagents include cupric oxide, ruthenium tetroxide and potassium permanganate. The

⁴ The derivatization of HOM has also been used for subsequent analysis by NMR or infrared spectroscopy to obtain well-resolved spectra, e.g. by silylation of groups with acidic protons.

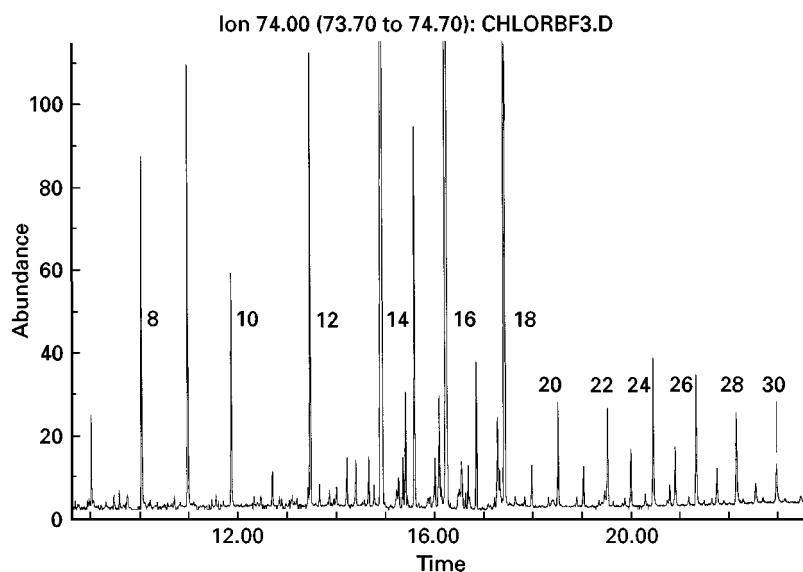


Figure 3 Fatty acid pattern (as methyl esters) of an HOM isolated from a sediment associated with coal wastewater, obtained after iodotrimethylsilane cleavage (using chlorotrimethylsilane–sodium iodide) and boron trifluoride catalysed methylation. Numbers indicate the carbon chain length of the homomorphic fatty acid.

hydrolysis is mainly catalysed either by sodium hydroxide or sulfuric/hydrochloric acid⁵. Another direction includes mild and selective enzymatic hydrolysis. As with thermochemolysis with TMAH, these approaches revealed products, including benzene mono-, di-, tri- and tetracarboxylic acids, furane di- and tricarboxylic acids, aliphatic mono-, di- and tribasic acids and (di-, tri- and tetracarboxyphenyl) glyoxylic acids, all of them preferably subjected to GC as MEs or trimethylsilyl ethers. CuO is known to oxidize the lignin macromolecule (cleavage of the β O-4 ether bond, as with TMAH thermochemolysis) and produces a series of *p*-hydroxyphenyl, guaiacyl and syringyl compounds.

3. Transesterification, e.g. using boron trifluoride-methanol. The yields from this milder approach are quite low, but the formation of by-products and the destruction of labile structures are minimized.

As with pyrolysis, chemical degradation may be full of pitfalls. Hexose sugars are known to dehydrate to hydroxymethylfurfural; pentoses give furfural in strong acids at elevated temperatures. Moreover, melanoidins may be formed from sugars in the presence of amino acids leading to enhanced (apparent)

aromaticity. Diols can be oxidized, including ring rupture, to form low molecular weight aliphatic acids. Gallic acid can be decarboxylated on heating in water, and so forth. Although the loss in weight of the HOM on chemical degradation gives yields between 3 and 30%⁶ of the mass of the starting polymer, the yields of products accessible to GC are significantly lower, in the range of 0.5–3%. A large percentage (about 25%) of the total organic carbon is lost as CO₂ by KMnO₄ oxidation. FTIR spectra give strong evidence that permethylation cannot remove all acidic protons. Thus, extrapolation to the macromolecular skeleton is quite biased.

Selective chemical degradation has also been used in a more restricted way to elucidate the fate of organic pollutants and metabolites in soils/sediments, which cannot be released by means of organic solvent extraction. This results in a better understanding of their incorporation into the macromolecular HOM and their remobilization potential. Pioneering work has been done by *Michaelis*, who cleaved bound polycyclic aromatic hydrocarbon (PAH) metabolites such as hydroxynaphthoic acids from the macromolecular HOM network using boron trichloride (capable of degrading ester and ether bonds) as well as by alkaline hydrolysis, and degraded phenolic entities from the HOM matrix by rhodium on charcoal

⁵ Hydrolysis proceeds faster and more efficiently if the HOM is dissolved in the hydrolytic reagent; thus, alkaline hydrolysis should be used with humic acids, which by definition are insoluble in acids.

⁶ Empirical findings suggest that a methylation procedure prior to degradation is beneficial towards yields of oxidative products of HOM.

hydrogenolysis. The type of bonding and linkage of pollutants/metabolites can be better elucidated using isotope-labelled Na^{18}OH , because only the carboxylic entity of the ester carries the heavier oxygen isotope, thus referring to products attached to the HOM matrix by ester bonds.

Although wet chemical degradation techniques as well as pyrolysis techniques involve some pitfalls and limitations, they can contribute to elucidation of the fundamentals of the diagenesis of organic compounds in soil and water. ^{13}C NMR results yield strong evidence that a large percentage (in general, about 60% in case of the HOM under study) of methyl groups is attached to hydrogen-free paraffinic carbon. These findings cannot be explained by building blocks consisting of alkanes or alkylbenzenes. Steranes and hopanes, considered to be the end products of a complex web of diagenetic reactions starting from functionalized bacteriohopanepolyols and serving as biomarkers in ancient sediments and petroleum, are assumed to account for that. Indeed, pentacyclic terpanes with 32–35 carbon atoms, confirmed by tracing $m/z = 191$ in the GC-MS mode, can be detected using both chemical and thermal degradation.

Future Developments

Conventional and TMAH pyrolysis, as well as controlled chemical degradation methods, applied together in combination with highly efficient GC-MS can give insight to the building blocks and the linkages between them in the polymeric HOM network. However, analytical pyrolysis has a significantly higher potential in revealing the chemical nature of simpler polymers, e.g. polyethylene and polystyrene, which give no or minor solid residue. Traditionally performed pyrolysis work with HOM conceals much significant information on the chemical nature of HOM by thermal degradation of functional groups and thermal rearrangements. Thermochemolysis with TMAH gives rise to complementary and more independent reactions in comparison

with conventional pyrolysis. Not much attention has been paid to improved specificity of bond cleavage in the structures. It will be important to understand the mechanisms of the cleavages, and to be able to relate the products identified to possible structures in the parent macromolecule.

See also: II/Chromatography: Gas: Derivatization; Detectors: Mass Spectrometry; Pyrolysis Gas Chromatography.

Further Reading

- Abbt-Braun G, Frimmel FH and Schulten HR (1989) Structural investigations of aquatic humic substances by pyrolysis-field ionisation mass spectrometry and pyrolysis-gas chromatography/mass spectrometry. *Water Research* 23: 1579.
- Hautala J, Peuravuori J and Pihlaja K (1998) Organic compounds formed by chemical degradation of lake aquatic humic matter. *Environment International* 24: 527.
- Hayes MHB, MacCarthy P, Malcolm RL and Swift RS (1989) The search of structure: setting the scene. In: Hayes MB *et al.* (eds) *Humic Substances II*, chap. 1, pp. 1–31. John Wiley.
- Kopinke FD and Remmler M (1995) Reactions of hydrocarbons during thermodesorption from sediments. *Thermochimica Acta* 263: 123.
- Lighthouse E (1998) Isotope and biosynthetic evidence for the origin of long-chain aliphatic lipids in soil. *Naturwissenschaften* 85: 76.
- Poerschmann J, Kopinke FD, Balcke G and Mothes S (1998) Pyrolysis pattern of anthropogenic and natural humic organic matter. *Journal of Microcolumn Separations* 10: 401.
- Richnow HH, Seifert R, Hefter J *et al.* (1997) Organic pollutants associated with macromolecular soil organic matter: mode of binding. *Organic Geochemistry* 26: 745.
- Saiz-Jimenez (1996) The chemical structure of humic substances: recent advances. In: Picollo A (ed.) *Humic Substances in Terrestrial Ecosystems*, ch. 1, pp. 1–44. Amsterdam: Elsevier.
- Schulten HR and Leinweber P (1996) Characterisation of humic and soil particles by analytical pyrolysis and computer modelling. *Journal of Analytical and Applied Pyrolysis* 38: 1.

Liquid Chromatography

D. K. Ryan, University of Lowell, Lowell, MA, USA

Copyright © 2000 Academic Press

Humic substances are complex mixtures of compounds and in order adequately to elucidate and

characterize the properties and reactions of humic substances, separation techniques are an absolute requirement. Initial work in this area employed low pressure liquid chromatography (LC) with extensive use of size exclusion chromatography (SEC). The advent and acceptance of high performance liquid

chromatography (HPLC) as well as its miniaturization and the development of column technologies, throughout the 1970s, has resulted in HPLC becoming the most widely used chromatographic technique for the separation of humic substances. The focus here will be on the HPLC of humic materials with only a passing reference to low pressure chromatographic methods.

The physical and chemical properties of humic substances are of obvious importance in their interaction with column materials and subsequent separation in chromatography. A brief description of germane humic characteristics will be presented first, followed by a discussion of the various chromatographic modes of separation, the important detectors employed and new horizons in the LC of humic substances.

Humic Properties

Humic substances are known by many names and can be found in measurable concentrations in almost every soil, water or sediment system on earth. Carbon-containing compounds are the common denominator from both plant and animal sources which break down under the normal sequence of death and microbial decomposition in the environment. All forms of organic carbon (OC) or organic matter (OM) that are dissolved and of natural origin are of interest here and form the broadest category, of which humic substances (HS) or the synonymous humic materials (HM) are the largest part. Nonhumic compounds under the OC classification include identifiable species such as amino acids, sugars, fatty acids and the like. Humic acids (HA) and fulvic acids (FA) are the two subunits of humic substances making up all water-soluble material in this class. The relationship between all of these categories is depicted in Figure 1.

Humic substances are macromolecular species ranging in molecular weight from about 1 to 100 kDa. They have historically not been considered polymeric in nature, lacking any confirmed monomeric unit, although this view has been challenged in recent years with the proposal of an approximately 700 Da monomer. Figure 2 shows a molecular model of the lowest energy building block conformation computed for a humic acid hexamer. Humic substances exhibit significant polydispersity and are polyelectrolytic, containing numerous carboxylic acid and ionizable phenolic groups. Very small amounts of amine functionality are sometimes present; however, essentially no sulfur groups are found associated with humic samples. Properties of humic substances that are relevant to chromatographic sep-

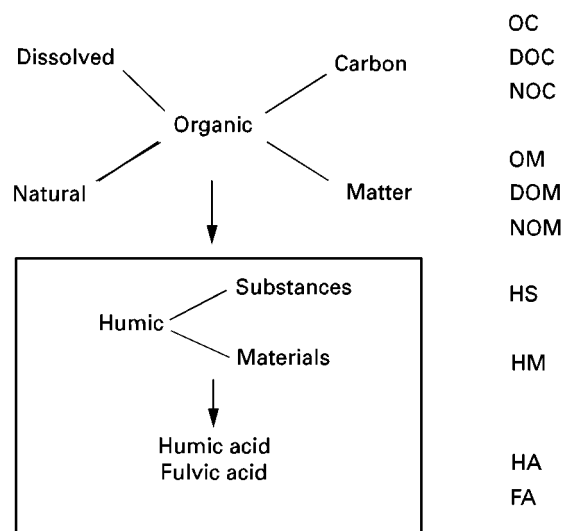


Figure 1 Terminology, acronyms and relationship for soluble organic carbon (OC) of natural origin. Humic and fulvic acid are the two categories of soluble humic substances or humic materials which are a subset of all organic materials in the environment.

arations are summarized in Table 1. Significant among these are the hydrophobicity or surface activity of humic substances causing them to adsorb and partition with appropriate materials, their acidity and polyelectrolytic character imparting water solubility and charge to the molecules allowing for ion exchange, and their range of molecular sizes and possibly shapes that makes feasible separations based on size.

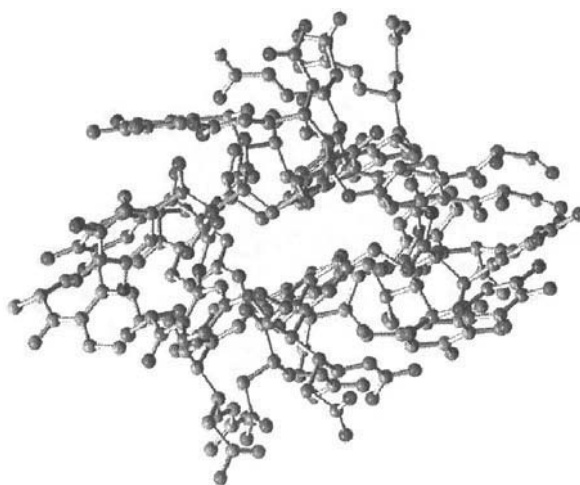


Figure 2 (See Colour Plate 87). Molecular model of the lowest energy conformations of humic acid building blocks linked to form a hexamer. Carbon atoms are green, oxygen atoms are red, nitrogen atoms are blue and hydrogen atoms are not shown. Reproduced with permission from Davies and Ghabbour (1999).

Table 1 Summary of characteristics for typical humic substances

Elemental composition	Approximately 50% C, 5% H, 45% O; very little N, no S
Ash content	Typically less than 0.5%
Molecular weight range	1–100 kDa
Purity	Complex mixture
Structure	Difficult to specify exactly
Functional groups	Aromatic and aliphatic carboxylic acids Phenolic OH and aliphatic OH Carbonyl groups Numerous aromatic rings Aliphatic chains Quinone/hydroquinone present Traces of bound metals, particularly Fe and Al
Acidity	Approximately 6 mmol g ⁻¹ from carboxyl groups
Solubility	Very soluble in water; generally, solubility increases with pH Poor solubility in most organic solvents
Other characteristics	Polydisperse Polyelectrolytic Surface active: hydrophobic portion with hydrophilic groups Metal complexation: binding of numerous metal ions Binding of organic molecules

Chromatographic Modes

Size Exclusion Chromatography

Some of the earliest LC separations of humic substances were based on the size exclusion mode of separation using distilled water, salt solutions or aqueous buffers as mobile phases. SEC studies showed that size separations were possible but, unfortunately, most attempts at SEC of humic substances gave poor resolution and marginal results. Chromatograms typically exhibited only one or two broad peaks with an occasional shoulder. Experiments resulting in several peaks by SEC have often been found by subsequent analysis to be the result of a mixed-mode separation. This comes about in low ionic strength mobile phases because of the repulsive forces between negatively charged humic substance molecules and negative charges on the surface of the column-packing materials. The actual separation is based partially on size and partially on charge, resulting in poor reproducibility and dramatic changes in the chromatography with slight changes in ionic strength, pH or solution composition. This complication completely eliminates the possibility of obtaining any molecular weight information from size exclusion – something that is normally a strong point of the method.

Once the problems with SEC of humic substances were better understood, improved packing materials such as the TSK gels (Toyo Soda, Tokyo, Japan) provided somewhat better resolution and reduced surface charge. However, the SEC of humic substances did not improve dramatically with these materials, primarily because of the nature of the humic substances themselves. Although humic substances have a seemingly broad size range, most samples have been preselected for size because of environmental conditions or by a particular isolation procedure, i.e. the method by which the sample was extracted from soil, sediment or water. In addition, each humic sample may contain a fairly uniform distribution of molecules over that range. These factors result in simple one- or two-peak chromatograms consisting of broad or poorly resolved peaks, such as those shown in Figure 3. The recent literature on humic substances has revealed little application of the SEC technique.

Ion Exchange

Ion exchange chromatography has found fairly limited application in the separation of humic

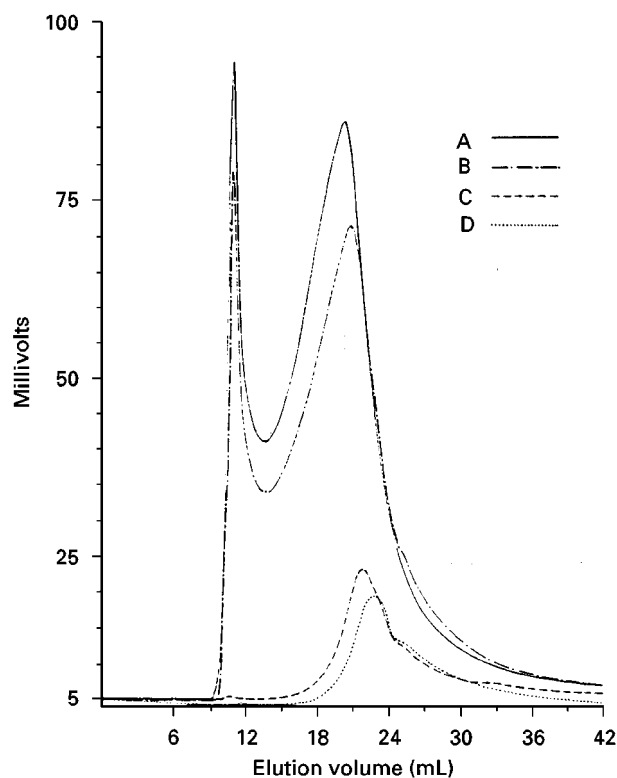


Figure 3 Size exclusion chromatograms of a humic acid sample on a TSK G3000SW (600 × 7.5 mm i.d.) with UV detection at 280 nm. Mobile-phase conditions are as follows: A, 0.05 mol L⁻¹ NaNO₃, pH 7; B, same as A with 4.6 × 10⁻⁷ mol L⁻¹, pH 6.97; C, same as A with pH adjusted to 5.54 with HCl; D, same as A with 4.6 × 10⁻⁷ mol L⁻¹ acetic acid, pH 5.69. Reproduced with permission from Conte and Piccolo (1999).

substances, possibly because of the very strong retention of humic molecules for most ion exchange packings. Early work with diethylaminoethyl (DEAE) functionalized supports demonstrated that ion exchange of humic substances is feasible, but rather harsh conditions must be used to approach quantitative elution of the retained material from the column. Some researchers advocated the use of 0.5 mol L^{-1} NaOH to obtain the best recoveries of humic substances from DEAE columns. Concern about the possible alteration of the humic substance molecules (hydrolysis, etc.) under these conditions has restricted its use. Ion exchange separations have been used extensively in the past for isolation and purification of humic substances from the environment. However, strongly basic conditions are also required for elution in this application and there has been a concerted effort in the area of humic substance isolation and purification to move towards less severe methods.

Reversed-phase HPLC

The general popularity of the reversed-phase mode for HPLC (RP-HPLC) separations in analytical chemistry is paralleled by its prominence as the chromatographic mode most applied to humic separations. One important reason for the development of this situation is the availability of several variables that can be adjusted to influence the separation. The percentage of organic modifier such as methanol, 2-propanol or acetonitrile can be regulated and held constant in isocratic separations or varied (either stepwise or continuously) in gradient elution. Ionic strength and buffer pH are commonly adjusted to improve resolution and even the length (C_1 to C_{18}) or type of stationary phase can be changed from alkyl to phenyl, diol or other types of functionality.

With all the flexibility available in RP-HPLC separations, it is often unclear upon initial examination why essentially all of the published chromatograms of humic substances exhibit broad, poorly resolved peaks that by some chromatographic standards would be unacceptable. The reason for this dilemma once again is linked to the nature of the mixture of molecules in humic substances. One view suggests that, although varied in properties, the molecules form a near continuum of species with characteristics so similar to one another that they are difficult to separate. The appearance of isolated peaks in the chromatogram is a function of greater numbers of molecules of certain types (in the continuum) over other molecules which elute in the valleys between peaks.

Since RP-HPLC separates on the basis of polarity, most chromatograms show two or three distinct re-

gions of peaks. Early in the chromatogram the most polar compounds elute, often as a jumble of sharp, but unresolved bands. Late in the chromatogram, the nonpolar species appear usually as very broad peaks with unresolved shoulders or side bands. Sometimes, a band of intermediate polarity is present midway through the chromatogram.

An important consideration in selecting a column for separating humic substances by RP-HPLC is the pore diameter of the packing material. Reversed-phase supports are available with a variety of pore sizes; however, larger pore diameters are more suitable for larger molecules such as humic substances. A common choice is a 30 nm pore diameter sold as a reversed-phase column for protein separations.

Ion Pair Reversed-phase Chromatography

Improvements in the RP-HPLC separation of many charged species can be realized by adding an ion-pairing reagent to the mobile phase. The ion-pairing reagent is commonly a tetrabutylammonium salt (in the cationic case) which can form an ion pair with the species of interest. Humic substances contain many ionizable carboxylic acid and phenolic groups, making them very suitable for this mode of chromatographic separation. **Figure 4** shows a representative ion pair reversed-phase (IP-RP-HPLC) chromatogram for the fulvic acid fraction of humic substances derived from soil. Although IP-RP-HPLC represents some improvement over RP-HPLC, the nature of the humic substances still gives rise to broad peaks that are less than completely resolved.

With regard to the exact mechanism of the separation in IP-RP-HPLC, at least two models exist. One perspective is that the ion pairing alters the polarity of the humic substance molecules, dramatically changing their retention characteristics on the reversed-phase column. A second theory supposes that the ion-pairing reagent partitions into the column leaving charged sites that allow for an ion exchange process with the humic substances as a means of separation. Reality is most probably somewhere between these two viewpoints. It should be noted that, once a RP-HPLC column has been subjected to an ion-pairing reagent, it is always an ion-pairing column.

Table 2 gives an overview of the HPLC modes discussed above. Representative publications are included for further reading in this area.

Detectors

Humic substances absorb UV and visible radiation at essentially all wavelengths and can therefore be readily monitored by absorbance detectors in HPLC. The

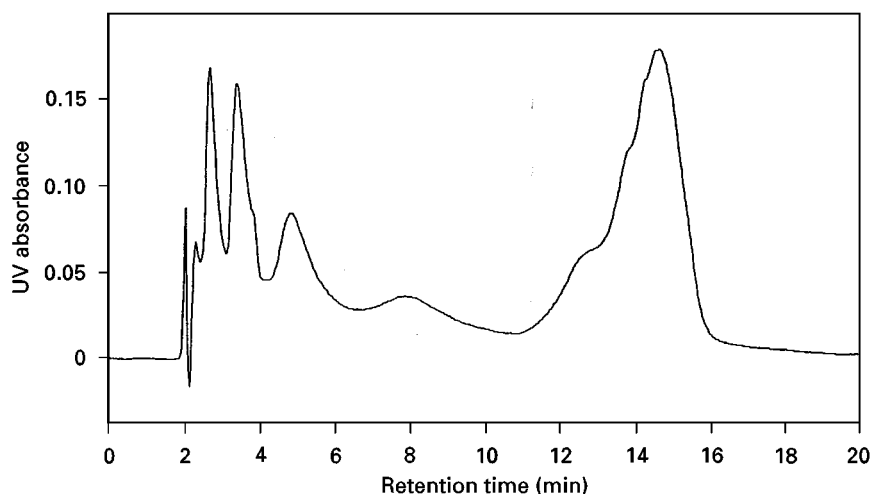


Figure 4 Ion pair reversed-phase chromatogram of Swanee Stream reference fulvic acid (SSRFA) separated on an SEG C₁₈ column using gradient elution beginning with 37% CH₃CN for 8 min followed by a linear gradient to 68.5% CH₃CN over 8 min at a flow rate of 1 mL min⁻¹. Tetrabutylammonium perchlorate was used as the ion-pairing reagent at a concentration of 50 mmol L⁻¹. UV absorbance at 254 nm was monitored for an 8 μ L injection of 0.048% (w/v) SSRFA.

absorbance spectrum of a typical humic substance sample is essentially featureless, looking somewhat like an exponential curve. Absorbance is high in the short wavelength region of the UV spectrum and drops quickly with increasing wavelength, tailing off into the red region of the visible spectrum. Therefore, almost any wavelength can be used to detect humic substances, but shorter wavelengths are more sensitive. Fixed wavelength measurements at 254 nm are the most common; however, variable wavelength detectors have been used at a variety of wavelengths with good success.

Photodiode array (PDA) monitoring of the complete UV-visible spectrum of the column effluent adds an additional dimension to HPLC, providing several advantages over conventional single wavelength detectors. PDA systems repeatedly collect spectra at a specified time interval (often once every second) throughout the life of the chromatogram. This spectral information is invaluable in method development, particularly when many unknown

compounds are present. Once the data are collected, several chromatograms can be generated, each with a different monitoring wavelength revealing features not visible in a single wavelength chromatogram. For example, a single well resolved peak at one wavelength may show a poorly resolved doublet at another wavelength. Similarly, peak purity can be determined by examining the spectra at several time intervals across a peak.

Finally, PDA detection can aid in the qualitative identification of the separated components by comparison of a peak's spectrum with the spectrum of known compounds. This approach has been used in some applications to elucidate certain structural features in separated fractions of humic substances. The general drawback with this application is that UV-Vis absorbance spectra are not conclusive evidence of a compound's identity and can only provide possible structural clues. When applied to the complex mixture of humic substances, only vague inferences can be made about possible structural components in

Table 2 Modes of liquid chromatography employed for separations of humic substances (HS)

Mode	Mechanism of separation	Reference
Size exclusion	Exclusion of larger HS molecules from certain pores based on size	Chin <i>et al.</i> (1994) Huber and Frimmel (1994)
Reversed-phase	Partitioning of hydrophobic portion of HS molecules into nonpolar stationary phase	Saleh <i>et al.</i> (1989)
Ion exchange	Exchange of anionic HS on cationic stationary phase	Andres <i>et al.</i> (1987)
Ion pair reversed-phase	Retention of ion-paired HS on nonpolar phase or ion exchange of HS on ion-pairing reagent-loaded phase	Butler and Ryan (1996)

the macromolecules that are contained within a peak. This type of data gives further evidence that moieties such as vanillic acid, catechol or other substituted aromatics are part of the structure of humic substances, but cannot provide unequivocal results.

The second and only other major detection method used for the HPLC of humic substances is fluorescence. Humic substances emit a broad fluorescence peak centred around 450 nm when excited by radiation in the 330–350 nm range. This fluorescence is not considered to be a very strong signal (high quantum yield) in comparison to other fluorescent species; however, sufficient sensitivity can be obtained with standard commercial fluorescence detectors to measure easily humic substances down to the low part-per-million level sufficient for most environmental measurements. Fluorescence is a selective means of detection because not all molecules fluoresce – a situation that is clearly true of the mixture of molecules in humic substances. HPLC experiments with both absorbance and fluorescence detection have shown that some components of humic substances absorb but do not fluoresce. This lack of fluorescence may result from one of at least two possibilities. The absence of the appropriate structural features (usually extended π electron system) in certain fractions of humic substances will render them non-fluorescent or the presence of fluorescence-quenching agents in a normally fluorescent fraction will likewise remove fluorescence. The most common fluorescence quenchers for humic substances are the paramagnetic metal ions, such as Cu^{2+} , Fe^{3+} , Ni^{2+} , Co^{2+} , Mn^{2+} , which form complexes at appropriate binding sites on the molecule. Recent studies have also shown that certain organic molecules can bind to humic substances either electrostatically or through hydrophobic interactions and also quench fluorescence.

Other Considerations

Humic substances are a fairly difficult class of compounds to work with because they are poorly characterized with respect to their chemical structure and many of their properties are not yet fully understood. Intra- and intermolecular hydrogen bonding, hydrophobic interactions and electrostatic effects surely play a role in what can be called the tertiary structure or shape of humic substance molecules. The variables of pH and ionic strength clearly play a role in determining molecular shape, which is very important with respect to HPLC separations; however, an understanding of the factors influencing shape is only now yielding to analysis through the use of molecular modelling.

Irreversible adsorption, concentration effects and solubility problems also plague the analysis of humic substances by HPLC. Although the fulvic acid fraction of humic substances is soluble at any pH, humic acid is not soluble at low pH and may have varying solubility depending on the exact solution conditions. Samples of isolated humic substances must be carefully dissolved and filtered before HPLC analysis and even then may not remain soluble throughout the separation because of changing gradient conditions.

Concentration effects are a related problem since high concentrations tend to favour aggregation and coagulation of humic substances, resulting in precipitation of the most nonpolar components in the sample. An important consideration when examining the published results in chromatographic studies of humic substances is the concentration of the solution injected into the chromatographic system. Many studies are conducted using as much as 500–1000 mg L⁻¹ of humic substances – a concentration level that is orders of magnitude higher than typical environmental levels in most cases. The results obtained in these instances may be influenced by concentration artifacts and are not likely to be representative of environmental conditions.

Irreversible adsorption is another difficulty that frequently occurs at the top of guard or analytical columns because of a high affinity of the column packing material for the humic substances. This mechanism may result in significant losses of sample material to the column and may skew results by selectively removing some compounds while not affecting others. The presence of bare silica for silica-based packings or other active sites can influence adsorption. In addition, the presence of sample components or impurities such as metal ions can facilitate interactions between humic substances and active sites on a column.

New Horizons

Although HPLC may be considered a mature technique, many advances have been made in recent years, primarily in the area of detectors, that have an impact on the chromatography of humic substances. One example is the use of carbon analysers as detectors for HPLC. Instruments that measure organic carbon in solution have long been used for the measurement of humic substances and other natural organics in nonchromatographic applications. It is only in the last decade that these instruments have been modified for use in HPLC. The advantages of dissolved organic carbon (DOC) detectors include their universal detection of all organic compounds

and their specificity for only carbon-containing species.

Two new approaches in the area of fluorescence detection of humic substances are the coupling of a fluorescence lifetime instrument to HPLC and post-column fluorescence quenching titrations as a means of measuring metal complex equilibria. Fluorescence lifetime measurements add yet another means of increasing the specificity of analysis, allowing improved qualitative determinations and generally increasing the amount of information obtained from fluorescence analysis of a sample. The coupling of phase modulation spectrofluorometry to HPLC results in a powerful method for measuring and resolving overlapping peaks as well as adding a dimension for identifying unknowns in a chromatogram. Although this type of detector is inherently expensive and will not see routine use, its application to humic substances, which have been shown to have three distinct fluorescence lifetimes, seems logical.

Post-column fluorescence quenching titration experiments have recently been employed in metal complexation studies to elucidate binding of metals to fractions of humic substances separated by HPLC. Quenching of the natural fluorescence by certain metal ions has become an accepted method for measuring equilibrium constants and other binding parameters for complexation of the metal by sites on humic substance molecules. Studying these equilibrium processes by HPLC has heretofore been very difficult because the chromatographic separation of the humic-metal complexes is adversely influenced by the presence of the metal ion. By separating the humic substances first without metal present, then adding metal ion via a post-column inline mixing tee, the complexes are formed just prior to their measurement by a conventional fluorescence detector. This approach alleviates any chromatographic problems associated with the presence of metal ions and allows valuable binding studies of metal ions with separated fractions of humic substances in a time-saving online mode.

Two of the most powerful instruments for measuring chemical structures of organic molecules are Fourier transform infrared spectroscopy (FTIR) and mass spectrometry (MS). A relatively new form of MS that has a major advantage in its application to macromolecules such as proteins is matrix-assisted laser desorption and ionization (MALDI) MS. The immense benefit of coupling a powerful separation technique such as HPLC with the unparalleled structural capabilities of FTIR and MS is obvious, particularly when applied to complex mixtures. However, there are significant difficulties encountered in the interfacing of these techniques which have hindered

advances in this area. A novel approach has been developed to meet this challenge which centres on the inherent ability of FTIR and MS to analyse solid samples. Column effluent which exits from the chromatograph is sprayed on to a slowly moving solid substrate under controlled conditions. Solvent is evaporated and the sample dried as the separated components are deposited sequentially. Once the chromatographic run is complete, the solid substrate with the deposited sample components is placed in a modified FTIR or MALDI MS unit for analysis. Sequential analysis along the track of deposited sample components yields a series of spectra similar in concept to PDA detection in HPLC, but this approach is far more useful in elucidating structural features and providing absolute qualitative confirmation of component's identity. The application of this technology to the analysis of humic substances with RP-HPLC has been pioneered.

Conclusion

The use of HPLC for separation of humic substances has been, and will continue to be, a challenging area in separation science. Additional information about the nature of humic substances will aid in the fine-tuning of this application of HPLC, as will improvements in column technology. Probably the most significant advances in the HPLC of humic substances will come with the utilization and development of more powerful detectors, particularly spectroscopic detectors. No doubt the complex, heterogeneous nature of humic substance samples will require a host of separation and detection strategies to be applied in the years to come before their analysis is considered in any way routine.

See Colour Plate 87.

See also: II/Chromatography: Liquid: Detectors: Fluorescence Detection; Detectors: Ultraviolet and Visible Detection; Ion Pair Liquid Chromatography; Mechanisms: Reversed Phases; Mechanisms; Size Exclusion Chromatography.

Further Reading

- Andres JM, Romero C and Gavilan JM (1987) Ion exchange chromatography of fulvic acids from lignite. *Fuel* 66: 827.
- Butler GC and Ryan DK (1996) Investigation of fulvic acid-Cu²⁺ complexation by ion-pair reversed-phase high-performance liquid chromatography with post-column fluorescence quenching titration. In: Gaffney JS, Marley NA and Clark SB (eds) *Humic and Fulvic Acids: Isolation, Structure and Environmental Role*, p. 140. Washington, DC: ACS Symposium Series 651.

- Chin YP, Aiken G and O'Loughlin E (1994) Molecular weight, polydispersity, and spectroscopic properties of aquatic humic substances. *Environmental Science and Technology* 28: 1853.
- Conte P and Piccolo A (1999) Conformational arrangement of dissolved humic substances. Influence of solution composition on association of humic molecules. *Environmental Science and Technology* 33: 1682.
- Davies G and Ghabbour EA (1999) Understanding life after death. *Chemistry and Industry* 7 June: 426.
- Huber SA and Frimmel FH (1994) Direct gel chromatographic characterization and quantification of marine dissolved organic carbon using high-sensitivity DOC detection. *Environmental Science and Technology* 28: 1194.
- Liu X and Ryan DK (1997) Analysis of fulvic acids using HPLC/UV coupled to FTIR spectroscopy. *Environmental Technology* 18: 417.
- Ryan DK, Thompson CP and Weber JH (1983) Comparison of Mn^{2+} , Co^{2+} , and Cu^{2+} binding to fulvic acid as measured by fluorescence quenching. *Canadian Journal of Chemistry* 61: 1505.
- Saleh FY, Ong WA and Chang DY (1989) Structural features of aquatic fulvic acids. Analytical and preparative reversed-phase high-performance liquid chromatography separation with photodiode array detection. *Analytical Chemistry* 61: 2792.
- Sein LT, Varnum JM and Jansen SA (1999) Conformational modeling of a new building block of humic acid: approaches to the lowest energy conformer. *Environmental Science and Technology* 33: 546.
- Smalley MB, Shaver JM and McGown LB (1993) On-the-fly fluorescence lifetime detection in HPLC using a multiharmonic Fourier transform phase-modulation spectrofluorometer. *Analytical Chemistry* 65: 3466.

HYDRODYNAMIC CHROMATOGRAPHY: PRACTICAL APPLICATIONS



A. Revillon, Centre National de la Recherche Scientifique, Vernaison, France

Copyright © 2000 Academic Press

Introduction

Either in research, the control or the production of chemicals, or during general observations in biochemistry, characterization is a primary necessity. Depending on the product, the nature, structure, size, shape, and molecular weight are some of the important parameters to be measured. For instance, the molecular weight distribution of polymers and particle size of latex/colloids (MWD and PSD, respectively) have to be known so that they can be correlated with properties. The data may be obtained using many techniques. These techniques are governed according to the various properties of a material and depend on the size range of the investigated material. Hydrodynamic chromatography (HDC) is one of these techniques and has found applications for sizing soluble or dispersed solid components. This article will discuss the size distribution of organic latex particles from the theoretical and practical points of view. Progress in packing columns with fine materials or in the use of fine capillary tubes has allowed rapid separation of species with high resolution. A second field of interest is polymers in solution. The combined effects of hydrodynamic and exclusion chromatography have extended possibilities for the separation of high-molecular-weight materials.

Hydrodynamic chromatography is used for diameter determination in the micron range (some nm to some μm). It will work for both solid and soluble samples, which are eluted according to their decreasing size. This leads to a visual picture of the size distribution. The main interest of HDC lies in the rapid separation (fractionation, which is an alternative name for this method: HDF) of the liquid or solid components present in the sample. Often low peak capacity and poor resolution are its limitations and involve the necessity for peak dispersion correction. Moreover, a quantitative study requires a double calibration. The first relates to elution volume and diameter of the analysed particles; the second gives a correspondence between the signal intensity and size of particles. This intensity depends on the nature of the detector and the operating conditions, for instance the choice of wavelength in UV. As an example, **Figure 1** shows the different absorbance curves of polystyrene (PS) latexes of different sizes. **Figure 2** shows the change in absorbance and scattering with wavelength and illustrates different peak contributions of PS particles to the chromatogram.

HDC operates similarly to size exclusion chromatography (SEC) and field flow fractionation (FFF), but needs one (inert) mobile phase and one (hydrodynamic) field only. The interesting principle of particles separation is the difference in their transport rates in a capillary, related to their location in the eluent. Large particles are preferentially in the centre of the capillary, where the flow rate is max-

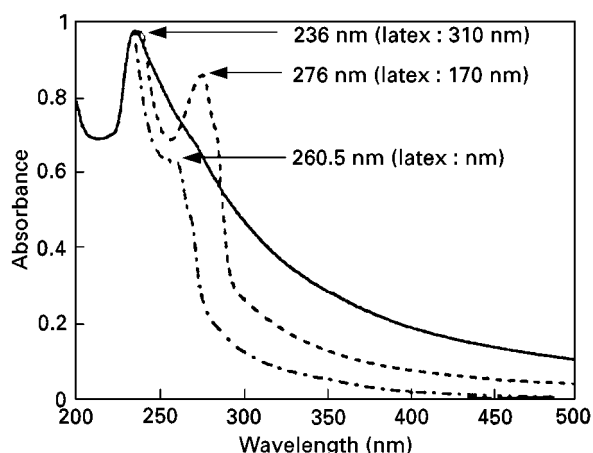


Figure 1 UV absorbance curves for polystyrene latex particles. (Reprinted from Nagasaki S, Tanaka S and Suzuki A (1993) Fast transport of colloidal particles through quartz-packed columns. *Journal of Nuclear Science and Technology* 30(11): 1136–1144.)

imum, so they are eluted faster than small ones, which are closer to the wall of the capillary, where the flow rate is zero. The ratio of the highest elution volume for a small molecule – called a marker – to that of a given particle is the separation factor (R_f). Besides the simplicity of the process, secondary advantages are the rapidity of measurement performed directly on the untreated medium and ease of operation of the equipment. Variation of operating parameters (flow rate, nature of eluent and additives, size of the capillary, etc.) allows a considerable range of possible applications. Chromatography is performed

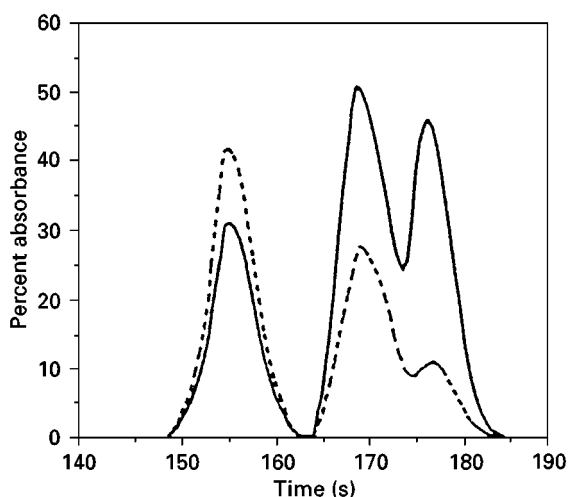


Figure 2 Effect of wavelength (—, 220 nm; ----, 254 nm) on the chromatogram of a trimodal mixture of polystyrene latexes (357, 176, 109 nm) on a capillary column $2\text{ m} \times 4\text{ }\mu\text{m}$, ionic strength 1 mM. (Reprinted from Dos Ramos JG and Silebi CA (1990) The determination of particle size distribution of submicrometer particles by capillary hydrodynamic fractionation. *Journal of Colloid and Interface Science* 135(1): 165–177.)

on two types of columns, open capillary or packed, where the interstitial space defines the channels. The use of very small particles (diameter $2\text{ }\mu\text{m}$) or fine capillaries (diameter $4\text{ }\mu\text{m}$) allows a high resolution. Relatively short capillary columns (3 m) lead to a rapid and efficient separation (5 min), as shown in Figure 3 for monodisperse polystyrene latexes.

This article focuses on the main applications of HDC and which are under constant evaluation. There is no effect of density and no limitation on the nature of the sample, but most studies are related to the field of polymers. Since there is no solvent limitation (soluble samples) or no solubility condition (solid samples), all polymer families have been examined. Most of the applications are relative to synthetic organic colloid separation in latex production and diameter measurements for quality control. As mentioned above, interesting perspectives are apparent by combining HDC and SEC with porous packings.

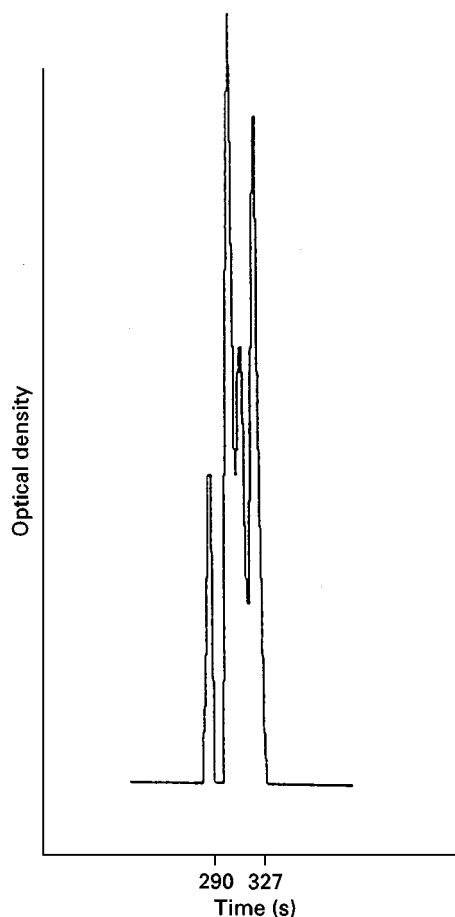


Figure 3 Fractogram of a mixture of four samples of Dow polystyrene latex of diameters 357, 234, 176 and 109 nm. 0.1 mM SLS, capillary $3\text{ m} \times 4\text{ }\mu\text{m}$. (Reprinted from Dos Ramos JG and Silebi CA (1989) An analysis of the separation of submicron particles by capillary hydrodynamic fractionation. *Journal of Colloid and Interface Science* 133(2): 302–320.)

Applications in Polymer Chemistry

Colloids/Latex

Some methods of polymer synthesis offer the possibility of preparing polymers with a defined average molecular weight with a narrow distribution (anionic initiation or modern controlled free-radical polymerization). This is important since some polymer properties are dependent on molecular weight and its distribution.

For certain applications it is the size which is the key parameter. For instance, it is the particle size which is important for rheological properties, film formation or protecting ability in relatively low-cost industrial coatings such as aqueous-phase paints and inks. Latexes of small particles have a lower viscosity than those of larger particles with the same percentage solids. They also have a better storage stability against sedimentation and further aggregation. In other applications, these 'water-borne' particles may also be high-value colloids for model compounds and reference materials. For instance, they are used as standards for calibration (membranes) or for packing chromatography columns. Surface modification allows many applications in biochemistry for diagnostic aids and purification. It is thus evident that accurate monitoring of diameter is important.

These particles are obtained in the free-radical emulsion polymerization heterogeneous process. Their diameter is around 100 nm, which can be dealt with in HDC. This process tends to be substituted by bulk and organic solvents processes, in order to reduce the use of solvents in the production of polymers. General interest in these particles is 'triple' fold: their regular and spherical shape, and the possibility of obtaining a predetermined diameter of a given value. This diameter does not depend on mechanical treatment, such as milling and sieving, but depends on the chemical and thermodynamic values of the process: size measurement is a way to determine the polymerization mechanism in relation to these parameters.

Polymerization kinetics As has been mentioned, a major use of HDC is related to colloids obtained by emulsion polymerization, a process which allows simultaneous high-polymerization rates and high-molecular weights. The rapidity of the HDC measurement is compatible with kinetic studies and monitoring during the polymerization. Eluted fractions may be characterized further by transmission electron microscopy (TEM) and analytical centrifugation to verify the effective existence of detected particles and to obtain a calibration curve. Photon correlation

spectroscopy (PCS) may be used for a simultaneous rapid analysis.

A normal emulsion system can be depicted as follows: a large fraction of the monomer is in large droplets (diameter around 1 μm); a small part of the monomer is dispersed in the aqueous phase either as an individual soluble molecule or as small aggregates stabilized by the surfactant, and called micelles (diameter around 5 nm). Various ionic and nonionic surfactants are used, besides steric ones, which are not as sensitive to electrolyte and pH effects. The initiator is in the aqueous phase: it is decomposed to active radicals by thermal activation or redox reaction. The primary radicals may add to soluble monomers molecules to form oligoradicals and/or enter into the micelle to give active particles. This is the first step of the polymerization up to a conversion of 5–10%: initiation or nucleation. The second step is the growth of these particles by consumption of the monomer contained in the large droplets. The number of particles remains constant up to 90% conversion, but their size increases. The rate of polymerization is constant during this second step. This rate (R_p) and number of particles (N) are governed by the concentration of monomer (M), initiator (I) and surfactant (S):

$$R_p = k_p [M] N/2 \quad \text{and} \quad N[I]^{0.4}[S]^{0.6}$$

k_p is the propagation rate constant.

Measurement of conversion and of particle size allows determination of the number of particles. A constant number of particles and an increase in their size are observed. The values may be correlated to concentration. Exponents may differ to those expected in the classical scheme, where particles are spherical and uniform in size. Some deviations may occur, such as additional nucleation by coagulation of precursor particles generating new particles and a second size distribution. They are of lower stability and have a slower rate of polymerization. Large aggregates may be formed by association of particles, as a result of insufficient stabilization. This leads to a broad or multimodal size distribution.

When industrial processes are discontinuous, the particles size of successive batches may differ. In order to correct this and obtain a constant quality, several batches are blended to deliver a uniform size distribution, corresponding to specific properties. Instead of performing physico-chemical measurements (rheology, surface tension) and end use tests, HDC is a rapid means of diagnosis.

Most of the literature on HDC is related to the separation of latexes. Conditions of elution – particularly the ionic strength – affect the separation,

but the surface charge density of the particles does not affect the separation factor. In contrast with polymers, the shear rate has little or no effect on particle size characterization. No deformation occurs when the particle is relatively rigid.

Modification of latexes To obtain large size latex, colloids obtained in a first step are polymerized further: successful results have been obtained with the method of Ugelstad.

Latexes are reactive to an extent depending on their stability. For instance, changes in size by the swelling of carboxylated styrene-butadiene latexes has been measured, according to changes in pH.

Flocculation of colloids in the presence of water-soluble ionic polymers or inorganic oxides has been observed by HDC in relation to other methods. Association of particulates under the effect of a thickener has been clearly demonstrated, though this association can be broken by intensive shear, and the same applies to aggregates.

Mini-emulsions

Mini-emulsions are oil droplets (50–500 nm) in water, stabilized by a surfactant (such as sodium lauryl sulfate) and a co-surfactant, which may be a long-chain alkane or a fatty alcohol with low water solubility. Their action is to reduce the oil diffusion from smaller to larger droplets. These mini-emulsions may also constitute an interesting polymerization system. Their stability depends on the relative concentration of components. An exponential decrease of droplet size has been observed when the concentration of cetyl alcohol is increased. The effect of the nature of the co-surfactant and ageing time has been studied. **Figure 4** shows chromatograms of a mini-emulsion at different times, corresponding to size differences: increase of diameter and decrease of dispersity occurs when cetyl alcohol is used. This is not observed when hexadecane is the co-surfactant.

Polymers

Dimensions of soluble polymers depend on molecular weight, nature of polymer, solvent type and temperature. A linear polymer is represented by an ideal random coil of a flexible chain, the radius of gyration being r_g . For actual polymers, requirements mean taking account of bond angles, hindered rotations and short-range intrachain interactions. Since polymer segments occupy space, this generates an 'exclusion volume', corresponding to an increase of dimensions; however 'unperturbed' dimensions, $\langle r_g^2 \rangle_0$, do not take solvent into account. Both interactions between

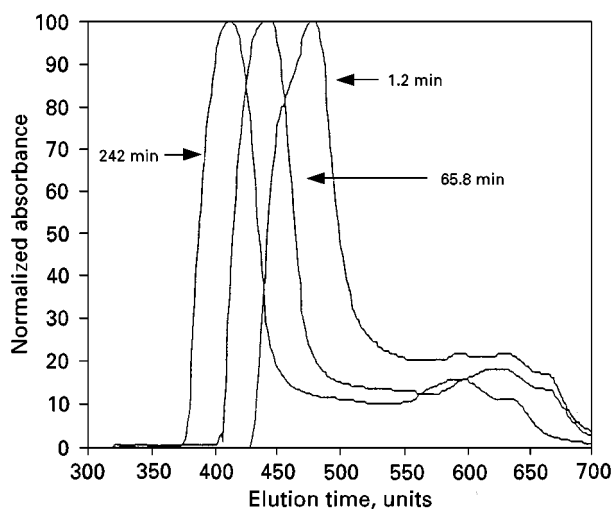


Figure 4 Fractograms at three different times for a toluene mini-emulsion prepared from a gel phase consisting of 10 mM SLS and 30 mM cetyl alcohol. (Reprinted from Miller CM, Venkatesan J, Silebi CA, Sudol ED and El-Aasser MS (1994) Characterisation of miniemulsion droplet size and stability using capillary hydrodynamic fractionation. *Journal of Colloid and Interface Science* 162: 11–18.)

the chains and between chain and solvent modify r_g . In a 'poor' solvent, these unperturbed dimensions mean that square of the radius of gyration $\langle r_g^2 \rangle_0$ is valid, since the polymer sphere is poor in the solvent. But in a 'good' solvent, it becomes $\langle r_g^2 \rangle = \alpha^2 \langle r_g^2 \rangle_0$, due to the expansion of the coil by the internal solvent molecules. For a given polymer, the unperturbed dimensions depend on solvent and temperature, corresponding to the θ conditions of Flory, with $\alpha = 1$. In these conditions, the a exponent of the Mark-Houwink viscosity law $[\eta] = KM^a$ is 0.5. Finally, applying classical theories of polymers in solution allows a relationship between size and molecular weight to be obtained. But the question is: what radius is to be considered in a chromatography experiment? In other words, is the apparent radius obtained in HDC a useful answer? Viscometric measurements show that polymer chains behave rather as non-free-draining (solvent immobilized in the interior of the chain) rather than a permeable coil. This means that the hard-sphere model is a reasonable approach. It may be represented by the hydrodynamic radius r_h , the value of which is about $0.7 r_g$.

Polymer molecules which are in a laminar flow near the wall in a tube are in a high stress domain and can be elongated and oriented. Those in the centre of the tube are in a low stress region, so that they differ in entropy. The entropy gradient in the tube leads to a migration of the molecules away from the wall, called 'stress-induced diffusion'. This is favoured by a high flow rate, small tube diameter and high

molecular weight. A second feature is a result of elongation: the cross-section of the chain is decreased and the molecule is eluted later. A third factor may affect the elution time: the fluid inertia induces a radial migration of the molecules towards an annular region of equilibrium, which is about at $0.6R$ (R is the capillary radius) of the centre of the tube (also called the 'tubular pinch effect'). This is more effective in capillary tubes than in packed columns.

Excellent results have been obtained for the separation of numerous polymers in solution, on columns packed with very small non-porous silica particles. As an example, a set of four polystyrenes (molecular weight differing by a ratio of 2) in THF was fully separated in less than 2 min (Figure 5). Two sets of polybutadienes (PB) and polyisoprenes (PIP) in THF at a lower flow rate were completely separated in 11 min. The maximum separation factor was about 1.3. An experimental calibration curve (molecular weight as a function of R_i) may be obtained for each polymer and fits theoretical predictions. A universal calibration curve is obtained when plotting relative size (chain radius r_p/R) as a function of $1/R_i$ (Figure 6). Alternatively, this means that different polymers of similar molecular weight may be separated, as shown in Figure 7. Other solvents of different thermodynamic properties are dioxane (PS, PB, PIP), toluene, methanol, ethyl methyl ketone and acetonitrile (PMMA), used in θ conditions (minimum interactions between chain and solvent, for a min-

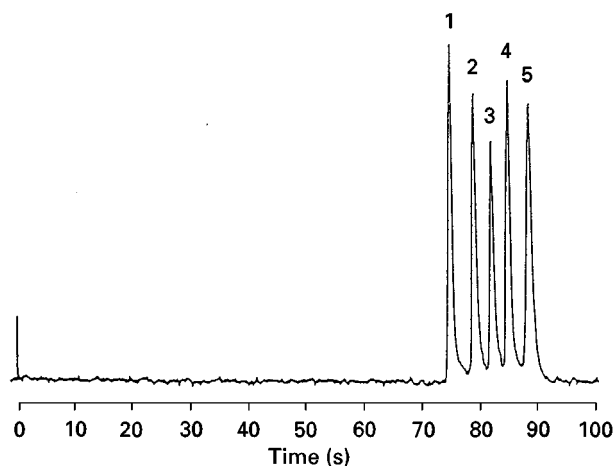


Figure 5 High-speed HDC of polystyrenes (1: 775 000; 2: 336 000; 3: 127 000; 4: 43 900; 5: toluene as marker) dissolved in THF on a column 150×4.6 mm, packed with $1.50\text{-}\mu\text{m}$ nonporous silica particles. UV detection. (Reprinted from Stegeman G, Kraak JC, Poppe H and Tijssen R (1993) Hydrodynamic chromatography of polymers in packed columns. *Journal of Chromatography A* 657: 283–303.)

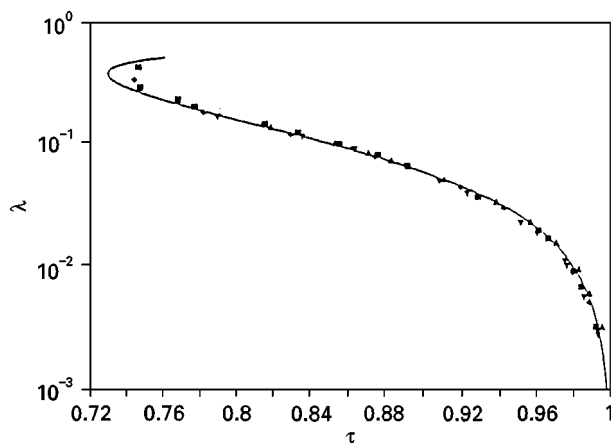


Figure 6 Universal calibration curve: $\lambda = r_p/R$ and $\tau = 1/R_i$. (Reprinted from Stegeman G, Kraak JC, Poppe H and Tijssen R (1993) Hydrodynamic chromatography of polymers in packed columns. *Journal of Chromatography A* 657: 283–303.)

imum coil size). The polymer size is effectively decreased, and the elution time is very sensitive to small changes in temperature around θ .

Combined HDC and SEC fractionation has been shown to expand the elution scale and allow complete separation of a wide range of polystyrenes, using porous silica (Figure 8) and polymeric packings. This offers interesting possibilities for elution of very high-molecular-weight materials. The

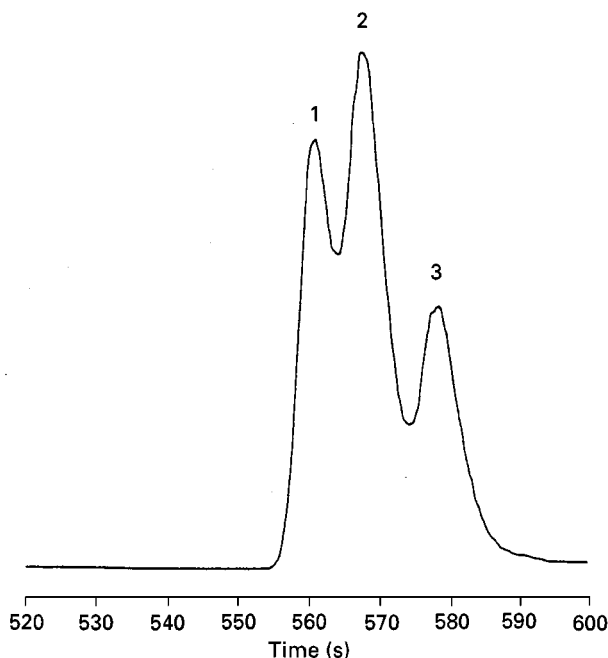


Figure 7 Three different polymers of similar molecular weight in THF. 1: PB 330 000; 2: PIP 295 000; 3: PS 336 000. (Reprinted from Stegeman G, Kraak JC, Poppe H and Tijssen RJ (1993) Hydrodynamic chromatography of polymers in packed columns. *Journal of Chromatography A*, 657: 283–303.)

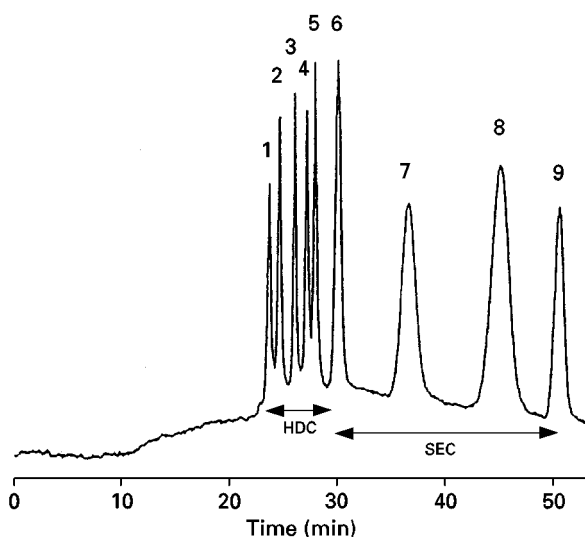


Figure 8 HDC-SEC separation of polystyrenes (10^{-3} molecular weight 1: 4000; 2: 2200; 3: 775; 4: 336; 5: 127; 6: 43.9; 7: 12.5; 8: 2.2; 9: toluene as marker) on three columns of 15 cm each, packed with Hypersil 3- μ m porous particles. (Reprinted from Stegeman G, Kraak JC, and Poppe H (1991) Hydrodynamic and size-exclusion chromatography of polymers of porous particles. *Journal of Chromatography* 550: 721-739.)

calibration curve on silica (**Figure 9**) clearly shows HDC and SEC domains (higher molecular weight and steeper slope for HDC). With narrow-pore cross-linked polystyrene, only one classical sigmoidal SEC curve is obtained.

Some authors have attempted to determine molecular weight or size for very large polymers, for instance water-soluble ones, which are used as viscosifiers in

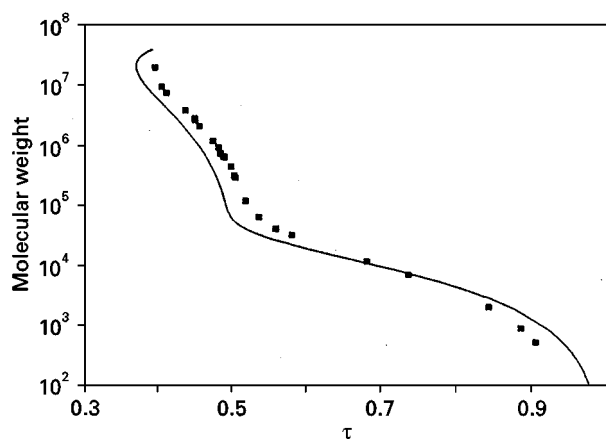


Figure 9 HDC-SEC calibration graph (molecular weight as a function of the ratio of the solvent to polymer migration velocity) with polystyrene on three columns of 15-cm each, packed with Hypersil 3- μ m porous particles. (Reprinted from Stegeman G, Kraak JC and Poppe H (1991) Hydrodynamic and size-exclusion chromatography of polymers on porous particles. *Journal of Chromatography* 550: 721-739.)

oil-recovery wells. The porous structure induces converging and diverging flow channels, where polymer solutions have non-Newtonian behaviour. At high flow rate, under pressure and passing through small pores, polymer coils may undergo chain extension and orientation which modify their size and viscosity.

Flow and dynamic behaviour of flexible and rigid macromolecules in a packed bed has been studied comparatively. Partially hydrolysed (10%) polyacrylamide (molecular weight higher than 12 million) was a flexible model of a random coil, xanthan polysaccharide (molecular weight over 2 million) a model for a rigid backbone and tobacco mosaic virus as a rodlike structure (length 0.7 μ m, diameter 15 nm). They have been eluted on a column packed with an ion exchange resin (diameter 11 μ m). Deformation of the initial flexible linear polymers occurs, since their apparent size changes with flow rate, at a value corresponding to unity for De , the Deborah number, defined as the ratio of hydrodynamic forces to Brownian forces. The polymers which have been strongly sheared or sonicated before the chromatographic analysis do not show this change in size, since the chain has been extensively broken. The effective size of rodlike polymers decreases when the flow rate increases: this is accounted for by orientation. For xanthans, two domains are observed when the flow rate increases: constant size, then a decrease after a flow value corresponding to the chain elongation (**Figure 10**). The slope (-0.5) of the high flow rate region fits that of the dumbbell model. Xanthan

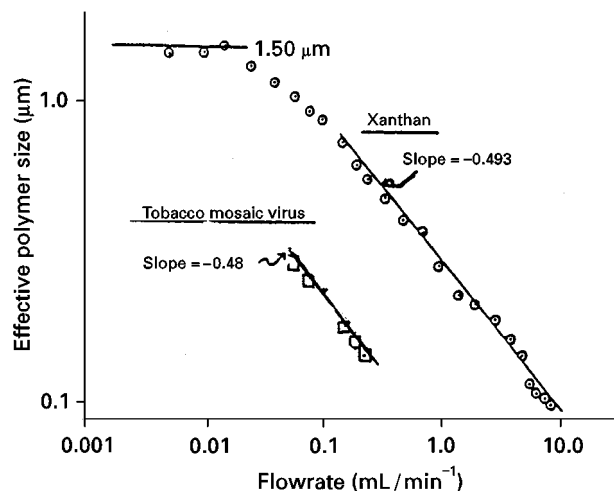


Figure 10 Effective size of xanthan and tobacco mosaic virus as the flow rate is varied in a column 248×10 mm packed with 11- μ m ion exchange particles; eluent with 2 g L $^{-1}$ nonionic surfactant and 2 mM Na $_3$. (Reprinted from Hoagland DA and Prud'homme RK (1989) Hydrodynamic chromatography as a probe of polymer dynamics during flow through porous media. *Macromolecules* 22: 775-781.)

polysaccharide behaviour has also been studied on nonporous SiC particles.

Biomaterials

Biomembranes are efficient separating materials. They are found in cells and are an excellent model for synthetic chemistry. They have many applications such as the separation of enantiomers, isotope enrichment, photosynthesis, and catalysis. Liposomes are used as drug-delivery systems and membranes, so their size and the amount of the transported material are important factors. Elution of liposomes from egg yolk lecithin has been performed on a column packed with porous inert glass, at different ionic strengths. An equivalent capillary radius R is given by the formula $R = d/[2 - 2(2 - R_f)^{1/2}]$, where d is the diameter of a colloidal particle, known from calibration with polystyrene standards. Recycling of the sample improves the separation (Figure 11).

Separation of natural products such as milk or globular proteins is also of interest. Preliminary results have been obtained for very large proteins on small nonporous glass spheres (Figure 12). Decreasing the ionic strength improves the separation. For common proteins, which require smaller particle sizes, the difficulty lies in the affinity of silica to proteins. The alternatives are to modify chemically the OH groups by grafting an inert moiety, or using an aqueous buffer, to repel proteins from the surface.

Inorganic Compounds

Silica or carbon black are widely used in various industries as fillers, the effect of which depends on the size. A variety of other compounds has

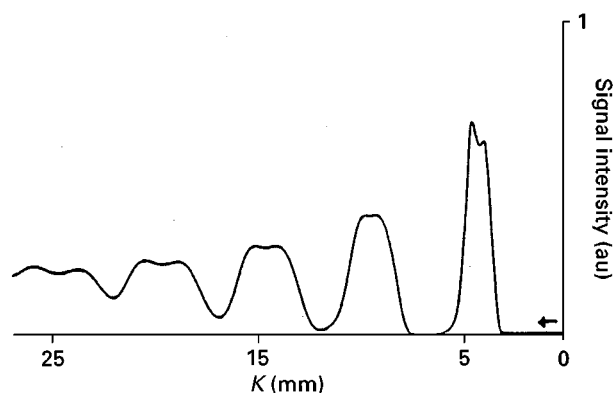


Figure 11 HDC of liposomes from egg yolk lecithin on inert glass particles (125–180 μm) in a $300 \times 15\text{-mm}$ column, eluent with 0.02 mM NaCl; filtration on 0.3- μm pore size, four recycles. (Reprinted from Molina FJ, Vila AO, Martos MJ and Figueruelo JE (1991) Estimation of the size of liposomes by modified HDC. *Journal of High Resolution Chromatography* 14: 590–592.)

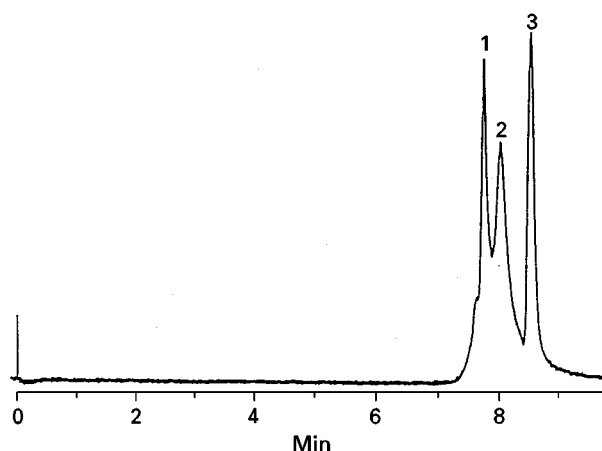


Figure 12 Separation of proteins on nonporous silica gel 2.1 μm particles, column $250 \times 4.6\text{ mm}$, sodium borate 5 mM, pH = 9. 1: thyroglobulin; 2: γ -globulin; 3: glycine. (Reprinted from Kraak JC, Oostervink R, Poppe H, Esser U and Unger KK (1989) Hydrodynamic chromatography of macromolecules on 2 μm nonporous spherical silica gel packings. *Chromatographia* 27(11/12): 585–590.)

been examined: paper fibres, cement, clay, metals and metal oxides of Fe, Ti, Al, silver halides. It has been found that a difference in density does not alter the elution order. The calibration based on polystyrene latexes remains valid for carbon black particles of density 1.86, and the results agree with those obtained by photon correlation spectroscopy.

Applications are also found in geology.

Conclusion

Despite its ability to provide useful results in size separations and determination, HDC is still only infrequently used. However, efforts are being made to improve its resolution and ease of use. Progress in synthesizing small size particles for packings and in narrow capillaries effectively allows rapid and excellent separation. Combined HDC and SEC offers new possibilities for determination of size and molecular weight of polymers in solution. HDC is also of interest in fundamental studies of flow behaviour in tubing or pores which are encountered in 'transport technology of materials': various fluids, solid particles, waste in rocks and soils, as well as in factories or pipes. In such work silica has the interesting advantage of being a hard spherical model for HDC mechanism studies.

See also: II/Chromatography: Liquid: Mechanisms: Size Exclusion Chromatography. Particle Size Separation: Theory and Instrumentation of Field Flow Fractionation.

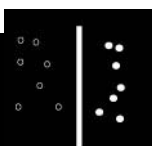
Further Reading

- Barth HG (ed.) (1984) *Modern Methods of Particle Size Analysis*. New York: John Wiley.
- Dos Ramos JG and Silebi CA (1990) Size analysis of simple and complex colloids in the submicron range using capillary hydrodynamic fractionation (CHDF). *Polymer Material Science Engineering* 62: 73–76.
- Guillaume JL, Pichot C and Revillon A (1985) Approaches cinétiques du mécanisme de la copolymérisation styrène-acrylate de butyle. *Die Makromolekulare Chemie Suppl.* 10/11 69–86.
- Revillon A and Boucher P (1989) Capillary hydrodynamic chromatography: optimization study. *Journal of Applied Polymer Science Symposium Edition* 43: 115.

Revillon A, Boucher P and Guiland JF (1991) Comparison of packed and capillary columns in hydrodynamic chromatography. *Journal of Applied Polymer Science: Symposium Edition* 48: 243–257.

Ugelstad J, Kaggerud KH, Hansen FK and Berge A (1979) Absorption of low-molecular weight compounds in aqueous dispersions of polymer-oligomer particles. 2. A two step swelling process of polymer particles giving an enormous increase in absorption capacity. *Die Makromolekulare Chemie* 180: 737–744.

HYDROGEN RECOVERY USING INORGANIC MEMBRANES



R. Hughes, University of Salford, Salford, UK

Copyright © 2000 Academic Press

Introduction

Global annual production and utilization of hydrogen now total some $6 \times 10^{11} \text{ Nm}^3$. Of this amount, approximately 50% is produced by steam reforming or partial oxidation of natural gas. Other sources include electrolysis of water and recovery from refinery off-gases. The main use of bulk hydrogen includes synthesis of ammonia, hydrotreating of heavy petroleum feedstocks, hydrogenation of vegetable oils and manufacture of transformer steels and other metallurgical heat treatment operations. More recent applications where high purity hydrogen is required include semiconductor processing and fuel cells. To obtain high purity several methods may be adopted, such as pressure swing adsorption and cryogenic technology. However, both these methods have disadvantages, including cost and degree of purity obtained; the cryogenic method gives purities ranging from 90 to 98% only.

Membranes can provide an efficient low cost means of separation and purification for hydrogen. Although polymeric membranes are well proven for gas separation, they are limited to temperatures not much greater than 250°C whereas, in many applications, high temperature processing is required. Inorganic membranes have shown considerable develop-

ment in recent years and, apart from their high temperature stability, they have in general much higher fluxes than polymeric membranes.

Inorganic membranes suitable for the recovery and purification of hydrogen may be divided into two classes, namely, porous and dense membranes. The former includes materials such as alumina, silica, zirconia and porous metals, for example, stainless steel. The dense membranes include palladium and its alloys, in which the unique permeation properties of palladium to hydrogen are utilized.

Porous Membranes

To achieve appropriate separations with this type of membrane, the pore size needs to be small. However, to achieve a suitable gas permeation rate through the membrane, the membrane should be as thin as possible. To meet this requirement, a composite structure is usually adopted in which a thin finely microporous separation layer is supported on a thicker more open microporous material. Such structures have now been developed by a number of procedures.

The various possible gas permeation mechanisms applicable to porous membranes are illustrated in **Figure 1**.

In this figure, the progression from Knudsen diffusion to molecular sieving is in parallel with increasing permselectivities (it should be noted that viscous flow gives no separation). The separation factor for all the processes depends strongly on the pore size and its distribution, the temperature, pressure and the

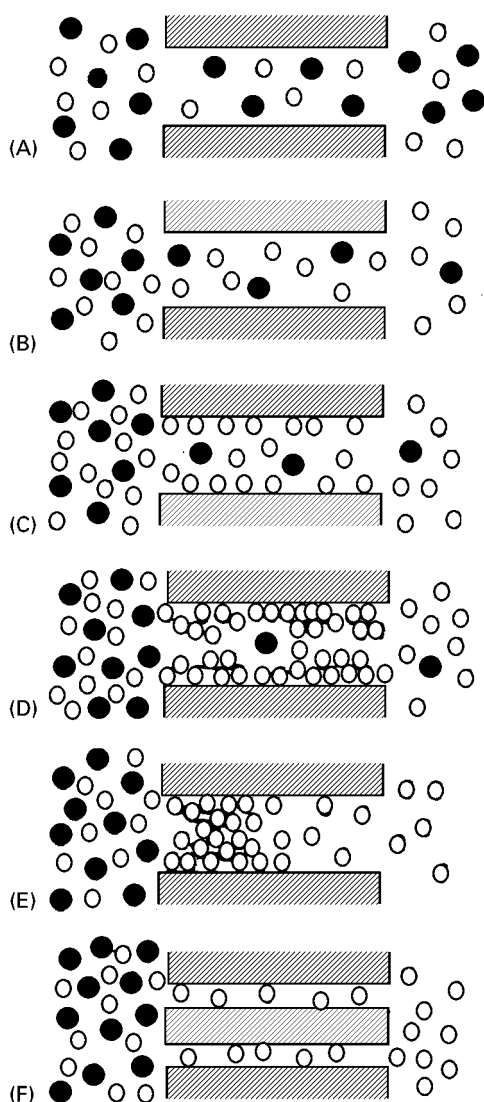


Figure 1 Transport mechanisms in porous membranes. (A) Viscous flow. Pore diameter is greater than gas mean free path – no separation. (B) Knudsen flow. Pore diameter is smaller than gas mean free path – separation is proportional to the square root of M_A/M_B . (C) Surface diffusion. Absorbed gas on the pore wall contributes to total gas flow. Transport of condensable vapour is enhanced. (D) Multilayer diffusion. Transport of absorbed gases is dominant and so condensable vapours have high transport rates. (E) Capillary condensation. Absorbed gas completely blocks pores. There is no transport of nonabsorbed gas. (F) Molecular sieving. Pores are so small that they begin to filter small molecules from large ones. Transport of small molecules is preferred. Modified with permission from Saracco G and Specchia V (1994) Catalytic inorganic membrane reactors: present experience and future opportunities. *Catalysis Review, Science and Engineering* 36: 305.

nature of the membrane and the permeating molecules. Because of these factors, porous membranes are more versatile in their applications compared with dense metal membranes, because they can be used for

separation of gases other than just hydrogen and oxygen only. Conversely, porous membranes show significantly lower selectivities compared with dense membranes.

Viscous flow occurs when the mean free path of the gaseous molecules is much less than the pore diameter. Under these conditions, molecule–molecule collisions are much more frequent than collisions between the molecules and the walls of the pores. The mean free path, λ , of a gas molecule is given by:

$$\lambda = kT/(2\sigma p) \quad [1]$$

where k is the Boltzmann constant, T the absolute temperature, p the absolute pressure and σ the collision diameter of the molecule. Thus, λ will increase with increase in temperature and with decrease in pressure. Calculated values of λ are shown in Table 1 for a number of gases. Since the pore diameter of many separation membranes is of the order of 1–4 nm it can be seen that mean free paths under conditions often encountered in many catalytic processes are greater than the pore diameter and therefore Knudsen diffusion can be the operating mechanism for many current membranes.

In Knudsen flow, as shown in Figure 1B, the molecules collide on average more frequently with the pore walls than with one another when the mean free path becomes much greater than the pore diameter and absolute pressure does not affect the flux if this flow is fully developed. With a binary mixture, the highest separation factor achievable is given by the ratio of the inverse of the square roots of the molecular weights. Hence, small molecules are preferentially transported across the membrane and the greatest potential is for separation of hydrogen from other gases. Even in this case, however, separation is limited: that for a hydrogen–nitrogen mixture is only 3.74 at best.

Table 1 Mean free paths for representative gases (nm)

Gas	Gas diameter (nm) σ	Temperature 500 K		Temperature 800 K	
		0.1 MPa	1.0 MPa	0.1 MPa	1.0 MPa
H ₂	0.29	183	18.3	293	2.9
CO	0.37	113	11.3	181	18.1
N ₂	0.37	111	11.1	177	17.7
CO ₂	0.39	102	10.2	164	16.4
C ₄ H ₁₀	0.50	62	6.2	100	10.0
C ₆ H ₁₂	0.61	42	4.2	67	6.7

Surface flow occurs (Figure 1C) when one of the permeating molecules can be preferentially physisorbed or chemisorbed on the pore walls and migrates along the surface. Surface diffusion increases the flux of the more strongly adsorbed components while reducing the contribution of the gas phase diffusion to total gas transport by decreasing pore diameter. Surface flow becomes more important as the pore size is reduced. Also, the effective pore diameter is further decreased by adsorption of the relevant species on the walls of the pores and thus obstructing the transfer of the other species through the free volume of the pores. As the temperature increases, most species will desorb from the surface and surface diffusion becomes less important.

Multilayer diffusion has been postulated to occur when molecule-surface interactions are very strong. The process is shown diagrammatically in Figure 1D. It may be regarded as an intermediate flow regime between surface flow and capillary condensation.

When the pores are small enough and one of the components of the gaseous mixture to be separated is a condensable vapour, absorbed vapour on the surface of the pore walls may be sufficient for the condensate to block gas-phase diffusion through the pore (Figure 1E). The condensate fills the pores and then evaporates at the permeate side, which has to be maintained at low pressure. In this case, only the condensed vapour permeates the membrane and nonabsorbed gases are almost totally retained by the membrane.

Molecular sieve transport occurs when pore diameters are small enough to permit only smaller molecules to permeate, while larger ones are excluded from entering these molecular-sized pores (Figure 1F). This type of process is frequently referred to as shape-selective diffusion. A necessary condition for effective separation by this means is that the pore size distribution is monodisperse and that the pores are very small – of the order of 0.5–1.0 nm.

From the above considerations it can be seen that a small pore size is necessary to obtain adequate separations. Since very finely porous membranes must necessarily have low permeabilities, useful fluxes are only obtained if the separating layer is made very thin. This has led to the evolution of asymmetric membranes in which the thin separation layer is supported on a wide pore matrix of similar material. Composite membranes have been developed in which different materials are used for the separation and support layers of the membrane. Molecular sieve membranes have been produced in this manner. An interesting development is the use of nanoporous carbon membranes for gas separation.

These membranes, which are produced by carbonization of polymers, have pore sizes in the molecular sieve range (0.5–0.6 nm) and operate by a combination of selective adsorption and surface flow. Rao and Sircar have shown that these nanoporous membranes can separate hydrogen from carbon dioxide and hydrocarbons with high selectivity. Experiments with silicalite zeolite for the separation of hydrogen and butane mixtures by Moulijn's group at Delft have shown that butane excludes hydrogen from the pores of the silicalite at room temperature by butane adsorption. However, at high temperature where adsorption effects are reduced, hydrogen permeation now predominates. These examples show that there is considerable scope for hydrogen separation from gas mixtures by using membranes with very small pore sizes and utilizing the adsorption and surface diffusion behaviour of the species involved.

Dense Membranes

A second type of hydrogen-separating membrane is the dense membranes made from various metals, metal alloys and metal oxides. Hydrogen permeates a number of metals at high temperatures, including tantalum, niobium, vanadium nickel, iron, copper, cobalt and platinum. Alloys of these and other metals also possess high permeation rates for hydrogen together with certain metal oxides such as perovskites, which permeate hydrogen ions at temperatures in excess of 700°C. However, the main materials developed for hydrogen permeation are palladium and its alloys. This is because of the very high level of hydrogen absorption possible with these materials. Pure palladium absorbs 600 times its volume of hydrogen at room temperature, with the various palladium alloys absorbing comparable quantities. Although metals such as niobium and tantalum, also possess the ability to absorb large quantities of hydrogen, the formation of surface oxide films inhibits the ingress of hydrogen into the bulk metal and consequently these metals cannot be used to permeate hydrogen as such. Attempts have been made to overcome this problem by deposition of thin layers of platinum or palladium but the results have not been entirely successful, due in part of the formation of intermetallic compounds.

Consequently, palladium and/or palladium alloys represent the main dense metals currently favoured for membranes for selective permeation of hydrogen because of the high hydrogen permeation rates achievable at temperatures less than 500°C. However, below a critical temperature of 300°C and a critical pressure of 20 bars, the hydrogen-palladium system exhibits two-phase behaviour. Early experiments with palladium membranes resulted in

mechanical failure due to the expansion and contraction of the metal lattice as hydrogen was absorbed and released. Alloying palladium with other elements such as silver, yttrium or cerium enables this difficulty to be overcome and an alloy of palladium with, for example, about 23% silver has been shown to be stable and have the optimum permeation rate for hydrogen.

Hydrogen Transport in Metal Membranes

Hydrogen transport through metal membranes is a multi-step process, as illustrated in **Figure 2**. Hydrogen molecules in the feed gas are adsorbed on to the metal surface where they dissociate into atoms. These atoms then diffuse through the metal to the downstream (permeate) side of the membrane where they recombine to form hydrogen molecules on the surface. These molecules are finally desorbed into the permeate gas stream. The process is selective, in that only hydrogen is transported through the membrane; other gases are excluded, so that in theory the membranes should have infinite selectivity. However, due to a number of factors, this does not occur, although very high selectivities can be attained.

Depending on which of the above steps is controlling, the exponent of the pressure driving force for the overall permeation will change. For diffusion control by hydrogen atoms, which process is normally attained at high temperatures, the overall hydrogen flux (J) will be given by:

$$J = K(p_h^{0.5} - p_l^{0.5}) \quad [2]$$

where p_h and p_l are the feed and permeate side pressures of hydrogen respectively.

However, if adsorption and/or dissociation of hydrogen into atoms is the controlling step then

the pressure exponents will tend to a value close to unity.

Metal Composite Membranes

Palladium-silver alloys have been used for a number of years for preparation of ultra-pure hydrogen for laboratory use. In recent years larger units have been made for the electronics industry. These membrane modules typically contain a number of small diameter alloy tubes with a metal wall thickness of about 50 μm . Sheet palladium alloys have also been used successfully for separation of hydrogen in reaction systems by Gryaznov and co-workers in Russia. However, the use of metal membranes alone has two serious disadvantages. If the permeation rate of hydrogen through the metal is diffusion-controlled, then the hydrogen flux is inversely proportional to metal thickness; most pure metal-alloy systems require a finite thickness to withstand the necessary pressure differential inherent in the separation process. Associated with this increased metal thickness is the material cost of palladium and its alloys.

Because of these factors, a number of methods have been proposed to overcome this problem, but essentially the common feature is to deposit the palladium on to a porous support material. The aim has been to obtain thin films of thickness ranging from 1 to 10 μm , but much thinner films have been produced by some investigators. The danger is that, with very thin films, the likelihood of pinholes being present increases considerably. Thin films in the micron range will give greatly increased fluxes, but the main difficulty is to produce films without cracks and to have good adherence to the support material. Substrates which have been used include porous glass, aluminas, silica, zirconia and stainless steel, although other porous materials have also been tried. The main

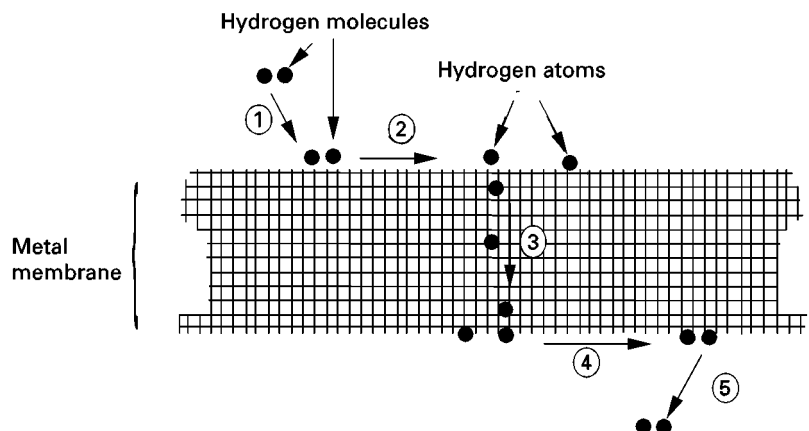


Figure 2 Permeation of hydrogen through metal membranes. 1, Sorption; 2, dissociation; 3, diffusion; 4, reassociation; 5, desorption.

techniques which have been developed for the deposition of thin films of palladium and palladium alloys on to porous substrates include:

1. magnetron sputtering
2. electroless plating
3. chemical vapour deposition
4. physical vapour deposition (thermal evaporation)
5. flame pyrolysis

There is some distinction in the way which palladium is deposited by these methods. The magnetron sputtering and vapour deposition methods tend to produce surface films whereas the chemical process of electroless plating can also act as a pore-plugging process. It has been found by a number of investigators, including the present author, that in comparing the suitability of α - and γ -alumina substrates for electroless plating, the wider pore α -alumina gives a more pinhole-free deposition. This has been attributed to the tendency of the electroless plating process to plug the pores; the more accessible wider pore mouths of the α -alumina facilitate entry of the depositing palladium.

In recent years the use of porous stainless steel as a support medium has been investigated since, although the pore sizes of stainless steel are currently larger than those of ceramic materials, this is compensated for by the robustness of the stainless steel and its potentially easier fabrication into an appropriate membrane module.

Use of composite membranes based on either ceramic or stainless steel supports is able to provide hydrogen permeation fluxes of $10^{-6} \text{ mol m}^{-2} \text{ s}^{-1} \text{ Pa}^{-1}$ or better with hydrogen-nitrogen selectivities in the range of 1000–5000. These results are suitable for a number of processes for hydrogen recovery, which are currently under evaluation.

Technical Challenges to the Use of Membranes for Hydrogen Recovery

Membranes used for separation of hydrogen from other gases at high temperature should possess the following features:

1. thermal and chemical resistance
2. crack-free
3. small pore diameters (porous membranes)
4. large surface areas for membrane modules
5. require high temperature seals
6. composite membranes must retain adherence of the separation layer under thermal cycling
7. fouling of the membranes must be avoided

Some of these problems are being overcome currently. A major problem is that of sealing the individual membrane units into a module. If cylindrical tubes

are to be used as membranes, then a shell-and-tube configuration as in conventional heat exchangers would seem to be the most favourable configuration, with the individual membrane tubes sealed into the end-plates of the shell. A stainless steel supported membrane tube would clearly have advantages in this case and would be preferable in terms of robustness compared to ceramic tubes.

Cost is a further factor. Although palladium is frequently cited as a major cost, it should be pointed out that, at present, the costs of porous ceramic or stainless steel support tubes are significant. No doubt these costs will decrease with increased production, but these represent a current constraint on applications.

Present Status and Potential Developments

Because of the increased demand for hydrogen as a clean fuel and for newer applications where very high purity is required (current semiconductor processing requires hydrogen with impurities of 10 p.p.b. or less), there will be a continued demand for processes to fill this need. Membrane technology can provide a significant input into this demand. Both porous and dense membranes can be utilized to provide recovery of hydrogen from process streams, but dense membranes are necessary at present to provide hydrogen of high purity. Although palladium and palladium alloys have been used almost entirely for production of pure hydrogen, other metals such as niobium, tantalum and vanadium possess, in theory, good permeating properties and are less expensive than palladium. The problem of the surface oxide layer inhibiting permeation of hydrogen is being tackled with some success and further efforts will undoubtedly lead to better performance from these materials.

With porous membranes, perhaps the most important developments are likely to occur with zeolite membranes. The development of these, either as individual membranes or in composite form on another support material, will undoubtedly open up a new area of application for inorganic membranes for hydrogen recovery and purification.

Further Reading

- Buxbaum RE and Kinney AB (1996) Hydrogen transport through tubular membranes of palladium-coated tantalum and niobium. *Industrial and Engineering Chemistry Research* 35: 530.
- Dixon AG (1999) *Innovations in Catalytic Inorganic Membrane Reactors, Catalysis*, vol. 14. Cambridge: Royal Society of Chemistry.

- Edlund DJ and McCarthy J (1995) The relationship between intermetallic diffusion and flux decline in compartmental membranes: implications for achieving long membrane lifetime. *Journal of Membrane Science* 107: 147.
- Gryaznov VM (1986) Hydrogen permeable membrane catalysts. An aid to the efficient production of ultra-pure chemicals and pharmaceuticals. *Platinum Metals Review* 30: 68.
- Hughes R (1996) Applications in gas and vapour phase separations. In: Scott K and Hughes R *Industrial Membrane Separation Technology*, pp. 114–150. London: Blackie Academic and Professional.
- Kapteijn F, Bakker WJW, Van der Graaf J *et al.* (1995) Permeation behaviour of a Silicalite-1 membrane. *Catalysis Today* 25: 213.
- Keizer K, Ulhorn RJR and Burggraaf TJ (1995) Gas separation using inorganic membranes. In: Noble RA and Stern SA (eds) *Membrane Separations Technology, Principles and Applications*, pp. 553–588. Amsterdam: Elsevier Science.
- Knapton AG (1977) Palladium alloys for hydrogen diffusion membranes – a review of high permeability materials. *Platinum Metals Review* 21: 44.
- Lewis FA (1967) *The Palladium-Hydrogen System*. London: Academic Press.
- Li A, Liang W and Hughes R (1998) Characterisation and permeation of palladium/stainless steel composite membranes. *Journal of Membrane Science* 149: 259.
- Rao MB and Sircar S (1993) Nanoporous carbon membrane for gas separation. *Gas Separation and Purification* 7: 279.

IMMOBILIZED BORONIC ACIDS: EXTRACTION



P. Martin and I. D. Wilson,
AstraZeneca Pharmaceuticals,
Macclesfield, Cheshire, UK

Copyright © 2000 Academic Press

Introduction

With the exceptions of antibody and molecular imprint-based methods, most solid-phase extractions rely on relatively nonspecific nonpolar van der Waals or ionic interactions. Another exception to the use of nonspecific interactions involves the use of reversible covalent bond formation with vicinal diols, or similar structures, in the target analyte with immobilized boronic acids. Clearly, the potential to exploit this type of interaction is limited but, where it can be exploited, highly specific solid-phase extraction (SPE) methods can result. Such methods, based on the use of boronic acids immobilized on materials, such as sepharose gels or phenylboronic acid (PBA) covalently linked to silica gel, have provided the basis for a number of SPE methods, as described below.

Mechanism of Interaction of Analytes with Immobilized PBA

The extraction mechanism that results in the formation of cyclic boronates is illustrated in **Figure 1**. In order for the reaction to proceed, the boronate must be in the reactive -B(OH)_3^- form, which is readily obtained by equilibrating the phase with an alkaline buffer. When the sample is applied, the covalent bond forms only with analytes possessing suitable

functional groups, e.g. vicinal diols, found in sugars or catechols. Other functional groups which can form covalent bonds with boronic acids include α -hydroxy acids, aromatic O-hydroxyacids and amides, 1,3-dihydroxy-, diketo-, triketo- and aminoalcohol-containing compounds. With formation of the covalent bond, the analyte is strongly bound to the phase, which may then be washed with strongly eluotropic solvents to remove nonspecifically retained contaminants (an alkaline pH must be maintained). Analytes can then be recovered using an acidic buffer/solvent, which hydrolyses the covalent bonds to liberate retained compounds and return the PBA to the -B(OH)_2 form.

As well as these specific interactions with PBA, a number of nonspecific interactions can also occur with residual silanols, the aminopropyl group via which the PBA is attached to the silica, and the phenyl ring itself, which offers the opportunity for π - π interactions. In addition, the boronic acid can act as a hydrogen bond donor, cations can also bind to the boronic acid, and there is the potential for the formation of charge-transfer complexes with unprotonated amines. All of these interactions may happen when performing an extraction, and care must be taken to ensure that the extraction scheme is optimized to the required boronate retention mechanism if the maximum specificity is to be obtained.

Buffer Selection

The first criterion to ensure a good extraction efficiency is to select a buffer for extraction on to

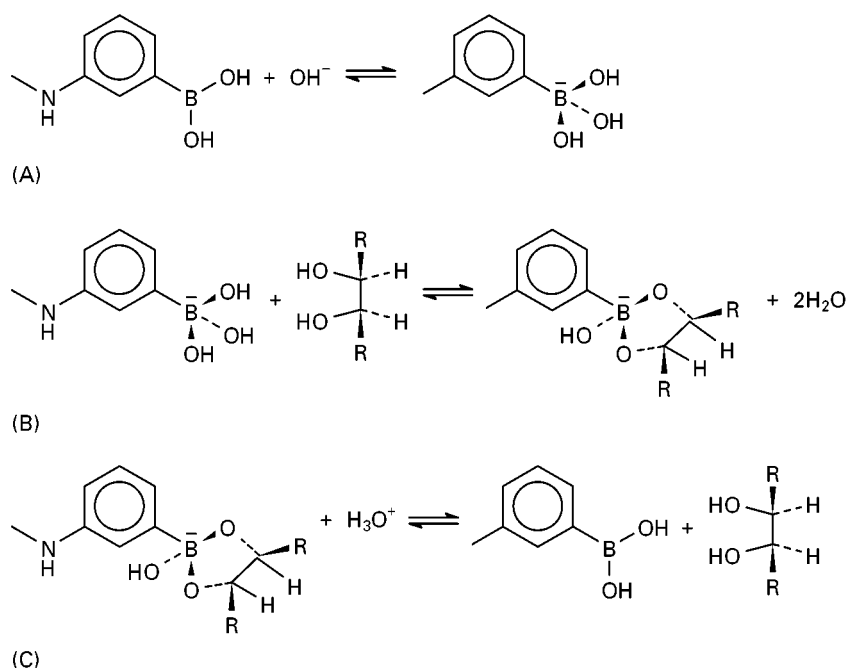


Figure 1 Mechanism of boronic acid extraction. (A) Activation of boronic acid in the presence of alkali; (B) formation of a covalent bond with a vicinal diol; (C) the use of acid to break the covalent bond and regenerate the boronic acid and the free diol.

PBA with an alkaline pH for the conditioning and sample application steps. Equilibration can be performed with, e.g. $0.1\text{--}1.5\text{ mol L}^{-1}$ buffer at pH 10–12 and then $0.01\text{--}0.05\text{ mol L}^{-1}$ buffer at pH 8–8.5. Zwitterionic buffers such as HEPES, glycine, diglycine and morpholine offer advantages and all have been used in this type of application. Clearly, buffers which can form covalent adducts with PBA are to be avoided, for the obvious reason that they eliminate covalent bond formation with the analyte. Such buffers include bicine, tricine, tris and 1',2',3'-ethanolamine.

Having obtained retention, analytes can be recovered by reducing the pH of the eluent to 5 or below. Typically acetic, trifluoroacetic and phosphoric acids may be used, with the addition of an organic modifier to help overcome nonpolar or silanophilic secondary interactions. Occasionally, the covalent adduct is sufficiently stable to require the addition of lactic or salicylic acid to the eluting buffer. Alternatively, elution with borate-containing buffers can be employed when acid-labile analytes are present.

Applications

Endogenous Biochemicals

Adenosine, catecholamines, dopamine, DOPA and related substances A major field of application in

the use of SPE with immobilized boronates (both gels and silica-based materials) is the extraction of various endogenous substances, especially catecholamines, l-dihydroxyphenylalanine (DOPA) and related materials, from biofluids. However, here we have concentrated on descriptions of the more recent procedures, generally involving the use of silica-based materials.

PBA gels have been employed in the extraction of nucleosides from biological samples for several studies, including the isolation of inosine and adenosine from human plasma. Methods have also been described for the simultaneous extraction of the adenosine and dopamine from human urine using a silica-based PBA phase. In this case extraction was performed using 100 mg PBA, activated by washing first with 5 mL of 0.1 mol L^{-1} formic acid followed by 5 mL pH 8.8 ammonium acetate buffer (0.25 mol L^{-1}). Urine (0.5 mL, pH 8.8) containing (\pm)-isoproterenol and 2-chloroadenosine, was allowed to flow through the sorbent bed until the liquid meniscus just reached the top of the layer, at which point 1 mL of pH 8.8 ammonium acetate (0.25 mol L^{-1}) was also applied to the cartridge. Elution was achieved with 1 mL of 0.1 mol L^{-1} HCl-methanol (4 : 1 v/v). This methodology allowed recoveries of 88–104% to be attained with good coefficients of variation (less than 5%).

An interesting two-stage SPE method has been devised for the isolation of DOPA from plasma and

urine using [^{14}C]-DOPA as an internal standard. Interfering urinary pigments (urochromes) were eliminated via an initial extraction on to a dual-layer cartridge consisting of an upper layer of strong cation exchanger (SCX) and a lower layer of Cl silica. After this cartridge had been conditioned with 5 mL methanol and HCl (0.2 mol L^{-1}) the urine sample (2.8 mL) was applied followed by a further two bed volumes of 0.2 mol L^{-1} HCl. The eluate was taken to pH 7.5–7.7 (1.5 mL of 2 mol L^{-1} Tris buffer), after which an aliquot was passed through 200 mg of PBA SPE column (conditioned with 1 mL of methanol and 1 mL of 0.2 mol L^{-1} Tris buffer). After removing of interferences with methanol (2 mL) and 0.1 mol L^{-1} Tris (1 mL), the analyte was eluted in 0.3 mL of 0.1 mol L^{-1} HCl. For plasma samples, it was necessary to remove plasma proteins prior to extraction. This was done via precipitation using ice-cold perchloric acid. The supernatant obtained after centrifugation was then passed through the PBA cartridge (at pH 7.5–7.7 with 2 mol L^{-1} Tris) and the analyte subsequently eluted, as described above. Overall recoveries of 80% for urine and 84% for plasma (SD 2–3%) were obtained (allowing 10–15 pg to be detected with high performance liquid chromatography (HPLC) electrochemical detection).

As well as DOPA itself, several methods have used PBA for extracting 5-S-*L*-cysteinyl-*L*-dopa (5-SCD) from urine. These methods have included a dual extraction, first on to a cation exchanger and then a PBA gel with 5-S-*D*-diastereoisomer as an internal standard. A more recent method using PBA on silica was also based on dual extraction with SCX and PBA. The urine samples, to which 5-S-*D*-cysteinyl-*L*-dopa (D-CD) had been added as an internal standard, were applied to an SCX column that had been washed sequentially with methanol (1.0 mL) and HCl (0.1 mol L^{-1} , 1 mL). After washing with HCl (0.1 mol L^{-1}) the SCX cartridges were placed in series with a PBA column (pretreated with methanol and then 1 mol L^{-1} dipotassium phosphate buffer). The target compounds were eluted from the SCX using the dipotassium hydrogen phosphate buffer. Compounds retained on the PBA cartridge were then eluted with 0.5 mL of 0.1 mol L^{-1} HCl (containing 10 mg L^{-1} of ascorbic acid), following a water wash step. Aliquots of the eluate were then analysed by HPLC.

More recently a new, fully automated method for 5-S-cysteinyl-dopa in plasma and urine has been proposed. In this method, the PBA cartridges were treated sequentially with heptane and acetone (1 mL of each) to remove impurities and were then conditioned with methanol (1 mL), HCl (0.3 mol L^{-1} ,

1 mL) and Tris buffer (10 mmol L^{-1} , 2 mL) followed by application of the appropriately buffered sample (1 mL of plasma or 1:100 diluted urine). The cartridges were then washed with 4 mL of 10 mmol L^{-1} Tris buffer prior to elution of the analyte with HCl (1 mL of 0.3 mol L^{-1}). Typical chromatograms from this work are illustrated in Figure 2.

Boric acid gels and silica-PBA have both been used to extract catecholamines from biological samples. The silica-based material has also been employed for the determination of noradrenaline and adrenaline in urine and found to be superior to conventional methods. In this method two SPE cartridges, a pentanesulfonic acid phase (PSA) and PBA were connected in series (the PBA cartridge had previously been washed with methanol (1 mL) and then HCl (0.1 mol L^{-1} , 1 mL)). Both cartridges were then washed sequentially with methanol (2 mL) and then aqueous ammonia (4 mL) and finally phosphate buffer (4 mL, 5 mmol L^{-1} pH 8.5). The urine sample (1 mL, pH 5 using ammonia) plus internal standard (dihydroxybenzylamine) were then applied followed by a wash with phosphate buffer (4 mL of pH 8.5 phosphate). After washing with a further 2 mL of the alkaline phosphate buffer, the PSA column was removed and the PBA cartridge was washed first with methanol (1 mL) and then acetonitrile-phosphate buffer (1 mL, 1:1 v/v). Recovery of the analytes was achieved using HCl (1 mL, 0.1 mol L^{-1}) and these were then analysed by HPLC with electrochemical detection.

In a similar method, urine (1 mL, diluted to 5 mL with water, pH 6.5–7.0) being assayed for dopamine, adrenaline and noradrenaline with 3,4-dihydroxybenzylamine added as internal standard was extracted using a combination of SCX and PBA. The SCX and PBA cartridges were initially treated with 1 mol L^{-1} HCl followed by methanol and 0.01 mol L^{-1} ammonium acetate buffer (pH 7.3), following which the sample was applied to the SCX column. This was washed with methanol and then ammonium acetate (0.01 mol L^{-1}): recovery of the analytes from this phase was achieved with $3 \times 500\text{ }\mu\text{L}$ of perchloric acid. This eluate was neutralized using a saturated solution of sodium carbonate and was then loaded on to the PBA cartridge which was first washed with methanol and then water. Finally the analyte was recovered for analysis, by HPLC with electrochemical detection, by elution with $2 \times 500\text{ }\mu\text{L}$ of 0.1 mol L^{-1} perchloric acid. Limits of detection of $1\text{ }\mu\text{g L}^{-1}$ for noradrenaline and $2\text{ }\mu\text{g L}^{-1}$ for dopamine were claimed.

Glycosylated amino acids In diabetes the glycosylated amino acid glucitolysine is formed when the

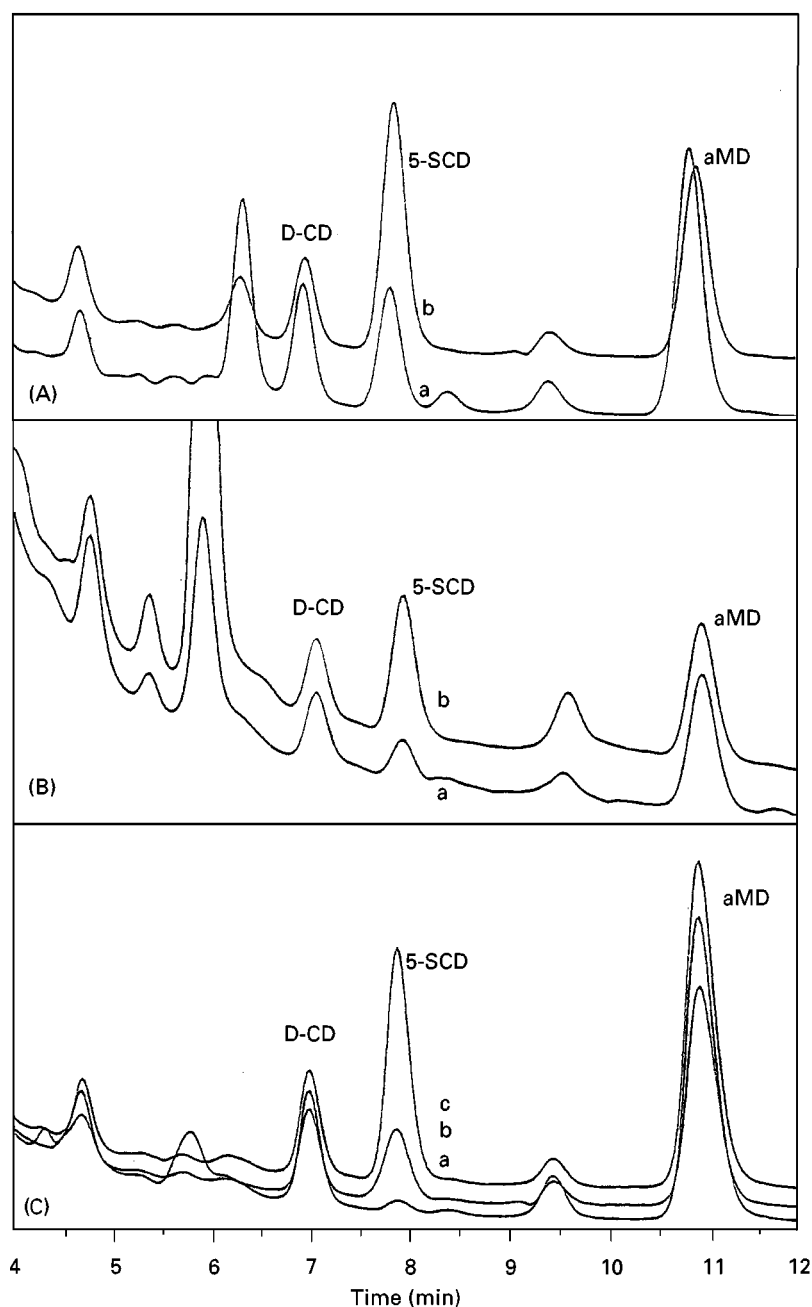


Figure 2 Chromatograms of 5-S-cysteinyl-dopa in PBA-extracted aqueous calibration standards plasma and urine. (A) Urine samples: (a) normal 5-SCD concentration ($320 \mu\text{g L}^{-1}$) and (b) pathological 5-SCD concentration ($1310 \mu\text{g L}^{-1}$). (B) Plasma samples: (a) normal 5-SCD concentration ($1.4 \mu\text{g L}^{-1}$) and (b) pathological 5-SCD concentration ($5.3 \mu\text{g L}^{-1}$). (C) Extracted aqueous calibration standards: 5-SCD concentration: (a) $0.4 \mu\text{g L}^{-1}$; (b) $3.2 \mu\text{g L}^{-1}$; (c) $8.0 \mu\text{g L}^{-1}$. aMD, 2-methyl-3-C3,4-dihydroxyphenyl-L-alanine. Reproduced with permission from Hartleb *et al.* (1999).

amino acid lysine in proteins reacts with glucose. An online extraction method for glucitolysine in protein hydrolysates with 'on-column' reaction with *o*-phthaldialdehyde (OPA) to allow HPLC with fluorescence detection has been described.

Glucitolysine extraction was achieved by washing the PBA phase with 0.1 mol L^{-1} HCl to remove

contaminants, followed by 0.1 mol L^{-1} NaOH, equilibration with pH 8.5 phosphate buffer (0.1 mol L^{-1}) and then application of the sample, also at pH 8.5. With the protein hydrolysates, interfering co-extracted amino acids were removed by washing with water or methanol. Recovery of glucitolysine was achieved by lowering the pH of the mobile phase.

Reduced oligosaccharides PBA has also been applied to the separation of oligosaccharides from their alditols and interfering amino acids and glycopeptides. The purification of an oligosaccharide–lipid conjugate (neoglycolipid) formed by the reductive amination of the sugar lactose with phosphatidylethanolamine dipalmitoyl (PPEADP) has also been demonstrated.

The columns were activated by treatment with methanol, HCl (0.1 mol L^{-1}), water and then NaOH (0.2 mol L^{-1}). Following washing with water ($2 \times 1 \text{ mL}$) samples were applied as aqueous solutions. Elution was performed by washing with water, acetic acid (0.1 mol L^{-1}) and finally HCl (0.1 mol L^{-1}) with the fractions eluted from the PBA analysed by thin-layer chromatography on silica. Under these conditions, oligosaccharides with glucose at the reducing end were not retained by the PBA columns, but the corresponding alditols were retained. Similar results were obtained for glycoprotein-derived octasaccharides and their corresponding alditols. The application of samples under alkaline conditions enabled the separation of the analytes from amino acids, peptides and glycopeptides, although there was some retention of nonreducing oligosaccharides.

In addition, methods were also provided that enabled the purification of oligosaccharide derivatives formed by reductive amination (resulting in the ring-opened sugars giving acyclic vicinal hydroxyl groups). Column activation in this example was performed using water, methanol and a 1 : 1 (v/v) mixture of methanol–chloroform to wash the column.

Reaction mixtures obtained after reductive amination were applied in methanol–chloroform (1 : 1 v/v), with subsequent elution (after various washes) in chloroform–methanol– 0.1 mol L^{-1} acetic acid (30 : 70 : 30 v/v).

Natural Products

Polyhydroxyflavones HPLC with sample preparation via extraction on to PBA cartridges has recently been applied to the analysis of a variety of dietary polyhydroxyflavones (quercetin, kaempferol, fisetin, rutin, myricetin and morin; see **Figure 3** for structures) present in vegetables, red wine and human blood plasma. The extraction involved conditioning the cartridges with aqueous acetonitrile (1 mL, 28% v/v) containing 1% trifluoroacetic acid followed by 1 mL water and 1 mL of phosphate buffer (0.5 mol L^{-1} , pH 8.5). The samples were then loaded on to the cartridge in phosphate buffer (pH 8.5). Following a wash step (1 mL of 10 mmol L^{-1} phosphate buffer, pH 8.5) the analytes were recovered in 2 mL of the aqueous acetonitrile solution used in the first step of the cartridge conditioning process (applied in four 0.5 mL aliquots). In general, good recoveries of the target compounds were obtained from matrices such as red wine and onions; recovery of, for example, quercetin was always greater than 90%. From human plasma the recovery of this compound was reduced to *c.* 80%, but with quite acceptable inter- and intraassay coefficients of variation. In **Figure 4** chromatograms for a variety of sample types are illustrated following sample preparation on PBA.

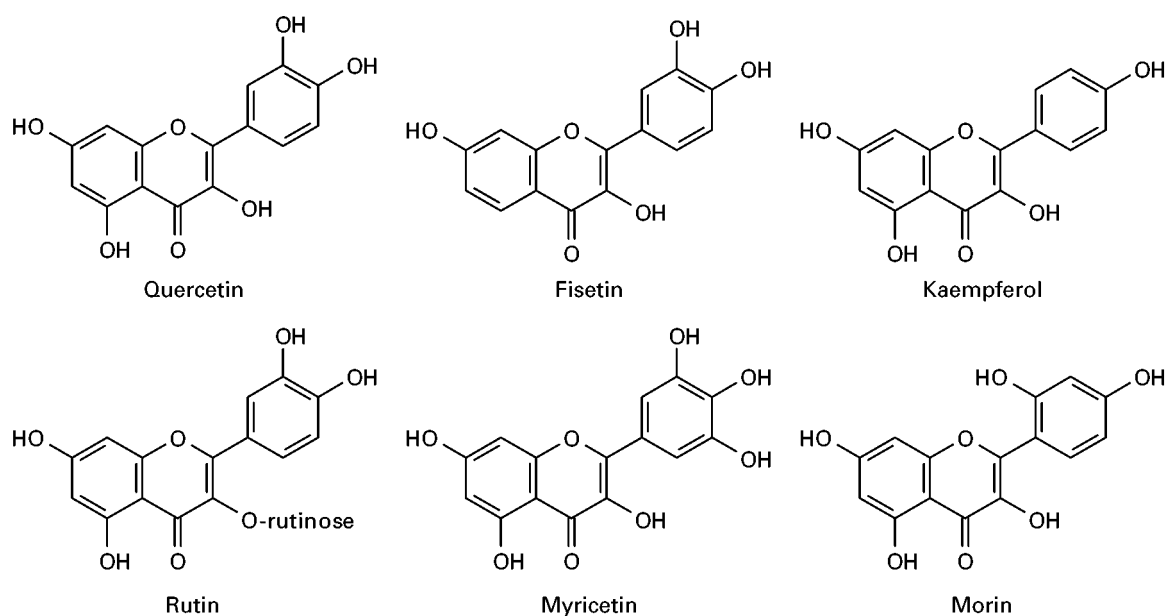


Figure 3 Structures of the dietary polyhydroxyflavones.

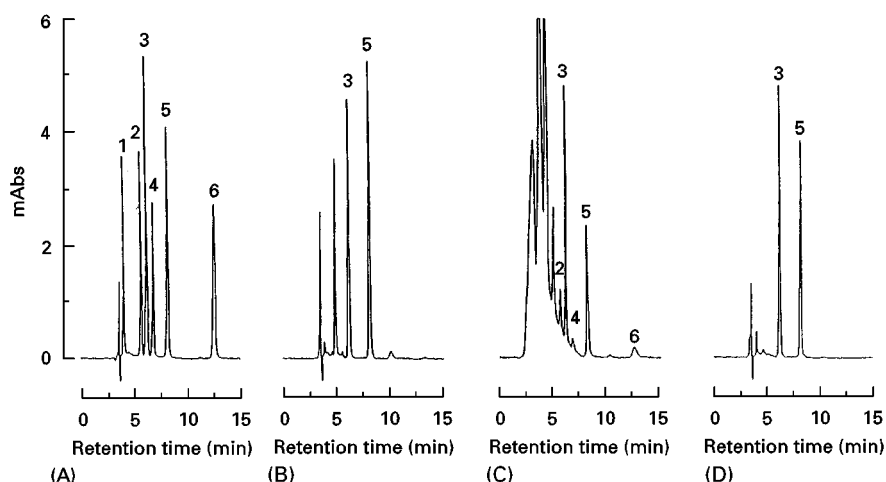


Figure 4 Chromatograms for a variety of sample types containing dietary polyhydroxyflavones following sample preparation on PBA. (A) Standard polyhydroxyflavones; (B) onion skin extract; (C) wine; (D) plasma spiked with quercetin. Peaks: 1, rutin; 2, myricetin; 3, fisetin; 4, morin; 5, quercetin; 6, kaempferol. Structures given in Figure 3. Reproduced with permission from Tsuchiya (1998).

It was noted that the absolute recoveries of quercetin, fisetin and rutin were better than those for the other compounds, and it was suggested that this could be explained by differences in the boronate complexes formed by 1,2 as opposed to 1,3 diols.

Ecdysteroids The ecdysteroids are the moulting hormones of insects and crustaceans. They are relatively polar polyhydroxy steroids (the structure of 20-hydroxyecdysone is given in Figure 5) which are widely distributed in nature. Indeed, over 250 ecdysteroids have been isolated from various sources, particularly plants, where they probably function as chemical defences against predatory insects. Many of the ecdysteroids contain one or more vicinal diols, most often encountered at C-2 and C-3 of the A ring of the steroid nucleus, and in the side chain at C-20 and C-22. PBA has been found to provide the basis for the selective extraction of those compounds in possession of a C-20,22 diol group, but not ecdysteroids containing only a C-2,3 structure.

In this instance the extraction of the C-20,22 diol-containing compounds involved activation of the PBA with ethanol (5 mL) and then an alkaline buffer (5 mL, *c.* pH 8). Borate (100 mmol L⁻¹ pH 8.0 or pH 8.2) or phosphate (100 mmol L⁻¹, pH 8.0) buffers gave essentially the same result. Under these conditions compounds such as ecdysone and 2-deoxyecdysone, which lack the C-20,22-diol, were extracted from the matrix but were readily recovered using alkaline methanol (70% methanol). The C-20,22-containing compounds were, in contrast, surprisingly well retained and even eluents composed of 90% methanol–1% trifluoroacetyl failed to recover more than 20% of these substances. Quantitative

recoveries of these strongly adsorbed ecdysteroids required buffers that contained either salicylic acid (25 mmol L⁻¹) or lactic acid (3% w/v) in 50–70% methanol. A typical chromatogram for 20-hydroxyecdysone from a plant extract is shown in Figure 5.

These differences in the extraction properties of the C-20,22-diol and the C-2,3-diol-containing ecdysteroids is interesting and may well result from the difference in the O–O atomic distances in the two structures. Thus, with the C-2,3 compounds, this distance is 28 pm but with the C-20,22 structures this narrows to 25.2 pm. It is thus possible therefore that a rigid 2,3-diol would be unable to form a cyclic boronate whereas with the less rigid C-20,22 a cyclic boronate is possible.

Drugs and Metabolites

β-Blockers

PBA has been used to extract β-blockers (a class of aminoalcohol-containing drugs) from aqueous solution, rat, and human plasma. The analytes included propranolol, epanolol, ICI 118551 and practolol (see structures in inset to Figure 6). The cartridges (100 mg PBA) were first conditioned with 1 mL methanol followed by 5 mL of glycine buffer, following which SPE was performed using 0.1 mol L⁻¹ glycine buffer at pH 8.2. Following sample application, nonspecifically retained substances were removed by washing with 1 mL of deionized water followed by 3 mL of methanol–water (40 : 60 v/v). The analytes were then recovered in 3 mL methanol–water trifluoroacetyl (50 : 50 : 1 v/v). The extraction was pH-dependent, with the greatest

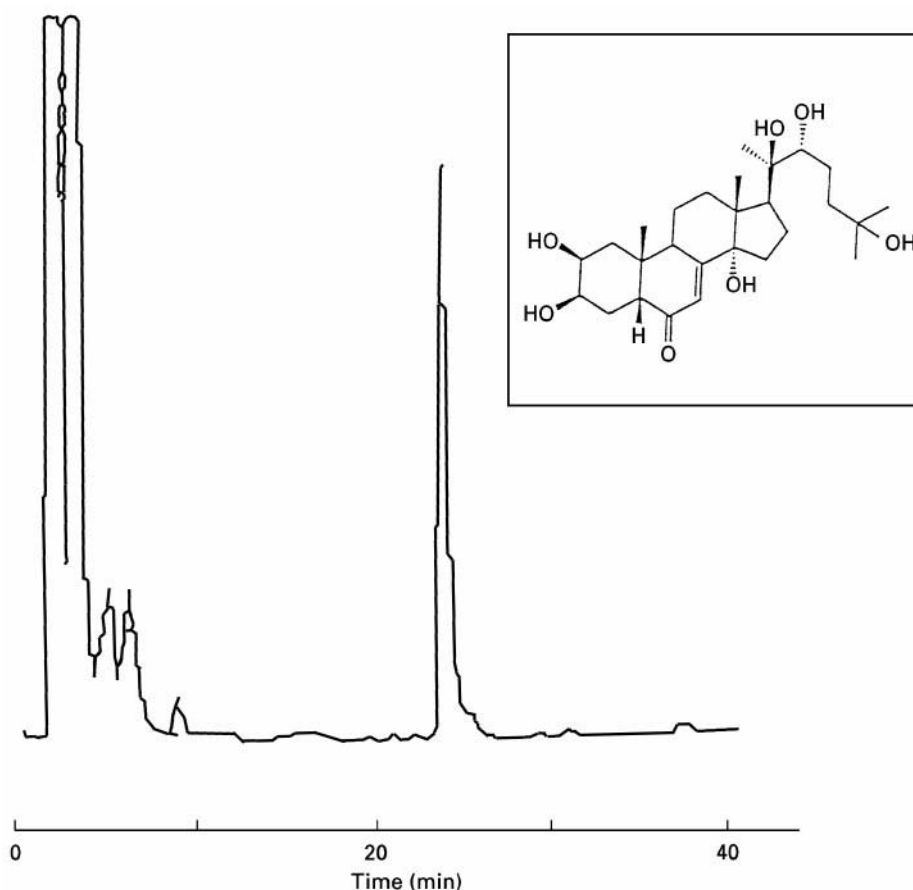


Figure 5 A typical chromatogram obtained for a PBA extract of a plant sample containing 20-hydroxyecdysone (see inset for structure).

extraction efficiency observed at pH 8 (Figure 6) but, in addition, structural features were also important. The extraction was most efficient for propranolol and ICI 118,551 (greater than 90%) with

only small losses at the application and wash steps. With practolol, losses at the application step were high (> 7%), and both practolol and epanolol showed losses at the wash step (8.8 and 16.5% re-

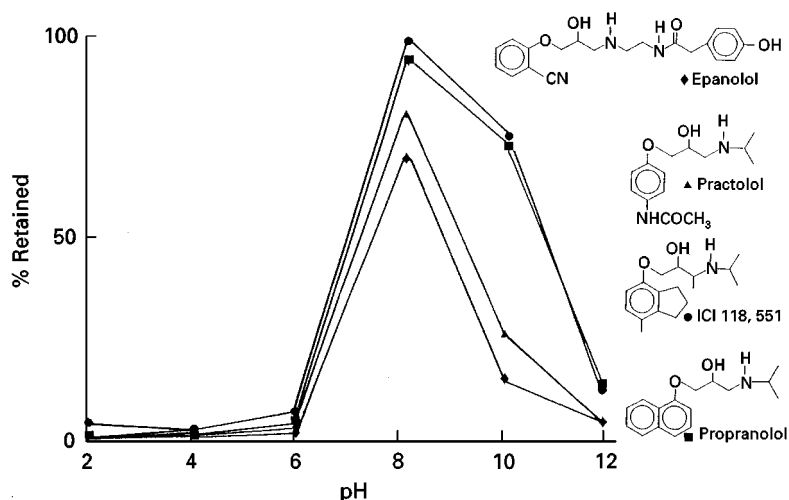


Figure 6 The effect of pH on the extraction of the β -blockers, propranolol, epanolol, ICI 118,551 and practolol on to PBA.

spectively). The latter could be reduced by decreasing the proportion of methanol in the solvent used for elution.

Some matrix effects were also noted for ep-anolol (but not propranolol, practolol and ICI118,551) when extraction was performed from rat plasma where losses at the application and wash steps were greater than from buffer. This effect, which probably resulted from protein binding, was reduced by diluting the sample with glycine buffer prior to extraction.

Glucuronides

Glucuronides are an important class of metabolites for xenobiotics such as drugs. In many analytical methods these conjugates are hydrolysed back to the aglycone followed by extraction. However, the glucuronides have the potential for SPE on PBA, enabling glucuronide-specific assays to be developed. A limited number of studies into the potential of this type of SPE using a range of model phenolic glucuronides, spiked into urine, have been performed.

The test analytes in these studies were phenolphthalien glucuronide, *p*-nitrophenylglucuronide, α -naphthylglucuronide and 6-bromo-2-naphthylglucuronide present in human urine at a concentration of 5 mmol L⁻¹. The extraction protocol developed for these compounds involved mixing 500 μ L urine with 1.5 mL of 100 mmol L⁻¹ 8.5 glycine buffer (pH 8.5) which was then applied to a PBA column that had been conditioned first with pH 10 glycine buffer (5 mL, 100 mmol L⁻¹) and then equilibrated with a further 5 mL glycine buffer at pH 5. Glucuronides that were retained on the PBA were then eluted with 5 mL of methanol-1% HCl (90:10 v/v). With this protocol the selective retention of some of the test compounds was demonstrated depending upon the structure of the analyte and the amount of PBA employed. With phenolphthalien glucuronide, good extraction was obtained with 300 mg PBA and complete extraction was demonstrated with cartridges containing 400 mg. Extraction on 100 and 200 mg cartridges was, however, incomplete. Good recoveries were seen in the methanol-HCl elution step. Phenolphthalien glucuronide and phenolphthalien sulfate were readily separated from each other using PBA. Good results for the extraction of 6-bromo-2-naphthyl- β -D-glucuronide were also obtained on 600 mg cartridges.

However, with both *p*-nitrophenol glucuronide and α -naphthylglucuronide extraction efficiency was not as good (20 and 50% respectively with 500 mg PBA cartridges).

Thus, whilst it was possible for certain structures to extract phenolic glucuronides on to PBA, and selectively to fractionate sulfates and glucuronides, the presence of glucuronic acid is not of itself sufficient to ensure extraction. Indeed, glucuronic acid itself was not retained under the extraction conditions used for the conjugates. Clearly the structure of the aglycone on to which the glucuronic acid is attached is also important. The exact structural features that would ensure good extraction of glucuronides have still to be elucidated, but π - π interactions may be important. It should also be noted that, whilst glucuronides possess vicinal diol groups with which to form boronate esters, it is also possible that the carboxylic acid and its adjacent hydroxyl group are responsible for the observed extraction.

Miscellaneous

Alizarin The tricyclic anthraquinone dye alizarin contains a *cis*-diol and has been used as a model compound for studying SPE with PBA. The cartridges were conditioned with methanol and then pH 8.6 HEPES buffer (0.1 mol L⁻¹). An aqueous solution of the dye (0.1%) was quantitatively retained, as a sharp band on the cartridge with elution subsequently achieved with methanol-HCl (0.1 mol L⁻¹) (3:1). Efficient extraction was only achieved at pH 7-10; however it was also shown that good extractions were also possible from solutions containing up to 70% of an organic solvent as long as they were alkaline. Indeed, as long as wash solvents were alkaline, it was possible to use solvents such as methanol, ethanol or acetonitrile without loss of the dye from the cartridge. The extraction of the analyte from plasma was only efficient if the sample was first extracted on to a C₁₈ phase. Elution from C₁₈ with an alkaline methanol buffer on to the PBA then resulted in good recoveries. Presumably protein binding was responsible for the poor result (see the β -blockers above).

Conclusions

For those compounds with the structural features that permit it, the possibility of selective extraction using immobilized phenylboronic acid may have potential benefits. Such a sorbent clearly has the potential to result in a relatively specific clean-up and it is perhaps surprising that there are relatively few published applications. However, it is evident from some of the examples provided above that the suitability of a particular analyte for extraction on to PBA can only be determined by experiment as the apparent possession of a suitable structure for cyclic boronate formation (e.g. a *cis*-diol) is no guarantee of success.

See also: II/Affinity Separation: Immobilized Boronates and Lectins. Chromatography: Liquid: Derivatization. Extraction: Solid-Phase Extraction. III/Ecdysteroids: Chromatography. Appendix 1/Essential Guides for Isolation/Purification of Drug Metabolites.

Further Reading

- Benedict CR and Risk M (1984) Determination of urinary and plasma dihydroxyphenylalanine by coupled-column high-performance liquid chromatography with C8 and C18 stationary phases. *Journal of Chromatography* 317: 27–34.
- Echizen H, Itoh R and Ishizaki T (1989) Adenosine and dopamine simultaneously determined in urine by reversed-phase HPLC, with on-line measurement of ultraviolet absorbance and electrochemical detection. *Clinical Chemistry* 35: 64–68.
- Hartleb J, Damm Y, Arndt R, Christophers E and Stockfleth E (1999) Determination of 5-s-cysteinyldopa in plasma and urine using a fully automatal solid-phase extraction-high-performance liquid chromatographic method for an improvement of specificity and sensitivity of this prognostic marker of malignant melanoma. *Journal of Chromatography B* 727: 31–42.
- Huang T, Wall J and Kabra P (1988) Improved solid-phase extraction and liquid chromatography with electrochemical detection of urinary catecholamines and 5-S-L-cysteiny-L-dopa. *Journal of Chromatography* 452: 409–418.
- Imai Y, Ito S, Maruta K and Fujita K (1988). Simultaneous determination of catecholamines and serotonin by liquid chromatography after treatment with boric acid gel. *Clinical Chemistry* 34: 528–530.
- Kagedal B and Pettersson A (1983) Liquid-chromatographic determination of 5-S-L-Cyseinyl-L-dopa with electrochemical detection in urine prepurified with a phenylboronate affinity gel. *Clinical Chemistry* 29: 2031–2034.
- Kupferschmidt R and Schmid R (1986) Organic dye compounds as an evaluation tool for sample extraction using bonded silicas. *Proceedings of the 3rd Annual International Symposium*, Tschia H, High-performance liquid chromatographic analysis of polyhydroxyflavones using solid-phase borate-complex extraction. *Journal of Chromatography B*, 720 (1998) 225–230.
- Martin P, Leadbetter B and Wilson ID (1993) Immobilized phenylboronic acids for the selective extraction of β -blocking drugs from aqueous solution and plasma. *Journal of Pharmaceutical and Biomedical Analysis* 11: 307–312.
- Maruta K, Fujita K, Ito S and Nagatsu T (1984). Liquid chromatography of plasma catecholamines, with electrochemical detection after treatment with boric acid gel. *Clinical Chemistry* 30: 1271–1273.
- Murphy SJ, Morgan ED and Wilson ID (1990) Selective separation of 20,22-dihydroxyecdysteroids from insect and plant material with immobilized phenylboronic acid. In: McCaffery A and Wilson ID (eds) *Chromatography and Isolation of Insect Hormones and Pheromones*, pp. 131–136. New York: Plenum.
- Oka K, Sekiya M, Osada H, Fujita K, Kato T and Nagatsu T (1982) Simultaneous fluorimetry of urinary dopamine, norepinephrine, and epinephrine compared with liquid chromatography with electrochemical detection. *Clinical Chemistry* 28: 646–649.
- Pfadenhauer EH and Tong S-D (1979) Determination of inosine and adenosine in human plasma using high-performance liquid chromatography and a boronate affinity gel. *Journal of Chromatography* 162: 585–590.
- Schmid R and Pollak A (1985) Specific extraction of a glycosylated amino acid from protein hydrolysates using boronic acid derivatised silica gel. Sample preparation and isolation using bonded silicas. In: *Proceedings of the 2nd International Symposium*, pp. 15–20, Analytichem International.
- Stolowitz ML (1985) Covalent chromatography: immobilized phenylboronic acid for sample preparation. Sample preparation and isolation using bonded silicas. *Proceedings of the 2nd International Symposium*. Analytichem International 41–44.
- Tschia H (1998) High-performance liquid chromatographic analysis of polyhydroxyflavones using solid-phase borate complex extraction. *Journal of Chromatography B* 720: 225–230.
- Tugnait M, Ghauri FYK, Wilson ID and Nicholson JK (1992) NMR monitored solid-phase extraction of phenolphthalein glucuronide on phenylboronic acid and C18 bonded phases. *Journal of Pharmaceutical and Biomedical Analysis* 9: 895–899.
- Tugnait M, Wilson FYK and Nicholson JK (1994) High resolution ^1H NMR spectroscopic monitoring of extraction of model glucuronides on phenylboronic acid and C18 bonded phases. In: Stevenson D and Wilson ID (eds) *Sample Preparation for Biomedical and Environmental Analysis*, pp. 127–138. New York: Plenum.
- Wu A and Gornet TG (1985) Preparation of urine samples for liquid-chromatographic determination of catecholamines bonded-phase phenylboronic acid, cation-exchange resin, and alumina adsorbents compared. *Clinical Chemistry* 31: 298–302.

IMMUNOAFFINITY EXTRACTION



D. Stevenson, University of Surrey, Guildford, UK
Copyright © 2000 Academic Press

Introduction

The mechanisms of separation in liquid chromatography are often classified as adsorption, partition, ion exchange and size exclusion. A further category could be included—affinity separations. Affinity chromatography uses very specific interactions between the compound of interest and a ligand bound to a chromatographic support to obtain separations. An early example of affinity separations was the use of an enzyme and its substrate. One particular type of affinity separation is immunoaffinity chromatography. In this case antibody–antigen interactions are used to obtain the separation. Either the antibody or the antigen can be bound to a support (immobilized). The current use of immunoaffinity extraction usually has the antibody immobilized (Figure 1). Immunoaffinity chromatography has often been used in the preparative mode where molecules of biological interest, which are difficult to recover by other methods, have been purified. Exam-

ples include enzymes, hormones, vaccines, interferons and antibodies.

Many modern analytical methods involve at least two distinct stages: preparation of a sample in a relatively clean form followed by instrumental analysis. This is particularly the case for the measurement of low concentrations of organic compounds in complex biological matrices such as blood, plasma, serum, urine, tissues and environmental matrices such as water, air, soil, foods, etc. One reason for the current interest in immunoaffinity extraction is its potential use as a highly specific variant of traditional solid-phase extraction in such analyses. In an ideal immunoextraction the sample is added to the column and only the target analyte is retained on the column. A wash step is then incorporated and potentially interfering material in the sample is washed from the column and discarded. The solvent is then changed and the elution solvent removes the target analyte from the column. The clean eluent is then analysed, usually by a modern instrumental method such as high performance liquid chromatography (HPLC) or gas chromatography (GC). This principle is shown in Figure 2. Immunoaffinity extraction is thus an attempt to combine the specificity of antibody-based methods with the separation and selective detection that can be obtained from instrumental chromatographic methods.

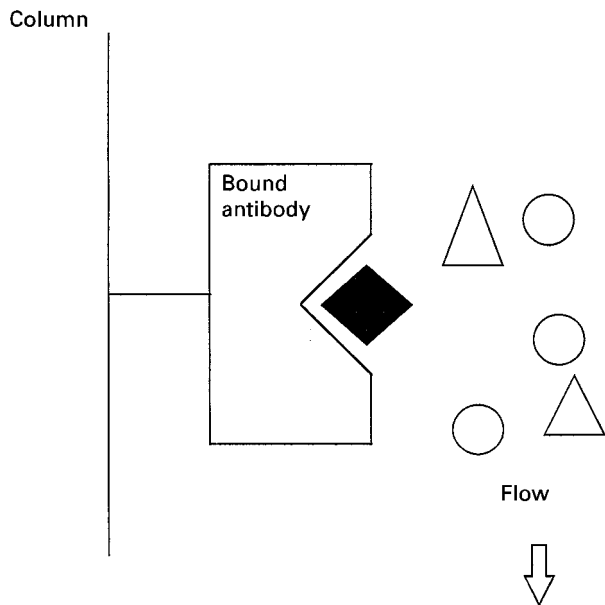


Figure 1 Principle of affinity extraction. Only analyte binds to the antibody. ♦, analyte; △, ○, unrelated compounds.

Solid-Phase Extraction

Solid-phase extraction is one of the most common forms of sample preparation in current use. In its usual format, it involves introducing a liquid sample to an extraction cartridge in a small syringe-shaped container. The cartridge contains a solid phase capable of extracting the analytes of interest and retaining them on the solid phase. The analyte is thus removed from a 'dirty' matrix. It is then eluted from the solid phase and injected into a GC or an HPLC. Such a procedure produces a cleaner sample and therefore less likelihood of peaks co-eluting with the analyte. The liquids are normally drawn through the cartridge under vacuum using a purpose-designed vacuum box, or using positive pressure at the head of the column. Solid-phase extraction is a simple form of liquid chromatography. A range of phases is commercially available, such as silica, C₁₈, C₈, C₅, C₂, phenyl, diol, amino bonded silica, ion exchange phases and polymer phases. Conventional solid-phase extraction

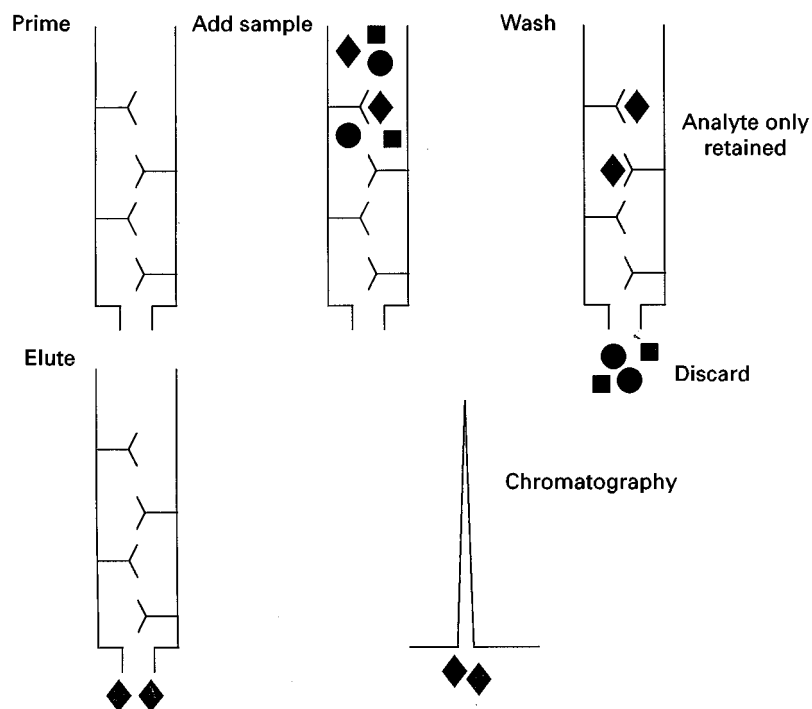


Figure 2 Idealized immunoextraction. Only analyte (♦) is retained through the wash step. This is then eluted and subsequently injected onto HPLC, GC, etc.

is easy to automate both online and offline. Commercially available phases have been used to analyse thousands of different compounds, but generally they are nonselective about which analytes they extract. A range of tailor-made phases have been developed, designed to extract only one or a few closely related analytes. Immunoaffinity extraction is an example of an attempt to develop highly specific solid-phase extraction procedures.

Antibodies

The key reagent for immunoextraction is the antibody which is immobilized on to a support. Antibodies are large biological molecules present in the serum of animals. They are produced by the immune system in response to foreign compounds, the so-called antibody-antigen response. Antibodies belong to a group of proteins called the immunoglobulins and have a relative molecular mass of about 150 000–900 000. Antibodies are normally only produced in response to compounds with a molecular mass of 1000 or above. As many of the compounds of interest in analytical chemistry are much smaller than this, they are chemically bonded to a carrier protein in order to elicit the immune response. For the antibody to be useful it must respond to the analyte, not

to the analyte-protein complex alone. In cases where the analyte does not contain a functional group suitable for bonding to a carrier protein, a structural analogue to the analyte is sometimes evaluated. As serum containing the antibodies is collected, it is referred to as antiserum. It will contain a number of different antibodies and is known as a polyclonal antibody.

In practice these antibodies will bind compounds bearing a close structural relationship to the compound of interest. This is known as cross-reactivity, and can be useful in immunoextraction as a group of compounds, such as phenylurea pesticides, can be extracted and then subsequently separated by HPLC. The forces involved in the antibody-antigen interaction are a mixture of ionic attraction, hydrogen bonding, hydrophobic attractions and van der Waals forces. Although individually they are relatively weak forces, in combination a relatively strong attraction is achieved. As a chemical reagent, antibodies are not very stable. They are easily denatured by extremes of pH and by organic solvents. They are much more stable under physiological conditions (i.e. close to pH 7 and in saline at about 1%). The main attraction of biological antibodies in analytical chemistry is their specificity, which arises due to biological recognition at the molecular level.

Table 1 Support materials used for antibody immobilization

Dextran (α -1,6-linked glucose)
Agarose (poly galactose and anhydro-galactose)
Cellulose (1,6-linked glucose chains)
Polyacrylimide
Alumina
Silica
Controlled pore glass

Immobilization of Antibody

Immunoextraction columns require the bonding of an antibody on to a suitable support while retaining the maximum amount of antibody activity. Some of the support materials used are shown in **Table 1** (for their particular characteristics, see Godfrey in Further Reading). Ideally, supports should show good flow characteristics, good chemical and mechanical stability, low nonspecific adsorption, low cost and suitable functional groups for bonding the antibody. As with conventional HPLC and solid-phase extraction, silica-based sorbents are the most popular for immunoextraction.

The methods used to couple antibodies to sorbents usually involve reaction with the carboxyl or amino groups on the antibodies. A range of different reagents is used to activate the sorbent on to which the antibody is bound. These include cyanogen bromide, carbonyl diimidazole, 1,4-butanediol diglycidioxy ether, divinyl sulfone, tresyl chloride and glutaraldehyde. Sorbents need to be thoroughly washed after bonding to remove residual reagents.

Optimization of Immunoextraction

Once an immunosorbent has been prepared, a known amount (by weight or volume) is added to a plastic or glass column with a retaining frit. As immunosorbents are relatively expensive to prepare (compared with commercially available solid-phase extraction columns), the minimum amount needed for a particular assay is used. Conditions are also chosen to allow the columns to be used many times. This means that gentle extraction conditions are favoured, otherwise the antibody will be denatured. However, when using immunoaffinity extraction as a clean-up method for chromatography, it is also desirable to elute the analyte in as small a volume as possible so that further preconcentration is unnecessary. A further consideration is the nature of the desorbing eluent with respect to the possibility of direct injection into an HPLC or GC. In principle there are many different variables requiring optimization for a successful immunoextraction (**Table 2**).

As the actual column preparation follows established protocols, much of the effort of developing a successful extraction protocol concentrates on the solvents used for conditioning and washing the column and on the solvent used for elution of analyte. Columns typically contain between 50 and 500 μL of antiserum. As antibodies originate from animal serum, physiological conditions are favourable for column washing.

A typical protocol would prime the column with phosphate-buffered saline at neutral pH. The sample would be loaded at a pH adjusted to fall in the range pH 5–9. Large sample volumes can be added and this allows concentration of the analyte on the column. The capacity of immunocolumns is usually dictated by the mass of analyte rather than the volume of sample. Biological samples such as plasma or serum often cause column blockage unless proteins are precipitated before the sample is added to the column. Flow rates up to about 5 mL min^{-1} are acceptable; otherwise, with higher flow rates the antibody–antigen interaction does not have sufficient time to ensure binding.

Once the analyte is bound on to the column it can be washed with phosphate-buffered saline at neutral pH. In order to elute the analyte in as small a volume as possible, without damaging the antibody, elution solvents are typically composed of phosphate-buffered saline at a low pH (down to pH 2) with the addition of a water-miscible solvent such as methanol or ethanol at a concentration of up to about 50%. At higher pH or lower concentration of organic modifier, the analyte elutes in a larger volume of elution solvent, which necessitates further concentration. This type of desorption is known as nonselective desorption. An alternative approach is to try selective desorption by adding a compound very similar in structure to the analyte in the elution solvent. This

Table 2 Parameters for optimization of immunoaffinity extraction

Type of support
Activation of support
Particle size of support
Pore size of support
Amount of antibody to immobilize
Immobilization chemistry
Quality and purity of antibody
Column dimensions
Column priming
Volume of sample to load
pH of sample
Wash solvent composition including pH
Elution solvent composition including pH
Flow rate
Regeneration conditions

approach has generally necessitated larger desorption volumes to obtain quantitative recovery than non-selective desorption and hence is not common.

One of the advantages of immunoaffinity extraction is that these procedures are usually carried out under aqueous conditions. As reversed-phase HPLC is often the favoured technique for subsequent analysis, the introduction of analyte dissolved in an aqueous medium is compatible with the mobile phase. Most applications of the technique involve extraction of drugs, endogenous compounds and pesticides. Examples of compounds for which immunoaffinity extraction has been reported are shown in Table 3.

One of the most successful applications of immunoaffinity has been the extraction of pesticides from water. Immunoextraction columns have been shown to be capable of preconcentrating up to 1 L of water containing the herbicides chlortoluron and isoproturon, yet still capable of desorption into low volumes (even as low as 1 mL) of elution solvent. Although lower sample volumes (such as 50–100 mL) are more likely to be used in practice, this feature of immunocolumns offers the possibility of large concentration factors and low overall detection limits. The cross-reactivity of antibodies to triazines and phenylureas has been used to immunoextract several compounds which were then subsequently separated and measured by HPLC.

The capacity of the immunocolumns is governed by the mass of analyte that can be retained before the column is overloaded rather than the volume of water passed through. The mass capacity of the column can be assessed by loading 1 mL aliquots of a standard solution of analyte and analysing fractions eluting from the column until the presence of analyte is detected. A simple calculation of the number of addi-

tions to the column times the amount added each time gives the mass breakthrough of analyte. An alternative approach involves overloading the column but then washing out excess analyte in solution, leaving bound analyte on the column. This is then eluted with the desorbing solution and the concentration and volume measured. A simple calculation gives the amount of analyte required to saturate the column.

The major advantage of immunoaffinity columns is the specificity that can be obtained. This is utilized to give cleaner chromatographic traces than using nonselective extraction such as liquid–liquid extraction or solid-phase extraction on silica or non-polar bonded silica.

Other Formats of Immunoaffinity Extraction

Immunoaffinity extraction has been carried out in formats other than solid-phase extraction. This has included high performance immunoaffinity chromatography and online HPLC column switching. In the former, immunosorbents are used as HPLC columns whereas in the latter, samples are extracted on an HPLC immunosorbent, preconcentrated and the flow then switched to a conventional HPLC column for analysis. Both methods attempt to base the separation on antibody–antigen interactions. In the case of column switching, complete automation can be achieved.

Molecular Imprinted Polymers

The major disadvantage with immunoaffinity extraction is the difficulty and expense in obtaining biological antibodies. An alternative approach is the use of molecular imprinted polymers as antibody mimics. These are synthesized in the chemistry laboratory and are consequently easier and less expensive to obtain. The target analyte (template) is mixed with a monomer such as methyl acrylic acid and a cross-linking agent such as ethylene glycol dimethacrylate. They are dissolved in a suitable solvent such as acetonitrile along with an initiator such as 2,2'-azobis-(2-methylpropionitrile) and heated or subjected to UV radiation. The polymer forms around the template within about 16 h. The polymer is ground into fine particles and then washed to remove the analyte template, thereby leaving cavities where the analyte can subsequently be bound. This polymer can then behave as an affinity column, mimicking the biologically derived immunoaffinity solid-phase extraction columns.

Table 3 Examples of immunoaffinity extraction

Aflatoxins
Albuterol
Atrazine
Carbofuran
Chloramphenicol
Ciprostene
Clenbuterol
Cytokinins
Isoproturon
Morphine
Ochratoxin A
Propranolol
Prostaglandins
Steroids
Thromboxane metabolites
Tenbolone
Zeranol

Columns derived from molecular imprinted polymers often show secondary interactions arising from the monomer, e.g. with methyl acrylic acid, cation exchange can occur. They show best specificity in the solvent in which they were originally dissolved, hence they are used with organic rather than aqueous solvents. Although easy to obtain and more stable to extremes of pH and organic solvents, they are not as specific as columns utilizing biologically derived antibodies. One problem with molecular imprinted polymers is the difficulty in washing out all traces of the analyte template. Remaining template leaches out when the columns are used for analysis, giving falsely high results. This problem is partially overcome by using a structural analogue to the analyte as the template. Provided the template can be separated from the analyte by HPLC, GC, etc. it will not interfere with the analysis. This approach does require cross-reactivity of the polymer, i.e. it must retain the analyte as well as the template.

The use of molecular imprinted polymers is an emerging field and new synthetic methods may improve the performance of these columns as well as other uses of the polymers. Examples of solid-phase extraction using molecular imprinted polymers include atrazine, pentamidine, propranolol, sameridine and tamoxifen.

Future Developments

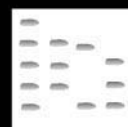
Immunoaffinity extraction has been demonstrated as being capable of selectively capturing analytes from complex matrices using antibody-antigen interactions. Techniques for preparing the columns and procedures for optimizing the retention and desorption of analyte are now well established. The availability of antisera to more compounds will expand the use of immunoextraction. As better procedures to produce antibodies or antibody fragments become available, the cost of antisera should come down. Although much of the work to date uses low molecular weight compounds as target analytes, immunoextraction might be even more valuable for the new products emerging from biotechnology which may present different problems with extraction using conventional liquid-liquid or solid-phase extraction methods. Better specificity from synthetic polymer antibody mimics should also see a growth in their utility in immunoaffinity-type extractions. Polymers that show specificity for analyte under aqueous conditions would be an advantage. Selective extraction at present comes at an extra cost in the production of the columns and is not yet available 'off the shelf'. It is likely to prove most useful

where simpler procedures cannot be used due to analyte instability or where particularly low detection levels are required. It should also be remembered that immunoaffinity extraction need not only be used with HPLC, GC or capillary electrophoresis.

Further Reading

- Burrin D (1995) Immunochemical techniques. In: Wilson K and Walker J (eds) *Principles and Techniques of Practical Biochemistry*, 4th edn, pp. 65-109. Cambridge: Cambridge University Press.
- de Frutos M (1995) Chromatography-immunology coupling, a powerful tool for environmental analysis. *Trends in Analytical Chemistry* 14: 133-140.
- Farjam A, Brugman EA, Henk L and Brinkman UAT (1991) On-line immunoaffinity sample pre-treatment for column liquid chromatography: evaluation of desorption techniques and operating conditions using an anti-estrogen immuno-pre-column as a model system. *Analyst* 116: 891-896.
- Godfrey MAJ (1997) Immunoaffinity and IgG receptor technologies. In: Matejtschuk P (ed.) *Affinity Separations: A Practical Approach*, pp. 141-195. Oxford: IRL Press.
- Holme DJ and Peck H (eds) (1993) *Analytical Biochemistry*, 2nd edn, pp. 233-260. Harlow: Longman.
- Janis LJ and Regnier FE (1988) Immunological-chromatographic analysis. *Journal of Chromatography* 444: 1-11.
- Martin-Esteban A, Kwasowski P and Stevenson D (1997) Immunoaffinity-based extraction of phenylurea herbicides using mixed antibodies against isoproturon and chlortoluron. *Chromatographia* 45: 364-368.
- Martin P, Wilson ID, Morgan DE *et al.* (1997) Evaluation of molecular-imprinted polymer for use in solid phase extraction of propranolol from biological fluids. *Analytical Communications* 34: 45-47.
- Phillips TM (1989) High-performance immunoaffinity chromatography. *Advances in Chromatography* 29: 134-173.
- Pichon V, Chen L and Hennion M-C (1995) On-line pre-concentration and liquid chromatographic analysis of phenylurea pesticides in environmental water using a silica-based immunosorbent. *Analytical Chimica Acta* 311: 429-436.
- Rashid BA, Aherne GW, Katmeh MF *et al.* (1998) Determination of morphine in urine by solid-phase immunoextraction and HPLC with electrochemical detection. *Journal of Chromatography A* 797: 245-250.
- van Ginkel LA, Stephany RW, van Rossum HJ and Zoontjes PW (1992) Perspectives in residue analysis; the use of immobilised antibodies in (multi) residue analysis. *Trends in Analytical Chemistry* 11: 294-298.
- Walt DR and Agayn VI (1994) The chemistry of enzyme and protein immobilisation with glutaraldehyde. *Trends in Analytical Chemistry* 13: 425-430.

IMPREGNATION TECHNIQUES: THIN-LAYER (PLANAR) CHROMATOGRAPHY



I. D. Wilson, AstraZeneca Pharmaceuticals,
Macclesfield, Cheshire, UK

Copyright © 2000 Academic Press

Introduction

The use of impregnated phases in thin-layer chromatography (TLC) has a long history, beginning in the very earliest days of the technique. As a consequence, much of the key literature in this field dates back to the 1960s and 1970s. The literature also contains a considerable number of examples of impregnation reagents where subsequently the methods have received little attention except in reviews of the subject.

The impregnation of the stationary phase in thin-layer, or planar, chromatography can be used to achieve a number of ends. These include changing the mode or selectivity of the chromatographic system, improving chromatographic performance and enhancing detectability. An example of the use of impregnation to change the type of chromatography would be the use of a nonpolar, water-immiscible material such as paraffin oil which can be used to enable reversed-phase separations to be performed on silica-gel TLC plates. Alternatively, plates impregnated with silver nitrate can be used to improve the separation of compounds containing double bonds (argentation chromatography). Similarly, boric acids or boronates are useful for compounds such as carbohydrates and sugars containing vicinal diols, and ion pair reagents provide a means for successfully separating polar ionic species. Although the use of impregnation techniques for enhancing detectability will not be considered in depth here, examples would include the incorporation of ammonium acetate followed by heating, which can result in the formation of intensely fluorescent derivatives, whilst paraffin oil impregnation can stabilize or enhance fluorescence and the radiolabelled substances can be detected using impregnation with a scintillant.

There are a variety of methods for obtaining impregnated layers, including the preparation of the TLC plate with slurries containing both the stationary phase and the impregnating reagent, pre- or post-chromatographic dipping, pre- or post-chromatographic development of the plate in a solvent containing the impregnating agent or spraying, and these are described below.

Impregnation Techniques

All of the techniques for impregnating TLC plates described below have been used at one time or another and are illustrated with examples in the subsequent sections on applications.

Spraying

Spraying the TLC plate is a simple and convenient method for applying the reagents used for detection in TLC and indeed is widely used for this type of application. It is, however, much less well suited to the impregnation of TLC plates in order to modify chromatography because of the difficulty of ensuring uniform coverage. It also requires much skill and expertise in order to ensure reproducible results from day to day. Both of these technical difficulties are clearly disadvantages, and spraying is therefore not recommended for routine applications in this area. Spraying is therefore probably best used, if at all, for one-off applications or for screening phases and impregnating reagents for a particular property during method development.

Dipping

Dipping plates in solutions of the impregnating reagent in a suitable (usually volatile) solvent is probably the simplest and most efficient method of ensuring even coverage of the stationary phase with the reagent of choice. Suitable dipping chambers, of the type used for immersing plates in solutions of chromogenic visualization reagents, are available from a number of manufacturers at modest cost. These chambers have relatively small volumes and so are not expensive in reagent. Some automated devices are also available that can be used to control the impregnation time accurately. Dipping, in general, because of the ease of control over parameters such as reagent concentration and impregnation time, should be considered to be the preferred method for impregnating TLC and HPTLC plates.

Pre-development

It is also a relatively easy matter to prepare TLC plates impregnated with the desired reagent by pre-development in a solution of reagent in a suitable solvent. This technique is also referred to as irrigation of the plates. The solvent used for this purpose needs to be sufficiently eluotropic to ensure that any

affinity of the reagent for the stationary phase is overcome or else, at worst, the plate will not be impregnated with the reagent which will stay at or near the origin (or else be distributed as a gradient of decreasing concentration up the plate). Nonmigration of the impregnating reagent is seen with, for example, the ion pair reagent cetrимide if dissolved in water and then used to coat reversed-phase TLC plates in the pre-development method. Because the reagent is relatively nonpolar it has a strong affinity for the stationary phase and remains at the origin. In such cases dipping is to be preferred.

Mixed Phases

Although with the advent of good quality commercial TLC and high performance TLC (HPTLC) products the preparation of TLC plates in the laboratory is no longer widely practised, one method of producing impregnated plates was to produce mixed phases. Thus, the bulk stationary phase (generally silica gel) was mixed with an appropriate amount of the impregnating reagent, a binding agent, slurried in a suitable solvent and spread as a layer on glass plates. After drying and activating (if necessary), the plates were then used as required. Some manufacturers provide a range of mixed phases (e.g. silver nitrate-impregnated plates, buffered layers, ammonium acetate-impregnated layers, etc.).

Specific Examples of Impregnation in TLC

Impregnation to Form Lipophilic Stationary Phases for Reversed-phase Separations

Before the introduction of good-quality bonded phases, the preparation of suitably hydrophobic stationary phases used to be a very popular method for obtaining layers with which to perform reversed-phase separations, and still has many advantages. This is readily achieved using liquid paraffin oil, undecane, *n*-decane, nitromethane, propylene glycol, silicone oil, decalin, Carbowax 400, formamide, 2-phenoxy- and 2-methoxyethanol, various mineral oils, and substances such as ethyl oleate and similar materials. In addition to modifying chromatography, impregnation with these materials can also be used to enhance or stabilize the fluorescence of suitable analytes, thus improving detection and quantification. However, it is the use of these materials to provide reversed-phase separations that is of interest here.

A typical example of the use of paraffin oil is provided by work on the reversed-phase separation of ecdysteroids (polar, polyhydroxylated steroids found in plants and arthropods). Here silica-gel TLC and

HPTLC plates were impregnated with a solution of 7.5% paraffin oil in dichloromethane (v/v) by dipping. The plates were air-dried and chromatography was performed using methanol-water mixtures. In an interesting variation on this general technique of impregnation, a variety of normal-phase separations, for nonsteroidal anti-inflammatory drugs, ecdysteroids, antipyrine and aminophenols, on silica gel were performed with the paraffin added to the mobile phase. Addition of 7.5% (v/v) of paraffin to the normal-phase solvent system did not affect chromatography but did enable the plate to be impregnated so that a subsequent reversed-phase separation in a second dimension could be undertaken immediately that the solvent from the normal-phase separation had evaporated. An example of this for the nonsteroidal anti-inflammatory compounds is shown in Figure 1. It should be noted that, with this type of impregnated plate it is also possible to perform the reversed-phase separation first, remove the nonpolar impregnating reagent with a suitable solvent (i.e. one that does not affect the analytes but does remove the impregnating reagent) and then perform a normal-phase separation in the second dimension. Alternatively, a similar outcome can be achieved by impregnation of that portion of the plate not used for

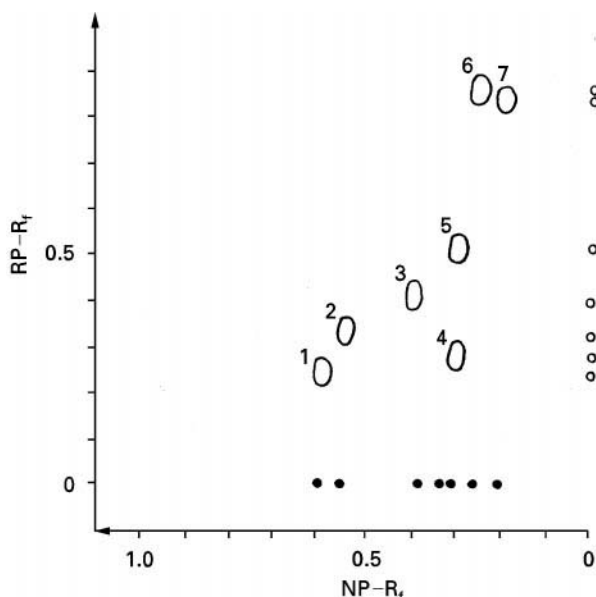


Figure 1 Two-dimensional separation of nonsteroidal drugs with paraffin impregnation during normal-phase (NP) separation in the first dimension to enable reversed-phase (RP)-TLC to be carried out in the second. 1, Ibuprofen; 2, ibufenac; 3, methyl analogue of isoxepac; 4, indomethacin; 5, isoxepac; 6, salicylic acid; 7, 5-methoxysalicylic acid. Details in Wilson ID (1984) Normal-phase thin-layer chromatography on silica gel with simultaneous paraffin impregnation for subsequent reversed-phase thin-layer chromatography in a second dimension. *Journal of Chromatography* 287: 183-188.

the separation in the first dimension, and examples of a normal-phase separation followed by impregnation with 2-phenoxyethanol or undecane for reversed-phase chromatography in the second dimension have been described.

Impregnation with Silver Nitrate

Argentation TLC also represents an important methodology and is considered in detail elsewhere in this work and so will only be briefly described here. The impregnation of TLC plates with silver nitrate has been used for many years as a means of improving the separation of unsaturated compounds, particularly certain lipids, based on the ability of silver ions to form charge transfer complexes with the π electrons of the carbon-carbon double bonds. In general, silica gel is used: the amount of silver nitrate used varies from as little as 2% up to 20 or 30% w/w depending upon the author and application. With silica gel, impregnation by both spraying (with a 10–20% solution in either water or methanol) and the preparation of mixed phases have been described. Following preparation it seems to be good practice either to use the plates the same day or else to store them in a sealed container in the dark until required. In general, non-polar solvent systems are employed (e.g. pentane, hexane-diethyl ether, chloroform-methanol, diethyl ether, light petroleum, etc.).

Whilst the use of silver nitrate-impregnated plates has generally been with normal-phase separations on silica gel, there has been recent work using reversed-phase (C_8 -bonded) layers dipped in solutions containing between 0.5 and 4% silver nitrate for 10 s. These plates were investigated for their ability to separate the *cis/trans* isomers of capsaicin, and comparison was made simply using the silver nitrate in the mobile phase (60 : 40 methanol-water v/v). With impregnation no effects were observed until the 2% (w/v) impregnating solvent was used, and even with 4% this was insufficient to provide the required resolution. In contrast, when present as a mobile-phase additive, even as low a concentration as 0.5% w/v was sufficient to give baseline resolution. It appears likely from this result that the high solubility of the silver nitrate in the mobile phase led to its rapid elution from the impregnated plate, with consequent loss of effect. Thus, interestingly, it seems from this work that the use of the silver nitrate in reversed-phase systems is only practicable when it is present as a mobile-phase additive.

Impregnation with Polyol and Sugar Complexing Reagents

The ability of borate ions to complex with suitable polyhydroxylated compounds such as carbohydrates

is well known and has provided the basis of a number of methods for their separation. TLC with layers impregnated with sodium arsenite, phosphotungstic, tungstoarsenate and molybdic acids have also been shown to have useful properties for the resolution of mixtures of oligo and monosaccharides.

Various methods have been used to prepare such layers, including both spraying and the preparation of mixed layers. Thus, in an early example of the use of boric acid, sodium borate and sodium arsenite plates were either sprayed with methanolic or aqueous solutions containing 10–20% of the impregnating reagent or plates were prepared by mixing 2.8 g of the reagent in 50 mL of water with 25 g of silica gel G to give a 10% (w/w) mixed layer. These layers were then used to separate the *erythro* and *threo* isomers of a variety of di- and trihydroxy long chain fatty acid esters.

Similar work on phosphotungstic and molybdic acid impregnated silica gel TLC plates showed them to be particularly useful for the separation of oligosaccharides giving complexes with higher R_f values than the corresponding boric acid complexes under similar conditions. In this case the plates were made by mixing 35 g of the chromatographic stationary phase (e.g. silica gel-alumina 1 : 1 or 3 : 1 or alumina) with 70 mL of an aqueous solution containing an appropriate amount of the impregnating reagent and spreading the plates as a 0.4 mm layer on to glass. The resulting plates were then dried at room temperature for 24 h, and heated for 1 h at 110°C before use. In general, the best results were obtained with TLC plates treated with phosphoric acid-sodium tungstate or saturated molybdic acid as impregnating reagents.

Impregnation with Liquid Ion Exchangers and Neutral Organophosphorous Compounds for Metal Ion Separations

The separation of inorganic ions has been an important application of TLC. Another area that has proved to be of some interest for the use of the impregnation technique as a means of improving analyte resolution in TLC has been the employment of the so-called liquid ion exchangers. This developed from the widespread use of this type of reagent in paper and column chromatography. A range of these liquid ion exchangers were used in early examples of this type of application. However, extensive experimentation suggested that adogen 464, alamine 336, amberlite LA1 and primene JM-T were suitable for this type of application. In these early studies a 0.1 mol L⁻¹ solution in chloroform was used for impregnation of the silica gel, with plates prepared from a suspension of the silica gel in this solution. Metal ions on TLC have also been resolved on layers

impregnated with neutral organophosphorous compounds such as tri-*n*-butyl phosphate and tri-*n*-octylphosphine oxide. The bulk of the early literature in this area was collated by Brinkman *et al.* (see Further Reading).

More recent examples of the use of impregnation for metal ion separations have included further examples of the use of primene JM-T, amberlite LA-1 and LA-2, alamine 336 and aliquat 336, tri-*n*-octylamine, tri-*n*-butyl phosphate and tri-*n*-butyl amine-impregnated silica gel TLC plates.

Impregnation with Ion Pair Reagents

The use of ion pair reagents is also discussed in detail elsewhere in this work and will therefore only be briefly described here. A number of workers have shown that ion pair reagents can be used as mobile-phase additives or following impregnation in the stationary phase for the subsequent chromatography of polar organic compounds. The methodology used depends to a large extent on the nature of the reagent, but also to some degree on the stationary phase. So, whilst both silica gel and alkyl-bonded layers can be treated with these reagents, the results are generally better with the bonded phases. In addition, it should be noted that low molecular mass ion pair reagents such as tetramethylammonium salts are so soluble that simply impregnating the stationary phase is generally ineffective as, with aqueous solvents, the reagent rapidly dissolves in the mobile phase when chromatography is initiated. This rapidly depletes the amount of reagent available for ion-pairing and results in a generally unsatisfactory chromatographic result. Other reagents, however, typically long chain sulfonic acids or quaternary ammonium compounds (e.g. sodium dodecyl sulfate or cetrимide) are only effective when the plate has been impregnated with the reagent (as a solution in a volatile organic solvent such as chloroform or ethanol) prior to chromatography. We have found that dipping is the most effective means of ensuring an even coating of the layer with these substances.

Impregnation with Chiral Selectors

Chiral separations in TLC have been accomplished using chiral stationary phases, chiral mobile-phase additives and by impregnating suitable TLC phases with chiral selectors. Probably the best characterized separation of this type is based on chiral ligand exchange where the chiral selector (2*S*, 4*R*, 2'*RS*)-4-hydroxy-1-(2'-hydroxydodecyl)proline/copper [II] acetate impregnated into C₁₈-bonded TLC or HPTLC plates. These plates are excellent for the separation of chiral amino acids and related compounds, and sub-

stances such as α -hydroxycarboxylic acids. Plates of this type are commercially available from several manufacturers (as the CHIR and Chiral Plate from Merck and Macherey Nagel, respectively). A typical series of separations on the CHIR HPTLC plate is shown in Figure 2. Alternative systems based on a similar mechanism involve the use of *N,N*-di-*n*-propyl-*L*-alanine or poly-1-phenylalaninamide copper complexes.

Another example of the impregnation approach to the chiral TLC separations involves the impregnation of diol-bonded HPTLC plates with the chiral ion pair reagent *N*-benzoxycarbonyl-glycyl-*L*-proline (ZGP). These plates are prepared by first washing with dichloromethane, then dipping in a 4 mmol L⁻¹ solution of ZGP and 0.4 mmol L⁻¹ ethanolamine. Following drying these plates can be used to separate the enantiomers of β -blockers such as propranolol using chloroform-ethanol solvent systems.

It is also possible to prepare a Pirkle-type stationary phase for chiral separations by dipping aminopropyl-bonded silica gel HPTLC plates into solutions of substances such as (*R*)-*N*-(3,5-dinitrobenzoyl)-phenylglycine or (*L*)-*N*-(3,5-dinitrobenzoyl)leucine

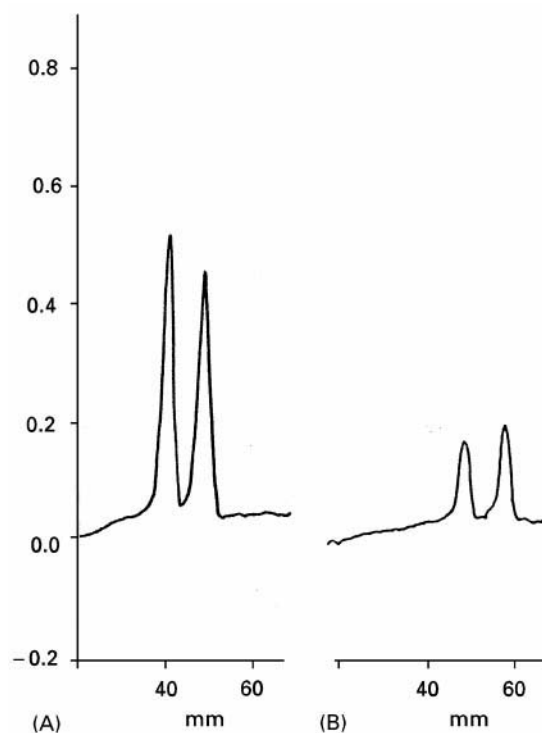


Figure 2 Separation of the enantiomers of (A) isoleucine and (B) leucine on the CHIR HPTLC plate (detection using ninhydrin) with a water-methanol-acetonitrile mobile phase (50:50:200 v/v). Details in Wilson ID, Spurway TD, Witherow L, Ruane RJ and Longden K (1990) Chiral separations by thin-layer chromatography. *Recent Advances in Chiral Separations*, pp. 159-168. New York: Plenum.

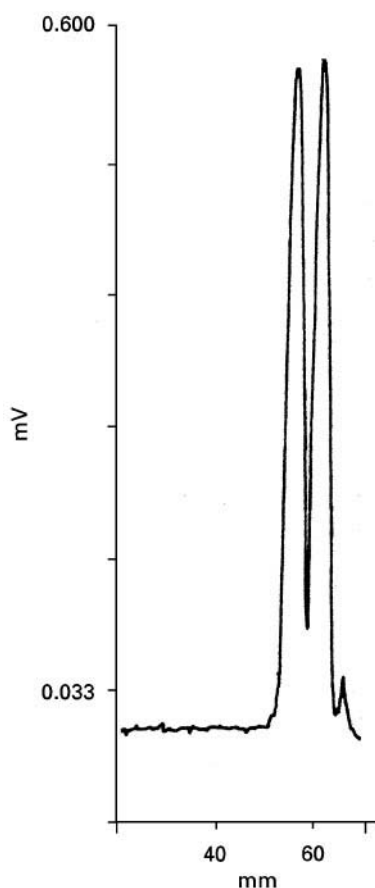


Figure 3 Separation of the enantiomers of 2,2,2-trifluoro-(9-anthryl)ethanol on aminopropyl bonded HPTLC plates modified by impregnation with *N*-(3,5-dinitrobenzoyl)-L-leucine to form an ionically bonded Pirkle-phase. Details in Witherow L, Spurway TD, Ruane RJ and Wilson ID (1991) Problems and solutions in chiral thin-layer chromatography: a two-phase 'Pirkle' modified amino-bonded plate. *Journal of Chromatography* 553: 479–501.

(0.5 mol L⁻¹). Since what is being formed is essentially an ionically bonded stationary phase, it is arguable that the plate is not being impregnated. However, the process that is performed, and the overall effects, are indistinguishable from conventional impregnation and the methodology is included for completeness. An example of a typical separation on such a modified plate is shown in Figure 3.

Impregnation with Oxalic Acid

The modification of TLC plates with oxalic acid has been performed to good effect for a range of solutes, including fatty acids, insecticides, nonionic detergents, azulenes and amines. In the example of the azulenes, the TLC plates were prepared by spreading the silica gel in a aqueous solution of 0.19 mol L⁻¹ oxalic acid, as immersion was found to give less satisfactory results. The plates were then

activated by allowing them to dry for several hours over desiccant silica gel (activation using heating in an oven gave similar but irreproducible results). This activation was quite critical for the achievement of a good separation, as plates that were too damp gave no resolution. For the TLC of certain acidic mycotoxins, the use of silica gel TLC plates that had been immersed in a 10% solution of oxalic acid in methanol for 2 min and then activated by heating at 110°C for 2 min enabled tailing to be eliminated and resulted in well-defined spots.

Impregnation with Inorganic Buffer Salts

The use of phases impregnated with sodium or potassium salts has been described for a number of solutes. Thus, conjugated dihydroxy bile acids were separated on silica gel plates that had been impregnated by dipping in a solution of potassium dihydrogen phosphate. However, a major application of this type of impregnation has been for carbohydrates. As examples, glucose, fructose and sucrose in molasses were resolved on silica gel HPTLC plates dipped in 0.2 mol L⁻¹ aqueous solution of monobasic potassium phosphate. In contrast, when this separation was attempted on nonimpregnated plates it failed. Similar results have been observed by other workers with this type of sample and in addition to potassium-based buffers, plates buffered with 0.15 mol L⁻¹ sodium dihydrogen phosphate (prepared by mixing Kieselghur with the buffer prior to spreading the plates) have also been used to separate sugars (fucose, xylose, ribose, etc). Other workers have also examined impregnation of silica gel, prepared by spreading the adsorbent in a solution of the appropriate salt, with a range of sodium salts (phosphates, acetate, sulfate, phenyl phosphate) for a wide range of carbohydrates, including mono- and oligosaccharides and uronic acids. From these studies the best separations of monosaccharides and uronic acids were obtained with plates impregnated with 0.2–0.3 mol L⁻¹ salt concentrations, whilst oligosaccharides gave the best results with 0.05–0.1 mol L⁻¹ salt solutions. Overall, from the published examples, it seems clear that the TLC separation of carbohydrates does benefit from the use of this type of impregnating reagent.

Charge Transfer Complexes for the Resolution of Polynuclear Aromatic Hydrocarbons

A range of compounds have been used to impregnate silica gel TLC plates in order to improve the

resolution of compounds such as the polynuclear aromatic compounds (fluoranthene, benzopyrene, etc.) based on the formation of charge transfer complexes with different electron acceptors. These reagents have included caffeine, tetracyanoethylene, 1,3,5-trinitrobenzene, picric acid, chloranil, bromanil, benzoquinone and similar compounds, 2,4,7-trinitrofluorenone, teramethyluric acid, urea, pyromellitic dianhydride, 9-dicyanomethylene-2,4,7-trinitrofluorenone, sodium desoxycholate, dimethylformamide, styphnic acid and various amino acids and nucleic acid bases. However, although a wide range of reagents have been impregnated into TLC plates in an attempt to enhance the separation of polynuclear aromatic hydrocarbons, not all have been equally effective: in one study picric acid was described as values, whilst styphnic acid showed some effect and trinitrofluorenone (on alumina) proved to be excellent. Some of the reagents listed above also proved to be heat- or light-sensitive further restricting their utility.

A recent example of the use of caffeine, shown by several groups to have a profound effect on the TLC of polynuclear aromatic hydrocarbons, as

a means of improving the HPTLC resolution of the polynuclear aromatic hydrocarbons, by charge transfer complex formation, involved preparing a solution of 4 g of the reagent in 96 mL of dichloromethane. Silica gel plates (with a preconcentration zone) were then dipped in this solution for 4 s and dried at 110°C for 30 min. Then, before sample application, the plates were pre-washed by running a blank chromatogram with dichloromethane as the mobile phase with subsequent reactivation at 110°C and then preconditioning the impregnated plate for 30 min at 100% relative humidity prior to sample application and chromatography. Following sample application, development was performed with diisopropyl ether-*n*-hexane (4:1) as the solvent in an unsaturated TLC tank. Although chromatography could be performed at room temperature, the best results (especially where quantification was to be performed) were obtained when the plates were developed at 22°C. The results of this type of separation, at room temperature and -22°C, are illustrated in Figure 4.

An added benefit of this type of system is that some of the reagents used for charge transfer chromatography also result in enhanced detection of the compounds of interest because of the highly coloured or even fluorescent complexes that are formed with reagents such as chloranil or pyromellitic dianhydride.

Miscellaneous Impregnation Reagents

As well as the areas described above, there are a large number of other applications of impregnation to modify the properties of the stationary phase in TLC. Some of these are briefly outlined below in order to give an indication of the extent of this type of work, but the list is by no means exhaustive.

Plates impregnated with ethylenediaminetetraacetic acid have been employed for the chromatography of certain antibiotics (e.g. anthracyclines and tetracycline), mycotoxins, citrinin and 8-hydroxyquinolone derivatives, and may confer benefits when the TLC of metal chelating compounds is performed.

TLC plates have also been impregnated with a variety of metal salts for particular compounds or classes of compounds. These include ferric chloride on Kieselguhr (oxine derivatives), zinc salts on silica gel and silanized silica gel (chlorinated anilines, carbamates), cadmium salts on silica gel (aromatic amines), manganese salts on silica gel (aromatic amines), copper sulfate on silica gel (hexosamines, glycosamines, barbiturates), thallium nitrate on silica gel (monoterpene hydrocarbons) and lithium

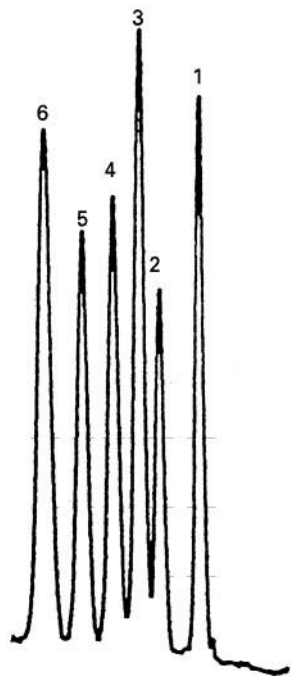


Figure 4 Fluorescence scan of a separation of polynuclear aromatic hydrocarbons (2 ng per spot, except 6 which was 10 ng per spot) on a caffeine-impregnated silica gel layer with chromatography performed at -20°C. 1, Benzo (ghi) perylene; 2, benzo (a) pyrene; 3, benzo (b) fluoranthene; 4, benzo(k)fluoranthene; 6, fluoranthene. Reproduced with permission from Funk W, Gluck V, Schuch B and Donnevert G (1989) Polynuclear aromatic hydrocarbons (PAHs): charge transfer chromatography and fluorimetric determination. *Journal of Planar Chromatography* 2: 28-32.

chloride-impregnated silica gel (pyrrolizidine alkaloids). Magnesium acetate has been used for phospholipids. In addition, lead salts have been employed as impregnating reagents to modify the separations of sugars and polyols. Recently, ammonium cerium (IV) nitrate was used for the separation of aromatic amines.

Other types of impregnation include the use of silica gel with phenol for aliphatic and aromatic amines following impregnation with 2% aqueous solution of the reagent. For the aromatic amines, phenol itself was found to be the most useful reagent, providing a significant improvement in spot shape was noted for a wide range of anilines compared to chromatography on the untreated stationary phase. In the case of aliphatic amines *o*-chlorophenol gave the best result. For both classes of compound this improvement in chromatography was assumed to be due to hydrogen bond formation between the reagent and the solutes. The chromatography of phenols on cellulose has also been modified by impregnation with 10% polyamide, and on silica gel with 20% polyamide. In addition, aniline-impregnated layers have been used for phenol derivatives whilst sodium nitrite-impregnated silica gel has also been shown to provide separations that could not be achieved on native silica gel. Carbonyl compounds were modified by derivatization to 2,4-dinitrophenylhydrazones on alumina TLC plates impregnated with silver nitrate (44%, w/w). Urea impregnation, described above for polynuclear aromatic hydrocarbons and related compounds, has also been used for the separation of lipid classes on silica gel plates.

Concluding Comments

As indicated in the introduction, impregnation techniques have been employed since the earliest days of TLC and their use greatly extends the versatility of TLC by enabling more selective separations or detec-

tion. To some extent the increasing availability of bonded layers has reduced the need for the preparation of silica gel layers impregnated with nonpolar materials such as paraffin oil in order to perform reversed-phase separations. However the usefulness of silver nitrate-impregnated phases for the separation of compounds containing double bonds remains undiminished, and similar observations could be made for many of the impregnation reagents described above. A continued role for impregnated stationary phases in TLC therefore seems likely.

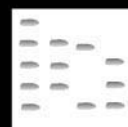
Further Reading

- Brinkman UA Th, De Vries G and Kuroda R (1973) Thin-layer chromatographic data for inorganic substances. *Journal of Chromatography* 85: 187–526.
- Funk W, Gluck V, Schuch B and Donnevert G (1989) Polynuclear aromatic hydrocarbons (PAHs): Charge transfer chromatography and fluorimetric determination. *Journal of Planar Chromatography* 2: 28–32.
- Gocan S (1990) Stationary phases in thin-layer chromatography. In: Grinberg N (ed.) *Modern Thin-layer Chromatography*. Chromatographic Science Series, vol. 52, pp. 5–138. New York: Marcel Dekker.
- Kirchner J (1967) *Thin-layer Chromatography: Techniques of Organic Chemistry*, vol. XII. New York: John Wiley.
- Morris LJ (1964) Specific separations by chromatography on impregnated adsorbents. In: James AT and Morris LJ (eds) *New Biochemical Separations*. London: Van Nostrand.
- Stahl E (1966) *Thin-layer Chromatography, a Laboratory Handbook*, 2nd edn. Berlin: Springer-Verlag.
- Wall P (1987) Argentation HPTLC as an effective separation technique for the *cis/trans* isomers of capsaicin. *Journal of Planar Chromatography* 10: 4–9.
- Wilson ID, Spurway TD, Witherow L *et al.* (1990) Chiral separations by thin-layer chromatography. In: Stevenson D and Wilson ID (eds) *Recent Advances in Chiral Separations*, pp. 159–168. New York: Plenum.

IMPRINTED POLYMERS: AFFINITY SEPARATION

See III/SELECTIVITY OF IMPRINTED POLYMERS: AFFINITY SEPARATION

IN-BORN METABOLIC DISORDERS: THIN-LAYER (PLANAR) CHROMATOGRAPHY



E. Marklová, Charles University, Hradec Králové,
Czech Republic

Copyright © 2000 Academic Press

The term inborn errors of metabolism or, more precisely, inherited metabolic diseases (IMD), is usually applied to a large group of relatively rare genetic disorders in the process of intermediary metabolism, transport defects or impaired receptors. The diagnostic procedure is complicated; the difficulty is the lack of sharp criteria for differential diagnosis, since the attendant symptoms are usually nonspecific. Comprehensive and specialized biochemical investigations therefore are the basis for the diagnosis of IMD. Using this approach, selective laboratory screening programmes can be prepared. The analytical programme includes a three-stage systematic procedure. Qualitative or semiquantitative procedures for urine metabolites are used when starting the investigation, the second step includes quantitative methods, while enzyme analysis or DNA testing belongs to the third stage, and completes the process of examination.

Multicomponent analysis of body fluids using gas and liquid chromatography combined with mass spectroscopy is the most important procedure used in the screening of IMD. However, at first one cannot do without simple and inexpensive methods like colour tests and thin-layer chromatography (TLC), which may give rapid qualitative information on metabolic conditions.

Selective laboratory screening concerns the analysis of individual groups of metabolites, usually those of amino acids and small peptides, catabolites of tryptophan, sugars, oligosaccharides, glycosaminoglycans, organic acids, purines and pyrimidines.

Separations are performed on pre-coated cellulose or silica gel high performance TLC (HPTLC) plastic or glass plates with or without fluorescent indicator F₂₅₄. The plates lay on a temperature-controlled surface (110–115°C), rapidly evaporating the elution solvent in the process of sample spotting. A volume, equivalent to a chosen amount of creatinine is used, when urine is applied.

Plates are developed with a mobile phase in either a horizontal DS chamber (Chromdes, Poland) or in a vertical pre-saturated glass tank. Chromatograms are dried and visualized under ultraviolet (UV) light of

$\lambda = 254$ and 366 nm and/or by spraying with a detection reagent. Reference standards are used for metabolite identification. Quantification is carried out by linear scanning with a TLC scanner, operated with a PC software package. Interpretation of results is made according to age, diet, therapy, clinical symptoms and elementary biochemical results.

Amino Acids

Two-dimensional ascending TLC on cellulose with ninhydrin detection is used as the first approach in the screening for amino acid metabolic disorders. As a rule, 10 μ L of plasma, serum, cerebrospinal or amniotic fluids (previously deproteinized with solid sulfosalicylic acid, 50 mg mL⁻¹) and a volume of urine, equivalent to 20 nmol of creatinine (previously desalted on Dowex-50WX8 in H⁺ form, eluted with 2 mol L⁻¹ ammonia) are applied to the 50 \times 50 mm HPTLC cellulose layer. The plate is then developed in the solvent systems 2-propanol–formic acid–water, 80 : 4 : 20, in the first dimension and *tert*-butanol–acetone–25% ammonia–water, 50 : 30 : 10 : 10, in the second dimension. Chromatograms are sprayed with ninhydrin reagent, observed within 1 h and the next day, then heated for 3 min at 80°C (Figure 1). Aspartylglycosamine (in patients with lysosomal storage disease) can be detected as a blue-green spot when lightly overstained with a mixture of concentrated acetic and hydrochloride acids, 4 : 1 and heated at 60°C for 5 min. For detection of proline and hydroxyproline isatin (0.2 g in 100 mL acetone + 5 mL acetic acid) is recommended. When abnormalities are suspected, multiple spraying, in addition to ninhydrin, can be used: Ehrlich reagent (for tryptophan, hydroxyproline, citrulline and homocitrulline), Pauly reagent (for histidine and tyrosine metabolites), Sakaguchi reagent (for arginine) or platinic iodide (for sulfur amino acids).

Mono- and Disaccharides

The best results of screening for sugar defects have been achieved using two-dimensional vertical TLC on silica gel glass plates with orcinol detection.

Filtered urine is diluted with 2-propanol, 1 : 1, and an aliquot, equivalent to 5 nmol of creatinine (or alternatively 5 μ L equivalent of plasma, serum or cerebrospinal fluid, deproteinized with solid sulfo-

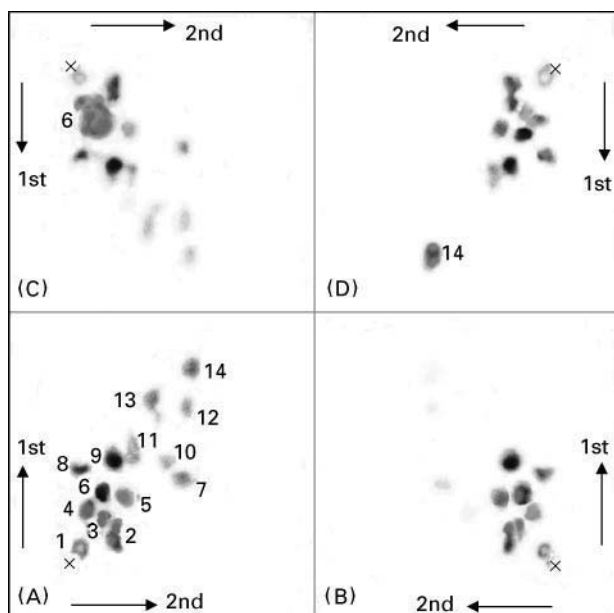


Figure 1 TLC of amino acids. The original 100 × 100 mm glass plate was divided into four by scraping off material. (A) Normal plasma; (B) normal urine (infant); (C) nonketotic hyperglycinaemia (urine, neonate); (D) leucinosia (urine, neonate). 1, Cys; 2, His + MeHis; 3, Lys; 4, Gln; 5, Ser; 6, Gly; 7, Tau; 8, Glu; 9, Ala; 10, Thr; 11, Tyr; 12, Phe; 13, Val; 14, Leu.

salicylic acid, 50 mg mL⁻¹) applied on the 50 × 50 mm layer. The plate is consecutively developed, with 0.5% boric acid in water-*n*-butanol-2-propanol, 20:30:50 (w/v) in the first direction and ethyl-acetate-acetic acid-water, 60:20:20 in the second direction. A freshly prepared mixture of orcinol (0.4% in ethanol, w/v) and concentrated sulfuric acid, 19:1, is used for detection. The plate is examined by transmitted light after 10 min warming at 100°C. Identification is made by comparison with standards, separated on the same plate (Figure 2).

Oligosaccharides

One-dimensional horizontal TLC on silica gel glass plates with fluorescent indicator F₂₅₄ combined with orcinol or resorcinol detection is used for screening of certain lysosomal storage diseases and adenylosuccinate lyase deficiency. A supernatant of centrifuged native urine is applied in an amount, derived from urinary creatinine and the age (μL of sample = 40 × *F* per concentration of creatinine in mmol L⁻¹; *F* = 0.75, 1, 1.5 and 2 for the ages < 1, 1–2, 2–8 and > 8 years, respectively). The plate is developed twice under saturated conditions with a freshly prepared mixture of *n*-butanol-acetic acid-water, 4.5:2:2, with drying in between. The chromatogram is observed under UV 254 nm light to look for two dark bands of succinyl purines (absorbing at 254 nm)

below raffinose. The oligosaccharides are then visualized by spraying with orcinol in the same way as described for mono- and disaccharides (Figure 3). Positive finding in UV light leads to rechromatography and detection with Pauly reagent and naphthoresorcinol, warmed for 10 min at 100°C. The same chromatographic procedure is convenient for screening of sialurias if using resorcinol reagent. For this a mixture of 1% resorcinol in 95% ethanol, w/v, and 2 mol L⁻¹ HCl, 1:9, with the addition of 0.1 mol L⁻¹ CuSO₄·5H₂O in water (0.025 mL per 10 mL of the mixture) is used. After spraying, the chromatograms are covered with glass and warmed at 120°C for 30 min. Pathological glycopeptides in urine (on α-*N*-acetylgalactosaminidase deficiency, aspartylglycosaminuria and fucosidosis) should first be detected by ninhydrin (see section on amino acids, above), then overstained with orcinol.

Glycosaminoglycans

One-dimensional multisolvent TLC on cellulose plastic sheet is one of the methods used for qualitative analysis of urinary glycosaminoglycans (GAGs, acid mucopolysaccharides), whenever the photometric screening test with azure A + B is repeatedly positive. GAGs are isolated from the sediment of centrifuged urine (10 mL aliquots of 24 h urine, adjusted to

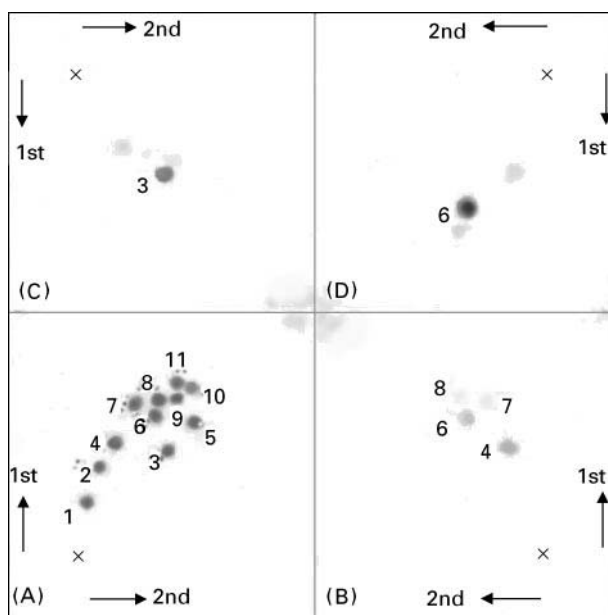


Figure 2 Separation of sugars (and oligosaccharides). The original 100 × 100 mm glass plate was divided into four by scraping off material. (A) Standard mixture; (B–D) urine samples: (B) normal neonate; (C) fructose intolerance (infant); (D) galactosaemia (neonate). 1, stachyose; 2, raffinose; 3, fructose; 4, lactose; 5, ribose; 6, galactose; 7, saccharose; 8, glucose; 9, xylose; 10, mannose; 11, arabinose.

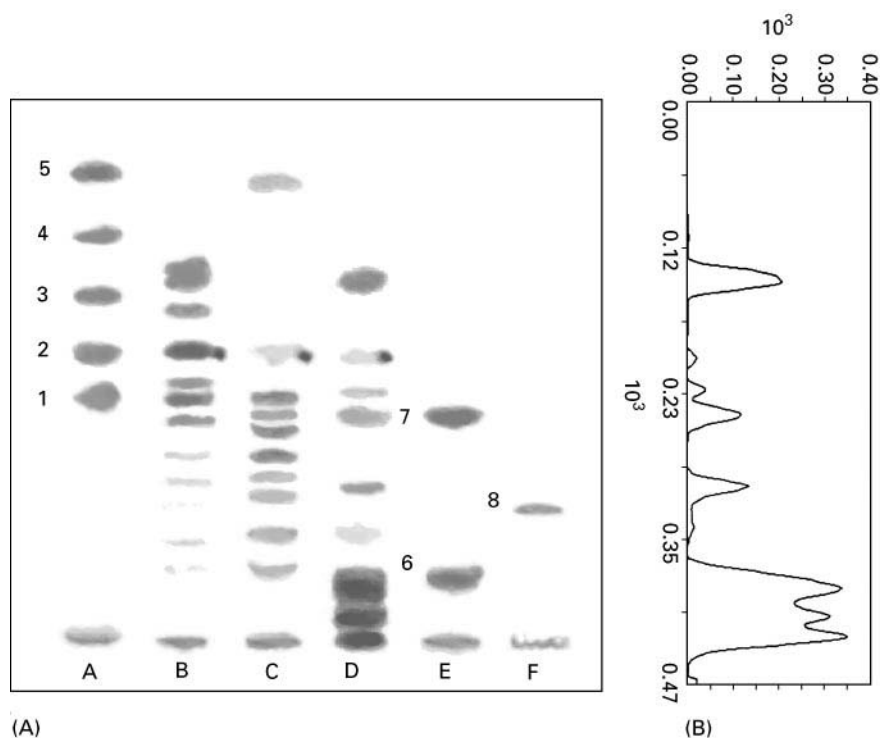


Figure 3 (A) TLC of oligosaccharides (and sugars), overlapping lactose as a standard. A, E, F, standards; B–D urine samples; A, normal infant; B, normal neonate; D, juvenile G_{M1} -gangliosidosis; F, overstained with resorcinol. 1, raffinose; 2, lactose; 3, glucose; 4, xylose; 5, ribose; 6, G_{M1} -octosaccharide; 7, glucotetrasaccharide; 8, sialic acid. (B) Densitogram of line D.

pH 5.5) by precipitation with 0.2 mL 5% aqueous cetylpyridinium chloride for 4 h in an iced-water bath. The dry precipitate is washed using 10 mL of 95% ethanol (saturated with sodium chloride) then diethyl ether, with centrifugation, decantation and drying in between. The precipitate is dissolved in 0.6 mol L⁻¹ sodium chloride (100 μ L) and 10 μ L aliquots are spotted on the layer. GAGs are successively separated (incremental distances of 2 cm for each run without intermediate drying) according to the solubility of their calcium salts in six solvents of decreasing ethanol concentration (1 mol L⁻¹ acetic acid–calcium acetate (g)–95% ethanol, v/w/v; I, 30 : 1 : 70; II, 40 : 2.5 : 60; III, 50 : 2.5 : 50; IV, 60 : 2.5 : 40; V, 70 : 2.5 : 30; VI, 100 : 5 : 0). After the sixth run, the plate is dried and immediately stained by immersing in toluidine blue in ethanol–acetic acid for 3 min. Excess stain is removed by rinsing in 10% acetic acid and the air-dried plate is evaluated by comparing with standards and using a densitometer (Figure 4).

Organic Acids

One-dimensional sequential TLC on cellulose glass plates in a horizontal arrangement with aniline–xylose detection is used in the screening for pathological organic acidurias.

Plasma, cerebrospinal fluid or vitreous humour is deproteinized with 95% ethanol, the supernatant is evaporated at 25°C under nitrogen, dissolved in water and the equivalent of 1 mL of the native material is further processed. A volume of urine, equivalent to 2.2 μ mol of creatinine, is made up to 1 mL with deionized water. All samples are then spiked with phenylbutyric acid as an internal standard, acidified to pH 1 with concentrated HCl and saturated with NaCl. Organic acids are extracted with 6 mL of diethyl ether–ethyl acetate mixture, 1 : 1 (vortexed, three times for 30 s). The supernatant is mixed with 100 μ L of 1 mol L⁻¹ ammonia solution in ethanol (to protect the volatile organic acids), concentrated under nitrogen at 25°C to 1 mL, and 20 μ L aliquots applied on the plate. Development is performed under saturated conditions in four consecutive steps (development distances increased in 1 cm steps in each run with intermediate drying), using the mobile-phase *n*-propanol–2 mol L⁻¹ ammonia, 7 : 3. The plate is sprayed with aniline–xylose reagent (xylose and aniline in methanol) and evaluated with a densitometer (Figure 5).

Purines and Pyrimidines

Two-dimensional TLC on cellulose glass plates in the horizontal arrangement with UV detection at

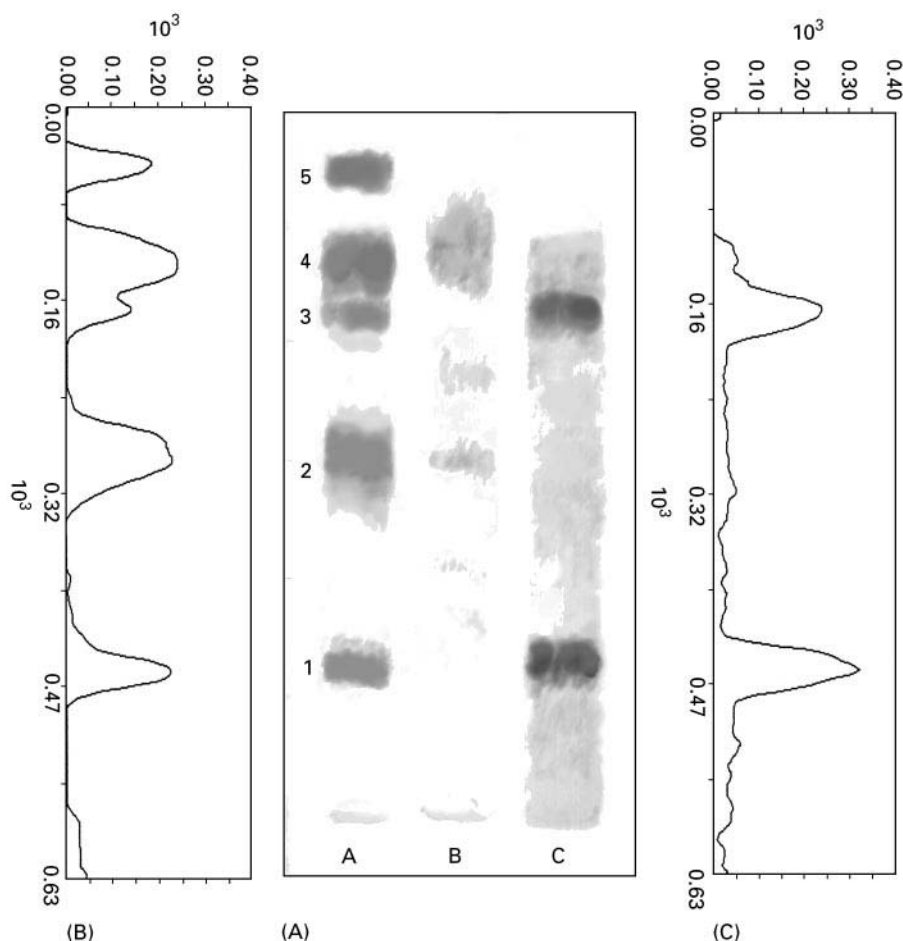


Figure 4 (A) TLC of glycosaminoglycans, multiple development. A, standards; B, control urine; C, mucopolysaccharidosis I-H. 1, dermatan-; 2, chondroitin-4-; 3, heparan-; 4, chondroitin-6-; and 5, keratan sulfates. (B) Densitogram of lane A; (C) densitogram of lane C.

254 nm is used to screen purine and pyrimidine defects. After 3 days on a low purine diet, 24 h urine is collected, warmed for 30 min at 50°C to dissolve precipitates and a filtered sample, equivalent to 50 μ mol creatinine, spotted on the layer. The mobile phase is *n*-butanol-methanol-water-25% ammonia, 40:20:20:1, developed twice with 15 min drying between each run for the first direction and 2 mol L⁻¹ ammonium sulfate in water for the second direction. Chromatograms are evaluated under UV light and by comparison with an age-control urine and the nucleoside and base standards, separated in parallel (Figure 6). For further identification, chromatograms are sprayed with mercuric acetate in 95% ethanol, then immediately with diphenylcarbazone in 95% ethanol and heated at 120°C for 10 min.

Tryptophan and its Metabolites

Screening method for both indolic and kynurenine metabolites of tryptophan (Trp) in urine is based on

Sep-Pak C₁₈ pretreatment, two-dimensional TLC on cellulose and detection at 254 and 366 nm, followed by staining with Ehrlich reagent. A volume of urine, equivalent to 2 μ mol of creatinine, is acidified to pH 3.5 and the clear supernatant applied on the Sep-Pak cartridge. Impurities from the sample are washed out, successively with sodium dodecyl sulfate (SDS) and SDS-methanol. The Trp metabolites are eluted with a mixture of 1 mol L⁻¹ ammonia and methanol (8:2). After evaporating the solvent under nitrogen the residue is dissolved in 250 μ L methanol. An aliquot of 20 μ L is applied on the dry cellulose layer, previously washed with de-ionized water. The plate is subjected to ascending development under saturated conditions at 4°C with two 0.2 mol L⁻¹ sodium acetate buffers: pH 6 for the first and pH 3.3 for the second direction. The air-dried plate is examined under UV light (Figure 7) and then sprayed with Ehrlich reagent. Comparing the urine sample with a mixture of standards, identification of 13 metabolites of tryptophan is possible.

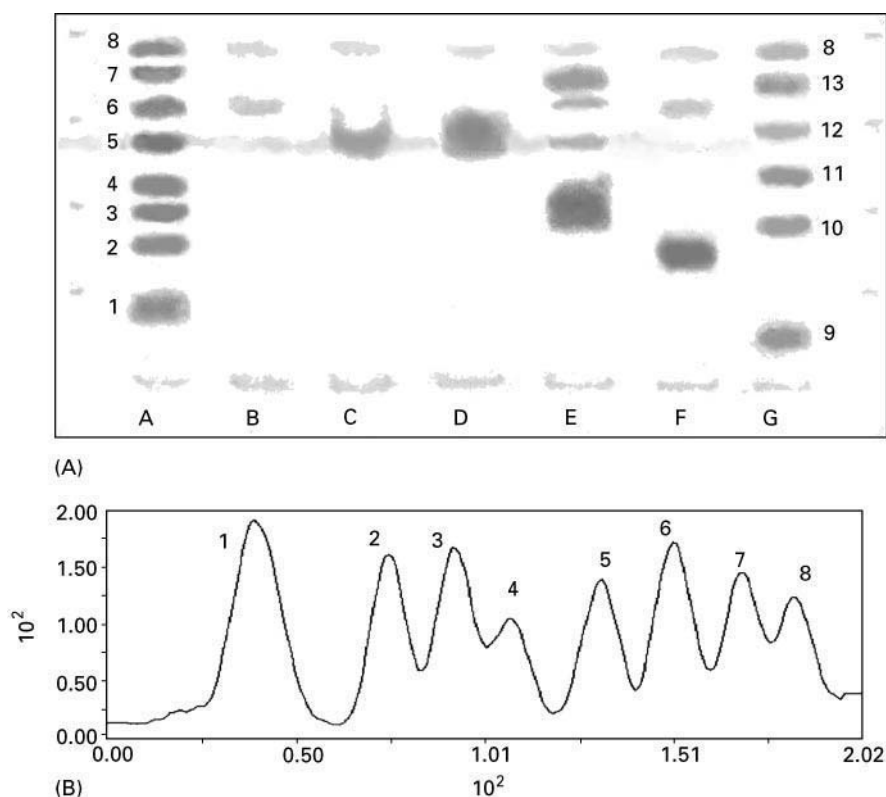


Figure 5 (A) TLC of organic acids, multiple development. A, standard mixture I; B, normal urine; C, normal plasma; D, lactic aciduria; E, 3-hydroxy-3-methylglutaric aciduria; F, methylmalonic aciduria; G, standard mixture II. 1, citric; 2, methylmalonic; 3, 3-hydroxy-3-methylglutaric; 4, ascorbic; 5, lactic; 6, hippuric; 7, isovaleric; 8, phenylbutyric (internal standard); 9, phosphoric; 10, adipic; 11, suberic; 12, sebacic; 13, 3-hydroxyisovaleric acids. (B) Densitogram of lane A.

Discussion

The protein-free filtrate from plasma and other material must be prepared rapidly to avoid binding of sulfur-containing amino acids to proteins. Some

changes occur rapidly at room temperature or even when stored at -20°C for a week (glutamine and asparagine, in particular, disappear).

There are several amino acid metabolic disorders which can easily be detected solely by TLC screening

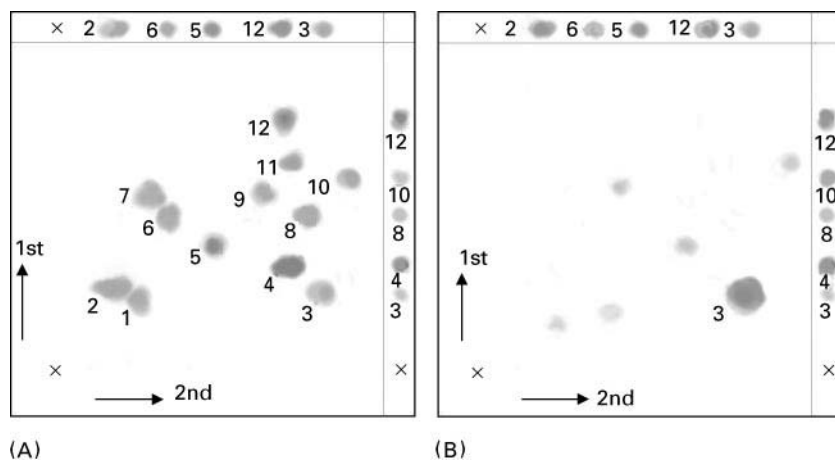


Figure 6 TLC of purines and pyrimidines. (A) Standards; (B) uric aciduria (adult). 1, xanthine; 2, guanine; 3, uric acid; 4, xantoxine; 5, hypoxanthine; 6, adenosine; 7, adenine; 8, orotic acid; 9, uracil; 10, cytosine; 11, inosine; 12, thymine.

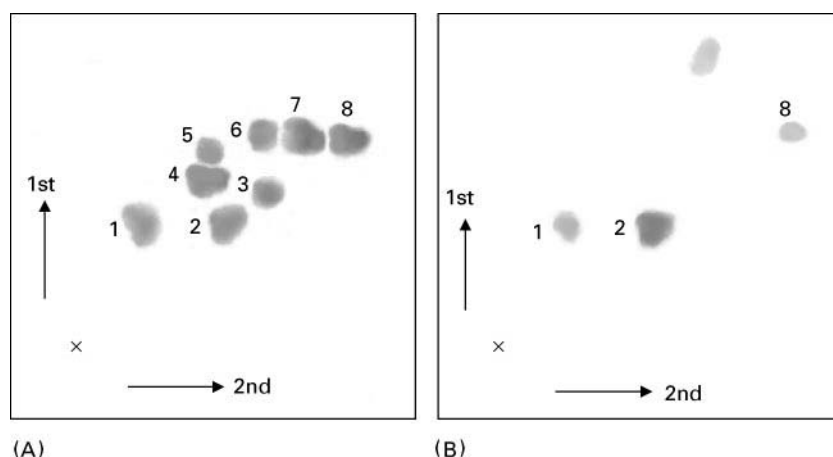


Figure 7 Separation of some indolic and kynurenine metabolites of tryptophan, UV 254 nm detection. (A) Standards, (B) xanthurenic aciduria (urine, child). 1, indolylacryloylglycine; 2, xanthurenic acid; 3, kynurenine; 4, kynurenic acid; 5, 5-hydroxyindolic acid; 6, 3-hydroxyanthranilic acid; 7, anthranilic acid; 8, indoxyl sulfate.

of urine, plasma or cerebrospinal fluid, such as leucinoses, phenylketonuria (where infants have not had newborn mass screening), hypermethioninaemic or -uric conditions, iminoglycinuria or cystinuria. An increase of glycine indicates primary nonketotic hyperglycinaemia or can be a secondary indication of an organic acid disease. Plasma glutamine is an important indicator of disorders of ammonia removal. Amniotic fluid is useful for prenatal detection of citrullinaemia, argininosuccinic aciduria or homocystinuria. High glycine in urine during therapy with valproate or ninhydrin-positive metabolites of antibiotics may confuse the interpretation of results.

On other occasions TLC only leads to a suspicion of IMD and a more precise method (amino acid analysis or HPLC) must be used for final diagnosis.

TLC is a simple screening technique for sugars, provided that their precursors are present in food. Under normal conditions no melituria is detectable. In neonates, traces of lactose and galactose appear in urine. Malabsorption, sugar intolerance, type I tyrosinosis and liver diseases, besides the genetic defects in metabolism of sugars, are the conditions related to pathological melituria. Two ribose-containing succinylpurines appear as blue-grey spots close to saccharose and galactose on chromatograms from urine and cerebrospinal fluid of patients with adenylosuccinase deficiency (IMD of purines).

Further investigation of sugar defects can be performed by specific enzyme assays, GC and HPLC.

Only slight banding with the most prominent glucose below raffinose-tetrasaccharide is detectable in normal urine when analysing oligosaccharides. Diagnosis may be difficult in neonates, where physiological lilac bands should be differentiated from the brownish ones excreted in mannosidosis, or from the pink-brown stripes seen under fucosidosis.

It is possible to combine a successive detection in UV light and spraying by ninhydrin, orcinol and resorcinol without losing sensitivity substantially. Some authors emphasize the importance of sample desalting; we have not found this necessary, desalting may lose some metabolites.

The final diagnosis can be achieved by enzyme activity assessment or structural analysis of the excreted oligosaccharides by gas chromatography-mass spectrometry (GC-MS) or nuclear magnetic resonance spectroscopy.

Most of the mucopolysaccharidoses (MPS) known so far present patterns of urinary GAGs which are clearly different from normal, even if the total urinary GAGs are not always present in excess (some cases of type III MPS), or the typical component does not react (keratan sulfate in MPS type IV). On the other hand, some pathological chromatograms may not reliably differentiate between MPS types I and VI, for example, without enzyme analysis. The main advantage of TLC of GAGs is to facilitate selection of the probable defective enzyme to be analysed for the definite diagnosis.

Urinary organic acid analysis is a vital diagnostic tool in the investigation of patients with suspected IMD, although not many laboratories perform TLC of organic acids. We consider this approach to be an important and convenient way of getting prompt orientation, allowing exclusion of negative samples in the first place. In healthy controls, organic acids are present at trace levels, the most prominent being hippuric acid. Pathological specimens are conspicuous by either unusual or very dark bands. Unclear or suspicious results are further checked by GC-MS, employing the remaining sample which is immediately lyophilized after an aliquot has been applied on the TLC layer.

Organic acid analysis may help in the diagnosis of saccharides, amino acids, fatty acids and respiratory chain defects.

Using two-dimensional TLC, some purine and pyrimidine defects can be revealed. Unfortunately, specific and sensitive visualization agents of these strongly UV-absorbing substances are not available. Large unusual spots in urine are easily detectable, but some false positives, due to other metabolites, drugs or food additives, should be carefully interpreted and verified by HPLC. HPLC-MS combined with an ion exchange pretreatment of urine is a promising method for the final diagnosis of these defects.

Metabolites of Trp are difficult to analyse because of their instability and low concentration in urine. To minimize losses, bright light should be avoided throughout the procedure. The method used is simple and reliable enough to detect increased excretion of Trp metabolites. In the case of any abnormality observed, the same pretreated urine sample is further processed by HPLC.

Conclusion

TLC might seem to be slightly overshadowed since the introduction of more sophisticated methods in the screening of IMD. However, these methods are not available everywhere and their cost may discourage their use for screening, so that they are only applied in rather advanced cases. Using TLC, more samples can be separated simultaneously on one plate under identical conditions, which decreases the price per analysis. Horizontal arrangement of plates can be economically employed for routine use because mobile-phase consumption is very low. Availability of pre-scored layers makes analyses more flexible, more rational and economical. Advantages of HPTLC pre-coated layers, compared to the standard ones which were previously used, consist in sharper separation, shorter migration distance, minimal diffusion and increased detection sensitivity.

Various TLC techniques in screening for IMD have been described. In general, we prefer such procedures, when the sample, analysed by TLC, may be subject to more detailed analysis by HPLC or GC-MS, if necessary. Using creatinine concentration as a basis for the volume option of the urine processed, misinterpretation of results can be minimized.

In children with unexplained neurological disease it is highly recommended that amino acid and sugar analysis of cerebrospinal fluid and urine before and after acid hydrolysis is performed systematically. In this way defects of purines or (N-acetylated) amino acids and peptides can be detected by virtue

of a large increase in aspartate, glycine or ribose levels.

TLC represents only one part of the whole IMD screening procedure and it is necessary to emphasize that negative TLC results do not prevent more detailed investigation if the patient shows continuous signs of an acute disease or progression of neurological symptoms.

It should be emphasized that negative findings are also important, because metabolic disease can be excluded.

Acknowledgement

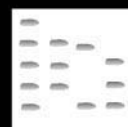
This work has been supported in part by the Ministry of Health, Czech Republic, Project No. 4097-3.

See also: **II/Chromatography: Thin-Layer (Planar):** Densitometry and Image Analysis; Instrumentation; Modes of Development: Conventional. **III/Acids:** Thin-Layer (Planar) Chromatography. **Amino Acids:** Thin-Layer (Planar) Chromatography. **Carbohydrates:** Thin-Layer (Planar) Chromatography. **Clinical Chemistry: Thin-Layer (Planar) Chromatography.** **Nucleic Acids:** Thin-Layer (Planar) Chromatography.

Further Reading

- Bender DA, Joseph MH, Kochen W and Steinhart H (eds) (1986) *Progress in Tryptophan and Serotonin Research*. Berlin: Walter de Gruyter.
- Chalmers RA and Lawson AM (1982) *Organic Acids in Man: Analytical Chemistry, Biochemistry and Diagnosis of Organic Acidurias*. London: Chapman & Hall.
- Duran M, Dorland L, Wadman SK and Berger R (1994) Group tests for selective screening of inborn errors of metabolism. *European Journal of Pediatrics* 153 (suppl 1): S27-S32.
- Hommes FA (ed.) (1991) *Techniques in Diagnostic Human Biochemical Genetics. A Laboratory Manual*. New York: Wiley-Liss.
- Kelly S (1977) *Biochemical Methods in Medical Genetics*. American Lecture Series. Springfield, IL: Charles C Thomas.
- Scriver CR, Beaudet AL, Sly WS and Valle D (eds) (1995) *The Metabolic and Molecular Basis of Inherited Disease*. New York: McGraw-Hill.
- Sherma J and Fried B (eds) (1990) *Handbook of Thin-layer Chromatography*. New York: Marcel Dekker.
- Shih V (1973) *Laboratory Techniques for the Detection of Hereditary Metabolic Disorders*. Cleveland, OH: CRC Press Uniscience.
- Smith I (ed.) (1969) *Chromatographic and Electrophoretic Techniques, Vol. I, Chromatography*, 3rd edn. Bath, UK: Heinemann-Medical.
- Touchstone JC (1992) *Practice of Thin Layer Chromatography*. New York: Wiley-Interscience.

INCLUSION COMPLEXATION: LIQUID CHROMATOGRAPHY



S. R. Gratz, B. M. Gamble and A. M. Stalcup,
University of Cincinnati, Cincinnati, OH, USA

Copyright © 2000 Academic Press

Introduction

Liquid chromatography (LC) may be simply described as an analytical technique used to separate the individual components of a solution based on their relative affinities for a liquid mobile phase and a stationary phase. There are numerous modes of LC (i.e. reversed-phase, normal-phase, ion exchange) that are commonly classified according to the mechanism by which separation occurs. One such mechanism involves the formation of inclusion complexes. An inclusion complex can be defined as an entity, consisting of two or more molecules, in which one molecule, the 'host', noncovalently encapsulates or includes a 'guest' molecule. In chromatography, differences in the strength of binding between guest molecules or analytes and a specific host allow for separation. The purpose of this article is to review recent applications of inclusion complexation in liquid chromatography. Although a variety of small molecule interactions with macromolecules or polymers have been ascribed to inclusion complexation, the focus of this article is on well-defined host molecules.

Host Molecules

Currently, there is a variety of compounds that can serve as a host molecule in an inclusion complex, most of which may be grouped into one of four classes. These classes include cyclodextrins, crown ethers, calix[n]arenes and macrocyclic antibiotics. A representative structure from each class of hosts is shown in Figure 1. One characteristic shared by each class of host molecules is the ability to include selectively compounds on the basis of size and shape.

It is important to point out that many inclusion host molecules possess at least one chiral centre (e.g. macrocyclic antibiotics and cyclodextrins) and that the vast majority of applications lie in the area of chiral separations. Chiral molecules are those that can exist as nonsuperimposable mirror images, or enantiomers. It has been demonstrated that the enan-

tiomers of many chiral compounds exhibit different bioactivities and/or biotoxicities. It has also been demonstrated that enantiomers may exhibit different complex stabilities when included in a given chiral host. This fact, combined with an increased awareness of the implications of chirality, has led to the exploitation of inclusion complexation for chromatographic chiral separations. For this reason the emphasis of this article is placed on chiral applications, but some achiral applications are also presented.

Briefly, cyclodextrins (CDs), which are natural products, are cyclic oligosaccharides consisting of D-glucose rings linked through α -(1, 4)-bonds. The glucose units are arranged in a toroidal structure best described as a truncated cone. The most common cyclodextrins are α -, β - and γ -CD which consist of six, seven and eight glucose rings, respectively. The interior of the cyclodextrin molecule is hydrophobic while the exterior is hydrophilic. Because a cyclodextrin consists of chiral D-glucose units, it constitutes a chiral host.

Crown ethers are perhaps best described as synthetic, heterocyclic macrocycles with repeating units of $(-X-C_2H_4-)$ where X is the heteroatom. In contrast to cyclodextrins, crown ethers are characterized by a hydrophobic exterior and a hydrophilic cavity. The cavity typically has a strong affinity for cationic species owing to electrostatic interactions between the cation and the heteroatoms of the crown ether. These characteristics of crown ethers have led to their use as phase transfer catalysts in organic synthesis.

Calix[n]arenes are synthetic, cyclic oligomers composed of phenolic units linked by methylene bridges. They may contain four to eight aryl moieties forming a macrocyclic structure with a central cavity. The inclusion interaction between calixarenes and various guest molecules is determined both by the cavity size and by the nature of the functional groups that act as binding sites. Although still relatively unexplored, the ability to functionalize calixarenes offers yet another method for the tailoring of chromatographic selectivity.

Finally, macrocyclic antibiotics typically possess numerous chiral centres that surround several pockets or cavities bridged by a series of aromatic rings. Like cyclodextrins, the macrocyclic antibiotics are also natural products. In contrast to other host molecules, native macrocyclic antibiotics incorporate ionizable moieties.

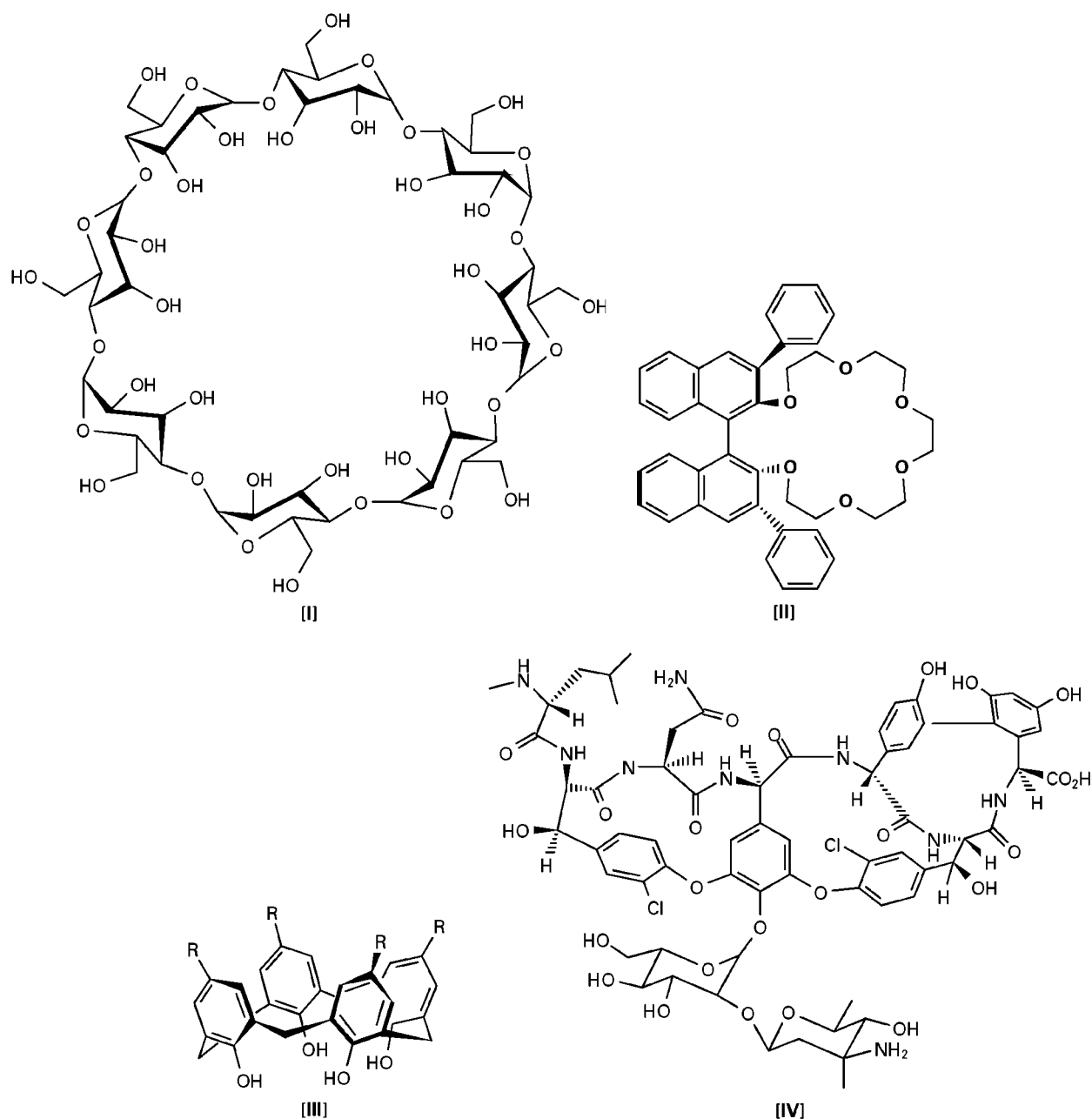


Figure 1 Representative structures of inclusion complex host molecules: [I], γ -CD; [II], a chiral crown ether; [III], a calix[4]arene; and [IV], vancomycin.

Currently there are two primary methods for exploiting inclusion complexation in LC. One method is the use of an inclusion host molecule as an immobilized ligand on a chromatographic sorbent. Stationary phases modified by cyclodextrin, crown ether, calixarene and macrocyclic antibiotic have all been reported. Alternatively, inclusion complex host molecules may be employed as mobile phase additives.

Historically, many of the hosts used to modify stationary phases originated as mobile phase additives, and thus will be considered first. Some advant-

ages and disadvantages of each method are outlined in Table 1.

Inclusion Complexation in the Mobile Phase

One approach to exploiting inclusion complexation in chromatography involves dissolving the host in the mobile phase. As indicated in Table 1, use of the host as a mobile-phase additive (MPA) instead of the cor-

Table 1 Advantages and disadvantages of using inclusion complex host molecules as mobile phase additives

<i>Advantages</i>	<i>Disadvantages/limitations</i>
Less expensive, conventional packed columns can be used	Possible interference with detection of analyte
Type and concentration of host are easily changed	Potential solubility problems
Wider variety of additives compared with stationary phases	Effect on mobile phase viscosity
Different selectivities relative to corresponding stationary phase	Impact on analyte recovery
	Large amounts of additive needed for column pre-equilibration

responding bonded stationary phase has a number of advantages and disadvantages, depending on the application. One of the primary reasons for utilizing the host as a MPA is that it offers more flexibility for the application, both in the type of host used and the concentration of the host. Unfortunately, the amount of additive needed to equilibrate chromatographic columns and to separate the samples can be very large, making this approach very costly. This is not a problem in thin-layer chromatography, since TLC plates do not require equilibration with the mobile phase. In either case, the presence of the additive in the mobile phase can complicate detection and analyte recovery.

Both cyclodextrins and macrocyclic antibiotics have been used extensively as MPAs, with cyclodextrins being the most widely used. Calixarenes and crown ethers have found more limited use as MPAs. The large absorption of the phenyl groups in the calixarene molecule makes it very difficult to detect the analyte by UV spectrophotometry owing to the high background. Crown ethers have been used to aid in the dissolution of buffers in strong organic systems and to assist in the partitioning of analytes

into the mobile phase. In one study, 18-crown-6 was used in the separation of carboxylated porphyrins. It was suggested that the crown ether could facilitate the partition of the porphyrins into the mobile phase through hydrophobic and polar interactions.

Cyclodextrins

Cyclodextrins are commonly used for the separation of enantiomers (chiral applications), but have also found use in the separation of geometric and structural isomers (e.g. α -pinene and β -pinene). Cyclodextrins can be used in their native form or as chemically modified additives. By derivatizing the outer rim hydroxyls of the cyclodextrin with various functional groups, the properties of the native cyclodextrins can be changed. Several representative examples of native and derivatized cyclodextrins, together with the types of molecules separated, are outlined in Table 2.

One of the main advantages to derivatization is the change in the solubility properties of cyclodextrins. Native β -CD, which is one of the most commonly used inclusion-type additives, has a very low solubility in aqueous-organic systems (solubility = 1.85 g

Table 2 Typical applications of native and derivatized cyclodextrins in liquid chromatography

<i>Cyclodextrin</i>	<i>Abbreviation</i>	<i>Applications</i>
Hydroxypropyl β -CD	HPBCD	Barbiturates, chlorophenols, amino acids, laser dyes, chlorophenols, hydantoins
Carboxymethyl β/γ -CD	CMCD	Steroidal drugs, amino acids
Water-soluble β -CD polymer	SCDP	Pesticides, barbiturates, chlorophenols, nitrostyrenes, tensides, cyclic hydrocarbons
Dimethyl carbamate β -CD	DMP	Radioligands
2,6-di- <i>O</i> -methyl β -CD	DIMEB	Barbiturates
Heptakis(2,3,6-tri- <i>O</i> -methyl) β -CD	TRIMEB	Tensides
Naphthylethyl carbamate β -CD	NEC-CD	Benzodiazepines, anesthetics, amines, amino acid esters, diuretics
Cationic β -CD		Amino acids, hydantoins
Acetyl β -CD		Anticancer drugs, aminoalkyl phosphonic acids, bronchodilators
Permethylated β -CD		Amino acids
Maltosyl β -CD		Amino acids, alkaloids
Sulfated β -CD		Anesthetics, antiarrhythmics, antimalarials, catecholamines, antidepressants, anticonvulsants, antihistamines
Native α -CD		Barbiturates, ArOH, tensides, terpenes
Native β -CD		Barbiturates, amino acids, PAHs, ArOH, aflatoxins, hydantoins, antiepileptic drugs, tensides, terpenes, alkaloids
Native γ -CD		Barbiturates, tensides, porphyrins, β -blockers

ArOH, aromatic alcohol.

per 100 mL of water, $\approx 16 \text{ mmol L}^{-1}$ solution). Solutions of derivatized cyclodextrins, however, can be made at concentrations as high as 400 mmol L^{-1} . It is important to note that these functionalized cyclodextrins are complex mixtures of reaction products. The increased solubility is a direct consequence of this product impurity. Unfortunately, the more concentrated cyclodextrin solutions have increased viscosity. Derivatization of cyclodextrins also affects its chromatographic selectivity, as a result of additional interactions made possible by the presence of various functional groups.

Liquid chromatography Thus far, of all the potential host molecules, cyclodextrins are the most extensively used MPAs in liquid chromatography. Most commonly, cyclodextrins are used as MPAs in the reversed-phase mode. The mobile phase typically consists of an aqueous buffer and an organic modifier. The cyclodextrin additive is included in the buffer component at concentrations appropriate to the application. In general, as the concentration of the cyclodextrin is increased, the enantioselectivity increases until an upper limit is reached. This is illustrated in Figure 2 for the separation of (\pm) - α -pinene. The organic component of the mobile phase should not form strong inclusion complexes with cyclodextrin as this will limit the interactions with the analyte(s) of interest. Large, bulky organic solvents should be avoided for this reason. Solvents typically used are methanol and acetonitrile, both of which form relatively weak inclusion complexes with cyclodextrins. Percentages of organic solvent used can be as low as 3% and as high as 45% in an isocratic mixture where gradients are not used. Typically, octadecylsilane (ODS) columns are used but other

bonded phases can be employed, depending on the application.

As mentioned, the use of cyclodextrins as MPAs allows the separation of enantiomers (e.g. (\pm) - α -pinene) and structural isomers. This allows the application of this method to many pharmaceuticals, pesticides and natural products. By varying the experimental parameters (type and concentration of cyclodextrin, percent organic solvent, etc.), information about the strength and stability of the complex can be obtained.

Mechanistic information about complex formation can also be obtained from the data. Frequently, a 1 : 1 host-guest complex is formed, but 2 : 1 complexes have been reported in the separation of terpenes and polycyclic aromatic hydrocarbons (PAHs).

Thin-layer chromatography Cyclodextrins can also be used as complex hosts in TLC. They are almost exclusively employed as MPAs rather than as bonded phases because there are no commercially available cyclodextrin bonded-phase TLC plates. The success of cyclodextrins may be partially attributed to their UV transparency.

Commercially available, reversed-phase plates are typically used. However, a 5% paraffin-in-hexane solution can be used to impregnate standard TLC plates for use as reversed-phase plates. The mobile phase is usually a water/organic solvent mixture with occasional use of buffers in the aqueous portion. As in column chromatography, the organic component is typically methanol or acetonitrile, and in some cases ethanol. The concentration of cyclodextrin in the mobile phase is usually less than 30 mmol L^{-1} and the choice of cyclodextrin concentration is governed by the same factors as discussed above for liquid chromatography. In general, as the concentration of the cyclodextrin is increased, the development time will increase due to the increased viscosity of the resulting solution.

The use of MPAs in TLC is often used to study the binding characteristics of various compounds to inclusion complex host molecules. This is typically accomplished using the following general equation (eqn [1]):

$$R_M = R_{M0} + bC \quad [1]$$

where R_M is the actual R_M value of an analyte determined at C (mmol L^{-1}) additive concentration; R_{M0} is the R_M value of an analyte extrapolated to zero additive concentration; b is the decrease in the R_M value caused by a 1 mmol L^{-1} increase of the additive concentration in the eluent (indicator of the complexing capacity); and C is the additive concentration in the eluent (mmol L^{-1}).

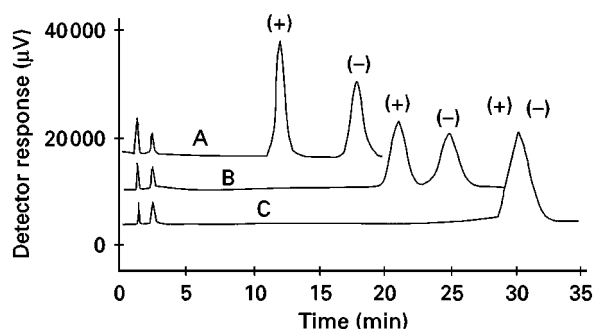


Figure 2 Separation of α -pinene enantiomers using α -CD as a mobile phase additive: (A) $16 \text{ mmol } \alpha\text{-CD}$; (B) $8 \text{ mmol } \alpha\text{-CD}$; (C) No $\alpha\text{-CD}$. (Adapted from Moeder C, O'Brien T, Thompson R and Bicker G (1996) Determination of stoichiometric coefficients and apparent formation constants for α - and β -CD complexes of terpenes using reversed-phase liquid chromatography. *Journal of Chromatography A* 736: 1–9).

The slope value, b , is linearly related to the stability of the host-guest complex. For example, a wide variety of pharmaceuticals, nonionic surfactants (tensides) and substituted aromatics have been investigated by this method. Frequently, information is needed about the steric and hydrophobic character of various analytes. Host-guest binding constants can provide information about inclusion within the cyclodextrin cavity. Cyclodextrins have also been used to study the effects of inclusion on the stability and transport of drugs. It is known that cyclodextrins can influence many of the biological properties of drugs when a host-guest complex is formed. The uptake, adsorption properties and degradation of the drug can be modified by complex formation.

Cserhádi and Forgács recently studied complex formation between carboxymethyl- γ -cyclodextrin and steroidal drugs. They found that the cyclodextrin mediated the hydrophobicity of the drugs suggesting that the complexed drug may have a modified efficacy.

Macrocyclic Antibiotics

In contrast to cyclodextrins, which have been used for chiral as well as achiral applications, macrocyclic antibiotic MPAs have been applied exclusively to enantiomeric separations. Macrocyclic antibiotics such as vancomycin and erythromycin have been used to resolve enantiomers by TLC. The first macrocyclic antibiotic to be used as a MPA was vancomycin by Armstrong and Zhou in 1994. It was used as a chiral selector in the TLC resolution of dansyl-amino acids, 6-aminoquinolyl- N -hydroxysuccinimidyl carbamate (AQC)-derivatized amino acids, and several pharmaceutical compounds. The composition of the mobile phase as well as the nature of the stationary phase were found to affect chiral resolution for these compounds. The mobile phase consisted of 0.6 mol L^{-1} NaCl with acetonitrile concentration between 17 and 40 vol%. The purpose of NaCl was to stabilize the binder on the TLC plates. For some of the derivatives, a 1% triethylammonium acetate buffer (pH 4.1) was also needed. It was found that diphenyl-type bonded phases provided the best resolution of the compounds studied. For all the amino acid derivatives, the D-enantiomer had a larger R_F value than the L-enantiomer.

Inclusion Complexation in the Stationary Phase

As mentioned previously, no commercially available TLC plates incorporate inclusion complexation ligands. However, conventional TLC plates have

been coated with various inclusion host molecules. For example, erythromycin was used to resolve a variety of dansyl-DL-amino acids. By impregnating the plate with 0.05% erythromycin, resolution of the enantiomers of the amino acids was achieved in a relatively short time (20–25 min). A mobile phase consisting of 0.5 mol L^{-1} NaCl, acetonitrile and methanol was used for the separation with one amino acid requiring the presence of acetic acid for separation. The amount of NaCl solution used was generally 7–25 times the amount of acetonitrile used. Methanol was required in very small amounts in some cases. The resolution of the enantiomers was affected by small changes in the mobile phase composition, as is the case with most chiral separations.

Cyclodextrin Phases

Among the inclusion-type stationary phases, the cyclodextrin phases have been the most widely used and the most successful, specifically in the area of chiral separations. Most chiral separations reported on native CD phases (α, β, γ) have been accomplished in the reversed-phase mode using aqueous buffers with small amounts of organic modifier. β -CD is the most commonly used of the native cyclodextrins. The applicability of CD phases has increased with the development of strategies for derivatizing these compounds. Functionalized cyclodextrins have also been used in the reversed-phase, normal-phase, and nonaqueous reversed-phase modes.

The functional groups on derivatized CDs can play a variety of roles in enhancing enantioselectivity. In some cases the substituent provides additional sites for interaction or may enlarge the CD cavity, allowing inclusion of larger analytes. Reported applications of the cyclodextrin phases are seemingly endless. However, several general conclusions can be drawn based on applications along with the theoretical work done in this area. First of all, inclusion complexation is believed to be a significant interaction only when CD-bonded phases, native or derivatized, are used in the reversed-phase mode. Next, inclusion complexation requires that at least some portion of the analyte fits structurally into the CD cavity. Typically, the presence of an aromatic ring in the analyte molecule satisfies this condition. Results indicate that chiral recognition is enhanced if the stereogenic centre lies between two π -systems or is incorporated in a ring. The presence of secondary hydroxyl groups at the rim of the CD cavity allows for hydrogen bonding with polar molecules. Amine and carboxyl functional groups have been shown to interact strongly with those hydroxyl groups on na-

tive CD phases, while nitrate, sulfate, phosphate and hydroxyl functional groups seem to prefer inclusion. Finally, both flow rate and temperature are known to affect CD-based chiral recognition in the reversed-phase mode. The enantioselective inclusion properties of native CDs have rendered them quite useful as chromatographic substrates, and the ability to derivatize these macrocyclic compounds has made them extremely versatile as inclusion complex host molecules.

Crown Ether Phases

The use of crown ethers as inclusion complexation stationary phases for LC originated with the work of Cram and co-workers during the mid-1970s. They observed that these compounds, specifically tetra-naphthylated 18-crown-6-ethers, could form inclusion complexes with alkylammonium compounds and used this idea to develop a chiral stationary phase for the separation of enantiomeric amines. Initially, crown ethers were covalently attached to a silica gel or polystyrene matrix until it was realized that they could be dynamically coated onto reversed-phase packing materials. Eventually, this chiral crown ether stationary phase was made commercially available. Numerous applications have demonstrated the ability of this phase to resolve most primary amino acids, amines, amino esters and amino alcohols. **Figure 3** shows a chromatogram in which a series of three racemic amino acids are separated using an ODS column coated with the chiral crown ether, compound [II]. With respect to enantiomeric separations, the crown ether phase is unique in that it does not require that analytes possess an aromatic ring for the achievement of chiral separation. Optimum performance of the crown ether is observed in acidic mobile phases that ensure protonation of the primary amine

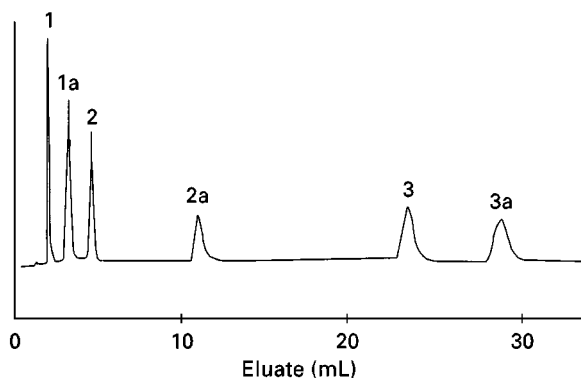


Figure 3 Enantiomeric separation of racemic amino acids: 1, D-arginine; 1a, L-arginine; 2, D-methionine; 2a, L-methionine; 3, D-tyrosine; and 3a, L-tyrosine. (Adapted from Shinbo *et al.*, 1987.)

functionality, which is included in the crown ether cavity. Typically, perchloric acid ($\cong 0.01 \text{ mol L}^{-1}$) with small amounts of acetonitrile or methanol is recommended as it provides better resolution and exhibits low UV absorption. A notable advantage of the crown ether phases is the commercial availability of both chiral configurations, so that the enantiomeric elution order can be readily changed.

Calix[n]arene Phases

Much like cyclodextrins, calixarenes are macrocyclic compounds that may be easily functionalized, which gives them great potential as stationary phase material. Unlike CDs, however, calixarenes have not yet been extensively employed in liquid chromatography, and therefore only a limited number of applications have been reported. The most successful applications have come with the calixarene chemically immobilized onto a silica gel matrix using a short hydrophilic spacer.

Successful separations of several classes of compounds including amino acids, polyaromatics, nucleosides and nucleobases using a *p*-tertbutyl calixarene-bonded phase indicated that this phase behaves primarily as a reverse-phase material. A typical chromatogram illustrating the separation of nucleosides on this phase is shown in **Figure 4**. In the same study, calixarene phases were reported to form strong inclusion complexes with sodium ions. The complexation with sodium presumably induces a conformational reorientation of the calixarene that increases its hydrophobic surface area, allowing for stronger interaction with hydrophobic analytes.

In another study using a calix[4]arene tetra-diethylamide phase, selective retention of Na^+ over other alkali metals and Ca^{2+} over Mg^{2+} was observed using only water as the mobile phase. Furthermore, addition of methanol to the mobile phase resulted in increased retention of NaCl while the retention of LiCl, KCl and CsCl was unaffected by methanol.

Macrocyclic Antibiotic Phases

Stationary phases based on macrocyclic antibiotics (MAs) such as vancomycin and teicoplanin were introduced by Armstrong in 1994. Now commercially available, and used almost exclusively for enantiomeric separations, these phases are typically referred to as the ChirobioticTM phases. **Figure 5** illustrates a chiral separation of bromocil, devrinol and coumachlor on a vancomycin stationary phase. Chiral selectivity with these phases is demonstrated in

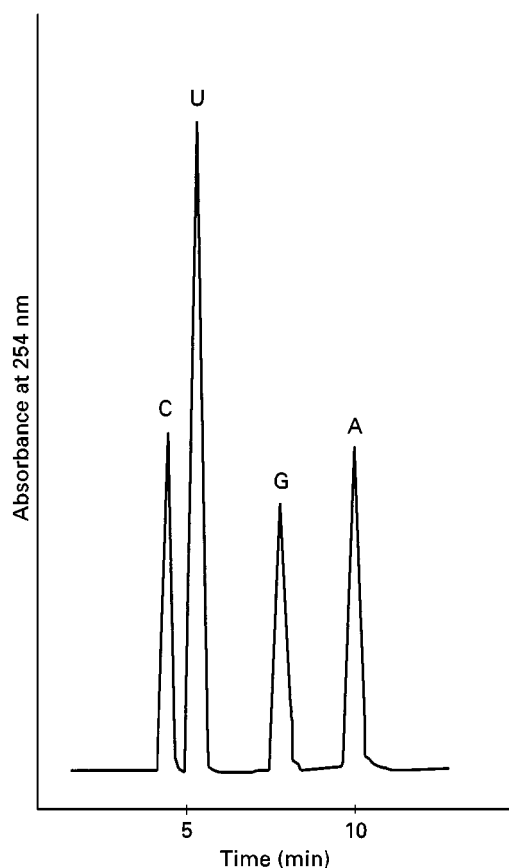


Figure 4 Separation of four nucleosides using a calixarene-bonded phase: cytidine (C), uridine (U), guanosine (G) and adenosine (A). (Adapted from Friebe *et al.*, 1995.)

the normal, polar organic and reversed-phase modes, allowing for the separation of a large variety of chiral analytes. The complexity of the antibiotic structures provides a number of potential interactions that may assist in separation, only one of which is inclusion complexation. Furthermore, an inclusion mechanism is likely to play a role only in the reversed-phase

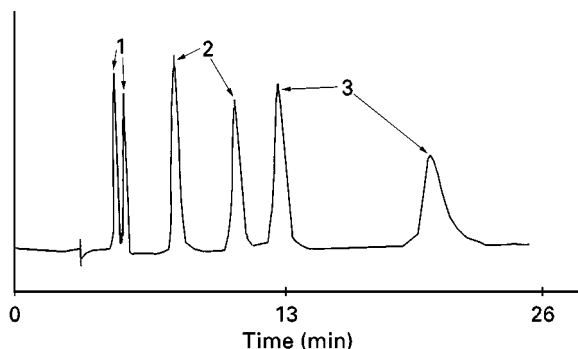


Figure 5 Enantiomeric separation of (1) bromocil, (2) devrinol and (3) coumachlor using a vancomycin stationary phase. (Adapted from Armstrong *et al.*, 1994.)

mode, hence this discussion will be limited to the reversed-phase characteristics of these phases.

A great deal of success has been attained with MA phases for the chiral separations of neutral molecules as well as amides and esters. Table 3 lists the conditions for several representative examples of chiral separations accomplished on a vancomycin-bonded phase.

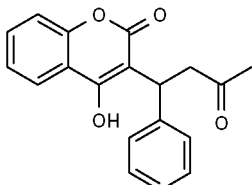
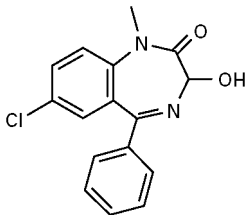
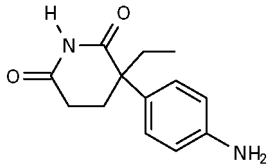
In terms of optimization and method development, retention can be controlled by adjusting the amount of organic modifier in the mobile phase. Selectivity is controlled by the type of buffer, the type of organic modifier and the pH. Both efficiency and selectivity are affected by the buffer type, ionic strength, flow rate and temperature. Tetrahydrofuran is reported to be the best overall starting organic modifier for efficiency and selectivity, but acetonitrile, methanol and ethanol have also been used with success.

It is important to note that these MAs can also be derivatized to alter enantioselectivity, which will undoubtedly increase the number of potential applications. Furthermore, the relatively small size of these molecules together with the fact that their structures are known increases the feasibility of performing mechanistic studies on chiral recognition.

Conclusions and the Future of Inclusion Complexation in Liquid Chromatography

The inclusion properties of several macrocyclic compounds with guest molecules have been extensively utilized in liquid chromatography. This has been accomplished by employing potential inclusion hosts as mobile-phase additives or as immobilized ligands on the chromatographic stationary phase. The presence of these macrocyclic host molecules in the mobile phase can interfere with analyte detection. Hence, most applications of inclusion complexation in liquid chromatography employ and will continue to employ immobilized ligands. While the commercial availability of the cyclodextrin, macrocyclic antibiotics and crown ether phases has no doubt contributed to their widespread exploitation, the calixarene phases may become more useful in the future as their properties become better understood. Certainly, the calixarene structure is more amenable to intelligent design than the naturally derived macrocyclic antibiotics or cyclodextrins. Inclusion complexation technology has been most extensively used in the area of chiral separations. Derivatization of macrocyclic compounds, such as cyclodextrins, macrocyclic antibiotics, crown ethers and calix[*n*]arenes has further enhanced their chromatographic utility.

Table 3 Applications of macrocyclic antibiotic-bonded phase

Compound	Structure	k (1st enantiomer)	α	Mobile phase	pH
Warfarin		1.98 2.27	1.70 1.44	10% ACN/ 90% buffer	7.0 4.1
Temazepam		1.17	1.06	10% ACN/90% buffer	7.0
Aminogluthethimide		0.79	1.15	10% ACN/90% buffer	7.0

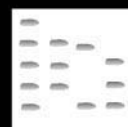
The buffer is 1% triethylammonium acetate. The column used was a 25 cm \times 4.6 mm i.d. vancomycin stationary phase.

See also: **III/Chiral Separations:** Capillary Electrophoresis; Cyclodextrins and Other Inclusion Complexation Approaches; Liquid Chromatography; Thin-Layer (Planar) Chromatography. **Essential Oils:** Gas Chromatography.

Further Reading

- Armstrong D and Zhou Y (1994) Use of a macrocyclic antibiotic as the chiral selector for enantiomeric separations by TLC. *Journal of Liquid Chromatography* 17: 1695–1707.
- Armstrong D, Tang Y, Chen S, Zhou Y, Bagwill C and Chen J (1994) Macrocyclic antibiotics as a new class of chiral selectors for liquid chromatography. *Analytical Chemistry* 66: 1473–1484.
- Bhushan R and Parshad V (1996) Thin-layer chromatographic separation of enantiomeric dansylamino acids using a macrocyclic antibiotic as a chiral selector. *Journal of Chromatography A* 736: 235–238.
- ChirobioticTM Handbook* (1996) Advanced Separation Technologies, Inc.
- Cserháti T and Valkó K (1994) *Chromatographic Determination of Molecular Interactions: Applications in Biochemistry, Chemistry and Biophysics*. Boca Raton, FL: CRC Press.
- Friebe S, Gebauer S, Krauss G, Goeremar G and Krueger J (1995) HPLC on calixarene bonded silica gels. I. Characterization and applications of the *p*-tert-butylcalix[4]arene bonded material. *Journal of Chromatographic Science* 33: 281–284.
- Glennon J, Horne E, Hall K et al. (1996) Silica-bonded calixarenes in chromatography. II. Chromatographic retention of metal ions and amino acid ester hydrochlorides. *Journal of Chromatography* 731: 47–55.
- Shinbo T, Yamaguchi T, Nishimura K and Sugiura M (1987) Chromatographic separation of racemic amino acids by use of chiral crown ether-coated reversed-phase packings. *Journal of Chromatography* 405: 145–153.
- Snopek J, Smolkaová-Keulemansová E, Cserháti T, Gahm K and Stalcup A (1996) In: Atwood J, Davies J, Macnicol D and Vogtle F (eds) *Comprehensive Supramolecular Chemistry*, pp. 515–573. Oxford: Pergamon.
- Stalcup A and Gahm K (1996) A sulfated cyclodextrin chiral stationary phase for high-performance liquid chromatography. *Analytical Chemistry* 68: 1369–1374.

IN-DEPTH DISTRIBUTION IN QUANTITATIVE TLC



I. Vovk and M. Prošek, National Institute of Chemistry, Ljubljana, Slovenia

Copyright © 2000 Academic Press

Among many techniques used for quantification of thin-layer chromatograms, slit-scanning densitometry is the most common. It gives the opportunity to choose between either reflectance or transmission mode according to the nature of the supporting material. For instance, glass-backed plates can only be used for transmission measurements above 320 nm due to absorption of the UV radiation, while aluminium-backed plates are opaque at all wavelengths.

The matrix of sample and stationary phase, which consists of small particles, is optically opaque and strongly light-scattering. Therefore, densitometric measurements of separated substances are much more difficult than equivalent photometric measurements in solution. A further problem with densitometry is the fact that it is unable to detect the vertical and radial concentration profiles of the separated substance within the spot as a result of diffusion and the chromatographic process.

Reflectance and transmission are particularly sensitive to changes in sorbent quality, thickness, spot shape and size, eluent and development conditions. To reduce the errors due to plate-to-plate variation, standards should always be applied to the same plate as the unknown samples. The errors due to migration differences as a result of edge effects, deviations in layer thickness and nonlinear solvent fronts can be further minimized using the data-pair technique introduced by Bethke and co-workers in 1974. This technique is based on an internal compensation, by pairing up the measurements of two spots on the same plate.

Most thin-layer chromatography (TLC) analysis is performed in the UV and visible spectral region by applying reflectance scanning densitometry. However, the results of reflectance measurements are restricted to the surface of the sorbent on the TLC plate and are therefore strongly dependent upon the in-depth distribution of the analysed compound inside the sorbent. Nonuniformity of the in-depth distribution of a compound inside the sorbent as a result of secondary chromatography can occur during the evaporation-drying stage. Differences in the in-depth concentration profiles of the samples and stan-

dards can cause significant errors and cannot be completely eliminated by the data-pair technique.

Theoretical Problems of Optical Scanning Densitometry

All optical methods for the quantitative evaluation of planar chromatograms are based on measuring the difference in optical response between blank regions of the stationary phase and regions with a separated substance. When monochromatic light falls on an opaque medium, some light may be reflected from the surface, some may be absorbed by the medium and converted to heat, and the remainder is diffusely reflected or transmitted by the medium. Regularly (specularly) reflected light does not give any useful information of the sample distributed within the sorbent, however, it can contribute to the noise signal in scanning densitometry as it cannot be distinguished from the diffusely reflected light. Quantification in TLC is based on measuring the diffusely reflected or transmitted light and assuming that the specularly reflected component from the sorbent is very small.

The propagation of light within an opaque medium is a very complex process that can be mathematically solved only by assuming certain simplifications. The transmission and reflectance of light in highly scattering media has been discussed by Chandrasekhar (1950) in his book on radiative transfer, where he gives the basic integro-differential radiation transport equation. As this equation has no analytical solution, all useful equations and theories have been developed by simplifying the actual case.

Continuum theories of absorption in opaque media, such as Kubelka-Munk's theory, are not appropriate for quantitative TLC. Although they describe the absorption and scattering properties of the medium, they do not take into account the interaction of light with individual particles in the layer and the very important problem of nonuniform in-depth distribution of a compound within the sorbent. Bodo, Johnson and Melamed have developed well-known discontinuum theories for the determination of absolute optical constants from the properties of individual sample particles. In 1968 Goldman and Godal published their paper on the theoretical basis of measurements by optical transmission and reflection in silica gel layers using a modified

Kubelka-Munk equation. The theoretical background of *in situ* evaluation of thin-layer chromatograms was described by Kortüm in 1969.

Theoretical studies of the problems in light scattering are important in order to reach an understanding of the measuring principle and to help the analyst to find more precise methods of evaluating the data. However, one of the main difficulties is the fact that the adsorbed substance is never homogeneously distributed over the whole sorbent which is required in theory for a relationship between reflectance and concentration of the adsorbed substance.

Multilayer Models

The effect of the concentration gradient of the substance on the intensity of the signal in reflectance and transmission measurements has been studied by a number of authors. Most have studied the theoretical aspect of this problem. Nevertheless, using different approaches, they have all come to the same conclusion. They showed that densitometric transmittance measurements and fluorescence measurements from the far (nonilluminated) side of a plate yield results which are almost independent of the in-depth distribution of the analysed material. In contrast, the densitometric reflectance and fluorescence measurements from the near (illuminated) side are strongly dependent on that distribution. They suggested using transmittance or fluorescence transmittance mode whenever there are reasons to suspect a non-homogeneous distribution of concentration or a changing coefficient of fluorescence of the separated material in the depth of the chromatogram.

However, as already pointed out, most densitometric measurements are performed in reflectance mode, and are therefore restricted only to the surface of the sorbent. It is for this reason that differences in the in-depth distribution of compounds (samples and standards) can cause erroneous results. Prošek and his co-workers have investigated the effect of the concentration gradient on the intensity of the diffusely transmitted and reflected light. They solved multilayer models using the mathematical theory of Bodo and Markov chains. In such a model a chromatographic band was placed in different sublayers (Figure 1). Although their equations do not offer any improvement from a practical point of view, they show the effect of the concentration gradient in the sorbent layer that the Kubelka-Munk theory cannot. The practical application of their theory was confirmed using the real models prepared from different kinds of layers (paper and TLC sorbents). The results obtained from these real models were in good agreement, confirming theoretical

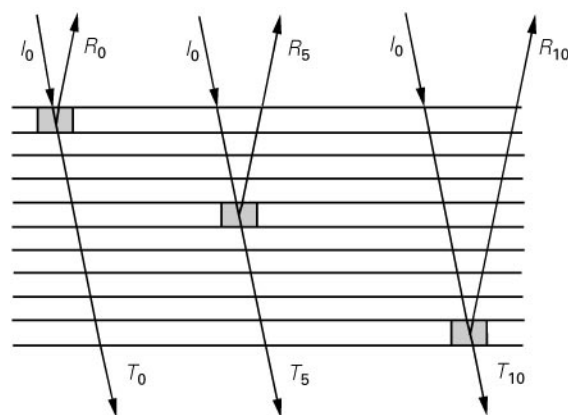


Figure 1 Schematic presentation of a multilayer model. I , incident beam; R , reflected beam; T , transmitted beam.

results and showing that reflectance densitometric measurements do not take into account the vertical subsurface concentration distribution.

Further investigations have been made with image analysing systems, an emerging detection technique in TLC. In the case of image analysing systems, higher radiation fluxes must be taken into account as the result of the illumination of a whole plate. Compared to slit-scanning densitometry, the intensity of diffuse light inside the illuminated layer is much higher, as higher numbers of reflected beams come from all parts of the layer. The results obtained by measuring multilayer models with a charge coupled device (CCD) camera (Figure 2) showed the effect of the position of the spot inside the layer on the signal. As can be seen from Figure 3, the intensity of the signal in the reflectance measurements is highly dependent on the position of the spot inside the layer. This has confirmed that differences in the in-depth distributions of standards and samples can cause significant errors in reflectance quantitative TLC. On the other hand, the position of the spot inside the layer has almost no effect on the signal in transmittance measurements.

Secondary Chromatography

While drying a TLC plate, molecules of compounds are moving with the evaporating mobile phase in the direction of the sorbent's surface. This process is called secondary chromatography and results in inhomogeneous vertical distribution of compounds inside the sorbent. This effect is bigger for compounds having high R_F values in the solvent being evaporated.

Variations of in-depth distribution have a big impact on densitometric reflectance measurements. This

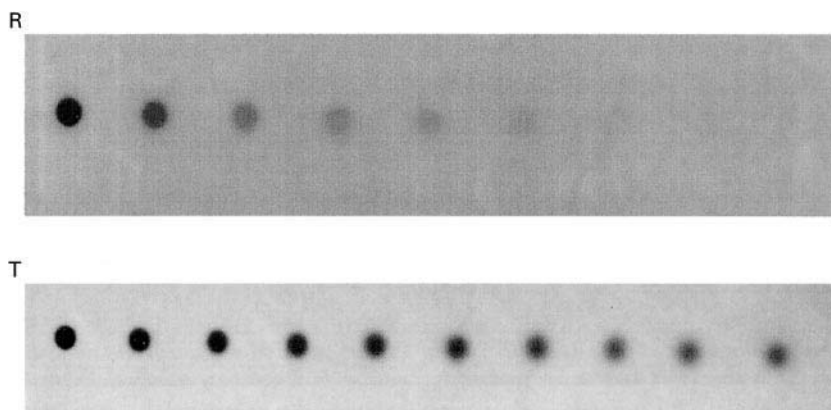


Figure 2 CCD images of a 10-layer model while measuring reflectance (R) and transmission (T) with a Camag video documentation system.

is one of the reasons for the nonlinearity of calibration curves and may lead to the erroneous interpretation of TLC chromatograms by reflectance densitometry. It is therefore very important to find drying conditions which will give TLC plates with the most homogeneous and consistent depth distribution of compounds.

Depth Profiling of TLC Plates by Photoacoustic Spectroscopy

Preliminary investigations of nondestructive depth profiling of TLC plates have been performed. The results obtained using different photothermal techniques, showed that photoacoustic spectroscopy (PAS) is most suitable for characterization of TLC

plates. Although PAS has been used previously for the qualitative and quantitative spectroscopic analysis of TLC plates, the first results of photoacoustic depth profiling of TLC plates have only recently been published.

PAS is a photothermal technique, which relies on the detection of pressure waves (sound) generated by the absorption of radiation in a periodically irradiated sample. It has the capability for *in situ* and nondestructive depth profiling of solid samples. This unique feature is due to the fact that the magnitude of the induced photothermal effect depends on the concentration and on the thermal diffusivity of a compound. The plot of the dependence of the photoacoustic (PA) signal on the modulation frequency provides information about the depth profile of the analysed compound.

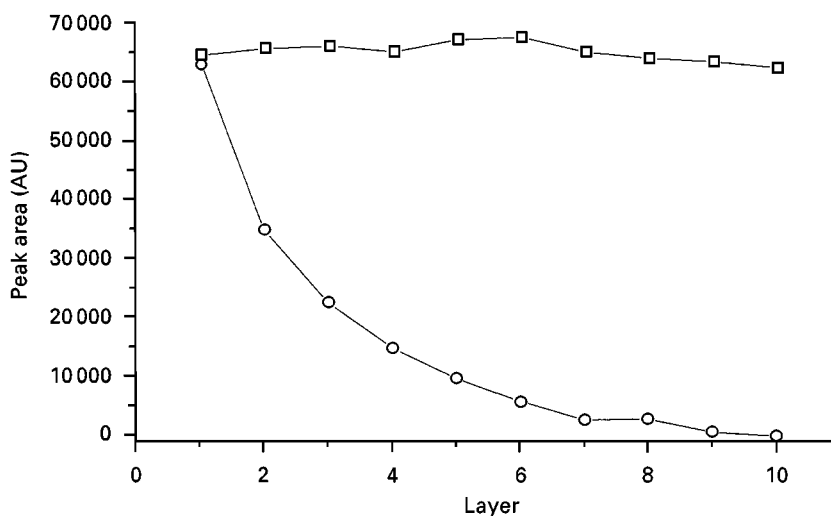


Figure 3 The effect of the spot position in the 10-layer model on the reflectance (circles) and transmission (squares) measurements with a Camag video documentation system.

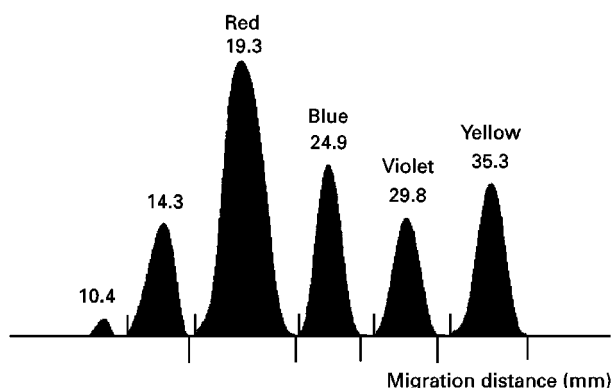


Figure 4 Densitogram obtained from Camag test dye mixture III. (Reproduced with permission from Vovk I, Franko M, Gibkes J, Prošek M and Bicanic D (1997) Depth profiling of TLC plates by photoacoustic spectroscopy. *Journal of Planar Chromatography* 10: 258. Copyright Research Institute for Medicinal Plants in cooperation with Springer Hungarica.)

The PA signals were analysed using the theory for a two-layer model consisting of the sorbent and the glass as the supporting material. Thermal diffusivity values (α) of the spots on TLC plates were obtained by curve fitting of normalized phase lags of PA signals. Different thicknesses of sample, corresponding to the thermal diffusion length μ , given as $\mu = \sqrt{(\alpha/\pi f)}$, were probed by varying the frequency (f) of the laser beam modulation.

The PA signals originating from different layers of a TLC plate were calculated by subtracting the values obtained at higher modulation frequencies

from those obtained at lower frequencies. From these two modulation frequencies and the previously obtained thermal diffusivities of each spot, the depth and thickness of each layer can be determined. Depending on the available range of modulation frequencies used in the PA measurements, the thickness of the probed layers varied from 23 to 37 μm . All the results were corrected for differences in layer thickness.

In-Depth Distribution of Compounds Inside the Sorbent and Quantitative TLC

The effect of nonhomogeneous in-depth distribution of compounds on quantitative TLC has been studied on TLC and high performance TLC (HPTLC) plates using the separation of a test dye mixture (Figure 4). The results of PA investigations showed that all compounds exhibited nonhomogeneous concentration profiles in a vertical direction. Although all the investigated compounds tended to concentrate in the upper 25% of a 250 μm thick layer, secondary chromatography can lead to deviations from this behaviour. Additionally, differences in the in-depth concentration distribution of different compounds on the same TLC plate were seen (Figures 5 and 6). While the yellow dye spots concentrated in the top 31 μm layer, the highest concentration in the violet spots was observed in the region between 39 and 61 μm . This indicates that the effects of secondary chromatography depend strongly on the properties of the compounds in each spot. The situation is different in the case of HPTLC plates, where

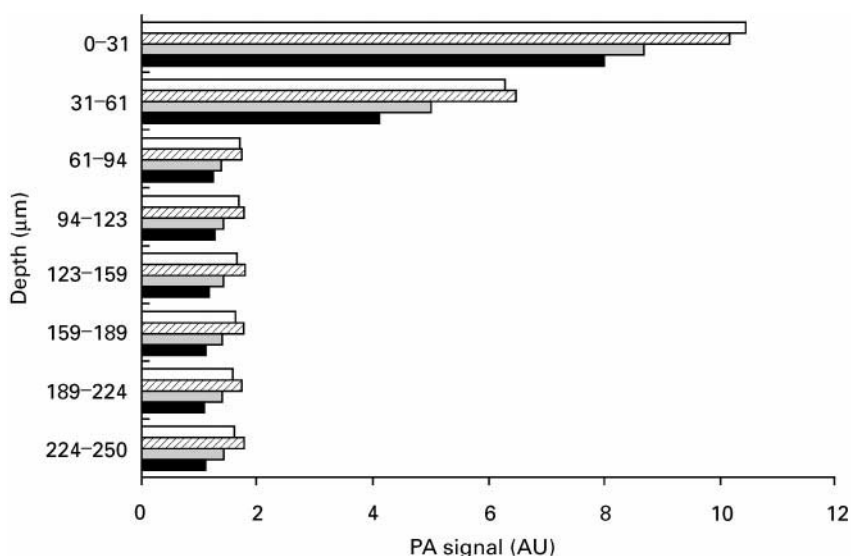


Figure 5 Depth distribution of the compound in yellow spots of equal concentration. Open column, track no. 4; cross-hatched column, track no. 3; dotted column, track no. 2; filled column, track no. 1. (Reproduced with permission from Vovk I, Franko M, Gibkes J, Prošek M and Bicanic D (1997) Photoacoustic investigations of secondary chromatographic effects on TLC plates. *Analytical Science* 13 (Suppl.): 191. Copyright The Japan Society for Analytical Chemistry.)

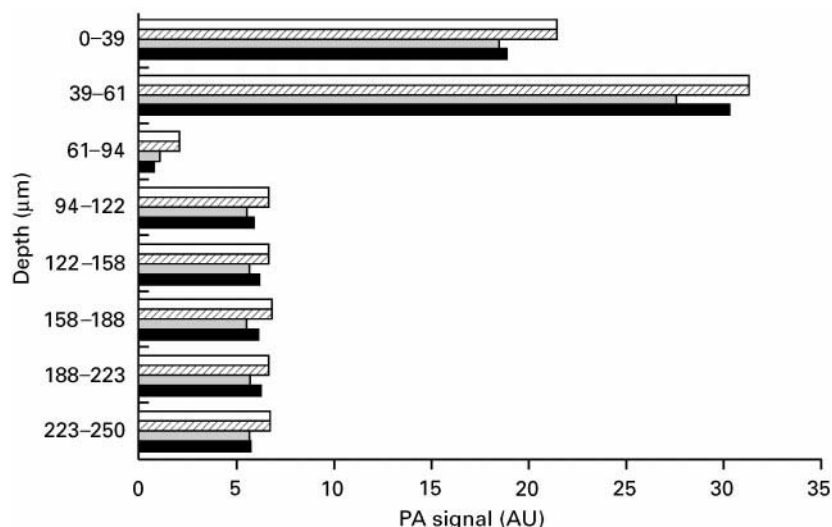


Figure 6 Depth distribution of the compound in violet spots of equal concentration. Open column, track no. 4; cross-hatched column, track no. 3; dotted column, track no. 2; filled column, track no. 1. (Reproduced with permission from Vovk I, Franko M, Gibkes J, Prošek M and Bicanic D (1997) Photoacoustic investigations of secondary chromatographic effects on TLC plates. *Analytical Science* 13 (Suppl.): 191. Copyright The Japan Society for Analytical Chemistry.)

even the violet spots tends to concentrate in the upper, 0–37 μm layer (**Figure 7**). Different in-depth distribution of compound inside the sorbent of TLC and HPTLC plates can be explained by 50 μm differences in the layer thickness. In the case of the thinner layer of the HPTLC plate, the evaporation of the mobile phase is faster and causes faster movement of the substance to the surface of the plate. Differences in PA signals from the same depths were observed for spots from different tracks. This

indicated that nonuniformity within one TLC plate could be the source of erroneous quantification in scanning densitometry (Figures 5–7). Additionally, when monitoring only the surface of the TLC plate, by reflectance densitometry, such irregular vertical concentration distribution can result in the nonlinearity of calibration curves (**Figure 8**). For the same reasons a nonlinear calibration curve is obtained by PAS, when the probed sorbent layer is too thin (top curve in **Figure 9**). Taking into account all the con-

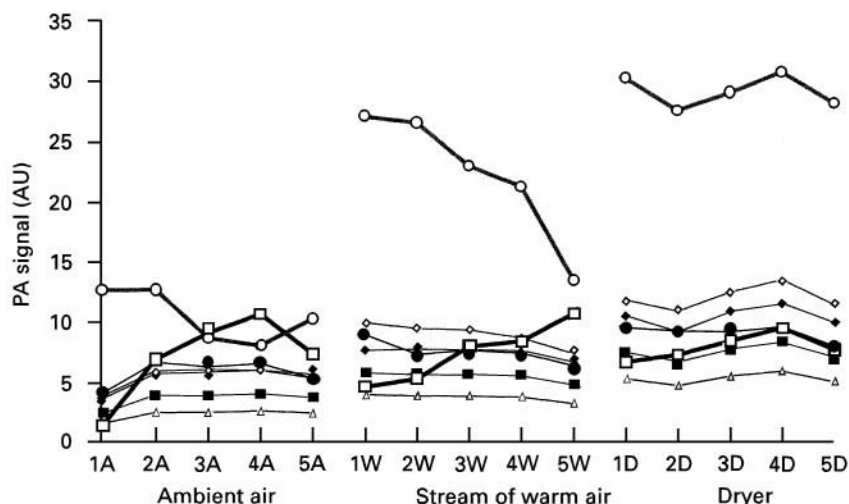


Figure 7 Depth distribution of the compound in violet spots on HPTLC plates dried in ambient air (A), in a stream of warm air (W) or in a dryer (D). Open circles, 0–37 μm ; open squares, 37–62 μm ; filled circles, 62–88 μm ; open diamonds, 88–125 μm ; open triangles, 125–148 μm ; filled squares, 148–176 μm . (Reproduced with permission from Vovk I, Franko M, Gibkes J, Prošek M and Bicanic D (1998) The effect of drying conditions on the in-depth distribution of compounds on TLC plates investigated by photoacoustic spectroscopy. *Journal of Chromatography* 11: 379. Copyright Research Institute for Medicinal Plants in cooperation with Springer Hungarica.)

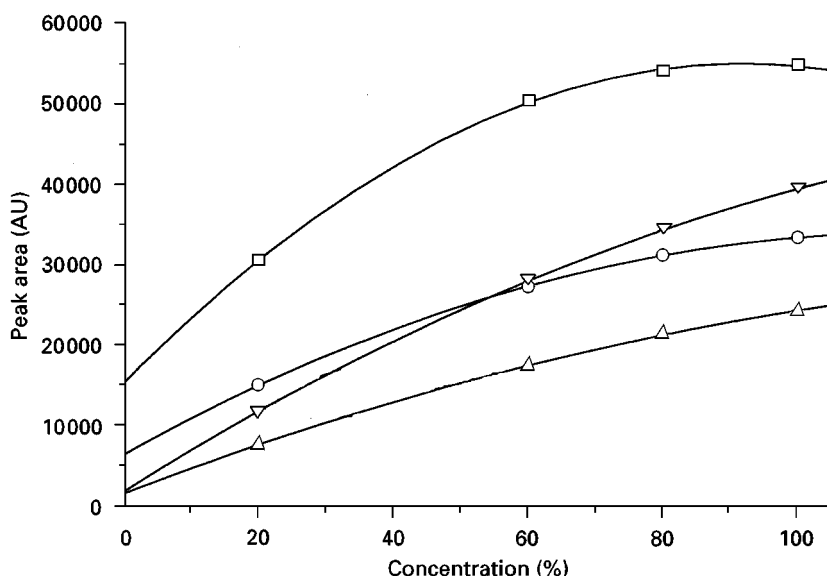


Figure 8 Calibration curves for the Camag test dye mixture III (squares, red spots; circles, blue spots; triangles, violet spots; inverted triangles, yellow spots) obtained by reflectance densitometry. (Reproduced with permission from Vovk I, Franko M, Gibkes J, Prošek M and Bicanic D (1997) Photoacoustic investigations of secondary chromatographic effects on TLC plates. *Analytical Science* 13 (Suppl.): 191. Copyright The Japan Society for Analytical Chemistry.)

siderable irregularities in vertical concentration distribution (61 μm) by PA probing of thicker sorbent layers (lower curves in Figure 9) leads to improved linearity of calibration curves compared to those obtained by reflectance densitometry.

Our investigations confirmed that in TLC not only accurate application, development and quantitative

evaluation, but also accurate drying are essential to obtain good results. Unfortunately, up to now the importance of this procedure has not been fully appreciated. The effects of drying process on the in-depth distribution of compounds inside the sorbent on HPTLC plates has therefore been investigated for drying in a dryer, in a stream of warm air

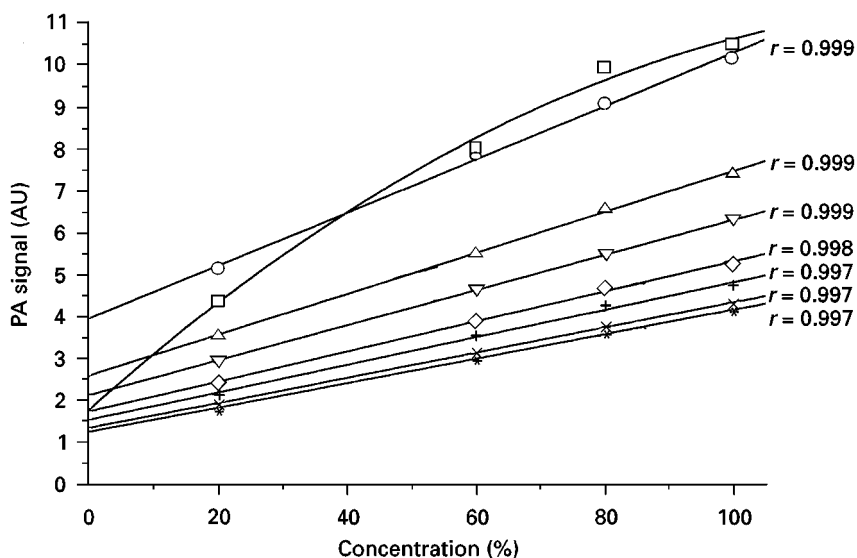


Figure 9 Calibration curves for the yellow spots obtained by PAS when probing different thicknesses of the sorbent. Squares, 0–36 μm ; circles, 0–61 μm ; triangles, 0–94 μm ; inverted triangles, 0–123 μm ; diamonds, 0–159 μm ; crosses, 0–185 μm ; multiplication signs, 0–225 μm ; asterisks, 0–250 μm . (Reproduced with permission from Vovk I, Franko M, Gibkes J, Prošek M and Bicanic D (1997) Photoacoustic investigations of secondary chromatographic effects on TLC plates. *Analytical Science* 13 (Suppl.): 191. Copyright The Japan Society for Analytical Chemistry.)

Table 1 Peak areas obtained by densitometric measurements of violet spots on three different HPTLC plates, dried in the ambient air (A) or in a stream of warm air (W) or in a dryer (D)

	<i>Peak areas (a.u.) for violet spots</i>						<i>RSD (%)</i>
	<i>Track 1</i>	<i>Track 2</i>	<i>Track 3</i>	<i>Track 4</i>	<i>Track 5</i>	<i>Mean</i>	
Ambient air	39 037	38 992	38 876	36 908	36 250	38 012.6	3.50
Warm air	38 242	38 886	38 788	37 889	35 311	37 823.2	3.86
Dryer	36 707	36 089	36 857	36 445	36 755	36 570.6	0.84

Reproduced with permission from Vovk I, Franko M, Gibkes J, Prošek M and Bicanic D (1998) The effect of drying conditions on the in-depth distribution of compounds on TLC plates investigated by photoacoustic spectroscopy. *Journal of Planar Chromatography* 11: 379. Copyright Research Institute for Medicinal Plants in cooperation with Springer Hungarica.

and in ambient air. The results obtained by PAS studies from different HPTLC plates were compared to those obtained by reflectance densitometry.

A comparison of the response areas was obtained for five violet dye spots from HPTLC plates dried in ambient air (A), in a stream of warm air (W) and in a dryer (D). The highest relative standard deviation (RSD) values were obtained for the plate dried in a stream of warm air (Table 1). The RSD for drying in a dryer was significantly lower than the RSD values for drying in the ambient air or in the stream of warm air. This can be explained by the nonuniform drying conditions across the HPTLC plate while drying in a stream of warm air.

The results of PA measurements are presented in Figure 7. For most of the tracks on all three HPTLC plates, the highest PA signals were detected in the top 37 µm thick layer. Significant differences in PA signals were observed under different drying conditions in the top 62 µm layer of the sorbent. Differences in the in-depth distribution of compounds due to variations of drying conditions across the same HPTLC plate are especially remarkable when the results for all five tracks from one plate (A, W or D) are compared (Figure 7). The largest variation was observed between tracks on the HPTLC plate dried in the stream of warm air. The most reasonable explanation for the large differences in PA signals observed between the plates dried in ambient air and those dried in a dryer or in the stream of warm air is the difference in radial distribution of the compound within the spots. When a TLC plate is dried in ambient air, the compound is radially distributed over a larger area as a result of diffusion. In the case of drying in the dryer and drying in a stream of warm air, the spots are shrinking due to migration of molecules in a radial direction towards the centre of the spot. This results in an increased concentration, and therefore higher PA signals (Figure 7), when the radius of the laser beam is smaller than the spot radius, as was the case. In the case of densitometric

measurements the probed area is larger than the diameter of a spot so that radial changes in concentration cannot be observed.

The magnitude of secondary chromatography, and consequently the vertical as well as the radial concentration distribution of compounds in the sorbent, depends on drying conditions. It also depends on the properties of the analytes and the type of TLC plate (TLC or HPTLC). Drying in a dryer gives the most reproducible results, while drying in a stream of warm air gives the least reproducible results.

Future Trends

We anticipate that in-depth distribution will have less effect on quantitative TLC in the future, because developments in the field of TLC plates is focused on producing thinner layers by using stationary phases with a smaller and more defined particle size. However, until this is achieved, further studies of secondary chromatography are necessary.

In addition, the wider use of image-analysing systems, mostly working in the visible part of the spectrum, will increase the number of methods using postchromatographic derivatization and quenching techniques. These procedures should also be tested by PAS to elucidate their effect on the in-depth and radial distribution of compounds on TLC plates.

See also: II/Chromatography: Thin-Layer (Planar): Densitometry and Image Analysis; Instrumentation.

Further Reading

Bein K and Pelzl J (1989) In: Analysis of surface exposed to plasmas by nondestructive photoacoustic and photo-thermal techniques. Auciello O and Flamm DL (eds) *Plasma Diagnostics: Surface Analysis and Interactions*, p. 211. New York: Academic Press.

- Gibkes J, Vovk I, Bolte J *et al.* (1997) Photothermal characterisation of TLC plates. *Journal of Chromatography A* 786: 163.
- Prošek M and Pukl M (1996) Basic principles of optical quantitation in TLC. In: Sherma J and Fried B (eds) *Handbook of Thin-layer Chromatography*, p. 273. New York: Marcel Dekker.
- Prošek M, Medja A, Kučan E *et al.* (1979) Quantitative evaluation of thin-layer chromatograms: The calculation of remission and transmission using multilayer model. *Journal of High Resolution Chromatography & Chromatographic Communications* 2: 517.
- Prošek M, Medja A, Kučan E *et al.* (1980) Quantitative evaluation of thin-layer chromatograms: The calculation of fluorescence using multilayer models. *Journal of High Resolution Chromatography & Chromatographic Communications* 3: 183.
- Vovk I, Franko M, Gibkes J *et al.* (1997) Depth profiling of TLC plates by photoacoustic spectroscopy. *Journal of Planar Chromatography* 10: 258.
- Vovk I, Franko M, Gibkes J *et al.* (1997) Photoacoustic investigations of secondary chromatographic effects on TLC plates. *Analytical Science* 13(suppl): 191.
- Vovk I, Franko M, Gibkes J *et al.* (1998) The effect of drying conditions on the in-depth distribution of compounds on TLC plates investigated by photoacoustic spectroscopy. *Journal of Planar Chromatography* 11: 379.

INDUSTRIAL ANALYTICAL APPLICATIONS: SUPERCRITICAL FLUID EXTRACTION



M. E. P. McNally, DuPont de Nemours,
Wilmington, DE, USA

Copyright © 2000 Academic Press

By the mid-1980s, routine analysis was accomplished in most industrial laboratories with the help of automated sampling and data-handling systems. The next major bottleneck caused by the burden of large sample loads that existed in many industrial environments was sample preparation and the method development time associated with it. Robots and automated systems were introduced to address these bottlenecks. Supercritical fluid extraction (SFE) was one of the automated systems introduced.

The initial introduction of SFE was unique, in that supercritical fluid chromatography (SFC) was developing at a parallel pace. Both introductions into the analytical community produced scientists who needed to learn the nuances of a totally new fluid, its capabilities, limitations, likeness to and difference from both gases and liquids.

SFE was embraced more readily in the industrial community than SFC. The reasons for this, in its utility as well as its developments, are considered in more detail in this overview.

Actual industrial applications of any analytical technology are sometimes well-guarded secrets. References can come from a variety of sources, not necessarily the published literature. Trends in the applications of SFE are no different. The most use has been in the food industry and the environmental area. Additional ap-

plications to a lesser extent are in polymer analysis, consumer products and pharmaceuticals.

Beyond the ability to conduct an analysis previously unachievable, the driving force for the adaptation of a technique into the industrial laboratory depends on a financial benefit. SFE has solved some problems that could not previously be solved. But it has mostly gained an industrial foothold by offering worthwhile cost savings over the already acceptable methodology, such as liquid extraction.

Instrumental Developments

In the development of SFE, industrial applications were the driving force to the advancement of commercial instrumentation. Initial offerings of commercial equipment involved cumbersome sample vessels with a myriad of problems. Not uncommonly, these were placed in single-vessel extraction units. At most, the instrumentation was capable of conducting SFC following the supercritical extraction. Speeds of analysis were typically measured by actual extraction time, and not overall sample handling, operator time or productivity. In this early equipment, productivity was not truly improved and industrial acceptance was slow. This equipment was only viable for those extraction methods that could not be conducted by another extraction solvent, i.e. a liquid or a gas. This led SFC, where both liquid and gas chromatography had a strong hold in the separation field, to be labelled as a niche technique. In the sample preparation field, where alternative automated extraction methods with liquids and gases were not as firmly

established, the competition was not as fierce for SFE.

Two paths were chosen. Work ensued to optimize the capabilities of supercritical fluids to encompass those compounds that might be more readily extracted by a liquid or a gas as opposed to a supercritical fluid. In addition, to compete with existing technology, albeit even classical liquid extraction, SFE needed to be able to routinely handle a larger volume of samples than was possible with these early instruments.

The first path necessitated a study of the theory and principles of supercritical fluids in terms of their solubilizing powers, matrix interactions, change with modifier or additive additions and their handling. These are generally considered academic endeavours, but much of this occurred in the industrial environment strictly out of need. Simply, it was cost-beneficial to use SFE over the classical technology. SFE was demonstrated to be a factor of 2–5 times cheaper per analysis but, more importantly, it was demonstrated to reduce classical liquid extraction method development time by 3–5 months. Reducing man-months in the process of reaching a product to market is a critical success factor in business. Not only is labour costly, but timing influences the introduction of product to market, the return of capital investiture and the ability to outpace the competition. This tremendous cost benefit resulted in industrial work on understanding some of the theoretical principles which would have otherwise been more slowly developed in academia.

Beyond the theoretical principles, the biggest single improvement, achieved through the second path, was the incorporation of the sample carousel. Easily adapted from the principle of commercial autosamplers, the carousel not only increased the total number of samples that could be analysed, but enabled unattended method development in the most labour-intensive portion of chemical analysis, the extraction step. Replicates of this have already spilled into other technologies, such as pressurized liquid extraction, but SFE was the first to utilize this feature in sample preparation.

A technique such as SFE is unlikely to survive in the industrial environment without the development of commercially available instrumentation. In the late 1980s, the market place had several key manufacturers developing and selling suitable equipment. More than a decade later, some of these have merged, some have reduced their efforts, some have retreated and concentrated on more commercially profitable areas. What remains are some well-designed pieces of instrumentation, directed at specific application areas, as in the fat analysers currently offered

by Leco and Isco/Suprex. In addition, there are small suppliers whose instrumentation tends to be less expensive but less amenable to adapting to large routine applications.

The development of SFE is by no means complete, nor can the technology be considered mature. Much of the theoretical questions have returned to academia, progress will be slower, but breakthroughs can still be expected. Much of the development in industrial supercritical fluids is currently in process and larger scale and analytical developments will follow these trends.

Industrial Applications

Successful applications have been readily demonstrated in some fields, specifically with environmental and food samples. Other applications have been more difficult to achieve and reproduce. The following applications outline some of the well-known uses of SFE.

Food Industry

Fat analysis Fats, lipids and oils have been extracted from a wide variety of foods from soybeans to oats, corn chips to brownies and meat to meat by-products and fish. Literature reports optimize the pressure and temperature of the extraction, the length of the extraction, the sample weight, the flow rate and the collection mode. Dynamic and static modes of extraction have also been investigated. Percentages of fat have been removed from sample matrices up to the 35% level; typically, gravimetric analysis follows the extraction procedure at these levels. Commercial manufacturers of foodstuffs are required by law to report percentage of fat on the package label. SFE has revolutionized this methodology. An American Society for Testing and Materials (ASTM) method for determining fat in certain selected foodstuffs has been accepted.

The nonpolar nature of fat, lipids and oils makes them extremely amenable to SFE. Liquid extraction of fat from foodstuffs is conducted using hexane solvent. Supercritical carbon dioxide has equivalent solubility properties, i.e. Hildebrand solubility parameter, to liquid hexane at low densities. Total fat analyses as well as the relationship of different lipid classes in foodstuffs have been determined. **Figure 1** shows the dynamic extraction profiles for the removal of triglycerides from 0.5 g of pork loin. As expected, higher densities give higher extraction efficiencies in shorter time periods. Although a time of 100 min may seem excessively long, compared to the classical techniques the time was orders of magnitude less. **Figure 2** compares SFE technology

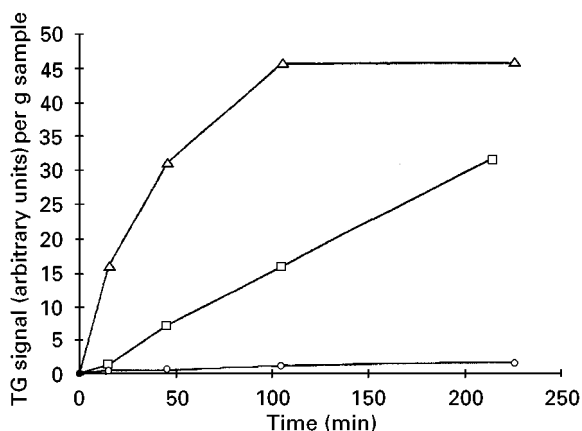


Figure 1 Extraction profiles for different densities. Circles, 105 bar (0.45 g mL^{-1}); squares, 134 bar (0.65 g mL^{-1}); triangles, 370 bar (0.91 g mL^{-1}). Pork loin 0.5 g. Dynamic extraction with pure CO_2 . Flow rate: 2 mL min^{-1} , temperature: 50°C , trap: octadecyl-silica, trap temperature: 50°C , nozzle temperature: 55°C , rinse solvent: cyclohexane at a flow rate of 1.0 mL min^{-1} , eluted volume: 1.4 mL .

versus the two classical methods for fat analysis: SBR (Schmid, Bondzynski and Rutzlaff) and the popular Bligh & Dyer (B&D) for six different samples. A paired sample *t*-test demonstrated no significant difference at the 95% confidence level for SFE versus the classical methods.

Decaffeination Commercial decaffeination of coffee, tea and cocoa using supercritical carbon dioxide has been the object of huge industrial effort. Patents have been issued since 1974 in this area, to assignees such as General Foods and Société d'Assistance Technique pour Produits Nestlé. In Germany, there is a plant able to decaffeinate approximately 27.3 million kg of product per year.

There is a substantial effort to make sure the process works and is cost-effective. It is also the first example of a commercial scale supercritical fluid process. Without a doubt, the analytical departments of the commercial operations are examining the effectiveness of supercritical fluids in both analysis and process development, but the work is rarely talked about outside individual commercial enterprises.

Not surprisingly, then, the first example of routine SFE in analysis was in the removal of caffeine from food products. Caffeine, a moderately polar molecule, would not structurally be chosen as likely to have a high solubility in supercritical carbon dioxide. The commercial and analytical scale extraction of caffeine from coffee requires the addition of water as does the extraction of caffeine using methylene chloride. Reports have suggested that there is a chemical bonding of caffeine to the coffee bean or that the moisture instigates a swelling to free the entrapped compound. In either case, this landmark extraction process had opened up the understanding of SFE; overcoming chemical interactions and access to the matrix in total are important features in the investigation of SFE.

Environmental Analysis

Soil analysis Environmental applications of SFE have attracted the largest effort. Soil has received the most attention; it is one of the most difficult matrices and one of the most frequently analysed. Soil types vary widely in both their chemical and physical properties, depending on their geographical origin and their unique history. All extraction methods for soil show wide variability of recoveries and standard deviations of $\pm 30\%$ are not uncommon. In general, the advent of SFE, which was the first analytical

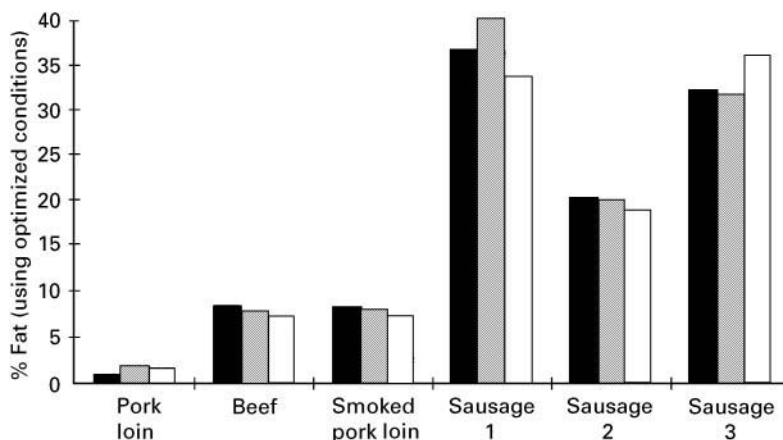


Figure 2 Comparison of total fat determination between SBR (filled columns), SFE (cross-hatched columns) and B&D (open columns). The samples were mixed with Hydromatrix (1 : 2 w/w) and 1 mL cyclohexane was added. Flow rate was 4.0 mL min^{-1} . 8% ethanol was used as modifier; the analytes were collected directly in vials; the rinse solvent pump was operated at 2 mL min^{-1} ; other conditions as outlined for Figure 1.

technology for automated soil extraction, reduced this variability to 10–20% within individual soil types. This reduced variability makes differences in extraction from different soils more apparent and gives rise to an understanding of the individual soil parameters controlling extraction.

Analytes of different polarities have been extracted with a wide range of supercritical fluid polarities. Unmodified carbon dioxide showed the best extraction reproducibility, while modified carbon dioxide demonstrated the ability to overcome active sites in the matrix or contribute to desirable matrix swelling. Additives, which show drastic effects in chromatographic retention, also show effects in SFE.

As with other extraction technologies, analytes in spiked samples are easier to recover than are real residues. Bound residues still exist with SFE, but with tighter precision a greater understanding of bound versus available residues has been obtained.

In terms of applications, wide variety of analytes from very nonpolar polychlorinated biphenyls (PCBs) to very polar herbicides have been extracted successfully. Again, optimized conditions show the wide range of polarizability that can be obtained with modified carbon dioxide mobile phases. **Table 1** gives a small example of the wide range of compounds that have been extracted from soils and the pertinent conditions. Multi-analyte methods are the norm, and coupled with liquid, gas and SFC, the methods are rugged.

Water analysis Aqueous samples have been extracted using supercritical fluids in several distinct methods. The first method is to place the liquid in the extraction vessel. The supercritical fluid either percolates through the matrix from a bottom entry port to a top exit or, in an opposite fashion, is introduced through the top of the vessel, contacting the sample for a specified period of time before it exits. Sulfonyleureas have been extracted from aqueous matrices using a system with a bottom entry and top exit. Flavour components of orange and lemon juice have used the top entry bottom exit format. Alternatively, some workers have passed the liquid either through a filter, pre-coated disc, or a separation cartridge. These trapping materials are then placed separately into extraction cartridges before introduction of the supercritical fluid. Success has been reported with all these techniques for a wide variety of environmental samples.

Agricultural products In this application area, matrices are complex and varied, detection levels are frequently at the parts per billion (p.p.b.) and parts per trillion (p.p.t.) level, and analyte similarity to the matrix is likely. All of these features lead to complex sample preparation and time-consuming method development. Food safety, environmental fate and product stewardship are major concerns for a competitive, consolidating industry. Successful extraction technologies need to demonstrate ease of use on

Table 1 Range of analytes successfully extracted by SFE from soils

Analyte	Soil	Supercritical fluid	Temperature	Pressure	Multi-residue method?
Total petroleum hydrocarbons (TPHs)	Diesel and gas contaminated	CO ₂	80°C	340 atm	Yes
Sulfonyleurea herbicides	All types	Methanol and water-modified CO ₂	60°C	300 atm	Yes
Ureas	All types	Methanol-modified CO ₂	100°C	300 atm	No
Organotin	Marine sediment, clay, topsoil	Methanol-modified CO ₂	60°C	450 atm	Yes
Polychlorinated biphenyls (PCBs) and polycyclic aromatic hydrocarbons (PAHs)	Railroad bed, storage dumpster soils and sediment	CO ₂	150°C	400 atm	Yes
Nitroaromatic and polycyclic aromatic hydrocarbons (PAHs)	Polluted industrial site and former ammunition plant soils	CO ₂ modified with triethylamine and trifluoroacetic acid in toluene	90°C	395 atm	Yes
Nonylphenol polyethoxylates (nonionic surfactants) and carboxylic acid metabolites	Sediment and sewage treatment plant sludge	Water-modified CO ₂	80°C	340 atm	Yes

a routine basis, ruggedness, reproducibility, accuracy and commercial availability of equipment. In addition, the current regulatory environment is insistent on advances in multi-residue analysis. These requirements and directives suggest that SFE is an obvious choice.

Herbicide, insecticide and fungicide extraction from soils by SFE has been demonstrated widely; conditions for some of these analytes are listed in Table 1. In addition to the work conducted on soils, plant and raw agricultural commodities have been routinely analysed. Most of the agrochemical classes have been extracted: organophosphates, phthalimides, organochlorines, phenols, carbamates, nitroanilines, oxazolidine, benzimidazoles, triazoles, sulfite esters, pyrethroids, imidazolines and sulfonylureas.

Frequently, sample pretreatment or processing must occur before sample extraction. Although this is time-consuming, this typically also occurs in most classical extraction methodologies. Grains and seeds are ground or milled into powders to expose the internal surface area to the extractant fluid; fruits and vegetables are chopped or diced; straws and hays may be cut or shred; oils may be treated as liquids or deposited on adsorbent surfaces. For some high water content species, drying agents such as Celite 545, Hydromatrix®, magnesium sulfate and molecular sieves have been used to lower the overall water content. They have been added to the extraction vessel before extraction or mixed with the sample during preparation. For very low moisture samples, the opposite sample preparation scheme has been pursued. As in the analysis of coffee beans described above, water has been added to dry samples such as wheat straw to swell the matrix and provide access to interstitial regions.

TCP, 3,5,6-trichloro-2-pyridinal, the major product of chlorpyrifos and chlorpyrifos methyl insecticides and trichlopyr herbicide, has been extracted from soil using SFE followed by detection via immunoassay. Effects of modifiers and additives with this extraction were dramatic, as seen in Table 2.

Pharmaceutical Applications

Some of the first reports of the use of analytical scale SFE were in the pharmaceutical industry. Specifically, benzoquinones, known as ubiquinones or co-enzyme Q (with a number which represents the number of side chain isoprenoid groups that are present, e.g. Q-6 has six side chains), were extracted from bacterial cell extracts. They have physical properties analogous to synthetic nonionic detergents, in that there is a polar aromatic end-group and a nonpolar oligomeric side chain. Because of the nature of these

Table 2 Effect of a co-solvent on the recovery of TCP from soil with SC-CO₂^a

Additive	Recovery (%)
None	15.4
Methanol	57.4
Methanol and ion-pairing reagent ^b	80.0

^a1 mL min⁻¹ CO₂ flow rate; 383 bar; 40°C; 30 min extraction; 1 mL methanol, 0.5 mL ion-pairing reagent.

^bIon-pairing reagent: 0.1 mol L⁻¹ methanolic solution of R-10 camphorsulfonic acid ammonium salt (Aldrich).

molecules, their solubility range is large; they are soluble in aqueous and hydrocarbon solvents. This property makes them easily amenable to extraction with either pure carbon dioxide or carbon dioxide systems.

As an example, an experimental human immunodeficiency virus (HIV) protease inhibitor drug (Figure 3), has been extracted from animal feed. Figure 4 shows the effects of extraction temperature and percent ethanol modifier on recovery, while Figure 5 illustrates the high performance liquid chromatography (HPLC) chromatograms of the animal feed extracts. These chromatograms illustrate the relatively clean background that can be obtained with SF extractions.

Workers from Agriculture and Agri-Food Canada gave an excellent example of a multi-residue methodology in the extraction of 22 organochlorine pesticides from eggs with a programme to screen routinely for these compounds. Figure 6 shows recoveries of the pesticides using CO₂ with and without methanol. Both solvents yielded adequate extraction results as well as drastic improvements in extraction time and solvent consumption over the existing Soxhlet extraction method. Background was significantly reduced with pure carbon dioxide.

Literature references show that fat- and water-soluble vitamins have been extracted from pharmaceutical formulations as well as food matrices. Traditionally, fat-soluble vitamin analyses require saponification followed by extraction with an organic

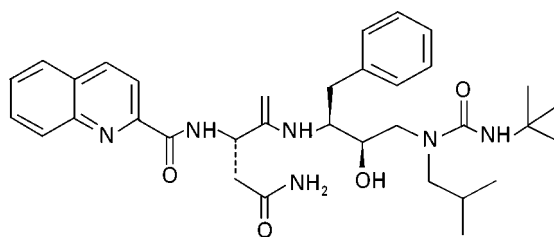


Figure 3 Structure of experimental drug SC-52151 extracted from animal feed using SFE.

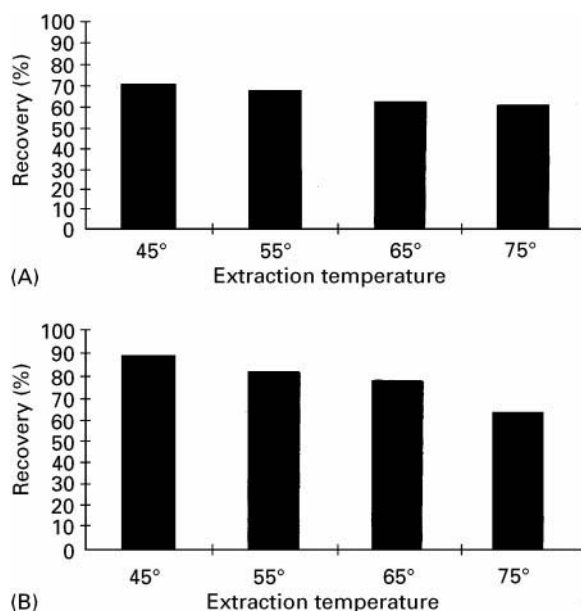


Figure 4 Extraction recoveries for SC-52151 from animal feed spiked at the 0.05% level. (A) 5%; (B) 10% ethanol modifier.

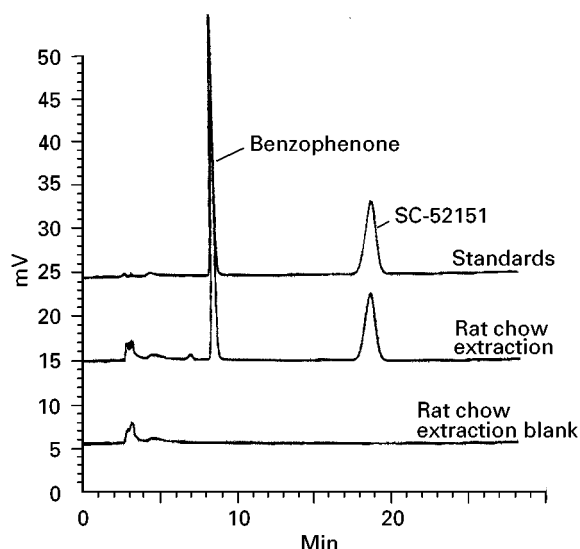


Figure 5 Reversed-phase HPLC traces of SFE animal feed extracts. Chromatographic conditions: column, Supelco C-8 DB (250 × 4.6 mm i.d.; 5 μ m particle size); mobile-phase flow rate, 1.0 mL min⁻¹; injection volume, 10 μ L; detection wavelength, 205 nm; mobile phase, 0.04 mol L⁻¹ sodium pentanesulfonate.

solvent. Solvent reduction and clean-up are generally also needed. SFE eliminates these steps. The water-soluble vitamins are more readily extracted with

modified carbon dioxide and minimal clean-up is required. Vitamins A₁, B₆, C, D₂, D₃ and K have all been successfully extracted using SFE.

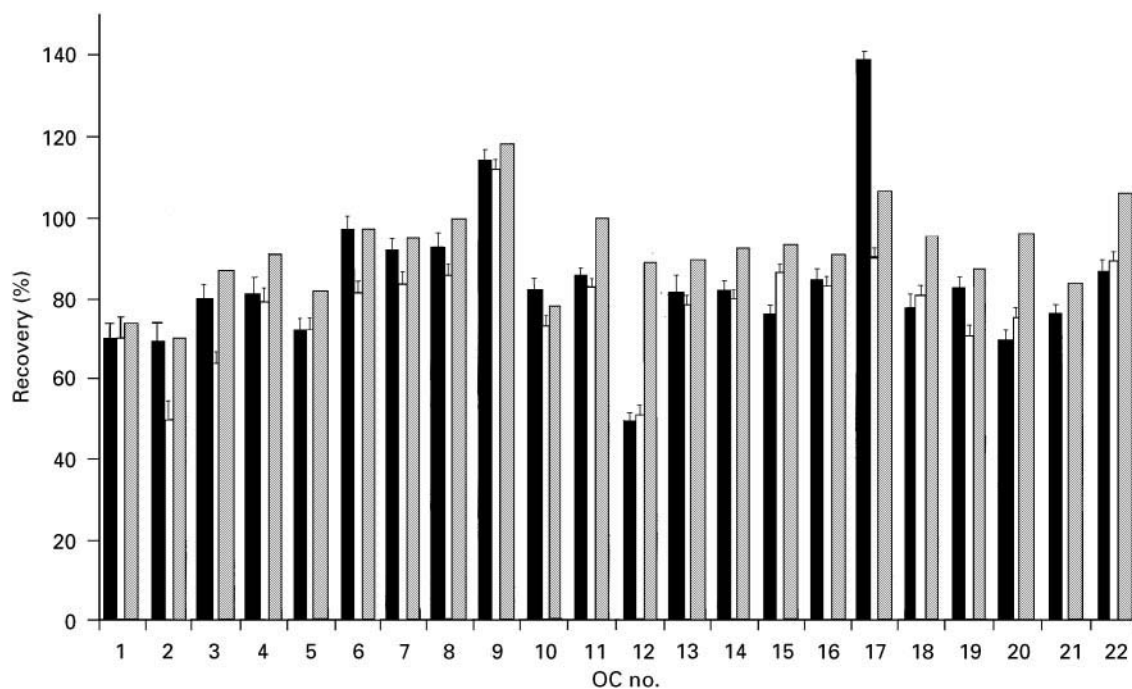


Figure 6 Recoveries of organochlorine pesticides from eggs using SFE with (filled columns) and without methanol (open columns) as modifier. Hatched columns represent spiked blanks. Error bars represent standard deviation of five replicates for methanol-modified extractions at three levels 3, 5 and 10% where concentration showed no significant difference. Organochlorine no. 1, hexachlorobenzene; 2, α -hexachlorobenzene; 3, lindane; 4, heptachlor; 5, aldrin; 6, ronnel; 7, β -hexachlorocyclohexane; 8, chlorpyrifos; 9, dicofol; 10, oxychlordane; 11, heptachlor epoxide; 12, α -endosulfan; 13, *trans*-chlordane; 14, *cis*-chlordane; 15, *p,p'*-DDE; 16, dieldrin; 17, endrin; 18, *o,p'*-DDT; 19, *p,p'*-tetrachlorodiphenylethane; 20, *p,p'* DDT; 21, mirex; 22, methoxychlor.

Herbal medicines have been characterized for industrial marketing in Japan using online SFE/SFC. A typical example is the case for atractylon, a characteristic component of *Atractylodes rhizome*. Rapid oxidation and degradation in UV light make manual methods difficult to execute with acceptable precision. The speed of the analysis by SFE coupled online with SFC make unstable, thermally labile and light-sensitive compounds easier to analyse.

Polymer Applications

The uses of supercritical fluids in industrial polymerization processes are many and varied. They include polymer fibre spinning, polymer-organic solvent-phase separation, fractionation, extraction of low molecular weight oligomers from polymers, high pressure polyethylene polymerization and fractionation and monomer purification. Backbone structure and slight differences in molecular weight can cause changes in polymer solubility properties. These differences are present in commercially prepared polymers and enable fractionation or extraction to be conducted on a large scale.

On the analytical scale, process monitoring of purity, oligomer content, oligomer and antioxidant extraction, additive concentration and removal of impurities have been conducted by SFE. Under supercritical conditions, the polymer matrix has been found to swell, in the same manner as has been described for soils. This has enabled SFE to accomplish analyses that were not previously possible by liquid extraction methods.

The most frequently reported area of SFE applications for polymers is the analysis of additives. Additives influence the physical nature of the polymer and come from a wide variety of classes. They can be low molecular weight and volatile or greater than 1 kDa with solubility in only some liquid solvents. Their analysis generally requires long, tedious multi-step procedures, which may include sample preprocessing, Soxhlet extraction, concentration and clean-up. The low viscosity and high solute diffusivity of supercritical fluids aids in the reduction and, in some cases, the elimination of these steps. The ability to determine the distribution of the additives within the polymeric grid has been demonstrated by several reports along with routine quantitative analysis. Commercial competitive product analysis is standard in industry and SFE has aided in the speed, ease and accuracy of this type of analysis.

The use of supercritical fluids in the polymer industry has opened up an area of knowledge that was previously closed; work continues to be actively conducted.

Additional Industrial Applications

In the fuel industry, stripping organics from minerals and shale rock has been conducted by SFE. Frequently, these methods used classical extraction methods that required several days. Equivalent results have been obtained in rapid extraction times of 15–30 min. Aromatic and aliphatic hydrocarbons (C_{10} – C_{35}), as well as naphthalene and asphaltene, are typical analytes that have been removed.

In the fibre industry, treatments with UV-stabilizers, removal and quantitation of residual dye components, and characterization of coatings, binders and adhesives have been conducted with the aid of SFE. Subsequent quantitative analysis either with SFC, LC, GC or mass spectrometry have all been successfully reported. The suggested procedures appear to be rugged enough to use for routine sample analysis.

Future Developments

The amount of research on SFE in the industrial environment is cyclical. Currently more work is being conducted on a larger scale in the areas of high temperature reactions, heterogeneous catalysis, reaction/separation schemes, antisolvent recrystallization and microencapsulation. However, research at the analytical scale continues. Without a doubt success with larger scale industrial processing leads to process monitoring and analysis. Analysis schemes, of necessity, frequently mimic the larger scale. This is one of the areas where SFE, and most likely supercritical chromatography, will continue to evolve with the pace controlled by need and economics. SFE, though novel in some locations, is no longer a new technology.

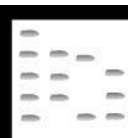
Low waste generation in SFE was originally touted as a huge payoff for exploiting the technique. Reduction in waste has been achieved with all automated sample preparation technologies, although the analytical laboratory has not been pushed to reduce solvent waste to the point that large scale processes have. The ability of a supercritical fluid to conduct the extraction of an analyte and leave no organic waste is a feature that can be exploited. The potential that it can be cleaned and recycled with minimum energy input makes it still more desirable. This is an area which could force the acceptance of supercritical technologies, including extraction, where it has been slow to take off.

See also: II/Extraction: Supercritical Fluid Extraction.

Further Reading

- Bright FV and McNally MEP (eds) (1992) *Supercritical Fluid Technology: Theoretical and Applied Approaches to Analytical Chemistry*. Washington: American Chemical Society.
- Charpentier BA and Sevenants MR (eds) (1988) *Supercritical Fluid Extraction and Chromatography: Techniques and Applications*. Washington: American Chemical Society.
- Johnston KP and Penninger JML (eds) (1989) *Supercritical Fluid Science and Technology*. Washington: American Chemical Society.
- Lee ML and Markides KE (eds) (1990) *Analytical Supercritical Fluid Chromatography and Extraction*. Provo: Chromatography Conferences.
- McHugh MA and Krukoni VJ (1994) *Supercritical Fluid Extraction: Principles and Practice*, 2nd edn. Stoneham: Butterworth-Heinemann.
- Smith RM and Howthorne SB (eds) (1997) *Supercritical Fluids in Chromatography and Extraction*. Reprinted from *Journal of Chromatography A* 785. Amsterdam: Elsevier.
- Westwood SA (ed.) (1993) *Supercritical Fluid Extraction and its Use in Chromatographic Sample Preparation*. Boca Raton: CRC Press.

INKS: FORENSIC ANALYSIS BY THIN-LAYER (PLANAR) CHROMATOGRAPHY



L. W. Pagano, M. J. Surrency and A. A. Cantu,
US Secret Service, Washington DC, USA

Copyright © 2000 Academic Press

Introduction

Because of the immense number of documents written, printed and copied each year, suspect documents generated by these methods have become common subjects for forensic examinations.

The forensic analysis of inks is performed to determine if inks are similar or different; to establish the authenticity of a document; to establish whether a document could have been produced on the purported date; or to determine the origin of a document. Although the chromatographic analysis of writing and stamp pad inks have been extensively documented, little has been written on the analysis of ink jet inks (jet inks) or photocopier/laser printer/LED printer toners, despite the volumes of such evidential documents under investigation.

All inks are composed of colorants in a vehicle. Today's inks include: writing, typewriting, stamp, printing, printer, jet and toner. The consistency of the vehicle ranges from liquids, such as those used in writing and jet inks; to paste, characteristic of some printing inks; to solids, such as those used in typewriting ribbons and toner.

This article only deals with inks whose colorants are separable by thin-layer chromatography (TLC). Such colorants include dyes and pigments that have some solubility in the extraction solvent. Since most printing inks use insoluble pigments as colorants, and therefore are not analysable by TLC, such inks are not considered here. Additionally, the jet inks and

toner under consideration are those used in full colour systems (YMCK).

The TLC separation of soluble inks involves six steps: sampling, extraction, spotting, developing, visualization/detection and interpretation.

A TLC method successfully used for the comparison of writing inks has translated well for the analysis of today's modern imaging media – jet ink and toner. Although colour toners are very different from classically defined 'ink', they are made up of separable dyes and TLC has proved useful in their analysis.

TLC is not an identification method unless used for comparison with a complete collection of standards. TLC is used in conjunction with a reference specimen library to match the manufacturer of an ink. These reference collections must contain samples of all inks manufactured throughout the world. Deficiencies in the library weaken the interpretation of a match and increase the number of nonmatches.

The most important criterion in the application of TLC to matching inks with library standard inks is that the inks under investigation and library inks be chromatographed under identical conditions using identical methods. A match becomes an identity only if the match is known to be unique and/or the library is complete.

Described in this article are procedures for analysing inks. The first step in an ink analysis is the identification of the ink type. This is best determined microscopically (**Figures 1–5**). This determination is critical because different chromatographic methods are used for different inks.

Once an ink is identified, the manufacturer may provide crucial information regarding the ink's formulation, earliest possible production date, and distribution.

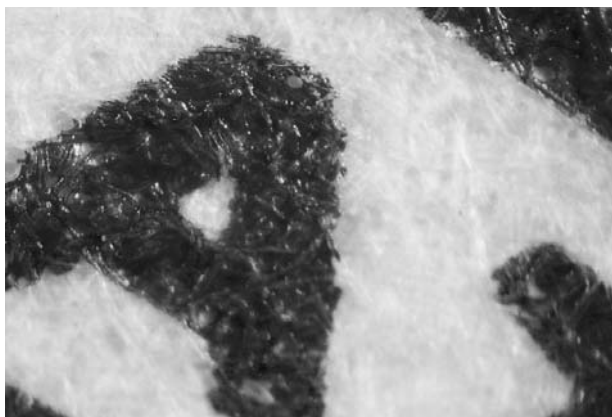


Figure 1 (See Colour Plate 88). Offset lithography photographed at 25 \times .

Jet Ink

Ink Jet Technology

Surprisingly, ink jet technology has been around for over 35 years, but only recently has it gained widespread use, most notably in desktop computer printers. This digital printing technology directs small droplets of ink to the substrate surface. Although there are several methods for accomplishing this, the two most common methods are continuous jets and drop-on-demand. Continuous jets create a stream of uniformly sized and spaced drops, which are deflected to produce an image. Drop-on-demand generates only the drops needed for image creation.

Fluid Jet Ink Chemistry

Most copiers/printers, which use ink jet technology, utilize a fluid, water-based ink. During the developmental stages of ink jet technology, researchers initially used fountain pen inks. These fountain pen inks caused corrosion on the print head surfaces, clogged

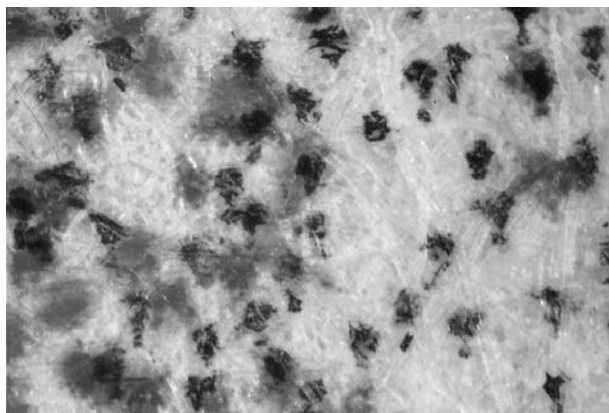


Figure 3 (See Colour Plate 90). Full colour ink jet photographed at 25 \times .

jet orifices, and had long drying times and excessive ink bleeding. Although these inks provided a starting point, it became apparent that this new technology would require specially formulated inks.

The early dyes were borrowed from the textile industry, then reworked and purified. Most of the organic dye counterions were replaced with larger ions, decreasing the activity and pH to a more suitable level and improving solubility, thus minimizing corrosion and crusting of the jet orifices. Along with the direct dyes, acid dyes and basic dyes used in textiles and food dyes were also adapted for ink jet systems. Organic dyes generally consist of three-dimensional compounds with ring structures having electron configurations that interact with incident radiation in the visible light range. Although these dyes must be soluble in water, they must be water-fast enough on the printed substrate to be used in an office environment. Amines and carboxylic functional groups were added to improve the binding of the dyes to the paper, and thus increase water-fastness.

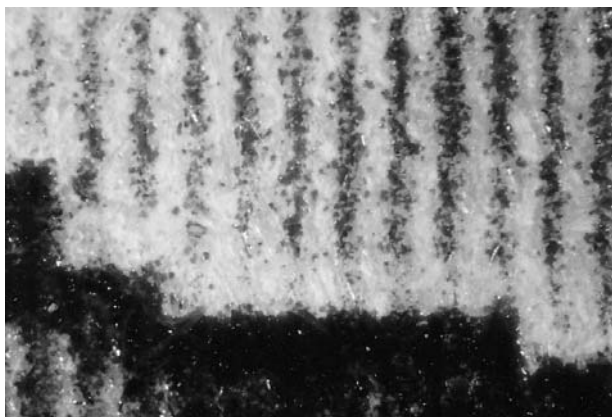


Figure 2 (See Colour Plate 89). Full colour toner photographed at 25 \times .



Figure 4 (See Colour Plate 91). Letterpress ink photographed at 25 \times .

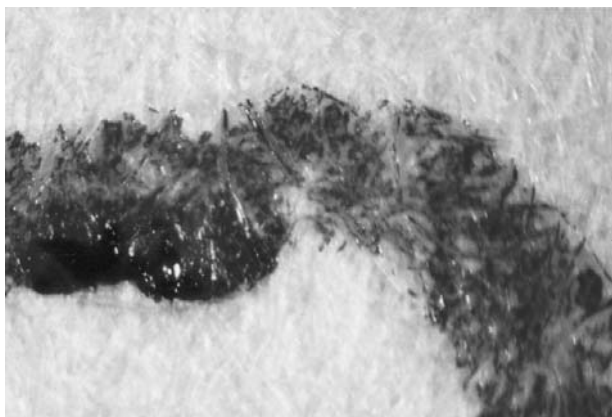


Figure 5 (See Colour Plate 92). Writing ink photographed at $25\times$.

Today, the majority of commercially available jet inks are specifically formulated by the manufacturers of the print-head and delivery systems, to several performance and aesthetic requirements. In addition, the ink must be chemically compatible with the components used to construct the ink reservoir and delivery and head assemblies; it must have sufficient relative density and surface tension to remain in the nozzle without leaking out of the orifice; and when ejected it must produce the desired drop shape and radius. The ink also needs to have good wetting properties, while maintaining rapid drying times, and must have chroma, hue and optical density suitable for producing colours pleasing to the end user. In addition, the ink must be nontoxic and environmentally safe.

Dyes are the most useful colorants for jet inks; however, pigments also have properties valuable to these systems. Pigments, which are insoluble and must be suspended in the ink, have many advantages over dyes, including optical density, light- and water-fastness and stability. The main disadvantage is the lack of commercially available pigments with particle sizes less than $1\text{ }\mu\text{m}$; most pigments are simply too large for use in ink jet systems. Advances in micropigments are producing more suitable pigments for use in ink jet systems.

To enhance ink performance, additives are incorporated. Often a low vapour pressure solvent, such as polyethylene glycol, is added to inhibit crusting. Other additives aid in buffering the solution, stabilizing the dyes (i.e. pyrrolidone), and wetting the paper (i.e. glycols, butyl ethers). To inhibit organic growth, biocides and fungicides are carefully selected and added to the formula. Like other water-based ink systems, bacteria and fungus thrive in jet inks.

The ink solution is a dynamic environment. Upon entering the delivery system or cartridge, the ink reacts with the polymers, foams and metals of the

container. Therefore, the ink in the printer or cartridge is no longer in its original state. The ink also changes composition, depending on its location in the cartridge and what materials are used. In systems that use low vapour pressure solvent(s) for crusting prevention, the actual chemical composition of the ink changes near the orifice as the solvent(s) evaporate.

Ink–Paper Interaction

In addition to the critical compatibility of the ink and print system, ink and substrate compatibility also plays a crucial role in print quality. The print quality is partially determined by the surface tension, viscosity, delivery angle and velocity of the ink and the sizing, surface energy and topography of the substrate. When paper is used as the substrate, print problems such as spread (dot-gain), absorption (bleed through the paper) and paper curl are quite apparent. Initially these problems were addressed by developing special paper coatings to control these factors, as well as to enhance contrast and to improve the colour gamut, optical density and water-fastness. Many of these coatings contain silica and starch and have a large surface pore volume to absorb large quantities of ink quickly. Other ink jet papers include multilayer configurations and polymerized coatings, designed to interact with the dyes, to adjust and render them insoluble in water and adjusting for the pH of the ink.

Analysing Jet Ink

Extraction solvent The solubility of the jet inks in their sampled state determines the solvent used for their extraction. Since the ink to be forensically examined is almost always on a document, the primary focus is the solubility of the ink in its dried state on a particular substrate. The most useful method is classical solubility testing by sampling and determining solubility in pure solvents, then binary combinations, in dimple plates. Once the best extraction solution has been determined, the solvents used should be chromatographic grade to avoid contamination. For jet inks an extraction solution of ethanol/water (1 : 1) has been found to be the most successful.

Solvent (mobile phase)/stationary phase Because of the complexity of the jet inks, the colorants generally cannot be separated using a single solvent. Therefore, solvent mixtures must be used. Chromatographically these solvents are chosen for their selectivity and strength. Additionally, the solvent should be made just before chromatographing. If the mobile phase is not made fresh, the concentrations will change as the higher vapour pressure solvents escape into the gas-

Table 1 Ink solvent system I

<i>Solvent</i>	<i>Eluotropic value (ϵ°) solvent strength on silica gel</i>	<i>Snyder group (selectivity)</i>	<i>Parts</i>
Ethyl acetate	4.4	VI	70
Absolute ethanol	4.3	II	35
Water	10.2	VIII	30

eous portion of the container. One solvent system, widely used for examining writing inks, has been found useful in the analysis of jet inks; this is solvent system I (Table 1). Additionally, solvent system V (Table 2) has been found to be another successful system.

The stationary phase, which is as important as the mobile phase, dictates the interactions between itself and the sample and solvent. Although there are several different stationary phases available (e.g. diol, reversed-phase, etc.) silica gel has proved to be most useful. Since some dyes have fluorescent characteristics, fluorescent indicators should be absent from the plate. It is highly advisable to clean the plates to remove any contaminants. This is performed by running the plate in the chosen solvent for the length of the plate and drying prior to spotting.

Sample preparation The substrate from which the inks are sampled is critical. Inks sampled from coated papers, which chemically and/or physically bind the ink, will chromatograph differently from the same ink printed on noncoated paper. Further, samples of ink taken directly from the cartridge versus drying the ink on a neutral substrate may also affect the chromatograms. Therefore, it may not be possible to analyse reliably documents produced on certain substrates by TLC.

Using a scalpel, ink should be removed from the uppermost layer of paper containing the ink. This method not only increases the ink-to-paper ratio, but also reduces potential contamination from ink on the reverse of the document. Samples must contain all of the imaging colours on the document, preferably in

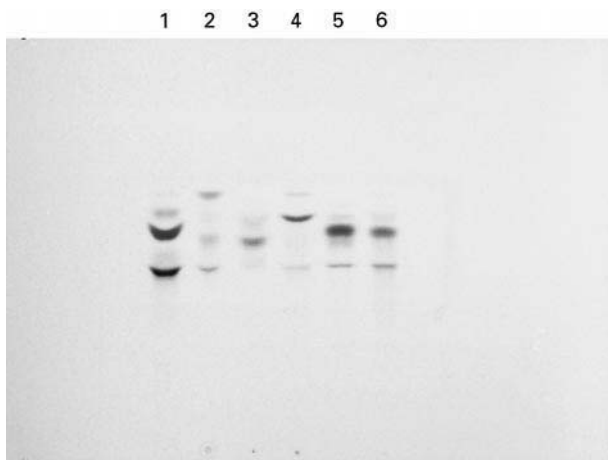
equal amounts. If the document does not contain all four of the process colours, changes to the library comparison and confirmation test methods are performed with only those colours found in the sample in question. Additionally, samples of plain areas of the paper must also be taken to identify any components contributed by the paper. Depending upon the subject of the document, little if no plain areas may exist for a proper substrate blank. This is often the case when the background of the original is not white. The scalpel method should help to minimize paper influence.

Extraction/spotting/development The amount of ethanol/water is dependent on the size of the sample. The concentration of the samples should be within the relative range of the library specimens. The extract is spotted using a Camag Nanomat with 1.0 μ L micropipettes at 1 cm from the bottom of a Whatman polyester silica gel plate. Once spotted, the plate is placed in a 95°C oven for 3 min to remove the extraction solvent. The plate is cooled to room temperature, then placed in a saturated vertical chamber containing solvent system I. The plate is allowed to develop to 4 cm from the origin, removed and dried.

Comparison/interpretation The developed plate is then compared with the chromatograms within the jet ink library and a list of possible matches is recorded. The possible library specimens are then sampled using the above mentioned method. The questioned ink and library specimens are spotted on a precleaned Whatman HPKF silica gel 60 plate. The plate is developed in a Camag saturated horizontal chamber containing solvent system I. After developing, the plate is dried. Once dry, the plate is interpreted under both UV and visible light (Figure 6).

Table 2 Ink solvent system V

<i>Solvent</i>	<i>Eluotropic value (ϵ°) solvent strength on silica gel</i>	<i>Snyder group (selectivity)</i>	<i>Parts</i>
Water	10.2	VIII	32
Acetic acid	6.0	IV	17
<i>N</i> -Butanol	3.9	II	41
Butyl acetate	–	–	10

**Figure 6** (See Colour Plate 96). Thin-layer chromatogram of full colour jet inks, solvent system I.

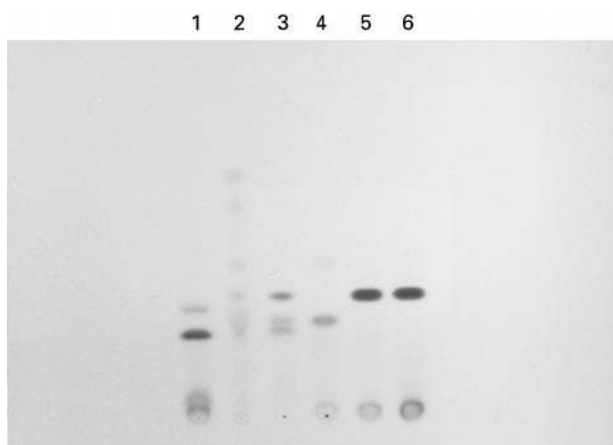


Figure 7 (See Colour Plate 97). Thin-layer chromatogram of full colour jet inks, solvent system V.

It should be noted that the interpretation of jet ink chromatograms is very different from interpretation of standard writing inks such as ball-point ink. Writing ink is eliminated if the relative dye concentrations are different between the questioned ink and a library specimen. This elimination is based on the fixed dye ratios within a writing ink, which is as characteristic as the dye composition itself. In ink jet systems, the concentrations of each of the four process colours varies according to the colour being reproduced; the relative concentrations of the dyes within the chromatograms will therefore also vary. As a result, relative concentration differences are not grounds for eliminating a jet ink specimen for consideration, as in the case of writing inks.

To confirm any matches to the library, a second plate with both the questioned sample and the matching library specimen is chromatographed using a Whatman HPLC silica gel 60 plate in solvent system V (Table 2). The match is then confirmed by interpreting the plate under both UV and visible light (Figure 7; see also Table 3).

If no matches are found, there may be deficiencies within the library or this may be caused by the use of

post-market inks, i.e. inks made to refill original cartridges. In the case of such inks, a new range of reactions take place. Even though post-market inks may be well represented in the library, when they are added to existing cartridges the interaction with the original ink and container components may alter their chromatograms to the extent that they do not resemble either the original ink or the post-market ink. For example, the post-market ink will initially force the original ink to the print-head. Farther back in the cartridge the old and new inks mix, forming gradients. The changes that occur are often greater than the sum of the components.

Writing Ink

Writing Ink Chemistry

All writing inks consists of colorants and a vehicle containing solvents and resin binders (ballpoint). Writing inks can generally be placed into two categories: ballpoint (Figure 8) and non-ballpoint inks (Figures 9 and 10). Non-ballpoint inks can be further subdivided into inks that are water-based (i.e. fountain pens, felt-tip markers, roller-ball) and those that are solvent-based ('permanent' markers). For ballpoint inks, the vehicle is commonly a mixture of glycol(s) (i.e. 2,3-butanediol, 1,2-propanediol), alcohols with low relative molecular mass (i.e. 2-phenoxy-ethanol, benzyl alcohol) and resin binders, which result in a paste-like consistency.

Most writing inks contain complex mixtures of mostly soluble dyes and occasionally suspended pigments (carbon or inorganic pigment), which result in unique formulations. Some of the more popular dyes and pigments are phthalocyanine blue, rhodamine, nigrosine and methyl violet.

Analysing Writing Ink

Extraction solvent The method for choosing an extraction solvent for writing ink is the same as that used for jet inks. For writing inks, extraction solvents

Table 3 Thin-layer chromatography of full colour jet inks as shown in Figures 6 and 7

Spot	Post-market Co.	Manufacturer	Model	Colours
1		Canon	BJC 620	YMCK
2		Epson	Stylus Colour 400	YMCK
3		Hewlett Packard	DeskJet 600	YMCK
4		Lexmark	2050	YMCK
5	American Ink Jet	Used in Hewlett Packard	DeskJet Series	YMCK
6	High Resolution	Used in Hewlett Packard	DeskJet Series	YMCK

Extraction solvent: ethanol/water.

Whatman HPLC Silica Gel 60.

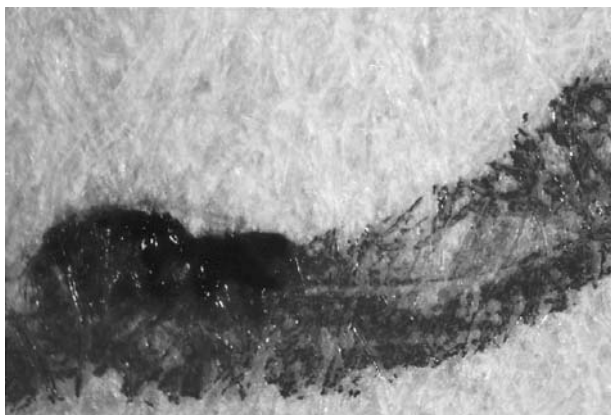


Figure 8 (See Colour Plate 93). Ballpoint writing ink photographed at 25 \times .

include ethanol/water for water-based and some solvent-based inks and pyridine for ballpoint and most solvent-based inks.

Solvent (mobile phase)/stationary phase Writing inks are complex mixtures and generally cannot be separated using a single solvent. Therefore, solvent mixtures are used to enhance separation of the colorants. Several different systems have been developed and tried. Solvent systems I and II (Table 1 and Table 4) are the most successful. Other solvent systems such as III and IV (Tables 5 and 6) can be more effective when inks are highly polar or contain Nigrosine.

Silica gel is the most useful stationary phase. The dyes and pigments used in writing inks may have fluorescent characteristics that are very helpful in their examination; fluorescent indicators should therefore be absent from the plate. Once again, the plates should be cleaned to remove any contaminants.



Figure 9 (See Colour Plate 94). Non-ballpoint writing ink (solvent-based) photographed at 25 \times .

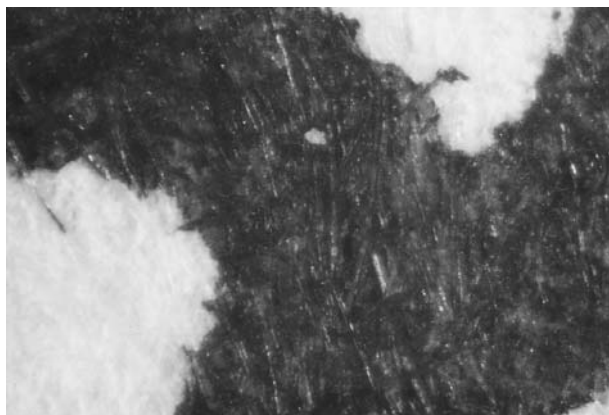


Figure 10 (See Colour Plate 95). Non-ballpoint writing ink (fountain pen) photographed at 25 \times .

Sample preparation Sampling is often accomplished by removal of the ink by use of a scalpel, a blunted 16–20 gauge hypodermic needle, or a commercially available forensic document sampling punch. If a scalpel is used, approximately 1 cm of an ink line is removed and placed into a vial. If the hypodermic needle or sampling device is used approximately ten plugs of ink (~ 0.1 μ g of ink) are removed from the document and transferred to a vial. As with ink jet analysis, samples of paper/substrate should be taken and examined to identify its contribution to the ink sample extract.

Extraction/spotting/development The ink is extracted by adding a minimum of appropriate extraction solvent and spotted onto the plate with 1.0 μ L micro-pipettes at 1 cm from the bottom of a Whatman polyester silica gel plate. Once spotted, the plate is placed in a 95°C oven for 3 min to remove the extraction solvent. The plate is cooled to room temperature, then placed in a saturated vertical chamber containing solvent system I. The plate is allowed to develop to 4 cm from the origin. The plate is removed and allowed to dry by evaporation.

Comparison/interpretation The developed plate is then compared with the chromatograms within the writing ink library and a list of possible matches is

Table 4 Ink solvent system II

<i>Solvent</i>	<i>Eluotropic value (ϵ°) solvent strength on silica gel</i>	<i>Snyder group (selectivity)</i>	<i>Parts</i>
N-Butanol	3.9	II	41
Absolute ethanol	4.3	II	35
Water	10.2	VIII	32

Table 5 Ink solvent system III

<i>Solvent</i>	<i>Eluotropic value (ϵ°) solvent strength on silica gel</i>	<i>Snyder group (selectivity)</i>	<i>Parts</i>
Cyclohexane	0.04	VII	10
Chlorobenzene	0.3	–	2
Absolute ethanol	4.3	II	1

recorded. The possible matches are sampled using the above mentioned method. The questioned ink and possible matching standards are then spotted on a precleaned Whatman HPKF silica gel 60 plate. The plate is developed in a horizontal chamber containing solvent system I. After developing, the plate is dried by evaporation and interpreted under both UV and visible light (**Figure 11**).

Unlike ink jet ink interpretation, the concentrations of the dye components from nonrefillable cartridge pens will not vary between the questioned document and the library samples. Therefore, relative concentration differences are grounds for eliminating an ink specimen.

To confirm any matches to the library, a second plate with both the questioned sample and the matching library specimen is chromatographed on a precleaned HPKF plate in solvent system II (Table 4). The match is then confirmed by interpreting the plate under both UV and visible light (**Figure 12**; see also Table 7).

Toner

Toner Technology

Electrophotography dates back to 1938 and has become the most widely used plateless printing technology. Electrophotography is a process that consists of a photoreceptive drum that is charged in darkness with a corona discharge and exposed to an original document through an optics system. The light reflected from the original image discharges the photoconductor where the light strikes it, creating a latent image on the drum corresponding to the dark areas on the original. This latent charged image is de-

Table 6 Ink solvent system IV (modified)

<i>Solvent</i>	<i>Eluotropic value (ϵ°) solvent strength on silica gel</i>	<i>Snyder group (selectivity)</i>	<i>Parts</i>
Ethyl acetate	4.4	VI	2
Absolute ethanol	4.3	II	2
Chlorobenzene	0.3	–	10

Two-phase liquid; the top phase is used as the solvent system.

**Figure 11** (See Colour Plate 98). Thin-layer chromatogram of ballpoint inks, solvent system I.

veloped with oppositely charged toner. The toner is transferred to a substrate and fixed. Today's digital electrophotographic machines use lasers or light emitting diodes (LED) driven by digital data to create the latent image on the photoreceptive drum.

Dry Toner Chemistry

Toners are electrostatically transferred to the paper or print substrate and are fused by heat, pressure or a combination of both. As with other inks, toners must meet certain print parameters, such as water- and light-fastness, but because of their unique way of imaging they must also meet a unique set of chemical and physical parameters, such as triboelectric properties.

Dry toners are very fine powders consisting primarily of a polymer resin binder and colorants. These colorants, pigments and dyes, are chosen primarily for their chroma, hue and colour purity. The most common pigments and dyes are carbon black,

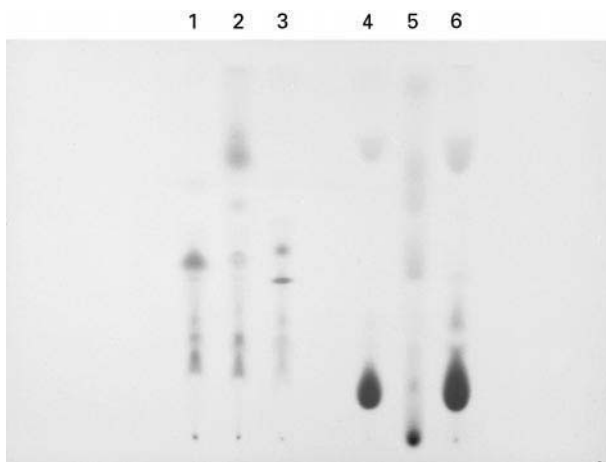
**Figure 12** (See Colour Plate 99). Thin-layer chromatogram of ballpoint inks, solvent system II.

Table 7 Thin-layer chromatography of ballpoint inks as shown in Figures 11 and 12

Spot	Manufacturer	Model	Colours
1	Papermate	Flexgrip	Blue
2	Skilcraft	Stick	Blue
3	Bic	Round Stic	Blue
4	Papermate	Flex Grip	Black
5	Skilcraft	Stick	Black
6	Bic	Round Stic	Black

Extraction solvent: pyridine.
Whatman HPKF Silica Gel 60.

nigrosines, copper phthalocyanines, azo-pigments and quinacridone.

The polymer or copolymer resin binder is chosen for its thermal characteristics such as glass transition temperature and flow viscosity. Polystyrene acrylates and epoxy polymers are used for hot roll and flash fusing. Small chain homologue polymers, e.g. polyethylene and polypropylene, and vinyl acetates are used for cold pressure and roll fusing. Polyester is used primarily for radiant fusing. Often additives are incorporated into the toners to alter physical properties: pigments and dyes are added for colour; magnetite salts are added to enhance control of the toner; ammonium salts are used for positive charge control; acidified carbon black and metal complexes are added for negative charge control; silica and zinc stearate are added as a lubricant and flow enhancement; and silicone oils and low weight polyethyl and polypropyl waxes are used as release agents to prevent the toner from adhering to the fusing roller.

Analysing Toner

Extraction solvent The method for choosing an extraction solvent for toner is the same as that used for jet and writing inks. It must first be determined in which solvent(s) the toner is soluble, then whether mixtures of solvents are needed to enhance solubility. Pure chloroform was found to be the most successful.

Solvent (mobile phase)/stationary phase Like jet and writing ink, toners generally cannot be separated using a single solvent. Therefore, solvent mixtures must be used to accomplish separation of the colorants. The most successful solvent system for toners are solvent systems I (Table 1) and modified IV (Table 6).

Silica gel is the most useful stationary phase. The dyes and pigments used in toners often have fluorescent characteristics that are very helpful in their examination, hence fluorescent indicators should be absent from the plate. Once again, the plates should be cleaned to remove any contaminants.

Sample preparation Sampling toner documents has advantages over jet ink documents. Although, as with ink jet documents, toner documents may have little or no clean paper areas, this is of little concern with toner sampling because the toner is removed from the document thermally. To remove the sample, a clean scanning electron microscope (SEM) aluminium stub placed over the sampling area is heated with a soldering iron. The heat causes some of the toner to be transferred to the stub. Since this method removes only the toner, paper interactions are avoided. Again, as with jet inks, all of the process colours should be sampled from the document in equal proportions. If the document does not contain all four of the process colours, changes to the library comparison and conformation test methods are performed with only those colours found in the sample.

Extraction/spotting/development The toner is washed from the stub with chloroform into a sampling vial. The toner wash is spotted onto the plate using 2.0 µL micropipettes at 1 cm from the bottom of a Whatman polyester silica gel plate. Once spotted, the plate is placed in a 95°C oven for 3 min to remove the extraction solvent. The plate is cooled to room temperature, then placed in a saturated vertical chamber containing solvent system I. The plate is allowed to develop to 4 cm from the origin, removed and allowed to dry by evaporation (Figure 13).

Comparison/interpretation The developed plate is then compared with the chromatograms within the toner library and a list of possible matches is recorded. The possible library specimens are sampled using the abovementioned method. The questioned toner and library specimens are then spotted on a precleaned Merck silica gel 60 plate. The plate is

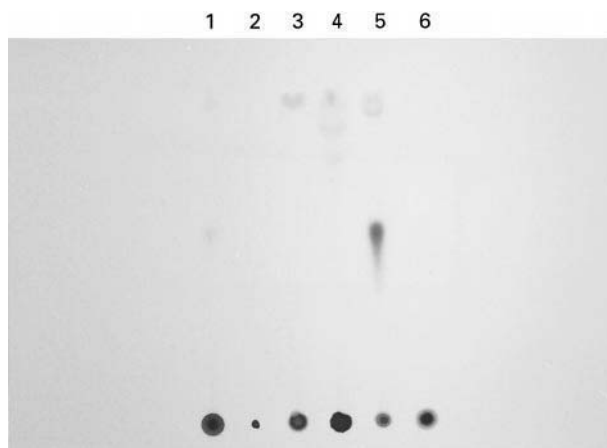


Figure 13 (See Colour Plate 100). Thin-layer chromatogram of full colour toner, solvent system I.

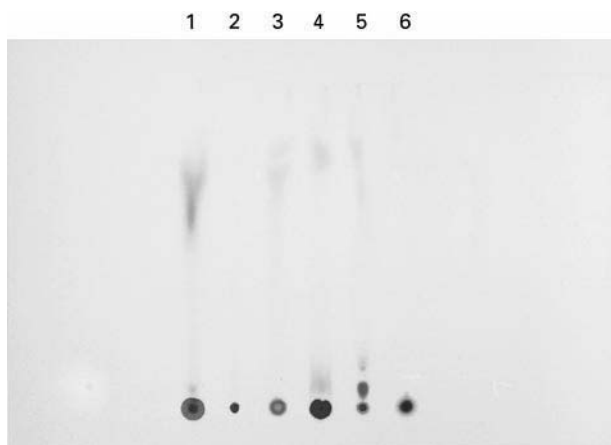


Figure 14 (See Colour Plate 101). Thin-layer chromatogram of full colour toner, solvent system IV.

developed in a Camag saturated horizontal chamber containing solvent system I. After developing, the plate is dried by evaporation. Once dry, the plate is interpreted under both UV and visible light.

As with jet ink interpretation, the concentrations of the dye components will vary owing to the varying concentrations of the four process colours between the questioned document and the library samples. Therefore, relative concentration differences are not grounds for eliminating a toner specimen, as in the case of writing inks.

To confirm any matches to the library, a second plate with both the sample and the matching library specimen is chromatographed using a Merck silica gel 60 plate, without fluorescent indicator, in modified solvent system IV (Table 6). The match is then confirmed by interpreting the plate under both UV and visible light (Figure 14; see also Table 8).

Conclusions

Through the use of colorant separation by TLC in conjunction with comparison libraries, the various original manufactures' inks can generally be distinguished from each other. At the time of this article,

Table 8 Thin-layer chromatography of full colour toner as shown in Figures 13 and 14

Spot	Manufacturer	Model	Colours
1	Canon	CLC 1000	YMCK
2	Konica	7728	YMCK
3	Minolta	CF 900	YMCK
4	Ricoh	8015	YMCK
5	Sharp	CX 7500	YMCK
6	Xerox	5775	YMCK

Extraction solvent: chloroform.
Merck Silica Gel 60.

total distinguishability is obtained for full colour jet inks and toners. The comparison of the colour components has proved to be more discriminating than the comparison of other components, such as resins within ballpoint inks and toner. The ability to discriminate inks, coupled with the low cost, ease and multiple samples per run, make TLC a powerful forensic tool for the analysis of modern documents produced by traditional and new inks.

See Colour Plates 88, 89, 90, 91, 92, 93, 94, 95, 96, 97, 98, 99, 100, 101.

See also: II/Chromatography: Thin-Layer (Planar): Instrumentation; Layers.

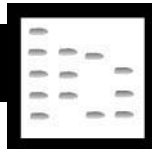
Further Reading

- American Society for Testing and Materials (ASTM) (1991) Standard Guide for Test Methods for Forensic Writing Ink Comparison. *ASTM STANDARD E1422-91*.
- Aginsky VN (1993) Comparative examination of inks by using instrumental thin-layer chromatography and microspectrophotometry. *Journal of Forensic Sciences* 38(5): 1111–1130.
- Andrasko J (1994) A simple method for sampling photocopy toners for examination by microreflectance Fourier transform infrared spectroscopy. *Journal of Forensic Sciences* 39(1): 226–230.
- Brunelle RL and Reed WR (1991) *Forensic Examination of Ink and Paper*, pp. 165–170. Springfield, IL: Charles C Thomas.
- Cantu AA (1995) A sketch of analytical methods for document dating. Part I. The static approach: determining age independent analytical profiles; and Part II. The dynamic approach: determining age dependent profiles. *International Journal of Forensic Document Examiners* 1(1): 40–51; and 2(3): 192–208.
- Diamond AS (1991) *Handbook of Imaging Materials*, pp. 548–562. New York: Marcel Dekker.
- Fishman DH (1997) Ink jet technology. *American Ink Maker* June: 36–39.
- Hackleman D (1985) Where the ink hits the paper *Hewlett-Packard Journal* May: 32.
- Maze C, Loren EJ, Kearl DA and Shields JP (1992) Ink and print cartridge development for the HP DeskJet 500 C/DeskWriter C Printer Family. *Hewlett-Packard Journal* August: 69–76.
- Pagano B (1985) *Identification of Photocopies by their Physical and Chemical Properties*. Canadian Society of Forensic Science.
- Pagano L (1991) *Colour Photocopy Analysis by Thin Layer Chromatography*. Mid-Atlantic Association of Forensic Science, Bethesda, Maryland, May 1991.
- Snyder LR (1968) *Principles of Adsorption Chromatography*, pp. 193–221. New York: Marcel Dekker.
- Solodar W (1998) Designing dyes for ink jets. *International Journal of Forensic Document Examiners* 4(1): 22–24.
- Tsujita J (1998) Copier/printer market research. J & F Associates, Inc., Great Neck, New York.

INORGANIC EXTRACTION: MOLECULAR RECOGNITION TECHNOLOGY

See III/MOLECULAR RECOGNITION TECHNOLOGY IN INORGANIC EXTRACTION

INSECTICIDES



Gas Chromatography

P. Brown, Central Science Laboratory, York, UK

Copyright © 1999 Crown Copyright

Developments in insecticide analysis have been closely linked to developments in gas chromatography (GC). Indeed, the invention of the electron-capture detector led to the discovery of residues of the persistent organochlorine insecticides in dead birds and this in turn raised concerns regarding pesticide residues in food and the environment. The range of applications of GC to insecticide analysis is very wide and the choice of technique must be appropriate for the intended purpose. The first requirement is to detect the compounds of interest; most GC detectors have some use in insecticide analysis. Different types of column are needed for different applications and the choice of injection technique is related to the analyte and the type of column. The ability to obtain a chromatogram from a solution of insecticides is just a starting point. The insecticides have to be extracted from a variety of samples and separated from many other co-extracted compounds which can interfere with the separation or degrade the column. There are four major classes of insecticides, each of which has its particular analytical requirements.

Applications of GC in Insecticide Analysis

Insecticides are biologically active compounds used principally in agriculture but also in public health applications. There is public concern over their production and use, their presence in food and their persistence in the environment. The requirement for insecticide analysis is wide-ranging. GC is better suited to residue analysis than measuring the high concentrations encountered in formulations. For GC analysis, the insecticides must be sufficiently volatile and thermally stable.

A manufacturer may be interested in a particular compound together with its metabolites and degradation products in biological systems and the environment. In cases of animal poisoning by an insecticide, the identification of the poison is the main task. Foods are monitored for many different insecticides and some degradation products; small residues around statutory limits must be identified and measured accurately in a wide variety of foods, each of which poses particular analytical challenges. Residues in water and air are even smaller and must be trapped and concentrated prior to measurement.

With such a variety of applications, it is essential that the analytical method is fit for its purpose.

Detectors for GC of Insecticides

A list of detectors and their application to insecticide analysis is shown in Table 1.

Columns and Injection Ports for GC of Insecticides

Packed Columns

GC of insecticides began with packed columns that gave low resolution and were limited by the temperature at which the nonbonded stationary phase began to bleed. To achieve sufficient resolution for identification and to obtain good peak shapes, a wide range of stationary phases was needed. Packed columns are not well suited to temperature programming and the sample is usually introduced by vaporization of a solution in a heated injection port. This is unsuitable for the thermally labile carbamates which have to be converted to more stable derivatives.

Capillary Columns

The introduction of fused silica capillary columns and bonded stationary phases brought higher resolution GC to routine analysis of insecticides. Higher

Table 1 Detectors used in the gas chromatography of insecticides

<i>Detector</i>	<i>Species detected</i>	<i>Insecticide classes</i>	<i>Comments</i>
FID (flame ionization) PID (photoionization)	Carbon compounds	All	With these detectors, difficult to identify the insecticides amongst the peaks from co-extracted compounds in residue analysis
ECD (electron capture)	Halogens and other electron-capturing species	Organochlorines, most pyrethroids, some OPs	Sensitive but not highly selective. Responds to some nonhalogenated compounds. Response affected by co-extractives
Electrolytic conductivity	Chlorine or sulfur or others	Organochlorines	More selective than ECD but less sensitive. Less robust. Requires more maintenance
NPD (nitrogen phosphorus)	Nitrogen and phosphorus	Organophosphates, carbamates	Responds to both elements. Slightly 'tunable'. Response changes slowly as salt bead ages. Response affected by co-extractives
Chemiluminescence	Nitrogen	Carbamates	Rarely used to date
FPD (flame photometric)	Phosphorus (with 526 nm filter)	Organophosphates some have phosphorus and sulfur	Very selective for phosphorus but large amounts of sulfur compounds may interfere
	Sulfur (394 nm)	Others with sulfur	Nonlinear response. Affected by bleed
AED (atomic emission)	Carbon, chlorine, nitrogen, sulfur, phosphorus, oxygen (not all at once)	All (but selective for chosen elements)	Versatile selective multielement detector but not as sensitive as some and costs more to buy and run
FTIR (Fourier transform infrared)	Functional groups that absorb infrared	Various, but only at high levels	Not sensitive enough for residue analysis
MS (mass spectrometry)			
Total ion chromatogram	All that ionize in MS	All	Same disadvantages as FID (above), but other modes are selective (below)
Selected ion(s)	Selected ions	All chosen compounds	Selective for compounds producing the chosen ions
Full spectrum	Mass spectrum	Identification of peak	Good identification if sufficiently sensitive
Negative-ion CI	Halogens (as ECD)	OCs, pyrethroids	Limited application
MS-MS	Fragmentation of ion	Co-eluting compounds or sparse spectrum	Aids identification in these difficult situations

OPs, organophosphates; OCs, organochlorines; CI, chemical ionization.

resolution, less active sites, temperature programming, cool on-column injection and the development of sensitive mass spectrometric detectors enabled many insecticides, including some that are thermally labile, to be analysed on a low polarity stationary phase (dimethyl polysiloxane, DB-1 or methylphenyl polysiloxane, DB-5, DB-17, etc.)

For fast analyses or for thermally labile compounds, a short wide-bore column (10 m × 0.53 mm i.d. with a 1 µm stationary phase thickness) works well in combination with semi-selective detectors (electron-capture, nitrogen-phosphorus and flame photometric detectors). If the analyte is sufficiently stable, a packed column injector can be converted for direct injection into a 0.53 mm capillary column by the addition of a liner with a volume of

about 1 mL and an appropriate reducing adapter. For cool on-column injection, a purpose-built port is necessary. A carrier gas (nitrogen or preferably helium or hydrogen) flow of about 5 mL min⁻¹ and a temperature gradient from 50 or 100°C at 5°C min⁻¹ to 250°C will be suitable for the analysis of most insecticides.

For higher resolution, a smaller bore (e.g. 0.25 mm internal diameter) and/or longer column is needed. Also, if the detector is a mass spectrometer, a low carrier flow around 1 mL min⁻¹ is preferred. Concentrated sample solutions are best analysed with a split injection technique where only a small proportion of the injected extract goes on to the column. For most insecticide analysis, splitless injection is used together with an initial column temperature low enough to

cold-trap the analytes and to condense the solvent if the solvent effect is to be employed.

Cool on-column injection is ideal for compounds that start to decompose in a hot injection port, but nonvolatile co-extracted solutes remaining in sample extracts will rapidly contaminate the column. A wide-bore retention gap will trap nonvolatiles and allow injection with a conventional syringe needle (instead of needing a fragile thin needle to inject directly into a small-bore column). Some carbamate insecticides can be analysed without derivatization on a nonpolar column with on-column injection.

Large volume injection is becoming popular for the analysis of low concentrations of insecticides in water samples. Volumes in excess of 100 μL of extract are injected into packing in an injection port liner from which the solvent is evaporated. The solutes are thermally desorbed on to the column where they are cold-trapped prior to the start of temperature-programmed GC analysis.

A thermal desorption and cold-trapping technique is also used for analysis of air samples from which contaminants have been trapped by passage through a tube of adsorbent.

Volatile insecticides used as fumigants in grain and other stored commodities may be analysed by head-space analysis; the volatile compounds are sampled from the air above the samples and passed in a gas stream to be trapped on the top of the GC column.

Analysis for Insecticides in Biological and Environmental Samples

Before insecticide residues can be analysed by GC, they have to be extracted from the samples containing them. These extracts contain many other co-extractives in addition to the insecticides and require a clean-up.

Extraction

The simple – and usual – way to check whether an analytical procedure will extract compounds of interest is to add a solution of the compounds to the exposed surfaces of sample (whole, chopped up or finely ground), allow the solvent to evaporate fully, then apply the analytical procedure. Residues that have been acquired by a plant or animal by systemic processes (transport via a plant's vascular system or the processes through gut and internal organs following ingestion by an animal) may be more difficult to extract than surface residues. Studies using radiolabelled compounds may be needed to determine whether such residues are extractable or bound.

Extracts are usually obtained by cutting the sample very finely (blending, homogenizing, milling, grinding, etc.) and extracting with an organic solvent. Extraction may be a one- or two-stage process aided by agitation (shaking, ultrasonication, homogenizing) followed by filtration or centrifugation (to separate solid and liquid). It may be continuous as in liquid–liquid extraction (for liquid samples) or in Soxhlet extraction, accelerated solvent extraction or supercritical fluid extraction (for solid samples).

Clean-up

The effects of co-extractives on GC include:

1. visible additional peaks on the chromatogram, perhaps unresolved from the analyte peak;
2. volatile substances that, although not themselves showing a detector response, elute with the analyte and affect the chromatography or the response of the detector to the analyte;
3. nonvolatile solutes deposited on injection, coating the injection liner and top of the column, changing the characteristics of the stationary phase in that region.

A clean-up from which a wide range of insecticides can be recovered will also recover many other co-extracted compounds. Some analysts use extracts with little or no clean-up, and selective detection such as GC-mass spectrometry (GC-MS). They compensate for chromatographic effects from co-extractives by the use of carefully chosen internal standards or prepare matrix-matched external standards in extracts of analyte-free sample material. An instrument used in this way will require frequent maintenance, but the overall result may be cost-effective.

Clean-up is a source of potential loss of analyte and adds extra time to analyses (but in recent years equipment for partial automation of this process has been introduced).

Gel permeation chromatography (GPC) is a technique that delays small molecules such as insecticides as they flow in and out of pores in the gel while larger molecules flow past in the solvent stream. The large molecules mainly form the nonvolatile material deposited at the GC injection port, so GPC is potentially a useful clean-up for insecticides in a wide range of sample matrices. The disadvantage of traditional GPC is that it uses large quantities of solvents (hundreds of millilitres) which have to be removed by evaporation. High performance GPC works on a smaller scale and can be automated, but the columns are expensive compared to analytical high performance liquid chromatography columns.

Column adsorption chromatography using quantities of between 1 g and 50 g of materials such as alumina, silica gel and Florisil was the traditional method for clean-up of extracts containing insecticides. These traditional columns have been largely superseded by small particle size materials in quantities from 100 mg to 1 g in cartridges, usually requiring a small pressure or vacuum to give a suitable flow rate. Cartridges of this type, including those with reversed-phase (C_{18}) and ion exchange packings, are now known as solid-phase extraction (SPE) cartridges. Equipment for automated operation of these cartridges is widely available.

Partition between two immiscible solvents, such as water and hexane, may be used to separate polar co-extractives from insecticides that are generally of low polarity. Originally separating funnels were used, but there are now cartridges of inert material that will absorb an aqueous solution but still allow efficient partition of insecticides into a water-immiscible solvent poured through the cartridge. A partition mechanism also operates with SPE cartridges containing bonded C_{18} packing material. Insecticides in aqueous solution are extracted by a partition process into the C_{18} and then eluted selectively from the cartridge by organic solvent mixtures of appropriate polarity.

There are other clean-up techniques developed for specific purposes. Sweep co-distillation is a process analogous to steam distillation, in which insecticides and other volatile materials are distilled out of heated liquid fat samples. Some of the organochlorine insecticides are resistant to chemical attack, so reaction of interfering compounds with strong acids or oxidizing agents has been used as a clean-up for these compounds.

The extraction and clean-up methods to be employed depend on the insecticide(s) to be analysed and the nature of the sample material. The analyst should consult the literature for a particular application, but if no suitable technique is described, some experimentation will be necessary.

Determination of Insecticides by GC

The requirements for GC determination depend on the purpose of the analysis. Generally, GC determination with a semi-selective detector or a single ion on a mass spectrometer requires additional confirmation, by an alternative technique or by measurement of other ions.

Organochlorines

Most of the insecticides of this type have been withdrawn from use in many countries, but residues per-

sist in the environment. Organochlorine insecticides are of several different chemical types but all contain chlorine atoms and are fat-soluble (non-polar). Lindane (hexachlorocyclohexane (γ -isomer), γ -HCH), dichlorodiphenyltrichloroethane (DDT) and dieldrin are examples (**Figure 1**). They are very slightly soluble in water, but are readily extractable into hexane from water or homogenized water-containing samples. Diethyl ether or ethyl acetate will also extract them from dry materials on which they are adsorbed. An alternative is to use a water-miscible solvent such as acetone to extract from water-containing samples; this is followed by partition between water and hexane. Supercritical fluid extraction with carbon dioxide as solvent and a C_{18} trap has also been used to extract organochlorine insecticides from relatively dry commodities. For clean-up of hexane extracts of fatty samples, chromatography on deactivated alumina or Florisil with further hexane elution recovers most of the organochlorines while leaving most co-extractives behind. GPC and sweep co-distillation are sometimes used to clean up extracts containing organochlorines. Although these insecticides are solids, care must be taken when evaporating extracts as, for example, γ -HCH is easily lost if a solution is evaporated to dryness.

All the organochlorine insecticides chromatograph well on dimethyl silicone stationary phases (DB-1, OV-1, etc.). Endrin and 1,1,1-trichloro-2,2-bis(4-chlorophenyl)ethane (p,p' -DDT) may break down or

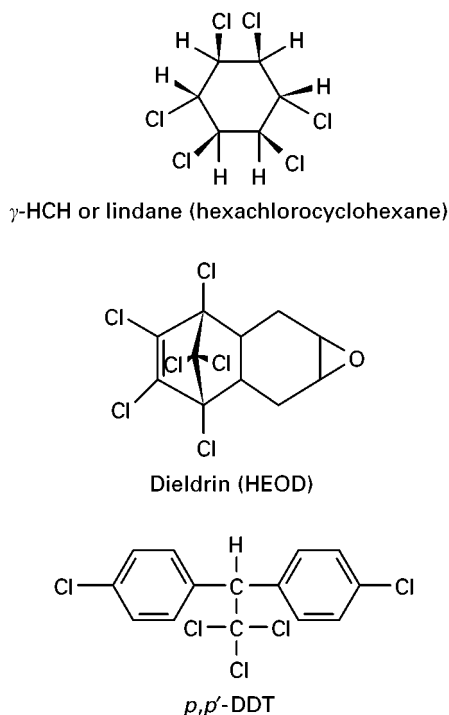


Figure 1 Organochlorine insecticides.

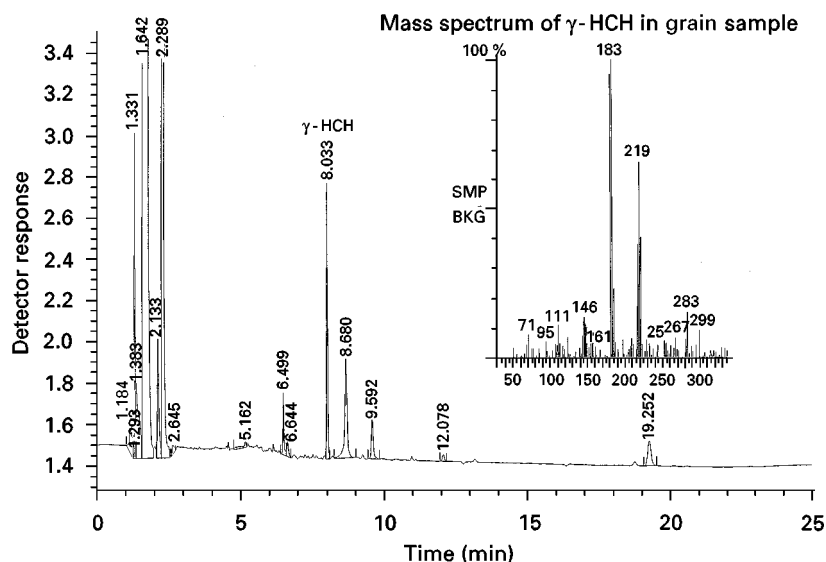


Figure 2 Chromatogram of extract of grain sample containing γ -HCH. Chromatogram of a cleaned-up extract of grain showing a residue of γ -HCH (0.7 mg kg^{-1}). $1 \mu\text{L}$ direct injection at 150°C on to $30 \text{ m} \times 0.53 \text{ mm i.d.}$, DB-1 column ($1.5 \mu\text{m}$ film thickness). Gradient from 100°C (1.0 min) at $25^\circ\text{C min}^{-1}$ to 225°C then at $2.5^\circ\text{C min}^{-1}$ to 265°C (3 min). Helium carrier gas. Hewlett Packard 5890 GC with ECD. GC-MS confirmation on $30 \text{ m} \times 0.25 \text{ mm i.d.}$ BPX5 column ($0.25 \mu\text{m}$ film thickness) in Finnigan GCQ instrument.

adsorb strongly if the injection liner and top of column become dirty or active. Splitless injection is usually used for residue analysis. A 20 m long, 0.53 mm i.d. column gives satisfactory resolution with a temperature programme from 100°C to 225°C . A chlorine-selective detector such as the very sensitive electron-capture detector or the less sensitive but more selective atomic emission detector may be used. For certainty of identification, a bench-top mass spectrometer is used to obtain a full mass spectrum; the chromatogram is monitored for selected ions at particular retention times to locate any organochlorine peaks (Figure 2). A capillary column has to be used to suit the maximum gas flow requirements of the mass spectrometer. For some of the organochlorines, negative-ion chemical ionization mass spectrometry is a successful detection technique.

Synthetic Pyrethroids

Synthetic pyrethroid insecticides have certain structural features in common. Permethrin, bifenthrin and fenvalerate are typical examples (Figure 3). They are only slightly more polar than the organochlorines and may be extracted in a similar way. Mixtures of, for example, hexane and ether will elute pyrethroids from Florisil clean-up columns or cartridges. Those synthetic pyrethroids that do not contain chlorine atoms contain other halogens or chemical groups that are electron-capturing. Retention times are longer than for the organochlorine compounds, so the temperature programme has to rise to 275°C (Figure 4). However, resolution of the isomers of some pyreth-

roids (e.g. cypermethrin) requires a higher resolution column (e.g. $30 \text{ m} \times 0.25 \text{ mm i.d.}$).

Carbamates

The carbamate insecticides are of two types, esters of *N*-methyl (or *N,N*-dimethyl) carbamic acid with

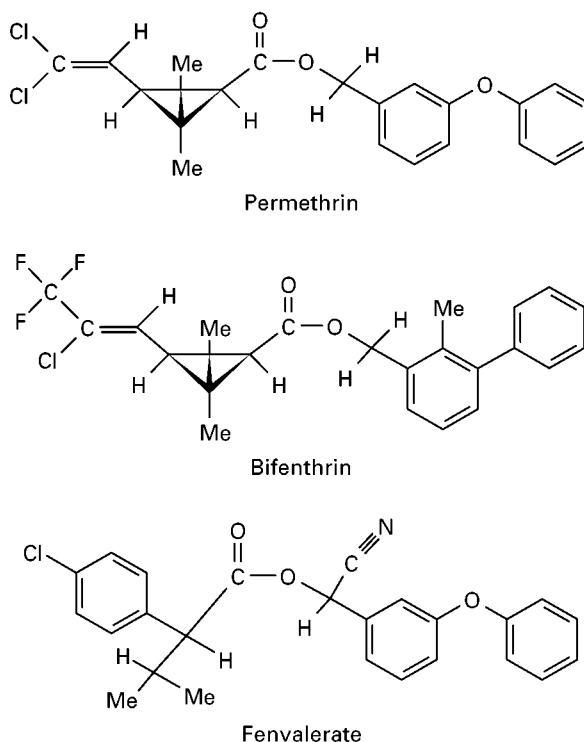


Figure 3 Synthetic pyrethroid insecticides.

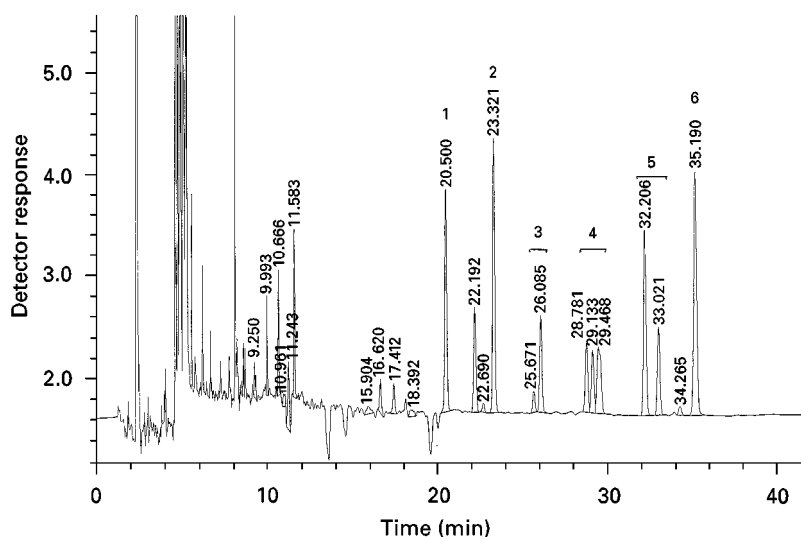


Figure 4 Chromatogram of six synthetic pyrethroids in honey bee extract. Chromatogram of cleaned-up supercritical fluid extract of honey bees spiked before extraction with six pyrethroids, each at 0.1 mg kg^{-1} . 1, Bifenthrin; 2, λ -cyhalothrin; 3, permethrin; 4, cypermethrin; 5, fenvalerate; 6, deltamethrin. $1 \mu\text{L}$ direct injection at 175°C on to $30 \text{ m} \times 0.53 \text{ mm i.d.}$, DB-1 column ($1.5 \mu\text{m}$ film thickness). Gradient from 50°C (1.0 min) at $25^\circ\text{C min}^{-1}$ to 225°C then at 2°C min^{-1} to 275°C (9 min). Helium carrier gas. Hewlett Packard 5890 GC with ECD.

either a phenol or an oxime. Carbaryl and pirimicarb are examples of the phenolic type. Aldicarb and methomyl are examples of the oxime type (Figure 5). They are extractable with diethyl ether, dichloro-

methane, ethyl acetate or acetone. Supercritical fluid extraction with carbon dioxide as extractant and a C_{18} trap is effective for dry or easily dried samples. Extracts containing carbamates may be cleaned up on columns or cartridges of silica gel, Florisil or very deactivated alumina eluted with hexane–diethyl ether mixtures or hexane with small additions of acetone. Gel permeation is an alternative clean-up technique that is useful for multiclass analyses.

The carbamate insecticides in general, and the oxime carbamates in particular, break down when heated. Before fused silica capillary GC columns and cool on-column injection became available, the carbamates were usually chromatographed as derivatives. A widely used derivatization procedure involved hydrolysis with hot aqueous sodium hydroxide solution, reaction of the phenol with 1-fluoro-2,4-dinitrobenzene and analysis on a dimethyl silicone packed column with electron-capture detection. Another procedure formed derivatives from intact carbamates and trifluoroacetic anhydride prior to GC analysis. Aldicarb, an oxime carbamate, and its toxic breakdown products may all be oxidized to aldicarb sulfone using peracetic acid or potassium permanganate. Aldicarb sulfone is chromatographed on a nonpolar column with a nitrogen-phosphorus detector (NPD), but with an injection port packed with glass wool at a temperature of 300°C where the carbamate breaks down and forms a nitrile from the oxime part of the molecule.

Carbamates of the phenolic type may be analysed successfully by using a nonpolar column of moderate length ($10\text{--}15 \text{ m} \times 0.53 \text{ mm i.d.}$) together with cool

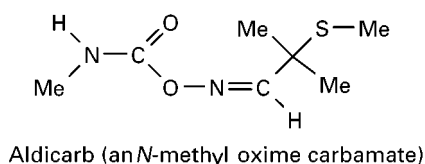
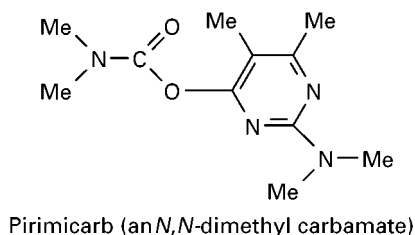
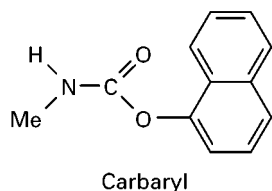
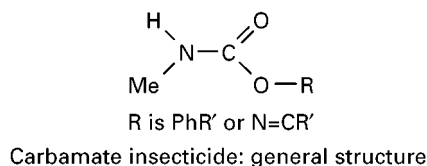


Figure 5 Carbamate insecticides.

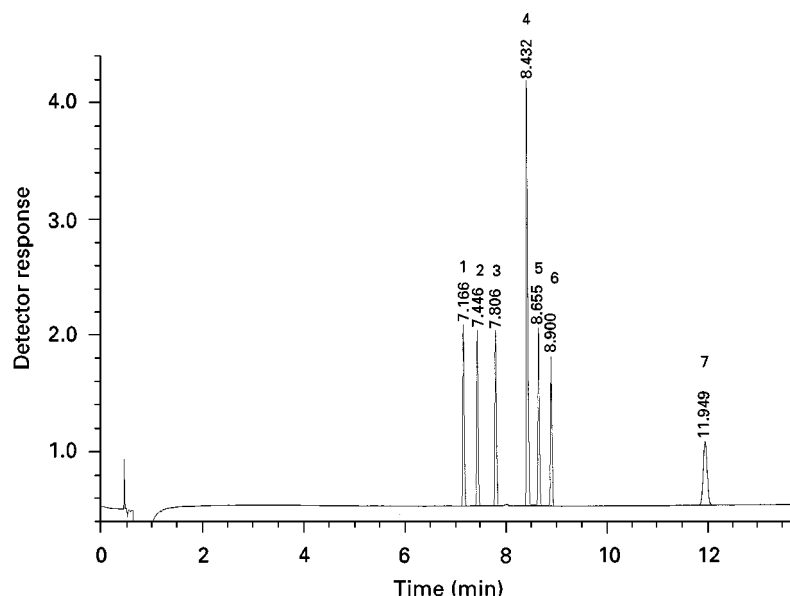


Figure 6 Chromatogram of seven *N*-methyl carbamates. 1, Propoxur; 2, bendiocarb; 3, carbofuran; 4, pirimicarb; 5, carbaryl; 6, methiocarb; 7, carbosulfan; 2 $\mu\text{g mL}^{-1}$ solution of each, 1 μL cool on-column injection at 50°C on to 15 m \times 0.53 mm i.d., DB-1 column (1.5 μm film thickness). Gradient from 50°C (0.5 min) at 20°C min^{-1} to 235°C (4 min). Helium carrier gas. Hewlett Packard 5890 GC with NPD. Note: Pirimicarb has four nitrogen atoms, so gives a larger response than the others.

on-column injection, a gentle temperature gradient and NPD (**Figure 6**). For analysis by GC-MS, small bore capillaries are used, coupled with a 0.53 mm i.d. retention gap. GC of most oxime carbamates is unsuccessful unless they are converted to derivatives. For oxime carbamates, and perhaps for many phenol carbamates, the preferred method of analysis is by liquid chromatography-MS (LC-MS) or by liquid chromatography with post-column conversion to a fluorescent derivative.

Organophosphates

The organophosphorus insecticides are esters of phosphoric acid (or its sulfur analogues) and are therefore often referred to as organophosphates to distinguish them from compounds with a C-P bond. There are several groups of chemically related organophosphates. Dichlorvos, malathion and parathion are examples (**Figure 7**). Organophosphates cover a wide polarity range from persistent and fat-soluble compounds such as carbophenothion to water-soluble and easily hydrolysed compounds such as mevinphos. Most are extractable from dried samples with dichloromethane, diethyl ether or ethyl acetate. As with carbamates, supercritical fluid extraction with carbon dioxide and a C_{18} trap will extract most of them from dry samples (or from samples that can be dried with sufficient drying agent). Clean-up depends on the compounds being analysed and the nature of the sample material. Silica

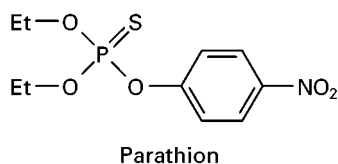
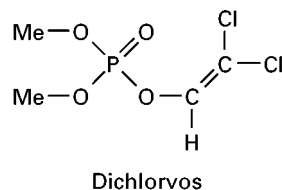
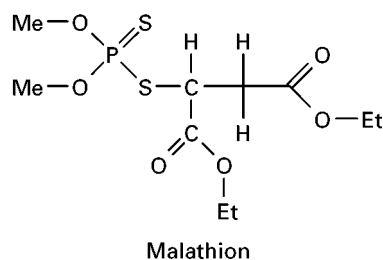
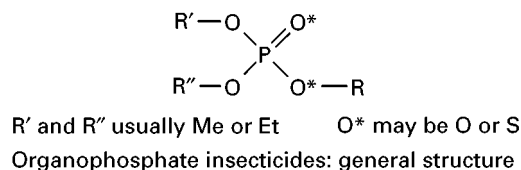


Figure 7 Organophosphate insecticides.

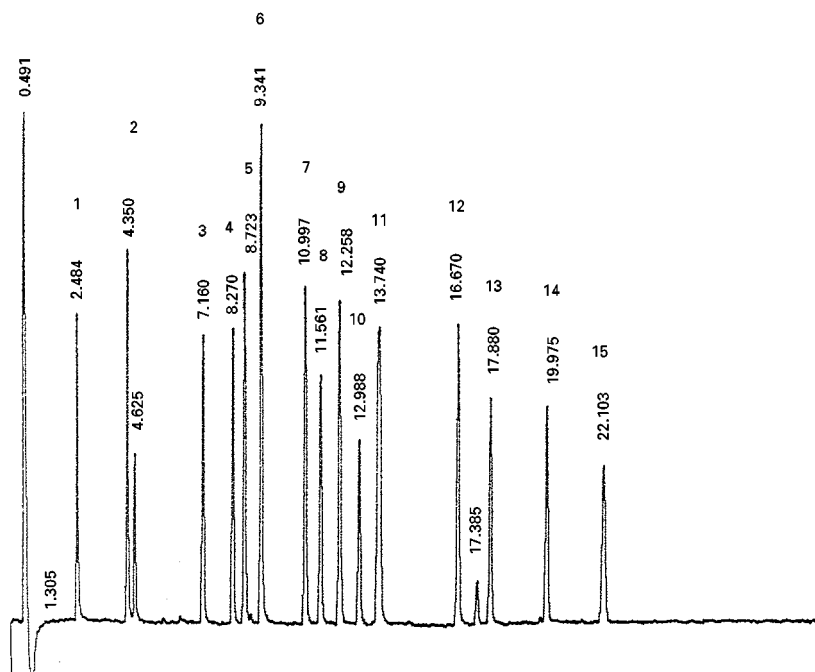


Figure 8 Chromatogram of 15 organophosphates in pheasant gizzard. Chromatogram of diethyl ether Soxhlet extract of pheasant gizzard contents, spiked before extraction with a mixture of 15 organophosphates, each at approximately 4 mg kg^{-1} . $2 \mu\text{L}$ direct injection at 225°C on to $15 \text{ m} \times 0.53 \text{ mm i.d.}$, DB-17 column ($1.0 \mu\text{m}$ film thickness). 1, Dichlorvos; 2, mevinphos (E + Z); 3, phorate; 4, diazinon; 5, fonofos; 6, dimethoate; 7, pirimiphos-methyl; 8, malathion; 9, fenthion; 10, chlorfenvinphos; 11, fosthiate; 12, carbophenothion; 13, triazophos; 14, phosalone; 15, azinphos-methyl. Gradient from 140°C (5 min) at $10^\circ\text{C min}^{-1}$ to 180°C then at 6°C min^{-1} to 270°C (10.5 min). Helium carrier gas. AI Cambridge Ai93 GC with Tracor FPD.

gel does not give a very effective multiresidue clean-up from fatty materials as many organophosphates are eluted with co-extractives. Active alumina will break down some organophosphates. Gel permeation is probably the best choice when analysing organophosphates covering a wide range of polarities.

Residue-level GC may be carried out using splitless or cool on-column injection with detection by mass spectrometry, flame photometric or atomic emission detector or NPD (of these, NPD is the least selective). Medium polarity columns (such as 50% phenyl) give good separation and peak shapes, but a more polar phase such as cyanopropyl is sometimes useful (avoid using it with an NPD). As for column length and diameter, although a $15 \text{ m} \times 0.53 \text{ mm i.d.}$ column will separate many organophosphates over a long slow temperature gradient, there are so many compounds of this type that some are bound to co-elute whatever the resolving power of the column (Figure 8).

Future Trends in the Analysis of Insecticides by GC

Capillary columns have largely replaced packed columns and precise electronic control of temperatures and gas pressures are standard features of modern gas chromatographs. The bench-top mass spectrometer is

now firmly established as the detector of choice for most applications. As computers increase in power, software for interpreting chromatograms and spectra and selecting results of interest will continue to develop and will become integrated with laboratory information management systems. The atomic emission detector may gradually displace the well-established element-selective detectors in a role complementary to GC-MS-MS in the larger analytical laboratories. The move away from GC for the thermally less stable compounds will continue as LC-MS is now sufficiently sensitive and robust for routine residue analysis. Large volume injection is becoming established as a standard technique in water analysis. The slow trend towards the analysis of smaller and smaller residues in food and environmental samples may take a step forward when large volume injection is used together with improved cartridge clean-up methods. For some sample types, solid-phase microextraction will routinely provide rapid transfer of analyte to the GC.

Automation of extraction and clean-up operations has been predicted as a major area of advance for the past 15 years. The laboratory robot has not taken over all laboratory work and the trend is towards laboratory instruments with added versatility and capacity for automation.

Supercritical fluid extraction is making slow progress, probably because of its high cost compared to traditional extraction methods. Perhaps eventually the gas chromatograph will control the extraction and clean-up of its own samples, recording all steps with a thorough audit trail. Trends in insecticide analysis will also depend on what new classes of compounds are approaching commercial use. Element-selective detectors may not be suitable, but GC-MS-MS and LC-MS-MS should be able to cope with just about anything.

See also: III/**Herbicides:** Gas Chromatography; Solid-Phase Extraction; Thin-Layer (Planar) Chromatography. **Insecticides:** Solid-Phase Extraction.

Further Reading

Bottomley P and Baker PG (1984) Multi-residue determination of organochlorine, organophosphorus and synthetic

pyrethroid pesticides in grain by gas-liquid and high-performance liquid chromatography. *Analyst* 109: 85–90.

Brown P, Charlton A, Cuthbert M, Barnett L, Green M, Gillies L, Shaw K and Fletcher M (1996) Identification of pesticide poisoning in wildlife. *Journal of Chromatography A* 754: 463–478.

Chamberlain SJ (1990) Determination of multi-pesticide residues in cereals, cereal products and animal feed using gel-permeation chromatography. *Analyst* 115: 1161–1165.

Cunniff P (ed.) (1995) *Official Methods of Analysis of AOAC International* (16th edn). Arlington: AOAC International.

McMahon BM and Hardin NF (eds) (1994) *Pesticide Analytical Manual* (3rd edn). USA: US Food and Drug Administration.

Meloan CE (ed.) (1996) *Pesticides Laboratory Training Manual*. Gaithersburg: AOAC International.

Tomlin CDS (ed.) (1999) *The Pesticide Manual* (11th edn). Farnham: British Crop Protection Council.

Solid-Phase Extraction

A. Przyjazny, Kettering University, Flint, MI, USA

Copyright © 2000 Academic Press

Introduction

Synthetic insecticides represent an almost universal environmental pollutant. Chemical structures of insecticides are very diverse, but major groups include organochlorine and organophosphorus compounds, methylcarbamates, and synthetic pyrethroids.

Organochlorine insecticides have been largely phased out of general use because of their toxicities and especially their persistence and accumulation in food chains. The structures of several common organochlorine insecticides are shown in **Figure 1**.

Organophosphorus insecticides have largely replaced organochlorine insecticides, because organophosphorus compounds readily undergo biodegradation and do not bioaccumulate. The structural formulas of some common organophosphorus insecticides are shown in **Figure 2**.

Carbamate insecticides are widely used for crop protection. Methylcarbamates are of environmental concern because of their high acute toxicity. **Figure 3** depicts the structures of several common carbamate insecticides.

Synthetic pyrethroids have been widely produced as insecticides during recent years. They have several advantages over organochlorine and organophos-

phorus insecticides, including greater photostability, enhanced insecticidal activity, and relatively low toxicity. The structures of common pyrethroids are shown in **Figure 4**.

As a result of their toxicity and carcinogenicity, insecticides are hazardous to human health and life. The major route of human exposure to insecticides is the gastrointestinal system. Besides regular use of polluted water, humans eat large amounts of food in which these pollutants have been accumulated, e.g., milk and dairy products, fish, poultry and meat, and fruits and vegetables.

Prior to 1960, an individual analytical procedure was used for almost every insecticide. As the number of insecticides in use increased, it became impractical to apply a large number of individual methods for all the insecticides that may be present. This has led to the development of multiresidue methods for the analysis of environmental samples. Ideally, multiresidue methods should provide rapid identification and quantification of as many different insecticides as possible at the required detection level.

The concentrations of insecticides in the environment are very low, typically in the parts-per-trillion to the parts-per-billion range. Furthermore, the sample matrices in which insecticides are usually determined are very complex in most cases. Consequently, extensive sample extraction, clean-up, and preconcentration are often required prior to the analysis.

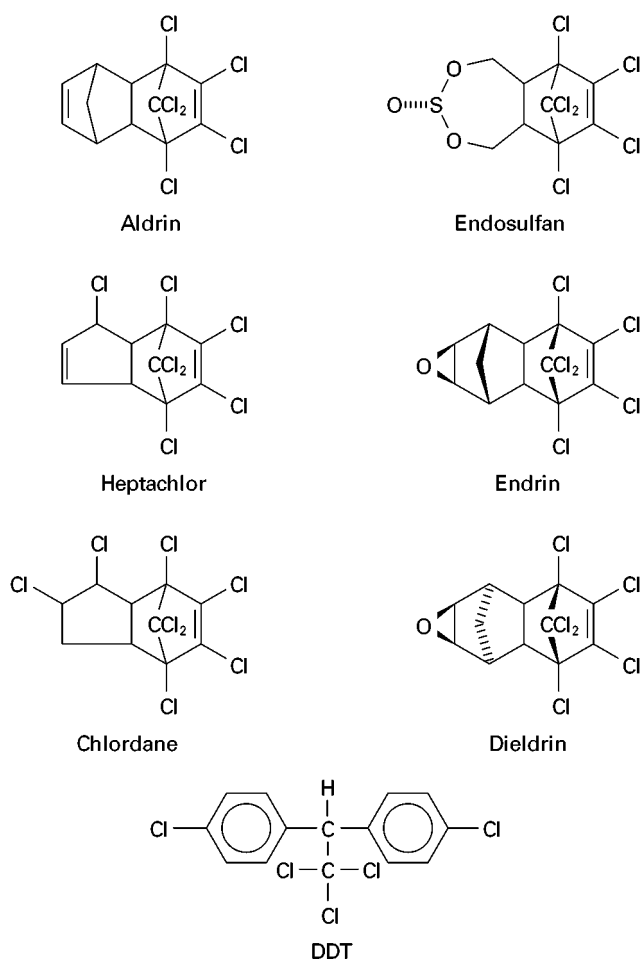


Figure 1 Structures of common organochlorine insecticides.

Comparison of Methods of Extraction for Insecticides

The most difficult and time-consuming step in the determination of insecticides in environmental samples is the extraction of the analytes from the matrix. Several methods are used to accomplish this task, including liquid-liquid extraction (LLE), solid-phase extraction (SPE), solid-phase microextraction (SPME), and supercritical fluid extraction (SFE).

Semivolatile compounds, such as insecticides, have been traditionally extracted by LLE using an organic solvent, such as methylene chloride. The main advantages of LLE are its simplicity and inexpensive equipment used. The procedure suffers from a number of disadvantages, including the use of large volumes of organic solvent which must be very pure (pesticide-grade), tediousness, difficulty with automation, and the formation of emulsions which are difficult to break. Also, the LLE is a multi-step procedure and is therefore prone to loss of analytes and/or contamination.

There is no doubt that solid-phase extraction has now become the method of choice for the extraction, clean-up, and preconcentration of insecticides from environmental, food, or biological samples. SPE drastically reduces amounts of organic solvents used and is not as time-consuming. It enables field sampling and does not suffer from emulsion problems. Other reasons for the growing number of procedures using SPE are the large choice of sorbents, including new polar sorbents capable of retaining more polar insecticides, the introduction of apparatus for automated SPE, which reduces time of analysis and increases sample throughput, and the possibility of automation of analytical procedures. However, SPE is not completely free from problems such as column overloading by passing samples with high content of contaminants, or early breakthrough caused by clogging of the pores by solids present in a sample. The cost of disposable SPE cartridges or discs may be significant in the case of a large number of analyses. Also, the interaction between sample matrix and analytes may result in low recoveries. SPE can carry contaminants into the final sample producing a high background.

Solid-phase microextraction is a new and simple extraction method which uses fused silica fibres coated with a polymeric liquid phase, such as polydimethylsiloxane, or a solid adsorbent, to extract analytes from gaseous, liquid or solid samples. The SPME process has only two steps: (1) partitioning of analytes between the fibre coating and the sample matrix, followed by (2) desorption of extracts into an analytical instrument: gas chromatograph or high-performance liquid chromatograph. SPME is different from SPE in that SPE isolates the majority of the analyte (> 90%) from a sample but only a small fraction of the sample (1–2%) is analysed, while SPME isolates only 2–20% of the analyte, but all of that sample is used in the analysis. SPME is solvent-free and it requires small amounts of samples. The SPME devices enable simple and direct introduction of concentrated samples into the analytical instruments. These devices are commercially available and the technique has been automated. The SPME technique has a wide linear dynamic range and low detection limits. Since SPME is usually used in the equilibrium rather than exhaustive extraction mode, recoveries are not 100%, but the precision and accuracy of the analytical methods using SPME are similar to those using other extraction procedures. The current limitation of SPME is a limited choice of available fibres, especially for the extraction of the more polar insecticides.

In the last six years, supercritical fluid extraction has proved to be an appropriate replacement for the

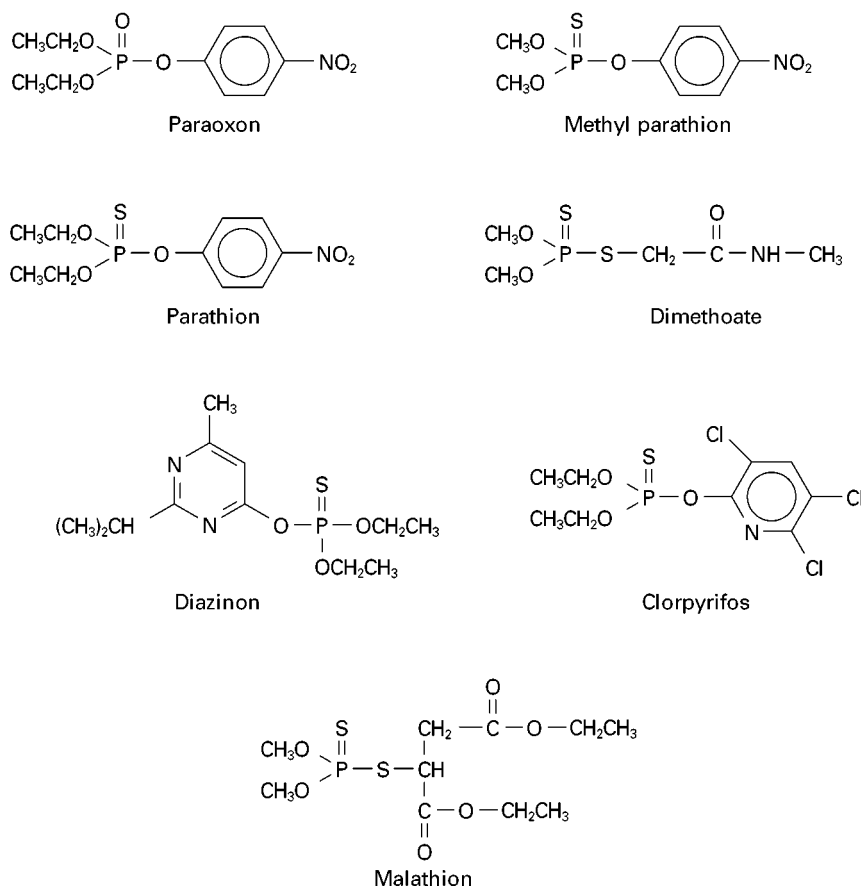


Figure 2 Structures of typical organophosphorus insecticides.

solvent extraction of insecticides from solid samples. SFE has gained acceptance in environmental analyses because it is a rapid, nonorganic solvent extraction technique that gives recoveries equal to, or even better than, traditional extraction procedures. SFE can be used directly or it can be coupled with solid-phase extraction (SPE-SFE). Direct SFE is mostly used for solid matrices (soil, sediment, food), while the tandem SPE-SFE is usually used for the extraction of insecticides from aqueous samples. The disadvantages of SFE include high costs associated with high-pressure fluid delivery system and high-purity gas source, both of which are heavy equipment that make field analysis difficult. However, the combination of solid-phase extraction and supercritical fluid extraction enables the performance of SPE directly in the field, using SPE sorbents, and carrying out the SFE step in the laboratory, thus eliminating the need for transporting the SFE equipment to the field.

In the near future, further improvements are to be expected with SPME, SPE, SFE and their combination (SPE-SFE). This should lead to the development of more standard methods for the determination of insecticides using these extraction techniques.

Application of SPE and SPME to Extraction and Preconcentration of Insecticides

Air Analysis

Increasing concern over the presence of insecticides in ambient and indoor air has led to the development of specific extraction methods for these pollutants. As a result of very low concentrations of insecticides in air (ng m^{-3} to $\mu\text{g m}^{-3}$), air sampling methods call for large sample volumes, ranging from about 1 m^3 to close to 1000 m^3 . In order to achieve those sample volumes in reasonable time, high sampling rates are required. Consequently, the sorbents used for air sampling should have low pneumatic resistance. The most typical extraction procedure makes use of polyurethane foam (PUF) as a lightweight, easy-to-use sampling material for these semivolatile compounds. Cylindrical PUF plugs effectively trap insecticides without creating excessive back pressure. Thus, high sampling rates are possible, which allows shorter sampling times and ensures more representative samples. These high sampling rates may also be required

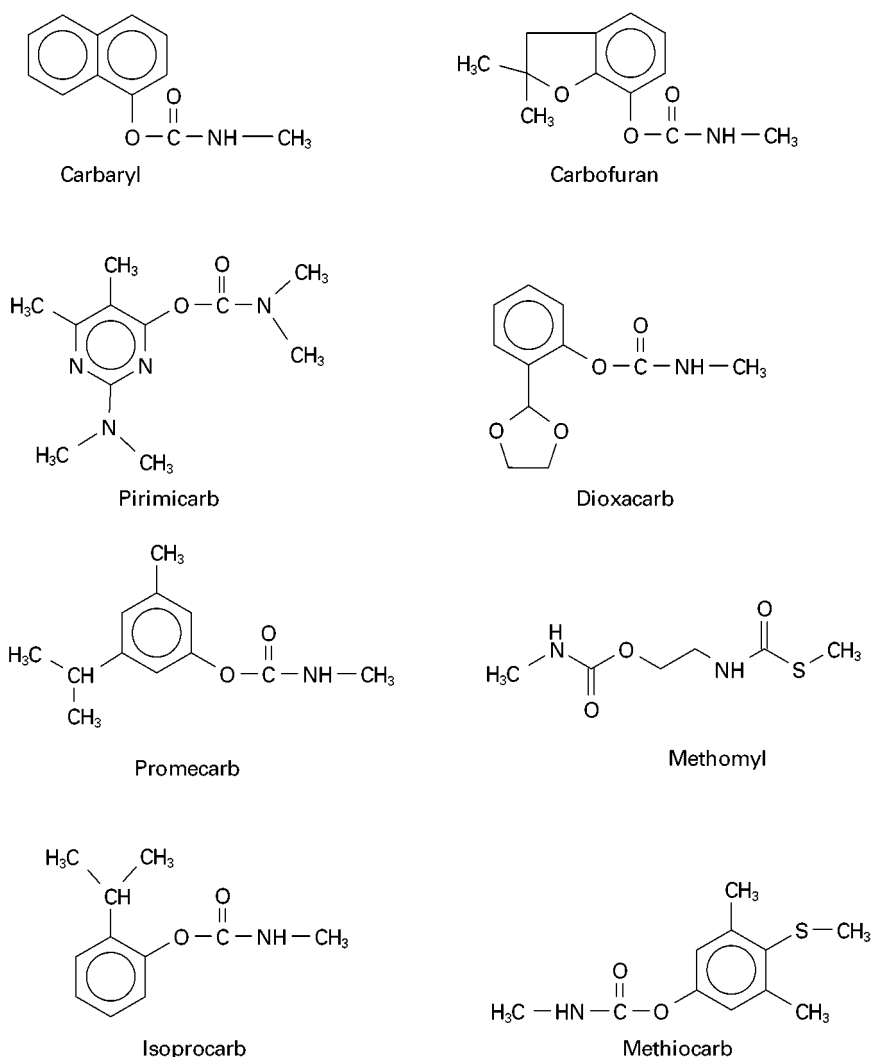


Figure 3 Structures of commonly used carbamate insecticides.

to attain needed detection limits. PUF plugs are sometimes used with an additional sorbent, such as Tenax TA or XAD-2 resin, to collect more volatile analytes. The air sample is usually first filtered through a microfibre filter, which traps aerosols and particulates. Then the air is drawn through the PUF cartridge. Following sample collection, the PUF sorbent is extracted by Soxhlet extraction with 5% diethyl ether in hexane and the insecticides are determined by gas chromatography with selective detection. For some insecticides, high performance liquid chromatography (HPLC) with an ultraviolet (UV) detector or electrochemical detector may also be the method of choice. If necessary, the extract may be cleaned up by SPE using Florisil or alumina and concentrated using a Kuderna-Danish apparatus. The above procedure can be applied to the multiresidue analysis of insecticides.

Applications using PUF to extract insecticides from air samples include a number of standard methods, including EPA Method IP-8, Method TO-4A and TO-10A. **Table 1** summarizes SPE conditions used for the extraction of insecticides from air samples.

XAD and Tenax resins have also been used for the isolation and analysis of insecticides from air samples. A method based on a high volume sampler with an XAD-2 resin trap was used to monitor 39 pesticides in ambient air. The volume of air sampled was 700 m³. After the extraction, pesticides were separately extracted with methylene chloride from the filter and XAD-2 resin. Extracts were concentrated and cleaned up by silica gel column chromatography and analysed by capillary gas chromatography/mass spectrometry with selected ion monitoring (cGC-MS-SIM). Organophosphorus and carbamate insecticides were detected at the 10 ng m⁻³ level.

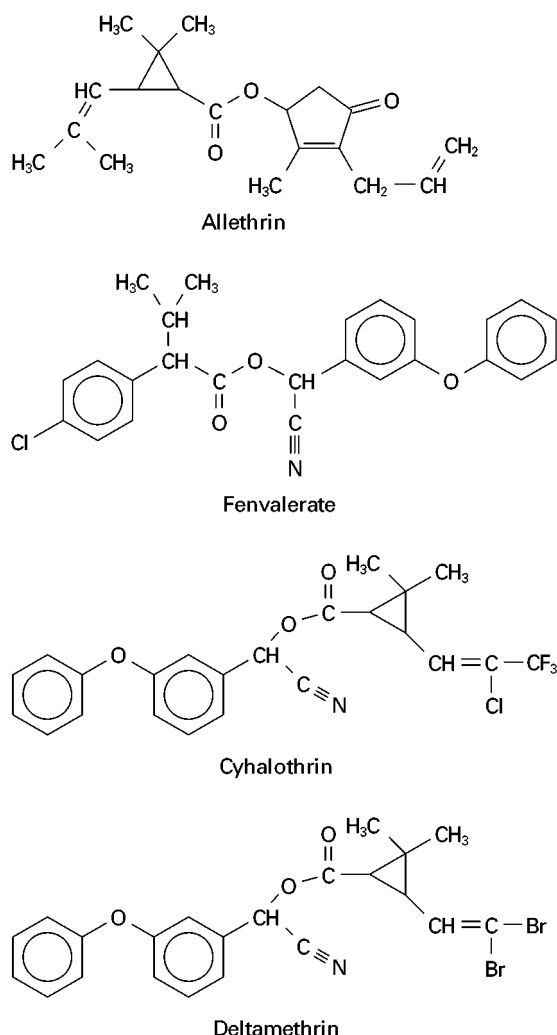


Figure 4 Structures of common pyrethroid insecticides.

An improved sampling method using SPE was developed for the multiresidue determination of pesticides in indoor air. The method involves adsorption of the pesticides in 1 m³ of air onto Tenax TA via an air-sampling pump, desorption with acetone, and determination by GC-MS. Limits of detection for the 23 pesticides studied (including organophosphorus insecticides) were on the order of ng m⁻³.

Recoveries of insecticides from XAD and Tenax resins can be improved by using supercritical fluid extraction to elute the analytes.

Water Analysis

The determination of insecticides in water samples is carried out by gas chromatography, liquid chromatography, or thin-layer chromatography. These chromatographic techniques require efficient isolation and concentration procedures, such as solid-phase extraction and solid-phase microextraction. Generally, the major role of SPE in water analysis is for trace enrichment of insecticides. The usual sample volume for trace enrichment varies from 100 mL to 1 L, although large-volume analysis by SPE is also possible. In the latter case, 10 to 100 L of water is passed through a column containing 1 to 10 L of XAD resin. This approach has been used to isolate and determine DDT from natural waters and the detection limit was in the order of pg L⁻¹.

The mechanism of sorption in trace enrichment is typically reversed phase, and the commonly used sorbents are C-18, C-8 or styrene-divinylbenzene (SDB) porous polymer. Trace enrichment using SPE can be accomplished in two modes: cartridge or disc. Both modes can be automated and be performed

Table 1 SPE conditions used in extraction of insecticides from air

Sample	Air (0.9 m ³) at 1–5 L min ⁻¹ for 4–24 h (low volume sampling (LVS)). Air (> 300 m ³) at 0.225 m ³ min ⁻¹ for 24 h (high volume sampling (HVS)).	
Analytes	Organochlorine (OC), organophosphorus (OP), methylcarbamates (MC), pyrethroids (PY). Concentration: 0.001–50 µg m ⁻³ .	
Sorbent	7.6 cm × 22 mm ID. PUF plug (density 0.0225 g mL ⁻¹) (LVS). 2.5 cm × 65 mm ID. PUF plug (HVS).	
Sorbent preparation	Using Soxhlet extractor, wash plug with acetone for 16 h, followed by ether–hexane (5 : 95) for 16 h. Vacuum dry 2–4 h at room temperature. Place in glass sampling cartridge and seal until sample collection.	
Elution of analytes	Using Soxhlet apparatus, extract plug with 300 mL of ether–hexane (5 : 95) for 16 h. Concentrate the extract to 5.0 mL using a Kuderna–Danish apparatus.	
Extract clean-up	For OC analysis, remove OP and MC with alumina. Use Florisil to achieve class separation.	
Determination	OC	cGC/ECD
	OP	cGC/FPD or NPD
	MC	cGC/NPD or reversed-phase HPLC
	Multiresidue	GC-MS

Table 2 SPE conditions used in extraction of organochlorine insecticides from water

Sample	River water (100 mL) with 1% methanol added
Analytes	28 organochlorine insecticides and their metabolites
Sorbent	500 mg C-18 cartridges
Sorbent preparation	Precondition with 5 mL each of acetone, methanol, and distilled water
Elution of analytes	Rinse the cartridge with 3 mL water, apply vacuum to remove water, and elute the analytes with 3 mL acetone
Determination	GC/ECD

either online or offline. The major advantage of discs over cartridges is that the former can use higher sample flow rates, which reduces the time necessary for extraction. On the other hand, the advantage of cartridges over discs is that the cartridges require a smaller volume of solvent to elute the analytes, which simplifies subsequent steps in the analytical procedure.

A typical SPE sequence using a C-18 cartridge consists of four steps. First, the SPE column is prepared to receive a water sample, by wetting with an organic solvent and by conditioning with water. Then, the aqueous sample is applied, and often the insecticides of interest are retained together with interferences from the sample matrix. Some of these interferences can then be removed by application of a washing solution. In the last step, the concentrated insecticides are desorbed with a small volume of organic solvent, which can then be partially evaporated to increase the enrichment factor. An example of such a procedure used for the extraction of organochlorine insecticides from water is shown in **Table 2**.

The US EPA has a number of standard methods for the analysis of organic pollutants in water, including insecticides, which make use of SPE. In Method 525.1, for example, analytes are extracted from a 1 L water sample using a C-18 SPE cartridge or disc. Next, the analytes are eluted from the cartridge or disc with a small quantity of methylene chloride, and concentrated further by evaporation of some of the solvent. The analytes are then quantified using GC-MS.

The US EPA has also approved various methods based on SPE discs containing either C-18 silica or styrene-divinylbenzene sorbent for the determination of organonitrogen and organophosphorus pesticides (Method 507) and of organochlorine insecticides (Method 508.1) in drinking and source waters. The use of SPE discs is particularly easy. The disc is placed in a filtration apparatus attached to a water-aspirator

vacuum source. Next, it is conditioned with 10 mL of methanol and 10 mL of distilled water, and the water sample is filtered through it. Then the extraction funnel and frit assembly is transferred to a second vacuum filtration flask containing a test tube. Three 5 mL aliquots of the eluting organic solvent are then drawn through the disc. The combined eluates are concentrated by evaporation and analysed by GC or HPLC.

There are many choices for eluting solvents in trace enrichment by C-18 solid-phase extraction. One of the most common solvents, removing the majority of hydrophobic insecticides sorbed on the resin, is ethyl acetate. If this eluent is followed by methanol, then this combination is compatible with both GC-MS and HPLC analysis. For very hydrophobic analytes, such as dichlorodiphenyltrichloroethane (DDT), a mixture of ethyl acetate–methylene chloride (1 : 1) is more effective than ethyl acetate alone.

Reversed-phase SPE is best suited for the extraction of nonpolar insecticides, such as organochlorine compounds. For polar pesticides, such as methylcarbamates or some organophosphorus compounds, different sorbents are preferred. Of those, two types are most common: graphitized carbon blacks (GCB) and styrene-divinylbenzene resins. Graphitized carbon black was successfully used to isolate carbamate and organophosphorus insecticides from water. Multi-residue methods have been developed for both polar and nonpolar insecticides in water for subsequent analysis by HPLC. Detection limits of 0.003 to 0.007 $\mu\text{g L}^{-1}$ were reported for a number of the analytes. A typical procedure for insecticide extraction from drinking water using a GCB sorbent is shown in **Table 3**. Usually, the preferred eluting solvent is a mixture of methylene chloride–methanol (80 : 20).

Table 3 SPE conditions used in extraction of carbamates and organophosphorus insecticides from water

Sample	Drinking water (100 mL to 1 L)
Analytes	Carbamates and organophosphorus insecticides
Sorbent	0.25 g ENVI-Carb
Sorbent preparation	Precondition with 5 mL methylene chloride–methanol (80 : 20), 1 mL methanol, and 10 mL 2% acetic acid in water
Elution of analytes	Elute the analytes with 0.8–1 mL methanol, followed by 2 \times 3.5 mL methylene chloride–methanol (80 : 20). Dry eluate to 400–500 μL . Reconstitute samples to 1 mL with methanol
Determination	HPLC with UV, DAD, or MS detection

DAD, diode array detector.

New polymeric sorbents, based on styrene-divinylbenzene copolymer, have proved their usefulness in the isolation of polar insecticides from water. These polymers (SDB from International Sorbent Technology or the Oasis HLB from Waters) have some hydrophilic nature to improve their wetting characteristics for good mass transfer, but they still have high capacities for polar analytes. The Oasis sorbent was used to isolate organophosphorus insecticides from tap water. Recoveries of the analytes ranged from 87 to 112%.

SPE clean-up and trace enrichment methods can be automated. In semiautomated methods, some operator intervention is required. In fully automated procedures, the entire SPE operation is carried out without user intervention, including online analysis by gas chromatography (GC) and HPLC. Automated online methods using SPE for the determination of carbamates and organophosphorus insecticides in water coupled with HPLC or GC have been developed. The methods offer all the inherent advantages of automatic methods, i.e. low sample and reagent consumption, minimal manipulation and contact with the reagents, accurate and reproducible results, and high throughput. The detection limits for the automated procedures were in the ng L^{-1} range for organophosphorus insecticides and between 0.01 and $1 \mu\text{g L}^{-1}$ for carbamates.

The majority of environmental applications of solid-phase microextraction have dealt with the isolation and determination of organic analytes in water samples. SPME has been successfully used for the determination of carbamates, as well as organochlorine and organophosphorus insecticides, in aqueous matrices. Usually, poly(dimethylsiloxane) (PDMS) fibres are used in the analysis of organochlorine insecticides; for organophosphorus insecticides, polyacrylate (PA) fibres are preferred, whereas for carbamates, either PDMS or PDMS/divinylbenzene (DVB) fibres are applied. A multiresidue procedure for the simultaneous determination of 60 pesticides in water has been developed. Either a PDMS-coated or a PA-coated fibre may be used to achieve detection limits in the low $\mu\text{g L}^{-1}$ range. The method had adequate precision and good linearity over the range 0.1–100 $\mu\text{g L}^{-1}$.

SPME is characterized by its simplicity, low cost, rapidity and sensitivity. An example of SPME procedure for the determination of organochlorine insecticides in water is shown in Table 4.

The compact nature of the SPME device and the simplicity of the procedure allow this method to be readily automated. The automated SPME instrument is available from Varian. Two online methods of determination using SPME have been described: one

Table 4 SPME conditions used in extraction of insecticides from water

Sample	4 mL water
Analytes	Organochlorine insecticides
Sorbent	100 μm polydimethylsiloxane fibre
Sorbent conditioning	Expose the fibre to the hot GC injection port (250°C) for at least 3 h
Extraction	Immerse the fibre into the sample for 15 minutes, stir rapidly
Elution of analytes	After extraction, insert the fibre into the GC injector port held at 260°C for five minutes
Determination	GC with ECD detection

for organochlorine insecticides and the other for organophosphorus insecticides. The former method used GC with electron-capture detector (ECD), while the latter method employed GC with nitrogen-phosphorus detector (NPD).

Soil and Sediment Analysis

Soils and sediments have much more complex matrices than air or groundwater. Consequently, the analysis of soil making use of SPE must be preceded by the extraction of the insecticides from a soil sample by an organic solvent or a mixture of solvents. A methanol/water mixture is often used for this purpose. Alternatively, accelerated solvent extraction can be used for the extraction of soils and sediments. Recently, however, supercritical fluid extraction has also been tried and found to be superior to liquid extraction in terms of reproducibility. The use of microwave-assisted solvent extraction (MASE) for the extraction of organochlorine insecticides from soil samples has been investigated. Compared to a conventional liquid extraction method, MASE yielded better or equal recoveries and superior repeatability. Extraction of insecticides from soil and sludge samples can also be accomplished by using subcritical water. Subcritical water is an excellent solvent to quantitatively extract both polar and nonpolar analytes from soils. Furthermore, subcritical water extractions can be highly selective and can be coupled with both SPE and SPME.

Following the extraction of insecticides from soils or sediments, SPE is used for both clean-up of the extract and for trace enrichment of the analytes. The procedures employed will be different for clean-up compared to those of trace enrichment. Two strategies are possible. The first is to remove interfering compounds by trapping them on the SPE cartridge and allowing the insecticides to pass through the cartridge for direct analysis or further enrichment (SPE clean-up). The second approach is to isolate the insecticides directly by SPE and elute them free

from the interferences or to wash the interferences off the SPE sorbent prior to elution (trace enrichment).

Polar sorbents are usually used to accomplish SPE clean-up of soil extracts. The most common sorbent is Florisil, which has been used widely for clean-up of soil extracts for the determination of various insecticides. Silica gel has also been used for this purpose, mostly in the determination of nonpolar analytes, such as organochlorine insecticides or pyrethroids. Alumina has been used less often, and only for the determination of organochlorine analytes. The clean-up step can also use SPE cartridges packed with silica gel modified with polar aminopropyl groups. This procedure has been applied to the determination of N-methylcarbamates in soils.

Clean-up of soil extracts can also be based on size-exclusion chromatography (SEC), which separates species by size rather than polarity. Clean-up by sorbents such as Florisil does not remove interferences of high molecular mass and polarity similar to that of the insecticides. In contrast, SEC removes materials of high molecular mass, such as humic substances from soil extracts. Currently, polystyrene columns are the most often used SEC sorbents. They are eluted with a number of different solvents, such as cyclohexane or cyclohexane-ethyl acetate.

When nonpolar sorbents, such as C-18 or C-8, are used, the clean-up of soil extracts can be incorporated in the SPE sequence just before the insecticide desorption. In this strategy, the soil extract is passed through the SPE cartridge or disc. Next, the sorbent is rinsed with a small volume of water containing an organic modifier, usually methanol. The interferences are removed, but the insecticides are retained. This step can only remove interferences that are more polar than the analytes, so the method can only be applied for the determination of nonpolar insecticides. Following the clean-up step, the insecticides are eluted from the SPE cartridge or disc using a small volume of an organic solvent, typically ethyl acetate, and this extract is further preconcentrated or directly analysed.

Table 5 summarizes SPE conditions used for the extraction of insecticides from soils and sediments.

When using polar sorbents, such as silica gel, alumina, Florisil, or silica gel with chemically bonded aminopropyl groups, SPE procedures can combine trace enrichment of insecticides and removal of interferences in soil extracts. In this strategy, the soil extract in a nonpolar solvent is passed through a column or cartridge containing a polar sorbent. Next, the analytes are eluted from the sorbent in a series of fractions using solvents of increasing polarity. For example, the effectiveness of Florisil, silica gel and alumina for the clean-up and trace enrichment of soil extracts containing organochlorine and organophosphorus insecticides has been compared. The results showed that silica gel was the best adsorbent. Nonpolar interferences were removed by a rinse with cyclohexane. An elution with ethyl acetate-hexane (5 : 95) followed by ethyl acetate resulted in the separation of the two classes of insecticides. The organochlorine insecticides were present in the first fraction, and the organophosphorus insecticides in the second fraction.

SPME has been used for the extraction of organochlorine insecticides from soil samples and soil solutions. The fibre was coated with polydimethylsiloxane. The method linearity and detection limits were tested in the 0.1–20.0 ng g⁻¹ range. SPME was found to be useful for screening of insecticides in contaminated soil samples, offering a simple alternative to established methods of analysis of insecticides in soil.

Analysis of Biological Materials

Biological matrices consist of body fluids, such as urine or plasma, and tissues. Biological fluids are viscous and may require pre-treatment, e.g. centrifugation, dilution or buffer addition, before SPE can be applied. Prior to extraction, tissue samples generally need to be blended or ground in order to disrupt the general architecture of the sample. Because of the complexity of matrices, SPE may have to

Table 5 SPE conditions used in extraction of insecticides from soil and sediment

Sample	Soil or sediment (20 g)
Analytes	Organochlorine (OC), organophosphorus (OP), methylcarbamates (MC), pyrethroids (PY)
Extractant	Water-methanol (10 : 90), water-acetone (50 : 50), hexane-acetone (90 : 10). Extract twice using Soxhlet, heated vial or accelerated solvent extractor. Dilute with distilled water and then process by SPE
Sorbent	360 mg of C-18 in a cartridge or 47 mm C-8 discs
Sorbent preparation	Precondition with 2 mL each of methanol, ethyl acetate, methanol, and distilled water
Elution of analytes	After sample addition, remove water from the sorbent by air, and elute with 2 mL of ethyl acetate
Determination	OC cGC/ECD or GC/MS OP cGC/FPD or NPD or GC/MS MC cGC/NPD or reversed phase HPLC Multiresidue GC-MS

be used for clean-up of sample extracts, as well as for trace enrichment.

Reversed-phase sorbents, such as C-18, are most commonly used for SPE of biological samples. The determination of insecticides in fluids does not require such extensive sample preparation as the analysis of insecticides in tissues. For example, in SPE methods for isolation and clean-up of organochlorine insecticides or synthetic pyrethroids from human urine or plasma, the samples only needed to be diluted prior to extraction, and the eluent did not require any further clean-up prior to gas chromatographic determination (see Table 6 for details). High recoveries, ranging from 90–102% for urine and 81–93% for plasma, were obtained.

The extraction of insecticides from tissue samples requires large volumes of organic solvents (100–500 mL), and extensive extract clean-up. The procedure is also very time-consuming. A novel procedure, so-called matrix solid-phase dispersion (MSPD), can reduce solvent use by 98% and increase sample throughput by 90%. This process involves the grinding of biological samples with bulk C-18 sorbent. The MSPD method consists of adding 0.5 g of sample to 2.0 g of C-18 packing and grinding the sample until a nearly homogeneous blend of sample components adsorbed onto the SPE material is obtained. The packing material is then transferred into a syringe barrel plugged with a filter paper disc. The column head is covered with a second disc and the contents are compressed with a plunger to a volume of 4.5 mL. The column may then be eluted with a solvent or a series of solvents for the analytes of interest. This procedure was used for the isolation of organochlorine and organophosphorus insecticides from a number of animal tissues. The analytes were eluted from the MSPD column with 8.0 mL of acetonitrile or acetonitrile–methanol (9 : 1) through a Florisil co-column. The resulting eluate was analysed directly by GC. The recoveries of the analytes

ranged from 60–114% for the concentrations examined.

Food and Natural Product Analysis

The determination of insecticides in food and natural products requires extracting the analytes from a complex matrix, either liquid or solid. Solids, such as food, must be homogenized and extracted with organic solvents or aqueous buffers before SPE. Interferences from the food products must be removed either during extraction or during SPE isolation. Homogenization can be carried out by grinding followed by solvent extraction and filtration, or by grinding and Soxhlet extraction. A recent improvement is accelerated solvent extraction (ASE), in which high temperature and pressure are used to push an organic solvent through a solid sample and to collect the eluate in a vial. Automated instrumentation capable of running 30 samples at once is available commercially. One sample is processed in 15 minutes with extraction efficiency equal to that produced by Soxhlet extraction in 12 h. Supercritical fluids can also be used for extraction of food. In this procedure, supercritical carbon dioxide is used to remove analytes from food without dissolving the matrix. Methanol is often added as a modifier to the supercritical CO₂ to enhance the solubility of analytes. Microwave-assisted solvent extraction and matrix solid-phase dispersion, fast and safe alternatives to traditional solvent extraction, can also be applied to food analysis.

The solvent used to extract insecticides should be compatible with the SPE method being used. In addition, it should not co-extract interferences. For samples with high content of nonpolar components (such as fats or oils), a nonpolar solvent such as hexane should be chosen. This, in turn, determines normal-phase SPE with Florisil, silica, alumina or a cyano (CN) sorbent. Samples with high water content are best extracted with polar solvents such as methanol, acetone, or acetonitrile. In this case, reversed-phase SPE (C-18 or C-8) is preferable.

A multiresidue method for the determination of 43 organophosphorus, 17 organochlorine, and 11 N-methyl carbamate insecticides in 10 g of plant or animal tissues has been developed. The insecticides are extracted with 5% ethanol in ethyl acetate. Samples with high lipid content are cleaned up by automated gel permeation chromatography with a 30% ethyl acetate in hexane eluent and inline silica gel minicolumns. Highly pigmented samples are cleaned up with class-specific SPE columns: Florisil for organochlorine insecticides, and aminopropyl for N-methyl carbamates. No further clean-up of

Table 6 SPE conditions used in extraction of insecticides from biological fluids

Sample	Human urine or plasma diluted with water (OP) or with 70% methanol (pyrethroids)	
Analytes	Pyrethroids, organophosphorus (OP)	
Sorbent	C-18 cartridges	
Sorbent preparation	Precondition with 2 mL each of methanol, ethyl acetate, methanol, and distilled water	
Elution of analytes	2 mL chloroform (pyrethroids) or chloroform–isopropanol (9 : 1) (OP).	
Determination	Pyrethroids	cGC/FID
	OP	cGC/FID

organophosphorus insecticide was necessary. Recovery of 71 insecticides ranged from 77 to 113%. The concentrated extracts were analysed by GC or liquid chromatography (LC) with specific detection.

Many multiresidue methods use acetonitrile extraction of the homogenized sample, reversed-phase SPE extraction of the analytes, and clean-up with an aminopropyl cartridge. In other cases, SPE is used for clean-up only. In this case, preparation of samples involves extraction with acetone and partitioning into methylene chloride–petroleum ether. This extract is cleaned up with an SPE aminopropyl column. The latter procedure has been automated by Gilson (Automated SPE clean-up (ASPEC)).

MSPD with C-18 silica has been used in multiresidue insecticide analysis in fruits and vegetables. The procedure is simple, inexpensive and rapid. Low detection limits (in the ppb range) and high recoveries (67–105%) were found for the investigated analytes.

In addition to using reversed-phase and normal-phase SPE for the clean-up and isolation of insecticides from foods and natural products, graphitized carbon black has also proved an excellent sorbent for this purpose. Table 7 shows SPE conditions for a rapid multiresidue clean-up and analysis of over 200 organochlorine, organophosphorus and

methylcarbamate insecticides in fruits and vegetables. Recoveries of the analytes ranged from 65 to 99.3%.

Future Developments

It is reasonable to expect continued development of the methods of isolation and preconcentration of insecticides based on SPE and SPME. The future for the latter technique looks particularly interesting, because simplification and increasing automation of preliminary analytical operations, particularly the extraction steps, is one of the modern trends in analytical chemistry. The analytical procedures using SPME have only two steps, can be easily automated, are rapid, simple, inexpensive, sensitive, and suitable for field analysis. New fibre coatings, more suitable for polar analytes, including those containing in-fibre derivatization reagents, should further extend the applicability of this technique.

In the extraction of insecticides from solid samples, such as food or biological materials, more procedures using MSPD are expected.

Future developments in solid-phase extraction will involve miniaturization of SPE procedures and considerably more online use of GC and HPLC. Sample handling will be minimized with automated systems. The use of automation will result in fast, easy, and reliable methods for SPE. To this end, syringe barrel designs and 96-well SPE plates will be used more extensively. Also, disposable pipette tips holding an extraction disc in the tip end, which are robotics compatible, will become more popular.

New SPE phases taking advantage of specific interactions will be introduced more widely. These include affinity SPE with antibodies bound to a solid substrate (immunosorbents) and the molecular-imprinted polymers.

Other uses of SPE, such as derivatization on SPE sorbents, will become more widely used. Also, the use of supercritical fluid extraction and subcritical water extraction for the elution of insecticides from sorbents will be given more attention. Compared to conventional solvents, SPE will enable more selective removal of interferences and more selective extractions of insecticides from matrix, and will minimize preparation of some complex samples (e.g. biological tissues) with the potential for developing completely automated SFE-SPE-SFE methods.

See also: II/Extraction: Analytical Extractions; Solid-Phase Extraction. III/Airborne Samples: Solid Phase Extraction. Environmental Applications: Pressurized Fluid Extraction; Solid-Phase Microextraction; Supercritical Fluid Extraction. Pesticides: Extraction from Water. Solid-Phase Micro-Extraction: Environmental Applications.

Table 7 SPE conditions used in extraction of insecticides from fruits and vegetables

1. Homogenize 50 g of chopped sample with 100 mL of acetonitrile
2. Add 10 g of NaCl. Homogenize for 5 minutes. Discard the lower aqueous layer
3. Condition C-18 tube with 5 mL of acetonitrile
4. Add 2 mL of acetonitrile extract from the sample; discard
5. Pass 13 mL of acetonitrile sample extract through the tube; collect
6. Add enough Na_2SO_4 to C-18 extracted sample to reach 15-mL mark. Cap the tube, shake well, and centrifuge for 5 minutes
7. Evaporate 10 mL of centrifuged sample to 0.5 mL
8. Add 1 cm Na_2SO_4 to the top of an ENVI-Carb (graphitized carbon black) tube
9. Condition the ENVI-Carb and LC- NH_2 tubes separately with 5 mL acetonitrile–toluene (3 : 1)
10. Connect the LC- NH_2 tube to the outlet of the ENVI-Carb tube
11. Condition with 5 mL of acetonitrile–toluene (3 : 1)
12. Add 0.5 mL of C-18 cleaned sample; allow to drain through both tubes by gravity; collect
13. Rinse the tubes with 1 mL acetonitrile–toluene (3 : 1). Continue eluting with 5 mL of solvent mixture
14. Rotoevaporate to approximately 2 mL. Add 10 mL of acetone. Evaporate again. Reconstitute to the desired volume
15. Organochlorine and organophosphorus insecticides are determined by GC/MS. Carbamates are determined by HPLC/postcolumn derivatization/fluorescence detection.

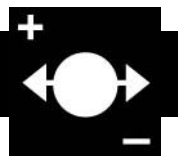
Further Reading

- Barcelo D (1993) *Environmental Analysis; Techniques and Instrumentation in Analytical Chemistry* 13. Amsterdam: Elsevier.
- Barcelo D and Hennion M-C *Trace Determination of Pesticides and Their Degradation Products in Water*. Oxford: Elsevier.
- Chau ASY and Afgan BK (1982) *Analysis of Pesticides in Water*, vol. 2, *Chlorine- and Phosphorus-containing Pesticides*. Boca Raton: CRC Press.
- Chau ASY and Afgan BK (1982) *Analysis of Pesticides in Water*, vol. 3, *Nitrogen-containing Pesticides*. Boca Raton: CRC Press.
- Das KG (1981) *Pesticide Analysis*. New York: Marcel Dekker.
- Font G, Mañes J, Moltó JC and Picó Y (1993) Solid-phase extraction in multi-residue pesticide analysis of water. *Journal of Chromatography* 642: 135.
- McDonald PD and Bouvier ESP (1995) *Solid phase Extraction: Applications Guide and Bibliography. A Resource for Sample Preparation Method Development*, 6th edn. Milford: Waters.
- McMahon BM and Sawyer LD (eds) (1985) *FDA Pesticide Analytical Manual*, vol. 1, Washington: FDA.
- Marcotte AL and Bradley M (eds) (1985) *FDA Pesticide Analytical Manual*, vol. 2, Washington: FDA.
- Pawliszyn J (1997) *Solid-Phase Microextraction: Theory and Practice*. New York: Wiley-VCH.
- Preston ST Jr and Pankratz R (1981) *A Guide to the Analysis of Pesticides by Gas Chromatography*, 3rd edn. Niles: Preston Publishers.
- Sherma J (1988) *Analytical Methods for Pesticides and Plant Growth Regulators*, vol. 16, *Specific Applications*. San Diego: Academic Press.
- Sherma J (ed.) (1989) *Analytical Methods for Pesticides and Plant Growth Regulators*, vol. 17, *Advanced Analytical Techniques*. San Diego: Academic Press.
- Simpson N (1997) *Solid Phase Extraction: Principles, Strategies, and Applications*. New York: Marcel Dekker.
- Thurman EM and Mills MS (1998) *Solid-Phase Extraction: Principles and Practice*. New York: John Wiley & Sons.

INSECTICIDES IN FOODSTUFFS

See **III / CARBAMATE INSECTICIDES IN FOODSTUFFS: CHROMATOGRAPHY AND IMMUNOASSAY**

ION ANALYSIS



Capillary Electrophoresis

M. Macka and P. R. Haddad, University of Tasmania, Hobart, Tasmania, Australia

Copyright © 2000 Academic Press

Introduction and Scope

Before the advent of capillary electrophoresis (CE), some impressive separations of inorganic species had been achieved by other electrophoretic methods, such as the separation of lanthanoids by paper electrophoresis using complexation with 2-hydroxyisobutyric acid (HIBA). With the introduction of capillary electrophoresis in 1981 by Jorgenson and Lukacs, separations of inorganic anions and cations started to appear quite early, but only sporadically until the late-1980s. There were several reasons for this. First, CE was a very new analytical technique

and some time was needed for the theoretical background and instrumentation to mature. The second factor was competition with alternative analytical techniques, mainly spectroscopic methods (atomic absorption spectrometry, inductively coupled plasma spectrometry), in the area of determinations of metals, and ion chromatography in the area of separation of inorganic anions. Third, the main potential of CE was seen to be in the separation of biopolymers and biologically active compounds including drugs, with inorganic analysis being regarded as a relatively minor application area of CE. Although the last two factors remain valid, CE has matured to the stage where applications are sought in all areas of analysis, including inorganic analysis. This development has been characterized by more research oriented towards solving the practical requirements of inorganic analysis. The important developments in inorganic analysis by CE are summarized in **Table 1**.

Anions and cations migrate in opposite directions when placed in an electric field. Typical commercial

Table 1 Some important developments in inorganic analysis by CE

Time	Development
1967	First separation of cations (Br^{3+} Cu^{2+}) by free solution electrophoresis (0.1 mol L^{-1} lactate) in a 3 mm axially rotating tube
1974	Separation of alkali metal cations in 200–500 mm Pyrex capillaries with potentiometric detection
1979	Separation of inorganic anions using 200 mm PTFE capillary and conductometric detection
1983	Separation of Cu^{2+} , Fe^{3+} using a simple acetic acid electrolyte and direct photometric detection at 254 nm
1987	Indirect detection of anions
1989	Use of pre-capillary formed PAR complexes for separation of Co^{II} , Cr^{III} , Ni^{II} , Fe^{III} MEC (electrolyte containing SDS, pH 8, 0.1 mmol L^{-1} PAR) and using direct detection in visible
1990	Indirect photometric detection of anions using chromate electrolyte at pH 8 and reversed EOF
1990	Separation of rare earths metals and Li, Na, K, Mg using HIBA and indirect UV detection using an electrolyte of 0.03 mol L^{-1} creatinine-HAc pH 4.8, 4 mmol L^{-1} HIBA
1995	Hyphenation with ICP-MS: separation and detection of Sr, Cu, Fe^{III} , Fe^{II} , Cr, As, Sn^{II} , Sn^{IV}
1997	ITP-CE online: separation of Fe^{III} as pre-capillary formed EDTA complex; BGE: 25 mmol L^{-1} MES + 10 mmol L^{-1} bis-tris-propane, pH 6.6; leading: 10 mmol L^{-1} HCl + 20 mmol L^{-1} L-histidine + 0.1% HPMC, pH 6.0; terminating: 5 mmol L^{-1} MES

MEC, micellar electrochromatography

CE instruments have one point of sample introduction and one point of detection, so the choice must be made as to the polarity of the electrodes placed at the injection and detection ends of the capillary in order to establish the direction of movement of ions. Further, the electroosmotic flow (EOF) caused by the application of the separation potential will sweep the ions either towards or away from the detector, according to the polarity of the electrodes and the surface charge on the capillary. While it is theoretically possible to design a CE system in which a high EOF flowing towards the detector is established, causing both anions and cations to flow towards the detector, the electrophoretic mobilities of most inorganic anions and cations are too high to allow this approach to be applied. It is therefore more common for inorganic anions and cations to be analysed separately and for their electrophoretic movement to be in the same direction as the EOF (i.e. towards the detector). This is termed 'co-electroosmotic' separation.

Separation of Inorganic Anions

Separation Strategy

The electrophoretic mobilities of inorganic anions are quite large in comparison to those of most organic anions (Figure 1). Consequently, the normal instrumental arrangement is to assign the negative side of the separation voltage to the electrode at the injection end (so that the electrophoretic migration of the analyte anions is towards the positive electrode at the detection end). Moreover, since the normal flow of EOF in a fused silica capillary is towards the cathode (i.e. in the direction opposite to the electrophoretic migration of anions in the above case), it is normally

necessary to suppress or reverse the EOF to give a rapid co-electroosmotic separation. Such EOF reversal can be achieved by dynamic modification of the fused silica capillary inner wall by adsorption of cationic compounds or by permanent (covalent bonding) of cationic groups onto the fused silica capillary inner wall to provide an overall positive charge on the wall. The dynamic modification method is used most commonly and can be achieved by adsorption of suitable cationic surfactants (such as C_{12} to C_{16} alkyltrimethylammonium salts) or of large molecules such as cationic polymers (e.g. polybrene, poly(N,N,N',N'-tetramethyl-N-trimethylenehexamethylenediammonium dibromide) by adding these to the background electrolyte (BGE) or by flushing the capillary between the runs. This is illustrated schematically in Figure 2.

After introduction of the sample into the capillary and application of the separation voltage, the anions migrate towards the cathode at the detection end in the order of their effective electrophoretic mobilities, which means that the anions migrating fastest will be detected first. The flow of the bulk BGE driven by the EOF towards the detector (co-EOF separation) allows anions of low electrophoretic mobility to be carried to the detector point more rapidly than would occur based only on their electrophoretic mobility in case of a suppressed-EOF separation. Therefore typical co-EOF separations of anions are characterized by rapid analysis times, as illustrated in Figure 3.

Separation Selectivity

The electrophoretic mobilities of inorganic anions cover a wide range from about $30 \times 10^{-9} \text{ m}^2 \text{ V}^{-1} \text{ s}^{-1}$ to over $100 \times 10^{-9} \text{ m}^2 \text{ V}^{-1} \text{ s}^{-1}$ (Figure 1). Inspection

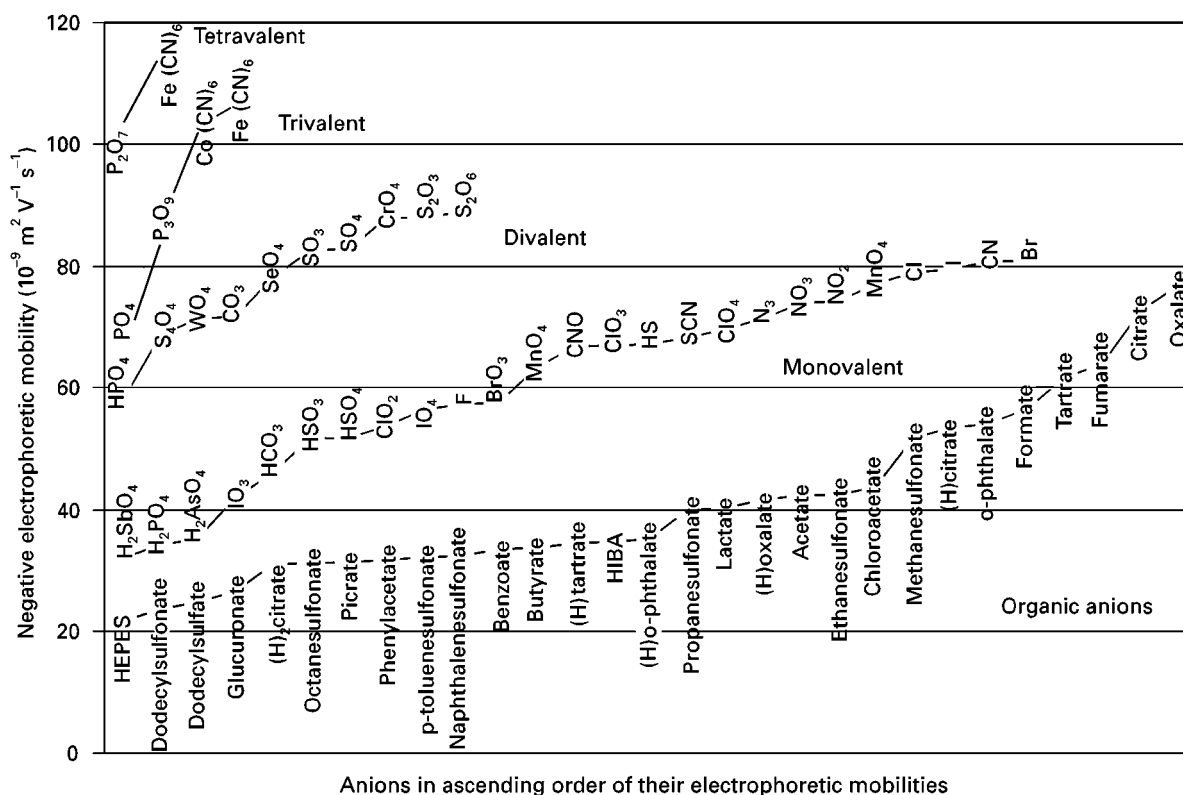


Figure 1 Electrophoretic mobilities of inorganic and some organic anions in ascending order of their mobilities. Key: (H), protonated form; (H)₂, diprotonated form, charges left out for simplicity. Electrophoretic mobilities were calculated from tabulated ionic conductances or taken from published values.

of Figure 1 shows that most inorganic anions have a unique value of electrophoretic mobility and should be straightforward to separate without the need to optimize the separation selectivity. However, in some cases electrophoretic mobilities of ions are similar

and steps need to be taken to manipulate selectivity in order to achieve a separation. The approaches available to achieve this goal are summarized in Table 2.

Probably the most universal tool for manipulating selectivity is to alter the solvation of the analyte anion

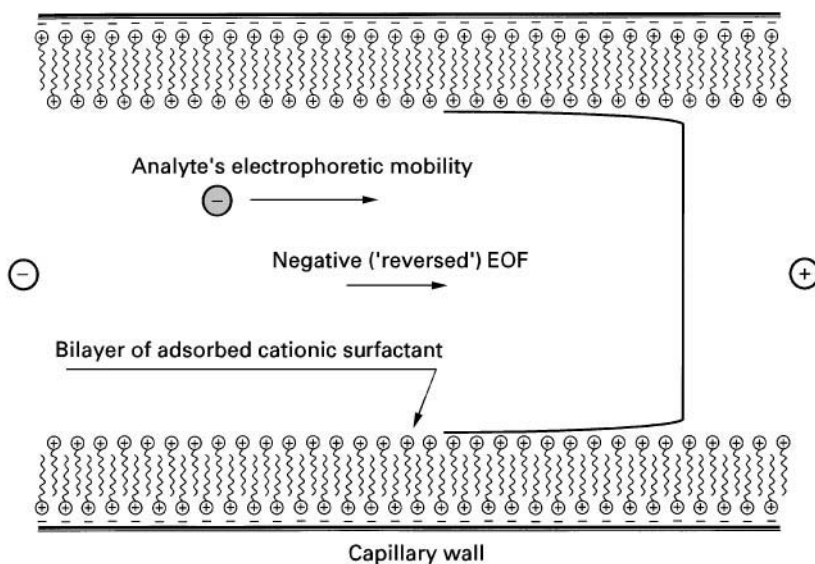


Figure 2 Schematic representation of co-electroosmotic separation of anions using EOF reversal.

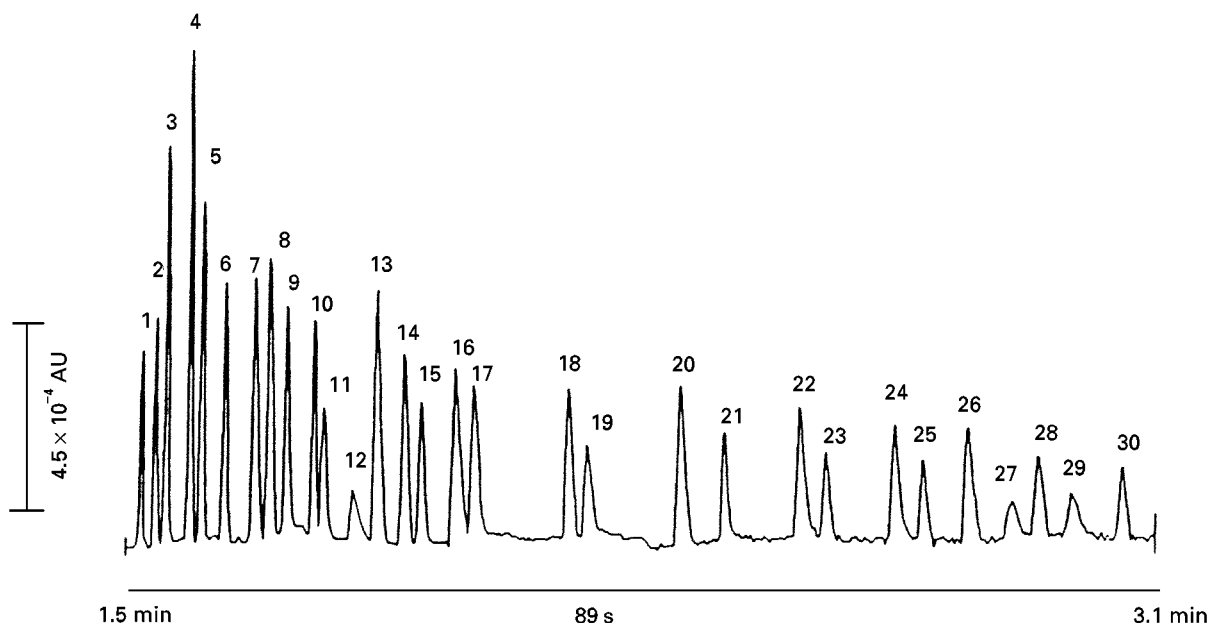


Figure 3 Separation of 30 anions using chromate BGE. Conditions: capillary, fused silica 75 μm i.d., 0.600 m length, 0.527 m to detector; BGE, 5 mmol L^{-1} chromate, 0.5 mmol L^{-1} tetradecyltrimethylammonium bromide (TTAB), pH 8.0; separation voltage, – 30 kV; detection, indirect at 254 nm; injection, electrokinetic at 1 kV for 15 s; sample, 0.3–1.7 ppm of each anion. Peak identification: 1, thiosulfate; 2, bromide; 3, chloride; 4, sulfate; 5, nitrite; 6, nitrate; 7, molybdate; 8, azide; 9, tungstate; 10, monofluorophosphate; 11, chlorate; 12, citrate; 13, fluoride; 14, formate; 15, phosphate; 16, phosphite; 17, chlorite; 18, galactarate; 19, carbonate; 20, acetate; 21, ethanesulfonate; 22, propionate; 23, propanesulfonate; 24, butyrate; 25, butanesulfonate; 26, valerate; 27, benzoate; 28, L-glutamate; 29, pentanesulfonate; 30, D-glucanate. (Reproduced with permission from Jones WR and Jandik P (1991) Controlled changes of selectivity in the separation of ions by capillary electrophoresis. *Journal of Chromatography* 546: 445–458.)

by adding organic solvents. For those anions that exhibit protonation equilibria in the pH range used in CE, substantial selectivity changes can be achieved by pH variations. The effective mobility of the analyte is defined as the weighted average of all the

mobilities of each of the forms, which for an acid H_nA undergoing protonation equilibria is

$$\bar{\mu}_A = \sum_{i=0}^n \mu_i \alpha_i \quad [1]$$

Table 2 Equilibria utilized for governing the separation selectivity

Anions/cations	Source of separation selectivity	Examples of BGE additives
Anions	Changes of effective mobility by utilizing protonation equilibria	pH optimization
	Changes of effective mobility by changes in solvation of the anions	Organic solvents
	Ion association of anions capable of hydrophobic interactions (e.g. I^- , SCN^-), with amphiphilic cations	Hexadecyltrimethylammonium
	Ion exchange interactions with polycationic molecules	Polybrene, polyethyleneimine
Cations	Complexation with an auxiliary ligand in partial complexation mode	HIBA, lactate, etc.
	Influence of the metal on the pK_a of a ligand group (total complexation mode)	PAR
	Dissociation of bound water molecules to mixed hydroxo–ligand–metal complexes (total complexation mode)	EDTA, CDTA and analogues
	Ion association of anionic complexes with amphiphilic cations, e.g. TBA^+ or hexamethonium (total complexation mode)	DHABS, CN^-
	IEEC (ion exchange electrochromatography), e.g. with poly(diallyldimethylammonium chloride), (total complexation mode)	EDTA, Quin2
	Changes of effective mobility by changes in solvation of the cations	Organic solvents

HIBA, 2-hydroxyisobutyric acid; PAR, pyridylazoresorcinol; EDTA, ethylenediaminetetraacetic acid; CDTA, trans-1,2-diaminocyclohexane-N,N,N',N'-tetraacetic acid; DHABS, 2,2'-dihydroxyazobenzene-5,5'-disulfonate; Quin, 2,8-amino-2-[(2-aminomethylphenoxy)methyl]-6-methoxyquinoline-N,N,N',N'-tetraacetic acid.

where μ_i is mobility and α_i is the fraction of the anion ion existing in form i .

For this approach to be successful, the BGE must be well buffered to avoid pH inhomogeneity within the migrating sample zone. Finally, ion exchange-type interactions between the analyte anions and some cationic water-soluble polymers may also be used to manipulate separation selectivity.

Detection of Anions

Direct and indirect photometric detection Most commercial CE instruments are equipped with a photometric detector and therefore direct and indirect photometric detection are the most commonly used detection methods in CE. Probably the most simple and robust detection technique in terms of baseline stability and lack of system peaks is direct photometric detection. Unfortunately this can be applied only to a few inorganic anions, such as iodate, bromide, thiocyanate, nitrate, nitrite, and some others.

Indirect detection has the prime advantage of being universal in its applicability and is the most frequently applied detection mode for CE separations of both inorganic anions and cations. An absorbing co-ion (commonly referred to as the probe ion) is added to the BGE and the detector monitors a suitable absorbing wavelength of the probe. Migrating bands of analytes displace the probe from the BGE and indirect detection is possible due to the resulting decrease in absorbance. The limit of detection (LOD) of a nonabsorbing analyte ion when detected by this process is given by:

$$c_{\text{LOD}} = \frac{c_p}{R \times D} = \frac{c_p \times N_{\text{BL}}}{R \times A} = \frac{N_{\text{BL}}}{R \times \varepsilon \times l} \quad [2]$$

where c_{LOD} is the concentration LOD, c_p is concentration of the probe co-ion in the BGE, R is the transfer (or displacement) ratio (that is, the average number of

probe co-ions displaced by one analyte ion), D is the dynamic reserve (the ratio of absorbance caused by the probe in the BGE to baseline noise), N_{BL} is the baseline noise, A is the absorbance caused by the probe in the BGE, ε is the molar absorptivity of the probe, and l is the effective pathlength.

The factors influencing detection sensitivity in indirect photometric detection are summarized in Table 3. As a general rule, the BGE should be well buffered to ensure optimal reproducibility, but at the same time the buffer must not add any competing co-ions to the BGE so that the probe ion is the only species displaced by the analyte (maximizing R) and detection sensitivity is therefore maximized. For indirect detection of anions it has been shown that this can be achieved either by using a buffering counter ion (i.e. one having the opposite charge sign to the probe) or by using buffering species of extremely low mobility, such as buffering ampholytes employed at a pH close to their pI . A further consideration in maximizing detection sensitivity is to ensure that the probe and the analyte have similar mobilities. Figure 4 shows the electrophoretic mobilities of some inorganic anions and some anionic probes. Typical concentration detection limits for indirect detection are in the low $\mu\text{mol L}^{-1}$ region, although sub- $\mu\text{mol L}^{-1}$ detection limits have been achieved by using highly absorbing dyes as probes.

Other detection methods Electrochemical detection methods, such as conductometric, amperometric and potentiometric detection methods, can be used in CE of inorganic anions with the first being the most successful. End-capillary detection, in which the detection electrodes are placed at the capillary outlet, has proved to be the optimal configuration. Commercial instrumentation for end-capillary conductometric detection has been introduced and is a useful approach for highly conductive analyte ions separated in a low conductivity BGE, such as 2-(N-

Table 3 Factors influencing sensitivity of indirect photometric detection

Factor	Methods of achievement
Minimal analyte peak width	Matching the mobilities of the analyte and the probe co-ion(s); minimizing solute-wall interactions
Maximal transfer ratio (R)	Matching the mobilities of analyte and probe co-ion(s); choice of BGEs without further co-ions which can compete with the probe (especially of similar mobilities)
Minimal baseline noise (N_{BL})	Minimal detector noise (usually by ensuring that the background absorbance is not too high); minimal 'chemical noise' (i.e. minimal solute-wall interactions of the analytes and/or probe)
Maximal absorptivity (ε) of the probe	Correct choice of the probe
Maximal effective pathlength (l)	Use of larger rather than smaller i.d. capillaries, use of extended pathlength capillary or z-cell

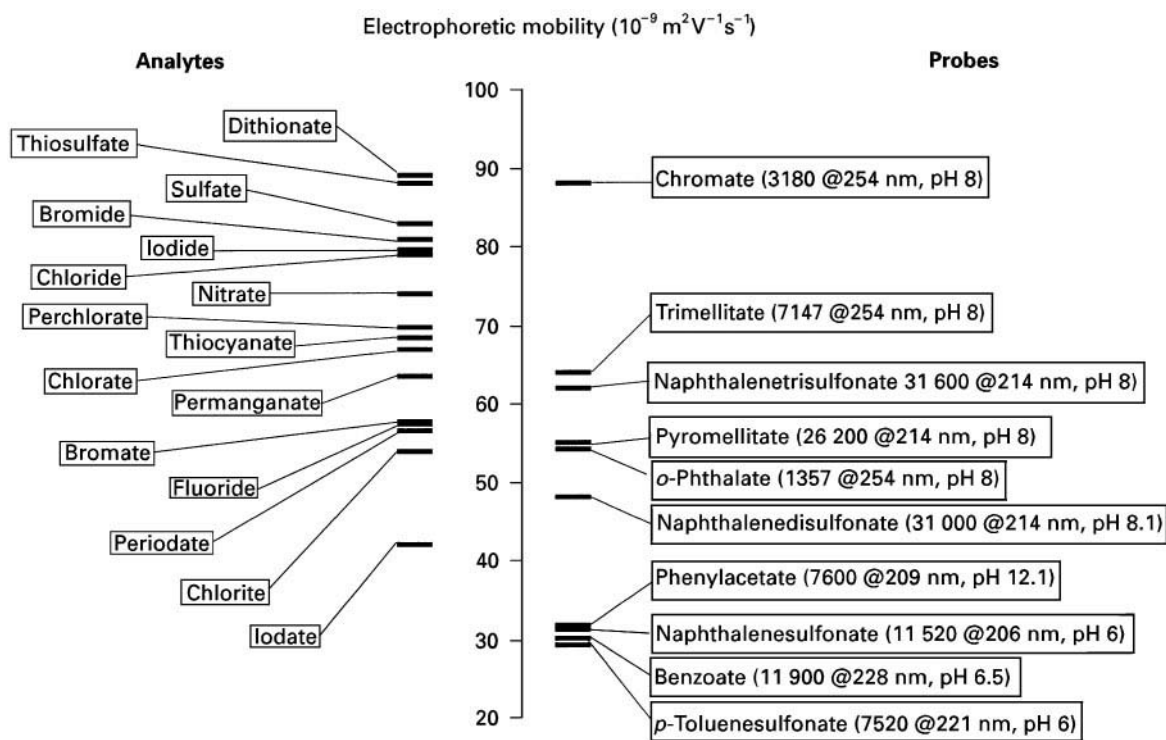


Figure 4 Matching of electrophoretic mobilities of some inorganic anionic analytes and probes. Given in brackets are molar absorptivity ($\text{L mol}^{-1} \text{cm}^{-1}$) at a wavelength (nm), and optionally a pH. (Data taken from Doble P and Haddad PR (1998) Indirect photometric detection of anions in capillary electrophoresis. *Journal of Chromatography A* 834: 189–212.)

cyclohexylamino)ethanesulfonic acid (CHES) buffer. The detection sensitivity is best for the most mobile anions and typical LODs are in the low $\mu\text{mol L}^{-1}$ range. End-capillary amperometric detection based on oxidation of anions such as nitrite, iodide, thiocyanate, azide or sulfite on gold, platinum or carbon fibre electrodes has been applied, with LODs down to the low nmol L^{-1} region. Finally, potentiometric detection using liquid membrane, solid-state coated wire or metallic copper electrodes has been applied to a range of anions. Concentration detection limits in the $\mu\text{mol L}^{-1}$ range have been achieved.

The use of information-rich detection techniques, such as mass spectrometry (MS), provides additional information that can be of advantage for analyte identification or to enhance the separation selectivity. The intriguing task of coupling CE to ICP-MS has been solved with the design of special nebulizers, such as the direct injection nebulizer, which introduces 100% of the sample to the plasma and does not cause any detectable peak broadening. Despite the disadvantages of high running costs and equipment complexity, CE interfaced to inductively coupled plasma mass spectrometry (CE-ICP-MS) has been successfully applied to speciation studies, such as of inorganic and organic species of selenium or arsenic,

for which LODs in the low ppt range have been reported.

Method Optimization

An important factor in the attainment of a robust CE method, delivering reproducible migration times and possessing some matrix tolerance, is correct buffering of BGEs. **Figure 5** shows the difference in tolerance towards an alkaline sample matrix for a buffered BGE and an unbuffered BGE, from which it can be seen that buffering is essential in the analysis of samples of this type.

With appropriate knowledge of the underlying principles of CE, such as methods for governing the separation selectivity or maximizing the sensitivity of indirect detection, methods for the separation of a limited number of analytes can often be developed without use of computer-based optimization procedures. In the case of inorganic anions the most frequently used BGE is sodium chromate (pH 8.0) containing a low concentration of a cationic surfactant such as tetradecyltrimethylammonium bromide for reversal of the EOF. The chromate ion acts as the probe for indirect photometric detection and has an electrophoretic mobility that is similar to those of many inorganic anions. Sensitive indirect

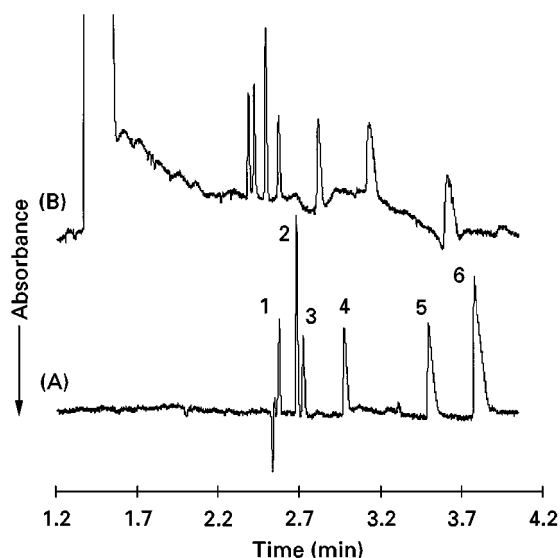


Figure 5 Tolerance to alkaline matrix illustrated using buffered (A), and unbuffered (B) chromate electrolytes. Conditions: capillary, fused silica 75 μm i.d., 0.600 m length, 0.500 m to detector; BGE, 5 mmol L^{-1} chromic trioxide, 20 mmol L^{-1} Tris, 0.5 mmol L^{-1} TTAB, pH 8.5 (a) or 5 mmol L^{-1} sodium chromate, 0.5 mmol L^{-1} TTAB, pH 8.5 (b); separation voltage, -20 kV; detection, indirect at 254 nm; injection, hydrostatic at 100 mm for 10 s; temperature, 25°C ; sample, 0.1 mmol L^{-1} of each anion in 50 mmol L^{-1} sodium hydroxide. Peak identification: 1, chloride; 2, sulfate; 3, nitrate; 4, chlorate; 5, phosphate; 6, carbonate. (Reproduced with permission from Doble P, Macka M, Andersson P and Haddad PR (1997) Buffered chromate electrolytes for separation and indirect absorbance detection of inorganic anions in capillary electrophoresis. *Analytical Communications* 34: 351–353.)

photometric detection at 254 nm can be achieved. Recently, buffered chromate electrolytes have been introduced using counterionic (cationic) buffers such as Tris or diethanolamine (Figure 5).

Sample Introduction and Sample Pretreatment

Sample introduction by electromigration methods is known to be matrix-dependent, therefore hydrostatic/hydrodynamic sample introduction is typically used. If electromigration injection is to be employed, matrix effects should be examined and standard addition rather than an external standard method should be used for calibration. Field-amplified stacking effects can be used for samples of lower ionic strength than the BGE, leading to lower concentration detection limits.

Real samples often require the application of simple procedures such as extraction, filtration to remove particular matter, or dilution, prior to the CE step and an online or at-line combination of such procedure(s) with CE is desirable. A dialysis/flow-

injection analysis (FIA) sample clean-up system coupled online to a CE allowed analysis of a number of anions in a variety of samples with complex matrixes such as milk, juice, slurries or liquors from the pulp and paper industry. In some cases, matrix removal (sample clean-up) combined with preconcentration of the analyte(s) may be necessary. Online isotachopheresis (ITP)-CE systems are capable of analysing anionic analytes in complex matrixes, but commercial instrumentation is not available widely. A general rule for the applicability of CITP-CE for sample clean-up is that the mobility of the analyte(s) should differ from the matrix ion(s) to be removed.

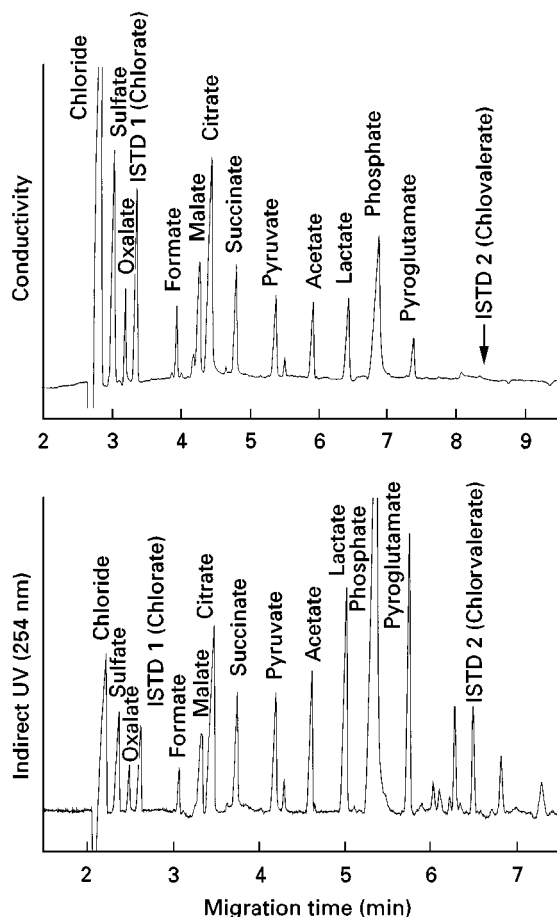


Figure 6 Separation of inorganic and anions and carboxylic acids in a beer sample using simultaneous nonsuppressed conductivity and indirect conductivity detection. Conditions: capillary, fused silica 50 μm i.d., 0.600 m length to end-capillary conductivity detector, 0.480 m to photometric detector; BGE, 7.5 mmol L^{-1} 4-aminobenzoic acid, 0.12 mmol L^{-1} TTAB, pH 5.75; separation voltage, -30 kV; detection, indirect at 254 nm; injection, hydrodynamic at 25 mbar for 12 s; sample, $10\times$ diluted stout. (Reproduced with permission from Klampfl CW and Katzmayer MU (1998) Determination of low-molecular-mass anionic compounds in beverage samples using capillary zone electrophoresis with simultaneous indirect ultra-violet and conductivity detection. *Journal of Chromatography A* 822: 117–123.)

Applications

A high proportion of the real samples analysed for inorganic anions by CE have been water samples (drinking water, mineral water, river water, ground water, well water, etc.), with fruit juices and beverages being another common type of sample. The fact that CE is not tolerant to high ionic strength samples is reflected in the infrequent application of CE to samples such as seawater, unless considerable dilution of the sample is undertaken. **Figure 6** shows a successful application of CE to the determination of inorganic anions using simultaneous indirect photometric and conductometric detection. This example also illustrates the fact that real samples usually require separation of inorganic anions from organic anions.

Cations

Separation Strategy

As for inorganic anions, most inorganic cations have electrophoretic mobilities that are too high to permit counter-EOF separation, so these species are usually separated co-electroosmotically. In this case the electrode with positive polarity is placed at the injection

side and when a bare fused silica capillary is used, the EOF is towards the detection side (cathode). Under these conditions the migration order is such that the analyte with the highest positive electrophoretic mobility migrates first and the analyte having the lowest positive mobility migrates last.

In contrast to the case for inorganic anions, many inorganic cations exhibit very similar mobilities, such as the whole group of rare earth metals or numerous transition metal ions (**Figure 7**). Therefore additional sources of separation selectivity to those available for anions are needed in order to separate these species. The main approach used is the addition of an auxiliary ligand to the BGE in order partially to complex the analyte cations (**Figure 8**). Provided the degree of complexation is different for each analyte cation, the effective charge and hence the effective mobility of each analyte will be unique and separation should be possible. These auxiliary ligands can be divided qualitatively into two groups according to the thermodynamic stability of the complexes formed with the analyte cations. **Table 4** summarizes the important characteristics of CE separation of metal ions using either weakly or strongly complexing auxiliary ligands.

Weakly complexing auxiliary ligands (such as HIBA or 19-crown-6) usually serve the sole purpose

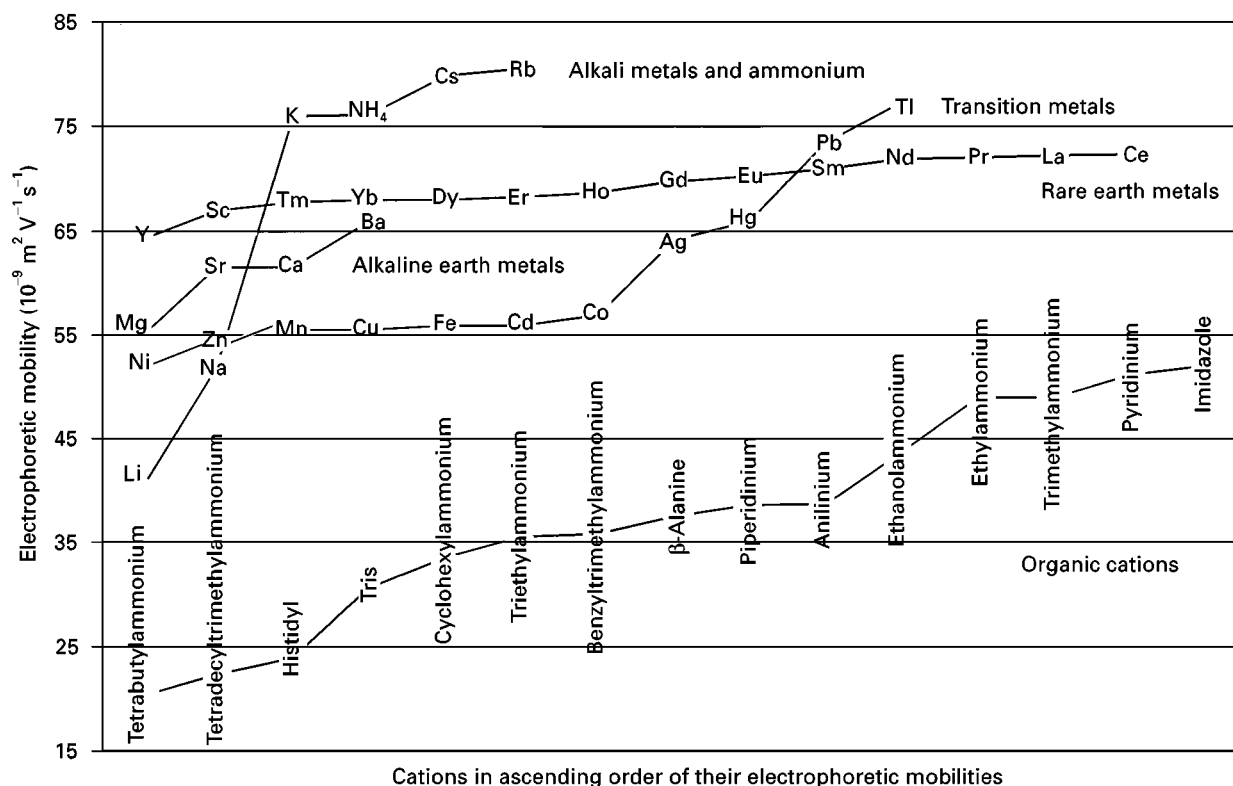


Figure 7 Electrophoretic mobilities of metal ions and some organic cations in ascending order to their mobilities. Ammonium was included with the alkaline metals because of its frequent importance in analysis of metal ions. Charges of metal cations have been left out for simplicity; transition metal ions divalent apart from monovalent Ag and Tl; organic cations all bear a charge of +1.

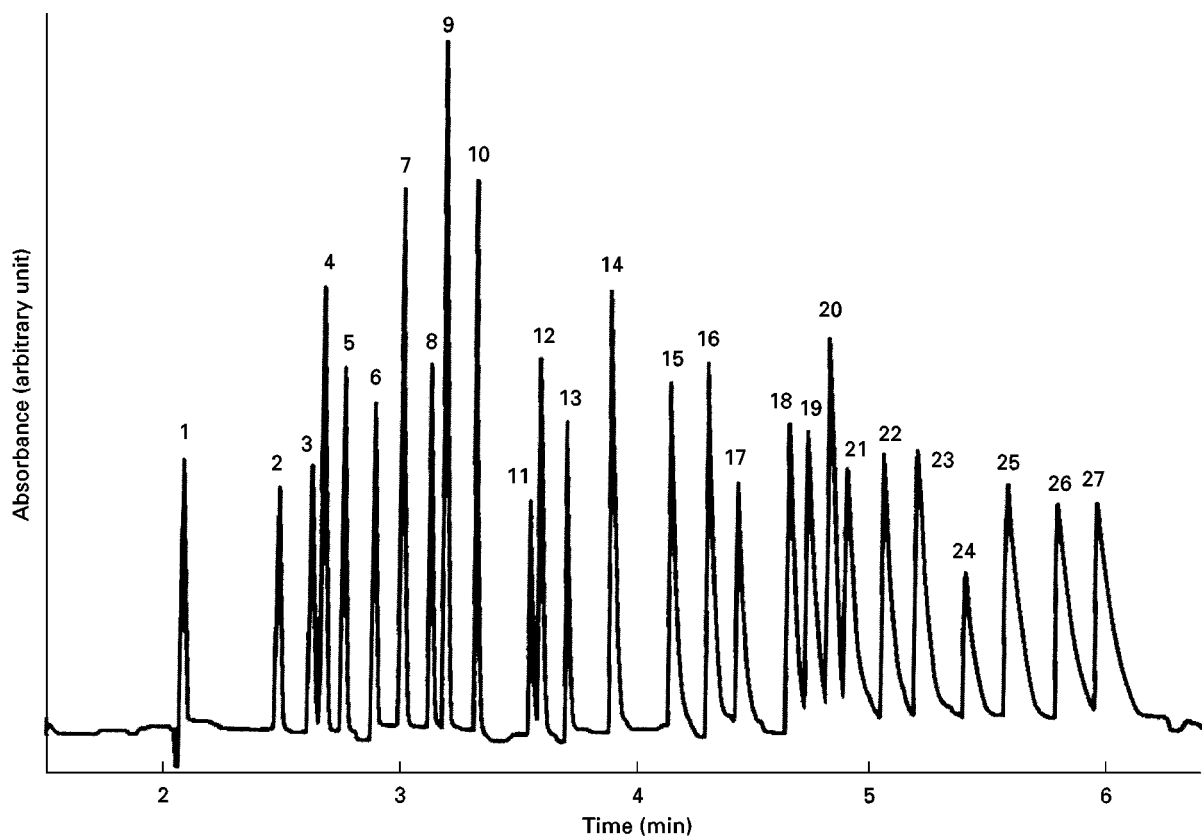


Figure 8 Separation of 27 alkali, alkaline earth, transition and rare earth metal ions in a single run using lactate as auxiliary ligand. Conditions: capillary, fused silica 75 μm i.d., 0.600 m length, 0.527 m to detector; BGE, 15 mmol L^{-1} lactic acid, 8 mmol L^{-1} 4-methylbenzylamine, 5% methanol, pH 4.25; separation voltage, 30 kV; detection, indirect at 214 nm; injection, hydrostatic at 100 mm for 30 s; sample, 1–5 ppm or each metal. Peak identification: 1, K^+ ; 2, Ba^{2+} ; 3, Sr^{2+} ; 4, Na^+ ; 5, Ca^{2+} ; 6, Mg^{2+} ; 7, Mn^{2+} ; 8, Cd^{2+} ; 9, Li^+ ; 10, Co^{2+} ; 11, Pb^{2+} ; 12, Ni^{2+} ; 13, Zn^{2+} ; 14, La^{3+} ; 15, Ce^{3+} ; 16, Pr^{3+} ; 17, Nd^{3+} ; 18, Sm^{3+} ; 19, Gd^{3+} ; 20, Cu^{2+} ; 21, Tb^{3+} ; 22, Dy^{3+} ; 23, Ho^{3+} ; 24, Er^{3+} ; 25, Tm^{3+} ; 26, Yb^{3+} ; 27, Lu^{3+} . (Reproduced with permission from Shi YC and Fritz JS (1993) Separation of metal ions by capillary electrophoresis with a complexing electrolyte. *Journal of Chromatography* 640: 473–479.)

of manipulating the separation selectivity and normally form part of the BGE into which samples containing free metal ions are injected. That is, *on-capillary complexation* is utilized (Figure 8). Since a substantial part of the metal exists as an uncomplexed cation, indirect absorption detection using a cationic absorbing probe contained within the BGE

is normally applied. Rapid complexation equilibria are necessary to enable manipulation of the selectivity of separation by varying parameters of the BGE such as the concentration of the auxiliary ligand and pH (Figure 8).

A completely different strategy is to use ligands forming stable, typically anionic complexes,

Table 4 Typical method properties according to the stability of the complex formed between the auxiliary ligand and the metal ion analyte

<i>Thermodynamic stability of the metal complex with the auxiliary ligand</i>	<i>Low</i>	<i>High</i>
Typical examples of the auxiliary ligand	HIBA, citric acid, lactic acid	CN^- , polydentate ligands such as EDTA and its analogues, metallochromic ligands
Degree of metal ion complexation	Partial	Total
Method of complex formation	On-capillary	Pre-capillary, often with on-capillary also used
Method of photometric detection	Indirect	Direct
Ease of selectivity manipulation	Straightforward	More difficult
Polarity of separation voltage on injection side	+	+, –

which are then separated as anions using the same approaches discussed earlier. Auxiliary ligands such as ethylenediaminetetraacetic acid (EDTA) or 2-pyridylazoresorcinol (PAR) may be used for this purpose and are usually added to the sample (that is, *precapillary complexation* is used). Often the BGE also contains a low concentration of the ligand in order to prevent the decomposition of less stable complexes. Most (or all) of the metal is complexed, so that detection using direct photometry is usually applicable. The complexation equilibria can be slow, but this then makes it difficult to alter the selectivity of separation and to retain good peak shapes. These separations are carried out in bare fused silica capillaries, fused silica capillaries with reversed EOF, or using other capillary wall chemistries. Depending on the charge of the metal complexes, the separation can be performed in either the co- or counter-electroosmotic modes, with either positive or negative separation potential applied on the injection side.

Metal ions are known to adsorb onto the surface of silica particles through interaction with silanol groups. In the case of polyvalent metal cations, this adsorption can be considered to be irreversible. Although the surface density of silanols on fused silica is lower by approximately an order of magnitude than for porous silica, it is well documented in CE using bare fused silica capillaries that metal ions present in the BGE (even as an impurity) can adsorb onto the capillary wall. The extent of adsorption is often reflected in changes to the EOF, with both suppression and reversal of EOF having been demonstrated. Despite these facts, coated capillaries have found relatively little use in separations of metal ions. In bare fused silica capillaries, the risk of adsorption of metal ions is counteracted by typically weakly acidic and complexing electrolytes.

Separation Selectivity

The most powerful and straightforward tool governing separation selectivity is control of the degree of complexation with the auxiliary ligand. For a metal ion present in several forms that are in equilibrium with rapid kinetics of interchange between the forms, the effective mobility of the analyte is given by the weighted average of the mobilities of each of the forms. For a metal ion M migrating in a BGE containing a ligand L forming complexes ML , ML_2 , ..., ML_n , the effective mobility of the metal can then be expressed as:

$$\bar{\mu}_M = \sum_{i=0}^n \mu_i \alpha_i = \frac{\sum_{i=0}^n \mu_i [ML_i]}{\sum_{i=0}^n [ML_i]} = \frac{\sum_{i=0}^n \mu_i \beta_i [L]^i}{\sum_{i=0}^n \beta_i [L]^i} \quad [3]$$

where μ_i is mobility and α_i is the fraction of metal ion existing in form i , $[ML_i]$ is the concentration of the complex ML_i , $[L]$ is the concentration of the form of ligand forming the complex and β is the overall stability constant ($ML_0 = M$, $\beta_0 = 1$).

A different situation occurs when utilizing auxiliary complexing ligands that form strong complexes with the metal ions. Since most of the metal ion is complexed under all BGE conditions, the complex formation/dissociation cannot be used to govern the separation selectivity as in the case of weakly complexing ligands. Apart from minor factors influencing the selectivity, such as solvation changes in various media, there are very few means to bring about a change in the charge/mass value of the analytes (and consequently a substantial change in selectivity). These include: (1) dissociation of functional groups on the ligand exhibiting protonation equilibria; (2) exchange of the remaining water molecules on the metal ion coordination sites not saturated by the ligand; and (3) ion association or ion exchange equilibria in the BGE solution (Table 4). The separation selectivity therefore varies considerably with the nature of the ligand used.

Detection

Direct and indirect photometric detection As with inorganic anions, direct and indirect photometric detection are the most commonly used detection methods in the separation of metal ions, being employed in about 85% of publications. Since most hydrated metal ions do not absorb at all, or have only weak absorption bands in the UV region above 185 nm, direct detection is normally possible only when the metal ions are complexed with an auxiliary ligand. Thus the auxiliary ligand, which in earlier discussion has been shown to play a crucial role in the separation of metal ions, also enhances the detectability of these species. Metallochromic ligands form highly absorbing ($\epsilon \sim 10^5 \text{ L mol}^{-1} \text{ cm}^{-1}$) coloured complexes with metal ions. When these complexes are stable and the separation results in well-shaped peaks, very good detection sensitivity can be obtained. For example, determination of transition metals in the form of complexes with PAR achieved concentration LODs in the order of $10^{-7} \text{ mol L}^{-1}$ or absolute LODs at fmol levels. Even lower LODs (80 nmol L^{-1} or 0.5 fmol for Zn) have been obtained for porphinate complexes ($\epsilon \sim 10^5 \text{ L mol}^{-1} \text{ cm}^{-1}$), but the detection method is less universal because different metal ions exhibit a range of absorption maxima and absorptivities.

The underlying principles for indirect photometric detection of inorganic cations are the same as for

inorganic anions (see above). Figure 9 illustrates matching of electrophoretic mobilities of some metal cations as analytes with some cationic probes.

Other detection methods Conductometric, amperometric and potentiometric detection methods can be utilized for inorganic cations and the same principles discussed apply. End-capillary conductometric detection has been used for a range of cations using low-conductive histidine-MES BGEs with similar success to anion analysis (LODs are in low $\mu\text{mol L}^{-1}$ range). End-capillary amperometric detection utilizing reduction of metal ions such as thallium, lead, cadmium, etc., and inorganic and organic mercury compounds on gold, platinum or mercury films, has been applied with low nmol L^{-1} range LODs. Potentiometric detection can also be used for metal ions and, as for anions, the solid-state electrodes show greatest promise.

CE coupled with electrospray mass spectrometry has achieved detection of about 30 metal ions by positive ion MS. Although chemical noise does not allow detection below ppb levels, LODs are generally

below those obtained for indirect photometric detection. Impressive LODs have been obtained by CE-ICP-MS, e.g. of 0.06 ppb for Sr^{II} (8 fg or 90 amol).

Method Optimization

The separation of up to 30 metal ions in one run using weakly complexing auxiliary ligands is a challenging analytical task and optimization of the BGE composition often requires the use of computer methods based on thermodynamic complexation models or the use of artificial neural networks. The BGEs used most frequently for metal ion analysis would normally utilize indirect photometric detection and a typical BGE contains a weakly complexing auxiliary ligand (such as HIBA) for governing separation selectivity for most transition metal ions and rare earth metals. It often also contains a crown-ether as a second auxiliary ligand to separate ammonium from potassium (see Figure 7) and an indirect detection cationic probe (such as imidazole, benzylamine, or creatinine) at pH ~ 4.5 –5.

While most authors have demonstrated the application of their developed separation to a real

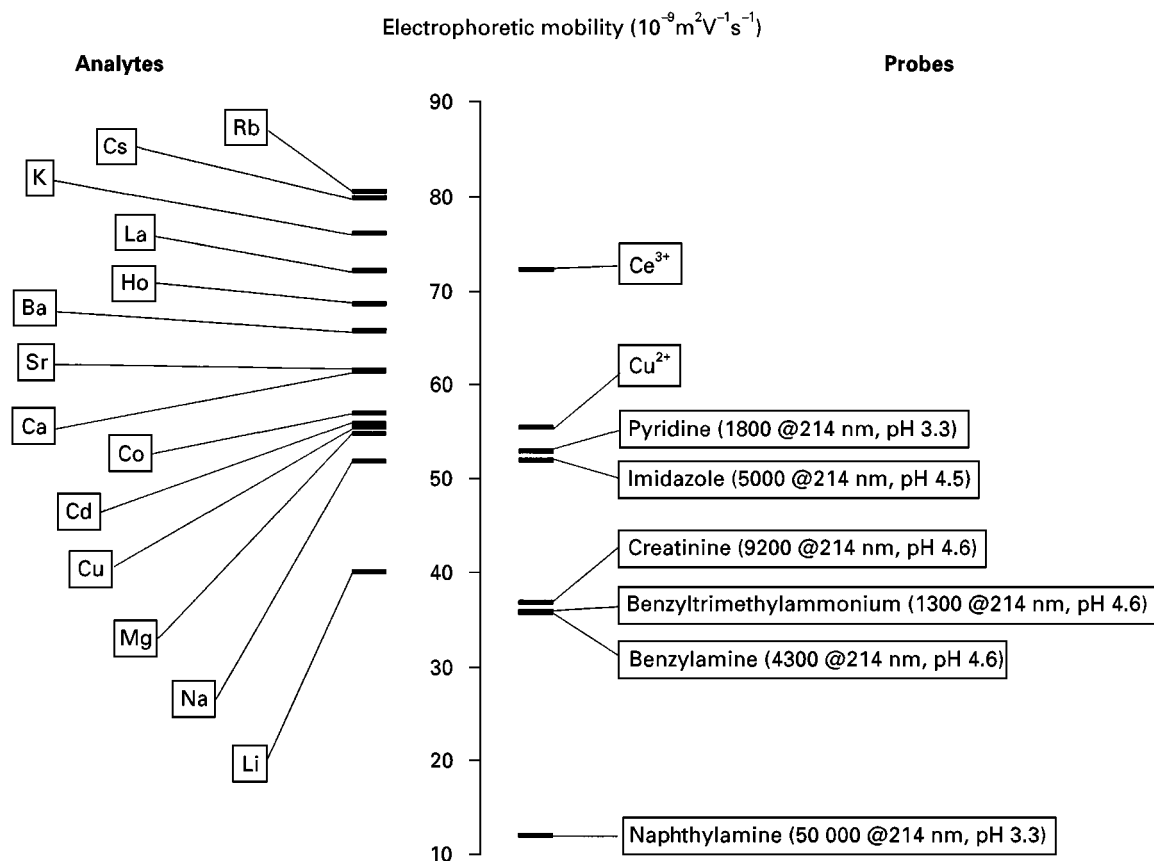


Figure 9 Matching of electrophoretic mobilities of some metal ion analytes and probes. Given in brackets are molar absorptivity ($\text{L mol}^{-1} \text{cm}^{-1}$) at a wavelength (nm), and optionally a pH. (Source of data: Beck W and Engelhardt H (1992) *Chromatographia* 313; Chen M and Cassidy RM (1993) Separation of metal ions by capillary electrophoresis. *Journal of Chromatography* 640: 425–431.)

sample of some kind, there have been relatively few studies on aspects of method validation, such as precision and accuracy. Typical precision for migration times, peak areas and peak heights show a relative standard deviation ranging from 3 to 10%.

Sample Introduction and Sample Pretreatment

In addition to the principles discussed earlier for anions, stacking effects can be achieved in the separation of metal ions using on-capillary complex formation in which oppositely migrating metal cations and ligand anions converge and react at the boundary between the injected sample plug and the BGE. A necessary condition to utilize the stacking by on-capillary complexation is fast complex formation. This approach was first demonstrated for four divalent metal complexes with PAR in which a plug of 1 mmol L^{-1} PAR was first injected into the capillary are then electromigration injection from a sample without added ligand was performed. This method with an optimized stacking procedure gave detection limits in the range of 10 nmol L^{-1} .

Ion exchange and chelating resins may be used to preconcentrate metal ions prior to CE determination in an offline configuration. Ion exchange materials are less successful for the selective preconcentration of heavy metals than chelating (iminodiacetate or dithiocarbamate) resins, or by the formation of metal chelates with an excess of the reagent, followed by adsorption of the chelate on a hydrophobic column.

Applications

As with anions, many of the real samples analysed have been various water samples, fruit juices and beverages and food. An example of an unusual application of CE to the analysis of high salinity samples is shown in Figure 10.

Simultaneous Separations of Anions and Cations

Despite the potential advantages of reduced analysis time and costs that arise from analysing both anions and cations in one run, separate analysis of both groups is still much easier and more robust. The simple fact that anions and cations migrate in opposite directions in an electric field means that a simultaneous analysis cannot be realized with one point of sample introduction and one point of detection.

However, there are two approaches that have proved successful. The first uses a sample injection simultaneously in two capillaries operated with the same BGE, with both capillaries equipped with independent detectors located near their ends. A relatively

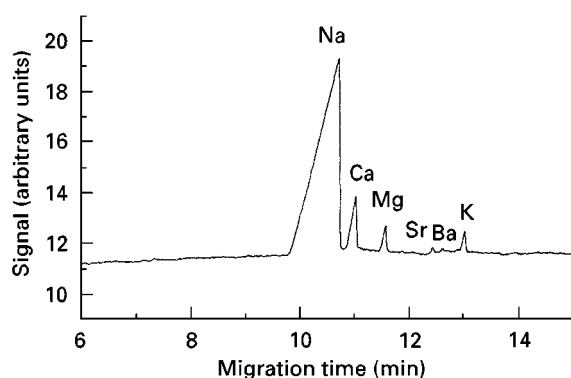


Figure 10 Separation of metal ions in a mixture of salt water and formation water using indirect photometric detection. Conditions: capillary, fused silica $75 \mu\text{m}$ i.d., 0.600 m length, 0.520 m to detector; BGE, 6.5 mmol L^{-1} HIBA, 5 mmol L^{-1} UVCAT-1 (Waters), 6.2 mmol L^{-1} 18-crown-6, 25% (v/v) methanol, apparent pH 4.8; separation voltage, 20 kV ; detection, indirect at 185 nm ; injection, hydrodynamic at 98 mm for 20 s ; sample, diluted by a factor of 125. (Reproduced with permission from Tangen A, Lund W and Frederiksen RB (1997) Determination of sodium, potassium, magnesium and calcium ions in mixtures of sea water and formation water by capillary electrophoresis. *Journal of Chromatography A* 767: 311–317.)

easier approach uses just one capillary, but sample is injected at both ends and the detector is located approximately in the middle of the capillary. This approach has been applied to the analysis of a range of real samples; an example is given in Figure 11.

It should be noted that when applying indirect detection using both an anionic and a cationic probe, the probes should be mixed in their free acid and free base forms to avoid the presence of competing ions in the BGE.

Future Developments

Control of the separation selectivity will be an area of development in CE of inorganic species. Utilization of ion exchange-type interactions with pseudostationary phases, and particles of sub- μm size, can introduce new selectivity into a CE separation. It is instructive to examine the separation selectivities achieved by ion chromatography and CE under standard conditions, as revealed by the elution or migration order of common analytes. In the case of IC, anions are eluted in the following order of retention times: $\text{F}^- < \text{Cl}^- < \text{NO}_2^- < \text{Br}^- < \text{NO}_3^- < \text{PO}_4^{3-} < \text{SO}_4^{2-} < \text{I}^-$. However, the migration times of these species in co-EOF CE are $\text{Br}^- < \text{Cl}^- < \text{SO}_4^{2-} < \text{NO}_2^- < \text{I}^- < \text{NO}_3^- < \text{F}^- < \text{PO}_4^{3-}$. A similar pattern emerges when the same comparison is made for inorganic cations, for which the IC retention times follow the order: $\text{Li}^+ < \text{Na}^+ < \text{NH}_4^+ < \text{K}^+ < \text{Mg}^{2+} < \text{Ca}^{2+} < \text{Sr}^{2+} < \text{Ba}^{2+}$, while migration times for co-EOF CE are

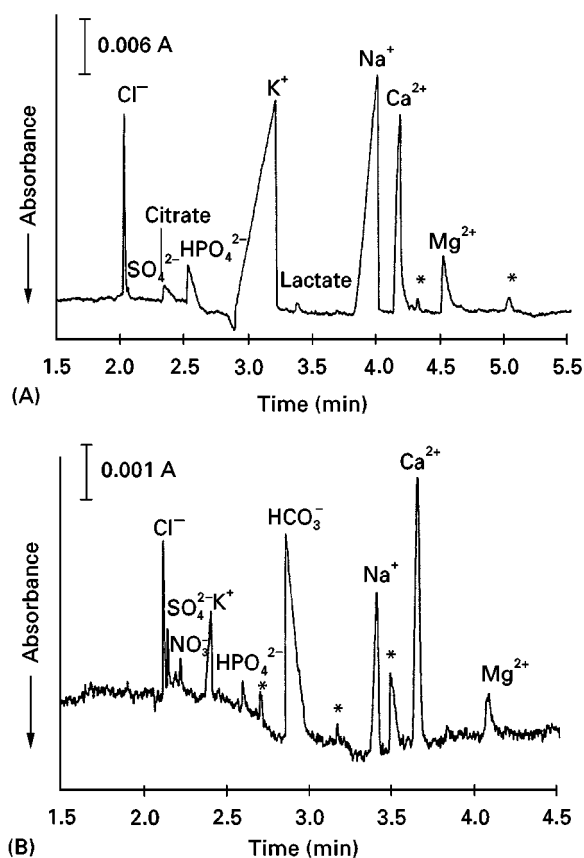


Figure 11 Simultaneous determination of inorganic anions and cations in milk (A) and mud (B) after offline dialysis. Conditions: capillary, fused silica 50 μm i.d., 0.500 m total length, 0.200 m to detection window from the anodic end; BGE, 6 mmol L^{-1} 4-aminopyridine, 2.7 mmol L^{-1} H_2CrO_4 , 30 $\mu\text{mol L}^{-1}$ CTAB, 2 mmol L^{-1} 18-crown-6, pH 8; separation voltage, 20 kV; detection, indirect at 262 nm; injection, hydrostatic at 50 mm for 10 s (cathode end) and 50 mm for 10 s (anode end) (A) or at 50 mm for 20 s (cathode end) and 100 mm for 40 s (anode end) (B); time between the injections, 60 s (A) or 30 s (B). (Reproduced with permission from Kuban P and Karlberg B (1998) Simultaneous determination of small cations and anions by capillary electrophoresis. *Analytical Chemistry* 70: 360–365.)

$\text{NH}_4^+ < \text{K}^+ < \text{Ba}^{2+} < \text{Sr}^{2+} < \text{Ca}^{2+} < \text{Na}^+ < \text{Mg}^{2+} < \text{Li}^+$. Complementary selectivities are again apparent. These selectivities suggest that a mixed-mode separation system in which the movement of analytes is influenced both by electromigration effects and ion exchange interactions might provide a means to manipulate selectivity in order to solve existing separation problems.

New developments can also be expected in the area of detection techniques. For instance, the use of highly absorbing cationic probes in carefully formulated BGEs that avoid competitive displacement has the potential to increase the sensitivity using indirect photometric detection. Further development

of other detection techniques can be anticipated, especially those compatible with the capillary dimensions and suitable for on- or end-capillary use and which do not necessitate elaborate changes to the capillary.

Finally, more advances in the area of online sample treatment and/or preconcentration techniques are likely to occur as CE becomes more of a routine tool for the determination of inorganic species in complex samples.

Further Reading

- Chiari M (1998) Selectivity in capillary electrophoretic separations of metals and ligands through complex formation. *Journal of Chromatography A* 805: 1–15.
- Dabek-Zlotorzynska E, Lai EPC and Timerbaev AR (1998) Capillary electrophoresis – the state-of-the-art in metal speciation studies. *Analytica Chimica Acta* 359: 1–26.
- Doble P and Haddad PR (1998) Indirect photometric detection of anion in capillary electrophoresis. *Journal of Chromatography A* 834: 189–212.
- Foret F, Křivánková L and Boček P (1993) *Capillary Zone Electrophoresis*. Weinheim: VCH.
- Fritz JS (1998) Determination of inorganic anions and metal cations. In: Camilleri P (ed.). *Capillary Electrophoresis, Theory and Practice*. Boca Raton, FL: CRC Press.
- Haddad PR (1997) Ion chromatography and capillary electrophoresis: a comparison of two technologies for the determination of inorganic ions. *Journal of Chromatography A* 770: 281–290.
- Haddad PR, Doble P and Macka M (1999) Developments in sample preparation and separation techniques for the determination of inorganic ions by ion chromatography and capillary electrophoresis. *Journal of Chromatography A* 856: 145–177.
- Jandik P and Bonn G (1993) *Capillary Electrophoresis of Small Molecules and Ions*. New York: VCH.
- Jones P (ed.) (1999) Electrophoresis of inorganic species, *Journal of Chromatography A* v. 834, Parts 1 + 2.
- Li SFY (1992) *Capillary Electrophoresis, Principles, Practice and Applications*. Amsterdam: Elsevier.
- Macka M, Haddad PR (1997) Determination of metal ions by capillary electrophoresis. *Electrophoresis* 18: 2482–2501.
- Mazzeo JR (1998) Capillary electrophoresis of inorganic anions. In: Khaledi MG (ed.). *High Performance Capillary Electrophoresis, Theory, Techniques and Applications*. New York: Wiley-Interscience.
- Pacáková K and Štulík V (1997) Capillary electrophoresis of inorganic anions and its comparison with ion chromatography. *Journal of Chromatography A* 789: 169–180.
- Timerbaev AR (1997) Strategies for selectivity control in capillary electrophoresis of metal species. *Journal of Chromatography A* 792: 495–518.
- Timerbaev AR (1997) Analysis of inorganic pollutants by capillary electrophoresis. *Electrophoresis* 18: 185–195.

Electrophoresis

See III / ION ANALYSIS / Capillary Electrophoresis

High-Speed Countercurrent Chromatography

E. Kitazume, Iwate University, Morioka, Iwate, Japan

Copyright © 2000 Academic Press

High-speed countercurrent chromatography (HSCCC), developed by Ito, is a useful method of separating many organic materials, such as biologically active substances, natural and synthetic peptides and various plant hormones. Like other countercurrent chromatography (CCC) methods, it is also free from problems based on solid supports, such as adsorption or irreversible binding and contamination of the sample.

HSCCC has been applied to preconcentration and separation of inorganic elements since the late 1980s and since then, inorganic elements, including rare earth elements, have been separated by HSCCC. Also the preconcentration and separation of inorganics from geological samples have been studied. The liquid systems for inorganics are more complicated than those for separation of organics, because they usually contain significant amounts of an extracting agent, which influences kinetic properties and viscosities of the whole two-phase system.

In order to achieve high sensitivity for analysing trace inorganic elements in a solution using atomic absorption spectrometry (AAS) or inductively coupled plasma atomic emission spectrometry (ICP-AES), conventional preconcentration methods such as evaporation, ion exchange and solvent extraction have been used. However, there are several problems in these methods for the determination of ultra trace elements, for example, peak broadening for ion exchange and a small enrichment factor for solvent extraction. It is difficult to achieve under 0.5 mL concentrated sample solutions by conventional methods. If there were effective methods to concentrate traces into 0.1 mL volume or less, absolute detection limits for trace analysis such as AAS, ICP-AES and ICP-mass spectrometry (ICP-MS) would be

greatly decreased, and matrix effects would be eliminated.

Recently, pH-zone refining CCC, which is a unique technique based on the neutralization reaction between the mobile and stationary phase, has been developed for the separation and enrichment of organic acids, basic derivatives of amino acids and acidic peptide derivatives. It can initiate chemical reactions in quite a limited thin area, the interface between the organic and aqueous phase. Therefore, if there is a reversible pH area between the mobile and stationary phase, the pH in the column can be continuously controlled. This means that another flow rate, concerned with pH and different from real flow rate, can be realized in the column. Impurities in sample solutions can be concentrated in the pH boundary in the column. As it can be successfully applied to the enrichment of inorganic trace elements in solution, it has great potential for on-line enrichment and subsequent analysis, when HSCCC is combined with instruments such as AAS, ICP-AES and ICP-MS.

Mechanism of Two-phase Separation in HSCCC

In HSCCC, a stationary sun gear is mounted around the central stationary axis of the centrifuge to prevent the flow tubes twisting. This gear arrangement gives a planetary motion of the column holder – one rotation about its own axis for one revolution around the central stationary axis of the centrifuge in the same direction.

Figure 1 shows a schematic diagram of two-phase separation in an HSCCC column. The heavier mobile phase (black) is introduced into the column from the right side (column head). The upper stationary phase (grey) is retained in the column by a rotational force field and Archimedean screw effect (ASE), in spite of being pushed to the column end by the mobile phase. For separation and enrichment of inorganic elements, the stationary phase commonly contains one or more extracting reagents, such as di(2-ethylhexyl)phosphoric acid (DEHPA), dissolved in the appropriate stationary organic phase. The mobile phase is commonly composed of inorganic acids and their salts. Water-soluble complexing reagents forming

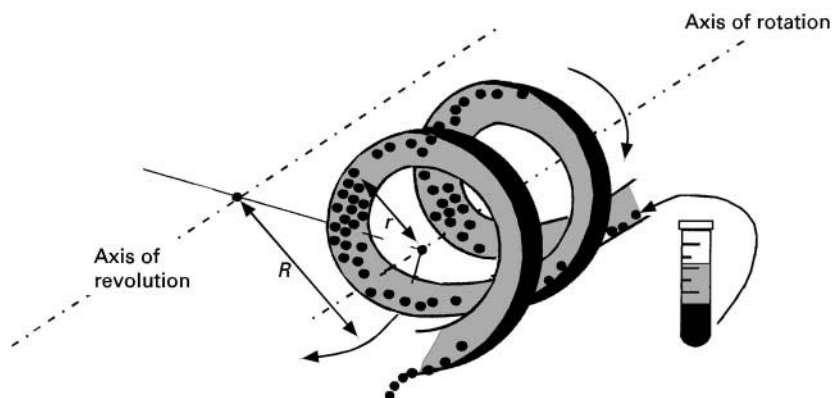


Figure 1 Schematic diagram of two-phase separation in HSCCC column. r , Rotation radius; R , revolution radius.

stable compounds with specified elements in the sample can also be used as an aqueous mobile phase. The column is revolved in the radius R and rotated with the radius r at the same time. When the coil column is facing the axis of revolution (top left in Figure 1), the two phases are vigorously mixed because of the weak force field. In contrast, when facing the outer side of the column, the mobile phase is clearly separated by a stronger force field than that at the inner side. The inner quarter turn of the coil is the most vigorous mixing area. As one phase usually occupies the column head by an Archimedean screw effect, another phase can be introduced as an eluent. After being introduced from the column head, the heavier mobile phase emerges from the end of the column (bottom left in Figure 1). When the column makes one revolution around the axis, it rotates once on the orbital of revolution. Therefore, as a specific point in the column, one turn in the coil proceeds towards the column head per revolution. At the same time, one cycle of each mixing and separation process at the specific point occurs in the column. As the HSCCC column rotates at over several hundred rpm, this is a rapid process. For example, there are 13 processes per second taking place at 800 rpm, giving efficient separation and mixing in the column.

Extracting Reagent for Separation of Inorganic Elements

As mentioned above, the existence of extracting reagent in the mobile phase is an essential factor in the separation of inorganic elements. It complicates the determination of several important factors, such as distribution coefficients, peak resolution and separation efficiency. Research reveals that the kinetic properties of a specific system used in HSCCC affect the separation efficiency. The mass transfer rate into the organic stationary phase is responsible for using either stepwise or isocratic elution. In addition, the value of the distribution coefficients, determined by batch extraction measurements on systems, are sometimes considerably different from the dynamic distribution coefficients calculated from the elution curve. Further theoretical and basic investigations are necessarily concerned with extraction kinetics, as well as the hydrodynamic behaviour of the two phases in the HSCCC column.

In Table 1, typical extracting reagents used for separation and enrichment of inorganic elements are summarized. Organophosphorus extractants are often used because of their solubility properties.

Table 1 Typical extracting reagents for separation and enrichment of inorganic elements using high-speed countercurrent chromatography

Extracting reagent	Two-phase system	Inorganic element
Di(2-ethylhexyl)phosphoric acid (DEHPA)	HCl, organic acid–heptane	Rare earth, heavy metals
2-Ethylhexylphosphonic acid mono-2-ethylhexyl ester (EHPA)	Carboxylic acid–toluene	Rare earth
Dinonyltin dichloride	HCl, HNO_3^- Methylisobutylketone (MIBK)	Ortho- and pyrophosphate
Cobalt dicarbonyl	HNO_3 -nitrobenzene	Cs and Sr
Tetraoctylethylenediamine (TOEDA)	HCl, HNO_3 , organic acid–chloroform	Alkali, alkaline earth, rare earth, heavy metals, Hf, Zr, Nb, Ta

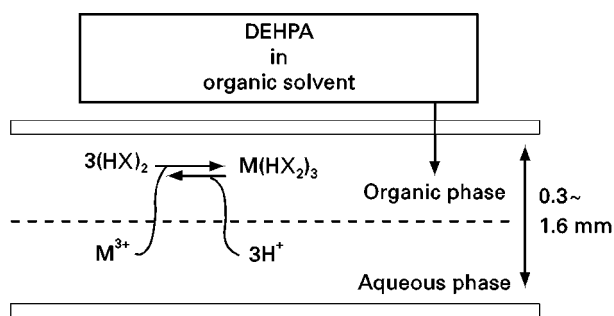


Figure 2 Extraction equilibrium in HSCCC column using di (2-ethylhexyl) phosphoric acid (DEHPA) as an extracting reagent for trivalent metal ion (M^{3+}). $(HX)_2$, dimer of DEHPA.

Figure 2 shows the equilibrium for extraction of trivalent metal ions, such as lanthanide, using the extracting reagent (DEHPA). DEHPA is commonly applied in industrial separation due to its high extractability and high separation factors between many inorganic elements, especially for rare earth elements. Trivalent metal ions (M^{3+}) are extracted as shown in Figure 2 in PTFE tubing of 0.3–1.6 mm in diameter. The long thin rectangles in Figure 2 show the wall of the PTFE tubing. $(HX)_2$ is a dimer of DEHPA. Metal ions in the aqueous phase are extracted into organic phase as $M(HX_2)_3$.

Mutual Separation of Inorganic Elements

Figure 3 shows a typical flow diagram of the instrumentation assembly for the separation of rare earth elements and other inorganic elements by HSCCC. In this case, the spectrophotometer is used as a detector for each element. If an alternative measurement system such as AAS, ICP-AES or ICP-MS is used, all the equipment depicted after the splitter is not required. Each separation is usually initiated by filling the en-

tire column with the stationary nonaqueous phase, followed by injection of an appropriate volume of the sample solution through the sampling port. Then, the mobile phase is eluted through the column at a flow rate of 0.1–5 mL min⁻¹ while the apparatus is rotated at several hundred rpm. In Figure 3, continuous detection of the inorganic elements is effected by means of a post-column reaction with an appropriate compound such as arsenazo III, and the elution curve is obtained by monitoring the effluent with a spectrophotometer. The effluent is divided into two streams with a tee adapter and a low-dead-volume pump (pump II). Pump II delivers a portion of the effluent at the required flow rate to the spectrophotometer and pump III adds reagent for post-column reaction to the effluent stream. The resulting stream first passed through a narrow mixing coil and then leads through an analytical flow cell in a spectrophotometer. The other effluent stream through the tee adapter is either collected or discarded.

Figure 4 shows a one-step separation of all 14 lanthanides (except for promethium) performed by applying an exponential gradient of hydrochloric acid in the mobile phase. The main problem in gradient elution is that the optimum range of the ligand concentration in the stationary phase is substantially different between the lighter and heavier groups of the rare earth elements. Because the separation of the heavy lanthanide elements, including thulium, ytterbium and lutetium, is more difficult, a ligand concentration of 0.003 mol L⁻¹ was selected for best resolution. With an isocratic separation mode, using a constant eluent concentration, even heavy lanthanide elements such as Tm, Yb and La are well separated.

Figure 5 shows a typical chromatogram of Ni(II), Co(II), Mg(II) and Cu(II) obtained by eluting with

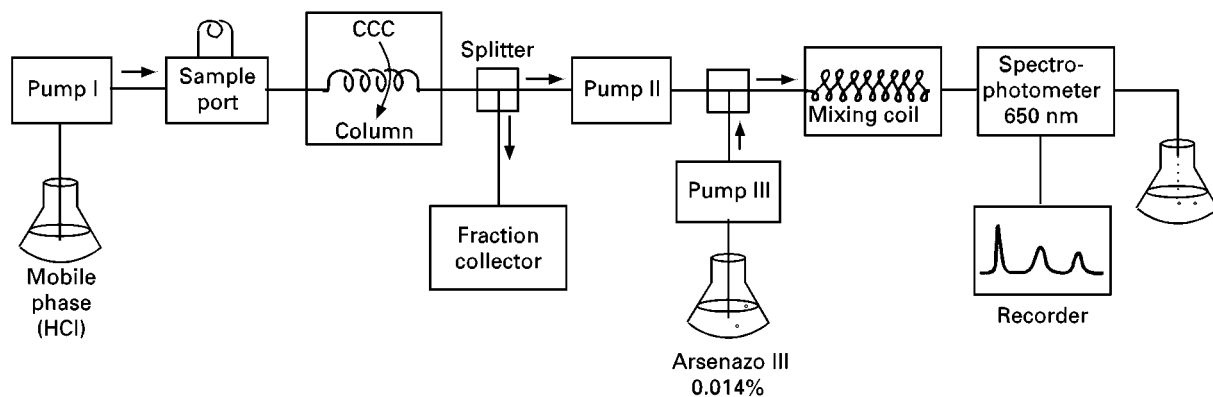


Figure 3 Flow diagram of instrumentation assembly for separation of rare earth elements by HSCCC. CCC, countercurrent chromatography.

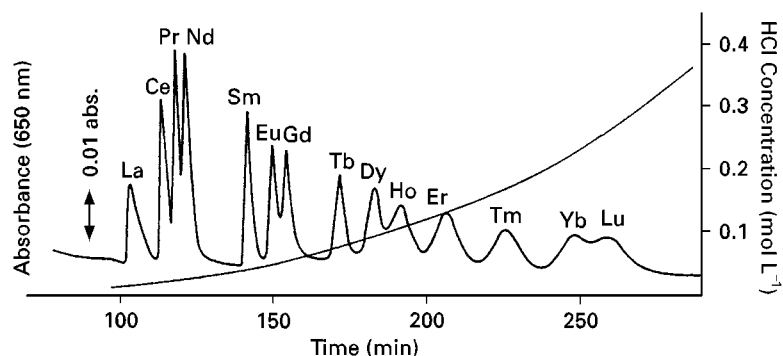


Figure 4 Gradient separation of 14 lanthanides obtained by HSCCC. Apparatus: HSCCC centrifuge with 7.6 cm revolution radius; column: three multilayer coils connected in series, 300 m \times 1.07 mm i.d., 270 mL capacity; stationary phase: 0.003 mol L⁻¹ DEHPA in *n*-heptane; mobile phase: exponential gradient of hydrochloric acid concentration from 0 to 0.3 mol L⁻¹, as indicated in the chromatogram; sample: 14 lanthanide chlorides, each 0.001 mol L⁻¹ in 100 μ L water; speed: 900 rpm; flow rate: 5 mL min⁻¹; pressure: 300 p.s.i.

7 mmol L⁻¹ citric acid at a flow rate of 5 mL min⁻¹. The efficiencies range from 1600 theoretical plates (Ni) to 200 (Cu).

Group Separation of Inorganic Elements

There are numerous methods, such as X-ray fluorescence (XRF), spectroscopy, AAS, AES and ICP-MS, for the determination of trace inorganics including rare earth elements. Of these methods, ICP-AES is one of the most popular for the determination of metals such as Ta, Zr, Hf, etc., including rare earth elements. However, there may be problems with spectral interference because of the many spectral lines. To ensure sufficient precision and accuracy,

especially for the determination of trace elements, separation of matrix elements, which interfere with the determination, must be undertaken. HSCCC has great potential as a separation technique which pre-concentrates trace elements before determination.

Figure 6 shows an example of the quantitative group separation of the rare earth elements from the constituents of rocks, which interfere with the determination of trace elements by ICP-AES. A 0.5 mol L⁻¹ solution of DEHPA in decane was used as the stationary phase. Alkaline, alkaline earth elements and iron(II) were separated from the total amount of rare earth elements at the first stage of the eluent concentration with 0.1 mol L⁻¹ hydrochloric acid. Then the total amount of rare earth elements, including yttrium, was eluted from the stationary

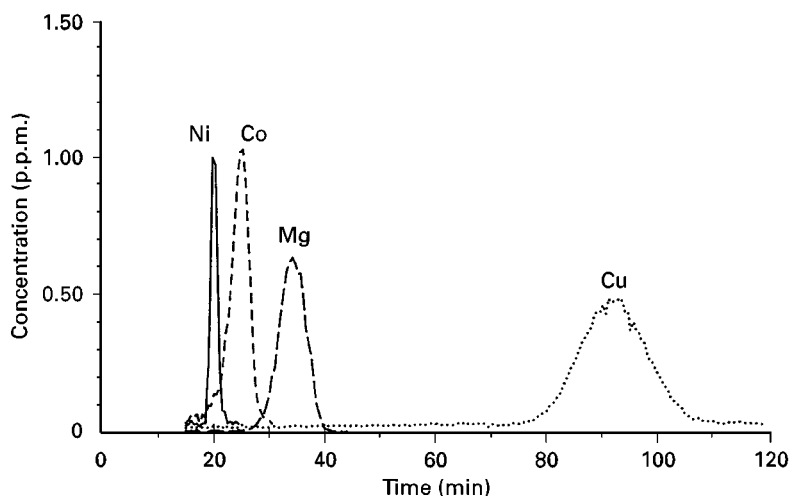


Figure 5 Isocratic separation of nickel, cobalt, magnesium and copper by HSCCC. Apparatus: HSCCC centrifuge with 10.0 cm revolution radius; column: one multilayer coil, 150 m \times 1.6 mm i.d., 300 mL capacity; stationary phase: 0.2 mol L⁻¹ DEHPA in heptane; mobile phase: 7 mmol L⁻¹ citric acid; sample 10 μ g Ni, each 20 μ g Co and Mg, 40 μ g Cu; speed: 800 rpm; flow rate: 5.0 mL min⁻¹; pressure: 140 p.s.i.; observed wavelength: 341.4 nm (Ni), 345.3 nm (Co), 280.2 nm (Mg), 324.7 nm (Cu).

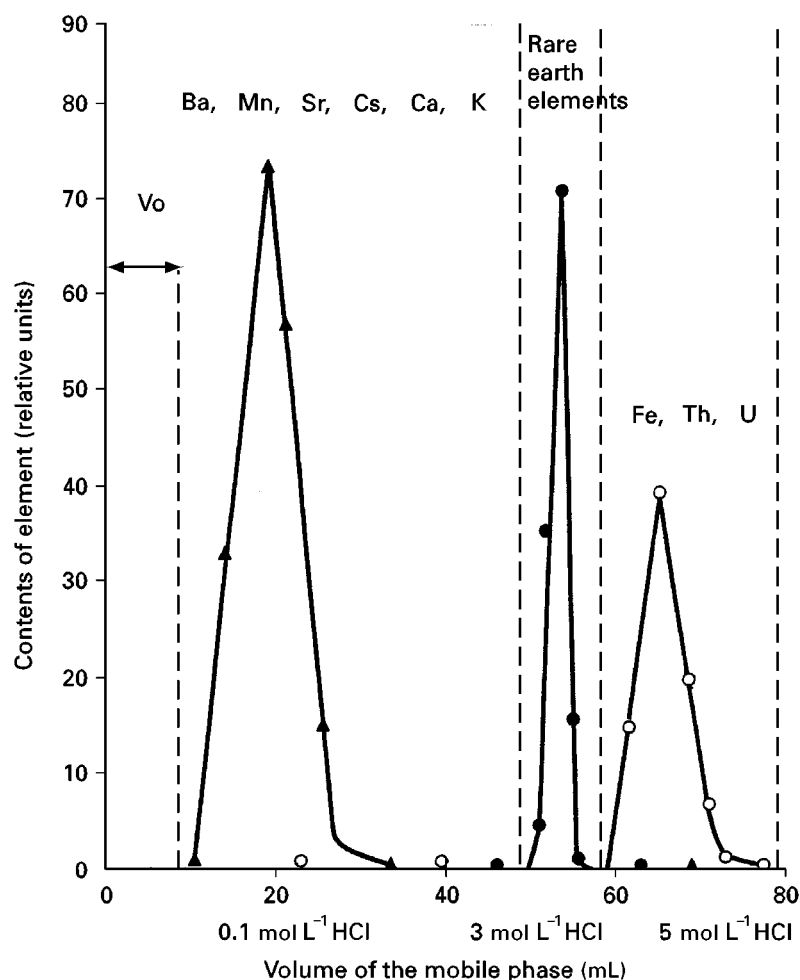


Figure 6 Example of quantitative group separation of the rare earth elements from the constituents of rocks. Apparatus: HSCCC centrifuge with 14.0 cm revolution radius; column: one monolayer coil, 1.13 m \times 1.5 mm i.d., 20 mL capacity; stationary phase: 0.5 mol L⁻¹ DEHPA in decane Kr: 30%; mobile phase: 1–0.1 mol L⁻¹ HCl, 2–3 mol L⁻¹ HCl, 3–5 mol L⁻¹ HCl; sample: Mn 0.3, Fe 6.4, Ca 8.2, Na 4.2, K 4.1 (%) and Ba 440, La 1350, Ce 2290, Nd 760, Pr 239, Sm 97, Eu 18.3, Gd 120, Tb 15, Dy 139, Ho 29, Er 88, Tm 12.5, Yb 71, Lu 8.6, Y 716, Cs 2.6, Sr 307, U 682, Th 940 (p.p.m.); speed: 350 rpm; flow rate: 2.0 mL min⁻¹. Kr, the retained stationary phase volume relative to the total column volume.

phase with 3 mol L⁻¹ hydrochloric acid. To elute other elements, including iron(III), from the stationary phase, 5 mol L⁻¹ hydrochloric acid was introduced into the column. Separation of the mixture was performed within 40 min at a pumping rate of the mobile phase of 2 mL min⁻¹.

Enrichment of Inorganic Elements

Large-scale Enrichment of Inorganics

HSCCC has great potential as an enrichment technique for trace elements before determination. Enrichment prior to determination can overcome problems such as interference, toxic or radioactive samples.

The p.p.b. level of metal ions in a 500 mL of the mobile phase was continuously concentrated into a small volume of the stationary phase retained in the column. Concentrated metal ions were simultaneously eluted with nitric acid and determined by a plasma atomic emission spectrometer. The recoveries of Ca, Cd, Mg, Mn, Pb and Zn were over 88% at the 10 p.p.b. level in 500 mL of the sample solution. The versatility of this method has been further demonstrated by the determination of trace metals in tap water and deionized water.

Rare earth elements have been enriched in a stationary phase of toluene: 2-ethylhexylphosphonic acid mono-2-ethylhexyl ester (EHPA) from a litre of aqueous solution, and eluted with a stepwise pH gradient.

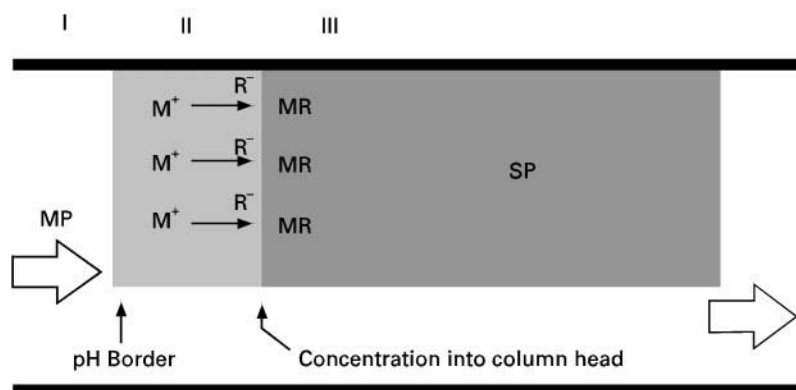


Figure 7 Concentration procedure just after revolving the HSCCC column. I, Mobile phase (MP) with HCl; II, sample with NH_3 ; III, stationary phase (SP) with NH_3 .

Large-scale enrichment is very useful to determine extremely low levels of metals in solution, when a large amount of sample is available.

Enrichment Using the pH-zone Refining Technique

Even if a large volume of sample is not available, enrichment techniques that concentrate trace metals in microlitre samples are sometimes quite useful because modern instrumental methods do not need a large sample size. Moreover, if trace metals separated from their major matrices can be concentrated in an extremely small area of the polytetrafluoroethylene (PTFE) tube in HSCCC, this would be ideal for flow-injection analysis. From this point of view, the recently developed pH-zone refining technique has great potential for enrichment of trace inorganic elements.

In pH-zone refining, a basic organic solution containing a complex-forming reagent such as DEHPA as

a stationary phase is used. After sample introduction into the column, metal ions stay close to the sharp pH border region in the small-bore PTFE tube. Then the trace inorganic ions in the sample are moved by the acid effluent (dilute HCl or HNO_3) to the tail of the column while concentrating in the sharp-moving pH interface, and finally eluted as small fractions containing concentrated inorganic ions.

This concentration procedure is shown in Figures 7 and 8. In Figure 7, sample ion is concentrated into the column head soon after the concentration procedure is started. After the stationary phase and the sample are introduced into the system, HSCCC is started at an appropriate revolution rate, followed by the mobile-phase pump. Metal or inorganic ions (M^+) are concentrated into the column head as MR. Zone III shows the stationary phase, which includes DEHPA and ammonia in an organic solvent such as ether or heptane. Zone II shows a sample phase with the pH adjusted by ammonia. When the column revolution is started, as the organic stationary phase is lighter than

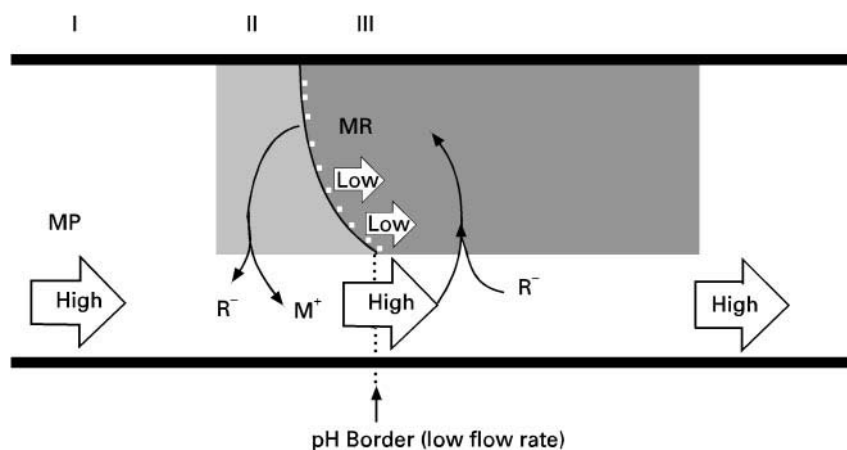


Figure 8 Concentration procedure at the pH interface in the HSCCC column. I, Mobile phase (MP) with HCl; II, stationary phase after being neutralized with HCl; III, stationary phase with NH_3 .

the mobile phase (diluted acid solution), it moves to the head of the column by ASE. The driving force based on ASE increases with the revolution speed of the column. Therefore, the stationary phase can be retained in the column by selecting an appropriate speed of revolution and pump rate, even if the mobile phase is introduced from the head into the column. The retention ratio of the stationary phase to the whole column can be varied from 20 to 70%, but is stable when all conditions including pump or revolution rate are constant. So, the position of the mobile phase is stable in the column when in operation. Inorganic ions (M^+) form complexes with ligand ions (R^-) and are mainly concentrated on the column head, shown as MR in Figure 7. Hydrogen and counter ions of the ligand are not shown in the figure.

Figure 8 shows a concentration procedure in the HSCCC column after all the ions in the sample are extracted on top of the zone III in Figure 7. After Zone II in Figure 7 (sample) has completely passed through the top of the stationary phase, ammonia in the stationary phase begins to be neutralized with hydrochloric acid in the mobile phase. The neutralization area, where reaction between the acid and the base has just finished, is shown as the pH border in Figure 8. The pH border proceeds from left to right. Also the concentrated ions proceed circulating (extracting and back-extracting process in Figure 8) around the pH interface. The rectangular zone (II + III) shows the total stationary phase.

The mobile phase that includes acid solution (hydrochloric acid in Figures 7 and 8) moves at a constant flow rate from the head of the column (left) to the tail of the column (right). The three arrows labelled High show a constant stream of the mobile phase.

As the mobile phase is an acidic solution, it reacts with ammonia in the stationary phase as it proceeds to the tail of the column in Figure 8. The left area (II) in the rectangular zone shows the stationary phase that has been saturated with hydrochloric acid. In the right area (III) in the rectangular zone, ammonia is not yet neutralized with hydrochloric acid. The dark gradation zone between areas II and III shows a pH interface, where the neutralization between acid and base has just finished. As the stationary phase and the mobile phase are mixed well in the HSCCC column, there must be a pH interface in the mobile phase.

The pH interface moves to the right (the same direction as the mobile phase); however, its flow rate is lower than that of the mobile phase because of the delay based on the neutralization. So, concentrated ions shown as MR on the top left of the zone III in

Figure 7 move slowly as shown by the flow rate arrow Low in Figure 8, and circulate around the pH interface by repeating extraction and back-extraction into the stationary phase and the mobile phase, respectively. The flow rate of the pH interface in the mobile phase is shown as the Low arrow in the stationary phase in Figure 8. The flow rate of the pH interface in the mobile phase may be made the same as that in the stationary phase by vigorous mixing in HSCCC column. The pH interface in the mobile phase is shown by the dotted line at the pH border in Figure 8. When the inorganic ions combined with ligand (MR) pass through the pH interface from zone III to zone II in the stationary phase, they are back-extracted into the mobile phase. Then, as the flow rate of the mobile phase is faster than that of the pH interface, the ions (M^+) pass through the pH border (shown by the black dotted line in Figure 8) from left to right in the mobile phase. Just after passing the pH border, the pH is rapidly rising, so, the ions react with the ligand again and are extracted back into the stationary phase. By repeating this cycle, the ions are moved to the tail (right) of the column without diffusion.

In the concentration mechanisms described above, there is no diffusion process observed as in elution procedures with ion exchange or other chromatographic separation methods, such as conventional HSCCC and HPLC. If there is no basic compound such as ammonia in the stationary phase, ions move to the tail with a different flow rate as a function of the distribution ratio between the stationary phase and the mobile phase. Many ions can be separated from each other in this way but because there is no sharp pH interface in the column, concentration is not effected, but only separation with diffusion.

Figure 9 shows the typical concentration results for a 10 p.p.m. solution of cadmium, magnesium and zinc. The injected sample solution contained 50 μg of each in 5 mL of 0.1 mol L⁻¹ tartaric acid solution adjusted to pH 8.8. The mobile phase was pumped at a flow rate of 0.05 mL min⁻¹. Revolutionary speed was 950 rpm. The eluent was collected every 2 min (0.1 mL fractions). The fractions were diluted 1 : 10 with water and the emission intensity for each element was measured by direct current plasma atomic emission spectrometer. The emission intensities for each element were increased 20-fold compared to the original sample solution. The results of this study demonstrate the high performance capabilities of the pH-zone refining technique. Trace elements in the sample solution can be successfully concentrated into a small volume with enormous enrichment.

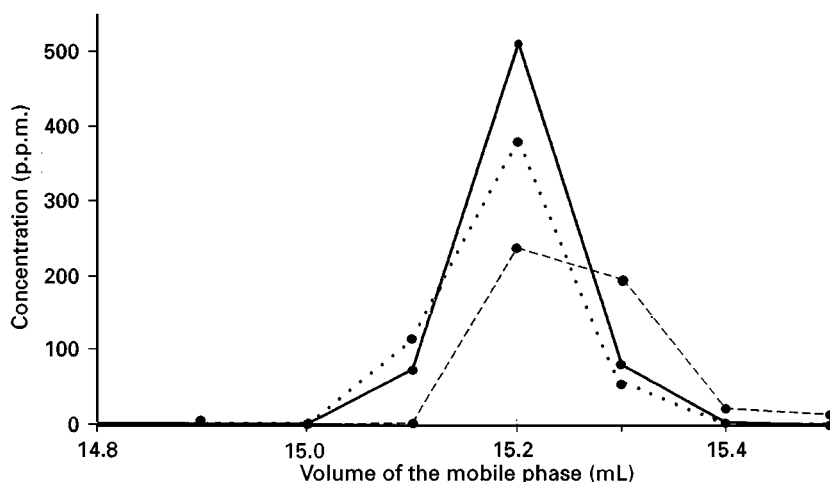


Figure 9 Typical concentration results for 10 p.p.m. solution of cadmium (continuous line), zinc (dashed line), magnesium (dotted line). Apparatus: HSCCC centrifuge with 10.0 cm revolution radius; column: one multilayer coil; sample: 5 mL of each 10 p.p.m. solution (pH 9.25) in 0.1 mol L^{-1} tartaric acid; mobile phase: 0.1 mol L^{-1} HCl saturated with ether; stationary phase: 6 mL of 0.2 mol L^{-1} DEHPA and 0.18 mol L^{-1} ammonia in ether; column: $0.5 \text{ mm i.d.} \times 32 \text{ m}$; flow rate: 0.05 mL min^{-1} ; speed: 950 rpm.

Conclusions

In contrast to HPLC, the unique feature of HSCCC is that there is no solid support in the column. As the distribution abilities including the capacity of the stationary phase are easy to control, HSCCC can be applied to the separation, enrichment and purification of inorganics over a wide range of concentration. In particular, enrichment of trace elements using pH-zone refining technique will be an ideal preconcentration method for subsequent determination by modern instrumental methods. HSCCC can be combined directly with the flow injection technique, and shows great potential for preconcentration of selected desired trace element prior to detection. On-line enrichment and subsequent analysis may thus take the place of conventional sample preparation using a beaker and separating funnel, in future investigations in this field.

See also: **III/Ion Analysis:** Capillary Electrophoresis; Liquid Chromatography; Thin-Layer (Planar) Chromatography.

Further Reading

Conway WD (1990) *Countercurrent Chromatography: Apparatus, Theory and Applications*. New York: VCH.

Fedotov PS, Maryutina TA, Grebneva ON *et al.* (1997) Use of countercurrent partition chromatography for the preconcentration and separation of inorganic compounds: group extraction of Zr, Hf, Nb, and Ta for their subsequent determination by inductively coupled plasma atomic emission spectrometry. *Journal of Analytical Chemistry* 52: 1034–1038.

Ito Y and Conway WD (1995) *High-Speed Countercurrent Chromatography*. New York: John Wiley.

Ito Y and Ma Y (1996) pH-Zone-refining countercurrent chromatography. *Journal of Chromatography A* 753: 1–36.

Kitazume E, Sato N, Saito Y and Ito Y (1993) Separation of heavy metals by high speed counter current chromatography. *Analytical Chemistry* 65: 2225–2228.

Kitazume E, Sato N and Ito Y (1998) Concentration of heavy metals by high-speed countercurrent chromatography. *Journal of Liquid Chromatography* 21: 251–261.

Mandava NB and Ito Y (1988) *Countercurrent Chromatography: Theory and Practice*. New York: Marcel Dekker.

Nakamura S, Hashimoto H and Akiba K (1997) Enrichment separation of rare earth elements by high-speed countercurrent chromatography in a multilayer column. *Journal of Liquid Chromatography A* 789: 381–387.

Liquid Chromatography

C. A. Lucy, The University of Alberta, Edmonton, Alberta, Canada

Copyright © 2000 Academic Press

Introduction

In general, inorganic ions cannot be detected using absorbance spectroscopy or electrochemistry. As a result, determinations of inorganic ions by liquid chromatography (LC) possess many characteristics distinct from determinations of organic compounds by LC. These differences are most noticeable in the detection methodologies used, but also feed back into the column design and operation. This article focuses on the distinct aspects of LC determinations of inorganic ions, and provides an introduction to approved methodologies for inorganic ion analysis. For further reading, the monograph by Haddad and Jackson and the recent special issue of *Journal of Chromatography A* (volume 789) devoted to chromatography of inorganic ions are strongly recommended.

Instrumentation for Inorganic Ion Analysis

General

Figure 1 shows a schematic diagram of a high performance liquid chromatograph (HPLC) for inorganic ion analysis. This instrument is commonly referred to as an ion chromatograph. The most distinguishing difference from a typical HPLC is the post-column reactor. Nonetheless, there are a number of other subtle differences. The pump, injector and tubing are essentially standard HPLC components. The only significant difference is that for inorganic ion analysis these components are generally constructed of metal-free materials, such as poly-

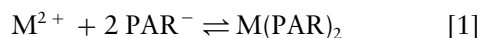
etheretherketone (PEEK). PEEK is extremely chemically inert, flexible, inexpensive and capable of withstanding high pressures.

Column

Separations of inorganic ions are performed using ion exchange. However, classical gel type (polystyrene-divinylbenzene) ion exchangers are not used. Such resins possess too high a capacity and the mass transfer is too slow to allow the low eluent strengths and high separation efficiencies required. Rather, columns for inorganic ion analysis are generally of two types. Firstly, and most commonly, the columns are packed with pellicular particles. Pellicular packings have a solid core with ion exchange sites only on the outer surface of the particle. Alternatively, dynamic ion exchange columns can be prepared from reversed-phase packings (C_{18}) by addition of an ion pair reagent to the mobile phase. In either case the ion exchange capacity of the columns is low, typically 20–200 μeq per column.

Post-column Reactor

As stated above, the most distinguishing feature of an HPLC for inorganic ion analysis is the post-column reactor. Its purpose is to facilitate detection of the inorganic ions. The simplest post-column reaction is the formation of a coloured product which can be measured with a spectrophotometer. For example, transition and lanthanide metal ions (M) can be monitored using post-column reaction with 4-(2-pyridylazo)resorcinol (PAR):



A reagent stream of excess PAR is added to the effluent from the ion exchange column. The

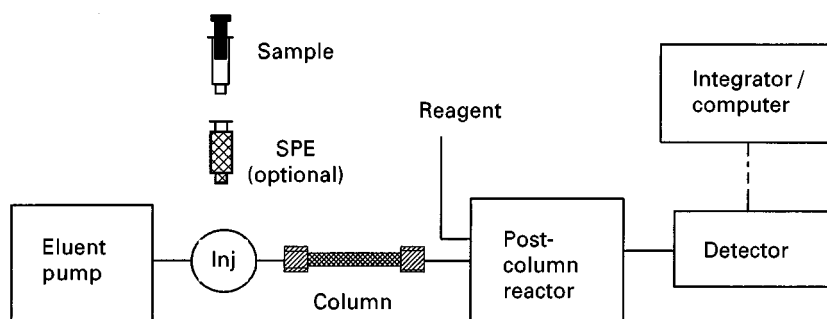
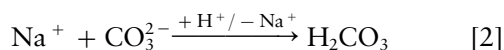


Figure 1 Schematic diagram of a high performance liquid chromatograph for analysis of inorganic ions. SPE, solid-phase extraction.

post-column reaction should ideally be instantaneous, as with PAR, allowing use of a simple T-connector as the post-column reactor. Once the colourless metal ions present are complexed by the PAR, the PAR absorbance undergoes a bathochromic shift. That is, in the absence of metal ions, the PAR reagent absorbs little light at ~ 510 nm, whereas metal-PAR complexes absorb intensely at this wavelength. This absorbance can be directly related to the metal ion concentration.

A more complex post-column reaction is suppression, which is used in conjunction with conductivity detection. All inorganic ions conduct electricity. Thus, conductivity is a universal detector for these species. However, the eluents used in ion exchange chromatography are also conducting. The function of the post-column suppressor is to eliminate (suppress) the background conductivity of the eluent, or at least reduce it to an insignificant level. Typical suppressors are membrane-based, although fibre- and column-based suppressors were used in older systems. The suppression process can be illustrated using the example of the determination of inorganic anions in a sodium carbonate eluent, as is used in Environmental Protection Agency (EPA) Method 300.0 and American Society for Testing and Materials (ASTM) Method D 4327. The membrane in a suppressor for anion chromatography is a cation exchange membrane. Eluent from the column flows on one side of the membrane, while a regenerant flows on the other side. The regenerant is typically H_2SO_4 . H^+ from the regenerant and Na^+ from the eluent freely exchange through the cation exchange membrane. Anions cannot pass through the membrane due to charge repulsion. As a result of exchange of H^+ for Na^+ in the eluent stream, the carbonate eluent is protonated, minimizing the background conductivity.



Carbonic acid is however a weak acid and does undergo some dissociation back to H^+ and HCO_3^- . However, this dissociation only results in a small residual (~ 15 μS) background conductivity. Samples do not possess this background conductivity. Thus, a 'water dip' is observed at the dead volume of the column (0.7 min in Figure 2) when the water from the sample elutes from the column. The weak acid character of carbonic acid can also cause some nonlinearity in calibration curves for inorganic anions when suppressed conductivity detection is used.

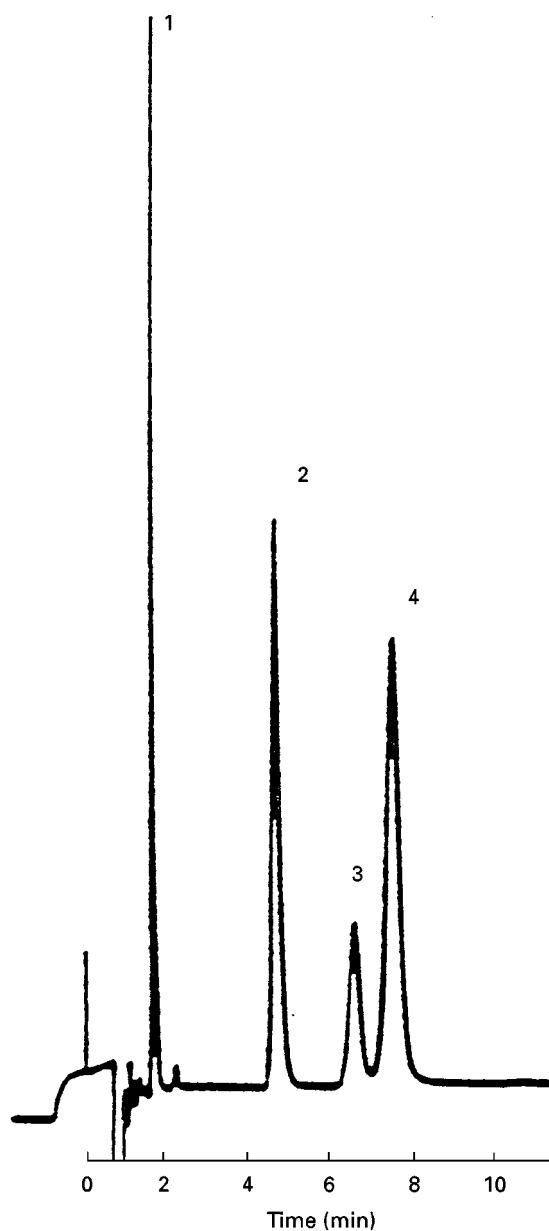


Figure 2 Separation of standard inorganic anions using pre-concentration as per ASTM method D 5542. Peaks: 1, $5 \mu\text{g L}^{-1}$ chloride; 2, $20 \mu\text{g L}^{-1}$ nitrate; 3, $20 \mu\text{g L}^{-1}$ phosphate; 4, $20 \mu\text{g L}^{-1}$ sulfate. Experimental conditions: column, Dionex AS4A; eluent, $0.75 \text{ mmol L}^{-1} \text{ NaHCO}_3/2.2 \text{ mmol L}^{-1} \text{ Na}_2\text{CO}_3$; flow rate, 2.0 mL min^{-1} ; detection, suppressed conductivity; injection volume, 10 mL on to a TAC-1 concentrator column. (Courtesy of ASTM.)

Special Considerations for Inorganic Ion Analysis

Water

Water used in the preparation of standards and eluents for routine determinations should be freshly distilled and deionized, and meet the specifications

for ASTM Type II water ($1 \text{ M}\Omega \cdot \text{cm}$). However, $1 \text{ M}\Omega \cdot \text{cm}$ water may contain up to 200 p.p.b. of any anion. Therefore, for trace anion analyses, ASTM Type I water ($18 \text{ M}\Omega \cdot \text{cm}$) is recommended. Modern deionization systems using nuclear-grade ion exchange resins to polish out inorganic impurities provide water of this grade which contains down to 20 p.p.t. chloride, 100 p.p.t. sodium and 50–60 p.p.t. ammonium.

Eluents

All eluents should be filtered through $0.2 \mu\text{m}$ membranes before use. Many ion chromatographic eluents are excellent growth media for algae. Therefore eluents should be stored at 4°C and not kept for longer than 1 month.

Sample Handling

Many samples possess acidic, alkaline or saline matrices which can disrupt liquid chromatographic determinations of inorganic ions. In such cases it is essential that the matrix components be removed prior to analysis. Solid-phase extraction (SPE) is a convenient means of eliminating such interferents. A SPE device is generally a small column or filter containing a chromatographic medium which fits on

to a sample syringe. Typical SPE cartridges for inorganic ion analysis contain cation exchange resin in the H^+ form to reduce sample pH, in the Ag^+ form to selectively precipitate halides and in the Ba^{2+} form to precipitate sulfate; anion exchange resin in the OH^- form to neutralize acidic samples; and hydrophobic materials such as polystyrene to remove hydrophobic matrix components. Passage of the sample through the SPE and directly into the injector provides a quick and convenient means of eliminating deleterious matrix components.

Methods for Inorganic Ion Analysis

A reliable source of methods for inorganic ion analysis is the approved regulatory methodologies. Table 1 provides a brief summary of approved methods from the US EPA and the ASTM. Other agencies, such as the National Institute for Occupational Safety and Health (US) and the Occupational Safety and Health Administration (US), also have approved methods for determination of air-borne species such as SO_2 , Br_2 , Cl_2 , NO_x and organoarsenics by conversion into aqueous inorganic ions and determination by ion chromatography.

Another rich source of information are vendor application notes. On-line listings of these application

Table 1 Regulatory methods for inorganic ion analysis by liquid chromatography

Method	Analytes ^a	Specified matrices
<i>EPA^b</i>		
218.6	Cr(VI)	Drinking water, groundwater, industrial wastewater effluents
300.0 A	F^- , Cl^- , NO_2^- , Br^- , NO_3^- , HPO_4^{2-} , SO_4^{2-}	Drinking water, surface water, wastewater, groundwater, reagent water, solids (after extraction), leachate
300.0 B	ClO_2^- , ClO_3^- , BrO_3^-	Drinking water and reagent water
300.6	Cl^- , NO_3^- , HPO_4^{2-} , SO_4^{2-}	Wet deposition (rain, snow, sleet, hail)
300.7	Na^+ , NH_4^+ , K^+ , Mg^{2+} , Ca^{2+}	Wet deposition (rain, snow, dew, sleet, hail)
A-1000	Cl^- , SO_4^{2-}	Drinking water
B-1012	NO_2^- , NO_3^-	Wastewater
<i>ASTM^c</i>		
D4327	F^- , Cl^- , NO_2^- , Br^- , NO_3^- , HPO_4^{2-} , SO_4^{2-}	Drinking water and wastewater
D4856	H_2SO_4	Workplace air samples
D5085	Cl^- , NO_3^- , SO_4^{2-}	Wet deposition (rain, snow, dew, sleet, hail)
D5257	Cr(VI)	Waste, drinking and surface waters
D5542 A	Cl^- , HPO_4^{2-} , SO_4^{2-}	High purity water
D5542 B	F^- , acetate, formate	High purity water
E1787	F^- , Cl^- , Br^- , ClO_3^- , NO_3^- , HPO_4^{2-} , SO_4^{2-}	Caustic soda (NaOH) and caustic potash (KOH)

^a Analytes listed in order of elution. Only analytes for which the method has been approved are listed. Other ions may be separated and detected using these methods.

^b EPA refers to the United States Environmental Protection Agency, Environmental Monitoring and Systems Laboratory, Cincinnati, OH 45268 USA. Copies of methods can be obtained from Superintendent of Documents, US Government Printing Office, Washington, DC 20402, USA.

^c STM refers to the American Society for Testing and Materials, 1916 Race Street, Philadelphia, PA 19103-1187 USA (telephone: (215) 299-5400; facsimile: (215) 977-9679). Methods are published in the *Annual Book of ASTM Standards*.

notes are available from a number of companies, such as Alltech Associates, Dionex Corporation, Metrohm and Waters Corporation.

Anions by Suppressed Conductivity

Many of the regulatory procedures listed in Table 1 for standard anions use suppressed conductivity ion chromatography and low capacity (20–35 µeq per column) ion exchange columns. Bicarbonate/carbonate eluents are used for the inorganic acid anions (EPA 300.0 and 300.6; ASTM D4327, D5085, D5542 A and E1787). Figure 2 shows the separation of standard anions using ASTM Method D 5542 with a bicarbonate/carbonate eluent on a Dionex AS4A column. Similar elution orders are observed with

other ion chromatographic columns. However, separation selectivities do vary with the column capacity, hydrophobicity and structure. Thus, the precise eluent concentrations and selectivities depend upon the specific column used.

Method B of the ASTM D 5542 protocol recommends the use of 5 mmol L⁻¹ sodium tetraborate, for separation of fluoride, acetate and formate. These anions are very weakly retained, and so a weak eluent is required to separate them from each other and from the water dip.

Detection limits for these regulatory methods are listed in Table 2. Using a 50 µL injection loop, low parts per billion (p.p.b., µg L⁻¹) are achieved using suppressed conductivity. This equates to less than

Table 2 Performance of regulatory methods for inorganic ion analysis by liquid chromatography with conductivity detection

Ion	Suppressed conductivity		Direct conductivity detection limit (p.p.m.)
	Approved range (p.p.m.)	Detection limit (p.p.m.)	
Direct injection			
Fluoride	0.3–8 ^a	0.01 ^a	0.04 ^b
Chloride	0.8–26 ^a	0.02 ^a	0.02 ^b
Nitrite	0.4–12 ^a	0.004 ^a	0.04 ^b
Bromide	0.6–21 ^a	0.01 ^a	0.06 ^b
Nitrate	0.4–14 ^a	0.002 ^a	0.04 ^b
o-phosphate	0.7–23 ^a	0.003 ^a	0.15 ^b
Sulfate	2.9–95 ^a	0.02 ^a	0.10 ^b
Chlorite ^c	Not stated	0.01	
Bromate ^c	Not stated	0.02	
Chlorate ^c	Not stated	0.003	
Sodium ^d	0.03–1.00	0.03	
Ammonium (as NH ₄ ⁺) ^d	0.03–2.00	0.03	
Potassium ^d	0.01–1.00	0.01	
Magnesium ^d	0.02–1.00	0.02	
Calcium ^d	0.02–3.00	0.02	
Preconcentration ^e			
Fluoride	0–0.014	0.0007	
Acetate	0–0.4	0.007	
Formate	0–0.35	0.006	
Chloride	0–0.024	0.0008	
Phosphate	0–0.04	Not determined	
Sulfate	0–0.6	0.002	

^a From ASTM D5085 and EPA 300.0 A Column, Dionex AS4A; eluent, 1.7 mmol L⁻¹ NaHCO₃/1.8 mmol L⁻¹ Na₂CO₃; flow rate, 2.0 mL min⁻¹; detection, suppressed conductivity; injection volume, 50 µL.

^b From EPA A-1000. Column, Waters IC-Pak Anion; eluent, 1.5 mmol L⁻¹ sodium gluconate/5.8 mmol L⁻¹ boric acid/1.3 mmol L⁻¹ sodium tetraborate/0.5% glycerine/2% butanol/6% acetonitrile (pH 8.5); flow rate, 1.2 mL min⁻¹; detection, direct conductivity; injection volume, 100 µL.

^c From US EPA method 300.0 B. Column, Dionex AS9A; eluent, 1.7 mmol L⁻¹ NaHCO₃/1.8 mmol L⁻¹ Na₂CO₃; flow rate, 1.0 mL min⁻¹; detection, suppressed conductivity; injection volume, 50 µL.

^d From US EPA method 300.7. Column, Dionex CS1; eluent, 0.005 mol L⁻¹ HCl for monovalent ions and 0.005 mol L⁻¹ HCl/0.004 mol L⁻¹ meta phenylenediamine dihydrochloride (MPDA-2HCl); flow rate, 2.3 mL min⁻¹; detection, suppressed conductivity; injection volume, 100 µL.

^e From ASTM D5542. Column, Dionex AS4A; flow rate, 2.0 mL min⁻¹; detection, suppressed conductivity; injection volume, 20 mL on to an AG-4A concentrator column. Eluent, 5 mmol L⁻¹ sodium tetraborate for F⁻, CH₃COO⁻ and HCOO⁻, 0.75 mmol L⁻¹ NaHCO₃/2.2 mmol L⁻¹ Na₂CO₃ for all other ions.

$1 \mu\text{mol L}^{-1}$ concentration in solution, or to less than 1 ng of anion injected. Much lower concentration detection limits can be achieved by preconcentrating the sample onto a small low capacity pre-column. In ASTM Method D5542 (Figure 2), 10 mL of high purity water is concentrated onto a pre-column. Such preconcentration can yield sub-p.p.b. detection limits. At such levels, proper handling of ultra pure water samples is essential to avoid contamination. Appropriate handling procedures are covered in ASTM Method D4453.

Anions by Direct Conductivity

Suppressed conductivity is the most common means of monitoring inorganic anions. However, approved methods also exist which do not use suppression. Rather these procedures measure the conductivity of the column effluent directly. EPA Method A-1000 has been approved for the determination of chloride and sulfate in drinking water. Figure 3A shows the separation achieved using a Waters IC-Pak anion column with a pH 8.5 borate/gluconate eluent.

Detection limits for direct conductivity detection are given in Table 2. In the analysis of drinking waters or other environmental samples with this direct conductivity method, high levels of carbonate, interfering metals (e.g. magnesium and calcium) and excess base may cause baseline disturbances. These interferences can be eliminated using an H^+ form SPE system.

Anions by Absorbance Detection

Anions by direct absorbance detection A number of inorganic anions absorb light in the low UV ($205\text{--}215 \text{ nm}$) range. In such cases it is possible to analyse these anions using a standard high performance liquid chromatograph possessing a UV detector. EPA Method B-1011 describes the analysis of nitrite and nitrate in water using absorbance detection at 214 nm . The molar absorptivity of these ions is quite strong (e.g. $9000 \text{ M}^{-1} \text{ cm}^{-1}$ for nitrate at 210 nm), yielding detection limits of 0.003 and 0.0003 mg L^{-1} for nitrite and nitrate respectively. UV detection provides comparable precision and

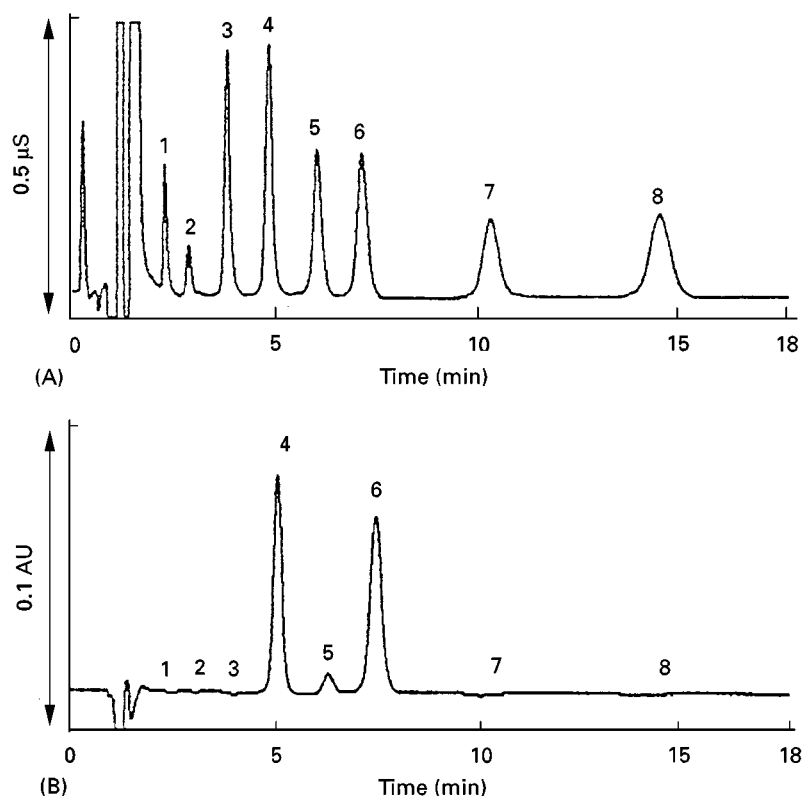


Figure 3 Separation and detection of standard inorganic anions using: (A) direct conductivity detection; (B) direct absorbance detection at 214 nm . Peaks: 1, $1 \mu\text{g L}^{-1}$ fluoride; 2, unknown concentration of bicarbonate (due to contamination by CO_2 in air); 3, $2 \mu\text{g L}^{-1}$ chloride; 4, $4 \mu\text{g L}^{-1}$ nitrite; 5, $4 \mu\text{g L}^{-1}$ bromide; 6, $4 \mu\text{g L}^{-1}$ nitrate; 7, $6 \mu\text{g L}^{-1}$ phosphate; 8, $4 \mu\text{g L}^{-1}$ sulfate. Experimental conditions: column, Waters IC-Pak A HR ($75 \times 4.6 \text{ mm}$; $6 \mu\text{m}$); eluent, borate-gluconate (pH 8.5); flow rate, 1.0 mL min^{-1} ; detection, direct absorbance at 214 nm followed in series by direct conductivity at 35°C ; injection, $100 \mu\text{L}$. (Courtesy of Waters.)

accuracy to suppressed conductivity for nitrate. Other anions such as F^- , Cl^- , ClO_4^- , HPO_4^{2-} and SO_4^{2-} do not absorb significantly above 195 nm, and so do not interfere, as can be seen in Figure 3B.

Other ions which absorb in the UV include Br^- (214 nm; 50 p.p.b. detection limit); BrO_3^- (210 nm; 50 p.p.b.); CrO_4^{2-} ($1600\text{ M}^{-1}\text{ cm}^{-1}$ at 365 nm; < 1 p.p.b.); I^- (226 nm; 50 p.p.b.); and IO_3^- (210 nm; 50 p.p.b.). However, there are no approved methods using UV absorbance detection for these ions.

Anions by indirect absorbance detection Indirect UV absorbance may also be used to detect inorganic anions. In indirect detection, the eluent is a strongly absorbing anion such as phthalate. Within the eluting peak, the analyte anion displaces an equivalent amount of the absorbing eluent anion. Thus, the absorbance decreases as each analyte elutes from the column. Often the leads on the detector are reversed when performing indirect detection, such that the peaks appear positive. Standard anions can be determined in 15 min with low p.p.b. detection limits using 0.8 mmol L^{-1} phthalate at pH 6.8 as eluent and indirect detection at 265 nm.

Post-column reaction detection In EPA Method 218.6 and ASTM Method D5257, hexavalent chro-

mium Cr(VI) is separated from Cr(III) and other reactive metal ions by anion exchange chromatography. Detection is by absorbance at 520 nm after post-column reaction with diphenylcarbohydrazide. This procedure is suitable for monitoring Cr(VI) from 1 to 1000 p.p.b.

Dasgupta has provided an exhaustive review of other methods for post-column reaction detection of anions.

Cations by suppressed conductivity EPA Method 300.7 is currently the only approved procedure for determination of inorganic cations using ion chromatography. This procedure was developed to determine monovalent and divalent cations in precipitation using ion chromatography with suppressed conductivity detection. As indicated in Table 2, detection limits for this procedure are in the low p.p.b. ($\mu\text{g L}^{-1}$) range. Cation exchange with suppressed conductivity is not limited to metal ions. **Figure 4** shows a separation of alkali metals, alkaline earth metals and some volatile amines.

Cations by Direct Conductivity

Alkali metals and alkaline earth metals can be detected using nonsuppressed conductivity detection. Using a

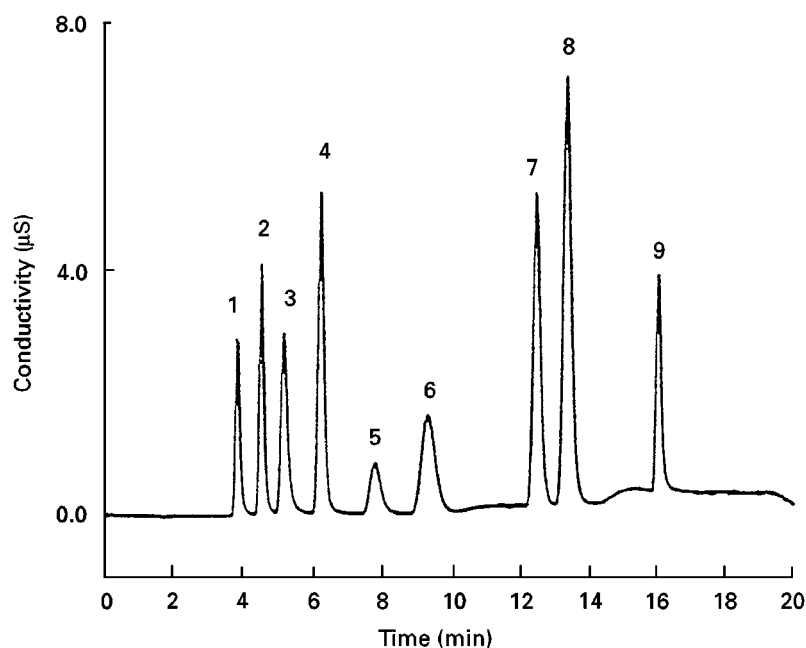


Figure 4 Separation of group I and II cations and volatile amines. Column: 25 cm \times 4 mm, 8–9 μm IonPac CS12A; mobile phase, step gradient of 16 mmol L^{-1} sulfuric acid–4% acetonitrile to 28 mmol L^{-1} sulfuric acid–4% acetonitrile to 50 mmol L^{-1} sulfuric acid–5% acetonitrile; flow rate, 1.0 mL min^{-1} ; detection, conductivity with suppression from a CSRS-II autosuppressor unit; temperature, 40°C . Sample: 1, lithium (0.5 p.p.m.); 2, sodium (2.0 p.p.m.); 3, ammonium (2.5 p.p.m.); 4, potassium (5.0 p.p.m.); 5, morpholine (10.0 p.p.m.); 6, 2-diethylaminoethanol (10.0 p.p.m.); 7, magnesium (2.5 p.p.m.); 8, calcium (5.0 p.p.m.); 9, cyclohexylamine (15.0 p.p.m.). (Courtesy of Dionex.)

3 mmol L⁻¹ HNO₃/0.1 mmol L⁻¹ ethylenediaminetetraacetic acid (EDTA) eluent on a Waters IC-Pak cation M/D column, linear response is observed down to 0.05 p.p.m. for Li⁺, Na⁺, NH₄⁺, K⁺, Mg²⁺ and Ca²⁺ in a 15 min separation. Other alkali metals, alkaline earth metals and amines can also be detected in this fashion.

Inorganic Cations by Absorbance Detection

Cations by direct and indirect absorbance detection

Simple inorganic cations generally cannot be effectively monitored by direct UV absorbance due to their low molar absorptivities. However, metal complexes with complexing ligands such as dithiocarbamates provide high molar absorptivities which yield low p.p.b. detection limits. Furthermore, these hydrophobic complexes can be separated using conventional reversed-phase columns. For instance, pre-derivatization of Ru³⁺, Pt²⁺, Pd²⁺ and Rh³⁺ with diethyldithiocarbamate enables their separation on a standard C₁₈ reversed-phase column with a methanol-water eluent and sensitive (p.p.b.) detection at 260 nm. This approach is most attractive when a post-column reaction detection system cannot be used and for the analysis of precious metals.

Indirect absorbance detection of alkali metals can be performed using eluents such as 4-methylbenzylamine (262 nm) and Cu²⁺ (252 nm). However, the detection limits are inferior to those obtained with suppressed conductivity.

Inorganic cations by post-column reaction detection The most common means of separating the first row transition metals by LC is on reversed-phase

(C₁₈) columns dynamically coated with C₈SO₃⁻ or low capacity ion exchangers. Complexing eluents such as tartrate and pyridine-2,6-dicarboxylate (PDCA) are used. Post-column reaction detection with PAR can be used for a wide range of metal ions including Pb²⁺, Fe³⁺, Cu²⁺, Ni²⁺, Zn²⁺, Co²⁺, Cd²⁺, Mn²⁺, Fe²⁺ and Hg²⁺ with detection limits in the low p.p.b. range for typical injection volumes. This is more than 100 times the sensitivity achievable with conductivity. Figure 5 shows a typical separation of transition metals by HPLC. A number of species (Fe³⁺, Cr³⁺, Sn⁴⁺) elute at the void volume (1.6 min in Figure 5) and so cannot be quantified. Degradation of the peak shape for copper is observed if trace organic acids are present in the water used to prepare the eluent.

High efficiency lanthanide separations are achieved using reversed-phase C₁₈ columns dynamically coated with C₈SO₃⁻ with gradient elution by α -hydroxyisobutyric acid. Elution is in the order of decreasing atomic mass (Lu → La). Post-column reaction detection with Arsenazo III with detection at 658 nm yields 1–5 p.p.b. detection limits using a 20 μ L injection.

Simultaneous separation of transition and lanthanide metals has been achieved based on the charge of the metal-PDCA complexes. Transition metals form monovalent or divalent anionic complexes with PDCA and so can be separated with a PDCA eluent on a Dionex CS5 column. Once all of the transition metals have eluted, the lanthanides, which form strongly retained trivalent anionic complexes with PDCA, are eluted with an oxalate-diglycolate eluent. Detection limits of 20–40 p.p.b. are observed for post-column reaction detection with PAR.

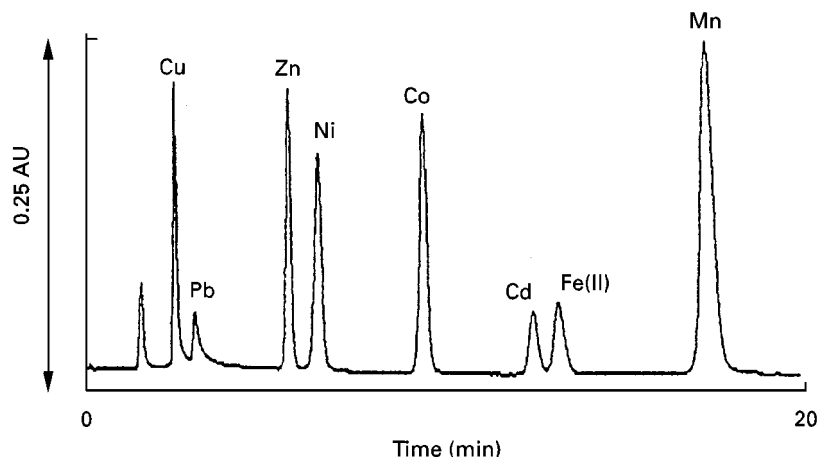


Figure 5 Separation of transition metals with post-column reaction detection. Experimental conditions: column, Waters Delta Pak C₁₈ (10 nm, 5 μ m); eluent, 2 mmol L⁻¹ sodium octanesulfonate, 35 mmol L⁻¹ sodium tartrate, 5% acetonitrile adjusted to pH 3.65 with NaOH; flow rate, 0.8 mL min⁻¹; detection, 500 nm after post-column addition of 0.5 mL min⁻¹ of 0.2 mmol L⁻¹ 4-(2-pyridylazo) resorcinol (PAR), 1 mol L⁻¹ acetic acid, 3 mol L⁻¹ ammonium hydroxide. (Courtesy of Waters.)

See also: II/Chromatography: Liquid: Derivatization; Mechanisms: Ion Chromatography.

Further Reading

- Chauret N and Hubert J (1989) Characterization of indirect photometry for the determination of inorganic anions in natural water by ion chromatography. *Journal of Chromatography* 469: 329–338.
- Dasgupta PK (1989) Postcolumn techniques: a critical perspective for ion chromatography. *Journal of Chromatographic Science* 27: 422–448.
- Haddad PR and Jackson PE (1990) *Ion Chromatography: Principles and Applications*. Amsterdam: Elsevier.
- Henderson IK, Saari-Nordhaus R and Anderson JM (1991) Sample preparation for ion chromatography by solid-

- phase extraction. *Journal of Chromatography* 546: 61–71.
- Krol J, Benvvenuti M and Romano J (1997) *Ion Analysis Methods for IC and CIA® and Practical Aspects of Capillary Ion Analysis Theory*. Milford, MA: Waters.
- Lucy CA (1996) Practical aspects of ion chromatographic determinations. *LC-GC* 14: 406–415.
- Rey MA and Pohl CA (1996) Novel cation-exchange stationary phase for the separation of amines and of six common inorganic cations. *Journal of Chromatography A* 739: 87–97.
- Robards K, Starr P and Patsalides E (1991) Metal determination and metal speciation by liquid chromatography: a review. *Analyst (London)* 116: 1247–1273.
- Romano JP and Krol J (1992) Regulated methods for ion analysis. *Journal of Chromatography A* 602: 205–211.

Thin-Layer (Planar) Chromatography

A. Mohammad, Aligarh Muslim University,
Aligarh, India

Copyright © 2000 Academic Press

Introduction

Thin-layer chromatography (TLC) is a subdivision of liquid chromatography in which the mobile phase (a liquid) migrates through the stationary phase (thin layer of porous sorbent on a flat inert surface) by capillary action. In 1938, two Russian workers, Izmailov and Schraiber, separated certain medicinal compounds on binder-free horizontal thin layers of alumina spread on a glass plate. Since the development was carried out by placing solvent drops on the glass plate containing sample and sorbent, their method was called drop chromatography. This method remained unnoticed for 10 years until two American chemists, Meinhard and Hall, used a mixture of aluminium oxide (adsorbent) and celite (binder) in a layer on a microscope slide to separate Fe^{2+} from Zn^{2+} . They called this technique surface chromatography and this was the first application of planar chromatography to the separation of inorganic ions. The real impetus for advancement of TLC started in 1951 with the work of Kirchner and his associates. Stahl introduced the term thin-layer chromatography in 1958 and standardized procedures, materials and nomenclature. The rapid growth of TLC slowed down during the 1970s with the rise in popularity of high performance liquid chromatography (HPLC) and ion chromatography (IC). However, recent improvements in TLC have removed many of its limitations.

High performance TLC (HPTLC) layers, being thinner and made of more uniform particle size sorbents, provide faster separations, reduced zone diffusion, lower detection limits, less solvent consumption and better separation efficiency. The distinct advantages of TLC over HPLC have been identified as low solvent consumption, low operational cost, easier sample preparation, more rapid throughput, greater detection possibilities and the use of disposable plates. TLC permits the simultaneous analysis of many samples in the same time required for one HPLC analysis and samples and standards are analysed by TLC under exactly the same conditions rather than serially, as in HPLC. Typically, 18–36 samples can be run on a single HPTLC plate with a development time of 3–20 min over a migration distance of 2–7 cm. However, the influence of environmental conditions on the reproducibility of R_F values and poor separation efficiency have been major disadvantages of TLC compared with HPLC and gas chromatography (GC).

TLC can be used for *qualitative* analysis, to identify the presence or absence of a particular substance in a mixture; *quantitative* analysis, to determine precisely and accurately the amount of a particular substance in a sample mixture; and *preparative* analysis, to purify and isolate a particular substance for subsequent use. All three applications require the common procedures of sample application, chromatographic separation and component visualization. However, analytical TLC differs from preparative TLC in that volumes and/or weights of samples are applied to thicker layers in the latter case.

Inorganic TLC

Though the first published reports on TLC described the separation of inorganic species, the importance of inorganic TLC did not receive recognition until the beginning of the 1960s when Seiler separated inorganic substances. After the work of Seiler, TLC of metal ions received a great impetus. Some of the major fields in which inorganic TLC has found applications include the analysis of biological, food, geological, industrial, pharmaceutical, soil, water and industrial waste water samples. The purpose of this article is to present briefly the current state-of-the-art procedures of TLC/HPTLC as applied to the analysis of inorganic ions.

Procedure

TLC is an offline process in which various steps are carried out independently (Figure 1). The basic TLC procedure involves the spotting of sample mixture (5–10 μL for conventional TLC and 1–2 μL for HPTLC) at about 1.5–2 cm above the lower edge of the layer, drying the spot completely at room temperature or at an elevated temperature, development of the plate, usually by one-dimensional ascending technique in a closed chamber (cylindrical or rectangular) to a distance of 8–10 cm, removing the plate from the developing chamber, removal of mobile phase from the layer by drying, detection of spots on the plate using a suitable detection reagent/procedure, measurement of R_F values of resolved spots and determination of the separated analyte. The differential migration of components in a mixture is due to varying degrees of affinity of the components for the stationary and mobile phases.

Sample Preparation

The sample solution to be analysed must be sufficiently concentrated to provide clear detection and/or be pure enough so that it can be separated as a discrete and compact zone. For low concentrations of analyte in a complex sample, preconcentration and clean-up procedures must frequently precede TLC.

Metal solutions are generally prepared by dissolving their corresponding salts in distilled water or 0.1 mol L⁻¹ HCl (or HNO₃) to a final metal concentration of 0.1–0.2 mol L⁻¹. Rare earth oxide solutions are prepared by fusion followed by dissolution in 0.5–6 mol L⁻¹ HNO₃ and anion solutions in distilled water, dilute acid or alkali are prepared from sodium, potassium and ammonium salts of the corresponding acids. Metal complexes are used as freshly

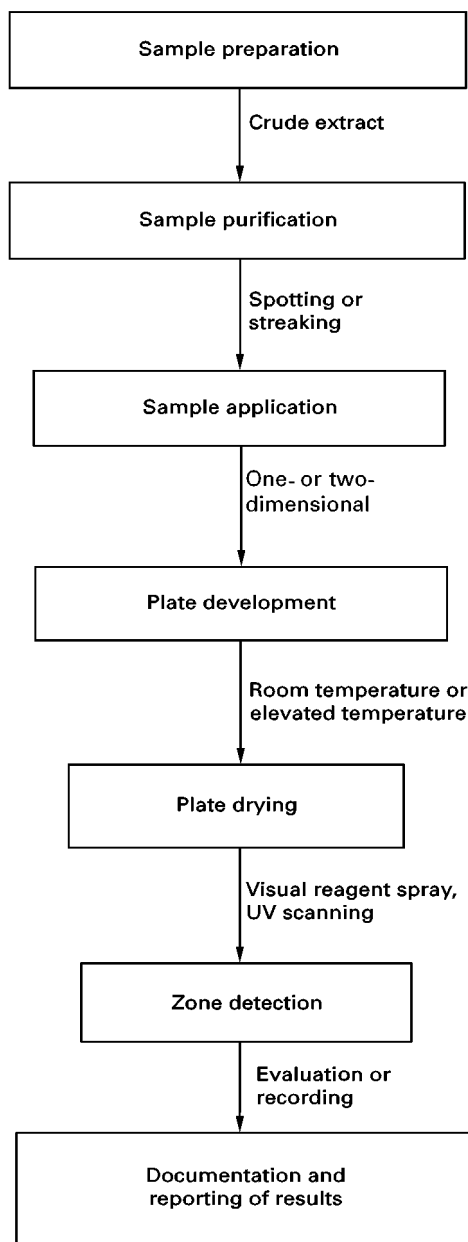


Figure 1 Schematic diagram showing the steps involved in a TLC process.

prepared solutions in ethanol, acetone, chloroform or distilled water. Specific standard methods are followed for sample preparation to identify and determine metal ions in biological, environmental, alloys, plants, foods, textile and geological samples.

TLC Plate Preparation

The current trend is to use commercially available pre-coated plates. The manual preparation of layers involves the coating of a slurry of the adsorbent (silica

gel, alumina, etc.) on to glass, aluminium or plastic sheets (20×20 or 20×10 cm) with the help of an applicator. The thickness of the dried layer of analytical purposes is kept to 0.1–0.3 mm. A binder (starch, gypsum, dextrin, polyvinyl alcohol) is usually added to the adsorbent to provide better adhesion, mechanical stability and durability. The addition of a fluorescent indicator compound is optional. Compared to conventional TLC, HPTLC layers are produced from sorbents of smaller and more uniform particle size (5–10 μm instead of 10–20 μm).

Sample Application

Definite volumes of samples are applied as spots or streaks using a micropipette, microsyringe or glass capillaries. A number of automatic spotters of various designs are available for sample application. The nano-applicator (Nanomat) is an example of a micrometer-controlled syringe which has a dynamic volume range of 50–230 nL. Another applicator (Linomat) allows sample application in narrow bands by a spray-on technique. The application of a sample as a streak or band provides more efficient separations because the efficiency of the separation on a TLC plate depends on the diameter of the spot along the direction of development. Thus, the best efficiency is achieved with the smallest diameter spot. Alternatively, the use of TLC plates with concentration zones converts the sample from the original spot into a band or streak. These plates consist of a bottom layer (2–2.5 cm) of a chromatographically inactive adsorbent (e.g. Kieselguhr) followed by the layer of an active adsorbent (silica or bonded silica). The advantages of sample application as a streak and the use of TLC plates with concentration zones are illustrated in Figure 2. The general aspects

of a sample application have been reviewed by Jaenchen.

Development Techniques

The migration of the mobile phases through the stationary phase (or sorbent layer) to effect separation of samples is called development. One-dimensional ascending development is the most commonly used mode in inorganic TLC. Other development techniques, such as multiple, stepwise, circular and two-dimensional development, have also been used to a limited extent. The migration distance for the mobile phase is kept to 10–12 cm for conventional TLC and 2–6 cm for HPTLC. Dzido has described the variants of the development techniques.

Chromatographic Systems

A combination of stationary and mobile phases constitutes a chromatographic system. The proper selection of stationary and mobile-phase conditions determines the effectiveness of a separation.

Stationary Phase (Layer Sorbent)

Many materials have been used as stationary phase in inorganic TLC but silica gel, an amorphous and porous adsorbent, has been the most favoured material, followed by alumina and cellulose. Thin layers of silica gel G (gypsum binder) and S (starch binder) with or without fluorescent indicator are frequently used. Silica gel is slightly acidic in nature and the silanol groups (Si–OH) can interact with solute molecules. On the other hand, alumina (aluminium oxide) is basic and more reactive than silica gel. Adsorption is the separation mechanism with both alumina

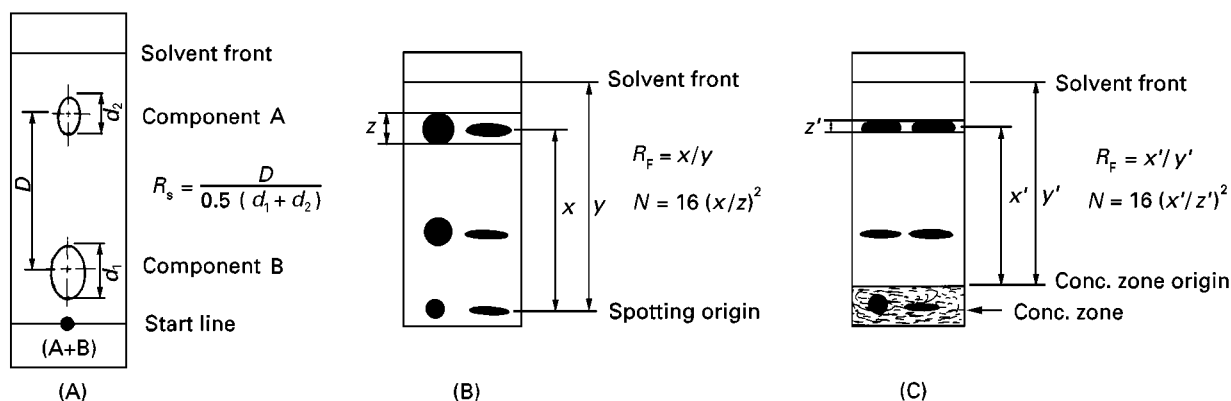


Figure 2 (A) Resolution of a two-component mixture on a TLC plate; (B) improved efficiency due to streaking; and (C) utility of concentration zone as a promoter of efficiency.

and silica gel. Cellulose, an organic material, is used as a sorbent to perform separations with increased sensitivity of detection and decreased development time compared to paper chromatography. The various layer materials may be broadly classified as:

1. nonsurface-modified or untreated sorbents;
2. impregnated or treated sorbents (organic and inorganic impregnants);
3. bonded or chemically modified sorbents (hydrophobic modified or reversed-phase and hydrophilic modified);
4. inorganic ion exchangers;
5. mixed sorbents.

More detailed information on pre-coated layers and sorbents that are commonly used in TLC is available elsewhere (see Further Reading).

The selective application of these different types of layer materials in inorganic TLC is summarized below.

Anions Silica gel, silica gel silica impregnated with fluorescein or inorganic salts, silica gel + antimonite acid/alumina/hydrous antimony(V) oxide/Zr(IV) molybdate, Sephadex, microcrystalline cellulose, surface-modified cellulose, cellulose + Kieselguhr/alumina, Kieselguhr, alumina, kaolin, hydrated stannic oxide and polyamide have all been used for the separation of anions.

Metal ions and rare earth elements The various layer materials used for the separation of metal ions, metal complexes and rare earth elements (REE) may, broadly, be classified as follows.

Nonsurface modified or untreated sorbents These include silica gel, alumina, cellulose, polyamide, polyacrylonitrile, Sephadex and Kieselguhr. Layers of chitin and its deacetylated derivative chitosan have been used to separate metal ions.

Impregnated or treated sorbents In general, silica gel impregnated with aqueous salt solutions, high molecular weight amines, organophosphorous compounds and organic chelating agents has been widely used for the separation of metal ions and REE. Metal complexes have been separated on silica gel impregnated with chlorobenzene, *p*-toluidine or surfactants and on layers of egg shell powder impregnated with Triton X-100.

Bonded or chemically modified sorbents Lipophilic C₁₈-bonded silica gel for REE and metal complexes, aminopropyl silica gel (NH₂) and octadecyl silica gel

(C₁₈) for lanthanide complexes of tetraphenyl porphyrin and surface-modified cellulose as well as cellulose derivatives for several metal ions have been used.

Mixed sorbents Combinations of silica gel and microcrystalline cellulose for noble metal ions and transition metal chlorosulfates, silica gel and microcrystalline cellulose containing ammonium nitrate for REE and silica gel and inorganic ion exchange gel mixtures for transition metal ions have been used.

Other sorbents Synthetic inorganic ion exchangers, porous glass sheets, soil and soil-flyash mixture, polychrome A, carbamide-formaldehyde copolymer and immobilized analogue of dibenzo-18-crown-6 on silica support for metal ions and diatomite for REE have also been used, but to a lesser extent.

The adsorbents in different forms (untreated, impregnated, chemically modified or mixed) preferred in the analysis of inorganic ions since 1973 are shown in Table 1.

Anions Silica gel > cellulose > alumina > inorganic ion exchangers > Kieselguhr > polyamide.

Cations/metal ions Silica gel > cellulose > inorganic ion exchangers > alumina > chitin and chitosan > diatomite > soil.

Metal complexes Silica gel > alumina > cellulose > polyacrylonitrile > Sephadex = polyamide.

The salting-out efficiency of mixed aminocarboxylate Co(III) complexes obtained on different adsorbents shows the sorbent precipitation in the order (with small discrepancies) polyacrylonitrile > cellulose > silica gel. Polyacrylonitrile is the most suitable sorbent for the separation of complexes. The HPTLC results of rare earth-tetraphenylporphyrin complexes show an increase in *R_F* values in the order of the atomic number on NH₂-bonded silica plates and a reverse trend, i.e. decrease in *R_F* values, with an

Table 1 Number of publications (%) on some sorbent layers appearing from 1973 to 1996

Layer material	Per cent publications		
	Metal ions	Metal complexes	Anions
Silica gel	49.6	75.6	50.5
Alumina	6.4	10.7	9.3
Cellulose	29.3	4.8	29.3
Inorganic ion exchanger	10.0		4.0
Chitin and chitosan	2.0		
Polyacrylonitrile		4.8	
Polyamide		~1.0	1.3

increase in atomic number is obtained on C₁₈-bonded silica layers.

Mobile Phase (Solvent System)

With a particular sorbent layer, the separation possibility of a complex mixture is greatly improved by the proper selection of the mobile phase. Mixtures of organic solvents containing an aqueous acid, base or a buffer are, in general, well suited for the separation of ionic species whereas anhydrous organic solvents are more useful for separating nonionic species. The following mobile phases have been used for inorganic TLC.

Inorganic solvents This includes solutions of mineral acids, bases, salts and mixtures of acids, bases and/or their salts.

Organic solvents This includes acids, bases, hydrocarbons, alcohols, amines, ketones, aldehydes, esters, phosphates and their mixtures in different proportions.

Mixed aqueous-organic solvents This includes organic solvents mixed with water, mineral acids, inorganic bases or dimethyl sulfoxide and buffered salt solutions.

Complexing solvents Solutions of surfactants (sodium dodecyl sulphate (SDS), cetyltrimethylammonium bromide (CTAB), Triton X-100) and ethylenediaminetetraacetic acid.

TLC with mobile phases of lower volatility gives better reproducibility compared to volatile mobile phases, although the latter have the advantage of quick evaporation from the sorbent layer after development.

Visualization

For the visualization of separated zones, physical, chemical or biological detection methods are commonly used. The physical detection methods are based on substance-specific properties and the most commonly employed methods of this group include the absorption or emission spectrophotometry, autoradiography and X-ray fluorescence. The chemical methods of detection involve spraying reagents capable of forming coloured compounds with the separated species on the plate or exposing the plate to vapour. Alternatively, the reagent can be incorporated in the mobile phase or in the adsorbent. In some cases, detection is completed by inspecting the TLC plate under ultraviolet light, after spraying with

a suitable reagent, or by exposing the plate to ammonia vapour. Bioautographic analysis, reprint methods and enzymatic tests can also be applied for detection purposes. Immunostaining and flame ionization detection methods have also been reported.

The detection methods and reagents used in inorganic TLC are summarized below.

Metal Ions

In addition to using conventional detection reagents such as dithizone, dimethylglyoxime, potassium ferrocyanide and 8-hydroxyquinoline, for cations, new reagents such as sulfochlorophenol azorhodamine, phenolazotriaminorhodamine and benzolazobenzol-azorhodamine have been proposed for selective detection of toxic heavy metals at nanogram levels. Radiometry is used to detect Pr(III), Pr(IV) and Tb(III). An elegant fluorescent method for the detection of Mg, Al, Ca, V, Cu, Zn, Ge, Y, Zr, Mo, Ag, Cd, In, La, Ce, Eu, Tb, Tl, Pb, and Bi at $3-3 \times 10^{-6}$ μmol levels has been reported whereby these cations are detected as coloured fluorescent zones generated simply on heating the chromatograms on porous glass sheets at 100–700°C for 15 min. Typical representative fluorescence spectra are shown in Figure 3.

Anions

For the detection of anions, saturated silver nitrate solution in methanol, 0.2–0.5% diphenylamine solution in 4 mol L⁻¹ H₂SO₄, 1% aqueous solution of potassium ferrocyanide, 0.5% alcoholic solution of pyrogallol, 10% FeCl₃ solution in 2 mol L⁻¹ HCl, 1% KI in 1.0 mol L⁻¹ HCl and mixture of aqueous KSCN and SnCl₂ in 1.0 mol L⁻¹ HCl, ammoniacal AgNO₃, aqueous bromocresol green, FeSO₄ + FeCl₃, alizarin, alizarin-zirconium lake, benzidine solution, (NH₄)₂ MoO₄ + SnCl₂ and 0.1% bromocresol purple containing dil. NH₄OH have been used. Autoradiography, scintillation counting and radiometric detection methods have also been applied. Several anions are detected on the basis of quenching effects: dark spots of the anions appeared on the bright greenish fluorescent background when the chromatograms are sprayed with aluminium(III)-morin fluorescent complex (prepared by dissolving 5 mg AlCl₃ and 5 mg of 2',3,4',5,7-pentahydroxyflavone (morin) in a mixture of 10 mL 30% CH₃COOH, 20 mL 98% ethanol and 20 mL water). The detected anions are IO₃⁻, IO₄⁻, CrO₄²⁻, PO₄³⁻, Cr₂O₇²⁻, NO₂⁻, NO₃⁻, SO₄²⁻, SO₃²⁻, Fe(CN)₆³⁻, Fe(CN)₆⁴⁻, and BrO₃⁻ (strong violet spots), F⁻, Cl⁻, Br⁻, I⁻, S²⁻, S₂O₃²⁻, VO₃⁻, VO₄³⁻, and MoO₄²⁻ (medium blue spots) and ClO₂⁻, ClO₃⁻, ClO₄⁻, SCN⁻ and WO₄²⁻ (weak yellow spots). Several anions producing intense blue colour with

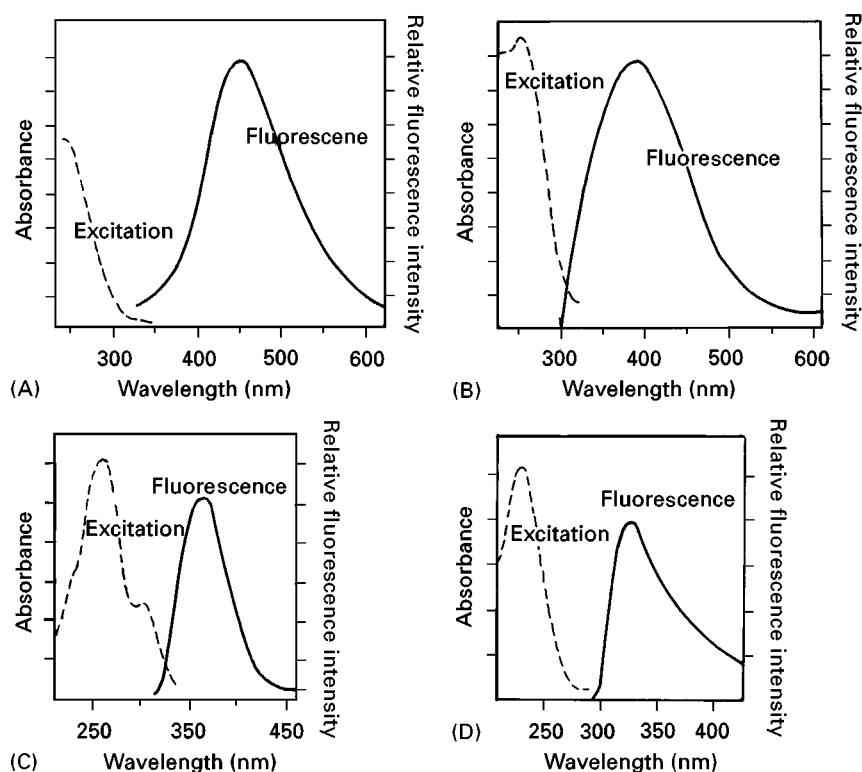


Figure 3 Fluorescence spectra of (A) copper, (B) lead, (C) cerium and (D) thallium ions heated on porous glass sheet. (Reproduced with permission from Yoshioka M *et al.* (1992) Fluorescence reactions of inorganic cations heated on a porous glass sheet for thin-layer chromatography. *Journal of Chromatography* 603: 223–229.)

0.2% Ph_2NH in H_2SO_4 are detected down to $0.1\ \mu\text{g}$ on silufol layers. Halides have been detected with alizarin-zirconium lake and AgNO_3 .

Rare Earth Elements

The REEs have been detected by first, spraying the plate with 0.1% arsenazo(III) solution and then with aqueous ammonia followed by gentle heating; second, heating at 70°C for 10 min after spraying with 0.02% chlorophosphonazo solution; and third, exposure of the plate to NH_3 after spraying with tribromochlorophosphonazo or xylenol orange solution. Saturated ethanolic solution of alizarin and dilute solutions (0.2–1%) of tribromoarsenazo have been used to detect REE.

Metal Complexes

Most of the complexes being coloured are visible without further treatment, e.g. $\text{Fe}(\text{phen})_3^{2+}$; $\text{Fe}(\text{bpy})_3^{2+}$; metal glyoxaldithiosemicarbazone; thiocarbonate complexes of Cu, Ni and Co; anil complexes of Cu, Mn, Fe and Zn; metal chelates of V, Co, Cr, Ni and Mn with 2,2'-dihydroxy-5,5'-dimethylazobenzene; trifluoroacetylacetonates of rare

earths; metal xanthates; metal chelates of 1-hydroxyphenazine; metal diethyldithiocarbamate complexes; metal dithizonates; transition metal monothio- β -diketonates; dithioacetylacetone; metal acetothioacetanilide. Metal oxinates, some geometrical isomeric complexes of Rh, Pt and Co, methylbenzylthiocarbonate metal chelates, Cu(II) carboxylates and Co (gly) are self-coloured but located under ultraviolet light. Trisethylenediamine Co(III) complexes are detected with sodium sulfide solution. β -Diketonates of Fe, Cr and Co, organotin compounds, alkali metal xanthates and piperidine dithiocarbamate complexes can be detected with iodine vapour. A fluorometric method has been used for the detection of heavy metal complexes with pyrene-substituted *N*-acylthiourea. Sometimes spots are detected by spraying coloured reagents such as pyrocatechol violet and copper sulfate as well as by immersing the TLC plates in a dilute solution of phenylfluorone reagent. *N,N*-diethyl-*N'*-benzoylthiourea-metal chelates have been detected by graphite furnace atomic absorption spectrometry and by UV detection. These techniques permit the sensitive detection of enriched platinum metals with detection limits in the nano- and picogram range (Table 2).

Table 2 Absolute detection limits for *N,N*-di ethyl-*N'*-benzoyl-thiourea chelates in chromatography

Element	HPTLC (ng)	HPLC (ng)	λ (nm)
Ru	0.22	10.018	275
Rh	0.21	10.006	261
Pd	0.08	10.008	274
Os	0.46	10.021	244
Ir	0.22	10.042	252
Pt	0.25	10.010	249

Data from Sehuster M (1992) Selective complexing agents for the trace enrichment of platinum metals. *Fresenius Journal of Analytical Chemistry* 342: 791–794.

Qualitative Analysis

Identification

In TLC the identification of separated compounds is primarily based on their mobility in a suitable solvent which is described by the R_F value of each compound, where:

$$R_F = \frac{\text{distance of spot migration from the origin}}{\text{distance of solvent front from origin}}$$

The factors which influence the magnitude of the R_F include the nature of the sorbent, layer thickness, activation temperature, chamber saturation, nature of the mobile phase, pH of the medium, room temperature, sample volume, relative humidity and mode of development. Another term, R_M , which is the logarithmic function of the R_F value, i.e. $R_M = \log(1/R_F - 1)$, is more useful as it bears a linear relationship to some TLC parameters or structural elements of the analyte. However, in cases of continuous and multiple development, where the solvent front is not measured, the term R_X :

$$R_X = \frac{\text{distance travelled by solute}}{\text{distance travelled by standard}}$$

is used.

If the retention data (R_F , R_M , or R_X values) of the compound to be identified are identical with those of the reference substance in three different solvent systems but on the same stationary phase or with the same solvent but on three different types of stationary phases, the two compounds can be regarded as identical with a good probability. However, for correct identification the chromatographic retention data are not enough and at least one spectroscopic method is necessary.

Table 3 hR_F ($R_F \times 100$) values, standard deviation (SD) of R_F values of metal ions present in industrial wastewater and dilution limits of metal ions in standard spiked water

Metal ion	hR_F value	SD of R_F value	Detection limit (μg)
Pb^{2+}	00	34×10^{-4}	7.78
Cd^{2+}	62	44×10^{-4}	6.00
Zn^{2+}	70	12.2×10^{-3}	0.46
Cu^{2+}	97	26×10^{-4}	5.23
Co^{2+}	97	12.4×10^{-3}	7.40
Ni^{2+}	97	58×10^{-4}	3.22

Stationary phase: silica gel G; mobile phase: 1.0 mol L⁻¹ sodium formate + 1.0 mol L⁻¹ KI (1 + 9). (Reproduced with permission from Mohammad A (1995) Identification, quantitative separation and recovery of copper from spiked water and industrial wastewater by TLC-atomic absorption and TLC-titrimetry. *Journal of Planar Chromatography – Modern TLC* 8: 463–466.)

Separation

The separated components of a mixture are detected and their R_F values recorded from the values of R_L (R_F of leading front) and R_T (R_F of trailing front). Some of the basic requirements for a good separation are (a) each spot should be compact ($R_L - R_T \leq 0.3$), (b) the difference in R_F values of two adjacent spots should be at least 0.1, (c) no complexation should occur between/among separable species and (d) chromatography of reference compounds and the

Table 4 Separation of thorium from uranium in presence of common anions

Anions	ΔR_F	K_{Th}	α	R_S
I^-	0.50	1.22	24.40	2.56
IO_3^-	0.41	0.96	10.60	2.34
Br^-	0.51	1.27	25.40	2.62
BrO_3^-	0.40	1.00	9.09	2.22
NO_3^-	0.40	1.00	9.09	2.00
Cl^-	0.48	1.38	27.60	2.74
SCN^-	0.25	0.54	4.91	1.25
S^{2-}	0.30	0.66	6.00	1.20

ΔR_F = Difference in the R_F values of UO_2^{2+} and Th^{4+} . K_{Th} = Capacity factor of Th^{4+} [$K_{Th} = (1 - R_F)/R_F$ for thorium]. α = Separation factor ($\alpha = K_{Th}/K_{UO_2}$). R_S = Resolution for the separation of Th^{4+} from UO_2^{2+} . [$R_S = D/0.5(d_1 + d_2)$]: D = distance between the centres of separated spots of Th^{4+} and UO_2^{2+} whereas d_1 and d_2 are their respective diameters. Stationary phase: silica gel; mobile phase: dimethylamine–acetone–formic acid (2 + 6 + 2, v/v). Reproduced with permission from Mohammad A and Fatima N (1988) A new solvent system for the separation of Th^{4+} , UO_2^{2+} and Zr^{4+} in the presence of common anions by thin layer chromatography. *Chromatographia* 25: 536–538.

Table 5 Separation of Zn–Cd–Hg mixture in spiked environmental samples

Metal ion	R_F values of separated ions			
	Seawater	Industrial wastewater	River water	Soil
Cd^{2+}	0.79	0.81	0.81	0.80
Hg^{2+}	0.96	0.90	0.96	0.98
Zn^{2+}	0.10	0.11	0.11	0.12

Stationary phase: silica gel G impregnated with 0.1% thorium nitrate; mobile phase: 1.0 mol L⁻¹ aqueous solution of sodium formate (pH 7.65). The presence of pesticides (malathion, carbaryl, carbofuran, bavistin and 2,4-dichlorophenoxy acetic acid) and anions (Cl^- , Br^- , I^- , SCN^- , MoO_4^{2-} and CrO_4^{2-}) did not hamper the separation of Zn^{2+} from Hg^{2+} and Cd^{2+} . Reproduced with permission from Mohammad A and Majid Khan MA (1992) *Proceedings of National Conference on Clean Environment Strategies, Planning and Management*. Lucknow, India, pp. 191–193. Lucknow: Legend India Environment Protection Pvt. Ltd.

mixture should be performed under identical experimental conditions. Selected examples of TLC/HPTLC separation of inorganic ions are given in Tables 3–5 and Figures 4–10. Bonded silica C₁₈ reversed-phase layers in combination with a methanol–lactate medium as mobile phase have been found to be most suitable for the separation of adjacent rare earths of middle atomic weight group (Figure 4). Carbamide–formaldehyde polymer (amino-

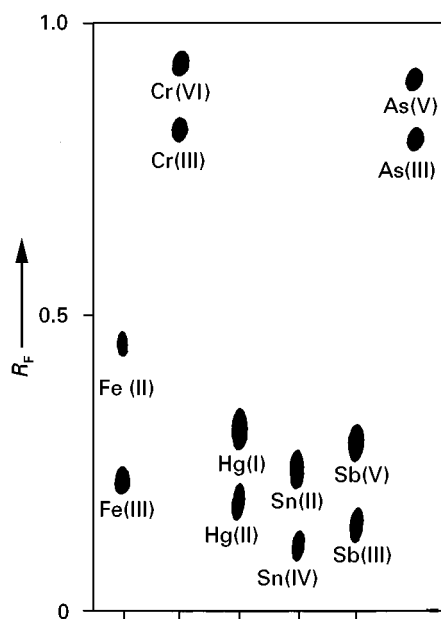


Figure 5 Chromatogram of the separation of some ions of different valency states on aminoplast layers developed with ethanol–2-propanol–5 mol L⁻¹ HCl (2 : 1 : 2). (Reproduced with permission from Perisic-Janjic NU, Petrovic SM and Podunavac S (1991) Thin-layer chromatography of metal ions on a new carbamide–formaldehyde polymer. *Chromatographia* 31: 281–284.)

plast) with acidic eluents is useful for the separation of metal ions of different valency states (Figure 5). Figures 6 and 7 show the separation of

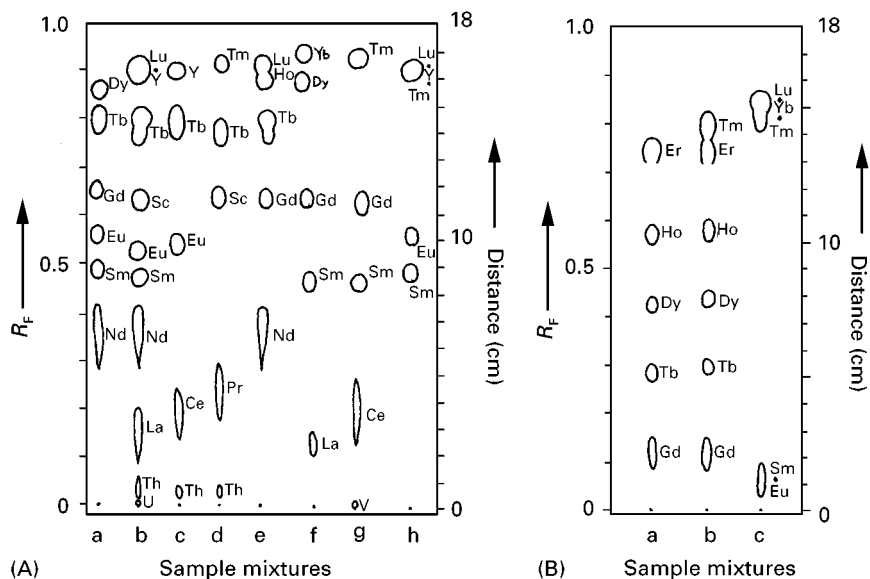


Figure 4 TLC separation of rare earth element on C₁₈-bonded silica with eluent systems (A) 1.0 mol L⁻¹ lactate in 50% methanol (pH adjusted to 6.35 before mixing with methanol) and (B) 0.5 mol L⁻¹ lactate in 50% methanol (pH adjusted to 6.35 before mixing with methanol). (Reproduced with permission from Kuroda R, Adachi M and Oguma K (1998) Reversed-phase thin-layer chromatography of rare earth elements. *Chromatographia* 25: 989–992.)

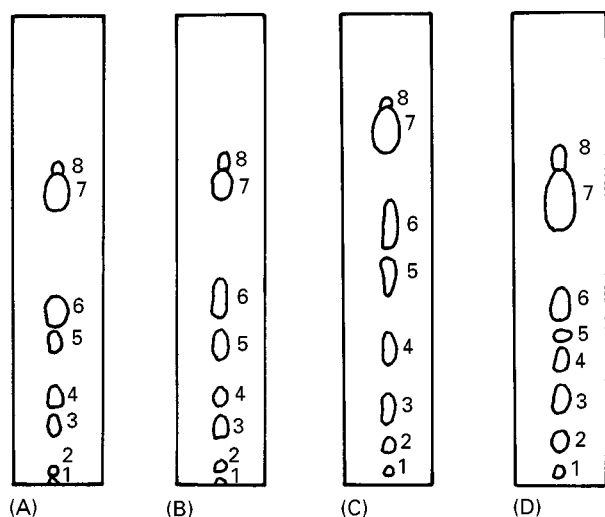


Figure 6 Separation of a mixture of diantipyrilmethane (DAM) salts. Mobile phase: acetone–chloroform (3 : 1 v/v). Reagents: (A) DAM; (B) MDAM; (C) HDAM; (D) PDAM. Anions: 1, SO_4^{2-} ; 2, Cl^- ; 3, Br^- ; 4, NO_3^- ; 5, SCN^- ; 6, I^- ; 7, ClO_4^- ; 8, reagent. (Reproduced with permission from Shadrin O, Zhivopistsev V and Timerbaev A (1993) Thin-layer chromatographic determination of inorganic anions as counter-ions of metal diantipyrilmethane cationic complexes and diantipyrilmethane cations. *Chromatographia* 35: 667–670.)

common anions in the form of metal diantipyrilmethane (DAM) complexes and salts of protonated DAM. The separation takes place on silica gel plates with elution by organic solvent–mineral acid or bi-

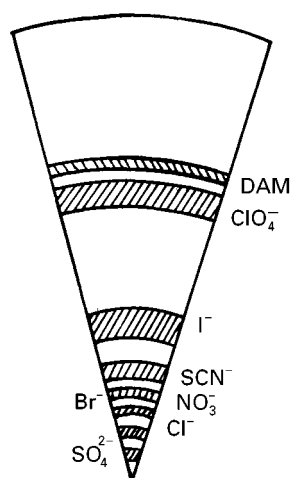


Figure 7 Sector of the radial thin-layer chromatogram of the mixture of diantipyrilmethane (DAM) salts. (Reproduced with permission from Shadrin O, Zhivopistsev V and Timerbaev A (1993) Thin-layer chromatographic determination of inorganic anions as counter-ions of metal diantipyrilmethane cationic complexes and diantipyrilmethane cations. *Chromatographia* 35: 667–670.)

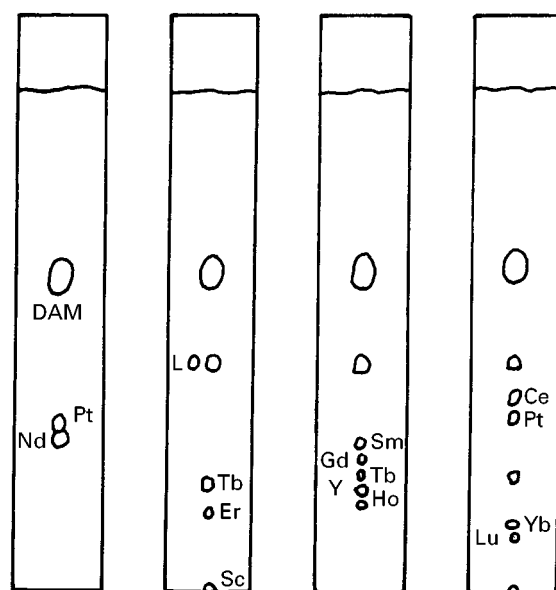


Figure 8 Separation of the mixture of diantipyril methanates of rare earth elements. TLC plate: silufol; mobile phase: *n*-propanol–0.7 mol L⁻¹ HCl (9 : 2). (Reproduced with permission from Timerbaev A, Shadrin O and Zhivopistsev V (1990) Diantipyrilmethane as complex-forming reagents in the thin-layer chromatographic determination of metals. *Chromatographia* 30: 436–441.)

nary organic solvent mixtures using ascending or radial development. Being highly coloured (iron complexes) or fluorescent under ultraviolet light (terbium complexes), chromatographic zones can easily be detected. Mixtures of REEs as diantipyrilmethanates are well resolved on silufol plates (Figure 8). A four-component mixture consisting of 4-methyl-2-pentanone, tetrahydrofuran, nitric acid and mono-2-ethylhexyl ester of 2-ethylhexylphosphoric acid (P 507) has been used for HPTLC resolution of 10 rare earths (Figure 9). HPTLC allows fast and effective separation of platinum group metals with *N,N*-diethyl-*N'*-4-(1-pyrene)butyrylthiourea (DE Py BuT) on silica gel layers using toluene as the mobile phase (Figure 10).

Quantitative Analysis

Methods for the quantitative evaluation of thin-layer chromatograms may be divided into two main categories: quantitation after elution from the layer and *in situ* quantitation on the layer. In the first, quantitation is performed after scraping off the separated analyte zone, collecting the sorbent and recovery of the substance by elution from the sorbent. Thereafter, the eluates are analysed by applying any suitable method of analysis, such as GC,

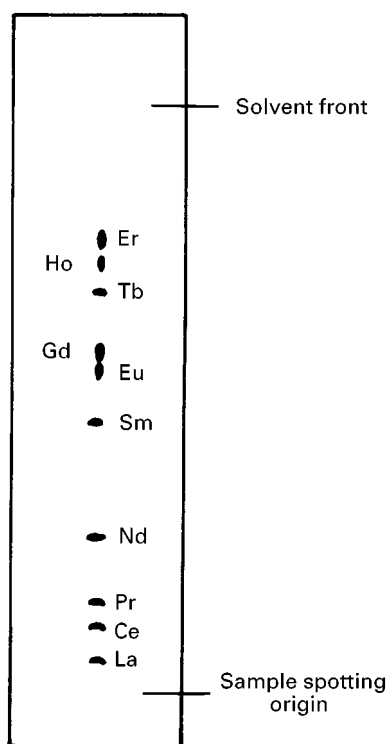


Figure 9 Chromatogram of the 10 rare earths using optimum mobile-phase conditions: 4-methyl-2-pentanone-THF-HNO₃-P 507 (3 : 1.5 : 0.46 : 0.46). (Reproduced with permission from Wang QS and Fan DP (1991) Optimization of separation of rare earths in high-performance thin-layer chromatography. *Journal of Chromatography* 587: 359-363.)

spectrophotometry or titrimetry. In the second, solutes are assayed directly on the layer with the help of visual, manual or instrumental measurement methods.

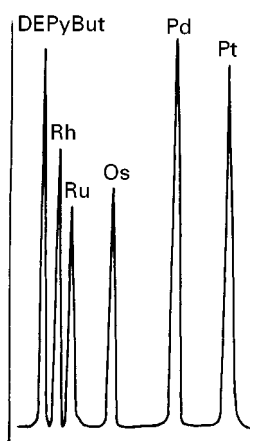


Figure 10 HPTLC separation of platinum group metals with DEP_y BuT. Eluent: toluene; relative humidity 5.0%, separation distance, 6 cm (Reproduced with permission from Schuster M and Unterreitmaier E (1993) Fluorometric detection of heavy metals with pyrene substituted *N*-acylthioureas. *Fresenius Journal of Analytical Chemistry* 346: 630-633.)

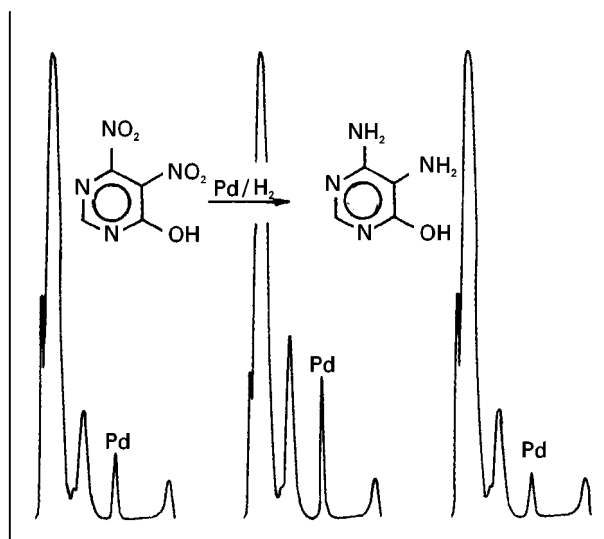


Figure 11 HPTLC determination of Pd in a synthesis solution. Ligand: *N,N*-di-*n*-hexyl-*N'*-benzoylthiourea. Stationary phase: silica gel 60, mobile phase: chloroform, relative humidity: 20%, separation distance: 3 cm detection: reflectance at 280 nm. (Reproduced with permission from Schuster M (1992) Selective complexing agents for the trace enrichment of platinum metals. *Fresenius Journal of Analytical Chemistry* 342: 791-794.)

In situ densitometry, a preferred technique for quantitative TLC, involves the measurement of visible or ultraviolet absorbance, fluorescence or fluorescence quenching directly on the layer. The measurements are made either through the plates (transmission), by reflection from the plate, or by reflection and transmission simultaneously, using either single-beam, double-beam, or single-beam-dual-wavelength

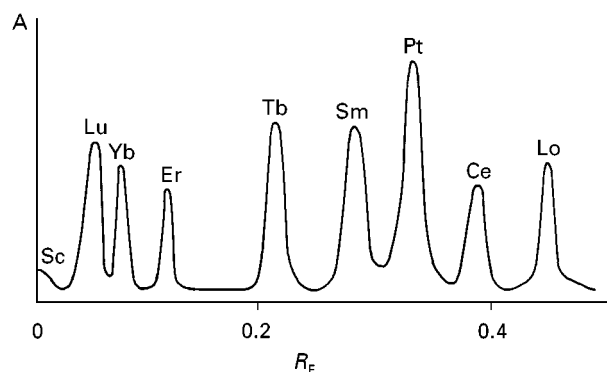


Figure 12 Densitogram of a mixture of rare earth element complexes. Stationary phase: silufol, mobile phase: *n*-propanol-0.7 mol L⁻¹ HCl (9 : 2); spraying reagent: 0.1% arsenazo III; wavelength: 590 nm. (Reproduced with permission from Timerbaev A, Shadrin O and Zhivopistsev V (1990) Diantipyrilmethane as complex-forming reagents in the thin-layer chromatographic determination of metals. *Chromatographia* 30: 436-441.)

Table 6 Quantitative and semiquantitative determination methods for inorganic ions

Method	Species determined
TLC-densitometry	B, Pb, Fe, Cu, Mn, Co, Ni, Mg, Zr, Mo, Ba, La, Ce, Sr, Se, Ti, Hg, phosphates, selenocyanate, U, Cd, Y, NO_2^- , NO_3^- , $\text{Fe}(\text{CN})_6^{3-}$, SCN^- , rare earth elements, Co(III)-1-(2-pyridylazo)-2-naphthol complex and bis carboxy ethyl germanium sesquioxide
TLC-spectrophotometry	Pb, Zn, Ni, Cu, Co, Zr, Pd, Mo, U, Hg(II), metal complexes, SCN^- , La, Ce, Pr, Nd, Cr(III), Fe(II), $\text{Cr}_2\text{O}_7^{2-}$ and $\text{Fe}(\text{CN})_6^{3-}$
TLC-UV spectroscopy	Hg(II), Cu, Cd
TLC-titrimetry	Cu, SCN^-
TLC-atomic absorption spectroscopy (AAS)	Cu, Zn, Fe, Ni, Pb, Mn
ICP-TLC-atomic emission spectroscopy (AES)	Rare earth elements, heavy metals
Neutron activation-circular TLC	Rare earth elements
Square wave-stripping voltammetry-TLC	Pb, Cd, Zn, Cu
TLC-photoacoustic measurement	Cobalt complex of 1-(2-pyridylazo)-2-naphthol
TLC-emission spectrometry	Alkaline earth metals
Visual colorimetry and peak spot-area measurement	Ti, Ni, Cu, Cr, Pb, Ag, Th, Tl(I), Al, Co, Zr, Fe(II), Fe(III), V, U, Cd, Zn, Ce, Hg, IO_4^- , Br^- , I^- , NO_2^- , Cl^- , NO_3^- , SCN^- , SO_4^{2-} , BrO_3^-

Source: *Chemical Abstracts* (1973–1996), USA.

scanning instruments. Modern optical densitometric scanners are linked to a computer and are capable of automated peak location, multiple wavelength scanning and spectral comparison of fractions in several operating modes (reflectance, absorption, transmission and fluorescence). Representative examples of HPTLC determination and densitometry are shown in **Figures 11** and **12**.

The combination of TLC with other analytical techniques has proved useful for the analysis of complex samples. Spectrophotometry, HPLC, inductively

coupled plasma-mass spectrometry and voltammetry in conjugation with TLC are the most commonly used techniques. However, infrared, thermal analysis and mass spectrometry have also been used.

For semiquantitative analysis, visual comparison and spot-size measurement methods are used. A definite volume of sample is chromatographed alongside standards containing the analyte. After detection, the amount of analyte in the sample is estimated by visual comparison of the size and intensity of the sample zone with the standards. This method works

Table 7 TLC results of the determination of Ti, Zr, Hf, La and Tb in various samples

Technique	Sample	Analyte	Determination results	
			Amount found (mean and SD)	Known amount (concentration)
Spot-area measurement method	Sulfite-cellulose liquor	Ti	31 ± 4 p.p.m.	35 p.p.m.
	High speed steel	Ti	25 ± 3 mg g ⁻¹	29.3 mg g ⁻¹
TLC-spectrophotometry	Synthetic mixture (Zr + Hf)	Zr	10.4 ± 0.3 µg	10 µg
		Hf	9.7 ± 0.2 µg	10 µg
	Mg-Al-Zr-Hf	Zr	1.1 ± 0.2 mg g ⁻¹	1.1 mg g ⁻¹
TLC-densitometry	Synthetic mixture	La	1.1 ± 0.1 µg	1.2 µg
		Tb	1.4 ± 0.1 µg	1.6 µg
	Lanthanum glass	La	179 ± 5 mg g ⁻¹	174 mg
		Tb		
	Monazite	La	4.0 ± 0.2 mg g ⁻¹	4.3 mg g ⁻¹
		Tb	1.1 ± 0.2 mg g ⁻¹	1.2 mg g ⁻¹

Reproduced with permission from Timerbaev A, Shadrin O and Zhivopistsev V (1990) Diantipyrilmethane as complex-forming reagent in the thin layer chromatographic determination of metals. *Chromatographia* 30: 436–441.

Table 8 Comparison of results of anions in water samples by TLC and ion chromatography (IC)

Sample	Technique	Determination results (p.p.m.)		
		SO_4^{2-}	Cl^-	NO_3^-
Ground water	TLC	34 ± 5	ND	10 ± 2
	IC	38.3	ND	12.8
Lake water	TLC	25 ± 4	29 ± 5	ND
	IC	27.2	28.0	ND
River water	TLC	9.8 ± 1.6	6.3 ± 1.2	ND
	IC	9.3	7.0	2.9

ND, not detected. Reproduced with permission from Shadrin O, Zhivopistsev V and Timerbaev A (1993) Thin-layer chromatographic determination of inorganic anions as counter-ions of metal-diantipyrilmethane cationic complexes and diantipyrilmethane cations. *Chromatographia* 35: 667–670.

well if the applied amounts of sample are kept close to the detection limit and the sample is accurately bracketed with standards. The shape and size of the spot produced are significantly influenced by the amount of analyte. A linear relationship between the size of the spot and the amount of analyte has been observed. This method has been used for semiquantitative estimation of titanium in steel and inorganic anions in water.

TLC techniques used and the species determined are listed in **Table 6**. TLC results of determination of certain species in real samples are shown in **Tables 7** and **8**, which indicate the versatility and accuracy of TLC.

Application

Some applications of inorganic TLC have been covered above. **Tables 9–11** list representative applications of TLC as used for the analysis of anionic, cationic and metal complex mixtures. In **Table 12** selective TLC applications related to the analysis of real samples (biological, food, geological, industrial, pharmaceutical, soil, water, wastewater and irradiated products) have been given.

Further Developments

Looking to the future, it is reasonable to expect increasing use of TLC and HPTLC for more application-oriented research in several fields (pharmaceutical, environmental, geological, forensic, agrochemical, textile, cosmetic and food sciences) because of the continued development of computer and microprocessor-based instrumental TLC. Layers with immobilized phases of wider range of selectivity, automation of sample application, hybrid mobile phases with improved chromatographic performance, online

Table 9 Stationary and mobile phases used in the analysis of certain anionic species

Anions	Stationary phase	Mobile phase
Hexacyanoferrate (II) and (III)	Silica gel G, alumina G	Polyhydric alcohols, formamide, DMF, methylamine, pyridine, water, ketones, esters and their mixtures in various ratios
Sulfur oxyanions	Silufol UV 254	Ethanol-dioxane-water-NH ₄ OH (30 + 60 + 50 + 25)
Oxyanions	Cellulose, microcrystalline cellulose containing fluorescent indicator	28% Aqueous ammonia-acetone- <i>n</i> -butanol (6 + 13 + 3), 28% aqueous ammonia-acetone (2 + 3), dioxane-water (3 + 2), acetone-acetic acid-water (20 + 1 + 20)
Halogen anions	Silica gel G, zirconium(IV) molybdate, cellulose	Basic and polar solvent systems, various alcohols mixed with aqueous ammonia
Phosphorous anions	Cellulose	Water-ethanol-2-methylpropanol-2-propanol-aqueous ammonia-trichloroacetic acid (150 + 175 + 75 + 107 + 2 + 25)
Arsenate, arsenite	Aluminium oxide	Aqueous solutions of KNO ₃ , Na ₂ CO ₃ , NaOAc, HOAc, K ₂ SO ₄ , K ₃ PO ₄ , NaF, acids and bases and buffer solutions
Oxyanions, chromate, dichromate, oxalate	Silica gel G impregnated with 0.1% aq. solutions of CuSO ₄ , ZnSO ₄ , NiCl ₂ , CoCl ₂ , Co(NH ₃) ₆ Cl	Acetone-DMSO or formic acid, acetone-DMSO-formic acid and acetone-mineral acid mixtures

DMF, dimethylformamide; DMSO, dimethylsulfoxide.

Table 10 Stationary and mobile phases used in the analysis of some cationic species

<i>Metal ions</i>	<i>Stationary phase</i>	<i>Mobile phase</i>
Alkali and alkaline metals	Microcrystalline cellulose, cellulose (MN-300) microcrystalline cellulose Lk, zinc ferrocyanide, tin(IV) arsenosilicate and arsenophosphate	Methanol–conc.HCl–water (8 + 1 + 1, 7 + 1 + 2), dioxane–2-propanol–conc. HCl–H ₂ O (7 + 7 + 5 + 8). HNO ₃ –methanol mixtures, buffered EDTA solutions, aqueous ammonium nitrate
Transition metals	Silica gel G, DEAE cellulose in chloride form, chitosan, chitin, silica gel impregnated with high molecular weight amines, cellulose	Aqueous solutions of HCl (1–5 mol L ^{−1}), LiCl (1–9 mol L ^{−1}), MgCl ₂ (2.5 mol L ^{−1}), CaCl ₂ (2.5 mol L ^{−1}) and saturated NaCl, Me ₂ CO–EtOAc–C ₆ H ₆ (7 + 1 + 3), 0.03 mol L ^{−1} citric acid, HNO ₃ at different concentrations
Light rare earth metals	Mixture of silica gel, starch and NH ₄ NO ₃ ; silica gel–NH ₄ NO ₃ –CM cellulose (5 : 0.64 : 0.16, w/w)	P ₂₀₄ –dioxane–EtOAc–HNO ₃ (1.1 + 2 + 2.4 + 4) tributylphosphate–THF–diethyl ether–HNO ₃ (1 + 9 + 9 + 1.5), trialkylmethyl ammonium chloride– <i>n</i> -octyl alcohol–petroleum ether–conc. HNO ₃ (60 + 7 + 25 + 1)
Heavy rare earth metals	Silica gel–NH ₄ NO ₃ –CM–cellulose (5.0 + 0.64 + 0.16, w/w); silica gel–starch–ammonium rhodanate (2.8 + 0.15 + 0.5, w/w)	Et ₂ O–THF–bis (2-ethylhexyl)phosphate–HNO ₃ , trimethylammonium chloride– <i>n</i> -octyl alcohol–petroleum ether–HCl (2 + 10 + 30 + 1, 2 + 6 + 30 + 1.2 and 2 + 7 + 30 + 1), bis (2 + ethylhexyl)phosphate–diisopropyl ether–diethyl ether–nitric acid (1 + 10 + 6 + 1.1), mono(2-ethylhexyl)phosphate–isopropyl ether–diethyl ether–nitric acid (1 + 8 + 8 + 1.1)
Lanthanides	Silanized silica gel (Merck) and polygram plate, silica gel impregnated with different concentrations of mono (2-ethyl hexyl) phosphate	3 mol L ^{−1} Tributyl phosphate in HNO ₃ –isooctane (2 + 8); THF–paraldehyde–HNO ₃ (2 + 7 + 1); 0.3 mol L ^{−1} triphenylphosphine oxide in paraldehyde–HNO ₃ (9 + 1); di-isopropyl ether–THF–HNO ₃ (10 + 6 + 1); HNO ₃ (0.05–3.0 mol L ^{−1})
Radionuclides ⁹⁰ Sr, ⁹⁰ Y, ¹⁴⁰ Ba, ¹⁴⁰ La	Silica gel (with and without gypsum binder)	Aqueous solutions of NaCl, KCl, NH ₄ Cl, CaCl ₂ , SrCl ₂ , and BaCl ₂
High valence metal ions	Silica gel impregnated with crystalline antimon(V) acid- <i>p</i> -sulfochlorophosphanazo	Potassium pyrophosphate solution
Mn(II), Mn(III)	Silica gel G	Eleven organic mobile phases consisting of hydrocarbons and their derivatives in different ratios
Transition metals	1,10-Phenanthroline (1%), DMG (1%), EDTA (2%) or β -naphthol (0.1%) impregnated silica gel	Pyridine–benzene–HOAc–H ₂ O (6 + 5 + 8 + 4), BuOH–benzene–formic acid (5 + 10 + 9), pyridine–benzene–HOAc–H ₂ O (5 + 5 + 4 + 1)

DEAE, diethylaminoethyl; THF, tetrahydrofuran; DMG, dimethylglyoxime; EDTA, ethylenediaminetetraacetic acid.

coupling of TLC with other sensitive techniques, better approaches in method development and application of detection reagents and greater use of instrumental densitometry can be expected. It is

hoped that the forced-flow layer methods with increased automation will be developed in the near future for faster separation of inorganic ions in real samples.

Table 11 Stationary and mobile phases used in the analysis of certain metal complexes

<i>Metal complexes</i>	<i>Stationary phase</i>	<i>Mobile phase</i>
Diethylthiocarbamates of Bi, Cu, Co, Ni	Silica gel G	Dichloromethane–petroleum ether (5 + 3)
Sulfate complexes of Pt, Pd, Rh, Ir	Commercial silufol plates (Kavalier, CSSR), silica gel KSK, silica gel	0.1, 1.0 and 6.0 NH_4SO_4 , 0.2 or 0.5 mol L^{-1} tetraoctylamine in benzene
β -Diketonates of Fe, Cr and Co	Silica gel (Merck)	CCl_4 , toluene, benzene, dichloromethane, diethyl ether
Xanthates of Cu, Ni, Co, Mo, Bi, Pb, Zn	Silica gel G	CCl_4 – CHCl_3 (10 + 1), toluene–benzene (10 + 1)
Anil complexes of Mn, Fe, Cu, Zn	Silica gel–starch (19 : 1)	Acetonitrile, methanol, ethanol, butanol, acetic acid or butanol–acetic acid (4 + 1, 3 + 2, 2 + 3, 1 + 4)
Metal oxinates (OX), (HOX), Cu (OX) ₂ , Zn (OX) ₂ , Al(OX) ₃ , Ga(OX) ₃ , In (OX) ₃	Styragel 60A (polystyrene–divinylbenzene copolymers), Merckogel OR-PVA 2000	CHCl_3 , <i>p</i> -dioxane, benzene, 10^{-3} – 10^{-1} mol L^{-1} HOX in CHCl_3 , 10^{-2} mol L^{-1} HOX in dioxane, 10^{-1} mol L^{-1} pyridine in CHCl_3
Mn, Co, Ni, Zn, Rh, Pd, Pt, Chelates of dithioacetyl-acetone	Silica gel	CCl_4 , 1,1,1-trichloroethane
Mixed amino carboxylato cobalt(III) complexes	Polyacrylonitrile	Aqueous ammonium sulfate solutions (1.1–3.48 mol dm^{-3})
Chlorosulfate complexes of transition metals and rare earths	Silica gel G–cellulose (2 : 1)	Sodium formate (1 mol L^{-1}) and ammonium sulfate (1 mol L^{-1})
Mercapto-4-methyl-5-phenylazopyrimidine complexes of Co, Ni, Pb, Cd, Cu	Surfactant-impregnated silica gel plate	Acetonitrile–xylene (70 : 30)

Table 12 Application of TLC to the analysis of real samples

<i>Species</i>	<i>Sample</i>	<i>Remark</i>
Se	Biological (tissues, blood, serum) environmental (drinking and surface water) and food stuffs	Isolation of Se from matrix, derivatization, extraction of Se-containing complex, TLC separation and fluorimetric determination. Detection limit 250 fg Se per spot
Cu, Fe	Serum	TLC separation and densitometric determination of Fe^{2+} , Fe^{3+} and Cu^{2+} complexed with 2-[(5-bromo-2-pyridinyl)azo]-5-(diethylamino) phenol in serum
Cd, Hg, Pb	Urine, blood	Separation on silica gel layer prior to spectrophotometric determination of Cd^{2+} , Pb^{2+} and Hg^{2+} in blood and urine samples
Heavy metals	Urine, blood, excrement	A sensitive detection of Zn^{2+} , Hg^{2+} , Cu^{2+} , Co^{2+} , Pb^{2+} , Ni^{2+} , Ag^+ and Bi^{3+} on silica gel layers (sensitivity 10^{-3} g L^{-1}) as dithizonates in biological samples
Hg	Animal, fish and plant tissues	Quantitative determination of mercury species (inorganic and methyl mercury) after extraction from tissues
Cu, Mg, Zn, Fe, Mn	Human faeces	Detection of metal–EDTA complexes on silica gel and cellulose layers
BrO_3^-	Food stuff	Extraction and purification using alumina column, separation on silica gel layer and densitometric determination of BrO_3^- in bread and flour dough. Detection limit of BrO_3^- was 0.1 $\mu\text{g g}^{-1}$ of bread
Fe, Mn, Co	Human milk	Extraction of metals from human milk with isobutyl methyl ketone–amyl acetate (2 : 1) and identification on cellulose layer

Table 12 *Continued*

<i>Species</i>	<i>Sample</i>	<i>Remark</i>
Polyphosphoric acids	Cheese, milk	Extraction with 25% trichloroacetic acid, separation and identification on polyamide layer developed with <i>n</i> -butanol–formic acid (1 : 1)
Polyphosphates	Soft drinks	Separation and determination of ortho- and polyphosphates in soft drinks using two-dimensional TLC and ion-exchange column chromatography
Si	Edible oils	Detection with rhodanine on silica gel layers developed with light petroleum–diethyl ether (98 : 2)
Rare earth metals	Rocks, monazite sand, ores, irradiated nuclear fuels	Determination by neutron activation analysis (determination limits $0.05\text{--}10\ \mu\text{g g}^{-1}$ for 10–30 mg sample) after preconcentration by circular TLC on Fixion 50×8 . Use of ICP-AES for determination of rare earths in concentrates obtained by means of TLC. Densitometric determination in monazite sand (linear range $0.015\text{--}0.60\ \mu\text{g}$ of individual rare earth) after TLC separation. The limits of detection for rare earths were 9–12 ng
Fe, Mn, Cu	Cotton materials	Detection of metal ions on microcrystalline cellulose plates developed with acetone–HCl–H ₂ O (8 : 1 : 2). TLC-spectrophotometry for determination of Mn traces in textile materials
NO_3^- , $\text{Fe}(\text{CN})_6^{3-}$	Molasses	TLC separation on silufol 254 plates developed with propanol–ammonia solution (2 : 1), detection with acidified diphenylamine and densitometric determination
La, Y	Alloys	Circular TLC with trioctylamine-treated cellulose layers as stationary phase and aqueous HCl as mobile phase for separation and spectrophotometric determination of La and Y (0.01–1.0%) in Mo-based alloys
Co	White wine	Fixation of Co^{2+} as 1-(2-pyridylazo)-2-naphthol complex on membrane filter followed by densitometric determination (concentration range in white wine $2.5\text{--}4.5\ \mu\text{g L}^{-1}$) by reflection absorbance of the complex
Fe(II)	Pharmaceuticals	Separation on microcrystalline cellulose layers, detection by 1,10-phenanthroline and determination by spectrophotometry
Mercury salts	Homeopathic drugs	Identification of chloride, nitrate, cyanide, sulfate and sulfide of Hg on silica gel G plates developed with acetone–chloroform–conc. HNO ₃ (4 : 5 : 1)
Mn	Pharmaceuticals	TLC separation and photodensitometric determination of Mn in vitamins and pharmaceuticals as PAN complex
Cr	$\text{Na}_2^{51}\text{CrO}_4$ injection	Determination of radiochemical purity of $\text{Na}_2^{51}\text{CrO}_4$ injections and γ -scintillation for quantitation of Cr-containing zones
NO_3^-	Feeds	Separation on alumina layer and spectrophotometric determination at 430 nm after extracting the coloured product formed with 3,4-xyleneol
Rare earths and fission products	Irradiated nuclear fuels	Two-dimensional TLC separation and enrichment followed by quantification by γ -spectroscopy

Table 12 *Continued*

<i>Species</i>	<i>Sample</i>	<i>Remark</i>
Co, Fe(III)	Cosmic dust	TLC separation and semiquantitative determination on the basis of spot size and colour intensity or by reflectance densitometry
⁸⁸ Sr, ⁹⁰ Sr	Soil	Extraction of strontium from soil with dicyclohexano-18-crown-6 in chloroform and TLC separation using circular procedure with silufol layer
Ta	Molybdenum-based alloys	TLC-AES for determination of Ta ($\geq 0.5\%$) in molybdenum alloys
Zn, Pb, Cu, Cd, Hg (organic and inorganic)	Plants	Detection (10–500 ng) using azo rhodanines as detector and nanogram determination by visual sorption-photometric method
Hg (organic and inorganic)	Water	HPTLC separation on silica gel layers and densitometric determination as dithizonates
Al, Be, Cr, Bi, Cu, Hg	Water	Extraction, TLC separation, detection (as Bi, Cu, Hg dithizonates, detection limit, 0.5 p.p.m.) and determination fluorimetrically (Al and Be as oxinates) and photometrically (Cr as diphenylcarbamide complex)
CuSO ₄ , CdSO ₄ , HgCl ₂ , AgNO ₃	Fresh and seawater	Evaporation, precipitation, micro-TLC separation and enzymatic detection
Fe, Cu, Hg, Cd, Co, Ni, Bi, Mn, Pb, Zn, Sn, Al, Cr, Be	Water	Extraction, TLC separation on silica gel layer developed with EtOH–1.0 mol L ⁻¹ HNO ₃ (99 : 1) and photometry in transmission mode. Detection limits 0.1–1 p.p.m. except Cr (8 p.p.m.)
Cu, Zn, Cr, Fe, Ni, Co, V	Electroplating wastewater	Simultaneous separation of metals and semiquantitative determination of Ni, Cu, Cr in wastewaters using cellulose with azopyrocatechol groups as layer material. Detection limit of metals in coloured zone was 0.05–2.0 µg
Co, Ni, Cu, Fe	Industrial and wastewaters	Visual semiquantitative determination of concentration of total heavy metals in wastewaters according to the intensity of coloured metal diethyl-dithiocarbamates formed directly on silufol plates. Determination of Cu and Ni at 5 mg L ⁻¹ in electroplating wastewater
Cu, Ni, Fe, Co	Electroplating wastewater	Quantitative trace analysis using 2-(5-bromo-2-pyridylazo)-5-diethyl aminophenol as complexing agent

EDTA, ethylenediaminetetraacetic acid; ICP-AES, inductively coupled plasma–atomic emission spectroscopy; PAN, 1-(2-pyridylazo)-2-naphthol.

See also: **II/Chromatography: Thin-Layer (Planar):** Densitometry and Image Analysis; Layers; Spray Reagents. **III/Impregnation Techniques: Thin-Layer (Planar) Chromatography. Ion Analysis:** Capillary Electrophoresis; High-Speed Counter Current Chromatography; Liquid Chromatography.

Further Reading

Fried B and Sherma J (eds) (1994) *Thin Layer Chromatography: Techniques and Applications*. New York: Marcel Dekker.

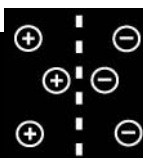
Gocan S (1990) Stationary phases in thin-layer chromatography. In: Grinberg N (ed.) *Modern Thin Layer Chromatography*, pp. 5–137. New York: Marcel Dekker.

Jork H, Funk W, Fisher W and Wimmer H (1990) *Thin Layer Chromatography, Reagents and Detection Methods*. Weinheim, Germany: VCH Verlagsgesellschaft.

Kuroda R and Volynets MP (1987) Thin-layer chromatography. In: Qureshi M (ed.) *CRC Handbook of Chromatography: Inorganics*. Boca Raton, FL: CRC Press.

- Lederer M (1994) *Chromatography for Inorganic Chemistry*. New York: John Wiley.
- MacDonald JC (ed.) (1994) *Inorganic Chromatographic Analysis*. New York: John Wiley.
- Mohammad A (1996) Inorganics and organometallics. In: Sherma J and Fried B (eds) *Handbook of Thin Layer Chromatography*, 2nd edn. New York: Marcel Dekker.
- Mohammad A and Tiwari S (1995) Thirty-five years thin-layer chromatography in the analysis of inorganic anions. *Separation Science Technology* 30: 3591–3628.
- Mohammad A, Fatima N, Ahmad J and Khan MAM (1993) Planar layer chromatography in the analysis of inorganic pollutants. *Journal of Chromatography* 652: 445–453.
- Mohammad A, Ajmal M, Anwar S and Iraqi E (1996) Twenty-two years report on the thin layer chromatography of inorganic mixtures: Observations and future prospects. *Journal of Planar Chromatography – Modern TLC* 9: 318–360.
- Poole CF and Poole SK (1991) *Chromatography Today*. Amsterdam: Elsevier.
- Touchstone JC (1992) *Practice of Thin Layer Chromatography*, 3rd edn. New York: Wiley-Interscience.

ION EXCHANGE RESINS: CHARACTERIZATION OF



L. S. Golden, Purolite International Ltd, Pontyclun, Mid-Glamorgan, Wales, UK

Copyright © 2000 Academic Press

Introduction

An ion exchange resin is an insoluble polymer matrix containing labile ions which are capable of exchanging with ions in the surrounding medium without any major physical change taking place in its structure. They are of two basic types, cation and anion exchangers. So-called cation exchange resins are in fact polymeric anions to which the labile cation is bound, and it is this cation which exchanges with other cations in solution. Likewise, anion exchange resins are polymeric cations with a labile, exchangeable anion.

The first synthetic ion exchange resins were developed by Adams and Holmes in 1935, based on a phenol-formaldehyde structure. The next most important development was the introduction of commercial ion exchange resins based on a cross-linked polystyrene matrix, and these resin types today still represent about 90% of the commercial resin market. More recently, polyacrylic resins have been introduced which have widened the scope and versatility of the synthetic ion exchange resins, and these represent most of the remaining 10% of the commercial market.

The development of synthetic polystyrene and polyacrylic resins has enabled these ion exchangers to be produced in spherical bead form, unlike the irregular-shaped particles of the phenol-formaldehyde types. In the majority of applications, the most effi-

cient treatment of a solution is obtained by passing this solution through a bed of ion exchange resin. A spherical bead shape offers optimum contact with the percolating solution without undue pressure drop across the bed, requiring only minimal inlet pressures.

The first polystyrene resins, introduced in 1947, were of what is now known as a *gel* type. Exchange takes place by diffusion of the ions through the resin structure to and from the ion exchange sites. The polymer chains are only separated by molecular distances, and the ease of penetration of the ions is very much influenced by the amount by which the resin structure can be swelled by the contacting solution. In 1956, Mikes and co-workers discovered a means of introducing pores (or holes) into the resin structure, which led to the introduction of *macroporous* resins, which further increased the scope of ion exchange techniques. These resins comprise a continuous polymer matrix interspersed with a continuous pore matrix.

Synthesis

Polymerization

Generally speaking, the synthesis of a modern ion exchange resin is a two-step process. In the first step, the spherical bead is produced by polymerization of styrene (or an acrylic monomer, usually methyl acrylate) plus a cross-linking agent (usually divinylbenzene, DVB) in an aqueous suspension. This technique of suspension polymerization is used extensively in the production of pearl (or bead) polymers, not specifically to make ion exchange resins, and is

dependent on the fact that the monomer is essentially insoluble in water. Thus, when stirred with water, the monomer will disperse into spherical droplets. Small quantities of various stabilizing ingredients are added to the water to make this dispersion more permanent.

An initiator is added to the monomer mixture which, on the application of heat, produces free radicals. These start a chain reaction with the monomer in which monomer units are progressively added to the growing polymer chains. Styrene contains just one double bond capable of reacting into the polymer chain. As a consequence, a polymer produced from styrene alone will comprise a large number of unconnected chains, and this hydrophobic polymer will be soluble in organic solvents such as aromatic hydrocarbons. Cross-linking agents, such as DVB, contain two or more reactive double bonds, each of which is capable of reacting in a separate polymer chain, ultimately leading to an 'infinite' single polymer chain network. Solvents will still be absorbed by the polymer chain and swell the polymer, but will not be able to dissolve it. The extent of the swelling is dependent on the proportion of DVB in the monomer: the more DVB, the less the polymer will swell.

The invention of macroporous resins has been briefly mentioned. The continuous pore structure within the resin matrix is produced by polymerizing the monomers in the presence of an inert diluent which is miscible with the monomers but essentially immiscible with the growing polymer chains. As the polymerization progresses, the mixture separates into two phases, one phase being the growing polymer, the other being the diluent plus a continuously decreasing amount of monomer. At the end of the polymerization, the diluent, which has not actually polymerized into the structure, is removed by distillation or washing, leaving the interconnecting network of pores.

Activation

The second stage of synthesis is to add a functional group to the polymer, which will contain the labile ion capable of exchange with ions in solution. The effect of this functional group is to make the polymer structure hydrophilic. The resin will now be swollen by water, but again cannot dissolve due to the polymer chain structure. The extent of this swelling by water is an important characteristic of an ion exchange resin, and controls its behaviour in many applications.

The sulfonic acid group of the strong acid cation resins is added by reaction of the polystyrene polymer with sulfuric acid at temperatures between 90 and

140°C. The amino group of the strong and weak base resins is added in two stages, firstly a chloromethylation to add a chloromethyl group to the polystyrene chain followed by addition of an amine to give the final quaternary or tertiary amino functionality. The choice of amine affects the resin properties, which will be discussed shortly.

Polyacrylic resins are produced as either weak acid cation resins with a carboxylic acid functional group (to which there is no polystyrene resin equivalent), or as strong or weak base anion resin whose properties are similar, but not identical, to those produced from polystyrene.

Classification of Ion Exchange Resins

Both cation and anion resins are available with strong and weak functional groups. The strong functional groups are ionized species within which the ionized labile ion can be replaced with an ion in solution. These resins will therefore easily exchange ions with dissolved salts. On the other hand, the weak functional groups are themselves nonionized and will therefore have very little ability to exchange with salts. Weakly functional anion resins will however readily remove anions from acidic solutions, and weakly acidic resins will readily remove calcium and magnesium from solutions of carbonates and bicarbonates.

Strongly basic resins are further subdivided into three categories. The most commonly encountered of these is the *strong base anion Type I* resin (often abbreviated to SBA I). The second most common category is the *strong base anion Type II* (SBA II), which is a weaker base than the Type I but still not weakly basic enough to be categorized as a weakly basic resin. The third category, *strong base anion Type III* (SBA III), is actually intermediate between these two types, and, although not as yet widely used, is being shown to combine useful characteristics of both.

In more recent years, a number of resins with special functional groups have been produced commercially. These are designed for removal of specific ions for special applications. One particular application is the use of a polystyrene resin with an aminophosphonic chelating group—this resin, in the sodium form, is used to remove calcium and other divalent ions from brine prior to the production of caustic soda by the membrane cell process. A conventional cation resin would be completely unable to remove these alkaline earths from concentrated salt solutions.

Resins in each category can be produced in both gel and macroporous forms.

Fundamental Ion Exchange Resin Characteristics

Irrespective of the resin type, there are certain fundamental parameters which characterize ion exchange resins, and determine how that resin will perform in its applications.

Moisture Retention

As mentioned earlier, an ion exchange resin is swollen by water but will not dissolve in it. The extent of this swelling is one factor which controls how the resin will perform in specific applications. A resin will absorb a certain amount of water, depending on the functional group, the ionic form and the amount of cross-linking. For a given resin type in a given ionic form, the swelling is entirely dependent on the amount of cross-linking.

Moisture retention is defined as the amount of water which is in equilibrium with the dry resin matrix. This water can be removed by hot air drying, but will be reabsorbed when the resin is put back in contact with excess water. The value of the moisture retention is easily determined by measuring the loss in weight of a fully swollen resin on drying, and expressing the moisture loss as a percentage of the total wet weight.

The importance of moisture retention in the performance of a resin should be fairly obvious. For the resin to operate, the ions in solution must have access to the active sites throughout the polymer structure, just as the ions which are displaced from these sites must be able to pass out of the resin back into solution. The more open the structure (i.e. the higher the moisture retention), the easier this will be.

The labile ion which is attached to the resin influences the hydrophilic nature of the structure, and so the moisture retention. For instance, at a given amount of cross-linking, a strong acid cation resin in the sodium form (i.e. with a Na^+ group attached to each sulfonic acid site on the structure) will have a significantly lower moisture retention than the same resin in the hydrogen form. Therefore, the ionic form must be stated along with the moisture retention.

Resin Capacity

The ability of an ion exchange resin to exchange ions is a function of the number of active groups that have been placed on the resin during the activation process. The overall term for this is the *capacity* of the resin, but this can be expressed and determined in a number of ways.

Dry weight capacity This measures the proportion of active sites in the dry resin matrix, and is expressed as equivalents per kilogram (or milliequivalents per gram, as some workers prefer). It is easily determined by weighing a dry sample of resin, rewetting it and displacing completely from the resin an ion which can be titrated in solution. This gives the total equivalents of sites on the dry resin, and is a direct measure of the extent of activation of the base polymer. For most applications, the figure obtained does not have any direct significance, since the resin is rarely used in its dry state except in certain specialized applications.

Total volume capacity Since resins are normally supplied and used wet (i.e. fully swollen in water), the capacity based on a volume of wet resin is more useful. It is, however, more difficult to measure a wet resin volume as accurately as dry resin weight, but essentially the test method is the same apart from measuring a known volume of resin rather than weight. The data is expressed in terms of equivalents per litre (or milliequivalents per millilitre).

Although the test value can now be related to the volume of resin installed in the resin treatment plant, it will still not tell the plant designer or user the capacity achievable when the unit is in practical operation.

Operating capacity This is the true practical parameter, but unfortunately it cannot be determined by a straightforward laboratory test. Since the operating capacity of a resin depends on many factors, such as the dimensions of the unit, the flow rate and quality of the liquid to be treated, the quality required of the effluent from the unit, the regenerant quantity and the operating temperature, etc., this capacity can only be calculated from data obtained by extensive laboratory testing of a resin type under simulated operating conditions. This data is usually provided in brochures supplied by the resin manufacturers, and more recently a number of these manufacturers have computer programs available to make these calculations quickly on data stored within the software.

Particle Size Distribution

As already described, modern ion exchange resins are in the form of spherical beads. The suspension polymerization technique does not produce beads of a uniform particle size, rather a distribution of sizes to give a resin within the range 0.3–1.2 mm. Most ion exchange applications have been developed around resins of this particle size range, but some special

applications do require the particles to be of a more specific size.

In the majority of applications, the ion exchange resin is contained in a vessel which is designed to allow the solution to be treated to pass through the resin bed and subsequently emerge from the unit. The resin has therefore to be retained within this unit by a suitable means, usually nozzles or slats of such an aperture that the solution can freely pass. Depending upon engineering design, these apertures will normally be about 0.2 mm wide, but in some designs can be as large as 0.4 mm. It is therefore essential that the ion exchange resin does not contain beads close to or less than this aperture size.

A number of resin applications require two resins to operate mixed together in the same unit. For regeneration, it is essential that these resins are separated. Strong acid cation resins have a density of about 1.25–1.30 g g⁻¹, whereas anion resins have a density of 1.07–1.10 g g⁻¹. Therefore, by applying backwash to lift and expand the resin bed, the cation resin beads will sink below the anion resin beads. A complete separation is readily achieved if the cation resin contains less coarse beads than the anion resin less fine beads.

Ions obviously have a greater path length to travel to the centre of a large bead compared to that of a small bead. This decreases the efficiency with which a larger bead can complete the ion exchange process. A number of applications have developed today in which beads of a more uniform size distribution, normally in the range 0.4–0.8 mm, are used, thereby eliminating the most coarse beads of the 'standard' size range.

For these reasons, measurement of particle size distribution of resins is important. The classical method is to use standard sieves, but due to limitations of sieve accuracy and availability, they are not best suited to measuring resins with narrower size distributions. Most resin manufacturers and larger users now use an instrumental technique based on a light extinction principle, such as the OMEGA (Fortress Dynamics, UK) or HIAC (Hiac-Rogco, USA).

Resin Volume Change

It was observed earlier that a given ion exchange resin will be in equilibrium with a different volume of water depending on its ionic form. Consequently, when the resin is treating the feed solution, the bed of resin will slowly swell or shrink as the ions are being exchanged. It is important for the plant design engineer to know the extent of this volume change in order to allow sufficient space for any increase in vol-

ume to be accommodated. It has been known for poorly designed plants to smash a resin, or even for the plant itself to be damaged, if this swelling factor has not been properly accounted for.

Other Resin Characteristics

There are a number of other parameters which have to be taken into account when designing an ion exchange plant, such as pH range and operating temperature. All resins of a given type will have virtually identical limitations on these parameters. The recommendations given by the resin manufacturers should be followed. It is worthy of note that SBA Type II resins are less thermally stable than their Type I counterparts, and that polyacrylic anion resins are less thermally stable than polystyrene ones with the same functionality.

Macroporous versus Gel Resins

In appearance, gel resin beads are usually transparent. Light entering the bead will pass through the homogeneous structure without being diffracted, therefore being visible from the other side of the bead. With a macroporous bead, there are numerous phase boundaries within the bead between the pores and resin matrix, at each of which the entering light will be refracted. Consequently, little or no light will emerge, giving the resin bead an opaque appearance.

Gel resins were in extensive use in ion exchange for many years before the invention of macroporous resins. These macroporous resins were found to have two main advantages over their gel counterparts – they were less susceptible to osmotic shock and less liable to organic fouling.

As just discussed, a resin will change in volume as it changes its ionic form. Moreover its volume will contract when it is in contact with strong electrolyte solutions which it will encounter during regeneration, and will rapidly swell again when this regenerant solution is washed off. These volume changes exert an osmotic stress across the boundary between resin and solution, which in the case of a gel resin is the resin bead boundary itself. These forces can weaken or even smash the resin bead. Although fragments of resin are still just as good as a whole bead in the exchange process, they will certainly impede the flow of liquid through the bed, increasing the pressure drop and decreasing the flow. Also, the small fragments can block the strainers of the unit, and even contaminate the treated solution.

A macroporous resin, by nature of its structure of interconnecting pores and matrix, comprises very

many small resin-solute interfaces, so although the osmotic force across the bead as a whole will be the same, it will be dispersed across all these small boundaries. Therefore, the stress on the bead will be much less, and there will be very much less chance of the resin bead being weakened or broken.

Most natural waters, as well as many organic solutions which ion exchange resins are used to treat, contain large and complex organic molecules. These will slowly penetrate a resin bead, particularly if the organic molecule itself contains an ionic charge. Because of their size, these molecules become entangled with the resin structure, and are not easily removed when the resin is regenerated. Consequently, these molecules build up within the resin, blocking access of the ions in solution to the exchange sites, with a resulting drop in resin capacity. This is known as *organic fouling*. The pore structure of macroporous resins allows greater freedom of passage of these organic molecules, so they are more freely released during regeneration. Anion resins based on an acrylic matrix, due to the nature of this matrix, are also less susceptible to organic fouling.

Unfortunately, macroporous resins also have a major disadvantage. Part of the resin bead, the pores, is purely water with no ion exchange properties. In order that the overall number of ion exchange sites within a given volume of resin is similar to a gel resin, the resin matrix itself has to contain less water – it will be more highly cross-linked. With such a matrix having a lower amount of water associated with the structure, ions will be able to move less freely, so causing the resin to exchange ions more slowly. In practical terms, this results in either reducing the rate at which the solution to be treated can be fed to the resin, or reducing the efficiency of the ion exchange process.

Since optimum efficiency of ion exchange (known as ion exchange *kinetics*) is an important factor in the design and operation of a treatment plant, gel resins will normally be preferred except in circumstances where the advantages of macroporous resins outweigh this major disadvantage.

Resin Regeneration

In most resin applications, the resin is used over many treatment cycles. Once the resin has become exhausted (in other words, when it is no longer removing the ions from solution at the threshold level required by the user), it is then regenerated with suitable chemicals to once again attach to the active group the mobile ion which will subsequently be released into the treated solution. In the case of cation resins in demineralization processes, this will be a mineral acid

and in the case of anion resins, an alkali, usually sodium hydroxide.

Not only do resins swell in water to a different extent when different ions are attached, they have a different affinity for the various ions, and in the case of treatment of solutions containing a mixture of ions, the resin sites will compete at different rates for the different ions. This is known as *selectivity*. Likewise, if an ion for which the resin has a higher selectivity is already attached to an active group, it will be much more difficult for an ion of a lower selectivity to displace it from the resin.

Consider a solution containing a cation B, and a cation resin in which all the sites are occupied by cation A. As a B ion penetrates through the bead, it will attach to an active site displacing an A ion in the process (Figure 1). Initially, since the resin contains only B ions, this released A ion can do nothing but emerge from the resin back into solution. However, as more and more sites within the bead take up B ions, there is a chance that the released A ion could displace another B ion which had already been taken up on a different site. The ease with which this would occur depends on the relative selectivity of ions A and B to the resin – if the resin is significantly more selective for the B ion, then this is less likely than if the resin were more selective for the A ion.

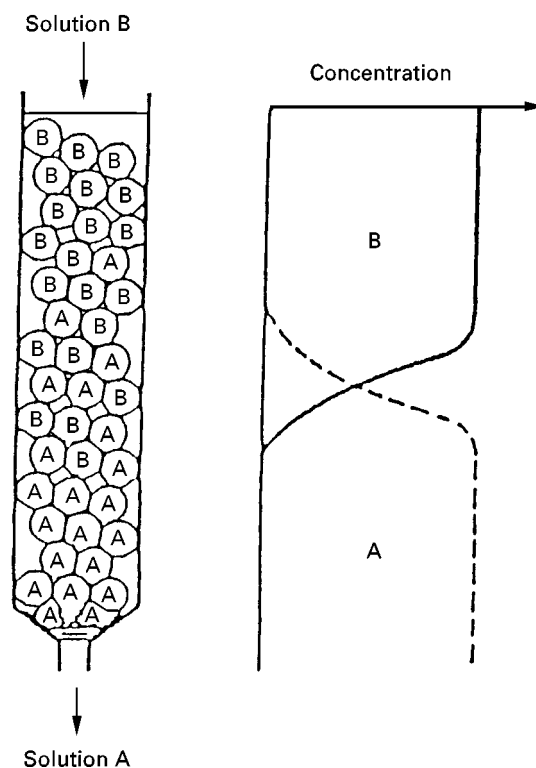


Figure 1 Ion exchange equilibrium.

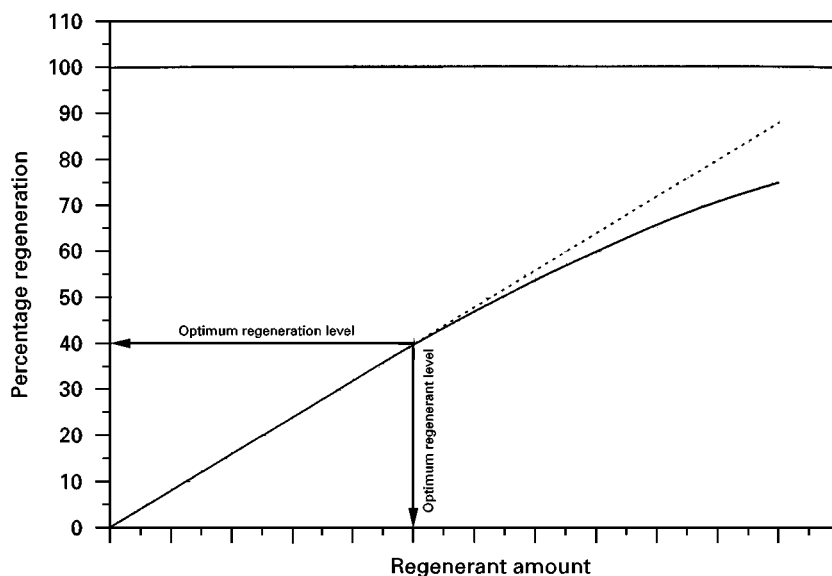


Figure 2 Typical regeneration curve. Dotted line, optimal; continuous line, practical.

When a resin is being regenerated, the more regenerant which is passed, the more completely will the resin be regenerated. However, because of this interchange of ions within the resin, the percentage of resin regenerated is not a linear function of the amount of regenerant (**Figure 2**). In other words, doubling the amount of regenerant used will not necessarily double the number of sites regenerated. Since the operational cost of an ion exchange resin plant is heavily influenced by the regenerant cost, it is

not usually practicable to regenerate a resin fully, rather to balance the percentage regeneration to the most economic use of the regenerant. Consequently, a quantity of regenerant much more than the point at which the regeneration curve loses linearity is unlikely to be used.

The shape of this regeneration curve will vary with different resins, depending not only on the nature of the active group and the moisture retention, but also on the structure of the resin matrix itself.

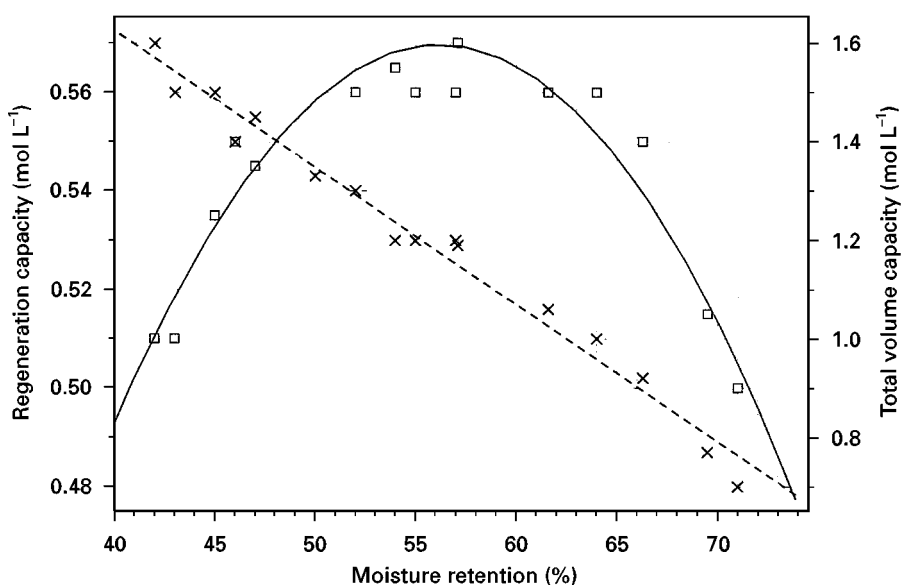


Figure 3 Comparison of regeneration (squares) and volume capacities (crosses) (on the same resin samples). SBA Type I gel resins regenerated with 65 g NaOH per litre resin.

Table 1 Typical regeneration efficiencies of different resin types

<i>Resin</i>	<i>Regeneration efficiency (%)</i>
SAC gel	50–60
SAC MP	45–55
WAC gel/MP	80–95
SBA I gel	35–45
SBA I MP	30–35
SBA II gel	60–70
SBA II MP	55–65
SBA III MP	45–55
WBA MP	80–95

Even two resins of the same functionality and total exchange capacity might regenerate differently.

Strongly acidic or strongly basic resins readily exchange ions from neutral salts. The exchange process is therefore an equilibrium, and the ion displaced from a resin site will be capable of exchanging with the ion on another site. In the case of a weakly functional resin, the exchange is more of neutralization reaction, and there is little chance of the released ion exchanging with another site on the resin. For this reason, the regenerability of a resin increases as its acidity or basicity decreases.

Regeneration capacity

In this test, a known volume of fully exhausted resin is put in a column, and a fixed amount of regenerant passed through. The type and quantity of regenerant would be appropriate to the application under consideration. The equivalents of ions displaced or adsorbed by the resin are determined, and the regeneration capacity can be expressed in terms of equivalents per litre of resin, or as a percentage of the total volume capacity of the resin (known as *regeneration efficiency*), which can conveniently be determined on the same measured volume of resin.

Figure 3 clearly shows the significance of moisture retention on the kinetic performance of a resin. As discussed earlier, a gel resin of a given type with a lower moisture retention will have a higher total capacity, but this higher capacity is not reflected by the regeneration capacity, and under many conditions the operating capacity, of the resin.

For the reasons discussed earlier, macroporous resins will generally have a lower regeneration efficiency than their gel counterparts. Table 1 gives an approximate indication of the regeneration efficiencies of the different categories of resin, using typical regeneration amounts of 60–80 g regenerant per litre of resin.

Conclusions

The main characteristics of ion exchange resins are summarized in Table 2.

Most current developments in ion exchange resin manufacture have been based on modifying production techniques to give more uniform bead distributions at lower production costs. One exception has been the introduction of a range of highly porous Macronet adsorbent resins which are finding applications in the removal of trace levels of organic contaminants in aqueous, and even gaseous, feed stocks, as well as replacing activated carbon in the removal of coloured bodies from sugar syrups.

There are some new developments of resins as pharmaceutical products or in the extraction of precious metals from spent ores. Newer and more exotic applications are continually being found for ion exchange resins outside the conventional water treatment field, but these generally use existing resin types or only slight modifications thereof.

See also: II/Ion Exchange: Historical Development; Inorganic Ion Exchangers; Organic Ion Exchangers; Organic Membranes; Theory of Ion Exchange.

Table 2 Typical characteristics of ion exchange resins

	<i>Strong acid</i>	<i>Weak acid</i>	<i>Strong base</i>	<i>Weak base</i>
Functional group	$-\text{SO}_3^-\text{H}^+$	$-\text{COOH}$	$-\text{CH}_2\text{N}^+\text{OH}^-$ $(\text{CH}_3)_3$	$-\text{CH}_2\text{N}(\text{CH}_3)_2$ $(\text{CH}_3)_2$
Effect of pH on exchange capacity	Largely independent	Negligible in acid solutions	Largely independent	Negligible in alkaline solutions
Resin salts	Stable	Hydrolyse on washing	Stable	Hydrolyse on washing
Regeneration	Excess strong acid required	Readily regenerated	Excess strong base required	Readily regenerated

Further Reading

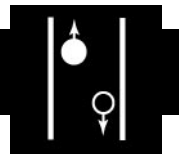
Adams, BA and Holmes EL (1935) *J. Soc. Chem. Ind.*, 54.
 Dale JA and Irving J (1992) Comparison of strong base resin types. In: Slater MJ (ed.) *Ion Exchange Advances – Proceeding of IEX'92*, pp. 33–40. London/New York: Elsevier Applied Science.
 Golden LS and Irving J (1972) Osmotic and mechanical strength in ion-exchange resins. *Chemistry and Industry*, 837–844.

Mikes J (1958) *J. Polym. Sci.*, 30, 615–23.
 Williamson WS and Irving J (1996) A preliminary comparison of Type II and Type III strong base anion resins at the new Plymouth power station, New Zealand. In: Grieg JA (ed.) *Ion Exchange Developments and Applications – Proceedings of IEX'96*, pp. 43–50. UK: The Royal Society of Chemistry.

ION EXCHANGE: ZEOLITES

See III / ZEOLITES: ION EXCHANGERS

ION FLOTATION



L. O. Filippov, Laboratoire Environnement et Minéralurgie, INPL-ENSG, Nancy, France

Copyright © 2000 Academic Press

Introduction

Sebba published a paper in 1959 in which he discussed a new method (ion flotation) for recovering solute from dilute solutions by adding surfactant, with subsequent adsorption of the solute onto bubbles. The principles of the process and the characteristics of the solute–surfactant product formed in solution were discussed in his monograph on ion flotation published in 1962. The method rapidly became popular and researchers in several countries have studied various aspects of the separation of metallic ions, trace elements, molecules, inorganic anions and organic matter from aqueous solutions. Many laboratory-scale studies have been carried out, most of them aimed at development, analytical applications, water purification, resource recycling, removing radionuclides from solutions, and recovering metals from sea water.

A comprehensive development of all aspects of the subject was presented in a monograph on adsorptive bubble separation techniques, edited by Lemlich in 1972, in which details and applications of ion and precipitate flotation methods were reported by Pinfeld.

The research group directed by Grieves made an important contribution to the theoretical and applied aspects of ion and precipitate flotation during the 1960s, particularly on wastewater treatment. They showed that flotation efficiency of long-chain surfactants was the result of physicochemical aspects of particle growth and dispersion. But the adsorption of surfactant onto the solid and gas phases was identified as a factor limiting bubble-particles attachment in some cases of ion flotation.

The adsorption of the surface-active solutes to the gas–liquid interface was studied by Rubin. An analysis based on the Gibbs and Langmuir isotherm and on an originally developed approach of long-chain ion adsorption in a solution containing several surface-active species was used to determine the effect of their concentrations on the ratio of distribution coefficients. This author also described the kinetic parameters for ion and precipitate flotation.

A detailed review of the precipitate and adsorbing colloid flotation technique with a comprehensive literature review appears in the monograph published in 1983 by Clarke and Wilson.

Golman has given a qualitative description of the chemical and kinetic aspects of ion flotation and some industrial applications, including the removal of molybdenum from solutions of hydrometallurgical flow-sheets. He has also given methods for treating foam products and purifying process residual solutions.

measured from samples of single and dual-phase materials, operated in a pressure-driven mode, plotted as a function of inverse temperature. This figure is intended to give some appreciation of the fluxes that are attainable; however, they are not normalized to a given partial pressure gradient or thickness of membrane, and thus the fluxes are not directly comparable. Taking a value of between 10 and $100 \text{ L m}^{-2} \text{ min}^{-1}$ as the level of oxygen flux needed for practical applications, it can be seen that the cobalt-containing single-phase materials give appreciable oxygen fluxes above about 900°C . It is interesting to note on this figure that the dual-phase material, fabricated from $(\text{Bi}_2\text{O}_3)_{0.75}(\text{Y}_2\text{O}_3)_{0.25}\text{-Ag}$ (35 v/v), approaches the lower bound of the practical fluxes at temperatures of 800°C .

It is not sensible to put data for electrical driven COGs on the same figure, given the restrictions mentioned above, however, some comparable figures are interesting. An equivalent flux of $15.8 \text{ L m}^{-2} \text{ min}^{-1}$ is

readily achievable with planar COG stack based on zirconia and operating at 1000°C . Similar performance has been reported for a system based on a CGO-operating temperature of 800°C .

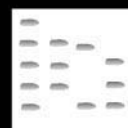
Further Reading

Bouwmeester HJM and Burggraaf AJ (1996) Dense ceramic membranes for oxygen separation. In: Burggraaf AJ and Cot L (eds) *Fundamentals of Inorganic Membrane Science and Technology*, pp. 435–528. New York: Elsevier.

Bouwmeester HJM and Burggraaf AJ (1997) Dense ceramic membranes for oxygen separation. In: Gellings PJ and Bouwmeester HJM (eds) *The CRC Handbook of Solid State Electrochemistry*, pp. 481–553. Boca Raton: CRC Press.

Steele BCH (1998) Ceramic ion conducting membranes and their technological applications. *C.R. Acad. Sci. Paris*, t.1, Serie II c, 533–543.

ION EXCLUSION CHROMATOGRAPHY: LIQUID CHROMATOGRAPHY



K. Tanaka, The National Industrial Research Institute of Nagoya, Nagoya, Japan

P. R. Haddad, University of Tasmania, Hobart, Australia

Copyright © 2000 Academic Press

Introduction

Ion exclusion chromatography (IEC) is a relatively old separation technique, attributed to Wheaton and Bauman, which is now staging an impressive comeback for the simultaneous determination of ionic species. IEC provides a useful technique for the separation of ionic and nonionic substances using an ion exchange stationary phase in which ionic substances are rejected by the resin while nonionic or partially ionized substances are retained and separated by partition between the liquid inside the resin particles and the liquid outside the particles. The ionic substances therefore pass quickly through the column, but nonionic (molecular) or partially ionized substances are held up and are eluted more slowly.

IEC is also referred to by several other names, including ion exclusion partition chromatography, ion chromatography-exclusion mode, and Donnan exclusion chromatography. In this article we use the term ion exclusion chromatography.

Generally, anions (usually anions of weak acids) are separated on a strongly acidic cation exchange resin in the hydrogen form and are eluted as the corresponding fully or partially protonated acids, while cations (usually protonated bases) are separated on a strongly basic anion exchange resin in the hydroxide form and are eluted as the corresponding bases. The eluents used are usually water, water/organic solvent mixtures, dilute (high conductivity) aqueous solutions of a strong acid, or dilute (low conductivity) aqueous solutions of a weak acid. A conductivity detector is commonly used to monitor the column effluent and, when the eluent conductivity is extremely high, a suitable suppressor system is generally used. UV-visible detection is also used as a selective detector in the determination of some aliphatic and aromatic carboxylic acids and some inorganic anions, such as nitrite and hydrogen sulfide. Using IEC, it is possible to separate weakly ionized anions such as fluoride, phosphate, nitrite, aliphatic carboxylic acids, aromatic carboxylic acids, bicarbonate, borate, aliphatic alcohols, sugars, amino acids, water, and others, as well as ammonium, amines, and others, based on a combination of the separation mechanisms of ion-exclusion, adsorption, and/or size-exclusion. Further discussion of these mechanisms may be found elsewhere in the encyclopedia.

More recently, a new concept in IEC has been developed in which a combination of a weakly acidic cation exchange resin and a weak-acid eluent is used for the separation of strong acid anions (such as sulfate, chloride and nitrate) and weak acid anions by an ion exclusion mechanism, together with the simultaneous separation of mono- and divalent cations by a cation exchange mechanism. The application of this method is described in this article.

Comprehensive reviews of IEC may be found in the texts of Haddad and Jackson, and of Gjerde and Fritz (see Further Reading). The goal of the present article is to explain the fundamental theory and some selected applications of IEC and to focus on some recent developments.

Background

Separation Mechanism

In conventional IEC of ionic and nonionic substances, a poly(styrene-divinylbenzene) (PS-DVB) based strongly acidic cation exchange resin in the hydrogen form is used exclusively as the separation column. The resin bed can be considered to consist of three distinct components:

1. a solid resin network with charged functional groups (the membrane);
2. occluded liquid within the resin beads (the stationary phase); and
3. the mobile liquid between the resin beads (the mobile phase or eluent).

The ion exchange resin acts as a hypothetical semipermeable membrane (a Donnan membrane) separating the two liquid phases (2) and (3). This membrane is permeable only for nonionic substances. When a mixture of analytes is injected onto the ion exchange column, anionic analytes are ion-excluded from the occluded liquid phase based on the Donnan membrane equilibrium established by the fixed negative charges on the cation exchange resin and therefore pass quickly through the column. On the other hand, nonionic substances may partition between the two liquid phases (2) and (3) and therefore pass more slowly through the column. Partially ionized analytes experience a lesser degree of repulsion by the membrane and are therefore eluted at retention times intermediate between fully ionized analytes and neutral analytes. This ion exclusion effect can be seen in **Figure 1A**, which shows the separation of aliphatic carboxylic acids.

In addition to this electrostatic ion exclusion effect, the separation process taking place on the surface of the resin particle may be influenced by hydro-

phobic adsorption and size exclusion effects, depending on the nature of the solute. These effects can be seen in **Figure 1B**, which shows the separation of sugars such as mono- and disaccharides by size exclusion, and the separation of alcohols such as methanol, ethanol, propanol and butanol by hydrophobic adsorption effects (**Figure 1C**).

Cation exchange resin columns with fairly large dimensions are often used for IEC because the retention volume (V_r) of the analyte is determined by the general equation:

$$V_r = V_0 + K_d V_i \quad [1]$$

where V_0 is the interstitial volume, V_i is the volume of eluent occluded within the pores of the resin beads, and K_d is a distribution coefficient ranging from 0 to 1. A large V_i value is needed to obtain good separations because of the narrow K_d range, assuming that only the ion exclusion effect is predominant in the separation of ionic and nonionic substances. This equation is essentially the same as the general equation for size exclusion chromatography.

When the V_r values of analytes measured on a strongly acidic cation exchange resin by elution with water are plotted against pK_{a1} (first dissociation constant), the plot shown in **Figure 2** is obtained. V_r values of strong acids, which are fully ionized, are independent of pK_{a1} , showing that the strong acid anions have been completely ion-excluded by the fixed sulfonate ions of the resin. V_r values of the weak acids such as phosphoric, hydrofluoric, formic, and acetic acids increase proportionally with pK_{a1} , which shows that the weak acids have been partially ion-excluded by the fixed sulfonate ions of the resin and there has been some permeation of these analytes into the occluded liquid phase inside the resin. This permeation correlated with the pK_{a1} values of the analytes between 1.3 and 6.4. The V_r values of very weak acids such as carbonic and boric acids are independent of pK_{a1} . From **Figure 2** and eqn [1], it is clear that the V_r values of the strong acids correspond to V_0 and the difference between V_r values of the strong acids and the very weak acids corresponds to V_i .

The K_d values of strong acids, weak acids, and very weak acids calculated from eqn [1] are between 0 and 1, except for weak acids having a hydrophobic nature, such as propionic, butyric and hydrogen sulfide. For these species, an adsorption effect is evident. As an example, propionic acid is eluted at a larger retention volume than expected from consideration of its pK_{a1} value alone, with the additional retention being attributable to hydrophobic adsorption of the analyte on the unfunctionalized regions of the stationary phase.

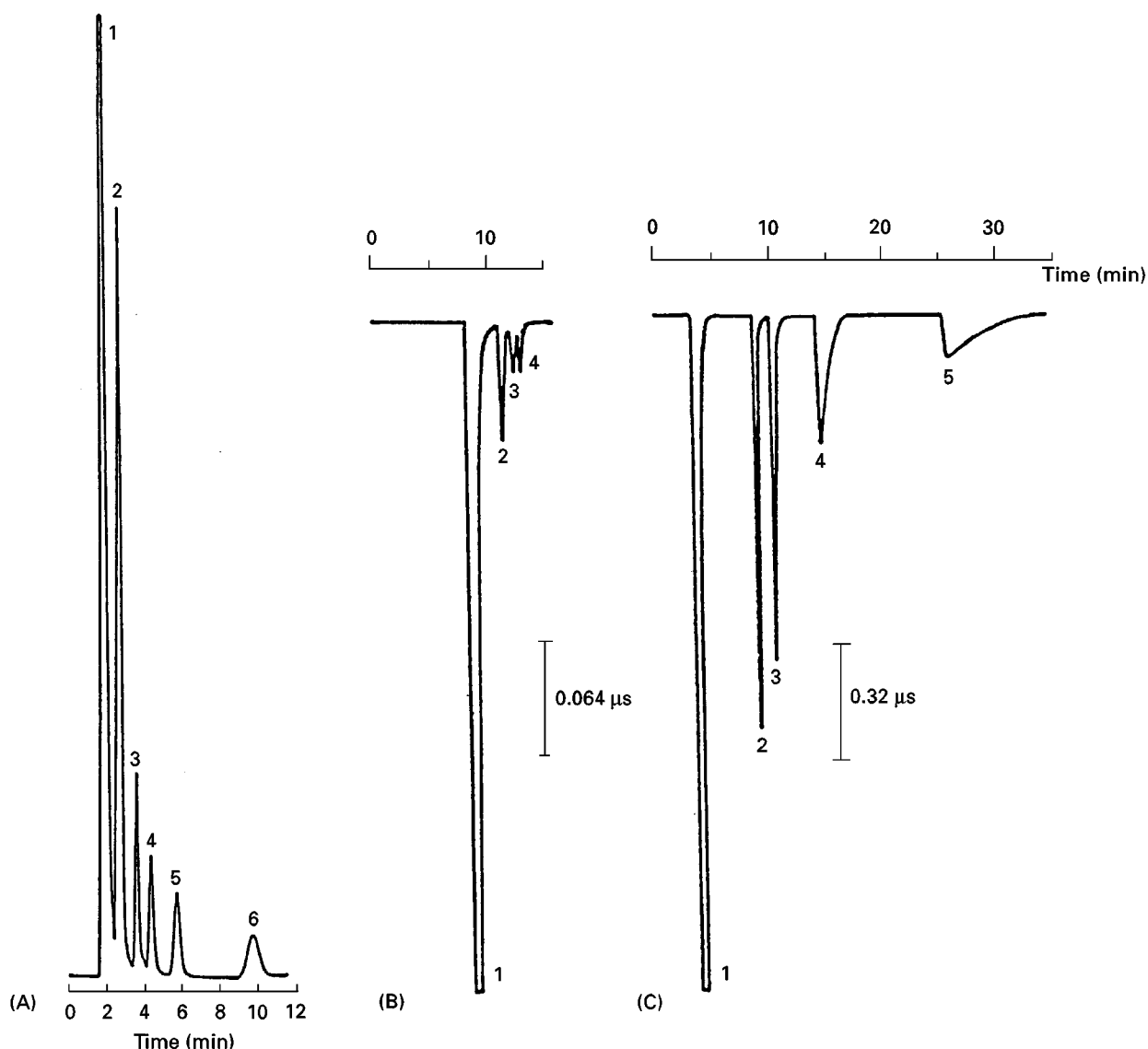


Figure 1 IEC separation of (A) aliphatic carboxylic acids by elution with 0.5 mmol L^{-1} benzoic acid/5% acetonitrile and (B) alcohols and (C) sugars by elution with 1 mmol L^{-1} sulfuric acid/water on a PS-DVB-based strongly acidic cation exchange resin column (8 mm i.d. \times 20 cm long).

(A) Peaks: 1, sulfuric acid (V_0); 2, formic acid; 3, acetic acid; 4, propionic acid; 5, butyric acid; 6, valeric acid. (B) Peaks: 1, dip; 2, sucrose; 3, glucose; 4, fructose. (C) Peaks: 1, dip; 2, methanol; 3, ethanol; 4, propanol; 5, butanol. (Figure 1A reproduced with permission from Fritz, 1988, and Figures 1B and 1C from Tanaka and Fritz 1986.)

In addition to the use of PS-DVB-based cation exchange resin, new IEC methods on polymethacrylate-based weakly acidic cation exchange resin and hydrophilic unfunctionalized silica gel have recently been developed to separate some of the more hydrophobic carboxylic acids. Figure 3 shows the IEC separation of some hydrophobic aliphatic and aromatic carboxylic acids on PS-DVB (Figure 3A) and polymethacrylate-based cation exchange resins (Figure 3B), and on unfunctionalized silica gel (Figure 3C), using 5 mmol L^{-1} sulfuric acid as eluent.

As can be seen from Figure 3, the V_r values of hydrophobic carboxylic acids increase with increasing hydrophobicity of the stationary phase (PS-DVB > polymethacrylate > silica).

Turning now to IEC of bases (cations) performed on strong anion exchange resins in the hydroxide form, some similar retention trends to those described above can be noted. Ionic analytes such as sodium and potassium ions are completely ion-excluded from the fixed positive charged resin phase and are eluted at a retention volume of V_0 , while nonionic

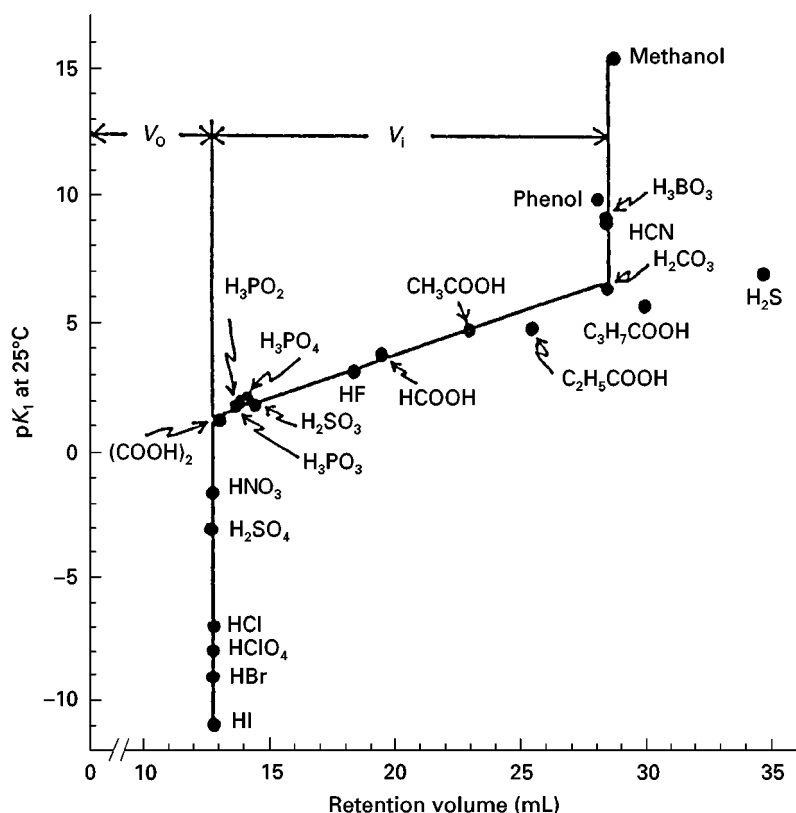


Figure 2 Relationship between retention volumes and their first dissociation constants for inorganic anions, carboxylic acids and nonionic substances on a PS-DVB-based strongly acidic cation exchange resin column (8 mm i.d. \times 55 cm long) by elution with water. (Reproduced with permission from Tanaka *et al.*, 1979.)

substances will permeate into the resin phase and are eluted at a retention volume of $V_0 + V_i$. Weak bases, such as ammonia and amines, are eluted at intermediate retention volumes, depending on their pK_b values and their hydrophobicity. As a result, weakly ionized cations can be separated from strongly ionized cations by the ion exclusion mechanism.

Instrumentation, Stationary Phases and Eluents

Ion exclusion chromatographic systems consist of the same components as any high performance liquid chromatography instrument. A UV detector is often used for the sensitive and selective detection of UV-absorbing substances such as aliphatic and aromatic carboxylic acids. However, this detector is insensitive to some aliphatic carboxylic acids, sugars and alcohols. Although a refractive index detector can be used as a bulk detector, the detection response is not high and the detector is flow- and temperature-sensitive. The most popular and universal detection method for IEC is conductivity. In order to decrease or suppress the eluent background conductivity, a membrane

suppressor system can be used (normally when the eluent is highly conducting), or alternatively a weak-acid eluent (aliphatic or aromatic carboxylic acids) of low conductivity can be used.

The most common resins used in ion exclusion chromatography are high capacity PS-DVB-based strongly acidic cation exchange resins of 5 μ m particle size. As discussed earlier, polymethacrylate-based weakly acidic cation exchange resin or unfunctionalized silica gel can also be employed.

Although the IEC separation of ionic and nonionic substances may be carried out simply by using water as the eluent, dilute aqueous solutions of some mineral acids or weak carboxylic acids give greatly improved peak shape and are therefore preferred for high resolution separations. Decreasing the pH of the eluent increases the retention of weakly ionized analytes such as carboxylic acids owing to a decrease in the fraction of the ionized analyte present. Therefore, the eluent pH is a very important factor in regulating retention volumes in IEC. Organic modifiers such as methanol and acetonitrile are often used to reduce hydrophobic interactions of the analytes with the resin. A further approach that may be used

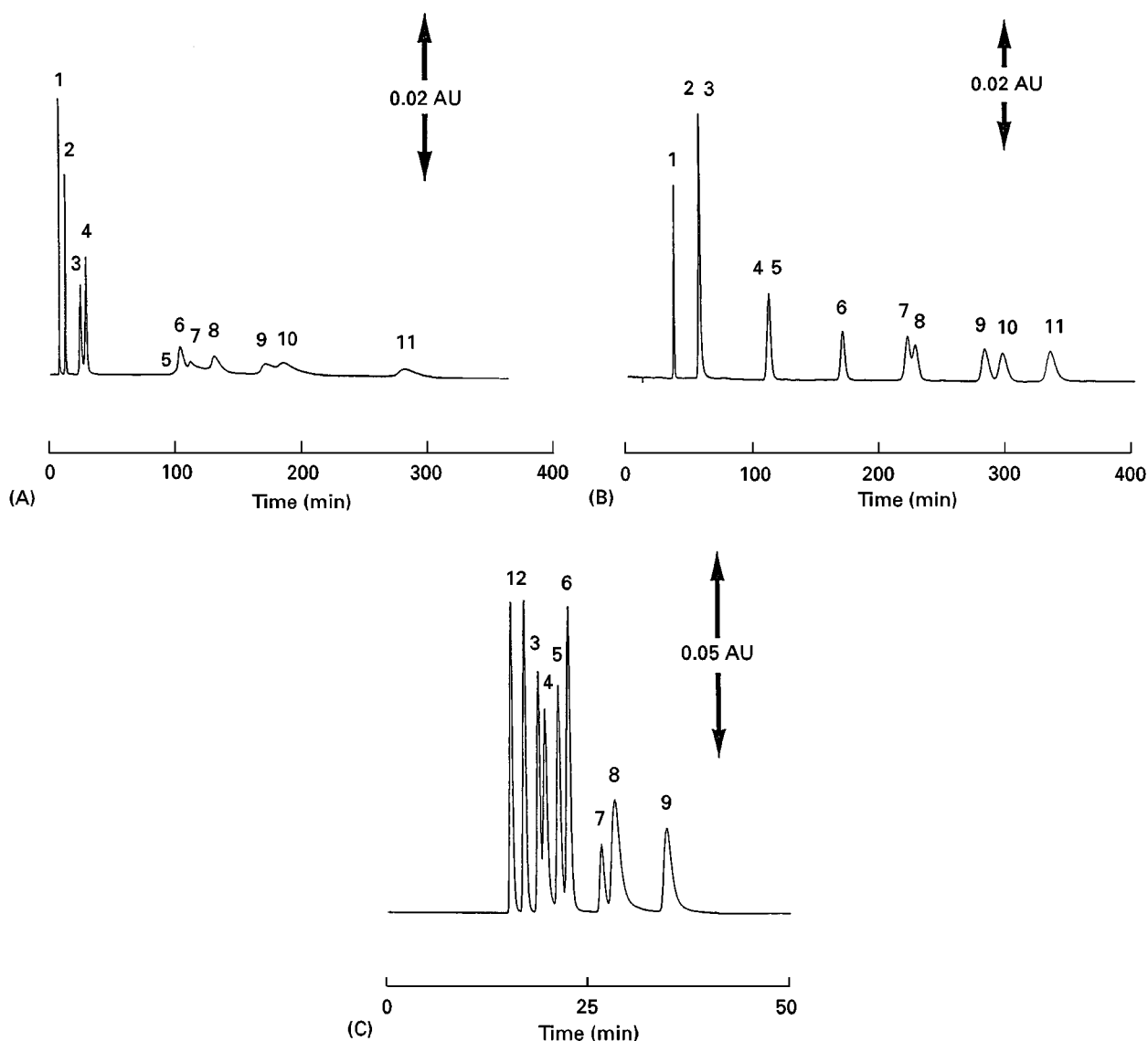


Figure 3 IEC separation of aromatic carboxylic acids on (A) PS-DVB-based strongly acidic cation exchange resin column, (B) polymethacrylate-based weakly acidic cation exchange resin, and (C) unfunctionalized silica gel by elution with 5 mmol L^{-1} sulfuric acid at 1 mL min^{-1} . Column size: $7.8 \text{ mm i.d.} \times 30 \text{ cm}$ long for all.

(A) Peaks: 1, pyromellitic acid; 2, trimellitic acid; 3, hemimellitic acid; 4, phthalic acid; 5, trimesic acid; 6, *m*-hydroxybenzoic acid; 7, phenol; 8, *p*-hydroxybenzoic acid; 9, terephthalic acid; 10, isophthalic acid; 11, benzoic acid. (B) Peaks: 1, hemimellitic; 2, pyromellitic acid; 3, phthalic acid; 4, trimellitic acid; 5, phenol; 6, benzoic acid; 7, *m*-hydroxybenzoic acid; 8, *p*-hydroxybenzoic acid; 9, isophthalic acid; 10, salicylic acid; 12, trimesic acid. (C) Peaks: 1, pyromellitic acid; 2, trimellitic acid; 3, hemimellitic acid; 4, terephthalic acid; 5, isophthalic acid; 6, phthalic acid; 7, phenol; 8, salicylic acid; 9, benzoic acid. (Reproduced with permission from Ohta *et al.*, 1996.)

to decrease the hydrophobic adsorption of analytes onto the resin is the addition of hydrophilic species, such as sugars, polyols and polyvinyl alcohol, to the eluent.

Optimization of Ion Exclusion Chromatographic Separation

To optimize an IEC separation, careful selection of the following experimental parameters must

be made:

1. the type of matrix used as the stationary phase (PS-DVB, polymethacrylate or silica);
2. the nature of the functional group (e.g. strong or weak acid);
3. the ion exchange capacity (low or high);
4. the nature of the eluent (e.g. strong or weak acids);
5. the pH of the eluent;

6. the amount of organic modifier present in the eluent; and
7. the type of detector used (universal or selective).

Selected Applications

Carboxylic Acids

Separation of carboxylic acids is probably the most common use of IEC. Carboxylic acids such as formic, acetic, propionic, butyric, valeric, citric, tartaric, oxalic, malonic, benzoic, salicylic, and others have been determined using UV and conductivity detection. **Table 1** lists some recent applications of IEC for these analytes. These methods have been applied to a wide variety of very complex sample matrices, such as biological materials, foods, beverages, pharmaceuticals, environmental materials and others. The separation is almost always performed on a PS-DVB-based cation exchange resin in the hydrogen form; examples of such separations may be found elsewhere in the encyclopedia. As an example of the use of alternative stationary phases, the separation of aliphatic carboxylic acids on a silica gel column by elution with 5 mmol L⁻¹ sulfuric acid is shown in **Figure 4**.

Weak Inorganic Acids and Bases

IEC has found increasing use for the determination of weakly ionized inorganic anions such as fluoride, nitrite, phosphate, sulfite, arsenite, arsenate, bicarbonate, borate and cyanide. This approach is very effective for the determination of weakly ionized anions in samples containing a high concentration of

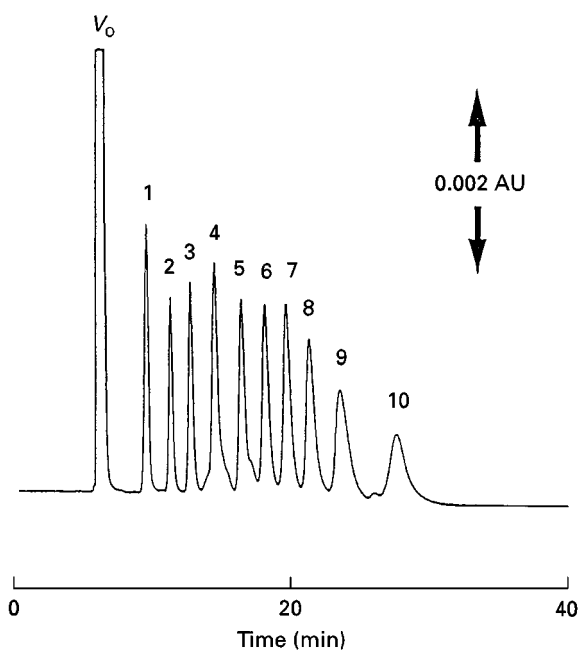


Figure 4 IEC separation of aliphatic carboxylic acids on silica gel column (7.8 mm i.d. \times 30 cm long) by elution with 0.05% heptanol/0.5 mmol L⁻¹ sulfuric acid at 1 mL min⁻¹. Peaks: V₀, nitric acid; 1, formic acid; 2, acetic acid; 3, propionic acid; 4, butyric acid; 5, valeric acid; 6, caproic acid; 7, heptanoic acid; 8, caprylic acid; 9, pelargonic acid; 10, capric acid. (Reproduced with permission from Ohta *et al.*, 1996.)

ionic species, e.g. seawater and wastewaters. **Figure 5** shows the separation of bicarbonate in tap waters by IEC with conductimetric detection by elution with water. The monitoring of bicarbonate ion is very important for the quality control of tap water and for

Table 1 Some applications of the determination of carboxylic acids by IEC

Sample	Column	Eluent	Detection ^a
Fermentation plants	Dionex HPICE-AS6	0.4/0.6 mmol L ⁻¹ heptafluoro-butyric acid	CD/S
Wine	Waters Radial Pak 5	0.2 mmol L ⁻¹ potassium dihydrogen phosphate	UV
Food	Shim-Pak SCR-102H	2 mmol L ⁻¹ toluenesulfonic acid	CD
Wine	TSKgel OA-Pak	0.75 mmol L ⁻¹ sulfuric acid	UV
Beverage	Shim-Pak IE	5 mmol L ⁻¹ sulfuric acid	UV
Silage liquor	Dionex IonPac-IEC AS-5	0.9/3.2 mmol L ⁻¹ perfluorobutyric acid	CD/S
Air	Dionex HPICE-AS1	2 mmol L ⁻¹ hydrochloric acid	CD/S
Ground water	Interaction Ion-300	0.2 mmol L ⁻¹ octansulfonic acid	CD/UV
Wine	Bio-Rad Aminex HPX 87-H	1 mmol L ⁻¹ camphorsulfonic acid	P/UV
Rainwater	Dionex HPICE-AS1	0.05 mmol L ⁻¹ sulfuric acid	CD
Rainwater	Hamilton PRPX-300	5 mmol L ⁻¹ sulfuric acid	UV
Air	Aminex-HPX 87H	0.25 mmol L ⁻¹ sulfuric acid/benzoic acid	CD
Bread/cake	TSKgel SCX	2 mmol L ⁻¹ phosphoric acid	UV
Antarctic ice	Bio-Rad HPX-87H	5 mmol L ⁻¹ methansulfonic acid	UV
Beverages	TSKgel SCX	5/10 mmol L ⁻¹ sulfuric acid	CD
Sewage	Yokogawa SCX-252	2 mmol L ⁻¹ sulfuric acid	CD/S
Rat plasma	Hitachi Gelpak C-620-10	0.3% phosphoric acid	FL

^aCD, conductivity; S, suppressor; UV, UV spectrometry; P, potentiometry; FL, fluorimetry.

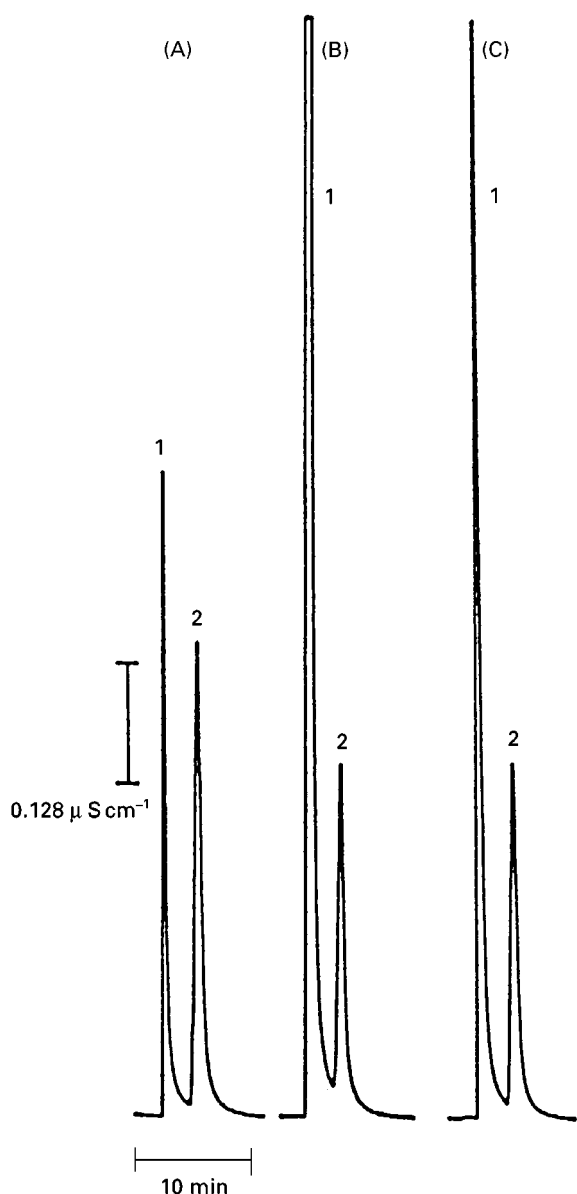


Figure 5 IEC separation of bicarbonate in tap waters on a PS-DVB-based strongly acidic cation exchange resin column (7.5 mm i.d. \times 10 cm long) by elution with water. (A) Raw tap water (10-fold dilution); (B) tap water after softening treatment; (C) tap water (10-fold dilution). Peaks: 1, strong acid anions; 2, bicarbonate ion. (Reproduced with permission from Tanaka and Fritz, 1987.)

the evaluation of the buffering capacity of natural waters.

Ethanolamines and ammonium ion may be successfully determined by IEC with UV or conductimetric detection on a PS-DVB-based strongly basic anion exchange resin in the hydroxide form. Industrial and environmental applications of the determination of ammonium ion are also common and include samples such as biological treatment process waters and ur-

ban river waters, as shown in Figure 6. Table 2 lists some of the recent applications of IEC in the analysis of weak inorganic acids and bases.

Strong Inorganic Acids

More recently, a simple and highly sensitive method involving simultaneous ion exclusion/cation exchange chromatography with conductimetric detection on a polymethacrylate-based weakly acidic cation exchange resin in the hydrogen form has been developed for the determination of inorganic strong acid anions such as sulfate, nitrate and chloride ions, and strong base cations such as sodium, ammonium, potassium, magnesium and calcium ions commonly found in acid rainwater. Use of a weak acid eluent (such as tartrate) permits both the anions and the cations to be determined, based on a simultaneous

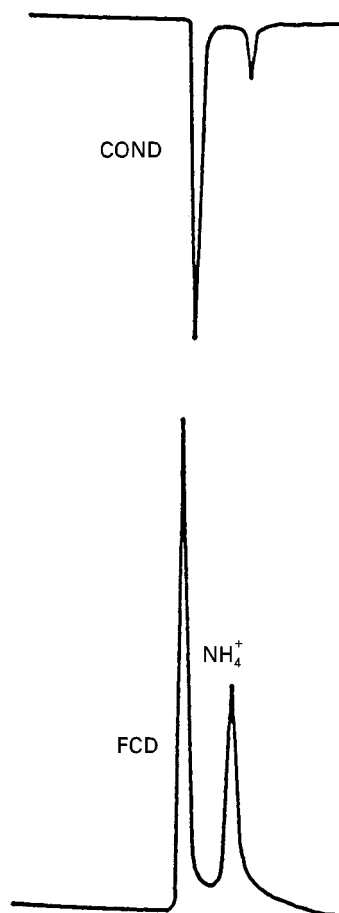


Figure 6 IEC separation of ammonium ion in biological treatment process water on a PS-DVB-based strongly basic anion exchange resin column (8 mm i.d. \times 550 mm long) by elution with water at 1 mL min⁻¹.

First peak is alkali- and alkaline earth metal cations. FCD, flow coulometric detector; COND, conductivity detector. (Reproduced with permission from Tanaka *et al.*, 1979.)

Table 2 Some applications of the determination of inorganic anions and cations by IEC

<i>Ion(s)</i>	<i>Sample</i>	<i>Column</i>	<i>Eluent</i>	<i>Detection^a</i>
F ⁻ , HCO ₃ ⁻	Beverages	Shim-pak SCR-102H	0.5 mmol L ⁻¹ toluene/sulfonic acid	CD
F ⁻	Wastewater	Hitachi-2613	20% methanol/water	CL/CD
HCO ₃ ⁻	Natural water	TSKgel SCX	Water	CD
HCO ₃ ⁻	Natural water	Develosil 30-5 (silica gel)	Water/borate	CD
NO ₃ ⁻ , NO ₂ ⁻	Wastewater	Hitachi 2613	10% methanol/water	UV
NO ₂ ⁻	Drinking water	Anion exclusion	5 mmol L ⁻¹ sulfuric acid	EC
As(V), As(III)	Sulfuric acid	Dionex HPICE AS-1	10 mmol L ⁻¹ phosphoric acid	UV
As(III)	Mineral water	Aminex HPX-85H	0.01 mol L ⁻¹ phosphoric acid	EC
Silica	Seawater	Dionex Ionpak ICE-AS1	Water	ICP-M
Silica	Natural water	Yokogawa SCX1-251	6.6 mmol L ⁻¹ perchloric acid	CL
Borate	–	Excelpak ICS-R3G/ICS-R 35	1 mmol L ⁻¹ sulfuric acid	VIS
Borate	Soil	Wescan Ion exclusion	0.3 mol L ⁻¹ D-sorbitol	CD
CN ⁻	Tap water	Sulfonated PS/DVB gel	1 mmol L ⁻¹ sulfuric acid	VIS
SO ₃ ²⁻	Beer	Dionex HPICE-AS1	10 mmol L ⁻¹ sulfuric acid	EC
PO ₄ ³⁻	Wastewater	Hitachi-2613	40% acetone/water	EC
SO ₄ ²⁻ , NO ₃ ⁻ , Cl ⁻ , Na ⁺ , NH ₄ ⁺ , K ⁺ , Mg ²⁺ , Ca ²⁺ ^b	Rainwater	TSKgel OA-PAK	5 mmol L ⁻¹ tartaric acid/7.5% methanol	CD
NH ₄ ⁺	Wastewater	Hitachi 2632	Water	CD/E

^aCD, conductivity; UV, UV spectrometry; EC, electrochemical; ICP-MS, inductively coupled plasma-mass spectrometry; CL, chemiluminescence; VIS, visible spectrometry.

^bSimultaneous ion-exclusion cation-exchange.

ion exclusion and cation exchange mechanism on the same stationary phase. The conductimetric detector responses are positive for the anions (which are separated by IEC and detected directly) and negative for

the cations (which are separated by ion exchange and are detected indirectly). The effectiveness of this method has been demonstrated in its application to acid rain, as shown in Figure 7.

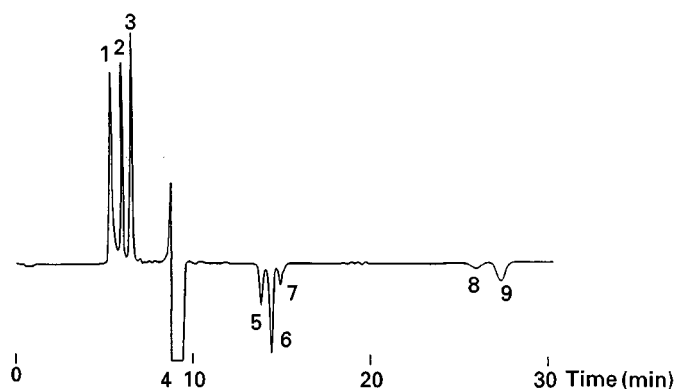


Figure 7 Simultaneous ion exclusion/cation exchange chromatographic separation of strong acid anions and mono- and divalent cations in acid rain at pH 4.7 on a polymethacrylate-based weakly acidic cation exchange resin column (7.8 mm i.d. × 300 cm long) by elution with 6 mmol L⁻¹ tartaric acid–7.5% methanol/water at 1.2 mL min⁻¹. Peaks: 1, SO₄²⁻; 2, Cl⁻; 3, NO₃⁻; 4, dip; 5, Na⁺; 6, NH₄⁺; 7, K⁺; 8, Mg²⁺; 9, Ca²⁺. (Reproduced with permission from Tanaka *et al.*, 1994.)

Table 3 Some applications of the determination of nonionic substances by IEC

Analyte	Sample	Column	Eluent	Detection ^a
Sugar	Wine, beer	TSKgel SCX	5 mmol L ⁻¹ sulfuric acid	CD
Sugar	–	Merck Polyspher OA-YH	10 mmol L ⁻¹ sulfuric acid	UV
Sugar	Juice, milk	Bio-Rad HPLX 87-H Aminex	0.1 mol L ⁻¹ sodium hydroxide	EC
Sugar	Corn syrup	PS-DVB sulfonate resin	Water	RI
Poloyol	–	Bio-Rad HPX-87H	Water	EC
Alcohol	Wine, beer	TSKgel SCX	5 mmol L ⁻¹ sulfuric acid	CD
Formaldehyde	Air	Rezex RFQ	1 mmol L ⁻¹ sulfuric acid	EC
Dimethyl sulfoxide	Seawater	Bio-Rad HPX-87H	5 mmol L ⁻¹ phosphoric acid	UV
Water	Organic solvents	Bio-Rad Aminex Q-150S	Acetonitrile/methanol	UV
<i>p</i> -Benzoquinone	Wastewater	TSKgel SCX	20% methanol	UV
Ketone	–	TSKgel SCX	5 mmol L ⁻¹ sulfuric acid	CD
Trichloroethanol	Plasma, urine	Aminex A-15	10 mmol L ⁻¹ K ₂ SO ₄ , 10 mmol L ⁻¹ KOH	RI

^aCD, conductivity; EC, electrochemical; UV, UV absorption; RI, refractive index.

Neutral Compounds

Neutral compounds such as sugars and alcohols can be separated by IEC, as shown earlier in Figure 1B and 1C. Table 3 lists some of the recent applications of IEC in this field. One of the more significant applications of IEC is its use for the determination of water. Using a short column packed with PS-DVB-based cation exchange resin in the hydrogen form and eluting with methanol containing a small amount of strong acid, a peak for water can be obtained with a spectrophotometric detector at 310 nm. This method is applicable to the determination of water in some organic solvents.

Conclusion

Despite the fact that IEC is a relatively old separation technique, new and diverse applications continue to emerge. IEC remains the method of choice for the separation of low molecular weight carboxylic acids. The separation mechanism of IEC is complicated by the fact that a wide range of processes are known to contribute to retention. At present there is no comprehensive mathematical retention model that accounts for all of the retention processes in IEC. For this reason, optimization of separations is generally performed on an empirical basis rather than through the use of computerized optimization routines such as those employed in many other forms of chromatography. However, there has been considerable recent activity in the study of retention processes in IEC and it can be expected that suitable computer optimization methods will soon appear.

See also: II/Chromatography:Liquid: Mechanisms: Ion Chromatography. III/Acids: Liquid Chromatography. Porous Polymers: Liquid Chromatography.

Further Reading

- Fortier NE and Fritz JS (1989) *Journal of Chromatography* 462: 323–332.
- Fritz JS (1988) *Journal of Chromatography* 439: 3–11.
- Gjerde D and Fritz JS (1987) *Ion Chromatography*, 2nd edn. New York: Huthig.
- Haddad PR and Jackson PE (1990) *Ion Chromatography – Principles and Applications*. Amsterdam: Elsevier.
- Haddad PR, Hao F and Glod BK (1994) *Journal of Chromatography A* 671: 3–9.
- Ohta K, Tanaka K and Haddad PR (1996) *Journal of Chromatography A* 739: 359–365; 782: 33–40.
- Tanaka K and Fritz JS (1986) *Journal of Chromatography* 361: 151–160.
- Tanaka K and Fritz JS (1987) *Journal of Chromatography* 409: 271–279.
- Tanaka K and Fritz JS (1987) *Analytical Chemistry* 59: 708–712.
- Tanaka K and Haddad PR (1996) *Trends in Analytical Chemistry* 15: 266–273.
- Tanaka K, Ishizuka T and Sunahara H (1979a) *Journal of Chromatography* 174: 153–157.
- Tanaka K, Ishizuka T and Sunahara H (1979b) *Journal of Chromatography* 177: 21–27.
- Tanaka K, Ohta K, Fritz JS, Miyanaga A and Matsushita S (1994) *Journal of Chromatography A* 671: 239–248.
- Tanaka K, Ohta K, Fritz JS, Lee Y-S and Shim S-B (1995) *Journal of Chromatography A* 706: 385–393.
- Tanaka K, Ohta K and Fritz JS (1996) *Journal of Chromatography A* 739: 317–325.
- Tanaka K, Ohta K and Fritz JS (1997) *Journal of Chromatography A* 770: 211–218.
- Weiss J (1995) *Ion Chromatography*. Weinheim: VCH Publishers.

Further Reading

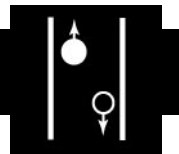
Adams, BA and Holmes EL (1935) *J. Soc. Chem. Ind.*, 54.
 Dale JA and Irving J (1992) Comparison of strong base resin types. In: Slater MJ (ed.) *Ion Exchange Advances – Proceeding of IEX'92*, pp. 33–40. London/New York: Elsevier Applied Science.
 Golden LS and Irving J (1972) Osmotic and mechanical strength in ion-exchange resins. *Chemistry and Industry*, 837–844.

Mikes J (1958) *J. Polym. Sci.*, 30, 615–23.
 Williamson WS and Irving J (1996) A preliminary comparison of Type II and Type III strong base anion resins at the new Plymouth power station, New Zealand. In: Grieg JA (ed.) *Ion Exchange Developments and Applications – Proceedings of IEX'96*, pp. 43–50. UK: The Royal Society of Chemistry.

ION EXCHANGE: ZEOLITES

See III / ZEOLITES: ION EXCHANGERS

ION FLOTATION



L. O. Filippov, Laboratoire Environnement et Minéralurgie, INPL-ENSG, Nancy, France

Copyright © 2000 Academic Press

Introduction

Sebba published a paper in 1959 in which he discussed a new method (ion flotation) for recovering solute from dilute solutions by adding surfactant, with subsequent adsorption of the solute onto bubbles. The principles of the process and the characteristics of the solute–surfactant product formed in solution were discussed in his monograph on ion flotation published in 1962. The method rapidly became popular and researchers in several countries have studied various aspects of the separation of metallic ions, trace elements, molecules, inorganic anions and organic matter from aqueous solutions. Many laboratory-scale studies have been carried out, most of them aimed at development, analytical applications, water purification, resource recycling, removing radionuclides from solutions, and recovering metals from sea water.

A comprehensive development of all aspects of the subject was presented in a monograph on adsorptive bubble separation techniques, edited by Lemlich in 1972, in which details and applications of ion and precipitate flotation methods were reported by Pinfeld.

The research group directed by Grieves made an important contribution to the theoretical and applied aspects of ion and precipitate flotation during the 1960s, particularly on wastewater treatment. They showed that flotation efficiency of long-chain surfactants was the result of physicochemical aspects of particle growth and dispersion. But the adsorption of surfactant onto the solid and gas phases was identified as a factor limiting bubble-particles attachment in some cases of ion flotation.

The adsorption of the surface-active solutes to the gas–liquid interface was studied by Rubin. An analysis based on the Gibbs and Langmuir isotherm and on an originally developed approach of long-chain ion adsorption in a solution containing several surface-active species was used to determine the effect of their concentrations on the ratio of distribution coefficients. This author also described the kinetic parameters for ion and precipitate flotation.

A detailed review of the precipitate and adsorbing colloid flotation technique with a comprehensive literature review appears in the monograph published in 1983 by Clarke and Wilson.

Golman has given a qualitative description of the chemical and kinetic aspects of ion flotation and some industrial applications, including the removal of molybdenum from solutions of hydrometallurgical flow-sheets. He has also given methods for treating foam products and purifying process residual solutions.

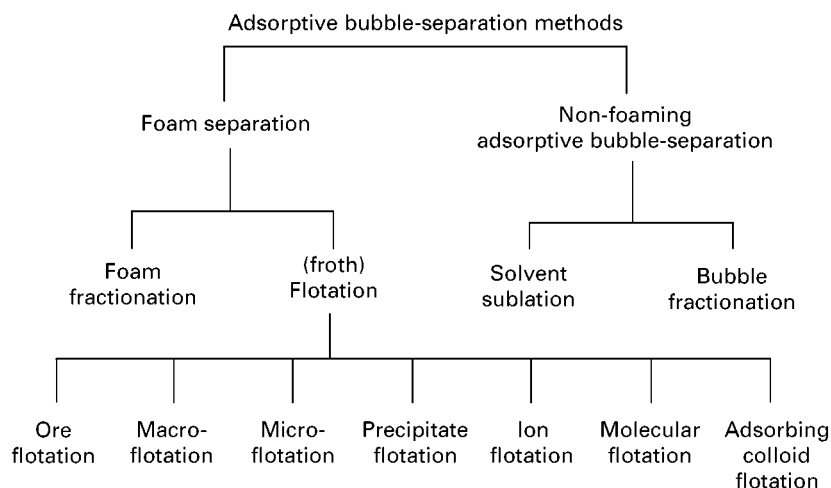


Figure 1 Schematic classification of the adsorptive bubble-separation techniques. (Reproduced with permission from R Lemlich (1972) *Adsorptive Bubble Separation Techniques*. New York: Academic Press. Copyright.)

Relatively few studies on this subject have been published recently. They focus mainly on extending the applications of the method. The progress made in column flotation techniques, especially with bubble generation systems, offers hydrodynamic conditions favourable for ion flotation. Filippov has reported on the results of recent pilot-scale studies applying this technique to precipitate and ion flotation. It was demonstrated that aggregate formation and destruction under low dissipation energy are the parameters controlling precipitate flotation. The combined use of column and bubble spargers in ion flotation provided a removal rate for metals equivalent to that of laboratory-scale trials.

Phenomenology and Classification

Separation by adsorption onto bubbles is based on the difference between the surface activities of the solute species. These species can be ionic, molecular, or colloidal, and their adsorption onto the bubble-liquid interface depends on their surface-active, adhesion or electric properties. A species that is not adsorbed onto bubbles can be made to do so by adding a surfactant to the solution.

The classification of methods based on these separation phenomena are shown in **Figure 1**. Lemlich called these processes ‘adsbubble (adsorptive bubble) separation methods’, while the term ‘adsbubble method’ was recommended by Sasaki, since the method involves both adsorption and adhesion. The classification of these techniques in **Figure 1** is based on the formation of the foam, which leads to two main groups:

- foam adsorptive separation and
- non-foaming bubble separation.

The nature of the entity is introduced later.

The Golman classification based on the phenomena at the various levels of process leads to another classification of ion recovery process (**Table 1**). This classification take into account:

- the type of phase that accumulates the floated species: foam, scum, organic or aqueous phase;
- the nature of the components to be adsorbed onto the bubble surface: ions or molecules, particles of the precipitate or carrier; and
- the collector use to modify the hydrophobic properties of the entities

Ion Flotation

Definition

Ion flotation, developed by Sebba, is a surface-inactive separation method that involves the removal of ions or molecules (*colligend*) from aqueous solution by adding surfactant, that is adsorbed onto the surface of rising bubbles. The surfactant-colligend product (*sublat*) may be formed in bulk solution or

Table 1 Classification of ion-recovery method

Flotation	Flotation			
	Froth	Foam	Solvent sublation	Bubble fractionation
Adsorptive		Without collector With collector		
Precipitate		Hydrophobic Hydrophobized		
Carrier		Hydrophobic Hydrophobized		

only at the higher concentrations produced by preferential adsorption on the bubble surface. The process is called *adsorption* ion flotation if the sublat is a soluble complex or a pair of ions. The process is *adhesion* ion flotation if the sublat forms a new phase in aqueous solution. A hydrophobic product (*scum*) is formed at the surface of the solution by destruction of the rising bubbles.

The formation of foam is not necessary for ion flotation. The hydrophobic nature of the scum makes it stable on the solution surface. A foam thin-layer phase may be needed to isolate the scum from the liquid phase and to evacuate it later to avoid it redissolving. Stable foam is a factor limiting the application of ion flotation, because it requires less foam formed or a lower gas rate. Solution entrainment also decreases the colligend concentration in the foam.

If the formation of a foam during ion flotation is undesirable or impossible (i.e. recovery of organic ions or quantitative separation), the process of *solvent sublation* is used. This method involves spreading a thin immiscible organic solvent layer on the surface of the water causing dissolution of the floating sublat.

Theory

There are several ways to describe ion flotation and to determine the quantity of surfactants required for optimal separation. One considers the bubble surface to be an ion exchanger owing to surfactant adsorption. The charge created is compensated for by the adsorption of inactive ions of opposite charge. Jorne and Rubin assumed that the radius of the hydrated ions determined the maximum approach of opposite ions to the bubble surface, based on the theory of a double electrical layer. Their theoretical calculations were confirmed experimentally. Another approach highlights the stability constants of soluble compounds (complexes and pairs of ions) formed by the surfactant with the colligend and an oppositely charged ion, according to Moore and Philipps. Some believe that a solid phase is formed (assumed to be two-dimensional) in the adsorption layer on the bubble surface. These assumptions mostly concern the adsorption mechanism of ion flotation.

Sebba and Golman used the product of the activities of the collector and colligend (L_A) to explain adhesion. The equilibrium of the system is determined by the constant of stability of sublat K_A and the solubility of its molecular form S_{AM} , when $L_A = K_A S_{AM}$. If we assume that a sublat flotation occurs as a colloid rather than molecules, the fraction P of the stoichiometric ratio Φ of collector/colligend molar concentrations is given according to

Golman by:

$$P = R + \frac{l}{m} \sqrt[m]{\frac{L_A}{f_{RX}^m f_A^l (1-R)^l C_A^{m+l}}} \quad [1]$$

where R is the rate of colligend recovery; f_{RX} , f_A are the surfactant RX and colligend A activity coefficients respectively; C_A is the colligend concentration; m and l are the stoichiometric coefficients of the reaction of sublation of A by RX.

The parameter $(L_A)_{P/R}$ calculated from this formula allows the deduction of the value of L_A that is needed to obtain a recovery R for a given Φ . This formula does not take into consideration changes in the ionic strength I with collector concentration. However, for the characteristic colligend concentrations and for Φ being practically stoichiometric the parameter I does not limit the application of this approach. This was confirmed by Golman for the ion flotation of various species.

The influence of the surface-active species concentration and solubility product P_s of sublat ($P_s = \text{constant}$ for $I = \text{constant}$) on the recovery of the colligend and the residual surfactant concentration is given in Figure 2. This confirms the experimental results. It is preferable to carry out ionic flotation in the concentration ranges of the collector so that $P = 1$ (values of Φ are stoichiometric). Colligend recovery when $P < 1$ is often reduced. The

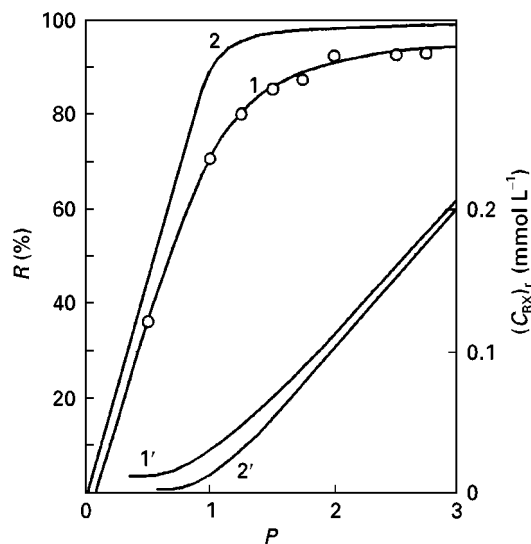


Figure 2 Colligend recovery R (1, 2) and surfactant residual concentration $C_{(RX)l}$ (1', 2') vs. surfactant consumption for a given sublat solubility product P_s : 1, 1' - $P_s = 10^{-9}$, 2, 2' - $P_s = 10^{-10}$. Solid lines, calculated results from eqn (1); \circ , experimental results of ion flotation of ReO_4^- with laurylammonium chloride, $L_A = 3.9 \times 10^{-7}$. (Adapted from AM Golman (1982) *Ionnaya Flotatsiya*, p. 42. Moscow: Nedra.)

considerable residual concentration of collector in the bulk solution when $P > 1$ decreases the process efficiency (economic). This makes it difficult to reuse a solution without purification and/or environmental problems. The excess collector also prevents flotation because of secondary adsorption onto bubbles and sublat surfaces if the sublat is solid, as demonstrated by Grieves and Golman.

Colligend: Collector Ratio

Ion flotation operates with dilute solutions of the colligend (10^{-5} to 10^{-3} mol L⁻¹). Higher colligend concentrations require significant collector consumption, increasing the operation costs. The ratio Φ of collector and colligend molar concentrations is one of the main parameters of ion flotation. The changes in the amount of colligend removed with Φ is shown in Figure 3, which are typical of ion-flotation systems.

As noted by Pinfeld, the ratio Φ required for complete flotation must be at least stoichiometric (Φ_{st}). This is true for the adhesion mechanism of ion flotation, but with adsorption, the amount of collector that can float without sublation depends on the bubble residence time in the liquid. The colligend cannot be completely removed in this case with a

stoichiometric Φ . The experimental results of Doyle, available in the literature, show that slightly more than stoichiometric amounts ($P = 1.1$ – 1.2) of sodium dodecyl sulfate were needed to reduce the heavy metals ion concentration to very low levels. Moreover, the curve behaviour around point $P = 1$ in Figure 3 could indicate the mechanism of ion flotation.

Role of Electrolytes and Anions

The role of electrolytes is significant during the collector-colligend and sublat–bubbles interaction. Their role must be taken into account because of their significant quantities in real industrial solutions. Electrolytes modify the ionic strength and can react with the collector. For $I = \text{constant}$, two cases are possible:

1. The opposite-charged ion forms a soluble product with the collector. The separation is more selective for higher colligend and for low opposite-charged ion concentrations. A higher collector concentration than that required by Φ also renders ion flotation more efficient.
2. The collector–colligend interaction product is insoluble. A critical concentration of the opposite ion can be defined, below which it does not react with the collector and consequently does not influence further colligend recovery.

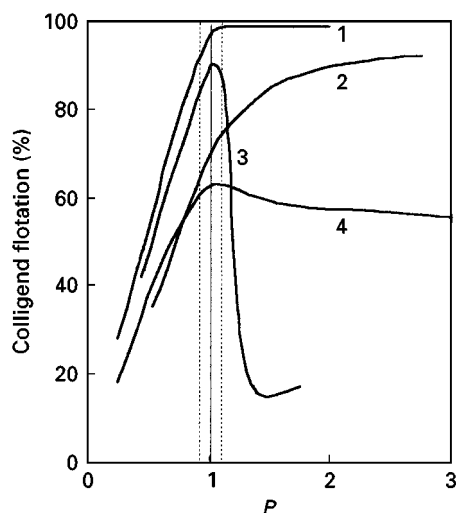


Figure 3 Dependence of the flotation of various colligends on the fraction (P) of collector : colligend ratio (Φ): (1) Ge^{3+} + tetradecylammonium chloride ($\Phi_{st} = 2$); (2) ReO_4^- + laurylammonium ($\Phi_{st} = 1$); (3) Cr^{6+} with hexadecylammonium bromide ($\Phi_{st} = 1.04$); (4) Ga^{3+} + amide oxime ($\Phi_{st} = 3$). (Adapted respectively from: (1,2) AM Golman (1983) *Fiziko-khimitscheskie Aspekty Ionnoi Flotatsii*, p. 245, Moscow: Nauka; (3) *The Chemical Engineering Journal* 9: R Grieves Foam Separations: A Review, 93, Copyright (1975), with permission from Elsevier Science; (4) with permission from A Masuyama et al. *Industrial Engineering Chemical Research* 29: 290, Copyright (1990) American Chemical Society.)

Changing the ionic strength by adding NaCl allows the selective separation of metal oxyanions (MeO^{4-} or MeO^{2-}) with hexadecyldimethylbenzylammonium chloride as collector (Figure 4). The recovery of oxyanion flotation as a function of $p[\text{NaCl}]$ illustrates the phenomena described above.

The change in ionic strength of the medium caused by adding anions reduces the effectiveness of ion flotation. The flotation of dichromate with a quaternary amine (adhesion mechanism) is blocked in the sequence, according to Grieves: $\text{PO}_4^{3-} > \text{SO}_4^{2-} > \text{Cl}^-$. The recovery of $\text{Fe}(\text{CN})_6^{4-}$ with a cationic collector is influenced by: $\text{CN}^- > \text{NO}_3^- > \text{Cl}^- > \text{SO}_4^{2-} > \text{CO}_3^{2-} > \text{PO}_4^{3-} > \text{P}_2\text{O}_7^{4-}$. This contradiction can be explained by the process taking place in each case.

The foam flotation of dichromate is controlled by the preliminary formation of a solid phase followed by adsorption onto bubbles (similar to precipitate flotation). The adsorption of differently charged ions influences surface hydration of the bubbles and the precipitate, the importance of which is directly related to the charge of the anion. Ferricyanide flotation is by solvent sublation. As was noted by Pinfeld, the smaller ionic radius of the anion, the more effective the collector competes with the colligend. The use of 2-octanol to collect the sublat on the solution

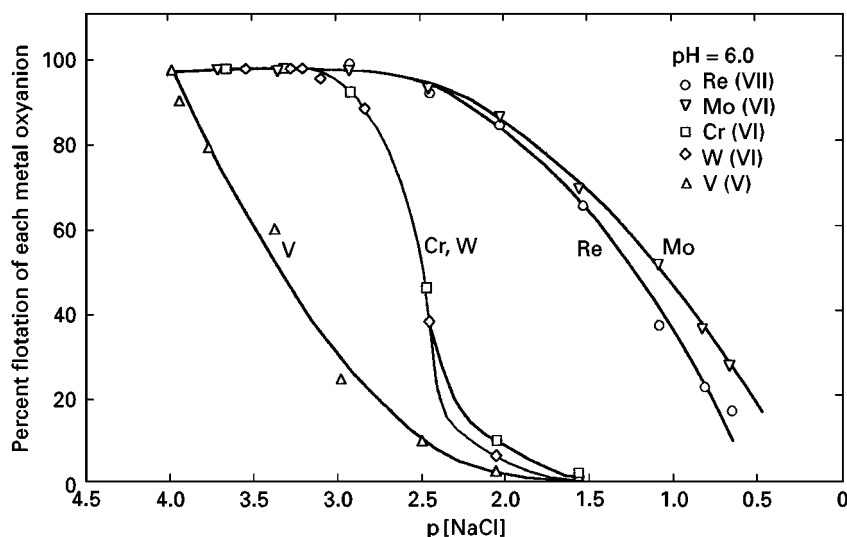


Figure 4 Effect of the negative logarithm of the sodium chloride concentration on the percentage flotation of each of five metal oxyanions. (Reprinted from *The Chemical Engineering Journal* 9: R Grieves Foam Separations: A Review, 93, Copyright (1975), with permission from Elsevier Science.)

surface can cause solvent to dissolve and become adsorbed onto the bubble surface instead of the collector. Under these conditions the lower charged anions neutralize the adsorbed collector, so that it is no longer available to float the colligend.

pH

Ion flotation is particularly sensitive to the pH because the pH determines the nature and the charge of the collector (the degree of ionization) and the colligend (hydrolysis), and causes variations in the ion-collecting mode. Pinfold also notes that the following phenomena that can take place when the pH changes:

- colligend hydroxides may form, and precipitate flotation may take place instead of ion flotation;
- extreme values of pH block flotation because the ionic strength is higher;
- the stability of scum could be affected because of sublat redispersion in the solution.

Temperature

The temperature influences all aspects of ion flotation, i.e. the collector and sublat solubility, the sublat particle size and the flotation results. Its role were confirmed by Grieves for the flotation of Cr^{6+} at $\text{pH} = 4.1$ with quaternary amine salts with hydrocarbon chains of C_{14} , C_{16} and C_{18} . The collector used acted as a precipitant, dispersing and flocculating agent depending on the temperature, determining the orientation of the collector molecules adsorbed on the sublat surface. The surfactant also acted as foaming agent because of the free collector adsorbed on the bubbles.

Optimal metal removal with C_{16} - and C_{18} -amine salts occurred with $\Phi = 1.04$ and 33 or 40°C . The abrupt drop in removal rate at higher values of Φ was explained by excess surfactant adsorbing to the particles, stabilizing them and preventing further aggregation. One of the most significant conclusions deduced from these experiments is that the particles of the precipitate $> 25\ \mu\text{m}$ are completely removed from solution, while almost no particles $< 7\ \mu\text{m}$ are floated.

Precipitate Flotation

According to Pinfold, precipitate flotation includes all processes in which an ionic species is precipitated in the liquid phase and is subsequently removed by attachment to the bubble surface. It is difficult to clearly distinguish between 'ion flotation' and 'precipitate flotation' when a collector is used as a precipitation agent.

If the colligend is first precipitated by a non-surface-active ion and made hydrophobic by adsorption of a surfactant, the process is termed *precipitate flotation of the first kind*. Many studies have been carried out on the removal of metal ions from aqueous solution (i.e. sea water) by this method. Heavy metals are generally precipitated with an alkali as the hydroxide and then removed by flotation with an ionic collector. The other insoluble salts (sulfide, carbonate, sulfate) can be precipitated.

The *precipitate flotation of the second kind* uses no surfactant for bubble-particle attachment because it suggests that the solid phase formed by interaction of two hydrophilic species (colligend and precipitation

agent) is hydrophobic. The following precipitants have been used for various metal ions: benzoinoxime (Mo, Cu), benzoylacetone (U), α -furyldioxime (Ni), hydroxyquinoline (Cu, Zn, U), α -nitroso- β -naphthol (Ag, Co, Pd), dodecylpyridinium with a collector (Sr, V), etc.

Kinetics

Ion flotation controlled by adhesion is a precipitate-like flotation because the sublat formed is a solid phase that can also be flocculated by adding active chemical agents or by the action of the collector. The two ionic flotation modes (adsorption and adhesion) may be distinguished at the level of particle–bubble interaction, depending on the nature of the sublat.

- The sublat formed is an ionic pair or a soluble complex (adsorption): the adsorption activity of these species on the bubbles determines the effectiveness of the process.
- The sublat is formed in the liquid phase as particles of 10^{-3} to 10^{-1} μm : the interaction of the sublat and the bubbles is controlled by the diffusion of the particles in the hydrodynamic fields of the bubbles.
- The sublat is a precipitate with micron- or millimetre-sized particle: the interaction results in sedimentation of the particles of negligible mass on the bubbles if the surface forces support the attachment of the entities.

The time necessary for 90–99% colligend recovery at colligend concentrations of 10^{-5} to 10^{-2} mol L^{-1} indicates that sublat flotation as a precipitate is kinetically preferable than flotation of the molecules (Figure 5). The flotation mechanism was concluded from independent experiments on the solubility product, microscopy, separation of the precipitated phase by centrifugation and filtration.

Few studies on the kinetics of ion flotation are published, while there are many papers on mineral particle flotation. However the kinetic parameters of the process determine the practical applications of flotation because they determine the scale-up procedure adopted.

Apparatus: Future Developments

Almost all ion flotation tests are carried out in cells (batch or continuous mode) equipped with a sintered-glass device to generate bubbles. The use of the column-type cells allows the user to: vary the introduction point of the collector and feed solution containing the colligend; vary the height of the foam;

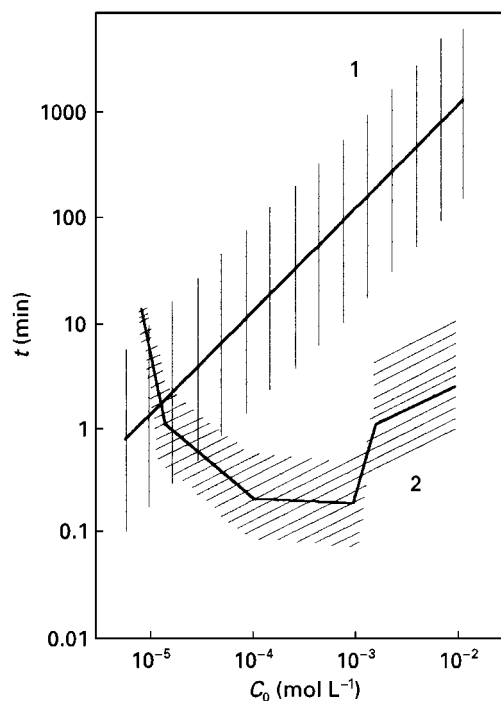


Figure 5 Comparison of the kinetic of adsorption and adhesion mechanism of ion flotation. (1) Adsorption mechanism; (2) adhesion mechanism. (Adapted from AM Golman (1982) *Ionnaya Flotatsiya*, p. 29. Moscow: Nedra.)

Colligend	Collector
Ba^{2+}	Laurylsulfonate-Na
$\text{Ag}(\text{S}_2\text{O}_3)^-$	Cetyldiethylbenzylammonium-Br
$\text{UO}_2(\text{CO}_3)_3^{4-}$	Cetyltrimethylammonium-Br
$\text{H}_3\text{W}_6\text{O}_{21}^{3-}$	Laurylammonium-Cl
$\text{H}_3\text{Mo}_7\text{O}_{24}^{3-}$	Cetylpyridinium acetate
	Cetyltrimethylammonium-Br
	Amine-C14
Ge^{3+}	Laurylammonium-Cl
	Cetyltrimethylammonium-Br

carry out sampling and/or *in situ* measurements if radioactive ‘tracers’ are used.

The most recent bubble-generating systems make column flotation a flexible tool for ion flotation.

A study of sublat formation and its structural organization showed that a column 75 mm in diameter and 3 m high could be used for ion flotation (Cr^{6+}) and for precipitate flotation (molybdenum). The bubble diameter determined the efficiency of separation by ion and precipitate flotation because of collision probability and aggregate stability in the microturbulence created by the rising bubbles. The flotation with small bubbles as in the dissolved-gas technique increases the collision probability. However, the low feed-flow rate of the process is a limiting parameter because of the low velocity of small rising

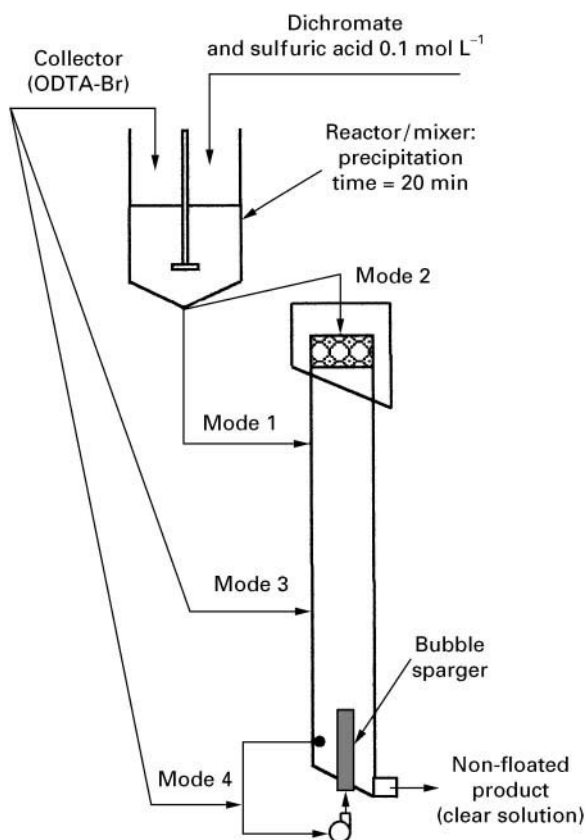


Figure 6 Ion flotation modes using column for Cr^{6+} recovery with ODTA-Br. Mode 1: precipitation–flotation. Mode 2: foam fractionating. Mode 3: ion flotation. Mode 4: precipitation on bubbles. (Reprinted from Filippov LO *et al.* Physicochemical mechanisms and ion flotation possibilities using column for Cr^{6+} recovery from sulphuric solutions, *International Journal Mineral Processing* 51: 229, Copyright (1997), with permission from Elsevier Science.)

bubbles. In addition, the flotation mechanism in this kind of technique, in which several small rising bubbles are trapped in a large precipitate floc structure, can cause transfer of the liquid present in the aggregate to the froth and reduce the separation efficiency.

Ion Flotation in a Column

The ion flotation of Cr^{6+} from sulfuric acid solutions (pH 1.5–2.0) with octadecyltrimethylammonium bromide (ODTA-Br) as collector is particularly difficult because a single chemical acts as precipitating, flocculating, dispersing and frothing agent. This is in addition to the problems of floating an element of negligible mass. It is thus nearly impossible for the precipitate to become adsorbed on bubbles because of an electrical charge of the same sign (owing to free collector) on the bubbles and precipitate particles. Several modes of ion flotation have been tested on a pilot scale (Figure 6).

In the classical mode of ion flotation (precipitation–flotation as described by Grieves), only the 200–240 μm diameter bubbles provide a low chromium recovery of 56.2–60.8%. An exceptionally stable, loaded froth with the liquid (7.0–19.0%) was carried over, which decreased the separation efficiency (Table 2). Some column/bubble generator assemblies can be used to solve the problems of bubble–precipitate electrostatic repulsion and collision. It has thus been possible to develop a new mode of ion flotation in which the chromium solution is introduced directly at the feeding point of column and the collector is introduced to the bubble generator. The strong surfactant properties of the collector caused to be adsorbed on the bubbles so that the chromium was precipitated on the gas phase. This new method gives about 81.6% Cr^{6+} removal by column flotation for a $\Phi = 1.2$ and a liquid residence time of 15–20 min. Retreatment of the solution can increase the total Cr recovery to 91.6%, with a Cr residual concentration of 4.5 mg L^{-1} , which corresponds to separation results by filtration.

Precipitate Column Flotation

The limiting conditions for molybdenum metal–organic precipitate flotation in columns are owing to aggregate stability under the turbulence created by upward movement of bubbles, which depends directly on the average bubble diameter. Pilot-scale flotation studies revealed the fundamental influence of the average bubble diameter and dissipation energy on molybdenum recovery in the form of precipitate obtained with the collector α -benzoin oxime for a molar concentration ratio of 2. It was therefore necessary to identify a bubble-size distribution and the gas hold-up in the column to ensure the flotation of low hydrophobic precipitate flocs, as they are extremely brittle with very low values of dissipated energy (0.01–0.05 W kg^{-1}). Destruction is conditioned by the aggregation mechanism (cluster–cluster type) and not only causes mean floc size to decrease from 150–350 μm to 30–50 μm , but also produces very fine particles that could elude collision with bubbles. Bubble spargers (Microcel, Flotaire, Imox) tested on a pilot scale provided the required values of these parameters for efficient column flotation (recovery up to 95%) of the precipitate for low superficial gas ($J_g = 0.22$ –0.55 cm s^{-1}) and feed flow rates ($J_l = 0.19$ –0.47 cm s^{-1}). An adjustment of the J_g/J_l ratio to optimal hydrodynamic conditions in counter-current pilot column corroborated laboratory-scale tests in the cell equipped with a fine porosity frit (No. 4).

Table 2 Main results on the hexavalent chromium removal by column flotation according to Figure 6^a

Ion-flotation mode	Chromium concentration in initial solution		Chromium residual concentration (mg L ⁻¹)	Chromium removal (%)	Stoichiometric ratio (Φ)	Average bubble diameter (mm)	Liquid entrainment (%)
	(mg L ⁻¹)	(mol L ⁻¹)					
Mode 1	52.3	10 ⁻³	22.9	56.2	2.0	0.23	12.5
Precipitation-flotation	52.3	10 ⁻³	20.5	60.8	2.0	0.21	7.5
	52.25	10 ⁻³	25.7	50.4	2.0	0.21	19.0
	52.24	10 ⁻³	21.0	59.8	1.2	0.22	6.6
Mode 2	52.52	10 ⁻³	17.7	66.3	2.0	—	4.5
Foam fractionating							
Mode 3	32.1	6 × 10 ⁻⁴	14.8	53.9	1.5	0.29	8.3
Ion flotation	52.38	10 ⁻³	33.0	37.0	1.2	0.27	6.2
Mode 4	23.6	4 × 10 ⁻⁴	8.0	66.1	1.2	0.36	4.2
Precipitation on bubbles	34.9	6 × 10 ⁻³	8.2	76.5	1.2	0.38	1.0
	52.33	10 ⁻³	8.7	83.0	2.0	0.33	1.7
	52.33	10 ⁻³	10.1	80.7	1.2	0.26	0.8
Retreatment of tail solution			4.4	91.6		0.32	—

^a(Reprinted from Filippov LO *et al.* Physicochemical mechanisms and ion flotation possibilities using column for Cr⁶⁺ recovery from sulphuric solutions, *International Journal Mineral Processing* 51: 229, Copyright (1997) with permission from Elsevier Science.)

Other Ion Flotation Related Processes Further Reading

Bubble Fractionation

This is the partial separation of components within a solution by the selective adsorption of surfactants, colloid or ultrafine particle species onto the bubble. The effect of separation is demonstrated by a concentration gradient along the column-like cell that allows removal of a colligend-rich solution from the top and depleted solution from the bottom of the cell. Separation efficiency clearly decreases with increasing column diameter as a result of axial diffusion of rising bubbles, which breaks up the concentration gradient.

Adsorbing Colloid Flotation or Carrier Flotation

This consists of the preliminary capture of colligend by the carrier particles (by adsorption, absorption, or co-precipitation), followed by charged-bubble flotation. Ion-exchange resin, activated charcoal, or the precipitate particles can be used as a carrier. The carrier particles can have flotation properties or be made hydrophobic by adding collector.

Molecular Flotation (Koisumi)

This is the recovery of molecules using a surfactant. The name molecular flotation is used for all flotation processes that involve the recovery of the molecular colligend or those analogous to ion flotation.

Clarke AN and Wilson DJ (1983) *Foam Flotation. Theory and Applications*. New York: Marcel Dekker.

Filippov LO, Joussemet R and Houot R (1997) Physicochemical mechanisms and ion flotation possibilities using column for Cr⁶⁺ recovery from sulphuric solutions. *International Journal of Mineral Processing* 51: 229.

Filippov LO, Joussemet R and Houot R (2000) Bubble spargers in column flotation: adaptation to precipitate flotation. *Minerals Engineering* 13: 37.

Grievies RB (1975) Foam separations: A review. *The Chemical Engineering Journal* 9: 93.

Grievies RB, Bhattacharya D and Ghosal JK (1976) Surfactant-colligend particle size effects on ion flotation: Influences of mixing time, temperature, and surfactant chain length. *Colloid and Polymer Science*, 254: 507.

Karger BL, Grievies RB, Lemlich R, Rubin AJ and Sebba F (1967) Nomenclature recommendations for adsorptive bubble separation methods. *Separation Science* 2: 401.

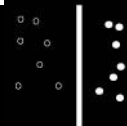
Lemlich R (ed.) (1972) *Adsorptive Bubble Separation Techniques*. New York, London: Academic Press.

Nicol SK, Galvin KP and Engel MD (1992) Ion flotation – potential application to mineral processing. *Minerals Engineering* 5: 1259.

Sebba F (1959) Concentration by ion flotation. *Nature* 184: 1062.

Sebba F (1962) *Ion Flotation*. Elsevier: Amsterdam, New York.

ION-CONDUCTING MEMBRANES: MEMBRANE SEPARATIONS



J. A. Kilner, Imperial College of Science,
Technology and Medicine, London, UK

Copyright © 2000 Academic Press

Introduction

Ceramic membranes are commonly used in separation processes involving the filtration of particulate matter from a fluid stream. This involves the use of controlled porosity ceramic materials, which essentially act as inert filters. More recently, dense ceramic membranes fabricated from ionic conductors have been proposed as active membranes for the high-temperature separation of oxygen from air for a variety of purposes.

The principle of using a dense ceramic ionic conductor to separate the ion-conducting species is, in itself, not new. The idea has been around since the turn of the century when Nernst first investigated solid electrolyte compositions for use as incandescent filaments in his glower devices. Since then ion-conducting ceramics have been used to separate a number of elements, for example oxygen, hydrogen and gallium, but mainly as a scientific curiosity and only on a laboratory scale. The current industrial interest in membrane separators was instigated by a Japanese group, who, in 1985, investigated dense oxide membranes, which were able to permeate substantial fluxes of oxygen at temperatures of 800–1000°C, with 100% selectivity. Since then there has been a rapid growth of both scientific and industrial interest in the use of these membranes for the separation of oxygen. The industrial interest has been driven by the possibility of providing compact oxygen separation plants for a number of applications including aerospace and medical, petrochemical and manufacturing industries.

This article describes a novel oxygen separation process, based on dense ion-conducting ceramic membranes. It is important to note that two different but related devices can be made from such membranes, both of which can be used in the oxygen separation process. In the first device, the driving force is supplied electrically and the membrane is made of an ionic conductor. In the second device, the driving force is supplied by a gradient in oxygen activity and the membrane consists of a mixed ionic electronic conductor. The materials used in the con-

struction of these devices and the devices themselves are described below.

Materials for Conducting Membranes

Ionic conduction in solids can be achieved in two main ways. Both require crystal structures in which there are a number of equivalent, partially occupied atomic sites. This condition of partial occupancy can occur either by the disordering of a low-temperature structure over two approximately equivalent sublattices, or by promoting large deviations from stoichiometry. Such oxygen ion-conducting materials can be further sub-divided into two groups: *electrolytes* that exhibit predominantly ionic conduction; and *mixed conductors*, materials in which there are both significant electronic and ionic contributions to the total conductivity. A useful concept to introduce at this point is the ionic transference number t_i . The ionic transference number is defined as the fractional contribution of the ionic component to the total conductivity. For a mixed conductor with both ionic (σ_i) and electronic (σ_e) conductivity, t_i is defined as:

$$t_i = \frac{\sigma_i}{\sigma_i + \sigma_e} \quad [1]$$

Clearly for solid electrolytes we require t_i to be very close to 1 and for mixed conductors $t_i < 1$.

The ionic conductivity of both types of material is thermally activated. The empirical relationship describing the ionic conductivity is given by:

$$\sigma = \frac{\sigma_0}{T} \exp\left\{\frac{-E_A}{kT}\right\} \quad [2]$$

where σ_0 is a constant pre-exponential factor, T is the absolute temperature, k the Boltzmann constant and E_A the observed activation energy for the process. Appreciable ionic conductivity for most oxygen conductors, greater than $10^{-1} \text{ S cm}^{-1}$, is only achievable at high temperatures (600–900°C) as the activation energies are always substantial (~ 50 – 100 kJ mol^{-1}).

Solid Electrolytes

Most practical oxide ion conductors are non-stoichiometric and are characterized by their ability

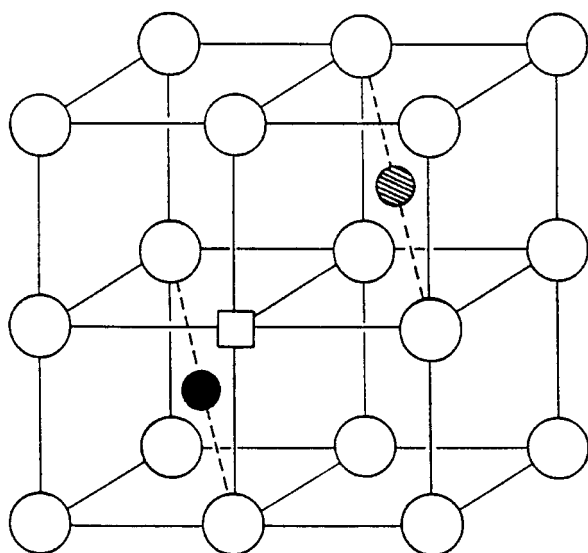


Figure 1 A half-unit cell of the fluorite structure showing a dopant cation and oxygen vacancy. ○, O²⁻ ion; ●, host cation (4⁺); □, vacancy; ●, dopant cation (2⁺ or 3⁺).

to accommodate large departures from the ideal oxygen stoichiometry, without breakdown of the crystal structure. For example, oxides of the fluorite structure shown in **Figure 1** display high ionic conductivities when doped with lower valent cations. In one such material, gadolinia doped ceria, the trivalent gadolinium substitutes for the tetravalent cerium ion, causing a charge imbalance in the lattice. The deficit of positive charge is balanced by the formation of oxygen vacancies, which restores the charge balance (see **Figure 1**). This process can be formalized into a defect equation using Kröger–Vink notation:



Ion transport (and hence charge transport) can take place in such materials by a mechanism involving ‘hopping’ into neighbouring vacant oxygen sites, provided the ion has sufficient energy to overcome the activation barrier, E_{m} , associated with the ionic migration. High ionic conductivity can be achieved by ensuring an optimum level of doping. Because of the relatively stable nature of the cations used in these materials there is a negligible electronic component to the conductivity, especially at high oxygen pressures.

Of the fluorite oxides, considerable attention has been given to the cubic stabilized zirconia (ZrO₂) system for application in both the ceramic oxygen generator (COG) and a closely related device, the solid oxide fuel cell (SOFC). Zirconia with 8 mol% Y₂O₃ (8-YSZ) adopts the fluorite structure and is

a pure ionic conductor over a wide range of oxygen partial pressures; however, as mentioned above, substantial ionic conductivity is only obtained at temperatures above 900°C. Ceria-gadolinia (CGO) displays similar ionic conductivity to YSZ but at much lower temperatures (~700°C), principally owing to a lower value of the activation energy observed for the conduction process. The main concern with CGO is that its electronic conductivity becomes substantial under reducing conditions due to the reduction of Ce⁴⁺ to Ce³⁺, which renders CGO unsuitable for high temperature applications where low partial oxygen pressures occur.

Of increasing interest is a new series of solid solutions which adopt the perovskite structure (see below) based on the parent compound LaGaO₃ (lanthanum gallates). Doped gallates of the type La_{1-x}Sr_xGa_{1-y}Mg_yO_{3-δ} (LSGM) have comparable ionic conductivity to CGO and do not appear to have any appreciable electronic conductivity. **Figure 2** shows a comparison of selected fluorite and perovskite ionic conductors as a function of temperature.

Mixed Conductors

Most of the mixed conductors of technological interest adopt the perovskite (ABO₃) structure (**Figure 3**). The structure is able to accommodate the substitution of many different cations into its framework, assuming the necessary ion size constraints are met. Again, non-stoichiometry is the key to achieving high transport rates of oxygen; however, in these materials, by definition, the electronic component of the conductivity is not negligible. Taking the perovskite-structured material lanthanum cobaltate (LaCoO₃) as an example, when a divalent cation such as strontium is substituted for trivalent lanthanum on the A-site, charge compensation takes place by a dual mechanism. This involves the creation of oxygen vacancies and a change in valency of the cobalt from Co³⁺ to Co⁴⁺. As described earlier, this substitution can be expressed in a defect equation using Kröger–Vink notation of the type:



where h^{\bullet} represents an electronic hole (Co⁴⁺). In this case both electronic compensation and vacancy compensation of the substitutional occurs, and t_i is usually substantially less than one.

One problem associated with the mixed conducting perovskite and perovskite-related materials is that the dual compensation mechanism leads to changing non-stoichiometry with temperature and atmosphere,

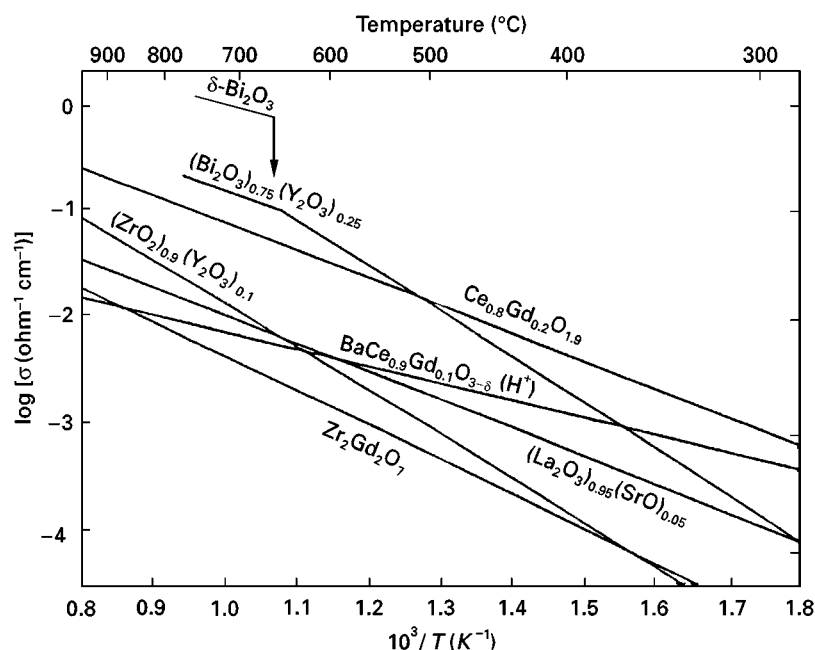


Figure 2 Oxygen ion conductivity of selected fluorite, fluorite-related and perovskite oxides.

i.e. the balance of vacancy and electronic compensation of the dopant changes with conditions. This manifests itself in a loss or gain of oxygen from the lattice. Most notable is the loss of oxygen with tem-

perature in a constant environment, and/or the sensitivity of the materials to oxygen activity at constant temperature. This loss of oxygen causes a large effective expansion coefficient, which can cause cracking of the membranes upon heating and/or upon the imposition of an oxygen activity gradient.

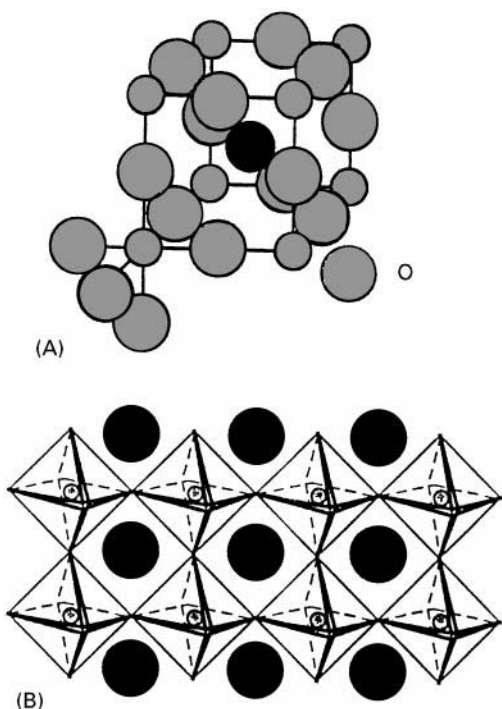


Figure 3 The perovskite structure. (A) Unit cell and (B) extended structure showing the corner-sharing BO_6 octahedra. ●, cation A; ●, cation B.

Dual Phase

Finding a single phase ceramic material that has high electronic and ionic conductivity while remaining mechanically and chemically stable is not a trivial matter—in fact, these requirements are often mutually exclusive. Materials that exhibit high oxygen ion fluxes also tend to possess high thermal expansion values, which can lead to catastrophic failure in a membrane subjected to a significant oxygen partial pressure gradient, as mentioned above. A way round this problem is to construct dual-phase membranes, effectively making a mixed conductor on a macroscopic scale (Figure 4). Such dual-phase materials consist of two separate phases, one an ionic conductor (e.g. YSZ) and the other an electronic conductor (Ag), which are mixed in suitable proportions to provide connectivity for both phases. The individual components are themselves stable at high temperature and in an oxygen pressure gradient. It is not as yet clear what is the best materials combination, or how to optimize the microstructures in order to maximize the oxygen flux that the membrane can transport.

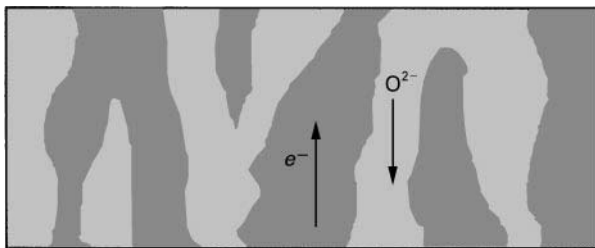


Figure 4 Schematic of a dual-phase membrane incorporating an ionic and electronic conducting phase.

Ion-Conducting Membrane Devices

Pressure Driven Devices

Pressure driven devices are perhaps the simplest form of ceramic oxygen generator. The membrane consists of a dense, gas-tight mixed ionic–electronic conductor (MIEC), which allows the transport of both oxygen ions and electronic species. The driving force for oxygen transport is a differential oxygen chemical potential applied across the membrane. This is achieved by applying a higher partial pressure of oxygen on the membrane feed side than on the permeate side (see **Figure 5**). The whole device may be operated well in excess of atmospheric pressure to achieve a pressurized permeate stream. The most practical design of such a device would be a series of thin-walled tubes. Obviously, the mechanical integrity of such a system is a major concern when very thin membranes are used, and some type of porous support would have to be employed in this case.

The device operates in the following manner. The first step is a surface reaction at the high-pressure surface of the membrane. The gaseous oxygen molecules interact with electrons at ‘active’ sites on the surface, they dissociate, become ionized and finally are incorporated into the oxide. The rate of this reaction is governed by the gas–solid surface ex-

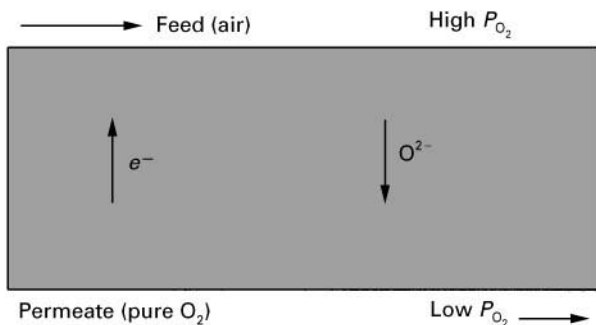


Figure 5 Schematic of a pressure-driven ceramic oxygen generator based on a mixed conducting oxide.

change coefficient, k . The second step is the diffusion of the oxide ions through the material to the lower pressure side where the reverse process occurs and oxygen is evolved, releasing electrons. The membrane in a pressure-driven device is electrically isolated, that is, there are no external electrical current paths. Thus, the membrane material must be a good electronic conductor to provide a return path for the electrons, providing a compensatory flux of electronic species to balance that of the oxygen ions. Normally, the level of electronic conductivity ($\approx 10^2$ – 10^3 S cm $^{-1}$) in these materials is much higher than the corresponding ionic conductivity (≈ 1 – 10^{-1} S cm $^{-1}$), i.e. $t_i \ll 1$, consequently it is the oxygen transport parameters that determine the achievable oxygen fluxes.

In this case, a simplifying model can be applied which allows some insight into the operation of the membranes. The ionic current through the membrane can be described in terms of the simple equivalent circuit shown in **Figure 6**. The apparent potential η is provided by the partial pressure drop across the membrane, and is defined using the Nernst equation:

$$\eta = \frac{RT}{4F} \ln \left\{ \frac{P'_{O_2}}{P''_{O_2}} \right\} \quad [5]$$

where P'_{O_2} and P''_{O_2} refer to the partial pressure of oxygen on each side of the membrane, T is the temperature, F is Faraday’s constant, and R is the gas constant. The membrane resistance (expressed as area specific resistance R_A (ohm cm 2)) is then described in terms of two components, the resistance of the bulk of the membrane to the passage of the ionic current R_0 and the resistance of the surface of the materials caused by the oxygen exchange process. This latter term is expressed as an equivalent electrode resistance R_E , assigned equally to both high and low pressure surfaces. The chief utility of this model is that it allows an easy visualization of the processes involved and it can be applied to the electrically driven separator with a slight modification. The ionic current density, $J_{O^{2-}}$ (A cm $^{-2}$), through the membrane of thickness L and of ionic conductivity σ can be expressed as:

$$J_{O^{2-}} = \frac{\eta}{(2R_E + R_0)} \quad [6]$$

$$= \frac{\eta}{\left(2R_E + \frac{L}{\sigma} \right)} \quad [7]$$

R_E can be expanded in terms of the surface exchange coefficient for the oxygen exchange process, k ,

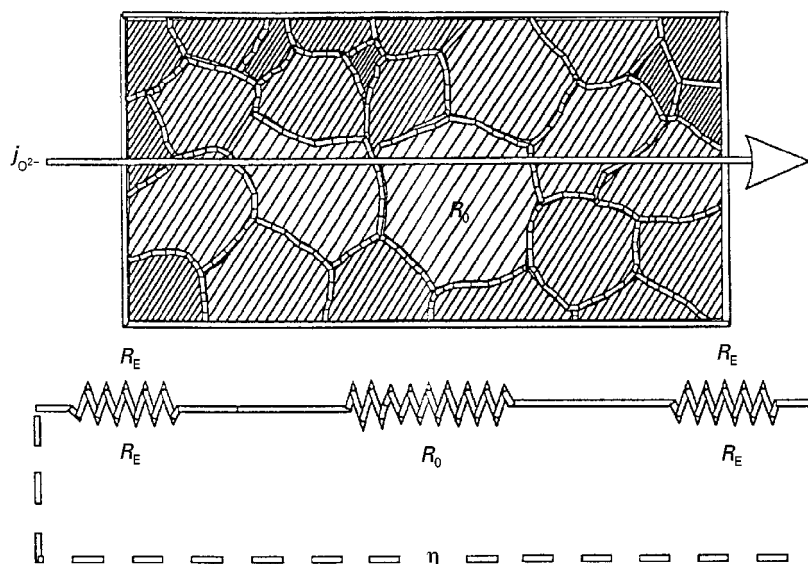


Figure 6 Equivalent circuit for a ceramic membrane device showing the ionic current.

and the diffusion coefficient, D :

$$J_{O^{2-}} = \frac{\eta}{\left\{ \frac{2D}{\sigma k} + \frac{L}{\sigma} \right\}} \quad [8]$$

The flux of oxygen through a pressure-driven device can be increased by making the membrane thinner (reducing R_0), but this is true only up to a certain point. The surface reaction kinetics ($\equiv R_E$) limit the ultimate flux of oxygen through a thin membrane, and beyond a certain characteristic limiting thickness, L_c , the flux remains constant. The numerical value of L_c is given by ratio D/k , which for most mixed conducting oxides of interest is approximately 100 μm , meaning that a supported thin film structure is probably required for an optimized permeation flux. A comparison of the oxygen fluxes achieved from a range of materials is discussed later.

Electrically Driven Devices

The electrically driven device consists of a solid electrolyte membrane with electrodes applied to each side to form a tri-layer structure (Figure 7). When an electrical potential is applied to the tri-layer, oxygen is reduced at the cathode, passes through the electrolyte as an O^{2-} ion and is evolved as oxygen at the anode. An external electrical connection allows the transfer of electrons from the anode to the cathode. The simple equivalent circuit used for the pressure-driven membrane is still applicable, however, R_0 now becomes the electrolyte ASR and R_E the polarization resistance of the electrodes (assumed to be identical).

The flux of oxygen produced by an electrically driven device is directly proportional to the current passing through the membrane ($1 \text{ A} \equiv 3.5 \text{ mL O}_2 \text{ min}^{-1}$), provided the ionic transference number is close to unity. Thus, the flux of oxygen for a given applied potential is governed by the resistance of the membrane (the sum of the electrolyte and electrode polarization resistances) and may be increased by either increasing the potential across the membrane or by reducing the resistance of the membrane. The extent to which the voltage can be increased depends largely on the stability of the electrolyte material. High applied potentials lead to the partial reduction of the electrolyte and the consequent increase in electronic conductivity, leading to a loss of efficiency, for example, in a material such as CGO.

The resistance of the membrane may be reduced by decreasing its thickness. Self-supporting electrolyte

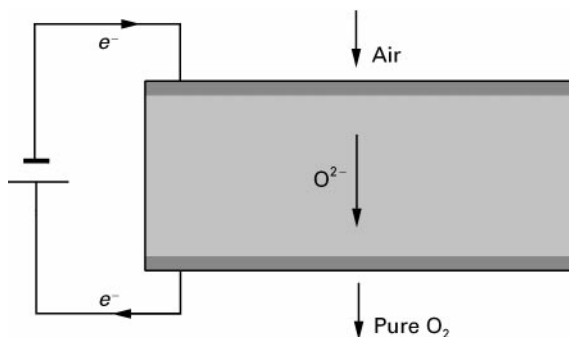


Figure 7 Schematic of an electrically driven ceramic oxygen generator based on a solid electrolyte. □, Ionic conductor; ■, mixed conductor.

membranes of the order of 100 μm are available. Thinner electrolytes are not sufficiently strong to support themselves, and therefore further reduction in electrolyte thickness can be achieved by preparing a dense film of the electrolyte on the surface of a porous electrode support. The gains that can be made from switching to thin layers are limited, analogous to the pressure-driven variant. This is because the largest contribution to the resistance of a membrane is usually the polarization resistance of the electrodes, R_E , particularly at the lower temperatures of operation. These are independent of the electrolyte thickness ($\equiv R_0$) and thus again the flux of oxygen is limited by the value of R_E .

It is interesting to note that electrode compositions for the electrically driven separator are similar to compositions used as membranes in pressure-driven devices, because the requirements are identical, i.e. a high electronic conductivity and the fast transport of oxygen. Again, the limiting factor turns out to be the kinetics of the surface oxygen exchange reaction at the electrode.

The advantages of electrically driven oxygen separation devices are that large fluxes of oxygen per unit area are possible. At 800°C, an electrical potential of only 0.7 V is equivalent to an oxygen partial pressure gradient ratio of 7×10^{30} . For applications in which the volume of a device is a key constraint, such as

medical and aerospace applications, an electrically driven device would be the favoured option. An added advantage of an electrically driven COG is that the technology is closely related to that of the solid oxide fuel cell (SOFC) currently under development, and appreciable 'spin-off' is expected. The size of the device can be further reduced if a planar geometry is adopted, similar to that of the planar SOFC. Finally, an electrically driven device is also able to produce oxygen at a higher pressure than the air feed-stock, provided the applied potential across the membrane exceeds the back electromotive force due to the partial pressure gradient of oxygen.

The main disadvantage of electrically driven devices is that they are invariably complicated multi-component devices. This has implications in terms of the thermal and chemical stability, and the compatibility of the various components at the elevated temperature of operation. The need to develop a high-temperature sealant, required for the planar geometry, is an added complication for these compact devices.

Oxygen Fluxes

Having shown the principle of the devices and having discussed the materials involved, it is of interest to look at the 'state of the art' in terms of the fluxes of oxygen that can be achieved. Figure 8 shows a range of fluxes

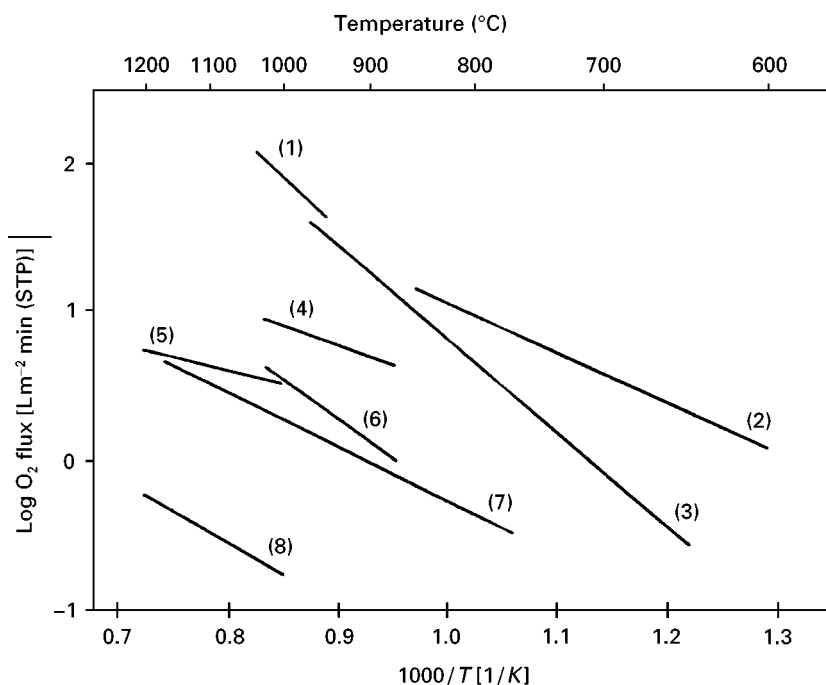


Figure 8 Arrhenius plots of oxygen permeation for: (1) $\text{SrFeCo}_{0.5}\text{O}_{3.25-\delta}$; (2) $(\text{Bi}_2\text{O}_3)_{0.75}(\text{Y}_2\text{O}_3)_{0.25}\text{-Ag}$ (35 v/v), 90 μm ; (3) $\text{SrCo}_{0.8}\text{Fe}_{0.2}\text{O}_{3-\delta}$; (4) $\text{La}_{0.2}\text{Sr}_{0.8}\text{Co}_{0.8}\text{Fe}_{0.2}\text{O}_{3-\delta}$; (5) $\text{La}_{0.3}\text{Sr}_{0.7}\text{CoO}_{3-\delta}$; (6) $\text{La}_{0.6}\text{Sr}_{0.4}\text{Co}_{0.2}\text{Fe}_{0.8}\text{O}_{3-\delta}$; (7) $\text{La}_{0.5}\text{Sr}_{0.5}\text{CoO}_{3-\delta}$; (8) YSZ-Pd (40 v/v), continuous Pd-phase.

measured from samples of single and dual-phase materials, operated in a pressure-driven mode, plotted as a function of inverse temperature. This figure is intended to give some appreciation of the fluxes that are attainable; however, they are not normalized to a given partial pressure gradient or thickness of membrane, and thus the fluxes are not directly comparable. Taking a value of between 10 and $100 \text{ L m}^{-2} \text{ min}^{-1}$ as the level of oxygen flux needed for practical applications, it can be seen that the cobalt-containing single-phase materials give appreciable oxygen fluxes above about 900°C . It is interesting to note on this figure that the dual-phase material, fabricated from $(\text{Bi}_2\text{O}_3)_{0.75}(\text{Y}_2\text{O}_3)_{0.25}\text{-Ag}$ (35 v/v), approaches the lower bound of the practical fluxes at temperatures of 800°C .

It is not sensible to put data for electrical driven COGs on the same figure, given the restrictions mentioned above, however, some comparable figures are interesting. An equivalent flux of $15.8 \text{ L m}^{-2} \text{ min}^{-1}$ is

readily achievable with planar COG stack based on zirconia and operating at 1000°C . Similar performance has been reported for a system based on a CGO-operating temperature of 800°C .

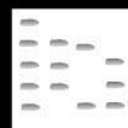
Further Reading

Bouwmeester HJM and Burggraaf AJ (1996) Dense ceramic membranes for oxygen separation. In: Burggraaf AJ and Cot L (eds) *Fundamentals of Inorganic Membrane Science and Technology*, pp. 435–528. New York: Elsevier.

Bouwmeester HJM and Burggraaf AJ (1997) Dense ceramic membranes for oxygen separation. In: Gellings PJ and Bouwmeester HJM (eds) *The CRC Handbook of Solid State Electrochemistry*, pp. 481–553. Boca Raton: CRC Press.

Steele BCH (1998) Ceramic ion conducting membranes and their technological applications. *C.R. Acad. Sci. Paris*, t.1, Serie II c, 533–543.

ION EXCLUSION CHROMATOGRAPHY: LIQUID CHROMATOGRAPHY



K. Tanaka, The National Industrial Research Institute of Nagoya, Nagoya, Japan

P. R. Haddad, University of Tasmania, Hobart, Australia

Copyright © 2000 Academic Press

Introduction

Ion exclusion chromatography (IEC) is a relatively old separation technique, attributed to Wheaton and Bauman, which is now staging an impressive comeback for the simultaneous determination of ionic species. IEC provides a useful technique for the separation of ionic and nonionic substances using an ion exchange stationary phase in which ionic substances are rejected by the resin while nonionic or partially ionized substances are retained and separated by partition between the liquid inside the resin particles and the liquid outside the particles. The ionic substances therefore pass quickly through the column, but nonionic (molecular) or partially ionized substances are held up and are eluted more slowly.

IEC is also referred to by several other names, including ion exclusion partition chromatography, ion chromatography-exclusion mode, and Donnan exclusion chromatography. In this article we use the term ion exclusion chromatography.

Generally, anions (usually anions of weak acids) are separated on a strongly acidic cation exchange resin in the hydrogen form and are eluted as the corresponding fully or partially protonated acids, while cations (usually protonated bases) are separated on a strongly basic anion exchange resin in the hydroxide form and are eluted as the corresponding bases. The eluents used are usually water, water/organic solvent mixtures, dilute (high conductivity) aqueous solutions of a strong acid, or dilute (low conductivity) aqueous solutions of a weak acid. A conductivity detector is commonly used to monitor the column effluent and, when the eluent conductivity is extremely high, a suitable suppressor system is generally used. UV-visible detection is also used as a selective detector in the determination of some aliphatic and aromatic carboxylic acids and some inorganic anions, such as nitrite and hydrogen sulfide. Using IEC, it is possible to separate weakly ionized anions such as fluoride, phosphate, nitrite, aliphatic carboxylic acids, aromatic carboxylic acids, bicarbonate, borate, aliphatic alcohols, sugars, amino acids, water, and others, as well as ammonium, amines, and others, based on a combination of the separation mechanisms of ion-exclusion, adsorption, and/or size-exclusion. Further discussion of these mechanisms may be found elsewhere in the encyclopedia.

ISOTOPE SEPARATIONS



Gas Centrifugation

V. D. Borisevich, Moscow State Engineering Physics Institute (Technical University), Moscow, Russia

H. G. Wood, University of Virginia, Charlottesville, VA, USA

Copyright © 2000 Academic Press

Introduction

The idea that a centrifugal field might be used to separate was first suggested by Lindemann and Aston

in 1919. In 1934 Beams and others at the University of Virginia developed a convection-free centrifuge for isotope separations, shown in **Figure 1**. Two years later Beams and Haynes demonstrated practical separation of chlorine isotopes. In 1938 the Nobel prize winner Urey suggested multiplying the separating effect between axis and periphery of a rotor produced by centrifugal forces by introducing countercurrent convection (like a fractionating column) within the spinning tube. At the end of the 1930s Groth and co-workers in Germany started to construct a high speed centrifuge for uranium isotope separation with axial countercurrent flow induced

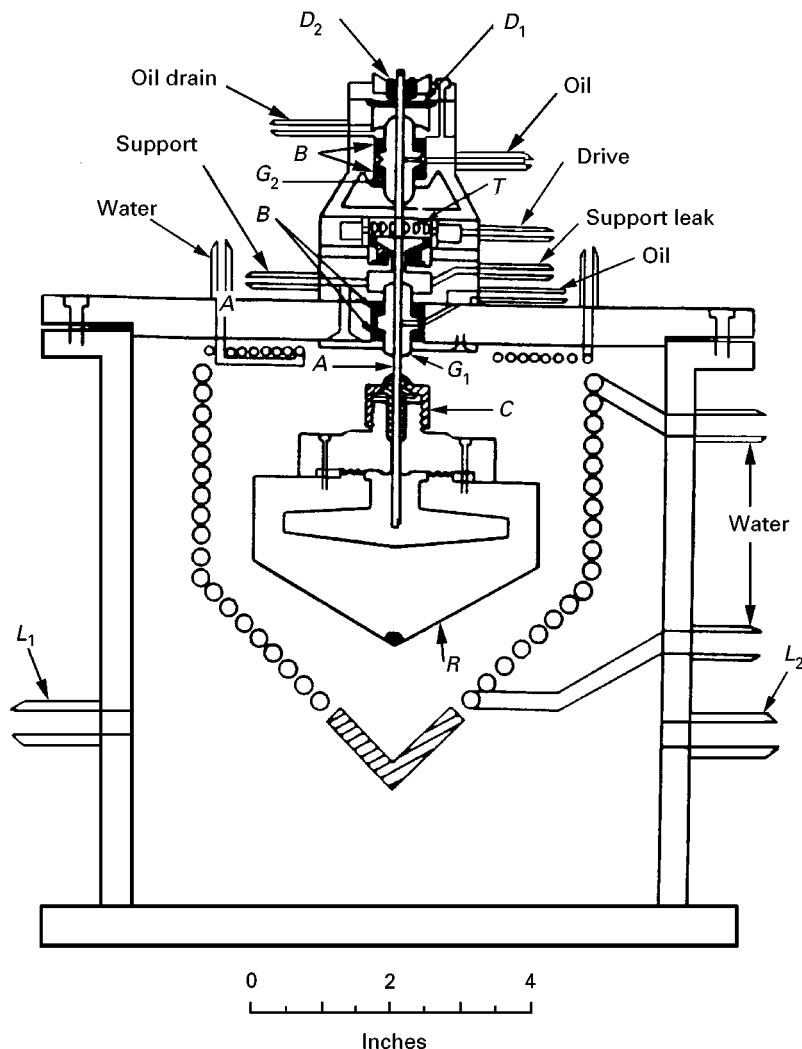


Figure 1 Schematic drawing of Beams' first successful evaporative centrifuge used to separate chlorine isotopes.

by heating the bottom of a rotor and cooling the top.

With the beginning of the Second World War in 1939, the separation of uranium isotopes became a subject of national importance. The experimental work on developing different types of gas centrifuges for uranium isotope separation was continued in Germany and was undertaken in the USA in the framework of the Manhattan Project. In that time, Dirac made fundamental contributions to the theory of the isotope separation process in a gas centrifuge, and Onsager's theory for calculation of separation efficiency in a thermal diffusion column was generalized for gas centrifuges by Cohen in 1951. They and their colleagues worked out a general mathematical model and demonstrated theoretically the ideal countercurrent flow profile to produce the maximum separation efficiency. Beginning in 1946, Steenbeck and Zippe contributed to the centrifuge development project in the USSR. Together with Russian co-workers, they developed a very elegant bearing system and adapted the scoop system of gas extraction not only to recover the gas from the rotor but also to generate the circulation flow to multiply the radial separating effect. After leaving the USSR in the mid 1950s, Zippe continued his activities in Germany and USA to reproduce the experiments that had been performed in USSR. In the USA, Zippe worked with Beams for about 2 years in the late 1950s. The Virginia short-bowl centrifuge, similar to the Russian design, was the result of their collaboration. A research and development programme for centrifugation was then pursued in the USA with the central effort located at the Department of Energy laboratories at Oak Ridge, Tennessee. In this programme, centrifuge rotors of an unprecedented length, of the order of 13 m were developed. The programme proved to be technically successful, but it was terminated in 1985 because of changes in US nuclear policies.

After the Second World War, centrifuge research programmes were initiated in several other countries: in the UK by Kronberger and Whitley; in France by Burgain and Le Manach; in Germany by Beyerle, Groth and Martin; in the Netherlands by Kistemaker and Los; in Japan by Kanagawa, Oyama and Takashima; and in Sweden by Landahl and associates.

The Soviet Union was the first country where this technology was developed on an industrial level. The first pilot plant, comprising 2500 gas centrifuges, was put into operation in 1957. The first industrial plant, which contained several tens of thousands of centrifuges, was commissioned in 1959. Soon after, USSR built an industrial plant with several hundred thou-

sand centrifuges configured in three levels and commissioned it in 1962–1964. Besides Russia, this method was commercialized at the end of the 1970s by the UK, Germany and the Netherlands collaborating and in the 1980s by Japan. At present, gas centrifugation is the most efficient, economic and reliable technology for production of enriched uranium.

Principles of Operation

The history of the development of a gas centrifuge for uranium isotope separation provides an excellent example of successfully overcoming numerous experimental and theoretical problems in the fields of physics of separation processes, gas dynamics, materials science, mechanical engineering and physical chemistry. The short-bowl centrifuge patented in 1957 by Zippe, Scheffel and Steenbeck is shown in Figure 2. The thin-walled vertical cylindrical rotor is suspended at the bottom by a low friction needle bearing and at the top by a frictionless magnetic bearing. It also uses damping bearings to resist vibrations at both ends of the rotor. In the case of the separation of uranium isotopes, uranium hexafluoride (UF_6) is introduced into the spinning rotor from a stationary central post and removed from stationary pipes called scoops located at either end of the

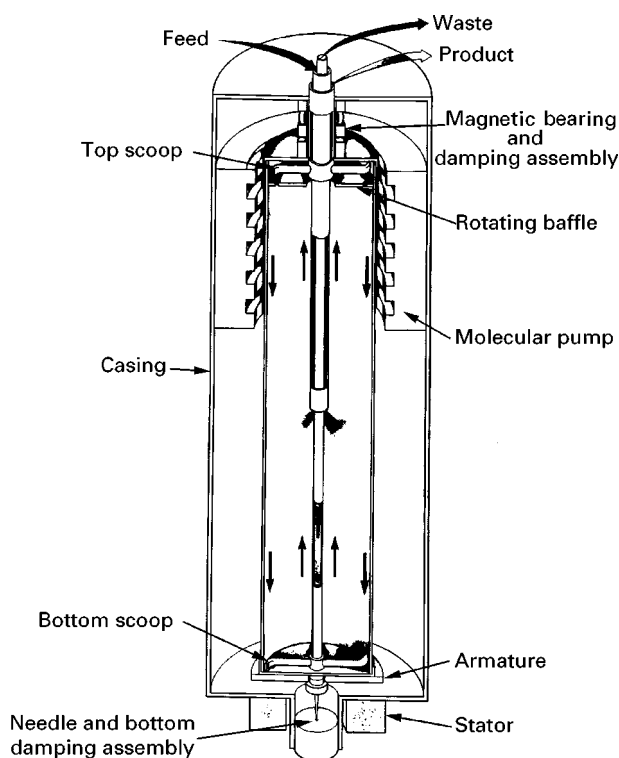


Figure 2 Schematic drawing of Zippe-type centrifuge.

rotor. In practice, the gas centrifuge is spun in a vacuum housing that is maintained by a Holweck-type spiral groove molecular pump. The very high peripheral speeds (for example, in the order of 600 m s^{-1}) generate centrifugal forces that compress the process gas into a thin stratified layer adjacent to the cylindrical wall of the rotor.

Separation Factor

The action of centrifugal forces causes a partial separation of isotopes along the rotor radius. If we consider the process gas to be a binary mixture of the two isotopic species $^{235}\text{UF}_6$ and $^{238}\text{UF}_6$, then the heavier molecules containing $^{238}\text{UF}_6$ will tend to be concentrated near the cylinder wall and the lighter molecules containing $^{235}\text{UF}_6$ will tend to be concentrated near the axis. Considering UF_6 as an ideal gas, a pressure gradient is developed which is governed by eqn [1]:

$$\frac{dp}{dr} = \frac{Mp}{RT}\omega^2 r \quad [1]$$

Here p is the pressure, M is the molecular weight of the gas, R is the gas constant, T is the absolute temperature, ω is the angular frequency of rotation and r is the radial coordinate. In the case of an isothermal centrifuge, the equation above is readily integrated to yield the following relation:

$$p(r) = p(0)(M\omega^2 r^2/2RT) \quad [2]$$

that gives the pressure $p(r)$ at any radial position r in terms of the pressure at the axis $p(0)$. For a mixture of two ideal gases of molecular weights, M_1 and M_2 , each gas would have a pressure governed by eqn [2] and the ratio of the two pressures gives the radial separation under equilibrium conditions (i.e. no axial gas circulation). An equilibrium separation factor between the two gases is therefore given by the expression:

$$\alpha_0 = \frac{x_1(0)/x_2(0)}{x_1(a)/x_2(a)} = \exp[(M_2 - M_1)\omega^2 a^2/2RT] \quad [3]$$

in which x_1 and x_2 are the concentrations of species 1 and 2, respectively, and a is the radius of the rotor.

The fundamental advantage of this technique over many other diffusion separation methods is that the primary isotope separation effect occurs at thermodynamic equilibrium. It should also be noted that the separation factor for the centrifuge process is a function of the absolute difference in the molecular weights of the components being separated. This is in contrast to various diffusion separation

processes where it is a function of the ratio of the molecular weights.

Separative Capacity

The stationary scoop at the top of the rotor induces a countercurrent flow by removing both mass and angular momentum, which induces pumping of the gas radially inward, forcing it to travel down near the axis and up along the cylinder wall. In order to prevent the influence of the scoop at the bottom, it is shielded by a baffle that rotates with the rotor and has holes which allow the gas to enter the scoop chamber and be removed from the centrifuge. This countercurrent flow produces a net transport of heavy isotopes to the top of the rotor and a net transport of light isotopes to the bottom, establishing a concentration gradient in the axial direction that is considerably greater than the primary (radial) isotope separation effect. Therefore, the gas removed by the bottom scoop is enriched in $^{235}\text{UF}_6$ (a product stream) and the gas removed by the top scoop is depleted in $^{235}\text{UF}_6$ (a waste stream).

As manufacturing technology has improved, higher rotational speeds have been achieved to obtain greater separation performance. At these higher speeds, shock waves develop in front of the stationary scoop, and the temperatures associated with these shock waves are high enough to cause decomposition of the process gas. It is important to note that the speed of sound in UF_6 at room temperature is approximately 90 m s^{-1} , and the peripheral speed of rotation of the process gas in modern centrifuges can be more than seven times greater than this. One design that avoids this decomposition problem is to shield the upper scoop with a rotating baffle with two concentric systems of holes. One system is located near the periphery to allow gas to enter the scoop, and the other system is located nearer the axis of rotation to induce internal circulation. Again, this internal circulation creates an axial separation factor many times that of the basic radial separation factor. The design of scoops and systems of holes in both baffles (their position and size) together with the temperature distribution on the side wall are used to control the internal circulation value and rate.

In 1941, Dirac demonstrated that a gas centrifuge, no matter how it is operated, has the maximum theoretical capacity:

$$\delta U_{\max} = \rho D \left(\frac{\Delta M \omega^2 a^2}{2RT} \right)^2 \pi Z/2 \quad [4]$$

where Z is the length of the rotor, ΔM is the difference in molecular weights, ρ is the density of the

Table 1 Maximum pressure ratio, radial separation factor and separative work at various peripheral speeds

ωa ($m\ s^{-1}$)	$p(a)/p(0)$ for $^{235}UF_6$	α_0	δU_{\max} kg SW per year	L/a^a
300	573	1.056	2.15	Does not exist
400	8×10^4	1.101	6.78	0.571
500	4.6×10^7	1.162	16.55	0.309
600	1.1×10^{11}	1.242	34.32	0.202
700	1.0×10^{15}	1.343	63.59	0.144

^a L/a : Ratio of radial distance for pressure to fall by 10^4 to centrifuge radius.

process gas, D is the coefficient of self-diffusion, and δU is the separative capacity in moles per unit time. Maximum pressure ratio, radial separation factor and separative work at various peripheral speeds of a gas centrifuge are presented in Table 1.

Design Principles

As is evident from eqn [4], the most important parameters in centrifuge technology are peripheral rotor speed and rotor length. The peripheral speed is limited by the strength of the rotor material. Hence, gas centrifuges require materials which have a high strength to density ratio. Such materials are aluminium alloys, titanium alloys, alloy steels or fibre composites. The centrifuge rotor can be made of more than one layer; for example, aluminium alloy covered with fibre composites. The materials problems include long-term fatigue and creep at high speeds. Because uranium hexafluoride forms hydrofluoric acid even with only a little moisture, corrosion is also a challenging problem area that must be addressed in the design.

The spinning rotor has certain natural frequencies determined by the materials of construction, the rotor length to diameter ratio, and the damping characteristics of the suspension systems. Centrifuges that operate at rotational frequencies below the lowest natural flexural frequency of the rotor are called subcritical centrifuges, and those that operate at rotational frequencies above the first natural frequency are called supercritical ones. As a rule, the rotors of supercritical machines consist of sections connected by bellows that act to reduce vibrations caused by resonant frequencies at certain operating speeds.

The Dirac maximum separative capacity has been derived for the case of an ideal circulation profile in a gas centrifuge. However, this ideal profile cannot be achieved in practice. The flow patterns that actually occur within a centrifuge rotor are governed by the

equations of fluid dynamics. The theoretical solution of these equations provides a basis for the optimization of the internal flow pattern that yields the maximum separation performance of a particular gas centrifuge design.

The flow pattern in a gas centrifuge can be divided into three regions in the radial direction, each with different flow features. Near the side wall, the flow is dominated by viscosity, and a strongly rarefied gas region (a vacuum core) is located near the axis of rotation. These two regions are connected by a transition region. The transition region as a rule occupies only a few per cent of the rotor radius, and its influence on separation is negligible. The vacuum core in modern centrifuges is spread over approximately three-quarters of the rotor radius. In this region the mean free path of the gas molecules is comparable with the rotor diameter. At these low pressures, the central core of the rotor cannot contribute to the isotope separation. As a result, the separation power of a gas centrifuge at high speeds increases only as the square of the peripheral speed instead of the fourth power, as given by the Dirac equation.

Cascade of Centrifuges

The separative work output of a single gas centrifuge is generally small compared to the total desired separative work. Hence, it is necessary to combine many centrifuges into a cascade to achieve the desired separation. Each stage of a cascade may have many centrifuges connected in parallel. This arrangement of the large number of centrifuges allows for simple replacement of a faulty individual centrifuge in the cascade. The considerable advantage of the centrifuges is that they need no special compressors for pumping gas through the cascade. The pressure difference required for pumping the gas through the cascade is generated by the dragging action of the scoops on the rotating gas. The cascade contains only centrifuges and piping. Thus, gas centrifuge enrichment of uranium uses only about 1/20th to 1/30th of the electricity per unit of separative work required by the gaseous diffusion process. The reliability of modern centrifuges allows them to operate nonstop for more than 15 years with a failure rate of only a few tenths of 1% per year. Once put into operation, gas centrifuges require no special preventive maintenance through their service lives, and the machines' separation characteristics remain practically constant over time. Provided that random failures occur, the fragments of the crashed machines can be left in the cascade because they will not have much effect on the overall cascade efficiency.

Separation of Nonuranium Isotopes

New Scientific Problems

More recently, interest has been shown in using gas centrifuges for other kinds of separations like stable isotopes or the isotopes of spent reactor uranium. For the stable isotopes, demand is growing in medicine and fundamental physics research, and the use of the gas centrifuge process makes it possible to produce isotopes economically when large (kilograms) quantities are needed. This is the case for the isotopes of xenon, krypton, tungsten, molybdenum, iron, tin, tellurium, sulfur, silicon, germanium, chromium and many others. The separation of stable isotopes by gas centrifuge has been underway for more than three decades in Russia. Currently, cascades of thousands of centrifuges are producing tens of kilograms of various isotopes. In another application, some countries have considered gas centrifuge technology as part of the reprocessing cycle of the re-enrichment of the spent uranium from power reactors which contains five isotopes: U^{232} , U^{234} , U^{235} , U^{236} and U^{238} .

A centrifuge designed for binary separations with uranium hexafluoride cannot be efficiently used for nonuranium isotope separation with different chemical compounds. Therefore, centrifuges with specific characteristics must be designed for particular separation problems. For some isotopes, specially synthesized gaseous chemical compounds must be prepared for use as the process gas. The basic condition for the applicability of the process gas in these newly designed centrifuges is that the gas vapour pressure is not less than 5–10 mmHg under normal operating temperatures. In addition to the condition that this substance should not corrode the structural material of the centrifuge, it has to be sufficiently resistant to temperature dissociation, and preferably must possess the maximum possible content of the desired element in the molecule. The list of such substances includes fluorides and oxyfluorides of metals and nonmetals, metal–organic and complex compounds, phosphorus hydrides, boron hydrides, Freons and some others. Significant differences in the chemical and physical properties of process gases leads to the necessity to create a set of gas centrifuge designs for various ranges of molecular masses. The internal circulating flow must be optimized for each of these designs.

The synthesis of volatile compounds suitable for process gases was not the only scientific problem the researchers faced when separating nonuranium isotopes. In contrast to natural uranium, most chemical elements are polyisotopic. This property leads to additional difficulties in enriching the intermediate components of the isotope mixture.

As perhaps the greatest achievement in the development of centrifuge technology for enrichment of nonuranium isotopes, one may consider the complex isotope separation for iron, carbon and oxygen as a pentacarbonyl of iron – $Fe(CO)_5$. This separation has been realized on an industrial scale at the electrochemical plant in the Krasnoyarsk region of Russia. All chemical elements included in the molecule structure are polyisotopic: iron contains four, carbon two, and oxygen three isotopes. A natural isotope abundance of $Fe(CO)_5$ represents a mixture of 284 types of molecules with different isotope distributions. These types are distributed through 20 components with molecular masses from 194 up to 213. Almost every one of them contains several isotopes for each of the chemical elements. This isotopic overlapping of iron isotopes with intermediate masses and heavy isotopes of carbon and oxygen limits the direct enrichment by a centrifuge cascade. However, this limitation has been removed by introducing into the separation process the isotope exchange between the molecules of pentacarbonyl of iron in so-called photoreactors. The combination of isotope separation in gas centrifuges with isotope exchange has allowed the achievement in a single process of a complex mix of highly enriched isotopes: ^{57}Fe with concentration more than 99%, ^{13}C and ^{18}O with concentrations up to 80%.

Advantages

The accumulated experience in separating isotopes of both light (boron, carbon, nitrogen and oxygen) and heavier chemical elements has shown gas centrifuge technology to be extremely promising. At the moment, isotopes of more than 20 chemical elements have been separated by gas centrifuges. The centrifuge cascade used for the separation of nonuranium isotopes usually has very low energy consumption and tens of times higher productivity than that of the electromagnetic installation and with a comparable output (Figure 3). Nonuranium isotope separation has been transformed into an independent area for development of gas centrifuge technology. It includes solving problems in the design of different types of centrifuges, in the theory of multicomponent isotope mixture separation, in chemical synthesis of process gases, in transformation of process gases with enriched isotopes required for use in chemical compounds, etc.

In many applications of isotope enrichment, rigid requirements on the isotope purity must be met, and undesired gas impurities must be reduced to a specified level. Gas centrifugation has also been recommended as an excellent practical tool to clean small

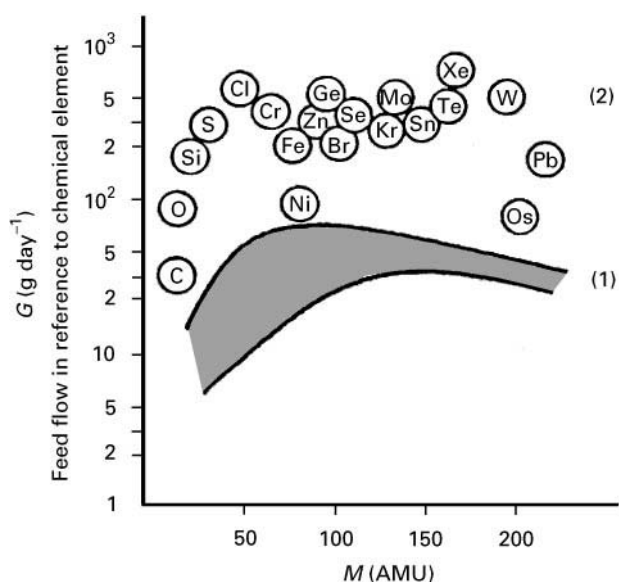


Figure 3 Illustration to compare the separation of nonuranium isotopes by electromagnetic separation (1) and by gas centrifuge (2). Production, G (g day^{-1} : feed flow into the installation), versus molecular mass, M , of the separating chemical element. Reproduced with permission from Goldstein *et al.* (1993).

gas impurities. An extremely important benefit of gas centrifuges is the opening of an era of economical large scale production of many stable isotopes that have applications in medicine, industry and fundamental science. For example, experiments on neutrino physics with large detectors that require tens of kg of enriched isotope have been made possible by the cost reductions achieved through the large scale production by gas centrifugation.

Future

The gas centrifuge is now a mature technology, but nevertheless the development potential has not been

exhausted. The separation efficiency of existing gas centrifuges for separation of uranium and nonuranium isotopes can be further improved. Additionally, the technology can be applied in the near future to the re-enrichment of uranium from spent nuclear fuel as well as to enriching tails (depleted uranium of separating plants) to the natural isotopic concentration or higher. In yet another area, experiments have been performed which show promising results for the application of gas centrifuge technology to purification of process gas from aerosol particles that can be used, for example, in the semiconductor industry.

See Colour Plate 102.

Further Reading

- Avery DG and Davies E (1973) *Uranium Enrichment by Gas Centrifuge*. London: Mills & Boon.
- Beams JW and Haynes FB (1936) The separation of isotopes by centrifuging. *Physical Review* 50: 491.
- Benedict M, Pigford LH and Levi HW (1981) *Nuclear Chemical Engineering*. New York: McGraw Hill.
- Cohen K (ed.) (1951) *The Theory of Isotope Separation as Applied to the Large-scale Production of U^{235}* . New York: McGraw-Hill.
- Goldstein S, Louvet P and Soulié E (eds) (1993) *Les Isotopes Stables Application-Production*. Paris: Centre d'Études de Saclay.
- Lindemann FA and Aston FW (1919) The possibility of separating isotopes. *Philosophical Magazine* 37: 523.
- London H (ed.) (1961) *Separation of Isotopes*. London: George Newnes.
- Olander DR (1972) Technical basis of the gas centrifuge. *Advances in Nuclear Science and Technology* 6: 105.
- Villani S (ed.) (1979) *Topics in Applied Physics: Uranium Enrichment*. New York: Springer-Verlag.
- Whitley S (1984) Review of the gas centrifuge until 1962. Parts 1 and 2. *Reviews of Modern Physics* 56: 43.

Liquid Chromatography

L. Lešetický, Charles University, Prague, Czech Republic

This article is reproduced from *Encyclopedia of Analytical Science*, Copyright © 1995 Academic Press

Introduction

The application of isotopes in science and especially in analytical chemistry is based on two rather contradictory assumptions. Tracer experiments require that

the isotopically modified and unmodified compounds behave in a very similar manner. A study of isotope effects must recognize, measure and interpret minute differences in the chemical and physical properties of compounds (isotopomers) that differ in their isotopic composition. These differences lead to different behaviour of isotopomers in all chromatographic processes, as has been demonstrated experimentally.

As early as 1938, Urey and coworkers published a paper on enrichment of ^6Li by ion exchange

chromatography and work in this field has been continuing to date. Gas-solid chromatography has been used for separation of the hydrogen isotopes, noble gases and some other gaseous elements and simple compounds. Low-molecular-mass volatile compounds labelled mainly with hydrogen isotopes have been separated by gas-liquid chromatography. During the late 1950s and the 1960s, papers were published concerning small but observable isotopic fractionation with liquid chromatography of isotopically labelled organic compounds. Over the last 20 years during which liquid chromatography (LC) has become a common analytical technique, many papers have been published dealing with separation of labelled compounds from their unlabelled counterparts. A review of these works, with a possible explanation of the mechanisms of the separation process, is presented.

Isotope Effects

Chromatography can be considered as a process in which the compounds to be separated interact with a stationary and a mobile phase. These mutual interactions differ in magnitude even for different isotopes of the same element. The magnitude of the interaction energy for an isotopic pair depends on many parameters that are discussed below.

It is possible to draw the following general conclusions from the experimental data on isotope effects on the physical properties of molecules.

1. The C-²H bond is shorter than the C-¹H bond (e.g. in ethane the C-H bond length is 111.2 pm; in hexadeuteroethane the C-²H bond length is 110.7 pm) and exhibits a higher electron density than the ¹H bond. The deuterium atom appears to be smaller than the hydrogen atom. There are small, but measurable differences in the dipole moments, e.g. $\mu(\text{CH}_3\text{-}^2\text{H}) = 3.7 \times 10^{-32} \text{ C m}$, $\mu(^1\text{HCl}) - \mu(^2\text{HCl}) = 1.7 \times 10^{-32} \text{ C m}$.
2. The C-²H bond has a polarizability lower than that of the C-¹H bond.
3. The C-²H stretching vibrational frequency (around 2200 cm⁻¹) is lower than the corresponding C-¹H frequency (around 3000 cm⁻¹).
4. Heavier isotopes have smaller atomic volumes; deuterated compounds have smaller molar volumes than the corresponding unlabelled compounds. The molar volume differences between, e.g. deuterated and unlabelled benzene are due to a molecular size effect caused by differences in the zero-point intermolecular motion of the molecules.
5. Deuterium (²H) is more electropositive than protium (¹H) and thus some isotope effects can

Table 1 Isotope effect on dissociation constants^a

Compound ^b	$\log(K_i/K_o)$
² HCOOH	0.035 ± 0.002
C ² H ₃ COOH	0.014 ± 0.002
(C ² H ₃) ₃ CCOOH	0.018 ± 0.001
C ₆ H ₅ COOH	0.010 ± 0.002
(2,6- ² H ₂)benzoic acid	0.003 ± 0.001
C ² H ₃ NH ₃ ⁺	0.051
(C ² H ₃) ₂ NH ₂ ⁺	0.117
(C ² H ₃) ₃ NH ⁺	0.207

^aWilli (1983), pp. 58–61.

^bOnly the isotope-modified compound is specified in the table.

be discussed in terms of inductive effects. This has been clearly demonstrated in the measurement of the secondary isotope effect on ionization equilibria of some deuterated carboxylic acids and protonated amines, as shown in Table 1.

6. Deuterated compounds are less lipophilic than the corresponding unlabelled compounds

All these experimentally demonstrated phenomena may influence chromatographic separation processes. Isotope effects on the chromatographic behaviour of compounds labelled with isotopes of heavier elements (carbon, nitrogen, oxygen, etc.) are so small that they can only be detected for simple compounds of low relative molecular mass. The following discussion is limited to deuterated and tritiated compounds and only a few examples are given of separations of heavier isotopes.

It should be pointed out that discussion of isotope effects in terms of inductive or other electronic effects is sometimes helpful but represents a gross simplification. A more exact description of the origin of the isotope effects uses the zero-point energy and the vibrational frequencies of the molecules in question.

Separation Processes

Two basic types of separation process can be distinguished. In systems with a polar stationary phase and nonpolar mobile phase (classical adsorption chromatography, normal-phase LC and chemically bonded polar stationary phase LC) the 'ordinary' (unlabelled) compounds are usually eluted first, i.e. the separation factor is less than unity ($\alpha = k_1/k_2 < 1$; subscripts 1, 2, 3 refer to protium, deuterium and tritium (³H), respectively). As mentioned above, deuterated or tritiated compounds are more polar and thus are more strongly bound to polar stationary phases.

Table 2 LC separation factors of some hydrocarbons versus their perdeuterated analogues

Compound	$\alpha = k_1/k_2$	Conditions ^{a,b}
[² H ₁₄]Hexane ^a	1.036	51
	1.049	40
[² H ₁₈]Octane ^a	1.054	51
[² H ₁₂]Cyclohexane ^a	1.044	33
[² H ₆]Benzene ^a	1.043	23
	1.048	18
[² H ₆]Benzene ^b	1.049	30
[² H ₈]Toluene ^a	1.046	33
	1.057	23
[² H ₈]Toluene ^b	1.052	40
[² H ₁₀]Phenanthrene ^b	1.067	70
[² H ₁₄]Durene ^b	1.071	70
[² H ₁₀]Biphenyl ^b	1.062	55

^aμ-Bondapak C₁₈ column; methanol in water (mol%); Tanaka (1977).

^bUltrasphere C₁₈ column; acetonitrile in water (v/v); Baweja (1987).

Partition chromatography and reversed-phase LC usually lead to the opposite result, i.e. a heavier isotopomer is eluted first ($\alpha > 1$). It has been suggested that a major contribution to the isotope effect is then a hydrophobic interaction. The fact that the separation factors are higher (see Table 2) when the mobile phase contains more water demonstrates that they are affected by more restricted motion of the C–H bonds (in solute), caused by a tighter solvation of the C–H bonds within the aqueous mobile phase relative to the hydrophobic stationary phase. On the other hand a less restricted motion of the C–H bonds in the stationary phase would tend to favour protium over deuterium, and this could contribute to the observed isotope effect.

Another important factor is the position of the label in a molecule. As these effects are essentially primary isotope effects, the best situation occurs when an isotopic atom is pushed out from the rest of a molecule, so that it is readily accessible for interaction. When the atom in question is in the shadow of a bulky group (e.g. *ortho* hydrogen in benzoic acid) or in an inconvenient configuration, hydrophobic interactions and adsorption can not take place or are greatly suppressed and no separation is attained. The other contributions, such as differences in solubility, molar volume and adsorption on the residual nonderivatized sites on the silica particles, seem to be of a far less importance for the magnitude of the isotope effect.

The above discussion deals with a direct interaction of an isotopic atom or bond with the stationary and mobile phases (primary isotope effect). However, there also exist chromatographic separations

based on secondary isotope effects. In molecules deuterated or tritiated in the position adjacent to an ionizable functional group, the magnitude of the isotope effect is often greatly enhanced. As follows from Table 1 α -deuterated amines are stronger bases than unlabelled amines, and α -deuterated acids are weaker acids than their protiated counterparts. In an elution system with a pH value near the pK_a values of the deuterated/unlabelled amine pair, this isotope-induced base strengthening would alter the ratio of protonated and unprotonated forms, leading to differences in the chromatographic mobility. However, at a pH much higher or much lower than the pK_a value where both labelled and unlabelled amines are completely protonated or unprotonated, the pK_a effect of isotopic substitution on the chromatographic separation is greatly suppressed. A similar effect was observed for labelled carboxylic acids.

Survey of Separations

Hydrocarbons and their Simple Derivatives

A separation of perdeuterated aliphatic and aromatic hydrocarbons has been performed on reversed-phase columns with similar results (Figure 1). A higher content of water in the mobile phase leads to higher separation factors (Table 2).

Chromatography of various isotopomers of benzoic acid shows a moderate effect of the number of deuterium atoms on the separation factor; however, an important effect is exerted by the position of the label (Table 3). Isotopomers containing deuterium in the *ortho* positions display lower isotopic separation than isotopomers with deuterium in

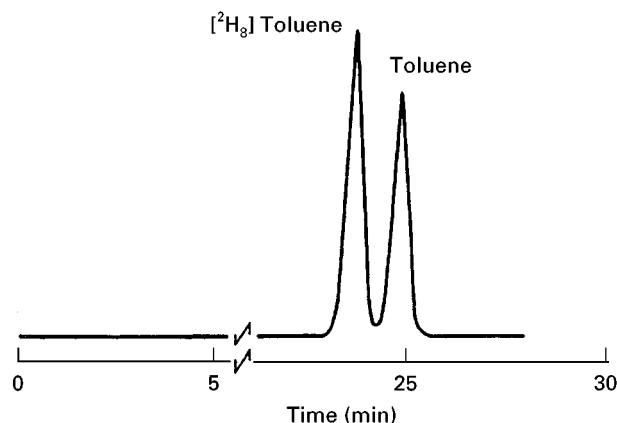


Figure 1 Reversed-phase LC separation of [²H₈]toluene and unlabelled toluene. Mobile phase: water–acetonitrile 60 : 40 (v/v). (From Baweja, 1987).

Table 3 LC separations factors of unlabelled versus deuterated carboxylic acids

Labelled compound	$\alpha = k_1/k_2$
[² H ₃₁]Palmitic acid	1.076 ^{a,b}
[² H ₂₃]Lauric acid	1.066 ^{a,c}
[² H ₅]Benzoic acid	1.040 ^{a,d}
	1.038 ^e
[3,4,5- ² H ₃]Benzoic acid	1.029 ^e
[2,3,5- ² H ₃]Benzoic acid	1.023 ^e
[3,4- ² H ₂]Benzoic acid	1.019 ^e
[3,5- ³ H ₂]Benzoic acid	1.019 ^e
[2,4- ² H ₂]Benzoic acid	1.013 ^e
[2,5- ² H ₂]Benzoic acid	1.010 ^e
[2,6- ² H ₂]Benzoic acid	< 1.010 ^e

^aμ-Bondapak C₁₈ column; Tanaka *et al.* (1977).^b64 mol%; CH₃OH-H₂O.^c51 mol%; CH₃OH-H₂O.^dH₂O, pH 2.51.^eHypersil C₁₈ column; CH₃OH-H₂O (3 : 7, v/v) + 1% HCOOH, Lockley *et al.* (1989).

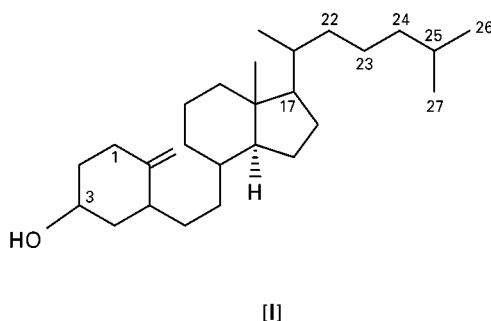
the *meta* or *para* positions. The isotope effects associated with the *ortho* positions are minimal, probably because interactions between the *ortho* C-¹H or C-²H bonds and the stationary phase are minimized by steric shielding of the carboxyl group. [9, 10, 12, 13-³H]Linoleic acid methyl ester and [9, 10, 12, 13-³H]oleic acid methyl ester were chromatographed on silica impregnated with silver nitrate, attaining partial separation from the appropriate [1-¹⁴C]methyl esters. The tritium atom bound on the olefinic carbon atoms affects the equilibrium constant of the formation of the silver-olefin complex.

Natural Substances

Tritium-labelled steroids have often been used for the elucidation of biochemical and physiological trans-

formations. During the chromatographic purification of such compounds, isotopic fractionation has often been observed. Good, sometimes baseline, separations of tritiated aldosterone, cortisone, oestrone, testosterone, prednisolone and oestradiol from their unlabelled or ¹⁴C-labelled analogues were obtained in reversed-phase LC, tritiated compounds being eluted first. Other techniques such as column partition chromatography and paper chromatography have also been successful.

Vitamin D₃ (cholecalciferol, [I]) is hydroxylated in living organisms to the 1,25-dihydroxy- or 24,25-



dihydroxy-derivatives. A significant chromatographic isotope effect was observed with both the derivatives labelled with tritium in positions 26 and 27, whereas labelling in positions 23 and 24 causes a substantially smaller effect. A similar behaviour was found in chromatography of the corresponding trimethylsilyl ethers (Table 4). As indicated in the table, the heavier isotopomers were eluted first on the reversed phase, and later than lighter isotopomers on the normal phase.

Catalytic hydrogenation with protium, deuterium and tritium of echinocandin B, a macrocyclic peptide

Table 4 LC separation factors of vitamin D₃ metabolites versus their tritiated counterparts

Vitamin D ₃ metabolite	$\alpha = k_1/k_3$	Eluent (v/v)
1,25-Dihydroxy-[23,24- ³ H]-TMS ^a	0.977 ^{b,c}	Hexane-CH ₂ Cl ₂ (85 : 15)
	0.989 ^{b,d}	Hexane-CH ₂ Cl ₂ -CH ₃ CN (90 : 10 : 0.035)
1,25-Dihydroxy-[23,24- ³ H]	0.991 ^{b,d}	Hexane-2-propanol
25(R),26-dihydroxy-[23,24- ³ H]-TMS ^a	0.965 ^{b,d}	Hexane-CH ₂ Cl ₂ (85 : 15)
1,25-Dihydroxy-[26,27- ³ H] ₆	0.983 ^{e,f}	Hexane-ethanol (94 : 6)
24,25-Dihydroxy-[26,27- ³ H] ₆	0.965 ^{e,f}	
25,26-Dihydroxy-[23,24- ³ H]	1.008 ^{e,g}	Methanol-water (3 : 1)
1,25-Dihydroxy-[26,27- ³ H] ₆	1.023 ^{e,g}	Methanol-water (1 : 1)

^aTMS = trimethylsilyl derivative.^bHalloran *et al.* (1984).^cZorbax-sil column.^dμ-Porasil column.^eWorth and Retallack (1988).^fEconosphere silica column.^gRadial-pak column.

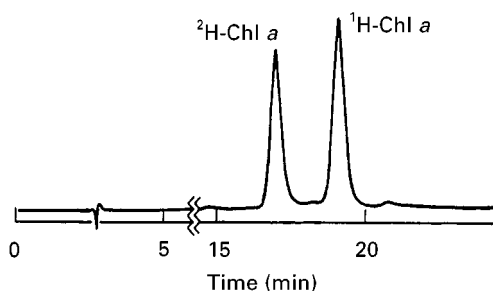
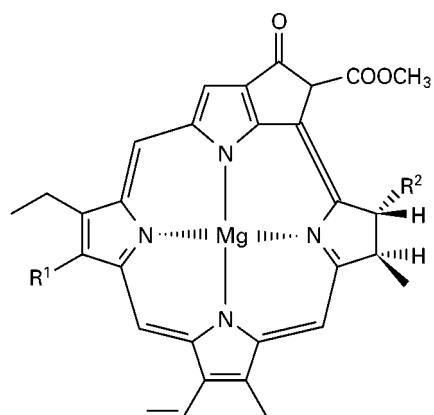
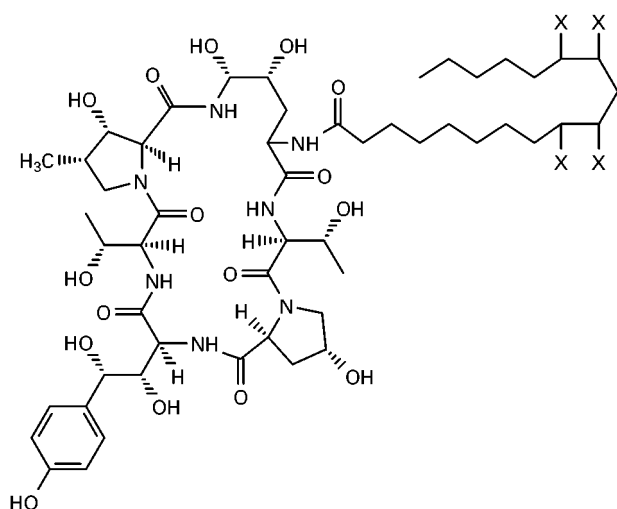


Figure 2 Reversed-phase separation of a deuterated chlorophyll *a* and undeuterated chlorophyll *a* on a 25 cm \times 4.6 mm i.d. C₁₈-Ultrasphere ODS column. Mobile phase: water-methanol-acetonitrile-tetrahydrofuran 5 : 28 : 38 : 23 (v/v/v/v). UV detector 663 nm. (From Baweja 1986.)



[III]



[III] X = ¹H, ²H or ³H

possessing antibiotic and antifungal properties, leads to the corresponding tetrahydroderivatives [III]. The isotope effect on the reversed-phase LC mobility was surprisingly large: $\alpha_2 = k_1/k_2 = 1.0190$ for the deuterated compound; $\alpha_3 = k_1/k_3 = 1.0233$ for the

tritiated compound. A Partisil 5 C₁₈ column and a mixture of 0.1% phosphoric acid (45%) with CH₃CN/THF/H₃PO₄ (90 : 20 : 0.1, v/v/v) (55%) as the eluent were used. Even though the chromatographic conditions described do not allow resolution of labelled and unlabelled species, such a possibility exists, e.g. when a column recycling system is used.

Reversed-phase LC of deuterated chlorophylls [III] obtained from green algae *Rhodospirillum rubrum* and *Rhodospirillum sphaeroides* grown in media containing 50%, 80%, 90% and 99.7% ²H₂O, exhibited baseline separation from isotopically unmodified chlorophyll. As usual, the labelled species were eluted first and the greater is the percentage of deuterium in the compound the faster it moved along the column (Figure 2, Table 5).

Drugs

[²H₁₀]Diphenylhydantoin (phenytoin [IV]) and [²H₁₀]-5H-dibenz[*b,f*]azepine-5-carboxamide (carbamazepine [V]) were separated from their unlabelled parent compounds by reversed-phase chromatography on a C₁₈ column with H₂O/CH₃CN/THF (80 : 16 : 4, v/v/v) as the eluent.

Table 5 LC separation factors of chlorophylls versus deuterated chlorophylls^a

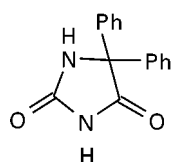
Labelled compound	$\alpha = k_1/k_2$	Eluent (A/B) ^b (v/v)
[² H]Chlorophyll <i>a</i>	1.132	5 : 95
[² H]Chlorophyll <i>a'</i>	1.158	5 : 95
[² H]Chlorophyll <i>b</i>	1.156	5 : 95
[² H]Bacteriochlorophyll <i>a</i> ^c	1.149	10 : 90
[² H]Bacteriochlorophyll <i>a</i> ^d	1.118	7 : 93
[² H]Pyrochlorophyll <i>a</i>	1.167	0 : 100

^aBaweja (1986).

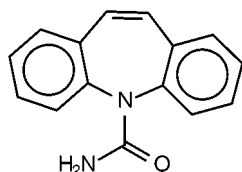
^bA = H₂O; B = methanol-acetonitrile-THF (30 : 40.5 : 24.5, by vol).

^cContains geranylgeranyl side-chain.

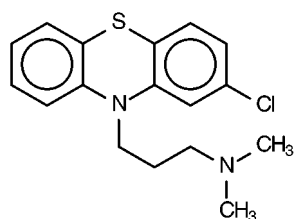
^dContains phytol side-chain.



[IV]



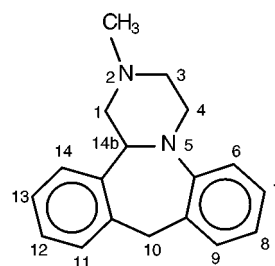
[V]



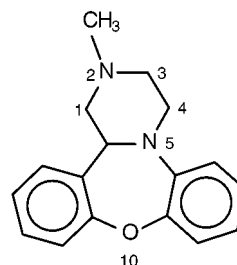
[VI]

Baseline separation was attained even when using extracted serum samples. The calculated resolution for the isotopomer pairs was 1.3. (Resolution $R_s = (t_2 - t_1)/[0.5(w_1 + w_2)]$.)

[CH₃-³H]Chlorpromazine [VI] and its metabolite [CH₃-³H]-7-hydroxychlorpromazine were separated on a chemically-bonded stationary phase (Spherisorb CN) from their unlabelled counterparts. Although the specific activity of tritiated compound was about 40 Ci mmol⁻¹ indicating approximately 1.5 tritium atoms per methyl group, the measured separation factors were rather high (Table 6). The separation factors depend strongly on the pH of the mobile phase, so that the isotope effect on the basicity of the dimethylamino group is probably significant. The labelled species was eluted later.



[VII]



[VIII]

An almost complete resolution was attained between unlabelled and di-, tri- or tetradeuterated drugs active on the central nervous system – 1,2,3,4,10,14b-hexahydro-2-methyldibenzo[*c,f*]pyrazino[1,2-*a*]azepine (mianserin [VII]) and 1,3,4,14b-tetrahydro-2,7-dimethyl-2H-dibenzo[*b,f*]pyrazino[1,2-*a*]-1,4-oxazepine (Org GC 94 [VIII]). [3,3,4,4-²H₄]Org GC 94 was chromatographed on a μ -Porasil column and n-hexane-2-propanol (90 : 10, v/v) to which 4% of ethanol and 0.1% of ammonia solution were added as the mobile phase. Various isotopomers of deuterated mianserin were chromatographed on LiChrosorb Si 60 and Spherisorb C₁₈ columns (Table 7). The deuterated compounds were always moving more slowly than the unlabelled ones. The greatest isotope effects have been found for compounds labelled on the piperazine ring (with the exception of position 14b) and on the methyl group,

Table 6 LC separation factors of chlorpromazine versus tritiated chlorpromazine^a

Labelled compound	$\alpha = k_1/k_3^b$	pH of eluent ^c
[CH ₃ - ³ H]Chlorpromazine	0.855	7
	0.901	6
	1.00	5
[CH ₃ - ³ H]-7-Hydroxychlorpromazine	0.847	7
	0.910	6
	0.952	5

^aYeung *et al.* (1984).

^bSpherisorb CN column.

^c10% 0.05 mol L⁻¹ sodium acetate buffer in methanol.

Table 7 LC separation factors of mianserin versus isotopomers of deuterated mianserin^a

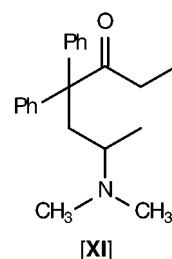
Labelled compound ^b	α_2 (LiChrosorb) ^c	α_2 (C ₁₈) ^d
[3,3,4,4- ² H ₄]Mianserin	0.893	0.935
[N-C ² H ₃]Mianserin	0.893	0.935
[3,3- ² H ₂]Mianserin	0.910	0.935
[1,1- ² H ₂]Mianserin	0.926	
[4,4- ² H ₂]Mianserin	0.971	

^aKaspersen *et al.* (1984).^bFor other isotopomers, namely [8-²H], [6,8-²H₂], [10,10-²H₂], [12-²H], [13-²H] and [14b-²H] no fractionation occurred.^cn-Hexane-2-propanol (9 : 1, v/v) + 0.1% NH₃, aq.^d0.1 mol L⁻¹ sodium acetate-acetonitrile (1 : 4, v/v).

indicating that the basicity change plays the most important role.

2-(N-Propyl-N-2-thienylethyl)-5-hydroxytetralinamine (N-0437 [IX]), an effective drug against Parkinson's disease and glaucoma, can be separated from its counterparts deuterated and tritiated at the propyl group. The corresponding diastereoisomeric glucuronides were prepared by enzymatic synthesis and separated in a reversed-phase LC system (Nova-Pak C₁₈). The separation factors were pH-dependent and relatively large, considering the remote positions of the labels from the nitrogen atom, e.g. $\alpha_2 = 1.033$; $\alpha_3 = 1.037$.

The above-mentioned effect of isotope substitution on the basicity of amines was demonstrated by thin-layer chromatography (TLC) of the popular antidepressant imipramine [X]. [²H₁₀]Imipramine labelled in both methyl groups and in aromatic rings and its parent compound were resolved on silica plates using different eluents, in which the pres-



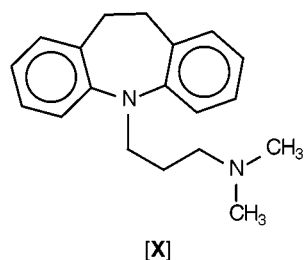
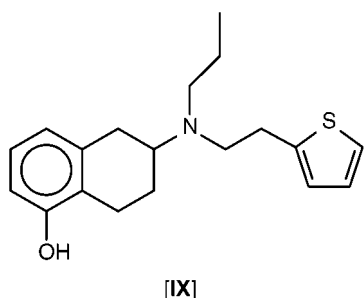
ence of ammonia was necessary; e.g. benzene-acetone-NH₃ (300 : 60 : 1, v/v/v); R_F [¹H] = 0.24; R_F [²H] = 0.18. Labelling on the benzene ring exerted no effect on the chromatographic mobility.

Similar TLC behaviour has been observed with (R,S)-6-[CH₃-²H₆]dimethylamino-4,4-diphenyl-heptan-3-one.HCl ([²H₆]methadone [XI]) (silica gel Merck; benzene-methanol-NH₃; 85 : 15 : 0.65, v/v/v); R_F [²H] = 0.58; R_F [¹H] = 0.79. Reversed-phase LC showed baseline resolution, whereas gas-liquid chromatography afforded no separation.

Isotopes of Heavier Elements

Liquid chromatographic separations of the isotopes of elements other than hydrogen have been rather rare. A high-efficiency liquid-liquid chromatography system consisting of porous silica microspheres covered with 25% (w/w) bis(2-ethylhexyl)phosphoric acid in dodecane as the stationary phase and nitric acid as the mobile phase obtained a certain enrichment of heavier isotopes of calcium in the front of the elution curve. Separation factors calculated by Glueckauf (1961) for ⁴²Ca, ⁴⁵Ca, ⁴⁸Ca versus ⁴⁰Ca were 1.0012–1.0029.

Better resolution was obtained when isotopic pairs of ¹⁴⁴Sm–¹⁵⁴Sm, ¹⁴⁰Ce–¹⁴²Ce, and ¹⁵¹Eu–¹⁵³Eu were chromatographed on LiChrosorb 60 with di-2-propylether-THF-65% HNO₃ (100 : 20 : 5, v/v/v). Heavier isotopes were always eluted first, the separation factors being two orders of magnitude higher than in ion exchange chromatography (1.030–1.085).



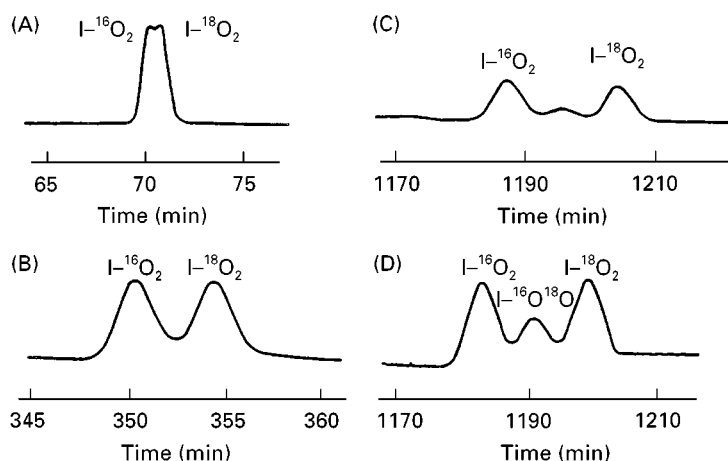


Figure 3 Separation of benzoic acid (I) isotopomers by recycle chromatography. Column: Cosmosil 5-C₁₈-P × 4, 15 cm × 4.6 mm i.d. Mobile phase: methanol-0.05 mol L⁻¹ acetate buffer (pH 4.83) 20 : 80 (v/v). Cycles: (A) 1, (B) 5, (C) and (D) 17. (From Tanaka, 1986.)

There are very few references in the literature to liquid chromatographic separations of organic compounds labelled with isotopes heavier than hydrogen. For example, Tanaka *et al.* (1986) demonstrated the oxygen isotope effect on the reversed-phase LC separation of ¹⁸O-labelled benzoic acid (Figure 3). They demonstrated that successful separation was due to differences in the dissociation constants between the labelled and parent compounds. The isotope effect was pH-dependent and attained a maximal value around pH 5 (Table 8). An equation was derived to determine the ¹⁸O isotope effect on the dissociation constants from LC data. This isotope effect was calculated to be $^{16}K_a/^{18}K_a = 1.020 \pm 0.002$. A very good, nearly baseline, resolution was attained in a recycle system for the pair benzoic acid – [¹⁸O₂] benzoic acid after five cycles, and for the mixture benzoic acid – [¹⁸O]benzoic acid – [¹⁸O₂]benzoic acid after 17 cycles. Similar results were obtained in chromatography of [¹⁸O₂]-4-chlorobenzoic acid and [OH-¹⁸O]-4-nitrophenol with their unlabelled counterparts. The ¹⁸O–H bond is stronger than the ¹⁶O–H bond so that ¹⁸O-labelled acids are weaker acids than unlabelled ones. Therefore, a longer retention time in reversed-phase LC was expected and found for the labelled carboxylic acid compared to the unlabelled acid.

The same procedure as above was successfully applied to the separation of aniline and [¹⁵N]aniline on the same column with 0.05 mol L⁻¹ acetate buffer containing 5% methanol and 0.01% triethylamine as the eluent. At pH 4.24 the separation factor was found to be $\alpha = k_{14}/k_{15} = 1.010$. The complete separation was accomplished after 20 cycles.

See also: II/Chromatography; Liquid: Mechanisms: Normal Phase; Mechanisms: Reversed Phases. III/Pharmaceuticals: Thin-Layer (Planar) Chromatography.

Further Reading

- Baweja R (1986) HPLC separation of deuterated photosynthetic pigments from their protio analogues. *Journal of Chromatography* 369: 125–131.
- Baweja R (1987) Application of reversed-phase HPLC for the separation of deuterium and hydrogen analogues of aromatic hydrocarbons. *Analytica Chimica Acta* 192: 345–348.
- Filer CN (1999) Isotopic fractionation of organic compounds in chromatography. *Journal of Labelled Compounds and Radiopharmaceuticals* 42: 169–197.
- Glueckauf E (1961) Isotope separation by chromatographic methods. In: London H (ed.) *Separation of Isotopes*, pp. 209–248. London: G. Newnes Ltd.

Table 8 Dependence on eluent pH of LC^a separation factors of benzoic acid versus [¹⁸O₂]benzoic acid^b

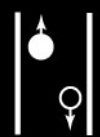
	Eluent pH							
	2.44	3.13	4.07	4.40	4.90	5.29	5.86	6.27
α	1.000	1.000	0.995	0.991	0.988	0.988	0.992	0.995

^aCosmosil C₁₈-P; methanol-0.05 mol L⁻¹ acetate buffer (20 : 80); 30°C.

^bTanaka *et al.* (1986).

- Halloran BP, Bikle DD and Whitney JD (1984) Separation of isotopically labelled vitamin D metabolites by HPLC. *Journal of Chromatography* 303: 229–233.
- Kaspersen FM, van Acquoy J, van de Laar GLM, Wagenaars GN and Funke CW (1984) Deuterium isotope effects in mianserin. *Recueil Travaux Chimique de Pay-Bas* 103: 32–36.
- Klein PD (1966) Occurrence and significance of isotope fractionation during analytical separation of large molecules. *Advances in Chromatography* 3: 3–65.
- Lešetický L (1985) Isotope separation by chromatographic methods [in Czech]. *Radioisotopy* 26: 113–126.
- Lockley WJS (1989) Regiochemical differences in the isotopic fractionation of deuterated benzoic acid isotopomers by reversed phase HPLC. *Journal of Chromatography* 483: 413–418.
- Simon H and Palm D (1966) Isotope effects in organic chemistry and biochemistry [in German]. *Angewandte Chemie* 78: 993–1007.
- Tanaka N, Araki M and Kimata K (1986) Separation of oxygen isotopic compounds by reversed-phase liquid chromatography. *Journal of Chromatography* 352: 307–314.
- Tanaka N and Thornton ER (1977) Structural and isotopic effects in hydrophobic binding measured by HPLC. A stable and highly precise model for hydrophobic interaction in biomembranes. *Journal of American Chemical Society* 99: 7300–7306.
- Willi AV (1983) *Isotope Effects in Chemical Reactions* [in German]. Stuttgart: G. Thieme.
- Worth GK and Retallack RW (1988) Tritium isotope effect in high-pressure liquid chromatography. *Analytical Biochemistry* 174: 137–141.
- Yeung PKF, Hubbard JW, Baker BW, Looker MR and Midha KK (1984) Isotopic fractionation of N-([³H]methyl)chlorpromazine and N-([³H]methyl)-7-hydroxychlorpromazine by reversed-phase high performance liquid chromatography. *Journal of Chromatography* 303: 412–416.

LEAD AND ZINC ORES: FLOTATION



M. Barbaro, Istituto Trattamento Minerali CNR,
Rome, Italy

Copyright © 2000 Academic Press

Outline of the Problem

Today, owing to the limitation of sources and supplies of mineral raw materials and the need to treat ores of increasingly lower grades, as well as those which are fine, complex mineralogically, and refractory, new flotation technology must be developed.

Flotation is in fact the most common process in metallic mineral separation and is the main way for recovering such valuable metals as lead (Pb) and zinc (Zn), or copper (Cu) from ores.

It is known that separation by flotation of useful minerals from gangue in an aqueous pulp happens when particles with polar, hydrophilic or wettable surfaces remain in the liquid phase, whilst particles with apolar hydrophobic or not wettable surfaces adhere to air bubbles. Collectors or depressing/activating reagents modify surface characteristics of minerals thus influencing affinity towards water. Thus, research into new separation technologies is mainly concerned with the search for new flotation reagents.

In fact the value of a flotation concentrate containing a given mineral, from which a desired metal is extracted by a metallurgical process, decreases with an increase in the presence of minerals containing metals other than the one of prime interest. It is thus necessary to design new specific collectors to separate the desired mineral from the gangue. Collectors generally employed in flotation are surfactants that form, for instance, electrostatic bonds with the solids (Leja 1982). Difficulty therefore arises when a particular metallic mineral, such as Pb or Zn mineral, has to be separated from an ore of complex composition or low grade (complex sulfide ores) or when the surface properties of the mineral (oxidized Pb and Zn ores) make the response to flotation extremely poor. To overcome this basic drawback in metal ore flotation, the possibility of using new compounds endowed with a strong affinity for metals themselves has been investigated. The search for new reagents for mineral flotation therefore aims to discover collectors (or depressants) capable of linking more selectively with a given element present in the ore.

The present work deals with the recovery of Pb and Zn by flotation and reviews the main problems faced by research engineers in this field.

Complex Pb-Zn Sulfide Ores

Complex sulfide ores have been defined as those ores for which it is difficult to recover one or more selective product of acceptable quality and economic value with minimal losses and at reasonable costs. Complex sulfide ores are fine-grained, intimate associations of chalcopyrite (CuFeS_2), sphalerite (ZnS) and galena (PbS), disseminated in dominant pyrite, and containing valuable amounts of minor elements.

Generally, collectors employed for sulfide recovery are of the thiol type, and the most commonly used are xanthates. A great number of studies have been carried out on xanthates, examining their adsorption mechanism by spectroscopic techniques such as infrared spectroscopy (Giesekke 1983, Kongolo *et al.* 1984, Little *et al.* 1961, Marabini *et al.* 1983), IR-ATR techniques (Mielczarski *et al.* 1987, Mielczarski *et al.* 1981), X-ray photoelectron spectroscopy (XPS) (Laajalehto *et al.* 1988, Page *et al.* 1989), and also by calorimetric techniques (Partyka *et al.* 1987, Arnaud *et al.* 1989).

However xanthates are active towards the whole class of sulfide minerals, rather than towards one individual mineral. Thus, in order to float a given mineral from a mixture of minerals belonging to the same sulfide class, modifiers are used in order to render the action of the collector more specific, and to improve separation efficiency (Finkelstein *et al.*, 1976).

However, there are many problems in this procedure and the desired results are not always obtained, especially in the case of minerals of a complex composition as in the case treated.

Hence the importance of seeking out collectors capable of linking selectively with one single given mineral rather than with the whole class. Selective linkage is possible if the collector structure incorporates active groups having specific affinity for certain cation characteristic of the mineral surface.

Thus, the search for new, more selective reagents for sulfide mineral flotation is mainly concerned with chelate-forming reagents. In fact, chelating reagents are particular complexing reagents consisting of large organic molecules capable of linking to the metal ion via two or more functional groups, with the formation of one or more rings, thus forming a very stable bond. The stability of metal chelates is influenced by many factors which govern the selectivity and specificity of the chelation reaction.

Examples of the use of chelating reagents in flotation were known from studies on traditional thiol collectors. In fact, both dixanthogen and thionocar-

bamate act as chelating reagents (Ackerman *et al.*, 1987).

There are many studies on chelating agents as collectors more selective than xanthates (Marabini *et al.*, Rinelli *et al.*, Usoni *et al.*, Barbaro *et al.*, Somasundaran) and a review on this topic has been published by Pradip (Pradip 1988). Use of reagents of chelate type offers the possibility of improving selectivity in the flotation separation of complex sulfide minerals (Marabini *et al.* 1990 and 1991).

Oxidized Zn and Pb Minerals

It is well known that there is a difference between sulfurized and oxidized minerals as regards their separation by flotation. It is easy to recover Zn from sphalerite and Pb from galena even using xanthate collectors but it is not the same for Zn from smithsonite (Zn CO_3) and Pb from cerussite (PbCO_3).

Flotation of Zn and Pb oxidized minerals is difficult because there are no known direct-acting collectors capable of producing single metal concentrates. The need for new specific collectors is felt particularly in the case of oxidized lead and zinc minerals because their surface – unlike that of the sulfide variety – is not easily rendered hydrophobic by the collectors generally used, to achieve efficient flotation. Furthermore, the solubility of these oxide minerals is high. Consequently the collector also interacts with metal cations which have gone into solution, thus greatly increasing the amount of reagent required for flotation. It is therefore common practice to sulfurize such minerals prior to flotation so as to prepare their surface to receive xanthates, the collectors generally adopted for concentrating sulfides. Generally the collectors normally used in beneficiation plants act only if the ore has been subjected to a preliminary sulfidization phase which is extremely delicate and critical. In fact, sulfurization calls for careful dosage to avoid rendering the mineral surface inert.

Thus classical collectors have an affinity towards given mineralogical classes, whilst chelating reagents – when chemically adsorbed on the mineral surface – have specificity towards given cations, independently from the mineralogical form of the solid.

However this approach also has two main disadvantages, firstly, excessive consumption (Marabini 1973, Marabini *et al.* 1983), and secondly, lack of an aliphatic chain which renders the mineral surface hydrophobic.

In fact the chelating reagents commercially available are almost all aromatic molecules without a long hydrocarbon chain; thus, although the chelated min-

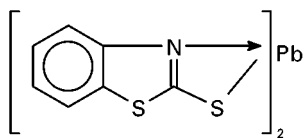


Figure 1 Structure of MBT-Pb chelate.

eral particle is fairly hydrophobic, it is not sufficiently aerophilic to ensure flotation. Studies on oxidized minerals (Usoni *et al.* 1971, Rinelli *et al.* 1973, Marabini 1975, Rinelli *et al.* 1976) were performed rendering particles hydrophobic by making contemporary available long-chain organic groups (as fuel-oil or oily frother) and chelating agents.

The first application of this concept is from 1973. A chelating reagent, namely 8-hydroxyquinoline (Figure 1) with fuel oil was used to float mixed oxide-sulfide minerals of Zn and Pb (Rinelli *et al.* 1973). Good recoveries have been attained on an ore containing 7.3% Zn with 1.4% as sphalerite, and 0.9% Pb with 1.4% as galena.

On the basis of the points made so far it is apparent that known chelating compounds form a class of reagents which can be used for the flotation of metallic ores, providing artificially the long chain organic portion by introducing a neutral oil (fuel oil). But the introduction of a new liquid phase into flotation pulp is damaging to the system as a whole and is not available on an industrial scale.

Studies, therefore, have been oriented towards the synthesis of new organic molecules containing both selective functional aromatic chelating groups and hydrophobic long alkyl chain portions. This is done by modifying known chelating collectors.

Indeed, much research was performed on the design of selective chelating collectors; this resulted in numerous structures being proposed and synthesized for laboratory-scale testing on lead/zinc ores prior to the performance of pilot-scale and plant-scale trials.

On the basis of a thermodynamic calculations for the selection of complexing collectors theoretically selective towards a cation (Marabini *et al.* 1983), two classes of reagents have been proposed by Marabini *et al.* (Marabini *et al.* 1988 and 1989, Nowak *et al.* 1991) for the flotation of oxidized Zn and Pb in a pilot plant. Much has been written on the role of the aliphatic chain in conventional collectors (Cases 1968, Predali 1968, Somasundaran 1964) but the work concerns new chelate-type reagents, of the mercaptobenzothiazole (MBT) and aminothiophenol (ATP) types having a mixed aromatic-aliphatic structure. The aromatic part contains specific functional

chelating groups that are selective towards the zinc or the lead of oxidized minerals (MBT is selective towards lead and ATP towards zinc) while the aliphatic part consists of a hydrocarbon chain which renders the surface-complex hydrophobic.

The collecting action of MBT is thus attributable to the formation of a surface film selectively chemisorbed on the mineral surface rendered hydrophobic by the aliphatic chain.

In fact in the case of hydrophilic oxidized minerals, the aromatic-heterocyclic portion of the MBT alone does not suffice to render the surface sufficiently hydrophobic to ensure flotation. Hence an aliphatic chain has to be introduced in the molecular structure. The aliphatic chain is necessary to ensure a hydrophobic condition and hence collecting power for the aromatic chelating (MBT or ATP) reagent.

It has been demonstrated that three carbon atoms is the minimum chain length needed to ensure collecting power that improves with aliphatic chain length. Performance is enhanced slightly by the presence of an ether oxygen atom.

Where reagents of the ATP type are concerned, these (as the Schiff bases derived therefrom) exert chelating action towards Zn (Barbaro *et al.* 1997). Chelation occurs through weak bonds with nitrogen and -SH as shown (Figure 2).

The formation of a chemisorbed surface film is sufficiently stable to account for the collecting action. The selectivity of molecules containing ATP and different aliphatic chains has been studied by flotation tests.

In this case the role of the aliphatic chain and of the ether oxygen is of more decisive importance than for MBT in assuring the stability of the adsorbed phase and thus floatability. The selectivity increases with the number of carbon atoms in the chain.

In particular, the presence of the oxygen in the chain enhances selectivity, whilst in MBT class reagents only chain length is effective. This difference can be explained by the different chemical structure of the two reagents. In the case of MBT, the effect of the aliphatic substituent is due mainly to its hydrophobicizing effect, and thus to its

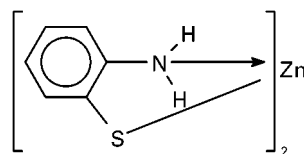


Figure 2 Structure of ATP-Zn chelate.

length which favours reciprocal attraction of the chains of the adsorbed layer.

By contrast, in the case of ATP, the effect of the aliphatic substituent is due not only to its hydrophobicizing effect, but also to its effect on reactivity of the aromatic polar head of the molecule. In fact the ATP chelating functional group has a weaker reactivity in comparison with MBT, and therefore is more sensitive to the effect of the substituent on its unique benzenic ring (whilst MBT has two aromatic structures). For this reason, in the case of ATP it is possible to observe that the presence of the oxygen in the chain greatly enhances selectivity. The positive effect of the R-O group in the para position *vis-à-vis* the nitrogen of ATP can be explained with the electron-releasing effect due to resonance of the oxygen with the benzene ring, which increases reactivity with the nitrogen group (Morrison 1973).

In the case of ATP, which forms a less stable bond with the mineral cation and which consists of a single benzene ring, the conjugative effect of the ether oxygen and the hyperconjugative effect of the alkyl groups are more evident than for MBT. Selectivity is improved by the insertion of oxygen in the chain and also by an increase in chain length. Here the effect of the alkyl chain on the aromatic functional group is more marked, permitting modulation of selectivity.

This research based on the design and synthesis of new flotation reagents opens new possibilities in the field of metallic Pb and Zn mineral recovery by flotation.

See also: II/Flotation: Hydrophobic Surface State Flotation.

Further Reading

- Ackerman PK, Harris GH, Klimpel R and Aplan FF (1987) Evaluation of flotation collectors for copper sulphides and pyrite. I. Common sulphydryl collectors, II. Non-sulphydryl collectors, III. Effect of xanthate chain length and branching. *Int. J. Min. Proc.* 21: 105–156.
- Arnaud M, Partyka S and Cases JM (1989) Ethylxanthate adsorption onto galena and sphalerite. *Coll. Surf.* 37: 235–244.
- Barbaro M, Herrera Urbina R, Cozza C *et al.* (1997) Flotation of oxidized minerals of copper using synthetic chelating reagents as collectors. *Int. J. Min. Proc.* 50: 275–287.
- Finkelstein NP and Allison SA (1976) The chemistry of activation, deactivation and depression in the flotation of zinc sulphides: a review. In Fuerstenau MC (ed.) *Flotation*, Gaudin AM memorial volume. New York: AIME.

- Giesekke EW (1983) A review of spectroscopic techniques applied to the study of interactions between minerals and reagents in flotation systems. *Int. J. Min. Proc.* 11: 19–56.
- Kongolo M, Cases JM, Burreau A and Predali JJ (1984) Spectroscopic study of potassium amylxanthate adsorption on finely ground galena. In Jones and Oblatt (eds) *Reagents in Mineral Industry*, pp. 79–87. Rome: IMM.
- Leja J (1982) *Surface Chemistry of Froth Flotation*. New York: Plenum.
- Marabini A, Barbaro M and Ciriachi M (1983) A calculation method for selection of complexing collectors having selective action on a cation. *Trans. IMM*, Sect. C 92: 20–26.
- Marabini A and Cozza C (1983) Determination of lead ethylxanthate on mineral surface by IR spectroscopy. *Spectrochimica Acta* 388: 215.
- Marabini AM and Rinelli G (1986) Flotation of lead-zinc ores. In *Advances in mineral processing. Proc Symp. honoring N. Arbiter*, N. Orleans, March 3–5, pp. 269–288.
- Marabini AM, Alesse V and Barbaro M (1988) New synthetic collectors for selective flotation of zinc and lead oxidised minerals. In Forssberg (ed.) *XVI Int. Min. Proc. Congr.*, Amsterdam: Elsevier, pp. 1197–1208.
- Marabini A, Barbaro M and Passariello B (1989) Flotation of cerussite with a synthetic chelating collector. *Int. J. Min. Proc.* 25: 20.
- Marabini A and Barbaro M (1990) Chelating reagents for flotation of sulphide minerals. In: *Sulphide Deposits – Their Origin and Processing*. London: Institution of Mining and Metallurgy.
- Marabini AM, Barbaro M and Alesse V (1991) New reagents in sulphide mineral flotation. *Int. J. Min. Proc.* 33: 291–306.
- Mielczarski J and Leppinen J (1987) Infrared reflection-absorption spectroscopy study of adsorption of xanthates on copper. *Surface Science* 187: 526–538.
- Nowak P, Barbaro M and Marabini A (1991) Flotation of oxidised lead minerals with derivatives of 2-mercaptobenzothiazole. Part 1: Chemical Equilibria in the System 6-methyl-2-mercaptobenzothiazole-lead salts. *Int. J. Min. Proc.* 32: 23–43.
- Page PW and Hazell LB (1989) X-ray photoelectron spectroscopy studies of potassium amylxanthate adsorption on precipitated PbS related to galena flotation. *Int. J. Min. Proc.* 25: 87–100.
- Partyka S, Arnaud M and Lindheimer M (1987) Adsorption of ethylxanthate onto galena at low surface coverage. *Coll. Surf.* 26: 141–153.
- Pradip (1988) Application of chelating agents in mineral processing. *Min. Met. Proc.* 80.
- Predali JJ (1968) Flotation of carbonates with salts of fatty acids. *IMM* 77: 140–147.
- Rinelli G and Marabini A (1973) Flotation of zinc and lead oxide-sulphide ores with chelating agents. *10th Int. Min. Proc. Congr.* London: IMM.

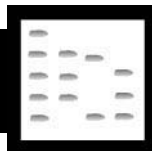
Rinelli G, Marabini AM and Alesse V (1976) Flotation of cassiterite with salicylaldehyde as a collector, Flotation, Gaudin AM Memorial Volume, Fuerstenau MC (ed.) vol. 1, p. 549.

Somasundaran P and Nagaraj PR (1984) Chemistry and applications of chelating agents in flotation and floccula-

tion. In Jones M and Oblatt R (eds) *Reagents in Mineral Industry*. London: IMM.

Usoni, L, Rinelli G and Marabini AM (1971) Chelating agents and fuel oil: a new way to flotation. *AIME Centennial Annual Meeting*. New York, Feb 26–March 3.

LIPIDS



Gas Chromatography

A. Kuksis, University of Toronto, Charles H Best Institute, Toronto, Canada

Copyright © 2000 Academic Press

Introduction

Natural lipids consist of complex mixtures of molecular species, which are found in association with cell membranes, lipoproteins and other subcellular structures. The composition differs among different cell and tissue types, reflecting the function of lipids in these body structures. Industrial and food products may be of plant, animal or synthetic origin. The gas chromatography (GC) of fatty acids by James and Martin in 1956 provided the first success in dealing with the complexity of the hydrolysis products of fats and oils. A few years later Kuksis and McCarthy developed methods for the resolution of intact triacylglycerols by high temperature GC.

Improved design of GC equipment, culminating in the development of reliable capillary columns, together with enzymic and chemical derivatization of samples now permits the separation of molecular species of all lipids on a routine basis. In modern analyses, conventional or high temperature GC serves as the final step in the multi-method resolution and quantification of individual components of a total lipid extract. The high molecular weight and low volatility, however, require constant vigilance in quantitative GC analysis of natural lipids.

Nonpolar Capillary Columns

Nonpolar capillary columns provide resolution based on the overall molecular weight of the lipid molecules. The nonpolar phases are typically polymethylsiloxane polymers with 5% phenyl groups. They are

stable to 350°C or higher temperatures. Other nonpolar phases for GC are provided by certain hydrocarbons, which are limited to much lower temperatures and are operated isothermally.

Polarizable Capillary Columns

The methylsiloxane liquid phases containing 50–65% phenyl groups become polar as the temperature increases above 290°C, as indicated by the longer retention of the unsaturated compared to saturated triacylglycerols. Below this temperature the liquid phase is nonpolar, as indicated by the earlier elution of the unsaturated compared to saturated fatty acid trimethylsilyl (TMS) esters. The polarizable liquid phases are stable up to 360°C. Since these liquid phases possess high temperature stability, they are well suited for the resolution of molecular species of seed oil and milk fat triacylglycerols.

However, columns at least 25 m long are needed to provide sufficient resolving power for the separation of the saturated and unsaturated species of natural diacyl and triacylglycerols, and ceramides.

Polar Capillary Columns

Capillary columns containing polar and very polar liquid phases are utilized mainly for the separation of saturated and unsaturated fatty acids as the methyl esters. The more stable polar capillary columns can be programmed to 280°C and used for the separation of the TMS ethers of diacylglycerols and ceramides as well as low molecular weight triacylglycerols.

Detection and Quantification of GC Peaks

The principal detector for the GC of lipids is the flame ionization detector (FID), but electron-capture detectors are also used (e.g. for pentafluorobenzyl esters). A number of authors have evaluated the quantitative GC analysis of fatty acids and triacylglycerols. GC with online electron impact (EI) mass

spectrometry (GC-EI-MS) yields largely qualitative information from which the structure of unknown molecules can nevertheless be deduced. However, both total ion current and single ion monitoring have been utilized for quantitative analyses using appropriate calibration curves.

Resolution of Neutral Lipids

Neutral lipids, including common triacylglycerols, are readily resolved according to their molecular weight or number of carbon atoms by high temperature GC. Mixtures of high and low molecular weight neutral lipids are best dealt with by temperature programming. These methods are also suitable for the GC of certain polar lipids provided the polar head groups have been removed or masked. The neutral lipid separations are usually performed on nonpolar liquid phases, but polarizable liquid phases of high temperature stability have also been employed for the separation of intact neutral lipids. In both instances some prefractionation of the lipid mixture is necessary for optimum analysis.

Isolation and Preparation of Derivatives

Usually this includes the removal of the polar lipids from the neutral compounds by thin-layer chromatography

(TLC), high performance liquid chromatography (HPLC) or simple adsorbent cartridges. Before GC, the free functional groups of the lipids must be protected in order to avoid dehydration and to increase volatility, as well as to improve other GC properties. This is readily accomplished by preparing TMS derivatives; in special instances other derivatives may be prepared. Free carboxyl groups may be methylated with diazomethane and alcohol groups may be acetylated with acetic anhydride in the presence of other ester bonds. Table 1 lists the more common reagents for derivatization of neutral lipids along with the reaction conditions. Polar lipids, such as glycerophospholipids, can be converted into neutral lipids by dephosphorylation. This can be readily accomplished by hydrolysis with phospholipase C (*Bacillus cereus*), which releases the phosphocholine moiety from phosphatidylcholine, lysophosphatidylcholine and sphingomyelin, and the phosphoethanolamine moiety of both diacyl and alkenylacylglycerophosphoethanolamines. The *B. cereus* enzyme also attacks the plasma inositol phosphatides to yield diacylglycerol moieties. Alternatively, the plasma phospholipids may be dephosphorylated by pyrolysis, acetolysis and silolysis, but the latter procedures lead to isomerization of the acylglycerols, incomplete conversion and partial destruction of the lipid samples.

Table 1 Preparation of derivatives for GC analysis of neutral lipids, fatty acids and prostanooids^a

Reagent	Ratio	Temperature	Time	Application
<i>Neutral lipids</i>				
Pyridine/HMDS/TMCS	12/5/2	Ambient	0.5–1 h	Trimethylsilyl ethers of acylglycerols and sterols
<i>t</i> -BDMCS/imidazole/dimethylformamide	1 : 2.5 in DMF	80°C	20 min	<i>tert</i> -Butyldimethylsilyl ethers of acylglycerols and sterols
Ac ₂ O/pyridine	1 : 10	80°C	1 h	Acetates of acylglycerols and sterols
PFB ₂ O/pyridine	1 : 10	80°C	1–2 h	Pentafluorobenzoates of acylglycerols and sterols
<i>Fatty acids</i>				
BF ₃ /MeOH	15%	Ambient	20 min	Methyl esters of free fatty acids
BF ₃ /MeOH	6–15%	60°C/reflux	2–10 min	Methyl esters of fats and oils
H ₂ SO ₄ /MeOH	6%	80°C/reflux	2 h	Methyl esters and dimethylacetals of fatty acids
HCl/MeOH	5%	60°C	0.5–2 h	Methyl esters of free and bound fatty acids
CH ₂ N ₂ /ether	Dilute	Ambient	5 min	Methyl esters of free fatty acids
KOH/MeOH/benzene	0.2–2 N	Ambient	0.5 min	Methyl esters of glyceryl esters
NaOH/MeOH	0.5–2 N	Refluxing	0.5–1 h	Methyl esters of steryl esters
2-NH ₂ -2-MePr (DMOX)		170°C	18 h	4,4-Dimethyloxazolines of unsaturated fatty acids
DEADMS/3-pyridyl carbinol		60°C	10 min, 10 min	Picolinyldimethylsilyl (PICSi) esters
(TFA) ₂ O/3-pyridyl carbinol	2 steps	50°C	1 h	Picolinyl esters of fatty acids
Oxalyl Cl/pyrrolidide	2 steps	Ambient	30 min	<i>N</i> -acyl pyrrolidides of fatty acids
<i>Prostanooids</i>				
PFBBr/ <i>N,N</i> -DIPETn/Meoxamine/BSTFA/pyridine	3 steps	Ambient, 60°C, and 60°C, resp.	10 min, 16 h, 15 min	PFB/MO/TMS derivatives of prostanooids, thromboxanes, hepoxilins

^aAbbreviations and experimental details are found in the text, in legends to figures and in references cited.

The dephosphorylated lipids are recovered by TLC or adsorbent cartridges and the exposed hydroxyl groups masked by acetylation or preparation of TMS derivatives. The diacyl, alkylacyl and alkenylacyl subclasses released from glycerophospholipids by phospholipase C can be readily resolved by normal-phase HPLC or TLC prior to the GC resolution of the molecular species of the *sn*-1,2-diradylglycerol moieties. Likewise, the method is suitable for the resolution of the molecular species of TMS ethers of the *sn*-1,2- and *sn*-2,3-diacylglycerol moieties of triacylglycerols derived by Grignard degradation, chiral-phase HPLC resolution as the dinitrophenylurethanes, and silolysis.

Total Neutral Lipid Profiling

Total neutral lipids are easily resolved into component lipid classes by GC on short (8–15 m) nonpolar capillary columns. Longer (25 m) polarizable capillary columns provide separations of molecular species. The components ranging from free fatty acids to triacylglycerols can be effectively quantified by tridecanoylglycerol added as an internal standard to the mixture prior to the GC analysis. **Table 2** lists the more common liquid phases for GC of neutral lipids along with the column conditions and selected applications.

Nonpolar capillary GLC **Figure 1** shows a GC separation of total lipids in plasma, following dephos-

phorylation and preparation of TMS derivatives, on a nonpolar capillary column along with that of a mixture of ceramides and monoacylglycerols released from the combined sphingomyelin and lysophosphatidylcholine fraction isolated by preliminary TLC. The separations on the nonpolar capillary column are limited to resolution by carbon number, although the unsaturated species are eluted slightly ahead of the saturates of the same carbon number. The ceramides (peaks 32–42) are eluted over the same temperature range as the diacylglycerols (peaks 34–40). GC separations similar to those obtained for the total plasma lipids are readily obtained for individual plasma lipoproteins and lymph chylomicrons, as well as for other total lipid extracts from natural sources that can be converted to neutral lipids. GC-MS of plasma total lipids provides confirmation of the peak identity. Mass chromatograms of characteristic fragment ions, retrieved from the total ion current by a computer, permit identification and quantification of overlapping molecular species of free fatty acids, their esters and amides, as well as free sterols and steryl esters.

Partial separation of saturated and unsaturated plasma cholesteryl esters has been reported on a nonpolar capillary column and identification confirmed by negative ammonia ionization mass spectrometry. GC-MS analysis of synthetic steryl esters by nonpolar capillary GLC and EI and chemical ionization has been reported. The GC separation of C₂₇ sterols has

Table 2 Commonly used liquid phases and columns for GC of neutral lipids^a

<i>Chemical composition</i>	<i>Commercial names</i>	<i>Column dimensions</i>	<i>Type of separation (temperature programme)</i>	<i>Applications</i>
Methylsilicone	BP-1 (OV-1, SE-30, SP-2100)	12 m × 0.22 mm i.d.	Carbon number (200–350°C)	Cholesteryl esters
5% Phenyl, 95% methylsilicone	SE-54 (DB-5, HP-5, BP-5, OV-5 ^b)	8 m × 0.32 mm i.d.	Carbon number (200–350°C)	Triacylglycerols, steryl esters
65% Phenyl, 35% methylsilicone	RSL-300 (OV-22, Rtx-65-TG)	25 m × 0.25 mm i.d.	Carbon and double bond number (40–360°C)	Triacylglycerols, steryl esters, ceramides
Methylsilicone	SE-52 (DB-, SE-54)	26 m × 0.3 mm i.d.	Carbon number (200–350°C)	Triacylglycerols, steryl esters
100% Dimethylsilicone	OV-1 (SP-2100, BP-1, DB-1)	5 m × 0.32 mm i.d.	Carbon number (100–350°C)	Triacylglycerol core aldehydes
100% Dimethylsilicone	OV-1 (SE-30, BP-1, SP-2100)	15 m × 0.3 mm i.d.	Carbon number (200–350°C)	Triacylglycerol core aldehydes
68% Cyanopropyl, 32% dimethylsiloxane	Rtx-2330 (SP-2330, SP-2560)	15 m × 0.32 mm i.d.	Carbon and double bond number (250°C, isothermal)	Diradylglycerol TMS and TBDMS ethers
100% Dimethylsilicone	SE-30 (SP-2100, DB-1, BP-1)	12 m × 0.25 mm i.d.	Carbon number (40–350°C)	Diradylglycerol TMS and TBDMS ethers

^aAbbreviations and experimental details are found in the text, in legends to figures and in references cited.

^bComparable liquid phases are given in brackets.

(Modified with permission from Restek Corporation (1998) *Chromatography Products*, International Version, pp. 544–545.)

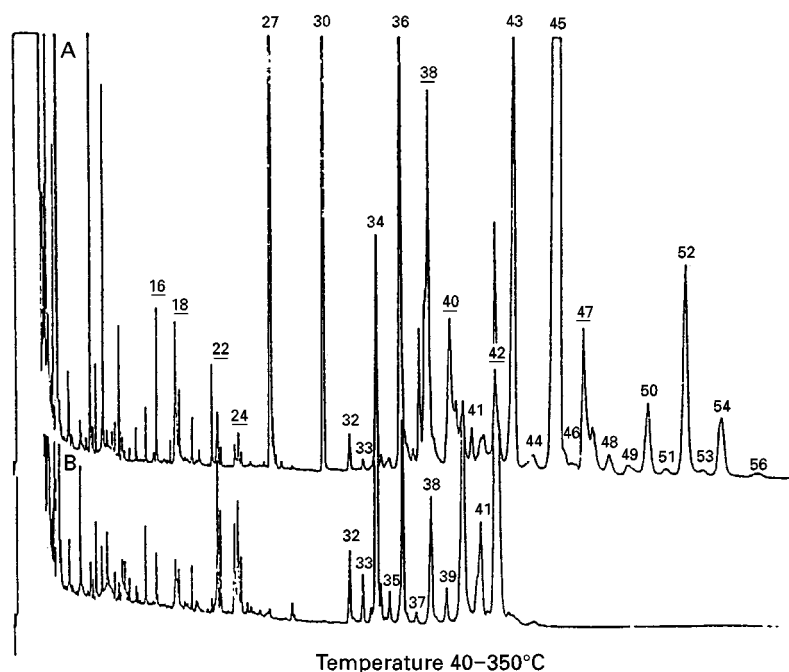


Figure 1 GC of total lipids of normal human plasma on a nonpolar capillary column. A, Total neutral lipids as obtained by dephosphorylation with phospholipase C; B, ceramides and monoacylglycerols released from sphingomyelin and lysophosphatidylcholine. Simplified peak identification: 16 and 18, free fatty acids; 22–24, monoacylglycerols; 27, free cholesterol; 30, tridecanoylglycerol (internal standard); 32–42, diacylglycerols and ceramides; 43–47, cholesteryl esters; 48–56, triacylglycerols. GC conditions: column, 5 m \times 0.25 mm i.d., 100% dimethylsilicone (SP-2100, Supelco); temperature, programmed, 170–350°C at 8°C min⁻¹ with hydrogen as carrier gas. (Reproduced with permission from Myher JJ and Kuksis A (1984) Determination of plasma total lipid profiles by capillary gas liquid chromatography. *Journal of Biochemical and Biophysical Methods* 10: 13–23.)

been reviewed and the retention times tabulated on DB-5 and CP-WAX columns for a large number of compounds as the TMS derivatives in relation to 5 α -cholestane.

Polarizable capillary GLC Figure 2 compares the plasma total lipid profiles as obtained by GC on (A) nonpolar and (B) polarizable capillary columns. The nonpolar column yields prominent peaks for free cholesterol, diacylglycerols and ceramides, cholesteryl esters and triacylglycerols. The lipid ester classes are resolved according to the total number of carbons. The polarizable column permits a separation of the glycerolipids and cholesteryl esters on the basis of both total carbon and double bond number. There is an extensive overlap among the molecular species of the diacylglycerols and ceramides but the cholesteryl esters are well resolved from each other and from the triacylglycerols of both higher and lower molecular weight. Characteristic lipid profiles are also obtained for the individual plasma lipoprotein classes. Cholesteryl arachidonate suffered some degradation and is incompletely recovered. The plasma triacylglycerols appear to be fully recovered, except for the more highly unsaturated long chain (56:4–66:18) species, which are only partially recovered.

Molecular Species of Diacylglycerols and Ceramides

The early GC analyses of molecular species of diacylglycerols were performed on nonpolar packed or capillary columns following a preliminary resolution based on unsaturation by argentation TLC. Polarizable capillary columns provide an improved resolution of the molecular species of diacylglycerols and especially of ceramides. Figure 3 compares the order of peak elution of diacylglycerols (partial Grignard deacylation products of lard triacylglycerols) and the ceramide moieties of plasma sphingomyelin. The diacylglycerol and ceramide peaks are eluted in order of increasing number of double bonds within a carbon number of each lipid class. Thus, the diacylglycerol 16:0–18:1 is eluted ahead of 16:0–18:2 and 18:0–18:1 is eluted ahead of 18:0–18:2, but 18:0–18:2 tends to overlap with 16:0–20:4. The ceramide d18:1–16:0 elutes earlier than the diacylglycerol 16:0/16:0 on the polarizable column, whereas on nonpolar columns they overlap.

The molecular species of diacylglycerols are best resolved by GC on polar capillary columns similar to those used for separation of fatty acid methyl esters. These columns provide especially detailed analyses of

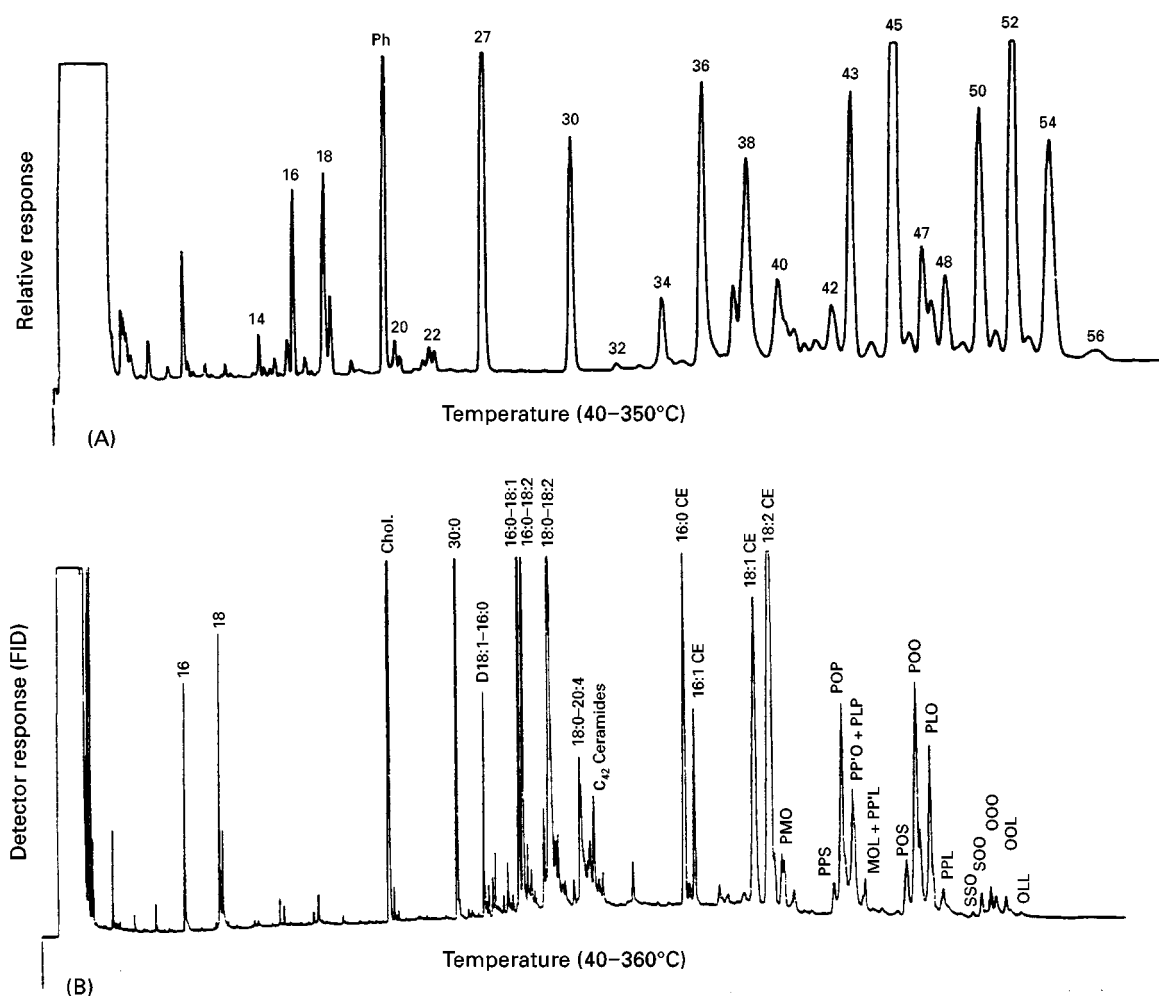


Figure 2 GC profiles of plasma total lipids on (A) nonpolar and (B) polarizable capillary columns. Peak identification: (A) as given in Figure 1; Ph, TMS ester of phthalic acid; (B) as given in the figure; L, linoleic; M, myristic; O, oleic; P, palmitic; S, stearic acids. GC conditions: (A) column, 5 m \times 0.25 mm i.d., dimethylsilicone (SP-2100, Supelco); temperature, programmed, 40–350°C at 8°C min⁻¹ with hydrogen as carrier; (B) column, 25 m \times 0.25 mm i.d., 65% phenylmethylsilicone (OV-22, Quadrex); temperature, programmed, 40–360°C at 50°C min⁻¹ to 150°C, then 10°C min⁻¹ to 310°C, and 2°C min⁻¹ to 360°C with hydrogen as carrier gas. (Reproduced with permission from Kuksis A, Myher JJ and Geher K (1993) Quantitation of plasma lipids by gas liquid chromatography on high temperature polarizable capillary columns. *Journal of Lipid Research* 34: 1029–1038.)

the TMS ethers of the diradylglycerol moieties of glycerophospholipids and triacylglycerols. **Figure 4** shows the resolution of the molecular species of the diacyl, alkylacyl and alkenylacyl subclasses of human plasma ethanolamine glycerophospholipids as obtained by polar capillary GC of the TMS ethers of the derived diradylglycerols. There are marked differences in the distribution of the chain length and unsaturation among the three subclasses of the plasma ethanolamine glycerophospholipids as anticipated from the fatty acid and diradylglycerol carbon number distribution. Polar capillary GC resolution of molecular species of the *sn*-1,2- and *sn*-2,3-diacylglycerols has been extensively utilized in structural

analyses of triacylglycerols. Tables have been compiled of GC retention factors of diradylglycerol TMS ethers on polar capillary columns.

Molecular Species of Triacylglycerols

GC is well suited for the separation of the molecular species of triacylglycerols. Nonpolar columns provided essentially carbon number or molecular weight resolution, while the polarizable liquid phases give effective separations of molecular species of saturated and unsaturated triacylglycerols. Polar capillary columns also provide separations based on both carbon and double bond number, but are limited to low molecular weight triacylglycerol mixtures.

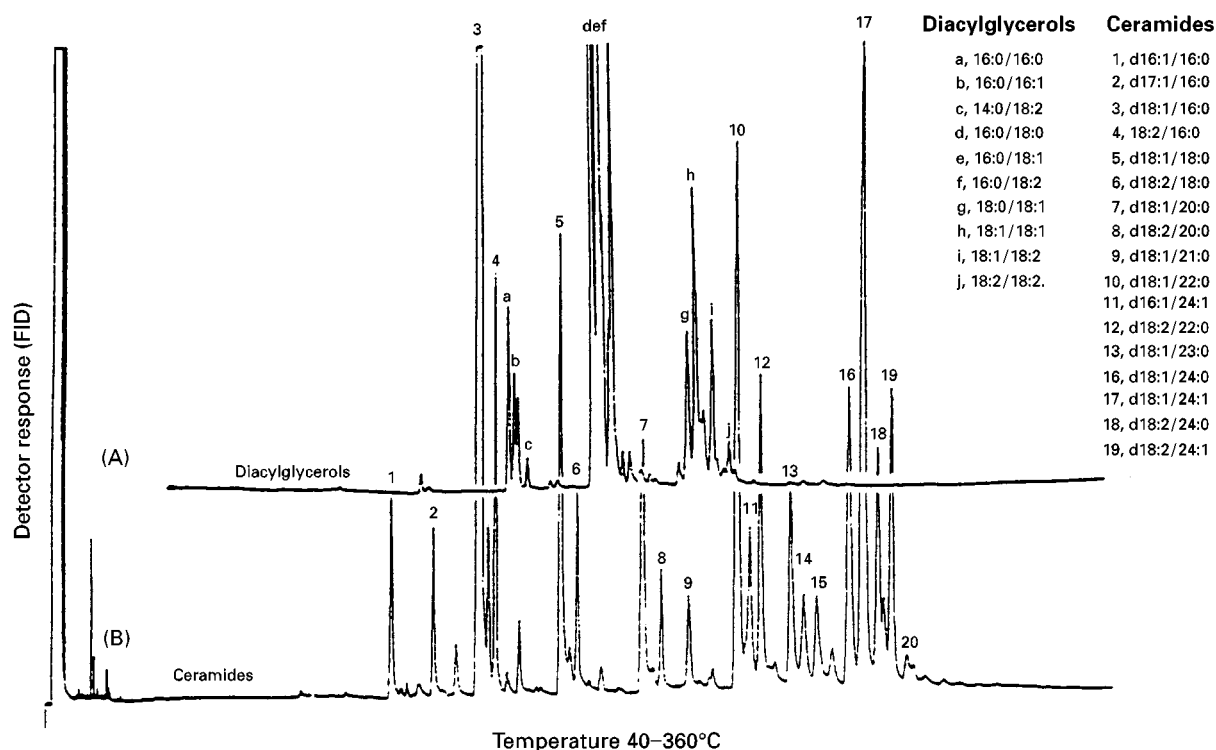


Figure 3 GC profiles of (A) common diacylglycerols and (B) the ceramides of plasma sphingomyelin as obtained on a polarizable capillary column. Peak identification is as given in figure. GC conditions are as given in Figure 2B. (Reproduced with permission from Kuksis A, Myher JJ and Geher K (1993) Quantitation of plasma lipids by gas liquid chromatography on high temperature polarizable capillary columns. *Journal of Lipid Research* 34: 1029-1038.)

Nonpolar liquid phases The first GC resolutions of molecular species of triacylglycerols were obtained on nonpolar packed columns of short length. **Figure 5** compares the separation of butteroil triacylglycerols obtained on a nonpolar packed column and on a capillary column. Both columns yield essentially carbon number resolution, although the capillary column shows some peak splitting due to separation of saturated and unsaturated species within a carbon number. A combination argentation TLC or HPLC with nonpolar GC separation is required for a more extensive separation of molecular species.

Nonpolar capillary GC columns have been effectively utilized for resolution of the reduction products of ozonized lard, rapeseed and palm oil triacylglycerols, as well as the reduction products of ozonized partially hydrogenated soybean oil. **Figure 6** shows the elution profile on a nonpolar column of the triacylglycerols of soyabean oil after reductive ozonolysis. The peaks are identified by the triplets of the fatty acids: palmitic (P), stearic (S) and the C₉ aldehyde (U) of the unsaturated fatty acid.

Polarizable liquid phases The usefulness of the polarizable liquid phases for the separation of saturated and unsaturated triacylglycerols was discovered by

Geeraert and Sandra in 1984. **Figure 7** shows the resolution of the molecular species of butteroil triacylglycerols. Peak identification presents a problem because of extensive resolution of isobaric species. However, preliminary resolution by argentation TLC in combination with GC-MS enabled the pattern of elution to be established. At the present time, the polarizable capillary column provides the most complete GC resolution of the molecular species of triacylglycerols.

The resolution of triacylglycerols seen in the GC-MS profiles is somewhat reduced in comparison to GC-FID. The reduced resolution complicates post-column processing of the GC-MS data due to lack of discrete peaks in parts of the total ion chromatogram. GC-MS quantification of milk fat triacylglycerols is improved by employing the Biller-Biemann enhancement technique to produce mass-resolved total ion chromatograms. The Biller-Biemann enhancement algorithm examines each mass that appears in successive scans in the TLC to detect masses that are rising and falling in intensity.

Polar liquid phases The polar capillary columns commonly employed for fatty acid methyl ester separation can resolve low molecular weight

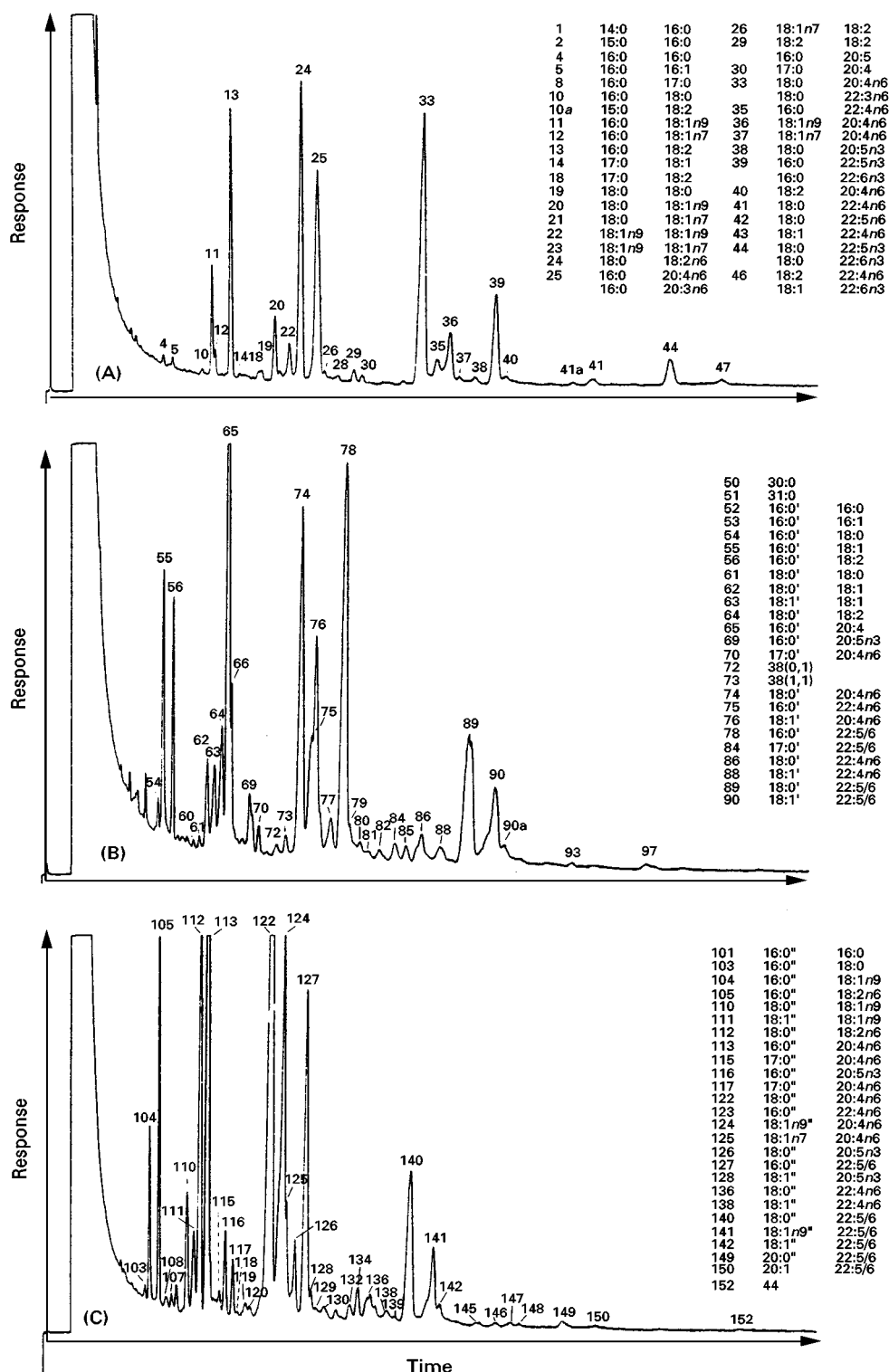


Figure 4 GC profiles of the TMS ethers diradylglycerol moieties of human plasma diradylglycerophosphoethanolamines (GPE). Peaks are identified in the figures. (A) Alkylacyl GPE; (B) alkenylacyl GPE; (C) diacyl GPE. Peak identification is given in the figures. GC conditions: column, 15 m \times 0.32 mm, i.d. 68% cyanopropyl/32% dimethylsiloxane (RTx 2330, Restek); temperature, isothermal, 25°C with hydrogen as carrier gas. (Reproduced with permission from Myher JJ, Kuksis A and Pind S (1989) Molecular species of glycerophospholipids and sphingomyelins of human plasma: comparison to red blood cells. *Lipids* 24: 408–418).

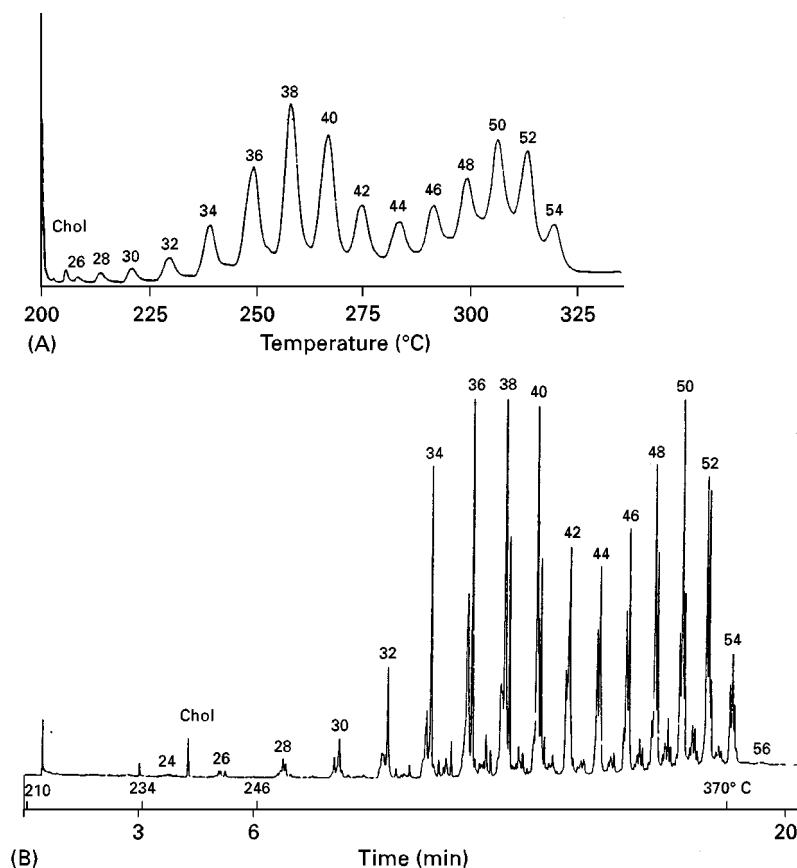


Figure 5 GC profiles of butteroil triacylglycerols as obtained on nonpolar columns. (A) Packed column; (B) capillary column. Peaks are identified by total acyl carbon as shown in the figures. GC conditions: (A) packed column, 50×0.25 cm, i.d. 2.5% SE-30, Applied Science; temperature, linearly programmed from 200 to 325°C with nitrogen as a carrier gas (Reproduced with permission from Kuksis A and McCarthy MJ (1962) *Canadian Journal of Biochemistry and Physiology* 40: 679–685.) (B) Capillary column, $25 \text{ m} \times 0.25 \text{ mm}$ i.d., methyl silicone (OV-1, Ohio Valley); temperature, programmed from 210 to 370°C in 20 min with hydrogen as a carrier gas. (Reproduced with permission from Geeraert, 1987.)

triacylglycerols and the diacetates of monoacylglycerols containing saturated and unsaturated fatty acids. Conventional polar capillary columns are not sufficiently stable at the high temperatures needed to elute long chain triacylglycerols.

Resolution of Fatty Acids

Fatty acids constitute the most extensively investigated class of lipids for GC separation, identification and quantification. Although the routines for the common fatty acids are well established, determination of minor fatty acids, including branched-chain and positional and configurational isomers, requires specialized approaches. Other problems arise from the presence of oxygenated functional groups in the fatty chains. Many of these fatty acids have been successfully identified by preparing nitrogenous derivatives in combination with GC-MS.

Isolation and Preparation of Derivatives

Proper isolation and preparation of derivatives are essential for both identification and quantification of fatty acids. The common procedures for isolating fatty acids consist of extracting lipids from biological materials, saponification and esterification of the recovered acids. Underivatized volatile fatty acids are difficult to quantify by GC because these highly polar compounds form hydrogen bonds that interact with the active sites on the column coatings and cause peak tailing and ghosting due to dimerization. These undesirable effects are avoided by converting the fatty acids into methyl esters or other volatile derivatives. Specially developed columns, however, may avoid both tailing and ghosting.

Preparation of methyl esters Table 1 also lists the more popular methods of derivatization of the common fatty acids for GC analysis. Formation of fatty

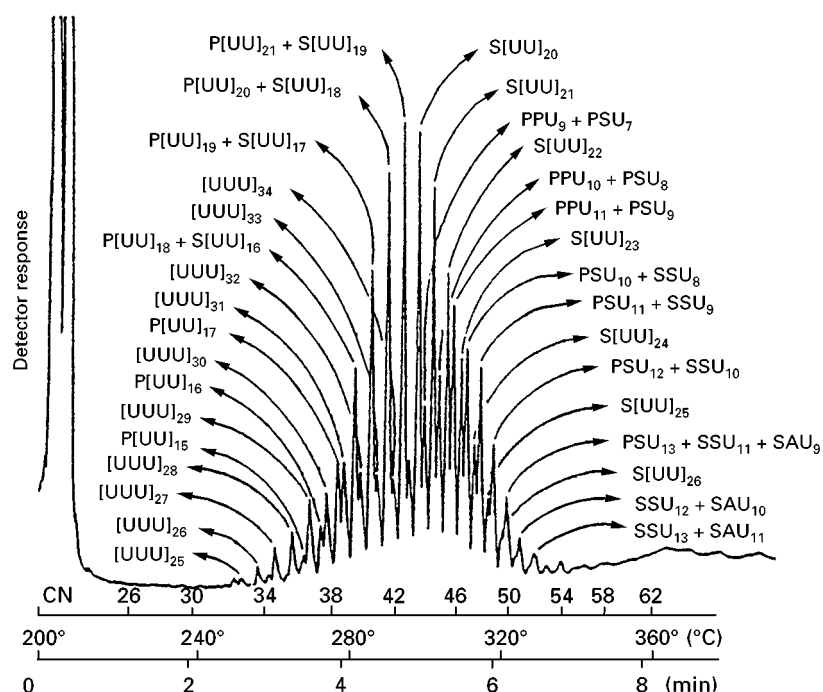


Figure 6 Non-polar capillary GC profile of the triacylglycerols of soybean oil after reductive ozonolysis. Peak identification is as given in figure: P, palmitic; S, stearic; U, unsaturated fatty acid residues. GC conditions: column 15 m \times 0.32 mm i.d. 100% methylsilicone (OV-1, Ohio Valley); temperature, 200°C (0.15 min) isothermal then 20°C min⁻¹ to 360°C with hydrogen as carrier gas. (Reproduced with permission from Geeraert E (1985) In: Sandra P (ed.) *Sample Introduction in Capillary Gas Chromatography*, vol. 1, pp. 133–158. Heidelberg: Alfred Hüetig Verlag.

acid methyl esters is usually accomplished in the presence of acid or alkaline catalysts. Acidic catalysts transesterify glycerolipids and other complex lipids as well as esterify any free fatty acids in the presence of

methanol. Inclusion of butylated hydroxytoluene as an antioxidant in the transesterification solution results in the formation of methoxy butylated hydroxytoluene, which emerges in the 14:0–16:0 fatty

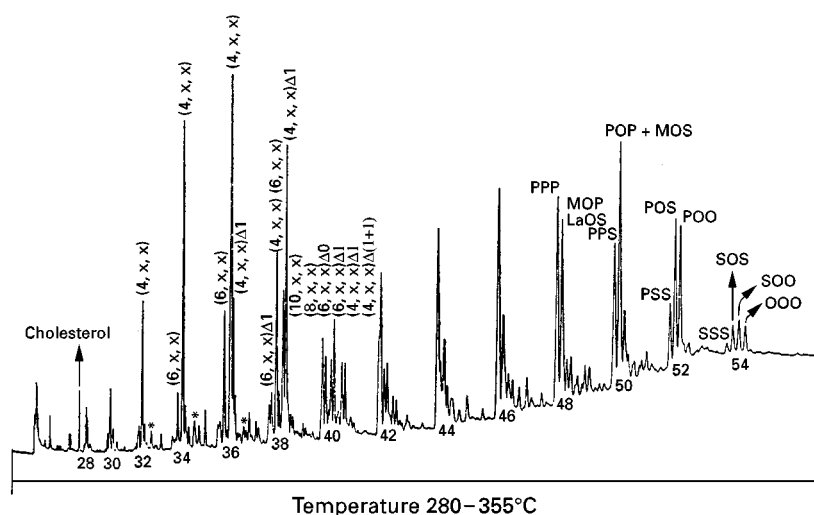


Figure 7 Polarizable capillary GC profile of butteroil triacylglycerols. Peak identification is as given in figure: P, palmitic; O, oleic; S, stearic; M, myristic acids; 28–54, total acyl carbon numbers; short chain triacylglycerols are shown as combinations with major long chain acids (x) of different degrees of unsaturation ($\Delta 0 - \Delta 1 + 1$) as identified elsewhere (Myher JJ, Kuksis A, Marai L and Sandra P (1988) *Journal of Chromatography* 452: 93–118.) GC conditions: column, 25 m \times 0.25 mm i.d., 50% phenylmethylsilicone (RSL-300, supplied by Sandra P); temperature, linearly programmed from 280 to 355°C over 30 min with hydrogen as the carrier gas. *Major acetate peaks. (Reproduced with permission from Geeraert E and Sandra P (1987) *Capillary GC of triglycerides in fats and oils using a high temperature phenylmethylsilicone stationary phase. Part II. The analysis of chocolate fats. Journal of the American Oil Chemist's Society* 64: 100–105.)

acid elution region. Phthalate esters have also been detected among plasma lipids, even when prepared in the absence of external contamination. The precise point of elution relative to fatty acid derivatives is dependent on the nature of the phthalate ester and the stationary phase, but typically it is in the same range as the C₁₈–C₂₂ fatty acids. In many instances it is convenient to perform the acid transmethylation *in situ*, e.g. in the presence of silica gel scrapings from a TLC plate.

Acid-catalysed transmethylation also leads to significant dehydration of the sterol moiety and degradation of conjugated fatty acids. The peaks formed during acid-catalysed methylation were identified as positional allylic methoxy isomers of 18:1 by GC-MS. Re-evaluation of the H₂SO₄–isopropanol reaction showed just as extensive isomerization of conjugated dienes as the HCl–MeOH method.

Alkaline catalysts transesterify neutral lipid esters in anhydrous methanol much faster (a few seconds to a few minutes), but they are unable to esterify free fatty acids, which constitutes a serious shortcoming. Furthermore, *N*-acyl lipids are not methylated. The presence of water leads to saponification. Alkaline reagents dissolve silica gel and cannot be employed with gel scrapings from TLC plates. Diazomethane can be prepared in ether solution by the action of alkali on a nitrosamide (e.g. *N*-methyl-*N*-nitroso-*p*-toluenesulfonamide) in the presence of alcohol. This reagent is commercially available as Diazald (Aldrich Chemical Co). Diazomethane is used for preparation of fatty acid methyl esters from lipids that have been first saponified. It has the disadvantages that it is highly toxic, explosive and likely to cause specific sensitivity.

Preparation of other derivatives Table 1 also lists a selection of reagents for derivatization of oxygenated fatty acids and prostanoids. Monohydroperoxy fatty acids are reduced to hydroxy acids after reaction for 1 h at room temperature with triphenylphosphine in diethyl ether prior to GC analysis of the methyl ester TMS ethers. The monohydroxy fatty acid methyl esters are hydrogenated for 5 min at room temperature in the presence of rhodium on alumina in methanol. They are converted to their TMS ether derivatives by reaction with *N*-methyl-*N*-trimethylsilyltrifluoroacetamide for 30 min at room temperature. *tert*-Butyldimethylsilyl ethers of secondary hydroxy fatty acid methyl esters are prepared by dissolving the sample in a mixture of dry toluene, dimethylformamide and pyridine, and adding *N*-*tert*-butyldimethylsilylimidazole and *N*-methyl-*tert*-butyldimethylsilyltrifluoroacetamide containing 1% *tert*-butyldimethylsilylchloride (TBDMS).

Of the many different derivatives described in the literature for GC analysis of prostaglandins, the pentafluorobenzoate–methoxime–TMS (PFB–MO–TMS) derivatives yield the most satisfactory results in terms of GC properties, electron-capture detection and MS response and stability. These derivatives show single well-shaped peaks for each compound, except for prostaglandin E₂–PFB–MO–TMS, whose *syn-anti* isomers can be seen as well-separated peaks.

Normal oxygenated and nonoxygenated fatty acids have been converted into nitrogenous derivatives for structural analyses by GC-MS. The picolinyl esters are prepared from the fatty acids by first converting them into acid chlorides by dissolving in thionyl chloride. The acid chlorides are then treated with a dilute solution of 3-pyridylcarbinol in acetonitrile. The picolinyl dimethylsilyl derivatives of fatty alcohols are prepared by dissolving the alcohol in dry pyridine, adding diethylaminodimethylsilyl-3-pyridylcarbinol and heating at 60°C for 10 min. The picolinyl esters of the epoxides are prepared by dissolving the epoxide in dry methylene chloride and adding a freshly prepared solution of 1,1'-carbonyldiimidazole followed by 3-pyridylcarbinol solution of triethylamine. The preparation of picolinyl esters via fatty acid chlorides cannot be used for derivatization of the epoxides because of their instability in acidic solutions.

The pyrrolidides are prepared from the lipid ester. The sample is heated with an excess of pyrrolidine in the presence of acetic acid for 30 min at 100°C. 4,4-Dimethylloxazoline derivatives also have useful properties for locating functional groups by MS, but quantitative preparation requires heating the methyl esters with 2-amino-2-methylpropanol at 180°C overnight.

Separation of Saturated and Unsaturated Fatty Acids

Table 3 lists the more popular liquid phases for the separation of saturated and unsaturated fatty acids and prostanoids. The Carbowax phases based on polyethylene glycol appear to provide the best general-purpose columns.

Normal chain fatty acids and dimethylacetals For equivalent chain length (ECL) measurements, the separations of saturated and unsaturated fatty acids are performed isothermally. Isothermal analyses give good ECL values and these are remarkably consistent for the bonded polyglycol columns. Extensive tables of ECL values have been compiled for the methyl ester derivatives of natural fatty acids on silicone,

Table 3 Common liquid phases for capillary GC of fatty acids and their oxygenated derivatives^a

Chemical composition	Commercial names	Column dimensions	Type of separation (temperature programme)	Applications
90% bis-Cyanopropyl/ 10% cyanopropylphenylsilicone	SP-2380 (OV-275/CP-Sil-88)	15 m × 0.32 mm i.d.	Carbon and double bond number (260–270°C)	Short chain triacylglycerols of butteroil distillates
Cross-bonded polyethylene glycol	Supelcowax-10 (Carbowax)	30 m × 0.25 mm i.d.	Saturates and polyunsaturates (185–220°C)	Fish oil fatty acids
Cross-bonded polyethylene glycol	Stabilwax (Carbowax CP 51)	60 m × 0.25 mm i.d.	Saturated and unsaturated esters (212°C, isothermal)	Seed oils and fats, marine oils
90% bis-cyanopropyl/10% cyanopropylphenyl	Rtx-2330 (CP-Sil-88, BPX-70) ^b	100 m × 0.25 mm i.d.	Δ^5 - Δ^{16} -isomers of <i>trans</i> -18:1 (160°C, isothermal)	<i>Trans</i> -18:1 of beef tallow and human milk
Biscyanopropyl, 68%/ dimethylsilicone, 32%	SP-2380 (BPX-70/CP-Sil-84)	50 m × 0.25 mm	Cyclic fatty acid methyl esters (180°C, isothermal)	Hydrogenated cyclic fatty acid monomers from vegetable oils
14% Cyanopropylphenyl/ 86% polysiloxane	CP Sil 19 (DB-1701)	25 m × 0.25 mm	Methyl ethers of isomeric hydroxy fatty acids (100–250°C)	Hydrogenated hydroperoxides of plasma lipids
2% Dimethylsilicone	OV-101	0.4 m × 3 mm, packed	Carbon number (315–330°C, isothermal)	TMS ethers of mycolic acids
95% Dimethyl/5% phenyl silicone	SE-54 (HP-5/ DB5/CP-Sil-8)	18 m × 0.28 mm	Double bond location (70–240°C)	Oxazoline derivatives of fish oil fatty acids
Dimethylpolysiloxane	DB-1 (SE-30/OV-1)	30 m × 0.25 mm	Epoxide location (200–250°C)	3-Pyridinylmethyl esters of epoxides
Dimethylpolysiloxane	DB-1 (SE-30/OV-1)	20 m × 0.25 mm	Methoxy PFB esters (100–310°C)	Urinary prostanoids
86% Dimethyl/14% cyano propylphenyl polysiloxane	DB-1701 (DB-5, CP-Sil 19CB)	15 m × 0.2 mm	F ₂ -isoprostane TMS ethers and PFB esters (190–300°C)	Arachidonic acid peroxidation products
86% Dimethyl/14% cyano propylphenyl polysiloxane	DB-1701 (DB-5, CP-Sil 19CB)	30 m × 0.25 mm	Methoxy PFB esters (18–300°C)	Eicosanoids in blood

^aAbbreviations and details of applications are given in the text, in legends to figures and in references cited.^bComparable liquid phases are given in brackets.(Modified with permission from Restek Corporation (1998) *Chromatography Products*, International Version, pp. 544–545).

Carbowax, Silar 5CP and CP-Sil 84 columns. **Figure 8** shows the resolution of the fatty acid methyl esters of menhaden oil on a 30 m polyethylene glycol (Famewax, Restek) column using temperature programming (190–225°C). This liquid phase is stable to 250°C. The elution order of the complex polyunsaturated fatty acid methyl esters is comparable to that obtained on other Carbowax columns.

Acid-catalysed transmethylation leads to conversion of vinyl ethers (when present) into dimethylacetals, which are eluted ahead of the fatty acids of corresponding carbon number. **Figure 9** shows the resolution of the fatty acid methyl esters and dimethylacetals derived from human erythrocyte membranes on a deactivated cyanopropylsiloxane column. Although the separation of many of the dimethylacetals and the methyl esters is incomplete, it is still possible to obtain a good indication of the

relative amounts of plasmalogens that may be present in the sample. Resolution of the major dimethylacetals and methyl esters on cyanopropylsiloxane columns has been obtained of one-third the length used by earlier workers. Prior to GC, the fatty acid methyl esters and dimethylacetals are resolved by normal-phase HPLC.

Identification of very long chain fatty acids An extensive series of long chain polyunsaturated fatty acids has been shown to occur in phosphatidylcholines of the vertebrate retina, where they make up a homologous series of even carbon polyenes having up to 36 carbon atoms. A detailed study has been made of these acids in bovine retina, where they were shown to belong to the same families as well-known fatty acids of the *n*-6 and *n*-3 series like arachidonate (20:4*n*-6), docosapentaenoate (22:5*n*-3) and docosa-

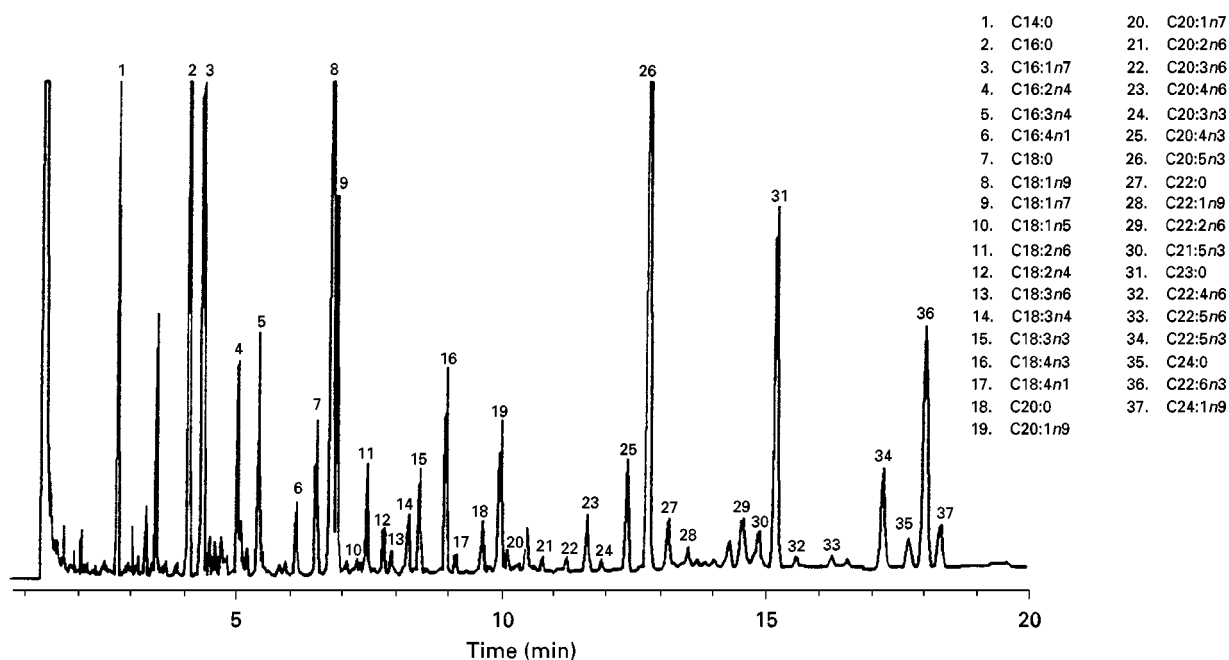


Figure 8 Polar capillary GC of fatty acid methyl ethers of menhaden oil. Peaks are identified in the figure. GC conditions: column, 30 m \times 0.25 mm i.d., 0.25 μ m cross-bonded polyethylene glycol (Famewax, Restek); temperature, 190°C (hold 4 min) then 4°C min⁻¹ to 225°C; carrier gas, helium; split injection 1 : 50 (Reproduced with permission from Restek Corporation (1998) *Chromatography Products*, International Version, p. 447).

hexaenoate (22:6n-3). The fatty acids were analysed by temperature-programmed GC using glass columns packed with 15% OV-225. The position of the double bonds in the long chain polyenes was determined by means of oxidative ozonolysis.

Separation of short chain fatty acids Because of their high volatility, the short chain fatty acids create difficulties in GC separation and quantification when present in mixtures with long chain acids. The volatility can be effectively reduced by preparing higher molecular weight esters (propionyl or butyl esters) which also provide a more comparable response in the FID. It also permits a clear resolution of the short chain fatty acids from the solvent front and identification and quantification of the short chain acids in the presence of long chain acids. Recently developed high speed capillary columns (20 m \times 0.10 mm i.d., 0.10 μ m film thickness DB-WAX or DB-225, Restek) have been found to give an effective separation and quantification of both short and long chain fatty acids as methyl esters. A total of 37 fatty acids can be analysed in less than 15 min.

Separation of Oxygenated Fatty Acids and Prostanoids

Oxygenated fatty acids occur in nature as a result of enzymatic and nonenzymatic oxidation, and because

of their physiological activity there is much interest in their analysis.

Fatty acid hydroperoxides are labile key intermediates in plant and mammalian lipid metabolism, acting as precursors of a variety of lipid-derived mediators such as prostaglandins and leukotrienes. Until recently, these analyses were usually done by GC, but now reversed-phase HPLC has been shown to have advantages for the analysis of the thermo-labile oxygenated derivatives of the fatty acids.

Hydroxides, epoxides, hydroperoxides and isoprostanes A 30 m nonpolar methylsiloxane column was used to measure the ECLs of hydrogenated derivatives of isomeric hydroxydocosahexaenoates. Mass spectra of hydrogenated compounds indicated the presence of hydroxyl groups at carbons 20, 16, 17, 13, 14, 10, 11, 7, 8 and 4. The isomers were apparently racemic mixtures.

GC-MS was used to identify the arachidonate epoxides/diols. The epoxide regioisomers of arachidonic acid as the methyl esters overlapped on nonpolar capillary columns. The isomeric epoxides were identified as their hydrolysis products, the dihydroxyicosatrienoic (DHET) acids, in the form of the PFB ester derivatives. The four regioisomers were not resolved by GC as PFB, TMS, TBDMS or Me esters. However, after being hydrolysed to the dihydroxyicosatrienoic acids, three of the four regio-

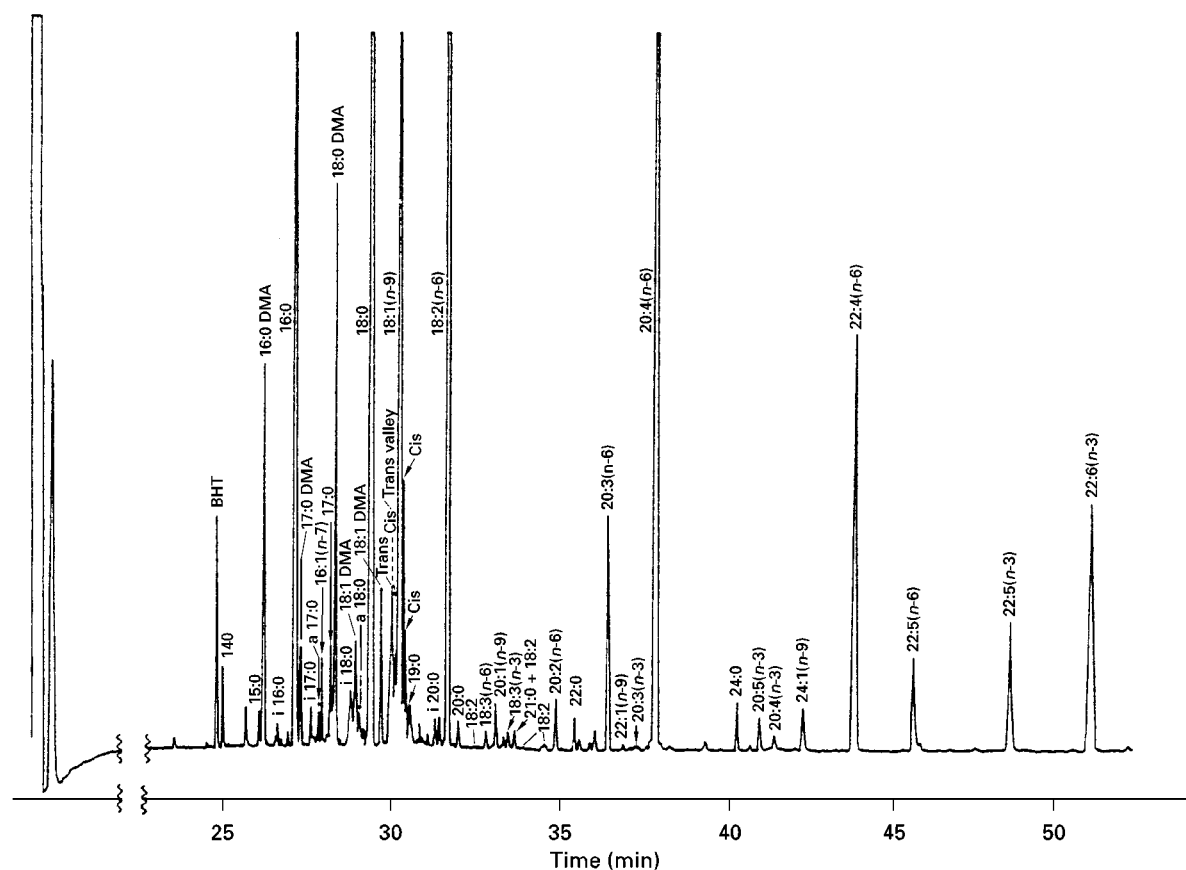


Figure 9 Polar capillary GC of fatty acid methyl esters and dimethylacetals of human erythrocyte membranes. Peaks are identified by short-hand notation as indicated in figure. GC conditions: column, 100 m \times 0.25 mm i.d., 0.2 μ m deactivated cyanopropylsiloxane (SP 2560, Supelco); temperature, 80°C (hold 2 min) then 8°C min⁻¹ to 220°C and hold for 32 min; carrier gas, helium; split injection 1 : 30. (Reproduced with permission from Alexander LR, Justice JB and Madden J (1985) Fatty acid composition of human erythrocyte membranes by capillary gas chromatography mass spectrometry. *Journal of Chromatography and Biochemical Applications* 342: 1–12.)

isomers were resolved as TMS ethers, PFB esters. The fourth regioisomer, 5,6-DHET, was resolved after being converted to a δ -lactone. The regioisomers of DHET were resolved as the (bis)-TBDMS, PFB esters on a 60 m nonpolar column operated isothermally at 300°C. The 8,9-DHET was followed by 11, 12-DHET, which was followed by 14,15-DHET.

TBDMS ethers have been used for GC-MS separation and identification of synthetic secondary hydroxy fatty acid isomers with carbon chain lengths of 16–20. With the exception of the spontaneous formation of γ - and δ -lactones of C₄-OH and C₅-OH fatty acids, the TBDMS ethers of all hydroxy fatty acid methyl esters in a mixture are readily identified by GC-MS, yielding information on chain length, location of the hydroxyl group and degree of unsaturation. The method has been applied to the identification of a complex mixture of bovine skim milk hydroxy fatty acids, of which 19 were newly identified. The separations were performed on a 30 m column coated with 100% methylsilicone. Hydroperox-

ides are not sufficiently stable for GC analysis. Therefore, the fatty acid ester hydroperoxides are reduced to the corresponding alcohols with triphenylphosphine and transmethylated with sodium methoxide before GC analysis. A 20 m \times 0.32 mm i.d. DB-1 column has been used for GC-MS analysis of linoleate and arachidonate peroxidation products. The hydroxy fatty acid methyl esters were isolated by TLC and converted into TMS ethers. By a combination of normal-phase HPLC and GC-MS, the linoleate oxidation products were identified as 9- and 13-OH derivatives and those arising from arachidonate oxidation as the 5-, 8-, 9-, 12- and 15-hydroxyicosatetraenoates.

Among the free radical catalysed peroxidation products of arachidonic acid, prostaglandin-like compounds named isoprostanes have been recognized which arise independent of the cyclooxygenase enzyme. The evidence has been reviewed for the natural occurrence of these compounds, their mechanism of formation and methods of determination. They have

GC properties similar to those of prostaglandin $F_{2\alpha}$, with which they may be confused. GC-MS has been recently employed for the measurement of plasma isoprostanes.

Prostaglandins The prostaglandins and thromboxanes are cyclo-oxygenase metabolites of arachidonic acid, which are involved in numerous pathophysiological pathways. High resolution GC in combination with mass spectrometry is generally recognized as the most specific and reliable method for qualitative and quantitative analysis of prostanoids. In fact, the use of high resolution GC is mandatory when the stable cyclo-oxygenase metabolites of arachidonic acid have to be analysed as a group. The application of GC-MS techniques to the analysis of prostaglandins and related substances has been reviewed, as well as the application of GC-MS to the analysis of other oxygenated fatty acids. Electron capture GC-MS analysis of the PFB-TMS derivatives has provided the most sensitive method for molecular mass determination. This method, however, does not provide structural information and even low energy collision-induced dissociation (CID) of the carboxylate anions from these derivatives does not yield structurally significant ions.

Figure 10A shows by means of authentic standards that a complete separation of all major metabolites of arachidonic acid via the cyclo-oxygenase pathway can be obtained in a relatively short time (30 min)

using a 30 m capillary column of OV-101-OV-17 (8:2). The selected ion monitoring profiles of the prostaglandins and thromboxanes were obtained with the PFB-MO-TMS derivatives at 220°C with helium as carrier gas. Figure 10B shows a chromatogram of the same substances detected by electron capture. A critical aspect of the application of high resolution GC in routine analyses of prostaglandins is that it requires greater purification of biological material.

Structural Identification

The location of double bonds and other modifications of the fatty chains is required for a complete characterization of the structure of the fatty acids. GC-MS techniques approach this problem by chemical modification prior to analysis.

Double-bond isomers Derivatization at the double bond to oxygenated compounds (carbonyl compounds and vicinal diols) leads to distinctive fragmentation patterns that allow determination of the points of unsaturation or epoxidation but this method leads to the formation of highly polar derivatives and an increase in molecular weight, which makes it unsuitable for the analysis of polyunsaturated fatty acids.

An alternative technique is based on derivatization of the terminal carboxylic group (remote site modification), whereby fatty acids are converted to *N*-acyl

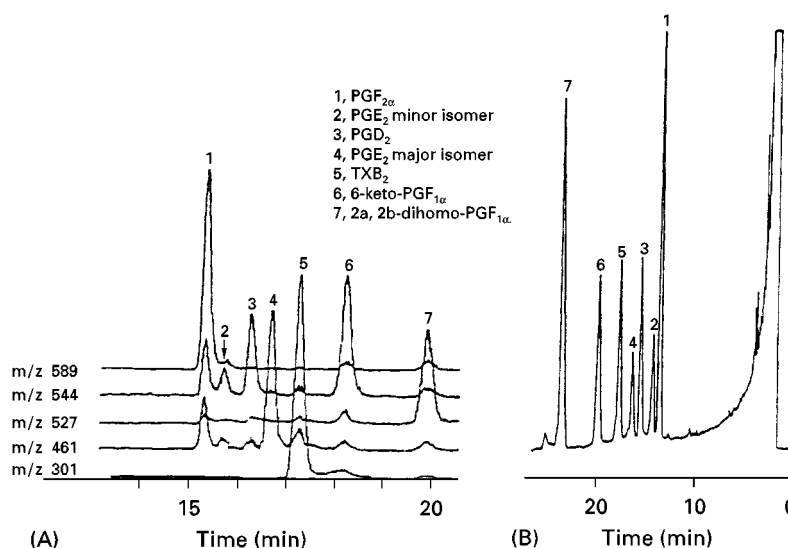


Figure 10 Polar capillary GC and selected ion monitoring (SIM) of authentic prostaglandins and major metabolites of arachidonic acid as PFB-MO-TMS derivatives. (A) SIM; (B) high resolution GC with electron capture detection. Peak identification is given in the figure. GC conditions: column, 30 m × 0.3 mm i.d., dimethylsiloxane/50% phenylmethylsiloxane 8:2 (OV-1/OV-17, Ohio Valley); temperature, 220°C isothermal; carrier gas, helium. (Reproduced with permission from Chiabrando C, Nosedà A and Fanelli R (1982) Separation of prostaglandins and thromboxane B₂ by high resolution gas chromatography coupled to mass spectrometry or electron capture detection. *Journal of Chromatography* 250: 100–108.)

pyrrolidides or picolinyl (3-hydroxymethylpyridinyl) esters that easily stabilize the ions containing the double bonds or substituents of the fatty chain. The pyrrolidides have been studied most often for the analysis of natural samples, but recently have been overtaken by the picolinyl esters or 4,4-dimethyloxazoline (DMOX) derivatives. Although distinctive modes of fragmentation can be obtained, the interpretation of spectra becomes substantially more difficult if the number of double bonds is greater than four. The picolinyl esters of isomeric unsaturated fatty acids give more abundant diagnostic ions than the pyrrolidides. **Figure 11** shows the capillary GC separations obtained with the picolinyl and pyrrolidide derivatives of pig testis fatty acids on OV-101 and BP-20 liquid phases, respectively. On the nonpolar methylsilicone (OV-101) column, the more unsaturated picolinyl esters emerge ahead of the less unsaturated and saturated fatty acids of the same acyl carbon number. On the polar BP 20, the pyrrolidide derivatives emerge in order of increasing unsaturation. The picolinyl esters require column temperatures about 50°C higher than methyl esters. The picolinyl esters are resolved according to number of double bonds on polar phases of high temperature stability, such as BPX-70 or Supelcowax 10, but

fatty acids of more than 20 acyl carbons may cause difficulty.

It has been shown that the DMOX derivatives of fatty acids are only slightly less volatile than the corresponding methyl esters and that they can be subjected to GC analysis on polar capillary columns to give resolutions based on degree of unsaturation. The GC separation has been carried out with the DMOX derivatives of fatty acids of rat testis and fish oil on a nonpolar methylsilicone (SE-54) column, from which the more unsaturated derivatives emerged ahead of the less unsaturated ones of the same acyl carbon number.

The picolinyl esters and DMOX derivatives can be separated by reversed-phase or argentation HPLC before GC-MS analysis, which is important for the detection of minor components in natural samples. These derivatives have high volatility and their mass spectra show easily recognizable diagnostic peaks for determination of the position of unsaturation. Tables have been prepared of characteristic ions in EI mass spectra of DMOX derivatives of 22 unsaturated fatty acids. The DMOX derivatives have been employed for successful identification of $\Delta 5$ -unsaturated polymethylene-interrupted fatty acids from conifer seed oils. Most analysts now prefer either picolinyl esters

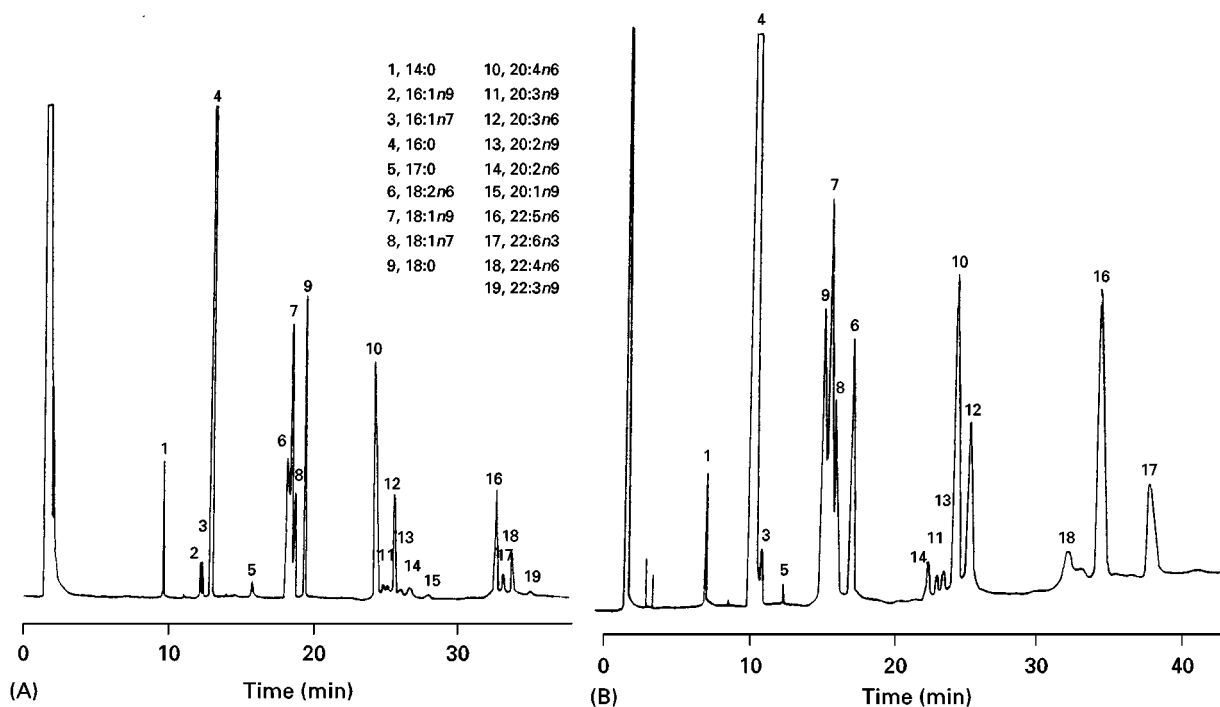


Figure 11 Capillary GC of (A) picolinyl and (B) pyrrolidide derivatives of pig testis fatty acids on nonpolar and polar phases. Peak identification is given in the figure. GC conditions: (A) column, 50 m \times 0.22 mm i.d., methylsilicone (OV-101, Ohio Valley); temperature, programmed from 195°C (hold 3 min) then 1°C min⁻¹ to 235°C; carrier gas, helium; (B) column, 12 m \times 0.22 i.d., polyethylene glycol (BP 20, SGE); temperature, programmed from 190°C (hold 3 min) then 1°C min⁻¹ to 230°C; carrier gas, helium. (Reproduced with permission from Christie WW, Brechany EY, Johnson SB and Holman RT (1986) A comparison of pyrrolidide and picolinyl ester derivatives for the identification of fatty acids in natural samples by gas chromatography-mass spectrometry. *Lipids* 21: 657-661.)

or DMOX derivatives for structural studies on fatty acids, but the pyrrolidides also provide informative mass spectra in many instances.

***cis/trans*-Isomers and conjugated acids** Identification of *cis/trans* isomers of unsaturated fatty acids cannot usually be achieved by GC-MS without reference substances. Satisfactory separations of the geometric isomers from margarine fatty acids and 44 synthetic C₁₈ unsaturated fatty acids have been obtained by GC on a 60 m capillary column coated with 100% cyanoethylsilicone (SP-2340). Overlaps occur between different double-bond systems and between some mono- and diethylenic, as well as between di- and triethylenic fatty acids. Because of these overlaps, the isomers cannot be determined by GC alone on the SP-2340 or on any other cyanosilicone phase. Prefractionation by silver ion TLC or HPLC is necessary. The GC separation of the *cis*- and *trans*-acids has been reported in milk samples using a 100 m capillary column coated with bis-cyanopropyl-32% dimethylsiloxane (SP-2560). The authors were able to calculate the total *trans* acid content by adding the relative percentage of all *trans* monounsaturated fatty acids and *cis/trans* linoleate and total conjugate dienes in the milk chromatograms. SP-2560 capillary columns were used to conduct an extensive investigation of the effect of various methods of methylation upon the estimation of the conjugated fatty acid content of bovine milk. Acid-catalysed methods caused extensive isomerization of conjugated dienes and formed allylic methoxy artefacts and are therefore not recommended for this purpose. Base-catalysed methods caused no isomerization of conjugated dienes and the formation of artefacts. GC-Fourier transform infrared-MS (GC/FTIR/MS) has been used to identify fatty acid methyl esters and differentiate between *cis/trans* isomers. In the FTIR spectra *cis/trans* isomers are identified by analysis of bands arising from C-H out-of-plane bending; for both fatty acid methyl esters and DMOX derivatives *cis*-1,2-disubstituted double bonds give a strong band near 720 cm⁻¹ and the corresponding *trans* isomers near 967 cm⁻¹. A greatly improved resolution of individual *trans*-18:1 isomers has been reported by capillary GC on a 100 m cyanopropyl polysiloxane (CP-Sil 88) column.

Epoxides The picolinyl esters are also adequate for the location of epoxide functions in linoleic, arachidonic and docosahexaenoic acids. The electron impact (EI) mass spectra of these derivatives show a molecular ion and a sequence of peaks, with two characteristic abundant ions that result from formal

cleavage of the carbon-carbon bonds at the oxirane ring. Both these ions retain the ester group. This fragmentation pattern allows the unequivocal identification of the separate epoxide isomers. The picolinyl esters of the epoxides are resolved on a 30 m methylsiloxane (DB-1) column, temperature-programmed from 220 to 300°C. These picolinyl esters provide characteristic GC-MS profiles that allow differentiation of the isomeric epoxides at nanogram levels.

Branched-chain and cyclic acids The methyl esters of branched and cyclic fatty acids are usually eluted ahead of their normal-chain counterparts. The methyl branched acids may be confused with straight-chain odd-carbon number isomers. Long (50 m) capillary columns with nonpolar (5% phenylmethylsilicone) stationary phases are preferred and cyclopropane acids are resolved from their monounsaturated counterparts. The position of the methyl branching and cyclopropane ring is not readily determined by GC-MS with EI even after preparation of pyrrolidide and picolinyl derivatives, although exceptions are known. Only small differences are seen among the DMOX derivatives, but they may be sufficient for distinction between close isomers.

It has been shown that low-energy CID of the molecular ions of fatty acid methyl esters obtained by electron ionization (70 eV) in the tandem quadrupole mass spectrometer yield a regular homologous series of carbomethoxy ions. This method can be used to determine methyl (or alkyl) branching positions, as shown by enhanced radical site cleavage at the alkyl branching positions of several methyl esters, including phytanic acid, isomethyl and anteiso-methyl branched acids and tuberculostearic acid. Analyses of various stable isotope variants support the hypothesis of alkyl radical migration to the carboxy carbonyl oxygen atom, with subsequent radical site directed cleavage, either with or without a cyclization event.

GC-MS Analyses of Stable Isotope-Labelled Lipids

In addition to identification of structures, GC-MS also provides the distribution and content of the stable isotope, both natural and enriched. Highly sensitive and reproducible estimates have been obtained for the isotopomer distribution by GC combined with isotope ratio mass spectrometry (isotopomer analysis). Furthermore, the utilization of appropriately labelled isotopic homologues as internal standards for the solute to be measured has greatly improved quantification by GC.

Isotopomer Analyses

Mass isotopomer distribution analysis (MIDA) uses stable isotopes with quantitative mass spectrometry. It is based on the principle that the isotope distribution or labelling pattern of a fatty acid (e.g. palmitic acid) synthesized from an isotopically perturbed monomeric precursor pool conforms to a binominal expansion. The proportion of unlabelled, single-labelled, double-labelled, and so on, molecular species of a fatty acid is a function of the probability that each precursor subunit is isotopically labelled in the fraction of newly synthesized fatty acid present. The advantages and disadvantages of this approach in studies of lipid metabolism have been discussed in the literature. Analogous combinatorial probability methods have long been used to measure endogenous synthesis of fatty acids. The analytical data for the biosynthesis of palmitic acid from [^2H -ethanol], [$^2\text{H}_2\text{O}$] or [^{13}C -acetate], for example, are provided by GC-MS analysis of the palmitic acid methyl ester and the methyl esters of any other fatty acids of interest. In this method every newly synthesized molecule is counted and the total synthesis calculated by summation of the newly formed molecules.

Definitive Methods

One of the major applications of GC-MS is in quantitative analysis with stable isotope dilution and selected ion monitoring. A known amount of a stable isotope-labelled variant of the molecule to be measured is added to the biological sample as an internal standard, followed by extraction, purification and chemical derivatization. The ions specific for the substance and the internal standard are then monitored. The ratio of the two ion abundances provides the quantitative measurement, which is independent of absolute sensitivity. The superiority of this approach has been demonstrated in the quantitative GC-MS analysis of prostaglandin $\text{F}_{2\alpha}$ in a biological extract using a deuterated derivative. Examples of this approach are provided by the highly sensitive measurement of thromboxane B_2 (TXB_2). Another group based their method on the use of low-blank ($^1\text{H} < 0.2\%$) tetradeuterated 18,18,19,19- $^2\text{H}_4$ TXB_2 , which they synthesized as the internal standard. After purification and HPLC, the samples were derivatized to give an open chain derivative of TXB_2 , a PFB-MO-TMS ether derivative, most suitable for negative ion chemical ionization mass spectrometry. In the selected ion monitoring mode, the detection limits per injection for pure standards and biological samples were 10 and 30 pg, respectively. GC was carried out on a 50 m \times 0.25 mm i.d. bonded SE-30 column. An antibody-mediated extraction method

for GC-MS analysis of thromboxane A_2 (TXA_2) urinary metabolites has been reported. An antibody (Ab) raised against TXB_2 (35% cross-reacting with 2,3-dinor- TXB_2) was coupled to CNBr-activated Sepharose 4B (Se) and used as a stationary phase for simultaneous extraction of both compounds from urine. Quantification was performed by GC-negative chemical ionization-MS, monitoring the carboxylate ion. The GC was performed on a 26 m cyanopropyl siloxane (CP-Sil 5CB) column.

The vasoconstrictor and platelet activator TXA_2 , the predominant product of arachidonic acid in the platelet, is a very reactive substance. It is rapidly converted by nonenzymatic hydrolysis to the stable TXB_2 . Detailed GC-MS analyses of the PFB-MO-TMS ether derivatives of the thromboxanes and their major metabolites have been described.

GC-MS with selected ion monitoring has been used to demonstrate the global changes in the prostaglandins and thromboxanes in rat circulation after administration of arachidonic acid. Figure 12 illustrates the measurements of the prostaglandins with multiple deuterium isotope dilution involving separation of pentafluorobenzyl esters, O-methyl oximes and TMS ether derivatives by high resolution GC and specific detection by NICI-MS in the selected ion mode. The selected ion monitoring profiles show the detection of reference prostaglandins (d_0 and d_4) and their 15 K and 15 KD metabolites: top chromatogram, total ion current; other chromatograms, selected ion mass chromatograms.

GC-MS-MS analyses

In GC-MS-MS, a specific ion is selected from the initial mass spectrum. The selected parent ion is allowed to enter a field-free reaction region, where it may undergo unimolecular or CID. The resulting fragments are analysed by a second mass spectrometer, which provides the MS-MS spectrum. Although commonly referred to as MS-MS, tandem mass spectrometric analysis is usually MS-CID-MS. The application of GC-MS-MS for the analysis of long chain carboxylic acids and their esters has proved enormously successful.

Conclusion

The complex nature and large number of molecular species with similar physicochemical properties make GC the preferred method of lipid analysis. GC provides the highest resolution and the shortest analysis time compared to other chromatographic techniques. GC with FID is highly sensitive and readily automated. Its applicability is limited by high temperature

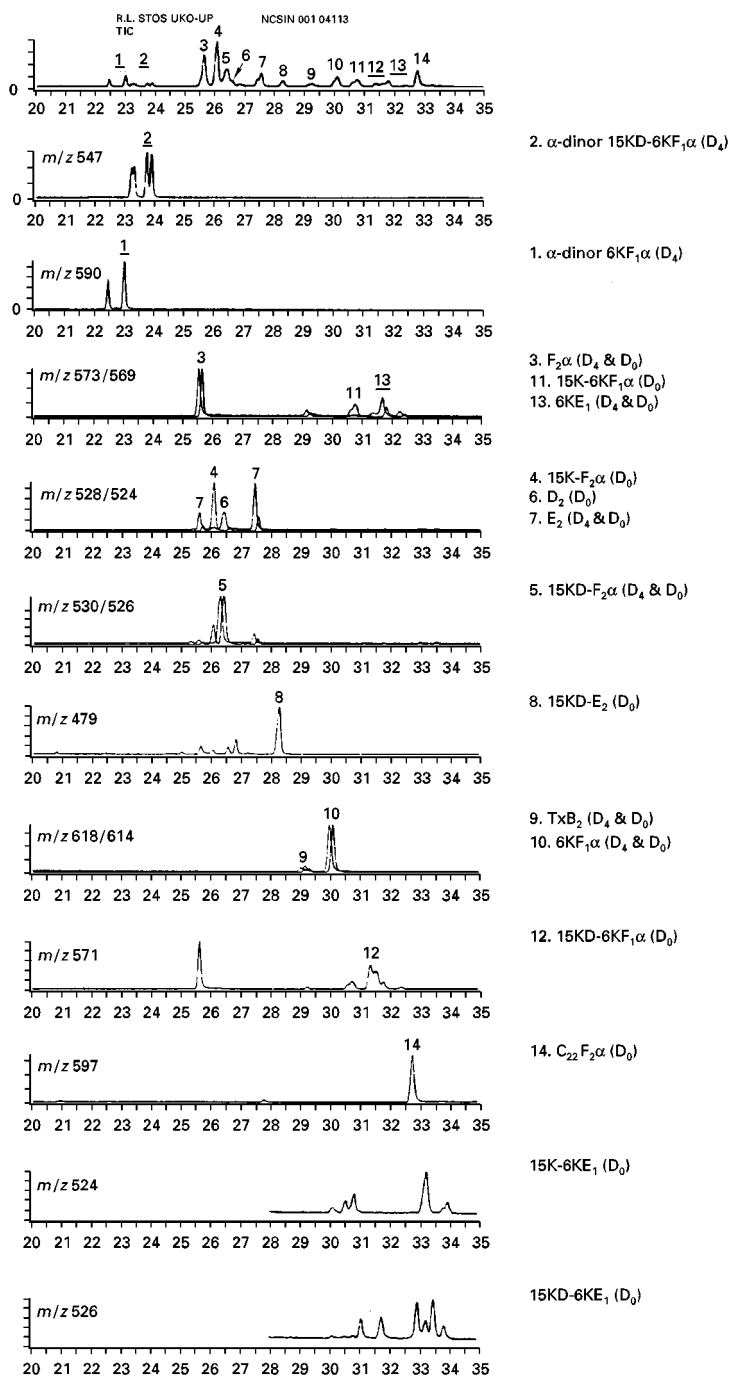


Figure 12 GC-negative chemical ionization-MS with selected ion monitoring of reference prostaglandins (D_0 and D_4) and their 15 K and 15 KD metabolites. Peak identification is given in the figure. GC conditions: column, 60 m \times 0.2 i.d., 0.25 μ m methyl silicone (DB-1, J & W); temperature, programmed from 100°C (hold for 2 min) to 280°C at 30°C min $^{-1}$; carrier gas, hydrogen. (Reproduced with permission from Pace-Asciak, 1987.)

stability and low volatility of the analytes, which may be overcome by enzymic and chemical modification of the samples. With appropriate strategy, automated GC provides a precise tool for the resolution and quantification of lipids ranging from fatty acids to triacylglycerols. Although appropriate GC strategy also provides identification of unknowns in relation

to standards, this must remain tentative unless combined with mass spectrometry. GC-MS of appropriate derivatives of fatty acids provides details of the molecular structure of the fatty acids and their esters. With continued development of liquid phases of increased thermal stability and lipid derivatives of increased volatility and informative mass spectra, GC

and GC-MS is likely to remain the method of choice for analyses of molecular species of most lipid classes for the immediate future.

See Colour Plate 103.

See also: **II/Chromatography: Gas:** Column Technology; Derivatization. **III/Lipids:** Liquid Chromatography; Thin-Layer (Planar) Chromatography.

Further Reading

- Ackman RG (1991) Application of gas-liquid chromatography to lipid separation and analysis: qualitative and quantitative analysis. In: Perkins EG (ed.) *Analyses of Fats, Oils and Lipoproteins*, pp. 270–300. Champaign, IL: American Oil Chemists' Society Press.
- Christie WW (1998) Gas chromatography-mass spectrometry methods for structural analysis of fatty acids. Review. *Lipids* 33: 343–353.
- Dobson G (1998) Cyclic fatty acids: qualitative and quantitative analysis. In: Hamilton RJ (ed.) *Lipid Analysis in Oils and Fats*, pp. 136–180. London: Blackie Academic & Professional.
- Eder K (1995) Review. Gas chromatographic analysis of fatty acid methyl esters. *Journal of Chromatography B* 671: 113–131.
- Geeraert E (1987) Polar capillary GLC of intact natural diacyl and triacylglycerols. In: Kuksis A (ed.) *Chromatography of Lipids in Biomedical Research and Clinical Diagnosis*, pp. 48–75. Amsterdam: Elsevier.
- Gerst N, Ruan B, Pang J *et al.* (1997) An updated look at the analysis of unsaturated C₂₇ sterols by gas chromatography and mass spectrometry. *Journal of Lipid Research* 38: 1685–1701.
- Harvey DJ (1992) Mass spectrometry of picolinyl and other nitrogen-containing derivatives of lipids. In: Christie WW (ed.) *Advances in Lipid Methodology*, vol. 1, pp. 19–80. Dundee, Scotland: Oily Press.
- Kuksis A (1994) GLC and HPLC of neutral glycerolipids. In: Shibamoto T (ed.) *Lipid Chromatographic Analysis*, pp. 177–222. New York: Marcel Dekker.
- Myher JJ and Kuksis A (1989) Relative gas-liquid chromatographic retention factors of trimethylsilyl ethers of diacylglycerols on polar capillary columns. *Journal of Chromatography* 471: 187–204.
- Myher JJ and Kuksis A (1995) General strategies in chromatographic analysis of lipids. *Journal of Chromatography B* 671: 3–33.
- Pace-Asciak CR (1987) Application of GC-MS techniques to the analysis of prostaglandins and related substances. In: Kuksis A (ed.) *Chromatography of Lipids in Biomedical Research and Clinical Diagnosis*. Journal of Chromatography Library, vol. 37, pp. 107–127. Amsterdam: Elsevier.
- Ruiz-Gutierrez V and Barron LJR (1995) Methods for the analysis of triacylglycerols. *Journal of Chromatography B* 671: 133–168.
- Spitzer V (1997) Structure analysis of fatty acids by gas chromatography-low resolution electron impact mass spectrometry of their 4,4-dimethyloxazoline derivatives – a review. *Progress in Lipid Research* 35: 387–408.
- Thompson RH (1996) Simplifying fatty acid analysis in multicomponent foods with a standard set of isothermal GLC conditions coupled with ECL determinations. *Journal of Chromatographic Science* 34: 495–504.
- Tvrzicka E and Mares P (1994) Gas-liquid chromatography of neutral lipids. In: Shibamoto T (ed.) *Lipid Chromatographic Analysis*, pp. 103–176. New York: Marcel Dekker.

Liquid Chromatography

A. Kuksis, University of Toronto, Charles H Best Institute, Toronto, Canada

Copyright © 2000 Academic Press

Introduction

Natural lipids consist of complex mixtures of molecular species, which are found in association with cell membranes, lipoproteins and other subcellular structures. The composition differs among different cell and tissue types, reflecting the function of lipids in these body structures. Much experimental effort and imagination has been expended in determining the exact composition of lipid species during dietary alterations and physiological activity.

The complex nature of natural lipids and their high solubility in organic solvents makes the separation and isolation of individual lipid classes and molecular species by most physical methods difficult or impossible. Only chromatographic methods have proven suitable for this. The earlier thin-layer and gas chromatographic routines have been complemented in recent years by high performance liquid chromatography (HPLC), which has proven to have nearly universal applicability.

Principles of Liquid Chromatography

Normal-phase Columns and Solvents

Normal-phase HPLC provides resolution based on the overall polarity of the lipid molecules. The

stationary phase is typically silica gel. The best column and mobile phase for a specific application are selected by trial and error or based on previous experience using thin-layer chromatography (TLC). More refined solvent selection is based on chemometric methods. The solvents selected for the mobile phase in either isocratic or gradient separations should be excellent lipid solubilizers and should not degrade the stationary phase. Therefore, the addition of buffering salts should be minimized and strong acids should be avoided. Other restrictions on the selection of the mobile phase may be imposed by the choice or availability of the detection system, e.g. ultraviolet (UV) and refractive index (RI) detectors.

Silver ion HPLC provides resolutions based on the number, position and configuration of the double bonds present in the lipid molecule. It complements other methods of separation. For this purpose silica gel columns are impregnated with silver nitrate or silver ions are immobilized on columns containing benzenesulfonic acid groups. Chlorinated solvents as the mobile phase, with acetone or acetonitrile as a polar modifier, afford especially good separations.

Reversed-phase Columns and Solvents

Reversed-phase HPLC is believed to separate lipid molecules based on their partition properties in a biphasic liquid-liquid system, although the exact mechanism is unknown. The most widely used and most important reversed phases for lipid analysis are silicas with relatively long hydrocarbon chains chemically bonded to the surface. Octyl- and octadecyl-bonded chains have been found to provide the best resolution of fatty acids and triacylglycerols.

Chiral-phase Columns and Solvents

HPLC on columns containing a stationary phase with chiral moieties bonded chemically to a silica matrix has proven well suited for the resolution of chiral glycerolipids. The approach has been to prepare 3,5-dinitrophenyl urethane (DNPU) derivatives of mono- and diacyl-*sn*-glycerols and related compounds, where the hydrogen atom on nitrogen in the urethane group is available for hydrogen bonding with the stationary phase. The 3,5-dinitrophenyl moieties of the urethanes contribute to charge-transfer interactions with functional groups having π electrons on the stationary phase; they are also advantageous for detection by UV absorption. A column with a polymer of (R)-(+)-1-(1-naphthyl)ethylamine moieties chemically bonded to silica gel (YMC-Pack A-KO3TM) has been applied to the resolution of diacyl-*sn*-glycerol

derivatives in a similar manner. The best solvents so far have been the hexane/dichloromethane/ethanol mixtures, which, for the purpose of online mass spectrometry, have been replaced by mixtures of hexane/dichloroethane/acetonitrile or isooctane/*tert*-butyl methyl ether/acetonitrile/isopropanol.

There are no foolproof recommendations for the selection of solvents. Previous success appears to be the best guide. However, the polarity of the solvents must be chosen so as not to destroy the hydrogen bonding responsible for the differential affinity between the enantiomers and the stationary phase.

Detectors and Quantification of Solutes

In early work, RI detectors were used in normal-phase HPLC. However, this detector is only applicable to isocratic elution, because RI detection is very sensitive to change in solvent composition. Short wavelength UV (205–210 nm) is also frequently employed for lipid detection but again suffers from sensitivity towards changes in solvent composition. However, UV absorption at longer wavelengths can be effectively used for the specific detection of UV-absorbing solutes. Furthermore, lipids with functional groups can be converted into UV-absorbing or fluorescing derivatives (e.g. free fatty acids, aminophospholipids), which have been widely exploited in reversed-phase HPLC. Many of these derivatives are sufficiently sensitive to permit detection of femtomole levels of the solute (see below).

In HPLC with flame ionization detection (FID), the analyte after solvent removal is burned in a flame and the ions formed are collected by applying an electric field. This nearly universal detector yields a linear relationship between the mass of the solute and peak area over a wide concentration range. More recently, the evaporative light-scattering detector (ELSD) has become the detector of choice in most analytical lipid separations. Like the FID, it is destructive, and must be employed with a stream splitter for peak collection.

It is generally agreed that all detectors require preliminary calibration with reference species to examine the response-structure relationship, and to determine the character of the calibration graph constructed in response-quantity dimensions to be able to work in the linear range. In principle, the quantification is based on measurements of peak area, normalization of the values and calculation of the relative percentage of each component.

Another detector for HPLC of universal application is provided by the mass spectrometer using a variety of ionization techniques to generate total or single ion current response. The use of this detector is

discussed along with the use of online mass spectrometry for peak identification (see below).

Liquid Chromatography–Mass Spectrometry/(LC-MS)

LC-MS

Online mass spectrometry allows one to obtain direct evidence about the nature of chromatographic peak, e.g. purity, molecular weight and characteristic fragment ions. This information, together with the knowledge of the relative retention time, is usually sufficient for peak identification. More complete identification may be obtained by MS-MS, which is based on the specific mass spectrometric fragmentation of primary ions. Recent reviews of LC-MS applications to lipid analyses are available (see Kuksis and Myher, 1995 and Kuksis, 1997 in Further Reading, below).

The online LC-MS analysis of lipids is accomplished using interfaces which eliminate the HPLC solvent and effect a reliable and efficient transfer of the solute to the ion source. An early method of interfacing HPLC and a mass spectrometer utilized a direct liquid inlet. Several successful applications to lipid analyses with chemical ionization mode were reported. In the positive ion mode, this method produced mass spectra similar to those recorded in electron impact mass spectrometry. Thus, for a triacylglycerol species, a pseudomolecular ion along with characteristic diacylglycerol-like ions were obtained. These ions are frequently sufficient to identify the molecular weight and degree of unsaturation of the component fatty acids. Furthermore, the regiodistribution of the fatty acids in acylglycerols can also be obtained by this ionization method. More recently, the softer ionization techniques, thermospray (TS), electrospray (ES) and atmospheric pressure chemical ionization (APCI) have been utilized for online monitoring of triacylglycerols resolved by HPLC. The latter techniques also allow direct LC-MS of the molecular species of intact glycerophospholipids, which yield largely or exclusively the pseudomolecular ions $[M + 1]^+$ and $[M - 1]^-$ respectively in the positive and negative ionization modes. This information is sufficient for tentative identification of molecular species when combined with knowledge of HPLC retention times and the overall composition of the fatty acids.

LC-MS-MS

Simple LC-MS is not sufficient to establish the exact composition of all molecular species, which requires the identification of the component fatty acids

in each parent acylglycerol molecule. The fast atom bombardment (FAB) and especially the ES ionization techniques are compatible with LC-MS-MS approaches and have been extensively utilized in polar lipid analysis. In many instances, flow ES-MS-MS has also proven adequate for identification of molecular species.

Pseudo MS-MS

LC-ES-MS ionization can be used to produce collision-induced dissociation (CID) spectra of singly charged species with greater sensitivity than can be achieved with flow ES-MS-MS systems. The HPLC effluent is carried into the ES source via a stainless-steel or fixed silica needle at flow rates of $1\text{--}40\ \mu\text{L min}^{-1}$. When analytes are present in the sprayed solution, molecular adduct ions from these analytes, typically protonated ions $[M + H]^+$, are formed. If a low voltage of 50–120 V is applied to the capillary exit, the molecular ion remains intact and the molecular weight of the analyte is obtained. If higher voltages are applied (e.g. 200–300 V) to the capillary exit, extensive and reproducible fragmentation of the molecular adduct ion is realized (pseudo MS-MS).

Isolation of Natural Lipids

In order to determine the composition of the lipid phase associated with a particular function it is necessary to isolate the appropriate subcellular structure and to determine the component lipid classes and molecular species. For the purpose of discussion the analyses are considered separately as those of neutral lipids, glycerophospholipids and sphingolipids, including glycosphingolipids.

Preparation of Lipid Extracts

The neutral lipids can be extracted from natural sources by means of benzene, chloroform and other non-polar solvents. More complete lipid isolation is obtained by extraction with more polar solvents, such as mixtures of chloroform and methanol. However, use of chloroform/methanol results in low recoveries of acidic phospholipids, lysophospholipids and non-esterified fatty acids, while acidified solvents generate lysophospholipid artefacts from tissues containing plasmalogens.

Purification and Preliminary Separation

Recently, organic solvent extraction has been replaced by solid-phase extraction. It is a simple, rapid technique and can be up to 12 times faster than liquid extraction when executed with commercially

Table 1 Separation scheme for fractionation of lipid classes from wheat flour using combined silica and aminopropyl solid-phase extraction columns

Absorbent	Solvents (volume ratio)	Volume (mL)	Lipid class eluted
Silica	Hexane/Et ₂ O (200 : 3)	15	SE
Silica	Hexane/Et ₂ O (96 : 4)	20	TG
Silica	Hexane/HOAc (100 : 0.2)	20	
Silica	Hexane/Et ₂ O/HOAc (100 : 2 : 0.2)	20	FFA
Silica	Hexane/ethyl acetate (95 : 5)	15	
Silica	Hexane/ethyl acetate (85 : 15)	15	1,2-DG, 1,2-DG
Silica	Et ₂ O/HOAc (100 : 0.2)	15	α -MG, β -MG
Silica	Et ₂ O/acetone (50 : 50)	20	MGDG, MGDG
Silica	Acetone	20	DGDG, DGDG
Silica	THF/ACN/isopropanol (40 : 35 : 25)	5	Trace GL
Silica	THF/ACN/isopropanol (30 : 35 : 35)	5	
Silica	THF/ACN/isopropanol (20 : 35 : 45)	5	NAPE
Silica	THF/ACN/MeOH (15 : 45 : 40)	5	NAPE, NAPE
Silica	THF/ACN/MeOH (15 : 35 : 50)	5	
Silica	THF/ACN/MeOH (10 : 35 : 55)	5	PC
Silica	THF/ACN/MeOH (5 : 35 : 60)	5	
Silica	CAN/MeOH (35 : 65)	5	lyso-PC
Aminopropyl	CHCl ₃ /MeOH/ammonium hydroxide (85 : 15 : 0.1)	25	
Aminopropyl	CHCl ₃ /MeOH/ammonium hydroxide (80 : 20 : 0.1)	20	NAPE
Aminopropyl	CHCl ₃ /MeOH/ammonium hydroxide (75 : 25 : 0.1)	20	
Aminopropyl	CHCl ₃ /MeOH/ammonium hydroxide (50 : 50 : 0.1)	20	NALPE
Aminopropyl	CHCl ₃ /MeOH/ammonium hydroxide (0 : 100 : 0.1)	20	

Et₂O, Diethyl ether; HOAc, acetic acid; THF, tetrahydrofuran; ACN, acetonitrile; MeOH, methanol; CHCl₃, chloroform. SE, steryl esters; TG, triacylglycerols; FFA, free fatty acids; DG, diacylglycerols; MG, monoacylglycerols; DGDG, diacylglycerol digalactoside; DGDG, diacylglycerol diglucoside; GL, glycolipid; NAPE, *N*-acyl phosphatidylethanolamine; NALPE, *N*-acyllyso phosphatidylethanolamine; lyso-PC, lysophosphatidylcholine. Modified with permission from Prieto JA *et al.*, 1992.

prepared cartridges. These cartridges have proven adequate for rapid removal of nonlipid components from total lipid extracts and for preliminary separation of both neutral and polar lipid classes. For this purpose, the cartridges are eluted by passing through them measured volumes of solvents of appropriate polarity. **Table 1** summarizes a separation scheme successfully applied to the fractionation of lipid classes from wheat flour that is also applicable to the resolution of most lipid classes from animal tissues. A major disadvantage of the solid-phase method is the difficulty of monitoring the separations, so that TLC must be frequently used to assess the results of such isolations.

The currently available techniques concerning extraction and characterization of the different lipids from biological specimens are designed for particular families and do not address consecutive isolation of lipid constituents in their totality. It must be pointed out that conventional TLC remains a convenient, rapid and reliable technique for lipid class isolation which permits efficient extraction of lipid components including gangliosides, without preferential loss of any one group and without the

uncertainty of working blindly. The protocol is applicable to biological samples of limited availability.

Derivatization

In order to improve resolution, detection and recovery, natural lipids may be subjected to derivatization prior to HPLC. Since neutral lipids are more readily resolved than polar lipids, the polar functional groups of natural lipids may be removed or masked prior to separation. Thus, the phospholipids may be subjected to dephosphorylation by phospholipase C and the resulting diacylglycerols silylated, acetylated or benzoylated before normal-phase or reversed-phase HPLC. This procedure allows improved resolution of the diacylglycerol classes by normal-phase HPLC and of molecular species by reversed-phase HPLC. The preparation of the benzoates also improves the UV detection of the molecular species by reversed-phase HPLC. The preparation of the benzoates also improves the UV detection of the molecular species, while a preparation of the pentafluorobenzoates improves the sensitivity of mass spectrometric detection of the lipid classes and molecular species. The diacylglycerols generated randomly from natural triacyl-

glycerols by Grignard degradation may be converted into the naphthylethyl urethane derivatives by an enantiomeric reagent prior to normal-phase separation of the resulting diastereomers. Using another approach to stereospecific analysis of triacylglycerols, the racemic diacylglycerols resulting from the Grignard degradation are converted into the dinitrophenyl urethanes of the diacylglycerols prior to separation of the enantiomers. In other instances, free fatty acids, free acylglycerols and aminophospholipids may be converted into UV-absorbing or fluorescent derivatives prior to reversed-phase HPLC. The total lipid extracts or any fraction of them may be hydrogenated, reduced with borohydride, peroxidized or ozonized prior to HPLC to provide reference materials or to improve the chromatographic behaviour of the solutes.

Separation of Neutral Lipids and Free Fatty Acids

Neutral lipids and free fatty acids are made up of monoacylglycerols, diacylglycerols, triacylglycerols, unesterified and esterified sterols, unesterified fatty acids and various other minor components of natural lipids, which migrate with neutral lipids just listed, e.g. tocopherols, alcohols, hydrocarbons, ketones, aldehydes and simple esters. This definition also includes neutral lipids derived from polar lipids by enzymic or chemical transformation (e.g. acylglycerols and ceramides), as well as the peroxidation products of lipids and prostanoids. These lipids possess excellent chromatographic properties.

Normal-phase Separations

Total lipid profiling on adsorption columns was practised in various forms long before the existence of any other comparable method. Reproducibility and quantification were the major problems which have now been resolved by the combination of HPLC and light scattering or mass spectrometric detection. **Figure 1** shows the separation of selected neutral and polar lipid standards and rat liver lipids by automated normal-phase HPLC using a light-scattering detector. Both neutral and phospholipid classes are well separated and this approach is suitable for use with ES-MS. Normal-phase HPLC is also well suited for the separation of natural and peroxidized fatty acid esters. **Figure 2** shows the separation of a mixture of standard oxosterols along with various other mixtures of oxosterols. The peaks were detected by UV at 205 nm.

Normal-phase HPLC can be employed for separation of the diastereomeric diacylglycerol naph-

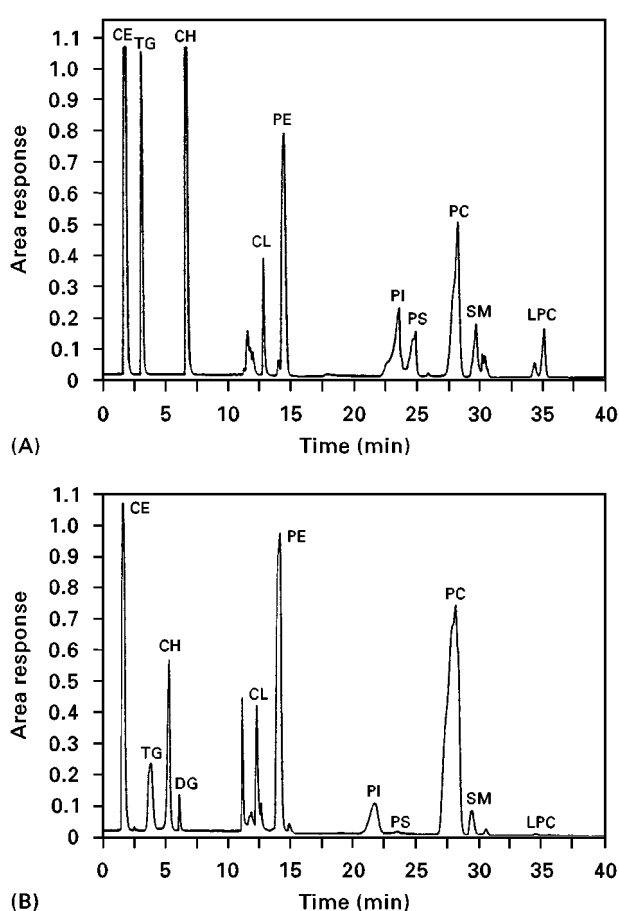


Figure 1 Separation of (A) standard and (B) rat liver lipids by automated normal-phase HPLC with light-scattering detection. Peak identification: CE, cholesteryl esters; TG, triacylglycerols; CH, unesterified cholesterol; DG, diacylglycerols; CL, cardiolipin; PE, phosphatidylethanolamine; PI, phosphatidylinositol; PS, phosphatidylserine; PC, phosphatidylcholine; SM, sphingomyelin; LPC, lysophosphatidyl choline. HPLC conditions: column, 5 μ m Ultrasphere Si (25 cm \times 4.5 mm); solvent, a binary gradient of three different solvent mixtures made up of hexane/tetrahydrofuran (99 : 1, v/v), isopropanol/chloroform (4 : 1, v/v) and isopropanol/water (1 : 1, v/v). (Reprinted with permission from Redden and Huang, 1991.)

thylethyl urethanes for the purpose of stereospecific analysis of the positional distribution of the fatty acids in natural triacylglycerols. **Figure 3** shows the separation of the diastereomeric diacylglycerols as the naphthylethyl urethanes. The *sn*-1,2- and *sn*-2,3-enantiomers are resolved with the elution order depending on the *S*- or *R*-configuration of the reagent. The diastereomeric naphthylethyl urethanes are prepared by reacting the free *sn*-1,2(2,3)-diacylglycerols with either the *S*- or *R*-isocyanate. The partial overlap between molecular species of enantiomeric diacylglycerols from natural sources does not compromise the identification and quantification of the species by ES-LC-MS.

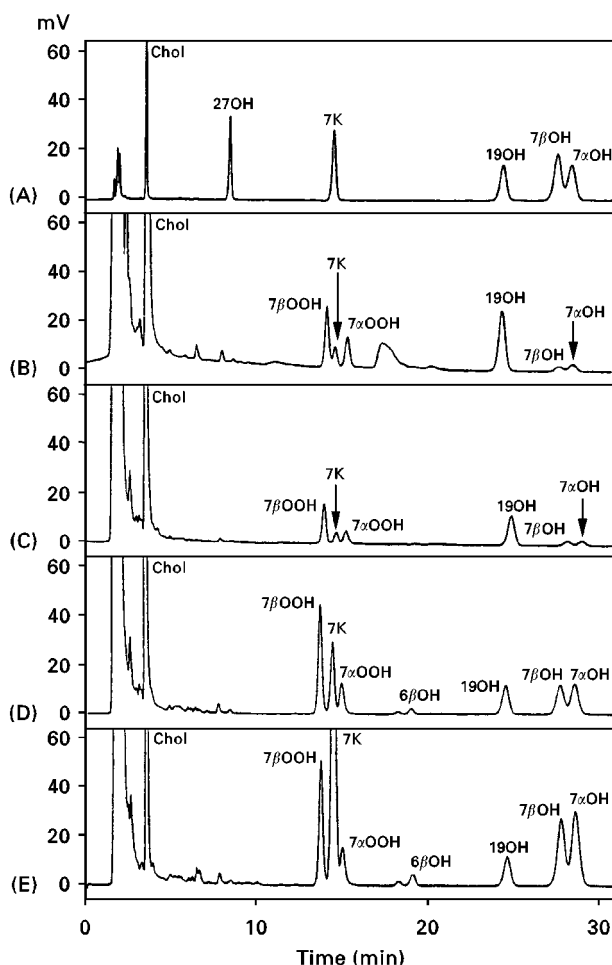


Figure 2 Normal-phase HPLC of (A) standard oxosterols and (B–E) oxidation products of cholesterol. B, Liposomal cholesterol oxidized with azoamidopropane at 37°C for 20 h; C–E, LDL cholesterol oxidized with Cu^{2+} for 4 h, 8 h and 24 h, respectively. Peak identification: Chol, cholesterol; 27OH, 27-hydroxycholesterol; 7K, 7-ketocholesterol; 19OH, 19-hydroxycholesterol (internal standard); 7βOH, 7β-hydroxycholesterol; 7αOH, 7α-hydroxycholesterol; 7βOOH, 7β-hydroperoxycholesterol; 7αOOH, 7α-hydroperoxycholesterol; 6βOH, 6β-hydroxycholesterol. HPLC conditions: two columns, 3 μm Ultramex (10 × 0.46 cm) in series with a 3 cm guard column; solvent, hexane/isopropanol/acetonitrile (95.8 : 3.90 : 0.30, by vol) at 1.5 mL min⁻¹. (Reprinted with permission from Brown AJ, Leong S-L, Dean RT and Jessup W (1997) 7-Hydroperoxycholesterol and its products in oxidized low density lipoprotein and human atherosclerotic plaque. *Journal of Lipid Research* 38: 1730–1745.)

Normal-phase HPLC is used for the separation of the leukotriene B₄ (LTB₄) metabolites, with a mobile phase consisting of hexane/isopropanol/acetic acid (96 : 4 : 0.1 by vol; **Figure 4**). The retention times of these compounds are closely related to their polarities, with LTB₄ having the longest and 10,11-dihydro-12-oxo-LTB₄ the shortest time. The 12-oxo-LTB₄ and 10,11-dihydro-LTB₄ have similar retention

times but can be distinguished from each other by their UV spectra. Normal-phase HPLC also separates the hydroxyeicosatetraenes (HETEs) and oxo-eicosatetraenes (oxo-ETEs) with a mobile phase of hexane/isopropanol/acetic acid (90.05 : 0.45 : 0.5 by vol), as shown in the same figure. As expected from its polarity, 15-oxo-ETE had a retention time considerably shorter than that of 15-HETE. The retention time of 12-oxo-ETE is also shorter than that of 12-HETE, but only marginally so.

Normal-phase HPLC on columns containing immobilized silver ions has been used for the fractionation of simple fatty acid esters and triacylglycerols according to the number and configuration of double bonds. **Figure 5** shows an Ag^+ -HPLC separation of a commercial mixture of conjugated linoleic acids (CLA). Using 0.1% acetonitrile in hexane, 12 peaks were obtained, which emerged into three groups of four peaks each. Evidence for the identity of the individual isomers was obtained by comparison with standards and by complementary chromatographic and MS techniques.

Reversed-phase Separations

Figure 6 shows the separation of the molecular species of randomized butterfat by reversed-phase HPLC with light-scattering detection. Butterfat constitutes one of the most difficult mixtures for any chromatographic separation. The analysis of a randomized sample has the advantage that all the

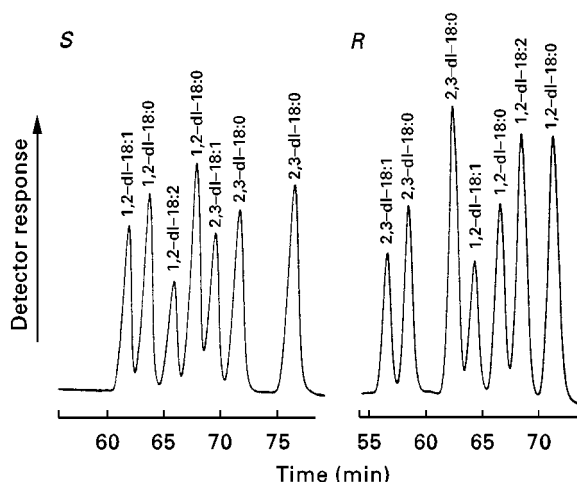


Figure 3 Normal-phase HPLC separation of 1,2- and 2,3-diacyl-*sn*-glycerols in the form of 1-(1-naphthyl)ethyl urethane derivatives. S: (S)-(+)-1-(1-naphthyl)ethyl urethanes; R: (R)-(1)-1-(1-naphthyl)ethyl urethanes. HPLC conditions: two columns, 3 μm Hypersil™ (250 × 4.6 mm i.d.) in series; solvents: hexane/isopropanol (99.5 : 0.5, v/v) at 0.8 mL min⁻¹ and UV detection at 280 nm. (Reproduced with permission from Laakso and Christie, 1990.)

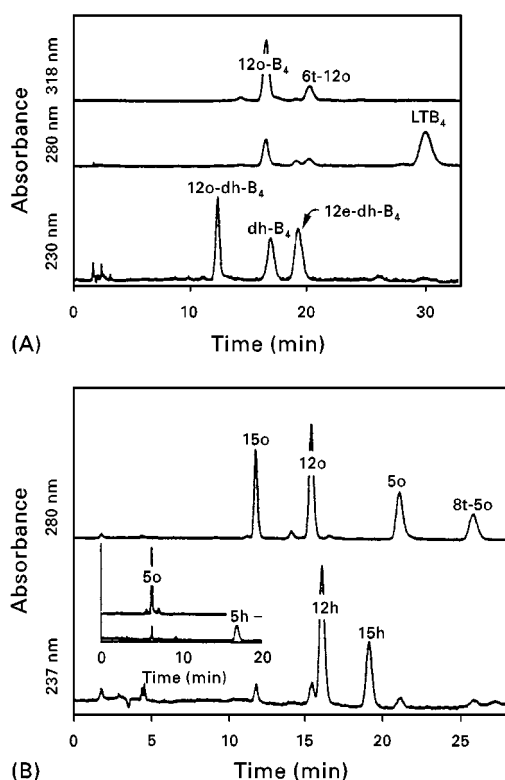


Figure 4 Normal-phase HPLC resolution of (A) LTB_4 , 12-oxo- LTB_4 (12o- B_4), 6-*trans*-12-oxo- LTB_4 (6t-12o), 10,11-dihydro- LTB_4 (dh- B_4), 12-oxo-10,11-dihydro- LTB_4 (12o-dh- B_4) and 12-epi-10,11-dihydro- LTB_4 (12e-dh- B_4) with hexane/isopropanol/acetic acid (96:4:0.1, v/v) and (B) HETEs and oxo-ETEs with hexane/isopropanol/acetic acid (99.05/0.45/0.5, v/v) as the mobile phase. The inset shows the normal-phase HPLC separation of 5-oxo-ETE and 5-HETE using a stronger mobile phase (hexane/isopropanol/acetic acid, 97.2:2:0.1, v/v). (Reproduced with permission from Powell *et al.* (1997) High-pressure liquid chromatography of oxo-eicosanoids derived from arachidonic acid. *Journal of Biochemistry* 247: 17–24.)

molecular species can be calculated on the basis of random distribution and sorted by number of acyl carbons and double bonds. Although there is nearly complete separation of the various triacylglycerol subclasses, numerous molecular species overlap. It is therefore necessary to employ MS to distinguish among the molecular species within each chromatographic peak. There is no resolution of enantiomers or regio-isomers.

Reversed-phase HPLC provides impressive separation of the complex fish oil triacylglycerols using either light-scattering or MS detection. Figure 7 shows the separation of a triacylglycerol mixture containing 43% docosahexaenoic acid by LC-ESI-MS. Some 33 major components are detected. An examination of the ions generated from each triacylglycerol peak revealed the presence of both

molecular and diacylglycerol-like fragment ions from which the triacylglycerol composition of each peak was determined. Figure 7B and 7C illustrates the identification of peaks 20 and 26 in the chromatographic profile. This extremely powerful method allows identification of species that have the same elution times but different elution times.

The triacylglycerol structures in the HPLC effluent can be determined by atmospheric pressure chemical ionization (APCI) using a corona discharge to ionize vaporized molecules to form both molecular and diacylglycerol-like fragment ions. Figure 8 compares the elution patterns recorded for a mixture of 35 triacylglycerols by reversed-phase HPLC with FID or APCI detection. Although different gradients of acetonitrile and dichloromethane were used in the two systems, the chromatographic patterns are similar.

Figure 9 relates the retention times of various synthetic oxotriacylglycerols to their theoretical carbon numbers used to aid identification of peroxidized

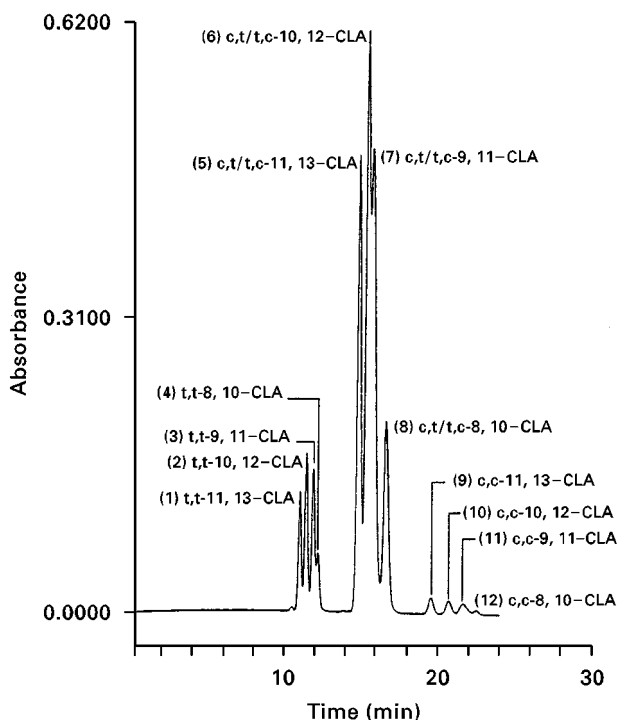


Figure 5 Silver ion HPLC of a commercial conjugated linoleic acid standard. Peak identification is as given in figure: CLA, conjugated linoleic acid. HPLC: column, 5 μm ChromSper, AgNO_3 (250 \times 4.6 mm i.d.); solvent, isocratic 0.1% acetonitrile in hexane. (Reproduced with permission from Sehat N, Yurawecz MP, Roach JAG *et al.* (1998) Silver ion HPLC separation and identification of conjugated linoleic acid isomers. *Lipids* 33: 217–221.)

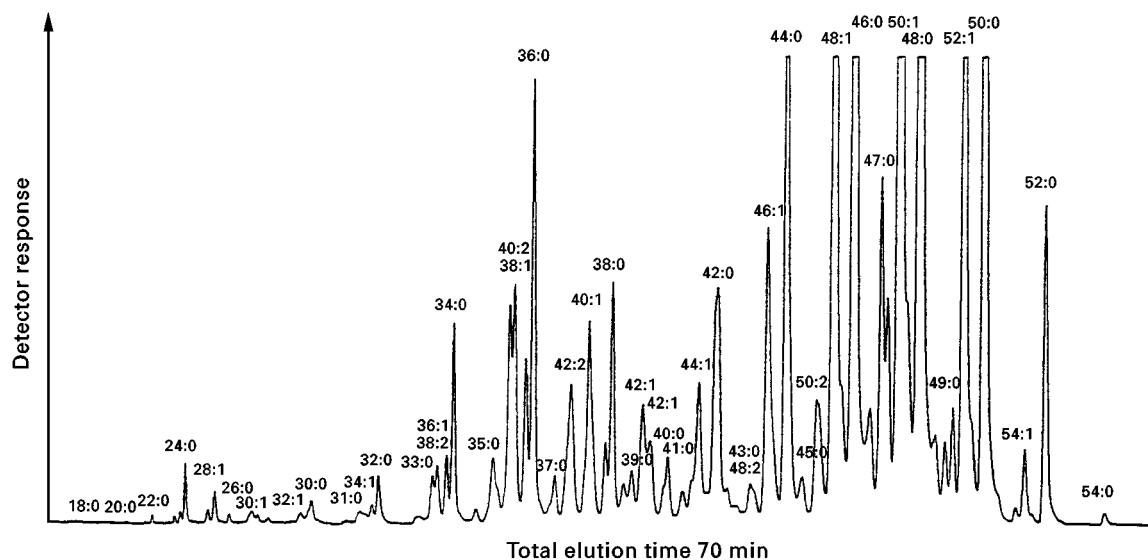


Figure 6 Reversed-phase HPLC elution profile of randomized butterfat triacylglycerols as monitored by light-scattering detection. Peak identification is given in the figure on the basis of total acyl carbon:double bond number. HPLC conditions: column, 5 μ m Supelcosil C₁₈ (250 \times 4.6 mm i.d.) solvent gradient: 10–90% isopropanol in acetonitrile in 90 min. (Reproduced with permission from Marai *et al.*, 1994.)

natural triacylglycerols by reversed-phase HPLC with ES-MS. The theoretical carbon numbers and correction factors for the oxidized and unsaturated triacylglycerols were calculated using the curve for the saturated triacylglycerols as a reference.

Tocopherols exist in nature as a complex mixture of 2-methyl-6-chromanol homologues and aromatic ring position isomers, each having a three-terpene-unit side chain at the C-2-position. These components of closely related structures can be separated by normal-phase HPLC on silica-based columns. However, the most extensive separations have been obtained by reversed-phase HPLC on a column of octadecyl polyvinyl alcohol sorbent. **Figure 10** shows the separation obtained for the α -, β -, γ -, δ - and ϵ -tocopherols on such a column with acetonitrile/water or methanol/water as the mobile phase.

Cholesterol, sitosterol and their metabolic precursors are also separated by reversed-phase HPLC. Conversion to UV-absorbing derivatives greatly facilitates their detection and quantification. Likewise, reversed-phase HPLC is suitable for the separation of cholesteryl esters. **Figure 11** demonstrates the separation of the cholesteryl esters in a lipid extract from cholesterol-loaded J774 macrophages showing esters ranging from eicosapentaenoate (docosahexaenoate) of cholesterol to stearate in order of their partition number. There are several minor peak overlaps. Normally, the cholesteryl esters in a total lipid extract would overlap with the triacylglycerols

also present in the mixture. This problem can be solved by a mild alkaline hydrolysis, which destroys the triacylglycerols without affecting the cholesteryl esters.

Similarly, reversed-phase HPLC can be employed for the separation of retinyl esters. **Figure 12** illustrates the separation of 15 synthetic retinyl esters with minimal overlap, except for retinyl linolenate, laurate and arachidonate, which are unlikely to occur together in a natural mixture.

Reversed-phase HPLC has been most extensively employed for the separation of the molecular species of diacylglycerols derived from glycerophospholipids by hydrolysis with phospholipase C and from triacylglycerols by hydrolysis with lipase or Grignard degradation. Both UV-absorbing and fluorescent derivatives are prepared to facilitate detection and quantification (**Table 2**). Reversed-phase HPLC is also excellent for the separation of the molecular species of the diacylglycerol DNPU derivatives recovered from chiral HPLC.

Finally, reversed-phase HPLC is suitable for the separation of fatty acids as UV-absorbing or fluorescent derivatives (**Table 3**) and may rival gas chromatography for specific applications. Thus, excellent separation and sensitive detection of the 9-anthrylmethyl esters and the 1-pyrenyldiazomethane derivatives of free fatty acids has been obtained (**Figure 13**). The method has been applied to the determination of endogenous fatty acids released from a cell culture upon stimulation.

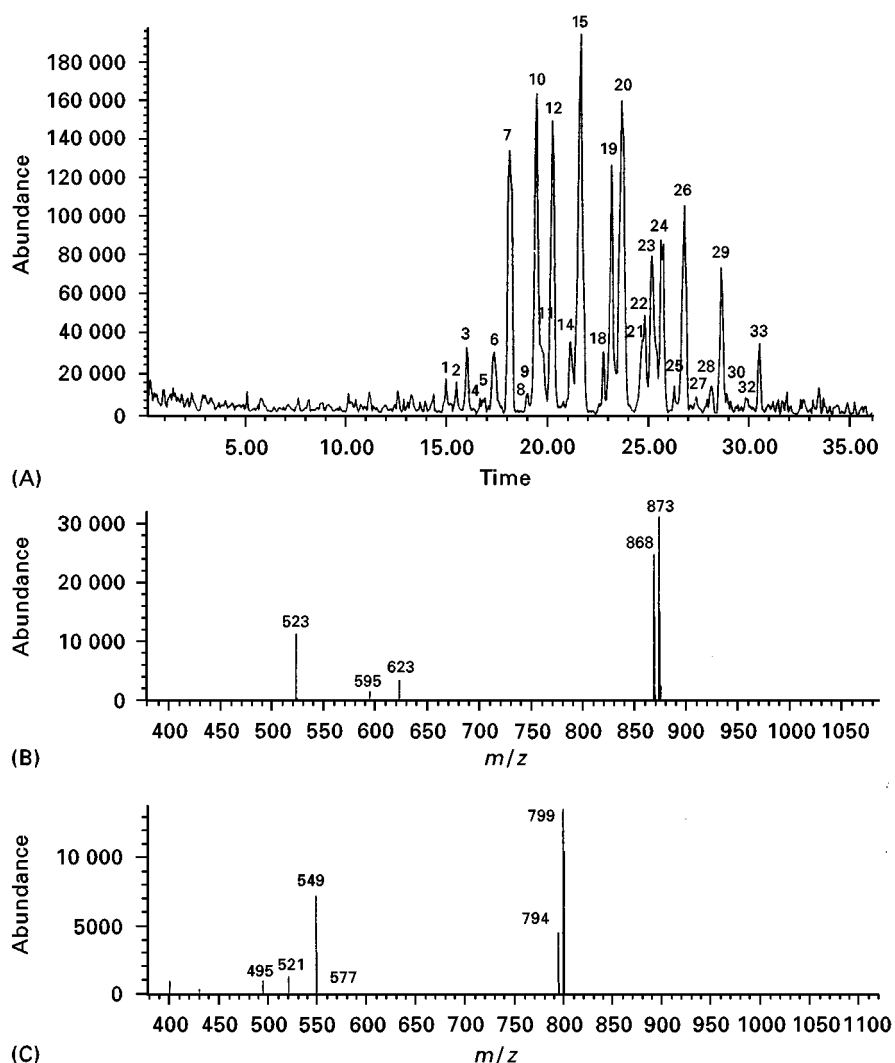


Figure 7 Reversed-phase HPLC of docosahexaenoic acid-rich oil with online ESI/MS. (A) Total positive ion current profile; (B) ESI-CID-MS of peak 20 (14 : 0/16 : 0/22 : 6): m/z 868, $[M + 18]^+$; m/z 873, $[M + 23]^+$; m/z 523, $[M\text{-RCOO}]^+$ (30 : 0 DG); m/z 595, $[M\text{-RCOO}]^+$ (36 : 6); m/z 623, $[M\text{-RCOO}]^+$ (38 : 6 DG); (C) ESI-CID-MS of peak 26 (14 : 0/14 : 0/18 : 1; 14 : 0/16 : 0/16 : 1): m/z 794, $[M + 18]^+$; m/z 799, $[M + 23]^+$; m/z 495, $[M\text{-RCOO}]^+$ (28 : 0 DG); m/z 521, $[M\text{-RCOO}]^+$ (30 : 1 DG); m/z 549, $[M\text{-RCOO}]^+$ (32 : 1 DG); m/z 577, $[M\text{-RCOO}]^+$ (34 : 1 DG). HPLC conditions: column, 5 μm Supelcosil LC-18 (250 \times 4.6 mm i.d.); solvent, linear gradient of 20–80% isopropanol in acetonitrile in 30 min; ESI-CID-MS conditions, capillary exit voltage 215 V. (Reproduced with permission from Myher *et al.*, 1997.)

Chiral-phase HPLC

Chiral HPLC permits the separation of enantiomeric diacylglycerols derived from Grignard degradation or lipase hydrolysis. **Figure 14** shows the separation of the *sn*-1,2(2,3)-diacylglycerols derived from Grignard degradation of a complex triacylglycerol mixture containing 43% docosahexaenoic acid; there is excellent separation of the enantiomers. With this chiral phase, the *sn*-2,3-enantiomers emerge last. There is considerable resolution of molecular species, especially within the longer-retained *sn*-2,3-enantiomers. The X-1,3-isomers not removed by borate TLC

emerge just ahead of, or overlap with, the *sn*-1,2-enantiomers. A chiral-phase LC-MS analysis of the 3,5-DNPU derivatives of the *sn*-1,2- and *sn*-2,3-diacylglycerols revealed the presence of a high proportion of species containing two long chain fatty acids per acylglycerol molecule, including 20 : 2–20 : 4 and 22 : 6–22 : 6.

Separation of Glycerophospholipids and Sphingomyelins

HPLC analysis of glycerophospholipids and sphingomyelins is usually performed with the total phos-

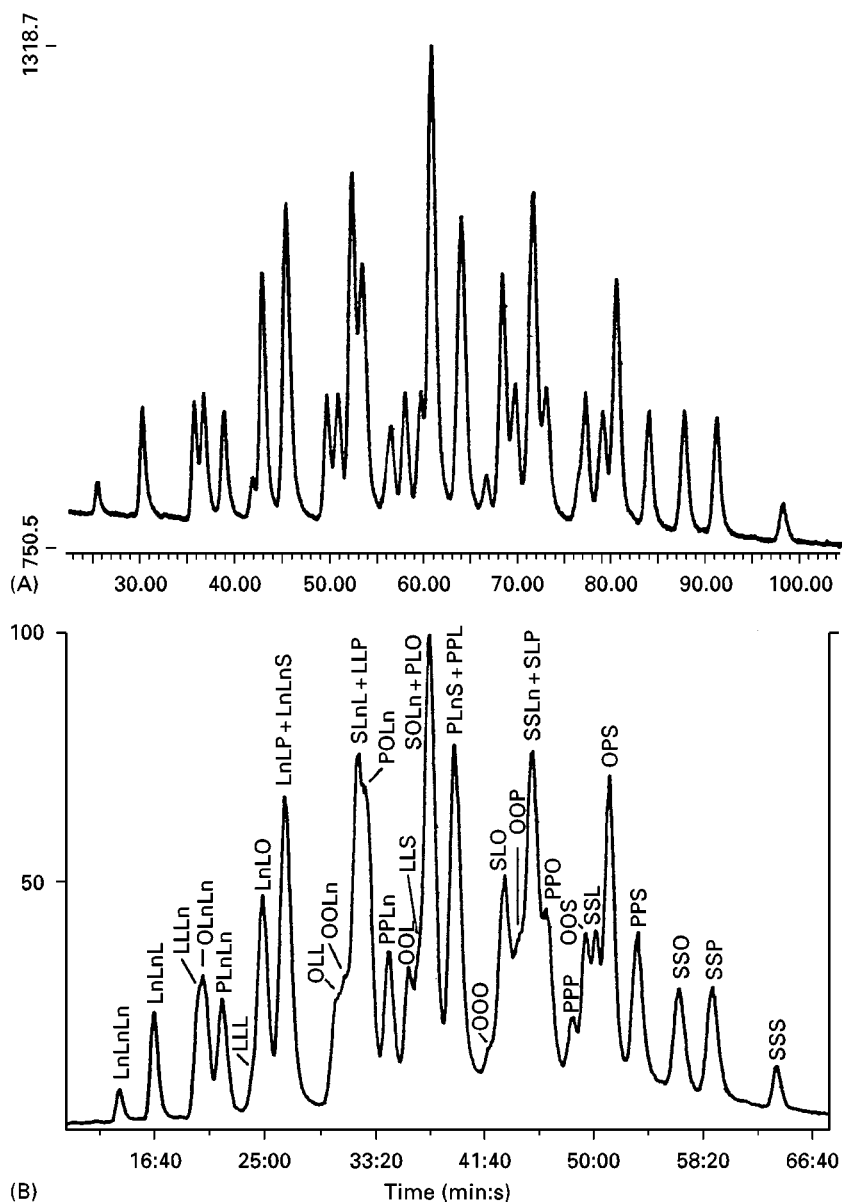


Figure 8 Reversed-phase HPLC separation of synthetic mixture of 36 triacylglycerols containing five randomly distributed fatty acids. Peaks are identified by component fatty acids: Ln, linolenic; L, linoleic; O, oleic; P, palmitic; S, stearic. HPLC conditions: column, 5 μ m Adsorbosphere C₁₈ (250 \times 4.6 mm, i.d.) in series with 10 μ m Adsorbosphere UHS C₁₈ (250 \times 4.6 mm); solvent, linear gradient of acetonitrile/dichloromethane 70 : 30 to 40 : 60, by vol, over 120 min; detector, FID. APCI conditions: initial acetonitrile/dichloromethane 65 : 35, v/v, followed by a 20–25 min linear gradient acetonitrile/dichloromethane 60 : 40, v/v, and held until 85 min. (Reproduced with permission from Byrdwell WC, Emken EA, Neff WE and Adlof RO (1996) Quantitative analysis of triglycerides using atmospheric pressure chemical ionization-mass-spectrometry. *Lipids* 31: 919–935.)

pholipid fraction recovered from the preliminary isolation of the lipid classes, unless it already involved the separation of the individual phospholipid classes. The purified phospholipid classes can be separated further into molecular species by HPLC using the original molecules or their enzymatic or chemical transformation products.

Normal-phase HPLC

Normal-phase HPLC is well suited for the separation of the phospholipids. Various silica gel columns yield excellent separations of the major phospholipid classes which, in many instances, also provide a readily discernible separation of the minor components.

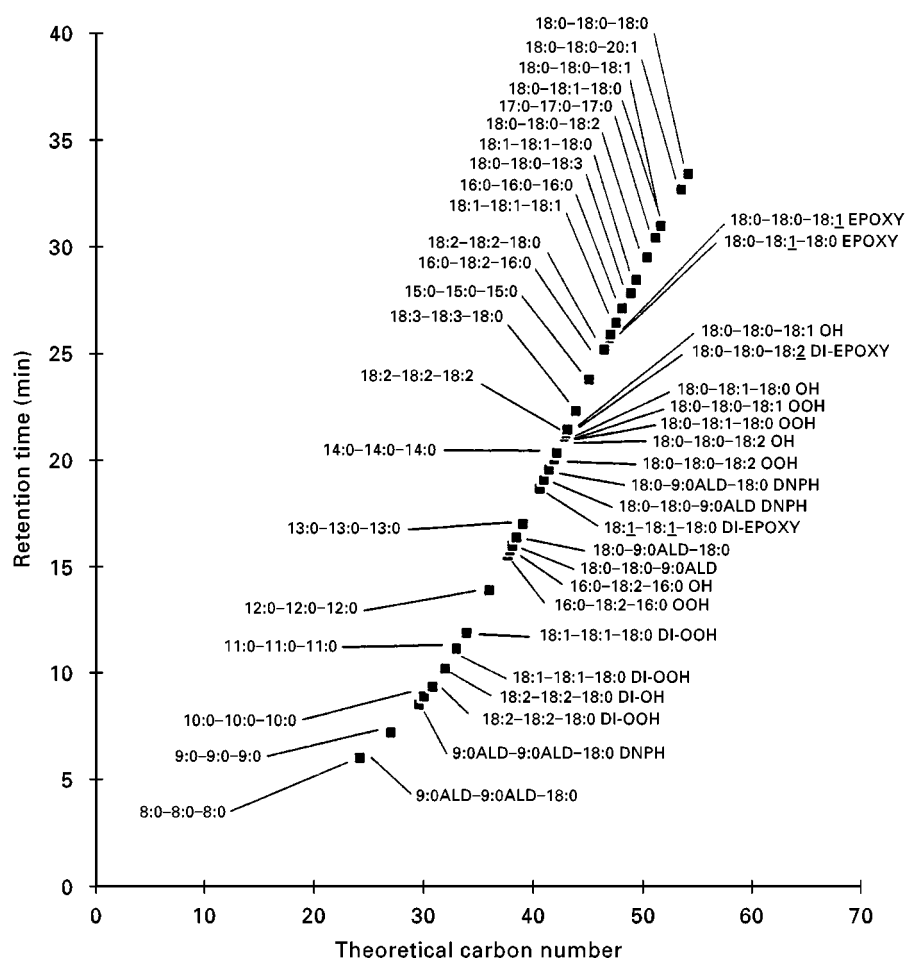


Figure 9 Plot of theoretical carbon numbers (TCN) versus retention times of reference oxo-triacylglycerols along with a series of saturated monoacid triacylglycerols. TCN and correction factors were calculated for oxotriacylglycerols and unsaturated triacylglycerols using the saturated triacylglycerols as a reference curve. (Reproduced with permission from Sjovald O *et al.*, 1997.)

Figure 15 shows the separation obtained with a silica gel column for the ethanolamine, choline, inositol and glycerol glycerophospholipids and sphingomyelin isolated from a subfraction of human high density lipoprotein preparation with online MS detection. In the positive ion mode only the choline-containing phospholipids are readily detected, although the ethanolamine glycerophospholipids can also be seen at low intensity. The acidic glycerol, inositol and serine phosphatides, along with any ethanolamine phospholipids, are best detected in the negative ion mode. The negative ion mode also registers the choline phospholipids as the chloride adducts. There is a complete baseline separation for all phospholipids without significant resolution of molecular species, except for SM, which is separated into long chain and short chain species.

Normal-phase HPLC with online MS can be used to assess the molecular species present in

the individual phospholipid classes. It is possible to obtain single ion chromatograms retrieved from the total positive ion current spectra for the major molecular species of the choline and ethanolamine phosphatides. In this normal-phase system the newly identified glycosylated diradylglycerophosphoethanolamine migrates with the front of the phosphatidylcholine peak. The single ion chromatograms retrieved by the computer from the total negative ion current permit accurate quantification of the major molecular species of the acidic glycerophospholipids.

Normal-phase HPLC can be used for the separation of the alkylacyl, alkenylacyl and diacyl subclasses of the ethanolamine glycerophospholipids as the trinitrophenyl derivatives. The diradyl subclasses of the choline glycerophospholipids cannot be separated by chromatography of the intact parent molecules. For this purpose, diradylglycerophosphocholines must be dephosphorylated and the re-

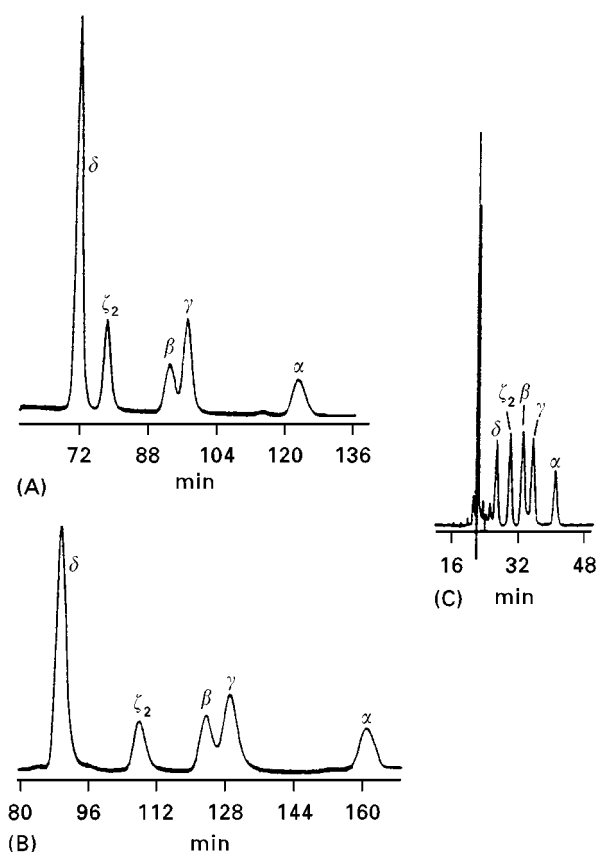


Figure 10 Reversed-phase HPLC separation of tocopherols. HPLC conditions: columns (A and B), 5 μ m Asahipak containing octadecyl polyvinyl alcohol phase; column C, 5 μ m Phenomenex Curosil-PFP phase (250 \times 4.6 mm i.d.); solvents: (A) acetonitrile/water (85 : 15, v/v); (B and C) methanol/water (87.5 : 12.5, by vol). (Reproduced with permission from Abidi and Mounts, 1997.)

sulting diradylglycerols converted into UV-absorbing or fluorescent derivatives (Table 2) prior to HPLC separation unless an ELSD system is used. The molecular species separation of the diradylglycerols is carried out by reversed-phase HPLC, as described for the diacylglycerols derived from triacylglycerols by Grignard degradation.

Reversed-phase HPLC

The total phospholipid mixture can also be separated on a reversed-phase column. Although this leads to extensive separation of the molecular species, there is little overlap among the different phospholipid classes. Both phospholipid classes and molecular species are readily identified and quantitated by online MS with ES ionization. Using 0.5% ammonium hydroxide in a water/methanol/hexane mixture on a C_{18} column, complex mixtures of phospholipid

classes and molecular species were identified mainly as protonated or natriated molecules.

The molecular species of the underivatized phospholipids can be separated by reversed-phase HPLC with a mixture of organic solvents and a counterion. The molecular species of intact aminophospholipids have previously been resolved as the UV-absorbing trinitrophenyl derivatives. The reversed-phase systems are also capable of separating the hydroxylated and hydroperoxidized glycerophospholipids from their unoxidized parent species.

Chiral-phase HPLC

The stereochemical configuration of phosphatidylglycerols has been assessed with chiral phases. Although natural phosphatidylglycerols possess two chiral carbons and are diastereoisomers, they are not readily separable by normal-phase columns. However, the bis-3,5-dinitrophenylurethanes can be separated by chiral-phase HPLC (Figure 16). The molecular species of all synthetic phosphatidylglycerol derivatives examined can be separated into diastereomeric peaks in a short time using a mobile phase of hexane/dichloromethane/methanol containing a small amount of trifluoroacetic acid.

Separation of Sphingolipids and Gangliosides

The neutral glycosphingolipids or cerebrosides are ceramide monohexosides, lactosides and higher sugar glycosides. The great complexity and number of new glycosphingolipid components being reported challenge the best contemporary methods of characterization. These lipids have been frequently investigated by FAB, chemical ionization and electron ionization MS with prior chromatographic separation. Likewise, the sulfatides and the sialic acid-containing glycosphingolipids (gangliosides) have been separated by HPLC prior to MS.

Normal-phase HPLC

A highly sensitive analytical method that allows the separation of ganglioside mixtures and quantification of individual nonderivatized gangliosides has been reported using Spherisorb- NH_2 . Gangliosides in the 2 pmol to 1 nmol range are separated on a 1 mm i.d. column with a gradient of acetonitrile/phosphate buffer. Figure 17 shows the resolution of standard gangliosides and gangliosides from the serum of a healthy human female and from human oligodendroglioma. Complete separations are obtained for GM3, GM2, GM1, GD3, GD1a, GD1b, GT1b and GQ1b. The

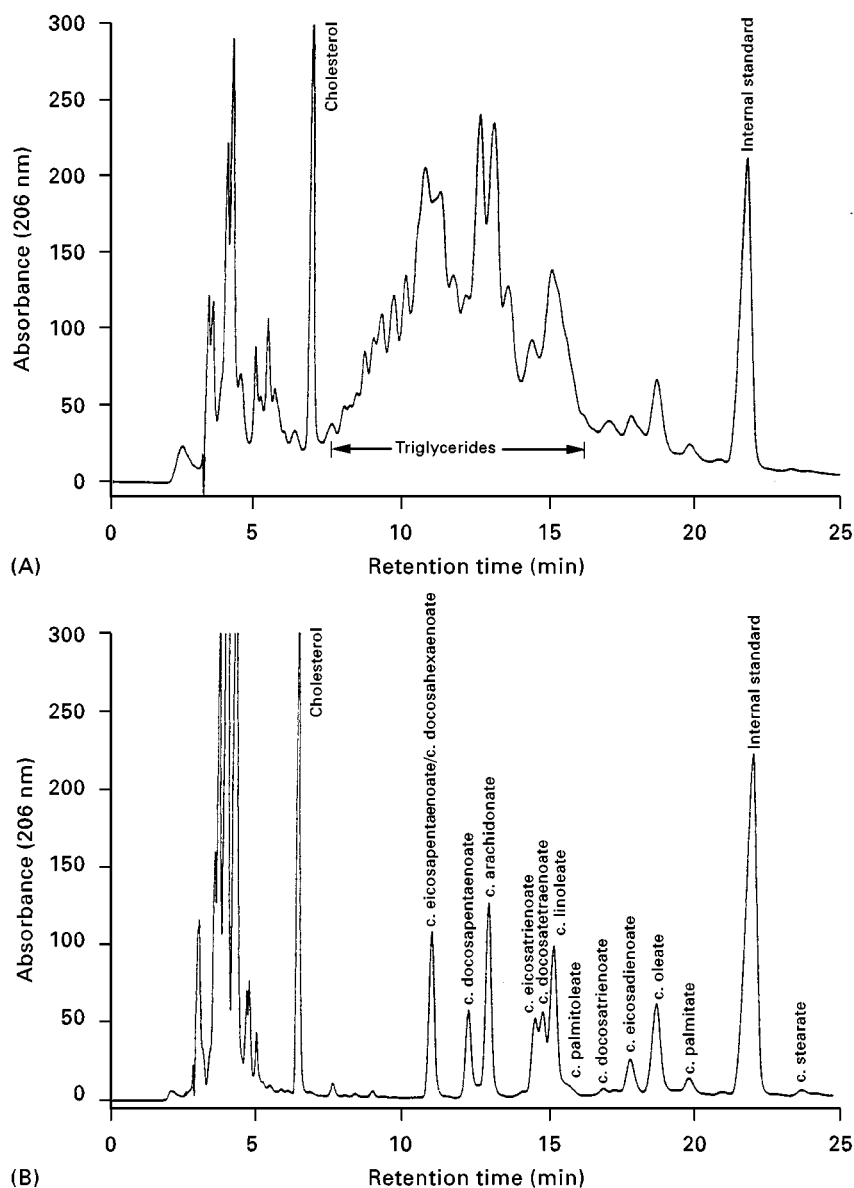


Figure 11 Reversed-phase HPLC of cholesteryl esters isolated from macrophages by lipid extraction and treatment of the extract with a dilute solution of ethanolic potassium hydroxide. Peak identification is given in the figure. HPLC conditions: column, 3 μ m Spherisorb ODS2 (250 \times 4 mm, i.d.); isocratic solvent, isopropanol/heptane/acetonitrile (35/12/52, by volume) and detected by UV absorption at 206 nm. (Reproduced with permission from Cullen P, Fobker M, Teglkamp K *et al.* (1997). An improved method for quantification of cholesterol and cholesteryl esters in human monocyte-derived macrophages by high performance liquid chromatography with identification of unassigned cholesteryl ester species by means of secondary ion mass spectrometry. *Journal of Lipid Research* 38: 401–409.)

new method of separation bypasses the earlier difficulties regarding baseline stability of the 195 nm absorption by using a high purity phosphate buffer.

Other workers have employed both FAB-MS and ES-MS to characterize monosialogangliosides of human myelogenous leukaemia HL60 cells and normal human leukocytes. The gangliosides were extracted and subjected to extensive segregation and examina-

tion of the selectin-binding ability of each fraction. Fractions were resolved on an Iatrobead column pre-equilibrated with isopropyl alcohol/hexane/water (55:40:5) and subjected to a linear gradient of isopropyl alcohol/hexane/water 55:40:5 to 55:25:20 with a flow rate of 1 mL min⁻¹. They were also reanalysed on a semipreparative Iatrobead column with a linear gradient of isopropyl alcohol/hexane/water 55:40:5 to 55:25:20 over

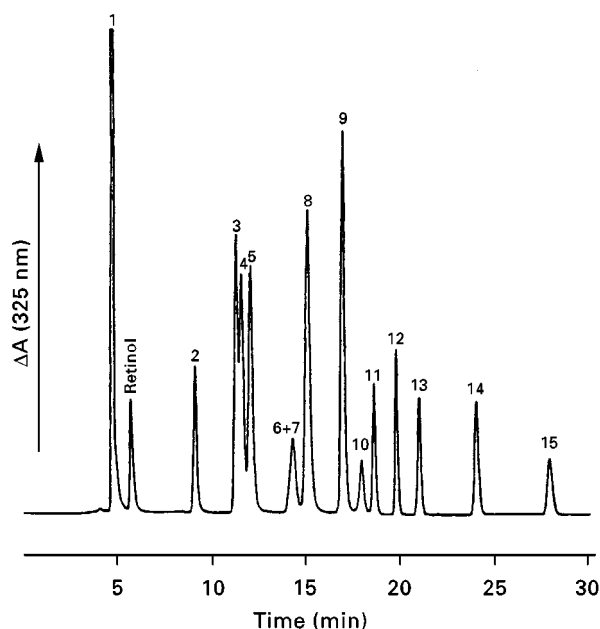


Figure 12 Reversed-phase HPLC of retinyl esters. Peak identification: 1, acetate; 2, caprate; 3, linolenate; 4, laurate; 5, arachidonate; 6/7, palmitoleate/linoleate; 8, myristate; 9, pentadecanoate; 10, oleate; 11, palmitate; 12, heptadecanoate; 13, stearate; 14, arachidate; 15, behenate. HPLC conditions: column, 5 μ m Suplex pKb 100 (250 \times 4.6 mm) with a 20 mm guard column; solvent, isocratic elution (14 min) with solvent A (acetonitrile/methanol/dichloromethane/hexane, 88 : 4 : 4 : 4, by volume) at 1 mL min⁻¹ followed by a linear gradient of 100% B (acetonitrile/methanol/dichloromethane/hexane, 70 : 10 : 10 : 10, by volume) over a 2 min period; isocratic elution with the final solvent composition continued for 14 min at 1.5 mL min⁻¹. Detection was at 325 nm. (Reproduced with permission from Wingerath T, Kirsch D, Spengler B *et al.* (1997) High performance liquid chromatography and laser desorption/ionization mass spectrometry of retinyl esters. *Analytical Chemistry* 69: 3855–3860.)

200 min with a flow rate of 0.5 mL min⁻¹. The final fractions from the normal-phase HPLC were analysed by TLC and the pure components subjected to negative and positive ion FAB-MS.

Table 2 Selected derivatives of diacyl and monoacylglycerols for UV and fluorescent detection

UV absorption	Fluorescent detection
Anthroyl derivatives	
Benzoates	
Dinitrobenzoates	
3,5-Dinitrophenylurethanes	Phenylurethanes
Naphthylethylurethanes	Naphthylurethanes
<i>p</i> -Nitrobenzoates	Anthrolyurethanes
Pentafluorobenzoates	

Modified with permission from Bell, 1997.

Table 3 Selected ester derivatives for UV and fluorescent detection of fatty acids

UV detection	Fluorescent detection
Anthrylmethyl	9-Anthrylmethyl
Benzyl	9-Aminophenanthrene
<i>p</i> -Bromophenacyl	4-Bromomethyl-7-acetoxycoumarin
<i>p</i> -Chlorophenacyl	9-Anthryldiazomethane
2-Naphthacyl	Dansyl-ethanolamine
<i>p</i> -Nitroanilides	4-Methyl-7-methoxycoumarin
<i>p</i> -Nitrobenzyl	4-Methyl-6,7-dimethoxycoumarin
<i>p</i> -Nitrophenacyl	4-Methyl-7-acetoxycoumarin
Pentafluorobenzyl	2-Naphthacyl
Phenacyl	
<i>p</i> -Phenphenacyl	

Modified with permission from Purdon, 1991.

Reversed-phase HPLC

Of the sphingolipids, the ceramides, cerebrosides and sphingomyelins have been most extensively studied by reversed-phase HPLC. Sphingomyelins obtained from bovine brain, chicken egg yolk and bovine milk fat were separated using a binary solvent system consisting of *n*-butanol/water isopropanol/isooctane on a C₁₈ column. The positive ion mass spectra exhibit prominent ions related to the amine base structure and fragments which can be utilized for identification of molecular species.

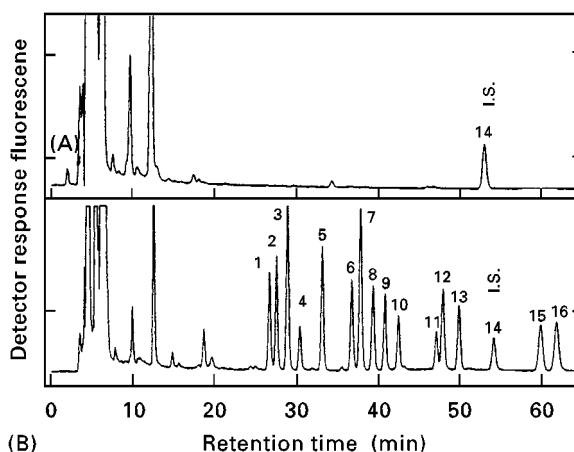


Figure 13 Reversed-phase separation of fatty acids as the 1-fluorescent pyrenyldiazomethane derivatives. Peak identification: 1, 20 : 5*n* - 3; 2, 14 : 1*n* - 9; 3, 18 : 3*n* - 3/18 : 3*n* - 6; 4, 22 : 6*n* - 3; 5, 20 : 4*n* - 6; 6, 14 : 0/16 : 2*n* - 9; 7, 18 : 2*n* - 6; 8, 20 : 3*n* - 6; 9, 22 : 4*n* - 6; 10, 24 : 5*n* - 6; 11, 18 : 1*n* - 9; 12, 16 : 0; 13, 24 : 4*n* - 6; 14, internal standard; 15, 20 : 1*n* - 9; 16, 18 : 0. HPLC conditions: column, 5 μ m LC-18 Supelcosil (250 \times 4.6 mm i.d.) with a Pelliguard precolumn (4.6 \times 20 mm) from Supelco; solvent: a gradient between water (solvent I) and acetonitrile (solvent II) was used as follows: 0–40 min, 90–100% solvent II and 40–70 min, isocratic 100% II at a flow rate of 1 mL min⁻¹. (Reproduced with permission from Brekke *et al.*, 1997.)

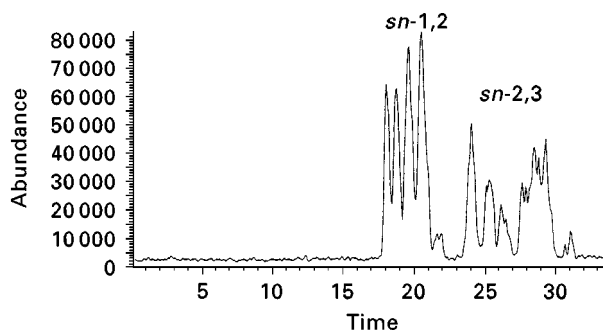


Figure 14 Chiral-phase HPLC of the dinitrophenyl urethane derivatives of the diacylglycerols from an oil rich in docosahexaenoic acid. *sn*-1-2-, *sn*-1,2-diacylglycerols; *sn*-2,3-, *sn*-2,3-diacylglycerols. HPLC conditions: chiral column, 25 cm \times 4.6 mm i.d. tube containing R-(+)-1-(1-naphthyl)-ethylamine polymeric phase chemically bonded to 30 nm wide-pore spherical silica (YMC-pack A-KO₃); solvent: isocratic hexane/dichloromethane/ethanol 40 : 10 : 1 by volume, at 0.5 mL min⁻¹; UV detector at 254 nm. (Reproduced with permission from Myher JJ, Kuksis A and Park PW (1996) Stereospecific analysis of docosahexaenoic acid-rich triacylglycerols by chiral-phase HPLC with on-line electrospray mass spectrometry. In: McDonald RE and Mossoba MM (eds) *New Techniques and Applications in Lipid Analysis*, pp. 100–120. Champaign, IL: American Oil Chemists' Society.)

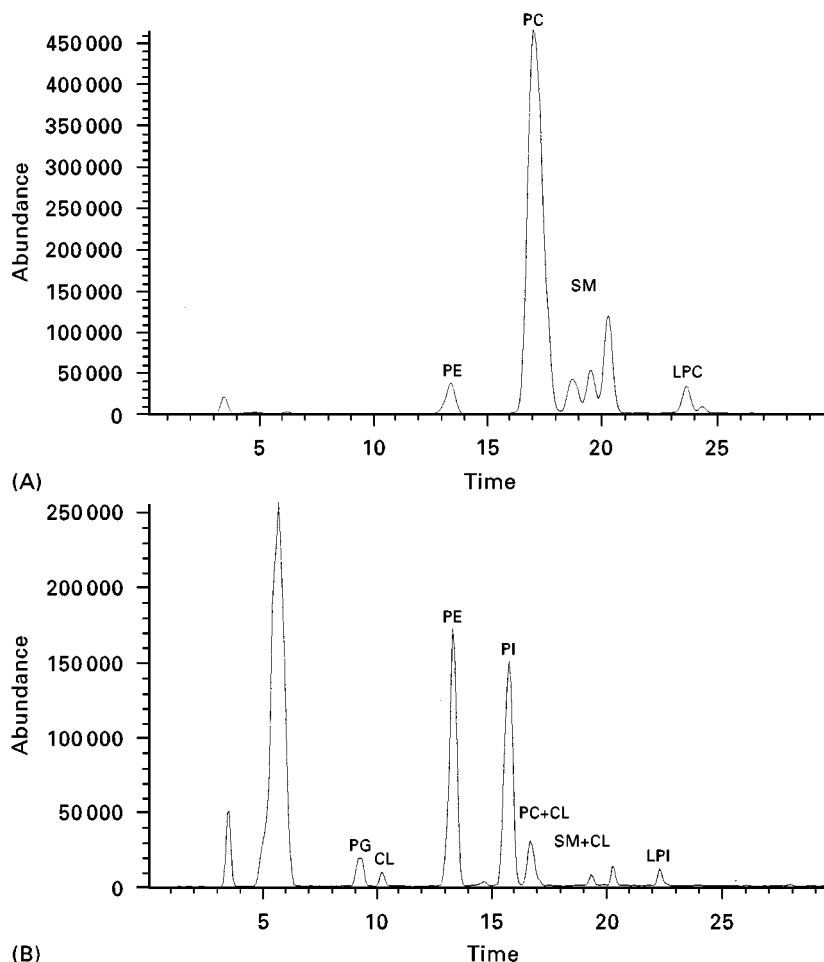


Figure 15 Normal-phase HPLC resolution of high density lipoprotein glycerophospholipids and sphingomyelins in (A) the positive and (B) negative ion mode as recorded by online electrospray mass spectrometry. Peak identification is as given in Figure 1; PAF, platelet-activating factor. HPLC conditions: column, 5 μ m Spherisorb (250 \times 4.6 mm i.d.); solvent, a linear gradient of 100% A (chloroform/methanol/30% ammonium hydroxide 80 : 19.5 : 0.5, by volume) to 100% B (chloroform/methanol/water/30% ammonium hydroxide 60 : 34 : 5.5 : 0.5, by volume) in 30 min. (Unpublished results of Kuksis A and Ravandi A, 1997.)

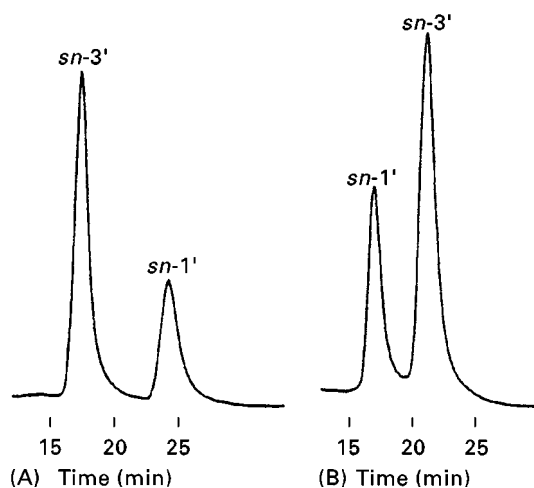


Figure 16 Chiral-phase HPLC resolution of the bis-3,5-dinitrophenylurethane derivatives of the diastereomeric 1,2-dilinoleoyl-*sn*-3-phospho-1'-*sn*-glycerol (*sn*-1') and 1,2-dilinoleoyl-*sn*-glycero-3-phospho-3'-*sn*-glycerol (*sn*-3) on liquid phases of opposite configuration. (A) (*R*)-(+)-1-(1-naphthyl)ethylamine column (YMC A-KO3); (B) (*S*)-(–)-1-(1-naphthyl)ethylamine column (YMC A-LO3); solvent, hexane/dichloromethane/methanol/trifluoroacetic acid (60/20/20/0.2, by volume) at 1.0 mL min^{–1}; column temperature 10°C. (Reproduced with permission from Itabashi and Kuksis, 1997.)

See also: II/Chromatography: Liquid: Derivatization; Detectors: Mass Spectrometry; Detectors: Ultraviolet and Visible Detection; Mechanisms: Chiral; Mechanisms: Normal Phase. III/Lipids: Thin-Layer (Planar) Chromatography. Silver Ion: Liquid Chromatography; Thin-Layer Planar Chromatography.

Further Reading

- Abidi SL and Mounts TL (1997) Reversed-phase high-performance liquid chromatographic separations of tocopherols. *Journal of Chromatography A* 782: 25–32.
- Bell MV (1997) Separations of molecular species of phospholipids by high-performance liquid chromatography. In: Christie WW (ed.) *Advances in Lipid Methodology – Four*, pp. 45–82. Dundee: Oily Press.
- Bligh EG and Dyer WJ (1959) A rapid method of total lipid extraction and purification. *Canadian Journal of Biochemistry and Physiology* 37: 911–917.
- Brekke O-L, Sagen E and Bjerve KS (1997) Tumor necrosis factor-induced releases of endogenous fatty acids analyzed by a highly sensitive high-performance liquid chromatography method. *Journal of Lipid Research* 38: 1913–1922.
- Dreyfus H, Guerold B, Freysz L and Hicks D (1997) Successive isolation and separation of the major lipid fractions including gangliosides from single biological samples. *Analytical Biochemistry* 249: 67–78.

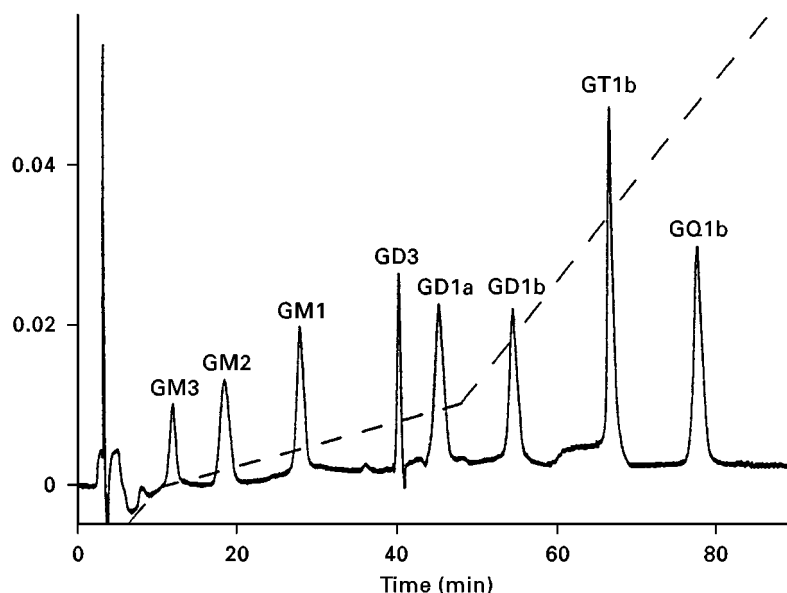


Figure 17 Normal-phase HPLC of standard gangliosides. Peak identification: GM3, GM2, GM1, GD3, GD1a, GD1b, GT1b and GQ1b denote gangliosides according to Svennerholm. HPLC conditions: column, microbore 3 μ m, Spherisorb-NH₂ (250 \times 1 mm i.d.). A guard column (1 \times 20 mm) was filled with the same material; solvent gradient: as indicated by dashed lines; it starts with 100% A, 0% B, and ends with 0% A, 100% B. Solvent A, acetonitrile/5 mmol L^{–1} phosphate buffer, pH 5.6 (83 : 17, v/v); solvent B: acetonitrile/20 mmol L^{–1} phosphate buffer, pH 5.6 (1 : 1, v/v) at 88 μ L min^{–1} at 20°C. (Reproduced with permission from Wagener R, Kobbe B and Stoffel W (1996) Quantification of gangliosides by microbore high performance liquid chromatography. *Journal of Lipid Research* 37: 1823–1829.)

- Folch J, Lees M and Sloane-Stanley GH (1957) A simple method for the isolation and purification of total lipids from animal tissues. *Journal of Biological Chemistry* 226: 497–509.
- Itabashi Y and Kuksis A (1997) Reassessment of stereochemical configuration of natural phosphatidylglycerols by chiral-phase high-performance liquid chromatography and electrospray mass spectrometry. *Analytical Biochemistry* 254: 49–56.
- Kaufmann P (1992) Chemometrics in lipid analysis. In: Christie WW (ed.) *Advances in Lipid Methodology – One*, pp. 149–180. Dundee: Oily Press.
- Kuksis A (1996) Analysis of positional isomers of glycerolipids by non-enzymatic methods. In: Christie WW (ed.) *Advances in Lipid Methodology – Three*, pp. 1–36. Dundee: Oily Press.
- Kuksis A (1997) Mass spectrometry of complex lipids. In: Hamilton RJ (ed.) *Lipid Analysis of Oils and Fats*, pp. 181–249. London: Chapman & Hall.
- Kuksis A and Myher JJ (1995) Application of tandem mass spectrometry for the analysis of long-chain carboxylic acids. *Journal of Chromatography B* 671: 35–70.
- Laakso P and Christie WW (1990) Chromatographic resolution of chiral diacylglycerol derivatives: potential in the stereospecific analysis of triacyl-*sn*-glycerols. *Lipids* 25: 349–353.
- Marai L, Kuksis A and Myher JJ (1994) Reversed-phase liquid chromatography-mass spectrometry of the uncommon triacylglycerol structures generated by randomization of butteroil. *Journal of Chromatography A* 672: 87–99.
- Moreau A (1996) Quantitative analysis of lipids by HPLC with flame-ionization detector or an evaporative light-scattering detector. In: Shibamoto T (ed.) *Lipid Chromatographic Analysis*, pp. 251–272. New York: Marcel Dekker.
- Myher JJ and Kuksis A (1995) General strategies in chromatographic analysis of lipids. *Journal of Chromatography B* 671: 3–33.
- Myher JJ, Kuksis A and Park PW (1997) Stereospecific analysis of docosahexaenoic acid-rich triacylglycerols by chiral-phase HPLC with on-line electrospray mass spectrometry. In: McDonald RE and Mossoba MM (eds) *New Techniques and Applications in Lipid Analysis*, pp. 100–120. Champaign, IL: American Oil Chemists' Society Press.
- Nikolova-Damyanova B (1997) Reversed-phase high-performance liquid chromatography: general principles and application to the analysis of fatty acids and triacylglycerols. In: Christie WW (ed.) *Advances in Lipid Methodology – Four*, vol. 8, pp. 193–251. Dundee, Scotland: Oily Press Lipid Library.
- Patton GM, Fasulo JM and Robins SJ (1982) Separation of phospholipids and individual molecular species of phospholipids by high-performance liquid chromatography. *Journal of Lipid Research* 23: 190–196.
- Powell WS, Wang L and Khanapure SP *et al.* (1997) High-pressure liquid chromatography of oxo-eicosanoids derived from arachidonic acid. *Analytical Biochemistry* 247: 17–24.
- Prieto JA, Ebri A and Collar C (1992) Optimized separation of nonpolar and polar lipid classes from wheat flour by solid-phase extraction. *Journal of American Oil Chemists' Society* 69: 387–391.
- Purdon MP (1991) Application of HPLC to lipid separation and analysis: mobile and stationary phase selection. In: Perkins EG (ed.) *Analyses of Fats, Oils and Lipoproteins*, pp. 166–191. Champaign, IL: American Oil Chemists' Society.
- Redden PR and Huang Y-S (1991) Automated separation and quantitation of lipid fractions by high-performance liquid chromatography and mass detection. *Journal of Chromatography Biomedical Applications* 567: 21–27.
- Sjovall O, Kuksis A, Marai L and Myher JJ (1997) Elution factors of synthetic oxotriacylglycerols as an aid in identification of peroxidized natural triacylglycerols by reverse-phase high performance liquid chromatography with electrospray mass spectrometry. *Lipids* 32: 1211–1218.
- Takagi T (1991) Chromatographic resolution of chiral lipid derivatives. *Progress in Lipid Research* 29: 277–298.

Thin-Layer (Planar) Chromatography

B. Fried, Lafayette College, Easton, PA, USA

Copyright © 2000 Academic Press

Introduction

Thin-layer chromatography (TLC) is widely used for the separation and identification of lipid classes with silica gel as the most frequently used stationary phase. Numerous mobile phases (solvent systems) are avail-

able for the separation of lipids and there are many nonspecific and specific detection reagents (visualization reagents) that are useful for detection.

There is no consensus as to the definition of a lipid. Kates considers lipids as compounds generally insoluble in water but soluble in a variety of organic solvents. He recognized the following classes of lipids: hydrocarbons, alcohols, aldehydes, fatty acids and derivatives such as glycerides, wax esters, phospholipids, glycolipids and sulfolipids. Gunstone and

Table 1 Lipids frequently separated by TLC

<i>Neutral lipids</i>	<i>Phospholipids</i>	<i>Glycolipids</i>
Diacylglycerols	Diphosphatidylglycerol	Gangliosides, e.g. monosialogangliosides; disialogangliosides; trisialogangliosides; tetrasialogangliosides
Free fatty acids Free sterols	Lysophosphatidylcholine Lysophosphatidylethanolamine	Plant and bacterial glycolipids, e.g. mono- and digalactosyldiacylglycerols
Monoacylglycerols Triacylglycerols	Phosphatidic acid Phosphatidylcholine	Sphingolipids, e.g. ceramides; sphingomyelin; cerebrosides; globosides; sulfatides
Wax esters	Phosphatidylethanolamine Phosphatidylglycerol Phosphatidylinositol Phosphatidylserine Phosphonolipids	

Hersl f consider that lipids are compounds based on fatty acids or closely related compounds such as the corresponding alcohols or sphingosine bases. Christie noted that a variety of diverse compounds usually soluble in organic solvents are classified as lipids and set up a convenient system of lipid classification that is followed here. His system considers the simple lipids (compounds that upon hydrolysis yield no more than two types of primary products per mole), also referred to as neutral or apolar lipids. According to Christie, the polar or complex lipids (compounds that upon hydrolysis yield three or more primary products per mole) are the glycerophospholipids (or simply phospholipids) and the glycolipids (also termed glyceroglycolipids or glycosphingolipids), including gangliosides. **Table 1** lists the major neutral lipids, phospholipids and glycolipids of interest in studies on the TLC of lipids.

Functions

Lipids are involved in many functions of animals, plants and microorganisms and these functions are often studied using TLC. Lipids are important as storage depots for energy reserve. In mammals the storage depot is usually in the form of adipose tissue and TLC analysis shows that the major storage lipids are triacylglycerols, free fatty acids and mixed glycerides. Less information is available on lipid storage in invertebrates but TLC studies have shown that storage sites exist in invertebrates, including chlorogagen tissue in earthworms, the digestive glands in snails and specialized organs called trophosomes in some nematodes. As shown by TLC, triacylglycerols are major storage components in invertebrates. Lipids

(mainly sterols, phosphoglycerides, glycolipids and sphingolipids) are important in the structural integrity of cells and comprise the major components of membranes. Phosphoglycerides in the membranes of nervous tissue are involved in the transmission of electrical signals. Phosphoinositides are involved in cellular communication. Neutral lipids serve as pheromones or carrier of pheromones in both invertebrates and vertebrates. TLC has been used extensively for at least tentative identification of these pheromones.

Christie has documented numerous lipid functions, including their role in abnormal lipid metabolism associated with various disorders; accumulation of lipids associated with coronary blood vessel and cardiac diseases; the importance of lipids in human welfare, including nutrition and disease; the role of lipids as important dietary factors and suppliers of calories for humans and animals; and the importance of lipids to the palatability of foods.

Glycolipids play an important role in cellular metabolism and TLC has helped to elucidate this role. Glycolipids occur at the external surfaces of cell membranes and help regulate cell growth; they also serve as receptors for toxins and hormones and modulate immune responses.

Sample Preparation

Lipid analysis should be done as soon as possible after samples have been obtained from plants and animals. If this is not possible, samples should be maintained at 4 C overnight or at  20 C for longer periods. Tissues that have been fixed in formalin, alcohol or other preservatives should not be used. Glass vessels

Table 2 Frequently used methods for sample preparation of lipids

<i>Lipid extraction technique</i>	<i>Comments</i>
<i>Vertebrate and invertebrate organ and tissue samples</i>	
Chloroform-methanol (2 : 1); typically 1 part of tissue or fluid to 20 parts of the solvent	Most widely used method of lipid extraction; useful for TLC of neutral and complex lipids
Chloroform-methanol-H ₂ O (1 : 2 : 0.8); following extraction, dilute the sample with 1 vol of chloroform and 1 vol of water to get a biphasic system	Particularly useful for extraction of more polar lipids such as gangliosides
Pre-extraction of brain tissue with 0.25% acetic acid followed by chloroform-methanol (2 : 1)	Nonlipid material first removed with the acetic acid; relatively pure lipid fraction then obtained by treatment with chloroform-methanol
Chloroform-methanol (1 : 2); typically 1 part of tissue to 3 parts of solvent mixture	Good for large amounts of tissue where complete recovery of lipid is not needed; does not use as much solvent as the previous extraction techniques
<i>Blood and amniotic fluids</i>	
Chloroform-isopropanol-water (7 : 11 : 2)	Extracts lipids but not pigments; lipids are not contaminated with blood pigments; neutral and complex lipids are quantitatively extracted
Amniotic fluid or blood plasma (about 1 mL) is added directly to a Spice C ₁₈ solid-phase extraction cartridge (Analtech, Newark, DE); the analyte is eluted with chloroform-methanol	Good separation of phospholipids achieved, since most extraneous material is removed; technique also useful for separating neutral lipids from steryl esters and phospholipids
<i>Plant tissues</i>	
Tissues first treated with isopropanol and then chloroform-isopropanol (1 : 1) prior to usual chloroform-methanol (2 : 1) extraction procedure	Isopropanol inhibits the action of plant lipases

are recommended for lipid analysis, along with aluminium foil or Teflon-lined lids. Plastic vessels should be avoided because they may dissolve in the organic solvents used during the TLC process. Most samples are extracted in mixtures of chloroform-methanol (Table 2) to remove quantitatively the lipids prior to subsequent chromatographic techniques. The first procedure listed in Table 2, usually referred to as the Folch extraction procedure, is the one most frequently used. In brief, this procedure generally uses a 20 : 1 ratio of chloroform-methanol (2 : 1) to sample so that, for example, if 100 mg of tissue is being extracted, 2 mL of chloroform-methanol is suitable for total lipid extraction. The tissue is usually extracted in a glass homogenizer and the extract passed through a glass wool filter; the lipid-containing filtrate is collected and used for TLC following concentration of the sample under nitrogen gas. Many variants of this extraction procedure are available.

Chromatographic Systems

The chromatographic system consists of the sample mixture (the analyte), the stationary phase (the sorbent) and the mobile phase (the development solvent). Along with the sample mixture, lipid standards (usually obtained from a commercial supplier) are

run at the same time. Development of the plate in a suitable mobile phase, from the origin to the solvent front, constitutes the essential part of the chromatographic process. Following development, the plate is allowed to dry and the analytes are detected (see detection, next section) and compared to the standards on the plate.

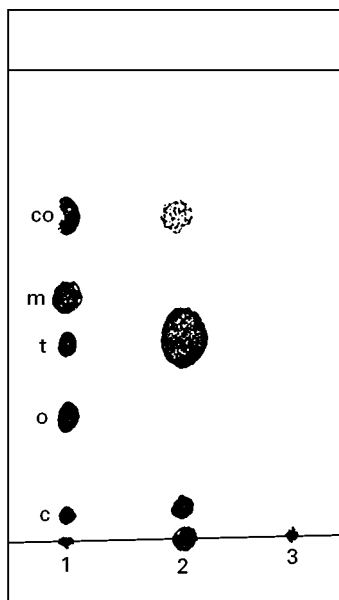
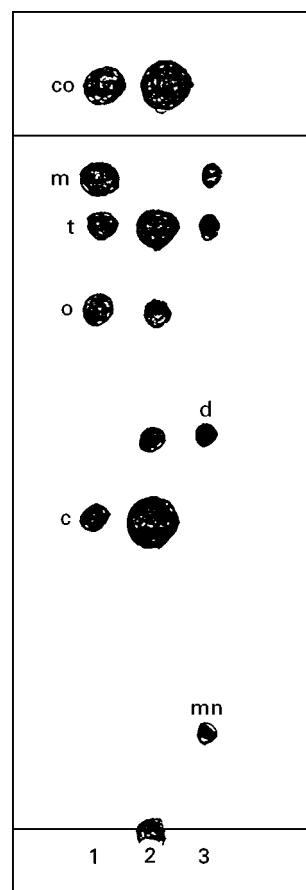
Numerous stationary phases are available for TLC, but the one of choice for lipid work is silica gel. There are many different types of silica gel plates and sheets and most workers use commercially prepared plates. Silica gel plates can be modified for particular purposes. For example, silver nitrate plates can be prepared and used to separate *cis*-enoic compounds based on unsaturation. Other examples exist that show how commercial and home-made silica gel plates can be altered for specialized lipid applications. The 1990s have seen considerable use of high performance thin-layer chromatography (HPTLC) for lipid analysis. HPTLC plates are made of fine silica particles of narrow size distribution, and have excellent resolving power. The quantity of sample applied to such plates can be reduced markedly from that applied to conventional TLC layers. Many samples can be analysed on the same plate with minimal amounts of mobile phase. HPTLC plates are now being used frequently in densitometric studies on lipids.

Table 3 R_F values of common neutral lipids separated in five frequently used solvent systems on silica gel

Compound	$R_F \times 100$				
	S_1	S_2	S_3	S_4	S_5
Cholesteryl esters	97	97	85	94	90
Triacylglycerols	63	79	70	60	82
Free fatty acids	42	21	62	39	50
Cholesterol	28	42	38	19	30
1,3-Diacylglycerols	24	66	46	21	40
1,2-Diacylglycerols	21	53	41	15	25
Monoacylglycerols	8	11	10	2	5

S_1 , hexane–diethyl ether–formic acid (80 : 20 : 2). S_2 , toluene–diethyl ether–ethyl acetate–acetic acid (80 : 10 : 10 : 0.2). S_3 , isopropyl ether–acetic acid (96 : 4) followed by petroleum ether–diethyl ether–acetic acid (90 : 10 : 1) in the same direction. S_4 , petroleum ether–diethyl ether–acetic acid (80 : 20 : 1). S_5 , heptane–isopropyl ether–acetic acid (60 : 40 : 4).

Numerous mobile phases are available for lipid TLC and most are used with a single development in the ascending mode. However, some systems have been designed for two or more developments in the same direction. A good example of this is the classical Skipski system (Table 3) that uses two developments

**Figure 1** Separation of a hen's egg yolk–saline extract on a silica gel sheet. Lipids were developed 10 cm from the origin in petroleum ether–diethyl ether–acetic acid (80 : 20 : 1) and detected by spraying with 5% phosphomolybdic acid in ethanol. Lane 1 contains a neutral lipid mix consisting of equal parts of cholesterol (c), oleic acid (o), triolein (t), methyl oleate (m) and cholesteryl oleate (co). Lane 2 shows the presence of triacylglycerols and free sterols as the predominant neutral lipids in the yolk–saline extract. Lane 3 contains saline alone that is neutral lipid-negative. (Reproduced with permission from Fried and Sherma (1999).)**Figure 2** Separation of a snail liver extract on a silica gel sheet using the dual solvent system of Skipski (see text). Lane 1 contains a neutral lipid mix as described in Figure 1. Lane 2 shows the separation of snail neutral lipids; note the abundance of free sterols and cholesteryl esters in this tissue. Lane 3 contains a neutral lipid mix with equal parts of monolein (mn), diolein (d), triolein (t), and methyl oleate (mm). (Reproduced with permission from Fried and Sherma (1999).)

in the same direction. Some mobile phases have been designed with two-dimensional TLC in mind, in which the second development is done after the plate is turned through a 90° angle.

Of the many unidimensional solvent systems available to resolve neutral lipids, the Mangold system and its modifications are most frequently used (Figure 1). This system consists of different combinations of petroleum ether (or hexanes), diethyl ether and acetic acid with a typical ratio of 80 : 20 : 1 v/v (petroleum ether–diethyl ether–acetic acid; Table 3). Changes in the ratios will affect R_F values of the neutral lipids being separated. Double development in the same direction as in the Skipski system is used to ensure good separation of glycerols from free fatty acids and free sterols (Figure 2). Although two-dimensional systems are infrequently used to separate neutral lipids, an example of such use is shown in

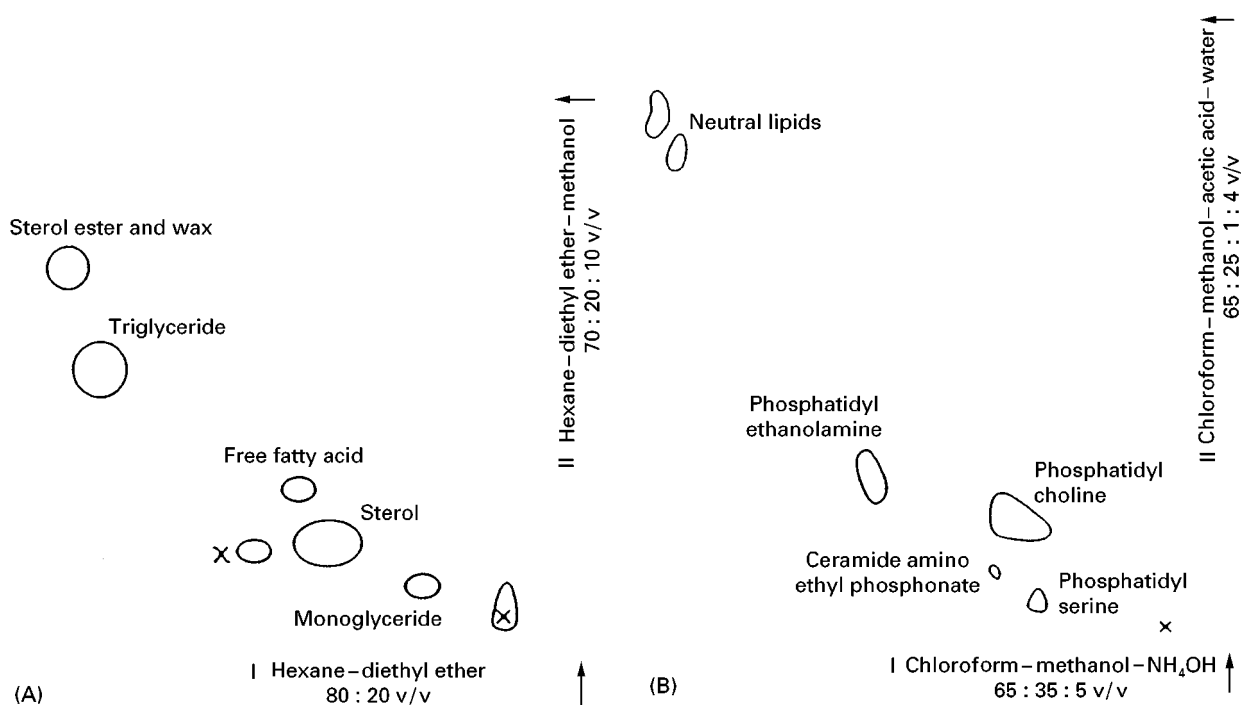


Figure 3(A) Chromatogram of the neutral lipids from an extract of the digestive gland-gonad (DGG) complex of the medically important snail *Biomphalaria glabrata*. The silica gel G plate was developed in the first direction in hexane-diethyl ether (80 : 20) and in the second direction in hexane-diethyl ether-methanol (70 : 20 : 10). Lipids were detected by spraying the plate with H_2SO_4 . (Reproduced with permission from Thompson SN (1987) *Comparative Biochemistry and Physiology* 87B: 357–361.) **(B)** Chromatogram of phospholipids from a similar extract as in Figure 3(A). The silica gel plate was developed in the first direction in chloroform-methanol- NH_4OH (65 : 35 : 5) and in the second direction in chloroform-methanol-water-acetic acid (65 : 25 : 4 : 1). Phospholipids were detected using various specific phospholipid detection reagents. (Reproduced with permission from Thompson SN (1987) *Comparative Biochemistry and Physiology* 87B: 357–361.)

Figure 3A, where a neutral lipid map is obtained. Two-dimensional development is used more frequently to resolve complex lipid mixtures and Figure 3B shows such a chromatogram resolving phospholipids in the medically important snail *Biom-*

phalaria glabrata. Table 4 shows the most widely used solvent systems for two-dimensional separations of complex lipids in animal and plant tissues.

Numerous one-dimensional systems for phospholipids are available. The commonly used ones for

Table 4 Four recommended solvent systems for two-dimensional separations of phospholipids and glycolipids on silica gel

System	Direction	Solvent composition and ratio	Comments
A	First	Chloroform-methanol-water (65 : 25 : 4)	Systems A and B are good for separating polar lipids of animal tissue on silica gel G; 10–15 complex lipids are separated
	Second	<i>n</i> -Butanol-acetic acid-water (60 : 20 : 20)	
B	First	Chloroform-methanol-28% aq. NH_3 (65 : 35 : 5)	
	Second	Chloroform-acetone-methanol-acetic acid-water (10 : 4 : 2 : 2 : 1)	
C	First	Chloroform-methanol-7 mol L^{-1} NH_4OH (65 : 30 : 4)	Good for separating bacterial polar lipids on silica gel G; 10–15 polar lipids are separated
	Second	Chloroform-methanol-acetic acid-water (170 : 25 : 25 : 6)	
D	First	Chloroform-methanol-0.2% aq. CaCl_2 (60 : 35 : 8)	Good for separating a wide variety of ganglioside species on HPTLC plates
	Second	<i>n</i> -Propanol-water-28% aq. NH_3 (75 : 25 : 5)	

separating phospholipids on silica gel are shown in Table 5. The most widely used system is that of Wagner (see S_5 in Table 5), consisting of chloroform-methanol-water (65 : 25 : 4 v/v). In this system, the neutral lipids are moved as one or several bands near the solvent front and the common phospholipids of plant and animal tissues are clearly resolved. Figure 4 shows a chromatogram of such a separation.

Glycolipid separation by unidimensional chromatography can be achieved in mobile phases consisting of various combinations of chloroform-methanol-water or chloroform-acetone-methanol-acetic acid-water. However, unidimensional separation of glycolipids is best done in the absence of phospholipids. Because glycolipids are difficult to separate completely by one-dimensional TLC, various two-dimensional procedures have been designed. A recommended two-dimensional system for glycolipids is chloroform-methanol-7 mol L⁻¹ ammonium hydroxide (65 : 30 : 4 v/v) in the first direction and chloroform-methanol-acetic acid-water (170 : 25 : 25 : 6 v/v) in the second direction.

One-dimensional TLC can be used to separate gangliosides with various combinations of chloroform-methanol-water or *n*-propanol-water as solvent systems. As noted for glycolipids, because of the diversity of oligosaccharides associated with gangliosides, it is difficult to achieve complete separation of these lipids using one-dimensional TLC. Thus, various maps have been prepared in which ganglioside species have been separated in two-dimensional systems. These maps follow the nomenclature of Svennerholm and use esoteric designations

Table 5 R_F values of common phospholipids separated in five frequently used solvent systems on silica gel

Compound	$R_F \times 100$				
	S_1	S_2	S_3	S_4	S_5
Diphosphatidylglycerol	91	94	—	—	—
Phosphatidylglycerol	—	—	90	78	—
Phosphatidylethanolamine	65	56	81	59	40
Phosphatidylserine	—	47	51	47	13
Phosphatidylinositol	—	34	34	52	13
Phosphatidylcholine	24	21	90	30	20
Lysophosphatidylcholine	6	6	—	—	6

S_1 , chloroform-methanol-water (25 : 10 : 1). S_2 , chloroform-methanol-acetic acid-water (25 : 15 : 4 : 2). S_3 , chloroform-light petroleum-methanol-acetic acid (50 : 3 : 16 : 1). S_4 , chloroform-ethanol-triethylamine-water (30 : 34 : 30 : 8). S_5 , chloroform-methanol-water (65 : 25 : 4).

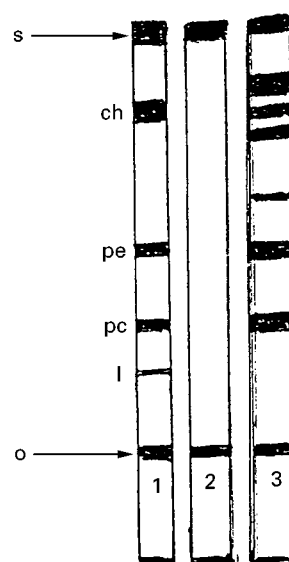


Figure 4 Separation of phospholipids extracted from snail-conditioned water (SCW) on a silica gel plate in the Wagner solvent system (see text). Lane 1 contains a standard with equal amounts of lysophosphatidylcholine (l), phosphatidylcholine (pc), phosphatidylethanolamine (pe) and cholesterol (ch). Lane 2 is a water blank without snails and is lipid-negative. Lane 3 contains SCW and shows that snails release significant amounts of phosphatidylcholine (pc) and phosphatidylethanolamine (pe), along with an unidentified component that migrates ahead of the pe. The bands near the solvent front are neutral lipids. Note the origin (o) and the solvent front (s). (Reproduced with permission from Fried and Sherma (1999).)

to indicate the nature of the gangliosides being separated. Details of this work are beyond the scope of this article. Experience, patience, and trial and error are needed to effect good separations of glycolipids and gangliosides with one- and two-dimensional TLC.

Detection

Following development, lipids are usually detected by a wide variety of detection (visualizing) agents either sprayed or dipped on to the plate. Detection reagents may be nondestructive and reversible such as iodine or destructive and nonreversible such as sulfuric acid. The afore-mentioned agents are considered general because they react with numerous different compound types. Table 6 provides a list of such general detection reagents frequently used to localize lipids on TLC plates. More or less specific detection reagents are used widely in TLC lipid studies and they generally indicate a particular compound or functional group, e.g. ninhydrin is used to localize amine groups associated with phospholipids such as phosphatidylserine or phosphoethanolamine. A list of spe-

Table 6 Five nonspecific reagents useful for the detection of lipids on TLC plates

Reagents	Procedure	Results
Iodine	Spray as 1% alcoholic solution or place a few crystals in the bottom of a closed tank	Dark-brown spots on a pale yellow or tan background in a few minutes
2',7'-Dichlorofluorescein	Spray with a 0.2% solution in 95% ethanol. Observe in UV light	Saturated and unsaturated polar lipids give green spots on purple background
Phosphomolybdic acid	Spray with a 5% solution in ethanol; heat at 100°C for 5–10 min	Blue-black spots on yellow background
Sulfuric acid	Spray with 50% aq. H ₂ SO ₄ ; heat as above	Black spots on a colourless background
Cupric acetate–phosphoric acid	Dissolve 3 g of cupric acetate in 100 ml of an 8% aq. phosphoric acid solution. Heat at 130–180°C for up to 30 min	Black spots on a colourless background

cific detection reagents frequently used in lipid TLC is shown in Table 7.

Quantification

There are many methods available for quantifying lipids using TLC. Some involve scraping and eluting lipids from the plate followed by spectrophotometric, gravimetric or chromatographic determination. The 1990s saw widespread use of direct *in situ* quantification, usually by densitometric methods, and an extensive literature is now available. Densitometry is performed in the reflection or transmittance mode with a specific brand of commercial densitometer. Any lipid that can be detected by ultraviolet or visible light is subject to densitometric analysis. Suitable standards, usually purchased from a commercial supplier, are needed and should match closely the compounds of interest. Quantification involves

bracketing the analyte between two standards, one of slightly lower concentration, and the second of slightly higher concentration. Standards can be used to construct a calibration curve.

A list of recent TLC lipid applications by densitometry for the quantification of lipids is shown in Table 8.

Concluding Remarks and Future Developments

The most extensive use of TLC is for the analysis of pharmaceuticals, followed by all aspects of lipid analysis. Silica gel TLC is an excellent tool for the separation and identification of neutral and complex lipid classes. Densitometry allows for the quantification of these compounds at least at the class level. Numerous specific detection reagents are helpful for identifying lipids. Moreover, techniques in which

Table 7 Specific chemical detection reagents for various lipids

Compound class	Reagent	Results
Cholesterol and cholesteryl esters	Ferric chloride	Cholesterol and cholesteryl esters appear as red-violet spots
Free fatty acids	2',7'-Dichlorofluorescein–aluminium chloride–ferric chloride	Free fatty acids give a rose colour
Lipids containing phosphorus	Molybdic oxide–molybdenum Zinzadze reagent	Phospholipids appear as blue spots on a white background within 10 min of spraying the plate
Choline-containing phospholipids (phosphatidylcholine and lysophosphatidylcholine)	Potassium iodide–bismuth subnitrate Dragendorff reagent	Choline-containing lipids appear in a few minutes as orange-red spots
Free amino groups (phosphatidyl-ethanolamine and phosphatidylserine)	Ninhydrin	Lipids with free amino groups show as red-violet spots
Glycolipids	α -Naphthol–sulfuric acid	Glycolipids (cerebrosides, sulfatides, gangliosides, and others) appear as yellow spots
Gangliosides	Resorcinol	Gangliosides appear as a violet-blue colour; other glycolipids appear as yellow spots

Table 8 Selected applications of densitometric TLC to the quantitative analysis of lipids

Material	Comments
Neutral lipids in egg yolk	HPTLC silica gel; Mangold solvent system of petroleum ether–diethyl ether–acetic acid (80 : 20 : 2) for determination of cholesterol, triacylglycerols, and free fatty acids, and <i>n</i> -hexane–petroleum ether–diethyl ether–acetic acid (50 : 20 : 5 : 1) for cholesteryl esters. Lipid detection and quantification as described for neutral lipids in <i>Biomphalaria glabrata</i> snails in this table
Neutral lipids in <i>Biomphalaria glabrata</i> snails	HPTLC silica gel plates; petroleum ether–diethyl ether–acetic acid (80 : 20 : 2) mobile phase; detection by spraying with 5% ethanolic phosphomolybdic acid; lipid zones measured by scanning at 700 nm with a Shimadzu CS 930 TL densitometer operated in the single-beam reflectance mode
Phospholipids in <i>Biomphalaria glabrata</i> snails	HPTLC silica gel plates; multiple developments in a chloroform–methanol–isopropanol–0.25% and KCl–ethyl acetate (30 : 9 : 25 : 6 : 18) mobile phase; detection by spraying with 10% cupric sulfate–8% phosphoric acid solution; phospholipids measured by reflectance scanning at 400 nm with a Shimadzu CS-930 densitometer in the single-lane/single-beam mode
Lecithin and sphingomyelin from amniotic fluid	Silica gel plates developed in chloroform–methanol–water (75 : 25 : 4); sprayed with phosphomolybdic acid; scanned in a densitometer at 450 nm in double-beam transmission mode; detection of each lipid at 0.2 µg level
Sphingolipids in the parasitic protozoan, <i>Blastocystis hominis</i>	Sphingolipids along with neutral lipids and phospholipids were quantified on HPTLC plates; sphingolipids resolved on plates with chloroform–methanol–water (70 : 22 : 3) and detected with the orcinol reagent; plates scanned with a Shimadzu Flying Spot densitometer operated in the reflectance mode at 580 nm
Brain gangliosides	Complex sample preparation; use of HPTLC plates; chloroform–methanol–0.22% CaCl ₂ (55 : 45 : 10) solvent system; detection by spraying with resorcinol–hydrochloric acid reagent; chromatogram scanned at 580 nm in transmission mode; separation and quantification of 4–8 brain gangliosides

plates can be impregnated with special agents have allowed for the separation and identification of molecular species within classes, e.g. molecular species of triacylglycerols.

A new area of work has used multiphase TLC, in which components are separated in two directions according to different parameters, e.g. conventional silica gel in one direction and reversed-phase in the other. This technique has proved useful in the analysis of triacylglycerols. The use of HPTLC-densitometry has revolutionized our ability to quantify lipids by relatively simple procedures. There are attempts underway to automate various aspects of the TLC process. Certainly with more automated methodology, TLC will be used more widely in the future by both chemists and biologists interested in lipid separations.

See also: II/Chromatography: Thin-Layer (Planar): Densitometry and Image Analysis; Layers; Spray Reagents. III/Lipids: Gas Chromatography; Liquid Chromatography.

Further Reading

- Christie WW (1982) *Lipid Analysis*, 2nd edn. Oxford: Pergamon.
- Christie WW (1987) *High Performance Liquid Chromatography and Lipids*. Oxford: Pergamon.
- Fried B and Sherma J (eds) (1996) *Practical Thin-layer Chromatography – A Multidisciplinary Approach*. Boca Raton: CRC.
- Fried B and Sherma J (1999) *Thin-layer Chromatography – Techniques and Applications*, 4th edn. New York: Marcel Dekker.
- Gunstone FD and Herslöf BG (1992) *A Lipid Glossary*. Ayr: Oily.
- Gunstone FD and Padley FB (eds) (1997) *Lipid Technologies and Applications*. New York: Marcel Dekker.
- Gurr MI and Harwood JL (1991) *Lipid Biochemistry – An Introduction*, 4th edn. London: Chapman & Hall.
- Hammond EW (ed.) (1993) *Chromatography for the Analysis of Lipids*. Boca Raton: CRC.
- Kates M (1986) *Techniques of Lipidology, Isolation, Analysis, and Identification of Lipids*, 2nd edn. Amsterdam: Elsevier.

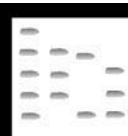
Mukherjee KD and Weber N (eds) (1993) *CRC Handbook of Chromatography – Analysis of Lipids*. Boca Raton: CRC.

Padley FB (ed.) (1996) *Advances in Applied Lipid Research: A Research Annual*, vol. 2. Greenwich: JAI.

Sherma J and Fried B (eds) (1996) *Handbook of Thin Layer Chromatography*, 2nd edn. New York: Marcel Dekker.

Shibamoto T (ed.) (1994) *Lipid Chromatographic Analysis*. Boca Raton: CRC.

LIQUID CHROMATOGRAPHY-GAS CHROMATOGRAPHY



L. Mondello, P. Dugo and G. Dugo,
University of Messina, Messina, Italy
K. D. Bartle and A. C. Lewis,
University of Leeds, Leeds, UK

Copyright © 2000 Academic Press

Introduction

High resolution gas chromatography (HRGC) is the most suitable technique for the analysis of volatile compounds. If the sample is a complex matrix, such as natural products, food products or environmental pollutants, direct gas chromatographic (GC) analysis is not advisable for several reasons, and a sample pretreatment is necessary. In fact, peaks of different classes of compounds may overlap, rendering the

qualitative and quantitative analysis of some compounds difficult. Moreover, if the compounds of interest are present only as trace amount, a preconcentration step is necessary before the GC analysis.

If the mixture is subjected to a preliminary separation by liquid chromatography (LC), the fraction so obtained can be analysed by GC. Offline coupling of LC and GC is laborious, involving numerous steps with the risk of contamination and possible greater loss of part of the sample than if online techniques were used. The online coupling of LC and GC offers a number of advantages compared to offline coupling: the amount of sample required is much lower; no sample work-up, evaporation or dilution is necessary and complex automated sample pretreatment is possible.

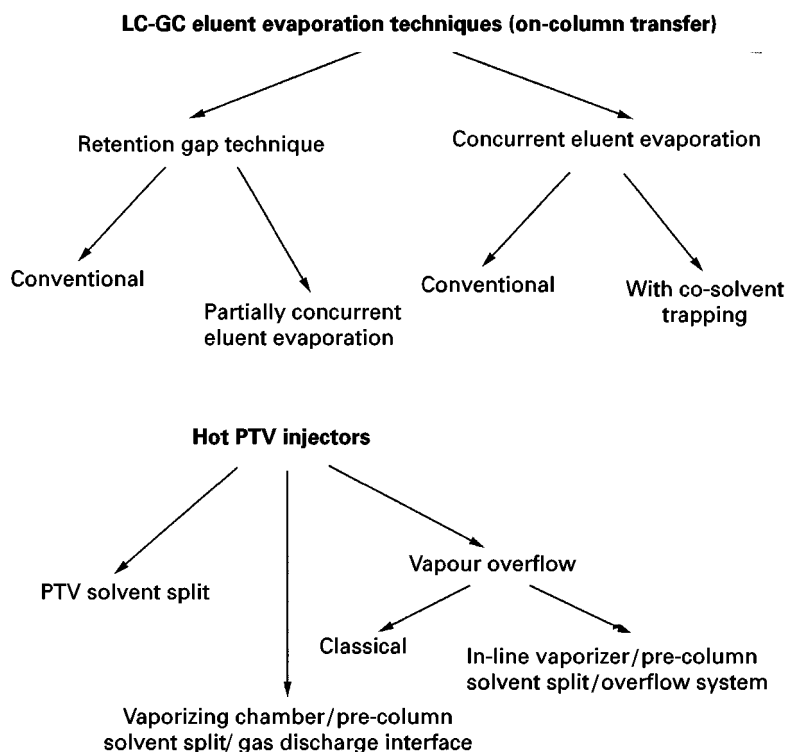


Figure 1 LC-GC transfer techniques. Possible mechanisms for LC-GC eluent evaporation.

The introduction of large amounts of solvent into a GC column requires the use of special techniques to separate the solvent from the sample selectively. At present, the principal techniques of eluent evaporation that allow transfer of large LC fraction into GC are based on the use of a modified on-column injector or on the use of a programmed temperature vaporizing (PTV) injector. **Figure 1** summarizes the transfer techniques used for online LC-GC coupling.

Concurrent Eluent Evaporation

Concurrent eluent evaporation is the most used technique, because of its simplicity and the possibility of transferring large amounts of solvent (up to 10 mL!). The technique involves complete evaporation of the eluent during its introduction into the GC system. This technique is suitable for the analysis of solutes with intermediate to high elution temperature, depending on the volatility of the eluent and on the volume of the LC fraction transferred.

When the sample solvent evaporates at the front end of the liquid, volatile compounds co-evaporate with the solvent and immediately start passing into the analytical column. The consequence is that, if the solvent vapours are vented through an early vapour exit, the volatile compounds are lost with the solvent vapour while, if venting is delayed, the most volatile compounds reach the detector even before the end of solvent evaporation. This causes a broadening of the initial band of solutes, which will give peaks that start with the solvent peak and spread out, masking some of the volatile peaks. Only high boiling substances, which migrate slowly during the transfer, will elute after the oven temperature increase, and will give sharp peaks. In practice, the first properly shaped peaks are eluted some 40–120°C above the transfer temperature.

The fraction to be analysed is contained in a loop, connected to a switching valve. The opening of the valve allows the sample in the loop to be driven by the carrier gas into the GC. Usually an early vapour exit is located after a few metres of deactivated precolumn and 3–4 m of retaining column (cut from the analytical column). The retaining pre-column provides a short zone where the solute can be focused in the stationary phase, so that volatile components will be trapped, avoiding their loss through the vapour exit. This is opened during solvent evaporation to reduce the amount of solvent that would reach the detector, and at the same time to increase the solvent evaporation rate.

Figure 2 shows the scheme of the loop-type interface.

Figure 3 shows an example of tocopherols, free sterols and esterified sterols determined in a single analytical run after acetylation. These compounds were pre-separated from the triacylglycerols by normal-phase LC.

Retention Gap

The retention gap method represents the best approach in the case of qualitative and quantitative analysis of samples containing highly volatile compounds. In fact, the retention gap technique allows the analysis of substances eluting immediately after the solvent peak, due to the reconcentration of these components by the so-called solvent effects (primarily solvent trapping). **Figure 4** shows the scheme of the retention gap transfer technique.

The term retention gap means a column inlet of a retention power lower than that of the analytical column. In the retention gap technique, the sample is introduced into the GC at a temperature below the boiling point of the LC eluent (corrected for the current inlet pressure). In this way, the solvent

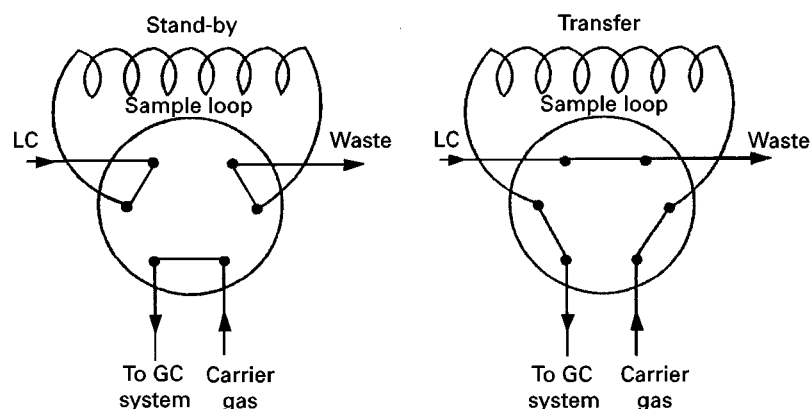


Figure 2 Loop interface scheme for concurrent eluent evaporation.

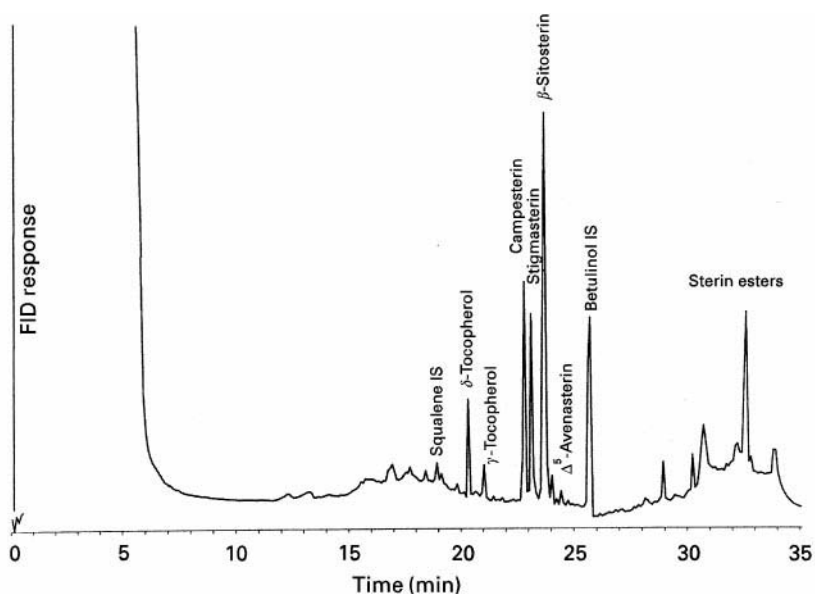


Figure 3 GC chromatogram of tocopherols, free sterols and esterified sterols transferred from the LC pre-separation system using the concurrent solvent evaporation technique. FID, Flame ionization detector. (Reproduced with permission from Lechner M and Lorber E (1998) *20th International Symposium on Capillary Chromatography*, Riva del Garda, Italy. Copyright P. Sandra and AJ Rackstraw.)

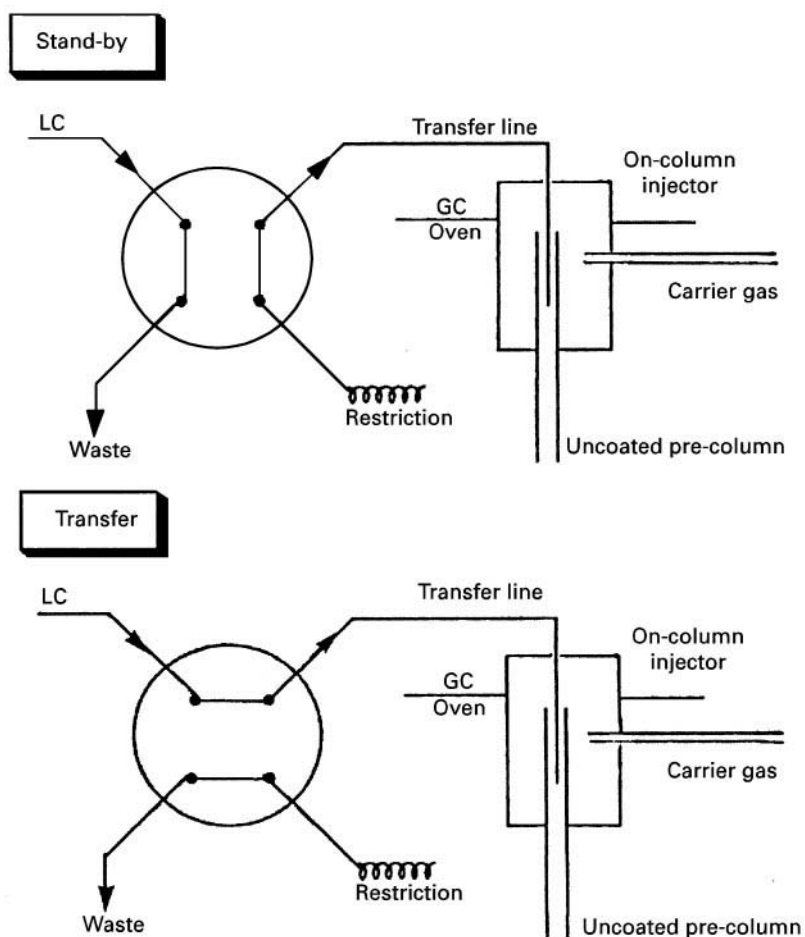


Figure 4 Retention gap scheme.

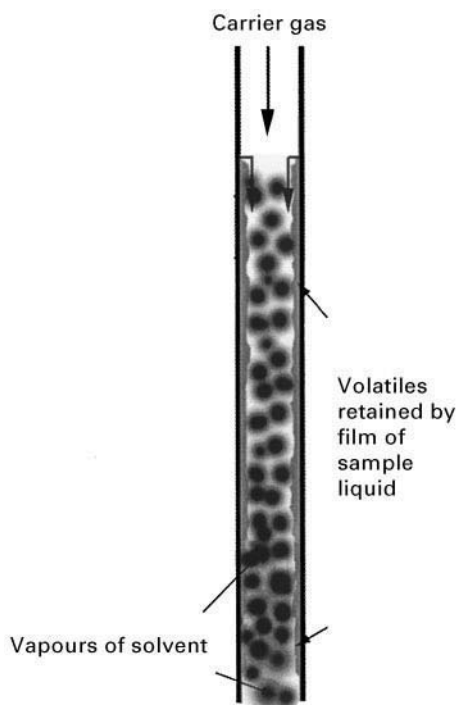


Figure 5 Solvent evaporation in a retention gap. The evaporation occurs from the rear part of the solvent.

vapours replace only part of the carrier gas, which continues to flow through the column. In the carrier stream, solvent evaporates from the rear towards the front of the sample layer (Figure 5). Under these conditions, the volatile compounds that are liberated from the solvent envelope start moving, but they are immediately trapped again by the solvent present ahead of the evaporation site (solvent-trapping effect). In this way, the volatile components can start moving in the carrier gas only when the process of solvent evaporation is complete.

A second effect, called phase soaking, occurs in the retention gap technique. This effect is obtained because the carrier gas is saturated by solvent vapours, so it swells the stationary phase with this amount of solvent. The consequence is that the column shows an increased retention power that can be used to trap the volatile compounds.

During the evaporation process, band broadening in space spreads the high boiling compounds. Two retention gap effects can reconcentrate these solute bands. First, compounds migrate more rapidly through the retention gap zone than through the main column; reconcentration depends on the ratio between the retention power in the pre-column and in the main column (phase-ratio focusing). Second, the compounds arrive at the entrance of the main column at a temperature at which they are practically unable to migrate, so they accumulate until the temperature

is increased, and concentrate. The limitation of the method is that, due to the poor capacity of uncoated pre-columns to retain liquid, only modest volumes can be transferred (100–150 μL of eluent) and long uncoated pre-columns are needed.

Two additional techniques have been developed to overcome the drawbacks of the techniques described above, with the aim of obtaining sharp peaks at elution temperatures below 120–150°C, for concurrent eluent evaporation, and to transfer large LC fractions, for the retention gap technique: partially concurrent solvent evaporation and co-solvent trapping.

Partially Concurrent Solvent Evaporation

Partially concurrent solvent evaporation allows working under conditions that still produce a zone flooded by the eluent (retention gap), providing solvent trapping. This causes a large amount of eluent to evaporate during its introduction (concurrently), so that shorter uncoated pre-columns or larger volumes of transferred fraction can be handled. In practice, an early vapour vent may be placed between the uncoated pre-column and the analytical column, but this makes closure of the vent critical for partial losses of early eluted peaks. A section of the analytical column may be installed after the uncoated pre-column but before the solvent vapour exit.

Figure 6 shows GC chromatograms obtained after pre-separation by normal-phase LC, applying the partially concurrent solvent evaporation. This application consists of the measurement of the enantiomeric ratio of linalol contained in sweet and bitter orange essential oil. This ratio characterizes each oil, differentiating them, so that the presence of the less valuable sweet orange oil can be detected in the more valuable bitter orange oil.

Co-solvent Trapping

Co-solvent trapping is used to obtain sharp solute peaks of correct size even for volatile compounds, with concurrent evaporation technique. A small amount of a higher boiling co-solvent is added to the main solvent (for example, *n*-heptane added to pentane), to prevent co-evaporation of the volatile compounds with the main solvent (Figure 7).

It is necessary to adjust the concentration of co-solvent so that some co-solvent is left behind as a liquid, while some is evaporated with the main solvent. In this way, the co-solvent remaining forms a layer of liquid film that evaporates from the rear to the front, as in the retention gap technique. The solutes are trapped by the solvent-trapping effect, and

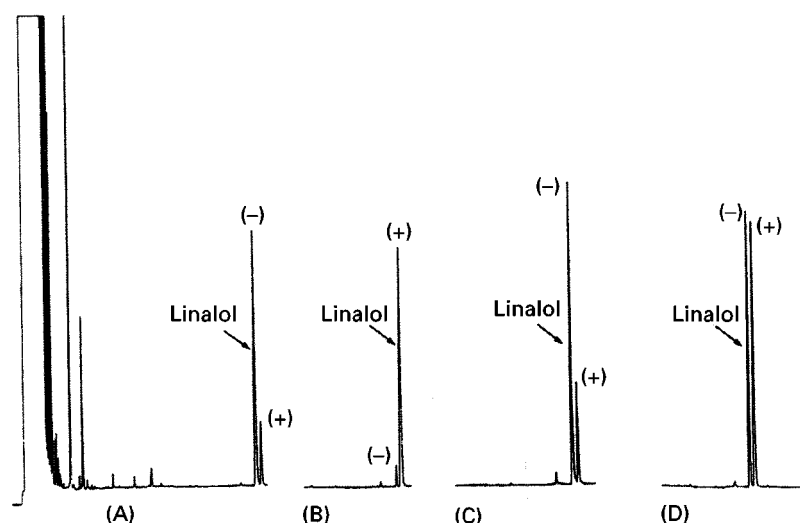


Figure 6 GC chiral separation of linalol from sweet orange, bitter orange and mixtures of the two essential oils, showing the different enantiomeric ratios. Linalol fraction was transferred from the LC system using the partially concurrent solvent evaporation technique. (A) Bitter orange; (B) sweet orange; (C) bitter orange 90%, sweet orange 10%; (D) bitter orange 70%, sweet orange 30%. (Reproduced with permission from Dugo G, Venzera A, Cotroneo A, Stagno d'Alcontres W, Mondello L and Bartle KD (1994) *Flavour and Fragrance Journal* 9: 99. Copyright John Wiley & Sons Limited.)

are released after the co-solvent has been evaporated. As can be seen, this technique shows some similarity to partially concurrent solvent evaporation. The main difference is that it is designed for the loop-type interface, while partially concurrent solvent evaporation works with an on-column interface. The optimization of the transfer conditions is not easy, so this technique has never been routinely applied to the transfer of normal-phase eluents, because the partially concurrent solvent evaporation technique is

easier to use. It can be the technique of choice for the transfer of water-containing solvents, because in contrast to retention gap techniques, concurrent eluent evaporation does not need wettability, and co-solvent trapping retains the volatile solute. Under these conditions, transfer occurs at 110–120°C, so the first compounds should elute at this temperature. Unfortunately, the problem is the lack of an uncoated pre-column resistant to condensed water. Studies on improving pre-column deactivation have been carried out, but the scant interest in reversed-phase LC coupled to GC prevented re-evaluation of this promising technique with improved methods of deactivation.

Vaporization with Hot Injectors

Together with the techniques described above, other techniques using hot injectors for the transfer from LC to GC, have been developed. PTV with solvent trapping in packed beds can be used successfully to transfer large volume fractions into the GC instead of into a capillary pre-column (uncoated, deactivated silica tubing). This technique shows some advantages compared to the techniques that use on-column sample introduction:

1. Packed beds retain more liquid per unit internal volume.
2. Wettability is no longer critical.
3. Packing material is more stable than deactivated silica tubing.
4. PTV is more easily heated than capillary column.

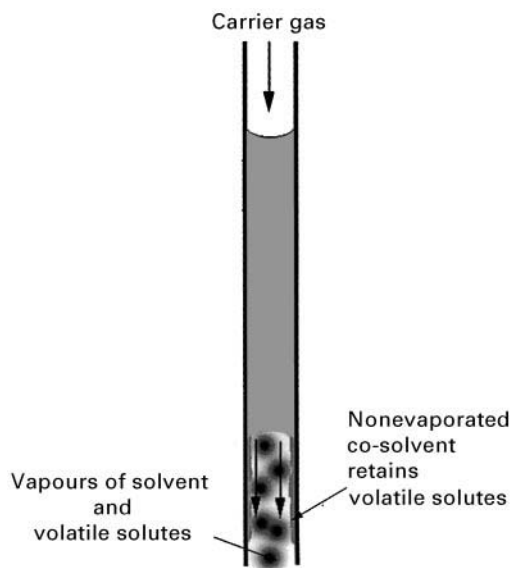


Figure 7 Concurrent eluent evaporation with co-solvent trapping effect. The volatile components are retained by the solvent film.

Because of the high retention power, the packed chambers have to be heated above the column temperature to release the solutes. This is a drawback in the analysis of thermally labile compounds, and high boiling compounds. In the PTV solvent split mode, the injection is made into a cool injector, and the solvent is largely removed via the split valve. Volatile compounds can evaporate with the solvent; many studies have been carried out to minimize the loss of volatiles, for example, reducing the temperature of the injector. On the other hand, high boiling compounds are difficult to release, due to the high retention power of the packing material. Introduction of large volumes in the PTV solvent-split mode was introduced in the 1970s and, since its introduction, many different approaches have been described.

The first configuration was a glass tube with a packed bed with a cool injector. The solvent vapours are discharged through the split valve. After solvent evaporation the split valve is closed and the injection chamber is heated to transfer the solutes into the column. Liners are usually packed with Tenax TA and Thermotrap TA. To increase trapping efficiency, liners with sintered porous glass beads were introduced.

Recently a new, fully automated online LC-GC coupling has been introduced. This interface consists

of a flow cell, where the fraction is sampled by a large volume autosampler, and automatically injected into a PTV device using the solvent vent mode. This technique was successfully applied to determine pesticide residues in complex natural matrices such as essential oils (Figure 8).

Vapour Overflow

The vapour overflow technique is intended for introducing samples into large volumes of solvent by syringe injection of dilute samples or by coupled LC-GC. The liquid is introduced into a packed (generally with Tenax) vaporizing chamber maintained above the solvent boiling point at a pressure which is near or below ambient. This technique is performed in the absence of carrier gas and vapours are discharged by expansion during evaporation (overflow). The vaporizing chamber is filled with packing material of a GC retention power for the volatile components. The carrier gas supply line is equipped with a switching valve, allowing the gas supply to be stopped during sample introduction. The sample is released by a syringe or a transfer line from the LC near the bottom of the vaporizing chamber. Vapours expand and, driven by the expansion, leave the system through the septum purge (Figure 9).

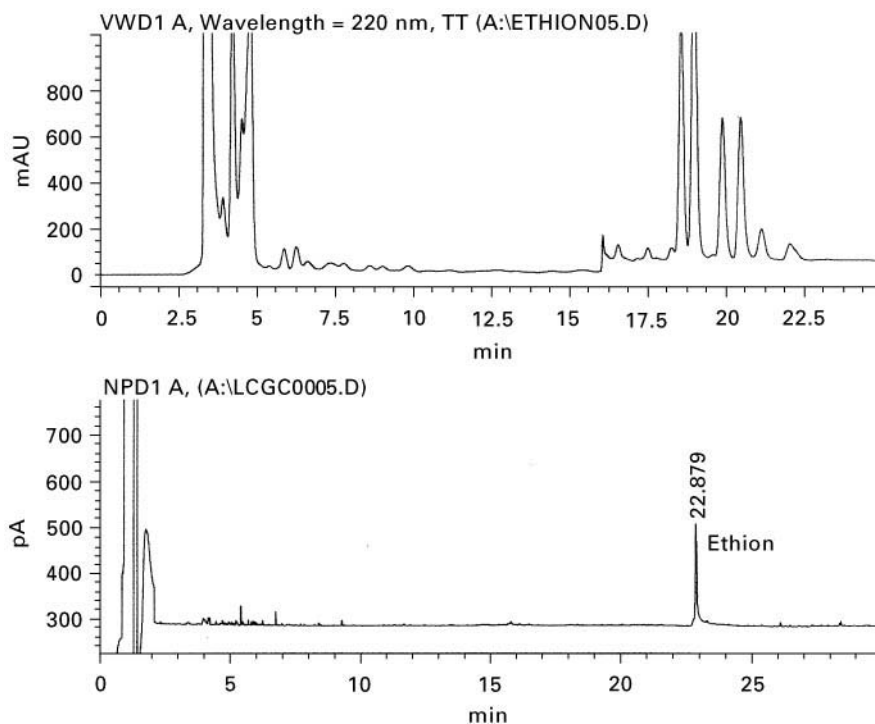


Figure 8 LC separation of (A) orange essential oil and (B) GC/NPD chromatogram of the fraction containing the pesticide ethion, transferred from the LC system, using the PTV interface type in the solvent vent mode. NPD, nitroge-n-phosphorous detector. (Reproduced with permission from David F, Correa RC and Sandra P (1998) *20th International Symposium on Capillary Chromatography*, Riva del Garda, Italy. Copyright P. Sandra and AJ Rackshaw.)

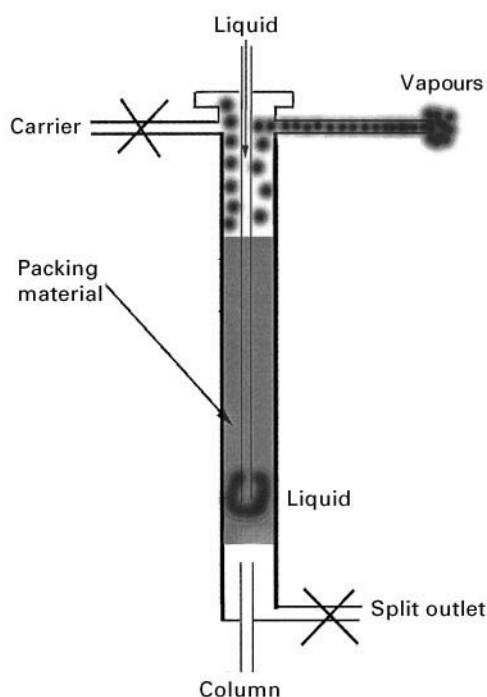


Figure 9 Vapour overflow interface. The solvent vapours are eliminated through the septum purge of the PTV injector.

After solvent evaporation is completed, the septum purge is closed, the injector is warmed up (PTV) and the trapped analytes are released into the column. More recently, this system has been modified for use with a conventional hot injector.

In-line Vaporizer/Pre-column Solvent-split/Overflow System

The in-line vaporizer/pre-column solvent-split/overflow system was developed by Grob for large volume liquid injection and for online LC-GC. This system is an overflow-based technique, but with an improvement for the retention of more volatile compounds. As can be seen from Figure 10, the vaporizer consisted of a transfer line (from the LC) of fused silica. Inside the vaporizer a 5 cm length of steel wire (untreated or deactivated) or of fused silica is inserted for complete evaporation of the liquid (250–350°C). Moreover the system is equipped with a retaining pre-column and an early vapour exit. The oven in this case is maintained at a low temperature (lower than with a loop interface) to improve retention of sample components by phase soaking. The improvement in the arrangement corresponds to about four extra carbon atoms retained (undecane instead of pentadecane).

Vaporizing Chamber/Pre-column Solvent-split/Gas Discharge Interface

The sample is injected by an autosampler or by online transfer from a high performance liquid chromatography (HPLC) into a heated device. The vaporizer is packed and maintained at a temperature suitable for solute evaporation. Compounds that are sensitive to high temperatures are injected into a PTV injector in

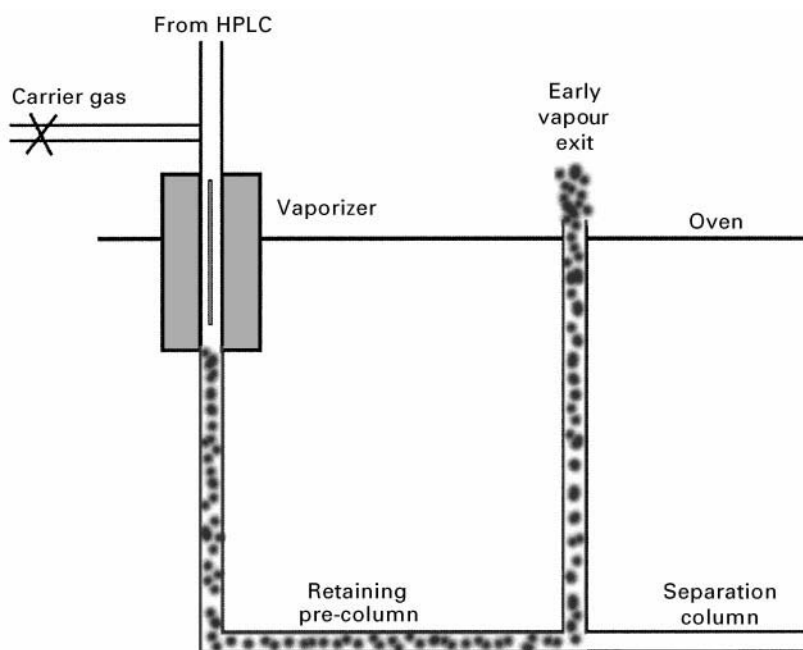


Figure 10 In line vaporizer/pre-column solvent-split/overflow system. The more volatile components are retained by the retention gap, letting the solvent out from the early vapour exit.

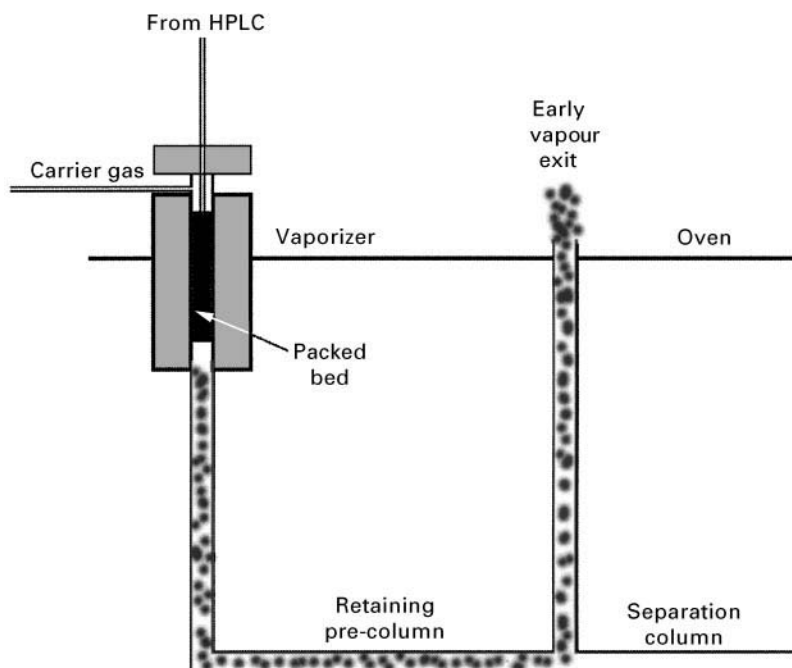


Figure 11 Vaporizing chamber/pre-column solvent-split/gas discharge interface. The vaporizer is packed and heated at a suitable temperature for solvent evaporation. The vapour exit can be positioned at the end of the retention gap.

order to evaporate the solvent first and then the solutes. As shown in **Figure 11**, the vapours are discharged through a pre-column and an early vapour exit. If solvent trapping is needed, an uncoated pre-column is installed after the injector and before the solvent vapour exit. Moreover, the use of a retaining pre-column is possible depending on how critical is the solvent vapour exit closure.

Conclusions

Coupled LC-GC is an excellent online method for sample preparation and clean-up. For the analysis of nonaqueous media the transfer technique of choice is certainly concurrent eluent evaporation using a loop-type interface. The main drawback of this technique is the loss of volatile solutes due to the solute co-evaporation with the solvent. If volatile compounds are present, transfer from LC to GC is best achieved by a retention gap technique. This on-column method yields sharp peaks starting from the programming of the GC oven temperature during eluent transfer. However, due to the limited capacity of uncoated pre-columns for liquid retention, the technique is only suited for the transfer of relatively small fractions. Larger fractions can be transferred by partially concurrent eluent evaporation since this includes the retention gap procedure. Presently, PTV solvent-split injection is considered as the method of choice for

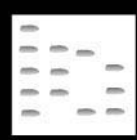
large volume injection of 'dirty' or water-containing samples. Finally, vaporizing chamber/pre-column solvent-split/gas discharge interface and in-line vaporizer/pre-column solvent-split/overflow systems seem to be promising techniques for LC-GC coupling in a wide range of applications.

See also: **I/Chromatography. II/Chromatography: Gas Column Technology:** Multidimensional Gas Chromatography; **Theory of Gas Chromatography. Chromatography: Liquid:** Multidimensional Chromatography; **Theory of Liquid Chromatography.**

Further Reading

- Grob K (1986) *On-column Injection in Capillary Gas Chromatography*. Heidelberg: Huethig.
- Grob K (1991) *On-line Coupled LC-GC*. Heidelberg: Huethig.
- Kelly GW and Bartle KD (1994) The use of combined LC-GC for the analysis of fuel products: a review. *Journal of High Resolution Chromatography* 17: 390.
- Mondello L, Dugo G and Bartle KD (1996) On-line micro-bore high performance liquid chromatography-capillary gas chromatography for food and water analyses. A review. *Journal of Microcolumn Separations* 8: 275.
- Vreuls JJ, de Jong GJ, Ghijsen RT and Brinkman UATH (1994) LC coupled on-line with GC: state of the art. *Journal of the Association of Official Analytical Chemists International* 77: 306.

MARINE TOXINS: CHROMATOGRAPHY



A. Gago-Martínez and J. A. Rodríguez-Vázquez,
Universidad de Vigo, Vigo, Spain

Copyright © 2000 Academic Press

Introduction

The marine environment may be seriously affected by contamination due to the massive proliferation of toxic phytoplanktonic species for example toxic algae or 'algal blooms', which appear at certain times of the year under the influence of various environmental factors. These phytoplanktonic microorganisms are essential food for filter-feeding bivalve shellfish as well as other types of marine seafood. This phenomenon is commonly known as a 'red tide'.

These toxic algal blooms cause important socioeconomic damage to those regions that depend on aquaculture or fisheries industry, owing to their environmental and human health impacts.

It is believed that the first reference to a harmful algal bloom appears in the Bible: '... all the waters in the river turned to blood, the fish died' (Exodus 7:20–21). One of the first recorded fatal cases of

human poisoning happened in 1793 in Poison Cove (British Columbia), caused by a group of alkaloids now called 'paralytic shellfish poisoning' toxins (PSP). Since this toxic event, a number of different toxic episodes have been reported in several places worldwide.

There are different type of shellfish poisoning: the main causative organisms and important toxicological effects are summarized in Table 1. In this article we will focus on the paralytic, diarrhoeic and amnesic shellfish poisoning (PSP, DSP and ASP) because they are responsible for most of the toxic events on the European Atlantic Coast and are also of general occurrence in many other places worldwide.

These toxins cause important human contamination and their impact has increased considerably over the last few years. For this reason, strict control of these toxins is necessary to prevent serious damage to health. The conventional mouse bioassay (still considered as official and routine methodology in most countries) is useful for determining most of the implicated toxins, but alternative analytical methods are desired, especially for research

Table 1 Main types of harmful algal blooms

Type of poisoning	Causative organism	Symptoms
Paralytic shellfish poisoning (PSP)	<i>Alexandrium catenella</i> <i>A. minutum</i> <i>A. tamarense</i> <i>Gymnodinium catenatum</i> <i>Pyrodinium bahamense</i>	Typical neurological symptoms. The severity of these symptoms is related to the ingested dose. Also symptoms like dizziness, nausea, vomiting, diarrhoea, muscular paralysis, respiratory difficulties, death through respiratory paralysis (in extreme cases).
Diarrhoeic shellfish poisoning (DSP)	<i>Dinophysis acuminata</i> <i>D. acuta</i> <i>D. fortii</i> <i>D. norvegica</i> <i>Prorocentrum lima</i>	Vomiting and diarrhoea typical of gastrointestinal disorders. Chronic exposure may cause tumour promotion, especially in the digestive system (stomach intestine and colon).
Amnesic shellfish poisoning (ASP)	<i>Pseudo-nitzschia multiseries</i> <i>Pseudo-nitzschia</i> <i>Pseudo-nitzschia australis</i>	Typical gastrointestinal disorders (nausea, vomiting, diarrhoea). Neurological symptoms, especially in older people and people with chronic illnesses – confusion, short-term memory loss.
Neurotoxic shellfish poisoning (NSP)	<i>Gymnodinium breve</i>	Headache, diarrhoea, muscle weakness, nausea and vomiting. Paraesthesia, respiratory difficulties, vision alterations, speech difficulties.
Ciguatera poisoning	<i>Gambierdiscus toxicus</i> <i>Prorocentrum lima</i>	Gastrointestinal disorders (diarrhoea, abdominal pain, nausea, vomiting), difficulty in balance, heart problems (low heart rate and blood pressure), death through respiratory failure (in extreme cases).

purposes where high sensitivity and specificity are required.

Owing to the complexity of the sample matrix, separation techniques are required to remove interferences and to increase the selectivity in the analytical response. During the 1990s considerable research has been focused on the development of chromatographic approaches for the analysis of PSP, DSP and ASP toxins. Liquid chromatography (LC) has been shown to be one of the most successful alternatives for the sensitive determination of these compounds using different detection modes. Capillary electrophoresis (CE) is another analytical alternative that has been recently developed for the analysis of PSP and ASP toxins and, as we will discuss later, this is a promising technique for the analysis of such compounds.

Separation Techniques for the Analysis of Marine Biotoxins

PSP Toxins

Paralytic shellfish poisoning (PSP) is a worldwide problem caused by consumption of shellfish that have accumulated potent neurotoxins produced by toxicogenic dinoflagellates. The PSP toxins include saxitoxin (STX) and several of its derivatives formed by addition of sulfo, hydrosulfate and *N*-1-hydroxyl groups (Figure 1).

The most common chemical method used for the analysis of PSP toxins is the combination of LC with online post-column oxidation and fluorescence detection, using two different isocratic and gradient

elution modes. This evolved from earlier work, which showed that STX could be easily oxidized to a fluorescence derivative by hydrogen peroxide under alkaline conditions. Hydrogen peroxide is not able to oxidize the *N*-1-hydroxylated derivatives, which are better oxidized by using periodate. This reagent is therefore commonly used in post-column oxidation systems in order to detect all PSP toxins. LC combined with post-column oxidation has resulted in a successful approach but unfortunately is not without difficulties, especially concerning the operation of the equipment. This has made it necessary to optimize parameters such as stationary phase, mobile phase, etc. An alternative LC method employing pre-chromatographic oxidation has been reported. This method results in improved separation and quantitation of most PSP analogues. Modification of the periodate oxidation reaction for the *N*-hydroxy-containing toxins has led to improved sensitivity and stability of the products, enabling overnight analysis.

All the high performance liquid chromatography (HPLC) methods mentioned have resulted in valid approach for the control of these toxic compounds, but although these methods offer good sensitivity and dynamic range, the sensitivity is dependent on parameters such as reagent concentration, reaction times, pH and temperature of the oxidation reaction. In addition to the elaborate procedure required to achieve reliable and reproducible results, the main drawback of the alkaline oxidation reaction is the reliance on fluorescence response factors for the different PSP toxins based on the only commercially available standard. Figure 2 shows an example of the

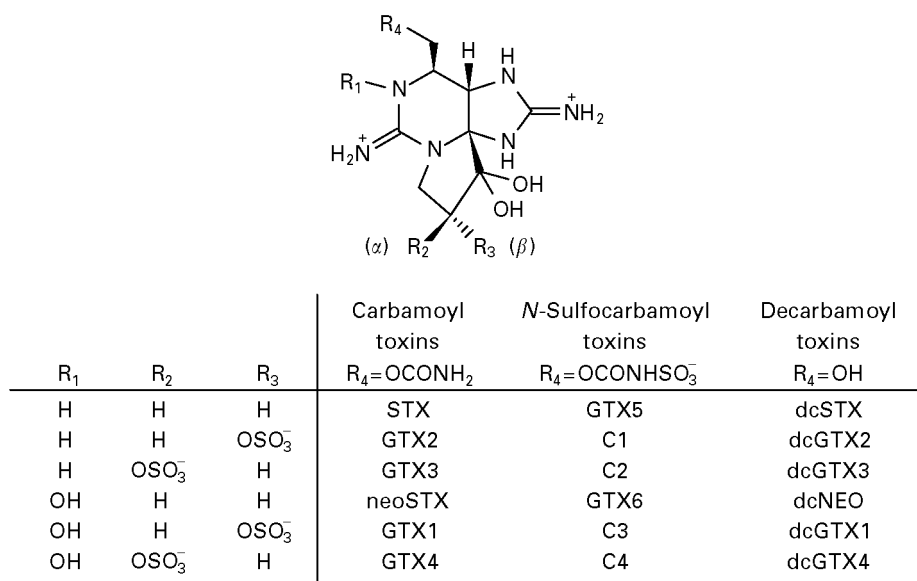


Figure 1 Chemical structure of PSP toxins.

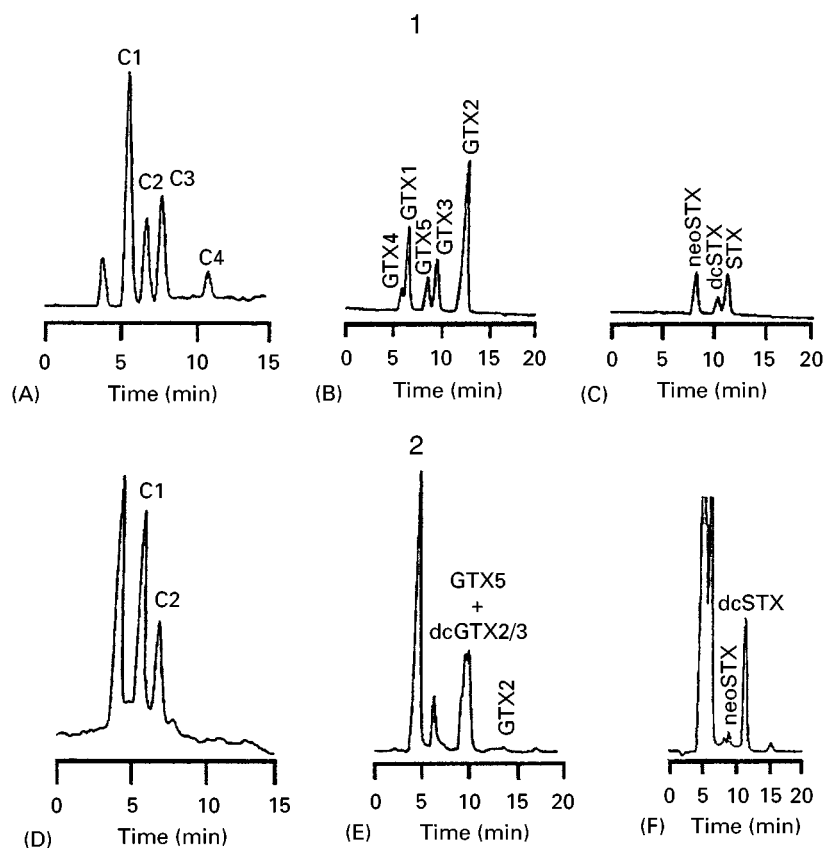


Figure 2 Chromatogram obtained for the PSP toxins profile by using post-column HPLC-FLD. (A) STX group; (B) GTX group; (C) C toxin group. 1, standard of PSP toxins; 2, mussel samples.

application of the LC technique with fluorescence detection for the analysis of PSP toxins in contaminated extracts of mussels for Galicia (northwest Spain). The conditions used to carry out this isocratic HPLC analysis with post-column oxidation are described in Table 2. Under these conditions good resolution was achieved for most of PSP toxins, with the exception of the gonyautoxin (GTX) group, owing to the presence of other GTX components with similar

retention times (this was confirmed using mass spectrometric detection).

The successful separation of these toxins by both ion exchange chromatography and cellulose acetate electrophoresis prompted investigations of the application of CE to their analysis. With the exception of the Ciguatera (C) toxins, which have neutral overall charge, all PSP toxins have positive charge under acidic conditions, and can be separated by elec-

Table 2 Conditions for the post-column HPLC-FLD analysis of PSP toxins

HPLC instrument	Perkin-Elmer series 10-LC
Mobile phase	Column: reversed-phase, prodigy 5 μm C ₈ Phenomenex 4.6 mm \times 15 cm
	Flow rate, 0.8 mL min ⁻¹
Mobil phase A (for C toxin group)	2 mmol L ⁻¹ tetrabutylammonium phosphate, pH 5.8
Mobile phase B (for GTX toxin group)	2 mmol L ⁻¹ sodium 1-heptanesulfonate in 10 mmol L ⁻¹ ammonium phosphate, pH 7.3
Mobile phase C (for STX group)	2 mmol L ⁻¹ sodium 1-heptanesulfonate in 30 mmol L ⁻¹ ammonium phosphate, pH 7.1, 5% v/v acetonitrile
Oxidizing reagent	7 mmol L ⁻¹ potassium periodate in 50 mmol L ⁻¹ potassium phosphate buffer, pH 9.0; flow rate: 0.4 mL min ⁻¹
Reaction system	In 10 m Teflon tubing (0.5 mm i.d.) at 65°C in water bath
Acid solution	0.5 mol L ⁻¹ acetic acid; flow rate: 0.4 mL min ⁻¹
Detection	Hitachi F1000 fluorescence detector, double monochromator. Excitation wavelength 330 nm; emission wavelength 390 nm

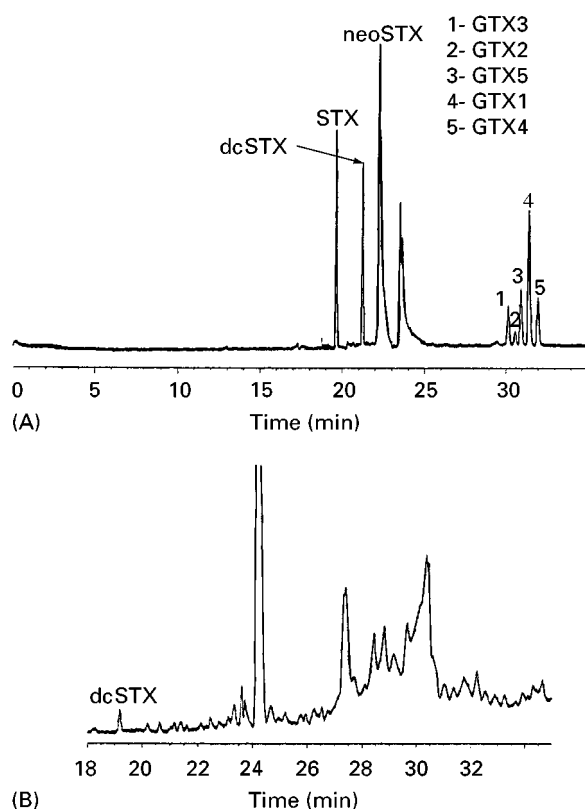


Figure 3 Electropherogram obtained for the PSP toxins profile by using CE-UV-DAD. (A) standard of PSP toxins; (B) mussel sample.

trophoresis. Capillary electrophoresis should provide an efficient separation of most PSP components; however, some of the inherent difficulties in analysing these compounds are the lack of a chromophore absorbing in the usual UV range as well as the lack of standards to confirm the electrophoretic peak identity.

To overcome situations where the electrophoretic peak identity presents some uncertainties, or standards are not available to correlate with the peaks of interest, it is necessary to use a complementary technique, such as mass spectrometric detection using

electrospray ionization. This technique has shown excellent sensitivity for PSP as well as for other marine toxins. Mass spectrometric detection coupled with CE has been used for the rapid and efficient determination of PSP toxins. This technique has also been applied for the analysis of real mussel samples and an efficient separation for most of PSP toxins was achieved.

An example of the application of CE to the analysis of PSP toxins in mussels is shown in **Figure 3**. Under the conditions described in **Table 3**, several contaminated Galician mussel samples were analysed by this technique. Clean-up of the samples was required to remove interferences, but after this clean-up good resolution was obtained for most PSP toxins with the exception of the C toxins, which are not ionized in acidic media. The potential of this technique in terms of sensitivity was clearly increased by using isotachopheresis. Resolution in terms of efficiency, by means of theoretical plates, was clearly higher than that achieved by using HPLC.

DSP Toxins

Since PSP toxins are potent neurotoxins, the term '*diarrhoeic shellfish poisoning*' (DSP) has been associated with a number of different groups of toxic compounds; these include polyether compounds such as okadaic acid (OA), dinophysistoxins (DTX1, DTX2, DTX3), pectenotoxins and the fused polyether yessotoxin. Toxicological studies have shown that okadaic acid and dinophysistoxins are potent phosphatase inhibitors; their common symptomatology is related with the occurrence of diarrhoea. The mechanism of action of the other compounds has not been fully established, but it seems that they do not cause diarrhoea; instead they are described as hepatotoxins. The main reason for including these toxins in the DSP group is probably their polyether structure (**Figure 4**).

DSP toxins are also produced by certain toxic dinoflagellates; the chemical structure of these toxins emerged following the isolation of new polyether toxin named okadaic acid, from the sponge *Hali-*

Table 3 Conditions for the CE-UV-DAD analysis of PSP toxins

CE-UV-D System	HP 30 CE (Hewlett-Packard); voltage 20 kV
Capillary	Polyvinyl alcohol (PVA) capillary (75 μ m i.d. and 104 cm length)
Background buffer	50 mmol L $^{-1}$ morpholine in water adjusted at pH 5 with formic acid
Injection	Sample injection into capillary was 20% of capillary volume. Pressure, 50 mbar; time, 120 s
ICTP	Voltage, 20 kV
	Leading buffer, 10 mmol L $^{-1}$ formic acid
	Terminating buffer, 50 mmol L $^{-1}$ morpholine in water adjusted at pH 5.0 with formic acid
	Time, 90 s
UVD detection	Wavelength 200 nm

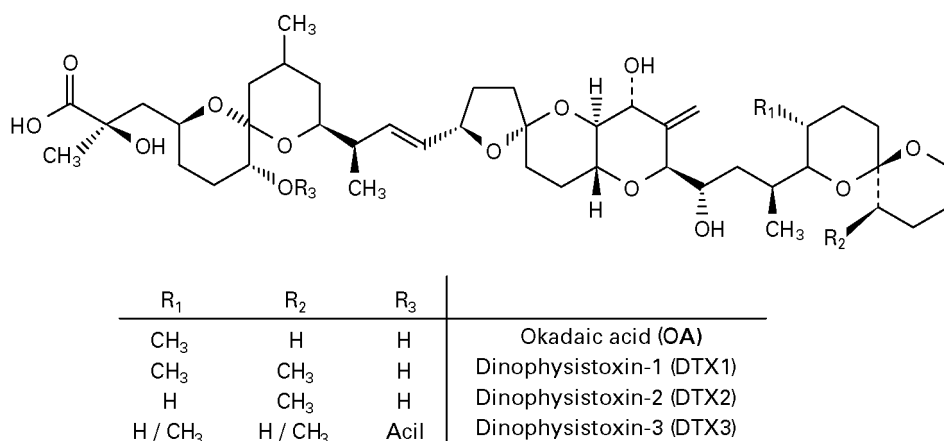


Figure 4 Chemical structure of DSP toxins.

chondria okadai. The similarities between okadaic acid and DTXs were quickly recognized. Several places worldwide have been affected by such toxic outbreaks since the first toxic event, which took place in the Netherlands in 1960. Although the toxic effects of okadaic acid are related to gastrointestinal disorders, these toxins have been shown to have the potential to bind to protein phosphatases. Consequently the toxicological activity of DSP toxins is also associated with the promotion of tumours, especially in the stomach, intestine and colon.

As for PSP toxins, mouse bioassay is the method commonly used for the analysis of DSP compounds, but the problems associated with this bioassay, such as long assay time, poor reproducibility and false positives, have instigated the search for alternative techniques. Since DSP toxins are lipid-soluble, organic solvents are required for their extraction. However, such lipid-soluble extracts are considerably more complex than aqueous extracts of the same organism and for this reason additional clean-up steps are required before analysis. DSP toxins can be detected by thin-layer chromatography (TLC), although the presence of interferences causes difficulties when using this technique.

DSP toxins may be separated by reversed-phase HPLC using an octadecylsilica (ODS) stationary phase and an acidified aqueous acetonitrile or methanol mobile phase. Detection can be accomplished with UV absorbance at 205–215 nm or with a refractive index detector, to give a detection level of about $10 \mu\text{g mL}^{-1}$ in solution, but the low selectivity of these detectors requires a high degree of clean-up prior to analysis. DSP toxins have a carboxyl group that is easily converted into a fluorescent ester derivative, which allows HPLC analysis with fluorescence detection. Pioneering work using this fluorescence

detection method uses 9-anthryldiazomethane (ADAM) as the derivatization reagent. Several other reagents have also been used for derivatization to try to overcome the problems of instability of ADAM; however, none has proven as selective and sensitive as ADAM. An HPLC method has been developed with fluorescence detection, using ADAM as derivatization reagent, which was synthesized *in situ* and used immediately. This method offers a reformulation of the previous *in situ* method. The ADAM method is very sensitive for DSP toxins, being able to detect 10 pg of the okadaic acid (OA) derivative injected on-column; the practical quantitation limit is about 10 ng g^{-1} tissue. **Figure 5** shows an example of the application of the *in situ* ADAM-HPLC analysis of standards and a real Galician mussel sample under the chromatographic conditions described in **Table 4**. This ADAM method is not suitable for the analysis of DTX-3 compounds owing to their high molecular weight and lipophilicity. They must first be converted back to OA, DTX-1 or DTX-2 via alkaline hydrolysis; nevertheless, these compounds can be directly analysed by mass spectrometric techniques.

Mass spectrometry is a powerful tool for the analysis of marine toxins. This technique can provide structural information, as well as offering high sensitivity and selectivity; this structural information is useful not only for the confirmation of toxin identity, but also for the identification of new toxins. The combination of HPLC with electrospray mass spectrometry (LC-ESMS) appears to be one of the most sensitive and rapid methods of analysis for DSP toxins. The detection limit found for this technique is about 1 ng g^{-1} in whole edible shellfish tissue. This mass spectrometric detection has been also applied for the analysis of Galician samples, allowing the first confirmation of DTX-2 in these mussels.

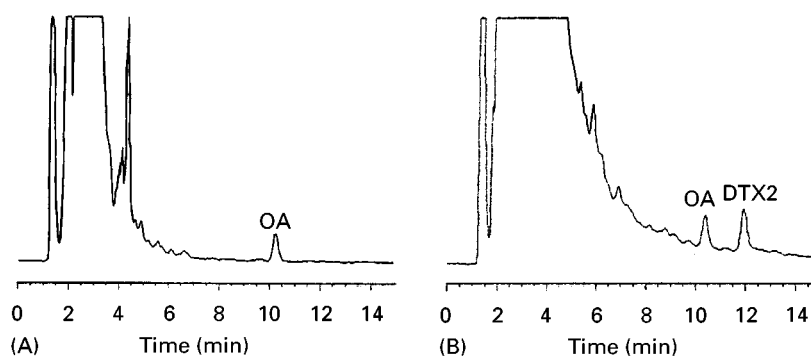


Figure 5 Chromatogram obtained for the DSP toxin profile by using ADAM-HPLC-FLD.

ASP Toxins

This new type of seafood toxicity was first described after a contamination that took place in Prince Edward Island, Canada, in 1987. None of the known shellfish toxins was implicated in this incident and eventually domoic acid was identified as the toxic agent. Amnesic shellfish poisoning was originally isolated from a red macroalga, *Chondria armata*, by Japanese researchers studying insecticidal properties of algal extracts. Most of the people affected by this intoxication experience gastroenteritis but many older people develop neurological symptoms including memory loss. Intraperitoneal injections of acidic aqueous extracts of mussels contaminated with domoic acid into mice cause death with unusual neurotoxic symptoms very different from those of paralytic shellfish poison and other known toxins.

Domoic acid (DA) is a known neurotoxin that is absorbed through the gastrointestinal system, causing damage in the central nervous system. The source of this toxin is a diatom, *Nitzschia pungens multiseriata*, which is ingested by shellfish such as mussels during normal filter feeding. The chemical structure of domoic acid is shown in **Figure 6**. This rare naturally occurring amino acid is a member of a group of potent neurotoxic amino acids that act as an agonist to glutamate, a neurotransmitter in the central nervous system. A number of DA isomers that show

varying degrees of toxicity have also been identified. Isomerization of DA can occur photochemically or thermally, the latter being significant in cooked seafood.

Like the toxins previously described, reliable methods for the analysis of DA and isomers in seafood products are extremely important for protection of public health. Domoic acid can be analysed semiquantitatively by TLC, but instrumental methods of analysis are most commonly used. HPLC or ion exchange chromatography using ultraviolet absorbance detection are the methods of choice. HPLC has been used since 1987 by Canadian regulatory agencies to prevent other incidents of shellfish poisoning, and is also the official method of analysis for domoic acid in most countries. Domoic acid may be extracted from shellfish tissues by boiling with water or by blending with aqueous methanol. The latter is most commonly used because it is better suited for trace analysis and combines well with a highly selective clean-up based on strong anion exchange. The detection of domoic acid is facilitated by its strong absorbance at 242 nm. The main problem of using this technique is associated with the presence of interferences, which can give false positives with crude extracts. This is the case of tryptophan and some of its derivatives. Since these compounds are often present in shellfish and elute close to domoic acid, SAX-SPE clean-up prior to HPLC-UV analysis avoids the problem caused by these

Table 4 Conditions for the ADAM-HPLC-FLD analysis of DSP toxins

HPLC system	Liquid chromatograph, HP-1050
Column	Reversed-phase column, HP-Hypersil ODS (4 mm i.d. × 25 cm, 5 μm)
Mobile phase	MeCN : H ₂ O (85 : 15)
Flow rate	1.0 mL min ⁻¹
Detection	Fluorescence detector, HP-1046A: excitation wavelength 254 nm emission wavelength 412 nm

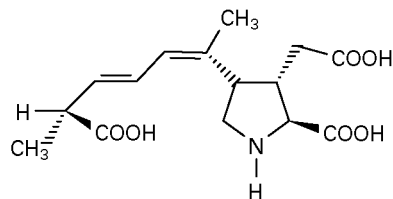


Figure 6 Chemical structure of domoic acid, main toxin responsible for ASP toxicity.

Table 5 Conditions for the HPLC-UV analysis of ASP toxins

HPLC system	Liquid chromatograph Jasco PU-980 pump
Column	Prodigy-ODS 5 μ m column (Phenomenex) 4.6 mm \times 25 cm
Mobile phase	10% v/v aqueous acetonitrile with 0.2 mol L ⁻¹ formic acid; flow rate, 1 mL min ⁻¹
UV detector	Perkin-Elmer LC-95 UV/Vis; wavelength 242 nm

interferences. An example of the application of the HPLC-UV technique for the analysis of domoic acid in standards, mussel tissue reference material and real contaminated bivalves under the chromatographic conditions described in Table 5 is shown in Figure 7.

A very sensitive alternative HPLC method using fluorescent detection has been proposed. This method uses 9-fluoronylmethyl chloroformate (FMOC) as derivatization reagent and the FMOC derivative is analysed with fluorescence detection.

Capillary electrophoresis offers the potential of fast high resolution separation of DA and its isomers and the possibility of trace analysis with very small amounts of sample. This method is also attractive in terms of being inexpensive and complementary to HPLC.

Extraction and clean-up procedures are priority steps in order to achieve the best chromatographic and electrophoretic resolution; when combined with a selective extraction and clean-up procedure, CE with UV detection is an excellent method for the separation and quantitative analysis of domoic acid and its isomers in shellfish tissues. Figure 8 shows the

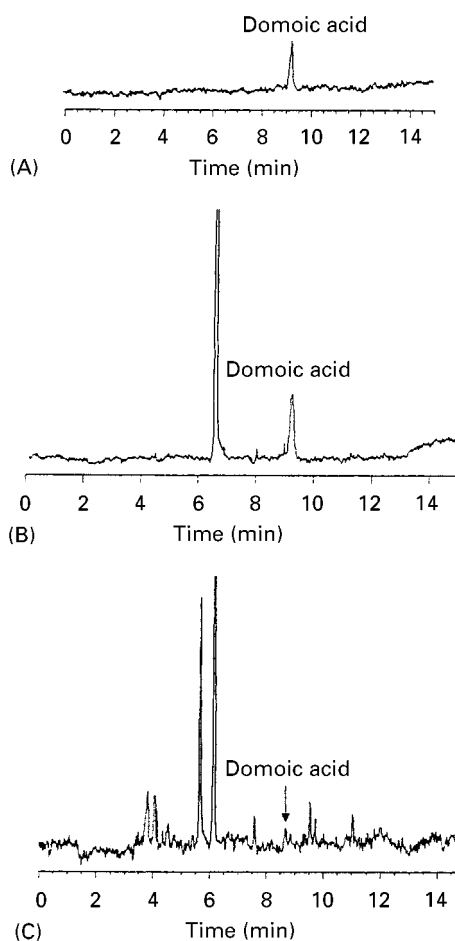


Figure 8 Electropherogram obtained for domoic acid by CE-UV-DAD. (A) Standard of domoic acid; (B) mussel tissue reference material (MUS-1); and (C) Galician mussel sample. (Reproduced with permission from James KJ *et al.* *Journal of Chromatography* 798: 147.)

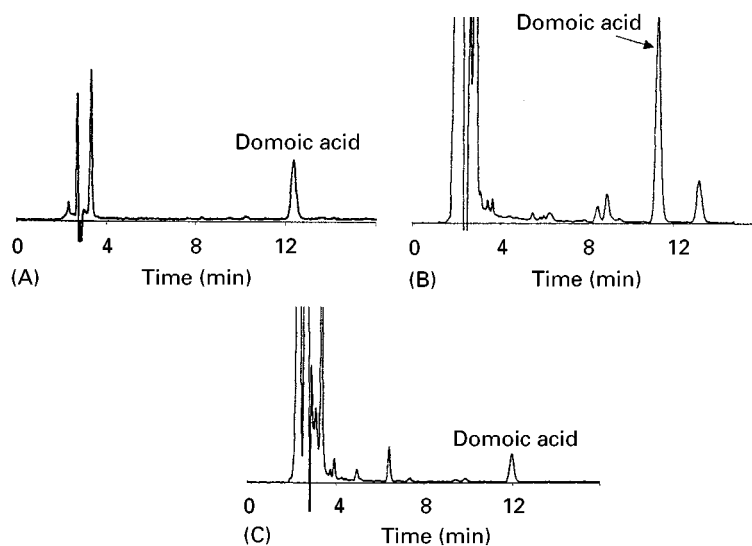


Figure 7 Chromatogram obtained for domoic acid by HPLC-UV. (A) Standard of domoic acid; (B) mussel tissue reference material (MUS-1); and (C) Galician mussel sample.

Table 6 Conditions for the CE-UV-DAD analysis of domoic acid

CE-DAD system	HP ^{3D} CE (Hewlett-Packard); voltage, 30 kV
Capillary	Bare fused silica capillary (50 µm i.d. × 66 cm length)
Background buffer	25 mmol L ⁻¹ borate at pH 9.2
DAD detector	Wavelength 242 nm
Injection	Pressure 50 mbar; time, 12 s

application of CE to the analysis of standard solution of domoic acid, mussel tissue reference material (MUS-1) and Galician mussel samples. The conditions for this CE analysis are summarized in **Table 6**.

The use of cyclodextrins allows an increase on the separation efficiency when compared with LC-UV-D. The better mass detection limit provided by this CE technique could be very useful for situations where limited sample size is available.

Future Trends

The techniques of HPLC and CE for the analysis of marine toxins provide the separation efficiency required for complicated matrices such as marine samples as well as the high resolution required to determine the toxins present in contaminated samples with very low detection limits. Extraction and clean-up steps prior to the chromatographic analysis are essential in order to obtain accurate quantitative results and also to prevent interferences that can cause false positives. New, fast and on-line automated procedure could give shorter and more accurate analyses. The possibility to combine this automation with simple methods is also desirable, especially for routine control purposes.

Taking into account the lack of standards for all toxins and also the appearance of new, unknown toxic compounds, the development of confirmatory techniques for their detection is an important research field. The development and optimization of coupling techniques, such as LC-MS or CE-MS, and the development of adequate interfaces as well as efficient ionization modes is a high priority.

See Colour Plate 104.

See also: II/Chromatography: Liquid: Detectors: Mass Spectrometry; Instrumentation; Mechanisms: Reversed Phases. **Electrophoresis:** Capillary Electrophoresis; Capillary Electrophoresis-Mass Spectrometry.

Further Reading

Bates HA and Rapoport H (1975) Chemical assay for saxitoxin, the paralytic shellfish poison. *Journal of Agriculture and Food Chemistry* 23: 237.

Bialojan C and Takai A (1988) Inhibitory effect of a marine-sponge toxin, okadaic acid on protein phosphatases specificity and kinetics. *Biochemical Journal* 256: 283–290.

Fujiki H, Suganuma M, Suguri H, Yoshizawa S, Takagi K, Uda N, Wakamatsu K, Yamada K and Murata M (1988) Diarrhetic shellfish toxin dinophysistoxin-1 is a potent tumour promoter on mouse skin. *Japanese Journal of Cancer Research* 79: 1089–1093.

Gago-Martinez A, Rodríguez-Vázquez JA, Quilliam MA and Thibault P (1996) Simultaneous occurrence of diarrhetic and paralytic shellfish poisoning toxins in Spanish mussels in 1993. *Natural Toxins* 4: 72–79.

Hallegraeffe GM, Anderson DM and Cambella AD (eds) (1995) *Manual on Harmful Marine Microalgae*. IOC Manuals and Guides No. 33, UNESCO.

Lawrence JF, Charbonneau CF, Menard C, Quilliam MA and Sim PG (1989) Liquid chromatographic determination of domoic acid in shellfish products using the paralytic shellfish poison extraction procedure of the Association of Official Analytical Chemists (AOAC). *Journal of Chromatography A* 462: 349–356.

Lawrence JF, Menard C and Cleroux Ch (1995) Evaluation of prechromatographic oxidation for liquid chromatographic determination of paralytic shellfish poisons in shellfish. *Journal of AOAC International* 78(2): 514–520.

Lee JS, Yanagi T, Kenma R and Yasumoto T (1987) Fluorimetric determination of diarrhetic shellfish toxins by high performance liquid chromatography. *Agricultural and Biological Chemistry* 51: 877–881.

Locke SJ and Thibault P (1994) Improvement in detection limits for the determination of paralytic shellfish poisoning toxins in shellfish tissues using capillary electrophoresis/electrospray mass spectrometry and discontinuous buffer systems. *Analytical Chemistry* 20: 3436–3446.

Oshima Y, Machida M, Sasaki K, Tamaoki Y and Yasumoto R (1984) Liquid chromatographic-fluorometric analysis of paralytic shellfish toxins. *Agricultural and Biological Chemistry* 48: 1707–1711.

Pocklington R, Milley JE, Bates SS, Bird CJ, De Freitas ASW, Quilliam MA (1990) Trace determination of domoic acid in seawater and plankton by high-performance liquid chromatography of the fluorenylmethoxycarbonyl (FMOC) derivative. *International Journal of Environmental and Analytical Chemistry* 38: 351–368.

Quilliam MA, Gago-Martínez A, Rodríguez-Vázquez JA (1998) Improved method for preparation and use of 9-anthryldiazomethane for derivatization of hydroxycarboxylic acids. Application to diarrhetic shellfish poisoning toxins. *Journal of Chromatography A* 807: 229–239.

Quilliam MA, Sim PG, McCulloch AW and McInnes AG (1989) High-performance liquid chromatography of domoic acid, a marine neurotoxin, with application to shellfish and plankton. *International Journal of Environmental and Analytical Chemistry* 36: 139–154.

Sullivan JJ (1990) High-performance liquid chromatographic method applied to paralytic shellfish poisoning research. In Hall S and Strichartz G (eds) *Marine Toxins*, pp. 66–77. ACS Symposium Series 418.

Sullivan JJ and Wekell MM (1987) In: Kramer DE and Liston J (eds) *Seafood Quality Determination*, p. 357. New York: Elsevier, North Holland.

Thibault P, Pleasance S and Laycock MV (1991) Analysis of paralytic shellfish poisons by capillary electrophoresis. *Journal of Chromatography A* 542: 483–501.

Wright JLC, Boyd RK, De Freitas ASW *et al.* (1989) Identification of domoic acid, a neuroexcitatory amino acid, in toxic mussels from eastern Prince Edward Island. *Canadian Journal of Chemistry* 67: 481–490.

Zhao JY, Thibault P and Quilliam MA (1997) Analysis of domoic acid and isomers in seafood by capillary electrophoresis. *Electrophoresis* 18: 268–276.

MECHANICAL TECHNIQUES: PARTICLE SIZE SEPARATION



A. I. A. Salama, Natural Resources Canada,
Devon, Alberta, Canada

Copyright © 1999 Minister of Natural Resources,
Canada

Introduction

Particles of many kinds and various sizes have played an important role in man's interaction with his physical environment. They abound in the soil and earth below; they are also present in water, air, chemical products, and many other sources. If particles were spherical or cubical, it would be easy to characterize them. Unfortunately, most of the particles present in our environment are of irregular size and shape. Therefore, it is desirable to try to develop methodologies and techniques to characterize particles of irregular size and shape, and this is the main objective of particle size analysis. Moreover, particle size analysis is important in studying particle behaviour in a medium as in many analytical sciences and industrial applications.

Particle size analysis in physical, chemical, and biological processes involves many concepts and techniques; however, this article focuses on the methods of particle size analysis utilizing mechanical techniques.

This article will first introduce some basic principles used in particle size analysis. This will be followed by a summary of the applicable particle size ranges for the different methods and the size ranges of most common particles found in industrial, chemical, environmental, and clinical applications. The most common mechanical techniques and methods used in particle size analysis will be briefly presented.

Particle Properties

Particle size analysis plays an important role in many analytical sciences and industrial applications. To assist in developing useful methodologies and tech-

niques it is essential to identify the main factors that control the behaviour of particles in a medium. Such factors include particle density, shape, size, size distribution, concentration, and surface characteristics, and the carrier medium dynamics (**Figure 1**). This article focuses on particle size analysis using mechanical techniques in relation to clinical, industrial, and environmental applications: therefore, the particles under consideration could be solid or liquid and the medium could be liquid or gas. In aerosol systems the medium is gas (air).

Density

Particles originating from a solid will have the same density as that of the parent material. However, if the material undergoes hydration or surface oxidization or if it agglomerates in clusters, its specific gravity will change. The particle density plays an important role in the separation of solids as in centrifugal and gravitational sedimentation, for example.

Particle Shape

Shape factors The method of formation influences the resultant particle shape. In comminution, attrition or disintegration, the generated particle resembles the parent material. On the other hand, if the method of formation is condensation from vapour, the smallest unitary particle may be spherical or cubical. In many cases condensation is followed immediately by solidi-

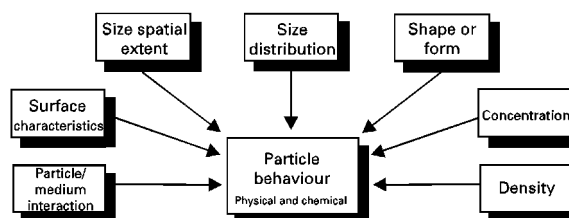


Figure 1 Main factors affecting particle behaviour in a medium.

fication and formation of chain-like aggregate (e.g. iron oxide fumes, carbon black).

Based on experimental data it has been found that for a collection of groups of particles having an average diameter D_{pi} for group i , the total surface area can be expressed as:

$$A_p = \alpha_s (\sum n_i D_{pi}^2) \quad [1]$$

where α_s is defined as the surface shape factor. The total volume can be expressed as:

$$V_p = \alpha_v (\sum n_i D_{pi}^3) \quad [2]$$

where α_v is defined as the volume shape factor. The surface and volume shape factors may be related to a combined shape factor k_p as:

$$k_p = \frac{\alpha_s}{\alpha_v} \quad [3]$$

In the case of spherical or cubical particles it can be shown that the shape factor is 6. For irregular particles, values vary from 6 to 10. Some other relationships can be obtained by using eqns [1]–[3]:

$$A_v = \frac{A_p}{V_p} = \frac{k_p}{D_p^*} \quad [4]$$

$$D_p^* = \frac{\sum n_i D_{pi}^3}{\sum n_i D_{pi}^2} \quad [5]$$

$$A_m = \frac{k_p}{\rho_p D_p^*} \quad [6]$$

where A_v = specific surface area (surface area per unit volume); D_p^* = specific surface diameter; A_m = surface area per unit mass; ρ_p = density of the particle material. The surface and volume information are used in estimating the equivalent spherical particle diameter which is used in studying particle behaviour in a medium.

Fractal geometry Mandelbrot introduced the basic concepts and theories of a new type of geometry called fractal geometry, in order to describe rugged structures. The main idea put forward by Mandelbrot is that the boundary of a rugged system can be described in its embedding space by a fractal dimension which describes its space filling effect. In the case of a fractal surface the estimate of surface area (A_λ) tends to increase without limit as the step size (resolution) λ of an elemental square decreases. This can be expressed as:

$$A_\lambda = k_a \lambda^{-(\delta-2)} \quad [7]$$

where k_a is a constant and the fractal dimension δ is greater than 2. Hence a plot of $\ln(A_\lambda)$ versus $\ln(\lambda)$ will have a slope of $[-(\delta-2)]$, where 'ln' designates a natural logarithm.

Kaye applied fractal geometry in his studies of the profiles of carbon black agglomerates. In subsequent studies he demonstrated the usefulness of fractal geometry in studying boundary and mass fractal dimensions of aerosol systems, fractal structures of fine particle systems, fragmentation, description of porous bodies and gas adsorption.

Surface Characteristics and Interfacial Phenomena

The surface characteristics of small particles include surface area, rate of evaporation and condensation, electrostatic charge, adsorption, adhesion and light scatter. In certain circumstances, changes in the environment of a particle during sampling and particle size analysis may change its size or state of aggregation or its surface characteristics. Such changes must be considered in the selection of a suitable sampling device or method for particle size analysis.

Surface area One of the important characteristics of small particles is the rapid increase in exposed surface area per unit mass as size decreases, which leads to increased chemical reaction rate. Fine powders of organic and inorganic oxidable materials (such as coal, iron, flour, sugar, and starch) burn vigorously or explode violently when in the form of an aerosol. Moreover, an increase in surface area increases the toxicity of some granular materials.

Evaporation and condensation Evaporation and condensation are diffusion mass transfer processes which proceed at rates proportional to the surface area exposed. The temperature and partial pressure in the vicinity of the surface control the time required for small particles (e.g. water) to evaporate into still air. The evaporation time is given by:

$$\tau = \frac{RT}{8M} \frac{\rho_p D_p^2}{D \Delta p} \quad [8]$$

where τ = evaporation time (s); ρ_p = density of particle material (kg m^{-3}); D_p = particle diameter (m); D = diffusion coefficient of vapour from particle ($\text{m}^2 \text{s}^{-1}$); Δp = difference between the particle pressure at the particle surface and in the surrounding fluid (N m^{-2}); R = gas constant ($8.3144 \text{ J mol}^{-1} \text{ K}^{-1}$); T = absolute temperature (K); M = molecular weight of evaporating particulate material. Finer particles can act as centres for

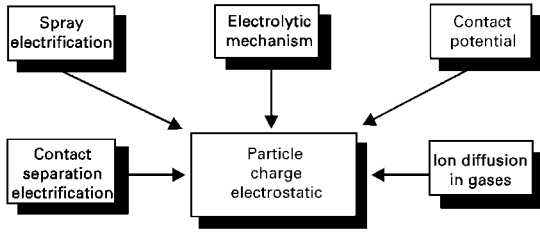


Figure 2 Mechanisms producing natural charge on particles.

condensation of moisture, leading to an increase in their size.

Electrostatic charge Electrostatic charge represents an excess or deficiency of electrons on the particle surface. This charge may be assumed to reside on the particle surface in an absorbed gas or moisture film. Mechanisms which produce natural charge on particle surfaces are shown in **Figure 2**. The electrostatic charge generated on a particle is proportional to the particle surface area, which is the principle used in the design of electrostatic classifiers and precipitators. Furthermore, the presence of electrostatic charge on particle surfaces controls the behaviour of particles in an electric field (see II/PARTICLE SIZE SEPARATION/Electrostatic Precipitation).

Scattering properties Scattering of radiation arises from inhomogeneities, such as dispersed dust or water drops, in the fluid medium. Scattering is often accompanied by absorption, and both scattering and absorption remove energy from the incident beams. The quantitative response of the intensity of transmitted and/or scattered beams can be used to characterize the size of a particle.

Kinetic Behaviour of Particles

The equivalent spherical particle diameter of an aggregate of irregularly-shaped particles can be determined by studying the inertial motion of particles in a medium. Such inertial motion can be found in many applications such as pulmonary deposition, design of industrial ventilation, particle collectors, and electrostatic precipitation. The various processes that affect particle motion in a field are shown in **Figure 3**.

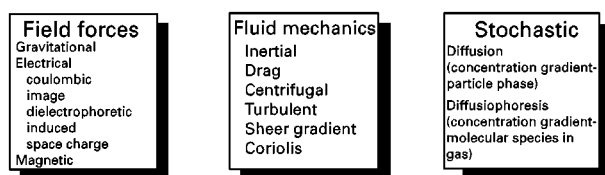


Figure 3 Processes affecting particle motion in a medium.

Medium Resistance

For a small spherical particle moving in a medium at low velocities (i.e. laminar flow), the drag (medium resistance) force acting on the particle is given by Stokes' Law as:

$$F_R = 3\pi\mu_m D_p V_{pm} = C_D \frac{\rho_m A V_{pm}^2}{2} \quad [9]$$

where F_R = medium resistance (N); D_p = particle diameter (m); ρ_m = medium density (kg m^{-3}); μ_m = medium viscosity ($\text{kg m}^{-1} \text{s}^{-1}$); V_{pm} = relative velocity between particle and medium (m s^{-1}); A = projected area of particle normal to its motion (m^2).

It is useful to relate the magnitudes of the inertial and viscous forces in the form of a dimensionless Reynolds' Number as:

$$Re_p = \frac{\rho_m D_p V_{pm}}{\mu_m} \quad [10]$$

The relationship between the drag coefficient C_D and the Reynolds' Number can be found in any fluid mechanics textbook. However, for spheres with $Re_p < 1$, $C_D = 24/Re_p$.

In finite containers a particle experiences an increase in the drag force due to two effects. First the fluid streamlines around the particle impinge on the container walls and are reflected back causing increased drag on the particle. The second effect occurs because the fluid is stationary at a finite distance from the particle, and there is a distortion of the flow pattern which reacts back on the particle. Taking into consideration these two effects, the drag force may be modified as:

$$F_R = 3\pi\mu_m D_p V_{pm} \left(1 + \frac{kD_p}{L} \right) \quad [11]$$

where L represents the distance from centre of particle to the container walls and $k = 0.563$ for a single wall or container bottom and $k = 2.104$ for a cylindrical container.

Particle Motion

Particle motion in a gravitational/drag field The linear motion of a particle in a direction X relative to time t and under the influence of the drag, gravitational, and buoyancy forces is governed by:

$$\frac{\pi}{6}\rho_p D_p^3 \left(\frac{d^2 X}{dt^2} \right) = \frac{\pi}{6}(\rho_p - \rho_m) D_p^3 g - 3\pi\mu_m D_p \frac{dX}{dt}$$

[12]

where g denotes gravitational acceleration. If the particle starts from zero velocity it will accelerate until it reaches a terminal velocity given by:

$$\left(\frac{dX}{dt}\right)_{t \rightarrow \infty} = V_{gt} = \left[\frac{D_p^2(\rho_p - \rho_m)}{18\mu_m}\right] \cdot g \quad [13]$$

from which the particle diameter can be expressed as:

$$D_p = \left[\frac{18\mu_m}{(\rho_p - \rho_m)g} \cdot V_{gt}\right]^{1/2} \quad [14]$$

Note that eqns [12] to [14] are applicable for $Re_p < 1$.

For a particle settling in air, it is usual to neglect the buoyancy correction, since ρ_p is of the order of unity, the air density is of the order of $10^{-3} \text{ g cm}^{-3}$, and viscosity of ambient air is $1.8 \times 10^{-5} \text{ kg m}^{-1} \text{ s}^{-1}$. Equation [13] reduces to:

$$V_{gt} = 3.03 \times 10^4 \rho_p D_p^2 \quad [15]$$

where V_{gt} , ρ_p , and D_p are expressed in m s^{-1} , kg m^{-3} , and m , respectively.

Particles with diameters less than or close to the mean free path of the fluid molecules begin to slip between molecules and settle at a higher velocity than that predicted by eqn [13] for settling velocity. Cunningham considered this so-called slip effect and introduced a correction term to the terminal settling velocity as:

$$V_{gtc} = C_c V_{gt} \quad [16]$$

$$C_c = \left(1 + \frac{2\alpha\lambda}{D_p}\right) \quad [17]$$

where C_c denotes the Cunningham slip correction factor, λ is the mean free path of medium molecules, and α is a constant of approximately one.

Particle motion in a rotational (centrifugal) field In a centrifugal field the radial motion of a particle at a distance R from the centre of rotation is governed by:

$$\frac{\pi}{6}\rho_p D_p^3 \left(\frac{d^2 R}{dt^2}\right) = \frac{\pi}{6}(\rho_p - \rho_m) D_p^3 \omega^2 R - 3\pi\mu_m D_p \frac{dR}{dt} \quad [18]$$

where ω is the angular velocity of the particle. Assuming that the particle movement outward is resisted by viscous drag, Stokes' law provides a reasonable approximation for the drag. Therefore, the terminal radial velocity at equilibrium is given by:

$$\left(\frac{dR}{dt}\right)_{t \rightarrow \infty} = V_{rt} = \left[\frac{D_p^2(\rho_p - \rho_m)}{18\mu_m}\right] \cdot \omega^2 R \quad [19]$$

which is equivalent to eqn [13].

To evaluate the performance of a centrifugal separation process, a separation factor ' SF ', defined as the ratio of centrifugal acceleration to gravitational acceleration:

$$SF \text{ or } g\text{-force} = \frac{\omega^2 R}{g} \quad [20]$$

is used. For dust-collecting cyclones (particles $> 100 \mu\text{m}$), $SF = 200$, while conventional centrifuges used in precipitation of submicron particles and large molecules in liquid suspension have $SF = 5000$. See II/PARTICLE SIZE SEPARATION/Hydrocyclones for Particle Size Separation.

Particle motion in an electrostatic field When particles larger than $1 \mu\text{m}$ are passed through a corona discharge as the result of bombardment charging, they acquire charges from electrons and adsorbed gas ions proportional to the surface area of the particle. The saturation charge acquired is given by:

$$Q_{pb} = ne = \pi\epsilon_0\epsilon_1\kappa D_p^2 E \quad [21]$$

$$\kappa = \frac{3\epsilon_2}{\epsilon_2 + 2\epsilon_1} \quad [22]$$

where Q_{pb} = saturation bombardment charge acquired (C); n = number of electron charges acquired; e = electron charge ($1.6022 \times 10^{-19} \text{ C}$); ϵ_0 = permittivity of vacuum ($8.8542 \times 10^{-12} \text{ F m}^{-1}$); ϵ_1 = relative permittivity of medium (gas); ϵ_2 = relative permittivity of particle material; E = external electric field strength (V m^{-1}). For particles less than $0.2 \mu\text{m}$, diffusion charging predominates and the charges acquired at time t are given approximately by:

$$Q_{pb} = ne = \frac{D_p k T}{2e} \ln \left(1 + \frac{\pi D_p V_i N_0 e^2}{2kT} t\right) \quad [23]$$

where Q_{pd} = diffusion charge acquired (C); k = Boltzmann constant ($1.3807 \times 10^{-23} \text{ J K}^{-1}$); T = absolute temperature (K); N_0 = ion density (ions m^{-3}); V_i = ion velocity (root mean square, m s^{-1}). Based on the acquired charge on the particle and assuming that air resistance is approximated by Stokes' Law, the particle terminal velocity in an electric field is given by:

$$V_{et} = C_c \left(\frac{EQ_p}{3\pi\mu_m D_p}\right) \quad [24]$$

where C_c = Cunningham slip correction factor; μ_m = medium (gas) viscosity; Q_p = acquired (bombardment or diffusion) charge on the particle.

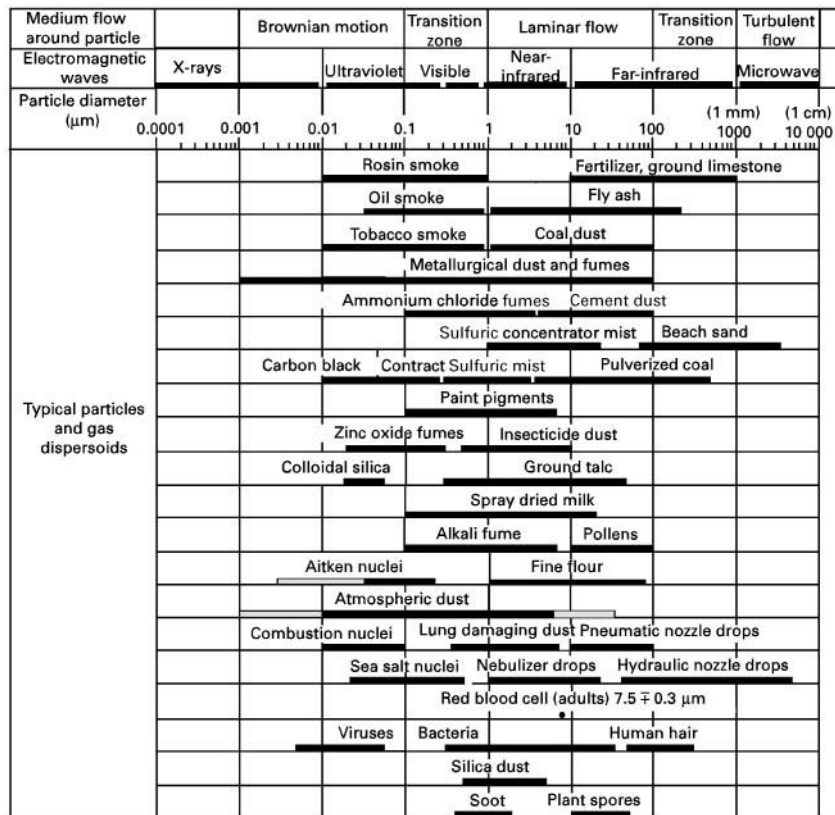


Figure 5 Typical particles and gas dispersoids.

Micromesh sieves are used to classify particles of size range 5–20 μm, while particles of size range 20–125 μm are classified in the standard woven wire sieves. Coarse particles (> 125 μm) are classified in

punched plate sieves. Punched plate sieves are commonly used in industrial applications where the openings are circular or rectangular; the sieves can take different configurations.

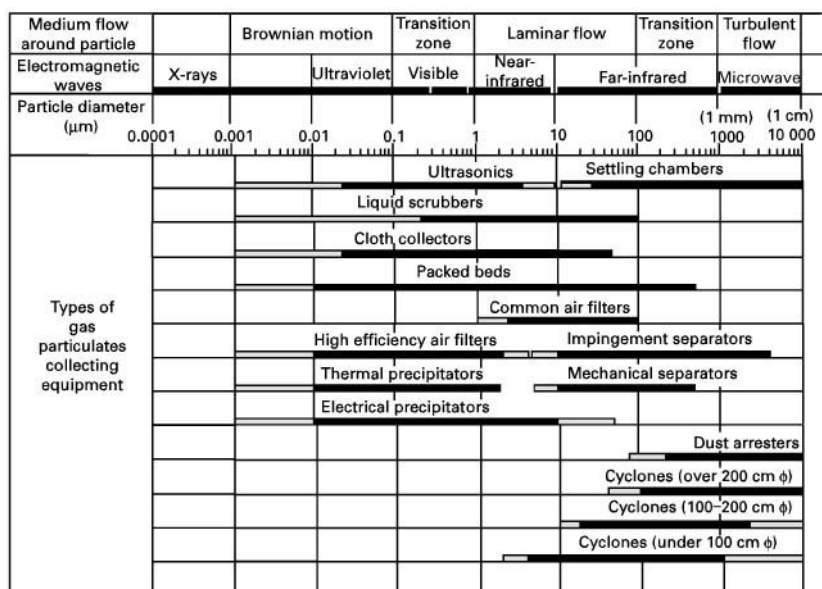


Figure 6 Different types of gas particulates collecting equipment (φ, diameter).

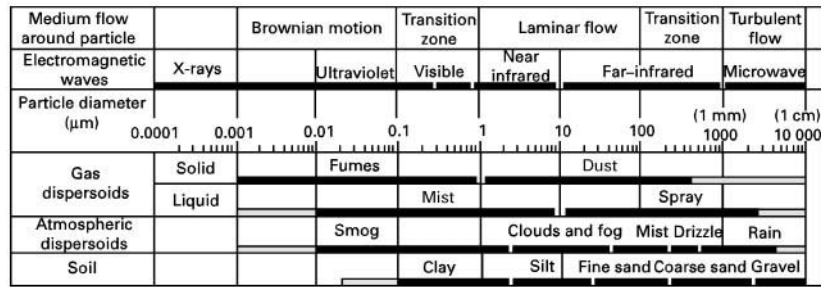


Figure 7 Some size range definitions.

The sieving test is conducted using up to 11 sieves stacked with progressively larger aperture openings towards the top, and placing the powder on the top sieve. A closed pan (receiver) is placed at the bottom. There are several schemes for shaking the sieves by mechanical or ultrasonic means. The residues in each sieve are recorded and expressed in percentage as cumulative values against the nominal sieve aperture values.

The common methods for fine sieving are machine, wet, hand and air-jet sieving. Wet-sieving is recommended for material originally suspended in a liquid and is necessary for powders which form aggregates when dry-sieved. In such tests the stack of sieves is filled with liquid and the sample is fed to the top sieve. Sieving is accomplished by rinsing, vibration, reciprocating action, vacuum, ultrasonication or a combination of these.

Table 1 presents the different international sieve standards and the corresponding sieve types. There are several sieve aperture progression ratios commonly available depending on the different international standards. In the USA, a progression ratio of $2^{1/2}$ is used. This ratio corresponds to successive particle groups of 2 : 1 particle surface ratio. The progression rate of $2^{1/3}$ ($10^{0.1}$) which has been adopted by the French corresponds to successive particle groups of 2 : 1 particle volume ratio. The progression ratios of $10^{0.1}$ and $10^{0.05}$ are recommended for narrow size distributions.

Table 1 International sieve standards

Country	Standard	Sieve type
Great Britain	BS 410	Woven wire
USA	ASTM E11	Woven wire
	ASTM E161-607	Micromesh (electroformed)
Germany	DIN 4188	Woven wire
	DIN 4187	Perforated plate
France	AFNOR NFX 11-501	Woven wire
International	ISO R565 1972(E)	Perforated plate

The probability of a particle passing through sieve apertures depends on the particles size distribution, the number of particles on the sieve (sieve loading), the method of sieve shaking, the dimension and shape of the particle, and the ratio of open area of sieve to total area. In addition, the sieving operation can be affected by the friability and cohesiveness of the powder.

Sedimentation

Sedimentation of fine powders in a suspension is an important tool in the determination of particle size distribution. **Table 2** presents a classification of the methods and techniques used in sedimentation (gravitational or centrifugal). To conduct particle size analysis using sedimentation, the suspension can be prepared using the line start (two-layer) or the homogeneous suspension techniques. In the two-layer technique, the powder is introduced at the top of a column of clear liquid. In the homogeneous suspension technique, the powder is uniformly dispersed in the liquid. As the particles start to settle the change in solids concentration at a particular fixed height with time or the sedimentation time rate is measured. The solids concentration or density measurements is used in the incremental methods, while the settling rate measurement is used in the cumulative methods. Incremental methods may be divided as fixed time and fixed depth methods, the latter being more popular, although a combination is sometimes used.

A powder is made up of three types of particles: primary particles, aggregates and agglomerates. The

Table 2 Sedimentation methods and techniques

Incremental methods	Cumulative methods
Solids concentration variation	Sedimentation rate
Line start	Line start
Homogeneous suspension	Homogeneous suspension
Suspension density variation	
List start	
Homogeneous suspension	

primary particles are crystalline or organic structures bound together by molecular bonding, while the aggregates are primary particles tightly bound together at their point of contact by atomic or molecular bonding. The force required to break these bonds is considerable. In case of agglomerates, the primary particles are loosely bound together with weak van der Waals forces. It is often necessary to disperse the powder in a liquid prior to analysis. Dispersion is affected by the use of wetting agents which break down the agglomerates to their constituent parts. This process is facilitated by mechanical or ultrasonic agitation.

Gravitational sedimentation In gravitational sedimentation there are four main techniques: volume sample, mass sample, manometry and sedimentation vessel-wall pressure sensing as shown schematically in Figure 8.

Incremental methods Based on the results of motion of a particle in a gravitational/drag field, it can be shown that the solids concentration of settling suspension at depth h can be related to the cumulative undersize mass distribution as:

$$\frac{C(h, t)}{C(h, 0)} = \frac{\int_{D_{\min}}^{D_t} f(D) dD}{\int_{D_{\min}}^{D_{\max}} f(D) dD} = \Psi \quad [27]$$

$$D_t = \left[\frac{18\mu_m}{(\rho_p - \rho_m)g} \cdot \frac{h}{t} \right]^{1/2} \quad [28]$$

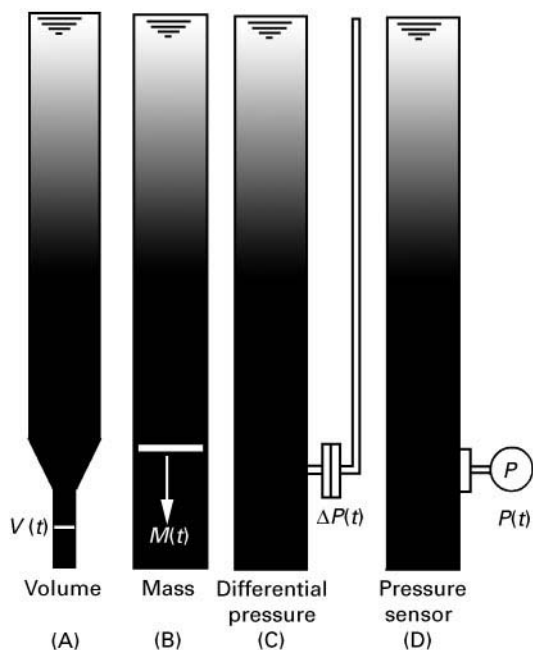


Figure 8 Main gravitational sedimentation techniques.

where $dm(D) = f(D)dD$ represents the mass fraction having particle size between D and $D + dD$. In eqns [27] and [28], it is assumed that the volume of particles (powder) in suspension is very small compared with the total volume of suspension. By plotting 100Ψ against the free-falling particle diameter D_t , the resulting curve shows the cumulative undersize percentage curve by mass.

Similarly, it can be shown that:

$$\frac{C(h, t)}{C(h, 0)} = \frac{\phi(h, t) - \rho_m}{\phi(h, 0) - \rho_m} = \Phi \quad [29]$$

where $\phi(h, 0)$ and $\phi(h, t)$ are the suspension density at a height h at $t = 0$ and $t = t$, respectively. By plotting 100Φ against D_t , the resulting curve shows the cumulative undersize percentage size curve.

The pipette method In this method, the changes in concentration occurring within a settling suspension are determined by drawing off definite volumes at a set of discrete intervals of time by means of a pipette. The solids concentration in the suspension is required to be between 0.2 and 1.0 vol%. If the concentration exceeds 1% the hindered settling adversely affects the results of the analysis. Initially the powder is made into a paste; this is followed by slow addition of the dispersing liquid, using a spatula plus mixing, to form a slurry. Further dispersion may be carried out in an ultrasonic bath. The suspension is washed into a sedimentation vessel. The analysis starts with violent agitation of the vessel avoiding the use of a stirrer. It is recommended that the container be continually inverted by hand for 1 min. Since initially the particles are not at rest, it is advisable to wait 1 min before withdrawing samples. The use of a time scale progression of 2 : 1 which produces a $2^{1/2}$ particle size progression is recommended. The collected samples are prepared to determine the solids concentration for particle size cumulative mass determination.

Hydrometers and divers The variation in density of settling suspension may be monitored with hydrometers, a method used widely in the cement industry. The method starts with a fully dispersed suspension and the densities at known depths are recorded as the solid phase settles out. The hydrometer technique is useful for quality control but not as an absolute method.

Divers are an extension of the hydrometer technique. They act as miniature hydrometers where each diver is calibrated to a particular density. Several divers of different densities are added to the fully dispersed suspension and each will settle at a height where its density is equal to the suspension around it.

Sealed in each diver is a copper ring which enables an external search coil to monitor and determine the location of the diver using high-frequency alternating current.

The specific gravity balance The specific gravity balance may be used to monitor the change within a settling suspension. Such a balance comprises two bobs, one in clear fluid and the other in the suspension being studied. The bobs are connected to the two arms of a beam balance. The depth of immersion of the bobs is adjustable. The change in buoyancy is counterbalanced by means of solenoids which are connected to a pen recorder. From the trace of the pen recorder, the particle size distribution can be calculated.

Cumulative methods Cumulative methods have an advantage over incremental methods in that the amount of sample required is small (about 0.5 g), which reduces the interaction between particles. This is a useful feature when only a small quantity of powder is available or when dealing with toxic materials.

Line start method In this case the size distribution may be directly determined by plotting the fractional weight settled against the free-falling diameter of particles. Special care needs to be exercised to eliminate the streaming problem, especially when the suspension at the top has higher density than the liquid.

Homogeneous suspension method Let us consider a powder with a mass distribution such that $dM = f(D)dD$, where dM represents the fractional mass of particles having a diameter between D and $D + dD$. Let us assume that the powder is completely dispersed in a liquid, and consider a suspension chamber of height h . It can be reasoned that mass per cent P which has settled out at time t is made up of two parts:

- (1) all the particles with a free-falling speed greater than that of D_t as given by Stokes' Law or some related law, where D_t is the size of particle which has a velocity of fall h/t ;
- (2) particles smaller than D_t which started off at some intermediate position in the chamber. The falling velocity of one of these smaller particles is v , the fraction of particles of this size that have fallen out at time t is (vt/h) .

This mechanism can be represented mathematically as:

$$P = \int_{D_t}^{D_{\max}} f(D) dD + \int_{D_{\min}}^{D_t} \frac{vt}{h} f(D) dD \quad [30]$$

which after some manipulation can be rewritten as:

$$P = M + t \frac{dP}{dt} \quad [31]$$

eqn [31] may be written in a different form as:

$$M = P - \frac{dP}{d \ln(t)} \quad [32]$$

Both eqns [31] and [32] can be used to determine M . The most obvious way is to tabulate t and P , and hence derive dP/dt , and finally M (cumulative percentage oversize) versus D_t . Equation [32] is recommended in cases of wide size distribution.

Centrifugal sedimentation Gravitational sedimentation for particle size analysis has limited flexibility. Firstly, the only means of varying the particle velocity is by selecting a medium with different density or viscosity. Secondly, gravitational sedimentation cannot handle particles smaller than 5 μm . Thirdly, most sedimentation devices suffer from the effects of convection, diffusion and Brownian motion. These difficulties can be reduced by speeding up the settling process by centrifuging the suspension. Furthermore, by the use of a centrifugal field, a substantially lower size limit and reduced analysis time can be achieved. As with gravitational methods the data may be cumulative or incremental and the sample may be homogeneous or two-layer.

Calculations of size distribution from centrifugal data are more difficult than calculations from gravitational data, since particle velocities increase as they move away from the axis of rotation (i.e. the particle velocity depends on its radial position). One way to overcome this difficulty is to use a relatively small settling radial zone at a far distance from the centre of rotation (i.e. the centrifugal force acting on all particles is approximately the same). Another solution is to use the line start technique. The most common techniques used in centrifugal sedimentation are schematically presented in Figure 9 where S and D designate source and detector, respectively.

Line start method Rewriting eqn [19] as:

$$V_{rt} = \frac{dR}{dt} = \left[\frac{D_t^2(\rho_p - \rho_m)}{18\mu_m} \right] \cdot \omega^2 R \quad [33]$$

together with separation of variables and integration of eqn [33], yields:

$$D_t = \left[\frac{18\mu_m}{(\rho_p - \rho_m)\omega^2 t} \cdot \ln\left(\frac{R}{S}\right) \right]^{1/2} \quad [34]$$

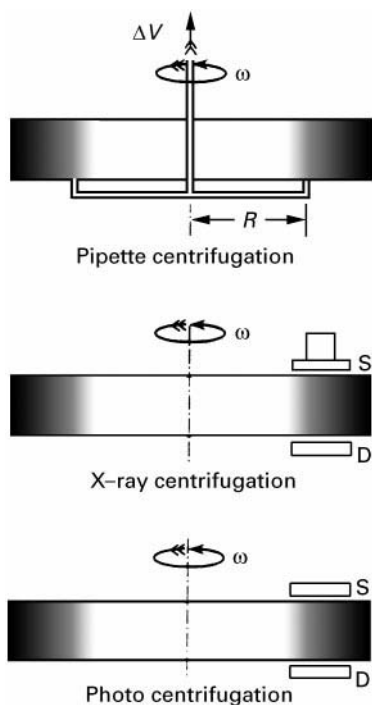


Figure 9 Main centrifugal sedimentation techniques.

where t is the time for a particle of size D_t to settle from the surface of the fill (at distance S from the centre of rotation) to a radial distance R . Hence, at time t , all particles at R will be of size D_t . Monitoring the per cent solids or density of the suspension at specified intervals of time will produce the particle size distribution which can be represented using cumulative values at different values of D_t .

Homogeneous suspension method Equation [34] still applies: however, at time t , all particles of size greater than D_t will have settled out radially to a distance R . Conversion of the sedimentation curve into a cumulative curve is not as simple in this case as for that of gravitational sedimentation. Difficulties involved in evaluating the sedimentation curve may be overcome in the case of a centrifugal field by assuming a constant centrifugal field, i.e. for $(R - S)$ interval is small enough to allow the approximation:

$$\ln\left(\frac{R}{S}\right) \approx \frac{(R - S)}{R} \quad [35]$$

when the value $(R - S)$ is one twentieth of R , the cumulative curve can be obtained directly by the pipette technique with an error of 1%.

Elutriation

In fluid classification, the effects of different forces on the movement of suspended particles control the separation of dispersed particles. As discussed in the kinetic behaviour of particles, the field forces are gravitation, as with elutriators, or centrifugal or Coriolis force in classifiers. The medium is usually water or air. In general all fluid classifiers can be divided into two classes, counterflow equilibrium (elutriation) and inverse flow separation. The elutriation is presented briefly below.

In the elutriation technique, the field and the drag forces act in opposite directions and particles leave the separation zone in one of two directions, depending on their size. Particles of a certain size stay in equilibrium in the separation zone. The grading is carried out in a series of vessels (cylindro-conical form) of successively increasing diameter. Hence, the fluid velocity decreases in each stage, the coarse particles being retained in the smallest vessel and the relatively finer particles in the following vessels. For air elutriation, the analysis is considered complete if the rate of change of weight in residues is less than 0.2% of the initial weight in half an hour, and for water elutriation the analysis ends when there is no sign of further classification.

Using Stokes' Law, the particle size retained in an intermediate vessel can be predicted approximately as

$$D_p = \left[\frac{18\mu_m}{(\rho_p - \rho_m)g} \cdot V_{\max} \right]^{1/2} \quad [36]$$

$$V_{\max} = 2V = 2\frac{Q}{A} \quad [37]$$

where Q = volumetric flow rate, A = vessel cross-sectional area at the equilibrium zone. In eqn [37] it is assumed that the flow profile in the vessel is parabolic. It is clear that elutriation is only suitable for rough dispersions. With small particles, sedimentation may be speeded up by using a centrifuge. This technique is utilized when classifying aerosols using a stream of air which flows in the direction opposite to the centrifugal force.

Electrostatic Precipitation

The electrostatic precipitator consists of an ionizing cathode at high potential surrounded by a collecting anode; typically, these anodes consist of concentric cylinders, the inner one often being a single wire. The gas suspension passes between the cylinders, picks up the charge, and travels to the anode where the charge is deposited. The transfer of electrons from one anode to the other constitutes an electric current. The mag-

nitude of this current is proportional to the number of particles deposited. Particle sizes can be determined by varying the flow rate or applied potential.

Classification in an electrostatic field by differences in charge is related explicitly to particle size. This type of instrument has been used for collecting aerosol bacteria. The instrument consists of a glass cylinder with a central electrode. The inner surface of the cylindrical glass is coated with a suitable material to act as the other electrode and to collect samples. The principal advantages of this type of instrument are high collection efficiency over a wide size range, low resistance and high flow-rate capacity.

Thermal Precipitation

Particles in a thermal gradient medium move in the direction of negative gradient, i.e. from hotter to colder regions. Based on this principle, the instrument typically consists of two parallel round microscopic glass plates and a heated wire in between as shown in **Figure 10**. The sample is drawn between the plates and the particles deposit on the glass plates and are collected for further analysis.

Normally a sample flow of $1\text{--}2\text{ cm}^3\text{ s}^{-1}$ is recommended and the collection efficiency is high for particles smaller than $5\text{ }\mu\text{m}$. The collecting device may be modified so that the sample is collected directly on an electron microscope grid. Modifications of the basic design include means of centering the wire in position, substitution of the wire by a ribbon to give more uniform deposits, and using inlet elutriators to exclude coarse particles. The practical application of thermal precipitation in gas cleaning plants has only rarely been attempted.

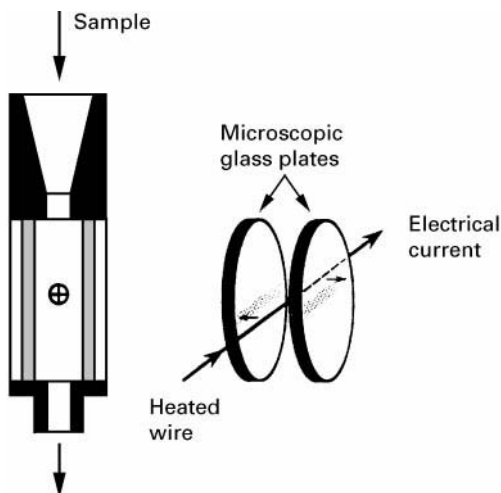


Figure 10 Thermal precipitation.

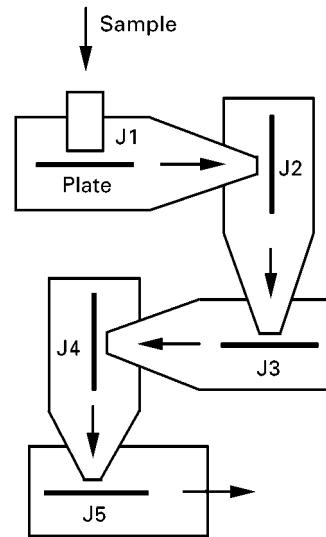


Figure 11 Cascade impactor.

Impaction

Impactor Inertial impaction devices cause an air sample to be drawn into a round or rectangular nozzle where the gas velocity is substantially increased. The jet from the nozzle is discharged against an adjacent flat surface, causing the air to diverge sharply. Particles in the air have more inertia than the air, and tend to continue forward as the air passes off to the sides, causing some of the particles to impact onto the surface. To prevent the particles from re-entrainment, a viscous material such as silicone fluid (or substrate) is used to coat the plate. The efficiency of impaction may be defined in terms of the dimensionless impaction factor as:

$$I = \left(\frac{C_c \rho_p D_{pa}^2 V_j}{18 \mu_m D_j} \right)^{1/2} \quad [38]$$

where D_{pa} = particle aerodynamic diameter; D_j = jet diameter or width; V_j = average air velocity at the jet outlet.

Classification of a particle cloud into discrete sizes using cascade impaction may be interpreted as measuring aerodynamic (equivalent spherical particle) diameter. Several impaction stages (cascade impactor) are used in the classification of a polydisperse cloud (see **Figure 11**). The stages are arranged to permit jet velocity to increase with each succeeding stage (by successive reduction in jet diameter or width), and to therefore cause particles of progressively smaller sizes to be impacted. In effect, the cascade impactor classifies particles according to their aerodynamic size. The aerodynamic diameter can be expressed in terms of Stokes'

diameter as:

$$D_{pa} = D_{Stokes} \rho_p^{1/2} \quad [39]$$

where D_{Stokes} is the measured diameter. The aerodynamic size is important because it controls the motion of a particle in an air stream. Therefore, it is significant for studies concerning lung inhalation, spray effectiveness, and gaseous cleaning devices. A special duty impactor (five-stage cascade impactor) has been developed for sampling and grading acid mists in the size range 0.3–3 μm .

Impinger Another sampling instrument, referred to as an impinger, also utilizes inertial impaction: however, deposition occurs at the bottom of a liquid-containing vessel. The downward-directed air-jet displaces the liquid and uncovers the bottom of the vessel. The particles that impinge against the wet surface are subsequently washed off by the liquid. The undeposited particles may be caught as air bubbles rise through the liquid. The particles are usually examined in the liquid suspension. Water is the most commonly used liquid.

Hydrodynamic Chromatography

Size information about colloidally suspended particles (0.01–1 μm) can be obtained by employing hydrodynamic chromatography (HDC). A medium (an aqueous solution) is pumped through a column packed with impermeable spheres. A pulse of colloidal suspension (0.2 cm^3) containing about 0.01 wt% polymer is injected into the flowing stream of the column entrance. The mobile phase from the column effluent is passed through a suitable detection system, such as a flow through spectrophotometer of the type used in liquid chromatography, and the detector response of the colloid is determined as a function of elution time. An extra step is needed to determine the concentration of solids in the eluted solution.

It has been observed that the larger particles elute faster than the small ones. It has also been found that the smaller the packing diameter the better the separation. Other factors which affect the rate of transportation through the bed are the size of bed particles, the ionic strength, and flow velocities, as well as the particle size of eluting particles.

In general, HDC has been successfully applied to the size characterization of a number of polymer lattices. The method is applicable to the size separation of particles between 0.02 and 1 μm , if they are rigid. Moreover, it is expected that HDC has wide applicability to sub- μm particles such as in lattices, carbon black, colloidal silica, paint, and photo-

graphic pigments, dyes, food colours, natural and artificial blood, and metallic fumes.

Another extension of HDC is to replace the packed bed with a long capillary. Capillary particle chromatography (CPC) requires 30 kPa pressure and has a separating range of 0.2–200 μm . In such techniques the particle transit time is a logarithmic function of particle size.

Liquid Particle Size Measurement Techniques

In the areas of combustion and chemical processes and in the pharmaceutical and agriculture industries, measurement of droplet size and velocity distributions is important. In one respect the measurement of droplets is easier than that of solid particles because droplets are usually spherical and smooth. In another respect the measurement of droplets is more difficult because they are not easy to collect and stabilize, and they may be volatile. Thus, an *in situ* measurement is usually preferable. The applications commonly used can be grouped as spray diagnostics (using ensemble scattering techniques and optical single-particle analysis) and spray measurement.

Acknowledgement

This work was supported in part by the Federal Panel on Energy Research and Development (PERD).

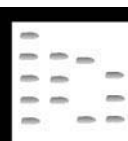
See also: II/Chromatography: Hydrodynamic Chromatography. **Flotation:** Cyclones for Oil/Water Separations; Historical Development; Oil and Water Separation. **Particle Size Separation:** Electrostatic Precipitation; Field Flow Fractionation; Thermal; Hydrocyclones for Particle Size Separations; Sieving/Screening.

Further Reading

- Allen T (1997) *Particle Size Measurement*, 5th edn. New York: Chapman and Hall.
- Barth HG (ed.) (1984) Modern methods of particle size analysis. In: *Chemical Analysis* (A Series of Monographs on Analytical Chemistry and its Application) pp. 1–75, vol. 73. New York: John Wiley.
- Barth HG and Sun ST (1985) Particle size analysis. *Analytical Chemistry* 57, 151R–175R.
- Barth HG, Sun ST and Nikol RM (1987) Particle size analysis. *Analytical Chemistry* 59: 142R–162R.
- Böhm J (1982) *Electrostatic Precipitators*. New York: Elsevier.
- Hirleman DE, Bachalo WD and Felton FG (eds) (1990) *Liquid Particle Size Measurement Techniques*, vol. 2. American Society for Testing and Materials, STP; 1083.
- Kaye BH (1981) *Direct Characterization of Particles*. New York: John Wiley.
- Kaye BH (1989) *A Random Walk Through Fractal Dimensions*. Weinheim, Germany: VCH Publishers.

- Mandelbrot BB (1983) *The Fractal Geometry of Nature*. San Francisco: W. Freeman Publishers.
- Miller BV and Lines R (1988) Recent advances in particle size measurement: a critical review. *Critical Reviews in Analytical Chemistry* 20(2): 75–116.
- Oglesby S Jr and Nichols GB (1978) *Electrostatic Precipitation*. New York: Marcel Dekker Inc.
- Provder T (ed.) (1998) Particle Size Distribution III, Assessment and Characterization. *ACS Symposium Series* 693, ACS.
- Salama AIA and Mikula RJ (1996) Particle and suspension characterization. In *Suspensions: Fundamentals and Applications in the Petroleum Industry*. Advances in Chemistry Series 251, ACS.
- Silverman L, Bellings CE and First MW (1971) *Particle Size Analysis in Industrial Hygiene*. New York: Academic Press.
- Syvitski James PM (1991) *Principles, Methods and Applications of Particle Size Analysis*. Cambridge: Cambridge University Press.

MEDICINAL HERB COMPOUNDS: HIGH-SPEED COUNTERCURRENT CHROMATOGRAPHY



T. Zhang, Beijing Institute of New Technology
Application, Beijing, China

Copyright © 2000 Academic Press

Introduction

Medicinal herbs are an important source of natural products for medicine. They include various chemical components ranging from fat-soluble to water-soluble compounds. The isolation of the biologically active components is the starting point of further research in chemistry and pharmacology as well as in the utilization of these compounds.

Traditional Chinese medicine is an extremely rich source of the experience acquired over a long period of time. In order to make greater use of traditional Chinese medicine, modern scientific methods are used to find the bioactive compounds in the traditional drugs and to use them as leading compounds for new drug design. New drugs developed in this way include anisodamine and the antimalarial agent Qinghaosu (artemisinin).

For separating and purifying bioactive compounds from medicinal herbs, modern chromatographic techniques, such as gas chromatography, high performance liquid chromatography, thin-layer chromatography and electrophoresis have significantly raised the technical level and have shortened the time required for research projects.

High speed countercurrent chromatography (HSCCC) has been recognized as an effective means for separation and purification of a wide variety of bioactive components. It is a liquid-liquid partition chromatography system based on a coil planet centrifuge system without the use of any solid support. This technique has developed rapidly during the past dec-

ade. It has been demonstrated to have preparative capabilities and unique properties for fractionating a variety of natural products and medicinal herbs.

Here some applications of the separation of bioactive compounds, such as alkaloids and flavonoids, in medicinal herbs by HSCCC are described.

Separations of Alkaloids

Separations of Alkaloids Extracted from *Stephania tetrandra* S. Moore

Dried roots of *Stephania tetrandra* S. Moor (Menispermaceae) or Fenfangji in Chinese is a traditional Chinese drug used for rheumatism and arthritis. The total active alkaloid content in the natural products is 2.3%. Three major alkaloids have been identified as tetrandrine (I, 1%), fangchinoline (II, 0.5%) and cyclanoline (III, 0.2%). I and II are inseparable by conventional methods, while III is well separated from the other two. As illustrated in **Figure 1**, I and II are both bisbenzylisoquinoline alkaloids, whereas III is a water-soluble quaternary protoberberine-type alkaloid.

A sample solution was prepared as a mixture of I and II with purified III to obtain a 10 : 5 : 2 weight ratio to simulate their composition in the natural drug. 3 mg of this sample was dissolved in 0.5 mL of the upper stationary phase of the selected solvent system. The solvent system was composed of n-hexane/ethyl acetate/methanol/water at two different volume ratios of 3 : 7 : 5 : 5 in the first experiment and 1 : 1 : 1 : 1 in the second. In both cases the lower phase was used as the mobile phase at a flow rate of 60 mL h⁻¹ in the normal elution mode. The apparatus used in these experiments was a Pharmatech Model CCC-2000 analytical countercurrent

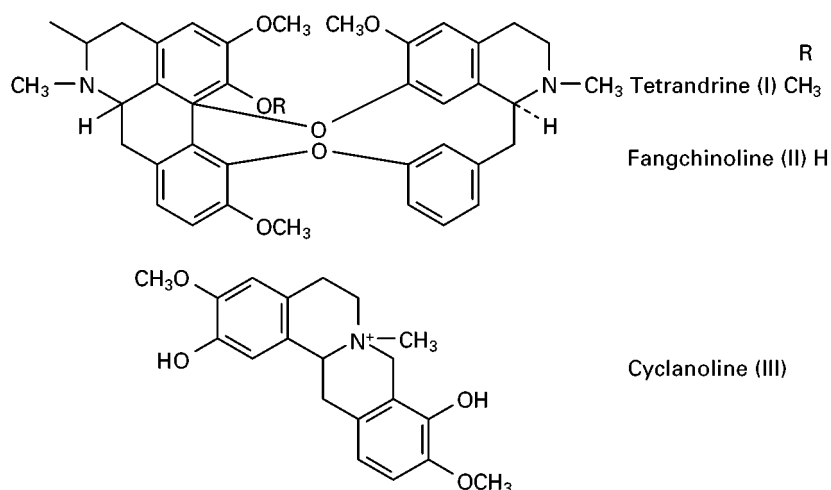


Figure 1 The chemical structures of tetrandrine(I), fangchinoline(II) and cyclanoline(III).

chromatograph made by Pharma-Tech Research Corp. It is equipped with a column holder at a 6.4 cm revolution radius. A multilayer coil prepared from a 70 m length of heavy wall 0.85 mm i.d. PTFE tubing is coaxially mounted on the holder. The total capacity of the column is 43 mL. The maximum speed of this centrifuge is 2000 rpm. The apparatus is equipped with a metering pump, a speed controller with a digital rpm display, and a pressure gauge.

Figure 2 shows the chromatogram obtained from the first experiment. In the normal elution mode,

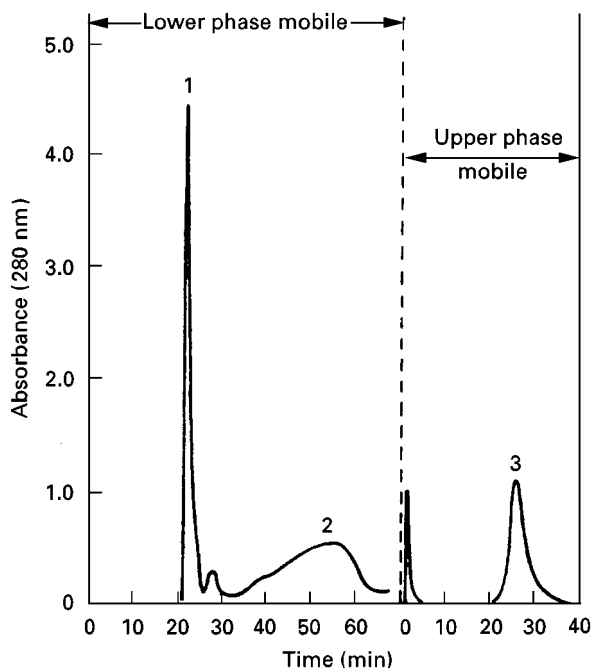


Figure 2 Chromatogram of the sample mixture of tetrandrine (1)–fangchinoline (2)–cyclanoline (3) (10 : 5 : 2). Solvent system n-hexane–ethyl acetate–methanol–water (3 : 7 : 5 : 5).

peaks 1 and 2 were completely resolved and collected in 70 min. This was followed by a reversed elution mode without interrupting the centrifuge run to collect the third peak in an additional 30 min. As shown in the chromatogram, a very small amount of impurity present between peaks 1 and 2 was also resolved.

The chromatogram obtained from the second experiment is shown in Figure 3. It demonstrates an alternative approach where the solvent composition was adjusted to modify the partition coefficients of the compounds to shorten the separation time without the use of a reversed elution mode.

A Finnigan MAT mass spectrometer was used to analyse the peak fractions to identify the compounds in peaks 2 and 3 in Figure 3 as purified fangchinoline and cyclanoline respectively.

Semipreparative Separation of Alkaloids from *Cephalotaxus fortunei* Hook f.

The alkaloids, isoharringtonine (I), homoharringtonine (II) and harringtonine (III) isolated from *Cephalotaxus fortunei* Hook f., possess anticancer potency. Among those compounds, (I) and (III) are isomers, and (II) and (III) differ only by a $-\text{CH}_2$ group (Figure 4).

A crude alkaloid powder was prepared from the leaves and branches of *C. fortunei* Hook f. 20 mg of the crude powder was dissolved in 1 mL of the solvent mixture (upper phase and lower phase) as the sample solution for each separation. The two-phase solvent system was composed of chloroform/0.07 M sodium phosphate buffer solution at the volume ratio of 1 : 1 (pH 5.0).

The apparatus used in these experiments was a GS-10A HSCCC made by Beijing Institute of New Technology Application. A pair of column holders

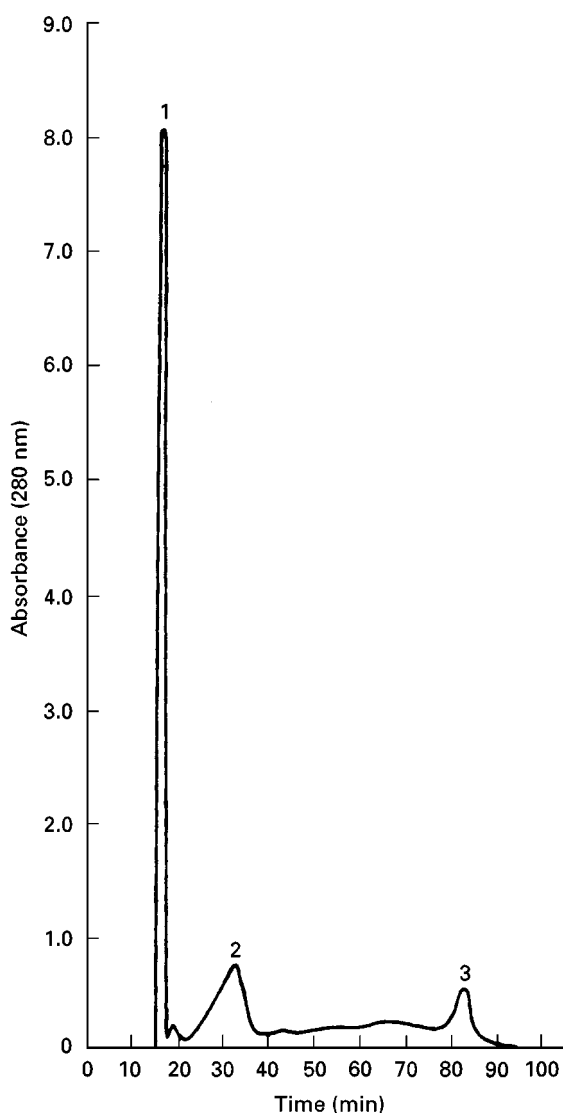


Figure 3 Chromatogram of the sample mixture of tetrandrine (1)-fangchinoline (2)-cyclanoline (3) (10 : 5 : 2). Solvent system n-hexane-ethyl acetate-methanol-water (1 : 1 : 1 : 1).

are held symmetrically on the rotary frame at a distance of 8 cm from the central axis of the centrifuge. The multilayer coil separation column was prepared by winding a 130 m length of 1.5 mm i.d. PTFE tubing directly on to the holder hub. The total capacity of the 14 layer column was 230 mL. The speed of this machine was regulated with a speed controller in a range between 0 and 1000 rpm, while 800 rpm was used as the optimum speed for the conventional two-phase solvent system.

In each separation, the column was first entirely filled with the stationary aqueous phase followed by injection of the sample solution. The apparatus was rotated at 800 rpm while the nonaqueous mobile phase was pumped into the column at a flow rate of

2 mL min⁻¹. Effluent from the outlet of the column was continuously monitored with a UV monitor at 254 nm and collected with a fraction collector at 2 min intervals. After a group of nonpolar compounds was eluted, the centrifuge was stopped while pumping was resumed to collect a polar compound still retained on the column. **Figure 5** shows the chromatogram obtained. Each fraction was analysed by TLC and the fractions corresponding to peaks 2, 4 and 6 were identified as isoharringtonine, homoharringtonine and harringtonine.

In order to increase the yield of the component homoharringtonine, 300 mg of crude extract was applied to produce 70 mg of the pure product. The method is useful for semipreparative separation of alkaloids and other natural products with similar polarity.

Separation of Flavonoids

Separation of Flavonoids in Crude Extract from Sea Buckthorn

The results of separations of a crude ethanol extract from dried fruits of sea buckthorn (*Hippophae rhamnoides*) are described. Five flavonoid constituents were successfully separated by P.C. Inc. A two-phase solvent system composed of chloroform-methanol-water at a 4 : 3 : 2 volume ratio was used. The sample solution was prepared by dissolving the crude ethanol extract in the solvent mixture of upper and lower phases at a concentration of 2.2 g %.

Separation was performed as follows: The coiled column was first entirely filled with the upper phase as the stationary phase followed by injection of sample solution containing 100 mg crude mixture through the sample port. The apparatus was rotated at the optimum speed of 800 rpm while the lower phase was pumped into the head end of the column as the mobile phase at 200 mL h⁻¹ flow rate. Effluent from the outlet end of the column was continuously monitored at 278 nm and fractionated into test tubes. An aliquot of each fraction was diluted with methanol and the absorbance was determined at 260 nm with a spectrophotometer. **Figure 6** shows the chromatogram obtained. Five flavonoid components were completely resolved from each other as symmetrical peaks and eluted in 2.5 h. Partition efficiencies computed from the equation $N = (4R/W)^2$ (where N is the efficiency expressed in terms of theoretical plates (TP), R is retention time of the peak maximum, W is the peak width expressed in the same unit as R) range from 800 TP (2nd peak) to 530 TP (5th peak). By calculating the partition coefficients of each peak and comparing the values

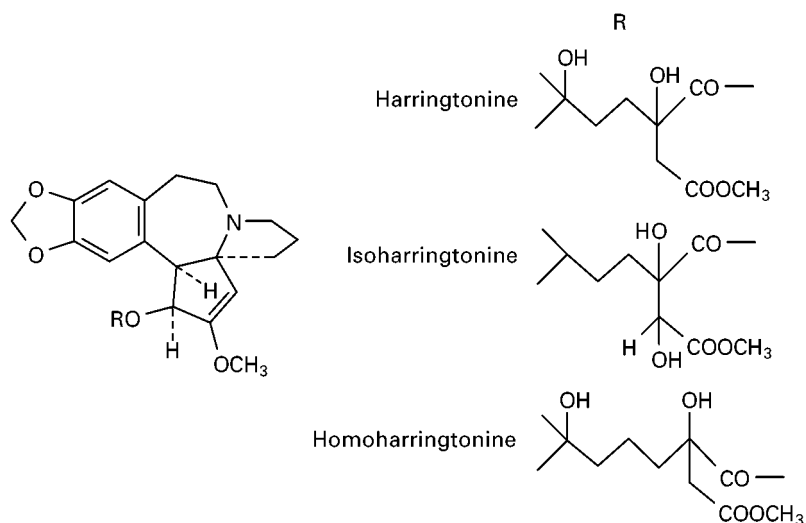


Figure 4 Chemical structures of harringtonine, isoharringtonine and homoharringtonine.

obtained with those of the pure compounds, quercetin and isorhamnetin peaks were identified as labeled in the chromatogram.

The same crude sample of ethanol extract from dried fruits of sea buckthorn can be separated with an analytical HSCCC for a series of rapid separations. The apparatus was a Pharma-Tech Model CCC-2000 made by Pharma-Tech Research Corp. The multilayer coiled column was prepared from a single piece of 0.85 mm i.d. heavy wall PTFE tubing. The total capacity of the column is 43 mL including 3 mL in the flow tubes. The revolution speed of the centrifuge can be continuously adjusted up to 2000 rpm. A LDC/Milton Roy Pump, a speed controller with digital rpm display and a pressure gauge are also included.

In these separations, 3 mg of sample of the flavonoid mixture were dissolved in 0.5 mL of solvent

mixture and loaded for each experiment. The centrifuge was rotated at the optimum speed of 1800 rpm. The effluent from the outlet of the column was continuously monitored with an LKB Uvicord S at 278 nm and then collected as 1 mL fractions with an LKB fraction collector. Each fraction was diluted with 2 mL of methanol and the absorbance was determined at 260 nm with a Zeiss spectrophotometer Model PM6.

Figure 7 shows the result of separation obtained at a flow rate of 60 mL h⁻¹. The high efficiency of the separation is evidenced by a minor peak present between the first and the second major peaks, which

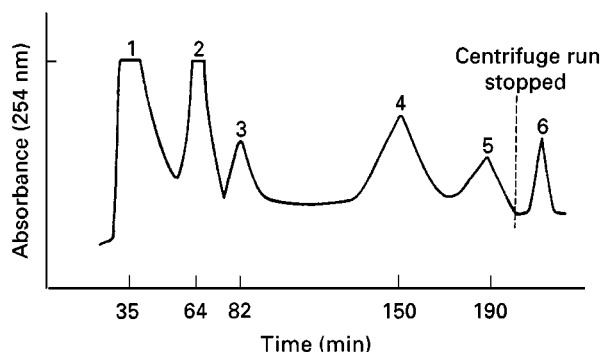


Figure 5 High speed CCC separation of harringtonine, isoharringtonine and homoharringtonine from a crude extract of *Cephalotaxus fortunei* Hook f. Peak 2, isoharringtonine; 4, homoharringtonine and 6, harringtonine.

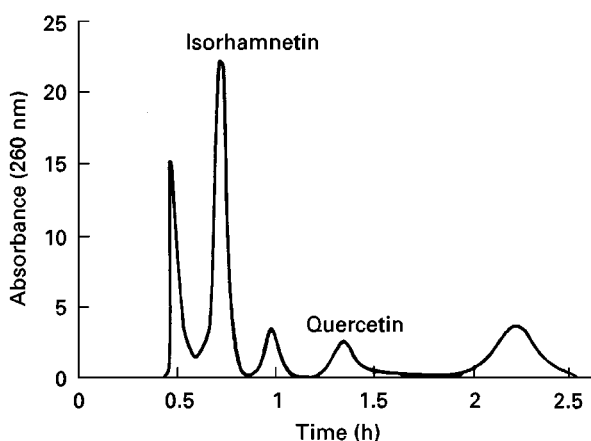


Figure 6 Counter-current chromatogram of flavonoids in crude extract from dried fruits of sea buckthorn by a multilayer coil planet centrifuge. Conditions for CCC: sample size, 100 mg; solvent system, chloroform-methanol-water (4:3:2); mobile phase, lower phase; flow rate, 200 mL h⁻¹; speed, 800 rpm; fraction volume, 6 mL.

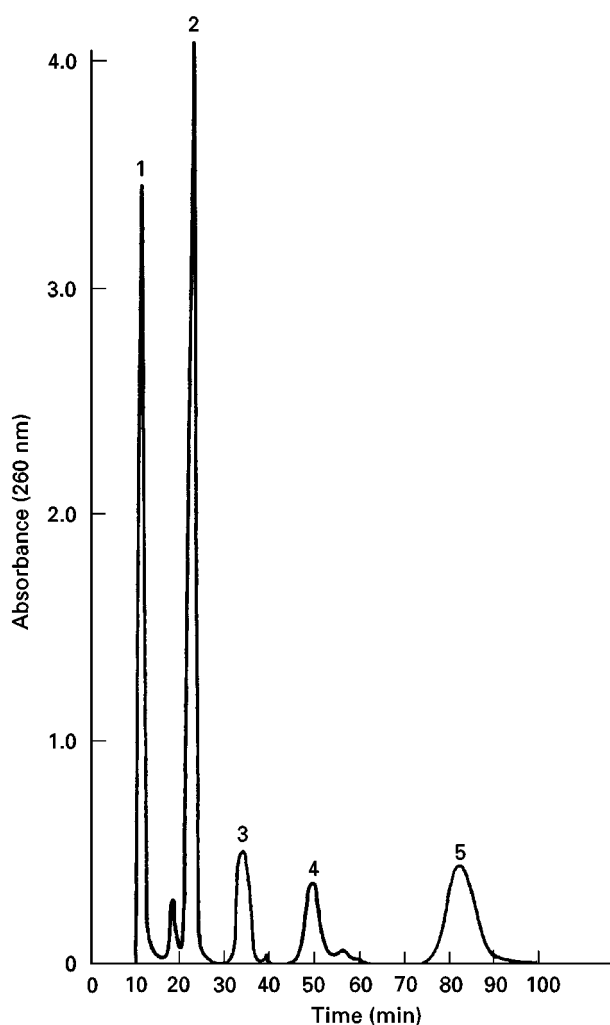


Figure 7 Chromatogram obtained from 3 mg extract by analytical countercurrent chromatography, flow rate of 60 mL min^{-1} .

was not detected in the semipreparative separation shown in Figure 6. Flow rates as high as 300 mL h^{-1} can be used to give a separation time of only 15 min, which is quite comparable with that of analytical HPLC.

The analytical HSCCC can be used to interface with MS to provide a new analytical methodology HSCCC-MS, combining the versatility and high resolution of HSCCC with the identification capability and low detection limit of mass spectrometry.

Preparative Separation of Kaempferol, Isorhamnetin and Quercetin from Extracts of *Ginkgo biloba* L.

Extracts of the leaves of *Ginkgo biloba* L. are used to increase peripheral and cerebral blood flow. *Ginkgo* extracts contain active compounds such as flavonoids and terpene lactones (ginkgolides and bilobalide).

They show effects on vascular and cerebral metabolic processes and inhibit platelet-activating factor. The standard compounds used to control the quality of *Ginkgo* extracts and its preparations, such as isorhamnetin, kaempferol and quercetin, the three major flavone aglycones in the leaves of *Ginkgo biloba* L., are expensive and difficult to obtain. Some commercial quercetin standards, usually used in quantitative analysis of total flavonoids, are not pure and contain isorhamnetin, kaempferol and impurities. The preparative separation and purification of flavonoids from plant materials by classical methods are tedious and usually require multiple chromatographic steps. HSCCC as a form of liquid-liquid partition chromatography without using a solid support matrix is very suitable for the separation of flavonoids.

HSCCC was performed using a Model GS-10A multilayer coil planet centrifuge made by the Beijing Institute of New Technology Application. A NS1007 constant-flow pump, a model 8823A UV monitor operating at 254 nm and a manual sample injection valve with a 35 mL loop, were used in the experiment. A Rainin Model SD-200 HPLC was used for analysis.

In these studies, a two-phase solvent system composed of chloroform-methanol-water at a volume ratio of 4 : 3 : 2 was used. The crude *Ginkgo* flavone aglycones were prepared by several steps, from the extract of *Ginkgo* leaves. A second sample was a commercial quercetin standard. The sample solutions were prepared by dissolving these two samples in equal volumes of upper and lower phases.

In each separation, the column was first entirely filled with the upper aqueous phase as stationary phase, and then the apparatus was rotated at 800 rpm, while the lower chloroform phase was pumped into the column at a flow rate of 2 mL min^{-1} . After the mobile phase front emerged and the two phases had established hydrodynamic equilibrium in the coil column, the sample solution containing 200 mg of crude *Ginkgo* flavone aglycones or commercial quercetin standard was introduced through the injection valve. HPLC analysis of the crude *Ginkgo* flavone aglycones is shown in Figure 8A. According to MS analysis, quercetin, kaempferol, isorhamnetin and some impurities were present. HPLC analysis of the commercial quercetin standard is shown in Figure 8B indicating that a larger amount of unknown impurity was present.

After repurification of the isorhamnetin peak by HSCCC, the purities of the three flavone aglycones were more than 99% according to the results of HPLC analysis. The identities of the three flavone aglycones were confirmed by MS analysis.

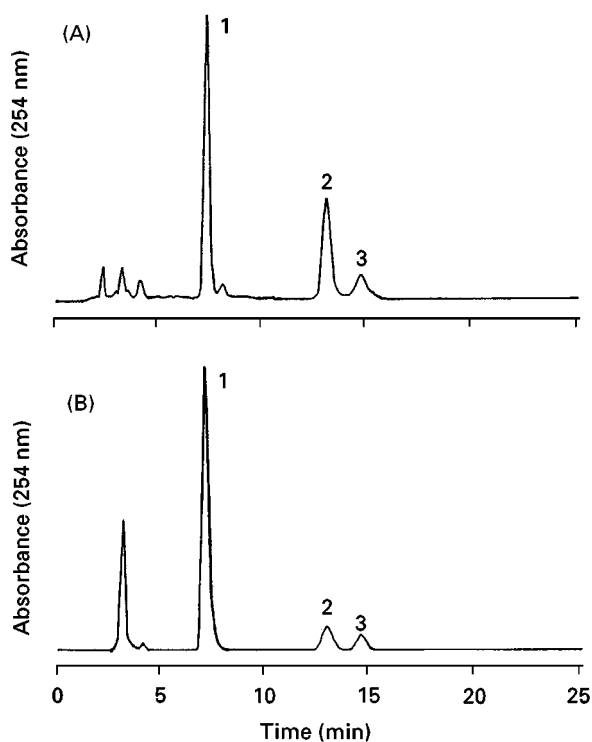


Figure 8 Chromatograms of the HPLC analyses of the crude *Ginkgo* flavone aglycones from the *Ginkgo* extracts (A) and the commercial quercetin standard (B). Mobile phase: methanol-0.04% H_3PO_4 (50:50, v/v); flow rate: 1.0 mL min^{-1} ; detection: 254 nm. Peak 1: quercetin; Peak 2: kaempferol; Peak 3: isorhamnetin.

Semipreparative Separation of Taxol Analogues

Taxol is a promising new anticancer drug. Currently, taxol intended for human consumption is mainly obtained from the bark of *Taxus*. Although taxol is the compound most commonly used in clinical treatment, numerous analogues have also been identified. Some of them are of similar biological activities to taxol, and some can be used as natural precursors to semisynthesize taxol by simply modifying the C13 side chains. Meanwhile, the study of these compounds may lead to the discovery of new alternatives with improved pharmaceutical properties or economic benefits. The separation and purification of taxol analogues by classical methods such as preparative TLC, open column chromatography and HPLC in general are complicated and have low recoveries. HSCCC can be used for the semipreparative separation of some taxol analogues such as cephalomannine and 7-epi-10-deacetyltaxol.

HSCCC was performed with a model GS-10A multilayer coil planet centrifuge made by the Beijing Institute of New Technology Application. The

chromatography system was the same as that described previously.

A crude extract containing 10% taxol from *Taxus yunnanensis* was pre-separated through a C_{18} column eluted by an acetonitrile–water gradient. After recovering the majority of the taxol and removing some other polar components, the fraction mainly containing cephalomannine, 7-epi-10-deacetyltaxol, residual taxol and an unknown compound was collected, concentrated and dried. The sample solution was prepared by dissolving the sample in the solvent mixture of upper and lower phases.

The two-phase solvent system, a quaternary system of n-hexane–ethyl acetate–ethanol–water was selected. In those studies a two-step separation was chosen. Firstly, the solvent system in 1:1:1:1 proportion was employed to separate the sample into two groups, A and B. Secondly, the system in 3:3:2:3 and 4:4:3:4 proportions was employed to separate the two compounds in A and B. In each separation, the coiled column was first entirely filled with the upper phase as the stationary phase. After the apparatus was rotated at 800 rpm, the lower phase was pumped into the column at a flow rate of 2 mL min^{-1} , while the sample solution was introduced via the injection valve. The effluent from the outlet of the column was continuously monitored at 254 nm. Twelve consecutive injections of 10–16 mg of sample mixture were performed without changing the stationary phase in the coiled column.

The four compounds were first separated into two groups as shown in Figure 9. Peak A contains mainly cephalomannine and taxol, while peak B contains mainly 7-epi-10-deacetyltaxol and the unknown compound. After 12 consecutive injections, 84.4 mg of A and 42.1 mg of B were obtained. Cephalomannine and taxol in peak A were well separated in the second step with the 3:3:2:3 solvent system

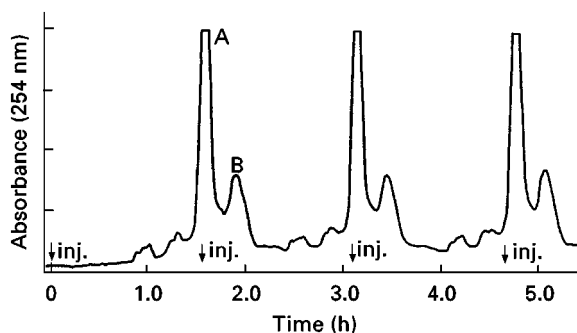


Figure 9 First step separation of taxol and its analogues by HSCCC with three consecutive injections. Solvent system: n-hexane–ethyl acetate–ethanol–water (1:1:1:1, v/v/v/v). A, cephalomannine + taxol; B, unknown + 7-epi-10-deacetyltaxol.

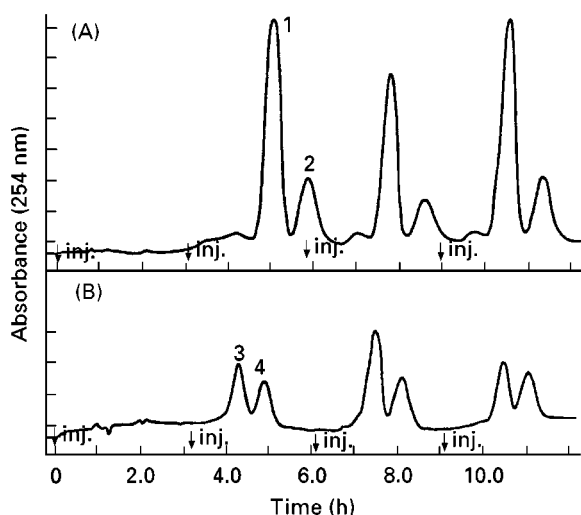


Figure 10 Second step separations of peak fractions (A) and (B) in Figure 9 by HSCCC with three consecutive injections. Solvent system: n-hexane–ethyl acetate–ethanol–water. (A) 3 : 3 : 2 : 3, (B) 4 : 4 : 3 : 4. 1, Cephalomannine; 2, taxol; 3, unknown; 4, 7-epi-10-deacetylaxol.

as shown in Figure 10. 49.3 mg of cephalomannine and 14.6 mg of taxol were obtained after six consecutive injections. The purities were about 99% and 87% respectively according to the results of HPLC analysis. Similarly with peak B, 7-epi-10-deacetylaxol and the unknown compound were separated

with the 4 : 4 : 3 : 4 solvent system as shown in Figure 10B: 12 mg of 7-epi-10-deacetylaxol and 10 mg of the unknown compound were obtained after three consecutive injections. The purities were about 85% according to the results of HPLC analysis.

Conclusions

Many applications of HSCCC such as the separation of alkaloids, flavonoids, hydroxyanthraquinone derivatives, etc., have been performed successfully. The main advantages of HSCCC are as follows:

1. Since no solid supports are used, all compounds in the sample solution are recovered. The crude sample can be injected directly into the column, which simplifies sample preparation.
2. Numerous two-phase solvent systems with a broad spectrum of polarity can be used with either the aqueous or organic phase as the mobile phase. Some examples are shown in Table 1.
3. The quantity of purified compound may range from milligrams to grams. Consecutive injection can be applied for large scale separation.
4. HSCCC will become widely used in the research and production of natural drugs, since the instrument is inexpensive, convenient to operate, solvent saving and has preparative capacity.

Table 1 Solvent systems for separation of some substances by high speed countercurrent chromatography

Substances separated	Solvent system
Alkaloids	nC ₆ H ₁₄ –EtOAc–MeOH–H ₂ O (1 : 1 : 1 : 1) nC ₆ H ₁₄ –EtOH–H ₂ O (6 : 5 : 5) CHCl ₃ –MeOH–H ₂ O (4 : 3 : 2) CHCl ₃ –MeOH–0.5% HBr–H ₂ O (5 : 5 : 3) Bu ⁿ OH–0.1 M NaCl (1 : 1)
Flavonoids	CHCl ₃ –MeOH–H ₂ O (7 : 13 : 8), (4 : 3 : 2)
Flavonoid glycosides	CHCl ₃ –EtOAc–MeOH–H ₂ O (2 : 4 : 1 : 4) EtOAc–Bu ⁿ OH–H ₂ O (2 : 1 : 2)
Indole	nC ₆ H ₁₄ –EtOAc–MeOH–H ₂ O (3 : 7 : 5 : 5), (1 : 1 : 1 : 1)
Xanthone glycosides	CHCl ₃ –MeOH–H ₂ O (4 : 4 : 3)
Lignans	nC ₆ H ₁₄ –CH ₃ CN–EtOAc–H ₂ O (8 : 7 : 5 : 1)
Lignan glycosides	CHCl ₃ –MeOH–H ₂ O (5 : 5 : 3) nC ₆ H ₁₄ –CH ₂ Cl ₂ –MeOH–H ₂ O (2 : 4 : 5 : 2)
Phenolic glycosides	CHCl ₃ –MeOH–H ₂ O (7 : 13 : 8) C ₆ H ₁₂ –Me ₂ CO–EtOH–H ₂ O (7 : 6 : 1 : 3) CHCl ₃ –MeOH–H ₂ O (7 : 13 : 8) Bu ⁿ OH–0.1 M NaCl (1 : 1)
Polyphenols	nC ₆ H ₁₄ –EtOAc–MeOH–H ₂ O (3 : 7 : 5 : 5)
Tannins	CHCl ₃ –MeOH–Bu ⁿ OH–H ₂ O (7 : 6 : 3 : 4)
Coumarins	CHCl ₃ –MeOH–Pr ⁱ OH–H ₂ O (5 : 6 : 1 : 4)
Saponins	CHCl ₃ –MeOH–H ₂ O (7 : 13 : 8)
Hydroxyanthraquinone derivatives	nC ₆ H ₁₄ –EtOAc–MeOH–H ₂ O (9 : 1 : 5 : 5)
25-Hydroxycholecalciferol	nC ₆ H ₁₄ –EtOAc–MeOH–H ₂ O (5 : 1 : 5 : 1)

See also: **II/Chromatography:** Countercurrent Chromatography and High-Speed Countercurrent Chromatography: Instrumentation. **Chromatography: Liquid:** Countercurrent Liquid Chromatography. **III/Alkaloids:** Gas Chromatography; High-Speed Countercurrent Chromatography; Liquid Chromatography; Thin-Layer (Planar) Chromatography.

Further Reading

Conway WD and Petroski RJ (1995) *Modern Countercurrent Chromatography*. American Chemical Society Symposium Series 593. Washington DC.

Ito Y (1986) *CRC Critical Reviews in Analytical Chemistry* 17: 65.

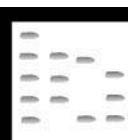
Ito Y and Conway WD (1996) *High-Speed Countercurrent Chromatography*. New York: John Wiley.

Mandava NB and Ito Y (1988) *Countercurrent Chromatography*. New York and Basel: Marcel Dekker.

Zhang TY (1991) *Countercurrent Chromatography*. Beijing: Beijing Science and Technology Press.

Zhang TY (1996) HSCCC on medicinal herbs. In: *High-Speed Countercurrent Chromatography*. New York: John Wiley.

MEDIUM-PRESSURE LIQUID CHROMATOGRAPHY



K. Hostettmann and C. Terreaux,
University of Lausanne, Lausanne, Switzerland

Copyright © 2000 Academic Press

Introduction

Medium-pressure liquid chromatography (MPLC) is one of the various preparative column chromatography techniques. Separation under pressure renders the use of smaller particle size supports possible and increases the diversity of usable stationary phases. MPLC was introduced in the 1970s as an efficient technique for preparative separation of organic compounds. MPLC overcame one major drawback of low pressure liquid chromatography (LPLC), i.e. the limited sample loading. This separation method is now routinely used beside or in combination with the other common preparative tools: open-column chromatography, flash chromatography, LPLC or preparative high performance liquid chromatography

(HPLC). The distinction between low pressure, medium pressure and high pressure LC is based on the pressure ranges applied in these techniques and the overlap is often considerable. MPLC allows purification of large compound quantities and, unlike open-column chromatography and flash chromatography, faster and improved separations are obtained. Packing of material with lower particle size under pressure enhances separation quality and moreover the solid phase can be reused. **Table 1** provides a comparative description of these different methods. Simplicity and availability of the instrumentation, together with recycling of packing materials and low maintenance costs, contribute to the attractiveness of this technique. More details about experimental conditions are given below.

Instrumentation

A schematic representation of a simple MPLC setup is shown in **Figure 1**. The instrumentation is made up of

Table 1 Comparative description of various preparative column chromatographic techniques

Technique	Stationary phase particle size (μm)	Pressure (bar)	Flow rate (mL min^{-1})	Sample amount (g)	Solvents	General
Open-column chromatography	63–200	Atmospheric	1–5	0.01–100	General solvent used	Frequent packing; RP not possible
Flash chromatography	40–63	1–2	2–10	0.01–100	General solvent used	Frequent packing
Low pressure LC	40–63	1–5	1–4	1–5	More solvent required	Prefilled Lobar columns
Medium pressure LC	15–40	5–20	3–16	0.05–100	More solvent required	Infrequent packing
Preparative HPLC	5–30	> 20	2–20	0.01–1	High purity solvent required	Higher resolution

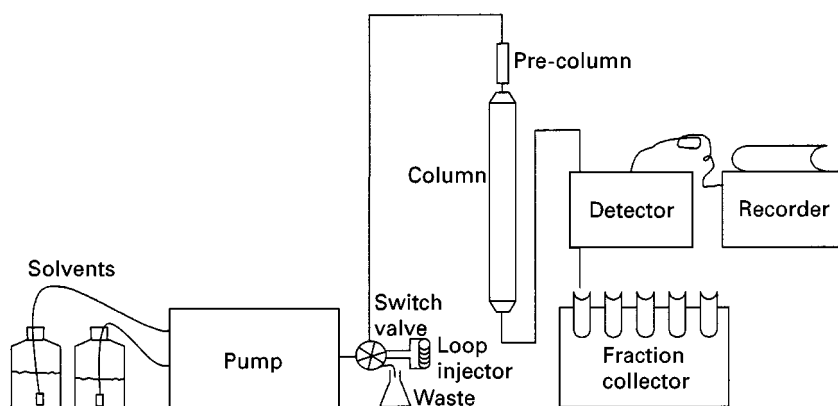


Figure 1 Typical MPLC instrumental setup.

a pump for solvent delivery, a sample injection system, and a self-packed column. Product separation can be followed either manually by monitoring with thin-layer chromatography (TLC) or automatically with a detector and a recorder connected to the column outlet. Separated compounds are collected by means of a fraction collector.

Pump

Chromatographic separation of 0.1–100 g sample within a few hours requires flow rates ranging from about 5 to 200 mL min⁻¹, with a maximal pressure of 40 bar. Several companies provide pumps suitable for MPLC. Criteria for selecting an MPLC pump include: flow rate range; presence or absence of a pulse-damper, which provides regular flow rates and pressures during separation and increases the reproducibility of the separation; presence of a pressure cut-off device; and presence of a gradient former. Some manufacturers provide pumps with exchangeable piston heads, thus allowing flow rates from 0.5 to 160 mL min⁻¹ with pressures up to 40 bar.

Column

The column is the central point when optimizing a preparative chromatographic separation and criteria such as amount of sample to be purified, amount of packing material and column length versus column diameter, have to be carefully considered. MPLC columns are generally made of thick glass coated with protective plastic and can withstand pressures up to 50 bar; however, some columns from some manufacturers cannot withstand pressures exceeding 20 bar. The columns vary in length as well as in internal diameter (i.d.) and sizes are expressed as filling volumes. Filling volumes range from 63 mL (9 mm i.d. × 100 mm) to 15 000 mL (105 mm i.d. ×

1760 mm) for the larger columns available. Selection of the column dimensions depends on the sample amount to be separated, ranging from 0.1 g with the smallest columns up to 100 g with large columns. Selectivity (α) and retention factor (k) are the prominent factors influencing resolution. Sample loading can greatly affect resolution. Therefore, when separations are 'easy' ($\alpha > 1.2$; high resolution between the eluted compounds), larger sample amounts can be loaded. Increasing the column diameter allows injection of a larger sample mass (higher throughput), but also makes use of smaller particle size material possible. On the other hand, increasing the column length results in higher resolution but has little or no effect on sample throughput. The back pressure increase with longer columns often implies the use of larger particle size material. The influence of column dimensions on resolution has been studied through the separation of standard mixtures. The correlation between resolution and amount of packing material was shown to be linear either when testing columns with identical internal diameter and different lengths or when varying the internal diameter in a set of columns of the same length. However, a lesser increase in resolution was observed with the use of larger internal diameter and a constant length. Consequently, longer columns are preferred in order to improve the separation of a given sample. The column system supplied by Büchi (Flawil, Switzerland) gives the possibility to couple columns together vary simply by means of a Teflon sealing joint, resulting in an increased resolving power.

Detector and Recorder

Monitoring of a MPLC separation can be performed by TLC of the collected fractions. Online detection is also routinely used with single-wavelength UV/Vis detectors. Most available UV detectors are designed for analytical purposes and are of little use for

preparative separations. Accommodation of high flow rates is a prerequisite for a preparative chromatographic detector. This results in a loss of sensitivity, which is compensated by the usual high concentration of the eluate. In fact, these concentrations are often so large when coming through the detection cell that the detector is overloaded. This problem can be solved by the use of detectors with a splitting system before the UV cell: one part of the sample goes directly from the column outlet to the fraction collector, while another part is diverted through the detector. Detectors with a pathlength < 0.1 mm are also very useful. Selection of a detection wavelength where absorption of the products is low can also be an alternative to avoid detection overload. The Gow-Mac 80-800 LC-UV detector is a specially designed detector for preparative separations: flow rates up to 500 mL min^{-1} are possible and the eluate arrives through a needle and passes as a thin film on a 6.5 cm wide quartz cell. Connection to a recorder allows visualization of the chromatographic separation.

Fraction Collector

Automatic collection of fractions can be performed by connecting a fraction collector to the column or detector outlet. The volume of the collected fractions is of course strongly dependent on the internal diameter of the column and the flow rate; it is in most cases time-monitored. Presence of a built-in peak detector or connection to an external one allows peak-monitored fraction collection. In its standard MPLC setup, the Büchi system provides a fraction collector with a total capacity of 240×20 mL tubes, 120×50 mL tubes or 48×250 mL tubes. This type of fraction collector has proved to be particularly suitable for MPLC.

Column Packing

Packing Material

Selection of the stationary phase is probably the most crucial parameter affecting separation quality. Several types of packing material are commonly used in MPLC and various factors have to be considered when choosing the packing material:

- particle size
- column length
- operating pressure
- type of sample
- cost.

With regard to cost-effectiveness, the most frequently utilized stationary phase is silica gel. Beside

its economic advantage, silica gel possesses other advantages such as a wide range of possible solvents as eluents, easy evaporation of the fractions and elution with high flow rates. The risk of irreversible adsorption is a possible major drawback of this support.

A wide range of particle sizes is commercially available. The smallest average particle size ($5\text{--}10 \mu\text{m}$) is used for analytical HPLC, while for preparative LC, stationary phases with sizes starting at $15 \mu\text{m}$ are the most convenient. Optimal separations are generally obtained with sizes around $20 \mu\text{m}$. The influence of particle size on resolution has been investigated. A large decrease in resolution was observed when the average particle size changed from $15 \mu\text{m}$ to $30 \mu\text{m}$. Using particle sizes of $52 \mu\text{m}$ or $130 \mu\text{m}$ resulted in a slower resolution decrease but the retention times increased significantly: 3 h more with an average particle size of $130 \mu\text{m}$ than with one of $15 \mu\text{m}$.

The use of modified silica gel phase (bonded phases) has become more common. These inherent advantages, such as a lower risk of sample decomposition and less irreversible adsorption, allowing an easier recycling of the column sorbent. Reversed-phase (such as RP-18, RP-8 or RP-4) or dihydroxypropylene-bonded (Diol, Merck, Germany) silica gels are frequently used for MPLC separations. Moreover, it is possible to use other commercially available bonded phases for MPLC separations.

Column Packing Methods

Different filling methods are described for packing MPLC columns. Filled columns should possess an optimal homogeneity and a good density. Two methods are most frequently used: dry filling and the slurry method.

Dry filling Dry filling is generally applied for silica gel. This method usually gives a 20% better packing density than the slurry method. The 'tap-and full' technique can be used with particle sizes larger than $20\text{--}30 \mu\text{m}$; however, when applying eluent pressure up to 40 bar, the packing density obtained may not be sufficient. Packing under nitrogen pressure allows use of $15 \mu\text{m}$ particle size silica gel and provides a high packing density. Filling is carried out manually by connecting a reservoir to the top of the column, which is then filled with dry stationary phase until it contains approximately enough phase to fill another 10% of the column (Figure 2). The system is then connected to a nitrogen cylinder and a 10 bar pressure is applied (with the column outlet open) until the level of packing material remains constant. The nitrogen valve can be closed and the pressure slowly goes down to atmospheric. Vacuum at the column exit can

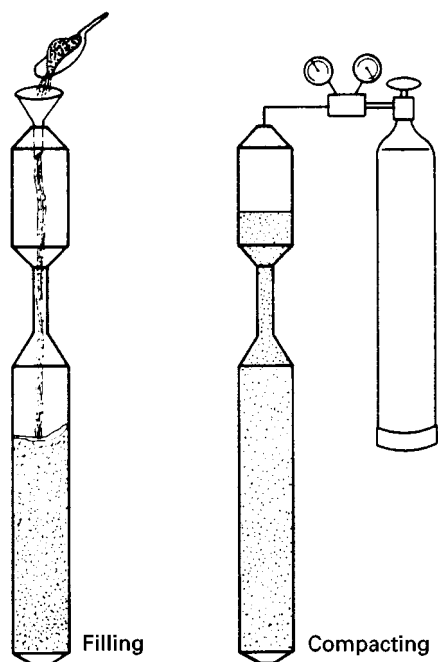


Figure 2 Dry filling of Büchi MPLC glass columns. (Reproduced with permission from Hostettmann *et al.*, 1997.)

be used as an alternative to nitrogen pressure. An automatic mechanism has been suggested to slowly and homogeneously fill the column ($3\text{--}4\text{ g min}^{-1}$). Passing mobile phase through the column induces compression of the stationary phase, which is compensated by the further addition of dry silica gel.

Slurry method The slurry method is an alternative method to pack silica gel, with the inconvenience of a lower packing density. However, slurry filling is the preferred method for packing bonded phases. The slurry is prepared by suspending homogeneously an appropriate amount of stationary phase in the eluent. The mixture is then poured into the column and the eluent is passed through the column until the stationary phase level is constant.

Column preparation and regeneration Before sample introduction, it is recommended that a separation test is performed with a standard mixture of compounds. A mixture of phthalic acid dimethyl-, diethyl- and dibutyl esters is convenient for testing silica gel columns, whereas the separation of benzene and naphthalene can be used for reversed-phase columns.

Usually, packing material is regenerated after each chromatographic separation. For silica gel supports, this can be performed by washing successively with methanol, ethyl acetate and *n*-hexane. However, after a certain time, the stationary phase should be

changed and the column repacked. Regular elution of a test mixture is a good method to determine column quality. Bonded-phase columns are generally easier to clean (for example with a mixture of methanol/tetrahydrofuran (1 : 1)) and thus have a longer working life. In order to prolong column lifetime, a pre-column can be used. Contaminating material remaining at the top of the column is thus eliminated after each MPLC separation.

Solvent Selection

Selection of the eluent system is also a crucial point in development and optimization of a MPLC separation. The ideal case would be successive direct testing of various solvent mixtures on the MPLC column. However, in routine practice such an approach is obviously impossible because of the waste of time due to column equilibration, together with loss of sample, etc. Two methods are mainly used for solvent selection: optimization by TLC or transposition of analytical HPLC conditions on MPLC.

Preliminary TLC allows rapid screening of numerous possible solvents and it is now well established how TLC results on silica gel plates can be transposed to silica gel columns. Solvent testing on silylated TLC plates can be used for reversed-phase columns. One important factor that has to be considered is that the surface areas of silica gel used in TLC is about twice that of the column packing material. Therefore, it is recommended that sample constituents display a retention factor (R_F) lower than 0.3 on the TLC plate. The major drawback of this method is the lower separation and resolution observed when reducing the solvent strength to obtain an $R_F \leq 0.3$. An alternative has been suggested to circumvent this problem: the use of overpressured-layer chromatography (OPLC) as a pilot method for MPLC. In a first step, a suitable multicomponent eluent with a good selectivity is searched for by means of TLC. Adjustment of the solvent strength and fine tuning are performed with OPLC. Unlike TLC, OPLC is a closed and equilibrated system and can be viewed as a 'planar column'. Because of these properties, direct transposition from OPLC to MPLC is an accurate and efficient method. Such an approach is also applicable to the other preparative pressure chromatography techniques using normal silica gel as stationary phase.

Because of the similarities of the phases used in analytical HPLC and preparative packing materials, separation optimization on an analytical HPLC column very often provides excellent results and transposition to MPLC is straightforward and direct. This is particularly evident for separations on

reversed-phase sorbents, where studies with TLC are more difficult. Due to the wider range of solvents available for normal-phase chromatography, preliminary tests on TLC are of major use prior to analytical HPLC optimization. Examples of transposition of analytical HPLC conditions to MPLC are given below.

Once the ideal conditions have been selected, a compromise has to be found between speed of separation and sample loading: decreasing the solvent strength (for example, by adding water to the solvent system in reversed-phase separations) will increase the separation between the different components and afford higher sample loading, but will require a considerable longer separation time. The influence of solvent strength on the resolution of a standard mixture has been studied and a linear decrease of resolution was observed when increasing the solvent strength. Running a gradient is also possible with MPLC, provided a suitable solvent delivery system is used. Peak sharpening can be obtained by a simple stepwise change of mobile phase composition.

Evaporation of large quantities of solvent takes place after fraction collection in order to concentrate the purified compounds. This procedure can cause the accumulation of considerable amounts of nonvolatile impurities from the solvent. As high purity solvents are very expensive, preliminary distillation of ordinary grade solvents to prepare the eluent can be a good compromise between solvent purity and quantity employed. Use of such lower grade solvents often implies an additional purification step by gel filtration, for example.

Sample Introduction

Several criteria have to be considered before sample injection on a MPLC column:

- sample preparation
- sample mass and volume
- solubility characteristics of the sample
- type of injection used.

If solubility is not a problem, the eluent should be chosen to dissolve the sample. However, even in such a case, care has to be taken to adjust the sample volume: a sample that is too dilute (injection of a large volume) results in decreased separation efficiency, while precipitation at the top of the column may be observed by injection of samples that are too concentrated. High concentrations of the sample may alter the viscosity of the solution, which is then very different from that of the mobile phase. High viscosity leads to severe tailing, while fronting may result from lower sample viscosity compared to the

mobile phase. Despite these inconveniences, injection of a small volume of a concentrated solution is usually preferred. Sample solubilization in a solvent different from the mobile phase is also possible, but special care has to be taken with such an approach: solubility after mixing the sample solution with mobile phase has to be checked in order to avoid sample precipitation on the top of the column. Samples can be injected either directly on the column through a septum, or by means of a sample loop. In both cases, injection success depends on the quality of the column packing to ensure a homogeneous distribution of the sample at the top of the column.

The various problems mentioned above are more frequently encountered with separations on reversed-phase columns. The mobile phase usually contains a large proportion of water and organic compounds are often encountered that are insoluble in water. Solid injection or solid introduction is an alternative to circumvent low sample solubility. The introduction mixture is prepared by mixing dry powdered sample with a suitable amount of column packing material. The sample can also be preadsorbed on stationary phase by removing the volatile solvent (e.g. dichloromethane, ethyl acetate, acetone, etc.) in which it was solubilized from the suspension containing the stationary phase. Homogeneity of the injection powder is a prerequisite for efficient separations. The proportions of the introduction mixture are generally one part sample mixed with two to five parts stationary phase. The prepared sample is then placed directly onto the column inside a small pre-column and the eluent is passed through the system for separation.

Applications: MPLC in Natural Product Isolation

MPLC has recently become widely used in the pharmaceutical, chemical and food industries, and many applications are found in natural product isolation. Both applications given below have been selected as examples of the transposition of analytical HPLC conditions to MPLC.

The methanol extract of *Halenia corniculata*, a Gentianaceae plant from Mongolia, was first passed through a Sephadex LH-20 gel column and the glycoside-rich fraction (300 mg) was then purified by MPLC on a reversed-phase RP-18 column, yielding six xanthone glycosides (1–6). The search for optimal conditions was performed by analytical HPLC (Figure 3A) and was followed by direct transposition to MPLC separation (Figure 3B).

The dichloromethane extract from the roots of *Tinospora crispa* (Menispermaceae) was first

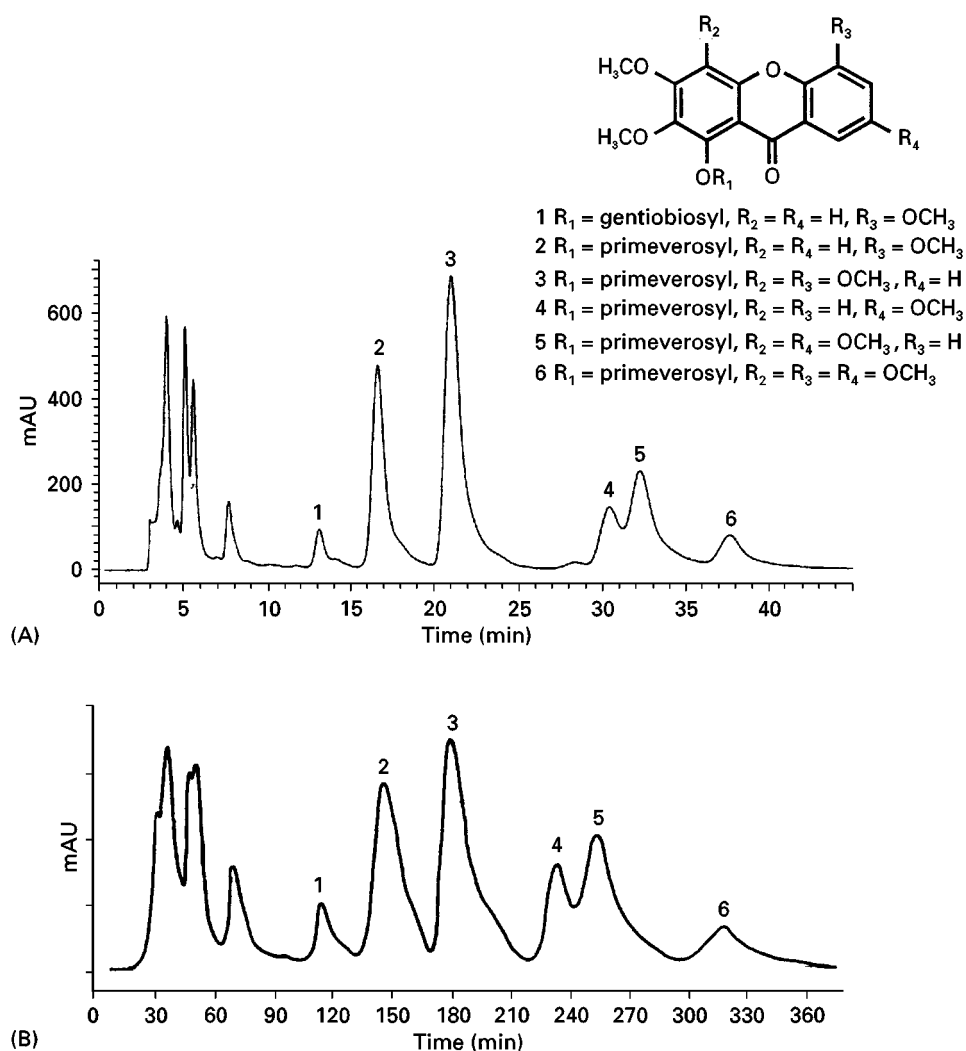


Figure 3 Transposition of conditions for the MPLC separation of xanthone glycosides from *Halenia corniculata* (Gentianaceae). (A) Analytical HPLC on a Lichrosorb 7 μm RP-18 (250 mm \times 4 mm) column with MeOH/H₂O 40 : 60 (v/v); flow rate 1 mL min⁻¹; (B) MPLC on Lichrosorb RP-18 (15–25 μm) with MeOH/H₂O 40 : 60 (v/v); flow rate 3 mL min⁻¹; column dimensions 460 mm \times 12 mm. (Reproduced with permission from Hostettmann *et al.*, 1997.)

fractionated by centrifugal partition chromatography and one fraction was submitted to analytical HPLC with an acetonitrile gradient (Figure 4A). Owing to the lower convenience of acetonitrile for preparative purposes (cost, toxicity), conditions were found with methanol on analytical HPLC (Figure 4B). The selected isocratic eluent system was transposed directly to MPLC and 6-h separation led to the isolation of three phenylpropane derivatives (7–9) (Figure 4C).

Conclusion

Since the early 1980s MPLC has been confirmed as an excellent preparative chromatographic tool that is

now routinely used in many laboratories. The extended use of various bonded phases in MPLC no longer restricts the use of this technique to the isolation of lipophilic substances with silica gel. For reasons of economy, recycling the stationary phase by simple washing or repacking of the column is of great interest in MPLC. Furthermore, a working experimental setup can be easily and rapidly assembled. The wide range of sample amounts that can be separated with this technique, together with the use of TLC and analytical HPLC in the search for optimal conditions, are also major benefits of this chromatographic method. However, good column packing and adequate sample preparation are prerequisites for successful separations. Further developments in MPLC

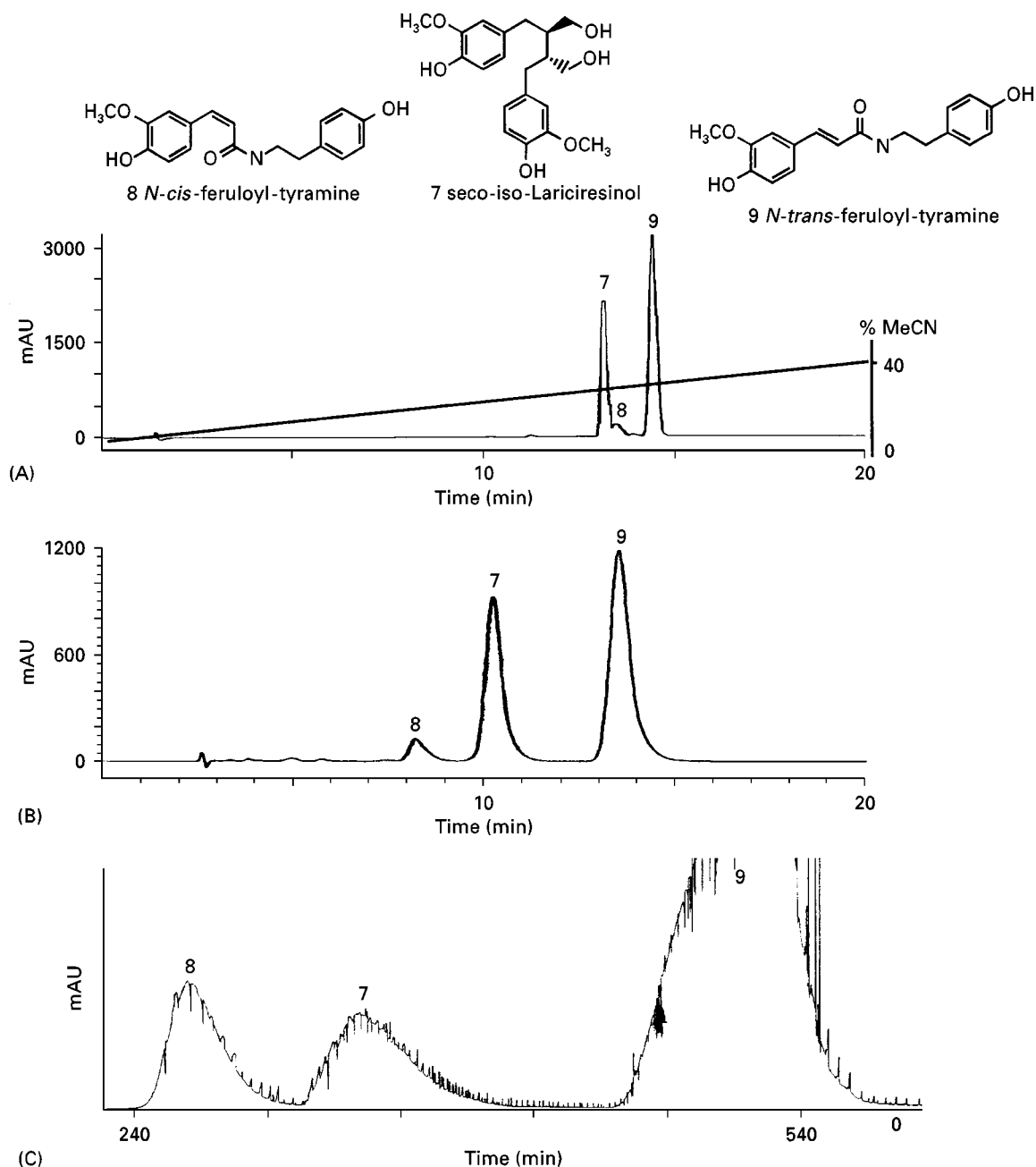


Figure 4 Transposition of analytical HPLC conditions for MPLC separation of phenylpropane derivatives from *Tinospora crispa* (Menispermaceae). (A) Analytical HPLC on a Lichrosorb 7 μ m RP-18 (250 mm \times 4 mm) column with a MeCN/water gradient 0 : 100 to 40 : 60 (v/v) in 20 min; flow rate 1 mL min⁻¹; (B) analytical HPLC on a Lichrosorb 7 μ m RP-18 (250 mm \times 4 mm) column with MeOH/water 40 : 60 in 20 min; flow rate 1 mL min⁻¹; (C) MPLC on Lichrosorb RP-18 (15–25 μ m) with MeOH/water 30 : 70; flow rate 4 mL min⁻¹; column dimensions 460 mm \times 12 mm.

will mainly concern detection problems with the optimization of detectors that can accommodate high sample loads.

See also: II/Chromatography: Liquid: Large-Scale Liquid Chromatography. III/Flash Chromatography. Natural Products: Liquid Chromatography; Thin-Layer (Planar) Chromatography.

Further Reading

- Cavin A, Hostettmann K, Dyatmyko W and Poterat O (1998) Antioxidant and lipophilic constituents of *Tinospora crispa*. *Planta Medica* 64: 393–396.
- Hostettmann K, Marston A and Hostettmann M (1997) *Preparative Chromatography Techniques – Applications in Natural Product Isolation*, 2nd edn. Berlin: Springer-Verlag.

- Leutert T and Von Arx E (1984) Präparative Mitteldruck-Flüssigkeitschromatographie. *Journal of Chromatography* 292: 333–344.
- Nyiredy S, Dallenbach-Toelke K, Zogg GC and Sticher O (1990) Strategies of mobile phase transfer from thin-layer to medium-pressure liquid chromatography with silica as the stationary phase. *Journal of Chromatography* 499: 453–462.
- Porsch B (1994) Some specific problems in the practice of preparative high-performance liquid chromatography. *Journal of Chromatography A* 658: 179–194.
- Rodriguez S, Wolfender J-L, Odontuya G, Purev O and Hostettmann K (1995) Xanthones, secoiridoids and flavonoids from *Halenia corniculata*. *Phytochemistry* 40: 1265–1272.
- Verzele M and Geeraert E (1980) Preparative liquid chromatography. *Journal of Chromatographic Science* 18, 559–570.
- Zogg GC, Nyiredy S and Sticher O (1989a) Operating conditions in preparative medium pressure liquid chromatography (MPLC). II. Influence of solvent strength and flow rate of the mobile phase, capacity and dimensions of the column. *Journal of Liquid Chromatography* 12, 2049–2065.
- Zogg GC, Nyiredy S and Sticher O (1989b) Operating conditions in preparative medium pressure liquid chromatography (MPLC). I. Influence of column preparation and particle size of silica. *Journal of Liquid Chromatography* 12, 2031–2048.

MEMBRANE CONTACTORS: MEMBRANE SEPARATIONS

J. G. Crespo, I. M. Coelho and R. M. C. Viegas,
Universidade Nova de Lisboa, Monte de Caparica,
Portugal

Copyright © 2000 Academic Press

Membrane-based processes are receiving recognition for their flexibility and efficiency. Processes like reverse osmosis, ultrafiltration and dialysis are already well developed and recently, membrane application to other separation processes, such as absorption and liquid-liquid extraction, have been gaining considerable attention.

In these latter processes, the porous membrane acts as contacting media for gas-liquid or liquid-liquid phases with comparable advantages to the traditional continuous contact equipment. While in conventional two-phase processes, dispersion of one phase into another immiscible phase is used in order to promote an efficient contact and increase the transport rate, membrane extraction is accomplished without dispersion of the two phases.

Consider a liquid-liquid extraction process and a microporous hydrophobic membrane with the aqueous-organic interface stabilized inside the membrane pores (Figure 1). Since the membrane is hydrophobic, the organic phase spontaneously wets the membrane and may permeate through the pores to the aqueous phase. This breakthrough problem can be controlled by applying a higher pressure on the phase that does not wet the pores. This higher pressure must not exceed a critical value, Δp_{cr} , otherwise the nonwetting fluid will

penetrate the pores and contaminate the other fluid phase.

If a hydrophilic membrane is used, the procedure is analogous, but in this case it is necessary to impose an organic phase pressure which is higher than that of the aqueous phase.

Although extraction can be conducted using a number of different membrane configurations, including flat-sheet, spiral-wound, rotating annular and hollow fibres, hollow fibres have received the most attention due to their high packing density: typical interfacial areas of contact per unit volume range from 1500 to 7000 m² m⁻³.

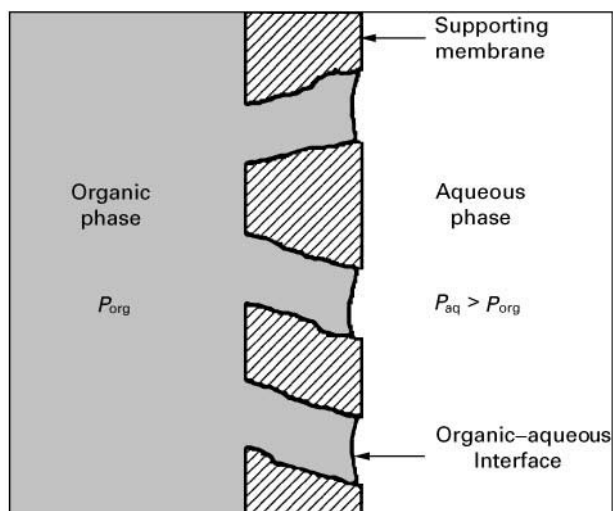


Figure 1 Organic-aqueous interface immobilized in a microporous hydrophobic membrane. P_{aq} , aqueous-phase pressure; P_{org} , organic-phase pressure.

The associated advantages of this configuration, which will be discussed in detail in the next section, have led to the development of an enormous range of processes, either with liquid-liquid phases or with gas-liquid phases.

Comparison between Membrane Contactors and Conventional Equipment

Advantages of Membrane Contactors

High contact area per unit volume Using a suitable module configuration such as a hollow fibre, membrane contactors can provide a contact area per unit volume which is 20–100 times higher than conventional equipment. The higher the interfacial area provided, the more efficient the contactor becomes and the smaller its size required for a given separation.

No loading and flooding constraints As the fluids to be contacted flow on the opposite sides of the membrane, both flow rates can be set independently. The available contact area remains constant even at very low or very high flow rates. This feature is particularly useful in applications where the required solvent/feed ratio is very low or very high, in contrast to conventional equipment, which is subjected to flooding at high flow rates and unloading at low ones.

Reduction of phase back-mixing When using membrane contactors, the mass transfer between the two phases occurs at the fluid-fluid interface immobilized at the mouth of the pores. This nondispersive contact minimizes emulsion formation and the occurrence of back-mixing is also reduced. By reducing back-mixing, a higher number of transfer units (NTU) can be achieved.

No need for density between the phases Unlike conventional dispersed-phase contactors, no density difference is required between fluids in liquid-liquid extraction because coalescence and separation of the dispersed phase are not necessary when using membrane contactors.

Reduced solvent hold-up Solvent hold-up is rather low when using membrane contactors; this may be important when using expensive solvents.

Modular design – direct scale-up The modular character of this equipment allows an easy straightforward scale-up procedure. Membrane operations

usually scale linearly and thus, when an application requires several contactors in series or parallel, this modular design allows a given process to be easily tested on a reduced scale.

Easy process integration As membrane contactors do not involve the dispersion of the two fluid streams, it is easy to combine them with other operation units. These hybrid processes can be highly advantageous from a technical and economic point of view. For example, a combined extraction/stripping process can be designed by coupling two membrane contactors in series, without the need for an intermediate coalescence step.

Limitations of Membrane Contactors

Additional membrane resistance Besides the mass transfer resistances associated with the boundary layers of the two fluid phases, the membrane provides a third resistance. While this additional resistance is often negligible it may, under some conditions, contribute significantly to the overall mass transfer resistance. It will be discussed later in this chapter a few heuristic rules to minimize this effect.

Fluid distribution in the shell side In hollow-fibre contactors the spatial distribution of the fibres is not perfectly uniform. This uneven distribution can induce fluid flow maldistribution in the shell side and, eventually, bypassing, especially when high flow rates are used. This problem may become particularly important when large scale modules are used.

Transmembrane pressure constraints The transmembrane pressure can become quite important in porous membrane contactors, because it may induce flow across the membrane (breakthrough), causing unwanted froth, foam and dispersion between the two phases. For this reason, the option between operation with co- or counter-current mode and the setting of the fluid flow velocity has to take into consideration the pressure drop profile developed along the module. This explains why laminar flow conditions are usually used.

Construction materials Membrane contactors employ polymeric membranes and potting adhesive resins to bond the fibre bundle to the module casing. These materials may have a limited compatibility with certain organic solvents, especially with aromatic compounds.

Linear up-scaling factor It was mentioned as an advantage that the scaling-up of membrane contac-

tors is rather simple and linear. On the other hand, this linearity is a serious drawback when comparing with traditional contacting equipment where the factor for scale-up cost is typically 0.6. This means that, if we want to double the capacity of a membrane contactor, the cost will be twice the original one, while for conventional equipment the cost will be $2^{0.6}$ of the original cost.

Membranes and Modules

Membrane Selection

Unlike most membrane operations, in membrane contactors the chemistry of the membrane is relatively unimportant, as it imparts no selectivity to the separation. The goal is to choose a membrane whose effect is not negative, i.e. that has no influence on mass transfer. Thus, the success of membrane contactors greatly depends on minimizing the membrane resistance to mass transfer. As a general rule, choose the membrane that is wet by the fluid to which the solute has more affinity (higher partition): if the solute partitions favourably to the solvent (organic), a hydrophobic membrane should be used; if it partitions favourably to the aqueous phase, then a hydrophilic membrane would be the best choice.

For gas-liquid contact two modes of operation are possible: wetted mode and dry mode. The wetted mode occurs when the pores are filled with liquid and the dry is when the pores are filled with gas: a hydrophilic membrane operates in wetted mode if the liquid phase is aqueous and in dry mode if it is organic, whilst a hydrophobic fibre will operate the inverse way. The dry mode is usually preferred to take advantage of the higher diffusivity of the solute in the gas phase, except in systems with an instantaneous interfacial reaction where the gas-phase resistance controls.

Still concerning the maximization of mass transfer, microporous membranes, typically with pore sizes between 0.05 and 1.0 μm and 20–100 μm thick have been used, in order to hinder solute diffusions as little as possible.

Hydrophobic membranes present the following advantages:

1. Higher pH and chemical stability
2. Reduced fouling with whole cells
3. Easier sterilizability

On the other hand, hydrophilic membranes are advantageous in the following conditions:

1. Systems with lysed cells or proteins, as they are likely to foul the membrane's surface to a lesser extent

2. Systems with very low interfacial tension. As hydrophilic membranes are commercially available with smaller pore sizes than the hydrophobic ones it can be easier to stabilize the interface (higher Δp_{cr}).

Module and Operating Mode Selection

Due to its high packing density (providing interfacial areas of contact up to 7000 $\text{m}^2 \text{m}^{-3}$), the hollow-fibre modules are the most attractive configuration.

Any design should be preceded by some preliminary considerations regarding the operating mode:

1. Should the feed stream flow in the tube or in the shell side of the module?
2. Should the extraction be carried out co- or counter-currently?
3. Should the operation be carried out in unsteady-state batch mode or in continuous mode?

As a general rule, the feed stream should circulate in the tube side whilst the extract should flow in the shell side. This observation stems from the fact that commercially available hollow-fibre modules still present deficient mass transfer in the shell side due to uneven distribution of the fibres, that can produce effects of channelling, bypassing and back-mixing on the shell side. With the aim of minimizing these problems, new modules have recently been marketed with baffles and better distribution of the fibres.

However, exception may be considered when dealing with feeds containing solids or a high degree of particles. Although cost considerations should be taken into consideration, a prior filtration is suggested.

Regarding co- or counter-current operation mode, although an attractive higher driving force could be attained with the latter, the stability of interface must be taken into consideration: when operating counter-currently, the transmembrane pressure difference along the module presents a higher variation which can interfere with the interface stability and even lead to breakthrough. The breakthrough pressure, Δp_{cr} , is determined by the pore size of the membrane, the interfacial tension between the two fluids and the contact angle, according to the Laplace equation:

$$\Delta p_{cr} = \frac{2\gamma \cos \theta}{r_p} \quad [1]$$

As to operating in batch recirculation or continuous contact mode, attention must be paid mainly towards the degree of extraction needed: the batch mode cannot achieve an extraction beyond the final equilibrium concentrations of both phases, while the

single-pass continuous counter-current operation can reach further extraction, depending on the fibre length and flow rates. For not such a high degree of extraction, the design equations must be looked at so as to choose the mode that minimizes the costs inherent in the desired extraction.

Commercially Available Membrane Contactors

The best known module is the Liqui-Cel® Extra-Flow, marketed by Celgard LLC (Figure 2). This module uses Celgard microporous polypropylene fibres, up to 22 500, that are woven into a fabric and wrapped around a central tube feeder that supplies the shell side fluid. It also contains a central shell side baffle that improves efficiency by minimizing shell side bypassing and provides a component of normal velocity to the membrane surface, which results in higher mass transfer coefficients than those achieved with strictly parallel flow. The larger modules can operate with liquid flow rates up to several thousand litres per minute.

Also, commercial hollow-fibre microfiltration and ultrafiltration modules with hydrophilic membranes, generally with parallel flow, can also be used as membrane contactors.

For bubble-free gas-liquid mass transfer applications, Membrane Corporation and W.L. Gore market modules with different nonporous membrane arrangements: the first with the fibres potted at one end only and individually sealed at the other end, so that all entering gas permeates the membrane; the second has the fibres arranged as a helix, offering higher shell side mass transfer coefficients than the parallel configuration.

Equipment Design

A hollow-fibre membrane contactor is a continuous contact equipment and so the well-known concept of mass transfer unit is also applied here:

$$L = HTU \cdot NTU \quad [2]$$

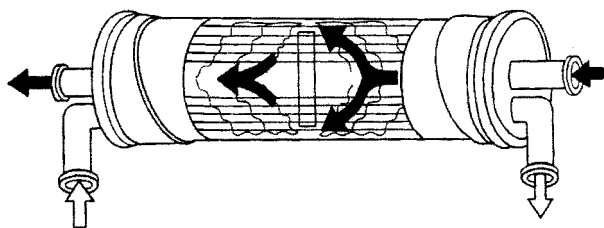


Figure 2 Schematic representation of a Liqui-Cel Extra-Flow membrane contactor.

where HTU is the height of the transfer unit and NTU is the number of transfer units necessary for a given separation. This equation allows the evaluation of the height or length of the contactor necessary to obtain the required extent of mass transfer.

The mathematical description of this design equation can be illustrated for an extraction process where the aqueous phase circulates in the tube side. In this case, a differential mass balance to the hollow-fibre module can be used to determine the change in solute concentration during a single pass:

$$-Q_{aq} \cdot dC_t = K_t \cdot dA_m \cdot (C_t - C_t^*) \quad [3]$$

where K_t is the overall mass transfer coefficient, Q_{aq} represents the aqueous-phase flow rate, A_m the membrane transfer area, equal to $\pi \cdot d_f \cdot L \cdot n_f$, where n_f is the number of fibres, and C_t is the solute concentration in the tube side phase. The superscript $*$ refers to the solute concentration in the tube side (aqueous phase) in equilibrium with the solute concentration in the shell side (organic phase).

Eqn [3] can be integrated for the fibre length. For the module inlet ($z = 0$) $C_t = C_t^{in}$ and for the outlet ($z = L$) $C_t = C_t^{out}$, where C_t^{in} and C_t^{out} are the solute concentrations entering and exiting the module, respectively:

$$L = HTU \cdot NTU = \frac{v_{aq}}{K_t a_i} \int_{C_t^{in}}^{C_t^{out}} \frac{dC_t}{C_t^* - C_t} \quad [4]$$

where v_{aq} is the fluid velocity circulating in the tube side, K_t is the module-averaged overall mass transfer coefficient and a_i is the interfacial area per unit module volume.

If a constant partition coefficient, P , can be assumed during the extraction process, integration of eqn [4] using $C_t^* = C_s/P$ where C_s , the solute concentration in the shell side phase, is obtained by mass balance, yields an analytical expression for the contactor length. The NTU expressions for a hydrophobic membrane with aqueous phase in fibre lumen and organic phase in the shell side, respectively for co-current flow and counter-current flow are the following:

$$NTU = \frac{1}{1 + \frac{Q_{aq}}{Q_{org}P}} \ln \frac{C_t^{out} - C_s^{out}/P}{C_t^{in} - C_s^{in}/P} \quad [5]$$

$$NTU = \frac{1}{1 - \frac{Q_{aq}}{Q_{org}P}} \ln \frac{C_t^{in} - C_s^{out}/P}{C_t^{out} - C_s^{in}/P} \quad [6]$$

For gas-liquid separations the partition coefficient may be replaced by H , Henry's law constant, and the aqueous and organic flow rates replaced by liquid and gas flow rates.

For systems with a variable partition coefficient it is necessary to introduce the equilibrium relation between C_t^* and C_s and a numerical integration is required.

Evaluation of Mass Transfer Coefficients

Three individual mass transfer resistances may be considered in membrane contactor extraction processes:

1. the inside tube boundary layer resistance
2. the membrane resistance to the solute diffusion through the pores
3. the shell side boundary layer resistance

The resistances are inversely proportional to the local mass transfer coefficients and a function of the system's geometry. Thus, for a hollow-fibre system when the membrane is wetted by the shell side phase, we obtain:

$$\frac{1}{K_t \cdot A_i} = \frac{1}{k_t \cdot A_i} + \frac{1}{P \cdot k_m \cdot A_{lm}} + \frac{1}{P \cdot k_s \cdot A_o} \quad [7]$$

where K_t represents the overall mass transfer coefficient (based on the tube side phase), k_t , k_m and k_s are

the local mass transfer coefficients on the tube side, membrane and shell side, respectively, and A_i , A_o and A_{lm} are the fibres' internal, external and logarithmic mean areas, respectively.

As the membrane may be hydrophobic or hydrophilic and the aqueous phase may circulate either in the fibre lumen or in the shell side, four different expressions for the overall mass transfer resistance for liquid-liquid extraction can be determined. Figure 3 shows the concentration profiles and the overall mass transfer resistances.

The tube side and the shell side mass transfer coefficients can be obtained experimentally and several correlations may be found in the literature.

Mass Transfer Correlations

Since laminar flux is predominant in hollow-fibre membrane contactors, a L  v  que type equation can be used to correlate both the tube side and the shell side mass transfer coefficients:

$$Sh_t = \alpha \cdot Sc_t^{bt} \cdot Re_t^{ct} \cdot \left(\frac{d_i}{1}\right)^{1/3} \quad [8]$$

$$Sh_s = \beta \cdot Sc_s^{bs} \cdot Re_s^{cs} \cdot \left(\frac{d_h}{1}\right) \quad [9]$$

where the subscripts t and s refer to the tube and shell sides, respectively, and α and β are constants. The

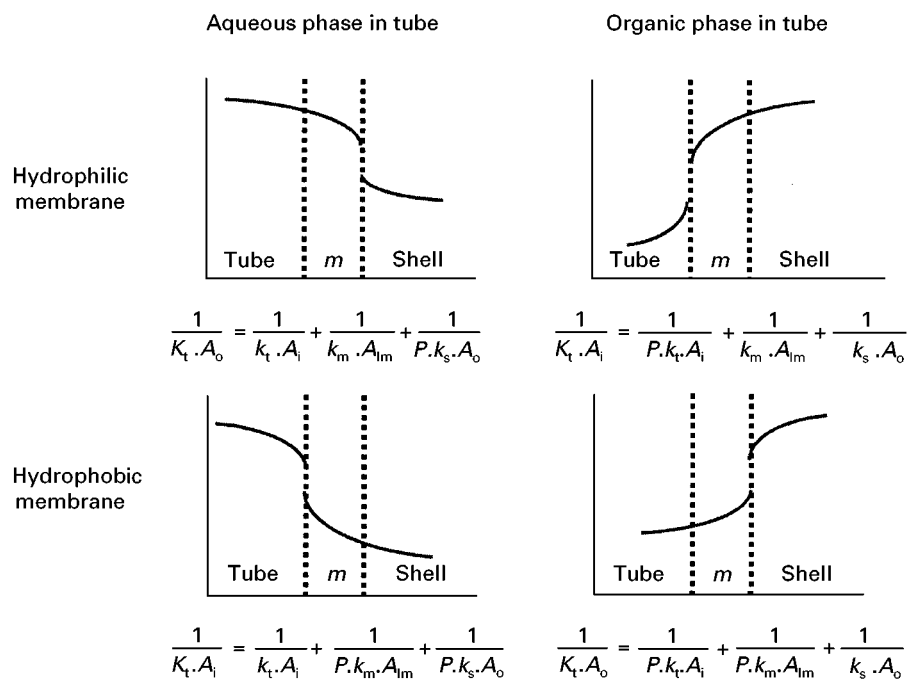


Figure 3 Concentration profiles and overall mass transfer resistance expressions for a chemical system with a solute partition coefficient favourable to the aqueous phase ($P < 1$).

Table 1 Mass transfer correlations for the tube side

Equation	Characteristics	Reference
$Sh = 1.62 Gz^{0.33} \quad Gz > 25$	Theoretical; laminar flux	Lévéque MC (1928) Les lois de transmission de chaleur par convection. <i>Annal. Mines</i> 13: 201
$Sh = 1.86 Gz^{0.33} \quad Gz > 100$	Empirical; laminar flux, heat transfer	Sieder EN and Tate GE (1936) Heat transfer and pressure drop of liquids in tubes. <i>Ind. Eng. Chem.</i> 28: 1429
$Sh = 1.64 Gz^{0.33} \quad 30 < Gz < 2000$	Hollow-fibre module; gas-liquid extraction	Yang MC and Cussler EL (1986) Designing hollow-fiber contactors. <i>AIChE J.</i> 32: 1910
$Sh = 1.5 Gz^{0.33}$	Hollow-fibre module; liquid-liquid extraction	Dahuron L and Cussler EL (1988) Protein extraction with hollow fibers. <i>AIChE J.</i> 34: 130
$Sh = 1.4 Gz^{0.33} \quad 50 < Gz < 1000$	Hydrophobic fibre; liquid-liquid extraction	Takeuchi H, Tahamashi K and Nakano EM (1990) Mass transfer in single oil containing microporous hollow fiber contactors. <i>Ind. Eng. Chem. Res.</i> 29: 1471
$Sh = 0.2 Re Sc^{0.33} (d_i/L)^{0.33} Gz < 65$	Hollow-fibre module; liquid-liquid extraction	Viegas RMC, Rodríguez M, Luque S, Alvarez JR, Coelho IM and Crespo JPSG (1998) Mass transfer correlations in membrane extraction: analysis of Wilson-Plot methodology. <i>J. Memb. Sci.</i> 145: 129

Gz : Graetz number = $Re Sc(d_i/L)$.

exponents of the Schmidt numbers (Sc), b_t and b_s , are usually 0.33; however, the exponents of the Reynolds numbers (Re), c_t and c_s , may be different from that value.

Tables 1 and 2 show some correlations collected from the literature for both tube side and shell side mass transfer coefficients in hollow-fibre membrane contactors.

Table 2 Mass transfer correlations for the shell side

Equation	Characteristics	Reference
$Sh = 1.25(Re d_h/L)^{0.93} Sc^{0.33}$	Hollow-fibre module; gas-liquid extraction	Yang MC and Cussler EL (1986) Designing hollow-fiber contactors. <i>AIChE J.</i> 32: 1910
$Sh = 8.8(d_h/L) Re Sc^{0.33} \quad Re < 100$	Hollow-fibre module; liquid-liquid extraction	Dahuron L and Cussler EL (1988) Protein extraction with hollow fibers. <i>AIChE L.</i> 34: 130
$Sh = 5.85(1 - \phi) d_h/L Re^{0.6} Sc^{0.33} \quad \phi < 0.2 \quad Re < 500$	Hollow-fibre module; liquid-liquid extraction	Prasad R and Sirkar KK (1988) Dispersion-free solvent extraction with microporous hollow fiber modules. <i>AIChE J.</i> 34: 177
$Sh = 0.85(d_h/L)^{0.25} (d_e/d_s)^{0.45} Re^{0.33} Sc^{0.33} \quad Re < 700$	Hydrophobic fibre; liquid-liquid extraction	Takeuchi H, Tahamashi K and Nakano EM (1990) Mass transfer in single oil containing microporous hollow fiber contactors. <i>Ind. Eng. Chem. Res.</i> 29: 1471
$Sh = 0.017 (d_e/d_s)^{0.57} Re^{0.8} Sc^{0.33} \quad 700 < Re < 2000$	Hydrophobic fibre; liquid-liquid extraction	Takeuchi <i>et al.</i> (1990)
$Sh = (0.53 - 0.58?) Re^{0.53} Sc^{0.33}$	Hollow-fibre module; gas-liquid extraction	Costello MJ, Fane AG, Hogan PA and Schofield RW (1993) The effect of shell side hydrodynamics on the performance of axial flow in hollow fibre modules. <i>J. Memb. Sci.</i> 80: 1
$Sh = 8.7 Re^{0.74} (d_h/L) Sc^{0.33} \quad Re < 50$	Hollow-fibre module; liquid-liquid extraction	Viegas RMC, Rodríguez M, Luque S, Alvarez JR, Coelho IM and Crespo JPSG (1998) Mass transfer correlations in membrane extraction: analysis of Wilson-Plot methodology. <i>J. Memb. Sci.</i> 145: 129

d_e , external fibre diameter; d_s shell diameter; d_h hydraulic diameter; ϕ packing factor = $n_t d_e^2/d_s^2$.

Concerning the tube side, in most published works an exponent of $c_t = 1/3$ is usually obtained for a higher tube side Reynolds numbers range. However, using tube side Reynolds numbers in a low range ($Re < 50$ and $Gz < 100$), values of $c_t = 1$ were reported.

For the shell side, the values of the exponent of the Reynolds number are $0.5 < c_s < 1$. Values of 0.5 for laminar flow and 0.6 for turbulent flow on the shell side of a shell and tube heat exchanger are reported. Deviation from these values may be due to the nonuniform distribution of the fibres and their deformation by action of organic solvents, both inducing an irregular flow due to the formation of stagnant zones, preferential pathways and deficient mixing.

Applications

Liquid-Liquid Extraction

Liquid-liquid extraction cover quite a broad range of applications, including metal extraction, wastewater treatment and extraction of pharmaceutical and other products of biotechnological interest, such as organic acids and proteins.

Recovery of metals from industrial process wastewater is important, not only because metals are valuable, but also because of environmental legislation restrictions. Several examples of metal extraction (Cu, Zn, Ni, Cr(VI), Cd) using membrane contactors, have been reported. Reactive extraction is usually employed and extractants such as organophosphorous compounds (TOPO, D₂EHPA), tertiary amines (tri-*n*-octylamine) and liquid ion exchangers (Aliquat 336) are used.

Extraction of pollutants from wastewater such as phenol, toluene and volatile organic compounds (VOCs) using methyl isobutyl ketone (MIBK), hexane and kerosene as solvents and also reactive extraction with several extractants were reported. A pilot-scale plant for extraction of chlorinated and aromatic compounds from industrial wastewaters in the Netherlands was in operation for periods up to 3 months, reducing contaminant levels to $10 \mu\text{g L}^{-1}$.

Reactive extraction of organic acids produced by fermentation, such as acetic, citric, lactic and succinic acid, were also reported. Extraction of amino acids using reversed micelles was also studied.

Protein extraction can be accomplished either by two-phase aqueous extraction or by reversed micelles. Problems of interface stabilization caused by emulsions due to the adsorption of surfactant to the membrane surface, thus lowering the interfacial tension, were reported. Careful control of the pressure difference across the membrane was required for a stable operation.

Gas-Liquid Contactors

In gas-liquid extraction with membrane contactors, most efforts have been conducted in the areas of gas absorption/stripping and of wastewater treatment. Other fields like dense gas extraction and semiconductor cleaning water have been the object of study more recently.

Commercial applications include the Pepsi bottling plant in West Virginia that has been operating a bubble-free membrane-based carbonation line since 1993, showing reduced foaming, improved yield, lower CO₂ pressures and increased filling speed at high temperatures. Also, several beer production plants are using this technology for CO₂ removal to obtain a dense foam head, while others remove oxygen from beer to preserve its flavour; the stripping of oxygen from water, which is then used to dilute beer, is also being applied. Other commercial applications include the treatment of boiler feedwater, stripping of CO₂ from anion exchange feed streams and ultrapure water production for semiconductor manufacture.

In wastewater treatment, air stripping of VOC has been studied using polypropylene hollow fibres to remove chloroform, tetrachloroethylene, carbon tetrachloride, 1,1,2-trichloroethane and trichloroethylene from aqueous streams. Also, several studies have reported the use of membrane contactors for bubble-free aeration in wastewater treatment. Advantages include the absence of foaming, higher aeration rates, lower power input and ability to handle solids.

A list of applications is summarized in Table 3.

Membrane Distillation

In membrane distillation a nonwetted hydrophobic microporous membrane separates two phases of different water chemical potential. The difference in the water chemical potential may be induced by a temperature difference of the aqueous

Table 3 Applications of membrane contactors on gas absorption/stripping processes

Application
SO ₂ , CO ₂ , CO and NO _x removal from flue gases
CO ₂ and H ₂ S removal from natural gas
CO ₂ removal from biogas
VOC removal from offgas
NH ₃ removal from air in intensive farmery
Recovery of volatile bioproducts
O ₂ transfer in blood oxygenation and in aerobic fermentation
Ultrapure water production for semiconductor manufacturing
Dense gas extraction
Separation of saturated/unsaturated (ethane/ethylene)

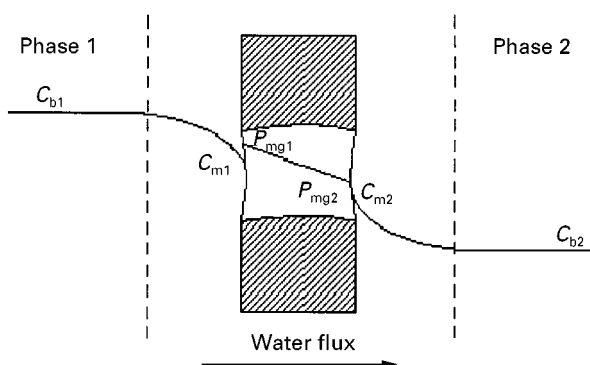


Figure 4 Schematic representation of water transport in osmotic distillation.

solutions corresponding to a difference in vapour pressure at both ends of the membrane. It may also be due to the different nature and concentration of the solute components of both phases, thus causing a different osmotic pressure of the two liquids. Since the osmotic pressure of an electrolyte solution is about 10 times higher than an equimolar solution of electrically uncharged particles, salt solutions (NaCl, CaCl_2 , KH_2PO_4) are efficient and relatively cheap systems to create high osmotic pressure differences. In both cases, water evaporates in the solution of higher chemical potential and the water vapour formed is transported across the membrane pores before being condensed in the solution of the lower water potential (Figure 4).

Solutions whose vapour pressure is relatively unaffected by the presence of the solute are ideal candidates for concentration using osmotic distillation. This includes solutions consisting primarily of sugars, such as fruit juices.

Two pilot-plant facilities located in Melbourne and Mildura (Australia) are successfully operating for concentration of fruit juices. Colour, flavour and aroma retention is good due to the lower operating temperature and stresses.

Grape juice concentrates used for production of high quality wines may also be concentrated by membrane distillation. Since these concentrates are stable for long periods of storage they can be shipped over long distances and high priced wines can be produced in regions where these grapes are not available or are too expensive.

Opportunities also exist for the concentration of pharmaceutical products, which are susceptible to thermal degradation.

Biphasic Membrane Bioreactors

Multilayer membrane bioreactors can readily be constructed from several membrane films to which different biocatalysts have been attached or from

combinations of permselective and catalytic membranes.

The use of permselective membranes in conjunction with catalytic films (or catalytic compartments) makes possible a high degree of control over the fluxes of the reaction participants, and hence over the course of reaction, that is impossible to achieve with catalyst particles. By using an adequate permselective membrane the fluids on either side of a membrane can be segregated, thus providing an additional degree of freedom in reactor design.

Most research work has been oriented to the development of biphasic membrane bioreactors where a microporous (hydrophobic or hydrophilic) membrane is used to separate an aqueous from an organic compartment. In this way, two immiscible liquid phases can be contacted across a membrane without one of the phases having to be dispersed in the other, as is required in most conventional multiphase reaction systems. In this type of reactor the biocatalyst may be linked to the membrane (Figure 5) or dispersed in one of the bulk phases.

The opportunity for development of biphasic membrane bioreactors is quite clear: the demand for selective removal of defined pollutants and the need for enantioselective transport and reaction for chiral synthesis in the pharmaceutical and food industries require new approaches in this field. Special attention has been devoted to the development of biphasic membrane bioreactors for enzymatic esterification and hydrolysis reactions.

Future Developments

Membrane contactors are unique equipment for promoting mass transfer while avoiding the dispersion of the fluid phases involved. This article has briefly reviewed the potential of membrane contactors in different areas of application and the problems which are still to be solved.

The industrial future of membrane contactors for liquid-liquid extraction processes, and in some defined situations for gas absorption, will depend very strongly on the ability to synthesize specific carriers or receptors with the potential to achieve recognition of individual solutes. Therefore, the trend will be the development of very selective carriers, in some cases with the ability for chiral recognition.

Membrane stability, in the sense of avoiding contamination between the two contacting fluids, is of major importance for the penetration of membrane contactors in some industrial markets. In particular, in the food and the pharmaceutical industries, trace contamination between the two fluid phases is a sufficiently strong reason to reject this type of process.

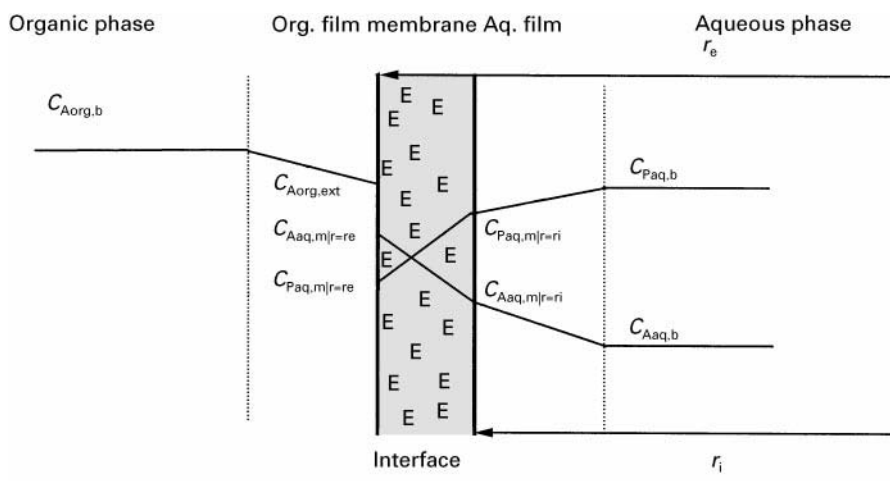


Figure 5 Representation of the enzymatic conversion of a substrate (subscript A) soluble in the organic phase to a product (subscript P) soluble in the aqueous phase. The enzyme is entrapped inside the porous structure of a hydrophilic membrane.

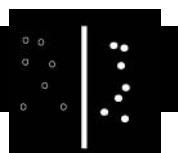
Development of organic solvents which are insoluble in water, nonvolatile and without the tendency to form emulsion would be highly desirable. Recently, the development of ionic liquids has been reported in the literature. These are entirely comprised of ions (complete absence of water), and are nonvolatile and insoluble in water. This type of solvent opens a world of new opportunities for liquid–liquid extraction and gas absorption using membrane contactors, without the risk of fluid cross-contamination. Also the use of dense gases and supercritical fluids has been suggested in membrane contactors. Again, the problem of contamination with the solvent phase could be eliminated.

Finally, new module design and new manufacturing materials will be welcome for certain type of applications, especially when viscous fluids and aggressive solvents are used. Further increases in membrane contactor performance are expected with the use of hollow-fibre fabrics and baffled modules.

Further Reading

- Cussler EL (1994) Hollow fiber contactors. In: Crespo JG and Boddeker KW (eds) *Membrane Processes in Separation and Purification*. Dordrecht: Kluwer Academic Publishers.
- Gabelman A and Hwang S-T (1999) Hollow fiber membrane contactors. *Journal of Membrane Science* 159: 61–106.
- Hogan PA, Canning RP, Petersen PA *et al.* (1998) A new option: osmotic distillation. *Chemical Engineering Progress* 49–61.
- Kunz W, Behabiles A and Ben-Aim R (1996) Osmotic evaporation through macroporous hydrophobic membranes: a survey of current research and applications. *Journal of Membrane Science* 121: 25–36.
- Matson SL and Quinn JA (1992) Membrane reactors. In: Ho WSW and Sirkar KK (eds) *Membrane Handbook*. New York: Chapman & Hall.
- Mulder M (1996) *Basic Principles of Membrane Technology*, 2nd edn. Dordrecht: Kluwer Academic Publishers.
- Prasad K and Sirkar KK (1992) Membrane-based solvent extraction. In: Ho WSW and Sirkar KK (eds) *Membrane Handbook*. New York: Chapman & Hall.
- Reed BW, Semmens MJ and Cussler EL (1995) Membrane contactors. In: Noble RD and Stern SA (eds) *Membrane Separations Technology. Principles and Applications*. Dordrecht: Kluwer Academic Publishers.
- Viegas RMC, Rodriguez M, Luque S *et al.* (1998) Mass transfer correlations in membrane extraction: analysis of Wilson-plot methodology. *Journal of Membrane Science* 145: 129.

MEMBRANE PREPARATION



Hollow-Fibre Membranes

M. van Bruijnsvoort and P. J. Schoenmakers,
University of Amsterdam, Amsterdam,
The Netherlands

Copyright © 2000 Academic Press

Introduction

Hollow-fibre membranes are an attractive alternative to conventional flat membranes in a growing number of important applications. Arguably, they have proliferated most in the biomedical and biochemical fields, thanks to their simple geometry and small dimensions in combination with their inherently high surface-to-volume ratio. Dialysis is the technique in which hollow-fibre membranes are most commonly employed.

There exist a number of extensive reviews on the technology, application and fabrication of membranes. A true classic is the book by Mulder, which contains a detailed overview of developments in the preparation of membranes and their use in purification. McKinney has provided a useful review of the preparation of organic hollow-fibre membranes. Tsapatsis has reviewed the preparation of inorganic membranes.

We have a particular interest in hollow fibres for polymer separations, with hollow-fibre flow field-flow fractionation (HF₅) as the analytical principle. Inorganic fibres are of great interest for polymers that require (strong) organic solvents. This article is biased due to this specific interest, our limited personal experience with different types of fibres and their preparation, and by our background as analytical chemists. The latter also provides us with an original perspective. To us there is an obvious analogy between the preparation of hollow-fibre membranes and open-tubular columns for chromatography. Both areas may benefit from such a comparison, presented in Table 1.

Types of Membranes

Basically, three types of membranes are distinguished:

- porous membranes;
- nonporous membranes; and
- liquid membranes.

All three types can be used in the hollow-fibre geometry. Porous membranes allow the passage of relatively large molecules. Depending on the size of the pores, one speaks of microfiltration (pore size > 100 nm), ultrafiltration (pore size < 100 nm), or nanofiltration (molecular weight cut-off > ca. 1000 Da). Nonporous membranes are permeable to very small molecules (gases). Liquid membranes are of interest because of the selectivity and flexibility they provide. A broad review of liquid membranes has been provided by Sastre and co-workers.

Hollow-fibre membranes are often the preferred geometry, offering distinct advantages over flat or tubular (diameter larger than 1 mm) membranes, for a number of reasons:

- high surface-to-volume ratio;
- conceptual simplicity;
- easy incorporation in flow streams;
- broad availability.

In preparing hollow-fibre membranes, we must try and capitalize on these advantages. For example, if the surface-to-volume ratio is a key parameter, then narrow-bore fibres are most interesting.

Membranes are used in many different ways in analytical chemistry. Most of their applications are in the areas of sampling and sample preparation, thanks to the fundamental ability of semipermeable

Table 1 Analogy between the properties of membranes and chromatographic columns

<i>Type of membrane selectivity</i>	<i>Chromatographic equivalent(s)</i>
Preferential interaction and adsorption from a gas, liquid or supercritical fluid	Gas chromatography with solid or polymeric stationary phases (GC) Normal-phase and reversed-phase liquid chromatography (LC) Supercritical-fluid chromatography (SFC)
Size selectivity (sieving effect)	Molar sieve columns (GC) Size exclusion chromatography (LC)
Charge selectivity	Ion exchange chromatography Ion exclusion chromatography
Affinity membranes	Affinity chromatography

membranes to differentiate between different materials (viz. matrix and analytes). This selectivity of the membrane can be based on molecular size, affinity, charge, or a combination of these properties. There are only a limited number of situations in which the actual analysis relies on the application of hollow-fibre membrane interfaces. These include the following:

- *Affinity chromatography.* Porous membranes combine a large surface area with a high permeability. By bonding specific groups to the surface, targeted species can be bound very strongly to the membrane. After the entire sample has been passed through the membrane, the analyte(s) can be removed. Affinity chromatography is of particular interest in the biochemical and biomedical areas. Since the membranes have a high permeability, the danger of degradation of vulnerable proteins is reduced. Moreover, the high fluxes possible allow more mass to be purified within the same period of time. Two extensive reviews (Roper and Josic) have been dedicated to this important field.
- *Extractions.* The intrinsic ability of hollow-fibre membranes to separate two distinct phases has found multiple applications in the field of extractions. Recently, Gabelman and Hwang published an extensive review on the subject of membrane contactors, i.e. membranes used to separate two immiscible phases.
- *Chiral separations.* The field of preparative chiral separations using hollow-fibre membranes is too interesting to remain unmentioned. In particular, in the pharmaceutical industry there is a great demand for the separation of racemic mixtures on a preparative scale. For example, a hollow-fibre supported liquid membrane can be used to separate two phases, with a chiral selector present in one of these. Alternatively, a chiral selector can be chemically bonded to the membrane surface, prepared in a manner similar to the membrane used for affinity chromatography.
- *Hollow-fibre flow field-flow fractionation (HF₅).* A technique in which the simplicity of hollow-fibre membranes is very advantageous is flow field-flow fractionation (flow FFF). The concept of flow FFF was brilliantly conceived by Giddings. In flow FFF, macromolecules or particles are injected into a channel with a porous wall and displaced by a flow perpendicular to its direction of movement. Based on the difference in average velocity lines that are occupied by particles with different diffusion characteristics (related to particle size or molecular mass), a fractionation is obtained. Ideally (i.e. for spherical particles), the re-

tention time is directly related to the diffusion coefficient of the analyte.

HF₅ was introduced by Carlshaf and Jönsson in 1988 as an instrumentally simple and cost-effective alternative to flow FFF channels with a flat configuration. However, during the 1990s only a limited number of papers have been dedicated to this promising technique. Flow FFF poses very high demands on the quality of the hollow-fibre membrane and, especially, on the fibre-to-fibre repeatability. This is definitely the most important reason for slow progress on the subject. Recently, Lee *et al.* showed an impressive fractionation of latex particles (Figure 1). For this type of fractionation their HF₅ system performed at least as good as alternative techniques, such as the more-established flat-channel flow FFF.

- *Isoelectric focusing.* In 1998, Korlach published an original article on pH-regulated electro-retention chromatography (ERC). This technique is quite similar to (electrical) FFF. A voltage is applied

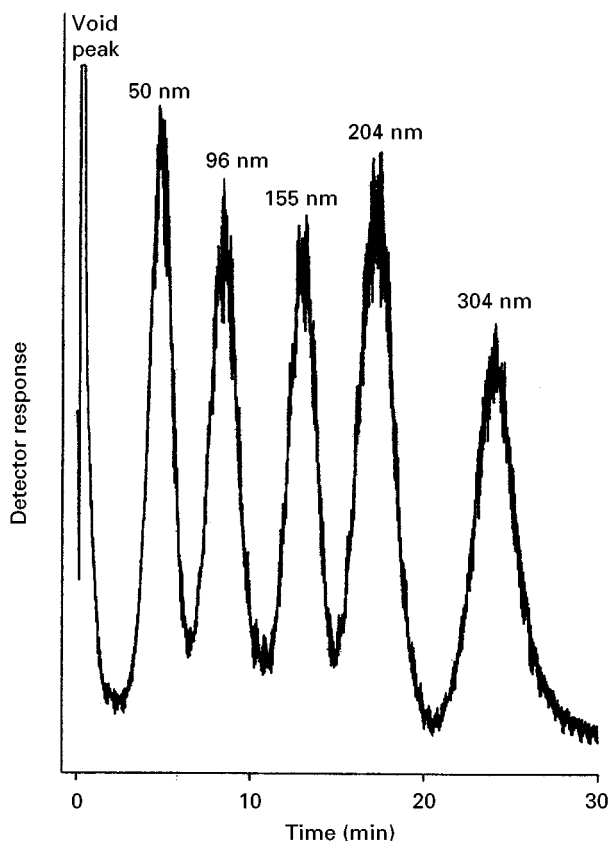


Figure 1 Hollow-fibre flow FFF fractogram showing the separation of polystyrene latex beads. (Reprinted with permission from Lee WJ, Min BR and Moon MH (1999) Improvement in particle separation by hollow fiber flow field-flow fractionation and the potential use in obtaining particle size distribution. *Analytical Chemistry* 81: 3446–3452.)

across the diameter of a hollow-fibre membrane. Subsequently, a pH gradient is applied in a fluid reservoir which surrounds the fibre. The gradient gradually diffuses into the hollow-fibre membrane. At some point (when the pH crosses the isoelectric point or pI value), the charge on the analyte reverses and the ions will start to migrate to the middle of the fibre, from where they will be rapidly eluted owing to the higher axial flow velocity. The bottleneck in the development of this technique, which is mainly applied to the separation of proteins, is adsorption of the analytes on the membrane.

Semipermeable membranes allow us to manipulate processes that take place at the interface between two (miscible or nonmiscible) phases. They can be used in the gas phase for sampling purposes (e.g. membrane-assisted headspace injection in GC, membrane inlet mass spectrometry, MIMS) or in the liquid phase for sample preparation (e.g. dialysis) or sample concentration. Membranes used for gas sampling usually consist of simple fibres made of polymeric materials, such as polysiloxanes. More sophisticated separations, such as affinity chromatography, require more sophisticated membranes with dedicated selectivities. Also when in contact with liquid phases, most of the fibres used in analytical chemistry are based on organic (polymeric) materials.

The most important characteristic of a membrane is its separation selectivity. Differences in permeability for different materials can be based on a sieving effect (size selectivity) or on the chemical structure of the membrane. Hydrophobic membranes are more permeable to (nonpolar) organic molecules, while hydrophilic membranes are more permeable to water. Membranes will also show adsorption effects. Certain materials (analytes or matrix components) may be preferentially contained in and on the membrane. In some cases this is a desired effect (affinity membranes are the obvious example). Where fibres are used for sampling or sample clean-up in analytical chemistry, adsorption effects are often undesirable.

Preparation of Hollow-Fibre Membranes

The art of hollow-fibre-membrane preparation has taken a high flight in recent years. Nowadays, hollow-fibre membranes are attainable in a fantastic variety of membrane and support materials, pore sizes, diameters, thicknesses, etc. An overview of the techniques involved in the preparation of hollow-fibre membranes is given below.

The various processes for preparing fibres tend to be rather complex, and certainly are laborious and time-consuming. The most difficult step is the optimization of the process, viz. ensuring repeatable (in-house) and ultimately reproducible (transferable) results. Hence, for small-scale applications of hollow-fibre membranes, including all practical applications within analytical chemistry, the most sensible approach to the technology is to obtain suitable fibres from a commercial source.

Preparing Fibres

Most commonly, polymer tubing is prepared by a process referred to as spinning. This can be seen as an extrusion process. A viscous polymer solution (or melted polymer) is pressed through a small hole, while a fluid (bore liquid) is pumped through the centre. This construction is known as a spinneret. It allows precise control of the fibre dimension, thickness, etc. On exiting the spinneret, the fibre is drawn through a coagulation bath, after which additional treatment steps may take place.

The coagulation bath may merely be used to solidify the polymer and stabilize the fibre, but it may also be used to deposit a membrane (see next section). Many different polymers can be processed this way and the porosity of the resulting microfiltration membrane is affected by a large number of parameters. A summary is provided in Table 2. In the case of porous fibres, the type of material used is usually of little relevance to the properties of the membrane. The latter are almost totally determined by the parameters of the pores (size distribution, shape) and the membrane thickness. The material is selected based on other criteria, such as compatibility with the materials (fluids) encountered in the application, mechanical strength and cost. A typical example of a hollow-fibre membrane is shown in Figure 2.

Membrane Films

Polymeric membrane films are usually formed by transferring a polymer from the liquid phase (solution, melt or suspension) to the solid phase. Such a process is known as *phase inversion*. Alternatively, membranes can be formed by *in situ* polymerization. Several processes will be considered below in some detail.

Liquid membranes from a special class of membrane films. They are prepared simply by immersing a microporous hollow fibre in a liquid. The liquid membrane, supported by the hollow fibre, separates two phases; by adding a selective carrier to the membrane (carrier-mediated transport), an increased selectivity can be obtained.

Table 2 Summary of variables affecting fibre properties

Variable	Values	Effects
Consumption of casting solution	Suspension of polymer in non-solvent ('dry spinning') Melted polymer ('melt spinning') Polymer solution ('wet spinning')	Great effect on fibre porosity (and other properties)
Spinning parameters	Extrusion rate (mass flux of solution) Tearing rate (speed of drawing the fibre) Bore fluid rate Distance between spinneret and coagulation solution Composition of coagulation bath Temperature at the various stages	Determines fibre dimensions (internal and external diameters) Significant effect on fibre porosity
Fibre treatments	Washing Chemical modifications	Removes contamination Determines selectivity

Film deposition techniques In order to create a film of a polymeric material on the inside of the fibre, the complete fibre can be filled with a solution of a polymer. Upon evaporation of the solvent, a film will be formed (*static coating*). The critical step is the evaporation of the solvent. This must take place slowly and regularly, in order to obtain a membrane with constant properties throughout the fibre. After a film has been deposited, it may be stabilized by heat treatment or by *in situ* cross-linking.

Instead of an evaporation step, a solvent displacement step may be introduced. In this case, a non-viscous liquid is pumped through the column containing the (viscous) film of polymer solution. The newly introduced liquid may either be a solvent or a non-solvent for the polymer, but it must dissolve the initial solvent. The solvent is then either extracted from the

film, or replaced by a non-solvent. In either case, phase inversion will occur and a solid polymeric layer is obtained.

A second method for depositing a film is to press a plug of a polymer solution or a liquid polymer through the fibre. Behind this plug, a polymeric film will be left on the wall (*dynamic coating*).

Important parameters determining the properties of the membrane include the solution thermodynamics of the specific polymer-solvent combination, the concentration of the polymer in the solution, the temperatures at various stages of the process, the rate of solvent evaporation (or the rate of replacement of the solvent by a non-solvent) and the presence of additives in the solution.

In situ polymerization Using the processes of static or dynamic coating described above, it is also possible to deposit a film of a solution containing monomers or polymer precursors (pre-polymers). This has the considerable advantage of a low solution viscosity, allowing the formation of relatively thick films without the need to apply high pressures. The residual solvent needs to be evaporated slowly and carefully after the polymerization to avoid cracks in the film or radial differences in film thickness.

Sol-gel deposition A promising class of membranes is that of the inorganic membranes, which are resistant to a wide variety of solvents, including potent organic solvents such as tetrahydrofuran or hexafluoro-isopropanol. The most common technique of preparation is sol-gel deposition on a ceramic support. This procedure was developed in the early 1980s by Burggraaf's group. A sol of nanometre-sized γ -alumina particles is deposited on the wall of the fibre from an aqueous solution containing a small percentage of polyvinyl alcohol. The deposited sol

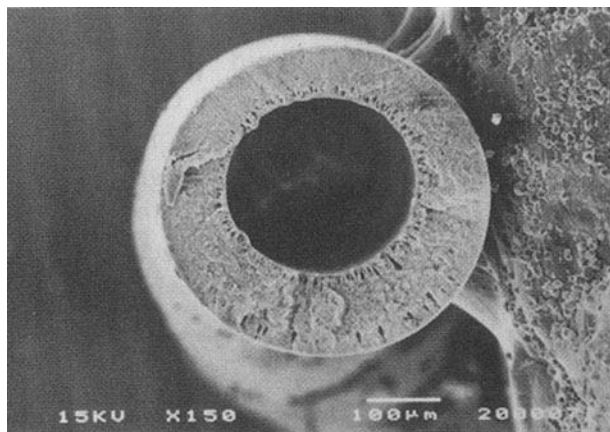


Figure 2 Typical scanning electron micrograph of an asymmetrical composite hollow-fibre membrane. (Reprinted with permission from Chung TS, Teoh SK and Hu X (1999) Formation of ultra-thin high-performance polyethersulfone hollow-fiber membranes. *Journal of Membrane Science* 133: 161–175.)

can be converted to a defect-free membrane by sintering.

Okubo pointed out in 1991 that for the preparation of membranes inside a narrow-bore ceramic hollow fibre (1.4 mm inner and 2.0 mm outer diameter) dynamic coating procedures (see Film Deposition Techniques, above) are required. By forcing the sol through the hollow fibre, a stable and thick defect-free layer can be obtained. Reducing the diameter of hollow-fibre membranes is important, as it results in an increase of the surface-to-volume ratio, so that very small volumes can be separated or purified. Many applications in medicine, biology and analytical chemistry stand to benefit.

Chemical Modification of Membranes

Polymers or reactive groups can be chemically bonded to suitable groups on the solid surface inside membrane pores. A large number of surface modification reagents are readily available and specific functional groups, to create the desired membrane selectivity, can be readily attached to such molecules. The process of chemically modifying membrane surfaces may also involve several reaction steps, which, however, may result in a less well-defined product.

Polymers can be attached to the surface ('grafted') through reactive functional groups, or through a pre-deposition radiation treatment. This process allows the creation of a great variety of selective membranes, which can be tailored for specific separations. These tailor-made phases allow affinity-type separations to be performed, in which extremely selective interactions are realized between the membrane surface and a selected analyte. Such interactions can be very strong, but desorption is possible by an appropriate change of conditions (displacing solvent or buffer).

Polymeric films can also be modified by introducing ionic groups, which drastically alters the properties of the membrane. Highly inert, nonpolar

polymeric membranes, such as polyethylene or polytetrafluoroethylene (Teflon®), can be modified to yield highly polar, ionic interfaces.

Hollow Fibres in Analytical Chemistry

As stated earlier, in most applications of hollow-fibre membranes in analytical science commercially available fibres are used. In only a limited number of cases (i.e. liquid membranes and affinity membranes) have analytical scientists reverted to in-house preparation. A nonexhaustive list of major suppliers of hollow-fibre membranes is provided in Table 3. Also, two suppliers of ceramic tubular membranes are listed in this table. Ceramic tubular membranes are not yet commercially available in diameters small enough ($d < 1$ mm) to be called fibres.

In Table 4 we present a selection of recently developed applications of hollow-fibre membranes in analytical chemistry, with emphasis on the types of fibres used and their preparation or commercial availability. Here, we concentrate on the use of hollow-fibre membranes directly coupled with analytical techniques. The case in which the membrane solely determines the separation process has been covered above. Omitted from this table are instruments featuring on-line couplings of either dialysis or filtration units to standard high performance liquid chromatography (HPLC) instruments. These techniques are already well established and commercially available. A very useful review on the state of the art in the on-line coupling of dialysis to HPLC and capillary electrophoresis (CE) has been provided by van de Merbel.

In ion chromatography, hollow-fibre membranes can be used either before the analytical separation column (pre-column) for sample preparation, or post-column to suppress the conductivity of the effluent (mobile phase) prior to conductivity detection. In an interesting article, Kaufmann described the insertion of a hollow-fibre membrane between an HPLC

Table 3 Some major suppliers of hollow-fibre membranes

<i>Producer</i>	<i>Location</i>	<i>Web address (April 2000)</i>
Dow-Corning	Midland, MI, USA	www.dowcorning.com
Hoechst Celgard	Wiesbaden, Germany	www.celgard.de
Minn Tech	Minneapolis, MN, USA	www.minntech.com
Millipore	Bedford, MA, USA	www.millipore.com
Sepracor	Marlborough, MA, USA	www.sepracor.com
A/G Technology	Needham, MA, USA	www.agtech.com
Tech-Sep ^a	Lyon, France	—
US Filter/Schumacher ^a	Asheville, NC, USA	schumacher-usa.com

^aSupplier of (tubular) ceramic membranes.

Table 4 A selection of applications of hollow-fibre membranes in analytical chemistry, connecting specific applications (techniques and analytes) with types and sources of membranes, and useful reviews*

	<i>Method</i>	<i>Compound</i>	<i>Author</i>	<i>Membrane type</i>	<i>Manufacturer</i>
Gas phase extractions	GC (MESI)	Volatile organic carbohydrates	Mitra (1996)	Silicon	Dow-Corning
			Yang (1994)	Silicon	Dow-Corning
	MIMS	Volatile organic carbohydrates	Ketola (1998)	Silicon	Dow-Corning
			Cisper (1995)	Silicon	Dow-Corning
			Srnivisan (1997)* Degn (1992)*		
Liquid phase pre-column	μ -LC	Bambuterol	Thordarsson (1996)	Polypropylene, 0.03 μ m	Hoechst, Celanese
	CE	Bambuterol	Palmarsdottir (1997)	Polypropylene, 0.2 μ m	AKZO Nobel
	CE	Organochlorides	Bao (1998)	Celgard X-10	AKZO Nobel
	CE	Proteins	Zhang (1997)	Cuprophane, 10 kDa	Hoechst Celanese
	CE	Methamphetamine	Pedersen (1999)	Polypropylene, 0.2 μ m	AKZO Nobel
	cIEF		Wu (1999)*		
Post-column	Reaction	Barbiturates	Haginaka (1987)	AFS-2	Dionex
		Bromate	Inoue (1997)	Nafion	Dupont
	Ion exchange	Small anions	Hanaoka (1982)	Nafion	Dupont
	Buffer exchange	Polyethylene glycol, proteins	Kaufmann (1993)	Cuprophane C1	Akzo Nobel
	Dialysis-electro-spray MS	Proteins	Lutz (1999)	Regenerated cellulose, 13 kDa	Spectrum Medical Instruments

Abbreviations: LC, liquid chromatography; CE, capillary electrophoresis; cIEF, capillary isoelectric focusing.

column and a detector for continuously exchanging buffer ions.

Following Davis, Haginaka's group has developed a hollow-fibre membrane-based post-column reactor. By immersing the fibre in, for example, an alkaline solution, the pH of the eluent can be altered to enable the detection of penicillins, amino acids, barbiturates, etc. However, since the process is diffusion-limited, a long fibre is usually required, leading to additional band broadening. Nonetheless, this is an elegant method to change the pH without the need to introduce an additional reagent stream and a post-column mixing coil.

Two important applications of hollow-fibre membranes are as sample preparation devices to extract specific analytes from a gaseous matrix. When the extracted components are directly fed into the ion source of a mass spectrometer, we speak of membrane-inlet mass spectrometry or MIMS. When the membrane serves as the inlet for a gas chromatograph various acronyms are used, of which MESI (membrane extraction with a sorbent interface) is the most common. The main objective of using membranes in these cases is to prevent large amounts of water (vapour) from entering the analytical instrument.

The membrane in MIMS can be used in different configurations. One of these involves a flat-disc membrane at the tip of a tubular probe, which is

inserted or immersed in the sample or sample stream. In most cases, however, a tubular membrane is used. Polysiloxane tubes (of surgical quality) are the most popular. The sample can either flow through this tube or be on the outside. In the first case, the membrane tube will be inside the mass spectrometer. In the second case, the membrane forms the interface between the mass spectrometer and the outside (chemical) world. A purge gas may pass through the inside of the tube, or it may just be connected to the mass spectrometer vacuum system.

The membrane tubes used for mass spectrometry are usually 1–2 mm in diameter. Using narrower tubes or fibres will not lead to lower detection limits, as the response of a mass spectrometric system increases with the amount (mass) of sample introduced per unit time. In principle, the mass flow of sample is proportional to the tube diameter, so that larger tube diameters are more favourable in this respect. A very large area can also be obtained by using flat, folded membranes. The use of hollow-fibre membranes for MIMS has the advantage that very small samples or sample streams suffice. An efficient parameter by which to affect the sensitivity of the system is the thickness of the membrane (tube wall). The selectivity of the system may be influenced by varying the tube materials. MIMS is most commonly applied to liquid samples, although the concept is

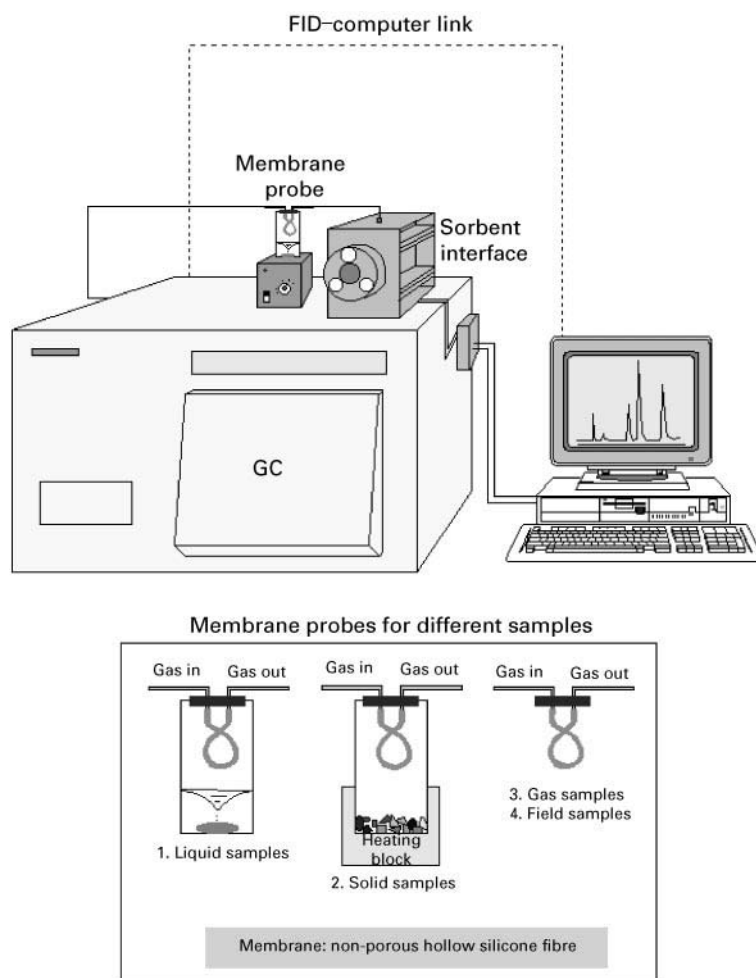


Figure 3 Principle of the MESI set-up. (With permission from the Web page <<http://sciborg.uwaterloo.ca/chemistry/pawliszyn/>>.)

equally valid for gaseous samples. The concept is very attractive for introducing components into the mass spectrometer from aqueous samples, such as those encountered in biotechnology (e.g. measuring the amounts of gases in fermentation broths) or in waste management, but can also be a practical tool in the laboratory. There are at this time relatively few known applications of MIMS for process monitoring, although this is one of the most promising areas.

The principle of MESI is illustrated in **Figure 3**. Analytes, following selective passage through the membrane, are trapped onto a sorbent interface. After a sufficient amount of the analytes has been accumulated, these components are desorbed. In GC this can be done by rapidly increasing the temperature (thermal desorption). Finally, the analytes are separated on the GC column. Most commonly, the membrane probe is used to sample a gaseous phase, either a gaseous sample or sample stream, or the

headspace of a liquid or solid sample. However, there is no fundamental reason why a liquid (e.g. aqueous) phase cannot be sampled directly. The technique can elegantly be used for the field analysis of air.

An interesting trend is the online coupling of hollow-fibre membranes to modern miniaturized separation techniques, where the intrinsic small volumes of hollow-fibre membranes come fully to their right. The hollow-fibre membrane introduces selectivity between analytes and matrix components (sample preparation), and can be used to concentrate the analytes prior to analysis. A liquid membrane device for sample preparation, developed by Mathiasson and Jönsson in 1996, is shown in **Figure 4**. The fibre is positioned in a small channel ($d < 1$ mm) that serves as the donor compartment. From the receptor compartment, i.e. the lumen of the fibre, small volumes can be manipulated towards the attached separation devices through narrow-bore capillaries. The device has been coupled to both μ -LC and CE, and has been

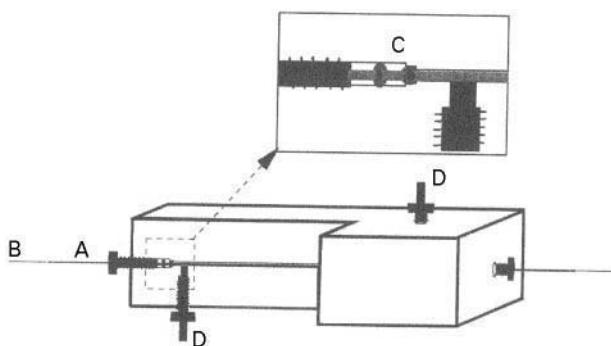


Figure 4 A liquid membrane device for sample preparation. A, hollow fibre (reaching through a hole drilled through the whole block); B, fused silica capillaries inserted in the ends of the fibre; C, O-rings for fixing the fibre and capillaries; D, connectors for the donor channel. (Reprinted with permission from Thordarson E, Palmarsdottir S, Mathiasson L and Jonsson JA (1996) Sample preparation using a miniaturized supported liquid membrane device connected on-line to packed capillary liquid chromatography. *Analytical Chemistry* 68: 2559–2563.)

employed for the analysis of drugs in a matrix of blood plasma.

See also: III/Membrane Preparation: Interfacial Composite Membranes; Phase Inversion Membranes.

Further Reading

- Degn H (1992) Membrane inlet mass spectrometry in pure and applied microbiology. *Journal of Microbiological Methods* 15: 185.
- Gabelman A and Hwang ST (1999) Hollow fibre membrane contactors. *Journal of Membrane Science* 159: 61.
- Giddings JC (1991) *Unified Separation Science*. New York: Wiley.
- McKinney R (1987) A practical approach to the preparation of hollow fibre membranes. *Desalination* 62: 37.
- Mulder M (1991) *Basic Principles of Membrane Technology*. Dordrecht: Kluwer.
- Roper DK and Lightfoot EN (1995) Separation of biomolecules using adsorptive membranes. *Journal of Chromatography A* 702: 3.
- Sastre AM, Kumar A, Shukla JP and Singh RK (1998) Improved techniques in liquid membrane separations: an overview. *Separation and Purification Methods* 27: 213.
- Tsapatzis M and Gavalas GR (1999) Synthesis of porous inorganic membranes. *MRS Bulletin* 24: 30.
- van de Merbel NC (1999) Membrane-based sample preparation coupled on-line to chromatography or electrophoresis. *Journal of Chromatography A* 856: 55.

Interfacial Composite Membranes

J. E. Tomaschke, Hydranautics Oceanside, CA, USA

Copyright © 2000 Academic Press

Introduction

The development of asymmetric cellulose acetate membranes in the 1960s was a breakthrough in membrane technology. These membranes consisted of a thin surface skin layer on a microporous support. The skin layer performed the separation required and because it was very thin fluxes were high. The microporous support provides the mechanical strength required. Following these developments Rozell *et al.* in 1967 described the preparation of the first interfacial (IFC) composite membranes. These membranes have since become the standard for reverse osmosis (RO) and nanofiltration (NF) applications.

IFC membranes have the same asymmetric status of the first-generation cellulose acetate membranes but are made by a very different procedure, shown schematically in Figure 1. In a first step a microporous polysulfone support membrane is impregnated with an aqueous solution containing a multifunctional amine. The impregnated membrane

is then contacted with a hexane solution containing a multifunctional acid chloride. Because the two solutions are immiscible the reactants can only combine at the membrane interface and so a thin polymer film layer forms at the surface. This layer performs the separation required.

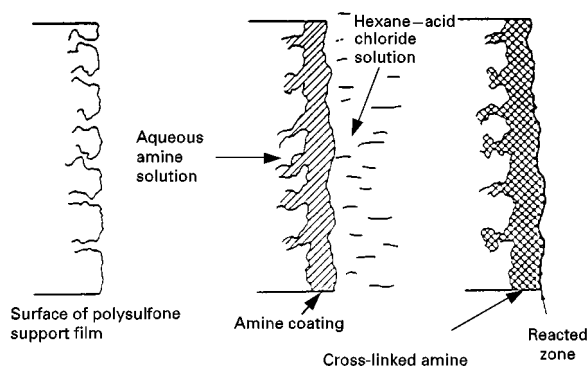


Figure 1 Schematic of the interfacial polymerization procedure. (From Cadotte JE and Petersen RJ (1981) Thin-film composite reverse osmosis membranes: origin, development and recent advances. In Turbak AF (ed.) *ACS Symposium Series 153*, Washington, DC, pp. 305–326.

IFC membrane development can be divided into two time periods. The earlier development from 1967 to approximately 1980 was characterized by work funded through the US Department of the Interior, whereas the majority of the development since 1980 has been industry funded. The early membrane preparations experienced a transition from the use of polymeric to monomeric amine reactants resulting in more durable products. Today the state-of-the-art IFC membrane chemistry consists of cross-linked aromatic polyamides derived from monomeric reactants. A review by Cadotte of composite RO membranes gives an account of the evolution of developments leading up to the commercialization of high performance membranes.

The basic interfacial method of membrane preparation using porous support has changed little since its inception though improvements in reactant chemistry and processing conditions have been made. The laboratory-scale preparation method remains a valuable initiation step in the development of IFC membranes because of its efficiency and simplicity. This method will be given a detailed discussion in the sections which follow.

Interfacial Polycondensation

Early Thin Film Synthesis

The origins of interfacial polycondensation reactions can be traced to Morgan of Du Pont who studied the interfacial polymerization of numerous polyamides and polyesters. He found the Schotten-Bauman reaction of diamines with acid chlorides to be an effective laboratory process, which was termed interfacial polycondensation. In this process, the irreversible polymerization of two highly reactive monomers takes place near the interface of the two phases of nonmiscible liquids, as demonstrated by the model system hexamethylenediamine sodium hydroxide-water/sebacoyl chloride-hydrocarbon solvent to produce Nylon 610. This model system is the basis for the discussion which follows.

When the two liquid phases containing diamine and acid chloride are brought together and the hydrocarbon or halogenated solvent, etc.) solvent is a non-solvent for the final polymer, a thin film of the polymer will be formed rapidly at the liquid interface. Generally this polymer is found to be tough and of high relative molecular mass. In a very short time interval equivalent amounts of reactants combine nearly quantitatively, with elimination of hydrogen chloride, and produce a thin film. In Nylon 610 polymerization, the optimal molar ratio of diamine to diacid chloride was found to be about 6.5, indicating the rate-limiting

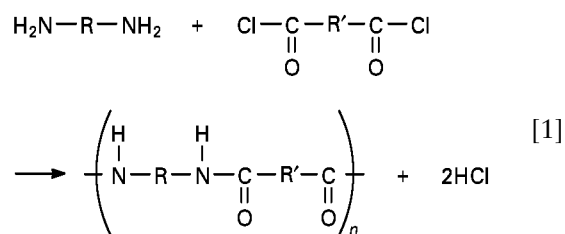
Table 1 Interfacial polycondensation variables

1. Reactivity of amine and acid chloride
2. Partition coefficient of amine water: organic solvent
3. Diffusion rate of amine into organic solvent
4. Concentration of reactants
5. Concentration ratio of reactants
6. Polymer film growth rate
7. Acid chloride hydrolysis rate
8. Polymer film permeability
9. Interfacial tension
10. Acid acceptor type
11. Surfactant type

feature of diamine diffusion across the interface and through the growing polymer film. Also noteworthy is the observation that polymer film growth occurs exclusively in the organic solvent phase owing to the extremely low solubility of acid chloride reactants in the aqueous phase. In general it is found that the mass transfer of the diamine is the rate-controlling step at all concentrations of reactants. The variables affecting interfacial polycondensation determined from experimentation are listed in Table 1.

Mechanism of Interfacial Polycondensation

The mechanism of membrane formation has been studied using the reaction between diamines and diacid chloride and can be generalized in eqn [1]:



Normally in the interfacial polymerization, sodium hydroxide or other suitable base is added to the aqueous phase as an acid acceptor to neutralize the hydrogen chloride formed and drive the reaction to completion. In some systems excess diamine reactant can serve as the acid acceptor since amine hydrochlorides are highly water soluble and at the same time insoluble in hydrocarbon solvents. In addition to the simple difunctional reactants shown in eqn [1], trifunctional and combinations of di- and trifunctional reactants may be used to achieve the desired degree of polymer cross-linking.

Initially the polymer film grows rapidly; growth then slows and finally a constant film thickness is reached. This is due to the inability of the amine reactant to diffuse through the polymer film to react with the acyl halide. Enkelmann and Wegner

described this process in eqn [2]:

$$\frac{dx}{dt} = K\frac{c}{x} - k'x \quad [2]$$

where x is the membrane thickness; c is the concentration of diamine; K is the diffusion coefficient of diamine through the membrane; and k' is the rate constant of the inhibiting reaction (\propto acid chloride hydrolysis).

When the limiting thickness x_{∞} of the film is reached, $dx/dt = 0$ and eqn [2] simplifies to $x_{\infty} = \sqrt{Kc/k'}$. The limiting film thickness is therefore proportional to the square root of the diamine concentration. Subsequently, Enkelmann and Wegner established as a solution of eqn [2] the rate law of membrane growth:

$$x' = \frac{x}{x_{\infty}} = [1 - \exp(-2k't)]^{1/2} \quad [3]$$

where x' is the reduced membrane thickness. Solving in terms of t (seconds) gives:

$$t = \log \frac{(1 - x')^2}{-2k'} \quad [4]$$

From this equation one can obtain values for early film growth from a period of seconds to over 10 min for more complete growth. It was found from this work that the limiting film thickness depended on both the absolute concentration and concentration ratio of the diamine and diacyl chloride reactants. Enkelmann also showed by X-ray diffraction techniques that in Nylon 610 membranes the polymer chains are ordered perpendicular to the interface. It was also concluded that membrane properties could be regulated by selecting particular reactive monomer ratio and concentrations, solvents and reaction times.

Early IFC Membranes

The IFC Membrane Structure

The development of IFC membranes is a logical outcome following the earlier development of asymmetric cellulose acetate (CA) membranes, as well as the previously discussed interfacial polycondensation work. The CA membrane is comprised of a soluble polymer or blend of polymers of varied cross-sectional morphology with the uppermost surface (skin) forming a permselective barrier. The IFC membrane, which is now the state-of-the art product, contains

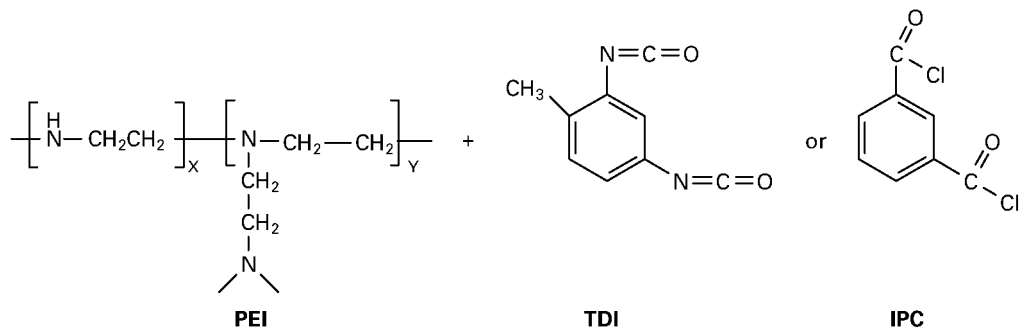
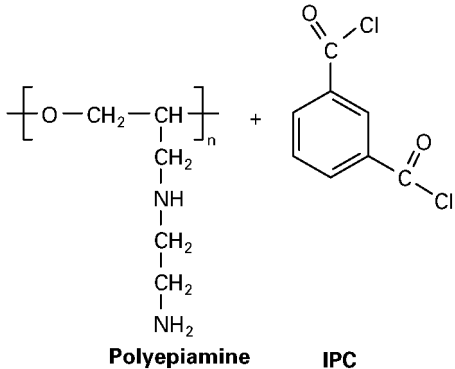
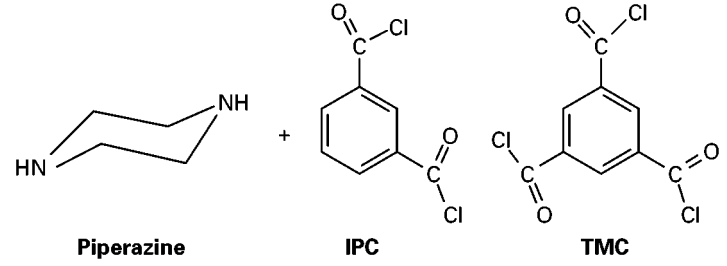
a microporous support layer of one polymer and a separate permselective skin or thin film of another polymer. The advantage of the IFC membrane is that the chemistry of the all-important permselective thin-film layer can be chosen independently from the underlying porous support material. Asymmetric membranes require polymers that are soluble in solvents necessary for the phase inversion process and this limits the number and type of polymers that can be utilized. Many useful crystalline, semicrystalline, and all cross-linked polymers are thus excluded from asymmetric membrane manufacture. The thin films of IFC membranes are in the range of 20–300 nm thick and when coupled with microporous supports of low hydrodynamic resistance provide membranes with unmatched productivity and solute retention.

NS-100 and PA-300 Membranes

In the discussions of IFC membranes that follow, technical milestones are highlighted with emphasis on commercially significant developments. The early period of membrane development shown in **Table 2** began in 1967 with the investigation of various aqueous diamine and hexane–diacyl chloride interfacial solutions upon polysulfone porous supports by Rozelle *et al.* at North Star Research Institute. These first IFC membranes had low salt rejections, probably due to lack of film integrity since the resultant polymers were not cross-linked. This pioneering work, however, is significant in that the essential elements for the preparation of IFC membranes were demonstrated. Shortly thereafter, in 1970, the first high salt-rejecting IFC membrane, NS-100, was also developed at North Star Research. This membrane was made from polyethylenimine (PEI) in the aqueous solution and toluene diisocyanate (TDI) in the hexane solution. The coated and drained polysulfone support was subsequently dried at 110°C to yield a dry composite membrane with greater than 99% salt rejection on a synthetic seawater feed at 1000 psig (6.9 MPa). A later related membrane, designated NS-101, substituted isophthaloyl chloride (IPC) for TDI as the cross-linker and provided similar results. The selective layers in these membranes consisted of cross-linked polyurea and polyamide films, respectively. The membranes demonstrated high permselectivity but were mechanically delicate and highly vulnerable to attack by chlorine disinfectant.

The sensitivity of early interfacial membranes to chlorine attack was a serious problem that has still not been completely solved. Chlorine is routinely added to water to prevent bacterial growth on the membrane surface. However, exposure to even p.p.m. levels of chlorine destroyed the permselective layer of IFC membranes within a few hours.

Table 2 Early interfacial composite membrane developments

Date	Development
1967	First IFC membranes investigated at North Star Research and Development Institute.
1970	NS-100 membrane
	 <p>PEI + TDI or IPC</p>
1975	PA-300 membrane
	 <p>Polyepiamine + IPC</p>
	NS-300 membrane
	 <p>Piperazine + IPC + TMC</p>

Another early membrane developed from a polyamine reactant was the PA-300 membrane by Riley *et al.* at UOP Fluid Systems Division in 1975. The advantage of this polyamide membrane prepared from IPC cross-linker was the lack of residual amines or amide functional groups in the polymer backbone, which exhibited improved chlorine tolerance. The performance of the PA-300 membrane was similar to that of the NS-100 and was the first IFC membrane to be utilized in a large-scale commercial desalination facility located in Jeddah, Saudi Arabia.

NS-300 Membrane

The last example of the earlier generation IFC membranes – the NS-300 – differed from its predecessors in that it was prepared from a difunctional *monomeric* amine, piperazine, and a trifunctional acyl chloride, TMC. This cross-linked polyamide membrane, developed at North Star division of Midwest Research Institute in 1975 by Cadotte *et al.*, demonstrated improved tolerance to chlorine compared to its predecessors due to absence of the

vulnerable amidic hydrogen. Later variants of this membrane included addition of the difunctional IPC acyl chloride, which resulted in increased salt rejection and decreased flux. As might be expected, this is probably due to the decrease in residual carboxylic acid functionality resulting from decrease of the trifunctional TMC cross-linker. Another interesting structural aspect of this polyamide is the nearly 90° out-of-plane orientation of the piperazine ring relative to the aromatic ring. This rigid polymer structure containing a high volume geometry may in part account for the high permeability of this membrane.

Contemporary IFC Membranes

Performance Goals

The goal of further membrane development was to maximize solvent passage while at the same time minimizing solute passage. In a typical reverse osmosis desalination application, this means developing membranes with high water permeability yet low salt passage. This effort applies to nanofiltration membranes as well, except in this case passage of monovalent salts and organics of low relative molecular mass is preferred. Since the two performance properties of solvent flux and solute retention are competing, it is found in practice that one generally observes a trade-off in these values with membrane optimization. Both the thin film chemistry and morphology determine its transport properties. Additional goals of recent IFC membrane development include durability, chlorine and other oxidant stability, and fouling resistance.

MPD-Based Membranes

Table 3 lists recent significant IFC membrane developments. Beginning with the wholly aromatic polyamide FT-30 membrane developed by Cadotte at Film-Tec in 1978, it is seen that all of the subsequent membrane examples rely on the aromatic diamine monomer *m*-phenylene diamine (MPD). With the exception of the A-15 membrane, all of the MPD-based membranes provide very high salt rejection and similar water fluxes. Consistent with the general trade-off principle, the A-15 yields higher water flux with commensurately lower salt rejection, making it what is commonly called in the industry a 'loose RO' membrane. The cross-linked aromatic polyamide remains the-state-of-the-art in IFC membrane chemistry. Membranes of this kind are durable, hydrolytically stable, temperature stable, and exhibit high transport properties. A range of commercially successful membranes encompassing nanofiltration, brackish RO and seawater RO applications have

been achieved with the basic MPD/TMC reactants. These and other modern IFC membranes are made essentially by the same techniques of interfacial polymerization onto porous polysulfone substrates as were their predecessors.

IFC Membrane Preparation

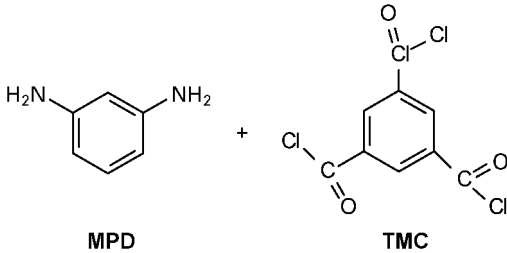
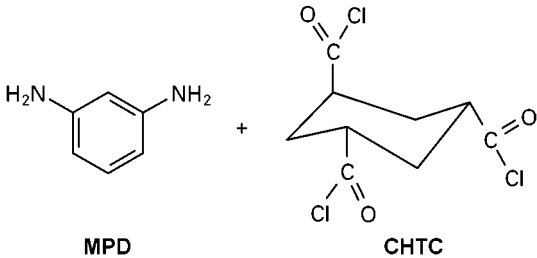
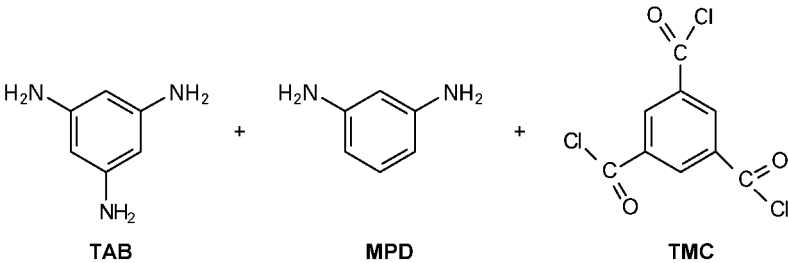
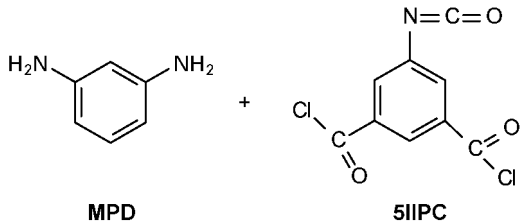
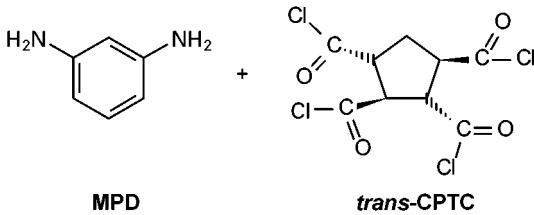
This section provides general information on how IFC membranes have been prepared and discusses guidelines for others to follow in preparing their own such membranes. The laboratory-scale preparations are discussed in an ordered sequence below with emphasis on techniques commonly practised in the desalination membrane industry for flat-sheet IFC membranes. The basic principles of these interfacial techniques are also applicable to the less commercially significant hollow fibre IFC membranes or other composite membrane formats.

Porous Support Preparation

The preferred polymer for use in porous support preparation is polysulfone, a moderately priced material with many desirable chemical and mechanical properties. In addition to strength and temperature stability, it is resistant to hydrolysis and oxidative attack. Its disadvantages, though relatively minor, are its hydrophobicity and lack of solvent resistance. The former property necessitates inclusion of surfactants or wetting agents for some aqueous coating methods used in IFC membrane manufacture and the latter property limits its applications to ones which are predominantly aqueous or contain nonaggressive solvents such as alcohols and aliphatic hydrocarbons. Nevertheless, polysulfone has been and remains the polymer of choice for the porous support of RO and NF IFC membranes.

Preparation of the polysulfone microporous support may be carried out using laboratory, pilot, or full-scale production equipment. Regardless of scale, all of these procedures involve conversion of a polymer in solvent solution to a porous solid layer in what is called the phase inversion process. As the water in the gelation or solidification bath replaces the solvent, the clear polysulfone solution, or casting solution, is transformed to an opaque plastic layer on to the surface coated. With laboratory preparation this is normally carried out by applying a 14–18% polysulfone solution in *N,N*-dimethylformamide (DMF) onto a flat glass plate using a Gardner blade or other suitable device set with a blade gap of 0.13–0.26 mm, then immersing the plate into a small tank of water. For better strength and ease of later processing, it is advisable to do the solution coating onto a calendered polyester fabric or related material attached to the

Table 3 Recent interfacial composite membrane developments

Date	Development
1978	FT-30 membrane (US 4 277 344)
	 <p style="text-align: center;">MPD + TMC</p>
1984	A-15 membrane (US 4 520 044)
	 <p style="text-align: center;">MPD + CHTC</p>
1986	SU-700 membrane (US 4 761 234)
	 <p style="text-align: center;">TAB + MPD + TMC</p>
1990	X-20 membrane (US 5 019 264)
	 <p style="text-align: center;">MPD + 5IIPC</p>
1991	NCM membrane (US 5 254 261)
	 <p style="text-align: center;">MPD + <i>trans</i>-CPTC</p>

glass plate. After several minutes, immersion time in the water bath to remove all solvent, the newly formed porous substrate is immersed again in a fresh water bath as a final rinse. This batchwise process can be scaled up and carried out as continuous processes employing pilot 1 foot (30 cm) wide or production 40-in wide (~ 100 cm) equipment. The advantages of utilizing the continuous process include not only the obvious efficiency but also better reproducibility in resultant porous support properties. However, it is sometimes necessary to pursue the laboratory batchwise process when experimenting with small quantities of costly new polymers or processing conditions that are not easily implemented on the larger-scale continuous equipment.

A typical polysulfone microporous support used in RO or NF IFC membrane fabrication is, by its pore size designation, an ultrafilter (UF) with surface pore sizes ranging from 0.005 to 0.05 μm . Since this size is an order of magnitude smaller than the interfacial film thickness, it easily supports the film even under operating pressures as high as 1000 psi (6.9 MPa). The thickness of the PS support must be sufficient to cover completely the carrier fabric surface plus irregularities caused by improper calendaring, debris and lack of flatness during the casting operation. In practice the net thickness of the PS layer ranges from 25 to 75 μm and that of the carrier fabric upon which it lies ranges between 75 and 150 μm . Scanning electron micrographs (SEM) of a typical PS porous support cross-section and top view are shown in Figure 2A and B, respectively. The anisotropic structure is plainly evident with the finest and most supportive pores residing in the upper surface of the support. The finished PS support is normally stored fully immersed in water or at least damp and protected from dust, debris and biological growth. In some cases it is necessary to include a biocide in the storage water, particularly if it is to be stored a long time. A simplified drawing of a continuous casting machine designed to manufacture PS porous supports in which a carrier fabric is used is given in Figure 3. A few additional comments regarding the porous support should be noted. In addition to polysulfone, other similar aromatic polyethers may be used such as polyether sulfone. However, these and other variants are significantly more expensive and, except for certain specialized applications, are generally not warranted. The final PS support should be rinsed free of the casting dope solvent otherwise this residual may fuse the porous structure when the IFC membrane is dried.

Aqueous Amine Reactant Application

The two basic formulations used in the RO IFC membrane industry contain the diamines piperazine

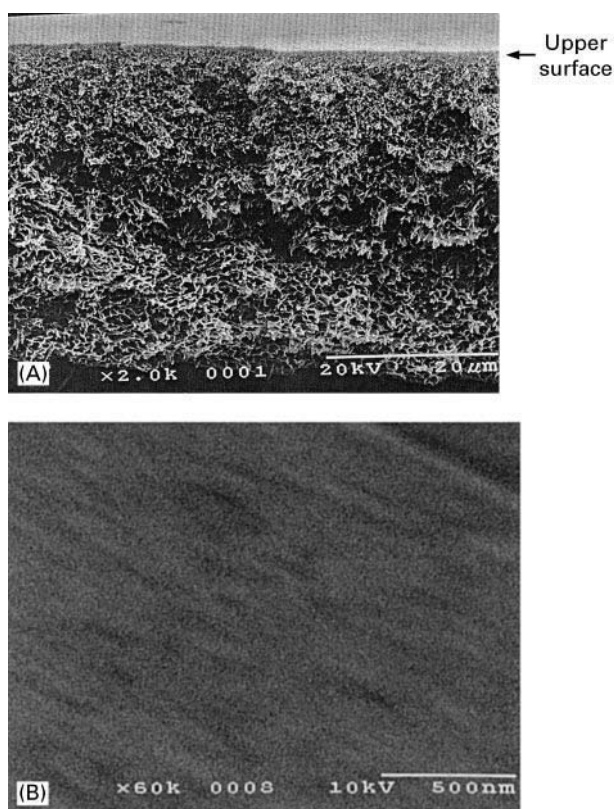


Figure 2 (A) SEM polysulfone porous support cross-section. (B) SEM polysulfone porous support (top view).

(Pip) or *m*-phenylenediamine (MPD). Because both the reactivity and solubility (partition coefficients) of these two monomers are different, it is necessary to utilize each at different absolute concentrations as well as different concentration ratios with the cross-linker. When using the Pip formulation it is usually necessary to include an acid acceptor such as sodium hydroxide (NaOH) to neutralize the hydrochloric acid by-product of the polyamidization reaction. This is not necessary when using MPD since it is a much weaker base than Pip and used in a higher excess concentration so that, excess MPD serves as its own acid acceptor. It is generally preferred also to include a surfactant in the aqueous amine formula to acid in the wetting and thus even coverage of the PS support. An anionic or neutral surfactant type is preferred.

There are many acceptable techniques for applying the aqueous amine solution to the PS support. Examples of these include dipping, pouring on, spraying, kiss coating, cloth coating, reverse roll coating, etc. A simple yet effective laboratory-scale method involves sandwiching a 6-in. (~ 15 cm) square piece of PS support between two plastic frames using metal clips to hold the two pieces together. An excess of amine solution is then poured onto the top surface of

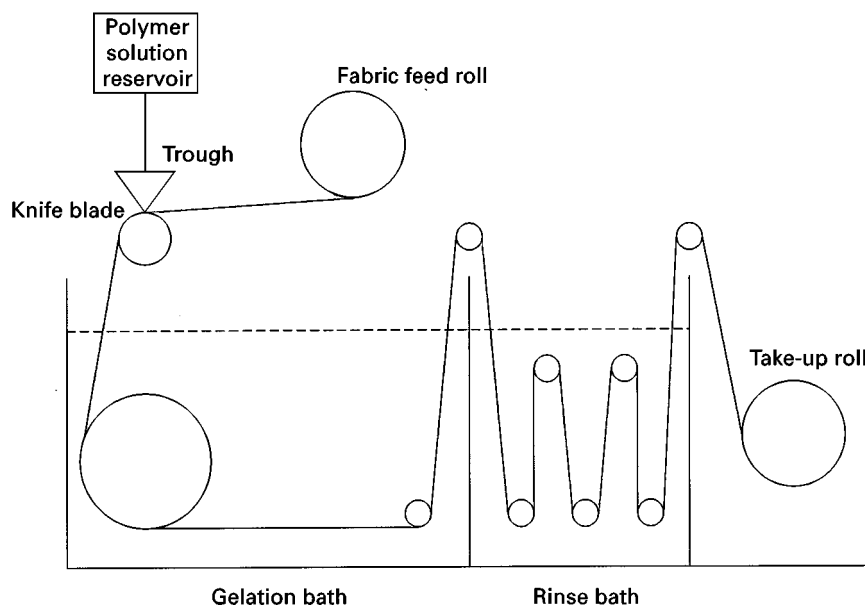


Figure 3 Continuous casting machine for porous support.

the PS support and after a brief time interval is drained off leaving an even, wet layer. Depending on the particular formulation the excess amine may be further removed by rubber roller, squeegee, or air knife. It is important that some degree of wetness remains prior to the contact with the cross-linker solution, otherwise the amine cannot transfer effectively via the water-solvent interface.

Cross-Linker Reactant Application

The choice of solvent for the acyl chloride reactant is dictated by the following requirements:

1. It must completely dissolve the acyl chloride (or other cross-linker) but not react with it.
2. It must be insoluble or virtually insoluble in water.
3. It must not dissolve or swell porous support.
4. It must have a sufficient volatility such that membrane-degrading temperatures are not required for its evaporation.

In practice, the only solvents meeting all of the above requirements are aliphatic hydrocarbons and chlorofluorocarbons (CFCs). There may also be some examples of hydrogenated chlorofluorocarbons (HCFCs) that are acceptable and at the same time are more environmentally friendly than the CFCs. For manufacturing purposes, further restrictions may include preferences for flash point above 100°F and (37.8°C) and low level toxicity. As mentioned previously, the concentration of cross-linker required will be different for the two types of diamines. The concentration of acyl chloride needed for the Pip

formulation is approximately five times that needed for the MPD formulation.

The method of cross-link solution application is generally limited to those which do not disrupt the biphasic nature of the interfacial reaction. If excessive disturbance to this step occurs, the growing polymer may be disrupted, leading to thin film discontinuity and ultimately to high salt passage through the defect regions. Dipping, pouring on gently, kiss coating, etc., are effective methods. For the laboratory-scale techniques, excess acyl chloride cross-link solution is gently poured onto the amine solution-coated PS support contained in the frame and kept horizontal for a brief period. The cross-link solution is then drained off vertically, leaving behind the delicate IFC film residing between thin aqueous and solvent layers. The final step involves some form of evaporation of these two solvents as described below.

Drying the IFC Membrane

Since the freshly polymerized thin film resides on a thin layer of water, this layer must be removed for the film to strongly adhere to the PS support surface. It is also desirable to remove the cross-link solvent so that the finished IFC membrane can be safely and conveniently handled in a dry state.

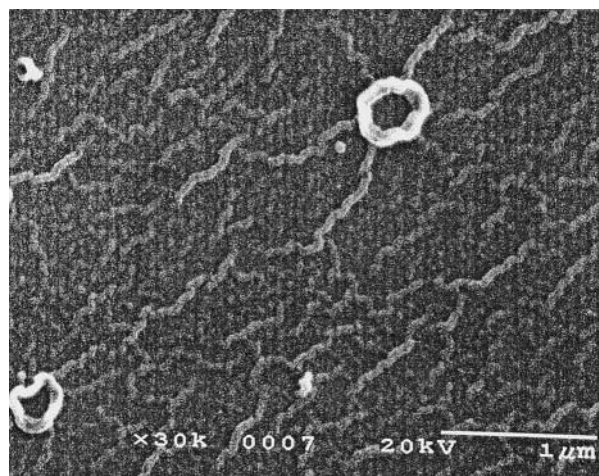
Depending on the volatility of the cross-link solvent and amount of moisture present under the IFC film layer, a temperature range of from ambient to 150°C is required. The higher temperature is a practical upper limit owing to tendency for discoloration and degradation of the IFC membrane. Though many

Table 4 IFC membrane optimization variables: simple approach

Aqueous solution	
1.	Amine monomer concentration
2.	Acid acceptor concentration
3.	Amount of solution applied to porous substrate
Organic solvent	
4.	Cross-link monomer concentration
5.	Cross-link solution contact time with amine solution
6.	Organic solvent volatility
7.	Drying temperature

forms of heating are possible forced air can be used with less heat because of the efficient mechanical effect it has on liquid evaporation. This can be an advantage for IFC membranes that are vulnerable to excessive dehydration. In general, it is found that lower boiling solvents combined with lower drying temperatures often result in membranes with higher fluxes and lower salt rejections than their higher boiling, higher drying temperature counterparts. Of course, longer time periods of drying can be employed in a similar manner with lower drying temperatures to achieve a similar effect, but the choice is ultimately dictated by mechanical and space requirements of the manufacturing equipment. For laboratory scale preparation, it is convenient to use forced hot air devices such as hair-dryers and/or laboratory convection ovens to dry the IFC membrane after the cross-link solution is drained off the frame. Because the thin film is not yet adhered to the PS support excessive air velocity is to be avoided.

The laboratory scale membrane preparation method described in previous sections is now recalled, combining the various steps together: Six inch (~ 15 -cm) square pieces of a polysulfone ultrafilter support are clamped between two Teflon® frames and coated on the upper surface with an aqueous solution of the amine monomer for several seconds; the excess solution is removed by any of the various methods previously mentioned. This freshly coated surface is immediately contacted with the cross-linker-solvent solution horizontally for a period of several seconds then drained vertically for several seconds and finally dried by either forced air and/or convection oven for several minutes. The precise conditions for each of the above steps will depend on the particular type of IFC membrane product that is desired, i.e. NF or RO application, and high productivity or high solute retention, etc., according to the development-performance relationships discussed in the previous sections. A listing of the major IFC membrane prepara-

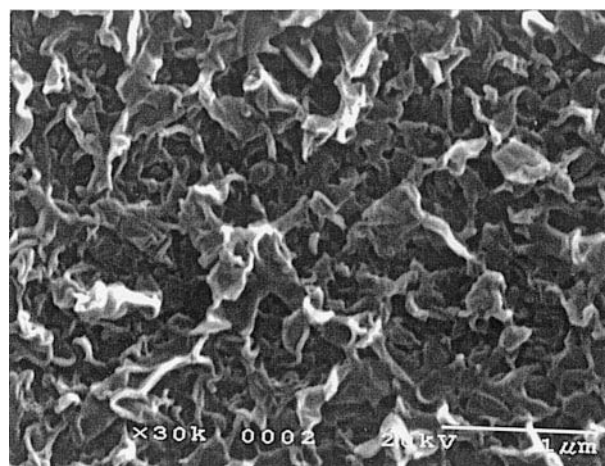
**Figure 4** SEM piperazine IFC membrane (top view).

tion variables is given in Table 4. SEM pictures of Pip- and MPD-based membranes are given in Figures 4 and 5, in which difference in surface roughness is seen. Figure 6 gives a simplified diagram of the continuous IFC membrane manufacturing process.

Testing and Optimization

Test Criteria

The membrane performance throughout the optimization process is obtained by testing on various saline or other solute feeds as appropriate for the particular type of membrane being developed. Examples of test feeds commonly used for RO and NF membrane evaluation are shown in Table 5. Because these feeds are in some respects arbitrary, one can easily substitute other concentrations of solutes, types

**Figure 5** SEM *m*-phenylenediamine IFC membrane (top view).

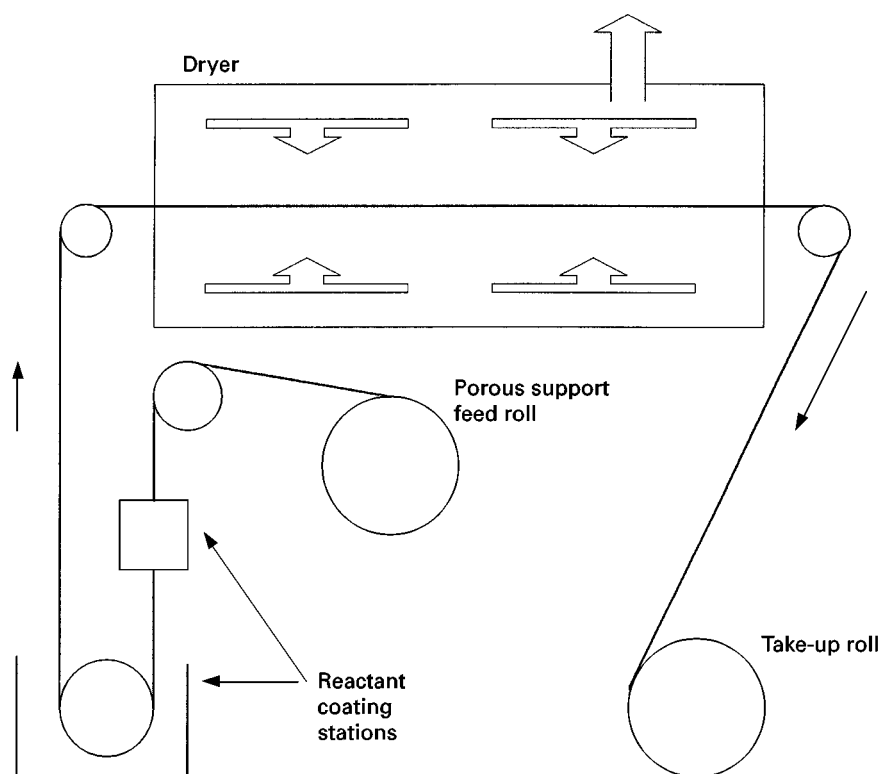


Figure 6 Continuous coating machine for IFC membrane.

of solutes, or test pressures to suit the desired application for the membrane.

The permeate quantity and quality are measured for each membrane sample tested and utilized as performance criteria. In the desalination industry, the former is termed membrane flux, with units of gallons/foot²-day (gfd) ($\times 40.8$ L/m²-day) and the latter as salt rejection (%). Flux measurements are made by collecting a volume of permeate under a controlled temperature and time interval. Knowing the active area of the membrane sample and utilizing a temperature correction factor for the viscosity of water, one can calculate the flux normalized to 25°C. Salt rejection is calculated from electroconductivity measurements of the permeates with correction for specific conductance as a function of sodium chloride concen-

tration, or via specific ion probe measurement. Salt rejection is finally calculated as

$$\left(1 - \frac{\text{permeate p.p.m.}}{\text{feed p.p.m.}}\right) \times 100$$

In the case of organic solutes, measurements of permeate and feed are done with a total organic carbon (TOC) analyser with rejection calculated in the same manner as before.

During the membrane development process it is often necessary to rank membranes based upon an objective evaluation. This is difficult because membrane flux and rejection both change. For example, how can a 20 gfd (815 L/m²-day) 99.0% membrane be ranked against a 15 gfd (611 L/m²-day)

Table 5 Test feeds for IFC RO and NF membranes

RO membranes			
35 000 ppm NaCl	1500 ppm NaCl	1500 ppm NaCl	1500 ppm isopropanol
800 psig	150–225 psig	1000 ppm CaCl ₂	150–225 psig
		150–225 psig	
NF membranes			
500 ppm NaCl	500 ppm MgSO ₄	500 ppm NaCl	500 ppm sucrose
75 psig	75 psig	300 ppm MgSO ₄	75 psig
		75 psig	

99.3% membrane, that is, one with a lower flux but higher rejection. A simple ranking method, if the salt rejection of the membrane is 75% or higher, is to take the ratio of flux/salt passage (F/SP) in which salt passage is simply $100 - \text{salt rejection}$. This value correlates well with the more sophisticated ranking calculation of A^2/B , in which A is the pure water permeability constant ($\text{g mol cm}^{-2} \text{s}^{-1} \text{atm}^{-1}$) and B is the salt transport coefficient (cm s^{-1}). In the discussion below, both a simple and a more sophisticated performance optimization example are presented for membrane development.

Simple Approach Optimization

If one has some development experience with a particular amine and cross-linker reactant system such that the workable range of reactant concentrations and processing conditions are at least roughly definable, or if highly optimized membrane performance is not essential, a simplified approach may be pursued. A listing of the recommended minimum number of optimization variables has been given in Table 4. The membrane optimization plan should be carried out in the order shown in this table since it is ordered from highest to the lowest criticality. This approach relies on selecting previously known conditions or educated estimates of some of the variables to be surveyed. The amine monomer concentration experiment would begin by comparing amine concentrations ranging, for example, from x to $3x$ with increments in-between while holding all other variables in Table 4 constant. This requires some discretion in selecting median values of the held constant variables based on prior knowledge. After determining the 'optimum' amine concentration one would proceed in order to the next variable and carry out the next experiment, holding all other variables constant except the acid acceptor concentration that is to be varied. This procedure continues until all the variables have been individually optimized. It is strongly recommended after a once-through optimization to reiterate this process at least once more since new values of many of the variables are likely to have been established. The second time through is likely to result in refinements of both the optimization variable values and the membrane performance.

It should be pointed out that this simple single-variable optimization approach can suffer errors due to interactive variables that can only be optimized in concert. For example, it is likely that, consistent with general principles of chemical reactants, when the amine concentration increases the need for cross-linker increases but so does that for the acid acceptor. In this example there is a three-variable interaction, not merely the two-variable one that the simple method exam-

ines. Thus it is often desirable to consider a more sophisticated approach to optimization in which the best combination of variables is found. A multivariable optimization process is offered below.

Self-Directing Optimization Approach (SDO)

In the SDO process, a regular simplex in K variables is constructed. The experiment can be initiated in K variables with $K + 1$ experiments and upon completion of the $K + 1$ experiments, the results are ranked from best to worst. In the case of IFC desalination membranes, ranking is performed using either F/SP or A^2/B calculations made from the flux and rejection results from a specified test feed type and operating pressure. An example of a Plackett-Burmann SDO plan containing 11 variables A–K in 12 experiments is presented in Table 6. Corresponding to the + and – symbols are high and low levels, respectively, to be selected for each variable A–K. The experiments 1–12 are carried out as one series in a random order. After completion of the first series of 12 experiments, the best eight cases, for example, will have the averages of each of the variables calculated. These average values are then multiplied by 2, then from these are subtracted each of the conditions of the four worst cases. The four new experiments created are then run and ranked against the previous eight best cases as before with subsequent elimination of the four worst cases. This process is repeated several times, each time eliminating the worst cases and creating new ones to be compared with the previous best. Eventually the variables will be found to converge such that the optimization is complete.

Future Developments

Within the polyamide family of chemistry used in IFC membrane preparation dramatic differences in transport properties can be obtained. It is believed that the thin film polymer chemistry and macrostructure play critical roles in determining these performance differences, thus it is expected that future development will rely heavily on the understanding of polymer structure–property relationships. Though there is relatively little such information available to date concerning membrane polymers, recent computer molecular modelling studies are beginning to show promise. Studies such as these and ones involving the mechanism of solvent/solute transport in permselective polymers will lead to future intelligent design of polymer membranes for specific separation processes. In addition to transport performance, there is still need for improvement in chlorine tolerance and fouling resistance by both RO and NF membranes.

Table 6 Plackett-Burman optimization plan

Exp.	Amine conc.	Acid accept. conc.	Amine applic.	Etc.	A.C. conc.	A.C. time	Sol. B.P.	Etc.	Etc.	Drying time	Etc.	Flux	Rej	A/B	Rank
1															
2	+	+	+	+	+	+	+	+	+	+	+	+	+	+	
3	+	+	+	+	+	+	+	+	+	+	+	+	+	+	
4	+	+	+	+	+	+	+	+	+	+	+	+	+	+	
5	+	+	+	+	+	+	+	+	+	+	+	+	+	+	
6	+	+	+	+	+	+	+	+	+	+	+	+	+	+	
7	+	+	+	+	+	+	+	+	+	+	+	+	+	+	
8	+	+	+	+	+	+	+	+	+	+	+	+	+	+	
9	+	+	+	+	+	+	+	+	+	+	+	+	+	+	
10	+	+	+	+	+	+	+	+	+	+	+	+	+	+	
11	+	+	+	+	+	+	+	+	+	+	+	+	+	+	
12	+	+	+	+	+	+	+	+	+	+	+	+	+	+	

There are performance gaps in presently available membrane products for the NF area of separations involving species with relative molecular masses ranging from 100 to 3000. It is foreseeable that markets will expand for NF membrane applications in high value separations for biotech, chemical, food, and pharmaceutical industries if well-defined relative molecular mass cutoffs can be achieved.

With respect to commercial IFC membrane manufacture, there is a need for improved uniformity and quality of carrier fabrics upon which the porous support is cast. Lack of control here can result in defects that are translated right through the completed composite membrane product. An additional future goal is the development of real-time membrane film integrity and/or performance measurement so that corrections to the process can be made during the course of the manufacture.

See also: II/Membrane Separations: Membrane Preparation; Reverse Osmosis; Ultrafiltration.

Further Reading

- Al-Gholaikah A, El Ramly N, Janyoon I and Seaton R (1978) The world's first large seawater reverse osmosis desalination plant, at Jeddah, Kingdom of Saudi Arabia. *Desalination* 27: 215–231.
- Cadotte JE (1984) In: Lloyd DR (ed.) *Evolution of Composite Reverse Osmosis Membranes, Materials Science of Synthetic Membranes*, p. 273. Washington, DC: ACS Symposium Series.
- Cadotte JE, Cobian KE, Forester RH and Petersen RJ (1976) *Continued Evaluation of Insitu-Formed Condensation Polymers for Reverse Osmosis Membranes*. NTIS Report No. PB 253193. Springfield: US Department of Interior.
- Cadotte JE, Petersen RJ, Larson RE and Erickson EE (1980) A new thin film composite membrane for seawater desalting applications. *Desalination* 32: 25–31. Amsterdam: Elsevier Science B.V.
- Enkelmann V and Wegner G (1976) Mechanism of interfacial polycondensation and the direct synthesis of stable polyamide membranes. *Makromolekulare Chemie* 177: 3177–3189.
- Enkelmann V and Wegner G (1972) *Makromolekulare Chemie* 157: 303.
- Hirose M, Minamizaki Y and Kamiyama Y (1997) The relationship between polymer molecular structure of RO membrane skin layers and their RO performances. *Journal of Membrane Science* 123: 153–163.
- Morgan PW, Kwolek S L and Wittbecker EL (1959) Interfacial polycondensation I and II. *Journal of Polymer Science* XL: 289–326.
- Riley RL, Fox RL, Lyons CE *et al.* (1976) Spiral-wound poly(ether amide) thin-film composite membrane systems. *Desalination* 19: 113–127.

Rozelle LT, Cadotte JE, Corneliussen RD and Erickson EE (1967) *Development of New Reverse Osmosis Membranes for Desalination*, Report No. PB-206329. Springfield, IL: VA National Technical Information Service.

Rozelle LT, Cadotte JE, Cobian KE and Kopp CV Jr (1977) In: Souriragan S (ed.) *Nonpolysaccharide Membranes for*

Reverse Osmosis. NS-100 Membranes for Reverse Osmosis and Synthetic Membranes, p. 249. Ottawa, Canada: National Research Council Canada.

Souriragan S (1970) *Reverse Osmosis*. New York: Academic Press.

Phase Inversion Membranes

M. Mulder, University of Twente, Enschede, The Netherlands

Copyright © 2000 Academic Press

Introduction

Phase inversion is the most versatile technique with which to prepare polymeric membranes. A variety of morphologies can be obtained that are suitable for different applications, from microfiltration membranes with very porous structures, to more dense reverse osmosis membranes, to gas separation and pervaporation membranes, with a complete defect-free structure. **Table 1** gives an overview of the techniques that are commonly applied for the preparation of synthetic polymeric membranes.

Most commercially available membranes are prepared by phase inversion. This is a process by which a polymer is transformed from a liquid or soluble state to a solid state. The concept of phase inversion covers a range of different techniques such as immersion precipitation or 'diffusion-induced phase separation', thermal-induced phase separation, 'vapour-phase' precipitation and precipitation by controlled evaporation. The technique of phase inversion has been known for quite some time; the first paper on the preparation of porous nitrocellulose membranes by phase inversion appeared in 1907.

Table 1 Frequently used techniques for the preparation of synthetic polymeric membranes

Process	Techniques
Microfiltration	Phase inversion, stretching, track-etching
Ultrafiltration	Phase inversion
Nanofiltration	Phase inversion, interfacial polymerization ^a
Reverse osmosis	Phase inversion, interfacial polymerization ^a
Pervaporation	Dipcoating ^a , plasma polymerization ^a
Gas separation	Phase inversion, dipcoating ^a , plasma polymerization ^a
Vapour permeation	Dipcoating ^a

^aSupport layer prepared by phase inversion.

After World War I the number of publications on membrane preparation and characterization increased significantly and led to the development of the first methods for producing porous nitrocellulose membranes in a reproducible way. The 'Membranfiltergesellschaft Sartorius-Werke' in Göttingen was the first company to produce microfiltration membranes on a commercial scale, based on the work of Zsigmondy. This early work on preparation and characterization was reviewed by Ferry in 1936.

Until World War II most membrane research was performed in Germany, but after the war the technology was transferred to USA. In 1960 Goetz developed a new method for the production of porous membranes. Some years later the Millipore Corporation was founded, which commercialized this production method. The membranes were typically microfiltration membranes and were still based on cellulosic materials. It was more than two decades before ultrafiltration membranes were developed. Alan Michaels, founder of the Amicon Corporation, promoted the development of ultrafiltration membranes. Until that time the research was still focused on cellulose as material but it became clear that due to the limited thermal and chemical stability other materials were required. This resulted in the development of various ultrafiltration membranes from polyacrylonitrile, polysulfone and polyvinylidene fluoride. Today polymeric materials are still the most commonly employed materials both in ultrafiltration and microfiltration. The early companies such as Sartorius and Schleicher and Schuell still exist and have expanded their membrane business to the technical market. Recently the market for the production of drinking water and industrial water from surface water has become important. Here both microfiltration/ultrafiltration and nanofiltration/reverse osmosis are either used as a single separation unit or in combination with each other or with another technique. The nanofiltration and reverse osmosis membranes are either thin film composites or, less commonly, asymmetric phase inversion membranes. In the case of composite membranes a phase inversion mem-

brane is usually used as support (see Table 1). For gas separation, vapour permeation and pervaporation composite membranes are generally applied with a porous support membrane prepared by phase inversion. Some gas separation membranes, such as polyphenylene oxide, are prepared by immersion precipitation, which results in completely defect-free asymmetric membrane.

Phase Inversion Membranes

Phase inversion is a process whereby a polymer is transformed in a controlled way from a solution state to a solid state. The concept of phase inversion covers a range of different techniques such as precipitation by controlled evaporation, thermal precipitation from the vapour phase and immersion precipitation. The majority of phase inversion membranes are prepared by immersion precipitation.

Precipitation from the Vapour Phase

This method was used as early as 1918 by Zsigmondy. A cast film, consisting of a polymer and a solvent, is placed in a vapour atmosphere where the vapour phase consists of a nonsolvent saturated with the solvent. The high solvent concentration in the vapour phase prevents the evaporation of solvent from the cast film. Membrane formation occurs because of the penetration (diffusion) of nonsolvent into the cast film. This results in a porous membrane without a top layer. With immersion precipitation an evaporation step in air is sometimes introduced and, if the solvent is miscible with water, precipitation from the vapour will start at this stage. An evaporation stage is often introduced in the case of hollow fibre preparation by immersion precipitation ('wet-dry spinning') exchange between the solvent and nonsolvent from the vapour phase, leading to precipitation.

Precipitation by Controlled Evaporation

In this method the polymer is dissolved in a mixture of solvent and nonsolvent where the solvent is more volatile than the nonsolvent. The composition shifts during evaporation to a higher nonsolvent and polymer content. This eventually leads to polymer precipitation, resulting in the formation of a skinned membrane.

Thermally Induced Phase Separation

A solution of polymer in a mixed or single solvent is cooled to enable phase separation to occur. Evaporation of the solvent often allows the formation of a skinned membrane. This method is frequently used to prepare microfiltration membranes, as will be discussed later.

Immersion Precipitation

Most commercially available membranes are prepared by immersion precipitation: a polymer solution (polymer plus solvent) is cast on a suitable support and immersed in a coagulation bath containing a nonsolvent. Precipitation occurs because of the exchange of solvent and nonsolvent. The membrane structure ultimately obtained results from a combination of mass transfer and phase separation.

All phase inversion processes are based on the same thermodynamic principles, as will be described in the next section.

Phase Separation

The change in Gibbs free enthalpy of mixing (dG) for a two-component system i and j , where the numbers of moles are n_i and n_j , respectively, is given by:

$$dG = V dP - S dT + \left(\frac{dG}{dn_i} \right)_{T,P,n_j} dn_i + \left(\frac{dG}{dn_j} \right)_{T,P,n_i} dn_j \quad [1]$$

Here V is the volume, S the entropy, P the pressure and T the temperature (K). The chemical potential of a component i , which is the partial molar free enthalpy, is defined as:

$$\mu_i = \left(\frac{\partial G}{\partial n_i} \right)_{P,T,n_j,n_k,\dots} \quad [2]$$

where μ_i is equal to the change in free enthalpy of a system containing n_i moles when the pressure, temperature and the number of moles of all the other components are held constant. For a multicomponent system eqn [1] becomes:

$$dG = V dP - S dT + \sum \mu_i dn_i \quad [3]$$

The chemical potential μ_i is defined at temperature T , pressure P , and composition x_i . For the pure component ($x_i = 1$), the chemical potential may be written as μ_i^0 .

The free enthalpy G_m of a mixture consisting of two components is given by the sum of the chemical potentials (the partial free enthalpy). If G_m is expressed per mole, then:

$$G_m = x_1 \mu_1 + x_2 \mu_2 \quad [4]$$

The dependence of the free enthalpy on the composition of the mixture is shown schematically in Figure 1. The value of the G_m at the y-axis represent

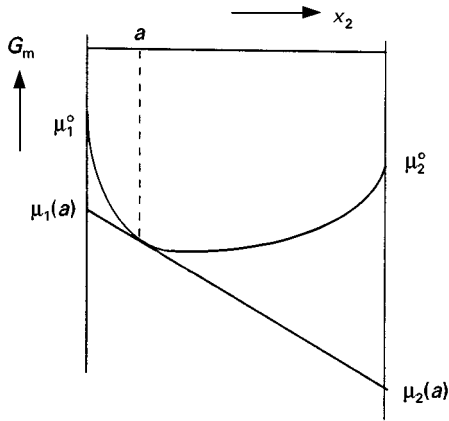


Figure 1 Schematic drawing of the free enthalpy of a mixture at temperature T as a function of the composition.

the chemical potential of the pure components, μ_1^0 and μ_2^0 , respectively.

For ideal solutions the free enthalpy of mixing per mole is given by:

$$\Delta G_m = RT(x_1 \ln x_1 + x_2 \ln x_2) \quad [5]$$

The solubility behaviour of polymer solutions differs completely from that of a solution containing components of low relative molecular mass because the entropy of mixing of the long polymeric chains is much lower. Flory and Huggins used a lattice model to describe the entropy of mixing of polymer solutions. In general for a binary system ΔG_m is given by:

$$\Delta G_m = RT(n_1 \ln \phi_1 + n_2 \ln \phi_2 + n_1 \phi_2 \chi) \quad [6]$$

where an additional term has been added that was originally derived as an enthalpic contribution and which contains the Flory-Huggins interaction param-

eter χ . In the original Flory theory χ was considered to be constant but for many systems it has been proven that this is not the case. In addition, χ is considered to be an excess free energy parameter containing all nonideality (including excess entropy). Differentiation of eqn [6] with respect to n_1 and n_2 , respectively, gives the partial molar free enthalpy difference of component 1 ($\Delta\mu_1$) and ($\Delta\mu_2$) upon mixing:

$$\begin{aligned} \Delta\mu_1 &= \mu_1 - \mu_1^0 = \left(\frac{\partial \Delta G_m}{\partial n_1} \right)_{P, T, n_2} \\ &= RT \left(\ln \phi_1 - \left(1 - \frac{V_1}{V_2} \right) \phi_2 + \chi \phi_2^2 \right) \end{aligned} \quad [7]$$

and:

$$\begin{aligned} \Delta\mu_2 &= \mu_2 - \mu_2^0 = \left(\frac{\partial \Delta G_m}{\partial n_2} \right)_{P, T, n_1} \\ &= RT \left(\ln \phi_2 - \left(1 - \frac{V_2}{V_1} \right) \phi_1 + \chi \frac{V_2}{V_1} \phi_1^2 \right) \end{aligned} \quad [8]$$

In the case of polymer solutions the entropy term is very small and a positive enthalpy of mixing will cause demixing. Decreasing the temperature often causes an increase in the enthalpy of mixing.

Figure 2 shows two plots of ΔG_m versus ϕ for two different temperatures. At temperature T_1 (Figure 2A), the system is completely miscible over the whole composition range. This is indicated by the tangent to the ΔG_m curve, which can be drawn at any composition. For example, at composition a the intercept at $\phi_2 = 0$ gives $\mu_1(a)$ (the chemical potential of component 1 in the mixture of composition a) and the intercept at $\phi_2 = 1$ gives $\mu_2(a)$. This means that the chemical potentials of both components 1 and 2 de-

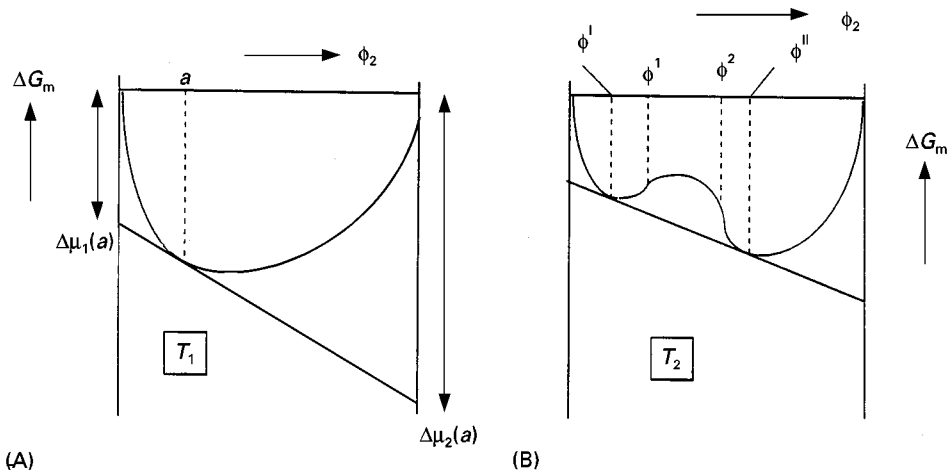


Figure 2 Free energy of mixing as a function of composition for a binary mixture. $T_2 < T_1$ ($H_m > 0$).

crease (or $\Delta\mu_i < 0$). At temperature T_2 (Figure 2B), the curve of ΔG_m exhibits an upward bend between ϕ^I and ϕ^{II} . These two points lie on the same tangent and are thus in equilibrium with each other. All the points on the tangent have the same derivative ($= \partial\Delta G_m / \partial n_i = \Delta\mu_i$), i.e. the chemical potentials are the same. In general, increasing the temperature leads to an increase in miscibility, which means that the enthalpy term becomes smaller. The two points on the tangent will approach each other and eventually they will coincide at the so-called critical point. This critical point is characterized by $(\partial^2\Delta G_m / \partial\phi_i^2) = 0$ and $(\partial^3\Delta G_m / \partial\phi_i^3) = 0$. Two points of inflection are also observed in Figure 2B, i.e. ϕ^1 and ϕ^2 . A point of inflection is the point at which a curve changes from being concave to convex, or vice versa. These points are characterized by $(\partial^2\Delta G_m / \partial\phi_i^2) = 0$. Plotting the locus of the minima in a ΔG_m versus ϕ diagram leads to the binodal curve. The locus of the inflection points is called the spinodal. A typical temperature-composition diagram is depicted in Figure 3.

The location of the miscibility gap for a given binary polymer-solvent system depends principally on the chain length of the polymer (see Figure 4). As the chain length increases the miscibility gap shifts towards the solvent axis as well as to higher temperatures. The critical point shifts towards the solvent

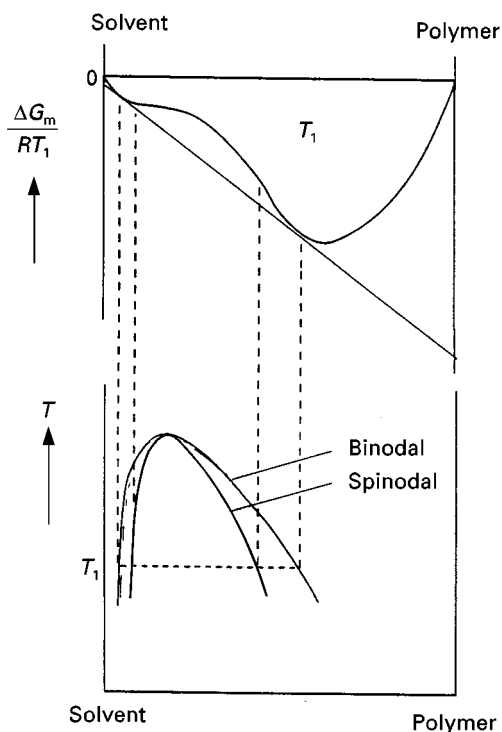


Figure 3 Temperature-composition phase diagram for a binary polymer-solvent system.

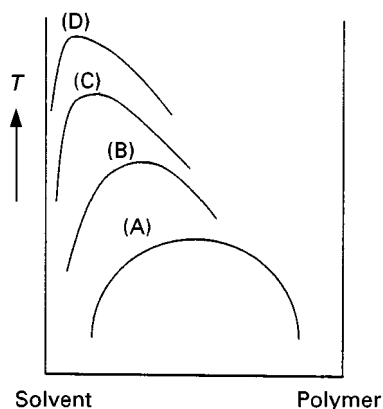


Figure 4 Schematic drawing of a binary mixture with a region of immiscibility. Binodal (A): mixture of two components of low relative molecular mass; binodals (B), (C), (D): mixtures of a solvent with low relative molecular mass and a polymer with increasing relative molecular mass.

axis, while the asymmetry of the binodal curve increases. The interaction between polymer and solvent is another important parameter, and this is expressed by the Flory-Huggins interaction parameter.

The location of the phase diagram in a binary or ternary system can be determined experimentally, e.g. by cloud point measurements, or theoretically by applying Flory-Huggins thermodynamics with suitable values for the interaction parameters.

Demixing Processes

Liquid-Liquid Demixing (Binary Systems)

To understand the mechanism of liquid-liquid demixing more easily, a binary system consisting of a polymer and a solvent will be considered. The starting point for preparing phase inversion membranes is a thermodynamically stable solution (see Figure 5), for example one with the composition A at a temperature T_1 (with $T_1 > T_c$). All compositions with a temperature $T > T_c$ are thermodynamically stable. As the temperature decreases demixing of the solution will occur when the binodal is reached. The solution demixes into two liquid phases and this is referred to as liquid-liquid demixing.

Suppose that the temperature is decreased from T_1 to T_2 . The composition A at temperature T_2 lies inside the demixing gap and is not stable thermodynamically. The curve of ΔG_m at temperature T_2 is also given in Figure 5. At temperature T_2 all compositions between ϕ^I and ϕ^{II} can reduce their free enthalpies of mixing by demixing into two phases with compositions ϕ^I and ϕ^{II} , respectively (see Figure 3). These two phases are in equilibrium with each other since they lie on the same tangent to the ΔG_m curve, i.e. the

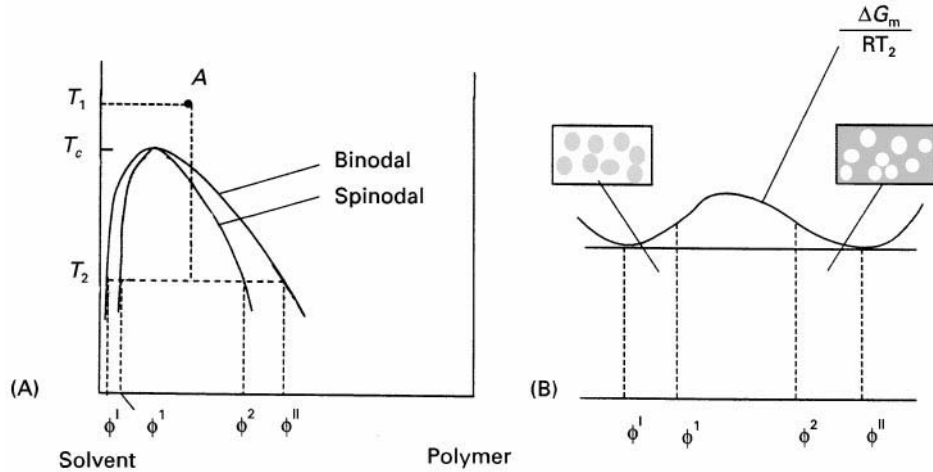


Figure 5 Demixing of a binary polymer solution by decreasing the temperature. T_c is the critical temperature.

chemical potential in phase ϕ^I must be equal to that of phase ϕ^{II} .

Figure 6 gives the curve of ΔG_m plotted against composition at a given temperature (e.g. T_2), together with the first and second derivative. Two regions can clearly be observed from the second derivative

(the lowest figure). Over the interval $\phi^1 < \phi < \phi^2$ the second derivative of ΔG_m with respect to ϕ is negative, implying that the solution is thermodynamically unstable and will demix spontaneously into very small interconnected regions of composition ϕ^I and ϕ^{II} :

$$\frac{\partial^2 \Delta G_m}{\partial \phi^2} < 0 \quad (\phi^1 < \phi < \phi^2) \quad [9]$$

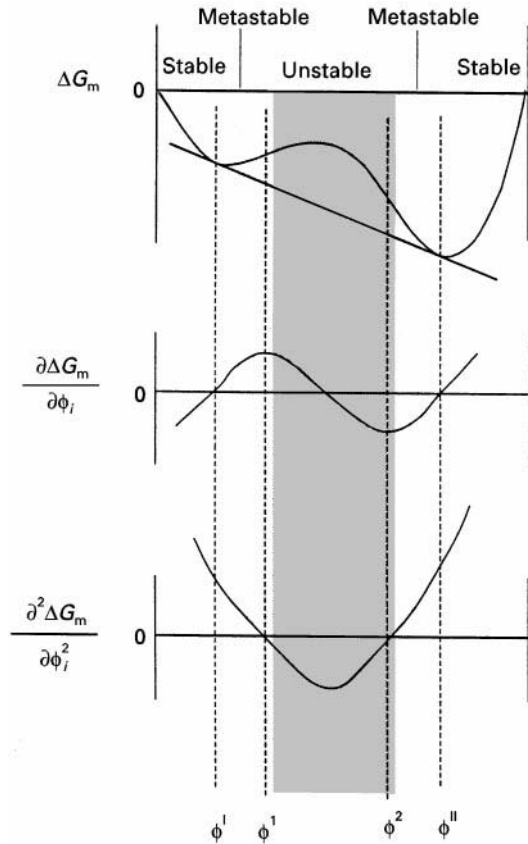


Figure 6 Plots of ΔG_m , the first derivative of ΔG_m and the second derivative of ΔG_m against ϕ .

The amplitude of small fluctuations in the local concentration increases in time, as shown schematically in Figure 7. In this way a lacy structured membrane is obtained, and the type of demixing observed is called spinodal demixing. Over the intervals $\phi^I < \phi < \phi^1$ and $\phi^2 < \phi < \phi^{II}$, the second derivative of ΔG_m with respect to ϕ is positive and the solution is metastable. This means that there is no driving force for spontaneous demixing and the solution is stable towards small fluctuations in composition. Demixing

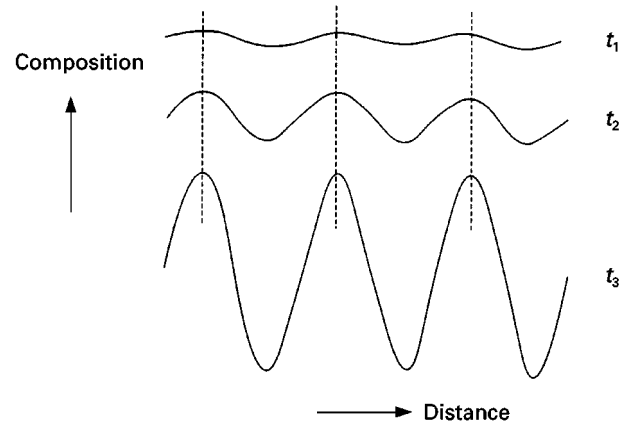


Figure 7 Spinodal demixing: increase in amplitude with increasing time ($t_3 > t_2 > t_1$).

can commence only when a stable nucleus has been formed. A nucleus is stable when it lowers the free enthalpy of the system; hence over the interval $\phi^I < \phi < \phi^I$ the nucleus must have a composition near ϕ^II , and over the interval $\phi^2 < \phi < \phi^II$ it must have a composition near ϕ^I :

$$\frac{\partial^2 \Delta G_m}{\partial \phi^2} > 0 \quad (\phi^I < \phi < \phi^I) \quad \text{and} \quad (\phi^2 < \phi < \phi^II) \quad [10]$$

After nucleation, these nuclei grow further in size by downhill diffusion whereas the composition of the continuous phase moves gradually towards that of the other equilibrium phase. The type of structure obtained after liquid-liquid demixing by nucleation and growth depends on the initial concentration.

Starting with a very dilute polymer solution (see Figure 5), the critical point will be passed on the left-hand side of the diagram and liquid-liquid demixing will start when the binodal curve is reached and a nucleus is formed with a composition near ϕ^II . The nucleus formed will grow further until thermodynamic equilibrium is reached (nucleation and growth of the polymer-rich phase). A two-phase system is formed consisting of concentrated polymer droplets of composition ϕ^II dispersed in a dilute polymer solution with composition ϕ^I . In this way a latex type of structure is obtained, which has little mechanical strength. When the starting point is a more concentrated solution (composition A in Figure 5), demixing will occur by nucleation and growth of the polymer-lean phase (composition ϕ^I). Droplets with a very low polymer concentration will now continue to grow until equilibrium has been reached.

As can be seen from Figure 5, the location of the critical point is close to the solvent axis. Hence the binodal curve for a polymer-solvent system will be reached on the right-hand side of the critical point, indicating that liquid-liquid demixing will occur by nucleation of the polymer-lean phase. These tiny droplets will grow further until the polymer-rich phase solidifies. If these droplets have the opportunity to coalesce before the polymer-rich phase has solidified, an open porous system will result.

Liquid-Liquid Demixing (Ternary Systems)

In addition to temperature changes, changes in composition brought about by the addition of a third component, a nonsolvent, can also cause demixing. Under these circumstances we have a ternary system consisting of a solvent, a nonsolvent and a polymer. The liquid-liquid demixing area must now be represented as a three-dimensional surface. The free enthalpy of mixing is a function of the composition, as can be seen from Figure 8, where the ΔG_m surface is depicted at a certain temperature. All pairs of compositions with a common tangent plane to the ΔG_m surface constitute the solid line projected in the phase diagram, the binodal. Figure 9 shows a schematic illustration of the temperature dependency of such a three-dimensional liquid-liquid demixing surface for a ternary system. The demixing area takes the form of a part of a beehive. As the temperature increases the demixing area decreases, and if the temperature is sufficiently high the components are miscible in all proportions. From this figure an isothermal cross-section can be obtained at any temperature as shown in Figure 10.

The corners of the triangle in Figure 10 represent the pure components polymer, solvent and

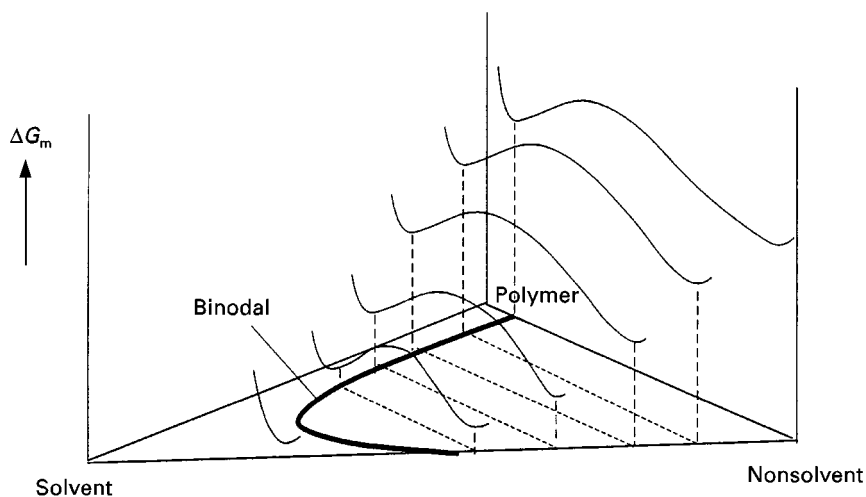


Figure 8 Schematic drawing of the free enthalpy of mixing (ΔG_m) as a function of the composition for a ternary system consisting of polymer, solvent and nonsolvent.

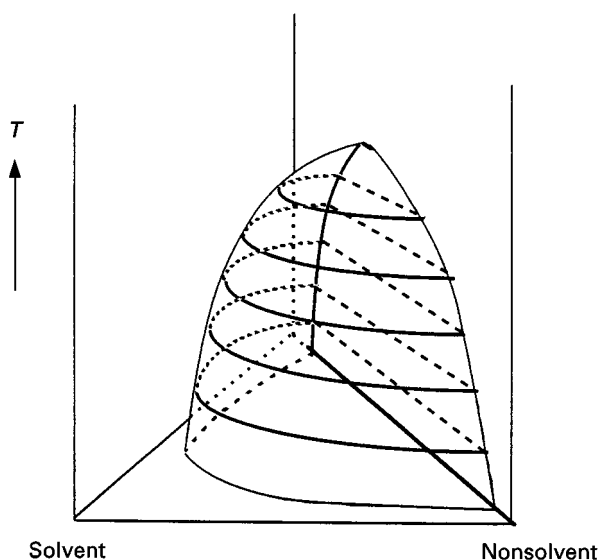


Figure 9 Three-dimensional representation of the binodal surface at various temperatures for a ternary system consisting of polymer, solvent and a nonsolvent.

nonsolvent. A point located on one of the sides of the triangle represents a mixture consisting of the two corner components. Any point within the triangle represents a mixture of the three components. In this region a spinodal curve and binodal curve can be observed. The tie lines connect points on the binodal curve that are in equilibrium. A composition within this two-phase region always lies on a tie line and splits into two phases represented by the two intersections between the tie line and the binodal curve. As in the binary system, one end point of the tie line is rich in polymer and the other end point is poor in polymer. The binodal curve may be calculated numerically. The tie lines connect the two coexisting phases that are in equilibrium with each other, and these

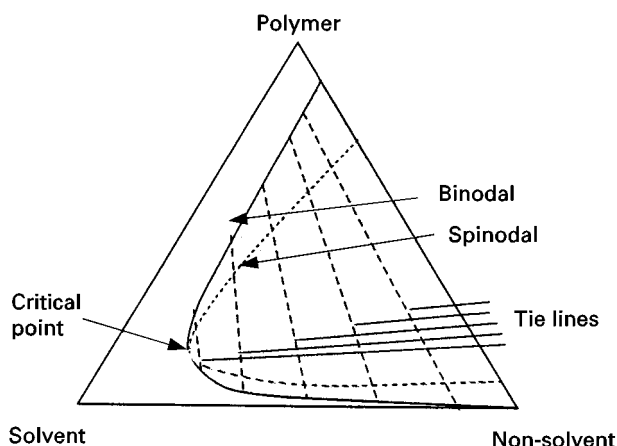


Figure 10 Schematic representation of a ternary system with a liquid-liquid demixing gap.

have the same chemical potential. By minimizing the following function the compositions of the end points may be obtained:

$$F = \sum f_i^2 \quad [11]$$

with $f_i = (\Delta\mu_i' - \Delta\mu_i'')$ and $i = 1, 2, 3$. The polymer-lean phase is indicated by a single prime (') and the polymer-rich phase is indicated by a double prime (").

The initial procedure for membrane formation from such ternary systems is always to prepare a homogeneous (thermodynamically stable) polymer solution. This will often correspond to a point on the polymer-solvent axis. However, it is also possible to add nonsolvent as long as all the components are still miscible. Demixing will occur by the addition of such an amount of nonsolvent that the solution becomes thermodynamically unstable.

When the binodal curve is reached liquid-liquid demixing will occur. As in the binary system, the side from which the critical point is approached is important. In general, the critical point is situated at low to very low polymer concentrations (see Figure 10). When the metastable miscibility gap is entered at compositions above the critical point, nucleation of the polymer-lean phase occurs. The tiny droplets formed consist of a mixture of solvent and nonsolvent with very little polymer dispersed in the polymer-rich phase, as described in the binary example (see Figure 5). These droplets can grow further until the surrounding continuous phase solidifies via crystallization, gelation or when the glass transition temperature has been passed (in the case of glassy polymers). Coalescence of the droplets before solidification leads to the formation of an open porous structure.

Solid-Liquid Demixing (Crystallization)

Many polymers are partially crystalline. They consist of an amorphous phase without any ordering and an ordered crystalline phase. Crystallization may occur if the temperature of the solution is below the melting point of the polymer. Figure 11 shows the free enthalpy of mixing (ΔG_m) for a binary system of polymer and solvent (or diluent) that shows no liquid-liquid demixing. However, below the melting point the chemical potential of the polymer in the solid state will be smaller than that in the solution. Therefore, the solution can lower its free enthalpy by phase separation into a pure crystalline solid state (ϕ_2) and a liquid state (ϕ_a in Figure 11) that are in equilibrium with each other ($\Delta\mu_{2,L} = \Delta\mu_{2,S}$). The corresponding melting temperature for this mixture ϕ_a is T_1 . This is shown schematically in Figure 11B. T_m^o is the melting point of the pure polymer and the melting

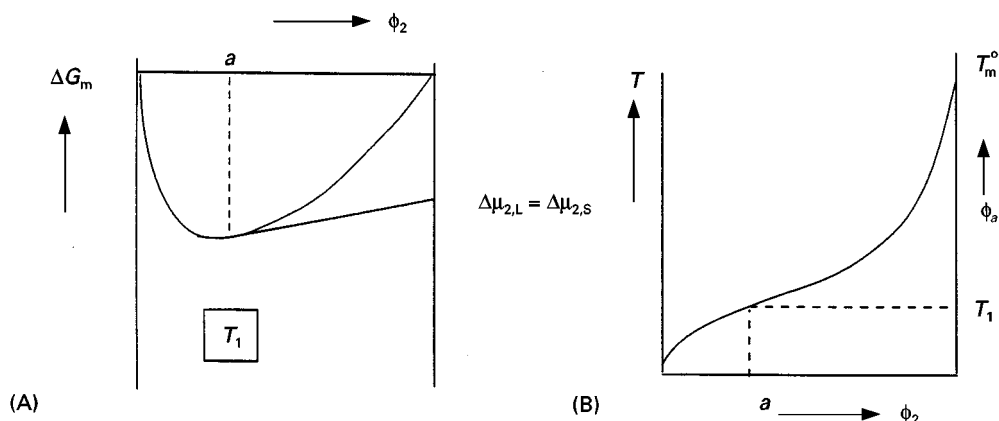


Figure 11 Schematic drawing of the free enthalpy of mixing for a binary system in which component 2 is able to crystallize (A) and the melting point curve as a function of the composition (B). ϕ_a is the volume fraction at point a .

point depression for a binary polymer-solvent system, as derived by Flory, is given below:

$$\frac{1}{T_m} - \frac{1}{T_m^o} = \frac{R}{\Delta H_f} \frac{V_2}{V_1} (\phi_1 - \chi\phi_1^2) \quad [12]$$

Here ϕ_1 is the volume fraction of solvent and χ is the polymer-solvent interaction parameter; T_m is the melting temperature of the diluted polymer; ΔH_f is the heat of fusion per mole of repeating units; and V_1 and V_2 are the molar volume of the solvent and of the polymer repeating unit, respectively.

For a ternary system with a semicrystalline polymer a similar ternary diagram can be constructed, as shown in Figure 12. However, it is somewhat more complex since solid-liquid demixing occurs in addition to liquid-liquid demixing. Except for the homogeneous region (I) where all components are miscible

with each other and a region where liquid-liquid demixing occurs (II), other phases can be observed. The curve PQ is the crystallization curve and a composition somewhere in the region of P-Q-polymer will contain crystalline pure polymer that is in equilibrium with a composition somewhere on the crystallization line PQ. A possible morphology of a semicrystalline polymer is shown schematically in Figure 13. Spherulitic structures are frequently observed in semicrystalline polymers.

Many morphologies are possible ranging from a completely crystalline to a completely amorphous conformation. The formation of crystalline regions in a given polymer depends on the time allowed for crystallization from the solution. In very dilute solutions the polymer chains can form single crystals of the lamellar type, whereas in medium and concentrated solutions more complex morphologies occur, e.g. dendrites and spherulites.

Membrane formation is generally a fast process and only polymers that are capable of crystallizing rapidly (e.g. polyethylene, polypropylene, aliphatic polyamides) will exhibit an appreciable amount of

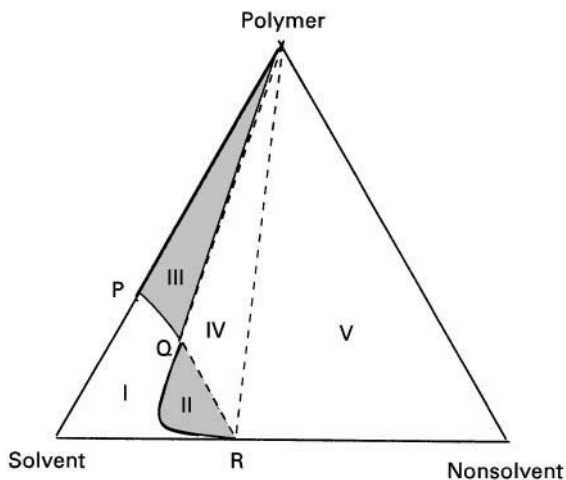


Figure 12 Ternary system of a semicrystalline polymer, solvent and nonsolvent system. I, homogeneous; II, liquid-liquid; III, Solid-liquid; IV, solid-liquid-liquid; V, solid-liquid.

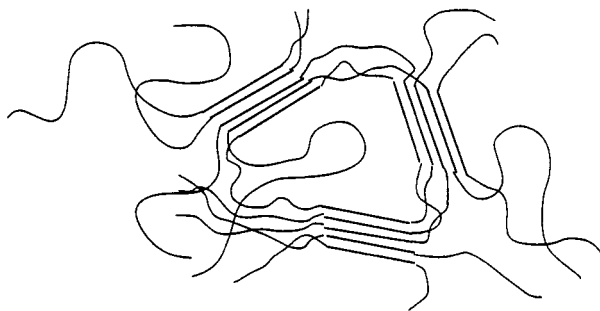


Figure 13 Morphology of a semicrystalline polymer (fringed micelle structure).

crystallinity. Other semicrystalline polymers contain a low to very low crystalline content after membrane formation. For example, PPO (2,6-dimethylphenylene oxide) shows a broad melting endotherm at 245°C. Ultrafiltration membranes derived from this polymer, prepared by phase inversion, hardly contain any crystalline material, indicating that membrane formation was too rapid to allow crystallization.

Gelation

Gelation is a phenomenon of considerable importance during membrane formation, especially for the formation of the top layer. It was mentioned in the previous section that a large number of semicrystalline polymers exhibit a low crystalline content in the final membrane because membrane formation is too fast. However, these polymers generally undergo another solidification process, i.e. gelation. Gelation can be defined as the formation of a three-dimensional network by chemical or physical cross-linking. Chemical cross-linking, the covalent bonding of polymer chains by means of a chemical reaction, will not be considered here.

When gelation occurs, a dilute or more viscous polymer solution is converted into a system of infinite viscosity, i.e. a gel. A gel may be considered as a highly elastic, rubber-like solid. A gelled solution does not demonstrate any flow when a tube containing the solution is tilted. Gelation is not a phase separation process, and it may also take place in a homogeneous system consisting of a polymer and a solvent. Many polymers used as membrane materials exhibit gelation behaviour, e.g. cellulose acetate, poly(phenylene oxide), polyacrylonitrile, poly(methyl) methacrylate, poly(vinyl chloride) and poly(vinyl alcohol). Physical gelation may occur by various mechanisms dependent on the type of polymer and solvent or solvent-nonsolvent mixture used. In the case of semicrystalline polymers especially, gelation is often initiated by the formation of microcrystallites. These microcrystallites, which are small ordered regions, are in fact the nuclei for the crystallization process but without the ability to grow further. However, if these microcrystallites can connect various polymeric chains together, a three-dimensional network will be formed. Because of their crystalline nature these gels are thermo-reversible, i.e. upon heating the crystallites melt and the solution can flow. Upon cooling, the solution again gels. The formation of helices often occurs during the gelation process. Gelation may also occur by other mechanisms, e.g. the addition of complexing ions (Cr^{3+}) or by hydrogen bonding.

Gelation is also possible in completely amorphous polymers (e.g. atactic polystyrene). In a number of systems the involvement of gelation in the membrane

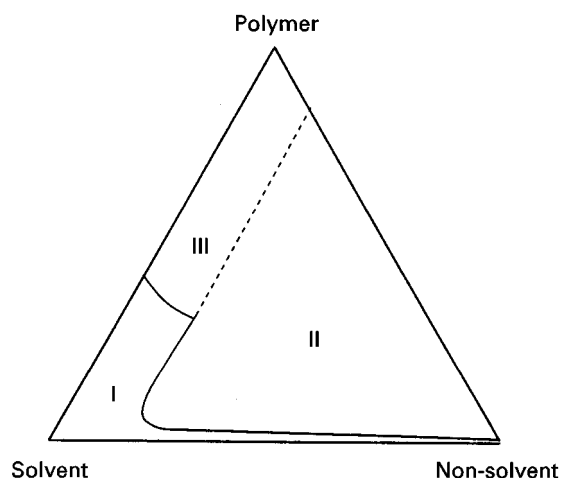


Figure 14 Isothermal cross-section of a ternary system containing a one-phase region (I), a two-phase region (II) and a gel region (III).

formation process often involves a sol-gel transition. This is shown schematically in **Figure 14**. As can be seen from this figure, a sol-gel transition occurs where the solution gels. The addition of a nonsolvent induces the formation of polymer-polymer bonds and gelation occurs at a lower polymer concentration. These sol-gel transitions have been observed in a number of systems, e.g. cellulose acetate/acetone/water, cellulose acetate/dioxane/water, poly(phenylene oxide)/trichloroethylene/octanol and poly(phenylene oxide)/trichloroethylene/methanol.

Vitrification

There are polymers that show neither crystallization nor gelation behaviour. Nevertheless, these polymers finally solidify during a phase inversion process. This solidification process may be defined as vitrification, which is the stage where the polymer chains are frozen in a glassy state, i.e. it is a phase where the glass transition temperature has been passed and the mobility of the polymer chains has been reduced drastically. In the absence of gelation or crystallization, vitrification is the mechanism of solidification in any membrane-forming system with an amorphous glassy polymer.

The glass transition of a polymer is reduced by the presence of an additive, i.e. a solvent or nonsolvent. This glass transition depression can be described by various theories, the Kelley-Bueche theory being widely used. A schematic phase diagram of the system PPO/trichloroethylene/methanol is shown in **Figure 15**. Four regions can be observed:

1. a one-phase region where all the components are miscible with each other;

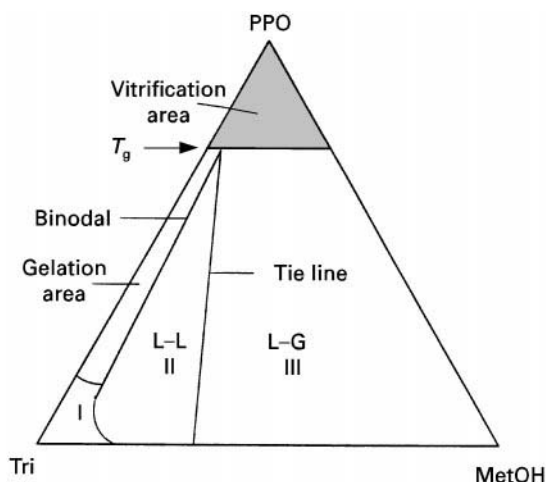


Figure 15 Schematic phase diagram of the quasi ternary system PPO/trichloroethylene/methanol.

2. a gel region where the polymer is able to form a three-dimensional network, providing that certain conditions have been established (a sol-gel transition for the system PPO/DMAc has been determined, however a minimum time of 1 h is necessary for gel formation whereas in immersion precipitation the timescale is much shorter);
3. a glassy region or vitrification region where the glass transition or the polymer has been passed. During immersion precipitation the diffusion of solvent and nonsolvent proceeds according to their corresponding driving forces independent of whether gelation occurs. The final solidification may be a combined gelation/vitrification process, or in absence of gelation vitrification will be the dominant process.
4. a two-phase region where liquid-liquid demixing occurs. In the figure only one tie line is given in which the polymer-rich phase has entered the vitrification area. On the left side of this tie line (II) the (equilibrium) system is still a liquid, whereas on the right side (III) vitrification of the polymer-rich phase had occurred.

Membrane Formation

Thermally Induced Phase Separation (TIPS)

Before describing immersion precipitation in detail, a short description of thermal precipitation or 'thermally induced phase separation' (TIPS) is given.

This process allows the ready preparation of porous membranes from a binary system consisting of a polymer and a solvent. Generally, the solvent has a high boiling point, e.g. sulfolane (tetramethylene sulfone, bp 287°C) or oil (e.g. nujol). The starting

point is a homogeneous solution, for example composition A at temperature T_1 (see Figure 5).

This solution is cooled slowly to the temperature T_2 . When the binodal curve is attained liquid-liquid demixing occurs and the solution separates into two phases, one rich in polymer and the other poor in polymer. When the temperature is decreased further to T_3 , the composition of the two phases follow the binodal curve and eventually the compositions ϕ^I and ϕ^{II} are obtained. At a certain temperature the polymer-rich phase solidifies by crystallization (polyethylene), gelation (cellulose acetate) or on passing the glass transition temperature (atactic polymethylacrylate). Frequently, semicrystalline polymers are used (polyethylene, polypropylene, aliphatic polyamides) which crystallize relatively fast, and hence a solid-liquid phase transition should be included.

Figure 16 shows how the liquid-liquid (L-L) demixing area and the solid-liquid (S-L) for a binary system. In the case of glassy amorphous polymers the melting line may be replaced by a vitrification line. This concept may be applied to various systems, Table 2 provides some examples of this thermally induced phase separation (TIPS) process.

Immersion Precipitation

An interesting question remains after all of these theoretical considerations: what factors are important in order to obtain the desired (asymmetric) morphology after immersion of a polymer-solvent mixture in a nonsolvent coagulation bath? Another interesting question is: why is a more open (porous) top layer obtained in some cases whereas in other cases a very dense (nonporous) top layer supported by an (open) sponge-like structure develops? To answer these questions and to promote an understanding of the basic principles leading to membrane formation

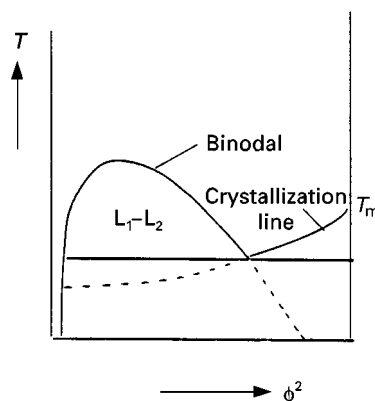


Figure 16 Construction of a T - ϕ diagram for a binary system polymer-solvent. The solidification line is the glass transition temperature line.

Table 2 Some examples of thermally-induced phase separation systems

Polymer	Solvent
Polypropylene	Mineral oil (nujol)
Polyethylene	Mineral oil (nujol)
Polyethylene	Dihydroxy tallow amine
Poly(methyl) methacrylate	Sulfolane
Cellulose acetate/PEG	Sulfolane
Cellulose acetate/PEG	Dioctyl phthalate
Nylon-6	Triethylene glycol
Nylon-12	Triethylene glycol
Poly(4-methyl pentene)	Mineral oil (nujol)

via immersion precipitation, a qualitative description will be given. For the sake of simplicity, the concept of membrane formation will be described in terms of three components: nonsolvent (1), solvent (2) and polymer (3). The effect of additives such as second polymer or material of low relative molecular mass will not be considered because the number of possibilities would then becomes so large and every (quaternary) or multicomponent system has its own complex thermodynamic and kinetic descriptions.

Immersion precipitation membranes in their most simple form are prepared in the following way. A polymer solution consisting of a polymer (3) and a solvent (2) is cast as a thin film upon a support (e.g. a glass plate) and then immersed in a nonsolvent (1) bath. The solvent diffuses into the coagulation bath (J_2) while the nonsolvent will diffuse into the cast film (J_1). After a given period of time the exchange of solvent and nonsolvent has proceeded so far that the solution becomes thermodynamically unstable and demixing takes place. Finally a solid polymeric film is obtained with an asymmetric structure. A schematic representation of the film–bath interface during immersion is shown in Figure 17.

The local composition at any point in the cast film depends on time. However, it is not possible to measure composition changes very accurately with time because the thickness of the film is only of the order of a few microns. Furthermore, membrane

formation can sometimes occur instantaneously, i.e. all the compositional changes must be measured as a function of place and time within a very small time interval. Nevertheless, these composition changes can be calculated. Such calculations provide a good insight into the influence of various parameters upon membrane structure and performance.

Different factors have a major effect upon membrane structure. These are:

- choice of polymer;
- choice of solvent and nonsolvent;
- composition of casting solution;
- composition of coagulation bath;
- gelation, vitrification and crystallization behaviour of the polymer;
- location of the liquid–liquid demixing gap;
- temperature of the casting solution and the coagulation bath; and
- evaporation time.

By varying one or more of these parameters, which are not independent of each other, the membrane structure can be changed from a very open porous form to a very dense nonporous variety.

Take polysulfone as an example. This is a polymer that is frequently used as a membrane material, both for microfiltration/ultrafiltration as well as a sublayer in composite membranes. These applications require an open porous structure, but in addition asymmetric membranes with a dense nonporous top layer can also be obtained that are useful for pervaporation or gas separation applications. Some examples are given in Table 3 that clearly demonstrate the influence of various parameters on the membrane structure when the same system, DMAc/polysulfone (PSf), is employed in each case. To understand how it is possible to obtain such different structures with one and the same system, it is necessary to consider how each of the variables



Figure 17 Schematic representation of a film–bath interface. Components: nonsolvent (1), solvent (2) and polymer (3). J_1 is the nonsolvent flux and J_2 the solvent flux.

Table 3 Influence of preparation procedure on membrane structure

Evaporation PSf/DMAc \Rightarrow pervaporation/gas separation
Precipitation of 15% PSf/DMAc/THF in water \Rightarrow gas separation ^a
Precipitation of 35% PSf/DMAc in water \Rightarrow pervaporation/gas separation ^b
Precipitation of 15% PSf/DMAc in water \Rightarrow ultrafiltration
Precipitation of 15% PSf/DMAc in water/DMAc \Rightarrow microfiltration ^c

^aAfter an initial evaporation step.

^bIt will be shown later that integrally skinned asymmetric membranes can be prepared with completely defect-free top layers.

^cTo obtain an open (interconnected) porous membrane, an additive, e.g. poly(vinyl pyrrolidone) must be added to the polymer solution.

affects the phase inversion process. The ultimate structure arises through two mechanisms: (1) a diffusion processes involving solvent and nonsolvent occurring during membrane formation; and (2) demixing processes.

Diffusional Aspects

Membrane formation by phase inversion techniques, e.g. immersion precipitation, is a nonequilibrium process that cannot be described by thermodynamics alone since kinetics have also to be considered. The composition of any point in the cast film is a function of place and time. To know what type of demixing process occurs and how it occurs, it is necessary to know the exact local composition at a given instant. However, this composition cannot be determined very accurately experimentally because the change in composition occurs extremely quickly (in often less than 1 s) and the film is very thin (less than 200 μm). However, it can be described theoretically. Cohen *et al.* were the first to describe mass transport in an immersion precipitation process. Since then many modified models have been published to describe better this highly nonideal complex multicomponent mass transfer system.

The change in composition may be considered to be determined by the diffusion of the solvent (J_2) and the nonsolvent (J_1) (see Figure 17) in a polymer fixed frame of reference. The fluxes J_1 and J_2 at any point in the cast film can be represented by a phenomenological relationship:

$$J_i = - \sum_{j=1}^2 L_{ij}(\phi_i, \phi_j) \frac{\partial \mu_j}{\partial x} \quad (i = 1, 2) \quad [13]$$

where $-\partial\mu/\partial x$, the gradient in the chemical potential, is the driving force for mass transfer of component i at any point in the film and L_{ij} is the permeability coefficient. From eqn [13] the following relations may be obtained for the nonsolvent flux (J_1) and the solvent flux (J_2):

$$J_1 = -L_{11} \frac{d\mu_1}{dx} - L_{12} \frac{d\mu_2}{dx} \quad [14]$$

$$J_2 = -L_{21} \frac{d\mu_1}{dx} - L_{22} \frac{d\mu_2}{dx} \quad [15]$$

As can be seen from the above equations, the fluxes in a given polymer/solvent/nonsolvent system are determined by the gradient in the chemical potential as driving force, while they also appear in the phenomenological coefficients. This implies that a knowledge of the chemical potentials, or better the

factors that determine the chemical potential, is of great importance. An expression for the free enthalpy of mixing has been given by Flory and Huggins. For a three-component system (polymer/solvent/nonsolvent), the Gibbs free energy of mixing (ΔG_m) is given by:

$$\Delta G_m = RT(n_1 \ln \phi_1 + n_2 \ln \phi_2 + n_3 \ln \phi_3 + \chi_{12}n_1\phi_2 + \chi_{13}n_1\phi_3 + \chi_{23}n_2\phi_3) \quad [16]$$

where R is the gas constant and T is the absolute temperature. The subscripts refer to nonsolvent (1), solvent (2) and polymer (3). The number of moles and the volume fraction of component i are n_i and ϕ_i , respectively. χ_{ij} is called the Flory-Huggins interaction parameter. In a ternary system there are three interaction parameters: χ_{13} (nonsolvent/polymer), χ_{23} (solvent/polymer) and χ_{12} (solvent/nonsolvent). χ_{12} can be obtained from data on excess free energy of mixing that have been compiled or from vapour-liquid equilibria. χ_{13} can be obtained from swelling measurements and χ_{23} can be obtained from vapour pressure or membrane osmometry. The interaction parameters account for the nonideality of the system and they contain an enthalpic as well as an entropic contribution. In the original Flory-Huggins theory they are assumed to be concentration independent, but several experiments have shown that these parameters generally depend on the composition. To account for such dependence the symbol χ is often replaced by another symbol, g , indicating concentration dependency.

From eqn [16] it is possible to derive the expressions for the chemical potentials of the components since:

$$\left(\frac{\partial \Delta G_m}{\partial n_i} \right)_{P,T,n_j} = \Delta \mu_i = \mu_i - \mu_i^0 \quad [17]$$

The eventual concentration dependency of the χ parameter must be taken into account in the differentiation procedure. The influence of the different interaction parameters χ (present in the driving forces) on the solvent flux and nonsolvent flux, and thus on the membrane structures obtained, will be described later.

The other terms present in the flux equations (eqns [16] and [17]) are phenomenological coefficients, and these must also be considered with respect to membrane formation. These coefficients are also mostly concentration dependent. There are two ways of expressing the phenomenological coefficients when the relationships for the chemical poten-

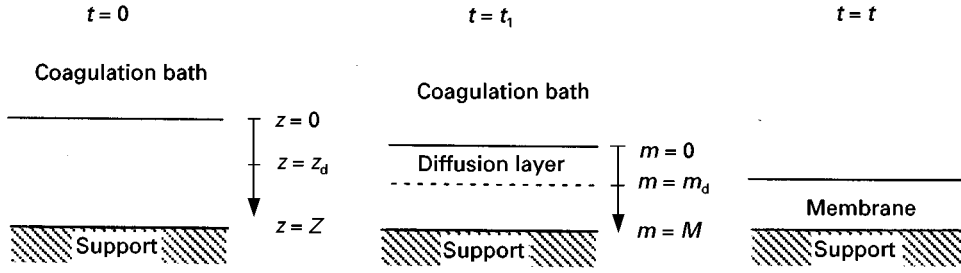


Figure 18 Schematic drawing of the immersion process at different times.

tials are known: (1) in diffusion coefficients; and (2) in friction coefficients.

In most cases there is a (large) difference between the casting thickness and the ultimate membrane thickness. This implies that during the formation process the boundary between the nonsolvent bath and the casting solution moves, as is shown in **Figure 18**. For this reason, it is necessary to introduce a position coordinate to correct for this moving boundary.

The immersion process starts at time $t = 0$. At all times $t > 0$, solvent will diffuse out of the film and nonsolvent will diffuse in. If there is a net volume outflow (solvent flux larger than nonsolvent flux) then the film-bath interface is shifted from $z = 0$, i.e. the actual thickness is reduced. This process will continue until equilibrium is reached (at time $t = t$) and the membrane has been formed. In order to describe diffusion processes involving a moving boundary adequately, a position coordinate m must be introduced (eqn [18]).

The film-bath interface is now always at position $m = 0$, independent of time. The position of the film-support interface is also independent of time (see **Figure 18**):

$$m(x, t) = \int_0^x \phi_3(x, t) dx \quad [18]$$

$$(dm)_t = \phi_3 (dx)_t \quad [19]$$

In the m -coordinate:

$$\frac{\partial(\phi_i/\phi_3)}{\partial t} = \frac{\partial J_i}{\partial m} \quad i = 1, 2 \quad [20]$$

Combination of eqns [18]–[20] yields:

$$\frac{\partial(\phi_1/\phi_3)}{\partial t} = \frac{\partial}{\partial m} \left[v_1 \phi_3 L_{11} \frac{\partial \mu_1}{\partial m} \right] + \frac{\partial}{\partial m} \left[v_1 \phi_3 L_{12} \frac{\partial \mu_2}{\partial m} \right] \quad [21]$$

$$\frac{\partial(\phi_2/\phi_3)}{\partial t} = \frac{\partial}{\partial m} \left[v_2 \phi_3 L_{21} \frac{\partial \mu_1}{\partial m} \right] + \frac{\partial}{\partial m} \left[v_2 \phi_3 L_{22} \frac{\partial \mu_2}{\partial m} \right] \quad [22]$$

The main factor determining the type of demixing process is the local concentration in the film. Using eqns [21] and [22] it is possible to calculate these concentrations (ϕ_1, ϕ_2, ϕ_3) as a function of time. Thus at any time and any place in a cast film the demixing process occurring can be calculated; in fact the concentrations are calculated as a function of place and elapsed time and the type of demixing process is deduced from these values. However, one should note that a number of assumptions and simplifications are involved in this model. Thus heat effects, occurrence of crystallization and relative molecular mass distributions are not taken into account. Nevertheless, it will be shown in the next section that the model allows the type of demixing to be established on a qualitative basis and is therefore useful as a first estimate. Furthermore, it allows an understanding of the fundamentals of membrane formation by phase inversion.

Mechanism of Membrane Formation

It is shown in this section that two types of demixing process resulting in two different types of membrane morphology can be distinguished:

- instantaneous liquid-liquid demixing, where the membrane is formed immediately;
- delayed onset of liquid-liquid demixing, where the membrane takes some time to form.

The occurrence of these two distinctly different mechanisms of membrane formation can be demonstrated in a number of ways: by calculating the concentration profiles; by light transmission measurements; and visually.

The best physical explanation is given by a calculation of the concentration profiles. To calculate the

concentration profiles in the polymer film during the delayed demixed type of phase inversion process, some assumptions and considerations must be made:

- diffusion in the polymer solution;
- diffusion in the coagulation bath – no convection occurs in the coagulation bath;
- thermodynamic equilibrium is established at the film–bath interface:

$$\mu_i(\text{film}) = \mu_i(\text{bath}) \quad i = 1, 2, 3;$$
- volume fluxes at the film–bath interface are equal, i.e.

$$J_i(\text{film}) = J_i(\text{bath}) \quad i = 1, 2.$$

In addition, the thermodynamic binary interaction parameters (the χ parameters or the concentration-dependent g parameters) that appear in the expressions for the chemical potentials must be determined experimentally.

- g_{12} , from calorimetric measurements yielding values of the excess free energy of mixing, from literature compilations of G^E and activity coefficients, from vapour–liquid equilibria and from Van Laar, Wilson, or Margules equations or from UNIFAC;
- g_{13} , from equilibrium swelling experiments or from inverse gas chromatography,
- g_{23} , from membrane osmometry or vapour pressure osmometry.

Two types of demixing process will now be distinguished that lead to different types of membrane structure. These two different types of demixing process may be characterized by the instant when liquid–liquid demixing sets in. Figure 19 shows the composition path of a polymer film schematically at

the very instant of immersion in a nonsolvent bath (at $t < 1$ s). The composition path gives the concentration at any point in the film at a particular time. For any other time, another compositional path will exist.

Because diffusion processes start at the film–bath interface, the change in composition is first noticed in the upper part of the film. This change can also be observed from the composition paths given in Figure 19. Point t gives the composition at the top of the film while point b gives the bottom composition. Point t is determined by the equilibrium relationship at the film–bath interface $\mu_i(\text{film}) = \mu_i(\text{bath})$. The composition at the bottom is still the initial concentration in both examples. In Figure 19A places in the film beneath the top layer t have crossed the binodal curve, indicating that liquid–liquid demixing starts immediately after immersion. In contrast, Figure 19B indicates that all compositions directly beneath the top layer still lie in the one-phase region and are still miscible. This means that no demixing occurs immediately after immersion. After a longer time interval, compositions beneath the top layer will cross the binodal curve and liquid–liquid demixing will start in this case also. Thus two distinctly different demixing processes can be distinguished and the resulting membrane morphologies are also completely different.

When liquid–liquid demixing occurs instantaneously, membranes with a relatively porous top layer are obtained. This demixing mechanism results in the formation of a porous membrane (microfiltration/ultrafiltration type). However, when liquid–liquid demixing sets in after a finite period of time, membranes with a relatively dense top layer are obtained. This demixing process results in the formation of dense membranes used for gas separation/perm vaporation. In both cases the thickness of the top

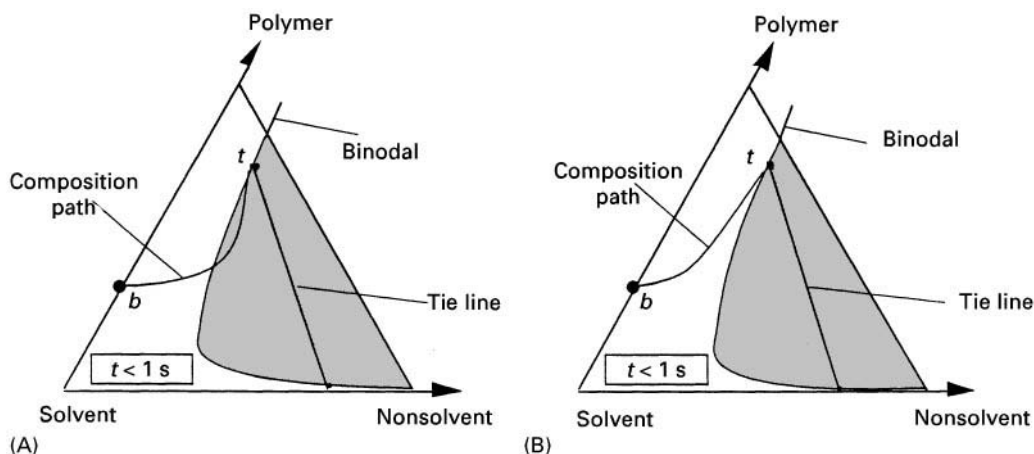


Figure 19 Schematic composition path of the cast film immediately after immersion; t is the top of the film and b is the bottom. Part (A) shows instantaneous liquid–liquid demixing whereas (B) shows the mechanism for the delayed onset of liquid–liquid demixing.

Table 4 Polymers that are frequently used as phase inversion membranes

Polymer	Process
Cellulose acetate	MF, UF, NF, RO, GS
Nitrocellulose	MF
Polysulfone	MF, UF
Polyethersulfone	MF, UF
Polyacrylonitrile	MF, UF
Polyvinylidene fluoride	MF, UF
Polyimide	UF, GS
Aliphatic polyamide	MF, UF
Aromatic polyamide	NF, RO
Polyphenylene oxide	GS

MF, microfiltration; UF, ultrafiltration; NF, nanofiltration; RO, reverse osmosis; GS, gas separation.

layer is dependent on a variety of membrane formation parameters (i.e. polymer concentration, coagulation procedure, additives, etc.).

Polymers for Phase Inversion Membranes

The preparation of phase inversion membranes has only been described briefly. It may be evident that many polymers can be applied as long as they are soluble in a suitable organic solvent. This is the only limitation. Nevertheless, owing to their mechanical, thermal and chemical properties some polymers are more frequently applied. Two of these so-called 'engineering polymers', polysulfone and polyethersulfone, are used as micro- and ultrafiltration membranes or as support material in composite membranes for nanofiltration, reverse osmosis and gas separation. These two polymers have very good film-forming properties and are soluble in a range of solvents. Beside these two polymers a wide variety of other polymers are applied; these are listed in Table 4.

Future Developments

Phase inversion will remain the most important technique for the preparation of polymeric membranes for microfiltration and ultrafiltration membranes and for use as support membranes in composite membranes for nanofiltration, reverse osmosis, gas separation, vapour permeation and pervaporation.

See also: **III/Membrane Preparation:** Hollow Fibre Membranes; Interfacial Composite Membranes

Further Reading

Arnauts J and Berghmans H (1987) Atactic gels of atactic polystyrene. *Polymer Communications* 28: 66–68.

Altena FW and Smolders CA (1982) Calculation of liquid–liquid phase separation in a ternary system of a polymer in a mixture of a solvent and a nonsolvent. *Macromolecules* 15: 1491–1497.

Altena FW, Smid J, Van den Berg JWA, Wijmans JG and Smolders CA (1985) Diffusion from solvent from a cast CA solution. *Polymer* 26: 1531.

Boom RM, Wienk IM, Boomgaard van den T and Smolders CA (1992) Microstructures in phase inversion membranes. Part 2, the role of the polymer additive. *Journal of Membrane Science* 73: 277–292.

Boom RM, Boomgaard van den T and Smolders CA (1994) Mass transfer and thermodynamics during immersion precipitation for a two-polymer system: evaluation with the systems PES-PVP-NMP-water. *Journal of Membrane Science* 90: 231–249.

Bulte AMW, Folkers B, Mulder MHV and Smolders CA (1993) Membranes of semi-crystalline aliphatic polyamide Nylon 4-6. Formation by diffusion induced phase separation. *Journal of Applied Polymer Science* 50: 13–26.

Caneba GT and Soong DS (1985) Polymer membrane formation through the thermal inversion process. 1. Experimental study of membrane formation. *Macromolecules* 18: 2538–2545.

Caneba GT and Soong DS (1985) Polymer membrane formation through the thermal inversion process. 2. Mathematical modeling of membrane structure formation. *Macromolecules* 18: 2545–2555.

Cheng L-P, Soh YS, Dwan A-H and Gryte CC (1994) An improved model for mass transfer during the formation of polymer membranes by the immersion precipitation process. *Journal of Polymer Science Part B, Polymer Physics* 32: 1413–1425.

Cohen C, Tanny GB and Prager EM (1979) Diffusion-controlled formation of porous structures in ternary polymer systems. *Journal of Polymer Science, Polymer Physics Edition* 17: 477–489.

Eykamp W (1995) Microfiltration and ultrafiltration. In: Noble RD and Stein A (eds) *Membrane Separation Technology, Principles and Applications*, pp. 1–25. Amsterdam: Elsevier.

Ferry D (1936) Ultrafilter membranes and ultrafiltration. *Chemical Reviews* 18: 373–455.

Flory PJ (1953) *Principles of Polymer Chemistry*. Ithaca, NY: Cornell University Press.

Gaides GE and McHugh AJ (1989) Gelation in an amorphous polymer: a discussion of its relation to membrane formation. *Polymer* 30: 2118–2123.

Guillotin M, Lemoyne C, Noel C and Monnerie L (1977) Physicochemical processes occurring during the formation of cellulose diacetate membranes. Research of criteria for optimizing membrane performance. IV. cellulose diacetate-acetone-organic additive casting solutions. *Desalination* 21: 165–170.

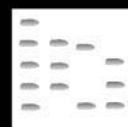
Kamide K and Matsuda S (1984) Phase equilibria of quasi ternary systems consisting of multi-component polymers in a binary solvent mixture. II Role of initial concentration and relative amount of polymers. *Polymer Journal* 7: 515–530.

- Koenhen DM, Mulder MHV and Smolders CA (1977) Phase separation phenomena during the formation of asymmetric membranes. *Journal of Applied Polymer Science* 21: 199–215.
- Lloyd DR and Kinzer KE (1991) Microporous membrane formation via thermally induced phase separation. II Liquid-liquid phase separation. *Journal of Membrane Science* 64: 1–11.
- McHugh AJ and Yilmaz L (1985) The diffusion equation for polymer membrane formation in ternary systems. *Journal of Polymer Science, Polymer Physics Edition* 23: 1271–1274.
- McHugh AJ and Tsay CS (1992) Dynamics of the phase inversion process. *Journal of Applied Polymer Science* 46: 2011–2021.
- Mulder MHV, Oude Hendrikman J, Wijmans JG and Smolder CA (1985) A rationale for the preparation of asymmetric pervaporation membranes. *Journal of Applied Polymer Science* 30: 2805–2830.
- Mulder MHV, Franken ACM and Smolders CA (1985) Preferential sorption versus preferential permeation. *Journal of Membrane Science* 22: 155–173.
- Mulder MHA (1996) *Basic Principles of Membrane Technology*. Dordrecht: Kluwer.
- Radovanovic P, Thiel SW and Hwang S-T (1992) Formation of asymmetric polysulfone membranes by immersion precipitation. Part II. The effects of casting solution and gelation bath compositions on membrane structure and skin formation. *Journal of Membrane Science* 65: 231.
- Radovanovic P, Thiel SW and Hwang S-T (1992) Formation of asymmetric polysulfone membranes by immersion precipitation. Part I. Modelling of mass transport during gelation. *Journal of Membrane Science* 65: 213–229.
- Reuvers AJ, Altena FW and Smolders CA (1986) Demixing and gelation behaviour of ternary cellulose acetate solutions studied by differential scanning calorimetry. *Journal of Polymer Science, Polymer Physics Edition* 24: 793–804.
- Reuvers AJ, Berg van den JWA and Smolders CA (1987) Formation of membranes by means of immersion precipitation. Part I. A model to describe mass transfer during immersion precipitation. *Journal of Membrane Science* 34: 45–65.
- Reuvers AJ and Smolders CA (1987) Formation of membranes by means of immersion precipitation. Part II. The mechanism of membranes prepared from the system cellulose acetate-acetone-water. *Journal of Membrane Science* 34: 67–86.
- Strathmann H, Koch K, Amar P and Baker RW (1975) The formation mechanism of asymmetric membranes. *Desalination* 16: 179–203.
- Tan HM, Moet A, Hiltner A and Baer E (1983) Thermoreversible gelation of atactic polystyrene solutions. *Macromolecules* 16: 28–34.
- Tsai FJ and Torkelson JM (1990) Roles of phase separation mechanism and coarsening in the formation of PMMA asymmetric membranes. *Macromolecules* 23: 775–784.
- Tsay CS and McHugh AJ (1990) Mass transfer modelling of asymmetric membrane formation by phase inversion. *Journal of Polymer Science* 28: 1327–1365.
- Tsay CS and McHugh AJ (1991) Mass transfer dynamics of the evaporation step in membrane formation by phase inversion. *Journal of Membrane Science* 64: 81–92.
- Tsay CS and McHugh AJ (1991) The combined effects of evaporation and quench steps on asymmetric membrane formation by phase inversion. *Journal of Polymer Science Part B, Polymer Physics* 29: 1261–1270.
- Vadalia HC, Lee HK, Myerson HS and Levon K (1994) Thermally induced phase separation in ternary crystallizable polymer solutions. *Journal of Membrane Science* 89: 37–50.
- Wisniak J and Tamir A (1978) *Mixing and Excess Thermodynamic Properties*. Amsterdam: Elsevier.
- Wijmans JG, Kant J, Mulder MHV and Smolders CA (1985) Phase separation phenomena in solutions of polysulfone in mixtures of a solvent and a nonsolvent: relationship with membrane formation. *Polymer* 26: 1539–1545.
- Wijmans JG, Rutten HJJ and Smolders CA (1985) Phase separation phenomena in solutions of PPO in mixtures of trichloroethylene, octanol and methanol: relation to membrane formation. *Journal of Polymer Science, Polymer Physics* 23: 1941–1955.
- Yilmaz L and McHugh AJ (1986) Analysis of solvent-non-solvent-polymer phase diagrams and their relevance to membrane formation modelling. *Journal of Applied Polymer Science* 31: 997–1018.
- Yilmaz L and McHugh AJ (1986) Modelling of asymmetric membrane formation. I. Critique of evaporation models and development of diffusion equation formalism for the quench period. *Journal of Membrane Science* 28: 287–310.
- Zeman L and Tkacik G (1988) Thermodynamic analysis of a membrane forming system water-N-methyl-2-pyrrolidone/polyethersulfone. *Journal of Membrane Science* 36: 119–140.

METABOLITES

See **III/DRUGS AND METABOLITES: Liquid Chromatography-Mass Spectrometry; Liquid Chromatography-Nuclear Magnetic Resonance-Mass Spectrometry**

METAL ANALYSIS: GAS AND LIQUID CHROMATOGRAPHY



P. C. Uden, University of Massachusetts,
Amherst, MA, USA

Copyright © 2000 Academic Press

Introduction

Since its inception as a separatory technique, gas-liquid chromatography (GLC) has had great impact in the quantitative resolution of mixtures of volatile compounds. Although the sister discipline of gas-solid chromatography (GSC) is used for inorganic gas analysis along with metalloid halides and hydrides, the potential of both GLC and GSC for inorganic compounds, metal complexes and organometallics has been less realized. The relative obscurity of inorganic gas chromatography derives from expectations that inorganic compounds are inherently of very low volatility and/or thermally unstable under GC conditions, are incompatible with column substrates, show undesirable reactivity making GC difficult, or are incompatible with conventional detectors. Some of these strictures apply, but there are many examples of GC of metallic and metalloid compounds including organometallics incorporating sigma or pi carbon to metal bonds, and metal complexes with coordinate bonds between oxygen, sulfur, nitrogen, phosphorus, or halogen, and the metal atom. Some metal oxides and halides may be eluted at high temperatures. Chemical derivatization methods may also enable successful elution. There is often considered to be a minimal group of chemical properties to be possessed by a compound before gas chromatography can be successful: volatility, thermal stability, monomeric form, neutrality, relatively low molecular weight, coordinative saturation and shielding of the metal atom(s) by bulky and inert organic functional groups. The compound should appear to the GC column as a simple organic species and free metal atoms should not be exposed to reactive sites. Inertness of column materials, injection and detection pathways are particularly important. Fused silica columns allow GC of previously inapplicable species. Detectors that are more compatible, selective or specific for inorganic compounds have opened the way for quantitative and sensitive analysis.

Liquid chromatography (LC) has been used extensively in thin-layer and ion exchange for metal ion

and compound separations. However high performance column chromatography (HPLC) with different column packings, instrumentation and detectors has given rise to many new capabilities. The literature of LC of inorganics and organometallics up to 1970 was presented by Michal with 700 references while that between 1970 and 1979 was surveyed by Schwedt with over 450 references. MacDonald's (1985) text *Inorganic Chromatographic Analysis* covers all LC and GC methods in a comprehensive review.

The various modes of HPLC allow a wider range of analytes to be chromatographed than in GC. Metal ions may be resolved by ion chromatography, or separated as ion pairs in a reversed-phase regime. Positively or negatively charged metal complexes may be similarly separated. Neutral metal complexes, chelates and organometallics may be chromatographed in reversed- or normal-phase systems. Metal-containing macromolecules such as metalloproteins may be separated by size exclusion. Chemical properties desirable in an inorganic compound for viable liquid partition chromatography include solvolytic stability, minimal adsorptive interactions and shielding of the metal by inert functional groups. As with GC, the analyte should appear to the column as an organic compound and free metal atoms should never be accessible to reactive sites. New detectors that are more compatible or specific for inorganic compounds have also made an impact in HPLC. Diode array UV, electrochemical detection and elemental and molecular mass spectroscopy have proven valuable. The inorganic chromatographer is often faced with a choice between GC and HPLC and each may be valuable in a complementary fashion. Supercritical fluid chromatography (SFC) has been little applied for metal compounds, successful applications following mostly from HPLC methodology.

The primary application of analytical chromatography in metals analysis is clearly in 'speciation' wherein the requirement is resolution and quantitation of specific chemical species incorporating the target metal. Situations occur (i) in which the chemical species is already amenable to the chosen chromatographic technique, and (ii) wherein it may be converted to such by physical or chemical means, as in pyrolysis, derivatization, etc. While total element analysis is less suited to chromatographic methods,

sometimes suitable derivatization techniques enable this as well.

Gas Chromatography

The classes of metallic substances for which GC is viable, either directly or by derivatization, are: binary metal and metalloid compounds such as halides, hydrides and oxides; sigma-bonded organometallic and organometalloid compounds such as alkyls and aryls; pi-bonded organometallics such as metal carbonyls and metallocenes; chelated metal complexes having nitrogen, oxygen, sulfur, phosphorus, etc., as ligand atoms. The text by Guiochon and Pommier (1973) *Gas Chromatography in Inorganics and Organometallics* provides an excellent summary of this topic augmented by Schwedt's coverage.

Binary Metal and Metalloid Compounds

Binary metal compounds with adequate vapour pressures and thermal stabilities at normal GC temperatures include main group hydrides and halides. At 1000°C or higher, some metal oxides have adequate properties.

Among hydrides, those of boron, silicon, germanium, tin, arsenic, antimony, bismuth, selenium and tellurium are viable having boiling points ranging from 112°C to -2°C. Low column temperatures and inert systems are needed. Element-selective spectral detectors are also advantageous. These separations are important for trace-level determinations in electronic grade organometallics. Organo-hydrides are also readily chromatographed. Analysis of environmentally significant arsenic and antimony compounds with microwave plasma emission detection involves reduction of alkylarsenic acids with sodium borohydride to alkylarsines.

Certain metal halides are sufficiently volatile for GC, but difficulty lies in their high reactivity in the vapour and condensed phases, necessitating precautions to ensure maximum inertness of the system. Among chlorides that have been gas chromatographed are those of titanium, aluminium, mercury, tin, iron, antimony, germanium, gallium, vanadium, silicon and arsenic. Problems arise from reaction with even methyl silicone oils and thus inert fluorocarbon packings have been favoured for reactive chlorides and oxychlorides including VOCl_3 , VCl_4 , PCl_3 and AsCl_3 . The less volatile metal bromides are very challenging and high temperature stationary phases such as alkali bromide salts coated on silica are needed. Some metal fluorides have low boiling points, e.g. tungsten (17.5°C), molybdenum (35°C), tellurium (35.5°C), rhenium (47.6°C) and uranium (56.2°C), for which low column temperatures are feasible. The

determination of alloys and metal oxides, carbides, etc., after conversion to fluorides by fluorination appears feasible.

One of the most extreme modifications of GC has been in the area of very high temperature GC for metal oxides, hydroxides and oxychlorides. Bachmann employed temperatures as high as 1500°C for the separation of oxides and hydroxides of technetium, rhenium, osmium and iridium. Quartz granules were used as the substrate and oxygen and oxygen/water mixtures as carrier gases with the necessary equipment modifications.

Organometallic Compounds

Crompton in *Gas Chromatography of Organometallic Compounds*, published in 1982, notes that during the preceding decade more than 1000 papers were published on this topic, relating to compounds of more than 50 elements. At least as many papers have been published since that time.

Sigma-bonded compounds GC is feasible for compounds of Al, Ga and In from Group III; Ge, Sn and Pb from Group IV; P, As, Sb and Bi from Group V; and Se and Te from Group VI. Also included are Hg and possibly Zn and Cd. The elements that have attracted most analytical interest have been silicon and lead, tin and mercury.

The organic functionalities are typically alkyl, aryl and substituted aryl groups; perfluoroalkyl and aryl groups, which typically impart enhanced volatility; and mixed alkyl-chloro and aryl-chloro systems. The two reported separations of aluminium alkyls leave doubts as to possible on-column decomposition. Trimethylgallium has been eluted along with $(\text{CH}_3)_2\text{GaCl}$ and CH_3GaCl_2 , but no GC of organometallic indium or thallium compounds has been reported. The GC characteristics of alkyl germanium, tin and lead compounds resemble those of silicon but with decreasing thermal stability. For alkylstannanes, on-column oxidation, hydrolysis or thermal degradation must be avoided. Selective detection has been widely used for organotin compounds, notably for environmental samples such as bis(tributyltin)oxide (TBTO) in marine paints, triphenylhydroxystannane pesticide after derivatization to triphenylmethylstannane, and tricyclohexylhydroxystannane in apple leaves after derivatization to tricyclohexylbromostannane.

GC of tetraalkyllead compounds is extensive and covers 30 years of developments. Crompton devotes 90 pages to discussion of organolead GC. The electron-capture detector is highly selective for tetraalkylleads, but is prone to contamination. Atomic spectral detection has been widely applied for lead-specific

detection, e.g. flame photometric detection with an oxygen-hydrogen flame at 405.8 nm and graphite furnace electrothermal atomic absorption detection at 283.3 nm. Chau quantitated methylethylleads in water, sediment and fish in an investigation of bio-alkylation processes, lead detection limits being between 0.01 and 0.025 $\mu\text{g g}^{-1}$ for solid samples. Plasma atomic emission detection for alkyl leads has been widely used; trimethyl- and triethyllead chlorides have been determined in water in the range of 10 ppb to 10 ppm and also derivatized by butyl Grignard reagent to form the trialkylbutylleads.

The alkyl and aryl derivatives of arsenic and antimony are more labile than those of Group IV elements, and require stringent GC conditions for successful elution. Bismuth compounds have not been chromatographed. Talmi determined As^{3+} and Sb^{3+} in environmental samples as triphenylarsine and triphenylstilbene, plasma emission detection giving limits of 20 pg and 50 pg, respectively.

GC of the environmentally significant organomercurials has attracted much attention, biomethylation of inorganic mercury being important. $(\text{CH}_3)_2\text{Hg}$ and CH_3HgCl have been separated on packed glass columns using plasma emission detection. Non-flame 'cold vapour', atomic absorption spectrophotometry detection has proved useful after catalytic conversion of organomercurials to elemental mercury.

Although they are not formally organometallics, many alkoxides share similar GC characteristics with alkyl compounds. Germanium, tin, titanium, zirconium and hafnium form stable volatile alkoxides, as do some Group III elements, notably aluminium. There have been GC separations reported of oxycarboxylate salts of beryllium and zinc.

Pi-bonded compounds The most gas chromatographed transition metal organometallics are those containing carbonyl, arene and cyclopentadienyl ligand moieties. Their elution characteristics are very favourable with only rare on-column degradation or adsorption reported. Effective separation of $\text{Fe}(\text{CO})_5$, $\text{Cr}(\text{CO})_6$, $\text{Mo}(\text{CO})_6$ and $\text{W}(\text{CO})_6$ is possible and methods may be employed for the highly toxic $\text{Ni}(\text{CO})_4$ since its high volatility permits ready elution. Many results have been reported for arene, cyclopentadienyl and related derivatives of metal carbonyls. Arenechromiumtricarbonyls and molybdenumtricarbonyls are easily gas chromatographed. Cyclopentadienylmanganesetricarbonyl ($\text{C}_5\text{H}_5\text{Mn}(\text{CO})_3$) and its derivatives are well suited to quantitative GC. Methylcyclopentadienylmanganesetricarbonyl, $(\text{CH}_3\text{C}_5\text{H}_4\text{Mn}(\text{CO})_3)\text{-MMT}$ has been determined in gasoline using various detectors. Capillary GC is effective for compounds of this class; spe-

cific element detection simplifies such separations and provides qualitative and quantitative proof of elution. Figure 1 shows such a capillary column separation with atomic emission detection of organometallics with differing metals and functionalities. Many of these organometallics are of interest as polymerization catalysts, etc.

Among GC of metallocenes, ferrocene, bis(cyclopentadienyl)iron, is the most familiar example. These compounds have favourable GC properties, ferrocene proving an ideal organometallic probe for determining column and system efficiency. Ferrocene derivatives chromatographed have included alkyl, vinyl, dialkyl, acetyl, diacetyl and hydroxymethyl compounds. GC behaviour is determined largely by the substituents; ruthenocene and osmocene have also been separated.

Metal Chelates

Neutral metal complexes deriving from a number of anionic ligands with oxygen, nitrogen, sulfur or phosphorus donor atoms, have been widely studied. The range of organic ligands that has been shown to be suitable for GC analysis has been limited, but a considerable amount of development and application has been done.

Beta-diketonates Beta-diketonates are readily formed with stability arising from multiple chelate rings. Ions with coordination numbers twice their oxidation state such as $\text{Al}(\text{III})$, $\text{Be}(\text{II})$ and $\text{Cr}(\text{III})$ form coordinatively saturated neutral complexes which are good for GC but the non-fluorinated beta-diketonates are generally of marginal thermal and chromatographic stability; they usually require column temperatures too high for thermal degradation to be completely absent. The major breakthrough in metal chelate GC involved fluorinated beta-diketone ligands, giving complexes of greater volatility and thermal stability. Moshier and Sievers gave the major impetus to this development, and a major portion of their monograph summarizes the analytical progress made to that time. Trifluoroacetylacetone (1,1,1-trifluoro-2,4-pentanedione-HTFA) and hexafluoroacetylacetone (1,1,1,5,5,5-hexafluoro-2,4-pentanedione-HHFA) have been the most widely studied and analytically developed of the fluorinated beta-diketonates. HTFA extended the range of metals that may be quantitated to include $\text{Ga}(\text{III})$, $\text{In}(\text{III})$, $\text{Sc}(\text{III})$, $\text{Rh}(\text{III})$ and $\text{V}(\text{IV})$. HTFA chelates of trivalent hexacoordinate metals such as $\text{Cr}(\text{III})$, $\text{Co}(\text{III})$, $\text{Al}(\text{III})$ and $\text{Fe}(\text{III})$ exhibit geometrical isomerism with facial (*cis*) and meridional (*trans*) forms present and interconverting. Numerous analytical applications of HTFA chelates are reviewed in detail by Moshier and

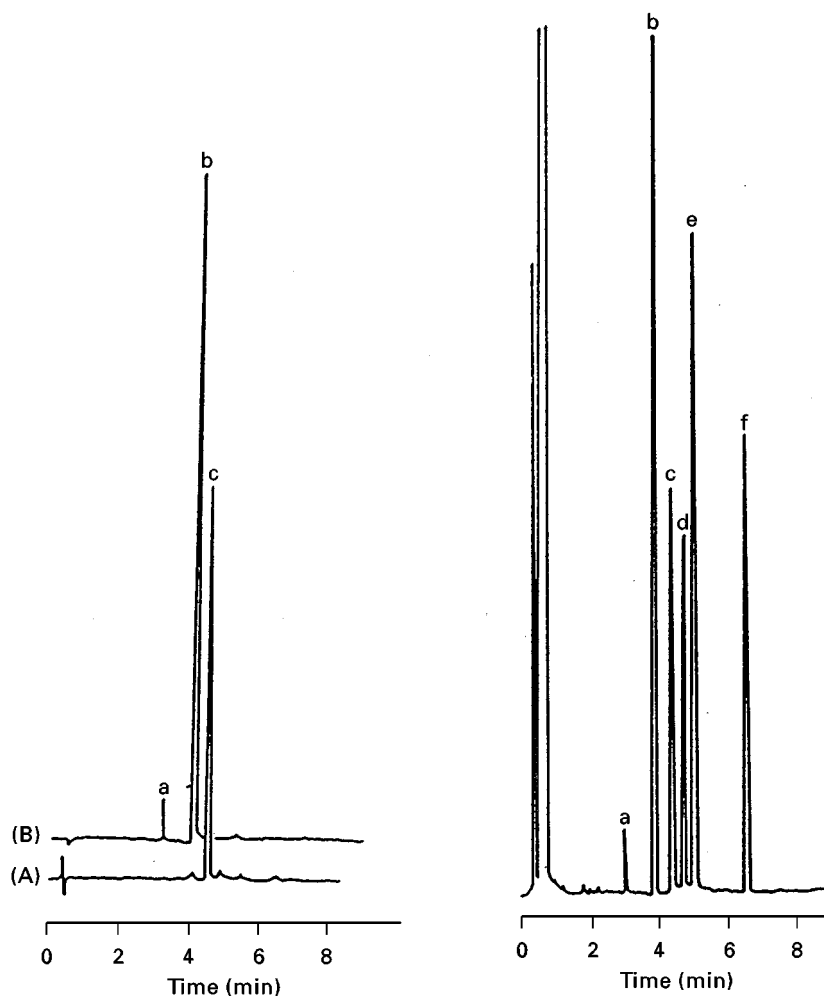


Figure 1 Microwave plasma atomic emission capillary GC detection of organometallics. Left: (A) chromium monitored at 267.7 nm (peak c) and (B) manganese monitored at 257.6 nm (peaks a and b). Right: carbon monitored at 247.9 nm for organometallic mixture. The six peaks afford 'universal' carbon detection. The identities of the eluted peaks are: (a) $C_5H_5Mn(CO)_3$, (b) $CH_3C_5H_4Mn(CO)_3$, (c) $C_5H_5Cr(NO)(CO)_2$ and $(C_5H_5)_2Ni$ (unresolved), (d) $C_5H_5V(CO)_4$, (e) $(C_5H_5)_2Fe$ and (f) $C_5H_5(CH_3)_5Co(CO)_2$. (Reproduced with permission from Estes SA *et al.* (1980). *Journal of Chromatography and Chromatographic Communications* 3: 471. Copyright John Wiley & Sons Ltd.)

Sievers, Uden and Henderson and in the texts of Guiochon and Pommier and Schwedt.

Since modifications of the beta-diketone structure may be made readily, various such ligands have been evaluated for GC. The two major adaptations have been the replacement of the methyl group by higher branched alkyl groups, notably *t*-butyl, and the incorporation of longer chain perfluoroalkyl groups in the ligand. Sievers used 1,1,1,2,2,3,3-heptafluoro-7,7-dimethyl-4,6-octanedione (heptafluoropropanoyl-pivalylmethane (HFOD or HHPM)) for lanthanide separations.

Alternative beta-difunctional chelates The major classes of such ligands are summarized in the schematic diagram in **Figure 2**. This indicates the mode of formation of the main alternative bidentate ligands

with sulfur donors and bidentate and tetradentate ligands with nitrogen donors.

Beta-thioketonates There are a number of advantages of these chelates. The metals showing favourable GC properties are those whose diketonates are generally unsatisfactory, such as the divalent metals nickel, palladium, platinum, zinc and cobalt. Nickel has been subjected to a complete quantitative analysis, as the monothiotrifluoroacetylacetonate.

Beta-ketoaminates The presence of the nitrogen atom in the ligand dictates an intermediate place between beta-diketonates and monothiokeetonates in terms of the metals which are readily complexed. The nickel group of metals is favourably complexed, but in addition stable chelates of copper(II) are formed,

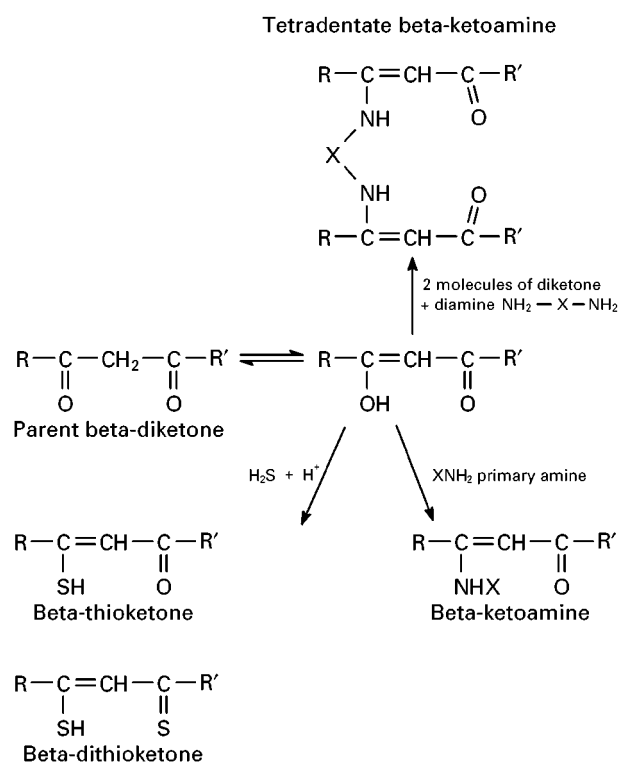


Figure 2 Formation of beta-difunctional ligands for metal gas chelate gas chromatography. (Reproduced with permission from Estes SA *et al.* (1980). *Journal of Chromatography and Chromatographic Communications* 3: 471. Copyright John Wiley & Sons Ltd.)

as are those of vanadyl (V(IV)O). The bidentate ketoamines are of only marginal GC stability to sub-microgram elution level, but tetradentate beta-ketoamine ligands form a useful group for GC of

Table 1 Representative tetradentate beta-ketoamine ligands used for chelate formation and gas chromatography of divalent transition metals

$ \begin{array}{c} \text{R}-\text{C}=\text{CH}-\text{C}-\text{R}' \\ \quad \quad \quad \\ \text{NH} \quad \quad \quad \text{O} \\ \diagup \quad \diagdown \\ \text{X} \\ \diagdown \quad \diagup \\ \text{NH} \quad \quad \quad \text{O} \\ \quad \quad \quad \\ \text{R}''-\text{C}=\text{CH}-\text{C}-\text{R}''' \end{array} $					
R	R'	R''	R'''	X	Ligand symbol
CH_3	CH_3	CH_3	CH_3	en	$\text{H}_2(\text{enAA}_2)$
CH_3	CH_3	CH_3	CH_3	pn	$\text{H}_2(\text{pnAA}_2)$
CH_3	CH_3	CH_3	CH_3	bn	$\text{H}_2(\text{bnAA}_2)$
CF_3	CH_3	CH_3	CF_3	en	$\text{H}_2(\text{enTFA}_2)$
CF_3	CH_3	CH_3	CF_3	pn	$\text{H}_2(\text{pnTFA}_2)$
CF_3	CH_3	CH_3	CF_3	bn	$\text{H}_2(\text{bnTFA}_2)$
$\text{C}(\text{CH}_3)_3$	CH_3	CH_3	$\text{C}(\text{CH}_3)_3$	en	$\text{H}_2(\text{enAPM}_2)$
$\text{C}(\text{CH}_3)_3$	CH_3	CH_3	$\text{C}(\text{CH}_3)_3$	pn	$\text{H}_2(\text{pnAPM}_2)$
CF_3	$\text{C}(\text{CH}_3)_3$	$\text{C}(\text{CH}_3)_3$	CF_3	en	$\text{H}_2(\text{enTPM}_2)$

en = CH_2-CH_2 ; pn = $\text{CH}(\text{CH}_3)-\text{CH}_2$; bn = $\text{CH}(\text{CH}_3)-\text{CH}(\text{CH}_3)$.

divalent transition metals. The addition of the extra five-membered ring stabilizes the complexes, which more than offsets their lowered volatility. Table 1 lists the tetradentate beta-ketoamine ligands that have been evaluated for GC of copper, nickel, palladium and vanadyl complexes. The fluorinated chelates have very great electron capturing abilities affording picogram level detection.

Dialkylthiocarbamates and dialkylthiophosphinates The metals complexed by these ligands are parallel to those chelated by the tetradentate beta-ketoamines for GC applications. Zinc, copper and nickel have been determined in marine bottom sediments and in sea sands and muds. In parallel to the development of fluorinated beta-diketone ligands, fluorinated dialkylthiocarbamates show analytical promise due to their increased volatility over non-fluorinated analogues. Tavlaridis and Neeb first investigated di(trifluoroethyl)dithiocarbamates, eluting zinc, nickel, cadmium, lead, antimony and bismuth complexes at 185°C . Sucre and Jennings reported effective capillary separation of these complexes of nickel and cobalt(III) on 5 metre fused silica columns. It appears likely that further refinement of high resolution columns will broaden the application of these versatile complexes for analytical GC.

Cardwell and McDonagh separated zinc, nickel, palladium and platinum 0,0'-dialkylthiophosphinates. These complexes are suitable for selective detection by flame photometry with monitoring of either the S_2 or HPO emission modes.

Metalloporphyrins One of the most important demonstrations of the expanded range of sample applications for inorganic GC brought about by high resolution fused silica capillary was of transition metal porphyrin complexes. Marriott achieved capillary GC elution of these closed macrocyclic ring copper, nickel, vanadyl and cobalt aetioporphyrin I, and octaethyl-porphyrin chelates with Kováts indices in the range 5200–5600.

Chromatographic Detection

Of particular value for metal compound chromatography are detectors giving 'selective' or 'specific' information on the eluates. Spectral property detectors such as the mass spectrometer (MS), the infrared spectrophotometer (IRS) and the atomic emission spectrometer (AES) fall into this class. The latter 'element selective' detectors are widely used: the microwave-induced plasma in particular for GC and the inductively coupled plasma mass spectrometer (ICPMS) for HPLC. These detector systems typically

offer nanogram level detection or lower for metal content of analytes. Metals may be determined directly or through derivatization procedures which render them more readily separable and detectable.

High Performance Liquid Chromatography

Size-Exclusion Chromatography (SEC)

SEC separates chemical species by molecular size and shape in a column containing particles of a rigid packing with a defined pore structure. Many applications to inorganic and organometallic species have been reported ranging in size from a few hundred to 10^5 Da or greater; from labile nickel complexes of alkyl substituted phosphorus esters to molecular clusters of inorganic colloids in the 1–50 μm range, aluminosilicate sols, humic acid metal complexes, metalloproteins and metalloproteins. Ferritin, an iron-containing protein which exists in a number of discrete forms, has been analysed using aqueous SEC, good repeatability being found for iron at the nanogram level. Trace levels of Cd, Zn and Cu metalloproteins in marine mussels were determined using SEC with sequenced UV absorption detection before the ICP. In the petroleum field, effective separation and determination of vanadium and nickel metalloporphyrins has been accomplished. Columns of pore size 10 nm in particular are a viable choice for many separation problems of inorganic chromatography.

Reversed-Phase High Performance Liquid Chromatography (RPHPLC)

RPHPLC of inorganic and organometallics may be characterized by the detector used and some examples are noted.

Atomic absorption (AA) The interfacing of column effluent and an AA spectrometer was attained in 1973, tetraalkyllead compounds being separated on C_{18} μ -Bondapak with 70% acetonitrile and 30% water. The superiority of AA detection over UV detection was shown, since gasoline samples have components that mask the tetraalkyl lead compounds.

Inductively coupled plasma (ICP) and direct current plasma (DCP) Plasma spectral detection for HPLC has emphasized the ICP and to some extent the DCP, in contrast to the dominance of the microwave-induced plasmas as element-selective GC detectors. Metal-specific detection is predominant and will probably remain so until more eluate-selective interface systems can be devised. The ICP became

commercially available in 1974 replacing atomic absorption spectroscopy as the method of choice for metal analysis. The technique and DCP has been coupled to HPLC for trace analysis and speciation of real-world samples such as arsenite, dimethyl arsenate and arsenate. A 130 ng mL^{-1} detection limit for arsenic in organoarsenic acids was found for 100 μL samples after hydride formation. Separation of mercury cations employed an alkyl sulfonate anion as ion pair reagent and, after hydride formation, gave detection limits of $50\text{--}100 \mu\text{g L}^{-1}$. A possible solution to overcome the difficulties in quantitative transfer of HPLC eluate involves a total injection microconcentric nebulizer (DIN) which can achieve almost 100% nebulization and transport efficiency. Detection limits down to 4 mg L^{-1} for zinc have been reported. The DCP gave detection for Cr(III) and Cr(VI) linear over at least three orders of magnitude with a detection limit of $10 \mu\text{g L}^{-1}$; applications include biological samples from ocean floor drillings, chemical dump sites, surface well water and waste water samples.

Visible and UV detection Spectrophotometric complexing reagents are widely used for visible spectral determination of many metals at low concentrations, but these complexes are seldom suited to HPLC. Pyridylazonaphthol complexes of copper, nickel and cobalt are separable by reversed-phase LC using acetonitrile/water/citrate buffer at pH 5 (80 : 18 : 2), 0.01 mol L^{-1} ammonium thiocyanate, and other such stable chelates are also amenable. In addition, non-absorbing species may be detected after conversion to chromophores by complexing, ion pairing or other chemical reactions. Neutral metal chelates such as beta-diketonates, beta-ketoaminates, dialkyldithiocarbamates and dialkyldithiophosphinates separable by GC may also be chromatographed by reversed-phase HPLC and less volatile complexes are also amenable to the technique.

Amperometric and differential pulse detection Dithiocarbamates of Cu(II), Ni(II), Co(II), Cr(III) and Cr(VI) have been detected amperometrically after HPLC separation. Although both the oxidation and reduction reactions of these organometallics are well defined, the ubiquitous presence of reducible oxygen dissolved in the polar solvent results in the oxidative process being more desirable. Knowledge of solvent, electrodes and electrochemistry is essential before a correct HPLC-EC protocol can be stated. Cancer chemotherapeutic drugs cisplatin, mitocynin C and mitoxanthrone are separable on C_{18} columns and are easily detected by oxidation, if the cisplatin oxidation

potential is shifted by 0.10 mol L^{-1} chloride to 0.80 V.

Detection selectivity may be improved by differential pulse detection as in the reversed-phase determination of alkyl- and aryl-mercurials, tri-*n*-butyl tin, triethyl tin and triphenyl tin.

Ion Pair Chromatography (IPC)

Combination of ion exchange and partition mechanisms and the performance of 5 and $10 \mu\text{m}$ C_{18} silica bonded phases give high performance ion separation in the direct and ion-paired modes. Pairing ions may be present in the mobile phase or retained on the surface. A C_{18} column coated with C_{20} alkyl sulfate gave baseline separation of Cu(II) , Co(II) and Mn(II) . The eluted metal ions were detected by absorption spectrophotometry at 530–540 nm after post-column reaction with 4-(2-pyridylazo)-resorcinol (PAR). Paired-ion HPLC separation of iron(II), nickel(II) and ruthenium as cationic 1,10-phenanthroline complexes with alkylsulfonic acids was achieved. Crown ethers can form stable complexes with metal cations, reversed-phase HPLC retention being dependent upon the relative size of the cation and the ring of crown ether. A typical elution order is $\text{Li}^+ < \text{Na}^+ < \text{Cs}^+ < \text{Rb}^+ < \text{K}^+$, and $\text{Mg}^{2+} < \text{Ca}^{2+} < \text{Sr}^{2+} < \text{Ba}^{2+}$.

Overall, the choice in inorganic column liquid chromatography is now between reversed-phase, including paired-ion, and ion chromatography, the former typically affording the better resolution.

HPLC-ICP-Mass Spectrometry (HPLC-ICP-MS)

The most extensively developed plasma mass spectral analytical technique is that of ICP-MS. The argon ICP acts as a mass spectral ion source; for a sample solution, after aerosol formation in a nebulizer and spray chamber, analyte is injected into the plasma where it undergoes desolvation, vaporization, atomization and ionization. A portion of the ions is sampled from the centre of the plasma and directed, through a low pressure interface, into the mass spectrometer. ICP-MS combines advantages of ICP-AES such as multi-element analysis, wide dynamic range and speed, with mass spectral acquisition, enhanced detection limits (typically $0.01\text{--}0.1 \text{ mg L}^{-1}$) and capability for isotopic analysis. In HPLC-ICP-MS detection limits as low as 100 pg/peak have been obtained for many elements. Ion exchange and ion pair chromatography were used for speciation of triorganotin species and arsenic speciation has been examined in a number of studies. The technique shows excellent prospects in biomedical and clinical studies in which analyte levels are usually below the capabilities of ICP emission

detection. Interfaced aqueous SEC with ICP-MS was used for element and isotope ratio detection of lead and copper in protein fractions of serum and blood cell haemolysate with molecular weight ranges from 11 kDa to $> 600 \text{ kDa}$ and detection limits in the $1\text{--}10 \mu\text{g L}^{-1}$ range for metallodrugs and their metabolites, measured in samples from patients undergoing gold drug therapy for arthritis. The elements mercury, arsenic, lead and tin have attracted most interest from the trace element environmental point of view.

Conclusions

High performance gas and liquid chromatography of metal compounds have always presented considerable challenges, but have in return provided many analytical and characterization insights, both qualitative and quantitative. In practical terms, the wider adoption of element-specific spectral detection depends on the continual development of commercial instrumentation to permit inter-laboratory comparisons of data and the development of 'recommended' methods of analysis which can be widely used. Many areas of analysis are subject to restrictions designed to ensure high levels of accuracy and precision. Fully integrated units which remove the need for analysts to interface their own GC, emission device and spectrometer may become as familiar in the future as GC-MS and GC-FTIR systems are today. Integrated HPLC and SFC systems will be longer delayed, but their eventual adoption is inevitable in view of the broad scope of these separation methods.

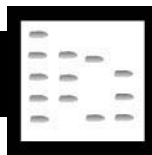
See also: II/Chromatography: Gas: Detectors: General (Flame Ionization Detectors and Thermal Conductivity Detectors); Detectors: Mass Spectrometry; Gas Chromatography-Infrared; Gas-Solid Gas Chromatography; Historical Development. Chromatography: Liquid: Detectors: Mass Spectrometry.

Further Reading

- Crompton TR (1982) *Gas Chromatography of Organometallic Compounds*. New York: Plenum Press.
- Guiochon G and Pommier C (1973) *Gas Chromatography in Inorganics and Organometallics*. Michigan: Ann Arbor.
- Krull IS (ed.) (1991) *Trace Metal Analysis and Speciation*. Journal of Chromatography Library, vol. 47. Amsterdam: Elsevier.
- Lederer M (ed.) (1984) *Separation Methods in Inorganic Chemistry*, Chromatographic Reviews, vol. 29. *Journal of Chromatography* 313: 1.
- McDonald JC (1985) *Inorganic Chromatographic Analysis*. New York: John Wiley.

- Michal J (1973) *Inorganic Chromatographic Analysis*. New York: Van Nostrand.
- Moshier RW and Sievers RE (1965) *Gas Chromatography of Metal Chelates*. Oxford, London: Pergamon.
- Schwedt G (1981) *Chromatographic Methods in Inorganic Analysis*. Heidelberg, New York: Huthig Verlag.
- Uden PC (1995) Element specific chromatographic detection by atomic absorption, plasma atomic emission and plasma mass spectrometry. *Journal of Chromatography* 703: 393.
- Uden PC and Henderson DE (1977) Determination of metals by gas chromatography of metal complexes – a review. *Analyst* 102: 889.

METAL COMPLEXES



Ion Chromatography

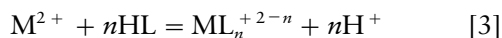
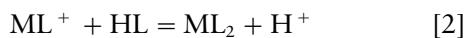
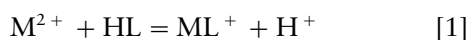
D. J. Pietrzyk, University of Iowa, Iowa City, IA, USA

Copyright © 2000 Academic Press

Introduction

Many different and clever methods have been reported in the literature for the separation of metal ions. Most involve chemical reactions in which complexes are formed between the hydrated metal ions and an inorganic or organic ligand. If an organic ligand is employed coordination is usually through oxygen, sulfur or nitrogen atoms, individually or in combination.

In a simplified representation the stepwise and overall formation of metal–ligand complexes can be represented by the following:



where M^{2+} is a divalent hydrated cation (acceptor) and HL is a monoprotic weak acid ligand (donor) that replaces the waters of coordination in a series of steps. The formation and dissociation of the metal–ligand (donor–acceptor) complexes proceeds, often rapidly, by a series of equilibrium reactions, each of which is defined by a formation constant. Because of the metal ion coordination number, the stepwise equilibria, the formation constant, and concentrations of the metal ion and ligand, a series of complexes (see the expression of the total equilibrium steps in eqn [3]) may coexist in the solution. When the ligand is neutral the charge of the resulting complexes are positive. However, the complexes may

associate with solution anions to produce neutral species. Ligands can also be anions, eqns [1]–[3], and thus the complexes that form can be cations, neutral or anionic, depending on the coordination number of the metal ion, the number of ligands bound to the metal ion, the formation constants for the complexes that form, and the metal ion and anionic ligand concentrations.

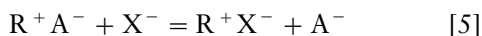
Conversion of a metal analyte into a complex is important in separations for two major reasons. First, the chemical and physical properties of the metal–ligand complex are sharply different than those of the metal ion hydrate. Solubility, ionic or polar character, and even volatility can be different. Formation constants for the metal–ligand complexes will differ and pH is often an important variable. Thus, the number of separation strategies that are applicable to the separation of metal ions are broadened and the number of variables that can be altered to bring about resolution in the separation of a complex mixture of metal ions is increased. Second, some metal–ligand complexes can be more easily detected, which improves quantitative estimation and even identification, than the metal ion hydrate. For example, metal–ligand complexes can be highly coloured, while some will fluoresce and/or have electrochemical properties that can be monitored.

Using complex formation between a ligand and metal ion to facilitate metal ion separations was an important strategy in the development of low efficiency liquid column chromatographic separations of metal ions, particularly in separations by ion exchange and partition column chromatography. Similarly, complex formation is a key elution parameter in high efficiency liquid column chromatographic separations. Each of these column strategies is briefly described in the following.

Ion Exchange

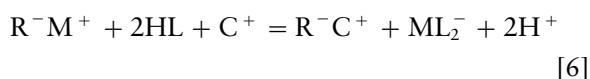
In ion exchange column chromatography the column is packed with either a cation exchanger, which will

exchange cations, or an anion exchanger, which will exchange anions. The exchangers are like insoluble electrolytes and exchange ions rapidly, reversibly and stoichiometrically. Cation exchange is represented in eqn [4] while eqn [5] illustrates anion exchange.



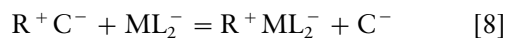
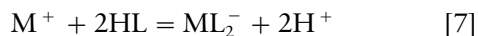
Here R is the ion exchanger matrix containing either an anionic or cationic ionogenic group, C^+ and A^- are co-cation and co-anion, respectively, and M^+ and X^- are the analyte cation and anion, respectively. The direction of the equilibrium in eqns [4] and [5] is determined by the selectivity coefficient for the exchanger towards the two competing ions. Thus, in the absence of mass action effects the exchanger will prefer the ion with the highest selectivity coefficient. For a mixture of analytes, for example a mixture of metal ions and a cation exchanger, the metal ion with the smallest selectivity coefficient would elute first and the metal ion with the largest selectivity coefficient would elute last when using a mobile phase containing an electrolyte that provides a cation of appropriate selectivity and concentration. To increase elution of the metal ion the electrolyte concentration in the mobile phase is increased, or a different electrolyte that provides a cation of higher selectivity is used.

While low efficiency metal ion separations are possible on cation exchangers, resolution is improved considerably when a ligand is included in the mobile phase and the separation occurs because of the properties of the metal complex. For example, elution of M^+ from the cation exchanger is enhanced with a mobile phase containing the ligand, HL, because of the formation of metal ion–ligand complexes. As shown in eqn [4], M^+ is retained on the cation exchanger through competition with the mobile phase cation C^+ . When the ligand is in the mobile phase, the ligand will form a complex with the metal ion, causing the equilibrium in eqn [4] to shift to the left with the formation of the metal ion–ligand complex. The overall effect of the ligand can be represented by eqn [6]:



From eqn [6] the best mobile phase ligand, assuming formation constants and solubility are favourable, will be one that forms anionic complexes with the metal ion.

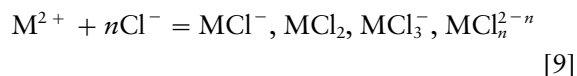
On the other hand, if the metal ion–ligand complex that forms is anionic, the complex can be retained by an anion exchanger, or



In this case the metal ion is subsequently removed from the anion exchanger by reversing the equilibrium in eqn [7], which is done by reducing the concentration of the ligand in the mobile phase. This causes the equilibrium in eqn [8] to shift to the left, thus removing the metal ion from the anion exchanger.

Low Efficiency Ion Exchange Separation of Metal Ions

In the 1940s ion exchange was recognized as an excellent strategy for the separation of metal ions. The advantages of including ligands in the mobile phase were soon realized and many different types of inorganic and organic ligands were evaluated to aid metal ion separations. Chloride ion was one inorganic ligand that was studied extensively. Many metal ions complex with Cl^- stepwise and the equilibria describing the stepwise formation of metal ion–chloride complexes are summarized by eqn [9]:



where the complexes that are present depend on the formation constants for the individual steps, the coordination number of the metal ion, and the Cl^- concentration. Depending on these factors, the metal analyte may be a cation, a neutral species or an anion. Thus, the charge of the metal-containing species may not only be altered but actually reversed and separation of the metals can become one of cations from anions.

Separation of metal ions is possible on either a strong acid cation exchanger or a strong base anion exchanger using a HCl mobile phase. With the cation exchanger increasing the HCl concentration shifts the equilibria represented by eqn [9] to the right, thus causing the metal analytes to elute from the cation exchange column as the metal chloro complexes (see eqns [4] and [6]). Those metals that form chloro complexes more readily (more favourable formation constants) will elute first.

The better resolution for metal ion separations is actually obtained when using a strong base type

anion exchanger with Cl^- as the mobile phase ligand. For the separation on an anion exchanger the mixture of metal ions is placed on the anion exchanger from a concentrated HCl solution. This converts the metal ions into chloro complexes (see eqn [9]) and these complexes are retained by the anion exchanger. The HCl concentration is then progressively reduced, the equilibria in eqn [9] shifts to the left, and the metal ions are removed from the column (see eqns [7] and [8]). In this case the more stable metal chloro complexes stay on the anion exchanger the longest and the least stable metal chloro complexes come off the earliest.

The retention of all the metal ions, some at several oxidation states, was determined on a strong base anion exchanger as a function of HCl concentration from $< 0.001 \text{ mol L}^{-1}$ to 12 mol L^{-1} HCl. These data allow one to predict elution order and conditions for the separation. Table 1 summarizes some of these results by listing the elution order for several metal ions on the anion exchanger from 12 mol L^{-1} HCl to dilute HCl. As HCl concentration in Table 1 is reduced, those metal ions above the HCl concentration listed are eluted while those below are retained on the exchanger. Many metal ion separations, including complex mixtures, are possible with the HCl eluent. Figure 1 shows the separation of the transition elements on a strong base anion exchanger by a successive decrease in mobile phase HCl concentration. The column was $26 \text{ cm} \times 0.29 \text{ cm}^2$ and about 6 mg of each cation was separated. Each metal ion was collected and its quantity was determined by chemical or instrumental methodology. Mn^{2+} was determined spectrographically, Fe^{3+} and Zn^{2+} were radioactive tracers and were determined by radioactivity, and Co^{2+} , Ni^{2+} , and Cu^{2+} were determined spectrophotometrically.

Table 1 Elution order for common metal ions on a strong base anion exchanger with an HCl mobile phase

Mobile phase HCl concentration (mol L^{-1})	Metal ion
12	Not retained: Ni^{2+} , Al^{3+} , lanthanoids, Th^{4+} Slight retention: Sc^{3+} , As^{5+} , Cr^{3+} , Mn^{2+}
9.5	Ti^{4+}
8	Hf^{4+}
7.5	Zr^{4+}
7	Fe^{2+}
6	U^{4+}
4.5	Co^{2+} , As^{3+}
3	Cu^{2+}
1	UO_2^{2+} , Fe^{3+}
0.02	Zn^{2+}
0.001	Cd^{2+}

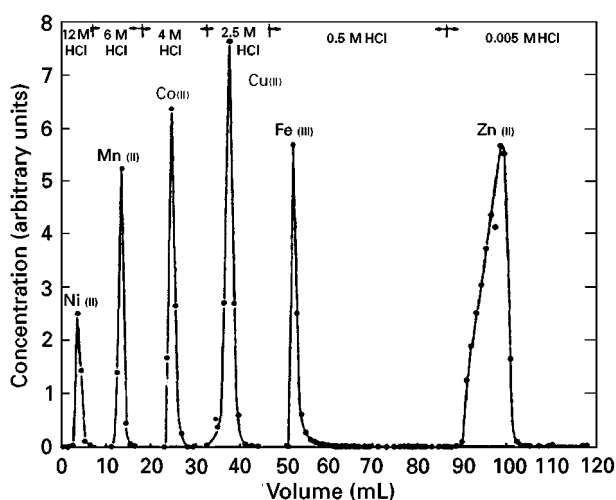


Figure 1 Separation of transition elements on a strong base anion exchanger from an HCl mobile phase. $\text{M} = \text{mol L}^{-1}$. (Reproduced from Kraus and Moore, 1953. Reprinted by permission of American Chemical Society.)

Success with chloride ion as the eluent ligand led to studies with many other inorganic ligands. Like Cl^- , F^- is also an important mobile phase ligand and was employed in a mobile phase that was 1 mol L^{-1} HF as a function of HCl concentration. The presence of the F^- is particularly useful because it forms complexes with Group IV and V elements such as Zr^{4+} , Hf^{4+} , Nb^{5+} and Ta^{5+} and aids their separation. Other inorganic ligands have also been shown to be useful but typically do not have the broad scope of applications characteristic of the HCl and HCl/HF elution systems. These ligands include NO_3^- , SO_4^{2-} , Br^- , I^- , SCN^- , CO_3^{2-} and CN^- . While the analytical applications of these ligands may be limited, several have been shown to be particularly useful in commercial recovery and purification applications, for example the isolation of uranium and thorium from low grade ores. Figure 2 illustrates an elution diagram that was used for the separation of a multicomponent high temperature alloy on a strong base anion exchanger using a combination of the HCl and HCl/HF elution scheme. Note that the column dimensions and sample size of 1 g are large and by today's standards this would be called a prep column and separation. Because each metal analyte was separated in such a large quantity each metal ion was determined by chemical methodology, namely by ethylenediaminetetraacetic acid (EDTA) titration or by gravimetry.

Organic ligands have been used in eluents to improve resolution in low efficiency ion exchange metal ion separations. Iminodiacetic acid, nitrilotriacetic acid and EDTA are examples of mobile phase ligands that have been used that form very stable complexes with many metal ions, while citric

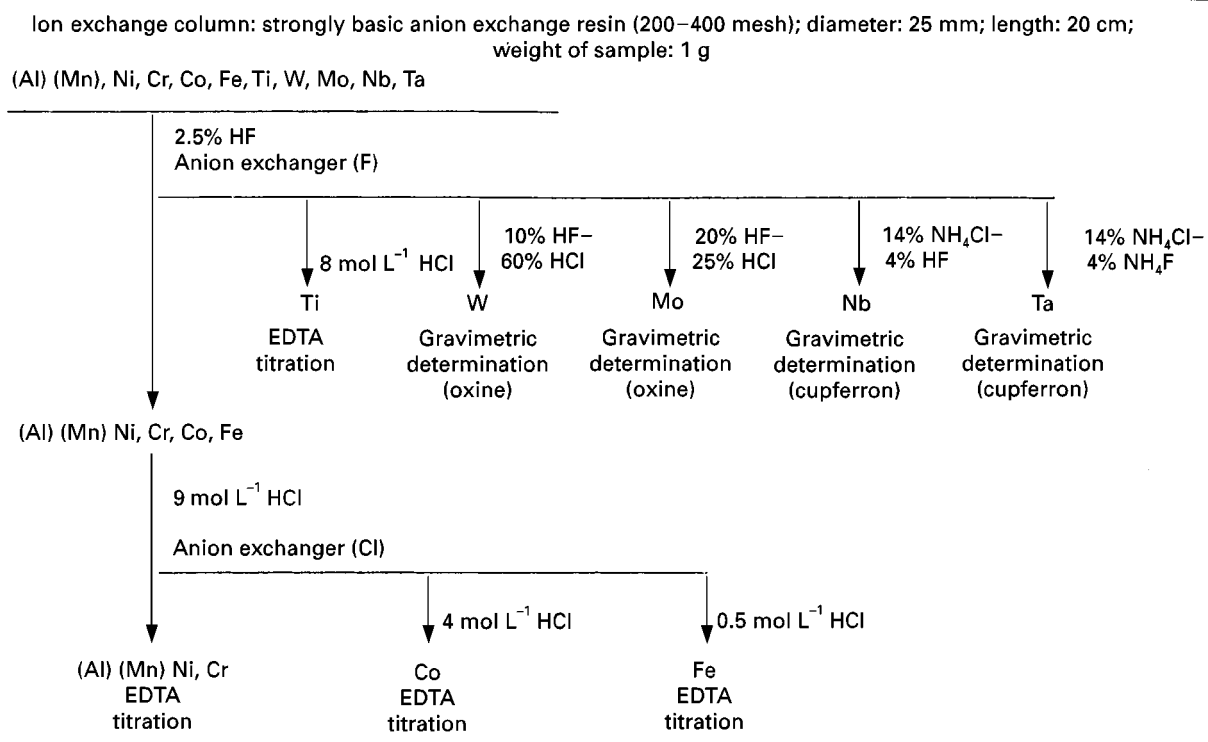


Figure 2 A flow diagram for the separation of a high temperature alloy on a strong base anion exchanger. The anion exchanger is a 40–75 μm , 2.5 cm \times 20 cm strong base anion exchange column and the sample size is about 1 g. (Reproduced from Wilkins, 1959. Reprinted by permission of Pergamon Press Ltd.)

acid, tartaric acid, malonic acid, oxalic acid, diglycolic acid and α -hydroxyisobutyric acid (HIBA) are examples of useful ligands that form metal ligand complexes of modest stability. In addition to formation constants, pH is also an important mobile phase variable that can be optimized to enhance resolution because all of these ligands are weak acids. Another mobile phase parameter that can be altered to influence elution is to use a mixed solvent for the mobile phase. The presence of the organic solvent in the mixture has a pronounced effect on the formation constants for the complexes as well as the exchange equilibrium with the exchanger. The type of organic solvent and its concentration then become variables in influencing elution time and resolution.

The unique complexing properties of organic ligands have been used to isolate and concentrate metals from ores and other geological samples. For example, one of the more successful applications of this kind was the isolation and separation of the lanthanoids on cation exchangers from mobile phases containing an organic ligand. Prior to this development individually pure lanthanoids were not readily available. Similar success was subsequently achieved in the isolation and purification of uranium and other actinoids, hafnium and zirconium, and many other less familiar metals from natural occurring ores and minerals.

Table 2 lists several elution conditions that have been used for the low efficiency separation of lanthanoids on anion or cation exchangers using a ligand in the mobile phase. The separation of the lanthanoids on a strong acid cation exchanger with lactate as the mobile phase ligand and a small pH increase during the elution is shown in Figure 3. Each lanthanoid was collected in a series of fractions and the lanthanoid in each fraction was determined spectrophotometrically by complex formation with 1-(2-pyridylazo)-2-naphthol (PAN). The pH and the formation constants for the lactate complexes determine the elution order. When HIBA is used as the ligand instead of lactate, the same elution order is obtained for the lanthanoids. In another example cation exchange was used to separate 35 metal ions into six separate groups by using mobile phase ligands citric acid, *N*-hydroxyethyl(ethylenedinitrilo)triacetic acid, EDTA, HCl and pH control in a predetermined elution programme.

Ligands in the Separation of Metal Ions by Partition Chromatography

Column liquid-liquid partition chromatography of metal ions can be one of two types. In one case the stationary phase is a nonaqueous immiscible solvent

Table 2 Mobile phase ligand conditions used for the separation of the lanthanoids on anion and cation exchangers

Mobile phase conditions	Exchanger	Application
HIBA at pH = 5.2	Cation	Early lanthanoids
HIBA at pH = 4.7	Cation	Lanthanoid radionuclides
HIBA, pH gradient from 3.4 to 4.0	Cation	Lanthanoids and fission products
0.24 mol L ⁻¹ lactate at 87°C	Cation	Lanthanoids
1.1–1.25 mol L ⁻¹ lactate and 3.1 to 3.25 pH gradient at 87°C	Cation	Lanthanoids
Ammonium lactate gradient at pH 5 and 95°C	Cation	Radiochemical separation of lanthanoids from fission products
26 mmol L ⁻¹ EDTA at pH 3.62 and 87°C	Cation	Ce, Pr, Nd, Sm, La
5–6 mol L ⁻¹ HNO ₃	Anion	La, Ce, Pr group separation
EDTA	Anion	Lanthanoids
Citrate	Anion	Lanthanoids

held up by an inert support and the mobile phase is usually an aqueous solution containing electrolyte, buffer, and a ligand. This type of column chromatography is called liquid–liquid reversed-phase partition chromatography (RPPC). The other strategy is the opposite – the stationary phase liquid is a polar or aqueous solvent held up by the inert support and the mobile phase is an immiscible organic solvent or solvent mixture of less polarity. In both cases the additives cause the metal ions to distribute between the two phases as the metal ions pass through the column. Separation occurs because of differences in the equilibrium positions imposed by the additives, namely the ligand, the resulting formation constants, the pH, and the properties of the two solvents that make up the two phases.

These techniques, which may also be carried out with solvent combinations that are partially miscible suffer from gradual changes in the stationary phase liquid over prolonged column use. This means it is difficult to maintain or reproduce a uniform,

constant stationary liquid phase, sometimes even in a single elution run and often over repeated runs. Even solvents that are thought to be completely immiscible will have a low level equilibrium distribution of one solvent into the other when they are brought together. Thus, the stationary liquid phase will be slowly removed (solvent bleed) from the inert support.

Because of solvent bleeding high efficiency liquid–liquid partition chromatography is rarely used and as a separation strategy it has been replaced by high efficiency reversed-phase and normal-phase column chromatography. Nevertheless, many difficult separations of metal ion mixtures are possible by RPPC and RPPC can be readily applied to cases where the chromatographer needs to separate large quantities of metal ions and is not faced with requirements of short analysis times, the best detection limits, and/or regulatory method controls. Several examples of RPPC described below illustrate the scope of using ligands in RPPC separations of metal ions.

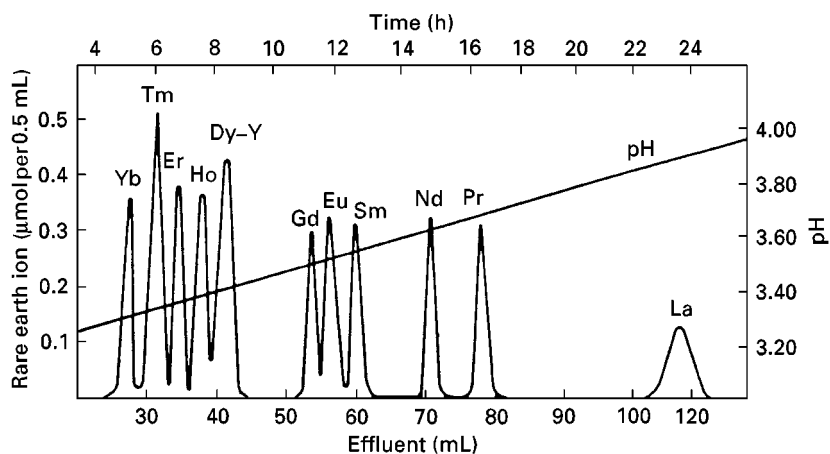


Figure 3 Separation of the lanthanoids on a strong acid cation exchanger. The cation exchanger column is a 40–75 μm, 0.5 cm × 100 cm column at 80°C and the mobile phase is a lactate buffer solution and pH gradient at about 0.7 mL min⁻¹. (Reproduced from Inczédy, 1966, p. 166. Reprinted by permission of Pergamon Press Ltd.)

Table 3 Selected applications of porous organic copolymers as support materials for the partition chromatographic separation of metal ions^a

<i>Metals</i>	<i>Porous polymer</i>	<i>Extraction system</i>
27 metal ions	XAD-2	Isopropyl ether/HCl Isobutylmethyl ketone/HCl Trioctylphosphine oxide/HCl Isobutylmethyl ketone/HBr Dioctyl sulfoxide/1,2-dichloroethane Aliquat 336 liquid anion exchanger/ toluene/H ₂ SO ₄
Ga, In, Th	XAD-2	Aliphatic α -hydroxyoxime/toluene
U ⁶⁺	XAD-2	5,8-Diethyl-7-hydroxydecane-6-one oxime/toluene
Mo ⁶⁺ , W ⁶⁺ , V ⁶⁺	XAD-2	HCl/H ₂ O
Cu	XAD-2	Kelex 100/H ₂ O
Mo ⁶⁺	XAD-2	Dithiozone/dibutyl phthalate
Au	XAD-2	Monothiobenzoylmethane/heptane
Fe, Cu	XAD-7	
Zn, Cd, Hg	Macroporous polystyrene-divinylbenzene	
Ni, Fe, Co	Ethylstyrene-divinylbenzene	

^aReproduced from Pietrzyk, 1989, p. 144. Reprinted by permission of Wiley-Interscience.

RPPC shares many features with solvent extraction and a wealth of information is available in the literature on the solvent extraction of metal–ligand complexes from one phase to another. In most cases a successful extraction depends on the properties of the complex that forms between the ligand and the metal ion. Complex formation constants, metal coordination, solubility of the ligand in the aqueous phase and the nonaqueous phase, solubility of the complex in each of the two phases, and pH are the main factors that determine the percent extraction and the selectivity in the extraction, and consequently the ability to resolve one metal ion from another. These same factors influence metal ion resolution in RPPC and must be optimized to obtain a successful separation.

Two of the more successful inert stationary phases for RPPC are polystyrene–divinylbenzene and acrylic acid-based macroporous copolymers. These are capable of holding up appreciable quantities of nonpolar organic solvents, many of which are desirable for partitioning procedures. Table 3 lists several RPPC quantitative metal ion separations that have been carried out where an inorganic or organic ligand is employed in the two-phase system to complex metal ions and bring about resolution on either the styrene or acrylic acid-type copolymers as the inert stationary phase.

Chelating Ion Exchanger

Instead of adding a ligand to the mobile phase, a chelating group can be chemically bound to a solid, inert matrix. In this case coordination occurs between the metal ion and the bound chelating group. Resolution is possible because of differences

in formation constants for the differential metal complexes that form with the stationary phase-bound chelating group, the mobile phase pH, and the ionic strength. Employing a second chelating group or ligand in the mobile phase to establish a competition between the bound chelating group and the mobile phase ligand towards the metal ion analytes is also an excellent elution procedure to effect resolution of the metal ion mixture.

Chelating ion exchangers often have several disadvantages, even though metal ion retention can be high and selectivity can be favourable. First, the kinetics for the exchange or dissociation of the metal ion from the chelating group bound to the stationary phase can be slow, and this causes poor elution behaviour. Second, few chelating ion exchangers are commercially available. One notable exception is a chelating ion exchanger that has the iminodiacetic acid group, $-\text{CH}_2\text{N}(\text{CH}_2\text{CO}_2\text{H})_2$, attached to a polystyrene–divinylbenzene copolymer. And third, because most chelating ion exchangers have to be synthesized in the laboratory, reproducibility from column to column is only fair. Furthermore, column efficiency in analytical separations is rarely exceptional because the kinetics are usually not favourable.

The major advantage of a chelating ion exchanger, which is very important to environmental and ultra-trace metal analysis, is that the exchanger can be used to isolate trace levels of metal ions from samples and/or to concentrate the trace metal ions prior to their determination. This has been proven to be particularly valuable for the isolation/concentration of metal ions other than the Group I metal ions, particularly transition metal ions, the lanthanoids and the actinoids. Often this can be done from solutions that may contain substantial quantities of

Table 4 Chelating ion exchangers

<i>Chelating group</i>	<i>Chelating group</i>
Anthranilic acid	<i>N</i> -substituted hydroxylamine
Arsonic acid	8-Hydroxyquinoline
Crown ether	Iminodiacetic acid
β -Diketone	Isothiuronium
Dimethylglyoxime	Nitrilotriacetic acid
Dithiocarbamate	Rescorinol
Dithiozone	Salicylic acid
Ethylenediaminetetraacetic acid	Thioglycolate
Hydroxyamic acid	

monovalent electrolyte, for example brine solution, boiler water and sea water. Table 4 lists several chelating ion exchangers that have been synthesized in the laboratory and some typical applications of these chelating ion exchangers.

High Efficiency Column Chromatographic Separation of Metal Ions and the Influence of Ligands on their Resolution

The analytical chemistry and role of the ligand in high efficiency or high performance liquid column chromatographic (HPLC) separations of metal ions is much the same as in low efficiency liquid column chromatographic separations. Mobile phase concentration of reagents including the ligand and metal ion analyte concentration are much lower due to more favourable chromatographic properties of high efficiency columns. Selectivity, retention, and particularly detection limits are improved. Formation constants, stepwise equilibria, coordination number, and formation of positive, anionic or neutral complexes are still crucial factors that influence separation. In addition, the rate of complex formation and dissociation is a major contributing factor because of the significant increase in linear velocity of the analyte in the high efficiency column.

Cation exchangers, anion exchangers, chelating exchangers, and reversed stationary phases are the major column stationary phases that are employed in high efficiency metal ion analyte separations. These modern, high efficiency stationary phase particles are available as small (5 and 10 μm), uniform, and spherical-sized particles of considerable physical strength that can be packed uniformly and reproducibly into columns to yield very favourable mass transfer, and thus high efficiency. All of these are properties that the column must possess in order to exhibit high efficiency. Columns that satisfy these criteria are commercially available.

Examples illustrating the scope of modern applications of ligands to improve the resolution in the separation of metal ions on high efficiency columns of cation and anion exchangers, reversed stationary phases and chelating exchangers are outlined in the following sections.

High Efficiency Cation Exchangers

Metal ions, particularly multivalent cations, are highly retained on high efficiency strong acid-type cation exchangers, even though exchange capacities may be very low. One approach to elute metal ions, particularly multivalent cations, from the cation exchanger is to use a mobile phase cation derived from ethylenediamine, $\text{H}_2\text{NCH}_2\text{CH}_2\text{NH}_2$, (En). In an acidic solution En, which is basic, will exist as the dication, $^+\text{H}_3\text{NCH}_2\text{CH}_2\text{NH}_3^+$ (H_2En^{2+}), providing the pH is low enough. Thus, the eluent strength of the mobile phase is determined by the mobile phase H_2En^{2+} concentration and metal ion analyte elution on a typical high efficient cation exchanger follows ordinary cation exchange. A second approach is to use a ligand in the mobile phase. A successful ligand is one that will form neutral or anionic complexes with the analyte metal ions that are stable (formation constants will influence elution order) and form and dissociate rapidly. It should be noted that although En is a ligand for many multivalent cations, in the diprotonated form its complexing ability is sharply reduced. When a ligand, for example citric acid, which forms complexes with metal ions, is included in the buffered mobile phase along with the H_2En^{2+} , resolution now depends on pH. This influences dissociation of citric acid (and also the eluent cation H_2En^{2+} and its potential complexing ability), the formation constants for the metal ion citrate complexes (and metal ion En complexes if they form), and the concentration of the citric acid ligand. The more stable the metal ion citrate complex and the higher the concentration of the citrate, the more quickly the metal ions are eluted. Figure 4 illustrates the high efficiency separation of several divalent metal ions on a strong acid high efficient cation exchanger using the combined effect of citrate as the ligand and H_2En^{2+} as a divalent mobile phase cation. A similar separation is possible using tartrate or oxalate rather than citrate as the mobile phase ligand.

Because complex formation constants differ, small differences in selectivity and elution order are obtained when the elution behaviour of citrate, tartrate and oxalate as ligands are compared. Consequently, metal ion elution order and selectivity for given metal ions, for example for transition metals, can be changed through the selection of the ligand.

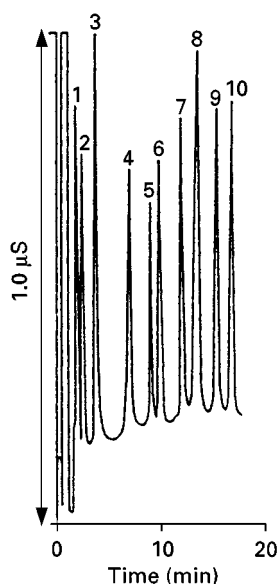


Figure 4 Separation of alkali, alkaline earth, and transition element metal ions on a cation exchanger. The column is a TSK IC cation SW column and the mobile phase is $3.5 \text{ mmol L}^{-1} \text{ H}_2\text{EN}^{2+}$, 10 mmol L^{-1} citric acid, pH 2.8, at a flow rate of 1.0 mL min^{-1} with conductivity detection. Peaks are: 1, Na^+ ; 2, K^+ ; 3, Cu^{2+} ; 4, Ni^{2+} ; 5, Co^{2+} ; 6, Zn^{2+} ; 7, Fe^{3+} ; 8, Mn^{2+} ; 9, Cd^{2+} ; 10, Ca^{2+} . (Reproduced from Timberbaev and Bonn (1993). Reprinted by permission of Elsevier Science Publishing.)

Figure 5 illustrates the separation of several transition metals using a mobile phase that contains both oxalate and citrate as ligands and gives an elution order slightly different from the order obtained in Figure 4. Metal ion complex formation is also very important in detection in high efficiency ion exchange separations of metal ions. In Figure 5 the metal ions are converted into complexes post-column online by reaction of the metal ion with 4-(2-pyridylazo)resorcinol (PAR) and the complex is detected by absorbance at 520 nm.

HIBA at pH 4.6 is a good ligand to use to separate lanthanoids on a cation exchanger. This separation is shown in Figure 6, where a gradient of $0.018\text{--}0.070 \text{ mol L}^{-1}$ HIBA is used for the elution of the lanthanoids on a Nucleosil SCX column, a sulfonated bonded phase-type cation exchanger. In Figure 6 detection was by a postcolumn reaction, which produces the highly coloured complex between the ligand, 3-(2-arsenophenylazo)-4,5-dihydroxy-2,7-naphthalene disulfonic acid trisodium salt (Arsenazo 1) and each of the lanthanoids as they are separated. If H_2En^{2+} is also included in the mobile phase with HIBA, separation of the first seven lanthanoids is obtained without employing an HIBA mobile phase gradient.

The properties of the cation exchanger used in the column will also influence the selectivity, even caus-

ing a reversal. For example, Figure 5 is a separation on a surface-sulfonated cation exchanger, while the cation exchanger used in Figure 4 is a surface/interior-sulfonated cation exchanger.

The latex-based exchanger affects elution order when ligands are used in the mobile phase because of the exchanger's composition. The latex-based cation exchanger, which is commercially available from the Dionex Corporation, for example Ion Pac CS5, is composed of a surface-sulfonated substrate as its central core, uniformly coated with a thin layer of aminated latex particles. This basic surface is then coated by a thin, uniform layer of sulfonated latex particles. The cation exchanger groups ($-\text{SO}_3\text{H}$) are on the surface while the aminated or anion exchange groups ($-\text{NR}_4^+$) are in the interior

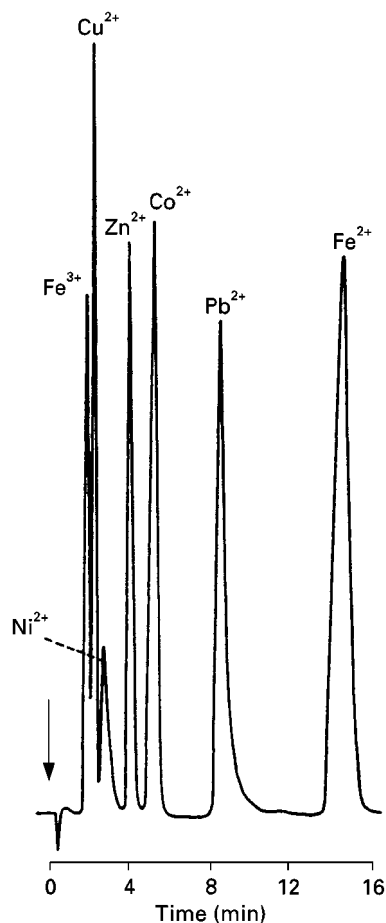


Figure 5 Separation of the transition element metal ions on a surface-sulfonated cation exchanger. The column is an Ion Pac CS2 column and the mobile phase is 0.01 mol L^{-1} oxalic acid, $0.0075 \text{ mol L}^{-1}$ citric acid, pH 4.2, at a flow rate of 1.0 mL min^{-1} . Detection is postcolumn absorbance at 520 nm after reaction with PAR. Sample injection is 50 μL containing 5 ppm Fe^{3+} , 0.5 ppm Cu^{2+} , 0.5 ppm Ni^{2+} , 0.5 ppm Zn^{2+} , 1 ppm Co^{2+} , 10 ppm Pb^{2+} , and 5 ppm Fe^{2+} . (Reproduced from Weiss, 1995, p. 197. Reprinted by permission of VCH Publishers.)

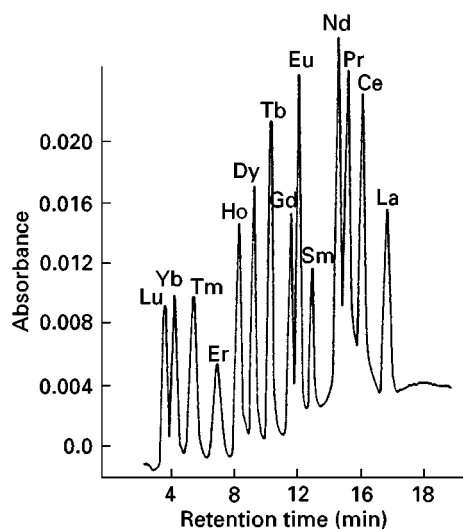


Figure 6 Separation of the lanthanoids on a sulfonated silica-bonded phase cation exchanger. The column is a 10 μm , 0.4 cm \times 10 cm, Nucleosil 10 SA column and the mobile phase is a linear gradient of 0.018 mol L⁻¹ to 0.070 mol L⁻¹ HIBA at pH 4.6. Sample injection is 10 μL containing about 10 $\mu\text{g mL}^{-1}$ of each lanthanoid. (Reproduced from Elchuk and Cassidy, 1979. Reprinted by permission of American Chemical Society.)

of the particle. Thus, the observed elution for metal ions on the Ion Pac CS5 will be influenced by both cation and anion exchange and the equilibria that favour cationic or anionic metal–complex formation. For example, the transition metal elution order in **Figure 7** on the Ion Pac CS5 column with oxalate as a mobile phase ligand is quite different from the order found in either **Figure 4** or **5** and is due to retention of anionic oxalate complexes that form between several of the transition metal ions and oxalate. When the Ion Pac CS5 column is used with a mobile phase containing pyridine-2,6-dicarboxylic acid (PDCA) as the ligand at pH 4.8, the elution order that is obtained is similar to that obtained by the sulfonated, nonlatex-type cation exchangers used in **Figures 4** and **5**.

High Efficiency Anion Exchangers

Some ligands will form very stable complexes with metal ions that are also anionic. It is often possible in these cases to separate the anionic metal–ligand complexes on high efficiency anion exchangers. For example, transition metal–PAR complexes are anionic and these complexes can be separated at high efficiency. Since the complexes are also highly coloured, detection of the separation is readily done at favourable detection limits by absorption. In another example the anionic complexes that form between multivalent cations and EDTA are anionic at the appropriate pH and can also be separated on

anion exchangers using an $\text{HCO}_3^-/\text{CO}_3^{2-}$ mobile phase that is common to ordinary ion chromatographic separation of anionic analytes. The basic requirement of the formation of a very stable anionic complex between the metal ion and the ligand is often a limiting factor and for this reason separation of metal ions in the presence of a ligand on a high efficiency cation exchanger is often a more versatile separation strategy.

The latex-based cation exchanger that possesses both cation and anion exchanger properties, such as the Ion Pac CS5, however, does provide a way to separate metal ion mixtures in the presence of mixed ligands where both cation and anion exchange are involved. This is illustrated in **Figure 8**, where both transition metals and lanthanoids are separated in one run on the high efficiency Ion Pac CS5 column using a complex gradient at the appropriate pH where the concentration of the ligands oxalic acid, diglycolic acid and PDCA are varied as a function of elution time. The PDCA causes the elution of the transition metals to be similar to that found on the

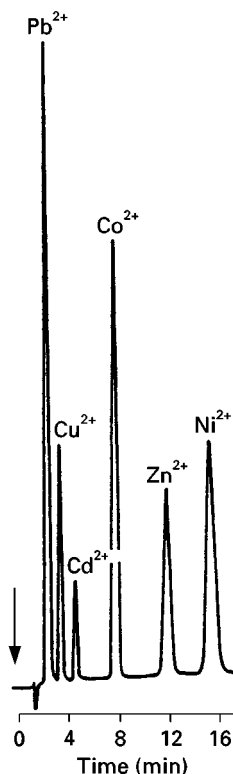


Figure 7 Separation of several transition element metal ions with oxalic acid as the mobile phase ligand. An Ion Pac CS5 column and a 0.5 mol L⁻¹ oxalic acid, pH 4.8, mobile phase at 1 mL min⁻¹ was used. Injection volume was 50 μL and contained 4 ppm Pb²⁺, 0.5 ppm Cu²⁺, 4 ppm Cd²⁺, 2 ppm Co²⁺, 2 ppm Zn²⁺, 4 ppm Ni²⁺. (Reproduced from Weiss, 1995, p. 199. Reprinted by permission of VCH Publishers.)

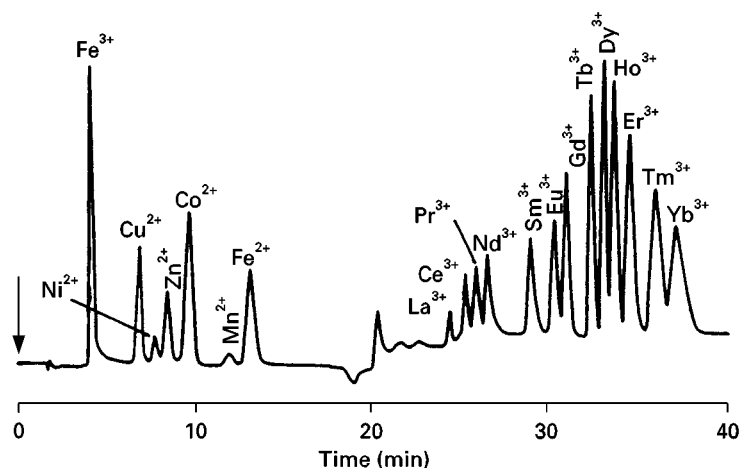
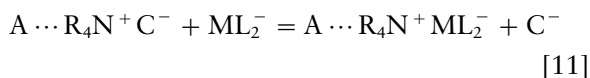
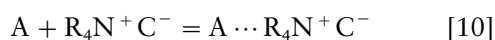


Figure 8 Separation of the transition elements and lanthanoid metal ions using a three-ligand mobile phase. An Ion Pac CS5 column and a mobile phase gradient of PDCA, oxalic acid, diglycolic acid, and LiOH for pH adjustment at 1 mL min^{-1} was used. Injection volume was $50 \mu\text{L}$ and contained 2 ppm Fe^{3+} , 1 ppm Cu^{2+} , 3 ppm Ni^{2+} , 4 ppm Zn^{2+} , 2 ppm Co^{2+} , 1 ppm Mn^{2+} , 3 ppm Fe^{2+} , 7 ppm of each lanthanoid. (Reproduced from Weiss, 1995, p. 205. Reprinted by permission from VCH Publishers.)

sulfonated cation exchanger (see Figure 5), while the lanthanoids remain on the column as trivalent anions. In the later stages of the gradient oxalic acid and diglycolic acid become more significant in concentration and cause the lanthanoids to be eluted in reverse order to that obtained by the high efficiency cation exchange separation of the lanthanoids (see Figure 6). If only the lanthanoids are to be separated, they can be separated in the order shown in Figure 8 on the Ion Pac CS5 column in about 25 min with the oxalic acid/diglycolic acid gradient. Detection is also made possible by the formation of metal complexes. In this example effluent from the column is combined with PAR to give the highly coloured metal ion–PAR complexes, which are readily detected by absorbance at 520 nm.

Reversed Phase

Separation of metal ions as anionic complexes on high efficiency reversed stationary phases, such as a C_{18} bonded phase silica or a polystyrene–divinylbenzene copolymer, requires a mobile phase that must also include an ion interaction reagent, for example a quaternary ammonium salt ($\text{R}_4\text{N}^+\text{C}^-$) having lipophilic character. The metal ion–ligand anionic complex interacts with the $\text{R}_4\text{N}^+\text{C}^-$, which in turn interacts with the reversed stationary phase, A, as shown below:



where M^{2+} is the metal ion analyte and ML_2^- represents the anionic metal–ligand complex. The direction of the equilibrium and subsequently the elution of the metal–ligand complex is controlled by the selection of the reversed stationary phase and the $\text{R}_4\text{N}^+\text{C}^-$ salt, the concentration of the $\text{R}_4\text{N}^+\text{C}^-$ salt, the counteranion X^- and its concentration via inert electrolyte, pH, solvent composition, the ligand, and the ligand concentration. This chromatographic strategy, or ion interaction chromatography (IIC), is known by several different terms and has been the subject of many studies to establish the nature of the interactions between the analyte, mobile phase components and stationary phase that are present. Clearly, several equilibria are involved and the success of the separation strategy in analytical applications requires careful control of all the equilibria.

Transition metal–PAR complexes are anionic and separations of these anionic complexes are possible on a reversed stationary phase. Other ligands can be used; the most useful ones are ligands that form kinetically stable anionic complexes with very high formation constants. Often the complexes are highly coloured and/or fluoresce and these properties allow sensitive detection.

Inorganic ligands that form very stable anionic complexes with metal ions can be used in a mobile phase that also contains a $\text{R}_4\text{N}^+\text{C}^-$ salt to separate the metal ions as complexes on a reversed stationary phase. Figure 9 illustrates the separation of transition metals as anionic cyanide complexes on a C_{18} reversed stationary phase column using a $\text{R}_4\text{N}^+\text{C}^-$ (Waters PICA additive) mobile phase. Detection in this separation is by absorbance at 214 nm.

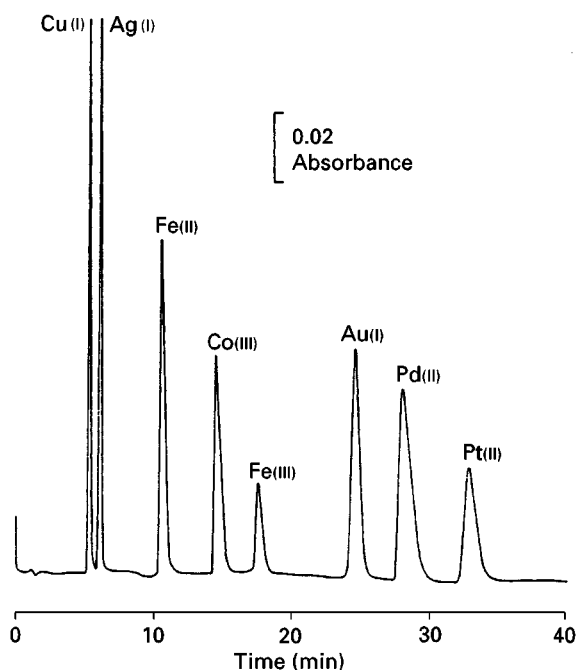
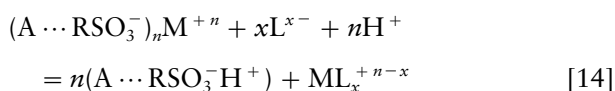
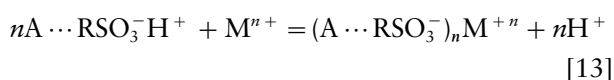
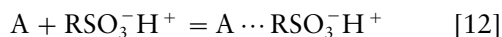


Figure 9 Ion interaction chromatographic separation of metal ions as cyano complexes. A 5 μm , 0.39 $\text{cm} \times 15 \text{ cm}$, Waters Nova Pak C_{18} column and an $\text{H}_2\text{O}/\text{CH}_3\text{CN}$ (23 : 77) 5 mmol L^{-1} tetramethylammonium hydroxide mobile phase at 1.0 mL min^{-1} was used. Sample injection was 10 μL and contained 0.15 $\mu\text{g Cu}^{1+}$, 1.5 $\mu\text{g Ag}^{1+}$, 0.02 $\mu\text{g Fe}^{2+}$, 0.2 $\mu\text{g Co}^{3+}$, 0.3 $\mu\text{g Fe}^{3+}$, 2.0 $\mu\text{g Au}^{1+}$, 0.4 $\mu\text{g Pd}^{2+}$, 0.2 $\mu\text{g Pt}^{2+}$ as cyano complexes. (Reproduced from Hilton and Haddad, 1986. Reprinted by permission from Elsevier Science Publishing.)

IIC with an anionic lipophilic reagent, such as an alkane sulfonic acid (RSO_3^-H^+), is also an important strategy for the high efficiency separation of metal ions. However, in this case the ligand in the mobile phase removes the metal ion from the reversed stationary phase according to the metal ion–ligand complex formation constants. The equilibria that are involved and which must be controlled for a successful separation are represented below (equilibria for complex formation are not shown – see eqns [1]–[3] where L is CN^-):



where A is the reversed stationary phase, RSO_3^-H^+ is the lipophilic ion interaction reagent, M^{n+} is the metal analyte ion, and L^{x-} is the mobile phase liquid.

Examples where this separation strategy has been successfully used are in the separation of transition metals or lanthanoids on a C_{18} stationary phase and octanesulfonic acid as the IIC reagent in the buffered mobile phase. The former metal analytes are eluted with tartrate in the RSO_3^-H^+ mobile phase and the elution order is Cu^{2+} , Pb^{2+} , Zn^{2+} , Ni^{2+} , Co^{2+} , Mn^{2+} , which differs from the tartrate elution of these cations on the sulfonated cation exchange column and the latex-based exchanger (see Figures 4, 5 and 7). The lanthanoids are separated by including the ligand HIBA in the RSO_3^-H^+ mobile phase and the elution order is the same as that indicated in Figure 6.

High Efficiency Chelating Exchangers

Few high efficiency chelating exchangers are commercially available. Even though various chelating groups have been chemically bonded to high efficiency silica or polystyrene–divinylbenzene copolymer particles, and metal ion retention is very high on these stationary phase particles, efficiencies generated on these columns are usually not comparable to efficiencies found for metal ion–ligand separations on ion exchangers or by reversed-phase ion interaction chromatography. In general, high efficiency is difficult to obtain, even when the core particle of the chelating exchanger meets high efficiency properties, because the complex between the metal ion and the bound chelating group often forms and dissociates slowly. Thus, metal ion analyte bands in elution can be broadened appreciably.

Using a ligand in the mobile phase to aid elution can sometimes reduce the analyte peak broadening. For example, the separation of transition metal ions on a high efficiency silica particle containing chemically bound iminodiacetic acid groups was achieved by using citrate, tartrate, nitrilotriacetic acid or PDCA in the buffered mobile phase. Since two complexing reactions are taking place, the metal ion elution order is dependent on the formation constant for the metal ion complex with the bound chelating group and with the mobile phase ligand in addition to pH. Other laboratory synthesized chelating exchangers where the chelating group (several of these are listed in Table 4) is bound to a high efficiency matrix, such as silica, have been evaluated for metal ion separations.

While metal ions can be separated on chelating ion exchangers, the more useful applications of chelating exchangers is still one of isolating and preconcentrating of metal ions from a complex sample matrix. Metal ions can be preconcentrated from biological samples, environmental samples and concentrated electrolyte solutions, such as seawater, brine and

other industrial waters, and strong alkali solutions. It is possible to automate fully the preconcentration and separation/analysis procedure. In an example of this trace levels of Mg^{2+} , Ca^{2+} and transition metals in biological and environmental samples are preconcentrated on two iminodiacetic acid-type chelating ion exchanger and one strong acid cation exchanger connected in series. The preconcentrated metal ions are then removed from the three columns and the concentrated metal ion mixture is separated on an analytical Ion Pac CS5 column by an elution programme that takes into account pH, ammonia/ammonium ion buffer concentration and PDCA concentration. Detection is by absorption after postcolumn reaction of the metal ions with PAR.

See also: II/Chromatography: Liquid: Mechanisms: Ion Chromatography. **Extraction:** Analytical Inorganic Extractions. **Ion Exchange:** Theory of Ion Exchange. III/Ion Analysis: Liquid Chromatography.

Further Reading

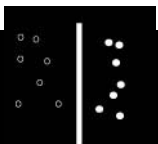
- Barkley DJ, Blanchette M, Cassidy RM and Elchuk S (1986) Dynamic chromatographic systems for the determination of rare earths and thorium in samples from uranium ore refining processes. *Analytical Chemistry* 58: 2222–2226.
- Cagniant D (1992) *Complexation Chromatography*. New York: Dekker.
- Elchuk S and Cassidy RM (1979) Separation of the lanthanides on high-efficiency bonded phases and conven-

- tional ion-exchange resins. *Analytical Chemistry* 5: 1434–1438.
- Haddad PR and Jackson PE (1990) *Ion Chromatography Principles and Applications*, p. 232. Amsterdam: Elsevier.
- Hilton DF and Haddad PR (1986) Determination of metal-cyano complexes by reversed phase ion-interaction high performance liquid chromatography and its application to the analysis of precious metals in gold processing solutions. *Journal of Chromatography* 361: 141–150.
- Inczedy J (1966) *Analytical Applications of Ion Exchangers*. Oxford: Pergamon Press.
- Kraus KA and Moore GE (1953) Anion exchange studies. VI. The divalent transition elements manganese to zinc in hydrochloric acid. *Journal of the American Chemical Society* 74: 1460–1462.
- Pietrzyk DJ (1989) Macroporous polymers. In Brown PR and Hartwick RA (eds) *High Performance Liquid Chromatography*, p. 244, New York: Wiley-Interscience.
- Siriraks A, Kingston HM and Riviello JM (1990) Chelation ion chromatography as a method for trace elemental analysis in complex environmental and biological samples. *Analytical Chemistry* 62: 1185–1193.
- Timberbaev AR and Bonn GK (1993) Complexation in ion chromatography – an overview of developments and trends in metal analysis. *Journal of Chromatography* 640: 195–206.
- Weiss J (1995) *Ion Chromatography*, 2nd edn, Weinheim: VCH.
- Wilkins DH (1959) The separation and determination of nickel, chromium, cobalt, iron, titanium, tungsten, molybdenum, niobium, and tantalum in a high temperature alloy by anion exchange. *Talanta* 2: 355–360.

Use in Gas Separation

See III/GAS SEPARATION BY METAL COMPLEXES: MEMBRANE SEPARATIONS

METAL MEMBRANES: MEMBRANE SEPARATIONS



Y. S. Lin and R. E. Buxbaum, University of Cincinnati, Cincinnati, OH, USA

Copyright © 2000 Academic Press

Introduction

The use of metal membranes for hydrogen separation was first demonstrated over a century ago. Graham discovered in 1866 that palladium absorbs a surprising

amount of hydrogen. Graham went on to show that palladium and palladium-silver membranes permeate only hydrogen, paving the way for the use of metal membranes for hydrogen extraction and purification. Much of the earlier knowledge in metal membranes is summarized in three reference books published in 1967–1968 (see Further Reading). Recent academic research is reviewed in several monographs on inorganic membranes and review articles. This article gives an overview of the general properties of metal membranes, followed with a description of methods that have been developed for membrane fabrication. Applications of the metal membranes in separation and chemical reaction processes and design of the metal membrane separation processes are described later in the article.

General Properties of Metallic Membranes

A surprising amount of hydrogen can be absorbed reversibly by palladium alloys and by many transition metals over a large temperature range. The absorption proceeds via interstitial incorporation in the metal, generally leaving the crystalline structure intact. Thus, for example, face-centered cubic palladium retains its structure to the metal hydride phase, with the hydrogen progressively occupying tetrahedral and octahedral sites. The nature of the chemical bonding is still not well understood, but a widely used model assumes that the hydride is an alloy (in the usual metallic sense) of hydrogen and the host metal. Electrons from the hydrogen progressively occupy the d-bands of the transition metal, and the hydrogen exists essentially as slightly shielded protons in the host lattice. The other model is based on a predominantly covalent bond between the metal and hydrogen. In this model molecular hydrogen is dissociated to become atomic hydrogen, which subsequently forms chemical-type bonds to the host metal.

Figure 1 shows hydrogen solubility relationships for several transition metals at different temperatures. At constant pressure, the hydrogen solubility of some metals increases with increasing temperature, while for some other metals it decreases. Figure 2 shows typical relationships of hydrogen solubility (presented in the atomic ratio of hydrogen to metal) versus hydrogen partial pressures at different temperatures. The dashed curve in Figure 2 encloses the two-phase region of the palladium hydride system with α -phase to its left and β -phase to its right. For all metals below their hydride phase transition, the solubility increases with hydrogen pressure. The most common relationship for this is

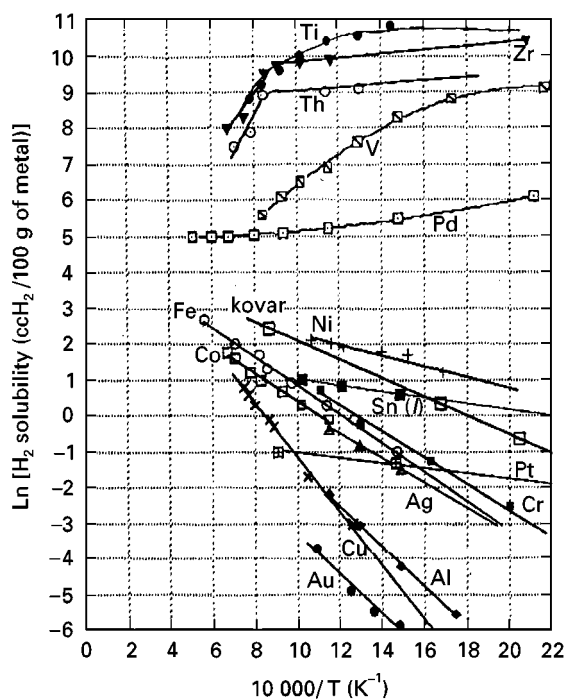


Figure 1 Hydrogen solubility of several transition metals at different temperatures ($P_{H_2} = 1$ atm). (Copyright REB Research & Consulting with permission.)

the Sievert's relation:

$$C = K_s P^{1/2} \quad [1]$$

That is to say that the hydrogen concentration, expressed as the ratio of hydrogen:metal or as the volume of hydrogen per gram of metal, is proportional to a temperature dependent constant (K_s) times the hydrogen pressure to the power $1/2$. The power $1/2$ in eqn [1] comes from the entropic effect of every molecule of hydrogen dissociating into two hydrogen atoms in the metal.

Aside from solubility, the most important qualities of a metal for use in metallic membranes are the hydrogen diffusivity in metal and the rates of dissociation and recombination reactions on the membrane surfaces. At the upstream membrane surface the surface reaction step consists of adsorption of H_2 , dissociation of this adsorbed H_2 into two hydrogen atoms (or charge-transfer reaction to form protons), and absorption of the atoms into the bulk metal. In the bulk there is a net transport of hydrogen atoms from high to low partial pressure sides along the concentration gradient. At the downstream membrane surface there is another surface reaction step including the formation of hydrogen molecules from hydrogen atoms (or protons) and desorption of hydrogen molecules from the surface to the gas phase.

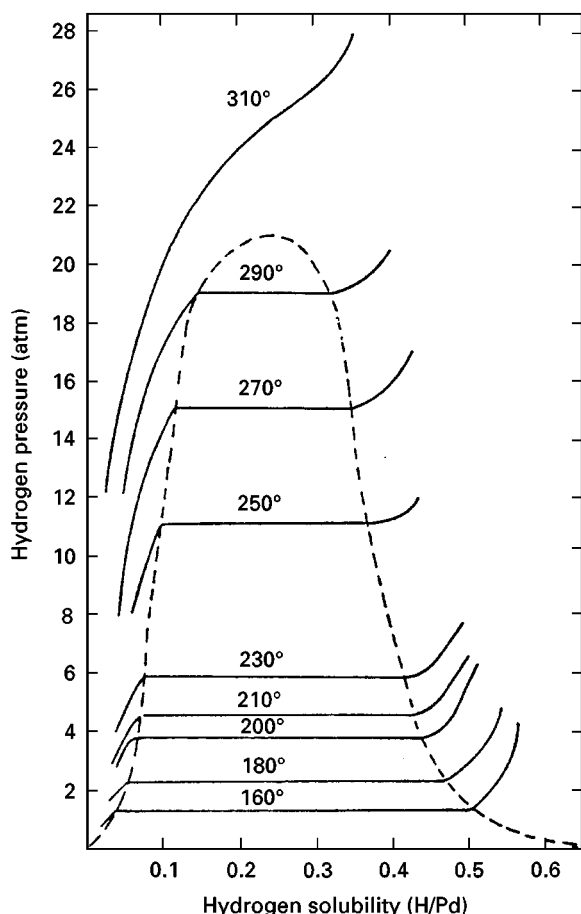


Figure 2 Hydrogen solubility of palladium at different hydrogen pressures and temperatures (°C) (From Lewis FA (1967) *The Palladium Hydrogen System*. Fig. 2.3, p. 17. New York: Academic Press.)

Based on the Mass Action Law, the following simplified equations can be obtained to describe the combined effects on hydrogen permeation flux:

$$J = K_R(P_{UH} - P_I) \quad [2]$$

$$J = (DK_s/2L) (P_I^{1/2} - P_{II}^{1/2}) \quad [3]$$

$$J = K_R(P_{II} - P_{DH}) \quad [4]$$

where P_{UH} is the upstream hydrogen pressure, P_{DH} is the downstream hydrogen pressure, P_I is the imaginary pressure in equilibrium with the upstream surface of the metal, and P_{II} is the imaginary pressure in equilibrium with the downstream surface. K_R is a lumped rate constant for the surface reaction step. In eqn [3], DK_s is the product diffusivity and Sievert's constant in the bulk metal membrane and L is the membrane thickness. Often $DK_s/2$ is called the hydrogen permeability and is plotted in Figure 3 for several metals. It should be noted that

metal membranes are practically impermeable to other gases such as helium or nitrogen due to their low solubility and diffusivity in the metals. Although for all the metals of interest to separation applications, the hydrogen diffusivity increases and solubility decreases with increasing temperature, we find for some metals (e.g. palladium) the permeability increases with temperature, while for others (e.g. tantalum, niobium) it decreases. The determining factor is the relative temperature dependency of diffusivity and solubility. Because of slow reaction steps (eqn [2] and eqn [4]), permeation membranes of Nb, V and Ta must be coated with palladium to be used for separation applications.

For most metal membranes, bulk diffusion is rate-limiting. That is, $(DK_s/2L)$ is typically smaller than K_R . For such membranes eqn [3] describes the flux with P_{II} and P_I replaced by P_{UH} and P_{DH} . In this case, the hydrogen permeance is inversely proportional to the membrane thickness with permeation flux exhibiting a $P_{H_2}^{1/2}$ dependence. This relationship is referred to as the Richardson's law. If the surface steps are rate-limiting, i.e. $(DK_s/2L)$ much larger than K_R , the hydrogen permeation flux is proportional to the transmembrane pressure drop. When resistances of both surface and bulk steps are equally important, the above equations are sometimes approximated with $P_{H_2}^{0.7}$ dependencies or similar simplified relations.

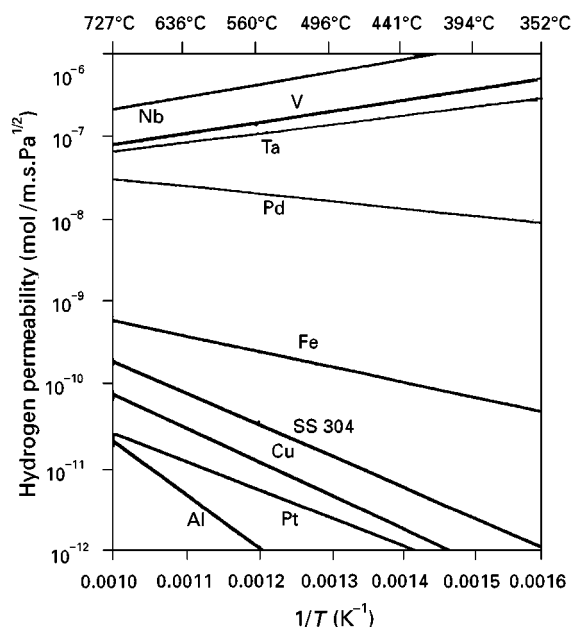


Figure 3 Hydrogen permeability of various transition metals at different temperatures. (Copyright REB Research & Consulting with permission.)

Another critical behaviour for any metallic membrane is durability. Figure 2 shows that below a critical temperature (310°C) palladium hydride can exist either in the α -phase or β -phase, depending on hydrogen pressure and temperature. Above the critical temperature, palladium hydride remains in the α -phase regardless of the hydrogen partial pressure. Both the α -phase and β -phase have the same face-centered cubic lattice structure, but the lattice constant of the latter is as much as 3% larger than the former. Thus, a hydrogen pressure swing below the critical temperature or a temperature swing (above the critical pressure) will cause large mechanical strains during phase transformation of the palladium hydride between the two phases. These lattice strains would destroy the mechanical integrity of a membrane made of palladium alone. This phenomenon is referred to as 'hydrogen embrittlement'. For practical application this is avoided by alloying the palladium and by lowering the hydrogen pressure sharply before the membrane cools to room temperature. The same problems and solutions are also applicable to Pd-coated transition metals.

Alloying palladium with silver results in a phase diagram with a decreased critical temperature and pressure. If we accept the metallic alloy model for metal-hydride systems, the role of silver can be explained as an electron-donating behaviour where electrons from silver and hydrogen atoms compete for filling the 4d-band of palladium. Since 4d-band filling is associated with β -phase formation, 40% silver prevents β -phase formation entirely although most common alloys do not employ quite so much silver. Once the 4d-band is filled, electrons from further hydrogen absorption contributes to 5s-band filling and the net effect is decrease in both critical temperature and pressure in the phase diagram. Common palladium-silver (23–25% silver) membranes and palladium-copper membranes can be operated at much lower temperatures than pure palladium membranes without significant hydrogen-embrittlement problems. This is especially true if care is taken at start-up and shutdown to avoid exposure of the membranes to high-pressure hydrogen at room temperature.

Metal membranes are susceptible to surface poisoning. Prolonged exposure of many metal membranes to sulfur or even carbon containing gases under some conditions could deactivate the membrane surface or change the bulk structure of thin metal membrane, affecting adversely the membrane permeation and separation properties. The current approach is to avoid this problem by removing poisoning impurities from the gas stream prior to the contact with the membrane surface. Modification of

the metal surface to improve its resistance to surface poisoning may provide an inherent solution to this problem. Research efforts in finding a suitable modification method have been limited, but are expected to increase in the future.

Fabrication of Metal Membranes

Casting/rolling is the current method for commercial production of palladium-based metal membranes. This method involves several steps. Membrane raw materials are melted at a high temperature to form ingots which go subsequently through hot or cold forging or pressing to produce tube or sheet. The final membrane has a thickness typically in the range of 50 to 75 μm (0.002–0.003 in). The metal membranes prepared by this method are polycrystalline with large grains (submicron or micron size). Furthermore, cold rolling often generates lattice dislocation and it can enhance hydrogen solubility in palladium and some of its alloys due to the accumulation of hydrogen around the dislocation. As a result, these polycrystalline metal membranes have very high hydrogen solubility.

Based on the Richardson equation (eqn [3]), thin metal membranes are more desired than thick ones in terms of hydrogen permeance and metal cost savings. The problem has been in forming such membranes and keeping them stable during temperature and pressure cycling. To improve the durability, thin metal membranes have been formed by coating on porous metallic or ceramic support. Several methods have emerged in the past decade for this including liquid-phase electroless plating and chemical vapour deposition (CVD).

Electroless plating involves autocatalysed decomposition of a selected metastable metal precursor such as $\text{Pd}(\text{NH}_3)_4\text{X}_2$ where X can be NO_3 , Cl or Br in alkaline aqueous solution at around 50°C. To avoid autodecomposition of the metal precursors a stabilizer such as ethylenediaminetetraacetic acid (EDTA) is often added. For nonmetallic supports, the surface (substrate) should be activated, e.g. by $\text{SnCl}_2/\text{PdCl}_2$ prior to electroless plating. Palladium or palladium-silver films with a thickness ranging from 5 to 30 μm have been prepared by this method on supports of porous alumina and stainless steel and on non-porous niobium, tantalum or vanadium alloy.

Thin metal membranes can also be prepared by CVD of metal salts and metal organic compounds, such as PdCl_2 and $\text{Pd}(\text{O}_2\text{C}_3\text{H}_7)_2$ and can also be produced by sputter coating of a solid metal. For CVD, the precursor vapour, with or without a reducing agent (hydrogen), is brought in contact with one surface of the porous support at a high temperature.

Reduction of the precursor occurs directly or by countercurrent exposure to the reducing agent at 200–400 °C. Palladium films as thin as 0.5 µm have been deposited on or inside porous alumina support this way. For sputter deposition a metal target of desired composition is placed apart from the substrate in a sputtering chamber filled with a working gas (argon) at low pressure (about 10^{-3} torr). A DC or radiofrequency AC electric-field gradient plasma is generated in the working gas and bombards the target. Fine metal particles or atoms dislodged from the target move towards the substrate and subsequently deposit. Thin palladium and palladium–silver membranes have been coated on porous γ -alumina and dense polymer substrates by this method.

Metal membranes prepared by the vapour methods are usually nanocrystalline with grain size in the range of a few tens of nanometers. Electroless-plated metal membranes appear to be more coarse-grained. For palladium on substrate membranes, the bulk diffusion step in the substrate is generally the rate-limiting step. Furthermore, fine-grained thin metal membranes appear to have a lower hydrogen permeability than coarse-grained thick metal membranes. Thus, while the metal cost for Pd-coated ceramics is typically much lower than for symmetric metal membranes, the flux is usually fairly similar and can even be lower than traditional metal membranes, and is typically proportional to the pressure dependence and not to $P_{H_2}^2$ as in eqn [3]. Similar membranes prepared by different methods can exhibit different dependency, and specific relationships should be obtained in order to design separation and reaction processes involving these metal membranes.

Metal Membrane Applications

The major large-scale application for metal membranes today is hydrogen purification, with most of that hydrogen used for integrated circuit manufacture. Different circuit technologies differ in the purity of hydrogen they require, and the current needs are between 5 nines (99.999%) and 8 nines (99.999999%) hydrogen, or 0.01 to 10 ppm impurities. The largest user, silicon-based semiconductor manufacture requires the lower levels of purity, and gallium arsenide the highest. These purity levels are expected to increase over time as transistor densities rise, doubling approximately every two years. Silicon applications should thus need 7 nines and gallium arsenide applications 9 nines hydrogen by 2005.

Metal membrane purification competes with adsorption technology for the market in electronic component manufacturing. The metal membrane market

is valued at only \$10 millions/year, but the ultrapure hydrogen delivery market is at least 100 times bigger suggesting significant room for growth in purifier sales. For electronic component manufacturing using cylinder hydrogen (the only choice in much of the Far East) there is no real alternative to membrane purification using tubular membranes of palladium–silver alloy (23–25% silver). The leading companies in this market are Johnson Matthey (75% market share) and Japan Pionics (25% market share.) Cylinder hydrogen is so impure that competing getter technology is not cost effective. Competing getter technology is often preferred with liquid hydrogen sources (available in the USA and Europe) because the pressure drop is lower and since the delivered hydrogen is purer, the cost is lower as well. Even here, membranes are often used for high value-added parts since getters tend to release small amounts of oxide dust as they saturate with impurities. This oxide can interfere with semiconductors manufacture and presents a safety hazard, e.g. released vanadium oxide dust is highly toxic with an exposure limit of 0.05 mg m^{-3} . Membranes are also safety favourites since the main getter alloys are flammable in contact with air at operating temperatures as high as 600°C.

A second major application for metal membrane purified hydrogen is as a carrier gas for gas chromatography. This is true particularly in Europe and the Far East where helium is scarce, but also in the USA for fast-response, high-sensitivity applications. The purity need here could be met by ultrapure cylinders, especially backed by a getter trap, but it is cost effective to use a membrane. An 'A-size' cylinder, containing 65 ft³ (STP) (1900 L (STP)) of ultrapure zero-grade hydrogen costs approximately \$220 currently. Continuous use as a carrier and reference gas consumes about 150 cm³ (STP) min⁻¹, emptying the cylinder in slightly over a week, and costing the customer \$10 000 annually. A membrane purifier of very modest size will allow the customer to use a much cheaper, lower grade of hydrogen, returning the purchase cost in six months or less.

Palladium membranes are also used for isotope enrichment providing a separation factor of about 1.4 for protium over deuterium, and about 1.7 for protium over tritium. While the hydrogen volume need for this application is small, the low separation factor ensures that quite a lot of membrane is needed.

A rather new line of metal membrane applications is for membrane reactors, mainly to generate hydrogen for fuel cells, but also to promote thermodynamically unfavourable reactions like methane splitting and ethylene production. A membrane reactor combines, in one unit, a catalytic reactor bed and a membrane separator to remove a desired

product (hydrogen) as it is formed. As a result membrane reactors drive the reaction towards completion and achieve advantages of enhanced catalyst use, higher feed space velocity and fewer side products.

Another benefit of membrane reactors, particularly for fuel cell applications that require high-purity hydrogen from source gases like methanol or gasoline, is that a membrane changes the way pressure affects extent of reaction and product recovery. Without the membrane in the reactor, a reforming reaction of this type would require low pressure operation to achieve high conversion, and would require a difficult hydrogen purification for the intended use. A membrane reactor allows the reaction to be driven by high pressures, greatly increasing the ease of hydrogen product recovery. At present, several membrane reactors are in trial and one at the pilot-plant scale for the production of hydrogen. Typical pressures of operation are at 17 atm, with operation temperatures dictated by the catalyst and material of construction. The size of the fuel cell market is currently small, but is believed to be rising fast.

Designs of Metal Membrane Separation Processes

Figure 4 shows the basic design of a hydrogen purifier. Prominently shown is a heat exchanger set between the input hydrogen feed and the purified hydrogen product. Heat recovery of this type is critical because the membranes typically operate at 350–400°C in an environment where the source gas and product application are near room temperature. Heat exchange cools the output gas and reduces the electric heating costs. Heat exchange also promotes temperature uniformity within the purifier; this is an important consideration since for most of the hydrogen permeable alloys a 100°C temperature gradient in

the membrane would mean that part of the membrane would have to operate at significantly below their optimal temperature for flux, and part of the membrane would operate at significantly above the optimal temperature for long life.

Figure 4 also shows a bleed valve to control the removal of impurities from the purifier, and a system to provide inert gas (nitrogen) flushing. Setting these systems is something of an art, since with too little bleed, impurities would build up in the purifier reducing the hydrogen output. Too much bleed, by contrast, results in a loss of heat and pressure resulting in a similar reduction in output. Most larger purifiers provide a nitrogen purge system as shown, to help extend the life of the membrane by reducing hydrogen embrittlement of the palladium alloys. This purge system can also be a source of problems as purging can result in hydrogen being sucked back into the purifier. If the sucked back hydrogen is contaminated with other electronic gases (particularly arsine) this will result in an irreversibly poisoned membrane.

There are basically two types of tubular membrane based commercial purifier designs: pressure-outside and pressure-inside. Until recently, large-scale hydrogen purification ($>100 \text{ L (STP) min}^{-1}$) was limited to pressure-outside design. Figure 5 shows schematic of a pressure-outside design. The inlet flow of fluid containing a mixed gas includes hydrogen flows over the outer surface of the metal membrane tubes housed inside a pressure vessel. The metal membrane tubes are operatively connected at one end to a header and the other end of the tubes are either capped or can be operatively attached to a floating head. Hydrogen permeates from outside into the inside of the metal membrane tubes, and leaves the membrane module through the outlet port. Pressure-outside designs (Johnson Matthey, Japan Pionics, and REB Research & Consulting) have longer life than the pressure-inside designs since the former do not require a braze seal at both ends of the membrane tube.

Pressure-inside designs, supplied by REB Research & Consulting, RSI and Power & Energy, are believed to output somewhat purer hydrogen because the impure gas flow past the membrane is more uniform than with pressure-outside designs. In the pressure-inside designs, the pressure drop and vibration effects in the tubes become excessive as tube lengths exceed 25–50 in. (63–127 cm). These effects could be effectively minimized by a scheme for placing several short lengths of Pd–Ag or similar tube in parallel while balancing the flow through each using matched, internally located flow restrictors. Forces of expansion and contraction by the membranes against the seals are believed to be a major

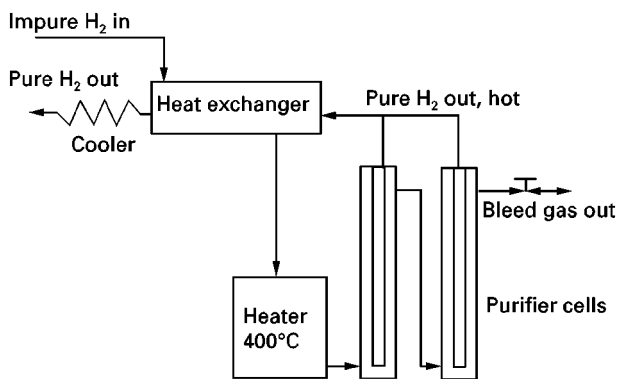


Figure 4 Schematic diagram of a metal membrane hydrogen purifier process. (Courtesy of Johnson Matthey, plc.)

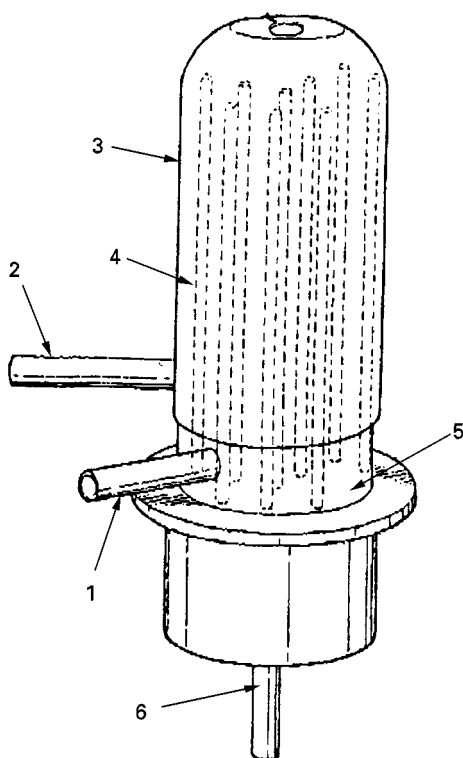


Figure 5 Schematic diagram of a pressure-outside design of metal membrane module: 1. Feed gas inlet. 2. Feed gas outlet. 3. Pressure vessel. 4. Metal membrane tubes. 5. Header. 6. Pure hydrogen outlet. (From US Patent 5,931,987, 1999.)

cause of fatigue failure in pressure-inside designs, as is burnthrough. Burnthrough is believed to be a bigger problem with pressure-inside designs since metals are inherently more stable in compression than in tension. That is a tube in compression will flow somewhat to heal a thin spot, but will flow away in tension turning a thin spot into a hole.

A third type of purifier using flat plates of Pd-Cu was recently demonstrated by Northwest Power. As flat plates can be made thinner than metal tubes the output flux with these membrane is exceptional. Unfortunately welded seals are much less reliable in this configuration than with tubes and instead graphite seals are used. The degree of purification from these devices is unacceptable for integrated circuit manufacture, but appears to be acceptable for use with fuel cells.

Almost all commercial metal membrane separation systems use the symmetric solid metal membranes fabricated by the conventional casting/rolling method. The only commercial attempt at using porous substrate supported metal membranes was in the 1950s and 1960s by Union Carbide who applied a thin layer of palladium-silver alloy on a porous ceramic substrate. By choosing the pore size and

thickness appropriately, metal cost per unit area could be decreased significantly while flux could be increased somewhat. The early membranes did not prove durable though, and had to be removed from service. Results with all of these alternatives is encouraging but it is fair to say that the commercial metal membrane market is still dominated by unsupported palladium alloys. The main reason is purity and durability: both the Pd-coated refractory metals and the Pd coated porous substrates have shown less cycling durability than typically associated with the solid Pd alloys, and the purity of hydrogen purified through the newer membranes has still to reach the very high levels of solid membrane purifiers. This latter is particularly significant for the high value added applications that dominate the metal membrane market currently.

Concluding Remarks

Metal membranes are the most hydrogen perm-selective inorganic membranes in the temperature range of 200–500°C. They are expected to remain so in the near future. Much progress has been made in understanding metal membrane properties and development of various methods for metal membrane fabrications. However, applications of metal membranes have been limited to hydrogen purification. In addition to the structural stability and cost problems, another major problem for metal membranes is their susceptibility to surface poisoning. This problem has to be solved in order for the metal membranes to gain wider acceptance in processes for separation of hydrogen containing gases of industrial importance.

Further Reading

- Armor JN (1998) Applications of catalytic inorganic membrane reactors to refinery products. *Journal of Membrane Science* 147: 217–233.
- Bhave RR (1991) *Inorganic Membranes. Synthesis, Characteristics and Applications*. New York: van Nostrand Reinhold.
- Burggraf AJ and Cot L (eds) (1995) *Fundamentals of Inorganic Membrane Science and Technology*. Amsterdam: Elsevier.
- Buxbaum RE (1999) Membrane reactor advantages for methanol reforming and similar reactions. *Separation Science and Technology* 34: 2113–2123.
- Buxbaum RE (1999) US Patent 5,888,273. *High Temperature Gas Purification System*. March 30.
- Buxbaum RE and Kinney AB (1996) Hydrogen transport through tubular membranes of palladium-coated tantalum and niobium. *I&EC Research* 35: 530–537.
- Hsieh HP (1996) *Inorganic Membranes for Separation and Reaction*. Amsterdam: Elsevier.

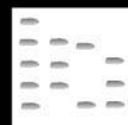
- Hwang ST and Kammermeyer K (1984) *Membranes in Separation*. Malabar, Florida: Rorbert E. Krieger.
- Lewis FA (1967) *The Palladium Hydrogen System*. London: Academic Press.
- Mueller WM, Blackledge JP and Libowitz GG (1968) *Metal Hydrides*. New York: Academic Press.
- Shu J, Grandjean BPA, Van Neste, A and Kaliaguine S (1991) Catalytic palladium-based membrane reactors.

A review. *Canadian Journal of Chemical Engineering* 69: 1036–1060.

Uemiya U (1999) State-of-the-art of supported metal membranes for gas separation. *Separation and Purification Methods* 28: 51–85.

Wise EM (1968) *Palladium Recovery, Properties and Uses*. London: Academic Press.

METAL UPTAKE ON MICROORGANISMS AND BIOMATERIALS: ION EXCHANGE



H. Eccles, British Nuclear Fuels, Preston, UK

Copyright © 2000 Academic Press

Introduction

Microorganisms and biomaterials can be used for the removal/recovery of metals from process liquors and liquid wastes. The mechanisms involved in capturing metals from solution by microorganisms and related materials are now commonly referred to as biosorption. Biosorption has been defined as the removal of metals or metalloid species, compounds and particulates from solution by biological material. It is one of the fields in environmental biotechnology, which is itself a small, but growing, component of the biotechnology industry (Figure 1).

The use of microorganisms to treat waste liquors on a commercial scale dates back to the end of the nineteenth century when the first communal sewage plants in Berlin, Hamburg, Munich, Paris and other major cities came into operation. In the intervening 100 years the use of microorganisms and plants to protect the environment has developed into a multi-billion dollar (US\$) industry. However, the foundations of this environmental biotechnology industry are still with the treatment of municipal/domestic effluents.

Although nature has demonstrated some subtle and intricate mechanisms for selectively controlling the mobility of pollutants in the environment, the conversion of this science to technology and to application has been very disappointing. In explaining this lack of application, it is important that these mechanisms

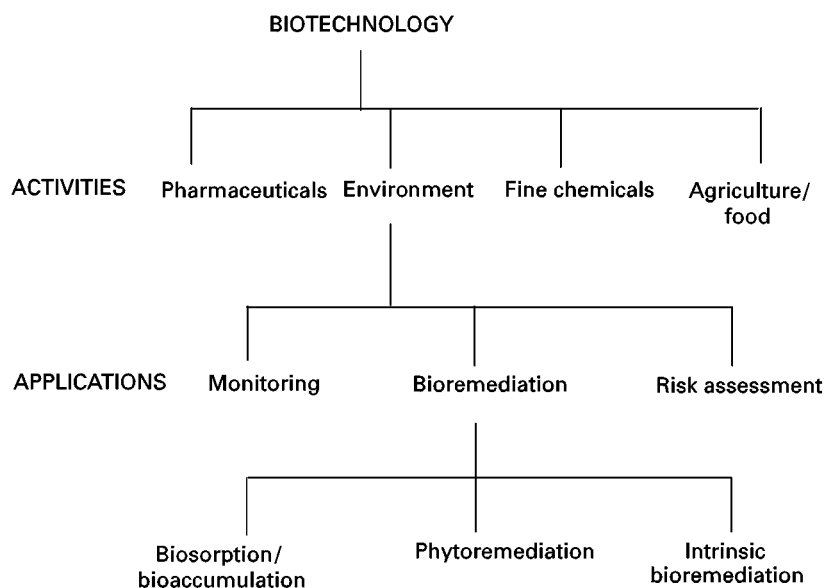


Figure 1 Biotechnology activities and applications. (This is an original developed by H Eccles.)

are appreciated; factors that influence their effectiveness need to be addressed to engineer robust and reliable processes.

Microorganisms and Biomaterials for Metal Removal

The biological systems studied for metal removal/recovery range from living microorganisms and dead cell systems to other biomaterials such as peat, coconut shells and eggshell membrane. All these systems have at least one common characteristic, namely their absorptive surfaces, and (in the case of living microorganisms within the cell structure) have at least one chemical moiety (functional group) that has an affinity for metal(s). This affinity can be accomplished by active and passive mechanisms that may act singly or in combination. The mechanisms can be microbiologically dependent, for example active transport across the cell membrane, or physicochemical and chemical-dominated reactions such as adsorption, cation exchange, complexation, chelation and precipitation. Essentially, active transport is a function of living cells, such as bacteria, algae and fungi. The remainder of the mechanisms are passive and may occur with living or dead cells or with other biomass.

Passive uptake mechanisms generally occur at the cell wall level (see Table 1) and the biomasses involved are generally tolerant to their environment. In their interactions with metals, dead cell systems and biomaterials behave as surrogate ion exchange materials. Ion exchange is a proven commercial technology that is widely used for the removal of metals from various liquors. Where major differences occur between biosorption and conventional ion exchange is when living microorganisms are involved, which results in the participation of other metal-removal mechanisms.

The basis for these differences and also for variations in metal-accumulation abilities is partly the result of cell surface characteristics. Microbial cell

Table 2 Cell wall macromolecules

<i>Cell wall macromolecules</i>	<i>Microorganism</i>
Polysaccharides, proteins, lipids, peptidoglycan	Bacteria
Mannan polysaccharides, chitin, galactosamine, proteins, lipids	Algae and fungi

walls are complex and are normally charged. Certain cell wall properties, such as the type of polar groups present and the charge within the cell wall macromolecules, may influence the metal capacity and selectivity. The types of macromolecules present in cell walls for bacteria, fungi and yeast are shown in Table 2.

Classification of bacteria, algae and fungi is based on aspects other than cell wall composition. Living organisms can be divided into two groups, prokaryotes and eukaryotes, based on cell structure. Bacteria belong to the prokaryote group, while algae and fungi belong to the eukaryotes. Further simple distinctions are that bacteria lack a nucleus and membrane-bound organelles and most bacteria have cell walls. Bacteria are without question the oldest and simplest organisms. Eukaryotic organisms have both a nucleus and membrane-bound organelles. Fungi are distinct from algae in that they have filamentous growth, lack chlorophyll and motile cells, and have chitin-rich cell walls (Figure 2).

Although these simple descriptions may be helpful in understanding the different behaviour of bacteria, fungi and algae with metals, they are by no means rigorous biological definitions, and the purist microbiologist may find them too superficial. It is probable, however, that the more rigorous and sophisticated explanations have contributed to the restrictive use of biotechnology in the environmental arena. This point will be discussed in more detail later.

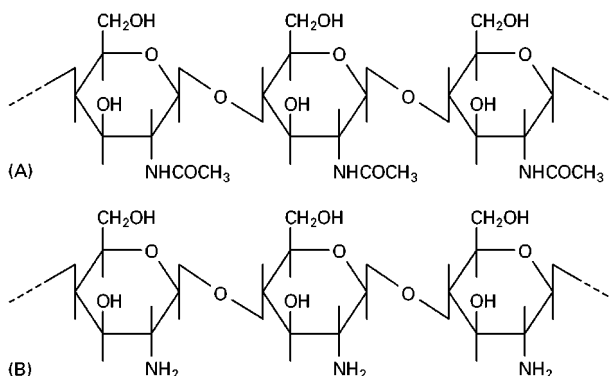


Figure 2 Chemical structure of (A) chitin and (B) chitosan. (Hardman DJ, McElowney S and Waite S (eds), *Pollution: Ecology and Biotreatment* (1993), p. 284, Addison Wesley Longman Ltd, UK.)

Table 1 Cell wall metal functional groups

<i>Cell wall functional group</i>	<i>Metal affinity</i>
Carboxyl	Ca, Mg, Cu, Zn
Imidazole	Cu, Pb
Sulfhydryl	Zn
Amino	Co, Ni, Cu
Phosphate	Ca, Mg, Fe, U
Sulfate	Ba, Ca, Sr
Thioether	Cu(I)
Amide	Cu, Co, Ni, Fe
Hydroxyl	Ca, Pb, Cu, Sr, Ba, Ni, Co, Zn

The complex nature of cell walls bestows some unique abilities on living microorganisms and to a lesser extent dead cell systems and biomaterials. Equally this complexity confers some serious drawbacks, as modelling of metal-removal mechanisms and predicting process efficiencies are extremely difficult when more than one metal functional group is available.

Notwithstanding these reservations, numerous microorganisms and biomaterials have been evaluated for a diversity of metals by many scientists worldwide. Some of the more definitive work is discussed in the following sections.

Dead Cell Systems and Biomaterials

Dead cell systems can be derived from living cells by subjecting them to a physical or chemical method to terminate the living cell metabolic activity. As growth conditions can confer some metal affinity characteristics on living cells, it is prudent to explain briefly the growth phase and the various parameters that may be controlled to achieve the desired goal. The more important growth phase conditions that can confer metal adsorption characteristics are:

1. time of cell harvesting;
2. composition of nutrient medium.

The growth of bacterial populations is normally limited either by the exhaustion of available nutrients or by the accumulation of toxic products of metabolism. This is particularly true for batch growth conditions. As a consequence, the rate of growth declines after the exponential phase and growth eventually stops. At this point a culture is defined as being in the stationary phase (Figure 3). The transition between the exponential phase and the stationary phase involves a period of unbalanced growth during which

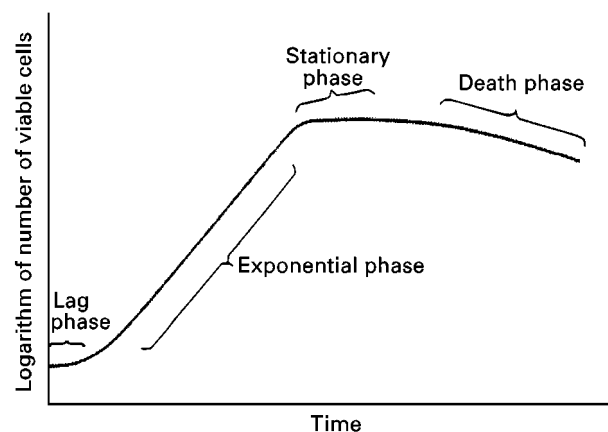


Figure 3 Generalized growth curve of a bacterial culture. Stanier RY, Ingraham JL, Wheelis ML and Painter PR (eds) *General Microbiology* (1986), 5th edition, p. 185, Prentice-Hall Inc, NJ.)

the various cellular components are synthesized at unequal rates. Consequently, cells in the stationary phase have a chemical composition that is different from that of the cells in the exponential phase. In general, cells in the stationary phase are small relative to cells in the exponential phase and they are more resistant to adverse physical and chemical agents.

Bacterial cells held in a nongrowing state eventually die, largely due to the depletion of the cellular reserves of energy. When cells are transferred from a culture in the stationary phase to a fresh medium of the same composition they undergo a change of chemical composition before they are capable of initiating growth. This period of change is called the lag phase.

Culture age affects the biosorption properties of microorganisms. For example, younger cells (12 h growth) of *Saccharomyces cerevisiae* removed approximately five times more uranium than older cells (24 h-growth).

The surface charge of living cells can vary both their age and with the nature and composition of the growth medium. With respect to metal adsorption, surface charge will have a predominant, if not the prime, influence. The cell wall surface charge is itself strongly affected by the pH value of the growth medium. This pH influence is due to the different ionogenic groups at the cell surface being susceptible to protonation/deprotonation reactions. Experimental evidence involving bacterial cells shows that carboxyl groups are present in excess over amino groups, and thus they dominate electrokinetic behaviour.

Physical methods that have been used to kill living cells include vacuum and freeze drying, boiling, autoclaving and mechanical disruption such as ultrasonics. Chemical methods include contacting the cells with various organic and inorganic compounds. The main aim of controlling the growth conditions coupled with the appropriate killing stage is to produce a biomaterial that has metal affinity properties superior to those of the parent living cell. The advantages of dead cells over living cells are:

- the metal removal process is largely independent of toxicity limitations;
- there are no requirements for growth media and nutrients;
- biosorbed metals can be eluted and the dead cells re-used;
- there is an ample and ready supply of some biomasses (dead cells);
- pretreatment of the biomass can enhance the metal biosorptive characteristics;
- the process is simpler and akin to ion exchange;

Table 3 Pretreatment methods to improve metal selectivity

Biomass type	Pretreatment method	Metal studied
<i>Penicillium digitalis</i>	0.1 mol L ⁻¹ sodium hydroxide	Ni, Cu, Zn, Cd, Pb
	Contacted with dimethyl sulfoxide for 90 min	U
	Trichloroacetic acid	U
<i>Saccharomyces cerevisiae</i>	10% (v/v) nitric acid, 30 min boiling	Cu
	10% (w/v) formaldehyde	Cd, Zn
	Detergent	Th
<i>Aspergillus niger</i>	Freeze-dried	U
	5% KOH	Cu, Cd, Zn, Co, Ni

- disposal of spent and/or excess nutrient media or surplus cells does not present a problem;
- the shelf-life of the dead biomass is nearly infinite.

If the required metal affinity characteristics have not been achieved at the harvesting stage and by the process used to kill the living cells, the dead biomass can be treated to enhance the key metal biosorptive properties such as metal capacity, metal selectivity and rate of uptake.

In Table 3 are reported some of the pretreatment methods employed and their effect on metal removal. Alkali treatment of fungal biomass has been shown to increase significantly the metal sorption capacity of *Aspergillus*, *Mucor* and *Penicillium*, and deacetylation of chitin in the cell wall to form chitosan-glucan complexes results in higher affinity for metal ions.

In what follows dead cell systems and biomaterials will be regarded as being equivalent, but any specific subtle differences will be highlighted. The biomaterials that have attracted most attention are those that are readily available in significant quantities, with or without pretreatment to enhance their metal uptake capability. To date these materials have included: peat, lignates, seaweed waste (dealginated seaweed), yeast from brewing operations, algal and

fungal biomasses and activated carbon from a variety of sources.

The last material is presently used commercially in the treatment of water for the removal of nonmetallic species; numerous papers have been published on the uses of activated carbon. In evaluating the above materials one feature regularly considered has been their particle size and the implications to scale-up. In their behaviour to metals these materials resemble ion exchange resins, which are invariably packed into columns. Thus laboratory studies have included the immobilization of biomaterials into particles of appropriate shape and size. Spherical particles 1–3 mm in diameter appear to be acceptable.

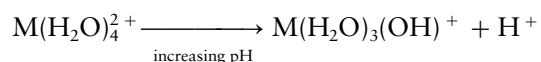
As the metal-removal processes are passive and of a chemical/physicochemical nature, the parameters considered are like those for ion exchange, namely pH, temperature, competing cations and metal speciation. These parameters are equally important to metal removal by living cell systems. Without doubt, pH is by far the most dominant influence on metal uptake. The optimal pH values for a variety of metals and biomaterials are presented in Table 4.

The efficiency of metal removal by the biomaterial as a function of pH will be related to: (1) the functional group involved and (2) metal speciation chemistry. At low pH values, i.e. about 3 or less,

Table 4 Optimal pH values for metal uptake by various biomaterials/microorganisms

Biomaterial / microorganism	Optimal pH value for metal removal	Metal(s)
Peat	1.5	Cr(vi)
	5.0	Cu(II)
	7.0	Ni(II)
Seaweed	4.0	Au
	5.0–6.0	Cu, Zn, Pb, Cd, Cr, Ni, Fe
<i>S. cerevisiae</i>	1.5	Mo(v)
	3.0–4.0	U(vi)
<i>Penicillium digitatum</i>	7.0	Cd
<i>Bacillus subtilis</i>	4.1	U
<i>Chlorella salina</i>	4.0	Tc(vii)
	8.0	Co

metal(s) uptake will be comparatively low as the metal(s) will be in competition with the hydrogen ion and most functional groups with an exchangeable hydrogen ion will be undissociated. On increasing the pH, competition with the hydrogen ion diminishes, dissociation of the hydrogen of the functional group increases and the speciation of the metal(s) changes from being a hydrated cation to hydroxy metal species thus:



This progressive displacement of the inner sphere of water molecules with increasing pH results in the metal ion becoming more amenable to adsorption by the biomaterial.

Temperature increases within a modest range, i.e. 20°C to 60°C, have little or no effect, either thermodynamically or kinetically, on metal removal for most biomaterial and metal systems. In general, optimal metal uptake will occur at 25°C for most dead cell systems and at a similar value (25–30°C) for biomaterials.

Metal affinity by many dead cell systems measured using single metal systems has been shown to comply with the Irving–Williams series. Most dead cell systems exhibit selectivity for heavier metals, such as Zn, Cu and Ni, over the lighter alkali metal ions. The selectivity of dead cell systems and biomaterials for a particular metal is highly dependent on the pH value of the solution under investigation and the functional group involved in the metal adsorption process. The determination of metal selectivity for dead cell systems and biomaterials is complicated in that more than one functional group may be involved in the biosorption process. These interactions (biosorption processes) may operate independently or may be interrelated. For example, Tsezas and Volesky indicated that three mechanisms are operative in uranyl ion biosorption by *Rhizopus arrhizus*. Two of the mechanisms occur simultaneously and rapidly (< 60 s to equilibrium). In the first process, uranyl ions coordinate with the amino nitrogen of the cell wall chitin, facilitating the second process in which the complexation sites acted as nucleation points for deposition of additional uranium. These two mechanisms accounted for 66% of the total uptake capacity (0.05 mmol U per g cell dry weight). The third process is considerably slower, only reaching equilibrium after 30 min, and involves the precipitation of uranyl hydroxide within the cell wall microcrystalline chitin.

Although most of the available literature is concerned with single metal experiments, a limited num-

ber of studies have involved binary metal systems or multimetal solutions. These studies demonstrate that copper generally has the highest binding capacity and exerts the largest competing effect.

The presence of anions in the metal solution under consideration will have an impact on metal biosorption, depending on the concentration of the anion and its metal-complexing ability. The more common anions, such as nitrate, chloride and sulfate, rarely affect the biosorption of metals when in near stoichiometric concentrations to the metal. Increasing their concentration will affect the biosorption (lower it), but this will depend on the ability of the metal to form anionic species. When the anion species such as EDTA²⁻, phosphate, citrate, etc., is capable of coordination/complexation with the metal, the metal capacity will be strongly reduced.

Living Cell Systems

Living cells systems offer some unique and subtle metal-accumulation mechanisms not possible with dead cell systems, biomaterials or conventional ion exchange resins. These active metal-accumulation mechanisms, in addition to the passive ones, are generally coupled with the metabolic activity of the algal, bacterial, fungal living cells.

Many organisms have developed detoxification mechanisms to overcome the detrimental effects of metals. For the purpose of this article two mechanisms will be taken as predominant, namely bioaccumulation and bioreduction. Although these mechanisms are generally encompassed by the term biotransformation, this terminology is far more appropriate to the treatment of organic pollutants using microorganisms, as these pollutants can be biodegraded to benign metabolic end products such as carbon dioxide and water. Metals are persistent and their toxicity is infinite. Microorganisms can only affect their physical and/or chemical state and transform them into more immobile forms that are less bioavailable to plants and other higher organisms. In achieving the biotransformation of metals, microorganisms are behaving as minute chemical factories generating chemicals, for example hydrogen sulfide, alkali and inorganic phosphate, or providing electrons from interconnected redox processes. These processes are summarized in Table 5. One process in particular will now be described in more detail.

In the natural environment the major mechanism for bacterial metal precipitation is through the formation of hydrogen sulfide and the immobilization of metal cations as metal sulfides. The bacteria involved in this process are the sulfate-reducing bacteria including members of the genera *Desulphovibrio*

Table 5 Metal bioaccumulation and bioreduction processes

Process	Metal-removal mechanism	Microorganism
Bioaccumulation	Sulfide precipitation	Sulfate-reducing bacteria
	Phosphate precipitation	<i>Citrobacter</i> sp.
	Hydroxide precipitation	<i>Alcaligenes eutrophus</i>
Bioreduction	Hydroxide/oxide precipitation	<i>Shewanella alga</i>
	Sulfide precipitation	Sulfate-reducing bacteria

and *Desulphotomaculum*. Sulfate-reducing bacteria (SRB) are widely distributed in anaerobic environments such as sediments and bogs. Sulfide production by sulfate-reducing bacteria is a consequence of their energy-generating processes. They couple the reduction of oxidized forms of sulfur, e.g. sulfates and sulfur, with the oxidation of reduced carbon in the form of simple organic molecules such as lactose or ethanol. The optimal chemical environment for effective sulfate reduction to sulfide is a pH value between 5.5 and 6.5 with a negative redox value of about 200–400 mV.

One of the underpinning features for the effectiveness of a SRB metal-removal process is the extremely low solubility product value for metal sulfides, as reported in Table 6. Other process advantages are:

- removal of metal anions such as chromate with initially the reduction of Cr(VI) to Cr(III) by the biogenic hydrogen sulfide;
- the ability of the microorganisms to nucleate the sulfide precipitation and thus assisting in the coagulation of metal sulfide particles;
- maintaining (slightly increasing) chemical neutrality of the process sulfate liquor due to the carbonate formed from oxidation of lactose or ethanol, or other suitable carbon sources, and sulfide from reduction of sulfate;
- the ability to remediate inorganic pollutants, for example toxic heavy metals and sulfate, as well as organic pollutants.

Table 6 Solubility product values for metal sulfides and hydroxides at 25°C

Metal	Hydroxide	Sulfide
Ag	2×10^{-8}	1.6×10^{-49}
Cu(II)	1×10^{-20}	8.5×10^{-45}
Zn	1×10^{-17}	1.2×10^{-23}
Ni(II)	1×10^{-15}	1.4×10^{-24}
Co(II)	1×10^{-15}	3.0×10^{-26}
Fe(II)	1×10^{-15}	3.7×10^{-19}
Cd(II)	1×10^{-14}	3.6×10^{-19}

These advantages may have been behind the development by Shell Research Ltd. of a biological process in preference to chemical ones for the removal of zinc, cadmium and sulfate from contaminated groundwater accumulating below a zinc smelter site. This process is the only biological metal-removal system employing specifically SRB operating on a commercial scale. The reasons for this unique situation is addressed in the next section.

The active metal biotransformation processes that rely on the precipitation of the offending metal(s) are not selective. The microorganisms require carefully controlled conditions both for their growth and to maintain enzyme activity, which are usually pH values ranging from 5.0 to 7.0, slightly aerobic 0 to +200 mV or anaerobic –200 mV to –400 mV.

Metals capable of forming insoluble hydroxides/oxides, phosphates or sulfides will precipitate effectively under these conditions. Consequently, competing cations that form such insoluble materials are only a problem in that they consume the precipitant, which in turn generally requires more carbon substrate. Interfering anion conditions will apply, similar to those already discussed above.

Although dead and living cell systems have been shown to have some unique capabilities for metal removal, the transfer to commercial technology has been very limited. The reasons for this will now be discussed.

Engineering and Process Considerations

Although dead cell systems, biomaterials and living cells have some distinct advantages compared with conventional ion exchange resins in the removal of metals from aqueous waste liquors, the number of recorded pilot-plant and commercial processes is extremely small, as illustrated in Table 7.

It would appear that even the rapid metal uptake by dead cell systems (less than 60 s for outer wall adsorption) combined with potentially cheap biosorbents and greater versatility of living cell systems such as SRB, capable of accommodating more than one

Table 7 Biological metal-removal pilot plants and commercial facilities

Process	Biomaterial/ microorganism	Target metal(s)	Process conditions
AMT-Bioclain	<i>Bacillus subtilis</i>	Pb, Zn	Pilot plant (PP) Capacity 20 BV h ⁻¹ Columns 18 L BV ⁻¹
Alga SORB	Algae	Cd, U, Pb, Hg	PP Capacity 10 BV h ⁻¹ Columns 0.4 L BV ⁻¹
BIOFIX	Various biomasses	Ni, Zn, Mn, Cd	PP Capacity 30 BV h ⁻¹ Columns 14.3 L BV ⁻¹
Shell Chemicals	Sulfate-reducing bacteria	Zn, Cd	PP Capacity 3 m ³ h ⁻¹ USAB 12 m ³ Commercial scale Capacity 300 m ³ h ⁻¹ USAB 1800 m ³

BV, bed volume; USAB, upflow anaerobic sludge blanket reactor.

pollutant such as sulfate and metals, are generally insufficient to convince potential users to install, or even consider, a biological process in preference to a chemical/physicochemical process.

In considering process technologies for removal of metals from waste liquors, certain criteria need careful and critical appraisal. These process criteria and their implications to biological systems are briefly reviewed.

Robustness

Dead cell systems and other biomaterials exhibit similar robust chemical properties to conventional ion exchange resins. They lack equality, however, because of their mechanical properties. Living organisms are significantly less robust as it is crucial to maintain cell growth and/or metabolic activity, which requires a carefully controlled environment. It is however possible, by judicious design, to arrange the biological stage of the process remote from and/or independent of the metal removal stage.

Selectivity

The metal selectivity of dead cell systems and biomaterials can be significantly improved by a variety of chemical treatments, but obviously at a cost and in some instances to the detriment of other process considerations, e.g. chemical treatment may result in a lowering of the total metal affinity.

However, metal selectivity may not be a prime consideration as effluents often contain several offending metals, in which case living cell systems are more appropriate as they are less discriminatory.

Compatibility

By definition effluent treatment processes have to be compatible with upstream, and in some instances downstream, operations. In many circumstances the compatibility requirement is exacerbated as effluent processes are retrofitted. Chemicals used in the biological metal-removal processes such as regeneration liquors for dead cell/biomaterial systems and excess sulfide and/or carbon substrate in SRB processes will require careful examination, in particular when water from the treated effluent is to be recycled.

Reliability

Site effluent treatment systems operate continuously, virtually 365 days a year. Biological processes are equal in reliability to their chemical competitors but may require greater control to ensure that environments are maintained, in particular for living cell metal removal processes.

Reliability can be enhanced by the installation of duplicate facilities and/or buffer storage, but with a cost penalty.

Simplicity

Modern automation has allowed effluent treatment facilities to be left unattended for significant periods. The greater the simplicity of metal removal, the lower the automation requirements. Dead cell/biomaterial systems are no more complicated than ion exchange resin processes, but this is not the case for living cells. Ensuring the activity of appropriate enzymes requires added process considerations.

Predictability

At the outset, effluent treatment designers will have to be confident that appropriate scientific and engineering information is available to meet all eventualities, in particular maloperation of the facility and the environmental impact this may have.

When more than one metal-removal mechanism may be participating, either synergistically or antagonistically, such information may not be readily available. Even when this information is available, predictability becomes more complex and difficult. Dead cell/biomaterial systems may fall into this category.

Efficiency

The biological process should have high metal-accumulation capacity and accumulation should be sufficiently rapid and efficient to compete with those of conventional technologies. In order to be competitive, the process should remove at least 99% of the target metals. There is clear evidence that biological systems can compete in efficiency with existing technologies, some reaching a sorption capacity of greater than 200 mg per g dry weight of dead cell systems.

The rate of heavy metal accumulation by biosorbents also compares favourably with existing separation techniques.

Versatility

Since waste streams are highly variable, the efficiency of metal removal should ideally be unaffected by other waste stream constituents and should be relatively stable to variations in pH. This presents one of the biggest challenges in the development of liquid waste treatment. The effect of pH on metal removal is often significant and varies with the biomass and metals. The presence of inorganic and organic components other than the target metal or metals common in waste streams. Such components have often been found to alter the efficiency of sorption. There are several possible mechanisms for this effect, ranging from direct competition for the binding sites resulting in lower uptake of target metal(s), to organic pollutants forming soluble complexes with metal(s) and thus reducing removal efficiency.

Economics

The dead cells/biomaterials and living cells should be cheap to grow and/or harvest. Clearly it is economically desirable to utilize waste biomass or material from other processes since the production cost will be

Table 8 Sources of waste biomass for use in heavy metal removal

Waste biomass	Source
Activated sludge, digested anaerobic sludge	Wastewater treatment
<i>Saccharomyces cerevisiae</i> (yeast)	Brewing
<i>Bacillus subtilis</i> (Gram-positive bacterium)	Enzyme production
<i>Penicillium chrysogenum</i> (fungus)	Penicillin production

reduced. Waste biomass is produced from a number of industrial processes (Table 8) but the use of waste biomass should not, however, be at the expense of process efficiency.

Realizing the Potential of Biosorption/Bioaccumulation of Metals

The understanding of the interactions of microorganisms with metals for a variety of applications such as health care, environmental protection and process technology (biocatalysis) has been pursued for nearly half a century. In this time numerous microorganisms have been isolated, characterized and evaluated for a diversity of metals. Notwithstanding this colossal effort, to date there are few installations, possibly no more than five major ones, that use microorganisms (excluding activated sludge processes) to remove and/or recover metals from waste waters/liquid wastes. Why is this? First, we need to consider what microorganisms are capable of – they are no different to their chemical counterparts, in that they cannot, for example, convert lead to gold or ‘eat’ plutonium! The perception of microorganism capabilities for dealing with metal pollutants is for the nonbiologists clouded by the great successes, reported worldwide, that these minute chemical factories have secured in dealing with oil spillages and land contaminated with a variety of organic pollutants. Without a doubt the microbial degradation of such pollutants is truly the ‘green ticket’, assuming of course that these pollutants are ultimately and quickly degraded to carbon dioxide and water.

One major reason hampering potential is the approach taken by microbiologists. In the past, and in many instances even today, screening for new microorganisms has been a major preoccupation and many person-years effort are expended in the laboratory with little thought as to how these microorganisms can/will be engineered into a technological process. The interaction between microbiologists and

workers in other scientific disciplines, in particular chemists, is now more strongly evident, largely because an array of scientific techniques is needed to characterize the microorganisms. The involvement of engineers is still lacking and consequently key questions are missed or omitted when considering the potential of microorganisms to treat complicated waste streams. Many engineers are surprised at the microbiologist's approach in tackling a seemingly new pollution problem. The technique of screening the polluted environment for thriving microorganisms is logical to the microbiologist, but curious to the engineer, who may not understand the subtleties of genera and strains.

It is this fusion of scientific and engineering approaches that is needed to enable bioremediation, and hence environmental biotechnology, to achieve its true potential.

Environmental legislation is now stringent and is likely to become even more so in the future. In this situation it is important not only that the process technology is understood, but also that the implications and consequences of perturbations to this technology can be accurately predicted. With environmental processes perturbations will undoubtedly arise, as to date there is no specification for effluents that is definitive.

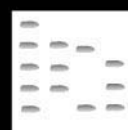
Unfortunately, in the present commercial environment, the quest for scientific knowledge is too often perceived as no longer valuable or affordable. In this respect the success of biotechnology in other areas, e.g. pharmaceuticals, may well have a positive benefit to other markets, persuading nonscientists that knowledge and intellectual property is valuable and ignorance is unaffordable.

See also: II/Ion Exchange: Theory of Ion Exchange. III/Biological Systems: Ion Exchange. Resins as Biosorbents: Ion Exchange.

Further Reading

- Brierley JA (1990) In: Volesky B (ed.) *Biosorption of Heavy Metals*, pp. 305–311. Boca Raton, FL: CRC Press.
- Darnall DW, Greene B, Hosea M, *et al.* (1986) In: Thompson R (ed.) *Trace Metal Removal from Aqueous Solutions*, pp. 1–24. Whitstable, Kent: Litho Ltd.
- Eccles H (1995) *International Biodeterioration and Biodegradation*, Special Issue, *Biosorption and Bioremediation*, vol. 35, pp. 5–16.
- Edyvean RGJ, Williams CJ, Wilson MM and Aderhold D (1997) In: Wase J and Forster C (eds.) *Biosorbents for Metal Ions*, pp. 165–182. London: Taylor & Francis.
- Gadd GM (1988) In: Rehm H-J (ed.) *Biotechnology-Special Microbial Processes*, vol. 6B, pp. 401–433. Weinheim: VCR.
- Hunt S (1986) In: Eccles H and Hunt S (eds) *Immobilisation of Ions by Biosorption*, pp. 15–46. Chichester: Ellis Horwood.
- Kuyucak N and Volesky B (1990) In: Volesky B (ed.) *Biosorption of Heavy Metals*, pp. 173–198. Boca Raton, CRC Press.
- Lovley DR, Phillips EJP, Gorby YA and Landa Y (1991) *Nature* 350: 413–416.
- Macaskie LE (1991) *CRC Critical Reviews in Biotechnology* 11: 41–112.
- McEldowney S (1990) *Applied Biochemistry and Biotechnology* 26(2): 159–180.
- Scheeren PJH, Koch RO, Buisman CJN, Barnes LJ and Versteegh JH (1992) *Transactions of the Institution of Mineralogy and Metallurgy, Section C* 101 (Sept/Oct): 190–199.
- Tsezos M (1997) In: Wase J and Forster C (eds) *Biosorbents for Metal Ions*, pp. 87–113. London: Taylor & Francis.

METALLOPROTEINS: CHROMATOGRAPHY



E. Parisi, CNR Institute of Protein Biochemistry and Enzymology, Naples, Italy

Copyright © 2000 Academic Press

Classification and Characteristics of Metalloproteins

Metals are known to play essential roles in catalysis, macromolecular structure and membrane stabilization as well as hormonal and genetic regulation. Metals present at very low concentrations in tissues and biological fluids are termed oligoelements. Usu-

ally they do not occur in the biological matter as free ions, but as metal-protein complexes. The term metalloprotein is used to define a large group of proteins containing one or more atoms of metal bound to specific sites in the polypeptide chain. The binding sites on the protein are provided by histidine nitrogens, glutamate or aspartate oxygens and cysteine sulfurs; the metal ligand is usually represented by calcium, selenium, iron, zinc, copper and other heavy metals.

Metalloproteins can be divided into two groups: biologically active metalloproteins and proteins with

no apparent biological activity. The first ones include metalloenzymes and zinc-containing DNA-binding proteins. Metalloenzymes are particularly suited to studies on metal-protein interaction aimed at a better understanding of the enzymatic mechanisms; their activity is measured by means of specific assays with an appropriate substrate. The metal can either stabilize the protein structure or be part of the active catalytic site; sometimes distinct atoms of the same metal may have structural or catalytic roles, depending on the site to which they are bound.

Metalloproteins that do not exhibit biological activity can be isolated by simply monitoring the metal. The most widely used technique for metal determination is atomic absorption spectrometry (AAS); however, alternative methods are also available, such as flame atomic emission spectrometry, plasma emission spectrometry, differential pulse polarography and the neutron activation analysis.

Metalloenzymes

Metalloenzyme Preparation

Metalloenzymes are widely represented in almost every group of enzymes. The methods used for the purification and separation of these enzymes from other components do not differ substantially from those usually employed for enzymes not containing metals as prosthetic groups. These methods include techniques such as gel permeation, ion exchange, affinity chromatography and high performance liquid chromatography (HPLC). The reader is referred to these specific topics for details on the chromatographic techniques.

The purification strategy varies from one enzyme to another; however, an effective procedure for some enzymes is affinity chromatography. Alcohol dehydrogenase, for example, can be extensively purified by affinity chromatography based on the interaction of the coenzyme with a Blue A column and subsequent elution of the enzyme with NAD^+ .

Good recovery of the metalloenzymes from chromatographic columns may depend on the precautions adopted during the separation procedures. In particular, special care is required to preserve the integrity of the metal-protein complex during chromatography by avoiding conditions that may affect metal binding. A loss of metal can occur in the presence of chelating agents such as ethylenediaminetetraacetic acid (EDTA) or as a result of decreasing the pH of the medium. Buffer complexation with metals may also affect metalloenzyme stability. The use of inorganic buffers should be avoided as they may remove metals

essential to enzymatic activity. To avoid problems of metal chelation, the use of Good buffers (made of *N*-substituted taurine and glycine) is useful. Certain substances usually added to protein solvents may affect the metal binding; high concentrations of reducing agents such as dithiothreitol may remove metals with low binding affinity. In these cases, the best choice is to use 0.5% (v/v) mercaptoethanol as a reducing agent, as this substance does not remove metals.

Separation of Protein and Metal Moieties

Metal-free enzymes are well-suited to the study of the interaction of protein and metal ions and the effect of such interaction on the structure and function of the enzyme. Separation of metal from protein is easily performed using chelating agents at a pH between 5.5 and 7.5. The most commonly used chelator for apoenzyme preparation is 1,10-phenanthroline, but it is a good rule to test several chelating agents for their efficacy. A list of chelating agents used to remove the metal from various metalloenzymes is given in Table 1. The use of EDTA as chelator is not recommended because it binds to protein and laboratory glassware; if its usage cannot be avoided, it is advisable to add a trace amount of ^{14}C -EDTA to check its complete removal.

The procedure for apoenzyme preparation requires that the enzyme, at a concentration of $0.1\text{--}1\text{ mmol L}^{-1}$, is dialysed against several volumes of chelator solution with several changes. Dialysis tubings may contain heavy metals, hence they should be heated at $70\text{--}80^\circ\text{C}$ for 2 h in metal-free water (see below) before use. Metal-free dialysis membranes (Spectra/por) are also commercially available. The chelator is removed by extensive dialysis against metal-free buffer (see below). If 1,10-phenanthroline or 8-hydroxyquinoline is used to chelate the metal, their removal can be monitored by following the optical densities of the dialysate, because these

Table 1 Chelating agents commonly used for the preparation of metal-depleted enzymes

Substance	Metal	Reference
Ethylenediamine-tetraacetic acid	$\text{Zn}^{2+} + \text{Mg}^{2+}$	McConn <i>et al.</i> (1964) <i>J. Biol. Chem.</i> 239: 3706
1,10-Phenanthroline	Zn^{2+}	Prescott <i>et al.</i> (1983) <i>Biochem. Biophys. Res. Commun.</i> 114: 646
Dipicolinic acid	Zn^{2+}	Maret (1989) <i>Biochemistry</i> 28: 9944
8-Hydroxyquinoline-5-sulfonic acid	Zn^{2+}	Jacob <i>et al.</i> (1998) <i>Proc. Natl. Acad. Sci. USA</i> 95: 3489

substances absorb light. The chelator can also be removed by gel filtration chromatography. A suitable chromatographic system is represented by a Bio-Gel P polyacrylamide pre-loaded column (Bio-Rad). For most proteins, an exclusion limit of 6000 may allow recovery of the apoenzyme in the void volume with little dilution of the sample.

An alternative procedure for apoenzyme preparation is provided by the use of Chelex 100. The sodium form of the resin, previously equilibrated in metal-free buffer, is mixed with the metalloenzyme solution at a ratio of about 20% in volume. If the metal is essential for catalytic activity, a time-dependent loss of enzyme activity may be observed during the treatment with Chelex 100. The advantage of this method is that the apoenzyme so prepared can be stored in the presence of the resin, thus avoiding its reactivation by adventitious metals.

In order to maintain the protein in a metal-free form, it is important to minimize the presence of contaminating metals. One of the first precautions for preventing an unwanted reassociation with metals is the use of metal-free water in all purification and separation procedures. Ultra pure water suitable for apoenzyme preparation can be obtained by repeated distillation or by using a Milli-Q apparatus (Millipore). The latter system can supply water with a metal content below the detection limits of sophisticated analytical methods such as AAS, provided the cartridge is changed frequently.

Although metal-free water is indispensable, sometimes its use is not sufficient to eliminate contamination unless polystyrene metal-free containers are used for its storage. Of course, even the use of high purity water will not avoid unwanted problems if reagents, glassware and buffers themselves are sources of contamination. The use of polystyrene labware must be preferred in place of polyethylene and polypropylene, because these may be sources of metal ions. The ubiquitous presence of metals such as zinc, mercury, iron and aluminium in many laboratory reagents is another factor that has to be controlled. It is advisable to remove these metals from buffers and solutions before using them in separation procedures. The most widely recommended methods for eliminating metals from aqueous media are dithizone extraction or treatment with a chelating resin.

Dithizone (diphenylthiocarbazone) is used as a complexing reagent to remove heavy metals from aqueous solutions by exploiting its high solubility in organic solvents compared to the low solubility in water. Dithizone may be recrystallized by dissolving 2 g of substance in 100 mL chloroform. The volume of this solution is then reduced to one-half by evaporation under a nitrogen stream. The crystals are col-

lected by filtration, washed with carbon tetrachloride and dried under vacuum. All the manipulations with organic solvents must be carried out in a hood. The solution to be extracted is shaken for 5 min with 0.1 vol of a freshly prepared dithizone solution (0.02% in chloroform) in a separatory funnel equipped with a Teflon stopcock (do not grease the stopcock). The extraction procedure must be repeated several times with different aliquots of dithizone solution. At the end, any trace of organic solvent present in the aqueous phase is removed under reduced pressure. This procedure works very well for ions such as Zn^{2+} , Cd^{2+} , Co^{2+} , Cu^{2+} , Fe^{2+} and Ni^{2+} , but is not as effective for Mn^{2+} . In addition, dithizone extraction cannot be used with buffers with a pH above 8, because at this pH dithizone solubility in water increases.

An alternative method uses a column of Chelex 100 as metal chelator. The resin is washed with 2 vol of 0.5 mol L^{-1} HCl, 5–6 vol of water and 2 vol of 0.5 mol L^{-1} NaOH. After a final wash with 5 vol of water, the resin is packed in a chromatographic column. The buffer to be demetallized is passed through the column at a flow rate of $10\text{--}20 \text{ mL min}^{-1} \text{ cm}^{-2}$, and collected after several bed volumes have been discarded.

Metalloproteins with no Enzymatic Activity

Detection of Metal-binding Proteins in Chromatographic Eluates

Most of the metalloproteins lacking catalytic activity are metal-binding proteins. In general, these molecules are characterized by a high metal-to-protein stoichiometry: usually from 4 to 7 atoms of heavy metal are bound to cysteinyl, glutamyl, aspartyl residues of the polypeptide chain. The best known among the metal-binding proteins are metallothioneins (MT), a family of cysteine-rich low molecular weight polypeptides present in all animal phyla, as well as in fungi, plants and cyanobacteria. Mammalian MT are single chain proteins made of 60 amino acids, including 20 cysteines arranged in two domains of metal-thiolate clusters containing 7 equivalents of metal (usually zinc, copper or cadmium).

Purification and separation of metal-binding proteins are performed by column chromatographic procedures, generally involving gel permeation and anion exchange methods and HPLC. As many metal-binding proteins do not exhibit evident biological activity, a widely used technique for monitoring chromatographic eluates is the determination of the metal by AAS. Flame AAS is mostly used for samples

in solution, provided the analyte concentration is in the order of p.p.m. ($1 \text{ p.p.m.} = 1 \text{ mg L}^{-1}$) and enough volume of sample (at least 1 mL) is available for analysis. If the analyte concentration is in the range of p.p.b. ($1 \text{ p.p.b.} = 1 \text{ } \mu\text{g L}^{-1}$), or if one wishes to minimize the volume of sample to be employed in the analysis, the technique of choice is the furnace AAS.

This technique, initially proposed by L'vov, became commercially available in 1969. A small amount of sample (20 μL) is introduced in a graphite furnace that is rapidly brought to high temperature by electrical heating. The sample is converted in atomic vapour and part of a light produced by a lamp containing the element to be analysed is absorbed by the analyte. In some cases, the sample is placed on a small platform added to the furnace to delay vaporization until the temperature within the furnace has reached a stable plateau. The addition of a matrix modifier may help to stabilize the analyte to high temperatures. A drastic reduction of the background influence is achieved by the Zeeman correction. The experimental conditions for the determination of the elements most commonly found in metalloproteins are reported in Table 2 for graphite furnace AAS.

In general, the quantification of the MT-bound metal in chromatographic eluates does not require pretreatment of the sample such as digestion with oxidizing agents or ashing. However, the extent of matrix interference should be evaluated by measuring the absorbance of a known standard in the presence of the sample (internal standard technique). If metal concentration is high, interference may be reduced by appropriate dilution of samples. The determination of volatile elements such as cadmium and mercury requires the addition of a modifier (Table 2).

Separation of Metallothionein from High Molecular Weight Proteins

The procedure currently employed for MT isolation is gel permeation chromatography. In a typical preparation, 1 vol of an ethanol chloroform solution (1.05/0.08 v/v) is added dropwise to 1 vol of a tissue

extract, previously centrifuged at 100 000 g. After the precipitate is centrifuged at 20 000 g for 15 min, the supernatant is mixed with 3 vol ethanol prechilled at -20°C and maintained at the same temperature overnight. The resulting pellet, collected by centrifugation at 20 000 g for 20 min, is dissolved in 20 mmol L^{-1} Tris/HCl buffer pH 8.6 and loaded on a Sephadex G-75 column equilibrated with 10 mmol L^{-1} Tris/HCl pH 8.6. The column is eluted with the equilibration buffer and the eluate is monitored for metal content. Such a procedure is particularly suitable for low molecular weight proteins like MT, because these can be easily separated from the bulk of high molecular weight proteins. MT usually elutes at the level of standard cytochrome *c* (mol wt about 12 000) because of molecular asymmetry (Figure 1).

One should be aware, however, that the original metal composition of MT may be altered by the presence of adventitious metals. As zinc usually found associated with tissue MT can be exchanged for other heavy metals with higher affinity for thiol groups, such as cadmium and copper ions, that may be present as contaminants in chromatographic media or glassware, it is advisable to render these sources metal-free before use. The methods for removing heavy metals from buffers have been described above. It is advisable to wash the gel permeation column with 3 bed vol of 2 mmol L^{-1} 1,10-phenanthroline to remove trace metals from the matrix. The column is then washed with metal-free buffer until disappearance of the absorbance at 320 nm.

Separation of Metallothionein Isoforms

Genetic polymorphism is a typical feature of metallothionein. One or more MT isoforms have been found in most animal tissues; their intracellular levels may vary from tissue to tissue. These isoforms are often very similar, with only a few amino acid substitutions in their amino acid sequences. Because they are so similar it is sometimes difficult to separate these proteins; however, if two isoforms have different

Table 2 Conditions for the determination of some elements by AAS with graphite furnace

Element	Wavelength (nm)	Atomization temperature ($^{\circ}\text{C}$)	Modifier	Graphite tube
Cd	288.8	1600	$0.2 \text{ mg NH}_4\text{H}_2\text{PO}_4 + 0.01 \text{ mg Mg(NO}_3)_2$	Pyrolytic/platform
Cu	324.8	2300	None	Pyrolytic/platform
Co	242.5	2500	$0.05 \text{ mg Mg(NO}_3)_2$	Pyrolytic/platform
V	318.5	2650	None	Pyrolytic/wall
Fe	248.3	2400	$0.05 \text{ mg Mg(NO}_3)_2$	Pyrolytic/platform
Hg	253.7	2000	$10 \text{ mg Te in } 1\% \text{ HCl}$	Uncoated/wall
Zn	213.9	1800	$0.006 \text{ mg Mg(NO}_3)_2$	Pyrolytic/platform
Se	196.0	2100	$0.05 \text{ mg Cu} + 0.01 \text{ mg Mg(NO}_3)_2$	Pyrolytic/platform

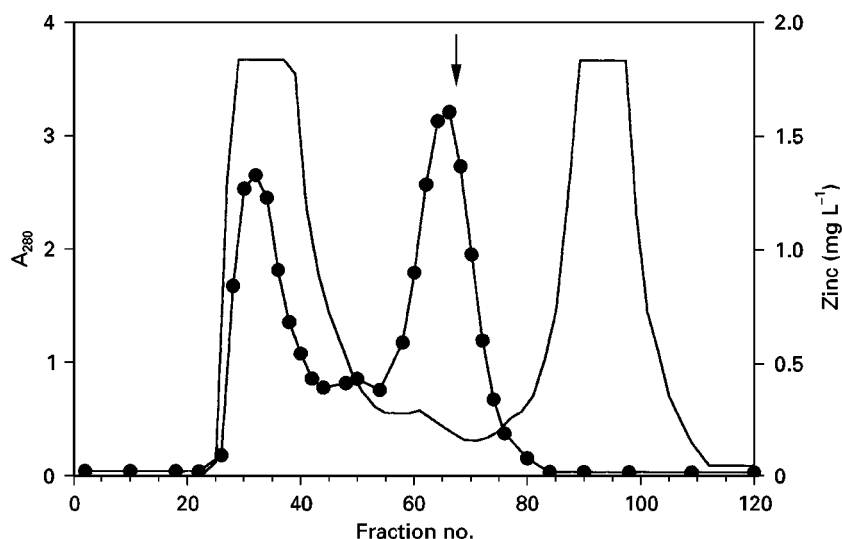


Figure 1 Separation of metallothionein by gel permeation chromatography. About 8 mL of extract containing 200 mg protein from fish liver was loaded on a Sephadex G-75 column (2.6×35 cm) previously equilibrated with 10 mmol L^{-1} Tris/HCl buffer pH 8.6. The column was eluted with the same buffer and fractions (2 mL) were monitored for absorbance at 280 nm (continuous line) and zinc content (circles). The arrow indicates the elution volume of standard rabbit liver metallothionein. Reproduced with permission from Scudiero R, Carginale V, Riggio M, Capasso C, Capasso A, Kille P, di Prisco G and Parisi E (1997) Difference in hepatic metallothionein content in Antarctic red-blooded and haemoglobinless fish: undetectable metallothionein levels in haemoglobinless fish is accompanied by accumulation of untranslated metallothionein mRNA. *Biochemical Journal* 322: 207–211.

net electric charges, they can be separated by anion-exchange chromatography. In **Figure 2** the elution profile from a diethylaminoethyl (DEAE)-cellulose column of two MT isoforms is shown. Metallothioneins were previously separated from high molecular weight

proteins by solvent precipitation followed by gel permeation chromatography on a Sephadex G-75 column under conditions similar to those described above. Anion exchange chromatography was performed as usual, by loading the sample on the column; this was

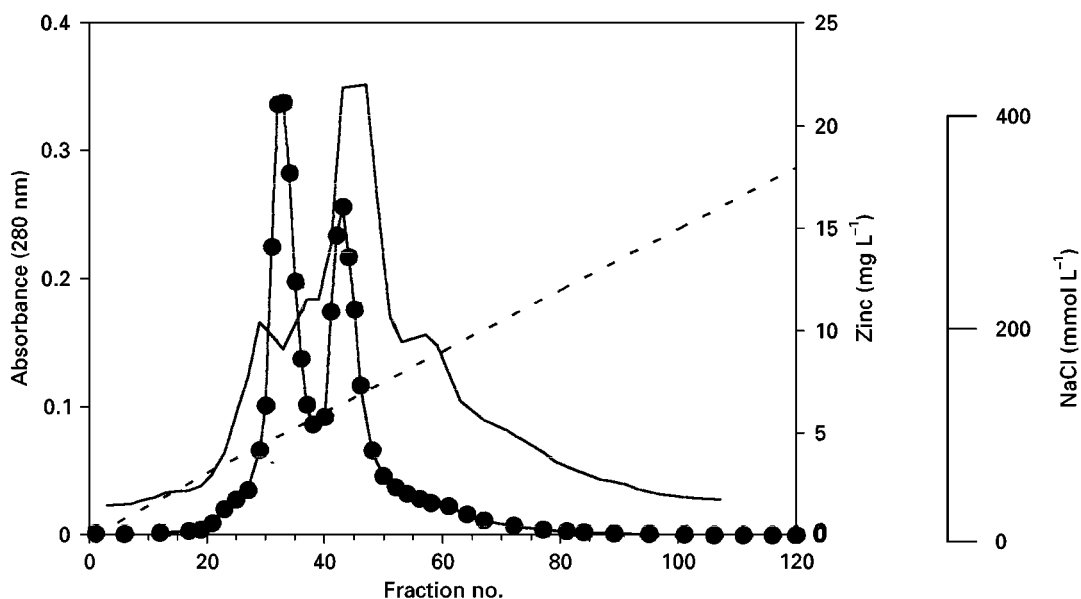


Figure 2 Separation of sea urchin metallothionein isoforms by anion exchange chromatography. The metallothionein-containing fractions from a Sephadex G-75 column were pooled and loaded on a DEAE-cellulose column (1.6×25 cm) equilibrated with 20 mmol L^{-1} Tris/HCl pH 8.6. The column was eluted with a linear gradient of NaCl (0 – 400 mmol L^{-1}) in equilibration buffer and fractions (3 mL) were monitored for absorbance at 280 nm (continuous line) and zinc content (circles). Reproduced with permission from Scudiero R, Capasso C, Carginale V, Riggio M, Capasso A, Ciaramella M, Filosa S and Parisi E (1997) PCR amplification and cloning of metallothionein cDNAs in temperate and Antarctic sea urchin characterized by a large difference in egg metallothionein content. *Cellular and Molecular Life Science* 53: 472–477.

Table 3 Chromatographic conditions for separation of metallothionein isoforms by HPLC

Column type	Elution buffers	Running conditions	Reference
TSK G 3000 SW (Yokyo Soda) (600 × 7.5 mm i.d.)	10 mmol L ⁻¹ Tris/HCl pH 8.6	20 min at a flow rate of 1.0 mL min ⁻¹	Suzuki <i>et al.</i> (1984) <i>J. Chromatogr.</i> 303: 131
LiChrosorb RP-18 (10 μm) (Bischoff Analysentechnik) (250 × 21 mm i.d.)	A: 25 mmol L ⁻¹ Tris/HCl pH 7.5 B: 60% CH ₃ CN in buffer A	One-step linear gradient: 0–100 min, 0–40% B at a flow rate of 2 mL min ⁻¹	Hunziker <i>et al.</i> (1985) <i>Biochem. J.</i> 231: 375
DEAE-5PW (Waters) (750 × 7.5 mm i.d.)	A: 10 mmol L ⁻¹ Tris/HCl pH 7.4 B: 200 mmol L ⁻¹ Tris/HCl pH 7.4	One step linear gradient: 0–12 min, 0–40% B at a flow rate of 1 mL min ⁻¹	Lehman <i>et al.</i> (1986) <i>Anal. Biochem.</i> 153: 305
Aquapore RP 300 (Brownlee Laboratories) (10 μm) (250 × 4.6 mm i.d.)	A: 10 mmol L ⁻¹ Tris/HCl pH 7.5 B: 60% CH ₃ CN in buffer A	One-step linear gradient: 0–100 min, 0–40% B at a flow rate of 1 mL min ⁻¹	Ebadi <i>et al.</i> (1989) <i>Neurochemical Res.</i> 14: 69
μBondapak C18 (Waters) (10 μm) (100 × 8 mm i.d.)	A: 10 mmol L ⁻¹ NaH ₂ PO ₄ pH 7.0 B: 40% CH ₃ CN in buffer A	Two-step linear gradient: 0–5 min, 0–10% B; 5–20 min, 10–25% B	Richards (1989) <i>J. Chromatogr.</i> 482: 87

washed with the low ionic strength buffer and eluted with a linear gradient of NaCl.

A suitable procedure for separation of MT isoforms is HPLC, and this can be performed with various types of column systems. Conditions most usually applied for the HPLC separation of MT are given in Table 3. Since MT are converted in the corresponding metal-free apoforms at acidic pH, the use of neutral buffer systems is recommended. A suitable system is a μBondapak C₁₈ column eluted with a two-step linear gradient of acetonitrile in phosphate buffer (Figure 3).

Preparation of Metal-free Metallothionein for Metal Reconstitution

Metal substitution in MT is a common procedure to produce a complex with a defined metal composition for structural studies. It must be remembered that certain metals form complexes with different coordination numbers: while Zn and Cd in MT are tetrahedrally coordinated, Cu forms tridentate complexes. To perform metal substitution it is necessary first to prepare the metal-free MT. In doing so, it is recommended that adventitious metals in reagents and glassware are avoided by following the procedures described above.

Metal-free MT can be prepared by lowering the pH of the protein solution to 2. Under these conditions, the metal moiety dissociates from the protein; the apothionein is then separated from the metal by gel permeation chromatography on a Sephadex G-25 column. An acidified sample of about 5 mL containing approximately 1.5 mg of protein can be separated

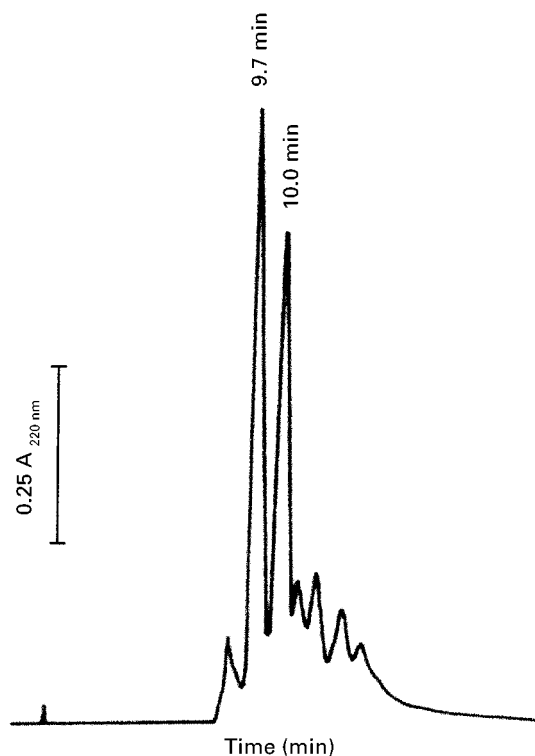


Figure 3 Separation of rabbit metallothionein isoforms by reversed-phase HPLC. The separation was performed on a μBondapak C₁₈ column using a two-step linear gradient of acetonitrile in 10 mmol L⁻¹ NaH₂PO₄ pH 7.0 at a flow rate of 3 mL min⁻¹ (0–6% from 0 to 5 min, 6–15% from 5 to 20 min). The amount of purified MT used in each run ranged from 50 to 100 μg. Modified with permission from Richards MP (1991) Purification and quantification of metallothioneins by reverse-phase high-performance liquid chromatography. *Methods in Enzymology* 205: 217.

from the metal on a 2×20 cm column in 0.1% trifluoroacetic acid, by recovering the apothionein in the void volume. The addition of a reducing agent is not required as the sulfhydryl groups of cysteines are maintained in the reduced form as long as the pH is acidic. The apothionein so prepared can be stored at -80°C in an atmosphere of argon in a sealed ampoule. Prolonged storage should be avoided, as apothionein has a strong tendency to be oxidized. Anaerobic conditions are strictly required to prevent oxidation of the sulfhydryl groups with formation of large protein aggregates. The concentration of the demetallized protein can be determined by titrating the sulfhydryl groups with Ellman's reagent (5,5'-dithiobis(2-nitrobenzoic acid)), or by measuring the absorbance at 220 nm and assuming an extinction coefficient of $7.9 \text{ mg cm}^{-1} \text{ mL}^{-1}$ at pH 2. Metals such as zinc and cadmium are completely removed from the protein at low pH, but the procedure is not as effective for copper.

Removal of copper from Cu-thionein requires the use of chelating agents such as diethyldithiocarbamate (DTC). A solution of Cu-MT, brought to pH 5 by adding $30 \mu\text{L}$ of 3 mol L^{-1} acetate buffer pH 5 per mL of solution, is mixed with solid DTC (1 mg mL^{-1} of MT solution) and incubated at room temperature for 1 h. The colloidal precipitate of Cu-DTC is then removed by filtration on a $0.22 \mu\text{m}$ Millipore filter, and the filtrate containing the apothionein is desalted on a Sephadex G-25 column equilibrated and eluted with 0.1% trifluoroacetic acid.

Metal substitution is performed by mixing an argon-purged acidic solution containing 20 mg apothionein with 7–8 equivalents of metal (Zn, Cd, Hg, Bi or Pb). The solution is then rapidly titrated to pH 8.6 (7.6 for Pb-MT) with an oxygen-free solution of 0.5 mol L^{-1} Tris base under fast stirring. Immediately after titration, the solution is mixed with a small aliquot of a Chelex 100 suspension in 20 mmol L^{-1} Tris/HCl pH 8.6 (7.6 for Pb-MT) and stirred for 5 min. The resin is then removed by centrifugation and the solution is concentrated by ultrafiltration. MT is purified by gel permeation chromatography on a Sephadex G-50 column equilibrated and eluted with 20 mmol L^{-1} Tris/HCl pH 8.6.

Reconstitution with Cu(I) is more troublesome as this ion has a marked tendency to oxidation. A stable form of Cu(I) can be prepared by dissolving Cu_2O in acetonitrile containing 2 mol L^{-1} HClO_4 at 100°C . The solution is evaporated at room temperature to obtain crystals. Reconstitution is carried out by mixing apometallothionein with increasing amounts of a solution of Cu(I)-acetonitrile at pH 2 followed by titration to pH 7 with Tris/acetate buffer. The whole procedure must be carried out under anaerobic conditions.

Conclusions

Developments in the field of metalloprotein research are strictly related to any future progress achieved in protein separation techniques. For metalloproteins, the main goals are reduction in the amount of the biomass required for their preparation, and decrease in separation time. Large amounts of protein are expected to be produced by expanding the use of recombinant DNA techniques combined with effective separation procedures such as affinity chromatography. Immunochemical methods can be applied for the detection of small protein quantities present in chromatographic eluates, and can be particularly useful for proteins lacking enzymatic activity. Techniques coupling HPLC and AAS may contribute to decreasing the time gap between sample separation and metal detection.

See also: II/Centrifugation: Analytical Centrifugation. **Chromatography: Liquid:** Mechanism: Size Exclusion Chromatography. **III/Peptides and Proteins:** Liquid Chromatography. **IV/Essential Guides for Isolation/Purification of Enzymes and Proteins.**

Further Reading

- D'Auria S, La Cara F, Nazzaro F *et al.* (1996) A thermophilic alcohol dehydrogenase from *Bacillus acidocaldarius* not reactive towards ketones. *Journal of Biochemistry* 120: 498.
- Deutscher MP (ed.) (1990) *Methods in Enzymology. Guide to Protein Purification*, vol. 182. New York: Academic Press.
- Ellman GL (1959) Tissue sulfhydryl groups. *Archives of Biochemistry and Biophysics* 82: 70.
- Klaassen CD (ed.) (1999) *Metallothionein IV*. Basel: Birkhäuser.
- Riordan JF and Vallee BL (eds) (1988) *Methods in Enzymology. Metallobiochemistry*, vol. 158. New York: Academic Press.
- Riordan JF and Vallee BL (eds) (1991) *Methods in Enzymology. Metallothionein and Related Molecules*, vol. 205. New York: Academic Press.
- Suzuki KT, Sunaga H and Yajima T (1984) Separation of metallothionein into isoforms by column switching on gel permeation chromatography and ion-exchange columns with high-performance liquid chromatography-atomic-absorption spectrophotometry. *Journal of Chromatography* 303: 131.
- Suzuki KT, Imura N and Kimura M (1993) *Metallothionein III*. Basel: Birkhäuser.
- Vallee BL (1960) Metal and enzyme interactions: correlation of composition, function and structure. In: Boyer PD, Lardy H and Myrbäck K (eds) *The Enzymes*, Vol. 3. New York: Academic Press.
- Vallee BL and Wacker EC (1970) Metalloproteins. In: H. Neurath (ed.), *The Proteins*, vol. 5. New York: Academic Press.

MICROORGANISMS: BUOYANT DENSITY CENTRIFUGATION

See III / FOOD MICROORGANISMS: BUOYANT DENSITY CENTRIFUGATION

MICROWAVE-ASSISTED EXTRACTION: ENVIRONMENTAL APPLICATIONS



G. N. LeBlanc, CEM Corporation, Matthews, NC, USA

Copyright © 2000 Academic Press

Speed and efficiency are always prime considerations of an analytical technique. In addition, we are seeing environmental considerations – ‘greening’ of methods – becoming another important factor. A solvent extraction technique that reduces extraction time, improves extraction efficiency and reduces solvent consumption by a factor of 10 is an important one. The latter is critical since it is estimated that about 100 million litres of organic solvent are used annually in organic analytical laboratories worldwide. The use of microwave heating for the extraction of compounds from a variety of sample matrices has been performed since 1985. This review article provides information on the development of the microwave-assisted extraction (MAE) technique, microwave instrumentation and its capabilities, and a perspective for extraction applications.

Development

Microwave heating was first introduced commercially in 1947. It took some time to catch on but it is now a standard item in most kitchens for cooking uses. Its use in the chemistry laboratory has significantly lagged behind domestic applications. Microwaves were first used in 1975 as a heating source for acid digestion under atmospheric conditions. The sample preparation step was reduced from 1–2 h to under 15 min, producing an overall reduction in analysis time. This work initiated the use of microwave energy as a heating source for the chemistry laboratory. Other applications include distillation, organic and inorganic synthesis, evaporation and solvent extraction.

The early applications for MAE were for the extraction of compounds with nutritional interest from

plant and animal tissues. From 1986 to 1990, Ganzler and co-workers published a series of four papers exploring the use of microwave energy to partition various compounds from soils, seeds, food and animal feeds as a sample preparation method prior to chromatographic analyses. The extraction step was performed under atmospheric conditions. They extracted a variety of compounds that included anti-nutritives, crude fat and pesticides. They used solvent schemes similar to their traditional Soxhlet technique to allow a direct comparison of the recoveries between the two techniques. The heating programme consisted of multiple 30 s microwave heating cycles (up to seven cycles) followed by a cooling step. This approach allowed observation of the samples in the microwave cavity to prevent sample boil-over.

The microwave extracts gave recoveries that were 100–120% of the Soxhlet technique. However, the MAE times were a factor of 100 less than the traditional Soxhlet approach. The authors postulated that improved extraction efficiency was due to the polar nature of the extracted compounds or the water contained in the materials. They also noted a decrease in extraction efficiency for the recovery of non-polar compounds when a nonpolar solvent was used.

The published work of Freitag and John in 1990 expanded the application and technique. These authors explored the use of microwave heating at elevated temperatures and pressure for the extraction of additives from polyolefins. The additives were antioxidants, Irganox 1010 and Irgafos 168, and the light stabilizer Chimassorb 81. The polyolefin matrices were polyethylene and polypropylene with a particle size of 20 mesh and a sample size of 1 g. The MAE was performed with 30 mL of 1,1,1-trichloroethane or a mixture of acetone and *n*-heptane. They obtained 90–100% recoveries of the additives with extraction times of 3–6 min without degradation of the analytes at the elevated temperatures of the extraction. This

compared favourably with the conventional 16 h Soxhlet or 0.5–2 h reprecipitation techniques.

Pare *et al.* from the Ministry of Environment of Canada introduced the microwave-assisted process (MAP™) through a US patent in 1991. In this work, Pare used microwave energy to extract a variety of essential components from natural products and foods, such as biologicals and consumer products. The primary examples are the extraction of essential oils from peppermint, garlic and cedar. The major feature of this work is the release mechanism for the compounds of interest from the substrate. The microwave energy was used to disrupt the glandular and vascular system of the tissue without damaging the surrounding tissue. The solvent was used to trap and dissolve the compounds released from the tissue.

In general, the mechanism involves localized heating of the free water present in the sample. Once the water is at or above its boiling point, the water causes the cell membrane to rupture. This water, as steam, transports the target analyte from the solid to the nonabsorbing solvent. In this type of work, the sample is a good dielectric while the solvent is a poor dielectric. The microwave process gave higher yields than the traditional steam distillation process. The authors postulated that the improved efficiency was due to the lower bulk temperatures and shorter extraction times.

In 1992, Bichi *et al.* published work from the pharmaceutical area based on MAE using closed-vessel technology with temperature-feedback control. They extracted pyrrolizidine alkaloids from dried plants using 25–50 mL of methanol. The extractions were performed over a temperature range of 65–100°C for 20–30 min. The MAE technique gave qualitatively and quantitatively identical chromatographic results relative to the samples extracted by the Soxhlet procedure with a significant reduction in extraction time and solvent consumption. The temperature feedback control provided highly reproducible extractions.

In 1993, Onuska and Terry published the first data on the use of MAE for pollutants from environmental samples. They successfully extracted organochlorine pesticide residues from soils and sediments using a 1 : 1 mixture of isooctane–acetonitrile using sealed vials. The samples were irradiated for five 30 s intervals. This produced faster and more reliable results than the conventional methods. They also studied the use of a nonpolar solvent, iso-octane, for the extraction of wet sediment samples. Pesticide residue recoveries increased as the moisture content increased to a maximum of 15% and then levelled off. This shows the importance of a polar co-solvent when using a nonpolar extracting solvent for MAE tech-

niques that are temperature-dependent. In 1994 Lopez-Avila *et al.* published their work to expand the use of MAE to 187 volatile and semivolatile organic compounds from soils. The compounds included polyaromatic compounds (PNA), phenols, organochlorine pesticides and organophosphorus pesticides. This work was performed using a temperature feedback-controlled microwave heating system with closed vessels. This demonstrated the viability of the technique for the extraction of many compounds of interest to the US Environmental Protection Agency with relatively small volumes of solvent and extraction times of only 10 min. This culminated in 1998 with the approval of the microwave extraction technique by the SW-846 Organic Methods Workgroup of incorporation into SW-846 as the latest of the 'green' methods.

In 1997 there were a number of significant extensions of the technology. Incorvia-Mattina *et al.* investigated the use of MAE to extract taxanes, used in ovarian and breast cancer research, from *Taxus* biomass. MAE offered significant time savings versus the standard shaking technique and improved yields versus synthetic approaches. Stout *et al.* combined MAE with liquid chromatography–electrospray ionization–mass spectrometry for the determination of imidazolinones in soils at concentrations of less than 1 p.p.b. McNair *et al.* reported the combination of MAE with solid-phase microextraction for the analysis of flavour ingredients at concentrations of 2–10 p.p.b. in solid food samples. This technique showed good selectivity for the target analytes in a variety of foods.

Instrumentation

MAE is the process of heating solid sample–solvent mixtures with microwave energy and the subsequent partitioning of the compounds of interest from the sample to the solvent. The most common approach is to perform the extraction in a sealed vessel that is microwave-transparent. This allows a temperature elevation significantly above the atmospheric boiling point of the solvent (Table 1) and hastens the extraction process.

The alternative approach is to perform the extraction in an open vessel at atmospheric conditions. This approach is common when the solvent is nonpolar or microwave-transparent and the sample is a biological or agriculture tissue that has a polar constituent, usually water. This is the basis for the patent issued to Environment Canada for the MAP™.

For the scope of this review article, we will limit the instrumentation discussion to the closed-vessel microwave heating system. In approaching MAE

Table 1 Solvent boiling point – closed vessel temperature comparison

Solvent	Boiling point (°C)	Closed vessel temperature (°C) ^a
Acetone	56.2 ^b	164
Acetone : Cyclohexane 7 : 3 vol/vol	52	160
Acetonitrile	81.6 ^b	194
Dichloromethane	39.8 ^b	140
Hexane	64.7 ^b	162 ^c
Methanol	68.7 ^b	151

^aAt 175 psig.^b*Lange's Handbook of Chemistry*, 14 edn. Dean JA (ed.) New York: McGraw-Hill, Inc., 1992: 11.10–11.12.^cUsing carboflon heating insert.

applications, it is first necessary to understand the analysts' objectives. These objectives include:

1. Selection of the optimum solvent for the analytes of interest.
2. Minimization of any steps prior to the extraction step.
3. The use of a minimum amount of solvent for the extraction step.
4. Effective and reproducible extraction conditions.
5. High sample throughput.
6. Safe operation.

Considering these objectives, a microwave-assisted extraction system was designed that was a derivative of the successful microwave acid digestion system. The key components are:

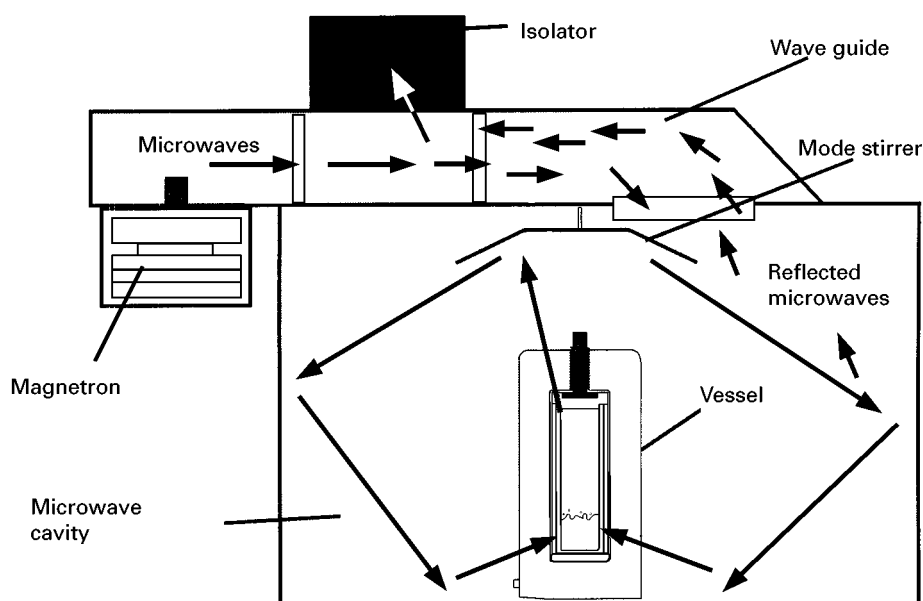
1. Microwave instrumentation
2. Solvent safety features

3. Vessel technology
4. Temperature control system
5. Indirect heating source (for heating nonpolar solvents)
6. Stirring mechanism

Each component is reviewed in terms of its technical merit and how it assists in meeting the analysts' objectives for the extraction step.

Microwave Instrumentation

Figure 1 shows the major components of the microwave system, including the magnetron, isolator, wave guide, cavity and mode stirrer. Microwave energy is generated by the magnetron, propagated down the wave guide and introduced into the cavity. The mode stirrer distributes the energy in various directions while the cavity acts as a containment housing for the energy until it is absorbed by the sample load within the cavity. The isolator protects the magnetron from

**Figure 1** Microwave system components.

reflected energy that would decrease its power output. A good analogy is a one-way mirror – it allows energy to go from the magnetron to the cavity but will not allow it to go from the cavity to the magnetron. A turntable can be used to rotate the sample load within the cavity to ensure even energy distribution.

Microwave heating is significantly different from conductive heating methods. Conductive heating is sample-independent. All samples placed inside a conduction heating oven will equilibrate to the programmed temperature. This can take quite some time. Microwave heating is sample-dependent. The temperature rise rate of samples will depend on their microwave-absorbing characteristics. The microwave design provides the ability to heat uniformly a large number of samples in a short period of time based on the sample load characteristics.

Solvent Safety Features

Due to the flammable characteristics of many organic solvents, there is a major safety issue when heating a solvent in a microwave field. This safety issue is magnified when heating these solvents in sealed vessels at temperatures up to 100°C above their atmospheric boiling point. The microwave system should have redundant safety features, each acting as a back-up to prevent possible fire or explosion from occurring inside the cavity. Instruments should be designed to eliminate possible ignition sources, to detect solvent leaks and to remove leaking solvent. **Figure 2** is an illustration of the interior of a commercially available microwave extraction system. The safety aspects are an exhaust fan which evacuates the cavity air

volume approximately once per second. If the exhaust fan fails or there is a block downstream of the fan, the air flow switch shuts down the system. The solvent detector monitors the cavity for the presence of solvent. The detector shuts the system down if solvent concentrations reach one-tenth of the lower explosive limit for acetone, sets off an alarm and posts a message for the operator. The cavity is Teflon-coated to minimize the potential of high energy discharges. The system door is designed to withstand an event equivalent to the explosion of 1 g of TNT. It will partially open, allowing gases to escape, and then the compression springs will pull it closed. This will contain any of the contents associated with a vessel-related event inside the system's cavity.

Vessel Technology

The closed vessels used for MAE are designed for temperatures up to 200°C and pressures of 200 psi (14 bar). The materials of construction for the components that are in contact with the sample-solvent mixture, either Teflon or glass, are inert to solvents. However, since these materials are relatively weak, an outer body is used that is much stronger – either a reinforced thermoplastic or a frame of polypropylene, or both. In addition, these materials of construction absorb a minimal amount of microwave energy. **Figure 3** illustrates a standard extraction vessel and a control extraction vessel. The vessels are composed of glass or Teflon liners, Teflon, PFA® seal cover, polyetherimide load disc and sealing screw, glass-filled polyetherimide sleeve and polypropylene support frame. The vessel has a built-in pressure relief

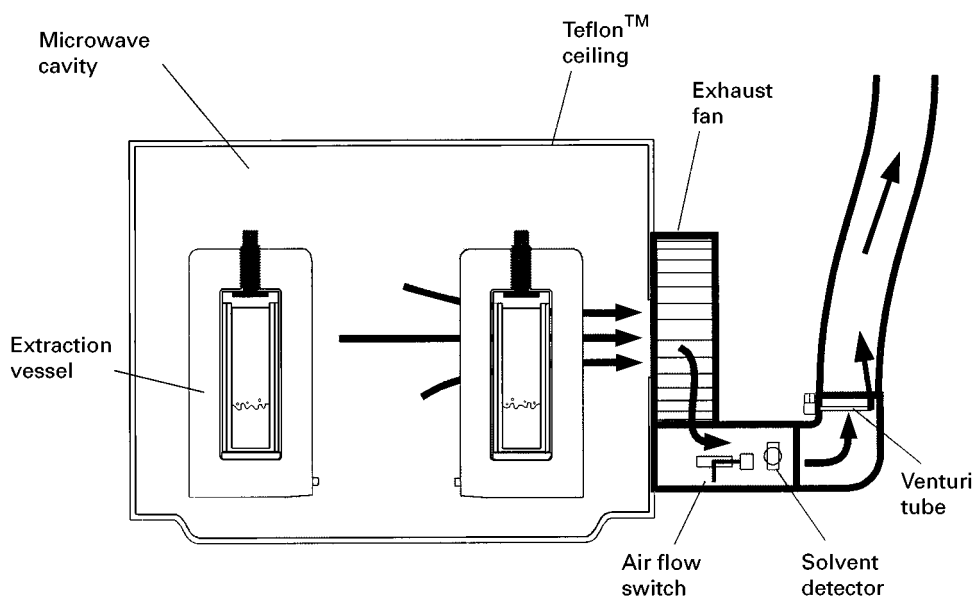


Figure 2 Safety exhaust and solvent detector.

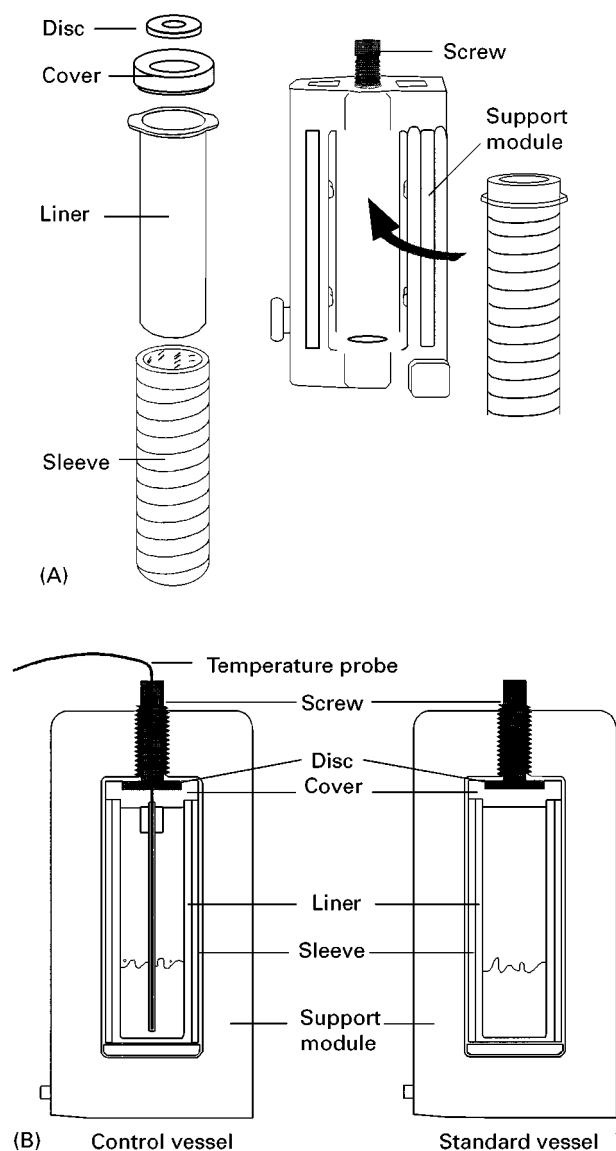


Figure 3 (A) Exploded view of a microwave extraction vessel. (B) Cut-away view of microwave extraction vessels.

mechanism for safety purposes. If the pressure inside the vessel exceeds the operating limits, the vessel will automatically vent. The control vessel is modified to accept a probe to monitor and control the extraction temperature. A turntable of 14 extraction vessels is placed into the instrument's cavity for batch processing. The ability to rapidly achieve elevated solvent temperatures under controlled conditions for a large batch of samples is a major advantage of the MAE technique.

Temperature Control System

Temperature control is necessary to optimize the extraction efficiency, prevent thermal degradation

of the target analytes, and to provide reproducible operating conditions. This is achieved with a temperature measurement system that is microwave-transparent so it does not cause any self-heating. The temperature probe is inserted directly into the control vessel to measure the temperature of the solvent-sample mixture. It is then used in a feedback control loop to regulate the microwave power output to achieve and maintain the operator-selected extraction temperature. This approach provides temperature control for one of the samples in the batch and assumes equivalent reaction conditions for all the other samples. This control technique is augmented with an indirect infrared temperature measurement system. The infrared sensor is located underneath the cavity floor. It monitors the temperature of each vessel as it passes over the sensor. This temperature reading is correlated to the direct temperature reading from the control vessel to provide temperature data for all of the samples in the batch.

Indirect Heating Source

In some extraction applications, the solvent of choice for the target analytes is nonpolar and therefore does not heat when exposed to the microwave field. This would normally preclude the use of the MAE technique unless the analyst is willing to alter the solvent scheme to include a polar co-solvent. This is not desirable since it alters the extraction efficiency (or selectivity). This problem is overcome with the use of an insert that is a chemically inert fluoropolymer filled with carbon black, a strong microwave absorber. The insert is placed into the vessel with the solvent-sample mixture. The insert absorbs microwave energy and transfers the thermal energy it generates to the mixture. The performance characteristics of the heating inserts for heating with *n*-hexane in a microwave field are seen in Table 2. The use of the heating insert allows transfer of existing methods to the MAE technique without a change in the solvent scheme.

Stirring Mechanism

Stirring increases the surface area contact between the sample and solvent. This offers the benefit of improved extraction efficiency and decreased solvent consumption. Stirring is achieved with the use of a rotating magnet below the cavity floor and the placement of a magnetic spinbar in the extraction vessel. The magnet creates a rotating magnetic field that couples with the spinbar in the vessel to create a stirring effect. The spinbars are either coated with an unfilled fluoropolymer for applications using polar solvents or a carbon black filled fluoropolymer for applications with nonpolar solvents.

Table 2 MAE heating rate for *n*-hexane using heating insert

Temperature set point (°C)	Time to temperature (min)		
	1 Vessel	6 Vessels	12 Vessels
100	1:45	2:45	3:45
125	2:30	4:15	6:15
150	3:35	6:15	9:30

Notes: Each vessel contained 50 mL of *n*-hexane and 1 heating insert. The starting temperature was 25°C. As a point of reference, 12 vessels containing 50 mL of acetone will reach 125°C in 5 min under equivalent conditions.

These components create a system to perform MAE. This technique has the capability to reduce extraction time, reduce solvent consumption and improve extraction efficiency. However, it does not come without a cost. The extraction step is but one of many necessary steps to obtain the final analytical result. The analyst must take into account the differences in using the MAE technique versus their existing approach. The primary difference is the finished sample form. It is the same sample-solvent mixture originally placed into the vessel. The analyst needs to separate the sample from the solvent at the completion of the extraction step. If the analyst can work with an aliquot of the solvent for analysis, this objection can be overcome with the use of a syringe filtration technique. A secondary consideration is the vessel manipulations used with MAE. These manipulations will be new for the analyst.

Applications

MAE has been applied to a wide variety of samples in which traditional Soxhlet extractions are performed. Table 3 gives a performance comparison of MAE versus conventional extraction techniques for a variety of sample types. For the scope of this work, we will limit the application discussion to the extraction of plastics and polymers, pesticides and environmental samples.

Plastics and Polymers

The additive package used in the production of polyolefins is designed to improve processing efficiency or to impart specific performance characteristics. The package can contain antioxidants, antistatic agents, slip agents, anti-block agents, UV stabilizers or antifogging agents. It is important for production efficiency and product quality that the appropriate amount of each additive is present. A fast and reliable method is needed to determine the additive concentration level. The conventional extraction approach is a reflux technique with an appropriate sol-

vent for 1–48 h followed by high performance liquid chromatography (HPLC) analysis. An alternative extraction technique is sonication for 30–60 min, but the gain in speed is offset by a loss in extraction efficiency. MAE has the ability to address the time and extraction deficiencies of the reflux and sonication techniques. Freitag and John first demonstrated the potential for MAE when they obtained excellent antioxidant recoveries from polypropylene and polyethylene.

Pesticides and Herbicides

Pesticides and herbicides are used to protect a wide variety of agricultural commodities. There is an interest in pesticides, herbicides and their degradation product concentrations in plant and animal tissues and soil and sediment samples. The underlying assumption is that extractable compounds are labile in the environment and constitute a threat to the environment if they are hazardous. Specific examples are from the work of Fish and Revesz on chlorinated pesticides from soils and the work of Stout's group on imidazolinone herbicides in plant tissues. Fish and Revesz showed chlorinated pesticide recoveries from a Certified Reference Soil greater than or equal to those achieved using the standard Environmental Protection Agency Soxhlet technique, method 3540. This was achieved with extraction times of only 20 min and solvent volumes of 50 mL. Stout *et al.* incorporated the use of MAE with liquid chromatography-electrospray ionization-mass spectrometry to shorten the clean-up procedure and method development time of residue methodologies for determining the imidazolinones and their metabolites in crops. This application area is of concern not only to the traditional commercial testing laboratory, but to agro-chemical producers.

Environmental

The organic side of the environmental laboratory market constitutes the majority of the analytical testing load. The extraction of priority pollutants, as well

Table 3 MAE versus conventional extraction techniques

Sample	Analyte	Microwave			Conventional		
		Solvent volume (mL)	Extraction time (min per sample) ^a	Concentration	Solvent volume (mL)	Extraction time (min per sample) ^a	Concentration
Environmental	Priority pollutants	25	7	–	300	1080	–
	TPH	30	7	943 mg kg ⁻¹	300	60	773 mg kg ⁻¹
	OCP	50	7	92.3% ^b	300	1080	83.4% ^b
	PCBs	25	7	47.7 µg g ⁻¹	250	1080	44.0 µg g ⁻¹
	Methylmercury	10	6	80 µg g ⁻¹	200	150	81 µg g ⁻¹
	Dioxins	30	8	565 pg g ⁻¹	300	1440	542 pg g ⁻¹
	Organotin	20	5	1.28 µg g ⁻¹	–		1.3 µg g ⁻¹
Plastics	Anti-oxidants	30	6	157 µg g ⁻¹	200	60	140 µg g ⁻¹
	Erucamide	30	6	480 µg g ⁻¹	200	60	491 µg g ⁻¹
	Oligomers	40	8.5	1.16%	190	1440	1.24%
	Plasticizer	30	8	11.80%	200	120	11.78%
	% Extractables	35	8	6.62%	150	960	6.60%
	% Oil	50	6	2.42%	135	250	2.40%
Agrochemical	PCNB	25	6	0.42 p.p.b.	300	60	0.36 p.p.b.
	Imidazolinone	20	5	11.2 p.p.b.	400	120	10 p.p.b.
Food	% Fat	40	7	49.02%	75	360	49.11%
	% Fat	35	6	8.73%	250	120	8.75%
Other	% Extractables	75	7	43.80%	200	120	39.00%
	% Wax	50	5	0.88%	150	60	0.71%
	% Extractables	60	7	0.55	250	1080	0.55%

^aIncludes weighing, reagent addition, vessel manipulation, heating and cooling time.^bValue is % recovery. TPH, total petroleum hydrocarbons; OCP, organochlorine pesticides; PCB, polychlorinated biphenyls; HDPE, high density polyethylene; LDPE, low density polyethylene; PET, polyethylene terephthalate; PCNB, pentachloronitrobenzene.

as other organic molecular species, from solid samples is a primary concern. The workload in the environmental laboratory is expected to increase significantly and will thus require extraction techniques that offer increased throughput, reduced solvent consumption, improved efficiency and reproducibility. MAE has the potential to address these needs. McMillin of US Environmental Protection Agency-Region VI demonstrated this in a comparison of various soil extraction techniques for semivolatile analysis. He used an abbreviated MAE technique consisting of a small modification to regular MAE. He worked with only 10 mL of solvent versus the conventional 30 mL. This eliminated the subsequent concentration step and allowed the sample to be injected straight from the extraction vessel into a GC. The abbreviated MAE provided better extraction efficiencies and reproducibility than the three conventional techniques. The extraction time averaged 16 min per sample with a solvent use of 10 mL per sample.

One difficulty in the use of MAE for the environmental laboratory market is Environmental Protection Agency approval. The methodology has been approved by the SW-846 Organic Methods Workgroup for incorporation into SW-846. However, the method has not been promulgated and thus can only be used when regulations do not specifically require SW-846 methods.

Future Developments

The instrumentation for MAE will continue to evolve, as will its potential applications. There will be developments in the vessel technology to address the separation issue of the sample and solvent after the extraction step. This will allow the technique to be a true replacement for the Soxhlet. There is also a need for larger vessel sizes. The current vessel has a working volume of 100 mL. There is a need to increase this to 250 mL and even higher for bulky samples and the inevitable push for lower detection limits. Finally, the microwave system's use should be extended to concentration of the sample after the extraction step. This will create a multi-tasking tool for the analytical laboratory.

MAE has focused on extraction applications from solid matrices. However, its speed and efficiency suggest that this technique will be used for isolating pharmaceutical compounds during the drug dis-

covery process. The recent addition of sample stirring suggests that it can be extended to liquid-liquid extraction applications. It could also be coupled with solid-phase microextraction to lower detection limits significantly. As MAE becomes more widely accepted and instrumentation evolves, we should see a significant increase in its applicability.

See also: II/Extraction: Microwave-Assisted Extraction. Environmental Applications: Soxhlet Extraction.

Further Reading

- Bichi C, Beliarab F and Rubiolo P (1992) Extraction of alkaloids from species of seneio. *Lab* 2000 6: 36-38.
- Fish J and Revesz R (1996) Microwave solvent extraction of chlorinated pesticides from soil. *LC-GC* 14(3): 230-234.
- Freitag W and John O (1990) Fast separation of stabilizers from polyolefins by microwave heating. *Die Angewandte Makromolekulare Chemie* 175: 181-185.
- Incorvia Mattina M, Iannucci Berger W and Denson C (1997) Microwave-assisted extraction of taxanes from taxus biomass. *Journal of Agricultural and Food Chemistry* 45: 4691-4696.
- Kingston H and Haswell S (eds) (1997) *Microwave-enhanced Chemistry*. Washington, DC: American Chemical Society.
- Kingston H and Jassie L (eds) (1988) *Introduction to Microwave Sample Preparation*. Washington, DC: American Chemical Society.
- Lesnik B (1998) Method 3546: microwave extraction for VOCs and SVOCs. *Environmental Testing and Analysis* 7(4): 20.
- Lopez-Avila V, Young R and Beckert W (1994) Microwave-assisted extraction of organic compounds from standard reference soils and sediments. *Analytical Chemistry* 66(7): 1097-1106.
- McNair R, Wang Y and Bonilla M (1997) Solid phase microextraction associated with microwave assisted extraction of food products. *Journal of High Resolution Chromatography* 20: 213-216.
- Onuska F and Terry K (1993) Extraction of pesticides from sediments using microwave technique. *Chromatographia* 36: 191-194.
- Stout S, Dacunha A and Safarpour M (1997) Simplified determination of imidazolinone herbicides in soil at parts-per-billion level by liquid chromatography/electron ionization tandem mass spectrometry. *Journal of AOAC International* 80(2): 426-432.

MOLECULAR IMPRINTS FOR SOLID-PHASE EXTRACTION



P. A. G. Cormack, University of Strathclyde,
Glasgow, UK

K. Haupt, INTS-INSERM, Paris, France

Copyright © 2000 Academic Press

Among the most important fields in analytical chemistry are medical, food and environmental analysis, where the target analytes are often present at very low concentrations in rather complex matrices. Methods currently used for analysis, such as liquid chromatography, gas chromatography or capillary electrophoresis, must therefore be preceded by a selective isolation and concentration step. Commonly used techniques for the extraction and clean up of analytes from environmental and biological samples are liquid-liquid extraction (LLE) and solid-phase extraction (SPE). Supercritical-fluid extraction (SFE) has also attracted interest, although it has not found widespread application thus far because of the specialized equipment required. The advantages of SPE compared with LLE are that it is faster, more reproducible, cleaner extracts are obtained, emulsion formation is not an issue, solvent consumption is reduced, and smaller sample sizes are required. It may also be cheaper than LLE when the costs for solvent disposal are taken into consideration. Moreover, SPE can be easily incorporated into automated analytical procedures. For a detailed introduction to SPE, the reader is directed to the relevant chapters in the Encyclopedia.

Solid phases currently employed for SPE include polystyrene divinylbenzene resins and chemically modified silica with either hydrophobic or ion-exchange groups. These materials generally yield satisfactory results if the conditions for extraction, washing and elution are carefully determined according to the chemical characteristics of the analytes and the other components in the sample. Nevertheless, due to the non-specificity of hydrophobic or ionic interactions, a large number of contaminants are often co-extracted, particularly if the sample matrix is very complex. A solution to this problem can be to use affinity sorbents, thus taking advantage of the specificity of biological recognition.

Theoretically, biomolecules like antibodies or receptors have the potential to meet the analytical demands for almost any target analyte since, with the

advent of phage display antibody libraries and recombinant antibodies, a suitable recognition element can be found in many cases, even if a natural receptor does not exist. Unfortunately, biomolecules also have a major drawback, which is their poor stability, particularly in the presence of organic solvents. Artificial receptors have therefore been gaining in importance as a possible alternative to natural systems. Molecular imprinting is becoming increasingly recognized as a versatile technique for the preparation of synthetic polymers bearing tailor-made recognition sites. These molecularly imprinted polymers (MIPs) are obtained by copolymerizing functional and cross-linking monomers in the presence of the analyte, which acts as a molecular template. The molecular imprinting technique is reviewed in more detail elsewhere in the Encyclopedia (*see* Affinity Separation/Imprint Polymers). Molecularly imprinted polymers combine the advantages of biological antibodies or receptors (very specific binding) with those of synthetic polymers (high physical and chemical stability, compatibility with both aqueous and organic solvents). Their use in sample preconcentration and clean up by solid-phase extraction is therefore highly attractive.

Analytical-Scale SPE

The applicability of imprinted polymers for SPE has been demonstrated on a number of compounds such as herbicides and drugs, which have been selectively extracted even from complex samples like beef liver extract, bile, blood serum and urine. **Figure 1** shows the principle of molecularly imprinted solid-phase extraction (MISPE). Typically, the sample is brought into contact with the imprinted polymer. This results in binding of the analyte and some impurities. Adsorption of the sample onto the polymer can be either from aqueous solution or from an organic or aqueous/organic solution after a solvent extraction step. The latter is often necessary to recover the analyte from solid or semi-solid samples, for example, soil or tissue. In both cases, the adsorption step is followed by a first elution step where impurities are washed away, whereas the specifically bound target analyte remains bound to the imprinted polymer. The last step is the elution of the analyte in concentrated and purified form using, for example, a competitor.

It has been shown that the target analyte can be recovered from samples at concentrations in the

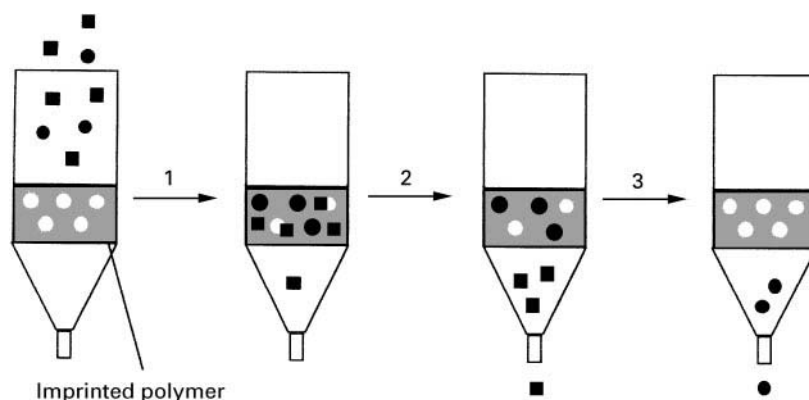


Figure 1 Principle of solid-phase extraction with an imprinted polymer. The sample is loaded onto the imprinted polymer, resulting in binding of both the analyte and some contaminants (step 1). A first elution step removes contaminants and the analyte remains in the specific binding sites (step 2). The analyte is then eluted from the polymer (step 3). ●, analyte; ■, other sample components.

lower $\mu\text{g dm}^{-3}$ to the mg dm^{-3} range. The lower limit is determined by the dissociation constant of the analyte binding to the polymer. The upper limit is set by the binding capacity of the polymer. If the quantity of polymer used for extraction is increased, more analyte will bind, although non-specific binding of contaminants will also increase considerably. It is therefore necessary to optimize the extraction protocol for a specific application in terms of the amount of polymer used, the sample load, and the adsorption, washing and elution conditions, etc.

The quantification of the herbicide atrazine in beef liver is a good example of the utility of imprinted polymers in SPE. In a first step, atrazine was extracted from liver tissue with chloroform. The imprinted polymer was then used to clean the chloroform extract and to further concentrate the analyte prior to quantification. In this specific example, the binding capacity of the polymer for atrazine in chloroform was found to be $19 \mu\text{mol g}^{-1}$. The analyte was eluted from the polymer with a suitable solvent (acetonitrile containing 10% acetic acid) and quantified, after drying and reconstitution in acetonitrile or buffer, by reversed-phase high performance liquid chromatography (RP-HPLC) or enzyme-linked immunosorbent assay (ELISA). When comparing the purified with the non-purified chloroform extracts in RP-HPLC, the SPE step with the imprinted polymer considerably improved the accuracy and precision of the HPLC method and lowered the detection limit from $20 \mu\text{g dm}^{-3}$ to $5 \mu\text{g dm}^{-3}$. This was achieved due to the removal of interfering components in the sample, resulting in baseline resolution of the atrazine peak. Furthermore, analyte recovery was increased from 60.9% to 88.7% (quantification by HPLC) and from 79.6 to 92.8% (quantification by ELISA).

Preparative-Scale SPE

What has been described thus far is, by and large, the use of molecular imprints as solid-phase extraction media in *analytical* applications, where the inherent selectivity of the imprints enables *efficient* clean up and/or preconcentration of samples prior to analyte quantification. Imprinted polymers are well suited to this purpose, and their functional capacity (the mass of analyte that can be bound per unit mass of polymer) places no undue restrictions on their widespread usage. In contrast, capacity is an important consideration in preparative-scale SPE, even if the solid-phase can be regenerated many times. Bearing in mind that the functional capacities of imprinted polymers prepared thus far have been moderately low, it is relatively easy to appreciate why only a few reports describing their potential use in preparative-scale work have appeared. However, there are certain niche applications that could conceivably be serviced by state-of-the-art materials where the low capacity is more than compensated for by the additional benefits that imprints confer, e.g. stability, selectivity, etc. In the long term it is certain that numerous opportunities will exist for the use of imprinted polymers in preparative-scale SPE once the low capacity issue has been addressed satisfactorily. They are well suited to product recovery from fermentation broths, production waste streams, and during chemical and enzymatic syntheses.

The term *facilitated chemical synthesis* in the context of preparative-scale SPE refers to chemical reactions that are performed and/or worked up in the presence of imprinted polymers. In the simplest case, this involves the addition of a polymer imprinted against the product to a vessel containing the crude reaction mixture. The imprint selectively binds the

product in preference to reactants, reagents, catalysts, etc., and is readily separated from the other components by virtue of its cross-linked insoluble character (the use of magnetic imprinted polymer particles or beads, which are available, would make this process even simpler). Alternatively, the crude reaction mixture can be passed through an appropriately sized SPE column, or the imprinted polymer can be placed in a product stream. Following selective adsorption, the product is washed out from the imprinted polymer and isolated. It can then be purified further if required. Another possibility for simple, inexpensive, and large-scale separations using imprinted-polymer particles is adsorptive bubble fractionation. The target compound is selectively adsorbed to the imprinted polymer in suspension within a cylindrical column containing a glass frit at the base of the column. Bubbles are formed when a gas is injected through the frit and they rise to the top of the column. Imprinted-polymer particles, which adhere to the gas bubbles, are transported to the top of the column where they accumulate and can then be easily recovered. It has been shown that enantiometric enrichment of L-phenylalanine anilide from a racemic solution can be achieved in this way, using an L-phenylalanine

anilide-imprinted polymer. Overall then, imprinted polymers appear to offer an efficient general method for product isolation and purification, at least in principle.

Bearing in mind the functional capacity limitations associated with imprinted polymers at present, it should be clear why preparative-scale MISPE is currently not an attractive option. For the time being, it is more practical to use state-of-the-art imprinted materials in the selective extraction of impurities that are present in low or trace concentrations in crude reaction mixtures, where the functional capacities of imprinted polymers place considerably fewer restrictions on their application. In the following example, a recently reported model system focused on the chemical synthesis of the artificial sweetener α -aspartame (Figure 2). In the synthetic sequence, Z-protected L-aspartic acid anhydride (2) was reacted with L-phenylalanine methyl ester (3) to give Z- α -aspartame (4). The α -aspartame product (1) was obtained following removal of the Z-protecting group from the intermediate (4). The key feature about this reaction sequence was that a by-product, Z- β -aspartame (5), was formed during the first step, which then had to be removed. The typical composition of the crude

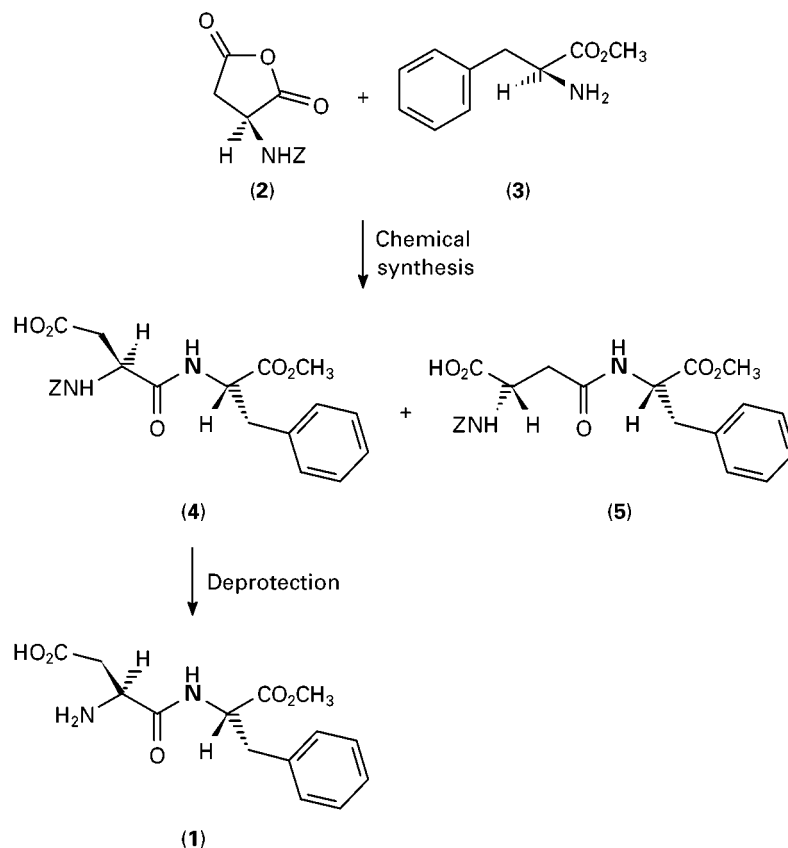


Figure 2 The chemical synthesis of α -aspartame. (1) α -aspartame, (2) Z-protected L-aspartic acid anhydride, (3) L-phenylalanine methyl ester, (4) Z- α -aspartame, (5) Z- β -aspartame.

reaction mixture was as follows: Z- α -aspartame, 59%; Z- β -aspartame, 19%; Z-L-aspartic acid, 22%. A polymer was imprinted against the by-product Z- β -aspartame (5) and used in the SPE mode for the selective removal of the by-product from the crude reaction mixture. After five passes through a solid-phase extraction column, the product purity was increased from 59 to 96%. In a control experiment using a nonimprinted polymer, the final purity achieved was only 86%.

It is also possible to use imprinted polymers advantageously *during* chemical reactions, to drive chemical equilibria in particular directions and thus influence product distributions in a controlled fashion. To prove this concept, the enzymatic condensation of Z-protected L-aspartic acid (6) with L-phenylalanine methyl ester (3) using the enzyme thermolysin was studied (see Figure 3). The equilibrium for this reaction, which normally lies to the left thus favouring reactants, can be driven to the right, in the direction of products by working in a nonsolvent for Z- α -aspartame. Another way of achieving the same effect would be to use a product-trap (product-sink) in the reaction itself, for example, a polymer imprinted against the product Z- α -aspartame. Indeed, when the reaction was carried out in the presence of

a Z- α -aspartame-imprinted polymer, the reaction yield was found to increase from 15 to 63%.

Present Limitations and Remedial Solutions

Any sorbent used in SPE must satisfy a range of performance criteria for a given application. Criteria that are of importance for imprinted polymers include: (1) Strong, selective, and reversible binding to the analyte; (2) fast mass-transfer kinetics; (3) high functional capacity; (4) minimal interaction of analyte with polymer backbone; (5) effective displacers available; (6) zero bleeding of template; (7) compatible with many solvents; (8) pressure resistant; (9) batch-to-batch reproducibility; (10) physical form of imprinted polymer; and (11) economics. Whilst imprints perform very well in many respects, there are certain limitations that need to be overcome in specific applications.

One of the most unsatisfactory features associated with the application of imprinted polymers as SPE sorbents in ultra-trace analysis is template leakage. Generally, once an imprinted polymer has been prepared, it is exhaustively extracted to remove the template from the polymer matrix. The difficulty in extracting 100% of the template molecule from an imprinted polymer has long been recognized, although until relatively recently it was widely believed that the few per cent of template remaining within the polymer was permanently entrapped. Recent work clearly demonstrates that this is not necessarily the case. What can and does occur is slow leakage of a portion of the remaining template from the polymer matrix over a period of time, even after exhaustive (solvent) extraction of the polymer beforehand. This template *leakage* or *bleeding* can have serious implications when the polymer is being used as an SPE sorbent in ultra-trace analysis, although is of much less concern in trace analysis.

Whilst a general solution to the bleeding problem is being sought by researchers across the globe, a possible method of circumventing the bleeding problem entirely is to use a template analogue during the imprinting step, rather than the template itself. One of the first demonstrations of this approach was described by Andersson *et al.* in a paper detailing the use of MISPE for the preconcentration of the drug sameridine (7) in human plasma, prior to its quantification via gas chromatography (GC). At the nanomolar concentration levels used in the study, leakage of template from the polymer matrix during sample handling was considerable and easily detectable via GC analysis. Bearing in mind the application and the concentration window, such leakage was completely

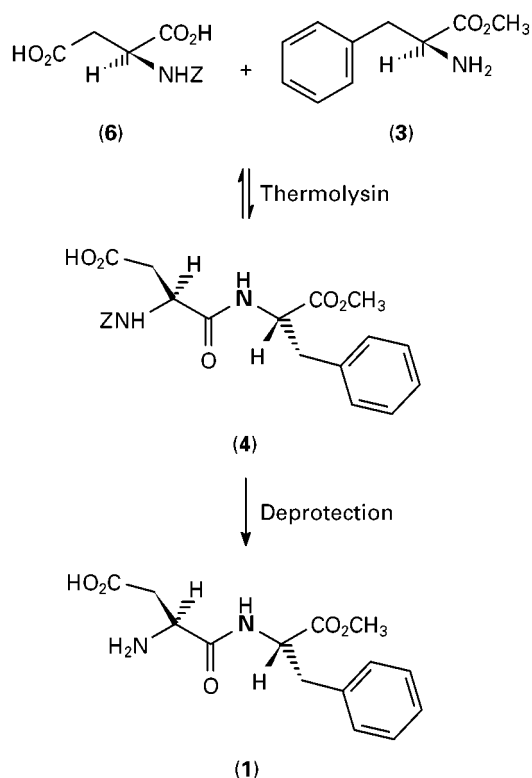


Figure 3 The enzymatic synthesis of α -aspartame. (1) α -aspartame, (3) L-phenylalanine methyl ester, (4) Z- α -aspartame, (6) Z-protected L-aspartic acid.

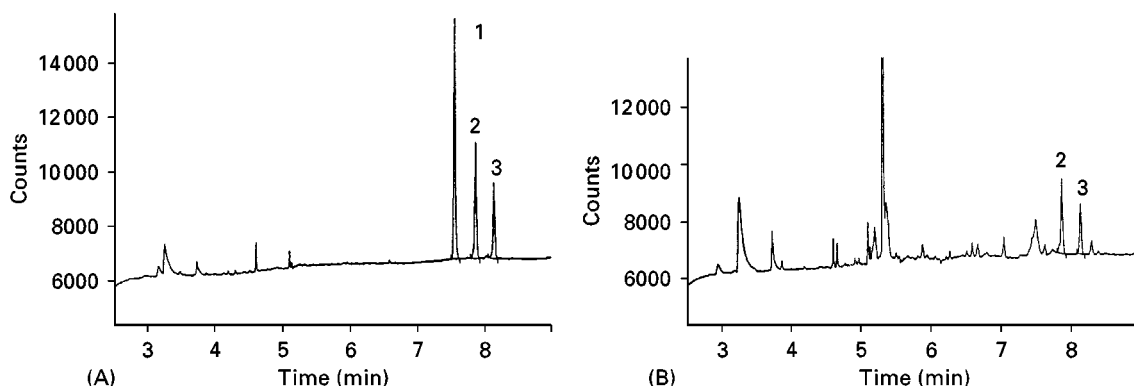
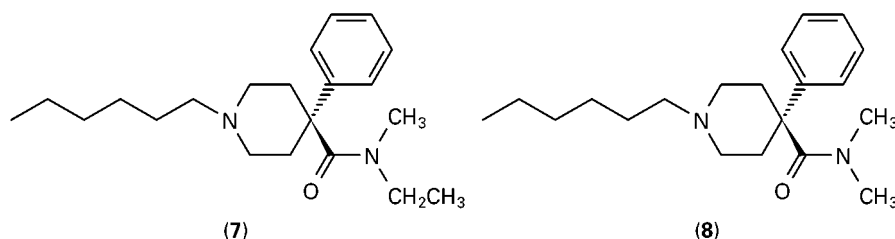


Figure 4 GC traces of human plasma samples spiked with sameridine and an internal standard, and subjected to (A) solid-phase extraction with an imprinted polymer and (B) standard liquid-liquid extraction. The peaks are (1) the template molecule (a close structural analogue of sameridine), (2) the analyte sameridine and (3) the internal standard. (Reproduced with permission from Andersson, Papricia and Arvidsson, 1997).



unacceptable because it led to large errors in the precision of the analytical measurement. Rather than take steps to minimize or eradicate leakage, a close structural analogue of sameridine (8) was used as the template molecule in the imprinting step, which yielded an imprinted polymer that still displayed a strong affinity for sameridine.

Following solid-phase extraction of sameridine from human plasma using this polymer, leakage of the analogue from the polymer matrix did occur, but sameridine and the analogue were readily resolved using GC and the sameridine was subsequently quantified. The results obtained were as good as those obtained via a standard liquid-liquid extraction method, with the added advantage that the plasma sample contained fewer matrix contaminants with MISPE than for LLE, i.e. the sample for assay was much cleaner (Figure 4).

The template-analogue method does rely upon the availability of a close structural analogue of the analyte, and also a strong affinity between the polymer imprinted against the analogue and the analyte. One or both of these criteria may not always be fulfilled, therefore new approaches are required to tackle the bleeding issue.

In a solid-phase extraction operation, one ideally wants strong binding of the analyte to the sorbent during the loading and washing steps, and rapid stripping of the analyte from the sorbent during the elu-

tion step, ideally in as small a volume as possible. Efficient loading and washing is therefore favoured by a strong affinity between the polymer and the analyte, whereas efficient elution is obtained when the affinity is moderate to weak. In some cases, MIPs can actually bind analytes too strongly, which means that stronger displacers or larger volumes of eluting solvent are required than would otherwise be considered ideal. In some circumstances, therefore, having an MIP of lower affinity but with the same selectivity would be desirable. One way of achieving this goal might be via thermal pretreatment of the polymer at high temperature prior to use, which can have the effect of killing off a proportion of the high-energy binding sites.

As indicated already, the low functional capacity of imprinted polymers does not unduly limit their potential in analytical applications, although it does place restrictions on their immediate value in preparative-scale solid-phase extractions. With the advent of new developments in the imprinting area, and the advantageous knock-on effect this is likely to have on capacities, it is expected that preparative-scale applications will become more feasible in the future. Scale-up of the polymerization process to an industrial scale must also be addressed. In future developments, the elaboration of imprinting methodologies in polar environments is also expected; at present, it is a challenge to prepare good imprints in these

'competitive' environments. Although it is possible to imprint certain templates in polar environments, polar solvents (e.g. water) tend to interfere to an unacceptable level with the non-covalent interactions between template and functional monomer that are often relied upon in imprinting protocols. What is more common and easier to deal with, however, is the use of imprints effectively in buffer and/or polar environments. Finally, the imprinting of larger templates (e.g. proteins) is rather challenging at present due to their 'fragile' nature. New synthetic developments should lead to progress in this area also.

Conclusions

Molecularly imprinted polymers constitute a new class of sorbents which combine the robust character of cross-linked polymers with the attractive properties of natural receptors. In sample clean up and concentration for trace and ultra-trace analysis, they offer distinct advantages over both liquid-liquid extraction and solid-phase extraction using classical sorbents and immunosorbents. Besides analytical applications, imprinted polymers are being increasingly considered for preparative-scale SPE applications, even though their present low functional capacity sets a limit on their widespread utility. However, concomitant with improvements in their capacity, it will become increasingly appealing to use imprinted polymers to remove products and/or by-products from reaction vessels/streams, and to influence directly the course of chemical reactions by 'equilibrium shifting'. Finally, it is worth noting that the area of molecular imprinting as a whole is undergoing rapid expansion at present. What this implies for MISPE is that one can expect tailored, high-performance imprinted polymers to become increasingly attractive and more widely available as methodologies improve and breakthroughs are made.

See also: II/Extraction: Solid-Phase Extraction. III/Immunoaffinity Extraction. Selectivity of Imprinted Polymers: Affinity Separation:

Further Reading

- Andersson LI, Papricia A and Arvidsson T (1997) A highly selective solid phase extraction sorbent for pre-concentration of sameridine made by molecular imprinting. *Chromatographia* 46: 57–62.
- Amstrong DW, Schneiderheinze JM, Hwang YS and Sellergren B (1998) Bubble fractionation of enantiomers from solution using molecularly imprinted polymers as collectors. *Analytical Chemistry* 70: 3717–3719.
- Bartsch RA and Maeda M (eds) (1998) Molecular and ionic recognition with imprinted polymers. *ACS Symposium Series* 703.
- Katz SE and Siewierski M (1992) Drug residue analysis using immunoaffinity chromatography. *Journal of Chromatography* 624: 403–409.
- Muldoon MT and Stanker LH (1997) Development and application of molecular imprinting technology of residue analysis. *ACS Symposium Series* 657: 314–330.
- Muldoon MT and Stanker LH (1997) Molecular imprinted solid phase extraction of atrazine from beef liver extracts. *Analytical Chemistry* 69: 803–808.
- Ramström O, Ye L, Krook M and Mosbach K (1998) Applications of molecularly imprinted materials as selective adsorbents: emphasis on enzymatic equilibrium shifting and library screening. *Chromatographia* 47: 465–469.
- Reid E, Hill H and Wilson I (1998) *Drug Development Assay Approaches, Including Molecular Imprinting and Biomarkers*. Guilford: Guilford Academic Associates.
- Sellergren B (1994) Direct drug determination by selective sample enrichment on an imprinted polymer. *Analytical Chemistry* 66: 1578–1582.
- Ye L, Ramström O and Mosbach K (1998) Molecularly imprinted polymeric absorbents for by-product removal. *Analytical Chemistry* 70: 2789–2795.

MOLECULAR RECOGNITION TECHNOLOGY IN INORGANIC EXTRACTION



J. D. Glennon, University College Cork, Cork, Ireland

Copyright © 2000 Academic Press

Selective ion recognition, binding and transport are important processes in living systems. From the active

sites of metalloproteins, such as amine oxidase, to lower molecular weight ligands like valinomycin, the K^+ -selective macrocyclic antibiotic, the underlying principles of such selective ion binding and utilization have for some time been the subject of intensive investigation and modelling by many researchers.

Table 1 Developments in macrocyclic host chemistry of major importance in ion recognition

von Baeyers (1872)	Origin of calixarenes in phenol-formaldehyde reactions
Meadow and Reid (1934)	Preparation of hexathia-18-crown-6 in low yield
Zinke and Ziegler: Niederl and Vogel (1940s)	Cyclic oligomeric structures assigned to products from phenol-formaldehyde reactions
Pedersen (1967)	Pioneering work on crown ethers, using picrate extraction
Rosen and Busch (1969)	Macrocyclic thioether ligands
Lehn, Sauvage and Diedrich (1969)	First macrobicyclic ligands, the cryptands
Gutsche (1978)	Introduced name calixarene and suggested potential as molecular receptors
Cram (1979)	Development of spherands, with more fixed pre-organized cavities for cation selectivity
Izatt and Christensen (1983)	Selective extraction of cesium ions by <i>p-tert</i> -butylcalixarenes in liquid membranes
Pedersen, Lehn and Cram (1987)	Nobel Prize in chemistry

Many new branches of chemistry have developed which aid the challenge, including supramolecular chemistry, the study of the formation and properties of larger molecular aggregates from the self-assembly of smaller complementary molecules through non-covalent intermolecular forces. Specifically, the creation of pre-organized cavities in synthetic host molecules for the selective reception of a neutral or ionic species is described as host-guest chemistry or molecular recognition, an approach gleaned from enzyme-substrate interactions. Macrocyclic ligands have received particular attention, as host molecules, since the pioneering work of Pedersen on the synthesis and metal extraction properties of crown ethers. This began a revolution in macrocyclic ligand and receptor design, acknowledged with the award of the Nobel Prize in chemistry in 1987 to three of the main contributing scientists, Pedersen, Lehn and Cram (Table 1), a revolution which continues today as new host molecules with unique selectivities of binding and mechanisms of release are produced.

Many macrocyclic ionophores are host molecules, which vary in the extent to which they are pre-organized for selective recognition of guest species and the fitting of guest to host in a complementary fashion. Some of the most important macrocyclic ligands are listed in Table 2. Cram recognized that the more highly organized the host was for binding and low

solvation, prior to complexation, the greater would be complex stability. Greater cation selectivity resulted, using fixed pre-organized host cavities of controlled size, provided by such macrocycles as cryptands and spherands. The chemical structures of representative macrocyclic host molecules are given in Figure 1, alongside the ions which have been shown to reside selectively in the guest cavities. The concepts that cavity size and shape could be tailor-made and fine-tuned to suit the selected cation diameter, and that donor atom choice determines the cation selectivity, have caught the imagination of many chemists over the last 30 years. In particular, separation scientists have been quick to demonstrate selective metal extractions, such as the separation of trace amounts of silver from mercury using 14-thiacrown-4 and the extraction of mercury and lead by 18-crown-6. Important studies were carried out on monocyclic aza crowns and cryptands, which are macrobicyclic compounds, where the complexed cation is completely enclosed by ligands, containing O and N, in a central cavity. More recently, attention has been focused on calixarenes, which are a class of functionalized metacyclophanes possessing convergent phenolic groups arranged around the periphery of a central aromatic cavity. These macrocycles have been described by Shinkai as the third host molecule after cyclodextrins and crowns as the first two major impact host molecules. The unique ionophoric properties of functionalized calixarenes have been clearly demonstrated using nuclear magnetic resonance (NMR) spectroscopy and liquid-liquid extraction studies. Functionalization, at the upper and lower rim, can lead to an enormous number of derivatives, water- or organic-soluble, with varied ionophoric selectivities.

In this review, representative examples of these molecular recognition reagents and their roles in selective metal ion extraction are presented. The emphasis is on illustrating through examples the influences that contribute to selectivity of complexation and extraction, and on the new materials and

Table 2 Macrocyclic ligands

<i>Molecular recognition ligands</i>	<i>Examples of metals complexed</i>
Crown ethers	Na, K, Rb, Cs
Thiacrowns	Ag, Au, Pt, Hg
Azacrowns	Cu, Ni
Cryptands	Na, K, Rb, Cs
Spherands, hemispherands, cryptaspherands	Li, Na, K, Rb, Cs
Calixarenes	Cs, Fe, Cu
Calixarenes (functionalized)	Na, Cs, Ca, Pb, Ag, Fe, UO_2^{2+}
Calixcrowns	K, Cs

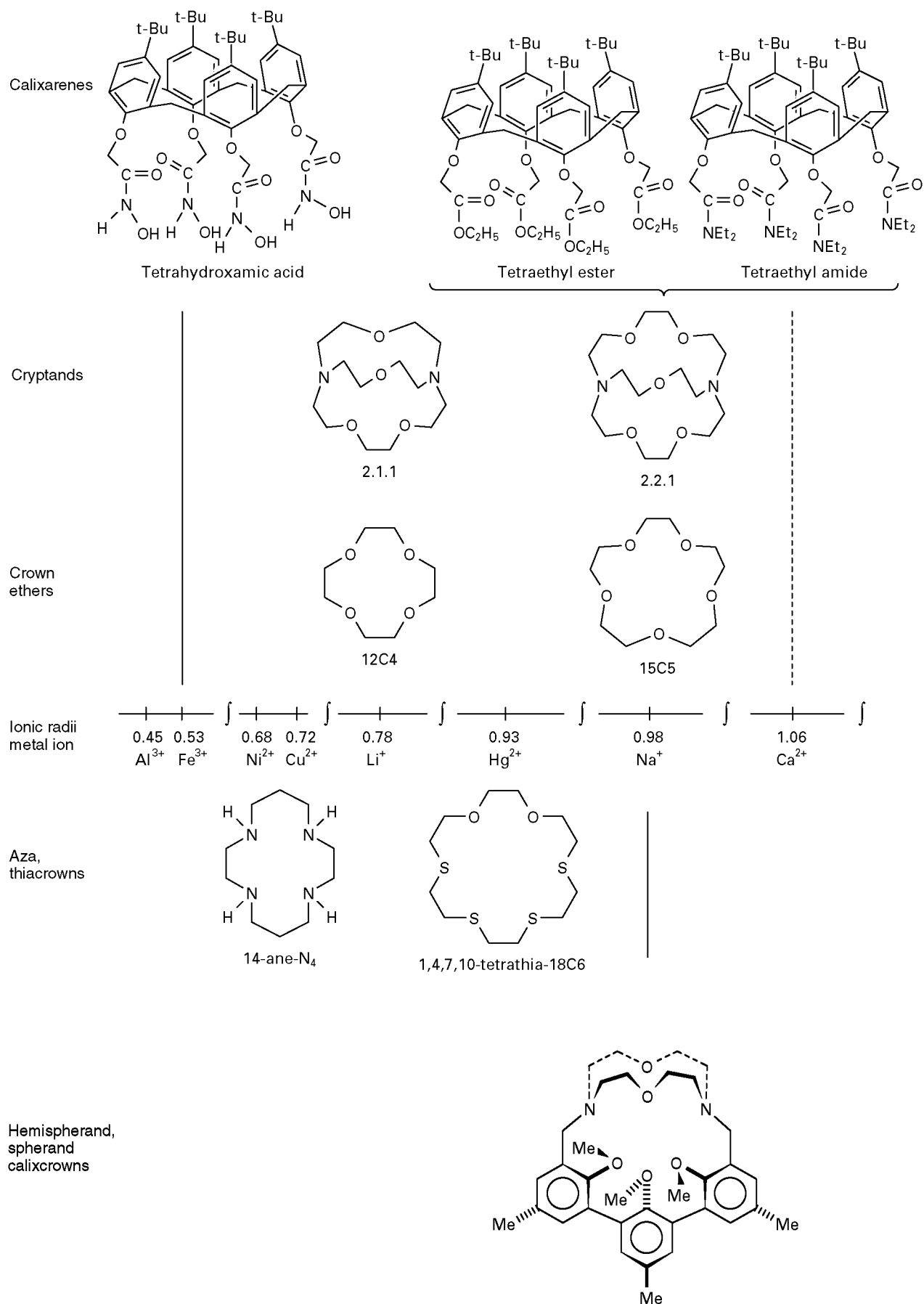


Figure 1 Macroyclic host molecules.

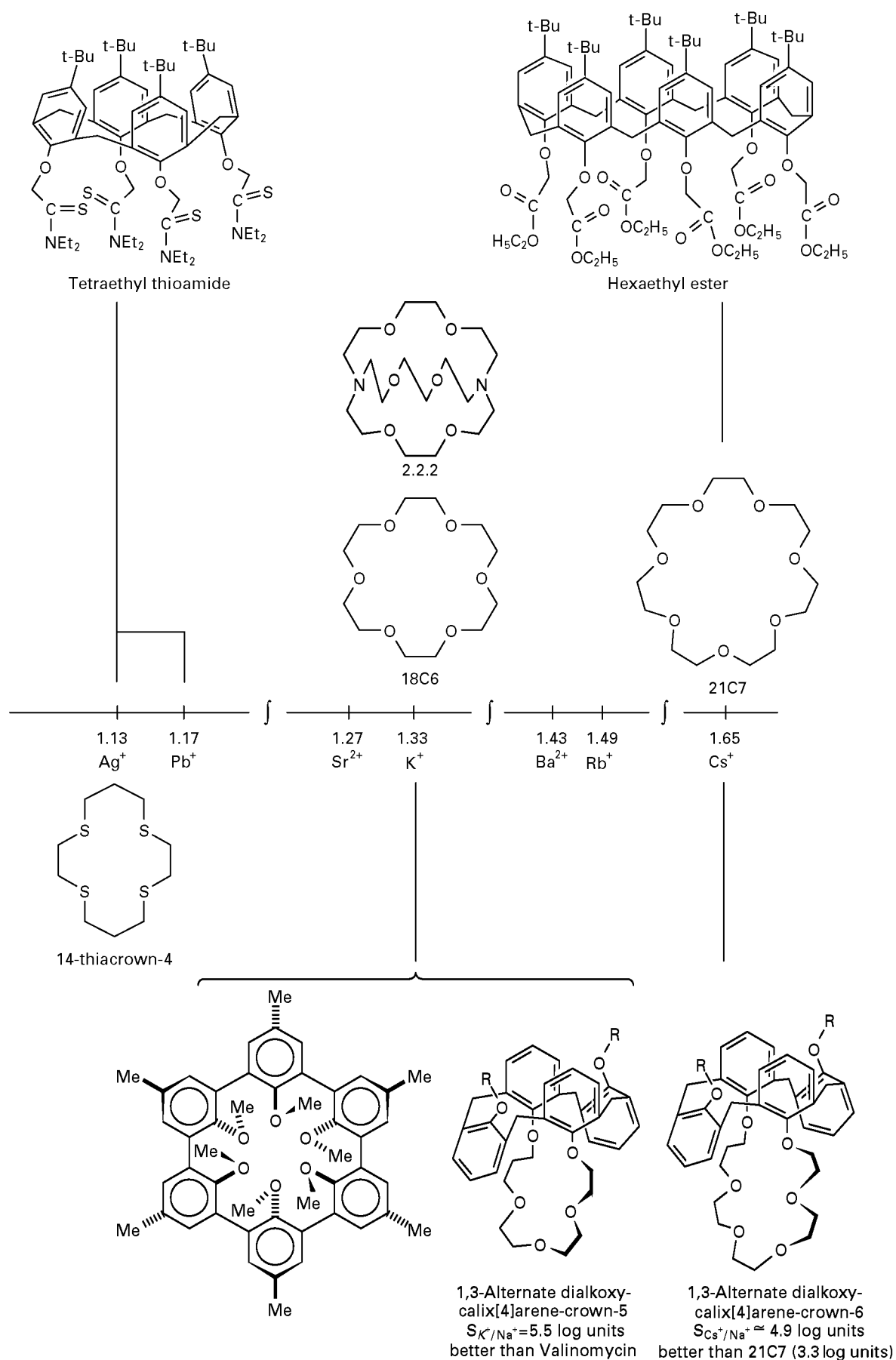


Figure 1 Continued

experimental approaches that have been adapted to demonstrate analytical and preparative-scale selective metal ion extraction using molecular recognition reagents.

Selectivity of Metal Ion Complexation

Determination of the selectivity of complexation is an important goal, since it gives further pointers to where the synthetic effort should focus, and it is a necessary step in assessing how far the synthetic design has progressed to meet the challenge presented by such natural ionophores as valinomycin.

The selectivity of molecular recognition ligands for metal ions is chiefly described in two ways, as the ratio of the measured stability constants for a pair of ions or from phase transfer and transport studies of selected cations from aqueous solution into organic solvents.

Ratio of Stability Constants

The stoichiometric stability constant K_s (sometimes symbol β) for the complexation of a metal ion, M , by a ligand, L , in solution at a constant ion strength, is defined as:

$$K_s = [ML]/[M][L]$$

in the simplest situation where a 1 : 1 complex is formed and where the square brackets refer to molarities of complex, free metal and free ligand in solution. This is commonly the situation when macrocyclic ligands are involved. Thus, when comparing the relative stabilities of complexation of two metal ions, M_1 and M_2 , with the same macrocyclic ligand, the ratio of the stoichiometric stability constants is a useful measure of selectivity:

$$\text{Complexation selectivity } S_{M_1/M_2} = K_s(M_1L)/K_s(M_2L)$$

Extraction Selectivity

The picrate extraction method introduced by Pederesen places the MR reagent in an organic solvent, such as dichloromethane, in contact with an aqueous metal picrate solution. If complexation occurs the metal ion extraction is monitored by spectrophotometry, following the co-extraction of the highly coloured picrate counterion ($\lambda_{\max} = 355 \text{ nm}$, $\epsilon = 14416 \text{ mol}^{-1} \text{ L cm}^{-1}$) into the organic solvent. The percentage cation extraction is calculated as the ratio $100 \times (A_0 - A)/A_0$, where A_0 is the measured absorbance of an aqueous blank metal picrate solution without complexation reagent and A is the absorbance recorded in the aqueous layer after equilibra-

tion. The method is particularly suited to the extraction of alkali and alkaline earths, but has also been applied to the assessment of the percentage extraction of transition metal ions. Thus, a liquid-liquid extraction method is used to determine the percentages of extraction for a series of metal ions and frequently tabulated or plotted against ionic radii to illustrate the ion preference of the reagent.

Selectivity of Molecular Recognition Ligands

Among the factors that contribute to the selectivity of metal complexation by macrocyclic receptors is the complementarity in size of the host cavity to the cation diameter. In Figure 1 this is readily seen with the crown ethers, where selectivity moves from Li^+ to Cs^+ as the host varies from 12-crown-4 up to the larger 21-crown-7. This matching of cation diameter and cavity size is also evident in the illustrated cryptand and calixarene series, with, for example, in the latter, Cs^+ selectivity being displayed by the calix[6]arene hexaester derivative. The principle of pre-organization of the host cavity is evident in the ion complexation by macrocycles such as the cryptands and spherands, which display greater complexing power than the earlier crown ethers. The influence of the nature of the donor atom on the selectivity of complexation is also evident in the illustrated macrocyclic compounds. The hard and soft acid-base theory of Pearson is a useful guideline as to the behaviour, with oxygen donor atoms considered to be hard bases and nitrogen and sulfur soft bases. Alkali and alkaline earth metal cations, considered hard acids, are preferred by hard bases, while soft acids such as heavy metals are preferred by soft bases. Shifts towards the complexation of soft cations such as Ag^+ , Pb^{2+} and Hg^{2+} are seen in the aza and thia crowns. It is also clearly seen in the versatile calixarene series, as for example among the tetrameric series where the change from ester to amide to thioamide moves the ion preference from Na^+ , to Ca^{2+} and on to Pb^{2+} and Ag^+ . Hancock has emphasized the role of chelate ring size within the macrocycle – an effect which influences the stability of complexation by such macrocycles as the azacrowns and the calixarene tetrahydroxamate, shown in Figure 1.

Of particular note is the influence of conformation on the stability and extraction of metal ions by molecular recognition compounds. This has been powerfully illustrated recently with calixcrowns, which are capable of cone, partial cone and 1,3-alternate conformations. Calixcrowns derived from calix[4]arenes, unsubstituted on the upper rim, can be fixed in the 1,3-alternate conformation, as shown in Figure 1.

Table 3 Percentage extraction and log β values for alkali and alkaline earth metal ion complexation by selected functionalized calixarene derivatives

Host macrocycle		Li	Na	K	Rb	Cs	Mg	Ca	Sr	Ba
<i>p</i> - <i>t</i> -Bu-Calix[4]arene-tetraethylester	%E	15	94.6	49.1	23.6	48.9				
$S_{Na/K} = 400$	Log β	2.6	5.0	2.4	3.1	2.7				
<i>p</i> - <i>t</i> -Bu-Calix[4]arene-tetraethylamide	%E	63	95.5	74	24	12	9	98	86	74
$S_{Ca/Mg} > 7.8$ log units	Log β	3.9	7.9	5.8	3.8	2.4	1.2	> 9	> 9	7.2
1,3-Dialkoxycalix[4]arene-crown-6	%E	2.5	2.6	13.8	41.7	63.5				
$S_{Cs/Na} > 4.9$ log units	Log β	< 1.5	< 1.5	4.3	6.0	6.4				
1,3-Dialkoxycalix[4]arene-crown-5		—	—	—	—	—				
$S_{K/Na} = 5.53$ log units	Log β	4.78	4.30	9.83	9.41	6.87				
Valinomycin		—	—	—	—	—				
	Log β	5.83	6.09	9.35	9.83	8.97				

Data compiled from Arnaud-Neu *et al.* (1989) and (1991), Dozol *et al.* (1997) and Casnati *et al.* (1996).
 Bold figures, highest selectivity and extraction.

While the extraction and complexation profiles are strongly dependent on the size of the crown, the behaviour is dependent on the conformation, with the highest extraction and complexation levels found for the 1,3-alternate ligands. Two striking selectivities have been achieved, as shown in Table 3. Remarkable Cs^+/Na^+ selectivity ($S_{Cs/Na} > 4.9$ log units) was obtained for the 1,3-alternate calix[4]-crowns-6, making applications to the extraction of caesium from radioactive waste possible. The conformation has a direct bearing on the relative stabilities, with cation- π interactions possible for caesium but not for the smaller sodium in the rigid conformation. In addition, 1,3-alternate-calix[4]arenecrown-5 conformers have been shown in extraction experiments from water to chloroform to have better K^+/Na^+ selectivity ($S_{K/Na} = 5.53$ log units) than the naturally occurring ionophore, valinomycin.

Numerous functionalized calixarenes and, more recently, calixcrowns have been studied for their ability to extract metal ions and the stabilities of the metal-ligand complexes measured. In general, changes in the extraction profiles as the ion is varied mirror the changes in stability of the complexes. Four representative examples chosen to illustrate the influences of donor atoms and conformation on extraction and selectivity are provided in Table 3, alongside stability data reported for valinomycin.

Molecular Recognition Ligands in Inorganic Extraction

Solvent Extraction of Metal Cations

The Pedersen picrate extraction method is particularly suited to alkali and alkaline earths; using it McKervey *et al.* were able to show that *p*-*t*-butyl-calix[4]arene esters and ketones were Na^+ -selective

over other alkali metal ions and that calixarene complexation of metal ions is determined by the cavity size and the type of functionalization.

In sample preparation prior to trace metal analysis, a well-established procedure is the extraction of transition and heavy metal ions such as Cu^{2+} and Pb^{2+} into methylisobutylketone using extraction reagents such as sodium diethyldithiocarbamate and dithizone. Extraction can be monitored by spectrophotometry, as many of the complexes are coloured, or by atomic absorption spectroscopy. While such liquid-liquid extraction methods using conventional extraction reagents achieve preconcentration and sample clean-up, today the challenge is for greater selectivity of extraction, even as far as the extraction of specific metal ions from complex matrices. This can be achieved by molecular recognition technology. As far back as 1983, Izatt *et al.* demonstrated selective extraction of Cs^+ through organic liquid membranes by macrocyclic *p*-*tert*-calix[n]arenes through the formation of neutral complexes following proton loss. Another illustrative example is the challenge of selective extraction of uranium from sea water, where lipophilic calix[6]arene carboxylates and phosphonates have been reported as uranophiles, capable of selective transport of UO_2^{2+} ions from water into organic media. In this manner, calixarenes functionalized with ionizable or chelating groups have been extensively studied over a range of pH for the extraction of transition and heavy metal ions from aqueous to organic solution. In particular, Shinkai has studied calix[5]- and calix[6]arenes with sulfonate, phosphonate, carboxylate and hydroxamate groups as uranophiles in extraction and transport experiments. The great strength of calixarenes as selective metal extraction reagents is that any chelating moiety can be attached to the macrocycle at the upper or lower rim for targeted metal ion extraction.

Extraction of Metal Ions using Molecular Recognition Solid Phases

The immobilization of extractants onto supports for solid-phase extraction has many advantages over liquid-liquid extraction, including minimization of the use of organic solvents and amenability to automation. Important approaches taken to immobilize extractants include dissolution in a support-held organic liquid and chemically bonded solid phases.

Supported liquid membrane enrichment technique The supported liquid membrane (SLM) enrichment technique involves using a solid membrane, such as porous polytetrafluoroethylene, which is impregnated with an organic solvent which acts as a stationary liquid positioned between two aqueous solutions (Figure 2A). When the membrane separator is configured to allow the use of flowing aqueous solutions, the technique can combine the selectivity and enrichment capabilities of liquid-liquid extraction with efficient matrix constituent removal for automated sample preparation. While the use of liquid membrane technology for extraction in industrial processes is well established, the use of SLM technology for analytical applications began in the mid 1980s for trace organic extraction. For trace metal extraction, recent examples have focused on the use of extractants such as 8-hydroxyquinoline and organophosphates. The use of a lipophilic diazo-18-crown-6 in an SLM for the separation of Cu^{2+} from natural water samples has been studied. SLM technology has in particular been used to complement liquid-liquid extraction studies in determining the selectivities of some of the more recently synthesized calixarene ligands. Further studies on the use of molecular recognition reagents in SLMs are likely to lead to further useful demonstrations of enhanced selectiv-

ities of extraction using molecular recognition ligands.

Solid-phase extraction technology This approach to the extraction of metal ions involves the partitioning or complexation of the metal species from the aqueous phase onto a solid phase, usually a polymer or silica. From literature reviews of solid-phase extraction, it is clear that chemically bonded phases derived from liquid chromatography are generally used for organic solute extraction. For metal ions, ion exchange and chelating phases have been widely used and have clear advantages over liquid sorbent-based approaches. How molecular recognition has impacted and can further impact on this approach to extraction will be seen from the next illustrative examples.

Silica-bond thiacycrown macrocycles Considerable work has been done on the chemical attachment of crown ethers to silica and polymeric supports for chromatographic separation of ions and chiral solutes. Separations of alkali and alkaline earths using water-based eluents have been demonstrated and ion-modulated separations carried out. For inorganic extraction, by far the greatest impact has been made with silica-bonded thiacycrown phases. Highly selective silica-bonded, sulfur-containing crown phases are commercially marketed in packed beds or columns as SuperLigTM and AnaLigTM (for industrial and analytical separations, respectively) by IBC Advanced Technologies (Provo, UT, USA). These molecular recognition materials have resulted from the research work of Izatt *et al.* at Brigham Young University, and have been applied to the extraction of targeted metals in complex matrices, such as the large scale removal of Pd^{2+} from AgNO_3 streams, the removal of Cs^+ , Sr^+ and Pb^{2+} from nuclear waste streams, and for analytical extractions, to the concentration and analysis of low level Hg^{2+} . The selectivity of silica-bound 1,4,7,10-tetrathia-18-crown-6 for Hg^{2+} over Ag^+ is reported as 10^6 ; in comparison, the selectivity of a typical ion exchange resin for Ag^+ over Hg^{2+} is 1.06.

Particle-loaded membranes The incorporation of solid-phase extraction particles into a web of microfibrils to form an extraction membrane with fast mass transfer kinetics has been described (Figure 2B). Highly selective and efficient removal of metal ions from solution is possible; for example, rapid sample processing and determination of radioactive strontium, counted from the surface of the membrane disc, can be achieved using EmporeTM Strontium Rad Disks, containing AnaLigTM molecular recognition technology.

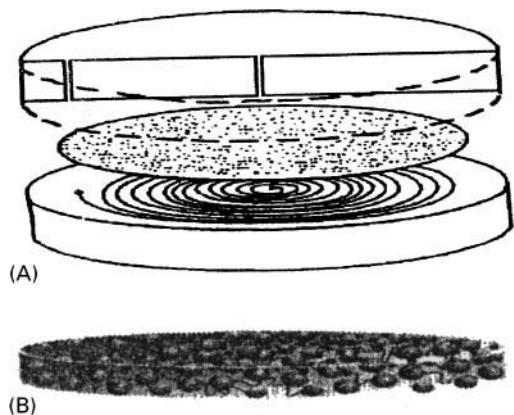


Figure 2 (A) Supported liquid membrane and (B) particle-loaded membrane.

Silica-bound molecular baskets for extraction and chromatography Molecular baskets, as calixarenes have been described, can be immobilized onto solid supports to yield new molecular recognition materials for extraction and chromatography. The obvious supports are polymer and silica phases. The nature of the surface silica-bound species in chemically bonded molecular baskets on silica has been elucidated using solid-state NMR spectroscopy. When packed as a chromatography column, a silica-bonded calix[4]arene tetraamide phase displayed significant retention of Ca^{2+} over Mg^{2+} , a result in keeping with the reported high complexation selectivity of the calixarene for Ca^{2+} over Mg^{2+} ions. For transition metal ion extraction, a macrocycle that combines the sequestering ability of siderophores with the ionophoric properties of calixarenes is another interesting example of these new phases. Calix[4]arene tetrahydroxamic acid can be chemically bonded to silica particles or partitioned onto a solid support. Metal uptake profiles as a function of pH have been determined using solid-phase extraction cartridges filled with these new molecular recognition phases and the phases have been characterized by diffuse reflectance infrared Fourier transform (DRIFT) and solid-state NMR spectroscopy. The molecular recognition phase is capable of selective removal of Pb^{2+} and Fe^{3+} from acidic aqueous solution with Ni^{2+} ,

Zn^{2+} , Co^{2+} , Mn^{2+} and Cd^{2+} . The complexation of Pb^{2+} takes place at a more acidic pH than is achievable with linear hydroxamic acids, as a result of host-guest complexation in the basket cavity. The structure of the silica-bonded molecular basket is schematically given in Figure 3, with coupling through two of the three available ethoxy groups on the derivatized upper rim. The sites for complexation of metal ions are shown on the lower rim. (It is acknowledged that there is a redundant hydroxamate group in the tetrahydroxamate when metal ions are complexed in an octahedral fashion.)

Supercritical Fluid Molecular Recognition Technology for the Extraction of Metal Ions

Instead of carrying out liquid-liquid extractions or solid-phase extractions for the pretreatment and preconcentration of metal ions from solid and liquid matrices, it is possible to send in a selective courier molecule to permeate through the sample, grab on to the targeted metal and deposit it in concentrated form into a collection vessel for further analysis. Such a technology utilizes the solvating power of supercritical CO_2 and the metal-ion complexing power and selectivity of organic ligands, and is currently the focus of considerable research attention. Several studies have been reported on the supercritical fluid extraction (SFE) of metal ions via the formation of

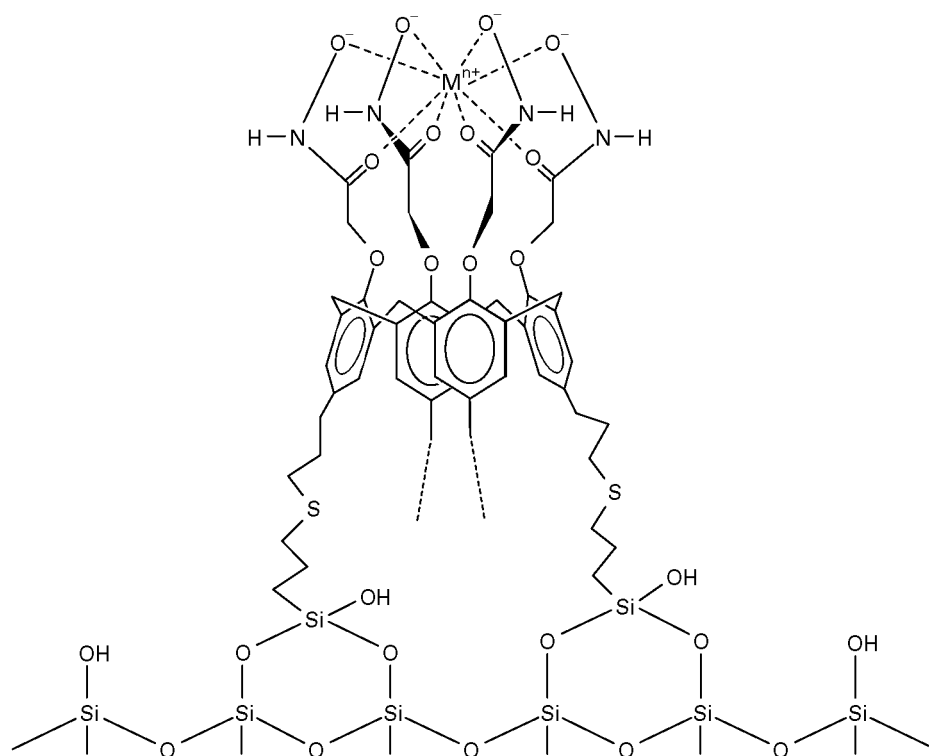


Figure 3 Proposed structure of silica-bonded calix[4]arene tetrahydroxamate phase.

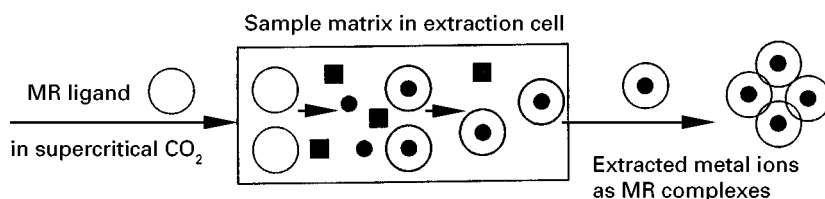


Figure 4 Schematic diagram of selective SFE of targeted metal ions using macrocyclic extractants. Filled circles, targeted metal ions; filled squares, diverse metal ions.

neutral metal–ligand complexes resulting in useful solubilities in supercritical CO_2 . These solubilities can be improved by several orders of magnitude by substituting fluorine for hydrogen in the chelating ligand. For example, β -diketones and dithiocarbamates have been fluorinated and successfully used as metal extraction reagents in SFE.

More advanced complexation in SFE is achievable using molecular recognition ligands, where enhanced selectivity of extraction is achievable by careful choice of donor atoms and host cavity size in a macrocyclic reagent, as illustrated in Figure 4.

Recently, such selective extractions using macrocyclic reagents in SFE has been demonstrated. The selective extraction of mercury from sand, and cellulose filter paper using ionizable dibenzobistriazolo crown ether in methanol-modified supercritical CO_2 has been reported. The synthesis and use of fluorinated molecular baskets for metal extraction in unmodified supercritical CO_2 has been described. Fluorinated calixarenes are the templates on which carefully selected chelating groups can be incorporated around the cavity to yield selective extractants for targeted metals. The ability of one such molecular basket, a fluorinated calix[4]arene tetrahydroxamate, selectivity to extract Fe^{3+} from metal mixtures on

cellulose paper has been monitored using atomic absorption analysis (Figure 5). Further examples of where targeted metal ions in a matrix, present as unwanted contaminants or as valuable metals to be recovered, are selectively complexed and removed by such macrocyclic extractants dissolved in supercritical CO_2 are likely in the future.

Future Developments

Molecular recognition ligands for metal extraction are likely in the future to be cage-like and pre-organized to provide the preferred symmetry of the targeted metal ion. Higher selectivities of extraction for cations and anions can be expected, by reagents which subsequently release the guest under an applied stimulus. Molecular recognition speciation, allowing preferential extraction of individual oxidation and chemical species, will receive more attention. In chemical analysis, the incorporation of molecular recognition into miniaturized extraction devices or layers followed by detection will be further examples of the powerful role of designed molecular recognition reagents in inorganic extraction.

See also: II/Affinity Separation: Immobilised Metal Ion Chromatography; Extraction: Analytical Inorganic Extractions; Solid-Phase Extraction; Supercritical Fluid Extraction. III/Ion Analysis: Liquid Chromatography; Metal Complexes: Ion Chromatography; Solid-Phase Extraction With Disks.

Further Reading

- Arnaud-Neu F, Collins EM, Deasy M *et al.* (1989) Synthesis, X-ray crystal structures, and cation-binding properties of alkyl calixaryl esters and ketones, a new family of macrocyclic molecular receptors. *Journal of the American Chemical Society* 111: 8681–8691.
- Arnaud-Neu F, Schwing-Weill M-J, Ziat K *et al.* (1991) Selective alkali and alkaline earth complexation by calixarene amides. *New Journal of Chemistry* 15: 33–37.
- Böhmer V (1995) Calixarenes, macrocycles with (almost) unlimited possibilities. *Angew. Chem. Int. Ed. Engl.* 34: 713–745.

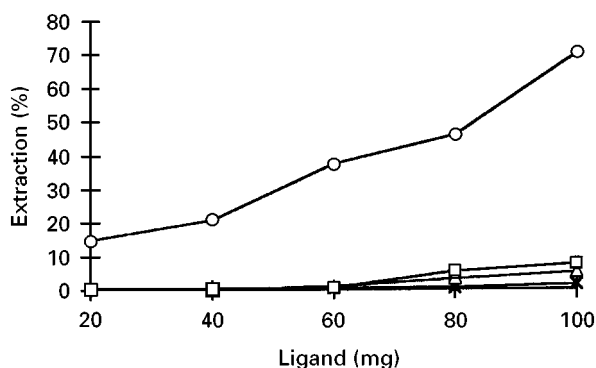


Figure 5 Percentage extraction of metal ions, as determined by atomic absorption analysis, versus mass of fluorinated calixarene tetrahydroxamate reagent used in the SFE of p.p.m. levels of Fe^{3+} (circles), Cu^{2+} (squares), Ni^{2+} (triangles) and Mn^{2+} (crosses) from spiked cellulose paper. 40 μL of water, 60°C, 350 atm, 30 min static and 15 min dynamic.

- Casnati A, Pochini A, Ungaro R *et al.* (1996) 1,3-Alternate calix[4]arene-crown-5 conformers: new synthetic ionophores with better K^+/Na^+ selectivity than valinomycin. *Chemistry-A European Journal* 2(4): 436–445.
- Cooper SR (1988) Crown thioether chemistry. *Accounts of Chemical Research* 21: 141–146.
- Dozol JF, Bohmer V, McKervery MA *et al.* (1997) EUR 17615 – New Macrocyclic Extractants for Radioactive Waste Treatment: Ionizable Crown Ethers and Functionalised Calixarenes. Luxembourg: Office for Official Publications of the European Communities 1997 – XII.
- Glennon JD, Hutchinson S, Harris SJ *et al.* (1997) Molecular baskets in supercritical CO_2 . *Analytical Chemistry* 69: 2207–2212.
- Hancock RK (1992) Chelate ring size and metal ion selection – the basis of selectivity for metal ions in open chain ligands and macrocycles. *Journal of Chemical Education* 69(8): 615–621.
- Ikeda A and Shinkai S (1997) Novel cavity design using calix[n]arene skeletons: towards molecular recognition and metal binding. *Chemical Reviews* 97: 1713–1734.
- Izatt RM (1997) Review of selective ion separations at BYU using liquid membrane and solid phase extraction procedures. *Journal of Inclusion Phenomena and Molecular Recognition in Chemistry* 29: 197–220.
- Jönsson JA and Mathiasson L (1992) Supported liquid membrane techniques for sample preparation and enrichment in environmental and biological analysis. *Trends in Analytical Chemistry* 11(3): 106–114.
- Kolthoff IM (1979) Applications of macrocyclic compounds in chemical analysis. *Analytical Chemistry* 51(5): 1R–22R.
- Krasnushkina EA and Zolotov YuA (1983) Macrocyclic extractants. *Trends in Analytical Chemistry* 2(7): 158–162.
- McKervery MA, Schwing MJ and Arnaud-Neu F (1996) Cation binding by calixarenes. *Comprehensive Supramolecular Chemistry* 1: 537–603.
- Pedersen CJ (1967) Cyclic polyethers and their complexes with metal salts. *Journal of American Chemical Society* 89: 7017.
- Wai CM and Wang S (1997) Supercritical fluid extraction: metals as complexes. *Journal of Chromatography A* 785: 369.
- Weber E and Bartsch RA (1989) *Crown Ethers and Analogs*. Chichester: John Wiley.

MULTIRESIDUE METHODS: EXTRACTION



S. J. Lehotay, Agricultural Research Service, Eastern Regional Research Center, Wyndmoor, PA, USA

F. J. Schenck, US Food and Drug Administration, Southeast Regional Laboratory, Atlanta, GA, USA

Copyright © 2000 Academic Press

Introduction

‘Killing two birds with one stone’ is a common expression that captures the essence of multiresidue methods of analysis. Multiresidue methods are almost always more efficient than separate single analyte methods for multiple analytes. However, a possible drawback of multiresidue methods that cover a wide polarity range or diversity of analytes is a potential loss of selectivity for individual analytes. The use of high efficiency analytical separation techniques and/or very selective detectors can compensate for a lack of selectivity in preceding steps, but as a general rule, a greater degree of selectivity leads to higher quality results. Multiresidue methods often involve a balancing act between the analytical scope of the method and the quality of the results for all analytes. It is sometimes difficult ‘to have your cake and eat it, too’.

Residues

In general, residues consist of synthetically derived chemicals that are not intended to occur in the sample, but may be present at trace concentrations as a by-product of a preliminary process related to the sample, or as a separate process altogether. Residues may be inorganic or organic, but inorganic compounds are generally analysed separately from organics. Multielemental analysis measures the natural occurrence of elements as well as any residues that may occur in the sample. Microorganisms and dirt may also be considered residues according to some definitions, but their analysis requires different techniques from organic compounds and they will not be considered further in this discussion. In the case of organic chemicals, many natural components are capable of being analysed in the same approach as the residue method, but these compounds are usually termed interferences, and great effort is often spent trying selectively to remove or avoid them (however, other chemists may be very interested in these matrix interferants).

The most common type of multiresidue application is the analysis of organic chemical contaminants in food and environmental samples. There are instances

when a residue is intended, such as a fungicide designed to extend product life, but for the large majority of situations, residues are not desired in the sample. Residues may consist of pesticides, drugs, industrial by-products and/or other pollutants. Within each of these categories are subcategories known as classes of analyte. For example, classes of insecticides include organophosphorus (OP), organochlorine (OC), carbamate, pyrethroid, and others; classes of pollutants include volatile organic compounds (VOC), polycyclic aromatic hydrocarbons (PAH), polychlorinated biphenyls (PCB) alkylphenol ethoxylates (APE) and others; and veterinary drugs include antibiotics (β -lactams, aminoglycosides and tetracyclines), antibacterials (nitrofurans, fluoroquinolones and sulfonamides), and anthelmintics (benzimidazoles, avermectins and milbemycins). Thus, multiresidue methods may be single-class or multiclass depending on the number of analytes and classes covered by the analytical scope of the method.

A few existing multiresidue methods may be used to analyse more than one type of residue (e.g. pesticides and industrial pollutants), but most applications generally require the analysis of a single residue category. Analytical needs do exist that would entail the monitoring of all types of residues in some sample matrices (e.g. certain foods), but different methods are usually conducted for the separate analysis of the different residue types. It is difficult enough to develop and perform multiclass, multiresidue methods, and very few multi-type, multiclass, multiresidue methods have been attempted. However, some overall analytical schemes may include a wide array of analyte types in the extraction procedure and then divide the extract into separate aliquots for different clean-up and analytical steps.

The Analytical Process

The analytical process goes through a series of steps which leads to the analytical results. Much like a chain that is only as strong as its weakest link, an analytical method is only as good as its weakest step. These steps consist of: (i) sample collection and handling; (ii) sample preparation (extraction, clean-up); (iii) analyte determination (analytical separation, detection); and (iv) reporting of results.

The primary consideration that must be addressed independently of the analytical steps, however, is the need for the data. The analytical method should be tailored to meet the minimum needs in terms of the scope of analytes to be detected, desired limits of detection (LOD) and acceptable precision and accuracy of the results. In many cases, the data needs will

require the best possible results for as many analytes as possible. However, no analytical method can detect all possible analytes in the same procedure, and all laboratories are constrained by available personnel, space, instrumentation and other resources. Thus, the analytes must be prioritized according to importance and weighed against the cost and availability of analytical methods for their detection. The analytical chemist considers the most efficient overall approach to determine the analytes of interest that meets the acceptable data quality requirements and fits within the laboratory budget. This process may involve trade-offs between the quality of results for a particular analyte balanced against the quality of results for one or more other analytes.

The first step in the analytical process involves sample collection and handling. Unless representative samples are collected of the appropriate matrix and the samples are treated properly to avoid losses of analytes or potential contamination, then the results may not provide the information necessary to meet the needs for the analysis. In fact, a false sense of security in misleading results is often the outcome unless each step in the analytical process is carefully considered and controlled. For example, excellent recoveries and reproducibilities may be achieved for the analysis of several OP insecticides in liver tissue, but nearly all OPs partition into fat tissue in animals, and very few appear in the liver. If the purpose of the analysis is to determine animal exposure to OPs and assess risk to humans, then fat tissue should be sampled, not liver. Otherwise, the analysis may accomplish nothing of real significance.

Extraction

Once the appropriate sample has been collected and handled properly, the next sequential step in the analytical process is the sample preparation procedure which is the subject of this article – *extraction*. Extraction is the separation of the analyte from the matrix. A few techniques, such as direct analysis of chemicals in liquids, may avoid the extraction step, but in most cases, the analytes must also be concentrated prior to analysis, which often necessitates an extraction process. The post-extraction steps in the analytical process may include clean-up of extracts and an analytical separation, but some sample preparation techniques incorporate clean-up and analyte separation into the extraction procedure. In other cases, the final analyte detection step may not require extra clean-up or analytical separation steps, but usually the price to pay for an approach that avoids clean-up steps is reduced ruggedness and higher instrument maintenance.

The type of extraction step that is used for a particular matrix depends on the nature of the matrix and analytes. Fundamentally, typical samples consist of solids, liquids and gases, or combinations thereof. Solids are usually not reasonably extracted with solids, and gases may not be extracted with gases (unless a solid membrane is placed between them), but all other combinations of liquid–solid, solid–gas, liquid–liquid and liquid–gas extractions are common in extraction techniques; supercritical fluids have also become a useful medium for extraction processes. With modern extraction techniques and the number of different solvents available, the control of pressure and temperature in the separation process has provided an essentially limitless number of possible separation conditions for the chemist to employ.

Extractions Involving Gases

For gaseous samples, the extraction process nearly always involves passing large volumes of sample through a solid phase or liquid trap. In solid-phase systems, the analytes are adsorbed on to the particle surfaces, and in liquids the analytes are partitioned into the liquid. In the case of low temperature trapping, the analytes may simply condense on to the cold surfaces. For the most volatile analytes, a combination of condensation and adsorption may be conducted by maintaining low temperature of an adsorptive surface. The analytes are concentrated in the trapping medium and may undergo clean-up or be directly analysed in a chromatographic system. The most common approach is probably to use active materials, such as Tenax, polyurethane foam, octadecylsilyl-derivatized silica, polymer resins, or a variety of other materials to adsorb the analytes.

The use of liquid trapping by bubbling the gas through a liquid is another easy approach to extracting air-borne substances, but evaporative losses of the liquid, greater temperature limitations and less convenience generally make large volume liquid trapping a less common approach. However, liquid coatings that are useful in gas chromatography (GC) are also useful at trapping analytes from gaseous samples. It is not uncommon to perform direct collection of gases from the atmosphere at the head of a GC column kept at relatively low temperature (typically -50°C to 50°C). The chemist must be careful, however, not to expose the column to temperatures outside its range of operation. Once the sample has been extracted/collected on the column, injection occurs by simply beginning the oven temperature programme to perform separation and analysis. Purge-and-trap techniques are another way of accomplishing this without introducing air into the GC system.

Thermal Desorption

Thermal desorption is an extraction technique which utilizes a flowing gas to extract a small heated solid or liquid sample. This process occurs during injection in GC systems and, in some cases, the approach is useful to separate thermally the analyte from the matrix for direct analysis in a flowing gas stream. The approach is not used widely in direct sample analysis, even for stable volatile and semivolatile analytes for a variety of practical reasons. For example, analyte–matrix interactions may be too strong in some cases, or matrix interferences may be too great.

Certain analytes are more prone to degradation during thermal desorption and, in multiresidue methods, these analytes may be deemed too important to sacrifice. Another potential pitfall may be that the sample size is too small to achieve the desired LOD. Thus, a liquid concentration step may be needed to increase the injected relative sample size, but then clean-up is usually required. Otherwise, thermal desorption can lead to a very rugged approach for sample introduction in GC analysis because the selectivity of the extraction matches the selectivity of the analysis. Unlike liquid sample introduction, nonvolatile components in the extract are not introduced into the GC column and the life of the chromatographic system is extended.

Solid-Phase Microextraction (SPME)

In the late 1980s, Pawliszyn and his group at the University of Waterloo in Canada invented a technique dubbed SPME, which conveniently takes advantage of the absorption and desorption processes between gases, liquids and solids. An SPME device is a small fibre rod that has been coated with a solid or liquid phase and which is contained in a pen-like sleeve. The coated fibre is exposed to the gaseous or liquid sample and then retracted into the sleeve for brief storage. Analysis may involve thermal desorption of the fibre in a GC injection port or solvent elution of the analytes from the fibre coating into a liquid chromatographic (LC) system.

SPME is applicable to extraction of liquid samples, but it has been most noteworthy for its effectiveness in the extraction of gases. In fact, one of its modes of operation for sampling liquids is to place the fibre in the headspace above the liquid sample in an enclosed volume. The analyte will eventually partition into the headspace and then into the coating on the fibre which can be desorbed into a chromatographic system for analysis.

The major advantage of SPME is ease of use. Other advantages include low cost and avoidance of hazardous solvents. At this time, only a few fibre coatings

are available, and this has limited the selectivity of SPME, but more coatings are expected to become available. The most common coating is polydimethylsiloxane (PDMS), which is also a common phase in GC columns.

Extractions Involving Only Liquids

Liquid-Liquid Extraction (LLE)

Water extraction is a common application for multi-residue methods. Water generally contains fewer matrix interferences than solid matrices and large volumes may often be extracted to decrease LOD. Before the widespread introduction of convenient solid-phase extraction (SPE) cartridges, LLE was the method of choice for extraction of water pollutants. Dichloromethane (DCM) is the most common solvent for extraction in LLE of water because: (i) it is only slightly miscible with water, (ii) it extracts an acceptably wide range of nonpolar analytes; (iii) it possesses a low boiling point to speed evaporation/concentration steps; and (iv) it is heavier than water and thus exists as the lower phase during partitioning in a separatory funnel or LLE glassware. Of course, other immiscible solvents are also used in LLE.

Traditionally, continuous LLE is conducted using specialized glassware which passes redistilled DCM through the water for an extended period of time (16–24 h). The extract collects with the DCM in a boiling flask where the DCM is removed by distillation. Otherwise, either manual or mechanical shaking is used to speed the extraction process (at the cost of more solvent volume and effort). In most cases, sample volume is limited to 1 L by the practical nature of the extraction process and size of the glassware. SPE has virtually displaced

LLE in water methods due to its greater versatility, convenience, solvent reduction and sample volume capacity.

Extractions Involving Liquids and Solids

The most common application in chemical residue analysis concerns the extraction of a solid sample using a liquid. A variety of liquid solvents are readily available to provide a medium for easy homogenization in a blending device. **Table 1** lists key properties of common liquids used in multiresidue methods. These parameters indicate the relative polarity of the solvent, volatility and miscibility with other liquids. In extraction processes, the tenet that like dissolves like (and conversely, opposites do *not* attract) is the primary consideration in choosing the extraction solvent. For example, hexane often provides a selective extraction for nonpolar analytes, and toluene may provide more selectivity for aromatic analytes. Practical considerations involving ease of evaporation, cost, safety and hazardous waste disposal also play a role in the selection of the extraction solvent. In situations involving acidic/basic analytes, pH is often the most critical property in the extraction and buffered aqueous solvents are often necessary. Another important consideration is the stability of the analytes in the extraction medium.

Soxhlet Extraction

In this technique, the sample is mixed with a dispersant and/or drying agent and placed in a permeable paper thimble. The extraction thimble is placed in a glass apparatus which is exposed to the extraction solvent. Fresh solvent enters the extraction section

Table 1 Selected properties of common solvents used in extractions

<i>Solvent</i>	<i>Polarity index</i>	<i>Dielectric constant^a</i>	<i>Boiling point (°C)</i>	<i>Viscosity (mN s⁻¹ m⁻²)</i>	<i>Density^b (g mL⁻¹)</i>	<i>Solubility in water (%w/w)</i>
Acetone	5.1	20.7	56.2	0.337	0.791	100
Acetonitrile	5.8	37.5	81.6	0.375	0.786	100
Cyclohexane	0.2	2.02	80.7	0.980	0.779	0.01
Dichloromethane	3.1	9.08	40.7	0.449	1.326	1.6
Diethyl ether	2.8	4.34	34.6	0.245	0.713	6.89
Ethanol	5.2	24.55	78.4	1.08	0.789	100
Ethyl acetate	4.4	6.02	77.2	0.455	0.901	8.7
Hexane	0.0	1.89	69.0	0.313	0.659	0.001
Iso-octane	—	1.94	99.2	0.504	0.692	—
Methanol	5.1	32.70	64.6	0.544	0.791	100
Toulene	2.4	2.57	110.8	0.587	0.866	0.051
Water	9.0	78.30	100.0	0.890	0.998	—

^aAt 25°C.

^bAt 20°C.

from the distillation section of the apparatus. When the solvent reaches a certain level, the extract siphons into a boiling flask where the extracted components are concentrated. The solvent is boiled and redistilled to fall back into the region where the sample is contained. In this way, the Soxhlet glassware is designed to repetitively conduct a number of extractions of the matrix with fresh (redistilled) solvent each time. This process is rather time-consuming (up to 16–24 h) to achieve adequate extraction efficiencies and takes up a great deal of glassware and laboratory space. Automated Soxhlet instruments have been introduced, but the Soxhlet approach is frequently regarded in modern laboratories as archaic.

Blending and Sonication

Blending the sample with the solvent is also an old-fashioned approach, but it is very fast, convenient and inexpensive. Thus, the use of blenders, choppers, shakers, probes and other mixing devices is not likely to disappear even as newer instrumental techniques are being introduced. In the case of matrices such as clay soils that tightly retain certain analytes, sonication using a high energy probe is an alternative method that can break matrix–analyte interactions. However, due to the higher energy input involved, sonication has a greater potential for degrading analytes than simple blending, but the approach can be useful for stable analytes.

Microwave-assisted Extraction (MAE)

MAE is a technique used in the 1990s for the extraction of organic residues in solid samples (microwave digestion has been used in the analysis of metals for several years). The approach simply involves placing the sample with the solvent in specialized containers and heating the solvent using microwave energy. The extraction process is more rapid than Soxhlet, and reduces solvent consumption, but it is more complicated and time-consuming than blending. As in the case of sonication, MAE may overcome retention of the analyte by the matrix, but analyte degradation can be a problem at higher temperatures in certain applications.

The selection of solvent, microwave energy applied and extraction time are the main parameters controlled in MAE. The user should use proper extraction vessels and equipment in MAE, because very high pressures can be generated and explosions may result if appropriate precautions are not taken. MAE instruments are available that conduct batch extractions to increase sample throughput, which is an advantage over automated instruments in other techniques that perform sequential extractions.

Pressurized Liquid Extraction (PLE)

PLE is another time-saving and solvent-reducing approach that was developed in the mid-1990s. The instrumental approach generally involves first dispersing the sample with an inert material (e.g. drying agent or sand) and placing the mixed sample in an extraction vessel. The general approach consists of introducing the solvent into the vessel followed by heating the vessel and a static extraction step (no flow). After this 0.5–20 min step, flow is initiated (dynamic extraction step) and the extract is collected in a vial. The process may be repeated if necessary to increase analyte recoveries. Although increased temperature is not a necessity in PLE, higher temperature is usually used to speed the extraction and break analyte–matrix interactions.

The order of importance of parameters for an application in PLE (and extraction in general) is typically: (1) solvent; (2) temperature; (3) time; (4) repetitions; (5) pressure. The same types of solvents can be used in PLE as in traditional approaches, but relatively viscous solvents, such as ethanol and water, can be difficult to permeate through the sample even at high pressures. Also, highly acidic and basic conditions can be damaging to instrument components, which limits the use of PLE in certain applications. The properties of solvents can change dramatically at different temperatures and pressures (the boiling point at room temperature is commonly exceeded in PLE and MAE), thus it may be possible to replace potentially more hazardous solvents with more benign solvents. Unfortunately, physicochemical properties of many common solvents are not yet known at the elevated temperatures and pressures possible in PLE and MAE.

Solid-Phase Extraction

SPE, sometimes referred to as liquid–solid extraction, is a popular technique for the isolation and separation of analytes from a liquid matrix. SPE columns, packed with small quantities of various chromatographic sorbents, are commercially available. SPE columns may contain polar sorbents such as silica, Florisil or alumina for normal-phase separations, and nonpolar bonded silica phases or polymers for reversed-phase separations. One of the most widely used types of SPE columns is packed with nonpolar octadecylsilyl-derivatized silica, or C₁₈. When liquids such as water, plasma and in some cases, milk, are eluted through C₁₈ SPE columns, nonpolar organic compounds such as certain pesticides, drugs or industrial pollutants will be adsorbed onto the column. These adsorbed analytes can be later eluted from the column with a relatively small amount of solvent.

SPE discs containing C_{18} are widely used for the isolation of contaminants from water. Large volumes (litres) of water can be fairly rapidly eluted through the discs, and organic compounds, such as OC pesticides, PCBs and PAHs will be retained. These trapped organic compounds can then be eluted from the SPE discs with organic solvents. In many cases, the choice of solvent, pH and SPE phase provides clean-up of matrix components during the extraction process.

Matrix Solid-phase Dispersion (MSPD)

MSPD is an extraction technique that entails mixing a sample of tissue or milk with an SPE sorbent. Stephen Barker and his group at Louisiana State University first developed the concept in the late 1980s. Typically, a small quantity (0.5 g) of liver, muscle, fat or milk is homogeneously dispersed with 2 g of C_{18} silica in a mortar and pestle. The C_{18} silica will disrupt the cells and disperse the contents over a large surface area, thereby exposing the entire sample to the extraction process. This homogeneous dispersion is then placed in a column, and the various components of the dispersion can be eluted from the column with a range of solvents. For example, lipids or fats can first be eluted from the column with hexane, while drugs, which are more polar, can be eluted with more polar solvents such as ethyl acetate and/or methanol. Thus, extraction and clean-up can be performed in a convenient procedure. Disadvantages of MSPD include the small sample size and potentially high cost of the solid-phase material.

Extractions Involving Supercritical Fluids

Supercritical Fluid Extraction (SFE)

SFE is an instrumental approach not unlike PLE, except a supercritical fluid is used as the extraction solvent rather than a liquid. SFE and PLE employ the same procedures for preparing samples and loading extraction vessels, and the same concepts of static and dynamic extractions are also pertinent. SFE typically requires higher pressure than PLE to maintain supercritical conditions and, for this reason, SFE usually requires a restrictor to better control flow and pressure of the extraction fluid. CO_2 is by far the most common solvent used in SFE due to its relatively low critical point (73 atm and $31^\circ C$), extraction properties, availability, gaseous natural state and safety.

A major advantage of SFE over liquid-based methods is that the extraction solvent becomes a gas after extraction and the analytes are conveniently concentrated in the collecting medium (solid-phase

trap or liquid). Liquid extraction methods nearly always require a concentration step after extraction. Another key advantage of SFE is that the density of the supercritical fluid and other physicochemical properties can be dramatically altered through control of temperature and pressure. This permits a somewhat higher degree of selectivity and versatility in the extraction process without having to use different solvents. In some cases, SFE can eliminate post-extraction clean-up steps, or at least make clean-up using SPE exceptionally convenient by using the SPE sorbent as a trapping medium in SFE. Due to its many practical advantages, SFE may be considered the first choice for extraction if it is able to meet the needs of the application.

However, SFE also has several disadvantages which have delayed the widespread implementation of the approach. The higher selectivity of SFE limits the range of analytes that can be extracted under the same conditions. Furthermore, SFE can have difficulty in overcoming analyte-matrix interactions in certain applications (soils in particular). Organic solvents (and water), often called modifiers in SFE, are sometimes added to the supercritical fluid to increase the polarity range of the extraction process and to help overcome analyte retention in the matrix. Other problems with SFE include the high cost of automated instruments, relatively small sample sizes and more involved method development process. SFE has been demonstrated to be effective in the extraction of a variety of residues from a variety of matrices, but it remains to be seen if the technique can overcome its drawbacks and become more widely implemented.

Conclusions

The analytical range of the overall analysis cannot exceed the analytical range of the extraction process, and in the case of multiresidue methods it is not uncommon to have a wide polarity range of analytes. For this reason, the use of rather exhaustive extraction conditions has been the traditional approach in multiresidue methods. The cost of a wide scope of analytes is often reduced selectivity, solvent-consuming and longer extractions, and additional clean-up of extracts. Ideally, however, the selectivity of the extraction process should match the polarity range of the targeted analytes, and no further clean-up would be required prior to analysis. Modern techniques may permit the realization of the ideal extraction process which is fast, automated, precise, efficient and safe. Furthermore, the variety of solvents and solid-phase sorbents, in combination with temperature and pressure control of modern instruments, can give the

chemist the ability to achieve the desired selectivity in a single, convenient extraction procedure.

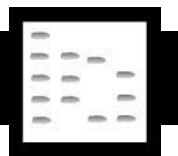
Due to the additional parameters of temperature and pressure that modern instrumental techniques provide, it has become more difficult to compartmentalize extraction techniques based on whether the extraction fluid is a dense gas, liquid, supercritical fluid, or combination thereof. Strictly speaking, pressurized fluid extraction PFE includes all types of pressurized extractions independent of the solvent's state of matter. Subcategories of PFE include SFE and PLE, but instrument companies have confused the terminology by marketing PLE as accelerated solvent extraction (ASETM) and enhanced solvent extraction (ESE). Other scientists have developed other terms to describe extraction techniques, such as enhanced fluidity extraction, which connotes a mixture of gas, liquid and/or supercritical fluid, and subcritical water extraction, which is meant to represent PLE using water at high temperatures. However, the unifying principles of extraction are the same no matter what instrument-makers or scientists may call a particular approach.

See also: **II/Chromatography: Gas:** Headspace Gas Chromatography. **Extraction:** Solid-Phase Extraction; Solid-Phase Microextraction; Solvent Based Separation; Supercritical Fluid Extraction. **III/Environmental Applications:** Soxhlet Extraction; **Microwave-Assisted Extraction: Environmental Applications. Solid-Phase Matrix Dispersion: Extraction.**

Further Reading

- Cairns T and Sherma J (eds) (1992) *Emerging Strategies for Pesticide Residue Analysis*. Boca Raton, FL: CRC Press.
- Environmental Protection Agency (1998) *Handbook of Environmental Methods*, 3rd edn. Schenectady, NY: Genium.
- Font G, Manes J, Molto JC and Pico Y (1993) Solid phase extraction multi-residue pesticide analysis of water. *Journal of Chromatography* 642: 135–161.
- Food and Drug Administration (1994) *Pesticide Analytical Manual*, vol. I: *Multiresidue Methods*, 3rd edn. Washington, DC: US Dept. of Health and Human Services.
- Lehotay SJ (1997) Supercritical fluid extraction of pesticides in foods. *Journal of Chromatography A* 785: 289–312.
- Lopez-Avila V, Young R, Benedicto J *et al.* (1995) Extraction of organic pollutants from solid samples using microwave energy. *Analytical Chemistry* 67: 2096–2102.
- Moats WA and Medina MB (eds) (1996) *Veterinary Drug Residues: Food Safety*. ACS Symposium Series 636. Washington, DC: American Chemical Society.
- Pawliszyn J (1997) *Solid Phase Microextraction: Theory and Practice*. New York: Wiley-VCH.
- Richter BE, Jones BA, Ezzell JL *et al.* (1996) Accelerated solvent extraction: a technique for sample preparation. *Analytical Chemistry* 68: 1033–1039.
- Walker CC, Lott HM and Barker SA (1993) Matrix solid-phase dispersion extraction and the analysis of drugs and environmental pollutants in aquatic species. *Journal of Chromatography* 642: 225–242.

NATURAL PRODUCTS



High-Speed Countercurrent Chromatography

A. Marston and K. Hostettmann, Institut de Pharmacognosie et Phytochimie, Lausanne University, Switzerland

Copyright © 2000 Academic Press

In high speed countercurrent chromatography (HSCCC) a sample is partitioned between two non-miscible liquid phases. One phase is held stationary by a centrifugal force (applied by spinning the separation element at high speed), while the second phase is pumped through the apparatus, hence the alternative term for the process centrifugal partition chromatography (CPC).

Unlike high performance liquid chromatography (HPLC), in which the stationary phase occupies 5–7% and the mobile phase about 75% of the column, the relative proportions in HSCCC are 50–75% for the stationary phase and 20–50% for the mobile phase. As a consequence, large sample loads are possible with HSCCC. Another important advantage of the absence of a solid support is that irreversible adsorption is avoided. There is total recovery of the injected sample and tailing is minimized. HSCCC is thus of special importance for the separation of sensitive and easily degraded samples. Although the efficiency of HSCCC separations is lower than that encountered in HPLC, the optimization of selectivity is the great advantage offered by the former technique.

The potential of HSCCC is further shown by the possibility of applying gradients for separations.

Solvent proportions can be changed during a chromatographic run. Furthermore, solvent elution can be reversed in the course of a separation by changing over stationary and mobile phases. Consequently, one of the characteristics of HSCCC is its extreme flexibility.

Most applications of HSCCC have been performed on two types of instrument. The first category, namely rotating coil instruments, consists of a polytetrafluoroethylene tube (column) wrapped around a spool. The spool is rotated around a central axis in such a way that it describes a planetary motion. Alternatively, hydrostatic equilibrium instruments can be employed. These have either cartridges or discs arranged around a central axis. The separation column, in effect, consists of a series of cells in the cartridges or discs.

Preparative Applications

HSCCC is becoming a routine preparative technique in both industrial and university laboratories. Sample sizes ranging from milligrams to grams (and even kilograms in specialized instruments) can be successfully chromatographed. An extensive range of separations by HSCCC has been published (see Further Reading).

Aqueous and nonaqueous solvent systems are used and the separation of compounds with a wide range of polarities is possible. Two-phase solvents are chosen according to the hydrophobicity of the sample. For polar compounds, *n*-butanol can be employed (e.g. ethyl acetate–butanol–water or chloroform–butanol–water systems), for moderately hydrophobic compounds chloroform (e.g. chloroform–methanol–water) solvent systems, and for more hydrophobic compounds, *n*-hexane (e.g. *n*-hexane–ethyl acetate–methanol–water) solvent systems. Some of the more frequently used solvent systems are shown in Table 1.

A number of representative separations by HSCCC are presented here, in order to give an idea of the possibilities available, together with the chromatographic conditions employed.

Plant-derived Natural Products

Flavonoids Many HSCCC separations of natural products involve polyphenols. The reason for this fact is that there is a tendency to ‘tail’ or even to adsorb irreversibly on conventional chromatographic supports (silica gel, polyamide etc.). This problem does not occur with all-liquid separation techniques and quantitative recovery of injected sample is achieved.

Separations of flavonoid aglycones and flavonoid glycosides have been performed mainly with chloro-

Table 1 Frequently used solvent systems for HSCCC

Sample	Solvent system
Polar	CHCl ₃ –MeOH– <i>n</i> -BuOH–H ₂ O 7 : 6 : 3 : 4
	<i>n</i> -BuOH– <i>n</i> -PrOH–H ₂ O 4 : 1 : 5
	<i>n</i> -BuOH– <i>n</i> -PrOH–H ₂ O 2 : 1 : 3
	EtOAc– <i>n</i> -BuOH–H ₂ O 3 : 2 : 5
Moderately polar	CHCl ₃ –MeOH–H ₂ O 4 : 3 : 2
	CHCl ₃ –MeOH–H ₂ O 5 : 6 : 4
	CHCl ₃ –MeOH–H ₂ O 10 : 10 : 6
	CHCl ₃ –MeOH–H ₂ O 13 : 7 : 8
	CHCl ₃ –MeOH–H ₂ O 7 : 13 : 8
	<i>n</i> -Hexane–EtOAc–MeOH–H ₂ O 1 : 1 : 1 : 1
Apolar	<i>n</i> -Hexane–EtOAc–MeOH–H ₂ O 10 : 5 : 5 : 1
	<i>n</i> -Hexane–CH ₃ CN–MeOH 8 : 5 : 2
	<i>n</i> -Hexane–CH ₃ CN–CH ₂ Cl ₂ 10 : 7 : 3

form–methanol–water or chloroform–methanol–propanol–water systems.

The time required for a particular separation can be reduced by incorporating reversed-phase (RP) operation into the procedure. Figure 1 shows the situation for the flavanone hesperitin (1) and the flavonols kaempferol (2) and quercetin (3). When eluting with the upper phase (mobile phase), the most polar component eluted first and the time for complete separation is over 8 h. Reversing the elution mode and changing to the lower phase as mobile phase at 70 min leads to completion of the separation in just over 2 h.

Alternatively, gradient operation can be used to speed up HSCCC. By pumping simultaneously the upper and lower phases of the two-phase solvent system by separate pumps, the proportions of the phases are changed in the coil during separation. In the example shown in Figure 2, the coil (capacity 360 mL) of the chromatograph was initially filled with equivalent amounts of upper and lower phases of the solvent used in Figure 1. The flavonoid mixture was then injected. By pumping upper phase at 4 mL min^{−1} and lower phase at 1 mL min^{−1} through the apparatus, the content of the lower phase in the coil was increased from 180 to 340 mL over 3 h. The separation time of the three flavonoids was thus reduced by 5 h, when compared with normal operation.

Xanthones This is another class of polyphenols to which liquid–liquid chromatography has successfully been applied. Extensive use of HSCCC was made for the separation of xanthones from a plant, *Hypericum roeperanum* (Guttiferae), from Zimbabwe. A dichloromethane extract of the roots gave a fraction (363 mg) rich in xanthones after initial chromatography. Separation of the individual xanthones from this

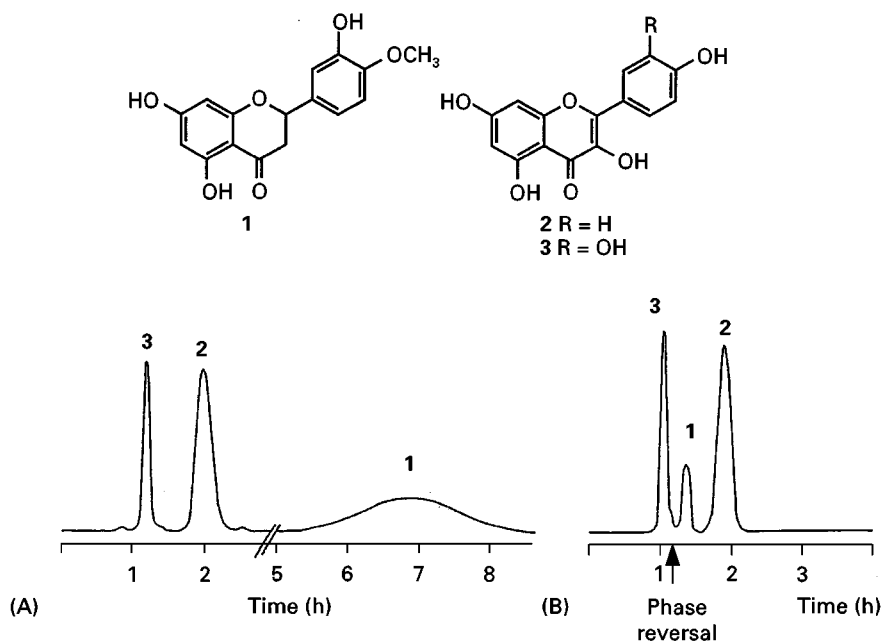


Figure 1 HSCCC separation of hesperetin (**1**), kaempferol (**2**) and quercetin (**3**) by normal and reversed-phase solvent elution. Instrument: multilayer countercurrent chromatograph (PC Inc.). Solvent system: CHCl_3 -MeOH- H_2O 5 : 6 : 4. Detection: 254 nm. (A) Upper phase as mobile phase; flow rate 3 mL min^{-1} ; rotational speed 700 rpm. (B) Upper phase as mobile phase to 70 min, then lower phase as mobile phase; flow rate 3 mL min^{-1} ; rotational speed 700 rpm. (Reproduced with permission from Marston A, Slacanian I and Hostettmann K (1990) Centrifugal partition chromatography in the separation of natural products. *Phytochemical Analysis* 1: 3–17. Copyright 1990, John Wiley and Sons Limited.)

fraction by other methods, including semipreparative HPLC, proved very difficult. However, HSCCC gave six fractions which, after final purification steps

provided eight xanthenes. For the HSCCC separation, the solvent hexane-EtOAc-MeOH- H_2O 1 : 1 : 1 : 1 was employed, with the upper phase as the mobile phase. One of the new xanthenes isolated, 5-O-dimethyl-paxanthonin (**4**), could only be satisfactorily separated by HSCCC.

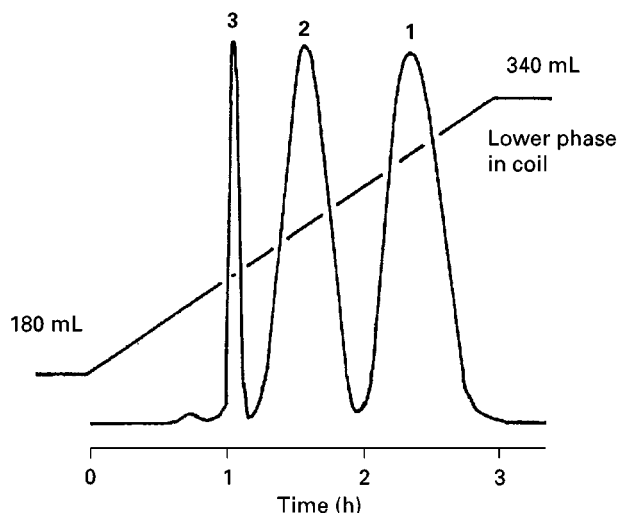
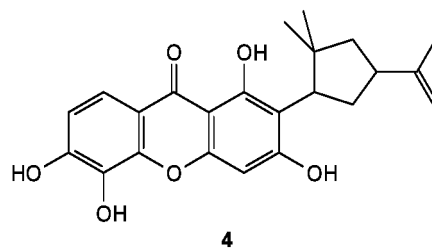
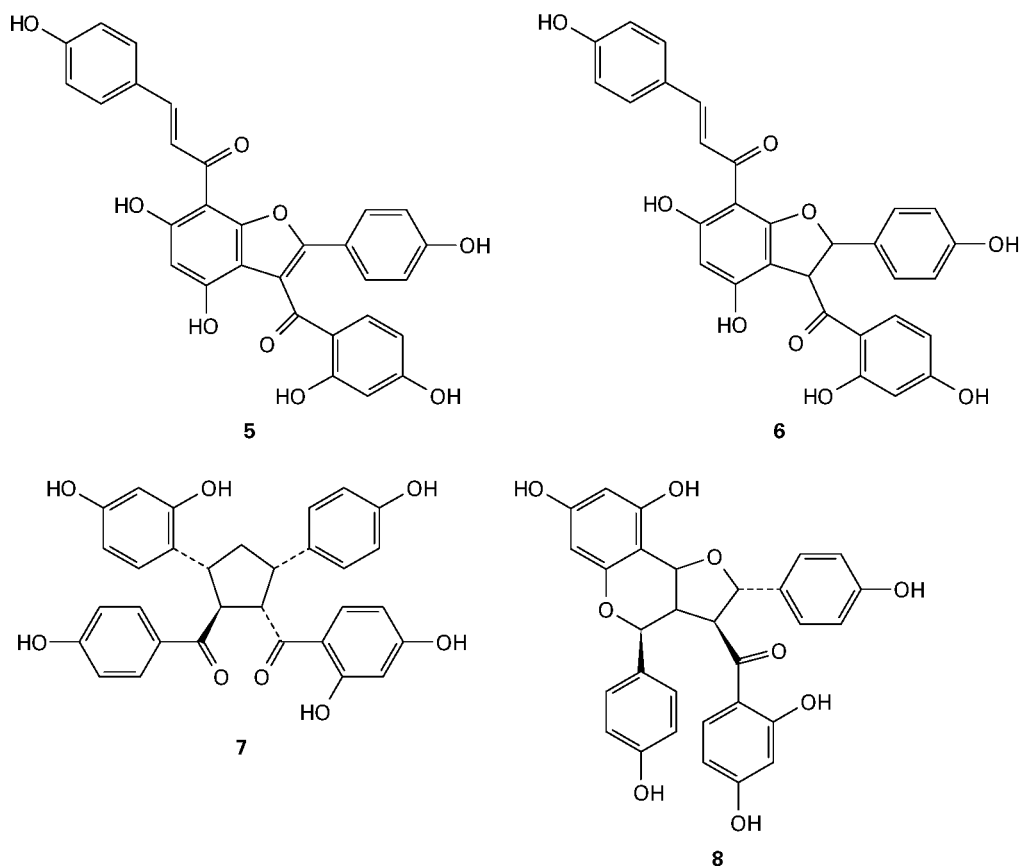


Figure 2 Gradient elution for the separation of flavonoids **1–3**. Instrument: multilayer countercurrent chromatograph (PC Inc.). Solvent system: CHCl_3 -MeOH- H_2O 5 : 6 : 4. Composition of mobile phase: upper phase at 4 mL min^{-1} , lower phase at 1 mL min^{-1} . (Reproduced with permission from Slacanian I, Marston A and Hostettmann K. (1989) Modifications to a high-speed countercurrent chromatograph for improved separation capability. *Journal of Chromatography* 482: 234–239. Copyright 1989, Elsevier Science.)



Chalcone derivatives A further example of the separation of polyphenols by HSCCC is provided by the isolation of chalcone derivatives **5–9** from *Brackenridgea zanguebarica*, a tree found in central Africa and belonging to the Ochnaceae family. This application of HSCCC also illustrates that large amounts of crude plant extract can potentially be handled.

Direct fractionation of 20 g of a methanol extract of the yellow bark layer from the tree is possible with the solvent system cyclohexane-ethyl acetate-methanol-water 8 : 8 : 6 : 6 (upper layer as mobile phase). The extract was dissolved in 20 mL of each phase and



introduced via a 60 mL sample loop. The separation column (660 mL) was first filled with 50% of each phase and then eluted with mobile phase. When steady run conditions had been achieved, the sample was injected. Seven fractions were obtained (A–G; Figure 3), three of these giving the antifungal polyphenols 5–8. Compound 5 crystallized from fraction

B, while compounds 6–8 were purified by a final low pressure liquid chromatography step on a C_{18} support. A novel, inactive, spiro derivative (9) was isolated from fraction E after low pressure liquid chromatography on a C_{18} stationary phase.

As can be seen, no more than two separation steps were required for each polyphenol isolated.

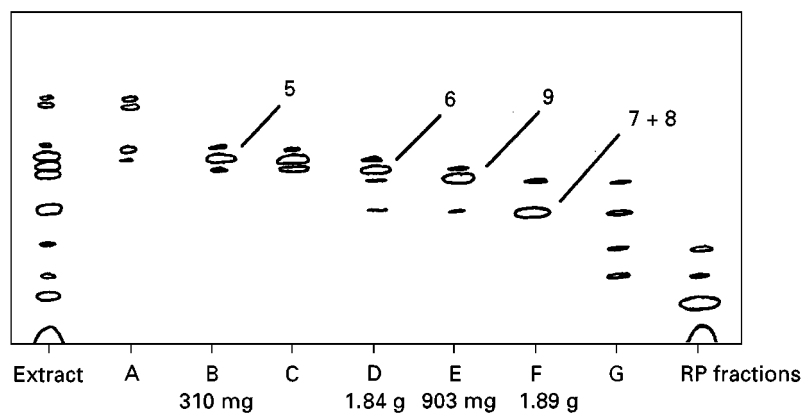
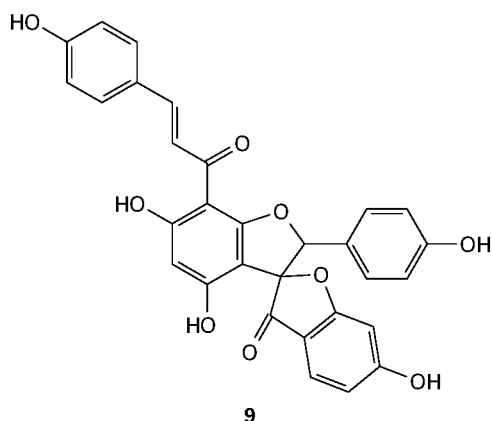


Figure 3 Thin-layer chromatography monitoring (solvent: lower phase of CHCl_3 – MeOH – H_2O 2 : 2 : 1) of fractions from the CCC-1000 HSCCC separation of *Brackenridgea zanguebarica* stem bark methanol extract. Solvent system: cyclohexane– EtOAc – MeOH – H_2O 8 : 8 : 6 : 6 (upper phase as mobile phase). Flow rate: 3 mL min^{-1} . Rotational speed: 1000 rpm. Detection: 254 nm. Sample size: 20 g.



Phenylpropanoids and coumarins It is possible to isolate natural products by HSCCC alone, as exemplified by the purification of phenylpropanoids and a furanocoumarin from a dichloromethane extract of the leaves of *Diplolephium buchanani* (Apiaceae). Initial fractionation gave semipure products (Figure 4). A subsequent liquid-liquid step, using a different nonaqueous solvent system in each case, gave pure myristicin (10, using hexane-*t*-butyl methyl ether-acetonitrile 5 : 1 : 5; upper layer as mobile phase) and a mixture of elemicin (11) and *trans*-isoelemicin (12) (using heptane-acetonitrile-methanol 6 : 3 : 1; upper layer as mobile phase). The furanocoumarin oxypeucedanin (13) was obtained by simple crystallization of the corresponding HSCCC

fraction. All four isolated compounds had both anti-fungal and larvicidal activities.

Lignans Initial fractionation of insecticidal neolignans from *Magnolia virginiana* (Magnoliaceae) by HSCCC was better, less expensive and more efficient than traditional open-column or more recent flash chromatographic methods. A hexane extract of the leaves was chromatographed with the lower layer of the solvent system hexane-acetonitrile-ethyl acetate-water 8 : 7 : 5 : 1 as mobile phase. This solvent contained only a small proportion of water to provide compatibility with the very lipophilic extract. Subsequent purification of the fractions provided a biphenyl ether (14) and two biphenyls (15, 16), which were not only insecticidal to *Aedes aegypti* (the vector of yellow fever) but also fungicidal, bactericidal and toxic to brine shrimp.

During the investigation of anti-human immunodeficiency virus type 1 lignans from creosote bush, *Larrea tridentata* (Zygophyllaceae), a cross-axis coil planet centrifuge was employed with aqueous phases containing sodium chloride, e.g. hexane-ethyl acetate-methanol-0.5% NaCl 6 : 4 : 5 : 5. The presence of salt reduced emulsification and gave improved stationary-phase retention.

Tannins Tannins include a wide variety of phenolic compounds, ranging from single glycosides of gallic

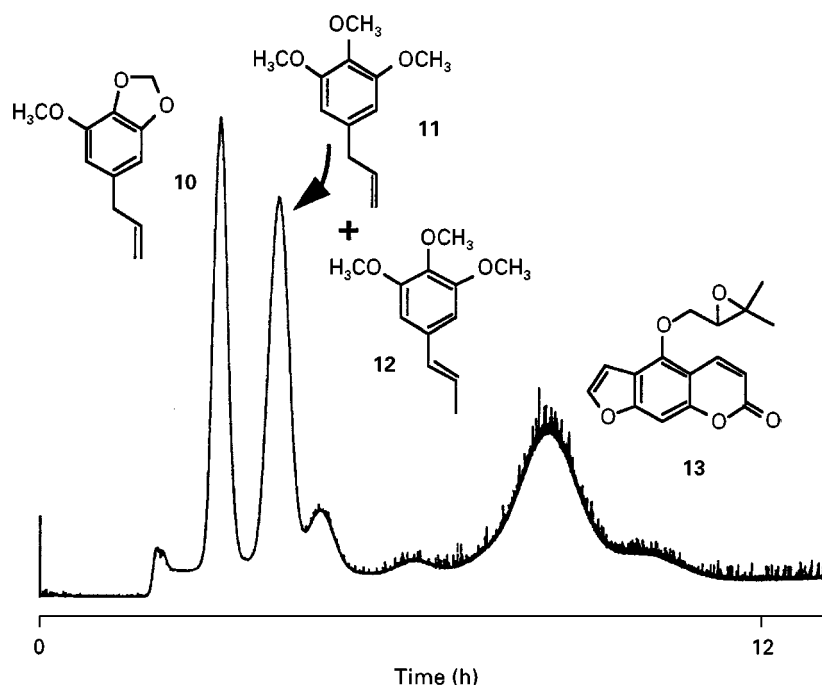
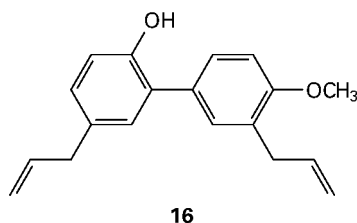
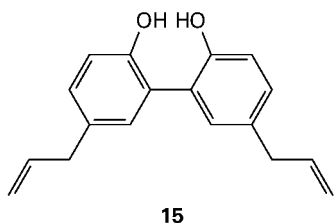
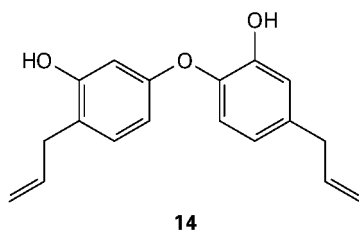


Figure 4 HSCCC initial fractionation on a CCC-1000 instrument of a dichloromethane extract of *Diplolephium buchanani* leaves. Solvent system: hexane-EtOAc-MeOH-H₂O 10 : 5 : 5 : 1 (upper phase as mobile phase). Flow rate 3 mL min⁻¹. Rotational speed: 1000 rpm. Detection: 254 nm. Sample size: 1.7 g.



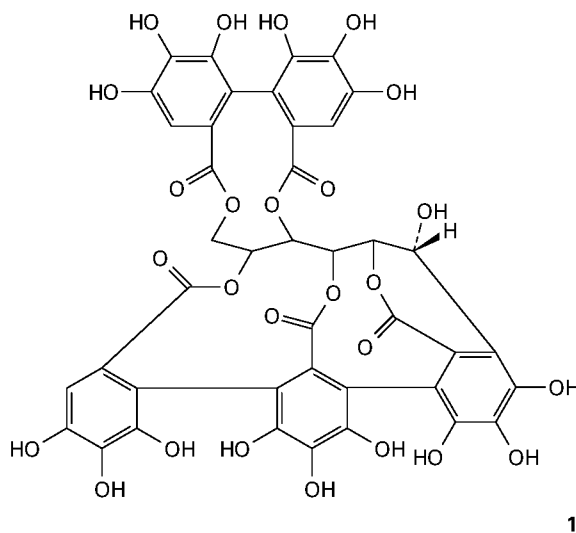
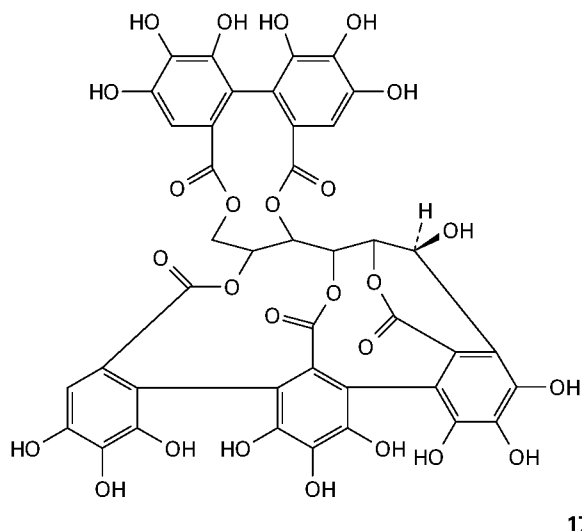
acid to complex condensed and polymerized derivatives of catechin, epicatechin and related compounds. Their separation poses special problems since there is often irreversible adsorption and even hydrolysis on solid supports. Preparative HPLC is accompanied by sample loss and deterioration or contamination of the column. HSCCC has proved to be an ideal technique for the resolution of these particular problems.

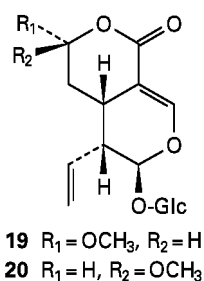
Among the examples of successful separations performed on cartridge instruments is the resolution of two diastereomers, castalgin (17) and vescalagin (18), which differ only in the configuration of a single hydroxyl group. They were extracted from *Lythrum anceps* (Lythraceae) leaves and chromatographed with the solvent system *n*-butanol-*n*-propanol-water (4 : 1 : 5), using the upper phase as the mobile phase.

The same solvent system was used to obtain a trimeric (nobotanin J; molecular weight 2764) and a tetrameric (nobotanin K; molecular weight 3742) hydrolysable tannin from the leaves of *Heterocentron roseum* (Melastomataceae). The isolation procedure involved chromatography on Toyopearl HW-40 (methanol-acetone-water gradient). Final purification of the two tannins was on an instrument with 12 cartridges (total capacity 240 mL; 700 rpm; flow rate 3 mL min⁻¹).

Monoterpene glycosides Among the examples of monoterpene glycosides that have been separated by HSCCC are two secoiridoid glycosides from the South American plant *Halenia campanulata* (Gentianaceae). Size exclusion chromatography of a crude methanol extract of the plant on Sephadex LH-20, followed by separation by HSCCC (1000 rpm) with the solvent system CHCl₃-MeOH-H₂O 9 : 12 : 8 (lower phase as mobile phase; flow rate 3 mL min⁻¹) gave the two glycosides (19, 20). Their separation is possible by HSCCC, despite the fact that they only differ in their configuration at C₇.

Triterpene glycosides Liquid-liquid chromatography is particularly suitable for the separation of highly polar compounds. Triterpene glycosides enter into this category and many successful isolations have





been performed using HSCCC either alone or in combination with other chromatographic methods. The direct separation of pure saponins from the crude methanol extract of *Hedera helix* (Araliaceae) berries has proved possible by this method. The extract was first partitioned between *n*-butanol and water. The *n*-butanol fraction was subjected to HSCCC, eluting with the lower layer of the solvent system $\text{CHCl}_3\text{-MeOH-H}_2\text{O}$ 7 : 13 : 8. Elution was monitored by thin-layer chromatography and gravimetry. Molluscicidal saponins **21–24**, with hederagenin as aglycone, were separated within 2 h by this technique (Figure 5).

Alkaloids The utility of CPC in separating alkaloids from gummy or tarry matrices has been shown in the preparative separation of pyrrolizidine alkaloids from different plant sources. After classical alkaloid extraction procedures, batches of up to 800 mg of extract could be chromatographed on a rotating coil apparatus (380 mL capacity). Potassium phosphate buffer (0.2 mol L^{-1}) at an appropriate pH was used as stationary phase, while the mobile phase was chloroform. With the buffered stationary phase, good solute resolution was achieved since structurally similar pyrrolizidine alkaloids differ in their pKa values.

HSCCC has been employed for the separation of the antitumour drug, camptothecin (**25**). From sources such as *Nothapodytes foetida* (Icacinaceae), camptothecin is often mixed with 9-methoxycamptothecin (**26**). These can be easily separated with the solvent systems $\text{CHCl}_3\text{-CCl}_4\text{-MeOH-H}_2\text{O}$ 2 : 2 : 3 : 1 or $\text{CH}_2\text{Cl}_2\text{-MeOH-H}_2\text{O}$ 5 : 3 : 1. The low solubility of the samples poses a problem with traditional chromatographic techniques. However, for the HSCCC separation, 500 mg of sample can be dissolved

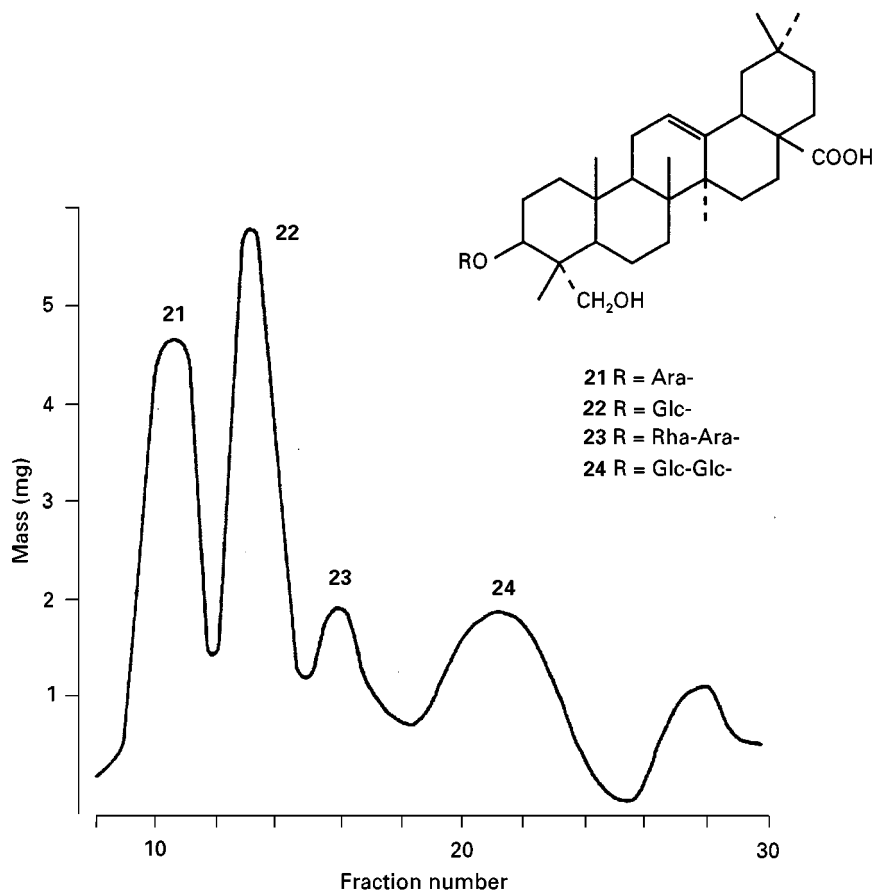
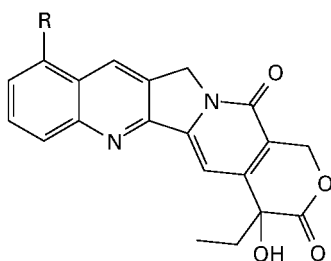


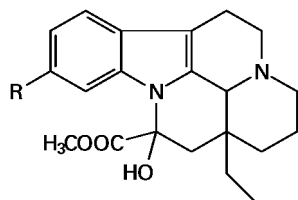
Figure 5 Separation of a methanol extract of *Hedera helix* berries on a Sanki CPC instrument. Solvent system: $\text{CHCl}_3\text{-MeOH-H}_2\text{O}$ 7 : 13 : 8 (lower phase as mobile phase). Flow rate 1.5 mL min^{-1} . Rotational speed: 700 rpm. Sample size: 100 mg.

in 70 mL lower phase and 10 mL upper phase (i.e. a large volume) for injection via a sample loop.



25 R=H (Camptothecin)
26 R=OCH₃ (9-Methoxycamptothecin)

Repetitive sample injections are possible for the separation of close-running compounds on rotating coil instruments. This has been shown for the separation of vincamine (27) and vincine (28) from *Vinca minor* (Apocynaceae). After 20 successive injections (at 42 min intervals), each of 1.7 mg sample mixture, 16.5 mg of 27 and 14 mg of 28 were obtained on a 230 mL rotating coil instrument. The solvent system was *n*-hexane-ethanol-water (6 : 5 : 5; lower phase as mobile phase). The resolution of the HSCCC system was not changed when the instrument was shut down overnight and restarted the next day with the same stationary phase in the column.



27 R=H (Vincamine)
28 R=OCH₃ (Vincine)

Marine Natural Products

The mild conditions achieved with HSCCC and the rapidity of the method are ideal for the separation of delicate marine natural products. Attempts at purification of antitumour ecteinascidins from the tunicate *Ecteinascidia turbinata*, for example, by normal-phase or RP chromatography leads to extensive loss of activity. HSCCC, however, proved to be an effective means of separating these light- and acid-sensitive alkaloids.

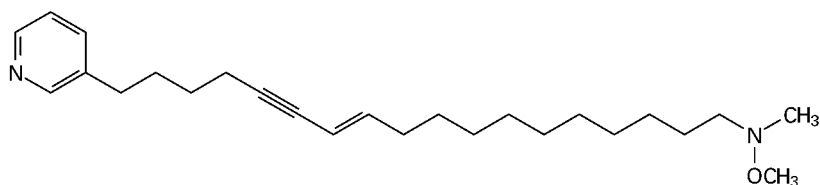
The pyrroloquinoline alkaloids isobatzellines A–C have been isolated from a *Batzella* sponge. They exhibited *in vitro* cytotoxicity against the P-388 leukaemia cell line and antifungal activity against *Candida albicans*. HSCCC with a rotating coil apparatus was used in their purification, following extraction and solvent partitioning. Elution was performed with the upper phase of the solvent system heptane–chloroform–methanol–water (2 : 7 : 6 : 3).

The nonaqueous solvent system heptane (or hexane)–dichloromethane–acetonitrile (10 : 3 : 7) has been applied to the separation of a variety of marine natural products, including a long chain methoxylamine pyridine, xestamine A (29), isolated from the sponge *Xestospongia wiedenmayeri*.

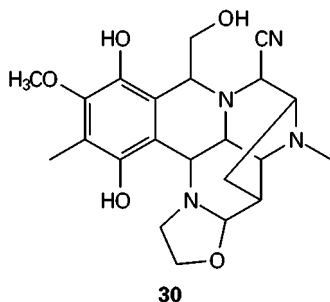
Antibiotics

Since its inception, HSCCC has been associated with the field of antibiotics. Liquid–liquid partition techniques are particularly suitable for their separation because bioactive metabolites are often produced in small amounts and have to be removed from other secondary metabolites and nonmetabolized media ingredients. Antibiotics are normally biosynthesized as mixtures of closely related congeners and many are labile molecules, thus requiring mild separation techniques with a high resolution.

To illustrate the applications of HSCCC to the separation of antibiotics, one example is provided by the sporavidins, which are water-soluble basic glycoside antibiotics with complex structures. These are unstable under basic conditions and exist as mixtures of closely related compounds. A sample comprising six sporavidins was resolved on a rotating coil countercurrent instrument (total capacity 325 mL; 800 rpm). Selection of the solvent system was based on partition coefficient data from chloroform–methanol–water, chloroform–ethanol–methanol–water and *n*-butanol–diethyl ether–water mixtures. After HPLC analysis, the final system adopted was *n*-butanol–diethyl ether–water (5 : 2 : 6). Sample was introduced by the so-called sandwich technique, in which sample was injected after filling with stationary phase and before mobile-phase elution. The six components were separated within 3.5 h, employing a total elution volume of 500 mL.



Streptomyces lusitanus produces the hydroquinone derivative **30** (cyanocycline C), which is extremely unstable and cannot be purified by semipreparative HPLC. However, isolation of this antibacterial compound was successfully performed on a rotating coil apparatus with the solvent system CHCl_3 -MeOH-iPrOH- H_2O 3 : 10 : 10 : 10.



Analytical Applications

Reducing the radius of revolution of a rotating coil and increasing the speed of rotation have produced highly efficient HSCCC systems with an effective analytical capability. Operational speeds lie between 2000 and 4000 rpm and the tube bore is less than 1 mm i.d. Efficient separations of micro-quantities of samples in a short time are thus possible. In general, the observed resolution and speed are comparable to those of HPLC. However, it is unlikely that HSCCC will displace HPLC for purely analytical applications. By comparison with analytical HPLC, the major advantage of HSCCC is that it is always possible to reverse the elution mode – this is useful for complex samples with a wide range of polarity. The other important use of analytical HSCCC is in the rapid selection of suitable solvent systems for scale-up to preparative applications.

The instruments available typically have a single rotating coil, with a total capacity of 5–40 mL. Flow rates are directly related to the selected solvent system and must be adapted in order to minimize back-pressure and leakage of the stationary phase. Although instruments are commercially available, many applications have been performed on prototype equipment.

While applications of analytical HSCCC to natural products are not numerous, many different classes of compounds have been separated: alkaloids, anthraquinones, coumarins, flavonoids, lignans, terpenoids and macrolides.

For example, the separation of a mixture of vincamine (**27**), the major alkaloid of *Vinca minor* (Apocynaceae) and vincine (11-methoxyvincamine) (**28**), has been performed by analytical HSCCC in hexane-ethanol-water (6 : 5 : 5) with a 0.85 mm i.d.

multilayer coil. Comparison of the separation with results obtained from analytical RP-HPLC showed that both methods gave baseline resolution, but it was possible to observe a small peak just preceding the vincine peak in analytical HSCCC which was not resolved by RP-HPLC. Analysis of the sample by HSCCC-mass spectrometry showed that the minor compound was probably an isomer of vincine.

A crude flavonoid mixture obtained from the ethanolic extract of the fruits of sea buckthorn (*Hippophae rhamnoides*, Elaeagnaceae) has been successfully separated with an analytical HSCCC instrument. The separation of a 3 mg mixture with chloroform-ethanol-water (4 : 3 : 2) was complete within 15 min when the mobile lower phase was pumped at a flow rate of 5 mL min⁻¹ (rotation speed 1800 rpm). The five main components of the fruit extract were resolved (including isorhamnetin, the principal flavonoid) within 8 min, a time scale wholly comparable to analytical HPLC separations. The instrument used has a 0.85 mm i.d. coil, with a 2.5 cm radius of revolution and a capacity of 8 mL.

Conclusion

The advantages of HSCCC favour a much wider use of this technique in the future: the absence of a solid chromatographic support avoids irreversible adsorption of samples; economics are favourable, as the consumption of solvent is up to 10 times less than conventional chromatographic techniques. Other features, such as the use of step and continuous gradients and the possibility of RP operation, add to the flexibility of the method. Very high sample loading is possible and large quantities of crude plant extracts can be injected without causing contamination problems. HSCCC, however, cannot be called a competitor to preparative-scale HPLC but it is rather a complementary technique. This complementarity can also be exploited when other chromatographic techniques fail to separate a given sample: HSCCC can be tried since its selectivity may be different.

It is still necessary to make improvements on the mechanical side. A variety of instruments are available but some are not yet reliable enough. Once larger scale production is underway, this sort of problem will be eliminated and the full potential of HSCCC will be realized.

See also: II/Chromatography: Liquid: Countercurrent Liquid. III/Alkaloids: Gas Chromatography; Liquid Chromatography; Thin Layer (Planar) Chromatography. **Antibiotics:** High-Speed Countercurrent Chromatography; Supercritical Fluid Chromatography. **Essential Oils:** Thin-Layer (Planar) Chromatography. **Natural Products:** High-Speed Countercurrent Chromatography;

Liquid Chromatography; Liquid Chromatography-Nuclear Magnetic Resonance; Supercritical Fluid Extraction; Thin Layer (Planar) Chromatography. **Terpenoids: Liquid Chromatography.**

Further Reading

- Conway WD (1990) *Countercurrent Chromatography: Apparatus, Theory and Applications*. New York: VCH Publishers.
- Foucault AP (ed.) (1995) *Centrifugal Partition Chromatography*. New York: Marcel Dekker.
- Hostettmann K, Marston A and Hostettmann M (1998) *Preparative Chromatography Techniques: Applications in Natural Product Isolation*, 2nd edn. Berlin: Springer.
- Ito Y and Conway WD (eds) (1996) *High-speed Countercurrent Chromatography*. New York: John Wiley.
- McAlpine JB and Hochlowski JE (1989) Countercurrent chromatography. In: Wagman GH and Cooper

- R (eds) *Natural Products Isolation – Separation Methods for Antimicrobials, Antivirals and Enzyme Inhibitors*, *Journal of Chromatography Library*, vol. 43, pp. 1–53. Amsterdam: Elsevier.
- Mandava NB and Ito Y (eds) (1988) *Countercurrent Chromatography: Theory and Practice*. New York: Marcel Dekker.
- Marston A and Hostettmann K (1994) Countercurrent chromatography as a preparative tool – applications and perspectives. *Journal of Chromatography A* 658: 315.
- Oka H, Harada K and Ito Y (1998) Separation of antibiotics by counter-current chromatography. *Journal of Chromatography A* 812: 35.
- Slacanin I, Marston A and Hostettmann K (1989) Modifications to a high-speed countercurrent chromatograph for improved separation capability. *Journal of Chromatography* 482: 234.

Liquid Chromatography

K. Hostettmann and J. L. Wolfender, Institut de Pharmacognosie et Phytochimie, Université de Lausanne, Lausanne, Switzerland

Copyright © 2000 Academic Press

Chemical investigation of plant constituents is strongly linked to the use of liquid chromatography (LC) at both the analytical and preparative level. Indeed, most of the secondary metabolites can be effi-

ciently separated or isolated by different liquid chromatographic techniques. The plant extracts are generally screened by different bioassays and submitted to fractionation by chromatography. The fractions obtained are further tested for their biological activities. This process is repeated until the isolation of a pure active constituent, which is finally identified by spectroscopic methods (bioactivity guided isolation; **Figure 1**).

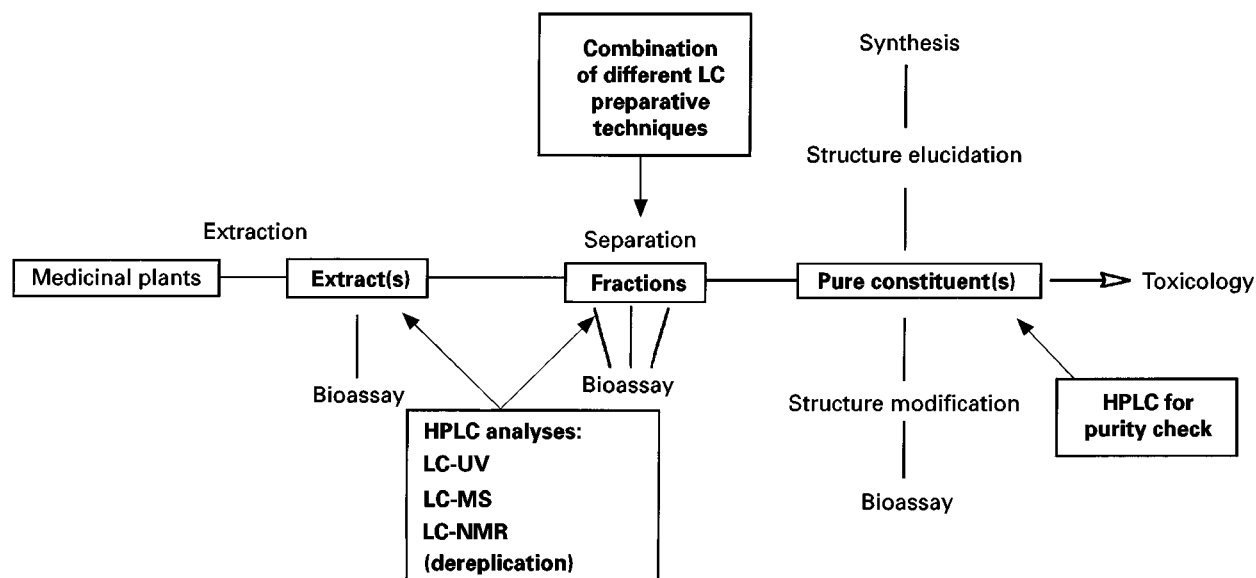


Figure 1 Procedure for obtaining the active principles from plants. LC techniques are used at the analytical and preparative level during the whole isolation procedure. HPLC hyphenated techniques play an important role in the early recognition of well-known compounds in the extract prior to isolation.

Generally the plant material is extracted by solvents of increasing polarity. This extraction step is very important because it allows a first rough fractionation of the plant constituents. Initial extraction with low polarity solvents yields the more lipophilic components, while alcoholic solvents give a larger spectrum of apolar and polar material. The plant extracts are usually very complex mixtures which contain hundreds or thousands of different constituents. Separation of all these constituents with a single chromatographic technique is often difficult to achieve. Thin-layer chromatography (TLC) and high performance liquid chromatography (HPLC) are the most commonly used techniques for a rapid check of the chemical composition of these extracts. If the isolation of a given constituent is required, a scale-up of the analytical separation conditions to preparative chromatography techniques is needed. These preparative techniques are generally open-column chromatography, low pressure LC (LPLC), medium pressure LC (MPLC) and semi-preparative HPLC. When irreversible adsorption problems or denaturation of natural products occur, countercurrent chromatography (CCC) techniques such as centrifugal partition chromatography (CPC) are preferred.

Analytical Techniques

High Performance Liquid Chromatography

Of all the LC chromatography techniques used in the analysis of plants, HPLC is probably the most useful and versatile. HPLC is used routinely in phytochemistry to pilot the preparative isolation of natural products (optimization of the experimental conditions, checking of the different fractions throughout the separation) and to control the final purity of the isolated compounds. For chemotaxonomic purposes, the botanical relationships between different species can be shown by chromatographic comparison of their chemical composition. Comparison of chromatograms, used as fingerprints, between authentic samples and unknowns permits identification of the unknown material and/or the search for adulteration.

HPLC of complex mixtures such as crude extracts is usually carried out on reversed-phase columns. For the separation of the different constituents, acetonitrile–water or methanol–water gradients are applied. Linear gradients are generally used but in the case of a very complex separation, a succession of isocratic and gradient steps may be necessary. For the suppression of tailing due to polyphenolic constituents, modifiers such as trifluoroacetic acid or acetic

acid are added, while for the separation of basic products such as alkaloids, amines or NH_4OH can be used. Crude extracts or fractions are usually injected without any sample preparation, but solid-phase extraction (SPE) prepurification or derivatization (usually to enhance the UV chromophore) can be performed in certain cases. The sample is preferably dissolved in the eluent but when solubility problems occur, as is often the case with plant extracts, stronger solvents such as tetrahydrofuran are used. When working with 4 mm i.d. columns, 50–200 μg of extract can be injected. In most cases, the separation is usually followed by UV detection because a majority of natural products possess UV chromophores. However, for the detection of constituents without a UV chromophore such as sugars, other techniques such as refractive index (RI), light scattering (LS) or electrochemical detection (ECD) are necessary.

A typical HPLC-UV chromatogram of the crude methanol extract of the roots of the African plant *Chironia krebsii* (Gentianaceae) is shown in **Figure 2**. The separation was achieved by applying a linear acetonitrile–water gradient on an RP-18 column. A good separation of the three main classes of constituents found in the plant was achieved.

HPLC Hyphenated Techniques

In many applications, it may be necessary not only to detect but also to identify compounds in extracts. With conventional detection methods such as UV, the identity of peaks can be confirmed only from their retention times, by comparison with authentic samples. In order to get more information on the metabolites of interest, there is a need for a multiple detection system offering the possibility of taking advantage of both chromatography as a separation method and spectroscopy techniques as detection and identification methods. HPLC has thus been coupled to various sophisticated detectors such as UV photodiode array detectors (LC-UV-DAD), mass spectrometers (LC-MS) or, more recently, to nuclear magnetic resonance instruments (LC-NMR).

When searching plant extracts for compounds with interesting properties, a multidimensional approach to their chromatographic analysis is of great significance. By combining HPLC online with UV, MS and NMR, a large amount of preliminary information can be obtained about the constituents of an extract before their isolation (**Figure 1**). In the case of polyphenols, for example, UV spectra recorded online give useful complementary information (type of chromophore or pattern of substitution) to that obtained with LC-MS and already provide a precise assignment of the peak of interest. When these data are not sufficient, LC-NMR can give a useful

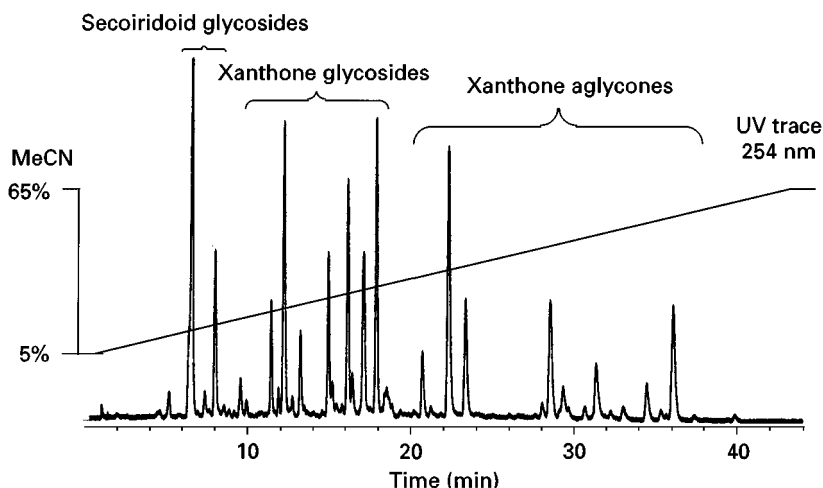


Figure 2 HPLC-UV analysis of the methanolic extract of the root of *Chironia krebsii* (Gentianaceae). HPLC: column, RP-18 NovaPak (4 μ m, 150 \times 3.9 mm i.d.); gradient, MeCN-H₂O (0.1% TFA) 5 : 95 \rightarrow 65 : 35 in 50 min (1 mL min⁻¹).

complement for a full structural identification online. This preliminary LC chemical screening avoids the useless isolation of known constituents and concentrates the search only on the compounds of potential further interest.

This approach is illustrated by the following example: a Gentianaceous plant, *Swertia calycina*, presenting interesting antifungal activities, was studied by LC-UV, LC-MS and LC-NMR. The LC-UV analysis of the dichloromethane extract was quite simple and exhibited three main peaks. The LC-UV spectra of these peaks permitted a first rapid online recognition of the various types of constituents of the extract. The LC-MS provided molecular weight information for each of these compounds (Figure 3).

These online data, together with chemotaxonomical considerations, allowed the identification of a xanthone (3) and a secoiridoid (1) in this plant. However, the structure of compound (2) could not be completely ascertained by LC-UV-MS alone, because its UV spectrum was characteristic for a quinonic chromophore and no compound of this type has been reported in the Gentianaceae family. The LC-MS of (2) exhibited a protonated $[M + H]^+$ ion at m/z 189, indicating a molecular weight of 188 amu. The LC-NMR analysis of the extract gave well resolved ¹H-NMR online spectra for the three major compounds. For the unknown (2), the online ¹H-NMR spectrum revealed the presence of a methoxyl group together with a quinonic ring proton while four other aromatic protons appeared at lower field (Figure 4). These online data were in good agreement with those of *O*-methyl lawsone, a known naphthoquinone. This type of compound has, however, never been reported in the Gentianaceae family.

Preparative Techniques

Preparative-scale separation is one of the most important operations carried out in a natural products laboratory. It is often tedious and time-consuming, especially when the mixture to be separated is complex. The nature of the separation problem varies considerably from the isolation of small quantities (mg or less), for structure determination purposes, to the isolation of very much larger amounts (hundreds of mg to kg quantities), for comprehensive biological testing or even for production of therapeutic agents.

The most important preparative techniques which have found application in the isolation and purification of natural products are listed in Table 1. A distinction has to be made between techniques using a solid stationary phase or a liquid fixed on an inert solid support and all-liquid partition techniques. For all these techniques, the use of solvents such as acetone or in some cases chloroform is inadvisable because in their presence natural products may undergo transformations.

Flash Chromatography/Open-column Chromatography

Open-column chromatography and flash chromatography are the most popular techniques for natural product isolation. Flash chromatography is a preparative air-driven liquid chromatographic technique with moderate resolution. It has the advantage over conventional open-column chromatography of minimizing sample loss and the risk of decomposition of natural products, due to the fast elution of the sample. These two techniques allow the use of various column sizes and permit the introduction of

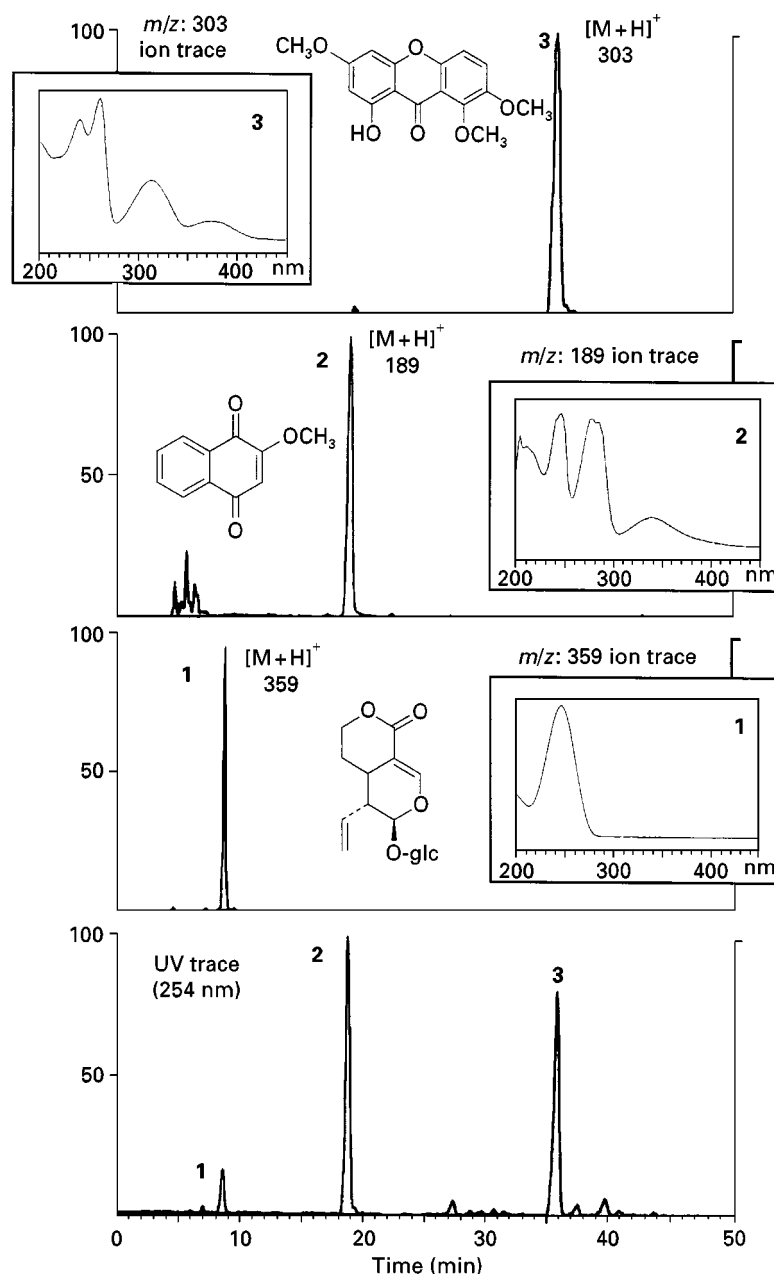


Figure 3 LC-UV and LC-thermospray (TSP)-MS analyses of the crude CH_2Cl_2 extract of *Swertia calycina* (Gentianaceae). For each major peak, the single ion LC-MS traces of the protonated molecular ions $[\text{M} + \text{H}]^+$ are displayed, together with the UV spectra obtained online.

mg to g quantities of sample. They are generally used with silica gel supports. As a rule of thumb, for natural product applications, around 30 mg sample loading per g of 50–200 μm support is feasible. When used only for filtration (first fractionation step of a crude plant extract), silica gel chromatography can be performed under overloaded conditions and quantities up to 100 mg g^{-1} of support can be loaded.

These techniques can be used at different steps in the isolation process of natural products. They are mostly well adapted to the separation of nonpolar to medium polarity plant extracts. In order to find the appropriate solvent system, preliminary TLC analyses are performed and the plate is sprayed with different reagents in order to detect the natural products of interest. For a given product, solvent systems producing R_F values between 0.2 and 0.3 are

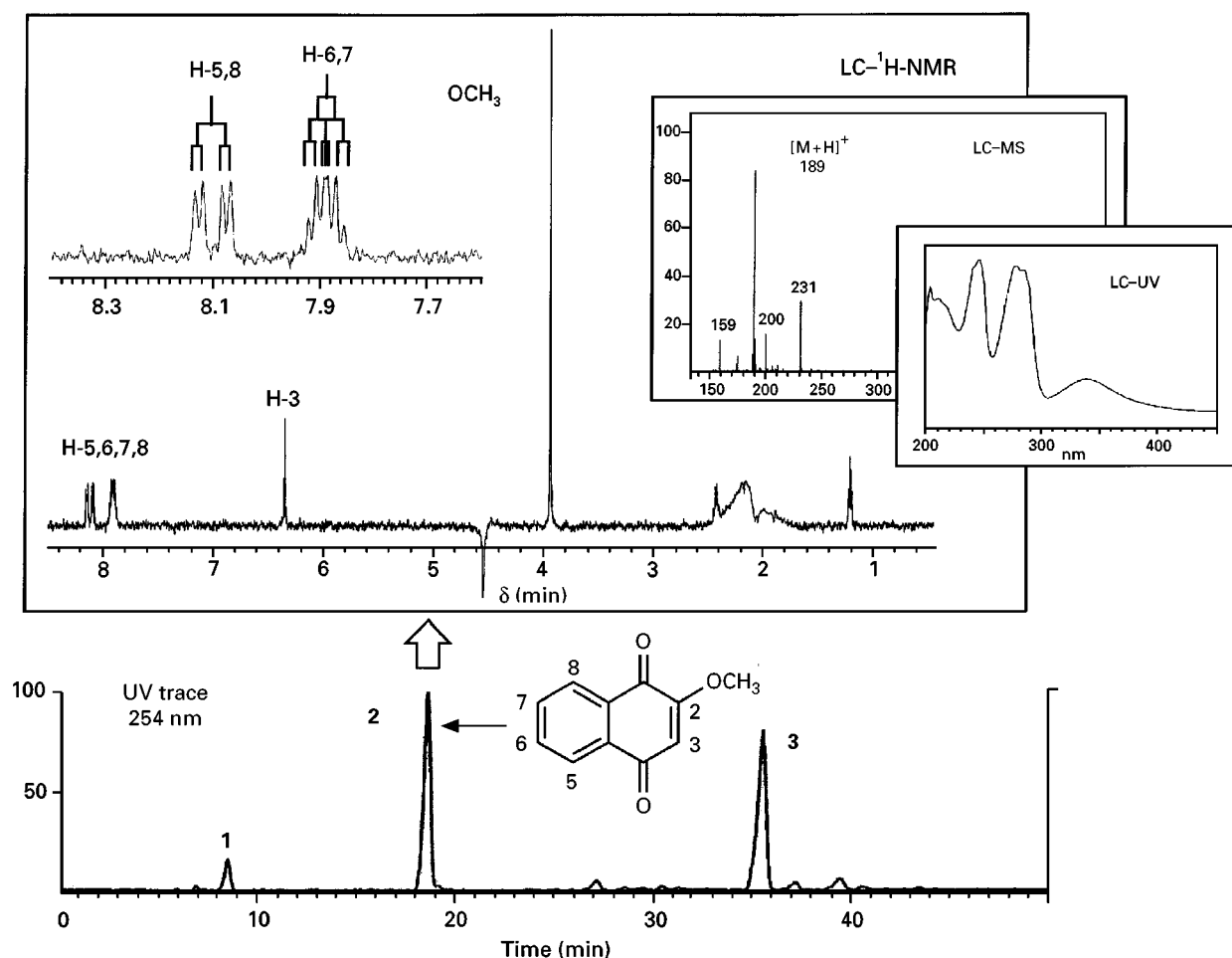


Figure 4 Summary of all the spectroscopic data obtained online by LC-UV, LC-MS and LC-NMR for the naphthoquinone (**2**) in the dichloromethane extract of *Swertia calycina* (Gentianaceae).

usually optimum for scale-up. When flash and open-column chromatography are used as first fractionation steps of crude plant extracts, solvent systems of increasing polarity are often employed. The fractions are checked by TLC at the outlet of the column and when compounds of a given polarity are eluted, the

solvent system is changed for a more polar one. This allows compounds of different polarities to be efficiently separated.

A typical step gradient solvent system for the separation of a dichloromethane extract by flash chromatography on silica gel is: chloroform–

Table 1 Preparative separation methods for plant constituents

Type	Technique	Abbreviation
Preparative thin-layer chromatography	Centrifugal TLC	CTLTC
Open-column chromatography		CC
Vacuum liquid chromatography		VLC
Pressure liquid chromatography	Flash	
	Low pressure LC	LPLC
	Medium pressure LC	MPLC
	High performance LC	HPLC
Liquid–liquid chromatography	Droplet countercurrent chromatography	DCCC
	Centrifugal partition chromatography	CPC

petroleum spirit (80 : 20), then pure chloroform, chloroform-methanol (80 : 20) and finally pure methanol for eluting the polar constituents.

Preparative Liquid Chromatography

Because of the complexity of the chemical composition of crude plant extracts, open-column chromatography or flash chromatography techniques alone often do not provide sufficient resolution for the isolation of pure natural products. The introduction of pressurized liquid chromatography in natural product chemistry has allowed the use of silica gel of smaller particle size and of bonded phases such as RP-8, RP-18 and diol, thus giving more versatility and better resolution.

Depending on the sample size and the resolution to be achieved, three techniques are generally used for phytochemical applications: LPLC, MPLC and semipreparative HPLC. Polar natural products such as glycosidic derivatives can mainly be separated on RP-8 or RP-18 bonded phases while compounds of intermediate polarity such as polyphenol aglycones, polyacetylenes and sesquiterpenes can be resolved on silica gel supports (Table 2).

Low and Medium Pressure Chromatography

LPLC makes use of columns containing packings of *c.* 40–60 μm , allowing high flow rates up to a pressure of 10 bar. Prepacked columns with various sizes and supports are available. MPLC accommodates much larger sample loads (100 mg–100 g) than LPLC (10 mg–1 g) and is designed to be operated at higher pressure (*c.* 5–40 bar). MPLC uses refillable columns of various sizes. Supports with particle sizes ranging from 15 to 200 μm can be used. MPLC is more versatile than LPLC but the basic operation of the two techniques is similar.

The chromatographic conditions for these techniques are selected by HPLC or by TLC. The

selectivity of the eluent is first optimized and then the composition of the mobile phase is adjusted to suit the preparative conditions. Retention factors (*k*) between 1 and 5 or *R_F* values < 0.4 are appropriate. Different representative solvent systems used for the separation of various classes of natural products are given in Table 2.

In some cases, similar resolution can be obtained by both LPLC or MPLC and analytical HPLC. This is of importance for the transposition of conditions from analytical to preparative level. It is illustrated here by the separation of iridoids and a phenylpropane glycoside from the root of *Sesamum angolense* (Pedaliaceae), a plant reputed to have antihaemorrhagic properties in African traditional medicine. Analytical HPLC of the relevant fractions is shown in Figure 5A and 5B. Baseline separation of phlomiol (4) and puchelloside-I (5) was possible with methanol-water (10 : 90). Verbascoside (6) was, however, only eluted with 32% methanol. These analytical conditions could be applied directly to a preparative separation on a Lobar LPLC column by performing a step-gradient elution from 10% to 32% methanol.

Following a similar procedure, several xanthone glycosides (7–12) from *Halenia corniculata* (Gentianaceae) were successfully isolated from an enriched fraction by MPLC in a single isocratic run (Figure 6).

Semipreparative HPLC

While analytical HPLC is useful for obtaining information about sample mixtures and does not rely on their recovery, the aim of semipreparative HPLC is to isolate pure substances. Compared to the other column LC techniques, HPLC can handle very small particle sizes (5–30 μm) which provide a large gain in separation efficiency. In phytochemical investigations, this technique is often used for final purification steps for a small number of compounds which are

Table 2 Representative solvent systems used for LPLC or MPLC

Substance class	Support	Eluent
Polyacetylenes	SiO ₂	Toluene-EtOAc (85 : 15)
Flavonoid aglycones	SiO ₂	C ₆ H ₁₄ -EtOAc, CHCl ₃ -MeOH
	DIOL	CHCl ₃ -MeOH-HOAc (950 : 50 : 1)
Flavonoid glycosides	RP-8	MeOH-H ₂ O gradient
Phenylpropanoid glycosides	RP-18	MeOH-H ₂ O gradient
Chromenes	SiO ₂	CHCl ₃ -C ₆ H ₁₄ -MeOH
Sesquiterpenes	SiO ₂	C ₆ H ₁₄ -EtOAc
Diterpenes	RP-18	MeOH-H ₂ O (1 : 1)
Triterpenes	RP-8	MeOH-H ₂ O (4 : 1)
Iridoid glycosides	RP-18	MeOH-H ₂ O gradient
Alkaloids	RP-8	MeOH-0.02 mol L ⁻¹ NH ₄ OAc (3 : 2)

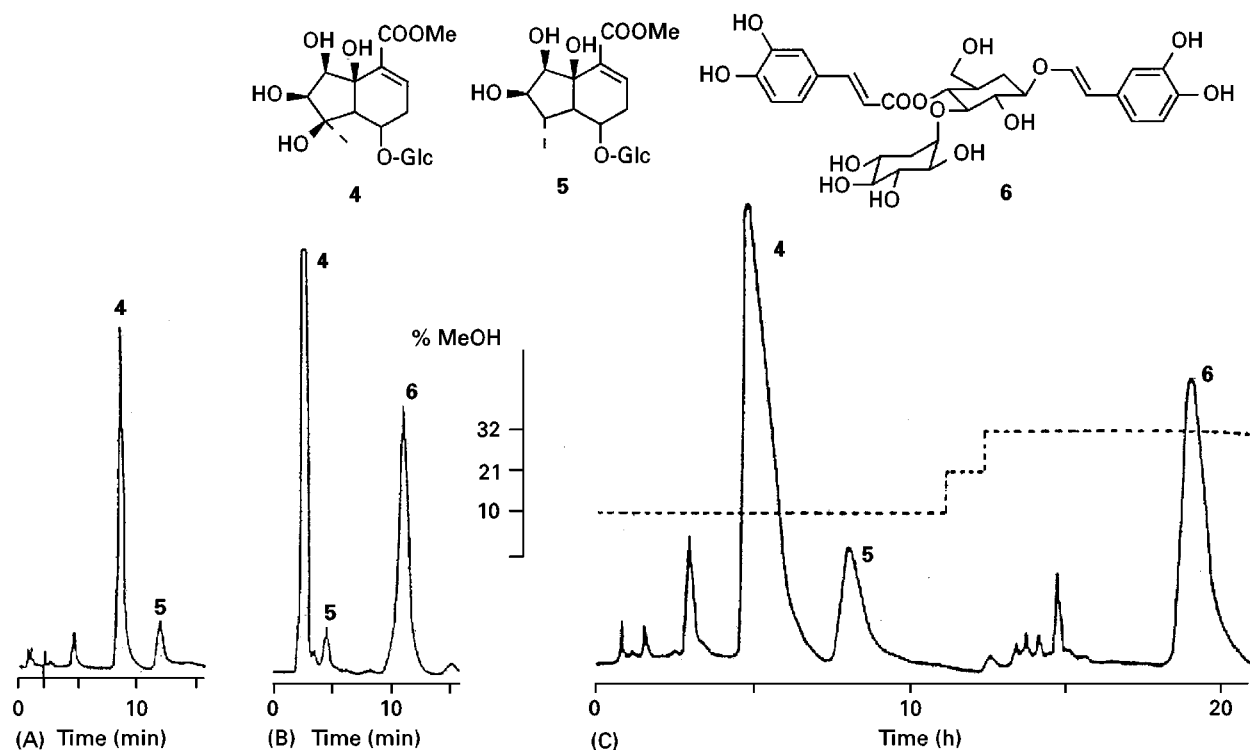


Figure 5 Isolation of iridoids from *Sesamum angolense*. (A) Analytical HPLC: column, LiChrosorb RP-8; eluent, MeOH-H₂O 10 : 90; detection, 254 nm. (B) Analytical HPLC: column, LiChrosorb RP-8 eluent, MeOH-H₂O 32 : 68; detection, 254 nm. (C) Preparative separation: column, Lobar RP-8 (310 × 25 mm i.d.); eluent, step gradient MeOH-H₂O 10 : 90 and 32 : 68; sample, 130 mg; detection, 254 nm.

difficult to separate. The loading capacity of the column is usually rather small (1–100 mg) and the isolation of a pure natural product often requires multiple injections of a given prepurified fraction. The number of applications of this technique to natural product isolation is very large.

Figure 7 shows the separation of closely related antifungal chromenes from *Hypericum revolutum* (Guttiferae) by semipreparative HPLC. The petroleum ether extract of the leaves and twigs after flash chromatography and LPLC on silica gel, gave an active fraction which appeared homogeneous by TLC. However, analytical HPLC on an RP-18 column showed the presence of two homologues (13 and 14). Since chromenes degrade in the presence of acid, forming the corresponding dichromenes, no acid was used in eluent for semipreparative separation. A total of 120 mg was separated by repetitive injections.

Centrifugal Partition Chromatography

The use of CCC represents an interesting complementary approach to LC on solid supports. This technique is an all-liquid method without the presence of a solid support and thus has the advantage over other liquid chromatographic methods of avoid-

ing irreversible adsorption of sample, allowing a quantitative recovery and minimizing the risk of sample denaturation. These points are extremely important when labile or polar natural products have to be isolated. Among the different countercurrent liquid chromatography techniques, CPC is probably the most popular technique because of its speed and ease of use. The choice of the solvent system can be guided by TLC and for rotating coils the best *R_F* range is 0.1–0.4. According to the type of instrument used – single coil, multiple coil or cartridge – the sample size ranges from 10 mg to 10 g. Selected examples of solvent systems used for the separation of various classes of natural products are given in Table 3.

In order to illustrate this approach, the separation of the active anthranoid pigments of *Psorospermum febrifugum* (Guttiferae), an African medicinal plant that exhibits strong growth inhibition of cancer cells and antimalarial activity, is shown in Figure 8. The lipophilic root bark extract of this plant was first separated by flash chromatography and LPLC but resulted in considerable material losses, owing to irreversible adsorption on the supports. However, in a single CPC step, three pure compounds (15, 16 and 17) and a mixture of a fourth anthranoid pigment

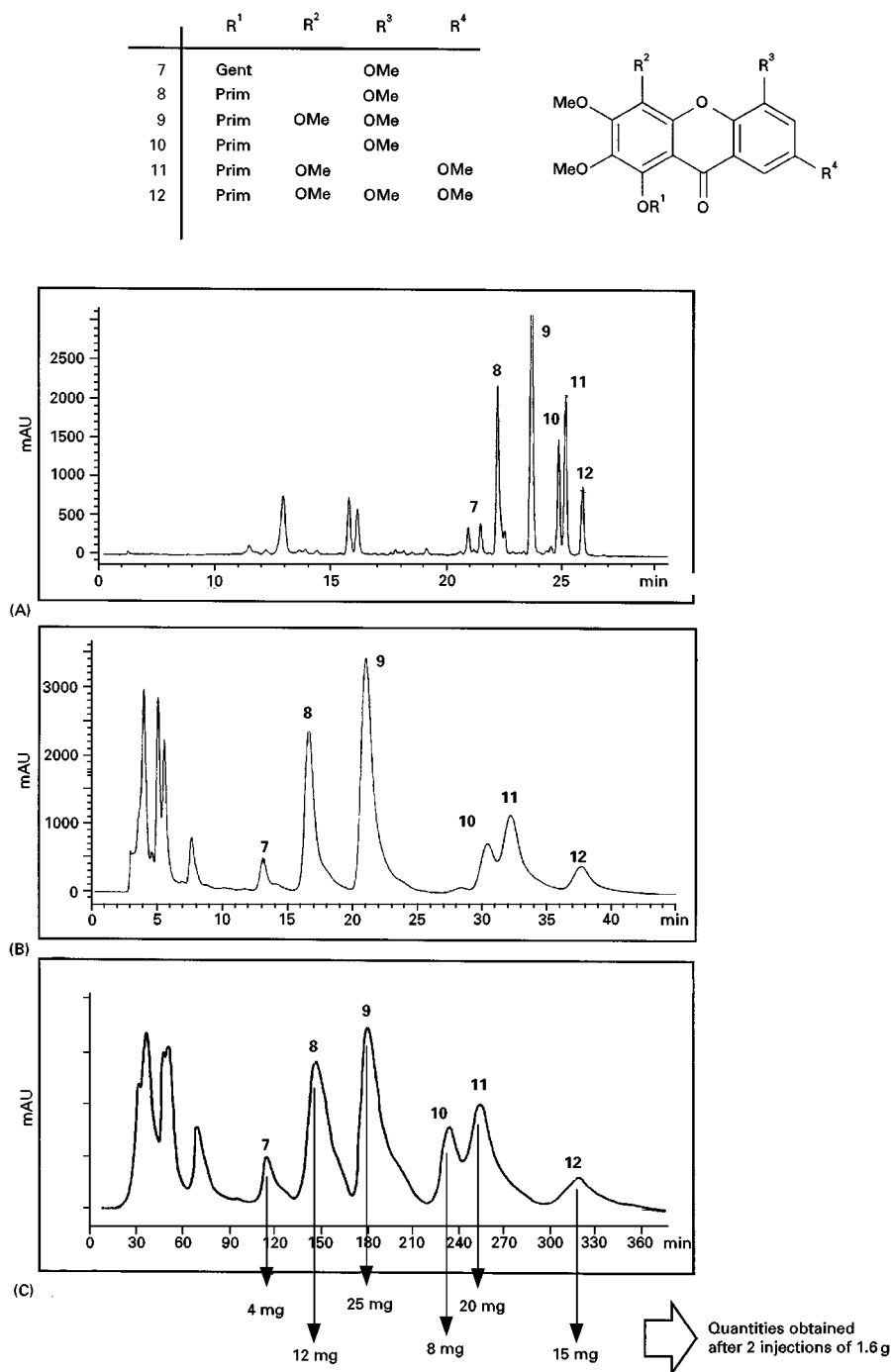


Figure 6 HPLC-MPLC transposition for the isolation of xanthone glycosides from an enriched fraction of *Halenia corniculata* (Gentianaceae) after separation by size exclusion chromatography on Sephadex LH-20 of the methanolic extract. (A) HPLC-gradient. Conditions: column: NovaPak RP-18 (3.9 × 150 mm); H₂O–MeCN; 5–65% MeCN in 50 min; 1 mL min⁻¹. (B) HPLC-isocratic. Conditions: column: LiChroCart; Lichrosorb RP-18 (7 μm); 4 × 250 mm; H₂O–MeOH (60 : 40); 1 mL min⁻¹. (C) MPLC-isocratic. Conditions: column: MPLC home-packed Lichrosorb Rp-18 (15–25 μm); 12 × 460 mm; H₂O–MeOH (60 : 40); 3 mL min⁻¹; 12 bar. Sample size 300 mg.

(18) with an unidentified constituent (19) were obtained without loss of product. A nonaqueous solvent system was used for the separation, which could be scaled up to a 500 mg sample size.

Combination of Methods

No single liquid chromatographic separation method is able to solve all separation problems and moreover

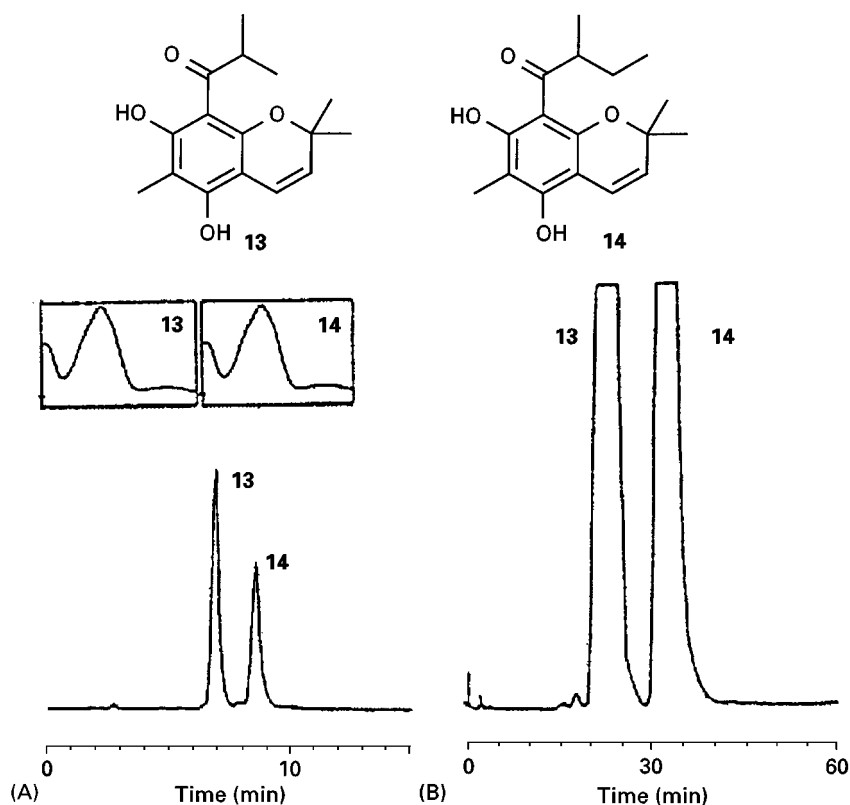


Figure 7 Separation of antifungal chromenes from *Hypericum revolutum* (Guttiferae). (A) Analytical HPLC: column, LiChrosorb RP-18 (250 × 4.6 mm i.d.); solvent, MeOH-H₂O 80 : 20; flow, 1.5 mL min⁻¹; detection, 254 nm. (B) Semipreparative HPLC: column, μ-Bondapak RP-18 (300 × 7.8 mm i.d.); solvent MeOH-H₂O 67 : 37; flow, 5 mL min⁻¹; detection, 254 nm.

it is very common to find multistep chromatographic operations for the isolation of pure natural products. Although it is possible to obtain a pure compound by a one- or two-step procedure,

a combination of techniques is normally required. Of course there are many different ways of putting together all the possible separation techniques, but in reality the choice of strategy is limited

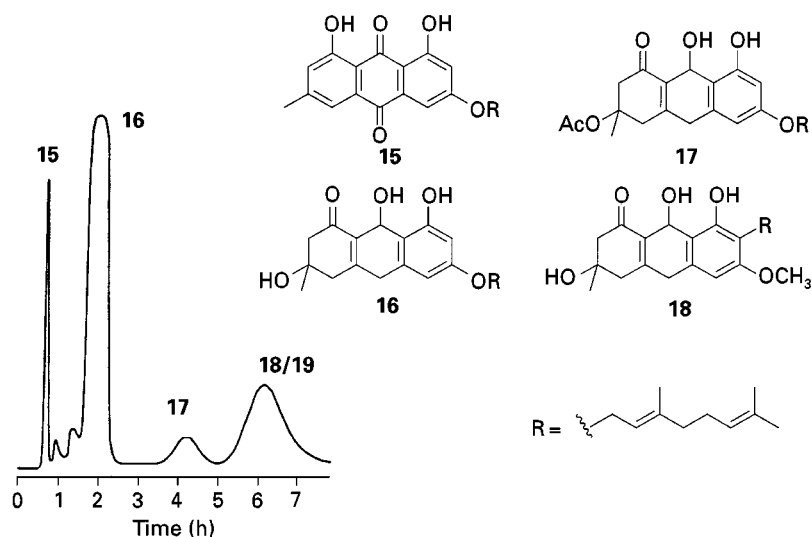


Figure 8 CPC separation of a light petroleum ether extract of *Psorospermum febrifugum* (Guttiferae) root bark. Solvent, *n*-C₆H₁₄-MeCN-MeOH (40 : 25 : 10, mobile phase = upper phase); flow, 5.5 mL min⁻¹; rotational speed, 1500 rpm; sample, 100 mg; detection, 254 nm.

Table 3 Representative solvent systems used for CPC separations

Substance class	Eluent
Flavonoids	CHCl ₃ -MeOH-H ₂ O 4 : 3 : 2
Xanthenes	Petrol ether-EtOAc-MeOH-H ₂ O 1 : 1 : 1 : 1
Tannins	<i>n</i> BuOH- <i>n</i> PrOH-H ₂ O 4 : 1 : 5
	<i>n</i> BuOH- <i>n</i> PrOH-H ₂ O 2 : 1 : 3
Saponins	CHCl ₃ -MeOH- <i>n</i> PrOH-H ₂ O 5 : 6 : 1 : 4
	CHCl ₃ -MeOH- <i>i</i> BuOH-H ₂ O 7 : 6 : 3 : 4
	CHCl ₃ -MeOH-H ₂ O 7 : 13 : 8
Polyacetylenes	Hexane-MeCN-TBME 10 : 10 : 1
Aporphine alkaloids	CHCl ₃ -MeOH-0.5% HOAc 5 : 5 : 3

by a number of constraints: the extraction method, the complexity of the extract, the sample preparation, the polarity, the stability, the solubility, the sample size and the complementarity of the separation techniques.

When choosing a separation strategy, it is often useful to pick steps which differ as much as possible in selectivity. During an isolation procedure, the scale of the operation decreases: as the purity of the product increases, there is a corresponding diminution of sample quantity. This implies that the initial fractionation steps are those which can separate large

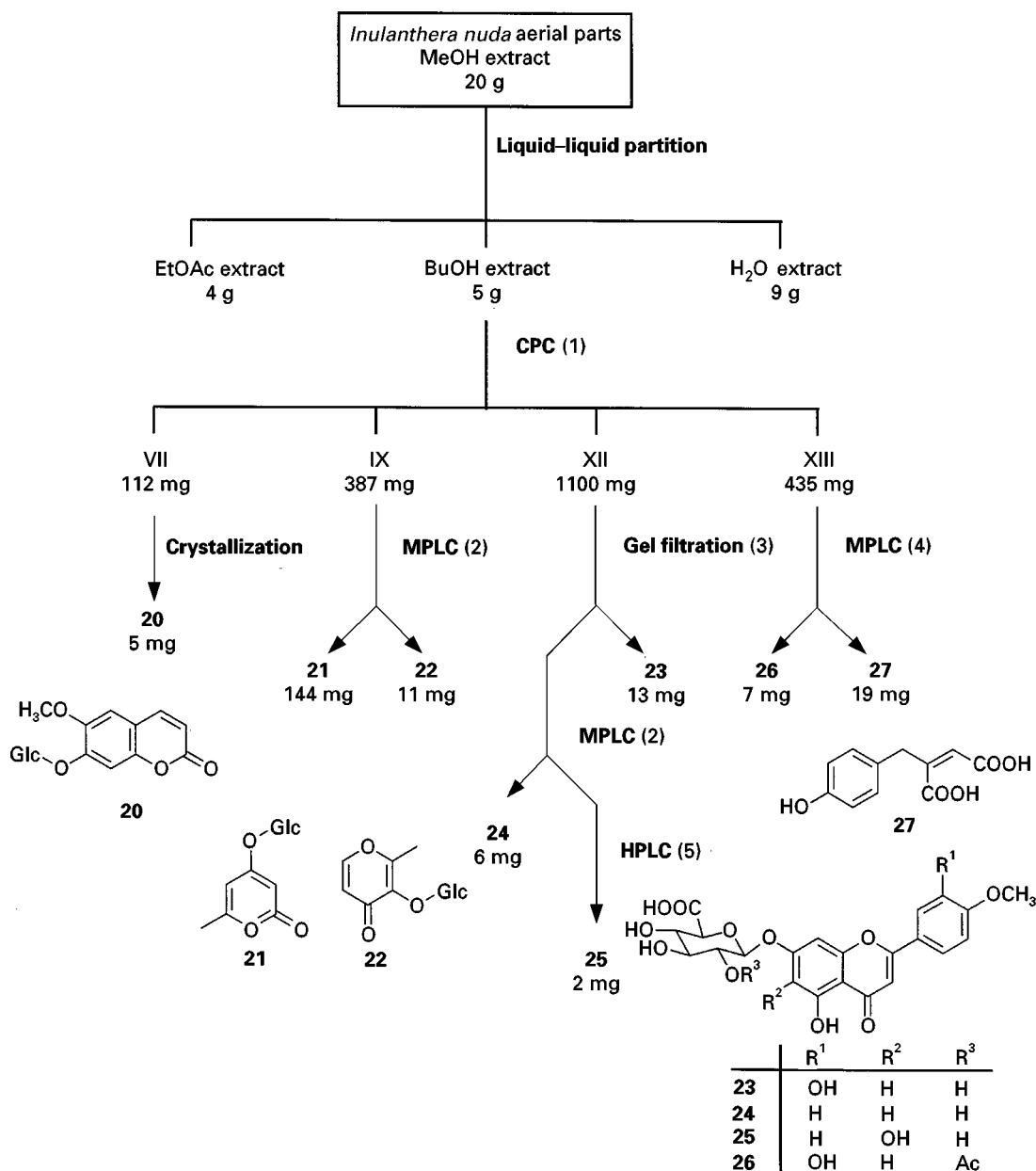


Figure 9 Strategy for the isolation of various aromatic constituents from *Inulanthera nuda* (Asteraceae). Conditions: 1, CHCl₃-MeOH-H₂O-*i*PrOH; 2, RP-18, MeOH-H₂O (1 : 9); 3, Sephadex LH-20, MeOH-H₂O (1 : 1); 4, RP-18, MeOH-H₂O (1 : 4); 5, RP-18, MeCN-H₂O (7 : 43).

amounts of material, e.g. column chromatography using relatively cheap stationary phases (silica, alumina, polyamide or XAD ion exchange resins), flash chromatography or CCC. Size exclusion chromatography (SEC) is also becoming increasingly popular as a first purification step. Subsequent chromatographic steps on smaller quantities can be performed with more expensive column packings and equipment. Semipreparative HPLC is often reserved for final purification.

The combination of different preparative chromatography techniques for the isolation of various aromatic compounds from *Inulathera nuda* (Asteraceae) is presented in Figure 9. A first liquid–liquid partition of the methanolic extract, dissolved in water, gave an enriched butanol extract which was further separated by CPC, affording 13 fractions. One of these fractions yielded (20) after recrystallization while the other constituents were further separated by MPLC or SEC. The final purification of flavonoid glycoside (25), for example, required a combination of SEC on Sephadex LH-20, followed by MPLC and semipreparative HPLC.

Conclusions

The introduction of modern liquid chromatographic methods has revolutionized the science of separation of natural products of plant origin. These new methods allow faster separations and facilitate the resolution of complex mixtures. As shown, techniques such as HPLC can be used both at the analytical and preparative level. At the analytical level and in combination with sophisticated detectors, structural information can be obtained online, while on the preparative scale closely related compounds can be successfully isolated.

The actual separation method or methods depend(s) on a number of factors relevant to the separation problem, but a judicious choice of strategy enables most targets to be reached. New methods and improvements are continually being introduced, with the result that the number of combinations available is steadily expanding, hopefully leading to a progressive simplification of the ever more complex separation problems that are being undertaken.

See also: II/Chromatography: Liquid: Detectors: Mass Spectrometry; Large-Scale Liquid Chromatography. **Extraction:** Solid-Phase Extraction. III/Flash Chromatography. **Medium-Pressure Liquid Chromatography. Natural Products:** High-Speed Countercurrent Chromatography; Thin-Layer (Planar) Chromatography. **Pigments:** Thin-Layer (Planar) Chromatography.

Further Reading

- Bidlingmeyer BA (1987) *Preparative Liquid Chromatography*. Amsterdam: Elsevier.
- Hostettmann K, Wolfender J-L and Rodriguez S (1997) Rapid detection and subsequent isolation of bioactive constituents of crude plant extracts. *Planta Medica* 63: 2.
- Hostettmann K, Marston A and Hostettmann M (1998) *Preparative Chromatography Techniques, Applications in Natural Product Isolation*. Berlin: Springer.
- Kingston DGI (1979) High performance liquid chromatography of natural products. *Journal of Natural Products* 42: 237.
- Marston A and Hostettmann K (1991) Modern separation methods. *Natural Product Reports* 8: 391.
- Marston A and Hostettmann K (1994) Counter-current chromatography as a preparative tool – application and perspectives. *Journal of Chromatography A* 658: 315.
- Wolfender J-L, Maillard M and Hostettmann K (1994). Thermospray liquid chromatography–mass spectrometry in phytochemical analysis. *Phytochemical Analysis* 5: 153.

Liquid Chromatography–Nuclear Magnetic Resonance

B. Schneider, Max Planck Institute for Chemical Ecology, Jena, Germany

Copyright © 2000 Academic Press

Hyphenation of chromatographic and spectroscopic methods is important in analytical chemistry and is of great value in modern natural product analysis. Gas chromatography–mass spectrometry (GC-MS) has been used for many years to analyse volatile compounds and derivatives of nonvolatile natural products. The development of liquid chromatogra-

phy–mass spectrometry (LC-MS) extended the scope of MS coupling techniques to allow analysis of non-volatile compounds without derivatization. Nuclear magnetic resonance (NMR) is less sensitive than MS but represents the most informative and most universal analytical technique for natural products. Thus, using a NMR spectrometer in coupling methods does not simply mean adding another detector but represents a new dimension in analytical natural product chemistry.

The combination of NMR and chromatographic, or electrophoretic, separation methods was made

possible by the introduction of high field spectrometers, with an increased dynamic receiver range, the development of suitable continuous-flow cell probes and solvent suppression techniques. High performance liquid chromatography (HPLC)-NMR was first described by Watanabe in 1979 and it is now an established method in the field of natural product research. A number of examples, mainly of plant natural products, are reviewed in this article, demonstrating the advantages and limitation of HPLC-NMR.

Methodology

Sample Preparation

As sensitivity of HPLC-NMR is currently in the microgram or even nanogram scale, the amount of tissue investigated can be dramatically reduced as compared with that required for conventional isolation of natural products. Small scale extractions using 0.5–1 g of dried plant tissue have been described as being sufficient to record HPLC- ^1H NMR spectra with an excellent signal-to-noise ratio. Natural products which are present in living tissue in only trace amounts (pg g^{-1} tissue) are now amenable to NMR analysis without isolation, either directly in the crude extract, or after employing simple work-up steps.

The procedures for sample preparation are essentially the same as those for normal analytical HPLC. Since extracts of biological tissues are normally complex mixtures of various substances covering a broad range of polarity, including both lipophilic and hydrophilic components, pre-purification or fractionation of the crude extract can often improve the chromatographic resolution. Enrichment of the desired natural product prevents overloading of the column by unwanted components and enhances the concentration of analytes above the detection limit. Due to the use of a NMR spectrometer as detector, deuterated solvents are strongly recommended for injecting the analyte into the chromatographic system.

HPLC

There are only a few special requirements for HPLC combined online with NMR. A pulsation-free HPLC pump to provide proper gradient formation and efficient solvent mixing should be used. The first detector cell (usually UV), which in HPLC-NMR is no longer at the end of the process, should be as small as possible to reduce peak broadening to a minimum. In general, reversed-phase chromatography is used for most HPLC-NMR applications in natural product

chemistry. Water and protonated organic solvents cause resonances in the NMR spectrum. These eluent signals might overlap with those of the analyte and thus prevent adequate spectrum evaluation. To minimize the intensity of solvent resonances, and to improve the detection limit, deuterated solvents are utilized. In practice, fully deuterated water (99% D_2O) is used in combination with nondeuterated HPLC-NMR-grade acetonitrile or methanol. The phenomenon of peak broadening, often occurring in longer isocratic HPLC runs, reduces the fraction of the peak transferred to the flow cell. To compensate for this broadening, solvent gradients are recommended for elution. Addition of trifluoroacetic acid or phosphoric acid also contributes to peak focusing and does not cause additional signals in the ^1H NMR spectrum. Due to the implicit requirements of NMR methodology (solvent suppression, lock solvent), reversed-phase gradients cannot begin below a minimum concentration of 1% of the organic component and are not useful when exceeding about 95%. Flow rates between 0.6 and 1.0 mL min^{-1} , usually employed in analytical HPLC, are also convenient under HPLC-NMR conditions. However, adaptation of flow rate to the particular HPLC-NMR mode (continuous-flow, stopped flow) is required. Recent developments, allowing the use of microbore and capillary columns, which require lower flow rates and consume smaller amounts of solvents, permit the economical use of completely deuterated eluents. In general, the highest sample amount possible should be injected to reduce measuring time. Even column overloading, and partial peak overlap in the UV trace, may be acceptable to some extent because only a fraction of the desired peak is located in the active volume of the flow cell during spectrum acquisition. It is important to note that the quality of chromatographic separation determines the success of the NMR measurement and, thus, should be executed as carefully as possible.

NMR

HPLC-NMR probes do not make use of conventional removable NMR tubes but contain a continuous-flow cell, fitted to the HPLC via a polyetheretherketone (PEEK) transfer capillary. The capillary connection should be as short as possible, otherwise the stray field of the NMR magnet has to be considered. As a compromise, the HPLC is usually positioned slightly outside the 5 mT line (corresponding to about 1.5 m for a 500 MHz magnet) of the stray field. A valve interface between the HPLC detector and the NMR probe allows selection of different modes, like continuous-flow, stopped-flow and storage

mode. The active volume of the flow cells is between 40 and 240 μL in size. In continuous-flow mode, the detector volume and the flow rate determine the residence time of the sample in the flow cell and thus have a significant impact on sensitivity. Capillary flow cells with a detection volume in the order of 50–900 nL have been developed for microbore and capillary HPLC. Since there is no sample rotation it is possible to fit the radiofrequency coils directly on the glass body of the flow cell. This arrangement affords an optimal filling factor and, consequently, results in extraordinarily high sensitivity of the HPLC-NMR probes.

Commercially available HPLC-NMR probes are designed as inverse detection probes and, therefore, are most efficient for acquiring ^1H NMR spectra. Figure 1 shows ^1H NMR spectra recorded in $\text{MeCN}-\text{D}_2\text{O}$ with and without solvent suppression. In the nonsuppressed spectrum only the eluent signals are visible. To visualize the resonances of the analyte, suppression of the solvent signals is necessary. This can be accomplished by presaturation or by the 'water suppression enhanced through T1 effects' (WET) sequence. WET is more efficient in con-

tinuous-flow measurement because it requires shorter delays in comparison with the presaturation technique. However, even most efficiently suppressed solvent signals cover a certain part of the spectrum and may overlay some of the resonances of the analyte. This general drawback of HPLC-NMR can be reduced by running the same sample again in another eluent system having different chemical shift values, e.g. using acetonitrile (δ 2.0)– D_2O in the first and methanol (δ 3.2)– D_2O in a second run. The sensitivity of HPLC-NMR significantly depends on the operation mode and a number of further factors discussed above and by other authors. For the stopped-flow technique, which is the most sensitive mode, the detection limit in routine analysis (500 MHz; 120 μL flow cell) is below 1 μg in reasonable times. Using a capillary column and a nanolitre flow cell, the detection limit is now in the nanogram range. The stopped-flow technique is also suitable for acquiring homonuclear correlation spectra (COSY, TOCSY, NOESY and ROESY) of samples below 10 μg . Moreover, gradient-assisted inverse-detected heteronuclear correlation spectroscopy (GHSQC and GHMBC)

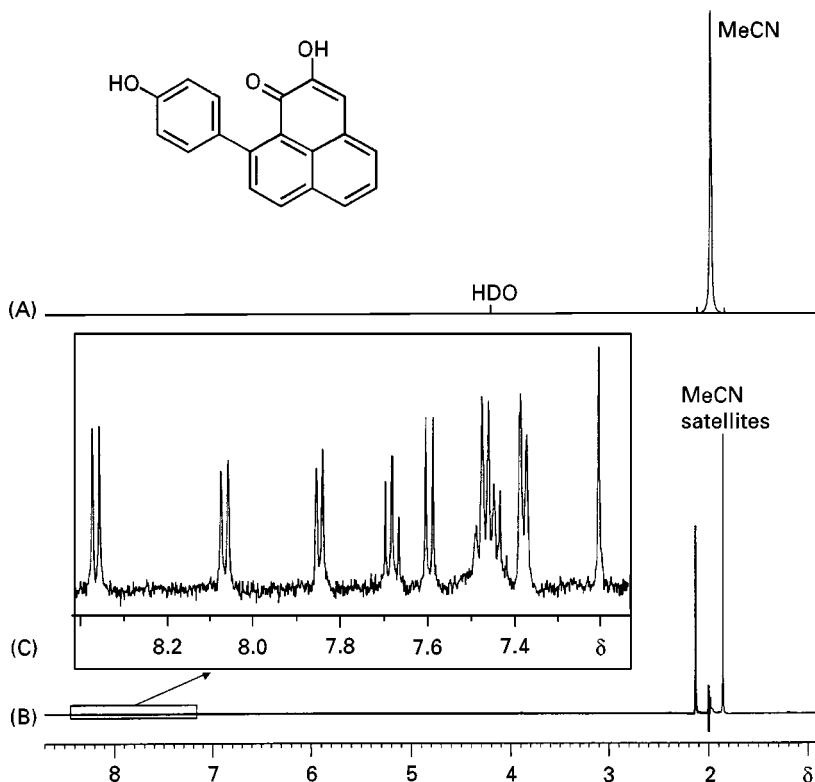


Figure 1 Stopped-flow HPLC- ^1H NMR spectra of an aromatic natural product measured in $\text{MeCN}-\text{D}_2\text{O}$. Spectrum (A), which was acquired without solvent suppression, exhibits the large signal of nondeuterated MeCN, small satellites of MeCN and the signal of HDO. Resonances of the analyte are not visible. Spectrum (B) was acquired using solvent suppression by double pre-saturation of MeCN and HDO. Spectrum (C) is an enlargement of (B), showing the well-resolved resonances in the aromatic part of the spectrum.

is also possible under HPLC-NMR conditions. The measurement in stopped-flow mode requires an accurate determination of the transfer time between the first detector, usually an UV or diode array detector, and the active volume of the flow cell. This is to ensure that the HPLC pump stops just at the moment when the top of the peak is in the magnet. Synchronization of HPLC and NMR is also required in fully automated mode that enables measurement of several peaks without further interaction of the operator.

The continuous-flow mode is much less sensitive than the stopped-flow technique but provides the opportunity to scan an extract rapidly for interesting natural products. Since the NMR resonances of the solvent depend on the composition ratio of the eluent, gradient elution requires continuous adaptation of the solvent suppression frequency to the moving signal. This suppression frequency is determined for each increment by the so-called scout scan prior to the WET sequence. In continuous-flow spectra the retention times (y axis) are plotted versus the chemical shifts (x axis). The extraction of traces from these unusual two-dimensional spectra yield one-dimensional ^1H spectra of the desired increment that can collectively be outlined as stacked plots.

Applications

Identification of Natural Products

An increasing number of applications of HPLC-NMR are devoted to the identification and structure elucidation of natural products. The main part of these investigations covers plant natural products as novel biologically active components for pharmacological and agricultural preparations. The aims and methodology of a number of these investigations are discussed in the following paragraphs. **Table 1** summarizes the classes of plant natural products and the plant families that have been analysed by hyphenated HPLC-NMR techniques.

Extracts equivalent to 250 mg of dried leaves of *Zaluzania grayana* (Asteraceae) were used for HPLC separation with direct measurement of ^1H NMR spectra in the online mode. Overlapping peaks could be separated more efficiently by the stopped-flow mode, collected in a sampling unit and analysed later by ^1H and 2D COSY measurements. These investigations provided information on the structure of two known and a novel sesquiterpene lactone of taxonomic relevance. Using a microsampling technique, glandular trichomes from the leaf surface of *Scalesia* species (Asteraceae) were collected. A sample combined from several species of the genus was used for

online HPLC-NMR analysis. Flavones and sesquiterpene lactones were identified by comparison with spectra of authentic reference compounds or literature data.

Unstable and structurally closely related bitter acids from dried female flowers of *Humulus lupulus* were extracted by supercritical carbon dioxide and analysed by HPLC-NMR in the stopped-flow mode without any degradation. Using an acetonitrile- D_2O eluent containing H_3PO_4 , well-resolved spectra of α - and β -hop acids were obtained despite column overloading (2.5 mg of extract was loaded on to an analytical reversed-phase column).

The online analysis of a CH_2Cl_2 extract of *Swertia calycina* (Gentianaceae) provided ^1H NMR spectra of all major constituents. Extraction of single traces from the 2D plot allowed a precise assignment of their specific resonances. Approximately $0.05\ \mu\text{mol}$ per peak was needed to obtain a ^1H NMR spectrum in the online mode using a 500 MHz NMR instrument. To improve the quality of the ^1H spectra and to measure a 2D COSY spectrum of one of the components, sweroside, the same extract was investigated in the stopped-flow mode. The detection limit for a ^1H NMR spectrum could be lowered by a factor of about 100 under stopped-flow conditions but longer acquisition times were required in comparison with the continuous-flow mode. In the case of the more complex methanol extract of another Gentianaceae species, *Gentiana ottonis*, clear ^1H NMR spectra of secoiridoids, flavones and xanthenes were only obtained in the stopped-flow mode. LC-UV and LC-MS data were also needed for full identification of compounds from both species.

Complementary HPLC-NMR and HPLC-MS studies were also performed on crude extracts and bioactive fractions from *Monetes engleri*. On-flow experiments indicated two major prenylated flavanone components in the CH_2Cl_2 extract of this plant but did not monitor minor components. A bioactive fraction obtained by medium pressure liquid chromatography (MPLC), containing these components, was subjected to stopped-flow HPLC-NMR analysis. ^1H NMR, 1D TOCSY, 2D NOESY and gradient-enhanced inverse ^1H , ^{13}C correlation experiments (GHSQC, GHMBC; **Figure 2**) were recorded from the enriched sample in a total acquisition time of 9.6 h. The WET sequence was used to suppress the eluent signals of the residual HDO resonance, the resonances of MeCN and its two ^{13}C satellites, and those of the propionitrile impurities of MeCN. The constitution of monotesone A, a new prenylated flavanone, was elucidated online using the strategy described. However, determination of the absolute configuration was only possible after isolation.

Table 1 Identification of plant natural products by HPLC-NMR

Species	Family	Natural products	HPLC	NMR	Reference
<i>Zaluzania grayana</i>	Asteraceae	Sesquiterpene lactones	RP-18, MeCN-D ₂ O, UV	500 MHz; online: ¹ H stopped-flow (peak sampling): ¹ H, 2D-COSY	Spring <i>et al.</i> (1995) <i>Phytochemistry</i> 39: 609
<i>Scalesia species^a</i>	Asteraceae	Flavanones, sesquiterpene lactones	RP-18, MeCN-D ₂ O, MeOH-D ₂ O, UV	500 MHz; online: ¹ H	Spring <i>et al.</i> (1997) <i>Phytochemistry</i> 46: 1369
<i>Humulus lupulus</i>	Moraceae	Lupulones	RP-18, MeCN-D ₂ O, UV	400 MHz; stopped-flow: ¹ H	Hötzl <i>et al.</i> (1996) <i>Chromatographia</i> 42: 499
<i>Swertia calycina</i>	Gentianaceae	Naphthoquinones, secoiridoids, xanthones	RP-18, MeCN-D ₂ O, UV	500 MHz; online: ¹ H; stopped-flow: ¹ H, 2D-COSY	} Wolfender <i>et al.</i> (1997) <i>Phytochem. Anal.</i> 8: 97
<i>Gentiana ottonis</i>	Gentianaceae	Flavones, secoiridoids, xanthones	RP-18, MeCN-D ₂ O, UV	500 MHz; stopped-flow: ¹ H	
<i>Monotes engleri</i>	Dipterocarpaceae	Flavanones	RP-18, MeCN-D ₂ O, UV	500 MHz; online: ¹ H; stopped-flow: ¹ H, 1D TOCSY, 2D NOESY, GHSQC, GHMBC	Garó <i>et al.</i> (1998) <i>Helv. Chim. Acta</i> 81: 754
<i>Lisianthus seemannii</i>	Gentianaceae	Secoiridoid dimer	RP-18, MeCN-D ₂ O, UV-DAD	500 MHz; stopped-flow: ¹ H	Rodriguez <i>et al.</i> (1998) <i>Helv. Chim. Acta</i> 81: 1393
<i>Vernonia fastigiata</i>	Asteraceae	glycosides Sesquiterpene lactones	RP-18, MeCN-D ₂ O MeOH-D ₂ O, UV	500 MHz; online: ¹ H; stopped-flow: ¹ H, 1D selective NOESY, 2D COSY, 2D NOESY	Vogler <i>et al.</i> (1998) <i>J. Natl. Prod.</i> 61: 175
<i>Terminalia macroptera</i>	Combretaceae	Sapogenines	RP-18, MeCN-D ₂ O, MeOH-D ₂ O, UV	500 MHz; online: ¹ H; stopped-flow: ¹ H, 1D selective NOESY, 2D COSY, 2D TOCSY, 2D NOESY	Vogler <i>et al.</i> (1998) <i>Natural Product Analysis</i> , Braunschweig/Wiesbaden: Vieweg, p. 143
<i>Rubia tinctorum</i>	Rubiaceae	Anthraquinones	RP-18, MeCN-D ₂ O, UV	500 MHz; stopped-flow: ¹ H	} Schneider <i>et al.</i> (1998) <i>Natural Product Analysis</i> , Braunschweig/Wiesbaden: Vieweg, p. 137
<i>Taxus baccata</i>	Taxaceae	Taxanes	RP-18, MeCN-D ₂ O, UV	500 MHz; stopped-flow: ¹ H	
<i>Taxus canadensis</i> <i>Taxus chinensis</i> var. <i>maiirei</i> <i>Taxus × media</i>	Taxaceae	Taxanes	RP-18, MeCN-D ₂ O, UV	500 MHz; stopped-flow: ¹ H, 2D TOCSY	Schneider <i>et al.</i> (1998) <i>Phytochem. Anal.</i> 9: 237
<i>Ancistrocladus guineensis</i>	Ancistrocladaceae	Naphthylisoquinolines	RP-18, MeCN-D ₂ O, UV	600 MHz; online: ¹ H; stopped-flow: ¹ H, 2D-TOCSY, 2D ROESY	Bringmann <i>et al.</i> (1998) <i>Anal. Chem.</i> 70: 2805

<i>Triphyophyllum peltatum</i>	Dioncophyllaceae	Naphthylisoquinolines	RP-18, MeCN-D ₂ O, UV	600 MHz; online: ¹ H; stopped-flow: 2D TOCSY, 2D ROESY	Bringmann et al. (1998) <i>Natural Product Analysis</i> , Braunschweig/Wiesbaden: Vieweg, p. 147
<i>Ancistrocladus likoko</i>	Ancistrocladaceae	Naphthylisoquinolines	RP-18, MeCN-D ₂ O, UV	600 MHz; stopped-flow: ¹ H, 2D TOCSY, 2D ROESY	Bringmann et al. (1999) <i>Magn. Res. Chem.</i> 37: 98
<i>Dioncophyllum thollonii</i>	Dioncophyllaceae	Naphthylisoquinolines, tetralones	RP-18, MeCN-D ₂ O, UV	600 MHz; online: ¹ H; ¹ H, 2D ROESY, ¹ H time slice	Bringmann et al. (1999) <i>J. Chromatogr. A</i> 837: 267
<i>Habropetalum dawei</i>	Dioncophyllaceae	Naphthylisoquinolines, isoquinolines	RP-18, MeCN-D ₂ O, UV, CD	600 MHz; online: ¹ H; stopped-flow: ¹ H, 2D TOCSY, 2D ROESY	Bringmann et al. (1999) <i>Anal. Chem.</i> 71: 2678
<i>Orophea enneandra</i>	Annonaceae	Lignans, tocopherols, polyacetylene	RP-18, MeCN-D ₂ O, UV	500 MHz; online: ¹ H	Cavin et al. (1998) <i>J. Natl. Prod.</i> 61: 1497
<i>Torreya jackii</i>	Taxaceae	Lignans	RP-18, MeCN-D ₂ O, UV	500 MHz; stopped-flow: ¹ H	Zhao et al. (1999) <i>J. Chromatogr. A</i> 837: 83
<i>Senecio vulgaris</i> ^a	Asteraceae	Pyrrrolizidines	RP-18, MeCN-D ₂ O, UV	500 MHz; online: ¹ H; stopped-flow: ¹ H, 2D COSY	Wolfender et al. (1998) <i>Current Organic Chemistry</i> 1: 575
<i>Cordia linnaei</i>	Boraginaceae	Meroterpenoid, naphthoquinones	RP-18, MeCN-D ₂ O, UV	500 MHz; online: ¹ H stopped-flow: ¹ H	Ioset et al. (1999) <i>Phytochem. Anal.</i> 10: 137
<i>Anigozanthos flavidus</i>	Haemodorraceae	Phenylphenalenones, stilbenes	RP-18, MeCN-D ₂ O, UV	500 MHz; stopped-flow: ¹ H, 2D TOCSY	Schneider et al. (1998) <i>Natural Product Analysis</i> , Braunschweig/Wiesbaden: Vieweg, p. 137; Hölscher and Schneider (1999) <i>Phytochemistry</i> 50: 155

^a Combined sample of several species of the genus; ^b and other *Senecio* species.

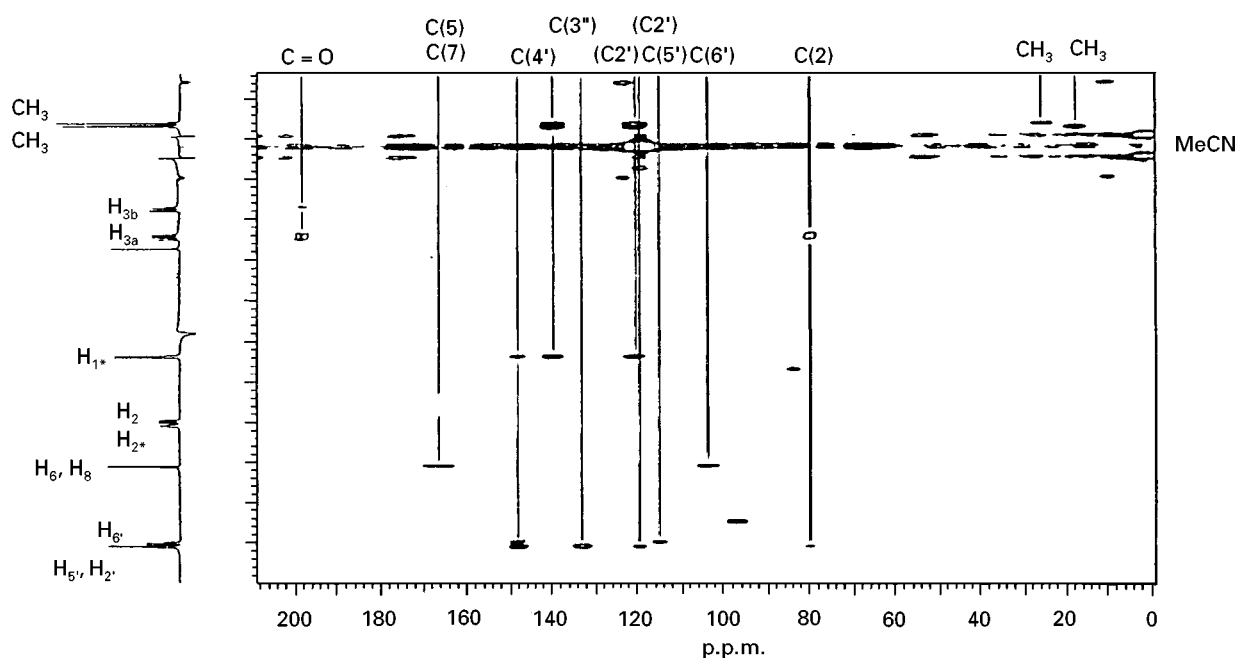


Figure 2 GHMBC spectrum of a prenylated flavanone acquired under HPLC-NMR conditions in 6 h 20 min. 1 mg of fraction injected. Reprinted with permission from Garo E, Wolfender JL, Hostettman K *et al.* (1998) Prenylated flavonones from *Monofes eglei*: on-line structure elucidation by LC/UV/NMR. *Helvetica Chimica Acta* 81: 754.

HPLC-NMR was shown as being the method of choice to assign the structure of a rapidly isomerizing dimeric secoiridoid glucoside carrying a (*Z*)-*p*-coumaroyl unit found in aerial parts of *Lisianthus seemannii* (Gentianaceae). The stopped-flow ^1H NMR spectrum of this unstable isomer was very similar to that measured for the isomerization product, as far as the monoterpene and glycosidic parts of the molecule were concerned. However, the resonances corresponding to the coumaroyl moieties exhibited signals of an (*E*)-double bond for the stable isomer and (*Z*)-double bond for the unstable one.

Less polar fractions of *Vernonia fastigiata* (Asteraceae) were investigated under continuous-flow conditions. In order to obtain information about signals hidden by suppressed peaks of the $\text{MeCN-D}_2\text{O}$ eluent, HPLC-NMR spectra were measured a second time in $\text{MeOH-D}_2\text{O}$. The combination of both complementary spectra allowed the assignment of all proton resonances of the corresponding sesquiterpene lactones in just two HPLC-NMR runs (Figure 3). 2D COSY spectra of selected compounds from the more polar fractions were measured in the stopped-flow mode. 2D NOESY and a 1D selective NOESY have been employed to clarify stereochemical features. Due to the selective excitation technique in the 1D NOESY, no solvent suppression was required. A similar array of methods was reported for HPLC-NMR

investigations on active triterpenoid sapogenines from *Terminalia macroptera* (Combretaceae).

An example of how natural products were identified by simply using HPLC- ^1H NMR was described for anthraquinones from hairy root cultures of *Rubia tinctorum* (Rubiaceae). First, the HPLC- ^1H NMR spectrum of a known anthraquinone, lucidine, was identified by comparison with an authentic standard and was then used to assign the structures of lucidin glycosides for which no reference compounds were available.

Partially purified extracts of *Taxus baccata* (Taxaceae) leaves were used in another example. Despite incomplete chromatographic separation, identification of two isomeric taxanes was clearly possible. Pre-purified extracts of only 0.5 mg air-dried needles of further *Taxus* species, *T. canadensis*, *T. chinensis* var. *mairei*, and *T. \times media* cv. *Hicksii*, were subjected to stopped-flow HPLC-NMR by ^1H and 2D TOCSY analysis. Taxol $^{\text{®}}$ and several other neutral and basic taxanes were identified by means of comparison with spectra of reference compounds or were deduced from related compounds. Due to the use of different solvents in HPLC-NMR and conventional NMR spectroscopy, differences of chemical shifts have to be considered. Comparing spectra measured by HPLC-NMR in $\text{MeCN-D}_2\text{O}$ with that of the same compound measured under conventional conditions in deuteriochloroform indicated that chem-

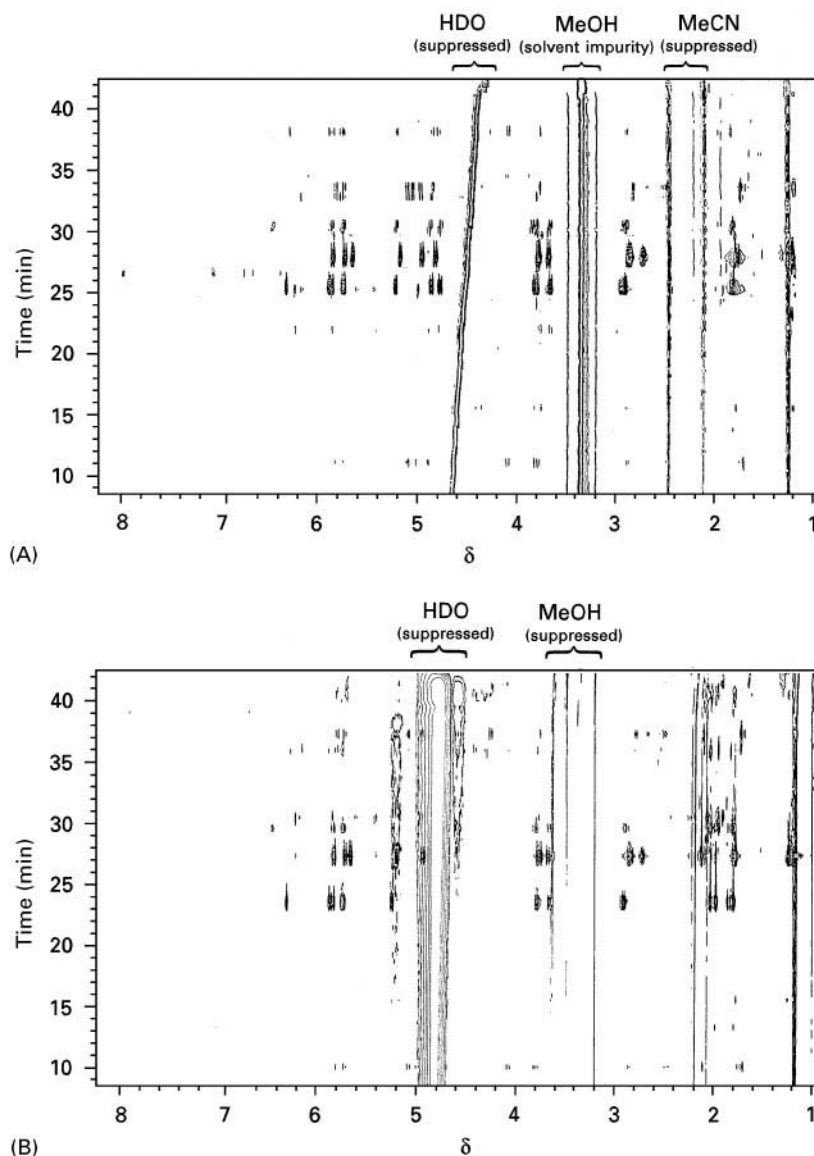


Figure 3 Comparison of 2D online HPLC-NMR plots of an extract of *Vernonia fastigiata* in (A) MeCN-D₂O and (B) MeOH-D₂O. Complementary HPLC-NMR eluents were used in order to provide information on signals hidden by suppressed resonances of each solvent. Adapted with permission from Vogler B, Conrad J, Hiller W, Klaiber I, Roos G and Sandor P (1998) Can LC-NMR serve as a tool for natural products elucidation? In: Schreier P, Herderich M, Humpf HU and Schwab W (eds) *Natural Product Analysis*, p. 143. Braunschweig/Wiesbaden: Vieweg.

ical shift differences did not exceed 0.2 p.p.m. However, due to the fact that some resonances were shifted upfield and others downfield, some signals appeared interchanged in sequence.

A series of HPLC-NMR analyses have been carried out at 600 MHz on naphthylisoquinolines from two plant families, the Diocophyllaceae and the Ancistrocladaceae. ¹H spectra extracted from the pseudo-2D continuous-flow diagram obtained under isocratic HPLC conditions using crude leaf extracts of *Ancistrocladus guineënsis* showed the typical signal pattern of naphthylisoquinolines. An optimized nonlinear

HPLC gradient was used for stopped-flow NMR analysis of a known alkaloid and two further closely related compounds. A 2D TOCSY of the HPLC fraction containing both compounds allowed the proton assignment of these isomers in a single NMR experiment. **Figure 4** shows 2D ROESY spectra of naphthylisoquinolines, the first example of the use of HPLC-NMR hyphenation to predict relative configuration. *Triphyophyllum peltatum* was analysed similarly. The major alkaloid of that species, dioncophylline A, was identified by ¹H, 2D TOCSY and 2D ROESY spectra. Additionally, two minor components

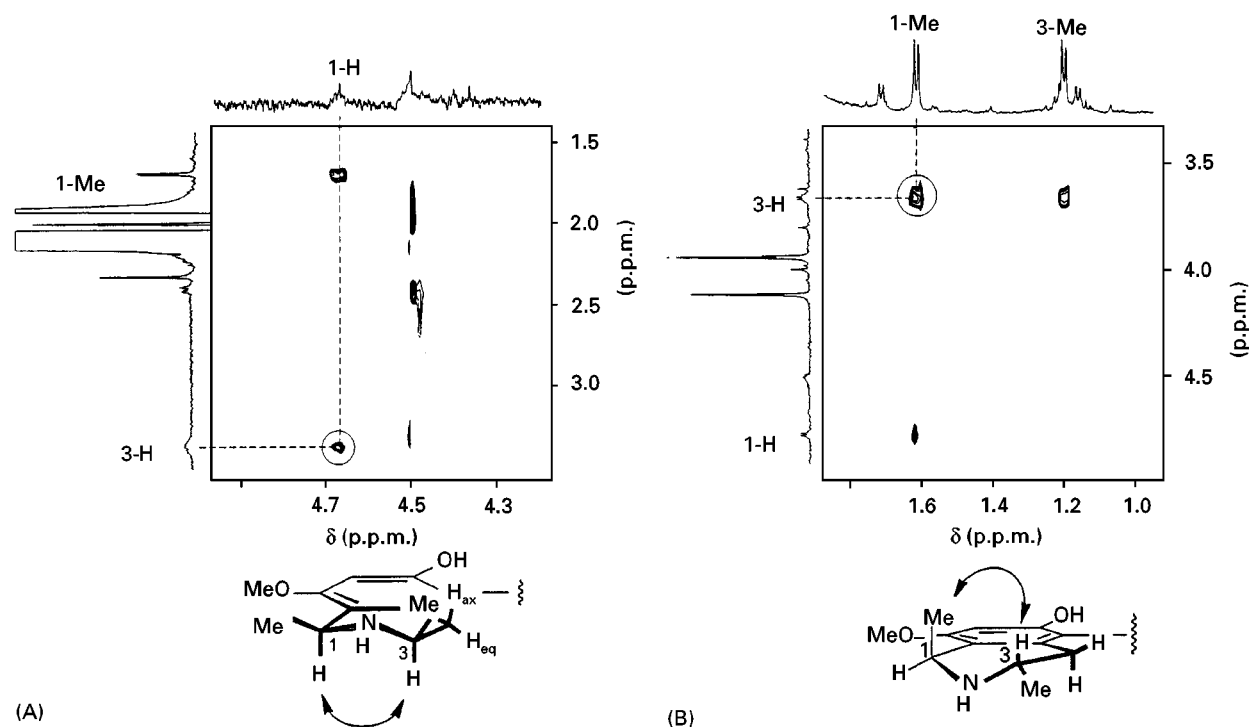


Figure 4 HPLC-NMR ROESY cross-peaks indicating the relative configuration at the isoquinoline moiety of diastereomeric naphthylisoquinoline alkaloids from *Ancistrocladus guineensis*. (A) Peak eluting at $t_R = 21.05$ min exhibits a correlation between ^3H and ^1H . (B) Peak eluting at $t_R = 21.60$ min shows a correlation between ^3H and ^1Me . Reproduced with permission from Bringmann G, Günther C, Schlauer J. *et al.* (1998) HPLC-NMR on-line coupling including the ROESY technique: direct characterization of naphthylisoquinoline alkaloids in crude plant extracts. *Analytical Chemistry* 70: 2805.

were identified in the same plant using an array of analytical methods, including HPLC-NMR. The constitution and relative configuration of new naphthylisoquinoline alkaloids from *Ancistrocladus likoko*, with a 5,8' coupling pattern, were also elucidated by application of 2D TOCSY and 2D ROESY experiments in the stopped-flow HPLC-NMR mode. Naphthylisoquinolines were also detected by online and stopped-flow HPLC-NMR techniques in *Dioncophyllum thollonii* (Dioncophyllaceae). Moreover, chromatographically unresolved diastereomeric tetralones with slightly different retention times were measured in a time-slice experiment. ^1H spectra were acquired in the stopped-flow mode at different positions of the chromatographic peak, and the diastereomers were distinguished by comparison of ^1H spectra of slices of pure and mixed components. The constitution and relative configuration of an isoquinoline and a naphthylisoquinoline from crude extracts of *Habropetalum dawei* (Dioncophyllaceae) were established by combined application of HPLC-NMR and HPLC-electrospray ionization (ESI)-MS-MS. Additional combinations with subsequent stopped-flow HPLC-circular dichroism (CD) experiments allowed deduction of the absolute configuration of these new metabolites.

While most HPLC-NMR studies make use of the stopped-flow option, either alone or after preliminary continuous-flow experiments, a variety of natural products from *Orophea enneandra* (Annonaceae) have been tentatively characterized by means of the continuous-flow technique without a subsequent stopped-flow run. Column overloading (2 mg) did not prevent proper separation of the components. The structures of three lignanes were identified by reference to literature data. In the cases of a tocopherol derivative and an unstable polyacetylene, targeted isolation and structure elucidation by complementary coupling techniques and conventional analytical methods were necessary.

A variety of lignanes were also identified from extracts of *Torreya jackii* (Taxaceae). Some of them were completely characterized by stopped-flow HPLC- ^1H NMR while in other examples isolation was required to confirm the structures by conventional NMR spectroscopy. After HPLC-NMR measurements, individual lignanes were collected and subjected to MS, which was considered to be an indispensable tool for complete structure assignment.

A study on *Senecio vulgaris* (Asteraceae) has allowed identification of a variety of pyrrolizidine

alkaloids and differentiation of certain isomeric macrocyclic diesters of that type. These compounds adopt *cis-trans* configurations and are not distinguishable by LC-MS. This example demonstrated again that complementary measurements in MeCN-D₂O and MeOH-D₂O are necessary to observe all resonances. Information obtained from the continuous-flow ¹H spectrum (24 scans per increment; column overloading by 3 mg of extract) were shown to be comparable to those from a corresponding stopped-flow spectrum.

Online and stopped-flow HPLC-NMR analysis of two minor isomeric meroterpenoid naphthoquinones from *Cordia linnaei* (Boraginaceae) yielded ¹H NMR spectra exhibiting identical signals in the aromatic region. Differences were only found in methyl signals when MeCN-D₂O and MeOH-D₂O were used as complementary HPLC-NMR eluents. One of the isomers, cordiaquinone C, carried a senecioid acid moiety while the other, being a new compound, was found to contain a tigloyl substituent instead.

Extracts of *Anigozanthos flavidus* (Haemodorraceae), a plant family accumulating phenylphenalenones and stilbenes in the roots, were investigated using stopped-flow HPLC-NMR. Comparison with spectra of references and literature data was used to differentiate between known and novel compounds. A number of known compounds were identified without isolation, while others had to be isolated, especially when possessing regions poor in hydrogen atoms.

Biosynthetic Applications

HPLC-NMR has been used in biosynthetic and enzymatic investigations of secondary plant products. Michellamines, representing dimeric naphthylisoquinoline alkaloids highly active against HIV, were formed biosynthetically by oxidative coupling of their inactive korupensamine monomers. This dimerization was catalysed by peroxidase preparations from three *Ancistrocladus* species (Ancistrocladaceae) and from *Triphyophyllum peltatum* (Dioncophyllaceae). The peroxidase was partially purified from *Ancistrocladus heyneanus* and characterized in more detail. The exclusive formation of a michellamine from its monomeric korupensamine precursor, shown in Figure 5, was confirmed by HPLC-MS and stopped-flow HPLC-¹H NMR experiments.

Details of the phenylpropanoid metabolism preceding later steps of the biosynthesis of phenylphenalenones from *Anigozanthos preissii* (Haemodorraceae) were elucidated by Schmitt and Schneider using the stopped-flow HPLC-NMR technique. Incorporation of dihydrophenylpropanoids into phenylpropanoids in root cultures of that plant was

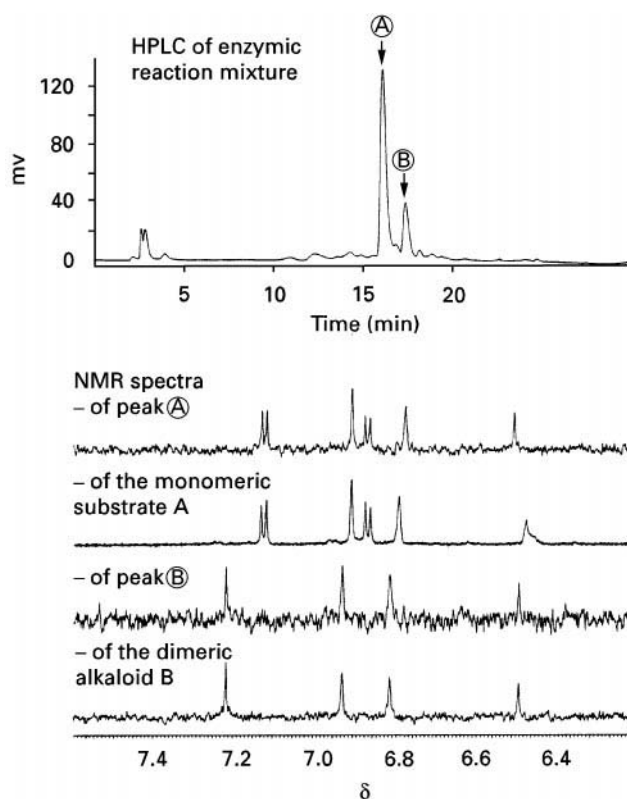


Figure 5 Stopped-flow HPLC-¹H NMR experiment confirming exclusive formation of a dimeric naphthylisoquinoline **B** from monomer **A** in the coupling reaction catalysed by peroxidase purified from *Ancistrocladus heyneanus*. Adapted with permission from Schlauer J, Rückert M, Herderich M *et al.* (1998) Characterization of enzymes from *Ancistrocladus* (Ancistrocladaceae) and *Triphyophyllum* (Dioncophyllaceae) catalyzing oxidative coupling of naphthylisoquinoline alkaloids. *Archives of Biochemistry and Biophysics* 350: 87.

proved by the coupling pattern in the HPLC-¹H NMR spectrum of *p*-coumaric acid biosynthesized from [2-¹³C]dihydrocinnamic acid (Figure 6). A number of simple phenolics, which are supposed to be formed from phenylpropanoids, were also detected in these experiments by HPLC-¹H NMR spectroscopy in the stopped-flow mode.

Applications Related to Natural Products

In areas related to natural product research, Careri and Mangia have reviewed the analysis of natural food components by HPLC-NMR. Lindon *et al.* have published an overview on HPLC-NMR in biomedical applications, and a small number of investigations have shown that the analysis of amino acids and peptide mixtures is also possible by HPLC-NMR.

The first HPLC-NMR analysis of biological macromolecules, published by Rückert *et al.*, utilized the combination of ion exchange chromatographic

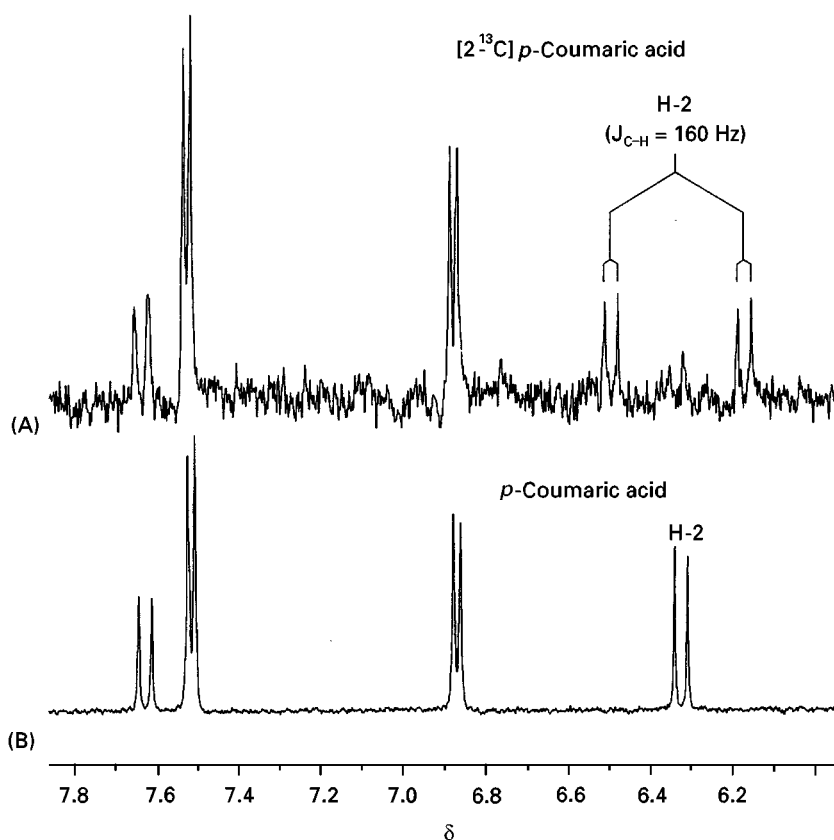


Figure 6 Stopped-flow HPLC- ^1H NMR experiment confirming biosynthetic incorporation of ^{13}C label into C-2 of p -coumaric acid. ^1H NMR spectra of (A) $[2-^{13}\text{C}]p\text{-coumaric acid}$ resulting from treatment of *Anigozanthos preissii* root cultures with $[2-^{13}\text{C}]$ dihydrocinamic acid and (B) nonlabelled reference.

separation with ^1H , 2D TOCSY and 2D NOESY spectroscopy to characterize small proteins in mixture. The authors expect that HPLC-NMR at very high field (750 and 800 MHz) and further enhancements in sensitivity should permit online experiments and heteronuclear 2D and 3D stopped-flow experiments in the future.

Summary and Future Developments

HPLC-NMR coupling has been developed into a valuable tool for natural product analysis. In general, the online technique is used to provide a rapid overview of the major components occurring in plants and other sources of natural products. The more sensitive stopped-flow method allows the detection and structure assignment of even minor components and enables the use of various homo- and heteronuclear correlation NMR experiments. However, unambiguous structure assignment of novel compounds of unexpected structural types requires information from other analytical methods, especially MS. Complete structure elucidation, together with stereochemical information, by multiple online com-

binations including NMR is possible but currently is rather the exception. Rapid development in analytical chemistry is expected to overcome present limitations of HPLC-NMR. The future scenario in a natural product laboratory could be an automated characterization of sources of natural products, starting with extraction and separation, followed by hyphenated instrumental analysis and finally computational structure elucidation. Additional combination with biological screening could avoid isolation of inactive compounds.

HPLC-NMR is an excellent approach to search for novel biologically active structures to be tested as new medicinal and agricultural agents, to identify known compounds without isolation, and to avoid unwanted re-isolation of known constituents from living organisms. Due to the large amount of structural information provided by NMR spectroscopy, its combination with HPLC and further spectroscopic techniques is also suitable when searching for new sources of rare natural products, for clarification of uncertain chemotaxonomic relationships and distribution of secondary compounds in various tissues. The introduction and routine application of capillary HPLC

and innovative fused capillary nanolitre flow cells in NMR probes, and further development in cryoprobe technology along with the use of improved processing procedures, will continue to enhance the sensitivity of HPLC-NMR coupling. As a microanalytical method, HPLC-NMR allows the detection of various groups of natural compounds and other biomolecules in the nanogram or even picogram range and, therefore, can contribute to the solution of problems of biochemical, physiological and chemoecological research.

See also: II/Chromatography: Liquid: Mechanisms: Reversed Phases; Nuclear Magnetic Resonance Detectors. III/Medium-Pressure Liquid Chromatography. Natural Products: Liquid Chromatography. Terpenoids: Liquid Chromatography.

Further Reading

- Albert K (1995) On-line use of NMR detection in separation chemistry. *Journal of Chromatography A* 703: 123.
- Albert K (1997) Supercritical fluid chromatography-proton nuclear magnetic resonance spectroscopy coupling. *Journal of Chromatography A* 785: 65.
- Behnke B, Schlotterbeck G, Tallerek U *et al.* (1996) Capillary HPLC-NMR coupling: high resolution ^1H NMR spectroscopy in the nanoliter scale. *Analytical Chemistry* 68: 1110.
- Careri M and Mangia A (1996) Multidimensional detection methods for separations and their application in food analysis. *Trends in Analytical Chemistry* 15: 538.
- Lindon JC, Nicholson JK, Sidelmann UG and Wilson ID (1997) Directly coupled HPLC-NMR and its application to drug metabolism. *Drug Metabolism Reviews* 29: 705.
- Pusecker K, Schewitz J, Gfrörer P *et al.* (1998) On line coupling of capillary electrochromatography, capillary electrophoresis, and capillary HPLC with nuclear magnetic resonance spectroscopy. *Analytical Chemistry* 70: 3280.
- Rückert M, Wohlfarth M and Bringmann G (1999) Characterization of protein mixtures by ion-exchange liquid chromatography coupled on-line to NMR spectroscopy. *Journal of Chromatography A* 840: 131.
- Seddon MJ, Spraul M, Wilson ID *et al.* (1994) Improvement in the characterization of minor drug metabolites from HPLC-NMR studies through the use of quantified maximum entropy processing of NMR spectra. *Journal of Pharmaceutical and Biomedical Analysis* 12: 419.
- Smallcombe SH, Patt SL and Keiffer PA (1995) Wet solvent suppression and its application to LC NMR and high resolution NMR spectroscopy. *Journal of Magnetic Resonance Series A* 117: 295.
- Schmitt B and Schneider B (1999) Dihydrocinnamic acids are involved in the biosynthesis of phenylphenalenones. *Phytochemistry* 52: 45.
- Schreier P, Herderich M, Humpf HU and Schwab W (eds) (1998) *Natural Product Analysis*. Braunschweig/Wiesbaden: Vieweg.
- Watanabe N, Niki E and Shimizu S (1979) An experiment on direct combination of high performance liquid chromatography with FT-NMR (LC-NMR). *Jeol News* 15A: 2.
- Wolfender JL, Ndjoko K and Hostettmann K (1998) LC/NMR in natural products chemistry. *Current Organic Chemistry* 1: 575.
- Wu N, Webb L, Peck TL and Sweedler JV (1995) On-line NMR detection of amino acids and peptides in micro-bore LC source. *Analytical Chemistry* 67: 3101.

Supercritical Fluid Chromatography

E. D. Morgan, Keele University, Staffordshire, UK

Copyright © 2000 Academic Press

The mild elution temperatures and the wide range of molecular masses it can accommodate makes supercritical fluid chromatography (SFC) particularly applicable to natural products. It is becoming the preferred method for the separation of enantiomers, and is especially useful for combined or hyphenated techniques. It forms a link between liquid chromatography (LC) and chromatography (GC), it has capabilities between the two and shares the instrumental set-ups of both, so both capillary column and packed column applications are recorded here.

The advantages and disadvantages of the method are debated elsewhere, but some of its strong points are indicated here. In all, 99% of supercritical fluid applications use supercritical carbon dioxide, since it has the great advantage that it is a nontoxic, non-flammable, pure, cheap mobile phase that presents no disposal problems. The greatest usefulness of SFC comes in connection with supercritical fluid extraction, which has received much attention for the isolation of natural products. If a substance can be extracted from plant or animal material with a supercritical fluid and some of the extract can be diverted to an online SFC, the course of the extraction can be followed very easily. Many of the applications of SFC recorded for natural products are of this type. The

greatest disadvantage of supercritical carbon dioxide is its relatively nonpolar nature. In its solvent powers, it resembles hexane at lower pressures, becoming slightly more polar at higher pressure. The polarity of the fluid can be increased by the addition of a small proportion of a highly polar organic solvent, miscible with the supercritical CO₂. This is most commonly methanol. The solubility of water in supercritical CO₂ is too low to be of much use to increase the polarity (but see below). The proportion of the so-called modifier solvent can range from 1 to 25%, but the critical point of the mixed fluid increases with the proportion of organic liquid and the advantages mentioned in this paragraph are steadily eroded with increasing proportion of modifier. In the chromatography of natural products, therefore, SFC is most useful for products of low polarity, such as terpenes, lipids and essential oils.

Free fatty acids, methyl esters, mono-, di-, and triglycerides can all be separated by SFC methods. The technique is particularly useful for triglycerides. Because triglycerides lack a useful UV absorption for high performance liquid chromatography (HPLC) and are at the limit of volatility for GC, they are not easy to separate and quantify without conversion to methyl esters. Using SFC with capillary columns and a flame ionization detector, they can be analysed directly. For capillary column determination of free fatty acids in an ethanol extract of *Sabal serrulata* two alternatives have been proposed: derivatization of the carboxyl group and saturating the CO₂ with water. Both methods produce a drastic improvement in resolution. Hydroxy acids are too polar for direct determination, and the separation of triglycerides is improved by the addition of a little methanol or acetonitrile, which then is detrimental to the use of a flame detector. It is possible to convert free carboxylic acids to their methyl esters in a flow-through system with CO₂ containing 10 mol% methanol at 80°C over a cation exchange resin in the H form. Capillary columns with a flame ionization detector have been used to separate the fatty acids and alcohols from hydrolysis of jojoba oil. The unhydrolysed portion of the wax esters could also be seen in the chromatogram. Wool wax alcohols from hydrogenated lanolin have been examined similarly. Using a microextractor, the triglycerides of a single cotton seed kernel were extracted by supercritical fluid extraction (SFE) and linked directly to SFC for analysis. In a rare example of application to insects, the same microcell (at 45°C and 20.2 MPa or 200 atm) has been used to extract the cuticular hydrocarbons and waxes from the cuticle of a dried fruit beetle *Carcophilus hemipterus*, which were then separated by capillary SFC. The results, probably

not optimized, were not as good as normally obtained by GC. Prostaglandins have been separated on a capillary column at 100°C with a CO₂ density gradient.

Staby and Mollerup have produced a comprehensive review of the separation and chromatography of fish oil constituents with supercritical fluids. These include triglycerides, free fatty acids, methyl and ethyl esters, cholesterol, α -tocopherol, phospholipids and squalene. The review is particularly directed towards pilot plant separations. Another review by Borch-Jensen and Mollerup in 1997 compared chromatographic systems for natural products like fats, seeds, oils and tissues.

The less polar steroids are usefully separated by SFC. Eleven steroids, including testosterone, oestrone, oestradiol, oestriol, cortisone and hydrocortisone, can be separated in less than 2 min with 6.1% methanol in CO₂ on a cyanopropyl HPLC column. Even bile acid conjugates (e.g. glycocholic acid and taurocholic acid) can be subjected to SFC. The ecdysteroids (insect moulting hormones, with a polyhydroxycholesterol structure) have been separated on packed columns under very similar conditions. Boronic ester derivatives of a diol functional group in some ecdysteroids improve selectivity for that group. The ecdysteroids, which have a strong UV chromophore, are also found in many plants of diverse type, and extracts of plants can be very quickly scanned for the presence of so-called phytoecdysteroids. With the coupling of a mass spectrometer to the SFC column, separation and identification of phytoecdysteroids can be performed in a matter of minutes.

Capillary SFC has been used to analyse the terpenes of some aromatic plants and the results compared with those obtainable by GC. Thyme (*Thymus vulgaris*) gave the same information as GC; for peppermint (*Mentha \times piperita*) and basil (*Ocimum basilicum*) the separation is much better by GC but SFC quantification is more reliable. The monoterpenes of lemon peel oil have been examined on a packed SFC column. Using two different silica columns (Nucleosil 100 and Spherisorb Si) linked in series with SFC Fourier transform infrared (FTIR; see later) eight sesquiterpenes (longicyclene, longifolene, aromadendrene, ledene, valencene, *cis*- and *trans*-calamenene and humulene) have been separated and identified, as have five sesquiterpenes from copaiba balsam and ylang-ylang oil under similar conditions.

Carotenes, with their strong visible and UV chromospheres, are ideal subjects for SFC. In spite of their low polarity, there are frequent reports that addition of a very small amount of an organic modifier improves selectivity. Vitamin A can exist in five pairs of *cis-trans* isomers which can be separated at

temperatures below 50°C, so avoiding any fear of isomerization.

More Polar Compounds

As already indicated, many examples of SFC of natural products are found where extraction with a supercritical fluid (SFE) and chromatography are coupled. A classic SFC separation, performed in 1982, was the separation of caffeine, theophylline and theobromine with CO₂-methanol. The pungent phenolic oil of ginger (*Zingiber rhizoma*) has been analysed for [6]-gingerol (see **structure**), [8]-gingerol and [10]-gingerol. SFE-SFC has been used in the extraction of ginkgolides (oxidized diterpenes from the leaves of *Ginkgo biloba*), paclitaxel (the antitumour agent Taxol) from *Taxus brevifolia*, and the anti-malarial artemisinin and its precursor artemisinic acid from *Artemisia annua*. The chromatography of artemisinin was carried out on both a capillary column with CO₂ (and 3% methanol) and a flame detector and on an aminopropyl packed column with a CO₂-methanol gradient (17.18 MPa and 40°C) and an evaporative light-scattering detector. The packed column method was faster: both compounds were eluted in 7 min as against 25 min by the capillary method. Paclitaxel has a strong UV absorption, but the ginkgolides do not, so the evaporative light-scattering detector is very helpful. Ginkgolide A has a molecular formula C₂₀H₂₄O₉, ginkgolide B C₂₀H₂₄O₁₀, paclitaxel C₄₇H₅₁NO₁₄, and artemisinin C₁₅H₂₂O₅, which shows that highly functionalized compounds can be suitable for SFC.

Limonoids from hexane extracts of the plants *Aphanamixis polystacha*, *Harpephyllum caffrum* and *Entandrophragma deleveyii* have been ana-

lysed by capillary SFC. A liquid crystal-modified polysiloxane phase that discriminated molecular shape was used in a capillary column to separate triterpene acids, including geometric isomers, from *Disoxylum peltigrewianum*. The natural insecticide azadirachtin (see **structure**) is usually analysed by reversed-phase HPLC, but because the extract obtained from Neem seeds usually contains a lot of less polar contaminants, including triglyceride oil, the column has to be flushed with pure methanol or acetonitrile at the end of each run, and total cycling time can be of the order of 1 h. With packed column SFC, using an aminopropyl silica or cyanopropyl silica column and CO₂-methanol (24 : 1, v/v) mobile phase at 20.6 MPa (3000 psi or 207 bar) at 55°C and at a flow rate of 2 mL min⁻¹, the oily impurities are eluted in the solvent front, good resolution and good peak shape are obtained, and the cycle time is about 20 min (**Figure 1**). The example illustrates how SFC in the right situation can have marked advantages over other chromatographic methods.

The cannabinoids and their metabolic products have been examined on capillary columns. SFC is perhaps not the most useful way to examine alkaloids, but a number of separations have been made. Six opium alkaloids (narcotine, papaverine, thebaine, ethylmorphine, codeine and morphine) have been separated from poppy straw on an aminopropyl column with CO₂-methanol-methylamine-water. Seven ergot alkaloids were separated from *Claviceps purpurea* and eight pyrrolizidine alkaloids from *Senecio ananymus*.

Flavonoids from citrus fruits that contain several methoxy groups (hexa- and heptamethoxyflavone, tangeretin, nobiletin, sinensetin and others) were separated on a silica column with CO₂-methanol.

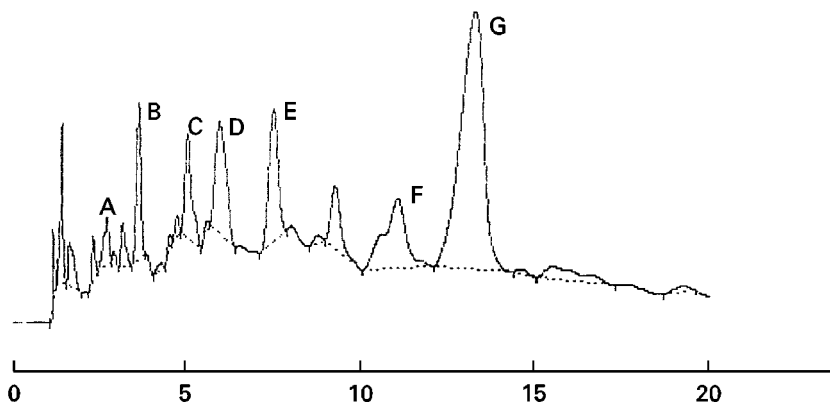


Figure 1 SFC chromatogram of an extract of triterpenoids from the seeds of *Azadirachta indica*, on a Spherisorb cyanopropyl column (150 × 4.6 mm i.d.) of 5 µm particle size, flow rate 2 cm³ min⁻¹ of CO₂-methanol (94 : 6) at 3000 psi (20.7 MPa) and 50°C with UV detection at 217 nm. Compounds are: A, nimbin; B, salannin; C, 6-desacetylsalannin; D, 3-desacetylnimbin; E, 3-tigloylazadirachtol; F, 3-acetyl-1-tigloylazadirachtinin; G, azadirachtin. Unpublished results of A.P. Jarvis and E.D. Morgan.

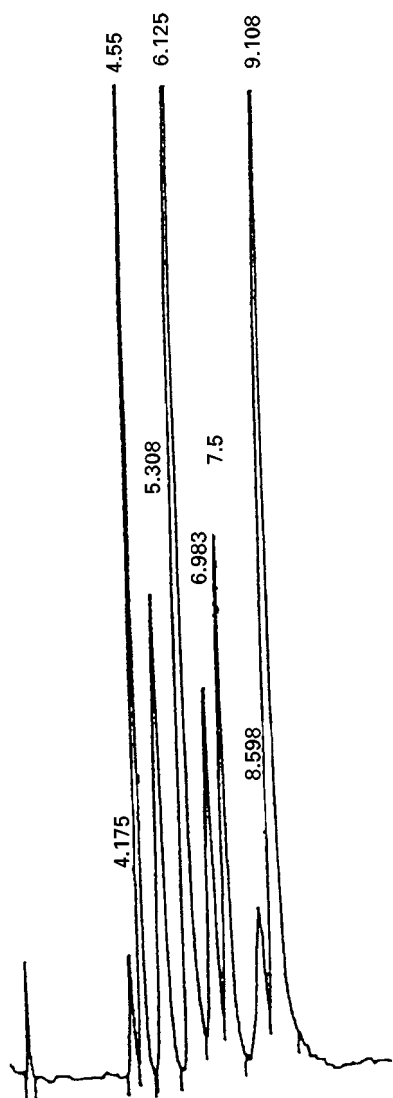


Figure 2 SFC of monosaccharides on Zorbax TMS column (250 \times 4.6 mm i.d.), flow rate 5 cm³ min⁻¹ of CO₂-modifier (80:20, v/v) at 200 bar (20 MPa) and 60°C. The modifier was methanol-water-triethylamine (91.5:8.0:0.5, v/v). Compounds in order of elution are D-ribose, m-erythrose, D-xylose, xylitol, L-sorbose, D-mannose, D-glucose and mannitol. (Reproduced with permission from Salvador A, Herbreteau B, Lafoose M and Dreux M (1997) Subcritical fluid chromatography of monosaccharides and polyols using silica and trimethylsilyl columns. *Journal of Chromatography A* 785: 195.)

A number of monosaccharides, polyols and glycolipids have been separated on silica and trimethylsilyl-bonded silica under subcritical conditions (41°C, 200 bar, and CO₂-methanol 80:20, or a modifier of methanol with 4% or 8% water; Figure 2).

An extensive review (in French) by Lubke cites 207 references on the advantages of SFC for the analysis of natural products.

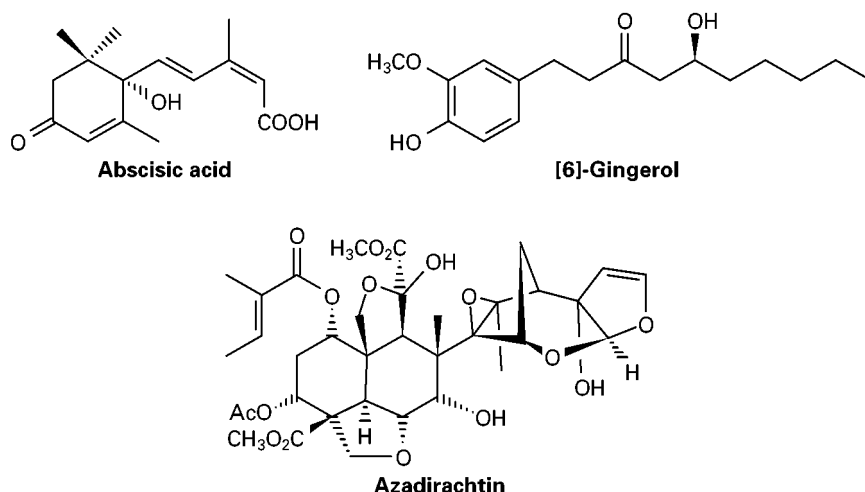
At the time of writing there is increasing interest in the use of subcritical water at 100–200°C as a mobile phase with divinylbenzene polymer columns for the chromatography of highly polar compounds like alcohols, phenols, amino acids and flavones. Clearly any compounds to be analysed must be stable to hydrolysis, as must the stationary phase. As temperature and pressure increase, water becomes less polar – at 200°C it is rather nonpolar – so by controlling these conditions a fluid phase of intermediate polarity similar to the water-methanol mixtures used in HPLC can be achieved.

Chiral Separations

Another advantage of SFC is in the separation of enantiomers. Chiral separations can be carried out at lower temperatures (often with greater efficiency than by GC on the same phases), and on larger molecules than with GC and with improved resolution over HPLC. The subject is still at a very early stage of development, with new discriminator phases appearing rapidly. If insufficient resolution is obtained under supercritical conditions, some investigators recommend subambient (and consequently subcritical) conditions. Separations have included the plant hormone abscisic acid (see **structure**), benzoin, ephedrine, mandelic acid, tropic acid (Figure 3), underivatized amino acids and their derivatives. For the separations shown in Figure 3, the composition of the mobile phase had the largest effect on retention, peak shape and enantioselectivity, with temperature the second most important influence. Tyrosine and tryptophan enantiomers are separated under subcritical conditions on a Chirobiotic T phase at 30°C and 200 bar isocratically with 40% modifier (methanol-water-glycerol, 92.8:7.0:0.2 v/v) in CO₂ with 0.1% triethylamine and 0.1% trifluoroacetic acid. Enantioseparations of five lignans were carried out on polyWhelk-O between 0°C and –42°C with 5–15% methanol in CO₂ with α values from 1.28 to 1.44. The potential of chiral separations of less volatile pheromones unsuitable for GC has not yet been explored.

Hyphenated Methods

All the predictable couplings of SFC to spectroscopic methods have been tried. SFC-FTIR has been used to look for isomerized fatty acids in the triglycerides of partially hydrogenated soya bean oil and in the free fatty acids after hydrolysis using a flow-through FTIR cell. SFC is more easily coupled to a mass spectrometer than HPLC, therefore many examples of SFC-mass spectrometry (MS) can be



found. The spectra resemble chemical ionization spectra, with prominent M^+ or $M + 1$ ions. Alkaloids of *Securidaca longipendunculata* have been separated by SFC-MS and SFC-MS-MS with a moving belt. Thermospray in the electron ionization mode with an SFC gradient was used for the indole alkaloids of *Catharanthus roseus* to identify 60 compounds. By SFC-UV 10 major alkaloids and 30–40 minor compounds were detected in the extract. A few antibiotics, including penicillin, cyclosporin, tetracyclin, oxytetracyclin and mitomycin C have been determined, in some cases after extraction from

blood. Ecdysteroid spectra can be varied by the operating conditions to give additional ions for $M-H_2O$, $M-2H_2O$, etc.

There are a number of examples of direct coupling between SFC and proton nuclear magnetic resonance (NMR) spectrometers. CO_2 has the great advantage of being transparent and only a small proportion of CD_3OD may be required. For polar compounds, subcritical D_2O can be used (see discussion above); it is both transparent and does not generate a very high pressure. The vapour pressure of water at $200^\circ C$ is only 1.55 MPa (225 psi or 15.5 bar). Resolution of

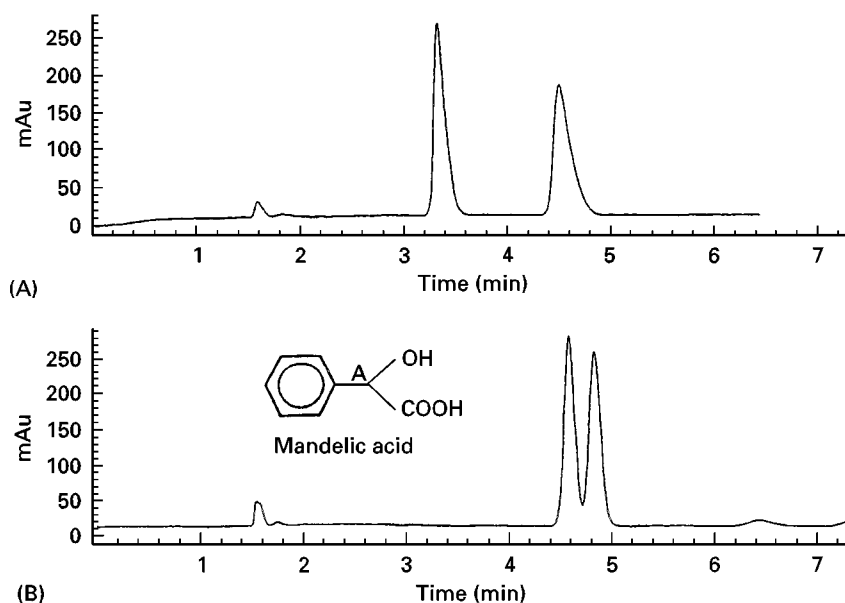


Figure 3 Separation of the enantiomers of mandelic acid on (A) Chiralpak OD (3,5-dimethylphenylcarbamate derivative of cellulose coated on $10\ \mu m$ silica gel) and (B) Chiralpak AD (3,5-dimethylphenylcarbamate derivative of amylose coated on $10\ \mu m$ silica gel). Both columns were $250 \times 4.6\ mm$ i.d., at flow rate $2\ cm^3\ min^{-1}$ of CO_2 -methanol containing 0.1% triethylamine and 0.1% trifluoroacetic acid and programmed from 5% modifier (5 min) to 30% at $5\ %\ min^{-1}$ at 200 bar (20 MPa) and $30^\circ C$. (Reproduced with permission from Medvedovici A, Sandra P, Toribio L and David F (1997) Chiral packed column subcritical fluid chromatography on polysaccharide and macrocyclic antibiotic chiral stationary phases. *Journal of Chromatography A* 785: 159.)

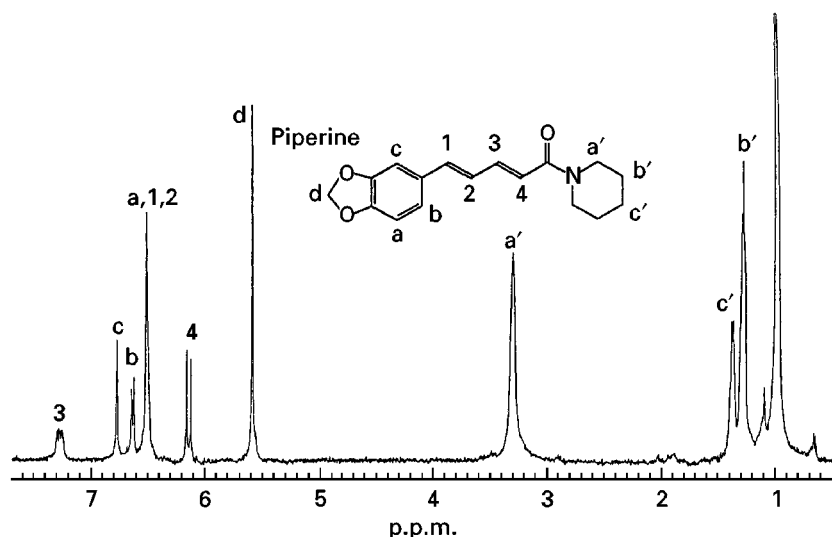


Figure 4 A stopped-flow ^1H NMR spectrum at 400 MHz of piperine extracted from pepper with supercritical CO_2 at $0.5\text{ cm}^3\text{ min}^{-1}$. Pressure was 294 bar (29.4 MPa), and temperature 44°C . (Reproduced with permission from Albert, 1997.)

the NMR spectra under continuous flow approaches the quality of conventional spectra. SFC-NMR has been applied to vitamins and a range of natural products, including extracts of coffee, hops and pepper (Figure 4). Two problems are, firstly, the dependence of NMR signals on pressure, and secondly, the increased spin-lattice relaxation times in a supercritical fluid.

Mycotoxins from *Fusarium roseum* culture extracts have been studied with a combination of SFC-UV and SFC-MS. Some experiments have been conducted with SFE-SFC-NMR-MS and we can expect to see more of such techniques and the hyphens extended.

Future Directions

SFC will not replace GC or HPLC, but predictions are dangerous. We already see new ideas coming forward, such as subcritical cryoseparations and use of superheated water as the mobile phase, that will extend its potential. In the field of polymers, surface active compounds are being used to render growing polymers soluble in supercritical CO_2 . The advantages of SFC are such that we can expect every opportunity to be seized to extend its possibilities, particularly in the areas of chiral separations and hyphenated methods.

Further Reading

- Albert K (1997) Supercritical fluid chromatography-proton nuclear magnetic resonance spectroscopy coupling. *Journal of Chromatography A* 785: 65.
- Anton K and Berger C (1998) *Supercritical Fluid Chromatography with Packed Columns. Techniques and Applications*. New York: Marcel Dekker.
- Arpino PJ and Haas P (1995) Recent developments in supercritical fluid chromatography-mass spectrometry coupling. *Journal of Chromatography A* 703: 479.
- Berger TA (1995) *Packed Column SFC*. RSC Monographs. London, UK: Royal Society of Chemistry.
- Berger TA (1997) Separation of polar solutes by packed column supercritical fluid chromatography. *Journal of Chromatography A* 785: 3.
- Bevan CD and Marshall PS (1994) The use of supercritical fluids in the isolation of natural products. *Natural Product Reports* 11: 451.
- Borch-Jensen C and Mollerup J (1997) Phase equilibria of fish oil in sub- and super-critical carbon dioxide. *Fluid Phase Equilibria* 138: 179.
- Charpentier BA and Sevenants MR (eds) (1988) *Supercritical Fluid Extraction and Chromatography. Techniques and Applications*. ACS Symposium Series 366. Washington: American Chemical Society.
- Chester TL, Pinkston JD and Raynie DE (1996) Supercritical fluid chromatography and extraction. *Analytical Chemistry* 68: 487R.
- Combs MT, Ashraf-Khorassani M and Taylor LT (1997) Packed column supercritical fluid chromatography-mass spectroscopy: a review. *Journal of Chromatography A* 785: 85.
- Greibrokk T (1995) Application of supercritical fluid extraction in multidimensional systems. *Journal of Chromatography A* 703: 523.
- Lubke M (1991) The advantages of supercritical fluid chromatography for analysing natural products. *Analysis* 19: 323.
- Staby A and Mollerup J (1993) Separation of constituents of fish oil using supercritical fluids - a review of experimental solubility, extraction, and chromatographic data. *Fluid Phase Equilibria* 91: 349.
- Williams KL and Sander LC (1997) Enantiomer separations on chiral stationary phases in supercritical fluid chromatography. *Journal of Chromatography A* 785: 149.

Supercritical Fluid Extraction

E. D. Morgan, University of Keele,
Staffordshire, UK

Copyright © 2000 Academic Press

There are two interesting points of the phase diagram of a pure substance: the triple point, where solid, liquid and gas are all in equilibrium, and the critical point, at which liquid and gas phases cease to have separate existence. At temperatures and pressures beyond the critical point there exists only the supercritical phase, with properties between those of a gas and a liquid, varying with conditions. For example, at high pressures a supercritical fluid has solubility and density properties close to those of the liquid, but with greater diffusibility and lower viscosity. High diffusibility and low viscosity improve mass transfer and so help to decrease extraction time. All this would be of only academic or research interest, were it not that one substance, carbon dioxide, which is cheap, readily available in a pure state, and non-toxic, has a readily accessible critical point (31.1°C, and 72.9 atm, 73.8 bar, 1071 psi, or 7.38 MPa). The density of supercritical carbon dioxide at various

values of temperature and pressure is given in Figure 1. Its vaporization on release of pressure avoids the step of concentrating a liquid solution after extraction.

The possibilities of using supercritical carbon dioxide as an extraction fluid were recognized first in industry in the 1950s and 1960s. It entered the laboratory in the 1980s at the same time pumps and control equipment were developed for supercritical fluid chromatography (SFC). Since then supercritical fluid extraction (SFE) has been explored with a wide variety of materials, and is generally recognized as a possible alternative to chlorinated or other toxic solvents for extraction of organic substances. There is no close competitor for carbon dioxide as a supercritical fluid for extraction. Other substances with easily accessible critical points are either too expensive (xenon), toxic (ammonia, nitrous oxide), flammable (ethane, pentane) or corrosive (ammonia). Extraction may be described as static (under pressure without flow of the supercritical fluid) or dynamic (the supercritical fluid flowing through the material to be extracted). Dynamic extraction is more common, but it can be preceded by a period of static extraction.

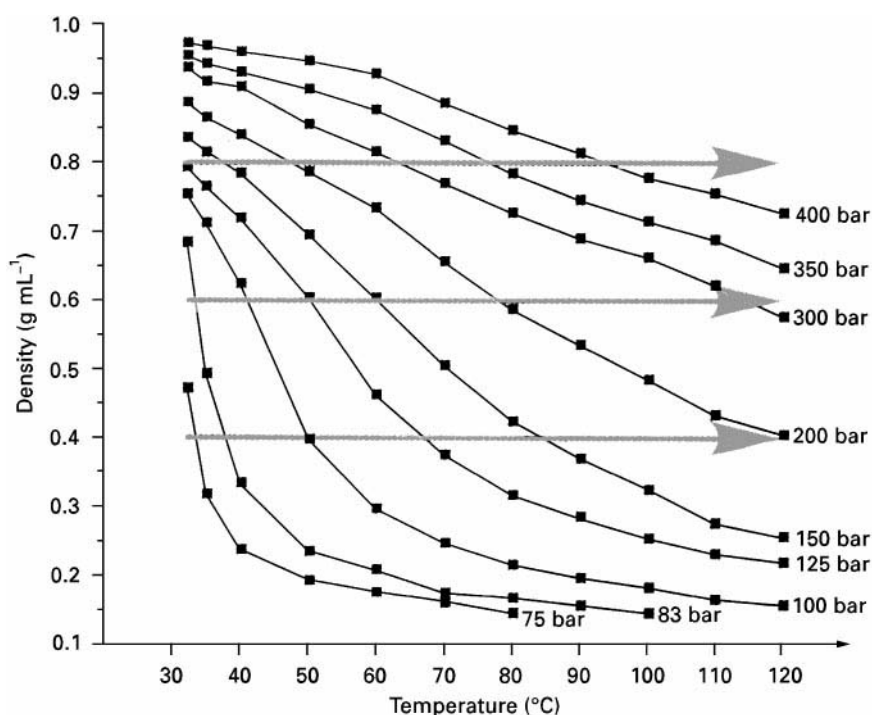


Figure 1 A plot of carbon dioxide density against pressure and temperature above the critical point. 10 bar = 1 MPa. Horizontal arrows represent constant densities of 0.4, 0.6 and 0.8. Fatty acids are extracted only above 0.4 g mL⁻¹, triglycerides above 0.6 g mL⁻¹. Reproduced with permission from Gere DR and Derrico EM (1994) *LC.GC International* 7: 325.

The subject roughly divides itself into two aspects: commercial-scale separation of valuable products (e.g. vitamins, drugs, flavours, fragrances, pigments) and laboratory-scale extraction for research or analysis of components. Bevan and Marshall have considered the design of large scale extractors. There are a number of commercial extractors available for small scale work. They usually have six or more chambers so that extractions can be carried out on several samples simultaneously or consecutively. Pressure can be maintained and controlled by an electronic valve or by use of a fixed restrictor, such as a length of silica capillary. After release of the pressure the extract can be collected on a solid adsorbent or the CO₂ bubbled through a solvent. Precautions have to be taken to prevent loss of material as an aerosol.

It is possible to build an extractor at modest cost. The chief needs are high pressure pumps (one for the CO₂, another for the modifier (if used, see below), a cooler for the CO₂, since it is pumped as a liquid, an old gas chromatography (GC) oven to maintain the desired temperature of the extraction, some empty high performance liquid chromatography (HPLC) columns for extraction chambers, a pressure gauge and some means of controlling and releasing the pressure. The simplest solution for this is a length of about 30–50 cm of silica capillary. Whatever the purpose of the extraction, it can be convenient to couple the equipment to a chromatographic system to monitor the course of extraction. Most convenient is on-line SFC. The composition of the extract can be sampled periodically by inserting a switching valve leading to the chromatograph. GC linked to the extraction is also much used, particularly for the extraction of essential oils and fragrances. The chromatograph can in turn be linked to a mass spectrometer. Now there is no end to the complexity of equipment that can be linked to the extraction. Albert has particularly explored the linking of SFE to nuclear magnetic resonance (NMR) spectroscopy, and gives examples that include natural products.

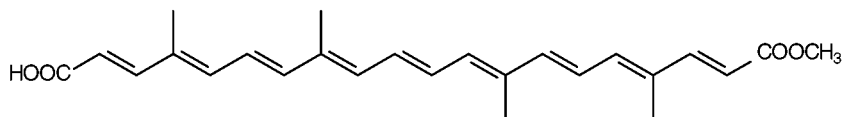
The solubility properties of supercritical CO₂ are close to those of hexane (polarity increases slightly with pressure), so its chief disadvantage is poor solubility for more polar substances. To extract lipids, the density needs to be above 0.4 g mL⁻¹ (see Figure 1),

for triglycerides it should be above 0.6 g mL⁻¹. The best way to improve solubility (if increasing pressure is not convenient) is to add a small proportion (5–10%) of a polar organic solvent, such as methanol. The organic solvent in this context is commonly called a modifier. The plant, animal or other material from which substances are being extracted is often called the matrix. The solubility of water in supercritical CO₂ is very low (0.4 mol% at 8.0 MPa, rising to 0.8 mol% of water at 20.0 MPa), but there are a number of examples where water has been used as a modifier for extraction of more polar compounds. The polarity of water drops remarkably as it approaches its critical point.

An early landmark in SFE was the commercial extraction of caffeine from coffee with CO₂. Caffeine is a relatively polar compound, so its extraction with the very apolar CO₂ is surprising. Hops and spices followed closely.

Lipids

Lipids from plant and animal sources are obvious targets for SFE, both on a commercial scale and as an analytical method in the laboratory. There are many reports of its use to extract fish oils (particularly to obtain concentrates of polyunsaturated acid glycerides), dairy products and seed oils. In many cases attempts are recorded to make selective extraction of valuable minor substances accompanying the oil, such as tocopherols, carotenes or sterols. The content of tocopherols is said to be significantly higher from rapeseed and soybeans by SFE. One can find examples of SFE of natural products in the reviews by Bevan and Marshall and by Jarvis and Morgan. The lipids of rapeseed and soybeans were extracted with CO₂ alone and with added propane or nitrous oxide. In another case, oil from a fungus *Mortierella ramanianae* was extracted with CO₂, N₂O, CHF₃ and SF₆. Extraction was best at 60°C and 157–295 bar with N₂O, followed by CO₂, CHF₃ and SF₆. Addition of 20% ethanol greatly increased the solubility of the oil and decreased its acidity. Some examples are listed in Table 1 with some of the conditions used for the extraction, although in most cases a range of differing conditions were explored. Unfortunately, there is a scarcity of information directly comparing efficiency of SFE with solvent extraction.



1 Bixin

Table 1 Examples of extraction of lipids with conditions used

Extracted	Matrix	Temperature (°C)	Pressure (MPa)	Additional information ^a
Bixin (1)	<i>Bixa orellana</i> (annatto)	40	60.62	4% Acetonitrile with 0.05% trifluoroacetic acid, yield 0.27%
Carotenes	<i>Daucus carota</i> (carrots)	40	60.6	5% CHCl ₃ 92.7%, 1 h
Carotenes	<i>Mauritia flexuosa</i> (buriti fruit)	40–55	30	80%
Carotenes and lutein	Leaf protein concentrate	40	30	
Fatty acid methyl esters	Fish oil	40	8.0	20 min
γ -Linolenic acid	<i>Oenothera paradoxa</i> (evening primrose) seed	40–60	20–70	30 min, 95%
Phospholipids	Rape seed (Canola)	70	55.2	10% EtOH
Phytosterols	Seed, corn oil, margarine			
Sterols	Egg yolk	45	17.7	a ^b , 1 h
Tocopherols	<i>Hordeum vulgare</i> (barley)	40	23.69	1 h, 4.38%, density 0.921
Triglycerides	Rapeseed, soybeans	20–40	25	a
Triglycerides	Ground rapeseed, linseed meal	90	34.3	
Triglycerides	Sunflower	42–80	15.2–35.4	20% EtOH

^aHigh percentages refer to total content, usually compared to that obtainable by solvent extraction; low percentages refer to total extracted as a percentage of total mass.

^bYield comparable to solvent extraction.

Glycolipids and phospholipids are less easily extracted and usually require the addition of methanol as modifier. Sterols and sterol esters are more difficult to extract than triglycerides, but have also been explored. By stepwise increases of pressure, the concentration of phytosterols in soybean extract increased 30 times, from corn fibre by 12 times and from corn bran by 37 times. Methods are available for the analytical determination of sterols in animal skin, meat and fat. SFE is particularly useful for unstable compounds such as γ -linolenic acid and carotenes. The latter have been extracted from leaf protein concentrates and carrots (see Table 1). Figure 2 shows a chromatogram of a carotene extract obtained from carrots. The content of tocopherols is greater in the oil of rapeseed and soybeans extracted by SFE than by solvent extraction. Fluorometric and electrochemical detectors with HPLC have been used to follow the extraction.

Lanolin has been extracted from wool using 20% acetone as modifier, giving comparable results to dichloromethane Soxhlet extraction, but it gave a cleaner product (less mineral salts and protein).

Essential Oils

Essential oils are an obvious target for SFE (Table 2), and this is probably the area that has received most attention in recent years, judging by the number of publications. Many compounds in essential oils are either highly unsaturated or subject to thermal or oxidative degradation, so that SFE offers a clear

advantage for them. One complication is that many plant oils have been obtained by steam distillation, which extracts the monoterpenes but leaves most of the sesquiterpenes behind. SFE removes monoterpenes and sesquiterpenes together, so that the composition and odour of the SFE product may be distinctly different. When the price paid for a

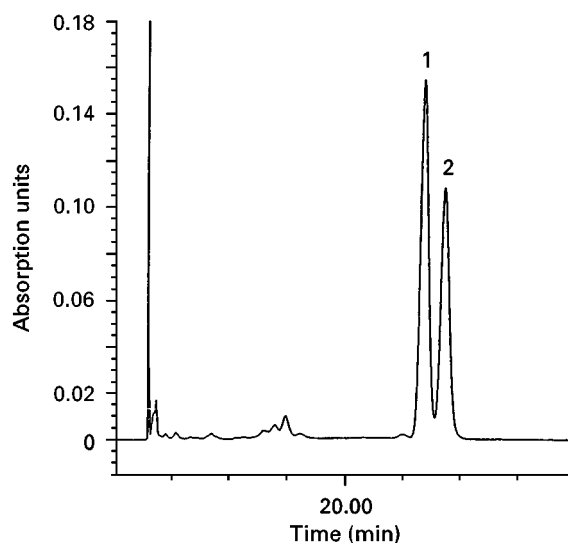


Figure 2 HPLC chromatogram of the SFE extract of carrots collected at 40°C and 50.5 MPa for 1 h with a flow rate of 600–750 mL min⁻¹ of CO₂. 1, α -carotene; 2, β -carotene. (Reproduced with permission from Chandra A and Nair MG (1997) *Phytochemical Analysis* 8: 244. Copyright John Wiley & Sons Ltd.)

Table 2 Examples of extraction of essential oils, flavours and fragrances with conditions

Extracted	Matrix	Temperature (°C)	Pressure (MPa)	Additional information
Onion flavour	<i>Allium cepa</i> (onion)	37	24.5	Flow 0.5 L min ⁻¹ , yield improved by EtOH modifier
Organo-sulfur compounds, cepaenes, allicin	<i>Allium tricoccum</i> (ramp)			
Root oil (118 compounds identified)	<i>Angelica archangelica</i>	40	12.0	1 h static, 2 h dynamic
Alkylpyrazines	<i>Arachis hypogaea</i> (roasted peanuts)	50	9.6	Density 0.35, lipids not extracted
Carvone, limonene	<i>Carum carvi</i> (caraway seed)	32	12.5	Time and flow rate affected yield
Capsacinoids	<i>Capsicum frutescens</i> (chili), <i>Capsicum annum</i> (paprika)	80		Density 0.75, H ₂ O, yield lower or equal to solvent extraction
Essential oil	<i>Cuminum cyminum</i> (cumin seed)	40	10.0	
Curcumin (3)	<i>Curcuma longa</i> (turmeric)	60	28.0	20% MeOH, 2 mL min ⁻¹
Neral, geranial, geraniol, nerolic and geranic acids	<i>Cymbopogon citratus</i> (lemongrass)			
β -Phellandrene, <i>p</i> -cymene, cryptone, spathulenol and 86 others	<i>Eucalyptus camaldulensis</i>			
Limonene, fenchone, methylchavicol, anethole	<i>Foeniculum vulgare</i> (fennel)	31–35	8.0–8.4	10.0%
Anethole	<i>Illicium verum</i> (star anis)	80		Density 0.35, 90% pure
Olive oil aroma (hexanal, 2-hexenal, hexanol, 3-hexenol and others)	Olive oil and olives	40–45	7.7–11.5	Static 1–5 min, dynamic 30 min
Essential oil (limonene)	Orange peel	20–50	8–28	Optimum for limonene (99.5%) 35°, 12.5 MPa; optimum for linalool, 35°, 8.0 MPa
Kavain, yonganin, methysticin and derivatives	<i>Piper methysticum</i> (kava)			
Essential oil	<i>Piper nigrum</i> (black pepper)	30–50	15–30	
Carnosic acid	<i>Rosmarinus officinalis</i> (rosemary)	37–47	10–16	
Eugenol, eugenol acetate, α - and β -caryophyllenes	<i>Syzygium aromaticum</i> (clove buds)	50	24	
Tanshinone IIA	<i>Salvia miltiorrhiza</i> (bunge)	60	24.5	0–10% MeOH
Pyrazines	<i>Theobroma cacao</i> (cocoa beans)	60	20.0	2% MeOH, 20 min

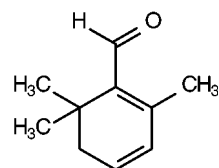
product depends upon odour, or content, this is important. Cedarwood oil obtained by SFE is closer in aroma to the original wood than steam-distilled oil. A disadvantage of SFE is that, at higher pressure, leaf waxes, which are not extracted by steam, are extracted as well. Freshly cut peppermint and spearmint plants extracted with supercritical and subcritical CO₂ (temperature 24–43°C) gave oils similar to that from steam distillation. A comparative study of essential oils and wax from lavender showed that the SFE extract contained three times as much linalyl acetate as the steam distillate; presumably the lower content was caused by hydrolysis. In the citrus industry it is reported that removing terpenes from citrus oil avoids oxidation to undesired products, while an

SFE product can be used to re-blend to give new flavour. SFE of rosemary leaves for 10 min gave similar yield to that of 4 h sonication with CH₂Cl₂ (Table 2). There is interest in the antioxidants obtainable from rosemary and sage, obtainable by a two-stage SFE extraction of the essential oil followed by the antioxidants. In a study of extraction of orange peel, the dried peel should be reduced to 2 mm particles for rapid extraction. For particles of 0.3 mm, 75% of the total oil was extracted with a ratio of 6 kg of CO₂ per kg of orange peel. In a study of effect of different modifiers on the SFE of lemongrass oil, GC-mass spectrometry (GC-MS) indicated a different profile of monoterpenes depending upon the modifier.

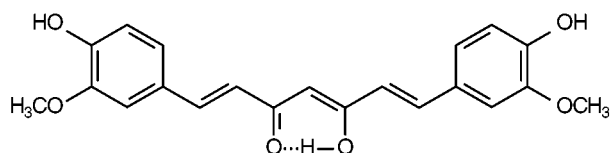
Flavours and Fragrances

The subject of flavours and fragrances overlaps with essential oils (Table 2). The mild conditions used for SFE with CO₂ can provide an accurate representation of the taste, colour and odour of natural substances found in herbs, spices, beverages and foods. Many studies have been of an analytical nature, to compare products obtained by different processes, to compare plant materials for quality, or to find the essential source of the desirable odour, as for example in the cases of coffee and olive oil. A brewed coffee aroma as similar as possible to the original brewed coffee has been obtained by SFE, monitored by smelling the product. Attempts have been made also to extract the aroma of virgin olive oil, from the oil and the olives, trap it on Tenax and analyse the product by GC-MS. SFE of cocoa beans with GC-MS analysis of the extract was used to assess the effect of storage on quality of the beans. Some alkylpyrazines were reduced after storage. There have been a number of studies of clove oil, none of which have reported a distinctly different yield between SFE and distillation methods. In many reports the yield is slightly lower by SFE. Hops have been the subject of study to produce bitter extracts for the brewing industry. The optimum conditions for an extract for the beer bitterness and aroma have been developed. Extraction of the leaves of hops gave no bitter extract. By adjusting the conditions the flavour of roasted peanuts could be collected without extracting the oil (Table 2).

Extraction of fennel seeds gave a higher yield by SFE (10.0%) than steam distillation (3.0%), about the same as extraction with hexane (10.6%), and less than ethanol extraction (15.4%), but the SFE and distilled products had a much more intense odour and taste than the solvent extracts. Cumin seed oil by SFE contained valuable components which would be thermally degraded by steam distillation. In the case of onion flavour oil SFE and liquid CO₂ extracts had the flavour of fresh onions, while the steam distillation solvent-extracted oil had a cooked onion flavour. The flavour of Emmentaler cheese during ripening has been followed by SFE and GC-MS, but further fractionation was needed because of the dominance of fatty acids, in order to analyse the less abundant alcohol, carbonyl and lactone aroma compounds. Guaca or quemadora (*Splilanthus americana*), with a slightly burning and numbing taste, is used in South American cooking. Comparison of steam-distilled and SFE extracts of leaves, stem and flowers showed significant differences (Figure 3). Eighty-eight compounds were identified in the extracts.



2 Safranal

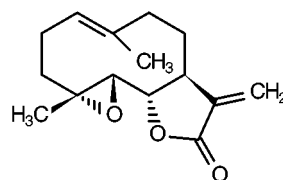


3 Curcumin

Saffron is such an expensive spice, that it is very liable to fraudulent imitation. The most important aroma compound, safranal (2), has been studied by isotope analysis. Synthetic safranal can easily be distinguished from the natural by ¹³C-isotope content. SFE gave a cleaner and faster method of obtaining an extract of volatiles than solvent extraction, but there was some isotopic fractionation depending upon extraction yield.

Medicinal Compounds and Alkaloids

There are many medicinal compounds in plants that are targets for SFE, but many of these are more polar substances and are therefore more difficult to extract efficiently. The conditions must be explored for each example at our present state of knowledge (Table 3). Feverfew (*Tanacetum parthenium*) is much in demand as a herbal remedy and other worthless dried plants of similar appearance are frequently sold as feverfew. The value of the plant can be checked by SFE with CO₂ for the content of parthenolide (4), the active ingredient. Artemisinin (5) is an antimalarial present in *Artemisia annua*. Texanes and baccatins have been extracted from ground needles and seeds of *Taxus* spp. with 3% ethanol modifier; ethyl acetate, methanol, dichloromethane and diethyl ether have all been used as modifier for this purpose. In all cases waxy materials are co-extracted, so hexane solvent extraction was used first



4 Parthenolide

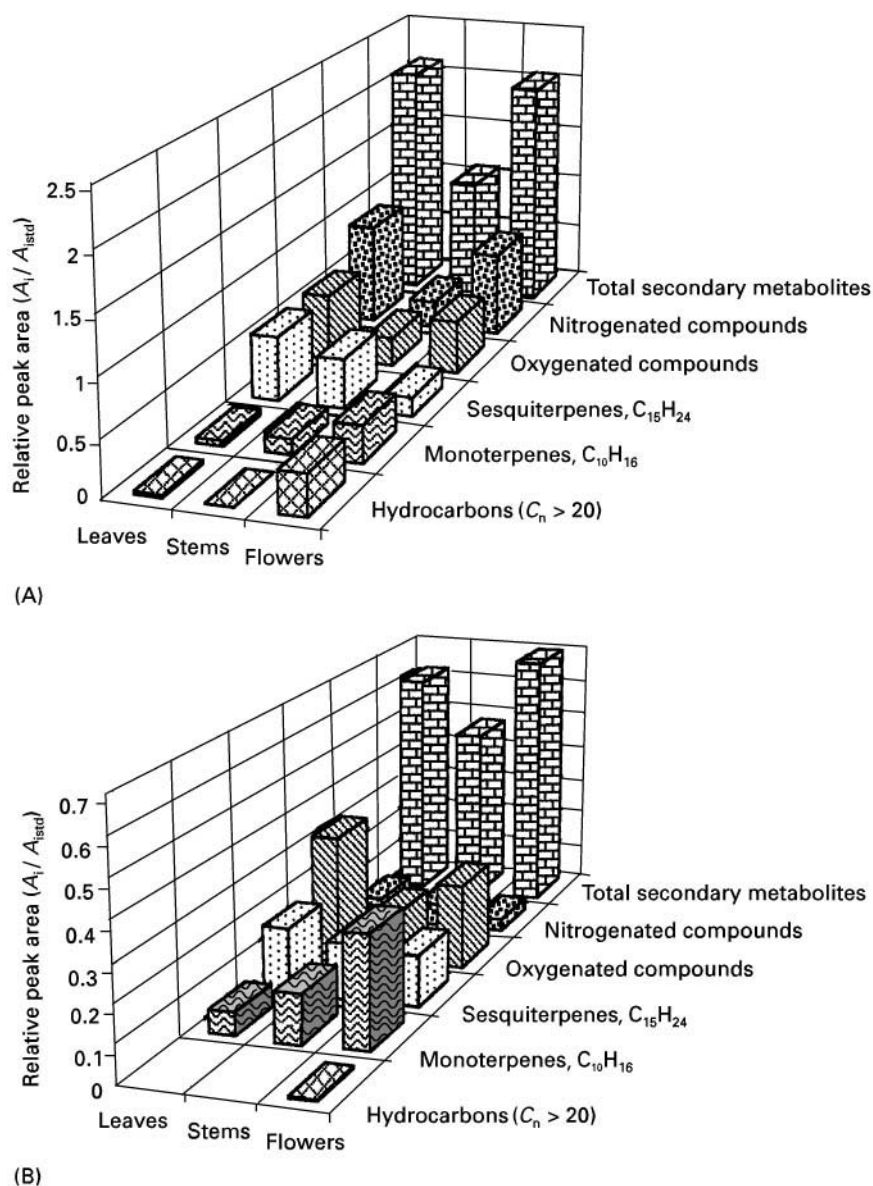
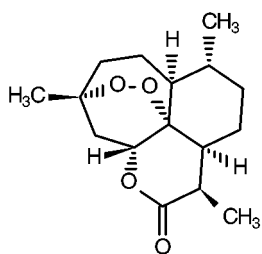


Figure 3 The composition of extracts obtained from different parts of the plant *Spilanthes americana* by (A) SFE and (B) simultaneous steam distillation-extraction. (Reproduced from Stashenko EE, Puertas MA and Combariza MY (1996) *Journal of Chromatography A* 752: 223 with permission from Elsevier Science.)



5 Artemisinin

to remove the waxes and then SFE was applied for the precursors of paclitaxel (taxol). Ginkgolides and bilobalides are extractable from *Ginkgo biloba* with 10% methanol added. There is a report of SFE of medicinal plants being directly coupled to a uterotonnic bioassay on abdominal muscle to discover possible substances to induce uterine contraction.

The bark of *Magnolia officinalis* is used in Chinese medicine for a number of purposes. A major active compound is magnolol (6), a neolignin. SFE was compared with solvent extraction with phytosols, a series of new nonchlorinated fluorocarbon

Table 3 Examples of extraction of medicinal compounds, alkaloids and polar compounds with conditions used

Extracted	Matrix	Temperature (°C)	Pressure (MPa)	Additional information
Atractylon (8)	<i>Atractylodes</i> rhizomes	40	10	2 mL min ⁻¹ , 20 s
Bile acids	Bovine bile	70	22	15% MeOH, 20 min, 88% recovery
Cedrelone (9)	<i>Cedrela toona</i>	40	40.0	30 min static, 40 min dynamic, 0.6 g sample wetted with 40 µL MeOH
Pyrethrins	<i>Chrysanthemum cinerariaefolium</i>	40	8.3	Most extracted in 3 h
Uterine contractants	<i>Clivia miniata</i> , <i>Ekebergia capensis</i> , <i>Grewia occidentalis</i> , <i>Asclepias fruticosa</i>		20–40	
Podophyllotoxin (6)	<i>Dysosma pleiantha</i> roots	40–80	13.6–34.0	With MeOH added, yield 95%
Phenols	Olive leaves	100	33.4	CO ₂ density 0.70, 10% MeOH, total 2 mL min ⁻¹ , 140 min
Glycosylated flavonoids	<i>Passiflora edulis</i> (passion fruit leaves)	75	10.1	15% MeOH, 5 min, 1.75%
Schisandrols, schisandrins (lignans)	<i>Schisandra chinensis</i>	40–80	13.6–34.0	80% of that from MeOH extraction
Flavonoids	<i>Scutellariae radix</i>	50	20.0	CO ₂ –MeOH–H ₂ O 20:2:0.9
Isoflavones	Soybean products	50	60	20% EtOH, 1 h, 93%
Theobromine, caffeine, cocoa butter	<i>Theobroma cacao</i> (cocoa)	40–90	8.0–30	EtOH modifier

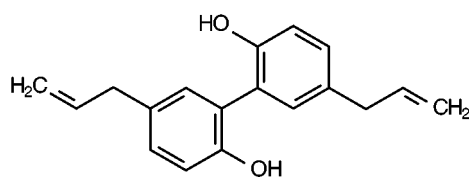
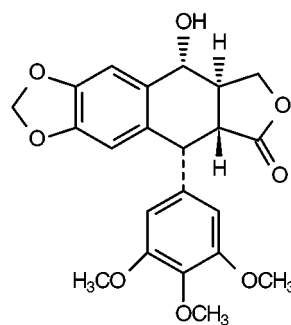
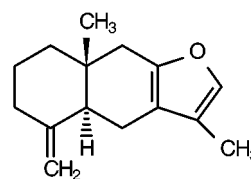
solvents of varying polarity. SFE with 10% added methanol gave the highest yield of magnolol (1.86%), and phytosol A gave the lowest (0.78%). Digoxin can be obtained from *Digitalis lanata* leaves by SFE, but the process is not very selective and various strategies have been tried to improve selectivity, including use of trifluoromethane and tetrafluoroethane as extractives, but no one alternative had a clear advantage.

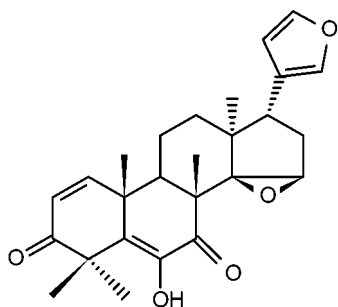
The antiviral compound podophyllotoxin (**7**) from *Dysosma pleiantha* and atractylon (**8**) from the oriental drug *Atractylodes* rhizome illustrate further the types of separations that have achieved. Atractylon, an oxidatively unstable compound, was extracted analytically in 20 s with a recovery 30% higher than by solvent extraction. The phototoxic furocoumarins (psoralen and derivatives) were extracted analytically from the vegetable celariac (*Apium graveolens*) by SFE, Soxhlet extraction with ethanol and sonication

with chloroform. SFE gave higher extractions (Figure 4).

Polar Compounds

The wide range of polar compounds of interest as natural products is a greater challenge to the power of

**6** Magnolol**7** Podophyllotoxin**8** Atractylon



9 Cedrolone

SFE. The success obtained varies considerably, and our understanding of the physical process of diffusion, cell wall penetration, rate of dissolution and solubility are too rudimentary to make predictions. Attempts to extract the tetranortriterpenoid azadirachtin ($C_{35}H_{44}O_{16}$) from neem (*Azadirachta indica*) seeds with or without added methanol did not give as high a yield as methanol solvent extraction. Attempts to remove triglyceride oil from the seeds first by selecting extraction conditions were not successful. Trichothecene mycotoxins at p.p.m. levels in wheat have been extracted for analytical purposes and determined online by chemical ionization-mass spectrometry (CI-MS).

McHugh and Krukonis have discussed the decaffeination of coffee extracts. The removal of nicotine from tobacco and snuff has also been achieved, chiefly for analysis. Some lignans and coumarins with lower numbers of hydroxyl groups

can be extracted. Hydroxypinoresorcinol was extracted from *Fraxinus japonica* and other *Fraxinus* species using CO_2 with water modifier. The extraction of lignans by SFE from *Forsythia* species was as good as solvent extraction with refluxing hexane or ethanol. SFE gave better extraction of flavanones and xanthones from the root bark of the Osage orange (*Maclura pomifera*), provided 20% methanol was used as modifier, than liquid extraction, and in much shorter time. An unusual example is the determination of the alkaloids berberine and palmatine in *Phellodendri* cortex using ion pair SFE. The ion-pairing agent was dioctyl sodium sulfosuccinate, with 10% methanol as the modifier. The extraction required only 10 min. Microcystins, toxic peptides, have been extracted from cyanobacteria with a ternary mixture of 90% CO_2 , 9.5% acetic acid and 0.5% water. Even the particulate material from hardwood smoke has been examined (the principal substances identified by GC-MS were guaiacol and syringol derivatives).

Where cost is mentioned, SFE is in many cases admitted to cost more at present than Soxhlet extraction, but some studies suggest that costs can be reduced with proper experiment design, even for poorly soluble natural products.

Looking Ahead

SFE is firmly established as an industrial process for the isolation of a small number of natural products. Patents exist for a larger number of examples. As new industrial plant is bought into operation, and old

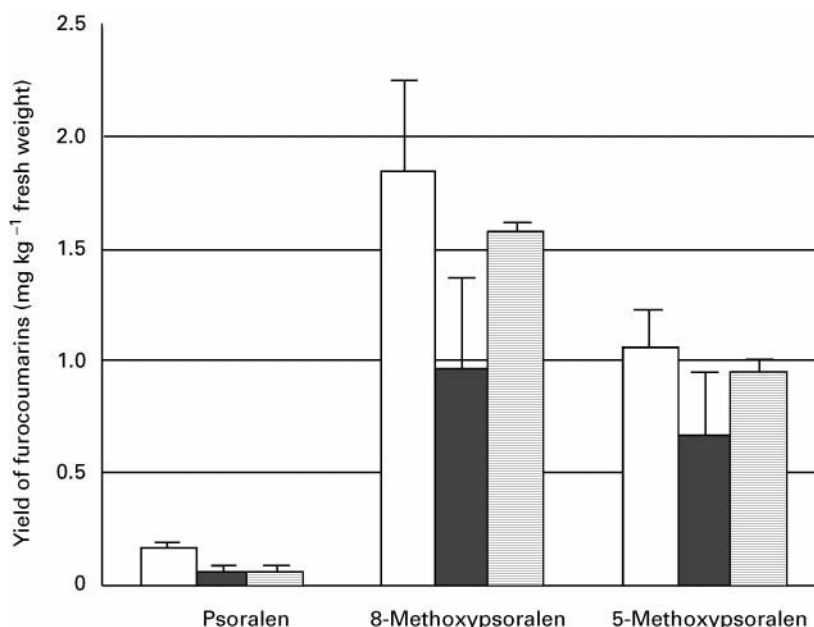


Figure 4 Comparison of extraction of three phototoxic furocoumarins from celeriac (*Apium graveolens*) by SFE (open columns), Soxhlet extraction (ethanol: filled columns) and sonication with chloroform (hatched columns). (Reproduced with permission from Järvenpää EP, Jestoi MN and Huopalahti R (1997) *Phytochemical Analysis* 8: 250. Copyright John Wiley & Sons Ltd.)

equipment removed, the number of examples will increase. Essential oils are going that way quickly. For polar substances, the published work shows that each material has to be examined to find the best conditions. It is difficult to assess how many natural products are being routinely extracted in this way, but the steady output of papers indicates continuing interest. As the chlorinated solvents are withdrawn, we can expect to see the use of SFE increase strongly. There is a ready market for some cheaper and less elaborate extraction equipment to meet this growing demand.

See also: II/Chromatography: Supercritical Fluid: Theory of Supercritical Fluid Chromatography. Extraction: Supercritical Fluid Extraction. III/Supercritical Fluid Extraction-Supercritical Fluid Chromatography.

Further Reading

Albert K (1997) Supercritical fluid chromatography-proton nuclear magnetic resonance spectroscopy coupling. *Journal of Chromatography A* 785: 65.

Bevan CD and Marshall PS (1994) The use of supercritical fluids in the isolation of natural products. *Natural Products Reports* 11: 451.

Jarvis AP and Morgan ED (1997) Isolation of plant products by supercritical-fluid extraction. *Phytochemical Analysis* 8: 217. [The whole of *Phytochemical Analysis* 1997; 8(5) is devoted to papers on supercritical fluid extraction.]

Kalampoukas G and Dervakos GA (1996) Process optimization for clean manufacturing: supercritical fluid extraction for β -carotene. *Computers and Chemical Engineering* 20: S1383.

McHugh MA and Krukonis VJ (1986) *Supercritical Fluid Extraction*. London: Butterworth.

Modey WK, Mulholland DA and Raynor MW (1996) Analytical supercritical fluid extraction of natural products. *Phytochemical Analysis* 7: 1.

Reverchon E (1997) Supercritical fluid extraction and fractionation of essential oils and related products. *Journal of Supercritical Fluids* 10: 1.

Smith RM and Hawthorne SB (1997) Supercritical fluids in chromatography and extraction. Special volume of *Journal of Chromatography A* 785.

Thin-Layer (Planar) Chromatography

J. Pothier, University of Tours, Tours, France

Copyright © 2000 Academic Press

Introduction

The use of thin-layer chromatography (TLC) for the analysis of plant extracts began in the 1960s, with the work of Stahl and Randerath. The continuing use, and further development of TLC in plant analysis is justified because of its rapidity and because of the availability of a number of different sorbents. TLC is also useful in plant analysis because it is possible to work on crude extracts, which is not the case with other analytical methods. In plant analysis, derivatization methods serve to increase sensitivity and selectivity in addition to providing evidence concerning the quality of the separation. A selection of the most important derivatization/detection methods are given in Table 1. As well as these advantages, TLC is very economical and can be employed for routine use because the consumption of solvent is very low, and it is possible to analyse numerous samples on the same plate. The literature on plant analysis by TLC is very extensive, with the most important contributions being those of Stahl, Randerath, Fried and Sherma, Harbone, and Wagner, who is our main reference on this topic. Most TLC

studies are listed in the different pharmacopoeias of the world, as reported by Wagner. The classes of plant compounds separated by TLC covered in this article are as follows:

- Alkaloids
- Glycosides: flavonoids, coumarins, anthocyanins, ginkgolides, anthraquinone glycosides, cardiac glycosides
- Saponins
- Essential oils
- Cannabinoids
- Valepotriates
- Bitter principles

Alkaloids

Most plant alkaloids are tertiary amines; others contain primary, secondary, or quaternary nitrogen (Figures 1–4). The basicity of individual alkaloids varies considerably; depending on which of the four types is represented. The pK_b values lie in a range 10–12 for weak bases like purines to 3–7 for stronger bases like opium alkaloids. These factors must be borne in mind for extraction, and also for derivatization. The sample sizes applied to the TLC plate must be calculated, according to the average alkaloid content of the specific extracts. The majority of workers

Table 1 Detection methods and spray reagents

Acetic anhydride	10 mL acetic anhydride, heated at 150°C for about 30 min and then inspected in UV light (365 nm)	Ginkgolides
Anisaldehyde-sulfuric acid	0.5 mL anisaldehyde with 10 mL glacial acetic acid, 85 mL methanol and 5 mL concentrated sulfuric acid, in that order. Spray and heat at 100°C for 5–10 min. Then evaluated in visible light or UV 365 nm; conservation limited, not usable when the reagent is red-violet	Terpenoids, propyl-propanoids, saponins, anthocyanins
Antimony(III) chloride (SbCl ₃)	20% solution of antimony chloride in chloroform, or ethanol sprayed and then heated for 5–6 min at 110°C	Cardiac glycosides, saponins
Chloramine-trichloroacetic acid	10 mL freshly prepared 3% aqueous chloramine T solution with 40 mL 25% ethanolic trichloroacetic acid, sprayed, then heated at 100°C for 5–10 min then evaluated in UV light (365 nm)	Cardiac glycosides
Dinitrophenylhydrazine	0.1 g, 2,4-dinitrophenylhydrazine in 100 mL methanol, followed by addition of 1 mL 36% hydrochloric acid; evaluation immediately in visible light	Ketones, aldehydes
Dragendorff (Munier-Macheboeuf) reagent	Solution A: 0.85 g basic bismuth nitrate in 10 mL glacial acetic acid and 40 mL water under heating. Solution B: 8 g potassium iodide in 30 mL water. Stock solutions A + B are mixed	Alkaloids
Dragendorff, followed by sodium nitrite	After spraying with Dragendorff, the plate is sprayed with 10% aqueous sodium nitrite. The coloured zones are brown	Alkaloids
Dragendorff (with hydrochloric acid)	5 g bismuth carbonate in 50 mL H ₂ O, then 10 mL hydrochloric acid and add 25 g potassium iodide, complete with water to 100 mL. The spray reagent is obtained by dilution of 1 mL in 25 mL HCN	Alkaloids, purines (caffeine, theobromine, theophylline)
Fast blue	Fast blue salt B in 100 mL. Spray then look in visible light. A second solution can be sprayed using 10% ethanolic acid, followed by inspection in visible light	Cannabinoids
Iodine	About 10 g solid iodine is spread in a chromatographic tank; the plate is placed into the tank and exposed to iodine vapour, yellow-brown zones are detected in visible light	Compounds with conjugated double bonds
Iodine-chloroform	0.5 g iodine in 100 mL chloroform; after spraying, the plate is warmed at 70°C during 5 min, the plate is evaluated after 20 min in visible or UV light (365 nm)	Ipecacuanha alkaloids
Iodine-hydrochloric acid	Solution A: 1 g potassium iodide and 1 g iodine in 100 mL ethanol. Solution B: 25 mL 25% HCl with 25 mL ethanol. Spray the plate with 5 mL of A followed by 5 mL of B	Purines
Iodoplatinate	0.3 g hydrogen hexachloroplatinate hydrate in 100 mL water with 100 mL 6% potassium iodide solution	Alkaloids (blue-violet)
Iron(III) chloride (FeCl ₃) Kedde reagent	10% in aqueous solution evaluation in visible light 5 mL freshly prepared 3% ethanolic 3,5-dinitrobenzoic acid with 5 mL 2 mol L ⁻¹ NaOH	Polyphenols Cardenolides
Liebermann reagent	5 mL acetic anhydride and 5 mL concentrated sulfuric acid is added carefully to 50 mL absolute ethanol, while cooling in ice. This agent must be freshly prepared. The plate is warmed at 100°C, 5–10 min and then inspected in UV light (365 nm)	Triterpenes, steroids (saponins)
Marquis reagent	3 mL formaldehyde in 100 mL concentrated sulfuric acid; evaluation in visible light	Morphine, codeine, thebaine
Neu (NP/PEG)	1% methanolic diphenylboric acid β -ethylaminoester (diphenylboryloxyethylamine, NP) followed by 5% ethanolic polyethylene glycol-4000 (PEG)	Flavonoids, anthocyanins

Table 1 Continued

Nitric acid (HNO ₃ concentrate) for alkaloids	After spraying the plate is heated 15 min at 120°C	Ajmaline, brucine
Nitric acid (HNO ₃) + KOH	After spraying, the plate is heated 15 min at 120°C. Then sprayed with 10% ethanolic KOH reagent. Red brown in visible light yellow-brown, brown fluorescence with UV light (365 nm)	Anthracenosides, sennosides
Phosphomolybdic acid reagent	20% ethanolic solution of phosphomolybdic acid spraying then heating at 100°C for 5 min	Essential oils
Potassium hydroxide (KOH) (Borntraeger reagent)	5% or 10% ethanolic potassium hydroxide. In visible light, anthraquinones coloured red; anthrones yellow in UV light (365 nm). Coumarins blue in UV light (365 nm)	Anthracenosides, coumarins
Vanillin-hydrochloric acid	1% in ethanol followed by 3 mL concentrated HCl. In visible light, heating 5 min at 100°C intensifies colours	Essential oils
Vanillin-phosphoric acid	1 g vanillin in 100 mL of 50% phosphoric acid. Heat 10–20 min at 120°C	Essential oils
Vanillin-sulfuric acid	1 g vanillin in 100 mL ethanol then add 2 mL of concentrated H ₂ SO ₄ . The plate is sprayed and heated at 100°C (10 min)	Essential oils
Van Urk reagent	0.2 g 4-dimethylaminobenzaldehyde in a cooled mixture of 35 mL water and 65 mL concentrated sulfuric acid. Then add 0.15 mL of a 10% aqueous iron(III) chloride solution	Indolic alkaloids, ergot alkaloids

use silica gel 60 F254 precoated TLC plates but aluminium oxide is also suitable. Many mobile phase systems contain chloroform, the eluting power of which may be decreased by addition of cyclohexane or increased by acetone, ethanol or methanol. The mobile phase is often made alkaline by the addition of ammonia or diethylamine to the less polar solvents but diethylamine is not easy to remove before spraying. The most commonly employed eluents are chloroform-methanol (90:10) and chloroform-diethylamine (90:10). It is also possible to use a screening system, suitable for the major alkaloids of most drugs employing a solvent mixture of toluene-ethyl acetate-diethylamine (70:20:10).

The detection of alkaloids is possible by quenching UV light at 254 nm and at 365 nm and by two main spray reagents Dragendorff and iodoplatinate (see Table 1). The chromatographic systems used for plant alkaloids and also the derivatization techniques used for identification are given in Table 2.

Glycosides

Glycosides are compounds that yield one or more sugars upon hydrolysis. Among the products of hydrolysis, the non-sugar components of the glycosides are known as aglycones. The classification of glycosides is a difficult matter and here the therapeutic use has been chosen.

Flavonoids

The flavonol glycosides and their aglycones are generally termed flavonoids. A large number of differ-

ent flavonoids are known to occur in nature, and these yellow pigments are widely distributed throughout the higher plants. The main constituents of flavonoid drugs are 2-phenyl- γ -benzopyrones. The various structural types of flavonoids differ in the degree of oxidation of the C ring. Most of these compounds are present in drugs as monoglycosides or diglycosides. It is possible to classify flavonoids into flavonols, flavones, flavanons, flavanols and flavanolignans in relation to substituents and the presence of double bonds (Figure 5).

There are numerous plants containing flavonoids and there are also numerous flavonoids and so here only the main plants and compounds are cited in Table 3.

Before TLC is possible, extracts of the plant must be made, and a general method for the extraction of flavonoids is as follows: 1 g of the powdered plant material is extracted with 10 mL methanol for 5 min at 60°C and then filtered. The methanolic extract is then analysed by TLC. When the plant contains lipids it is often necessary to use hexane to defat the powder prior to methanolic extraction and TLC. It is also worth noting that when analysing flavonoids, it is often better to examine the aglycones present in hydrolysed plant extracts. Having obtained a suitable extract, it is then possible to separate the various components using TLC and a variety of chromatographic systems have been devised for this purpose.

It is possible to screen flavonoids on silica gel TLC plates with the following solvent: ethyl acetate-formic acid-glacial acetic acid-water (100:11:11:26).

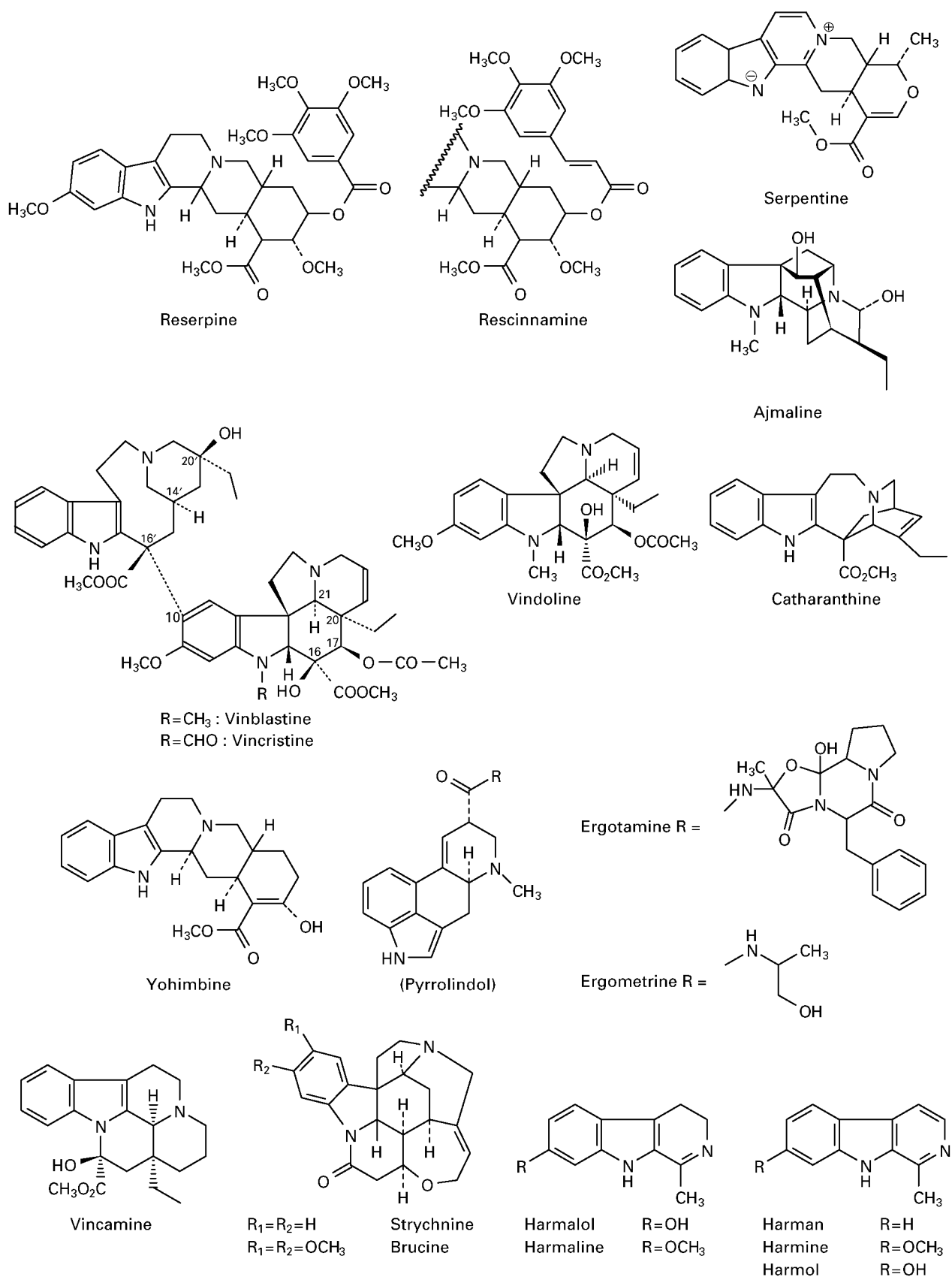
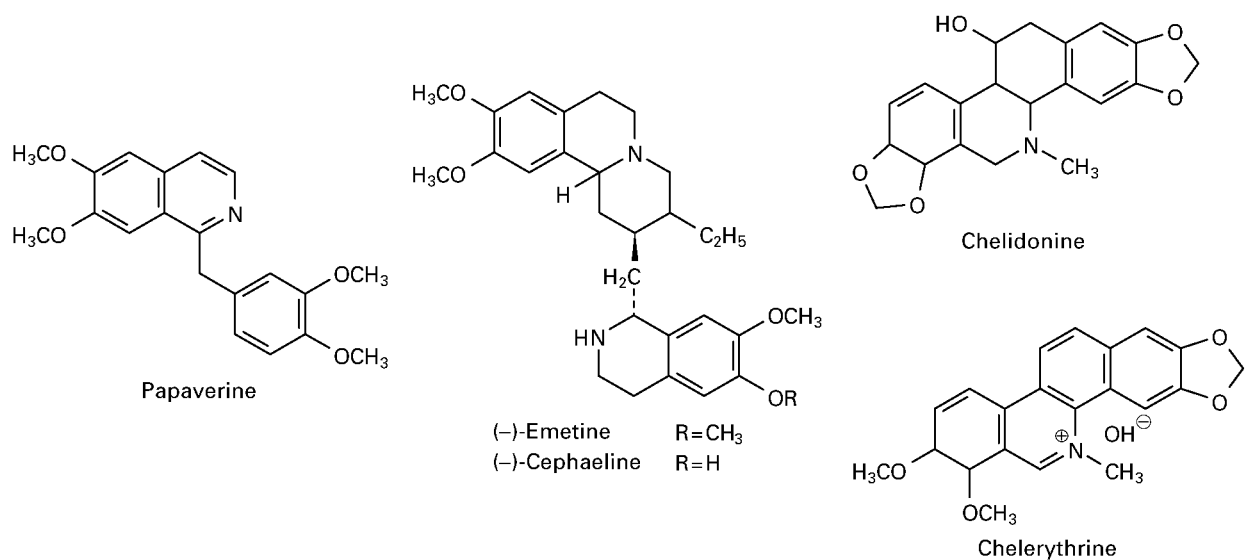
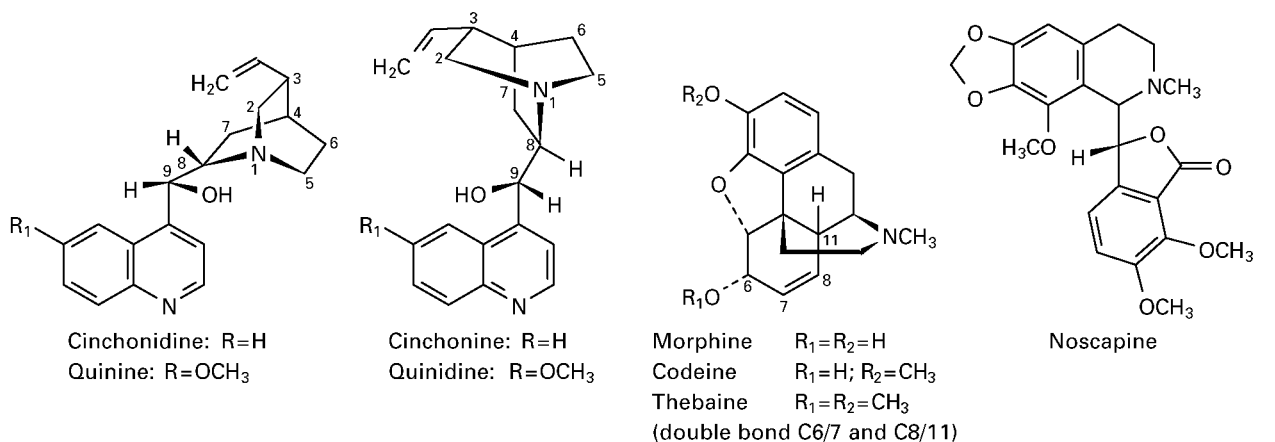
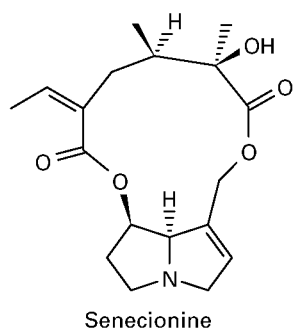


Figure 1 Alkaloids: indoles.

Quinoline/isoquinoline



Pyrrolizidine



Tropane

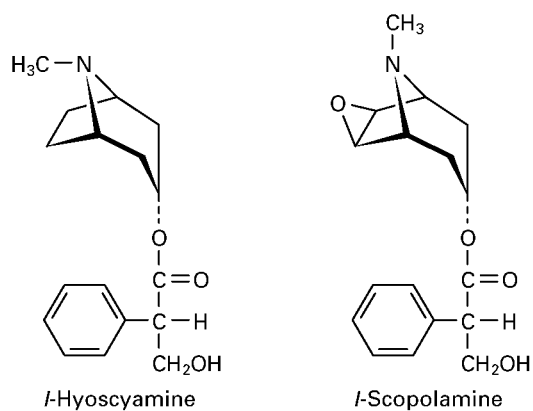
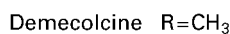
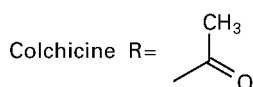
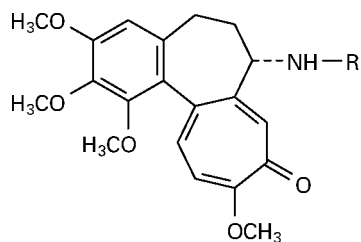
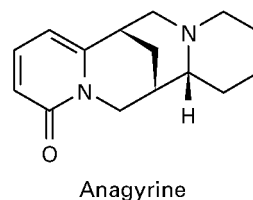
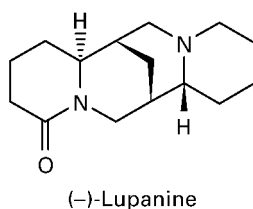
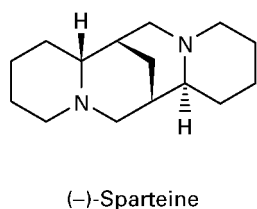
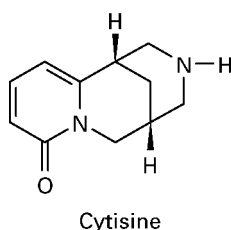
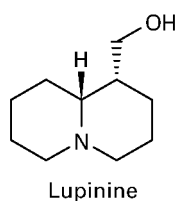
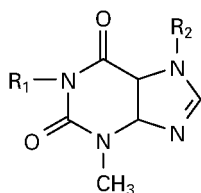


Figure 2 Alkaloids: quinoline/isoquinoline, pyrrolizidine and tropane.

With addition of methyl ethyl ketone (MEK) to give the solvent ethyl acetate–formic acid–glacial acetic acid–MEK–water (50 : 7 : 3 : 30 : 10) it is possible to separate rutin and vitexine-2-O-rhamnoside. Numer-

ous other eluents are also used, such as chloroform–acetone–formic acid (75 : 16.5 : 8.5) for flavanolignans of milk thistle (*Silybum marianum*) and amentoflavone from black haw (*Viburnum*

Tropolone**Quinolizidine****Purines**

	R ₁	R ₂
Caffeine	CH ₃	CH ₃
Theobromine	H	CH ₃
Theophylline	CH ₃	H

Figure 3 Alkaloids: tropolone, quinolizidine and purines.

prunifolium). Chloroform–ethyl acetate (60 : 40) has been used for the flavonoid aglycones of *Orthosiphon aristatus*.

Flavonoid aglycones In addition, the following eluents can be used to separate the aglycones of flavonoids: benzene–pyridine–formic acid (72 : 18 : 10) and toluene–ethyl formate–formic acid (50 : 40 : 10). Toluene–dioxane–glacial acetic acid (90 : 25 : 4) and a further list of suitable sorbents and solvent systems for flavonoids and their aglycones is given in **Table 4**.

Flavonoids can be detected on TLC plates containing a fluorescent indicator because they cause fluorescence quenching when irradiated with UV light at 254 nm, or 365 nm depending on the structural type. Flavonoids also show dark yellow, green or blue fluorescence, which is intensified and changed by the use of various spray reagents. With the spray reagent diphenylboryloxyethanolamine/polyethylene glycol (NP/PEG), flavonoids and biflavonoids give yellow–orange and green fluorescence when irradiated at 365 nm. Acetic acid reagent gives various blue fluorescent zones after heating.

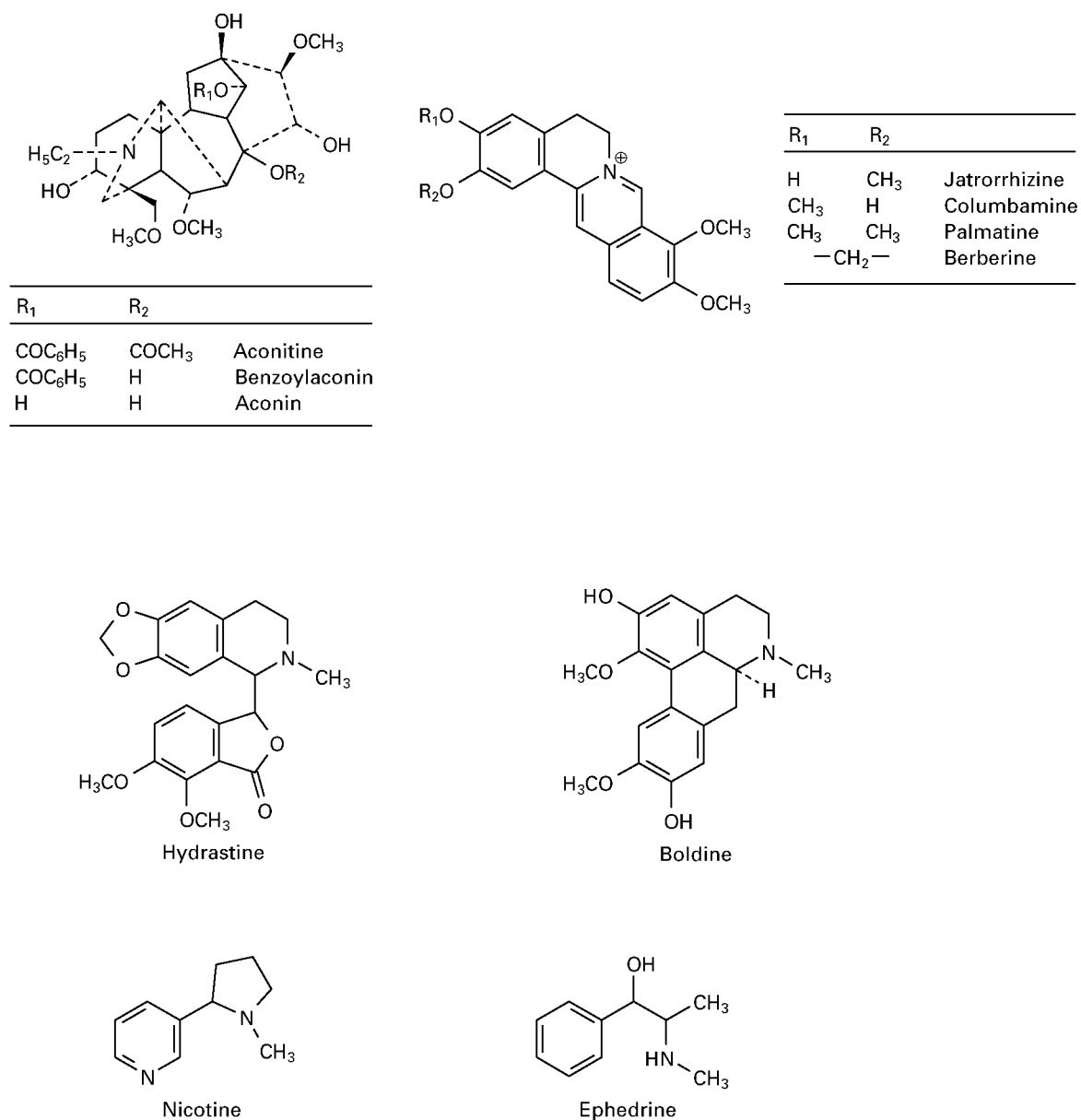


Figure 4 Miscellaneous alkaloids.

Coumarins

Coumarins are derivatives of benzo- α -pyrones (Figure 6).

- *Simple coumarins* consist of coumarin and compounds substituted with OH in umbelliferon, or OCH₃ in scopoletin, and both present in tonka beans (*Coumarouna odorata*), woodruff (*Asperula odorata*) and melilot (*Melilotus officinalis*) or in position C6- and C7-scopoletin which is common in Solanaceae C5 and C8 like fraxin, isofraxidin, fraxetin three compounds of ash bark (*Fraxinus excelsior*).

- *Complex coumarins* belong to two families of plants, the Solanaceae and especially the Apiaceae. C-prenylated coumarins like umbelliprenin are found in angelica root (*Angelica archangelica*). The furanocoumarins possess a furan ring fused at C6 and C7 like psoralen from rue (*Ruta graveolens*), imperatorin, bergapten in ammi (*Ammi majus*), angelica and burnet root (*Pimpinella major*), or a furan ring fused at C7–C8 like angelicin in angelica. Pyranocoumarins have an additional pyran ring at C7–C8, for example visnadin, samidin from ammi (Figure 6).

Table 2 Alkaloids

Group	Eluents	Reagents	Compounds
Quinoline/isoquinoline			
Cinchona (bark): <i>Cinchona</i> sp., <i>Cinchona succirubra</i> , <i>Cinchona ledgeriana</i>	Chloroform–acetone– methanol–ammonia (60 : 20 : 20 : 10) Chloroform diethylamine (90 : 10) Toluene–ethyl acetate–diethylamine (70 : 20 : 10)	10% ethanol H ₂ SO ₄ , then UV 365 nm 10% H ₂ SO ₄ or 10% HCOOH, then iodoplatinate	Quinine, quinidine, strong fluorescence Quinine, quinidine cinchonine, cinchonidine main alkaloids, dihydrocompounds and epiquinine basis give coloration; pink to blue with iodoplatinate
Opium (<i>Opium</i>)	Toluene–acetone–ethanol– ammonia (45 : 45 : 7 : 3) Cyclohexane–ethylenediamine (80 : 20) Chloroform–acetone– diethylamine (50 : 40 : 10) Chloroform–methanol (90 : 10) Toluene–ethyl acetate–diethylamine (70 : 20 : 10)	Dragendorff and NaNO ₂ Iodoplatinate Marquis reagent NP/PEG, then UV 365 nm	Morphine, codeine, noscapine, papaverine thebaine; all major alkaloids give orange–brown coloration Pink coloration with papaverine, noscapine, thebaine Blue with morphine and codeine Violet for codeine and morphine Except codeine, the main alkaloids give a blue fluorescence
Ipecac (<i>Cephaelis ipecacuanha</i>)	Toluene–ethyl acetate– diethylamine (70 : 20 : 10)	UV 365 nm Iodine reagent Dragendorff	Cepheline, emetine, fluorescence light blue Cepheline, bright blue emetine yellow–white The major alkaloids give orange–brown coloration
Celandine (<i>Chelidonium majus</i>)	Propanol–water–formic acid (90 : 9 : 1)	UV 365 nm Dragendorff	Bright yellow fluorescence of coptisine, sanguinarine; weak yellow–green for chelidonine, chelerytrine Brown. Not stable with main alkaloids
Pyrrolizidine			
Golden senecio (<i>Senecio vulgaris</i>)	Chloroform–methanol– ammonia–pentane (82 : 14 : 2.6 : 20) Acetone–methanol–ammonia (40 : 30 : 20)	UV 254 nm	Senecionine, Senecionine <i>N</i> -oxide, agmatine
Tropane			
Belladonna (<i>Atropa belladonna</i>), Thorn apple (<i>Datura stramonium</i>), Henbane (<i>Hyoscyamus niger</i>)	Toluene–ethyl acetate– diethylamine (70 : 20 : 10) Acetone–water–ammonia (90 : 7 : 3)	Dragendorff Iodoplatinate	Scopolamine, (–)-hyoscyamine or atropine
Tropolone			
Meadow saffron (<i>Colchicum autumnale</i>)	Chloroform–methanol (95 : 5) Benzene–ethyl acetate– diethylamine–methanol–water (15 : 12 : 3 : 6 : 12) Chloroform–acetone– diethylamine (80 : 10 : 10)	UV light (254 nm) Dragendorff, 10% ethanol Hydrochloric acid gives a yellow coloration	Colchicine, demecolcine, 3-demethylcolchicine

Table 2 Continued

Group	Eluents	Reagents	Compounds
Indole alkaloids			
Rauwolfia: <i>Rauwolfia</i> sp., <i>Rauwolfia vomitoria</i> , <i>Rauwolfia serpentina</i>	Toluene–ethyl acetate–diethylamine (70 : 20 : 10)	UV 254 nm	Ajmaline: prominent quenching
	Heptane–methyl ethyl ketone–methanol (53 : 34 : 8)	Dragendorff (orange–brown)	All alkaloids, ajmaline, serpentine, rescinnamine, rauwolcine give orange colours
	Cyclohexane–diethyl ether (60 : 40)	Nitric acid	Ajmaline give red colour
Catharanthus leaves (<i>Catharanthus</i> sp.)	Ethyl acetate–ethanol–benzene–ammonia (100 : 5 : 5 : 3) Chloroform–methanol (90 : 10) two dimensional: direction 1, ethyl acetate–methanol (80 : 20); direction 2, dichloromethane–methanol (12 : 1)	Dragendorff	Vinblastine, vincristine, vindoline Catharanthine, and other minor alkaloids give a brown coloration
Yohimbe bark (<i>Pausinystalia yohimbe</i>)	Toluene–ethyl acetate–diethylamine (70 : 20 : 10)	UV 365 nm	Yohimbine (blue fluorescence)
		Dragendorff	Yohimbine, pseudoyohimbine, coryantheine (orange zones)
Ergot (<i>Claviceps purpurea</i>)	Toluene–ethyl acetate–diethylamine (70 : 20 : 10) Toluene–chloroform–ethanol (28.5 : 57 : 14.5)	Van Urk	Ergocristine, ergotamine, ergometrine give blue zone
Common periwinkle leaves (<i>Vinca minor</i>)	Ethyl acetate–methanol (90 : 10)	UV 254 nm	Vincamine, vincaminine, vincamajine, vincine give blue–green fluorescence
		Dragendorff	Weak brown, with major alkaloids
Nux vomica (<i>Strychnos nux vomica</i>) Ignatius beans (<i>Strychnos ignatii</i>)	Toluene–ethyl acetate–diethylamine (70 : 20 : 10)	UV 254 nm	Strychnine, brucine give strong blue fluorescence
		Dragendorff	Brown for brucine, strychnine and minor orange–brown zones for pseudostrychnine, and α,β -colubrines for nux vomica
		Iodoplatinate	Blue zones with brucine and strychnine
		Nitric acid	Brucine give a red colour
Syrian rue (<i>Peganum harmana</i>)	Chloroform–acetone–diethylamine (50 : 40 : 10) Chloroform–methanol–ammonia 10% (80 : 40 : 1.5)	UV 365 nm	Harmanol, harmaline, harmine, harmone, harmone, give a strong blue fluorescence
Miscellaneous alkaloids			
Aconite (<i>Aconitum napellus</i>)	Ether–chloroform–ammonia (25 : 10 : 1) Cyclohexane–ethyl acetate–ethylenediamine (80 : 10 : 10) Hexane–chloroform (60 : 40) Chloroform–methanol (80 : 20)	UV 254 nm Dragendorff NaNO ₂	Aconitine, mesaconitine, hypoaconitine, give orange colours

Table 2 Continued

Group	Eluents	Reagents	Compounds
Barberry (<i>Berberis vulgaris</i>)	n-Butanol–formic acid–water (90 : 1 : 9)	Dragendorff	Berberine, protoberberine, jateorrhizine, palmitine give orange colours
	n-Butanol–ethyl acetate–formic acid–water (30 : 50 : 10 : 10)	Without treatment	Berberine, yellow in visible light
Hydrastis (<i>Hydrastis canadensis</i>)	(See barberry, <i>Berberis vulgaris</i>)	UV: hydrastine, blue–white fluorescence with Dragendorff	Berberine, hydrastine
Boldo (<i>Peumus boldus</i>)	Toluene–ethyl acetate (93 : 7)	Dragendorff	Aporphinic alkaloids, boldine
Tobacco (<i>Nicotiana tabacum</i>)	Toluene–ethyl acetate–diethylamine (70 : 20 : 10)	UV for nicotine, Dragendorff	Nicotine, normicotine, anabasine, give red–orange colours
Desert tea (ma huang) (<i>Ephedra</i> sp.)	Toluene–chloroform–ethanol (28.5 : 47 : 14.5)	Ninhydrin (violet–red for ephedrine)	Ephedrine, norephedrine, pseudoephedrine give orange colours
Quinolizidine			
Lupines (<i>Lupinus</i> sp.)	Chloroform–methanol ammonia (85 : 14 : 7)	UV and iodine vapours, Dragendorff	Lupanine, sparteine, cytisine, <i>N</i> -methylcytisine,
Broom tops (<i>Sarothamnus</i> sp.)	Chloroform–methanol (80 : 20)	Iodoplatinate	hydroxylupanine, matrine
	Cyclohexane–diethylamine (70 : 30)	Heating the plate to 100°C, then UV 254 nm	Fluorescence blue
	Toluene–acetone–ethanol–ammonia (30 : 40 : 12 : 4)	Note: quantification by densitometry (565 nm) after derivatization by Dragendorff	
	Cyclohexane–dichloromethane–diethylamine (40 : 40 : 20)		
Purines			
Coffee (<i>Coffea</i> sp.)	Ethyl acetate–methanol–water (100 : 13.5 : 10)	UV light (254 nm)	Fluorescence quenching for caffeine, theobromine,
Thea (<i>Thea sinensis</i>)			theophylline
Cocoa (<i>Theobroma cacao</i>)	Ethyl acetate–formic acid–glacial acetic acid–water (100 : 11 : 11 : 26)	Dragendorff, acidic iodine–hydrochloric acid reagent	range coloration
Mate (<i>Ilex paraguayensis</i>)			Dark brown coloration
Guarana (<i>Paullinia cupana</i>)			

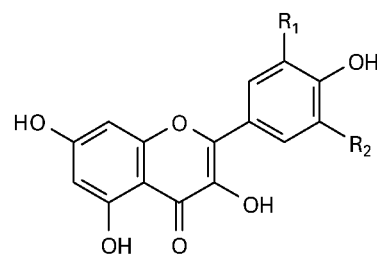
For analysis by TLC, it is necessary to first prepare an extract and for this 1 g is extracted with 10 mL methanol for 30 min under reflux on a water bath. After filtration the solution is evaporated to about 1 mL before application to the plate. For separation on silica gel TLC plates, the following eluents are used: toluene–ether (10 : 10; saturated with 10% acetic acid) – this eluent is used for coumarin/aglycones; and ethyl acetate–formic acid–glacial acetic acid–water (10 : 11 : 11 : 26) for glycosides. Following chromatography, the coumarins can be detected by irradiation with UV light as there is distinct fluorescence quenching for all coumarins at 254 nm and 365 nm. Simple coumarins give blue or blue green fluorescence, and furano and pyranocoumarins yellow, brown, blue, or blue–green fluorescence. The non-substituted chromones show less intense fluorescence: visnagin (pale blue);

khellin (yellow brown). They can also be detected by using spray reagents and these include NP/PEG and KOH.

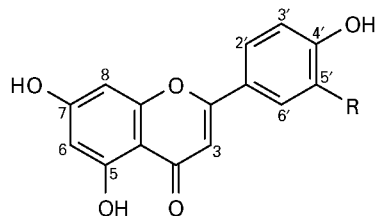
Anthocyanins

Anthocyanins are the most significant group of coloured substances in plants; they are responsible for the pink, mauve, red, violet, and blue colours of flowers and other plant parts. They are present in plants as glycosides of flavylium salts in petals and leaves. In the fruits of higher plants, they are mostly present as glycosides of hydroxylated 2-phenylbenzopyrylium (**Figure 7**). Anthocyanins found in numerous plants used therapeutically include the following: hibiscus (*Hibiscus sabdariffa*) (hibiscin); corn flowers (*Centaurea cyanus*) (cyanin; pelargonin); common mallow (*Malva sylvestris*) (malvin

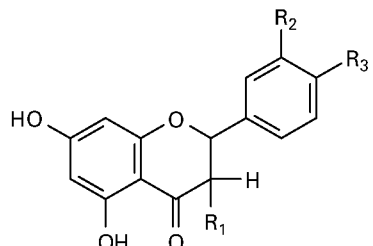
Flavonols

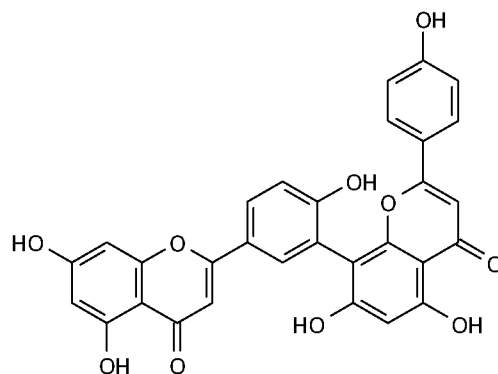
	R ₁	R ₂	Aglycone	Quercetin
	OH	H	Quercetin	Q-3-O-glucoside
	H	H	Kaempferol	(isoquercitrin)
	OH	OH	Myricetin	Q-3-O-rhamnoside
	OCH ₃	H	Isorhamnetin	(quercitrin)
				Q-3-O-galactoside
				(hyperoside)
				Q-3-O-rutinoside
				(rutin)
				Q-4'-O-glucoside
				(spiraeoside)

Flavones

	Aglycone	Glycoside
	Apigenin R=H	A-8-C-glucoside (vitexin) A-6-C-glucoside (isovitexin) A-7-O-apiosyl-glucoside (apiin) A-6- α -L-arabinopyranoside-8-C-glucoside (schaftoside)
	Luteolin R=OH	L-5-O-glucoside (galuteolin) L-8-C-glucoside (orientin) L-6-C-glucoside (iso-orientin)

Flavanones

	R ₁	R ₂	R ₃	
	H	H	OH	Naringenin
	H	OH	OH	Naringin
	H	OCH ₃	OH	Eriodyctiol
	H	OH	OCH ₃	Eriocitrin
				Homocriodyctiol
				Hesperetin
				Neohesperidin
				Hesperidin



Amentoflavone

Figure 5 Flavonoids.

Table 3 Plant flavonoids: eluents

<i>Plant</i>	<i>Eluents</i>	<i>Compounds</i>
Arnica (<i>Arnica montana</i>)	Ethyl acetate–glacial acetic–formic acid–water (100 : 11 : 11 : 26)	Quercetin-3-O-glucoside and 3-O-glucogalacturonide, luteonin-7-O-glucoside, kaempferol-3-O-glucoside
Ginkgo leaves (<i>Ginkgo biloba</i>)	Ethyl acetate–glacial acetic–formic acid–water (100 : 11 : 11 : 26) Chloroform–acetone–formic acid (75 : 16.5 : 8.5) Toluene–acetone (70 : 30)	Quercetin, kaempferol and isorhamnetin glycosides: flavonol acylglycosides Biflavonoids: amentoflavone, bilobetin, ginkgoetin, isoginkgoetin Ginkgolides a, b, c, catechin and epicatechin
Acacia flowers (<i>Robinia pseudoacacia</i>)	Ethyl acetate–formic acid–glacial acetic acid–water (100 : 11 : 11 : 26)	Kaempferol-3-O-rhamnosylgalactosyl-7-rhamnoside (robinin) Acacetin-7-O-rutinoside, acaciin
Roman camomile (<i>Chamaemelum nobile</i>)	Ethyl acetate–formic acid–glacial acetic acid–water (100 : 11 : 11 : 26)	Apigenin-7-O-glycoside, 7-aposil glucoside (apiin) Quercitrin
Marigold flowers (<i>Calendula officinalis</i>)	Ethyl acetate–formic acid–glacial acetic acid–water (100 : 11 : 11 : 26)	Isorhamnetin glycosides Isorhamnetin-3-O-glucoside (narcissin)
Hawthorn flowers, leaves (<i>Crataegus</i> sp.)	Ethyl acetate–formic acid–glacial acetic acid–water (100 : 11 : 11 : 26)	Quercetin glycosides: rutin, hyperoside spiraeoside Flavon-C-glycosides: vitexin, isovitexin rhamnoside
Coltsfoot (<i>Tussilago farfara</i>)	Ethyl acetate–formic acid–glacial acetic acid–water (100 : 11 : 11 : 26)	Quercetin glucosides, rutin, hyperoside isoquercetin
German chamomile flowers (<i>Matricaria chamomilla</i>)	Ethyl acetate–formic acid–glacial acetic acid–water (100 : 11 : 11 : 26)	Flavonoid aglycones, apigenin-7-O-glucoside, luteolin-7-O-glucoside
Meadow-sweet (<i>Filipendula ulmaria</i>)	Ethyl acetate–formic acid–glacial acetic acid–water (100 : 11 : 11 : 26)	Quercetin-4'-O-glucoside (spiraeoside) Hyperoside Kaempferol glycosides
Lime flowers (<i>Tilia</i> sp.)	Ethyl acetate–formic acid–glacial acetic acid–water (100 : 11 : 11 : 26)	Quercetin glycosides: quercitrin, isoquercitrin Kaempferol glycosides
Mullein flowers (<i>Verbascum album</i>)	Ethyl acetate–formic acid–glacial acetic acid–water (100 : 11 : 11 : 26)	Kaempferol, rutine, hesperidin, apigenin
Blackcurrant (<i>Ribes nigrum</i>)	Ethyl acetate–formic acid–glacial acetic acid–water (100 : 11 : 11 : 26)	Quercetin, kaempferol, myricetin and isorhamnetin glycosides
Round-headed bush clover (<i>Lespedeza capitata</i>)	Ethyl acetate–formic acid–glacial acetic acid–water (100 : 11 : 11 : 26)	Flavon-C-glycosides: orientin, iso-orientin, vitexin, isovitexin
Passion flower (<i>Passiflora incarnata</i>)	Ethyl acetate–formic acid–glacial acetic acid–water (100 : 11 : 11 : 26)	Flavon-C-glycosides: isovitexin, vitexin, orientin, iso-orientin Flavon-O-glycosides: rutin, hyperoside, isoquercitrin
Lemon and other Aurantiaceae (<i>Citrus</i> sp.)	Ethyl acetate–formic acid–glacial acetic acid–water (100 : 11 : 11 : 26)	Flavanon glycosides, eriocitrin, naringin, hesperidin
Sophora buds (<i>Sorophora japonica</i>)	Ethyl acetate–formic acid–glacial acetic acid–water (100 : 11 : 11 : 26)	Flavonol glycosides: rutin

Table 4 Plant flavonoids: sorbents/eluents

Plant/sorbent	Eluents ^a	Compounds
Silica gel		
Elm (<i>Ulmus</i> sp.)	Ethyl acetate–formic acid–acetic acid–water (100 : 11 : 11 : 27)	Quercetin glycoside, kaempferol glycoside
<i>Lipocedrus</i>	Chloroform–methanol–formic acid (90 : 10 : 1)	Flavonol glycoside
<i>Calendula officinalis</i> (flowers)	Benzene–methanol–acetic acid (90 : 16 : 8)	Flavonol glycoside
Henry anisetree (<i>Illicium henryii</i>) (root cortex)	Butanol–acetic acid–water–methanol (40 : 20 : 10 : 50)	Flavonoids
<i>Sedum sediform</i>	Toluene–acetone–formic acid (60 : 60 : 12)	Phloroglucinol glycoside
<i>Olea europea</i>	Ethyl acetate–formic acid–water (60 : 10 : 10)	Flavonoids
Polyamide (aglycones)		
<i>Alnus glutinosa</i>	Toluene–petroleum ether–MEK–methanol (50 : 25 : 11 : 13)	Flavonoid aglycones
<i>Keckiella</i>	Benzene–MEK–methanol (80 : 13 : 7)	Flavonoid aglycones
<i>Viguiera</i> sp.	Toluene–MEK–methanol (60 : 25 : 15)	Flavonoid aglycones
Polyamide (flavonoids)		
<i>Lastenia californica</i>	Water–butanol–acetone–dioxane (70 : 15 : 10 : 5)	Flavonoids
<i>Rosa</i> cultivars	Methanol–acetic acid–water (90 : 5 : 5)	Flavonoids
<i>Cleome</i> sp.	Methylene chloride–benzene–methanol (75 : 5 : 5)	Flavonoids
	Benzene–petroleum ether–MEK–methanol (60 : 60 : 7 : 7 or 60 : 30 : 7 : 7)	
	Benzene–MEK–methanol (40 : 30 : 30)	
<i>Illicium henryii</i>	Butanol–acetic acid–methanol–water (40 : 10 : 20 : 50)	Flavonoids

^aMEK = methyl ethyl ketone.

and delphinidin glycosides); hollyhock (*Althea rosea*) (delphinidin-3-glycoside, malvidin-3-glycoside); bilberry (*Vaccinium myrtillus*) (delphinidin-3-glycoside = myrtillin A).

For analysis, anthocyanins must be extracted from plants with solvents containing acetic or hydrochloric acid. Plants are extracted for 15 min with methanol–HCl 25% (9 : 1) and the filtrates are subsequently used for chromatography. For TLC on silica gel, the following eluents are commonly used: ethyl acetate–glacial acetic acid–formic acid–water (100 : 11 : 11 : 26); and n-butanol–glacial acetic acid–water (40 : 10 : 20 or 40 : 10 : 50). Because these compounds are coloured, detection is possible visually without the need for chemical treatment or the developed TLC plates can be sprayed with anisaldehyde–H₂SO₄ reagent.

Anthraquinone glycosides

A number of glycosides with aglycones related to anthracene are present in such drugs as cascara (*Cascara sagrada*), aloes (*Aloe* sp.), alder buckhorn (*Rhamnus frangula*), rhubarb (*Rheum officinalis*) and senna (*Cassia senna*). These drugs are employed as cathartics. On hydrolysis, the glycosides yield aglycones which are di-, tri-, or tetrahydroxy-anthraquinones or derivatives of these compounds (Figure 8). The anthraquinones possess phenolic

groups on C1 and C8 and keto groups on C9 and C10; in the anthrones and anthranol, only C9 carries an oxygen function. Most compounds in this group are present in the plant as O-glycosides. In the O- and C-glycosides, the only sugars found are glucose, rhamnose and apiose.

Prior to TLC, the powdered plant material is extracted for 5 min with methanol (1 g of plant in 100 mL) then filtered. It is necessary to hydrolyse the extract to characterize the aglycones and for this 1 g of powder plant is heated under reflux with X mL 7.5% hydrochloric acid for 15 min. After cooling, the mixture is extracted by shaking with X mL of chloroform or ether. The organic phase is then taken and concentrated to about 1 mL, and then used for TLC. Chromatography is performed on silica gel precoated plates with light petroleum–ethyl acetate–formic acid (75 : 25 : 1) or ethyl acetate–methanol–water (100 : 13.5 : 10) for all anthracene drug extracts except for senna. In this case, n-propanol–ethyl acetate–water–glacial acetic acid (40 : 40 : 29 : 1) is used.

For the non-laxative dehydrodianthrones of St John's wort (*Hypericum perforatum*) (Figure 8), TLC is performed with the eluent toluene–ethyl formate–formic acid (50 : 40 : 10).

Following TLC, all anthracene derivatives can be readily detected because they quench fluorescence

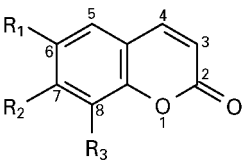
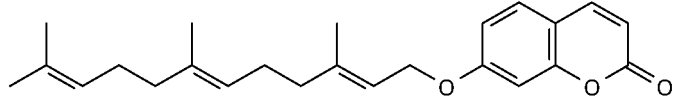
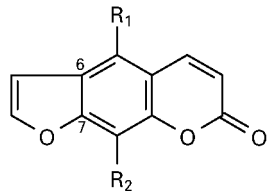
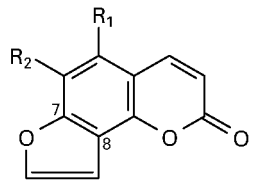
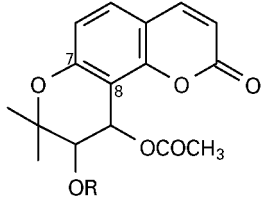
	R ₁	R ₂	R ₃	
	H	H	H	Coumarin
	H	OH	H	Umbelliferone
	OH	OH	H	Aesculetin
	OCH ₃	OH	H	Scopoletin
	OCH ₃	OH	OH	Fraxetin
	OCH ₃	OH	OCH ₃	Isofraxidin
	OCH ₃	OH	O-gluc	Fraxin
 Umbelliprenin				
7,6-Furanocoumarins	R ₁	R ₂		
	H	H		Psoralen
	H	OCH ₃		Xanthotoxin
	H	OH		Xanthotoxol
	OCH ₃	H		Bergapten
7,8-Furanocoumarins	R ₁	R ₂		
	H	H		Angelicin
	OCH ₃	H		Isobergapten
Pyranocoumarins	R			
	—CO—CH=C(CH ₃) ₂			Samidin
	—CO—CH ₂ —CH(CH ₃) ₂			Dihydrosamidin
	—CO—CH—C ₂ H ₅			Visnadin
	CH ₃			

Figure 6 Coumarins.

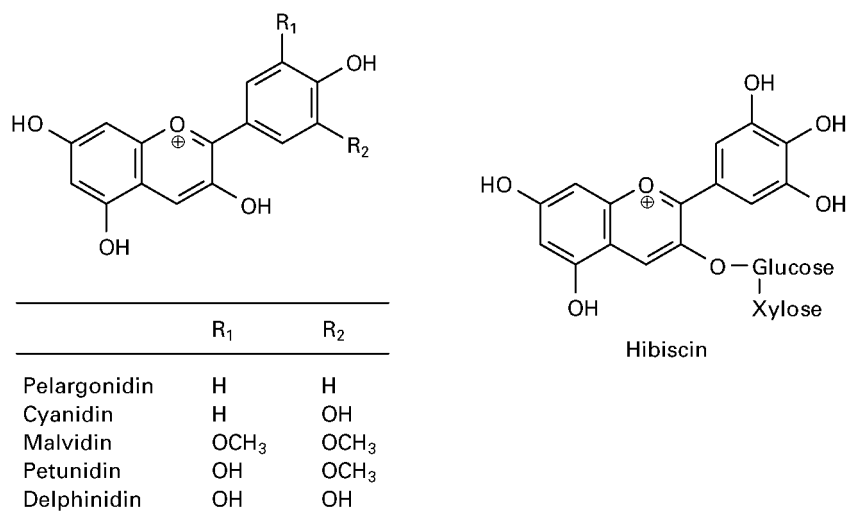


Figure 7 Anthocyanins.

when irradiated at UV 254 nm and give yellow or red-brown fluorescence. Different specific reagents are also used for detection (see the Appendix). Thus anthraquinone appears red in the visible after spraying with KOH. With NP/PEG, anthrones and anthranones give intense yellow fluorescence when irradiated at 365 nm. For the characterization of senosides, the TLC plate is sprayed with HNO₃ and then heated for 10 min at 120°C. Before spraying with ethanolic KOH, these appear brown-red in UV 365 nm and brown in visible light. Hypericin gives red fluorescence when irradiated at 365 nm.

Cardiac glycosides

There are some steroids present in nature, known as the cardiac glycosides, which are characterized by the highly specific and powerful action that they exert upon cardiac muscle. These steroids occur as glycosides with sugars in the 3-position of the steroid nucleus. The steroid aglycones or genins are of two types, either a cardenolide or a bufadienolide.

The steroids are structurally derived from the tetracyclic 10,13-dimethylcyclopentanoperhydrophenanthrene ring system. They possess a γ -lactone ring for the cardenolide or a δ -lactone ring for the bufadienolide attached in the position at C17. The sugar residues are derived from deoxy- and/or C3-O-methylated sugars, and they are linked glycosidically by the C3-OH groups of the steroid aglycones (Figure 9). The main plants containing cardenolides are white foxglove (*Digitalis lanata*), red foxglove (*Digitalis purpurea*), oleander (*Nerium oleander*), strophanthus (*Strophanthus gratus*; *Strophanthus kombe*), adonis (*Adonis vernalis*) and lily of the valley (*Convallaria majalis*). The main plants containing bufadienolides

are hellebores (*Helleborus* sp.) and squill (*Urginea maritima*).

For analysis, 1–10 g of powered plant is extracted by heating for 15 min under reflux with 20 mL 50% ethanol, with the addition of 10 mL 10% lead(II) acetate solution. After cooling and filtration, the solution is extracted twice with 15 mL dichloromethane. The combined lower organic phases are then filtered over anhydrous sodium sulfate and evaporated to dryness. The residue is dissolved in 1 mL of dichloromethane-ethanol (1 : 1) and the solution obtained is used for chromatography.

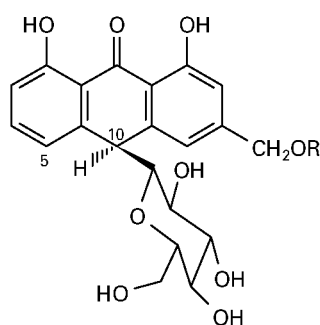
The TLC of the cardiac glycosides is accomplished on silica gel with the following solvents: ethyl acetate-methanol-water (100 : 13.5 : 10) or (81 : 11 : 8) and ethyl acetate-methanol-ethanol-water (81 : 11 : 4 : 8); and the lower phase of chloroform-methanol-water (35 : 25 : 10) for Hellebore bufadienolides.

The separated analytes can be detected under UV light at 254 nm as there is weak fluorescence quenching for cardenolides which is more distinct for bufadienolides. Spray reagents for detection include antimony chloride in chloroform and heating at 100°C, chloramine T, sulfuric acid and Kedde reagent (see the Appendix).

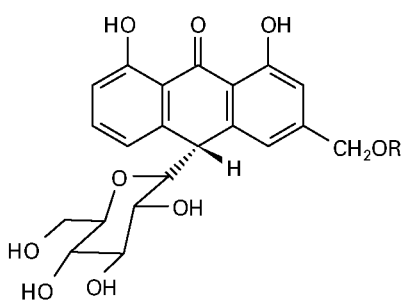
Saponins

The formation of persistent foams during the extraction or concentration of plant extracts indicates the presence of saponins. The saponins are mainly triterpene derivatives, with similar amounts of steroid present. The most important plants are described in Table 5. Ginseng roots (*Panax ginseng*) contain triterpene glycosides: the ginsenosides a, b, c, d, e, f,

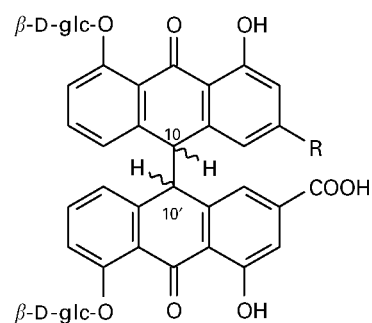
Anthraquinone glycosides



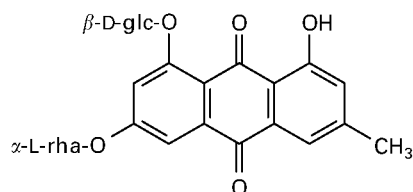
R=H, aloine A
R=α-L-Rha, aloinoside A



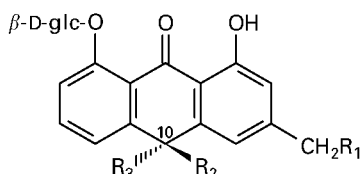
R=H, aloine B
R=α-L-Rha, aloinoside B



R	C-10	C-10'	
COOH	R	R	sennoside A
COOH	R	S	sennoside B
CH ₂ OH	R	R	sennoside C
CH ₂ OH	R	S	sennoside D

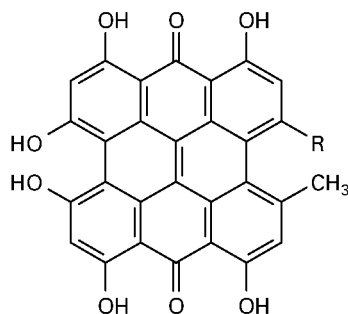


Glucofranguloside A



R₁=OH, R₂=β-D-gluc, R₃=H, cascaroside A
R₁=OH, R₂=H, R₃=β-D-gluc, cascaroside B
R₁=H, R₂=β-D-gluc, R₃=H, cascaroside C
R₁=H, R₂=H, R₃=β-D-gluc, cascaroside D

Dehydrodianthrone



R=CH₃, hypericine
R=CH₂OH, pseudohypericine

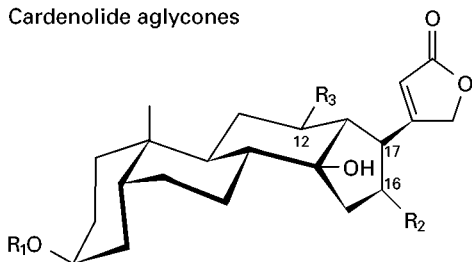
Figure 8 Anthraquinones.

g, h. Horse chestnuts (*Aesculus hippocastanum*) contain the pentacyclic triterpenes glycosides aescine and aescinol, liquorice roots (*Glycyrrhiza glabra*) contain saponins aglycone from the glycyrrhetic acid, milkwort

root (*Polygala senega*) triterpene ester saponins 'senegenines', red soapwood root (*Saponaria officinalis*) triterpene saponins, Indian pennywort (*Centella asiatica*) asiaticoside A, B, 'madecassoside'

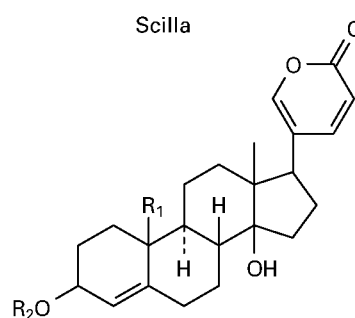
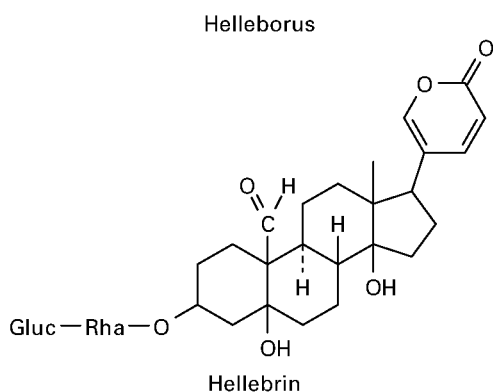
Cardenolides

<i>Digitalis lanatae</i> and <i>Digitalis purpureae</i>		R ₁	R ₂	R ₃
Cardenolide aglycones	Digitoxigenin	H	H	H
	Gitoxigenin	H	OH	H
	Digoxigenin	H	H	OH
	Diginatigenin	H	OH	OH
	Gitaloxigenin	H	O—CHO	H



	R ₁	R ₂	R ₃	
 <i>Adonis</i>	OH	H	CHO	K-Strophanthidin (S)
	H	OH	CHO	Adonitoxigenin (A)
	H	OH	CH ₂ OH	Adonitoxigenol (-rhamnoside)
	OH	OH	CHO	Strophadogenin (-diginoside)
<i>Strophanthus</i>	OH	H	CHO	Cymar (S-cymaroside), helveticoside (S-β-D-digitoxide)
				k-Strophanthidin (S) Erysimoside (S-digitoxoside-glucoside), k-strophanthin-β, k-strophanthoside

Bufadienolides



	R ₁	R ₂
Scillarenin	CH ₃	H (Aglycon)
Proscillaridin A	CH ₃	Rham
Scilliphaeoside	H	Rham
Scillaren A	CH ₃	Gluc-Rham
Glucoscillaren A	CH ₃	Gluc-Gluc-Rham

Figure 9 Cardiac glycosides.

Table 5 Saponosids

Plants	Eluents	Reagents	Compounds
Ginseng roots (<i>Panax ginseng</i>)	Chloroform-methanol-water (70 : 30 : 40) Butanol-ethyl acetate-water (40 : 10 : 10)	Vanillin-phosphoric acid gives red zones in the visible and red; fluorescence in UV 365 nm Sulfuric acid then heated 110°C, 7 min	Triterpene glycosides, ginsenosides Rx (x = a, b ₁ , b ₂ , d, e, f, g ₁ , h) Derived from dammarane (protopanaxatriol, panaxadiol)
Eleutherococcus roots (<i>Eleutherococcus senticosus</i>)	1,2-Dichloroethane- ethanol-methanol-water (65 : 22 : 22 : 7)	Vanillin-sulfuric acid detection at UV 285 nm	Triterpenes: eleutherosides
Liquorice roots (<i>Glycyrrhiza glabra</i>)	Chloroform-glacial acetic acid-methanol-water (60 : 32 : 12 : 8) Ethyl acetate-ethanol-water- ammonia (65 : 25 : 9 : 1)	Anisaldehyde-sulfuric acid	Saponosids: glycyrrhizin, glycyrrhizic acid Aglycone: glycyrrhetic acid
Milkwort roots (<i>Polygala senega</i>)	Chloroform-glacial acetic acid-methanol-water (60 : 32 : 12 : 8)	Anisaldehyde-sulfuric acid: five red saponin zones	Triterpene ester saponins = senegenins
Red soapwood (<i>Saponaria officinalis</i>)	Chloroform-glacial acetic acid-methanol-water (60 : 32 : 12 : 8)	Anisaldehyde-sulfuric acid give six violet zones and one brown band	Triterpene saponins derived from gypsogenin (quillaic acid)
Butcher's broom (<i>Ruscus aculeatus</i>)	Chloroform-glacial acetic acid-methanol-water (60 : 32 : 12 : 8)	Anisaldehyde-sulfuric acid: six to eight yellow or green bands	Steroid saponins = neoruscogenin glycosides Aglycones: ruscogenin and neoruscogenin
Sarsapilla (<i>Smilax</i> sp.)	Chloroform-glacial acetic acid-methanol-water (60 : 32 : 12 : 8)	Anisaldehyde-sulfuric acid: six yellow-brown saponins	Steroid saponins: smilax saponin, spirostanol-saponin Aglycones: sarsapogenin and its isomer smilagenin
Indian pennywort (<i>Centella asiatica</i>)	Chloroform-glacial acetic acid-methanol-water (60 : 32 : 12 : 8)	Anisaldehyde-sulfuric acid: violet-blue in fluorescence. Brown-violet zone	Esters saponins Madecassoside, a mixture of asiaticoside A and B
Soap bark (<i>Quillaja saponaria</i>)	Chloroform-glacial acetic acid-methanol-water (60 : 32 : 12 : 8)	Anisaldehyde-sulfuric acid: brown-to-violet zones	Quillaja saponins constitute a mixture of hydroxy gypsogenins
Horse chestnut seeds (<i>Aesculus hippocastanum</i>)	Chloroform-glacial acetic acid-methanol-water (60 : 32 : 12 : 8) Propanol-ethyl acetate-water (40 : 30 : 30)	Anisaldehyde-sulfuric acid gives main blue-violet-black of aescins Iron(III) chloride at UV 540 nm	Pentacyclic triterpene glycosides, aescine, aescinol β -Aescine

and soap bark (*Quillaja saponaria*) quillaja saponins (Figure 10).

Steroid saponins are present in Butcher's broom (*Ruscus aculeatus*) like ruscogenin and *Sarsaparilla* *smilax* sp. smilax saponins.

In order to obtain a suitable sample for TLC the plant powder is extracted by heating for 10 min under reflux with 10 mL of 70% ethanol. After filtration

and evaporation, this solution is used for TLC. Ginseng radix is extracted with 90% ethanol under the same conditions.

Chromatographic solvents for the separation of these compounds on silica gel include chloroform-glacial acetic acid-methanol-water (64 : 32 : 12 : 8) which is suitable for separation of numerous saponin mixtures. For ginsenosides

chloroform-methanol-water (70 : 34 : 4) is used whilst ethyl acetate-ethanol-water-ammonia (65 : 25 : 9 : 1) is useful for glycyrrhetic acid.

Once separated, the various analytes can be seen by inspection under UV light at 254 or 365 nm for glycyrrhizin and glycyrrhetic acid. Spraying with vanillin-sulfuric acid reagent gives a range of colours for the saponins in the visible spectrum mainly blue, blue-violet and sometimes red and yellow-brown zones. The anisaldehyde-sulfuric acid reagent gives the same colours as vanillin. Vanillin-phosphoric acid reagent with ginsenosides gives red-violet colours in the visible spectrum, and reddish or blue fluorescence when viewed under UV light at 365 nm.

Essential Oils

Essential oils are the odorous principles found in various plant parts (Table 6) because they evaporate when exposed to the air at room temperature, they are called 'volatile oils', 'ethereal oils' or 'essential oils'; the last term is applied since volatile oils represent the 'essences' or odoriferous constituent of the plants. Odorous principles consist either of (a) terpenes, i.e. alcohols (borneol, geraniol, linalool, menthol), aldehydes (anisaldehyde, citral), ketones (carvone fenchone, menthone, thujone), esters (bornyl acetate, linalyl acetate, menthyl acetate oxides, 1,8-cineole) or (b) phenylpropane derivatives i.e. anethole apiole, eugenol and safrole (Figure 11). Es-

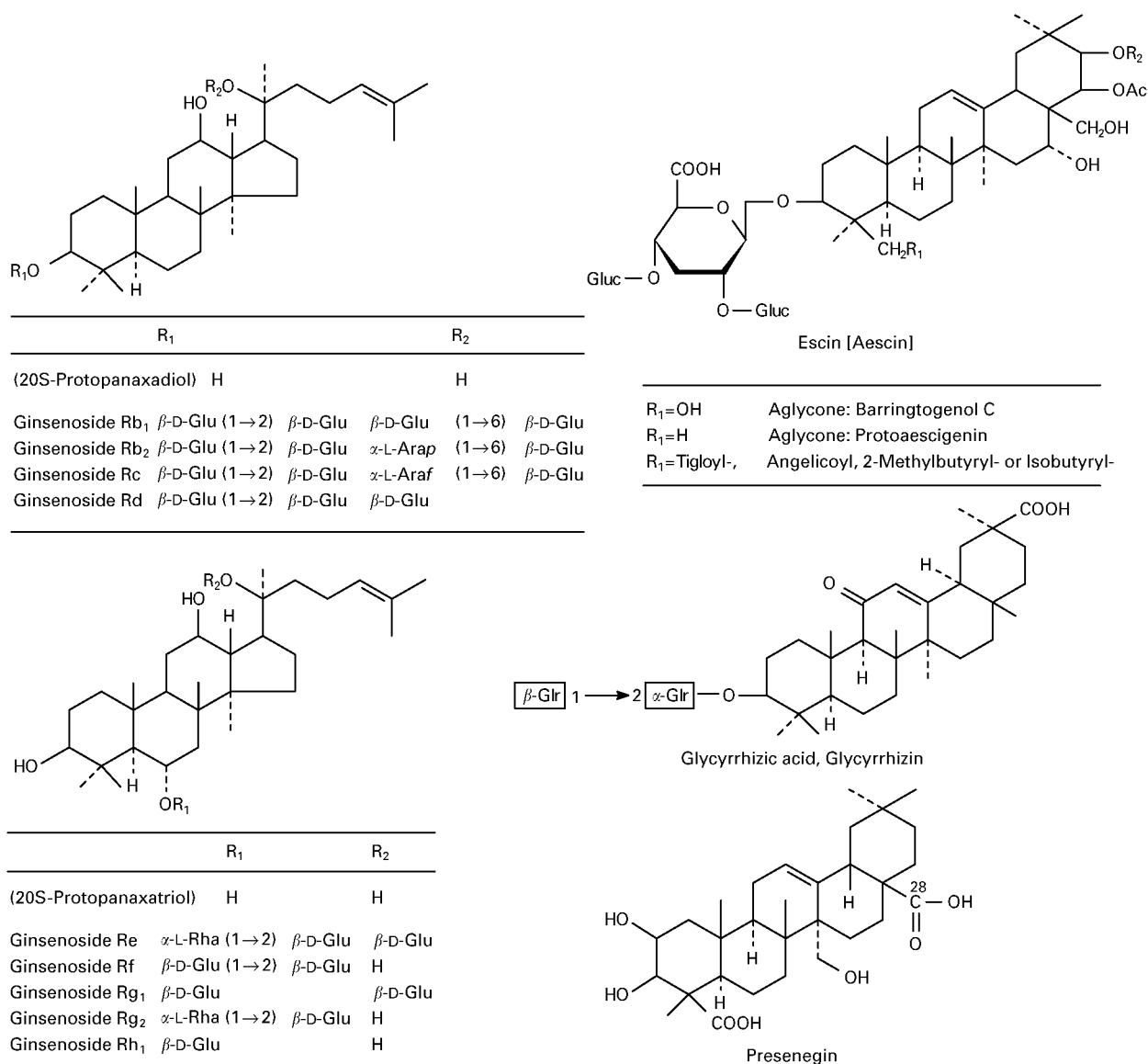


Figure 10 Saponins.

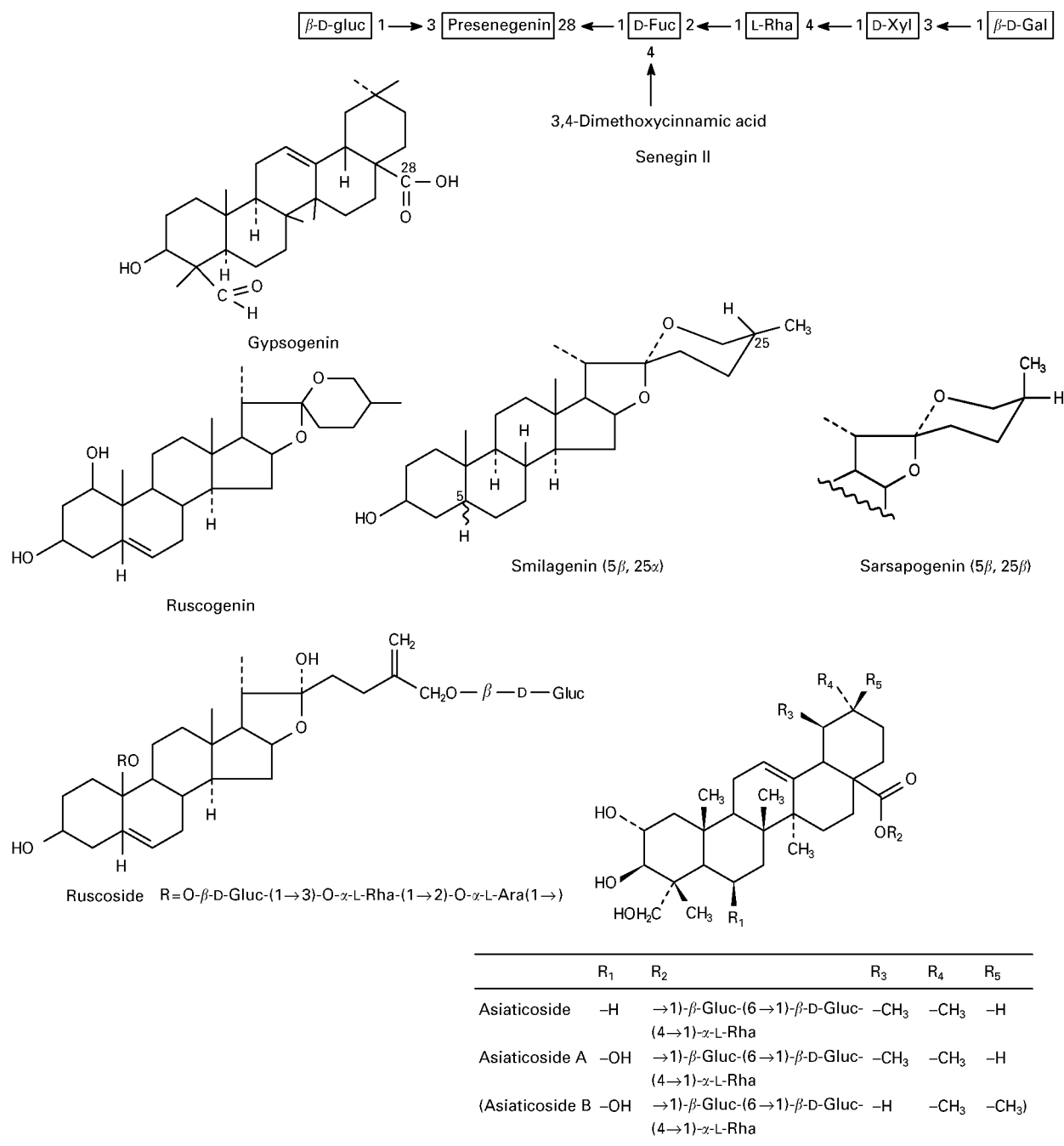


Figure 10 Continued.

essential oils are soluble in ethanol and toluene and are mostly obtained by steam distillation of plant material.

For the preparation of extracts, a micro-steam distillation method is used to obtain the essential oil; a standard method is described in some pharmacopoeias. The essential oil is recovered in toluene or xylene and constitutes the sample to be analysed by TLC, but it is also possible to isolate it with hexane, ether or acetone.

Silica gel is the most widely used sorbent for the essential oils, with solvents such as benzene or toluene, chloroform, methylene chloride ethyl acetate for development. Because of its toxicity, however, benzene can no longer be recommended as a solvent for TLC. The eluent toluene-ethyl acetate (93 : 7) is suitable for the analysis and comparison of all of the important essential oils. Different eluents can be employed in special cases, e.g. toluene (*Pimpinella*

Table 6 Essential oils

<i>Plant family</i>	<i>Plants</i>	<i>Main compounds</i>	<i>Colour with vanillin-sulfuric acid</i>
Apiaceae	Anise (<i>Pimpinella anisum</i>)	<i>Trans</i> -anethole	Red-brown
	Fennel seed (<i>Foeniculum vulgare</i>)	<i>Trans</i> -anethole	Red-brown
	Parsley fruits (<i>Petroselinum crispum</i>)	Apiol	Violet-brown
		Myristin	Violet-brown
	Caraway fruits (<i>Carvum carvi</i>)	Carvone	Red-violet
	Coriander fruits (<i>Coriandrum sativum</i>)	Linalool	Blue
Asteraceae	Camomile flowers (<i>Chamomilla reticula</i>)	Chamazulene	Red-violet
		Bisabolol	Violet
	Roman camomile (<i>Chamaemelum nobile</i>)	Easters of angelicin	Grey-violet
	Worm seed (<i>Artemisia cina</i>)	1,8-cineole, thujone	Blue
Lamiaceae	Peppermint leaves (<i>Mentha</i> sp.)	Menthol	Blue
		Menthone	
	Rosemary leaves (<i>Rosmarinus officinalis</i>)	1,8-cineole	Green
		Borneol, pinene, camphene	Blue
	Lemon balm (<i>Melissa officinalis</i>)	Citronellal	Blue-violet
		Citral	Black-blue
		Citronellol	Violet-blue
			Black-blue
	Lavander flowers (<i>Lavandula officinalis</i>)	Linalool	Blue
		Nerol	Blue
		Borneol	Blue-violet
	Basil (<i>Ocinum basilicum</i>)	Methyl chavicol	Red
	Thyme (<i>Thymus vulgaris</i>)	Thymol	Red-violet
		Carvacrol	Red
		Linalool	Blue
	Sage leaves (<i>Salvia officinalis</i>)	Thujone	Pink-violet
		1,8-Cineole	Blue
		Borneol	Blue-violet
	Greek sage (<i>Salvia triloba</i>)	1,8-Cineole	Blue
		Thujone	Pink-violet
Lauraceae	Cinnamon bark (<i>Cinnamomum zeylanicum</i>)	Cinnamaldehyde	Grey-blue
	Chinese cinnamon (<i>Cinnamomum aromaticum</i>)	Cinnamaldehyde	Grey-blue
Myrtaceae	Cloves (<i>Syzygium aromaticum</i>)	Eugenol	Yellow-brown
	Blue gum leaves (<i>Eucalyptus globulus</i>)	1,8-Cineole = eucalyptol	Blue
Rutaceae	Bitter orange peel (<i>Citrus aurantium</i> sp.)	Limonene	Grey-violet
		Citral	Blue-violet
	Bergamot (<i>Citrus aurantium</i> var. <i>amara</i>)	Limonene	Grey-violet
		Citral	Blue-violet
	Orange flowers (<i>Citrus sinensis</i>)	Linalyl acetate	Blue
		Linalool	Blue
	Lemon peel (<i>Citrus limon</i>)	Limonen	Grey-violet
		Citral	Violet-blue

anisum), chloroform (*Melissa officinalis*), methylene chloride (*Pimpinella*, *Juniperus*, *Lavandula*, *Rosmarinus*, and *Salvia*), toluene-ethyl acetate-

(*Eucalyptus*, *Mentha*), chloroform-toluene (75 : 25) for *Thymus vulgaris* and *Chamomilla recutita* (Table 2).

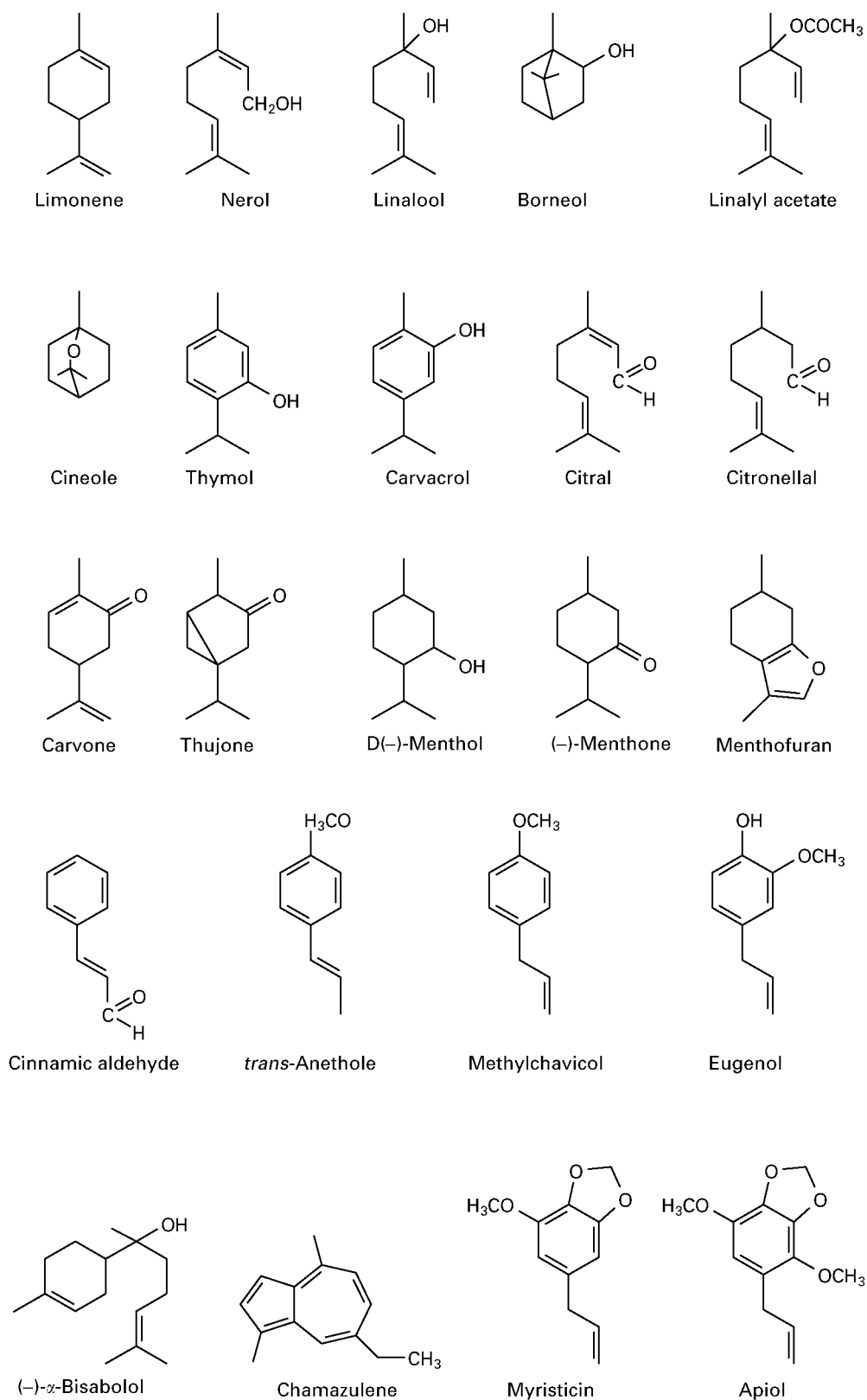


Figure 11 Essential oils.

Under UV light at 254 nm, compounds containing at least two conjugated double bonds quench fluorescence and appear as dark zones against the light-green fluorescent background of the TLC plate. This is the case for the derivatives of phenylpropane (anethole, safrole, apiol, myristicin, eugenol) and compounds such as thymol. The spraying reagents that can be used for the essential oils are (see Appendix) anisaldehyde-sulfuric acid, which gives blue, green, red and brown coloration, and phosphomolybdic acid, which gives uniform blue zones on a yellow background. However, the reagent most widely used for these compounds is vanillin-sulfuric acid which gives a range of different colours (Table 6).

Cannabinoids

The cannabinoids are found in Indian hemp (marihuana; *Cannabis sativa* var. *indica*) (Figure 12). The cannabinoids are benzopyran derivatives but only $\Delta^9,10$ -tetrahydro cannabinol (THC) shows hallucinogenic activity. The type and quantity of the constituents present in the plant depends on the geographical origin and climatic conditions. Marihuana is the flowering or seed-carrying, dried branch tips of the female plant. Hashish is the resin from the leaves and flower of the female plant. The most important cannabinoids are cannabidiol, cannabidiol acid, cannabinol, and Δ^9 -THC.

For chromatography, the powdered plant material is extracted with chloroform or hexane and separation can be performed on silica gel TLC plates with hexane-diethyl ether (80 : 20) or hexane-dioxane (90 : 10).

The cannabinoids can be detected by irradiation under UV (254-nm) light as they show fluorescence quenching. With the Fast blue reagent the cannabinoids form violet-red, orange-red or carmine zones; standard thymol gives an orange zone.

Valepotriates

The main active constituents of these drugs, the valepotriates are triesters of a terpenoid, trihydric alcohol. This alcohol has the structure of an iridoid cyclopentanopyran with an attached epoxide ring. Valepotriates are present in valerian rhizome (*Valeriana officinalis*). The drug is extracted with dichloromethane at 60°C then filtered and evaporated to dryness. The chromatographic system is silica gel with toluene-ethyl acetate (75 : 25) or n-hexane-methyl ethyl ketone (80 : 20) as eluents. Under UV light (254 nm) they give a yellow fluorescence and in the visible region with the dinitrophenylhydrazine reagent, after heating, green-grey or blue zones appear. The valepotriates characterized in this way are valtrate, isovaltrate, and acevaltrate.

Bitter Principles

The bitter principles are other compounds in plants which can be characterized by TLC. Plants with bitter principles include gentian, hops, condurango, artichoke and bryony root. Most of them possess a terpenoid structure and can be characterized in TLC with ethyl acetate-methanol-water (77 : 15 : 8) and then derivatization with vanillin-sulfuric reagent. However, these compounds are less important

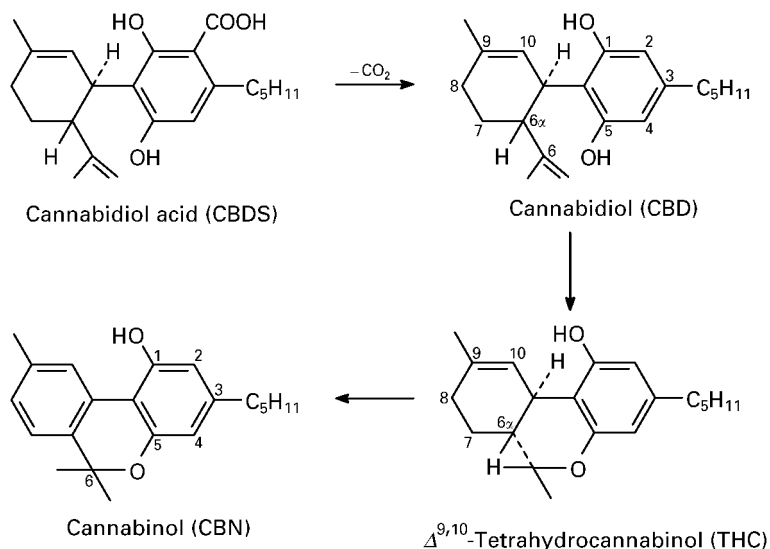


Figure 12 Cannabinoids.

than the compounds mentioned elsewhere in this chapter.

Conclusion

TLC has many advantages for the analysis of herbal products, especially phytopharmaceuticals, for the identification of plants and the quantification of certain marker substances. Planar chromatography has advantages because it allows a parallel evaluation and comparison of multiple samples. In addition, various chromatographic separation systems can be combined with a multitude of specific and non-specific derivatizing agents. Even in samples having complex matrixes such as the pharmaceutical preparations of extracts of plants, sample preparation can be kept simple because of the use of the stationary phase for only one analysis. Unlike column chromatography, contamination of the chromatographic system by carryover cannot occur. In many instances the chemical composition of the herb is not completely known and for many plants, there are often no established methods of analysis available so that a rapid screening technique like TLC is very valuable. Constituents of herbals that belong to very different classes of chemical compounds can often create difficulties in detection, but with this in mind, TLC can offer many advantages.

See Colour Plates 105, 106.

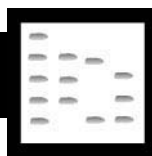
See also: III/**Alkaloids:** High Speed Counter Current Chromatography; Liquid Chromatography; Thin-Layer (Planar) Chromatography. **Citrus Oils:** Liquid Chromatography. **Essential Oils:** Distillation; Gas Chromato-

graphy; Thin-Layer (Planar) Chromatography. **Pigments:** Liquid Chromatography; Thin-Layer (Planar) Chromatography. **Terpenoids:** Liquid Chromatography. **Appendix 17/Thin-Layer (Planar) Chromatography: Detection.**

Further Reading

- Anonymous (1998) Camag bibliography service. CD ROM. Muttentz, Switzerland: Camag.
- Baerheim Svendsen A and Verpoorte R (1983) *Chromatography of Alkaloids. Part A: Thin Layer Chromatography*. Elsevier: Amsterdam.
- Bruneton J (1999) *Pharmacognosy, (Phytochemistry Medicinal Plants)*, 2nd edn. Paris: Tec and Doc.
- Fried B and Sherma J (1994) *Thin Layer Chromatography: Technique and Applications*. New York: Marcel Dekker.
- Fried B and Sherma J (1996) *Practical Thin Layer Chromatography*, pp. 31–47. Boca Raton: CRC Press.
- Geiss F (1987) *Fundamentals of Thin Layer Chromatography*. Heidelberg: Hüthig.
- Harbone JB (1973) *Phytochemical Methods. A Guide to Modern Techniques of Plant Analysis*. London: Chapman and Hall.
- Jork H, Funk W, Fisher W and Wimmer H (1990) *Thin Layer Chromatography Reagents and Detection Methods*, Vol 1a. Weinheim: VCH.
- Randerath K (1967) *Dünnschicht Chromatographie*, 2nd edn. Berlin: Springer Verlag.
- Stahl E (1967) *Dünnschicht Chromatographie*, 2nd edn. Berlin: Springer Verlag.
- Touchstone J (1992) *Practical Thin Layer Chromatography*, 3rd edn. London: John Wiley.
- Wagner K, Bladt S and Zgainski EM (1966) *Plant Drug Analysis*. Berlin: Springer Verlag.
- Wichtl M (1994) *Herbal Drugs and Pharmaceuticals*. Boca Raton: CRC Press.

NEUROTOXINS: CHROMATOGRAPHY



K. J. James and A. Furey, Cork Institute of Technology, Cork, Ireland

Copyright © 2000 Academic Press

Chromatography has had a major impact on the discovery and detection of potent, naturally occurring neurotoxins. The neurotoxins discussed in this article were selected because they significantly impact on human health as a result of intoxications from bites and stings or the consumption of contaminated food and water. Many of these toxins target receptors that have implications for the development of potential therapeutic agents. In the neurotoxin topics that have

been highlighted here, the role of chromatography in toxin discovery, purification and analysis is emphasized.

Neurotoxins from Marine and Freshwater Algae

It was only in the latter part of the 20th century that scientists appreciated that certain species of microalgae can cause sporadic toxic events that can lead to serious illness, with occasional deaths, in humans as well as farmed and domestic animals. When high populations of toxin-producing microalgae occur

Table 1 Representative neurotoxins that are found in microalgae and marine food

<i>Toxin</i>	<i>Toxin potency, LD₅₀ µg kg⁻¹</i>	<i>Poisoning syndrome</i>	<i>Food type</i>	<i>Typical LC method</i>
Saxitoxin	3	Paralytic shellfish poisoning (PSP)	Shellfish, freshwaters	LC-FL
Azaspiracids	140–200	Azaspiracid poisoning (AZP)	Shellfish	LC-MS
Anatoxin-a	200	'Very fast death factor'	Freshwaters	LC-UV, LC-FL
Anatoxin-a(s)	20	–	Freshwaters	LC-MS
Tetrodotoxin	8	Puffer fish poisoning	Puffer fish, crabs	LC-FL
Brevetoxin-a	95	Neurological shellfish poisoning (NSP)	Shellfish	LC-UV
Ciguatoxin	0.45	Ciguatera	Finfish	LC-MS

LD₅₀, lethal dose at 50% mortality, for 14–20 g mouse, when delivered intraperitoneally (IP).

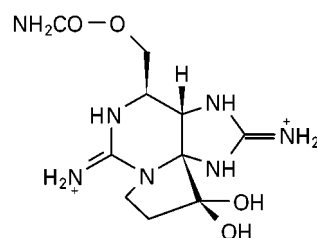
they are termed harmful algal blooms (HABs) and there is compelling evidence to suggest that there is a global increase in the frequency of such events. Molluscs are the marine animals most susceptible to this toxicity, especially the filter-feeding varieties such as mussels, clams, scallops and oysters, which accumulate these toxins to hazardous concentrations. However, potent neurotoxins can also occur in finfish, toxins can accumulate in food plants, while skin absorption of toxins from bacteria is also possible. The comparative potencies of the main neurotoxins that are found in microalgae and marine food are shown in **Table 1**. Their high toxicities, together with the worldwide occurrence of these toxins, have led to a requirement for sensitive analytical methods for their determination. Ciguatoxin is a lipid-soluble toxin and occurs in the flesh of finfish in tropical and subtropical waters. It exerts its effect by activating voltage-dependent sodium channels, producing both gastrointestinal and neurological symptoms with occasional fatalities. Other neurotoxins that act on sodium channels include (1) tetrodotoxin, first discovered in puffer fish, (2) saxitoxin, responsible for paralytic shellfish poisoning (PSP) and (3) brevetoxins, responsible for neurological shellfish poisoning (NSP). A new human toxic syndrome, azaspiracid shellfish poisoning (AZP), which is caused by the consumption of mussels, has recently been identified in Europe. Cyanobacteria (blue-green algae) can produce both hepatotoxins and neurotoxins and represent a serious hazard because of their contamination of freshwater lakes and reservoirs used by animals and for human consumption. Anatoxin-a is the most common neurotoxin in freshwaters but PSP toxins have also been reported. Chromatography continues to play an important role, not only in the discovery of neurotoxins, but also in the development of analytical methods that are used for their quantitative determination for regulatory control and for forensic investigation of intoxications. Highly sensi-

tive chromatographic detection methods, especially using fluorescence (liquid chromatography–fluorescence, LC-FL) and mass spectrometry (liquid chromatography–mass spectrometry, LC-MS), have been particularly important and have been critical for the identification of the microalgae responsible for producing specific neurotoxins.

Neurotoxins from Cyanobacteria (Blue-Green Algae)

There have been reports since the 19th century of animal mortalities associated with drinking water contaminated by cyanobacteria. These phenomena have occurred throughout the world and have been attributed to both hepatotoxic microcystins and to neurotoxins which are produced by some species of cyanobacteria. There are three classes of neurotoxins that are commonly found in cyanobacteria: (1) saxitoxin and analogues, (2) anatoxin-a(s), (3) anatoxin-a and analogues. These compounds are shown in **Figures 1–3**.

Saxitoxin and analogues The most spectacular neurotoxic event due to cyanobacteria occurred in Australia in 1991 when a toxic bloom in the Darling river resulted in the deaths of 1600 sheep and other animals. These intoxications were attributed mainly to neurotoxins belonging to the saxitoxin group, which were previously identified as PSP toxins. These toxins are discussed elsewhere. The investigation of

**Figure 1** Saxitoxin.

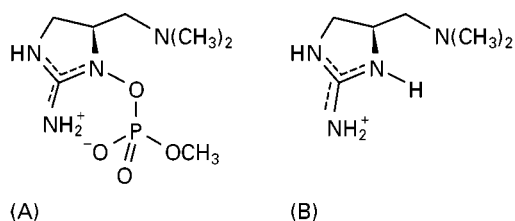


Figure 2 (A) Anatoxin-a(s), m/z 253.1; (B) fragment ion, m/z 143.1.

these events relied heavily on the application of the fluorimetric high performance liquid chromatography (HPLC) method (LC-FL) for saxitoxins, developed by Oshima. This method uses paired ion reagents with three sets of isocratic reversed-phase chromatographic conditions to separate 18 analogues, which are detected by post-column oxidation and form highly fluorescent products. In addition to the PSP toxins that have previously been identified in shellfish, a number of new PSP analogues have recently been isolated from cyanobacteria.

Anatoxin-a(s) Anatoxin-a(s) is a unique organophosphate toxin and it is a potent cholinesterase inhibitor. This neurotoxin has been identified in cyanobacteria in North America and in Europe where it has been fatal to dogs and birds. However, this toxin is difficult to detect as the chromatographic sensitivity using ultraviolet light (LC-UV) is very poor and it is probably more widespread in nature than has so far been discovered. Anatoxin-a(s) is unstable, particularly at slightly basic pH, but has been determined using fast atom bombardment-mass spectrometry (FAB-MS). However, even a 'soft' ionization technique

such as electrospray LC-MS produces mainly the fragment ion at m/z 143.1 (Figure 2B), due to loss of the phosphate moiety. Fortunately, this ion is sufficiently characteristic to allow the screening of water and algae samples for the presence of anatoxin-a(s).

Anatoxin-a and analogues Anatoxin-a (Figure 3A, R = CH₃) was the first cyanobacterial toxin to be structurally elucidated and it is a potent nicotinic agonist which acts as a depolarizing neuromuscular blocking agent. Typical symptoms in animals include muscle fasciculations, gasping and convulsions, with death due to respiratory arrest within minutes after drinking contaminated water. In fact, fatalities to animals, including cattle and dogs, were so rapid that before the identification of anatoxin-a this toxin was referred to as 'very fast death factor'. A related toxin, homoanatoxin-a (Figure 3A, R = C₂H₅), was isolated recently in Norway.

Several chromatographic methods are available for the analysis of anatoxin-a in cyanobacterial bloom material, including LC-UV and LC-MS using electrospray ionization. Derivatizations of anatoxins, followed by gas chromatography (GC) with electron capture or MS detection have also been successful. A highly sensitive LC-FL method has been developed by the authors for the determination of anatoxin-a, using derivatization with 4-fluoro-7-nitro-2,1,3-benzoxadiazole (NBD-F). This has been applied to the analysis of the anatoxins and their degradation products, the dihydro (Figure 3B) and epoxy (Figure 3C) analogues, which result from the reduction or oxidation of the alkene moiety. These degradation products are not detected by the commonly used LC-UV method as they do not have the α,β -unsaturated ketone that is present in the parent toxins.

The determination of anatoxin-a in raw waters poses greater analytical problems mainly due to the low natural concentration of this toxin. However, Harada has developed an efficient solid-phase extraction (SPE) procedure in which anatoxin-a and analogues are efficiently extracted from water using a weak cation exchange phase. After trapping the anatoxins on the SPE cartridge, which is washed with methanol-water, they are readily eluted using acidic methanol since they are basic compounds. All of these anatoxins can be derivatized by reaction with NBD-F (Figure 4), at room temperature for several minutes, to produce highly fluorescent products that are readily separated using isocratic reversed-phase LC-FL. A typical chromatogram showing the separation of the NBD derivatives of anatoxin-a, homoanatoxin-a and their degradation products is shown in Figure 5A. The detection limit for anatoxin-a

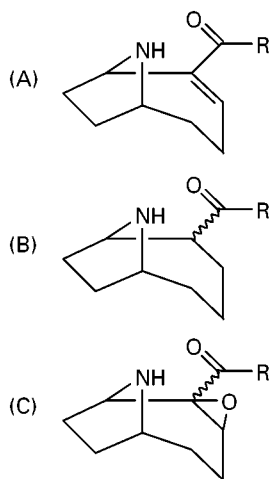


Figure 3 (A) Anatoxin-a (R = CH₃), homoanatoxin-a (R = CH₂CH₃); (B) dihydroanatoxin-a (R = CH₃), dihydrohomoanatoxin-a (R = CH₂CH₃); (C) epoxyanatoxin-a (R = CH₃), epoxyhomoanatoxin-a (R = CH₂CH₃).

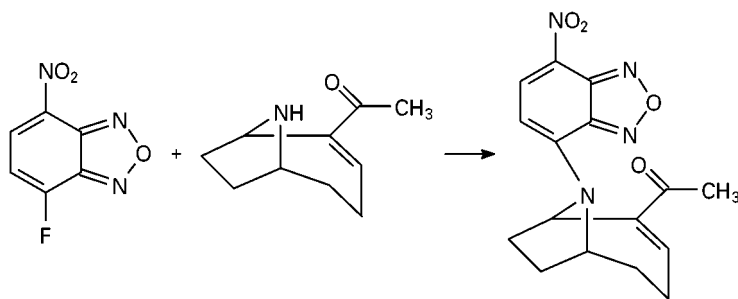


Figure 4 Reaction of anatoxin-a with NBD-F to produce a fluorescent product.

is 0.02 ng mL^{-1} , which allows this method to be applied to the routine monitoring of water supplies as well as for the forensic investigation of toxic incidents. This method was used to investigate the deaths of two dogs near Lough Derg, Ireland, two weeks after the event. Figure 5B shows a chromatogram from the investigation in which the dihydroanatoxin-a isomers are separated and are present in higher levels than anatoxin-a. Frequently, the detection of dihydroanatoxins in old samples may be the only evidence to implicate anatoxins in an intoxication event as anatoxin-a is unstable and readily decomposes at basic pH and in light.

Azaspiracid Poisoning (AZP) – A New Human Toxic Syndrome

Azaspiracid (formerly KT-3) is a marine toxin responsible for a new toxic syndrome, AZP. The first confirmed occurrence of this toxicity was in November 1995 in the Netherlands when at least eight people reported severe illness after the consumption of cultured mussels from the west coast of Ireland (Killary Harbour). Although human symptoms, which included vomiting, severe diarrhoea and stomach cramps, were similar to diarrhetic shellfish poisoning (DSP), only insignificant levels of DSP toxins were detected using LC-FL. The isolation of the major toxin was difficult, which is typical when dealing with a complex matrix such as shellfish tissue, and relied on the use of a variety of preparative chromatographic phases, as described by Satake and co-workers. Starting with 20 kg of mussel meat, the extract from several solvent extraction procedures was first subjected to adsorption chromatography using silica, followed by gel permeation chromatography. Next, carboxymethyl (CM) and diethylaminoethyl (DEAE) weak ion exchange phases were used and the final purification again used gel permeation to give 2 mg of azaspiracid.

Azaspiracid is characterized by a trispiro assembly and an azaspiro ring moiety that is unique in nature (Figure 6). In 1997 azaspiracid was again responsible

for a toxic incident, which occurred in Arranmore Island, Ireland, with more than 12 local human intoxications. There have been several other reported incidents, in Italy and France, and two analogues of azaspiracid have also been isolated, namely methylazaspiracid (AZ-2) and demethylazaspiracid (AZ-3). There have only been limited toxicological studies of azaspiracids. Mice administered high doses of azaspiracid died after short periods, showing neurotoxic symptoms, while morphopathological studies showed that the target organs are the liver, spleen and digestive tract.

Azaspiracids, like most other shellfish toxins, are produced by dinoflagellates but the causative organism is as yet unknown. However, unlike other types of shellfish toxicity, natural depuration of azaspiracids is very slow and toxins can persist in shellfish for as long as eight months. The development of analytical methods to determine azaspiracids in seafood is therefore a priority research topic and LC-MS has proved invaluable for the monitoring and management of toxic outbreaks. Figure 7 shows the chromatograms obtained from a crude extract from mussels using electrospray ion-trap mass spectrometry, without using any clean-up procedure. To achieve further confirmation of toxin identity, liquid chromatography–collision-induced dissociation–mass spectrometry (LC-CID-MS), with a collision energy of 40%, gave a characteristic fragmentation due to sequential loss of water molecules, as shown in Figure 8.

Venoms from Snakes and Spiders

Neurotoxic Peptides

More than 90% of the snake venoms produced by mambas, cobras and tiger snakes (which all belong to the family *Elapidae*), contain small protein molecules that are responsible for a wide range of toxicological and pharmacological activities. The complex mixtures of polypeptides that are present in most snake

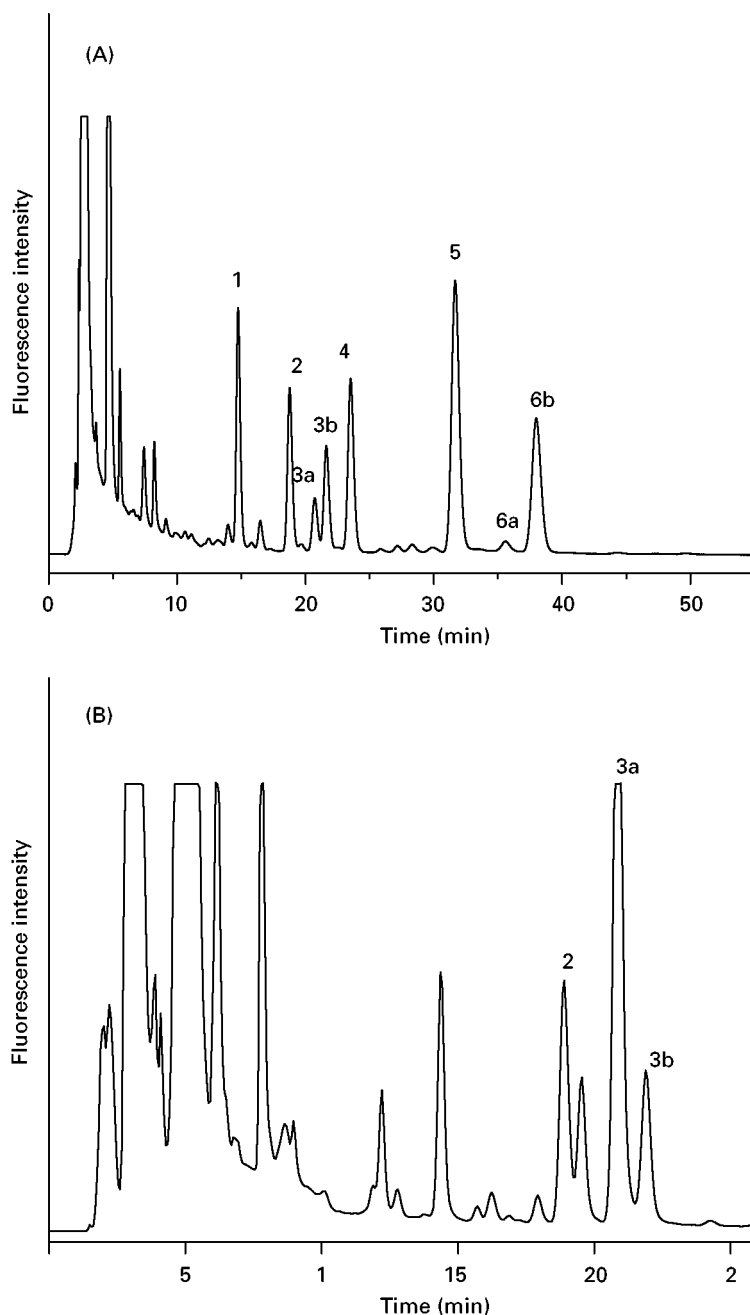


Figure 5 (A) Chromatogram from the fluorimetric HPLC analysis of anatoxin standards following derivatization with NBD-F. 1, NBD-anatoxin-a epoxide (14.7 min, 4.1 ng); 2, NBD-anatoxin-a (18.7 min, 3.5 ng); 3a, NBD-dihydroanatoxin-a isomer 1 (20.7 min, 1.2 ng); 3b, NBD-dihydroanatoxin-a isomer 2 (21.6 min, 2.5 ng); 4, NBD-homoanatoxin-a epoxide (23.5 min, 4.3 ng); 5, NBD-homoanatoxin-a (31.6 min, 8.8 ng); 6a, NBD-dihydrohomoanatoxin-a isomer 1 (35.5 min, 0.4 ng); 6b, NBD-dihydrohomoanatoxin-a isomer 2 (37.9 min, 5.2 ng). Reproduced with permission from James KJ *et al.* (1998) *Journal of Chromatography* 798: 147–157. (B) Chromatogram obtained using a water sample from Lough Derg, Ireland, showing the presence of NBD derivatized anatoxins. This water contained anatoxin-a ($2.1 \mu\text{g L}^{-1}$), dihydroanatoxin-a isomer 1 ($49 \mu\text{g L}^{-1}$) and dihydroanatoxin-a isomer 2 ($1.6 \mu\text{g L}^{-1}$). HPLC conditions: $5 \mu\text{m}$ Prodigy C_{18} column ($250 \times 3.2 \text{ mm}$); temperature, 35°C ; mobile phase, acetonitrile–water (45 : 55, v/v); flow rate, 0.5 mL min^{-1} ; fluorescence detection, λ_{ex} 470 nm, λ_{em} 530 nm.

venoms can be generally divided into neurotoxins and cardiotoxins (6000–10 000 amu), together with phospholipases A_2 (c. 13 000 amu) and larger enzymes. Often, the toxic effects of these peptides

result from a synergistic effect of the polypeptides rather than from a high intrinsic toxicity of individual compounds, and they have attracted interest for their potential therapeutic applications.

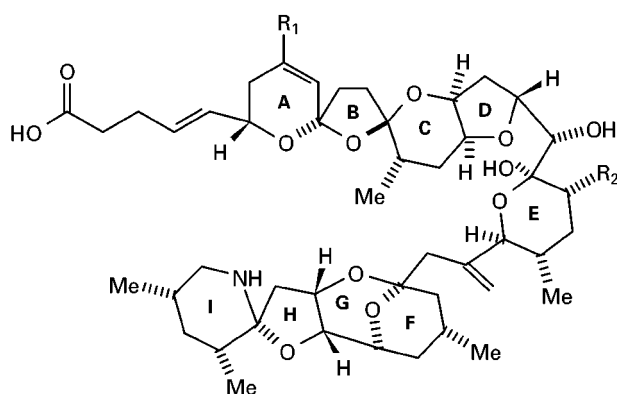


Figure 6 Azaspiracid (AZ-1, $R_1 = H$, $R_2 = Me$), methylazaspiracid (AZ-2, $R_1 = R_2 = Me$), demethylazaspiracid (AZ-3, $R_1 = R_2 = H$).

The analysis of snake venoms has traditionally relied on chromatographic separations using gel filtration and ion exchange phases, with protein size determined using methods such as sodium dodecyl sulfate–polyacrylamide gel electrophoresis (SDS-PAGE). Subsequent sequencing of the amino acids in the isolated proteins can be carried out by automated Edman degradation with a gas phase microsequencer.

Using these techniques, the isolation of 28 peptides from the venom of the black mamba snake has been reported, most of which are structurally related cationic peptides, called dendrodotoxins, with similar activities. However, the application of capillary electrophoresis–electrospray ionization–mass spectrometry (CE-ESI-MS) has been shown to be a particularly effective technique for the separation and analysis of such complex mixtures of small proteins as are found in these venoms. A problem that is often encountered when separating basic peptides is the retention of a net positive charge that leads to peak broadening due to the sorption of analytes to the negatively charged column wall. Several column wall derivatizing reagents have been reported to minimize this problem and it has been shown by Tomer and co-workers that when CE is carried out using a fused silica column derivatized with 3-aminopropyltrimethoxysilane (APS), the charge on the capillary wall becomes positive. Excess negative ions in solution drive the electroosmotic flow from a high negative potential to ground, and positively charged analyte ions are repelled by the column wall. ESI-MS is particularly useful for the analysis of large protein analytes, as these become multiply charged. The m/z

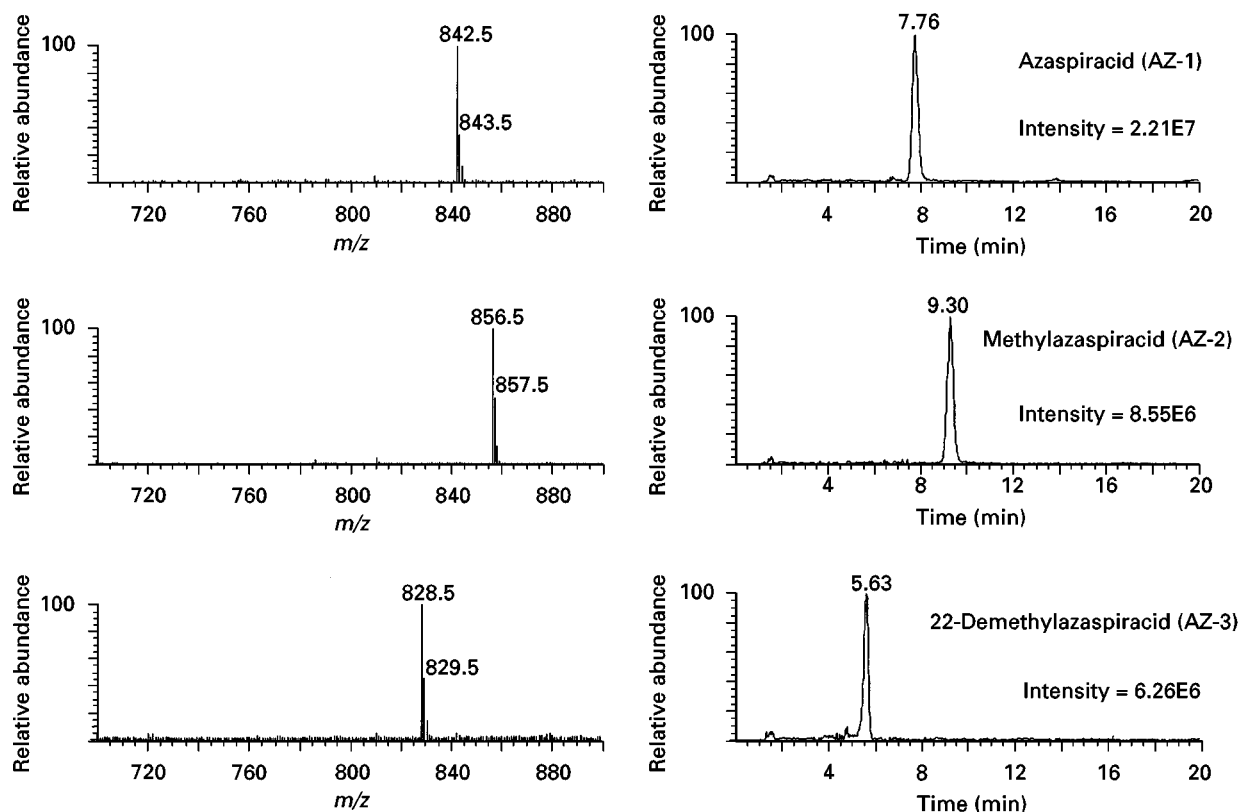


Figure 7 Electrospray LC-MS analysis of a toxic shellfish sample implicated in human intoxication. Azaspiracid ($14.7 \mu\text{g g}^{-1}$), methylazaspiracid ($13 \mu\text{g g}^{-1}$), 22-demethylazaspiracid ($8 \mu\text{g g}^{-1}$). Chromatographic conditions: C_{18} Luna column ($5 \mu\text{m}$, $250 \times 3.2 \text{ mm}$, Phenomenex); 25°C ; acetonitrile–water (70 : 30) containing 0.50% TFA; Flow rate 0.2 mL min^{-1} .

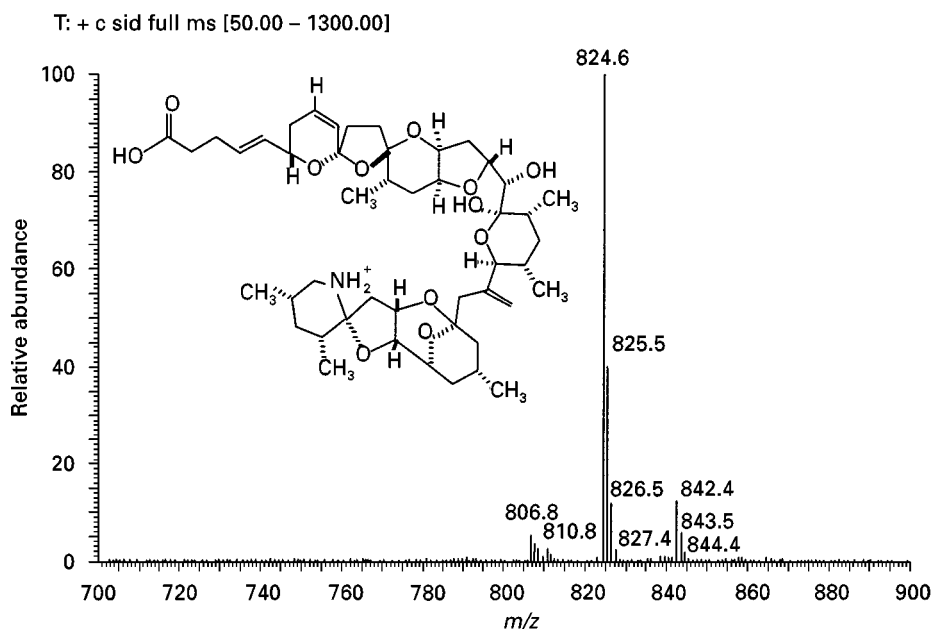


Figure 8 Mass spectrum obtained by LC-CID-MS of azaspiracid at 40% collision energy showing fragment ions for $[M + H - H_2O]^+$ and $[M + H - 2H_2O]^+$ at m/z 824.5 and 806.4, respectively.

ratio (determined by the mass spectrometer) is consequently reduced, which permits the determination of higher charged large molecules using spectrometers with significantly lower mass ranges. For example, the CE-ESI-MS analysis of the black mamba snake venom showed two dominant ions in the spectrum at m/z 1020 and 1090 which were related to the $[M + 7H]^{7+}$ and $[M + 6H]^{6+}$ ions of toxin 1 (7133.5 amu), previously shown to be the predominant dendrotoxin.

Acylpolyamine Neurotoxins from Spider Venoms

The tendency among humans to avoid contact with spiders is attributed, in part, to the ability of some species to deliver potent venoms. This venomous capability is used largely to paralyze or kill prey, particularly insects, but also affects a wide range of invertebrate and vertebrate animals. Neurotoxins are important as tools in neurochemical research and to investigate the functioning of neural receptors and ion channel modulators. Chemical studies on spider venoms have been hampered by the fact that many proteins, polypeptides and polyamines are often present in samples that are difficult to acquire in sufficient quantities. Special interest has been shown in acylpolyamines, low molecular weight toxins from spiders that antagonize specific glutamate receptors, since there are few other examples of this activity. Neural functions affected include memory and motor control and these toxins are important in studies to design potential therapeutic agents.

Acylpolyamines were first discovered in the 1980s and some examples are shown in **Figure 9**. They contain an aromatic ring connected to chains containing amide and amine moieties with some also incorporating amino acids, particularly arginine. The lengths of the polyamine chains vary considerably, as they can contain from 7 to 43 atoms, and they are linked to various phenol or indole rings. Examples of toxins with a dihydroxybenzene ring include NSTX-3 (Figure 9A-2, X = C) and JSTX-3 (Figure 9A-3, X = C).

Several chromatographic techniques have been applied to separate these complex mixtures, which can contain as many as 50 acylpolyamines in a single spider venom sample. Preparative HPLC can be used directly to separate toxins in an aqueous extract of spider venom using photodiode-array UV detection. However, tandem LC, combining UV detection with on-line fluorescence detection, following reaction with *o*-phthalaldehyde (OPA), has proved valuable for the detection of minor components. For these separations, a linear gradient of water (containing 0.1% trifluoroacetic acid), for example 5–60% acetonitrile, can be used for reversed-phase chromatography. Fractions containing active constituents typically require up to three further preparative LC steps, with both ion exchange and octadecyl-silica (ODS) columns, to purify toxins to homogeneity. Bioassays of fractions to detect toxin activity are also frequently used in these studies and an example is the assay of histamine release from rat peritoneal

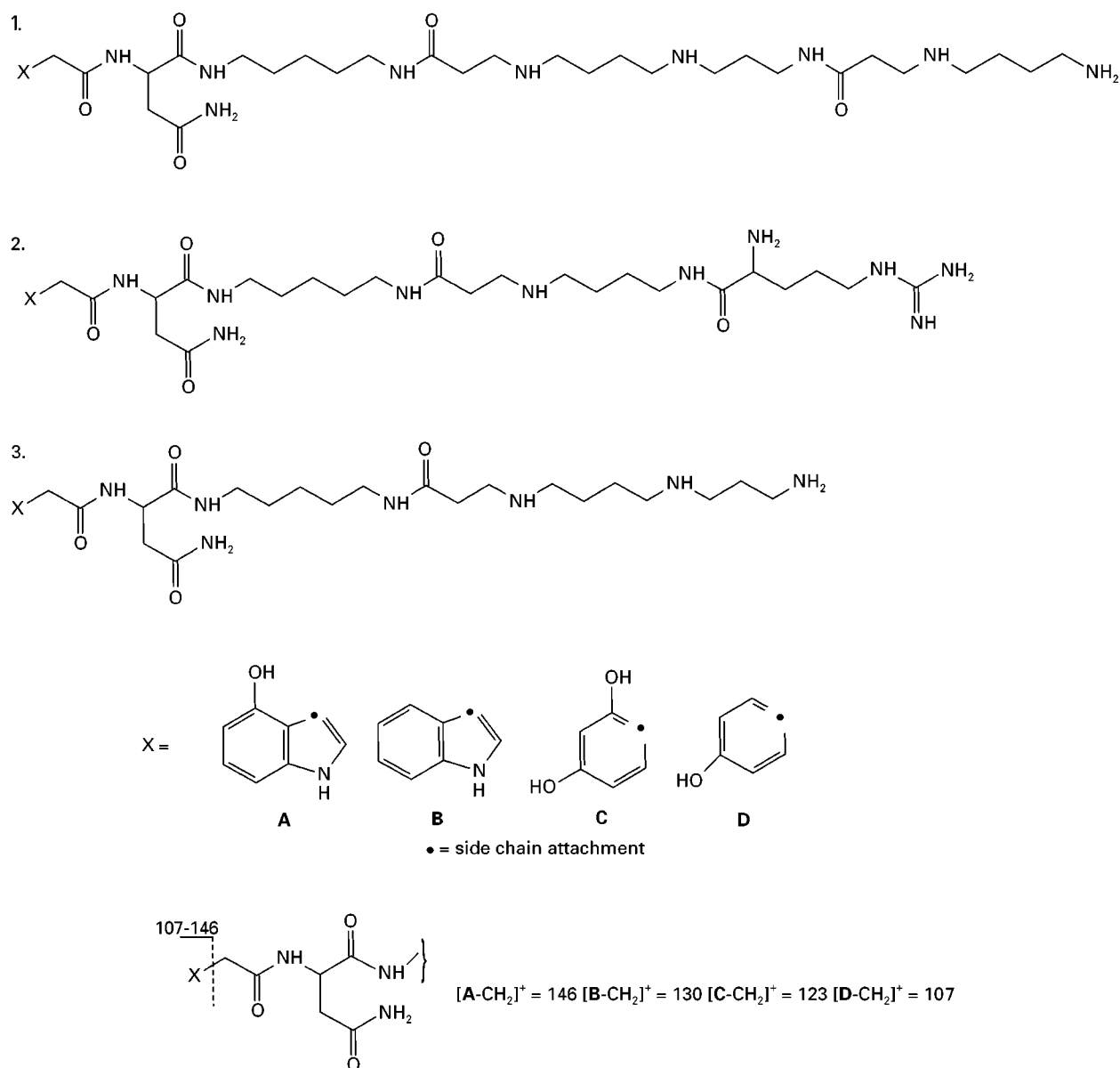


Figure 9 Structures of acylpolyamine toxins from spiders.

mast cells. Toxin identification requires NMR and/or hydrolysis of toxins to amino acids and amines, but for structural confirmation of very small quantities of toxins synthesis has also been employed.

In recent years, major advances have been made possible by the use of μ -column LC with FAB-MS. **Figure 10** shows the two-dimensional MS chromatogram from a spider venom extract obtained using on-line μ -column LC-FAB-MS. The acylpolyamines in this venom have an arginine terminal group with structures similar to those in Figure 9A–2A, –2B and –2C. Further structural information can be obtained

using collision-induced dissociation (CID) tandem mass spectrometry (MS-MS) which is often sufficient for the full structural elucidation of these toxins. The aromatic ring in each toxin is readily identified from the strong MS signal because fragmentation at the carbon adjacent to the ring produces ions of m/z 107 (phenol), 123 (dihydroxybenzene), 130 (indole) or 146 (hydroxyindole), as illustrated in Figure 9B. From such studies, over 40 acylpolyamines have been identified in a crude spider venom extract. A combination of LC-MS and matrix-assisted laser desorption/ionization (MALDI) MS has emerged as

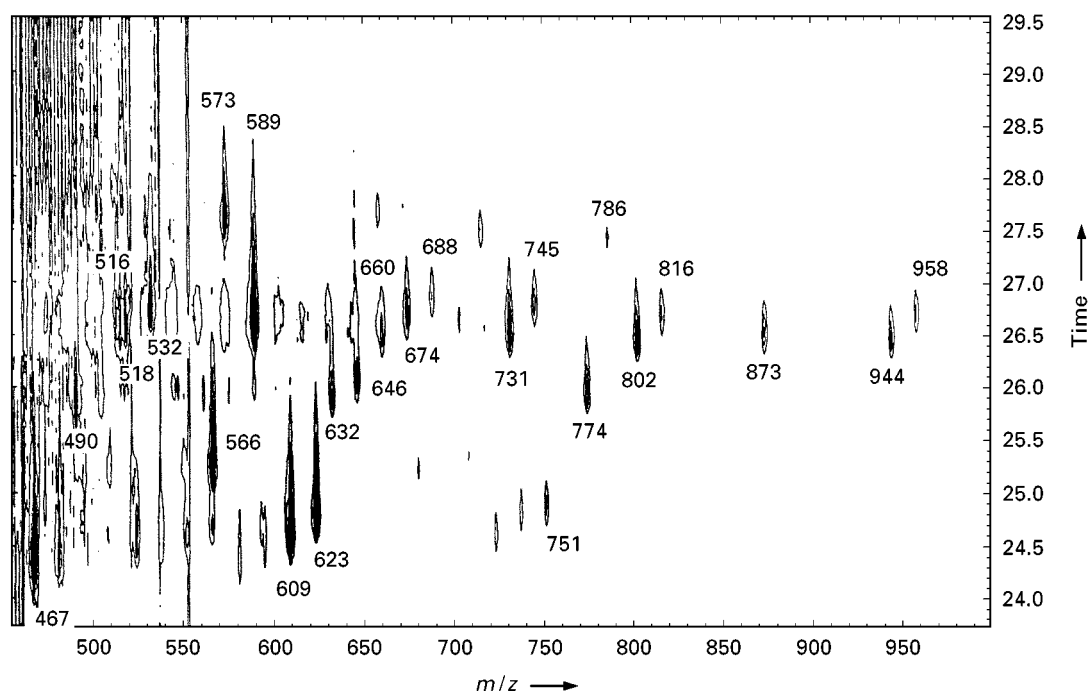


Figure 10 Two-dimensional MS chromatogram display of protonated molecular ions $[M + H]^+$ obtained from spider venom (*Nephilengys cruenta*) extracts using on-line μ -column LC-FAB-MS. (Reproduced with permission from Palma MS *et al.* (1997) *Natural Toxins* 5: 47.)

a powerful technique for the analysis of small samples of venom containing complex mixtures of these toxins.

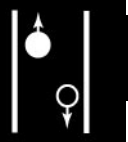
See Colour Plate 107.

See also: **II/Chromatography: Gas:** Derivatization; Detectors: Mass Spectrometry. **Chromatography: Liquid:** Detectors: Fluorescence Detection; Detectors: Mass Spectrometry. **Electrophoresis:** Capillary Electrophoresis-Mass Spectrometry; One-dimensional Sodium Dodecyl Sulphate Polyacrylamide Gel Electrophoresis. **III/Toxins: Chromatography. Venoms: Chromatography.**

Further Reading

- Botana LM, Rodriguez-Vieytes M, Alfonso A and Louzao MC (1996) Phycotoxins: paralytic shellfish poisoning and diarrhetic shellfish poisoning. In: Noller LML (ed.) *Handbook of Food Analysis*, vol. 2, pp 1147–1169. New York: Marcel Dekker.
- Chorus I and Bartram J, eds (1999) *Toxic Cyanobacteria in Water*. World Health Organisation. London: E&FN Spon.
- Codd GA, Jefferies TM, Keevil CW and Potter E, eds (1994) *Detection Methods for Cyanobacterial Toxins*. Cambridge: Royal Society of Chemistry.
- Falconer I, ed. (1993) *Algal Toxins in Seafood and Drinking Water*. London: Academic Press.
- Hu AT, ed. (1988) *Handbook of Natural Toxins*, vol. 3 *Marine Toxins and Venoms*. New York: Marcel Dekker.
- James KJ, Furey A, Sherlock IR, *et al.* (1998) Sensitive determination of anatoxin-a, homoanatoxin-a and their degradation products by liquid chromatography with fluorimetric detection. *Journal of Chromatography* 789: 147–157.
- McCormick KD and Meinwald J (1993) Neurotoxic acylpolyamines from spider venoms. *Journal of Chemical Ecology* 19: 2411–2413.
- Oshima Y (1995) Postcolumn derivatisation liquid chromatographic method for paralytic shellfish toxins. *J AOAC Int.* 78: 528–532.
- Palma MS, Itagaki, Y, Fujita T, Naoki H and Nakajima T (1997) Mass spectrometric structure determination of spider toxins: arginine-containing acylpolyamines from venoms of Brazilian garden spider. *Nephilengys cruenta*. *Natural Toxins* 5: 47–57.
- Perkins JR, Parker CE and Tomer KB (1993) The characterisation of snake venoms using capillary electrophoresis in conjunction with electrospray mass spectrometry: Black Mambas. *Electrophoresis* 14: 458.
- Reguera B, Blanco J, Fernández, ML and Wyatt T, eds (1998) *Harmful Algae*. Santiago de Compostela: Xunta de Galicia and Intergovernmental Oceanographic Commission of UNESCO.
- Satake M, Ofuji K, Naoki H, *et al.* (1998) Azaspiracid, a new marine toxin having unique spiro ring assemblies, isolated from Irish mussels, *Mytilus edulis*. *Journal of the American Chemical Society* 120: 9967–9968.
- Schäfer A, Benz H, Fieler W, *et al.* (1994) Polyamine toxins from spiders and wasps. In: Cordell GA and Brossi A (eds) *The Alkaloids: Chemistry and Pharmacology*, vol. 45, pp 1–125. San Diego: Academic Press.

NICKEL AND COBALT ORES: FLOTATION



G. V. Rao, Regional Research Laboratory, Council of Scientific and Industrial Research, Bhubaneswar, India

Copyright © 2000 Academic Press

Introduction

Most of the world's nickel is extracted from the mineral pentlandite, $(\text{Ni, Fe})_9\text{S}_8$, which frequently occurs in ores containing predominantly pyrrhotite and various non-sulfides, some of which contain magnesium (Table 1). The nickel content in such sulfide ores is generally low (0.2–3%) and varies from place to place in the same deposit. The low nickel content of the present-day nickel sulfide ores renders them unsuitable for either direct smelting or hydrometallurgical extraction, thus requiring beneficiation.

The usual method of nickel extraction from sulfide ores is through the production of nickel matte after enriching the nickel content of the ore. This is commonly carried out by magnetic separation, flotation, or a combination of both after the ore is comminuted to below 200 μm in size. The enrichment depends upon the degree of rejection of the other sulfide and non-sulfide gangue. The maximum grade of nickel achieved by flotation is around 28% Ni.

Problems Associated with Sulfide Mineral Flotation

The main problem encountered is selectivity of pyrrhotite and also in some cases chalcopyrite during flotation. A clean and satisfactory separation of pentlandite from pyrrhotite by flotation is difficult in practice since pyrrhotite typically contains intergrown inclusions of pentlandite as well as nickel in solid solution. In fact pyrrhotite often contains 0.5–1% Ni that cannot be separated by physical methods. The common occurrence of both monoclinic (magnetic) and the hexagonal (nonmagnetic) forms of pyrrhotite in association with pentlandite also poses problems. Another type of alteration which adversely affects flotation recoveries is that tochilinite has flotation properties similar to that of pyrrhotite. As a consequence it either reports to the flotation tailings, thereby decreasing the nickel recovery, or, if it is effectively floated, a significant amount of pyrrhotite accompanies it, diluting the nickel grade in the concentrate.

There is a distinct difference in silicate mineralogy between types of host rock, which have their own problems with respect to rejection of gangue by

flotation. Talc and other naturally hydrophobic magnesia-bearing minerals have a tendency to float with sulfides, resulting in a concentrate exceptionally high in magnesia. The presence of magnesia causes viscosity problems in the slag during smelting. Magnesia also promotes conditions favourable to hetero-coagulation of minerals, especially fine sulfides with coarse gangue minerals, thus leading to nickel loss.

Flotation Practice in Nickel Sulfide Deposits

Nickel sulfide minerals such as pentlandite can, in general, be separated from their gangue by flotation using a thiol group of collectors like xanthates and alkyl dithiophosphates in the presence of variety of activators, depressants and dispersants. Since nickel sulfides contain other sulfides such as pyrrhotite, pentlandite and chalcopyrite, the enrichment of nickel is generally carried out by two methods:

1. production of bulk concentrate containing all sulfides together as smelter feed;
2. production of bulk chalcopyrite–pentlandite concentrate by preferentially depressing the pyrrhotite followed by selective flotation of chalcopyrite and pentlandite.

Although bulk flotation of all sulfides is relatively simple the presence of pyrrhotite, which contains minor amounts of nickel but substantial amounts of sulfur (Table 2), causes excessive sulfur dioxide emissions during smelting of the concentrate.

Since most of the sulfur contained in the flotation concentrate is emitted from pyrrhotite, the rejection of pyrrhotite is important, especially in Canada, owing to stringent limits imposed on SO_2 emissions from smelters in that country. The pyrrhotite from the Canadian ores in the Sudbury region occurs in two crystallographic forms having distinct characteristics. The monoclinic pyrrhotite, being magnetic, can be partly rejected by magnetic separation, while the hexagonal pyrrhotite is separated by flotation.

Pyrrhotite is known to float poorly in alkaline media; therefore the general practice is to selectively float pentlandite from pyrrhotite, by maintaining a highly alkaline pH with cyanide as depressant and using thiols like xanthates or dithiophosphates as collectors. Although it is possible to reject significant

Table 1 Principal nickel and nickeliferous minerals in nickel sulfide deposits

	Formula	Nickel content (%)
Nickel minerals		
<i>Primary</i>		
Pentlandite	(Ni,Fe) ₉ S ₈	25–41
Millerite	NiS	65
Heazlewoodite	Ni ₃ S ₂	73
Gerardorfite	(Ni,Co,Fe)AsS	15–35
Nickeline	NiAs	44
Awaruite	Ni-Fe	25–75
<i>Secondary</i>		
Violarite	Ni ₂ FeS ₄	33–40
Bravoite	(Ni,Fe)S ₂	17–24
Haapalaite	4(Fe,Ni)S·3(Mg,Fe)OH ₂	
Annabergite	(Ni,Co) ₃ (AsO ₄) ₂ ·8H ₂ O	
Nickeliferous minerals		
<i>Primary</i>		
Pyrrhotite	Fe _(1-x) S	Up to 1.5
Mackinawite	(Fe,Ni) ₉ S ₈	Up to 9
Arsenopyrite	FeAsS	Up to 0.5
<i>Secondary</i>		
Pyrite	FeS ₂	Up to 12
Marcasite	FeS ₂	Up to 6
Smythite	Fe _{3.25} S ₄	Up to 5
Tochilinite	6Fe _{0.9} S·5(Mg,Fe)(OH) ₂	Up to 5
Magnetite	Fe ₃ O ₄	Up to 1

(Reprinted with permission from The Minerals, Metals and Materials Society (TMS).)

amounts of pyrrhotite in this way, the concomitant pentlandite losses into flotation tailings are highly unsatisfactory, in addition to the problem of water contamination due to cyanide.

A typical example of a nickel sulfide plant operating with highly floatable talcose gangue is at Trojan mine in Zimbabwe. The Zimbabwean sulfide deposits contain very low grades of nickel (0.6%) and copper (0.04–0.4%). The easily floatable non-sulfide minerals dilute the grade of the concentrate and also result in nickel losses into the tailings. This problem can be overcome by using depressants like carboxymethylcellulose (CMC) and guar gum deriva-

tives, although their cost accounts for as much as 60% of the reagent cost incurred in the plant.

Developments in Flotation

Flotation of Nickel Sulfide Minerals

Collectorless flotation It is known that chalcopyrite and pyrrhotite can be floated without collectors at electrode potentials of +400 mV and +50 mV respectively, and pyrite does not float even at +700 mV. The underlying mechanism causing hydrophobicity, although obscure, is attributed to surface oxidation, formation of elemental sulfur and partial dissolution of mineral surface, leaving a sulfur-rich layer.

Collectorless flotation studies on three lean nickel sulfide ores, from Outokumpu Finnmines Oy (Enonkoski (0.31% Ni and 0.14% Cu), Vammala (0.9% Ni and 0.45% Cu) and Hitura (0.32% Ni and 0.11% Cu)), ground in steel and ceramic mills at a pH range of 3–12 using polypropylene ether as frother revealed interesting details.

The pentlandite, chalcopyrite and pyrrhotite from Enonkoski ore ground in a steel mill floated easily without a collector at low pH values of 3–5 (Figure 1). The floatability of these three minerals was improved when the same ore was ground in a ceramic mill (Figure 2). This suggests that collectorless flotation in acidic pH can be adopted as a low-cost pre-concentration phase to obtain a bulk sulfide concentrate.

Effect of sulfur dioxide It is possible to effectively separate Cu–Ni ores from pyrrhotite gangue in the absence of a collector, but with SO₂ and an effective complexing agent such as diethylenetriamine (DETA) and a frother. The depressant action of SO₂, which is greatly enhanced in the presence of DETA, does not affect the recovery of chalcopyrite. Figure 3 shows that 93% of chalcopyrite can be recovered in 12 min in the presence of SO₂, but the co-recovery of 12% pentlandite and 23%

Table 2 Distribution of Ni and S in sulfide ores

Ore source	Nickel distribution (%)		Sulfur distribution (%)		
	Pentlandite	Pyrrhotite	Pentlandite	Chalcopyrite	Pyrrhotite
Sudbury	87.0	13.0	12.5	9.8	77.7
Thompson	94.8	5.20	20.1	1.5	78.4
Shebandowan	91.8	8.20	16.0	7.6	76.4

(Reprinted from Agar GE (1991) with permission from Elsevier Science.)

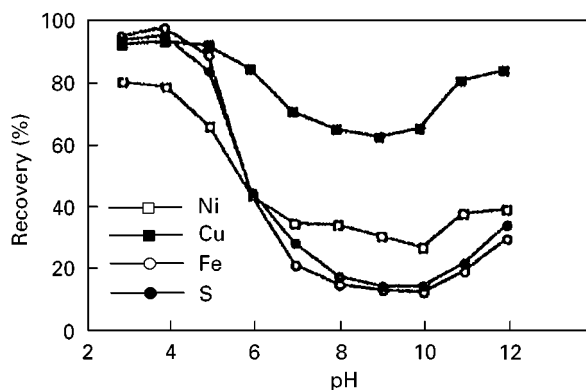


Figure 1 Effect of pH on collectorless flotation recoveries on Enonkoski noritic ore after grinding in steel mill. (Reprinted from Heiskanen *et al.* (1991) with permission from Elsevier Science.)

pyrrhotite makes the grade unacceptable. The overall recovery of pentlandite and pyrrhotite could be restricted to 4.1% and 2.5% respectively by introducing DETA in combination with SO_2 (Figure 4).

The differential separation of pentlandite and pyrrhotite from the resulting flotation tailings with sodium isobutyl xanthate collector and Dow froth -250 can also be achieved in the presence of SO_2 and DETA. By using 1.4 kg SO_2 per tonne of ore in combination with 300 g DETA per tonne a concentrate with an overall pentlandite recovery of about 89% could be produced, while restricting pyrrhotite recovery to less than 12.5% (Figure 5).

Problems due to process water The difficulty of selective depression of pyrrhotite at Canadian plants was found to be due to the process water containing heavy metal ions such as Ni^{2+} , Cu^{2+} , Ag^{2+} , which were causing the inadvertent activation. By using a small amount of DETA the separation effi-

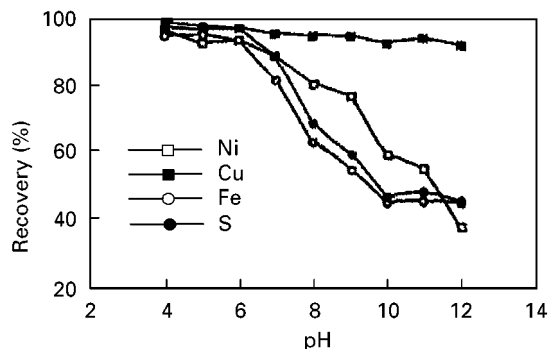


Figure 2 Effect of pH on collectorless flotation recoveries on Enonkoski noritic ore after grinding in ceramic mill. (Reprinted from Heiskanen *et al.* (1991) with permission from Elsevier Science.)

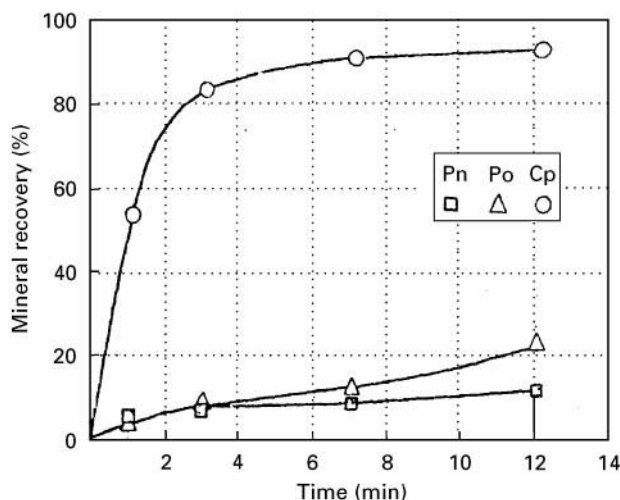


Figure 3 Collectorless flotation kinetics after treatment with sulfur dioxide ($1.1 \text{ kg t}^{-1} \text{ SO}_2$; 35 g t^{-1} Dow froth -250, pH ≈ 9.5). (Reprinted with permission from the Canadian Institute of Mining, Metallurgy and Petroleum.)

ency was greatly improved (Figure 6); however, the depressing effect is more effective when the ore is oxidized.

The activation products formed on pyrrhotite may be sulfides of Ni, Cu and Ag, which are usually insoluble under reducing conditions. When the mineral is oxidized, the activation products convert to oxides, increasing the solubility in the presence of DETA and thus causing its depression.

Effect of pulp potential Pentlandite can be floated selectively from pyrrhotite by maintaining the pulp

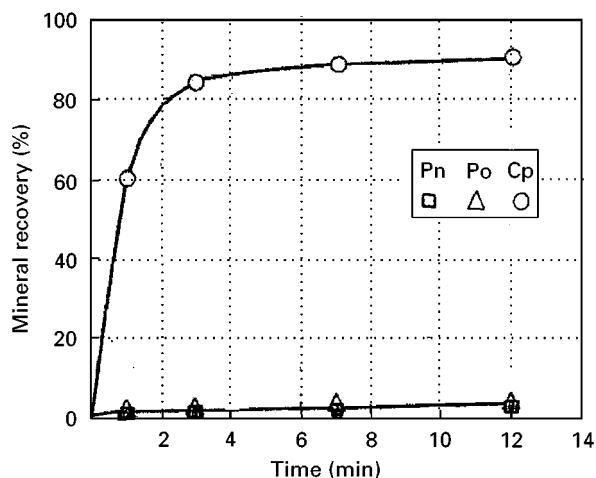


Figure 4 Collectorless flotation kinetics after treatment with sulfur dioxide and DETA ($1.1 \text{ kg t}^{-1} \text{ SO}_2$; 200 g t^{-1} DETA; 35 g t^{-1} Dow froth -250, pH ≈ 9.5). (Reprinted with permission from the Canadian Institute of Mining, Metallurgy and Petroleum.)

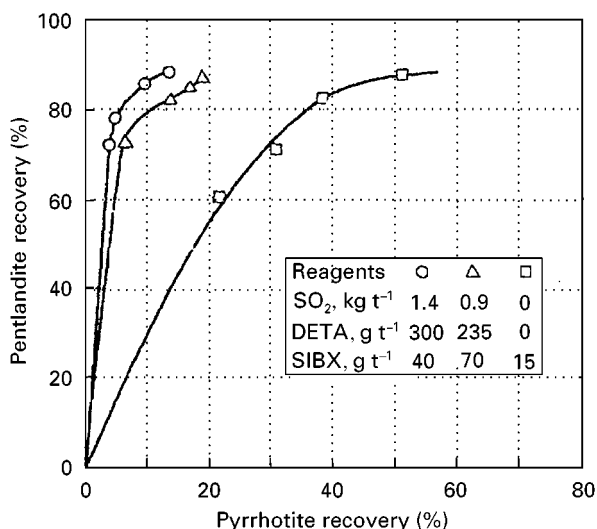


Figure 5 Flotation selectivity in the separation of pentlandite from pyrrhotite using sulfur dioxide and diethylenetriamine with sodium isobutyl xanthate (pH \approx 9.2, 25 g t⁻¹ Dow froth - 250). (Reprinted with permission from the Canadian Institute of Mining, Metallurgy and Petroleum.)

pH at a sufficiently alkaline value and with minimal quantities of collector. Careful grinding and classification are essential for retrieving the coarse pentlandite while restricting the entry of pyrrhotite into the concentrate. Interestingly, the influence of pulp potential on flotation recovery of pentlandite and pyrrhotite is virtually the same (Figure 7), and the possibility of achieving satisfactory selective flotation from such mineral mixtures by means of differential pulp potential can be ruled out.

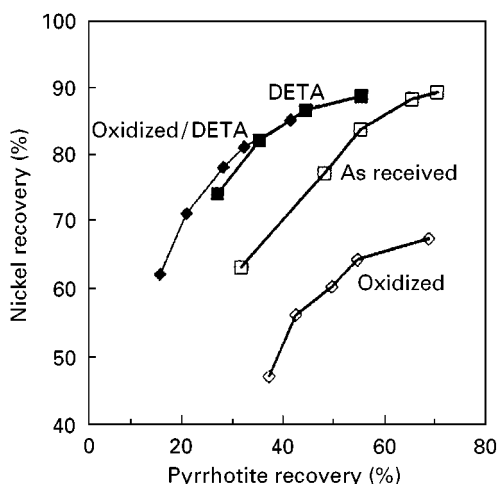


Figure 6 Flotation results obtained with Clarabelle ore from Canada in the presence and absence of DETA, with amyl xanthate collector. (Reprinted from Yoon *et al.* (1995) with permission from Elsevier Science.)

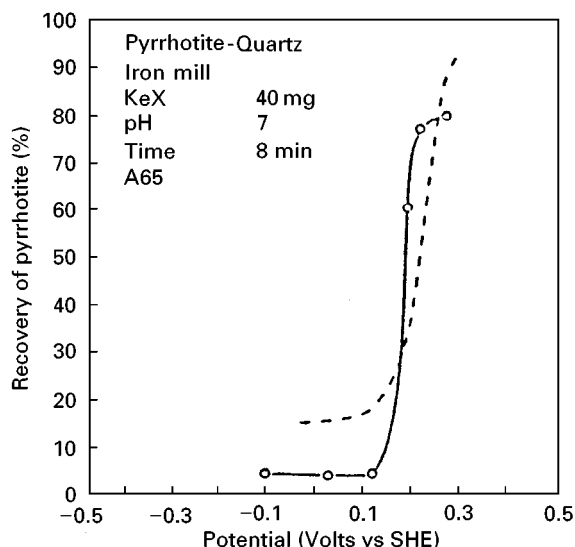


Figure 7 Influence of pulp potential on the flotation of pyrrhotite with potassium ethyl xanthate at pH 7. (The broken curve shows the corresponding data for pentlandite.) (Reprinted from Senior GD, Shannon LK and Trahar WJ (1994) The flotation of pentlandite from pyrrhotite with particular reference to the effects of particle size. *International Journal of Mineral Processing* 42: 169–190 with permission from Elsevier Science.)

Recovery of Valuable Slimes

By High Intensity Conditioning

The recovery of valuable metal being lost in slimes is of paramount importance. It has been estimated that recovering 15% of the metal lost in the less than 10 μ m fines in Canada would increase revenue by approximately \$100 m.

High intensity conditioning of slimes in the presence of collector and frother substantially improves the flotation kinetics of pentlandite slimes. The floatability of fine particles by high intensity conditioning, however, largely depends on the nature of the ore and the power input per unit volume of pulp treated. Maximum recoveries are obtained at a power input exceeding 1.5 kWh m⁻³ of pulp. High intensity conditioning of slurry adopted at the Trojan mill in Zimbabwe has improved nickel recoveries by 2–4%, owing to the increased flotation response of oxidized and tarnished nickel-bearing sulfides.

Depression and Activation by Slimy Gangue Minerals

Many hydrophobic silicate minerals such as talc, chlorite, kaolinite and serpentinite activate other minerals by forming slime coatings. It is also known that the serpentine slimes, containing chrysotile and

lizardite, form slime coatings on unoxidized pentlandite and such coatings depress nickel flotation. The formation of these slime coatings is directly related to the magnitude and sign of surface charges of the slimes and sulfide particles.

Crysotile is known to depress nickel sulfide more than lizardite. Addition of small amounts of chrysotile to the flotation pulp (0.05 g L^{-1}) dramatically decreases pentlandite flotation recovery, from 90% to 5%.

Dispersion of Slime Coatings

The reagents generally known to modify the slime surface charge and reduce their adverse influence on pentlandite flotation are dextrin, sodium pyrophosphate, sodium silicate, sodium carbonate, guar gum and CMC. Among these reagents CMC has been found to be the best, despite the high concentration required (more than 2 kg t^{-1}). CMC treatment of an Australian ore containing a number of magnesium silicate minerals improved the flotation rate of pentlandite when using amyl xanthate as a collector. The carbonate ions derived from soda ash enhanced dispersion in the pulp, while CMC facilitated the removal of slime particles from pentlandite, thereby allowing the xanthate to coat the surface. The pentlandite fines flotation was found to be improved with either soda ash or CMC but the synergistic effect of both proved beneficial for intermediate sizes.

Effect of Saline Water

The extent of slime coating is related to the zeta potential, being greatest when slime and particles have a high zeta potential of opposite sign. The zeta potential of the particles can be decreased by increasing the concentration of counterions. A highly saline pulp produces a high concentration of counterions, Na^+ , and Cl^- , which influence the slime dispersion, besides enhancing hydrophobicity due to modification of the hydration layer around the mineral particles and air bubbles.

In the presence of 10% saline solution, fine nickel sulfide flotation is promoted, whereas flotation with 1 kg t^{-1} CMC does not result in upgrading the nickel sulfides. Flotation tests on the whole feed and cyclone overflow of a transition ore, from Western Australia, in saline pulp gave better results (Figure 8) than the addition of 1 kg t^{-1} of CMC.

Separation of Nickel from High Nickel Matte

The separation of chalcocite (Cu_2S) and heazlewoodite (Ni_3S_2) from high nickel matte can be

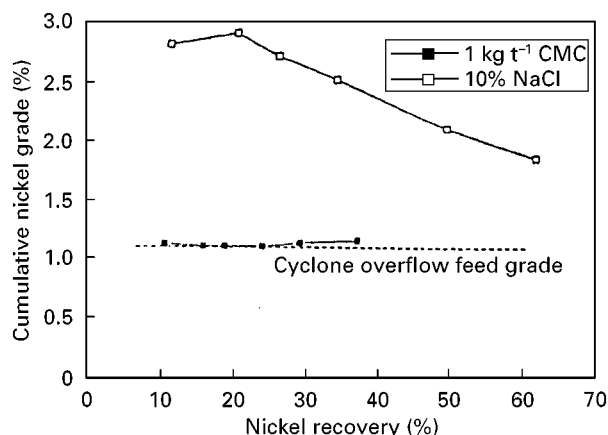


Figure 8 Comparison of dispersant regimes on nickel recovery from cyclone overflow material with CMC and NaCl. (Reprinted from Wellham *et al.* (1992) with permission from Elsevier Science.)

achieved by maintaining the proper pH and pulp potential while using xanthates as collectors. The flotation recovery of Cu_2S and Ni_3S_2 has been studied by adjusting the oxidation-reduction potential of the flotation pulp with $(\text{NH}_4)_2\text{S}_2\text{O}_8$ and KMnO_4 . The recovery of Ni_3S_2 is almost zero either at pH 8.5 where $E_h > 500 \text{ mV}$ or at pH 11.2 with $E_h > 400 \text{ mV}$, whereas the potential has little effect on Cu_2S at pH 8.5. The depression of Ni_3S_2 can be improved by employing $\text{Ca}(\text{ClO})_2$, as modifier of potential, and Ca^{2+} ions. As the potential of Ni_3S_2 is increased, with increase in dosage of $\text{Ca}(\text{ClO})_2$ the recovery decreased, but the potential appears to have little effect on the flotation behaviour of Cu_2S (Figure 9).

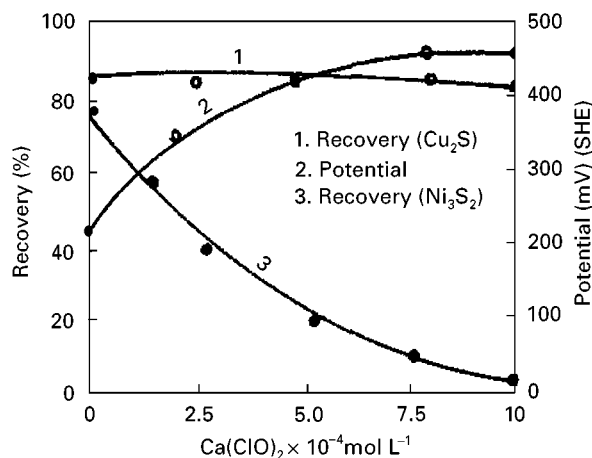


Figure 9 Flotation recovery of Cu_2S and Ni_3S_2 and E_h as a function of $\text{Ca}(\text{ClO})_2$ in the presence of a mixture of butyl xanthate and ethyl xanthate ($10^{-4} \text{ mol L}^{-1}$). (Reprinted with permission from International Academic Press.)

Lateritic Nickel Resources

Lateritic nickel resources are formed when peridotite, an igneous rock comprising predominantly the mineral olivine, which contains around 0.25% Ni, are exposed to prolonged and intense chemical weathering. During such prolonged weathering, the magnesium and silica are leached out of the rock to leave a residue rich in ferric oxide, nickel and other minor constituents such as aluminium and chromium. The type of weathering which dissolves silica and metallic elements from rocks to produce limonite and silicate nickel ores occurs most frequently in tropical climates with a high rainfall, and with decomposing vegetable matter to provide organic acids and carbon dioxide in the ground water.

Lateritic nickel deposits are classified on the basis of differences in the essential make-up of the profiles. The differences between limonitic and silicate minerals influence the methods by which they are treated for nickel recovery.

Developments in Laterite Flotation

Flotation studies on an ore from New Caledonia with a variety of collectors did not give any substantial upgrading with appreciable recoveries (Table 3). Laboratory investigations on garnierite samples from the Pomalaa mine, Indonesia, indicated that by using sodium oleate in combination with a chelating reagent like dimethylglyoxime or α -diphenylglyoxime the flotability of garnierite could be markedly increased at high pH. Between pH 11 and 12 stable nickel chelate complexes are believed to be formed, causing maximum flotability (Figure 10). However,

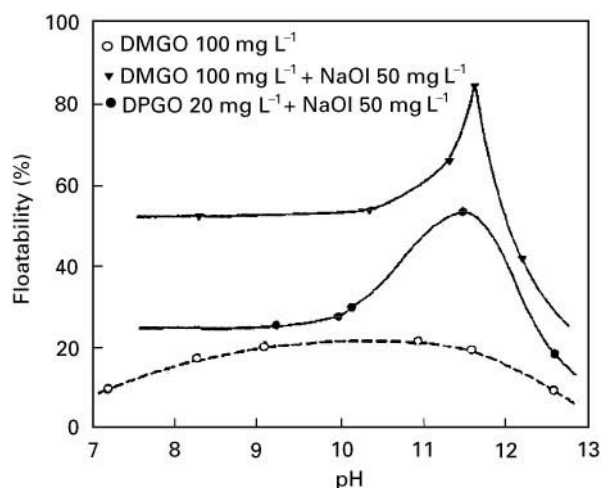


Figure 10 Effect of pH on the floatability of garnierite using dimethylglyoxime (DMGO) or α -diphenylglyoxime (DPGO) as chelating reagents along with sodium oleate. (Reprinted from Nakahiro Y, Saburi H and Wakamatsu T (1987) Fundamental study on the flotation of garnierite using chelating reagents and anionic collectors. *International Journal of Mineral Processing* 19: 69–76 with permission from Elsevier Science.)

other anionic collectors like mercaptobenzothiazole and sodium diethyldithiocarbamate show no favourable effects on garnierite collection even when the same chelating reagents are used in combination.

Treatment of Limonitic Ores

In India, substantial quantities of nickel-bearing lateritic material containing 0.5% Ni are available at Sukinda, Orissa, which is the country's largest chromite deposit. During chromite mining, nearly 10 t of

Table 3 Significant minerals in nickel laterites

Minerals	Formula	% Ni
<i>Peridotite rock</i>		
Olivine	(Mg,Fe,Ni) ₂ SiO ₄	0.25
Orthopyroxene	(Mg,Fe)SiO ₃	0.05
Serpentine	Mg ₃ Si ₂ O ₅ (OH) ₄	0.25
<i>Saprolite zone</i>		
Nickeliferous serpentine	(Mg,Fe,Ni) ₃ Si ₂ O ₅ (OH) ₄	1–10
Garnierite	(Ni,Mg) ₃ Si ₄ O ₁₀ (OH) ₂	10–24
<i>Intermediate zone</i>		
Nontronite	(Ca,Na,K) _{0.5} (Fe ³⁺ ,Ni,Mg,Al) ₄ (Si,Al) ₈ O ₂₀ (OH) ₄	0–5
Quartz	SiO ₂	0
<i>Limonite zone</i>		
Goethite	(Fe,Al,Ni)OOH	0.5–1.5
Asbolite	Mn,Fe,Co,Ni oxide	1–10

(Reprinted with permission from The Minerals, Metals and Materials Society (TMS).)

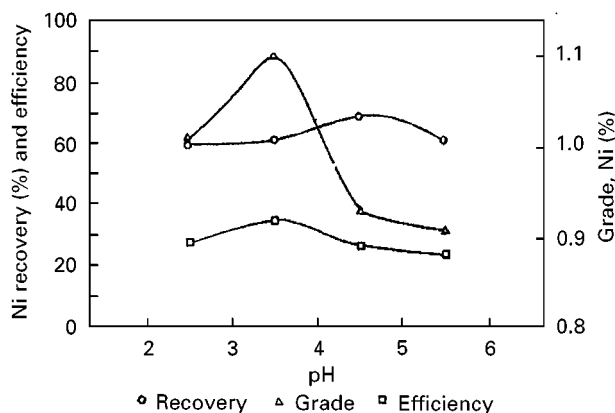


Figure 11 Effect of pH with sodium petroleum sulfonate collector (0.4 kg t^{-1}). (Reprinted with permission from Society for Mining, Metallurgy and Exploration, Inc.)

waste overburden, containing on average 0.5% Ni, 0.02% Co and 25% Fe, are currently being rejected for every tonne of chromite mined. The nickel in such waste materials is found to be in association with goethite, which is the predominant iron mineral and tends to become enriched in the fines along with iron.

Flotation of goethite has been attempted to enrich nickel in proportion to iron enrichment. The nickel could be enriched to above 1.1% Ni with around 75% recovery at pH between 3.5 and 5 on a variety of samples studied by using a commercial grade (SPS 430) anionic petroleum sulfonate collector. The flotation response of the lateritic nickel-bearing iron with different collectors and their mixtures can be seen in Figures 11 and 12. The flow chart suggested for enriching nickel to above 1.1% from lean lateritic chromite overburden is given in Figure 13.

The pertinent details concerning the flotation response of a variety of samples drawn from a wide cross-section of the overburden dumps, including scrubbing, are given in Table 4.

Cobalt

Cobalt is present in many rocks, soils and sea water in very low concentration and exploitable deposits occur only in a few places. As a result cobalt-containing ores are not mined primarily for their cobalt content, but rather cobalt is produced as a by-product, particularly from the production of copper, nickel, silver, gold, lead and zinc. The cobalt minerals which are exploited mostly for their recovery as by-products are given in Table 5.

The only beneficiation plant put up exclusively to recover cobalt is in Morocco, treating the complex cobalt-bearing ores from the Bou-Azzer deposit. The principal ores at Bou-Azzer are skutterudite and

erythrine. The specific gravity of these cobalt-bearing minerals being high (5.7–6.8), they are recovered first by gravity concentration followed by flotation of the middlings of the gravity circuit and the fines using amyl xanthate collector subsequent to activation with sodium sulfide and copper sulfate. A mixed cobalt concentrate containing 10% Co can be obtained by combination of gravity and flotation from a feed containing 0.9% Co.

Cobaltite can be separated from pyrite, chalcopyrite and pyrrhotite by initial separation of chalcopyrite, followed by an acidic bulk flotation of all the remaining sulfides using amyl xanthate. Pyrite and pyrrhotite are subsequently floated by depressing the cobaltite with monocalcium aryl sulfonate. Another known flotation separation of cobaltite, from a similar ore containing the same type of minerals, is by direct flotation of all the sulfides other than cobaltite at mildly alkaline pH followed by flotation of cobaltite from tailings with ethyl xanthate at acidic pH after activation with copper sulfate.

By utilizing nitrosonaphthol-based collectors, the flotation of two oxide minerals – erythrite ($\text{Co}_3(\text{AsO}_4)_2 \cdot 8\text{H}_2\text{O}$) and smolyaninovite (Co_3Ni ,

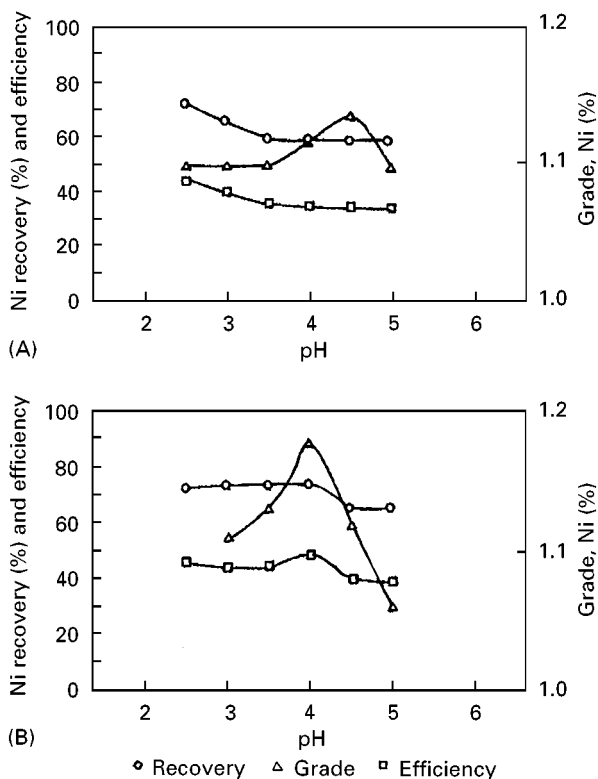


Figure 12 (A) Effect of pH with Flotator® P195 collector (0.25 kg t^{-1}). (B) Effect of pH with a mixture of SPS 430 and Flotator® P195 (1 : 1 at 0.25 kg t^{-1}). (Reprinted with permission from Society for Mining, Metallurgy and Exploration, Inc.)

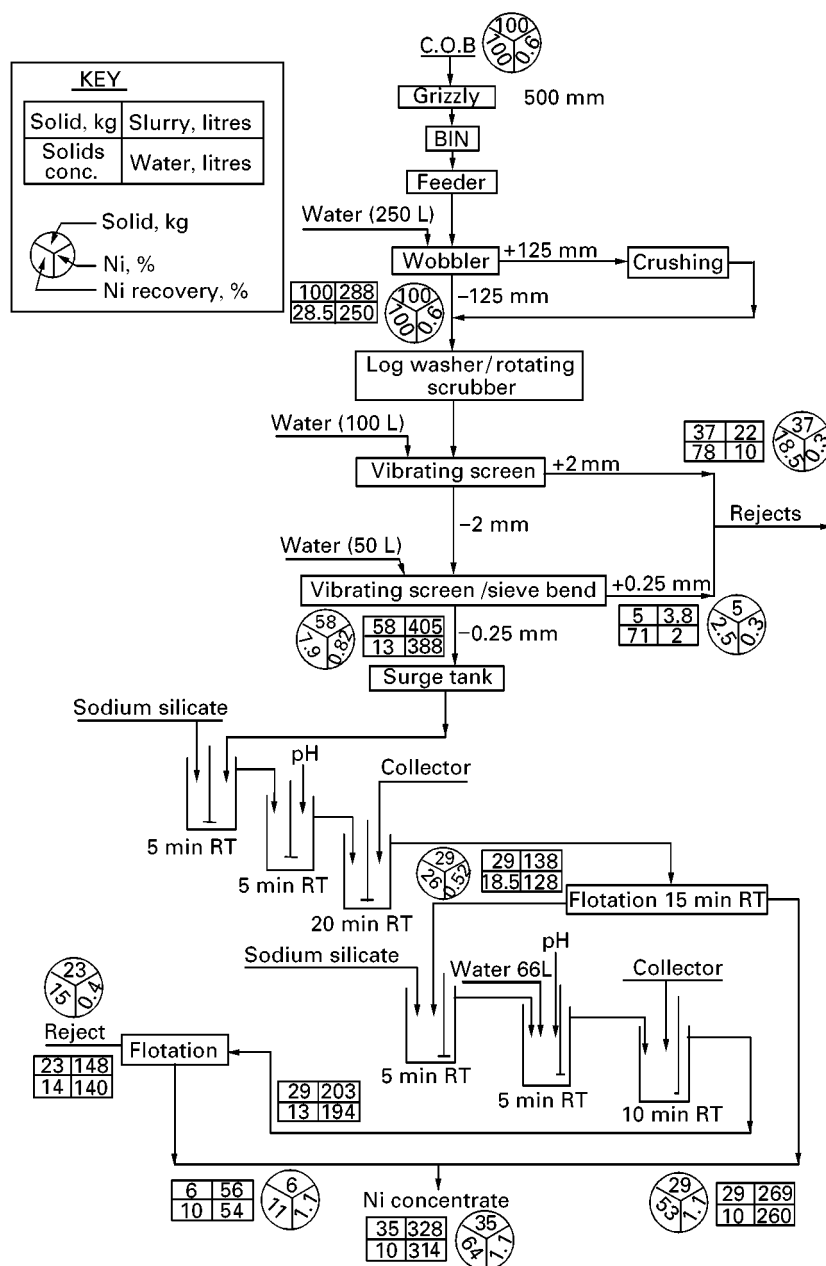


Figure 13 Flow chart to pre-concentrate nickel from lateritic chromite overburden material from Sukinda, India.

$\text{Ca,Mg}_3(\text{Fe,Al})_2(\text{AsO}_4)_4 \cdot 11\text{H}_2\text{O}$ – and a sulfide mineral – arsenosulfide cobaltite (CoAsS) – could be improved.

The flotation response of cobaltite (CoAsS) from Mount Cobalt with nitrosophthol indicated an optimum response between pH 8 to 9 (Figure 14) whereas its flotation response with xanthates is known to be best at pH 4–4.5.

The flotation results obtained with xanthate and nitrosophthol can be seen in Table 6. Nitrosophthol collectors are found to be pH-dependent

and specific for cobalt-bearing minerals. The availability of cobalt ions on or near the mineral surface may be the determining factor for the selectivity of nitrosophthol collectors. Alkyl group attachment on to the naphthalene ring increases the hydrophobicity of the cobalt-bearing minerals on to which these compounds adsorb, thereby increasing the collecting capability of nitrosophthol, but at the expense of selectivity.

A combination of xanthates and nitrosophthol collectors is suitable for the recovery of cobalt sulfide

Table 4 Flotation results on nickeliferous chromite overburden (COB) materials of Sukinda

COB assay		Flotation feed assay ^a		% Ni expected in product ^b	% Ni obtained in product	Fe/Ni in flotation feed
Ni (%)	Fe (%)	Ni (%)	Fe (%)			
0.58	28.5	0.87	38.5	1.13	1.10	44.2
0.40	19.0	0.82	35.7	1.15	1.08	43.5
0.78	28.0	1.20	42.0	1.43	1.35	35.0
0.55	22.0	0.90	40.0	1.13	1.15	44.4
0.57	32.0	0.78	40.6	0.96	0.91	52.0
0.36	14.9	0.57	23.0	1.24	1.11	40.0

^aThe fines obtained after scrubbing the COB (– 210 µm size).

^b% Ni expected in product = (% Ni in feed/% Fe in feed) × 50.

COB, chromite overburden.

(Reprinted with permission from Society for Mining, Metallurgy and Exploration, Inc.)

deposits that are partly oxidized, whereas nitrosonaphthol collector alone is effective for oxide cobalt deposits.

Conclusions

The nickel extraction process is dictated by the mineralogical assemblage of the ore. Pyrrhotite rejection has been of no real importance in many mills treating sulfide ores except in countries having strict restrictions on SO₂ emission. Pyrrhotite rejection from pentlandite is not very satisfactory in the plants adopting differential flotation, but recent investigations indicate the possibility of employing SO₂ and DETA besides adopting starvation flotation. The problems often encountered in sulfide flotation are the fast floating magnesia-bearing minerals and coatings of crysotile and lizardite. Such problems can be addressed successfully by adding soda ash, CMC or sodium chloride. Plants where SO₂ emissions are not

a problem can adopt collectorless flotation at acidic pH as a cost-effective pre-concentration process. New flotation reagents like nitrosonaphthol can be adopted in circuits containing oxidized sulfide ores.

There seems little prospect of upgrading nickel from oxide ores since the nickel values are finely dispersed. Marginal upgrading is possible by using dioxime collectors. In view of the contemporary technological practices being followed elsewhere in the world and the Ni content of ores utilized by such processes, flotation of limonitic ores with anionic collectors like petroleum sulfonates is likely to play

Table 5 Principal cobalt minerals

Mineral	Formula	Cobalt content (%)
Cattierite	CoS ₂ (pure)	47.8
Linnaeite	Co ₃ S ₄ (pure)	58.0
Siegenite	(Co,Ni) ₃ S ₄	20.4–26.0
Carrollite	(Co ₂ Cu)S ₄	35.2–36.0
Cobaltite	(Co,Fe)AsS	26.0–32.4
Safflorite	(Co,Fe)AsS ₂	13–18.6
Smaltite	(Ca,Ni)As ₂	21
Glaucodot	(Co,Fe)AsS	12–31.6
Skutterudite	(Co,Fe)As ₃	10.9–20.9
Heterogenite	CoO(OH) (pure)	64.1
Asbolite	Co	0.5–5.0
Erythrite	(Co,Ni) ₃ (AsO ₄) ₂ · 8H ₂ O	18.7–26.3
Gersdorffite	(Ni,Co)AsS	Low
Pentlandite	(Fe,Ni,Co) ₉ S ₈	Up to 1.5
Pyrite	(Fe,Ni,Co)S ₂	Up to 13

(Reprinted with permission from VCH Verlagsgesellschaft.)

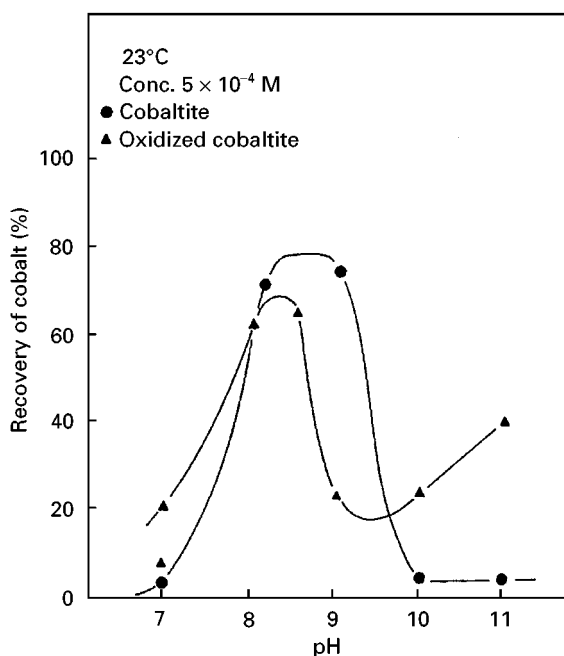


Figure 14 Recovery of cobalt from cobaltite-containing sample as a function of pH with 1-nitroso-2-naphthol as collector (– 105 + 75 µm). (Reprinted with permission from The Institution for Mining and Metallurgy.)

Table 6 Comparison of flotation results of Mount Cobalt sulfarsenide cobalt-mineralized sample with nitrosonaphthols and xanthates

Flotation products	pH	Collector	Wt (%)	Co (%)	Recovery (%)
Rougher concentrate	8.2	NN	19.0	16.16	88.7
Scavenger concentrate	8.5	BNN	18.6	1.69	9.0
Scavenger tailing			62.4	0.13	2.20
Calculated head				3.47	
Rougher concentrate	4.5	SEX	9.0	30.74	82.6
Scavenger concentrate	4.4	PAX	1.80	19.68	10.5
Scavenger tailing			89.2	0.26	6.9
Calculated head				3.35	
Rougher concentrate	4.20	PAX	9.50	31.13	96.4
Scavenger concentrate	8.5	NN	2.70	3.22	2.8
Scavenger tailing			87.8	0.03	0.8
Calculated head				3.09	

NN, 1-nitroso-2-naphthol; BNN, tert-butyl-1-nitroso-2-naphthol; SEX, sodium ethyl xanthate; PAX, potassium amyl xanthate. Conditioning time, 20 min; flotation time, 5 min; collector concentration, 5×10^{-4} M; frother, MIBC; % solids, 10; feed, 100% – 105 μ m. (Reprinted with permission from The Institution for Mining and Metallurgy.)

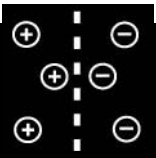
a vital role in raising the nickel content to above 1.1% from lean limonitic deposits abundantly available in various tropical zones. Processing such flotation concentrate by hydrometallurgical routes needs to be explored.

Cobalt minerals are generally recovered as by-products during the extraction of zinc, copper, nickel, silver etc. Flotation of cobalt sulfide ores can be best achieved at acidic pH (~ 4) with xanthate collectors and at pH of about 7.5 for oxide ores with nitrosonaphthol chelating reagents, while their mixture is recommended for oxidized sulfide ores.

Further Reading

- Agar GE (1991) Flotation of chalcopyrite, pentlandite, pyrrhotite ores. *International Journal of Mineral Processing* 33: 1–19.
- Alcock RA (1988) The character of the occurrence of primary resources available to the nickel industry. In: Tyroler GP and Landolt CA (eds) *Extractive Metallurgy of Nickel and Cobalt*, pp. 67–90. Warrendale, Pennsylvania: The Minerals, Metals and Materials Society.
- Engel MD, Middlebrook PD and Jameson GJ (1997) Advances in study of high intensity conditioning as a means of improving mineral flotation performance. *Minerals Engineering* 10(1): 55–68.
- Heiskanen K, Kirjavainen V and Laapas H (1991) Possibilities of collectorless flotation in the treatment of pentlandite ores. *International Journal of Mineral Processing* 33: 263–274.
- Kelebek S, Wells PF and Fekete SO (1996) Differential flotation of chalcopyrite, pentlandite and pyrrhotite in nickel-copper sulfide ores. *Canadian Metallurgical Quarterly* 35(4): 329–336.
- Kerfoot DGE (1991) Nickel. In: Elvers B, Hawkins S and Schultz G (eds) *Ullmann's Encyclopedia of Industrial Chemistry*, pp. 157–219. Weinheim: VCH.
- Mackiw VN (1985) Nickel and cobalt. In: Weiss NL (ed.) *SME Mineral Processing Handbook*, vol. 2, pp. A17-1–A17-58. Littleton, CO: SME American Institute of Mining, Metallurgical and Petroleum Engineers.
- Pietrobon MC, Grano SR, Sobieraj S and Ralston J (1997) Recovery mechanisms for pentlandite and MgO-bearing gangue minerals in nickel ores from Western Australia. *Minerals Engineering* 10(8): 775–786.
- Rao GV and Sastri SRS (1996) Novel approach for enriching nickel content in lean lateritic chromite overburden. *Minerals and Metallurgical Processing* 13(2): 77–81.
- Teoh EC, Lawson F and Han KN (1982) Selective flotation of nickel and cobalt bearing minerals with use of specific dioximes surfactants. *Transactions of the Institution of Mining and Metallurgy. Section C: Mineral Processing and Extractive Metallurgy* 91: 142–152.
- Wellham EJ, Elber L and Yan DS (1992) The role of carboxy methyl cellulose in the flotation of nickel sulfide transition ore. *Minerals Engineering* 5(3–5): 381–395.
- Wezhong Xing and Jian Zhong Yu (1993) Beneficiation technology of copper–nickel sulfide ores in China. In: Chongyue Fu, Huanhua He and Chuanfu Zhang (eds) *Proceedings of the International Conference on Mining and Metallurgy of Complex Nickel Ores*, pp. 43–52. China: International Academic Press.
- Yoon RH, Basilio CI, Marticorena MA, Kerr AN and Stratton-Crawley R (1995) A study of the pyrrhotite depression mechanism by diethylenetriamine. *Minerals Engineering* 8(7): 807–816.

NOVEL INORGANIC MATERIALS: ION EXCHANGE



D. J. Jones, Université Montpellier,
Montpellier, France

Copyright © 2000 Academic Press

Introduction

The modification of open-structured solids by ion exchange is a versatile and powerful synthetic route to new compounds. These may be either novel inorganic phases that cannot be prepared directly using high temperature ceramic routes, or composite systems incorporating an additional organic or inorganic component. In both cases the methods used are part of *chimie douce*, a rare example of a scientific French term that has penetrated into common international usage.

From both a conceptual and a practical point of view, it is useful to distinguish those solids that, by the arrangement of their constituent atoms in space, form a rigid, open-structured network and that readily undergo ion exchange reactions only to within the limit of the size constraint of the window openings of the structure, and those in which the framework is made up of two-dimensional layers that may be prised apart if sufficient energy can be provided to overcome the van der Waals or hydrogen bonding interactions. Typical examples of the former are provided by microporous zeolites, such as zeolite A, while smectite clays, such as montmorillonite, exemplify the latter. Here, as in layered oxides, phosphates and other classes of bidimensional solids, the structure adapts itself depending on the incoming molecule, and the variable parameter represented by the interlayer spacing allows an enormous variety of species to be ion exchanged or intercalated. While more classically, ion exchange or intercalation was a single-step process, much recent work is characterized by the development and use of pre-expansion or exfoliation techniques, and reprecipitation of the dispersed layers in the presence of the desired intercalant ion, molecule or polymer. These methods have significantly broadened the range of new nanocomposite materials that can be prepared, which display properties including second harmonic generation (in the case of intercalation of dyes), chiral recognition, electronic conductivity (in the case of ion exchange of electroactive molecules or polymers), protonic conductivity, micro- and meso-porosity for catalysis and sorption, etc.

The term 'intercalation' will be used in its strictest sense here, to mean the topotactic and reversible insertion of a guest species into a host layered compound; this term has been more generally applied to host matrices of any dimensionality.

Host-Structures for Ion Exchange Reactions

To a first approximation, solids of fixed pore size are three-dimensional structures. In zeolites, and zeotypes with ultralarge pores and having alumino- or gallo-phosphate framework compositions, the window frames to the pores are composed of tetrahedrally coordinated atoms, the number of which defines the size of the entry aperture. Zeolite and zeotype molecular sieves are characterized by their high crystallinity and narrow pore size distribution dominantly in the micropore range, i.e. pore diameter below 2 nm, but more recently extending up into the low mesopore region. Charge imbalance created, in the simplest cases, by inclusion of aluminium in a silica framework, is counterbalanced by intrapore cations, and the Si/Al ratio therefore defines the number of exchangeable ions, or ion exchange capacity, usually expressed as the number of milliequivalents (of exchangeable ion) per gram (of ion exchanger). While the modification of zeolites and zeotypes is a starting point for new inorganic syntheses, zeolite ion exchange properties have long been exploited for water softening in detergents and their Brønsted acidity has been used by the petroleum industry in fluid catalytic cracking and other processes.

This enormous historical use and the economical necessity to crack progressively heavier fractions provided the impetus for the synthesis of ion exchanging materials having a pore size reaching more firmly into the mesopore range, and the plethora of activity associated with all aspects of surfactant-assisted syntheses of mesoporous solids attests to the significance of the discovery of this liquid crystal templating, or cooperative nucleation approach. If the surface acidity has since proved to be disappointing, the narrow and controllable mesopore distribution readily attainable using these routes represents a major advance with applications in many fields. Of the hexagonal, cubic and lamellar phases known, only the ion exchange capacity and unidimensional channels of

the first have been used in the synthesis of composite new materials. Potential host structures for modification by ion exchange include the macroporous silicates or aluminosilicates (zircono-, titano-, etc.) silicates formed, for example, by sol-gel routes. However, these are generally amorphous compounds, and this article will be restricted to crystalline host matrices.

Compounds that crystallize in a layered arrangement have no permanent porosity, and the structures adapt in at least one dimension – that perpendicular to the stacking axis of the layers – on ion exchange or intercalation. Layer-structured crystals can be divided into those having neutral layers, which have no ion exchange properties and in which the driving force for any intercalation reaction is an electron transfer process, and those with either positively or negatively charged layers, which are anion and cation exchangers, respectively. The best-known anion exchangers are the layered double hydroxides $[M_1^{II}_{1-x}M_x^{III}(\text{OH})_2]^{x+} [X_{x/m}^{m-} \cdot n\text{H}_2\text{O}]^{x-}$ and hydroxy double salts $M^II M^III(\text{OH})_3X$, where X is an exchangeable anion, such as OAc^- , Br^- , CO_3^{2-} , etc. In the first of these, charge imbalance in the parent brucite, $\text{Mg}(\text{OH})_2$, crystal structure is induced by partial substitution of M^II by M^III and X occupies the interlayer region. The situation is different in the series based on the botallackite structure $\text{Cu}_2(\text{OH})_3\text{Br}$, as the anion forms part of the coordination sphere of the metal atoms, and its replacement may involve a dissolution–reprecipitation mechanism. Layered silicates (e.g. smectite clays), layered niobate or titanate perovskite structures, layered silicic acids (magadiite, kenyaite, etc.), layered sulfates and phosphates are all known cation exchangers. These may be prepared directly in their hydrogen form, as is the case with α -metal(IV) hydrogen phosphates, or in a form containing an interlayer alkali metal ion, readily exchanged for the proton in acidic solutions. These are solid acids and may display, in addition to the catalytic properties already referred to above in the context of zeolite host matrices, high, water-assisted protonic conductivity. Indeed, ion exchange with inorganic layered matrices can be perceived in the more general framework of ion transfer/transport and ionic mobility.

This section would not be complete without mentioning two additional important classes of ion exchanging materials, which find their place quite naturally between those two extremes of three- and two-dimensionality described above. In one class a permanently porous structure is formed from a layered structure by pillaring, in which process some of the initial ion exchange capacity is retained, and in the other, a layered solid is formed from an initially three-dimensional framework by the clustering of

structural defects induced by ion exchange. These two classes will be discussed in greater detail below.

Synthesis of Metastable Microporous Layered or Framework Materials

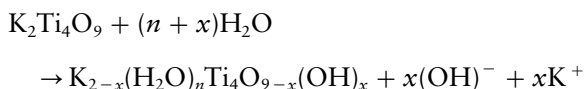
The classical approach to the synthesis of many solid state compounds is to mix individual elements or simple solid compounds together and fire them at elevated temperature. Here, the diffusion of atomic/ionic species through reactants and products controls product formation. Nonclassical routes to the preparation of inorganic solids, including the full range of solution chemistry, sol-gel chemistry, insertion and intercalation chemistry techniques of synthesis, have gained increasing importance because they offer alternative means by which both classical materials and novel compositions may be prepared. Of particular interest in the present context is the use of topochemical pathways whereby a solid prepared by high temperature ceramic methods is the precursor for a thermodynamically unstable but kinetically stable phase. This usually involves the extraction or insertion of a mobile species from/into a rigid framework, either by ion exchange or a redox process.

Often, the mobile species is an alkali metal ion. The material takes on industrial importance in the particular case of lithium, with the potential and actual use of lithium insertion compounds as electrodes in lithium batteries, in particular for portable electronic devices and for electric vehicles. For example, the spinel form of manganese dioxide known as λ - MnO_2 cannot be obtained directly by classical methods, nor is it stable at high temperatures, but it is prepared by extraction of lithium either chemically or electrochemically from its lithiated congener LiMn_2O_4 . Generally, in order to maintain charge balance, this process occurs with oxidation of Mn^{III} in the mixed valence ($\text{Mn}^{III}/\text{Mn}^{IV}$) precursor to give λ - Mn^{IV}O_2 . This oxidative extraction can provide cell voltages of c. 4 V. X-ray absorption spectroscopy (near-edge and fine structure) have provided much information on the changes in oxidation state and accompanying local structural modifications induced by the loss of the Jahn–Teller ion Mn^{III} and resulting increase in local symmetry. Lithium-rich spinel manganates $\text{Li}_{1+x}\text{Mn}_{2-x}\text{O}_4$, with $0 < x < 0.33$, are also known. In these materials lithium occupies octahedral sites left vacant by the lower manganese content and electrical neutrality is achieved by an increase of the average oxidation state from 3.5 in LiMn_2O_4 to 4 in $\text{Li}_{1.33}\text{Mn}_{1.67}\text{O}_4$. Oxidative removal is no longer possible, and ion exchange with protons occurs when lithium is removed chemically in acid solution. The octahedral sites vacated by manganese, and not occu-

pied by lithium in the acid exchanged samples, result in lamellar-type lattice defects in the spinel structure in which weakly bound water could be trapped. There is no direct synthetic route to either protonated or nonprotonated λ - MnO_2 .

Indeed, for obvious reasons, high temperature routes often preclude the formation of hydroxylated or hydrated inorganic compounds. Amongst others, protonated dicalcium triniobate $\text{HCa}_2\text{Nb}_3\text{O}_{10}$ and the trititanate $\text{H}_2\text{Ti}_3\text{O}_7$ are simply prepared in acid solution by ion exchange of potassium and lithium, respectively. The materials formed are solid acids, with important implications for eventual proton conductivity or catalytic activity; other modifications may be imposed depending on the dimensionality of the solid. Thus $\text{HCa}_2\text{Nb}_3\text{O}_{10}$ can be further derivatized by acid-base reaction with alkylamines, and by pillar- ing. These last aspects will be further developed below. The so-called γ -form of zirconium phosphate, $\gamma\text{-ZrPO}_4(\text{H}_2\text{PO}_4) \cdot 2\text{H}_2\text{O}(\gamma\text{-ZrP})$, is metastable with respect to the α -form, $\alpha\text{-Zr}(\text{HPO}_4)_2 \cdot \text{H}_2\text{O}$, and protonated γ -ZrP can only be obtained via ion exchange in acid solution of sodium or ammonium ions in the corresponding precursor prepared at 80–180°C from zirconyl chloride, sodium or ammonium hydrogen phosphates, and phosphoric or hydrochloric acid.

Other possibilities are opened up when the topotactic step is followed by dehydroxylation–condensation. An interesting example is provided by a particular form of titanium dioxide that can be prepared from potassium tetratitanate, $\text{K}_2\text{Ti}_4\text{O}_9$. The latter is formed at 950°C, but is hygroscopic and sensitive to acid hydrolysis. In water, potassium ions are eliminated:



and, when $x = 2$, thermolysis at 500°C yields $\text{TiO}_2(\text{B})$, where the index B indicates the structural relationship to the bronze Na_xTiO_2 (Wadsley bronze). When $x = 1$, then the octatitanate is formed, $\text{K}_2\text{Ti}_8\text{O}_{17}$. The structure of this is identical to that of the potassium richer phase $\text{K}_3\text{Ti}_8\text{O}_{17}$ (Watts bronze), which can be prepared by a classical high temperature route. This is illustrated in Figure 1.

Rather than extraction, a starting compound can also be modified by further insertion of a mobile species. Thus, in addition to the removal of lithium from LiMn_2O_4 described above, lithium may be further reversibly inserted with reduction of Mn^{IV} to give $\text{Li}_2\text{Mn}_2\text{O}_4$. This intercalation can be performed electrochemically, at an average voltage of 3 V, or chemically, using butyllithium or lithium iodide. From

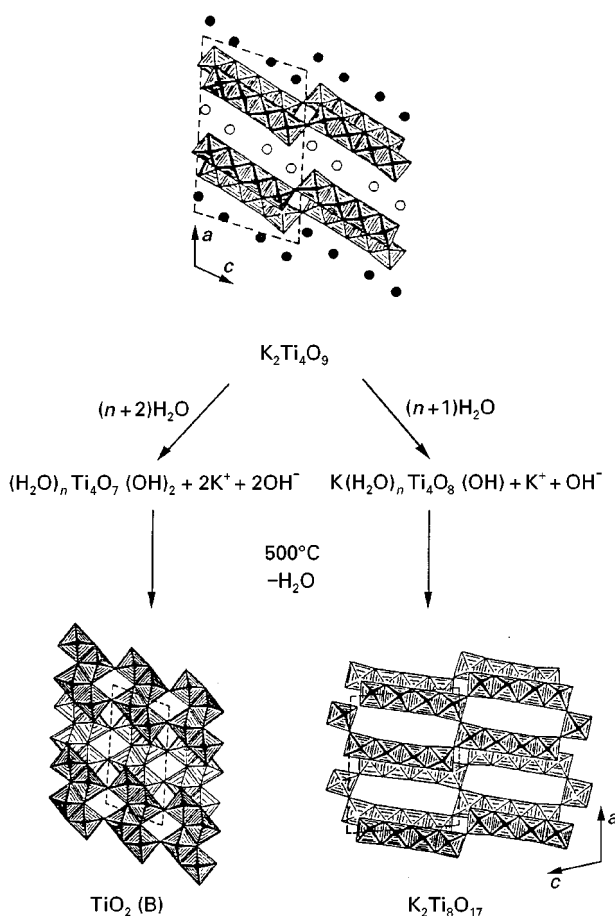


Figure 1 Soft chemical route from dipotassium tetratitanate to a form of titania [$\text{TiO}_2(\text{B})$] and dipotassium octatitanate.

a structural point of view, the local distortions around Jahn–Teller Mn^{III} ions in octahedral sites are no longer suppressed by the presence of non–Jahn–Teller Mn^{IV} , and the unit cell becomes increasingly tetragonally distorted due to cooperative elongation of the J–T Mn^3+O_6 octahedra along the c -axis of the crystal. Although the tetragonal structure is crystallographically different from the precursor cubic structure, they are related in that the linkage of edge-sharing MnO_6 octahedra in the three-dimensional $[\text{Mn}_2\text{O}_4]$ spinel sublattice is conserved.

Use of Ion Exchange and Intercalation for the Synthesis of Materials with New Compositions

The modifications of open-structured two- or three-dimensional hosts by ion exchange with functionalized organic (monomeric, polymeric), inorganic (simple ions, inorganic complexes, polynuclear ions) or organometallic species to give nanocomposite

solids of new composition and tailored structure is an increasingly powerful route to materials displaying a range of enhanced or induced physical (mechanical, optical, electrical, magnetic, textural) or chemical (catalytic, molecular or chiral recognition) properties. Of these, perhaps most attention has been given over recent years in two areas, that of the insertion, or formation *in situ*, of polymers or extended aggregates in the interlayer or intrapore regions of inorganic hosts, and that of the synthesis of pillared layered solids.

Molecular Recognition

The separation of enantiomers on a preparative, rather than analytical, scale is an increasingly important objective, in particular for the pharmaceutical industry. Ion exchanging, microporous solids represent one route currently being explored for the separation of chiral molecules, either making use of a chiral inorganic solid or by modifying the host structure by ion exchange in a first stage such that it recognizes, and becomes specific for, the uptake of one enantiomer from a racemic solution. This is an exciting area of study that deserves to receive much attention in the future.

Intercalated Polymers and Extended Aggregates

During the 1990s considerable interest has focused on the association of ion exchanging host matrices and polymers (or extended aggregates), inspired from both fundamental and more applied viewpoints. As well as being considered to be model systems for interface studies, such constrained environments are expected to enforce a higher degree of polymer ordering, and be conducive to the isolation of polymer chains. Polymer-inorganic host nanocomposites can be discussed, *inter alia*, in relation to the nature of the property induced or enhanced. Currently, two important areas can be distinguished corresponding to materials displaying either mechanical or electrical (ionic, electronic) properties. For example, unprecedented mechanical properties of nylon-clay nanocomposites have been observed, involving a doubling of the tensile modulus and strength, and an increase of the heat distortion temperature by up to 100°C. On intercalation of polymer electrolytes, typically poly(ethylene oxide) (PEO), into a host structure, the oxyethylene units replace water in the coordination sphere of interlayer Li^+ or Na^+ ions and the normally soluble polymer is heterogenized and protected from chemical aggression. Thermal stability is improved, and the materials display good ionic conductivity over a broader temperature range than PEO-salt electrolytes. The association of host matrices with

electroactive polyaniline, polypyrrole and organic metals such as tetrathiafulvalene provide an original source of electronically conducting materials and has inspired research directed at building devices from molecular assemblies. In addition, it can be predicted that in the future, matrices occluding chromophore aggregates will play a role in the field of second harmonic generation; however, as yet the number of examples of nanocomposite solids displaying nonlinear optical properties is limited.

Inorganic host structure-polymer (or aggregate) nanocomposites can also be discussed in relation to the synthetic method used to intercalate or form the polymer *in situ*. From a conceptual point of view the simplest, direct ion exchange, has been used to insert hydrophilic polymers such as PEO, poly(ethylene-imine) (PEI), poly(ethylene glycol) (PEG), poly(phosphazene), gelatin, lysozyme and protamine from solution into layered solids including montmorillonite, fluorohectorite, divanadium pentoxide, transition metal phosphorus trichalcogenides and zirconium phosphate. This strategy requires a compatible polymer-host solvent system. An alternative related method lies in the use of direct intercalation from polymer melts in which the solid polymer (polystyrene, polyamides, polyesters, polycarbonate) and the inorganic matrix are heated to above the softening point of the polymer. The hydrophobicity of the polymer and of the interlayer environment is a key experimental factor, and the latter can be modified prior to intercalation from the melt, e.g. by ion exchange of interlayer Na^+ , etc., for surfactant ions. The intercalated organic-inorganic hybrids formed have an interlayer separation of 1–3 nm, but another, rarer, situation exists when the miscibility of the inorganic and organic systems is high, in which the layered host is exfoliated and individual layers are separated by 10–15 nm. Third, in the absence of any exchange reaction with the host solid, a phase-separated composite is formed, where packets of nonmodified host matrix are embedded in a polymer matrix (Figure 2).

Other synthetic routes make use of ion exchange with a monomer and *in situ* polymerization in the interlayer or intrapore region. Here, distinction can be made between the polymerization of assembled monomers and a redox intercalative polymerization. In the former, monomer species bearing reactive groups that might be, for example, acetylenic, nitrile, functionalized aromatic molecules or condensable moieties, are ion exchanged in a first stage into the inorganic host. In the case of a layered host structure, the charged surface leads to a particular orientation of the monomer units that may favour a given polymerization pathway in the subsequent polymerization

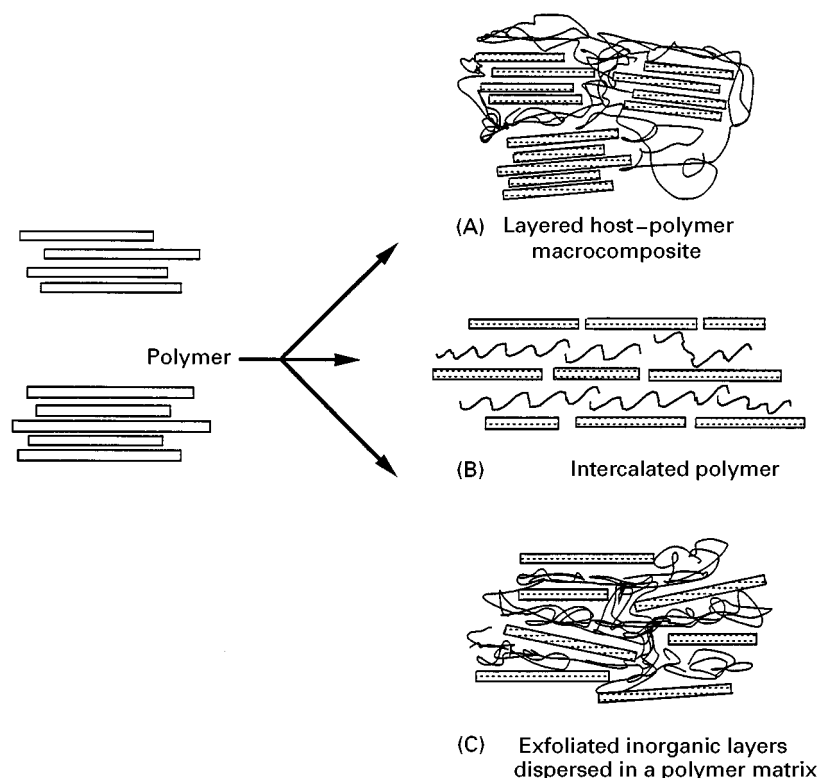


Figure 2 Schematic representation of the continuum in inorganic layered host structures and polymer arrangements between (A) phase-separated regime; (B) intercalated polymer; and (C) polymer dispersion of exfoliated inorganic layers.

step induced thermally, radiatively or chemically. Thus cation exchange of aminocaproic acid into montmorillonite or zirconium phosphate, or anion exchange from acrylic acid into layered double hydroxides, lead to nylon-6 and to polyacrylate, respectively, as the monomers are condensed and water is split off when the temperature is raised to *c.* 200°C. Propargylamine ($\text{HC}\equiv\text{CCH}_2\text{NH}_2$) and di-propargylamine [$\text{HC}\equiv\text{CCH}_2(\text{NH})$]₂ readily intercalate with proton transfer into metal(IV) phosphates, and γ -radiation or thermal treatment under inert atmosphere produces polymers of polyacetylenic character. ^{13}C NMR is of particular utility, as a probe spectroscopic technique for the interlayer region, in following the loss of monomer and identifying the nature of the polymer formed. An interesting example is provided by ion exchange of *p*-xylylene- α -dimethylsulfoxonium for Li^+ or Na^+ in M_xMoO_3 . On thermal treatment at 100–250°C, dimethylsulfide is eliminated and interlayer poly(*p*-phenylenevinylene) generated. Chemical oxidation (atmospheric oxygen, ammonium peroxide, etc.) has also been used to initiate the polymerization process, e.g. of anilinium in zeolite-Y, mordenite and ordered mesoporous aluminosilicate MCM-41, and of methyl methacrylate in montmorillonite.

The polymer intercalate may also serve as a precursor phase; a potentially important development lies in the use of clay-polymer intercalation nanocomposites as precursors for graphite films. Such template carbonization uses the inorganic matrix to orient the organic species as it evolves from the ion exchanged monomer to a polymer to a carbon. Destruction of the template and subsequent heat treatment leads to flexible graphite films.

Intercalative polymerization can occur when the matrix has electron transfer properties. These may be inherent to the host solid, as in FeOCl , V_2O_5 , etc., or may be conferred on a redox-inactive matrix by ion exchange with appropriate transition metal ions. Thus following ion exchange of Cu^{2+} or Fe^{3+} into mordenite, zeolite-Y, montmorillonite, zirconium phosphate, ordered mesoporous aluminosilicate MCM-41, etc., electron donor molecules such as aniline (Figure 3) and pyrrole are oxidized, ion exchanged and undergo polymerization concomitantly, and the metal ion is reduced and, in some cases, eliminated as electrically neutral colloidal particles. Electroactive molecules such as tetrathiafulvalene (TTF) have also been assembled in γ -zirconium phosphate using this same approach.

TTF provides an example of an electron donor molecule that can only be inserted in an ion

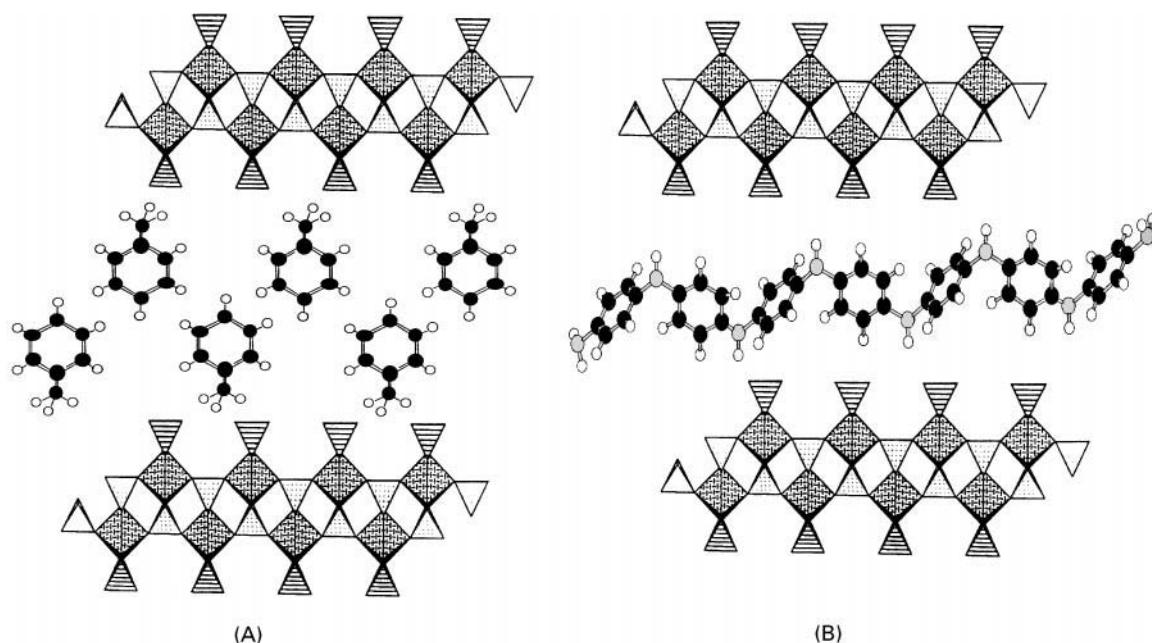


Figure 3 Schematic diagram showing layers of (A) $\gamma\text{-ZrPO}_4 \cdot \text{HPO}_4 \cdot (\text{anilinium})$, (B) $\gamma\text{-ZrPO}_4 \cdot \text{HPO}_4 \cdot (\text{PANI})$.

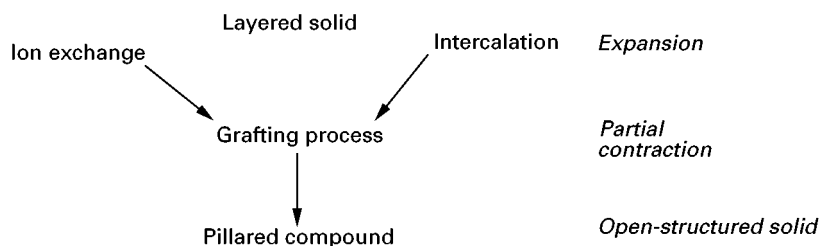
exchanging matrix if oxidized. Indeed, from the point of view of associated electrical properties, partial oxidation of TTF is required. These two conditions have been combined recently by oxidizing TTF with bromine to $\text{TTF}^{0.72+}$, which can then be ion exchanged with species used to pre-expand the interlayer region in host α - and γ -ZrP. The TTF units do not lie parallel to the plane of the phosphate layers and, although not a polymer system, they are nevertheless stacked into extended aggregates and provide the π -orbital overlap necessary for conduction.

Pillared Layered Solids

Reference was made above to the requirement by the petroleum industry during the 1970s for acid catalysts of pore size in the mesopore region, distinctly greater than that of the zeolites available at that time. Although templated routes to larger pore zeolites had not yet been successful, the modification of

preformed layered solids by ‘pillaring’ was to give rise to a new area of chemistry and a new type of porous solid. The calculated surface area of a two-dimensional solid is high, $960 \text{ m}^2 \text{ g}^{-1}$ for example for α -zirconium phosphate, although nitrogen BET (Brunauer, Emmett, Teller) measurements indicate a surface area of *c.* $5 \text{ m}^2 \text{ g}^{-1}$ only. To render at least part of the surface area accessible, the layers must be permanently separated using inorganic spacers introduced by ion exchange or intercalation. To consolidate the structure and liberate interlayer regions occupied by organic moieties, hydroxyl groups or water, the expanded phase is then treated thermally or chemically (Scheme 1 and Figure 4).

The presence of inorganic species acting as pillars and interacting strongly with the layers gives rise to thermally stable materials of high surface area (BET surface areas typically between 150 and $400 \text{ m}^2 \text{ g}^{-1}$) and pore volume accessible for adsorption and separation, catalysis and ion exchange. An important area



Scheme 1 Formation of a pillared compound from a layered solid.

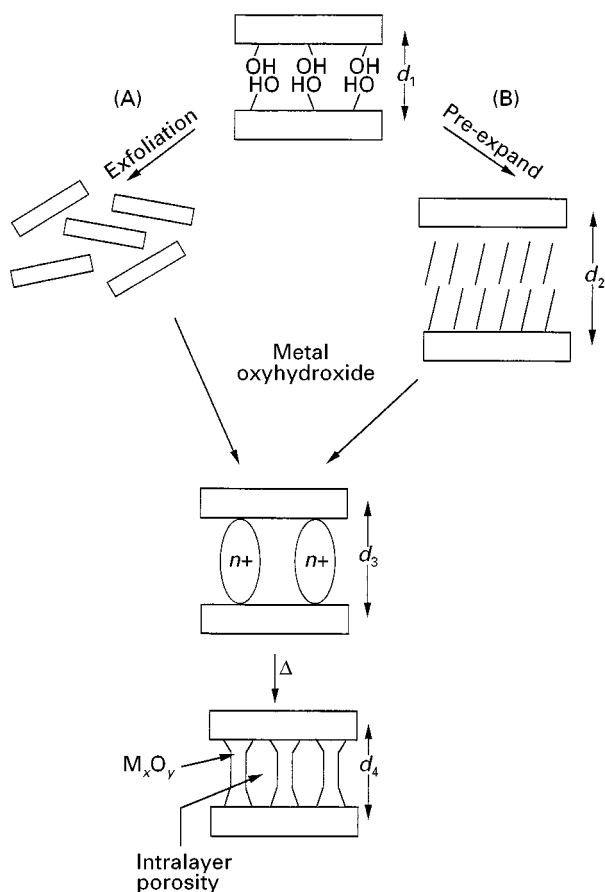


Figure 4 Synthesis of pillared layered structures by ion exchange and grafting from (A) swelling matrices and (B) host structures of high layer charge density.

represented by metal phosphonates is beyond the scope of this article by virtue of the synthetic routes to this class of pillared solid.

The extent of uptake of the pillar precursor species, a direct result of the ion exchange capacity of the host matrix, is a key parameter influencing the ultimate textural properties of the pillared solid, since it con-

trols the lateral spacing of the pillars. Indeed, the synthesis of porous solids from higher layer charge density solids was only achieved some 15 years after the first results published on smectite clays. In addition, the layer charge density of smectite clays is sufficiently low that they swell spontaneously in water and the ion exchange of generally bulky, polynuclear inorganic ions still occurs readily. In contrast, for non-clay substrates of higher layer charge density a pre-expansion or exfoliation step is the general rule. This is summarized in Table 1.

A further requirement is that the pillaring species should be regularly arranged in the interlayer region, in order to generate a solid of narrow pore size distribution. While this regular distribution is achieved at the precursor stage by the registry between host and guest ions, sintering of the metal oxide particle on thermal treatment and degradation of the host structure itself both contribute to producing a broader – and frequently bimodal (spanning the micro- and small meso-pore range) – pore size distribution than is characteristic, say, of zeolites. Additional criteria for the matrix are therefore that it must be sufficiently rigid that it does not collapse in regions between the pillars on dehydration and that the layer charges must be uniformly distributed. In this respect, synthetic clays and non-clay substrates have received particular attention recently since, in addition, these provide the possibility of varying the layer charge density, e.g. by changing the Si/Al ratio or by partially replacing sites for ion exchange with nonexchangeable groups. Nevertheless, when the host matrix has small platelet diameter or when it undergoes an exfoliation stage in the synthesis, reassembly of the layers following ion exchange with the pillaring solution can lead to the situation where edge-to-face stacking predominates ('house-of-cards' arrangement), which has more developed mesoporosity (Figure 5).

Most of the two-dimensional matrices mentioned above have been used as a starting point for pillared

Table 1 Comparison of properties of smectite clays and nonswelling host lattices and consequences on the formation of porous, and not just cross-linked, layered solids

<i>Smectite clays</i>	<i>Non-clay substrates</i>
Low layer charge density	High layer charge density
Spontaneously swell in water	No spontaneous swelling in water; exfoliation (infrequent) under defined conditions not necessarily compatible with existence of polynuclear inorganic species
Pillaring by direct ion exchange with aqueous solution of polynuclear inorganic pillaring species	No direct intercalation → must pre-expand and then ion-exchange, e.g. butylamine/ Al_3^{+}
Inserted species are well spaced	Crowded interlayer

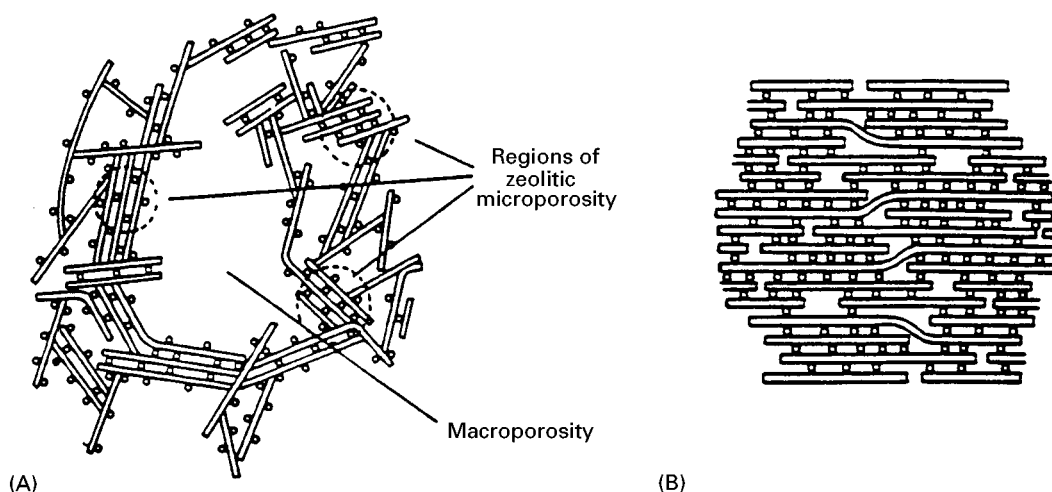


Figure 5 (A) House-of-cards arrangement of the layers of a pillared solid where flocculation after delamination has led to predominant edge-to-face stacking. (B) regular pillared solid with predominant edge-to-edge stacking morphology.

layered structures. A broad spectrum of pillaring species exists based on polynuclear metal hydroxo or oxo complex ions obtained by the hydrolysis of metal salts, such as the aluminium Keggin ion $[\text{Al}_{13}\text{O}_4(\text{OH})_{24}(\text{H}_2\text{O})_{12}]^{7+}$, their gallium and iron analogues, and heteronuclear combinations. These include aluminium Keggin ion modified by the addition of rare earth ions, $[\text{Cr}_3(\text{OH})_4(\text{H}_2\text{O})_9]^{5+}$, $[\text{Zr}(\text{OH})_8(\text{H}_2\text{O})]^{8+}$, metal chloride cluster ions $[\text{M}_6\text{Cl}_{12}]^{2+}$, $\text{M} = \text{Nb}, \text{Ta}$, organometallic oligomers, e.g. $[\text{H}_2\text{N}(\text{CH}_2)_3\text{Si}_{1.5}]_8$, silicon tris(acetylacetonate), positively charged colloidal particles of titania or silica and, in the case of cationic layers, polyoxometallate ions. The variety of pillaring ions and layered hosts available provides enormous flexibility for creating numerous chemical combinations. This opportunity arises precisely because the route to pillared solids is via ion exchange, which allows variety in framework chemical and atom concentrations not yet attainable in other porous solids, in particular in the family of M41S mesoporous silicates. However, in large part because of the low degree of crystallinity of pillared layered solids, little direct structural information is available using X-ray diffraction and the relationship between structure and properties remains to be explored. Furthermore, in the case of complex polynuclear ions, the dominant species in solution may not be the same as that stabilized in the interlayer region. Local structural information around the metal atoms of the layer and the pillaring species can be obtained using magic angle spinning nuclear magnetic resonance (MAS-NMR) and X-ray absorption spectroscopies.

Some of the ion exchange capacity used in assembling the pillaring species is regenerated during the

calcination stage. This retained ion exchange capacity is important, since it provides the opportunity for a Brønsted acidity additional to the Lewis acidity generally conferred by the inorganic oxide particles forming the pillars. It can be exploited to further modify the chemical composition of the solids, and so tailor them for a particular application, in particular in catalysis. In addition, pillared layered solids can be seen as a new type of confining matrix for the organization and quantization of polymers and metal clusters or sulfides, and pillared materials derivatized in this way have been termed nano/nanocomposites.

Finally, mention should be made of a new development in a related area making use of sol-gel and intercalation chemistry, and surfactant-directed synthesis. Porous clay heterostructures are formed by reacting cationic surfactant exchanged fluorohectorite, vermiculite or rectorite with neutral amine/tetraethoxysilane to give a structure in which silica-lined cavities impart permanent porosity to the interlayer region.

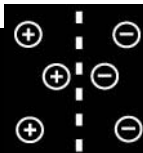
See also: II/Ion Exchange: Catalysis: Organic Ion Exchangers; Historical Development; Inorganic Ion Exchangers; Novel Layered Materials: Non-Phosphates; Organic Ion Exchangers; Theory of Ion Exchange.

Further Reading

Ammundsen B, Jones DJ, Rozière J and Burns GR (1996) Effect of chemical extraction of lithium on the local structure of spinel lithium manganese oxides determined by X-ray absorption spectroscopy. *Chemistry of Materials* 8: 2799–2808.

- Alberti G and Bein T (eds) (1996) *Solid State Supramolecular Chemistry: two and three dimensional inorganic networks*, Vol. 7 in Atwood JL, Davies JED, Macnicol F and Vögtle F (eds) *Comprehensive Supramolecular Chemistry*. Amsterdam: Elsevier.
- Aranda P and Ruiz-Hitzky W (1992) Poly(ethylene oxide)-silicate intercalation materials. *Chemistry of Materials* 4: 1395-1403.
- Beck JS, Vartuli JC, Roth WJ *et al.* (1992) A new family of mesoporous molecular sieves prepared with liquid crystal templates. *Journal of the American Chemical Society* 114: 10834-10843.
- Clearfield A (ed.) (1982) *Inorganic Ion Exchange Materials*. Boca Raton, FL: CRC Press.
- Galarneau A, Borodawalla A and Pinnavaia TJ (1995) Porous clay heterostructures formed by gallery-templated synthesis. *Nature* 374: 529.
- Garcia ME, Naffin JL, Deng N and Mallouk TE (1995) Preparative scale separation of enantiomers using intercalated α -zirconium phosphate. *Chemistry of Materials* 7: 1968-1973.
- Giannelis EP (1996) Polymer layered silicate nanocomposites. *Advanced Materials* 8: 29-35.
- Jones DJ, El Mejjad R and Rozière J (1992) Intercalation and polymerization of aniline in layered protonic conductors. In: Bein T (ed.) *Supramolecular Architecture, Synthetic Control in Thin Films and Solids*, ACS Symposium Series 499, pp. 220-230. Washington, DC: American Chemical Society.
- Nazar LF, Zhang Z and Zinkweg D (1992) Insertion of poly(*para*-phenylenevinylene) in layered MoO_3 . *Journal of the American Chemical Society* 114: 6239-6240.
- Ohtsuka K (1997) Preparation and properties of two-dimensional microporous pillared interlayered solids. *Chemistry of Materials* 9: 2039-2050.
- Olivera-Pastor P, Maireles-Torres P, Rodríguez-Castellón E *et al.* (1996) Nanostructured inorganically pillared layered metal(IV) phosphates. *Chemistry of Materials* 8: 1758-1769.
- Rouxel J (1992) Design and chemical reactivity of low-dimensional solids: some soft chemistry routes to new solids. In: Bein T (ed.) *Supramolecular Architecture, Synthetic Control in Thin Films and Solids*, ACS Symposium Series 499, pp. 88-113. Washington, DC: American Chemical Society.
- Schöllhorn R (1996) Intercalation systems as nanostructured functional materials. *Chemistry of Materials* 8: 1747-1757.
- Wang L, Schindler J, Kannewurf CR and Kanatzidis MG (1997) Lamellar polymer- Li_xMoO_3 nanocomposites via encapsulative precipitation. *Journal of Materials Chemistry* 7: 1277-1283.

THE NUCLEAR INDUSTRY: ION EXCHANGE



J. Lehto, University of Helsinki, Helsinki, Finland

Copyright © 2000 Academic Press

Introduction

Ion exchange is used in nearly all phases of the nuclear fuel cycle beginning in the early stages of uranium ore treatment where ion exchange is one of the major processes used: uranium is removed from ore leach liquors using anion exchange resins.

At nuclear power plants, ordinary organic ion exchange resins are mainly used for the removal of ionic and particulate contaminants from the primary circuit, condensate and fuel storage pond waters. Ion exchange resins are also used for the solidification of low- and medium-activity nuclear waste solutions. The number of applications of selective inorganic ion exchangers in the separation of radionuclides from nuclear waste solutions has been increasing since the mid-1980s.

In nuclear fuel reprocessing plants, the main separation method is solvent extraction. Ion ex-

change is, however, used for the solidification of low- and medium-activity waste solutions, as well as for the partitioning of radioactive elements for further use.

This article reviews all the most important areas of the utilization of ion exchangers in the nuclear power industry. Special attention is paid to ion exchange processes, which involve radionuclide removal functions, and to new developments in selective ion exchange materials.

Ion Exchange Materials Used in the Nuclear Industry

Nuclear Grade Ion Exchange Resins

Organic ion exchangers used at nuclear power plants are based on conventional poly(styrene-divinylbenzene) resins with sulfonic acid ($-\text{SO}_3^-$) and quaternary ammonium ($-\text{N}(\text{CH}_3)_3^+$) functional groups for cations and anions, respectively. Nuclear grade resins,

Lehto J (1993) Ion exchange in the nuclear power industry. In: Dyer A, Hudson HG and Williams PA (eds) *Ion Exchange Processes: Advances and Applications*, p. 39. Cambridge, UK: The Royal Society of Chemistry.

Lehto J and Harjula R (1997) Selective separation of radionuclides from nuclear waste solutions with inorganic ion exchangers, *React Funct Polym* (in press).

Navratil JD (1989) Ion exchange technology in spent fuel reprocessing. *Journal of Nuclear Sciences and Technology*, 26: 735.

Shultz WW, Wheelwright EJ, Godbee H, Mallory CW, Burney GA and Wallace RM (1984) Ion exchange and adsorption in nuclear chemical engineering. In: *AIChE Symposium Series* 80(233): 96.

NUCLEIC ACIDS



Centrifugation

A. Marziali, University of British Columbia, Vancouver, Canada

Copyright © 2000 Academic Press

Introduction

Centrifugation has been applied to nucleic acid isolation and purification through numerous protocols which, at some level, contain elements of one or more of three basic techniques: isopycnic or density equilibrium separation, phenol-chloroform extraction, and differential precipitation. Even if we consider only the protocols that are in current use, numerous variations on these appear in the literature. These variations result from the intended use of the product, the required purity from specific contaminants, the cost and throughput goals of the technique, and often the author's personal preferences. This article will make no attempt to cover all variations but will instead illustrate by example the basic forms of centrifuge-based techniques for nucleic acid separation as they are presently used. A rough guide to these three basic techniques and their applications is contained in Table 1. Each of these will subsequently be described separately.

Recent demands imposed on nucleic acid purifications by large scale DNA sequencing operations have led to the development, and increased use of filtration-based purification methods for high throughput separations. Though the cost of the filter membranes required for these separations is much higher than the cost of centrifugation, the throughput and ease of automation of the membrane based methods make them preferable in many situations. Recent developments in automation of centrifugation, discussed in the last section of this article, may reverse this trend.

Isopycnic Separations

General Principle

Isopycnic separations rely on the balancing of the buoyant and centrifugal forces acting on a submerged sample during centrifugation. When a sample of density ρ_s and effective volume V is placed in a medium of density ρ_m in the presence of a centrifugal field a , the sample feels an upward buoyant force $F_b = \rho_m Va$, and an opposing centrifugal force $F_c = \rho_s Va$. Consequently, the sample will move 'up' toward the rotation axis if $\rho_s < \rho_m$ and 'down' if $\rho_s > \rho_m$. This motion terminates when the sample reaches the boundary of the medium or when it enters a region of the medium where $\rho_s = \rho_m$. Based on this principle, if a sample container is filled with a medium whose density increases gradually in the downward direction, a sample injected in this medium will migrate to the region of the medium that matches the sample density (provided such a region exists). This location is known as the isopycnic point of the sample.

Samples may therefore be separated based on their densities provided a medium is found that can be formed into a density gradient and whose density range includes that of the sample. One of the criteria in the selection of separation media for a specific sample is to ensure that this condition is met.

After a substantial migration period (often over a day), the sample fractions of different densities can be observed as bands within the medium. Extraction of these bands is performed by puncturing the centrifuge tube with a hypodermic needle and withdrawing the desired band. The resolution provided by this method is a function of the separation medium and the relative density difference in the fractions to be separated.

In the case of nucleic acids, RNA and DNA exhibit very different densities in aqueous solutions and therefore can be separated. Cesium salt solutions are typically used as the separation medium since in

Table 1 Three common methods of nucleic acid separation employing centrifugation

<i>Separation type</i>	<i>Application</i>
Isopycnic centrifugation: Gradients of cesium salts –	High purity, low throughput DNA purification. Separation of DNA, RNA, and DNA–RNA hybrids. Separation of DNA by conformation. Plasmid DNA purification. Nucleic acid separation by base composition
Non-ionic media gradients – (Metrizamide, Nycodenz)	High purity RNA purification
Phenol–chloroform extraction	Separation of nucleic acids from proteins
Differential precipitation	Concentration of nucleic acids, removal of some salts. High throughput, medium purity nucleic acid purification

a centrifugal acceleration field they spontaneously form into a density gradient whose range can include that of DNA. RNA typically exhibits higher density than the maximum cesium gradient density and pellets at the bottom of the centrifuge tube. DNA may also be fractionated according to a number of variables which affect its buoyant density. Single stranded DNA and double stranded DNA differ in their degree of hydration and therefore exhibit different buoyancies, allowing them to be separated into two different bands in Cs_2SO_4 (or NaI) gradients. Also, the base composition (G + C content) of DNA linearly affects its buoyancy allowing separation of DNA from different organisms, and, in some cases, even separation of DNA from different regions of the same eukaryotic genome (Figure 1).

The addition of intercalating molecules such as ethidium bromide to the gradient may be used to separate DNA based on its conformation. Linear and relaxed circular DNA allow a larger amount of ethidium bromide to intercalate than supercoiled DNA, leading to decreased density and band separation. In the example described below, this result is used to separate supercoiled plasmid DNA from genomic and nicked circular plasmid DNA.

Separation of RNA is difficult to perform in cesium salt solutions because of its density and tendency to form a precipitate. Consequently, separation of RNA is now performed in nonionic media such as Metrizamide and Nycodenz. Table 2 lists some commonly used density gradient media and their associated use.

A common example of the use of cesium chloride gradients is illustrated in the isolation of plasmid DNA. Note that this is an abbreviated protocol: the

references at the end of this article should be consulted for further details.

Phenol Extraction for Separating DNA/Proteins

A common method for separating nucleic acids from proteins is extraction by phenol or phenol:chloroform. In this technique, solutions containing protein and nucleic acids are combined with an equal part of phenol or phenol:chloroform and mixed into an emulsion. Since phenol and chloroform are solvents for denatured proteins while nucleic acids are soluble in the aqueous phase, centrifugation of the phases results in separation of nucleic acids from proteins. In some cases, multiple extractions may be required and may be followed by extractions in pure chloroform and by ethanol precipitation depending on the required purity of the nucleic acid sample. A simple example of this technique is the purification of DNA from M13 bacteriophage for purposes of DNA sequencing. An abbreviated protocol is given in Figure 2.

Differential Precipitation Methods

Ethanol or Isopropanol Precipitation

Perhaps the simplest way to concentrate nucleic acids by centrifugation is precipitation in ethanol or isopropanol solutions. This technique takes advantage of the fact that nucleic acids can form a solid precipitate in these solutions when their negative charge is neutralized by the presence of monovalent cations. A common example of this is ethanol precipitation of DNA in which an aqueous DNA sample is mixed with ethanol and a small amount of salt (often sodium acetate). After incubation, a solid precipitate of the sodium salt of DNA is formed which can be centrifuged into a pellet. Repeated washing of this pellet with 70%–80% ethanol solutions helps remove residual salts.

Though ethanol precipitation is not useful in separating nucleic acids from many contaminants, this form of purification is the final step in many nucleic acid purification schemes as it tends to both concentrate the nucleic acid and remove any remaining salts or contaminants used in previous separations and extractions. In some cases, salt contaminants already present in the sample can be used to aid precipitation without further addition of sodium acetate (or other salts). The simplicity of this protocol has made it a cornerstone of high throughput nucleic acid purification. Table 3 is a rough guide to the choice of salt used in the precipitation.

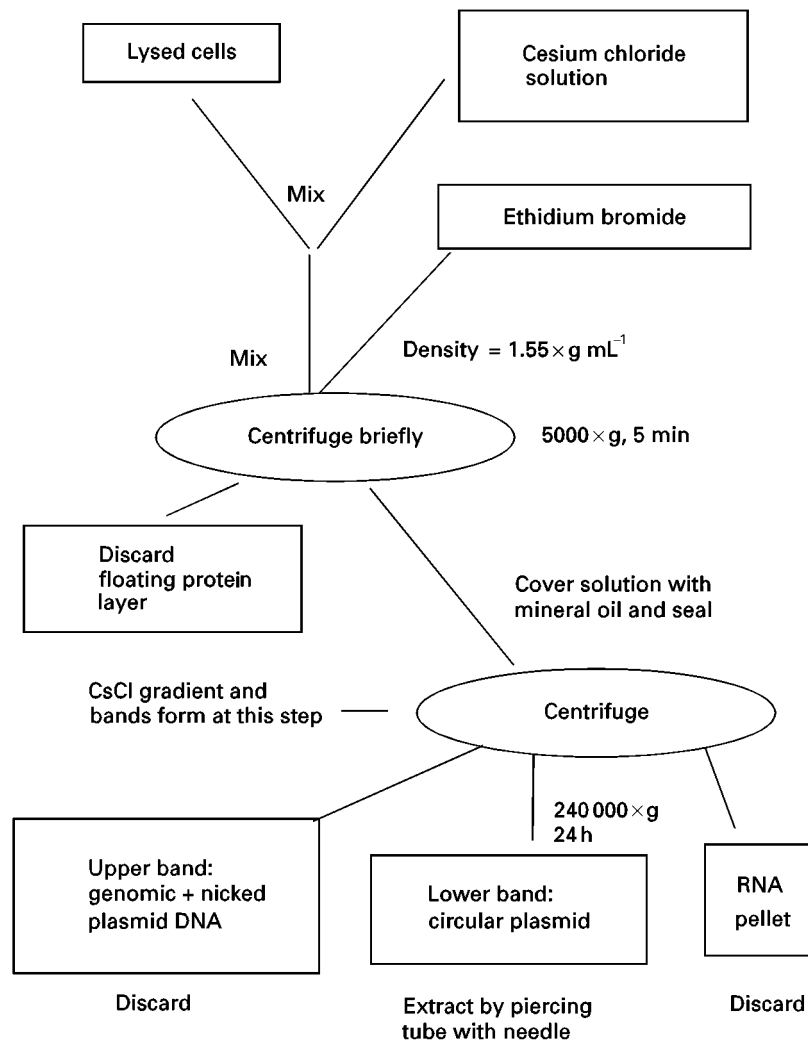


Figure 1 Plasmid DNA purification by CsCl – Ethidium bromide continuous gradient.

Precipitation of nucleic acids from buffers containing high concentrations of EDTA or phosphate ions may result in co-precipitation of these substances. Also, precipitation of small nucleic acid strands (<100 nucleotides) may be improved by the addition of carriers such as glycogen, by the addition of MgCl_2 , or by increased duration and speed of the

centrifugation ($100\,000 \times g$, 1–2 hours). Centrifugations for nucleic acid precipitations are typically carried out at $0-4^\circ\text{C}$, though for substantial concentrations ($>40 \text{ ng } \mu\text{L}^{-1}$) of long strands (such as DNA template for sequencing) incubation and centrifugation can also be carried out at room temperature.

The generic protocol shown in **Figure 3** is an example of ethanol precipitation for final concentration of DNA from a plasmid or M13 preparation.

Discarding of the ethanol supernatant is a common source of problems during precipitations performed in microtitre plates for two reasons. First of all, the pellet is not tightly bound to the sample plate as the centrifugation can only be performed at $3500 \times g$. Secondly, the ethanol is usually removed by inverting the entire microtitre plate and gently shaking or tapping it on a bench. Not surprisingly, inexperienced manual execution of this step can lead to loss of the DNA pellets with the ethanol.

Table 2 Some density gradient media commonly used for nucleic acid separation

Separation medium	Application
CsCl	Isolation of plasmid DNA. Separation of DNA by conformation. Separation of DNA by base composition
NaI	Separation of single vs. double stranded DNA
Metrizamide, Nycodenz	Fractionation of RNA

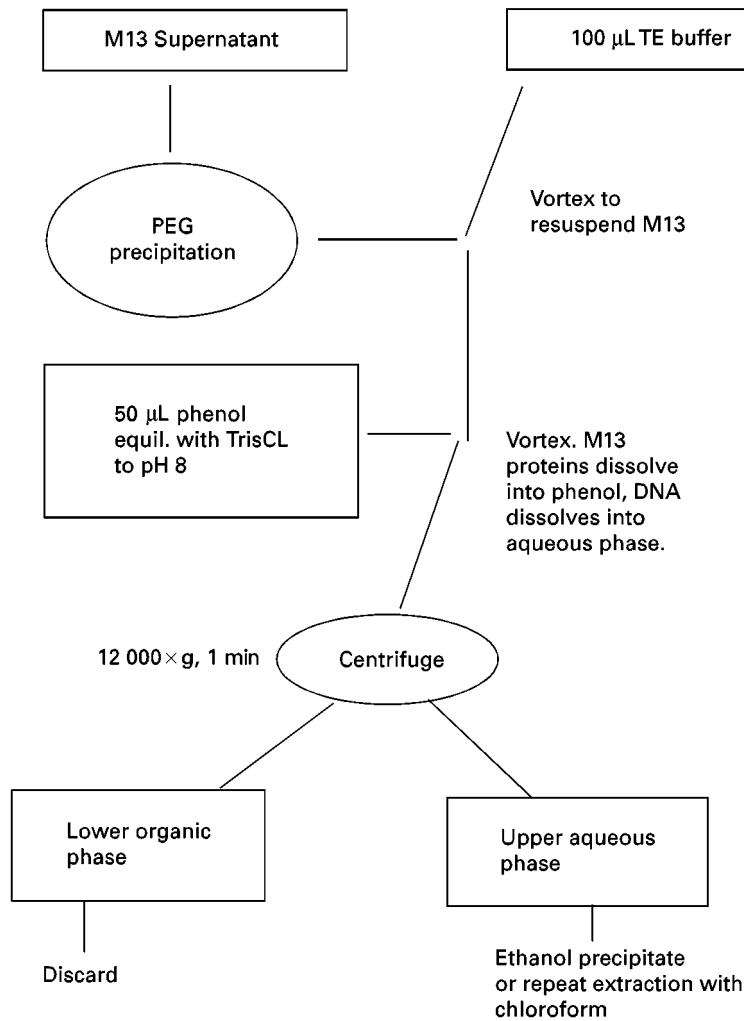


Figure 2 M13 DNA purification by phenol:chloroform extraction.

After the initial precipitation, the pellet can be resuspended in TE buffer to the desired concentration, or, if particularly low salt concentration is

desired in the final product, a further ethanol wash can be performed. This is done by washing the pellet in 70% ethanol and centrifuging for a further five minutes before again discarding the ethanol.

Table 3 Salt solutions used for nucleic acid precipitation

<i>Salt</i>	<i>Final concentration</i>	<i>Advantage/application</i>
Ammonium acetate	2.0–2.5 M	Reduces co-precipitation of dNTPs
Lithium chloride	0.8 M	Works with high concentrations of ethanol (as used in RNA precipitation)
Sodium chloride	0.2 M	Allows SDS to remain soluble in ethanol Used with samples containing SDS
Sodium acetate	0.3 M	Used for routine RNA and DNA precipitations

Isopropanol may be used in place of ethanol. In this case, only one volume of isopropanol should be used per volume of DNA solution. This is usually less desirable as residual isopropanol is more difficult to remove and more likely to cause coprecipitation of salts.

Precipitation of RNA is performed as for DNA except that 2.5 to 3 volumes of ethanol should be used per volume of RNA solution.

Plasmid Preparations by Differential Precipitation

Another form of differential precipitation is commonly used for the separation of small nucleic

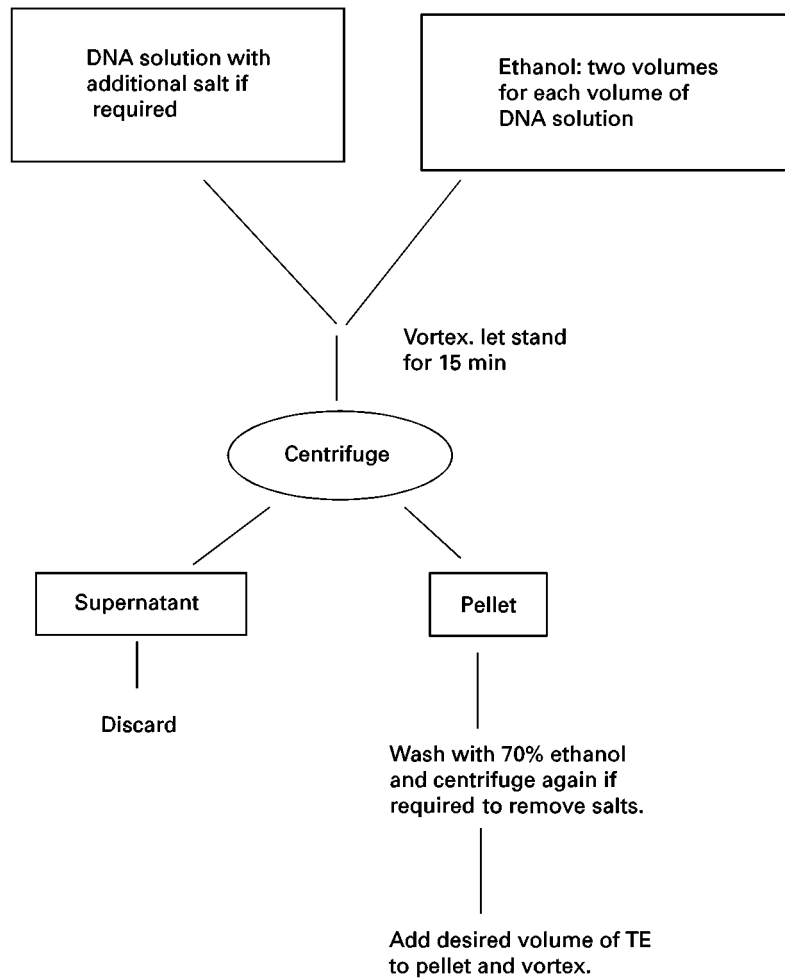


Figure 3 Ethanol precipitation of DNA.

acid molecules such as plasmid DNA from genomic DNA, RNA and protein contaminants. One example of this technique is the frequently used alkaline lysis preparation for the purification of plasmid DNA from *E. coli*. The technique takes advantage of the fact that the large genomic DNA strands from lysed bacterial cells will precipitate much more easily than the smaller plasmid molecules. Consequently, a mixture can be generated in which the genomic DNA can be pelleted, allowing the plasmid DNA to be extracted with the supernatant. The generic technique is shown in **Figure 4**.

Nucleic Acid Separation at High Throughput

Present and future efforts in the development of novel nucleic acid purification methods are likely to be aimed at satisfying the demand for inexpensive and high speed purification of a large number of

samples simultaneously. This is particularly true in applications related to large scale DNA sequencing and analysis. Currently, large-scale sequencing labs are expanding their operations to reach sequencing rates of 50 000 to 100 000 DNA samples per day. Though density gradient separations such as CsCl have historically provided the highest purity DNA, they are far too laborious to be employed at this rate. Furthermore, because of the inherently parallel operation in these cases, any DNA purification schemes must be compatible with standard microtitre plate formats.

Large scale operations have therefore depended largely on a variety of simpler purification methods including membrane purifications, magnetic bead separations, and precipitation based separations. The first two of these rely on preferential binding of the desired nucleic acid to a membrane such as glass fibre, or to a slurry of beads which can be isolated magnetically. Both these methods are easily scaled to highly parallel operation through the use of conventional

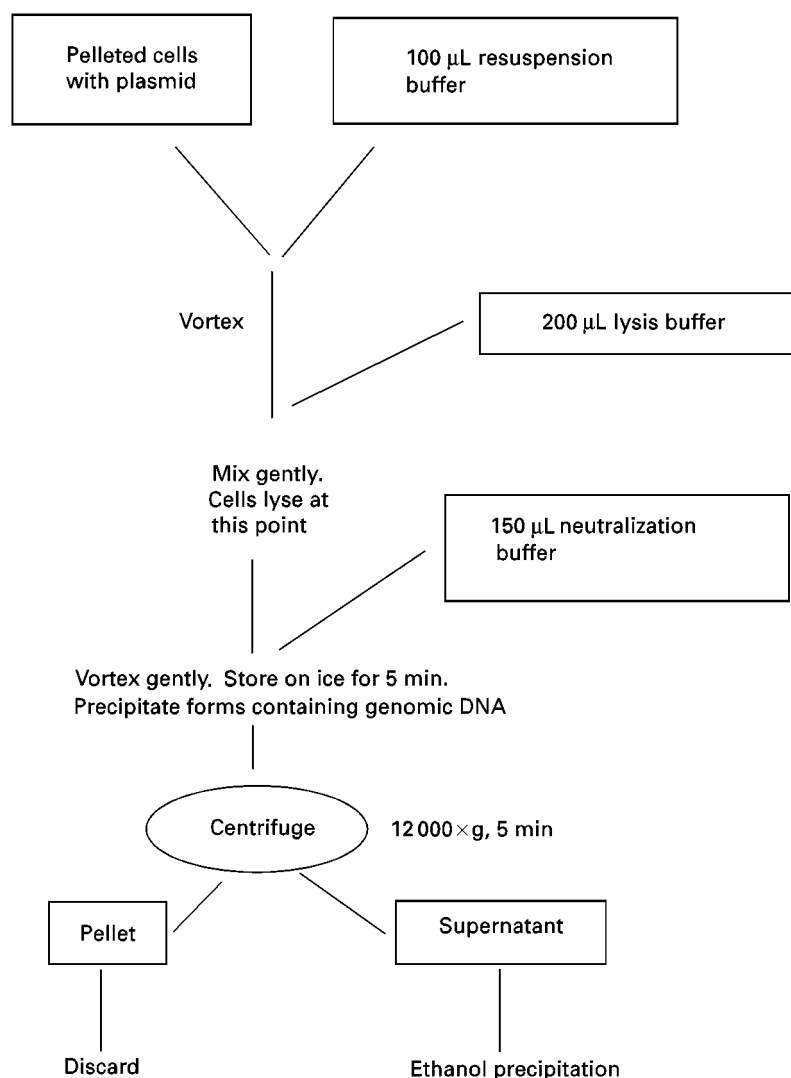


Figure 4 Plasmid purification by differential precipitation.

microtitre plates (for bead separations) and microtitre membrane plates (now available with up to 384 sample wells per plate). Furthermore these two methods are easily automated, and numerous instruments now exist that can perform filter membrane or magnetic bead based separations with very little labour cost and at high throughput. The only drawback to these methods has typically been the cost associated with either the magnetic beads or the disposable filter membranes.

Precipitation based purification methods, though inherently less expensive because of the lack of disposables involved, have been somewhat harder to adapt to large scale operation because of the human effort required to set-up and operate a conventional centrifuge. Though centrifugation of high density microtitre plates is routinely performed, unat-

tended automation of this process has been avoided until recently, and many large sequencing labs simply rely on manual execution of centrifuge based protocols.

Automation of Nucleic Acid Separation by Centrifugation

Two methods for performing high throughput automated centrifugation have emerged which allow the construction of automated instruments for performing centrifugation-based purification protocols.

Automated, indexing centrifuges The first of these methods is based on automation of centrifugation in the same fashion as it is performed manually. This involves simply automating the placing and removal of sample plates or tubes in and out of a standard

centrifuge. The difficulty involved with this method is that standard centrifuge rotors are not designed to stop at a repeatable indexed orientation. Consequently, the robotic arm which places and removes the samples from the samples from the centrifuge, cannot know the location of the samples at the end of a run.

The solution to this problem is to index the rotor position by means of an electronic sensor or a mechanical stop. One example of this type of solution is a plasmid preparation instrument developed at the Lawrence Berkeley National Laboratory (LBNL). This instrument consists of a robotic gantry equipped with a pipetting and gripping tool which can access a work surface that includes an indexing centrifuge. To prepare the centrifuge for robotic access, a pneumatic actuator opens the lid while another actuator is extended to interfere with tabs attached to the rotating rotor shaft. These tabs, when pressed against this actuator, define a well-indexed position for the rotor buckets. To ensure contact between these tabs and the actuator, the rotor is turned by an external friction coupling which can slip once the tab is in contact with the actuator. With the rotor positioned in this fashion, the robotic tool can reliably enter the centrifuge and locate the rotor bucket or sample plate.

With an instrument of this type, plasmid purification at the rate of 192 samples in 2.5–4 h can be performed. Final DNA purification occurs by ethanol precipitation, automated within the centrifuge described.

Similar methods have been used to automate centrifugation in other instruments including the commercially available Autogen 740 and Autogen 850 instruments. These instruments also contain automated centrifuges and are capable of various DNA and RNA purifications at rates up to 48 samples per 4–6 h.

Miniature, arrayable centrifuges A second approach to automation of centrifugation for high throughput DNA purifications has recently been developed at the Stanford DNA Sequencing and Technology Center. The goal of this approach is to remove the inherent radial acceleration limit ($\sim 3500 \times g$) imposed on microtitre plate centrifugation by the structural weakness of the sample plate. It is because of this strength limit that centrifugation of DNA samples in microtitre plates typically requires 20–30 min per separation. By centrifuging the samples directly within a reusable, high strength rotor, accelerations of over $20\,000 \times g$ can be reached, substantially decreasing pelleting times. To implement this at high throughput, a large number of small rotors operating in parallel is required.



Figure 5 (See Colour Plate 108) Titanium belt driven and air driven rotors used in the arrayable flow-through centrifuge. A penny is shown for scale.

The Stanford group's implementation of this concept consists of blocks of 96 individual, high speed rotors, arrayed on the same spacing as a standard 96 well microtitre plate. The rotors (Figure 5) can be spun at up to 70 000 rpm in both directions about their central axis by means of either compressed air or a motor driven belt.

In the belt driven version of the device, all 96 rotors turn simultaneously at identical rotation speeds, thus ensuring protocol uniformity across all samples. The rotors are manufactured from titanium, and are washable and reusable. The inner cross section of these rotors is wider in the middle (axially) than at the ends, thus guaranteeing that pellets will form in a specific area away from the inlet and outlet. The general principle of operation is as follows (Figure 6).

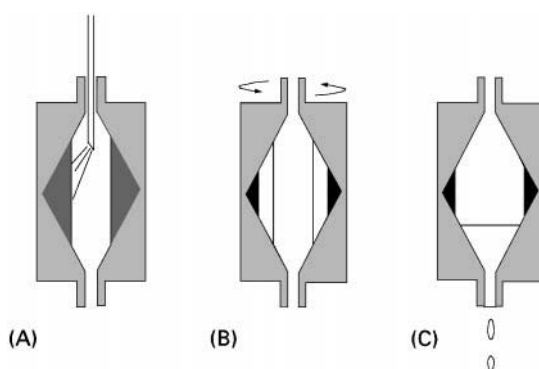


Figure 6 Principle of operation of arrayable flow-through centrifuge: (A) Sample is injected through the upper axial orifice into the spinning rotor. The centrifugal field instantly presses the sample against the inside wall of the rotor preventing it from exiting through the bottom orifice. (B) Rapid spinning of the rotor separates sample phases – any solid precipitate is pressed into the widest part of the rotor. (C) The rotor is stopped and the supernatant drips out the bottom orifice. The pellet can be re-suspended by injecting a small amount (100 μ L) of buffer into the rotor and agitating the rotor through repeated clockwise and counterclockwise accelerations. This procedure can also be used to clean the rotor and prepare it for the next sample to be separated.

The small size of this flow-through centrifuge allows highly parallel operation, smaller sedimentation drift distances, and high angular velocities. These high velocities in turn translate to large sedimentation forces which, coupled with the short drift distance, lead to much shorter separation times than a conventional microtitre plate centrifuge. Calculations based on *E. coli* sedimentation indicate a 40 fold decrease in pelleting time over a conventional centrifuge.

Applications of this technology to nucleic acid separation are being exploited primarily in the area of plasmid DNA purification for sequencing purposes. Instruments are being constructed based on this technology which should be capable of purifying over 500 plasmid DNA samples from cell cultures within one hour using an alkaline lysis protocol. In this protocol, two separations are required, one to clear the cell lysate, followed by ethanol precipitation to collect the DNA. With this protocol in mind, a multi-stage version of this flow-through centrifuge system (where the supernatant from one array of rotors drips into the input of a second array) is being developed at Stanford.

See Colour Plate 108.

See also: II/Centrifugation: Theory of Centrifugation.

Further Reading

- Birnie GD and Rickwood D (1978) *Centrifugal Separations in Molecular and Cell Biology*. London: Butterworth.
- Ford TC and Graham JM (1991) *An Introduction to Centrifugation*. Oxford: BIOS Scientific Publishers.
- Marziali A, Willis TD and Davis RW (1999) *An Arrayable Flow-Through Microcentrifuge for High Throughput Instrumentation*. Proc. Natl. Acad. Sci., USA. 5 Jan.
- Parish JH (1972) *Principles and Practice of Experiments with Nucleic Acids*. New York: John Wiley & Sons.
- Rickwood D (1984) *Centrifugation (Second Edition)*. Oxford: IRL Press.
- Rickwood D, Ford TC and Steensgaard J (1994) *Centrifugation – Essential Data*. New York: John Wiley & Sons.
- Sambrook J, Fritsch EF and Maniatis T (1989) *Molecular Cloning. A Laboratory Manual. Second Edition*. USA: Cold Spring Harbor Laboratory Press.
- Sheeler P (1981) *Centrifugation in Biology and Medical Science*. New York: John Wiley & Sons.

Extraction

S. J. Walker and K. E. Vrana, Wake Forest University, Winston-Salem, NC, USA

Copyright © 2000 Academic Press

Introduction

The recent explosion of information from recombinant DNA technology and the human genome initiative has come about in response to a number of key technological advances. These include the discovery and characterization of restriction endonucleases, the development of plasmid and phage vectors, and the creation of high throughput DNA sequencing methodologies. Less dramatic, but no less important, has been the development and refinement of protocols for extracting, purifying, and characterizing the various nucleic acids from complex biological mixtures. The present chapter reviews these procedures with particular emphasis on the unique characteristics and methodological constraints involved in dealing with deoxyribonucleic acid (DNA) vs. ribonucleic acid (RNA).

Figure 1 establishes the experimental hurdles to the isolation of purified nucleic acids. A eukaryotic cell contains a variety of biological macromolecules of

which the genetic material (nucleic acids) represents a minor component. The investigator is therefore faced with the daunting task of separating proteins, lipids, and nucleic acids from each other. Indeed, many applications require fractionating the genetic material into DNA and RNA and even subfractionating the RNA into ribosomal and messenger RNA species. These last two tasks are complicated by the fact that chromosomal DNA is a fragile, double-stranded molecule of very high molecular weight (3 billion total base pairs). RNA, on the other hand, while much smaller (75–10 000 nucleotides), is a single-stranded molecule that is exquisitely sensitive to enzymatic degradation. Fortunately, each biological fraction within a cell bears unique biophysical characteristics (charge, lipophilicity, chemical makeup, etc.) and these characteristics provide convenient mechanisms for resolving the macromolecules from one another.

In general, various nucleic acid isolations follow a common procedure. Cells, tissues, or organs are homogenized under conditions designed to protect the nucleic acid integrity, while simultaneously disrupting other macromolecules. This is followed by a relatively simple organic extraction (phenol-based) and selective precipitation from ethanol. The resulting preparations are then characterized by

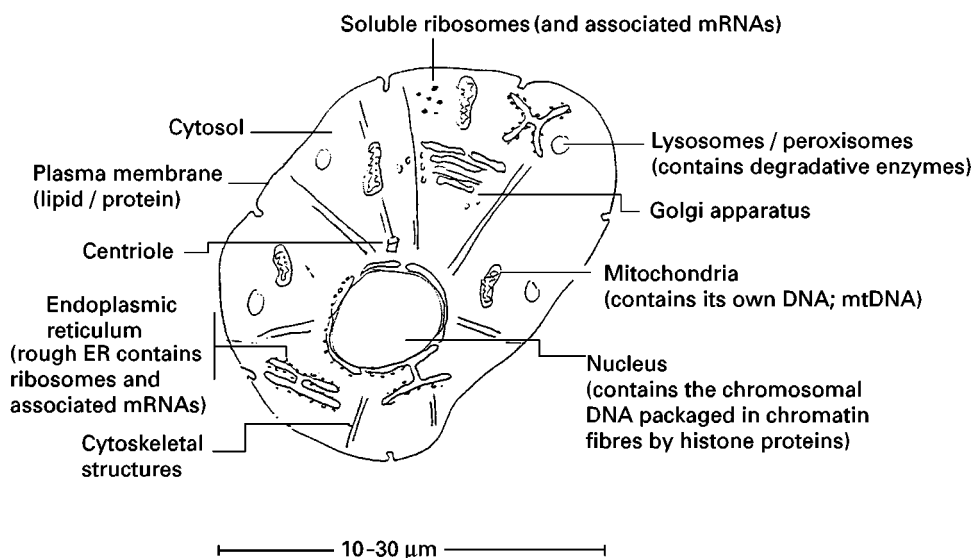


Figure 1 The technical hurdles in isolating nucleic acids from an animal cell. The cell is composed of a complex mixture of macromolecules (proteins, lipids, carbohydrates and nucleic acids) present in a number of different compartments. This is also true of the nucleic acids, where DNA is predominantly housed in the nucleus (with a small proportion of mitochondrial genes present within these organelles). The DNA is packaged in a complex mixture of nucleic acid and protein. The messenger RNA is present in the cytoplasm as free nucleic acid, as well as mRNA bound to soluble and membrane-bound ribosomes. The ribosomes themselves are composed of proteins and the structural ribosomal RNA molecules (18S and 28S rRNAs). Finally, the lysosomes are specialized organelles that sequester degradative enzymes from the rest of the cellular contents. The experimental challenge is therefore to disrupt the cell (while inactivating the degradative enzymes) and extract pure nucleic acids from the complex mixture of diverse macromolecules.

spectrophotometric and size fractionation methodologies (gel electrophoresis).

Organic (Phenol-Based) Extraction and Ethanol Precipitation

Before turning our attention to the peculiarities and specifics of DNA versus RNA isolation, we will consider two common features of nucleic acid isolation in general, namely, organic extraction with phenol-based solutions and the precipitation of nucleic acids with ethanol. A fundamental observation was made over 40 years ago that a simple organic extraction can resolve nucleic acids from nearly all other cellular macromolecules. Notably, mixing an aqueous homogenate of cells/tissues with phenol results in the extraction of the hydrophobic lipids into the organic phase and the denaturation, partial extraction and precipitation of protein. Therefore, if such an aqueous-organic emulsion is resolved – generally by low speed centrifugation – three specific compartments will be generated. The heavy, organic phase will be found at the bottom, the aqueous phase (containing the nucleic acids) will be found at the top, and a precipitate of insoluble protein will be found in a thin interface between the disparate solutions. This very simple approach has become a mainstay of the mod-

ern molecular biology laboratory and permits the economical and efficient preparation of nucleic acids.

Several modifications of the approach have been made in the years since that initial observation. First, it was found that inclusion of an equal volume of chloroform (CHCl_3) improves phase separation of the aqueous and organic compartments. Moreover, it ‘drives’ residual water from the phenol phase, thus limiting reductions in the volume of the aqueous phase. Finally, inclusion of small amounts of isoamyl alcohol reduces or prevents foaming of the solution during emulsion. As a result, many common protocols require the use of PCI (phenol-chloroform-isoamyl alcohol), in a 25:24:1 ratio, for the extraction of nucleic acids from complex mixtures.

Once nucleic acids (both DNA and RNA) have been resolved from other macromolecules, they frequently need to be concentrated prior to further experimental manipulation. This can be readily accomplished by ethanol precipitation. The addition of high concentrations of monovalent cations to a solution of nucleic acid polymers neutralizes their phosphate backbone. These large macromolecules are then only barely maintained in solution. Keep in mind that even small tRNA molecules (75 nucleotides) are

25 000 Da in size; eukaryotic chromosomes, on the other hand, are on the order of 50 billion Da. The subsequent addition of ethanol to such a solution produces structural transitions in the nucleic acids, with their subsequent precipitation from solution. The precipitates are collected by centrifugation and then washed with ethanol to dissolve the salt and the preparation is then redissolved in a buffer of choice. Most monovalent cations are suitable for the precipitation, although sodium acetate, ammonium acetate and sodium chloride are used, in that order of preference. As will be discussed, there are specialized applications in which lithium is used in the selective precipitation of RNA. Typically, the salt concentration of a solution is raised to ≥ 0.3 M and two volumes of ethanol added (to raise the final ethanol concentration to 67%). Following a varying period of precipitation (depending on the specific application), the DNA or RNA is collected, extracted with 75%, salt-free ethanol and then used.

DNA Purification

DNA can be isolated from whole blood, and from virtually any tissue or collection of cells. Selecting which protocol best suits one's needs will be dependent upon three basic criteria: (1) the starting material (both the biological source and the amount); (2) the desired size of the resultant DNA; and (3) the quantity of DNA needed. With almost any starting material, if the end-point application can accommodate chromosomal DNA that has been sheared somewhat, the investigator has the greatest flexibility in the selection of methodologies. In addition, as a result of the explosion in molecular biology-related research and development over the last 10–15 years, there are numerous kits available through companies such as Promega and Qiagen that supply reagents and complete protocols for purifying DNA. There are also reagents that allow the researcher to isolate RNA, DNA and proteins from the same starting material. In this section, we discuss the general principles involved in DNA extraction and briefly describe some of the more popular commercially available reagents

Genomic DNA (Mammalian)

To begin a DNA purification, if the starting material is whole blood or cultured cells, the first step is to concentrate the cells. This is accomplished by rinsing the cells in an appropriate buffer, followed by centrifugation and removal of the liquid phase. For tissue preparations, those that have been snap frozen (in liquid nitrogen) can either be ground to a fine powder while still frozen using a mortar and pestle,

or disrupted using any of a number of manual or mechanical homogenization devices. The desired size of the resultant DNA and the tenacity of the tissue type determines if relatively mild (e.g. Teflon to glass, hand-held homogenizers) or more severe (mechanical homogenizers such as the Brinkman Polytron) devices are required. The goal of this first step of the isolation is to disrupt cell–cell interactions and to produce some cell lysis. The next step, independent of the starting material, is the release of the intercellular contents from the structures that maintain internal compartmentalization (e.g. nuclear membranes). Once the cells have been homogenized, final lysis is typically accomplished by enzymatic digestion with proteinase K (a broad specificity serine protease) followed by extraction of the DNA in an equal volume of phenol. Interestingly, proteinase K is most active in high concentrations of detergent (typically sodium dodecyl sulfate, SDS) and elevated temperatures. Therefore, investigators generally need not worry about nucleases as a source of confounding activities because they are inactivated under these conditions.

Depending upon the purity and size of DNA required, subsequent extractions can be performed (with pooling of the aqueous phase each time) followed by dialysis (to recover high molecular weight DNA, e.g. > 200 kb) or by precipitation of the DNA with two volumes of ethanol. After several washings of the pellet with 70% ethanol, the dried DNA pellet can be resuspended in water or buffer and assessed spectrophotometrically for quantity and quality by determining its absorbance at 260 and 280 nm. DNA that is relatively free of contaminating proteins or phenol will have a ratio greater than 1.75.

There are now a number of reagents being marketed that allow for 'single-step' separation of DNA, RNA and protein (e.g. Tri Reagent, Molecular Research Center, Inc.; TRIzol, Gibco-BRL). The initial cell disruption phase is identical to what has already been described, with the caveat that the cells are resuspended (or homogenized) in a solution of phenol and guanidine thiocyanate. The homogenate from this resuspension is separated into phases by mixing with either bromochloropropane or chloroform. DNA is found almost exclusively at the interface between the liquid phases, while RNA is in the aqueous phase and proteins are in organic phase. These reagents provide a quick, convenient and reliable means to isolate nucleic acids from samples of nearly any origin.

The extraction of genomic DNA from plant cells and bacterial cells is nearly identical to what has already been described, with one exception. Both plant cells and some strains of bacteria are rich in

polysaccharides – compounds that must be effectively removed from preparations to ensure high quality DNA for cloning and sequencing. To accomplish this, following treatment of a cell preparation with detergent and proteinase K, the NaCl concentration is adjusted to 0.7 M and 1% cetyltrimethylammonium bromide (CTAB) is added to the cell lysate. This compound complexes with both polysaccharides and with residual proteins such that a chloroform extraction removes the polysaccharides, proteins, and cell debris. The high molecular weight DNA can then be precipitated from the supernatant with ethanol.

Plasmid DNA (Bacterial)

The cloning of a mammalian gene of interest into a bacterial plasmid vector, with subsequent amplification in bacterial cell culture and purification of this amplified plasmid DNA, has been a hallmark of molecular biology for 20 years. Isolation of plasmid DNA is a routine practice for any laboratory actively engaged in recombinant DNA research. The basic methodology has not changed significantly since the original alkaline lysis procedure was first described. Briefly, an overnight culture of bacterial cells, carrying a plasmid vector of interest, is first concentrated by centrifugation followed by aspiration of the growth medium. The cells are then resuspended in a Tris-EDTA buffer containing $100\ \mu\text{g mL}^{-1}$ RNase A, lysed in a 0.2 M sodium hydroxide and 1% SDS solution, and neutralized with 1.3 M potassium acetate solution. After a centrifugation step, the cleared lysate is mixed with a DNA-binding resin. This can then be poured onto a minicolumn that traps the DNA/resin mixture upon application of a vacuum or upon centrifugation (by placing the minicolumn into a microfuge tube). The column is washed several times with a Tris-EDTA solution containing potassium acetate and 55% ethanol and the DNA is eluted from the column in either water or buffer (e.g. Tris-EDTA). DNA, prepared in this fashion, is suitable for enzymatic digestion, cloning, or sequence analysis. Quantification of plasmid DNA can be accomplished as described earlier in this section.

Following the extraction and purification of DNA, it is characterized in a variety of ways. It is quantified by measuring the absorbance at 260 nm. The extinction coefficient of pure DNA is approximately $1\ \text{OD}_{260}/50\ \mu\text{g mL}^{-1}$. The structural integrity of the nucleic acid can be analysed by resolving the molecular weight species by agarose or polyacrylamide gel electrophoresis. The resolved nucleic acids can then be visualized with a fluorescent intercalating dye (e.g. ethidium bromide).

RNA Purification

It seems ironic that one of the key resources for the analysis of gene expression – the RNA – is exquisitely sensitive to degradative enzymes naturally found within the cells (the ribonucleases, RNases). Moreover, the human body produces robust levels of RNase within the secretions of the body as a barrier to external microorganisms. This is particularly true of the sweat, and nucleases are a ubiquitous problem on the fingers of an investigator. Finally, the most commonly-used enzyme, RNase A, is virtually impossible to ‘kill’. That is, it has been known for many years that RNase A can be boiled and disrupted but it spontaneously refolds into an active conformation and reestablishes its enzymatic activity. Therefore, the traditional means of sterilizing materials for an experiment – autoclaving – is largely ineffective in handling this problem. Efforts must be taken to start with no environmental contaminants and then treat the materials with very strong reagents to inactivate any adventitious contamination problems.

Homogenization in Chaotropic Agents

The secret of successfully isolating RNA is the rapid inactivation of degrading enzymes and the resolution of the nucleic acid. This is generally accomplished by disrupting the fresh tissues (or freshly frozen tissue) in a solution composed of a very strong chaotropic agent. The chemical of choice is a guanidinium salt (generally as an isothiocyanate salt). This is a very strong disruptive compound that is not oxidizing and so does no damage to the nucleic acid. Note that RNA is naturally single-stranded and so will be perturbed if its secondary structure is transiently disrupted. Referring again to Figure 1, The reader will see that in the intact cell, the degradative enzymes are sequestered from the RNA within the lysosomes. The problem is therefore to protect the nucleic acids from the enzymes during the extraction process. This is generally accomplished by disrupting the cells (whether fresh or still frozen) directly in the chaotropic agent. The key is to prevent any freezing–thawing cycles or other physical manipulations that will disrupt the subcellular organelles and release the degradative nucleases to attack the RNA. From this point on, the extraction is similar to isolation of DNA. Namely, the homogenate is extracted with phenol or PCI, the aqueous solution is extracted with chloroform to remove traces of phenol, and the nucleic acids are precipitated with monovalent cation and ethanol. One notable exception is the use of lithium salt instead of sodium or ammonium. In practice, lithium selectively precipitates RNA and so

aids in the removal of small amounts of DNA contamination.

The resulting purified RNA is once again quantified by measuring the absorbance at 260 nm (extinction coefficient of $1 \text{ OD}_{260}/40 \mu\text{g mL}^{-1}$) and the quality assessed by the $\text{OD}_{260}/\text{OD}_{280}$ ratio (pure RNA has a value ≥ 2.0). Following denaturing agarose gel electrophoresis, a typical cellular RNA preparation will present two prominent species representing the structural ribosomal RNAs (16S and 23S for prokaryotic cells; 18S and 28S for eukaryotic cells).

Isolation of Poly-A⁺ Containing RNA

For many purposes, an investigator will be interested only in the messenger RNA fraction, and because the structural ribosomal RNAs represent 98% or greater of the total, measures must be taken to purify the mRNA. This is accomplished by taking advantage of the fact that most (but not all) eukaryotic mRNA molecules are distinguished by the presence of a homopolymeric adenylate sequence at the extreme 3' end of the macromolecule (the poly A⁺ tail). This stretch of 100–200 residues acts to stabilize the mRNA; however, it also serves as a convenient mechanism for purifying this particular nucleic acid species. Most of the applications are predicated on an affinity column chromatography with oligo-deoxythymidine residues of between 12 and 18 nucleotides in length (oligo-dT_{12–18}). The poly A⁺ tail binds via complementary hydrogen binding to the oligo-dT and the structural RNAs fail to hybridize and bind. Conditions are changed so as to disrupt the nucleic acid interactions and the mRNA is released (desorbed) from the affinity matrix. Note that almost all mRNA species contain a poly A⁺ tail and so this separation approach does not differentiate between specific mRNA species.

Summary/Future Directions

Nucleic acid extraction from biological samples was one of the enabling technologies in the development of molecular biology. It has remained largely un-

changed for the past 20 years and, in its present state, continues to be a mainstay of the field. Most of the common advances have been in the automation of the process and the creation of high throughput technical platforms. The challenge for the coming years will be the further refinement of these automated applications and the creation of solid-state systems. These approaches will involve the liberation of nucleic acids from the biological samples, capture of the specific chemical form (DNA or RNA) on a solid matrix, and the subsequent analysis of the nucleic acid in that physical environment without further manipulation. Regardless of these potential technical advances, however, the essential principles will remain unchanged and the separation of nucleic acids from complex mixtures of macromolecules will be a requisite step in the characterization of genomic systems.

See also: II/Membrane Separations: Donnan Dialysis. III/Nucleic Acids: Centrifugation.

Further Reading

- Ausubel FM, Brent R, Kingston RE, Moore DD, Seidmann JG, Smith JA and Struhl K (1987) *Current Protocols in Molecular Biology*. Chichester: John Wiley and Sons.
- Chirgwin JJ, Przbyla AE, MacDonald RJ and Rutter WJ (1979) Isolation of biologically active ribonucleic acid from sources enriched in ribonuclease. *Biochemistry* 18: 5294–5299.
- Chomczynski P and Mackey K (1995) Substitution of chloroform by bromochloropropane in the single-step method of RNA isolation. *Analytical Biochemistry* 225: 163–164.
- Chomczynski P and Sacchi N (1987) Single-step method of RNA isolation by acid guanidine thiocyanate-phenol-chloroform extraction. *Analytical Biochemistry* 162: 156–159.
- Kirby KS (1957) A new method for the isolation of deoxyribonucleic acids: Evidence on the nature of bonds between deoxyribonucleic acid and protein. *Biochemistry Journal* 66: 495–504.
- Sambrook J, Fritsch EF and Manitis T (1989) *Molecular Cloning: A Laboratory Manual*. Cold Spring Harbor: Cold Spring Harbor Laboratory Press.

Liquid Chromatography

C. W. Gehrke, University of Missouri,
Columbia, MO, USA

K. C. Kuo, Indiana University Medical Center,
Indianapolis, IN, USA

Copyright © 2000 Academic Press

Introduction

Investigations in nucleic acid biochemistry are directed toward a better understanding of how the chemical structure of nucleic acids correlated with their unique biological functions. This information

can then be used to gain a deeper insight into how cells normally regulate their metabolic activities, allows speculation on how they evolved their respective biological role(s), and potentially permits correlation of the altered structures of nucleic acids in abnormal or diseased states to biological function. An understanding of how cells behave normally and in the diseased state provides the basis for the development of rational therapeutics and improved diagnostic tools. Studies are now being undertaken in many laboratories on nucleic acid metabolites as cancer markers, and of chemical carcinogens and mutagens adducted to nucleic acids for assessment of human exposure to environmental insults. Methodological limitations have hampered the advancement and exploitation of using modified nucleosides and their signals in routine tests in clinical chemistry or as important determinant life molecules in biochemical research. The development of high resolution chromatographic methods for qualitative identification and quantitative measurement of an array of nucleosides and to obtain chemical *information on* nucleic acid components has been a challenge to analytical biochemists since the beginning of the 1960s and has evolved into a powerful tool since the mid-1980s.

Our laboratory has made extensive investigations on reversed-phase high performance liquid chromatography and ultraviolet-photodiode array detection (RP-HPLC-UV) nucleoside analysis and has developed comprehensive chromatographic methods and quantitative enzymatic RNA hydrolysis procedures. Sixty-seven known nucleosides can be identified and 31 ribonucleosides; six deoxynucleosides can be quantified directly in a single chromatographic run from an enzymatic hydrolysate of RNAs, DNAs, and in physiological fluids. In collaborative efforts with scientists across the world we have applied these methods in a number of interesting investigations. We briefly introduce RP-HPLC-UV for deoxynucleosides and ribonucleosides and place emphasis on applications in three areas:

1. RP-HPLC-UV methods for total nucleoside composition of RNAs and DNAs;
2. modified nucleosides as cancer markers and in normal metabolism; and
3. preparative isolation of unknown nucleosides in nucleic acids for structural characterization.

RP-HPLC of Nucleosides

Chromatography Information on HPLC instrumentation; chromatographic parameters for high resolution, high speed, and high sensitive separation of nucleosides; analytical and semipreparative enzy-

matic hydrolysis of nucleic acids; and clean-up procedures (ultrafiltration procedure and phenylboronate gel column clean-up) for ribonucleosides in physiological fluids have been presented in the literature (see 'Further Reading' section).

It is a challenge to the analytical biochemist to separate and measure such a large number of nucleosides simultaneously in a complex biological matrix. One of the major problems for nucleoside chromatography is to obtain the needed reference molecules so that the information for the essential qualitative and quantitative analytical references can be established. There are only about 20 modified ribonucleosides that can be obtained through commercial sources. We have standardized the chromatographic retention times, obtained RP-HPLC-UV spectra and determined the molar response factors for a large number of ribonucleosides. Scientists in their respective laboratories need to standardize and calibrate their analytical system for modified nucleoside analysis in a broad range of biological matrices. To overcome this limitation, we have selected three unfractionated transfer RNAs (tRNAs) – *Escherichia coli*, brewer's yeast, and calf liver – as reference sources of the nucleosides. Each of these tRNAs contain unique as well as common nucleosides and provide an array of modified nucleosides that are often encountered by researchers. Some minor differences in the modified nucleoside profile may be observed in these three tRNAs from different sources, especially for *E. coli* tRNAs. This problem can be resolved by using a reliable supplier or by standardization of a selected lot of tRNAs obtained in large quantity and of good homogeneity. **Figure 1** shows the 254 nm chromatograms from the high resolution separation of the nucleosides in the three reference tRNAs. The nucleoside peaks are identified by an assigned index number, which essentially corresponds to their respective elution order. **Table 1** gives the IUPAC names, one-letter symbol, and the index number of the nucleosides that have been determined by RP-HPLC-UV. Other ribonucleosides, which are not yet characterized by RP-HPLC-UV, are also included in this table. A total of 67 ribonucleosides have been chromatographically and spectrometrically characterized.

RP-HPLC-UV Methods for Total Nucleosides Composition of RNAs and DNAs

Nucleoside chromatography protocols for a broad array of RNAs and DNAs have been applied extensively. In general, RNA nucleoside chromatography

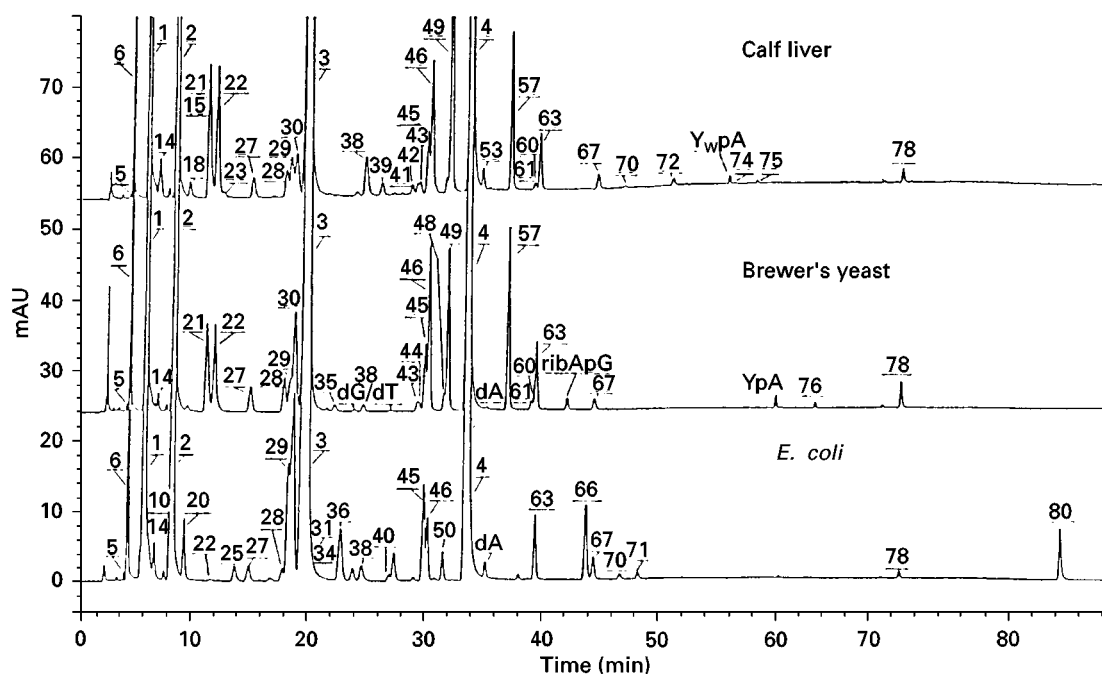


Figure 1 HPLC chromatography of reference nucleosides from unfractionated calf liver, brewer's yeast, and *E. coli* tRNAs.

requires emphasis on resolution and flexibility, and for DNA the emphasis is on accuracy and speed. There is also an ever-increasing need in biochemical analysis for high sensitivity. Recent progress in instrumentation and column technology has increased LC-UV sensitivity more than 10-fold so that low picograms of nucleosides can be quantitated routinely.

Unfractionated tRNA constitutes one of the most complicated mixtures of biopolymers known and high resolution is required for this analysis (Figure 1).

Isoacceptor tRNAs are usually available only in very small amounts (less than a few micrograms); however, an advantage with single-species tRNAs is that they are less complicated in composition. For analysis of single-species tRNAs, an intermediate resolution and higher sensitivity protocol (high speed) are generally used. An accurate identification and quantitation of the total nucleoside composition are very important in providing supplementary and confirmatory information in support of tRNA sequence studies. Figure 2 shows the separation of nucleosides in tRNA^{Leu} from bovine serum. Table 2 gives the comparison of quantitative results from five isoacceptor tRNAs obtained by RP-HPLC-UV and compared to sequence analysis. The lower m⁷G value is indicative of the instability of m⁷G at alkaline pH during enzymatic hydrolysis. It is of interest that differences of one residue number for uridine in tRNA^{Phe} and uridine and guanosine values in tRNA^{Val} were

observed from the two analytical methods. Table 3 gives the mol% values of all the nucleosides in four bovine isoaccepting tRNAs. These four tRNAs were isolated in Dr Gerard Keith's group at the Institute for Molecular and Cellular Biology (IBMC) in Strasbourg, France. Their sequences were not yet determined at the time of HPLC analysis. These mammalian tRNAs have considerably more modifications than the tRNAs from *E. coli* (Table 2) and two unknown modified nucleosides were observed in tRNA^{Leu}.

Ribosomal RNA Nucleoside Analysis

Ribosomal RNA (rRNA) is a high molecular weight RNA. In *E. coli* the 70S rRNA has a molecular weight of 2.75×10^6 amu and the small subunits, 16S rRNA and 23S rRNA, have 1542 and 4718 residues, respectively. Only 10 methylated nucleosides have been reported in the 16S and 23S rRNAs. To accomplish the chromatography of rRNA for composition analysis it is necessary to separate and measure one modified nucleoside residue in ca. 5000 nucleotides. This demands a high column capacity so that a large amount of sample (100 μ g or more) can be injected without loss of resolution. The high resolution and high speed chromatographic protocols described for tRNA nucleoside composition analysis all have adequate capacity to meet this requirement for rRNA

Table 1 Nomenclature of ribonucleosides and index numbers

<i>IUPAC name</i>	<i>One-letter symbol</i>	<i>Index no.</i>
<i>Adenosines</i>		
Adenosine	A	4
2'-O-Methyladenosine	Am	61
1-Methyladenosine	m ¹ A	21
1-Methyl-2'-O-methyladenosine	m ¹ Am	
2-Methyladenosine	m ² A	66
2-Thioadenosine	s ² A	
2-Methylthioadenosine	ms ² A	
3-Methyladenosine	m ³ A	
1,3-Dimethyladenosine	m ¹ m ³ A	
5'-Methylthioadenosine	ms ⁵ A	
1,N ⁶ -Dimethyladenosine	m ¹ m ⁶ A	
N ⁶ -(N-Formyl- α -aminoacyl)adenosine	f ⁶ A	
N ⁶ -Methyladenosine	m ⁶ A	67
N ⁶ -Methyl-2-methylthioadenosine	ms ² m ⁶ A	
N ⁶ ,N ⁶ -Dimethyladenosine	m ₂ ⁶ A	74
N ⁶ -Methyl-2'-O-methyladenosine	m ⁶ Am	71
2-Hydroxyadenosine	O ² A (isoG)	
N ⁶ -Carbamoyladenosine	nc ⁶ A	
N ⁶ -Threoninocarbonyladenosine	tc ⁶ A (t ⁶ A)	63
N ⁶ -Methyl-N ⁶ -threoninocarbonyladenosine	mtc ⁶ A (mt ⁶ A)	70
N ⁶ -Threoninocarbonyl-2-methylthioadenosine	ms ² tc ⁶ A	72
N ⁶ -Glycinocarbonyladenosine	gc ⁶ A (g ⁶ A)	50
N ⁶ -Methyl-N ⁶ -glycinocarbonyladenosine	mgc ⁶ A (mg ⁶ A)	
N ⁶ -(Δ 2-Isopentenyl)adenosine	i ⁶ A	78
N ⁶ -(Δ 2-Isopentenyl)-2-methylthioadenosine	ms ² i ⁶ A	80
N ⁶ -(cis-4-Hydroxyisopentenyl)adenosine	cis oi ⁶ A	
N ⁶ -(4-Hydroxyisopentenyl)-2-methylthioadenosine	ms ² oi ⁶ A	79
9-(2'-O-Ribosyl- β -D-ribofuranosyl)adenine	rA	
<i>Inosines</i>		
Inosine	I	29
1-Methylinosine	m ¹ I	43
2-Methylinosine	m ² I	
7-Methylinosine	m ⁷ I	16
9- β -D-Ribofuranosylpurine (nebularine)	neb	
7- β -D-Ribofuranosylhypoxanthine		
<i>Cytidines</i>		
Cytidine	C	1
2'-O-Methylcytidine	C _m	27
2-Lysinocytidine (lysidine)	k ² C	
2-Thiocytidine	s ² C	20
3-Methylcytidine	m ³ C	18
N ⁴ -Methylcytidine	m ⁴ C	22
N ⁴ -Methyl-2'-O-methylcytidine	m ⁴ C _m	
N ⁴ -Hydroxymethylcytidine	om ⁴ C	
N ⁴ -Methyl-2-thio-2'-O-methylcytidine	m ⁴ s ² C _m	
N ⁴ -Acetylcytidine	ac ⁴ C	48
5-Methylcytidine	m ⁵ C	23
5-Methyl-2'-O-methylcytidine	m ⁵ C _m	
5-Hydroxymethylcytidine	om ⁵ C	12
<i>Guanosines</i>		
Guanosine	G	3
2'-O-Methylguanosine	G _m	45
1-Methylguanosine	m ¹ G	46
N ² -Methylguanosine	m ² G	49
3-Methylguanosine	m ³ G	
7-Methylguanosine	m ⁷ G	28
N ² ,N ² -Dimethylguanosine	m ₂ ² G	57
N ² ,N ² -Dimethyl-2'-O-methylguanosine	m ₂ ² G _m	

Table 1 *Continued*

<i>IUPAC name</i>	<i>One-letter symbol</i>	<i>Index no.</i>
<i>N</i> ² , <i>N</i> ² -7'- <i>O</i> -Methyltrimethylguanosine	m ² m ⁷ G	
Queuosine	Q	40
β-D-Mannosylqueuosine	manQ	41
β-D-Galactosylqueuosine	galQ	42
<i>Xanthosines</i>		
Xanthosine	X	32
1-Methylxanthosine	m ¹ X	
7-Methylxanthosine	m ⁷ X	
<i>Uridines</i>		
Uridine	U	2
2-Thiouridine	s ² U	33
2-Thio-2'- <i>O</i> -methyluridine	s ² Um	
2-Selenouridine	Se ² U	
3-(3-Amino-3-carboxypropyl)uridine	acp ³ U (nbt ³ U)	32
3-Methyluridine	m ³ U	37
4-Thiouridine	s ⁴ U	36
2,4-Dithiouridine	s ² s ⁴ U	
4-Thiouridine disulfide	(s ⁴ U) ²	
5-(β-D-Ribofuranosyl)uracil (pseudouridine)	Ψ	6
5-(2'- <i>O</i> -Methyl-β-D-ribofuranosyl)uracil (2'-O-methylpseudouridine)	Ψ _m	39
5-(β-D-Ribofuranosyl)- <i>N</i> ¹ -methyluracil (1-methylpseuduridine)	m ¹ Ψ	17
5-(2'- <i>O</i> -Methyl-β-D-ribofuranosyl)- <i>N</i> ¹ -methyluracil (1-methyl-2'- <i>O</i> -methylpseudouridine)	m ¹ Ψ _m	
5,6-Dihydrouridine	hU (D)	5
5-Methyl-5, 6-dihydrouridine	m ⁵ hU (m ⁵ D)	
5-methyluridine	m ⁵ U (T)	30
5-Methyl-2'- <i>O</i> -methyluridine	m ⁵ U _m (T _m)	53
5-Methyl-2-thiouridine	m ⁵ s ² U (s ² T)	52
5-Hydroxyuridine	h ⁵ U	11
5-Carboxyhydroxymethyluridine	chm ⁵ U	
5-Carboxymethyluridine	cm ⁵ U	7
5-Carboxymethyl-2-thiouridine	cm ⁵ s ² U	
5-Methoxyuridine	mo ⁵ U	34
5-Methoxy-2-thiouridine	mo ⁵ s ² U	55
5-Aminomethyluridine	nm ⁵ U	
5-Aminomethyl-2-thiouridine	nm ⁵ s ² U	
5-Methylaminomethyluridine	mnm ⁵ U	9
5-Methylaminomethyl-2'- <i>O</i> -methyluridine	mnm ⁵ Um	
5-Methylaminomethyl-2-thiouridine	mnm ⁵ s ² U	25
5-Methylaminomethyl-2-selenouridine	mnm ⁵ Se ² U	
5-Carboxymethylaminomethyluridine	cmnm ⁵ U	8
5-Carboxymethylaminomethyl-2'- <i>O</i> -methyuridine	cmnm ⁵ Um	
5-Carboxymethylaminomethyl-2-thiouridine	cmnm ⁵ s ² U	24
5-Carbamoylmethyluridine	ncm ⁵ U	14
5-Carbamoylmethyl-2'- <i>O</i> -methyluridine	ncm ⁵ Um	
5-Carbamoylmethyl-2-thiouridine	ncm ⁵ s ² U	
5-Methoxycarbonylmethyluridine	mcm ⁵ U	44
5-Methoxycarbonylmethyl-2-thiouridine	mcm ⁵ s ² U	60
5-Methylcarboxymethoxyuridine	mcmo ⁵ U	54
5-Methylcarboxymethoxy-2-thiouridine	mcmo ⁵ s ² U	68
6-Carboxyuridine (oridine)	c ⁶ U (O)	
Hydroxywybutosine	YOH, OyW	75
Wybutosine	Yt, yW	76
Wyosine	Y, W	77

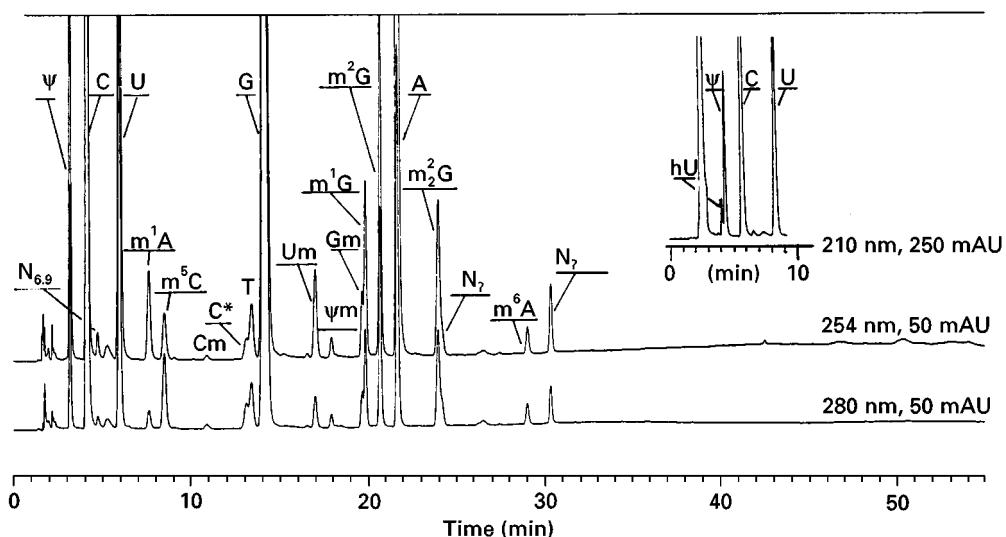


Figure 2 HPLC of nucleosides in tRNA^{Leu} from bovine serum.

analysis. Chromatograms of these respective hydrolysates are presented in **Figure 3** and **Figure 4** and the quantitative results are presented in **Table 4**. Some deoxyribonucleosides were found in the enzy-

matic hydrolysates of the tRNA samples. However, their presence does not interfere with the measurement of any known modified ribonucleoside. This separation demonstrates the high selectivity of the

Table 2 RP-HPLC-UV for total composition of isoaccepting tRNAs

Residue per 76 residues										
Yeast tRNA ^{Phe}		E. coli tRNA ^{Phe}		E. coli tRNA ^{Glu}		E. coli tRNA ^{Met}		E. coli tRNA ^{Val}		
HPLC	Lit.	HPLC	Lit.	HPLC	Lit.	HPLC	Lit.	HPLC	Lit.	
<i>Major nucleoside</i>										
C	15.8	15	20.6	21	27.1	27	25.1	25	23.2	23
U	12.1	12	8.8	8	9.0	9	8.3	8	10.1	9
G	18.3	18	22.8	23	21.9	22	23.6	24	22.1	23
A	16.0	17	14.0	14	12.9	13	13.6	14	13.8	14
<i>Modified nucleoside</i>										
hU	2.16	2	2.39	2			1.08	1	1.05	1
ψ	2.05	2	2.80	3	2.02	2	1.00	1	1.18	1
m ¹ A	0.91	1								
mn ^m s ⁵ U					1.24	1				
m ⁵ C	1.98	2								
Cm	0.80	1					0.89	1		
m ⁷ G	0.76	1	0.69	1			0.71	1	0.58	1
m ⁵ U	1.01	1	1.01	1	1.00	1	1.00	1	1.00	1
s ⁴ U			0.92	1			0.75	1	0.74	1
Gm	1.00	1								
m ² G	0.99	1								
m ² A					1 ^a	1				
m ⁶ A									1 ^a	1
ms ² i ⁶ A			1.01	1						
o ⁵ U									1 ^b	1

^aNot quantitated, assumed to be one residue.

^bNot identified, assumed to be one residue if present.

Table 3 RPLC-UV analysis of nucleoside composition in bovine isoaccepting tRNAs

Nucleosides	Mol% of nucleosides			
	Pro-tRNA	Lys-tRNA	Thr-tRNA	Leu-tRNA
<i>Major nucleosides</i>				
C	24.1	25.0	23.4	23.6
U	12.8	10.9	14.1	14.8
G	27.6	27.8	24.7	22.9
A	14.9	15.9	16.1	17.6
<i>Modified nucleosides</i>				
hU	3.08	3.97	4.21	nc
Ψ	5.92	6.35	2.46	4.98
mcm ⁵ U	nd	nd	nd	2.84
m ³ C	nd	1.36	1.05	nd
m ¹ A	1.07	0.94	0.94	1.12
m ⁵ C	3.48	0.32	3.31	1.19
Cm	0.35	0.05	0.90	nd
m ⁷ G	0.39	0.05	0.01	nd
I	0.73	0.01	0.95	1.30
m ⁵ U(T)	nd	1.21	0.04	1.20
Um	0.99	0.11	0.04	1.19
Gm	0.38	0.01	1.10	0.43
m ¹ G	2.65	1.30	1.17	1.12
ac ⁴ C	nd	nd	nd	0.82
m ² G	1.13	1.97	2.33	2.35
m ₂ ² G	0.08	0.15	1.11	1.19
t ⁶ A	nd	2.00	2.17	nd
m ⁶ A	0.42	0.42	0.44	0.10
Unknown 1				nc
Unknown 2				nc
Total	100.5	99.72	100.5	99.33

nd, not detected.

nc, not calculated. mcm⁵U was calculated using factor for Urd. Unknown 1 is probably an unknown nucleoside. Could be a modified Ado. Unknown 2 is probably an unknown nucleoside. Could be a modified Cyt.

RP-HPLC so that the respective deoxy- and ribonucleoside are differentiated. RP-HPLC showed qualitative and quantitative differences of modification in both 16S rRNA and 23S rRNA as compared to the literature values. In 16S rRNA we found one additional residue of m⁵C, and m²G. Two nucleosides, Gm and m⁴Cm, were not found. From 23S rRNA, four additional residues of Ψ, two of m⁴C, one of m⁵C, two of m²G, and one of m²A, were found by RPLC. A number of other modifications as shown in Table 4 are in good agreement with the literature values.

Messenger RNA Nucleoside Analysis

Messenger RNAs from viral and eukaryotic cells contain a unique structure known as 'caps' that consist of an inverted 7-methylguanosine (m⁷ Guo) linked to

the penultimate nucleoside through a 5'-5' triphosphate bridge. These mRNAs usually have a very low amount of internal nucleoside modification (< 1/1000). A highly selective RP-HPLC-UV separation using a micro anion exchange column was developed for isolation of the cap structures to enhance the resolution and sensitivity of the separation and measurement.

Deoxynucleoside in DNAs

The determination of the molar composition of the major and modified deoxynucleosides in high molecular weight DNAs requires a high degree of accuracy and sensitivity. Modified nucleosides in the DNA such as 5-methyldeoxycytidine (m⁵dc) 6-methyldeoxyadenosine (m⁶dA) and 4-methyldeoxycytidine (m⁴dC) are normally present at 0.1 to 2 mol% level. Several separation systems were developed and used in our laboratory. The method that we use is dependent on the sample matrices (i.e. presence of RNA, deoxyinosine (dl), inosine (I), nucleobases, and other UV peaks) and amount of DNA sample available. An optimum amount of DNA is 10 µg. The best chromatographic system for the separation of deoxynucleosides is a two-buffer, single ramp gradient using a 150 × 4.6 mm Supelcosil® LC-18S column. With this column a complete separation can be achieved in less than 15 min. Dual wavelength quantitation and high quality data reduction software are essential for the analysis. The deoxynucleoside reference compounds obtained from commercial sources do not have the required purity to obtain the accuracy pair ratio, i.e. (dC + m⁵dC)/dG = 1.000 and dT/(dA + m⁶dA) = 1.000, from high molecular weight DNAs. Quantitation of the nucleoside composition of a large number of isolated DNA oligomer fragments and synthesized oligomers requires a high sensitivity. In this case, a 5 cm or 3 cm regular bore (3.9–4.6 mm) with 3 or 5 µm particle size columns used in an isocratic separation mode provides the separation in less than 10 min with a five-fold increase in sensitivity. Refer to the published HPLC protocols for quantitation of major and modified nucleosides in DNA. Precision and linearity of the method are presented in Tables 5 and 6. The high resolution separation of ribo- and deoxynucleosides is presented in Figure 5.

Modified Nucleosides as Cancer Markers and in Normal Metabolism

Borek stated that the hope of finding some unique metabolic products or unique components of malignant cells circulating in body fluids which can be

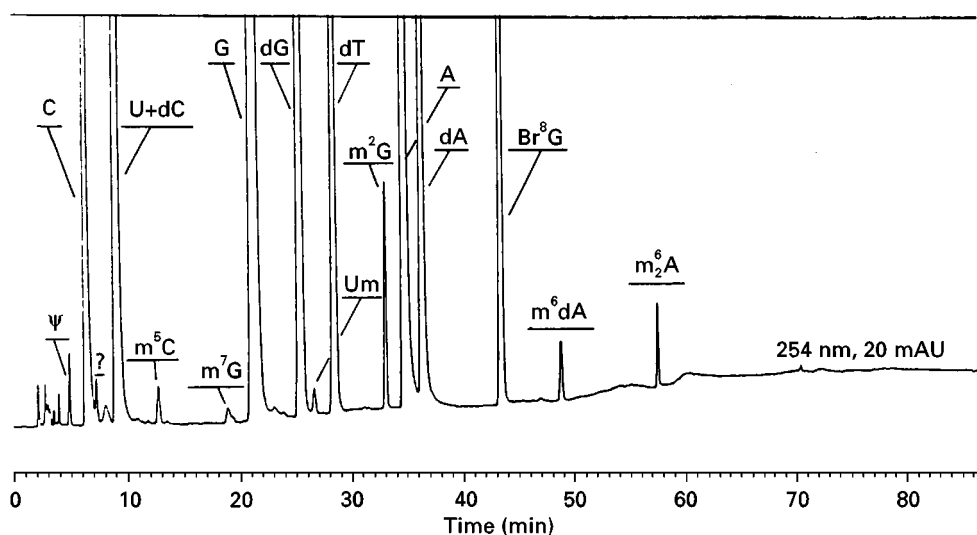


Figure 3 HPLC of nucleosides in *E. coli* 16S rRNA.

measured is as old as modern biochemistry. The term 'tumour marker' has been coined by Dr Morton K. Schwartz of the Sloan Kettering Institute for such a product. Before we consider whether we have fulfilled such a hope, we ought to define what a tumour marker should be. The requirements for an effective tumour marker are manifold; it ought to be specified for malignancy – it should provide a minimum of false-positives and false-negatives; it ought to indicate the extensiveness of the malignancy and it should preferably diminish or hopefully disappear after effective therapy.

At an international conference held in Vienna (1982) under the auspices of the Society for Early

Detection of Cancer, someone calculated that there were close to 90 reported different tumour markers. It can be stated, however, that unfortunately none of these putative tumour markers meet even partly the qualifications we have set above.

A problem is that most of the tumour markers in use today are proteins. Proteins are the peripheral end products of the molecular mechanisms of every cell. A mammalian cell is endowed with the capability of producing perhaps 10 000 or more different proteins. Unless we chance upon a protein which is either causal of a malignancy or which is a universally aberrant concomitant of malignant tissues, looking for protein products which will qualify as tumour

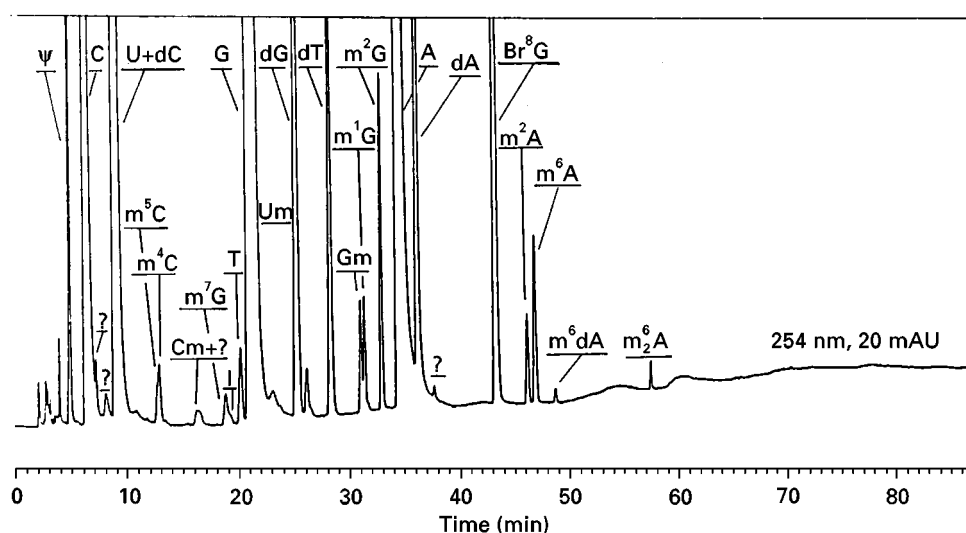


Figure 4 HPLC of nucleosides in *E. coli* 23S rRNA.

Table 4 RP-HPLC-UV quantitation nucleosides in *E. coli* 16S and 23S rRNA

Nucleosides	Mol% in 16S rRNA		Mol% in 23S rRNA	
	HPLC	Lit. ^a	HPLC	Lit. ^b
C	23.0	22.8	22.2	
U	20.9	20.4	20.4	
G	30.4	31.6	30.7	
A	25.1	25.2	26.0	
Total	99.4	100.0	99.3	
<i>Residues/mol in</i>				
Ψ	1.3	0.0	7.8	3.0
m ⁵ C	2.0	1.0		
m ⁴ C			1.9	0.0
m ⁷ G	0.5	1.0	0.7	1.0
Cm + ?			0.9	1.0
T			1.7	1.0
m ³ U	0.8	1.0	0.9	1.0
Gm	0.0	1.0	0.9	1.0
m ⁴ Cm	0.0	1.0		
m ¹ G			0.8	1.0
m ² G	2.9	2.0	2.3	0.0
m ² A			0.9	0.0
m ⁶ A			2.1	2.0
m ⁸ A	1.6	2.0	0.2	0.0

^aLiterature values from Noller HF (1984) Structure of ribosomal RNA. In Richardson CC, Boyer PD and Meista A (eds) *Annual Review of Biochemistry* 53: 119–162.

^bLiterature values obtained from Gutell RR, Weiser B, Woese CR and Noller HF (1985) Comparative anatomy of 16-S-like ribosomal RNA. *Progress in Nucleic Acid Research and Molecular Biology* 32: 155–216.

^cm⁷G is partially lost during hydrolysis.

^dThe 210 nm signal was examined; no hU was observed.

markers in terms of the requirements listed above is hopeless.

A promising marker is the tRNAs of tumour tissue. The finding of aberrant tRNA-methylating enzymes in tumour tissue prompted the study of the tRNAs themselves. Surprisingly, only a few of the tRNAs in

Table 6 Linearity of RP-HPLC-UV from analysis of calf thymus DNA

μg of DNA injected	Mol% of deoxynucleoside ^a				
	dC	m ⁵ dC	dG	dT	dA
8.5	20.85	1.47	22.38	27.59	27.68
5.0	20.93	1.51	22.41	27.70	27.44
2.5	20.86	1.55	22.58	27.64	27.41
1.25	20.81	1.52	22.54	27.89	27.38
0.50	20.78	1.67	22.45	27.65	27.46
Average	20.85	1.54	22.47	27.69	27.48
SD	0.051	0.068	0.076	0.10	0.10
%RSD	0.24	4.4	0.34	0.38	0.38

^aSee notes to Table 5.

the malignant tumour were found to be different in structure from those in the normal tissue counterpart. Dr Guy Dirheimer of Strasbourg isolated 18 different tumour-specific tRNAs and found modification on them different from those in normal counterparts. On the other hand, we have determined with the aid of Japanese colleagues that the primary sequence is the same. Perhaps to enable it to perform its many functions, tRNA is endowed with an extraordinarily complex structure. Its primary sequence consists of about 80 of the four major bases found in other RNAs: adenine, cytosine, guanine and uracil. In addition to these major bases, tRNA contains a large variety of modified bases that are unique to it. The modified bases increase in number with the complexity of the organism. Thus, for example, *E. coli* tRNA may contain only two or three, yeast tRNA may contain five or six, and mammalian tRNA may contain modified bases constituting as much as 20% of the total. It has also been shown that the tRNA methyltransferases are abnormally hyperactive in every malignant tissue. Borek found that the level of excretion of the nucleosides in urine when followed before, during, and after therapy in a malignancy that responds well to chemotherapy, that within five days of commencement of therapy in six patients with Burkitt's lymphoma, that the excretion levels in urine returned to normal and remained normal as long as the subjects were in remission.

There have been reports since the early 1950s that cancer patients excrete elevated levels of methylated purines and pyrimidines as well as other modified nucleosides. Ample evidence had indicated that increased tRNA methylase activity in neoplastic cells was a common and consistent finding, and increased excretion of modified bases in urine from cancer patients and tumour-bearing animals had also been reported. Methylation of the bases in tRNA had been

Table 5 Precision of RP-HPLC-UV for DNA total composition analysis

	Mol% of deoxynucleoside ^a				
	dC	m ⁵ dC	dG	dT	dA
Average	20.94	1.52	22.42	27.59	27.65
SD	0.0080	0.022	0.022	0.035	0.043
%, RSD (N = 16)	0.038	1.43	0.096	0.13	0.15

^aAverage values from four hydrolysates; four analyses were made from each hydrolysate over a period of 2 days. Sample: DNA calf thymus DNA. SD: population standard deviation; %, RSD: relative standard deviation as a percentage.

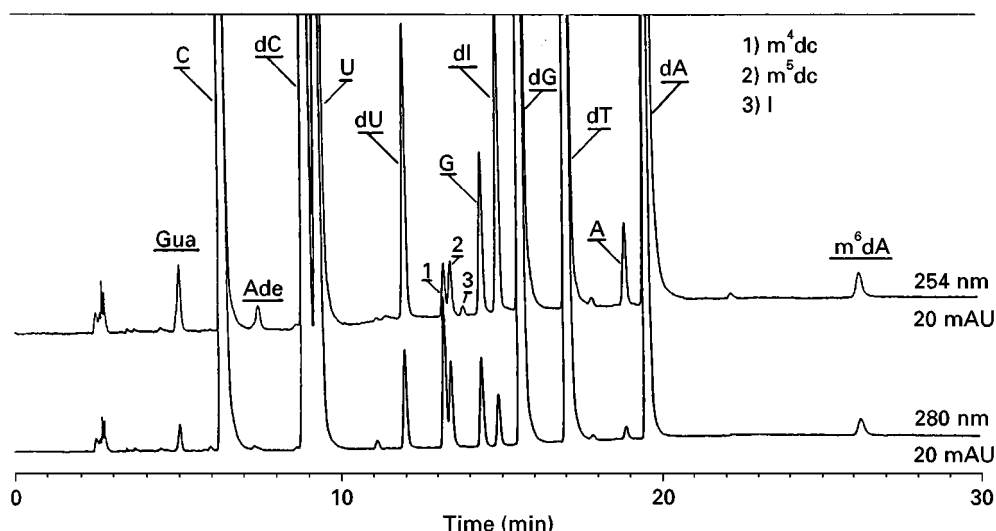


Figure 5 High resolution chromatography of ribonucleosides and deoxynucleosides.

found to occur after the macromolecule is formed, and of particular interest was that these methylated compounds were not reincorporated into the tRNA molecule but thought to be excreted intact. It has been suggested that the high turnover of a subpopulation of tRNA is the major reason for increased excretion of modified nucleosides by cancer patients. The measurement of modified ribonucleosides in body fluids as biological markers of cancer resulted largely from the studies of tRNAs by the late Dr Ernest Borek. In 1974, Dr Gordon Zubrod, then director of the National Cancer Institute (NCI), appreciated the possible value of this concept. A contract was awarded by the NCI to our laboratory at the University of Missouri to develop high resolution quantitative chromatographic methods of modified nucleosides for use in tumour marker studies. Under the leadership of Professor Charles W. Gehrke gas chromatographic and RP-HPLC-UV methods were developed for measuring modified nucleosides in urine. Later the method was further improved for measuring serum nucleosides. The RP-HPLC-UV method is far better than the gas chromatographic method for highly water-soluble nucleosides, and hence it was used in analysis for a majority of the clinical studies. **Figure 6** and **Figure 7** show the separations for ribonucleosides in human urine and serum from a patient with lung cancer and acute myelogenous leukaemia, respectively. **Figure 8** presents the recovery of nucleosides from spiked serum and normal serum.

Our research on tRNA catabolites in urine and serum has centred on analysis of the modified nucleosides following isolation of the nucleosides by

boronate gel affinity chromatography. Advances in the isolation, identification and measurement of modified nucleosides have been striking, and are now providing greater insights into the value of modified nucleosides as potential tumour markers in following the course of cancer and treatment. Numerous research groups in the USA, Europe, and Japan have studied modified nucleosides and their potential relationships to cancer. A comprehensive review was presented by Zumwalt *et al.* Trewyn and Grever have provided an excellent review of urinary nucleosides in patients with leukaemia. They reviewed the available literature and discussed laboratory analyses, including methods, reference values, and multivariate analyses; clinical studies covering nonmalignant disease and infection, acute leukaemia (childhood and adult) and chronic leukaemias. They concluded that measurement of urinary nucleoside excretion offers a potential tool for monitoring disease activity in patients with acute lymphoblastic leukaemia, chronic myelo-cytic leukaemia, and perhaps chronic lymphocytic leukaemia. They also point out that additional work is necessary in following serial determinations of nucleosides at frequent intervals in patients with different types of leukaemia to assess the true value of these compounds as an accurate monitor of disease activity within the individual patient. We initiated investigations to study the correlation of the levels of serum-modified ribonucleosides with clinical status of the patient. Longitudinal serum samples were collected from leukaemia, lymphoma, and lung cancer patients. Four modified nucleosides Ψ , m_2^2G , t^6A , and m^1I , were selected to study the relationship of their levels in serum versus the course

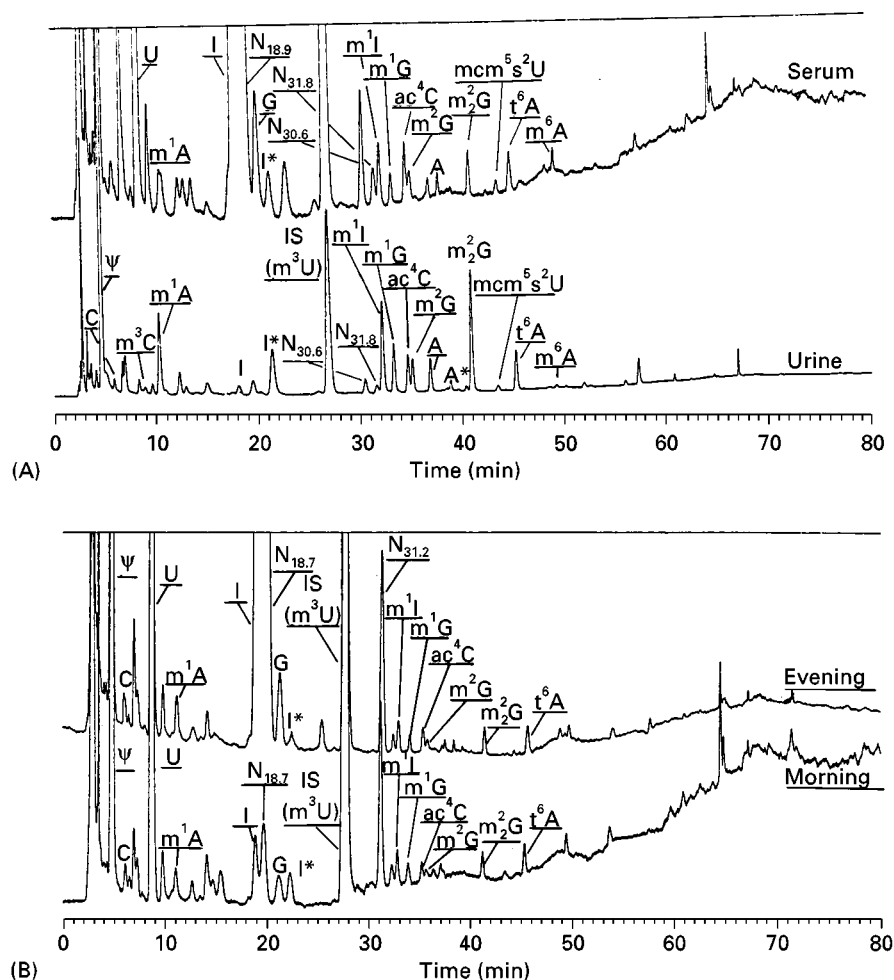


Figure 6 RP-HPLC-UV separations of nucleosides in (A) human urine and (B) serum from a lung cancer patient and a chromatogram for a morning and evening sample.

of disease. Serum pseudouridine levels showed a direct relationship to total RNA turnover. N^2,N^2 -Dimethylguanosine and N^6 -threoinocarbonyladenine, which are only found in tRNA, showed that their concentrations in serum reflects the state of tRNA catabolism. 1-Methylinosine is a very interesting modified nucleoside. The concentration of serum m^1I in the normal population is quite high ($65 \pm 21 \text{ nmol mL}^{-1}$) and is one of the commonly elevated nucleosides found in cancer patients.

The origin of serum 1-methylinosine is not completely clear at this time. It can be accounted for partially from direct tRNA turnover and deamination of m^1A by adenosine deaminase in serum. We also studied longitudinal collected normal serum samples and found that the four target nucleosides levels in serum are constant during one day (7.30 a.m., 12.00 noon and 5.00 p.m.), and over 14 days. For cancer patients we plotted the ratio of each nucleoside to the average concentration found from 94 normal subjects

as a percentage. The results of the longitudinal studies from one selected leukaemia patient, one lymphoma, and one with lung cancer are presented here. The modified nucleoside level from the respective patients over time are presented in Figure 9, Figure 10 and Figure 11. The patient description and correlation of clinical status and modified nucleoside levels are as follows.

Patient MP-K (Acute Myelogenous Leukaemia): Patient Description (Figure 9)

A 31-year-old white male smoker was admitted on 12 June 1991 with fever. Work-up showed severe leucocytoses, with increased white cell count up to 244 000. The patient went into pulmonary oedema; a bone marrow test was performed and leucophoresis started. Bone marrow showed acute myelogenous leukaemia. Chemotherapy and antibiotics were given. Sample collection was started 10 days after

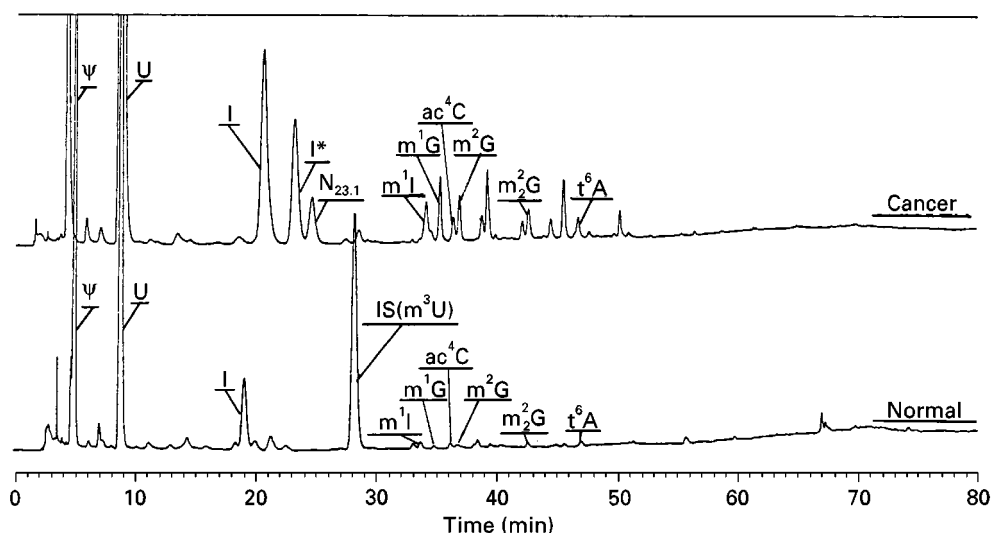


Figure 7 RP-HPLC-UV separations of nucleosides from patient with acute myelogenous leukemia versus normal.

diagnosis. The patient recovered and on 2 July 1991 a bone marrow test was again done and there was no evidence of leukaemia. However, 2 weeks later a repeated bone marrow showed relapse of disease. Chemotherapy was again given on 18 July 1991. A bone marrow 2 weeks after treatment (day 38) showed persistent disease. In the meantime the patient developed appendicitis and surgery was performed but the patient died postoperatively.

Clinical status and modified nucleoside levels (Figure 9) We started collecting samples on this patient right after induction chemotherapy was given. A bone marrow test done by the time sample no. 2

was drawn showed no evidence of leukaemia. However, there was already a slight increase in modified nucleoside levels. Relapse of the disease was clinically suspected and confirmed by bone marrow and there was a marked increase in all modified nucleoside levels. Reinduction chemotherapy was given and correspondingly there was a decrease in levels of modified nucleosides. A bone marrow test was performed at day 38 of the study, which showed presence of leukaemic cells at a time when modified nucleoside levels were also increasing. From this date, a good clinical correlation of the level of markers increased with clinical deterioration of the patient.

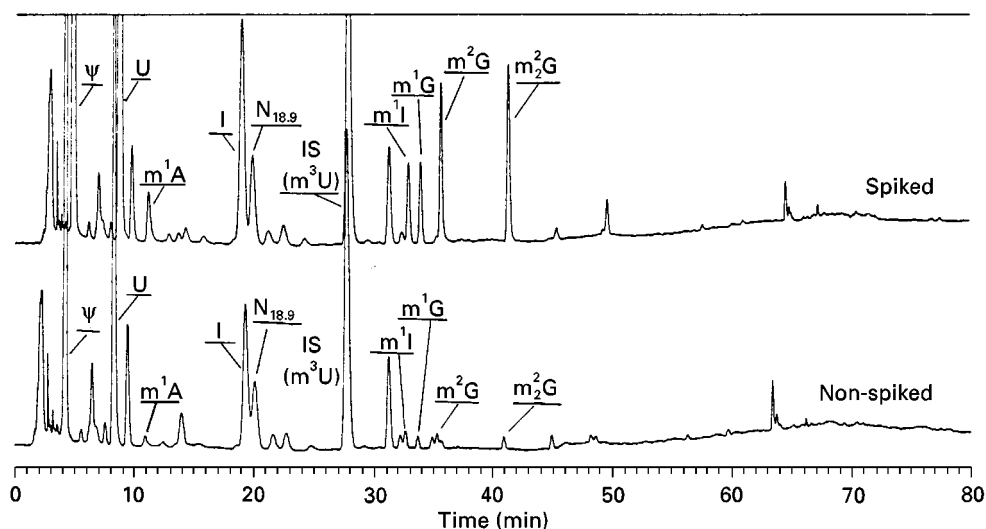


Figure 8 Recovery of nucleosides from spiked and normal serum.

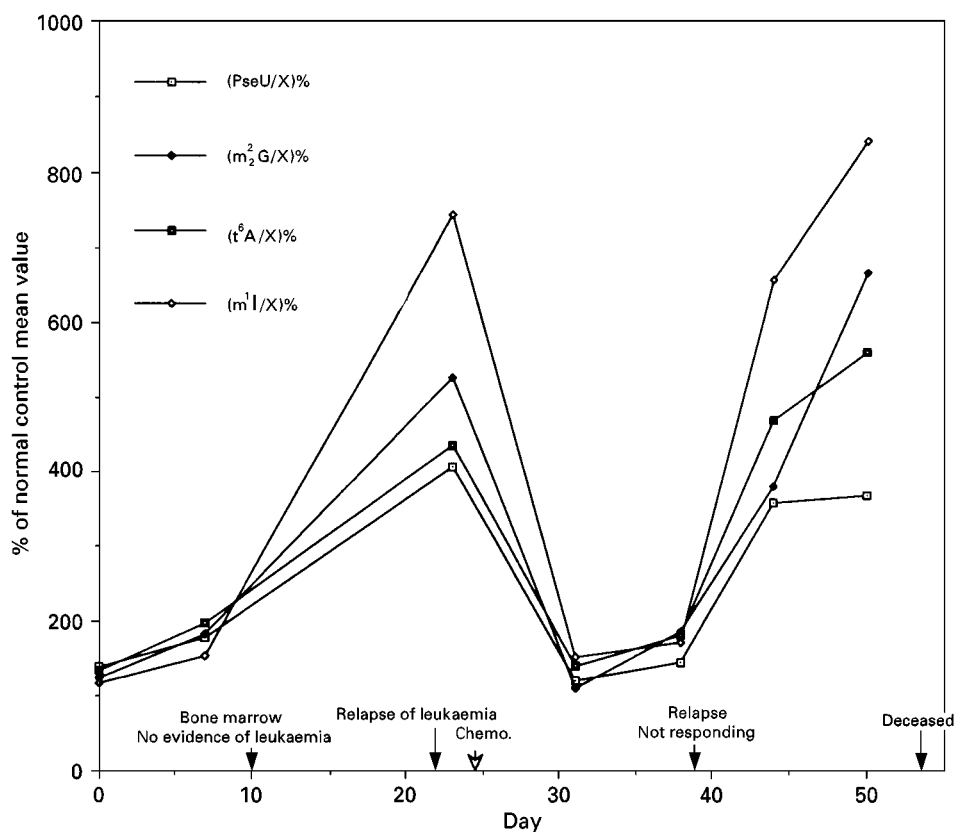


Figure 9 Serum-modified nucleoside levels as cancer biomarkers in patient with acute myelogenous leukaemia.

**Patient MP-Y (Non-Hodgkin Lymphoma):
Patient Description (Figure 10)**

A 60-year-old white female smoker presented on 1 June 1991 with weakness in the lower extremities and magnetic resonance imaging (MRI) showed evidence of cord impression. Biopsy showed non-Hodgkin lymphoma, large cell type. Postoperatively the patient received radiation therapy. The patient was started on chemotherapy after assessment of disease. On physical examination she had axillary adenopathy and computed axial tomography (CAT) scan of the chest showed chest wall disease and a pleural effusion. CAT scan of the abdomen showed metastasis to the lumbar spine. Sample collection started on 20 September 1991 while the patient was on therapy. Evaluation of her disease showed response by physical examination (axillary lymph node decreased size), neurological examination improving and by CAT scan with decreased pleural fluid. CAT scan of the abdomen showed no evidence of disease. The patient continued the same regimen of chemotherapy. In February (day 140) the patient went into respiratory distress and increased pleural effusion was detected. However, cytology and bronchos-

copy found no evidence of lymphoma. Chemotherapy was continued as soon as the patient recovered. Shortly after the patient was again admitted to hospital with fever. The patient also complained of a chest wall mass that had been growing in the last few weeks. The patient died shortly after this from cardiorespiratory arrest before any treatment was given. Autopsy showed lymphoma.

Clinical status and modified nucleoside levels (Figure 10) By the time the patient was included in the study she was already on chemotherapy and clinically responding. Modified nucleoside levels were quite steady until day 175, when there was a gradual increase and a peak around day 250 of the study. Clinically the patient was having lung problems and an infiltrate and new plural effusion by lymphoma was never documented; however, all four modified nucleoside levels increased to 250–350% of the normal control mean values. The modified nucleoside levels continued to increase and remained higher. The patient died from cardiorespiratory arrest. Lymphoma was later proved present by biopsy in the chest wall mass. There was a good clinical correlation of

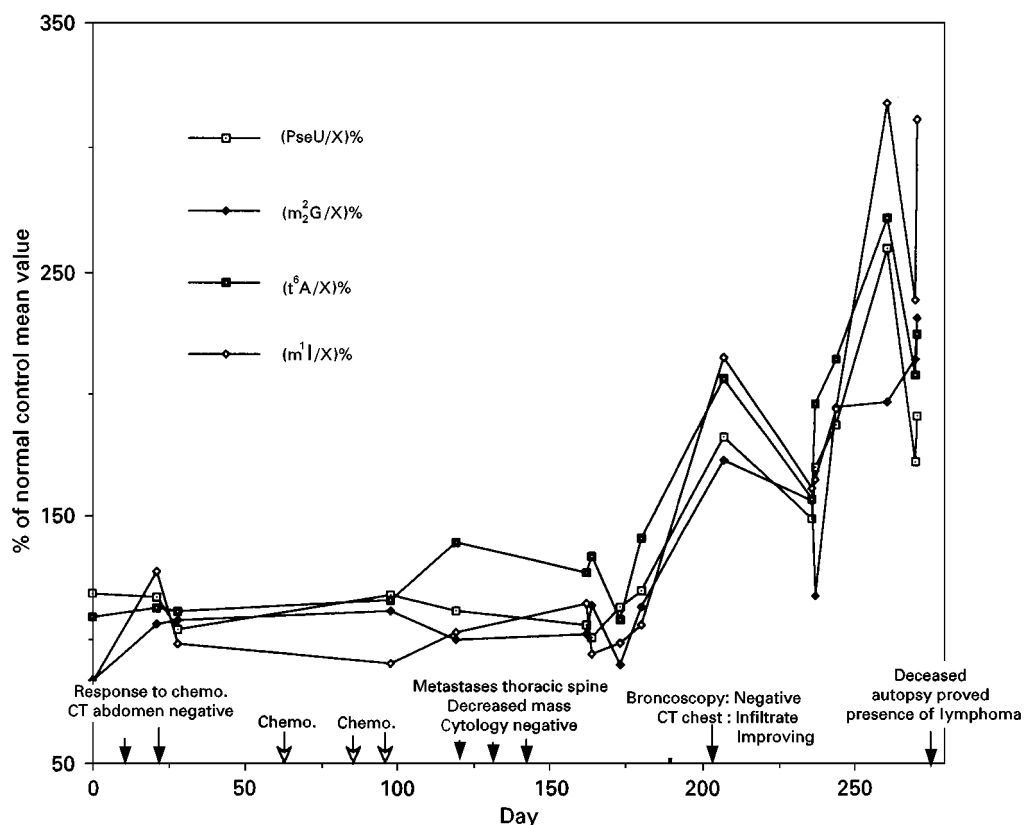


Figure 10 Serum-modified nucleoside levels as cancer biomarkers in lymphoma patient.

the four serum modified nucleosides levels and lymphoma.

Patient LRH (Adenocarcinoma of the Lung): Patient Description (Figure 11)

A 58-year-old white male smoker presented in April 1993. Biopsy and MRI showed poorly differentiated adenocarcinoma of the lung with metastases to the adrenal gland (adrenal mass) and no pleural effusion. Chemotherapy was started on 26 May 1993. This patient was not responding to chemotherapy and his clinical status was gradually deteriorating. In October 1993 (week 23) the patient was in the end stage of the disease.

Clinical status and modified nucleoside levels (Figure 11) This patient was not responding to treatments. His clinical status was continually deteriorating. The progression of disease correlated with increased levels of modified nucleosides. When the disease reached the end stage, the levels of all four modified nucleosides were > 300% higher than the normal control mean values. In this case the modified

nucleoside levels clearly correlated with the progress of the disease.

Preparative Isolation of Unknown Nucleosides in Nucleic Acids for Structural Characterization

Knowledge of the chemical structure of nucleoside modifications in nucleic acids is essential for increasing our understanding of their chemical structure and biological function relationships. tRNA is one of the most heterogeneous biopolymers known. It not only has a variety of functions within the cell, but also contains a much larger proportion of modified nucleosides than other nucleic acids; more than 60 modified nucleosides have been characterized in tRNA. With our newly developed RP-HPLC-UV nucleoside chromatography methodology, providing its enhanced resolution and sensitivity, many new modified nucleosides have been detected and identified. As tRNA research investigations are conducted on more complex organisms it is highly likely that additional modified nucleosides will be discovered, as we have

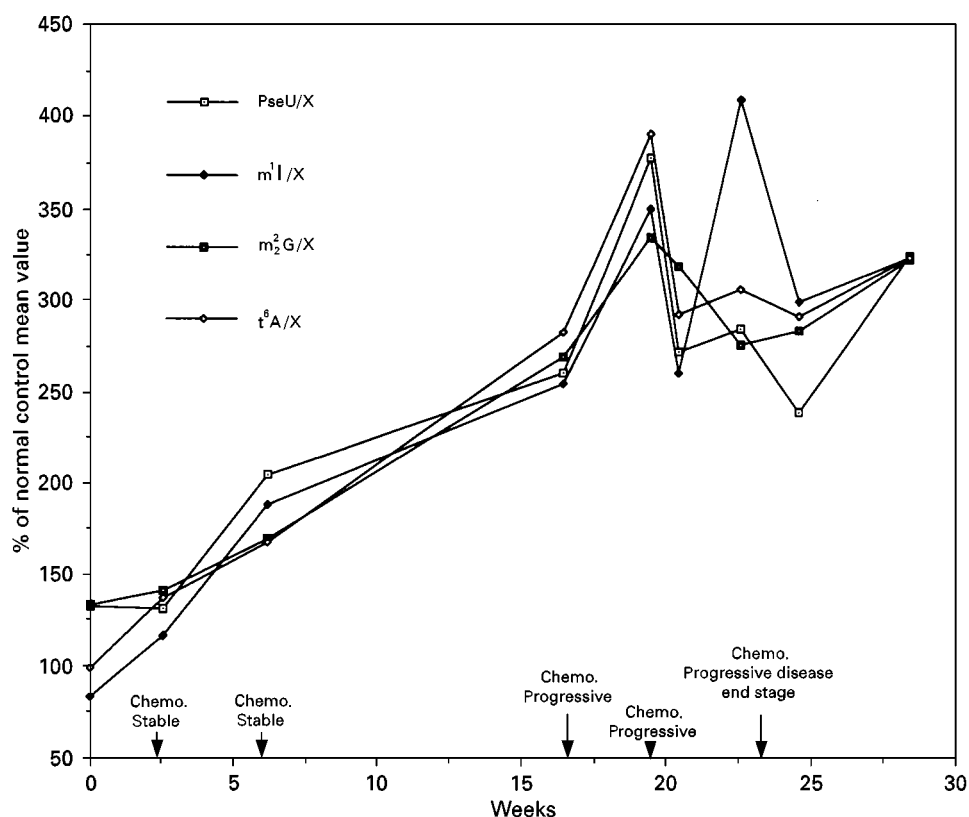


Figure 11 Serum-modified nucleoside levels as cancer biomarkers in patient with adenocarcinoma of the lung.

observed many unidentified nucleosides in urine and serum. The information on modified nucleosides in human tRNAs is limited, and further investigation should be conducted.

For purification of specific tRNAs, various types of chromatographic and electrophoretic procedures have been used. Because of the complexity of the initial mixture, the first purification step is generally not for high selectivity but for high capacity. We therefore used the countercurrent distribution (CCD) method, which is mild and serves as a first preparation step with a high capacity. This CCD method has been adapted from Holley and Merrill and by Dirheimer and Ebel. This technique permits separation of quantities of tRNAs as high as 5–6 g.

In our research we introduced standard RPLC-UV methodologies for the analysis of nucleosides and nucleoside composition of RNAs, detailed the chromatographic protocols, developed the ‘nucleoside columns’, and gave the essential requirements needed in the HPLC instrumentation. Three optimized systems with particular emphasis placed on resolution, speed, and sensitivity are described. In addition, three unfractionated tRNAs were selected: *E. coli*, yeast, and calf liver as sources of ‘reference nucleosides’ to establish the performance of the

chromatography; also a quantitative enzymatic hydrolysis protocol to release exotically modified nucleosides from tRNAs was described. We have addressed the analytical characterization of nucleosides in nucleic acids, and chromatography and modification of nucleosides from the perspective of additional chromatographic methodologies for isolation of the nucleic acids, quantitative enzymatic hydrolysis, high resolution preparative HPLC, and affinity chromatography to obtain the pure single-species nucleosides for UV absorption spectroscopy and interfaced mass spectrometry identification. In addition, we described experiments on the determination of the structure–spectrum relationships, composition, and conformation using an array of advanced analytical techniques of HPLC-UV, FT-IR, nuclear magnetic resonance and mass spectrometry (MS), as well as structure–RP-HPLC retention relationships. In these studies, a consortium of scientists from different institutions have combined their expertise and present a comprehensive discussion of the isolation and analytical–structural characterization of tRNAs, oligonucleotides, and nucleosides in RNA and DNA. Two modified nucleosides, A* and G* in yeast initiator tRNA (initiator tRNA^{Met}) at positions 64 and 65 in the T-Ψ stem were identified as an unmodified

guanosine at position 65, and for A* as O- β -D-ribofuranosyl-(1''-2')-adenosine in position 64. We elucidated that the final structure for A* at position 64 in yeast initiator tRNA^{Met} was established as an O-ribofuranosyl-(1''-2')-adenosine-5''-phosphate linked by a 3'5'-phosphodiester bond to G at the position 65.

An unknown U* nucleoside in position 34 isolated from yeast mitochondrial tRNA^{Leu} was characterized as cmnm⁵U by HPLC-UV-MS.

Also, we have confirmed m³U, an unknown modified uridine, in the 16S colicin fragment from *E. coli* rRNA, and report the structural characterization of a catabolite in canine urine as 5-hydroxymethylcytidine (om⁵C).

This report describes the 'research tools' we have developed and are using in analytical characterization of modified nucleosides and dinucleosides in RNAs and which will be of value to others in molecular biology investigations.

A good clinical correlation was observed in patient management using four cancer modified nucleoside biomarkers in following the course of disease and treatment.

See also: II/Chromatography: Liquid: Detectors: Ultra-violet and Visible Detection; Mechanisms: Reversed Phases.

Further Reading

- Borek E (1971) Introductions to symposium: tRNA and rRNA modification 1. Differentiation and neoplasia. *Cancer Research* 31: 596-597.
- Borek E (1972) The morass of tumor markers. *Bulletin of Molecular Biology and Medicine* 10: 103-117.
- Borek E and Kerr SJ (1972) Atypical transfer RNAs and their origin in neoplastic cells. *Advances in Cancer Research* 15: 163-192.
- Borek E, Baliga BS, Gehrke CW, Kuo KC and Waalkes TP (1977) High turnover rate of transfer RNA in tumor tissue. *Cancer Research* 37: 3362-3366.
- Desgres J, Keith G, Kuo KC and Gehrke CW (1989) Presence of phosphorylated O-ribosyladenosine in T- Ψ stem

of yeast methionine initiator tRNA. *Nucleic Acids Research* 17: 865-882.

- Dirheimer G and Ebel JP (1967) Fractionnement des rRNA de Levure de biere par distribution en countre-courant. *Bulletin de la Société Chimique et Biologique* 49: 1679-1687.
- Gehrke CW and Kuo KC (1989) Ribonucleoside analysis by reversed-phase high performance liquid chromatography. *Journal of Chromatography* 471: 3-36.
- Gehrke CW, McClune RA, Gama-Sosa MA, Ehrlich M and Kuo KC (1984) Quantitative RP-HPLC of major and modified nucleosides in DNA. *Journal of Chromatography* 301: 199-219.
- Gehrke CW and Kuo K (eds) (1990) *Chromatography and Modification of Nucleosides*. Amsterdam: Elsevier.
- Holley RW and Merrill SH (1959) Counter-current distribution of an active ribonucleic acid. *Journal of the American Chemical Society* 55: 735.
- Kuchino Y, Borek E, Grunberger D *et al.* (1982) Changes of post-transcriptional modification of large base in tumor-specific tRNA^{Phe}. *Nucleic Acids Research* 10: 6421-6432.
- Kuo KC, McCune RA, Gehrke CW, Midgett R and Ehrlich M (1980) Quantitative reversed-phase high performance liquid chromatographic determination of major and modified deoxyribonucleosides in DNA. *Nucleic Acids Research* 8: 4763-4776.
- Kuo KC, Smith CE, Shi Z, Agris PF and Gehrke CW (1986) Quantitative measurement of mRNA cap 0 and cap 1 structures by high-performance liquid chromatography. *Journal of Chromatography and Biomedical Applications* 378: 361-374.
- Kuo KC, Esposito F, McEntire JE and Gehrke CW (1987) Nucleoside profiles by HPLC-UV in serum and urine of controls and cancer patients. In: Cimino F, Birkmayer GD, Klavins JV, Pimentel E and Salvatore F (eds) *Human Tumor Markers*. Berlin: Gruyter, pp. 519-544.
- Martin RP, Sibley A, Gehrke CW *et al.* (1990) 5-Carboxymethylaminomethyluridine is found in the anticodon of yeast mitochondrial tRNAs recognizing two-codon families ending in a purine. *Biochemistry* 29(4): 956-959.
- Trewyn RW and Grever MR (1986) Urinary nucleosides in leukemia: laboratory and clinical applications. *CRC Critical Reviews in Clinical Laboratory Sciences* 24: 555.

Thin-Layer (Planar) Chromatography

J. J. Steinberg, Albert Einstein College of Medicine, Yeshiva University, New York, NY, USA

Copyright © 2000 Academic Press

Introduction

Thin-layer (TLC; or planar chromatography) is well suited to the separation of nucleic acids. One of the

most important chromatographic systems for nucleic acids – ion exchange chromatography – received great impetus with the development of poly(ethylene imine)-HCl prepared cellulose (PEI), which became available in the early 1960s. The studies that followed laid the foundation for the analytical and preparative TLC of nucleic acids. Many types of plate are presently available for TLC, but most reports are limited to PEI-cellulose, ODS (octadecylsilica), and silica gel in simple one-dimensional systems.

Gel electrophoresis has diminished the need for TLC of large oligonucleotides and the inability to have stable thick (2 mm or more) chromatographic plates has diminished the development of preparative TLC. High performance liquid chromatography (HPLC) has become important for smaller oligomer separations, and especially important for preparative chromatography. TLC and HPLC together can serve for initial investigations, but usually require further analytical instrumentation or chemical characterization. Coupled UV and Fourier transform infrared (FTIR) have added to the power of chemical characterization by HPLC and these systems are now becoming available in TLC. HPLC, however, is limited when employing highly radioactive molecules as extensive cleaning and decontamination of the whole HPLC system is required. In the hands of expert experimentalists TLC offers outstanding flexibility that matches HPLC, with less labour and cost.

Sorbents

Considerations for sorbents are: physical and chemical properties, pore diameter, pore volume, surface area, particle size distribution and mean size. Adsorption is the main mode of chromatography employed. Weak physical interactions in TLC include van der Waals forces, dipole-dipole forces and hydrogen bonding. Cellulose ion exchange further employs polyethyleneimine ($-\text{CH}_2-\text{CH}_2-\text{NH}$)_n for more specific separations. Typically, polar solvents are employed for polar solutes with hydrophobic phases. Solvents are based on an elutropic classification with elution power increasing with polarity. The speed of elution also depends on the viscosity of the eluent.

Cellulose is used when ion exchange properties are not needed. It is most often used for the separation of sugars, amino acids and similar compounds. A popular sorbent for the separation of nucleic acid derivatives, it readily separates pyrimidines (higher R_F) from purines. Commercial grade microcrystalline cellulose (Avicel) has been used for the retention of guanine (base or nucleoside) in either acidic (HCl; formic acid) or basic (ammonia) solvents.

Diethylaminoethylcellulose (DEAE) has the functional group incorporated into the paper. It is an anion exchanger that is generally used to separate proteins and enzymes and similar materials, but is also used for nucleic acids, nucleotides, deoxynucleotides and nucleosides. Separation on DEAE-cellulose is not as sharp as on PEI-cellulose, but there is a considerable amount of information on the separation of nucleic acids on these layers.

There are many published tables that contrast TLC separations with various solvents and demonstrate the utility of cellulose in the relative retention of amino groups, regardless of purine/pyrimidine structure, in either acid (HCl, isobutyric acid) or ammonium hydroxide mixtures. The presence of ammonium carbonate (and to a lesser extent formate) affects purine/pyrimidine separations, with R_F values greater for pyrimidines.

ECTEOA is the abbreviation for the epichlorohydrin and triethanolamine groups that are combined with cellulose. DEAE-cellulose and ECTEOA-cellulose layers have about the same ability to resolve nucleic acid derivatives. ECTEOA-cellulose is especially useful for the separation of nucleic acids, nucleotides and nucleosides as an anion exchanger and is also good for the rapid separation of pyrimidines from purines.

ITLC (instant TLC) plates are glass microfibre sheets. The addition of silicic acid or silica gel gives the additional designation of SA or SG, respectively. Multiple solvent systems used with these plates allow the retention of adenine and its associated structures.

Silica gel has been used extensively, although it was not used in the early development of the TLC of nucleic acids. It is also used for the separation of amino acids and proteins. It is especially advantageous in separating pyrimidine from purines.

G is the designation for CaSO_4 binder (gypsum). Silica-G has been used to resolve pyridine nucleotides, uridine diphosphate (UDP) derivatives of hexosamines and acetylhexosamines. Silica-G is used for preparation of larger quantities of bases, nucleosides and many of their derivatives.

Reversed-phase (RP; ODS or C_{18}) performs essentially as silica gel. The opportunity of developing a strategy on RP-TLC and transferring it to a similar HPLC system is possible, but not always successful. The utilization for TLC of commonly available premixed HPLC solvents (methanol, acetonitrile, tetrahydrofuran, phosphates) is very convenient and allows information to be obtained quickly. RP-TLC, as opposed to its HPLC counterpart, cannot be as easily employed over a wide range of pH values.

Much of the knowledge of PEI-cellulose has come from the work of Randerath. This material has been

extensively studied and used in the separation of nucleic acid bases, nucleosides and nucleotides, with good separation and resolution. It has also been used for the separation of RNA and DNA hydrolysates, and for large scale preparations among other applications. It remains the most versatile paper for the separation of deoxynucleotide monophosphates (dNMP).

High performance (HP) TLC is constantly undergoing improvements; it offers smaller layers, more uniform and smaller sorbent particles, thinner layers and faster development. HPTLC can be utilized for nucleic acid identification, but is not commonly used. Typically, HPTLC offers quantities of product that are too small for identification by GC, FTIR or NMR.

Preparative TLC is a rapid technique where the analyte is streaked across a plate, and separation commences on a layer 1–5 mm thick. The nucleic acid of interest is scraped off the plate and eluted accordingly. Papers for centrifugal layer chromatography offer an alternative preparative technique. Chiralplates have had excellent results in separating enantiomers and halogenated compounds, and can also play a role in separation of nucleic acids.

Solvents

These are discussed in detail in the publications given in the Further Reading section. Tactically, an initial screen of unknowns or products on TLC is carried out as a preparation for the development of an HPLC method. This is helpful, and the rule of thumb is that 20 one-dimensional TLC runs with different solvents will determine the best eluent.

Directionality, including ascending, descending, two- and multi-dimensional, circular and drip chromatography have all been employed either to improve separations or to increase sample throughput. Automated anti-circular TLC systems where the solvent is applied at the periphery and flows inward toward the centre offer improved ability to examine fractions with R_F values near 1.

Results are essentially empirical, with advantages for most techniques based on analysis time for a specific set of analytes. Excellent reproducibility and success has been obtained with two- or multi-dimensional TLC, which greatly enhances the number of theoretical plates available, and hence the ultimate separation. Significant progress in gradient TLC will also impact on nucleic acid separations.

TLC has great flexibility – concentration, viscosity, polarity, pH, ionic strength, composition of gas phase and temperature are all important and controllable. Educated trial and error is not inappropriate to devel-

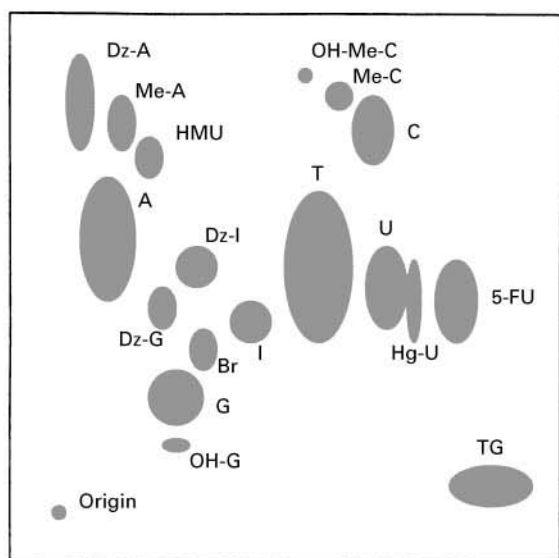
op initial TLC characterization of analytes. The strategy of many separation techniques emphasizes the chemical differential migration, e.g. hydroxyl, ammonium groups, of the various dNMPs with selective retention. The solvent affects all components of a mixture equally as a nonselective driving force. Further resolution of dNMPs from DNA can be accomplished by selective removal of particular compounds, or groups of compounds; to emphasize or diminish a specific dNMP we would consider competing with an analogue, e.g. deaza-dGMP for dGMP adducts, or depurinating to emphasize pyrimidines (see Figures 1 and 2). This strategy allows us to maintain simplicity in the solvent system.

In optimizing planar chromatography, computer programs exist that are very helpful in developing choices for solvents. Demixing remains a major problem in predicting retention and the ultimate experimental outcome. Again, 20 chromatograms are sufficient to define experimental variables for optimum resolution. Solvent selectivity has been discussed in terms of proton donation, acceptance or dipole interactions. Many mixtures of solvents exist, yet a reliable few can serve almost all purposes. We have listed the common solvents for TLC as a guide in Table 1.

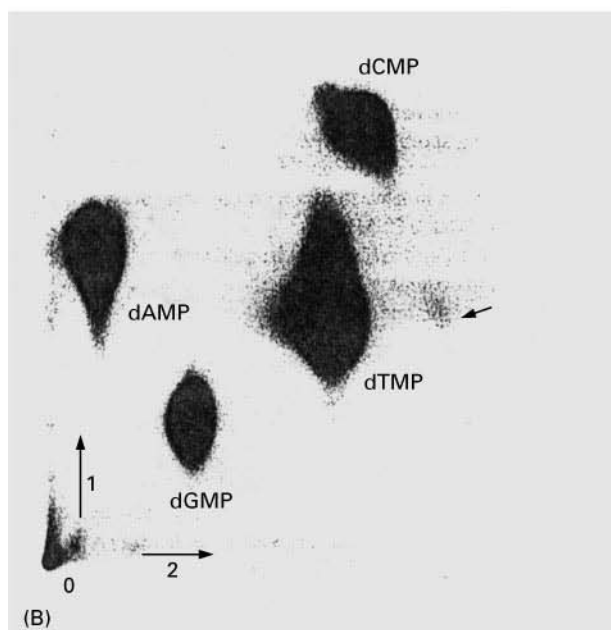
Uniformity of Techniques

A general problem with TLC is the paucity of uniform guidelines that can direct investigators in different laboratories. Any serious investigator in TLC systems must establish rigorous and reproducible techniques. Few papers give in detail all the parameters necessary to reproduce successfully experimental TLC protocols. Much of this is pragmatic, especially given simple unidimensional systems where only one known chemical, with established controls, is confirmed. Most typically, these are pharmaceutical-based studies, which simply confirm one known pharmaceutical that conforms to the available control.

Success in characterizing true unknowns in complicated bi- or multidirectional systems (two-dimensional TLC) requires the publication and listing of uniform criteria. Attempts have been made to validate TLC techniques by directing attention to a number of concerns including R_F reproducibility, the role of the mobile phase, the stationary phase, the quality and quantification of zones, the method of elution and the estimation of spots. It is suggested that published TLC papers should attempt a more uniform approach to stating clearly experimental materials, methods and conditions. In view of the need for interlaboratory reproducibility, listed below are the



(A)



(B)

Figure 1 (A) Stylized representation of nucleic acid separations. (B) Normal enzymatic and ^{32}P -labelled digest of placental DNA.

chromatographic conditions necessary for the successful separation of dNMPs on PEI-cellulose:

1. Solvents (composition): first dimension, acetic acid (1.0 mol L^{-1} , pH 3.5 with NaOH); second dimension, $5.6 \text{ mol L}^{-1} (\text{NH}_4)_2\text{SO}_4$, $0.12 \text{ mol L}^{-1} \text{Na}_2\text{EDTA}$, $0.035 \text{ mol L}^{-1} (\text{NH}_4)\text{HSO}_4$ to pH 4.0. Stable over 2 weeks.
2. Layer (brand, grade): PEI-cellulose, Sigma.
 - Size, geometry: square, $200 \text{ mm} \times 200 \text{ mm}$.
 - Method of storage: refrigerator at 4°C .

- Preparation: no pre-run; constant room temperature and humidity.
 - Treatment: cool air-dried (dehumidified) during spotting.
 - Heterogeneity (R_F lower with thicker paper): $> 1\text{--}3\%$ variation over each TLC.
3. Developing tank (make, size): Sigma Inc; $275 \text{ mm} \times 275 \text{ mm} \times 75 \text{ mm}$ with lid.
 4. Application amount: $1.0\text{--}10.0 \mu\text{L}$ (or 20 000–100 000 CPM (counts per minute)).
 5. Drying (origin, plate, after first dimension): at 1 cm, 1 cm x, y axis; cold dryer.
 6. Direction of development: ascending, both dimensions.
 7. Distance of origin from solvent reservoir (closer for higher R_F): 1.0 cm.
 8. Depth of immersion: 5 mm.
 9. Volume of solvent in reservoir: 15 mL.
 10. Duration of development (h): first dimension, 4 h; second dimension, 15 h.
 11. Temperature: 17°C ; 50–60% humidity constant.
 12. Equilibrium humidity in tank: complete prior to TLC.
 13. Character of solvent front: observe as regular, linear.

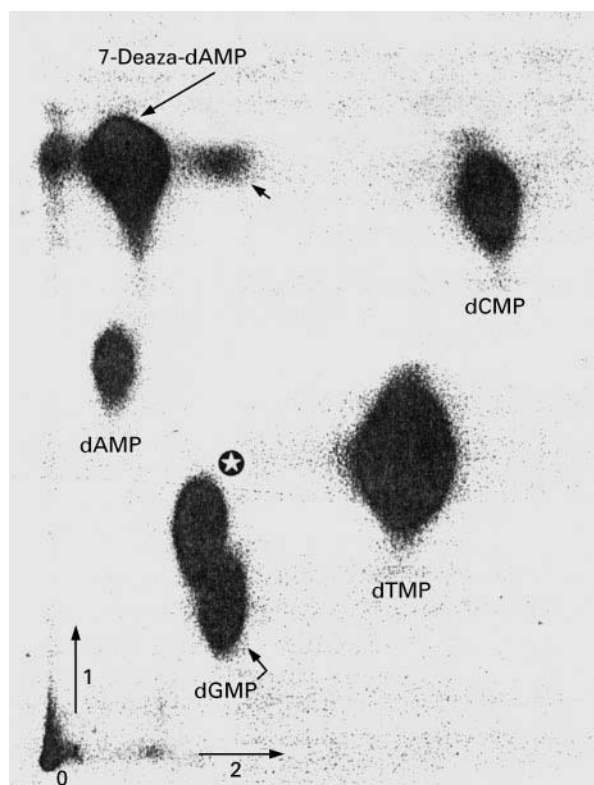


Figure 2 DNA analogue-labelled digest: deaza-dAMP replacing dAMP.

14. Comparison of R_F versus R_X : consistency of chemical migration versus relative standard – less than 3% variability. All R_F values given as ' R_X ' with x, y coordinates. NB: Conversion of R_X to R_F requires all numbers divided by 19 cm. (If R_F values are given these are usually multiplied by 100 = hR_F .)

Most parameters in TLC are quantifiable, and all quantitative information should be listed. A greater attempt by investigators, reviewers and editors to adhere to these standards will increase both the likelihood of chromatographic success, its reproducibility, and sensitivity.

Sensitivity

In our 2D-TLC system for dNMPs we attempt to discover and analyse altered nucleic acids (adducts) or synthetic nucleic acids used as pharmaceuticals (analogues). The technique can ultimately detect one radioactive adduct per 10^8 nucleotides, which is as sensitive as any analytical system available. At this stage we radiolabel 0.2 μ g of DNA with 32 P to 6.0×10^6 DPM (disintegrations per minute). We assay from 2.0×10^4 to 1.0×10^6 DPM and can reliably detect as few as 50 DPM over background. This allows a mathematical minimum detection of one adduct per 10^5 – 10^8 nucleotides. Yet, many unique analytes can be detected at up to one per 10^8 – 10^{10} dNMP (as few as 25 DPM above background). An example of detectability can be seen by the complicated pattern of adducts formed by DNA in buffer remaining refrigerated for a prolonged period and obvious DNA reactivity with water and oxygen as noted by the proliferation of adducts at 72 h autoradiography. Furthermore, we have detected adduct incorporation when we have altered and 'contaminated' the dNMP reaction mixture pool with less than 1 nmol of a foreign dNMP during enzymatic incorporation (see Table 2). These lower values are within the range for detecting modifications by environmental, drug and ageing processes, e.g. methylated or deaminated dNMPs.

Reliability

Control dNMPs and DNA are run with every batch of samples. Experience with this technique shows that variations of R_F values ranging from 1 to 5% can be achieved in over 2000 analyses. The Ambis (computerized radioactive scanning of TLC) statistically correlates consistently with laser densitometry, but mean values can vary in densitometry by $\pm 6.5\%$ overall. There are also qualitative differences be-

tween densitometry and scintillation counting, specifically where densitometry is unable to account for all the 'spots' that it detects as a 'smear', though the human eye can easily distinguish borders, zones and spots. However, the Ambis is more successful in quantifying smear areas by counting smear CPM. A statistical analysis of Ambis data versus densitometry provides a correlation coefficient of 0.93, $p < 0.001$, $n = 23$ pairs, providing the formula: Ambis DPM = $62.4 (\text{mm}^2 \text{ area from densitometry}) - 17\,410$. The Ambis is more successful in detecting dUMP (see Figure 3) and other less discrete dNMPs than densitometry. Yet densitometry shows up borders between migration patterns of close dNMPs better, especially methylated dNMPs. Other variations in CPM reflect quenching of radioactivity from the TLC plates. At low DPM, quenching blocks 90% of counts detectable, but at high DPM, quenching blocks only 50% of counts. These differences are mathematically quantifiable, and the formulae generated have high predictability. TLC data must be presented as quantitative and statistical values to further increase reliability of techniques, and correlate inter laboratory discrepancies.

Analyte Identification

The major ability to both elute and identify any nucleic acid resides in its functional groups and heterocyclic rings. Any approach to identification of unknown or modified nucleic acids should begin with characterizing functional groups, and subsequently using this information to improve separation. Furthermore, functional groups offer sites of chemical alteration and simple bench-top techniques, can confirm structure. tRNA has served as the primary impetus for developing accurate and reproducible techniques to separate methylated nucleosides. It is not possible to summarize in this article the literature that exists on the chemistry of nucleic acids.

In consideration of both choice of TLC paper and likely nucleic acid identification, a few observations apply. In general hydrophobic modifications and methylation decrease R_F , hydrophilic modifications, e.g. succinylations, increase R_F . Low versus high negative nucleic acid charges are alterable and dependent on TLC and solvent system. Other strategies may be first to react chemically with nucleic acids prior to chromatography.

Sugars such as pentose ring riboses and deoxyriboses react readily. The sugars are uncharged at physiological pH, and lose a proton at pH 12. The major advantage of the phosphodiester bond is that it is cleaved with extreme acid or alkali. The charge and number of the phosphates ultimately confer their

Table 2 Purine/pyrimidine detection schema

<i>Moiety</i>	<i>Reagent/reaction</i>	<i>Result: nucleic acids</i>
Nucleoside mono-, di- and triphosphates	Ammonium molybdate–perchloric acid	Blue spots
Caffeine	Chloramine-ammonia	Rose-red coloured spots
Xanthine derivatives	Chlorine-ammonia	Xanthine derivatives – violet
Deoxyribonucleosides, deoxyribo-, mono-, di- and triphosphates	Cysteine–sulfuric acid	Purines – green fluorescence
Purines	Eosine–mercury chloride	Purines – red violet best seen under UV light
Purines	Mercuric acetate–diphenyl carbazole	'Shadows' on violet background (circle after appearance not stable)
Purines and pyrimidine bases	Mercuric nitrate–ammonium sulfide	Black spots
Oxidized pyridine nucleotides, adenine-containing compounds	Potassium cyanide	Oxidized pyridine nucleotides – fluorescent zones; adenine-containing compounds
Adenine, guanine, hypoxanthine, xanthine and derivatives from cytosine and derivatives from chloride, bromide and iodide from histidine	Silver nitrate–bromophenol blue	Adenine, guanine, hypoxanthine, xanthine, and derivatives – blue spots Cytosine and derivatives – royal blue; chloride, bromide, iodide – violet
Purines	Silver nitrate–sodium dichromate	Red spots
Sulfur derivatives of purines and pyrimidines	Thiocarbamide reaction	Green or blue spots
Guanine and xanthine and compounds from other naturally occurring purine and pyrimidine derivatives (except urate)	UV light + exposure to HCl	Dark spots against fluorescence of paper (except uric acid) guanine and xanthine exposed to HCl–strong fluorescence

mobility on chromatography. The monoester phosphate has two ionizable OH groups, and is in relative equilibrium at physiological pH.

Studies have been carried out on the lipophilic characteristics of xanthine and adenosine derivatives. These are potentially important for large classes of drugs, including chloroadenosine. Lipophilic characteristics can be studied with silicone-coated or C_{18} TLC plates. Methanol/phosphate buffer, pH 7, with a methanol content ranging from 30 to 80% have been used. Equations have been obtained to allow maximum allowable separations of 44 purines.

Separation of hydroxy-2'-deoxyguanosine-3'-monophosphate is carried out in 1.5 mol L^{-1} ammonium formate (pH 3.5), and then 0.4 mol L^{-1} ammonium sulfate. Though good separation of C_8 -hydroxy-dGMP is obtained, most dNMPs remain in the midline, with significant artefacts in the second dimension. Aside from ageing, metabolism of DES (the hormonal drug diethylstilbesterol) also forms C_8 -hydroxy-dGMP.

Novel separations of anomeric α (pharmacological) purines can be carried out on copper acetate Chiral-plates with methanol/water/ACN and visualization under UV light.

Others use silica gel separations of noncyclic radioactive [^3H] adenosine as neuromodulators, and only use one-dimensional separation. The solvents are various mixtures of butanol/ammonia/water/acetic acid. Separation takes 3–4 h. Typical separations un-

equivocally demonstrate cAMP, inosine, adenosine and adenine. UV sensitivity is down to 5 nmol. Plant cytokinins (adenine) are separated on silica gel in ethanol/ammonium borate, butanol/ammonia or butanol/water. Measured ATP is obtainable from degraded meat via 5% cold perchloric acid on silica gel and isobutanol/amy alcohol/ethoxyethanol/ammonia/water (mature solvents for 48 h).

Guanine can be separated from other nucleic acids on PEI-cellulose with triethylammonium bicarbonate (TEAB) 0.5 mol L^{-1} pH 7.6. Good separation of cyclics, phosphates and nucleosides is evident. Cyclic purines are separated by PEI with ammonium acetate/hydroxide/ethanol eluent at pH 9.0 in one dimension, ascending from triphosphates to nucleobases. Cyclic purines are also separated with PEI in 0.4 mol L^{-1} acetic acid, then 0.125 mol L^{-1} LiCl. GTP is separated with PEI and Luciferase, water and then 1.4 mol L^{-1} LiCl for 50 min. Assay is by scintillation counter.

Alkylated deoxyuracil separation is carried out with RPTLC in methanol/propanol/water/dichloroethane. Water/ethanol has greatest effects on longer chains. Here TLC demonstrates quantitative structure–activity relationships (QSAR).

Thymine dimer separation has been successful on silica gel with one-dimensional chloroform/methanol/water and two-dimensional ethyl acetate/propanol/water, then sprayed with cysteine/sulfuric acid. Separation is evident, but almost all in midline.

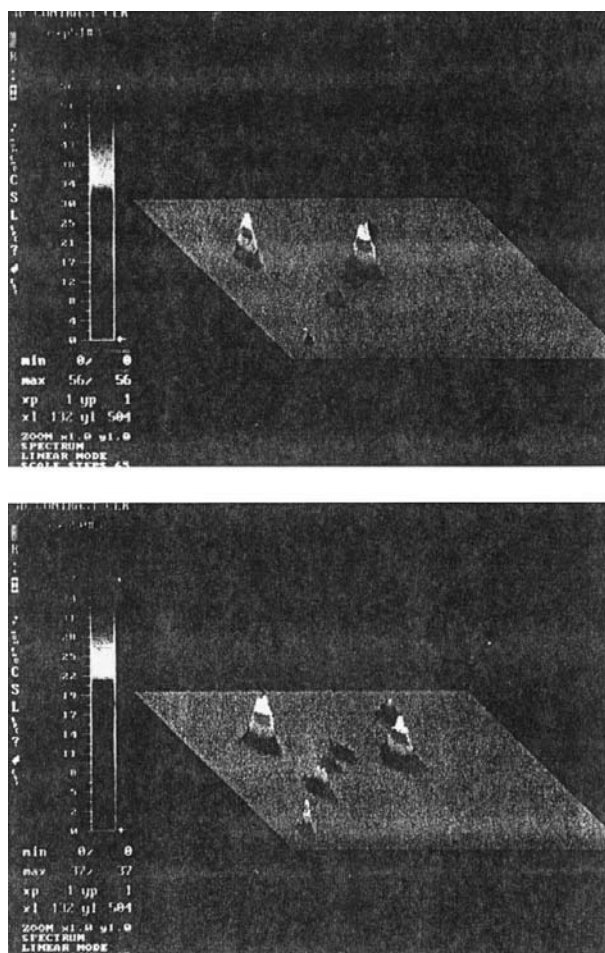


Figure 3 Three-dimensional ^{32}P computer reconstruction of DNA digest and DNA digest with chemically introduced dUMP.

Thymine dimers are also separable via cellulose and *n*-butanol/water, and 2D-ammonium sulfate/sodium acetate/propanol. Adhesive tape can be used to remove cellulose for scintillation counting.

'Bench-top' chemistry can be successfully employed for chemical identification of nucleic acids with derivatization by dimethylaminonaphthalene-5-sulfonyl chloride (DANS-Cl) formic acid (6%), acetate/ethanol/ammonium hydroxide, or ethyl acetate/ethanol/ammonium hydroxide used on a polyamide sheet. Also borohydride is used in post-labelling reduction [^3H].

Halogenated uracils can be separated on silica HPTLC plates. Solvents are chloroform/ethanol/water \pm acetate. As many as 27 pyrimidine analogues have been separated. Cellulose TLC and various combinations of butanol/ammonia/ethyl acetate/formic acid/sodium phosphate/propanol/isoamyl alcohol were used. New analogues are regularly discovered by 2D-TLC with PEI in isobutyric acid/water/ammonium hydroxide (first dimension) and ammonium

sulfate/isopropanol/sodium acetate (second dimension). Among these is 'pdJ', a nucleotide. Hydrazine is used to destroy other pyrimidine rings. These modified nucleotides are resistant to post-labelling.

Diol detection occurs with methyl red in ethanol, boric acid and acetone. These conditions are good for polar sugars; arabinosyl, ribosyl and deoxyribosyl are well handled with PEI in LiCl. Acyclonucleosides are powerful antiviral agents, e.g. acyclovir for herpes. These analogues lack one or more atoms on the pentofuranose ring. Separation strategies can be developed to take advantage of the alterations in the sugar.

Typical specimens from biological sources contain mixtures of purines and pyrimidines. Thin TLC layers (0.1 mm thick) give no elongated spots when used. The separations are fast (10 min) with good efficiency (5000 theoretical plates) at R_F values under 5.5 cm. Ammonium sulfate (0.2–5.0 mol L^{-1}) solutions are used as eluents; other salts (many less ionized than $(\text{NH}_2)_4\text{SO}_4$) contribute little. pH (borax, acetate, HCl, ammonium) contributes little to separations achieved with ammonium sulfate.

TLC has been used to separate nucleotides from cell culture. TLC gives high resolution, but low load capacity and cumbersome sample-handling procedures. CEL 300 plates and butanol/acetic/water or ethanol/ammonium acetate (pH 5) effect good separations. Colorimetric quantitation is possible with ninhydrin-cadmium. TLC is most effective for nucleotides of relative molecular mass below 4000. Plant viral RNA has been chromatographed with cellulose TLC with *n*-butyric/ammonia/water in one dimension, and ammonium sulfate/sodium acetate/isopropanol in the second. The system easily separates 2' versus 3' NMPs. Methylated RNA is separated by 2D-TLC on plates consisting of varying percentages of silica gel/cellulose with acetonitrile (ACN) ethyl acetate/propanol/butanol/water/ammonium hydroxide eluents. Many of these simpler systems line the NMPs in the midline. Pyrimidine/guanine dinucleotides are well separated on PEI with 0.8 LiCl/acetic acid.

An additional challenge to biomedical applications of TLC relates to the separations of cyclic nucleotides from noncyclic phosphates. Alumina TLC and ammonium acetate, pH adjusted with ammonium hydroxide, has been used to effect these separations. 3'-5'-cGMP uses borate impregnated silica in butanol/methanol/ethyl acetate/ammonium hydroxide. Cyclic pyridines/purines are separated on cation exchange layers, pretreated with HCl, as opposed to the popular anion (PEI) systems, with an eluent of 0.05 mol L^{-1} oxalic acid.

The utility of gel electrophoresis for the separation of long chain oligonucleotides has relegated TLC to

smaller chain species. Intermediate chain oligonucleotides are readily handled by HPLC, but many smaller ones are not. This is the province of TLC. Silica gel TLC has been important in oligomer separations well up to decamers.

tRNA digests can be effectively separated, based on the nucleobase irrespective of adenines. PEI-cellulose in butanol/methanol/water, then formic acid in water, is used. For TLC that is salt-sensitive, PEI plates and 0.5% formic acid in an ascending fashion (occasionally using urea, which reduces smear) are worthwhile. 0.15 mol L^{-1} Li/formate, pH 3.0, achieves separations with as little as 5 DPM after 3 weeks autoradiography. In 2D-TLC systems, one can also add urea/formic acid/pyridine. 2D-TLC is carried out with 22% formic acid in the first dimension and with 0.1 mol L^{-1} formic + pyridine to pH 4.3 in the second dimension. Variation in TLC batches giving different binding capacities and relative primary, secondary and tertiary amine separation were observed but it was felt the results were internally consistent. The best pH is at 4.3, and investigators were successful up to 50 nucleotides.

Avicel cellulose can be used in 2D to 3D with isopropanol/ammonium hydroxide, isobutyric/ammonium hydroxide/EDTA, or ammonium acetate with detection by ethanol/scanning slit UV of the plates. Up to the C_{18} isomer were nicely resolved in a stepwise fashion. Silica gel and ammonium acetate separates up to the C_{12} isomer, and achieves good distinction.

Fingerprint Analyses

In practice all conceivable nucleic acids with altered moieties that form, whether from oxygen stress, aldehydes or other reactive species, cannot be immediately chemically defined on a routine basis. Most investigators in the field of nucleic acid adducts define a particular pattern that is specific to a chemical alteration, mutagen or carcinogen. In ageing research, these are designated 'indigenous' spots. One can employ as much specific chemical characterization as possible, but ultimately may rely on fingerprint analyses. Many of our published figures demonstrate examples of a fingerprint chromatogram (Figure 1).

Detectors and Instrumentation

The main detection techniques are colorimetry and visual inspection, zone elution (scraping) for HPLC, spectrometry and GC, or voltammetry, densitometry and radiochemical techniques. More recent methods include computerized radiochemical, laser densitometric and phosphorimager techniques.

Identification of an unknown analyte requires R_F values that are reproducible to $\pm 3\%$. The geometry of the unknown must conform to the known, under the same chromatographic conditions. Co-chromatography of known and unknowns is always required.

Table 2 lists chromogenic reactions; a great deal of nucleic acid colorimetric information is available from published sources. Common reagents include mercuric acetate (purine and pyrimidines), Ehrlich reagent for *N*-carbamyl amino acids formed after alkali hydrolysis (NaOH), and Pauly reagent for imidazole rings.

Fluorescence remains a standard technique. TLC plates are impregnated with UV fluorescent material at 254 nm (typically zinc silicate). Upon exposure, the nucleic acids absorb at 254 nm and therefore quench, so that they appear black against a blue-green background of fluorescence. The errors in quantification by UV remain high (30%). Some scanning detectors employ UV, which can be applied to TLC plates and gives better quantitative data.

Sensitivity is enhanced by fluorescence techniques but typically these techniques require derivitization (pre- or post-chromatography), which is well described in nucleic acid chemistry.

Fourier transform infrared detection is available for TLC. Many papers had high IR absorbance and were inadequate for direct IR measurement. Papers are now available that allow direct measurement. GC is best employed in conjunction with zone elution, and certainly has application to nucleic acids, though lipids have been more extensively studied.

Mass spectrometry (MS) is readily applied to nucleic acids, but typically after zonal elution to avoid interfering solutes. Present developments in coupled MS-TLC must take into account the sorbent, solvent and analyte – which will not exceed 0.25% w/w based on sample and sorbent. The apparatus requires the ability to extract, elute or volatilize analyte directly from the TLC plate. These instruments will be a boon to the ability to detect and characterize analytes. Investigators have defined nucleic acid photoproducts, radical-induced products, those modified by xenobiotic biotransformation, new and naturally occurring nucleosides especially found in RNA, methylated bases and stable isotopes. Interfaces between MS and liquid chromatography systems have also been extensively investigated.

A large amount of data has been accumulated based on laser densitometry using autoradiographically developed X-ray film from 2D-TLC chromatograms that house the separation of radioactive dNMPs. The exposure times chosen give the ability to label unknowns at high counts, in as little as 2 h, but

typically runs take 24–72 h. Many runs of 96 h to weeks reveal groups of adducts that are reproducible, and many undescribed. Present densitometric techniques can range from a few minutes for unidimensional analyses to 2 h for complete analyses of a 20 cm × 20 cm autoradiogram. Comparison of techniques with direct scintillation counting – the other gold standard – approach r values of 0.99, and similarly correlate with the best quantifying techniques.

Scintillation Counting

The coupling of sensitive (25 DPM above background), rapid (15 min for a 20 cm × 20 cm plate) scintillation counting with computerization represents a major advance in TLC quantification. It allows *in situ* measurement of radioactivity and quantitative reconstruction of the nucleic acids in two or three dimensions. The ready ability to compare TLC plates, generate tables for comparison and rapidly apply statistical or analytical methods by computer is immense. This has revealed quantifiable relationship in nucleic acid and DNA chemistry that were previously quite complicated to examine.

Scintillation counting and densitometry both have very significant advantages and disadvantages. Clearly the ability to quantify a plate immediately after a run and drying makes scintillation counting the ‘first-look’ method. Yet densitometry allows one to examine, by eye, parts of the chromatogram that may be viewed as background by scintillation counting. These techniques are complementary and will be more extensively used in the future.

Phosphoroimager

Recently, sensitive, rapid phosphoroimagers have been made available that give excellent quantitative data. They employ phosphors able to capture radiation energy from various sources comparable to autoradiography in less than 8% of the time. They not only deliver standard R_F values, but also a mass of quantitative information. The better ability to subtract controls, carry out statistical analyses and enhance minute adducts may revolutionize adduct and analogue detection of nucleic acids.

Immunoassay

This technique, similar to Western blotting, allows colorimetric reactions to occur after binding by antibodies that recognize nucleic acid adducts, and subsequent recognition by enzyme-linked antibodies that cause colorimetric reactions with the application of the appropriate substrate. Little experience is at hand

on these techniques, but they increase the specificity of reaction adducts of interest.

Summary and Future Developments

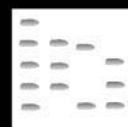
Uniformity in approach is required in TLC chromatography. This article has highlighted information drawn from the wider nucleic acids literature and has referred the reader to new techniques that have been successful in the author’s laboratory. These will enhance nucleic acid TLC and the characterization of unknowns, especially where expensive equipment is not available. Greater quantification of data by methods that are now well accepted is needed. The TLC of nucleic acids still remains significantly underused, and it is hoped that this article has offered the investigator a ready source to follow for analytical investigations.

See also: II/Chromatography: Thin-Layer (Planar): Densitometry and Image Analysis; Mass Spectrometry; Modes of Development: Conventional; Modes of Development: Forced Flow, Overpressured Layer Chromatography and Centrifugal; Preparative Thin-Layer (Planar) Chromatography; Radioactivity Detection; Spray Reagents. III/Deoxyribonucleic Acid Profiling: Capillary Electrophoresis. Impregnation Techniques: Thin-Layer (Planar) Chromatography. Nucleic Acids: Extraction; Liquid Chromatography. Appendix: 2/Essential Guides to Method Development in Two-Dimensional Electrophoresis.

Further Reading

- Carey FA and Sundberg RJ (1992) *Advanced Organic Chemistry*, 3rd edn. New York: Plenum Press.
- Grinberg A (1990) *Modern Thin Layer Chromatography*. New York: Marcel Dekker.
- Kochectov NK and Budovskii EI (1972) *Organic Chemistry of Nucleic Acids*. New York: Plenum Press.
- Randerath K and Struck H (1961) Thin layer chromatography: separation of nucleic acid derivatives in cellulose layers. *Journal of Chromatography* 6: 365–367.
- Sherma J and Fried B (eds.) (1996) *Thin-Layer Chromatography*, 2nd edn, revised. New York: Marcel Dekker.
- Singer B and Grunberger D (1983) *Molecular Biology of Mutagens and Carcinogens*. New York: Plenum Press.
- Stahl E (ed.) (1990) *Thin Layer Chromatography: A Laboratory Handbook*, 2nd edn. London and New York: Springer Verlag.
- Steinberg JJ, Cajigas A and Oliver G (1996) *Nucleic Acid and their Derivatives, Thin-Layer Chromatography*, 2nd edn. New York: Marcel Dekker.
- Touchstone JC (1992) *Practice of Thin Layer Chromatography*, 3rd edn. New York: Wiley Press.
- Zweig G and Sherma J (eds.) (1972) *Handbook of Chromatography*. Cleveland, OH: CRC Press.

OCCUPATIONAL HYGIENE: GAS CHROMATOGRAPHY



M. Harper, University of Alabama at
Birmingham, Birmingham, AL, USA

Copyright © 2000 Academic Press

Introduction

Industrial or occupational hygiene has been defined as the anticipation, recognition, evaluation and control of environmental factors or stresses arising in or from the workplace that may cause sickness, impaired health or significant discomfort. The factors causing stress encountered in the workplace are typically divided into 'physical' and 'chemical', although, increasingly, a biological component has been recognized as, for example, with infectious diseases.

Chemicals can occur as gases, vapours and mists and as solids in the form of dusts and fumes. Their hazard potential is related to their ability to react with or be absorbed by the skin or lungs. The physiological response to exposure is related to its frequency, duration and severity, the route of exposure, and the chemical make-up of the substance, as well as factors relating to individual susceptibility. Gases and vapours can cause problems in the lungs by irritation, or can be absorbed into the bloodstream to cause problems elsewhere in the body. While such absorption is most likely in the lungs, substantial uptake of vapour is also possible through the skin. Liquids and solids also may be absorbed through the skin with local irritation or systemic effects, while aerosols can be deposited in various regions of the pulmonary system. In the lungs, certain dusts cause problems associated with their physical characteristics, while others are soluble and may be absorbed. Very fine particles may also enter the body and be transported elsewhere. Liquid droplets may cause irritation or be absorbed. Absorption of any chemical into the body may cause acute or chronic health effects in organs or tissues distant from the site of absorption. The most important classes of chemicals are the permanent gases, organic chemicals, inorganic acids and the heavy metals. Exposure limits for these chemicals are published by government and other agencies.

Monitoring of the environment is required to determine the nature and quantity of chemicals present, and also to evaluate the effectiveness of control measures. Monitoring is typically carried out through sampling, either of the air being breathed, or of

surfaces which the skin or clothing may contact, or of the workers themselves through analysis of breath, blood or urine. Protocols have been established to standardize the methods of sampling and analysis. These methods are generally available, although they are often updated to meet the changing needs of hygiene investigations so that it is important to maintain a current awareness of the literature. Gas chromatography (GC) is one of a number of techniques used in the analysis of samples. It is used to separate the hazardous chemicals one from another, or from the matrix in which they are presented for analysis. GC is most often a laboratory analytical tool, but field-portable units are also available.

Factors in the Selection of Sampling and Analysis Methods

The ideal method would be specific, sensitive, and free from interference. In addition, it would provide real-time continuous output as well as time-integrated results. Finally, it would be simple and cheap to operate. It is rarely possible to satisfy all these criteria in currently available technology and compromise is often necessary.

Air Sampling

There is substantial variation of hazardous chemical concentration in both space and time. To obtain accurate information concerning the airborne dose to the worker, it is necessary to sample air from the 'breathing zone'. Personal monitors therefore require an inlet port or sensor close to the face. Temporal variability can be covered by taking a time-integrated sample. Regulated concentration limits normally are expressed in terms of 8-h (work-shift) averages, although short-term limits are also employed for compounds with more acute toxicity. The time period for short-term averaging is typically 15 min in the USA, although other periods (e.g. 30 min) may be in use elsewhere. In addition, some regulations call for ceiling limits that cannot be exceeded under any circumstances. Although time periods for ceiling limit determinations are not stated, implying an instantaneous warning, in practice all monitoring equipment involves some time lapse. Equipment used for short-term sampling is often used to monitor ceiling values.

The simplest method for taking an air sample is to trap the air in an inert container. The air can be analysed either in the laboratory or in a field-portable gas chromatograph, by direct injection using a gas-tight syringe or gas sampling loop. Alternatively the chemical content can be concentrated by secondary trapping using a sorbent-filled or cryogenically cooled trap, and then released by rapid heating. The containers used include glass syringes or bottles, bags made of various polymers (e.g. Tedlar®, Teflon®, Mylar®, Saran®) or metal containers (stainless steel that has been electropolished, treated by the SUMMA® process or lined with fused silica). However, all such containers are bulky, even though smaller canisters have been manufactured recently to hold 200–500 mL of air and which can be worn on a belt or harness. There are issues of sample stability with whole-air samples. For example, many aromatic compounds are not stable in Tedlar bags over periods greater than 24 h, and their stability depends on the type of fitting used, with polypropylene providing greater stability than stainless steel. 1,3-Butadiene, on the other hand, is very stable in Tedlar bags, while dimethylformamide disappears very rapidly. Sulfur compounds are more stable in fused-silica lined canisters than in polished stainless steel. Tedlar bags should probably not be re-used as their integrity may be compromised, although they frequently are in practice. The expense of canisters ensures multiple re-use although carry-over to future samples is an issue when working from high concentrations to low, and contamination with oil mist renders a canister useless. There are also issues of sample recovery, due to photochemical reaction in transparent bags, or through moisture condensation on the interior of canisters.

The widespread development of sampling equipment to meet the combined needs of being lightweight, unobtrusive and carried by the worker, and of being able to provide time-weighted average results, has led to a simple method for a wide range of gases and vapours using a battery-operated pump to pull air through a tube filled with a sorbent (Figures 1 and 2). Changing the type or quantity of sorbent extends the range of vapours that can be collected. Another advantage is adjustable flow rate that can be raised to obtain sufficient sample to exceed detection limits at low concentrations or lowered to reduce the sample so that breakthrough does not occur at high concentrations.

Sorbents generally can be classified as being of two types: those that react with the chemical of interest and those that use adsorption to collect airborne vapour molecules. The former type is preferred for gases that are not readily condensed at room temper-

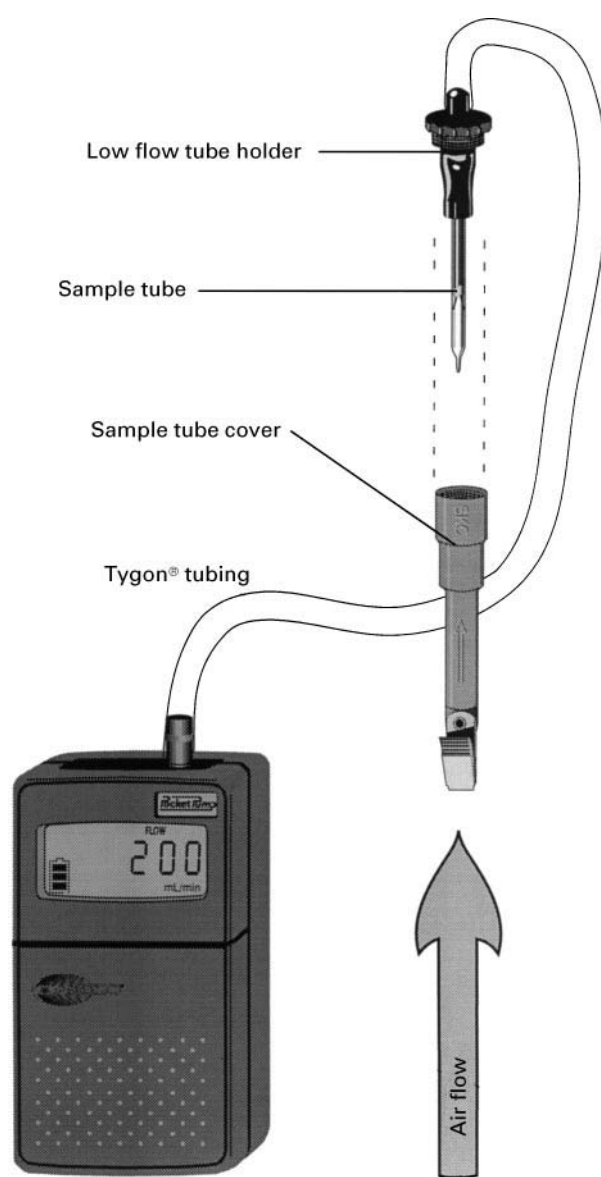


Figure 1 Typical personal air sampling train comprising sorbent tube and air-mover (pump). This is the commonest method of sampling worker exposure to hazardous gases and vapours.

atures, for chemicals that are unstable or reactive, or where the reaction product can be detected with a better sensitivity. Some examples are reaction of aldehydes to stable hydrazone derivatives with analysis by GC or high performance liquid chromatography (HPLC), and the reaction of ethylene oxide with hydrobromic acid to form bromoethanol, which gives a good response with an electron-capture detector.

The second type of sorbent, using microporous materials with high surface area, is more common. Activated carbons can have surface areas as high as $1000 \text{ m}^2 \text{ g}^{-1}$ or more, with a network of large pores



Figure 2 Personal air sampling train attached to a worker.

leading to successively smaller pores with diameters in the nanometre range. Molecules that enter this region are affected by forces extending from the pore walls and from other molecules held in close proximity to them. Adsorption is strong and essentially complete at the low concentrations encountered in the air. Transport from the air stream to the sorbent is by molecular diffusion, and both diffusion and adsorption are relatively rapid. Thus only a small quantity of sorbent is required (as little as 100 mg) for effective removal of molecules from the air. The adsorbed chemicals are liberated from the charcoal after sampling by application of a polar solvent, commonly carbon disulfide.

Other sorbents are used routinely for particular applications. Many of these are the same polymeric resin materials used in chromatographic column packings. The range of sorbents is large, and complicated by the number of trade names used (e.g. Porapak® N or Q, Chromosorb® 102, 104 or 106, Amberlite® XAD-2, XAD-4 or XAD-7, or Tenax®



Figure 3 Diffusive sampler attached to a worker. This method is more acceptable to workers but the uptake rate varies from chemical to chemical and cannot be altered by field hygienists.

TA or GR). One specific use for these sorbents is in thermal desorption, where the application of heat rather than a solvent is used to remove the collected chemicals. Graphitized carbon blacks are also used in this application.

An alternative to the use of pumps is to allow the molecules of the chemical being sampled simply to diffuse to the sorbent surface (Figure 3). Several styles of diffusive sampler are available, some of which develop colour reactions for on-site analysis, and others which contain the same types of sorbent used in the pumped tubes, and which are analysed in a similar manner.

Semi-volatile chemicals are normally sampled using a filter prior to the sorbent tube. A range of filters is available, including glass or quartz fibre, cellulose ester and polymeric membranes. The filter is extracted with a solvent, which may be the same as that used for the sorbent. This same arrangement is used where mists of volatile components are encountered.

Biological Sampling

Many occupational hygiene methods involve the analysis of breath, urine or blood samples. GC analysis may involve the chemical of interest or a metabolite such as the phenol content of urine used as a monitor of benzene exposure. While breath sampling is the least invasive, it may not be the best estimate of exposure over a period of time, and is often the most variable. Urinary analysis is also quite variable, and correction for concentration is often made using the analysis of the creatinine component. Blood is the most difficult fluid to take on a

Table 1 Organic chemicals with biological exposure indices

<i>Chemical</i>	<i>Measured marker</i>
<i>Organic chemicals monitored in urine</i>	
Acetone	Acetone
Aniline	<i>p</i> -Aminophenol
Benzene	<i>s</i> -Phenylmercapturic acid
Carbon disulfide	2-Thiothiazolidine-4-carboxylic acid
Chlorobenzene	4-Chlorocatechol or <i>p</i> -Chlorophenol
<i>N,N</i> -Dimethylacetamide	<i>N</i> -Methylacetamide
<i>N,N</i> -Dimethylformamide	<i>N</i> -Methylformamide
2-Ethoxyethanol and 2-ethoxyethyl acetate	2-Ethoxyacetic acid
Ethyl benzene	Mandelic acid
Furfural	Furoic acid
<i>n</i> -Hexane	2,5-Hexanedione
Methanol	Methanol
2-Methoxyethanol and 2-methoxyethyl acetate	2-Methoxyacetic acid
1,1,1-trichloroethane	Trichloroacetic acid or trichloroethanol
4,4'-Methylene bis(2-chloroaniline) (MBOCA)	MBOCA
Methyl ethyl ketone	Methyl ethyl ketone
Methyl isobutyl ketone	Methyl isobutyl ketone
Nitrobenzene	<i>p</i> -Nitrophenol
Parathion	<i>p</i> -Nitrophenol
Pentachlorophenol	Pentachlorophenol
Perchloroethylene	Trichloroacetic acid
Phenol	Phenol
Styrene	Mandelic acid or phenylglyoxylic acid
Tetrahydrofuran	Tetrahydrofuran ^a
Toluene	Hippuric acid or <i>o</i> -cresol ^a
Trichloroethylene	Trichloroacetic acid or trichloroethanol
Xylenes	Methylhippuric acid
<i>Organic chemicals monitored in blood (venous unless otherwise specified)</i>	
1,1,1-trichloroethane	Trichloroethanol
Pentachlorophenol	Pentachlorophenol (in plasma)
Perchloroethylene	Perchloroethylene
Styrene	Styrene
Toluene	Toluene
Trichloroethylene	Trichloroethylene or trichloroethanol
<i>Organic chemical measured in breath (end exhaled air)</i>	
Ethyl benzene	Ethyl benzene
<i>n</i> -Hexane	<i>n</i> -Hexane
1,1,1-trichloroethane	1,1,1-trichloroethane
Perchloroethylene	Perchloroethylene
Trichloroethylene	Trichloroethylene

^aNotice of intended change (1998).1998 Threshold Limit Value (TLVs[®]) and Biological Exposure Indices (BEIs[®]) book.

Reprinted with permission of ACGIH. The TLV/BEI Booklet is updated annually.

regular basis, but it is used, for example, in the regulation of exposure to lead. The American Conference of Governmental Hygienists (ACGIH[®]) TLV booklet also includes a listing of Biological Exposure Indices (BEI[®]s). A list of current BEIs and the marker compounds is given in **Table 1**.

Breath samples may be collected in special containers, or passed through sorbent tubes to concentrate the chemicals of interest. The sample can then be introduced into a gas chromatograph using a gas-

sampling loop, or through solvent or thermal desorption of the sorbent. The humidity of the exhaled breath is an interfering factor, as is also the presence of chemicals manufactured by normal biological processes within the body. Blood and urine samples are more difficult to analyse chromatographically because of the matrix. Urine samples can be injected into a GC if the injection liner is replaced frequently, but blood contains surfactants and is a much more difficult medium. Liquid-liquid or liquid-solid

extraction, static and dynamic head space analysis, or solid-phase microextraction have all been used as sample preparation techniques. Many metabolites are highly polar, water-soluble compounds and HPLC is often the preferred analytical technique, especially where the presence of aromatic rings allows ultraviolet detectors to be used. However, many of the compounds listed can be analysed by GC as they are, or after derivatization. The final choice of method may depend on a number of factors.

Special care must be taken in the timing of the sample in relation to the work-periods, and also in the taking of the sample. For example breath samples should be of end-exhaled air, and blood samples should be of venous rather than capillary blood. In addition, some standards are based on total urinary excretion and others on urinary concentration. The sample container and the presence of sample preservatives are also important.

Sources of Methods

The US National Institute for Occupational Safety and Health (NIOSH) has been responsible for the *NIOSH Manual of Analytical Methods* (NMAM), now in its fourth edition. The NMAM is the largest repository of methods in the world, and many of its methods have been adopted by government agencies in other countries, such as the Health and Safety Laboratory of the UK. **Table 2** gives a list of commonly used NIOSH methods together with the chromatographic columns used (most methods use carbon disulfide, sometimes with a polar modifier, as the desorbing solution and flame ionization detection).

Validation of Methods

The validation of methods should encompass all stages of the method, including both the sampling and analysis steps. The NMAM contains details of the NIOSH method validation objectives, and a detailed validation manual for pumped sampling methods has been published (see Further Reading section). In addition, the NIOSH has supported the ASTM Standard D6246 for evaluating the performance of diffusive samplers. The US Occupational Safety and Health Administration (OSHA) Methods Manual contains similar documentation. The UK Health and Safety Executive also has standard method validation protocols (e.g. MDHS 27 for diffusive samplers). **Table 3** lists the American Society for Testing and Materials (ASTM) standards covering the analysis of air samples.

Sorbent Selection for Air Sampling Methods

The choice of chromatographic analysis procedure is intimately associated with the selection of the sorbent and the desorption procedure. Both the column type and the detector possibilities depend on the type of sample finally presented for analysis. While published methods give guidance, experienced analysts can develop or modify procedures to meet most eventualities. For example, the analysis of benzene may vary depending on whether benzene has been collected as part of a simple or complex mixture, and whether it is necessary to quantify only the benzene or all components, whether the sample was collected on charcoal or a polymer sorbent, whether the desorption is with a simple solvent or a mixture or by heat, and whether detection is by flame ionization (FID), photoionization (PID) or mass spectrometry (MS).

Charcoal is the most widely used sorbent for organic vapours. Various sources of charcoal are used, but in all cases the porosity has been enhanced by activation. Charcoals normally require solvent desorption. Anasorb® 747 is a popular charcoal from petroleum precursors that has wide application in the OSHA methods. Amborsorb®s are charcoals derived from controlled carbonization of organic polymers.

Porous polymers include cross-linked styrene and divinyl benzenes, which can have relatively large pores (Chromosorb 102, Amberlite XAD-2) or smaller micropores (Chromosorb 106, Porapak or Haysep Q, Amberlite XAD-4). Also used are polar sorbents derived from acrylonitrile (Chromosorb 104, Amberlite XAD-7) or pyrrolidones (Porapak N, R). Tenax has a very small surface area and is normally only used for sampling low concentrations. It has the advantage of having a very low adsorption capacity for water. Because of its higher surface area and adsorption capacity, hydrophobicity, and compatibility with both solvent desorption and thermal desorption, Chromosorb 106 has been generally regarded as the most suitable polymer for occupational hygiene sampling. However, if thermal desorption is used the upper temperature limit of Chromosorb 106 is only 250°C, compared with 350°C for Tenax or Carbotrap® (a graphitized carbon), rendering it unsuitable for the collection of semi-volatile components. Styrene polymers such as chromosorb 106 also tend to have significant background when used for thermal desorption of the low concentrations found in ambient or residential indoor air, so that Tenax or Carbotrap are better.

The graphitized carbons mentioned above are available in different surface areas (e.g. Carbotrap C is approximately 10 m² g⁻¹ and Carbotrap B is

Table 2 Methods from the *NIOSH Manual of Analytical Methods* (all columns are 3.2 mm i.d. × 3 m packed columns unless otherwise specified)

<i>Method name</i>	<i>Method no.</i>	<i>Column used</i>	<i>Alternatives</i>
Hydrocarbons BP 36–126°C	1500	20% SP-2100	
Benzene			50/80 mesh Porapak P
Cyclohexane			50/80 mesh Porapak Q
Cyclohexene			50/80 mesh Porapak Q
<i>n</i> -Heptane			10% OV-101
<i>n</i> -Hexane			10% FFAP
Methylcyclohexane			10% FFAP
<i>n</i> -Octane			10% FFAP
<i>n</i> -Pentane			10% FFAP
Toluene			50/80 mesh Porapak Q
Hydrocarbons aromatic	1501	10% OV-275	
Benzene			50/80 mesh Porapak P
<i>p</i> - <i>t</i> -Butyltoluene			10% FFAP
Cumene			10% FFAP
Ethylbenzene			10% FFAP
α -Methylstyrene			10% FFAP
Naphthalene			10% OV-101
Styrene			10% FFAP
Toluene			50/80 mesh Porapak Q
Vinyltoluene (<i>o</i> , <i>m</i> and <i>p</i>)			10% FFAP
Xylene (<i>o</i> , <i>m</i> and <i>p</i>)			50/80 mesh Porapak Q
Hydrocarbons halogenated	1003		
Benzyl chloride		10% SP-1000	
Bromoform		10% SP-1000	
Carbon tetrachloride		10% SP-1000 ^a	
Chlorobenzene		10% SP-1000	
Chlorobromomethane		10% SP-1000	
Chloroform		10% SP-1000 ^a	
<i>o</i> -Dichlorobenzene		10% OV-101	
<i>p</i> -Dichlorobenzene		10% SP-1000	
1,1-Dichloroethane		10% SP-1000	
1,2-Dichloroethylene		10% SP-1000	
Ethylene dichloride		10% OV-101	
Hexachloroethane		3 m × 6 mm o.d. glass, 3% SP-2250	
1,1,1-Trichloroethane		10% OV-101	
Tetrachloroethylene		10% OV-101	
1,1,2-Trichloroethane		10% OV-101	
1,2,3-Trichloropropane		10% FFAP	
			SP-2100
			SP-2100 0.1% Carbowax
			DB-1 capillary
Naphthas	1550	10% SP-2100	DB-1 capillary
Petroleum ether			
Rubber solvent			
Petroleum naphtha			
VM&P naphtha			
Mineral spirits			
Stoddard solvent			
Kerosene			
Coal tar naphtha			
Esters 1	1450	5% FFAP	10% SP-1000
<i>n</i> -Amyl acetate			
<i>sec</i> -Amyl acetate			
<i>n</i> -Butyl acetate			
<i>sec</i> -Butyl acetate			
<i>t</i> -Butyl acetate			
2-Ethoxyethyl acetate			
Ethyl acrylate			

Table 2 *Continued*

<i>Method name</i>	<i>Method no.</i>	<i>Column used</i>	<i>Alternatives</i>
Isoamyl acetate Isobutyl acetate Methyl isoamyl acetate <i>n</i> -Propyl acetate			
Ketones 1	1300	Glass, 3.5 m × 6 mm i.d. 10% SP-2100 0.1% Carbowax	10% SP-2100 or DB-1 capillary
Acetone Cyclohexanone Diisobutyl ketone 2-Hexanone Methyl isobutyl ketone 2-Pentanone			
Alcohols 1	1400	Glass, 2 m × 4 mm i.d. 0.2% Carbowax	10% FFAP
Ethanol Isopropyl alcohol <i>t</i> -Butyl alcohol			
Alcohols 2	1401	Glass, 3 m × 2 mm i.d. 10% SP-1000	10% FFAP
<i>n</i> -Butyl alcohol <i>sec</i> -Butyl alcohol Isobutyl alcohol <i>n</i> -Propyl alcohol			

^a6 m column.

approximately 100 m² g⁻¹) and are used with thermal desorption in environmental applications. They have been used less often in occupational hygiene investigations, although the NIOSH has recently included a semi-quantitative screening method involving tubes containing multiple layers of sorbents including graphitized carbons in combination with carbon molecular sieves. Carbon molecular sieves,

such as the Carboxen® series, can be used to sample the most volatile compounds, but have the disadvantage of also trapping large amounts of water vapour from atmospheres of high humidity.

Silica gel is a highly polar and quite strong adsorbent, useful for very polar compounds such as methanol or amines. Strong adsorption of water is a problem with using this sorbent for other chemicals. Because of this adsorption of water, silica gel is used in specific applications, such as the collection of methanol with subsequent desorption by water and analysis on a packed Tenax column with FID.

Table 3 ASTM standards (1998) covering chromatographic analysis of air samples

<i>Standard</i>	<i>Area of application</i>
<i>Test methods</i>	
D4947	Chlordane and heptachlor
D6209	Gaseous and particulate polycyclic hydrocarbons
D4413 and 5578	Ethylene oxide
D5075	Nicotine and 3-ethenylpyridine
D4766	Vinyl chloride
D5466	VOCs (canister method)
<i>Practices</i>	
D3686 and 3687	VOCs (charcoal tube method)
D4861	Pesticides and polychlorinated biphenyls
D6060	Sampling process vents with a portable gas chromatograph
D6196	Selection of sorbents for thermal desorption

VOC, volatile organic compound.

Solvent versus Thermal Desorption

There are significant drawbacks to the use of solvents for the recovery of chemicals from sorbent samples, not the least of which is the added hygiene and safety burden of handling a solvent such as carbon disulfide. Solvents do not always give 100% recovery, and recoveries significantly less than 75% may be associated with increased variability in the precision of recovery. It may be difficult to optimize a solvent for best recovery of a mixture of polar and nonpolar chemicals, and the solvent may interfere with chemicals in the mixture. There are special problems relating to the adsorption of water from atmospheres of high humidity, and its subsequent release from the sorbent on addition of the desorbing solvent. For

example, charcoal can absorb large quantities of water (hundreds of milligrams per gram) from atmospheres of humidity greater than 50%. This water is displaced by carbon disulfide but does not mix with it. Polar compounds such as acetone can partition into the separate water phase causing an apparent drop in recovery. Several options have been developed to deal with polar compounds, including adding a polar modifier (e.g. 2-propanol or dimethylformamide) to carbon disulfide, or switching to an altogether different solvent (e.g. 95% dichloromethane/5% methanol). However, it is difficult to substitute entirely for carbon disulfide because of its small response with the FID and its good recovery of nonpolar compounds. New carbon sorbents such as Anasorb 747 exhibit much better adsorption and desorption properties under these conditions. When using polymer sorbents, care must be taken in the choice of recovery solvent. While styrene polymers are compatible with most solvent systems, Tenax will swell in some solvents, and pyrolydine polymers may dissolve.

An alternative to solvent desorption is thermal desorption. In this technique the sorbent tube is heated while a stream of carrier gas removes the collected vapours. Because this transfer can take several minutes the recovered vapours are usually focused in a secondary trap. There are several varieties of secondary trap in common use, including large sorbent traps at ambient temperature, open capillary tubes cooled cryogenically, and narrow-bore sorbent traps cooled to sub-ambient temperatures by Peltier cooling. The latter method provides for rapid transfer of the analytes to the column, with effective transfer of compounds in the range C_2 – C_{30} , and without risk of ice blockage or condensation of permanent gases such as oxygen. Some specialized analyses of thermally labile compounds such as nerve agents or vesicants may require derivatization prior to desorption.

Thermal desorption has existed since the mid-1970s, but has not significantly replaced solvent desorption in most countries for several reasons. Efficient thermal desorption requires a sorbent with less attraction for the vapours of interest than charcoal. The use of sorbents with lower surface areas and smaller capacity can lead to premature breakthrough of the sample during the sampling period. Sorbent tubes for solvent desorption are designed with a 'back-up' sorbent section that can be analysed to detect such breakthrough but sorbent tubes for thermal desorption are not. There are also quality assurance issues that must be addressed, for example, in calibrating the analysis (standards must be added as solutions to blank tubes and then the solvent re-

moved), using internal standards (more easily added to a solvent) or making multiple analyses (which would normally require taking multiple samples). Water management can also be a problem with thermal desorption of real-world samples. The transfer of desorbed water onto a capillary chromatographic column can alter the pressure gradient across the column and the polarity of the system, changing both retention time and peak area. Where sorbent tubes contain hydrophilic sorbents their performance can be improved by drying the sample with 300 mL of helium prior to desorption. Thermal desorption is often used for the analysis of canister samples, with the contents of the canister being drawn through the secondary trap or focusing tube, which is then desorbed and analysed. Water management may also be necessary in the analysis of canister samples. The UK Health and Safety Laboratory is the main source of published thermal desorption methods.

One important major advantage of thermal desorption is the possibility of increasing the quantity of sample that can be placed on the chromatographic column, by means of the secondary focusing trap. Recent developments in optimizing the technology now allow complete on-column injection of the entire sample, raising detection limits as much as two orders of magnitude over solvent injections. This is very useful for ambient and indoor air investigations at ppb levels, and also is making the system attractive for workplace analyses where there are chemicals with exposure limits at 1 ppm or below (e.g. benzene). When using thermal desorption for such trace analyses particular attention must be paid to the background levels of the sorbent (typically no more than 1 ng per component and 10 ng total) and handling, transport and storage procedures for the tubes. Thermal desorption also has potential applications in the analysis of biological samples, either through sorbent trapping from breath, or from direct heating of blood or urine samples. Both solvent and thermal desorption systems can be automated.

Types of Columns

When methods were being selected and validated in the early 1970s capillary chromatography was not far advanced commercially. Nor was it particularly necessary, since neither sensitivity nor selectivity was an issue. Typical occupational exposure limits at that time ranged from 10 to 1000 parts per million by volume of air for an 8-h time-weighted average. Assuming a full-shift sample using a sample tube operated at 20 mL min^{-1} (approximately 10 L of air), the tube could contain up to 10 mg of sampled chemical. Even if this were diluted in several millilitres of

solvent, a single injection into the gas chromatograph typically contained micrograms of the chemical. In addition, chemicals were less often used in complex blends, so that interfering peaks were less common. Typically, the only separation required was between the solvent, a single chemical in the sample and an internal standard. This was achieved easily with 1/8th inch (3.2 mm) packed columns, even in isothermal mode, and this procedure could be extended to cover many simple solvent mixtures used in industrial applications. A selection of the columns used in the NMAM is given in Table 2.

Packed columns continue to be used today for permanent gases, such as the sulfur gases (sulfur dioxide, sulfur trioxide, hydrogen sulfide, carbonyl sulfide, carbon disulfide and mercaptans), or for very volatile compounds such as 1,3-butadiene. The packings are typically zeolite or carbon molecular sieves, or, in the case of the two examples just given, alumina-PLOT columns have been used. However, as occupational exposure limits continue to fall (on average by an order of magnitude between 1980 and 1990), and the number of regulated chemicals increases and complex mixtures become more common, there is a distinct move towards the use of capillary columns, which is supported by laboratories wishing to speed up analytical procedures. This has been recognized by the NIOSH, who intend to begin a programme of updating the methods in the NMAM to include capillary columns. The typical modern occupational hygiene laboratory will have a collection of capillary columns from 15 to 100 m length, both microbore (0.32 mm) and megabore (0.53 mm), with different films and thicknesses. A standard all-purpose column might be a DB-1 or DB-5 or equivalent from other manufacturers. A typical example of a complex analysis is the determination of trace benzene (American Conference of Governmental Industrial Hygienists threshold limit value (TLV) for 1999 is 0.5 ppm) in the presence of gasoline (see Figure 4).

Types of Detectors

The flame ionization detector has been the traditional detector of choice in industrial hygiene analyses. It has a very wide linear range. With packed columns, limits of quantitation range typically from 2 to 20 ng of chemical per injection. The sharper peaks obtained with capillary columns can allow quantitation at lower concentrations, but this must be balanced against the smaller sample loading. Sample loading can be increased with megabore capillary columns, or by preconcentration at the injection stage. Overall limits of quantitation of 0.1–1 ng per injection are possible. Halogenated hydrocarbons do not provide

as many ions in the flame and therefore have smaller detector responses. In addition, reactions with remnant ions from the carbon disulfide solvent can alter the response of halogenated hydrocarbons at low concentrations. Photoionization detectors (PIDs) are often used with portable gas chromatographs since only a single source of gas is required; however, care must be exercised in keeping the lamp clean in field use. The PID is also useful for the detection of aromatic hydrocarbons in the presence of aliphatic hydrocarbons (e.g. benzene in gasoline). The electron-capture detector (ECD) is often preferred for halogenated solvents, but the ECD is not compatible with large quantities of carbon disulfide solvent and other solvent recovery systems (e.g. hexane, ethyl acetate, toluene) do not provide as efficient recovery from charcoal sorbents.

Mass spectrometry (MS) has become popular for the analysis of trace organic components in the atmosphere through methods promulgated by the EPA. The development of quadrupole detectors has allowed the rapid scan of spectra in the timescale of a capillary peak. When the spectra are matched to a reference library, compound identification is possible, especially when this information is cross-referenced to specific compound retention times from Kováts indices. However, because MS detectors have been costly to purchase and maintain, while FIDs have had adequate sensitivity and the compounds of interest are known in advance, MS methods have not been developed for occupational hygiene analyses. This is changing and a recent example from the NMAM (method 2539) is a screening method for aldehydes (Figures 5 and 6). In investigations of the quality of ambient or indoor air, the dilution of the sample by solvent desorption effectively puts most contaminants below the limits of quantitation of both the FID and MS. The mass spectrometer therefore is most suitable in combination with thermal desorption for sampling multiple unknown contaminants at low concentrations. For this application a semi-quantitative NIOSH screening method (method 2549) has been developed. MS in single-ion mode can increase detection limits by a factor of 10 or more. Two examples are given showing the usefulness of the MS detector in compound identification and quantitation. Both involve the analysis of benzene in complex samples. In Figure 4 the single peak at the retention time of benzene is resolved in the MS scan as a mixture of benzene and another compound (possibly cyclohexane). In Figure 7 the single peak is resolved into benzene and butanol. In both cases benzene could be quantified at low concentrations without interference by measuring the m/z 78 ion in single ion mode.

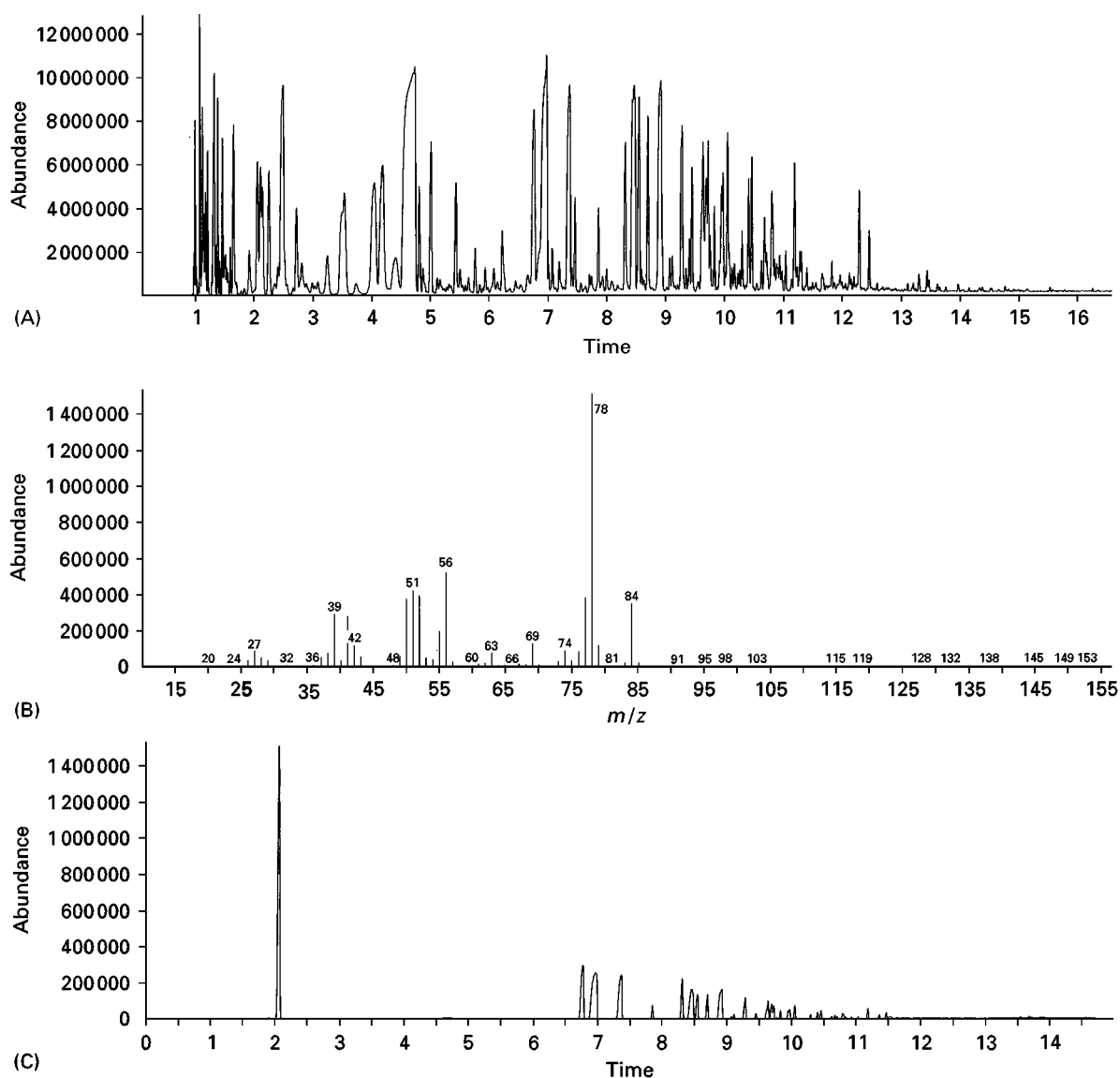


Figure 4 Determination of benzene in gasoline using GC-MS. The GC column was a 5% phenylmethylsiloxane HP-5MS. (A) Total ion chromatogram (note an FID trace would be similar). Retention time of benzene is 2.06 min. (B) Mass spectrum of peak at 2.06 min resolves interference from a C_6H_{12} compound. (C) Single ion scan at m/z 78 can be used to quantify benzene.

Other alternatives to the FID are normally used in trace-level compound-specific analyses, and detection limits may be enhanced by derivatization. For example, formaldehyde may be determined as a derivative with hydroxymethylpiperidine using a nitrogen-phosphorous detector. Sulfur compounds are often detected using a flame photometric detector (FPD).

Quality Assurance

The number of samples taken per investigation will depend on the number of exposed workers and the perceived extent of any problem and may vary from

one to several hundred. The best choice of laboratory for analysing occupational hygiene samples is one that specializes in such samples and accepts them on a routine basis. Laboratories may voluntarily participate in Proficiency Analytical Testing (PAT) schemes or, once they have established proficiency in these schemes, request accreditation by various recognized bodies. In the USA the proficiency samples for organic solvents include aliphatic, aromatic and chlorinated hydrocarbons, alcohols, ketones and esters. Many other countries have similar proficiency testing and accreditation programmes. For example, the UK Health and Safety Laboratory operates the Workplace Analysis Scheme for Proficiency (WASP).

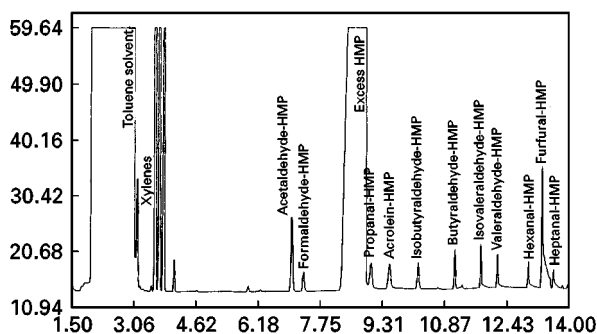


Figure 5 Determination of multiple aldehydes as their derivatives with 2-hydroxymethylpiperidine. Total ion chromatogram of aldehyde mix from spiked sorbent tube separated on a 15 m DB-1301 column.

In addition to documentation of methods and practices, the following specific elements are considered appropriate for good analytical practice:

- **Initial calibration verification.** This is based on a range of standards diluted from a stock solution. Multiple points encompassing the expected sample range are used to create a calibration curve. If the samples fall outside this range, further standards are prepared. The response of the detector to the standards, and their correlation coefficient, should be within control limits. Field-portable detectors may use packaged calibration gases.
- **Continuing calibration verification.** At least one of the standards used for the initial calibration is repeated each 10–20 injections (or more frequently if considered desirable).
- **Internal standards.** An internal standard is useful to compensate for minor variations in the sample size injected into the GC, but because it may mask a chemical of interest internal standards are not always employed where the sample is not well characterized.
- **Reagent blanks.** The solvent used to make up standards and desorb samples is checked for contamination. This procedure is essential if low concentrations of analyte are to be determined.
- **Matrix blanks.** The sampling medium is checked for contamination.
- **Matrix spikes.** A known quantity of the analyte is added to a blank sample medium, which is carried through the full analytical procedure to ensure proper recovery.
- **Replicates.** Used to ensure the precision of analysis. Particularly useful at low sample concentrations.
- **External standards.** Known concentrations of the chemical of interest obtained from a source other than the laboratory. Standard mixtures of com-

monly analysed chemicals are obtainable from speciality sources.

Other quality assurance methods used less often include: using a surrogate (a compound that behaves similarly to that of interest, but which can be separated, such as a deuterated analogue, which is used in the same way as a matrix spike with actual samples), matrix additions (direct addition of known quantities of the chemical of interest, which are subtracted from the final result) and splitting the sample (division of the sample for separate analyses).

Portable Gas Chromatographs

The detectors used in GC, especially the FID and the PID, are often used as stand-alone instruments for 'total' hydrocarbon analysis. They are calibrated to a standard concentration of an alkane in air. These detectors may also be used with a portable gas chromatograph to transfer laboratory analytical techniques to the field. Time-integrated samples can be collected using a sampling bag and are introduced using a gas-tight syringe. Built-in sampling pumps can give semi-'real time' measurements. Some instruments operate at ambient temperatures, but are limited to gases and very volatile compounds; most have some capability for temperature programming. Both packed and capillary column instruments are available, but since their introduction in the early 1980s wide-bore capillary columns have become standard. A detection limit of 0.1 ppb is claimed by one manufacturer (probably for an ECD), but most are higher, up to 0.1 ppm using PIDs or FIDs. Some are available with an option for different detector or injector types. Most can be linked to a personal computer. Many are mains powered but some use rechargeable batteries with a life of around 8 h or better. All are relatively heavy (< 20 kg), and none are truly considered 'personal' samplers. There are significant issues of user training and field calibration, and compressed gases (for carrier gas or instrument calibration) and radioactive sources (e.g. ECDs) cannot be transported on commercial aircraft. A very recently developed instrument uses ambient air as the carrier gas. While detection limits and separations are not as good as with helium, no compressed gases are required for instrument operation if the detector is a PID, or an FID with hydrogen generated by electrolysis of water.

To date, portable gas chromatographs have not been used for compliance monitoring by the OSHA, nor have they replaced traditional personal sampling methods, although the NIOSH has developed several analytical methods that use a portable gas chromatographs for analysis of exhaled breath, or

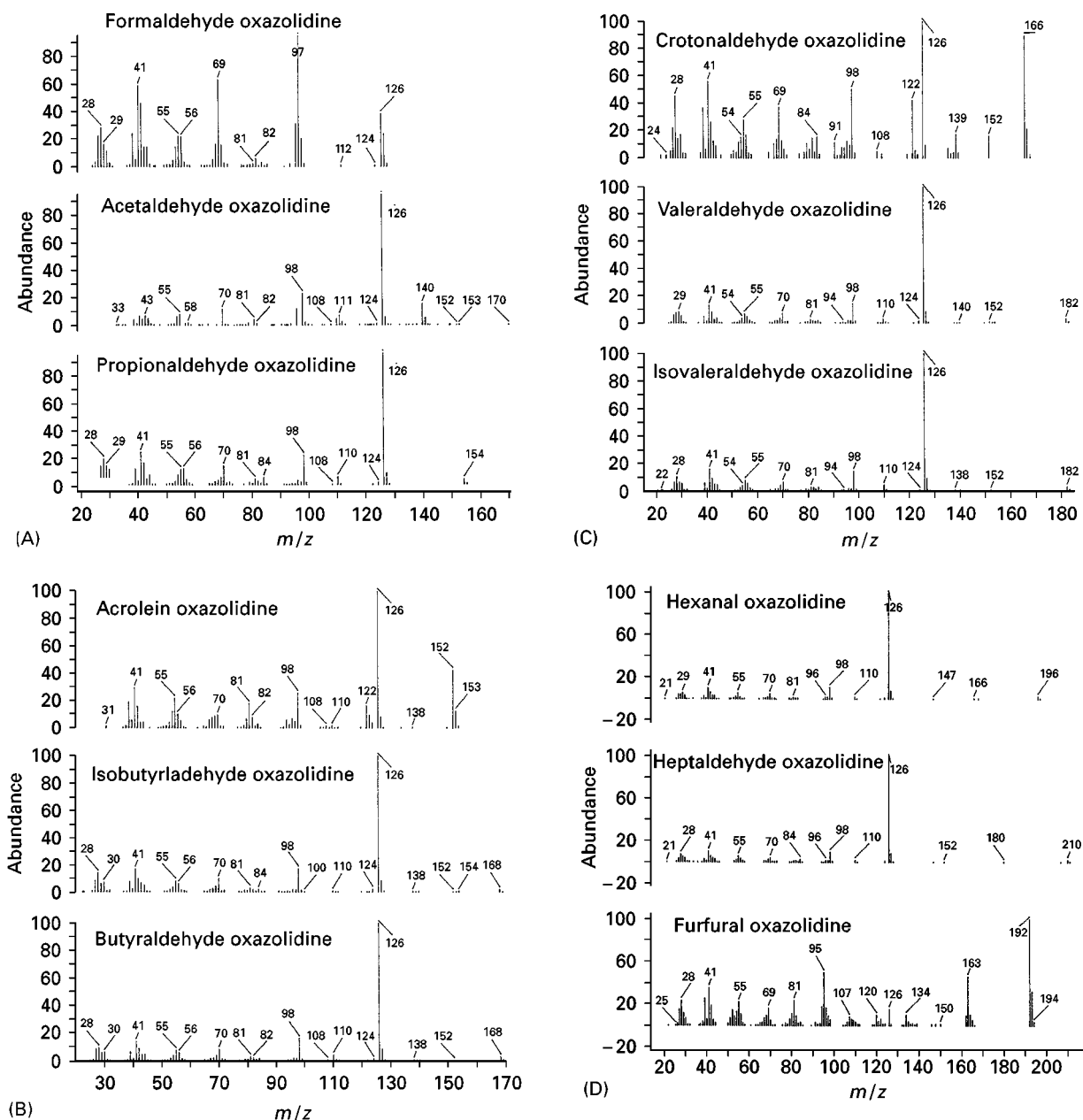


Figure 6 Determination of multiple aldehydes as their derivatives with 2-hydroxymethylpiperidine. Individual reference spectra using a 70 eV HP 5970 mass selective detector at 20–400 a.m.u. scan (30 m DB-1 column).

polluted air, or in ventilation studies (3700 for benzene, 3702 for ethylene oxide and 3701 for trichloroethylene using a PID, 6603 for carbon dioxide (TCD) and 6602 for sulfur hexafluoride (ECD)). In all cases these methods require samples to be collected in bags before analysis. Portable gas chromatographs have the advantage of near real-time response, which can be combined with observation of the work activity, for example by video monitoring, to gauge the effect of different work practices and control measures. Other applications include exhaled

breath analysis, measuring the penetration of organic chemicals through protective clothing, providing assurance of safe entry into confined spaces, and monitoring at hazardous waste sites and spills.

The Future

Traditional occupational hygiene sampling and analysis is already facing problems with sensitivity. As an example one can cite the NIOSH method for acrylonitrile. The NIOSH recommended exposure

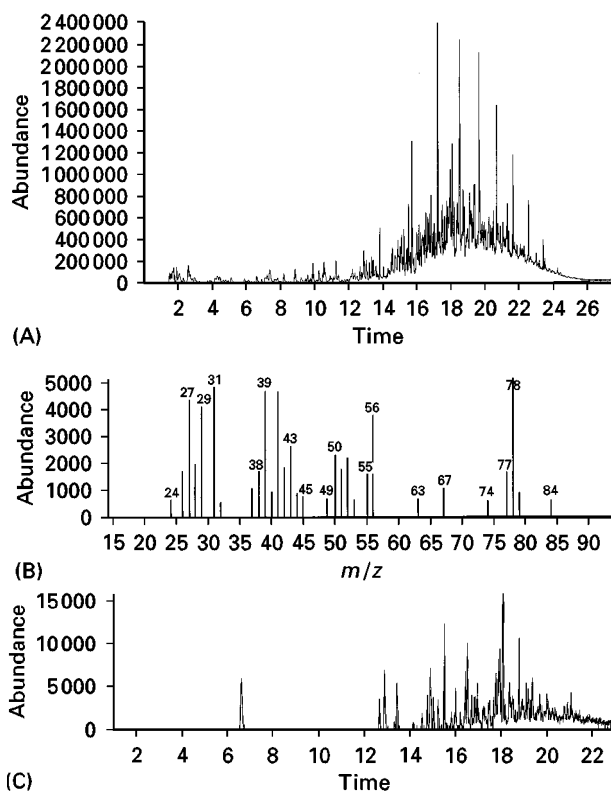


Figure 7 Air sample taken during asphalt paving operations analysed by TD-GC-MS (30 m DB-1 column). (A) Total ion chromatogram. Retention time of benzene is 6.6 min. (B) Mass spectrum of peak at 6.6 min showing the presence of butanal in addition to benzene. (C) Single ion chromatogram of m/z 78 benzene ion, eliminating other hydrocarbon interferences.

limit is 1 ppm, but the lower limit of the method is only slightly less at 0.7 ppm. Several other chemicals (e.g. benzene, 1,3-butadiene, vinyl chloride, ethylene oxide, etc.) have exposure limits close to the lower limit of their method range. In almost no case has an exposure limit been raised – the limit for benzene fell from 100 ppm (1946) to 25 ppm (1961) to 10 ppm (1978), and the current Threshold Limit Value® (TLV) is 0.5 ppm. Clearly the challenge is to find more sensitive methods of detection. One route is to use capillary chromatography, another is to use thermal desorption, and another is to use MS detection. The combination of all three can yield a sensitivity of around 0.1 ng per sample (equivalent to $0.03 \mu\text{g m}^{-3}$, or 0.1 ppb, for a 3-L sample). One problem with such a combination is the cost, which can be as much as ten times that of the analysis of a conventional charcoal tube by solvent desorption and GC-FID. The advent of fast GC systems may lower the cost by allowing a greater daily sample throughput.

Another issue for the field is the long turn-around time for the result (sometimes weeks). Detectors that can give on-site results are clearly preferable. With

micro-miniaturization (the ‘GC-on-a-chip’) this may become achievable in the near future.

Acknowledgements

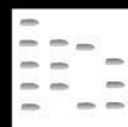
The author is indebted to Dr Eugene Kennedy and Dr Ardith Grote (NIOSH, Cincinnati, OH, USA) for the use of Figures 4–7.

See also: II/Chromatography: Gas: Detectors: Mass Spectrometry; Detectors: Selective; Gas Chromatography-infrared; Headspace Gas Chromatography; Multi-dimensional Gas Chromatography; Sampling Systems. III/Solid-Phase Microextraction: Environmental Applications; Overview.

Further Reading

- Baselt RC (1988) *Biological Methods for Industrial Chemicals*, 2nd edn. Littleton, MA: Year Book Medical Publishers.
- Cohen BV and Hering SV (1995) *Air Sampling Instruments for Evaluation of Atmospheric Contaminants*, 8th edn. Cincinnati, OH: American Conference of Governmental Industrial Hygienists.
- Kennedy ER *et al.* (1995) *Guidelines for Air Sampling and Analytical Method Development and Evaluation* (DHHS [NIOSH] Pub. No. 95-117. Cincinnati, OH: NIOSH.
- Kneip TJ and Crable JV (eds) (1988) *Methods for Biological Monitoring: A Manual for Assessing Human Exposure to Hazardous Substances*. Washington, DC: American Public Health Association.
- Lauwerys RR and Hoet P (1993) *Industrial Chemical Exposure: Guidelines for Biological Monitoring*, 2nd edn. Boca Raton, FL: Lewis Publishers.
- National Institute for Occupational Safety and Health (1994) *NIOSH Manual of Analytical Methods*, 4th edn (DHHS[NIOSH] Pub. No. 94-113). Cincinnati, OH: NIOSH.
- Ness SA (1994) *Surface and Dermal Monitoring for Toxic Exposures*. New York: Van Nostrand Reinhold.
- Occupational Safety and Health Administration (1985) *OSHA Analytical Methods Manual*. Salt Lake City, UT: US Department of Labor, OSHA Technical Center.
- Que Hee SS (ed.) (1993) *Biological Monitoring: An Introduction*. New York: Van Nostrand Reinhold.
- US Environmental Protection Agency, Office of Solid Waste and Emergency Response (1996) *Test Methods for Evaluating Solid Waste Physical/Chemical Methods* (SW-846), 3rd edn, final update III. Washington, DC: US Environmental Protection Agency.
- Winberry WT *et al.* (1988) *Compendium of Methods for the Determination of Toxic Organic Compounds in Ambient Air* (EPA/600/4-89/017). Washington, DC: US Environmental Protection Agency.
- Winberry WT *et al.* (1990) *Compendium of Methods for the Determination of Air Pollutants in Indoor Air* (EPA/600/4-90/010). Washington, DC: US Environmental Protection Agency.

OILS, FATS AND WAXES: SUPERCRITICAL FLUID CHROMATOGRAPHY



F. David, A. Medvedovici and P. Sandra,
Research Institute for Chromatography,
Kortrijk, Belgium

Copyright © 2000 Academic Press

Introduction

The analysis and characterization of lipids and waxes is of great importance in the food industry, pharmaceutical and cosmetic industry, in surfactant and detergent technology and in natural product research. Lipid analysts have always been on the forefront of developments in separation sciences and new techniques in chromatography have often been developed for the separation of lipids. The first application of gas chromatography, for instance, was the separation of fatty acids by James and Martin. Since then, all chromatographic techniques, including capillary gas chromatography (CGC), high performance liquid chromatography (HPLC), thin layer chromatography (TLC), capillary zone electrophoresis (CZE), micellar electrokinetic chromatography (MEKC), capillary electrochromatography (CEC) and supercritical fluid chromatography (SFC) have been applied to the analysis of lipids and also waxes which have similar physico-chemical characteristics.

It is not possible to give a complete overview of the possibilities and limitations of each of these techniques in comparison to supercritical fluid chromatography for these analytes. For a detailed description of the use of supercritical fluids in the analysis of oils, fats and waxes, we refer to a number of recently published books listed in the Further Reading. The possibilities of both capillary column supercritical fluid chromatography (cSFC) and packed column supercritical fluid chromatography (pSFC) in the analysis of lipids and related compounds will be illustrated. The experiences gained in the authors' laboratories over the years are summarized.

The Analytical Challenge

According to Christie, lipids can be defined as 'fatty acids and their derivatives, and substances related biosynthetically or functionally to these compounds'. This is a rather broad definition and covers a large

number of organic substances. In general, two lipid classes can be distinguished: simple lipids, yielding maximum two primary hydrolysis products after saponification; and complex lipids, yielding three or more hydrolysis products. Triglycerides, natural waxes and sterol esters are examples of simple lipids as they yield fatty acids and glycerol, fatty acids and an aliphatic alcohol or fatty acids and a sterol, respectively, on saponification. Phosphatidylethanolamine (a phospholipid) on the other hand, is a complex lipid as it yields glycerol, phosphoric acid, fatty acids and ethanolamine on saponification.

Lipid mixtures as they occur in natural fats, oils and waxes, are quite complex in their composition. A vegetable oil, for instance, mainly consists of triglycerides, but also contains free fatty acids, monoglycerides, diglycerides, sterols and sterol esters. Within these classes, different combinations of fatty acids are possible. All constituents contribute to the specific characteristics of the lipidic nature and are therefore important to analyse. No single analytical technique can, however, offer sufficient resolution power to separate all possible constituents. The different analytical techniques are therefore more complementary to each other than competitive. In the authors' laboratories, all these chromatographic techniques are therefore used to unravel the complexity of lipids.

The most important types of lipid analyses will be discussed below

Lipid Analysis

Separation of Fatty Acids

The type of fatty acids in fats, oil and waxes determine the physical (melting and boiling point, viscosity) and chemical (nutritional, fragrance) properties of the product. Therefore the determination of the fatty acid composition is often the first step in lipid characterization. Fatty acids need to be separated according to chain length, unsaturation and in some cases also according to the location of the unsaturation and the *cis/trans* configurations. For fatty acid profiling, CGC is the most widely used technique. The lipids are saponified and methylated into the fatty acid methyl esters (FAMES) before analysis. In comparison to CGC, no other technique can provide the same resolution per unit of time. Christie has given an overview of GC separations of fatty acids,

including the determination of *trans* isomers. For the analysis of *cis/trans* isomers, HPLC or SFC on silver-doped columns or argentation HPLC using a mobile phase containing silver ions offers, however, more powerful alternatives.

Analysis of Triglycerides

The analysis of oils and fats without saponification is becoming more and more important as it provides typical fingerprints for each oil and fat. The triglycerides need to be separated according to the number of carbon atoms in the fatty acid chains (carbon number, (CN), separation). In a carbon number separation, the tristearin (SSS), triolein (OOO) and trilinolein (LLL) elute as one peak. CGC and cSFC can perform carbon number separations. In addition, it is also interesting to differentiate triglycerides according to unsaturation. For this type of analysis, CGC, HPLC, SFC and CEC have been used.

Profile of Mono-, Di- and Triglycerides

Additional information is also obtained by the analysis of mono- and diglycerides. This is especially important for the characterization of emulsifiers and food additives. Several emulsifiers are esters of fatty acids or fatty alcohols and glycerol, sorbitol, sorbic acid, tartaric acid or lactic acid. Also some polymer additives (slip and antistatic agents) are based on mono- and diglycerides. Often, only saturated fatty acids are used here, and a carbon number separation is sufficient. For this analysis, also CGC, HPLC and SFC can be applied.

Sterol and Sterol Ester Analysis

Sterol and sterol esters are minor constituents in oils and fats, but they are important for the quality of the products. Olive oil quality, for instance, can be monitored by the analysis of the sterol profiles. Sterols and sterol esters can be analysed by CGC, HPLC and SFC. Since the relative concentrations of sterolic compounds are low ($\text{ppm} = \text{mg kg}^{-1}$), prefractionation and enrichment are needed. Prefractionation can be done by classical techniques, such as saponification and liquid-liquid extraction, column chromatography or solid-phase extraction. Recently HPLC and SFC fractionation have been developed and the application of these techniques allows automation and on-line coupling to GC or GC-MS.

Phospholipids

Phospholipids form a special class of lipids. They are composed of a glycerol molecule substituted by one or two fatty acids and one additional polar group. The latter group can be choline (phosphatidylcholine

or lecithin), ethanolamine, serine or inositol. Phospholipids are very polar and ionic. None the less, the fatty acid chains give to phospholipids hydrophobic properties, making them very useful as emulsifiers. The analysis of intact phospholipids by CGC or SFC is not possible due to the limited temperature stability of the solutes. Phospholipids can only be analysed by HPLC or MEKC.

Other Oleochemicals

According to the definition of Christie, other organic compounds also containing fatty acid chains can be considered as lipids. This includes waxes (mostly esters between long-chain fatty acids and long-chain fatty alcohols), ethoxylated alcohols and glycolipids. Depending on the molecular weight, CGC, HPLC or SFC can be used.

In this article examples of separation by SFC are presented for the classes of organic solutes mentioned. An overview of the nomenclature used in lipid analysis is given in the Appendix.

Supercritical Fluid Chromatography

Supercritical fluid chromatography (SFC) is a separation technique similar to gas and liquid chromatography, but using a supercritical fluid as mobile phase. If a liquid or a gas is used above its critical temperature and pressure, it changes to a supercritical fluid. The characteristics of supercritical fluids are intermediate between those of gases and liquids. A supercritical fluid can be considered as a dense gas. The lower viscosity and high diffusivity in comparison to a liquid make supercritical fluids interesting for chromatography (faster stationary phase-mobile phase mass transfer), while the higher density, in comparison to a gas, allows the solubilization and transport of the solutes through the column at lower temperatures. Moreover, the solubilization power can be modified by changing the density through temperature and/or pressure. Selective extraction (supercritical fluid extraction) and gradient supercritical fluid chromatography are possible. The low critical temperature (31.3°C) and low critical pressure (72.9 atm), together with the low toxicity and high availability, make carbon dioxide (CO_2) the only practical usable supercritical fluid.

SFC was first performed using packed columns (pSFC). Only in the late 1980s did a first generation of dedicated SFC equipment become available. At that time, however, most SFC research work was focusing on capillary SFC (cSFC) using ultranarrow bore columns ($25\text{--}100 \mu\text{m i.d.}$), pure carbon dioxide as mobile phase, (in most cases) a syringe type pump,

a fixed restrictor and typically a GC detector (mostly FID). In this article, some examples of lipid analysis by cSFC separations will be given. In the mid 1990s, a second generation of SFC instruments became available. These instruments are more dedicated to pSFC and consist of a reciprocating supercritical fluid pump, a modifier pump (modifiers are not used with capillary columns), a variable restrictor and typically an HPLC detector. pSFC has been used more successfully than cSFC for lipid analysis. Detailed information on SFC theory and instrumentation is given in Anton and Berger. See also Further Reading.

Capillary Supercritical Fluid Chromatography for the Analysis of Lipids

The analysis of neutral lipids, such as triglycerides, is one of the first successful applications of cSFC. Using an apolar capillary column (SE-54, 5% phenylmethylsilicone), good carbon number separations are obtained. This is illustrated in Figure 1 with the analysis of palm kernel oil.

The triglycerides from CN 28 (combination of, for instance, two decanoic acid and one octanoic acid chain) to CN 54 (combination of three C_{18} fatty acids) are separated in a 30 min analysis time. For most applications, cSFC and high-temperature capillary gas chromatography (HT-CGC) provide similar quantitative data. In HT-CGC, injection and column temperature programming are however, critical, and it has been observed that highly unsaturated triglycerides (trilinolein, trilinolenin) tend to polymerize in the column at 330–360°C. cSFC offers an advantage in this respect since the analysis temperature is much lower (100–150°C). In cSFC with FID detection, the response factors of saturated and unsaturated triglycerides are very similar and calibration is easy. Especially for the analysis of oils with a high degree of unsaturation (e.g. fish oils containing mostly 22:6 n-3 docosahexaenoic acid and 20:5 n-3 eicosapentaenoic acid), cSFC offers an advantage over HT-CGC although complete separation of the lipids is not possible without a multidimensional approach.

The analysis of triglycerides according to carbon number and unsaturation, is much more difficult. The highest resolution can be obtained using HT-CGC on a diphenyldimethylsilicone phase (more than 35% phenyl substitution, e.g. OV-17, HP-50 +). As demonstrated by Geeraert, the combination of the high efficiency of the capillary column with the high selectivity of the stationary phase at 330–360°C, gives a detailed triglyceride profile. cSFC using polar cyanopropyl silicone columns (25% cyano substitution,

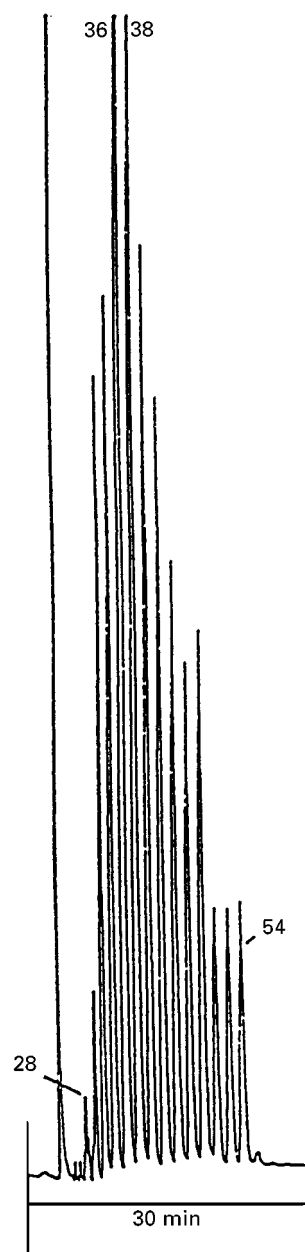


Figure 1 Carbon number separation of palm kernel oil by cSFC. Column: 10 m \times 100 μ m i.d \times 0.2 μ m SE-54. Temperature: 170°C. Pressure programmed from 19 to 29 MPa in 30 min.

e.g. OV-225, SB cyano-25) has also been used for this separation. A separation according to unsaturation of a mixture of triglyceride reference compounds is given in Figure 2.

For natural lipid mixtures, this separation is, however, insufficient to resolve all possible fatty acid combinations and several co-elutions occur. The lower resolution obtained with cSFC in comparison to HT-CGC is a result of the strong dependence of the column efficiency on the supercritical fluid mobile phase velocity. Although a 10 m L \times 50 μ m i.d.

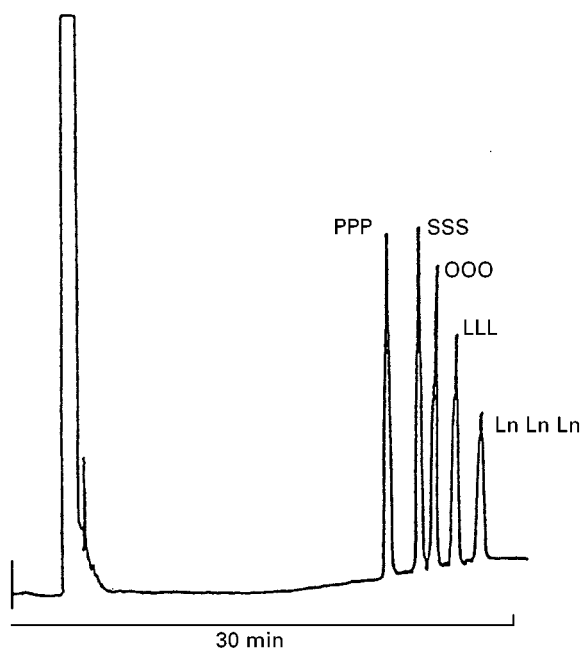


Figure 2 cSFC analysis of triglyceride standards on a polar column. Column: 10 m \times 100 μ m i.d. \times 0.1 μ m OV-225. Temperature: 150°C. Pressure programmed from 15 to 30 MPa at 0.5 MPa min⁻¹.

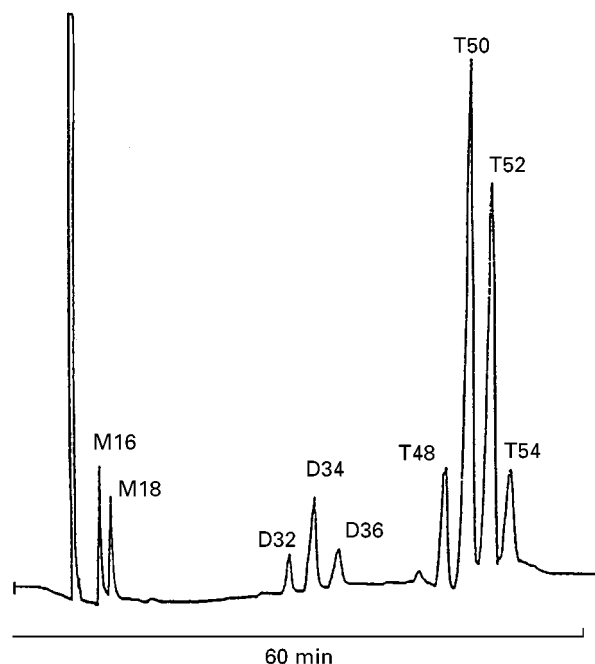


Figure 3 cSFC analysis of palm oil mono- (M), di- (D) and triglycerides (T). Column: 20 m \times 100 μ m i.d. \times 0.2 μ m SE-54. Temperature: 150°C. Pressure programmed from 15 to 25 MPa at 1 MPa min⁻¹, then to 30 MPa at 0.1 MPa min⁻¹.

column, theoretically should correspond to an effective plate number (N) 200 000, this efficiency cannot be applied in practice. The optimum linear velocity is only 0.2 cm s⁻¹ and this would result in a 83 min void time and a 15 hr analysis time for a solute with capacity factor $k = 10$. In practice, the narrow bore columns are used in cSFC at much higher velocities, resulting in effective plate numbers smaller than 10 000. This is even lower than in pSFC (see below). H.J. van Oosten has published a detailed study on the qualitative and quantitative aspects of cSFC for the analysis of triglycerides.

Another interesting application of cSFC is the separation of mono-, di-, and triglycerides. For GC analysis, the mono- and diglycerides need derivatization into the trimethylsilyl derivatives. With SFC, they can be analysed without derivatization. A typical chromatogram is shown in **Figure 3**.

Glycerol monopalmitate (M16), glycerol monostearate (M18), glycerol dipalmitate (D32), palmitoylstearyl glycerol (D34), glycerol distearate (D36) and the triglycerides are well separated according to their carbon number. For complex mono-, di- and triglyceride mixtures, such as some types of emulsifiers, the higher resolving power of HT-CGC is, however, needed.

cSFC has also been used for the analysis of waxes, sterols and sterol esters and ethoxylated alcohols. An example of a beeswax analysis is given in **Figure 4**.

The analysis of phospholipids by cSFC has also been described. For this analysis, the phospholipids are derivatized using diazomethane methylation (phosphoric acid group), acylation (amine or alcohol functionality) and/or demethylation (quaternary ammonium group). Using an apolar column, the phospholipids could be separated according to the carbon number. Group-type separations of phospholipids could not be realized by cSFC.

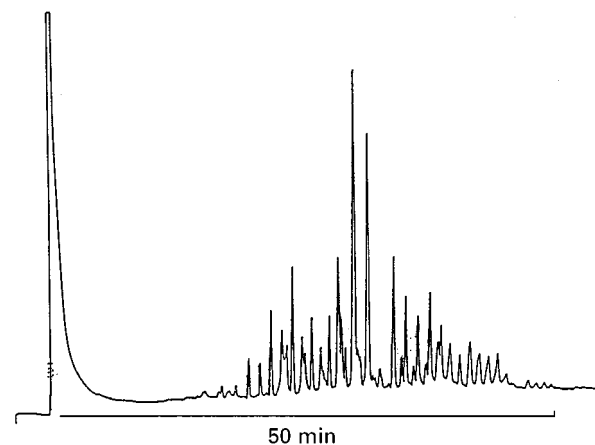


Figure 4 cSFC analysis of beeswax. Column: 10 m \times 50 μ m i.d. OV-1. Temperature: 100°C. Pressure programmed from 10 MPa (7.5 min) to 30 MPa at 0.4 MPa min⁻¹.

Although interesting separations could be obtained, cSFC is not widely used in routine laboratories for lipid separations. The main restriction is the robustness of the instrumentation. Column installation, restrictor maintenance and injection problems make state-of-the-art cSFC insufficiently robust for routine work.

Packed Column Supercritical Fluid Chromatography for the Analysis of Lipids

A few years after the introduction of cSFC, a second generation of SFC instrumentation was introduced on the market. This equipment was primarily dedicated to pSFC and the performance was based on specially designed reciprocating supercritical fluid pumps and new restrictor technology. The use of modifiers extended the applicability of SFC and the variable restrictors are much more robust than fixed restrictors (used in combination with capillary columns). The same performance as standard HPLC equipment in terms of repeatability, stability and robustness was realized.

Interesting pSFC separations of lipids can be made on conventional HPLC columns. Octadecyl silica (ODS), the most universal HPLC phase (reversed phase HPLC) can also be used in pSFC. The term 'reversed phase supercritical fluid chromatography (RP-SFC)', however, we consider inadequate, due to either the adsorption of carbon dioxide as a high-density layer or adsorption of the polar modifier on the stationary phase surface. Consequently, separations are actually achieved according to a normal phase mechanism. Therefore we prefer the term 'pSFC-ODS' for separations in supercritical conditions realized on ODS stationary phases rather than RP-SFC.

Triglycerides are separated on ODS columns according to the carbon number, but the presence of double bonds reduces retention. Separation of triglycerides by means of non-aqueous reversed phase high pressure liquid chromatography (NARP-HPLC) can be realized according to the equivalent chain number (ECN), whereby $ECN = CN - [2 \times NDB]$ in which CN is the carbon number and NDB the number of double bonds.

Separation of triglycerides using pSFC-ODS is achieved according to the separation number (SN), whereby the separation number equals carbon number (CN) minus the number of double bonds (NDB), thus $SN = CN - NDB$.

An example of such a separation is given in Figure 5 for the analysis of peanut oil. In this separation, the peak at SN 48 corresponds to LLL and

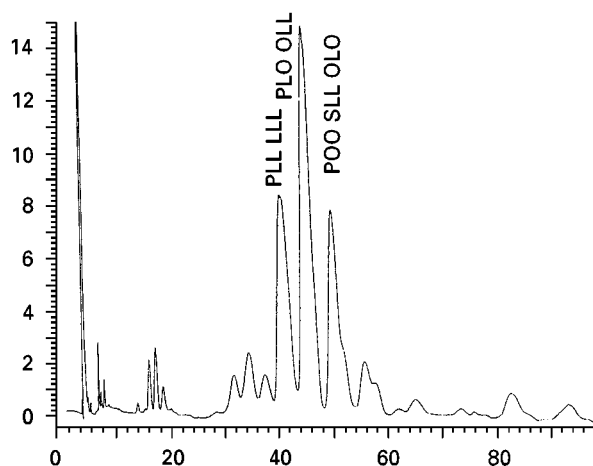


Figure 5 pSFC-ODS fractionation of triglycerides from peanut oil. Column: Adsorbosphere C18 (25 cm \times 4.6 mm i.d. \times 5 μ m) serially coupled to Shandon ODS Ultrabase (25 cm \times 4.6 mm i.d. \times 5 μ m). Temperature: 25°C. Flow rate: 2 mL min⁻¹. Modifier: methanol 2.5%, isocratic. Pressure: 150 bar. Detection: UV 210 nm. Injection volume: 5 μ L. Sample concentration: 100 mg mL⁻¹.

PLL, SN 49 corresponds to OLL and PLO and SN 50 to OLO + SLL + POO.

In comparison to HPLC, pSFC has the advantage of a much lower pressure drop across the column due to the lower viscosity of the mobile phase. While the efficiency of the column in pSFC is equal to the efficiency in HPLC, serial coupling of several columns is feasible in pSFC. This results in much higher total effective plate number (N = sum of plate number of each column). One of the best packed column SFC separations of triglycerides has used seven 12-cm columns in series (84-cm column length in total, 5- μ m ODS packing material, $N = 200\,000$). A typical separation is shown in Figure 6. In comparison to the separation shown in Figure 5, this chromatogram exhibits increased resolution. Both the efficiency and selectivity are increased in comparison to the SN separation shown in Figure 5. Group separation is made this time according to the ECN number, exactly as in NARP-HPLC. Resolution within a group is illustrated by the separation of PLL, POLn, OLL and OOLn, all characterized by ECN 44.

The change in the elution order can be explained either by the use of a more polar modifier (methanol-acetonitrile mixture) and by the use of subcritical elution conditions (16°C).

Another very interesting separation is obtained by pSFC using a silver-doped stationary phase. On this stationary phase, separations according to unsaturation and to some extent according to the geometrical configuration are obtained. The separation mechanism can be explained by two processes: (1) the over-

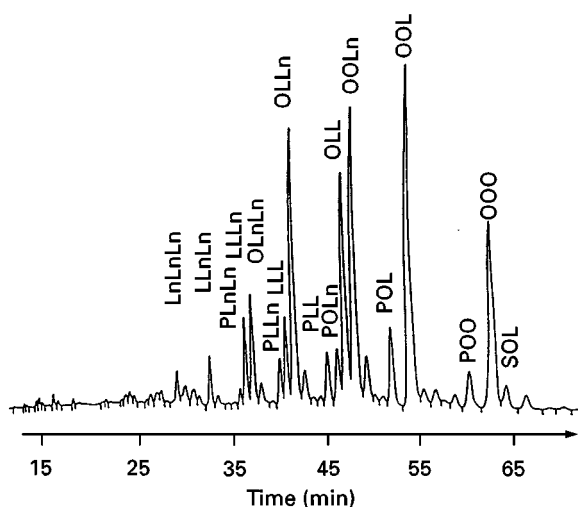


Figure 6 pSFC-ODS separation of triglycerides from rapeseed oil. Column: Hypersil ODS (12 cm \times 4.6 mm i.d. \times 5 μ m) seven columns serially. Temperature: 16°C. Flow rate: 3 mL min⁻¹. Modifier: acetonitrile-methanol mixture 9 : 1, 6%, isocratic. Pressure: 100 bar. Detection: UV 210 nm. (Reproduced from Leselier E and Tchaplai A (1996) Mise au point de l'analyse des triglycerides en chromatographie subcritique sur colonnes remplies. *Proceedings du 3ème Colloque sur les Fluides Supercritiques, Grasse, France*, pp. 115-126.)

lapping of the π orbitals belonging to the unsaturated site of the solute with the 5s orbital of the silver ion and (2) the interaction between an antibonding π^* orbital of the unsaturated site of the solute with a 4d-filled orbital of the silver ion.

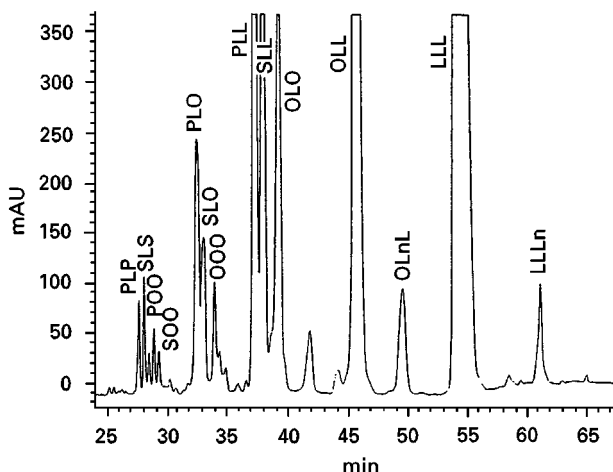


Figure 7 pSFC-SI separation of triglycerides in sunflower oil. Column: Silver-loaded Nucleosil 100-5 SA (25 cm \times 4.6 mm i.d. \times 5 μ m). Temperature: 65°C. Flow rate: 1 mL min⁻¹. Modifier: acetonitrile-isopropanol mixture 6:4, programmed from 1.2% (2 min) to 7.2% (28 min) at 0.3% min⁻¹, then to 12.2% at 0.54% min⁻¹, 2.5%. Pressure: programmed from 150 bar (2 min) to 300 bar at 1.5 bar min⁻¹. Detection: UV 210 nm. Injection volume: 5 μ L. Sample concentration: 100 mg mL⁻¹.

Recently, stable silver ion HPLC columns could be made by using silica-based cation exchange columns as support for silver ions. The ions are linked to the silica support via ionic bonds to phenylsulfonic acid groups chemically bonded to the silica.

Such columns have been successfully used in our laboratory both in HPLC and in pSFC. In pSFC, excellent triglyceride separations are obtained. This is illustrated in **Figure 7**, showing the analysis of sunflower oil. Within each group with the same number of double bonds, an additional separation according to chain length is observed. When solutes are characterized by the same number of double bonds, a higher retention corresponds to a higher carbon number, e.g. PLL elutes before SLL. Finally, an additional separation is obtained between lipids with the same number of double bonds and carbon number, but containing a different number of unsaturated fatty acids. Thus, SLL, containing only two unsaturated fatty acids elutes before OOL, which contains three unsaturated fatty acids.

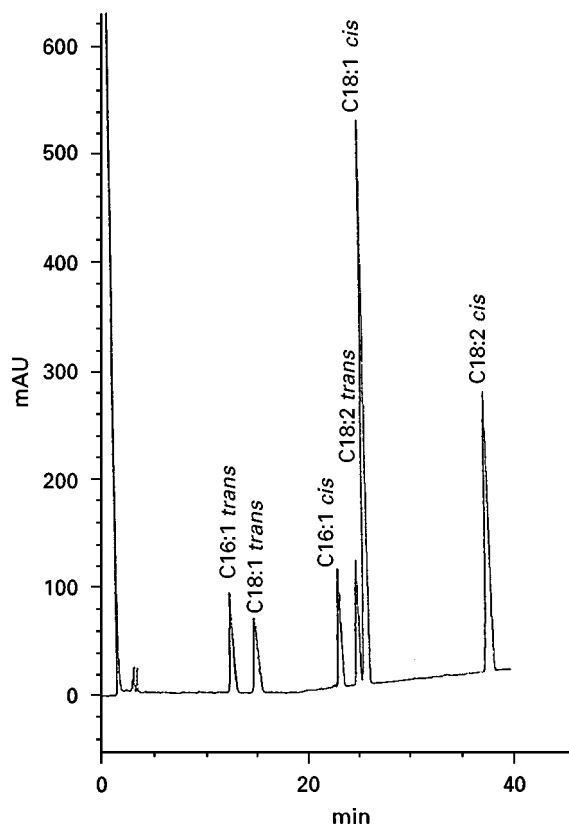


Figure 8 pSFC-SI separation of a standard mixture of geometrical isomers of fatty acids as methyl esters (FAMES). Column: Silver-loaded Nucleosil 100-5 SA (25 cm × 4.6 mm i.d. × 5 μm). Temperature: 80°C. Flow rate: 2 mL min⁻¹. Modifier: acetonitrile-isopropanol mixture 6 : 4, programmed from 0.5% (15 min) with a gradient of 0.1% min⁻¹, 2.5%. Pressure: 250 bar. Detection: UV 210 nm. Injection volume: 5 μL.

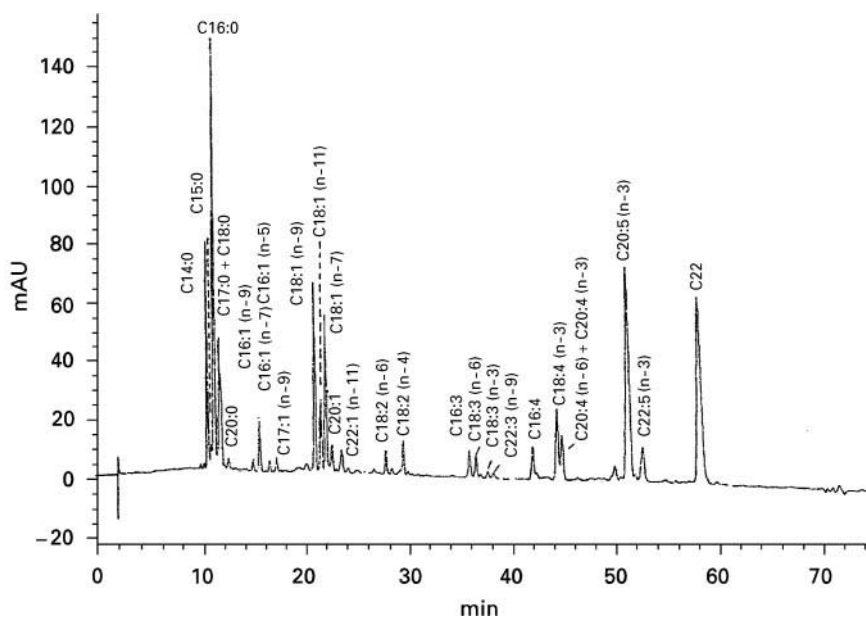


Figure 9 pSFC-SI separation of fatty acids as phenacyl esters (FAPes) from sardine oil. Column: Silver-loaded Nucleosil 100-5 SA (25 cm \times 4.6 mm i.d. \times 5 μ m). Temperature: 80°C. Flow rate: 2 mL min⁻¹. Modifier: acetonitrile–isopropanol mixture 6 : 4, programmed from 1% (2 min) to 41% at 0.2% min⁻¹. Pressure: 250 bar. Detection: UV 254 nm. Injection volume: 5 μ L.

As can be deduced from Figures 5 and 7, the pSFC-ODS separation and the silver ion pSFC separations are complementary to each other. Very detailed triglyceride analysis can therefore be obtained by using a multidimensional approach. First a SN separation is obtained on an ODS column. The fractions of different SN number are collected and re-analysed by silver ion SFC. pSFC is especially suitable for fraction collection, since the largest part of the mobile phase is a gas after decompression and concentrated fractions are obtained.

On silver-doped stationary phases, a separation of geometrical isomers of fatty acids can also be achieved. In **Figure 8**, a standard mixture of C16:1 *cis-trans*, C18:1 *cis-trans* and C18:2 *cis-trans* fatty acid methyl esters (FAMES) was separated. In comparison to cSFC, detection in pSFC is normally done by UV detection, because of the use of modifiers which are not compatible with FID detection. In comparison with HPLC, pSFC allows the use of low wavelengths. In the case of fatty acids, derivatization of the carboxyl group with phenacyl bromide (2-bromoacetophenone) allows detection at higher wavelengths which results in higher sensitivity. **Figure 9** shows the separation of fatty acids from sardine oil as phenacyl ester derivatives (fatty acid phenacyl esters, FAPes) on a silver-doped stationary phase.

Another very interesting detector for pSFC is the evaporative light-scattering detector. This detector is especially useful in lipid analysis since the response

factors are less dependent on the number of double bonds and very similar for saturated and unsaturated lipids.

Packed-column SFC has also been applied to other oleochemicals including sterols, sterol esters and waxes. Fractionation of free sterols from the complex matrix of vegetable oils can be achieved in a short analysis time by pSFC on an aminopropyl silica-gel (APSG) column as shown in **Figure 10**. This separation, in combination with collection of the sterol

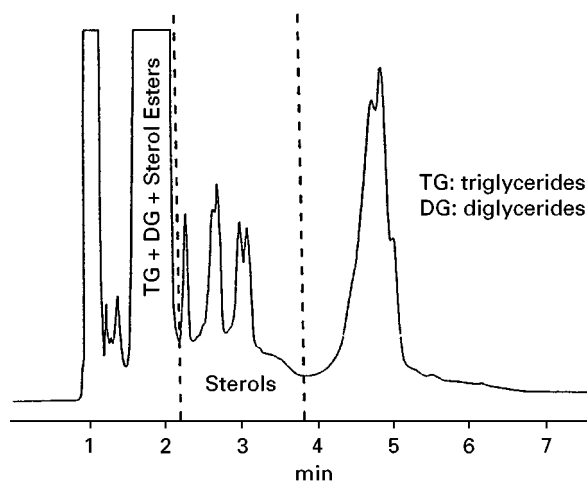


Figure 10 Isolation of the sterolic fraction in sunflower oil by pSFC. Column: Aminopropyl silica-gel APSG (20 cm \times 4.6 mm i.d. \times 5 μ m). Temperature: 70°C. Flow rate: 2 mL min⁻¹. Modifier: methanol 10% isocratic. Pressure: 150 bar. Detection: UV 210 nm. Injection volume: 5 μ L. Sample concentration: 10%.

fraction and subsequent CGC-MS analysis, was used for the characterization of vegetable oils.

Future Outlook

The next step in the use of pSFC in the analysis of oils, fats and waxes is interfacing the technique to spectroscopic detectors such as mass spectrometry or nuclear magnetic resonance spectrometry.

Supercritical fluid chromatography interfaced to mass spectrometry (SFC-MS) has already become a valuable technique in the hands of specialists. State-of-the-art pSFC-MSD interfacing has recently been reviewed by Combs *et al.*

The separation of triglycerides in vegetable oils by interfacing pSFC on a silver-doped stationary phase to atmospheric pressure chemical ionization-mass selective detection (APCI-MSD) has been described. The coupling was made using a commercially available LC interface, without any modification. No loss of resolution was noted, while sensitivity was 100 times higher compared to UV detection. The molecular $[M-H]^+$ ions could be elucidated in the mass spectra. However, the lower the degree of unsaturation, the more fragmentation occurred. Elucidation of the position of the fatty acids on the glycerol backbone (POP versus PPO for example) was feasible.

The combination of pSFC with NMR also offers a bright perspective. The mobile phase, mainly consisting of carbon dioxide, does not interfere with the 1H spectra. pSFC-NMR has been reviewed by Albert.

Last, but not least, the preparative-scale features of SFC are worth mentioning. Process-scale pSFC has been applied for the production of high purity ω -3 fatty acids and their ethyl esters from fish oils. A preparative pSFC approach for the production of pure eicosapentaenoic acid has been described, highlighting again its tremendous economic impact.

Appendix: Nomenclature in Lipid Analysis

For carbon number separations, triglycerides are coded as Tnn, indicating a triglyceride with a total of nn carbon atoms in the fatty acid chains (sum of three fatty acids). T54 can thus be tristearin, triolein or another combination of three C_{18} fatty acids or C_{16} , C_{18} , C_{20} . In the same way, monoglycerides are indicated as Mnn with nn the number of carbon atoms in the fatty acid and diglycerides are indicated by Dnn, with nn the sum of the carbon atoms in the two fatty acid chains.

For detailed separations, the triglycerides are coded XYZ, indicating the fatty acid substitutes in the molecule. Abbreviations for common fatty acids are listed

Table 1 Abbreviations used for common fatty acids

Abbreviation	Fatty acid name	Carbon number : number of double bonds
P	Palmitic acid	16 : 0
S	Stearic acid	18 : 0
O	Oleic acid	18 : 1
L	Linoleic acid	18 : 2
Ln	Linolenic acid	18 : 3

Table 2 Shorthand designation used for common fatty acids

Systematic name	Trivial name	Shorthand designation
<i>cis</i> -9-Tetradecenoic acid	Myristoleic acid	C14 : 1 (n-5)
<i>cis</i> -9-Hexadecenoic acid	Palmitoleic acid	C16 : 1 (n-7)
<i>cis</i> -6-Octadecenoic acid	Petroselinic acid	C18 : 1(n-12)
<i>cis</i> -9-Octadecenoic acid	Oleic acid	C18 : 1 (n-9)
<i>cis</i> -11-Octadecenoic acid	<i>cis</i> -Vaccenic acid	C18 : 1 (n-7)
<i>cis</i> -9-Eicosenoic acid	Gadoleic acid	C20 : 1 (n-11)
<i>cis</i> -11-Eicosenoic acid	Gondoic acid	C20 : 1 (n-9)
<i>cis</i> -13-Docosenoic acid	Erucic acid	C22 : 1 (n-9)
<i>cis</i> -15-Tetracosenoic acid	Nervonic acid	C24 : 1 (n)

in Table 1. SLO, for instance, corresponds to a triglyceride with a stearin-linolein-olein fatty acid combination.

For detailed separations of fatty acids, each analyte is identified as Cmm : p (n - q), where mm corresponds to the number of carbon atoms in the fatty acid molecule, p is the number of double bonds and q is the number of carbon atoms from the double bond in the terminal region of the molecule. C 18:1 (n-9), for instance, is 9-octadecenoic acid (one double bond in 9 position from terminal side of molecule). The relation between the systematic name, the trivial name and the short designation mentioned above for common fatty acids is given in Table 2.

Further Reading

- Albert K (1997) Supercritical fluid chromatography-proton nuclear magnetic resonance spectroscopy coupling. *Journal of Chromatography A* 785: 65-83.
- Anton K and Berger C (eds) (1997) *Supercritical Fluid Chromatography with Packed Columns. Techniques and Applications*. Science series, vol. 75. New York: Marcel Dekker.
- Caude M and Thiebaut D (eds) (1999) *Practical Supercritical Fluid Chromatography and Extraction*. Amsterdam: Harwood Academic Publishers.
- Christie WW (1989) *Gas Chromatography and Lipids A Practical Guide*. Ayr: The Oily Press.
- Christie WW (ed.) (1992) *Advances in Lipid Methodology*, vols 1-5. Ayr: The Oily Press.

- Combs MT, Ashraf Khorassani M and Taylor LT (1997) Packed column supercritical fluid chromatography-mass spectroscopy A review. *Journal of Chromatography A* 785: 85–100.
- Geeraert E and Sandra P (1985) Capillary gas chromatography of triglycerides in fats and oil using a high temperature phenylmethylsilicone stationary phase. *Journal of High Resolution Chromatography* 8: 415–422.
- King JW and List GR (eds) (1996) *Supercritical Fluid Technology in Oil and Lipid Chemistry*. Champaign, Illinois: AOCS Press.
- Smith R (ed.) (1988) *Supercritical Fluid Chromatography*. RSC Chromatography Monographs. London: The Royal Society of Chemistry.
- Smith RM (ed.) (1995) *Packed Column Supercritical Fluid Chromatography*. RSC Chromatography Monographs. London: The Royal Society of Chemistry.
- van Oosten HJ, Klooster JR, Vandeginste BGM and De Galan L (1991) Capillary supercritical fluid chromatography for analysis of oils and fats. *Fat Science Technology* 93: 481–485.

OILS: EXTRACTION BY SOLVENT BASED METHODS

See III/FATS/Extraction by Solvent Based Methods

OLIGOMERS: THIN-LAYER (PLANAR) CHROMATOGRAPHY

See III/SYNTHETIC POLYMERS/Thin-Layer (Planar) Chromatography

ON-LINE SAMPLE PREPARATION: SUPERCRITICAL FLUID EXTRACTION



J. M. Levy, Levytech, Gibsonia,
PA, USA

Copyright © 2000 Academic Press

Introduction

Over the past few years, there have been several advances in the use of new sample-preparation strategies prior to chromatographic analyses. These include supercritical fluid extraction (SFE), solid-phase microextraction (SPME) and accelerated solvent extraction (ASE). Each of these techniques is relatively new and will be used in more analytical strategies. SPME, for example, stands out in the realm of sample preparation in that the technique is solventless. ASE is also particularly exciting since the technique represents a modern version of long-established Soxhlet extractions. Therefore, by elevating temperatures and pressures to keep the liquid solvent from vaporizing, ASE approaches can be thought of as a 'universal' sample-preparation tools. The advantage of SFE is the fact that a supercritical fluid (i.e. carbon dioxide)

is utilized with its blend of liquid and gaseous properties to achieve selective extraction of target analytes without major interference (depending on the sample). Of these three techniques, only SPME and SFE can be considered selective tools and they are also the only ones that can be interfaced directly to a chromatograph. The discussion in this article will focus on the use of SFE as a viable and selective strategy for sample preparation.

SFE continues to evolve as it is applied to a more and more diverse range of sample matrices. In the early years, much emphasis was placed on using SFE for environmental methods but, this has now blossomed into the wide application of SFE for food and agricultural analyses, polymer characterization, and pharmaceutical assays.

One of the distinct advantages of SFE (besides the physical properties of liquid-like density, gas-like viscosity, no surface tension and intermediate diffusivity) is the ability to directly couple the extraction effluent from a sample matrix to an analytical chromatograph for quantitative or qualitative determination.

In analytical chemistry, sample preparation is often the most error-prone step, requiring arduous and sometimes lengthy procedures before the actual sample can be analysed. SFE directly addresses the problem and provides analysts with the option of directly coupling the sample preparation procedure to the various forms of column chromatography to effectively achieve the analytical objectives. An added advantage is that the nature of the online interfacing of SFE does not exclusively limit the use of the chromatographic instrument to only SFE sample introduction. The flexibility exists whereby the analyst can use SFE in an offline collection mode as well as online. Offline SFE gives the analyst the most capability for manipulation in method development and analytical characterization, since the extracted effluent can be collected and then taken to any analytical instrument (i.e. GC, LC, SFC, MS, NMR, IR, UV).

This chapter will describe the use of online SFE/GC and SFE/SFC in terms of theory of operation, interface mechanics, instrumentation and application examples. In addition, some examples of selectivity enhancements in SFE will be described.

On-line Interfacing Mechanics

A generalized scheme of online SFE is shown in Figure 1. A SFE system delivery pump compresses the primary extraction fluid (usually carbon dioxide) and solubilizes the analytes from a matrix which is contained in a heated extraction vessel. These solubilized

analytes are then transferred online to an analytical chromatograph (i.e. GC, SFC or HPLC). The transfer line is used to control the volume of supercritical fluid that is flowing through the sample matrix. Depending on the analytical need, there is considerable flexibility obtainable when interfacing SFE online to a capillary GC. For many determinations, flame ionization and mass spectrometric detectors have been employed. However, it is also possible to utilize the more selective and sensitive detectors such as nitrogen-phosphorus and electron-capture detectors, depending on the application. In all of these cases, the detectors have a very low response to CO₂, depending for the most part on the impurities present in the commercial supply of CO₂. Most of the published online SFE/GC applications have utilized capillary columns ranging from 0.20-mm internal diameter to 0.53-mm internal diameter and have encompassed the full range of GC stationary phase coatings. To date, there have been no reports of SFE fluids stripping off capillary column stationary phase coatings after online interfacing.

As a means of sample introduction to GC, online SFE presents itself as an alternative to other means of sample introduction such as headspace, purge and trap, thermal desorption, pyrolysis, and even conventional syringe injection. Figure 2 shows a comparison of online SFE/GC with conventional syringe injection using eucalyptus leaves and a fuel-contaminated sediment sample. The two modes of online SFE/GC, namely, split and on-column, were utilized. As can be seen, the GC peak shapes and amplitudes were comparable for online SFE and conventional syringe injection. A noticeable difference in the chromatograms is the absence of a solvent peak from the flame ionization detector. In comparison to headspace, purge and trap and thermal desorption, SFE has the potential to encompass a wide range of volatile to non-volatile analytes, depending on the sample and the extraction conditions that solubilize the entire sample (e.g. certain polymer matrices).

Figure 3 shows a generalized schematic diagram of a typical online SFE/GC. A typical procedure for performing online SFE/GC involves first loading (usually weighing out) a small sample into an extraction vessel, depending on analyte sensitivities and analytical objectives. After weighing out a sample, the end caps of the vessel are tightened and the extraction cell is placed in the extraction oven. After pressure and thermal equilibration for the charged extraction vessel in the static mode (closed outlet of vessel to CO₂ flow), an electronic high-pressure switching valve changes position and shifts the extraction to the dynamic mode (opened outlet of the vessel for flow) transferring the extraction effluent through a heated

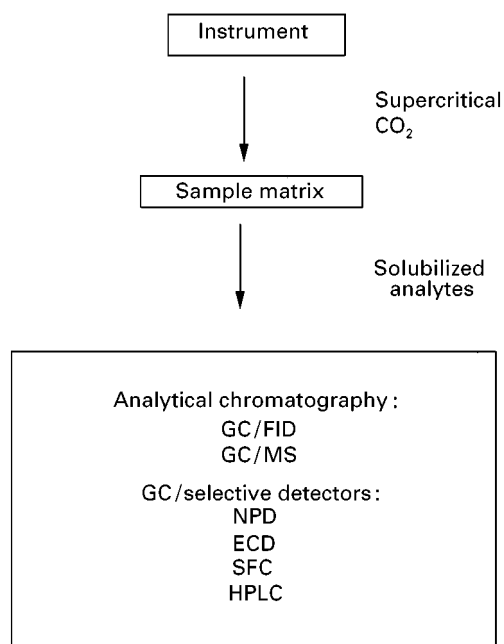


Figure 1 Generalized scheme for online SFE.

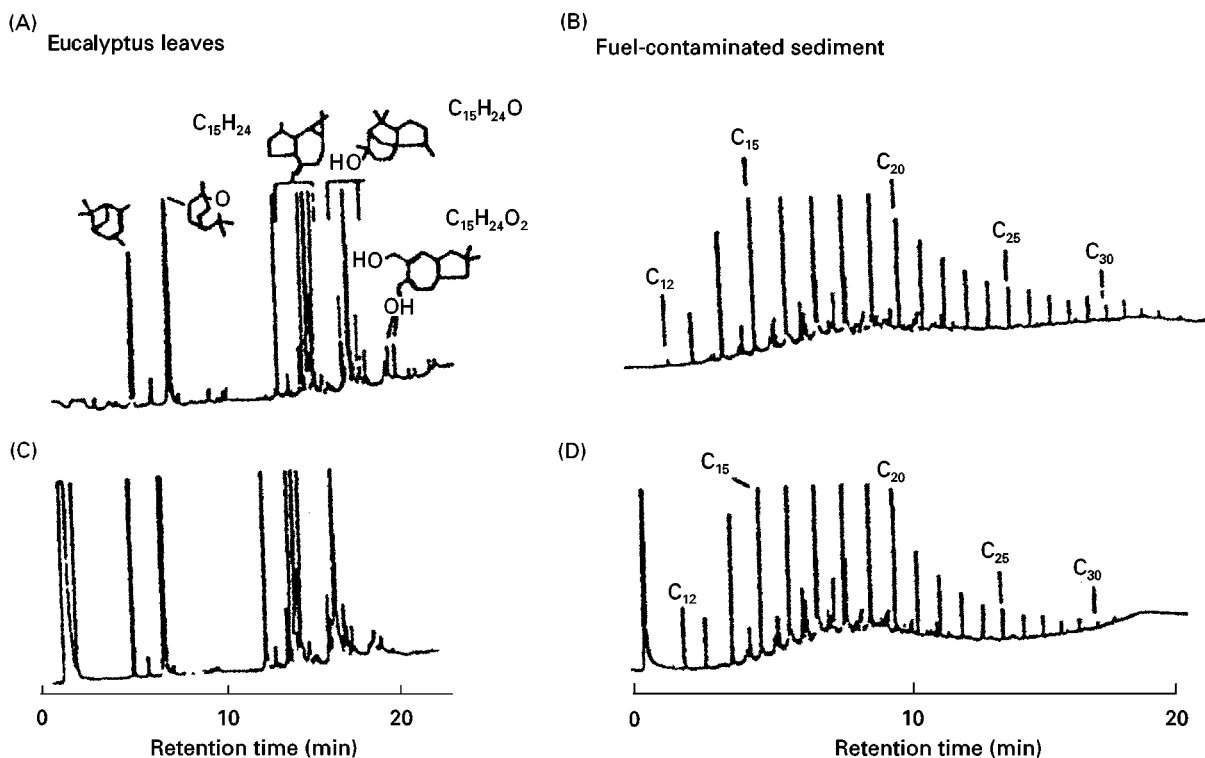


Figure 2 Comparison of chromatographic peak shapes obtained using (A) on-column SFE/GC and (B) split SFE/GC with (C) conventional on-column and (D) split GC injections of methylene chloride extracts. Reproduced with permission from Hawthorne SB *et al.* (1989) *Journal of Chromatographic Science* 27: 347–354 and Hawthorne SB *et al.* (1990) *Journal of Chromatographic Science* 28: 2–8.

transfer line (made of fused silica or stainless steel) directly into a capillary GC injection port as shown in Figure 3.

The flow through the transfer line is regulated by restricting (crimping) the stainless-steel line or by using small inner-diameter fused silica. The decompressed CO_2 , gaseous flow typically ranges from 35 to 300 mL min^{-1} depending on the extraction vessel void volume (i.e., sample size). To achieve highly efficient extractions, three to five void volumes of

supercritical fluid need to be flushed through the charged extraction vessel. The decompressed gas flow into the GC needs to be set at each extraction pressure setpoint to achieve efficient extractions.

Two modes of online SFE/GC exist, namely split SFE/GC and on-column SFE/GC. Figure 4 is a pictorial representation of what is occurring during SFE introduction into GC. During split SFE/GC, the solubilized analytes exit the extraction vessel through a stainless steel (1/32 in \times 0.007 in internal diameter) transfer line which is inserted directly through the septum and septum cap of an unmodified split/splitless capillary injection port. The supercritical fluid state is maintained until it reaches the tip of the transfer line (i.e. restrictor) and decompresses directly inside the heated injection port. So therefore, in theory, the analytes are purposely not allowed to fall out of solution until they are completely transferred to the GC injection port. The heat of the injection port aids in minimizing the expansive cooling of the supercritical fluid upon decompression. After decompression, the analytes vaporize inside the heated injection port, mix with the GC carrier gas, are homogenized inside the existing glass split-injection port liner, and decompressed gaseous CO_2 (and

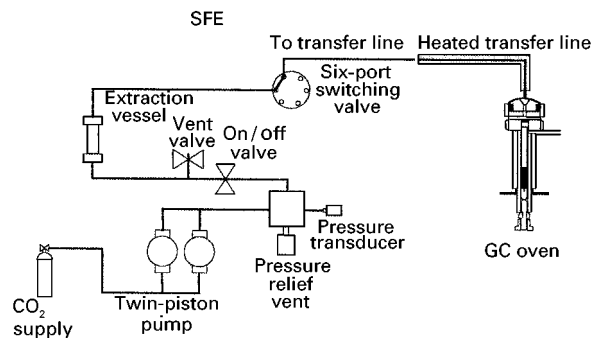


Figure 3 Generalized online SFE/GC interface: schematic diagram.

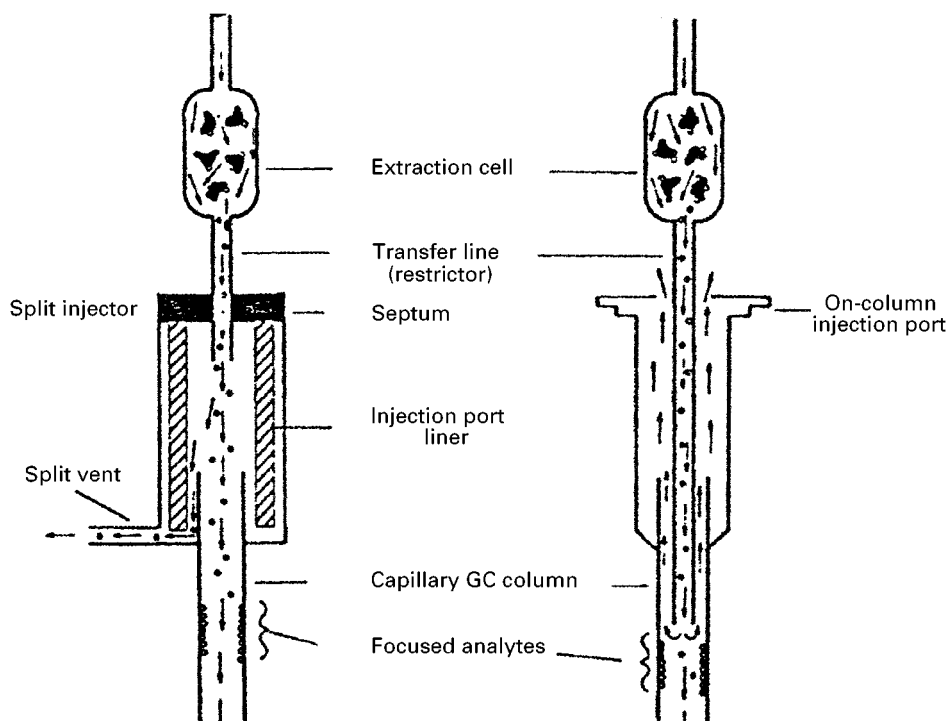


Figure 4 Pictorial representation of online SFE/GC interfacing. Left, split SFE/GC; right, on-column SFE/GC.

analytes) flows out of the split vent during the dynamic extraction transfer mode. This is reproducible and potentially quantitative since the split ratio does not change from run to run. The development of temperature-programmable injection ports has allowed even further advances in focusing techniques after SFE deposition.

During on-column SFE/GC, the solubilized analytes exit the extraction vessel through a fused silica transfer line (10–50 μm internal diameter) which is inserted directly into an on-column capillary injection port. All of the solubilized analytes and decompressed gaseous CO_2 enter the GC capillary column, maximizing the sensitivity of an analysis (analogous to on-column syringe GC injection). For this reason, however, the fused silica transfer line needs to be physically removed after the dynamic extraction transfer mode since the decompressed CO_2 would essentially become the GC carrier gas and possibly extinguish a flame ionization detector. In split SFE/GC, the transfer line normally remains inserted in the injection port during the entire analytical run. The majority of published applications have been accomplished using online split SFE/GC. In general, split SFE/GC is better suited for generalized method development and characterization of a variety of different samples.

For both online split and on-column SFE/GC, the stationary phase of the GC capillary column is

responsible for focusing the extracted analytes. Depending on the volatility range of the analytes, additional cooling (i.e. a cooled injection port) may be necessary to achieve sharp chromatographic peak shapes. This can be accomplished with a temperature-programmable injection port or by cooling the entire GC oven. An example of this is shown in Figure 5, demonstrating the effect of the cryogenic trapping temperature on the SFE/GC characterization of BTEX and n-alkanes from Tenax-TA. During the extraction, the GC capillary column was maintained at -50 , -25 , 5 or 25°C . After each extraction the GC oven was heated to 40°C at $50^\circ\text{C min}^{-1}$ and then at 8°C min^{-1} to 300°C . The lower the setting of the GC oven temperature, sharper chromatographic peak shapes were obtained for the earlier eluting (more volatile) species. Maintaining the GC oven temperature at -50°C yielded the best chromatographic performance. In practice, at temperatures below -50°C , plugging of the transfer line occurs because of the freezing of the decompressed CO_2 inside the capillary column. The duration of the dynamic extraction transfer mode is usually the same as the duration of the initial (cryogenically cooled) temperature of the GC oven. After the dynamic transfer, normal GC temperature programming is performed and analytical GC results are obtained. This same routine can be applied if a temperature-programmable injection port is available.

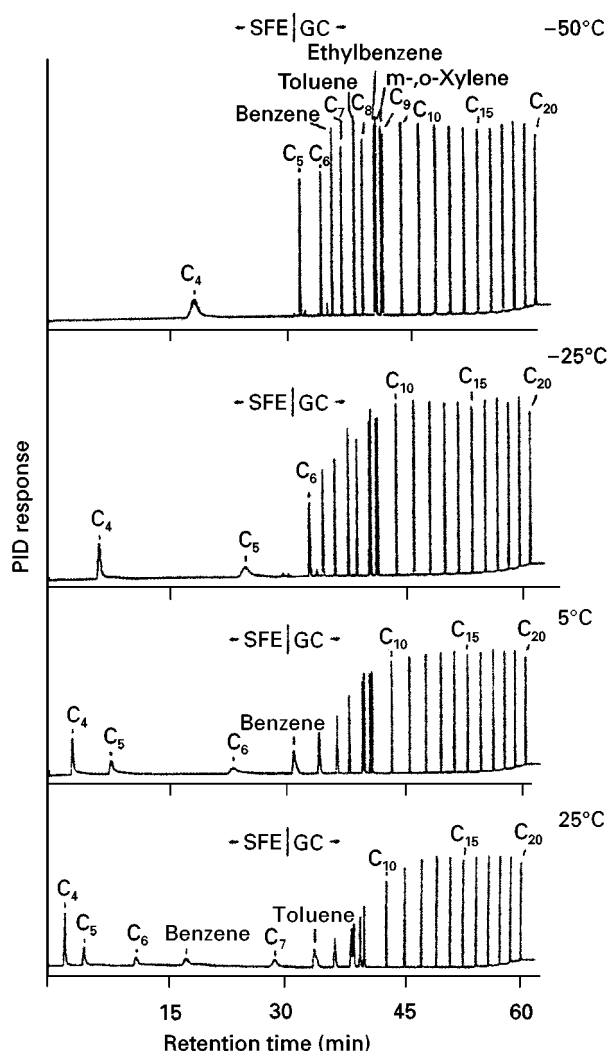


Figure 5 Effect of cryogenic trapping temperature on the online SFE/GC/FID analysis of rosemary. Reproduced with permission from Burford MD and Hawthorne SB (1994) *Journal of Chromatography A* 685: 79–94.

Figures 6–8 represent several example applications displaying the advantages of utilizing online SFE/GC. In each of these cases, flame ionization detection (FID) was utilized for the target analyte characterizations. In Figure 6, a rapid field survey was conducted using online SFE/GC to determine the carbon number range for total petroleum hydrocarbons (TPH) in soil. A fouled isocracker catalyst from a refinery was analysed and the aromatic component contamination was determined using online SFE/GC-MS, shown in Figure 7. In Figure 8, orange oil was spiked into an extraction vessel filled with hydromatrix (i.e., pelleted diatomaceous earth) and rapidly extracted. In this, online SFE with CO₂ as the extraction fluid was invaluable since early eluting components in the orange oil were not overwhelmed by the response from classical liquid solvents.

Selectivity in On-line SFE/GC

Compared to conventional liquid extractions like Soxhlet or ASE, a distinct advantage of SFE is the ability to tune the operational extraction parameters to achieve the selective extraction of certain analytes from a complex sample. An obvious approach in controlling SFE selectivity is by varying extraction temperatures and pressures. These parameters directly control extraction densities which in turn affect the threshold solubilities or mobilities of specific analytes. Certain classes of compounds, in theory, have distinct threshold solubilities. For example, a qualitative SFE/GC characterization of polynuclear aromatic hydrocarbons (PAHs) at different extraction pressures has been performed. In going from low to high SFE pressures, a noticeable difference, despite some overlap, was experienced in the distribution of the chromatograms by retention time and peak amplitude, indicating the potential for online SFE class fractionation. At 80 atm, two-ring, alkylated two-ring, three-ring, and lower alkylated three-ring PAHs are extracted. At 125 atm, the extracted fraction consists of alkylated three-ring, four-ring and some alkylated four-ring PAHs. At the highest pressure, 200 atm, alkylated four-ring and larger PAHs are extracted. The ability to tune selectivities by varying SFE densities is not only dependent on the target analytes of interest but also on the sample matrix. This is due to the contributions of other SFE mechanisms besides solubility, namely diffusion and adsorption effects.

Another means of enhancing SFE selectivities and efficiencies is by the use of modifiers such as methanol. These modifiers enhance extraction efficiencies by affecting solubilities, diffusion rates or surface adsorption, depending on the sample matrix and the target analytes. In SFE, modifiers can be added to the primary supercritical fluid by using dual-supply pumps or by uniquely adding a specific volume of modifier directly to the extraction vessel with the sample. In online SFE/GC, depending on the modifier identity, the modifier may elute in the GC as a discrete peak together with the extracted analytes. Depending on the modifier concentration, a retention gap or thick-film capillary column may be needed to separate the large (solvent-like) modifier peak and focus the target analyte peaks. Some modifiers such as formic acid, do not have an appreciable response with conventional flame ionization detectors. Figure 9 shows the results for the online SFE/GC-FID characterization of sucrose esters in ground tobacco with and without BSTFA (N,O-bis(trimethylsilyl)trifluoroacetamide) as a derivatizing agent. In this case, BSTFA was added for derivatization during the

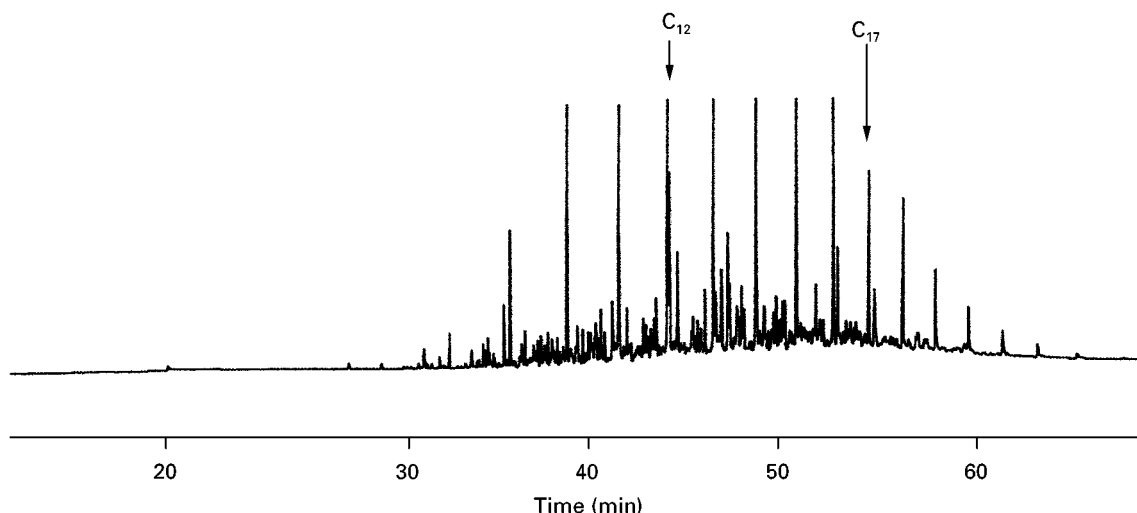


Figure 6 Online SFE/GC determination of total petroleum hydrocarbons in soil (diesel fuel range).

extraction but also functioned as a modifier as well. It is clearly evident when comparing the two chromatograms that the BSTFA derivatized the sucrose esters during the SFE step, and therefore improved the detectability of these compounds. **Table 1** lists another example of the use of modifiers in online SFE/GC to enhance the extraction efficiency of selected aromatics analytes from a petroleum residue. The percentage recoveries for the selected aromatics were low when using only supercritical CO₂ for SFE and were distinctly enhanced when different modifiers were added to the residue in the extraction vessel. A period of static equilibration was required under the outlined extraction conditions, for the full modifier effect. Moreover, by varying only the modifier identities (keeping the modifier concentrations con-

stant at 7%) obvious differences in percentage recoveries were obtained. Propylene carbonate and benzene achieved comparable efficiencies as opposed to the lower efficiencies obtained with methanol for this particular sample matrix and analyte.

Further selectivities can be obtained in online SFE/GC by the use of alternative supercritical fluids such as sulfur hexafluoride (SF₆) and nitrous oxide (N₂O). The use of these supercritical fluids in online SFE has been limited compared to CO₂, but has demonstrated certain distinct advantages due to their physical properties.

Different adsorbents can also be used to selectively immobilize interfering analytes from a complex sample before analytical determinations. Adsorbents, such as Celite, sodium sulfate, magnesium sulfate,

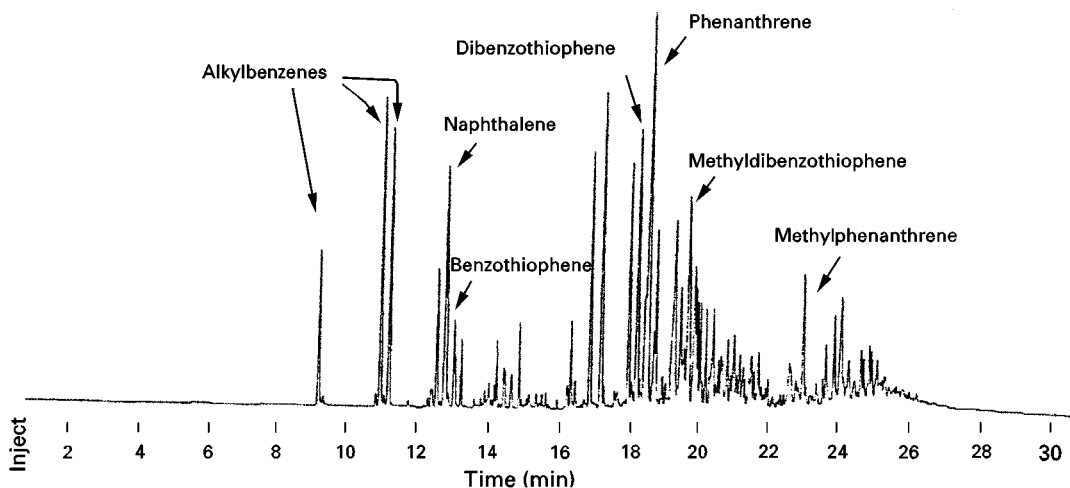


Figure 7 SFE/GC of a fouled isocracker catalyst. Reproduced from Hawthorne SB.

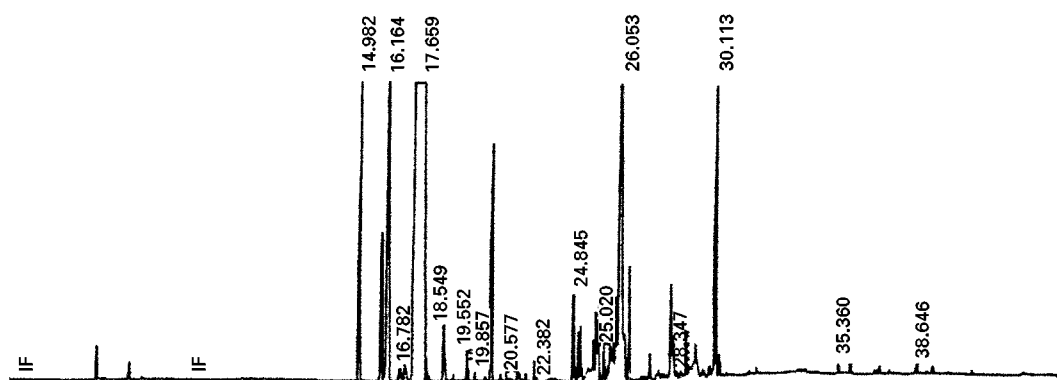


Figure 8 Online SFE/GC characterization of Orange Oil.

Florisil, alumina, polyurethane foam, and hydromatrix (diatomaceous earth) have been used in online SFE applications to remove interfering analytes and water. An obvious disadvantage could be situations where target analytes are irreversibly bound to the adsorbents or where interferences are introduced by the adsorbent. Adsorbents have been utilized by mixing them with proportionate amounts of sample before introduction into an extraction vessel or by utilizing two extraction vessels in series, the first containing the sample, and the second containing adsorbent before the GC.

On-line SFE/SFC

Supercritical fluid chromatography (SFC) has been used widely as an analytical tool for the separation of relatively nonpolar, thermally unstable and high molecular weight solutes beyond the range of GC. The physical properties of supercritical fluids have unique characteristics to solve many problems, where both GC and high performance liquid chromatography (HPLC) fail. The online modes of SFE/SFC have several distinct advantages that are beyond the scope of either technique when used separately. These

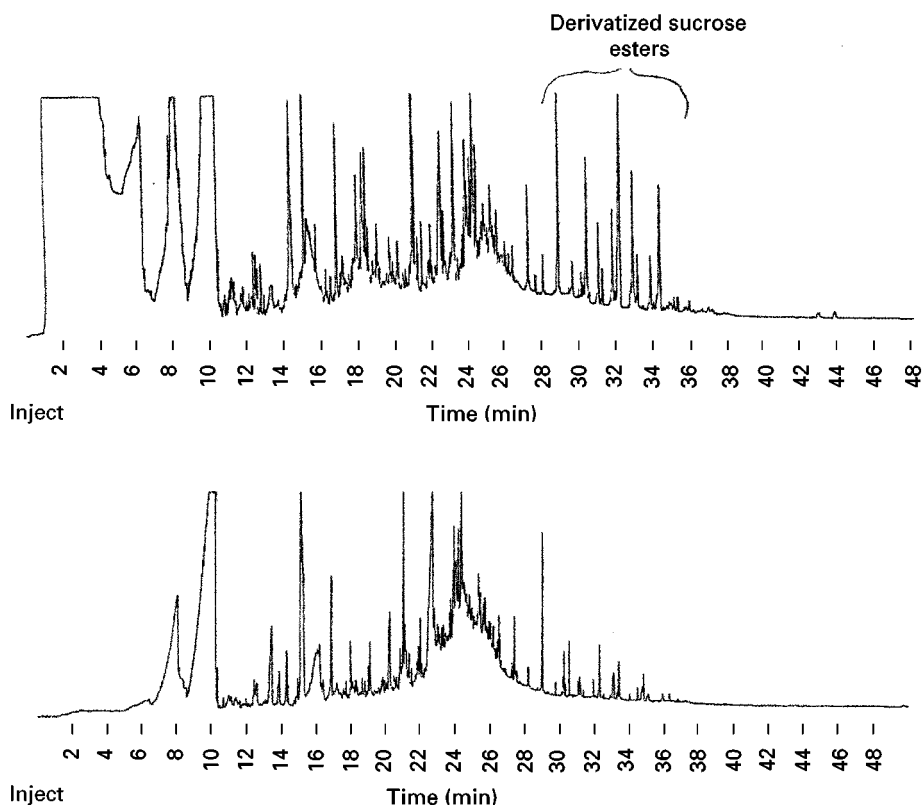


Figure 9 Online SFE/GC of ground tobacco. Top, BSTFA added; bottom, without BSTFA.

Table 1 Use of modifiers in online SFE^a/GC^b: percentage target analyte yields

Compound	Modifier			
	Benzene	Methanol	Propylene carbonate	CO ₂
Ethylbenzene	101%	76%	98%	45%
Cumene	101%	86%	98%	40%
2-Chloronaphthalene	100%	93%	101%	73%
1,2,4-Trimethylbenzene	99%	87%	98%	38%

^aSFE: 300 mg of petroleum residue, 425 atm, 65°C, 10 min static, 7 min dynamic.

^bGC: 30 × 0.25 mm I.D. DB-1, inlet programmed from 0°C to 300°C at 600°C min⁻¹, 30°C (7 min) to 325°C at 7°C min⁻¹.

advantages are (a) trace analysis capability, (b) preparation with minimal sample contamination, (c) higher reproducibility, (d) increased productivity, and (e) online automation of the sample preparation step with the chromatographic analysis step. In the online mode, a high pressure extraction cell and the extracted components are trapped or focused in a device prior to SFC analysis. SFE/HPLC has been practised by several groups but has been demonstrated in only limited applications. This is largely due to the fact that coupling to GC and SFC is much more straightforward compared to coupling to HPLC. One main limitation is the fact that the LC mobile phase needs to be gas-free since bubbles can cause problems for most LC detectors.

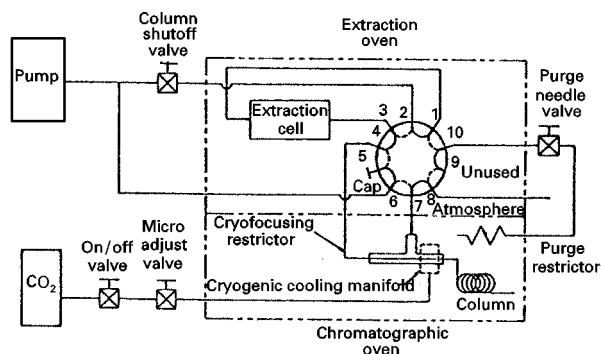
SFE/SFC Interface Mechanics

The arrangements in these hyphenated techniques usually involved several valves, one or two pumps and ovens. A simple approach has been applied to perform online SFE/SFC in both static (after pressurization of the extraction cell, extraction is allowed without passing any flow of supercritical fluid through the cell) and dynamic (after pressurization of the extraction cell, supercritical fluid continuously flows through the outlet of the cell) modes. Another method which has been used frequently for online SFE/SFC is the use of a second supply pump to pressurize the extraction vessel and the sample while the first supply pump is used solely to obtain chromatographic separation. Applying the second pump for extraction usually creates less technical problems and more freedom since both modes of extraction can be achieved and the chromatographic system is independent of the extraction system.

Other approaches that have been used to perform online SFE/SFC have been systems with multiple switching valves that permit collection of the extrac-

ted sample in a cooled adsorbent trap. After extraction and collection, the valves are switched and the cryogenic trap temperature is increased. By switching the valves and heating the trap, the supercritical fluid carries the extracted materials onto the analytical column. **Figure 10** shows an online SFE/SFC system which uses a cryofocusing region to collect the extracted material. In this system, the selector valve is first placed to the column position. During this period the temperature of the cooled region is adjusted to a desired level. Next, the valve is switched to the extraction vessel where the supercritical fluid of the desired density removes the extracted material from the region. During the decompression of CO₂, at the tip of the restrictor, the selector valve is switched to the column position and the supercritical fluid moves the analytes from the trap flow to the column. Meanwhile, the trap is also heated to the necessary temperature to help move the analytes onto the column.

Another system which uses a cryofocused trap to perform online high pressure SFE/SFC is shown in **Figure 11**. The system is comprised of three different valves (ten-port/two-position, five-port/four-position and four-port/two-position selector valves) and a zero dead-volume tee. During the extraction period, the mobile phase from the pump enters the tee. Tubing from one outlet of the tee leads the mobile phase to the injector valve for use only in conventional SFC applications. Tubing from the other outlet of the tee goes through the ten-port valve to the extraction vessel and then into the five-port selector valve. From the ten-port valve, the extracted analytes are held at a specified extraction temperature with industrial grade, dry carbon dioxide. All of the extracted material is then collected in the cryofocusing trap. The decompressed CO₂ gas from the trap is then vented through the ten-port valve into the oven atmosphere. After completion of the extraction, the pump is equilibrated for SFC. Upon reaching equilibrium, the ten-port and five-port selector valves are switched simul-

**Figure 10** SFE/SFC system and a cryogenic cooling trap with multiple valves.

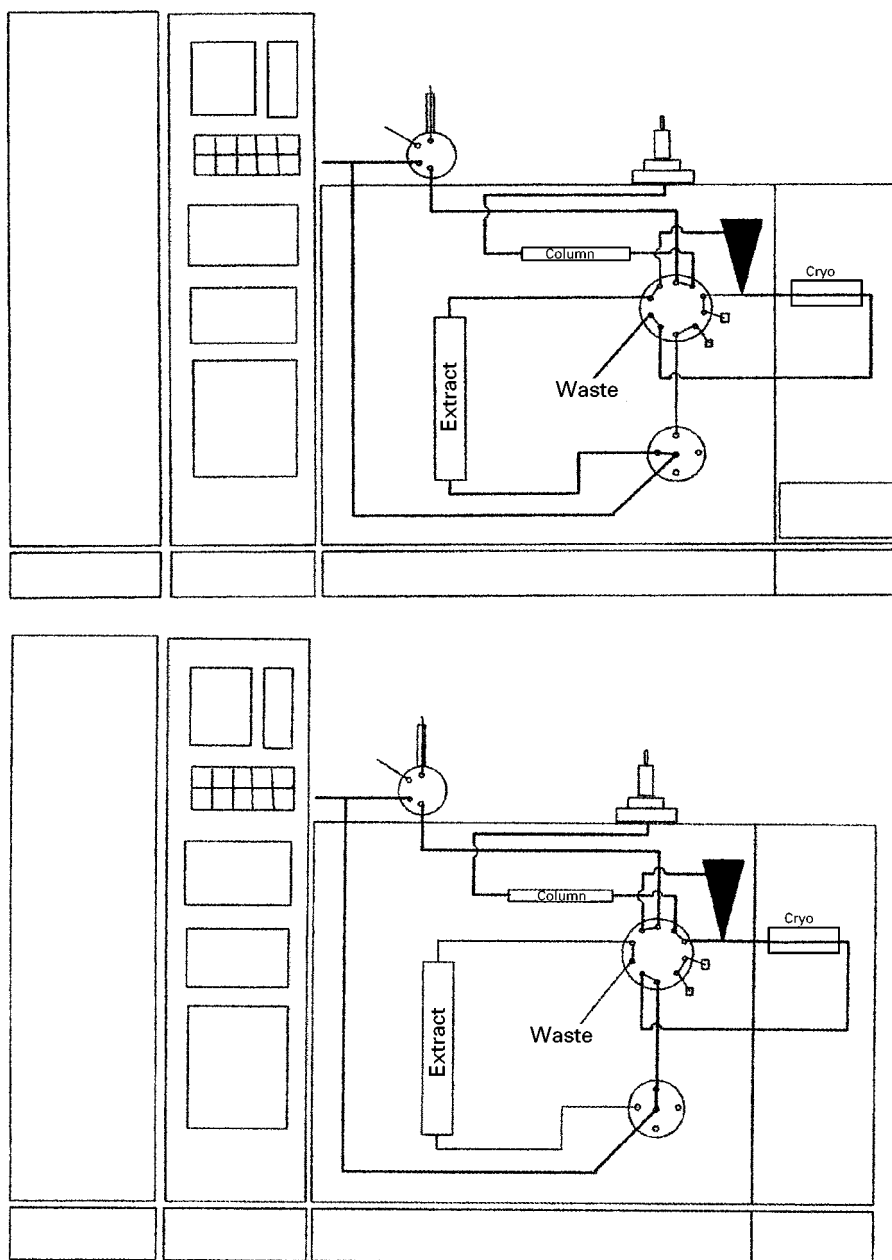


Figure 11 SFE/SFC system and cryogenic trap with multiple valves in extraction (top) and injection (bottom) modes.

taneously (Figure 11). In this configuration, mobile phase passes through the tee, the injection valve, and the ten-port valve into the cryofocused trap, which is then ballistically heated to the specified injection temperature. After backflushing, the mobile phase carries the extracted components from the trap back to the ten-port valve into the chromatographic column. Additional CO_2 flow from the other outlet of the tee to the cryofocused trap restrictor prevents backflushing of the extracted material into the restrictor.

Most of the SFE/SFC devices described above are designed to obtain qualitative results. A later design

gave quantitative results for different hydrocarbon standards using an online SFE/SFC system. The results showed that the amount of material extracted was directly proportional to the volume of sample placed in the extraction vessel. Later they demonstrated the quantitative analysis for different additives in low-density polyethylene using an FID.

A very elegant use of online SFE/SFC is shown in Figure 12 which is a chromatogram of five different additives extracted from low-density polyethylene. For this experiment, a polymer was placed in the extraction vessel, extracted (450 atm, 100°C),

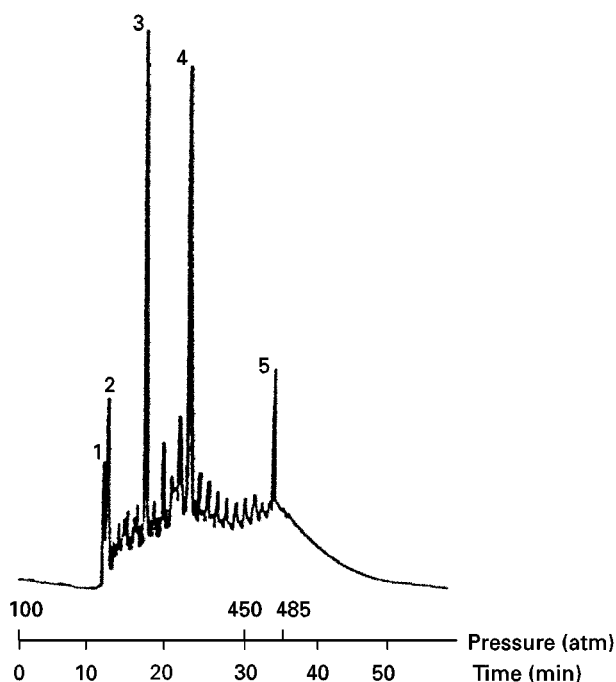


Figure 12 Online SFE/SFC of different additives from low-density polyethylene. 1, BHT; 2, BHEB; 3, Isonox 129; 4, Irganox 1076; 5, Irganox 1010. (Reproduced from Levy JM and Ashraf-Khorassani M (1992) *Journal of Chromatography Library Series* 53: with permission from Elsevier Science.)

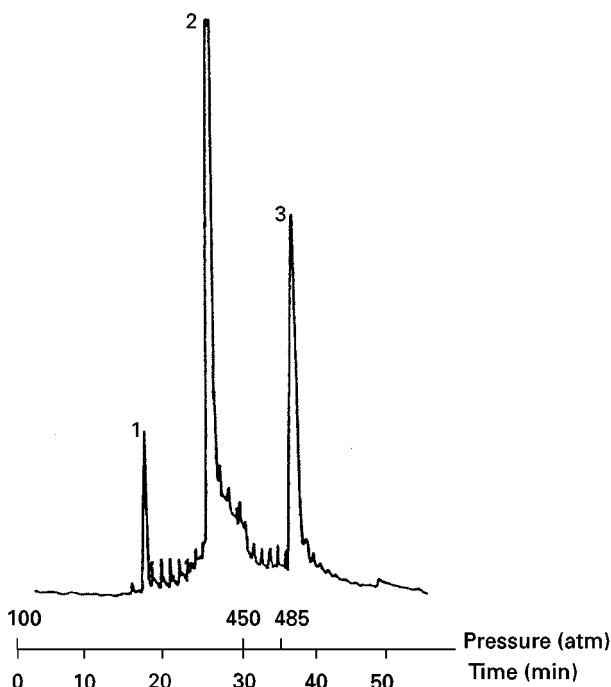


Figure 13 Online SFE/SFC of additives from polyethylene concentrate. 1, Irgafos 168; 2, Cyasorb 3346; 3, Cyanox 1790. (Reproduced from Levy JM and Ashraf-Khorassani (1992) *Journal of Chromatography Library Series* 53: with permission from Elsevier Science.)

collected and cryofocused at -25°C . After extraction and collection, the trap was backflushed and the extracted component was flushed into the analytical SFC poly(ethylene glycol) (PEG) column. Each additive was identified and quantitated at the 200–300 ppm level. **Figure 13** shows the extraction and separation of three different additives from another polyethylene sample. Again, after extraction (450 atm, 100°C) and collection (-25°C), the extracted components were backflushed into the SFC octadecyl column, with each additive being determined at the 100–200 ppm level. Besides, polymer applications, online SFE/SFC also has been used for the characterization of caffeine in teas, as shown in **Figure 14**.

Conclusions

Both directly coupled SFE/GC and SFE/SFC fall into the realm of problem-solving tools that can be

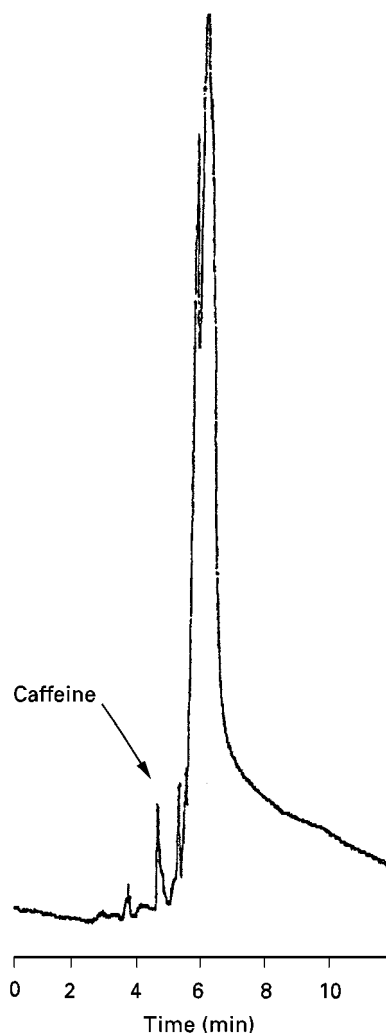


Figure 14 Online SFE/SFC of tea.

effectively utilized by analytical chemists for qualitative or quantitative characterizations or determinations. For GC, SFE presents itself as a selective sample introduction means for liquid or solid matrices with volatile and nonvolatile analytes. The nature of SFE instrumentation provides an added feature with the potential capability of sample preparation in the field with analytical determinations using an online GC/MS. Online SFE/SFC complements SFE/GC when target analytes are thermally labile or beyond the volatility range of GC. An added feature with SFE/SFC is the wide range of method development capability since SFC can be interfaced to a full array of GC and LC detectors (e.g., flame ionization, ultraviolet absorbance, mass spectrometer, infrared, nitrogen-phosphorus and sulfur chemiluminescence). As SFE technology further evolves, additional capabilities will be added and refined in the area of selectivity enhancement (i.e., modifiers, absorbents, *in situ* derivatization) and operational parameter optimization (what conditions to use for specific analytes and sample matrices).

See also: II/Chromatography: Supercritical Fluid: Instrumentation. **Extraction:** Supercritical Fluid Extraction. III/Supercritical Fluid Extraction-Supercritical Fluid Chromatography.

Further Reading

- Anderson MR, Swanson JT, Porter NL and Richtey BE (1989) *Journal of Chromatographic Science* 21: 371-377.
- Ashraf-Khorassani M and Levy JM (1990) *Journal of High Resolution Chromatography & Chromatographic Communications* 13: 742-747.
- Ashraf-Khorassani M, Kumar ML, Koebler DJ and Williams GP (1990) *Journal of Chromatographic Science* 28: 599-604.
- Berger TA (1995) *Packed Column SFC*. London: Royal Society of Chemistry.
- Burford MD, Hawthorne SB and Miller DJ (1994) *Journal of Chromatography A* 685: 79-94.
- Charpentier BA and Sevenants MR (eds) (1988) *Supercritical Fluid Extraction and Chromatography. Techniques and Applications*. ACS Symposium Series 366. Washington DC: American Chemical Society.
- Hawthorne SB (1990) *Analytical Chemistry* 62(11): 633A-624A.
- Hawthorne SB and Miller DJ (1986) *Journal of Chromatographic Science* 24: 258-264.
- Hawthorne SB and Miller DJ (1987) *Journal of Chromatography* 403: 63-67.
- Hawthorne SB, Krieger MS and Miller DJ (1988) *Analytical Chemistry* 60: 472-477.
- Hawthorne SB, Krieger MS and Miller DJ (1989) *Analytical Chemistry* 61: 736-740.
- Hawthorne SB, Miller DJ and Krieger MS (1989) *Journal of Chromatographic Science* 27: 347-354.
- Hawthorne SB, Miller DJ and Langenfeld JJ (1990) *Journal of Chromatographic Science* 28: 2-8.
- Levy JM and Ashraf-Khorassani M (1992) Hyphenated techniques in SFC and SFE. *Journal of Chromatography, Library Series* 53.
- Levy JM and Guzowski JP (1988) *Fresenius Zeitschrift für Analytische Chemie* 330: 207-210.
- Levy JM and Rosselli AC (1988) *Chromatographia* 28: 613-616.
- Levy JM, Guzowski JP and Huhak WE (1987) *Journal of High Resolution Chromatography & Chromatographic Communications* 10: 337-347.
- Levy JM, Cavalier RA, Bosch TN, Rynaski AF and Huhak WE (1989) *Journal of Chromatography* 27: 341-346.
- Levy JM, Rosselli AC, Boyer DS and Cross K (1990) *Journal of High Resolution Chromatography & Chromatographic Communications* 13: 416-421.
- Roberts I and Lynch T (1995) In: Adlard ER (ed.) *Chromatography in the Petroleum Industry*. Amsterdam: Elsevier.
- Skelton RJ Jr, Johnson CC and Taylor LT (1986) *Chromatographia* 21: 3-12.
- Westwood SA (ed.) (1993) *Supercritical Fluid Extraction and its Uses in Chromatographic Sample Preparation*. London: Blackie Academic & Professional.
- Wright BW, Frye SR, McMinn DG and Smith RD (1987) *Analytical Chemistry* 59: 640-644.
- Xie QL, Markides KE and Lee ML (1989) *Journal of Chromatographic Science* 27: 365-370.

OPIATES

See III/HEROIN: LIQUID CHROMATOGRAPHY AND CAPILLARY ELECTROPHORESIS

ORGANELLES



Centrifugation

J. A. Garner, University of Southern California,
Keck School of Medicine, Los Angeles, CA, USA

Copyright © 2000 Academic Press

Introduction

Centrifugation techniques are commonly used to fractionate and separate intracellular organelles of many cell types. Here, common reasons for separation of those organelles, as well as brief description of different types of subcellular organelles, are presented. This is followed by a description of the physical principles upon which centrifugal separations are based, and common methods applied for this purpose. Last, a brief description of the types of equipment available for these separations, as well as the advantages and disadvantages of different tools, will be presented. The reader is directed to additional reviews in the Further Reading section for more detailed information. Another source of valuable information is the literature provided by manufacturers of centrifuges, rotors, and separation media.

Subcellular Organelles

Higher eucaryotic cells contain numerous intracellular (or subcellular) organelles (**Figure 1**). These are structurally distinct entities located within the boundaries of the cell's plasma membrane and are generally associated with one or more specific cellular functions. Indeed, one of the distinguishing features of eucaryotic cells as compared with prokaryotes, is that they have attained the ability to compartmentalize their cellular functions into these organelle 'packages'. This has allowed eucaryotic cells to evolve into larger cells, cells that can have highly specialized functional domains by limiting organelles to particular cellular regions, and eventually allowed the evolution of specific cell types, tissue types and complex organisms.

Subcellular organelles can generally be divided into two broad classes: the membrane-bounded organelles and cytoplasmic organelles. Membrane-bounded organelles are structures enclosed within one or more lipid-based membranes. These organelles include vesicular structures of different sizes, such as the cell's

nucleus, mitochondria, lysosomes, peroxisomes, vacuoles, secretory vesicles, endosomes, and less well-defined vesicular structures. The Golgi apparatus and endoplasmic reticulum are large, complex structures that, during the process of disruption of the cell to release organelles, are usually broken and reform into smaller vesicles (termed 'microsomes') in a wide range of sizes. Certain plasma membrane fractions from certain cells may also be obtained during subcellular fractionation owing to the presence of highly specialized plasma membrane domains that may differ structurally and functionally (see Mircheff in the Further Reading).

Separate from the membrane-bounded organelles are the cytoplasmic organelles, distinct structural entities that are not enclosed within intracellular membranes. Examples of cytoplasmic organelles include the intracellular filament systems, such as microtubules, microfilaments, and intermediate filaments. Other cytoplasmic organelles are free ribosomes (not membrane-associated) and specialized cellular inclusions. Stretching the definition of cytoplasmic organelles slightly would allow the inclusion of multi-enzyme complexes found in the cytoplasm and separable by centrifugal and other techniques in this class.

Last, centrifugal techniques may be used to enrich parts of cells that have highly specialized functional domains. Examples of these subcellular fractions include synaptosomes (pinched-off neuron terminals and associated postsynaptic structures from the central nervous system) or the brush border of intestinal epithelial cells. These are complex parts of cells that are functionally distinct, and their isolation by centrifugal techniques allows for increased ease of their study.

For an in-depth description of the structure and function of all of the intracellular organelles described above, the reader is referred to the cell biology text by Alberts *et al.*

Purpose of Separating Subcellular Organelles

The separation of subcellular organelles by centrifugal techniques allows the enrichment (but not usually the purification) of these organelles. This enrichment may then serve as a starting point for use of other techniques that can more effectively isolate organelles. Obtaining an enriched sample may also be the first step towards biochemical purification of

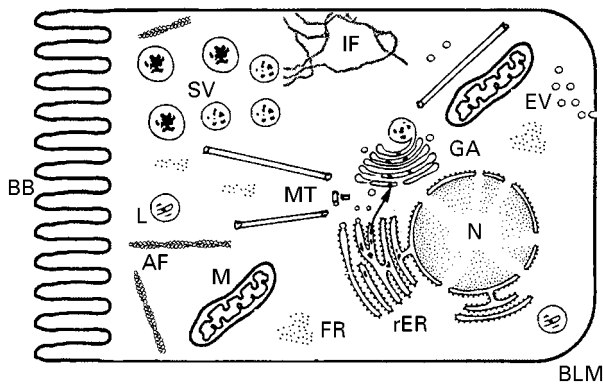


Figure 1 Diagram of a cell with subcellular organelles. A stylized diagram of an epithelial cell is shown with various common intracellular organelles drawn inside. Membrane-bounded organelles include the nucleus (N), the rough endoplasmic reticulum (rER), the Golgi Apparatus (GA), mitochondria (M), immature and maturing secretory vesicles (SV), endocytic vesicles (EV), and lysosomes (L). Cytoplasmic organelles include free ribosomes (FR), actin filaments (AF), microtubules (MT), and intermediate filaments (IF). Specialized regions of the plasma membrane include the brush border (BB) of the cell and the basolateral membrane of the cell (BLM).

individual proteins, glycoproteins, or other macromolecules that may be of considerable functional significance. Preparative centrifugation of lysed cells is a common technique that is used to perform the primary crude enrichment of these molecules.

A separate feature of interest to many cell and molecular biologists has to do with intracellular processing of macromolecules, whether they be destined for export from the cell or are specifically targeted to a particular domain of interest. Centrifugation techniques that allow separation of the various intracellular organelles such as the Golgi apparatus, the endoplasmic reticulum and various secretory vesicle pathways can be used to identify the compartment a particular molecule of interest is entering at various times after initiation of transcription. Combination of these centrifugal techniques with timed processing of a tagged protein or other cellular product can allow detailed elucidation of the intracellular route and compartments inhabited by that protein and its ultimate target location.

Homogenization of Cells to Free Subcellular Organelles

Organelles do not randomly float in the cytoplasm of cells; they are instead highly organized in a cytoplasmic matrix of very high protein concentration. The cytoplasmic matrix is a proteinaceous web or net of varying viscosity that organizes the organelles and maintains them within specialized functional do-

main of the cell. Before beginning to enrich for certain subcellular organelles, it is necessary first to break open the plasma membrane, and disrupt the matrix that holds the organelles. This is done by the process of homogenization of cells or tissues, and dilution of the cellular contents with at least 10 volumes of aqueous buffer prior to any centrifugation.

Tissue or cells of interest plus neutral aqueous buffer and protease inhibitors are placed in a ground glass/glass, glass/Teflon®, or Dounce cell homogenizer. A ground glass/glass homogenizer disrupts cells but also will likely damage nuclei. This causes the release of large amounts of highly viscous nucleic acids (which can severely compromise the subsequent isolation of subcellular organelles). A glass/Teflon® or Dounce homogenizer (using the loose pestle followed by the tight pestle) should break open cells but leave nuclei intact. The latter is the more desirable for subsequent subcellular fractionation of organelles.

If a large quantity of material must be processed, or a tissue of origin has large amounts of connective tissue within it (such as muscle) then other types of tissue or cell disruptors may be used. Examples are the Omnimixer® (Sorvall Instruments, Inc.) or Polytron® (Brinkmann Instruments, Inc.) in which a motor-driven propeller drives the sample through small apertures in the shaft to cause cell disruption.

Fractionation of Subcellular Organelles

The type of centrifugation technique used to separate organelles after homogenization will be determined by the physical properties of the desired organelles, and generally will depend on the sedimentation rate of the organelle of interest in a medium of defined density and viscosity. The sedimentation rate of any particular organelle obeys the principal of Stokes' law as it refers to the settling of a sphere in a gravitational field, as follows:

$$1/6\pi d^3(\rho_p - \rho_l)g = 3\pi d\mu v$$

where v = sedimentation rate or velocity of the sphere, d = diameter of the sphere, ρ_p = particle density, ρ_l = liquid density, μ = viscosity of liquid medium, and g = gravitational force.

'Sedimentation rate', or the rate at which an organelle moves through a medium of defined density and viscosity in a centrifugal field, is a function of the intrinsic buoyant density (density being mass per unit volume), the shape of the organelle in the medium, and the centrifugal force exerted on the or-

ganelle. The shape of the organelle plays a role in that a highly asymmetric organelle may sediment more slowly than a tight spherical organelle of the same mass. Sedimentation rate is determined by the following:

$$v = dr/dt = (s)(\omega^2 r)$$

where v = sedimentation rate, s = sedimentation coefficient in seconds or Svedberg units, r = the distance between the particle and the centre of rotation (cm), ω = the rotor speed in radians s^{-1} , and dr/dt = the rate of movement of the particle (cm s^{-1}).

The sedimentation rate of an organelle is proportional to the relative centrifugal force (RCF) on that organelle. It is determined by the following:

$$RCF = 1.12r(\text{rpm}/1000)^2$$

where rpm is the revolutions per minute, and r , or radius, is the distance from the centre of rotation to periphery of rotation. The maximum centrifugal force would be experienced at the bottom of the centrifuge tube (r_{max}), and the minimum centrifugal force would be experienced at the top of the centrifuge tube (r_{min}), and the average at r_{ave} .

The sedimentation rate is proportional to the size of that particle; hence, the sedimentation rate of a cell's nucleus is usually higher than that of a smaller mitochondrion or endocytic vesicle of similar density. Each population of organelles has an average buoyant density. However, this average value may be of limited value in that the range in variation in both structure and buoyant density for individuals within the population of organelles can be quite substantial. Table 1 lists buoyant densities for common membrane-bounded subcellular organelles, and it demonstrates the similarity in buoyant density among membrane classes. As a result of this similarity – and

this is an important point – it is virtually impossible to completely purify an individual organelle from all other organelles on the basis of its buoyant density alone, although a given type of organelle may be significantly enriched by these processes (which may be sufficient for certain studies).

An exception to this rule can be found for certain organelles such as microtubules (major polymeric cytoskeletal structures in cells), which can be purified to near homogeneity by centrifugal techniques. However, in these cases, one must usually make use of techniques that take advantage of that organelle's unique biological properties. For example, microtubule polymers and tubulin (the constituent protein subunit) have substantially different buoyant densities. Sample conditions can be easily altered so that they either favour assembly of the tubulin into the polymer, which pellets during centrifugation, or disassembly of the polymer into tubulin subunits, which remain in solution. Thus microtubules can be purified away from other organelles by 'cycling' the tubulin between its assembled and disassembled states and using centrifugation to separate the fractions appropriately.

In addition to the intrinsic buoyant density of organelles, it should also be appreciated that the buoyant density of a particular organelle may be altered in response to the osmolarity of the medium. For example, the high osmolarity of sucrose solutions in a sucrose gradient can cause a depletion of water from mitochondria, resulting in their shrinkage and a concomitant increase in buoyant density. This is sufficiently significant to account for differences in mitochondrial fractionation patterns in sucrose solutions as compared with media of high density but low osmolarity such as Ficoll®. On occasion, this feature of certain intracellular organelles can be exploited to help in their enrichment.

Types of Centrifugation Used for Organelle Enrichment

The enrichment of subcellular organelles may be provided by any one or a combination of different centrifugal techniques, including differential, rate zonal, or isopycnic centrifugation. These types of centrifugation would be termed 'preparative', as their ultimate goal is the enrichment of organelles. Analytic ultracentrifugation, where the goal is to determine the physical nature of a particle, is discussed elsewhere in the chapter.

Differential centrifugation (Figures 2 and 3) uses gross differences in buoyant density to sequentially pellet or sediment organelles of decreasing buoyant density. Starting with low centrifugal force spins for

Table 1 Densities of common membrane-bounded organelles in sucrose solutions^a

Organelle	Density (g cm ⁻³)
Golgi apparatus	1.06–1.10
Plasma membrane fractions	1.16
Smooth endoplasmic reticulum	1.16
Mitochondria	1.19
Lysosomes	1.21
Peroxisomes	1.23
Soluble proteins	1.30
Ribosomes	1.60–1.75

^aData were compiled from Sober HA (ed.) (1968) *Handbook of Biochemistry*, 2nd edn. Cleveland: The Chemical Rubber Co. Also Birnie GD and Rickwood D (eds) (1978) *Centrifugal Separations in Molecular and Cell Biology*. London: Butterworths.

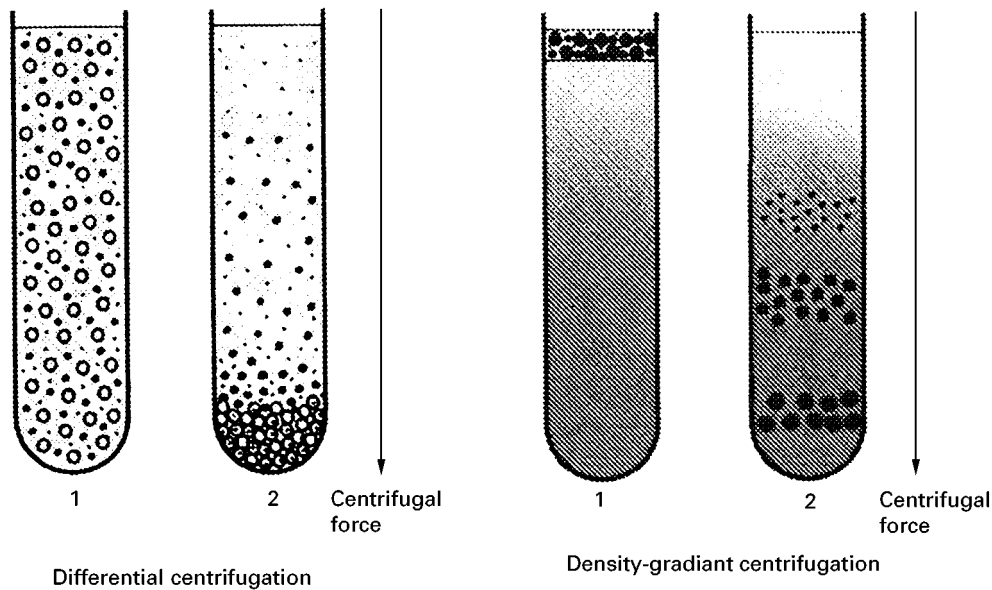


Figure 2 The principles of differential and density-gradient centrifugation. Differential centrifugation operates on the principle that denser particles sediment more rapidly and at lower g forces than lighter particles. Density-gradient centrifugation allows a mixture of particles or organelles of different densities to be separated: they band in a density gradient at the zone of the medium that has the same density as the particles.

short times, to remove the densest organelles from a sample homogenate, increased centrifugal force and length of time pellets lighter organelles. The first material pelleted from a homogenate at approximately $1000\text{--}1500 \times$ the force of gravity, g , for 10–15 min are nuclei, along with cellular and extracellular debris remaining in the homogenate. The supernate from this spin would be subsequently spun at approximately $10\,000 \times g$ for 20–30 min, to pellet mitochondria, lysosomes, and organelles of similar buoyant density. Microsomes, or small vesicles, pellet from the supernate of the mitochondrial spin after centrifugation at approximately $100\,000 \times g$ for several hours. Centrifugation speeds and times may be considerably lower for specific microsomal fractions, as determined empirically.

As mentioned above, use of these differential centrifugation steps is not sufficient to purify individual organelle types, primarily because of the range in size of the population. In addition, the mechanics of differential centrifugation allow for substantial trapping of lighter organelles within the pellets of heavier organelles. This latter can, to a certain extent, be compensated for by vigorous resuspension of the pellet and repetition of the centrifugation step. Effective resuspension of pellets into homogenous samples is imperative if those pellets are to be either subjected to further gradient fractionation or alternative treatment. If lumps are present, the sample will not fractionate according to individual organelle buoyant density. Use of a 3–10 mL syringe attached to a 4-inch,

14-gauge blunt-ended Popper Laboratory Pipetting cannula (Fisher Scientific, Inc.) allows thorough resuspensions. The same tool may be used in layering sample on gradients or retrieving fractions from the centre of density gradients as described below.

Each of the resuspended pellets and supernates obtained in the scheme described above (Figure 3) can be subjected to further centrifugation, usually by isopycnic or rate-zonal separation on density gradients, to more completely separate desired populations of organelles.

Isopycnic Centrifugation

In isopycnic centrifugation, using a continuous gradient, a fairly homogeneous population of organelles will ‘band’ in the gradient at their actual buoyant density over several hours. This method of separation is independent of time, and relies solely on the actual buoyant density of the particle. Banded organelles or particles can be recovered from the gradient by subjecting it to fractionation (either by punching a hole in the bottom of the tube and draining it, or by taking specific volumes of fractions from the top of the gradient). If bands are visible, they may be removed individually with a syringe with a long needle.

Rate-zonal Centrifugation

In rate-zonal centrifugation, the sample to be analysed is layered on a preformed density gradient and subjected to centrifugal force for a defined length of

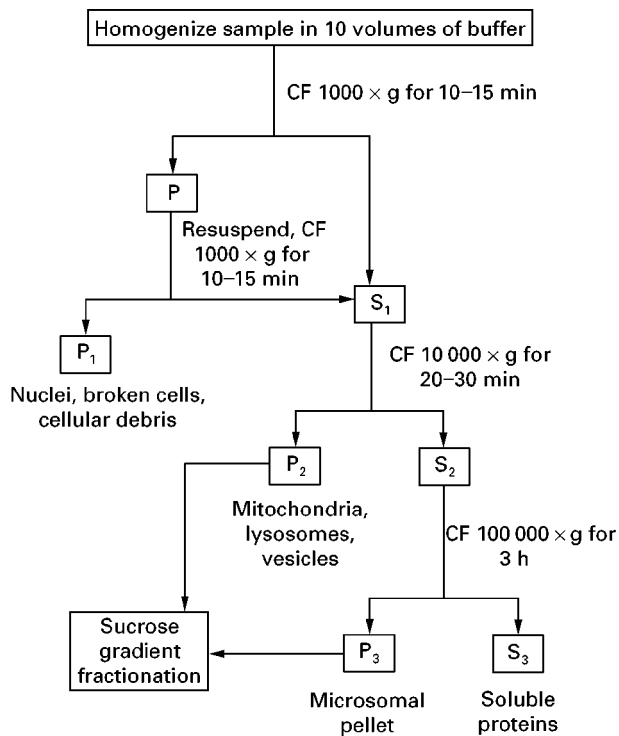


Figure 3 Differential centrifugation. A flow chart showing a common scheme for the differential centrifugation of a cellular homogenate. The first pellet is resuspended and recentrifuged, and the two supernates are combined as S_1 . Both the microsomal and mitochondrial pellets may be further fractionated on sucrose density gradients or by other mechanisms. CF = centrifuge.

time. The particles sediment through the gradient at a rate that is a function of their sedimentation coefficient. Once sufficient separation of the desired organelles is achieved, the run is terminated, and once again, banded organelles can be obtained by fractionation of the gradient.

Depending upon the medium used, density gradients may either be self-generated, or may be formed within the centrifuge tube prior to sample administration (see later). Media that can generate their own gradient in a centrifugal field are usually mixed with samples at a density equivalent to the mid-density of the desired gradient, prior to gradient formation. Alternatively, preformed density gradients can be generated from a two-chambered gradient mixer, and sample layered on top of, or within, the gradient prior to centrifugation (Figure 4). Preformed gradients may also be made by layering decreasing densities of medium in 'steps' rather than a continuous gradient in a tube, then allowing diffusion over time to produce the gradient.

Equipment

Preparative or high-speed centrifuge A high-speed centrifuge (e.g. Beckman J21) will spin samples at

speeds up to 20 000 rpm, with g forces of up to 48 000 (JA-20 rotor). With other rotors, both speed and centrifugal force vary. Rotors for use in this centrifuge can vary substantially in radius and volume of sample carried. High-speed centrifuges are generally refrigerated but do not achieve a vacuum. In differential centrifugation, the process of cellular fractionation up to the mitochondrial spin is usually performed in a high-speed centrifuge.

Preparative ultracentrifuge A preparative ultracentrifuge (e.g. Beckman L8-80M[®]) is a centrifuge capable of spinning a sample at up to 80 000 rpm, and, depending again upon the rotor radius, at maximal centrifugal forces in the hundreds of thousands $\times g$. Ultracentrifuges spin rotors under vacuum, limiting frictional forces upon the rotor, and are refrigerated. There are numerous rotor types, varying in style and volume, that can be used in an ultracentrifuge. Centrifugal force placed upon an organelle is an important aspect of its fractionation, and, as described earlier, centrifugal force varies with the radius of the circle in which the sample is spun. Since rotors have varying radii, a simple nomogram can be used (Figure 5) to determine the rpm necessary to achieve the same centrifugal force in two different rotors.

Rotors

The rotor used in a protocol is chosen on the basis of the type of centrifugation being performed (e.g. rate zonal or density gradient), the g forces necessary, and the capacity of the rotor tubes. The manufacturer's literature is an excellent source for further information about the specifics of individual rotor types. Three different types of rotors are commonly used in the fractionation of subcellular organelles: swinging-bucket rotors, fixed-angle rotors, and vertical or near-vertical tube rotors (Figure 6). Continuous-flow rotors may also be used for certain large-scale applications.

In fixed-angle or vertical tube rotors, the sample orientation is fixed in space, and the liquid contents reorient during acceleration and deceleration. The angle at which fixed-angle rotors hold the tubes can vary among rotors up to completely vertical in vertical tube rotors. Fixed-angle rotors are excellent for pelleting material, since the pellets move both downward and outward to accumulate in a small restricted zone at the outer base of the tube. Fixed-angle and vertical tube rotors are often used for isopycnic runs. They are capable of superior separation of sample densities because of the large cross-sectional area of material banded, and the change in orientation of the sample during acceleration and deceleration does not

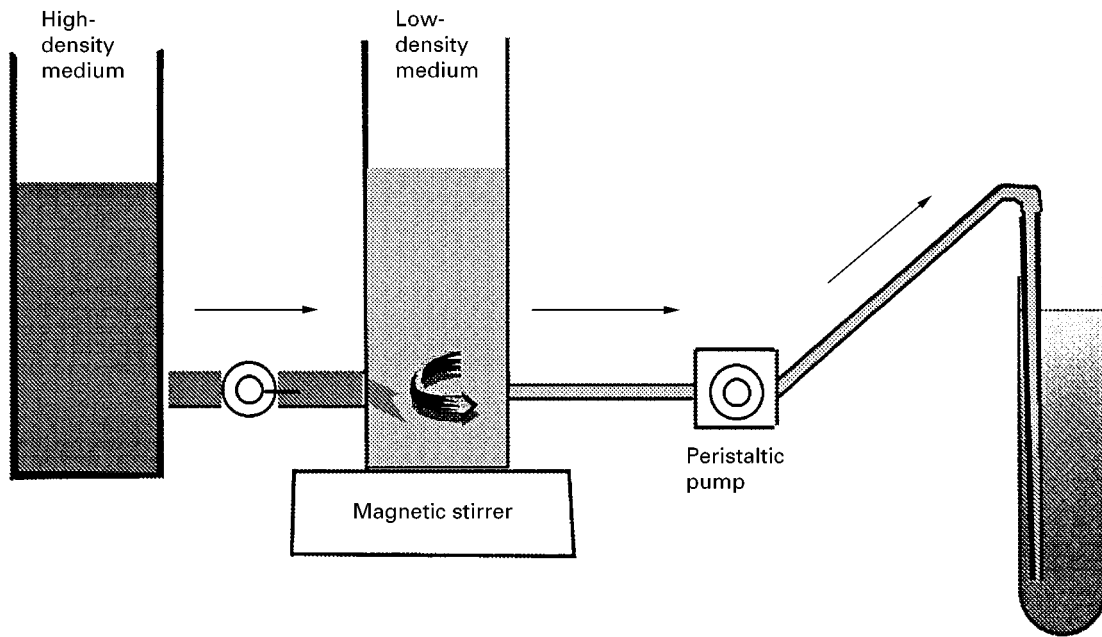


Figure 4 Generation of density gradients. A defined volume of high concentration medium is put in one chamber that is connected through a stopcock with a second chamber. A defined volume of low concentration medium is put in the second chamber. The second chamber contains a mixing bar. Fluid is drawn out of the second chamber into the bottom of the centrifuge tube by gravity or peristaltic pump, and concurrently drawn from the first chamber into the second. The medium concentration thus increases continuously, with the heavier medium displacing the lighter medium upwards as it enters the bottom of the gradient tube. Sample is usually carefully layered in lighter medium on the top of the gradient, with particles travelling to their buoyant density after being subjected to centrifugal force. Samples may be alternatively layered within the central part of the gradient, then organelles travel up or down the gradient to reach their own buoyant density.

appear to affect the relative separation of materials. Fixed-angle and vertical tube rotors can achieve equilibrium more rapidly than swinging-bucket rotors because of the decreased path length, resulting in a much shorter run.

Swinging-bucket rotors are most commonly used for density-gradient centrifugation. In accelerating swinging-bucket rotors, the buckets containing the samples swing outward until horizontal, where they remain for the entire run. They return to their original position on deceleration. Thus the tube is always oriented in the direction of centrifugal force. This effectively reduces artifactual problems introduced by wall effects. Swinging buckets also usually have a relatively long path length, which allows increased spatial separation of the contents. However, this increased resolution of the contents comes at a slight cost in terms of separation time. The volume of the sample which can be applied to the gradient in a swinging-bucket rotor is a function of the cross-sectional area of the tube. If too large a sample volume is applied, there is insufficient radial distance to allow effective separation of the subcellular particles. Similarly, there is a limit on the sample concentration that is effectively applied to a tube; if the concentration is too high, 'streaming' of the sample may result.

Zonal rotors can handle sample sizes of 50 to 100 times that of swinging-bucket rotors and are highly useful for large-scale purification of a variety of different types of particles. These rotors have an internal large cylindrical chamber that is divided into sectors by vanes attached to the central core. There is additionally a rotating seal assembly which allows fluid to be pumped in or out of the cavity while the rotor is spinning. Particles are purified on the basis of their rate-zonal separation. Buffer of known density is pumped in either the central core or at the periphery and fractions are collected exiting through the edge port or at the rotor centre.

Examples of Media Used for Fractionation

Most membrane-bound organelles have a density that is not widely variant from the buffer itself. In addition, the biological nature of most organelles requires that they be maintained in medium that will not alter their biological properties in a way that masks function. This has necessitated the development of media that are consistent with maintaining biological function yet can differentiate buoyant densities that are only marginally different from each

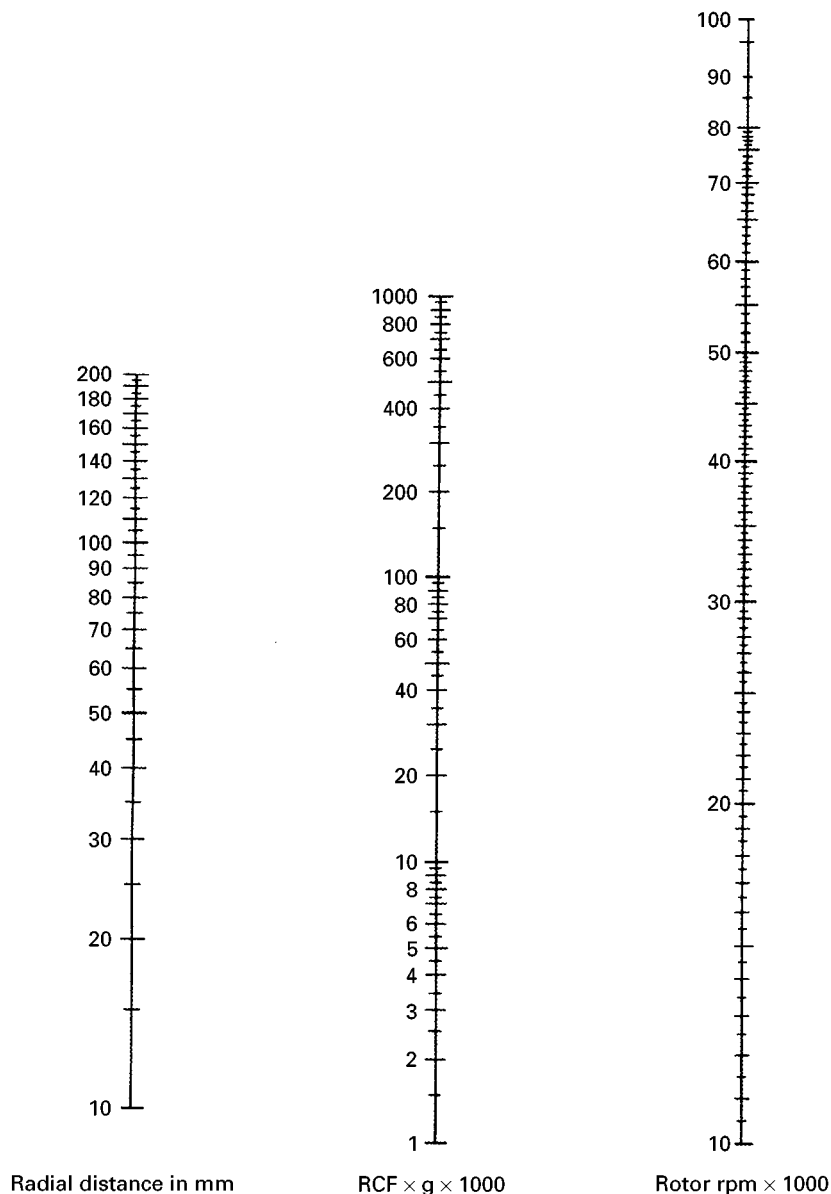


Figure 5 Nomogram. A nomogram is an invaluable diagram which allows one to compute the rpm necessary in order to achieve the same RCF in two rotors with different r values. Use a straight edge to connect the values known in two of the columns, and the appropriate value for the third column can be read where the straight edge intersects it. (Data compiled from *Beckman Rotors and Tubes for Preparative Ultracentrifuges, a User's Manual*, Spinco Business Unit Technical Publications, Palo Alto, CA, USA, 1993.)

other. These media are usually dissolved in neutral, aqueous buffers (phosphate, Tris, etc.) of physiological osmolarity.

A good separation medium (a) can establish a gradient over the appropriate density range, (b) does not affect biological activities of interest, (c) is isosmotic in the presence of sensitive organelles, and (d) does not interfere with assays that may be necessary for the characterization of particular bands. The medium should be easily removable from the sample either by dialysis or by dilution and pelleting of the

band, and the medium material should not bind irreversibly to biological samples. It is further helpful if the medium does not absorb light in the UV or visible range because fractionation of gradients may require monitoring. A last consideration is cost and availability.

Sucrose, sorbitol and, to some extent, cesium chloride are the three media most commonly used for subcellular fractionation. Sucrose and sorbitol are often used because they are fairly neutral, they can be easily removed from the sample of interest by dialysis

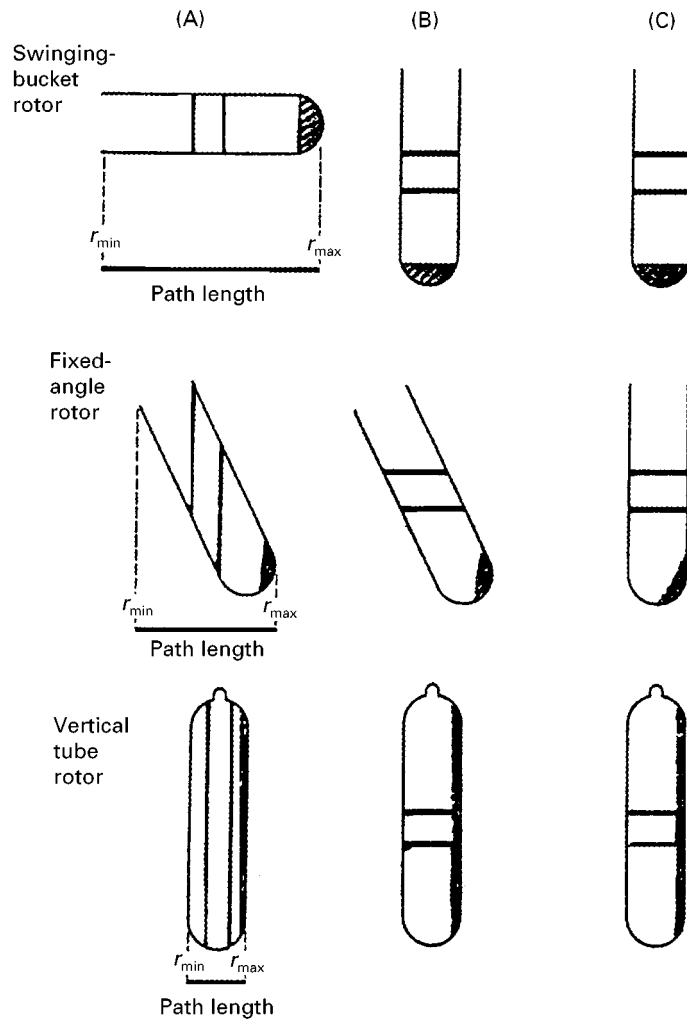


Figure 6 A comparison of gradient samples run in swinging-bucket, fixed-angle, and vertical rotors. This diagram shows the location of sample bands in centrifuge tubes during the centrifugation (A), at rest in the rotor (B), and at rest outside the rotor (C) for each type of rotor commonly used to separate subcellular organelles. Swinging-bucket rotors have the longest path length, can achieve the widest separation of sample bands, and the samples are always oriented in the direction of centrifugal force. Thus, there is little, if any, disruption of the bands. Run lengths, however, are longer because of the increased pathlength. Fixed-angle rotors allow for efficient pelleting within a short time over a shorter path length. Vertical tubes require shortest time for separation as they have a very short path length, and achieve good separation because of the large cross-sectional area of the sample within the tube. However, sample can mix with materials pelleted against the outside wall. (Reprinted as modified with permission from *Beckman Rotors and Tubes for Preparative Ultracentrifuges: a User's Manual*, Spinco Business Unit Technical Publications, Palo Alto, CA, USA, 1993.)

or by dilution and re-centrifugation, and are relatively inexpensive. Cesium chloride is more often used for isolation of macromolecules than organelles, but has the added advantage that it self-generates gradients in a centrifugal field. The refractive index of both sucrose and cesium chloride can be measured with a refractometer, which allows one to determine the actual density of each fraction recovered from a gradient (Tables 2 and 3). Alternatively, use of markers of known buoyant density in control gradients (Pharmacia Density Marker Beads) or oscillating densitometers can be used to determine density.

If osmolarity is a factor, in that the organelle to be separated can be made to swell or shrink in hypo- or hyperosmotic media respectively, a medium that is high in density but composed of extremely large molecules should be chosen, thus increasing density but decreasing osmolarity. Examples of such media are Ficoll® (Pharmacia), a synthetic polymer of copolymerized sucrose and epichlorohydrin of average molecular weight 400 000 daltons, Percoll® (Pharmacia), a colloidal suspension of polyvinylpyrrolidone-coated silica, and Nycodenz® (Nycomed), a non-ionic, tri-iodinated derivative of benzoic acid. All of these media are higher in molecular weight

Table 2 Sucrose density, refractive index and concentration^a

Percentage concentration (w/v)	Density (g mL ⁻¹)	Refractive index	Percentage concentration (w/v)	Density (g mL ⁻¹)	Refractive index
0	0.9982	1.3330	34	1.1463	1.3883
1	1.0021	1.3344	35	1.1513	1.3902
2	1.0060	1.3359	36	1.1562	1.3920
3	1.0099	1.3374	37	1.1612	1.3939
4	1.0139	1.3388	38	1.1663	1.3958
5	1.0179	1.3403	39	1.1713	1.3978
6	1.0219	1.3418	40	1.1764	1.3997
7	1.0259	1.3433	41	1.1816	1.4016
8	1.0299	1.3448	42	1.1868	1.4036
9	1.0340	1.3464	43	1.1920	1.4056
10	1.0381	1.3479	44	1.1972	1.4076
11	1.0423	1.3494	45	1.2025	1.4096
12	1.0465	1.3510	46	1.2079	1.4117
13	1.0507	1.3526	47	1.2132	1.4137
14	1.0549	1.3541	48	1.2186	1.4158
15	1.0592	1.3557	49	1.2241	1.4179
16	1.0635	1.3573	50	1.2296	1.4200
17	1.0678	1.3590	51	1.2351	1.4221
18	1.0721	1.3606	52	1.2406	1.4242
19	1.0765	1.3622	53	1.2462	1.4264
20	1.0810	1.3639	54	1.2519	1.4285
21	1.0854	1.3655	55	1.2575	1.4307
22	1.0899	1.3672	56	1.2632	1.4329
23	1.0944	1.3689	57	1.2690	1.4351
24	1.0990	1.3706	58	1.2748	1.4373
25	1.1036	1.3723	59	1.2806	1.4396
26	1.1082	1.3740	60	1.2865	1.4418
27	1.1128	1.3758	61	1.2924	1.4441
28	1.1175	1.3775	62	1.2983	1.4464
29	1.1222	1.3793	63	1.3043	1.4486
30	1.1270	1.3811	64	1.3103	1.4509
31	1.1318	1.3829	65	1.3163	1.4532
32	1.1366	1.3847	66	1.3224	1.4558
33	1.1415	1.3865	67	1.3286	1.4581

^aData were compiled from the US National Research Council (1933) In Washburn EW (ed.) *International Critical Tables of Numerical Data, Physics, Chemistry and Technology*. New York: McGraw-Hill.

than sucrose, and each has its own intrinsic advantages. Ficoll® is neutral, can achieve concentrations up to 50% covering a density range up to 1.2 g mL⁻¹, and does not penetrate biological membranes. Ficoll® is, however, difficult to remove from the sample by dialysis because of its large molecular weight. Percoll® is non-toxic and can be used over wider density ranges (up to 1.3 g mL⁻¹). Percoll® has the added advantage of being a medium that self-generates gradients in a centrifugal field, and the gradients formed are isosmotic throughout. However, Percoll® has the disadvantage that it is difficult to remove from the sample by dilution and recentrifugation, or by dialysis. In addition, Percoll®, Ficoll® and

metrizamide (similar to Nycodenz®) are precipitated at low pH, eliminating the possibility of purification of protein from samples by acid precipitation. Nycodenz®, with a density range up to 1.4, can be used to effectively fractionate subcellular particles (particularly small ones). Its advantages include its solubility at low pH, its self-forming gradients, and its lack of interference with enzyme assays. Its relatively low molecular weight (821) allows removal by dialysis. All of these media are significantly more expensive than sucrose or sorbitol.

Tables 2–5 provide data concerning density, refractive index, and concentration of different commonly used media.

Table 3 Cesium chloride density, refractive index and concentration^a

Percentage concentration (w/v)	Density (g mL ⁻¹)	Refractive index	Percentage concentration (w/v)	Density (g mL ⁻¹)	Refractive index
1	1.0047	1.3333	34	1.336	1.3657
2	1.0125	1.3340	35	1.350	1.3670
3	1.0204	1.3348	36	1.363	1.3683
4	1.0284	1.3356	37	1.377	1.3696
5	1.0365	1.3364	38	1.391	1.3709
6	1.0447	1.3372	39	1.406	1.3722
7	1.0531	1.3380	40	1.420	1.3735
8	1.0615	1.3388	41	1.435	1.3750
9	1.0700	1.3397	42	1.450	1.3764
10	1.0788	1.3405	43	1.465	1.3778
11	1.0877	1.3414	44	1.481	1.3792
12	1.0967	1.3423	45	1.4969	1.3807
13	1.1059	1.3432	46	1.513	1.3822
14	1.1151	1.3441	47	1.529	1.3837
15	1.1245	1.3450	48	1.546	1.3852
16	1.1340	1.3459	49	1.564	1.3868
17	1.1437	1.3468	50	1.583	1.3885
18	1.1536	1.3478	51	1.601	1.3903
19	1.1637	1.3488	52	1.619	1.3920
20	1.1739	1.3498	53	1.638	1.3937
21	1.1843	1.3508	54	1.658	1.3955
22	1.1948	1.3518	55	1.6778	1.3973
23	1.2055	1.3529	56	1.699	1.3992
24	1.2164	1.3539	57	1.720	1.4012
25	1.2275	1.3550	58	1.741	1.4032
26	1.2387	1.3561	59	1.763	1.4052
27	1.2502	1.3572	60	1.7846	1.4072
28	1.2619	1.3584	61	1.808	1.4093
29	1.2738	1.3596	62	1.831	1.4115
30	1.2858	1.3607	63	1.856	1.4137
31	1.298	1.3619	64	1.880	1.4160
32	1.311	1.3631	65	1.905	1.4183
33	1.324	1.3644			

^aData were compiled from the US National Research Council (1933) In Washburn EW (ed.) *International Critical Tables of Numerical Data, Physics, Chemistry and Technology*. New York: McGraw-Hill.

Table 4 Density and refractive index of Ficoll® solutions^a

Percentage concentration (w/w)	Density (g mL ⁻¹)
0	1.000
10	1.035
20	1.073
30	1.115
40	1.160
50	1.203

^aData computed from manufacturer's literature (Amersham Pharmacia Biotech, Uppsala, Sweden).

Table 5 Properties of Nycodenz® solutions^a

Percentage concentration (w/v)	Molar concentration	Refractive index (20°C)	Density (g mL ⁻¹) (20°C)
0	0	1.3330	0.999
10	0.122	1.3494	1.052
20	0.244	1.3659	1.105
30	0.365	1.3824	1.159
40	0.487	1.3988	1.212
50	0.609	1.4153	1.265
60	0.731	1.4318	1.319
70	0.853	1.4482	1.372
80	0.974	1.4647	1.426

^aData modified from Rickwood D, Ford T and Graham J (1982) *Analytical Biochemistry* 123: 23–31.

Summary

In this review, the principles behind, and the utility of, fractionation of subcellular organelles by centrifugal techniques have been explored. Common methods used, and a review of the advantages and disadvantages of certain experimental tools (centrifuges, rotors, and aqueous media used for fractionation) were also reviewed and tables and graphs useful for designing protocols were also provided.

See also: II/Centrifugation: Large-Scale Centrifugation; Theory of Centrifugation.

Further Reading

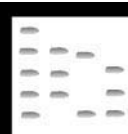
- Alberts B, Bray D, Lewis J, Raff M, Roberts K and Watson JD (1994) *The Molecular Biology of the Cell*, 3rd edn. New York and London: Garland Publishing.
- Chervenka CH and Elrod LH (1972) *A Manual of Methods for Large Scale Zonal Centrifugation*. Palo Alto, CA: Spinco Division of Beckman Instruments, Inc.
- DeDuve C (1964) Principles of tissue fractionation. *Journal of Theoretical Biology* 6: 33–59.

- Griffith OM (1986) *Techniques of Preparative, Zonal, and Continuous Flow Ultracentrifugation*, 5th edn. Palo Alto, CA: Applications Research Department, Spinco Division, Beckman Instruments, Inc.
- Luby-Phelps K (1994) Physical properties of cytoplasm. *Current Opinion in Cell Biology* 6: 3–9.
- McKeithan TW and Rosenbaum JL (1984) The biochemistry of microtubules. A review. *Cell & Muscle Motility* 5: 255–288.
- Mircheff AK (1989) Isolation of plasma membranes from polar cells and tissues: apical/basolateral separation, purity and function. *Methods in Enzymology* 172: 18–34.
- Mircheff AK (1996) Methods and experimental analysis of isolated epithelial cell membranes. In: Wills NK, Reuss L and Lewis SA (eds) *Epithelial Transport: A Guide to Methods and Experimental Analysis*, pp. 190–211. London: Chapman and Hall.
- Pasquali C, Fialka I and Huber LA (1999) Subcellular fractionation, electromigration analysis and mapping of organelles. *Journal of Chromatography B* 722: 89–102.
- Rickwood D, Ford T and Graham J (1982) Nycodenz®: a new nonionic iodinated gradient medium. *Analytical Biochemistry* 123: 23–31.

Field Flow Fractionation

See III/CELLS AND CELL ORGANELLES: FIELD FLOW FRACTIONATION

PAINTS AND COATINGS: PYROLYSIS: GAS CHROMATOGRAPHY



T. P. Wampler, CDS Analytical, Inc.,
Oxford, PA, USA

Copyright © 2000 Academic Press

Because they are complex polymeric materials, usually compounded with coloured or opaque fillers, paints and coatings, especially when dry, pose a difficult analytical problem. Gas chromatography in particular, and mass spectrometry, may seem unlikely tools for the analysis of such materials, but when combined with pyrolysis as a sample introduction technique, they may be used routinely. Via pyrolysis, the polymers used in paints and coatings are fragmented to produce molecules small enough to be compatible with gas

chromatography-mass spectrometry (GC-MS), but still characteristic of the original material. Natural polymers, including plant resins and drying oils, as well as synthetic polymers like polyesters, acrylics and polyurethanes, have been studied extensively, and may be easily differentiated using this technique.

Pyrolysis

The general purpose of paints and coatings is to apply a protective or decorative film of material on to a substrate. The range of materials which may be used to form such a film is extremely wide, as is the range of techniques used to apply it. Soluble materials may be dissolved in a suitable solvent and applied as a thin

coat which produces a film as the solvent evaporates, as in the case of many varnishes and lacquers. On the other hand, materials may be applied which react in place, linking into a complex polymer network. Materials may even be applied as a powder which is subsequently melted into a film. The paint or coating may include many different constituents, both organic and inorganic, to give it the required physical and visual properties, including opacity, flexibility, colour, resistance to water, shine, durability and so on.

Once applied and set, paints and coatings have one characteristic in common: the molecules which comprise the finished product are almost always much too large to be analysed by GC. In fact, chemical analysis of dried paint is a difficult challenge by any technique, since the sample material is such a complex mixture of different polymers, additives, pigments and fillers. Analytical pyrolysis, however, permits the use of GC and MS in the investigation of these materials by breaking the large molecules into fragments small enough to be compatible with these instruments. Samples are typically heated rapidly to temperatures in the range of 600–800°C. At these temperatures, the organic macromolecules undergo bond dissociations based on the relative strengths of the bonds employed in the compound. Consequently, the molecule will fragment in a reproducible way, consistent with the chemistry of the compound, and form products which are directly indicative of the composition. This is true for simple homopolymers such as polystyrene, but also true for complex systems involving multiple monomers and various constituents. Frequently, the small molecules formed include the monomer or monomers of polymers, in addition to indicative products specific for various polymer types.

Instrumentation

The following sections discuss specific types of paints and coatings, with example pyrograms for many of these types. Unless indicated in the figure legends, all of the chromatograms were produced using the instrument parameters described here.

Pyrolysis

Samples were pyrolysed using a platinum coil filament autosampler (model 2500 autosampler, CDS Analytical Inc, Oxford, PA, USA). Approximately 100 µg of sample material was placed into a quartz tube and held in place using quartz wool. The samples were placed online with the GC carrier flow, and then heated to the indicated temperatures for the specified times, typically 750°C for 15 s.

Gas Chromatography–Mass Spectrometry

A model 6890 (Hewlett-Packard, Wilmington, DE) gas chromatograph was equipped with a HP-5 column (30 m long, 0.25 mm diameter, 0.25 µm film) operated with a 75:1 split ratio and helium as the carrier gas, in the constant pressure mode at 5.9 psi. The oven initial temperature was 40°C for 2 min, then programmed at 6°C min⁻¹ to 300°C, held for 5 min. A mass selective detector (model 5972A, Hewlett-Packard, Wilmington, DE) provided the mass spectra. Scans were taken at a rate of 2.4 s⁻¹ over the mass range of 35–550.

Paints and Varnishes

Varnishes

Clear, decorative or protective finishes are formulated and applied in a variety of ways. A varnish may be as simple as a plant resin (such as mastic, sandarac or dammar) or shellac (secreted by insects) dissolved in a solvent. A film of the solid organic material is left on the surface of the object varnished after the solvent evaporates. More likely, the formula includes drying oils – unsaturated fatty acids which polymerize when exposed to air – plus natural or synthetic resins, thinners and other additives. When pyrolysed, the dried varnish film creates indicative molecules from the various constituents, revealing much about its composition. The natural resin dammar, for example, is comprised extensively of triterpenes, made from three terpene units or six isoprene units. When pyrolysed, dammars generate chromatograms (pyrograms) showing groups of terpenes, as do the other plant resins used in making varnishes. **Figure 1** is a pyrogram of Kremmer dammar, which was heated to 650°C for 15 s. The peaks at about 25 min are sesquiterpenes, having three isoprene units, and the materials eluting at about 45 min are diterpenes (two terpene or four isoprene units). Other terpenoid resins used in making varnishes behave in a similar way, producing characteristic chromatograms permitting them to be differentiated. By contrast, when shellac is pyrolysed, it reveals a mixture of complex fatty acids, esters and olides, as shown in **Figure 2**.

Polyurethanes are formed from the reaction of a diisocyanate with a di- or polyfunctional alcohol. When pyrolysed, the most characteristic material formed is the regeneration of the diisocyanate. This is the case whether the polyurethane is a foam rubber-type polymer, or used as part of a paint or varnish. Hexane diisocyanate and toluene diisocyanate (TDI) are two commonly used polyurethane constituents, but others, both aromatic and aliphatic, are encountered as well. **Figure 3** is a pyrogram obtained by

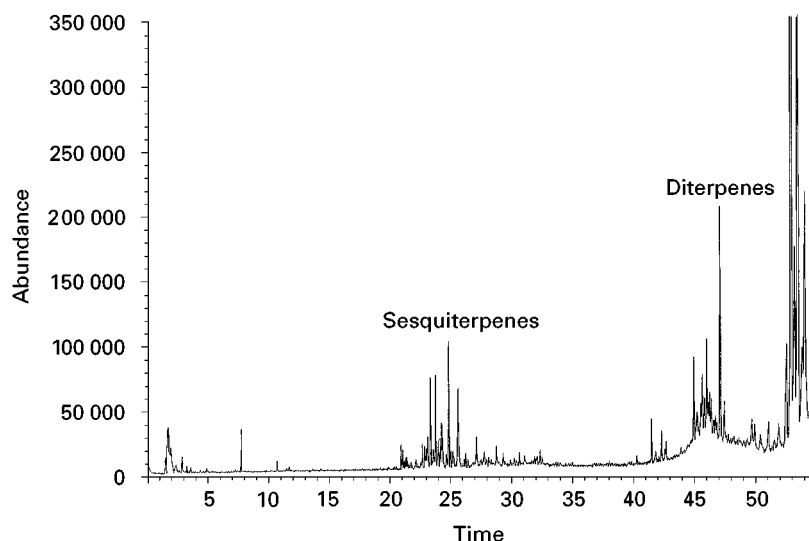


Figure 1 Kremmer dammar pyrolysed at 650°C for 15 s.

heating a sample of a polyurethane film to 700°C for 20 s, in which the large peak at 21 min is identified as TDI.

Oil finishes, based on large amounts of drying oils, are popular for furniture. Tung oil in particular is high in C₁₈ polyunsaturated fatty acids, which polymerize when exposed to oxygen. Pyrolysis products from pure tung oil include some of the unsaturated acids, plus hydrocarbons, both aromatic and aliphatic, formed from the long chain of the acid. Commercial tung oil finish products are likely to contain other polymerizing agents as well. **Figure 4** shows the pyrogram of a recently dried film produced from a commercial tung oil product. The peaks at 32 and 36 are unsaturated fatty acids seen in pure tung oil, but there is also a peak at 21 min marked T,

which is TDI, showing that this product incorporated polyurethane as well. Exterior waterproofing finishes may also incorporate drying oils, and other things as well. The pyrogram shown in **Figure 5**, from a wood waterproofing product, reveals both long chain fatty acids (for example, the largest peak at 37 min) as well as a series of hydrocarbons eluting from 38 to 45 min.

House Paints

Alkyd Glyceryl phthalate polyesters have been used for many years to make paints for a wide range of uses, including interior and exterior housepaint. The reaction of the difunctional acid and the polyfunctional alcohol creates the polyester film. When pyrolysed, the ester linkage of the polyester is cleaved,

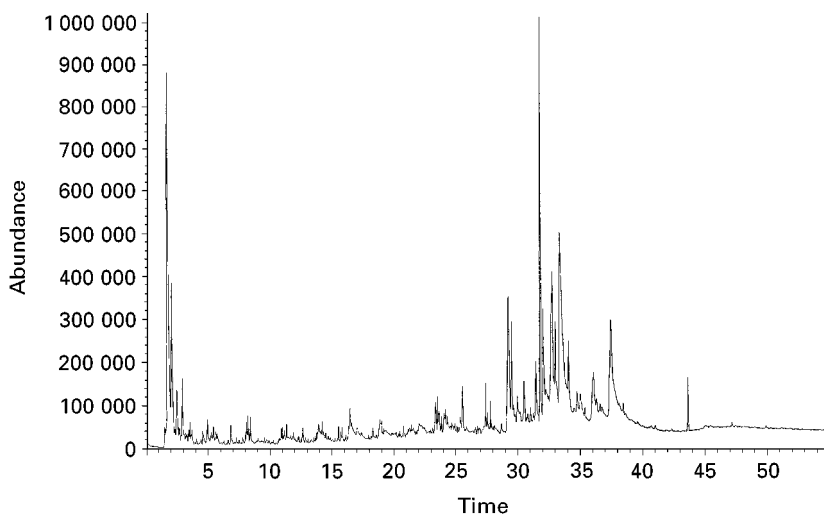


Figure 2 Pyrolysis of shellac at 700°C for 15 s.

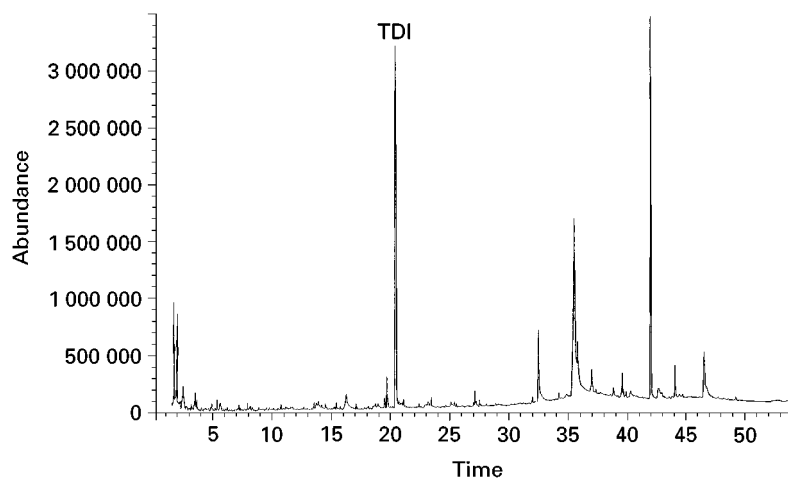


Figure 3 Pyrolysis of a polyurethane film at 750°C for 20 s. TDI at about 21 min is toluene diisocyanate.

resulting in the formation of phthalic anhydride, the characteristic pyrolysate for these paints. An example of this is shown in **Figure 6**, produced from a light green interior semi-gloss trim paint. The large peak at 20 min is phthalic anhydride, the most abundant pyrolysis product. Smaller constituents elute before this peak, mostly oxygenated degradation products from the alcohol portion of the polyester. In addition, peaks are generated from the drying oils in the formulation, in this case eluting at about 33 min (C_{16}) and a small peak at 36 min (C_{18}).

Latex Latex housepaints are substantially different. These water-based emulsions are almost always formulated using a variety of different polymers

and copolymers, offering an essentially unlimited range of formulations. Typical polymers used include polyvinylacetate (PVA), polymethylmethacrylate (PMMA), polystyrene and polybutylacrylate (PBA) as well as higher acrylics. When pyrolysed, many of these polymers regenerate sufficient monomer to be identified in the pyrolysate. This is true for PMMA, polystyrene, PBA and other acrylates and especially for methacrylates. Acrylates, like PBA, and polystyrene also produce higher oligomers, especially the dimer and trimer. In cases of copolymers, there may be mixed dimers and trimers as well, if the different monomers are part of the same polymer chain. PVA, however, does not produce monomer. Because of the relative bond weakness, acetic acid is split from the

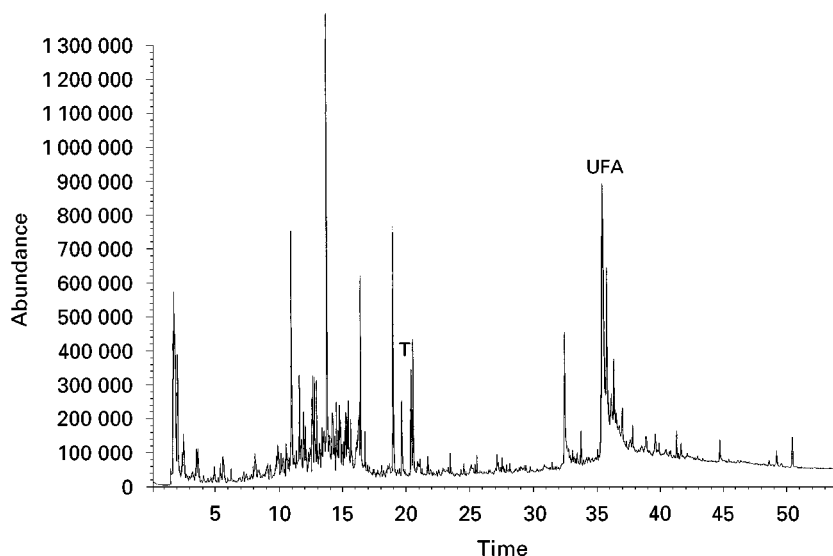


Figure 4 Pyrolysis of dried tung oil finish. Peak labelled T is toluene diisocyanate; UFA is a C_{18} unsaturated fatty acid.

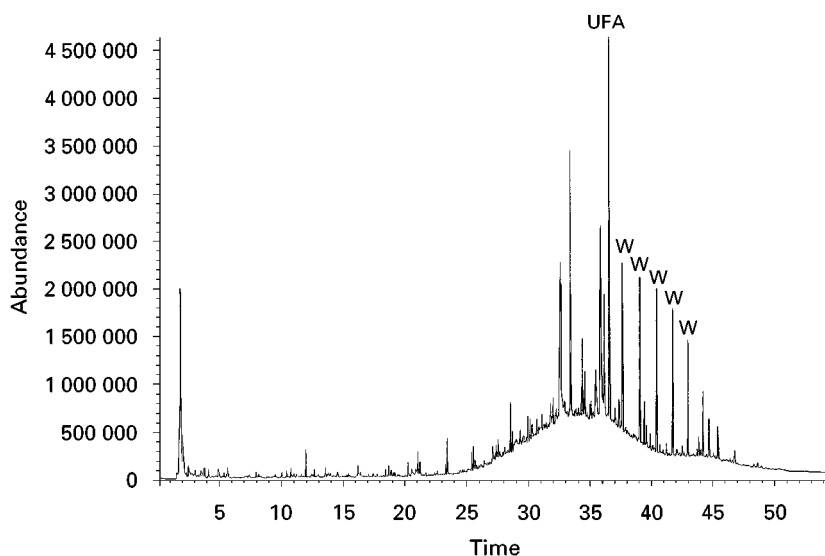


Figure 5 Pyrolysis of a waterproofing film at 750°C for 20 s. Peak marked UFA is a C₁₈ unsaturated fatty acid. The peaks marked with a W are from a hydrocarbon wax.

polymer backbone before the chain is broken. As the acetic acid leaves the polymer, the backbone becomes highly unsaturated. Consequently, when the chain finally does break, it generates aromatics. Therefore, instead of vinyl acetate monomer, the pyrolysis products include acetic acid, benzene, toluene and other substituted aromatics.

The pyrogram of a flat green latex wall paint shown in **Figure 7** illustrates much of this. The paint is largely PVA, as shown by the large acetic acid peak eluting at about 3 min. Peak number 2 is one of the aromatics formed from the PVA chain (toluene). In

addition, the paint included styrene and butyl acrylate, which elute at about 8 min. The white latex analysed in **Figure 8** is significantly different. For this paint, the largest peak is styrene, with the amounts of styrene and butyl acrylate both substantially increased relative to the PVA, and therefore dimers and trimers of these monomers may be seen eluting later in the chromatogram. In addition, there is a peak for methyl methacrylate as well.

Spray paint The flat black, indoor/outdoor spray paint shown in **Figure 9** was deposited from a spray

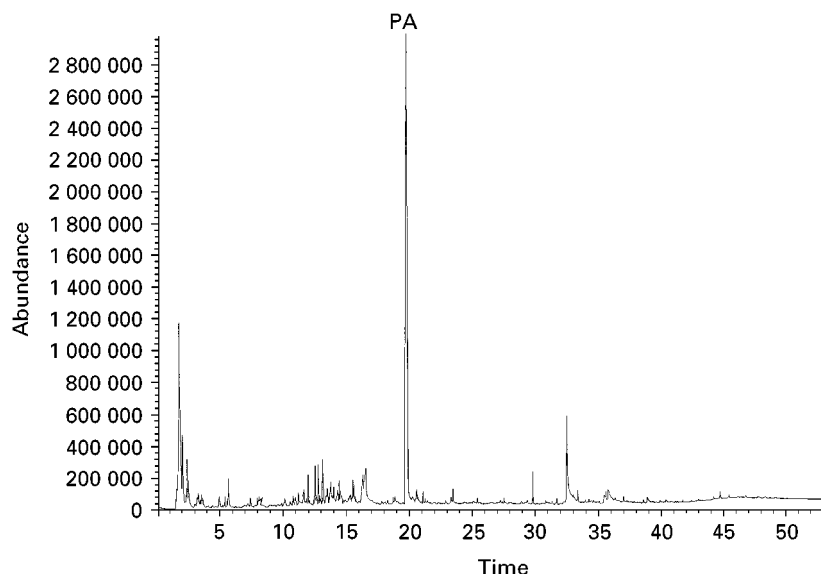


Figure 6 Pyrogram of a glyceryl phthalate alkyd housepaint. The peak labelled PA is phthalic anhydride.

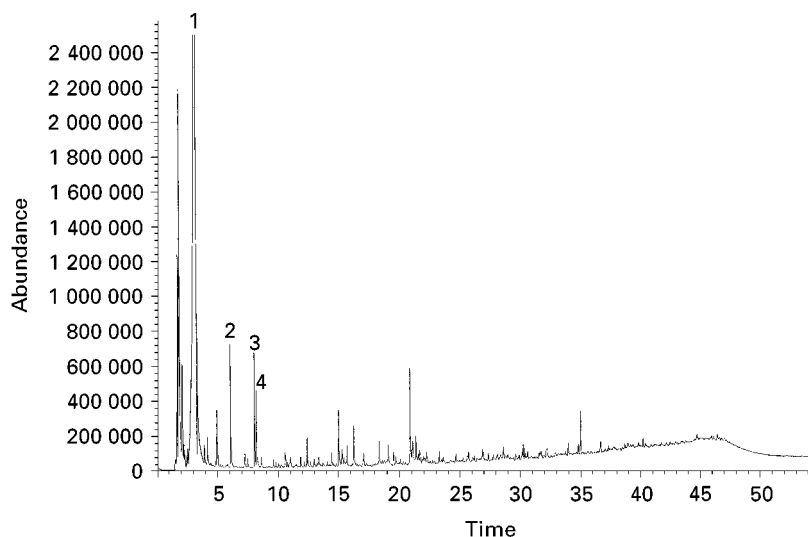


Figure 7 Pyrolysis of a latex paint at 750°C. 1, Acetic acid (from PVA); 2, toluene; 3, styrene; 4, butyl acrylate.

which contained acetone and xylenes. In fact, the peak at about 7 min is a xylene, probably retained in the paint matrix and released as the sample was heated. The pyrogram shows methyl methacrylate (4 min) phthalic anhydride (20 min) and a series of peaks between 32 and 37 min derived from drying oils, especially a C_{18} fatty acid.

Beverage container paint The paint pyrolysed to produce the chromatogram in **Figure 10** was scraped from an aluminium can which contained a carbonated soft drink. The paint was formulated using mostly methyl methacrylate, with some butyl acrylate and a little styrene.

In all of the paint examples here, only the major polymer constituents have been stressed. Paints, of course, contain many other ingredients, such as stabilizers, catalysts, solvents and additives, and peaks from some of these may appear in the chromatogram. In addition, there are pigment and materials to make the paint opaque. Many of these are inorganic, and although they may be present in large quantities (for example, TiO_2), their presence rarely affects the progress of the pyrolysis in creating identifiable fragments from the polymers.

Automotive paints Through the 1950s, automobile paints were likely to be glyceryl phthalate polyesters.

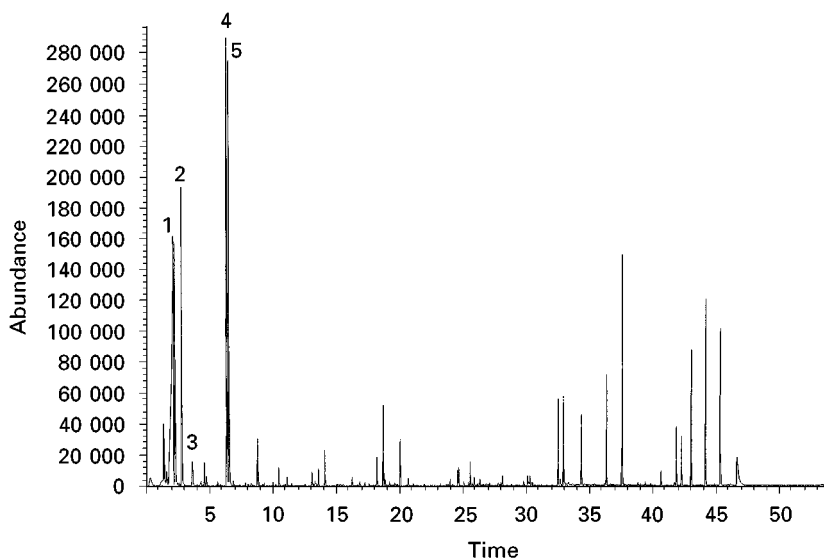


Figure 8 Pyrogram of latex paint at 700°C. 1, Acetic acid; 2, methyl methacrylate; 3, toluene; 4, styrene; 5, butyl acrylate.

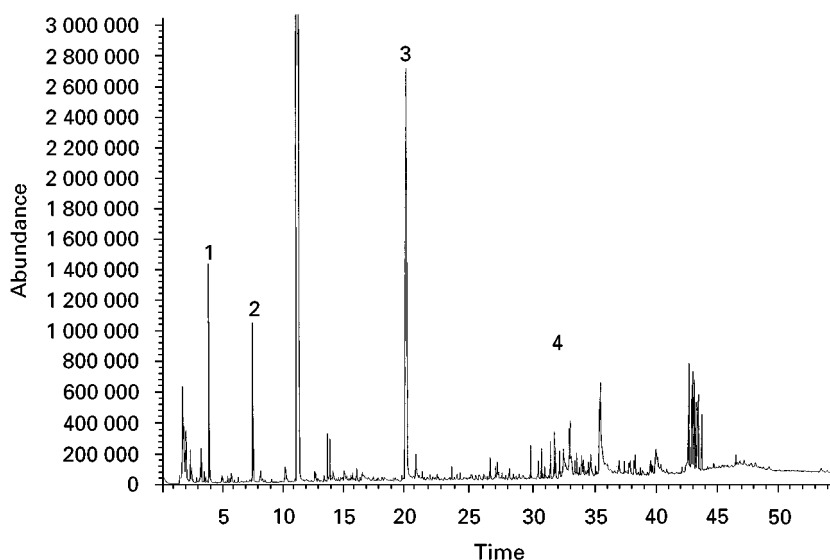


Figure 9 Pyrolysis of a flat black spray paint. 1, Methyl methacrylate; 2, xylene; 3, phthalic anhydride; 4, drying oils.

As described above, these phthalate polyesters pyrolyse to produce a characteristic peak for phthalic anhydride, plus other small molecules from the polymer. To control shrinkage and provide flexibility, plasticizers were added to these paints, generally in the form of a phthalate ester. When the paint sample is pyrolysed, it is typical to find that the plasticizer has been volatilized intact, and consequently it shows up in the pyrogram as well, even though strictly speaking it is a thermally desorbed molecule, not a pyrolysis product. This can be seen in the pyrogram shown in **Figure 11**. The paint is a black du Pont product used on a 1955 Chevrolet, and the sample pyrogram it produced has a large peak for phthalic anhydride at

about 19 min, and peak for the plasticizer (dibutyl phthalate) at 31 min. In the 1960s these paints were replaced with other formulations, initially using mostly PMMA with a phthalate plasticizer. In the 1970s other monomers were added to the mix, including styrene, butyl acrylate and butyl methacrylate. Since polymers using these monomers produce significant amounts of monomer when pyrolysed, pyrograms of such an automotive finish look like the example in **Figure 12**, where peak 1 is methyl methacrylate, 2 is styrene, 3 is butyl acrylate, 4 is butyl methacrylate and 5 is butyl benzyl phthalate.

It must be pointed out that automotive finishes may be very complex systems, incorporating multiple

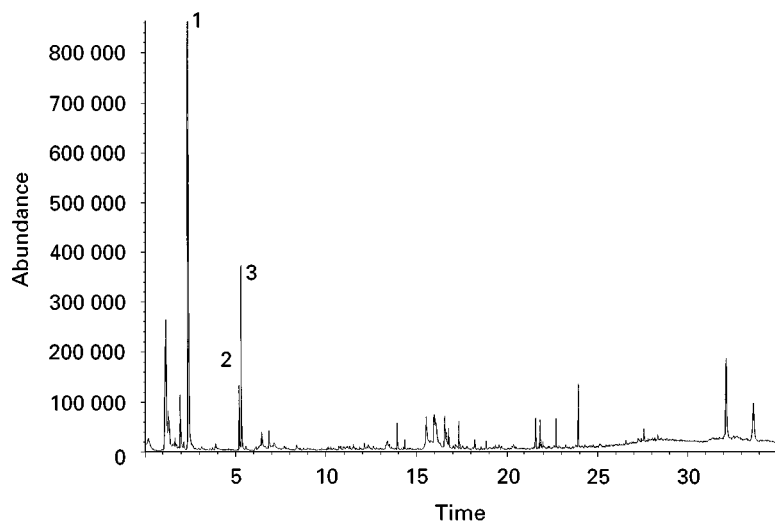


Figure 10 Paint from an aluminum soda can. 1, Methyl methacrylate; 2, styrene; 3, butyl acrylate. GC programme 40°C for 2 min, then 10°C min⁻¹ to 300°C.

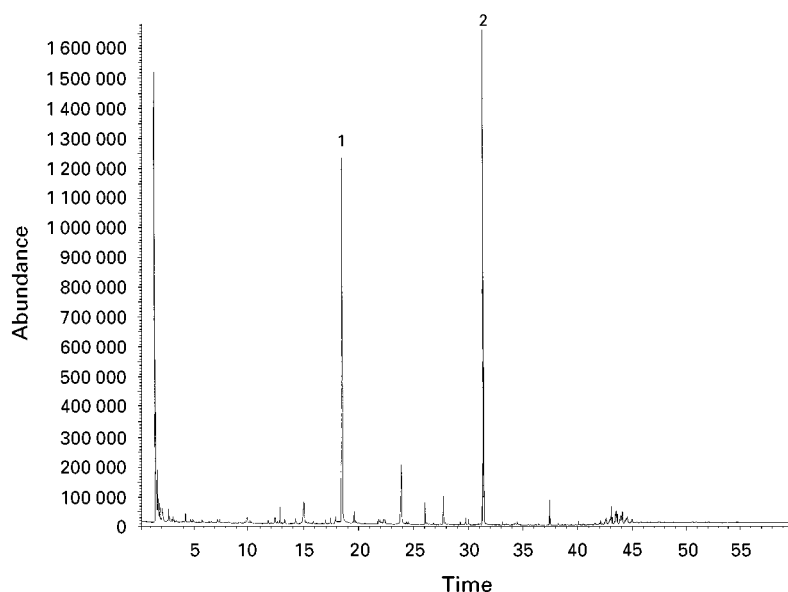


Figure 11 Paint from a 1955 black Chevrolet. 1, Phthalic anhydride; 2, dibutyl phthalate, a plasticizer.

layers, each of which is probably a different paint formulation. Further, these layers may be cross-linked with specific reagents, filled, coloured, etc. The examples shown here will deal primarily with the polymer composition of the paints, but information is frequently present concerning additives, especially plasticizers and light stabilizers, as well.

In an effort to reduce the amount of solvent vented to the air when a car is painted, manufacturers have developed paints with a higher solids load (and consequently less solvent per application). These paints are usually solutions of smaller polymer molecules, which

are linked together during drying to form larger, cross-linked polymers. The standard monomers (methyl methacrylate, styrene, butyl acrylate, butyl methacrylate) are still used, but others are added to provide sites for cross-linking. These are frequently hydroxy compounds, and the OH functionality is used to form urethane, epoxy or other bonds during cross-linking. Hydroxyethyl methacrylate and hydroxypropyl methacrylates are used in the paint polymer chain to provide these sites. When paints incorporating the hydroxy methacrylates are pyrolysed, these monomers are produced just as the others are, and the pyrogram looks like

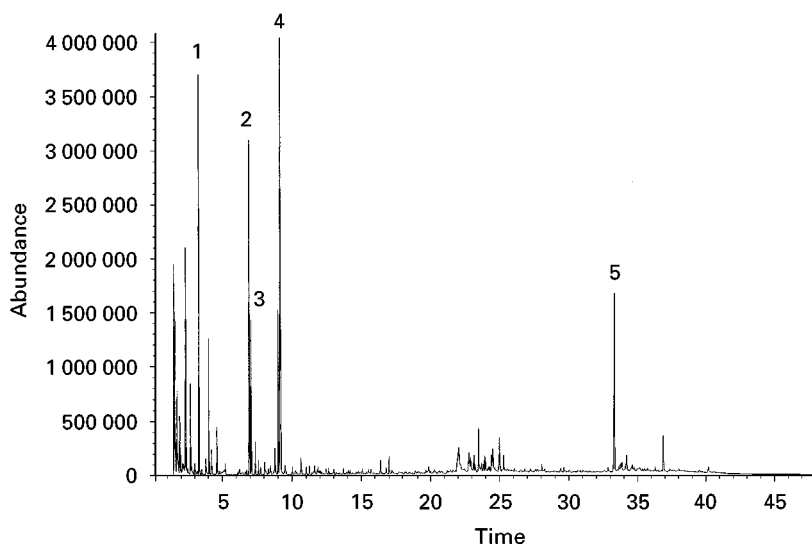


Figure 12 Pyrogram of automobile paint including multiple monomers. 1, Methyl methacrylate; 2, styrene; 3, butyl acrylate; 4, butyl methacrylate; 5, butyl benzyl phthalate (plasticizer).

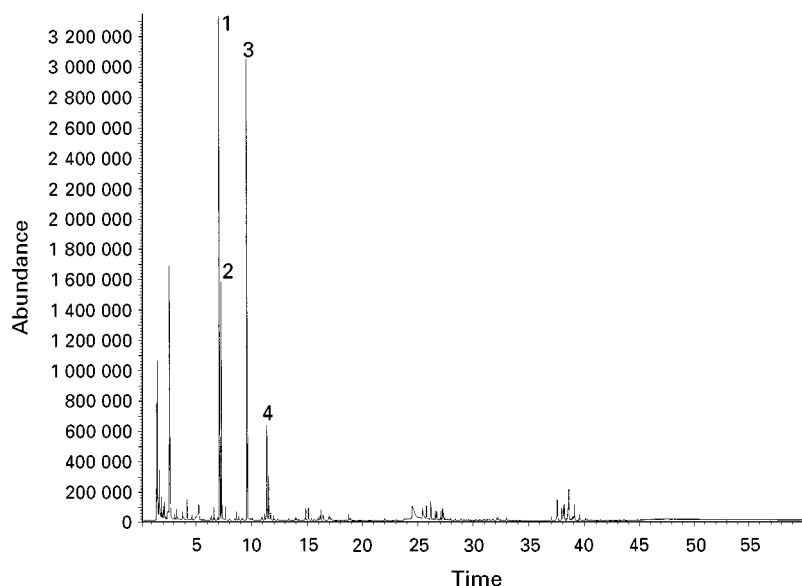


Figure 13 Pyrolysis of black acrylic enamel car finish. 1, Styrene; 2, butyl acrylate; 3, butyl methacrylate; 4, hydroxy propyl methacrylate.

Figure 13, in which styrene (peak 1), butyl acrylate (2) and butyl methacrylate (3) are major pyrolysis products. Peak 4 is 2-hydroxy propyl methacrylate, a common monomer added to provide cross-linking sites.

It is not unusual to see evidence of other polymers and polymer constituents in automotive finishes, either as the cross-linkers or from one of the many paint layers. Urethanes and epoxies are frequently used, and the characteristic compounds from these materials are frequently identifiable. The paint shown in **Figure 14** employed a urethane in addition to the monomers already discussed. When pyrolysed, it re-

veals methyl methacrylate, styrene, butyl acrylate and butyl methacrylate (peaks 1–4 in the pyrogram) and also shows TDI (peak 5 at about 17 min). Epoxies are frequently made using bisphenol A, which is regenerated on pyrolysis and provides a good indicator. The very complex pyrogram of a 1993 red car paint shown in **Figure 15** includes a peak at 31 min for bisphenol A, evidence of an epoxy formulation, in addition to standard monomers and a large peak of phthalic anhydride at about 17 min.

As a further step in improving the performance of automotive finishes, manufacturers are incorporating

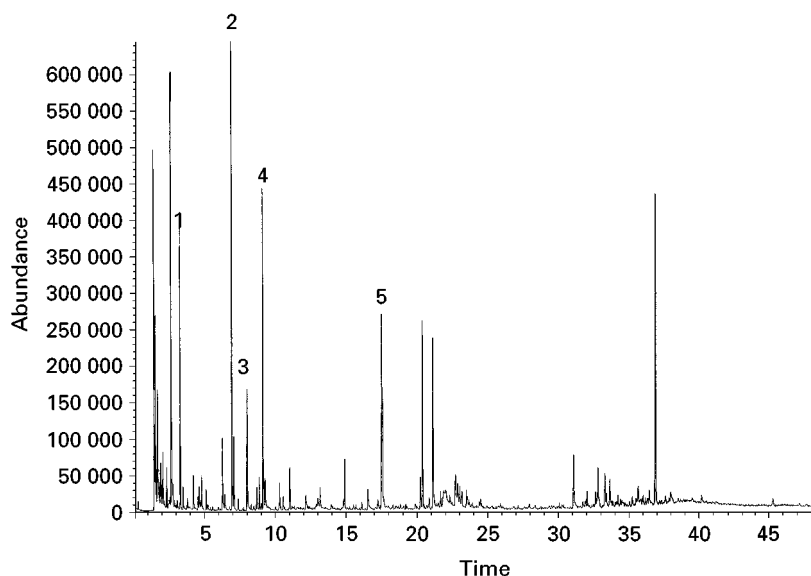


Figure 14 Pyrogram of automotive finish including urethane bonds. 1, Methyl methacrylate; 2, styrene; 3, butyl acrylate; 4, butyl methacrylate; 5, toluene diisocyanate (TDI).

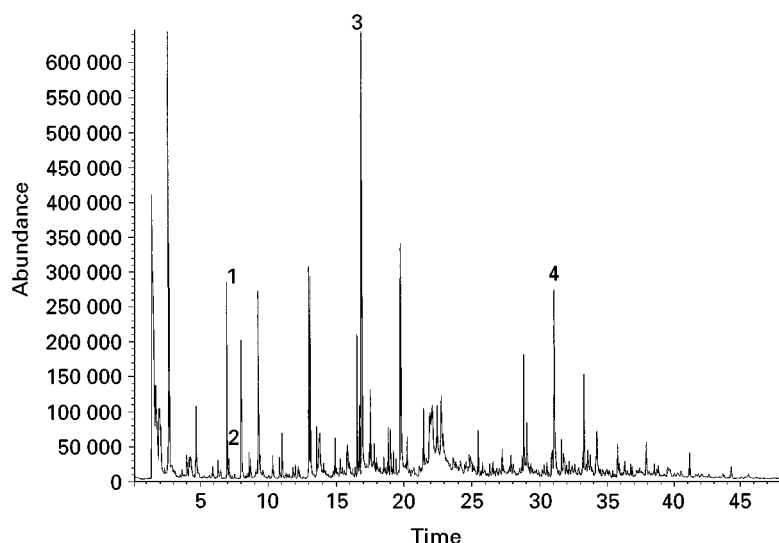


Figure 15 Read automobile paint with epoxy constituents. 1, Styrene; 2, butyl acrylate; 3, phthalic anhydride; 4, bis-phenol A (from epoxy).

the plasticizing agents into the polymer itself, instead of using an additive like a phthalate ester. Consequently, pyrograms of paints produced in the 1990s are likely to show no phthalate plasticizers, but to have peaks for long chain methacrylates instead. These methacrylates with long aliphatic substituents become part of the paint polymer, with the aliphatic tail providing flexibility in a way which will not be lost from the polymer by evaporation. **Figure 16** shows a pyrogram of a paint which used a substantial amount of styrene (1), made flexible by the addition of octyl methacrylate (2) which elutes at about 17 min, and is the largest peak in the chromatogram.

Paper Coatings

Papers are coated with a variety of polymeric materials to provide qualities such as gloss for magazines and waterproofing for food packaging, in addition to decorative and functional uses of inks and toners from printers and photocopiers. Although it is sometimes difficult to separate the coating from the paper fibres, this may not be required for many analyses. This is because the polymer coating and the paper will be pyrolysed essentially independently of each other, and the resulting pyrogram will contain information about each of the constituents. The pyrolysis products of cellulose are well documented, and consist of many oxygenated materials such as furans,

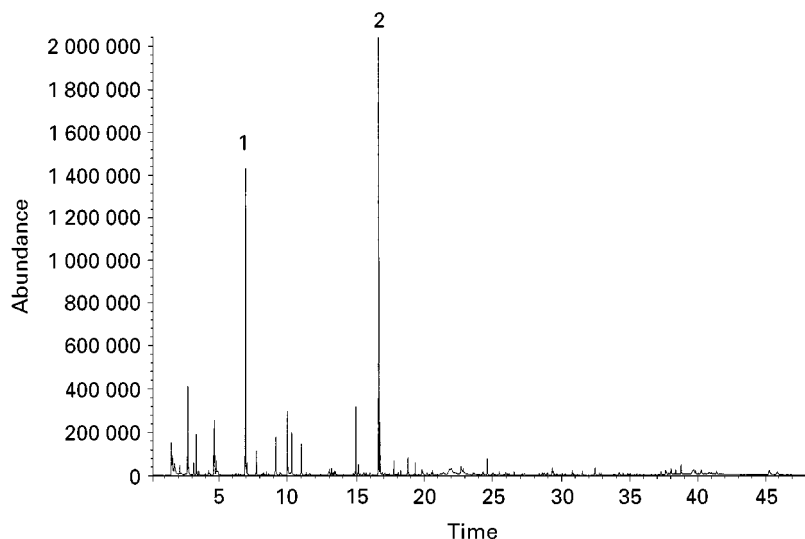


Figure 16 Automobile paint with long alkyl chain methacrylate. 1, Styrene; 2, octyl methacrylate.

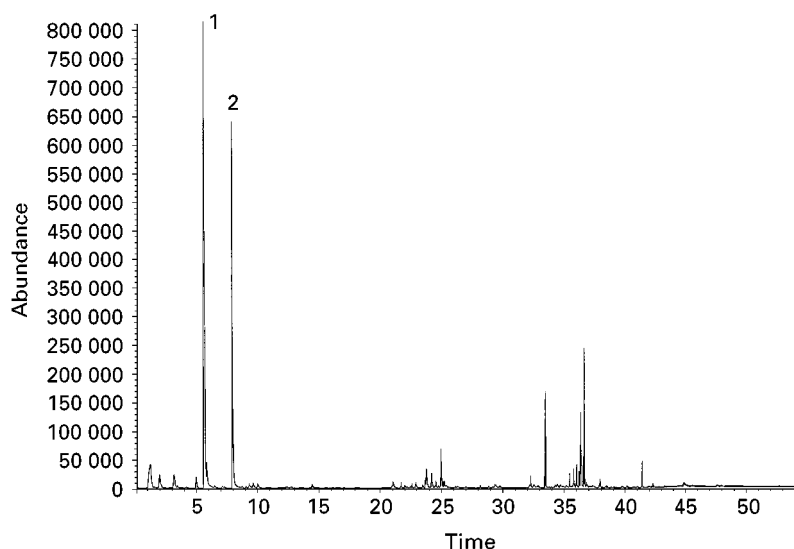


Figure 17 Coating for freezer carton. 1, Styrene; 2, α -methyl styrene.

plus levoglucosan, whereas the products from most coatings include monomers like styrene, acrylics and hydrocarbons, so differentiating them is generally straightforward. **Figure 17**, for example, shows the products of pyrolysing a coating used on cardboard boxes made for storing frozen foods. The two large peaks, eluting at about 6 and 8 min, are styrene and α -methylstyrene, respectively. When a piece of a box coated with this polymer is pyrolysed, the result is the pyrogram shown in **Figure 18**. Most of the peaks are cellulose pyrolysates, including furancarboxaldehyde (1), hydroxymethylfurancarboxaldehyde (4) and levoglucosan (5). The monomers styrene and α -methylstyrene, however, are superimposed on the cellulose products, and are seen as peaks

2 and 3. The furans, especially furancarboxaldehydes and levoglucosan, are reliable markers for cellulose and should be seen in any paper, coated or not.

In **Figure 19** they can be seen again, this time from a piece of glossy magazine paper. Since the paper is thinner than the cardboard box, the relative amount of the coating is larger here, and the polymer constituents forming the glossy finish show up readily. In this case, the coating is a copolymer of styrene, butadiene and methyl methacrylate, and each of the monomers represents one of the major peaks in the pyrogram.

Polyolefins are frequently used as coatings or laminates on to papers for a variety of purposes. The

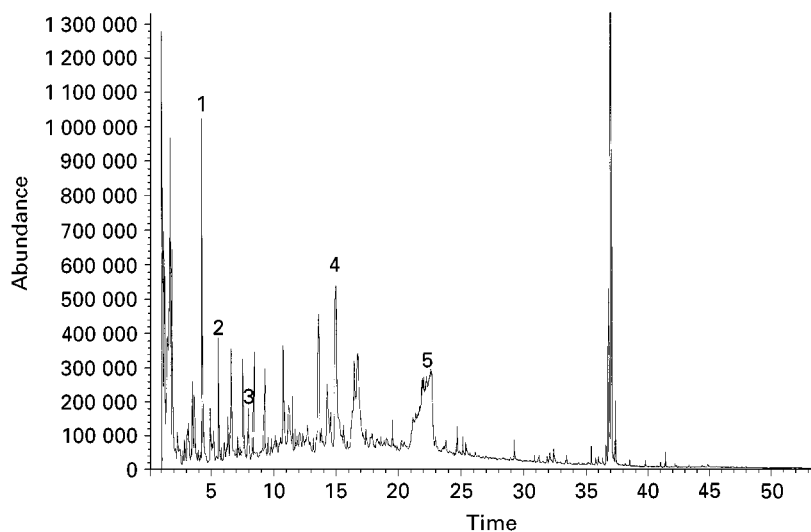


Figure 18 Pyrolysis of cardboard with coating shown in **Figure 17**. 1, Furancarboxaldehyde; 2, styrene; 3, α -methylstyrene; 4, hydroxymethylfurancarboxaldehyde; 5, levoglucosan.

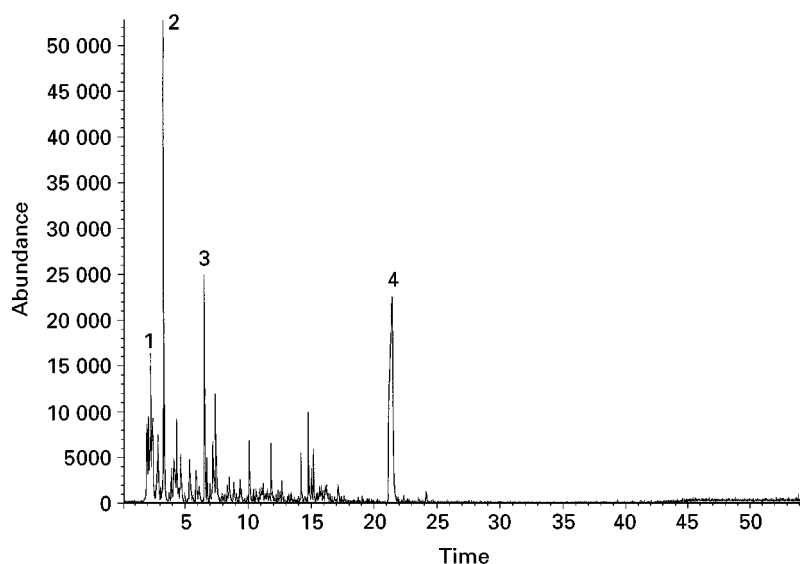


Figure 19 Pyrogram of a piece of glossy coated paper stock. 1, Butadiene; 2, methyl methacrylate; 3, styrene; 4, levoglucosan.

glossy coating on a photograph is likely to be polyethylene, as is the protective film on paper used as freezer-wrap. When polyethylene is pyrolysed, it is broken into many long chain hydrocarbons, including alkanes, alkenes and dienes. These polymer fragments elute in a series of triplet peaks, making a characteristic pattern for polyethylene. When a piece of paper coated with polyethylene is pyrolysed, the cellulose peaks are again seen, co-eluting with the polyethylene hydrocarbon fragments. **Figure 20** shows an example of this, being the pyrogram of a piece of coated freezer paper. Most of the larger peaks before 18 min are from cellulose, and the poorly shaped peak at 22 min is levoglucosan. All of the

triplet peaks, including the one at 18 min and almost everything after 24 min, are normal hydrocarbons indicative of polyethylene pyrolysis.

Glass surfaces are also frequently covered with a coating, such as a silk screen ink for decorative pieces, a film for colouring or shading, or a layer to provide a working surface. **Figure 21** shows an interesting application of glass coating, in which laboratory glass slides were coated with a Teflon material to create wells for aqueous reagents. When Teflon is pyrolysed, it reverts almost entirely to monomer, tetrafluoroethylene. The coating which had been applied to the glass consisted largely of Teflon, plus a styrene/ethyl acrylate copolymer. When pyrolysed,

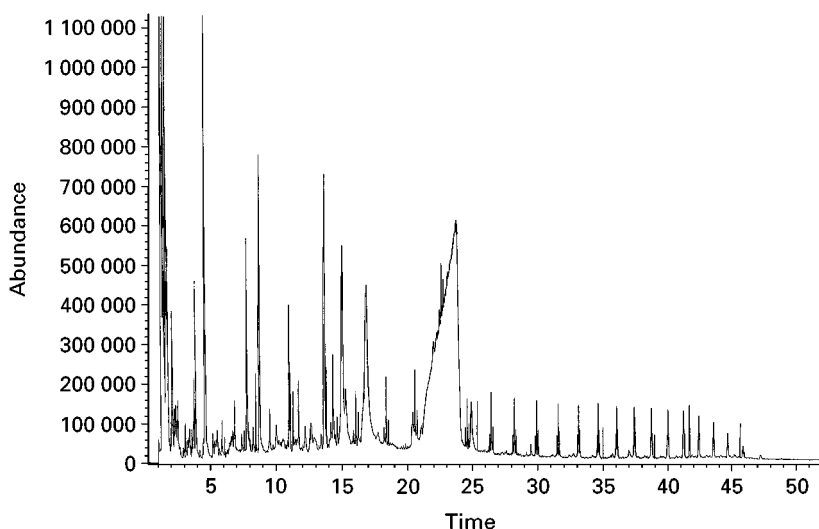


Figure 20 Pyrolysis of freezer paper (polyethylene-coated cellulose paper) at 750°C for 15 s.

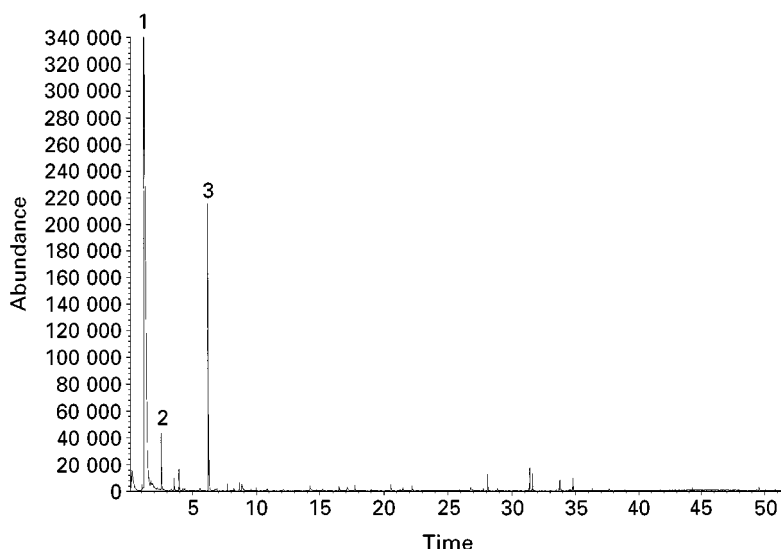


Figure 21 Coating applied to glass, pyrolysed at 750°C for 20 s. 1, Tetrafluoroethylene; 2, ethyl acrylate; 3, styrene.

a simple chromatogram results, revealing peaks for all three monomers, tetrafluoroethylene, ethylacrylate and styrene.

Future Developments

The development of more complex, specialty or high performance coatings will reinforce the need for detailed analysis in both quality control and product development laboratories. Pyrolysis-capillary GC-MS should become increasingly relied upon to unravel these complex polymer matrices. The development of fast GC techniques will do much to expand the use of this technique, since the time required to produce a well resolved pyrogram is perhaps the greatest drawback. The introduction of several automated systems for pyrolysis-GC-MS has already made the technique routine, enhancing reproducibility and efficiency of instrument use.

See also: II/Chromatography: Gas: Detectors: Mass Spectrometry; Pyrolysis Gas Chromatography. III/Art Conservation: Use of Chromatography in.

Further Reading

Blazso M (1997) Review: Recent trends in analytical and applied pyrolysis of polymers. *Journal of Analytical and Applied Pyrolysis* 39: 1.

Brauer GM (1970) Pyrolysis-gas chromatographic techniques for polymer identification. In: Slade PE and Jenkins LT (eds) *Techniques and Methods of Polymer Evaluation*, vol. II, p. 41. New York: Marcel Dekker.

Irwin WJ (1982) *Analytical Pyrolysis: A Comprehensive Guide*. New York: Marcel Dekker.

Liebman SA and Levy EJ (eds) (1985) *Pyrolysis and GC in Polymer Analysis*. New York: Marcel Dekker.

Shedrinsky AM, Wampler TP and Baer NS (1988) The identification of dammar, mastic, sandarac and copals by pyrolysis gas chromatography. *Wiener Berichte uber Naturwissenschaft in der Kunst* 4(5): 12.

Simonsick WJ (1992) Mass spectrometric techniques for coatings characterization. *Analysis of Paints and Related Materials: Current Techniques for Solving Coating Problems*, pp. 22-38. Standard Technical Publication 1119. American Society for Testing and Materials.

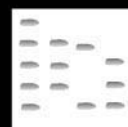
Voorhees KJ (ed.) (1984) *Analytical Pyrolysis Techniques and Applications*. London: Butterworths.

Wampler TP (ed.) (1995) *Applied Pyrolysis Handbook*. New York: Marcel Dekker.

Wampler TP, Bishea GA and Simonsick WJ (1997) Recent changes in automotive paint formulation using pyrolysis-gas chromatography/mass spectrometry for identification. *Journal of Analytical and Applied Pyrolysis* 40(14):79.

Wheals BB (1980) Analytical pyrolysis techniques in forensic science. *Journal of Analytical and Applied Pyrolysis* 2: 277.

PARTICULATE CHARACTERIZATION: INVERSE GAS CHROMATOGRAPHY



D. Butler and D. R. Williams, Surface Measurement Systems, London, UK

Copyright © 2000 Academic Press

Introduction

Inverse gas chromatography (IGC) represents a unique refinement of a classic chromatographic method in which an unknown solid material such as a powder, fibre or film may be characterized. By reversing the traditional role of unknown mobile phases and known reference stationary phases, the gas-solid chromatographic retention processes may be used to characterize an unknown particulate sample by eluting a series of known gas or vapour molecules through a column packed with the sample materials. IGC is the only chromatographic technique in which a solid-state material may be characterized in its native state. Despite the fact that over 500 papers have been published over the last 8 years using IGC, the technique is still not well known nor well appreciated by many scientists. However, this article will highlight the opportunities that IGC offers for surface and materials characterization generally as well as briefly reviewing the principles and main IGC methodologies. Finally, recent trends in material characterization applications will be briefly reviewed.

History

The intrinsic relationship between gas-solid chromatography and the adsorption isotherm was established by a number of workers starting in the 1940s and going through the 1950s. Gluckauf, Martin, James, Gregg, Purnell, Wilson, Wicke and Stock all contributed to our early understanding of gas-solid chromatographic retention/adsorption processes which forms the basis of analytical gas chromatography (GC) as we know it today.

The first systematic use of GC as a technique for characterizing solid-state materials was pioneered by Russian scientists in the early 1960s led by Professor Kiselev at Moscow University who also coined the terminology IGC. Their work was motivated by an interest in understanding the fundamental nature of gas-solid retention behaviour for high energy solid surfaces including carbons, zeolites, silica, alumina and catalyst materials as well as other porous solids.

Their work resulted in a very detailed fundamental understanding of the gas-phase adsorption processes on these particulate materials which were additionally being evaluated as stationary phases for traditional analytical chromatography. Their work allowed a detailed understanding of the adsorption processes including heats of adsorption, diffusion processes, adsorption processes, specific surface interactions and surface areas. Work was undertaken at both low and high solute concentrations.

Through the 1960s and 1970s research activity on IGC moved on to other classes of materials for study, most notably polymers. New refinements in both experimental technique as well as data analysis were pioneered. Many studies of polymer glass transition temperatures, small molecule diffusion, polymer-polymer interactions and crystallinity were first reported in this period. Workers such as Guillet, Conder, Smidsrod, Laub, Schrieber and Gray were all productive during this period.

During the 1980s and 1990s we have seen a much wider range of materials being studied using IGC. Initially this commenced with surface studies on fibres and filler particles for advanced materials, and more recently we have seen growing interest in IGC for food and pharmaceutical characterization. Techniques have remained very much unchanged during this period with virtually all work published being based on low solute concentrations. Refined analyses have been developed to determine the surface energy and acid-base properties of particulate materials as well as methods for determining polymer-polymer interaction constants and solubility parameters. Workers including Gray, Lawrence, Duda, Papirer, Schultz, Balard, Munk, DiPaola-Baranyi have all published significant work during this period. The recent availability of commercial IGC equipment which can perform a wide new range of experimental IGC methods is certain to catalyse growth in this technique in the new millennium.

Instrumentation

Virtually all of the published work on IGC has been undertaken on either home-built or modified commercial GC equipment. Though both analytical and physicochemical measurement approaches such as IGC are intrinsically very similar, the demands for

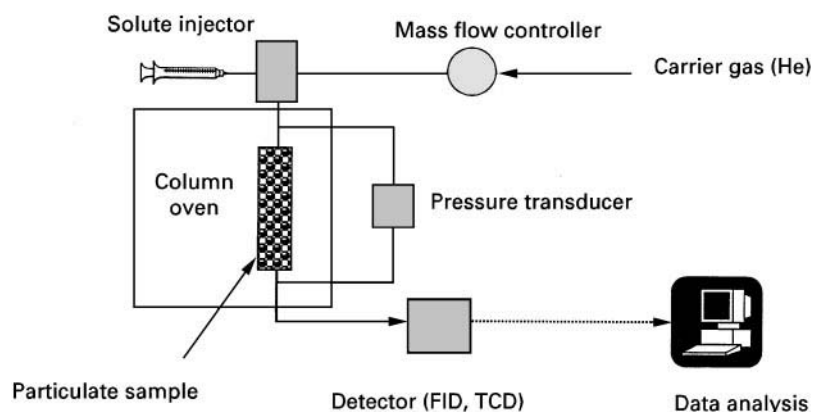


Figure 1 Typical schematic of an IGC system for infinite dilution studies. FID, Flame ionization detector; TCD, thermal conductivity detector.

accurate and precise retention data for physicochemical measurement have required additional experimental refinement not normal nor standard for analytical GC equipment.

Ideally, well-designed IGC equipment for low solute concentrations should incorporate:

1. thermal conductivity mass flow controllers
2. pressure sensors for measuring pressure drop along the column
3. computerized data acquisition of detector signals
4. full statistical analysis of solute peak/boundary shapes

Figure 1 shows a typical schematic diagram of an IGC system for infinite dilution studies used by the author.

To undertake work at high solute concentrations – finite concentration (FC) work – much more complex experimental instrumentation must be employed. The main feature of FC studies is the need to be able to generate both simple, and sometimes complex, concentration profiles of multiple solutes at concentrations, perhaps as high as P/P_0 of 0.95. This necessitates the generation of solute vapours with very stable concentration profiles. Condor and Purcell, amongst other workers, have developed appropriate GC systems to undertake such studies. Current commercial systems incorporate similar instrumental approaches as well as other experimental refinements.

Theory

IGC methods fall into two primary categories. The most common case is infinite dilution (ID) studies in which the solute concentration is low, normally less than $0.01 P/P_0$. In this case the solute molecules behave independently and retention behaviour is thus in the Henry's law region. At higher concentrations,

when solute–solute interactions become significant, then Henry's law is no longer valid and we refer to FC techniques. These later methods require special experimental techniques as well as complex data analysis.

Infinite Dilution

IGC studies under ID conditions represent over 95% of all IGC papers published in the last 10 years. Subsequently this section will especially highlight the ID approach.

Figure 2 shows four overlaid chromatograms obtained for alkane vapour species interacting with a GC column packed with crystalline fibres at 40°C under conditions of infinite dilution. The quantity t_M is the time for an inert non-interacting species to sweep through the packed column. This time is known as the experimental dead time and is typically measured using methane or nitrogen. This retention time t_M , multiplied by the carrier gas flow rate, F , approximates the dead volume, V_M , within the system. This dead volume consists of the internal volume of the instrumentation plumbing as well as dead space within the sample column.

As the hydrocarbon chain length increases, so does the ability of the solute species to interact with the fibre surface. This results in increasing retention times for the solute molecules. This trend is clearly shown in the peaks shown for hexane through octane. The increased residence time in the GC column results in broader and less intense solute peaks due to increased longitudinal diffusive broadening. The peaks nevertheless maintain their Gaussian shape.

The retention time, t_R , per unit of sample mass for an adsorbing solute vapour allows the net retention volume, V_N , to be determined using eqn [1]:

$$V_N = j t_R F(T/273.15) - j t_M F(T/273.15) \quad [1]$$

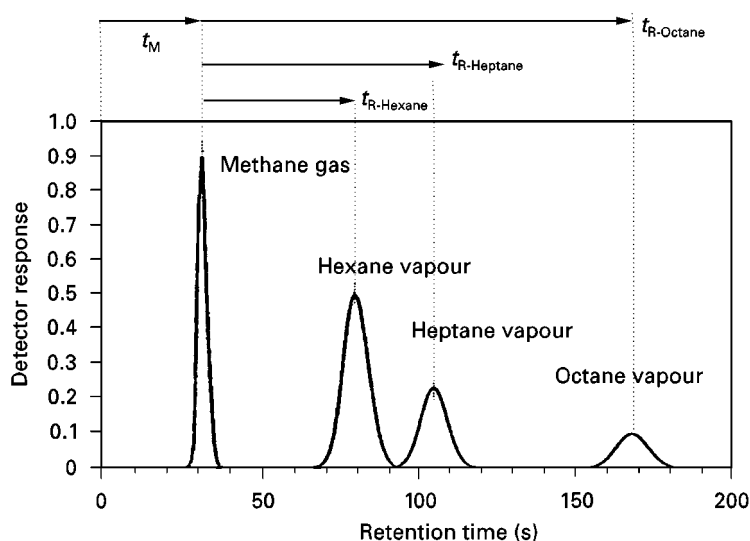


Figure 2 Overlaid chromatograms for alkane vapours on crystalline fibre surface.

where F is the carrier gas flow rate, T is the column temperature, t_M is the dead time and j is a correction term allowing for the pressure changes along the column.

The retention process for the solute with the stationary phase is determined by the solute partitioning between the stationary and mobile phases at the relevant temperature, pressure and concentration. For the case in which the retention process is due to solid-vapour adsorption, solute partitioning between the mobile and stationary phases is given by the appropriate adsorption isotherm. At low solute concentrations ($< 0.01P/P_0$) the adsorption isotherm is typically linear and this region is commonly described as the Henry's law region. In this region solute molecules adsorbing on to a surface are independent and nearest neighbour interactions are not significant. Gaussian-shaped chromatograms, as shown in Figure 2, result in the case of adsorption in the Henry's law region.

In this linear region of the adsorption isotherm, the net retention volume V_N may be related directly to the surface area of the sample A and the partitioning coefficient K_S in the case of surface retention of the solute:

$$V_N = AK_S \quad [2]$$

In the case in which both surface and bulk retention mechanisms operate, we must modify eqn [2]:

$$V_N = AK_S + VK_B \quad [3]$$

where the second term relates to bulk sorption into a volume V with a solubility K_B . K_S is also the slope of

the adsorption isotherm at infinite dilution and is simply defined as the ratio of the solute concentration q in the stationary phase to the solute concentration c in the mobile phase:

$$K_S = q/c \quad [4]$$

If a dynamic experimental technique is being used to study equilibrium processes, certain precautions need to be performed to confirm the equilibrium nature of the retention data. The simplest and most useful tests to perform are experiments with at least two different flow rates to confirm that the V_N is independent of the carrier gas flow rate.

It is thus apparent that the net retention volume V_N is directly proportional to the slope of the adsorption isotherm and thus the equilibrium constant for the adsorption process. Consequently, standard thermodynamic analysis may be applied to the data. For example, from the temperature-dependent partitioning coefficient K_S the heat of adsorption ΔH_A° using eqn [5] may be determined. Choice of appropriate standard states for the adsorbed species allows both free energies of adsorption ΔG_A° and entropies of adsorption ΔS_A° to be determined as well:

$$q_d = -\Delta H_A^\circ = R d(\ln K_S)/d(1/T) \quad [5]$$

$$\Delta G_A^\circ = -RT \ln(K_S p_{s,g}/\pi_s) \quad [6]$$

$$\Delta S_A^\circ = -(q_d + \Delta G_A^\circ)/T \quad [7]$$

A study of V_N as a function of temperature thus allows a detailed study of surface adsorption thermodynamics to be undertaken.

Measuring the retention behaviour of a series of alkane probes allows the dispersive (long range) component of the surface energy of the surface, γ_s^d to be estimated. By estimating the change in retention volume as one increases the size of the alkane probe, the differential free energy of adsorption for an imaginary $-\text{CH}_2-$ species can be determined. Using the assumption that an infinite surface of $-\text{CH}_2-$ groups is equivalent to a poly(ethylene) surface and with the use of the Fowkes' geometric mean work of adhesion analysis, γ_s^d may be estimated using eqn [8]:

$$\gamma_s^d = (4/\gamma_{s-v})((\Delta G_A^{\text{CH}_2})/(Na_{\text{CH}_2}))^2 \quad [8]$$

where N is Avogadro's constant, a_{CH_2} is the area of a $-\text{CH}_2-$ group and γ_{s-v} is the surface energy of polyethylene. This simple ratio measurement has become very popular, not least because there is no need to know the exact surface area for the sample.

The above physicochemical properties represent some of the basic IGC measurement types. There exists an extensive range of much more complex analyses which are beyond the scope of this article, including retention by bulk rather than surface retention mechanisms. Other methods include:

1. acid-base interaction constant-donor/acceptor numbers
2. free energies for specific chemical interactions
3. polymer-polymer (Flory-Huggins) interaction constants
4. solubility constants
5. diffusion constants
6. glass transition temperature of polymeric materials

Finite Concentration

Though very little work has been published using FC techniques in the past 10 years, there exists a substantial body of research using these approaches from the preceding 20 years. This work has proven the power and utility of these IGC methods. Like ID, FC is not simply a method but rather a family of experimental approaches linked simply by the use of high solute concentrations. Unlike ID, however, the shapes of the FC chromatograms are rarely Gaussian, but rather take on very complex and nonsymmetrical shapes. Conder and Young's book is still the definitive review of FC methods and should be studied for more detail (see Further Reading).

The fundamental equation from which FC work is based is given below:

$$V_N = A(1 - j\gamma_0)d_q/d_c \quad [9]$$

where γ_0 is the mole fraction of solute in the gas phase at the column inlet and d_q/d_c is the slope of the adsorption isotherm at concentration c .

In this section a brief review of the major FC methods will be provided as well as a general list of the major classes of information which can be determined using FC methods.

The simplest FC method is known as the frontal analysis (FA) approach. In this case a step change in solute concentration is introduced into the IGC column. This concentration boundary will migrate along the column and the time at which the boundary is seen by the detector (minus dead time) will depend upon how much such solute is adsorbed by the stationary phase. A knowledge of the solute concentration and the carrier gas flow rate allows the amount of solute adsorbed to be determined. By undertaking this measurement at differing solute concentrations, an adsorption isotherm may be determined.

Another useful technique is the frontal analysis by a characteristic point (FACP). In this case the shape of the boundary produced by a step change in concentration is analysed. The shape of the tailing of this FC chromatogram can be analysed to provide an adsorption isotherm from one chromatogram via recourse to various analyses based around eqn [9].

For both FACP and FA, very specially modified GC equipment must be used. These modifications are nontrivial and have in turn limited the recent use of these methods. One of the most common FC methods reported in the literature is elution of a characteristic point (ECP). The popularity of this method is simply because it can be undertaken with a standard GC injection system. The technique involves injecting a solute, typically a liquid in one large injection, down the IGC column. The resulting large solute peak will migrate along the column, resulting in the production of a highly nonsymmetrical peak. Analysis of the boundary shape based on eqn [9], not unlike the FACP methods, can allow the adsorption isotherm to be determined from a single or a family of chromatograms.

The final major class of FC techniques is elution on a plateau (EP). In this technique a steady-state concentration profile is established along the IGC column. With an essentially constant concentration profile along the column, a small positive or negative variation in concentration is introduced and the time for the perturbation to propagate along the column is determined (Figure 3). This net retention volume will correspond to the K_s for the plateau concentration c under investigation. By undertaking experiments at different concentrations, an adsorption isotherm may be accurately constructed. This method has the major

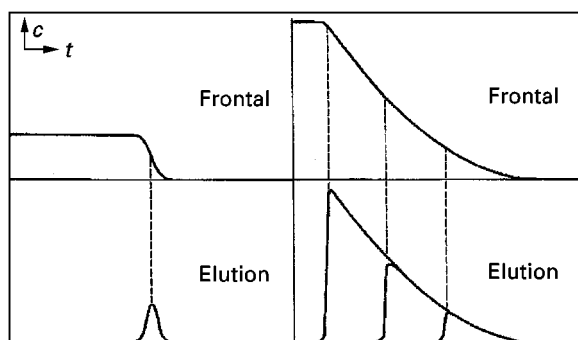


Figure 3 The relationship between frontal and elution chromatograms (after Conder).

advantage over other FC methods that the experiment is undertaken under conditions of essentially constant solute concentration.

Finite concentration methods can be used to determine the following:

1. adsorption isotherms
2. competitive adsorption phenomena
3. porosity and diffusion
4. total uptake/break-through profiles

Applications

Fibres and Filler Particles

The last 20 years have seen a substantial amount of research published on the surface characterization of fibre and filler particles. Invariably these materials are for incorporation in advanced composite materials for which the interfacial properties are known to depend on the surface properties of the reinforcing entities. Measurements of the thermodynamics of adsorption for both weak and strong adsorbing probes are well established for carbon, glass, aramid, cellulose and polyethylene fibres. In many cases their acid-base properties have also been reported. Many high energy inorganic particulate materials have also been investigated, including silica, activated carbon, alumina, bentonite and calcium carbonate. In many cases surface properties have been investigated as a function of heat treatments, surface chemical modifications as well as comminution operations such as milling. Most studies reported have used ID techniques, though FC techniques are also reported periodically.

Pharmaceuticals

The last 5 years have seen a very rapid rise in the interest of the pharmaceutical industry in the use of IGC for the characterization of pharmaceutical ma-

terials. The importance of solid dosage forms and the rapid development of novel and complex approaches to solid-state drug delivery have fuelled this interest. Work has already been reported for highly crystalline materials including α -lactose monohydrate, salbutamol sulfate, caffeine, theophylline and microcrystalline cellulose. These studies have focused on changes in surface energies associated with these materials using ID techniques. Such IGC work has already been demonstrated to be a valuable technique for quantifying batch-to-batch variations in pharmaceutical powders not readily, if at all, identifiable using any other experimental approach. The development of IGC instrumentation with multiple solute capabilities has led to work being recently reported for the surface energy of pharmaceutical powders as a function of relative humidity. Such data are also important for understanding practical storage and stability behaviour of pharmaceutical materials. A rapid expansion of work in this area can be expected over the next few years.

Food

IGC work on food materials has been very sporadic during the last 10 years. In many ways this reflects the complex and multicomponent nature of these materials. However, some trends are becoming apparent in this industry. Use of IGC in combination with mass spectroscopic techniques shows great promise for determining the evolution of volatile flavour species from food systems. The ability of IGC to be used for small molecule/polymer solubility has led to the increasing use of IGC for studying base food materials such as starch.

Polymers

Recent highlights include the use of IGC for measuring the permeability of packaging materials to gases and other small solute molecules. Techniques have also been developed for determining the diffusion constants for small molecules, especially for capillary columns coated with polymeric materials. These studies highlight some of the most complex IGC phenomena when both surface and bulk retention mechanisms are operative. Use of IGC to measure the glass transition temperature (T_g) for polymeric materials still attracts significant research interest. IGC is especially sensitive to such a transition due to a change in the retention mechanism from surface dominated below T_g to bulk retention above T_g . T_g has also been measured for thin polymeric coatings which cannot be easily analysed using traditional thermal techniques. Work has also been reported on mesophase transitions for liquid crystalline polymers.

Porous Materials

Porous materials are one of the most complex materials to analyse by any technique, including IGC. This complexity is due to the combination of heterogeneous surface sites and an intricate system of internal and external surfaces. Progress has been made in developing methods for estimating surface basicity and acidity as well as deriving adsorption energy distribution functions. The ability to differentiate solute adsorption due to micropore filling versus surface adsorption has been demonstrated using IGC. This ability allows the true external surface area to be estimated, which is difficult to accomplish with traditional static techniques. Developments in the characterization of these materials have been facilitated by the use of traditional IGC methods combined with thermal ramped desorption approaches which allow information on a wide range of adsorption energies to be determined.

Other Materials

Work has been reported on the use of IGC to characterize coal, sand, conducting polymers, soils and crude oils.

Conclusions

IGC has been shown to be a powerful technique for studying physicochemical interactions between solutes and solid-state materials, especially those at the surface. Indeed, the more extensive use of the technique has clearly been hampered by the lack of commercially available IGC equipment during the past 30 years. Though the number of techniques for surface characterization has increased substantially in the last 20 years (SIMS, XPS, etc.), most of these methods do not provide thermodynamic but rather analytical information. The realization that thermodynamic information about solid-state-solute interactions is important and the very recent advent of commercial IGC instrumentation is likely to result in

a significant increase in research using IGC during the next 10 years.

Acknowledgements

Discussions with Dr D. Fetsch and Dr F. Thielmann are gratefully acknowledged.

See also: III/Reverse-Flow Gas Chromatography.

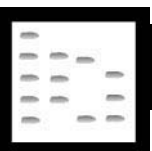
Further Reading

- Al-Saigh ZY (1997) The characterization of polymer blends by inverse gas chromatography. *Trends in Polymer Science* 5: 97–102.
- Conder CL and Young CL (1979) *Physicochemical Measurement by Gas Chromatography*. Chichester: John Wiley.
- Kiselev AV and Yaskin YI (1969) *Gas-Adsorption Chromatography*. New York: Plenum Press.
- Lloyd DR, Ward TC and Schreiber HP (eds) (1989) *Inverse Gas Chromatography*. ACS Symposium Series 391. Washington: American Chemical Society.
- Mukhopadhyay P and Schreiber HP (1995) Aspects of acid-base interactions and the use of inverse gas chromatography. *Colloids and Surfaces* 100: 47–71.
- Papirer E and Balard H (1999) Inverse gas chromatography: a method for evaluation of the interaction potential of solid surface. In: Pefferkorn E (ed.) *Interfacial Phenomena in Chromatography*, pp. 145–171. New York: Marcel Dekker.
- Pefferkorn E (ed.) (1999) *Interfacial Phenomena in Chromatography*. New York: Marcel Dekker.
- Voelkel A (1996) Inverse gas chromatography in the examination of acid-base and some other properties of solid materials. *Studies in Surface Science and Catalysis* 99: 465–477.
- Williams DR (1990) Inverse gas chromatography of fibres and filler particles. In: Ishida H (ed.) *Controlled Interfaces in Composite Materials*, pp. 219–232. New York: Elsevier.
- Williams DR (1994) Inverse gas chromatography. In: Ishida H (ed.) *Characterisation of Composite Materials*, pp. 80–104. Boston: Butterworth-Heinemann.

PEPTIDES AND AMINO ACIDS: CAPILLARY ELECTROPHORESIS

See III/AMINO ACIDS AND PEPTIDES: CAPILLARY ELECTROPHORESIS

PEPTIDES AND PROTEINS



Liquid Chromatography

C. T. Mant and R. S. Hodges, University of Alberta, Edmonton, Alberta, Canada

Copyright © 2000 Academic Press

Introduction

High performance liquid chromatography (HPLC) has proved extremely versatile in aiding the isolation of peptides from a wide variety of sources, including complex proteolytic and/or chemical cleavage mixtures of proteins as well as crude mixtures arising from the ever-increasing employment of solid-phase peptide synthesis. The complexity of such peptide mixtures may vary considerably depending on the source. Thus, for instance, peptides obtained from biological tissues are often found in very small quantities and may require extensive purification, while impurities arising from peptide synthesis are usually closely related to the peptide of interest (deletion, terminated or chemically modified peptides), missing perhaps only one amino acid residue, and may be difficult to separate. The development of high performance separation techniques has enabled the much more efficient utilization of peptide size (size exclusion chromatography or SEC) and net charge (ion exchange chromatography or IEC) compared to the much inferior and slower separations achievable by classical SEC and IEC. In addition, reversed-phase chromatography (RPC), a technique that does not have a classical predecessor, has proved to be an excellent means of analysing peptides based on their relative hydrophobic/hydrophilic characteristics.

With the requirement for efficient separation protocols constantly fueling demands for improvements in HPLC instrumentation and packings, it is perhaps not surprising that researchers have generally overlooked the potentially useful mixed-mode properties of high performance packings which, with careful manipulation of mobile-phase conditions, can offer a novel addition to the HPLC arsenal. In our experience, all HPLC packings have exhibited some deviation from ideal solute retention behaviour; thus, SEC packings often exhibit some hydrophobic and ionic characteristics, IEC packings exhibit hydropho-

bic character to a greater or lesser extent and RPC packings frequently also exhibit some ion exchange properties. Mobile phases may then be designed to minimize or eliminate such mixed-mode characteristics which, if left unchecked, can lead to poor resolution and broad, tailing peaks. The mixed hydrophobic and charged characteristics of peptides make these molecules particularly susceptible to such nonideal retention behaviour. However, the reverse is that certain so-called nonideal packing characteristics – in the sense that they represent an unintended, nonspecific property of a column packing – may significantly enhance the resolving power of that packing.

As noted above, the hydrophobic/hydrophilic characteristics of peptides, a result of the nonpolar/polar nature of the side chains making up the peptide, are well recognized, particularly in terms of peptide elution from a reversed-phase column in order of increasing peptide hydrophobicity. What has not been so well recognized until relatively recently, however, is that since ion exchange stationary phases are designed to be as hydrophilic (or as neutral) as possible to avoid hydrophobic interactions, such hydrophilic characteristics may be used to advantage if harnessed properly. The present article describes, and illustrates with practical examples, how the ionic nature of a strong cation exchange matrix may be overlaid with hydrophilic characteristics, thus effecting peptide separations by a combined hydrophilic/cation exchange mechanism. This novel mixed-mode approach, termed hydrophilic interaction–cation exchange chromatography (HILIC-CXC) offers drastically different selectivity to RPC, underlining its value as a complementary approach.

General Principles and Conditions of HILIC-CXC

The term hydrophilic interaction chromatography (HILIC) was originally coined to describe separations based on solute hydrophilicity. Thus, separation by HILIC, in a manner similar to normal-phase chromatography (to which it is related), depends on hydrophilic interactions between the solutes and a hydrophilic stationary phase, i.e. solutes are eluted in order of increasing overall hydrophilicity (decreasing hydrophobicity). Characteristic of HILIC-CXC separations is the presence of a high initial organic

modifier (e.g. acetonitrile) concentration in the mobile phase which, concomitant with overcoming any undesirable hydrophobic column behaviour, serves to promote hydrophilic interactions between the solute and the stationary phase, specifically a strong cation exchange stationary phase with significant hydrophilic characteristics. Such characteristics generally only become apparent once any matrix hydrophobicity has been suppressed. Hydrophilic interactions between peptides and the cation exchange packing are then overlayed on the ionic interactions between basic (potentially positively charged) peptides and the negatively charged packing.

Different ion exchange matrices exhibit differing degrees of hydrophobic characteristics. In order to gain the full benefit of the HILIC mode, it is important to overcome unwanted hydrophobic properties of the matrix with as low a level of organic modifier as possible – the ion exchange matrix should be as hydrophilic as possible. In this way, there is a greater organic modifier range open to the researcher to effect mixed-mode HILIC-CXC peptide separations. In our hands, the PolySulfoethyl A strong cation exchange column (based on a polypeptide coating, poly[2-sulfoethylaspartamide], covalently bonded to silica) has proven to be very hydrophilic, hence its use in the separations shown in the current article.

Typical conditions for mixed-mode HILIC-CXC are a linear increasing sodium perchlorate (NaClO_4) gradient ($2\text{--}20\text{ mmol L}^{-1}\text{ NaClO}_4\text{ min}^{-1}$) at pH 3–7, with the mobile phase containing 15–80% acetonitrile (ACN). Thus, the cation exchange column separates peptides based on net positive charge and this separation mode is then complemented by the presence of ACN overcoming undesirable hydrophobic interactions and promoting desirable hydrophilic interactions. NaClO_4 is suitable for this mixed-mode approach due to its excellent solubility in aqueous solution even in the presence of high concentrations of organic modifier. Where the charged characteristics of the components of a specific peptide mixture are unknown, relatively low pH conditions are a good starting point in order to maximize the basic character of the peptide solutes and, hence, enhance ionic interactions with the negatively charged strong cation exchange matrix. Thus, at pH 3, any acidic (potentially negatively charged) residues (aspartic acid, glutamic acid) will be mainly in the protonated, neutral form. In addition, a full positive charge on the basic residue histidine ($\text{pK}_a = 6.5$) is also assured at low pH. Although perhaps a less obvious concern, there is also a need to be cautious with the pH of the mobile phase when considering basic residues such as lysine ($\text{pK}_a \sim 10$) and arginine ($\text{pK}_a \sim 12$). This caution arises from reduction in pK_a of such basic resi-

dues frequently observed in a nonpolar environment, represented in the present case by the nonpolar (relative to water) organic modifier ACN. Thus, due to the presence of high concentrations of ACN (up to 90%) characteristic in HILIC-CXC mobile phases, the use of relatively low pH conditions to ensure full protonation (i.e. a full positive charge) of basic side chains is a wise precaution. As an additional benefit, silica-based ion exchange columns tend to be more stable over a period of time at pH 3 compared to pH values around neutrality.

The general principles of HILIC-CXC are well demonstrated in **Figure 1** which compares the separation of four random coil peptides, denoted S2, S3, S4 and S5 (**Table 1**), by RPC (top), CXC (middle) and HILIC-CXC (bottom). This four-peptide mixture contains peptides with the same net positive charge (+2) and subtly increasing hydrophobicity ($\text{S2} < \text{S3} < \text{S4} < \text{S5}$). Note that the only difference between the CXC and HILIC-CXC runs is the presence of 10% (v/v) ACN in the former compared to 80% (v/v) in the latter.

From **Figure 1**, peptides are as expected, eluted from the RPC column (top) in order of increasing hydrophobicity. Under characteristic cation exchange conditions (middle), the presence of 10% (v/v) ACN helps to eliminate unwanted hydrophobic interactions between solutes and the stationary phase, and the four peptides are very poorly resolved, as expected given the identical net charge on the peptides. Note, however, that the low concentration of ACN (10%) has already induced hydrophilic interactions with the matrix in that the elution order is already opposite to that of RPC (the most hydrophobic peptide is eluted first and the most hydrophilic last). In comparison, under HILIC-CXC conditions (bottom), the elution order remains the same but the peptides are now well resolved. Clearly, to effect a separation of these peptides on the cation exchange column, an increased concentration (80% (v/v)) of ACN is required in the mobile phase in order to promote hydrophilic interactions with the stationary phase to complement the ionic interactions.

Optimization of HILIC-CXC Run Conditions

While flow rates of $0.5\text{--}2.0\text{ mL min}^{-1}$ are generally favoured for analytical ion exchange separations and, by extension, mixed-mode HILIC-CXC runs, the effect of varying flow rates is somewhat limited. In contrast, variations in gradient rate (increasing counterion concentration per unit time) have the potential for large effects on the efficiency of separation. In addition, one option available to HILIC-

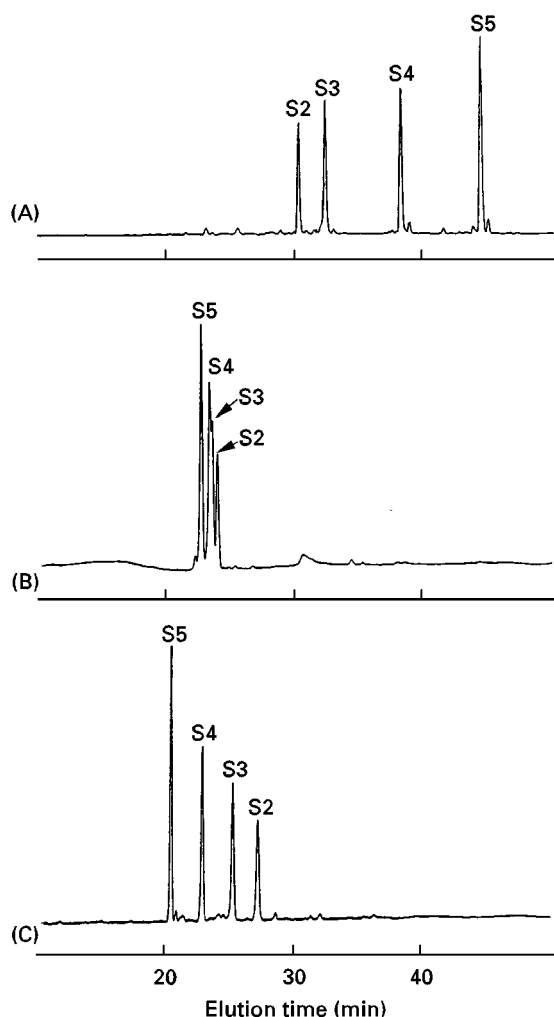


Figure 1 General principles of HILIC-CXC versus RPC: (A) RPC; (B) CXC; (C) HILIC/CXC. Columns: Zorbax SB300-C₈ reversed-phase column (150 × 4.6 mm i.d., 5 μm particle size, 30 nm pore size) from Hewlett-Packard PolySulfoethyl a strong cation exchange column (200 × 4.6 mm i.d., 5 μm, 30 nm) from PolyLC. Conditions: RPC, linear AB gradient (0.5% acetonitrile min⁻¹) at a flow rate of 1 ml min⁻¹, where eluent A is 20 mmol L⁻¹ aq. triethylammonium phosphate (TEAP), pH 3, and eluent B is eluent A containing 60% (v/v) acetonitrile, both eluents containing 100 mmol L⁻¹ NaClO₄; CXC, linear AB gradient 5 mmol L⁻¹ NaClO₄/min⁻¹, following 5 min isocratic elution with eluent A at a flow rate of 1 ml min⁻¹, where eluent A is 20 mmol L⁻¹ aq. TEAP, pH 3, containing 10% (v/v) acetonitrile and eluent B is eluent A containing 400 mmol L⁻¹ NaClO₄. HILIC/CXC, same conditions as for CXC, except for 80% (v/v) acetonitrile in eluents A and B; all runs carried out at 30°C and peaks detected by absorbance at 210 nm. (Reproduced with permission from Mant *et al.*, 1998a.)

CXC, but not to separations based solely on an ion exchange mechanism, is to vary the ACN concentration in the mobile phase in order to modulate the magnitude of hydrophilic interactions overlaying the ion exchange process.

Variation of Salt Gradient Rate

Figure 2 shows the effect of varying gradient rate of NaClO₄ (under conditions of a consistent and high ACN concentration) on the HILIC-CXC elution profile of a mixture of six cyclic, amphipathic β-sheet peptides. These peptides offer a particularly stringent test of the capabilities of the HILIC-CXC approach in that only the two residues making up the hydrophilic face (the face binding preferentially to the ion exchange matrix) of the β-sheet are varied (Table 1); the overall net charge of all the peptides is identical (+2); note that the hydrophobic face of all six peptide analogues, made up of leucine and valine residues (Table 1), is constant. From Figure 2, reducing the gradient rate from 5 mmol L⁻¹ NaClO₄ min⁻¹ to 2.5 mmol L⁻¹ min⁻¹ and, finally, to 1 mmol L⁻¹ min⁻¹ clearly affects the efficiency of the separation with, interestingly, optimal separation in this mixed mode being achieved at the intermediate rate of 2.5 mmol L⁻¹ min⁻¹. Thus, while reducing the gradient from 5 mmol L⁻¹ min⁻¹ (top) to 2.5 mmol L⁻¹ min⁻¹ (middle) achieved an expected improvement in resolution (peptides Dap and Arg are co-eluted at the higher gradient rate), further reduction to 1 mmol L⁻¹ min⁻¹ (bottom) results in a deterioration of the separation, with peptides Orn and Dab now co-eluted. Such results, while illustrating the efficacy of varying salt gradient rate, also serve to indicate the complexity of peptide retention behaviour when responding to variations in run parameters.

Variation of Acetonitrile Concentration

Figure 3 demonstrates the effect of ACN concentration on the elution of a mixture of 12 peptides with negligible secondary structure; the numbers denote the number of potentially positively charged groups on the peptides (Table 1). With 20% ACN in the mobile phase (Figure 3A), the overall elution order of all 12 peptides is essentially based on increasing net positive charge (+1 < +2 < +3 < +4) – ionic interactions dominate the separation process. At 50% ACN (Figure 3B), ionic interactions are still dominant since peptides are still generally eluted in order of increasing net positive charge. However, a hydrophilic interaction mechanism also becomes more substantial, as evidenced by the improvement in the separation of peptides of like charge. Also, note the elution of peptide 14 before the lesser charged (but more hydrophilic) b3 and a3, a clear example of how more highly charged peptides may still be eluted prior to less highly charged peptides if the latter are significantly more hydrophilic than the former. A further increase in ACN concentration to 90% (Figure 3C)

Table 1 Synthetic peptides used in this study

Figure	Peptide sequence ^a	Peptide notation
<i>Random coil peptides</i>		
1, 3, 4	Ac- R -G-G-G-L-G-L-G- K -amide	S2, e2
1, 3, 4	Ac- R -G-A-G-G-L-G-L-G- K -amide	S3, f3
1, 3, 4	Ac- R -G-V-G-G-L-G-L-G- K -amide	S4, g4
1	Ac- R -G-V-V-G-L-G-L-G- K -amide	S5
3, 4	Ac- R -G-V-Y-G-L-G-L-G- K -amide	h3
3, 4	NH ₂ - R -G-G-G-G-L-G-L-G- K -amide	a3
3, 4	NH ₂ - R -G-A-G-G-L-G-L-G- K -amide	b3
3, 4	NH ₂ - R -G-V-G-G-L-G-L-G- K -amide	c3
3, 4	NH ₂ - R -G-V-Y-G-L-G-L-G- K -amide	d3
3, 4	Ac-G-G-G-L-G-G-A-G-G-L- K -amide	i1
3, 4	Ac- K -Y-G-L-G-G-A-G-G-L- K -amide	j2
3, 4	Ac-G-G-A-L- K -A-L- K -G-L- K -amide	k3
3, 4	Ac- K -Y-A-L- K -A-L- K -G-L- K -amide	l4
<i>Cyclic and constrained peptides^b</i>		
2, 6	<u>V-H-L-Y-P-V-H-L-Y-P</u>	His
2, 6	<u>V-R-L-Y-P-V-R-L-Y-P</u>	Arg
2, 6	<u>V-K-L-Y-P-V-K-L-Y-P</u>	Lys
2, 6	<u>V-O-L-Y-P-V-O-L-Y-P</u>	Orn
2, 6	<u>V-Dap-L-Y-P-V-Dap-L-Y-P</u>	Dap
2, 6	<u>V-Dab-L-Y-P-V-Dab-L-Y-P</u>	Dab
5	<u>V-K-L-K-V-Y-P-L-K-V-K-L-Y-P</u>	GS14 (V1, K2, etc.)
8A	Ac- K -C- K -S-T-Q-D-E-Q-F-I-P- K -G-C-S- K	03138
<i>Helical peptides</i>		
7	Ac-E-L-E- K -L-L-L-E-L-E- K -L-L- K -E-L-E- K -amide	LL7
7	Ac-E-L-E- K -L-L-V-E-L-E- K -L-L- K -E-L-E- K -amide	LV7
7	Ac-E-L-E- K -L-L-S-S-L-E- K -L-L- K -E-L-E- K -amide	LS7
7	Ac-E-L-E- K -L-L-T-T-L-E- K -L-L- K -E-L-E- K -amide	LT7
8B	Ac-Q-C-G-A-L-Q- K -Q-V-G-A-L-E- K -E-E-G-A-L-E- K -Q-V-G-A-L-Q- K -Q-V-G-A-L-Q- K -amide	01118
9, 10	Ac- K -I-S-A-L- K -E- K -I-S-A-L- K -E- K -I-S-A-L- K -E- K -I-S-A-L- K -amide	J1

^a Peptide sequences are shown using the one-letter code for amino acid residues, except Dap denoting diaminopropionic acid and Dab denoting diaminobutyric acid; Ac = *N*^α-acetyl and amide = *C*^α-amide; potentially positively charged residues and groups are shown in **bold**.

^b Underlined residues represent D-amino acids; lines linking N- and C-termini of linear sequences represent cyclic nature of these peptides; peptide 03138 contains an intrachain disulfide bridge, represented by line linking Cys residues.

shows the most dramatic change in column selectivity with the hydrophilic interactions now dominating the separation process, producing a much different elution profile compared to those seen at lower ACN concentrations. For instance, peptide i1 (+1 net charge) is eluted after the less hydrophilic h2 (+2 net charge); similarly, e2 (+2 net charge) is eluted after the much less hydrophilic k3 and, most dramatically, peptide l4 (+4 net charge) is eluted before the more hydrophilic c3, b3 and a3 (+3 net charge).

The flexibility of HILIC-CXC is also demonstrated in Figure 3D, where a double gradient (increasing salt gradient with concomitant decreasing ACN gradient) is employed to effect the separation, thus maintaining dominant hydrophilic (over ionic) interactions while reducing analysis time (relative to the chromatogram

shown in Figure 3C) but retaining good column selectivity. From Figure 3D, this is achieved by a lower level of ACN in buffer B (50% as opposed to 90% in buffer A), which leads to a decrease in peptide retention relative to that effected by maintaining 90% acetonitrile in both mobile-phase buffers (Figure 3C). The peptide elution order obtained with this combined salt and ACN gradient is almost identical (save for a reversal of e2 and k3) to that shown in Figure 3C, but is obtained in about two-thirds of the time and with sharper peaks.

Although the results shown in Figures 2 and 3 are derived from mixtures of only a limited range of peptides, they do at least provide a useful summary of the major optimization options available. Indeed, the double-gradient approach shown in Figure 3D is

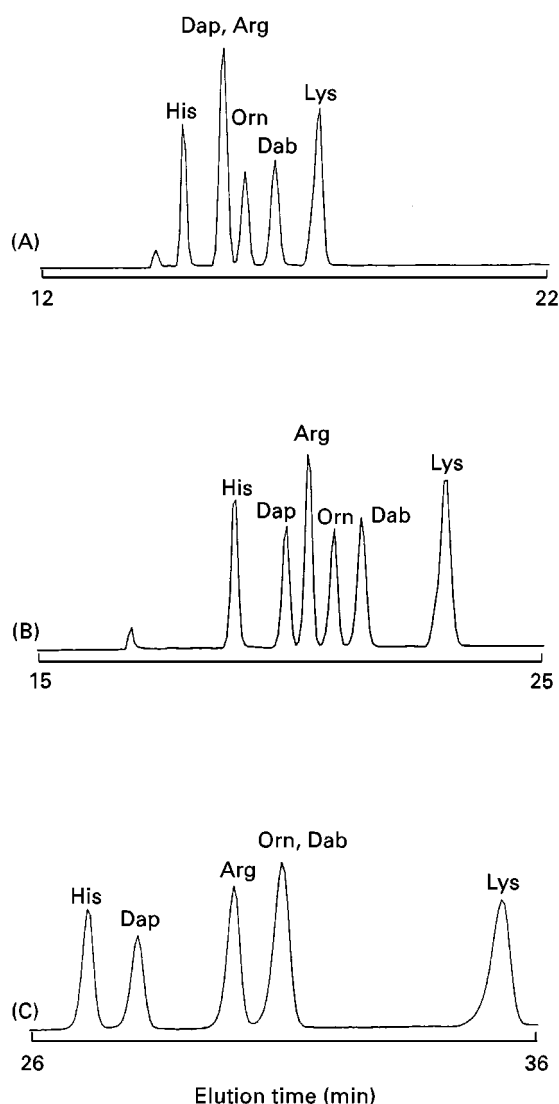


Figure 2 Effect of salt gradient steepness on HILIC-CXC of peptides. CXC column: see Figure 1. Conditions: same as HILIC-CXC conditions in Figure 1, save for 90% (v/v) acetonitrile in eluent A and 80% (v/v) acetonitrile in eluent B; linear AB gradients at (A) 5 mmol L⁻¹ min⁻¹; (B) 2.5 mmol L⁻¹ min⁻¹; (C) 1 mmol L⁻¹ min⁻¹. (Reproduced with permission from Mant *et al.*, 1998b.)

a good starting point when first applying mixed-mode HILIC-CXC to a peptide mixture of interest. Initial run conditions similar to those described for Figure 3D, save for a lower pH (e.g. pH 3) to ensure the maximum degree of positively charged character of the peptides, are recommended. The observed elution profile can be subsequently optimized by varying gradient rate and/or mobile-phase ACN concentration as required; in addition, if acidic (potentially negatively charged) residues are present in the peptides, the pH can also be manipulated to modulate the positively charged character of the peptides and,

hence, vary the strength of ionic interactions between peptides and the cation exchange matrix.

Practical Applications of HILIC-CXC for Peptide Separations

In order to appreciate fully the unique selectivity advantages of HILIC-CXC for peptide separations,

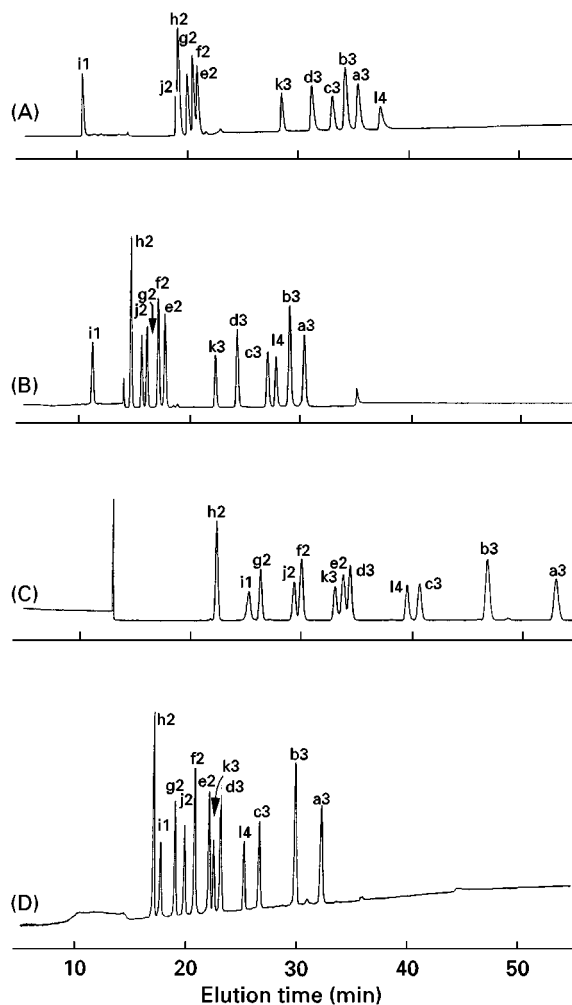


Figure 3 Effect of acetonitrile concentration on HILIC-CXC of peptides. CXC column: see Figure 1. Conditions: (panels A–C), linear AB increasing salt gradient (2% B min⁻¹, equivalent to 5 mmol L⁻¹ NaClO₄ min⁻¹, starting with 100% A at a flow rate of 1 ml min⁻¹, where A is 5 mmol L⁻¹ aqueous TEAP, pH 7, and B is A plus 0.25 mol L⁻¹ NaClO₄, pH 7, both A and B containing 20% (panel A), 50% (panel B) or 90% (panel C) (v/v) acetonitrile; panel D, linear AB gradient) 2% B min⁻¹, equivalent to a linear increasing salt gradient of 5 mmol L⁻¹ NaClO₄ min⁻¹ and a linear decreasing acetonitrile gradient of 0.8% acetonitrile min⁻¹, starting with 100% A at a flow rate of 1 ml min⁻¹, where A is 5 mmol L⁻¹ aqueous TEAP, pH 7, containing 90% (v/v) acetonitrile and B is 5 mmol L⁻¹ aqueous TEAP, pH 7, containing 0.25 mol L⁻¹ NaClO₄ and 50% (v/v) acetonitrile; all runs carried out at 26°C and peaks detected at 210 nm. (Reproduced with permission from Zhu *et al.*, 1992.)

it is important to demonstrate the resolution of mixtures of peptides with different characteristics, e.g. random coil peptides, peptides with a defined secondary structure, constrained peptides, etc. Such a range of peptides is well represented by those presented in Table 1. In addition, the value of the HILIC-CXC is also better appreciated if its ability to resolve peptide mixtures is compared to that of the RPC mode.

HILIC-CXC is a Complementary Mode to RPC for Peptide Separations

Figure 4 compares the RPC and HILIC-CXC elution profiles of the same mixture of peptides with negligible secondary structure used in Figure 3. In fact, the HILIC-CXC double-gradient system at pH 7 (increasing salt gradient, decreasing ACN gradient) resulting in the elution profile shown in Figure 3D is here being compared to RPC at pH 7 (Figure 4A: including the presence of $250 \text{ mmol L}^{-1} \text{ NaClO}_4$ to suppress any

undesirable ionic interactions between negatively charged free silanols on the silica surface and any positively charged residues) in order to create as direct a comparison as possible between the two modes. From Figure 4A, the elution profile shown represents a relative measure of the hydrophobicity of the 12 peptides, from the least hydrophobic to the most hydrophobic as expressed by their increasing RPC elution times. Under HILIC-CXC conditions (Figure 4B), instead of a simple reversal of peptide elution, cation exchange interactions overlayed on interactions involving the hydrophilic/hydrophobic nature of the peptides now lead to useful selectivity differences between the two modes, major examples of which are denoted by arrows in Figure 4. The resolution of the peptide mixture is satisfactory using either RPC or HILIC-CXC, although that achieved by HILIC-CXC is superior and the complementary aspects of the two modes are quite clear.

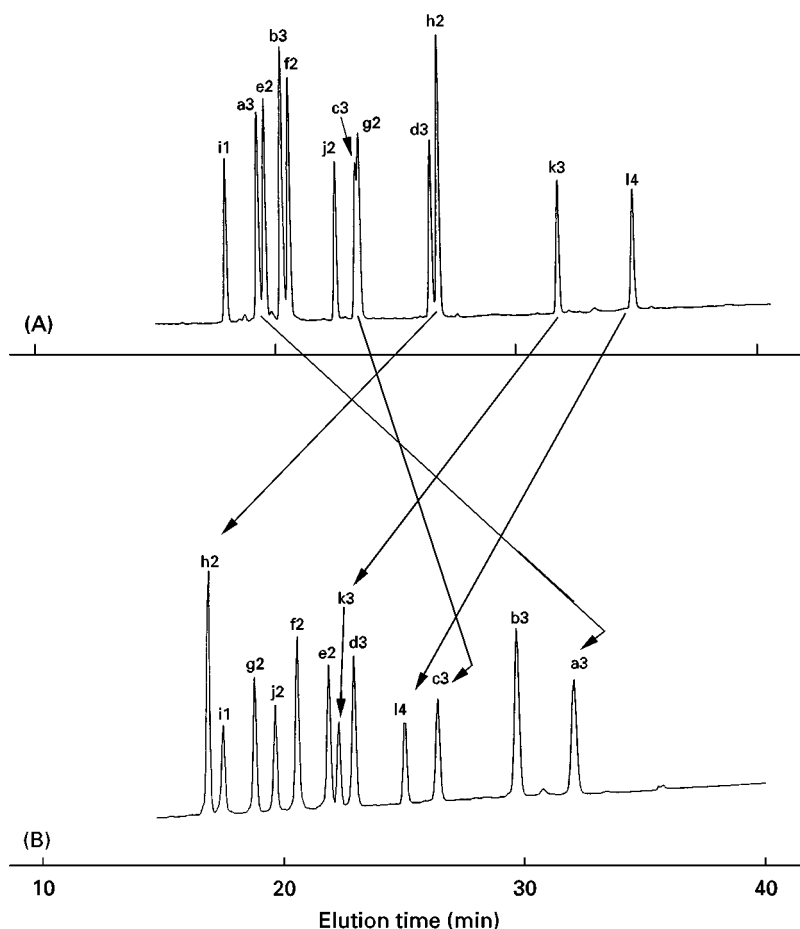


Figure 4 (A) RPC versus (B) HILIC-CXC of peptides with negligible secondary structure. Columns: see Figure 1. Conditions: RPC, linear AB gradient ($1\% \text{ acetonitrile min}^{-1}$) at a flow rate of 1 mL min^{-1} , where eluent A is $10 \text{ mmol L}^{-1} \text{ aq. } (\text{NH}_4)_2\text{HPO}_4$, pH 7, and eluent B is eluent A containing $50\% \text{ (v/v) acetonitrile}$, both eluents containing $200 \text{ mmol L}^{-1} \text{ NaClO}_4$; HILIC-CXC, same conditions as Figure 3 panel D; runs carried out at 26°C and peaks detected at 210 nm . Numbers above the peptide peaks denote the number of potentially positive charges they contain. (Reproduced with permission from Mant and Hodges, 1996.)

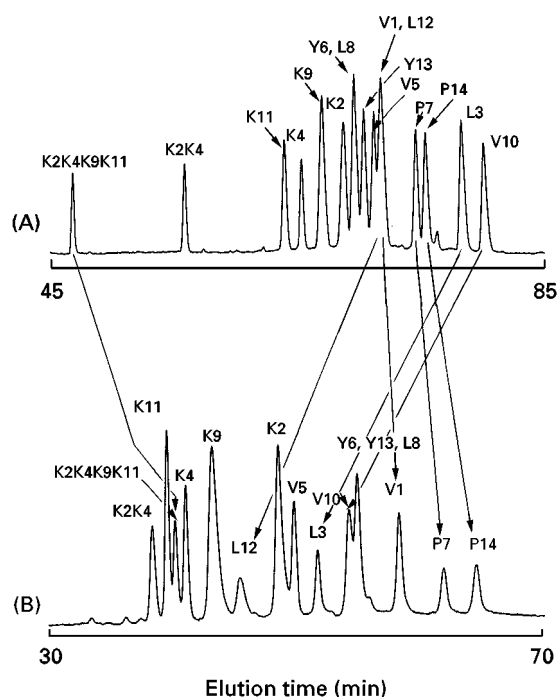


Figure 5 (A) RPC versus (B) HILIC-CXC of cyclic peptides. Columns: see Figure 4. Conditions: RPC, linear AB gradient (0.5% acetonitrile min^{-1}) at a flow rate of 1 mL min^{-1} and a temperature of 70°C , where eluent A is 0.05% aq. trifluoroacetic acid (TFA) and eluent B is 0.05% TFA in acetonitrile; HILIC-CXC, linear AB gradient $2.5 \text{ mmol L}^{-1} \text{ NaClO}_4 \text{ min}^{-1}$, following 5 min isocratic elution with 100% eluent A at a flow rate of 1 mL min^{-1} and a temperature of 30°C , where eluent A is 20 mmol L^{-1} TEAP, pH 3, and eluent B is eluent A containing $400 \text{ mmol L}^{-1} \text{ NaClO}_4$, with eluents A and B also containing, respectively, 90% and 80% (v/v) acetonitrile. Peaks were detected at 210 nm . (Reproduced with permission from Mant *et al.*, 1998.)

Even more dramatic selectivity changes are illustrated in Figure 5, which compares the RPC and HILIC-CXC chromatograms for a mixture of cyclic 14-residue analogues of gramicidin S, an amphipathic β -sheet peptide. Each residue in the native GS14 sequence (Table 1) has been systematically replaced with its enantiomer, i.e. 14 diastereomers; two additional analogues are included with either double (peptide K2K4) or quadruple (peptide K2K4K9K11) L-Lys to D-Lys substitutions. The result of each enantiomeric substitution within the framework of GS14 disrupts the β -sheet structure to varying degrees, depending on the position of the substitution. Due to their isomeric nature, the 16 diastereomeric analogues have the same intrinsic hydrophobicity; thus, the differences in their RPC elution times (Figure 5A) are due to their effective hydrophobicities, i.e. the ability of a particular analogue to form a preferred hydrophobic binding domain and present this hydrophobic face to the reversed-phase matrix. From Figure 5B, the analogues with the longer reten-

tion times can present a relatively greater hydrophobic face to the reversed-phase matrix compared to analogues with low retention times which cannot present such a hydrophobic face due to more severe disruption of β -sheet structure and, hence, amphipathicity. In an analogous manner to RPC, since all 16 peptides have the same inherent hydrophilicity, their relative positions in the HILIC-CXC elution order (Figure 5B) must also be dependent on the relative disruption of β -sheet structure and amphipathicity and, hence, their effective hydrophilicities, i.e. the ability of a particular analogue to form a preferred hydrophilic binding domain and present this hydrophilic face to the ion exchange matrix.

The two elution profiles shown in Figure 5 are markedly different, reflecting profound differences in the selectivity of the two modes. Despite the complexity of the peptide elution shifts between RPC and HILIC-CXC, the more dramatic selectivity shifts (denoted by arrows) are readily apparent. Thus, peptides V1 and L12 are completely co-eluted by RPC but widely separated by HILIC-CXC; peptides L3 and V10 are the last eluted peptides during RPC, but are eluted towards the middle of the HILIC-CXC chromatogram; peptide K2K4K9K11 is eluted early during RPC, but moves significantly later in retention time relative to the other peptides during HILIC-CXC. Although both modes achieve reasonable separation of the 16-peptide mixture, this is an excellent example of where a two-column approach (e.g. HILIC-CXC followed by RPC of collected HILIC-CXC fractions), taking advantage of complementary chromatographic selectivities, is required to achieve optimal separation.

Figure 6 compares the relative effectiveness of RPC and HILIC-CXC in separating 10-residue amphipathic cyclic β -sheet analogues of gramicidin S, where substitutions have only been made on the hydrophilic face of the peptides (Table 1). Since the hydrophobic preferred binding domain of all six analogues is constant, i.e. all substitutions have been made in the hydrophilic face which tends to be oriented away from the reversed-phase stationary phase, the poor resolution of the peptides by RPC (Figure 6A) is not surprising; in contrast, these peptides are much better separated by HILIC-CXC (Figure 6B), since the preferential binding of the hydrophilic face of the peptides to the cation exchange matrix now enhances the separation. The arrows again denote relative positions of the peptide analogues between the HILIC-CXC and RPC runs in order to highlight selectivity differences between the two modes.

A similar effect of amphipathic secondary structure on the relative utility of HILIC-CXC and RPC is shown in Figure 7, which compares the relative

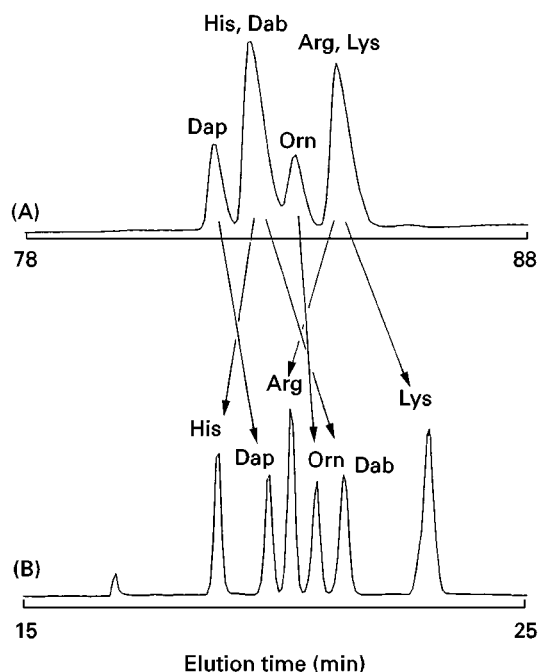


Figure 6 (A) RPC versus (B) HILIC-CXC of cyclic, amphipathic β -sheet peptides. Columns: see Figure 1. Conditions: RPC, same as Figure 1 save for 50% (v/v) acetonitrile in eluent B; HILIC-CXC, same as Figure 2 for 2.5 mmol L⁻¹ NaClO₄ min⁻¹ run. Peaks were detected at 210 nm. (Reproduced with permission from Mant *et al.*, 1998.)

effectiveness of the two modes in separating amphipathic α -helical peptide analogues LL7, LV7, LT7 and LS7 (Table 1), where substitutions have only been made in the hydrophilic face of the helices. From Figure 7A, in RPC the identical hydrophobic-preferred binding domains of the peptides bind to the hydrophobic matrix, resulting in co-elution of all four peptides under RPC conditions. Therefore substitutions in the hydrophilic face, which is oriented away from the reversed-phase matrix, have little effect on the RPC retention behaviour. In contrast to RPC, all four peptides are well resolved by HILIC-CXC (Figure 7B), even though they all have the same net positive charge, with the substitution sites in the hydrophilic faces able to interact intimately with the ion exchange matrix and, hence, influence the retention behaviour of the four analogues. Note that elution is in order of decreasing hydrophobicity, with the Leu analogue being eluted first, followed by the Val, Thr and Ser analogues, exactly as expected based on the most hydrophilic peptide being eluted last in HILIC.

HILIC-CXC for Purification and Analysis of Solid-phase Synthetic Products

In addition to RPC being the method of choice for most preparative separations of peptides, it is also

commonly employed analytically to check the purity of a purified product. However, a single peak obtained during RPC is not necessarily a guarantee of peptide purity. Thus, a complementary method, such as HILIC-CXC, is required for a more accurate assessment of peak purity as well as offering an alternative approach to obtaining the required purity.

Figure 8A outlines the purification and analysis of a 35-residue cysteine-containing synthetic peptide (peptide 01118 from Table 1). The RPC elution profile of the reduced crude peptide (top) suggests a successful synthesis, i.e. a major single peak with relatively few impurities. Analysis of the subsequently RPC-purified major component by RPC (middle) shows a single, symmetrical peak. The lack of any shoulder on the peak, obtained on a very efficient column, suggests excellent peptide purity. However, mass spectrometry of this peptide showed not only the expected product mass, but a second strong signal exhibiting a peptide mass 103 units less than expected, indicating deletion of the Cys residue at position 2 of the peptide (Table 1). Although it might have been expected that deletion of a relatively hydrophobic residue such as Cys would be detected by RPC, apparently the loss of this residue has been masked by the diminishing contribution a residue

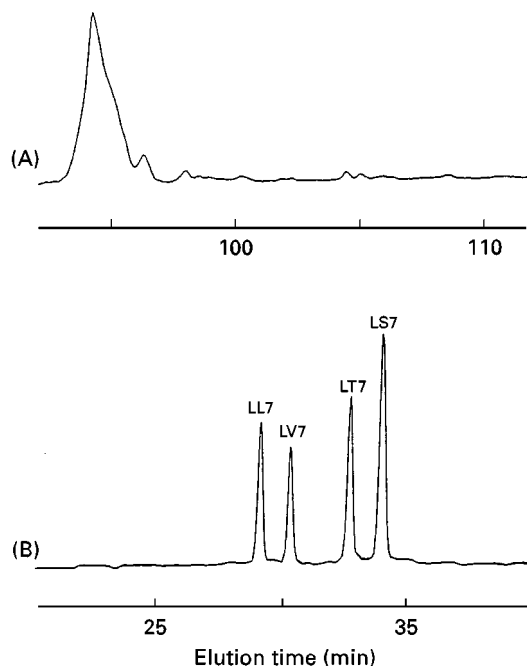


Figure 7 (A) RPC versus (B) HILIC-CXC of amphipathic α -helical peptides where substitutions have been made in the hydrophilic face. Columns: see Figure 1. Conditions: RPC, same as Figure 5; HILIC-CXC, same as HILIC-CXC run in Figure 1. Peaks were detected at 210 nm. (Reproduced with permission from Mant *et al.*, 1998.)

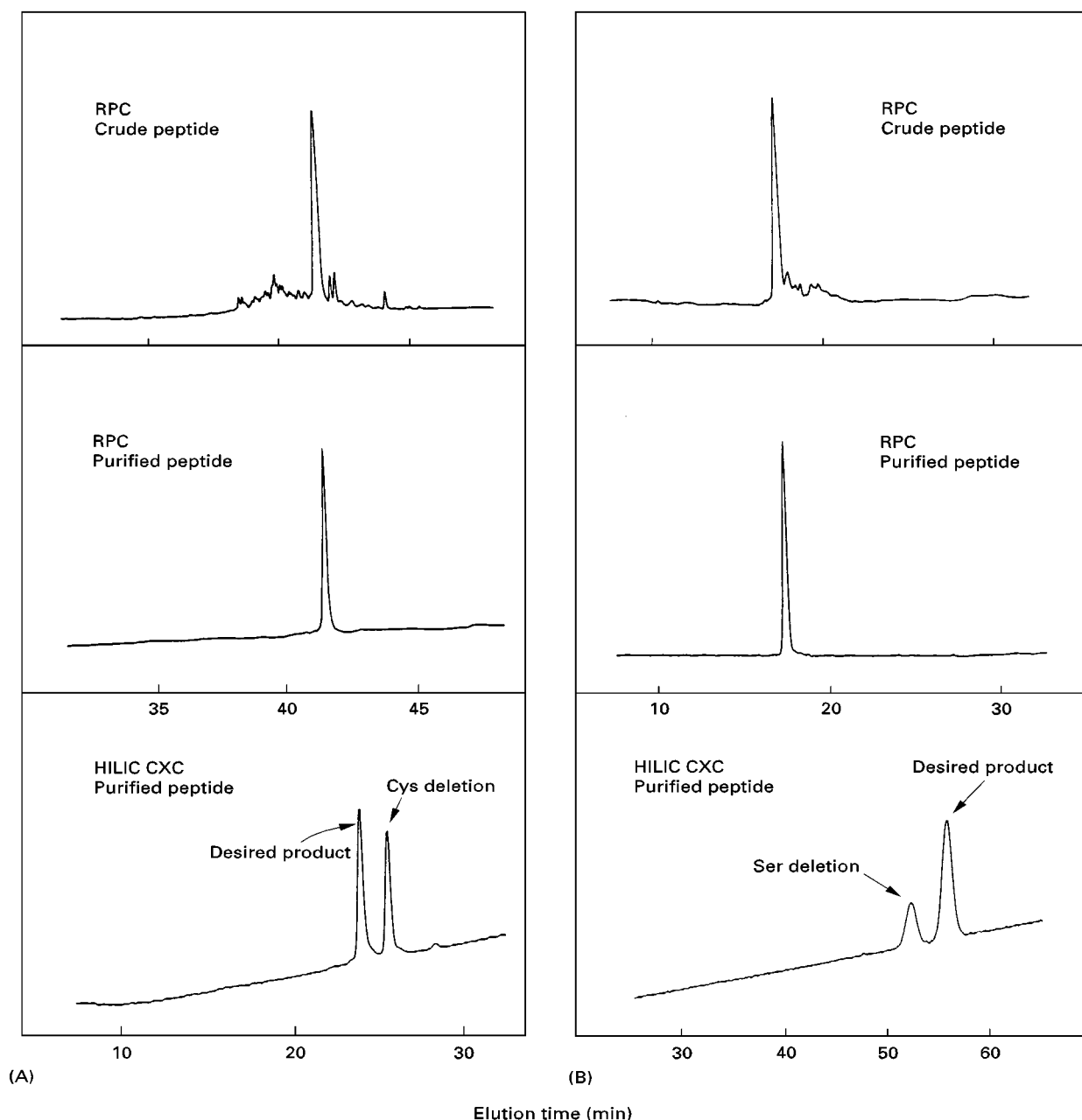


Figure 8 Analysis and purification of synthetic peptides by RPC and HILIC-CXC. (A) 35-residue Cys-containing α -helical peptide; (B) 17-residue intrachain disulfide-bridged peptide. Column: see Figure 1. Conditions: RPC, same as Figure 5 save for a gradient rate of 1% acetonitrile min^{-1} ; HILIC/CXC, linear AB gradient ($2.5 \text{ mmol L}^{-1} \text{ NaClO}_4 \text{ min}^{-1}$ from $30 \text{ mmol L}^{-1} \text{ NaClO}_4$, following 10 min isocratic elution with $30 \text{ mmol L}^{-1} \text{ NaClO}_4$) at a flow rate of 1 ml min^{-1} and a temperature of 26°C , where eluent A is 5 mmol L^{-1} aq. TEAP, pH 7, containing 65% (v/v) acetonitrile and eluent B is eluent A containing $400 \text{ mmol L}^{-1} \text{ NaClO}_4$. Peaks were detected at 210 nm. (Reproduced with permission from Mant *et al.*, 1997.)

makes to the overall hydrophobicity/hydrophilicity with increasing peptide chain length together with any other conformation effects specific to the peptide. **Figure 8A** bottom now illustrates the excellent separation of the two peptides when HILIC-CXC is applied to the purified peptide shown in the middle RPC profile. The loss of the Cys residue makes the peptide more hydrophilic (i.e. less hydrophobic), hence the

later elution of the Cys-deletion impurity. Note that neither IEC nor SEC is suitable as a complementary purification mode for this particular mixture owing to the identical net charge and essentially identical size of the two peptides. From **Figure 8A** a suitable purification protocol is HILIC-CXC of the crude peptide mixture followed by RPC of the desired product for desalting and final purification.

Figure 8B outlines the purification and analysis of a 17-residue synthetic peptide containing an intrachain disulphide bridge (peptide 03138 from Table 1). Following purification of the crude oxidized peptide mixture (top) by RPC, analysis of the purified product showed a single symmetrical peak (middle), indicating, in a similar manner to Figure 8A middle, excellent peptide purity. However, mass spectrometry of this single peak again showed, in addition to the expected mass, a second signal; in this case, this second signal exhibited a peptide mass 87 units less than the desired product, indicating deletion of one of the Ser residues. In RPC terms, Ser is classed as only a slightly hydrophilic group and hence contributes little to the retention behaviour of a peptide during RPC; thus, it is not surprising that the deletion product is difficult to detect, let alone resolve, by RPC. This is particularly true considering (as was subsequently determined) the position of the residue within the intrachain disulphide bridge as well as the 17-residue length of the peptide (see comments above concerning peptide chain length effects). IEC and SEC are again not suitable for isolation of the desired peptide product. However, Figure 8B bottom again illustrates the efficacy of the HILIC-CXC approach to resolving two peptides inseparable by RPC. Indeed, this mixed-mode approach appears to enhance the hydrophilic contribution of a Ser residue, as the Ser-deletion impurity is now baseline-resolved from the desired product. The Ser-deletion peptide is eluted prior to the desired product, since loss of this residue has made the peptide less hydrophilic (i.e. more hydrophobic) than the native peptide. In a similar fashion to the purification problem outlined in Figure 8A for the Cys-containing product, peptide 03138 is also best purified by an initial HILIC-CXC step followed by RPC of the desired peptide product.

Another excellent example of the utility of mixed-mode HILIC-CXC is illustrated in Figure 9 which follows the protocol required to purify a synthetic 21-residue α -helical peptide (denoted J1 in Table 1) from the peptide crude mixture. From the RPC elution profile (top) of the crude peptide, a major peak is obtained with a number of more hydrophilic and hydrophobic impurities, some of which are eluted very close to the main component. Subsequent attempts to improve the isolation of this main peak by varying the pH and/or the ion-pairing reagent used in the RPC mobile phase were unsuccessful, thus ruling out the possibility of an efficient one-step purification by RPC. Application of mixed-mode HILIC-CXC to the crude mixture resulted in the middle elution profile which shows a major peak as well as several other smaller, yet substantial, peptide components. Collection of the major peak followed by RPC produced the

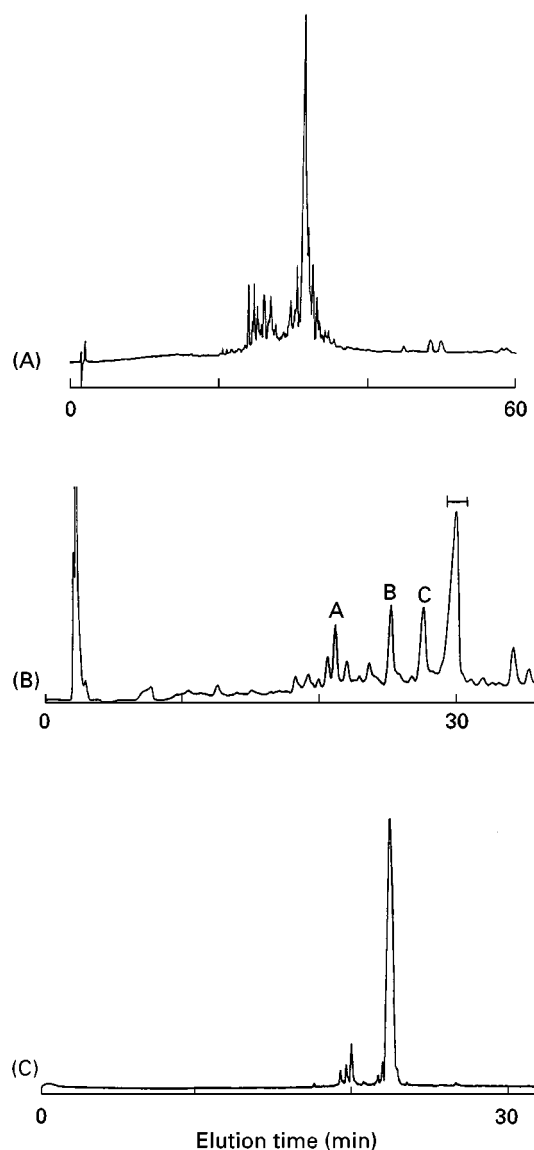


Figure 9 Two-step HILIC-CXC and RPC purification protocol for synthetic peptide. (A) RPC of crude peptide; (B) HILIC/CXC of crude peptide; (C) RPC of HILIC/CXC main peak. Columns: see Figure 1. Conditions: RPC, linear AB gradient (1% acetonitrile min^{-1}) at a flow rate of 1 mL min^{-1} , where eluent A is 0.05% aq. trifluoroacetic acid (TFA) and eluent B is 0.05% TFA in acetonitrile; HILIC-CXC, linear AB gradient $2.5 \text{ mmol L}^{-1} \text{ NaClO}_4 \text{ min}^{-1}$, following 10 min isocratic elution with eluent A at a flow rate of 1 mL min^{-1} , where eluent A is 10 mmol L^{-1} aq. TEAP, pH 6.5, containing 65% (v/v) acetonitrile and eluent B is eluent A containing $350 \text{ mmol L}^{-1} \text{ NaClO}_4$; all runs were carried out at 30°C and peaks were detected at 210 nm. The fraction denoted by the bar in the HILIC-CXC elution profile (panel B) was collected and subsequently purified by RPC (panel C).

bottom elution profile, with the major purified peak shown subsequently by mass spectrometry to be the desired product. Clearly, this two-step protocol was very successful in solving a difficult purification problem. Note that the middle separation, which efficient-

ly removed from the desired product the impurities eluted close to this peptide during RPC (top), could not be achieved by IEC alone, i.e. the high ACN level characteristic of HILIC-CXC was vital to the separation.

A closer look at the HILIC-CXC separation (middle profile), specifically taking note of the three major impurities (denoted A, B and C), again highlights the unique selectivity properties of this mixed-mode approach. Peak A contains Lys-deletion peptide and is thus easily resolved from the desired product due not only to the loss of a positively charged residue but also to the concomitant significant loss of hydrophilicity represented by this decrease in charge character. In contrast, peaks B and C are not deletion products, i.e. they exhibit the same net charge as the product, but are in fact peptides representing modifications of the desired peptide where random acetylation of Ser residues has occurred. Subsequent investigation identified peak B as a peptide analogue with acetylation of a single Ser at position 3 of the sequence (Table 1); peak C represents a peptide analogue with acetylation of a single Ser at position 10 or position 17 of the sequence or possibly a mixture of these two modified analogues. Thus, not only is HILIC-CXC able to resolve these Ser-modified analogues from the desired product, but it is also able to distinguish between the subtle differences in hydrophilicity/hydrophobicity arising from the sequence position of modification.

An explanation for the marked superiority of HILIC-CXC to resolve the Ser-modified impurities from peptide J1 may be gleaned from Figure 10 which presents the sequence of peptide J1 as a helical net with the residues between the lines representing a wide, relatively hydrophilic face compared to the narrow hydrophobic face made up of Ile and Leu residues. The Ser residues (boxed to highlight positions of potential acetylation) lie in this wide hydrophilic face and would thus be expected to interact closely with the ion exchange matrix; conversely, they would be generally oriented away from a reversed-phase matrix, leading to a lesser effect of Ser-modification during RPC. Note that the environment (i.e. residues) surrounding Ser 10 and Ser 17 is identical while that of Ser 3 is quite different, probably accounting for the HILIC-CXC resolution of the Ser 3-modified peptide from that of analogues arising from acetylation at either of the other two positions.

Future Prospects

Clearly, HILIC-CXC offers a valuable, complementary alternative to RPC for peptide separations; indeed, such an approach often rivals RPC for

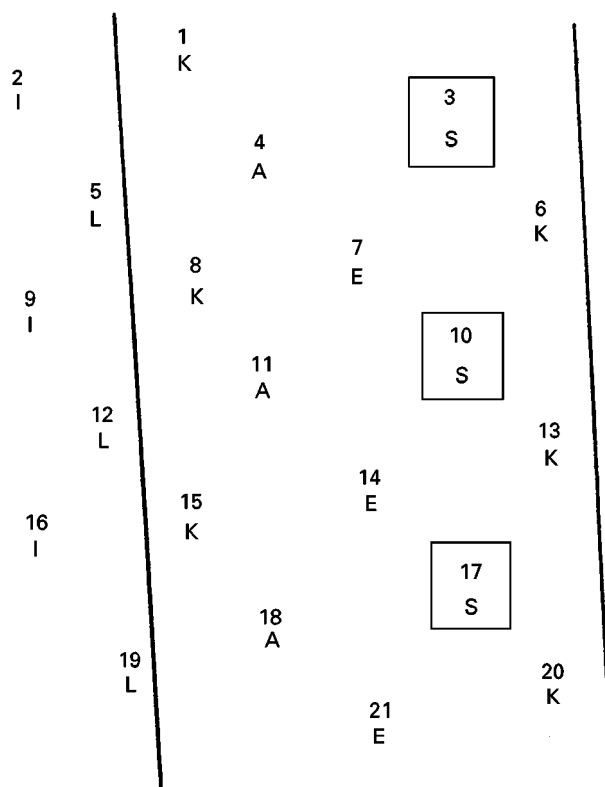


Figure 10 Sequence of synthetic amphipathic peptide J1 presented as an α -helical net. The radius of the α -helix is taken as 0.25 nm with 3.6 residues per turn, a residue translation of 0.15 nm and thus a pitch of 0.54 nm. The area between the lines represents the more hydrophilic face of the peptide, with the Leu and Ile residues representing the narrow hydrophobic face. The boxed Ser residues represent potential sites of side chain acetylation.

resolution of specific peptide mixtures. While the present article offers only a brief overview of the potential of HILIC-CXC for separation of peptides, it has already been successfully employed for protein separations where RPC alone was unable to effect the required resolution. In addition, since the need to identify peptide mixture components as well as to separate and quantify them is great, e.g. HPLC in conjunction with electrospray mass spectrometry (HPLC-MS), the utility of HILIC-CXC separations will be enhanced even further with the development of volatile mobile phases.

See also: II/Chromatography: Liquid: Mechanisms: Ion Chromatography; Mechanisms: Reversed Phases; Mechanisms: Size Exclusion Chromatography.

Further Reading

Alpert AJ (1990) Hydrophilic-interaction chromatography for the separation of peptides, nucleic acids and other

- polar compounds. *Journal of Chromatography* 499: 177.
- Lindner H, Sarg B and Helliger W (1997) Application of hydrophilic-interaction liquid chromatography to the separation of phosphorylated H1 histones. *Journal of Chromatography* 728: 55.
- Mant CT and Hodges RS (eds) (1991) *High-performance Liquid Chromatography of Peptides and Proteins: Separation, Analysis, and Conformation*. Boca Raton: CRC Press.
- Mant CT and Hodges RS (1996) Analysis of peptides by high-performance liquid chromatography. *Methods in Enzymology* 271: 3.
- Mant CT, Kondejewski LH, Cachia PJ, Monera OD and Hodges RS (1997) Analysis of synthetic peptides by high-performance liquid chromatography. *Methods in Enzymology* 289: 426.
- Mant CT, Litowski JR and Hodges RS (1998) Hydrophilic interaction/cation-exchange chromatography for separation of amphipathic α -helical peptides. *Journal of Chromatography* 816: 65.
- Mant CT, Kondejewski LH and Hodges RS (1998) Hydrophilic interaction/cation-exchange chromatography for separation of cyclic peptides. *Journal of Chromatography* 816: 79.
- Zhu B-Y, Mant CT and Hodges RS (1991) Hydrophilic-interaction chromatography of peptides on hydrophilic and strong cation-exchange columns. *Journal of Chromatography* 548: 13.
- Zhu B-Y, Mant CT and Hodges RS (1992) Mixed-mode hydrophilic and ionic interaction chromatography rivals reversed-phase liquid chromatography for the separation of peptides. *Journal of Chromatography* 594: 75.

Thin-Layer (Planar) Chromatography

R. Bhushan, University of Roorkee, Roorkee, UP, India
J. Martens, Universität Oldenburg, Oldenburg, Germany

Copyright © 2000 Academic Press

Introduction

Thin-layer chromatography (TLC) has found extensive application in protein chemistry including recovery of peptides in microgram and nanogram quantities for further primary structural analysis, identification of peptides in partial hydrolysates, in correlating the chromatographic properties of the intact peptides with those of individual amino acids, peptide mapping to characterize or to identify a protein available in very small quantities, resolution of diastereomeric and enantiomeric peptides without any derivatization, fractionation of proteins on the ultramicro scale, testing the optical homogeneity of synthetic peptides, and determination of relative molecular masses.

Application of TLC to the following aspects of peptide studies have also been reported: experimental studies of solute retention and support matrix effects in reversed-phase TLC (RP-TLC) of peptides; a rapid thin-layer immunochromatography method using monoclonal antibodies of two distinct specificities for quantitation of protein antigens; non-stoichiometric models for theoretical treatment of the chromatographic process on ion exchange phases; determination of amino acid configuration of synthetic peptide analogues on Chiralplate® with MeCN/MeOH/H₂O (4:1:1), prepared from the

racemic aromatic amino acids; dependence of the silanophyl effect on the chemical structure of peptides and on the type of mobile phase; study of the salting out behaviour of some peptides with aromatic groups by adsorption TLC on cellulose; separation of peptides on Empore TLC sheets and blotting onto polyvinylidene difluoride (PVDF) membranes with subsequent gas-phase sequencing; analysis of peptide and protein hydrolysates by 2D cellulose TLC and densitometry and its application to luteinizing hormone.

A knowledge of the behaviour of peptides and proteins with both the mobile and stationary phases, particularly with respect to information about kinetics of diffusion, adsorption and desorption, denaturation or conformation changes, is required. Optimization of chromatographic separations of peptides and proteins means a complete resolution of all components in a minimum time, on a preparative scale and with the retention of bioactivity. Various principles of liquid chromatography have successfully been applied to TLC resolution of peptides and proteins, e.g. reversed-phase, size exclusion, ion exchange, etc. The different thin-layer materials used for the purpose include silica gel, cellulose, mixtures of silica gel and cellulose, hydroxyapatite and cross-linked dextran gel filtration media like Sephadex® (various grades from Pharmacia, Uppsala, Sweden). The ordinary porous silica-based stationary phases containing chemically bonded alkyl chains of varying lengths have several disadvantages such as low stability at alkaline pH values (pH > 8), secondary equilibria caused by low diffusion kinetics within the pores,

and ion-exchange effects due to ionized underivatized silanol groups. Therefore, alternative stationary phases are being developed, e.g. coated silica phases, polymer-based phases, and nonporous materials. The separation and purification of peptides and proteins by ion exchange offers advantages because of mild separation conditions providing higher bioactivity recovery.

Sample Preparation

Depending on the nature and source, the proteins may be digested before applying them to thin-layer plates; some of the methods reported in the literature are described below.

1. Proteins are dissolved in ammonium bicarbonate (0.5%, pH 8.0) and digested with trypsin (1% w/w) for 4 h at 37°C. Chymotrypsin (1% w/w) may be added for trypsin–chymotrypsin digest and the digestion continued for a further 4 h. The peptides are recovered by freeze-drying.
2. Proteins may either be alkylated with iodoacetic acid or oxidized with performic acid to render them susceptible to enzymatic digestion. The treated proteins are then dissolved in ammonium bicarbonate buffer (0.05 mol L⁻¹, pH 8.4) to a concentration of 2 mg mL⁻¹ and TPCK-treated trypsin (1-(1-tosylamide-2-phenylethyl chloromethyl ketone)) is added to give a final enzyme-to-substrate ratio of 1 : 75. The digest is incubated for 5 h at 30°C, freeze-dried, and redissolved in 10% isopropanol for application to the plates.

For TLC of smaller peptides, the samples have either been synthesized or obtained commercially. The stock solutions (0.025 mol L⁻¹) are prepared in aqueous 2-propanol (10%) and are kept refrigerated when not in use. For proteins, solutions can be prepared in dilute saline solutions or in an appropriate buffer.

Preparation of Thin-Layer Plates

Commercially available precoated silica or cellulose plates have generally been used. Sometimes these plates have uneven coatings that can be checked by holding the plates against a light box and looking for dark streaks or patches that indicate uneven thickness. Such plates should be rejected or used for initial trial runs only. The following method has been widely used for making plates with cellulose powder. Preparation of thin-layer plates from Sephadex is also described.

Thin-Layer Plates from Cellulose

Cellulose powder is slurried with methanol/water (4 : 1, 200 mL). The slurry is poured into a Büchner funnel and is washed successively with 2-propanol/water/acetic acid (3 : 1 : 1, 300 mL); methanol/water (1 : 3, 200 mL); methanol/1 mol L⁻¹ HCl (3 : 2, 200 mL); water (200 mL), and finally with methanol (200 mL). The powder is dried overnight *in vacuo* before use. The purified cellulose powder (15 g) is spread as a slurry over five plates (20 × 20 cm) at an initial thickness of 400 µm. The coated plates are allowed to dry overnight in a horizontal position before use.

Thin-Layer Plates from Gel Filtration Media

Sephadex G-100 (6 g) or Sephadex G-200 is suspended in 100 mL of the solvent (e.g. 0.5 mol L⁻¹ NaCl solution). Care should be taken to ensure that no aggregates are present in the final gel suspension. The dextran gels usually take 48 h to proceed to complete swelling. Thoroughly cleaned and dry glass plates (10 cm × 20 cm) are coated with a 0.9 mm-thick layer of a suitable thin-layer spreader. The plates are kept in a closed vessel containing a dish of the solvent and stored in the horizontal position for at least 18 h before use. The layers may be stored for fairly long periods in a wet chamber; if they dry out or show cracking, a very mild spray with buffer solution is applied to regenerate the layers.

Development of Chromatograms

The silica gel or cellulose-based chromatograms are developed in the usual manner, while the development of gel plates is carried out as shown in Figure 1.

Various solvent systems, support materials, and detection procedures for the TLC of a variety of proteins and peptides have been summarized in

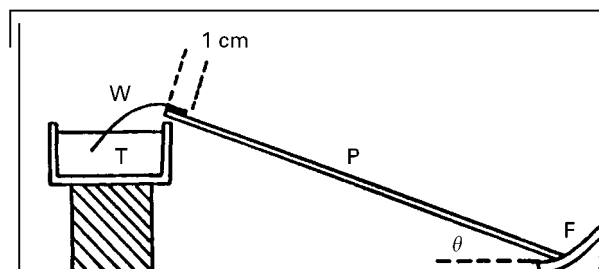


Figure 1 Apparatus for thin-layer chromatography of proteins. Solvent (0.5 M NaCl) is led to plate P by means of Whatman No. 3 filter paper wick W. The wick should overlap about 1 cm onto the gel layer. T is the solvent trough.

Table 1. The R_F values for some of these systems have been recorded in Tables 2–6.

For two-dimensional peptide mapping, conventional chromatography follows electrophoresis. The plate is dampened with electrophoresis buffer, taking care not to smudge the applied sample, and run at 1000 V for 40–90 min, for 20 cm × 20 cm plates. The electrophoresis plate is removed from the apparatus and dried overnight in a fume hood (there should be no smell of acetic acid on the plates). The plate is then developed using a suitable chromatographic solvent (Table 1). The composition of the solvent is critical for the mobility of peptides. More organic solvent in the mixture tends to increase the relative mobility of the hydrophobic peptides, since the stationary phase is hydrophilic. Some of the solvent systems used for two-dimensional work are mentioned in Table 7.

Detection of Peptides on Thin-Layer Chromatograms

Various peptides and proteins are located on the thin layer chromatograms by using ninhydrin, fluorescamine, o-phthalaldehyde, iodine vapours or UV. Quantitation is performed by densitometric scanning or by spectrophotometry after eluting the peptides; immunochromatography using monoclonal antibodies has also been used for quantification.

Detection on Cellulose or Silica Gel Plates

The plates can be viewed using a long-wavelength (366 nm) UV source or stained with a suitable reagent as described in Table 1. Certain other detection methods are described below.

1. *Morin reaction.* The dried chromatograms are sprayed with a 0.05% solution of morin (3,5,7,2',4-pentahydroxyflavone) in methanol, and heated for 2 min at 100°C. The *N*-protected amino acids and peptide derivatives give yellowish-green fluorescence on a green fluorescent background, or dark absorption spots under UV. The detection limit is about 2 µg per spot.
2. *Iodine starch reaction.* The chromatogram is placed in an iodine vapour atmosphere for 5 min. The excess iodine is removed by leaving the plate in the open air, and then the layer is sprayed with 1% aqueous starch solution. The peptides (and amino acids) give blue spots.

Detection on Gel Layers

The gel layer is covered with dry filter paper (Whatman 3 mm), avoiding bubble formation and is carefully smoothed down over it. The layer and the paper

are dried together at 120°C or the paper is carefully peeled off the layer and dried at 110°C.

The proteins on the paper are detected by the usual paper chromatographic methods. The dried paper is immersed for 15 min in Amido black 10 B (0.6 g) dissolved in a mixture of methanol or ethanol (750 mL), water (450 mL), and glacial acetic acid (100 mL) and washed three times with 1% acetic acid for 30 min each time. Alternatively, the paper is stained in 1% solution of Bromophenol blue saturated with mercuric chloride for 5 min and then washed five times with 0.5% acetic acid for 30 min each time.

Recovery of Peptides

After detection, the peptide spots on the cellulose or silica gel thin layers are carefully scraped and are transferred to 150 mm long Pasteur pipettes that have been tightly plugged with one-quarter of a glass fibre membrane filter (20 mm diameter, Sartorius SM 13400) and prewashed with 2 mL of 6 mol L⁻¹ HCl; 200 µL of 6 mol L⁻¹ HCl containing 0.02% β -mercaptoethanol is added to each of the Pasteur pipettes and the peptide is extracted at room temperature for 15 min. The HCl is then forced through the filter with nitrogen (1 atm).

TLC of Diastereomeric and Enantiomeric Dipeptides

Successful separation of dipeptide diastereomers, either as the free peptides or as the *N*-protected methyl esters, has been reported. Starting from pure L-methionine and DL-alanine, Np-S-L-Met-DL-Ala-O-Np and Np-S-L-Met-L-Met-DL-Ala-O-Np were synthesized and the separation of diastereomeric *p*-nitrophenyl (Np) esters of *N*-protected di- and tripeptides was achieved on silica gel F₂₅₄ precoated (Merck) plates. TLC separation of diastereomeric dipeptides has been well documented.

Typical examples of the separation of enantiomeric dipeptides on Chiralplates® are given in Table 5. It was observed that the antipodes with C-terminal L-configuration always gave a smaller R_F value than the corresponding enantiomeric dipeptide with C-terminal D-configuration. The method also resolves diastereomeric dipeptides. A comparison of resolution of four isomeric Try-Try, Ala-Ala, Phe-Phe, Tyr-Tyr, Lys-Ala, and Asp-Ala mixtures on Chiralplates® and on microcrystalline cellulose plates showed that the separation of L,L and D,D pairs of all tested dipeptides was better on microcrystalline cellulose plates while L,D, and D,L pairs were better separated on Chiralplates® (Figure 2A, B).

Table 1 Solvent systems, support materials, and detection procedures for TLC of proteins and peptides

No.	Protein/peptide	Developing system	Detection
1	Carbazo peptides	(a) <i>n</i> -Butanol/acetone/acetic acid/5% NH_4OH /water (9 : 3 : 2 : 4) (b) <i>n</i> -Butanol/acetone/5% NH_4OH (11 : 6 : 3) (c) <i>n</i> -Butanol/acetone/pyridine/water (15 : 3 : 10 : 12) (d) <i>n</i> -Butanol/acetone/5% NH_4OH /H ₂ O two-phase mixture (6 : 1 : 1 : 2) CHCl_3 (34%) NH_4OH /ethanol (2 : 1 : 2)	0.2% Ninhydrin spray (<i>n</i> -Butanol/2 N acetic acid, 95 : 5) followed by a spray of a saturated solution of $\text{K}_2\text{Cr}_2\text{O}_7$ in conc. H_2SO_4
2	Leu-Try-Leu		Dried for 2 h at 60°C, sprayed with 1% (v/v) triethylamine in acetone followed by 0.1% fluorescamine in acetone
3	Np-S-L-Met-DL-Ala-O-Np, Np-S-L-Met-L-DL-Ala-O-Np, Np-S-Met-Ala-Met-OMe	Solvents and hR_F given in Table 3	Iodine
4	<i>N</i> -t-butoxy peptides	Ethanol/pyridine/water/acetone (5 : 5 : 3 : 1)	Exposure to chlorine followed by spraying with α -toluidine reagent or dicarboxidine reagent
5	Lysino alanine	(a) Butanol/anhydrous acetic acid/water (4 : 1 : 1) (b) Phenol/water (3 : 1)	Ninhydrin
6	Peptides from proteases	(a) Chloroform/methanol (3 : 1) (b) Chloroform/methanol/acetone (45 : 4 : 1)	(a) Aqueous 2% sodium nitroprusside (b) 4% Ninhydrin in acetone/pyridine/acetone (97 : 3 : 2) (c) 1-Naphthol/NaBrO (Sakaguchi reagent) 0.5% Ninhydrin in acetone
7	Insulin	(a) 0.1 N HCl/96% ethanol (1 : 1) (b) 0.5 N HCl/ethanol/acetone (5 : 3 : 0.5)	0.5% Ninhydrin in acetone, heated at 100°C
8	Pepsin, trypsin and α -chymotrypsin	(a) 0.1 N HCl/ethanol (1 : 1) (b) 0.5 N HCl/ethanol/acetone (5 : 3 : 0.5)	Ninhydrin
9	Angiotensin	(a) <i>n</i> -Butanol/acetone/water (4 : 1 : 1) (b) <i>n</i> -Butanol/pyridine/water (15 : 10 : 3)	UV
10	Bradykinin	<i>iso</i> -Propanol/methyl acetate/conc. ammonia (9 : 7 : 4)	UV after exposure to dioxane vapours
11	Dansyl peptides from ATP-creative phosphotransferase	Methyl acetate/ <i>iso</i> -propanol/conc. ammonia (9 : 7 : 4)	Chlorine/toluidine
12	Glycopeptides from <i>Escherichia coli</i> and <i>Bacillus megaterium</i>	<i>n</i> -Butanol/pyridine/acetone/water (130 : 20 : 6 : 24)	P_2O_5 , 130°C
13	Lipopeptides from <i>Nocardia asteroides</i>	Chloroform/methanol (1 : 1)	Chlorine/toluidine, KMnO_4
14	Cyclotriptides from <i>Aspergillus ochraceus</i>	Five different solvent systems	Ninhydrin/chlorine/toluidine
15	Basic polypeptides	(a) <i>n</i> -Butanol/25% ammonia/water (34 : 3 : 3) (b) Chloroform/methanol (9 : 1)	0.5% Ninhydrin in acetone, heated at 100°C for 10 min
16	Lipase, diastase, papain, emulsin, invertase	96% Ethanol/0.1 N HCl (1 : 1)	Radioactivity
17	Lipopeptides from <i>E. coli</i>	Chloroform/methanol/water (68 : 25 : 4)	

Table 1 Continued

No.	Protein/peptide	Developing system	Detection
18	Angiotensin antagonists	(a) Chloroform/acetone (5 : 1) (b) <i>n</i> -Butanol/acetic acid/water (4 : 1 : 1)	Ninhydrin
19	Vasopressin and xylocin, tripeptide amides	Butanol/acetic acid/water (4 : 1 : 1)	UV
20	<i>N</i> -methyl oligopeptides	(a) Chloroform/methanol (9 : 1) (b) Chloroform/acetone (8 : 2 or 9 : 1)	Chlorine/toluidine, UV, iodine UV, iodine
21	Dansyl peptides of lipoproteins	Three different solvent systems	Ninhydrin
22	Glycoprotein-derived oligosaccharides	Propanol/acetic acid/water (3 : 3 : 2)	Orcinol
23	Various peptides	Chloroform/methanol/aq. 17% ammonia (2 : 2 : 1)	Sprayed with 0.1% solution of 4-chloro-7-nitrobenzofuran in ethanol, followed by 50% methanol (adjusted to pH 11 with (NaOH)
24	Enantiomeric and diastereomeric dipeptides (on Chiralplate)	Solvents and hR_F given in Table 5	0.1%
25	<i>Boc</i> - β -Ala-Try-Met-Asp-Phe	Chloroform/methanol/acetic acid (18 : 2 : 1); sec-butanol/3% ammonia (25 : 11 and 3 : 1); ethanol/acetic acid/water (20 : 6 : 11); <i>n</i> -butanol/acetic acid/water (4 : 1 : 5, upper phase)	Ninhydrin, Ehrlich reagent, fluorescamine reagent
26	Oligopeptides (8 standard samples)	(a) <i>iso</i> -Amyl alcohol/ethanol/anhyd. acetic acid/pyridine/water (175 : 50 : 13 : 175 : 150) (b) <i>iso</i> -Propyl alcohol/ethanol/aq. ammonia (4 : 4 : 3)	Ninhydrin
27	Lysino alanine	(a) <i>iso</i> -Propyl alcohol/1 M HCl (3 : 1) (b) <i>tert</i> -Butyl alcohol/acetone/methanol/water/conc. ammonia (4 : 4 : 1 : 14 : 5); electrophoresis in glacial acetic acid/98% formic acid/water (17 : 5 : 28, pH 2)	Ninhydrin
28	Ribonuclease B, globin, R17-bacteriophage coat protein, carboxymethylated protein, subunits from BI component of TYMV; tryptic digest of glyceraldehyde 3-phosphate dehydrogenase of yeast	(a) <i>n</i> -butanol/pyridine/acetic acid/water (15 : 12 : 3 : 12) (b) <i>iso</i> -Butanol/pyridine/water (7 : 7 : 6) (c) <i>iso</i> -Amyl alcohol/pyridine/water (7 : 7 : 6) (d) Butanol/acetic acid/water (5 : 1 : 4), upper phase	Cd-Ninhydrin spray followed by heating at 60°C
29	Dipeptides with Leu/Ile as <i>N</i> -terminal residues	Solvent and hR_F given in Table 4	Cd-Ninhydrin spray followed by densitometry
30	Several di- and tripeptides (see Table 2)	Solvents and hR_F given in Table 2	Cd-Ninhydrin spray followed by heating at 60°C for 15 min
31	S-Carboxymethyl insulin chain-A, Ala-Leu-Gly, Leu-Leu-Val-Tyr, Glu-Gly-Phe	(a) Pyridine/acetic acid/water/acetone (2 : 4 : 79 : 15) at pH 4.4, electrophoresis (b) <i>n</i> -Butanol/pyridine/acetic acid/water (915 : 10 : 3 : 12)	(a) 0.3% Ninhydrin in collidine/acetic acid/ethanol (3 + 100 + 87) (b) 1% Fluorescamine (w/v) in acetone (c) 0.05% α -Phthalaldehyde in methanol (w/v) containing 0.2% β -mercaptoethanol and 0.09% Brij-35; sheets pre- and postsprayed with 10% triethylamine in methylene chloride

Table 1 Continued

No.	Protein/peptide	Developing system	Detection
32	Tryptic peptides from polyoma virus	(a) Acetic acid/0.5% pyridine, pH 3.5 (25 V cm ⁻¹) for electrophoresis (b) <i>n</i> -Butanol/acetic acid/water/pyridine (5 : 1 : 4 : 1)	Ninhydrin spray
33	Ribonuclease S protein	(a) 1.25 mol L ⁻¹ Pyridine acetate buffer, pH 6.45, 400 V for electrophoresis (b) Butanol/acetic acid/pyridine/water (30 : 6 : 20 : 24), TLC	Cd-Ninhydrin
34	Actinomycinhydrolysate	(a) Formic acid/acetic acid, pH 6.0 10 mA, electrophoresis (b) Butanol/water/acetic acid (5 : 4 : 1) TLC	Cu-Ninhydrin, fluorescamine
35	Acid hydrolysates of collagen	(a) <i>iso</i> -Propanol/butanone/1 mol L ⁻¹ HCl (12 : 3 : 5) (b) 2-Methyl-2 butanol/butanone/acetone/methanol/conc. ammonia (5 : 4 : 7 : 1 : 4)	Cd-Ninhydrin, <i>o</i> -phthalaldehyde
36	Cystine peptides	Butanol/acetic acid/water (71 : 7 : 22)	Ninhydrin
37	Streptococcal peptides	Aq. 10% trichloroacetic acid	Ninhydrin
38	Enantiomeric dipeptides, Try-Try, Ala-Ala, Phe-Phe, Tyr-Tyr, Lys-Ala, Asp-Ala (synthesized)	Pyridine/water (2 : 1 or 4 : 1) at -10°C	Ninhydrin
39	Bovine serum-albumin, bovine γ -globulin, α -chymotrypsin, cytochrome c, haemoglobin, lysozyme, myoglobin, ovalbumin, ovomucoid, pepsin, ribonuclease, thyroglobulin, trypsin (Sephadex G-100, G-200)	Solvent and <i>R_f</i> given in Table 6	Staining in 0.2% Ponceau S in 10% aq. acetic acid for 30 min followed by washing with water
40	Ornithine carbamoylphosphate transferase (Sephadex G-200, G-200 superfine)	0.5 mol L ⁻¹ NaCl	Amido black 10B in methanol/water/glacial acetic acid (5 : 4 : 1)
41	α -Chymotrypsin, aldose, catalase, bovine serum albumin, ovalbumin, lysozyme, phosphorylase b, β -galactosidase, alkaline phosphatase, lactate dehydrogenase, glyceraldehyde phosphate dehydrogenase (Sephadex G-75 and G-100)	6 mol L ⁻¹ guanidine hydrochloride (descending chromatography)	On paper, by spraying with diazotized sulfanilic acid
42	Small peptides on aluminium-backed thick silica gel	-	Fluorescence
43	Cystine and its peptides on polyamide or silica gel	-	Spraying with dilute 2-nitro-5-sulfothiobenzoate
44	Peptides from soya bean meals on KHSO ₄ -coated silica gel plates	Butanol/dioxane/water (4 : 5 : 1)	Treated with saturated thiobarbituric acid solution 85% H ₃ PO ₄ (1 : 1), then with ethanolic naphthoresorcinol/20% H ₂ SO ₄ (10 : 1), heated at 105°C
45	Phenyl alanine peptides on ammonium tungstophosphate-coated silica gel	0.1 mol L ⁻¹ Nitric acid/1 mol L ⁻¹ ammonium nitrate	

Table 1 Continued

No.	Protein/peptide	Developing system	Detection
46	Small peptides	Suspended over aq. 2,4,6-trimethyl pyrylium tetrafluoroborate and alkaline with 0.5 mL of triethyl amine then adjusted to pH 3 by acetic acid (chamber temp 80°C)	SIMS
47	Peptides on silica gel 60H	Water or aq. methanol	Ninhydrin
48	Oleoyl-L-alanyl-L-alanine	Water/MeCN (7 : 3), pH 5.0	Ninhydrin
49	Peptides on cellulose, impregnated cellulose or alumina layers (reversed-phase)	Propan-1-ol as organic component	—
50	Enantiomeric peptides on Chir® plate	—	—
51	Peptide from <i>Schumanniohyton magnificum</i> with anti-cobra venom activity on silica, or silica impregnated with 5% liq. paraffin in petrol ether	Acetone/methanol/10% ammonia (3 : 1 : 1); butanol/methanol/10% ammonia (3 : 1 : 1); chloroform/methanol (1 : 1)	Spraying with Dragendorff reagent, 5% ferric chloride, or 2% ninhydrin in acetone
52	HBsAG (hepatitis B virus) segments in soln on silica	Ethyl acetate + stock soln of pyridine/acetic acid/water (20 : 6 : 11) in various proportions	Spraying with toluidine/KI after chlorination
53	Protein antigens	A sandwich assay format using monoclonal antibodies of two distinct specificities, on covalently immobilized to a defined detection zone on a porous membrane while other serves as a label. Sample is mixed with the coating, and the mixture is then passed along a porous membrane in detection zone.	Monoclonal antibodies immobilized to a defined zone on a porous membrane; blue colour
54	Thyrotropin hormone, on silica	Chloroform/methanol (9 : 1), or ethyl acetate + stock soln of pyridine/acetone/water (20 : 5 : 11) in ratio 6 : 4.	—

Layer material for S. nos 1–25, 42–45, 51–52, 54, silica gel, for S. nos 26–38, cellulose; for S. nos 39–41, Sephadex; for S. no. 49 cellulose or alumina; and for S. no. 50, Chir® plate.

Table 2 $^a hR_F$ values of peptides from L-amino acids after one-dimensional TLC on cellulose

Peptides	Solvent systems				
	A	B	C	D	E
Ala-Ala	65	26	55	68	58
Ala-Asp	56	1	45	44	19
Ala-Glu	64	5	58	56	29
Ala-Gly	50	17	36	46	46
Ala-Phe	94	52	86	84	85
Ala-Ser	52	17	36	41	49
Gly-Ala	52	18	37	43	46
Gly-Asp	43	0	30	29	13
Gly-Gly	34	13	22	29	34
Gly-His	7	16	5	16	32
Gly-Ile	81	49	65	80	75
Gly-Leu	82	51	67	87	80
Gly-Lys	14	11	2	21	27
Gly-Phe	75	50	65	76	67
Gly-Pro	47	17	39	45	44
Gly-Ser	32	13	22	28	26
Gly-Tyr	68	28	45	64	51
Gly-Val	72	36	56	73	62
Leu-Ala	97	56	88	90	89
Leu-Gly	82	52	67	84	83
Leu-Val	100	77	98	96	95
Val-Gly	67	38	56	70	69
Val-Leu	100	80	98	100	95
Ala-Gly-Gly	47	13	34	39	43
Glu-Cys-Gly	16	0	7	7	0
Gly-Gly-Gly	32	8	20	31	30
Val-Gly-Gly	65	28	52	65	61

^a hR_F is the R_F value multiplied by 100.

Solvent systems: A, 2-propanol/butanone/1 M HCl (60 : 15 : 25); B, 2-methyl butan-2-ol/butanone/propanone/methanol/water/ammonia (10 : 4 : 2 : 1 : 3 : 1); C, 2-propanol/water (3 : 1); D, 2-propanol/water/acetic acid (15 : 4 : 1); E, 2-propanol/water/ammonia (15 : 4 : 1). All proportions are v/v.

Separation of Peptides on Reversed-Phase Plates Impregnated with Ion Pair Reagents

Successful separations of a large number of di- and tripeptides, and some tetra- and pentapeptides, on home-made silanized silica gel plates and reversed-phase (RP-2, RP-8, RP-18) plates impregnated with dodecylbenzenesulfonic acid, anionic and cationic detergents such as triethanolaminedodecylbenzene sulfonate (DBS), sodium dioctylsulfosuccinate (Na-DSS), and *N*-dodecylpyridinium chloride (*N*-DPC), and on ammonium tungstophosphate layers have been reported in the literature. The separation conditions and hR_F values of some polypeptides of moderate size and of similar structure on home-made layers of silanized silica gel and RP-2 plates are recorded in Table 8. The separation of such pep-

Table 3 hR_F values for dipeptides and tripeptides

Peptides	hR_F	Solvent
Np-S-Met-Ala-O-Np		
L-L	77	
L-D	67	A
Np-S-Met-Met-Ala-O-Np		
L-L-L	58	
L-L-D	66	B
Np-S-Met-Ala-Met-OMe		
L-L-L	56	
L-D-L	52	C

Solvents: A, acetic acid/diethyl ether (1.5 : 20, v/v); B, acetic acid/diethyl ether (0.2 : 20, v/v); C, diethyl ether/iso-propanol (20 : 0.25, v/v). Np = p-nitro phenyl-.

tides is, however, a difficult problem of analytical importance.

The different solvent systems and chromatographic conditions used for these separations are summarized in Table 9. The description of the peptides and their structures is omitted. These systems may thus provide helpful guidance for choosing or developing a solvent system according to the actual requirement of the experiment.

Table 4 Chromatographic behaviour of dipeptides from L-amino acids on thin layers of cellulose

Peptides	hR_F			Colour yield ($\text{mm}^2 \mu\text{mol}^{-1}$) $\times 10^{-4}$	
	A	B	C	405 nm	490 nm
Ile-Ala	90	68	56	3.5	7.8
Ile-Gly	84	53	46	3.7	5.2
Ile-Glu	94	13	13	10.1	23.0
Ile-Leu	100	88	86	1.6	14.6
Ile-Lys	58	50	41	86.6	22.5
Ile-Met	94	79	80	3.7	8.4
Ile-Phe	100	81	89	4.5	13.6
Ile-Pro	89	60	63	2.9	3.5
Ile-Ser	87	53	38	5.8	13.7
Ile-Try	100	83	83	2.6	10.8
Ile-Val	100	80	83	5.8	14.5
Leu-Ala	97	58	–	2.9	5.1
Leu-Gly	82	52	0	2.9	5.6
Leu-Leu	99	66	83	3.8	8.5
Leu-Met	100	71	75	9.6	15.1
Leu-Phe	99	73	79	6.9	10.5
Leu-Ser	88	61	41	4.5	9.8
Leu-Try	100	73	77	7.7	13.0
Leu-Tyr	97	67	66	8.9	10.8
Leu-Val	100	77	–	3.1	5.0

Solvents: A, 2-propanol/butanone/1 mol L⁻¹ HCl (12 : 3 : 5); B, 2-methyl-2-butanol/butanone/propanone/methanol/water/0.88 NH₃ solution (10 : 4 : 2 : 1 : 3 : 1); C, *n*-butanol/butanone/water/0.88 NH₃ (80 : 5 : 17 : 3).

Table 5 Resolution of enantiomeric and diastereomeric dipeptides

Enantiomeric dipeptide		hR_F values			
		A		B	
L-isomer	D-isomer	L	D	L	D
Gly-L-Phe,	Gly-D-Phe			57	63
Gly-L-Leu,	Gly-D-Leu			53	60
Gly-L-Ile,	Gly-D-Ile			54	61
Gly-L-Val,	Gly-D-Val			58	62
Gly-L-Try	Gly-D-Try			48	55
D-Leu-L-Leu,	L-Leu-D-Leu	19	26	48	57
D-Ala-L-Phe,	L-Ala-D-Phe	21	26	59	65
D-Met-L-Met,	L-Met-D-Met	29	33	64	71

Diastereomeric dipeptides hR_F in eluent B

Diastereomeric dipeptides	hR_F in eluent B
L-Leu-L-Leu	45
L-Leu-D-Leu	53
L-Ala-L-Ala	64
L-Ala-D-Ala	70
L-Ala-L-Phe	59
L-Ala-D-Phe	65
L-Met-L-Met	62
L-Met-D-Met	72

Solvent system: A, methanol/water/acetonitrile (1 : 1 : 4, v/v); B, methanol/water/acetonitrile (5 : 5 : 3, v/v). Length of run 13 cm. Detection: 0.1% ninhydrin reagent.

Table 6 $^aR_{Hb}$ values of proteins on Sephadex plates

Protein	Molecular weight $\times 10^{-2}$	$^aR_{Hb}$	
		A	B
Cytochrome-C	13.0	0.68	0.74
Ribonuclease	13.6	0.68	0.74
Lysozyme	14.5	0.65	0.70
Myoglobin	16.9	0.79	0.80
α -Chymotrypsin	22.5	0.87	0.87
Trypsin	23.8	0.83	0.86
Ovomucoid	27.0	0.94	1.03
Pepsin	35.0	0.99	1.04
Ovalbumin	45.0	1.03	1.04
Haemoglobin	68.0	1.00	1.00
Bovine serum albumin	65.0	1.28	1.54
Bovine γ -globulin	180.0	1.28	1.54
Thyroglobulin	650.0	1.33	1.83
Macroglobulin	1000		1.86

$^aR_{Hb} = d_p/d_{Hb}$, where d_p and d_{Hb} are the distances traversed by the test protein and by hemoglobin, respectively.

A, plates of Sephadex G-100, developed in 0.5 mol L⁻¹ NaCl solution; B, plates of Sephadex G-200, developed in 0.5 mol L⁻¹ NaCl solution.

Table 7 Conditions for fingerprinting tryptic peptides on silica gel G thin-layer plates (20 cm \times 20 cm \times 0.1–0.25 mm)

First dimension: electrophoresis

pH 3.5, pyridine/acetic acid/water (2 : 20 : 978, v/v) 1000 V, 45 min

pH 6.5, pyridine/acetic acid/water (100 : 3 : 897, v/v) 1000 V, 40 min

pH 4.7, *n*-butanol/pyridine/acetic acid/water (2 : 1 : 1 : 18, v/v)

Second dimension: chromatography at 25°C

Chloroform/methanol/ammonium hydroxide (2 : 2 : 1, v/v)

n-Propanol/ammonium hydroxide (7 : 3, v/v)

n-Butanol/pyridine/acetic acid/water (97 : 75 : 15 : 60, v/v), pH 5.3

Determination of Relative Molecular Mass of Proteins

Since there is a close correlation between the logarithm of the relative molecular mass of a protein and its chromatographic behaviour (the distance covered in a constant time on a given layer), TLC of proteins and polypeptide chains on cross-linked dextran gel provides a method that allows rapid estimation of relative molecular masses of polypeptides. Relative molecular masses of several polypeptides estimated via TLC on Sephadex G-75 and G-100 plates developed with 6 mol L⁻¹ guanidine hydrochloride are shown in Table 10. Sephadex G-75 is used for the chromatography of polypeptide chains with relative

Table 8 hR_F values of polypeptides on home made layers of silanized silica gel and on RP-2 plates

Compound	Silanized silica gel		RP-2	
	A	B	B	C
Angiotensin III inhibitor	47	76	75	81
Angiotensin III	16	55	53	71
Angiotensin II	37	75	73	79
Angiotensin I	22	63	59	75
Melittin	00	00	00	52
Glucagon	00	33	26	72
Insulin B chain	00	36	31	72
Actinomycin C ₁	00	03	02	25
Actinomycin V	00	04	03	22
Actinomycin I	00	08	05	32

A, 1 mol L⁻¹ acetic acid in 30% methanol; B, 1 mol L⁻¹ acetic acid + 3% potassium chloride in 50% methanol; C, 3% potassium chloride in water/methanol/tetrahydrofuran (4 : 3 : 3). Migration distance was 11 cm for home-made layers and 6 cm for RP-2 plates. Actinomycins were yellow; other compounds were located by 1% ninhydrin in pyridine/acetic acid (5 : 1). Actinomycins I and V differ from C₁ by having one of the two prolines replaced by 4-hydroxy- and 4-ketoproline, respectively.

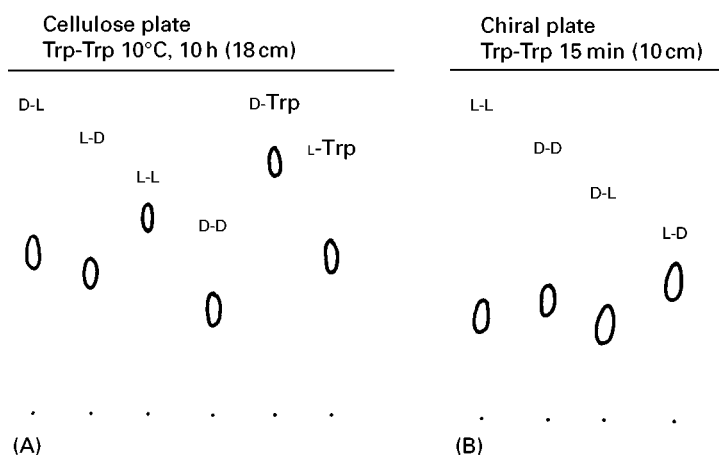


Figure 2 Chromatograms of Trp-Trp isomers. (A) Microcrystalline cellulose plate; eluent, pyridine/water (2 : 1). (B) Chiral plate; eluent, methanol/water/acetonitrile (50 : 50 : 200).

Table 9 TLC conditions for the separation of peptides on impregnated and RP silica gel plates

- RP-2, RP-8, RP-18, plates impregnated with 4% HDBS
 - 1 mol L⁻¹ acetic acid in methanol/water (1 : 1)
 - 1 mol L⁻¹ acetic + 0.2 mol L⁻¹ HCl in methanol/water (1 : 1); at high methanol percentage, i.e. methanol/water (4 : 1), the *R_F* values increased and more polar peptides gave elongated spots. The RP plates cannot be used with aqueous organic eluents containing more than 30% water.
- Untreated thin layers of silanized silica gel or impregnated with different detergents
 - Water/methanol/acetic acid (64.3 + 30 + 5.7), for untreated plates
 - 0.1 mol L⁻¹ or 0.05 mol L⁻¹ HCl + 1 mol L⁻¹ acetic acid in 30% methanol (pH 1.25 or 1.55); 0.1 mol L⁻¹ NaCl + 1 mol L⁻¹ acetic acid in 30% methanol (pH 2.75 or 3.30); 0.1 mol L⁻¹ sodium acetate + 0.1 mol L⁻¹ acetic acid in 30% methanol (pH 5.10); 1 mol L⁻¹ sodium acetate in 30% methanol (pH 8.15), for plates impregnated with 4% HDBS.
 - Water/acetic acid (7 : 3 or 1 : 1), for plates impregnated with 4% HDBS.
 - 0.1 mol L⁻¹ acetic acid + 0.1 mol L⁻¹ sodium acetate in 30% methanol, 1 mol L⁻¹ acetic acid in 30% methanol; 1 mol L⁻¹ sodium acetate in 30% methanol, for plates impregnated with 4% N-DPC. Alkaline elements, which cannot be used in RP column chromatography, can be used here. Separation on layers impregnated with N-DPC is better with an eluent of pH 5.10 than with an eluent of pH 2.75.
- Layers of ammonium tungstophosphate + CaSO₄ · (1/2)H₂O in the ratio 4 : 2
 - Aqueous solutions of ammonium nitrate (1 mol L⁻¹, 2 mol L⁻¹)

These plates provided compact spots and good resolutions. Mainly di-, tri-, tetra- and homopeptides were resolved by the above methods. The peptides were detected by spraying the wet layers with a solution of 1% ninhydrin in pyridine/glacial acetic acid (5 : 1) and then heating the layers at 100° for 5 min.

HDBS, Dodecylbenzenesulfonic acid; N-DPC, N-dodecylpyridinium chloride.

Table 10 Relative molecular masses of proteins on Sephadex plates

Protein	<i>M_r</i>	No. of PC	<i>M_r</i> of PC	<i>M_r</i> results (SD)
Lysozyme	14 500	1	14 500	17 500(520)
Lactate dehydrogenase	12 600	4	31 500	31 000(500)
Glyceraldehyde phosphate dehydrogenase	140 000	4	35 500	35 500(1200)
Alkaline phosphatase	41 000	1	41 000	41 500(800)
Phosphorylase b	188 000	2	94 000	98 000(500)
β-Galactosidase	135 000	1	135 000	132 000(400)

SD, standard deviation; PC, polypeptide chain.
Results are mean of 15 runs.

molecular masses less than 100 000, while Sephadex G-100 is used for higher molecular mass proteins. The solutions of proteins are prepared in guanidine hydrochloride (10 mg mL^{-1}), and cytochrome-*c* (10 mg mL^{-1}) is used as an internal standard. Descending chromatography is carried out at room temperature under an inclination angle of 25° to the horizontal. After 3 h of development the quotient R_s protein/ R_s cytochrome *c* is calculated for each protein–cytochrome *c* combination. A standard calibration line is obtained by plotting the log relative molecular masses of standards against protein–cytochrome quotient; the relative molecular masses of the unknown proteins are calculated from this plot.

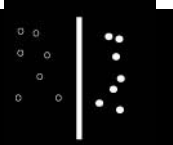
See also II/Affinity Separation: Immunoaffinity Chromatography. **Chromatography:** Size Exclusion Chromatography of Polymers. **Chromatography: Thin-Layer (Planar):** Densitometry and Image Analysis; Ion Pair Thin-Layer (Planar) Chromatography; Layers; Spray Reagents. **III/Amino Acids and Derivatives:** Chiral Separations.

Impregnation Techniques: Thin-Layer (Planar) Chromatography. Appendix: 1/Essential Guides for Isolation/Purification of Enzymes and Proteins.

Further Reading

- Arendt A, Kotodziejczyk A and Solotowska T (1976) Separation of diastereoisomers of protected dipeptides by thin-layer chromatography. *Chromatographia* 9: 123–126.
- Bhushan R and Martens J (1996) Peptides and proteins. In: Sherma J and Fried B (eds) *Handbook of Thin Layer Chromatography*, 2nd edn. New York: Marcel Dekker.
- Bhushan R, Mahesh VK and Mallikharjun PV (1989) TLC of peptides and proteins: a review. *Biomedical Chromatography* 3: 95–104.
- Lepri L, Desideri PG, Heimler D and Giannessi S (1983) High performance thin-layer chromatography of diastereomeric di-, and tri-peptides on ready for use plates of silanised silica gel and on ammonium tungstophosphate layer. *Journal of Chromatography* 265: 328–334.

PERVAPORATION: MEMBRANE SEPARATIONS



S. P. Chopade, Michigan State University,
East Lansing, MI, USA

S. M. Mahajani, Monash University, Clayton,
Victoria, Australia

Copyright © 2000 Academic Press

Introduction

The future of membranes in liquid–liquid separation lies in their potential to replace conventional unit operations such as distillation and cryogenic separation. Pervaporation, which has elements in common with reverse osmosis and membrane gas separation, is a liquid–liquid membrane separation process that can be employed for aqueous–organic or organic–organic separations. The most developed area of pervaporation is the separation of aqueous–organic mixtures but a vast potential lies in the area of organic–organic separations, specifically in the separation of azeotropic organic mixtures, where conventional separation processes tend to be complex and uneconomical.

The first pervaporation studies were carried out in late 1950 by Binning and coworkers at American Oil. However the process was not commercialized owing

to lack of technology to prepare a membrane that would withstand the commercial application. By the 1980s, membrane technology was advanced to the extent that a commercially viable pervaporation technology could be developed. However, the only commercialized applications today are the alcohol dehydration and separation of volatile organics from aqueous solutions. A few pilot-plant studies have been carried out on the industrially more significant organic–organic separations.

The applications of pervaporation can be categorized as follows: (1) dehydration of organic solvents; (2) removal of volatile organic compounds from aqueous streams; and (3) separation of organic–organic mixtures. There is a tremendous amount of literature on the first two applications. Pervaporation has been successful in these applications because the properties of organic components are very different from water and exhibit distinct membrane permeation properties. The feed solutions are also relatively non-aggressive and do not chemically degrade the membrane. However, in the case of separation of organic–organic mixtures, it is much more difficult to select membranes that would exhibit selectivities for one component over the other. This article

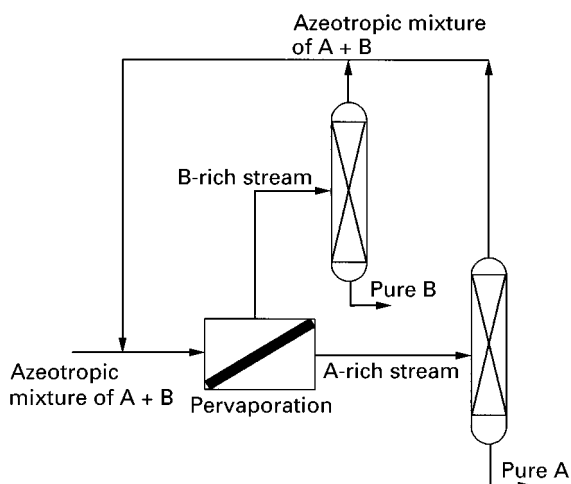


Figure 1 Schematic of pervaporation-distillation scheme for azeotrope separation.

is focused on this type of organic-organic separation. In a typical pervaporation process, even though the membrane selectivity is high, the mass flux achieved is fairly low ($2 \text{ kg m}^{-2} \text{ h}^{-1}$). Thus pervaporation is most advantageously used, when combined with another operation such as distillation. A schematic of such a hybrid process scheme is shown in **Figure 1**. An azeotropic mixture $A + B$ is subjected to one-stage pervaporation to give a permeate rich in A and retentate rich in B. Both the streams are individually subjected to fractional distillation to yield pure A and pure B, and a recycle stream of azeotropic mixture of $A + B$.

In pervaporation, the liquid mixture is brought in contact with one side of the membrane and permeated product is removed from the other side by applying vacuum (**Figure 2A**). Alternatively, the vapour product can also be removed by use of a carrier gas (**Figure 2B**). The permeate is then cooled and the organic phase condensed and collected to obtain the product.

The ability of a pervaporation membrane to perform separation is usually characterized by a separation factor defined as:

$$\alpha_{ab} = \frac{C_{a_p}/C_{b_p}}{C_{a_f}/C_{b_f}} \quad [1]$$

where, C_a , C_b are concentrations of A and B, and the subscripts p and f designate permeate and feed, respectively. The separation factor depends upon the operating conditions of the pervaporation processes and the solubility and affinity of the compounds in the feed solution towards the membrane. The selectivity can be of two types: solubility selectivity and

diffusivity selectivity. In most of the organic separations, dense membranes are employed and the diffusivity selectivity is generally low. Hence, of importance here is the solubility selectivity. For high solubility, membranes should have high affinity for one component and little affinity for the other component. However, excessive affinity for one component causes significant swelling of the membrane leading to loss in selectivity and mechanical strength. In the case of organic-organic separations, the membrane selection is particularly difficult. Several different methods such as polymer alloys, crosslinking, concentrated emulsion polymerization, microphase separation, copolymerization, and plasma graft filling polymerization have been proposed to prepare the membranes with the desired properties.

Selection of Membrane for Pervaporation

The choice of membrane to perform a particular separation is determined by the membrane's stability, productivity, and selectivity. Membrane productivity is the measure of the quantity of a component that permeates through a specific area of membrane in a given unit time and depends on the intrinsic permeability and the thickness of the membrane. The ability of a membrane to separate the desired component is characterized by its selectivity. Selectivity depends on the preferential sorption and relative permeability of the components. There is usually a trade-off between membrane permeability and selectivity. In 1993, Huang and Feng introduced a composite number called a pervaporation separation index (PSI) to take into account both these aspects.

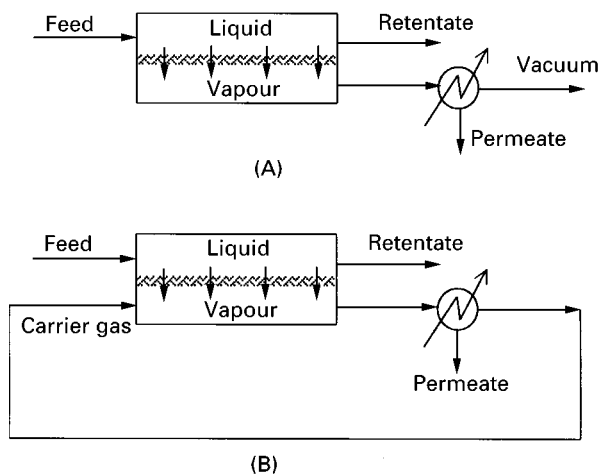


Figure 2 Schematic of pervaporation process. (A) By vacuum. (B) By carrier gas.

The stability of the membrane strongly depends on chemical, mechanical, and thermal properties of the membrane and the type of the environment.

Although the use of pervaporation for the separation of organic–organic mixtures represents a large opportunity for energy and cost savings, it is the least developed application of pervaporation. This is because of problems associated with the choice of proper membrane for the concerned application. Organic–organic separations involve relatively harsh conditions and the stability of the membranes under these conditions is often low. The polymeric membranes that are commonly used for aqueous systems are not stable in organic environment. This is an area of active research.

Once the stable membrane material is identified, attention should be focused on obtaining maximum separation with large production rate. As mentioned earlier, separation is achieved by virtue of the difference between the permeability or the solubility (affinity) values of the component in the membrane. The permeability in the membrane depends on the molecular size, and small molecules tend to permeate faster through the membrane. However, their permeation can be restricted by selecting a membrane material that offers less solubility to these components. Hence, the polarity of the membrane can conveniently be manipulated in such a way that it offers preferential treatment for the components to be separated on the permeate side. For instance, to improve the permselectivity towards certain non-polar organics, the membrane can be filled with organophilic adsorbents.

Materials used for pervaporation membranes are normally polymeric in nature. Polymeric membranes can be classified in three different categories: glassy

polymer membranes, elastomeric polymer membranes and ionic polymer membranes. Glassy polymers are water-selective whereas elastomeric polymers are organo-selective. However, for organic–organic separations, the selection of material becomes highly system-specific and is based on relative polarity and molecular size of the components to be separated. Hence, all the polymer membrane types have shown selectivity to certain components in organic–organic mixtures. Hydrophilic–hydrophobic composite membranes containing polystyrene as the dispersed phase and polyacrylamide as the continuous phase have shown tremendous selectivity towards aromatic difluoride compared to aliphatic ones. Membranes made from cellulose esters, polyethylene, and poly(vinylidene difluoride) modified to contain various Werner complexes, have been successfully used on a laboratory scale for separation of isomer mixtures such as *p*-xylene–*o*-xylene. Ionic membranes of perfluorosulfonic acid have been found to be effective for the selective pervaporation of relatively polar organic compounds such as alcohols. A list of organic–organic separations attempted by pervaporation is shown in Table 1.

In the interest of improving the membrane productivity, either membrane structures are modified or a different configuration such as a hollow-fibre membrane is used. The membrane structure can be altered by introducing an asymmetry during the membrane preparation procedure and most industrially important membranes are asymmetric. These membranes have a thin dense selective surface layer supported on a much thicker microporous layer. When the support material and layer material are different, then the membranes are called composite membranes. One of the advantages of the com-

Table 1 Examples of organic–organic separation by pervaporation

Type of system	Example	Membrane(s) used ^a
Aromatic–alcohol	Benzene–methanol, ethanol, propanol	Polyethylene, cellulose acetate
	Toluene– <i>n</i> -butanol	Polypropylene, polyethylene
Aromatic–naphthalene	Benzene–cyclohexane	PVA, acrylonitrile copolymers, plasma grafted, composite
Aromatic–paraffin	Benzene– <i>n</i> -hexane	Polyethylene
	Toluene– <i>n</i> -heptane	Polyethylene
Mixture of isomers	<i>o,m,p</i> -xylene	Polyethylene, PVF
Alcohol–paraffin	Ethanol–hexane	PTFE–PVP
Alcohol–naphthalene	Ethanol–cyclohexane	PTFE–PVP
Alcohol–ketone	Methanol–acetone	PTFE–PVP
Halogenated hydrocarbons	Dichloroethane–trichloroethylene	Polystyrene–butadiene
Reactive systems	Methanol–MTBE	Organophilic plasma polymerized
	Ethanol–ETBE	Organophilic plasma polymerized
	Methanol–dimethylcarbonate	Organophilic composite

^aPTFE–PVP: poly(tetrafluoroethylene)-*N*-vinylpyrrolidone; PVF: poly(vinylidene difluoride) modified by including Werner complexes.

posite membranes is that different polymers may be used as the barrier layer and the porous support, which allows a combination of properties that may not be available in a single material. The hollow-fibre membrane configuration is constructed similarly to a shell-and-tube heat exchanger. This configuration provides advantages over a flat plate-and-frame configuration such as large membrane area per unit volume, self-supporting ability, etc.

Applications

We will discuss here a few commercially important organic-organic systems that have potential of adapting pervaporation-assisted separation schemes.

Pervaporation-Distillation

Pervaporation-distillation process for MTBE production Methyl-*t*-butyl-ether (MTBE) is manufactured through the reaction of isobutylene from the C_4 fraction with methanol. The reaction is limited by equilibrium. The current technologies use a combination of reaction and either normal distillation or reactive distillation. The former process can exploit the potential of pervaporation before, during or after the distillation step to recover methanol from the reaction mixture. **Figure 3** shows the two possible configurations, which use pervaporation as an intermediate step in MTBE manufacture.

The first configuration uses pervaporation to separate methanol from the reactor effluent (**Figure 3A**).

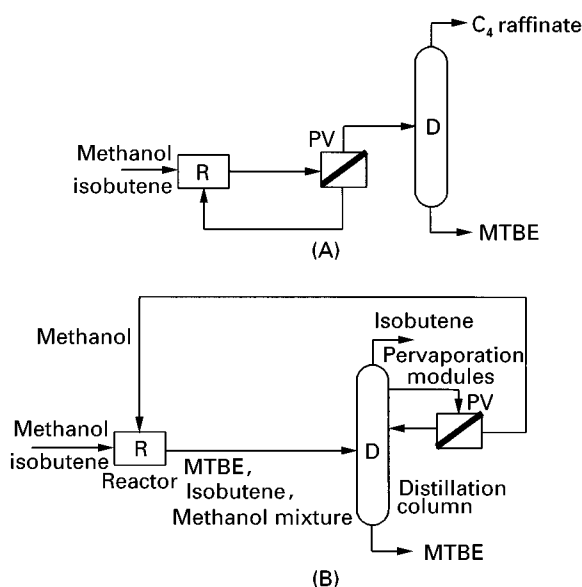


Figure 3 Different configurations of hybrid pervaporation-based MTBE processes.

The methanol-rich permeate is fed back to the reactor. This increases the overall conversion and also reduces the load on the methanol recovery unit. Moreover, this modification is easily possible in an existing MTBE plant without any major investment. The second configuration involves the withdrawal of a side-stream from the rectifying section of the distillation column to subject it to pervaporation (**Figure 3B**). Methanol from this stream can be separated and the retentate is again fed back to the distillation column. By doing this, the load on methanol recovery can be substantially reduced. Both configurations have been proved to be beneficial in view of reducing the investment cost by about 5–20%. The second configuration appears to be attractive compared to one that incorporates pervaporation before distillation. It involves low flow rates, low amount of methanol to be separated and a large driving force owing to high methanol concentration. Hence a membrane with a small surface area serves the purpose. A variation of the second scheme is also possible where the top product of the distillation column is liquefied and fed to the pervaporation unit to separate the methanol. The methanol-rich permeate is recycled back to the reactor. A highly permselective asymmetric aromatic polyimide membrane is used with a separation factor greater than 200. As a separate methanol recovery unit is not required, the process is more promising than the two options mentioned above.

A general advantage that is realized by adopting the hybrid process using pervaporation is the considerable savings in energy (especially steam) consumption. An organophilic (methanol-philic) plasma-polymerized PERVAP 1137 membrane (Sulzer Chemtech/GFT) has been suggested for this operation.

Pervaporation-distillation process for ETBE production Typically ethyl *t*-butyl ether (ETBE) is produced by acid-catalysed etherification of isobutylene with ethanol. The products are separated by distillation, the top product being the C_4 fraction and the bottom consisting of ethanol and ETBE. Pervaporation can be incorporated into this process to purify the bottom of the distillation column wherein ethanol is separated from ETBE (**Figure 4**). An organophilic (ethanol-philic) copolymer PERVAP 2051 membrane is used for this purpose and this brings down the ethanol content in the ETBE product stream to less than 1% w/w. A significant reduction in operating cost is realized with the help of the hybrid process. Pervaporation can also be used to recover ethanol from the top product of distillation. The liquid retentate may be fed back to the distillation through

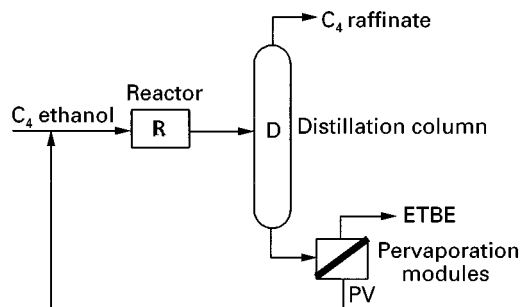


Figure 4 Hybrid pervaporation process for ETBE.

the column feed. The hybrid process is more economical than the conventional process.

Separation of Benzene–Cyclohexane

Cyclohexane is industrially produced by hydrogenation of benzene. They have close boiling points (within 1°C) and also form an azeotrope and hence cannot be separated by simple distillation. With the right choice of membrane, the separation can be achieved via the pervaporation route. However, the similar molecular size of benzene and cyclohexane makes the selection of a pervaporation membrane challenging. Poly(vinyl alcohol), acrylonitrile/methyl methacrylate, acrylonitrile/vinyl acetate, polymer metal complex membranes, plasma-grafted polymer membranes, and composite membranes of acrylic acid/styrene have all been employed with each having their own advantages/disadvantages. The process has been successfully demonstrated on a laboratory scale but there is no commercial process so far. Rautenbach and Albrecht made a comparative study of different separation schemes for this system. A comparison of a cascade of pervaporation processes with extractive distillation using furfural shows that the pervaporation process is more capital intensive. However, the conventional two-column extractive distillation process does not give the desired purity of the benzene and cyclohexane stream. A hybrid pervaporation–extractive distillation process shown in **Figure 5** proves to be the economically attractive alternative and gives the highest purity product. Furfural is used as an extractive carrier to carry benzene down in the first column. The bottom of the first column contains benzene and furfural, which are separated to obtain 99.5% pure benzene in the second column. The top product of the first column is subjected to a one-stage pervaporation where benzene is selectively removed to obtain 99.2% cyclohexane. The hybrid process can save up to 20% of the overall costs of the extractive distillation process.

Dimethyl Carbonate–Methanol Separation

Dimethyl carbonate (DMC) finds use in gasoline products as a fuel oxygenate and can be blended with alcohols or MTBE. It can serve as an MTBE substitute or as a phase enhancer in gasoline containing alcohol. DMC is prepared industrially by the reaction of methanol with carbon monoxide and oxygen. The process produces a mixture of methanol and DMC, which cannot be separated by simple distillation owing to the formation of an azeotrope. In the conventional process, a two-pressure distillation scheme is employed to split the azeotrope. The degree of separation achieved is nevertheless insufficient to meet the product specifications so a supplementary physical separation process such as crystallization is needed to obtain the desired product purity. Another route is to employ extractive distillation, where water is preferably used as an extractant. This means the separation of water–methanol needs to be carried out to recover the methanol. Owing to the high specific and latent heat of water, this process becomes very energy intensive.

Pervaporation combined with distillation can be advantageously employed to separate the methanol–DMC azeotrope as shown in **Figure 6**. The azeotropic methanol–DMC mixture is subjected to pervaporation. The retentate is 45% DMC, which is further separated by a distillation column into 99% DMC at the bottom and a near-azeotropic methanol–DMC mixture at the top. The top stream is recycled to the pervaporation. The further advantage of this scheme is that the top composition at the distillation column is not required to be azeotropic. This further brings down the number of stages required in the rectifying section of the column. This, combined with the elimination of high-pressure column, brings down the investment cost by 60% from the conventional process to the pervaporation–distillation hybrid process. Organophilic composite

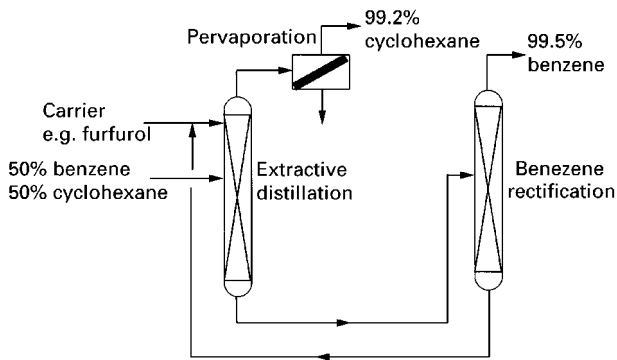


Figure 5 Hybrid process for separation of benzene–cyclohexane.

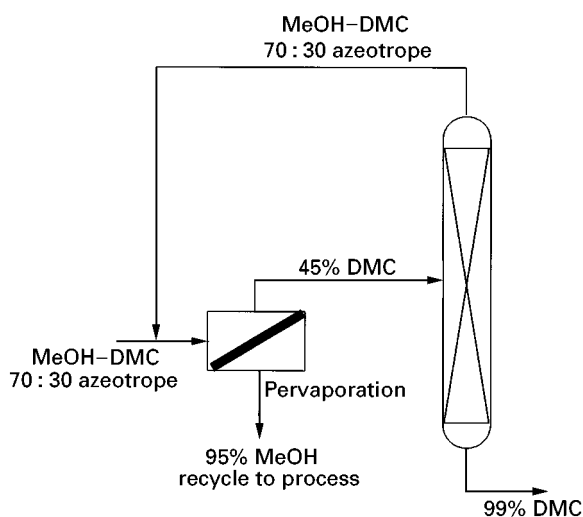


Figure 6 Pervaporation-distillation hybrid process for DMC.

membranes are used to carry out the pervaporation separation.

Separation of Aromatics-Saturates

The separation of aromatics from saturates is of considerable importance in the petrochemical industry. The boiling range of the aromatics and saturates is the same and hence simple distillation fails to separate the products. Pervaporation can be efficiently employed for this separation. A copolymer of polyimide-aliphatic polyester is advantageously used as a membrane. The polyimide provides the stability at high temperature whereas the polyester provides for the selectivity to aromatics. Other membranes that can be used for this application are polyurea urethane, polyurethane imides, and polyester imides. The process shown in **Figure 7** gives high selectivity towards the aromatics. A part of the aromatic permeate (25–40%) is recycled back to the pervaporation stage where it is mixed with the fresh feed. This scheme gives unexpectedly high selectivity than when the feed is exclusively either fresh feed or recycle permeate. Heavy cat naphtha can be separated by the

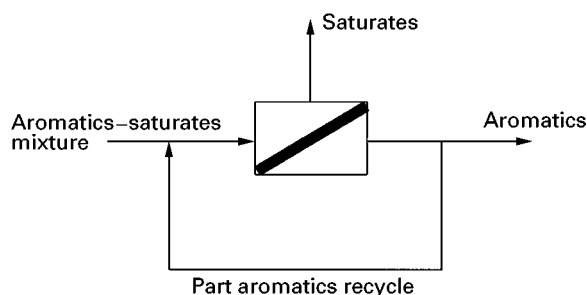


Figure 7 Pervaporation scheme for the separation of aromatics-saturates.

above process into aromatic-rich permeate for high-octane gasoline use and aromatic lean retentate suitable for diesel fuel. The process can also be applied to intermediate cut naphtha, diesel oil, gas oil, and light aromatic streams boiling in the C_5 range.

Conclusion

Pervaporation of organic-organic mixtures has the great potential of replacing conventional processes. The key areas of applications are separation of azeotropes and close boiling mixtures. However, the challenge for pervaporation to prevail in organic-organic separation is enormous, as there is a lot of inertia of the industry to change from the conventional distillation processes. Finding a suitable membrane is the most important hurdle in devising a pervaporation system. Hence, the major thrusts in this field should be towards developing new membranes with high flux, selectivity, and stability. At the same time, to warrant commercialization, high surface area modules must be developed. With emerging trends in membrane research and newer techniques such as asymmetric and composite membranes, the day is not too far off when pervaporation will be the preferred process. As outlined earlier, pervaporation combined with conventional separation is the way forward in most of the applications. Hence, overall integrated process development needs to be given equal importance. Ultimately, in order to achieve a complete success, membrane development efforts should be backed by more theoretical research for a better understanding of the complicated phenomenon of pervaporation.

Further Reading

- Aminabhavi TM, Khinavar RS, Harogoppad SB and Aithal US (1994) Pervaporation separation of organic-aqueous and organic-organic binary mixtures. *Journal of Macromolecular Science - Reviews in Macromolecular Chemistry and Physics* C34(2): 139.
- Feng X and Huang RYM (1997) Liquid separation by membrane pervaporation: a review. *Industrial and Engineering Chemistry Research* 36: 1048.
- Huang RYM and Feng X (1993) Dehydration of isopropanol by pervaporation using aromatic polyetherimide membranes. *Separation Science and Technology* 28: 2035.
- Lipnizki F, Field RW and Ten Po-Kiong (1999) Pervaporation-based hybrid processes: design, applications and economics. *Journal of Membrane Science* 153: 183.
- Rautenbach R and Albrecht R (1985) The separation potential of pervaporation. Part 2. Process design and economics. *Journal of Membrane Science* 25: 25.
- Zhang S and Drioli E (1995) Pervaporation membranes. *Separation Science and Technology* 30(1): 1.

PESTICIDES



Extraction from Water

M.-C. Hennion and V. Pichon, Laboratoire
Environnement et Chimie Analytique, Paris, France

Copyright © 2000 Academic Press

Introduction

Pesticides and their metabolites have received particular attention in the last few years in environmental trace organic analysis because they are regularly detected in surface and ground waters especially throughout Europe and North America as a consequence of their widespread use for agricultural and nonagricultural purposes. Several priority lists have been published to protect the quality of drinking and surface waters.

Pesticides, as organic compounds, are usually determined by chromatographic and related techniques. However, they are present in the environment at trace levels and despite advances in separation and quantification, no sample can be directly analysed and an extraction and concentration step is required, whatever the matrix. The detection levels required for monitoring pesticides in drinking water at a regulatory level depend on the particular country. In the USA, a priority list has been established on the basis of the toxicity of the analytes which contains about 25 pesticides and metabolites with a health advisory level in the range $1\text{--}700\text{ }\mu\text{g L}^{-1}$. Europe has more drastic regulations since the concentration of each pesticide should be lower than $0.1\text{ }\mu\text{g L}^{-1}$, and quantification at this level requires detection limits of $0.01\text{ }\mu\text{g L}^{-1}$ for the analytical procedure. For the monitoring of ground and surface water, several parameters have been taken into account such as quantities used, water solubility, hydrolysis half-life and soil adsorption coefficient. In surface water, in the USA, the recent National Pesticide Survey (NPS) list includes almost 150 pesticides with many degradation products; in Europe, a priority list was published in 1992 which contained 55 compounds.

Therefore, in order to reduce the price and time of environmental monitoring, it is relevant to perform multiresidue analysis which includes modern polar pesticides and their degradation products. Sample preparation remains the weakest link and the time-

determining step in the whole procedure for trace analysis of pesticides. Before implementing any strategy it is important to consider the strong interdependence of the various steps of the whole procedure, i.e. sample handling, separation and detection. There is no unique strategy for the sample handling step, because it depends on the nature of the pesticides to be determined (e.g. volatility and polarity), on the nature of the matrix and on the degree of preconcentration necessary. Interference removal is a critical step which is strongly related to the concentration of the analyte of interest and of the matrix. It is evident that the strategy for determining pesticide below the micrograms per litre level in drinking water may be different from that used in a very polluted river.

The methods for extraction and concentration of pesticides are mainly liquid-liquid extraction and solid-phase extraction. One key problem in pesticide analysis comes from the diversity of their chemical functional groups with varying polarity and physico-chemical properties.

Liquid-Liquid Extraction

Liquid-liquid extraction (LLE) is the simplest extraction method and is described in US EPA (Environmental Protection Agency) official methods. The large choice of solvents which provide a wide range of solubility and selective properties, is often given as an advantage of the method. But, in fact, each solvent is not really specific for a class of compounds. Hexane and cyclohexane are typical solvents for extracting nonpolar compounds, such as organochlorine and some organophosphorus pesticides, whereas dichloromethane and chloroform are the common solvents used for the extraction of medium-polarity pesticides. EPA method 507 allows the determination of 46-nitrogen- and phosphorus-containing pesticides in water, with an extraction of a 1 L sample of water with 200 mL of dichloromethane, followed by an evaporation step, a reconcentration in 5 mL of methyl t-butyl ether (MTBE) and an analysis step using GC with a nitrogen-phosphorus detector (NPD). Detection limits are estimated in the range $0.1\text{--}4.5\text{ }\mu\text{g L}^{-1}$, depending on the analyte. EPA method 508 uses a similar extraction step for chlorinated pesticides in ground water using GC electron capture detector (ECD) with detection limits in the range $0.02\text{--}1.3\text{ }\mu\text{g L}^{-1}$. The detection limits of these two methods are in agreement with Health Advisory

Levels in the USA. Many European laboratories use LLE methods which are derived from the EPA methods; the enrichment factor can be easily increased by greatly reducing the final volume which allows detection limits closer to the EU regulatory level of $0.1 \mu\text{g L}^{-1}$ for each pesticide.

However, due to the trend shown by the EPA for reducing the consumption of organic solvents, new methods involve micro-LLE extraction. As an example, EPA method 504 for the determination of organochlorine pesticides in water requires only 2 mL of dichloromethane or hexane for a 35 mL aqueous sample volume with detection limits in the range $0.08\text{--}7 \mu\text{g L}^{-1}$. Micro-LLE of this sort cannot be adapted to meet the EU detection limits.

LLE allows a fractionation into acidic pesticides and basic/neutral fraction with successive extractions at different pH values. However, extraction of relatively polar and water-soluble organic compounds is difficult. The recovery obtained from 1 L of water using dichloromethane is 90% for atrazine but only 16% and 46% for deisopropyl- and deethylatrazine. When using a mixture of dichloromethane and ethyl acetate with 2 M ammonium formate these metabolites of atrazine are extracted with recoveries of 62% and 87% respectively.

The main advantages of LLE are its simplicity and requirements for simple equipment, but the glassware must be carefully washed and stored under rigorous conditions. LLE is not free from practical problems (such as formation of emulsion) which are difficult to break. The disposal, use and evaporation of large volumes of solvent, often toxic and flammable, are the main drawbacks. These organic solvents should be of pesticide grade which makes them rather expensive. Automation requires the use of robots and LLE is typically an offline procedure, with risks of loss and contamination during transfer and evaporation steps. Therefore, the trends in reducing the use of organic solvents in analytical laboratories and the low performances in extracting polar compounds explain the increasing replacement of LLE by solid-phase extraction.

Solid-Phase Extraction

Recent Developments of SPE Formats

Offline SPE materials are mainly disposable cartridges and disc membranes. The recent developments tend to increase the sample throughput and to use solid-phase sorbents able to broaden the polarity range of analytes.

Limitations of packed SPE conventional cartridges and discs include restricted flow rates and plugging of the top frit when handling water containing sus-

pended solids, such as surface water. Therefore, the percolation of natural samples can take a long time for a typical 500 mL volume unless the sample has been carefully filtered beforehand. Various approaches have been developed to solve this problem. One consists in depth filters which can be placed above the cartridge or membrane extraction disc, or which are now integrated in some SPE cartridges providing fast flow rates. Empore discs have recently become available with sorbent trapped in a PTFE matrix. These discs are also included in cartridges, known as disc cartridges. New discs, which consist of a thin bed of microparticles supported in a laminar structure, allow the percolation of 1 L of surface water without any previous filtration in less than 5 min.

With regard to sorbent technology, many are now specified as specially made for broadening the polarity range of analytes. These include not-end-capped C_{18} silicas and monofunctional C_{18} silicas, the aim being to increase the number of unmodified silanol groups on the bonded silica surface in order to provide secondary polar interactions with basic polar solutes. Cross-linked styrene-divinylbenzene (SDVB) copolymers with high specific areas in the range $500\text{--}1200 \text{ m}^2 \text{ g}^{-1}$ are now available from all manufacturers in cartridges and/or discs. Typical amounts of sorbent are 100–200 mg and the cartridge designs have been optimized for rapidly processing large volumes of water. Carbonaceous sorbents have also been shown to extract very polar analytes.

Automation

A typical SPE sequence includes four steps: (i) conditioning of the sorbent; (ii) application of the sample; (iii) rinsing and clean up of the sample; and (iv) desorption of the analytes to be separated. These steps can be performed sequentially for up to 24 cartridges at the same time using extraction units working under positive or negative pressure. The whole sequence can also be easily automated using devices which can accept any commercial cartridges or extraction discs. Examples are the ASPEC from Gilson, Microlab from Hamilton, AutoTrace and RapidTrace from Zymark. The possibility exists with some of these devices for automatic injection of an aliquot of the final extract into the chromatographic system. Complete automation also exists which couples SPE directly with online LC analysis (ASPEC XL from Gilson; Prospekt from Spark Holland; OSP-2 from Merck). These last two pieces of equipment improve productivity since the next sample is automatically prepared while the previous sample is being analysed.

Selection of the Sorbent for Multiresidue Extraction

LC has been shown to be suitable for multiresidue separation of many compounds over a wide range of polarity without previous derivatization and examples can be found in the literature, the most impressive one being the multiresidue separation of 72 pesticides in one run published by Di Corcia and Marchetti. Identification of compounds is widely performed with UV diode array detectors which can provide the whole spectrum of the analytes. Fluorescence is also used because of its sensitivity for the detection of *n*-methyl carbamates, following a post-column derivatization reaction. LC with mass spectrometry is also increasingly used in environmental laboratories.

The extraction of analytes from water requires the selection of an extraction sorbent which will provide a 90–100% recovery with the sample volume required for the necessary quantification. According to the detection limits obtained with conventional LC-UV diode array detectors or MS interfaces, typical sample volumes using offline extraction procedures are in the range 300–500 mL in order to provide detection limits in drinking water as low as 0.01–0.03 $\mu\text{g L}^{-1}$ and 0.1 $\mu\text{g L}^{-1}$ in surface waters for transport and fate studies.

The same sorbents as those used in reversed-phase LC are utilized and there is an analogy between the SPE processes and classical elution chromatography. Processes involved in SPE are a frontal chromatographic process during the extraction step and displacement chromatography during the desorption step. It is then possible to predict and optimize the main SPE parameters from data generated by LC. Among the various tools for selecting the sorbent and predicting the recovery according to the percolated sample volume, the most important is the retention factor of the analyte in water, k_w . Therefore, developing a SPE method only requires knowledge of the retention behaviour of the analytes with the extraction sorbent in LC with water as mobile phase, as measured by k_w . Both breakthrough curves and recovery curves have been modelled according to the sample volume. With an amount of sorbent of 500 mg, a recovery in the range 90–100% will require a sorbent providing $\log k_w > 3$ for the analytes. Whatever the SPE format, disc or cartridge, the process is the same and the criteria for the selection of the sorbents are similar. It is just necessary to know the amount of sorbent.

A good stability has been observed for analytes on SPE sorbents which allows the percolation of samples on site and further analysis in the laboratory.

Multiresidue Extractions Using *n*-Octadecyl Silicas

Prediction from the water–octanol partition coefficient of the compound Octadecyl- and octyl-bonded silicas have been the universal extraction sorbents for many years. Since the retention mechanism is primarily governed by hydrophobic interactions between the analyte and the carbonaceous moieties of the alkyl chains grafted to the silica surface, a relation has been observed between the retention factors of the analytes and their water–octanol partition coefficient (K_{ow}). Therefore, k_w values can be approximated without any additional measurements from K_{ow} values which were reported in a recent edition of the *Pesticide Manual*.

Limitation for the extraction of polar pesticides in a multiresidue mixture For LC purposes, trifunctional silanes are preferred over monochlorosilanes for the bonding synthesis because a layer or multiple carbon–siloxane covalent bonds on the silica surface is formed. The objective in SPE is to increase to a maximum hydrophobic interactions and the surface coverage so that rather highly porous silica is usually selected, with an average surface area above 500 $\text{m}^2 \text{g}^{-1}$ and with average carbon content of 17–18% for *n*-alkyl silicas. These C_{18} silicas will provide the highest retention for the more polar analytes. Like LC phases, the SPE alkyl silicas were first end-capped but, in order to enhance secondary interactions, the number of residual silanol groups has been increased by eliminating end-capping procedures, or by using monofunctional silane and no end-capping. Hydrogen bonding interactions and, especially, ionic interactions with polar basic compounds after pH adjustment can be increased and that is the reason for the broader range of polarity which can be achieved by these silicas specially designed for polar analytes. However, even if an increase of recoveries for some polar basic analytes has been observed, the increase in $\log k_w$ values is small at 0.2–0.5 in log units.

The limitation in using C_{18} silicas is in the extraction of polar pesticides and/or metabolites, which are characterized by $\log K_{ow}$ below 2. To give an example, recoveries of deisopropylatrazine and phenol ($\log K_{ow}$ values of 1.2 and 1.5 respectively) are lower than 20% with a sample volume of 500 mL and using an extraction disc containing 450 mg of C_{18} silica. Increasing the amount of sorbent to 1 g in the cartridge, gives a recovery of deisopropylatrazine of 52% and 44% from a sample volume of 1 L using respectively C_{18} Polar Plus from J.T Baker and LiChrolut RP-18 from Merck.

Application to drinking water samples Figure 1 illustrates the potential of C_{18} silica for determining many pesticides over a wide range of polarity in

drinking water at $0.1 \mu\text{g L}^{-1}$. The triazines and phenylureas have been selected because they include some polar analytes such as the degradation products

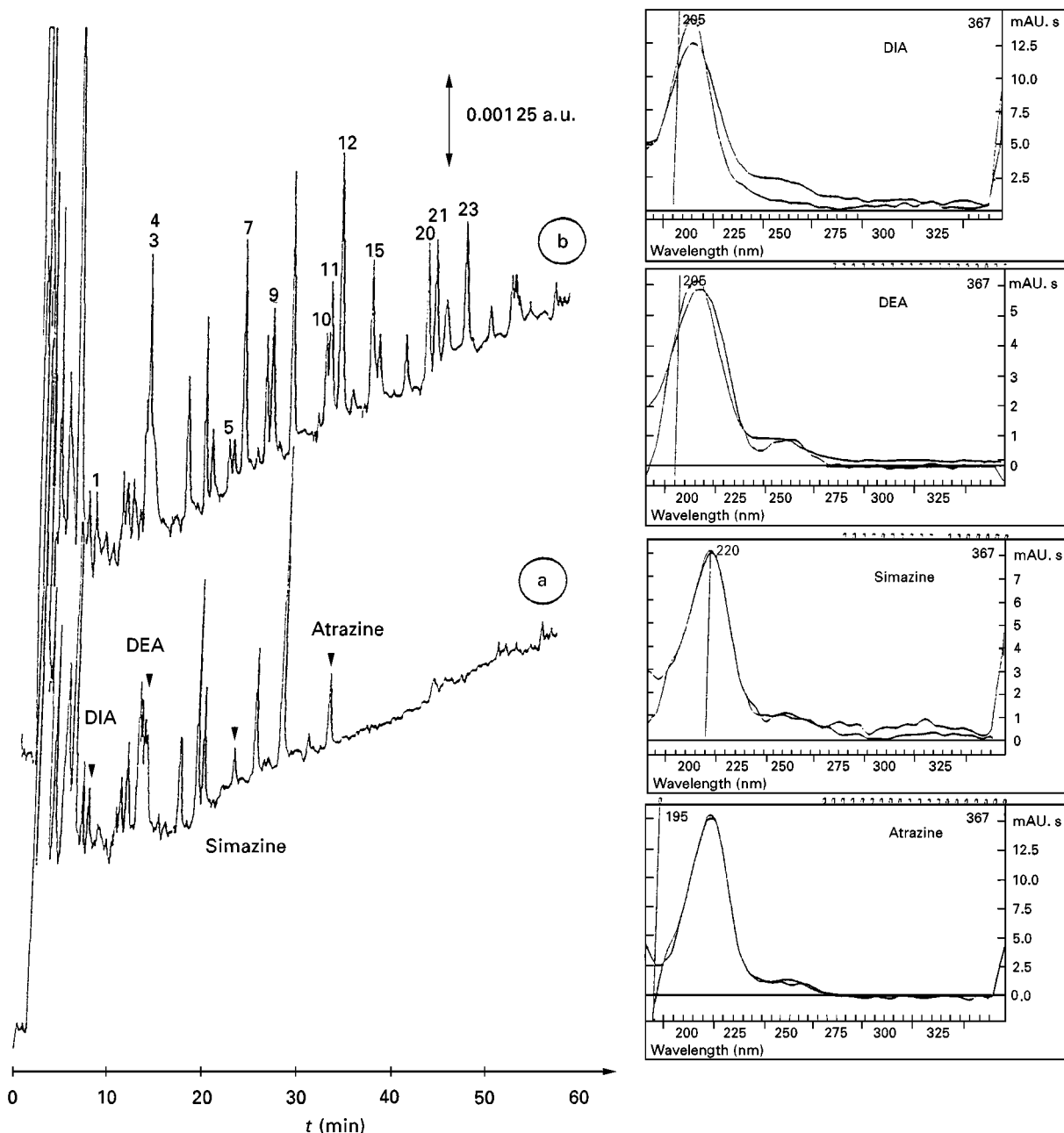


Figure 1 Chromatogram corresponding to the preconcentration of 500 mL of drinking water and spectra of the peaks identified using the UV DAD software: (a) non-spiked and (b) spiked with $0.1 \mu\text{g L}^{-1}$ of each analyte.

Preconcentration using a 500 mg C_{18} silica cartridge, desorption with 4 mL of methanol, evaporation to dryness, and addition of 500 μL of an acetonitrile/water mixture (20/80, v/v). Injection of 50 μL . Analytical column: Supelcosil LC-18-DB 25 cm \times 4.6 mm i.d.; acetonitrile gradient with 0.005 M phosphate buffer at pH 7; UV detection at 220 nm. Peaks: 1, DIA; 2, fenuron; 3, OHA; 4, DEA; 5, hexazinone; 6, metoxuron; 7, simazine; 8, monuron; 9, cyanazine; 10, metabenzthiazuron; 11, simetryne; 12, atrazine; 13, chlortoluron; 14, fluometuron; 15, prometon; 16, monolinuron; 17, isoproturon; 18, diuron; 19, difenoxuron; 20, sebutylazine; 21, propazine; 22, buturon; 23, terbutylazine; 24, linuron; 25, chlorbromuron; 26, chloroxuron; 27, difluzbenzuron; 28, neburon. (Reproduced from *International Journal of Environmental and Analytical Chemistry* 65, Pichon V, Cau Dit Coumes C, Chen L and Hennion M-C, Solid-phase extraction, clean-up and LC for routine multiresidue analysis of neutral and acidic pesticides in natural waters in one run, pp. 11–25, Copyright (1996), with permission from Gordon and Breach, Science Publishers.)

of atrazine, i.e. deisopropylatrazine (DIA), hydroxyatrazine (OHA) and deethylatrazine (DEA), and fenuron or metoxuron (with $\log k_w$ around 2.5 or lower), many moderately polar compounds and rather apolar pesticides such as neburon ($\log K_{ow}$ 4.3). The separation was not optimized because the occurrence of each compound in the same sample is unlikely. Co-eluted analytes do not belong to the same group and can easily be differentiated by the UV diode array detector. The chromatogram in Figure 1b represents the chromatogram obtained for an extract from 500 mL of drinking water spiked with $0.1 \mu\text{g L}^{-1}$ of each pesticide. Recoveries were above 85–90% for each analyte, except the early eluted peaks 1 to 4 for which recoveries were 26, 51, 68 and 68%. Recoveries of peaks 7 and 12 were higher, due to the presence of these compounds in the sample, as shown in Figure 1a where a nonspiked sample was analysed under the same experimental conditions. The occurrence of simazine (peak 7) and atrazine (peak 12) was confirmed by comparison of retention times and of UV spectra from the library of the DAD at concentrations of $0.016 \pm 0.003 \mu\text{g L}^{-1}$ and $0.12 \pm 0.02 \mu\text{g L}^{-1}$ respectively. The match between the retention times and the two UV spectra was excellent so that no further confirmation was required. The peaks which showed up at 7.9 and at 13.3 min may be deisopropylatrazine and deethylatrazine, but the match was not good and another method is required for confirmation.

Multiresidue extraction including acidic pesticides: pH and matrix effects Acidic herbicides are very slightly retained by C_{18} silica in their ionic form so that they can be extracted using a C_{18} silica cartridge provided the sample has been previously acidified before percolation. Table 1 shows the low extraction recoveries measured for some acidic herbicides when percolating 500 mL of spiked drinking water at pH 7 and the much better results when acidified at pH 2 or 3 with perchloric acid. When natural water

Table 1 Recoveries (%) of acidic herbicides at different pH used for the preconcentration of samples (500 mL) of drinking water spiked with $0.5 \mu\text{g L}^{-1}$ of each analyte using a 500 mg C_{18} cartridge

Compound	pK_a	pH2	pH3	pH7
Dicamba	1.94	89	46	2
Bentazone	3.2	100	100	6
Ioxynil	3.96	98	83	31
MCPP	3.07	104	108	27
2,4-DB	4.8	98	92	38
2,4,5-TP		100	78	10
Dinoterb	5.0	72	49	30

samples are acidified at pH 2, there is an interfering peak due to humic and fulvic acids as shown when comparing the chromatograms of Figure 2a and b. The strong acidity of humic and fulvic acids (pK_a around 3) explains why interferences are only detected at acidic pH. This co-extraction of humic and fulvic acids requires an optimization of the mobile phase gradient in order to elute the first compounds after the interfering peak, so that most of the pesticides can still be determined at the $0.1 \mu\text{g L}^{-1}$ level in drinking water samples. In Figure 2b, only the very polar ones will show up in the interfering peak if the mobile phase gradient is adjusted in order that most of the peaks are eluted after 20 min. Surface water contains higher amounts of humic and fulvic acids and determination of pesticides at the $0.1 \mu\text{g L}^{-1}$ level becomes impossible, as shown in Figure 2c. An additional clean-up step using a Florisil cartridge was applied to the extract obtained after desorption from the C_{18} cartridge and detection limits could be improved as shown in Figure 3b. However setting up the analytical conditions for this step is not straightforward but laborious, time-consuming and generates additional losses in recovery.

Multiresidue Extractions Using Apolar Styrene-Divinylbenzene (SDVB) Copolymers

Potential for extraction of very polar analytes as compared with C_{18} silicas In recent years, ultra-clean highly cross-linked styrene-divinylbenzene (SDVB) polymers with relatively high specific surface areas have been introduced by most manufacturers of disposable cartridges and have shown high capability for the extraction of polar analytes. This is demonstrated by 100% recoveries for phenol and deisopropylatrazine from a sample volume of 1 L and using 200 mg of SDVB sorbents. Table 2 compares the retention factors in water, which have been measured or estimated for a C_{18} silica and SDVB with different specific surface areas. The higher retention of SDVB sorbents over C_{18} silicas is due to strong π - π interactions between analytes and the SDVB matrix in addition to common hydrophobic interactions. The effect of the surface area is very important and an increase in retention by a factor of 20 to 100 may be observed when the specific area of the SDVB sorbent increases from 400 to $1000 \text{ m}^2 \text{ g}^{-1}$.

Therefore, highly cross-linked SDVBs are the sorbents of choice for multiresidue extraction of a mixture containing highly polar analytes.

Application to the determination of acidic, neutral and basic pesticides in the same run with removal of humic and fulvic acid interferences The retention of acidic pesticides was studied at neutral pH in order to

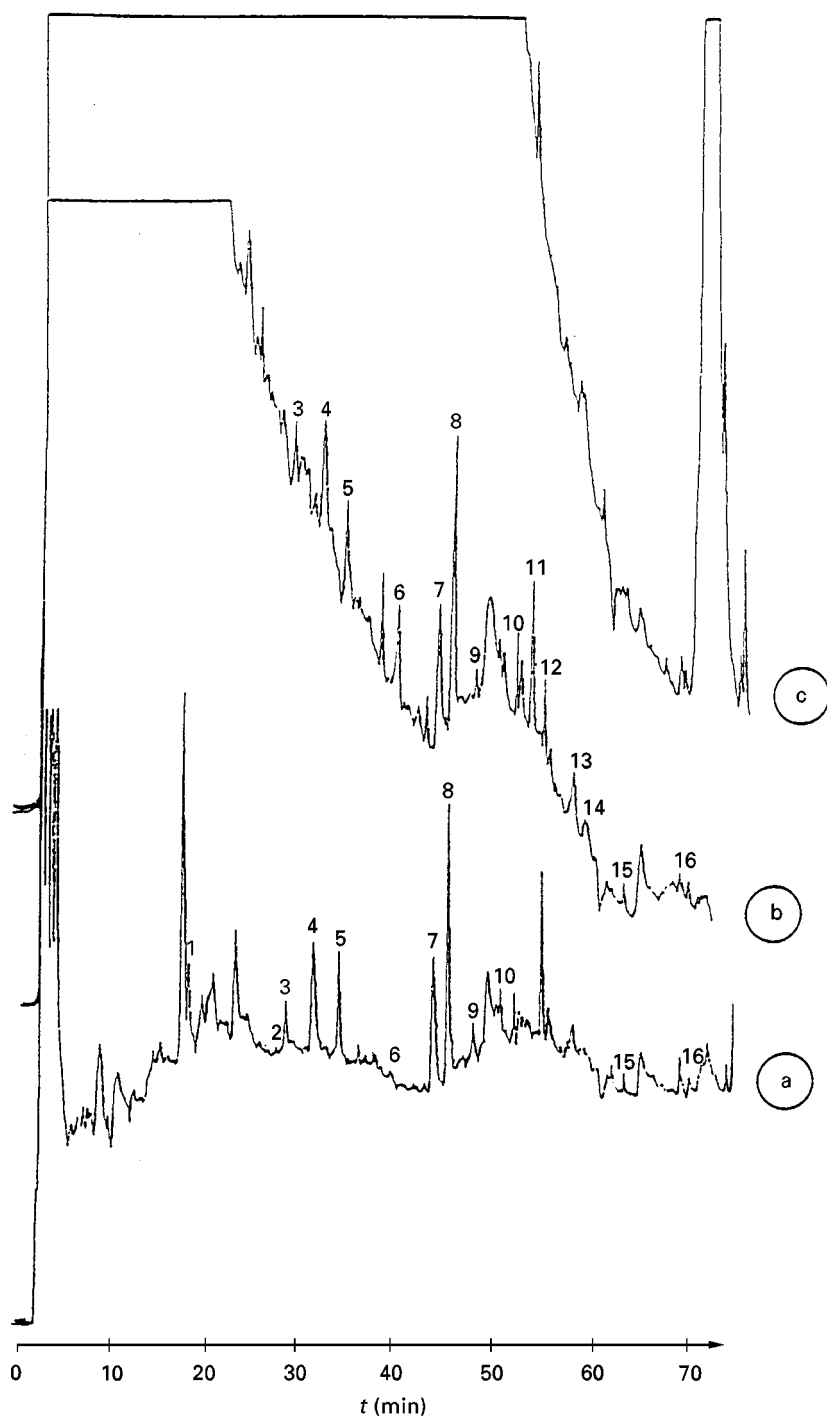


Figure 2 Effect of sample pH and of the sample matrix on the pre-concentration of 500 mL of (a) drinking water spiked with $0.1 \mu\text{g L}^{-1}$ of each analyte at pH 7; (b) drinking water spiked with $0.1 \mu\text{g L}^{-1}$ of each analyte at pH 2; and (c) River Seine water spiked with $0.1 \mu\text{g L}^{-1}$ of each analyte at pH 2.

Preconcentration using a 500 mg C_{18} silica cartridge, desorption with 3 mL of methanol, evaporation to dryness, and addition of 500 μL of a dichloromethane/water mixture (20/80, v/v). Analytical column: Bakerbond narrow pore C_{18} silica, 25 cm \times 4.6 mm i.d.; acetonitrile gradient with 0.005 M phosphate buffer at pH 3. UV detection at 220 nm. Peaks: 1, chloridazon; 2, aldicarb; 3, metoxuron; 4, simazine; 5, cyanazine; 6, bentazone; 7, atrazine; 8, carbaryl; 9, isoproturon; 10, difenoxuron; 11, ioxynil; 12, MCPP; 13, 2,4-DB; 14, 2,4,5-TP; 15, metolachlor; 16, dinoterb. (Adapted from *International Journal of Environmental and Analytical Chemistry* 65, Pichon V, Cau Dit Coumes C, Chen L and Hennion M-C, Solid-phase extraction, clean-up and LC for routine multiresidue analysis of neutral and acidic pesticides in natural waters in one run, pp. 11–25, Copyright (1996), with permission from Gordon and Breach, Science Publishers.)

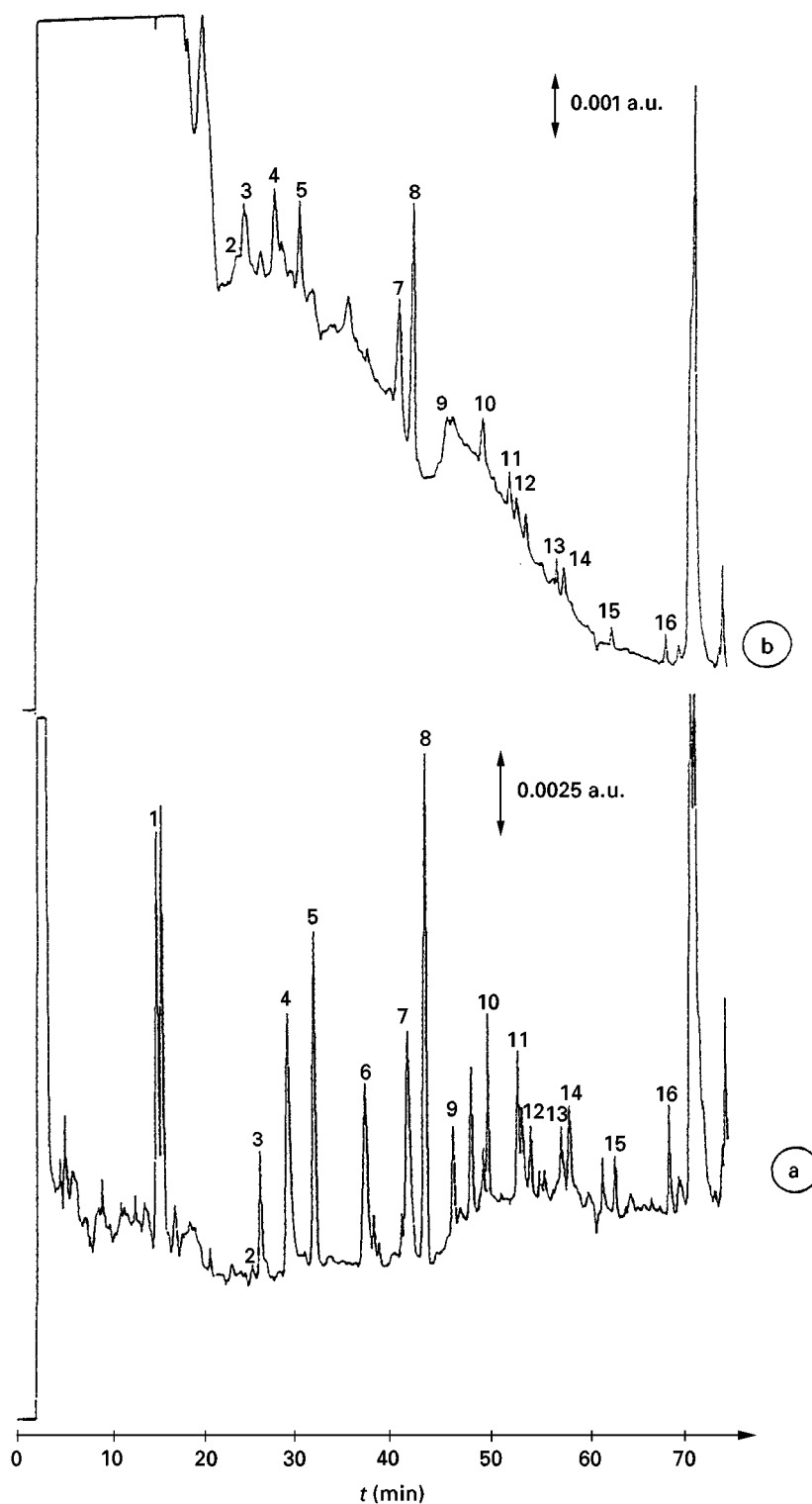


Figure 3 Preconcentration of 500 mL of Seine River water spiked at $0.5 \mu\text{g L}^{-1}$ and acidified at pH 2 (b) without and (a) with a clean-up step on Florisil. Analytical conditions and numbering of peaks as in Figure 2. (Reproduced from *International Journal of Environmental and Analytical Chemistry* 65, Pichon V, Cau Dit Coumes C, Chen L and Hennion M-C, Solid-phase extraction, clean-up and LC for routine multiresidue analysis and neutral and acidic pesticides in natural waters in one run, pp 11–25, Copyright (1996), with permission from Gordon and Breach, Science Publishers.)

decrease the amount of co-extracted humic and fulvic acids in surface waters. The recoveries of the acidic pesticides reported in Table 1 using a C_{18} silica cartridge were also measured using a 200 mg SDVB cartridge and a sample volume of 500 mL of drinking water spiked with $0.1 \mu\text{g L}^{-1}$ of the acidic analytes and adjusted to pH 7. The recoveries of dicamba

which was lower than 3% on a 500 mg C_{18} cartridge under the same extraction conditions was increased to 78% on SDVB and the recoveries of all other acidic compounds were found to be higher than 85–90%. As on C_{18} silicas, humic and fulvic interferences were shown to be co-extracted at pH 3 whereas they are not at pH 7 as shown by Figure 4. The fact they are

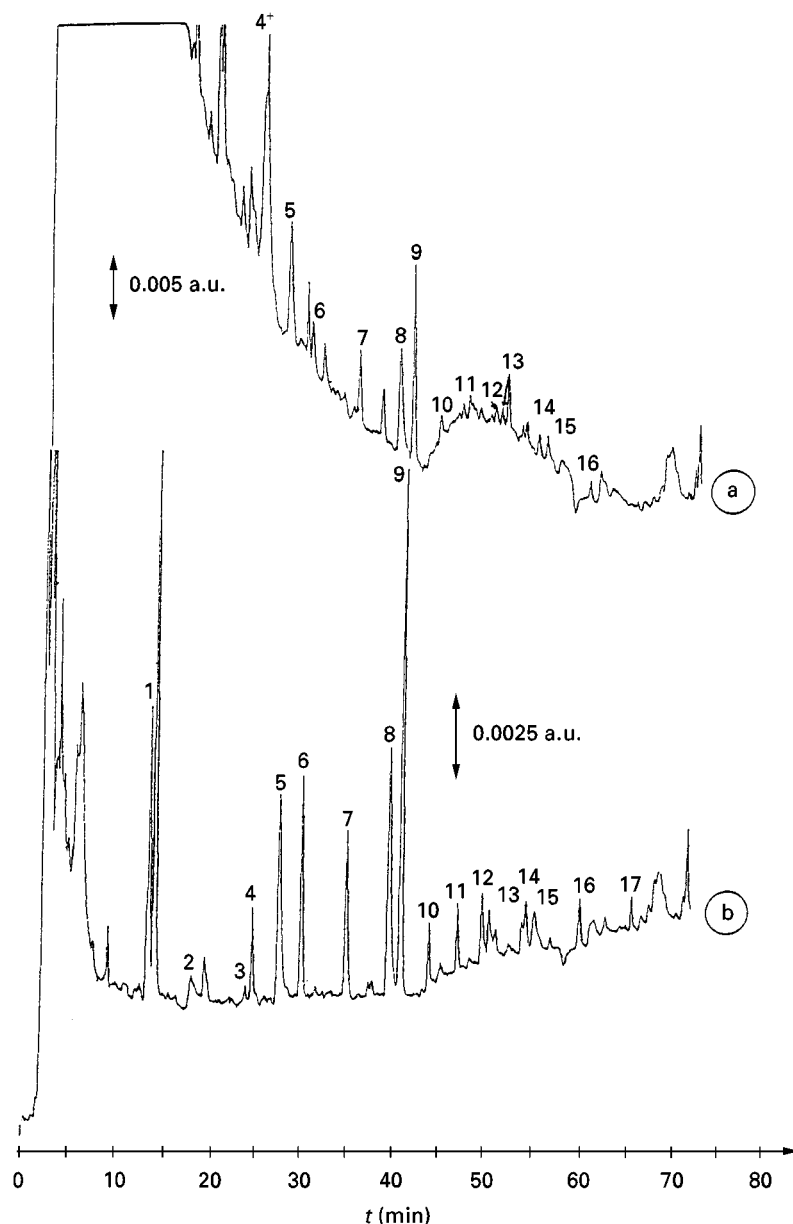


Figure 4 Effect of pH of the sample on the pre-concentration of 500 mL of drinking water spiked at $0.1 \mu\text{g L}^{-1}$ with various acidic, neutral and basic pesticides: (a) pH 3 and (b) pH 7 using a 200 mg SDB cartridge.

Desorption with 4 mL of methanol, evaporation to dryness, and addition of 200 μL of an acetonitrile/water mixture (20/80, v/v). Analytical column: Bakerbond narrow pore C_{18} silica, 25 cm \times 4.6 mm i.d.; acetonitrile gradient with 0.005 M phosphate buffer at pH 3. UV detection at 220 nm. Peaks: 1, chloridazon; 2, dicamba; 3, aldicarb; 4, metoxuron; 5, simazine; 6, cyanazine; 7, bentazone; 8, atrazine; 9, carbaryl; 10, isoproturon; 11, ioxynil; 12, MCP; 13, difenoxuran; 14, 2,4-DB; 15, 2,4,5-TP; 16, metolachlor; 17, dinoterb. (Reprinted from *Journal of Chromatography A* 737 Pichon V, Cau Dit Coumes C, Chen L, Guenu S and Hennion M-C. Simple removal of humic and fulvic acid interferences using polymeric sorbents for the simultaneous solid-phase extraction of polar acidic, neutral and basic pesticides, pp. 25–35, Copyright (1996), with permission from Elsevier Science.)

Table 2 Comparison of $\log k_w$ obtained for various sorbents and polar analytes and measured or estimated from LC data

Analytes	$\log K_{ow}$	$\log k_w$			
		<i>C</i> ₁₈ silica ^a	PRP-1 (415 m ² g ⁻¹)	SDVB (350 m ² g ⁻¹)	SDVB (1060 m ² g ⁻¹)
Oxamyl	0.3	1.7 ± 0.1	nd	2.8 ± 0.1	4.1 ± 0.2
Chloridazon	1.2	2.3 ± 0.1	nd	3.8 ± 0.2	nd
Deisopropylatrazine	1.2	2.3 ± 0.1	3.1 ± 0.1	3.2 ± 0.2	4.4 ± 0.2
Phenol	1.5	1.9 ± 0.1	nd	3.0 ± 0.1	nd
Aldicarb	1.4	2.5 ± 0.1	nd	4.0 ± 0.2	5.3 ± 0.2
Deethylatrazine	1.5	2.7 ± 0.1	3.5 ± 0.3	3.5 ± 0.2	4.8 ± 0.3
Simazine	2.3	3.4 ± 0.1	> 4	4.1 ± 0.2	5.9 ± 0.3
2-Chlorophenol	2.4	2.9 ± 0.1	> 4	3.6 ± 0.2	nd

^a*C*₁₈ silica in Empore disc from J. T. Baker, specific surface area 510 m² g⁻¹, carbon loading 17–18% C, end-capped; nd, not determined.

still not retained at pH 7 is due to their high polarity because of the numerous ionized groups and/or to their different configuration at pH 7 and their possible occurrence in the colloidal fraction. However, the consequence of a high retention of acidic pesticides in their ionic form together with the absence of retention of humic and fulvic interferences gives the remarkable possibility of determining acidic and neutral pesticides in surface water samples without any clean-up at the low 0.1 µg L⁻¹ concentration level as shown in Figure 5.

Use of Porous Graphitic Carbon for the Extraction of very Polar Metabolites

The most commonly used carbonaceous sorbents are graphitized carbon blacks (GCB). Their higher efficiency over *C*₁₈ silica for trapping polar pesticides has been extensively shown by the group of Di Corcia *et al.* GCB is not pressure resistant enough to be used in LC so that no data indicating the LC behaviour of solutes are available. In recent years, a porous graphitic carbon (PGC) has been available in SPE cartridges. It has been derived from that made for LC (under the trade mark Hypercarb). PGC has been shown to be particularly efficient for the extraction of some very polar analytes which cannot be extracted by the SDB polymers, such as for instance di- and tri-hydroxyphenols, aminophenols, and other aromatic derivatives containing several polar functional substituents. They have been shown to extract the highly polar degradation products of atrazine including cyanuric acid. As an example Figure 6 shows the determination of the degradation products of atrazine, DEA and DIA as well as the didealkylated metabolite deethyl-deisopropylatrazine (DDA) in ground water. Recoveries were in the range 90–95% for each analyte using a SPE cartridge packed with

200 mg of Hypercarb and a sample volume of 500 mL. DDA is a very polar metabolite, with a $\log K_{ow}$ value of 0, and its occurrence in ground water has never been shown, due to the difficulty of extraction and analysis. It was shown that in soil DEA is stable whereas DIA is rapidly transformed into DDA. Our results have confirmed this hypothesis because DEA is detected in high amounts, DIA at

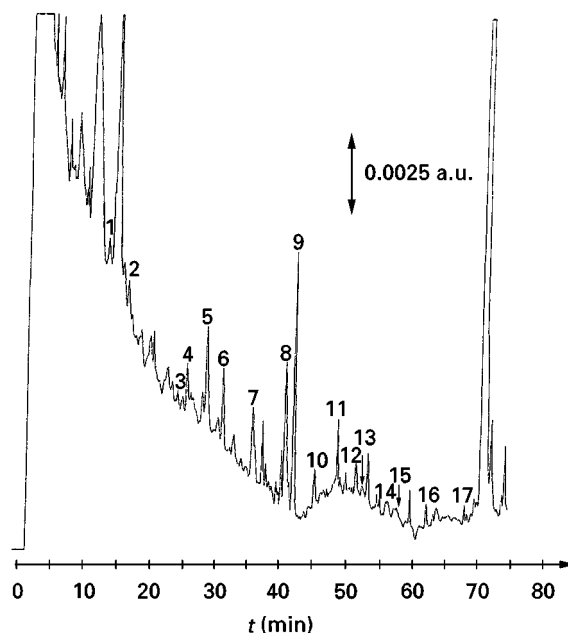


Figure 5 Preconcentration of 500 mL of River Seine water spiked with 0.1 µg L⁻¹ of herbicides at pH 7. Experimental conditions as in Figure 4b. (Reprinted from *Journal of Chromatography A* 737 Pichon V, Cau Dit Coumes C, Chen L, Guenu S and Hennion M-C. Simple removal of humic and fulvic acid interferences using polymeric sorbents for the simultaneous solid-phase extraction of polar acidic, neutral and basic pesticides, pp. 25–35, Copyright (1996), with permission from Elsevier Science.)

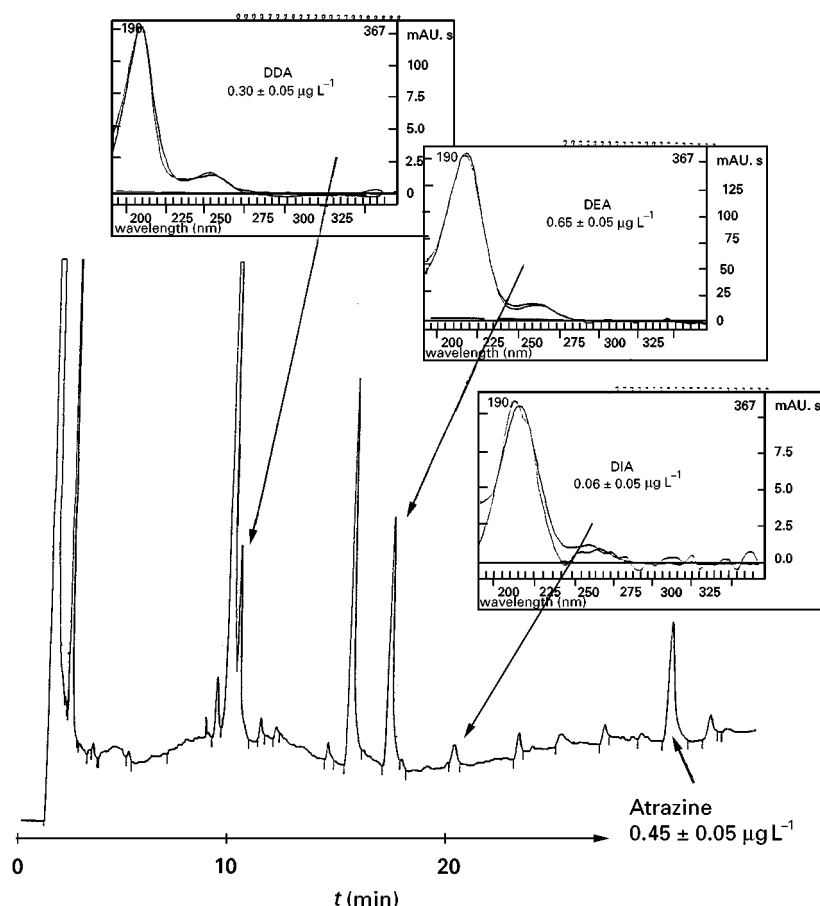


Figure 6 Preconcentration of 500 mL of ground water and spectra of the peaks identified using the UV DAD software. Preconcentration using a 200 mg Hypercarb cartridge. Analytical column: Hypercarb, 10 cm \times 4.6 mm i.d.; acetonitrile gradient with 0.005 M phosphate buffer at pH 7. UV detection at 220 nm.

trace level and DDA has half the concentration of DEA. This last figure illustrates the persistence and importance of the degradation products in ground water, since the sum of the concentration of metabolites is twice the concentration of the parent compound atrazine.

Further Trends

Research for sample preparation is a very active area at the moment, partly explained by the need for reducing as much as possible the use, disposal and release in the environment of toxic solvents, together with a reduction of the total analysis cost. In Europe, chemists are faced with the drastic drinking water regulatory level of 0.1 $\mu\text{g L}^{-1}$ for each pesticide. Therefore, trends are for setting up multiresidue analysis.

Trends are also for simplifying the labour of sample preparation, increasing its reliability and

eliminating the clean-up step of aqueous samples by decreasing as much as possible the amount of interfering components extracted from complex matrices. Regarding these last two aspects, the new polymeric extraction sorbents have a remarkable potential. Sorbents based on immunaffinity extraction are also promising for their high selectivity, and extraction, concentration and clean-up are performed in the same step.

See also: II/Extraction: Analytical Extractions: Solid-Phase Extraction. III/Porous Graphitic Carbon: Liquid Chromatography: Solid Phase Extraction with Discs.

Further Reading

Barcelo D (1993) Environmental Protection Agency and other methods for the determination priority pesticides and their transformation products in water. A review. *Journal of Chromatography* 643: 117.

- Barcelo D and Hennion MC (1995) On-line sample handling strategies for the trace-level determination of pesticides and their degradation products in environmental waters. A review. *Analytica Chimica Acta* 318: 1.
- Barcelo D and Hennion MC (1997) *Trace Determination of Pesticides and Their Degradation Products in Water*. Amsterdam: Elsevier.
- Barcelo D, Chiron S, Lacorte S, Martinez E, Salau JS and Hennion MC (1994) Solid-phase sample preparation and stability of pesticides in water using Empore disks. *Trends in Analytical Chemistry* 13: 352.
- Font J, Manes J, Molto JC and Pico Y (1993) Solid-phase extraction in multiresidue pesticide analysis. A review. *Journal of Chromatography* 642: 135.
- Lacorte S, Ehresmann N and Barcelo D (1995) Stability of organophosphorus pesticides on disposable solid-phase extraction precolumns. *Environmental Science and Technology* 29: 2834.
- Mayer M, Poole SK and Poole CF (1995) Retention characteristics of octadecylsiloxane-bonded silica and porous polymer particle-loaded membranes for solid-phase extraction. *Journal of Chromatography A* 697: 979.
- Miller KG and Poole CF (1994) Methodological approach for evaluating operational parameters and the characterization of a popular sorbent for solid-phase extraction by HPLC. *Journal of High Resolution Chromatography* 17: 125.
- Pichon V, Chen L, Guenu S and Hennion MC (1995) Comparison of sorbents for the solid-phase extraction of the highly polar degradation products of atrazine (including ammeline, ammelide and cyanuric acid). *Journal of Chromatography A* 711: 257.
- Pichon V, Cau-dit-Coumes C, Chen L, Guenu S, Hennion MC (1996) Simple removal of humic and fulvic acid interferences using polymeric sorbents for the simultaneous solid-phase extraction of polar acidic, neutral and basic pesticides. *Journal of Chromatography A* 737: 257.
- Pichon V, Cau-dit-Coumes C, Chen L, Hennion MC (1996) Solid-phase extraction, clean-up and liquid chromatography for routine multiresidue analysis of neutral and acidic pesticides in natural water in one run. *International Journal of Environmental and Analytical Chemistry* 65: 11.
- Pichon V, Charpak M, Hennion MC (1998) Multiresidue analysis of pesticides using new laminar extraction disks and liquid chromatography and application to the French Priority List. *Journal of Chromatography A* 795: 83.
- Slobodnik J, Groenewegen MGM, Brower ER, Lingman H and Brinkman UATH (1993) Fully automated multiresidue method for trace level monitoring of polar pesticides by liquid chromatography. *Journal of Chromatography* 642: 359.
- Tomlin C (ed.) (1994) *The Pesticide Manual*, 10th edn. Crop Protection Publications.

Gas Chromatography

M.-R. Lee and B.-H. Hwang, National Chung-Hsing University, Taichung, Taiwan, Republic of China

Copyright © 2000 Academic Press

Introduction

A pesticide is usually defined as any organism or substance that is manufactured for direct or indirect control or prevention of any pest. Pesticides often alter the growth, development or characteristics of insects and plants. Most pesticides are synthetic chemicals that can be classified into six classes, according to their chemical type: organochlorine compounds, organophosphorus compounds, carbamates, phenoxyalkanoic acid derivatives, substituted ureas and triazines. Currently, several hundred pesticides are widely applied to a broad variety of crops to reduce losses from weeds, insects and diseases. Herbicides are employed in agriculture for pre- and post-emergent weed control of corn, wheat, barley and sorghum; they are also used on railways and roadside

verges. In general, organochlorine compounds are resistant to hydrolysis, and those that undergo photochemical reaction tend to form compounds with a persistence comparable to, or greater than, their parent compounds. Some organochlorine pesticides have been banned due to their toxicity, persistence and bioaccumulation in environmental matrices. Owing to the environmental impact of pesticides, several priority lists, also called 'black' or 'red' lists, have been published to protect the quality of surface and tap water. Thirty-nine pesticides are listed in priority order in the 76/464 EEC (European Economic Community) Council Directive on pollution caused by certain dangerous substances discharged into the aquatic environment of the community. The US Environmental Protection Agency (EPA) has established drinking water regulations and health advisory levels for individual pesticides.

Since the publication of Rachel Carson's book *Silent Spring* in 1962, many countries have legislated for public health protection. Such regulations have ultimately focused on protecting the general public

from pesticide residues. An illegal residue is defined as one that is above US EPA tolerance, one for which the 76/464/EEC Directive on the Quality of Water Intended for Human Consumption sets a maximum admissible concentration (MAC), or one that rises above the detection limit listed in the Department of Food and Agriculture's Multiresidue Pesticide Screen. The surveillance of various bodies of water is one of several important activities that provide information on present pollutant levels and future trends in waters. Monitoring pesticide residues in water is one of the important parameters in surveillance activity and environmental study. Regardless of the timing of the application, most pesticides applied to the soil are only lightly incorporated into the soil. Minimizing the risks of above-ground environmental contamination and reducing the hazard to nontarget organisms are very important for human health. Monitoring of pesticide residues in food of animal origin might also indicate a major source of exposure for humans. Therefore, pesticide residue determination has become a critical part of environmental analysis.

Many kinds of pesticides have been released into the environment, making it impossible to separate all pesticides in a single analysis. Thus, the analytical procedure for monitoring pesticide residues must be fast, easy, applicable to a number of different sample classes with only slight modification, and sufficiently sensitive and selective.

Many analytical procedures for analysing pesticide residues have been proposed in the development of multiclass, multiresidue; single-class, multiresidue; and single-residue methods, for a wide variety of sample types. Most pesticide residue analyses have been performed using multiresidue methods involving solvent extraction of the analytes from the sample matrix. Multidimensional analytical systems combining gas chromatography (GC) and high performance liquid chromatography (HPLC) with multiple detectors give many multiresidue methods. Qualitative and quantitative determination by GC with element-selective detectors and confirmation of results using an ancillary method such as mass spectrometry (MS) is the predominant method in pesticide residue analysis. The accuracy and precision of pesticide analyses depend on both sample preparation and instrumental performance. The chromatographic technique requires efficient isolation and concentration procedures. This study presents information on the analysis of pesticides using GC and introduces methods for sample preparation including various types of extraction techniques and derivatization procedures. The effectiveness of the techniques described are demonstrated by determining pesticide residues in real samples.

Sampling, Extraction, Clean-up and Derivatization

Pesticide residue analysis determines not only the parent compounds, but also their metabolites and degradation products. As many investigations have confirmed, determining pesticide residues in the range below ng mL^{-1} is difficult and extremely complex because of the need to isolate, accurately identify, and measure such minute quantities in large amounts of extraneous material. Gas chromatography is the most widely adopted technique in pesticide residue analysis. Pesticides that are amenable to direct analysis by means of GC should preferably be determined by means of this method because it separates well, is fast, and has available many selective and sensitive detectors. The sample generally cannot be analysed directly by using GC for pesticide residues; extraction is required to isolate the target contaminants from the sample matrix.

Clean-up is also necessary to isolate the target pesticides from interfering co-extractives before injection into a GC column. In pesticide extraction, classical solvent extraction method is the conventional method. Conventional extraction and matrix solid-phase dispersion methods have been used for organochlorine pesticides (OCPs) in fish muscle. Carbon dioxide is used as an extractant in high pressure Soxhlet extraction for determining organochlorine pesticides in olive oil, vegetable and fish tissue samples. Solid-phase extraction is extensively employed for the trace enrichment of pesticide residues from complex matrices. Common adsorbents are charcoal and porous polymers. Charcoal is widely used to extract low relative molecular mass polar pesticides and their metabolites, which are highly retained in water.

The homogeneous structure of polymers results in greater reproducibility in enrichment experiments. The most widely used types of polymers are 2,6-diphenyl-*p*-phenylene oxide (Tenax GC), acrylate polymers (Separon SE, XAD-8), ethylvinylbenzene-divinylbenzene (Porapak Q) and styrene-divinylbenzene copolymers (Polysorbs, Amberlite, XAD-2, PRP-1). The bonded silicas, including C_{18} , C_8 , cyano and amino, have been widely applied for the preconcentration of various types of pesticides from water samples. Octadecyl-bonded SPE has been proposed by the US EPA in Method 525.

A wide range of polarities of pesticide residues can be separated from sample coextractants by optimizing the SPE elution solvent. Homogeneous sample pulp, prepared from vegetables and fruits, is adsorbed on the surface of activated Florisil, which is then extracted in a glass column with ethyl acetate or

methylene chloride mixed with acetone. Kadenczki found a recovery rate of over 80% for pesticide residues, including carbamate, organochlorine, organophosphate, synthetic pyrethroid, triazine and miscellaneous pesticides. The recovery is also independent of the sample material. Snyder investigated the use of a supercritical fluid extraction method to extract 12 organochlorine and organophosphate pesticides from four soils: sand, clay, top soil and river sediment. The soils were extracted at a pressure of 350 atm and a temperature of 50°C with supercritical CO₂ modified with 3% methanol. The recovery of pesticides was greater than 85% for each of the matrices.

Solid-phase microextraction (SPME) has been introduced by Pawliszyn and his group. The mechanism of SPME is mainly based on adsorbing analytes from aqueous solutions onto a fused silica fibre coated with a polymeric adsorbent. An equilibrium occurs of analyte concentration between the sample and the solid-phase fibre coating. Extracted compounds are then thermally desorbed in the injector of the gas chromatographic system. Sampling in the SPME method can be done rapidly, directly, and without any solvent. Pawliszyn selected a 100 µm poly(dimethylsiloxane) (PDMS) fibre to extract ametryn, parathion, prometryn, simetry and terbutryn pesticides. Different modes of absorption were evaluated included static, magnetic stirring, fibre vibration and flow-through extraction cell methods. Montury has investigated using the SPME technique with 100 µm PDMS, to determine the residues of insecticides and fungicides commonly used for vineyard protection at the level of 20 µg L⁻¹.

Carbamates and some pesticides that have high polarity and low vapour pressure are generally not amenable to direct GC analysis. Derivatization is a convenient means of obtaining better chromatographic separations with increasing volatility and detector sensitivity, particularly with the electron capture detector (ECD). A chemical derivatization technique is also a highly effective procedure for confirming a pesticide residue's identity. By using this approach, the resulting derivatives examined by GC provide specific identification. Dehydrochlorination with KOH or NaOH is used to confirm the residues of DDT and its analogues. Reductive dechlorination with CrCl₂ is applied to identify heptachlor, endrin, metabolites of endrin, and some organophosphorus pesticides. For determining carbamate pesticides, silylation and acylation are the most widely applied derivatization procedures. Some halogenated silylating reagents are chloromethyldimethylchlorosilane, bromomethyldimethylchlorosilane, and 1,3-bis(chloromethyltetramethyldisilazane). The acyla-

tion reagents are trichloroacetic anhydride, pentafluoropropionic anhydride, trichloroacetyl chloride, heptafluorobutyric anhydride and trifluoroacetic anhydride.

Environmental Applications

The maximum levels of pesticide residue allowed in the European Union (EU) are 0.1 µg L⁻¹ in drinking water and 1–3 µg L⁻¹ in surface water. Pico presented a procedure for analysing water samples using online, solid-phase extraction gas chromatography. A cartridge packed with styrene-divinylbenzene polymer was used in sampling and ethyl acetate was used as the elution solvent. Organophosphorous pesticides and several triazines in tap water were tested using a GC flame photometric (FPD), flame ionization (FID), or nitrogen-phosphorous (NPD) detector. When a 10 mL sample of the tap water was analysed, the detection limit for all pesticides was lower than 0.1 µg L⁻¹. NPD and FPD are very much more sensitive and selective than FID. Hence, the SPE-GC-NPD system has been used widely for the analysis of pesticides, particularly organophosphorus pesticides in surface water samples. Tan compared solvent extraction using hexane and Freon TF (trichlorotrifluoroethane) and solid-phase extraction using octadecyl (C₁₈)-bonded porous silica, to determine the presence of organochlorine pesticide residues in water. It was concluded that the recoveries and precision using the SPE method for detecting organochlorine pesticides were poorer than those using the extraction method.

We have developed a methylation post-derivatization method on the fibre following SPME with GC-MS to analyse acidic herbicides from an aqueous sample. The acidic herbicides included 2-(4-chloro-2-methylphenoxy)propionic acid (MCP), 2-methoxy-3,6-dichlorobenzolic acid (dicamba), 4-chloro-2-methylphenoxyacetic acid (MCPA), 2-(2,4-dichlorophenoxy)propionic acid (2,4-DP), 2,4-dichlorophenoxyacetic acid (2,4-D), 2-(2,4,5-trichlorophenoxy)propionic acid (2,4,5-TP), 2,4,5-trichlorophenoxyacetic acid (2,4,5-T), 2-(*sec*-butyl)-4,6-dinitrophenol (dinoseb), and 2-(2,4-dichlorophenoxy)butyric acid (2,4-DB). A polyacrylate (PA)-coated SPME fibre yielded a higher extraction efficiency than that obtained with PDMS. The selected ion monitoring (SIM) mode in MS was used to quantitatively analyse the sample. **Figure 1** displays the mass chromatogram of the 100 µg L⁻¹ acidic herbicides solution determined in this way.

Detection limits at the level of 10–30 ng L⁻¹ are achieved for all herbicides by using this technique. Linearity is obtained over a wide range, with pre-

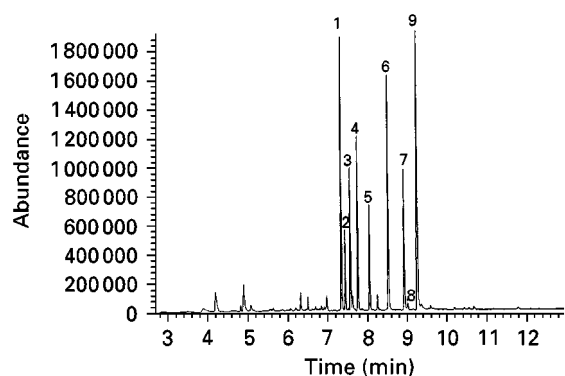


Figure 1 Mass chromatogram of $100 \mu\text{g L}^{-1}$ acidic herbicides solution by post-derivatization following SPME with PA fibre in GC-MS analysis. Peaks: 1, MCPP; 2, dicamba; 3, MCPA; 4, 2,4-DP; 5, 2,4-D; 6, 2,4,5-TP; 7, 2,4,5-T; 8, dinoseb; 9, 2,4-DB.

cision below 12% relative standard deviation (RSD). In addition, various degradation compounds of acidic herbicides in basic solution including 2,4-dichlorophenol, 2,4,5-trichlorophenol and 4-chloro-3-methylphenol have been detected.

Durand has studied the confirmation of chlorotriazine pesticides, their degradation products, and organophosphorus pesticides in soil samples, using GC-MS with electron impact and positive and negative chemical ionization. Sample pretreatment of soil samples was carried out via Soxhlet extraction for 12 h with methanol. Glass columns filled with 2 g of Florisil effected clean-up. The elution solvent was hexane. Residue levels of chlorotriazine pesticides and organophosphorus pesticides were determined in soil samples at levels from 5 ng g^{-1} to $9 \mu\text{g g}^{-1}$. Snyder compared supercritical fluid extraction with classical sonication and Soxhlet extraction for organophosphorus and organochlorine pesticides from soils. Supercritical fluid extraction was found to have the best overall precision over either the Soxhlet or the sonication extractions, and was also less labour-intensive. We have compared different methods of mass spectrometry including GC-MS (EI, CI), GC-MS-MS, and GC-ECD to determine ethion from soil. The largest recoveries (over 96%) were achieved with a 1:1 mixture of methanol and acetone as extraction solvent for 3 h in Soxhlet extraction. The limit of detection of ethion for all techniques is below the nanogram level. The mass chromatogram of GC-MS-MS selected reaction monitoring (SRM, m/z 384 \rightarrow m/z 231) in electron impact ionization mode, of a soil sample containing 0.5 ng g^{-1} ethion, is illustrated in Figure 2. The best ethion detection limit (170 pg g^{-1} of soil) was obtained using this technique.

Agricultural Applications

Leoni described a multiresidue method for the quantitative analysis of 28 organophosphorus pesticides in vegetable and animal foods using GC. The pesticides were extracted with different solvents from either fatty or nonfatty foods. Clean-up was carried out on active carbon-celite and on disposable minicolumns of bonded-phase silica, according to fat and pigment content. A wide-bore column (SPB-5) with flame photometric detection, operated in phosphorus mode, was chosen for GC analysis. The recovery tests obtained were 81–85% for apples, whole milk, pasta and eggs, and 89% for olive oil. Schenck described a procedure for screening organochlorine and organophosphorus pesticide residues in eggs using an SPE clean-up and GC detection. The pesticides were extracted from the eggs using acetonitrile. A tandem C_{18} and a Florisil SPE column were used for extract clean-up with recoveries ranging from 80% to 90%. The limit of quantitation was $0.005 \mu\text{g mL}^{-1}$ for organochlorine pesticides and $0.01 \mu\text{g mL}^{-1}$ for organophosphorus pesticides. Torres proposed a multiresidue extraction method based on matrix solid-phase dispersion (MSPD) for the extraction and GC screening of 18 insecticides including aldrin, ethion, and dicofol, from oranges. The limits of detection were from 2 to $171 \mu\text{g kg}^{-1}$, which is about 10 times lower than the maximum residue level established by the European Community. Sulfuric acid pretreatment for the simultaneous GC screening of organochlorine and organophosphorus pesticides in herbal essential oils was studied by Yoon. A mixed phase of 17% (v/v) of sulfuric acid to organic solvent (hexane/ethyl ether 9:1, v/v) and a reaction time of 30 s was used to carry out steam distillation to extract pesticides from herbs; this was followed by GC-FID. The recovery of the studied pesticides was in the range of 75% to 111% for organochlorine pesticides

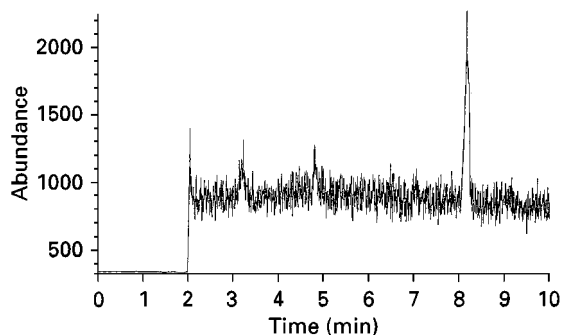


Figure 2 Mass chromatogram of a soil sample containing 0.5 ng g^{-1} ethion produced by using GC-MS-MS selected reaction monitoring (m/z 384 \rightarrow 231) in EI mode.

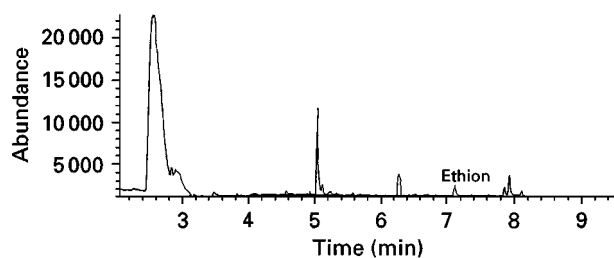


Figure 3 Mass chromatogram of a real orange sample for monitoring ethion in GC-MS analysis. A C_{18} SPE cartridge was used to extract ethion from oranges. A mixed solvent of hexane and dichloromethane, in a ratio of 1 : 1, was used as the elution solvent. A capillary fused silica DB5-MS column was used in the GC-MS analysis.

and 72% to 116% for organophosphorus pesticides. A SPME method was developed and validated by Simpli'cio to determine the level of organophosphorus pesticides, including diazinon, fenthion and triazophos, in fruits and fruit juice using an FPD in phosphorus mode. Limits of detection of the method for fruit and fruit juice matrices were below $2 \mu\text{g kg}^{-1}$ for all pesticides. Monitoring of ethion residues and its degradation compounds in oranges, using C_{18} SPE cartridges for extraction followed by GC-MS and GC-MS-MS, was studied in our laboratory. **Figure 3** presents the mass chromatogram of a real orange sample obtained using selected ion monitoring (m/z 384 of ethion).

Next, a comparison was made of GC-MS and GC-MS-MS with various ionization modes. The EI mode in GC-MS with selected ion monitoring was the best method, obtaining a $0.96 \mu\text{g g}^{-1}$ limit of detection. Various extraction methods, including Soxhlet extraction, SPE and SPME, were used to study the extraction of 19 organochlorine pesticides found in Chinese herbal medicines. GC-ECD and GC-MS were evaluated to determine the presence of the pesticides. **Figure 4** presents the analysis of 200 ng g^{-1} of spiked pesticides by using SPME-GC-ECD. The limits of detection for all organochlorine pesticides are below ng g^{-1} .

Biological Applications

Petty investigated a method for the analysis of nine organochlorine pesticides in wildlife urine. The urine samples collected from a single domestic dog were spiked with a standard mixture containing lindane, aldrin, chlordane, DDE, endrin and DDT. The extraction of organochlorine pesticides from urine was performed on a C_{18} SPE column. The method's limits of detection ranged from 1.4 to $2.7 \mu\text{g L}^{-1}$ when using an ECD.

Lott proposed a multiresidue isolation technique using matrix solid-phase dispersion (MSPD) and GC-ECD for screening 14 organochlorine pesticides in crayfish hepatopancreas. In the MSPD extraction, 0.5 g of the homogenized fish tissue was blended with 2 g of C_{18} silica, and the resulting mixture was then transferred to a 10 mL syringe-barrel column that contained 2 g of activated Florisil. Pesticides were eluted by gravity flow with 8 mL of acetonitrile. Two microlitres of the elute was directly analysed by GC. The results showed that the MSPD technique combined with GC-ECD enabled the successful extraction and determination of the 14 organochlorine pesticides at $125\text{--}2000 \text{ ng g}^{-1}$ levels.

Diserens has proposed the extraction and clean-up for multiresidue determination of pesticides in lanolin. Lanolin, a waxy material extracted from wool, is one of the raw materials used in cosmetic products. The diatomaceous earth in an Extrelut column was used to adsorb a light petroleum solution containing lanolin. The acetonitrile extract was passed through an SPE cartridge containing a C_{18} column. Organophosphorus pesticides were determined by GC using FPD in the phosphorus mode. Organochlorine pesticides were determined by GC-ECD after extraction and clean-up in a Florisil column. The limits of detection for the various pesticides are about $5 \mu\text{g kg}^{-1}$ for organochlorine compounds and $50 \mu\text{g kg}^{-1}$ for organophosphorus pesticides.

We have evaluated GC-MS with selected ion monitoring for determining organochlorine pesticides in fish. Petroleum ether was used to extract pesticide residue from 2 g of fish tissue. The gas chromatogram

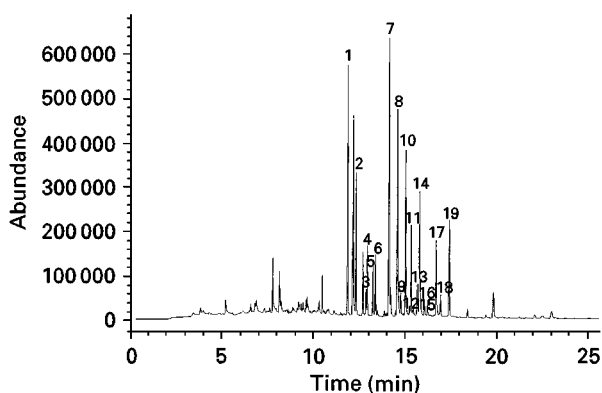


Figure 4 Gas chromatogram of spiked 200 ng g^{-1} 19 organochlorine pesticides in a herbal medicine formula analysed by SPME GC-ECD. Peaks: 1, α -BHC; 2, γ -BHC; 3, β -BHC; 4, heptachlor; 5, δ -BHC; 6, aldrin; 7, heptachlor epoxide; 8, endosulfan I; 9, p,p' -DDE; 10, dieldrin; 11, endrin; 12, o,p' -DDT; 13, p,p' -DDD; 14, endosulfan II; 15, p,p' -DDT; 16, endrin aldehyde; 17, endosulfan sulfate; 18, Methoxychlor; 19, endrin ketone.

from a shad fish captured from the Taiwan Strait gave limits of detection for the organochlorine pesticides in fish below ng g^{-1} . The concentration of *p,p'*-DDE was detected at 90 ng g^{-1} .

Future Prospects

In recent years, new and improved methods and technologies to analyse pesticide residues have rapidly evolved. Analytical methods for most residue pesticides have detection and quantification limits at the low parts per billion to parts per trillion for water analysis, and low parts per million to parts per billion for other samples such as crops, soils and biological matrices. Many preconcentration methods have been developed in clean-up procedures, including exhaustive solvent extraction, automated Soxhlet extraction, microwave-assisted extraction, MSPD extraction, SPE using microcolumns, cartridges, and Empore discs, and SPME. Qualitative and quantitative determination by GC with element-selective detectors, and confirmation of results using MS, continues to be the predominant technique for multiresidue pesticide analysis. MS has been widely used for confirmation of trace pesticide identification and quantitation. Tandem mass spectrometry (MS-MS) is replacing the conventional approaches to confirmation and GC added to the MS-MS will increase the specificity obtained. Now that ion trap mass spectrometry has been introduced, pesticide residue confirmation can be obtained through experiments involving MS-MS or MS^n on compounds of high relative molecular mass, to yield a pyramid of related product ions. With mass spectrometry developments the MS-MS technique will become inexpensive, and eventually the GC-MS-MS technique will be the conventional means of analysing pesticide in most classes of sample matrices.

See also: **II / Chromatography: Gas:** Detectors: Mass Spectrometry; Detectors: Selective. **Extraction:** Analytical Extractions; Solid-Phase Extraction; Solid-Phase Microextraction; Supercritical Fluid Extraction. **III / Herbicides:** Gas Chromatography; Solid-Phase Extraction; Thin-Layer (Planar) Chromatography. **Pesticides:** Extraction from Water; Supercritical Fluid Chromatography; Thin-Layer (Planar) Chromatography.

Further Reading

- Barceló D (1993) Environmental Protection Agency and other methods for the determination of priority pesticides and their transformation products in water. *Journal of Chromatography* 643: 117–143.
- Cairs T and Sherma J (1992) *Emerging Strategies for Pesticide Analysis: A Volume in the Series Modern Methods for Pesticide Analysis*. Boca Raton, FL: CRC.
- Edwards CA (1976) *Persistent Pesticides in the Environment*, 2nd edn. Boca Raton, FL: CRC.
- Frehse H (1991) *Pesticide Chemistry: Advances in International Research, Development, and Legislation*. Weinheim: VCH.
- Racke KD and Coats JR (1990) *Enhanced Biodegradation of Pesticides in the Environment*. Washington, DC: American Chemical Society.
- Racke KD and Leslie AR (1993) *Pesticides in Urban Environments: Fate and Significance*. Washington, DC: American Chemical Society.
- Richter O, Dieckkrüger B and Nörtersheuser P (1996) *Environmental Fate Modelling of Pesticides: From the Laboratory to the Field Scale*. Weinheim: VCH.
- Rosen JD (ed.) (1987) *Applications of New Mass Spectrometry Techniques in Pesticide Chemistry*. New York: John Wiley.
- Sherma J (1991) Pesticides. *Analytical Chemistry* 63: 118R–130R.
- Somasundaram L and Coats JR (1991) *Pesticide Transformation Products: Fate and Significance in the Environment*. Washington, DC: American Chemical Society.

Supercritical Fluid Chromatography

M. E. P. McNally, E.I. DuPont de Nemours and Co., Inc., Wilmington, DE, USA

Copyright © 2000 Academic Press

Introduction

Supercritical fluid chromatography (SFC) is a useful tool in the analysis of pesticides and herbicides. Typically, this is done with liquid or gas chromatography and there are basic advantages and disadvantages to each of these methods of analysis. For LC, the liquid

phase offers the unique advantage of a wide range of solubilities but detection interfaces tend to be the limiting factor. GC has the ability to be more easily interfaced to specific detection capabilities but has significant limitations in the area of solubility; compounds must be able to be readily volatilized. For agriculturally active compounds, the lack of a universal detector for HPLC limits the scope of its applicability to compounds which do not contain UV chromophores. GC is limited to thermally stable volatile compounds since they must move through the

chromatographic column in the gaseous state. Not all pesticides and herbicides contain a chromophore, others are thermally labile, or are not volatile, and therefore require derivatization for GC analysis. The analysis of pesticides and herbicides by supercritical fluid chromatography is a reasonable alternative to LC and GC. SFC offers the ability to be coupled to a wide variety of detectors that are both LC and GC compatible. In addition, the solubilizing powers of a supercritical fluid at low operating temperatures can easily mimic those achieved with liquids, thus making SFC more applicable to a wider range of pesticide and herbicide classes than either LC or GC.

Since the mid-80s, the advantages of SFC in pesticide and herbicide analysis have been well documented. SFC has also been used to solve separation problems. In the main stream of pesticide and herbicide analysis however, SFC remains a niche technique that is employed when classical LC and GC analysis are not successful in solving a problem. Even in those examples where SFE may be used to remove the herbicidal or pesticidal analyte of interest, the follow-up technique is still predominantly gas or liquid chromatography.

This report outlines typical examples of the use of supercritical fluids for the chromatographic analysis of pesticides and herbicides by pesticide class. Table 1 lists these pesticides, their common and trade names, mode of action and pesticide class.

Carbamates and Methyl Carbamates

Carbamate pesticides were rapidly analysed with flame ionization detection by Wright and Smith. The compounds investigated were propoxur, chlorpropham, carbaryl, and phenmedipham and baseline resolution was achieved in less than 1.5 min. To achieve this rapid separation, the authors used a short capillary column ($0.9\text{ m} \times 25\text{ }\mu\text{m}$ i.d.) coated with 5% phenyl polymethylsiloxane that had been cross-linked with azo-tert-butane. This type of rapid separation represents one of the other distinct advantages of SFC. The high diffusivities of supercritical fluids allow for rapid equilibration, as the compounds of interest travel through the chromatographic column achieving higher separation factors in less time. Overall analysis times are therefore reduced. In this separation, pure carbon dioxide was used as the mobile phase with pressure programming rates of 100 atm min^{-1} . The baseline resolution of propoxur, dicamba, carbaryl, 2,4-D, silvex, and phenmedipham was achieved later in approximately 120s by these same authors, again demonstrating the rapid analysis of carbamate pesticides by SFC. For this mixture of

six pesticides, the separation was achieved on a $1.5\text{ m} \times 25\text{ }\mu\text{m}$, 5% phenyl polymethylsiloxane column with pressure programming at 50 atm min^{-1} . This mixture was further expanded with the addition of picloram and chloramben and baseline resolution was obtained on a 1.5 m capillary column in approximately 120s, demonstrating consistently the rapid analysis times that can be achieved using SFC for carbamates.

In more typical separation timeframes, Richter reported the separation of four carbamate pesticides on a more standard size column $15\text{ m} \times 50\text{ }\mu\text{m}$ i.d. fused silica column with an SE-33 stationary phase ($0.25\text{ }\mu\text{m}$ film thickness). Aldicarb, methomyl, diflubenuron, and phenmedipham were baseline resolved in a little more than 20 min.

UV detection at 254 nm was used to analyse carbamate pesticides by Games and co-workers using analytical-scale packed columns with modified carbon dioxide. The pesticides analysed were chlorpropham, pirimcarb, methiocarb, carbaryl, phenmedipham and asulam. Resolution was achieved in approximately 5 min on a $10\text{ cm} \times 4.6\text{ mm}$ i.d. LiChrosorb column. 12% methanol-modified carbon dioxide was the mobile phase and the flow rate was programmed to help achieve the rapid separation by increasing the rate from 2 mL min^{-1} to 4 mL min^{-1} after the first 2 min.

Although nitrous oxide, especially when mixed with alcohol modifiers, has since been shown to be a safety hazard under supercritical conditions, initially investigators explored the use of nitrous oxide as an alternative to carbon dioxide to obtain alternative separation mechanisms. Capillary SFC for the separation of free amines and their carbamate and amide derivatives was investigated by Mathiasson *et al.* with nitrous oxide as the mobile phase. A thermionic nitrogen-phosphorus detector was used and its performance optimized by systematic variation of the makeup gas flow rate (nitrogen), the hydrogen and air flow rates, and the bead current. The effects of increasing nitrous oxide pressure on detector response were explored and a dependence of peak area on the system pressure was observed. This same effect on detector response was seen with the addition of methanol modifier to the nitrous oxide. Concentrations of methanol above 0.8% resulted in a significant loss in signal from the detector.

Aldicarb, methomyl, mesurol, oxamyl, carbofuran, and carbaryl were analysed by capillary SFC by Richter and coworkers in parsley extracts. The column was a $10\text{ m} \times 50\text{ }\mu\text{m}$ i.d. SB-methyl-100 and a nitrogen-phosphorus detector was used. Practical limits of detection were achieved, the pesticides were determined in the parsley extract at levels of approximately 2 ppb.

Table 1 Compound classes of herbicides, insecticides and pesticides

<i>Compound common name</i>	<i>Trade name</i>	<i>Mode of action</i>	<i>Compound class</i>
α -BHC or Benzene Hexachloride		Ingested insecticide	Organochlorine insecticide
Alachlor	Lasso TM	Cell division inhibitor	2-Chloroacetanilide herbicide
Aldicarb	Temik	Cholinesterase inhibitor	Carbamoyloxime insecticide
Aldrin	Octalene		Organochlorine insecticide
Atrazine	Gesaprim	Photosynthetic electron transport inhibitor	1,3,5-Triazine
β -BHC or Benzene hexachloride		Ingested insecticide	Organochlorine insecticide
Bendiocarb	Ficam, Garvox, Seedox	Cholinesterase inhibitor	Methyl carbamate insecticide
Captafal	Difolatan	Protective non-systemic fungicide	Phthalimide fungicide
Captan	Orthocide TM	Protective spray, root or dip fungicide	Phthalimide fungicide
Carbaryl	Sevin	Cholinesterase inhibitor	Methyl carbamate insecticide
Carbofuran	Furadan, Curaterr, Yaltox	Cholinesterase inhibitor	Carbamate insecticide
Carbophenothion	Trithion	Acaricide	Organophosphorus insecticide
Chlorbromuron	Maloran	Photosynthetic electron transport inhibitor	Urea herbicide
Chlordane	Octachlor	Non-systemic contact and ingested insecticide	Chlorinated hydrocarbon insecticide
Chlorpyrifos	Dursban, Lorsban	Cholinesterase inhibitor	Organophosphorus insecticide
DDD	Rhothane		Organochlorine insecticide
DDE	Gesarol, Guersarol TM	Non-systemic ingested contact insecticide	Organochlorine insecticide
DDT	Gesarol, Guesarol, Neocid	Non-systemic ingested and contact insecticide	Organochlorine insecticide
Dieldrin	Octalox		Organochlorine insecticide
Diflubenzuron	Dimilin	Chitin synthesis inhibitor	Benzoylurea insecticides
Dioxathion	Delnav		Organophosphorus insecticide
Disulfoton	Di-Syston, Dithiosystox, Frumin AL, Solvirex	Cholinesterase inhibitor	Organophosphorus insecticide
Diuron	Karmex	Photosynthesis inhibitor	Urea
Ethyl parathion	Thiophos, Bladan, Folidol, Fosferno, Niran TM	Cholinesterase inhibitor	Organophosphorus insecticide

Table 1 Continued

Compound common name	Trade name	Mode of action	Compound class
Fenchlorphos	Nankor Trolene Korlan	Systemic insecticide	Organophosphorus insecticide
Fenitrothion	Accothion, Cytel, Cyfen, Folithion, Sumithion	Cholinesterase inhibitor	Organophosphorus insecticide
γ -BHC or benzene hexachloride	Lindane, Gammexane	Ingested insecticide	Organophosphorus insecticide
Hexachlorobenzene, HCB	Voronit C	Selective fungicide used to control <i>Tilletia caries</i> on wheat	Organochlorine fungicide
Malathion, Carbofos Metalaxyl	Cythion Apron, Ridomil, Fubol	Cholinesterase inhibitor Systemic fungicide	Organophosphorus insecticide Acetalanine
Methidathion	Supracide Ultracide	Cholinesterase inhibitor	Organophosphorus insecticide
Methomyl	Lannate, Nudrin TM	Cholinesterase inhibitor	Carbamoyloxime insecticide
Methoxychlor	Marlate	Contact and stomach insecticide	Bridged-di-phenyl insecticide
Methyl parathion	Trithion	Cholinesterase inhibitor	Organophosphorus insecticide
Metobromuron	Patoran	Photosynthetic electron transport inhibitor	Urea herbicide
Oxamyl	Vydate	Cholinesterase inhibitor	Carbamoyloxime insecticide
Parathion	Thiophos, Bladan, Folidol, Fosferno, Niran	Cholinesterase inhibitor	Organophosphorus insecticide
Pentachlorophenol	Dowacide G, Santobrite	Termite control	Phenolic herbicide, insecticide and fungicide
Phenmedipham	Betanal	Photosynthetic electron transport inhibitor	Bicarbamate herbicide
Phorate	Thimet, Agrimet TM	Cholinesterase inhibitor	Organophosphorus insecticide
Tetrachlorvinphos	Gardona, Rabond,	Cholinesterase inhibitor	Organophosphorus insecticide
Tetradifon	Tedion V-18	Non-systemic acaricide	Bridged diphenyl acaricide
Thiodicarb	Larvin, Semevin	Cholinesterase inhibitor	Carbamoyloxime insecticide
Tri-allate	Avadex BW, Far-Go	Cell elongation inhibitor	Thiocarbamate herbicide

The separation of the thermally labile acid and carbamate pesticides propoxur, BPMC (fenobucarb), propachlor, carbofuran, alachlor, carbaryl, linuron, and diuron was achieved by Wright *et al.* using

SFC/MS with ammonia chemical ionization. Capillary SFC was used for sample introduction into the MS instrument. Resolution of all compounds except BPMC and propachlor was obtained on

a 10 m \times 50 μ m 5% phenyl methylpolysiloxane stationary phase. Ammonia provided softer ionization with an (M + 18) + molecular ion and little fragmentation, while methane chemical ionization resulted in an (M + 1) + molecular ion and increased fragmentation when the two reagent gases were compared. These same authors conducted additional work comparing the same reagent gases for the chemical ionization of a larger group of carbamate and acid pesticides. Again, capillary SFC was used as a means of sample introduction. The separated and identified carbamate pesticides were: aldicarb, aldicarb sulfoxide, aldicarb sulfone, carbaryl, BPMC, propoxur, chlorpropham, carbofuran, asulam, desmedipham, and penmedipham. The acid pesticides explored were 2,4-D, 2,3-D methyl ester, dicamba, picotam, Silvex and Silvex methyl ester. The capillary columns were short (2 m \times 50 μ m i.d.) the pressure ramps rapid (50 atm min⁻¹). Spectra obtained using ammonia resembled thermospray HPLC/MS spectra. The general rule for carbamates was that the ammonium adduct ion was the base peak. The absence of significant thermal degradation was indicated since the molecular species was present.

Carbofuran, its 3-keto, and 3-hydroxy metabolites extracted from the gullet of a bird were analysed by multidimensional SFC/SFC. A 1.0 μ L aliquot of bird extract was injected allowing for detection limits for both metabolites and carbofuran at levels in the range 1 to 10 ng. A flow-switching interface demonstrated the use of two 50- μ m-i.d. capillary columns in tandem. In this example, a biphenyl column was first in the series, a glyme column second. The use of solvent venting allowed for the injection of large volumes.

A multichannel UV detector for capillary SFC was used to analyse the pesticides bendiocarb and carbaryl and the herbicides alachlor, diuron and metalaxyl. A photodiode array spectrophotometer acquired the UV spectra. The detector flow cell volume was 710 nL made from a fused silica capillary (0.32 mm i.d.) with the polyimide coating removed. The capillary column a 12 m \times 100 μ m i.d. 5% phenylmethyl polysiloxane achieved baseline resolution in 31 min. Full spectra over the range 190 to 310 nm were collected at the peak apexes for each compound. Excellent sensitivity was achieved, for example the limit of detection of bendiocarb (S/N = 5) was 3.8 ng.

Triazines

Both packed and capillary column SFC have been successfully used for the analysis of triazine herbicides. To achieve good signal/noise ratios at concentrations as low as 5 ppm, Ashraf and coworkers

reported using solvent-vented injections of as much as 1.0 μ L samples onto a 2 m \times 110 μ m i.d. retention gap. The gap was connected through a venting valve to a 10 m \times 50 μ m i.d. fused silica capillary SFC column. The valve was switched to the inject position for a controlled amount of time when as little as 0.2 μ L of sample was delivered, or for the full length of the chromatographic run for the delivery of 1.0 μ L of sample. During the injection process, the sample loop was purged with nitrogen gas. After injection, the repositioned venting valve passed the flow of nitrogen through to the vent, concentrating the injected compounds on the pre-column. Another switch of the venting valve brought the analytical column in-line for the chromatographic analysis. This injection technique was successful for up to 20 ppm solutions of the two triazine herbicides, atrazine and cyanazine. Two pyrethroids and one benzophenylurea compound were also successfully injected using this technique.

Packed column SFC was used by Taylor *et al.* to investigate the behaviour of triazine and triazole herbicides. Carbon dioxide flow rate, outlet pressure, and oven temperature were explored using an analytical scale, 25 cm \times 4.6 mm i.d., Deltabond CN column. Baseline resolution of the eight compounds of interest was obtained in approximately six minutes again illustrating the rapid equilibration and elution possible with supercritical fluids. In an atypical flow delivery method, the flow of carbon dioxide was held constant, while the flow of methanol was increased during the chromatographic run. Over the course of the six minute chromatographic run, the methanol concentration was increased from 2.4% to approximately 30%. The outlet pressure during the separation was 270 atm (4000 psi) and the oven temperature was held constant at 60°C. There is little question that supercritical conditions were not maintained during the analysis. Specifically, once the methanol concentration reached levels at or above 12 to 15%, sub-critical or enhanced fluidity chromatography were the most likely mobile phases affecting the separation. Despite the change in mobile phase state throughout the chromatographic process, the separation was successfully achieved.

Concentration ranges from 2.5 ppb to 25 ppm were examined by Ashraf *et al.* using a 'three electrode' thermionic detector. Both the phosphorus and nitrogen selective modes were explored with capillary SFC as the means of sample introduction. The compounds of interest included two triazine herbicides, two pyrethroids, a benzophenylurea, and a chlorophenyl vinyl diethylphosphone. The capillary SFC column was a 10 m \times 50 μ m i.d. biphenyl methyl polysiloxane. Significant baseline rise was observed during pressure programming. To reduce this effect,

optimization experiments for hydrogen, air, and nitrogen flow rates (as makeup gas), and the position of the alkali source in relation to the flame tip were conducted. In the phosphorus mode, detection in the picogram range was demonstrated for the vinyl phosphone. Detection was only slightly improved over what could be obtained with flame ionization detection when nitrogen-containing compounds, such as the triazines, were examined in the phosphorus mode. In the nitrogen mode, the background current was much lower. This did not result in a less severe baseline increase with pressure programming. This detector was found to demonstrate enhanced sensitivity in the nitrogen mode, with detection limits in the range 0.6 to 60 pg.

SFC/MS and GC/MS were both easily connected with capillary SFC via a capillary-direct interface. The interface used required no modification of the mass spectrometer. Hawthorne and Miller reported the analysis of a triazine herbicide metabolite using capillary SFC/MS and obtaining spectra collected in the CI mode with methane as the reagent gas.

A minimum detection limit of approximately 35 pg (S/N = 3) was obtained for a triazole fungicide metabolite on a 5 m × 50 μm SB-methyl-100 column. An electron capture detector was utilized for this capillary SFC analysis. Pressure programming from 100 to 350 atm (1500 to 5100 psi) at 40 atm min⁻¹ was performed without a substantial increase in detector background signal. Makeup gas of 10% methane in argon was used with a detector operating temperature of 350°C. The optimum conditions for system operation were found with makeup gas flow rate of 15 mL min⁻¹, and the restrictor positioned approximately 3 cm from the column nut at the entrance to the detector.

The effects of 'enhanced fluidity' mobile phases on s-triazines: ammeline, hydroxyatrazine, desethyl-desisopropyl atrazine, atrazine, terbutyne and terbutylazine have been shown. **Figure 1** shows the names, structures and pK_a values of these herbicides. Enhanced fluidity chromatography uses carbon dioxide at lower percentages and mobile phase modifiers such as methanol at higher percentages than SFC. This yields gains in diffusivity and viscosity over liquid chromatography but not to the level obtained with SFC. **Figure 2** shows the chromatographic separation of four of these triazines at elevated pressures and temperatures with three different mobile phase compositions. **Table 2** shows the chromatographic efficiencies and retention times of analytes with different mobile phase conditions. These values are taken from the chromatograms illustrated in **Figure 2**. Ultimately, for these triazine herbicides the viscosity reduction of the 'enhanced fluidity' mobile phase yielded higher optimum flow rates, higher efficiency, shorter analysis time, and decreased pressure drop. These are the same advantages seen when a supercritical fluid mobile phase is used, but to a lesser extent. The example has been included in this review of SFC to be inclusive and to illustrate to the reader that many examples in the literature which claim to be 'supercritical', fall in and out of the supercritical region of a phase diagram. Even so, advantages over liquid chromatographic separations can be seen.

Ureas and Sulfonylureas

Much work has been carried out using supercritical techniques on ureas and sulfonylureas. This class of herbicides was newly introduced in the early 1980s.

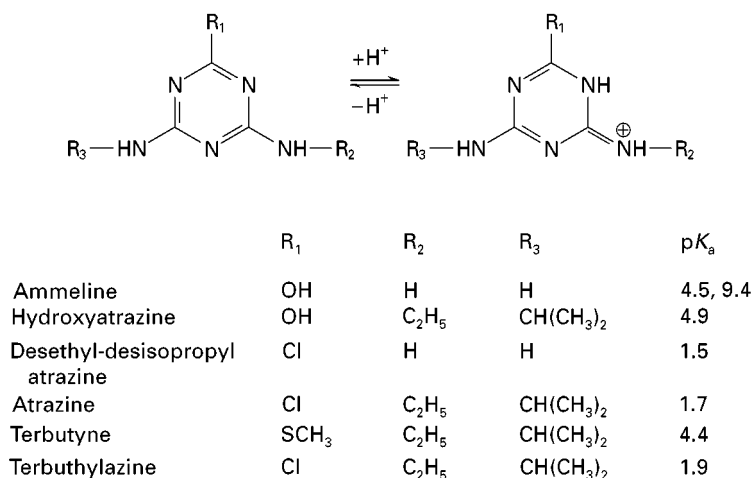


Figure 1 Chemical structures and pK_a values of triazine herbicides.

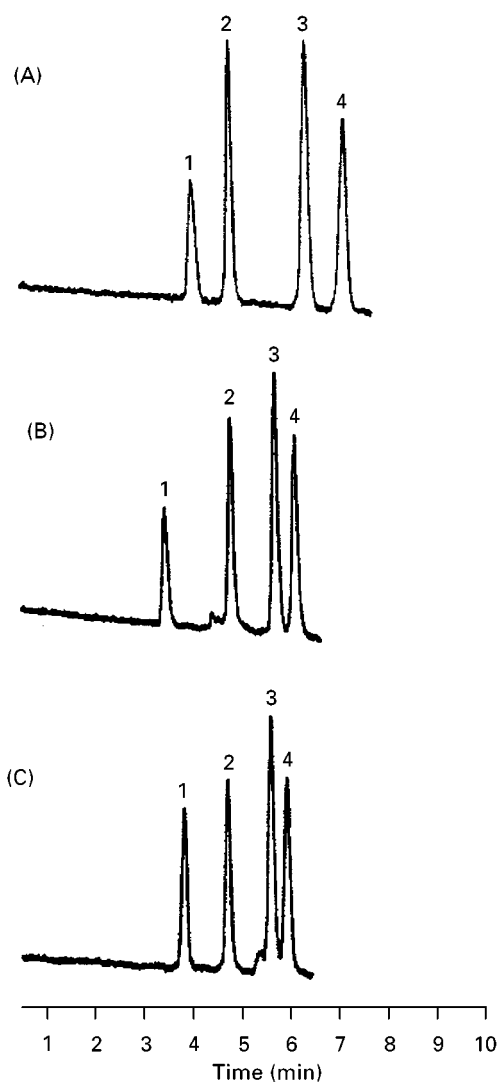


Figure 2 Chromatograms at 238 atm, 0.35 mL min⁻¹ for different mobile phase conditions: (A) 64:36 mol% methanol-H₂O; (B) 51:29:20 methanol-H₂O-CO₂; (C) 51:29:20 methanol-H₂O-CHF₃. Peaks: 1. hydroxyatrazine; 2. desethyl-deisopropyl atrazine, 3. atrazine, 4. terbutylazine.

They have low use rates in the agricultural arena and so require low analytical detection limits and they are thermally labile. The desired low detection limits make liquid chromatography more difficult and the thermal lability make GC inappropriate. Wheeler and McNally compared packed and capillary supercritical fluid chromatography with HPLC using representative ureas and sulfonylureas. Five herbicides were analysed by the three techniques. For both the capillary and the packed column SFC experiments and LC, UV detection was used. Limits of detection, reproducibility, and linearity of response were compared. The compounds investigated were the moderately polar herbicides, Oust®, Glean®, Harmony®, Karmex® and

Nustar®. Oust®, Glean® and Harmony® are sulfonyl urea herbicides. Karmex® or diuron is a phenyl methyl urea, and Nustar® is a silicon fungicide. Results indicated that faster analysis, lower detection limits, and greater injection-to-injection reproducibility were obtainable with packed column SFC. No appreciable difference in the linearity of response between the three techniques was observed. Using capillary SFC with FID detection, short capillary columns were used to examine these same compounds. Relative standard deviations for peak area were 3 to 5% range. The linear range was found to be fairly compound dependent, and detection limits were reported in the range 20 to 80 µg mL⁻¹.

Baseline resolution of dimethylcarbanilide, dimethylphenylurea (linuron), diphenylmethylurea (diuron), monuron, and carbanilide was achieved in eight minutes. Shah and Taylor used an analytical scale packed cyanopropyl column. Using a methanol modified carbon dioxide mobile phase, the separation was achieved holding the methanol concentration constant at 2%, and the flow rate at 3 mL min⁻¹. Ureas, sulfonylureas and their manufacturing precursors have been separated using packed and capillary SFC columns, a carbon dioxide mobile phase and an on-line FTIR detector. The column used in the urea separation was a packed 10 cm × 1 mm i.d. cyano column. Capillary columns and split-less injections of 0.1 µL were employed for precursors at concentrations of approximately 3 mg mL⁻¹. The ureas studied were: dimethylphenyl urea, diphenylmethyl urea, monuron, and carbanilide. On the packed column, baseline resolution of all compounds except for the partially resolved dimethylcarbanilide and dimethylphenyl urea, was obtained. Peak assignments were made based on retention time and spectral interpretation comparison with pure standards. After attempts to develop the separation on the packed CN column failed, capillary SFC columns were used to separate the benzamide-anilide mixture. The baseline resolution of six precursors was achieved in approximately 25 min.

The packed SFC retention behaviour of a variety of urea and sulfonyl urea precursors was studied with modified carbon dioxide mobile phase by McNally and co-workers. Methyl, phenyl, nitro, amide, carboxamide and chloro functional group positioning were examined to gain an understanding of retention characteristics. Extensive modifier interactions were investigated in this study, using methanol, ethanol, isopropanol, hexanol and tetrahydrofuran at 2% w/v in carbon dioxide. A silica stationary phase was chosen to simulate polar matrices, i.e. soil and plant materials. Comparisons with supercritical fluid extraction retention were drawn. This was the first

Table 2 Efficiencies and retention times of analytes with different mobile phase conditions at the same flow rate: 0.35 mL min^{-1} ^a

Peak	Mobile phase (mol%), flow rate					
	64/36 methanol/H ₂ O, 0.37 mL min^{-1}		51/29/20 methanol/H ₂ O/CO ₂ , 0.35 mL min^{-1}		51/29/20 methanol/H ₂ O/CHF ₃ , 0.37 mL min^{-1}	
	Efficiency	<i>t</i> (min)	Efficiency	<i>t</i> (min)	Efficiency	<i>t</i> (min)
1	3714	4.05	4271	3.54	4908	3.81
2	8054	4.83	8932	4.80	9254	4.70
3	9672	6.4	10870	5.72	11588	5.59
4	10306	7.2	11332	6.14	11738	5.92

^aPeak numbers are the same as in Figure 2. The values provided are averages of at least three replicated chromatograms with RSD $\leq 5\%$.

comparison of the two made in the literature. Since that time, several extensive reports have proven this correlation to be true. In this functional group study, specific interactions were observed which were attributed to the polarity of the compound, steric interactions between individual functional groups of the molecules, the functional group molecular make-up, and the polarity of the modifier used.

A benchtop thermospray mass spectrometer has been coupled with packed column SFC for the detection of the packed column SFC separation of ureas. The column used to separate dimethylcarbanilide, dimethylphenyl urea, diphenylmethyl urea, monuron, diuron, and carbanilide was a 1-mm i.d. cyanopropyl column. Significant baseline rise with pressure programming was noted and attributed to hydrocarbon contamination in the carbon dioxide mobile phase. This was eliminated in the selective ion monitoring (SIM) mode of the mass spectrometer.

Diuron was the target analyte in a study which examined the effect of repeller potential on spectra obtained by SFC/MS using a thermospray interface. The influence of the repeller potential on the degree of fragmentation was studied. An analytical scale (4.6 mm i.d.) packed column was used for sample introduction with 2% methanol carbon dioxide mobile phase. Spectra of diuron at low repeller potentials resembled CI spectra while at high repeller potentials the result was close to the EI spectra of diuron. High vaporizer temperature led to the thermal decomposition of diuron.

As has been stated, the advantages of SFC are that separation is achieved rapidly, with a high number of theoretical plates, leading to resolving powers that are far superior to those found in liquid chromatography. The use of SFC for the separation of a wide range of sulfonylurea compounds has been demonstrated in the analysis of environmental water samples. Preceded by a simple concentration step on an SPE cartridge, as low as 0.5 ng mL^{-1} detection levels

in the original sample were achieved reproducibly. No additional sample clean-up was required. This was not the case with capillary electrophoresis and liquid chromatography. Figures 3(A), 3(B) and 3(C), show the SFC/UV chromatograms obtained for spiked Milli-Q water, and spiked river and spike creek water respectively. As is illustrated, chromatographic interference was not seen in any of the chromatograms. The SFC conditions coupled six standard $5 \mu\text{m}$ packed analytical columns in series, one Zorbax® ODS, $4.6 \text{ mm} \times 25 \text{ cm}$, and five Zorbax Silica also $4.6 \text{ mm} \times 25 \text{ cm}$. The mobile phase was a carbon dioxide methanol gradient, initial methanol percentage 1% at 90 bar held constant for four minutes, then ramped to 7% at 150 bar at 10 min, then held at 150 bar but ramped to 16% methanol in an additional ten minutes. The temperature was 60°C , flow rate 2.00 mL min^{-1} . Retention times were in the 30 to 40 minute range. This was quick considering the total length of the six columns. An example chromatogram of twelve separated sulfonylurea compounds is illustrated in Figure 4. Again, no interference is seen in the creek water, in the retention time of interest.

Organophosphorus Pesticides

Malathion, phoxim, ethion, dimethoate, and azinphos-methyl in onion and tomato extracts have been separated by packed capillary SFC with a phosphorus-selective thermionic detector. Attempts at separating these compounds with pure carbon dioxide were unsuccessful; methanol and 2-propanol were used as modifiers. 1.5% methanol resulted in baseline resolution in nine minutes. 3.5% 2-propanol also achieved baseline resolution but inferior peak shape. The packed column was a $5 \mu\text{m}$ C-18 $15 \text{ cm} \times 0.32 \text{ mm}$ i.d. packed. The detector performance was optimized with regard to mobile phase composition, hydrogen and air flow rates, and the

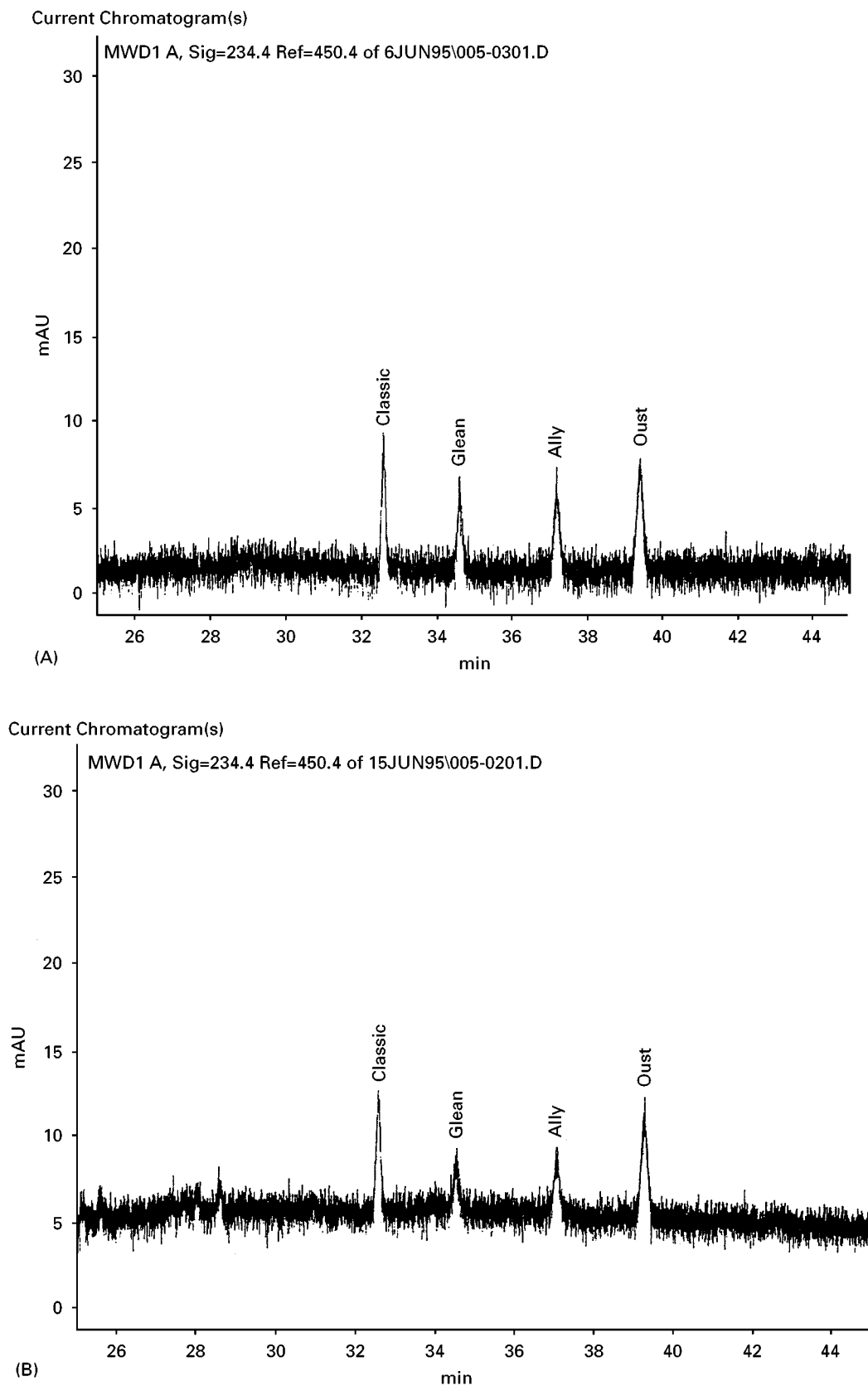


Figure 3 (A) Millo-O water at 0.5 ppb. (B) White Clay Creek water at 0.5 ppb. (C) Brandywine River water at 0.5 ppb.

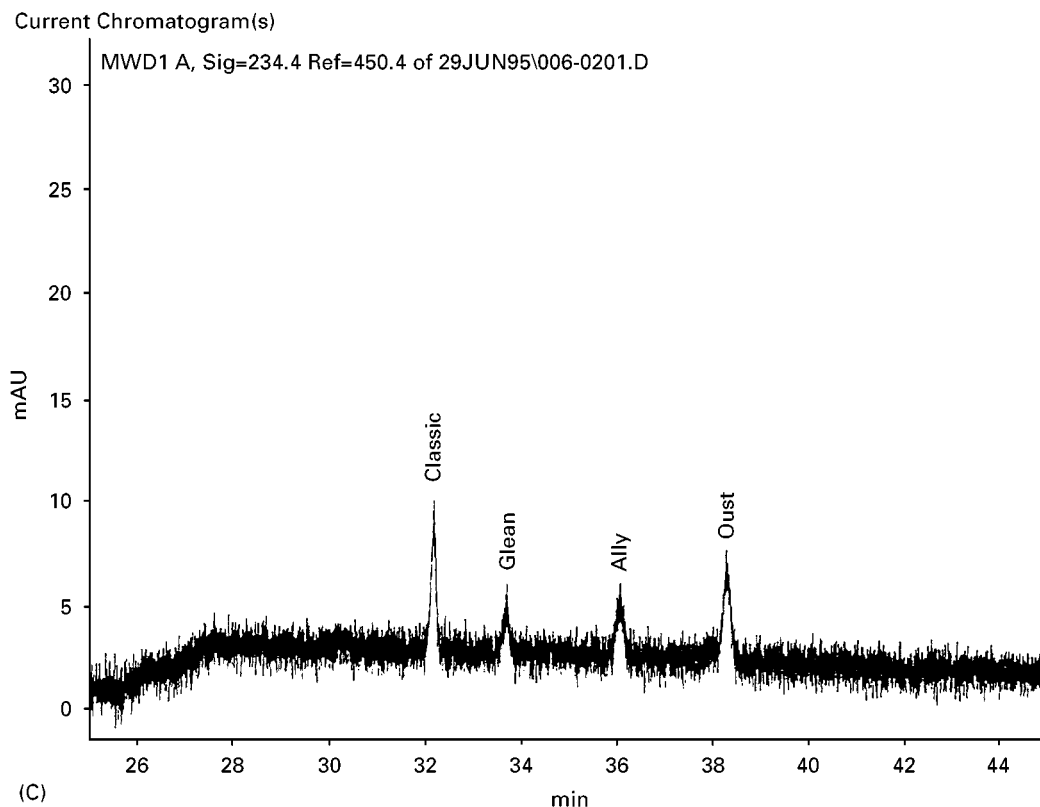


Figure 3 Continued

distance between the detector jet and bead. Standard calibration plots were compared for standards dissolved in acetone and into tomato and onion extracts. Slopes of the calibration curves were unchanged, suggesting an absence of matrix effects. Limits of detection for these organophosphorus insecticides ranged from 15 to 62 pg with methanol modifier.

The organophosphate pesticides chlorpyrifos, chlorpyrifos methyl, iodofenphos, leptophod, methidanthion, tetrachlorvinphos, phosmet, and famphur were separated using microbore packed column SFC with mass spectrometric detection. The separation was achieved with an amino column and 2% 2-propanol modified carbon dioxide. Baseline resolution was achieved in approximately 7 min except for chlorpyrifos and chlorpyrifos methyl. A high flow rate (HFR) interface between the SFC system and the mass spectrometer allowed for the use of packed columns. CI spectra were collected using ammonia or 2-propanol as the reagent gas. 94 pg on-column detection of chlorpyrifos in the selected ion monitoring mode yielded a S/N ratio of 21. An extract of cherries spiked with this mixture of insecticides was analysed utilizing this method.

Sulfur chemiluminescence detection with capillary SFC has been demonstrated for the analysis of

malathion, carbophenothion, dioxathion, fenitrothion, and methyl and ethyl parathion. Restrictor tip positioning in relation to the chemiluminescence chamber was found to have a large effect on the quality of the chromatographic separation.

The capillary SFC was carried out on a 3.5 m \times 100 μ m DB-5 fused silica column with pure carbon dioxide mobile phase. The analysis of malathion from a commercial formulation was demonstrated. Detection limits were compound specific for malathion; 4.5 mg or 77 pgs^{-1} was reported while 39 ng (65 pgs^{-1}) was demonstrated for methyl parathion.

Phorate, Di-Syston, malathion, and ethion were investigated using capillary SFC and a microwave-induced plasma for detection. The 10 m \times 50 μ m, SB-cyanopropyl-50 capillary SFC column was used to introduce the pesticide samples into the plasma, using nitrous oxide as the mobile phase. Detection was conducted at the sulfur line. Baseline disturbances with both positive and negative slopes were observed at differing helium flow rates. An optimum helium flow rate for sulfur line monitoring was determined. With the use of nitrous oxide as a mobile phase, interference from CN-band emission was found with most of the lines investigated. Sensitivities were com-

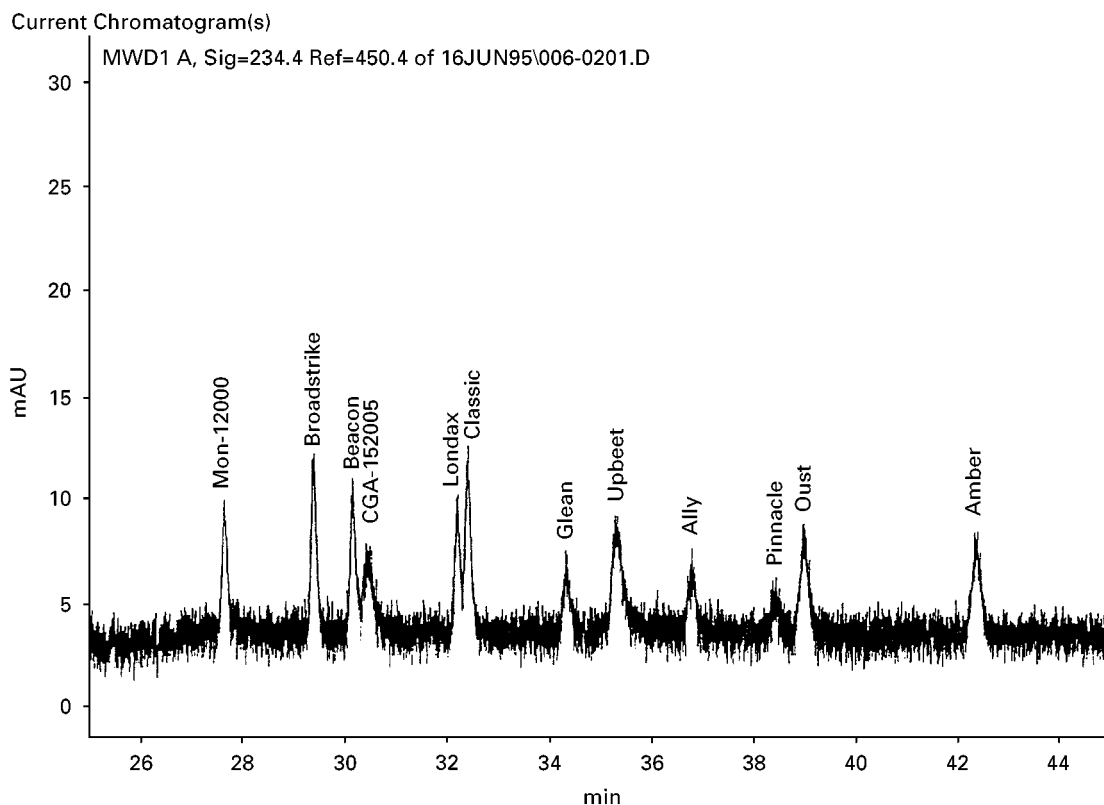


Figure 4 White Clay Creek water at 1.0 ppb.

pound and mobile phase dependent. The sensitivity reported for sulfur with carbon dioxide as the mobile phase was 73 pg s^{-1} .

The separation of two organophosphorus insecticides (i.e. methidathion and chlorpyrifos) and a carbamate insecticide (i.e. carbofuran) was demonstrated by capillary SFC coupled with flame ionization and radio-frequency plasma detectors. When a FID was used, all three compounds were detected. When the RFP detector was used, either the chlorpyrifos or both the chlorpyrifos and the methidathion were detected, depending on whether the wavelength of chlorine emission or sulfur emission was being monitored. Short capillary columns, 2 to 3 m \times 50 μm , and slow flow rates were used to prevent the introduction of too much mobile phase, and subsequent quenching of the plasma. The emission spectra of carbon dioxide and nitrous oxide did not show significant background or interference in the regions of interest for sulfur and chlorine.

Organochlorine Pesticides

A comparison between micro-column liquid chromatography and capillary SFC was conducted for the analysis of a series of organochlorine and

other select pesticides from water samples. Small injection volumes in the SFC analysis limited the sensitivity, but the savings in analysis time was significant, 50 min compared to 10 h.

Acceptable recoveries of 2,4,5-T, 2,4-D, p,p'-DDD, methoxychlor, atrazine, dioctylphthalate, pyrene, pentachlorophenol, cabazole, and hexachlorobenzene were demonstrated for the microbore LC isolation method using UV detection. The capillary SFC separation with a 10 m \times 50 μm , SE-30 column and FID detection showed interfering peaks when SepPak cartridges were used. To eliminate this, water samples were preconcentrated through lyophilization. Both lake and river water samples were studied.

Detection limits of 0.64 pg were reported for Chlordane, a chlorinated hydrocarbon, Tri-allate, a thiocarbamate herbicide using capillary SFC and ECD detection. Arochlor 1254, and Arochlor 2565 were also separated and detected from the mixture. A 6 m \times 50 μm capillary column and frit restrictors to provide back pressure to the system were used. Optimum make-up gas flow rate (10% methane/argon) was determined to be between 20 and 30 mL min^{-1} . Detector temperature affected the sensitivity in a compound-dependent manner. Separations of seven

thermally labile pesticides including metobromuron, fenitrothion, fenchlorphos, chlorbromuron, tetra-chlorvinphos, tetradifon and diruon were accomplished in approximately 20 minutes.

Fourier transform mass spectrometry has been used for the detection of lindane, aldrin, DDE, dieldrin, DDD, DDT and methoxychlor in a mixture separated by SFC. Previously, this had been difficult due to the extreme difference in pressure requirements between the mass spectrometer and the supercritical fluid chromatograph. Relatively long capillary columns, $20\text{ m} \times 100\text{ }\mu\text{m}$, were used for this work. Typical chromatographic detection limits were in the low-nanogram range, although the sensitivity for aldrin and dieldrin was not as great due to the extent of fragmentation.

Carbofuran, α -BHC, γ -BHC, β -BHC, chlordane, and DDT were separated by capillary ($6\text{ m} \times 50\text{ }\mu\text{m}$) SFC and detected with the use of a double focusing mass spectrometer. The interface developed was a direct heated probe. Spectra were collected in the negative-ion chemical ionization mode with methane as the reagent gas. The mass on column per compound was in the subnanogram range.

Chlordane was examined by capillary SFC and RFP detection using the emission wavelength for chlorine. The capillary SFC conditions are the same as those outlined in the organophosphorus section for methidathion and chlorpyrifos and a carbamate insecticide, carbofuran. The presence of DDT in milk was examined similarly. Using FID, milk extracts yield a complex chromatogram due to the triglycerides. Triglycerides are not detected by RPD, and a single peak for DDT is easily detected in milk. α - and β -BHC, chlordane, and methoxychlor were also separated and detected by RPD in the chlorine mode. Nitrous oxide was used as the mobile phase in this separation. Detection limits changed with the pressure of the capillary SFC system; higher detection limits were seen at higher pressures. Sulfur detection limits of 60 pg s^{-1} were obtained at 100 atm, while this limit rose to 178 pg s^{-1} at 400 atm.

Phthalimide Fungicides

Capillary SFC with electron-capture detection was unsuccessfully attempted for captafol and captan, although these compounds had been previously detected in SFC/FID experiments. This failure was attributed to the inability of these high melting compounds to be vaporized in the detector cavity of the ECD. The chromatographic mode is not the cause of this failed attempt as much as is the choice of detector.

Carbamoyloxime Insecticides

Aldicarb and methomyl, two carbamoyloxime insecticides, diflubenzuron, a benzoylurea and phenmedipham, a dicarbamate herbicide were separated on capillary columns ($15\text{ m} \times 50\text{ }\mu\text{m}$ ID) with a nitrogen-phosphorus detector. Similar separations of the four compounds were obtained when carbon dioxide and nitrous oxides were used as the mobile phase. Upon the addition of 1% THF as a modifier, changes in retention were observed, with the later eluting peaks, diflubenzuron and phenmedipham, showing larger changes in retention.

These same four pesticides were separated by capillary ($10\text{ m} \times 100\text{ }\mu\text{m}$) SFC with FTIR (Fourier transform infrared) detection. The flow cell interface used was connected to the chromatographic column and to the restrictor by lengths of $100\text{ }\mu\text{m}$ fused silica capillary tubing, the same ID as the capillary separation column. 200 nL injection volumes of 5 mg mL^{-1} of each component yielded spectral quality that was sufficient to provide structural information for these compounds. A 22:1 split ratio was utilized. 'Gram-Schmidt Plus' reconstruction techniques removed interference caused by changing density of the carbon dioxide with pressure programming. Spectral subtraction techniques were used to remove CO_2 features from the obtained IR spectra.

The use of dual-flame photometric detector with capillary SFC for the detection of the sulfur and phosphorus containing compounds: Oxamyl, parathion, chlorpyrifos, and Larvin. Modifications were made to the detector to make it compatible with supercritical mobile phases. The capillary SFC column was a $15\text{ m} \times 75\text{ }\mu\text{m}$ i.d.. Detection limits were superior in the phosphorus mode, only slight baseline disturbance with pressure programming was noted over the range 50 to 200 atm (700 to 2900 psi). The detection limit of 0.5 ng ($S/N = 2$) was reported for parathion. In the sulfur mode more significant baseline disturbances were observed over the same pressure range. A baseline correction programme was used; even with this only a detection limit of 25 ng ($S/N = 2$) for benzo[b]thiophene was observed.

Pyrethrins

Six naturally occurring pyrethrin insecticides isolated from chrysanthemums were separated by capillary SFC. The pyrethrins were: cinerin I and II, jasmolin I and II, and pyrethrins I and II. Separation by a biphenyl column provided baseline resolution of the six compounds insecticides followed by on-line FTIR analysis. The separation of the six compounds by GC resulted in the degradation of pyrethrins I and II; therefore SFC/FTIR provided a way to analyse these

compounds without degradation. The SFC/FTIR spectra were able to distinguish between the structurally similar pyrethrins continuing to maintain the structural information provided by GC/IR analysis.

Future Developments

The future of SFC in pesticide and environmental analysis is not predictable. Currently more work is being reported in supercritical fluid extraction than in chromatography. However, research continues in a few locations with a few select individuals. The future of SFC seems to lie with chiral separations and pharmaceutical analysis and not with the environmentally oriented work presented in this review. This is not to suggest that the work presented here is without value. Advances into enhanced fluidity chromatography were most likely initiated from the work in SFC. As with other analytical techniques, success in one area leads to attempts in others.

Low waste generation in SFC is not enough to carry the technique into the arena where it can compete equally with LC and GC, the investment in training and equipment is too large a barrier to be overcome with what has fallen into the category of being a 'niche' technique. Liquid and gas chromatography are well cemented into environmental analysis. SFC of pesticides will continue to go beyond academic exercises to solve real problems, but most like

ly only when LC and GC do not yield a satisfactory result.

Further Reading

- Bright FV and McNally MEP (1992) *Supercritical Fluid Technology: Theoretical and Applied Approaches to Analytical Chemistry*. Washington: American Chemical Society.
- Brown PR and Grushka E (1994) *Environmental Applications of Supercritical Fluid Chromatography*. Advances in Chromatography, vol. 34, ch. 5. New York: Marcel Dekker, Inc.
- Charpentier BA and Sevenants MR (1988) *Supercritical Fluid Extraction and Chromatography: Techniques and Applications*. Washington: American Chemical Society.
- Johnston KP and Penninger (1989) *Supercritical Fluid Science and Technology*. Washington: American Chemical Society.
- Lee ML and Markides KE (1990) *Analytical Supercritical Fluid Chromatography and Extraction*. Provo: Chromatography Conferences.
- Smith RM (1988) *Supercritical fluid chromatography*. London: The Royal Society of Chemistry.
- Smith RM and Hawthorne SB (1997) *Supercritical fluids in chromatography and extraction*. Reprinted from *Journal of Chromatography A*, vol. 785. Amsterdam: Elsevier.
- Westwood SA (1993) *Supercritical Fluid Extraction and Its Use in Chromatographic Sample Preparation*. Boca Raton: CRC Press, Inc.
- White CM (1988) *Modern Supercritical Fluid Chromatography*. Heidelberg, Huthig Verlag.

Thin-Layer (Planar) Chromatography

J. Bładek and A. Rostkowski, Military University of Technology, Warsaw, Poland

Copyright © 2000 Academic Press

Introduction

Pesticides are a group of chemicals designed for killing weeds, pest control and plant growth regulation. They are poisons by design. Some of them also demonstrate carcinogenic potential and/or teratogenic activity. Pesticides (or products of their transformation in the environment) can penetrate soil, water, air and also food and fodder. As a result, pesticides are currently present in all parts of the environment. Many of them undergo degradation, but others are persistent and may accumulate in the food chain.

Development of residue analysis for pesticides is driven by toxicological purposes or by the need to

identify residues. In the first case, the compounds are identified as being potentially hazardous to human health or to the environment. In the second case, the determination of residues is mainly aimed at inspecting and monitoring of food or environmental samples. Thin layer chromatography (TLC), including its modern developments (high-performance adsorbents, application of new, automatic techniques of spotting and development of chromatograms, spray-on technique of sample application), is still used for such analyses, especially in combination with selective biochemical detection methods or multidimensional methods although gas chromatography and high-performance liquid chromatography with selective detectors (ECD, NPD, AED or MS) are more important.

There is now a considerable literature describing pesticide analysis by TLC, with environmental and food monitoring, generally being the main aim in such

research (see Fodor-Csorba in Further Reading). There are also numerous works of cognitive character, concerning investigation of the most advantageous chromatographic systems, separation techniques and methods of visualization and quantification. Assessment of physical and chemical properties of pesticides, e.g. their mobility, bioaccumulation and biotransformation, is also an important area of TLC study.

General Principles of Pesticide Analyses

The high selectivity, high detectability and reliability of analysis under fairly simple conditions contribute to the effective use of TLC for pesticide applications. Unfortunately, in the great majority of cases, pesticides need to be determined in complex matrices at extremely low concentrations over a wide polarity range. Therefore the analysis of samples without some preliminary preparation is almost impossible. Separation of pesticides in such samples to determine chemical identity and achieve detection and quantification should be followed by obtaining representative samples, sample clean-up and analytes enrichment.

Sample Preparation

Sample preparation techniques for analysis of pesticide residues by TLC are similar to those applied in the analysis of other pollutants. In the case of liquid matrices (water, milk, oil), liquid-liquid extraction (LLE) and, more recently, solid phase extraction (SPE) are most often used. For instance, C₁₈ cartridges are useful for the extraction and purification of phenylurea herbicides, N-methylcarbamate and organophosphorous insecticides from water. For solid matrices (soil, meat, fruit and vegetable) liquid extraction is the most effective, although SPE has also been used after liquid extraction. Nowadays there is an increase in the application of supercritical fluid extraction, especially for the isolation of pesticides from solid matrices. This technique is useful for the trace analysis of pesticides because of much reduced amount of co-extracted interfering material.

It should be emphasized that TLC has no limitations in the scope of solvents that can be used for sample preparation, since solvent is removed and does not take part in the chromatographic process. The choice of TLC solvent is limited only by the physico-chemical properties of particular groups of pesticides. For example, carbamates are relatively labile chemicals so that during their extraction, strong bases are to be avoided to prevent losses due to chemical reaction. Extraction is usually carried out with acetonitrile or methanol (solubility in petroleum

solvents is limited). A small amount of water often allows actively absorbed pesticides to be released into the solvent. Strongly retained pesticides may be removed by elution with a mixture of water and methanol (1 : 4, v/v) and then partitioned into methylene chloride or eluted directly with ethyl acetate if the extract is clean. Extraction of organophosphorous or organochlorine pesticides is similar. These substances are much less labile than the carbamate pesticides and may, therefore, be retained on more active sorbents.

The solvent chosen to extract residues of pesticides depends not only on the solubility of the chemical, but also on the nature of the information required. This feature has special meaning in the analysis residues of pesticides from plant tissue. For example, the determination of residues for the purpose of establishing of safe re-entry times of workers after crops have been sprayed, requires a surface extraction of residue. On the other hand, determination of pesticide residues in fruits or vegetables to ensure the safety of food for consumers usually requires homogenization of the whole sample to extract the total impurities.

The goal of clean-up is to remove as much interfering, co-extracted substances and to lose as little of the pesticides as possible. Clean-up of samples depends on the type of matrix, detection limits required and the visualization technique employed. Usually about 80% of water samples had not been cleaned, but almost all analyses of pesticides in soil and food samples requires at least some clean-up. Selective methods of pesticide visualization such as fluorescence or enzymatic methods may minimize the need of clean-up.

Development Techniques

The majority of pesticide separations are performed on un-modified sorbents such as silica gel, cellulose aluminium oxide and polyamide. Modified sorbents (amino-NH₂ octyl-RP-C₈, and octadecyl-RP-C₁₈ or impregnated silica gel) are also used (Table 1).

The composition of the mobile phase is the second parameter, defining the conditions for chromatographic separation. During pesticide analysis in normal phase systems, mixtures of organic solvents are often applied. In reversed-phase systems mixtures of polar solvents (e.g. methanol, acetonitrile) with water, organic acids (e.g. acetic or formic acid) or ammonia are used. In some cases, organic salts or ion exchangers are dissolved in the mobile phase to improve the selectivity of the system.

All works concerning research into the best chromatographic systems are commonly named 'behaviour'. An investigation of the relation between pesticide structure and retention provides informa-

Table 1 Examples of chromatographic systems and techniques of development used in pesticide analyses

Analytes	Chromatographic systems		Technique of development
	Stationary phase	Mobile phase	
Pesticides of different classes	HPTLC silica	Gradient based on <i>tert</i> -butylmethyl ether + 5% acetonitrile, hexane, formic acid and ammonia	AMD
Pesticides of different classes	HPTLC silica	Gradient based on acetonitrile, dichloromethane and hexane	AMD
Pesticides of different classes	Silica gel impregnated by paraffin oil	Aqueous sodium chloride solution modified by β -cyclodextrin polymer	Classical TLC
Triazine herbicides	HPLC silica	Chloroform : ethyl acetate (1 : 3)	OPLC
Carbamates	RPC-18	Acetonitrile : water (17 : 3) or chloroform : acetonitrile : acetone (4 : 1 : 1)	Classical TLC
Cyanophenyl herbicides	Silica bonded β -cyclodextrin	Water : methanol (7 : 3) or glycine : methanol	Sandwich DS chamber

tion about the character of interactions in the chromatographic system and the possibility of prediction of their separation. Such works concern the behaviour of different groups of pesticides on silica gel, impregnated silica gel, reversed-phases, water insoluble β -cyclodextrin polymer, etc. Perišić-Janjić and co-workers have carried out research on the chromatographic behaviour of four groups of *s*-triazine derivatives on aminoplast (a carbamide-formaldehyde polymer) and cellulose. Chromatograms were developed with three aqueous mobile phases. The basic aim of the investigation was the evaluation of aminoplast (cellulose was used as comparative adsorbent) for the separation of triazines. Because the *s*-triazines are weak bases, the influence of mobile phase pH on the chromatographic retention was also examined. The authors demonstrated that retention behaviour of *s*-triazine derivatives on aminoplast and cellulose is similar. The greatest changes in R_F values occur in the pH region of protonation and dissociation of the triazine derivatives. It was also shown, that changes in retention factor, k , with pH allows the determination of ionization constants of the analytes.

One-dimensional ascending or horizontal techniques have usually been applied for the separation of pesticides in a closed chamber; multiple and two-dimensional development techniques have been rarely used. The new instrumental techniques such as forced flow planar chromatography (FFPC), automated multiple development (AMD) and gradient

development techniques are being used more frequently. The work of Mazurek and Witkiewicz is an example of the investigation of good separation techniques for pesticides. The direct aim of the work was the analysis of organophosphorous warfare agents, but they were analysed in the presence of 22 pesticides. The main features of the work are the application of the Prisma model for the mobile phase optimization, two-dimensional development, a biochemical method of visualization and separation by overpressure TLC (OPLC). The authors demonstrated faster separations in pressure chambers compared with classical TLC. It leads to a decreased spot diffusion and an increase in the number of theoretical plates. It was also shown that complete separation of all components of the mixture is possible only by two-dimensional OPLC (Figure 1). Examples of pesticides separation using automated multiple development (AMD) and gradient development technique are presented below.

Detection, Identification and Quantification

Pesticides are visualized using chemical or biochemical, physicochemical and physical methods. Chemical methods are based on wetting the adsorbent by solvents or aerosols of different agents, which react with the pesticides, resulting in coloured products. Fluorescence and enzymatic methods are particularly useful in pesticide investigations. They are dis-

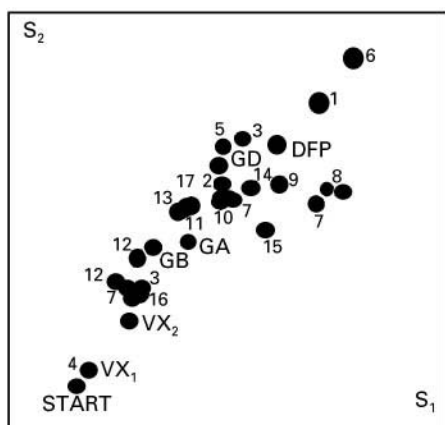


Figure 1 Two-dimensional OPLC separation of pesticides in the presence of organophosphorous warfare agents. Stationary phase – silica gel (TLC 10 × 10 cm); mobile phase: first direction (S_1) diisopropyl ether–benzene–tetrahydrofuran–n-hexane (10 + 7 + 5 + 11, v/v); second direction (S_2) tetrahydrofuran–n-hexane (2 + 3, v/v). Development distance – 6 cm; total development time – 30 min. Visualizing reagent – enzymatic. 1 = Co-Ral; 2 = DDVP; 3 = diazinon; 4 = disyston; 5 = ethion; 6 = fenclor-phos; 7 = gution; 8 = malathion; 9 = monitor; 10 = naled; 11 = thimet; 12 = trichlorphon; 13 = zolone; 14 = carbaryl; 15 = thiram; 16 = fenuron; 17 = linuron. (Reproduced with permission from Mazurek, 1991.)

tinguished by high sensitivity and specificity and allow the analysis of pesticides in the presence of background impurities that do not interfere. In enzymatic detection chromatograms are first sprayed with

an enzyme solution, then, after appropriate incubation, components altered by enzyme are detected by reaction with a suitable reagent. This method is characterized by very low detection limits and sometimes it allows analysis of pesticides without resorting to enrichment of the sample. Radiometric visualization methods are used for detection of radiolabelled pesticides. Radiometric methods are mainly applied to studies of pesticide metabolism in plants and animals, the uptake of pesticides by plants from soil and the fate of pesticides in the environment. The principal methods for the detection and quantification of radiolabelled pesticides separated on TLC plates are autoradiography, scraping followed by scintillation counting, and direct measurement using radiation detectors. The common pesticide visualization methods are presented in Table 2.

Lawrence, Frei, Mallet, and their co-workers focused attention on the visualization and quantification of pesticides by fluorescence methods. A comprehensive account of their works was presented by Hurtubise (see Further Reading). Most fluorescence analyses of pesticides require pre-treatment of the compounds to convert them to a fluorescent species. Certain organophosphorous pesticides fluoresce after just heating others (e.g. carbaryl or benzomyl) form fluorescent anions as a result of hydrolysis, and others (e.g. organothiophosphorous compounds) can be quantified in the presence of metal chelating compounds. Sulfur-containing pesti-

Table 2 Reagents for visualization of pesticides

Class of pesticide	Reagent
Organochlorine	Sodium hydroxide-cobalt (II)-acetate- <i>o</i> -tolidine <i>N,N</i> -Dimethyl-1,4-phenylenediamine
Organophosphorous	4-Nitrobenzenediazonium tetrafluoroborate Mercury (II) salt-diphenylcarbazone 4-(4-Nitrobenzyl)piridyne Enzymatic methods
Carbamate	Bratton–Marshall reagent Fast Blue salt 4-(Dimethyloamino)-benzaldehyde-sulfuric acid <i>N,N,N',N'</i> -Tetramethyl-1,4-phenylenediamine 4-Nitrobenzenediazonium tetrafluoroborate
Phenoxy acid	2,6-Dichloroquinone-4-chloroimide
s-Triazine derivatives	<i>N,N,N',N'</i> -Tetramethyl-1,4-phenylenediamine Chlorine-4,4'-tetramethyldiaminodiphenylmethane Chlorine- <i>o</i> -tolidine-potassium iodide Tetrabromophenolphthalein ethyl ester-silver nitrate-citric acid
Urea derivatives	<i>N,N,N',N'</i> -Tetramethyl-1,4-phenylenediamine Bratton–Marshall reagent

cides are determined quantitatively by pH-sensitive fluorescent reagents. The best fluorogenic reagents are dansyl chloride and fluorecamine. Fluorescence allows detection of certain pesticides at the level of 10 ng and linearity in the range 10 ng to 10 µg.

In the review articles written by Sherma, several new spray reagents, recently introduced for the selective detection of pesticides, are presented. For instance 20% sodium hydroxide, 5% cupric acetate, 1% phosphomolybdic acid followed by 0.1% *o*-toluidyne in acetic acid was proposed for the determination pyrethroid insecticides containing a nitrile group. These form blue spots with a detection limits of 1 µg without interference from organophosphorous, organochlorine and carbamate insecticides. Synthetic pyrethroids (fenvalerate, cypermethrin, fenprothrin) can be visualized as pink-coloured spots at 1 µg by their alkaline hydrolysis to liberate HCN, which reduces 2-(4-iodophenyl)-3-(4-nitrophenyl)-5-phenyl-tetrazonium chloride to formazan in the presence of phenazonium methosulfate. Organophosphorous, organochlorine and carbamate insecticides do not interfere. Another example is the application of 2-trichloromethylbenzimidazole to determination pesticides containing either an azine or an azole ring. Excellent detection limits (20 ng to 10 µg) and very high selectivity makes this agent as very useful chromogenic agent for identification as well as for detection of these compounds.

Quantitative analyses of pesticides are performed mainly by UV-VIS densitometric measurement or by fluorescence. Quantitative analyses of pesticides can also be performed by combining TLC with other analytical techniques, e.g. TLC/HPLC, TLC/GC, TLC/MS, etc. Theoretical considerations, the correct approach to multidimensional methods development, instrumental requirements and contemporary applications of these approaches have been reviewed by Poole *et al.*

Applications

The agricultural use of pesticides gives rise to most analysis. Instrumental TLC has been applied for sensitive and fully quantitative analyses of environmental samples and control of food. Applications in forensic toxicology are less common. A feature of these analyses are investigations of pesticide residues in very completed matrices. Samples of vegetables, meat, food or biological material (for forensic toxicology) are analysed identically (Table 3).

Monitoring of the Environment

Butz and Stan have demonstrated the application of the AMD technique for the monitoring of environmental samples and the strategy of the whole proced-

ure, which has become a German Standard (DIN 38407 part II). Pesticides isolated from water are spotted on the layer with standards, and separated using gradient elution. Gradient elution allows the separation of pesticides belonging to different classes of compounds such as phenylureas, carbamates, triazines, phenoxy-carboxylic acids, and others. In total, 283 pesticides were analysed and only eighteen of them give detection limits of more than 100 ng and can therefore not be analysed from one litre of drinking water without further treatment. Two examples of drinking water spiked at the 100 ng L⁻¹ level are presented to demonstrate the merits of the method. Further research confirmed that the AMD technique can be easily applied to screen for pesticide residues in drinking water and ideally supplements other analytical techniques (Figure 2).

In the AMD technique in the first ten isocratic development steps, the starting zones are focused into sharpened bands. The elution gradient starts with an alkaline solvent mixture and ends with an acidic solvent. In this way it is possible to move or fix particular compound classes, such as acids or amines. The pH change provides better peak shapes and improves separation performance. Figure 3 shows a densitogram of a pesticide mixture separated using a gradient (UV absorption measurement with multiple wavelength scan). The limit of detection of most pesticides was 10 ng. However, it should be emphasized that in real samples the resulting spectra of the peak may be altered by overlapping matrix compounds, so that a pesticide, although present may not be recognizable. In such cases the authors recommend another gradient to confirm positive results.

TLC/AMD and SPE have been used for the analyses of pesticide residues in strongly contaminated samples of soil (Figure 4). Chromatograms were developed in a normal-phase system by AMD gradient elution. Limitations of detectability were compensated for by the application of relatively large volumes (by use of a spray-on technique) of analysed solutions. Quantitative assessment (linear relationship $A = f(c)$, where A is densitometric peak area, c mass of pesticide in band formulated in ng) was achieved by UV absorption measurement scanning of the chromatograms by a 'zig-zag' technique (Table 4).

Recovery and error of the method was estimated; the recovery level was 80% and the R.S.D. was less than 9%. The result presented confirm the advantages of modern TLC, which result principally from equipment development. It was demonstrated that the greatest benefits in the trace analysis of pesticides are achieved by the use of the 'spray-on' technique of sample application.

Table 3 Examples of TLC application to pesticide analysis in different matrices

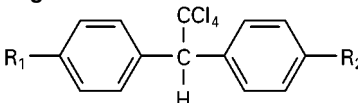
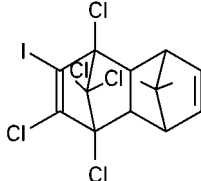
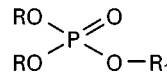
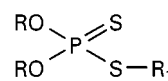
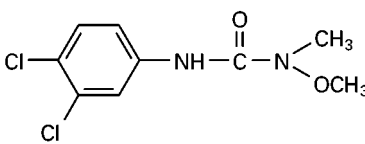
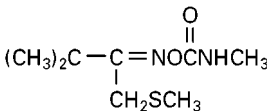
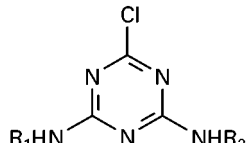
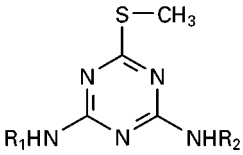
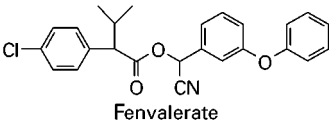
Class of pesticide and examples of its structure	Analyte	Matrix	Chromatographic system	
			Stationary phase	Mobile phase
Organochlorine				
<div></div> <p>Metoxychlor: $R_1 = R_2 = \text{OCH}_3$ DDT: $R_1 = R_2 = \text{Cl}$</p>	Metoxychlor in presence of DDT, isomers, γ -HCH, toxaphene, dieldrin, aldrin, etc. DDT and DDE DCP	Water Plants Poultry	Silica gel Silica gel Silufol	Hexane–acetone (9 : 1) Hexane–ethyl ether (17 : 3) Hexane–benzene–ethyl acetate (6 : 4 : 1)
<div></div> <p>Aldrin</p>	DDP, DDT, parathion, metoxychlor Aldrin, dieldrin	Water Water	HPTLC Silica gel	Gradient based on dichloromethane and hexane Heptane
Organophosphorous				
<div></div> <p>Dichlorfos: $R = \text{CH}_3$, $R = \text{CHCCl}_2$</p>	Metaphos Chlorpyrifos metabolites	Vegetables Banana pulp	Silica gel + gypsum + Zn Silica gel	Hexane–acetone (4 : 1) Hexane–chloroform (4 : 1)
<div></div> <p>Malation: $R = \text{C}_2\text{H}_5$, $R_1 = \text{CH}(\text{CH}_2\text{COOC}_2\text{H}_5)\text{COOC}_7\text{H}_9$</p>	Bromofos Methidation	Peanut crops Clinical samples	RPC-18 W RPC-18	Acetic acid–chloroform–isooctane (1 : 4 : 15) Acetonitrile–water (3 : 1)
Carbamates				
<div></div> <p>Linuron</p>	Diflubenzuron Diuron, isopropuron, linuron, metoxuron, monolinuron, nrburon	Water Plant	HPLC HPTLC	Ethyl acetate–toluene (1 : 3) Gradient based on acetonitrile, dichloromethane, acetic acid, toluene and hexane
<div></div> <p>Thiofanox</p>	Metoxuron and its breakdown product Aldicarb and thiofanox	Potato Sugar beet	RPC-18 RPC-18	Acetonitrile–water (17 : 3) Chloroform–acetonitrile–acetone (4 : 1 : 1)
Triazines				
<div></div> <p>Simazine: $R_1 = R_2 = \text{C}_2\text{H}_5$</p>	Metribuzin	Soil	Silufol	Chloroform–ethyl ether (2 : 1)

Table 3 Continued

Class of pesticide and examples of its structure	Analyte	Matrix	Chromatographic system	
			Stationary phase	Mobile phase
 Desmetryne: R ₁ = CH ₃ , R ₂ = CH(NH ₃) ₂	Simazine, atrazine, promazine, prometon, desmetryne, ametryne, terbutryne	Water	Zn carbonate	Benzene–acetone (19 : 1)
Pyrethroids  Fenvalerate	Halogenated pyrethroid insecticide and its <i>trans</i> -isomers of permethrin and cypermethrin from valerate	Fruits and plants	Silufol	Hexane–chloroform (3 : 2)

Investigations of Pesticides in the Environment

In environmental research not only the level of pesticide residues is controlled but also their behaviour in different matrices. In such research TLC is used for the measurement of the mobility of pesticides, their bioaccumulation and biodegradation.

Residues of pesticides introduced into the environment are adsorbed onto soil particles and may end up as sediments at the bottom of lakes and rivers. Therefore, knowledge of the mobility of pesticides in soil is an essential element of environmental investigations. Measurements of pesticide mobility are usually performed using STLC (soil thin-layer chromatography). In this technique a stationary phase is prepared from a soil sample, in which the mobility of pesticides is to be determined. Solutions of persistent pesticides (sometimes radiolabelled pesticides) are spotted onto

the prepared layer and then developed with water as the mobile phase. STLC is also used for the evaluation of the influence of exogenous organic matter on the mobilities of pesticides in the soil. For example, examination of the mobility of diazinon and linuron demonstrated that simultaneous addition of organic compounds and other pesticides to the soil in agricultural practice may alter the mobility of sparingly soluble pesticides.

In another example researchers exposed Bluegill Sunfish to [¹⁴C] metolachlor at a concentration of 1 mg L⁻¹ for 34 days in a flow-through system. After that time all the fish were removed from the tank and dissected into tissues. After extraction and clean-up, eluates were spotted (together with unlabelled standards) onto layers, and then separated by two-dimensional development. Radioactive zones were detected using X-ray film. The non-radiolabelled

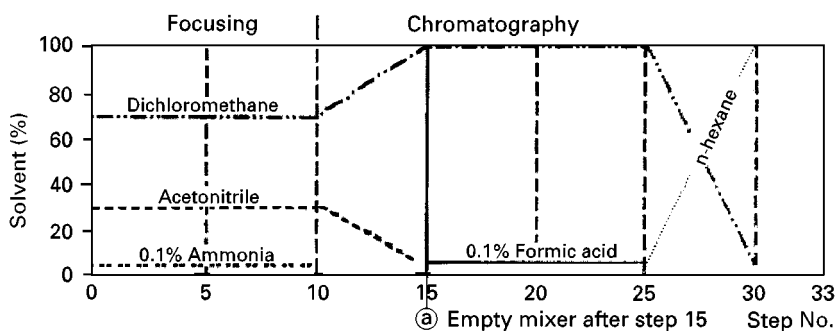


Figure 2 Gradient example for pesticide screening in DIN 38407 part 11. (Reproduced from Morlock, 1996 with permission from Elsevier Science.)

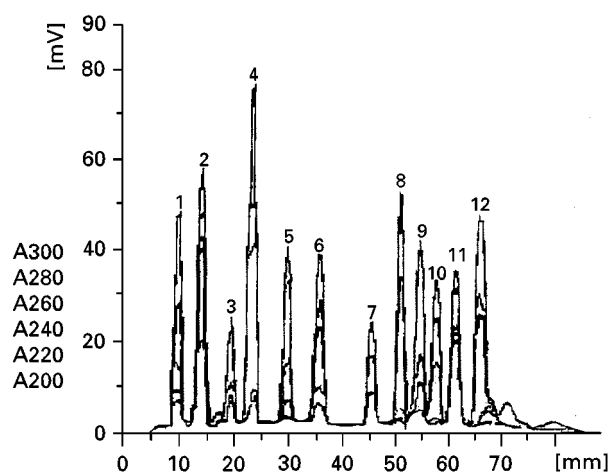


Figure 3 Multi-wavelength of a pesticide mixture separated according to the gradient in Figure 2. 1 = hydroxyatrazin, 2 = formetan, 3 = triadimenol, 4 = matalaxyl, 5 = isoproturon, 6 = diuron, 7 = dimethylaminosulfanilide, 8 = methidathion, 9 = 2,4-*p*-isobutyl ester, 10 = endrin, 11 = 2,2-*bis*-(4-chlorophenyl)-1,1-dichloroethane. (Reproduced from Morlock, 1996 with permission from Elsevier Science.)

standards were visualized with UV light. Detection of known metabolites was performed by the removal of radioactive zones and scintillation counting (in this case TLC was used as a clean-up technique). Unknown metabolites were identified using FAB/MS and NMR. The result showed that the pathways of the transformation of metolachlor by Bluegill Sunfish are very similar to those observed in animals, soils, and plants. In a similar way, examinations of bioaccumulation of pesticides may be performed.

TLC as a Clean-up Technique

An application of TLC as a clean-up technique is based on the separation of components of analysed mixture on TLC followed by layers introduction of analytes directly to the detector of other analytical instrument (on-line technique) or the removal of the analytes together with adsorbent and its elution with appropriate solvent (off-line technique). Identification of pesticides or their metabolites is performed

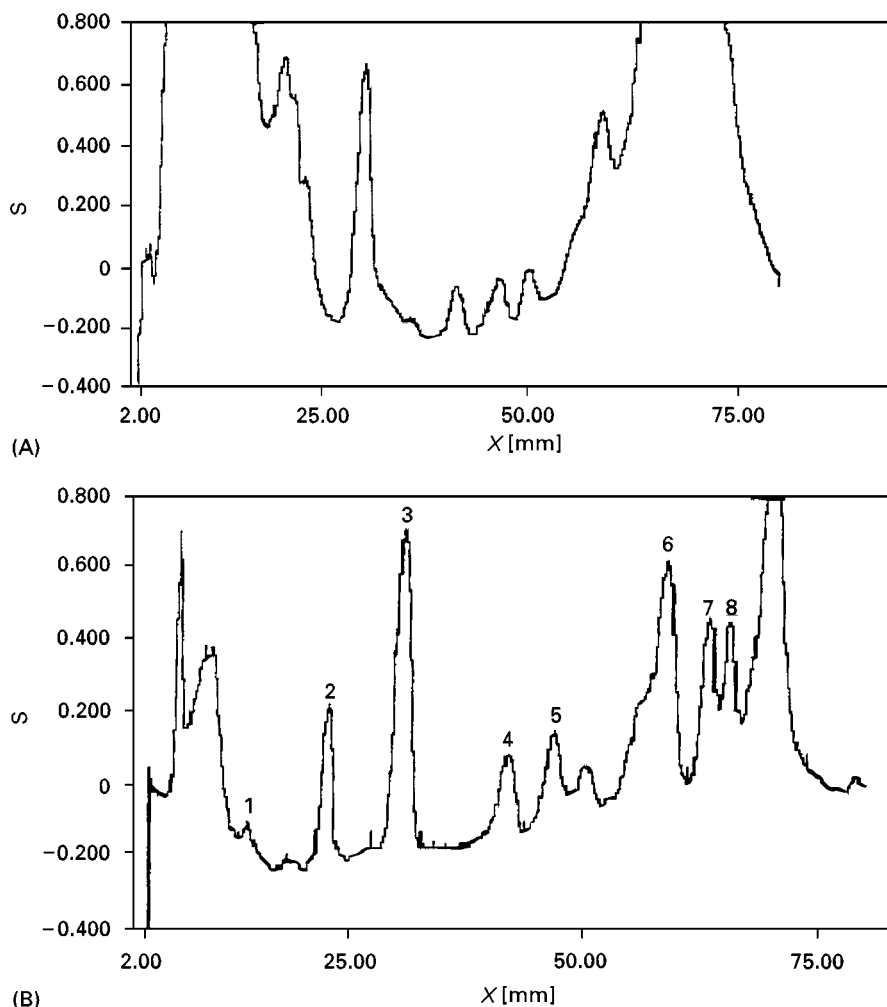


Figure 4 Chromatograms of soil sample: (A) before purification, (B) after purification by SPE. S = absorbance, x = distance of bands. Peaks: 1 = oxamyl, 2 = pirimicarb, 3 = carbaryl, 4 = phosalone, 5 = malathion, 6 = fenitrothion, 7 = tetradifon, 8 = metoxychlor. (Reproduced with permission from Bładek, 1996.)

Table 4 Parameters of quantification

Type of pesticide	λ_{\max} (nm)	Calibration curves			Detection limits		
		$A = f(c)$	Correlation coefficient	Max. range of linearity (ng/band)	In band (ng)	RSD (%)	In soil ($\mu\text{g kg}^{-1}$)
Oxamyl	220	$A = 3939c + 183$	0.9932	1200	150	6.1	7.7
Carbaryl	265	$A = 21793c + 1561$	0.9961	800	70	5.6	3.3
Pirimicarb	220	$A = 92115c + 1010$	0.9993	200	25	9.0	1.2
Malathion	200	$A = 5556c + 9970$	0.9958	4000	400	3.1	20.0
Phosalone	210	$A = 11695c + 1420$	0.9964	2000	200	4.4	10.0
Methoxychlor	220	$A = 63653c + 1955$	0.9991	500	50	8.7	2.4
Tetradifon	220	$A = 75175c + 580$	0.9994	500	50	8.0	2.5
Fenitroton	280	$A = 84782c + 1821$	0.9981	500	50	9.0	2.6

(Reproduced from Błażek, 1996 with permission from Elsevier Science.)

mainly by GC/MS, FTIR or NMR. The work in Bluegill Sunfish mentioned above is an example of such an application of TLC in pesticide analyses.

Conclusions

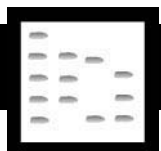
In the history of applications of TLC for pesticide analysis two periods (pre- and post- 1980s) may be distinguished. Within the first period, analyses were performed on home-made layers using equipment allowing for detection of substances at the μg level. During that period most chromatographic systems and methods of visualization of pesticides were developed. The second period is mainly connected with development of instrumental TLC which has enabled application of the technique for analysis of pesticides at the desired level, appropriate to the needs of food and environmental analysis.

It has not been possible to cover all applications of TLC in pesticide analysis extensively and therefore, only the demonstration of the method's abilities are presented here. TLC can be used for the clean-up of samples, for performing simple semi-quantitative screening analyses and, in the case of instrumental TLC, for the full quantitative analyses of pesticides.

Further Reading

- Błażek J, Rostkowski A and Miszczak M (1996) Application of instrumental thin-layer chromatography and solid phase extraction to the analyses of pesticide residues in grossly contaminated samples of soil. *Journal of Chromatography A* 754: 273–278.
- Butz S and Stan HJ (1995) Screening of 265 pesticides in drinking water by thin-layer chromatography with automated multiple development. *Analytical Chemistry* 67: 620–630.
- Cruz SM, Scott MN and Merrit AK (1993) Metabolism of ^{14}C metolachlor in bluegill sunfish. *Journal of Agriculture and Food Chemistry* 41: 662.
- Fodor-Csorba K (1996) Pesticides. *Handbook of Thin Layer Chromatography* (eds Sherma J and Fried B), pp. 753–817. New York: Marcel Dekker.
- German standard methods for the examination of water waste and sludge. Berlin: German Standard Institute (Deutsches Institut Für Normung, DIN) DIN 38407, Part II.
- Hurtubise RJ (1981) Pesticide analysis. In: *Solid Surface Luminescence Analysis* (ed.: Guilbault), pp. 151–175. New York: Marcel Dekker.
- Mazurek M and Witkiewicz Z (1991) The analysis of organophosphorus warfare agents in the presence of pesticides by overpressured thin layer chromatography. *Journal of Planar Chromatography* 4: 379–384.
- Morlock GE (1996) Analysis of pesticide residues in drinking water by planar chromatography. *Journal of Chromatography A* 754: 423–430.
- Perišić-Janjić NU, Jevrić LR, Bončić-Carić GA, Jovanović BŽ and Ilić SR (1995) The chromatographic behaviour of some s-triazine derivatives on various supports. *Journal of Chromatography A* 703: 573–612.
- Poole CF and Poole SK (1995) Multidimensionality in planar chromatography. *Journal of Chromatography A* 703: 573.
- Sánchez-Camazano M, Sánchez-Martín MJ, Poveda E and Iglesias-Jiménez E (1996) Study of the effect of oxogenous organic matter on the mobility of pesticides in soil using soil thin-layer chromatography. *Journal of Chromatography A* 754: 279–284.
- Sherma J (1997) Determination of pesticides by thin-layer chromatography. *Journal of Planar Chromatography* 10: 80–89.

PETROLEUM PRODUCTS



Gas Chromatography

J. P. Durand, Institut Français du Pétrole,
Cedex, France

Copyright © 2000 Academic Press

Introduction

Gas chromatography (GC) is an analytical technique that is widely used for characterizing hydrocarbons, and numerous advances in this method have originated in petroleum industry laboratories. Moreover, its use has markedly increased in the last few years with the progress in instrumentation and the relatively low cost of the equipment.

Its applications cover the exploration, production and refining of crude petroleum. These have developed around four major types of methods: analysis of gaseous hydrocarbons, analysis of liquid hydrocarbons, analysis of traces of heteroatomic compounds, and simulated distillation.

Advances in Instrumentation

Since the 1980s, while there has been little progress in the theory of chromatography, the instrumentation has constantly evolved. There have been major improvements in the reliability of equipment and columns, new specific detectors have been developed, and increasingly powerful computers have been used for data processing and controlling the equipment. The use of electronic pressure and flow rate regulators with increasingly stable capillary columns has made it possible to produce chromatograms that are much more reproducible. Microcomputing has simplified the analyst's work (in some cases a little too much, up to the point of forgetting the basics) and has opened the way to automation, standardization of complex methods and the development of correlation methods. Detailed analysis of gasoline and simulated distillation are the two methods that have undergone the greatest evolution. In the analysis of gaseous hydrocarbons, the most important step has been the replacement of packed columns by porous layer open-tubular columns with far greater efficiency and stability. In addition to improvements in the sensitivity and stability of the major types of selective detectors (flame photometry and electron capture),

two others – atomic emission and chemiluminescence – are now commercially available.

In the last two to three years, the new advances in technology have been in the fields of rapid analysis and equipment miniaturization. With microcolumns (100 μm i.d.) or multimicrocapillaries with very fast flow rates and programmed temperatures, gaseous hydrocarbon analysis times can be reduced to 1–2 min. However, such conditions do not allow sufficient resolution for analysing heavier hydrocarbons; here rapid chromatography is used as a screening tool, or to decrease the analysis time for simulated distillation. All these methods are now in the development stage. The recent commercial availability of portable and compact chromatographs meets the need for on-site analyses, giving reduction in sampling problems.

Gaseous Hydrocarbon Analysis

The analysis of gaseous hydrocarbons is generally carried out with porous layer capillary columns (gas-solid chromatography). These efficient columns are now very stable and are used in control laboratories. The most widely employed adsorbents are alumina and adsorbent polymers. Alumina capillary columns provide good resolution for the most difficult separation encountered in petrochemical laboratories, that of isobutene and butene-1.

Molecular sieves are used to separate the permanent gases (O_2 , N_2 , H_2 , CO , etc.). To analyse these and hydrocarbons with a single injection, multi-column chromatographs with switching valves have been developed. Natural gas, gases from crude petroleum and refinery gases are the main applications for which methods have been developed and standardized (ASTM D1945-81, IP 345/80, IP 344/88, ISO 6974-84). Gas analysis has considerable economic importance, both for natural gas, allowing the determination of the calorific value from chromatographic analysis (ISO 6977-84), and for the petrochemical feeds from the steam cracking process (ethylene, propylene and butadiene), owing to the large volumes of these gases now on the market.

Liquid Hydrocarbon Analysis

Detailed Analysis of Light Hydrocarbons

Although the separation of several hundred constituents of gasoline has been carried out for more than

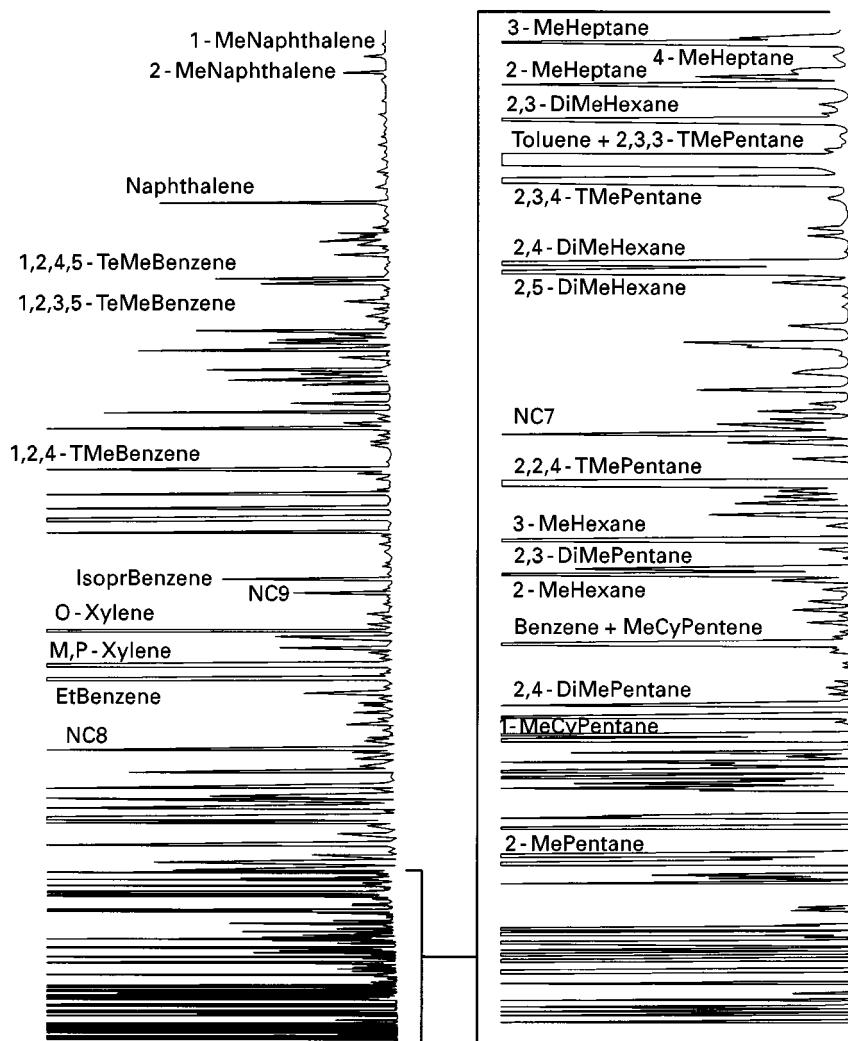


Figure 1 Chromatogram of a commercial gasoline following the NF N07-086 standard. Operating conditions: column, 50 m \times 0.20 mm i.d.; stationary phase 0.5 μ m OV1; oven, 35°C for 10 min, then 1.1°C min⁻¹ up to 114°C, and 1.7°C min⁻¹ to 250°C, held 5 min; detector, 280°C; carrier gas, helium at a constant flow of 0.8 mL min⁻¹.

30 years, the methods have been standardized only relatively recently (ASTM D5134-90, NF07-086). The chromatogram of a commercial gasoline, obtained as specified in the French standard NF M07-086, is shown in **Figure 1**. By using a procedure standardizing a number of parameters and specifications, capillary chromatographic methods with temperature programming are reproducible from one chromatographic system to another and identification of complex chromatograms can be automated. This automation has led to the development of numerous applications in the petroleum field. The large amounts of data supplied by the detailed analysis are normalized, after processing, to determine the physical properties (molecular weight, gross calorific value, octane number, etc.), to optimize the thermodynamic or kinetic models, and to predict the quality of the conversion products.

In refining, the two main processes, reforming and catalytic cracking, require increasingly detailed information regarding the gasoline range fraction. The complete detailed analysis data for the naphtha feed and effluents from the reforming units make following and modelling the conversion and optimization of the control of the units possible. A major application field for automated capillary chromatography is in the use of micro-pilot plants involving small amounts of feeds and effluents. The methods developed for the catalytic cracking micro-pilot plants allow detailed analysis of the gasoline cut and determination of octane numbers directly on the total effluent (final boiling point 580°C) by using a pre-column to eliminate the heavier compounds.

Commercial gasolines are formulated using around 10 petroleum basestocks. New environmental con-

straints mean that the resulting mixtures require more rigorous optimization. With all the constraints concerning benzene, other aromatics and olefins, together with the additional octane number requirements brought about by the progressive elimination of lead from fuels, there is an increasing demand for the detailed characterization of basestocks and mixtures. Analyses are now carried out on a regular basis in control laboratories.

One of the main causes of errors in modelling the behaviour of fluids in petroleum reservoirs has been the lack of reliable analytical data. Using a thermodynamic model based on an equation of state for calculating the properties of these fluids requires accurate knowledge of the molecular weights and their distribution. The large amount of information provided by the detailed and direct analysis of the fraction up to C_{20} with the molecular weight distribution has modified the methodology of describing reservoir fluids.

Characterization of the C_3 – C_{15} fraction of oils and extracts from source rocks is an important parameter for studying the origin and migration of hydrocarbons. Until recently only a profile or fingerprint was available, but now this fraction can be quantified by automated capillary methods. Various parameters (paraffin, aromatic numbers, etc.) have been obtained from the detailed analysis to follow variations in chemical composition and show biodegradation or leaching phenomena. Soil pollution by hydrocarbons, particularly fuels, requires pollutant monitoring. The replacement of global methods, like solvent extraction, by detailed analysis of the fuel, can provide a better follow-up of the decontamination operations. Figure 1 shows a chromatogram of commercial gasoline following the NF N07-086 standard.

Hydrocarbon Type Analysis of Light Hydrocarbons

Hydrocarbon type analysis (Paraffins/Isoparaffins/Aromatics/Naphthenes/Olefins (PIANO)) can be obtained from detailed analysis with a data system that identifies each of the peaks and combines them into their respective groups. Because there are some co-elutions, this analysis may not be accurate with gasolines containing significant amounts of olefinic and naphthenic constituents eluted before *n*-octane.

Some methods of type analysis have been developed with the multidimensional GC technique; these are commonly referred to as PIANO analysis. A four-column system with automatic valve switching and cold traps has been utilized to determine normal paraffins, isoparaffins, naphthenes, olefins and aromatics. A polar column separates aromatics and non-aromatics, a 13X molecular sieve column

separates paraffins and naphthenes, while a 5A molecular sieve column separates normal paraffins and isoparaffins. The unsaturated components are retained in an olefin trap, released by heating the trap and then hydrogenated. These separations allow determination of the distribution by hydrocarbon type and carbon number.

Heavy Hydrocarbon Liquid Analysis

The high resolution of capillary columns, which provides separation of a major fraction of the hydrocarbons with boiling points up to 200°C, is not sufficient for the heavier petroleum cuts owing to their increasing complexity. Although detailed information is not directly available, GC is nevertheless very extensively used. The chromatogram can serve as a qualitative plot for determining the presence of specific compounds or classes of compounds. Quantification of normal paraffins in crude petroleum (compounds that are clearly distinguished from the unresolved material) and waxes can be made. However, the most important applications concern the characterization and quantification of the fractions in hydrocarbon types, obtained, in particular, by liquid chromatography (LC). In most cases, the compounds are identified by mass spectrometry (see below). The development of online coupling of high performance liquid chromatography (HPLC) and GC has led to several petroleum applications: measurement of aromatics in gas oils, and measurement of polyaromatics in diesel engine exhausts and mineral oils.

GC/MS Coupling

Mass spectrometry (MS) coupled with GC (GC-MS) is now the main identification technique. From bench equipment (increasingly numerous) to more sophisticated systems providing high resolution measurements, the identification is facilitated by computer processing of libraries containing thousands of mass spectra. This technique has made an essential contribution to analysis of hydrocarbons, in particular for the detailed analysis of fuels and their bases, geochemical studies and pollution problems. Up to around 1000 compounds have been identified in oils. For two decades numerous data for different columns, retention times or indices of hydrocarbons identified by GC-MS have been published for compounds in gasolines and kerosenes. For the medium distillates, where direct detailed analysis is not possible, the distribution per carbon number of the MS analysis can be obtained by combining the separation by boiling point and carbon number from GC

with the analysis of hydrocarbon type from MS. Methods have been developed specifically for monitoring hydroprocessing treatments in order to provide evidence of mechanisms and to have access to the reaction kinetics. The use of GC-MS in geochemistry has been a major step in the study of the transformation of organic matter during sedimentation: this has involved going from comparison of chromatograms to the identification of molecular structures and the search for biochemical markers. This has become a standard method for following these markers in oils.

Heteroatomic Compounds Analysis

The elements most often looked for in petroleum products are sulfur, nitrogen, oxygen and the halogens. The analyst has available several single- or multi-element detectors.

Sulfur

The most widely used detector for many years has been the flame photometric detector (FPD). In spite of its limitations (non-linearity, variable response, quenching), methods have been standardized for the light petroleum cuts. The recent development of a more sensitive chemiluminescence detector for sulfur without these limitations has allowed extension of the application field to heavier cuts, such as gas oils and crude oils. The chromatograms of sulfur compounds from a catalytically cracked gas oil before and after hydroprocessing obtained with this detector are shown in Figure 2. Comparison of the two chromatograms shows the changes in the sulfur compounds during the hydroprocessing.

Nitrogen

The situation is identical to that of sulfur, the nitrogen-phosphorus detector (NPD) also having limitations (variable response, relatively low selectivity). The arrival of a chemiluminescence detector for nitrogen has provided access to semi-quantitative analysis of nitrogen compounds in gasoline and gas oil cuts from conversion processes.

Oxygen

The development of a detector specific to oxygen (O-FID) has met the need for the measurement of oxygenated compounds such as methyl *t*-butyl ether in commercial gasolines. Several methods have been standardized (EN 1601-96, ASTM D5599-93). Due to its low sample capacity, this detector cannot be used for measuring traces of oxygen.

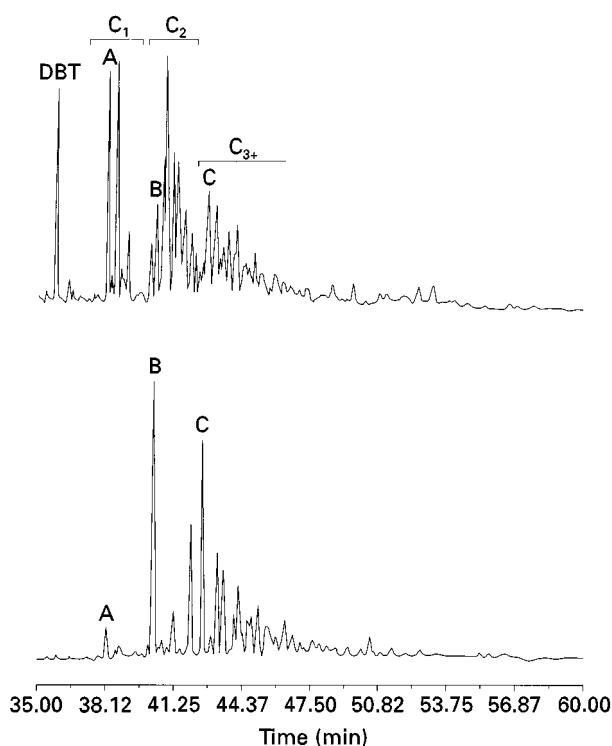


Figure 2 Chromatogram of sulfur compounds from a catalytic cracking gas oil (LCO) before and after hydroprocessing obtained with a chemiluminescent detector. Operating conditions: column, 30 m × 0.32 mm i.d.; stationary phase 4 μm SPB-1; oven, 60°C to 320°C at 5°C min⁻¹. DBT, dibenzothiophene; C₁, methyl; C₂, dimethyl or ethyl; C₃₊, three or more branched carbons.

Halogens

The electron-capture (ECD) and electrochemical detectors are used to determine the halogens. The ECD is very sensitive when the molecule is poly-halogenated; sulfur hexafluoride, used as a tracer, can be directly detected at the p.p.b. level. The main applications concern chlorofluorocarbon gases, chlorinated solvents and polychlorinated biphenyls (PCBs).

Multielement Detectors

While all the specific detectors mentioned above can detect only one element at a time, the atomic emission detector is multielement, with some restrictions concerning the number of elements that can be detected per analysis and the sensitivity to some of these elements. This is a powerful identification tool (complementary to MS). The main applications are measurement of oxygen compounds in gasolines, multielement simulated distillation (H, C, S), and the determination of nickel and vanadium in crude oils.

Simulated Distillation

Simulated distillation (SD) by GC has been the subject of numerous studies for 30 years. It is a technique that advantageously replaces traditional distillation methods for rapid checking of product yields. The principle is simple: the sample is injected into a column, which separates hydrocarbons according to their boiling points; using a mixture of normal paraffins with known boiling points, the correspondence between the retention time and boiling point is established and then the weight %–boiling point curve can be constructed. However, the implementation is more difficult. The first problem concerns the choice of the stationary phase to obtain good agreement with the real distillation curves; the second is the stability of this phase at the maximum temperatures used. There are many interdependent parameters involved in these two problems. Although several methods have been standardized (ASTM D3710-90, ASTM D2887-93, ASTM D5307-92), their applications give rise to a number of difficulties in routine use. Operating conditions, column performance, frequency of calibration runs and blanks, quantification, and raw data processing are the parameters to be controlled to achieve the level of precision given by the standard methods. Column performance is affected by noneluting residues. The problem can be resolved by installing a pre-column with a backflush and calculating sample recovery with an internal standard.

The arrival in the last few years of very stable metal columns and the use of electronic pressure and flow regulators have provided better control of the experimental parameters. These advances have extended the final determined boiling point up to 650°C with

conventional methods and to 720°C with high temperature simulated distillation (HTSD). The chromatogram of a light crude oil with a final boiling point of 650°C, obtained with a metal column, is shown in **Figure 3**. The range of boiling points of petroleum products is thus almost completely covered by using two methods, since HTSD can operate only with cuts having boiling points above 150°C. Consequently, for samples containing light compounds, heavy compounds and non-recoverable residues, a fractionated distillation yielding two cuts is necessary.

Simulated distillation can be used to determine gasoline dilution of used engine oils (ASTM D3525), to analyse the oil-soluble fraction of particulates emitted by diesel engines (estimation of the proportion attributable to the fuel and lube), and to estimate engine oil volatility (ASTM D5480).

Conclusion

The high resolving power of GC makes it a major analytical tool for characterizing the very complex mixtures that constitute petroleum products. The recent development of correlation methods in near-infrared spectroscopy (NIR) for characterizing light hydrocarbons could challenge the dominant position of chromatography in this field because of the speed of the NIR techniques. However, GC will always remain the method giving the most detailed information. With the present evolution of fast chromatography, its disadvantage of a longer analysis time is disappearing. Although GC is not as fast as spectroscopic methods, analyses in a few minutes with microequipment will ensure that it continues to be

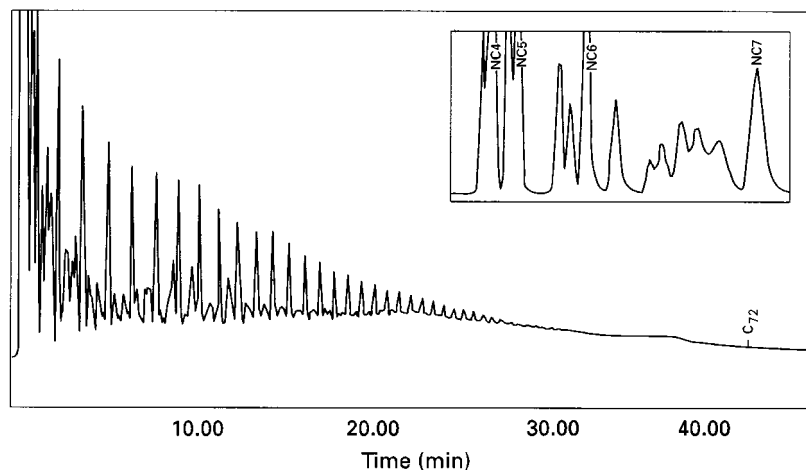


Figure 3 Chromatogram of a light crude oil with a final boiling point of 650°C. Operating conditions: column, 10 m, deactivated metal; stationary phase 0.5 μm OV1; oven, 35°C for 1 min, then 10°C min^{-1} up to 390°C, held 14 min; detector, 400°C; carrier gas, helium at a constant flow of 10 mL min^{-1} .

a powerful tool for the detailed analysis of hydrocarbons.

See also: **I/Chromatography. II/Chromatography: Gas:** Column Technology; Detectors: General (Flame Ionization Detectors and Thermal Conductivity Detectors; Detectors; Mass Spectrometry; Historical Development; Multidimensional Gas Chromatography; Theory of Gas Chromatography.

Further Reading

Adlard ER (ed.) (1995) *Chromatography in the Petroleum Industry*. Amsterdam: Elsevier.
Benner RL and Stedman DH (1989) *Analytical Chemistry* 61: 1268.

Di Sanzo F and Chawla B (1992) *Journal of Chromatography* 271: 589.
Dressler M (1986) *Selective Gas Chromatography Detectors*. Amsterdam: Elsevier.
Durand JP, Béboulène JJ and Ducrozet A (1995) *Analysis* 23: 481.
Grob K (1991) *On-line Coupled LC-GC*. Heidelberg: Hüthig Buch Verlag.
Grob RL (ed.) (1995) *Modern Practice of Gas Chromatography*. New York: Wiley.
Korth J, Ellis J, Crisp PT and Hutton AC (1998) *Fuel* 67: 1331.
Lin R and Wilk ZA (1995) *Fuel* 74: 1512–1521.
Quimby BD and Sullivan JJ (1990) *Analytical Chemistry* 62: 1027.

Liquid Chromatography

V. L. Cebolla, L. Membrado and J. Vela,
Instituto de Carboquímica, Consejo Superior de
Investigaciones Científicas (CSIC), Zaragoza, Spain
Copyright © 2000 Academic Press

Introduction

Techniques based on liquid chromatography are used in the petroleum industry for process monitoring, compliance with environmental regulations, the evaluation of product quality, catalyst performance and feed processability, as well as for determining hazardous compounds, and understanding and solving basic research problems.

Chromatographic techniques and methods used for analysing petroleum products are chosen depending on their boiling point range, which is related to their carbon number. In order to simplify the further discussion, classification of petroleum products into light, middle and heavy distillates is considered throughout this work.

Techniques based on capillary gas chromatography (GC) can perform molecular characterization of some light distillates, such as gasolines and others. However, this technique has limitations when it comes to analysing heavier distillates. As the complexity of petroleum products rapidly increases with the increasing boiling range of distillates, liquid chromatographic techniques play a crucial role in the analysis of middle and heavy distillates. They are also complementary to GC for analysing light distillates. Most of the applications of liquid chromatography to petroleum products include separation, identification and, in some cases, quantification of individual components; separation, quantification, and, sometimes,

preparative isolation of hydrocarbon types; in addition to molecular size distribution and average molecular weight determination.

In general, complete molecular separation of the components of petroleum distillates is not possible using liquid chromatography owing to their complex nature and the limited resolution of current techniques. As the boiling range of the product to be analysed increases, the greater its complexity due to the increase in the number of isomers and the broader variety of compound types present. Furthermore, the concentration of polar compounds (e.g. heterocyclic compounds) increases as the products become heavier. Therefore, the heavier the product, the poorer the chromatographic resolution obtained, and the more difficult it is to achieve good separations. In most cases, extensive separations are meaningless in the petroleum industry, but determination of particular target compounds in various distillates is sometimes useful.

Determination of hydrocarbon types (which includes separation and quantification) of all types of distillates is usually carried out by liquid chromatography. Hydrocarbon types in petroleum products can be roughly summarized into saturates (n-paraffins, branched paraffins, and cycloalkanes or naphthenes), olefins (alkenes and cycloalkenes), aromatics (hydrocarbons containing one or more rings of the benzenoid structure), and polars (which include heterocycles and/or high molecular weight material). This simple scheme becomes more complicated with increasing sample boiling range because of the many possible combinations of compound types (e.g. alkylaromatics, aromatic olefins, etc.). Therefore, separation designs may vary depending on nature of the sample and information required by the analyst.

Liquid chromatographic techniques used for the above-mentioned purposes are based on open-column liquid chromatography (LC), high performance liquid chromatography (HPLC), size-exclusion chromatography (SEC), and thin layer chromatography (TLC), as well as multidimensional techniques.

Open-column Liquid Chromatography (LC)

Liquid chromatography has been used for many years to carry out gravimetric determination of hydrocarbon types. This usually consists of separation on normal adsorption phases such as silica gel or alumina. This technique has also been used for preparative isolation of hydrocarbon types, either to carry out further characterization of isolated fractions, or to use the isolated fractions as external standards for calibrating other instrumental techniques (e.g. HPLC), which are in turn employed for hydrocarbon-type determination.

LC-based standard tests for hydrocarbon-type analysis were developed for use by the petroleum industry at a time when other instrumental chromatographic techniques were not yet available. The main advantage of these was that simple glassware was used. Some of these standard tests are still in common use because product specification analyses and referee methods require basic testing procedures (Table 1). For research purposes, low pressure to medium pressure LC is used rather than open-column LC in order

to increase separation efficiency to some extent. Other modifications to standard tests may involve the use of detectors to monitor eluents or the use of different stationary phases depending on the analytical objective.

In general, all open-column or low pressure LC methods are lengthy, labour intensive, expensive (they require high solvent consumption), and the columns need to be repacked for each determination.

Light distillates The fluorescent indicator adsorption (FIA) method (ASTM D1319) has been in use for a long time (Table 1). Light distillates are separated, using silica gel as stationary phase in a precision bore column and isopropyl alcohol as eluent, into saturates, olefins and aromatics. The use of fluorescent dyes, previously added to the gel, makes it possible to calculate the volume percentage of each hydrocarbon type from the length of each zone in the column, without eluting the zones out of the column. It must be taken into account that uncontrolled losses of some light hydrocarbons may be produced during elution, and samples containing C₃ or lighter hydrocarbons and/or more than 5% v/v C₄ and C₅ hydrocarbons must be depentanized (see ASTM method D2001).

There are many drawbacks to the FIA method. Apart from the operational ones (related to improper packing of the column and incomplete elution of hydrocarbons by isopropyl alcohol), it provides poor precision, especially for olefins at concentrations typi-

Table 1 Examples of standard tests based on open-column liquid chromatography

<i>Standard method</i>	<i>Scope</i>	<i>Boiling range (°C)</i>	<i>Comments</i>
ASTM D1319 ^a ; IP 156 ^b	Hydrocarbon types in liquid petroleum products by fluorescent indicator adsorption	< 315	Displacement development. Use of fluorescent dyes. Silica gel (100–200 mesh), isopropyl alcohol. Vol % of saturates, olefins, aromatics.
ASTM D2002	Methods for isolation of representative saturates fraction from low-olefinic petroleum naphthas	< 232	Displacement development. Use of fluorescent dyes. Silica gel (100–200 mesh), isopropyl alcohol.
ASTM D2003	Methods for isolation of representative saturates fraction from high-olefinic petroleum naphthas	< 221	Displacement development. Use of fluorescent dyes. Silica gel (100–200 mesh), isopropyl alcohol.
ASTM D2007	Method for characteristic groups in rubber extender and processing oils by the clay-gel adsorption chromatographic method	< 260	Applicable to samples with < 0.1% asphaltenes. Clay gel and silica gel. Elution using n-pentane and toluene/acetone (50/50)
ASTM D2549	Method for separation of representative aromatics and non-aromatic fractions of high boiling oils by elution chromatography	232–538	Bauxite and silica gel. Elution using n-pentane, diethylether, chloroform and ethanol

^aAmerican Society for Testing of Materials, Philadelphia, USA.

^bInstitute of Petroleum, London, UK.

cally found in gasolines and it does not detect oxygenated compounds blended into gasoline (they are in the aromatic zone).

Middle and heavy distillates The ASTM D2007 standard is used and is still the reference when a hydrocarbon-type determination is developed using other techniques. This method provides sample separation into saturates, aromatics, resins, and asphaltenes or uneluted (SARA). It consists of the elution of n-pentane and toluene/acetone (50 : 50, v/v) through a double column which contains clay in its upper section and clay plus silica gel in its lower section. Its application requires a previous removal of n-pentane insolubles (asphaltenes). In general, the use of chromatographic columns for these kinds of product may produce irreversible adsorption of the heaviest and/or more polar compounds on to the stationary phase, which affects quantitation.

LC-based methods have also been used for a long time for determining and isolating nitrogen, sulfur and oxygen compounds in different types of petroleum distillates. Apart from silica gel, procedures include successive separations using alumina and cation exchange phases, as well as complexation packings.

Standard methods based on LC usually work using fixed volumes of eluent for the various fractions. Therefore, possible cross-contamination of fractions and errors in quantification of hydrocarbon types may occur. Conventional detection provides poor information because of column overloading. Monitoring of the eluent can be carried out using offline analytical techniques (e.g. TLC-FID).

High Performance Liquid Chromatography (HPLC)

HPLC gives a much better resolution than LC. It is a less time-consuming technique, and requires a smaller amount of sample. Percentages of peaks are usually quantified after calibration, without the errors associated with solvent evaporation and sample manipulation. However, in all column-based methods, some heavy and/or polar compounds can be irreversibly adsorbed, producing column deterioration and, therefore, incomplete elution. This can be mitigated by an adequate choice of stationary and mobile phases, and the proper use of backflushing.

Applications of HPLC include hydrocarbon-type determination (separation and quantification) and preparative isolation of hydrocarbon types: separation, identification and, in some cases, quantitative determination of single components (usually one or several target compounds).

Hydrocarbon-type Determinations

Typical analytical and preparative HPLC normal-phase columns are mostly used for hydrocarbon-type separations.

Light distillates Separation into saturates, olefins and aromatics is of most interest, and classical adsorbents, such as silica gel or alumina have been used. This analysis has been carried out on gasolines using a silica gel column, a fluorocarbon as mobile phase and refractive index (RI) detection. The low polarity of the eluent used allows the separation of saturates from olefins. Aromatics are backflushed from the column (Figure 1).

The use of silica containing bonded groups capable of forming charge transfer complexes has allowed the

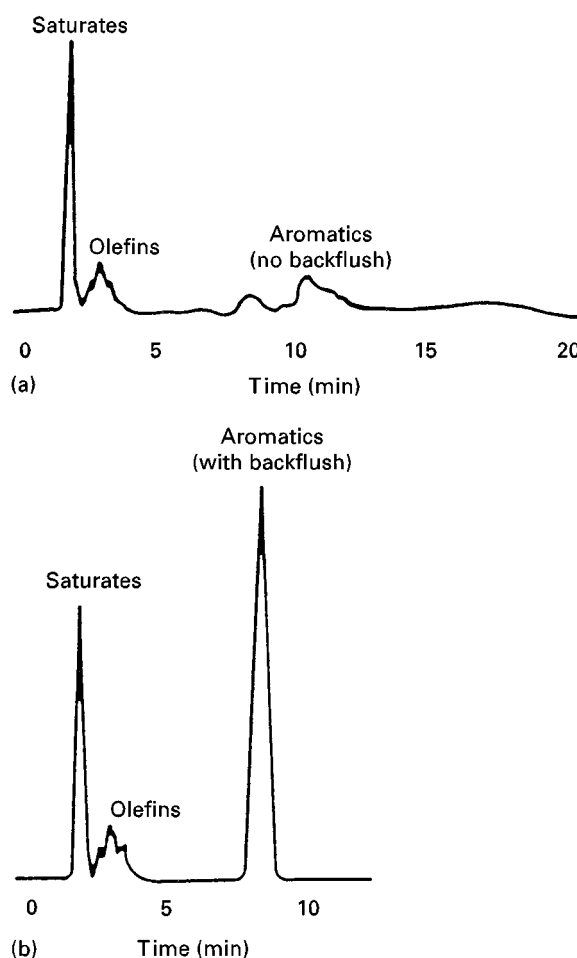


Figure 1 Chromatogram of a heavy gasoline distillate with and without flow reversal. Column, μ -Porasil, 30 cm \times 4 mm; mobile phase, FC-78; flow rate, 3.5 mL min⁻¹; sample size, 3 μ L; detector, RI (R-401) attenuation \times 16. (Reprinted from *Journal of Chromatographic Science* 13. Suatoni JC, Garber HR and Davis BE (1975) Hydrocarbon group types in gasoline-range material by high performance liquid chromatography, 367–371. With kind permission from Preston Publications, A Division of Preston Industries, Inc.)

additional resolution of naphthenes from paraffins to be achieved in light distillates.

Middle distillates Separations according to number of aromatic rings (mono-, di- and polyaromatics), typically of more interest for middle and heavier distillates, have been carried out using silica gel and also the above-mentioned charge-transfer stationary phases. For this purpose, three groups of silica-bonded acceptors have been mostly utilized: nitroaromatics (e.g. commercially available dinitroanilinopropyl silica, DNAP, and 8-(2,4,6-trinitroanilino)octyl, TNAO), tetrachlorophthalimido groups, and caffeine and related compounds. Polar amino- or cyano-bonded silica have also been used extensively in the petroleum industry (e.g. IP391 standard) for this separation, using heptane or hexane as mobile phase and RI detection. Thus, saturates, mono-, di- and polyaromatics are separated using backflushing and the three last groups quantified. Likewise, the content of saturates, olefins and polyaromatic hydrocarbons (PAHs) in a variety of light and middle distillates has been successfully determined by argentation chromatography using both coated and bonded stationary phases.

Heavy distillates Besides analysis of saturates, aromatics and polar compounds, other hydrocarbon-type determinations which involve PAHs have been performed on practically all types of heavy distillates using both nitroaromatic phases and tetrachloroph-

thalimidopropyl-bonded silica. However, in all these cases, resolution is not very good and quantitative analysis is only possible in a few cases. In spite of this, these methods are useful for process monitoring or comparative purposes (e.g. determination of PAHs in used lubricating oils before and after oxidation treatments).

Determination of Individual Compounds

Individual carcinogenic PAHs have usually been determined in almost all types of distillates, after a previous cleaning-up step, using reversed-phase columns, taking advantage of the selectivity and sensitivity of fluorescence detection. Electrochemical detection has also been used for this purpose, by Ce(IV) oxidation of PAHs to quinones.

Other representative applications of HPLC are summarized in Table 2. Reversed-phase HPLC has been used as an alternative to GC in order to quantitatively determine benzene and toluene, and various oxygenates (ethanol, MTBE, ETBE, TAME) in gasolines (Figure 2). Other determinations of targeted compounds in light distillates include silica gel normal-phase separations (coumarin in kerosenes, 2,4-dimethyl-6-t-butylphenol antioxidant in light distillates), and charge-transfer HPLC (determination of ppm amounts of aniline, quinoline, pyridine and isoquinoline in kerosene and diesel).

Where middle distillates are concerned, both normal phase and reversed phase have been used to separate a broad variety of compounds, which

Table 2 Some representative applications of HPLC to petroleum analysis

<i>Samples</i>	<i>Determinations</i>	<i>Stationary phase, mobile phase and detection</i>
Light distillates	Selected oxygenates in gasolines	RP ^a ; water/acetonitrile (backflushing hydrocarbons to waste); RI
	Benzene and toluene	RP; water/acetonitrile (remaining gasoline backflushed to waste); RI
	Aromatic N compounds	DNAP and other charge-transfer; dichloromethane; UV
	Coumarin in kerosenes (IP 374)	silicagel; 2-propanol in n-hexane; UV
	2,4-Dimethyl-6-t-butylphenol antioxidant in light distillates (IP 343)	NP ^b and compatible eluents; UV
Middle distillates	Individual PAHs	RP (after cleaning up) and compatible eluents; fluorescence and others
	Identification of N compounds in diesel	DNAP and other charge transfer; dichloromethane; UV
	Dyes and markers in diesel	RP and compatible eluents; UV
	Alkyl nitrate cetane diesel improvers	Silica gel and compatible eluents; Infrared detection
Heavy distillates	Phenalenones	RP; UV
	PAHs in heavy oils	NP and charge transfer; normal-phase eluents; UV, RI
	Furfural in lubricants	RP; water/methanol; UV
	More than 50 additives in lubricants	Normal and reversed phase; compatible eluents; UV, RI, ELSD

^aReversed phase.

^bNormal phase.

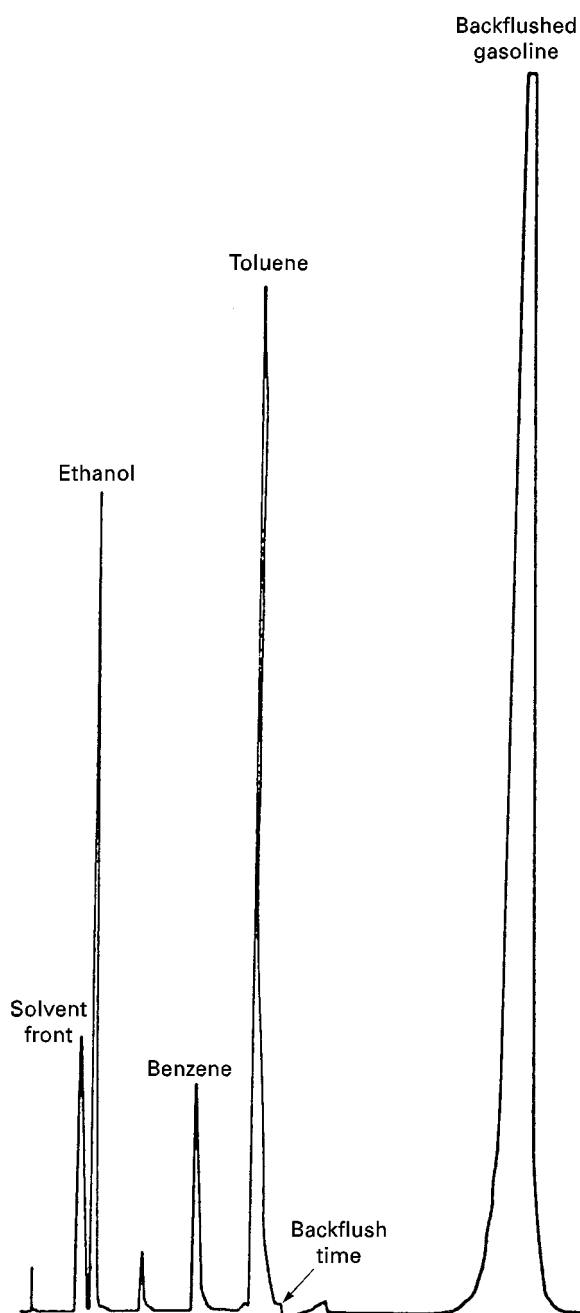


Figure 2 Chromatogram of lead-free gasoline with ethanol. See the following reference for conditions. (Reprinted from *Journal of Chromatographic Science* 23. Pauls RE (1985) Determination of high octane components: methyl *t*-butyl ether, benzene, toluene, and ethanol in gasoline by liquid chromatography, 437–441. With kind permission of Preston Publications, A Division of Preston Industries, Inc.)

include dyes and coloured diesel markers, alkyl nitrate cetane diesel improvers, phenalenones, aza-arenes and alkylaromatic amines. In the case of lubricants, more than 50 additives which include antioxidants and antiwear agents, ashless dispersants,

and viscosity improvers have also been separated using the above-mentioned phases and quantified using UV, refractive index (RI) and evaporative light scattering (ELS) detection.

Detection and Quantification

Problems in detection come from the lack of a system which provides uniform response factors for all hydrocarbon types. Moreover, response factors for a given family vary from fuel to fuel. For this reason, hydrocarbon types from the sample to be analysed are usually preparatively isolated, and used as external standards for calibration.

UV cannot detect saturates, and responses of compounds are strongly dependent on chemical structure. RI is mostly used in the petroleum industry in spite of its technical disadvantages of baseline drift, slow stabilization, influence of temperature changes, negative peaks, and impossibility of using gradient elution. In general, variations in response factors for compounds are lower for RI than for UV. The use of RI (e.g. IP 391 standard for saturates, mono-, di- and polyaromatics) is justified because it uses pure aromatic compounds for external calibration. In effect, since the refractive index of each aromatic family varies over a much narrower range than that of the total aromatic fraction, the response of each family is quite well matched using several pure standards (*o*-xylene, 1-methylnaphthalene and phenanthrene). However, saturates are not accurately determined because of the large variation of refractive index possible for saturates and the small difference between saturates RI and that of the commonly used mobile phases (e.g. hexane).

The use of ELS detection is becoming more frequent in petroleum HPLC. It presents practical advantages over RI, better performance and the possibility of using gradient elution. However, it is not a true universal detector and some small volatile aromatics (e.g. methylnaphthalenes) are not detected even under mild working conditions. ELS working parameters can be optimized to obtain, in some cases, uniform responses of different compounds. However, responses depend in part on solute densities.

The dielectric-constant detector (DC) and FID have been reported to provide uniform response factors for hydrocarbon types. However, for the former, contradictory results have been published, and, in the case of FID, technical problems do not yet appear to have been solved. Mass spectrometry (MS) detectors, using different types of HPLC interfaces, have also been used although their application seems, at the moment, to be limited to a more in-depth characterization of separated fractions and to the identification of individual compounds.

Size-exclusion Chromatography (SEC)

SEC is a molecular sieving technique that separates molecules according to their selective permeation into the pores of a gel stationary phase on the basis of differences in their size in solution. Solute permeation into the gel increases with decreasing molecular size, resulting in longer elution. However, not only size but also chemical effects are present in the elution of petrochemical samples and related molecules.

Molecular size distributions SEC is a low resolution technique that allows qualitative or semiquantitative molecular size distributions (MSD) of high molecular weight heavy fractions (e.g. lubricant base oils, paraffin waxes, heavy petroleum fractions, asphalts, etc.) to be obtained in order to assess the effects of process variables. Conversion of MSD into molecular weight distributions (MWD) is usually determined by calibration using narrow polystyrene standards or fractions from the petroleum samples themselves. To cover low molecular weight ends, normal paraffins or PAH are also used. However, these determinations carry a high degree of uncertainty. Likewise, SEC has been used for obtaining estimates of average molecular weight of oil products. In general, molecular weights of petroleum constituents can vary between 30 000 and 100 Da.

Columns and mobile phases SEC is usually carried out using a series of relatively small pore size (100–1000 Å) polystyrene-divinylbenzene (PS-DVB) polymers. Among other packings, poly(divinylbenzene) and Sephadex (a dextran-based polymer) columns are also popular. The use of small particle size (3 µm) packings, and of mixed pore distribution in single columns has been recently introduced. Preparative SEC columns, using either open-column or HPLC technology, have also been used for sample clean-up to remove small molecules from high molecular weight materials or vice versa.

Inter- or intra-association of sample molecules or their interaction on the column should be minimized by selecting an appropriate solvent. The most common mobile phases are tetrahydrofuran, toluene, chloroform, pyridine and quinoline.

Detection Semiquantitative profiles of size distribution have been obtained using differential RI, ELS, UV diode-array, fluorescence, and FID detection. SEC coupled with atomic absorption or emission such as inductively coupled plasma atomic emission (ICP-AES) or atomic emission detectors (AED) has been applied to obtain elemental profiles (for Fe, Ni, V or S) from petroleum samples.

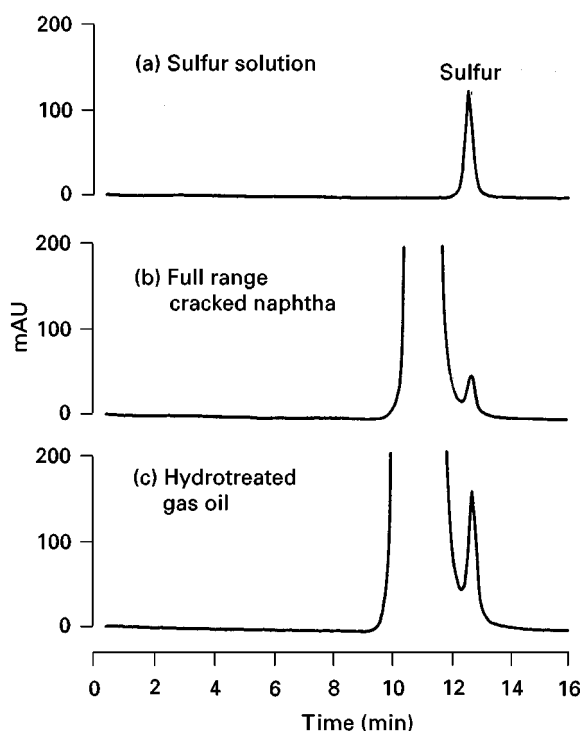


Figure 3 Evidence for the presence of elemental sulfur in hydrotreated cracked naphtha and gas oil obtained from pilot unit runs. (Reprinted from *Journal of Chromatography A* 740. Barman BN (1996) Determination of elemental sulfur by size-exclusion chromatography. Optimization and petrochemical applications, 237–244. With kind permission from Elsevier Science-NL.)

Use of non-size effects These can be used for particular separations; interesting applications relative to light and middle distillates have been developed. Thus, water and C₁–C₃ alcohols can be determined in gasolines using a series of PS-DVB columns. With the same type of stationary phase, determination of pericondensed PAHs in different distillates, and of elemental sulfur in naphthas and gas oil, have been developed which take advantage of elution beyond the total permeation limit of SEC (Figure 3).

Thin Layer Chromatography (TLC)

TLC is a simple, rapid, robust and inexpensive technique but it is not usually considered as quantitative or sufficiently sensitive. However, progress in plate manufacture (including small-sized HPTLC plates), in sample application devices, in development instrumentation, and in automated UV and fluorescence scanning densitometers, should allow improvements in separation and quantification of petroleum-derived samples to be achieved. Advantages of TLC for petroleum analysis are high sample throughput, simultaneous processing of standards

and samples, and the possibility of analysing the whole sample without previous fractionation or deasphalting.

Planar Chromatography

Conventional TLC silica gel and alumina plates (with development using solvents of increasing polarity) have been mostly used for qualitative or semiquantitative hydrocarbon-type analysis, and also for preparative isolation of hydrocarbon families in heavy distillates for further analysis or gravimetric determination of collected fractions.

In general, non-quantitative analyses have involved visual detection of colourless substances using inspection under UV illumination (if they absorb in the UV region or they exhibit fluorescence by UV excitation) or the use of chromogenic or fluorogenic spray reagents. Thus, semiquantitative adulteration of gasolines with kerosenes can be detected using silica gel plates and n-heptane as eluent.

Quantitative hydrocarbon-type analysis is possible using UV fluorescence scanners although there are only a few papers on this in the literature. Aromatic and polar peaks of petroleum bitumens have been quantified using UV scanning, and saturates using fluorescence scanning after impregnation of the plates with berberine salts. Modern scanners present the advantage of providing structural data of peaks (UV spectra). The possibility of a future growing application of TLC to the analysis of light and middle distillates depends on the control of vaporization of compounds during development and drying steps.

TLC-FID

This technique combines the advantages of TLC with the possibility of quantitation using an FID. TLC-FID has been quantitatively applied to hydrocarbon-type determination (e.g. SARA, saturates, aromatics, resins and asphaltenes) of all types of heavy distillates (lubricants, residua, asphalts, heavy oils, etc.). In these cases, FID responses are quite uniform although calibration cannot be discarded *a priori*.

Separations are carried out on Chromarods which consist of reusable quartz rods sintered with 5 μm silica gel or alumina. Saturates, alkylaromatics, aromatics, polars or resins, and asphaltenes have been separated. Olefins have also been separated in some heavy distillates by impregnating silica rods with AgNO_3 . Solvent development is carried out as in planar chromatography.

However, TLC-FID presents several disadvantages with regard to planar chromatography such as the destructive nature of FID, the impossibility of obtain-

ing structural data from FID detection, and the possible influence of sample volatility in quantification which makes it difficult to apply this technique to light and some middle distillates.

Multidimensional Liquid Chromatographic-based Techniques

A multidimensional system generates its resolving power mainly from the selectivity differences of the separating modes used. The most important multidimensional systems in petroleum chemistry are based on HPLC-HPLC and HPLC-GC.

HPLC-HPLC

Separation schemes include combinations of two or more columns. Normal-, reversed-, charge-transfer, argentation- and size-exclusion phases have been used to separate fractions of specific polarity or size in a broad variety of distillates. Hydrocarbon-type determinations of all types of distillates have been carried out. It is very common to use a polar normal phase as a first column. Thus, polar compounds (resins, asphaltenes) are retained on the packing and recovered using backflushing. Selection of the second column depends on the particular families to be separated (e.g. olefins from saturates, aromatics from saturates). Automated column selection and switching systems can improve method development and sample analysis.

HPLC-GC

GC is the most desirable final chromatographic step after HPLC fractionation in order to carry out either the analysis of selected separated fractions of hydrocarbons (e.g. by normal-phase HPLC), or the analysis of low molecular weight components in high molecular weight samples (SEC-GC). However, the final boiling point determines whether or not GC can be applied to the entire sample.

Packed capillary HPLC columns or conventional 4.6 mm i.d. HPLC columns are equally viable as long as the correct transfer method is chosen. Both loop-type and on-column interfaces have been used for analysis of saturates and aromatic fractions in gasolines, kerosene and diesel; for analysis of PAHs in light distillates, middle distillates and lubricating oils; and for determination of chlorinated benzenes in fuel oil. The loop-type interface involves complete evaporation of the HPLC eluent during its introduction in the GC. It allows a transfer of large LC fractions (100–1000 μL), and an easier internal standard quantitation (using an extra loop) to be carried out. It is

especially suitable for nonvolatile samples. A better approach to qualitative and quantitative analysis of volatile samples is through methods based on an on-column interface. However, the retention gap method uses long uncoated pre-columns and only allows modest volumes of HPLC fractions to be transferred. The partially concurrent evaporation method, where only a part of the HPLC eluent is evaporated, works with larger fraction volumes (approx. 200 μ L) and with shorter uncoated precolumns.

Future Trends

The development of new, more accurate techniques based on liquid chromatography (especially HPLC, TLC, and new multidimensional or hyphenated techniques) will be increasingly important owing to legislation calling for the reduction of aromatic content in fuels. Therefore, these techniques will continue to play a crucial role in the petroleum industry for the choice of process conditions and the evaluation of fuel quality.

See also: **II/Chromatography:** Liquid Chromatography-Gas Chromatography. **Chromatography: Gas:** High Temperature Gas Chromatography; High-Speed Gas Chromatography. **Chromatography: Liquid:** Detectors: Ultraviolet and Visible Detection; Large-Scale Liquid Chromatography; Mechanisms: Normal Phases; Mechanisms: Size Exclusion Chromatography; Multidimensional Chromatography. **III/Bitumens:** Liquid Chromatography. **Crude Oil:** Liquid Chromatography. **Flame Ionization Detection:** Thin-Layer (Planar) Chromatography. **Flash Chromatography.** **Geochemical Analysis:** Gas

Chromatography. Liquid Chromatography-Gas Chromatography. Medium-Pressure Liquid Chromatography. Petroleum Products: Gas Chromatography.

Further Reading

- Adlard ER (ed.) (1995) *Chromatography in the Petroleum Industry*. Amsterdam: Elsevier.
- Annual Book of ASTM Standards, vols 05.01 and 05.02. *Petroleum Products, Lubricants and Fossil Fuels*. ASTM, Philadelphia PA 19103-1187, USA (issued annually).
- Cagniant D (ed.) (1992) *Complexation Chromatography*. New York: Marcel Dekker.
- Cortés HJ (ed.) (1990) *Multidimensional Chromatography*. New York: Marcel Dekker.
- Drews AW (ed.) (1989) *Manual on Hydrocarbon Analysis*, 4th edn. Philadelphia: American Society for Testing of Materials.
- Herod AA (1994) A review of the uses of planar chromatography in the coal and oil industries. *Journal of Planar Chromatography* 7: 180-196.
- Kelly GW and Bartle KD (1994) The use of combined LC-GC for the analysis of fuel products: a review. *Journal of High Resolution Chromatography* 17: 390-397.
- Pauls RE (1995) Chromatographic characterization of gasoline. *Advances in Chromatography* 35: 259.
- Ranny M (1987) *Thin-layer Chromatography with Flame Ionization Detection*. Dordrecht: D. Reidel.
- Standard Methods for Analysis and Testing of Petroleum and Related Products* 1992, vol. 2. Institute of Petroleum, London, 1992.
- Yau WW, Kirkland JJ and Bly DD (1979) *Modern Size-Exclusion Liquid Chromatography. Practice of Gel Permeation and Gel Filtration Chromatography*. New York: John Wiley.

Thin-Layer (Planar) Chromatography

A. A. Herod and M.-J. Lazaro,
Imperial College, London, UK

Copyright © 2000 Academic Press

Introduction

Thin-layer chromatography (TLC) has strengths not applicable to other chromatographic methods. These can be summarized as cheapness of materials, low volume requirement for solvents, the ability to use any mixture of solvents, and, most important, the intractable materials of a complex sample are re-

tained within the surface area of the chromatographic plate and may be recovered. In addition, chromatographic failures can be disposed of without damaging the budget. Such considerations do not apply to gas chromatography or liquid chromatography, where involatiles (in GC) or insolubles (in LC) are lost on the column or inlet system with the possibility of permanent damage to the column performance. The difference in cost of thin-layer plates and chromatographic columns ranges from a factor of 100 for GC capillary columns, up to a factor of 1000 for preparative HPLC columns. Whereas TLC has most often

been used to examine individual compounds, it has found use (as TLC with flame ionization detection using silica rods) in the examination of crude oils and more recently as a preparative method to separate the high molecular mass fractions of coal and biomass liquids and petroleum vacuum residues for examination free from the smaller, more volatile components.

Uses of Thin-Layer Chromatography

Thin-layer chromatography has been applied to tars and oils in three ways: (1) to identify individual compounds or groups of compounds such as polycyclic aromatic hydrocarbons (PAHs); (2) to measure types of compounds such as oils, maltenes, asphaltenes and preasphaltenes in crudes by the TLC-FID method; and (3) as a fractionation method for examination by other techniques such as NMR or laser ionization mass spectrometry. These uses are considered in more detail below.

Identification of Individual Compounds or Groups of Compounds

Analytical TLC of coal tar has been achieved using silica gel plates and development by a manual method using the series of solvents – tetrahydrofuran, chloroform/methanol (4 : 1 v/v), toluene and pentane. The separated components have been recovered and examined by probe mass spectrometry directly with no prior extraction from the silica. A typical analytical separation is shown in **Figure 1**. The standard compounds on the plate included pyrogallol, perylene and rubrene, with a coal extract produced in a bomb with tetralin solvent. Mass spectra of recovered fractions are shown below.

Measurement of Compound Types

The separation and quantification of compound types – oils, maltenes, asphaltenes and preasphaltenes (terms derived from solvent solubility fractionation)

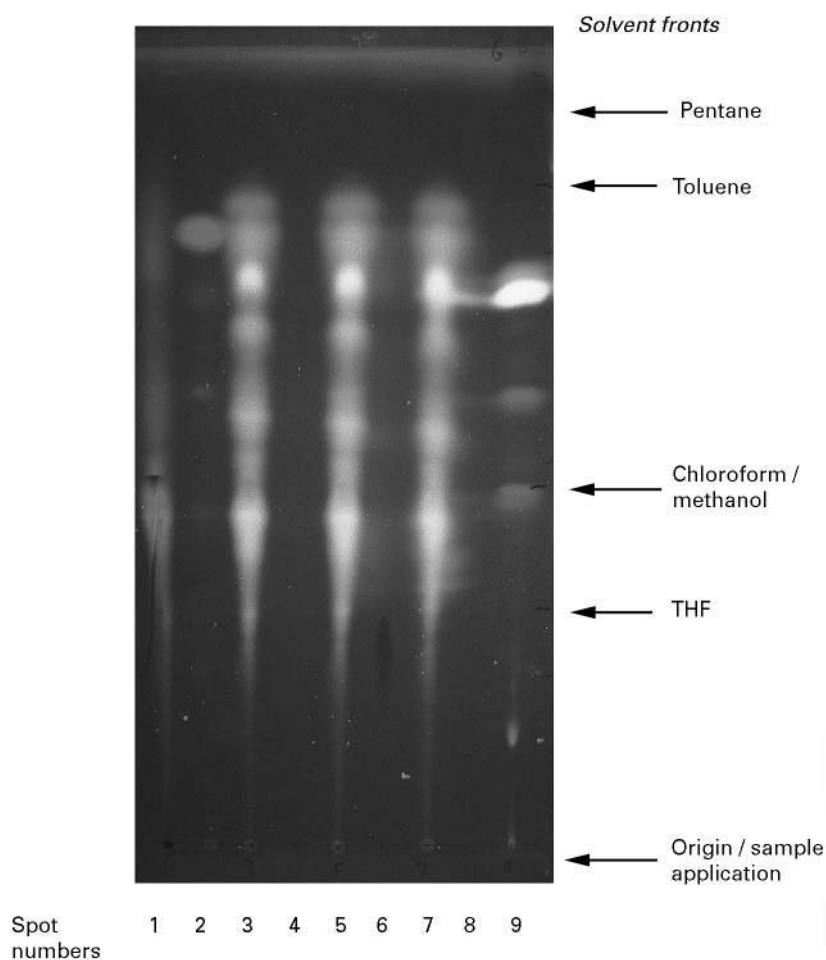


Figure 1 (See Colour Plate 109) Analytical development of coal tar pitch, tetrahydrofuran solubles, on silica developed in tetrahydrofuran, chloroform/methanol (4 : 1 v/v), toluene and pentane. Pitch at lanes 3, 5 and 7; perylene at lane 2; rubrene at lane 9; pyrogallol at lane 6; coal extract at lane 1. Whatman K6 silica; solvent fronts THF 55 mm, chloroform/methanol 83 mm, toluene 153 mm and pentane 178 mm.

– in oils and coal derived liquids may be achieved using the combination of TLC on rods with flame ionization detection (FID). The normal equipment used for this is the Iatroscan Chromatograph with Chromarods to effect the separation. Rods are cleaned and prepared by passage through a hydrogen/air flame, sample is deposited near one end of the rod and development proceeds as for a plate, using an appropriate solvent sequence. The developed and dried rod is passed through the flame detector to evaluate the separated fractions; calibration of the response factors of the different types of fraction is essential to give quantitative information. The sample is destroyed by the detection method but, as only small quantities of sample are used, several developments can be made at the same time to allow repeatability checks. Figure 2 shows details of different development sequences to obtain adequate separation of a coal tar pitch. The initial sequence was not satisfactory owing to the aromatic character of the pitch. The final sequence indicated that the hexane development had no effect on the separation of the pitch, since hexane would separate aliphatics, which are absent from the pitch.

Separation of Fractions for Examination by Other Techniques

In this mode, TLC has opened a route to the isolation of fractions of coal-derived liquids and tars from biomass as well as petroleum vacuum residues. The essence of the method is the application of sample either in solution or as a suspension or slurry in a volatile solvent. Pyridine has been used for slurring or dissolving all of these sample types; 1-methyl 2-pyrrolidone (NMP) is capable of dissolving coal and biomass tars, but is involatile (boiling point 202°C) and cannot be removed easily from the plate. After addition to the longer edge of a plate as spots or as a band along the bottom of the plate, usually 10 cm × 20 cm coated with silica gel, the pyridine is allowed to evaporate. Figure 3 shows a typical preparative development of a synthetic naphthalene mesophase pitch using tetrahydrofuran and toluene, with application of sample in a pyridine slurry. After separation the colours of the bands were black (immobile), brown (mobile in tetrahydrofuran but immobile in toluene) and orange (mobile in both solvents).

Development solvents used include pyridine followed by acetonitrile, pyridine followed by *N,N*-dimethylformamide and tetrahydrofuran followed by toluene. In each case, the first solvent used is the more polar of the two and development is not more than half way up the plate, less than 5 cm. After drying, the

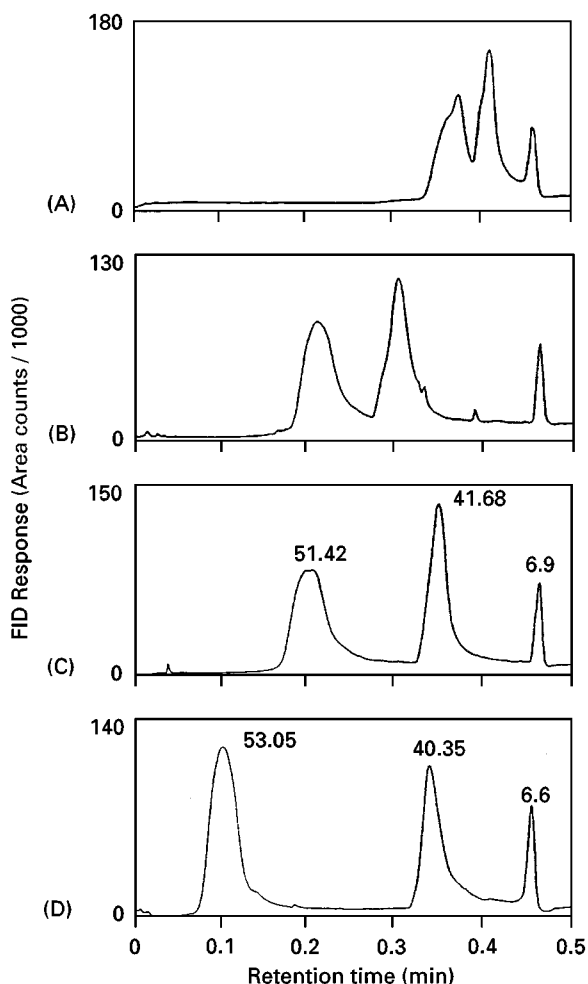


Figure 2 TLC-FID chromatograms corresponding to the following development sequences: (A) 38 min *n*-hexane, 3 min toluene, 30 s dichloromethane (DCM)-MeOH; (B) 38 min *n*-hexane, 20 min toluene, 5 min DCM-MeOH; (C) 45 min *n*-hexane, 20 min toluene, 3 min DCM-MeOH; (D) 35 min toluene, 3 min DCM-MeOH. Numbers correspond to area percentages. (TLC-FID reproduced with permission from Cebolla VL, Vela J, Membrado L and Ferrando AC (1996) *Chromatographia* 42(5/6) March 1996, © Friedr. Vieweg & Sohn Verlagsgesellschaft mbH.)

plate is developed in the second solvent to a distance approximately twice that of the first, but less than 10 cm. In some cases, the development has been achieved using a manual multiple development technique in which the plate is removed from the tank after the solvent front has passed the sample application zone (or the solvent front of the previous solvent), dried and reinserted into the same solvent to continue the development. By this method, the possibility of the mobile material being partially retained by the immobile fraction is reduced.

To avoid contamination of the tar fractions, the plates are usually washed before use with the first

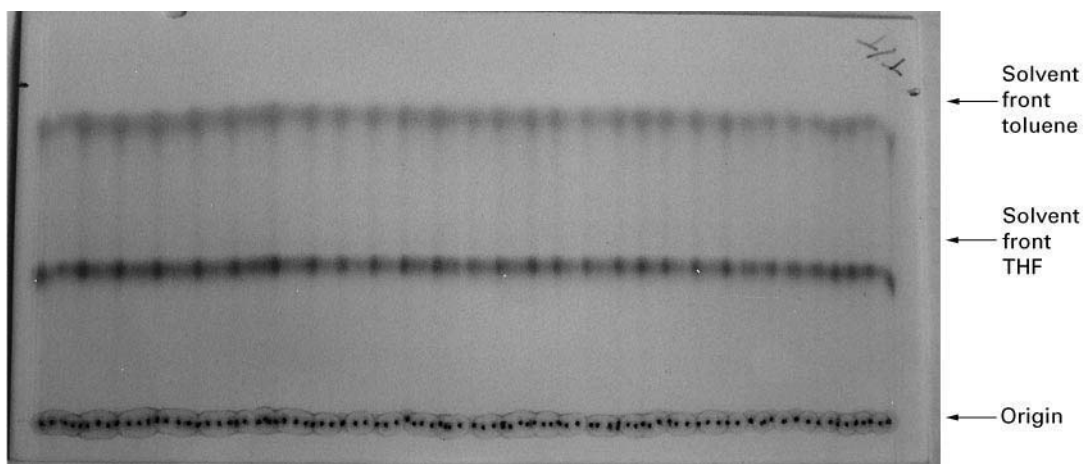


Figure 3 (See Colour Plate 110) Preparative development of a synthetic naphthalene mesophase pitch applied in pyridine slurry and developed in tetrahydrofuran and toluene.

solvent to be used in the development, either pyridine or tetrahydrofuran. This is achieved by placing the fresh plate into a development tank containing the solvent and allowing the solvent front to rise almost to the top of the plate. In the subsequent preparative or analytical development, the final solvent front is not allowed to reach the washing-solvent front and, in consequence, the height of the plate used for the separation is probably not more than two-thirds of the available plate height, with allowance for the sample application zone being above the initial level of the solvent when first placed into the development tank.

As indicated earlier, after development three zones are normally visible (black, dark brown and orange or yellow). These zones are recovered by scraping the coated silica into a glass vial and extracting with NMP at room temperature, with ultrasonic agitation if necessary. The extract may be recovered either by decanting the solvent from the silica, using a syringe, or by adding the slurry to a glass syringe equipped with a filter tip (0.6 μm). In this case, the physical pressure necessary to force the solvent through the filter may cause the filter to be blown off the syringe, with loss of sample. The complete removal of black, low mobility material from the silica is difficult to achieve and the residual silica may be dark in appearance; however, the recovered material is unlike the other fractions in molecular mass and spectroscopic behaviour (see below). The solutions derived by solvent extraction may be concentrated by vacuum evaporation or used as recovered. NMP is a difficult solvent to remove completely, but water washing of the almost dried fraction may achieve removal since NMP is very soluble in water.

Instrumentation

For TLC on plates as described here, the equipment needed is minimal: simple development tanks lined with absorbent paper to produce an atmosphere in the closed vessel that is in vapour equilibrium with the solvent pool in the tank, to reduce evaporation from the advancing solvent front on the plate. The plates themselves may be used as commercially supplied, requiring only a solvent wash to remove impurities from the area of the plate to be used for the separation.

More complex automated chromatographic development instruments may be used but the simple separation of tars into three fractions can be achieved without them.

TLC-FID requires specialist equipment since the chromatographic rods require passage through the detector flame by a controlled mechanical technique. The Iatroscan Chromatograph with Chromarod silica rods has been developed for this analysis.

Analyses by Other Methods

Material from analytical spots or bulk fractions recovered from thin layer plates may be analysed by a variety of analytical techniques. In particular, mass spectrometric methods can be applied since they require very little sample. Also, several different mass spectrometric techniques can be applied to either one recovered spot or a bulk fraction. In this section, the analysis of fractions obtained by preparative TLC by probe mass spectrometry, matrix-assisted laser desorption mass spectrometry (MALDI-MS), size exclusion chromatography (SEC) and UV-fluorescence spectroscopy (UV-F) are discussed.

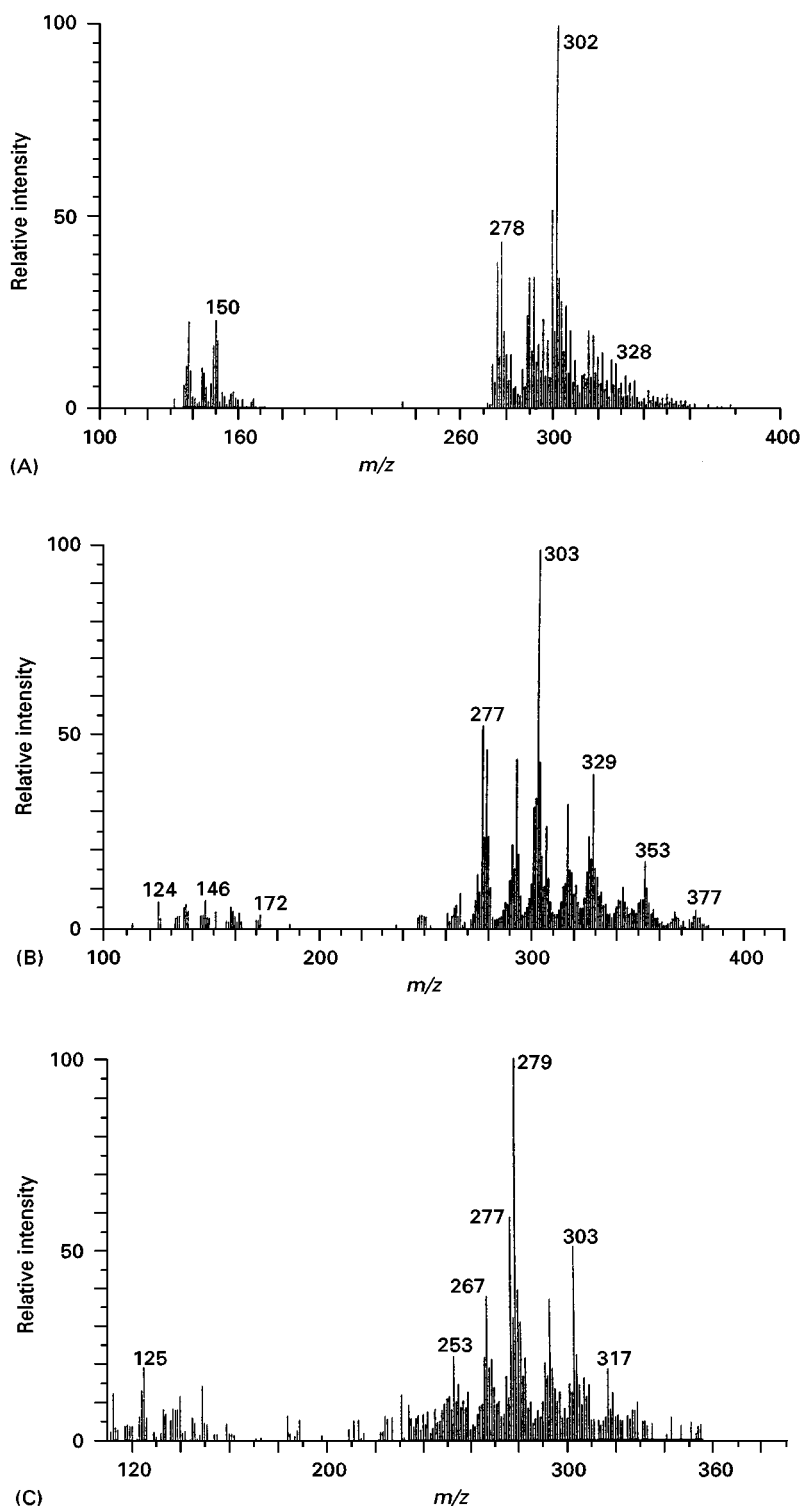


Figure 4 Probe mass spectra of TLC spots from an analytical development of coal tar pitch. Plots are normalized intensity versus mass number (m/z). (A) Fraction 2, aromatics; (B) fraction 5, neutral nitrogen heterocyclic aromatics; and (C) fraction 9, basic nitrogen heterocyclic aromatics. (Mass spectra reproduced from Herod AA and Kandiyoti R (1995) Fractionation by planar chromatography of a coal tar pitch for characterisation by size-exclusion chromatography, UV fluorescence and direct-probe mass spectrometry. *Journal of Chromatography A* 708: 143–160, © 1995, with kind permission of Elsevier Science NL.

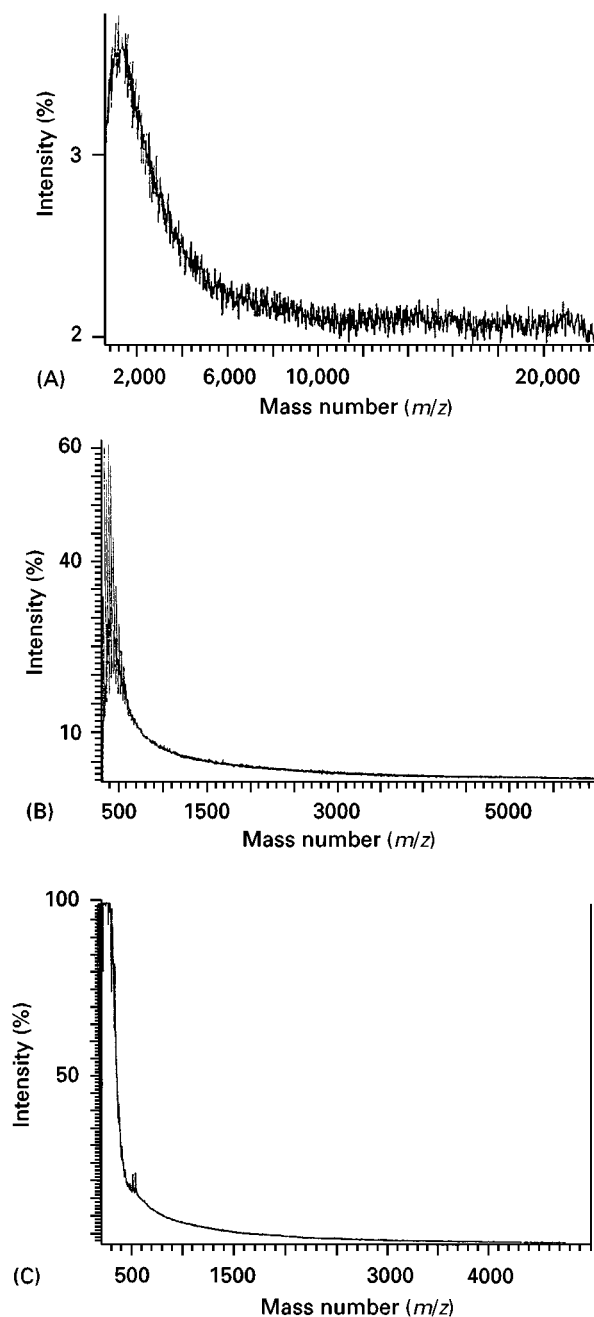


Figure 5 MALDI-mass spectra of coal tar pitch fractions from development in pyridine/acetonitrile. (A) Immobile fraction; (B) fraction mobile in pyridine only; (C) fraction mobile in pyridine and acetonitrile. (Reproduced with permission from Herod AA *et al.* (1996) Matrix-assisted laser desorption/ionization mass spectrometry of pitch fractions separated by planar chromatography. *Rapid Communications in Mass Spectrometry* 10: 171–177, © John Wiley & Sons Ltd.)

Probe Mass Spectrometry (Probe-MS)

This method can be used without extraction of the fraction from the silica. The range of molecular mass achieved depends on the volatility of sample in vac-

uum and the probe temperature; for fractions of pitch an upper mass of around m/z 600 is possible. The examination of spectra of spots in combination with R_F values of standards can permit the identification of compound types – aromatics, pyridinic and pyrrolic nitrogen heterocyclic aromatics. The absence of signal for the material left at the origin indicates that

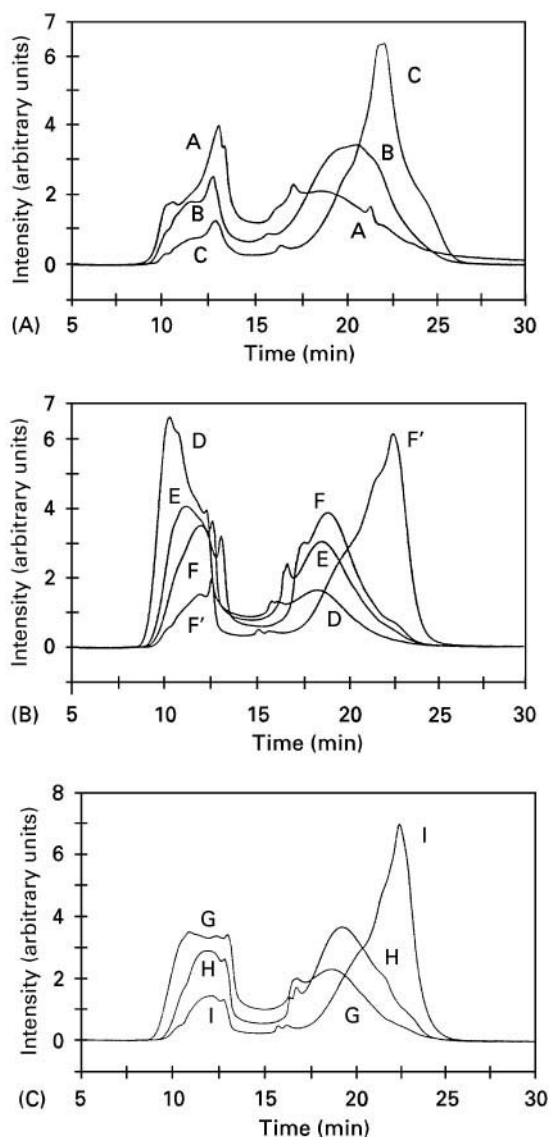


Figure 6 SEC profiles at 350 nm UV absorbance of pitch fractions. (A) Fractions A immobile in pyridine, B mobile in pyridine and C mobile in pyridine and acetonitrile; (B) fractions D immobile in pyridine, E mobile in pyridine, F mobile in pyridine and partly mobile in dimethylformamide and F' mobile in pyridine and dimethylformamide; (C) fractions G immobile in tetrahydrofuran, H mobile in tetrahydrofuran and I mobile in tetrahydrofuran and toluene. (Reproduced with permission from Herod AA *et al.* (1996) Matrix-assisted laser desorption/ionization mass spectrometry of pitch fractions separated by planar chromatography. *Rapid Communications in Mass Spectrometry* 10: 171–177, © John Wiley & Sons Ltd.)

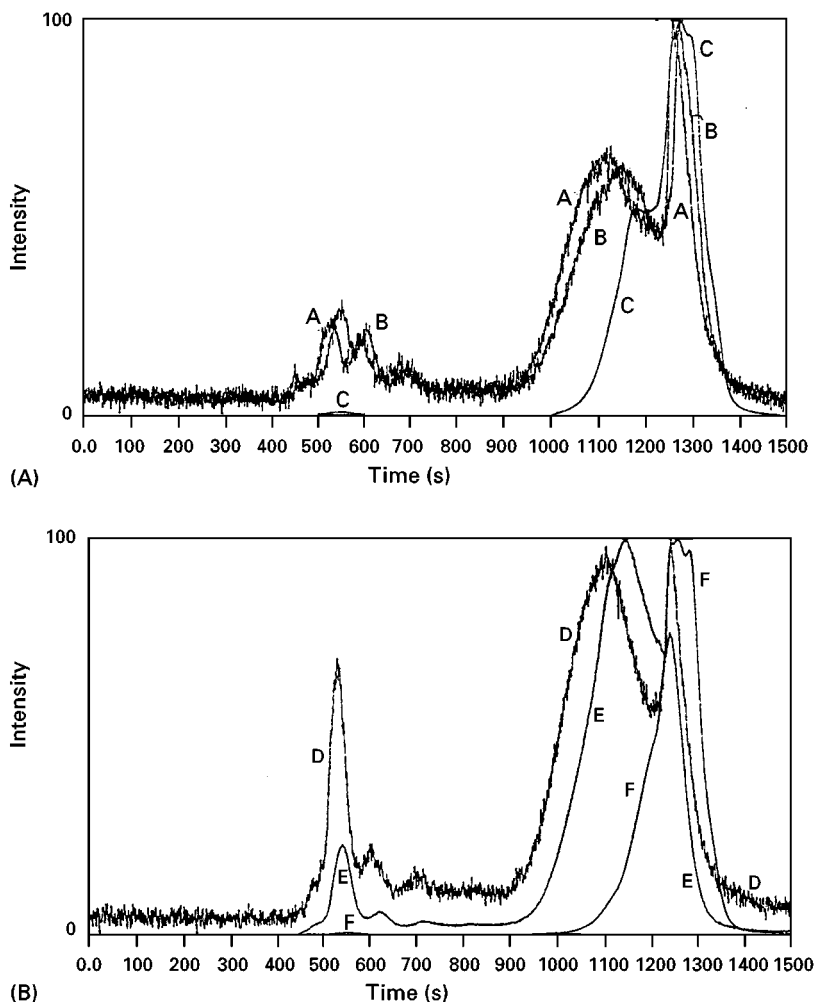


Figure 7 SEC profiles of pitch in NMP solvent of (A) fractions A, B and C from TLC in pyridine and dimethylformamide and (B) fractions D, E and F from TLC in tetrahydrofuran and toluene; detection by UV fluorescence with excitation at 320 nm and emission at 380 nm (fractions C and F) or 480 nm (fractions A, B, D and E). Fractions A and D are immobile; fractions B and E are partly mobile; fractions C and F are very mobile. (Reproduced with permission from Herod AA and Kandiyoti R (1996) Fractionation of coal tar pitch by planar chromatography for the characterisation of large molecular mass materials. *Journal of Planar Chromatography* 9: 16–24, © Research Institute for Medicinal Plants, H-2011, Budakalasz, Hungary.)

it contains large, involatile molecules rather than aggregates of small polar molecules.

Figure 4 shows mass spectra for some spots recovered from an analytical separation of a coal tar, following a separation similar to that shown in Figure 1. Fractions 1 (mobile in pentane) and 2–4 (mobile in toluene close to toluene front) gave molecular ions for polynuclear aromatic hydrocarbons ranging from fluorene (m/z 166) to m/z 482, corresponding to a dimethyl tetrabenzobinaphthyl type. Fractions 5, 6 and 7 correspond to the range of mobility between aromatics in the toluene zone and the chloroform/methanol solvent front and show evidence of the presence of nitrogen-containing heterocyclics. Fractions 8–11 were taken from material

mobile in chloroform/methanol but not mobile in toluene and correspond to basic nitrogen heterocyclic aromatics. The probe mass spectra of thin-layer fractions have allowed the identification of isomer classes rather than individual isomers but have extended the mass range of identified nitrogen PAH to nearly m/z 500. The identification of neutral and basic nitrogen components can be achieved during one rapid, simple and inexpensive separation with the use of standards to define the separation. Also, interference from the ^{13}C isotope peak of the more abundant polycyclic aromatics which have molecular masses one unit less than the nitrogen heterocyclics, is avoided, as opposed to the situation in GC-MS where both types elute together.

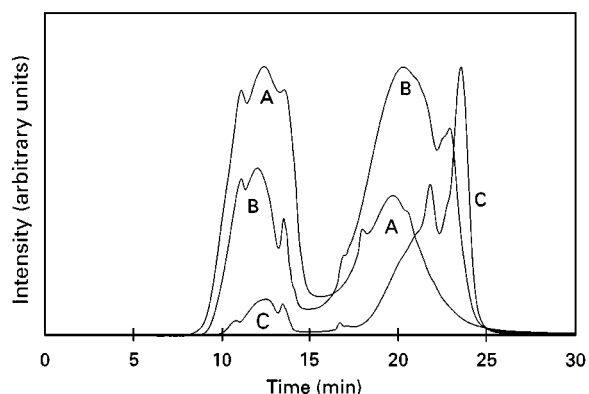


Figure 8 SEC profiles in NMP of TLC fractions of Point of Ayr liquefaction pilot plant coal digest. Fractions A immobile in pyridine, B mobile in pyridine, C mobile in pyridine and acetonitrile; UV absorbance detection at 350 nm. (Reproduced with permission from Herod AJ *et al.* (1996) Planar chromatography as a method of fractionation of a coal liquefaction extract for Mössbauer spectroscopy. *Journal of Planar Chromatography* 9: 361–367, © Research Institute for Medicinal Plants, H-2011, Budakalasz, Hungary.)

Matrix Assisted Laser Desorption Mass Spectrometry (MALDI-MS)

The application of MALDI-MS to coal-derived fractions is at an early stage. Much of the published work corresponds to laser ablation MS, where the fractions are examined with no added matrix but with the small molecules of the sample itself acting as the matrix. In the absence of small molecules (indicated by SEC) to form an effective matrix for kerogen extracts, no significant mass spectrum can be generated for the large molecules; addition of suitable matrix materials allows the generation of mass spectra, however. The upper limits observed for coal-derived materials by MALDI are in excess of 100 000 u but so far, it has not proved possible to generate mass spectra from the TLC-immobile fractions containing the largest molecules. Similarly, the techniques and matrix materials used to generate spectra for coal-derived fractions have not proved successful with immobile fractions from either biomass tars or petroleum vacuum residues.

One essential requirement for producing good mass spectra is the reduction of polydispersity (ratio of mass average to number average molecular mass) of fractions. **Figure 5** shows the MALDI-mass spectra of coal tar pitch fractions from development in pyridine and acetonitrile: (A) immobile fraction; (B) fraction mobile in pyridine only; and (C) fraction mobile in pyridine and acetonitrile. Increasing the mobility leads to shifts of molecular masses to smaller values and to changes in the shapes of spectra; the spectra become narrower and sharper with increasing mobil-

ity. Comparing relative intensity scales, intensities of immobile fraction spectra were only 1–4%, whereas the spectra of mobile fractions gave signal at full scale (100%). Smaller-mass molecules appear to be preferentially ionized and desorbed, thus skewing the molecular ion distribution in favour of the smaller molecules.

Size Exclusion Chromatography (SEC)

Size exclusion chromatography has been used extensively for the examination of oils and tars from coal, biomass and petroleum. Until recently, tetrahydrofuran (THF) was the solvent most used, for example for asphalts for road tars. In work with coal tar, we have shown that the use of THF gives erroneous results since the high-mass portion of the tar is lost to the guard column, which gradually blocks. It can be

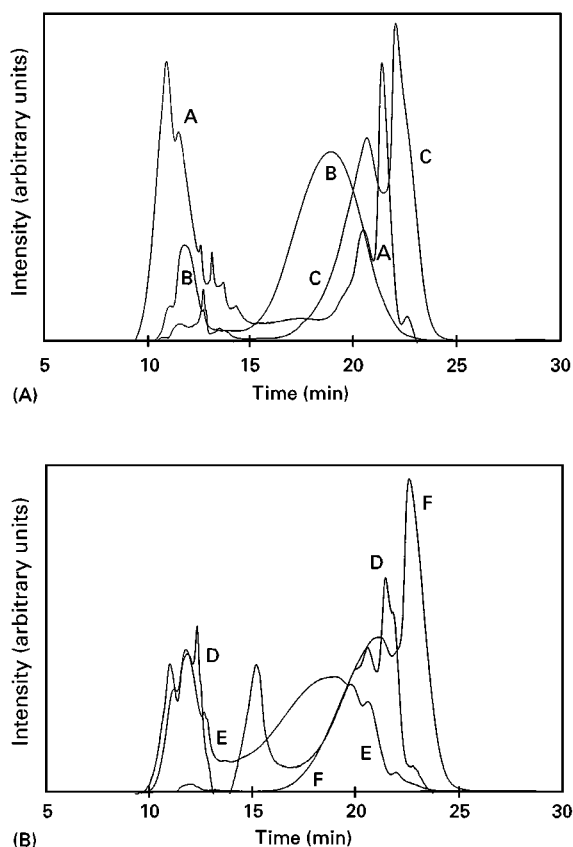


Figure 9 SEC profiles of Stockholm tar (a commercial pine-wood tar) fractions. (A) A immobile in pyridine, B mobile in pyridine and C mobile in pyridine and acetonitrile; (B) D immobile in tetrahydrofuran, E mobile in tetrahydrofuran and F mobile in tetrahydrofuran and toluene. UV absorbance at 300 nm. (Reproduced from the work of Lazaro MJ, Domin M, Herod AA and Kandiyoti R (1999) Fractionation of a wood for pitch by planar chromatography for the characterisation of large molecular mass materials. *Journal of Chromatography A* 840: 107–115; not previously shown in this form.)

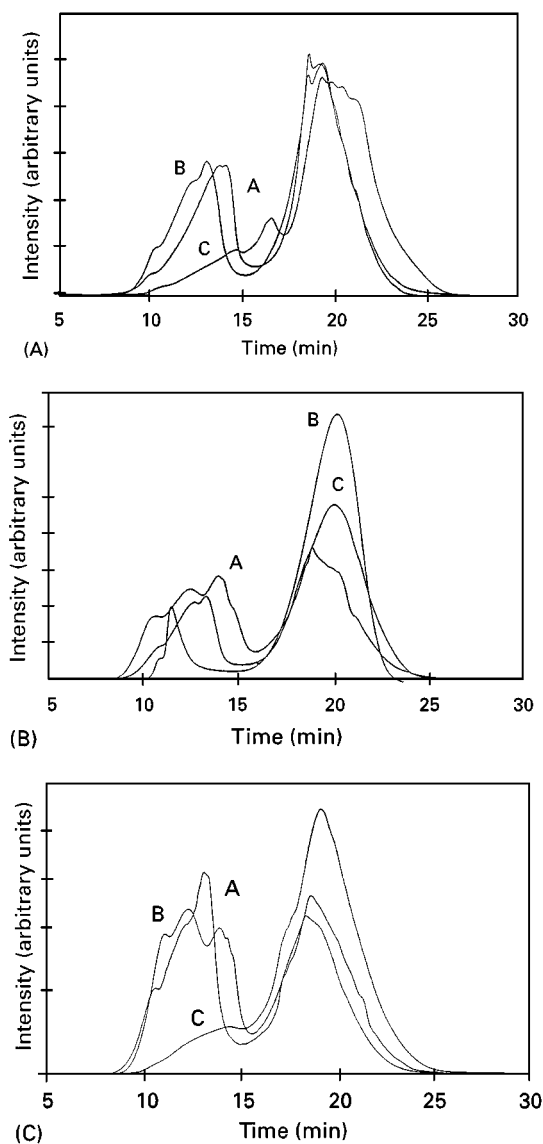


Figure 10 SEC profiles of petroleum vacuum residues. Fractions from TLC of (A) residue 1 in pyridine and acetonitrile, (B) residue 2 in pyridine and acetonitrile, (C) residue 1 in THF and toluene; curves are A immobile, B mobile in first solvent and C mobile in both solvents. (Reproduced from Deelchand J-P Naqvi Z, Dubau C, Shearman J, Lazaro MJ, Herod AA, Read H and Kandiyoti R (1999) Planar chromatographic separation of petroleum residues and coal-derived liquids. *Journal of Chromatography A* 830: 397-414; Copyright Elsevier Science.

cleaned using 1-methyl-2-pyrrolidinone (NMP) and restored to a usable state. In addition, THF does not completely dissolve the coal-derived materials. In the work described here, NMP has been used to dissolve tars and as an eluent for SEC. Although NMP dissolves coal tars and biomass liquids completely, it is

a poor solvent for alkanes and therefore petroleum-derived materials may be only partially soluble. However, the use of TLC fractionation allows the removal of alkanes from the aromatics by applying a final development of pentane. If UV absorbance is the method of detection for SEC, then alkanes are not observed.

SEC chromatograms of coal tars, biomass tars and petroleum vacuum residues are shown in Figures 6–10. All of the chromatograms show at least two major peaks, the first near the exclusion limit of the column and the second corresponding to material resolved by the column. The signal for the excluded material is thought to correspond to material the column is unable to resolve. If resolved, this material will appear as a long trailing distribution of apparently larger-mass material. More important though is the increasing proportion of excluded material in the TLC fractions with increasing immobility. This indicates that the TLC separation is on the basis of molecular size and not just polarity. Indeed, the definition of polarity for the fractions of tars described as oils, maltenes, asphaltenes and preasphaltenes on the basis of solubility or insolubility in particular solvents may apply equally well as a measure of increasing molecular

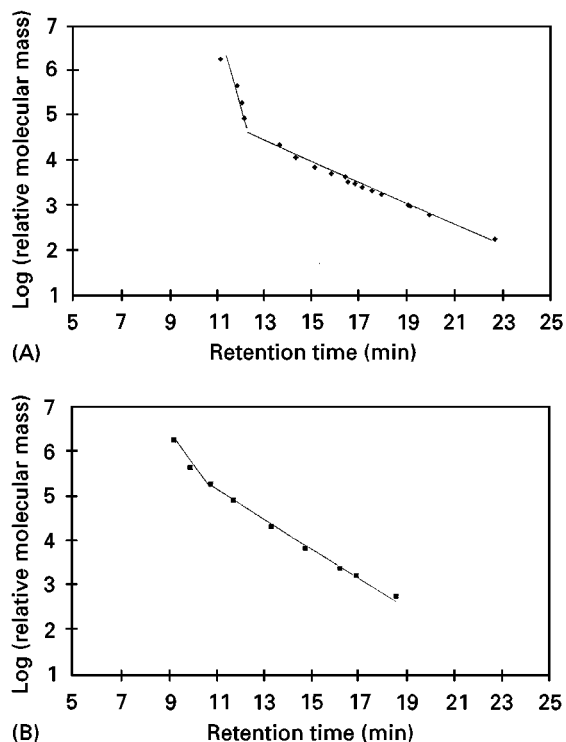


Figure 11 Calibration graphs for two SEC columns using polystyrene standards; \log_{10} molecular mass versus elution time. (A) Mixed E column and (B) Mixed D column from Polymer Laboratories Ltd, Church Stretton, UK.

mass or size. In SEC, the sequence of solvent-derived fractions shows a trend towards increasing molecular size from oil to preasphaltene. The combination of evidence from SEC, TLC, solvent solubility and MALDI-MS indicates that the immobile fractions do contain the largest molecular masses present in the tars from different sources. The SEC profile of the

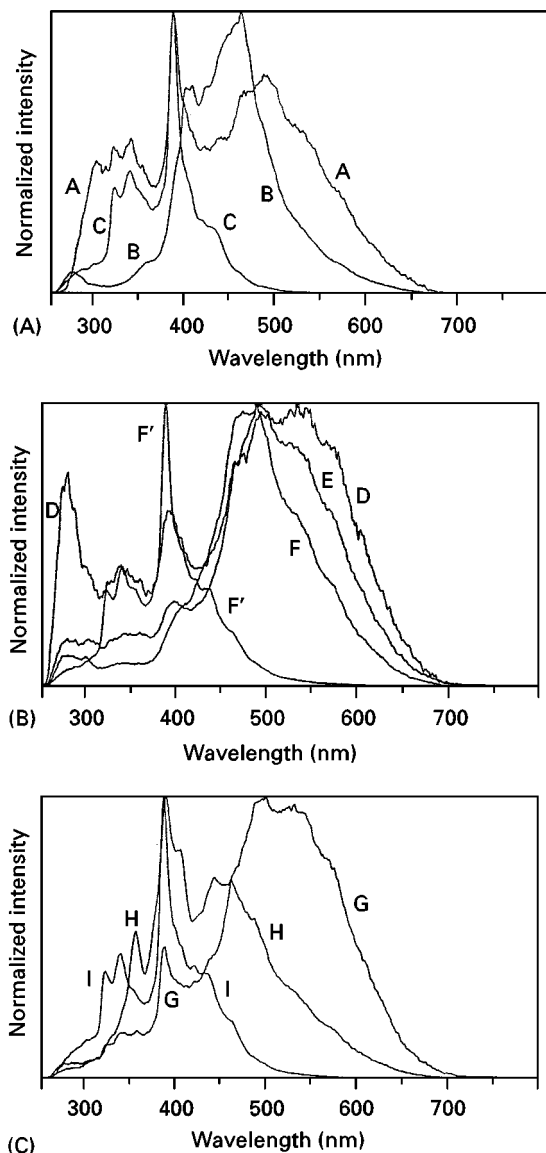


Figure 12 UV-fluorescence synchronous spectra of coal tar pitch fractions. (A) A immobile in pyridine, B mobile in pyridine, C mobile in pyridine and acetonitrile; (B) D immobile in pyridine, E mobile in pyridine, immobile in dimethylformamide, F partly mobile in dimethylformamide and F' mobile in dimethylformamide; (C) G immobile in tetrahydrofuran, H mobile in tetrahydrofuran, immobile in toluene and I, mobile in toluene. (Reproduced with permission from Herod AA *et al.* (1996) Matrix-assisted laser desorption/ionization mass spectrometry of pitch fractions separated by planar chromatography. *Rapid Communications in Mass Spectrometry* 10: 171–177, © John Wiley & Sons Ltd.

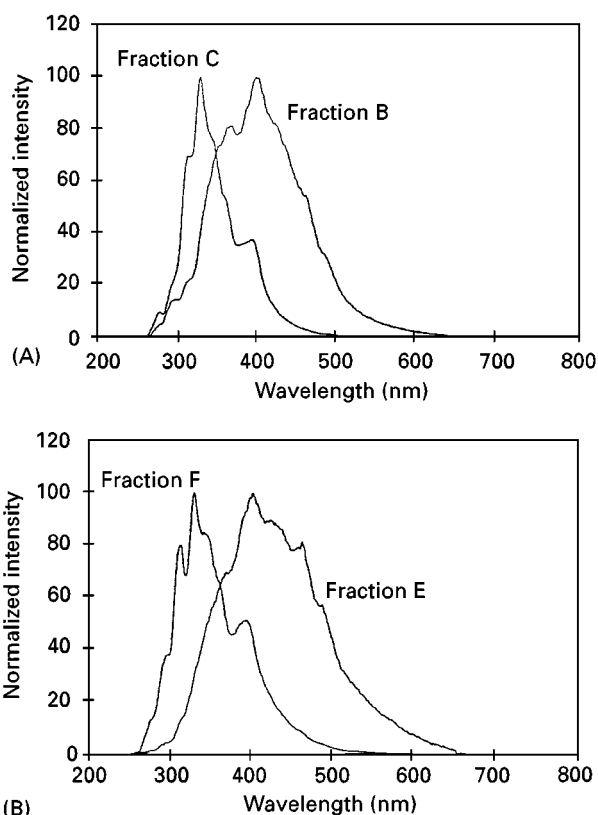


Figure 13 UV-fluorescence synchronous spectra of Stockholm tar fractions. (A) B mobile in pyridine and C mobile in pyridine and acetonitrile, the immobile fraction A did not show fluorescence; (B) E mobile in THF and F mobile in THF and toluene, the immobile fraction D did not show fluorescence. (Reproduced from the work of Lazaro MJ, Domin M, Herod AA and Kandiyoti R (1999) Fractionation of a wood for pitch by planar chromatography for the characterisation of large molecular mass material. *Journal of Chromatography A* 840: 107–115; not previously shown in this form.)

whole pitch shows a relatively smaller peak of excluded material compared with the immobile fractions. This points to the masking effect of the greater concentration of smaller masses and more mobile material, and emphasizes the utility of the planar chromatographic separation.

Calibration of the column separation is normally achieved using polymer standards; in this work polystyrene standards have been used. The calibration then appears to apply to polycyclic aromatic hydrocarbons and their N, S and O derivatives up to masses of approximately 1000 u. At higher masses, two problems apply: (1) there are no standard PAH available; and (2) the structures of the tar molecules are totally unknown. Calibration curves based on polystyrenes up to relative mass 1.84 million are shown in **Figure 11** for two columns. The linear regions from low mass (A) 20 000 u or (B) 200 00 u correspond to

the working region in which solute molecules penetrate the pores of the column packing and separate by size. The linear relation for larger polystyrenes at shorter elution times may correspond to separation in the space between the particles of the packing and molecules eluting in this region are described as excluded from the porosity; the discontinuity is described as the exclusion limit of the column.

UV-Fluorescence Spectroscopy (UV-F)

UV-fluorescence spectroscopy does not measure molecular size directly, but shifts of fluorescence maximum intensity to longer wavelengths indicate an increasing aromatic cluster size since the fluorescence originates from the largest aromatic system within a molecule, fed by energy absorbed by the smaller pendant aromatic groups. Such shifts to longer wavelengths point to increasing molecular size. Decreasing fluorescence quantum yields are a consequence of increased molecular size and complexity since there are more pathways for the electronic exci-

tation to progress to vibrational and thermal energy rather than being lost as fluorescence.

UV-F spectra of coal- and biomass-derived liquids and petroleum residues are shown in **Figures 12–14**. In coal-derived tars, the fluorescence intensity of the materials showing reduced mobility in TLC (and being largely excluded from the SEC porosity) decreases and the maximum shifts towards red wavelengths, indicating that these fractions contain large molecules. With biomass tars, immobile fractions do not show any fluorescence at all, indicating the presence of very high molecular mass material.

The fractions mobile in both solvents showed relatively strong fluorescence intensities, the position of the peaks at lower wavelengths suggesting the presence of relatively smaller polynuclear aromatic ring systems and probably also the presence of lower molecular mass material. Similarly fractions mobile in one solvent gave less intense fluorescence than fractions mobile in both solvents. TLC fractions of petroleum vacuum residues show no similar shift to red wavelengths with increasing immobility, or markedly reduced quantum yield but tend to cover the same range of wavelengths with shifts of intensity of peaks within that range. However, SEC of the immobile fractions indicates that the lack of mobility results from molecular size.

Conclusions

Several examples of the fractionation by TLC of coal- and biomass-derived liquids and petroleum residues have been shown. TLC improves the isolation and characterization of large molecular mass fractions in oils and tars for examination by other techniques such as probe mass spectrometry, MALDI-MS, SEC and UV-F. The separation is relatively rapid and inexpensive and requires only small volumes of solvents. The fractionation has led to structural information not readily available by direct characterization of the original mixture. Molecular-mass distributions, determined by SEC and MALDI, increase with decreasing mobility of the fractions in thin layer chromatography. UV-F spectroscopy has distinguished structural features by showing the presence of large polycyclic aromatic systems that increase in proportion to decrease in mobility of fractions. Detailed structures of the largest molecules remain unknown. Probe mass spectra have allowed the identification of isomer class and extended the mass range of identified nitrogen PAH to nearly m/z 500, allowing the identification of neutral and basic nitrogen types as well as the major components through one rapid, simple and inexpensive separation.

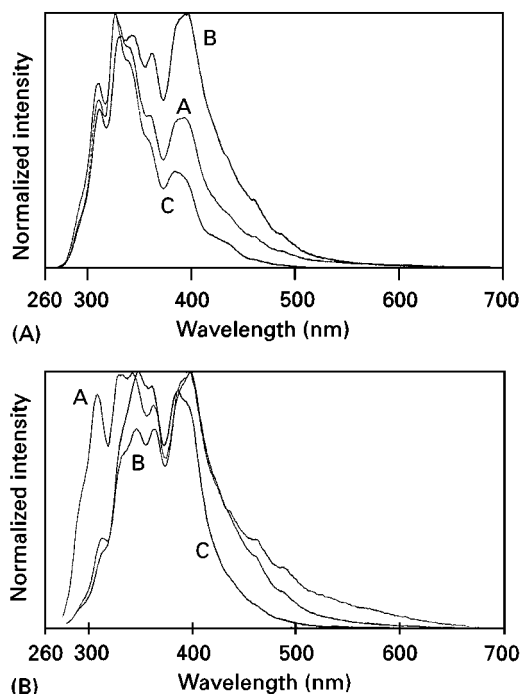


Figure 14 UV-fluorescence synchronous spectra of petroleum residues. (A) Sample 1 and (B) sample 2 (A immobile in pyridine, B immobile in acetonitrile and C mobile in pyridine and acetonitrile). (Reproduced from Deelchand J-P, Naqvi Z, Dubau C, Shearman J, Lazaro MJ, Herod AA, Read H and Kandiyoti R (1999) Planar chromatographic separation of petroleum residues and coal-derived liquids. *Journal of Chromatography A* 830: 397–414; Copyright Elsevier Science.

See Colour Plates 109, 110.

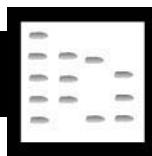
See also: **II/Chromatography: Liquid:** Mechanisms: Size Exclusion Chromatography. **III/Bitumens: Liquid Chromatography. Crude Oil: Liquid Chromatography. Flame Ionization Detection: Thin-Layer (Planar) Chromatography. Geochemical Analysis: Gas Chromatography. Polycyclic Aromatic Hydrocarbons:** Gas Chromatography; Solid-Phase Extraction; Supercritical Fluid Chromatography; Thin-Layer (Planar) Chromatography.

Further Reading

- Davison RR, Glover CJ, Burr BL and Bullin JA (1995) SEC of asphalts. In: Chi-san Wu (ed.) *Handbook of Size Exclusion Chromatography*, ch. 8, pp. 211–247. New York: Marcel Dekker.
- Herod AA (1994) A review of the uses of planar chromatography in the coal and oil industries. *Journal of Planar Chromatography* 7(3): 180–196.

- Herod AA (1998) Azaarenes and thiaarenes. In: Neilson AH (ed.) *The Handbook of Environmental Chemistry*, vol 3. I: PAHS and Related Compounds, Chemistry, ch. 7, p. 271. Berlin: Springer-Verlag.
- Jork H, Funk W, Fischer W and Wimmer H (1990) *Thin Layer Chromatography: Reagents and Detection methods*, vol. 1a. Weinheim, Germany: VCH Verlagsgesellschaft.
- Lakowicz JR (1983) *Principles of Fluorescence Spectroscopy*. New York: Plenum Press.
- Somsen GW, Morden W and Wilson ID (1995) Planar chromatography coupled with spectroscopic techniques, a review. *Journal of Chromatography A* 703: 613–665.
- Touchstone JC (1992) *Practice of Thin Layer Chromatography*, 3rd edn. New York: John Wiley & Sons.
- Wolffbeis OS (1993) *Fluorescence Spectroscopy – New Methods and Applications*. Berlin: Springer-Verlag.

PHARMACEUTICALS



Basic Drugs: Liquid Chromatography

B. Law, AstraZeneca Pharmaceuticals, Mereside, Alderley Park, Macclesfield, UK

Copyright © 2000 Academic Press

Introduction

High performance liquid chromatography (HPLC) is the most important technique for the separation, analysis and quantification of a wide range of drug types. Although there are a variety of approaches available for the chromatography of basic drugs, analysis of these compounds is still one of the main challenges for the practising chromatographer in the pharmaceutical industry. The general approaches have remained the same since the early days of HPLC, but there have been many refinements and developments since the late 1960s. In the main these have involved modification and improvements to the stationary phase, which are still continuing today.

This article focusses on the main methods of separation and analysis of basic drugs that are currently in use. Consideration is given to the relative pros and cons of the different approaches, as well as the development and evolution of the techniques.

Liquid–Solid Chromatography

Liquid–solid, or normal-phase chromatography (LSC) was one of the first approaches employed for the separation of bases in modern LC. Its use, however, has decreased dramatically since the 1970s and it is now rarely employed for the routine separation of basic drug molecules.

LSC was originally carried out using native silica or alumina, with the former being preferred for the separation of bases. Recently, there has been a gradual shift towards the use of polar bonded phases such as cyanopropyl, amino or diol, the last two showing preferential retention of bases compared with cyanopropyl. These bonded materials overcome some of the problems associated with silica phases such as deactivation by water and long equilibration times. The problem of deactivation is particularly acute in the area of bioanalysis, where it can be difficult to obtain extracts that are totally dry. To a certain degree this problem can be overcome by the inclusion in the eluent of a small amount (1% v/v) of water or a short-chain alcohol.

Eluents for LSC typically consist of mixtures of a nonpolar hydrocarbon, such as hexane or isooctane, and a polar modifier, e.g. dichloromethane, 2-propanol, methyl *t*-butyl ether or ethyl acetate. Frequently, the addition of an amine modifier such as triethylamine may be necessary to give satisfactory peak shapes.

LSC does complement reversed-phase separations, in that the selectivity is very different, with the order of elution usually being reversed. Unlike the more widely used reversed-phase HPLC (RP-HPLC; see below), it is particularly suited to the separation of geometric isomers.

Reversed-phase HPLC

RP-HPLC for pharmaceutical analysis took off in the early 1970s with the introduction of commercially available microparticulate bonded packings. Although it rapidly became the dominant mode of chromatography in the pharmaceutical area, it quickly became apparent that the chromatography of basic compounds was not a straightforward matter. Despite this, RP-HPLC still figures prominently in both literature and pharmacopeia methods.

The analysis of basic solutes using RP-HPLC methods presents a number of problems, principally because the analyte is retained by a number of retention mechanisms (some of which are poorly understood) in addition to the expected hydrophobic interaction. These include: hydrogen bonding, π - π interactions, ion exchange, ion pair formation and salting out. It is the multiplicity of these retention mechanisms that often leads to poor chromatographic performance, characterized by low peak efficiencies, tailing or asymmetric peaks and retention times that are dependent on the mass of compound injected.

Many of these phenomena can be traced back to the presence of unreacted silanols on the bonded silica surface. Despite the use of forcing conditions during the bonding process, there always remains a significant number of unreacted silanols, around 60% of the total. Silanols are acidic and if ionized can function as ion exchange sites. They are also polar and are able to interact with solutes via hydrogen bonding. While hydrogen bonding is not considered to be a serious problem, ion exchange can be particularly troublesome. From an energetics point of view this is easy to understand since the energy involved in coulombic or ionic interactions is around 20 times greater than that of hydrophobic interactions. Much of the development of RP-HPLC phases has been directed at minimizing the number (or type) of silanols, or at least minimizing their influence.

The interaction of a basic solute with the residual silanols is dependent on the pK_a of the base and the stereochemistry around the basic centre. The higher the pK_a and the lower the steric hindrance around the basic centre, the greater the interaction with silanols. Thus pyridine, which is a relatively weak base (pK_a

5.25), is also probably the smallest and least hindered aromatic base and can be particularly difficult to chromatograph on reversed-phase materials.

A number of general strategies involving both changes to the mobile phase and the stationary phase have been employed to improve the chromatography of bases. Each of these is discussed below.

Stationary Phase Modifications

End-capping

For many years manufacturers attempted to eliminate the residual silanols through a process known as end-capping. Following the primary bonding procedure, the stationary phase is further reacted with a small silylating reagent such as trimethylchlorosilane (TMCS) or hexamethyldisilazane, both of which generate trimethylsilyl groups ($(CH_3)_3Si-$). The rationale for their use is that the small size of the trimethylsilyl group should allow access to the silanols, which are inaccessible to bulkier primary reagents such as octadecyldimethylchlorosilane. However, this approach has never been fully successful, and even after exhaustive end-capping, unreacted silanols always remain. It is also believed that some silanols are so reactive that although they can be end-capped, they rapidly hydrolyse in aqueous organic mobile phases (especially at acid pH) to regenerate the silanol.

Polymer-coated Phases

In this approach a polymer coat is formed over the surface of the silica. If desired this can be further modified by the addition of C_{18} groups, for example. Although partially successful in blocking access to the silanols, this approach also leads to reduced efficiency, presumably through poor mass transfer caused by blocking of the silica pores. Although packings based on this approach are commercially available, they are not widely used.

Sterically Protected Phases

Another approach to minimizing silanol interactions is through the use of sterically hindered silylating reagents, such as diisopropyloctadecylchlorosilane. The rationale here is that the bulky isopropyl groups (in contrast to the more commonly employed methyl groups) should result in steric occlusion of any residual silanols. This approach has only been partially successful in reducing analyte-silanol interactions and has not been widely adopted. However, it would appear to be more successful in stabilizing the bonded phase and allowing the use of a wider range of pH.

Base-deactivated Phases

In the mid-1980s it was demonstrated that it was the type, rather than the number of silanols that was responsible for the secondary interactions. A poor silica is characterized by an uneven distribution of silanols with varying and strong acidity – so-called Type A materials. In contrast, good silicas (Type B) are characterized by a large population of hydrogen-bonded, low-acidity silanols.

This discovery led to the development of the so-called base-deactivated phases, which were claimed to be superior to standard materials for the separation and analysis of bases. **Figure 1** presents three chromatograms showing the separation of a series of basic drugs using three reversed-phase packings. The first is a standard C_{18} material, the second is partially deactivated (typical of end-capped materials), and the third is a modern base-deactivated material. The improvement in peak shape and efficiency across these three types is clearly evident.

The purity of the silica that is used to make the bonded-phase material is also considered to be important in the analysis of basic drugs. Silicas with high purity and very low metal content, particularly aluminium and iron, have been shown to give improved performance. These metallic impurities can

act in one of two ways: directly as centres for chelation, or indirectly through their polarization of silanols, thereby increasing their acidity or activity.

Much of the technology that has gone into the development of modern reversed-phase materials is proprietary. However, most of these stationary phases are probably made by employing one or several of the following approaches: fully rehydroxylated silicas with an even distribution of low acidity silanols; high purity silicas; sterically hindered silylating reagents; or more recently silylating reagents incorporating a polar linkage (e.g. carbamates). It is important to note that a column that gives particularly good performance with one compound may be totally unsuited to the analysis of another compound. This is clearly seen from the data in **Table 1**, which compares the performance of four commercial columns based on the tailing observed for a series of basic drugs. All the columns were claimed to be suitable for the analysis of bases. For example, column I is clearly the worst with atenolol and chlorpheniramine, giving rise to the most severe tailing peaks. With amiloride, however, column I is almost as good as column IV, the best, and column II stands out as being quite different. With pyridine as a simple test marker, all the columns give a similar poor performance. Before selecting a column, therefore, it is

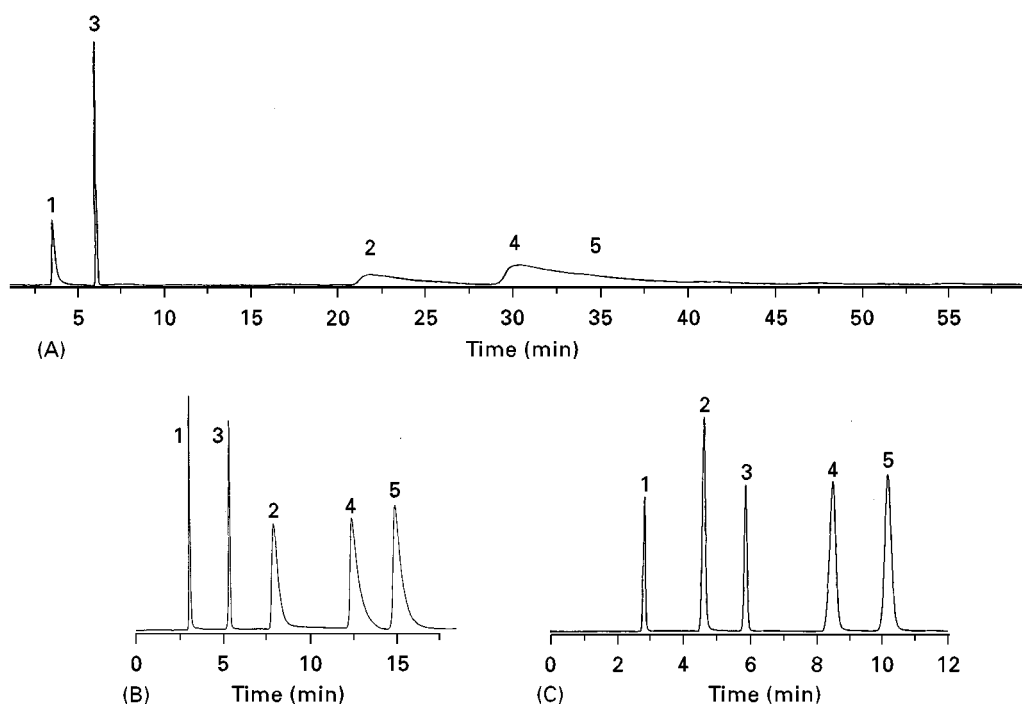


Figure 1 A comparison of the chromatography of a range of basic compounds on three C_{18} reversed-phase packings: (A) a conventional material, (B) a semi-deactivated material and (C) base-deactivated material. Eluent: methanol/ KH_2PO_4 (25 mmol L^{-1} , pH 6.0) (80/20). Flow rate: 1 mL min^{-1} . Identification: 1, norephedrine; 2, nortriptyline; 3, toluene (neutral test marker); 4, imipramine; 5, amitriptyline. (Reproduced with permission from Hichrom, Reading, UK.)

Table 1 The tailing factor for a range of basic compounds on four base-deactivated reversed-phase columns

Compound	Tailing factor on different columns			
	I	II	III	IV
Atenolol	2.6	1.7	1.3	1.2
Pyridine	2.2	2.5	2.1	2.7
Pindolol	1.7	2.2	1.4	1.3
Amiloride	1.2	1.7	1.2	1.1
Cycloguanil	2.2	1.9	1.4	1.2
Chlorpheniramine	6.8	3.1	3.1	1.6

Eluent methanol/water, containing ammonium acetate (0.1 mol L^{-1}), pH approximately 7.1. (Reproduced from Law *et al.*, 1998, with permission from Elsevier Science.)

important to try it out with the given analyte using a variety of conditions, since some columns seem to perform better with acidic eluents while others work best at neutral pH. The use of a number of parameters such as retention, efficiency and peak tailing are necessary if a true measure of column performance with regard to a particular analyte is to be gained.

Most manufacturers and distributors of HPLC materials supply base-deactivated materials.

Polymeric Phases

In an attempt to eliminate the effects of silanols totally some manufacturers moved away from silica completely and developed polymeric phases based on styrene-divinylbenzene. These materials are claimed to offer pure reversed-phase chromatography devoid of the secondary interactions that so bedevil chromatography on silica-based materials. They also offer a significant advantage in that they are fully stable over the pH range 1–14. This allows chromatography of basic drugs in the unionized form at high pH, which is impossible with standard silica-based materials.

These materials, however, were not without disadvantages. Some of the early materials underwent swelling when moving from high aqueous to high organic eluents, resulting in back-pressure changes and column blocking. Surprisingly, however, they also suffered from secondary interactions that resulted in poor performance. It has been claimed that the grafting of alkyl chains (typically C_{18}) onto the polymer phase is a useful method of minimizing these undesirable interactions. The major disadvantage of these materials for most analytes, including basic drugs, is the poor peak efficiencies attributed to slow mass transfer. These materials have not found widespread general use, although they are used for some particular applications, such as the analysis of quater-

nary amines, where their high retentivity compared with comparable silica phases is particularly useful.

Eluent Modifications

Organic Modifier

It is a generally observed phenomenon that of the three commonly used organic modifiers – methanol, acetonitrile and tetrahydrofuran – the first gives the most symmetrical peaks with basic compounds. This is usually explained by the fact that methanol has both hydrogen bond acceptor and donor properties, in contrast to the other two solvents, which have only acceptor properties. Thus, methanol is able to interact and effectively block residual silanols to a greater extent.

Eluent Buffers

Phosphate buffers are commonly used in HPLC eluents, especially for reversed-phase work. Of the two counterions mainly used, potassium has greater affinity for the silanol ion exchange sites than sodium. Thus the use of potassium phosphate is recommended, since this will result in a small but significant improvement in peak shape. It follows also that the use of stronger buffers (100 mmol L^{-1}) should be more effective than buffers of lower concentration.

Eluent pH

The eluent pH can also have a marked effect on peak shape. Since the undesirable interactions are ionic, then an improvement in chromatographic performance should be achieved by suppressing the ionization of either the base or the silanol. Because many basic compounds of pharmaceutical interest are relatively strong bases ($\text{pK}_a > 8.5$), an eluent pH of around 10.5 would be required to suppress their ionization. Since many silica-based stationary phases undergo dissolution at $\text{pH} > 7.5$ –8, this approach is impractical. More commonly, therefore, the eluent pH is reduced to around 2 to 3 through the addition of trifluoroacetic acid or phosphoric acid in an attempt to suppress the ionization of the silanols. This approach is not always fully successful because a small population of silanols are often quite acidic with pK_a values < 1 . Acidified eluents, however, do complement the use of silanol-blocking and ion pair reagents (see below).

Silanol-blocking Agents

Silanol-blocking agents, which normally take the form of a lipophilic amine, can be considered as a special type of eluent additive. They are usually

included in the eluent at a concentration of around 25 mmol L^{-1} . If secondary or tertiary amines are used, then the eluent pH needs to be adjusted to ensure full ionization of the amine. Where quaternary amines are used the eluent can be at any pH, although a slightly acidic eluent would be recommended to minimize the number of ionized silanols.

The large excess of the protonated amine in the eluent effectively blocks or masks the residual silanols, making them less accessible to interaction with the basic analyte. A number of systematic studies have been carried out on the use of silanol-blocking agents. From these a number of general conclusions can be drawn. First, the silanol-blocking properties of alkylamines decreases in order primary < secondary < tertiary \leq quaternary. Compounds of the type $(\text{CH}_3)_3\text{N}^+\text{R}$ or $(\text{CH}_3)_2\text{N}^+\text{HR}$, where R is a long alkyl chain, are the most effective. There is no consensus as to the optimal length of the alkyl chains; some workers recommend triethylamine ($30\text{--}50 \text{ mmol L}^{-1}$) while others prefer dimethyloctylamine ($5\text{--}10 \text{ mmol L}^{-1}$). As well as improving peak shape and efficiency, the use of masking agents can also lead to a significant reduction in retention for basic solutes. Silanol-blocking agents can also be used with base-deactivated materials, where significant improvements can be observed with some basic drugs.

Dynamically Modified Silica

Introduced by Hansen in the early 1980s, this approach involves the creation of a dynamic reversed phase. A bare silica column is used with an aqueous/organic eluent containing a long-chain quaternary ammonium compound. Initially the eluent is passed through the column until equilibrium is reached, and the quaternary ammonium compound forms an adsorbed monolayer on the silica surface. This approach has been shown to give good peak shapes for strong bases (Figure 2) and to give separations difficult to achieve using base-deactivated materials. A major and somewhat surprising attribute of the system is the excellent reproducibility in selectivity, even when changing from one brand of silica to another. Thus this approach is particularly suited to those assays where long-term reproducibility is essential, such as in pharmaceutical quality control. Despite these advantages this method has not become widely used, possibly due to the limitations with respect to UV detection, particularly at short wavelength. The lack of compatibility with mass spectrometry, currently the favoured means of detection in the pharmaceutical industry, probably means that it will never become popular.

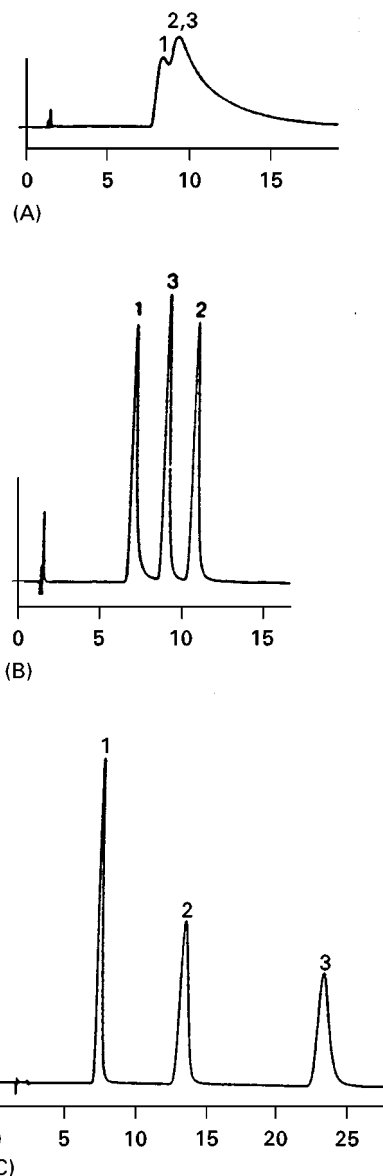


Figure 2 The separation of imipramine and metabolites under three sets of conditions. (A) Column, LiChrosorb RP-18 ($120 \text{ mm} \times 4.6 \text{ mm}$); eluent, methanol/water/phosphate buffer (0.2 mol L^{-1} , pH 4) (60 : 35 : 5). (B) As for (A) but with the addition of dodecyltrimethylammonium bromide (2.5 mmol L^{-1}) and sodium dodecanesulfonate (5 mmol L^{-1}). (C) Column, LiChrosorb Si 60 ($120 \text{ mm} \times 4.6 \text{ mm}$); eluent, methanol/water/phosphate buffer (0.2 mol L^{-1} , pH 7) (55 : 40 : 5) with the addition of cetyltrimethylammonium bromide (2.5 mmol L^{-1}). Identification: 1, imipramine-*N*-oxide; 2, desipramine; 3, imipramine. (Reproduced from Hansen SH, Helboe P and Thomsen M (1987) Separation of basic drug substances by reversed-phase high-performance liquid chromatography on dynamically modified silica and on bonded-phase materials. *Journal of Chromatography* 409: 71–80, with permission from Elsevier Science.)

Ion Pairing HPLC (IP-HPLC)

This is an approach developed during the early 1980s and pioneered by Schill and co-workers. It is parti-

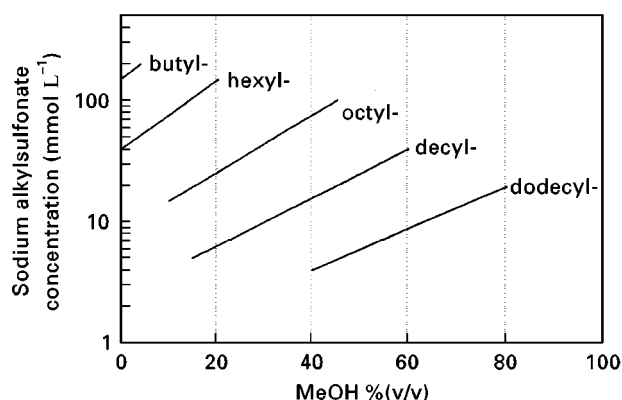


Figure 3 Recommended maximum mobile-phase concentrations of alkyl sulfonate pairing ions and their application range as a function of the mobile-phase methanol concentration. (Reproduced from Bartha A, Vigh G and Vorga-Puchony Z (1990) Basis for the rational selection of the hydrophobicity and concentration of the ion-pairing reagent in reversed-phase ion-pair high-performance liquid chromatography. *Journal of Chromatography* 499: 423–434, with permission from Elsevier Science.)

cularly useful for the separation and analysis of polar bases such as drugs containing quaternary amine groups, which are usually difficult to analyse under standard reversed-phase conditions because their high polarity leads to poor retention. Because of the general improvement in the quality of reversed-phase materials (end-capped, base-deactivated) the use of IP-HPLC has declined somewhat. Typical ion pair reagents are perchlorate or more commonly alkyl sulfonates (e.g. pentane, heptane or dodecane). The organic ion pair reagents are normally added at concentrations of around 10 to 100 mmol L⁻¹ and, to ensure full ionization of the basic drug, the eluent is normally acidified to a pH of around 2–3. The longer the alkyl chain of the pairing ion, the greater the retention. Excellent control of selectivity with respect to other bases, as well as neutral or acidic compounds, is possible. This flexibility can also make optimization of the system complex, since as well as organic modifier type, modifier concentration and eluent pH, the nature and concentration of the ion pair reagent, as well as the concentration of the buffer, all have an effect on the separation. The optimization of such systems have been extensively studied. Figure 3 shows how the nature and concentration of the pairing ion are dictated by the methanol concentration in the eluent.

In a number of applications, a quaternary ammonium ion has also been added to the eluent to further improve the peak shape of the basic analytes.

Ion Exchange HPLC (IE-HPLC)

Ion exchange is a useful, if under utilized, mode of chromatographing basic solutes. With this form of

chromatography the ionic interactions, which prove so troublesome in RP-HPLC, are actually employed as the major retention mechanism. Two general approaches are available, the first employing native silica as the stationary phase and the second utilizing bonded phases bearing a specific ion exchange group.

Ion Exchange Using Native Silica

As stated earlier, the silanol groups on the surface of silica gel are weakly acidic with a bulk pK_a of around 4. Consequently at pH values greater than 4 the silanols become ionized and they are able to act as ion exchange sites. Silica is typically used with eluents consisting of a mixture of an organic modifier (methanol or acetonitrile) and an aqueous buffer at a pH > 7. A variety of buffers have been employed, but ammonium acetate is particularly useful since it has low UV absorbance, high volatility and is noncorrosive. A good general purpose eluent is methanol/ammonium acetate buffer (9:1 v/v, pH 9.1). When employed with Spherisorb S5W silica this system shows excellent performance for the analysis of strongly basic drugs with pK_a values > 8. Most bases, including some quaternary ammonium compounds, give excellent peak shapes (< 1.2) asymmetry and high efficiencies (N = 50 000 plates m⁻¹). Despite the use of a high eluent pH the silica stationary phase shows excellent stability and the columns can be used for many months with no loss in performance. This unexpected stability of the silica is attributed to the use of a high proportion of organic modifier in the eluent and ammonia as the base, rather than sodium, potassium or a strong organic base, which are generally more aggressive.

This approach is particularly good for drug screening since a wide range of drug types elute in a relatively narrow retention range (Figure 4). Thus gradient elution, which would be needed to chromatograph a similar set of compounds under RP-HPLC conditions, is avoided. Retention is found to be dependent on the solute pK_a with the more basic compounds being more highly retained. Since the pK_a of basic drugs often does not change radically when the drug is metabolized, the system is useful for the analysis of metabolites in biological fluids. To a certain degree the retention of the metabolites is predictable, with most metabolites eluting after the parent compound in contrast to RP-HPLC.

The major limitation of this approach is its restriction to the analysis of strong bases with pK_a values > 8. The column-to-column reproducibility can also be a problem as 'ageing' of the silica, whether in the dry state or packed into a wet column, can result in significant selectivity differences.

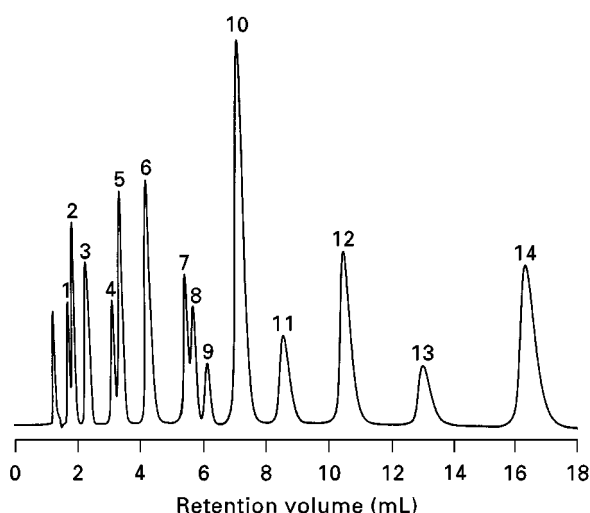


Figure 4 The separation of a range of bases using a Spherisorb S5W column (100 mm \times 4.6 mm) and an eluent consisting of methanol/ammonium acetate buffer (9 : 1, v/v) with an apparent pH of 9.1. Identification: 1, tetracaine; 2, tamoxifen; 3, diphenhydramine; 4, amiloride; 5, thioridazine; 6, chlorpheniramine; 7, *N*-methylamphetamine; 8, debrisoquine; 9, 4-hydroxydebrisoquine; 10, quinacrine; 11, strychnine; 12, betahistine; 13, benzethonium; 14, pyrantel. (Reproduced from Law, 1990.)

Ion Exchange Using Bonded Phases

Although introduced not long after hydrocarbon-bonded phases, these materials have never really caught on for the separation of drugs. To a degree this may be due to the perceived complexity of ion exchange as a mode of separation, with the need to control the ionization of both analyte and stationary phase. However, the use of strong cation exchanger (SCX) materials, such as propylsulfonic acid, which are highly acidic ($pK_a < 1$) and effectively ionized at all pH values, makes the development of separations relatively straightforward.

Recently there has been renewed interest in bonded phase ion exchange materials with a number of reports appearing on applications of the propylsulfonic acid phases. To ensure full ionization of both weak and strong bases, acidic eluents should be employed, and to give good efficiencies and good selectivity, a high organic modifier concentration is recommended. Using a Spherisorb 5 μ m SCX column with an eluent consisting of methanol/water/trifluoroacetic acid (800 : 200 : 2.3 v/v) containing ammonium formate (20 mmol L⁻¹) it has proved possible to chromatograph a very wide range of basic drugs. The system shows acceptable retention for strong bases such as the β -blockers ($pK_a \sim 9.5$) through to weak bases such as diazepam with a pK_a of only 3.4 (Figure 5). Like the silica-based system described

above, this approach also gives very good performance with high efficiencies (up to 70 000 plates m⁻¹) and good peak symmetries. The retention is controlled in the main by the concentration of the ammonium formate buffer. Furthermore, through systematic modification of the eluent pH or organic modifier concentration, it is possible to change selectivity in a predictable manner.

One advantage of both the above ion exchange approaches is that the eluent constituents are relatively volatile ensuring compatibility with mass spectrometric detection.

Future Developments

RP-HPLC, utilizing silica-based materials, is likely to continue as the dominant technique for the analysis of pharmaceuticals including basic drugs. Despite their problems and limitations, silica-based materials are still able to outperform polymeric phases. Although the development of polymer-based materials is likely to continue, our knowledge and understanding of silica – despite its use in HPLC for over 30 years – is still growing. A number of academic groups and chromatography companies are actively researching silica. Although major breakthroughs in the

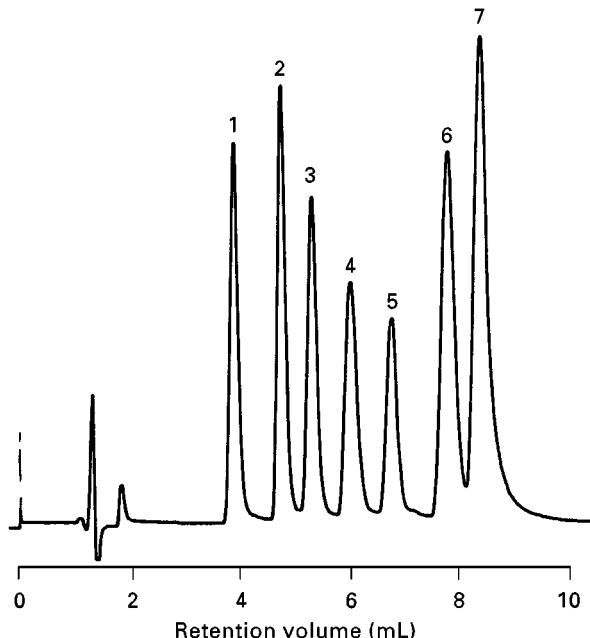


Figure 5 The separation of a range of basic drugs using a Spherisorb 5SCX column (100 mm \times 4.6 mm) and an eluent consisting of methanol/water/trifluoroacetic acid (TFA) (800 : 200 : 2.3, v/v) containing ammonium formate (0.02 mol L⁻¹), with an apparent pH of 2.45. Identification: 1, halofantrine; 2, minoxidil; 3, haloperidol; 4, reserpine; 5, cimetidine; 6, verapamil; 7, clomipramine. (Reproduced from Law and Appleby, 1996.)

methods of production and quality of silica are unlikely, a process of refinement can be expected, leading to even better deactivated materials.

While it would be encouraging to believe that the benefits of some of the other approaches will be recognized and exploited, the conservative nature of the pharmaceutical analyst – partially driven by the heavily regulated nature of the industry – and the dominance of reversed-phase methods make this unlikely.

See also: II/Chromatography: Liquid: Column Technology; Ion Pair Liquid Chromatography; Mechanisms: Ion Chromatography; Mechanisms: Normal Phase; Mechanisms: Reversed Phases. III/Porous Polymers: Liquid Chromatography.

Further Reading

- Gasco-Lopez AI, Santos-Montes A and Izquierdo-Hornillos R (1997) The effect of different amines added to eluents as silanol masking agents on the chromatographic behaviour of some diuretics in reversed-phase high-performance liquid chromatography using C18 packings. *Journal of Chromatographic Science* 35: 525–535.
- Hansen SH, Helboe P and Thomsen M (1988) Separation of basic drugs by high-performance liquid chromatography using dynamically modified silica. *Trends in Analytical Chemistry* 7: 389–393.
- Law B (1990) The use of silica with reversed-phase type eluents for the analysis of basic drugs and metabolites. *Trends in Analytical Chemistry* 9: 31–36.
- Law B and Appleby JRG (1996) Re-evaluation of strong cation-exchange high-performance liquid chromatography for the analysis of basic drugs. *Journal of Chromatography A* 725: 335–341.
- Law B, Houghton SJ and Ballard P (1998) An approach to the evaluation and comparison of reversed-phase high-performance liquid chromatography stationary phases. *Journal of Pharmaceutical and Biomedical Analysis* 17: 443–453.
- McCalley DV (1996) Effect of organic solvent modifier and nature of the solute on the performance of bonded silica reversed-phase columns for the analysis of strongly basic compounds by high-performance liquid chromatography. *Journal of Chromatography A* 738: 169–179.
- Nawrocki J (1997) The silanol group and its role in liquid chromatography. *Journal of Chromatography A* 779: 29–71.
- Snyder LR, Kirkland JJ and Glajch JL (1997) *Practical HPLC Method Development*, 2nd edn. New York: John Wiley & Sons.
- Vervoort RJM, Maris FA and Hindriks H (1992) Comparison of high-performance liquid chromatographic methods for the analysis of basic drugs. *Journal of Chromatography* 623: 207–220.

Capillary Electrophoresis

K. D. Altria and S. M. Bryant, GlaxoWellcome Research Centre, Hertfordshire, UK

Copyright © 2000 Academic Press

Introduction

In recent years the analysis of pharmaceuticals has been predominantly performed by high performance liquid chromatography (HPLC), which offers a number of advantages over other alternative techniques. These advantages include automated and precise sample injection devices, sensitive detection and high capacity autosamplers. HPLC is supported by other techniques such as thin-layer chromatography (TLC) and gas chromatography (GC). In the late 1980s a further technique, that of capillary electrophoresis (CE), became recognized as a viable alternative and complementary technique to HPLC. Modern CE instruments offer some of the same features as HPLC in terms of automation and autosampler capacity, although precision and sensitivity are not as good.

The wide range of application areas for CE within pharmaceutical analysis mirror well those of HPLC. These areas include the determination of drug-related impurities, chiral separations, main peak assay, stoichiometric determinations and the analysis of vitamins. The majority of pharmaceuticals are synthetic organic molecules that are well suited to analysis by HPLC or CE. There is an increasing move in pharmaceutical companies to the development of new pharmaceuticals that are based on biomolecules such as peptides and DNA. Traditionally these biomolecules have been analysed using electrophoretic techniques; for this reason CE has been widely applied to the analysis of biomolecule pharmaceuticals.

One of the attractive features of CE is that method development can be relatively simple for uncomplicated separations of ionizable pharmaceuticals. For example the majority of pharmaceuticals are basic drug salts. Use of a low pH electrolyte causes these basic drugs to protonate and become cations, and thus allows separation by CE. There are also a number of drugs with acidic functionalities that can

be separated by CE as anions using high-pH electrolytes. Neutral solutes require the use of micellar electrokinetic chromatography (MEKC) methods. Water-insoluble drugs can be separated in CE using traditional aqueous-based electrolytes but there is an increasing tendency towards the use of nonaqueous solvent systems in CE. The ease of method development is also a key feature in the use of CE for chiral separations, as a range of chiral additives can be quickly and effectively assessed in automated unattended injection sequences.

The use of indirect UV detection for the detection of small inorganic and/or organic cations and anions is widespread. These applications include determination of metal ion contents and inorganic anions such as sulfate and chloride. Traditionally determination of these species is performed by ion exchange chromatography but CE offers specific advantages in terms of ease of operation and reduced time and cost of consumables.

In this article the various application areas of CE in drug analysis are covered with some illustrative examples of reported applications. The discussion also includes some details regarding the analytical performance levels described for these analyses.

Determination of Drug-related Impurities

Capillary electrophoresis is increasingly being viewed as an alternative, complementary technique to HPLC for the determination of drug-related impurities. A number of applications have been reported, many with detection of the impurities at the 0.1% level or lower. Often low UV wavelengths (190–200 nm) are used to improve the detection limits obtained. The ability of CE to give a different selectivity to HPLC and/or TLC provides a further means to characterize the impurity content and profiles in drugs.

The separation of structurally similar drug-related impurities is difficult as the drugs and the related impurities often have very similar electrophoretic mobilities. Therefore the separation conditions must be optimized to enable a good resolution to be obtained, especially as low detection limits are generally required for the related impurities in the presence of a large drug peak. The pH of the separation is the most important optimization factor for separation of ionic species. However, the concentration and type of surfactant used is the most important factor for resolution of neutral and/or charged species by MEKC. Other factors that can be optimized in method development include the addition of ion-pair reagents and cyclodextrin and the ionic strength and type of electrolyte. These factors influence the shape of the main

peak and appropriate optimization may allow resolution of a closely exiting impurity. For instance, various types and concentrations of ion-pair reagent have been employed in conjunction with cyclodextrin in the optimization of the separation of remoxipride and related impurities. **Figure 1** shows the separation achieved of remoxipride and eight related impurities using a relatively complicated pH 3 phosphate buffer which contained 40 mM hydroxypropyl beta cyclodextrin and 20 mM tetrabutylammonium bromide.

Many examples of the use of CE for the analysis of drug-related impurities have been published that have shown CE to be a useful complementary technique to support HPLC. These methods have been validated and are in routine use in many pharmaceutical companies. These include a CE method that has been used to monitor the stability of a cephalosporin in solution. Validation included specificity, linearity and repeatability by different analysts on different days. Migration time precision was less than 1% RSD (relative standard deviation). Injections were performed from sample solutions every 30 min to monitor the solution stability online. The cephalosporin (Roche compound RO 23-9424) was found to be twice as stable in an L-arginine/sodium benzoate/saline solution than when prepared in water.

Chiral Separations

Undoubtedly the most frequently used selectors in free solution CE are cyclodextrins (CDs). Other possibilities include crown ethers, carbohydrates, proteins and chiral antibiotics. The majority of pharmaceutical applications have involved the use of CDs. The most widely used approaches in MEKC are mixtures of sodium dodecyl sulfate (SDS) and CDs or bile salts, which are naturally occurring chiral surfactants.

There have been many quantitative applications of CE to the separation of drug enantiomers and these have included several reports of the validation of these methods. Method validation for chiral CE methods is similar to that undertaken for validation of an HPLC method. In the validation of a CE method, aspects such as the precision of injection, detection limits, and method repeatability on different capillaries using different operators and reagents are important. As in other separative techniques, comigration of related impurities with either of the enantiomer peaks is possible. Therefore it is necessary to establish the migration position of all available related substances in method selectivity studies. This procedure has been performed in a number of chiral CE methods including the chiral separation of a cholesterol-lowering agent (**Figure 2**). The ability of the

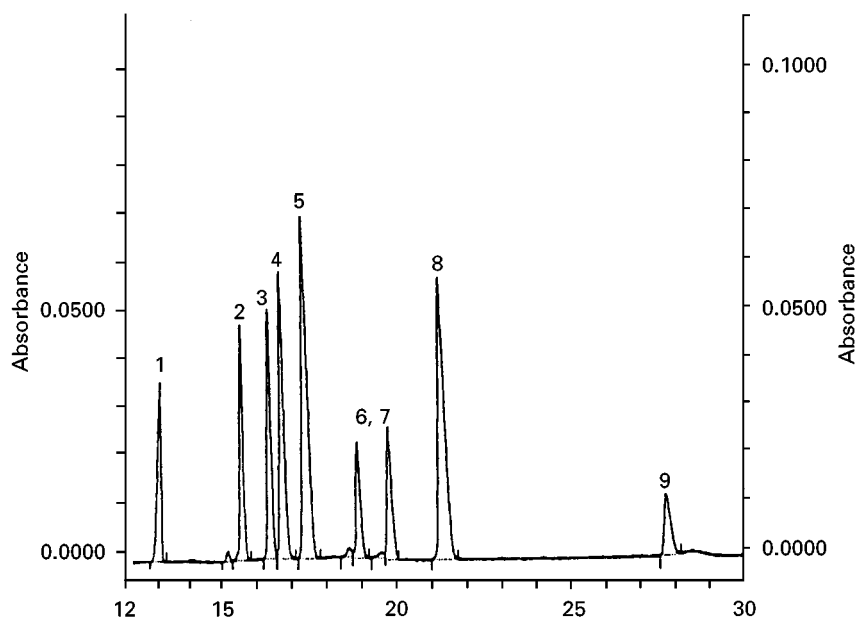


Figure 1 Effect on resolution of remoxipride analogues by variation of the tetrabutylammonium ion (TBA^+) concentration (0.1 mmol L^{-1}) in the presence of hydroxypropyl- β -cyclodextrin (HP- β -CD; 40 mmol L^{-1}) using a phosphate buffer at pH 3.0. The TBA^+ concentrations were (A) 10 mmol L^{-1} and (B) 20 mmol L^{-1} . The peaks are: 1, FLA 708; 2, FLA 739; 3, FLA 83; 4, FLB 526; 5, FLA 731 (remoxipride); 6, NCR 513; 8 = FLA 740; and 9, FLA 797 (x -scale in min). (Reproduced from Stalberg O, Brotell H and Westerlund D (1995) *Chromatographia* 40: 697–704, with permission from Elsevier Science.)

method to quantify accurately the enantiomeric impurity is also an important part of method validation and is often demonstrated by recovery experiments in which accurately known amounts of the impurity are spiked into standards of reference material. **Table 1** shows recovery data obtained during validation of a method for enantio-purity determination of a cholesterol-lowering drug.

Main Component Assay

The use of CE for main component assay is possible as commercially available instruments offer a high degree of automation and are capable of unattended injection sequences by use of PC-controlled autosamplers. The injection precision demands in many pharmaceutical companies is stringent for separative

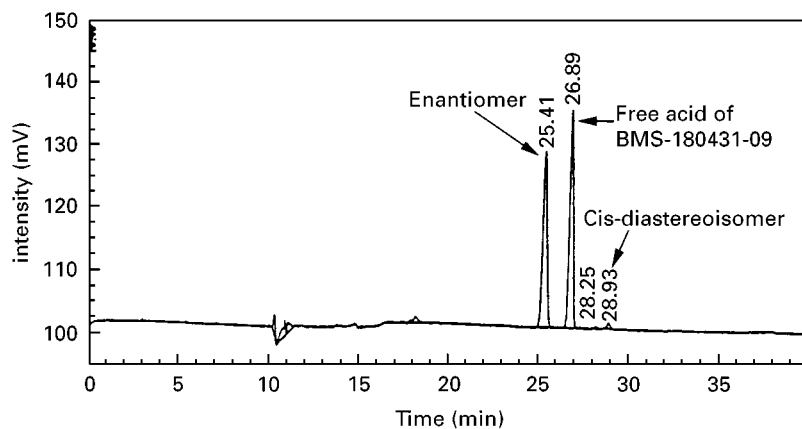


Figure 2 CD-MEKC of a racemic mixture of BMS-180431-09 with some trace *cis*-diastereoisomer added. Conditions: 0.01 mol L^{-1} ($1.5 \text{ g per } 100 \text{ mL}$) hydroxypropyl- β -cyclodextrin, 0.1 mol L^{-1} sodium borate, 0.03 mol L^{-1} SDS, pH 9.3, 20 kV, current $\sim 65 \mu\text{A}$, 50 cm effective capillary length, $50 \mu\text{m}$ capillary width, UV adsorption detection at 200 nm; sample was 0.3 mg mL^{-1} in water. (Reproduced with kind permission from Noroski JE, Mayo DJ and Moran M (1995) *Journal of Pharmaceutical and Biomedical Analysis* 13: 45–52.)

Table 1 Percentage recovery of enantiomer added to BMS-180431-09

Spike (% w/w)	Found	Recovery
0.36	0.37	102.7
0.65	0.65	100.5
0.80	0.84	104.6
1.10	1.11	100.9

Reproduced from Noroski JE, Mayo DJ and Moran M (1995) *Journal of Pharmaceutical and Biomedical Analysis* 13: 45–52, with permission from Elsevier Science.

techniques such as HPLC and CE and figures such as 1–1.5% RSD are common practice. This can be routinely obtained by HPLC but this is not always the case for CE as the injection volumes are very small (1–20 nL) and can be variable. The use of internal standards to eliminate injection volume-related errors can dramatically improve the precision in CE and allow the required precision requirements to be achieved. For example internal standards were used in the validation of a simple pH 2.5, 25 mmol L⁻¹ phosphate buffer for assay of a wide range of basic drugs. The method was shown to have good sensitivity, linearity (correlations > 0.999) with RSD values of 0.3–2.0% for peak area ratios. The robustness of the method to deviations in the method settings was satisfactorily assessed using an experimental design. Shelf-lives of electrolyte and sample solutions were assessed (3 months and 14 days, respectively). Good precision was obtained using either aminobenzoic acid or imidazole as the internal standard. Good agreement between CE data and the label claim for tablets was obtained (Table 2).

An MEKC method was successfully validated according to US Pharmacopoeia guidelines for analysis of hydrochlorothiazide and chlorothiazide. The

method involved use of a 20 mmol L⁻¹ borate buffer containing 30 mmol L⁻¹ SDS. A 100 µm capillary was employed to give large peak areas in order to minimize integration-related errors. Careful control of the method settings such as injection time, temperature and sample concentration enabled values below 1% RSD to be routinely obtained with no internal standard. Recoveries ranged from 99.5–100.6% absorbance unit full scale (AUFS) for hydrochlorothiazide over the range 50–150% of target concentration. Detector linearities were greater than 0.998. Analyses were successfully repeated on different days by different analysts using different capillaries to demonstrate robustness.

Stoichiometric Determinations by CE

During development of a new drug, a range of different salts may be synthesized to compare pharmaceutical properties such as solubility, stability and crystallinity. The ratio of the drug to counterion is known as the drug stoichiometry and this needs to be characterized analytically. The typical stoichiometry is a 1 : 1 drug : counterion mixture; however, 2 : 1 and 1 : 2 compositions are frequently manufactured, depending upon the ionic nature of the drug and/or counterion. There is a clear analytical need to quantify drug : counterion levels to demonstrate that the correct salt version has been manufactured and that the required stoichiometry can be reliably achieved batch-to-batch when the final drug salt has been selected.

The counterion of basic drugs include inorganic ions such as sulfate and chloride or organic ions such as maleate, fumarate, acetate or succinate. Cations analysed involve a range of metal ions including Na⁺, K⁺, Mg²⁺, Ca²⁺ and simple low molecular weight amines. Since these analytes possess little or no chromophore, indirect UV detection is generally necessary. However, some larger anionic counterions such as benzoates and simple organic acids can possess sufficient UV absorption to allow direct UV detection. Alternatively, metal ions may be complexed on-capillary to form metal chelates, which can then be detected by direct UV measurement.

The quantitative aspects of a CE method for the determination of calcium in calcium acamprosate has been validated. Standard solutions of calcium carbonate and test solutions of calcium acamprosate containing 100 ppm of Ca²⁺ and Mg²⁺ (internal standard) were determined by indirect detection at 214 nm. Table 3 shows the determination of calcium in calcium acamprosate and the results compare favourably with the theoretical content.

Table 2 Assay results by CE for tablets and drug substance

<i>Label claim</i>	<i>Analysis</i>	
Lamiduvine content (mg per table)		
150	HPLC	152.2
	CE	155.6
100	CE	104.0
Histamine acid content (% w/w)		
	CE	
	Sample 1	100.3, 100.2
	Sample 2	100.8, 100.7
	Average	100.5

Reproduced from Altria KD, Frake P, Gill I *et al.* (1995) *Journal of Pharmaceutical and Biomedical Analysis* 13: 951–957, with permission from Elsevier Science.

Table 3 Comparison of CE and titration results for the calcium content in calcium acamprosate drug substance

Batch	Theoretical content	CZE	EDTA titration
C110	10.01% m/m	10.01% m/m (10.00, 10.04)	9.98% mass/mass
OTA 37	10.01% m/m	9.98% m/m (9.96, 10.01)	10.08% mass/mass

CZE, capillary zone electrophoresis; EDTA, ethylene diamine-tetracetic acid; % m/m. Reproduced from Fabre H, Blanchin MD, Julien E *et al.* (1997) *Journal of Chromatography A* 772: 265–269, with permission from Elsevier Science.

Levels of chloride and sulfate have been determined using electrolyte containing chromate and tetradecyltrimethylammonium bromide (TTAB). Sample solutions were prepared to give 100 ppm of chloride as sulfate as appropriate. AnalaR grade salts such as NaCl were used as reference standards. **Table 4** shows the good agreement between the average CE results, microanalysis data and the theoretical content. Peak areas were used to calculate % w/w in samples of three different drug substances. Improved data for injection have been obtained using an internal standard. A detection limit of $0.5 \mu\text{g mL}^{-1}$ was reported for standard anions.

Separation and detection of a range of organic acids is possible using phthalate as the background absorber (Figure 3). The method has been validated for the quantitation of both succinate and maleate content in drug substance batches.

Vitamin Analysis

The majority of vitamin determinations are currently performed by HPLC with UV detection. These HPLC methods involve gradient elution and often extensive

Table 4 Comparison of CE and microanalysis/theoretical results for chloride and sulfate content

Batch		Theoretical concentration	Microanalysis	CE results
Chloride (% w/w)				
GRD1	A	8.0	–	8.0, 7.9
GRD2	A	9.6	9.5	9.3, 9.3
	B	9.6	9.6	9.4, 9.4
	C	9.6	9.5	9.2, 9.7
	D	9.6	9.4	9.9, 9.6
	E	9.6	9.5	9.3, 9.5
Sulfate (% w/w)				
GRD3	A day 1	16.6		16.7
	A day 2	16.6		16.8

GRD, Glaxo Research and Development. Reproduced with kind permission from Altria KD, Goodall DM and Rogan MM (1994) *Chromatographia* 38: 637–642.

sample work-up prior to analysis to remove matrix interferences. The majority of vitamins are water-soluble acidic compounds and can be readily determined by free solution CE using high pH electrolytes. Water-insoluble and neutral vitamins require the use of MEKC. Many of the vitamins are acids or contain groups that ionize at high pH and therefore borate or phosphate buffers in the pH range 7–9 have been used extensively.

The CE and MEKC methods have been compared with the USP HPLC method to determine various B group vitamins in capsules, tablets and syrups. **Table 5** shows the data obtained by the three techniques to be equivalent. The use of an internal standard (paracetamol) improved the CE and MEKC precision from 7–10% RSD to 1%. Accuracy and repeatability of the MEKC method was demonstrated by spiking appropriate levels of the vitamins into artificially prepared mixtures of the tablet excipients.

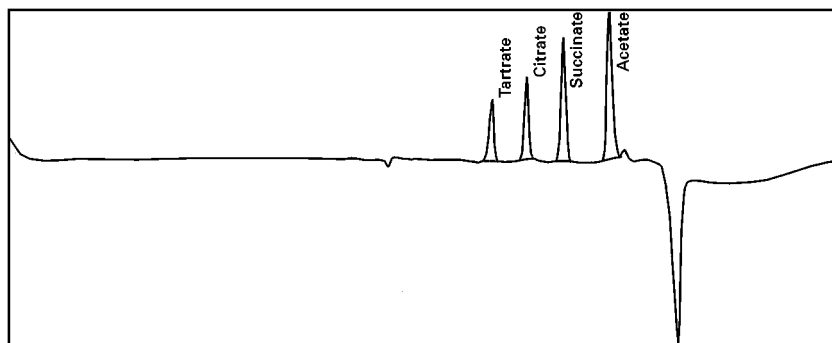


Figure 3 Separation of a selection of organic acids using phthalate as the background absorber. Separation conditions: fused silica capillary $27 \text{ cm} \times 75 \mu\text{m}$; buffer, 50 mmol L^{-1} , 4-morpholineethanesulfonic acid (Mes), 0.5 mmol L^{-1} TTAB and 5 mmol L^{-1} phthalate adjusted to pH 5.2; voltage -3.0 kV ; wavelength 254 nm indirect detection (detector signal reversed); temperature 30°C . (Reproduced with kind permission from Altria KD, Assi KH, Bryant SM and Clark BJ (1997) *Chromatographia* 44: 367–371.)

Table 5 Cross-validation of vitamin assay results by CE, MEKC and HPLC

Sample	Analyte	Results as % label claim		
		CE	MEKC	HPLC
Tablet	B ₁ (15 mg)	118.7 ± 1.7	123.6 ± 2.6	123.8 ± 3.6
	PP (50 mg)	110.8 ± 3.1	108.0 ± 1.2	108.7 ± 2.1
	B ₂ (15 mg)	99.0 ± 2.2	99.4 ± 2.1	103.9 ± 0.7
	B ₆ (10 mg)	110.9 ± 3.3	113.7 ± 1.7	112.4 ± 3.2
Syrup (5 mL)	B ₁ (10 mg)	117.2 ± 4.0	112.4 ± 1.3	111.6 ± 1.6
	PP (20 mg)	111.2 ± 1.4	109.4 ± 0.9	111.5 ± 3.4
	B ₂ (1 mg)	115.4 ± 1.5	119.3 ± 2.9	117.2 ± 2.2
	B ₆ (5 mg)	109.9 ± 1.4	106.2 ± 3.1	113.2 ± 3.9
Soft capsule	B ₁ (10 mg)	122.0 ± 2.2	126.6 ± 1.7	n/a
	PP (30 mg)	111.3 ± 1.8	108.6 ± 1.7	n/a
	B ₂ (7 mg)	112.1 ± 3.1	114.9 ± 1.6	n/a
	B ₆ (5 mg)	108.6 ± 1.8	108.2 ± 1.6	n/a

n/a, not analysed. Reproduced with permission from Boonkerd S, Detaevernier MR and Michotte Y (1994) *Journal of Chromatography A* 670: 209–214.

Six replicate samples were analysed on each of four separate days and acceptable data were obtained for average recovery and precision from the pooled assay results.

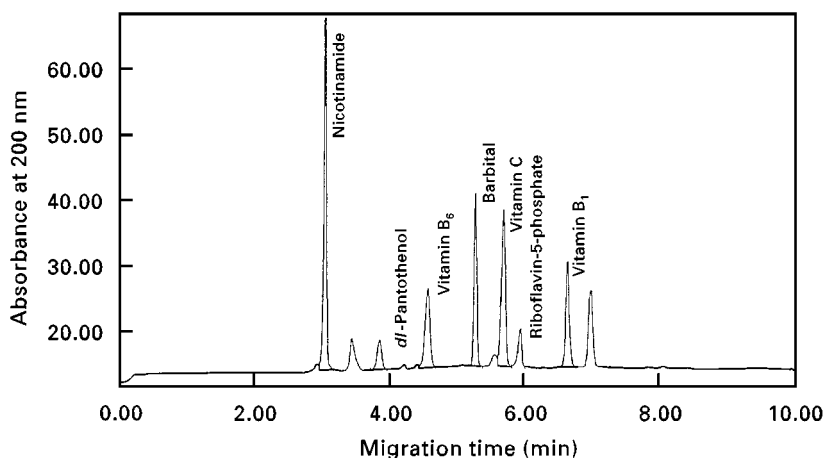
Figure 4 shows the separation of a range of common vitamins in a pharmaceutical preparation. The components are separated using a micellar electrolyte containing the surfactant SDS with acetonitrile and cyclodextrin modifiers. Detection is at 200 nm.

Levels of vitamins B₁, B₃, B₆, B₂, and C in injection solutions have been determined using an MEKC method with ethylaminobenzoate as an internal standard to give RSD values for precision of less than 2%. Agreement with label claims ranged from 98.8% to 104% for the five components.

Regulatory Aspects

The acceptance of CE methods by regulatory authorities has been highlighted in a confidential survey of a number of major UK and US pharmaceutical companies. All CE methods submitted had been accepted without technical query. The companies surveyed indicated that they had no reluctance to submit appropriate CE data in submissions. The survey was conducted in mid 1994 and the number of submitted methods has certainly increased since then. For example, a stability indicating MEKC method for the analysis of BMS-188484 has been successfully included in a regulatory submission from Bristol-Myers-Squibb.

Pharmacopoeia have also recognized the advancing application of CE within pharmaceutical companies

**Figure 4** Separation of a range of vitamins.

and a draft USP general chapter on CE has been published (*Pharm Forum* 1996) in anticipation of future monographs containing CE analytical methods.

Conclusions

The use of CE in the analysis of pharmaceuticals is now becoming firmly established as a useful complement and alternative to the more widely employed technique of HPLC. The major attractions of CE are that considerable cost and time savings are possible, especially in the areas of chiral analysis and in the determination of solutes having limited or no chromophore. The recent advent of the use of nonaqueous solvents in CE should extend further the application range of the technique. Routine CE methods have been established in many industrial laboratories and CE methods have been successfully submitted to regulatory authorities.

Further Reading

- Altria KD (1997) In: *Analysis of Pharmaceutical by Capillary Electrophoresis*. Weisbaden: Vieweg Press.
 Altria KD (1998) *PharmEurope* 10: 524–526.
 Altria KD, Frake P, Gill I *et al.* (1995) Validated capillary electrophoresis method for the assay of a range of basic

- drugs and excipients. *Journal of Pharmaceutical and Biomedical Analysis* 13: 951–957.
 Boonkerd S, Detaevernier MR and Michotte Y (1994) Use of capillary electrophoresis for the determination of vitamins of the B group in pharmaceutical preparations. *Journal of Chromatography A* 670: 209–214.
 Bretnall AE, Hodgkinson MM and Clarke GS (1997) Micellar electrokinetic chromatography stability indicating assay and content uniformity determination for a cholesterol-lowering drug product. *Journal of Pharmaceutical and Biomedical Analysis* 15: 1071–1075.
 Fujiwara S, Iwase S and Honda S (1998) Analysis of water-soluble vitamins by micellar electrokinetic capillary chromatography. *Journal of Chromatography* 447: 133–140.
 Nickerson B, Cunningham B and Scypinski S (1995) The use of capillary electrophoresis to monitor the stability of a dual-action cephalosporin in solution. *Journal of Pharmaceutical and Biomedical Analysis* 14: 73–83.
 Noroski JE, Mayo DJ and Moran M (1995) Determination of the enantiomer of a cholesterol-lowering drug by cyclodextrin-modified micellar electrokinetic chromatography. *Journal of Pharmaceutical and Biomedical Analysis* 13: 45–52.
 Thomas BR, Fang XG, Chen X, Tyrell RJ and Ghodbane S (1994) Validated micellar electrokinetic capillary chromatography method for quality control of the drug substances hydrochlorothiazide and chlorothiazide. *Journal of Chromatography* 657: 383–394.

Chiral Separations: Liquid Chromatography

W. J. Lough, University of Sunderland,
 Sunderland, UK

Copyright © 2000 Academic Press

Introduction

Between the mid-1980s and the mid-1990s great advances were made in the development of commercially-available methodologies for the separation of enantiomers. These developments were undoubtedly catalysed by the need to determine the enantiomer content of chiral drug substances, chiral drug products and samples of chiral drugs in biological fluids in the pharmaceutical research and development environment. It had long been recognized that, since it is possible to distinguish between enantiomers in a chiral environment, enantiomers might be expected to have different effects on the body which contains potential chiral 'selectors' such as proteins, peptides, carbohydrates and enzymes. The action of a drug on

the body or of the body on the drug involves many processes including the following:

- active transport
- plasma binding
- tissue binding
- receptor protein binding
- drug metabolism
- active secretion.

These and many of the other processes involve or may involve mediation by a protein or enzyme so that there is no shortage of opportunities for chiral discrimination to take place. As a consequence it is actually quite rare for enantiomers to have very similar pharmacological and toxicological properties. They must therefore be treated as if they were different drugs, and their use in combination in a drug product in a fixed 50 : 50 ratio as the racemate must be justified to the governmental regulatory bodies which issue licences to companies to produce and market drugs. Not only is this usually not justifiable,

but also when it is justifiable the burden of justification might be such that it is even conceivable that it might be more convenient to proceed with a single enantiomer in any case.

The classic case of thalidomide, developed as a non-addictive alternative to barbiturates, is frequently cited as an illustration of the extreme case, where the desired pharmacological activity resides in one enantiomer and the other enantiomer has all the undesirable toxic effects. This is in fact an oversimplification of the true situation and the emphasis on this one case does nothing to allude to the wide range of other possible cases that might arise. There is no doubting though that the thalidomide case served not only to highlight the potential problems inherent in developing racemic drugs but also it triggered off the greater awareness of drug safety that led to the extensive regulatory frameworks that today control the production and sale of pharmaceuticals. Just as there was a time lag before there was a readily available capability to resolve enantiomers, so there was a time lag before single enantiomer chiral synthetic drugs were being brought onto the market.

Application Areas

Many of the naturally-occurring chiral drugs and chiral drugs derived from naturally-occurring subunits contain multiple chiral centres. Penicillin antibiotics and steroids are cases in point. For such compounds it would be exceptional for there to be a need to determine the enantiomer of the drug as an impurity as this would involve inversion of the stereochemistry at all chiral centres. What is more likely to be an impurity is an epimer where there is inversion at one of the chiral centres only. Since the chiral drug and one of its epimers are diastereomers they may be separated by high performance liquid chromatography (HPLC) on an achiral column.

For a different reason a chiral separation is also not usually required for the drug substance of a chiral drug marketed as the racemate, a 50 : 50 mixture of the enantiomers. If there is no chiral intervention in the synthesis there would be little reason to suspect that anything other than a 50 : 50 mixture was present. Accordingly in pharmacopoeial monographs it is usually sufficient to establish for the drug substance that e.g. the optical rotation lies between $+0.15^\circ$ and -0.15° . Chiral LC would only be required if 'chiral switch' were being contemplated. This might happen if it was thought that a significantly better drug could be had by substituting a single enantiomer for the racemate in cases when the racemic drug had been developed and licensed before the significance of

chirality in drugs had been fully appreciated and before chiral resolution had become commonplace. The first step in the chiral switch decision making process, even before resolving, isolating and testing the individual enantiomers, would often be to study the fate of the individual enantiomers in the body following dosing with the racemate. It is therefore necessary to have a method capable of determining low levels of each enantiomer in biological fluids. To study the enantiomers in this way in the presence of the other enantiomer does not necessarily give a close approximation to the pharmacokinetics of the enantiomers when they are dosed on their own, but it does give an early indication as to whether there is a major difference in the way each enantiomer interacts with the body.

The main area in which enantiospecific LC methods are called for is in the research, development and production of synthetic single enantiomer drugs. This category mainly consists of drugs which arise directly from the selection of the most suitable enantiomer of a new chemical entity but will also include those which arise from a chiral switch. The actual applications of chiral LC which are important and most commonly carried out are described below.

Preparative Resolution of Individual Enantiomers

Clearly the individual enantiomers need to be isolated before they can be tested for their pharmacological action. This is very often done by semi-preparative LC since often only milligram quantities are needed. Preparative even up to Kg scale is an option for the actual production of a drug substance but most often a stereospecific synthetic route is more commercially viable.

Trace Enantiomer Determination in a Drug Substance

The trace enantiomer must be treated like any other related substance and therefore must be quantified down to levels of 0.1% w/w. This is usually carried out as a separate exercise from the determination of other related substances.

Chiral Drug Bioanalysis

As already indicated, a chiral method for the determination of enantiomers plays an important role in the decision on which enantiomer should be developed as a drug candidate. For a new chemical entity this will take place in the discovery phase of pharmaceutical research and development but a few studies might still be needed in early development to ensure that there is no interconversion between enantiomers taking place in the body.

There are a few other instances where a chiral assay might be needed but, for example, the determination of trace enantiomer in a formulated product would only be needed if it were known that it was a potential degradant.

Method Development

Now that the current scenario involves a strong preference for the development of single enantiomer drugs, the types of chiral analytical methods that are required has changed. However the first step in method development is as always to achieve chiral resolution. This has never been a matter of trial and error. By the late 1980s there was already a large number of chiral stationary phases (CSP) available for direct resolution by chiral LC. Despite this it was possible to group these together in classes by their mode of action and from this deduce which types of enantiomeric drugs might be separable using each class. For example, the acidic drug ibuprofen is highly protein bound in plasma and it is therefore no surprise that its enantiomers may be separated on a column containing an albumin CSP since albumin is the major binding plasma protein for acidic drugs. As CSP became more effective and more sophisticated by incorporating multiple modes of interaction, such simple predictions were no longer possible.

Fortunately there were 'intelligent' approaches that could be used to address this paradoxical situation. These are outlined below.

NMR Modelling

If splitting of the signals for the analyte is observed when its ^1H NMR spectrum in the presence of the chiral selector that is used in the chiral HPLC column is recorded, then if the solvent used in ^1H NMR is the same or similar to that which might be used in HPLC then it might be expected that chiral resolution will be observed in HPLC.

Molecular Modelling

The molecular orbitals involved in the transient diastereomeric complexes formed between the individual enantiomers and the chiral selector determine whether there is a large enough energy difference for the selector to be able to distinguish between the enantiomers at ambient temperature. While it is one thing to simulate selector approaching select and in a vacuum, it is an altogether more difficult matter to construct a meaningful simulation that incorporates mobile phase molecules, neighbouring chiral 'strands' on a CSP and the supporting stationary phase.

Databases

The most well known of these is *Chirbase*. Whether or not a separation will take place may be predicted by comparing with information on similar selector-selectand situations held on the database. This approach is reliant on the quality of the information held on the database and suffers from the weakness that it might be a subtle difference between the chiral drug being studied and a similar one described on the database that might be responsible for a quite marked difference in behaviour towards the chiral selector being considered.

Expert Systems

These systems are more versatile than databases in that they make decisions and learn from experience with each problem encountered. Again, each new problem might be subtly different from the one that has gone before and it might be this subtle difference that is critical with respect to which is the best chiral selector to use.

While these approaches have remained popular in academic circles, screening approaches have been more widely adopted in pharmaceutical research and development. This might typically involve the LC of the racemate being studied on three or four different chiral columns in a column-switching manifold, using a range of different mobile phases. Ideally in one overnight run the racemate would be analysed on each column using each of the mobile phases. The conditions which had shown the best resolution would then be identified by the computer controlling the system in order that they be further refined, if necessary, using mobile phase optimization so that by the morning the chiral method development would be complete. The increasingly widespread use of such screens may be attributed to the fact that the CSP used in them are now more effective to the extent that the screens are usually highly successful, with 'hit rates' for chiral resolution in the range 80–100% being quite common. Their acceptance in drug development in particular arises also because of the availability of highly automated instrumentation and the fact that in this environment, the purchase of a range of chiral LC columns which would generally be regarded as expensive is cost effective in the context of the benefit derived and the overall costs involved in pharmaceutical research and development. Modelling and database approaches have been overtaken because now it is just as quick to do the actual experiments.

Derivatized cellulose CSP with organic mobile phases usually play an important role in such screens. For example the use of ChiralCel OD, ChiralPak

AD, ChiralPak AS and the Whelk-O CSP with *n*-hexane-propan-2-ol (85 : 15, v/v) containing 0.5% triethylamine and *n*-hexane-propan-2-ol (85 : 15, v/v) containing 0.5% trifluoroacetic acid as the mobile phase is highly effective. Remarkable though the success rate of such a screen might be it would be the complete answer to all chiral method development problems, since it would not be ideal for giving optimum conditions for very polar compounds and would not be suitable in practice for samples presented as salts or as aqueous solutions. For these cases a screen using a cyclodextrin CSP and different macrocyclic antibiotic CSP with polar organic and aqueous-organic mobile phases would likely be more appropriate. Such a screen is often as effective as the type involving organic mobile phases and, for the polar organic mobile phase in particular, the final optimization can be quite simple.

Of course, achieving the chiral separation is not the end of the story. There are additional difficulties peculiar to each type of application.

Preparative Resolution of Individual Enantiomers

An additional difficulty in preparative resolution is the issue of time and money. Therefore as high as possible a sample load will be applied to the column. This leads to loss of efficiency and subsequent loss of resolution. Although loss of baseline resolution can be compensated for by collecting or 'shaving off' a leading part of the first peak and the second part of the second peak with the portion collected where the peaks overlap being recycled later, it is a general rule that it is better to start off with very high chiral resolution before commencing with scale-up.

The range of approaches to preparative chiral LC is dealt with elsewhere in this Encyclopedia. However the approach of choice will depend on the circumstances. In the 'drug discovery' phase of pharmaceutical research and development it will often be sufficient to obtain mg-quantities of each enantiomer for pharmacological testing or perhaps g-quantities if preliminary information on pharmacokinetics or toxicology is required before proceeding to early 'development'. Under these circumstances chemists are usually prepared to put up with the cost of using a semi-preparative (~7 mm i.d.) or preparative (16–22 mm i.d.) derivatized polysaccharide column, as this works out more economical than taking the time that might be needed to develop a 'cheaper' method.

The economics in a Pilot Plant or Production environment are entirely different. Conventional preparative chiral LC on scaled-up versions of analytical columns would be too expensive in terms not only of

money but also time (which of course is money!). In this scenario the simulated moving-bed approach to preparative work, in which the mobile phase is cycled round a closed system of connected preparative chiral columns and resolved enantiomers are periodically drawn from the system at set points, is becoming increasingly popular. However, old habits die hard and if organic chemists cannot devise a stereoselective synthesis they may then still revert to a fractional crystallization to isolate the large quantities of one enantiomer that are required.

Trace Enantiomer Determination in Drug Substance

As for preparative chiral LC, there are additional problems that need to be dealt with over and above simply achieving chiral resolution. Generally it will be necessary to be able to determine down to 0.1% of the trace unwanted enantiomer in the bulk drug substance. Since peaks in HPLC are more often than not slightly asymmetric with a degree of peak tailing, this determination of enantiomeric impurity is more difficult when the impurity peak elutes after the main peak. As with the problem with scale-up in preparative chiral LC, one approach is to attempt to obtain a separation that is significantly better than baseline resolution. In this way the impurity peak is well clear of the tail of the main peak with the result that its area may be more accurately integrated. An alternative approach is to use the chiral stationary phase or chiral mobile phase based on the antepode of the chiral selector enantiomer used initially. Under these circumstances the enantiomeric impurity peak will elute first and will be much easier to determine. Switching the chirality of the selector in this way may be carried out for small molecule chiral selectors such as ligand-exchange, synthetic multiple interaction or Pirkle-type, ion-pair and crown ether selectors. However it is a weakness of the broader spectrum chiral selectors based on larger molecules, e.g. proteins, cyclodextrins, derivatized polysaccharides and macrocyclic antibiotics, that such a simple reversal of retention order is not possible.

Another difficulty is that the enantiomeric impurity must also be resolved from other structurally-related impurities. In general this is possible but it is more difficult to separate all structurally-related impurities from one another with a method using a chiral stationary phase or mobile phase additive. It is for this reason, and the fact that it is not prudent to use expensive chiral stationary phases more than is absolutely necessary, that the determination of trace enantiomeric impurity is almost always performed as a separate test.

Chiral Drug Bioanalysis

The difficulties over and above that of achieving a chiral separation are much more apparent for chiral drug bioanalysis than for the other two application areas that have been discussed. In any determination of drugs in biological fluids, problems arise because the levels of drug are invariably low and the matrix is invariably complex. Often also, for example in clinical trials to assess the safety and efficacy of a drug on patients, sample numbers may be very high. However this latter issue does not normally apply to chiral drug bioanalysis since, as has already been indicated, a method which is not stereoselective may be used if it can be shown in early development that the drug does not racemize or invert to its opposite enantiomer when in the body. Accordingly, some of the complex, automated methods involving column switching mooted in the early days of chiral drug bioanalysis when there were still many racemic drugs in the development phase are no longer appropriate. What is needed is simple methods that don't take too long to develop. As it is not sensible to load 'dirty' samples from biological fluids onto expensive chiral columns, the most common approach is to use extensive sample pre-treatment. This would involve concentration as well as clean-up so that the levels of drug loaded onto the column would be well above the limit of quantitation.

While the use of chemical derivatization is another approach that may be adopted to ensure that the chiral drug and its enantiomer, if present, are easily detected, chiral derivatization followed by achiral LC is an approach that needs to be used with caution. There is now greater awareness of potential difficulties such as racemization during the derivatization reaction, kinetic resolution caused by different reaction rates for the enantiomers and differing detector responses for the diastereomeric products. Apart from the racemization issue and the fact that an extra step is involved in the analytical procedure, there are no such drawbacks when achiral derivatization is used followed by chiral LC. Further, when the derivatizing agent contains a π -electron rich aromatic ring system and the chiral stationary phase used is a synthetic multiple interaction or Pirkle-type containing a π -electron deficient aromatic ring system in the chiral selector, then very good chiral resolution as well as easy detectability may be anticipated.

A more recent approach to chiral drug bioanalysis that fulfils all the requirements is the use of solid phase extraction (SPE) followed by direct injection of a large volume of the SPE eluate onto a microbore LC containing the porous graphitic packing material Hy-

percarb^R with a mobile phase containing a chiral mobile phase additive. Low limits of quantitation are ensured by the focussing effect that takes place because the eluate from a C-18 or phenyl-SPE cartridge is less strongly eluting than the mobile phase in the microbore LC column. Hypercarb^R is used because it is both highly retentive, thereby requiring a mobile phase that is more strongly eluting than that required to elute the analyte from the C-18 or phenyl-SPE cartridge, and is a very effective achiral support for use in methods that use a chiral mobile phase additive. The latter property is also at least in part due to its high retentivity.

Future Perspectives

Chiral LC of drugs is one of the scientific success stories of the late 20th century. It is now a mature area of research even although it only really began in the 1980s. While it would be useful to have more economical preparative chiral LC methods and to be able to determine enantiomeric and other structurally-related impurities simultaneously, it has to be said that these are not critical needs and that the major advances have almost certainly already taken place.

See also: III/Chiral Separations: Chiral Derivatization; Liquid Chromatography.

Further Reading

- Ahuja S (ed.) (1997) *Chiral Separations; Applications and Technology*. American Chemical Society.
- Ariens EJ, Wuis EW and Veringa EJ (eds) (1988) Stereoselectivity and bioactive xenobiotics. A pre-Pasteur attitude in medicinal chemistry, pharmacokinetics and clinical pharmacology. *Biochemical Pharmacology* 37: 9–18.
- Booth TD, Lough WJ, Saeed M, Noctor TAG and Wainer IW (1997) An investigation into the enantiospecific recognition mechanisms operating on three amylose-based stationary phase: effects of backbone and carbamate side chain chiralities. *Chirality* 9: 173–177.
- Laganier S (1997) Current regulatory guidelines of stereoisomeric drugs: North American, European and Japanese points of view. In: *The Impact of Stereochemistry on Drug Development and Use*, pp. 545–565.
- Lough WJ (ed.) (1989) *Chiral Liquid Chromatography*. Blackie Publishing Group.
- Lough WJ (1998) Chiral resolution for pharmaceutical R & D – beyond the final frontiers? *European Pharmacology Review* 3: 48–55.
- Lough WJ and Noctor TAG (1994) Multi-column LC approaches to chiral bioanalysis. In: Riley CM, Wainer IW and Lough WJ (eds) *Biomedical and Pharmaceutical*

- Applications of Liquid Chromatography*, pp. 241–257. Oxford: Pergamon Press.
- Millership JS and Fitzpatrick A (1993) Commonly used chiral drugs: a survey. *Chirality* 5: 573–576.
- Prangle AS, Hughes S, Noctor TAG and Lough WJ (1998) Chiral drug bioanalysis with on-column sample-focus-
ing. *Journal of Pharmaceuticals and Pharmacology* 50, 93.
- Prangle AS, Noctor TAG and Lough WJ (1998) Chiral bioanalysis of warfarin using microbore LC with peak compression. *Journal of Pharmacology and Biomedical Analysis* 16: 1205–1212.

Chromatographic Separations

J. Vessman, AstraZeneca R&D Mölndal, Mölndal, Sweden

This article is reproduced from *Encyclopedia of Analytical Science*, Copyright © 1995 Academic Press

Overview

Pharmaceutical analysis is traditionally defined as analytical chemistry dealing with drugs both as bulk drug substances and as pharmaceutical products (formulations). However, in academia, as well as in the pharmaceutical industry, other branches of analytical chemistry are also involved, viz. bioanalytical chemistry, drug metabolism studies and analytical biotechnology. The development of drugs in the pharmaceutical industry is a long-term process, often taking more than a decade from the start of a research project to the appearance of a drug on the market. That process involves several decision points, such as the choice of the candidate drug after the preclinical screening phase, the investigational new drug (IND) application before testing the compound for the first time in man, and finally the new drug application (NDA) which summarizes the data obtained from all the studies needed for marketing approval of the drug as a medicine. In all these steps, especially the IND and NDA, the amount of data generated is enormous. Analytical chemists take part in many of the studies that constitute this documentation. Substance quality and its specifications are based on substance analysis, and that knowledge is later used for quality control during full-scale production. Product analysis involves dealing with the various formulations and starts after the IND has been approved. The results from such work lead to specifications that form the basis for the quality control of the product. For both substances and formulations there is an increasing interest in the introduction of process analytical chemistry.

Biomolecules, i.e. macromolecules such as proteins or hormones, either produced by isolation from biological sources or by means of biotechnology, must also be subjected to careful analytical control. Thus

whilst the analytical tasks required for biomolecules are somewhat different from those of ordinary pharmaceuticals when it comes to regulation and documentation of their quality and properties they definitely belong to the same group.

There are a number of regulations that have to be followed in the development of pharmaceuticals as well as in their production. Regulatory approval is required prior to the IND and before marketing is licensed (NDA). Today clinical trials also undergo scrutiny by the authorities.

An important part of the development process is safety evaluation, primarily the toxicology tests, which run from 6 to 24 months in different species. During this time bioanalytical studies are performed as well as control of the formulations used in the tests. After approval for marketing, the authorities exercise control of products on the market and require post production stability data. Public interest in the quality of drugs is also reflected in the compilation of substance monographs in compendia that are known as pharmacopoeias. In addition to collections of substance monographs these pharmacopoeias contain general analytical methods and some also contain monographic requirements on the formulation of the substances.

This article provides an overview of mainly substance and product analysis (traditional pharmaceutical analysis), as used in the pharmaceutical industry. The support of other branches of analytical chemistry will be mentioned.

Bulk Drug and Pharmaceutical Products

Common Features

Identity testing Identity testing is used to verify that the drug substance is what it is stated to be or that the formulation contains the correct compounds. Infrared (IR) spectra are used quite extensively in industry, whereas the pharmacopoeias often have a set of alternative tests. These can be colour reactions, melting point of a compound or derivative, optical

rotation values or ultraviolet (UV) spectral data such as maximum wavelength and absorptivity. Today chromatographic data are also used to support identity tests.

Impurities Impurities or degradates require separation methods and are usually studied at the level from 0.1–2% (purity patterns) or 0.1–5% (stability profiles). This means that the analytes have to be quantified in up to a 1000-fold excess of the major compound. In practice qualitative work is performed at still lower levels. This sometimes creates problems in the chromatographic methods as minute amounts of related substances may be hidden under the peak of the drug itself. This is the background for the interest in peak purity tests. With the advent of diode-array detection in liquid chromatography (LC) compounds with different chromophores may be differentiated, either through spectral comparison or by absorbance ratioing at selected wavelengths. However, a peak impurity present at below 1% may be difficult to detect. The use of mass spectral data for the verification of peak purity is still better and has been practised in gas chromatography–mass spectrometry (GC-MS). However, peak purity tests are inferior to the use of complementary separation systems.

Selected analytes Selected analytes sometimes have to be analysed at ppm levels. Typical examples are aromatic amines, nitrosamines, reactive intermediates left from the synthesis, or certain solvent residues, i.e. all components that are known to be noxious and thus must be controlled separately.

Compendial analysis Pharmacopoeias are the official collections of drug standards. They all include requirements for drug substances but only a few have monographs for products (formulations). Harmonization efforts between the compendia for the three big markets, Europe, Japan and the US, have recently been started. There is an agreement now that the major pharmacopoeias are in principle intended for the pharmaceutical industry and the authorities and not for community pharmacies.

Bulk Drug Analysis

Physicochemical characterization Physicochemical characterization yields a number of important parameters that can be used in the control of the quality of a substance. Typical properties are melting point and other thermal data, acid-base behaviour with pK_a values, redox potentials, polymorphism, solubility and spectral information.

Purity tests Purity tests are in particular focused on related substances such as homologues, analogues, by-products from the synthesis or degradates. Enantiomeric purity has been a more common test since the early 1980s. Chromatography has revolutionized our ability to determine substance purity and is currently the most important check, giving essentially the finger-print of a synthesis. An example of a separation of some potential impurities that have been added to a metoprolol sample is given in **Figure 1**. For qualitative studies LC-MS is beginning to establish its role as the primary on-line analytical tool for the elucidation of unknown structures among the impurities. From a toxicological point of view the impurity profile of the substance batch used in safety studies should form a reference for the full-scale production material. This means that in later batches impurities in amounts that deviate from those found in the batches used for toxicology should be avoided. The high standard and good reproducibility required of the purity profile is clearly evident from that perspective. There are some other tests that also contribute to the general impression of the quality of a substance, i.e. tests for protolytic impurities, content of chloride, sulfated ash or residue upon ignition that gives the inorganic content. These tests reflect the performance of the purification process in general, but their importance will probably diminish in the future. For inorganic ionic analytes the older methods can be replaced by ion chromatography.

Heavy metals and arsenic Heavy metals are routinely determined, often with one or other form of sulfide precipitation. These tests are performed from the viewpoint of safety and the general limits ($1\text{--}30\text{ }\mu\text{g mL}^{-1}$ (g^{-1})) are now more often related to the dose. For metals such as mercury, lead, cadmium or nickel, atomic absorption spectrometry or other instrumental methods are often prescribed. Copper and other transition metals can act as catalysts in certain degradation reactions and thus require special attention. Surprisingly, arsenic tests that were important at the beginning of this century are still considered necessary.

Potency assay Common for all bulk drugs is an assay of potency. This can be an aqueous or nonaqueous titration based on protolytic properties or on some other property. Many compounds lack functional groups suitable for titration and here chromatographic methods (LC in particular) are often used. However, titrations are preferable as their precision is, in general, superior.

Biomolecules Biomolecules such as proteins represent a special type of bulk drug. Depending on the

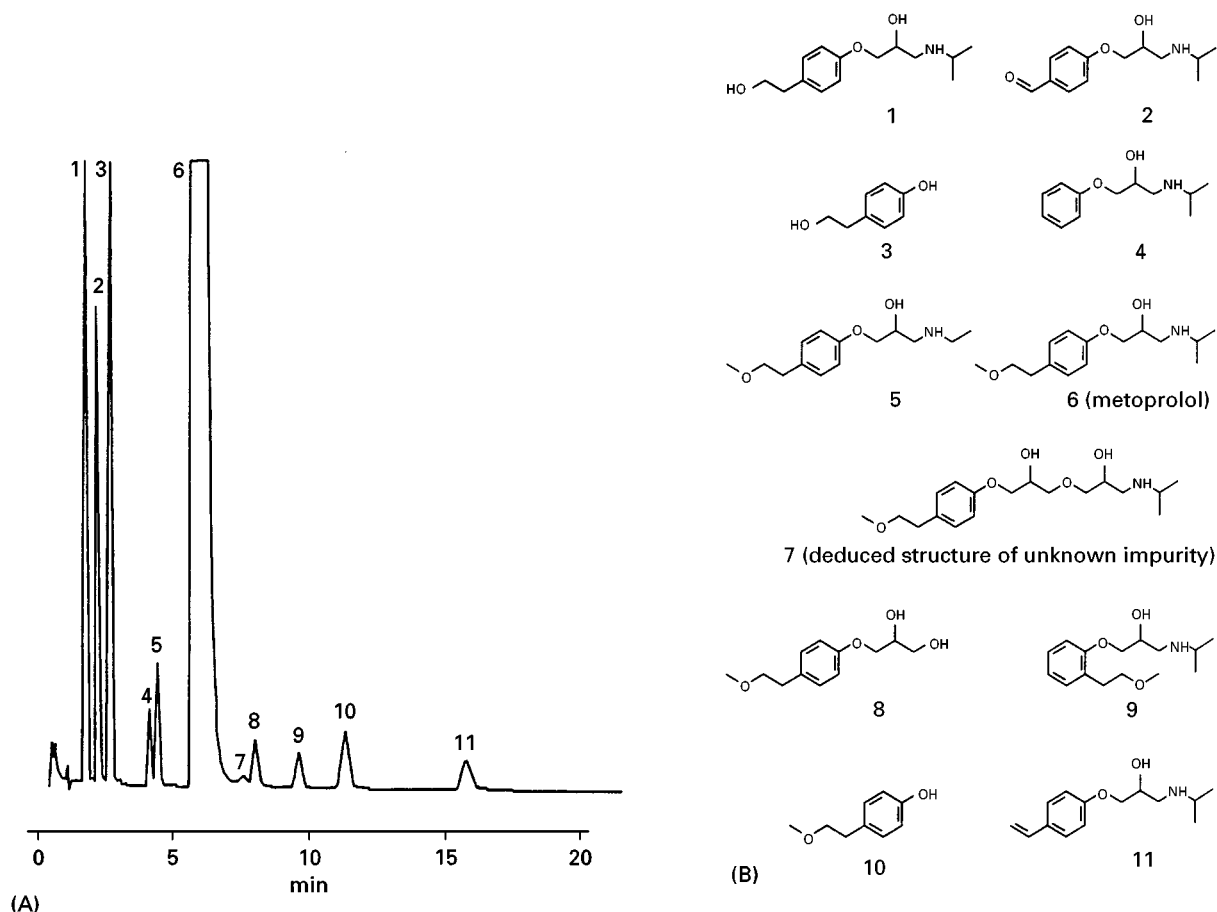


Figure 1 (A) Separation by LC of metoprolol and some of its potential impurities that have been added in amounts from 0.01 to 0.4% to a pure sample. Peak 6, Metoprolol; peak 7, an unknown impurity. Peaks 1–11, see structures in (B). Column: 125 mm long and 4 mm i.d. filled with 5 μ m C-8 particles (Li Chrospher RP-Select B). Mobile phase: Acetonitrile, 17% in ammonium phosphate buffer 0.05 mol L⁻¹, pH 3.2. Detection at 280 nm. (With thanks to Lars A. Svensson, Astra Hässle, Sweden.)

source, various chromatographic tests are used to show the absence of contaminating proteins remaining from the purification process. The separation methods used have a more biochemical character and differ from those for compounds of synthetic origin. Immunochemical techniques are very often used as complements. Typical tests include separation of dimers, trimers etc. from the biomolecule itself. Molecular size determination by size-exclusion chromatography is common and will probably be supplemented by mass spectrometry in the future.

Biotechnological products have some advantages over products from human or animal origin with respect to the risk of transferred diseases, but they have some special requirements. In particular, when parenteral use is intended, the absence of host proteins has to be guaranteed as well as DNA residues from the vector used for expression. Such matters often need the attention of specialist laboratories.

Bioassay Many biomolecules have, over the years, been assayed using methods where biological activity in an animal, organ or receptor is assessed, i.e. a bioassay. The traditional opinion has been that such bioassays cannot be replaced by physicochemical methods as the latter do not reflect the biological activity. Bioassays, no matter how well characterized they are, have certain disadvantages with respect to precision, time and cost compared to instrumental methods. The pharmaceutical industry has therefore been able to show that, for several of its biotechnological products, e.g. insulin and human growth hormone, chromatographic methods (LC in particular) can give the same information. Moreover, proteins from different species can be chromatographically separated and degradation products well quantified. This is not possible in quantitative bioassays where only the sum of activities is obtained. A similar paradigm shift has also taken place for antibiotics, where LC methods give information not

available from microbiological assays. However, it should be noted that for many biomolecules there are, as yet, no alternatives to bioassay.

Excipients

There are a great number of materials that are used to transform a substance from an active compound to a medicine useful for a patient in a therapeutic situation. These compounds, or excipients, are becoming more and more important in the construction of modern drug delivery systems. Many excipients are macromolecules and have been used for decades in traditional remedies. With modern drug delivery systems the old requirements may not always fit those necessary for the technologically advanced products of today. This has become increasingly evident in recent years. Moreover, the requirements on excipients in the various pharmacopoeias are not always consistent with each other and are often rather vague. This has been recognized at an international level and efforts at harmonization are proceeding. Polymeric excipients are generally characterized by some average physicochemical property such as viscosity. Studies of the distribution of relative molecular mass are rarely performed on such excipients due to the lack of suitable methods. The majority of the excipients used today, however, have relative molecular masses in the same range as the active compounds. The tests for safety and purity are similar to those of the drugs.

Excipients could usefully be classified or tested according to their properties at three levels, viz. molecular, particular and bulk properties. Those are tested for by the manufacturer of a dosage form. It is not clear which of those properties should be covered by the official compendia. Testing of functionality, i.e. at particulate or bulk level, does not seem to be possible yet. Typical tests are bulk density, specific surface area, flowability and particle size distribution. However, the standardization of methodology in compendia, without specification limits, would probably be of help for both vendor and buyer. As excipients are becoming more and more complex, their analytical characterization will be more important. Interesting opportunities lie ahead, particularly with macromolecular separation, MS and spectrometric methods such as near-infrared (near-IR) spectrometry.

Pharmaceutical Products

A medicine is much more than simply a drug substance, and huge efforts are put into the development of biopharmaceutically optimized drug delivery systems. Analytical chemists contribute to that process by analysing the experimental formulations with re-

spect to various properties such as homogeneity, content, stability and release of the active agent in dissolution testing but also through bioanalysis to create data for *in vitro* – *in vivo* correlations.

Solid dosage forms Solid dosage forms, e.g. tablets and capsules, are by far the most common for several reasons. The production of relevant doses is easy to accomplish, and scale-up is usually a standard technological process. All divided dosage forms have strict requirements for uniformity of content, i.e. a statistical sampling of the batch should show a uniform distribution of the active component. This requirement is especially important for units with very small amounts of the active component, i.e. from a few μg per dose to 50 mg. This has often led to automated analytical methods to cope with the large number of samples.

The pharmacokinetic performance of a drug influences the construction of a formulation. This has nowadays led to a dominance of drug delivery systems that provide a controlled or modified release of the drugs, defined as extended or delayed release. Release-controlling polymers are used to build up a barrier that prevents immediate release of a compound. In this way high peak plasma concentrations of drugs are avoided and usually only one dose per day is necessary. The characteristic properties of the formula are evaluated in *in vivo* tests where blood samples are analysed often by extremely sensitive bioanalytical methods.

However, for routine quality control it is usual to rely on *in vitro* models, which obviously have to be correlated with the *in vivo* data. Dissolution testing has been standardized in the pharmacopoeias for a long time with respect to release media, apparatus and other conditions. However, in modified release formulations the prescribed conditions might have to be changed. This is the responsibility of the analytical chemist, whilst still having the routine testing conditions in mind, i.e. quality control (QC) methods should also be practically feasible.

Parenterals Parenterals are dosage forms intended for injection into the body. Water is normally used as the solvent. The special tests for parenterals include sterility and absence of particles as well as endotoxins that can give fever reactions. The old test that was performed on rabbits is nowadays often replaced by a test based on the reaction of endotoxins with a lysate from *Limulus amoebocyte* (LAL-test) that is less time-consuming and more exact. Sterility testing is complicated from a sampling point of view because of the random appearance of microbial contaminants. A thorough in-process validation is the best way to

ensure that the products are sterile. In large volume parenterals' requirements on limits for particle contamination have created a need to analyse for particles down to the size of a few micrometres, usually by light-blocking or by conductivity techniques. For compounds which are sparingly soluble in water other solvents or co-solvents can be used creating problems of quite a different kind for both formulator and analyst, such as evaluation of precipitation phenomena and interactions with packaging materials.

Other dosage forms Other dosage forms are needed for topical administration such as creams, ointments and patches. The latter should usually deliver the drug over an extended period of time and thus require reliable *in vitro* release testing and as a consequence also *in vivo* data.

Sometimes other routes of administration are necessary. Thus suppositories are used for rectal delivery and sprays for the nasal route. Sublingual delivery can be advantageous, e.g. for nitrate esters. For asthma the use of inhalators has increased considerably as reliable hi-tech delivery systems have been developed. Here the uniformity of the inhaled dose (usually a few μg), as well as the narrowness of the particle size distribution, must be safeguarded.

The analytical problems of these dosage forms have to do both with the type of excipients used and their characterization and quality as well as the function of the delivery system.

Toxicological formulations Toxicological formulations appear in the early project work in short-term toxicology tests performed before testing in humans (pre IND) and later on during long-term carcinogenicity studies before approaching the authorities for marketing approval (pre NDA). The reason for mentioning them here is that at this early stage a full understanding of the properties of a drug is not always available, and most important, the animal feed into which the drug may be blended is a very difficult matrix in which to analyse a drug. Yet, the analyst has to determine the homogeneity and the stability of such formulated animal feeds during the use of the material. Here the rules of Good Laboratory Practice (GLP) are emphasized with careful validation of analytical methods.

Packaging materials Packaging materials are also part of the medicine presented to the patient. They are usually polymers that have properties chosen to give drug the product protection during storage and handling. Usually multilayer materials are used, as in blister packages for tablets, with some layers being a barrier towards moisture penetration.

Plastic bottles are becoming more common now. For many products, particularly parenterals, there is a risk of interaction between the polymeric material and the active component, especially if the latter has a lipophilic character. Rubber stoppers in parenterals are likewise prone to trap organic molecules from, and also leak stabilizers into the solution. Biomolecules in solution may adsorb onto these surfaces and this may be especially significant if the amounts in solution are minute. From these comments it is clear that stability testing must also be performed in the consumer package under appropriate conditions of temperature, humidity and light.

Stability studies Stability studies constitute a major task for the analytical chemical laboratory. The aims of initial physicochemical studies and investigations of incompatibilities, i.e. preformulation studies, are to identify the weak points of a compound, in order to avoid vulnerable conditions in the formulation. An example of an incompatibility reaction in a formulation containing three active ingredients and stored under accelerated conditions is given in **Figure 2**. The structure of the degradate was elucidated with electrospray LC-MS and verified as shown in **Figure 3**. Heat, moisture, oxygen and light may all influence stability.

Tests have to be performed under standardized conditions with respect to temperature and humidity. Accelerated tests can be used to isolate the weak points, but in the documentation submitted to the authorities long-term stability data under normal conditions are required. In these studies stability indicating assays are important and usually LC is the method of choice as the measurement of the drug content should not be disturbed by interfering components. Early degradation is, however, more reliably monitored through the degradates as the precision in the determination of a degradate is less demanding than the measurement of the corresponding decrease in the parent compound.

Full-scale production Full-scale production is the final step in the research process. Scaling up from the pharmaceutical development laboratory via the pilot plant to full-scale production is not without problems. This is one of the reasons for the requirement by the authorities that stability studies should be performed and reported for the first three production batches. The transfer (scaling up) can be facilitated by thorough process controls that give an understanding of those parameters which must be controlled. As pharmaceutical formulations are more complicated today than ever before it is clear that process analytical chemistry will play an important role in the

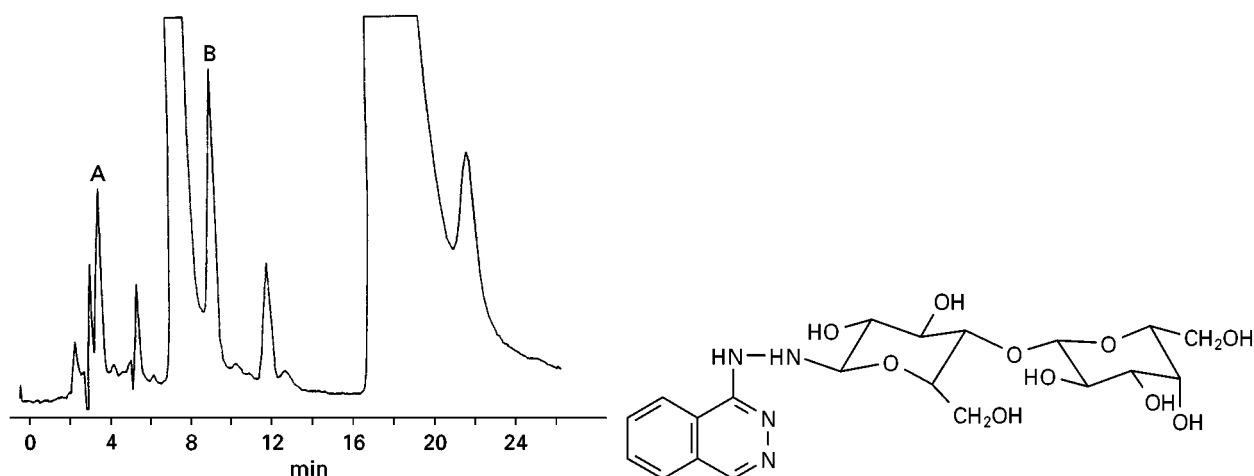


Figure 2 Separation by LC of degradates from a formulation containing hydralazine. After storage at accelerated conditions components A and B started to grow the peaks. They were both the result of an incompatibility with lactose. The structure of B was elucidated by LC-MS as shown in Figure 3. (With thanks to Rose-Marie Janson, Astra Hässle, Sweden.)

future. In this way it will hopefully be possible to control the process by feedback reactions before severe deviations occur. Noninvasive techniques such as near-IR and ultrasonic methods provide interesting possibilities in this context.

Specifications and Quality Control (QC)

Specifications

The quality requirements of a substance in bulk and those of a pharmaceutical formulation are compiled

in specifications. In these documents the requirements on the various quality parameters are given as minimum or maximum limits or ranges. Formulations often have requirements on technical properties such as dissolution rate, disintegration and hardness for tablets. All those requirements are the result of comprehensive studies in the R&D phase, where the knowledge of the properties of the drug is gathered, resulting in the optimized formulation of the active component. The analytical and technical test methods that are linked to the specifications will have evolved during the R&D process and can, at the NDA stage, be transferred to QC laboratories.

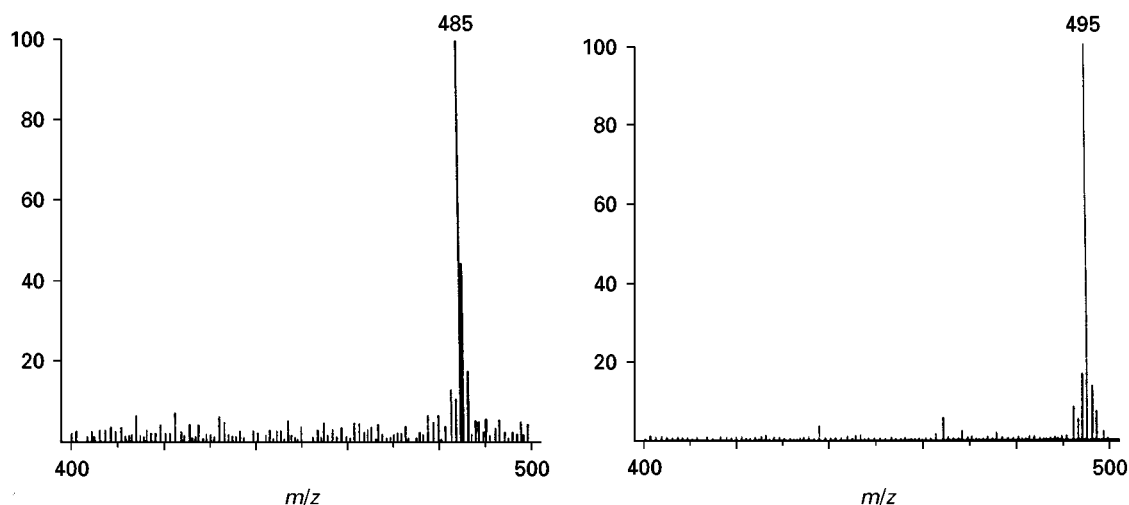


Figure 3 Mass spectra of degraded B in Figure 2. Electrospray LC-MS was used with a 0.5 m fused silica capillary column, i.d. 250 μm . The packing material was 5 μm C-18 Chromasil and the mobile phase was 60% acetonitrile in 5 mmol L^{-1} ammonium acetate with a flow rate of 1.5 $\mu\text{L min}^{-1}$. The left-hand panel mass spectrum was obtained with the mobile phase consisting of water and the right-hand panel with the use of heavy water (deuterium oxide) instead. The mass number difference is due to nine hydrogen atoms exchanged with deuterium plus the ion charge H^+ being changed to D^+ . (With thanks to Karl-Erik Karlsson, Astra Hässle, Sweden.)

It is important to bear in mind that what is used in clinical trials should be reproduced in full-scale production. Of special importance is the particular batch, or so-called biobatch, which is studied *in vivo* and compared with *in vitro* properties as in dissolution testing to establish a correlation *in vivo* – *in vitro*. This batch is of critical importance for the future and its documentation has to be thorough. The bioavailability, as documented in the biobatch, is the foundation for the coming market presentation. Equally important are the substance batches used in safety studies, and requirements on the knowledge of their quality are very exacting. Also, there is a distinction between release and check specifications. The requirements at the release usually are somewhat tighter than those at a control performed any time during the entire lifetime of a medicine (check specification). In order to be aware at an early stage of deviations from the intended range of a quality parameter in a process the industry works with internal specifications that are tighter than the external ones.

Reference Substances

Most methods require some form of chemical reference substances (CRS), which have already been characterized in an IND more thoroughly than in normal specifications, for example, by adding thermo analytical data and spectrometric data for structural evidence, e.g. infrared, nuclear magnetic resonance and ultraviolet. Compendial methods have official CRS, which are available for customers all over the world. It is important to remember that a reference substance can be used for different purposes, not all of them requiring extensive testing. So a CRS for identity testing is less demanding from a purity point of view. For daily work a less expensive working standard can be calibrated vs. a CRS.

Quality Control (QC)

Full-scale production is checked in the QC laboratories according to the specifications and test methods approved by the authorities. Decisions by QC management cannot be overruled by any person in the organization, which puts a particular onus on the competence and judgement of the person in charge of QC. In addition to the chemical and biological tests that comprise QC the organization can introduce preventive measures to avoid quality impairment. This activity is defined as integrated or total QC and is further outlined in Good Manufacturing Practice (GMP) (see Regulatory Aspects). It cannot be emphasized enough that chemical control at the end of

a process can never replace high standards in the process itself. This is sometimes so evident that release in certain cases can be given based on the documentation and control in the process steps. This is called parametric release. Parametric release has been accepted by the authorities in those cases where end control does not fully reflect failures in the production. This has been most evident in many biotechnological processes, where the absence of host proteins, DNA residues or virus particles has been approved through a thorough validation procedure where the purification step is challenged. The analytical methodology is not adequate in this situation at the end control.

Process analytical chemistry may, in the near future, play a similar role in showing that a process does not run beyond prescribed limits. This not only gives better quality in products, but also fewer failures and thus reduced costs. Verification of identity is required at several stages during the process, not only at the end. This can be done in many ways and it is important to remember that the sum of the tests performed during a process also contributes to that verification. Biotechnological products are a special case in that the identity of the recombinant protein with that of the native one has to be established. Thus, it is important that the correct order of the sequence of amino acids is verified. Peptide mapping provides one way of showing this by comparing the chromatographic pattern of peptide fragments obtained after enzymatic cleavage. Capillary electrophoresis (CE) complements LC in this role. In this area there are new and interesting possibilities with mass spectrometric techniques that allow molecular ions to be determined up to and above 200 kDa.

Regulatory Aspects

Good Manufacturing Practice (GMP) was mentioned above and has been a cornerstone of pharmaceutical production and control since the 1970s. These regulations state clearly what has to be done to safeguard quality from the beginning of the production process to the end, viz. documentation, staff qualifications, standard of facilities, technical standards, handling of material, labelling, etc. Control guidelines are mentioned but not in the same detail as in Good Laboratory Practice (GLP). These rules state that all documentation of analytical methods should fulfil certain performance criteria, that instruments should have maintenance records and that their performance and those of the method should be documented. Every analyst should in principle document an analytical method and its aims.

Validation of Analytical Methods

Validation of an analytical method establishes in laboratory studies that the performance characteristics of the method meet the requirements for the intended application, thus the method does what it is expected to do. In the *United States Pharmacopeia* (USP) the following items are listed: precision, accuracy, limit of detection, limit of quantification, selectivity, range, linearity and ruggedness. Of these, accuracy is probably the most difficult to document or obtain, at least for solid formulations. This has to do with the fact that recovery experiments are difficult to design in such a way that they resemble the process conditions. The reactions there can create interactions which are not obtained in an experiment where the analyte has only been mixed or spiked to the sample.

Selectivity is another factor in the validation process that is much discussed. Many authorities require a selective method in a product release specification and mean that a chromatographic procedure has to be carried out even if a simple UV method is free from interferences. Here cost effectiveness should be the guide and analysts should therefore use their scientific arguments to justify using the simpler method. Validation procedures are equally important in the documentation of bioanalytical methods.

International harmonization Harmonization efforts are now being made at an international level. Of special importance is the possibility of having the same guidelines worldwide on how stability studies should be performed and reported. The same is true of guidelines on how to study impurities, especially where the limits should be set and at what level identification is needed. Similar efforts are seen for dissolution testing and how to correlate *in vivo* and *in vitro* data. The question of bioavailability and bioequivalence is an important one and a common view on these issues would be welcome, even if recommendations on how to perform a bioanalytical method will probably never appear in a pharmacopoeia. In recent years the interest in chiral drugs has increased and we can now also see an interest in harmonization for these compounds.

Emerging Techniques in Pharmaceutical Analysis

Analytical chemistry is one of the disciplines most frequently involved in the R&D work performed in the pharmaceutical industry. This makes the industry very analysis intensive, which explains the high level of interest in testing new methods in order to get further information. It is also clear that this interest in

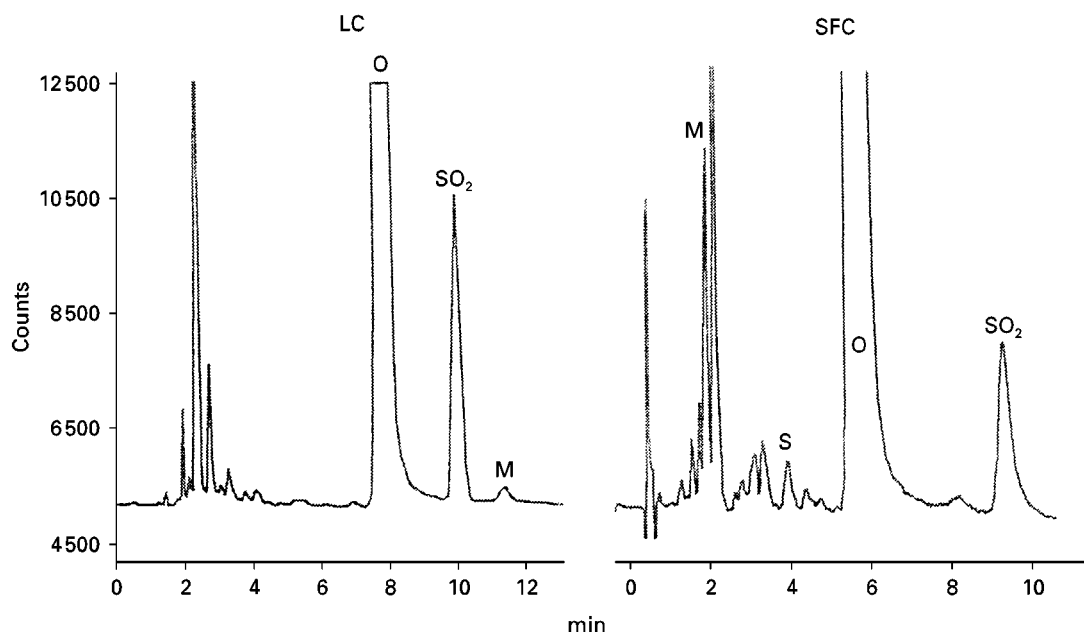


Figure 4 Separation by LC and SFC of omeprazole and some related compounds. Conditions for LC: column 100 mm long and 4.6 mm i.d. filled with 3 μm C-18 (Chrompak Microsphere). Mobile phase: acetonitrile, 26%, in phosphate buffer 0.01 mol L⁻¹ and pH 7.4 containing tetrabutylammonium 1.0 mmol L⁻¹. Flow rate: 1.0 mL min⁻¹. Conditions for SFC: column 125 mm long and 4 mm i.d. with 5 μm Li Chrosorb NH₂. Mobile phase: carbon dioxide 2.0 mL min⁻¹ with methanol containing 1% triethylamine at 120 μL min⁻¹. Temperature: 40°C. Pressure: 175 bar. Test compounds: O = omeprazole (a sulfoxide); S = reduced form, a sulfide; SO₂ = oxidized form, a sulfone, and M = two isomers of *N*-methylated omeprazole (only separated by SFC). (With thanks to Olle Gyllenhaal and Svante Johansson, Astra Hässle, Sweden.)

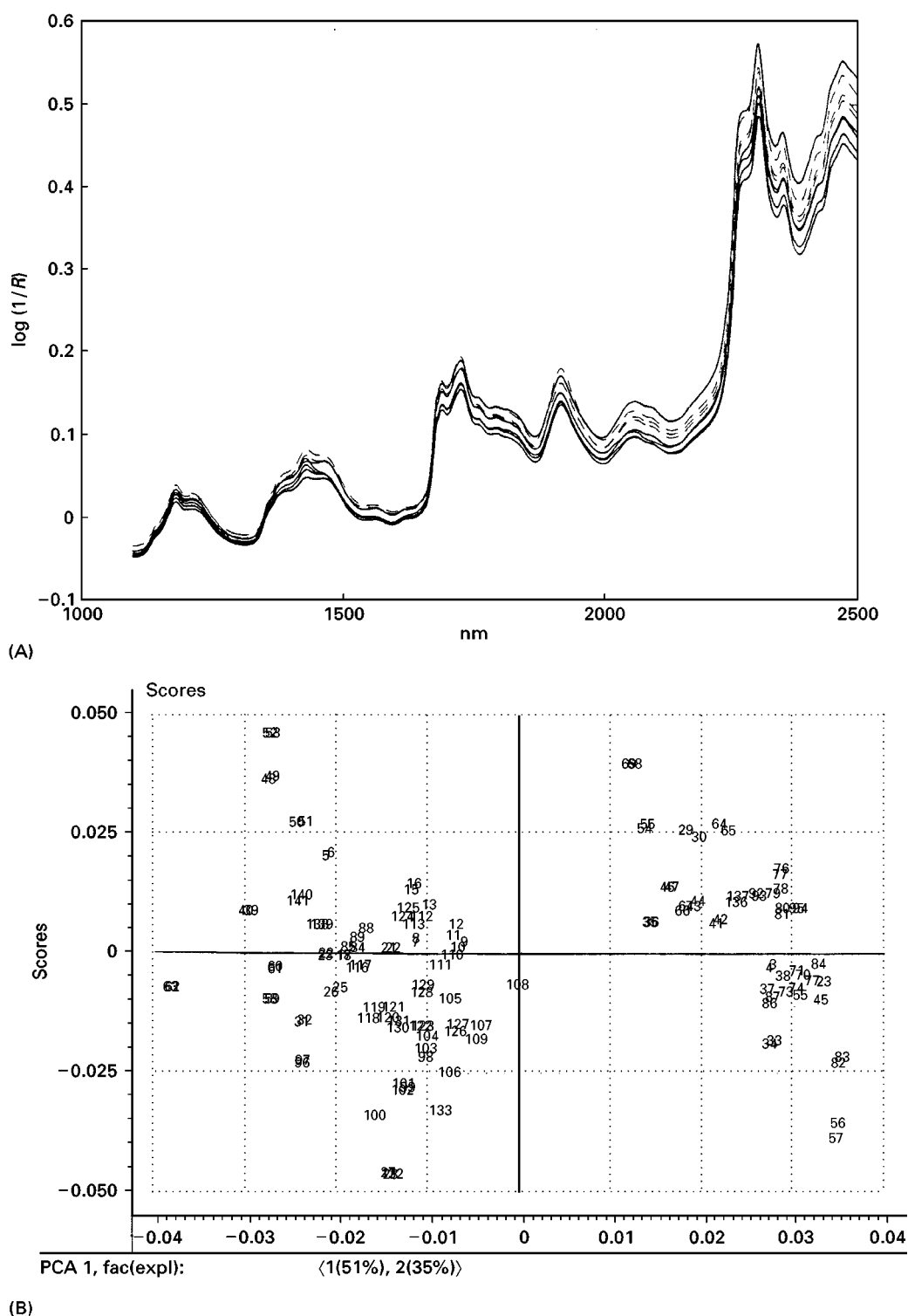


Figure 5 (A) Reflectance spectra in the near-IR of a number of ethyl celluloses obtained from two vendors. (B) Principal component projection of the spectra in (A) after multiplicative signal correction. The left cluster is from vendor 1 and the right one from vendor 2. (With thanks to Mats Josefson, Astra Hässle, Sweden.)

learning, and using the latest techniques, stems from a desire to obtain reliable information more quickly, or to obtain complementary data.

The research process is a long-term commitment and requires high standards in the results from the very beginning. The quality of the results relies

on competent analytical chemists, but also on the availability of good instrumentation, which is often evident in the laboratories of the research intensive pharmaceutical industry. Separation techniques, especially LC, have had an enormous impact on pharmaceutical analysis. The combination of LC with MS has further extended the possibilities of the techniques as qualitative data can very often be obtained on-line. Can we foresee a similar development in years to come? The development of new techniques usually proceeds in a stepwise fashion and, at present, mass spectrometric techniques are taking a giant step towards the analysis of macromolecules in a reliable way. This revolutionary process has just begun to show promising results with relative molecular masses of more than 200 kDa being determined using time of flight drift tubes. Whether or not these instrumental possibilities can be combined on-line with separation methods, especially CE, remains to be seen. These MS extensions will have great impact on biotechnology products and macromolecular compounds used as excipients.

Another area where rapid development is taking place is Raman spectrometry. New technology has opened interesting possibilities for this old technique. Many opportunities lie ahead both in regular and in process analysis.

Separation methods will see continued growth, particularly the capillary techniques. Capillary chromatography is particularly useful when expensive mobile phases are used. A good example of LC-MS using packed fused silica columns 250 μm in diameter is given in Figure 3. Here heavy water was used interchangeably with an aqueous phase. Hydrogens bound to heteroatoms (O, N, S) were then replaced with deuterium, which was easily revealed in the mass spectrometer. This tells the analyst how many labile hydrogens the molecule has (in the case of the example this was 10). For macromolecules up to particles, the use of field flow fractionation (FFF) techniques can be expected to increase. Complementary information to LC will come from CE and supercritical-fluid chromatography (SFC). The latter technique will probably find a place in product analysis, especially in the packed column version, where polar compounds can be analysed. Packed column SFC is an interesting complement to LC, showing more rapid and efficient separations. An example is given in Figure 4, where omeprazole and some related compounds are separated. The sulfide form is eluted at about 25 min in LC, i.e. twice the retention in SFC. Capillary electrophoresis has recently become

a useful separation method in the pharmaceutical industry, not least for biotechnological applications.

Chemometric methods will have an impact on many types of technique, particularly in areas where properties which are not easily measurable (such as taste, texture, etc.) have to be correlated with physicochemical parameters. In this context, near-IR has started to gain prominence within the pharmaceutical industry. An example from the analysis of a number of cellulose ether samples with reflective near-IR is shown in Figure 5. The individual spectra do not show much in the way of differences. The spectra were corrected for different light penetration depths by multiplicative signal correction (MSC). Then the entire spectra were projected by principal components analysis (PCA) as points on a plane. The samples could be grouped into two clusters in this plane, one for each vendor. The calibration of this technique is entirely dependent on multivariate analysis or chemometrics and this combination will grow in use. In the same way process analytical chemistry is going to proceed based on multivariate data. Many noninvasive approaches rely on near-IR and multivariate calibration. New approaches combined with techniques that will stand harsh process conditions will also be introduced. Clearly, in the future new principles of measurement may also be necessary and the analytical chemist will have much to contribute here.

See also: III/Pharmaceuticals: Basic Drugs: Liquid Chromatography; Neutral and Acidic Drugs: Liquid Chromatography; Supercritical Fluid Chromatography; Thin-Layer (Planar) Chromatography. III/Proteins: High-Speed Countercurrent Chromatography.

Further Reading

- Beckett AH and Stenlake JB (1988) *Practical Pharmaceutical Chemistry*, 4th edn, parts 1 and 2. London: Athlone Press.
- Connors KA (1982) *A Textbook of Pharmaceutical Analysis*. Chichester: John Wiley.
- Munson JW (1981) *Pharmaceutical Analysis: Modern Methods*, part A. New York and Basel: Marcel Dekker.
- Schill G, Ehrsson H, Vessman J and Westerlund D (1984) *Separation Methods for Drugs and Related Compounds*, 2nd edn, pp. 187–198. Stockholm: Swedish Pharmaceutical Press.
- Schirmer RE (1991) *Modern Methods of Pharmaceutical Analysis*, 2nd edn, vols I and II. Boca Raton, Ann Arbor: CRC Press.

Crystallization

W. Beckmann and U. Budde, Schering AG,
Berlin, Germany

Copyright © 2000 Academic Press

Two decades ago, crystallization was called both an art and a science. However, the field is improving quickly. The crystallization of pharmaceuticals is still sometimes regarded an art and rather a mystery. However, crystallization processes are widely used throughout the production processes of the active ingredient of a drug product, and a lot of knowledge is nowadays available.

For the crystallization of drug substances several aspects have to be considered, as the crystallization process is the last step in the chemical manufacture of pharmaceuticals. The crystallization determines a number of important properties of the drug substance, namely the purity and residual solvent content, the polymorphic form, crystal size and size distribution, and it affects downstream processes such as drying, ease of comminution and formulation of the final drug product.

The crystallization of all drug intermediates have the same goals and follows the same procedures as for other organic substances and thus will not be discussed here separately.

General Considerations for the Development of the Crystallization Process

In general, the demands on the crystallization of a drug substance differ according to the final use, e.g. if the product is used in oral dosage forms, in ointments or in liquid formulations. However, for the sake of simplicity, it is assumed here that the crystallized drug substance is to be used in an oral dosage form.

Figure 1 shows a typical crystallization process of a drug substance and the downstream processes up to the formulation of the drug product. The crystallization and the properties of the product have a great influence on all the following steps.

Impurities

Foreign and related compounds The requirements on the purity of a drug substance are strict; guidelines require a purity of typically >98%. Individual impurities with a known structure have to be below 0.5% and unidentified impurities have to be below 0.1 or

0.05%. In addition, the toxicological effect of all impurities must have been assessed in the first toxicological tests, i.e. no new impurity is allowed that has not been present in the batch used for toxicological experiments.

The purification of a drug substance via crystallization cannot be predicted easily. While foreign impurities can mostly be easily reduced, related substances like impurities stemming from side reactions in the synthesis behave in an unpredictable way. In general, the purification via crystallization will decrease with an increase in the yield, especially if the yields are >90–95%.

Residual solvent content Beside obvious solvent properties such as a certain solubility for the drug substance and an appropriate purification to yield ratio, the choice of the solvent for the crystallization of a drug substance is governed by the permissible limitations placed on the residual solvent content of the drug substance. All typical solvents have been classified according to their toxicity and tolerated daily uptakes of a solvent have been established, that are not to be exceeded by the drug product.

Three classes of solvents are distinguished: (i) those that should be avoided; (ii) those that have a limit to their daily uptake; and (iii) those for which no limits have been set up so far. Examples are benzene and dichloroethane for class 1, methanol and dichloromethane for class 2 and ethanol, ethyl acetate and acetone for class 3. In addition, good manufacturing practice (GMP) requires the manufacturer to limit the residual solvent to the lowest content possible.

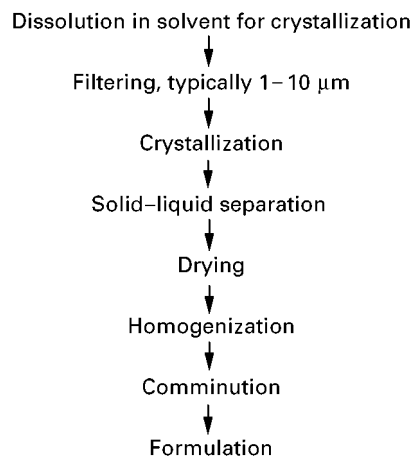


Figure 1 Typical crystallization and downstream processes up to formulation.

Table 1 Productivity, yield and development prerequisites for the separation of isomers via crystallization, enzymatic resolution and chromatography

Parameter	Crystallization	Enzymatic resolution	Chromatography
Productivity	High	Low	Medium
Selectivity	Varies	High	Very high
Prerequisite	High	High	Low
Development time	High	High	Low to medium

Two types of limits for the residual solvent content of a drug are distinguished. Case 1 is a dosage-independent concentration limit and Case 2 is a limit for the total uptake through the drug product, that must not be exceeded by the solvent content of the drug substance and the excipients.

The mechanisms of incorporation of solvent into the crystals can be described as follows:

- The solvent is incorporated into the lattice at fixed positions during the crystallization (solvate formation). In this case, the incorporation cannot be avoided directly. In some cases, a solvent of crystallization is removed or replaced by water.
- The solvent is incorporated into the lattice as three-dimensional inclusions. The formation of inclusions is facilitated by the speed of crystallization, thus, the amount of residual solvent can be decreased by lowering the rate of crystallization. For some systems, the tendency to form three-dimensional inclusions of solvent increases with the crystal size.

If a problem with the residual solvent content of a drug arises, the clear remedy is a change of solvent.

Separation of isomers An increasing number of pharmaceutical active ingredients are either isomers or enantiomers. Typically, different isomers of a chemical compound exhibit different biological or

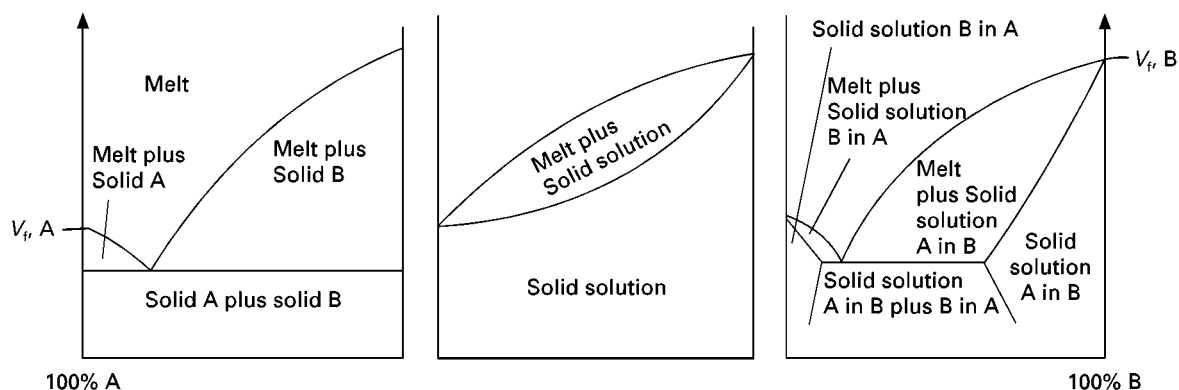
therapeutic activities, with one of the isomers being the carrier of the activity. In some cases, the second isomer can even have an adverse biological activity. In any case, the inactive isomer constitutes an unnecessary load to the body. Thus, a separation of isomers is almost a prerequisite for the production of a drug.

Isomers can be separated by enzymatic resolution, chromatography or crystallization. **Table 1** summarizes and compares productivity, yield and development prerequisites of the three separation techniques.

The success (or possibility) of the separation of isomers via crystallization depends on the phase diagram of the two compounds.

Figure 2 shows typical phase diagrams of isomers, i.e. eutectics, solid solutions and partial solubility in the solid state. A separation of isomers in a single step is only feasible for eutectic systems. Systems forming solid solutions have to be purified in multiple steps, as for example in zone refining which is only feasible if the substance is stable in the molten state. For systems exhibiting partial miscibility in the solid state, the separation cannot be better than the partial miscibility concentrations.

In principle, isomers forming eutectics can be separated directly via crystallization. However, without using special techniques, the crystallization can only be carried out until the concentration of the mother liquor has reached the composition of the eutectic mixture. To improve the yield two ways are often pursued:

**Figure 2** Typical phase diagrams for isomers: eutectics, complete miscibility in the solid state and partial miscibility in the solid.

- Forming diastereomeric salt derivatives of the isomer will often direct the eutectic composition towards one of the isomers. This will increase the yield and productivity of the crystallization process considerably.
- The desired isomer is enriched via preparative HPLC followed by crystallization. The chromatographic technique achieves a high degree of enrichment but the amount of solvent to be handled is considerable. Crystallization is carried out at high concentrations and thus more effectively. Attempts have been made to find the optimal cost effective division between the separation via preparative HPLC and crystallization.

Solid-State Forms

Polymorphism Before a crystallization process is developed, the solid-state polymorphism of the substance has to be elucidated. Less than 50% of the drug substances described in monographs crystallize in a single polymorphic form; the majority form polymorphs, pseudomorphs, or both. The polymorphic form of a drug can influence a number of its properties such as the following:

- The solubility and the dissolution rate and consequently the bioavailability. Although typical differences in solubility between polymorphs are of the order of ≤ 2 , the differences in solubility between pseudomorphs are somewhat higher. The largest differences exist between amorphous and crystalline material.
- The habit (the external appearance) of the crystals which in turn influences the mechanical properties of the drug during further processing such as the ease of comminution.
- The chemical stability.

Thus the regulatory agencies ask for the reproducible production of the specified polymorphic form. In the case that a drug can form more than one polymorph, a choice of the polymorphic form must be made.

Amorphous compounds Amorphous solids are a metastable form of the drug substance that can crystallize at any instant. In this respect, an amorphous form can only be second choice as solid-state form for a drug substance.

The stability of amorphous material can be characterized by its glass-transition temperature T_g , which can be determined by differential scanning calorimetry (DSC). Below the glass-transition temperature, the molecules are practically frozen; above it they have a finite mobility making the conversion into a crystalline form possible.

The glass-transition temperature and thus the stability of amorphous materials can be decreased by residual solvent.

Salts A number of properties of the chemical compound can call for the use of a salt as the drug substance. An insufficient chemical stability of the parent compound can be overcome by the formation of a salt, e.g. amines sensitive to oxidation can be stabilized by forming a hydrochloride. Other properties calling for salt formation include low melting points or unfavourable solid-state properties such as a tendency to form amorphous material or too many polymorphs.

Finally, in case of an insufficient solubility in water or gastro-enteric fluids it is sometimes tried to avoid this problem by the formation of salts.

Salts of sparingly-soluble parent compounds can lead to the precipitation of the parent compound when the salt is dissolved in water. This poses considerable problems if it occurs during formulation like wet granulation.

Salts are typically formed by precipitation or reaction crystallization, i.e. by adding an acid or a base to a solution of the drug substance. Of course, each salt constitutes a new drug substance, that has to be treated accordingly as a new chemical entity.

Clathrates Chemical instability of parent compounds can also be overcome by the formation of clathrates typically of α -, β - or γ -cyclodextrin. The parent molecule partially enters the large voids of the cyclodextrin (see **Figure 3**). It is thus shielded from the environment, especially the excipients.

The clathrate is typically formed by precipitation i.e. by adding the parent compound dissolved in a water-miscible organic solvent to an aqueous solution of the cyclodextrin.

Choice of solid-state form The selection of the optimal solid-state form is an important step in the

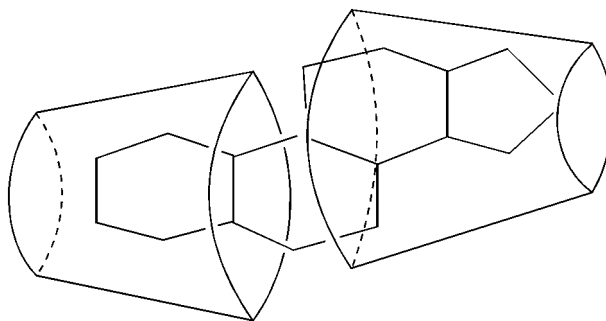


Figure 3 Schematic picture of the clathrate formation of a steroid by two β -cyclodextrin molecules.

• Number of solid-state forms
• Hygroscopicity
• Chemical stability
• Reproducible production
• Pharmacokinetics (dissolution rates)
• Toxicological properties
• Comminution
• Stability against excipients

Figure 4 Properties of the different solid-state forms of a drug to be considered when choosing the optimum form to be used in the final product.

development of the crystallization process of a drug. The form, once decided upon, has to be used in all relevant clinical and pharmaceutical tests and it must be certain that this form can be crystallized in a reproducible way, and that it can be formulated into the drug product.

A number of basic physico-chemical and pharmaceutical properties of the different forms that are considered for selection are listed in **Figure 4**, and can be tested and used in the process of decision making.

A drug substance that occurs only in a single polymorphic form is preferred; if not available, the stable polymorph is preferred. The techniques to infer the relative stability of polymorphs include solubility measurements, storage in suspensions and DSC experiments to construct enthalpy–temperature diagrams.

Crystal size and habit

Crystal size and habit of a drug can vary considerably. Thin needles, platelets and rhombohedral crystals are found. The crystal habit can influence all processes after crystallization

- during work-up, the de-watering in the centrifuge, the washing of the filter cake and the drying are affected;
- in the formulation, behaviour during micronization or flow during direct tableting are affected.

Micrographs of the drug substance and crystal size distributions can help in understanding the behaviour of the product crystallized under different conditions.

Habit The external appearance of crystals is called habit. The crystal habit can be influenced by the growth conditions. For example, crystals of the A modification of Abecarnil, a β -carboline derivative, grown after spontaneous nucleation at high supersaturations exhibit an avicular habit, while those grown at moderate supersaturations after seeding are still needle like but thicker and more rod-like (**Figure 5**).

Other factors determining the crystal habit are the solvent and the impurity profile of the material to be crystallized. The impurity level that influences the habit – and other properties – can be as low as ppm. **Figure 6** shows the habits of a steroid crystallized from two different solvents, one more protic (solvent I) and the other more aprotic (solvent II). Of course, the different habits lead to a different behaviour in downstream processing.

Crystal size distribution For the formulation of oral dosage forms, the desired crystal size distribution is

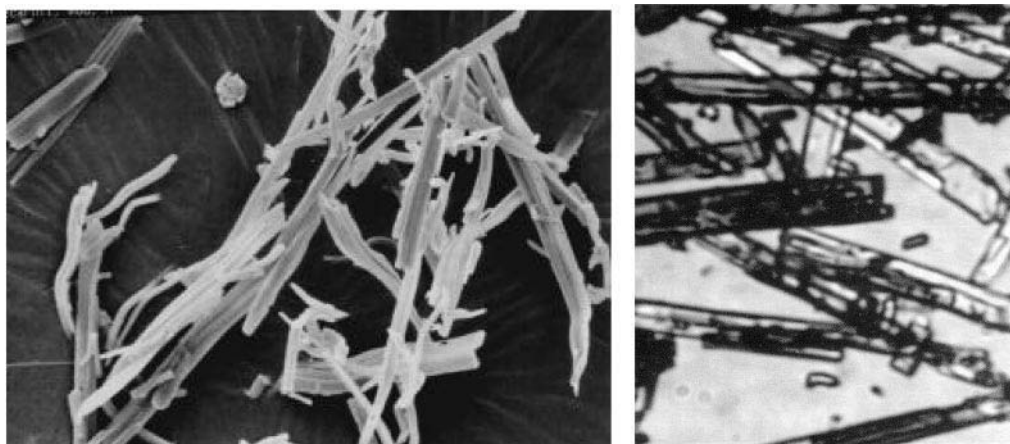


Figure 5 (See Colour Plate 111) Habit of Abecarnil grown from methanol after spontaneous nucleation at relatively high supersaturations (left) and grown at moderately low supersaturations after the addition of seeds (right).

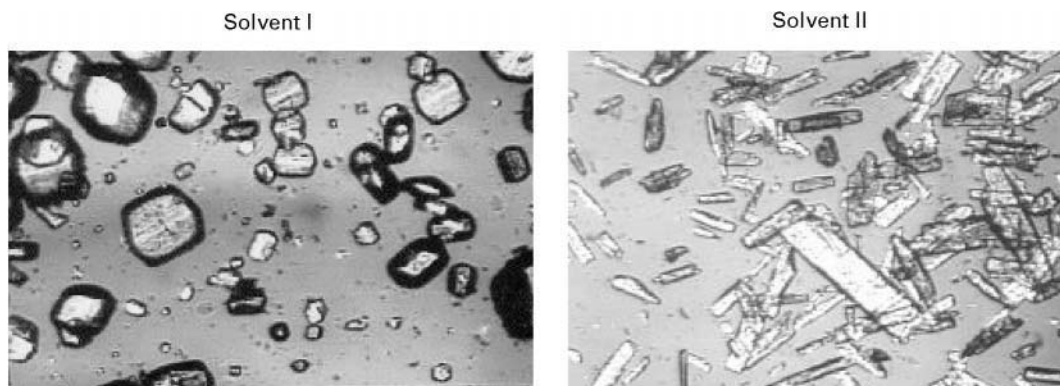


Figure 6 (See Colour Plate 112) Habit of a steroid crystallized from two different solvents.

mainly imposed by the demands for blend and content uniformity. For low-dosage formulations, such as steroids in contraceptives, the maximum crystal size is $\leq 10\ \mu\text{m}$. These crystal sizes cannot be attained via classical crystallization techniques. Thus, the standard procedure is crystallization and drying followed by a comminution, e.g. via jet-milling. It has been reported that the milling process is also dependent on the crystal size and the homogeneity of the crystal size to ensure a homogeneous milling process.

The size distribution obtained in a jet mill is decisively determined by the cut size of the cyclone of the mill. When the drug substance is to be used without comminution, the crystal size distribution will typically be broader. Small crystals, $\leq 10\text{--}100\ \mu\text{m}$, can only be achieved via precipitation, larger crystals by evaporative or cooling crystallization. If large crystals are desired, the best way to control the process is via seeding. Here, care must be taken not to destroy the crystals during the crystallization process through the power input of the stirrer or during work-up, especially in agitation dryers.

Care must be taken to avoid agglomeration during crystallization and drying, as this process is erratic and in precipitation processes agglomeration is almost unavoidable. For the formulation of liquid dosage forms, the dissolution rate can limit the permissible crystal size, although the requirements are not really strict.

Development of the Crystallization Process

In most cases, a drug substance will be crystallized from solution in a batch process. The techniques most often employed are cooling, evaporative, drowning-out and reaction crystallizations. Glass-lined as well as stainless-steel vessels are used. These classical crys-

tallization techniques and their implications will be discussed in detail. Certain properties of the drug substance may call for a crystallization from the melt, via spray drying or through the use of novel techniques for particle formation. These techniques will be discussed more briefly later.

Laboratory Development of Crystallization Technique

Supersaturation, nucleation and growth The crystallization involves two basic steps, nucleation and growth. The driving force for both processes is the relative supersaturation, typically defined as $\sigma = \Delta c / c_{\text{sat}}$, where $\Delta c = c - c_{\text{sat}}$, the difference between the actual concentration c and the saturation concentration c_{sat} . Depending on the magnitude of the supersaturation, at which the nucleation occurs, nucleation and growth will have different importance:

- at high supersaturation, nucleation will be the dominant process, the number of nuclei formed is large so that the increase in size via growth and thus the particles found are small;
- at low supersaturation, the number of nuclei is small so that growth dominates and coarse crystals will be obtained.

The first process is usually called precipitation, the second one crystallization. In both processes, nucleation can either be deliberate by seeding or involuntary by primary, spontaneous nucleation. As far as spontaneous nucleation concerned, heterogeneous nucleation by foreign particles in the solution will dominate. In case of easily or moderately soluble substances secondary nucleation caused by addition of the parent crystals in general dominates the nucleation process, once crystals of a sufficiently large size are present.

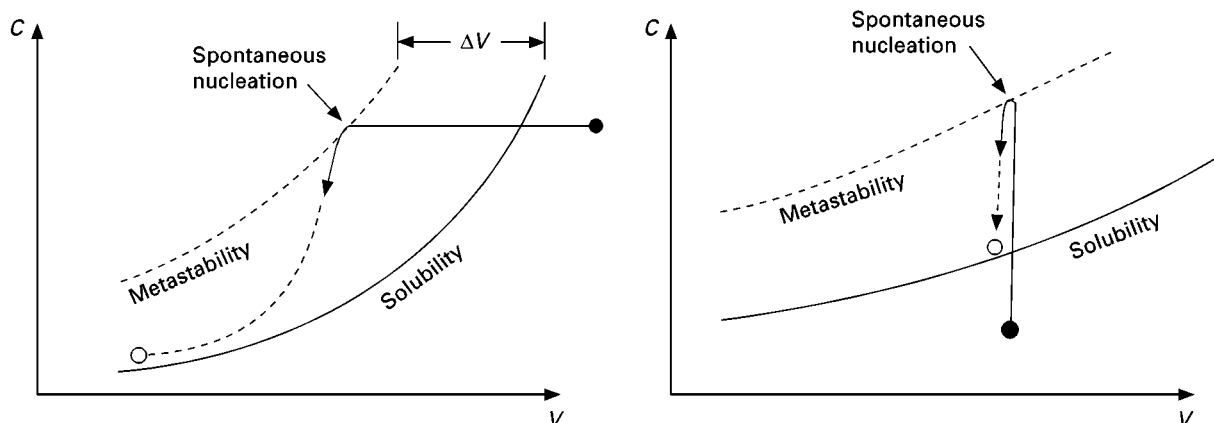


Figure 7 Typical solubility and metastability curves for a drug substance.

Solubility and metastability Two basic pieces of information on the system are necessary for a successful development of a crystallization process, the solubility curve and degree a solution can be supersaturated before spontaneous nucleation occurs.

The solubility defines the equilibrium state of the substance dissolved in the mother liquor, and the metastable zone is a concentration region, where a supersaturated mother phase can exist for a certain period of time without spontaneous nucleation. This latter region has typically a width of the order of 10°C and owing to the relatively large metastable zone, the amount of material coming out of solution under spontaneous nucleation without further cooling can be of the order of 10–30% of the entire mass, which is a considerable value. **Figure 7** shows typical solubility curves and metastable lines. The left-hand system lends itself to cooling crystallization, the right hand one to a evaporative crystallization because of the slope of the solubility curve.

For a drowning-out crystallization, a primary solvent in which the drug substance has a high solubility and a secondary, or anti-solvent, which has a negligible solubility are needed. **Figure 8** shows three typical curves for the mixing.

If the solubility has a concave curvature, i.e. the secondary solvent acts as an anti-solvent a drowning-out crystallization is feasible as shown in curve B. For curves A and C, crystallization by addition of an anti-solvent is not possible.

For precipitation by mixing of reactants or the formation of salts, the solubility is given by the solubility product, i.e. $a + b \rightarrow \text{product} \downarrow$ and $K = [a][b]$ (**Figure 9**).

For moderate formation constants, the solubility at $[a] = [b]$ is quite low. This implies high to very high supersaturations upon mixing, which can lead to small or very small crystals, which in turn can cause

problems in downstream processes, $\sigma = \Delta c/c_{\text{eq}}$. If c_{eq} is very low, σ will become very high. But this on its own has nothing directly to do with small crystals. Small crystals result from the lack of growth limits in the solution (even at high σ values). Apart from that abundant nucleation also leads to small crystals, but this is also true for easily soluble compounds.

Influence of impurity and purity of material An often underestimated effect is caused by changes that may be made during the lifetime of the synthesis and its implications for the crystallization process. Variations in the impurity profile can influence both the width of the metastable zone and thus the degree of supersaturation at which spontaneous nucleation occurs, and the polymorph obtained during via spontaneous nucleation. It can also influence the rate of polymorphic transformation during work-up and the habit and crystal size. Although the effects of a changing impurity level on the behaviour of a drug substance are difficult to anticipate during the first stages of development, there is a need for a careful investigation of these effects.

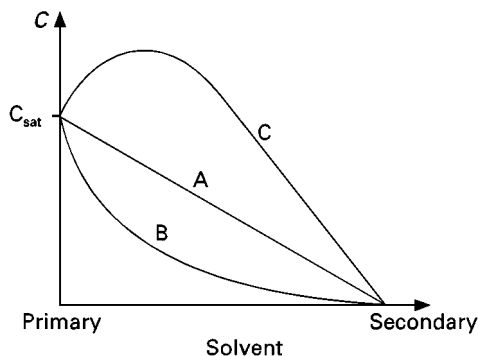


Figure 8 Typical solubility curves for a drug substance in a mixture of a primary and a secondary solvent.

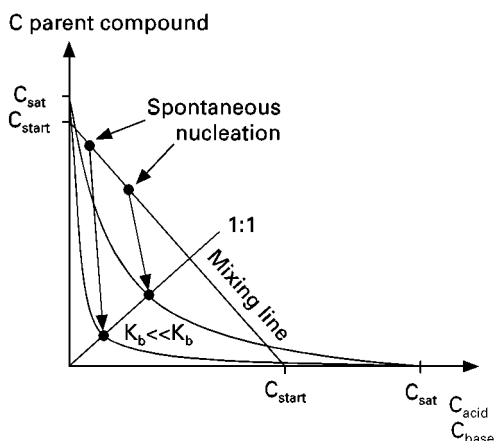


Figure 9 Solubility for a ionic reaction crystallization such as the formation of the salt. The supersaturation at moderate formation constants reaches a high value.

Choice of solvent and of the crystallization technique The choice of solvent for the crystallization of a drug substance is governed by (i) the need to use a Class 3 or Class 2 solvent and (ii) a solvent that does not interact with the drug substance. These considerations limit the solvents allowed to very few, preferably such as ethanol, ethyl acetate and water.

A cooling crystallization is the first choice, if the temperature dependence of the solubility permits it. It is the most straightforward technique for the crystallization, as the temperature, is easily controlled. In most cases, the temperature dependence will be such, that >90–95% of the material dissolved will crystallize upon cooling from a temperature close to the boiling point down to ambient temperatures. Final temperatures down to -10°C can easily be handled; lower temperatures may significantly increase production costs.

If the solubility changes only gradually with temperature, evaporative crystallization, either at ambient or at reduced pressure may be chosen. To increase yield it is often followed by a cooling step.

If the solubility of the drug in the organic solvent is high, and if the solvent cannot be changed and it is

miscible with water, anti-solvent precipitation with water can be used. Since a drowning-out crystallization leads to solvent mixtures that have to be treated afterwards, this technique should be avoided when possible.

Rate of crystallization The rate of crystallization should not exceed values that cause too much uptake of solvent via inclusions. For a cooling crystallization, natural cooling profiles should be avoided, as most of the material crystallizes too fast. Linear cooling rates are a first approximation. The rates can be classified as slow, realistic, fast and crash cooling for rates of < 5 , < 10 , < 15 and $> 15^{\circ}\text{C h}^{-1}$, respectively.

Instead of linear rates, a controlled rate of crystallization should be used where possible; this is especially important for drowning-out crystallizations, for neutralization reaction crystallizations or for the formation of salts. In these cases, even a moderate dosage of the anti-solvent or the acid or base can lead to very high supersaturation which in turn can cause the formation of oils or amorphous material. Often most of the yield is produced during the addition of the first amount of the secondary solvent.

Thus either a very slow dosing or when exactly stepwise dosing with time interval between are appropriate tools to avoid too high supersaturation and the adverse effects usually observed for nucleation and growth at high supersaturation.

At the point of addition, high local supersaturation is generated so that mixing has to be optimized (see **Figure 10**).

Programmes for cooling, evaporative and drowning-out crystallization are derived by requiring the crystallization to proceed with a constant rate of deposition of mass or with a constant linear growth rate. **Figure 11** presents curves for a drug substance having a temperature dependence of the solubility of 40 kJ mol^{-1} . The solubility decreases by a factor of 10 with a change in temperature from 70 to 20°C . However, the calculations yield only the profile, the absolute times are not given.

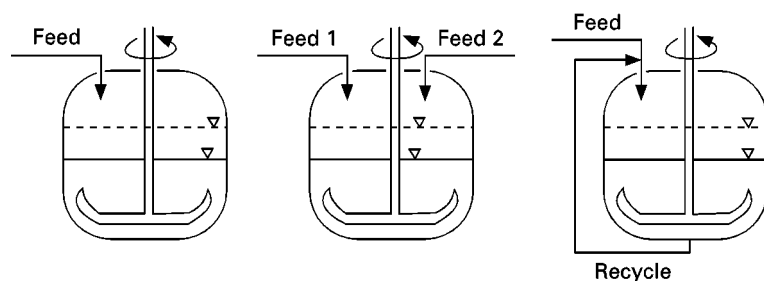


Figure 10 Mixing schemes for precipitation. Dosing of the anti-solvent into the primary solvent (left) is to be avoided. A parallel dosing of both solutions (middle) is better and even better is a dilution scheme (right).

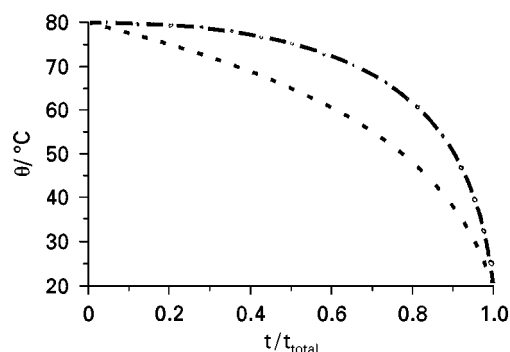


Figure 11 Suggestion for a cooling programme for a drug having a high solubility dependence on temperature. The lower curve is for a constant flux of mass, the upper for a constant rate of crystallization. --- Constant growth rate; --- Constant flux of mass.

Seeding is more likely to succeed for cooling and evaporative crystallizations but rather difficult in drowning-out crystallizations, or in precipitation because these processes are dominated by primary nucleation around the inlets that can hardly be avoided.

Scale-up Crystallization parameters arrived at in the laboratory have to be scaled up for production and this must always be borne in mind. In the laboratory, typically glassware or small crystallization vessels are used. In production, vessels are either glass or glass lined, or are made of stainless steel. The vessels are equipped with a cooling/heating jacket and a distillation device. Stirrers are normally impellers or of the anchor type. Few vessels are baffled, the only device acting in this respect is often the temperature probe.

The scale-up factors from laboratory to production are in the order of $100\text{ mL}^{-1}\text{ L}$ to several 100 L or 1000 L, factors considered high for crystallization operations. The stirrer action can be scaled up using either constant tip velocity or constant power input, as is the case for all crystallization operations.

A problem often encountered in production but seldom in the laboratory is the formation of encrustation during distillation. This is to be avoided, as it can create hot spots and can act as a source of seeds. In this case, the outcome of the crystallization is entirely unpredictable. Encrustations during distillations can be avoided using reflux schemes.

Work-up The classical procedure for the work-up of the crystallized drug substance is centrifugation and washing followed by drying on a tray dryer. This procedure involves a number of transfer steps, where the product can be contaminated or where the product can contaminate the environment.

The number of transfer steps can be minimized by using the filter type dryer shown in **Figure 12**. The device is used for the solid-liquid separation, washing and finally drying. The heat is transferred both through the outer wall and the stirrer. The stirrer facilitates the washing and the drying. However, if this stirrer is used inappropriately, it can act as a milling device and can generate fines down to $<10\text{ }\mu\text{m}$.

Other Crystallization Techniques

Direct contact cooling (DCC) In the direct contact cooling (DCC) process a solution of the drug substance in a primary solvent at a temperature close to saturation is mixed with a liquid coolant, rapidly creating supersaturation, consequently followed by crystallization of the drug substance. Coolants include immiscible as well as miscible liquids and liquidified gases. Recently, solid CO_2 at -60°C has been used as coolant. Coolants that are gaseous under ambient conditions offer the advantage that they can easily be separated from the mother liquor. Depending on the heat capacities and the ratio of mixing very high supersaturations and thus fine particles can be obtained. **Figure 13** shows a SEM micrograph of Abecarnil crystallized by using solid CO_2 coolant.

Spray drying In spray drying, a solution of the drug substance in an appropriate solvent is sprayed into

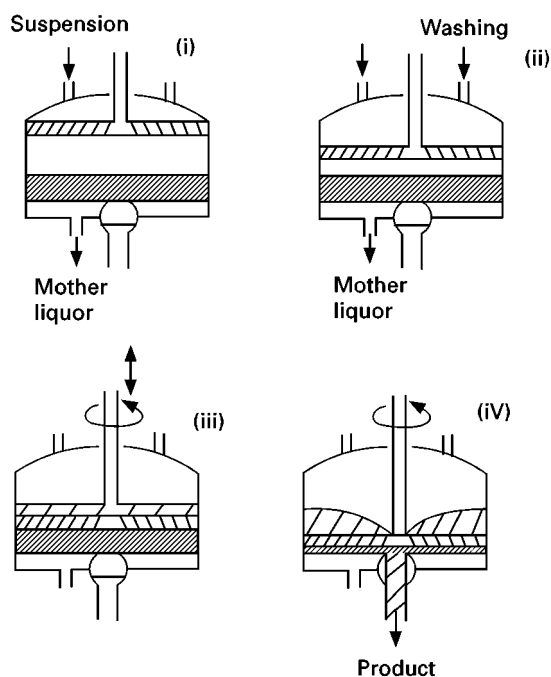


Figure 12 Schematic drawing of a filter dryer, in the states (i) solid-liquid separation, (ii) washing and (iii) drying. The heating is via both the surface of the dryer and the stirrer and (iv) product discharge.

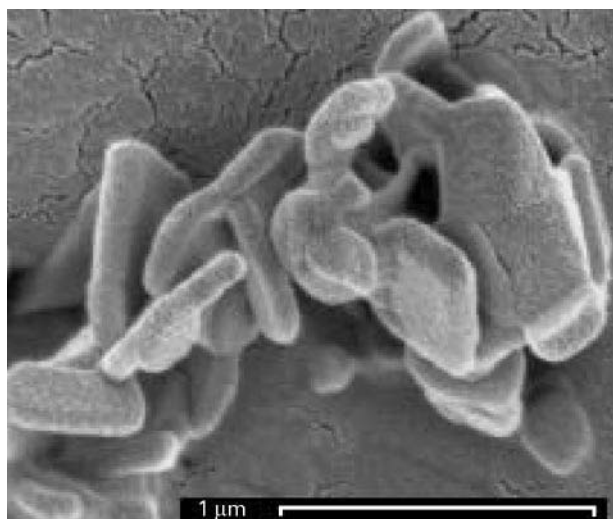


Figure 13 SEM image of Abecarnil obtained by using solid CO₂ as direct contact coolant.

a hot stream of gas that carries the heat both for the evaporation of the solvent and the drying of the product. Although the temperature of the gas stream lies between 200 and 300°C, the maximum temperature that the drug substance is exposed to is close to or less than the boiling point of the solvent. The short residence times also limit the thermal stress.

The particle size attained through spray drying is of the order of micrometres. The habit of the particles obtained strongly depends on the system, typical particle shapes are shown in **Figure 14**. The left micrograph shows well-defined spherical particles, that are fully separated. The right micrograph shows felted needles obtained with a different substance.

In most cases, spray drying will be from organic solvents. In these cases, safety against explosions can be achieved either by keeping the amount of solvent in the stream of air below the explosive limit or by using nitrogen as an inert drying gas.

The solid-state form obtained can be amorphous or crystalline depending on the substance and the drying conditions. The fast evaporation of the solvent can lead to amorphous material. However, if the glass transition temperature of the drug substance is less or equal to the temperature regime in the dryer, a transformation into a crystalline product may occur. This transformation may be facilitated by residual amounts of solvent.

Melt crystallization Melt crystallization techniques are rarely applied for the crystallization of drug substances, as many have a high melting point, typically $\geq 150^\circ\text{C}$, a temperature at which these compounds have a tendency to become unstable if exposed to these temperatures for prolonged periods of time.

Techniques of particle formation The requirement to produce small particles of a drug substance has led to the development of alternative processes of particle formation via a precipitation technique. These processes are as follows:

- RESS: the Rapid Expansion of Solutions of the drug in Supercritical CO₂, or other fluids. This technique is hampered by the low solubility of most drug substances in supercritical fluids. Although modifiers can increase the solubility, they have to be removed effectively to prevent agglomeration or ripening.

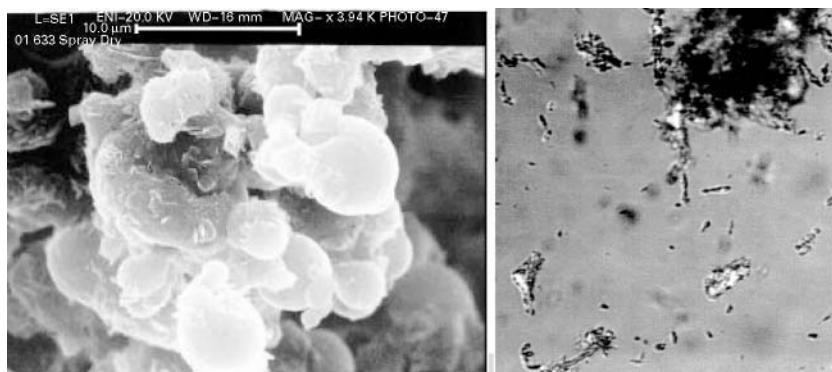


Figure 14 (See Colour Plate 113) Shape of particles obtained via spray drying. The left micrograph shows well-separated spherical particles typically obtained. Note the indentations on one side. The right micrograph shows felted needles that are in addition interwoven. Both products are fully crystalline.

- PCA: the precipitation of the drug substance from a solution in a primary solvent with the aid of a Compressed Anti-solvent, namely CO₂.
- SEDS: Supercritical solution Enhanced Dispersion of Solutions. A solution of the drug in a primary solvent is mixed in a nozzle with a stream of supercritical CO₂ that acts both as dispersant and anti-solvent. The particles form immediately and are collected on filter plates. This technique offers a number of very intriguing advantages such as very small particle size, very low residual solvent contents, or a low surface charge of the particles facilitating the formulation process.

It has been reported, that proteins or peptides crystallized via this technique fully retain their biological activity.

With these processes, crystal sizes down to and below 1 µm can be attained. So far, all these processes work in batch mode with small batch sizes, although attempts are being made to increase the batch size.

The particle formation, nucleation and growth, in all three techniques is rapid. Information on the nucleation and growth process are only emerging and more work needs to be done. Due to the nucleation and growth under very high supersaturations, the polymorphic form obtained might not be the stable one.

Acknowledgements

The authors are indebted to a number of colleagues who helped during the years, namely W.H. Otto and M. Schirmer for their help in crystallization experiments. Other helpful colleagues include T. Backensfeld, S. Erb, P. Höfert, S. Küppers, G. Mann, R. Mertins, P. Nisch, M. Ottnad, R. Richter and G. Winter.

See Colour Plates 111, 112, 113.

See also: II/Crystallization: Control of Crystallizers and Dynamic Behaviour; Polymorphism. III/Supercritical Fluid Crystallization.

Further Reading

- Beckmann W, Budde U and Nickisch K (1998) Development of a seeding technique for the crystallization of the metastable. A modification of Abecarnil. *Organic Process Research and Development* 2: 298–304.
- Blehaut J and Nicoud RM (1998) Recent aspects in simulated moving bed. *Analysis Mag* 26: M60–M70.
- Boistelle R, Klein JP and Guyot-Hermann AM (1996) Éléments de cristallographie et de cristallogenèse à l'usage des industriels de la chimie et de la pharmacie. *S.T.P. Pharma Pratiques* 6: 111–140.
- Brittain HG (ed.) (1995) *Physical Characterisation of Pharmaceutical Solids*. New York: Marcel Dekker.
- Byrn A *et al.* (1995) Pharmaceutical solids: a strategic approach to regulatory considerations. *Pharmaceutical Research* 12: 945–954.
- Grant DJW and Hiuch T (1990) *Solubility Behavior of Organic Compounds*. Chichester: John Wiley.
- ICH-guidelines are found on the internet at www.eudra.org/emea.html. Guidelines Q3C discuss residual solvent content, Q3A the purity of drug substance and Q7A GMP considerations.
- Jaques J, Collett A and Wilen SH (1994) *Enantiomers, Racemates, and Resolutions*. Malabar, Fla: Krieger.
- Masters K (1991) *Spray Drying Handbook*, 5th edn. Burut House, Harlow, Essex: Longman.
- Mersman A (ed.) (1995) *Crystallization Technology Handbook*, 1st edn. New York: Marcel Dekker.
- Mullin JW (1993) *Crystallization*, 3rd edn. London: Butterworth-Heinemann.
- Szejtli J (1982) *Cyclodextrins and their Inclusion Complexes*. Budapest Akademiai Kisdo.

Neutral and Acidic Drugs: Liquid Chromatography

R. K. Gilpin, Wright State University, Dayton, OH, USA

C. S. Gilpin, Ohio University, St. Clairsville, OH, USA

Copyright © 2000 Academic Press

Introduction

Although the general topic of the high performance liquid chromatographic (HPLC) analysis of neutral and acid drugs encompasses a broad range of com-

pounds that include antibacterial agents to vitamin supplements, many of the more common acid compounds are therapeutically active as analgesics, antipyretics, and antiinflammatories (e.g., aspirin, diclofenac, flurbiprofen, ibuprofen, indomethacin, ketoprofen, meclofenamic acid, mefenamic acid, naproxen, tolmetin and other compounds shown in Table 1). In many cases, this group of compounds are relatively small molecules and are structurally simple, containing only one or two aromatic rings and a single ionizable carboxyl group. Many of the common

Table 1 Recently published HPLC methodology for common acid drugs

Analyte	Procedure
General	<p>The simultaneous analysis of twelve common nonsteroidal antiinflammatory drugs has been carried out by reversed-phase chromatography on a C18 column using acetonitrile–phosphate buffer as the eluent and detection at either 230 or 320 nm. The method has been used to evaluate the level of the analytes in human urine samples [5].</p> <p>A fully automated on-line dialysis sample preparation procedure has been developed for assaying several nonsteroidal antiinflammatories in human plasma. In addition different strategies for improving analyte loss due to drug–protein binding are discussed [6].</p> <p>A systematic investigation of the enantioselective separation of 28 α-alkylarylcarboxylic acids on an amylose tris(3,5-dimethylphenylcarbamate) chiral station phase has been carried out and the resulting retention data correlated to a series of molecular descriptors [7].</p> <p>A [2.2.2]-bicyclooctane-based stationary has been developed for the chiral resolution of various profen enantiomers which functions via combination of hydrogen bonding, π–π face-to-face stacking, π–π face-to-edge interactions [8].</p>
Aspirin	<p>A high performance liquid chromatographic (HPLC) method has been developed for the simultaneous determination of aspirin and salicylic acid in transdermal perfusates. The compounds are separated on a C8 column 65 : 35 water–acetonitrile containing 0.2% phosphoric acid. For certain samples, a gradient was introduced by increasing the acetonitrile content of the mobile phase after the salicylic acid had eluted [9].</p> <p>Aspirin and salicylic acid have been determined in skin and plasma samples by an isocratic reversed-phase method that uses a C18 column and 75 : 25 pH 2.5 phosphate buffer–acetonitrile as the eluent [10].</p> <p>Gradient elution reversed-phase methods have been developed for measuring aspirin and warfarin in combination tablet formulations and in the presence of potentially related impurities that uses a C8 column operated at 40°C. In the first instance the starting conditions, which are maintained for 11 minutes, are 68 : 17 : 15 water adjusted to pH 2.6 with formic acid–methanol–acetonitrile. This is followed by a linear gradient over 15 minutes to 56 : 17 : 27 of the respective solvents and a hold time of an additional 38 minutes. When assaying for possible related substances, a second gradient step is used to 13 : 17 : 70 [11].</p> <p>An isocratic reversed-phase assay has been reported for measuring aspirin, salicylic acid, and warfarin sodium. The separations are carried out on a C18 column using 23 : 5 : 5 : 67 acetonitrile–tetrahydrofuran–glacial acetic acid–water as the eluent with UV detection at 282 nm. The method has been used to study tablet dissolution [12].</p> <p>An alternate isocratic reversed-phase method has been developed for measuring the analyte in model solution aerosols. It uses a C8 column with 44 : 5 : 5 methanol–THF–1 M phosphoric acid qs to 100 with water as the eluent and UV detection at 275 [13].</p>
Diclofenac	<p>An isocratic reversed-phase method has been reported for measuring the analyte and flurbiprofen in plasma. It uses a C18 column and 35 : 65 acetonitrile–0.1 M sodium acetate adjusted to pH 6.3 with glacial acetic acid as the eluent and detection at 278 nm [14].</p> <p>The analyte has been detected fluorometrically as its photodecomposition product, carbazole-1 acetic acid, after on-line post column UV irradiation. Excitation and emission wavelengths of 286 nm and 360 nm are used respectively. The photoderivative is formed via loss of both chlorine substituents and ring closure [15].</p> <p>Solid-phase extraction in combination with isocratic reversed-phase chromatography has been used to measure the analyte as well as indomethacin and phenylbutazone in human urine. The separations were performed on a C18 column using 42 : 58 acetonitrile–10 mM pH 4 acetate buffer as the eluent and detection at 210 nm [16].</p> <p>The analyte has been assayed in the presence of oxybuprocaine in human aqueous humor by reversed-phase HPLC-EC using a C8 column coated with a hydrophilic polyoxyethylenepolymer. The detection limit for the analyte is 500 pg [17].</p> <p>Pharmaceutical formulations containing the analyte, cyanocobalamin, and betamethasone have been assayed on a C18 column operated at 34°C employing 60 : 40 acetonitrile–water adjusted to pH 3.45 with acetic acid as the eluent and detection at 240 nm [18].</p> <p>See general methodology above [5].</p>
Felbinac	See general methodology above [5].
Fenbufen	See general methodology above [5].
Fenoprofen	See general methodology above [6].

Table 1 *Continued*

Analyte	Procedure
Flurbiprofen	See general [5,6] and diclofenac [14] methodology above.
Ibuprofen	<p>A reversed-phase method has been developed for studying the analyte and five metabolites that uses a 1.5 mm i.d. semi-microcolumn and a linear gradient over 70 minutes from 2:98 acetonitrile–phosphate buffer (pH 2.5 0.05 M) to 60:40 of the respective components. Both UV and EC detection were used to obtain information about glucuronation [19].</p> <p>The analyte has been assayed in erythrocytes and plasma by an isocratic reversed-phase procedure following its liquid–liquid extraction with methylene chloride. The separation is carried out on a C18 column with 22:10 methanol–water acidified with perchloric acid to pH 3 as the eluent and UV detection at 222 nm [20].</p> <p>Two cellulose-based chiral phases (Chiralcel OD and Chiralcel OJ) have been evaluated for their ability to resolve various aliphatic ibuprofen esters and the latter material in combination with nonaqueous eluents provided effective resolution of most of the esters [21].</p> <p>The retention properties of a molecularly imprinted 4-vinylpyridine/ethylene glycol dimethacrylate polymer for (S)-ibuprofen have been evaluated using aqueous eluents. The novel packing, which is prepared via a multi-step swelling and thermal polymerization method, also has been used to partially resolve the enantiomers of ibuprofen metabolites, 2-hydroxy- and 2-carboxyibuprofen [22].</p> <p>Both zonal elution and high-performance affinity techniques have been used to characterize the interaction of enantiomers of ibuprofen with immobilized human serum albumin [23].</p> <p>The stereo specific analysis of two major metabolites of ibuprofen (hydroxyibuprofen and carboxyibuprofen) in urine has been carried out using a sequential achiral–chiral HPLC approach. The achiral separation was carried out under normal-phase conditions using a silica column and 98.2:1.8 hexane–ethanol with 0.05% trifluoroacetic acid (THF) as the eluent. The fraction containing the two metabolites is collected, evaporated to dryness, and redissolved in 92:8 hexane–ethanol with 0.05% THF (i.e. the chiral eluent). Subsequently, the chiral separation is performed on a Chiralpak AD CSP column [24].</p> <p>A method has been reported for simultaneously determining the four major metabolites of the analyte in biological fluids. It uses a silica column and N-cetyl-N,N,N-trimethylammonium hydroxide dissolved in the eluent to dynamically modify it [25].</p> <p>A column-switching system has been developed for measuring ibuprofen directly in plasma that employs three sequential separation steps: (1) the deproteinization and fractionation of 100 mL plasma samples with a polymer-coated mixed-function phase column, (2) concentration with an intermediate column, and (3) a final analytical separation. The reported dynamic range for the analyte is 0.1–250 mg mL⁻¹ with intra-day and inter-day variation of less than 5.6% and 6.5% respectively and a detection limit of 25 ng mL⁻¹ [26].</p> <p>See general methodology above [5,6].</p>
Indomethacin	<p>The analyte has been assayed in plasma samples on a C18 column operated at 50°C in combination with 50:50 acetonitrile–6 mM phosphoric acid as the eluent and detection at 205 nm [27].</p> <p>A study has been carried out to examine the loss of the analyte as well as ibuprofen and flufenamic acid in valve injectors for samples in non-eluting solvents [28]. Likewise, the assessment of injection volume limits when using on-column focusing with microbore LC has been evaluated [29].</p> <p>See general methodology [5] as well as methodology for diclofenac [16] above.</p>
Ketoprofen	<p>An isocratic method has been developed for measuring the analyte in tissue samples following a two-step extraction procedure which involves an initial extraction into methylene chloride and back extraction following acidification with HCl into 95:5 isooctane–isopropanol. Subsequently, HPLC separation is carried out on a C18 column using 43:57 acetonitrile–water containing 0.1% glacial acetic acid and 0.03% triethylamine [30].</p> <p>Zonal elution in combination with a novel mathematical approach has been used to characterize the mechanisms involved in the stereoselective binding of ketoprofen enantiomers to immobilized human serum albumin [31].</p> <p>A stereospecific HPLC assay has been reported for the analyte in human plasma and urine that employs an amylose carbamate column and 80:20 hexane–isopropanol with 0.1% trifluoroacetic acid as the eluent [32].</p> <p>See general methodology above [5,6].</p>
Loxoprofen	See general methodology above [5].
Mefenamic acid	See general methodology above [5].

Table 1 *Continued*

Analyte	Procedure
Naproxen	Recently uniform-sized molecularly imprinted polymers for (S)-naproxen have been prepared using 4-vinylpyridine and ethylene glycol dimethacrylate as functional monomer and cross-linker respectively [33]. Subsequently, this material was modified further with a hydrophilic external layer via treating it with a 1 : 1 mixture of glycerol monomethacrylate and glycerol dimethacrylate. Likewise, molecularly imprinted polymers for the analyte have been prepared using 4-vinylpyridine and ethylenedimethacrylate [34]. In this latter study two different polymerization approaches were tested and materials prepared by the thermal route were found to have better chiral selectivity. See general methodology above [5,6].
Piroxicam	See general methodology above [5].
Sulindac	See general methodology above [5].

profens and compounds like ibuprofen and xenbucic fit this general description as illustrated in **Figure 1**. However in some cases, with compounds such as indomethacin, caprofen, tolmetin, and zomepirac, additional functional groups are present which influence the chemical equilibria of the solutes and hence make generalization about separation conditions more difficult.

The most common of the non-steroidal analgesic/anti-inflammatories is aspirin, which is sold throughout the world as an over-the-counter (OTC) product and in combination with other non-acid analgesics as well as various other cough-cold agents. However in more recent years, compounds like ketoprofen and ibuprofen, which were first introduced as prescription products for the treatment of arthritis and related inflammatory disorders, are now available in OTC dosage forms and popular for their analgesic properties. When considered as a group, the number of pharmaceutically important acid analgesics/antiinflammatories is relatively small, but because of their widespread therapeutic usage, hundreds of assay procedures have been reported for these compounds, many of which are HPLC based.

In terms of the neutral drugs, perhaps the most common of these are hormones/steroids, certain vitamins (e.g. A, D and E), the pharmaceutical co-additives (e.g. alkyl parabens), and other miscellaneous compounds like the anticoagulant, warfarin, the coronary vasodilator, visnadine, and the antineoplastic agent, carubicin. Some of the more common examples of non-ionizable pharmaceutically active compounds are listed in **Tables 2** and **3** along with the accompanying analytical methodology that has appeared more recently. A number of these have been assayed by HPLC in combination with either mass spectrometry or an alternate detection technique to more commonly used UV monitoring. Also, unlike ionizable drugs that typically require buffers to obtain sufficient solute phase interaction, the neutral

drugs are often separated using neat binary hydroorganic eluents in combination with either a C8 or C18 stationary phase. However, unlike the acid drugs, which contain at least one aromatic ring and are easily detectable using standard UV monitoring at 254 nm, a large number of them (i.e. the steroids) contain only a carbonyl group(s) (λ_{max} about 210 nm) and are less favourably detectable by UV monitoring.

Because of the very large number of HPLC procedures that have appeared for neutral and acid drugs, as well as for the related metabolites and degradation products of these, it is not possible to do an extensive review of them in the space limitations of the current chapter. Rather, a more general discussion of important principles and strategies in developing HPLC methods is presented, accompanied by representative analytical procedures for a number of the more important compounds that have appeared in the recent literature. However, for additional information the reader is referred to the comprehensive biennial reviews, *Pharmaceutical and Related Drugs*, that have appeared in *Analytical Chemistry*.

General Trends and Considerations

Over the last three decades HPLC-based methods have become increasingly popular and currently are the most widely used procedures for assaying pharmaceutical compounds. Their growing acceptance has resulted from the inherent versatility and reliability of the methodology, improvements in hardware, and ease of use and automation. Likewise, fundamental sample considerations such as thermal instability, low volatility, and matrix complexity have been important contributing factors.

The selection of the appropriate separation mode is dependent on the solubility and size of the analyte. Since most of the acid and neutral drugs are relatively small analytes that can be dissolved in either water or hydroorganic solvents, and are either neutral or their

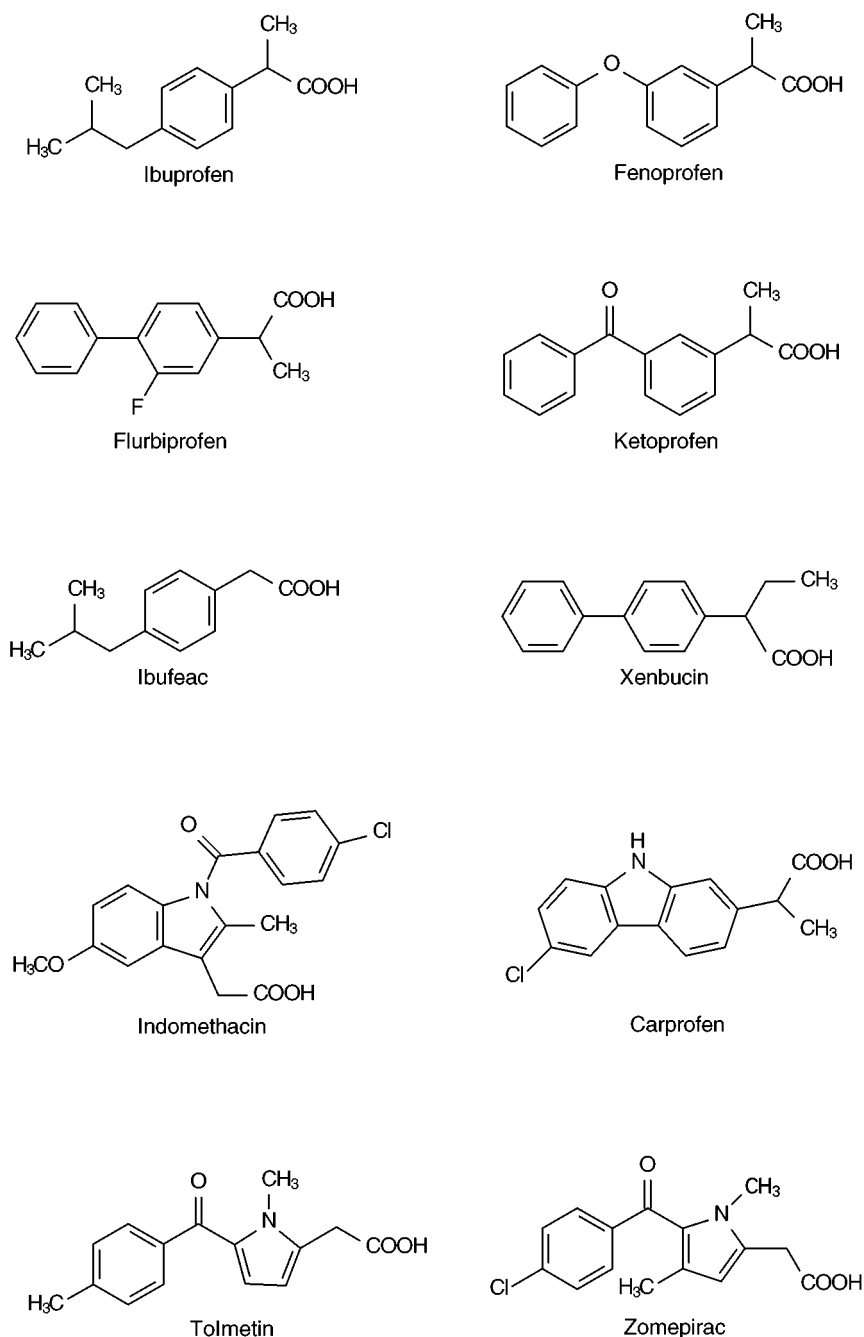


Figure 1 Examples of some common acid drugs.

chemical equilibria can be favourably controlled, reversed-phase (RP) procedures dominate the literature. However, in cases where structural differences are small (e.g. certain steroids, closely related impurities, or degradation products that result in only very minor changes to the analyte hydrophobicity) normal-phase conditions may provide better selectivity. In addition, if the intended application is to measure the level of a single active ingredient and to assure that it is

within acceptable standards during manufacture of the formulated product, then simplicity, reliability, speed, and cost become important factors in selecting the overall approach. Typically in this situation, assays based on the use of isocratic eluents are more effective than those based on gradient elution conditions since they are easier to carry out by the less trained practitioner. Alternatively, if the analytical problem involves more complex samples or less

Table 2 Recently published HPLC methodology for steroids

Analyte	Procedure
General	<p>Several reversed-phase HPLC methods have been developed for assaying a variety of corticoid alcohols and their corresponding esters and acetals derivatives. All are carried out with a C18 column in combination with several aqueous–acetonitrile eluents, either deoxycorticosterone or methylprednisolone as internal standards, and UV detection. In addition to the parent analytes studied (i.e. fluorocortisone and fluorocortisone acetate, triamcinolone and triamcinolone acetoneide, dexamethasone and dexamethasone phosphate, 21-hydroxydeflazocort and deflazacort, betamethasone and betamethasone valerate), the methods have been used to examine the hydrolysis of the analytes in aqueous media at different pH and temperature conditions [35].</p> <p>Several conjugated and unconjugated estrogens and related impurities have been assayed by reversed-phase chromatography in combination with postcolumn online photochemical derivatization via UV irradiation (254 nm) of the column effluent prior to fluorescence detection (excitation 280 nm; emission 410 or 312 nm). The photo induced modifications were useful for the identification of the various estrogens. The method has been used to evaluate raw materials and pharmaceutical formulations [36].</p> <p>The influence of temperature on the high-performance chromatographic separation of steroids using eluents containing β-cyclodextrin has been studied [37].</p> <p>The analysis of several binary drug mixtures have been carried out using either C18 or cyano bonded phases in combination with on-line post-column photochemical derivatization [38]. In another study, the simultaneous determination of glucocorticoids in plasma and urine using HPLC in combination with precolumn fluorimetric derivatization with 9-anthroyl nitrile has been considered [39].</p> <p>The quantitative structure-chromatographic retention relationship of underivatized equine estrogens have been investigated [40].</p> <p>The feasibility of using a combined liquid chromatographic–thermospray mass spectrometric–isotope dilution approach for measuring corticosteroids in human plasma has been evaluated. The selection of the eluent composition and its effect on the MS results are discussed [41].</p> <p>The use of particle-loaded membranes to extract steroids prior to their HPLC analysis has been considered in terms of improvements in analyte stability and detection [42].</p>
Beclomethasone	<p>Metered-dose inhalers containing the analyte have been studied a simple isocratic method that uses a C8 column and 50 : 50 acetonitrile–water as the eluent [43].</p> <p>HPLC methodology as well as other related assay procedures have been evaluated as a means of measuring the active ingredients and excipients found in commercial nasal sprays. The samples studied were highly viscous and contained a large number of particles in suspension. As such, special emphasis was paid to sample cleanup prior to analysis. Of the techniques examined, liquid chromatography was found best in terms of reproducibility and speed for assaying beclomethasone dipropionate, fluticasone dipropionate and benzalkonium chloride [44].</p>
Betamethasone	<p>Different hyphenated liquid chromatographic (LC) and mass spectrometric (MS) techniques have been evaluated for their use as fast direct analytical methods of measuring betamethasone in hydrolysed and non-hydrolysed urine. Following both the LC, thermospray, and mass spectrometric parameters separately several combined approaches were examined which included LC in combination MS–MS, coupled-column LC (LC–LC) combined with single quadrupole MS, and LC–LC–MS–MS. Neither of the three-step configurations (LC–MS–MS and LC–LC–MS) did not give satisfactory results. However, LC–LC–MS–MS analysis was found to meet the requirements of high sample throughput speed, selectivity, and sensitivity [45].</p> <p>See general methodology above [35].</p>
Cortisol	See general methodology above [41].
Cortisone	<p>Electrochemically modulated HPLC, a technique developed by Deinhammer and co-workers, has been used to assay four common steroids including the analyte. The separations were carried out using a stainless-steel column containing both a tubular Nafion cation-exchange membrane and packing of porous graphitic carbon spheres, a mixture of 50 : 50 acetonitrile–water containing 0.1M-HClO₄/0.1M-LiClO₄ as the eluent, an open-circuit potential of + 0.44 V vs. Ag/AgCl/saturated NaCl and detection at 258 nm. The unique aspect of this technique is the ability to adjust analyte retention by manipulating the applied column potential [46].</p> <p>See general methodology above [41].</p>
Deflazacort	See general methodology above [35].
Dexamethasone	<p>On-line coupled immunoaffinity chromatography-reversed-phase high-performance liquid chromatography particle beam interfaced quadrupole ion trap mass spectrometry has been used to measure dexamethasone and flumethasone [47].</p> <p>See general methodology above [35].</p>

Table 2 *Continued*

Analyte	Procedure
Fluorocortisone	See general methodology above [35].
Fluticasone	<p>The purity of batches of bulk drug substance has been evaluated via a combination of directly coupled HPLC–NMR spectroscopy and HPLC–MS. The separations are carried out on a C18 column using a multilevel gradient produced with D₂O and acetonitrile [48].</p> <p>High-performance liquid chromatography/atmospheric pressure chemical ionization mass spectrometry has been used to quantify fluticasone propionate in human plasma. The eluent was 50 : 50 water–ethanol and the mass spectrometer was set to monitor masses of 473.2 and 501.2 <i>m/z</i>, which correspond to the internal standard (i.e. the 22R epimer of budesonide) and the analyte respectively [49]. This same analyte also has been measured in plasma using an automated solid-phase extraction liquid chromatography tandem mass spectrometric approach [50].</p> <p>See methodology for beclomethasone above [44].</p>
Hydrocortisone	<p>The analyte has been assayed in gel formulations by a reversed-phase isocratic procedure using a C18 column and 60 : 40 methanol–pH 7.5 0.02 M phosphate buffer as the eluent [51].</p> <p>A normal-phase procedure has been developed for simultaneously measuring prednisolone and hydrocortisone in human serum. A silica column is used in combination with 266 : 120 : 26 : 0.8 n-hexane–dichloromethane–methanol–acetic acid as the eluent [52].</p> <p>See methodology for cortisone above [46].</p>
Lenonorgestrel	The orally active, progestational agent, levonorgestrel (l) in transdermal patches has been extracted with methanol and separated isocratically on a C18 column with 55 : 45 acetonitrile–water as the eluent and detection at 225 nm. The average recovery of 1 mg of the analyte from patches was 99% with an RSD of 0.4% [53].
Prednisolone	See general methodology [41] as well as methodology for cortisone [46] and hydrocortisone [52] above.
Prednisone	See general methodology [41] and methodology for cortisone [46] above.
Triamcinolone	An isocratic reversed-phase method has been reported for measuring triamcinolone acetonide in ointment preparations. The separations are carried out with a C18 column and either 35 : 65 acetonitrile–water or 55 : 44 : 1 methanol–water–acetic acid [54].
Triamcinolone	See general methodology above [46].

routine usage such as that encountered during drug discovery and product development, then specificity, versatility, and flexibility are the most important factors and gradient and multilevel elution, combination column, and novel detection approaches may not only be more convenient, but necessary. Additionally, gradient elution and alternate detection approaches may provide an important advantage in the detection and identification of trace impurities, especially if they vary significantly in their structures and polarity.

As noted above, an important trend in drug discovery and development has been the ever expanding usage of HPLC and the development of separation procedures that are based on reversed-phase conditions. An inspection of the recent pharmaceutical literature reveals that by far the most typical set of RP conditions used to measure neutral and acidic drugs employ either 150 or 250 mm conventional bore columns packed with either octadecyl or octyl 5 to 10 μ m porous silica-based stationary phases in combination with either water–methanol or water–acetonitrile as eluents. Typically, octyl bonded phases

are used for more hydrophobic analytes or if the analyte is easily resolved on an octadecyl phase, to reduce the amount of organic co-solvent in the hydroorganic eluent. An alternate approach to reducing the chain length of the bonded groups is to use shorter columns. For the neutral drugs, other retention modifying agents (i.e. those that are added to the eluent to suppress unfavourable equilibria) are not needed and for many of the common acid drugs, such as the non-steroidal analgesics/antiinflammatories (see Table 1), the most common eluent modifiers are simple buffers added to minimize ionization.

Chemical Equilibria and Methods Development

In the case of neutral drugs, pH control of the eluent is unnecessary. The reason for this is theoretically illustrated in Figure 2 by the series of dashed lines labeled 1', 2', 3' and 4' (i.e. constant $\ln k'$ vs. eluent pH) for a homologous series of alkyl esters, such as

Table 3 Recently published HPLC methodology for miscellaneous acid and neutral pharmaceutical agents

Analyte	Procedure
Ascorbic acid	<p>The stability of the analyte as well as ascorbyl palmitate and magnesium ascorbyl phosphate have been studied using an amino column and either 40:60 acetonitrile–pH 4 phosphate buffer or 70:30 methanol–pH 3.5 phosphate buffer as the eluents [55].</p> <p>A review with 70 references has been published that considers the use of different detection methods as well as other HPLC conditions for assaying L-ascorbic acid, its dehydro oxidation product, D-isoascorbic acid, and its dehydro oxidation product [56].</p>
Etoposide	<p>A reversed-phase method, which uses a phenyl column, 23:77 acetonitrile–25 mM citric acid–50 mM sodium (pH 2.4) buffer as the eluent and electrochemical detection, has been developed for simultaneously assaying etoposide and its <i>O</i>-demethylated metabolite, etoposide catechol in human plasma. Prior to carrying out the chromatographic separation, the samples are extracted using chloroform and methanol. In addition, the long term stability of etoposide and etoposide catechol in human plasma containing ascorbic acid and stored at 27°C has been demonstrated and the procedure has been used to study the analytes pharmacokinetics in plasma following etoposide administration [57].</p> <p>Several combined HPLC–fluorimetric detection procedures have been developed for measuring the analyte and related compounds in physiological media [58–61].</p>
Parabens	<p>Alkyl esters of <i>p</i>-hydroxybenzoic acid have been separated on a C18 column using 60:40 methanol–water as the eluent and detection at 254 nm [62].</p>
Retinoic acid	<p>A gradient elution method has been developed for measuring 9-<i>cis</i>-retinoic acid and its major metabolite, 4-<i>oxo</i>-9-<i>cis</i>-retinoic acid in human plasma. The analytes are first extracted with methyl-<i>tert</i>-butyl-ether and then separated on a C18 column by employing a multilevel gradient approach. The gradient components are pH 2.7 acetate buffer and methanol and detection is at 348 nm. The method is selective against endogenous compounds and potential metabolites (retinol, all <i>trans</i>-, 13-<i>cis</i>-, and 4-hydroxy-9-<i>cis</i>-retinoic acid) [63].</p> <p>Normal-phase liquid chromatography/mass spectrometry has been used to study the photo degradation of retinoic acid. The chromatographic separations were performed on a silica column using 96.5:3.5 hexane–tetrahydrofuran containing 0.015% acetic acid as the eluent. Isomerization to form 5,6-epoxides occurred more readily in solution than in the solid form and 13-<i>cis</i> retinoic acid oxidized more readily than the all-<i>trans</i> isomer [64].</p>
Vitamin A	<p>UV, electrochemical, and particle beam mass spectrometry have been evaluated for use in assaying vitamins A and E in infant formula and related samples. Separations were carried on both a standard and micro bore C8 columns using hydroorganic eluents [65].</p>
Vitamin E	<p>See methodology for vitamin A above [65].</p>

alkyl esters of *p*-hydroxybenzoic acid (i.e. methyl, ethyl, propyl, and butyl paraben). Shown in **Figure 3** is a representative chromatogram of the separation of this series of analytes carried out on a short column containing an octyldecyl reversed-phase packing using a simple binary hydroorganic eluent. Likewise, this separation demonstrates how retention is influenced by simple hydrophobic changes in the molecule and a plot of $\ln k'$ vs. carbon number is linear with a slope related to the incremental methylene selectivity. The addition of a polar substituent (e.g. a hydroxyl group) will result in a shift to shorter retention.

For many of the more common acid drugs, the most often used eluent modifiers are simple buffers that are added to control the protonation/deprotonation of the ionizable carboxyl group and hence to alter the reversed-phase retention properties of the analyte. A simple rule for reversed-phase separations

is that by decreasing the extent of dissociation of the analyte one increases its interaction with the stationary phase, hence increasing its retention and the possibility of resolving like compounds. This also is illustrated in **Figure 2**, which shows how eluent pH influences the retention of a series of homologous acids with the general structure RCOOH , where R would be the alkyl chain in fatty acids or it would include all structural features in the molecule except the carboxyl group (e.g. as shown in Figure 1 where the basic structure of ibufec is compared to the structure of ibuprofen which contains an additional methyl group). In the deprotonated form (RCOO^-), the acid drug elutes quickly from the column, whereas in the protonated form (RCOOH), it is retained to an increasing degree based on the hydrophobicity of the molecule. As in the case of the neutral compounds, the incremental addition of carbons to R results in a predictable incremental increase in

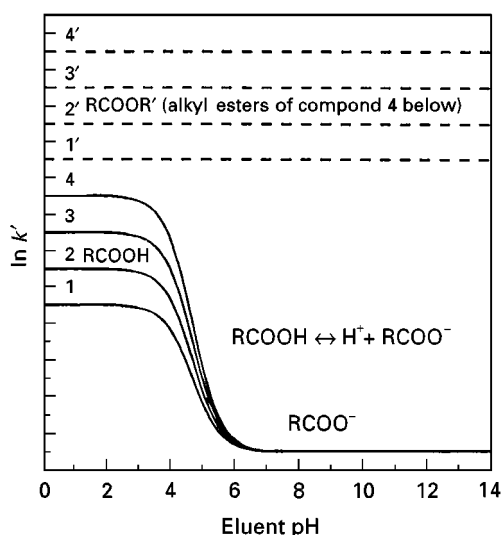


Figure 2 Influence of eluent pH on the retention properties of neutral (dashed lines) and simple monoprotic acid (solid lines) drugs. Curves 1–4 show the incremental change in $\ln k'$ as a function of incremental addition of carbon to simple ionizable solutes, and 1'–4' show the continued incremental change when carbons are added to the alkyl ester portion of monoprotic compounds represented by solid line 4.

retention. This is illustrated by the family of retention curves in **Figure 2** (solid lines labeled 1–4). In the fully protonated form, as in the case of the neutral compounds, the relationship between retention and size (i.e. carbon number) of the aliphatic portion of the homologue is logarithmic.

Typically, the preferred set of conditions for the separation of simple acid drugs (i.e. monoprotic compounds) is in the plateau region of the curves shown

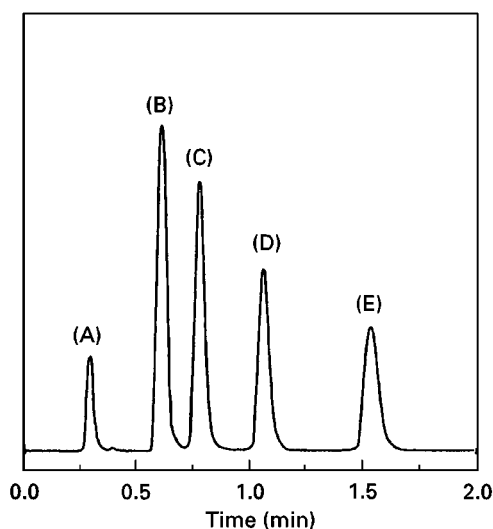


Figure 3 Reversed-phase separation of paraben homologues. Solutes: (A) unretained peak, (B) methyl paraben, (C) ethyl paraben, (D) propyl paraben, and (E) butyl paraben.

in **Figure 2**. Experimentally, this is accomplished by adjusting the pH of the eluent to about 1 to 1.2 pH units below the pK_a of the carboxyl group which is approximately 4.7. When the eluent is buffered to about 3.5, the solute exists predominately in its uncharged form and its retention is governed by the hydrophobic interactions between the nonpolar portion of the molecule and the immobilized alkyl chains of the bonded phase. However, once the eluent pH is adjusted to this region, further adjustments to lower pH will have little effect on the quality of the separation, but will lead to increased chances of phase instability and decreases in the long term performance of the column. A working range for most silica-based bonded phases is 3.0 to 8.5 which is within a useful range for resolving most acidic drugs without the addition of more exotic eluent additives.

As the analyte becomes more complex in terms of the presence of multiple functionality and other structural features, it is often not possible to predict in advance many of the subtleties controlling retention. Considering some of the related non-steroidal analgesic/anti-inflammatories appearing in **Figure 1**, it is possible to predict that ibuprofen will elute before ibuprofen, since the molecules are structurally very similar except ibuprofen contains an additional methyl carbon. However, it is much more difficult to predict how long indomethacin will be retained compared to tolmetin or the elution order of ketoprofen, fenoprofen, and flurbiprofen. Nevertheless for the latter set of compounds, since they are structurally similar, it is reasonable to suggest that an assay developed for ketoprofen might be a useful starting point for fenoprofen. Additionally, it is reasonable to suggest that the pH of the eluent for separating the first six compounds in **Figure 1**, which are all monoprotic acids should be in the 3.5 range, since the only important structural feature requiring eluent buffering, is the carboxyl group.

Representative Methodology

Summarized respectively in **Tables 1–3** are HPLC methods that have appeared recently for assaying some of the more common (1) non-steroidal anti-inflammatories/analgesics, (2) steroids, and (3) other miscellaneous neutral and acid drugs. These represent only a fraction of the numerous analytical procedures that have appeared and many of them are useful for measuring the analyte in biological materials as well as in formulated products. Shown respectively in **Figures 4–7** are representative separations of common non-steroidal anti-inflammatory drugs, aspirin and salicylic acid, several important steroids, and the fat-soluble vitamins A, D and E. In all cases the

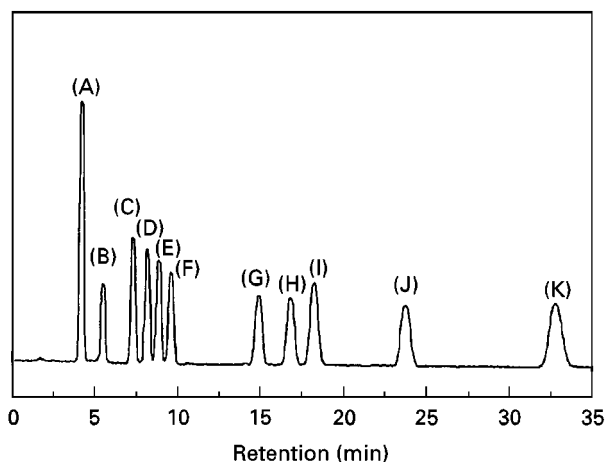


Figure 4 Reversed-phase separation of common nonsteroidal antiinflammatory drugs. Conditions: C_{18} column using 42:58 acetonitrile–phosphate buffer (pH 5.0) as the eluent. Solutes: (A) sulindac, (B) loxoprofen, (C) ketoprofen, (D) naproxen, (E) felbinac, (F) fenbufen, (G) flurbiprofen, (H) diclofenac, (I) indomethacin, (J) ibuprofen, and (K) mefenamic acid. (Chromatogram redrawn from Hirai, Matsumoto and Kishi, 1997.)

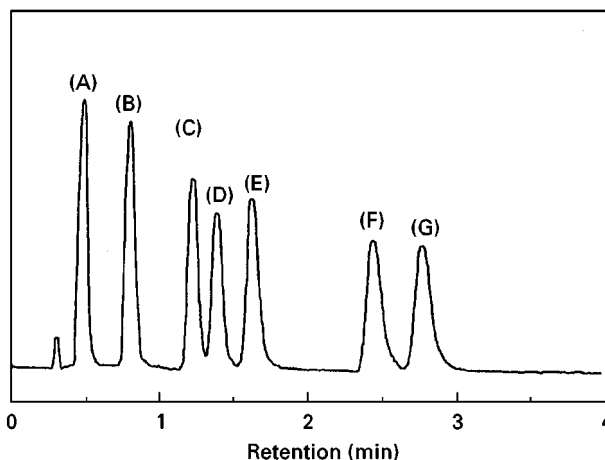


Figure 6 Reversed-phase separation of common steroids. Conditions: C_{18} column using 20:80 acetonitrile–phosphate buffer (pH 3.0). Solutes: (A) hydrocortisone, (B) corticosterone, (C) 11- α -hydroxyprogesterone, (D) unidentified compound, (E) 11-keto progesterone, (F) deoxycorticosterone, (G) 17- α -hydroxyprogesterone. (Chromatogram redrawn from *J. Chromatogr. Sci.* 1995, 33: 411.)

chromatograms were obtained under reversed-phase conditions using either an octyl or octadecyl column. In the first three examples standard bore columns were used in combination with UV detection and in the latter vitamin assay the separation was performed on a narrower 2.0 mm i.d. column using both UV and electrochemical detection.

In addition to the relatively common approaches in terms of separation mode and operating conditions

discussed above, other important considerations have been addressed in the literature. These include analyte-cleanup prior to carrying out the HPLC separation, evaluation of optical purity, and the development of novel phases such as molecularly imprinted polymers as well as the use of alternate detection techniques like mass spectrometry and fluorescence to improve sensitivity and selectivity. In the latter instance, post-column photo-decomposition/derivatization has been used in methods developed for simple acid drugs such

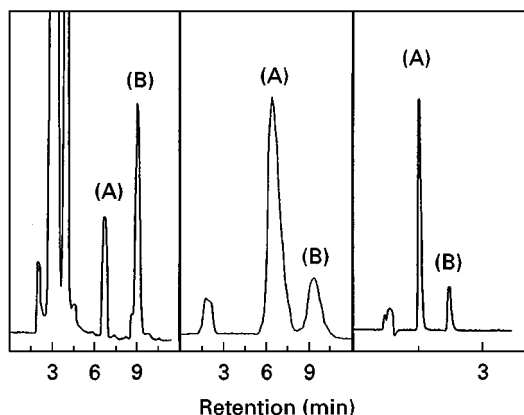


Figure 5 Reversed-phase separations of aspirin and salicylic acid. Conditions: left: C_8 column using 35:65 acetonitrile–water containing 0.2% orthophosphoric acid, centre: C_{18} column 25:75 acetonitrile–phosphate buffer (pH 2.5), right: C_{18} column 23:5:5:67 acetonitrile–tetrahydrofuran–glacial acetic acid–water. Solutes: (A) aspirin and (B) salicylic acid. (Chromatograms redrawn from McMahon, O'Connor, Fitzgerald, leRoy and Kelly, 1998, Pirola, Bareggi and DeBenedictus, 1998, McCormick, Gibson and Diana, 1997, respectively.)

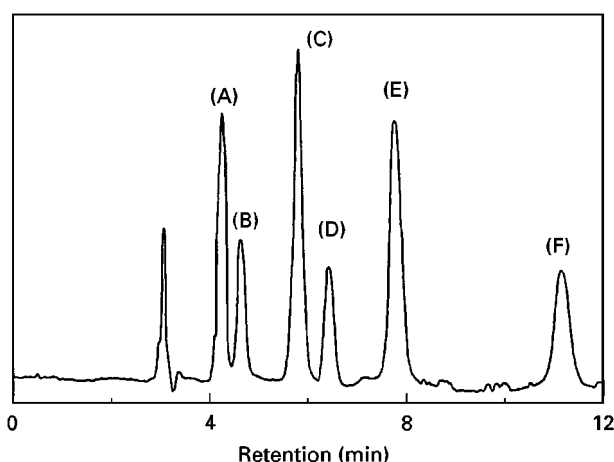


Figure 7 Reversed-phase separation of fat-soluble vitamins. Conditions: C_8 column using 92:8 methanol–water. Solutes: (A) vitamin A, (B) vitamin A acetate, (C) vitamin D_3 , (D) vitamin E, (E) vitamin E acetate, and (F) vitamin A palmitate. (Chromatogram redrawn from Andreoli, Careri, Manini, Mori and Musci, 1997.)

as diclofenac, conjugated and unconjugated estrogens and related impurities, and binary drug mixtures containing either betamethasone, hydrocortisone, desonide, dexamethasone, or triamcinolone.

Further Reading

- [1] Gilpin RK and Pachla LA (1999) *Analytical Chemistry* 71: 217R–233R.
- [2] Gilpin RK, Jaroniec M and Lin S (1990) *Chromatographia* 30: 393.
- [3] Jaroniec M, Lin S and Gilpin RK (1990) *Analytical Chemistry* 62: 2092.
- [4] Horvath C and Mellander W (1997) *J. Chromatogr. Sci.* 15: 393.
- [5] Hirai T, Matsumoto S and Kishi I (1997) *Journal of Chromatography B: Biomedical Sciences and Applications* 692: 375–388.
- [6] Herraiz-Hernandez R, van de Merbel NC and Brinkman UATH (1995) *Journal of Chromatography B: Biomedical Sciences and Applications* 666: 127–137.
- [7] Booth TD and Wainer IW (1995) *Journal of Chromatography A* 737: 157–169.
- [8] Pirkle WH and Yuelong L (1996) *Journal of Chromatography A* 736: 31–38.
- [9] McMahon GP, O'Connor SJ, Fitzgerald DJ, leRoy S and Kelly MT (1998) *Journal of Chromatography B: Biomedical Sciences and Applications* 707: 322–327.
- [10] Pirola R, Bareggi SR and DeBenedittis G (1998) *Journal of Chromatography B: Biomedical Sciences and Applications* 705: 309–315.
- [11] Montgomery ER, Taylor S, Segretario J, Engler E and Sebastian D (1996) *Journal of Pharmaceutical and Biomedical Analysis* 15: 73–82.
- [12] McCormick TJ, Gibson AB and Diana FJ (1997) *Journal of Pharmaceutical and Biomedical Analysis* 15: 1881–1891.
- [13] Blondino FE and Byron PR (1995) *Journal of Pharmaceutical and Biomedical Analysis* 13: 111–119.
- [14] Giagoudakis G and Markantonis SL (1998) *Journal of Pharmaceutical and Biomedical Analysis* 17: 897–901.
- [15] Kuhlmann O and Krauss G (1997) *Journal of Pharmaceutical and Biomedical Analysis* 16: 553–559.
- [16] Bakkali A, Corta E, Berrueta LA, Gallo B and Vincente F (1999) *Journal of Chromatography B: Biomedical Sciences and Applications* 729: 139–145.
- [17] Kuhlmann O, Stoldt G, Struck H and Krauss G (1998) *Journal of Pharmaceutical and Biomedical Analysis* 17: 1351–1356.
- [18] Gonzalez L, Yuln G and Volonte MG (1999) *Journal of Pharmaceutical and Biomedical Analysis* 20: 487–492.
- [19] Kimura T, Shiota O and Ohtsu Y (1997) *Journal of Pharmaceutical and Biomedical Analysis* 15: 1521–1526.
- [20] Sochor J, Klimes J, Sedlacek J and Zahradnick M (1995) *Journal of Pharmaceutical and Biomedical Analysis* 13: 899–903.
- [21] Ducret A, Trani M, Pepin P and Lortie R (1998) *Journal of Pharmaceutical and Biomedical Analysis* 16: 1225–1231.
- [22] Haginaka J, Sanbe H and Takehira H (1999) *Journal of Chromatography A* 857: 117–125.
- [23] Hage DS, Noctor TAG and Wainer IW (1995) *Journal of Chromatography A* 693: 23–32.
- [24] Tan SC, Jackson SHD, Swift CG and Hutt AJ (1997) *Journal of Chromatography B: Biomedical Sciences and Applications* 701: 53–63.
- [25] Kepp DR, Sidelmann UG, Tjornelund J and Hansen SH (1997) *Journal of Chromatography B: Biomedical Sciences and Applications* 696: 235–241.
- [26] Kang SH, Chang S, Do K, Chi S and Doo SC (1998) *Journal of Chromatography B: Biomedical Sciences and Applications* 712: 153–160.
- [27] Sato J, Amizuka T, Niida Y, Umetsu M and Ito K (1997) *Journal of Chromatography B: Biomedical Sciences and Applications* 692: 241–244.
- [28] Lough WJ, Mills MJ and Maltas J (1996) *Journal of Chromatography A* 726: 67–75.
- [29] Mills MJ, Maltas J and Lough WJ (1997) *Journal of Chromatography A* 759: 1–11.
- [30] Panus PC, Tober-Meyer B and Ferslew KE (1998) *Journal of Chromatography B: Biomedical Sciences and Applications* 705: 295–302.
- [31] Zhivkova ZD and Russeva VN (1998) *Journal of Chromatography B: Biomedical Sciences and Applications* 714: 277–283.
- [32] Carr RA, Caille G, Ngoc AH and Foster RT (1995) *Journal of Chromatography B: Biomedical Sciences and Applications* 668: 175–181.
- [33] Haginaka J, Takehira H, Hosoya K and Tanaka N (1999) *Journal of Chromatography A* 849: 331–339.
- [34] Haginaka J, Takehira H, Hosoya K and Tanaka N (1998) *Journal of Chromatography A* 816: 113–121.
- [35] Gonzalo-Lumbreras R, Santos-Montes A, Garcia-Moreno E and Izquierdo-Hornillos R (1997) *Journal of Chromatographic Science* 35: 439–445.
- [36] Gatti R, Gotti R, Gioia MG and Cavrini V (1998) *Journal of Pharmaceutical and Biomedical Analysis* 17: 337–347.
- [37] Zarzycki PK, Wierzbowska M and Lamparczyk H (1996) *Journal of Pharmaceutical and Biomedical Analysis* 14: 1305–1311.
- [38] Di Pietra AM, Andrisano V, Gotti R and Cavrini V (1996) *Journal of Pharmaceutical and Biomedical Analysis* 14: 1191–1199.
- [39] Shibata N, Hayakawa T, Takada K, Hoshino N, Minouchi T and Yamaji A (1998) *Journal of Chromatography B: Biomedical Sciences and Applications* 706: 191–199.
- [40] Novakovic J, Pacakova V, Sevcik J and Cserhati T (1996) *Journal of Chromatography B: Biomedical Sciences and Applications* 681: 115–123.
- [41] Shibasaki H, Furuta T and Kasuya Y (1997) *Journal of Chromatography B: Biomedical Sciences and Applications* 692: 7–14.

- [42] Lensmeyer GL, Onsager C, Carlson IH and Wiebe DA (1995) *Journal of Chromatography A* 691: 239–246.
- [43] LeBelle M, Pike RK, Graham SJ, Ormsby ED and Bogard H (1996) *Journal of Pharmaceutical and Biomedical Analysis* 14: 793–800.
- [44] Bernal JL, del Nozal MJ, Martin MT and Diez-Masa JC and Cifuentes (1998) *Journal of Chromatography A* 823: 423–431.
- [45] Polettini A, Bouland GM and Montagna M (1998) *Journal of Chromatography B: Biomedical Sciences and Applications* 713: 339–352.
- [46] Ting E-Y and Porter MD (1997) *Analytical Chemistry* 69: 675–678.
- [47] Creaser CS, Feely SJ, Houghton E and Seymour M (1998) *Journal of Chromatography A* 794: 37–43.
- [48] Mistry N, Ismail IM, Smith MS, Nicholson JK and Lindon JC (1997) *Journal of Pharmaceutical and Biomedical Analysis* 16: 697–705.
- [49] Li YN, Tattam BN, Brown KF and Seale JP (1997) *Journal of Pharmaceutical and Biomedical Analysis* 16: 447–452.
- [50] Callejas SL, Biddlecombe RA, Jones AE, Joyce KB, Pereira AI and Pleasance S (1998) *Journal of Chromatography B: Biomedical Sciences and Applications* 718: 243–250.
- [51] Galmier MJ, Beyssac E, Petit J, Aiache JM and Lartigue C (1999) *Journal of Pharmaceutical and Biomedical Analysis* 20: 405–409.
- [52] Doppenschmitt SA, Scheidel B, Harrison F and Surmann JP (1995) *Journal of Chromatography B: Biomedical Sciences and Applications* 674: 237–246.
- [53] Prabhakar B and Deshpande S (1997) *Indian Drugs* 34: 699–701.
- [54] Kedor-Hackmann ERM, Gianotto EAS and Santoro MI RM (1997) *Analytical Letters* 30: 1861–1871.
- [55] Austria R, Semenzato A and Bettero A (1997) *Journal of Pharmaceutical and Biomedical Analysis* 15: 795–801.
- [56] Barthelemy JP (1996) *Analisis* 24: 95–103.
- [57] Cai X, Woo MH, Edick MJ and Relling MV (1999) *Journal of Chromatography B: Biomedical Sciences and Applications* 728: 241–250.
- [58] Liliemark E, Pettersson B, Peterson C and Liliemark J (1995) *Journal of Chromatography B: Biomedical Sciences and Applications* 669: 311–317.
- [59] Stremetzne S, Jaehde U and Schunack W (1997) *Journal of Chromatography B: Biomedical Sciences and Applications* 703: 209–215.
- [60] Manouilov KK, McGuire TR, Gordon BG and Gwilt PR (1998) *Journal of Chromatography B: Biomedical Sciences and Applications* 707: 342–346.
- [61] Robieux I, Aita P, Sorio R, Toffoli G and Boicchi M (1996) *Journal of Chromatography B: Biomedical Sciences and Applications* 686: 35–41.
- [62] Thomassin M, Cavalli E, Guillaume Y and Guinchard C (1997) *Journal of Pharmaceutical and Biomedical Analysis* 15: 831–838.
- [63] Dzerk AM, Carlson A, Loewen GR, Shirley MA and Lee JW (1998) *Journal of Pharmaceutical and Biomedical Analysis* 16: 1013–1019.
- [64] Bempong DK, Honigberg IL and Meltzer NM (1995) *Journal of Pharmaceutical and Biomedical Analysis* 13: 285–291.
- [65] Andreoli R, Careri M, Manini P, Mori G and Musci M (1997) *Chromatographia* 44: 605–612.
- [66] Atlas of Chromatograms section (1995) *Journal of Chromatographic Science* 33: 411.

Supercritical Fluid Chromatography

W. H. Wilson, Hewlett-Packard Co., Wilmington, DE, USA

Copyright © 2000 Academic Press

Introduction

The role of supercritical fluid chromatography (SFC) for the pharmaceutical scientist is based on its enhanced performance compared with high-performance liquid chromatography (HPLC). These advantages are speed, selectivity, and efficiency. Since diffusion is faster in a fluid than a normal liquid, SFC typically is five to ten times faster than HPLC. The mobile phase is less polar than the stationary phase in most SFC analyses so that the separation mechanism is similar to normal-phase HPLC. Thus, SFC can serve as a powerful complement to the vast majority of reversed-phase HPLC analyses. In terms of efficiency, SFC does not necessarily make the column more efficient.

However, the tenfold lower viscosity of the mobile phase allows columns to be joined together. As many as eleven 20 cm × 4.6 mm 5-μm packed columns have been linked to yield over 250 000 theoretical plates. Packed capillary columns have been made even longer.

In order to demonstrate the utility of SFC for pharmaceutical analysis, the range of SFC in this field needs to be understood. A brief review of mobile phases, columns, and solutes (see the SFC instrumentation section) will suggest the current limits. The modes of application are summarized, indicating current and future usage. Finally, a thorough but by no means exhaustive listing of successful solute-specific applications serve as a reference for more detailed investigation.

Range of SFC

Mobile Phases

Carbon dioxide is by far the most popular choice as the primary mobile phase component. Since most

compounds of pharmaceutical interest are more polar than carbon dioxide, a polar component will be needed in the mobile phase. Organic modifiers such as methanol, ethanol, and acetonitrile have been added to carbon dioxide to increase its elution strength. For strongly polar analytes such as amines or acids, a third component, called an additive, is needed to improve peak shape. Typical additives are primary amines for bases and trifluoroacetic acid for acids.

Solutes

SFC can separate a wide range of pharmaceutical solutes. From nonpolar fatty acid methyl esters to multifunctional acids and bases; SFC overlaps the application 'spaces' of gas chromatography (GC) and HPLC. Pharmaceuticals that are soluble only in aqueous solutions are not likely candidates for SFC. For example, purines and pyrimidines can be eluted from packed column SFC. These building blocks of DNA and RNA are polar, basic moieties but can be chromatographed, although DNA itself, has not been eluted by SFC. Similarly, amino acids can be readily analysed but proteins are not typically feasible. Recent work, however, suggests that short peptides can be eluted; further studies are in order.

Columns

The diffusivity of analytes in supercritical fluids is sufficiently high to allow both capillary and packed columns to be used. Both column types have strengths and weaknesses (refer to the instrumentation chapter). For most pharmaceutical applications, capillary columns do not offer sufficient retention time and area reproducibility to be implemented in routine use. However, some enantiomer separations are well suited to capillary SFC and warrant consideration of the technique.

Packed columns have been the predominant mode of operation for most pharmaceutical analyses. Column diameters from 50 μm up to preparative scale have been used. Particle diameters as small as 1.5 μm have found a use in packed column SFC. Since the mechanism for analyte retention is akin to normal-phase HPLC, typical stationary phases are cyanopropyl, aminopropyl, and diol-functionalized supports. Less polar columns such as octyl and octadecyl are also used. Support materials of silica, alumina, zirconia, and polymeric materials have been employed with successful results. Perhaps the most prominent application of packed column SFC is chiral separations. The majority of chiral stationary phases have been used in packed column SFC with beneficial results (refer to the chiral separations chapter).

Detectors

Numerous detectors have been modified and developed for SFC. The most prominent condensed phase detector is UV-Vis. Other condensed phase detectors are fluorescence, FTIR, radiometric, and electrochemical. Gas phase detectors such as mass spectrometry, flame ionization, and others have been interfaced to SFC.

Pharmaceutical Applications

Achiral Separations

The fundamental advantages of SFC are a normal-phase retention mechanism, rapid analysis times, tunable selectivity, and high efficiency. Since the stationary phase is more polar than the mobile phase, SFC is most similar to normal phase HPLC. Solute separation is based on their polarity and functional groups rather than their hydrophobicity. Consequently, it is an excellent complement to reversed-phase HPLC. In addition, retention time stability is similar to reversed-phase HPLC. The effects of trace amounts of water in the mobile phase are essentially insignificant for SFC when compared with normal-phase HPLC, particularly for polar pharmaceutical compounds. For example, a mixture of steroids shows the elution profile from a silica column (Figure 1). The steroids elute based on the number of polar functional groups in the structure. For example, estrone (one ketone, one alcohol) elutes before estradiol (two alcohols) which elutes before estriol (three alcohols). Note the rapid speed of analysis. The column is run at 2.5 mL min^{-1} . In HPLC, the column would be run at five to ten times lower flow rate. As

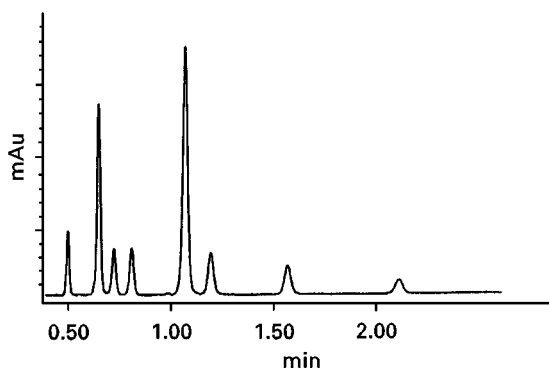


Figure 1 Steroid analysis by packed column SFC. Column 2.1 \times 250 mm Lichrosphere Si-60 (5 μm particles); oven 70°C; flow rate 2.5 mL min^{-1} ; outlet pressure 200 bar; modifier 20% methanol in carbon dioxide; UV detection at 210 nm. Elution order: progesterone, methyltestosterone, testosterone, estrone, estradiol, cortisone, hydrocortisone, and estriol. Courtesy Dr TA Berger, Berger Instruments.

Table 1 Achiral pharmaceutical separations

Family	Solutes	Reference
Alkaloids	Codeine, cryptopine, morphine, narcotine, thebaine	<i>Journal of Chromatography</i> 437: 351
Amphetamines	Methamphetamine, amphetamine, phenethylamine, ephedrine, norephedrine	<i>Journal of Chromatography</i> 515: 385
Antibiotics	Cephalosporins	Smith RM ed. <i>Supercritical Fluid Chromatography</i> , London: Royal Society of Chemistry (1988) p 180
	Erythromycin	<i>Journal of Chromatography</i> 454: 243
	Sulfonamides	<i>Journal of Chromatography</i> 363: 147
Anticancer	Taxicins	HRC 16: 666
Antidepressants	Amitriptyline, nortriptyline, protriptyline, imipramine, desipramine	<i>Journal of Pharmaceutical Science</i> (1994) 83: 281
Antipsychotics	Triflupromazine, carphenazine, methotrimeprazine, promazine, perphenazine, chlorprothixene, deserpine, thiothixene, reserpine, acetophenazine, ethopropazine, promethazine, propiomazine, molindone	<i>Journal of Pharmaceutical Science</i> (1994) 83: 287
Barbiturates	Barbitone, butobarbitone, Amylobarbitone, pentobarbitone, talbutal, quinalbarbitone, methohexitone, phenobarbitone, heptabarbitone	<i>Journal of Chromatography</i> 481: 63
Benzodiazepines	Ketazolam, diazepam, nordazepam, clonazepam, chlordiazepoxide, lorazepam, estazolam, temazepam, triazolam, lorazepam, lorazepam	<i>Journal of Chromatography</i> 483: 51
Beta blockers	Betaxolol, cycloprolol, metoprolol, nadolol, pindolol, propranolol	<i>Journal of Chromatography</i> 539: 55
	Timolol, atenolol, betaxolol, pindolol, bupranolol, pronethalol, oxprenolol	<i>Analysis for Drugs and Metabolites</i> . Cambridge: Royal Society of Chemistry, (1990) p. 257
Calcium channel blockers (Dihydropyridines)	Felodipine	<i>Journal of Pharmacology and Biomedical Analysis</i> (1994) 12: 1003
Ergot alkaloids	Agroclavine, festuclavine, elymoclavine, noragroclavine, chanoclavine I, chanoclavine II, norchanoclavine II, bromocriptine mesilate, ergocryptine	<i>Journal of Chromatography</i> 363: 147
Gingkolides	Bilobalide, ginkgolide A, ginkgolide B, ginkgolide C, ginkgolide J	<i>Supercritical Fluid Chromatography with Packed Columns</i> . New York: Marcel Dekker, p. 116.
H2 receptor antagonist	Ranitidine and metabolites	<i>Journal of Chromatography</i> 683: 402
NSAIDs	Phenylbutazone and metabolite	<i>Journal of Pharmacology and Biomedical Analysis</i> (1995) 13: 59
Purines	Mercaptopurine, trimethoprim, trifluridine, zidovudine	HRC 13: 393
Sesquiterpenes	Many	<i>Journal of Chromatography</i> 779: 307
Steroids	Many	<i>Chromatographia</i> (1995) 40: 58
		<i>Journal of Chromatography</i> 363: 147
Stimulants	Cocaine, amphetamine, methamphetamine, benzphetamine, phenmetrazine, phendimetrazine, methylphenidate, ephedrine, phenylephrine, hydroxyamphetamine, nylidrine, phenylpropanolamine, mephentermine, naphazoline, xylometazoline, tetrahydrozoline	<i>Journal of Pharmaceutical Science</i> (1994) 84: 489
Xanthines	Caffeine, theophylline, theobromine	<i>Journal of Chromatography</i> 363: 147

cited previously, columns can be linked to increase efficiency or tune selectivity. In the latter case, columns of different stationary phase can be joined to change selectivity. An example of this appears in the chiral section.

Table 1 contains a summary of achiral pharmaceutical separations. Where practical, the actual sol-

utes chromatographed are listed. The majority of these separations have been done on packed columns. SFC easily analyses basic compounds such as phenothiazine antipsychotics, tricyclic antidepressants, and stimulants. Nevertheless analysis of acids is also possible. Berger has demonstrated the elution of benzene derivatives with up to six carboxylic acid functional

groups. A ternary mobile phase of carbon dioxide, methanol, and trifluoroacetic acid was required to elute these strong acids.

An extremely valuable application of SFC is as a compound purity measurement tool. Gyllenhal *et al.* demonstrate the utility of SFC on four separate pharmaceuticals. All four examples indicate that SFC either equalled or improved the existing HPLC methods. For instance, packed column SFC was able to separate two impurities from metoprolol that HPLC was unable to achieve. Once again, the complementary nature of a reproducible, normal phase-like separation enhances the more traditional reverse phase HPLC results.

Chiral separations

Perhaps the most important role SFC currently plays in pharmaceutical analysis is as a chiral resolution technique (refer to Chiral Separations/Supercritical Fluid Chromatography). In this arena, the normal-phase retention mechanism is a tremendous asset. Since most chiral separations rely on polar solute-stationary phase interactions, a normal-phase environment is much more conducive to chiral recognition. Normal-phase HPLC chiral separations typically can be replaced by packed column SFC and enjoy the benefits of faster analysis times, lower solvent consumption, and more reproducible retention times. SFC also offers greater efficiency by allowing columns to be coupled.

Similar and dissimilar stationary phases can be coupled together to permit selectivity tuning.

Figure 2 shows an achiral/chiral column pair used to separate ibuprofen enantiomers in a urine matrix. The sample is initially injected onto the cyano column. The large peak at approximately 1 min is ibuprofen. When this peak has passed into the switching valve, the valve is turned and the loop contents are injected into the chiral column. The advantage of this approach is that on the achiral column, both enantiomers will coelute. With the valve arrangement used, the more polar urine components are never introduced into the chiral column. The peaks at approximately 7 min are the ibuprofen enantiomers. Note that ibuprofen is sold as the racemate of the enantiomers. The larger second peak is the S form of ibuprofen, while the barely visible first peak is the R form. In the body, the R form is inverted to the S form. Sandra *et al.* investigated a 'universal' chiral column by coupling three different chiral columns in series. In 90% of the successful separations on a single phase, the column triad was able to perform as well.

Preparative Separations

A natural extension of SFC is as a preparative separation technique. The column capacity is a function of the packing material and is essentially equivalent to liquid chromatographic systems. Consequently, scale-up procedures are similar. A major advantage for SFC is the solvent. Upon expansion, the mobile phase becomes gaseous or gaseous with a small amount of liquid phase, simplifying the recovery of analytes. The bulk of the mobile phase is nontoxic

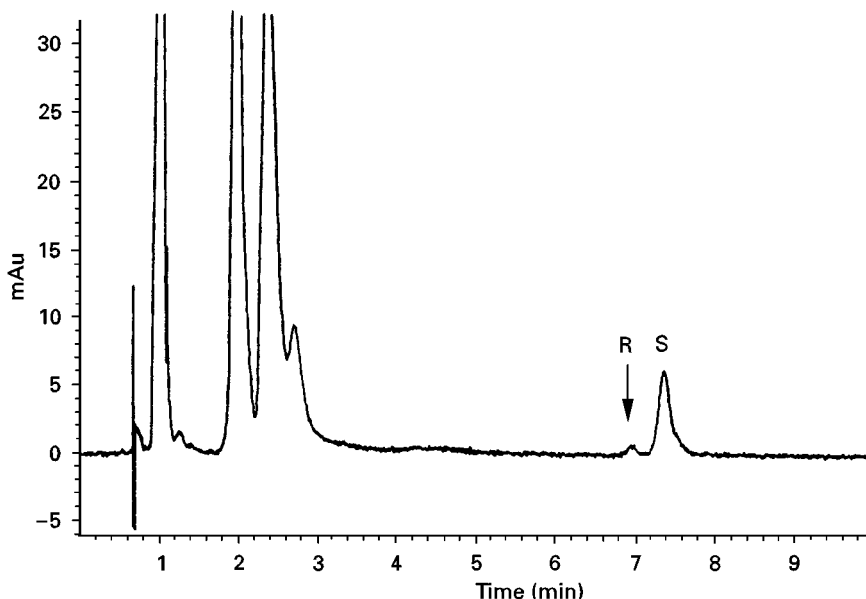


Figure 2 Chiral separation of ibuprofen in a biological matrix. Columns 4 × 125 mm Lichrosphere CN (5 μm particles) and 4.6 × 250 mm Chiralpak AD (10 μm particles); oven 35°C, flow rate 2 mL min⁻¹; outlet pressure 150 bar; modifier 5% methanol in carbon dioxide, UV detection at 210 nm; injection volume 5 μL. Courtesy Dr TA Berger, Berger Instruments.

(carbon dioxide) and, at large enough scale, can be recycled.

The differences between using normal liquids and supercritical fluids for preparative separations present advantages and disadvantages in both cases. For isocratic mobile phases, HPLC is probably easier in terms of mobile phase handling (e.g. no back-pressure regulator required). Mobile phase recycling is straightforward in HPLC since the column effluent is merely redirected to the pump inlet reservoir. SFC requires some repressurization apparatus at the outlet of the back-pressure regulator in order to recycle the mobile phase. However, SFC can use pressure as a separation variable whereas HPLC cannot. Although pressure programming in SFC is not as powerful as composition programming, it still affords the user an additional degree of flexibility. Recovery to initial chromatographic conditions from a pressure programme in SFC is very rapid. For composition programming or in HPLC terms, 'gradient programming', HPLC is more difficult to use. The time for column recovery is substantially longer in HPLC than in SFC, particularly for normal-phase separations. In addition, mobile phase recycling is complicated in gradient HPLC. The mobile phase depressurization actually benefits SFC in this scenario. By depressurizing the mobile phase, the concentration of modifier can be reduced to some low, reproducible value. This fluid can then be repressurized and fed to the pumping system with the modifier added to restore the desired initial composition. Column re-equilibration is very fast in SFC, thus minimizing recovery time.

Jusforgues *et al.* have described three applications of preparative SFC which demonstrate some of the merits of this approach. The excellent retention

time and area reproducibility possible with SFC is demonstrated with an insecticide. For the discrete peaks, the retention time reproducibility ranges from 0.17% to 0.19% relative standard deviation. In terms of peak area, the range is 1.17–1.54% relative standard deviation. An additional example given by these authors shows the separation of enantiomers by preparative SFC. The separation cycle takes less than 5 min and the yield of > 99% purity compounds is 29 g day⁻¹.

Laboratory-scale preparative separations, typically in the milligram range, are attractive in conjunction with combinatorial chemistry. The aforementioned rapid analysis time, simple mobile phase elimination, and loading capacity make SFC an attractive option for small-scale purification.

Rapid Screening

The extensive growth of combinatorial chemistry has brought about significant changes in pharmaceutical analysis. Synthetic production is now discussed in terms of thousands of compounds per year. With this explosion of organic syntheses, the companion techniques must also develop to handle the load. Parallel synthesis must be met with rapid, parallel analysis to maintain the pace. SFC is well suited for interfacing with this demanding need.

The current workhorse for combinatorial analysis is still reversed-phase HPLC. As discussed previously, packed column SFC is both complementary to reversed-phase HPLC and potentially an order of magnitude faster. Not only is this speed apparent in the analysis times but more importantly, in the total cycle time on the system. **Figure 3** illustrates the impressive speed of gradient elution by packed column SFC. The

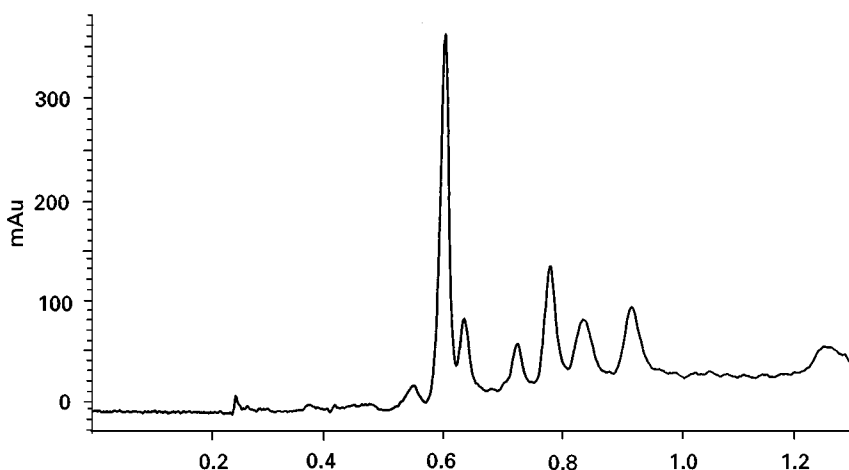


Figure 3 High-speed packed column SFC for combinatorial screening. Column 4 × 125 mm Lichrosphere CN (5 µm particles); oven 35°C; column flow 4 mL min⁻¹; outlet pressure 120 bar; 15–65% modifier (methanol + 0.4% isopropylamine) programmed at 45% min⁻¹ in carbon dioxide, UV detection at 230 nm; 10 µL injection from a 96-well plate. Courtesy Dr TA Berger, Berger Instruments.

column is a 125 mm \times 4 mm \times 5 μ m Lichrosphere cyano (these are typical column dimensions for a standard HPLC separation). The sample is drawn directly from a titre plate and injected. The modifier is programmed from 15% to 65% at 45% min⁻¹. The analysis takes 1.2 min to complete and an additional 0.68 min to re-equilibrate. Consequently, the system is able to run over 760 samples per day. On a similar column by reversed-phase HPLC, the system is capable of two to three runs per hour or at best, 72 samples per day.

Note that the chromatogram shows several peaks in the sample. Since the goal of this synthesis was a single component, there are some obvious complications. With the column used, the system has sufficient peak capacity to separate the seven components identified. For a similar speed of analysis by HPLC, the column would have to be substantially shorter or have much smaller particles. In either case, the peak capacity would not be the same at the SFC separation. As a result, the HPLC system may be unable to resolve all of the peaks. The speed and efficiency of SFC is better suited to these high volume analyses than HPLC.

Summary

The rapid analysis speed, complementary selectivity, and achievable high efficiency of SFC make it a valu-

able technique for pharmaceutical analysis. Because of its normal-phase-like retention mechanism, SFC affords users of reversed-phase HPLC an orthogonal separation system. In addition, chiral separations are clearly a strong application for SFC. The renewed interest in SFC for laboratory-scale purifications and combinatorial screening has breathed new life into this technique.

A valid point raised by Wilson *et al.* is that the current literature still demonstrates the potential of SFC rather than fully developed methods. This situation has begun to change. Although the literature may not reflect it yet, more and more pharmaceutical workers are using SFC as a routine technique.

Further Reading

- Anton K and Berger C (eds) (1997) *Supercritical Fluid Chromatography with Packed Columns, Techniques and Applications*. New York: Marcel Dekker.
- Berger TA (1995) *Packed Column SFC*. Cambridge: RSC Chromatography Monographs.
- Dean JR (ed.) (1993) *Applications of Supercritical Fluids in Industrial Analysis*. Boca Raton: CRC Press.
- Smith RM (ed.) (1988) *Supercritical Fluid Chromatography*. Cambridge: RSC Chromatography Monographs.

Thin-Layer (Planar) Chromatography

B. Renger, Byk Gulden, Konstanz, Germany

Copyright © 2000 Academic Press

In 1938, Izmailov and Schraiber used aluminium-coated plates to separate coloured plant extracts. Further development of thin-layer chromatography (TLC) as a semiquantitative analytical technique and a tool for identity testing took place in the mid-1950s, especially by Stahl. Soon after this pioneering work, TLC found its way into pharmaceutical analysis.

Surveys of the analytical literature from the late 1980s to the mid-1990s show that approximately 25–30% of all articles published in the field of TLC described pharmaceutical applications. These figures may give some idea about the status of TLC in pharmaceutical analyses.

The rapid development of liquid chromatography (LC, especially high performance liquid chromatography (HPLC)) in the mid-1970s has made LC the

predominant analytical method in pharmaceutical analysis. Nevertheless, even today TLC must be considered the most widely used pharmacopoeial chromatographic technique.

TLC in the Pharmacopoeias

An early example of pharmacopoeial use of TLC (Table 1) was for impurity testing of corticosteroids in the *British Pharmacopoeia* (BP) addendum 1966 and as a general method featured in the BP of 1968. A typical specification for an active pharmaceutical ingredient until then would require verification of identity and then rely on a usually nonspecific assay supplemented by traditional limit tests, e.g. for heavy metals and chloride. For most organic substances a reasonably sharp melting point was a crude but generally accepted measure of purity. The introduction of TLC to the BP 1968 had great expectations of this technique, as it refers to 'greatly increased

Table 1 TLC in the pharmacopoeias

1964	DAB 7 – GDR: general method
1966	BP addendum: corticosteroids
1968	BP: general method
1980	DAB 8 – add. – FRG: general method
1985	DAB 9 – FRG: 'quantitative' determination of glycyrrhizic acid in liquorice root
1998	DAB – 1998 monograph 'soja lecithin': assay of phosphatidylcholine via quantitative TLC
1999	EP addendum 1999: revised general monograph TLC including quantitative TLC

DAB, German Pharmacopoeia; FRG, Federal Republic of Germany; GDR, German Democratic Republic; EP, European Pharmacopoeia.

emphasis placed on detection and control of impurities [from] manufacture or degradation ... made possible by the rapid development of TLC as a reliable means of detecting and assessing small quantities'.

In its basic form, as developed then, TLC is simple, rapid, robust and inexpensive and can be performed in nearly every analytical environment. Therefore it is still widely used in national and international pharmacopoeias for identity testing of active pharmaceutical ingredients and excipients, especially of compounds of natural origin like plant extracts or herbal preparations. In its semiquantitative mode, where spots of reference test solutions are usually visually matched against the impurity spots in the chromatogram of the undiluted test sample, it is still the widest used chromatographic technique to con-

trol impurities in either active pharmaceutical ingredients or drug products.

High performance TLC (HPTLC), with layers composed of particles with smaller diameters and narrow particle size distributions, gives greater separation efficiency and improved detection limits. Automated scanning densitometers have led to instrumental quantitative TLC, but neither of these developments has found its way into the national and international pharmacopoeias until recently.

Today, most of the TLC procedures included in pharmacopoeial monographs must be considered to represent an obsolete form of this technique, leading to the misconception that TLC *per se* is merely a qualitative or at best semiquantitative technique lacking in accuracy and sensitivity (**Figure 1**).

But even when performed under state-of-the-art conditions, separation power and sensitivity are generally lower for TLC than for HPLC. As a consequence, there is a general shift away from semiquantitative TLC to quantitative HPLC for the control of impurities in new or revised pharmacopoeial monographs. This development is especially justified by the requirement of the guidelines of the International Conference on Harmonization (ICH), to control unknown impurities down to a threshold limit of 0.1% – originally intended for new chemical entities only – but today also applied to well-known active pharmaceutical ingredients, listed in pharmacopoeias. This general shift away from TLC to HPLC for the control of impurities and related substances must be considered irreversible.

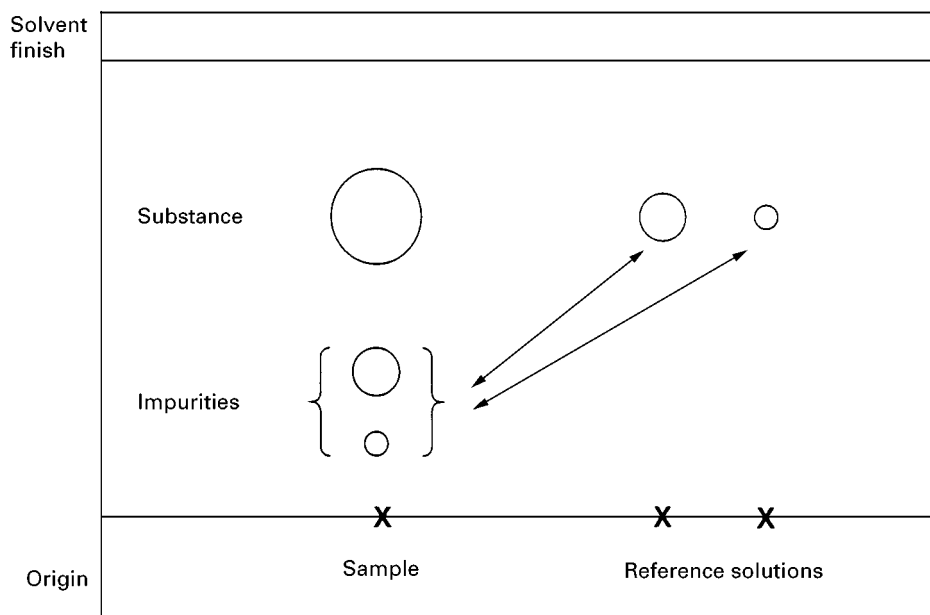
**Figure 1** Pharmacopoeial use of TLC: testing for related substances.

Table 2 Quantitative TLC in the general monograph TLC of the Addendum 1555 of the European Pharmacopoeia: features

Plates	Laboratory-prepared plates abandoned; commercially available plates referred to in reagent section
Performance test	Plates are tested using a mixture of Sudan red, methyl orange, bromocresol and methyl red for separation efficacy and/or with benzoic acid for fluorescence quenching
Preconditioning	Washing or impregnating of plates, if appropriate
Development	Vertical and horizontal development described
Visual estimation	Described for related substances tests and identification
Verification of separation power	Described for related substances tests and identification
Verification of detection power	Described for related substances tests
Quantitative measurement	Described for substances responding to UV-visible irradiation (remission or fluorescence) or containing radionuclides using three-point calibration (approx. 80, 100, 120% of expected value) and scanning densitometry
Resolution factor	Results are only valid if the resolution (R_s) between measured peak in the chromatograms is greater than 1.0
Signal-to-noise ratio	Described for determination of the detection limit (DL)

However, the progress in quality of sorbent materials, pre-coated plates and instrumentation that has led to a remarkable improvement in the reliability of instrumental quantitative TLC, has led to its recent introduction as a general pharmacopoeial method. The revised general monograph 2.2.27 *TLC* of the addendum 1999 of the *European Pharmacopoeia* for the first time includes a description of quantitative TLC via automated scanning densitometry and lists the required performance parameters *resolution* and *limit of detection* (Table 2).

The first example of the pharmacopoeial use of fully automated quantitative TLC is the assay for phosphatidylcholine in the monograph *Soya Lecithin* of the addendum to the *German Pharmacopoeia DAB* (1998).

Potential Applications of TLC/HPTLC

For many years TLC was not considered to be a reliable quantitative technique and it was displaced by the techniques of gas chromatography, introduced as a general method in the *BP* of 1968 and, in the mid-1970s by LC, especially HPLC, which today is the most popular technique for assays and purity testing (Table 3).

It must be emphasized that only approximately 20% of analytical work in the pharmaceutical industry is controlled by pharmacopoeias. The remaining 80% of analytical problems, such as analytical work in research and development, reaction and process control, stability testing, analytical control of cleaning and its validation may be solved by every available analytical technique, assuming that the corresponding validation and performance data prove that it is suitable for the intended use.

When used with plates containing fluorescence indicators that allow detection of UV-active substances

by UV irradiation for identification, the existence of more than 1000 specific derivatization agents represents a major advantage of TLC over other chromatographic techniques.

Hyphenated techniques, or combinations of TLC with spectrometric techniques like Fourier transform near infrared spectroscopy (FT-NIR), Fourier transform infrared spectroscopy (FTIR), diffuse reflection infrared Fourier transformation (DRIFT), Raman/surface enhanced Raman spectroscopy (SERS) or mass spectrometry (MS) with different ionization techniques, are reserved for special applications and are not as commonly used as simple visualization.

For fast, rough quantifications – either in purity and related substance testing or for assays – TLC coupled with visual examination and/or with the emerging technique of video densitometry must be considered the most flexible and economic alternative of all chromatographic techniques.

But TLC is no longer the traditional, uncomplicated but less reliable technique. Reliable, technically mature automated instruments are available for individual steps like sample application, development, derivatization, scanning and quantitation.

For assays and content testing, TLC with scanning densitometry must be considered a realistic alternative to other chromatographic techniques concerning analytes with problematic detection characteristics. Also it is suitable with crude or dirty sample matrices, especially when particulate impurities like plant extracts of finished pharmaceuticals raise problems with other analytical techniques.

Sometimes the weakness of TLC – its lower separation power – can be an advantage: when components consisting of mixtures of oligomers or having different chain length distributions have to be assayed in different matrices.

Table 3 Potential applications of TLC/HPTLC in pharmaceutical analysis

Type of analytical procedure	Field of application	Principle(s)
Qualitative/identification (API)	Quality control of components, active pharmaceutical ingredients (API), finished pharmaceuticals Single container identification Quality control of herbal/vegetable drugs and fermentation products At-site and port-of-entry testing Forensic and drug of abuse screening	Parallel chromatography of sample and reference standard or reference sample, evaluation and comparison of R_F values, spot size and colour (after derivatization) Evaluation and comparison of R_F values using different mobile-phase systems with data from libraries, specific derivatization if required, <i>in situ</i> or offline spectroscopy of selected spots/bands
Semiquantitative purity test (limit test)	Quality control of components, API, finished pharmaceuticals Quality control of herbal/vegetable drugs and fermentation products At-site and port-of-entry testing: check for adulterations and contaminations	Parallel chromatography of sample and diluted (1 : 50, 1 : 60, 1 : 200) test solution or solutions of potential impurities. Visual match of spot size and intensity (after derivatization if required) with following estimation of impurity/related substances content. Increased reliability and precision using video densitometry.
Semiquantitative assay/content testing	Reaction/process/cleaning control or optimization in: API synthesis Pharmaceutical manufacturing Fermentation Plant/herbal extraction Assay of herbal/vegetable drugs and extracts	Parallel chromatography of reaction mixture or rinse solution and educt/starting materials/previous sample/previous rinse solution. Visual estimation and/or video integration and estimation of process reaction/cleaning progress Parallel chromatography of sample and different concentrations of lead component/reference sample. Visual evaluation and/or video integration after derivatization if required.
Quantitative assay/content testing/impurity/related substances testing	Quality control of APIs and finished drugs Quality control of herbal drugs/extracts and fermentation products Assays and purity testing in stability studies (development, ongoing, follow-up) Bioanalytics: bioavailability studies, pharmacokinetic studies Reaction/process control or optimization: impurity profiles	Parallel chromatography of sample and different concentrations of reference standard and/or dilutions of main component and/or reference sample. Pre- or postchromatographic derivatization if required, preferred: automated spotting, development under controlled conditions, quantitative evaluation via calibration function using peak area or peak height after scanning densitometry (or video integration if applicable)

Validation and Performance Characteristics

Like any other analytical technique, TLC used in pharmaceutical quality control or in stability studies and later stages of pharmaceutical development (clinical trial batches) has to be validated in line with the latest guidelines of the ICH. As planar chromatography allows the simultaneous analysis of up to 24 samples on one plate, the time and effort required to validate a procedure are distinctly lower than for other chromatographic techniques.

Performance data verify that, under optimized conditions, quantitative TLC or HPTLC results are comparable to those of LC. A prerequisite is parallel testing of two sample weightings with double-spotting (resulting in four spots for every unknown) and – mandatory according to the monograph in the *European Pharmacopoeia* – a three-point calibration (e.g. 80, 100, 120% of label claim in assays) for linear and preferably four-point calibration for nonlinear calibration models. Except for fluorescence measurements, calibration functions in TLC are generally nonlinear. Narrow specification limits and working

Table 4 Comparison of performance characteristics of TLC, HPTLC and HPLC

Separation power	Technique	Performance
Separation number	TLC	~ 10
	HPTLC	~ 15–20
	HPLC	~ 150
Sensitivity		
Detection limit (UV absorption)	TLC	~ 1–5 µg
	HPTLC	~ 0.2–0.5 µg
	HPLC	~ 0.05–0.3 µg
Precision		
RSD interm. precision (assay)	TLC	~ 1.5–3.0%
	HPTLC	~ 1.0–2.0%
	HPLC	~ 0.8–1.5%

RSD, random standard deviation; interm. precision, day-to-day variability.

ranges in pharmaceutical analytical chemistry however often make it possible to use quasi-linear calibration functions over the limited concentration ranges to avoid calibration via higher polynomial functions.

Generally, selectivity, separation power and sensitivity (expressed as quantitation limit) are lower for TLC or HPTLC than for LC. For assays, measurement uncertainty and precision data from validation experiments are comparable, whereas for quantification of impurities and related substances, the higher variability and measurement uncertainty and the resulting higher quantitation limit normally make HPLC the preferred analytical technique. TLC may be the method of choice if the detection characteristics of the analyte does not encourage the use of LC, e.g. for phospholipids that require light-scattering detection in LC.

Table 4 gives a rough estimation of selected performance characteristics of TLC–HPTLC.

Features and Advantages of TLC

There is a general shift away from TLC to HPLC for the control of impurities in new or revised pharmacopoeial monographs. Planar chromatography has a number of features and advantages (Table 5) so that, for some of the applications listed above, this technique must be considered to be at least an alternative to other chromatographic methods.

Actual Use of TLC in Pharmaceutical Analyses

As outlined in Table 3, TLC may theoretically be used for nearly every analytical task in the pharma-

ceutical industry. However, the general lower performance characteristics compared to LC on one hand and the special features (outlined in Table 5) on the other hand have resulted in some specifically traditional applications of TLC. These are identification, especially for port-of-entry testing, single container testing and for samples of natural origin like plant extracts or fermentation products. In its semiquantitative mode it is used for fast on-site testing. Applications in pharmacokinetic or bioavailability studies as well as quantitative determinations of impurities or related substances and assays of active pharmaceutical ingredients are still exceptions, mostly limited to cases where the matrix or the detection features of the compounds are to be determined, or the matrix excludes or limits the use of other chromatographic techniques.

Table 6 lists the main applications of TLC in pharmaceutical analysis today. For most of these applications, TLC is either mandatory or at least recommended by the respective pharmacopoeias and compendiums or encouraged by regulatory authorities.

Economic and Environmental Considerations

Most separations by TLC are performed in a normal-phase mode, using unmodified silica gel pre-coated layers, whereas HPLC in pharmaceutical analysis is nearly always used in the reversed-phase mode. Therefore, Table 6 lists predominantly examples where the straight-phase mode of TLC must be considered more appropriate than reversed-phase or examples where normal-phase TLC acts as a supple-

Table 5 Advantages and features of TLC/HPTLC

Simplicity of handling, easy to learn technically
Flexibility, short preparation time needed prior to analysis
Broad choice of mobile-phase systems
Numerous (> 1000) sensitive and selective reagents for detection and/or visualization
No obligation for elution of the analyte
Whole chromatographic information is stored on the plate and can be (re)evaluated
Detection and/or quantitation steps can easily be repeated using different parameters
Simultaneous yet independent analysis/samples of several samples and reference standards on one plate offers a high sample throughput and an increased reliability of results (in-system calibration)
Procedures are generally robust, allowing easy transfer and adoption
The single use of the plates offers the ability to handle crude, complex or dirty samples, even those with particulate impurities
Modular structure

Table 6 Main applications of TLC in pharmaceutical analyses (qualitative, semiquantitative and quantitative)

Identity testing of raw materials, components and drugs in quality control, on-site or at port-of-entry
Single container identification if spectroscopic techniques (e.g. near infrared (NIR)) not suitable or available
Identity, purity testing and assay of herbal/vegetable material, extracts and drugs
Single, rapid on-site/port-of-entry testing for adulterated and faked drugs
Purity and related substance testing or assays if analyte has problematic detection characteristics (polyglycol derivatives, quaternary ammonium salts, phospholipids) and/or the materials require laborious and error-prone sample workup steps in other chromatographic techniques
Additional straight-phase technique parallel to RP-HPLC or other techniques for proving procedure selectivity in validation, for second assays of reference standards, in stability testing to prove that primary technique indicates stability and in forced degradation studies to give better mass balance

mentary or additional technique run in conjunction with reversed-phase HPLC (Figure 2).

There is a main field of application, however, where TLC and HPLC may be regarded as competing techniques. These are assays and content determinations of finished pharmaceutical products. HPLC has been the most popular analytical technique for these determinations for many years (and, like TLC, the most popular compendial technique for impurity and related substances testing) within the last few years. But papers dealing with TLC in pharmaceutical analysis are focusing more and more on final product assay and content testing, especially on content uniformity testing of tablets.

This application combines the technique's inherent advantages, its ability to accept complex or dirty sample matrices without requiring time-consuming sample clean-up steps, and its ability to run several samples on one plate in parallel and to be readily available without requiring system set-up and equilibration times.

In addition, TLC generally requires fewer solvents and chemicals than HPLC procedures.

Reports on the costs of performing multiple drug analyses conclude that cost reductions using TLC or HPTLC instead of LC (HPLC) can be significant. This is especially the case when many repetitive analyses have to be performed at one time and automated HPLC systems are not economic, as the total number of batches is too low or manufacturing is not evenly distributed throughout the year. If the obtainable separation performance parameters are considered sufficient, that is, if the TLC procedures have precisions within the required limits and a random standard deviation (RSD) of 2%, as required by the USP,

then planar chromatography offers an alternative that costs less, is faster and has less impact on the environment. In addition, this type of TLC can in certain cases be performed even in hospitals, pharmacy laboratories or ports of entry, warehouses or

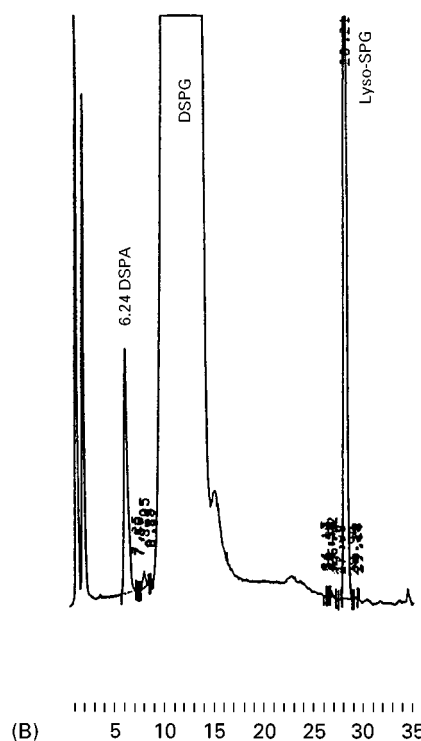
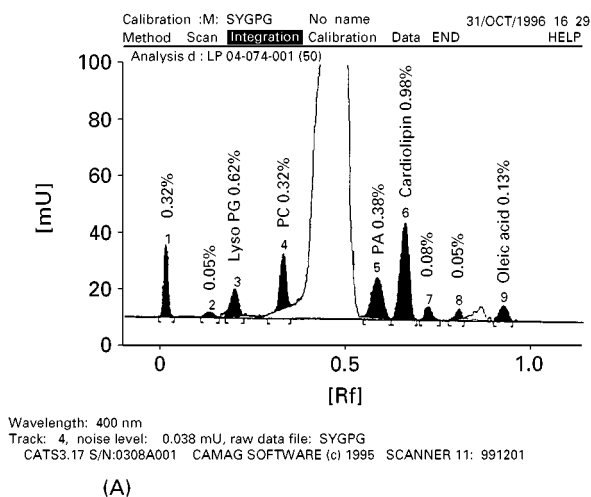


Figure 2 Comparison of HPLC and HPTLC analyses of phospholipids. (A) HPTLC, copper (II) sulfate/phosphoric acid derivatization and scanning densitometry. (B) HPLC, light-scattering detection. (A) Lyso PG, lyso phosphatidyl glycerol; PC, phosphatidyl choline; PA, phosphatidic acid; main component, 1-palmitoyl-2-oleyl-3-phosphatidyl glycerol; %, peak area compared to main component. (B) DSPA, phosphatidic acid; lyso LPG, lyso phosphatidyl glycerol; main component, 1,2-distearoylphosphatidyl glycerol (DSPG).

small control laboratories. However, although most of the published applications in the field have their origin not in the highly HPLC-oriented first world, the approach must not be considered to be only valuable and suitable for simple control laboratories with very limited assets.

Pharmaceutical analytical laboratories work under enormous economic and time pressure. Sample throughput has to be increased and lead times decreased, both without any consequence to the reliability of the results and at best without increase in personnel and operational costs. Therefore it must be recommended that TLC is considered as a possible replacement or substitute for compendial or noncompendial HPLC assays and content uniformity testing, especially for tablets.

Future Perspectives

A shift away from the traditional, semiquantitative TLC compendial purity testing of active pharmaceutical ingredients must be expected. Instead, a higher level quantitative TLC will be recommended and promoted by various national/international regulatory agencies for on-site and port-of-entry testing of pharmaceuticals. This development will be stimulated by the development of modern video imaging systems. Originally developed for documentation, modern closed-circuit device cameras are now combined with powerful software to collect the information stored on a plate in a very short time. Although not yet generally as precise and accurate as scanning densitometry, latest published results indicate that at least in the UV-region, video imaging can produce assay results that are equivalent to those derived by scanning densitometry. The lower price of video integration systems makes them the ultimate choice for rapid quantitative TLC applications.

The use of scanning densitometry will be limited to more delicate analytical tasks like stability or quality

control testing procedures such as assays or content testing of finished pharmaceuticals, especially tablets, where TLC will expand because of its economical and environmental advantages, compared to HPTLC.

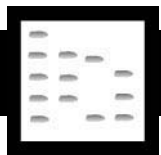
Highly sophisticated hyphenated techniques or combinations of TLC with spectrometric techniques such as FT-NIR, FT-IR, Raman or MS with different ionization mechanisms and MS-MS will be improved, but they will remain special technical solutions to special problems and must not be expected to become routine methods.

See also: II/Chromatography: Thin-Layer Planar: Densitometry and Image Analysis; Historical Development; Instrumentation; Layers; Mass Spectrometry; Modes of Development: Conventional; Modes of Development: Forced Flow, Overpressured Layer Chromatography and Centrifugal. III/Pharmaceuticals: Basic Drugs: Liquid Chromatography; Capillary Electrophoresis; Neutral and Acidic Drugs: Liquid Chromatography; Thin-Layer Chromatography-Vibration Spectroscopy.

Further Reading

- Jork H, Funk W, Fischer W and Wimmer H (1990 and 1994) *Thin Layer Chromatography, Reagents and Detection Methods*, vols 1 and 2. Weinheim: VCH.
- Renger B (1998) Contemporary thin-layer chromatography in pharmaceutical quality control. *Journal of AOAC International* 81: 333–339.
- Sethi PD (1996) *HPTLC Quantitative Analysis of Pharmaceutical Formulations*. New Delhi: CBS Publishers.
- Sherma J and Fried B (1991) *Handbook of Thin Layer Chromatography*, New York: Marcel Dekker.
- Sherma J and Fried B (1994) *Thin Layer Chromatography, Techniques and Application*, New York: Marcel Dekker.
- Szepesi G and Nyiredi S (1992) Planar chromatography: current status and future perspectives in pharmaceutical analysis. *Journal of Pharmaceutical and Biomedical Analysis* 10: 1007–1015.

PHENOLS



Gas Chromatography

M.-R. Lee, National Chung-Hsing University,
Taichung, Taiwan, Republic of China

Copyright © 2000 Academic Press

Phenolic compounds are extensively used in the chemical industry. Some simple phenolic species are known to be products of vascular plant metabolism, and also contribute to the polymeric structures of tannins and lignin. In addition to their use as intermediates in industry and in the production of dyes, plastics and pharmaceuticals, chlorophenols have

been extensively utilized as preservative agents, pesticides, antiseptics and disinfectants. Chlorophenols can also be obtained by hydrolysis, oxidation and microbial degradation of chlorinated pesticides, and can be produced when phenol-contaminated water is chlorinated for purification. The US Environmental Protection Agency (EPA) listed 11 phenols as priority pollutants, including phenol, 2-nitrophenol (2-NP), 4-nitrophenol (4-NP), 2-chlorophenol (2-CP), 2,4-dinitrophenol (2,4-DNP), 2,4-dichlorophenol (2,4-DCP), 2,4-dimethylphenol (2,4-DMP), 2-methyl-4,6-dinitrophenol (2-M-4,6-DMP), 4-chloro-3-methylphenol (4-C-3-MP), 2,4,6-trichlorophenol (2,4,6-TCP) and pentachlorophenol (PCP). Several phenolic compounds are also listed in the European Community (EC) Directive 76/464/EEC regarding dangerous substances discharged into the aquatic environment. For drinking purposes, EC Directive 75/440/EEC states that maximum levels of phenolic compounds in surface water should be within the range 1–10 ng mL⁻¹. Therefore, rapid and reliable methods must be developed to analyse these compounds.

Owing to its high sensitivity and resolving power, chromatography is the most commonly used analytical technique to determine phenols. Previous investigations have developed gas chromatography (GC), high performance liquid chromatography (HPLC), capillary electrophoresis (CE) and supercritical fluid chromatography (SFC) to monitor these pollutants. Government-approved analytical methods, e.g. US EPA 604 and 625 (acid-extractable section), are based on gas chromatography using electron capture or mass spectrometry detection.

Gas chromatography is the most widely used technique in analytical chemistry. The merits of gas chromatography include its speed, precision and accuracy. Gas chromatography is appropriate for separating and analysing nonpolar volatile materials but it is limited in application to materials that exert vapour pressures of at least 10 mmHg at the column operating temperature. Also, owing to their high polarity, phenols tend to produce broad-tailed peaks, and this effect increases as the column ages. In order to obtain more favourable chromatographic peaks, less polar derivatives of phenols are often prepared. When GC is applied to determine trace amounts of phenols in water or other samples a pre-concentration or extraction step is frequently required. Proper sampling largely determines the validity of an analytical sample for trace analysis. Various pre-concentration techniques have been developed for phenol analysis. The sensitivity of GC for phenol analysis depends markedly on the detector used. Sample preparation methods, including various types of extraction tech-

niques and derivatization procedures, are described below. The effectiveness of the techniques is demonstrated by investigations on real samples.

Sample Preparation

As many investigations have confirmed, determining phenolic compounds in water or other matrices in the range below 1 ng mL⁻¹ is extremely difficult. The extraction and preconcentration of a mixture of phenols present difficulties owing to their wide range of polarities. In addition, volatilization may cause losses in preconcentration because of their relatively high vapour pressure. The conventional preconcentration technique is liquid-liquid extraction (LLE) for aqueous samples. The US EPA method for the analysis of phenols in water (EPA 604 and 625, acid-extractable section), consists of acidification of the sample to pH 2, followed by dichloromethane extraction. Merits of LLE include its simplicity and the need for inexpensive equipment. Nevertheless, despite its extensive use, LLE has many drawbacks, such as emulsion formation and different extraction efficiencies for different compounds. In addition, the method requires a large amount of solvent, and is slow and laborious. It is also hazardous to health since it uses toxic organic solvents that are also relatively expensive in terms of disposal. Solid-phase extraction (SPE) protocols are more commonly used than conventional LLE procedures, thereby reducing loss of analytes and the use of large amount toxic solvents. The complete extraction is performed in a series of stages, including washing, conditioning, eluting and drying. Many SPE materials are used in the preconcentration of phenols from aqueous samples including Empore disks, cartridges or small precolumns. Sorbents, including C₁₈, C₁₀, C₈, C₂, CH, CN and RLRP-S (styrene-divinylbenzene copolymer), have been used to investigate the extraction efficiency of phenols in water. The C₁₈-based sorbents have the property of low breakthrough volume of the more polar analytes and are therefore inappropriate for the simultaneous preconcentration of polar and nonpolar compounds. Notably, the breakthrough problem occurs for catechol, phenol and 4-NP extracted with C₁₈ sorbent. According to a previous investigation, a polymeric material such as Amberlite XAD-2 or XAD-4 or PRP is the most appropriate sorbent, yielding recoveries of up to 80% for most phenolic compounds; however, the breakthrough problem for some phenols still occurs. To overcome this problem, polymeric phases with high cross-linking have been proposed, e.g. by using the packing materials based on styrene-divinylbenzene copolymer, such as Isolute ENV⁺, Lichrolut EN,

Envi-chrom, PLRR-S and Porapak RPX. However, SPE can be expensive because the cartridges are normally discarded after one extraction. Moreover, the extraction still uses organic solvents that potentially threaten health and the surrounding environment.

Solid-phase microextraction (SPME) does not require the use of an organic solvent. The mechanism of SPME is based on an equilibrium of analytes between the sample and the solid phase coating on a quartz fibre. The analytes are directly determined by thermal desorption from the fibre into a GC. SPME has been extensively applied to extract trace organic compounds from aqueous samples owing to its solvent-free methodology, simplicity and rapidity. The feasibility of applying SPME to extract phenols from a complex matrix with polyacrylate (PA)- or poly(dimethylsiloxane) (PDMS)-coated fibres has been thoroughly evaluated. Extraction optimization procedures have been systematically studied, involving the pH of the sample, the desorption time and salting-out. Supercritical fluid extraction (SFE) and Soxhlet extraction techniques have been used for the solid samples. The extraction of 11 phenolic compounds from a river sediment by methanol- CO_2 mixtures under supercritical conditions and Soxhlet extraction with methylene chloride have been evaluated.

In the GC analysis of high polarity and vapour pressure phenols, a derivatization step is frequently executed to provide the mixture with better chromatographic characteristics. Until now, the derivatives used for this purpose have been based on the formation of esters, ethers and silyl derivatives. The derivatizing agents used are acetic anhydride, diazomethane, 2,4-dinitrobenzene, heptafluorobutylimidazole, pentafluorobenzoyl chloride, pentafluorobenzoyl bromide and silanizing agents. Acetylating agents have been widely used for the derivatization of phenols. Phenols can be acetylated in the aqueous organic sample or after extraction. EPA method 8041 recommends the derivatization of phenols to methylated phenols using diazomethane but diazomethane gas is extremely toxic, irritating and carcinogenic, so derivatization must be handled in a hood and with safety equipment.

Environmental Applications

Analysing phenol residues in environmental samples by GC has been the subject of extensive investigations. A novel means of determining eight chlorophenols in tap water was reported: it involved the direct acetylation of the chlorophenols with acetic anhydride in the presence of K_2CO_3 . A graphitized carbon cartridge was used for extraction and precon-

centration. Chlorophenols were quantitatively measured by a microwave-induced plasma atomic emission detector at the sub-p.p.b. level in tap water. A methylphenylsilicone capillary column was used for separation.

The purge-and-trap technique and laboratory-made pulsed-spray techniques to extract five chlorophenols in water have been evaluated. The absorbent tubes were packed with 100 mg Tenax TA (0.2 μm). The absorbent tubes were attached to the injector port of a GC and heated to 200°C for 3 min to desorb the trapped analytes. GC separation was followed by MS detection and quantitation in the selected ion monitoring (SIM) mode. **Figure 1** depicts the gas chromatogram of spray-and-trap GC-MS of a water sample containing 100 $\mu\text{g L}^{-1}$ chlorophenols and 20 $\mu\text{g L}^{-1}$ internal standard (2,4,6-tribromophenol). Low ng L^{-1} levels of detection were obtained for the studied chlorophenols.

The optimization of SPME conditions for the determination of phenols was investigated. The SPME method, based on a polyacrylate-coated fibre, gave a detection limit at 32–0.01 $\mu\text{g L}^{-1}$ level for GC-flame ionization detector (GC-FID) and GC-mass spectrometry (GC-MS) using saturated sodium chloride solution at pH 2. Applying the method to analyse a sewage sample indicated that the matrix significantly influenced the extraction of heavier chlorinated phenols. The feasibility of SPME-GC-MS was examined for detecting phenolic compounds in waste water and the effects of humic acid and surfactants on recovery were studied. SPME using pencil lead as a sorbent for analysis of 2-CP in water was also investigated. The detection limit for the determination of chlorophenols by GC-ECD (electron-capture detection) was 1 ng mL^{-1} . According to their results, the dissolved humic substances (10 mg L^{-1}) did not affect the analysis. Analysis of chlorophenols from an aqueous sample by GC-MS following SPME and reaction with diazomethane has been studied. A silica fibre coated with polyacrylate yielded good extraction efficiency. **Figure 2** displays the mass chromatogram of chlorophenols derivatized with diazomethane after SPME, with detection limits at the level of ng L^{-1} .

The direct determination phenols in water using headspace-gas chromatography (HS-GC) has been developed. A method has been proposed based on the GC headspace analysis of phenols in solids as acetate derivatives. The acetate derivatives were directly prepared in the wet solid samples by acetic anhydride in the presence of KHCO_3 and separated on a diisodecylphthalate capillary column with FID. The detection limit ranged between 0.03 and 0.08 $\mu\text{g g}^{-1}$. We have evaluated SPME with a polyacrylate fibre

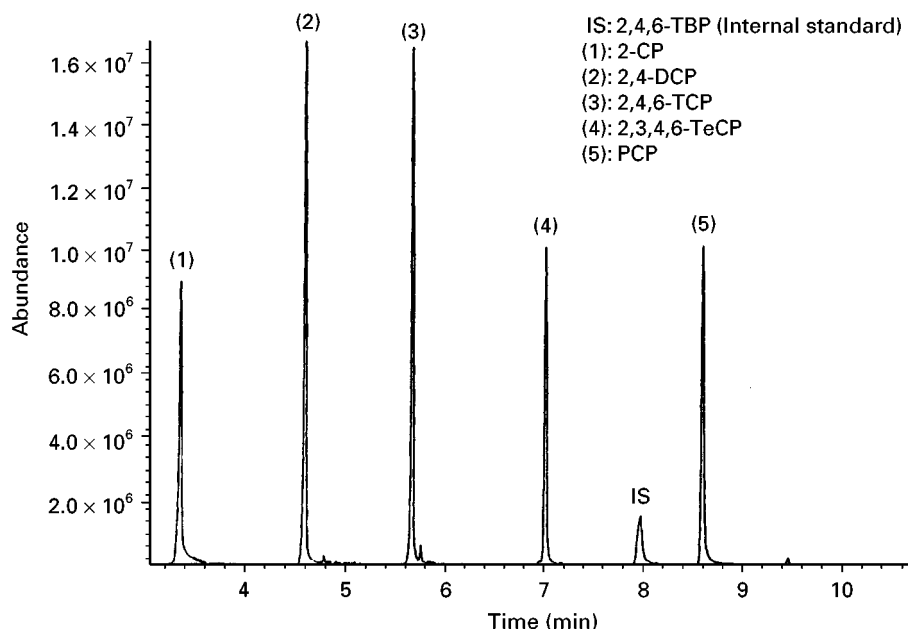


Figure 1 Chromatogram of pulsed spary-and-trap GC-MS of a water sample containing $100 \mu\text{g L}^{-1}$ chlorophenols and $20 \mu\text{g L}^{-1}$ internal standard (2,4,6-tribromophenol).

coupled with GC-MS (electron impact ionization and negative chemical ionization) to determine chlorophenols in landfill leachates and soil. The chlorophenols were analysed without any derivatization.

The method is precise and can be used over a wide linear range, with detection limits of 1 ng L^{-1} levels of chlorophenols in water. The chlorophenols were determined in soil contaminated with PCP from

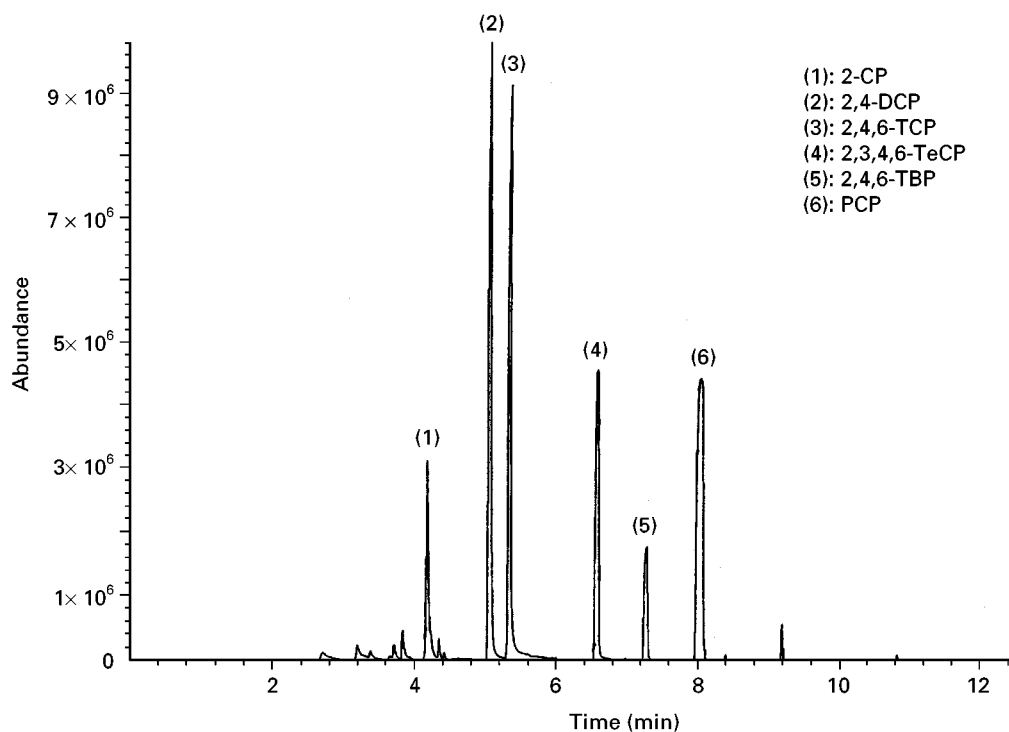


Figure 2 Chromatogram of $100 \mu\text{g L}^{-1}$ chlorophenols by post-derivatization following SPME with diazomethane produced using GC-MS (SIM).

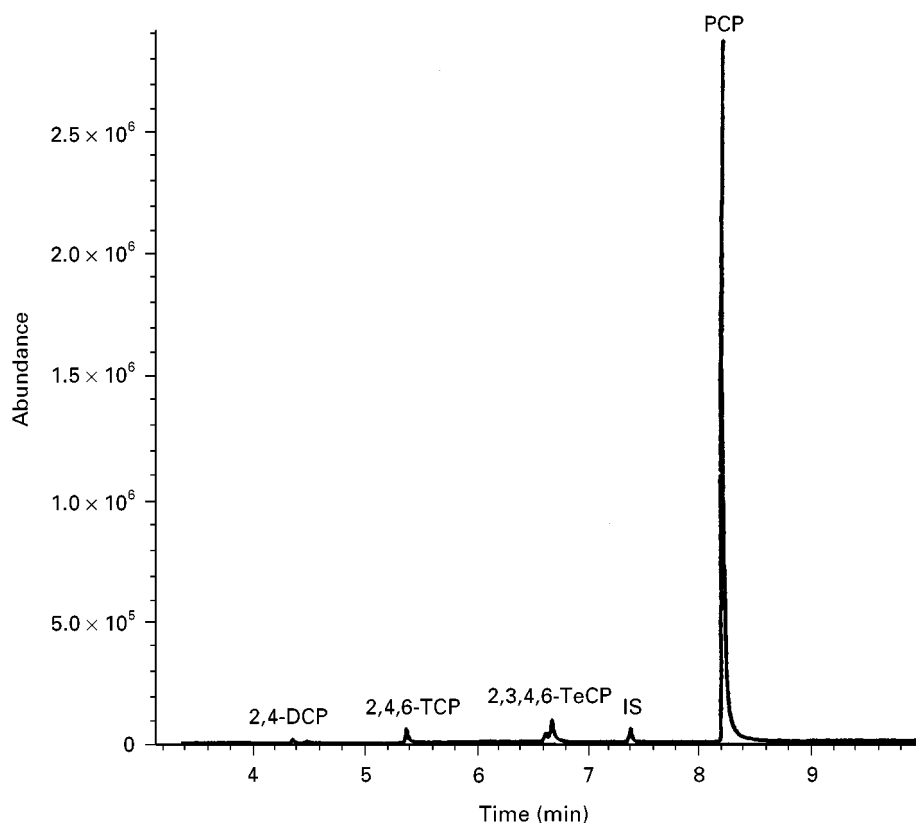


Figure 3 Mass ion chromatogram (TIC) of a real soil sample. (Reproduced from Lee MR (1998) *Journal of Chromatography A* 806: 323, with permission from Elsevier Science.)

a chemical manufacturing plant. **Figure 3** depicts the mass ion chromatogram of a real soil sample. Chlorophenols detected were 2,4-DCP, 2,4,6-TCP, 2,3,4,6-tetrachlorophenol (2,3,4,6-TeCP) and PCP. The internal standard was 2,4,6-tribromophenol. The PCP detected in the soil was estimated to be $534 \mu\text{g g}^{-1}$.

Biological Fluid Analysis

The monitoring of phenols in human urine and other biological samples is used as an indication of occupational exposure or exposure to environmental contamination. The efficiency of extracting analytes from complex matrices, particularly urine samples, affects the detection level. Selecting the optimum sample preparation method is a prerequisite for trace analysis of phenols in urine. Many methods of extraction combined with chromatographic techniques have been proposed to determine phenols in urine. One method determined the urinary chlorophenols as acetyl derivatives after hot acid hydrolysis, then extracted them using LLE with toluene. The chlorophenol derivatives were then determined by GC-MS using selected ion monitoring. The method was used to monitor the urine of sawmill workers who are still

occupationally exposed to chlorophenols because of a contaminated work environment. The limit of quantification was in the level of $3.6 \mu\text{g g}^{-1}$ creatinine for all the studied chlorophenols. A sensitive and selective method was developed for the quantitation of total *o*-phenylphenol (free plus conjugates) found in human urine samples. Conjugates of *o*-phenylphenol were acid-hydrolysed to free *o*-phenylphenol, extracted into toluene and derivatized to the pentafluorobenzol ester derivative. The analysis was performed via negative ion chemical ionization-GC-MS (NCI-GC-MS). In this case, the lower limit of quantification was 1 ng mL^{-1} urine.

As the result of the degradation of proteins and amino acids, the presence of some phenols, such as phenol, *p*-cresol, *p*-ethylphenol and catechol in free and conjugated forms, is commonly found in normal urine at the 5–20 p.p.m. level. The variety and amount of phenols excreted into urine are quite individual and vary with nutrition, smoking habits and intake of antibiotics. In dietary studies, it is required to monitor the relationship between nutrition and the levels of the phenols in faeces and urine samples. In occupational hygiene determination of phenol in urine after exposure to benzene or toluene is to detect

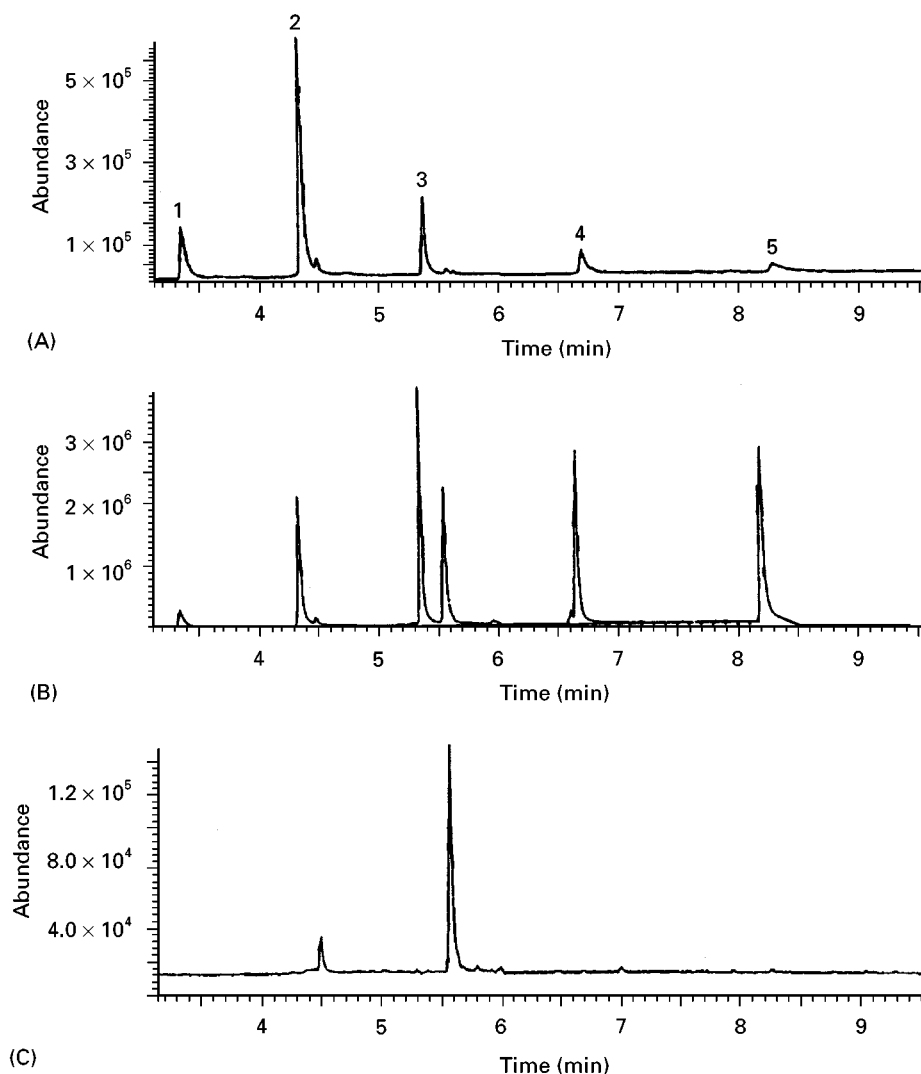


Figure 4 Mass chromatogram of (A) $25 \mu\text{g L}^{-1}$ chlorophenols in urine at pH 7, (B) at pH 1 and (C) blank urine, produced by SPME-GC-MS. Peaks are assigned as 1, 2-chlorophenol; 2, 2,4-dichlorophenol; 3, 2,4,6-trichlorophenol; 4, 2,3,4,6-tetrachlorophenol; 5, pentachlorophenol. (Reproduced from Lee MR (1998) *Journal of Chromatography B* 707: 95, with permission from Elsevier Science.)

the increased levels of phenol and *p*-cresol. Hydrolysis of urine samples with concentrated sulfuric acid during stream distillation followed by GC has been described. The condensate is buffered with H_3BO_3 -NaOH and acetylated with acetic anhydride. The derivatives of all cresols and xylenols were completely separated on an SE-54 capillary column. In this case, acid hydrolysis of phenolic conjugates must be combined with steam distillation, which is not performed offline. Acid hydrolysis of phenol conjugates in urine by concentrated H_3PO_4 , followed by extraction and acetylation, then GC on an OV-1 or OV-17 packed column with FID has been used to monitor normal levels of phenol and *p*-cresol or phenol and *o*-cresol after exposure to benzene or toluene vapours. The detection limit is 1 mg L^{-1} , which is

adequate for the purpose. The feasibility of combining SPE on Separcol SI C_{18} with GC-ECD to determine chlorophenols and cresols in human urine after acid hydrolysis has been discussed. Before GC determination, the isolated compounds were derivatized with pentafluorobenzyl bromide. The limit of determination of phenols varied from 5 to 20 ng mL^{-1} . Using this method, 52 from occupationally and nonoccupationally exposed groups were examined for the presence of chlorophenols in urine.

The feasibility of applying SPME and GC-MS to determine chlorophenols in urine has been evaluated. The amount of an analyte extracted relies heavily on the conditions of the SPME. **Figure 4** shows that the extraction is enhanced by decreasing the pH of the urine solution from 7 to 1.

According to these results, the optimum SPME experimental procedures to extract chlorophenols in urine were with a polyacrylate-coated fibre at pH 1, extraction time 50 min and desorption into the GC injector at 290°C for 2 min. The technique offers a low ng L^{-1} sensitivity to determine trace amounts of chlorophenols in a urine sample containing high levels of interference. The method has been successfully used to analyse urine samples of workers in a sawmill where chlorophenol-containing anti-stain agents were previously used. Analysis indicated that chlorophenols were found in 9 out of 10 urine samples. The concentration of chlorophenols ranged from $0.02 \mu\text{g L}^{-1}$ (PCP) to $1.50 \mu\text{g L}^{-1}$ (2,4-DCP).

Future Prospects

Phenols, particularly chlorophenols, are toxic at concentrations of a few $\mu\text{g L}^{-1}$ and are also persistent. Determining trace amounts of phenols is not easy for real samples that consist of extremely complex matrices. Methods for monitoring trace amount of phenols in real samples must be sensitive and selective, and should be rapid and simple. A mixture can be separated by GC into its individual components and, at the same time, the amount of each compound present can be determined. Furthermore, analysis can be performed with various detectors at a moderate cost. The applications presented here demonstrate the effectiveness of GC to analyse quantitatively trace levels of phenols in complex mixtures. Although various GC methods for phenol analysis have been widely used, novel techniques and sample pretreatment methods are continually being introduced. Simple retention times are not very reproducible and linking with a mass spectrometer as a detector is desirable for unambiguous identification. This approach has the merits of speed, sensitivity and selectivity. The MS-MS technique will become less expensive in the future

and, eventually, the preferred means of analysing phenols when coupled to GC. Currently GC-MS-MS is more expensive than GC-MS but offers an extra separation stage to resolve the problem of analysing mixtures not amenable to GC-MS.

See also: II/Chromatography: Gas: Column Technology; Derivatization; Detectors: Mass Spectrometry; Detectors: Selective; III/Phenols: Liquid Chromatography; Solid-Phase Extraction; Thin-Layer (Planar) Chromatography.

Further Reading

- Allowway BJ and Ayres DC (1997) *Chemical Principles of Environmental Pollution*, 2nd edn, pp. 113–123. London: Chapman & Hall.
- Bruner F (1993) *Gas Chromatographic Environmental Analysis*, pp. 181–223. New York: VCH.
- Budde WL and Eichelberger JW (1979) *Organics Analysis Using Gas Chromatography/Mass Spectrometry – A Techniques and Procedures Manual*. Michigan: Ann Arbor Science.
- Ettre LS (1973) Phenols. In: Snell FD and Ettre LS (eds) *Encyclopedia of Industrial Chemical Analysis*, vol. 17, pp. 1–50. New York: Wiley.
- Fielding M and Horth H (1988) The formation and removal of chemical mutagens during drinking water treatment. In: Angeletti G and Bjørseth A (eds) *Organic Micropollutants in the Aquatic Environment*, pp. 285–292. Dordrecht: Kluwer.
- Fishbein L (1972) *Chromatography of Environmental Hazards*, vol. 1, pp. 214–333. Amsterdam: Elsevier.
- Joy EF and Bernard AJ Jr (1973) Chlorophenols. In: Snell FD and Ettre LS (eds) *Encyclopedia of Industrial Chemical Analysis*, vol. 19, pp. 511–528. New York: Wiley.
- Soniassy R, Sandra P and Schlett C (1994) *Water Analysis Organic Micropollutants*, pp. 141–162. Waldbronn: Hewlett-Packard.
- Suffet IH and Malaiyandi M (1997) *Organic Pollutants in Water Sampling, Analysis and Toxicity Testing*, pp. 64–81. Washington DC: American Chemical Society.

Liquid Chromatography

R. M. Marcé and F. Borrull, Universitat Rovira i Virgili, Tarragona, Spain

Copyright © 2000 Academic Press

Phenols include a considerable range of substances which possess an aromatic ring with one or more hydroxyl substituents. These compounds are present in many different types of sample, which means that

the determination of phenolic compounds is of wide interest.

These compounds may be natural or synthetic. They are present in all plant tissues and are frequently the most abundant secondary metabolites in fruits, in which they sometimes reach high concentrations. Phenolic compounds may also be found in combinations to form flavones and glucosides in trees and plants.

Apart from their natural origin, phenols are also breakdown products from natural compounds such as lignins, tannins and humic substances. Chlorinated nitrophenols are the main degradation products of many chlorinated phenoxy acid herbicides and organophosphorus pesticides.

Phenolic compounds are extensively used in diverse products, such as plastics, dyes, antioxidants, cosmetics, pharmaceuticals and paper.

Some phenolic compounds are claimed to have medicinal properties, and are used in ointments and creams because of their antifungal, disinfectant and anaesthetic properties. Some compounds, namely caffeic, chlorogenic, ferulic, gallic and ellagic acids, have been found to be pharmacologically active as antioxidant, antimutagenic and anticarcinogenic agents.

As a result of emission accidents and other releases, phenolics are present in the environment and chlorophenols particularly constitute an environmental problem owing to their possible presence in rivers, lakes and seas where they may enter the food chain. Some phenols are toxic to humans and aquatic organisms and can cause serious taste and odour contamination even at very low levels.

Thus, the types of sample in which phenolic compounds are to be determined are diverse and include biological fluids (serum, whole blood, urine), industrial products and process streams, medicinal creams and ointments, dyes and environmental samples such as air or water (including wastewater, surface water and tap water).

Table 1 shows the main classes of phenolics in fruits and **Table 2** shows the phenolic compounds included on the priority pollutants list of the European Community and the US Environment Protection Agency (EPA).

The determination of individual phenolic compounds requires chromatographic techniques because of the large number of compounds with similar structures. Of these techniques, gas chromatography involves the derivatization of most phenolic compounds, which increases the time of analysis and introduces the possibility of additional errors. Supercritical fluid chromatography does not significantly improve their analysis compared to the other chromatographic techniques and an organic modifier, such as methanol, must be added to CO₂ for the mobile phase. Capillary electrophoresis, by both capillary zone electrophoresis and micellar electrokinetic chromatography, may be used in the determination of phenolic compounds but its limited concentration sensitivity, even when online preconcentration techniques are used, has so far restricted its application.

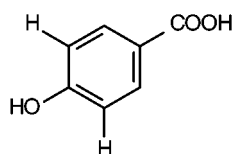
Thus, the recommended technique for determining phenolic compounds is either gas or liquid chromatography, the latter being the most used.

In some kinds of sample, the concentration of phenols may be very low and the detection systems not sensitive enough to detect them, so a preconcentration step is often required. Some samples also require a clean-up step in order to prevent possible interferences from the matrix.

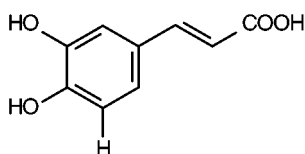
Table 1 Main classes of phenolics in fruits

Number of carbon atoms	Basic skeleton	Class	Example	Fruit (example)
7	C ₆ -C ₁	Hydroxybenzoic acids	<i>p</i> -Hydroxybenzoic	Strawberry
9	C ₆ -C ₃	Coumarins	Scopolin	Citrus
	—	Hydroxycinnamic acids	Caffeic	Apple
10	C ₆ -C ₄	Naphthoquinones	Juglone	Walnut
13	C ₆ -C ₁ -C ₆	Xanthenes	Magniferin	Mango
14	C ₆ -C ₂ -C ₆	Stilbenes	Resveratrol	Grape
15	C ₆ -C ₃ -C ₆	Flavonoids	Cyanidine	Cherry
		Isoflavonoids	Daidzein	French bean
<i>n</i>		Lignins		Stone fruits
		Tannins		Persimmon

Examples



p-Hydroxybenzoic acid



Caffeic acid

Table 2 Phenolic compounds included in priority pollutants list of the EC and US EPA (method 604 and 8041)*Commission of the European Communities (directive 76/464/EC)*

2-Amino-4-chlorophenol
 4-Chloro-3-methylphenol
 2-Chlorophenol
 3-Chlorophenol
 4-Chlorophenol
 Pentachlorophenol
 Trichlorophenols

US EPA list of priority pollutants (EPA 8041)

Phenol	4-Chloro-3-methylphenol
2-Methylphenol	3-Methylphenol
4-Methylphenol	2,4-Dimethylphenol
2-Chlorophenol	2,4-Dichlorophenol
2,6-Dichlorophenol	2,4,6-Trichlorophenol
2,4,5-Trichlorophenol	2,3,4,5-Tetrachlorophenol
2,3,4,6-Tetrachlorophenol	2,3,5,6-Tetrachlorophenol
Pentachlorophenol	2-Nitrophenol
4-Nitrophenol	2,4-Dinitrophenol
Dinoseb	2-Cyclohexyl-4,6-dinitrophenol
4,6-Dinitro-2-methylphenol	

Liquid Chromatography Separation

Reversed-phase separation is by far the most efficient technique for separating phenolic compounds. Several kinds of column have been used, although C_{18} -bonded silica seems to be the preferred stationary phase. When 29 phenolic compounds with chloro-, nitro-, hydroxy-, methoxy-, ethoxy-, aldehyde-, and carboxylic functionalities were separated in different columns (a polymer functionalized silica, a polystyrene divinylbenzene polymer, a carbonaceous phase and a silica C_{18}), the best results were obtained with the C_{18} silica. The best overall separation is obtained with the C_{18} column, but a carbon column may be better for the more polar compounds.

When the C_{18} , diphenyl and propyl nitrile columns are used with different gradient elutions, the best resolution is also obtained on a C_{18} stationary phase.

It should be pointed out that, depending on the supplier, the characteristics of the column may differ slightly. It is also important to take the dimensions of the columns into account. Several lengths (between 100 and 300 mm) of stainless-steel columns of 4.6 mm i.d. are commonly used, but microbore columns have also been used to reduce solvent consumption, shorten analysis time, increase sensitivity and allow the injection of smaller sample volumes. However, microbore columns are limited because of the higher interference from the matrix components and the changes in flow rates, both of which considerably shorten the life span of the column.

Phenolic compounds can be separated by isocratic or by gradient elution. Gradient elution is generally

based on the modification of the organic solvent, mainly methanol or acetonitrile. Gradient elution is usually preferred when phenols covering a wide range of polarity are to be determined. However, it may take longer to stabilize the analytical column and there may be changes in the baseline due to the changes of the mobile phase.

When isocratic elution is used, separation is good for the more polar compounds but dispersion is significant in the late eluted peaks, which means a decrease in sensitivity. So in some cases, such as the determination of phenols of environmental concern, two elutions at different percentages of organic solvent are recommended when isocratic elution is used, due to the different polarity of phenol and pentachlorophenol. For isocratic elution, the instrumentation is simpler since only one pump is necessary. Isocratic separation is preferred when electrochemical detection is used because gradient elution involves a significant decrease in sensitivity. However, for most applications gradient elution is used.

Figure 1 shows a chromatogram of a standard solution of seven phenolic compounds under isocratic elution.

The composition of the mobile phase depends on the type of detector used. In general, the pH of the mobile phase and the percentage of organic solvent are the most important parameters to be optimized.

The pH of the mobile phase is known to influence the retention of phenols on the column depending on their protonation, dissociation or partial dissociation. Partial dissociation might lead to additional peak broadening and asymmetric peaks due to co-elution of the acid solute of the component and its conjugate base. The influence of this effect depends on the K_a values of the compounds. The most common pHs used for the separation of phenolic compounds are between 2.5 and 3, where the analytes are separated in their acidic form, and 5–7, when some of the phenolic compounds are in their dissociated form. Depending on the phenolic compounds to be separated, one pH value or another may give better separations. It is also usually recommended to work with buffer solutions to adjust the pH of the mobile phase. Acetic acid is the most used acid to adjust the pH, although sulfuric acid is also used, and buffer solutions of phosphate are the most used. Table 3 summarizes some pH and buffer solutions, analytical columns and detection conditions used for the determination of phenolic compounds in different samples.

Some phenolic compounds can also be determined by ion interaction reversed-phase HPLC. The method is based on the ability of phenolic compounds to form ion pairs with alkylammonium ions and, for instance,

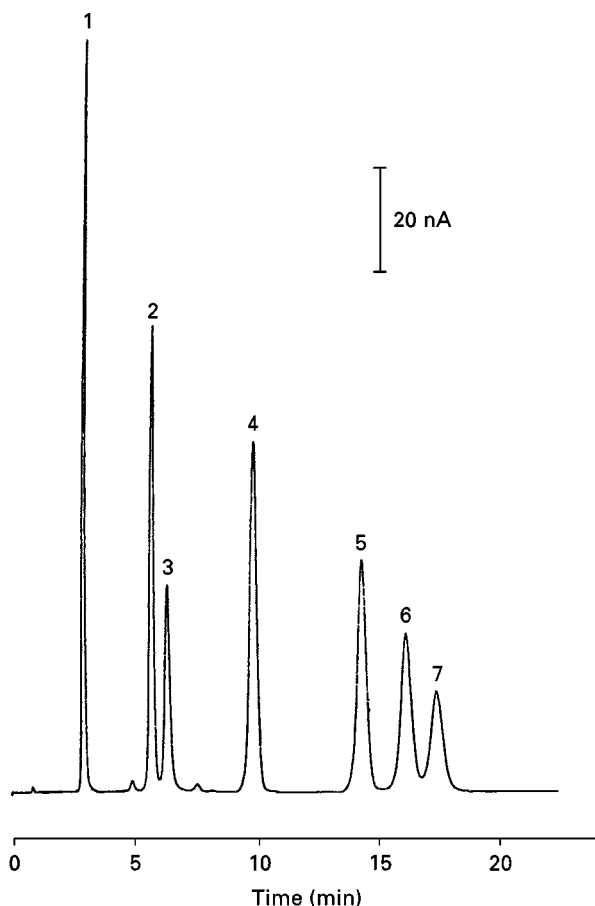


Figure 1 Chromatogram of a standard solution (20 ng for each compound). Analytical column: 125 × 4 mm i.d. LiChrospher 100 RP-18. Mobile phase: 30 mmol L⁻¹ sodium monohydrogen-phosphate/sodium dihydrogen phosphate, pH 7.0–acetonitrile-methanol (64:19:17, v/v/v) at 1.4 mL min⁻¹. Coulometric detection, applied potential 750 mV vs Pd. Peaks: 1, phenol; 2, *o*-chlorophenol; 3, 2,4,6-trichlorophenol; 4, 2,4-dimethylphenol; 5, 4-chloro-3-methylphenol; 6, 2,4-dichlorophenol; 7, pentachlorophenol. (Reprinted with permission from Galcerán MT *et al.* (1995) *Analytica Chimica Acta* 304: 75.)

the 11 EPA priority phenolics may be determined with a mobile phase of water–acetonitrile solution of octylammonium *o*-phosphate at pH 8.

Phenols may be separated by micellar reversed-phase liquid chromatography. For instance, phenolic compounds and their corresponding glucuronides have been determined in urine by isocratic elution using a mobile phase which contains acetonitrile and cetyltrimethylammonium bromide. The use of this micellar agent means that the selectivity of the analytes must be high relative to the urine matrix components and it allows the glucuronides and parent compounds to be simultaneously analysed without the need for gradient elution.

Some compounds may also be added to the mobile phase in order to form complexes with the phenolic

compounds and enhance the detection response: for instance, α -cyclodextrin can be added to the mobile phase in order to enhance the fluorescent properties of phenolic compounds.

Detection

The method of detection which is most used in liquid chromatography for the determination of phenolic compounds is UV spectrophotometry, although in recent years electrochemical detection, fluorescence, chemiluminescence and mass spectrometry have been used to increase the sensitivity and selectivity. Their application is described below.

UV Spectroscopy

This is the most widely used technique and each group of phenolic compounds is characterized by one or several UV light absorption maxima. For instance, phenol and chlorophenol derivatives are usually detected at 280 nm, whereas nitrophenols and pentachlorophenol are usually detected at 310 nm. As regards other phenolic compounds, 220 and 275 nm are characteristic of flavanols and hydrocalchones, while 260 and 350 nm are characteristic of flavonols.

Diode array detectors (DAD) are recommended because spectral libraries can be used for confirmation purposes. In complex matrices, identifying spectra by comparison is extremely useful and DAD enables each peak to be measured at its maximum wavelength of absorbance, which means an increase in sensitivity. DAD also makes it possible to detect overlapped peaks when their spectra are different enough.

Phenolic compounds may also be derivatized pre- or post-column in order to enhance their absorptivity in the UV-visible region but derivatization is not commonly used because of the increase in complexity of the method.

Electrochemical Detection

Electrochemical detection (EC) is more sensitive than UV detection for such phenols as phenol and chlorophenols and common breakdown products from lignin such as vanillin, syringaldehyde and *p*-coumaric acid. However, sensitivity does not increase significantly for nitrophenols. The electrochemical conditions depend on the oxidation and/or reduction potential of the solute. The operational potential in most cases is a compromise between the optimal faradaic current and the lowest level of background current for each solute. The electrochemical oxidation of phenolics requires the use of high applied potentials – around 1 V versus a standard calomel

Table 3 High performance liquid chromatography conditions for the determination of phenolic compounds

Compounds	Column	Mobile phase	Detector	Comments	Reference
18 EPA priority phenolics	Waters C-18 150 × 3.9 mm i.d.	Gradient: A 1% acetic acid B MeOH acetonitrile (1/3)	UV: 310 nm PCP and mononitrophenols 280 nm rest of compounds	TSP for confirmation Natural waters off-SPE	Puig and Barceló (1995)
11 Phenolic compounds	Spherisorb ODS-2 250 × 4 mm i.d.	Gradient: A 1% acetic acid with 0.05 g L ⁻¹ KCl B MeOH	UV: 316 nm 4-NP 280 nm rest of compounds EC: 1 V	Environmental waters online SPE	Pocurull <i>et al.</i> (1996)
18 EPA priority phenolics	Hypersil green ENV C ₁₈ 150 × 4.6 mm i.d.	Gradient: A 1% acetic acid B MeOH acetonitrile (1 : 1) 1% acetic acid	APCl 30 V cone voltage	Post-column addition MeOH containing 0.1 mol L ⁻¹ TEA	Puig <i>et al.</i> (1997)
13 Phenolic compounds	Hypersil C ₁₈ 125 × 4 mm i.d.	Isocratic: 30 mmol L ⁻¹ acetate/acetic acid (pH = 5.3)-acetonitrile-MeOH (60 : 30 : 10)	EC (dual electrode) 750 mV (vs. Pd)	Environmental waters offline SPE	Galcerán and Jáuregui (1995)
Hydroxybenzoic acids Hydroxycinnamic acids	Spherisorb ODS-2 250 × 1.1 mm i.d.	Gradient: A phosphate buffer pH2.4 B MeOH	UV 280 nm hydroxybenzoic acid 320 nm hydroxycinnamic acid	Wine samples SPE	Buiarelli <i>et al.</i> (1995)
Hydroxybenzoic acids Hydroxybenzaldehydes	Lichrospher RP-C-18 250 × 4 mm i.d.	Gradient: A MeOH-acetic acid-H ₂ O (5 : 2 : 93) B MeOH-acetic acid-H ₂ O (90 : 2 : 8)	DAD 240–390 nm	Brandy samples	Barroso <i>et al.</i> (1996)
Hydroxybenzoic acids Hydroxybenzaldehydes	Waters Nova Pak 150 × 3.9 mm i.d.	Isocratic: MeOH-H ₂ O (0.1% acetic acid, 0.2m mol L ⁻¹ (C ₂ H ₅) ₄ Ni, pH 5.7)	ESP 56 V cone voltage	Fibre samples LLE	Giocchini <i>et al.</i> (1996)
Caffeic, chlorogenic, ferulic and gallic acids	Lichrospher 100 RP-18 150 × 3.9 mm i.d.	Isocratic: H ₂ O-ethyl acetate-acetic acid (95.6 : 4.1 : 0.3)	UV 280, 320, 360 nm	Juices LLE	Shahrzad and Bitsch (1996)

Puig D and Barceló D (1995) *Chromatographia* 40: 435. Pocurull E, Marcé RM and Borrull F (1996) *Journal of Chromatography A* 738: 1. Puig D, Grassenbauer M and Barceló D (1997) *Analytical Chemistry* 69: 2756. Galcerán MT and Jáuregui O (1995) *Analytica Chimica Acta* 304: 75. Buiarelli F, Cartoni G, Coccioli F and Levetsovitu Z (1995) *Journal of Chromatography A* 695: 229. Barroso CG, Rodríguez MC, Guillen DA and Pérez-Bustamante JA (1996) *Journal of Chromatography A* 724: 125. Giocchini AM, Roda A, Galletti GC, *et al.* (1996) *Journal of Chromatography A* 730: 31. Shahrzad S and Bitsch I (1996) *Journal of Chromatography A* 741: 223.

Table 4 Detection limits ($\mu\text{g L}^{-1}$) in groundwater using online procedures with UV and electrochemical detection

Compound	UV	EC
Phenol	10	0.02
4-Methylphenol	1.5	0.01
2,4-Dimethylphenol	0.8	0.03
2-Nitrophenol	1.2	2
4-Nitrophenol	0.8 ^a	3
2,4-Nitrophenol	0.5	3
4-Chloro-3-methylphenol	2	0.01
2-Chlorophenol	1.5	0.05
3-Chlorophenol	1.7	0.05
4-Chlorophenol	1.5	0.05
2,4-Dichlorophenol	2	0.03
2,4,6-Trichlorophenol	2	0.03
2,3,5-Trichlorophenol	2	0.03
2,3,4-Trichlorophenol	2	0.03
3,4,5-Trichlorophenol	2	0.05
Pentachlorophenol	1 ^a	0.03

Sorbent: PLRP-S; UV detection, 230 nm (^a310 nm); EC detection, 1 V; sample volume, 10 mL. Reprinted from Puig and Barceló (1995), with permission from Elsevier Science.

electrode which opens up the possibility of fouling the electrodes. Two meta hydroxyl groups in the ring will increase the oxidation potential by some 500 mV. Such a high potential value makes it possible for other matrix compounds to be oxidized, thus increasing the background current.

The increase in sensitivity is very important when isocratic elution is used, although it is lower for gradient elution. Another problem encountered with the use of high applied potentials is the competition between the oxidation of phenols and their electro-polymerization which takes place at the electrode surface, thus fouling the surface and giving rise to a decline in signal response with time.

Table 4 compares the limits of detection obtained in groundwater using online solid-phase extraction-liquid chromatography with UV and electrochemical detection. It shows lower limits of detection for most phenols with electrochemical detection, although for nitrophenols, as already mentioned, limits of detection are lower with UV detection.

Pulsed amperometric detection (PAD) is more stable and its greater sensitivity for phenolic compounds makes it highly appropriate for detecting them. Using a working potential which is sufficiently positive to oxidize the phenols electrochemically, the current obtained is proportional to the concentration of the analyte. As the electrochemical conversion results in electrode fouling, a high oxidative potential pulse is applied immediately after the elution of the analytes which strips the fouling products from the electrode. The pulse is followed by another pulse

which is lower than the working potential to reduce impurities and clean the electrode surface. This self-cleaning method allows the user to carry out a large number of analyses without cleaning the electrode.

It has been demonstrated that the PAD technique may be used with 200 injections of severely contaminated river water containing di-, tri-, tetra- and pentachlorophenols at a global concentration of about 5 ppm.

The use of chemically modified electrodes (CME) circumvents some of the disadvantages of phenol detection.

A multielectrode electrochemical detector consists of four coulometric array cell modules with four electrochemical detection cells; each may also be used for detecting phenols. The detectors with porous graphite working sensors and palladium reference and counter electrodes are arranged in series after the analytical column. The advantages of this system are that each compound is detected at its highest sensitivity potential and that each peak can be confirmed by comparing the matching ratio *R* of the standard and the actual sample. *R* is the ratio between the response from the subdominant channel.

Coulometric array detection is designed so that the eluent flows through a porous graphite electrode having a large cell constant which in turn increases the sensitivity and the signal stability. Unlike common electrochemical detectors in which the electrode typically reacts to 10% or less of the injected sample, coulometric sensors convert 100% of the analyte because phenols oxidize in the high porosity electrode.

Fluorescence and Chemiluminescence

Fluorescence and chemiluminescence detection are known to be very selective and sensitive. Phenols themselves are not fluorescent but they may be converted into a fluorescent compound through a derivatization reaction or by the addition of additives to the mobile phase, in order to make the phenols fluoresce.

The chemical reaction can be in the pre- or the post-column mode. Phenols can be detected by a post-column derivatization procedure, photochemical decomposition of the dansyl derivatives of the phenolic compounds and fluorescence detection. The UV irradiation leads to the formation of highly fluorescent dansyl derivatives which are several orders of magnitude more sensitive than nonirradiated derivatives.

Phenolic compounds can also be determined fluorimetrically by measuring cerium(III), which is the result of oxidizing phenols with cerium(IV) and low limits of detection can be reached.

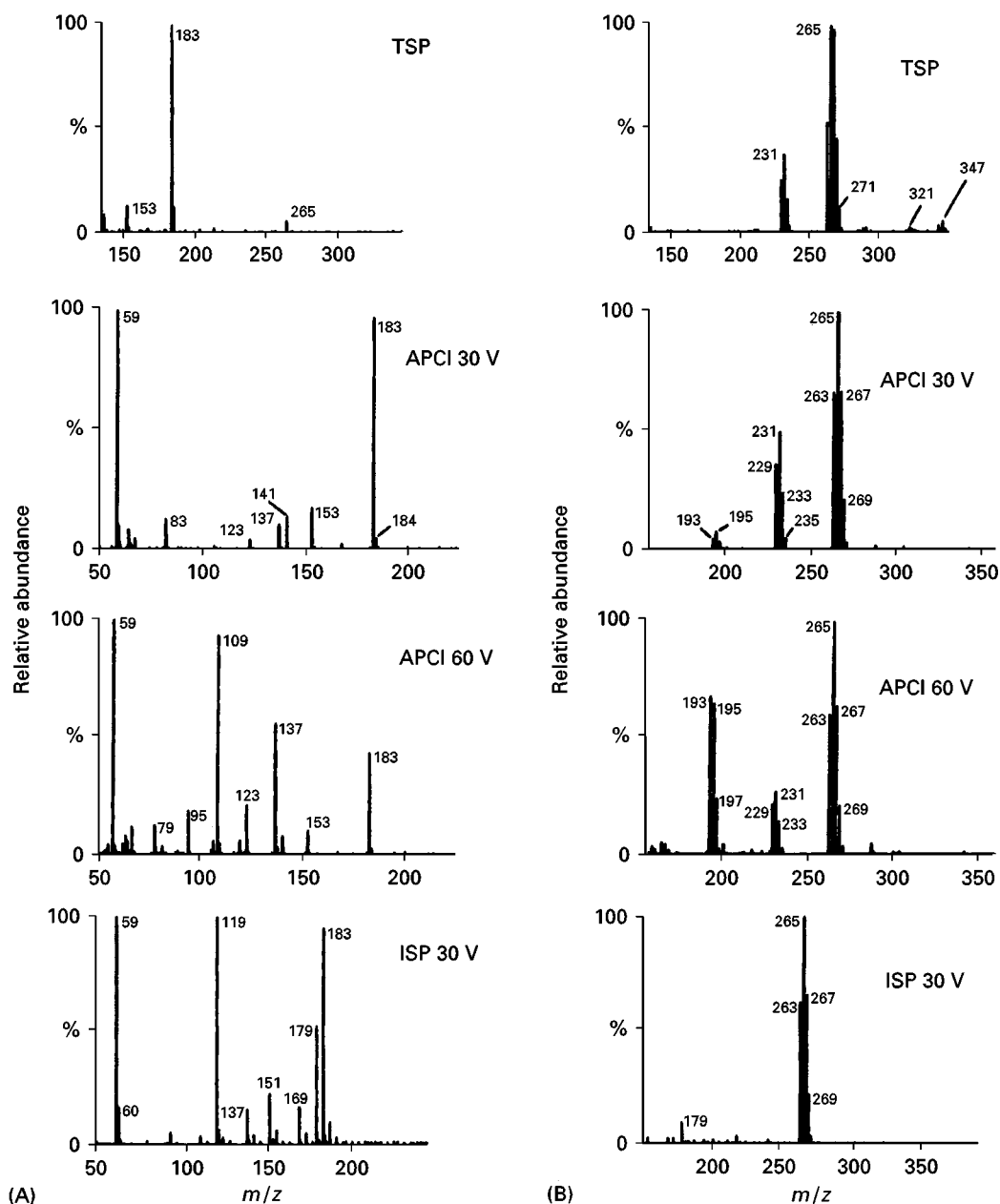


Figure 2 Mass spectra obtained in flow injection analysis using TSP, APCI (30 V cone voltage), APCI (60 V cone voltage) and ISP (30 V cone voltage) for (A) 2,4-dinitrophenol and (B) pentachlorophenol. Conditions: TSP, 1 mL min⁻¹ methanol (1 µg mL⁻¹ analyte)–water (1% acetic acid) 1:1 and post-column addition of 0.2 mL min⁻¹ 50 mmol L⁻¹ ammonium acetate; APCI, 1 mL min⁻¹ methanol (1 µg mL⁻¹ analyte)–water (1% acetic acid) 1:1; ISP: 0.3 mL min⁻¹ [methanol (1 µg mL⁻¹ analyte)–water (1% acetic acid)–methanol (0.1 mol L⁻¹ TEA)]. (Reprinted with permission from Puig *et al.* (1996). *Journal of Mass Spectrometry* 31: 1297.)

α -Cyclodextrin can be added to the mobile phase to form inclusion complexes with analytes, such as *p*-hydroxybenzoic, ferulic and vanillic acids and methyl paraben. The inclusion complexes fluoresce allowing detection limits of 1–5 ng L⁻¹.

Chemiluminescence detection may give low detection levels, in the range of 10–100 times lower than for fluorescence detection. The generally preferred detection system is the peroxyoxalate chemilumines-

cence system. The alkyl-, nitro- and chlorophenols can be detected by using both pre- or post-column derivatization. The method consists of dansylation, photolysis of substituted phenols and peroxyoxalate chemiluminescence detection.

Mass Spectrometry

Mass spectrometry (MS) has become an increasingly attractive technique as a result of the rapid

Table 5 Instrumental detection limits in SIM mode using LC-MS

Compound	MDLs (ng)		
	TSP	APCI	ISP
Catechol	2	0.004	0.740
Phenol	ND	ND	0.175
2-Nitrophenol	1.5	0.050	0.045
4-Nitrophenol	0.4	0.002	0.120
2,4-Dinitrophenol	0.7	0.004	0.256
2-Amino-4-chlorophenol	3.1	0.050	0.500
4-Chloro-3-methylphenol	4.5	ND	3
4-Methylphenol	ND	ND	0.400
2,4-Dimethylphenol	ND	ND	6
2-Chlorophenol	5	0.085	3
3-Chlorophenol	4	0.045	2
4-Chlorophenol	4	0.040	2
2,4-Dichlorophenol	3	0.007	1.310
2,4,6-Trichlorophenol	0.95	0.004	0.330
2,3,5-Trichlorophenol	0.90	0.003	0.350
2,4,5-Trichlorophenol	0.90	0.003	0.300
3,4,5-Trichlorophenol	0.90	0.002	0.300
Pentachlorophenol	0.5	0.001	0.100

MDL, method detection limit; ND, not detected up to 2000 ng. Reprinted from Puig and Barceló (1996), with permission from Elsevier Science.

developments and improvements in interfaces to couple MS to high performance liquid chromatography (HPLC) in recent years. The interfaces which are most used are those based on ionization at atmospheric pressure such as electrospray (ESP), ionspray (ISP) and atmospheric pressure chemical ionization (APCI), although thermospray (TSP) has also been widely used in the recent past.

The TSP interface provides a good response in the negative ion mode for the phenolic compounds on the US EPA list of priority pollutants except for phenol, 4-methylphenol and 2,4 dimethylphenol because they cannot be deprotonated by current buffers even at a high buffer concentration level. The positive ionization (PI) mode shows no signal response for the chlorophenols of environmental interest since the ammonium ions of the mobile phase are not able to protonate them. This is circumvented in the negative ionization (NI) mode where the high intensity of $[M-H]^-$ is the result of the electron-attracting chlorine group in the aromatic moiety. Other phenolic compounds, such as 4-hydroxycoumarin, 7-hydroxycoumarin and 3,5-dimethoxyphenol, exhibit good responses under the PI mode of operation and some of the main peaks are $[M-H]^+$ and $[NH_4]^+$.

The main advantages of atmospheric pressure interfaces are the resulting higher sensitivity (especially when using APCI), robustness and ease of use. What is more, by increasing the extraction voltage,

structural information can be obtained via collision-induced dissociation using a simple quadrupole instrument.

An ES interface may be used to analyse phenolic compounds. It is compatible with conventional solvent mixtures used for normal or reversed-phase HPLC, up to 80% of which can be water, but only volatile buffers or counterions may be used. The flow rate should be kept low, which is easily done by post-column splitting or by using a semimicro- or micro-column.

Plant phenolic compounds may be determined by HPLC-ES-MS. They are separated in a phenyl column by ion-pairing with tetraethylammonium iodide and are then identified in the negative ion mode, in which only their deprotonated molecules $[M-H]^-$ are generated.

APCI and ISP interfaces give $[M-H]^-$ as the main ion with an extraction voltage in the range 20–30 V. It should be pointed out that raising the cone voltage leads to a decrease in sensitivity so this parameter should be carefully optimized to get a good compromise between both factors.

An ISP interface may also be used, but since an acidic pH is normally required for the chromatographic separation of phenolic compounds, a buffer must be added post-column in order to generate ions in solution when performing LC-ISP-MS experiments. This is done by using either KOH or triethylamine. By far the most interesting feature of the ISP interface is the detection of phenol, 4-methylphenol and 2,4-dimethylphenol, although a methanol percentage above 85% is required. This is accomplished by using porous graphitized carbon (PGC) columns where excessive retention allows these analytes to be resolved using 100% methanol as mobile phase.

Figure 2 shows the different mass spectra for 2,4-dinitrophenol and pentachlorophenol obtained in flow injection analysis using TSP, APCI at two cone voltage values and ISP. It can be seen that the compounds are fragmented differently in each case.

Table 5 shows the limits of detection for different interfaces obtained under selected ion monitoring (SIM). It can be seen that APCI is more sensitive than the other interfaces by one or two orders of magnitude.

Sample Handling Techniques

The determination of phenolic compounds usually requires pretreatment of the sample prior to injection into the liquid chromatograph. This pretreatment has two main goals: to clean up the sample, particularly when complex matrices are to be analysed, and to concentrate the phenolic compounds when these are present at low levels in the sample.

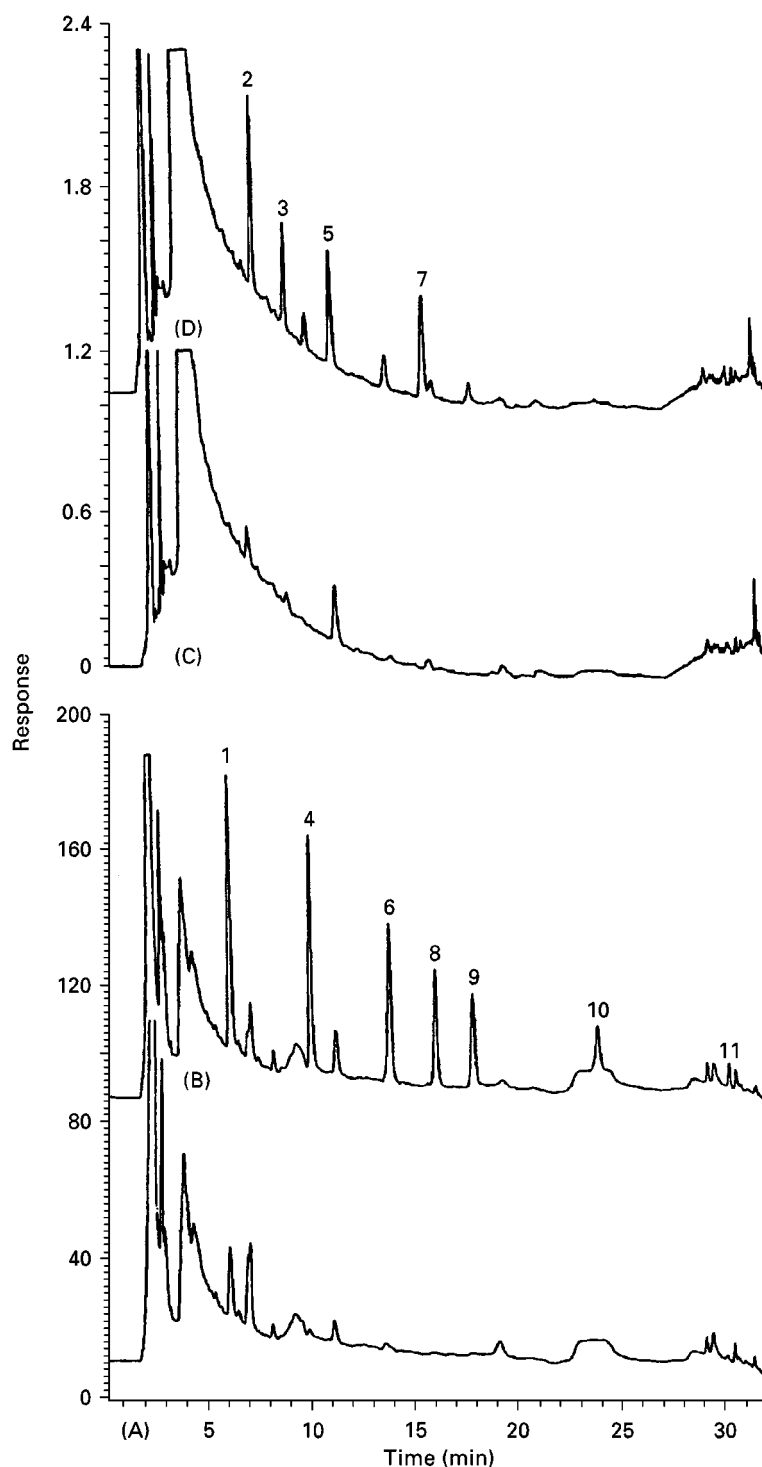


Figure 3 Chromatograms obtained by online trace enrichment with a PLRP (polystyrene-divinylbenzene sorbent) pre-column and an electrochemical detector (A,B) or a UV detector (C,D) of 10 mL. (A) Ebro river water; (B) Ebro river water spiked at $1 \mu\text{g L}^{-1}$ with each phenol; (C) Ebro river water; (D) Ebro river water spiked at $1 \mu\text{g L}^{-1}$ with each phenol. 1, Phenol; 2, 4-nitrophenol; 3, 2,4-dinitrophenol; 4, 2-chlorophenol; 5, 2-nitrophenol; 6, 2,4-dimethylphenol; 7, 2-methyl-4,6-dinitrophenol; 8, 4-chloro-3-methylphenol; 9, 2,4-dichlorophenol; 10, 2,4,6-trichlorophenol; 11, pentachlorophenol. (Reprinted from Pocurull *et al.* 1996, with permission from Elsevier Science.)

The easiest way to handle a sample is to combine a concentration with a membrane filtration or ultra-filtration step. This may reduce the level of interfering compounds and eliminates solids and colloids. Liquid-liquid extraction is still a very common sample-handling technique, although it requires a

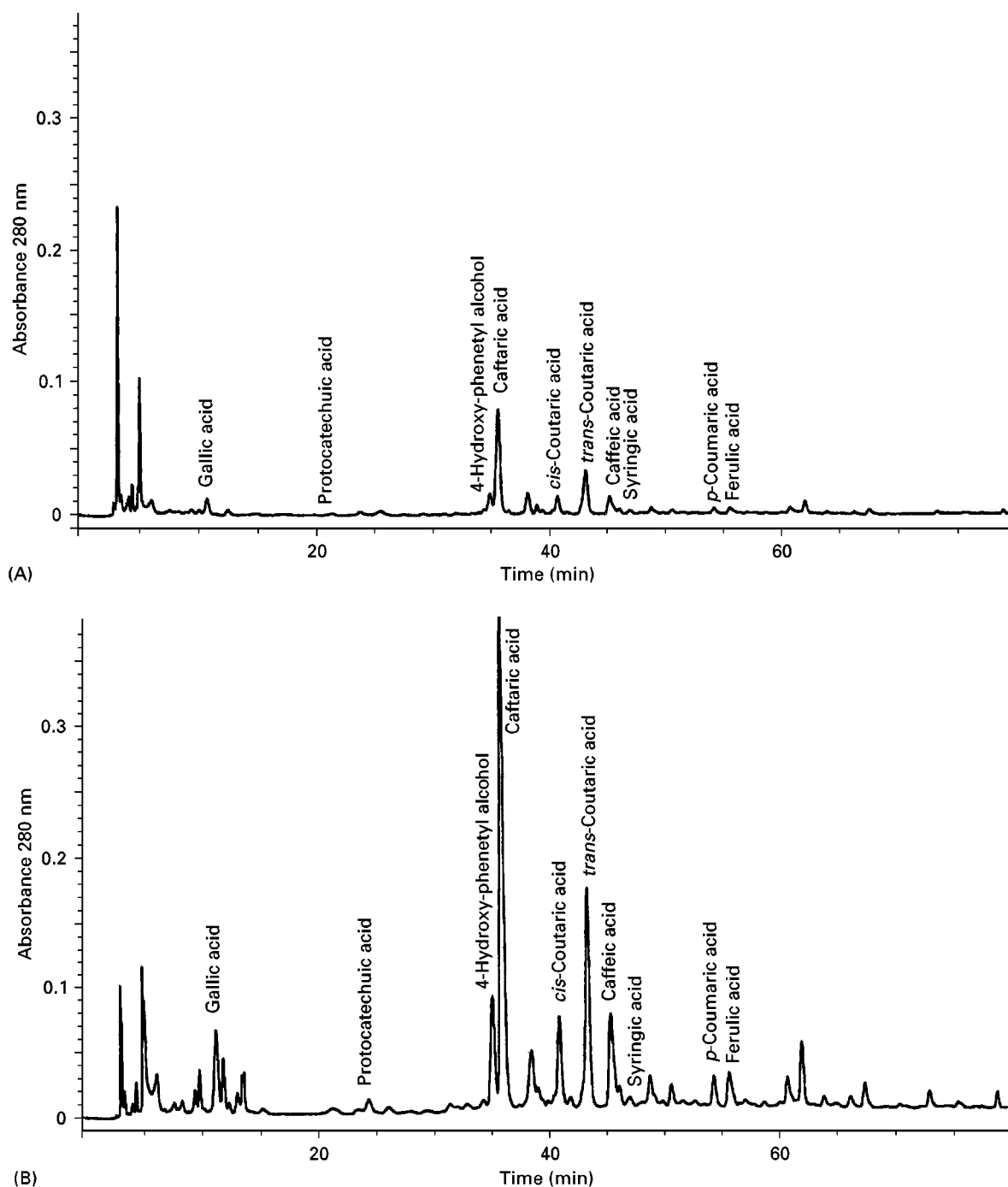


Figure 4 Chromatograms (280 nm) of 20 µL of sherry by direct injection (A) and of 5 mL of sherry after online solid-phase extraction with a polystyrenedivinylbenzene LiChrolut EN (B). (Reprinted from Chilla *et al.* (1996), with permission from Elsevier Science.)

large amount of organic solvents, which is a disadvantage from the environmental point of view.

The most widely used sample clean-up in biological and environmental samples is solid-phase extraction (SPE), which can be used in the offline mode or as an automated online coupling. Online coupling has some very important advantages, such as the automation of the system, lower organic solvent consump-

tion and less handling of the sample. Phenolic compounds can be determined by online SPE reversed-phase LC (SPE-RPLC) with good results as regards limits of detection and precision.

Sorbents such as bonded silica and the polymeric phases can be used in SPE. The low breakthrough volume of most polar phenols in the common sorbents, such as C₁₈-bonded silica and styrene-divinylbenzene,

is considerably increased when highly cross-linked polymer sorbents or chemically modified polymers are used.

The phenolics of environmental concern can be determined at levels required by legislation by using online SPE-RPLC and different sorbents can be used, although the best ones are the highly cross-linked polymeric sorbents.

Figure 3 shows the chromatograms of 10 mL of river water sample obtained by online trace enrichment with a styrene-divinylbenzene (PLRPs) precolumn and HPLC with electrochemical and UV detectors. The figure also shows the chromatograms of the same sample spiked at $1 \mu\text{g L}^{-1}$ of each phenol.

As regards other kinds of sample, online SPE-RPLC has been successfully applied to the determination of phenolic compounds in beverages, urine and so on.

Figure 4 shows the chromatograms of a sherry, obtained after direct injection of 20 μL (A) and after online SPE of 5 mL of sample (B) and HPLC with UV detection at 280 nm.

In summary, liquid chromatography is a suitable technique for determining phenolic compounds in different kinds of samples. Different detection techniques may be used, some of which, such as EC, enable low levels of phenols to be detected. Mass spectrometry, mainly with APCI, is good for confirming the presence of a phenol in samples at low levels. SPE is the sample-handling technique which is most used for both preconcentration and clean-up of the samples. The combination of this technique, in both the off- and online mode, enables phenols to be detected at low $\mu\text{g L}^{-1}$.

See also: II/Chromatography: Liquid: Derivatization; Detectors: Mass Spectrometry; Detectors: Ultraviolet and Visible Detectors. Extraction: Solid-Phase Extraction. III/Phenols: Gas Chromatography; Solid-Phase Extraction.

Further Reading

- Chilla C, Guillén DA, Barroso CG and Pérez-Bustamante JA (1996) Automated on-line solid-phase extraction-high-performance-liquid chromatography-diode array detection of phenolic compounds in sherry wines. *Journal of Chromatography A* 750: 209.
- Macheix JJ, Fleuriet A and Billot J (1990) *Fruit Phenolics*. Boca Raton, FL: CRC Press.
- Marko-Varga GA (1993) Liquid chromatographic determination of phenols and substituted derivatives in water samples. In: Barceló D (ed.) *Environmental Analysis. Techniques, Applications and Quality Assurance*, p. 225. Amsterdam: Elsevier.
- Marko-Varga GA and Barceló D (1992) Liquid chromatographic retention and separation of phenols and related aromatic compounds on reversed phase columns. *Chromatographia* 34: 146.
- Patterson JM and Smith WT (1995) Phenols. In: Townshend A (ed.) *Encyclopedia of Analytical Science*, vol. 7, p. 3928. London: Academic Press.
- Pocurull E, Sánchez G, Borrull F and Marcé RM (1995) Automated on-line trace enrichment and determination of phenolic compounds in environmental waters by high-performance liquid chromatography. *Journal of Chromatography A* 696: 31.
- Pocurull E, Marcé RM and Borrull F (1996) Determination of phenolic compounds in natural water by liquid chromatography with UV and electrochemical detections after on-line trace enrichment. *Journal of Chromatography A* 738: 1.
- Puig D and Barceló D (1995) Comparative study of on-line solid phase extraction followed by UV and electrochemical detection in liquid chromatography for the determination of priority phenols in river water samples. *Analytica Chimica Acta* 311: 63.
- Puig D and Barceló D (1996) Determination of phenolic compounds in water and waste water. *Trends in Analytical Chemistry* 15: 362.
- Puig D, Barceló D, Silgoner I and Grasserbauer M (1996) Comparison of three different liquid chromatography-mass spectrometry interfacing techniques for the determination of priority phenolic compounds in water. *Journal of Mass Spectrometry* 31: 1297.

Solid-Phase Extraction

J. Bładek and M. Śliwakowski, Military University of Technology, Warsaw, Poland

Copyright © 2000 Academic Press

Introduction

Nowadays, sample preparation plays the major role in analysis, as the increasing complexity of samples

frequently makes direct analysis impossible. With particular samples, this act is often the limiting factor in the analysis. The aims of sample preparation are as follows: to put the sample in the appropriate physical state for analysis; to clean up the analytes (separate the interference from analytes), and enrichment of analytes. There are many methods of sample preparation which lead to correct analytical results. Features and applications of these methods are presented in numerous compilations and monographs. In this

article, only techniques in which solid-phase extraction (SPE) or solid-phase microextraction (SPME) are applied to samples containing phenols are presented.

Phenols form the group of aromatic compounds with one or more hydroxyl groups. These chemicals are produced as waste in oil refineries, coke plants and some chemical manufacturing, such as the pulp and paper, antioxidant, plastics and dye industries. They also occur in the environment as biodegradation products of humic substances, tannins and lignin. Nitro- and chlorophenols are the main degradation products of many organophosphorous insecticides and chlorinated phenoxyacid herbicides.

The need of analyses focused on the content of phenol results from the fact that phenols, especially chlorophenols, are toxic at concentration levels of a few $\mu\text{g L}^{-1}$. Even at very low concentrations, phenols affect the taste and odour of fishes and drinking water. A number of phenol compounds are listed (e.g. by the European Community, US Environmental Protection Agency (EPA)) as priority pollutants. Recent regulations enacted in many European countries state that phenols cannot be present in water destined for human consumption at individual levels exceeding $0.1 \mu\text{g L}^{-1}$. This means that analytical methods capable of detecting phenols at tens of ng L^{-1} are necessary. These methods should also be able to detect phenols at $1\text{--}3 \mu\text{g L}^{-1}$ levels in surface water samples, because several phenols are toxic to aquatic life. There are various methods to determine phenols in samples. Most important are:

- Spectrophotometric methods based on the reaction of 4-aminoantipyrine with phenols (in this method only total phenols can be determined);
- Gas chromatography with derivatization and electron-capture detection (standard EPA method);
- Liquid chromatography with UV, amperometry, mass spectrometry, fluorescence or chemiluminescence (after derivatization) detection;
- Thin-layer chromatography (usually used as a screening method).

Unfortunately, each of the above analytical procedures is inadequate for monitoring traces of phenols in complex matrices. Each requires enrichment and clean-up techniques. In many laboratories, the procedures for phenol trace enrichment are carried out by means of distillation or liquid-liquid extraction. The disadvantages of these methods, such as enrichment of contaminants, time, emulsion forma-

tion, and the use of relatively large amount of solvents, are well known. Consequently, SPE and SPME were established as promising alternative sample preparation techniques.

Specificity SPE of Phenols

As a first approach, SPE can be described as a simple chromatographic process with aqueous media as the mobile phase and the sorbent as the stationary phase. During the enrichment step, the analytes are retained by the sorbent and not eluted by water. Advantages of the method are low cost, minimal consumption of organic solvent and convenience. The techniques can be incorporated easily into fully online set-ups, facilitating automation. Various solid phases with different selectivity, such as octadecyl- or phenyl-bonded silicas, ion exchange materials, polymer resins, porous graphitic carbon, and graphitized carbon black, are used for extraction with varying results. The specificity of extracting phenols by SPE must first consider all the following parameters:

- Phenol and substituted-phenols are acids. Extraction depends on the degree of ionization and can be controlled by the sample pH. Adjusting the pH of the solution or solvent to be used for elution of about 2 units away from the pK_a affords the possibility of achieving quantitative retention and elution of the analyte. For instance, adjustment of the pH of the solution containing 2,4-dinitrophenol (pK_a 4.09) to two pH units above the pK_a of analyte results in approximately 99% ionization. The analyte is deprotonated and forms the conjugate base, which can be retained by anion exchange sorbents. Consequently, the pH of the elution solvent should be 2 pH units below pK_a values. At this pH the analytes are no longer negatively charged and can be eluted from the sorbent. Similarly, at $\text{pH} = 7$, samples containing, e.g. phenol (pK_a 9.89) or 2,4-dimethylphenol (pK_a 10.63), acid-base equilibrium of these substances shifts significantly toward the neutral form, which is readily retained on nonpolar phases.
- Phenols, like polar analytes, are slightly volatile and can be partially degraded when heated. Online SPE procedures are often more convenient to analyse these substances. Online coupling of SPE to liquid or gas chromatography of phenols is easily performed in many laboratories with the automated devices commercially available. In these systems, the extraction pre-column is placed in the sample-loop position of a six-port switching valve. After conditioning, sample application and clean-

ing, the pre-column is coupled to an analytical column by switching the valve to the inject position. Phenols are then eluted directly from the SPE pre-column by a suitable mobile phase, which also permits their chromatographic separation. Advantages of online SPE are that there is no risk of contamination or loss of analyte as there is no sample manipulation between preconcentration and analysis; quantitative results are expected; and the entire sample is transferred and analysed, allowing small sample volume to be used.

- The characteristic matrix for phenols is water. The presence of relatively large amounts of humic substances in aqueous samples can make SPE techniques less effective in extracting phenols. Formation of chemical complexes with fulvic acids and saturation of adsorbent sorption sites by these acids (which are rather scarcely retained by adsorbents) can lead to considerable analytes losses.
- The need for derivatization of phenolic samples is motivated by improved sensitivity and gas chromatographic performance. Derivatization with acetic anhydride to form phenol acetates is one of the simplest and most practical methods. This method does not require extraction of the phenols to organic solvent prior to the addition of the derivatizing reagent.

SPE of Phenols by Reversed Phases Based on Silica Gel

Synthetic silica with a nominal pore diameter of 6 nm and a particle size distribution of 40–63 μm is used for the synthesis of the chemical-bonded stationary phases. A broad range of phases for selective sample preparation are available. This range covers nonpolar, medium polar and strongly polar phases (ion exchangers).

Work concerning applications of reversed-phase SPE (RP-SPE: using octadecyl- or phenyl-bonded silicas as adsorbents) for extraction of phenols from water have lost practical utility. Additionally, if the matrix contains lipophilic compounds, selective isolation of such phenols using reversed phases based on silica gel is difficult. In these cases, isolation using an anion exchange mechanism is more selective.

From a number of publications concerning the efficiency of different phases for the isolation of phenols, two (both by Puig and Barceló) demand more attention. The first concerns the application of reversed phases based on silica gel in offline and online systems. Offline experiments were performed using

C_{18} extraction discs and, for comparison purposes, styrene-divinylbenzene (SDB) discs. After disc activation with 10 mL of acetone and 10 mL methanol, 1 L of groundwater spiked with phenol at $5 \mu\text{g L}^{-1}$ and acidified to pH 2 was passed through the discs. Analytes were eluted using three aliquots of methanol of 20 mL total volume. Eluates were concentrated to 1 mL and analysed by liquid chromatography (LC-UV) and liquid chromatography-mass spectrometry (LC-MS) methods. Online SPE-LC was carried out on stainless steel pre-columns (10 \times 2 mm). Extraction efficiency was determined for the following phases, based on silica gel: C_{18} , $\text{C}_{18}\text{-OH}$, C_8 , phenyl, cyclohexyl and, for comparison purposes, CN and polystyrene divinylbenzene sorbent (PLRP-S). Pre-columns were conditioned with 10 mL methanol and 5 mL water (pH 3). After extraction of spiked samples, acidified to pH 2, and washing the sorbent with 2 mL of water, phenols were eluted by passing the mobile phase (mixture of water and methanol-acetonitrile 1 : 3 containing 1% acetic acid) directly through the analytical column. The authors evaluated recoveries (Table 1), breakthrough volume, matrix effects and the influence of extraction column dimensions on band broadening. The size of pre-column is an important parameter in the coupling methods because the profile of concentrated analytes transferred to the analytical column should ideally be as narrow as possible at the beginning of the separation. It was shown that the more non-polar sorbents (C_{18} and C_8) gave good results for the more nonpolar phenols (e.g. trichlorophenol and pentachlorophenol). With these phases the concentrated volume, prior to breakthrough of the other target compounds, was less than 10 mL. The results concerning the remaining phenols were only slightly improved by using monofunctional $\text{C}_{18}\text{-OH}$.

SPE of Phenols on Polymeric Phases

At the beginning of the 1970s, a new nonionic styrene-divinylbenzene copolymer, with a particle size distribution appropriate for sample preparation (40–120 μm), was introduced by Junk *et al.* Due to its very large surface area (approximately $1200 \text{ m}^2 \text{ g}^{-1}$), its adsorption capacity for organic compounds is excellent. That adsorbent contains a relatively large number of active aromatic sites capable of interactions with the aromatic phenols, which considerably improves the enrichment of these analytes. The other advantage of the styrene-divinylbenzene copolymer is excellent chemical and mechanical stability. As previously mentioned, Puig and Barceló performed a comparative study of the performance of four sorbents for online SPE followed by LC of phenol

Table 1 Mean percentage recoveries and standard coefficients of variation (CV) of phenols in different sorbents in ground water when working with online procedures using a 10 × 2 mm i.d. stainless-steel pre-column

Compound	Sorbent						
	<i>C</i> ₁₈	<i>C</i> ₁₈ /OH		Cyclohexyl		PLRP-S	
	Concentration (μg L ⁻¹) 5	0.5	5	0.5	5	0.5	5
Catechol	< 20	< 20	< 20	< 20	< 20	< 20	< 20
Phenol	< 20	< 20	< 20	< 20	27 ± 8	< 20	37 ± 6
4-Methylphenol	25 ± 6	42 ± 7	54 ± 6	59 ± 5	68 ± 6	69 ± 5	88 ± 6
2,4-Dimethylphenol	57 ± 5	61 ± 3	75 ± 4	67 ± 4	77 ± 5	81 ± 3	96 ± 4
2-Nitrophenol	31 ± 8	50 ± 5	63 ± 4	46 ± 6	61 ± 4	76 ± 4	95 ± 5
4-Nitrophenol	33 ± 7	44 ± 6	56 ± 6	42 ± 5	59 ± 6	78 ± 5	89 ± 7
2,4-Dinitrophenol	30 ± 6	40 ± 5	53 ± 5	40 ± 6	53 ± 5	100 ± 4	99 ± 4
2-Amino-4-chlorophenol	< 20	< 20	< 20	< 20	< 20	< 20	< 20
4-Chloro-3-methylphenol	52 ± 5	58 ± 4	76 ± 3	55 ± 5	70 ± 4	85 ± 6	94 ± 5
2-Chlorophenol	< 20	49 ± 5	52 ± 4	66 ± 4	78 ± 5	76 ± 4	85 ± 4
3-Chlorophenol	< 20	35 ± 6	48 ± 5	68 ± 5	81 ± 5	78 ± 7	90 ± 6
4-Chlorophenol	< 20	41 ± 5	53 ± 4	65 ± 4	73 ± 5	85 ± 6	93 ± 6
2,4-Dichlorophenol	41 ± 5	73 ± 4	85 ± 5	71 ± 7	85 ± 6	81 ± 5	95 ± 3
2,4,6-Trichlorophenol	62 ± 5	72 ± 4	87 ± 6	92 ± 4	97 ± 4	96 ± 5	98 ± 4
2,3,5-Trichlorophenol	70 ± 4	75 ± 4	81 ± 4	90 ± 4	98 ± 5	94 ± 6	99 ± 5
2,3,4-Trichlorophenol	71 ± 5	74 ± 3	87 ± 5	91 ± 6	101 ± 5	95 ± 7	100 ± 5
3,4,5-Trichlorophenol	75 ± 4	78 ± 5	88 ± 4	95 ± 4	98 ± 5	93 ± 5	102 ± 5
Pentachlorophenol	87 ± 4	89 ± 4	97 ± 3	97 ± 5	99 ± 5	100 ± 5	99 ± 3

Spiking level: 0.5 and 5 μg L⁻¹ (*n* = 6 for each phenolic). Sample volume: 10 and 100 mL for 5 and 0.5 μg L⁻¹ concentration respectively. Reproduced with permission from Puig and Barceló (1995).

compounds in water. Three of these PLRP-S, LiChrolut EN and Isolut ENV) were phases based on styrene-divinylbenzene copolymer; the fourth was porous graphitic carbon (PGC) (Table 2), detection limits (to 0.1 μg L⁻¹) and breakthrough volumes. Improved breakthrough values were obtained with LiChrolut EN and Isolut ENV. PGC gave good results only for aminophenols. It was demonstrated that acidification of the sample is necessary to avoid binding of some phenols to humic substances and to prevent their partial deprotonation.

SPE of Phenols on Carbon Phases

The selective retention of phenols contained in water can be realized using PGCs or graphitized carbon blacks (GCBs).

It was demonstrated that retention of some polar compounds in water could be high when using PGC. In one experiment an online technique, coupling SPE and LC, was applied to the analysis of water-soluble organic pollutants, such as aminophenols. (These products are degradation products of aniline and some pesticides and their extraction from water is difficult owing to their high polarity. The authors demonstrated that a PGC pre-column cannot be

coupled online with the widely used and efficient *C*₁₈ analytical column, but could be used with a PGC analytical column. Separations on *C*₁₈ is achieved with water-rich mobile phases, which are unable to desorb analytes that are more retained by PGC pre-column. Band broadening, the influence of the matrix, and recoveries were evaluated. For example, retention of 4-aminophenol on PGC, which is not retained on *C*₁₈ and only slightly on PRP-1, was 10 times higher in compared with PRP-1.

The other carbon materials recommended for phenol extraction are GCBs. They are nonporous sorbents with surface areas ranging from 8 to 100 m² g⁻¹. The adsorbent contains chemical heterogeneities on its surface. In the presence of water, these surface to form positively charged impurities. Thus GCB behaves both as a nonspecific sorbent and an anion exchanger. This feature is used for rapid and simple isolation of acidic analytes from co-extracted base-neutral species by differential elution. Elution by neutral eluents allows for transfer to solution of base-neutral and very weak acidic compounds. The most acidic compounds (e.g. phenols having *pK*_a values lower than 7) remain on the adsorbent and may be transferred to the solution by the acidified eluent. Commercially referred to as Carbograph 1 or Car-

Table 2 Mean percentage recoveries \pm standard deviation of phenol compounds in groundwater using different sorbent and working with online liquid–solid extraction (LSE) using a 10 \times 2 mm i.d. stainless-steel pre-column

Compound	Sorbent			
	PLRP-S	LiChrolut EN	Isolute ENV	PGC
Catechol	< 20	55 \pm 9	57 \pm 8	61 \pm 7
Phenol	34 \pm 5	67 \pm 7	62 \pm 7	54 \pm 6
4-Methylphenol	69 \pm 6	75 \pm 6	82 \pm 5	52 \pm 7
2,4-Dimethylphenol	81 \pm 4	98 \pm 4	92 \pm 4	n.d.
2-Nitrophenol	76 \pm 5	88 \pm 5	88 \pm 5	n.d.
4-Nitrophenol	78 \pm 5	84 \pm 6	100 \pm 4	n.d.
2,4-Dinitrophenol	100 \pm 4	102 \pm 5	98 \pm 4	n.d.
2-Amino-4-chlorophenol	< 20	< 20	< 20	87 \pm 6
4-Chloro-3-methylphenol	85 \pm 5	92 \pm 6	88 \pm 5	n.d.
2-Chlorophenol	76 \pm 4	86 \pm 6	81 \pm 4	85 \pm 7
3-Chlorophenol	78 \pm 6	83 \pm 5	79 \pm 5	88 \pm 6
4-Chlorophenol	85 \pm 6	84 \pm 5	80 \pm 4	88 \pm 5
2,4-Dichlorophenol	81 \pm 3	94 \pm 5	92 \pm 3	n.d.
2,4,6-Trichlorophenol	96 \pm 4	103 \pm 5	99 \pm 5	n.d.
2,3,5-Trichlorophenol	94 \pm 5	96 \pm 4	101 \pm 6	n.d.
2,3,4-Trichlorophenol	95 \pm 5	101 \pm 4	105 \pm 6	n.d.
3,4,5-Trichlorophenol	93 \pm 5	99 \pm 4	98 \pm 4	n.d.
Pentachlorophenol	100 \pm 4	100 \pm 3	99 \pm 5	n.d.

Reproduced from Puig and Barceló (1996), with permission from Elsevier Science.

bopack, GCB has proved to be a valuable sorbant for SPE. However, it was demonstrated that Carbograph 4 is more efficient than Carbograph 1 in extracting very polar compounds from large volumes of water (Table 3). A robust and selective liquid chromatography method was developed enabling rapid determination of 11 US EPA phenols in samples in the ng L⁻¹ range. The method involved extraction of phenols by a reversible 0.5 g Carbograph 4 cartridge and re-extraction by an eluent containing a quaternary ammonium salt. Phenols were directly analysed by LC-UV, after derivatization to appropriate acetyl derivatives. Recovery of phenols was higher than 90%.

SPE of Phenols on Anion Exchangers

For phenol analysis, synthetic anion exchangers (polymers and chemical-bonded silicas) are generally applied because of their durability and chemical resistance. The typical functional groups of strong or weak basic anion exchangers are $-\text{CH}_2-\text{N}^+(\text{CH}_3)_3$ and $-\text{N}^+\text{H}(\text{R})_2^-$ respectively.

An application of ion exchangers for selective determination of phenols in water by a two-trap tandem extraction system followed by LC has been proposed. The first extraction column was filled with 300 mg GCB and the second with 50 mg of a strong anion exchanger (SAX, commercially referred to as Sephadex QAE A-25). After the water sample had

been passed through the GCB cartridge, the latter was connected to the SAX cartridge. Base-neutral species adsorbed on GCB were removed by a neutral eluent. Co-eluted, very weakly acidic phenols were selectively re-adsorbed on the SAX sorbants. Next, avoiding disconnection of the cartridges, an acidified eluent was allowed to flow through the two cartridges to recover the most acidic phenols from the GCB and the least acidic phenols from the SAX. After partial removal of the solvent, the final extract was analysed by LC-UV. Recoveries of 17 phenols added to 2 L of drinking water were higher than 90%.

Recoveries from 1 L of tap water and seawaters are presented in Table 4. In one process it was possible to concentrate both more and less polar phenols. The method is characterized by high selectivity; only acidic organic compounds can interfere with the phenols. Anionic surfactants (frequently occurring in aqueous environmental samples) are not eluted, because the formic acid contained in the second mobile phase is unable to displace the anionic surfactants from positively charged sorption sites populating the GCB surface.

Solid-phase Microextraction of Phenols

SPME can be used to concentrate volatile, semivolatile and nonvolatile phenols in both liquid

Table 3 Recovery of phenol on extracting 4 L of drinking water by cartridges containing two different GCB sorbent materials

Compound	Recovery (%) ^a		
	Carbograph 1	Carbograph 4	
	Forward elution	Forward elution	Backflush elution
Phenol	26 ^b	95	96
4-Nitrophenol	93	65	99
2-Chlorophenol	53	97	98
2,4-Dinitrophenol	93	15	96
2-Nitrophenol	97	97	98
2,4-Dimethylphenol	63	98	100
4-Chloro-3-methylphenol	98	96	99
2,4-Dichlorophenol	96	98	98
4,6-Dinitro-2-methylphenol	97	10	95
2,4,6-Trichlorophenol	93	96	98
Pentachlorophenol	100	36	101

^aMean values obtained from duplicate measurements.

^bRecoveries of phenols remained unaltered in the backflushing mode.

Reproduced with permission from Di Corcia *et al.* (1996).

and gaseous samples. This method, in which sorbent-coated silica fibres are used to extract analytes, is superior to other sample preparation methods. The fibre is introduced into the sample or headspace and phenols (or other organic substances) establish equilibrium and partition on to the phase. Next, the analytes are thermally desorbed from the fibre to the gas chromatograph. SPME is a fast, simple and sensitive technique which does not require the use of solvents. The method is significantly simpler than conventional SPE, thereby reducing the potential for loss of analyte during the extraction process. Most of the SPME methods are based on a poly(dimethylsiloxane) coating, which is relatively nonpolar. In the case of phenol extraction, it is necessary to use a more polar phase or a derivatization procedure to reduce their polarity and improve chromatographic properties.

The basis of SPME optimization for the determination of phenols was established by Buchholz and Pawliszyn. The subject of the research was to evaluate the derivatization step by increasing the affinity of the phenols for the poly(dimethylsiloxane) coating, comparison of the affinity of phenols for the poly(dimethylsiloxane) coating and a more selective, polar coating (a poly(acrylate)), the influence of acid and salt on the enhancement of phenols, evaluation of time equilibration on the equilibrium distribution constant between a solid-phase coating and water and an evaluation of the above parameters on carry-over. Headspace analysis of phenols was also evaluated. The most important conclusions are:

- The poly(dimethylsiloxane) coating is not suitable for extracting phenol; some chlorophenols and nitrophenols could not be extracted in large enough amounts to be detected by GC.
- The derivatization procedure created compounds with higher affinity for the poly(dimethylsiloxane) coating; the amount of acetate extracted for most of the target analytes was several times greater than the free form (2-nitrophenol was the only compound for which the amount of derivative extracted was less than the free phenol). It was demonstrated that the *in situ* derivatization can be performed directly in the polymeric coating.
- Phenol acetates have significantly better peak shape than the free phenols.
- Poly(acrylate) coating was successful in extracting both polar and nonpolar compounds; the fibre only slightly favours the polar phenols over its nonpolar analogues.
- Only 15 min is required for all analytes to equilibrate with the poly(dimethylsiloxane) coating; with poly(acrylate)-coated fibres, 40 min was required. That can be explained by the fact that the poly(dimethylsiloxane) phase is a liquid, whereas the poly(acrylate) phase is a solid.
- When the extraction is performed under saturated salt condition, 5.5 times more phenol was extracted compared to the control sample (sample of the same concentration at neutral pH and with no salt added).
- The salting-out effect was observed for high pK_a phenols; this results in a positive increase in the

Table 4 Recovery of phenol on extracting 1 L of tap water and seawater by the proposed method compared with those from two other extraction methods

Compound	Recovery (%) ^a					
	Anion exchanger		C ₁₈		This method	
	Tap	Sea	Tap	Sea	Tap	Sea
Guaiacol	12	5	3	8	98	93
<i>p</i> -Nitrophenol	96	56	6	9	99	98
<i>p</i> -Cresol	27	7	8	10	97	92
6-Chlorovanillin	94	33	20	28	100	99
<i>o</i> -Chlorophenol	97	14	6	11	98	95
2,4-Dinitrophenol	98	95	7	13	96	98
<i>o</i> -Nitrophenol	93	47	7	9	97	97
2,4-Dimethylphenol	44	14	20	36	98	97
Bromoxynil	97	89	68	84	101	101
2,4-Dichlorophenol	94	73	20	32	99	100
4,6-Dinitro- <i>o</i> -cresol	98	93	40	56	95	95
loxynil	102	96	101	98	100	100
2,4,6-Trichlorophenol	98	89	88	85	98	98
3,4,5-Trichlorosyringol	99	90	93	94	96	97
Tetrachlorophenol	100	93	98	98	99	100
Dinoseb	99	94	96	97	101	01
Pentachlorophenol	101	97	99	100	97	97

^aMean values obtained from triplicate measurements. Reproduced with permission from Di Corcia *et al.* (1993).

amount extracted for these phenols; for phenols which have a considerable portion of their molecules in the ionized form, the salting-out effect is a negative factor.

- Matrix significantly affects the extraction of phenols, especially nitrophenols and heavier chlorinated phenols. These effects can be overcome by normalization to extreme acid and salt conditions. Headspace is another method of reducing matrix influence.
- If the fibre is directly exposed to samples which are high in particulate matter, material from the matrix could coat the solid phase and interfere with extraction. To avoid this, the headspace above the liquid should be sampled. The success of this method depends on the transfer of analytes from the aqueous phase to the headspace. Most of the target phenols could be enriched in the headspace by decreasing their solubility in the aqueous phase through saturation with sodium chloride and acidification to pH below 1. However, even with these extreme conditions, most phenols needed 1–2 h to reach equilibrium.

Conclusions

The trace determination of phenols in environmental samples requires specific strategies. Analytical methods need to be sensitive selective, rapid and

simple. Both SPE and SPME techniques with a variety of sorbents for enrichment and purification are used. In the last decade, several online systems for SPE-LC or SPE-GC have been published. Online SPE procedures provide greater sensitivity, lower sample volumes, lower consumption of organic solvent, higher automation and better reproducibility. SPME is rarely applied and seems to vary with phenol concentration.

See also: II/Extraction: Solid-Phase Extraction. III/Solid Phase Microextraction: Environmental Applications.

Further Reading

- Buchholz KD and Pawliszyn J (1994) Optimization of solid-phase microextraction conditions for determination of phenols. *Analytical Chemistry* 66: 160.
- Di Corcia A, Marchese S and Samperi R (1993) Selective determination of phenols in water by a two-trap tandem extraction system followed by liquid chromatography. *Journal of Chromatography* 642: 175.
- Di Corcia A, Bellioni A, Madbouly MD and Marchese S (1996) Trace determination of phenols in natural waters. Extraction by a new graphitized carbon black cartridge followed by liquid chromatography and re-analysis after phenol derivatization. *Journal of Chromatography* 733: 383.
- Guenu S and Hennion MC (1994) On-line sample handling of water-soluble organic pollutants in aqueous samples

- using porous graphitic carbon. *Journal of Chromatography* 665: 243.
- Junk GA, Richard JJ, Grieser MD *et al.* (1974) Use of Macroreticular resins in the analysis of water for trace organic contaminants. *Journal of Chromatography* 99: 745.
- Puig D and Barceló D (1995) Off-line and on-line solid-phase extraction followed by liquid chromatography for the determination of priority phenols in natural waters. *Chromatographia* 40: 435.
- Puig D and Barceló D (1996) Comparison of different sorbent materials for on-line liquid-solid extraction followed by liquid chromatographic determination of priority phenol compounds in environmental water. *Journal of Chromatography* 733: 371.

Thin-Layer (Planar) Chromatography

J. H. P. Tyman, Institute of Physical and Environmental Sciences, Brunel University, Middlesex, UK

Copyright © 2000 Academic Press

Introduction

Phenols have played an important part in thin-layer chromatography (TLC) since its inception as a general separatory method. The phenolic group occurs in a wide variety of natural replenishable organic compounds from the amino acids (tyrosine), the alkaloids (morphine), the steroids (estrone), glycosides (arbutin, carminic acid, flavonols), perfume ingredients (methyl salicylate, eugenol), phenolic lipids (cashew phenols, urushiol) and the tetracyclines to the cannabinoids. Fractions derived from fossil fuels by distillation or by synthesis contain phenol itself, the cresols, xlenols and polynuclear compounds. Many purely synthetic products, notably drugs (aspirin, paracetamol), technical products (*t*-butylphenol, nonylphenol, and other intermediates such as chloro- and nitrophenols extend the range of substances as candidates for TLC.

The classical separations of structural isomers of monohydric, dihydric and polyhydric phenols and their derivatives have generally formed the basis for subsequent applications to mixtures of more complex compounds. All these initial studies were essentially qualitative and have led over the past four decades to quantitative work aimed at the determination of a single phenolic substance in a mixture or of the total phenolic composition.

The original TLC adsorption method with silica gel was soon supplemented by the partition technique by coating the adsorbent with a paraffinic compound or by silanization. These reversed-phase (RP) approaches have, with the introduction of excellent commercial plates, led to the routine use of alkylsilylbonded silica gel with C₁₈, C₈ or C₂ silyl groups.

In a similar fashion, with the development of uniform particle size adsorbents high performance TLC

(HPTLC), combined techniques such as TLC-ultraviolet (TLC-UV), TLC-mass spectrometry (TLC-MS), (TLC-GLC) and TLC-high performance liquid chromatography (TLC-HPLC) have all been applied to the study of phenolic materials.

A wide variety of adsorbent layers have been investigated for the analysis of phenols, including silica gel, alumina, cellulose and polyamides as well as mixtures in certain cases with other inorganic materials such as calcium hydroxide or impregnated with organic additives. The use of argentation TLC with phenolic lipids is well established but other ions, for example Fe(III) and Cu(II), have found limited application.

Solvents from the whole elutropic range have been employed and frequently basic conditions have been found advantageous by the use of ammonia or by the addition of an organic base, although solvents acidified with formic acid have an application. With the availability of silica gel G₂₅₄, visualization of phenolic substrates is straightforward, although with non-indicating silica gel, the use of dichlorofluorescein, rhodamine 6G or a wide selection of spray reagents has become common practice and almost completely displaced the use of sulfuric acid and thermal charring. Documentation by means of photocopying, photography or by the use of dyeline paper and an ammoniated atmosphere are all effective methods.

In the following examples, the analytical scale TLC separations of a range of isomeric compounds are tabulated. At the preparative scale increased sample loading leads to a loss of resolution and indeed the loading/resolution factor should be examined in all cases.

Separation of Structural Isomers of Phenols and Phenolic Acids

The *R_F* values of an extensive range of phenolic compounds of synthetic and natural origin have been given in the literature listed in the Further Reading

section, notably in the Tables in Tyman (1996) and Hanai (1982).

Cresols

The separation of structural isomers represents an effective test of a chromatographic method and this is particularly relevant to TLC where a considerable body of work has been devoted to the *o*-, *m*- and *p*-derivatives of phenol. Thus, in Table 1 some results, from experiments covering a period of nearly four decades, are shown on the cresols. Marginal differences of R_F values are seen in solvent systems a–f, h, and less so in i. Remarkably, it is only recently that an acceptable separation has been achieved with system g involving silica gel G, although in this case a second run would be desirable if phenol itself were present in a commercial sample.

Ethylphenols

The *o*-, *m*- and *p*-isomer of the homologous ethylphenol might similarly be separated. Table 2 indicates four other systems which have been examined and only in system a with alumina is the separation well defined. A crucial factor of importance in isomer separations is the relative R_F values of the *m*- and *p*-isomers since a steric influence aids the differentiation of the *o*-isomer.

In the case of higher homologues, for example the isomeric *t*-butylphenols, silica gel (type 60) with benzene appears to be marginally more effective than alumina with diisopropyl ether or cellulose (by RP with aqueous ethanol), giving for the *o*-, *m*- and *p*-isomers R_F values of 54, 22 and 16 respectively.

Chlorophenols

The R_F values of the isomeric monochlorophenols are shown in Table 3. This series has been widely

Table 2 R_F Values of phenol and isomeric ethylphenols on various layers

Compound	Conditions			
	a	b	c	d
Phenol	13	54	73	79.5
2-Ethylphenol	32	77	25	40
3-Ethylphenol	14	—	32	48.5
4-Ethylphenol	24	61	28	45.5

^aTyman (1996a): diisopropyl ether, alumina₂₅₄. ^bHanai (1982): benzene–ethyl acetate, 95 : 5, silica gel FG. ^cTyman (1996a): 8 mol L⁻¹ ammonia in 20% methanol, silanized silica gel impregnated with triethanolamine salt. ^dTyman (1996a): ethanol–water, 75 : 25, cellulose, reversed phase.

studied by adsorption methods (b–e, g) and by partition procedures (a, f, h) and, generally, greater resolution has been found with the latter. Nevertheless, by the use of basic layers (b) or with basic solvents (c) almost comparable results are achieved. As with many isomeric compounds, the 3- and 4-isomers present the main problem.

Nitrophenols

The separation of the isomeric nitrophenols depicted in Table 4 presents relatively little difficulty and generally adsorption conditions (b–e) have proved as effective as others; the use of impregnated silanized silica gel (f) does not seem to aid the *o*-/*p*- compound separation. The increased polarity of the nitro group compared with the chloro substituent appears to help the separation of the 3- and 4-isomers.

Table 1 R_F Values of phenol and isomeric methylphenols (cresols) on various layers

Compound	Conditions								
	a	b	c	d	e	f	g	h	i
Phenol	43	63	46	34	30	63	37	63	79
<i>o</i> -Cresol	52	92	60	33	31	74	53	50	55
<i>m</i> -Cresol	45	84	51	29	38	63	36	50	63
<i>p</i> -Cresol	49	79	49	31	33	65	46	55	57

^aPetrowitz (1969): benzene–methanol, 95:5, silica gel G. ^bHanai (1982): benzene–methanol 90 : 10, alumina–calcium hydroxide 40 : 20. ^cTruter (1963): chloroform, silica gel G–starch. ^dHanai (1982): 20% methyl-*t*-butyl ether in hexane, silica gel G. ^eBund *et al.* (1995): methyl-*t*-butyl ether–hexane, 10 : 90, silica gel RP-18. ^fPetrovic *et al.* (1992): silica gel impregnated with Cu(II) and with Al(III), chloroform–acetone, 95 : 5. ^gBaranowska and Skotniczna (1994): chloroform–isopropanol, 49 : 1.5, silica gel G. ^hBaranowska and Skotniczna (1994): benzene–isopropanol, 50 : 4. ⁱTyman (1996a): 8 mol L⁻¹ ammonia in 20% methanol, silanized silica gel impregnated with dodecylbenzene sulfonate triethanolamine salt.

Table 3 hR_F Values of phenol and isomeric chlorophenols on various layers

Compound	Conditions							
	a	b	c	d	e	f	g	h
Phenol	30	66		16	47	73	79	
2-Chlorophenol	48	30	21	42	50	93	53	77
3-Chlorophenol	34	20	34	20	47	82	43	50
4-Chlorophenol	28	27	41	16	43	67	46	37

^aBund *et al.* (1995): methyl-*t*-butyl ether-hexane, 10 : 90, silica gel RP-18. ^bHanai (1982): benzene-methanol, 90 : 10, alumina-calcium hydroxide. ^cHanai (1982): toluene-piperidine, 5 : 2, silica gel GF₂₅₄. ^dTyman (1996a): benzene, silica gel G. ^eTyman (1996a): diethyl ether-*n*-hexane, 1 : 1, silica gel G. ^fTyman (1996a): system 5A, 1 M (pH 11.30) ammonia in 30% methanol, silanized silica gel. ^gTyman (1996a): ethanol-water, 75 : 25, cellulose, reversed phase. ^hLepri *et al.* (1982): 1 M (pH 11.30) ammonia + 0.1 mol⁻¹ ammonium acetate in 20% methanol, silica gel RP-18, impregnated with 4% dodecylbenzene sulfonic acid.

Aminophenols

The isomeric aminophenols have been separated as shown in Table 5 on a diverse range of adsorbents and solvent systems, all of which have yielded acceptable separations, although system b, one of the most recently examined, is to be preferred above the others.

Dihydroxybenzenes

In a similar way, the dihydroxybenzenes have been studied widely and the same system as used for the aminophenols (Table 5, condition a) has afforded the best separation of the three isomers, as depicted in Table 6.

Hydroxybenzaldehydes and Hydroxyketones

In the carbonyl series, comparatively little work has been carried out on either the hydroxybenzaldehydes or ketones. Table 7 indicates that no single system

affects the separation of all three isomers and the use of system a with e would be desirable.

In the ketone series, 2- and 4-hydroxybenzophenones appear to be readily separable from benzophenone itself on silica gel GF in benzene, with hR_F values of 53, 0 and 63 respectively. In benzene-piperidine (9 : 1), the corresponding values were 59, 9 and 77.

Phenolic Acids

Experimentation on the separation of isomeric phenolic acids has been widespread and a number of systems have been introduced, as shown in Table 8. The prevalent use of mildly acidic or basic solvent systems is seen compared with previous separations. In system a the formic acid enhances the separation of the 2-isomer through increased H-bonding, while in b-d the use of a basic solvent generally improves the resolution of all the isomers. The acetic acid component of systems e and f is insufficient to influence the separation of the 3- and 4-isomers.

Table 4 hR_F Values of nitrophenols on various layers

Compound	Conditions					
	a	b	c	d	e	f
Phenol	30		48	29	74	
2-Nitrophenol	64	96	75	57	79	83
3-Nitrophenol	20	80	43	14	62	68
4-Nitrophenol	12	65	35	8	46	89

^aBund *et al.* (1995): diethyl ether-*n*-hexane, 1 : 1, silica gel G. ^bHanai (1982): benzene-ethyl acetate, 90 : 10, zinc carbonate-silica gel, 30 : 20. ^cHanai (1982): benzene-methanol, 95 : 5, silica gel G₂₅₄. ^dHanai (1982): 20% diisopropyl ether in hexane, silica gel 60. ^eTyman (1996a): diisopropyl ether, silica gel 60. ^fTyman (1996a): system 4B.

Some Qualitative Separations of Mixtures of Phenolic Derivatives

Natural Phenolic Acids

Many natural phenolic acids have a useful pharmacological activity and plant sources containing them have a phytotherapeutic function. The two-dimensional TLC separation of reference mixtures or of the plant extracts of *Polygonum amphibium* has been effected first by development with benzene-methanol-acetonitrile-acetic acid (80 : 10 : 5 : 5) and, after removal of the eluent by evaporation,

Table 5 hR_F Values of isomeric aminophenols on various layers

Compound	Conditions							
	a	b	c	d	e	f	g	h
Phenol	32	90	91	58	22	19		
2-Aminophenol	53	50	68		31	34	30	55
3-Aminophenol	63	37	57	80	39	43	25	49
4-Aminophenol	69	14	52	86	53	50	19	41

^aBund *et al.* (1995): methanol–water, 50 : 50 RP-18. ^bBund *et al.* (1995): hexane–methyl *t*-butyl ether, 40 : 60. ^cPetrovic *et al.* (1992): toluene–chloroform–acetone, 40 : 25 : 25, silica gel GF + Cu(II) or Al(III). ^dTyman (1996a): 0.21 mol L⁻¹ NaCl–formamide–acetonitrile, 41 : 15 : 44, silica gel C₁₈. ^eHanai (1982): 0.5 mol L⁻¹ ammonia in 50% ethanol, Biorad AG3-X4A. ^fHanai (1982): water–methanol, 4 : 1, BD-cellulose. ^gHanai (1982): benzene–methylethyl ketone, 90 : 10, zinc carbonate–silica gel 30 : 20. ^hHanai (1982): benzene–methanol, 95 : 5, silica gel GF.

a second development at right angles is carried out with sodium formate–formic acid–water (10 : 1 : 200, w/v/v). The result of the first development is shown in Figure 1A and of a second development in Figure 1B. The formulae of the 14 acids are shown in Figure 2.

Methylation of 3-Pentadecylphenol

The methylol derivatives of 3-pentadecylphenol are of interest for the solvent extraction of the borate ion and are obtained by the methylation of 3-pentadecylphenol with formaldehyde, a reaction which affords mainly the 4- and 6-methylols, a minor proportion of the 2-isomer, the 2,4-, 2,6- and 2,4-dimethylols and some 2,4,6-trimethylol. The reaction mixture of isomeric compounds has been separated on silica gel G with light petroleum (60–80°C)–diethyl ether–dimethylformamide–acetic acid (75 : 85 : 5 : 1), as depicted in Figure 3. It is imperative to confirm the identity of bands by spectroscopic means and by the use of synthetic reference compounds in the 2-, 4- and 6-methylol series obtained in

the present instance by reduction of the corresponding phenolic acid or aldehyde.

Phenolic Components and Constituents of *Anacardium occidentale* (Cashew)

Mixtures of phenols and phenolic acids such as occur in the shell of the cashew are used as precursors for the manufacture of certain formaldehyde resins. They have been separated with diethyl ether–light petroleum (40–60°C)–formic acid (30 : 70 : 1), as shown in Figure 4 on silver-impregnated silica gel G, which also affords a separation of the saturated, 8Z-monoene, 8Z,11Z-diene and 8Z,11Z,14-triene constituents of each component phenol. In the absence of silver ion, the four main component phenols cardol, 2-methylcardol, cardanol and anacardic acid (each containing four constituents, $n = 0, 2, 4, 6$) have hR_F values 20, 36, 58 and 76 respectively. By contrast, in an ammoniated solvent with multiple development,

Table 6 hR_F Values of dihydric phenols on various layers

Compound	Conditions					
	a	b	c	d	e	f
Phenol	32	63	74	36	59	
1,2-Dihydroxybenzene	47	40	49		29	45
1,3-Dihydroxybenzene	55	30	39	58	36	40
1,4-Dihydroxybenzene	64		43	67	48	32

^aBund *et al.* (1995): methanol–water, 50 : 50 RP-18.

^bBaranowska and Skotniczna (1994): benzene–isopropanol, 50 : 40, silica gel G. ^cTyman (1996a): diisopropyl ether, silica gel 60. ^dTyman (1996a): system 1A, silanized silica gel. ^eHanai (1982): biorad AG3,X4A, 0.5 ammonia in 95% ethanol. ^fHanai (1982): benzene–ethyl acetate, 90 : 10, zinc carbonate–silica gel, 30 : 20.

Table 7 hR_F Values of isomeric hydroxybenzaldehydes on various layers

Compound	Conditions					
	a	b	c	d	e	f
Phenol					26	
2-Hydroxybenzaldehyde	63	52	63	71	59	70
3-Hydroxybenzaldehyde	79	57	69	78	9	66.5
4-Hydroxybenzaldehyde	64	56	68	76		66.5

^aTyman (1996a): 2% formic acid. ^bTyman (1996a): 20% KCl. ^cTyman (1996a): iPrOH–NH₄OH–H₂O, 8 : 1 : 1. ^dTyman (1996a): 10% AcOH. ^eHanai (1982): silica gel 60F, 20% Et₂O–hexane. ^fHanai (1982): polyamide, butan-2-one–acetophenone–50% acetic acid, 5 : 5 : 4.

Table 8 hR_F Values of isomeric phenolic acids on various layers

Compound	Conditions					
	a	b	c	d	e	f
Benzoic acid		70		53		
2-Hydroxybenzoic acid	70	82	63	55	59	75
3-Hydroxybenzoic acid	37	59	21	31	39	67
4-Hydroxybenzoic acid	27	50	34	17	38	66

^aTyman (1996a): 2% formic acid, cellulose. ^bTyman (1996a): ethanol-ethyl acetate-ammonia, 9:3:2, silica gel G impregnated with silver oxide. ^cHanai (1982): isopropanol-benzene-conc. ammonia, 3:1:1. ^dHanai (1982): ethanol-butanol-water-conc. ammonia, 49:30:15:15, rice starch. ^eHanai (1982): upper phase of benzene-acetic acid-water, 10:15:5, silica gel. ^fHanai (1982): toluene-acetic acid-water, 70:20:1, silica gel G.

a system used subsequently for quantitative analysis and described later, the phenolic acid anacardic acid was retained at low hR_F and separated from the three other phenols.

Resorcinolic Compounds from Rye

The homologous cardol constituents in rye (*Cereale scale*) have been separated by the use of a two-way development involving a preliminary separation (direction 1) of the saturated, monoene and diene members on argentated silica gel with benzene-ethyl acetate (85:15) and then, after removal of the silver ion and impregnation of the silica gel with paraffin

oil, RP separation of the C_{13} to C_{29} homologues by development (direction 2) with acetone-methanol-water (60:15:25), as shown in Figure 5.

Factors Influencing the Separations of Phenolic Compounds

Although, as with many classes of organic compound, the nature of the adsorbent, of the functional groups and of the position of the solvent or solvent mixture in the relative elutropic series are dominant influences, phenols have a unique property in respect of the intramolecular hydrogen bonding of a considerable number of the *o*-functional groups with the hydroxyl group. The hR_F values of *o*-substituted phenols on silica gel under adsorption conditions extend over a wider numerical range than those of the corresponding *m*- and *p*-isomers. Strongly hydrogen-bonding groups such as NO_2 , CHO and Cl head the series, as do bulky alkyl groups which by contrast exert a purely steric effect.

This is seen particularly with 2,6-compounds with nonpolar substituents such as the 2,6-di-*t*-butyl derivatives which are important antioxidants. These very nonpolar compounds are also actually less polar than their methyl ethers. Table 9 depicts the hR_F values for a number of 2,6-disubstituted compounds. A steric factor operates in the 2,6-dialkylphenol series, where 2,6-dimethyl, 2,6-diethyl, 2,6-diisopropyl, 2,6-diallyl and 2,6-di-*sec*-butylphenol have hR_F values of 43, 63, 86, 54, 94 respectively compared with phenol, 9, and the 2,6-di-*t*-butylphenol, 94, on cellulose plates

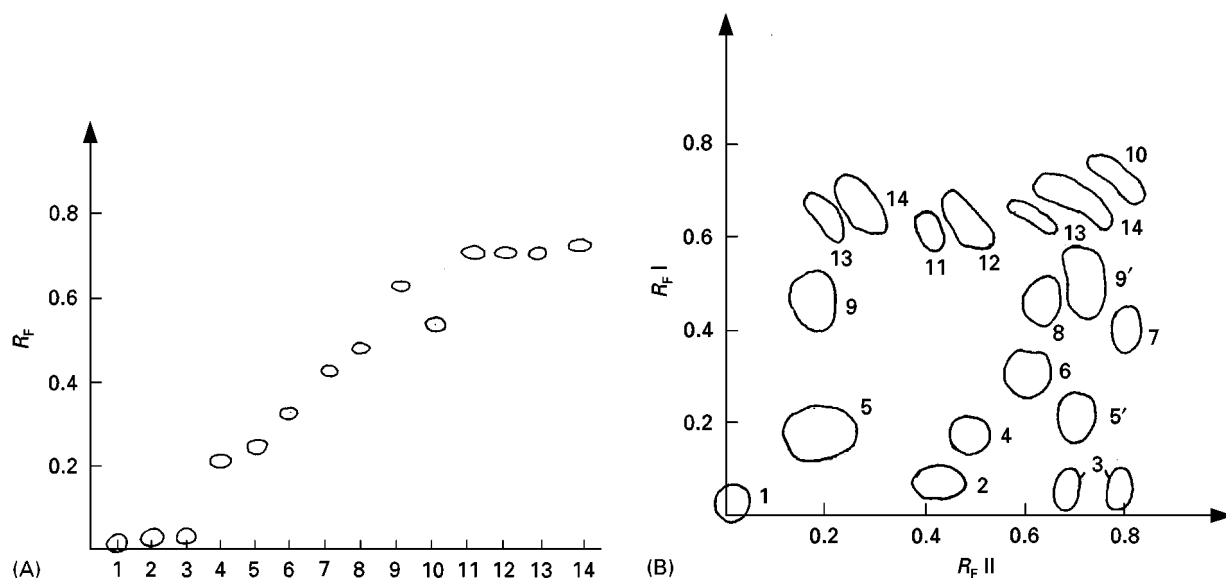


Figure 1 (A) One-dimensional separation of phenolic acids 1–14 (formulae as in Figure 2). 5' and 14' represent *cis* isomers. (Reproduced with permission from Smolarz and Waksmundzka-Hajnos, 1993.) (B) Two-dimensional separation of phenolic acids 1–14. (Reproduced with permission from Smolarz and Waksmundzka-Hajnos, 1993.)

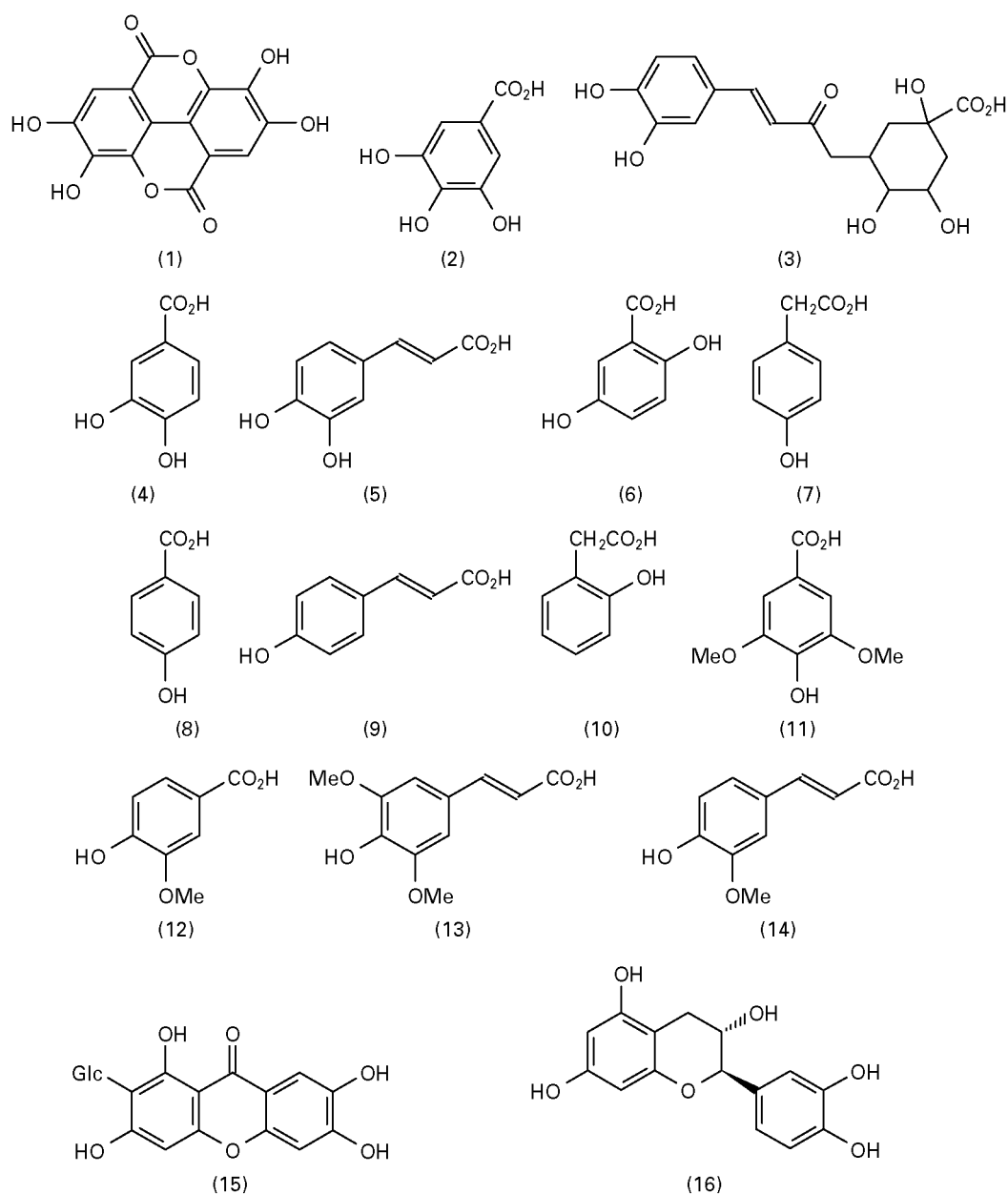


Figure 2 Formulae of phenolic acids 1–14.

impregnated with *N*-methylformamide and developed in hexane (Table 9).

With the *m*- and *p*-series, the bR_F values of all compounds are nearly parallel. The NO_2 , CHO and Cl groups now simply exert a polar effect (and an electronic effect on the phenolic acidity) while alkyl groups have a minor steric role. The isomeric phenolic acids behave similarly with respect to hydrogen bonding. 2,3- 2,4- and 2,5-Disubstituted compounds compare with the monosubstituted 2-series while 3,4- and 3,5-disubstituted compounds compare with 4-monosubstituted phenols.

Although current theory has no predictive use for structural assignment of polysubstituted compounds from their bR_F values, nevertheless the vast number of such values available from the literature affords a guide to the selection of an appropriate system. There is little doubt that solvent selection is the most important influence, as illustrated in **Table 1** where, with virtually the same adsorbent in entries (c) and (g), a period of 40 years separates a relatively poor from an excellent resolution, obtained simply by the addition of isopropanol to the same solvent.

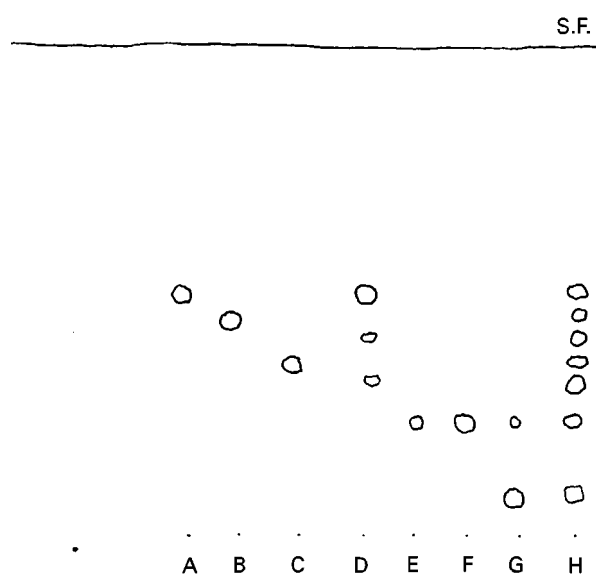


Figure 3 Separation of methylol derivatives of 3-pentadecylphenol. A, 2-methylol; B, 6-methylol; C, 4-methylol; D, mixture of 2-methylol, 2,6-dimethylol and 2,4-dimethylol; E, 4,6-dimethylol; F, 4,6-dimethylol; G, 2,4,6-trimethylol; H, mixture of all the synthetic methylols. (Adapted with permission from Tyman, 1996a.)

This crucial role of the solvent is seen in the R_F values of certain hydroxyanthraquinones, depicted in **Figure 6**, where the advantage of hydrogen bonding in affording a separation of compounds 1 and 2 from 3 and 4 is sacrificed with the use of the polar solvents *n*-butanol or ethyl acetate. It is perhaps relevant to reiterate the value of the Stahl triangle (**Figure 7**) for separations to be effected under adsorption conditions.

Quantitative Separation of Mixtures of Phenolic Compounds

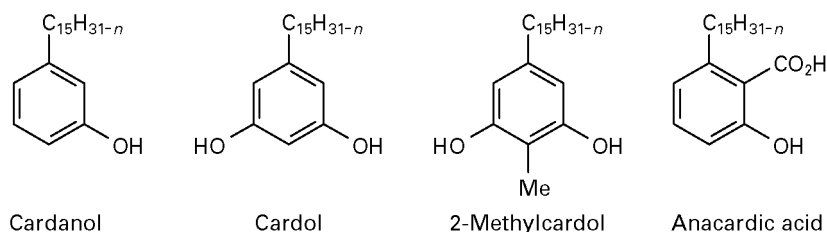
A variety of applications of TLC to the analysis of phenolic compounds in biochemical, environmental, industrial and consumer products has been summarized by Tyman (1996). In the following descriptions a selected range of quantitative studies are given. In the first the phenolic components of natural

cashew nut-shell liquid (CNSL), comprising anacardic acid, cardol, 2-methylcardol and cardanol, have been determined by the preferred method of densitometry, 'on the plate' and also by UV spectrophotometry 'off the plate'. The natural product is essentially a mixture of a phenol, a resorcinol, a hindered resorcinol and a phenolic acid. Its composition is required to assess the effectiveness of its industrial thermal decarboxylation at 200°C for obtaining technical CNSL, a product widely used in friction dusts for use in automobile brake and clutch systems.

Composition of Natural Cashew Nut-shell Liquid from *Anacardium occidentale* by Densitometry

Following lengthy experimentation, multiple development was used, initially with light petroleum (40–60°C)–diethyl ether–ammonia solution (50:50:5) to separate cardanol, 2-methylcardol from cardol/ammonium anacardate and then with diethyl ether–ammonia (90:10) to separate cardol and ammonium anacardate. The hR_F values were ammonium anacardate (0), cardol (36), 2-methylcardol (61) and cardanol (71). Subsequently, for the analysis of technical CNSL, which contains predominantly cardanol, cardol and 2-methylcardol, the alternative solvent system light petroleum–diethyl ether–formic acid (70:30:1) was employed, in which the hR_F values are 58, 20 and 36 respectively.

The natural product was obtained from frozen raw cashew nuts by cracking followed by solvent extraction and recovery at ambient temperature. Commercial silica gel G plates (20 × 20 cm) were used and multiple development in an ammoniated solvent system with 10, 20 and 30 µL of the unknown sample applied alongside 10, 16, 20, 24 and 30 µL of a standard solution containing anacardic acid, cardol, 2-methylcardol and cardanol. After development, removal of the solvent, visualization with iodine, the use of a cover plate and both horizontal and vertical scanning, the areas of all the bands were obtained by integration. A typical plate is illustrated in **Figure 8**.



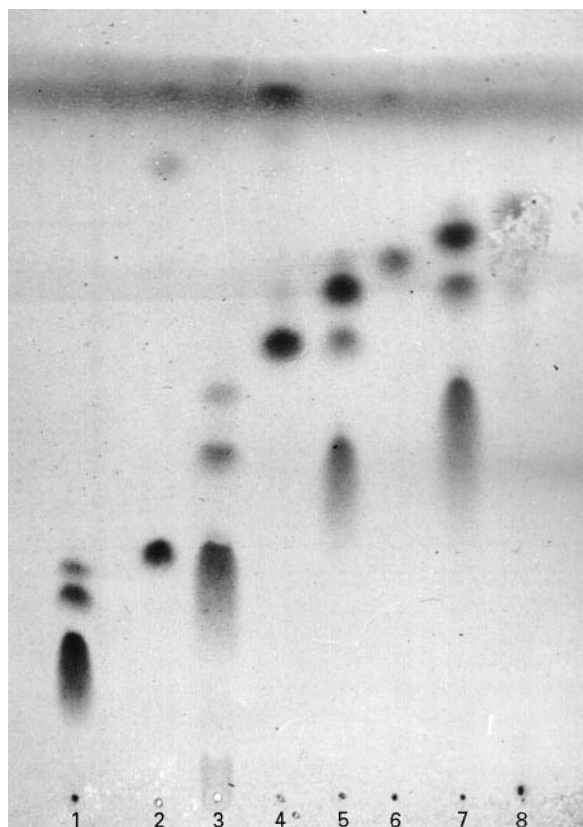


Figure 4 TLC of cashew phenols before and after hydrogenation on silica gel G with 10% silver nitrate. Samples 1, 3, 5 and 7 are cardol, 2-methylcardol, cardanol and anacardic acid. Samples 2, 4, 6 and 8 are the hydrogenated samples showing absence of unsaturated constituents. Detection with sulfuric acid and charring. (Adapted with permission from Tyman, 1996a.)

Plots of area by densitometry versus volume (μL) of the standard solution for each standard phenolic component gave a series of straight lines conforming to the relation $y = mx$, to which the least-squares method was applied in order to determine accurately the slope m .

From the resultant plots and the areas by densitometry, the volumes (equivalent μL) of the unknown solution were ascertained. By simple proportionation relative to the known weights of the four phenols in the volume of standard solution used, the weights of the four component phenols in the unknown were then found. Table 10 depicts some results of two runs from a total of nine experiments. The average recovery (natural CNSL found/weight taken) was 98.0%.

Elution and Indirect Spectrophotometry

In the 'off the plate' method the same ammoniated system was used with multiple development, the

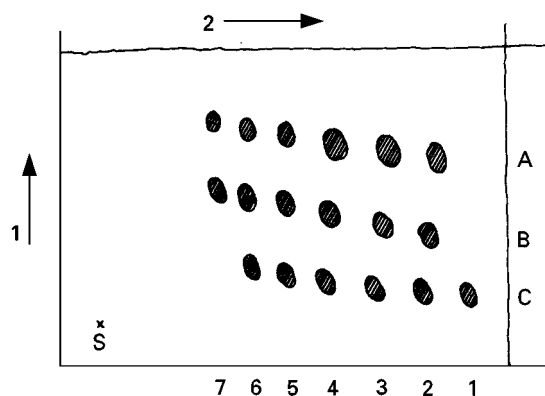


Figure 5 Two dimensional separation of 5-alkenylresorcinol homologues. Development 1 was first to 5 cm and then to 8 cm. Development 2 was at right angles. Detection was with Fast Blue B. A, saturated; B, monoene, C, diene constituents; S, starting point. Numbers 1–7 represent C_{13} to C_{25} respectively. (Adapted with permission from Tyman, 1996a.)

bands were visualized with Rhodamine 6G, removed from the plate and then eluted to recover the phenolic components which, after freeing from indicator by acidification, were made up to standard volume and examined by UV spectrophotometry. From the epsilon values $[(E\ 1\% \ 1\text{ cm} \times \text{mol. wt})/10]$ found, after correction for the purity of the phenols from the values of pure standards, the weights of the four component phenols were obtained and hence the percentage composition. The UV absorption of the four phenols is depicted in Figure 9.

It is of interest to compare the compositional analyses of natural CNSL by densitometry, gas chromatography (GC) and high performance liquid chromatography (HPCL) as depicted in Table 11.

Table 9 hR_F Values of hindered phenols and their methyl ethers on silica gel G in light petroleum, 40–60°C (LP)/chloroform (C)

Compound	Conditions				
	a	b	c	d	e
2,6-Di- <i>t</i> -butyl-4-methylphenol	36	64	75	83	84
2,6-Di- <i>t</i> -butyl-4-methylanisole	27	57	75	83	84
2- <i>t</i> -Butyl-6-methoxy-4-methylphenol	12	31	44	66	76
2- <i>t</i> -Butyl-6-methoxy-4-methylanisole	4	20	32	55	66
2-Methoxy-4,6-di- <i>t</i> -butylphenol	14	41	52	68	73
2-Methoxy-4,6-di- <i>t</i> -butylanisole	8	29	38	57	64
2-Methoxy-6-pentadecylphenol	11	29	38	60	70
2-Methoxy-6-pentadecylanisole	65	17	24	48	65

Adapted with permission from Tyman 1996a. ^aLp 100; ^bLP-C, 80 : 20; ^cLP-C, 60 : 40; ^dLP-C, 40 : 60; ^e100.

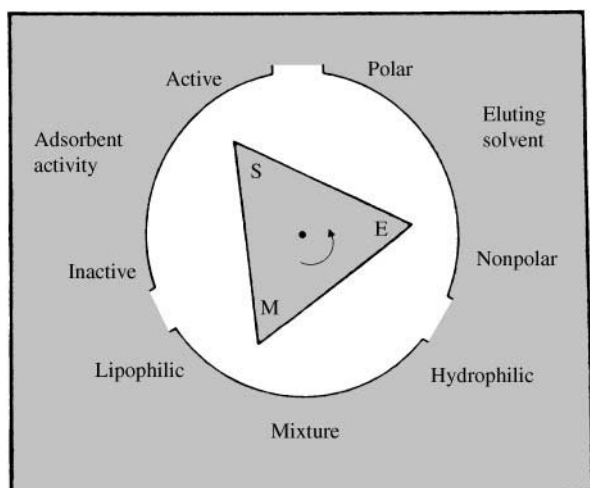


Figure 6 Separation of hydrogen-bonded derivatives of 1,8-dihydroxy and of 1-hydroxyanthraquinones. S, starting point; M, mixture; E, eluant. (Reproduced with permission from Tyman and Morris, 1967.)

TLC methods have also been employed with the phenolic lipid urushiol from *Rhus vernicifera*.

Determination of Phenolic Compounds, Mangiferin, Colladin and Colladonin in *Colladonia triquetra*

The natural product mangiferin (15), 2- β -D-glucopyranosyl-1,3,6,7-tetrahydroxy-9H-xanthene-9-one, which possesses mono hydrogen-bonded resorcinol

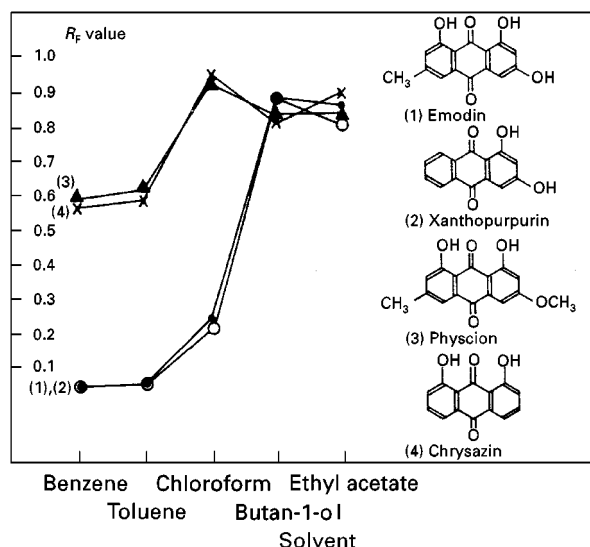


Figure 7 The Stahl triangle. Open circles, (1) emodin; closed circles, (2) xanthopurpurin; triangles, (3) Physcion; crosses, (4) chrysazin. (Reproduced with permission from Tyman and Morris, 1967.)

and catechol moieties in its structure, occurs as the major component in the Bulgarian medicinal plant *Colladonia triquetra* and is useful for cardiotonic, spasmolytic, diuretic and in other phytotherapeutic applications. In connection with agricultural production an improved analysis was developed for mangiferin by TLC and compared with an HPLC method. Colladin and colladonin are minor components in the natural product extracted.

Seeds of the natural product (2 g) were extracted with hot methanol and after recovery by concentration the residual material was dissolved in dioxan–water (1 : 1) filtered and then made up to a volume of 25 cm³, from which an aliquot was diluted 10-fold with dioxan–methanol (1 : 1) to give solution II. A standard solution of pure mangiferin (0.0100 g) was prepared in dioxan–methanol (1 : 1) (100 cm³).

Silica gel 60 F₂₅₄ plates were used and 1.0, 2.0, 3.0 and 4.0 μ L of solution II applied alongside 5.0, 6.0, 7.0, 8.0 and 9.0 μ L of the standard solution of pure mangiferin and developed with the solvent ethyl acetate–formic acid–water (67 : 13 : 20) to a distance of 10 cm. After drying, the bands were scanned for their fluorescence under UV illumination with Helena Laboratories Cliniscan densitometer and quantification followed from the peak areas obtained by integration. In a similar way, using standard solutions of colladin and colladonin alongside solutions of the natural extract with the solvent benzene–methyl ethyl

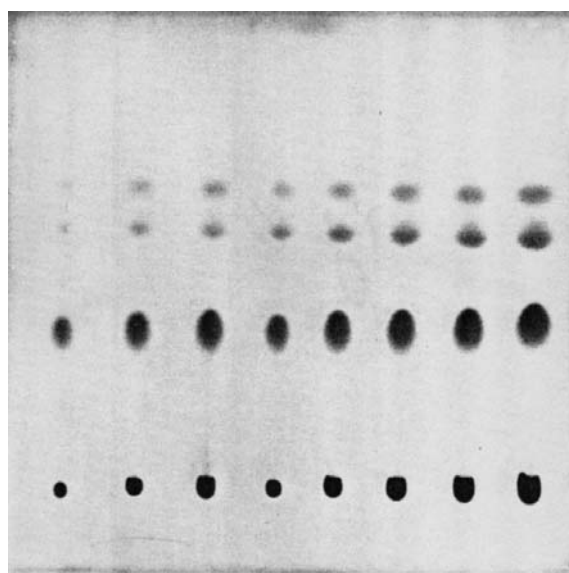


Figure 8 Separation of cashew phenols in an ammoniated system. R_f values of cardanol, 2-methylcardol, cardol and ammonium anacardate in descending order and from left to right, three samples of the unknown and then five of a standard solution. (Reproduced with permission from Pusey, 1969.)

Table 10 Percentage composition of component phenols in natural cashew nut-shell liquid (CNSL) by 'on the plate' densitometry

Vol. CNSL Standard (μ L)	Equiv. μ L from area/volume plots				wt. (g) component phenol				Total (g)
	A	B	C	D	A	B	C	D	
20	12.16	13.20	5.88	8.76	0.1442	0.0420	0.0060	0.0098	0.2020
%					71.38	20.79	2.97	4.86	
20	12.08	13.60	6.24	9.04	0.1432	0.0432	0.0064	0.0101	0.2029
%					70.57	21.31	3.13	4.99	
Average of 7 runs					71.33	20.28	3.25	5.12	

^aAnacardic acid; ^bcardol; ^c2-methylcardol; ^dcardanol. Adapted with permission from Pusey (1969).

ketone-formic acid (9:1:1) and densitometric evaluation as before, their percentage occurrence in the natural product was determined. Comparison with an HPLC method based on the use of LiChrosorb RP-18 was made and the results are shown in Table 12.

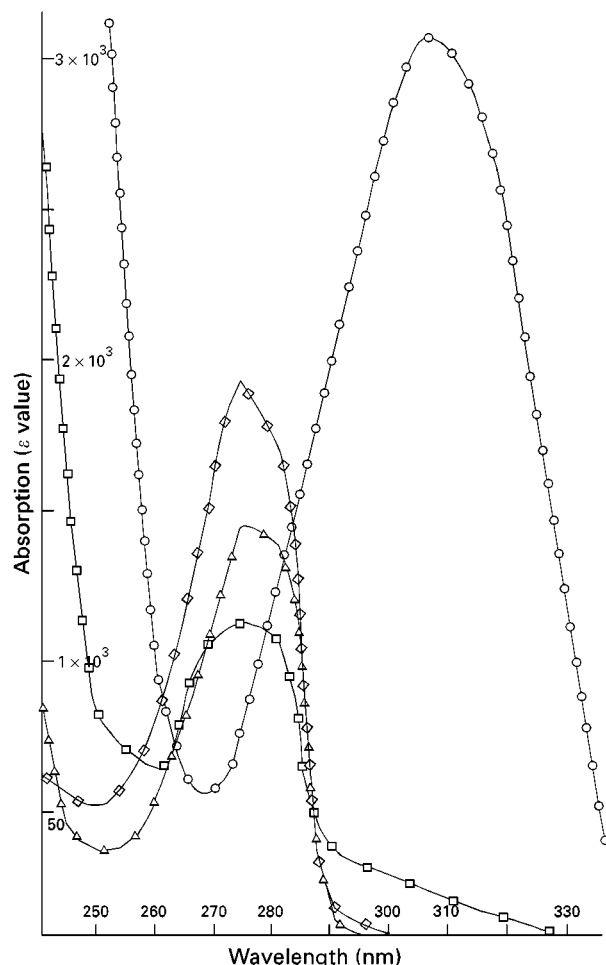


Figure 9 UV absorption spectra of the component phenols of natural cashew nut-shell liquid. circles, Anacardic acid; squares, cardanol; triangles, cardol; diamonds, 2-methylcardol. (Reproduced with permission from Pusey, 1969.)

Determination of the Flavan, Catechin in Cube Gambir, from *Uncaria gambir*

Cube gambir, which is obtained industrially by drying the aqueous extract of twigs and leaves of *Uncaria gambir*, has uses in dyeing and tanning, as an astringent and more recently for its antiulcer activity attributed to its component catechin, (2R,3S)-(+)-3,3',4',5,7-pentahydroxyflavan, a compound with resorcinol and catechol structural groupings. It has to be distinguished from black catechu, which contains (2R,3S)-(-)-epicatechin and for its analysis TLC and HPLC methods have been evaluated.

With commercial HPTLC plates of silica gel 60 F₂₅₄ and the solvent chloroform-ethyl acetate-formic acid (50:40:10), catechin (*b*R_F 34) and epicatechin (*b*R_F 40) are separated, although some decomposition was detected in prolonged experiments. By using cellulose F with the solvent, 1-butanol-acetic acid-water (40:10:50, upper phase taken), based on earlier work, an improved separation was obtained (catechin, *b*R_F 64 and epicatechin 78) and decomposition avoided. Nevertheless, degradation can be avoided on silica gel by prompt development after spot application. The pure standards catechin, epicatechin and 4-hydroxybenzoic acid were used in aliquots of 1 μ L alongside 1 μ L applications of the crude extract of cube gambir which was first dissolved in methanol-water (1:1) containing 1% acetic acid and filtered. After development to 10 cm, and evaporation of the solvent, bands were detected by UV irradiation at 277 nm and measured with a Shimadzu high speed TLC scanner CS-920.

From linear calibration plots of area/concentration and six determinations based on the integrations of 18 spots, cube gambir was found from the TLC method to contain $48.21 \pm 1.6\%$ catechin compared with $50.59 \pm 0.58\%$ by HPLC. The difference of approximately 2.4% was attributed to incomplete separation by HPLC and TLC densitometry was concluded to be useful for rapid analysis and for industrial monitoring.

Table 11 Comparison of percentage compositional analyses of natural cashew nut-shell liquid (*Anacardium occidentale*) by different method

Method	Anacardic acid	Cardol	2-Methylcardol	Cardanol
HPLC	71.65 ± 0.493	22.17 ± 0.398	1.08 ± 0.049	5.13 ± 0.374
GC	71.51 ± 0.230	22.34 ± 0.110	2.75 ± 0.720	3.27 ± 0.110
Densitometry	71.33 ± 1.25	20.28 ± 0.710	3.25 ± 0.720	5.12 ± 0.740

Adapted with permission from Pusey (1969).

Determination of Phenolic Acids in Plant Materials

Phenolic acids occur widely in combined form as esters or glycosides and for their liberation and subsequent quantitative distribution in the plant kingdom, enzymic and basic hydrolysis have been employed. Generally, comparable results are obtained by these two procedures. In the basic method the recovered phenolic acids are percolated in aqueous solution through a polyamide column and then eluted to obtain all the phenolic acids except salicylic acid and gentisic acid which are eluted with methanolic ammonia. The main phenolic acids are recovered with ethyl acetate, concentrated and made up to volume in methanol (10 cm³, solution A) and the material recovered with methanolic ammonia is similarly treated and made up in methanol (10 cm³, solution B). The method is an 'off the plate' procedure with quantification by UV spectrophotometry and absorbance at the optimum wavelength compared to the absorbance of pure reference solutions.

Silica gel G was used with solvent 1 (dichloromethane-acetic acid-water: 2 : 1 : 1) for the phenolic acids have one hydroxyl group while solvent 2 (benzene-acetic acid: (45 : 4) was used for phenolic acids with hydroxyl and methoxyl groups and for salicylic acid. Application of known volumes of A and of the standard mixture on one plate was followed by development with solvent 1 and likewise solvent 2 was used with B and the standards on another plate. After drying, the chromatograms bands are detected by examination under UV light and by spraying with methanolic ferric chloride. It was found convenient and satisfactory in practice to cover the portion of the

plate devoted to the unknown phenolic acids (A or B) and to spray the identification band with ferric chloride. The phenolic acids in the bands from the unknowns A or B were then marked out, removed by scraping, eluted with methanol and made up to volume for spectral examination under the usual conditions. Table 13 shows the spectral and R_F values for a range of phenolic acids.

For quantification, concentration/UV absorbance plots for each phenolic acid were obtained.

Determination of Chloro and Nitrophenols in Water Supplies

Phenolic compounds are widespread in the environment, either from natural sources, or from synthetic operations, and thus may be present in drinking, surface or ground waters. The US Environmental Protection Agency has quoted the compounds 2,4-dimethyl-, 4-chloro-3-methyl-, 2-chloro-, 2,4-dichloro-, 2,4,6-trichloro-, 2-nitro-, 4-nitro-, 2,4-dinitro-, 4,6-dinitro-2-methyl- and pentachlorophenols as priority pollutants. German drinking water regulations call for a limiting value of 0.0005 mg L⁻¹, while in the World Health Organization recommendations for drinking water, maximum standard values are fixed at 0.0001 mg L⁻¹ for total chlorophenols. A comprehensive examination of the TLC properties of 39 phenols on aluminium-backed RP-18 F₂₅₄ plates in 12 solvent systems has served as a basis for the detection of significant phenolic pollutants in water supplies.

Water is spiked with the phenols at a concentration of 1 mg L⁻¹ (0.0001%), adjusted to pH 2, and then sucked under vacuum through a small pretreated LiChrolut EN column over a period of 3–4 h. The column is dried with a stream of nitrogen for 15–30 min, and the phenols eluted with ethyl acetate (2 × 0.5 cm³) and made up to 1 cm³ with ethyl acetate. Samples of 2 µL are applied on to silica gel 60 F₂₅₄ RP-18 plates (10 × 20 cm) and developed with dichloromethane-*n*-hexane (50 + 50, w/v) for 20 min. Detection is by UV absorbance at 224 nm with a Camag TLC/HPTLC Scanner II. Figure 10

Table 12 Percentage composition of mangiferin, colladin and colladonin in *Colladonia triquetra* by TLC and by HPLC methods

Compound	TLC	HPLC
Mangiferin	2.96 ± 0.079	3.03 ± 0.131
Colladin	0.105 ± 0.008	0.106 ± 0.004
Colladonin	0.595 ± 0.011	0.604 ± 0.006

Adapted with permission from Tyman (1996b).

Table 13 UV spectral maxima (methanol), calibration factors (CF*) and hR_F values of phenolic acids (solvents 1 and 2)

<i>Phenolic acid</i>	<i>Substituent</i>	<i>CF</i>	<i>Max (nm)</i>	<i>hR_F</i>	
				<i>Solvent 1</i>	<i>Solvent 2</i>
<i>Hydroxy acid</i>					
Salicylic	2-OH	1.74	305	100	67
3-Hydroxybenzoic	3-OH	2.60	298	79	33
4-Hydroxybenzoic	4-OH	0.49	253	86	33
2,3-Dihydroxybenzoic	2,3-OH	2.43	318	89	34
2,4-Dihydroxybenzoic	2,4-OH	1.34	295	78	30
Gentisic	2,5-OH	1.78	330	63	25
2,6-Dihydroxybenzoic	2,6-OH	2.47	317	33	14
Protocatechuic	3,4-OH	0.82	258	44	16
3,5-Dihydroxybenzoic	3,5-OH	2.88	310	20	8
Gallic	3,4,5-OH	0.89	271	11	6
Phloroglucine	2,4,6-OH	0.61	261	10	5
Vanillic	3-OMe, 4-OH	0.81	258	100	58
Syringic	3,5-OMe, 4-OH	0.88	272	100	44
2-Hydroxycinnamic	2-OH	0.98	325	95	34
3-Hydroxycinnamic	3-OH	0.44	276	89	33
Caffeic	3,4-OH	0.56	325	51	14
Ferulic	3-OMe, 4-OH	0.58	320	100	54
Isoferulic	3-OH, 4-OMe	0.64	322	100	49
Sinapic	3,5-OMe, 4-OH	0.61	322	100	39

CF*: concentration ($\text{mg } 100 \text{ cm}^{-3}$) corresponding to an absorbance of 0.5 g cm^{-2} . Adapted with permission from Vanhaelen *et al.* (1984).

shows the chromatogram obtained with a mixture of five phenols (hR_F values given in brackets), 4-nitrophenol (4.7), 4-chloro-3-methylphenol (16.8) 2,4-dimethylphenol (21.9), 2,4-dinitrophenol (27.1) and 4-nitrophenol (60.3). Their visual and spectral detection limits and recoveries from the column extraction process are shown in Table 14 along with some values of other phenols which have been similarly processed.

Derivatization of phenols has also been employed to obtain the enhanced absorbance resulting from the

formation of coloured derivatives, although the resolution of the resultant compounds may then be diminished.

Conclusions

Although the TLC separation of phenols is well established for qualitative analysis, it is clear that excellent quantitative analysis can be achieved with the vast range of solvent systems, commercial plates and detection equipment currently available. HPTLC and

Table 14 Detection limits and percentage recovery of some pollutant phenols

Compound	Detection limit (ng)		Wavelength (nm)	Recovery (%)
	Visual	Spectral		
2-Nitrophenol	100	20	278	86
4-Nitrophenol	100	20	281	97
2,4-Dinitrophenol	100	20	267	99
2-Chlorophenol	1000	100	220	
2,4-Dichlorophenol	400	100	204	97
2,4,6-Trichlorophenol	400	100	207	
Pentachlorophenol	200	20	216	81
4-Chloro-3-methylphenol	400	100	200	97
4-Chloro-2-methylphenol	100	20	224	89
2,4-Dimethylphenol	400	100	223	73
4,6-Dinitro-2-methylphenol	100	20	276	
Phenol	400	200	274	95

Adapted with permission from Bund *et al.* (1995).

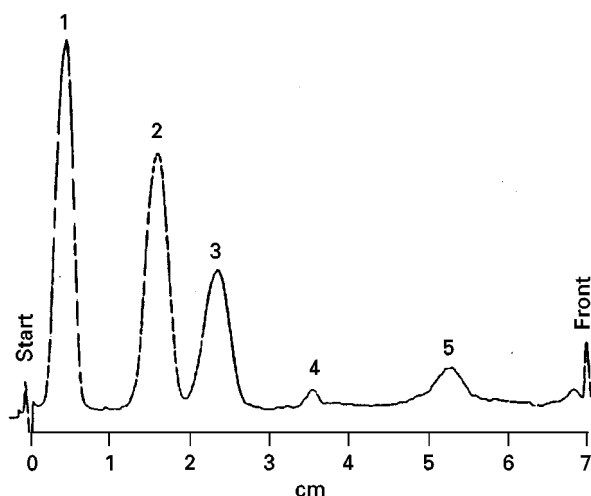


Figure 10 Separation of five phenols (extracted from spiked water) on silica gel RP-18 with UV detection. (Reproduced with permission from Bund *et al.*, 1995.)

RP approaches will extend the range of separative possibilities. Layers impregnated with silver and with other inorganic ions afford the opportunity for selective separations of unsaturated constituents of alkenylphenols and *cis/trans* isomers and of benzenoid compounds respectively. Combination of TLC with other chromatographic and/or spectroscopic techniques 'on' or 'off the plate' is likely to offer an economic approach to the analysis of complex mixtures of synthetic and natural phenols.

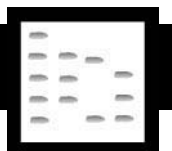
See also: II/Chromatography: Thin-Layer (Planar): Densitometry and Image Analysis; Layers; Mass Spectrometry; Spray Reagents. III/Impregnation Techniques: Thin-Layer (Planar) Chromatography. Phenols: Gas Chromatography; Liquid Chromatography; Solid-Phase Extraction. Silver Ion: Thin-Layer (Planar) Chromatography.

Further Reading

- Baranowska I and Skotniczna A (1994) Behaviour of phenols in normal and reversed-phase thin-layer chromatography. *Chromatographia* 39: 564–568.
- Bund O, Fischer W and Hauck HE (1995) The chromatographic properties of 39 phenolic compounds on a RP-18 stationary phase. *Journal of Planar Chromatography* 8: 300–305.

- Hanai T (1982) Phenols and organic acids. In: Zweig G and Sherma J (eds) *Handbook of Chromatography*, pp. 127–158. Tables TLC-1–TLC-15. Boca Raton, FL, USA: CRC Press.
- Lepri L, Desideri PG and Heimler D (1982) High-performance thin-layer chromatography of chloro-, bromo- and alkylphenols on ready-for-use plates of silanized silica gel alone and impregnated with anionic detergents. *Journal of Chromatography* 248: 308–311.
- Petrović M, Kaštelan-Macan M and Horvat AJM (1992) Thin-layer chromatographic behaviour of substituted phenolic compounds on silica gel layers impregnated with Al(III) and Cu(II). *Journal of Chromatography* 607: 163–167.
- Petrowitz H-J (1969) Synthetic organic products. In: Stahl E (ed.), *Thin-layer Chromatography*, pp. 657–685. London: George Allen and Unwin.
- Pusey DFG (1969) Thin-layer chromatography and the organic chemist. *Chemistry in Britain* 5: 408–412.
- Schmidlein H and Herrman K (1975) Quantitative analysis for phenolic acids by thin-layer chromatography. *Journal of Chromatography* 115: 123–128.
- Simova M, Tomov E, Pangarova T and Pavlova N (1986) Determination of phenolic compounds in *Colladonia triquetra* L. *Journal of Chromatography* 351: 379–382.
- Smolarz HD and Waksmundzka-Hajnos M (1993) Two-dimensional TLC of phenolic acids on cellulose. *Journal of Planar Chromatography* 6: 278–281.
- Tyman JHP (1978) *Journal of Chromatography* 166: 159–182.
- Tyman JHP (1987) Analysis of long chain phenols. In: Treiber LR (ed.) *Quantitative Thin-layer Chromatography and its Industrial Applications*, ch. 5, pp. 125–161. New York: Marcel Dekker.
- Tyman JHP (1996a) Phenols, aromatic carboxylic acids and indoles. In: Sherma J and Fried BJ (eds) *Handbook of Thin-layer Chromatography*, 2nd edn, ch. 25, pp. 877–905 (Tables 1–19). New York: Marcel Dekker.
- Tyman JHP and Morris LJ (1967) The composition of cashew nut-shell liquid (CNSL) and the detection of a novel phenolic ingredient. *Journal of Chromatography* 27: 287–288.
- Vanhaelen M, Vanhaelen-Fastré TR, Niebes P and Jans MJ (1984) Thin-layer chromatography-densitometry and high performance liquid chromatography of catechin in cube gambir. *Chromatography* 294: 476–479.

PHEROMONES



Gas Chromatography

N. G. Agelopoulos and L. J. Wadhams,
AFRC, Rothamsted, Experimental Station,
Harpenden, Herts, UK

Copyright © 2000 Academic Press

Organisms are able to communicate with each other by means of signal chemicals, or semiochemicals. These are chemicals mediating interactions between individuals, either within the same species (pheromones) or from different species (allelochemicals). Semiochemicals have been most extensively studied for insects, particularly social insects and insects of economic importance. The study of semiochemicals, and the interactions they mediate, is part of chemical ecology and contributes to the understanding of behaviour, development and evolution of organisms.

Semiochemicals are classified according to the relationships between the organisms involved. Pheromones are secreted and released by an organism and cause a specific response in a receiving organism of the same species, whilst allelochemicals are produced by one species and cause a response in a different species. Allelochemicals are further subdivided into allomones, kairomones, synomones and apneumones. Allomones elicit a response that is favourable to the emitter (e.g. defensive secretions utilized against enemies), kairomones favour the receiver (e.g. chemicals that attract parasites or predators), synomones are beneficial to both the emitter and receiver (e.g. floral scents that attract pollinators) and apneumones arise from a nonliving source (e.g. rotting meat odours).

In insects, pheromones are usually produced in specialized glands and perceived by sense organs on the antenna. Their existence has been known since early times. In 1914, the eminent French naturalist and entomologist Fabre reported that a single female of the emperor moth, *Saturnia pavonia*, kept in a wire cage on a window sill, was able to attract a great number of males from kilometres away. However, the first identification of a pheromone was only achieved in 1959. The work was started in 1939 and required the isolation of tens of thousands of excised pheromone glands before the pheromone structure of bombykol [(E,Z)-

10,12-hexadecadien-1-ol] was finally identified. Since then, improvements in isolation and identification techniques have made pheromone identification a simpler and faster procedure, utilizing only a few insects. A large number of pheromones have now been identified for organisms ranging from algae to primates.

Most pheromones fall into three main groups: sex pheromones that influence mate location and courtship behaviour; alarm pheromones that warn neighbours of impending danger; pheromones that influence spacing patterns, e.g. aggregation pheromones. Some pheromones derive specificity from their molecular structure. However, many contain compounds that are common to pheromones from different species or are components of other semiochemical systems. In these cases, specificity can be achieved by employing mixtures having unique relative proportions, with spatial or temporal separation of the organisms often adding to specificity. Although it was thought initially that pheromones would be single components, it is now clear that most are multicomponent systems and that, in many cases, behavioural effects are not mediated by the pheromone alone but require the presence of other semiochemicals. Thus, aggregation of bark beetles on a suitable host tree is mediated by a complex of semiochemicals derived from conspecifics attacking the tree, and from secondary metabolites released by the tree itself.

Structures as simple as ethanol can be employed as pheromone components. However, within the constraints required for aerial transport, considerable specificity can be achieved within one empirical formula by a combination of structural isomerism and stereoisomerism, encompassing both optical and geometrical isomerism. Thus, for the lepidopterous sex pheromones, where the basic structures usually comprise only C₁₂–C₁₆ straight carbon chains with functionalities of alcohol, aldehyde and acetate, considerable diversity is obtained by a combination of the position, degree and geometrical isomerism of unsaturated double bonds.

Insect pheromones can employ a range of structures, from fatty acid-based components to polyketides and polyisoprenoids (Figure 1). Polyketides can be simple compounds, for example 4-methyl-3,5-heptanedione (Figure 1, structure 1) the aggregation pheromone of the pea and bean weevil, *Sitona lineatus*, or structures with several chiral centres such

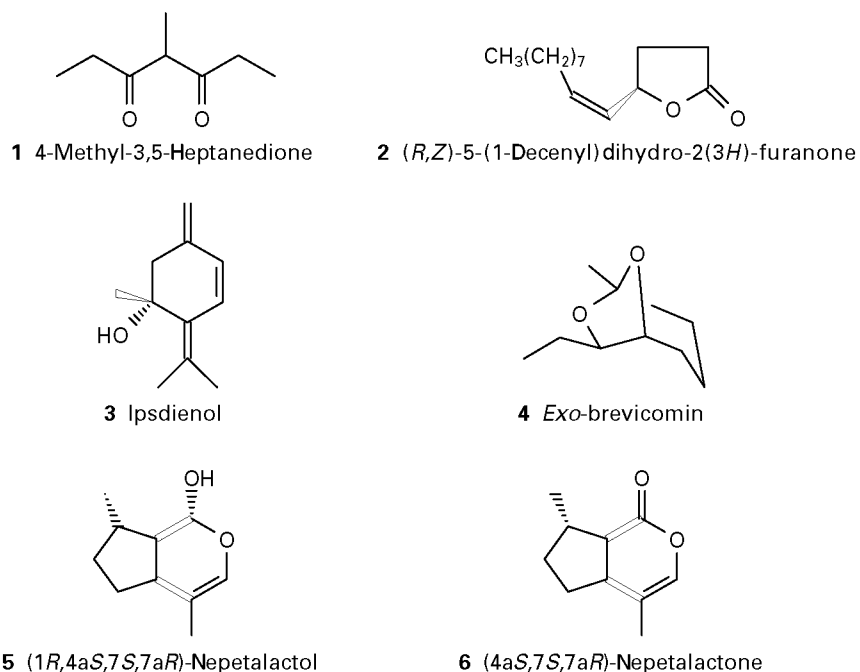


Figure 1 Diversity of structures employed as pheromones. **1** The aggregation pheromone of the pea and bean weevil (*Sitona lineatus*); **2** the sex pheromone of the Japanese beetle (*Popillia japonica*); **3** the aggregation pheromone of the pine engraver (*Ips pini*); **4** the aggregation pheromone of a number of pine beetles; **5** and **6** the sex pheromone of many aphid species.

as *exo*-brevicommin (Figure 1, structure 4), a component of the aggregation pheromone of a number of bark beetles, including the mountain pine beetle, *Dendroctonus ponderosae*. Simple terpenoids can also be employed, for example (*E*)-citral in the Nasonov pheromone of the honeybee, or highly chiral cyclopentanoid structures comprising the sex pheromones produced by sexual female aphids. For many aphid species, two biosynthetically related compounds are involved, a nepetalactol and a nepetalactone. There are 16 and 8 possible isomers respectively, but only the (1*R*,4*aS*,7*S*,7*aR*)-nepetalactol (Figure 1, structure 5) and the (4*aS*,7*S*,7*aR*)-nepetalactone (Figure 1, structure 6) are behaviourally active.

Isolation Techniques

This is a key stage in the identification of semiochemicals and the techniques used will determine, to a large extent, the subsequent analytical techniques, particularly in terms of sample introduction into the gas chromatograph (GC). Most of the insect pheromones so far identified have been extracted using solvents with a range of polarities and were obtained from whole insects, specific parts of insects (e.g. pheromone glands) or the frass (i.e. the refuse and excrement) produced by feeding insects. In some instances, the pheromone is released from a droplet which can be readily collected. For example, matur-

ing eggs of the mosquito *Culex quinquefasciatus*, a vector of the parasite responsible for the tropical disease filariasis, produce a droplet containing a volatile oviposition pheromone that attracts gravid females of the same species to lay eggs nearby. In this case, sample preparation is a simple matter of collecting the droplets in a fine capillary tube. Extracts made from whole insects or pheromone glands are able, in most cases, to provide a sample containing the compounds present in the pheromone gland, but may show qualitative and quantitative differences from the naturally emitted semiochemical blend. Ratios are a fundamental aspect of many semiochemical systems. For a number of aphid species, the sexual females (oviparae) attract winged males by releasing a sex pheromone from porous plaques on their hind tibiae. Using solvent extraction of the female tibiae, it was demonstrated that the sex pheromone of the vetch aphid, *Megoura viciae*, comprises a synergistic mixture of the monoterpenoids (4*aS*,7*S*,7*aR*)-nepetalactone and (1*R*,4*aS*,7*S*,7*aR*)-nepetalactol. However, with an air entrainment technique, collecting volatiles from the air above calling oviparous *M. viciae*, it was found that the nepetalactone was released in significantly higher concentrations than was found in the leg extracts (Figure 2). Whilst only a small amount of the nepetalactone (1–2 ng per aphid) was obtained from the leg extract, the amount produced by calling females was 200 ng per aphid.

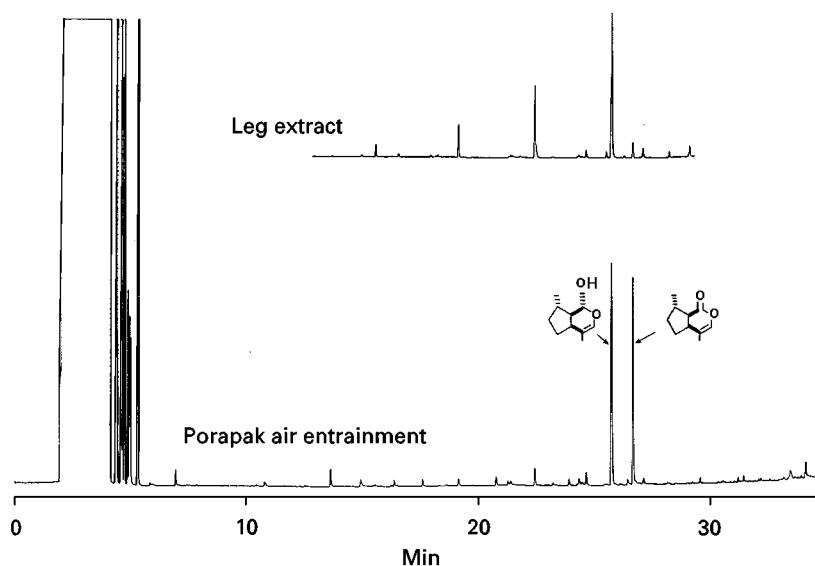


Figure 2 GC of pheromone components produced by sexual female aphids (oviparae): amounts obtained by air entrainment and (inset) solvent extraction of excised hind tibiae.

These findings suggested that, during calling, production of nepetalactol is continuous and that a proportion of the nepetalactol is sequentially oxidized to nepetalactone. These two compounds, in different ratios, were shown to be the main components comprising the sex pheromones of many aphid species.

The problems associated with solvent extraction can be overcome by using dynamic entrainment systems, where the organism emitting the semiochemicals is contained in a glass chamber through which is passed a stream of highly purified air. The volatiles produced are swept from the system and collected in a trap, usually a porous polymer, activated charcoal or a cryogenic trapping system. They can then be recovered from the trap by either solvent or thermal desorption. The advantages of using such a system are that not only are the semiochemicals isolated in the proportions emitted by the organism, but also the extracts obtained are free from contaminants associated with straight solvent extraction and are thus directly amenable to analysis by GC. In addition, since the sampling is not destructive, it can be used to investigate the time course of semiochemical production.

Solid-phase microextraction (SPME) is a relatively new isolation technique that has been developed for the extraction and concentration of a wide range of volatile and semivolatile organic compounds from various matrices such as air, water and soil. The technique can be utilized for direct immersion into liquid samples and for sampling the headspace of liquid and solid samples. SPME uses a polymer-

coated fibre to absorb chemicals from the matrices, relying on a three-phase equilibrium between the sample, its vapour and the fibre. Samples are desorbed from the SPME fibre by thermal desorption in the GC injector. A number of fibres have been produced using different types of coating, e.g. polydimethylsiloxane (100 μm) for volatile chemicals, carbowax/DVB for alcohols and other polar compounds and polyacrylate for semivolatile compounds. Although the technique is still in a developmental stage, its ability to collect insect pheromones has already been demonstrated. However, SPME is not without its drawbacks, particularly when used for quantification, since adsorption on to the fibre is related to the chemical properties of the compound, with some compounds being adsorbed more readily than others. The time needed for a compound to equilibrate with the fibre is related to the structure of the compound, and experimental conditions such as temperature and humidity can affect the adsorptive capacity of the fibre. Despite these limitations, SPME has several major advantages in that it is rapid, nondestructive and allows sequential samples to be taken.

Sample Introduction

Analysis of complex samples places a great demand on the inlet (injection) system of the GC. The injection techniques used in capillary GC are split/splitless, direct, cold on-column and temperature-programmed vaporization. Considerable emphasis has been placed upon developing improved sample introduction techniques, minimizing sample de-

composition or isomerization, and the delivery of all components of the sample into the column in the same proportions as in the original mixture. Cold on-column injection techniques, where the sample is introduced directly on to the capillary column, can largely overcome these problems. However, this imposes considerable constraints on the initial isolation techniques, since it is essential that the sample is free from high molecular weight contaminants. Another versatile and popular technique is programmed-temperature vaporization, where the sample is introduced into a cold injector port followed by a rapid temperature rise, thus achieving vaporization.

The use of solvents can present problems for the chemical ecologist. Even highly purified solvents, when analysed on a modern high efficiency capillary GC system, show considerable levels of impurities. In addition, very volatile components can be masked by the solvent peak. Hence, in many cases, especially when working at extreme sensitivities, it is preferable to work with solvent-free systems and a number of injection systems for this have been developed. Although many were initially designed for use with packed columns, there is no fundamental difficulty in adapting them for use with capillary GC. In one of these solid sample injection systems, the material to be analysed is sealed inside a glass capillary, which is then placed inside the heated injector for a few minutes to allow the sample to volatilize, or for a biological sample to heat through. The tube is then crushed with a plunger and the volatile material is swept directly on to the column by the carrier gas. The advantages of this technique are simplicity of operation, reduced chance of contamination and no dilution. Even highly volatile compounds such as methanol and acetaldehyde can be recognized and quantified.

Thermal desorption provides another method of introducing samples on to the GC column without the use of solvents. Volatiles collected by dynamic air entrainment systems on to porous polymer traps can be removed either by solvent elution, or by thermal desorption in the GC injector. In the latter instance, all of the sample is introduced on to the GC column, thus increasing sensitivity and allowing analysis of compounds with short retention times. However, thermal desorption is not without its own drawbacks, particularly the thermal instability of some compounds.

GC Columns

Modern capillary GC columns have great resolving power and offer a high speed of analysis, greater sensitivity and the capacity to elute a greater range of

components, providing that the molecules of solute to be analysed are thermally stable, inert in terms of reacting with the capillary column and have sufficient volatility. As with all GC analyses, the most important parameters to be considered in selecting the best column are the stationary phase, internal diameter, film thickness and length. The stationary phase used in the column has the greatest effect in separation. Depending on the chemical properties of the compound, some compounds separate better on some stationary phases than on others. However, since semiochemical analyses are usually performed on complex mixtures comprising compounds with a wide range of boiling points and functionalities, the choice of column is frequently a compromise. This is not usually a problem since the high efficiency of modern capillary columns ensures that most analyses can be performed on a limited range of phases. Indeed, the stationary phases most commonly used in pheromone research are nonpolar (e.g. 100% polydimethylsiloxane), polar (e.g. polyethylene glycol) or medium polarity (e.g. poly[diphenyldimethylsiloxane] copolymer). GC columns with polar phases are invaluable for the separation of many pheromones, particularly fatty acid-derived lepidopterous pheromones.

Animal – and particularly insect – olfactory receptor systems are highly specialized and are frequently able to distinguish between enantiomers. Thus, in human olfaction, the two enantiomers of carvone (*p*-mentha-6,8-dien-2-one), a chiral cyclic ketone with one asymmetric carbon atom, have very different odours. One has the odour of caraway [(*R*)-carvone] and the other of spearmint [(*S*)-carvone]. Chirality plays a key role in insect chemical ecology and biological activity is often dependent on the enantiomeric composition of a chiral compound, and situations exist where the ‘non-natural’ enantiomer is inactive or, more problematically, may even elicit a repellent response. Japonilure, the female-produced sex pheromone of the Japanese beetle, *Popillia japonica*, comprises (*R*)-(Z)-5-(1-decenyl)dihydro-2-(3*H*)-furanone (Figure 1, structure 2) and males require high enantiomeric purity of the (*R*)-isomer to be attracted to the sex pheromone. However, males also possess receptors for the (*S*)-isomer which, when perceived simultaneously with the (*R*)-enantiomer, has an inhibitory effect, and only a few per cent of the wrong enantiomer can inhibit the response to the natural pheromone. Geographical variation in the production of, and response to, the enantiomers of the aggregation pheromone ipsdienol (Figure 1, structure 3) has been demonstrated for the pine engraver, *Ips pini*, in eastern and western populations in the USA. Thus, determination of the chirality of such

pheromones is of paramount importance in chemical ecology. However, until recently, such determinations have been limited to the sampling of large numbers of insects for determination of optical rotation by conventional methods, e.g. Fourier transform nuclear magnetic resonance.

GC techniques are preferred for enantiomer composition studies since they are very sensitive, require less sophisticated instrumentation and can be applied even to small amounts of impure biological samples. Chiral GC phases, where optical resolution is achieved through reversible diastereomeric association between the chiral environment and the solute enantiomer by means of molecular interactions such as hydrogen bonding, inclusion phenomena, transition metals or charge transfer interactions, have been used for the determination of the enantiomeric composition of pheromones. One class of widely distributed pheromone components are the spiroketals isolated from various insects such as bees, wasps and beetles. The first such pheromone to be identified was chalcogran, or 2-ethyl-1,6-dioxaspiro(4,4)nonane, the pheromone of the beetle *Pityogenes chalographus*, which was resolved by complexation GC with a capillary column coated with nickel(II)-bis(6-heptafluorobutyl)-(R)-pulegonate.

Although some chiral columns, e.g. the cyclodextrins, are now available commercially, they are relatively expensive and column performance can deteriorate quite rapidly. A convenient and attractive alternative to the direct separation of enantiomers is the GC separation of a diastereomeric derivative formed with an optically pure derivatizing agent, on achiral stationary phases which are less expensive and more generally available. A number of derivatives are available, particularly for alcohols, of which some of the most effective are the *N*-trifluoroacetyl (*S*)-alanyl esters, *N*-trifluoroacetyl-(*S*)-prolyl esters and (*R*)-*trans*-chrysanthemoyl esters. Using the latter derivatives, it is possible to obtain baseline separation of the chrysanthemate esters of 3-octanol on a simple OV-1 column. With highly purified reagents, it is possible to convert chiral alcohols and latent alcohols into separable diastereomers, enabling chiral determinations to be made on unpurified extracts of individual insects. Information on variation of pheromone chirality may have profound implications, both for population studies and for investigating the impact of pest management programmes.

Detectors

There are many types of detectors used in GC which have different degrees of selectivity. Of these, the flame ionization detector (FID) gives a response for

almost all carbon-containing compounds. Allied to this, it is rugged and relatively insensitive to operating variables and has a low dead volume and an extremely wide linear range of response. These properties have ensured that it is by far the most commonly used of all detectors in chemical ecology. Another widely used detector is the mass spectrometer and, indeed, advances in understanding the subject have been achieved largely as a result of developments in this field.

GS-mass spectrometry (GC-MS) is now the method of choice for initial semiochemical identification and, in many instances, is the only technique available and able to provide structural information at the very low sample levels usually encountered in such studies. Mass spectrometers can range from sophisticated instruments with a variety of soft ionization techniques, very high resolving power and extended mass ranges, to small bench-top instruments with limited mass ranges and other capabilities. GC-MS can also be used in quantification and selected ion monitoring (SIM) is a widely accepted quantitative technique based on monitoring the ion abundance of selected m/z values. The sensitivity of SIM for a given compound may be 1000 times as great when monitoring selected ions as when scanning the complete mass spectrum.

In addition to the universal detectors, a number of selective detectors are used. Typically, the extracts obtained from insect or plant sources may contain several hundred components, the vast majority of which are not behaviourally active. The location of the active components in such cases presents a considerable problem for chemical ecologists. This was often attempted in the past by preparative GC of the sample, followed by testing of each of the fractions in a laboratory behavioural assay. By repetitive fractionation and bioassay, it was hoped that fractions containing a single active compound could be obtained for subsequent identification studies. However, this procedure was exceedingly time-consuming and, since many pheromone systems comprise more than one compound, often fruitless. Thus, considerable efforts have been directed towards the development of selective detectors that can be coupled directly to the GC to allow rapid location of biologically active components in complex natural product extracts.

Insects perceive volatile semiochemicals via olfactory receptors, usually located on the antenna. These olfactory cells are extremely sensitive and are tuned to the detection of semiochemicals involved in the insect's chemical ecology. When stimulated, these receptors transform the chemical signal into a series of electrical events which are then passed directly to the

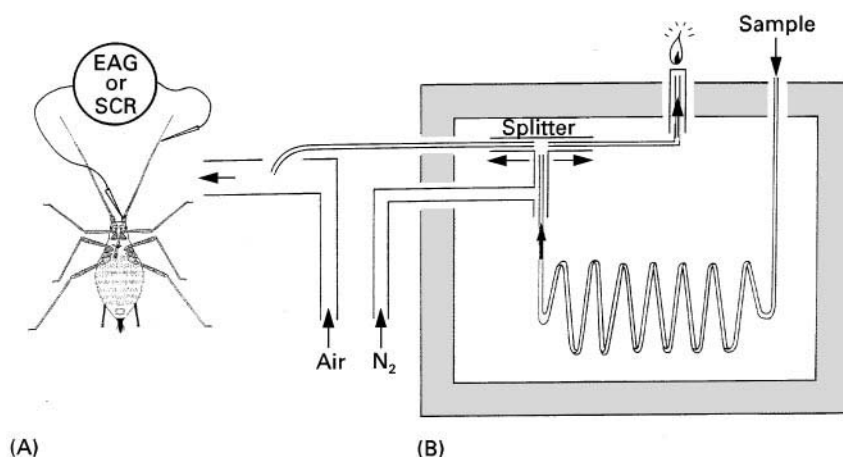


Figure 3 The coupled GC–electrophysiology system. (A) Antennal detector; (B) GC detector. EAG, electroantennogram; SCR, single-cell response.

insect's central nervous system. By placing electrodes in the antenna, it is possible to record these electrical events. At the simplest level, this can be achieved by excising the antenna and suspending it between two electrodes connected to an amplifier system. The so-called electroantennogram, obtained from the antenna on stimulation with an appropriate semiochemical, can then be displayed on an oscilloscope, chart recorder or computer screen. At a more sophisticated level, the responses from the individual olfactory neurons on the antenna can also be recorded (single-cell responses). These electrophysio-

logical preparations have a relatively long lifetime, ranging from tens of minutes to several hours, and thus offer considerable potential for the development of highly specific GC detectors. By linking these preparations to high resolution gas chromatography, i.e. splitting the effluent from the GC column and presenting it simultaneously to the FID of the GC and to the antennal preparation (Figure 3), it is possible to locate biologically active compounds even within highly complex extracts. Since modern high resolution GC columns typically have peak widths of only a few seconds, considerable care must be taken to ensure

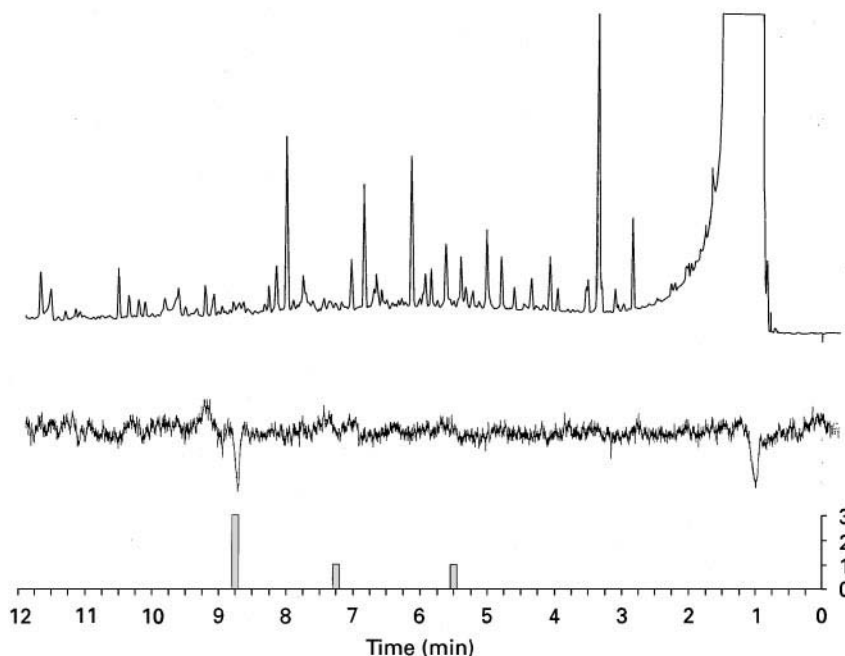


Figure 4 Coupled GC–electroantennogram and GC–behavioural assay with males of the aphid parasitoid *Praon volucre*. Upper trace: GC of volatiles from virgin females; middle trace: electroantennogram response from one male; lower columns: behavioural responses (number of males, out of five tested, showing wing-fanning activity).

that components eluting from the column arrive simultaneously at the two detectors.

Coupled GC-electrophysiological techniques have provided a powerful tool in the chemical ecologist's armoury, enabling accurate targeting of specific peaks for subsequent identification by GC-MS. Indeed, the accuracy of these systems is such that, even where no GC-MS peak is observed, it may still be possible to extract sufficient information from the MS data system to allow a tentative identification to be achieved. By adding marker peaks to the sample that elute either side of the electrophysiologically active component, or by using other compounds present in the original sample which show up on the GC-MS trace,

the researcher can pinpoint accurately the region in the GC-MS chromatogram where the electrophysiologically active peak should elute. Manual interrogation of the data system can then identify specific ions that peak at the expected scan numbers. Such identifications, on picograms of material, would not be possible without the accurate information on where to look in the chromatogram that is provided by coupled GC-electrophysiological studies.

Although electrophysiological activity of a compound suggests that it is involved in some aspect of the insect's chemical ecology, it gives no indication of the behavioural role. Confirmation of the behavioural relevance of a particular component in the chromato-

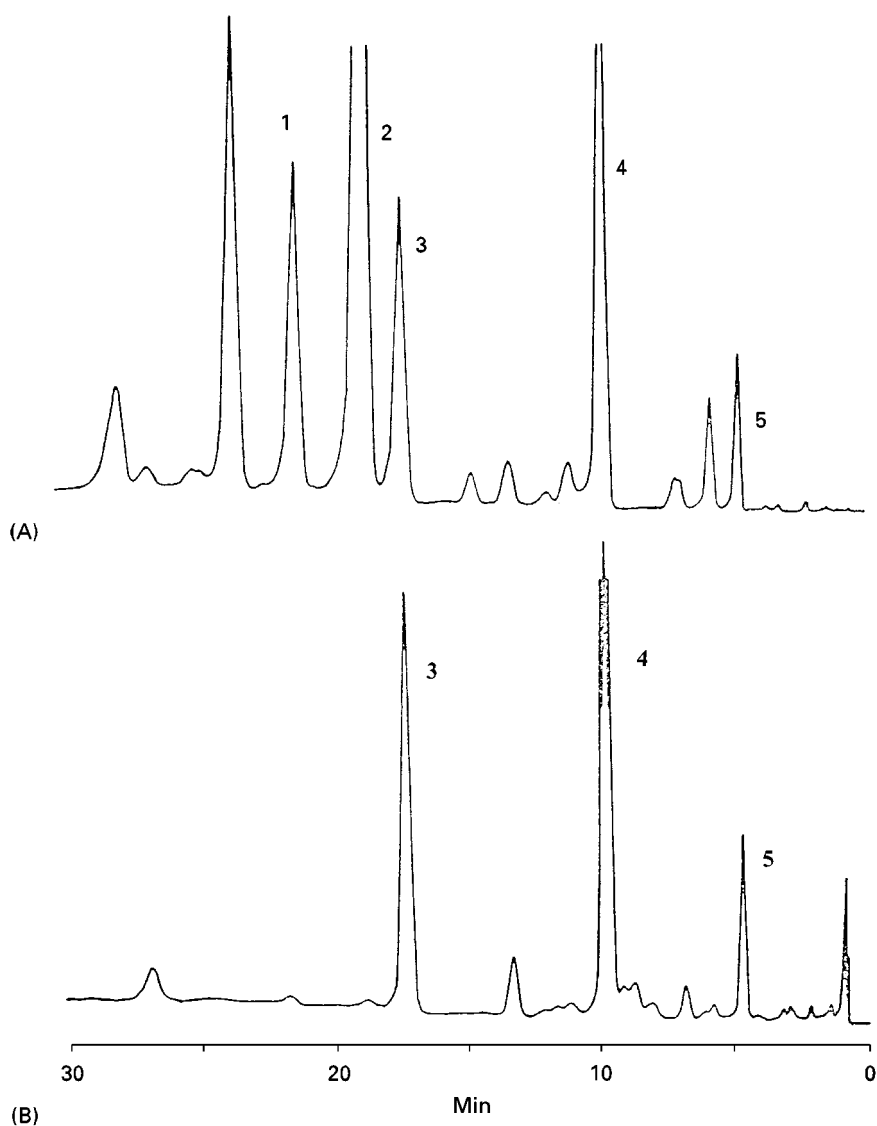


Figure 5 Reaction chromatography. Bromination of alkenes. (A) Gas chromatogram of the Dufour gland contents of the ant *Myrmica rubra*, obtained using solid sampling technique with a packed column (2.75 m \times 4 mm of 10% polyethylene glycol adipate on gas chrom M.). (B) A gland from another worker treated with bromine during injection with the solid sampling technique. 1, α -Farnesene; 2, 8-heptadecene; 3, heptadecane; 4, pentadecane; 5, tridecane.

gram can be obtained by linking the GC to a simple behavioural assay, for example the wing-fanning response elicited from male aphid parasitoids by the female sex pheromone (Figure 4). By monitoring the responses of individuals or groups of insects in the bioassay chamber as they are exposed to the effluent from the GC, it is possible to locate, quite accurately, the elution time of the semiochemical. This technique was widely used in the 1970s, particularly in studies on lepidopterous sex pheromones. More recently, this approach has been used to investigate the role of learning in mixture recognition by foraging honeybees.

Reaction Gas Chromatography

GC-MS is the main identification tool for chemical ecologists, but frequently does not provide sufficient information for a full characterization of the compounds of interest. Thus, in terms of lepidopterous sex pheromones, which usually comprise long chain fatty acid derivatives with varying degrees of unsaturation, MS frequently cannot locate the positions of double bonds, nor distinguish between (*Z*)- and (*E*)-isomers. Microscale reactions conducted before chromatography, or even on-column, can be used to provide information about the class of compound and its functional group, or even to convert them into more stable derivatives. It is possible to carry out a surprising number of reactions on nanogram quantities of material where the reaction is reproducible, quantitative and gives simple products. Various methods have been described for hydrogenation, ozonolysis, epoxidation, reduction, hydrolysis and esterification on nanogram sample levels, or even the use of subtraction loops or specific reactions to remove particular classes of compounds from the mixture (Figure 5).

Conclusions

For the chemical ecologist, GC is not just a technique that enables high resolution and separation of

complex natural product extracts. It can also provide considerable structural information. At the simplest level, noting the retention times of compounds of interest on polar and nonpolar stationary phases can give information on the molecular mass and polarity of a compound. However, when appropriate microscale reactions are included in the repertoire, the GC can prove to be a considerable aid in the identification of semiochemicals. When combined with MS, the availability of structural information is increased considerably.

See also: II/Chromatography: Gas: Column Technology; Detectors: Mass Spectrometry; Headspace Gas Chromatography. III/Chiral Separations: Gas Chromatography.

Further Reading

- Allenmark S (ed.) (1991) *Chromatographic Enantioseparation Methods and Application*. England: Ellis Horwood.
- Attygalle AB and Morgan ED (1988) Pheromones in nanogram quantities: structure determination by combined microchemical and gas chromatographic methods. *Angewandte Chemie* 27: 460.
- Baugh PJ (ed.) (1993) *Gas Chromatography: A Practical Approach*. New York: Oxford University Press.
- Cardé RT and Bell WJ (eds) (1995) *Chemical Ecology of Insects* 2. New York: Chapman & Hall.
- Hummel HE and Miller TA (eds) (1984) *Techniques in Pheromone Research*. New York: Springer-Verlag Inc.
- McCaffery AR and Wilson ID (eds) (1990) *Chromatography and Isolation of Insect Hormones and Pheromones*. New York: Plenum Press.
- Millar JG and Haynes KF (eds) (1998) *Methods in Chemical Ecology: Chemical Methods*. New York: Chapman & Hall.
- Nordlund DA and Lewis W (1976) Terminology of chemical releasing stimuli in intraspecific and interspecific interactions. *Journal of Chemical Ecology* 2: 221.
- Pickett JA, Wadhams LJ, Woodcock CM and Hardie J (1992) The chemical ecology of aphids. *Annual Review of Entomology* 37: 67.
- Sandra P (ed.) (1985) *Sample Introduction in Capillary Gas Chromatography*, vol. 1. Heidelberg: Dr Alfred Huethig Verlag.

Thin-Layer (Planar) Chromatography

E. D. Morgan, Keele University, Staffordshire, UK

Copyright © 2000 Academic Press

Thin-layer chromatography (TLC) in the study of pheromones is more a subject of potentials than of

wide application. Its use, some examples of its application in general and specific problems, and some sources where the reader can find procedures to follow are described here.

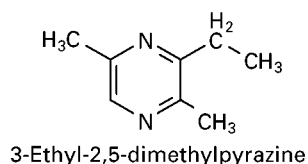
There is a constant argument between those who advocate simpler methods and techniques (often the

older practitioners) and those (sometimes the younger scientists) who believe that the latest and most elaborate and expensive equipment gives the best result in the shortest time. TLC lies in the thick of this argument. Its inherent simplicity, low cost, rapidity and ready interpretation are among its great advantages. Its detractors draw attention to its limited resolution and relatively poor limit of detection. Nevertheless, it is a useful and time-saving technique, worthy of consideration, and there are several recent books devoted entirely to the subject. The technique can be very simple, with hand-applied mixtures and simple spectroscopic, chemical or just bioassay detection methods, or it can be as instrumentally complex as one wishes, with automatic application, scanning densitometers, linking to nuclear magnetic resonance (NMR) and mass spectrometers. A new automatic device is available for collecting bands of silica from a TLC plate and transferring them by suction to solid-phase extraction (SPE) cartridges, which are then extracted with solvent.

Wilson has done much to show the capabilities of TLC allied to other techniques. Modern NMR spectroscopic methods make it possible to place the silica band containing the compound of interest directly into the NMR tube and obtain high resolution spectra. Mass spectroscopists were reluctant at first to put fine silica powder from TLC plates directly into their instruments but now commercial devices are available for doing just this. Highly polar compounds are not suitable for electron ionization-mass spectrometry (EI-MS) by direct insertion of the silica band from TLC, but several groups have shown that fast atom bombardment-mass spectrometry (FAB-MS) can be performed directly on this material, and that with suitable instruments, fragmentation information can be obtained by thin-layer chromatography-tandem mass spectrometry (TLC-MS-MS). Fell has written a comprehensive review on TLC in the study of insects (divided into carbohydrates, lipids, ecdysteroids and terpenoids, amines and pigments). Advocates of TLC, however, have not had a great influence on the field of pheromone studies, but TLC can have great advantages in preliminary studies of new pheromones.

Whatever one places on a TLC plate can be recovered (provided it does not decompose in the meantime), but with both gas chromatography (GC) and high performance liquid chromatography (HPLC) compounds can be either lost in the solvent front or never eluted from the column. Without a good quantitative bioassay or the use of radio-labelled samples the loss would not be detected and the research would be defective. With a simple bioassay, TLC can quickly yield information. An example from personal experience is illustrative. At the beginning of a study of the

Structure I



trail pheromones of *Myrmica* ants, no candidate peaks could be seen in a GC of an extract of the glands. To make sure the material was stable enough to purify, several poison glands known from bioassays to be the source of the pheromone were placed at the origin of a TLC plate, and chromatographed with hexane-acetone (7 : 3). Then the silica from the origin to the solvent front was divided into several bands, which were scraped from the plate, and eluted with acetone or methanol and the extracts submitted to a simple bioassay. There was far too little material there to be visualized by a chemical test. The active band containing the pheromone was readily recognized by a positive bioassay; the other bands were inactive (Figure 1). There was no correlation evident between activity and visualized bands because there was so little of the pheromone present. By trying a few other solvent systems, a good idea of the polarity of the pheromone was quickly obtained. By a few further TLC experiments (adding NaBH₄, NaOH or HCl) it was quickly established that the substance did not contain a reducible ketone group, was not acidic, but was basic. This knowledge greatly encouraged and simplified the subsequent isolation and identification of the pheromone (3-ethyl-2,5-dimethylpyrazine; structure I) with GC-MS. A little chemical imagination can devise other simple reactions that can be used with TLC to learn about functional groups. Once the simple TLC with bioassay has been mastered, more advanced techniques suggest themselves.

Insects

Since many pheromones are readily volatile and transmitted through the air, gas chromatography has been the technique of first resort. It is too often forgotten that some pheromones are not volatile. A good example of a totally involatile pheromone is the oviposition-deterrent pheromone (structure II) of the cherry fruit fly *Rhagoletis cerasi*, identified by a large group led by Hurter, and for which a great deal of TLC was used.

When the female fly lays her egg inside the cherry, she places the pheromone on the cherry surface to warn other flies that this cherry is already occupied. It must remain there for the life of the larva, and withstand sunlight and rain. Isolation began with 7.3 g of female fly faeces, extracted with methanol and

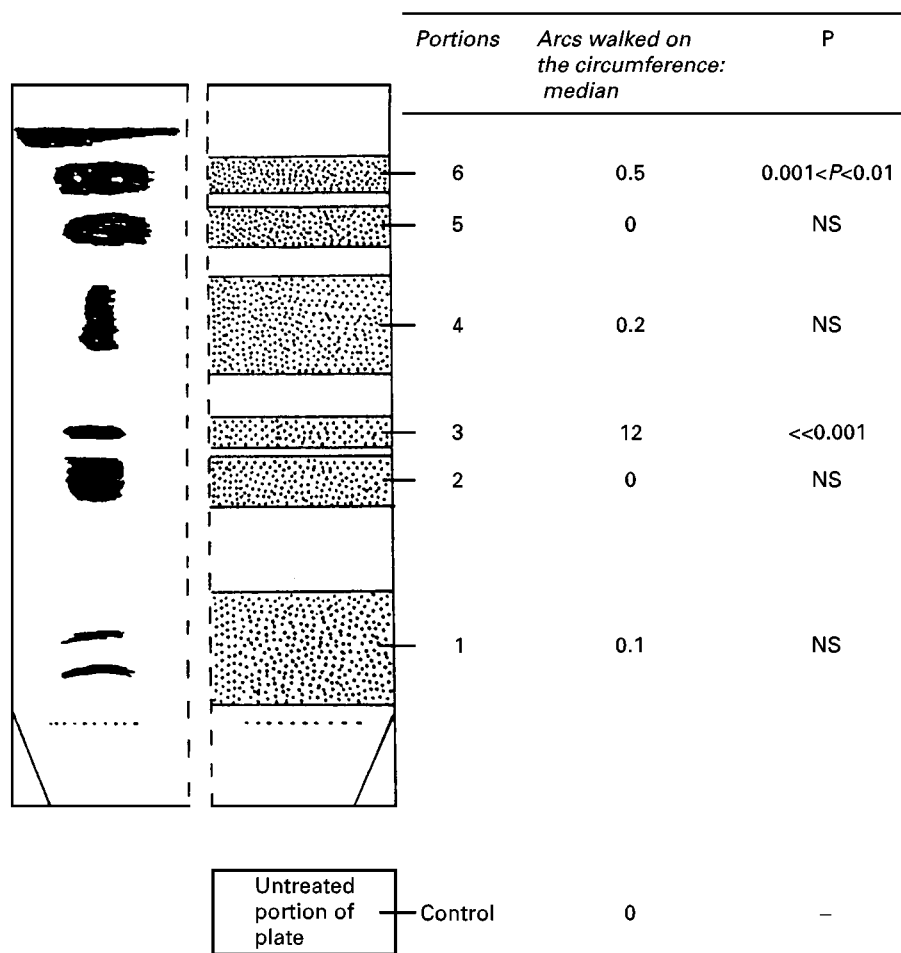


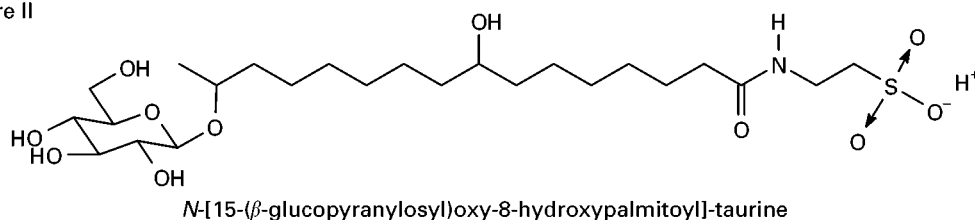
Figure 1 Thin-layer chromatogram of poison glands of *Myrmica rubra* ants applied to the origin of a silica plate and eluted three times with hexane–acetone (85 : 15). The plate was partly sprayed with phosphomolybdic acid for visualizing, and partly cut and the silica removed for elution of activity as shown. The activity of the fractions as indicated by worker ants following a circular trail is also shown. *P*, Level of probability; NS, nonsignificant difference for $P = 0.01$. (Reproduced with permission from Cammaerts-Tricot *et al.* (1997) Isolation of the trail pheromone of the ant *Myrmica rubra*. *Journal of Insect Physiology* 23: 421.)

cleaned up on a cellulose powder column. Preparative TLC on PSC cellulose, developed with ethanol–water (1 : 1), and cutting 0.1 R_F bands located all the activity in the 0.9–1.0 R_F band. This was subjected to HPLC and the active band was further separated on Antec OPTI-UP C-12 plates, developed with methanol, and the activity was found this time in the 0.5–0.7 R_F band. Later, when the pure pheromone was obtained, the taurine fragment was identified by

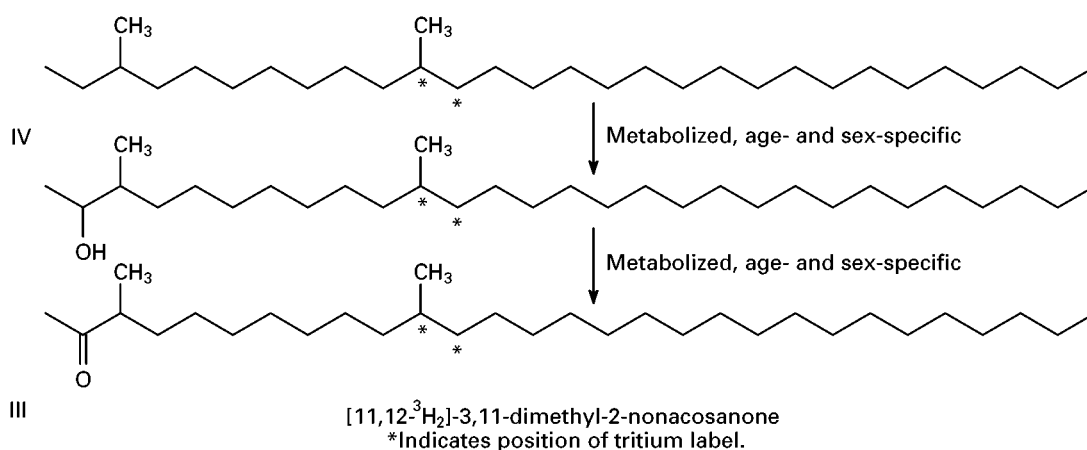
TLC on Merck Silicagel 60F₂₅₄, using *n*-butanol–99% acetic acid–water (8 : 3 : 1), and *n*-propanol–25% aqueous ammonia (8 : 2) and visualizing with Cl₂, I₂ and N,N,N',N'-tetramethyl-4,4'-diaminodiphenylmethane.

The sex attractant pheromones of Lepidoptera are not stored in the pheromone-producing gland but are synthesized and released as required. Aldehydes are the immediate precursors in *Manduca sexta*, but

Structure II



Structures III and IV



to find which of the lipid classes was the source of the aldehydes, conventional lipid TLC was used effectively. Reversed-phase TLC has been used in the actual identification of lepidopteran sex pheromones too. Merck RP-8F_{254S} plates with acetonitrile–water (9 : 1) were used by Ando and others to separate C₁₂ to C₁₆ alcohols, aldehydes and acetates. Chromatograms were presented; this demonstrates how it is a useful tool in determining the chain length and number of double bonds. Separation of the *cis-trans* isomers so common in lepidopteran pheromones is very simple by argentation TLC.

Sex pheromone activity of the brown-legged grain mite *Aleuroglyphus ovatus* (strictly, mites are not insects) was not observed by Kuwahara in either a crude hexane extract or in column chromatography fractions. But when carefully separated from masking alarm pheromone activity of citral by TLC, the activity was readily recognized and the pheromone identified as 2-hydroxy-6-methylbenzaldehyde. The different pheromones of the camel tick and the dog tick were first studied by TLC, which showed them to be in the cholesteryl ester fraction of the surface lipids of the ticks, then HPLC was used to identify the exact compounds. Two-dimensional reversed-phase high performance thin-layer chromatography (RP-HPTLC) was used in the final stage of purification of a group of long chain branched and unbranched alcohols and acetates in looking for the female-produced sex pheromone of the screwworm fly, a serious pest of cattle. Plates were eluted once with hexane–ether (94 : 6) in one direction, then five times with hexane–benzene (96 : 4) in the second direction.

TLC is an excellent way to study the biosynthesis and metabolism of pheromones and precursors using autoradiography. The biosynthesis of the sex pheromone (3,11-dimethylnonacosan-2-one; struc-

ture III) of the German cockroach was studied through radio-TLC and radio-GC of a tritiated hydrocarbon precursor, 3,11-dimethylnonacosane (structure IV). When the hydrocarbon was applied to the surface of the insects, it was poorly converted to the ketone (structure III), but also to the intermediate alcohol. The alcohol, when applied, was efficiently converted to the ketone (Figure 2).

The effect of age and day length on the production of the main component ((*Z*)-11-hexadecenal) of the sex pheromone of the important grain pest *Helicoverpa zea* was quantified by TLC and GC. Radioactivity in the TLC fractions was monitored by scraping off bands of the silica for scintillation counting. Later the direct nervous control of the synthesis of this compound was demonstrated with radio-TLC, radio-HPLC and column chromatography. Further studies of the stimulation of pheromone production in glands of *H. armigera* and production of its fatty acid precursors were both measured by TLC. Similar methods were used to correlate the amounts of pheromone aldehydes and their triacyl glycerol precursors in the glands of the tobacco hornworm *M. sexta*.

Other Animals

TLC can be still more useful in the separation of the complex mixtures often encountered in mammalian pheromones. Female mole rats (blind, solitary rodents), when they are on heat, are attracted to substances in the urine of adult males which they would otherwise avoid. The urine was extracted with dichloromethane and the activity was shown by TLC to be correlated with the sterol and fatty acid ethyl ester fraction, but TLC also showed that this was only part of the activity found in the urine.

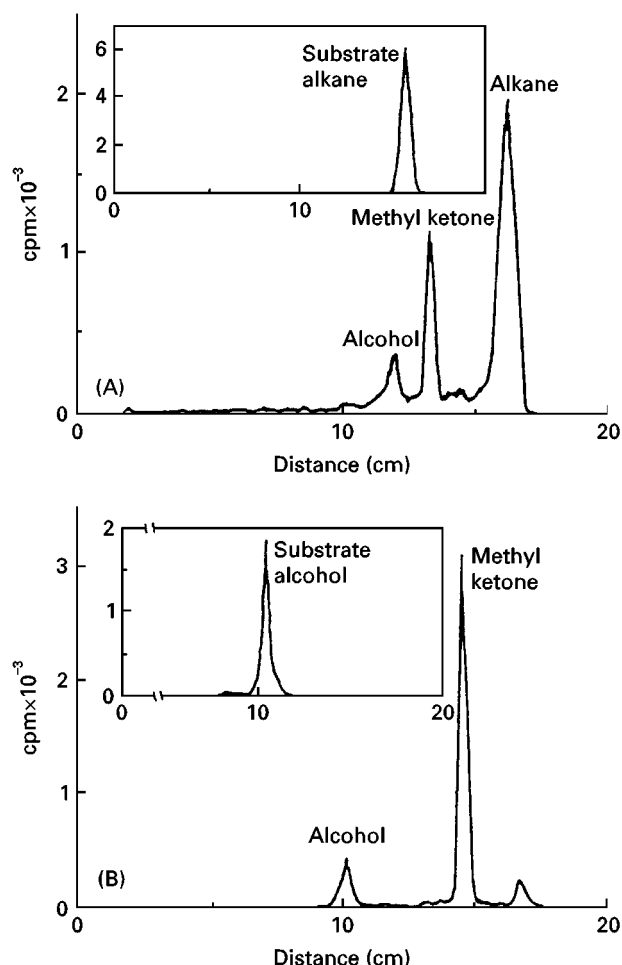


Figure 2 (A) Radio-TLC of cuticular extracts from female German cockroaches treated with $[11,12-^3\text{H}_2]-3,11$ -dimethyl-nonacosane (inset: TLC of the pure alkane used). (B) Similar TLC of products when female insects were treated with $[11,12-^3\text{H}_2]-3,11$ -dimethyl-2-nonacosanol (inset: TLC of pure alcohol used). (Reproduced with permission from Chase *et al.* (1992) Biosynthesis and endocrine control of the production of the German-cockroach sex-pheromone 3,11-dimethylnonacosan-2-one. *Proceedings of the National Academy of Sciences of the USA* 89: 6050.)

Tigers, like domestic cats, mark territory by spraying a marking pheromone upwards and backwards with their urine. The more volatile components are held from too rapid evaporation by lipid fixatives. The composition of the fixative has been studied by TLC and separated into cholesteryl esters, wax esters, tri-, di- and mono-glycerides, free fatty acids, sterols and phospholipids. The nature of the components could then be determined by transesterification and GC.

Marine Animals

Even fish pheromones have yielded to a study by TLC. The male yellowfin sculpin from Lake Baikal

releases a sexual pheromone with its milt to attract females. An ether extract of male urine was separated into fractions, much as described above for *Myrmica* ants, and the active fractions from TLC were further purified by HPLC, and mass spectrometry identified testosterone and 11β -hydroxytestosterone. A third component was probably farnesol. TLC was used similarly to identify androgens in the serum of male Australian lungfish, and showed that testosterone was the main androgen. The exploration of maturation pheromones in goldfish has been studied through metabolism of $[^3\text{H}]-17\alpha$ -hydroxyprogesterone by ovarian follicles and following the products with autoradiography of TLC plates. Even corals produce pheromones at reproduction time. The identification in, and metabolism of, $[^3\text{H}]$ progesterone and $[^3\text{H}]$ androstenedione by Antarctic soft corals was studied by TLC with multiple elution. The metabolites are thought to be part of their chemical signalling or defensive metabolites.

Enantiomers

Enantiomer identification and separation are very important in pheromone isolation and synthesis, although no example of TLC used for this purpose can be found. Lepri's review of enantiomer separation by TLC gives many examples of its use that could be applied in pheromone studies.

Concluding Comments

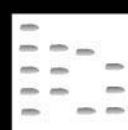
Everyone knows about TLC, and everyone will have used it in their undergraduate days. All the techniques are in place for the greater use of TLC in pheromone research. All that is needed is for investigators to bear it in mind. It can save a great deal of time and effort in the preliminary stages of an investigation, give some indication of the characteristics of the compound being investigated, and provide a guide to the best instrumental method for further separation or purification. Mass spectrometry has long been able to handle the material from a single TLC band; with modern NMR instruments, there can be enough material on a single plate to obtain a good spectrum. The future of TLC in pheromone work could be bright: its greatest enemy is inertia.

See also: II/Chromatography: Thin-Layer (Planar): Mass Spectrometry. III/Chiral Separations: Thin-Layer (Planar) Chromatography. **Pheromones:** Gas Chromatography.

Further Reading

- Ando T, Hasegawa Y and Uchiyama M (1986) Separation of lepidopterous sex-pheromones by reversed-phase thin-layer chromatography and high-performance liquid-chromatography. *Agricultural and Biological Chemistry* 50: 2935.
- Bertsch WS, Hara S, Kaiser RE and Zlatkis A (eds) (1987) *Instrumental HPTLC*. Heidelberg: Hütig.
- Cammaerts-Tricot M-C, Morgan ED and Tyler RC (1977) Isolation of the trail pheromone of the ant *Myrmica rubra*. *Journal of Insect Physiology* 23: 421.
- Chase J, Touhara K, Prestwich GD *et al.* (1992) Biosynthesis and endocrine control of the production of the German-cockroach sex-pheromone 3,11-dimethylnonacosan-2-one. *Proceedings of the National Academy of Sciences of the USA* 89: 6050.
- Fell RD (1996) Thin layer chromatography in the study of entomology. In: Fried B and Sherma J (eds) *Practical Thin-layer Chromatography*, ch. 5, p. 71. Boca Raton: CRC Press.
- Hurter J, Boller EF, Stadler E *et al.* (1987) Oviposition-deterrent pheromone in *Rhagoletis cerasi* L. – purification and determination of the chemical constitution. *Experientia* 43: 157.
- Katsel PL, Dmitrieva TM, Valeyev RB and Koslov YP (1992) Sex pheromones of male yellowfin Baikal sculpin (*Cottomephorus grawingki*) – isolation and chemical studies. *Journal of Chemical Ecology* 18: 2003.
- Kuwahara Y, Sato M, Koshii T and Suzuki T (1992) Chemical ecology of astigmatid mites. 32. 2-Hydroxy-6-methyl-benzaldehyde, the sex-pheromone of the brown-legged grain mite *Aleuroglyphus ovatus* (Troupeau) (Acarina: Acaridae). *Applied Entomology and Zoology* 27: 253.
- Lepri L (1997) Enantiomer separation by thin layer chromatography. *Journal of Planar Chromatography* 10: 320.
- Lessman CA (1991) Metabolism of progesterones during *in vitro* meiotic maturation of follicle-enclosed oocytes of the goldfish (*Carassius auratus*). *Journal of Experimental Zoology* 259: 59.
- Poddar-Sarkar M (1996) The fixative lipid of tiger pheromone. *Journal of Lipid Mediators and Cell Signalling* 15: 89.
- Sherma J and Freid B (eds) (1991) *Handbook of Thin-layer Chromatography*. New York: Marcel Dekker.
- Somsen GW, Morden W and Wilson ID (1995) Planar chromatography coupled with spectroscopic techniques. *Journal of Chromatography A* 703: 613.
- Wall PE (1997) Argentation thin layer chromatography. *Journal of Planar Chromatography* 10: 4.
- Wilson ID (1996) Thin-layer chromatography: a neglected technique. *Therapeutic Drug Monitoring* 18: 484.
- Wilson ID and Morden W (1996) Advances and applications in the use of HPTLC-MS-MS. *Journal of Planar Chromatography* 9: 84.

PHYSICOCHEMICAL MEASUREMENTS: GAS CHROMATOGRAPHY



J. R. Conder, University of Wales, Swansea, UK

Copyright © 2000 Academic Press

Introduction

Chromatography has been used for making physicochemical measurements for as long as it has been used for chemical analysis. When Martin and Synge introduced liquid-liquid chromatography in 1941 they also described how they used it to determine the distribution coefficient of the solute between the two (mobile and stationary) liquid phases.

In the early publications on gas-solid chromatography (GSC), by Wicke in 1940 and 1947 and Cremer and Prior in 1947 and 1951, the use for chemical separation is described simultaneously with physicochemical applications to the measurement of adsorption isotherms and free energies of adsorption. The earliest physicochemical measurements by gas-liquid chromatography (GLC) date from 1955 and 1956,

when several authors described how to measure boiling points, partition coefficients and heats and entropies of solution for a volatile solute dissolved in a nonvolatile solvent. Since then, the scope of gas chromatographic (GC) techniques of physicochemical measurement has branched out in many different directions and now extends into a great variety of fields. These techniques are used by chemists and chemical engineers in many different specialist areas.

It is estimated that several thousand research papers have been published to date on the physicochemical applications of GC. Some of these applications have analogues in liquid chromatography, which is the subject of a separate article (Physico-Chemical Measurements).

Types of Measurement

The different types of physicochemical properties which can be measured by GC are classified in

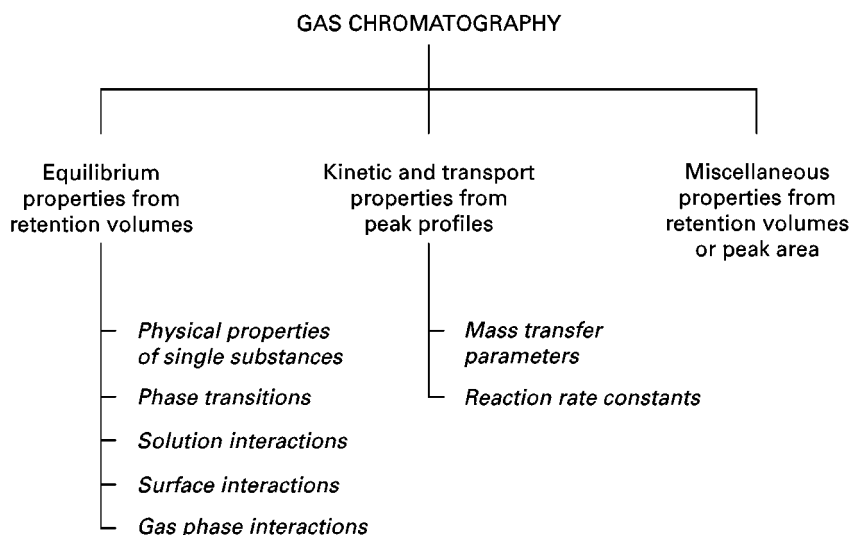


Figure 1 Classification of the physicochemical applications of gas chromatography. (Reproduced with permission from Conder, 1992.)

Figure 1 and listed in Table 1. They fall into three categories: equilibrium properties, kinetic and transport properties, and miscellaneous properties.

Equilibrium Properties

The largest category of properties measurable by GC is equilibrium properties obtained by measuring retention volumes. The equilibrium parameters relate to the distribution of a solute between a moving carrier gas and a stationary phase which may be liquid, solid or interfacial. (The term 'solute' is used here for all these cases.) The solute is usually injected as a small, discrete sample and its retention volume is determined. For example the activity coefficient γ of a volatile solute in a liquid stationary phase coated on an inert solid support can be determined by simply measuring the retention volume V_N of the solute and using the equation:

$$\gamma = \frac{RTW_L}{V_N p_1^0 M_L} \quad [1]$$

where R is the universal gas constant ($8.314 \text{ kJ kmol}^{-1} \text{ K}^{-1}$), T is the temperature (K), p_1^0 the saturation vapour pressure (kN m^{-2}) of the pure solute, W_L the mass of stationary phase in the column (kg) and M_L its molecular weight (kg kmol^{-1}). For the most accurate measurements this equation is modified to incorporate a gas imperfection correction.

Besides activity coefficients, other parameters describing interactions in solution can be determined from measurements of retention volume and appropriate theoretical analyses, as listed under solution

interactions in Table 1. Similarly, one can use retention measurements on suitably chosen systems of solute, stationary phase, support and mobile phase to study many surface interactions, phase transitions and physical properties of single substances, again listed in the table. A useful technique in some of these cases is inverse chromatography, where the solute is used merely as a probe to explore the behaviour of the stationary phase. This technique has been much used in investigations of polymer solutions, solid surfaces, and the various types of phase transitions listed in Table 1. Interactions between components in the gas phase are measured by varying the pressure at which the column is operated.

Kinetic and Transport Properties

Many kinetic and transport properties can be determined from the extent to which they cause a migrating solute peak to broaden as it moves along the column, or more generally from the solute concentration-time profile recorded at the column outlet. Thus, the height H (in units of length of column) equivalent to a theoretical plate can be determined by measuring the second moment σ of the peak (in time units) and the retention time t_R and using the equation

$$H = L \left(\frac{\sigma}{t_R} \right)^2 \quad [2]$$

where L is the length of the column. It is known that H varies with carrier gas velocity according to equations such as the van Deemter equation which includes parameters such as the diffusivities of the solute in the carrier gas and liquid phase and the film

Table 1 Physicochemical parameters measured by gas chromatography*Physical properties of single substances*

Latent heat
Boiling point
Vapour pressure

Phase transitions

Liquid crystals
Melting, pre-melting and post-melting transitions
Glass transition in polymers
Adsorbed liquid films
Solid-solid transitions

Solution interactions

Partition coefficient
Activity coefficient
Enthalpy and entropy changes
Complexing constants
Hydrogen bond strength
Polymer solution interactions
Solubility of gases in liquids
Solubility of liquids in liquids, solubility of (volatile) solids in liquids
Setschenow constants
Liquid-liquid distribution coefficient
Multicomponent gas-liquid equilibria
Multicomponent gas-solid equilibria

Surface interactions

Gas-solid adsorption coefficient
Surface heterogeneity
Gas-liquid interface adsorption coefficient

Gas phase interactions

Second virial coefficient of gas mixtures

Mass transfer parameters

Diffusivity in gases
Diffusivity in liquids
Diffusivity in micropores
Interfacial resistances
Adsorption and desorption rate constants
Obstruction factor
Extra-particle voidage

Reaction rate constants

In liquids
On surfaces

Miscellaneous properties

Molecular weight and average molecular weight
Surface area
Pore size distribution
Liquid film thickness
Polymer crystallinity
Structural assignment
Void zones in packed beds and rock cores
Calorific value

Table reproduced with permission from Conder, 1992.

thickness of the liquid phase. Consequently, these parameters can be obtained by determining H as a function of gas velocity.

Reaction rate constants are measured by several techniques. Some involve stopping or reversing the

flow through the column. Others involve determining the solute concentration-time profile at the column outlet (Figure 2).

Miscellaneous Properties

The third and last category is a miscellaneous group of properties which can be obtained from either the retention volume, the peak profile, or the area under the recorded peak. These include molecular weights, surface areas and polymer crystallinity, as listed in Table 1.

In all the categories of physicochemical measurement so far described, the property studied is derived from measurements based on the chromatographic processes occurring in the column. There are also a few types of physical measurement in which GC is used purely as a tool of chemical analysis. These are not covered in this article though it should be pointed out that, in some cases, the analytical approach is well established, e.g. in studies of the kinetics of gaseous reactions, or of vapour-liquid equilibria by headspace analysis.

Status of GC Methods

Of the three categories of GC measurement just described, the study of equilibrium properties is the largest. This area depends on the theory of chromatographic retention which is firmly founded. Equilibrium properties are usually measurable with greater precision than other GC properties. Precisions as high as 0.05% are attainable, depending on the application and the quality of the equipment used.

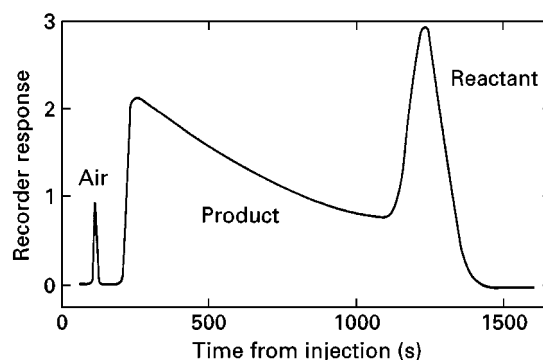


Figure 2 Illustration of the product curve method for determining reaction rate constants. The reaction is the decomposition of dicyclopentadiene in the liquid Silicone DC 550 at 190°C. The chromatogram is produced after a sample of dicyclopentadiene (reactant) is injected into a GLC column with Silicone DC 550 as the stationary phase. The reactant is adsorbed more strongly than the products and so elutes later. According to the theory of the product curve method the rate constant is found from the slope of a logarithmic plot of the product curve in the chromatogram. (Reproduced with permission from Langer and Patton, 1973.)

In contrast, measurements of transport properties such as diffusivities are much affected by the form of peak broadening model used to analyse the data. For instance, the original van Deemter equation has been superseded by more elaborate models whose relative merits have been much debated. Early studies of transport processes by GC were therefore mostly restricted to applications motivated particularly by the needs of GC itself, such as improving the efficiency of separation in analytical, preparative and production GC. Since then, however, the technique has also found wider application to rate measurements where it sometimes possesses singular advantages. Thus, certain forms of GC measurement of diffusivities provide some of the best diffusion coefficient data currently available. As a further example, studying reactions by conducting them in a chromatographic column offers the unique feature of simultaneous reaction and separation, allowing forward and back reactions to be studied directly without mutual interference, as shown in Figure 2.

Among methods of physicochemical measurement, GC offers an unusually wide range of application. Three particular roles may be distinguished:

- GC often provides an alternative to other techniques, with different advantages and disadvantages.
- GC has proved a fruitful means of discovery of new generalizations based on large volumes of data.
- GC can be combined synergistically with other techniques to shed new light on the phenomenon under study.

Examples of the first role are numerous. Thus, the most important concentration region for studying molecular interactions in solution is infinite dilution of the solute component. Non-GC methods, which depend on measuring vapour pressure, suffer from diminishing precision of measurement as infinite dilution is approached. The GC method, which depends on measurement of retention, is not inherently concentration dependent. Simple elution chromatography lends itself particularly well to infinite dilution, while several chromatographic methods, involving both elution and frontal modes of operation, are available to cover a wide concentration range up to a high mole ratio of solute in the mobile phase (Figure 3). As a second example, determination of mixed second virial coefficients of gas mixtures by non-GC methods, such as compressibility measurements or from pressure or volume changes on mixing, require an accurate knowledge of the second virial coefficients of both pure components. GC provides an alternative method which not only avoids this need but is more accurate.

In the second role, GC has led to the discovery of a number of valuable generalizations about the behaviour of chemical systems. For instance, it has been found that the partition coefficient of a solute in a binary mixture of two involatile liquids is very often a linear function of the volume fraction or molarity of either binary component. This has been shown to hold, with a few exceptions, for over 400 different systems (Figure 4). Similarly, studies have shown that the thermal behaviour of a variety of polymethylenic liquids spread on silica-type surfaces closely mimics their behaviour on the surface of water. This indicates the formation of orientated monomolecular films whose transitions have accordingly been explored by GC. In cases such as these, the value of GC lies in its speed and simplicity. Alternative methods, such as vapour pressure measurement or infrared, ultraviolet or magnetic resonance spectroscopy, are less practical for collecting the large volumes of data required. Another field of application is the correlation of retention with structure and pharmacological behaviour (QSRR).

Sometimes, results obtained by GC and other methods appear to differ. This has been observed, for example, in studies of phase transitions and adsorption at gas-liquid interfaces. In such cases the value of chromatography lies in the scientific progress achieved by trying to understand why different methods of studying apparently the same property give different results. By combining chromatographic, surface tension and gravimetric solubility measurements, for example, Martire, Pecsok and Purnell in 1965 were able to obtain unambiguous values of the average thickness of the liquid film on a porous support and resolve previous differences over the surface area and distribution of liquid on the support.

Advantages of GC Methods

As an alternative to other means of studying physicochemical behaviour, GC has its own advantages and disadvantages which depend on the applications concerned. However, certain characteristic advantages and disadvantages can be discerned. The principal advantages are enumerated below.

Speed

GC experiments are relatively fast. Local equilibrium is achieved very rapidly in the column because the interfacial area between the mobile and stationary phases is very large and path lengths for mass transfer are short. Solutes therefore usually pass through the column in minutes or even seconds. The virtue of speed provides many advantages. It is particularly valuable for solutes which are thermally unstable or have only short radioactive half-lives.

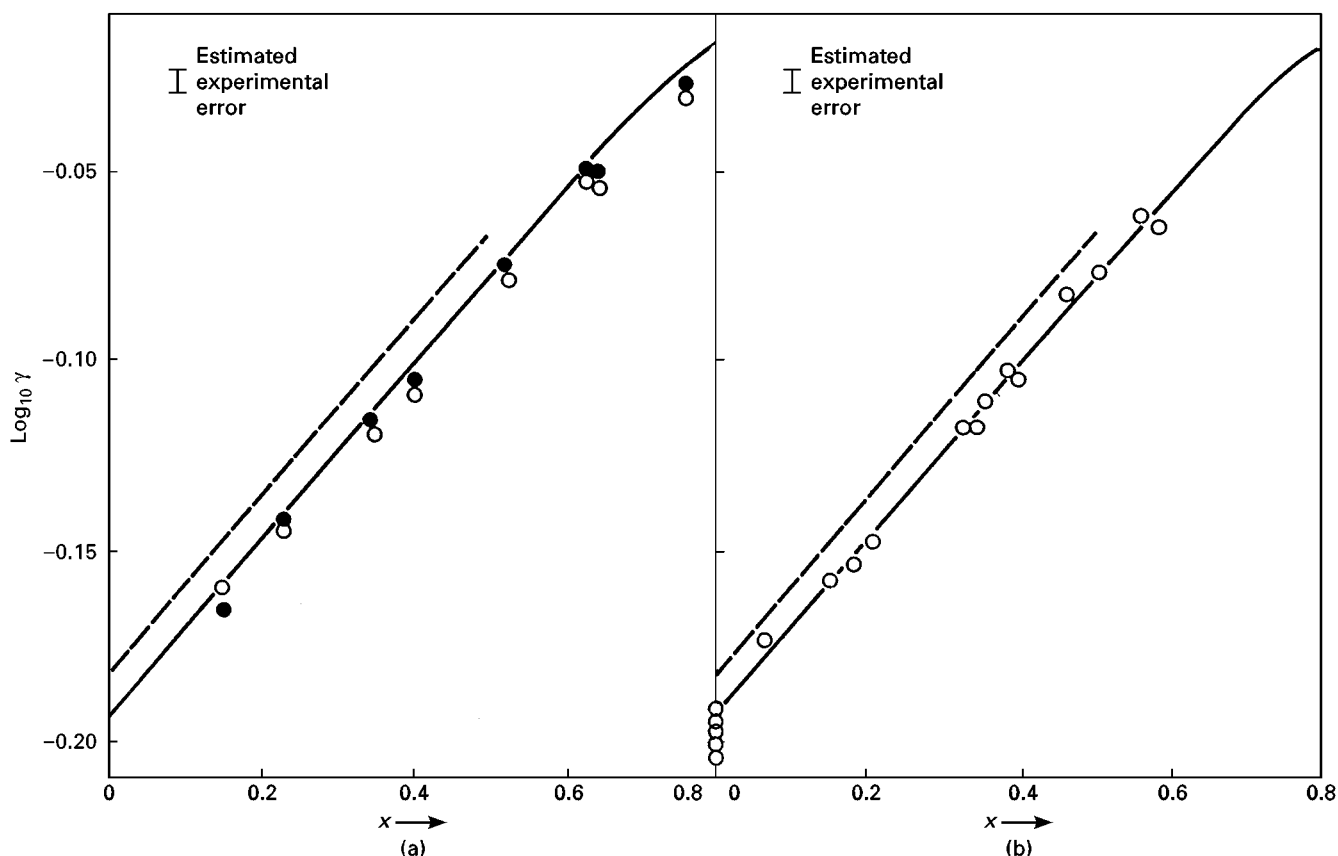


Figure 3 Example of activity coefficients in solution studied at finite solute concentrations: comparison of GC and static (gravimetric) results. The logarithm of the activity coefficient γ of the solute *n*-hexane in squalane stationary phase is plotted against mole fraction x of *n*-hexane at 30°C. (a) Chromatographic technique of frontal analysis (FA) using frontal breakthrough curves for: O diffuse front (sorption), ● self-sharpening front (desorption). (b) Chromatographic technique of elution on a plateau (EP) of constant solute concentration. Continuous curve: best line, extrapolated to $x = 0$, through static data of Ashworth and Everett (1960) obtained with squalane supported on Celite. Broken curve: static data of Martire, Pecsok and Purnell (1965) obtained with unsupported (bulk) squalane. The separation of about 2½% in γ for the two static plots is small but experimentally significant and is believed to be due to the use of different samples of squalane. The results of the GC techniques are in excellent agreement with each other, with the static data of Ashworth and Everett (1960) and with further static measurements by Ashworth (1973). (Reproduced with permission from Conder and Purnell (1969) *Transactions of the Faraday Society* 65: 839. Copyright Royal Society of Chemistry.)

Experimental time can often be saved by injecting a mixture of several solutes of differing retentions in one run. Work requiring large amounts of data can be conducted within a reasonable timescale.

Contact times can be kept short. When adsorption on catalysts is studied by static methods, the problem is to observe it despite the accompanying presence of decomposition. The temperature has to be far below the normal operating temperature of the catalyst to avoid excessive decomposition during the experiment. With elution GSC the temperature can be near the normal operating temperature because of the short contact time between 'solute' (adsorbate) and adsorbent at each point in the column. Low contact time is also beneficial in studying adsorption on polymer surfaces. Here static measurements do not distinguish between surface adsorption and bulk adsorption. GSC allows the rapid adsorption process

to be examined without interference from the slower adsorption process.

Small Amounts of Material Required

GC measurements at infinite dilution require only very small amounts of solute, e.g. 100 µg, but as little as 10^{-11} g can be used if necessary. This is a particular advantage for solutes that are available only in trace amounts. The amount of stationary phase needed is also relatively small – 2 g of liquid is typical in a packed column but 1 mg of liquid can be used in a capillary (open tubular) column.

Impure and Mixed Solutes

Solute mixtures or impurities are usually separated on the column, and so can be run without previous purification.

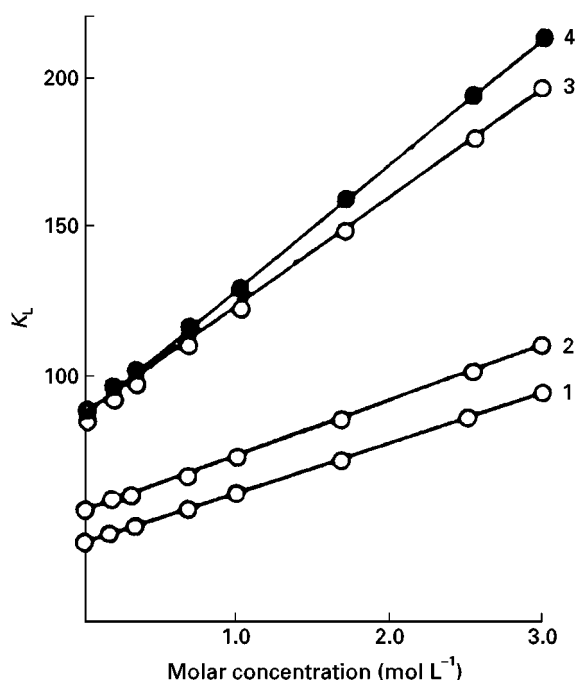


Figure 4 Example of linear plots of gas-liquid distribution coefficient K_L of solutes against molar concentration (mol L^{-1}) of di-*n*-butyltetrachlorophthalate in squalane at 80.3°C . Data of Eon, Pommier and Guiochon. The solutes are: (1) 2-methylfuran, (2) 2,5-dihydrofuran, (3) benzene and (4) thiophen. (Reproduced with permission from Purnell and Vargas de Andrade (1975) *Journal of the American Chemical Society* 97: 3585. Copyright American Chemical Society.)

Reactive Solutes

GC methods are often preferred for reactive solutes because separation of reactants and products on the column allows the forward reaction to be studied alone without interference from the reverse reaction or from autocatalysis or product inhibition. Additionally, contact times are short, quantities small and fewer difficulties are encountered with reaction with the materials of construction of the equipment.

Wide Temperature and Pressure Range

Change of temperature is much more easily accomplished in a chromatograph than in most volumetric or gravimetric techniques. Additionally, because the column is of small diameter and compact, extremes of temperature and pressure can be achieved more readily than by many other techniques, e.g. below 100 K, above 1200 K, or up to 2000 bar.

Characteristics of GC Methods

Despite the advantages of GC methods, there are also several characteristic limitations inherent in the technique which need to be appreciated for reliable

measurement. Much effort has been expended in overcoming these limitations. On the whole considerable success has been achieved, though often at the expense of complicating the technique. We will consider five characteristics of the method: interference between interactions under study, stationary phase volatility, the number of components in the system studied, the influence of the 'inert' carrier gas and the influence of the support.

Interference Between Interactions Under Study

The remarkable versatility of the method seen in Table 1 is partly due to the large number of components characteristically present in a chromatographic column. A GLC column contains at least three bulk phases (gas, liquid and solid) and two interfacial phases (gas-liquid and liquid-solid; the gas-solid interface is seldom problematic in GLC). Potentially, therefore, the study of one interaction may be complicated by the presence of another. Common examples of interfering processes are adsorption on the solid support and/or adsorption at the gas-liquid interface during studies of interactions in solution. The adsorption increases the retention volume from which the solution parameters are to be determined. Sometimes it is possible to avoid or minimize the interference by suitable choice of support. If not, procedures have been devised involving varying the loading of liquid phase on the support and plotting the data in such a way as to determine both the solution and adsorption parameters.

Influence of the Solid Support

This is the commonest example of the interference problem just described. Physicochemical measurements are usually made with packed columns. In GLC a solid support is used to hold the stationary phase as a liquid of high surface area. It is seldom safe to treat the support as completely inert. Adsorption of solute by the support often causes 'tailing' of polar solutes. It is not always appreciated that support adsorption may still affect solute retention even when no tailing is observed. Reproducibility of the support was a serious bar to reproducible data in early GC work. Support adsorption can be detected and eliminated by varying the liquid loading and analysing the data appropriately. This is a desirable procedure in all GLC measurements of solution equilibria unless there is already good evidence that adsorption by the support is negligible. It is usually found that support adsorption can be neglected with nonpolar organic solutes. In other cases one can either greatly reduce the effect by chemically reacting the support surface with a silanizing agent, or eliminate the effect by

appropriate data analysis of measurements at different liquid loadings.

Volatility of the Stationary Phase

By its nature, GC is well suited to studying binary systems involving one volatile component, the solute, and one involatile component, the liquid or solid stationary phase. The technique may be extended to volatile stationary phases with vapour pressures up to about 3 bar, either by the well-established approach of pre-saturating the carrier gas with vapour of the stationary phase, or by a technique of nonsteady-state gas chromatography recently developed for the purpose.

Multicomponent Systems

In simple chromatography with an inert carrier gas, there are often only two active components, the volatile solute and a single-component, involatile, stationary phase, together forming a binary system. Two types of multicomponent system can also be studied. In the first, there are two or more involatile components in the stationary phase. This type of multicomponent system is met in studying complexing behaviour in solution. It presents no new problems of technique though the analysis of the data is of great thermodynamic interest. In the other type of multicomponent system more than one volatile component is involved in the liquid phase interaction. In this case one of the two volatile components must be introduced at a steady concentration into the carrier before entry to the column, and the other solute is injected as a discrete sample. This method has been used to study multicomponent gas-liquid and gas-solid equilibria at high pressures.

Influence of the 'Inert' Carrier Gas

Although the carrier gas is often thought of as inert, several interactions involving the carrier and solute occur in the gas phase. The combined contribution to the measured retention of solute is of the order of 1–5%. This is usually known as the gas imperfection correction. It needs to be calculated and corrected for in studies of adsorption or solution equilibria making any claim to accuracy. The correction was often omitted or incorrectly calculated in early studies and invalid versions of the correction are still sometimes quoted in current publications.

Apparatus Requirements

Most physicochemical measurements by GC are conducted with packed rather than open tubular (capillary) columns. The very high resolution offered by

open tubular columns is of little benefit for most physical measurements. Determination of the mass of stationary phase in the column is easier and more accurate with packed columns.

The type of GC apparatus needed for physicochemical measurements depends on the precision of measurement desired, which varies with the application. A commercial instrument is often suitable for simple physical properties such as latent heats, boiling points and vapour pressures, where the role of GC is to provide a method of obtaining large amounts of data rapidly. The control of column temperature may be of high precision but poor accuracy with a commercial chromatograph, but with improved instrumentation of pressure and flow rate, is also appropriate for most measurements at infinite dilution of the solute. For work at finite concentrations of the solute, however, it is necessary either to inject especially large samples of solute or to pass into the column a steady concentration of solute in the mobile phase. Various forms of finite concentration technique have been developed. Almost all require a purpose-built instrument or a specially modified commercial unit. Studies of gas phase interactions, which entail elevated pressures, also require specially built GC equipment.

Measurement of Separation Process Data

In the design of process plant a variety of data is needed on the properties of substances, particularly in designing separation and reaction processes. Chemical engineers are not always as aware as chemists of the suitability of GC methods for obtaining property data, but the potential is considerable. Of the parameters listed in Table 1, those particularly relevant to process engineering include physical properties of single substances, activity coefficients in solution, gas solubilities, liquid-liquid distribution coefficients, multicomponent equilibria, adsorption coefficients, diffusivities, mass transfer parameters, reaction rate constants and some of the miscellaneous properties.

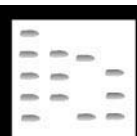
See also: II/Chromatography Gas: Column Technology; Historical Development; Theory of Gas Chromatography.

Further Reading

- Berezkin VG (1991) *Gas-Liquid-Solid Chromatography*. New York: Marcel Dekker.
- Conder JR (1992) Physicochemical measurement by chromatography: overview and solution thermodynamics. In: Dondi F and Guiochon G (eds) *Proceed-*

- ings of the NATO Advanced Study Institute on Theoretical Advances in Chromatography, Ferrara, 18–30 August 1991, pp. 315–337. Dordrecht: Kluwer Academic Publishers.
- Conder JR and Young CL (1979) *Physicochemical Measurement by Gas Chromatography*. Chichester: John Wiley.
- Gray DG (1977) Gas chromatographic measurements of polymer structure and interactions. *Progress in Polymer Science* 5: 1.
- Jönsson JA (1987) *Chromatographic Theory and Basic Principles*. New York: Marcel Dekker.
- Katsanos NA (1988) Reversed-flow gas chromatography applied to physico-chemical measurements. *Journal of Chromatography* 446: 39.
- Langer SH and Patton JE (1973) Chemical reactor applications of the gas chromatographic column. In: Purnell JH (ed.) *New Developments in Gas Chromatography*, pp. 293–373. New York: John Wiley.
- Laub RJ and Pecsok RL (1978) *Physicochemical Applications of Gas Chromatography*. New York: John Wiley.
- Locke DC (1976) Physicochemical measurements using chromatography. In: Giddings JC, Grushka E, Cazes J and Brown PR (eds) *Advances in Chromatography*, vol. 14, p. 87. New York: Marcel Dekker.
- Paryiczak T (1986) *Gas Chromatography in Adsorption and Catalysis*. Chichester: Ellis Horwood.
- Phillips CSG (1973) Chromatography and intermolecular forces. *Berichte Bunsen-Gesellschaft Physikalische Chemie* 77: 171. (In English)
- Phillips CSG (1985) Chromatography beyond analysis. In: Bruner F (ed.) *AJP Martin Honorary Symposium*, Urbino, 1985, p. 333. Amsterdam: Elsevier.
- Purnell JH (1962) *Gas Chromatography*, ch. 14. New York: John Wiley.
- Purnell JH (ed.) (1973) *New Developments in Gas Chromatography*. New York: John Wiley.
- Young CL (1968) The use of gas-liquid chromatography for the determination of thermodynamic properties. *Chromatographic Reviews* 10: 129.

pH-ZONE REFINING COUNTERCURRENT CHROMATOGRAPHY



Y. Ito, National Institutes of Health, Bethesda, MD, USA

Copyright © 2000 Academic Press

What is pH-zone-refining Countercurrent Chromatography (CCC)

This countercurrent chromatography (CCC) technique distributes large quantities of ionic analytes (acids and/or bases) into a train of rectangular peaks of very high concentrations with high purity. The method utilizes ionic interaction between analytes to shift their partition coefficients according to pK_a and hydrophobicity.

Development of pH-zone-refining CCC

In liquid chromatography, isocratic elution usually produces symmetrical peaks where the peak width increases with retention time. In the course of purification of BrAcT_3 (*N*-bromoacetyl-3,3',5-triiodo-L-thyronine) by high-speed countercurrent chromatography (HSCCC), it was found that the product formed an unusually sharp peak corresponding to over 2000 theoretical plates, while the preceding impurity peak showed a normal width of about 500 plates. The cause of this sharp peak formation was

finally found when the collected fractions were manually analysed for pH. As shown in Figure 1, the pH-curve showed a gradual decline after the solvent

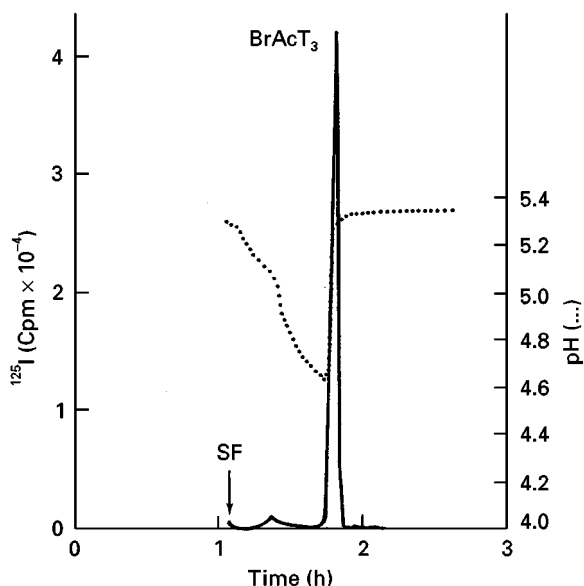


Figure 1 Disclosure of the cause of sharp peak formation by manual pH measurement. Sample: CCC-purified BrAcT_3 (approximately 0.1 mmol) + blank bromoacetylation mixture. The elution of the sharp peak coincides with the abrupt rise of the pH suggesting the acid in the sample solution as the cause of the peak sharpening.

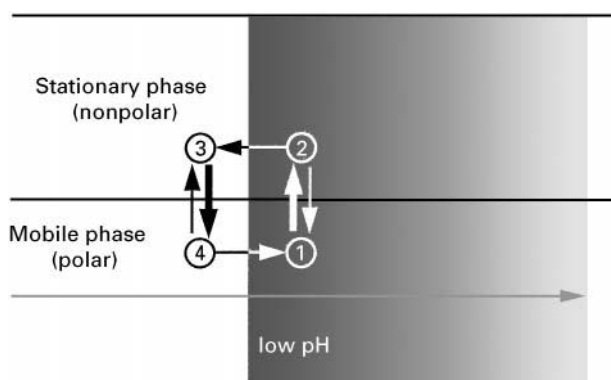


Figure 2 Schematic illustration of the peak-sharpening process in the separation column. A portion of the column contains non-polar stationary phase in the upper half and the polar mobile phase in the lower half. The acid analyte circles around the sharp retainer border by repeating protonation and deprotonation as described in the text.

front followed by an abrupt rise which coincided with the elution of the sharp product peak. Mass spectro-metric analysis of the sample solution showed the presence of bromoacetic acid, a reaction product of BrAcT_3 synthesis. Here, bromoacetic acid acts as a 'retainer' acid since it prevents elution of the analyte. Other organic acids such as trifluoroacetic acid (TFA) and acetic acid also can produce this effect, if introduced in the sample solution and/or the organic stationary phase. It must not be added to the mobile phase which should instead contain a base such as ammonia which acts as an 'eluter' base in the opposite sense of the 'retainer' acid.

A portion of the separation column shown in **Figure 2** indicates that the organic stationary phase is in the upper half and the aqueous mobile phase in the lower half. As described by its non-linear isotherm, the retainer acid forms a sharp rear boundary which moves through the column at a rate lower than that of the mobile phase. When the acid analyte is present in the mobile phase at position 1 (**Figure 2**), it becomes protonated due to the low pH and partitions into the organic stationary phase at position 2. As the basic mobile phase moves forward, the analyte is exposed to a higher pH at position 3 where it is deprotonated (ionized) and transferred to the lower aqueous phase at position 4. In the aqueous mobile phase the analyte migrates quickly through the sharp retainer border to repeat the cycle. Consequently, the analyte is always confined to a narrow region around the retainer border and elutes as a sharp peak together with that border.

In order to trap the analyte peak around the retainer border, one requirement must be satisfied. In **Figure 3** K_r represents the partition coefficient (sol-

ute concentration in the stationary phase divided by that in the mobile phase) of the retainer acid, and K_a and K_b for those of the analyte at acidic and basic conditions, respectively. If K_r is greater than K_a and K_b , the analyte elutes earlier than the retainer border forming a broad peak (peak 1). If K_r is smaller than K_a and K_b , the analyte elutes after the retainer border again with a broad peak (peak 3). Peak sharpening takes place only when K_r falls between K_a and K_b (peak 2).

This method allows the use of multiple retainer acids as spacers to separate sharp analyte peaks at their boundaries. **Figure 4** shows a separation of three dinitrophenyl (DNP)-amino acids by the spacer acids. The separation was performed with a two-phase solvent system composed of methyl *t*-butyl ether/water where TFA and three spacer acids were added to the upper organic stationary phase and ammonia (eluter base) to the lower aqueous mobile phase. Polar DNP-aspartic acid (DNP-asp) was eluted between acetic acid and propionic acid, DNP-alanine (DNP-ala) between propionic acid and *n*-butyric acid, and the more hydrophobic DNP-leucine (DNP-leu) after *n*-butyric acid.

This 'pH-peak-focusing' CCC has useful applications such as the concentration and detection of minor components and the improvement of analytical separations by shifting the retention time of the analyte away from non-ionic impurities. However, the most important application is found in preparative-scale separations. When the sample size of the DNP-amino acids in the above separation was in-

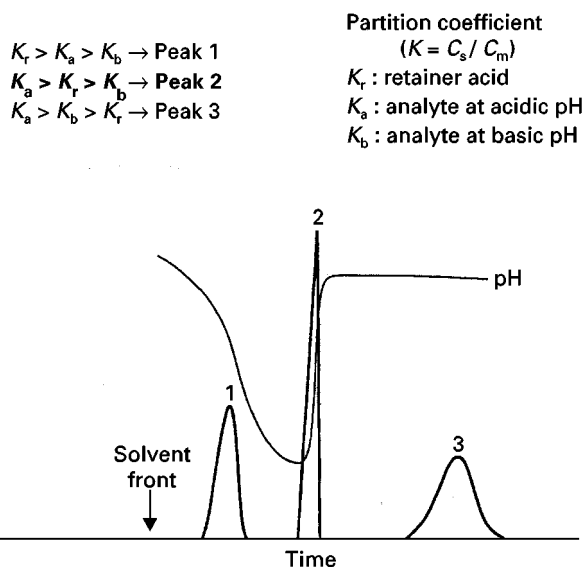


Figure 3 General requirement of sharp peak formation. Peak 1 is obtained when both K_a and K_b are smaller than K_r , while peak 3 is obtained when both K_a and K_b are greater than K_r . Sharp peak 2 is formed when K_r falls between K_a and K_b , as indicated above.

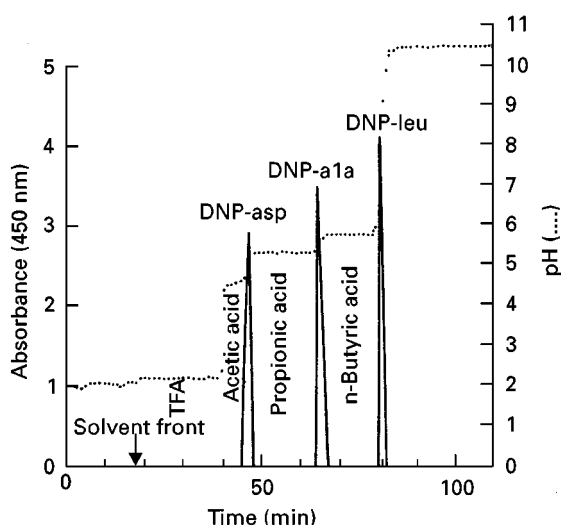


Figure 4 Separation of DNP-amino acids by spacer acids. Three spacer acids introduced in the stationary phase form pH-zones to isolate sharp analyte peaks at their boundaries. Solvent system: methyl *t*-butyl ether–acetonitrile–water (4 : 1 : 5); retainer acids: TFA, acetic acid, propionic acid, and *n*-butyric acid, each $0.4 \mu\text{L mL}^{-1}$ in the organic stationary phase; eluter base: 0.1% ammonia in the aqueous mobile phase (pH 10.77); sample: DNP-L-aspartic acid, DNP-L-alanine and DNP-L-leucine each 1 mg; flow-rate: 3 mL min^{-1} ; revolution: 800 rpm; retention of the stationary phase = 81.0%.

creased by 100-fold from 1 to 100 mg, under otherwise identical conditions, the upper chromatogram shown in Figure 5 was obtained. Each component formed a highly concentrated rectangular peak associated with a specific pH as shown by the dotted line. The elimination of the three spacer acids (Figure 5, lower) resulted in fusion of these three peaks while preserving their original rectangular shapes as demonstrated by well-defined pH-zones and K_{std} values measured with a standard solvent system (chloroform–acetic acid–0.1 M HCl at a volume ratio of 2 : 2 : 1) as shown in the lower chromatogram.

This new modification of the HSCCC method produces characteristic pH-zones according to pK_a and hydrophobicity of analytes and for this reason it has been named ‘pH-zone-refining CCC’. It shares many features with displacement chromatography and provides several advantages over the conventional HSCCC technique such as increased sample loading capacity, high concentration of fractions, concentration and detection of minor components, and detection and precise localization of rectangular major peaks by monitoring the effluent pH even though the analytes have no chromophore. Of course, unlike standard HSCCC, it depends on the ability of an analytes to exist in two different forms, one hydrophobic and one hydrophilic.

Mechanism of pH-zone-refining CCC

Model Experiment

The mechanism of pH-zone-refining CCC may be demonstrated by the following model experiments. Figure 6 shows preparation of solvent phases to initiate the experiment for separating acidic analytes. About equal volumes of ether and water are equilibrated in a separatory funnel and the two phases separated. A retainer acid such as TFA is added to the upper organic phase (shaded) while an eluter base such as ammonia is added to the lower aqueous phase. In each experiment the column is first entirely filled with the stationary phase. This is followed by injection of sample solution containing three acidic

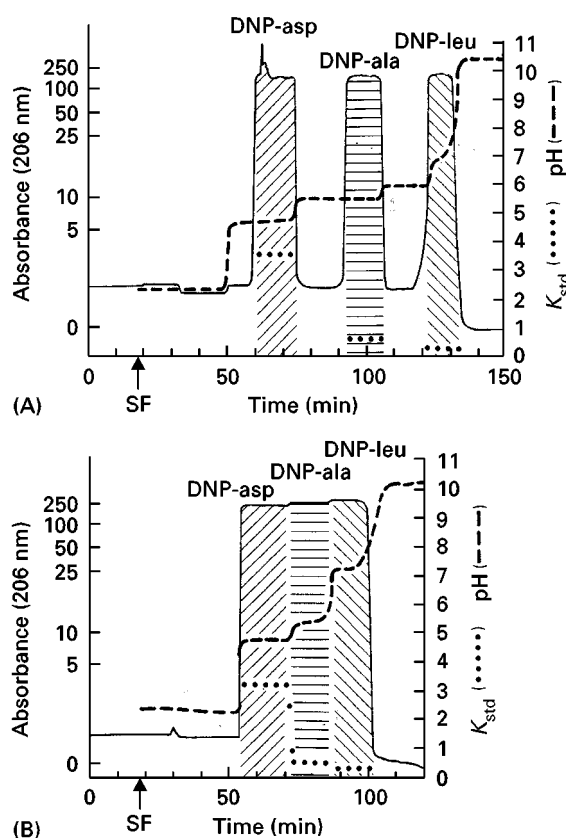


Figure 5 pH-zone-refining CCC of DNP-amino acids with (A) and without (B) spacer acid in the stationary phase. (A) Rectangular peaks of three DNP-amino acids were widely separated from each other by the spacer acids (acetic acid, propionic acid and *n*-butyric acid). (B) Elimination of the spacer acids resulted in fusion of the rectangular peaks with minimum overlapping as demonstrated by associated pH values and partition coefficient values (K_{std}). Experimental conditions are identical to those in Figure 4, except that the sample size was increased to 100 mg for each component. The K_{std} values were obtained by partitioning an aliquot of each fraction to the standard solvent system composed of chloroform–acetic acid–0.1 M HCl (2 : 2 : 1) (SF = solvent front).

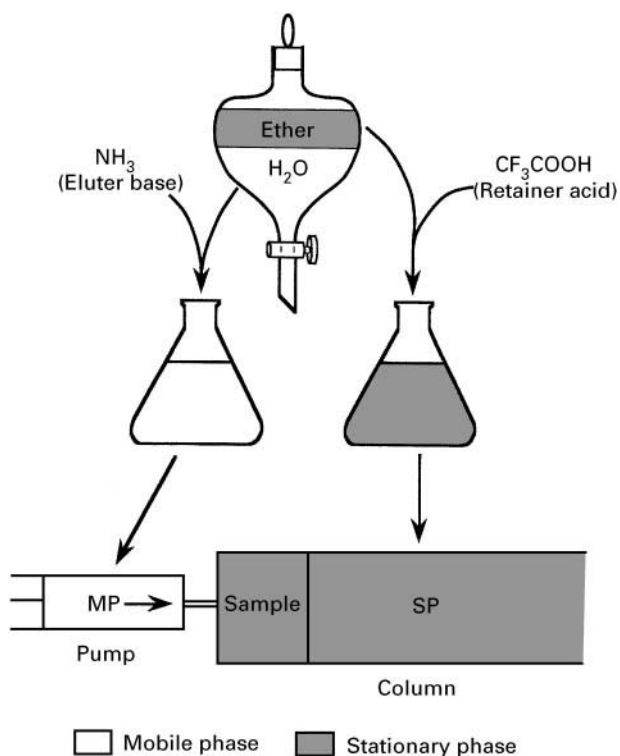


Figure 6 Model experiment for pH-zone-refining CCC for separation of carboxylic acids: preparation of solvent phases.

analytes. The mobile phase then is pumped into the column and the column rotated at a desired rate.

Figure 7 (upper diagram) illustrates the result of the experiment where a portion of the separation column shows the organic stationary phase (shaded) in the upper half and the aqueous mobile phase in the lower half. As described by its nonlinear isotherm, the retainer acid, TFA, forms a sharp boundary which moves through the column space occupied by the mobile phase at a rate considerably lower than that of the mobile phase. Three analytes, S_1 , S_2 , and S_3 , competitively form solute zones behind the sharp TFA border according to their pK_a and hydrophobicity. S_1 , with the lowest pK_a and hydrophobicity, is located immediately behind the TFA border, while S_3 with the highest pK_a and hydrophobicity is located at the end of the solute zones where it forms a sharp rear border.

As indicated by curved arrows, proton transfer takes place at each zone boundary governed by the difference in pH between the neighbouring zones. The loss of the solute from the mobile phase to the stationary phase at the zone front is compensated for by its return at the back of each zone, while ammonium ions in the aqueous phase serve as counterions for all species. After reaching equilibrium all three solute zones move at the same rate as that of the TFA border, while constantly maintaining their indi-

vidual widths and pH. Charged minor components present in each zone are efficiently eliminated either forward or backward according to their partition coefficients (pK_a and hydrophobicity) and eventually accumulate at the zone boundaries. Consequently, the three analytes elute as a train of rectangular peaks with sharp impurity peaks at their narrow boundaries as illustrated in the lower diagram of **Figure 7**.

A similar experiment can be performed by using the acidified organic phase as the mobile phase. In this displacement elution mode the sharp retainer border is formed behind the solute zones, and the order of the elution for three solutes are reversed, forming a downward staircase pattern of the pH curve.

Distribution Equilibrium of Solute and Retainer Acid Within the Separation Column

Figure 8 shows the simplified distribution equilibrium of TFA (CF_3COOH) and solute S ($RCOOH$) between the stationary organic phase and the flowing aqueous phase on the assumption that the concentration of ionized components in the organic phase is negligible. The pH of the mobile phase in the solute zone (zone S) on the left-hand side of the sharp TFA border is given from the following three equations:

$$K_{D-s} = [RCOOH_{org}]/[RCOOH_{aq}] \quad [1]$$

$$K_s = [RCOOH_{org}]/([RCOOH_{aq}] + [RCOO^-_{aq}]) \quad [2]$$

$$K_{a-s} = [RCOO^-_{aq}] [H^+_{aq}]/[RCOOH_{aq}] \quad [3]$$

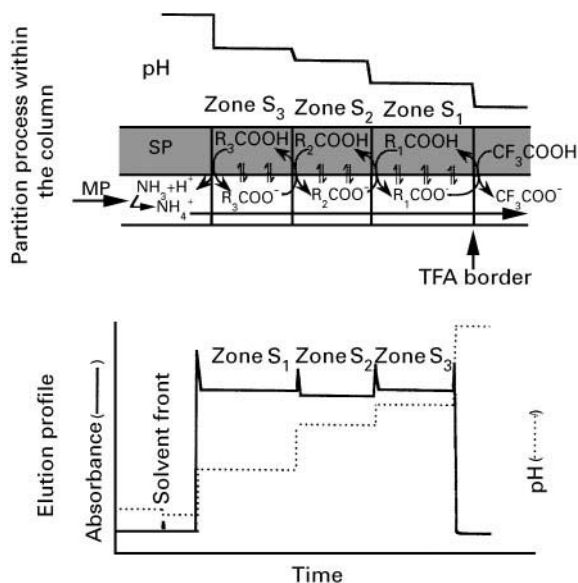


Figure 7 Model experiment for pH-zone-refining CCC for separation of carboxylic acids: partition process within the column and elution profile.

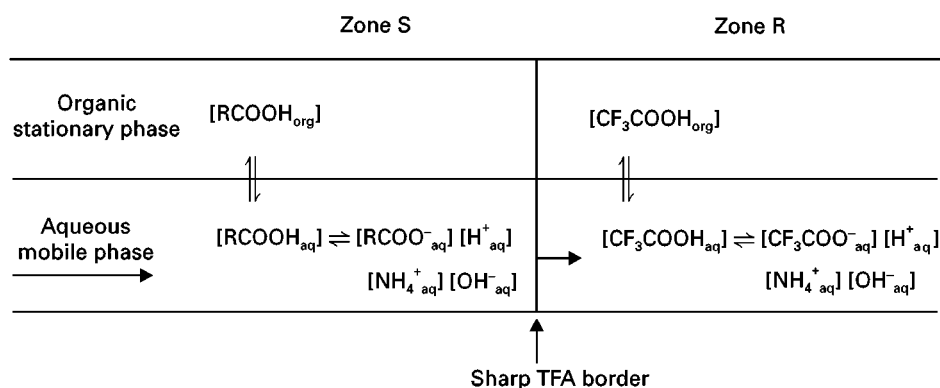


Figure 8 Distribution equilibrium of various species on both sides of the sharp TFA retainer border in the separation column.

where K_{D-s} is the partition ratio of solute S (RCOOH) and K_{D-s} , the dissociation constant of the solute. These equations reduce to

$$\text{pH}_{z-s} = \text{p}K_a + \log \left\{ (K_{D-s}/K_s) - 1 \right\} \quad [4]$$

where pH_{z-s} is pH of the mobile phase in the solute zone. As shown in the above equation, the pH of the solute zone is determined by the $\text{p}K_a$ and hydrophobicity (K_{D-s}) of the solute as well as its partition coefficient (K_s).

Figure 9 shows the relationship between the pH of the mobile phase and the solute partition coefficient (K) within the column (left) and the profile of pH-zones eluted (right). These curves may be drawn from eqn [4] by inserting the actual values of K_{D-s} and $\text{p}K_a$ for the solutes. If these parameters are not available, each curve can be obtained experimentally by dissolv-

ing various amounts of solute in the solvent system (containing the eluter base but no retainer acid), and measuring the pH of the lower aqueous phase and the solute concentration in both phases. Then the diagram can be constructed by plotting the pH on the ordinate against K (the solute concentration in the upper organic phase divided by that of the lower aqueous phase) on the abscissa. As described by the non-linear isotherm, K increases with increasing amounts of solute which causes a decrease in pH. In Figure 9 (left) five pH curves are arranged from the top to bottom in the order of decreasing $\text{p}K_a$ of the solutes where the lowest curve represents that of the retainer acid with the lowest $\text{p}K_a$. The vertical line drawn through the critical K value, called the operating line, intersects each pH curve and determines the pH level in the corresponding solute zone eluted as shown in the diagram on the right.

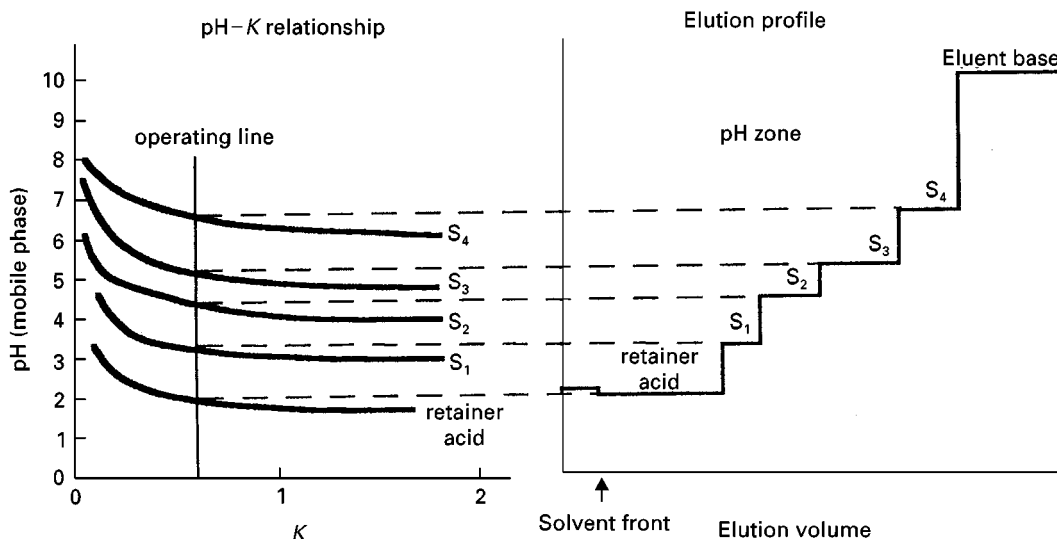


Figure 9 Relationship between pH/ K curves and eluted pH-zones.

This pH vs K diagram is useful for predicting the experimental results including the order of solute elution, the pH level of each solute zone, and the feasibility of the separation. A good separation is expected from a set of pH curves which show well-separated curves with even distributions.

pH-zone-refining CCC vs Displacement Chromatography on a Solid Support

As described earlier pH-zone-refining CCC closely resembles displacement chromatography in many aspects, including formation of highly concentrated rectangular peaks, concentration of minor components at the boundaries of the major peaks and isotachic movement (moving at the same rate) of all solute zones. However, an important difference between the two is that in pH-zone-refining CCC a retainer or an eluter agent transfers the analytes from the stationary phase to the mobile phase by either protonation or deprotonation, which changes the partition coefficient of the analytes. In displacement chromatography on a solid support, the displacer displaces analytes by transferring it from the solid support to the mobile phase. Another important difference between the two methods is the concentration of the analyte in the mobile phase. In displacement chromatography, concentration of the analyte is determined by its adsorption onto the solid support. Consequently, the earlier eluting analyte shows a lower concentration than the later eluting analytes. In pH-zone-refining CCC, on the other hand, the analyte concentration is mainly determined by the molar concentration of the counterion in the aqueous phase, and therefore all monovalent analytes are eluted at similar molar concentrations in the aqueous mobile phase. Similarities and differences between the two techniques are summarized in Table 1.

Application of pH-zone-refining CCC

The applications of pH-zone-refining CCC are presented here under two subheadings: standard and affinity separations. pH-zone-refining CCC separation is usually performed with a retainer agent in the stationary phase and an eluter agent in the mobile phase. However, the separation of certain groups of compounds requires an additional agent, a ligand, in the stationary phase. Such groups include enantiomers, highly polar analytes such as catecholamines and sulfonated dyes, and zwitterions such as amino acids and peptides. Samples, solvent systems and essential ingredients such as retainers, eluters and ligands used in various applications for the standard and affinity pH-zone-refining CCC techniques are summarized in Tables 2 and 3, respectively.

The following examples of pH-zone-refining-CCC separations have been performed using a HSCCC centrifuge equipped with a semi-analytical multilayer coil of 1.6 mm internal diameter having a total capacity of about 320 mL. In the conventional HSCCC technique the sample loading capacity of this column is limited to a few hundred milligrams.

Standard Separations

Amino acid derivatives Three chromatograms of DNP-amino acids shown in Figure 10 demonstrate the capability of pH-zone-refining CCC. All separations were performed with the same solvent system composed of methyl *t*-butyl ether–acetonitrile–water at a volume ratio of 4 : 1 : 5 where a 200 μ L quantity of TFA (retainer acid) was added to the sample solution, and 0.1% v/v aqueous ammonia (28%) (eluter base) to the aqueous mobile phase to raise the pH to 10.5.

The top chromatogram was obtained from 6 mg of the sample mixture consisting of six different

Table 1 Comparison between pH-zone-refining CCC and displacement chromatography

	pH-zone-refining CCC		Displacement chromatography using solid support
	Standard mode	Displacement mode	
Key reagents	Retainer	Eluter	Displacer
Solute transfer (phase)	Mobile \rightarrow Stationary	Stationary \rightarrow Mobile	Stationary \rightarrow Mobile
Action location	Front of solute bands	Back of solute bands	Back of solute bands
Formation of solute bands	A train of individual solute bands with minimum overlapping		
Travelling rate of solute bands	All solute bands move together at the same rate as that of the key reagent.		
K^* in solute bands	Same as and determined by that of the key reagent for all solutes		
Impurities	Concentrated at the boundaries of the solute bands		
Peak profile	A train of rectangular peaks associated with sharp impurity peaks at their boundaries		
Solute concentration in mobile phase is determined by	Concentration of counterions in aqueous phase		Solute affinity to stationary phase
Elution order is determined by	Solute pK_a and hydrophobicity		Solute affinity to stationary phase

* K is the partition coefficient expressed by solute concentration in the stationary phase divided by that in the mobile phase.

Table 2 Samples and solvent systems applied to standard pH-zone-refining CCC

Sample*	Solvent systems (volume ratio) [†]	A pair of acid/base reagents [‡]	
		Retainer	Eluter
DNP-amino acids (up to 1 g)	MBE/AcN/H ₂ O (4 : 1 : 5)	TFA (200 μ L/SS)	NH ₃ (0.1%/MP)
	MBE/AcN/H ₂ O (4 : 1 : 5)	TFA (0.04%/SP)	NH ₃ (0.1%/MP)
	MBE/AcN/H ₂ O (4 : 1 : 5)	TFA, spacer acids (each 0.04%/SP)	NH ₃ (0.1%/MP)
	MBE/H ₂ O (DPCCC)	NH ₃ (22 mM/SP)	TFA (10.8 mM/MP)
	MBE/H ₂ O (DPCCC)	NH ₃ (44 mM/SP)	TFA (10.8 mM/MP)
	MBE/H ₂ O (DPCCC)	NH ₃ (22 mM/SP)	TFA (10.8 mM/MP) (Spacer acids/MP or SS)
Proline (OBzl) (1 g)	MBE/H ₂ O	TEA (10 mM/SP)	HCl (10 mM/MP)
Amino acid (OBzl) (0.7 g)	MBE/H ₂ O	TEA (10 mM/SP)	HCl (10 mM/MP)
Amino acid (OBzl) (10 g)	MBE/H ₂ O	TEA (5 mM/SP)	HCl (20 mM/MP)
CBZ-dipeptides (0.8 g)	MBE/AcN/H ₂ O (2 : 2 : 3)	TFA (16 mM/SP)	NH ₃ (5.5 mM/MP)
CBZ-dipeptides (3 g)	MBE/AcN/H ₂ O (2 : 2 : 3)	TFA (16 mM/SP)	NH ₃ (5.5 mM/MP)
CBZ-tripeptides (0.8 g)	BuOH/MBE/AcN/H ₂ O (2 : 2 : 1 : 5)	TFA (16 mM/SP)	NH ₃ (2.7 mM/MP)
Dipetide- β NA (0.3 g)	MBE/AcN/H ₂ O (2 : 2 : 3)	TEA (5 mM/SP)	HCl (5 mM/MP)
Indole auxins (1.6 g)	MBE/H ₂ O	TFA (0.04%/SP)	NH ₃ (0.1%/MP)
TCF (0.01–1 g)	DEE/AcN/10 mM AcONH ₄ (4 : 1 : 5)	TFA (200 μ L/SS)	MP
Red #3 (0.5 g)	DEE/AcN/10 mM AcONH ₄ (4 : 1 : 5)	TFA (200 μ L/SS)	MP
Orange #5 (0.01–5 g)	DEE/AcN/10 mM AcONH ₄ (4 : 1 : 5)	TFA (200 μ L/SS)	MP
Orange #10 (0.35 g)	DEE/AcN/10 mM AcONH ₄ (4 : 1 : 5)	TFA (200 μ L/SS)	MP
Red #28 (0.1–6 g)	DEE/AcN/10 mM AcONH ₄ (4 : 1 : 5)	TFA (200 μ L/SS)	MP
Eosin YS (0.3 g)	DEE/AcN/10 mM AcONH ₄ (4 : 1 : 5)	TFA (200 μ L/SS)	MP
Amaryllis alkaloids (3 g)	MBE/H ₂ O	TEA (5 mM/SP)	HCl (5 mM/MP)
	MBE/H ₂ O (DPCCC)	HCl (10 mM/SP)	TEA (10 mM/MP)
Vinca alkaloids (0.3 g)	MBE/H ₂ O (DPCCC)	HCl (5 mM/SP)	TEA (5 mM/MP)
Structural isomers (15 g)	MBE/AcN/H ₂ O (4 : 1 : 5)	TFA (0.32%/SP)	NH ₃ (0.8%/MP)
Stereoisomers (0.4 g)	Hex/EtOAc/MeOH/H ₂ O (1 : 1 : 1 : 1)	TFA, octanoic acid (each 0.04%/SP)	NH ₃ (0.025%/MP)
Fish oil (0.5 g)	Hex/EtOH/H ₂ O (4 : 1 : 5)	TFA (10 mM/SP)	NH ₃ (0.1%/MP)

*DNP: dinitrophenyl; CBZ: carbobenzoxy; OBzl: benzyl esters; β NA: naphthyl amide; TCF: tetrachlorofluorescein; amaryllis alkaloids: crinine, powelline and crinamine; vinca alkaloids: vincamine and vincine; structural isomers: 2- and 6-nitro-3-acetamido-4-chlorobenzoic acid; Stereoisomers: 4-methoxymethyl-1-methyl-cyclohexane carboxylic acid; fish oil: mixture of docosahexaenoic acid and eicosapentaenoic acid.

[†]The upper organic phase was used as the stationary phase (SP) and the lower aqueous phase, the mobile phase (MP) except in DPCCC where the above relationship is reversed. MBE: methyl-*t*-butyl ether; AcN: acetonitrile; BuOH: *n*-butanol; Hex: hexane; EtOAc: ethyl acetate; MeOH: methanol; AcONH₄: ammonium acetate; DEE: diethyl ether; DPCCC: displacement mode.

[‡]TFA: trifluoroacetic acid; AcOH: acetic acid; SP: in stationary phase; MP: in mobile phase; SS: in sample solution; TEA: triethylamine.

DNP-amino acids. All components were eluted together as a sharp single peak without any visible evidence of separation. When the sample size was increased 100 times, i.e. from 6 to 600 mg, the ultra-violet (UV) trace at 206 nm produced a highly concentrated rectangular peak which was divided into six flat pH-zones (dotted line) as shown in the middle chromatogram. The partition coefficient of fractions measured with a standard solvent system composed of chloroform–acetic acid–0.1 M HCl revealed that each pH-zone corresponds to one species as indicated in the chromatogram. The bottom chromatogram illustrates the separation of 500 mg each of DNP-glutamic acid and DNP-valine under similar conditions. Each component formed a long plateau associated with its specific pH where the length of each

plateau increased in proportion to the applied sample size. A sharp transition between the two plateaus indicates minimum overlap between the two peaks. A gradual decline of pH curves in both pH-zones was apparently caused by a steady increase of the travelling rate of the retainer acid border and the following solute zones through the column, since the retainer acid was added exclusively to the sample solution.

pH-Zone-refining CCC can be equally well applied to the separation of basic compounds using a retainer base such as triethylamine and an eluter acid such as hydrochloric acid. This was first demonstrated by the separation of amino acid benzyl esters. **Figure 11** shows a chromatogram of a set of amino acid benzyl esters using a two-phase solvent system composed of methyl *t*-butyl ether and water where triethylamine

Table 3 Samples and solvent systems applied to affinity pH-zone-refining CCC

Sample*	Solvent systems† (volume ratio)	A set of key reagents‡		
		Retainer	Eluter	Ligand
(±)-DNB-leucine (2 g)	MBE/H ₂ O	TFA (40 mM/SP)	NH ₃ (20 mM/MP)	DPA (40 mM/SP)
(±)-DNB-valine (2 g)	MBE/H ₂ O	TFA (40 mM/SP)	NH ₃ (20 mM/MP)	DPA (40 mM/SP)
Catecholamines (3 g)	MBE/H ₂ O	NH ₄ OAc (200 mM/SP)	HCl (50 mM/MP)	DEHPA (20%/SP)
Dipeptides (1 g)	MBE/AcN/50 mM HCl (4 : 1 : 5) (SP)	TEA (20 mM/SP)		DEHPA (10%/SP)
Dipeptides (1 g)	MBE/AcN/H ₂ O (4 : 1 : 5) (MP)		HCl (20 mM/MP)	
	MBE/BuOH/AcN/50 mM HCl (2 : 2 : 1 : 5) (SP)	TEA (20 mM/SP)		DEHPA (30%/SP)
	MBE/BuOH/AcN/H ₂ O (2 : 2 : 1 : 5) (MP)		HCl (20 mM/MP)	
Bacitracins (5 g)	MBE/50 mM HCl (1 : 1) (SP)	TEA (40 mM/SP)		DEHPA (10%/SP)
	MBE/H ₂ O (MP)		HCl (20 mM/MP)	
FD&C Yellow No. 6 (2 g)	MBE/AcN/H ₂ O (2 : 2 : 3)	H ₂ SO ₄ (0.2%/SP)	NH ₃ (0.4%/MP)	TDA (5%/SP)

*DNB: dinitrobenzoyl.

†MBE: methyl *t*-butyl ether; AcN: acetonitrile; BuOH: *n*-butanol.‡TFA: trifluoroacetic acid; NH₄OAc: ammonium acetate; TEA: triethylamine; DPA: N-dodecanoyl-L-proline-3,5-dimethylanilide; DEHPA: di-(2-ethylhexyl) phosphoric acid; TDA: tridodecylamine; SP: organic stationary phase; MP: aqueous mobile phase.

(10 mM) was added to the organic stationary phase and hydrochloric acid (10 mM) to the aqueous mobile phase. Seven components were well resolved in 3 h.

The preparative separations of three amino acid benzyl esters are shown in **Figure 12** where three sample sizes of 0.6 g (A), 3 g (B) and 6 g (C) were separated with the same solvent system composed of methyl *t*-butyl ether–water, where 5 mM triethylamine was added to the organic stationary phase and 20 mM HCl to the aqueous mobile phase. Comparison of these three chromatograms clearly shows that the increase of the sample size results in a proportional increase of the peak width whereas the width of the mixing zones remains the same as indicated by the sharp transition of the standard *K* values between the peaks (*x*-line). This again demonstrates the great potential of the technique for preparative-scale separations.

Peptide derivatives Peptides can be fractionated easily by pH-zone-refining CCC in a manner similar to that for the amino acid derivatives described above, if either amino or carboxylic terminal is blocked. **Figure 13** shows separations of a set of Z or CBZ (carbobenzoyloxy)-dipeptides by pH-zone-refining CCC using a two-phase solvent system composed of methyl *t*-butyl ether–acetonitrile–water (2 : 2 : 3, v/v) with 16 mM TFA in the organic stationary phase and 5.5 mM ammonia in the aqueous mobile phase. Eight components, each 100 mg, were well resolved within 4 h. A gram-quantity separation of three components, Z-gly-gly, Z-gly-ala and Z-gly-leu, was also successfully performed with a similar solvent system.

Alkaloids Many alkaloids may be effectively separated by pH-zone-refining CCC using triethylamine in the organic phase and HCl in the aqueous phase. **Figure 14** shows chromatograms of alkaloids from a crude amaryllis extract. The separation was performed with a two-phase solvent system composed of methyl *t*-butyl ether–water. The upper chromatogram was obtained by eluting with an aqueous phase and the lower chromatogram by eluting with an organic phase (displacement mode). In both elution modes three components were well resolved. The sample size was 3 g in each separation. Elution with the organic phase yields a free base in an organic solvent which is easily evaporated. For unstable alkaloids, aqueous phase elution may be preferred because the sample is collected in the salt form that is often more stable.

Figure 15 shows a chromatogram obtained from a crude extract of *Vinca minor* by the displacement mode of pH-zone-refining CCC. Two major components, vincine and vincamine, were separated and each eluted as a free base in about 2 h. Irregularity of the pH curve was caused by instability of the pH reading obtained from the organic mobile phase.

Miscellaneous separations The method can be very useful for purification of structural isomers from a crude synthetic reaction. **Figure 16** shows a separation of 2- and 6-nitro-4-chloro-3-methoxybenzoic acids by pH-zone-refining CCC. An 11.7 g amount of the crude reaction mixture was resolved into two peaks in 3 h, the 6-nitro isomer (3.1 g) and 2-nitro isomer (5.9 g) with a mixing zone (0.7 g). One of the

pH-zone refining CCC of DNP amino acids

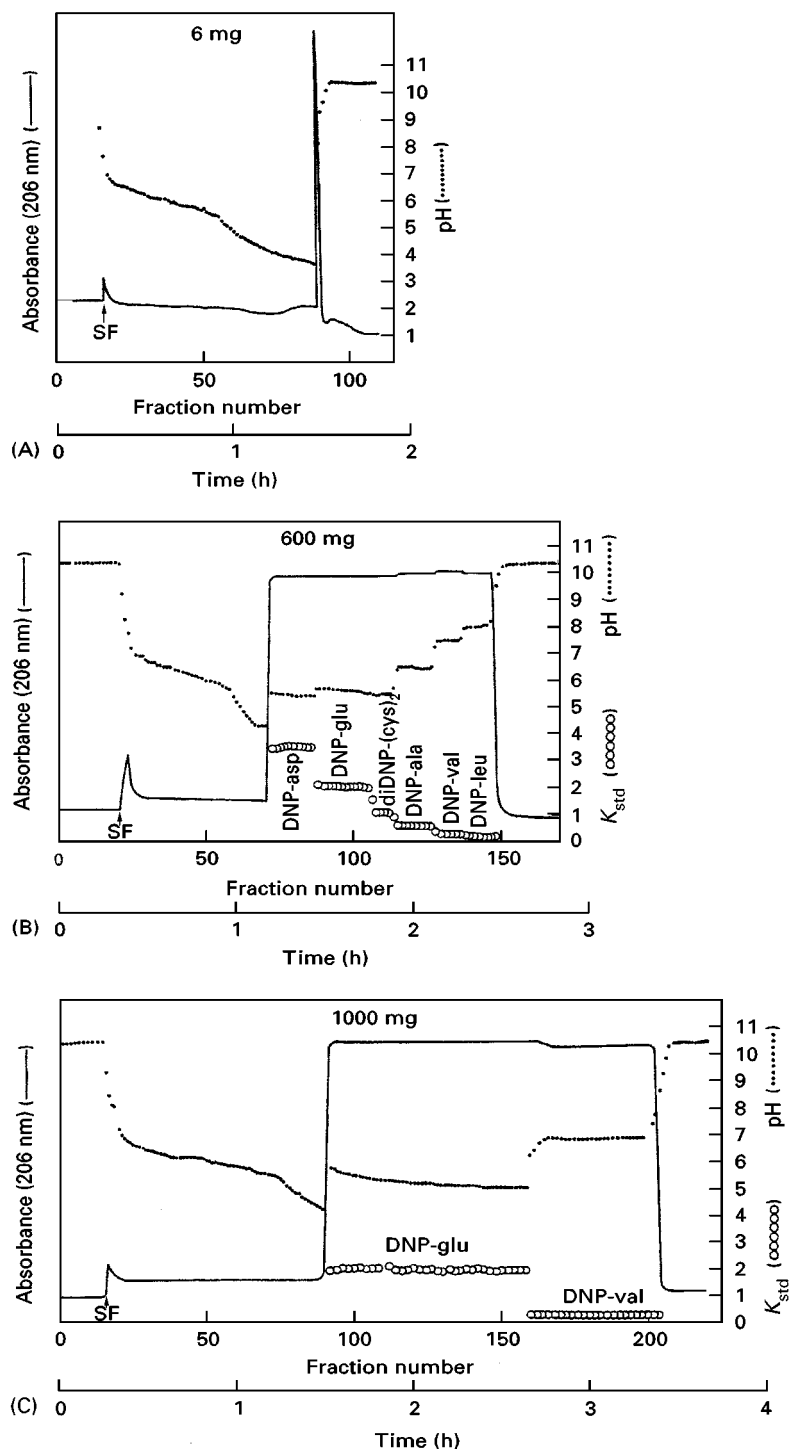


Figure 10 Chromatogram of DNP-amino acids. Top: separation of a small amount (6 mg) of six different DNP-amino acids. Middle: separation of large amounts (600 mg) of the above six DNP-amino acids. Bottom: separation of large quantities of DNP-L-glutamic acid and DNP-L-valine (500 mg of each). SF = solvent front. Solvent system: methyl *t*-butyl ether–acetonitrile–water (4 : 1 : 5) where 0.1% aqueous NH_3 (approximately 14 mM) was added to the aqueous mobile phase (pH 10.5) and 200 μL TFA was added to the sample solution; flow-rate: 3 mL min^{-1} ; detection: 206 nm; revolution: 800 rpm.

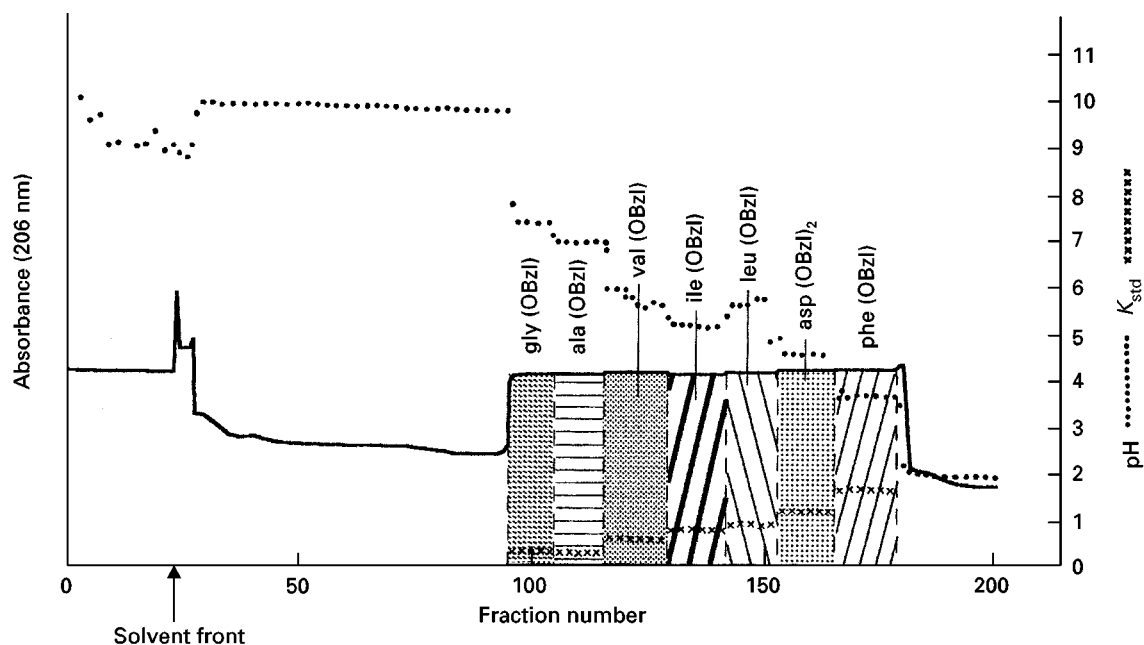


Figure 11 Separation of seven amino acid benzyl esters by pH-zone-refining CCC. Solvent system: methyl *t*-butyl ether/water, 10 mM triethylamine in upper organic stationary phase and 10 mM hydrochloric acid in lower aqueous phase; sample: a mixture of seven amino acid benzyl esters as indicated in the chromatogram, 100 mg each dissolved in 20 mL solvent; flow-rate: 3 mL min⁻¹; detection: 206 nm; revolution: 800 rpm; retention of stationary phase: 71.2%.

advantages of pH-zone-refining CCC is that compounds with no chromophore can be conveniently monitored by pH alone: the fractions of major components are located in their flat pH-zones and those of minor components at their boundaries, since in accord with eqn [4] they are unlikely to have identical or compensating pK_a and hydrophobicity. This potential is demonstrated in the separation of the stereoisomers of 1-methyl-4-methoxymethylcyclohexane carboxylic acid, using octanoic acid as a spacer. As shown in Figure 17, the two isomers were eluted after the octanoic acid each forming a pH-zone with a relatively narrow mixing zone. The collected fractions were analysed by gas chromatography-mass spectrometry (GC-MS) of their esters as indicated in the upper part of the figure.

The pH-zone-refining CCC separations of hydroxyxanthene dyes and sulfonated dyes are described under separation of dyes (high-speed countercurrent chromatography).

Affinity Separations

Enantiomers In CCC, which uses no solid support in the column, the chiral selector is simply dissolved in the liquid stationary phase to carry out the separation by either conventional or pH-zone-refining CCC.

The chromatogram in Figure 18 was obtained from 2 g of a DNB-leucine racemate using an affinity

ligand, *N*-dodecanoyl-L-proline-3,5-dimethylanilide (DPA) in the stationary phase. The racemic mixture was resolved in highly concentrated rectangular peaks with minimum overlap. The fractions were analysed by analytical CCC as indicated in the diagram, using the same chiral selector, and also with CD and optical rotation instruments. This technique should be very useful in the pharmaceutical industry where an ever-increasing number of drugs are now required to be produced in chirally pure forms.

Catecholamines Catecholamines containing two or more hydroxyl groups strongly favour partition into the aqueous phase even in a polar butanol two-phase solvent system. However, the use of a ligand such as di(2-ethylhexyl)phosphoric acid (DEHPA) in the organic stationary phase radically improves their partition behaviour so that pH-zone-refining CCC of a mixture of 100 mg each of four polar catecholamines and two related compounds using the above ligand in the stationary phase can be well resolved in 3 h.

Peptides For pH-zone-refining CCC of free peptides a series of experiments was performed using DEHPA as a ligand in the stationary phase. A set of three dipeptides with a broad range in hydrophobicity was separated with a solvent system composed of methyl *t*-butyl ether, acetonitrile and water at a volume ratio

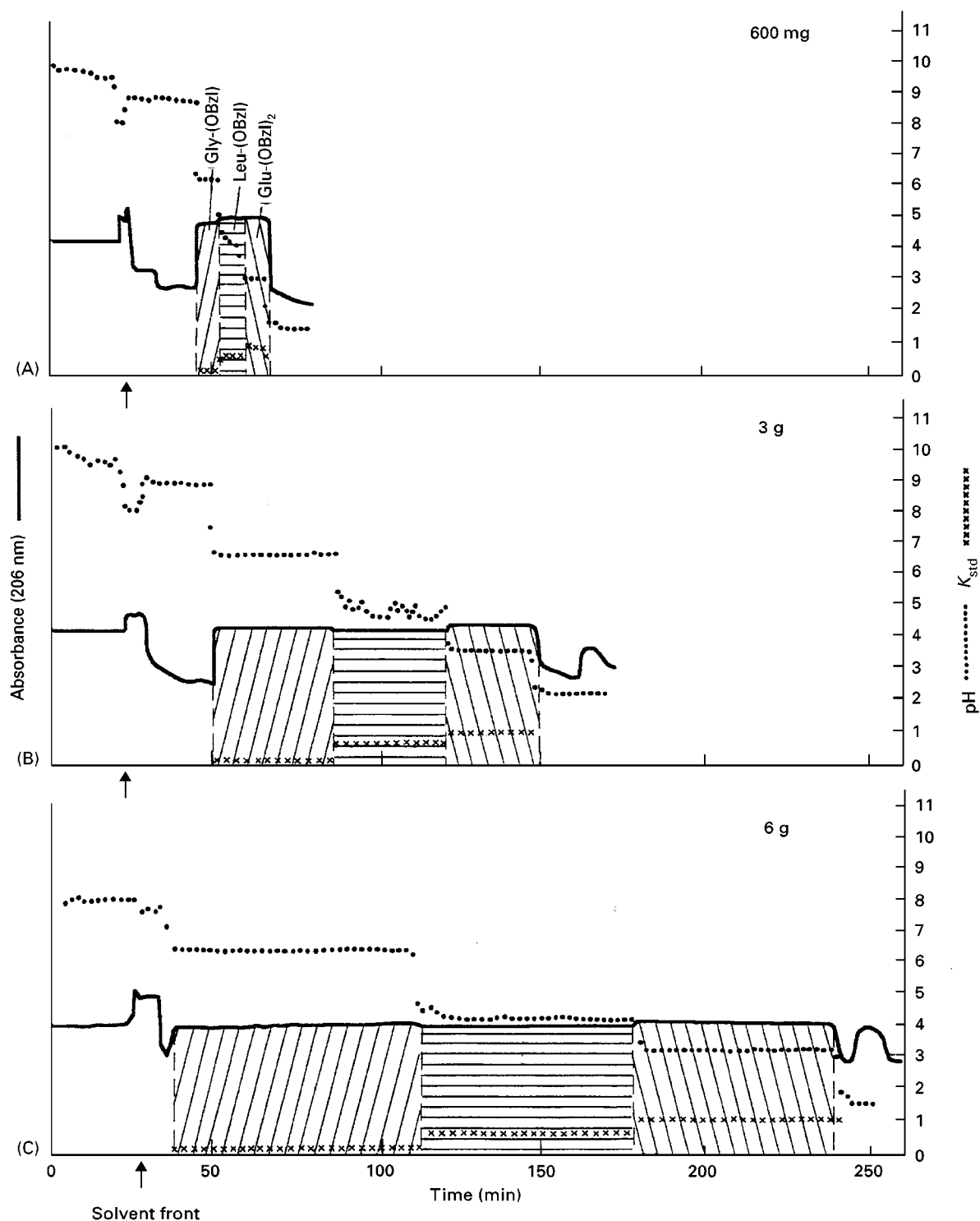


Figure 12 Separation of three amino acid benzyl esters by pH-zone-refining CCC. Solvent system: methyl *t*-butyl ether/water, 5 mM triethylamine in organic stationary phase and 20 mM hydrochloric acid in aqueous mobile phase; sample: gly(OBzl)·Tos, leu(OBzl)·Tos and glu(OBzl)·Tos, each 0.2 g (A), 1 g (B) and 2 g (C); flow-rate: 3 mL min⁻¹; detection 206 nm; revolution: 800 rpm; retention of stationary phase: 76.5% (A), 63.3% (B) and 77.8% (C).

of 4 : 1 : 5 where triethylamine and various amount of the ligand were added to the organic stationary phase and HCl to the aqueous mobile phase. The

results are shown in the left three chromatograms in **Figure 19**. At a 10% ligand concentration, the second and third peaks were fused together while the polar

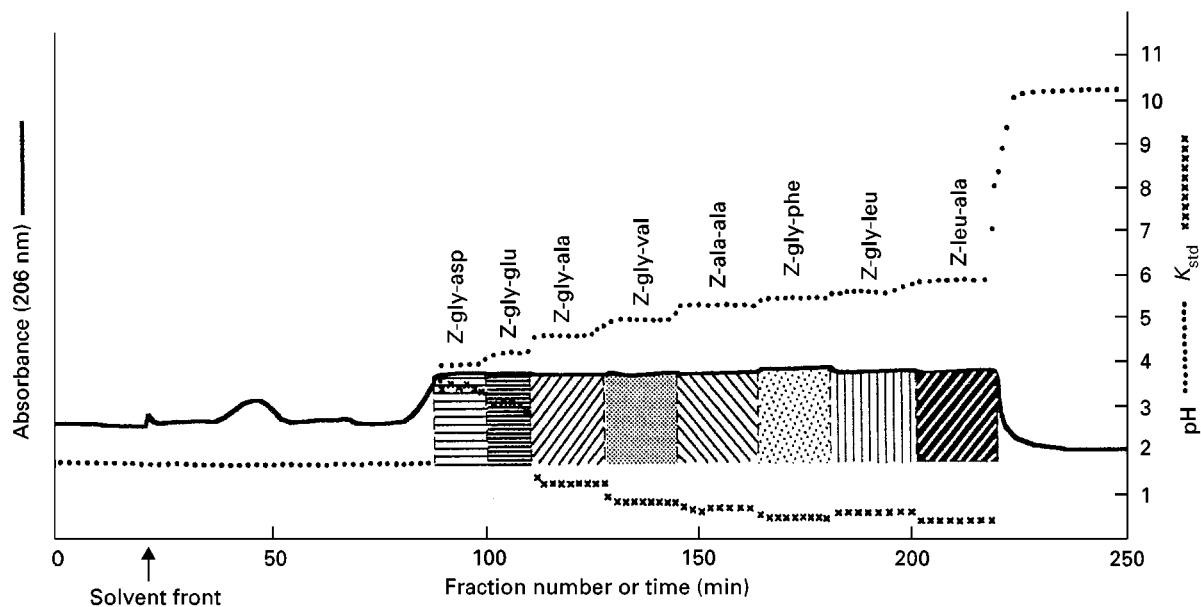


Figure 13 Separation of eight CBZ(Z)-dipeptides by pH-zone-refining CCC. Solvent system: methyl *t*-butyl ether–acetonitrile–water (2 : 2 : 3, v/v), 16 mM TFA in organic stationary phase (pH 1.83) and 5.5 mM NH_3 in aqueous mobile phase (pH 10.62); sample: eight CBZ-dipeptides as indicated in the chromatogram, each 100 mg dissolved in 50 mL solvent (25 mL each phase); flow-rate: 3.3 mL min^{-1} in the head-to-tail elution mode; detection: 206 nm; revolution: 800 rpm (first 66 mL eluted at 600 rpm to prevent the carryover of the stationary phase); stationary phase retention: 65.1%.

tyrosyl-glycine peak was eluted earlier. Increasing the ligand concentration to 20–30% resulted in fusion of the first and second peaks while the hydrophobic tyrosyl-leucine peak was isolated and eluted much

later. Increasing the polarity of the solvent system by modifying the phase composition improved the sharpness of the fused first and second peaks as shown in the right-hand chromatogram. The results

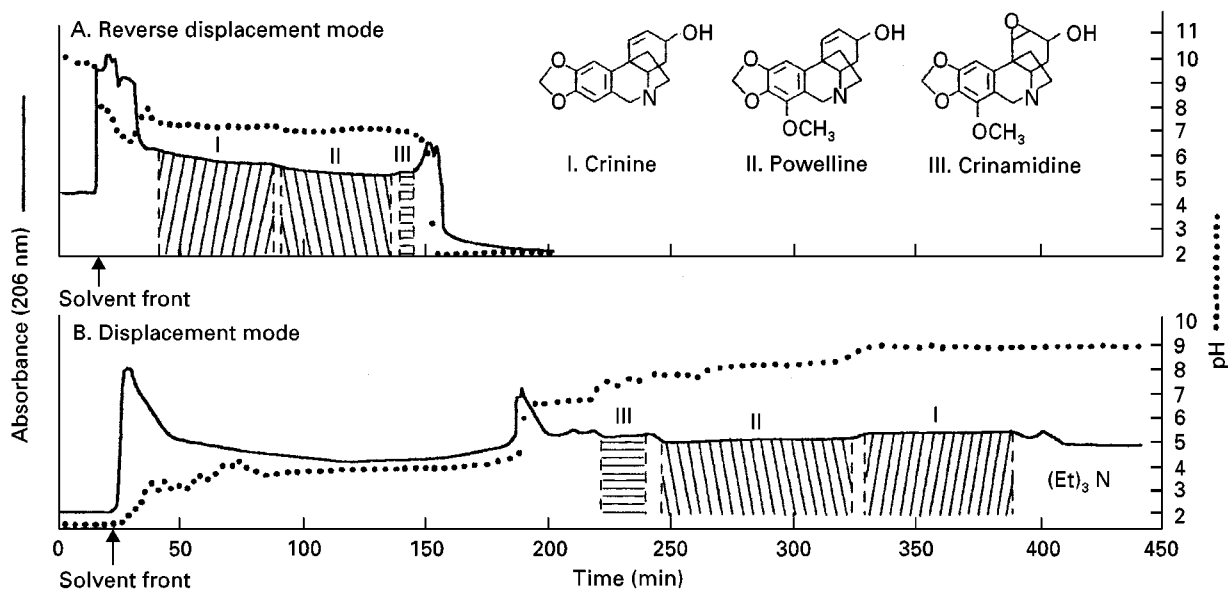


Figure 14 Chromatograms of crude alkaloid extract of solvent *Crinum moorei* obtained by standard mode (A) and displacement mode (B) of pH-zone-refining CCC. Solvent system: methyl *t*-butyl ether/water; stationary phase: (A) organic phase (5 mM triethylamine) and (B) aqueous phase (10 mM HCl); mobile phase: (A) aqueous phase (5 mM HCl) and (B) organic phase (10 mM triethylamine); flow-rate: 3.3 mL min^{-1} ; sample: crude alkaloid extract of *Crinum moorei*, 3 g dissolved in 30 mL of each phase; detection: 206 nm; revolution: (A) 800 rpm (600 rpm until 66 mL of mobile phase was eluted) and (B) 600 rpm throughout.

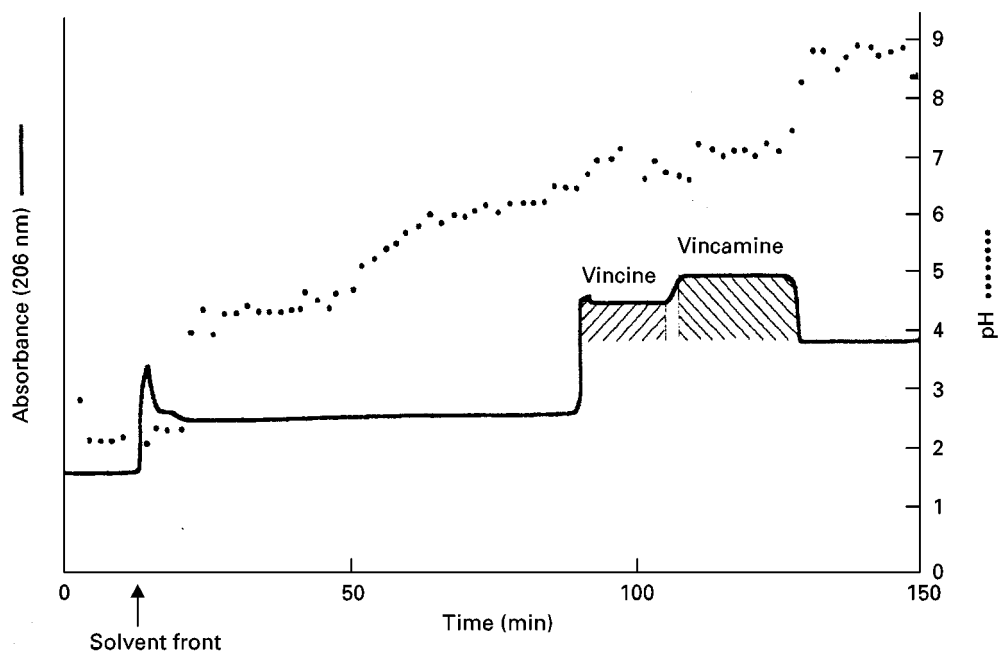


Figure 15 Separation of alkaloids from *Vinca minor* by pH-zone-refining CCC using displacement mode. Solvent system: methyl *t*-butyl ether/water, 5 mM triethylamine in organic mobile phase and 5 mM HCl in aqueous stationary phase; flow-rate: 3.3 mL min^{-1} in tail-to-head elution mode; sample: crude alkaloid extract of *Vinca minor*, 300 mg dissolved in 30 mL of solvent system (equal volumes of each phase); detection: 206 nm; revolution: 800 rpm; retention of stationary phase: 90.4%.

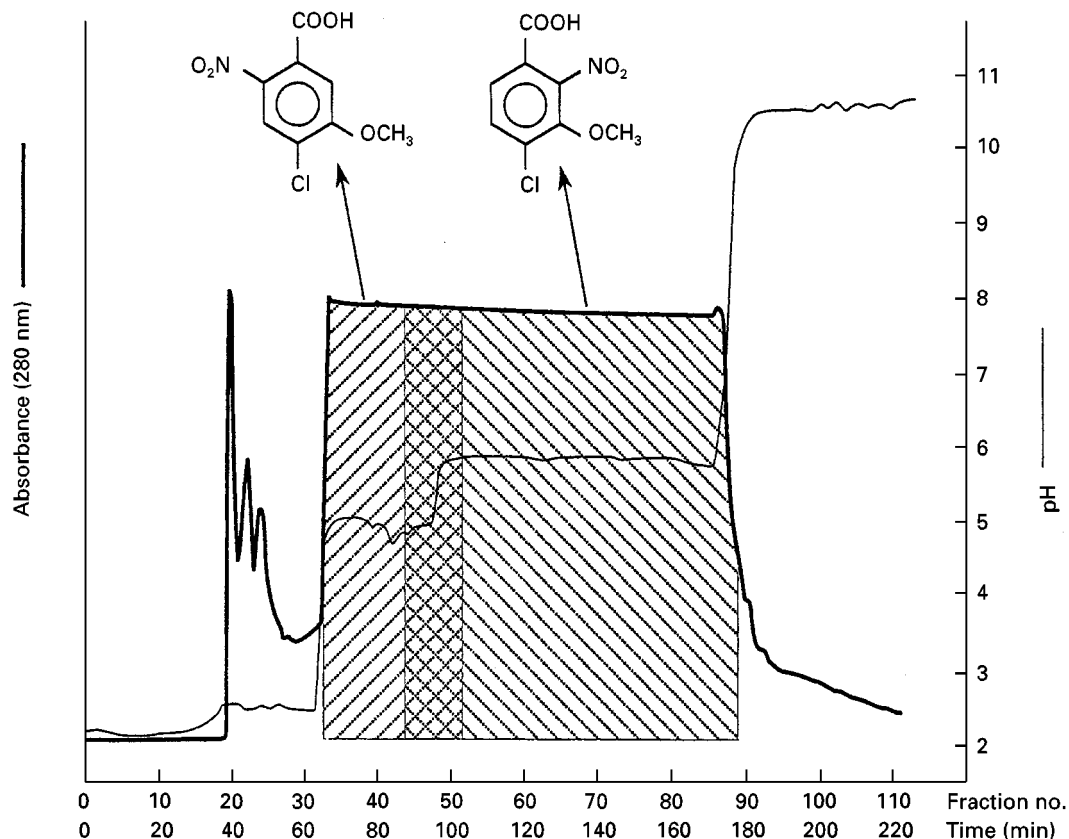


Figure 16 Separation of crude reaction mixture of 2- and 6-nitro-4-chloro-3-methoxybenzoic acids by pH-zone-refining CCC. Solvent system: methyl *t*-butyl ether-acetonitrile-water (4 : 1 : 5), TFA was added to the upper organic stationary phase at 0.3% (12 mM, pH 2.2) and ammonia 0.8% (100 mM, pH 10.6) to the lower aqueous mobile phase; sample: crude reaction mixture (11.7 g) of two isomers indicated in the figure; flow-rate: 3 mL min^{-1} ; detection: 280 nm; revolution: 800 rpm.

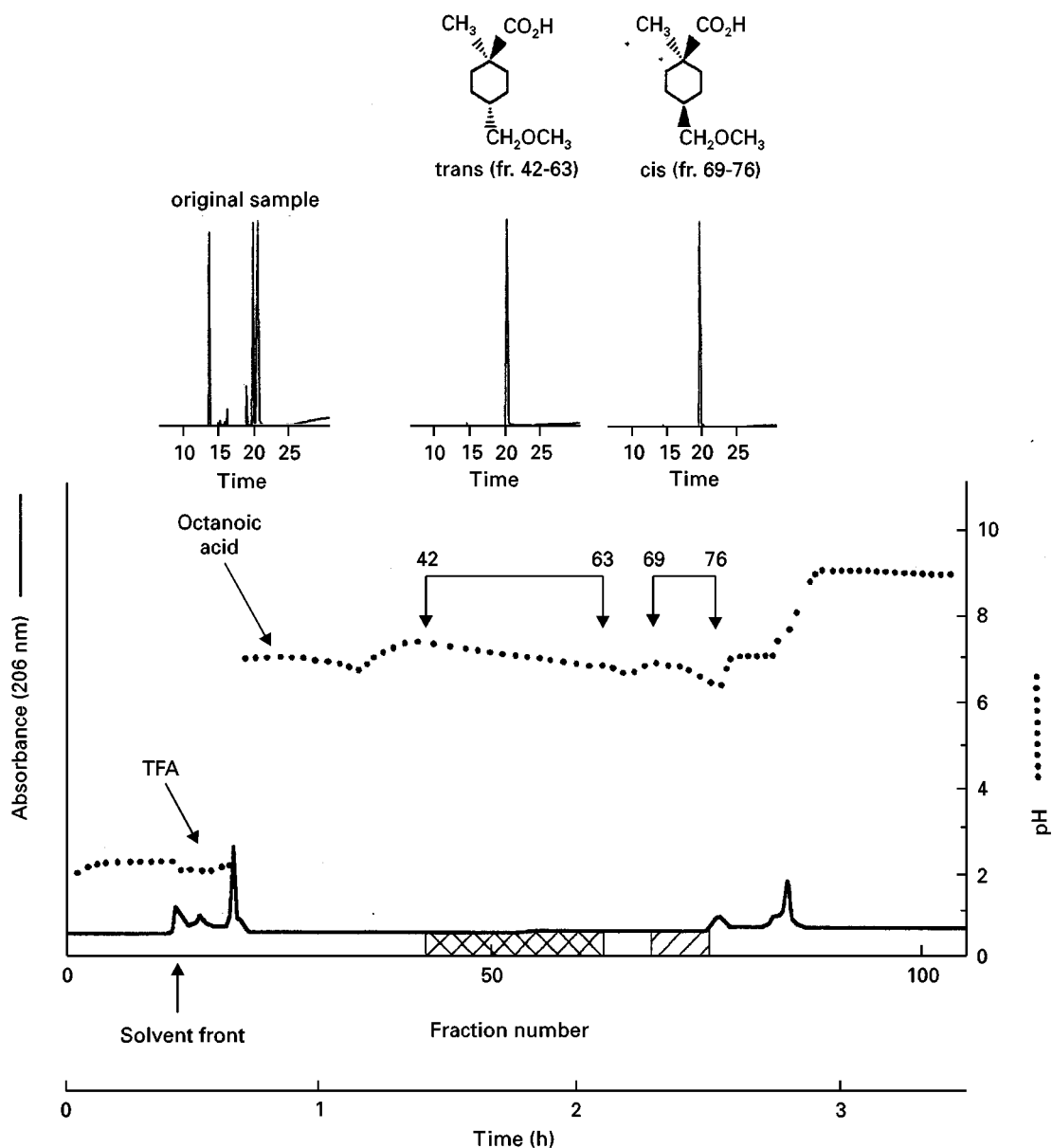


Figure 17 Separation of *trans*- and *cis*-stereoisomers of 1-methyl-4-methoxymethylcyclohexanecarboxylic acid by pH-zone-refining CCC using octanoic acid as a spacer. Solvent system: methyl *t*-butyl ether–acetonitrile–water (4 : 1 : 5), 0.32% TFA in organic stationary phase (pH 1.74), and 0.8% aqueous ammonia in aqueous mobile phase (pH 11.2); flow-rate: 3 mL min⁻¹ in head-to-tail elution mode; sample: crude nitration product of 3-acetamido-4-chlorobenzoic acid (15 g) dissolved in 100 mL in equal volumes of each phase and the pH adjusted to 8.7 with aqueous ammonia; detection: 206 nm; revolution: 800 rpm (600 rpm until 66 mL of mobile phase was eluted). In analysis of fractions by GC/MS as indicated above the main chromatogram, the acids were converted to their methylesters for chromatographic purposes.

of these preliminary studies indicated that both ligand concentration and solvent composition should be adjusted according the hydrophobicity of the peptides. Under optimized conditions, pH-zone-refining CCC of dipeptides was successful. As shown in **Figure 20**, both polar and non-polar groups of dipeptides, each consisting of two isomeric pairs, were well resolved in 3–4 h.

Five grams of bacitracin complex consisting of multiple components were subjected to pH-zone-refining CCC under optimized conditions similar to those applied to the hydrophobic dipeptides (**Figure 21**). The UV trace at 280 nm showed multiple peaks while the pH-curve yielded flat zones at around pH 2. As indicated by HPLC analysis, two major components, bacitracins A and F, were isolated.

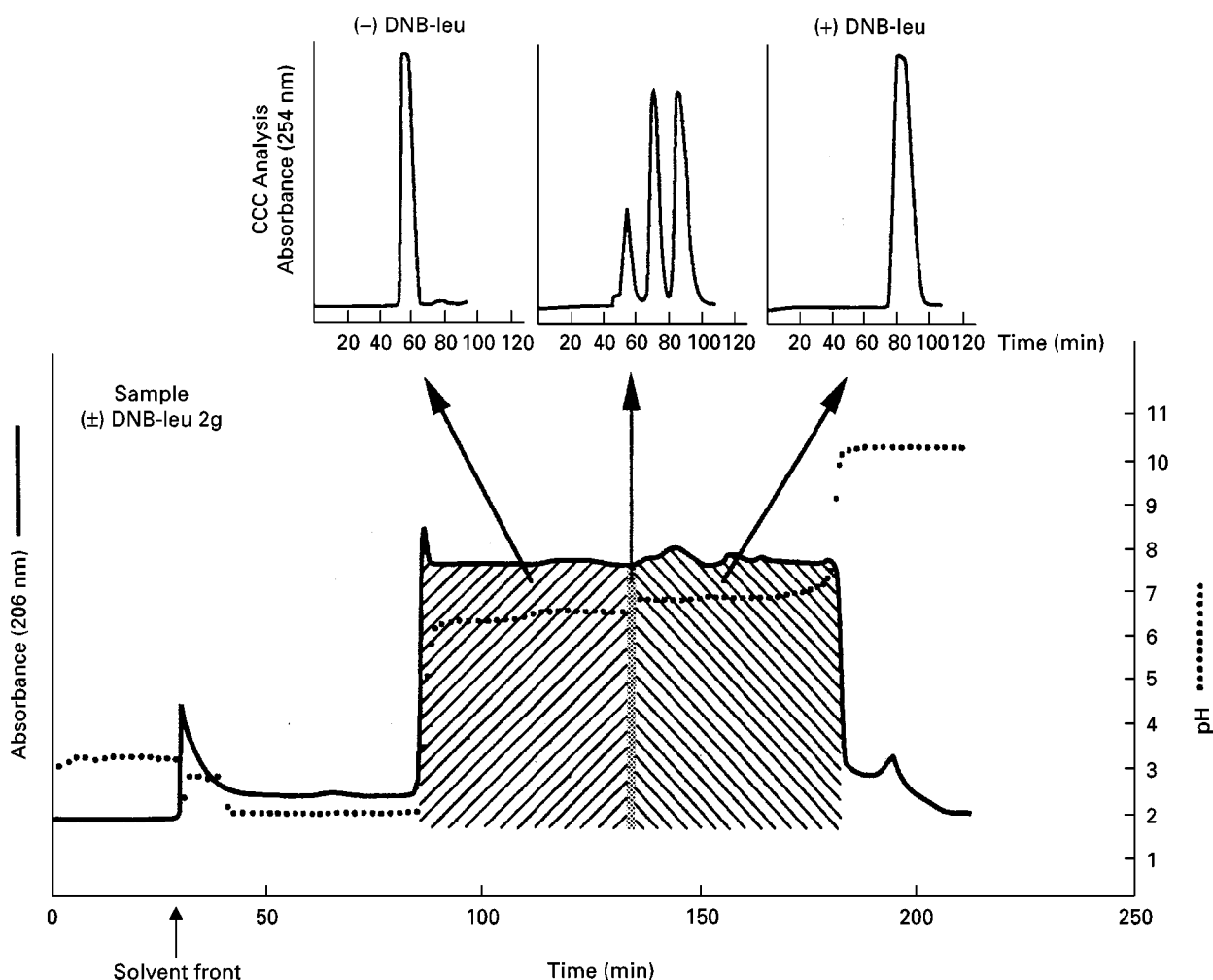


Figure 18 Chiral separation of (±)-DNB-leucine by pH-zone-refining CCC using DPA as a ligand. CCC conditions: solvent system: methyl *t*-butyl ether/water, TFA (40 mM) + ligand DPA (40 mM) in organic stationary phase and ammonia (20 mM) in aqueous mobile phase; sample: (±)-DNB-leucine 2 g; flow-rate: 3 mL min⁻¹ in head-to-tail elution mode; detection: 206 nm; revolution: 800 rpm. Analytical CCC was carried out with the same column using the conventional HSCCC technique under the following conditions: solvent system: hexane-ethyl acetate-methanol-10 mM HCl (8 : 2 : 5 : 5), organic stationary phase containing DPA (20 mM); flow-rate: 3 mL min⁻¹ in head-to-tail elution mode; detection: 254 nm; revolution: 800 rpm.

Detailed technical guidance for performing pH-zone-refining CCC including the choice of two-phase solvent systems, the preparation of sample solution, separation procedures, and so on has been given in the literature.

Advantages of pH-zone-refining CCC

The applications described here demonstrate the advantages of the pH-zone-refining CCC method over the conventional HSCCC technique as well as over many other commonly employed chromatographic procedures. These include:

1. Sample loading capacity is increased over 10 times for a given column.
2. Fractions are highly concentrated.
3. Increase in sample size produces a higher percentage of pure fractions.
4. Minor components are concentrated and detected at the boundaries of the major peaks.
5. Sample with no chromophore can be effectively monitored by pH.

On the other hand, pH-zone-refining CCC has the following limitations: the analytes must be ionizable and, if they have similar hydrophobicities, their pK_a s should differ by 0.2 or greater. In addition, the sample size should be at least 0.1 mmol and preferably more, for each species, so it is not applicable to trace quantities. This limitation could be overcome if the column diameter were able to be sufficiently

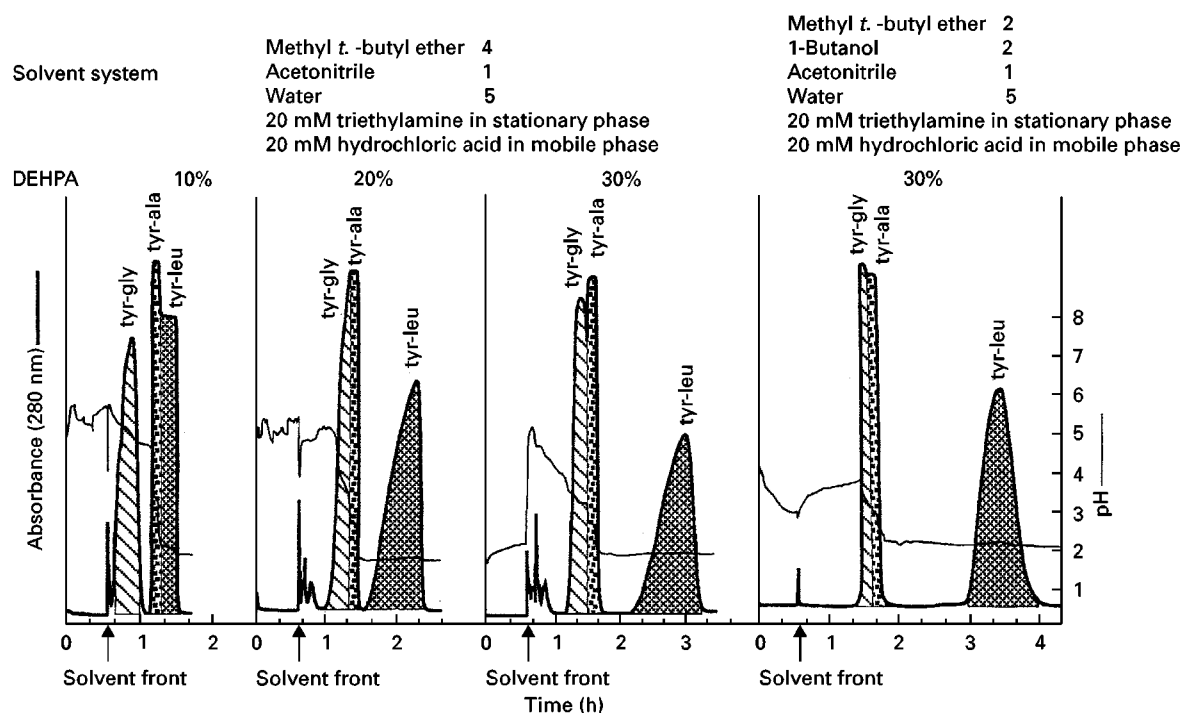


Figure 19 Separation of 3 dipeptides by pH-zone-refining CCC using DEHPA in the stationary phase. Sample: three dipeptides indicated in the chromatogram, each 100 mg; flow-rate: 3 mL min^{-1} in head-to-tail elution mode; detection: 280 nm; revolution: 800 rpm.

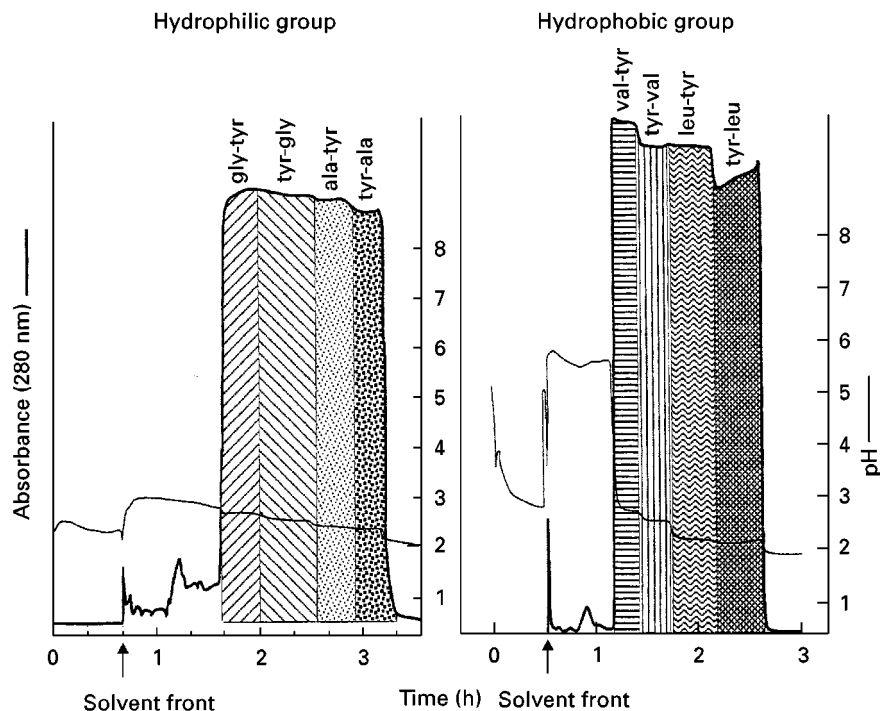


Figure 20 Separation of dipeptides by pH-zone-refining CCC. Hydrophobic (right) and hydrophilic (left) groups of dipeptides each consisting of two isomeric pairs were separated under the optimized conditions. Solvent systems: hydrophobic group: methyl *t*-butyl ether–acetonitrile–water (4 : 1 : 5) 20 mM triethylamine and 10% DEHPA in organic stationary phase and 20 mM HCl in aqueous mobile phase, hydrophilic group: methyl *t*-butyl ether–*n*-butanol–acetonitrile–water (2 : 2 : 1 : 5) 20 mM triethylamine and 30% DEHPA in organic stationary phase and 20 mM HCl in aqueous mobile phase; flow-rate: 3 mL min^{-1} in head-to-tail elution mode; sample: dipeptides indicated in the chromatogram, total amount of 1 g for each group; detection: 280 nm; revolution: 800 rpm.

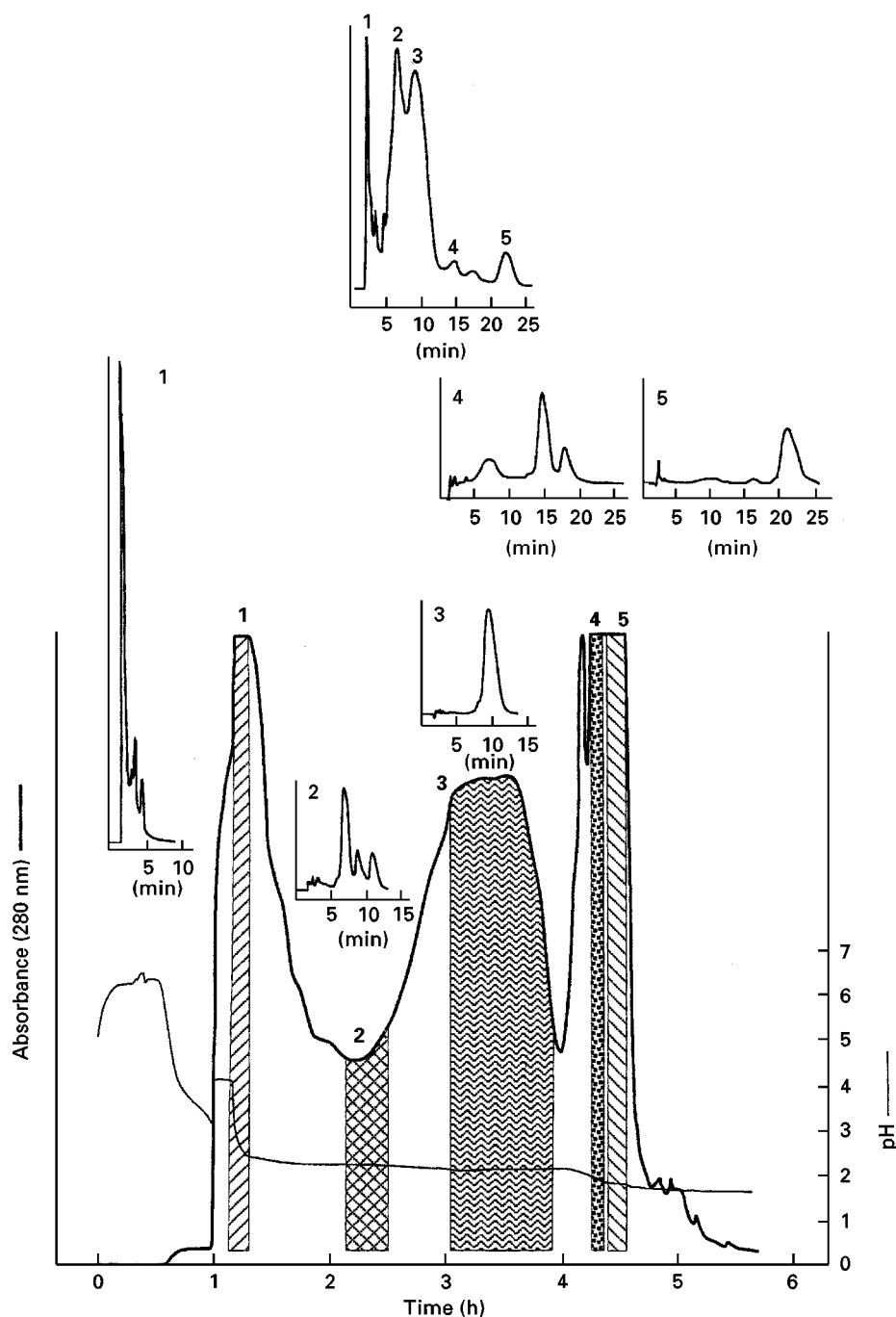


Figure 21 Preparative separation of bacitracin complex by pH-zone-refining CCC. Solvent system: methyl *t*-butyl ether-acetonitrile-water (4 : 1 : 5), 40 mM triethylamine and 10% DEHPA in organic stationary phase, and 20 mM HCl in aqueous mobile phase; flow-rate: 3 mL min⁻¹; sample: 5 g of bacitracin dissolved in 40 mL of solvent (20 mL each phase); detection: 280 nm; revolution: 800 rpm.

reduced. Of course, the technique can be used to concentrate trace quantities by the pH-peak-focusing CCC mentioned earlier.

The above features of pH-zone-refining CCC suggest that the method possesses great potential for preparative-scale research separations. Because of its unique ability to handle large-scale separations, the

method should find particular application in many industrial processes.

Acknowledgement

The author is indebted to Dr Henry M Fales for editing the manuscript.

See also: **II/Chromatography:** Countercurrent Chromatography and High-Speed Countercurrent Chromatography: Instrumentation. **Chromatography: Liquid:** Countercurrent Liquid Chromatography. **III/Alkaloids:** Gas Chromatography; Liquid Chromatography; Thin-Layer (Planar) Chromatography. **Amino Acids:** Gas Chromatography; Liquid Chromatography; Thin-Layer (Planar) Chromatography. **Chiral Separations. Amino Acids and Peptides: Capillary Electrophoresis. Antibiotics:** High-Speed Countercurrent Chromatography. **Chiral Separations:** Amino Acids and Derivatives; Liquid Chromatography. **Dyes:** High-Speed Countercurrent Chromatography; Liquid Chromatography; Thin-Layer (Planar) Chromatography. **Ion Analysis:** High-Speed Countercurrent Chromatography. **Natural Products:** High-Speed Countercurrent Chromatography. **Proteins:** High-Speed Countercurrent Chromatography.

Further Reading

Horváth C, Nahum A and Frenz JH (1981) High-performance displacement chromatography. *Journal of Chromatography* 218: 365–393.

Ito Y (1996) In: Ito Y and Conway WD (eds) *High-Speed Countercurrent Chromatography*, pp. 121–175. New York: John Wiley.

Ito Y and Ma Y (1994) *Journal of Chromatography* 672: 101–108.

Ito Y and Ma Y (1996) pH-Zone-refining countercurrent chromatography. *Journal of Chromatography A* 753: 1–36.

Ito Y, Shibusawa Y, Fales HM and Cahnmann HJ (1992) Separations of basic amino acid benzyl esters by pH-zone-refining countercurrent chromatography. *Journal of Chromatography* 625: 177–181.

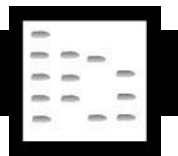
Ito Y, Shinomiya K, Fales HM, Weisz A and Scher AL (1995) In: Conway WD and Petroski RJ (eds) *Modern Countercurrent Chromatography*, pp. 154–183. American Chemical Society.

Ma Y and Ito Y (1994) Studies on an abnormally sharpened elution peak observed in countercurrent chromatography. *Journal of Chromatography* 678: 233–240.

Ma Y and Ito Y (1995) Separation of peptide derivatives by pH-zone-refining countercurrent chromatography. *Journal of Chromatography* 702: 197–206.

Ma Y and Ito Y (1997) *Analytica Chimica Acta* 352: 411–427. Weisz A, Scher AL, Shinomiya K, Fales HM and Ito Y (1994) *Journal of the American Chemical Society* 116: 704–708.

PIGMENTS



Liquid Chromatography

S. Roy, Université du Québec à Rimouski,
Rimouski, Québec, Canada

Copyright © 2000 Academic Press

Introduction

Thin-layer chromatography (TLC) represented a key development in aquatic sciences because it enabled the routine separation and quantitation of algal chlorophylls, carotenoids and their breakdown products (Table 1 and Figure 1) to be obtained. These pigments can be used as markers for algal taxa, processes such as grazing or cell senescence and water masses. However, TLC methods are not easy to automate, are difficult to use in field situations and have gradually given way to liquid chromatography (LC) methods.

High performance LC (HPLC) analysis of pigments has been developed over the last 20 years. Both normal-phase (NP) and reversed-phase (RP) techniques have been used, with preference for the RP mode due to the relatively low polarity of the analysed compounds. The NP mode is now mostly used for the separation of specific pigments (e.g. monovinyl from

divinyl chlorophylls) while RP-HPLC is preferred when a complete separation of all major chlorophylls and carotenoids is required. The analysis of phycobiliproteins, the other major group of algal pigments, is not yet done by chromatographic separation on a routine basis.

Within the various RP-HPLC methods, gradient elution has generally been preferred over isocratic for full pigment separation. Ion-pairing reagents, or phase buffering, have been included in a number of techniques to improve the resolution of the more polar pigments. Three groups of pigments present particular difficulties in their separation: the pigment pair lutein–zeaxanthin, the various members of the chlorophyll *c* group and the monovinyl and divinyl forms of chlorophyll *a* and *b*. Improved separation of zeaxanthin and lutein has been achieved using a nonend-capped C_{18} column (see below) and a combination of acetonitrile, methanol and ethyl acetate as mobile phase. Resolution of chlorophyll c_3 from the other compounds in the chlorophyll *c* group has been obtained by including an ammonium acetate buffer in the initial methanol mobile phase. Separation of all three forms of chlorophyll *c* has been achieved on a polyethylene column using aqueous acetone as mobile phase, as well as by using a very high ion strength solvent in combination with a high carbon loaded

Table 1 Major algal chlorophyll and carotenoid pigments

Name	Molecular formula	Occurrence
<i>Chlorophylls</i>		
Chlorophyll <i>a</i> (monovinyl)	C ₅₅ H ₇₂ N ₄ O ₅ Mg	All photosynthetic algae and higher plants
Divinyl chlorophyll <i>a</i>	C ₅₅ H ₇₀ N ₄ O ₅ Mg	Some prochlorophytes
Chlorophyll <i>b</i> (monovinyl)	C ₅₅ H ₇₀ N ₄ O ₆ Mg	Green algae, symbiotic prochlorophytes and higher plants
Divinyl chlorophyll <i>b</i>	C ₅₅ H ₆₈ N ₄ O ₆ Mg	Some prochlorophytes
Chlorophyll <i>c</i> ₁	C ₃₅ H ₃₀ N ₄ O ₅ Mg	Chromophyte algae, brown seaweeds
Chlorophyll <i>c</i> ₂	C ₃₅ H ₂₈ N ₄ O ₅ Mg	Chromophyte algae, brown seaweeds
Chlorophyll <i>c</i> ₃	C ₃₆ H ₂₈ N ₄ O ₇ Mg	Some prymnesiophytes, chrysophytes and diatoms
Mg-3,8-divinyl phytylporphyrin-132-methyl carboxylate	C ₃₅ H ₃₀ N ₄ O ₅ Mg	Some prasinophytes
<i>Chlorophyll degradation products</i>		
Chlorophyllide <i>a</i>	C ₃₅ H ₃₄ N ₄ O ₅ Mg	Senescent algae
Pheophytin <i>a</i>	C ₅₅ H ₇₄ N ₄ O ₅	Algal and plant detritus (also small concentration in photosynthetic reaction centres)
Pheophorbide <i>a</i> + same types of degradation products for the other chlorophylls	C ₃₅ H ₃₆ N ₄ O ₅	Zooplankton faecal pellets and marine detritus
<i>Carotenoids</i>		
Alloxanthin	C ₄₀ H ₅₂ O ₂	Cryptophytes
Astaxanthin	C ₄₀ H ₅₂ O ₄	Some green algae + marine animals
19'-Butanoyloxyfucoxanthin	C ₄₆ H ₆₄ O ₈	Pelagophytes, some prymnesiophytes and dinoflagellates
β,γ-Carotene	C ₄₀ H ₅₆	Minor pigment in green and red algae and in cryptophytes
β,β-Carotene	C ₄₀ H ₅₆	Green and chromophyte algae and higher plants
Crococanthin	C ₄₀ H ₅₄ O	Cryptophytes
Diadinoxanthin	C ₄₀ H ₅₄ O ₃	Diatoms, prymnesiophytes, some chrysophytes and dinoflagellates
Echinenone	C ₄₀ H ₅₄ O	Cyanobacteria + some green algae
Fucoxanthin	C ₄₂ H ₅₈ O ₆	Diatoms, prymnesiophytes, brown seaweeds, some dinoflagellates
19'-Hexanoyloxyfucoxanthin	C ₄₈ H ₆₈ O ₈	Many prymnesiophytes, some dinoflagellates
Lutein	C ₄₀ H ₅₆ O ₂	Green algae, red seaweeds, higher plants
Neoxanthin	C ₄₀ H ₅₆ O ₄	Brown seaweeds, chrysophytes, green algae, higher plants
Peridinin	C ₃₉ H ₅₀ O ₇	Photosynthetic dinoflagellates
Prasinocanthin	C ₄₀ H ₅₆ O ₄	Some prasinophytes
Siphonein	C ₅₂ H ₇₈ O ₅	Green algae and siphonous green seaweeds
Vaucheriaxanthin (ester)	C ₄₀ H ₅₆ O ₅	Xanthophytes and eustigmatophytes
Violaxanthin	C ₄₀ H ₅₆ O ₄	Green algae, brown seaweeds and higher plants
Zeaxanthin	C ₄₀ H ₅₆ O ₂	Cyanobacteria, green algae, prochlorophytes, most chrysophytes and raphidophytes

fully end-capped C₁₈ column. The resolution of mono- from divinyl chlorophyll *a* and *b* can be obtained on a C₈ column or by varying the temperature of a polymeric C₁₈ column (see below).

The most complete, up-to-date information about the analysis of pigments, particularly for the use of aquatic scientists, can be found in a recent Scientific Committee on Oceanic Research (SCOR) UNESCO monograph edited by Jeffrey *et al.* This book covers sample collection, methods for pigment extraction and analysis, with emphasis on HPLC methods, comparisons with nonchromatographic methods, preparation of pigment standards and a key for identification of the various algal pigments.

Selection of Columns

Most methods attempting to separate the majority of pigments in a single step have used RP-HPLC with C₁₈ columns (Figure 2). Presently, the most popular C₁₈ columns for pigment analysis are the end-capped,

monomer-coated C₁₈ columns (Table 2), although these may not be the best for the separation of polar carotenoids. End-capping deactivates the remaining free silanol groups after the monomeric coverage. Columns from different companies differ in their carbon load (amount of bound C₁₈) and the type and extent of end-capping.

The separation of monovinyl from divinyl chlorophyll *a* and *b* was first achieved on NP silica columns, but these methods did not become very popular because of the reactivity of the stationary phase, the incompatibility of the extraction solvents with the technique and the lack of resolution of the polar pigments. These were replaced by C₈ columns, which can separate mono- from divinyl chlorophyll *a* and *b* but do not resolve all the chlorophyll *c* compounds (Figure 3).

The latest improvement in this field has been the development of columns which have multiple levels of C₁₈ bound to the silica (often called polymeric octadecylsilica columns). These allow the most

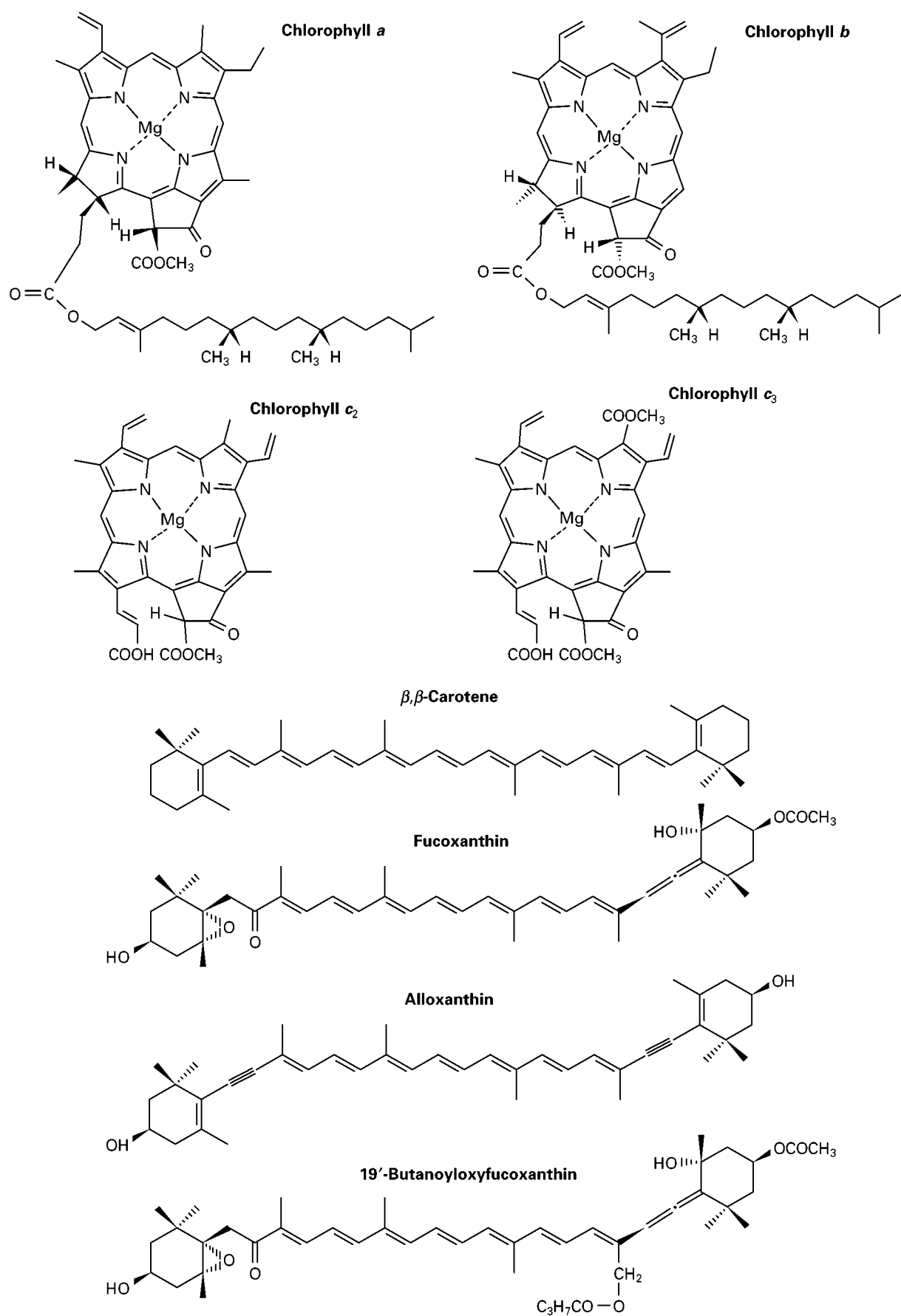


Figure 1 Chemical structures of major algal chlorophylls and carotenoids.

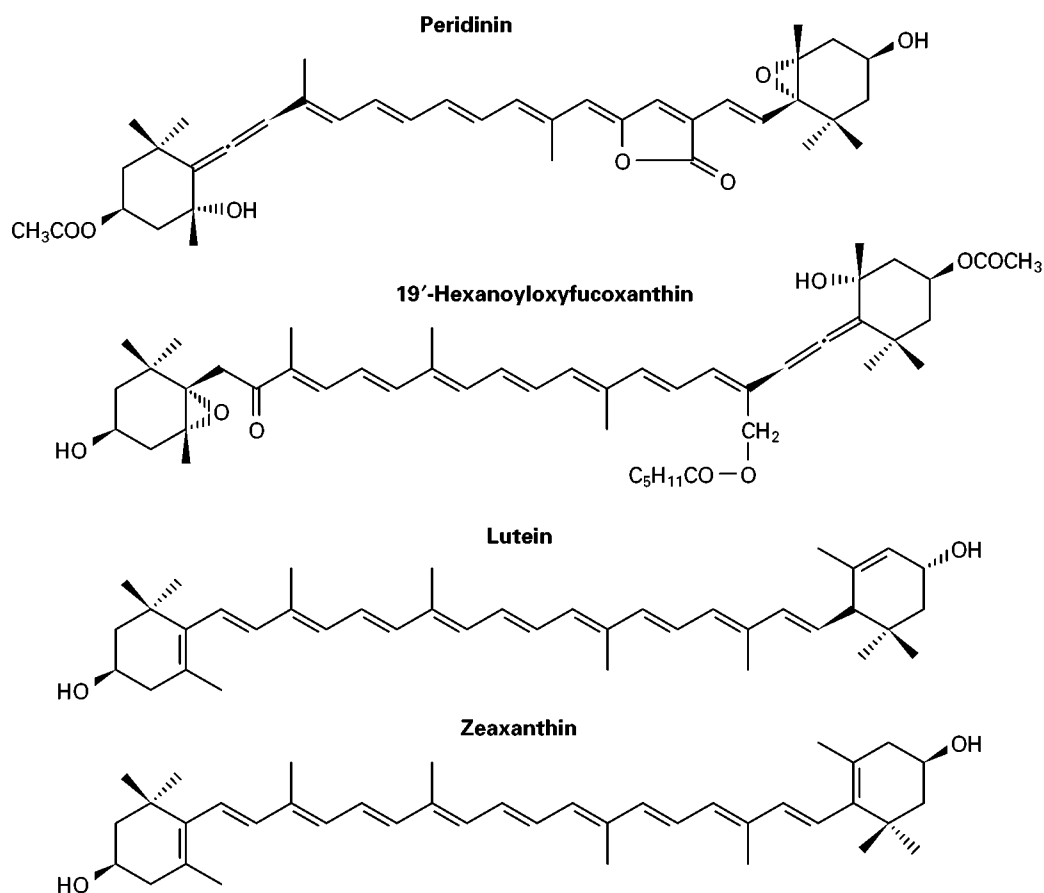


Figure 1 *Continued*

complete separation of chlorophylls and carotenoids but these coatings are more sensitive to temperature than monomeric columns, and hence the columns need to be thermostated. The work on marine pigments conducted in the laboratory of Zapata and Garrido has been instrumental in these developments

(Figure 4). Recently, research scientists in the field of food science have developed a polymeric triacontyl (C_{30}) column which provides adequate retention of polar carotenoids (e.g. good separation of lutein and zeaxanthin) as well as much improved separation of the nonpolar carotenes (Figure 5).

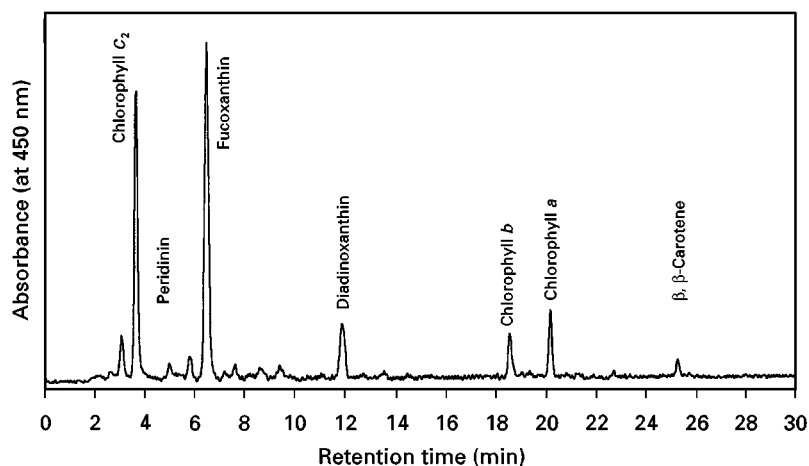


Figure 2 Analysis of pigments from ice algae from the Arctic (Roy, unpublished). Column 5 μ m. Spherisorb ODS-2 (C_{18}). Separation conditions: 50 : 50 of (85% methanol–15% ammonium acetate 0.5 mol L⁻¹) : (90% acetonitrile–10% water) to 30 : 70 of (90% acetonitrile–10% water) : ethyl acetate over 33 min; 0.8 mL min⁻¹. Temperature 27°C.

Table 2 Selection of columns for HPLC pigment analysis

Type of column	Carbon load	End-capping	Dimensions (mm)	Particle size (μm)	Type of analysis
<i>Reversed-phase (monomeric)</i>					
Spherisorb ODS-2 (C_{18})	12%	Yes	250 \times 4.6	5	Algal pigments
Ultrasphere C_{18}	12%	Yes	250 \times 4.6	5	Plant pigments
Zorbax ODS	20%	No	250 \times 4.6	5	Lutein/zeaxanthin
RSil C_{18}	16%	Yes	150 \times 4.6	5	Chlorophyll c_1 , c_2 , c_3
Hypersil MOS-2 (C_8)	6–7%	Yes	100 \times 4.6	3	MV and DV chlorophyll and lutein/zeaxanthin
<i>Reversed-phase (polymeric)</i>					
Vydac 201 TP	9%	No	250 \times 4.6	5	MV and DV chlorophyll and chlorophyll c_1 , c_2 , c_3
Asahipak ODP-50	17%	No	250 \times 4.6	5	MV and DV chlorophyll
Lichrospher PAH	21%	No	250 \times 4.6	5	Chlorophyll c_3 , MgDVP, phytol chlorophyll c
<i>Normal-phase</i>					
Rosil	10%	No	150 \times 4.6	5	MV and DV chlorophyll a and b

MV, Monovinyl; DV, divinyl; MgDVP, Mg-3,8-divinyl phytylporphyrin-132-methyl carboxylate.

Mobile Phases

The most common mobile phases for pigment analysis currently use two to three solvents in a gradient

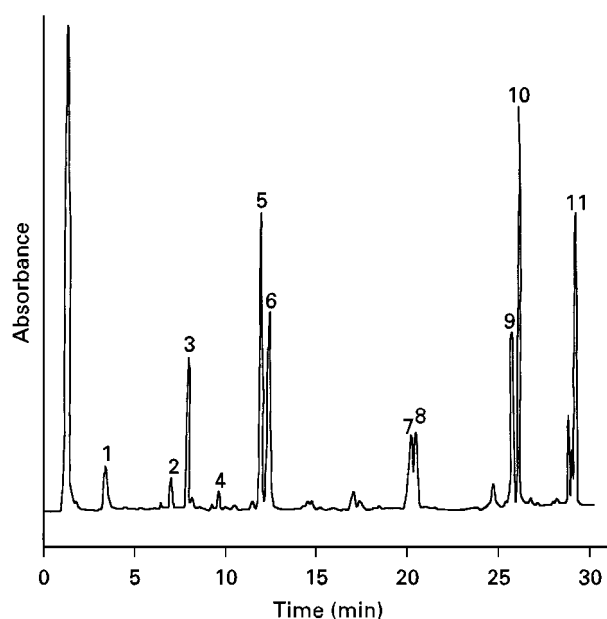


Figure 3 Analysis of pigments from algal cultures (*Dunaliella tertiolecta*, *Synechococcus* sp. and *Prochlorococcus* sp.). Column (3 μm) Shandon Hypersil MOS2 (C_8). Separation conditions: 75 : 25 of (70% methanol–30% ammonium acetate 1 mol L^{-1}): methanol to 100% methanol over 32 min; 1 mL min^{-1} . Peaks detected at 440 nm: 1, chlorophyll c -like; 2, neoxanthin; 3, violaxanthin; 4, antheraxanthin; 5, zeaxanthin; 6, lutein; 7, divinyl chlorophyll b ; 8, chlorophyll b ; 9, divinyl chlorophyll a ; 10, chlorophyll a ; 11, α - and β -carotene. (Reproduced with permission from Barlow RG, Cummings DG and Gibb SW (1997) Improved resolution of mono- and divinyl chlorophylls a and b and zeaxanthin and lutein in phytoplankton extracts using reverse phase C_8 HPLC. *Marine Ecology Progress Series (Inter-Research)* 161: 303–307.)

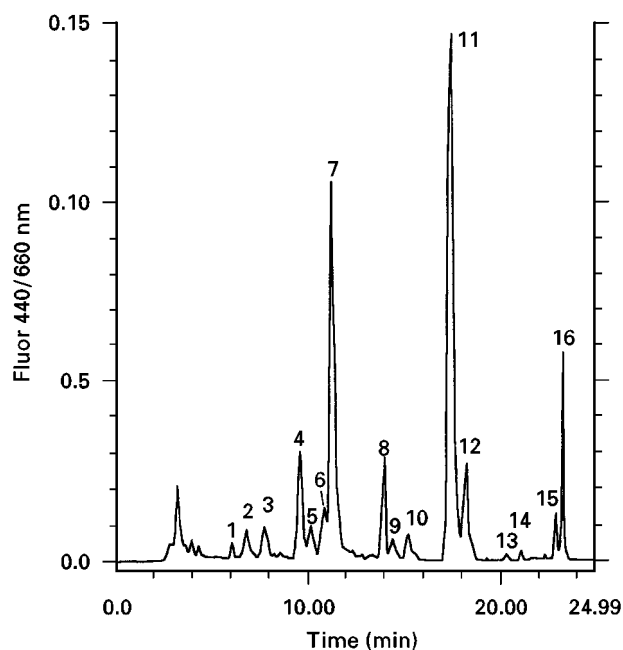


Figure 4 Analysis of pigments from marine phytoplankton. Column (5 μm) Vydac 201 TP. Separation conditions: 65 : 35 of (45% methanol–35% acetonitrile–20% aqueous pyridine, 0.25 mol L^{-1}): acetone to 100% acetone over 24 min; 1.2 mL min^{-1} . Temperature 27°C. Peaks detected by their fluorescence (excitation = 440 nm, emission = 660 nm): 1, chlorophyll c -like; 2, chlorophyll c -like; 3, divinyl protochlorophyllide a ; 4, chlorophyll c_1 ; 5, monovinyl chlorophyll c_3 ; divinyl chlorophyll c_3 ; 7, chlorophyll c_2 ; 8, chlorophyll b ; 9, chlorophyll b_2 ; 10, chlorophyll a allomer; 11, chlorophyll a ; 12, chlorophyll a_2 ; 13, chlorophyll a isomer; 14, chlorophyll a_2 isomer; 15, phytol-substituted chlorophyll c -like pigment; 16, phytol-substituted chlorophyll c -like pigment. (Reproduced with permission from Garrido JL and Zapata M (1997) Reversed-phase high-performance liquid chromatographic separation of mono- and divinyl chlorophyll forms using pyridine-containing mobile phases and a polymeric octadecylsilica column. *Chromatographia* 44: 43–49.)

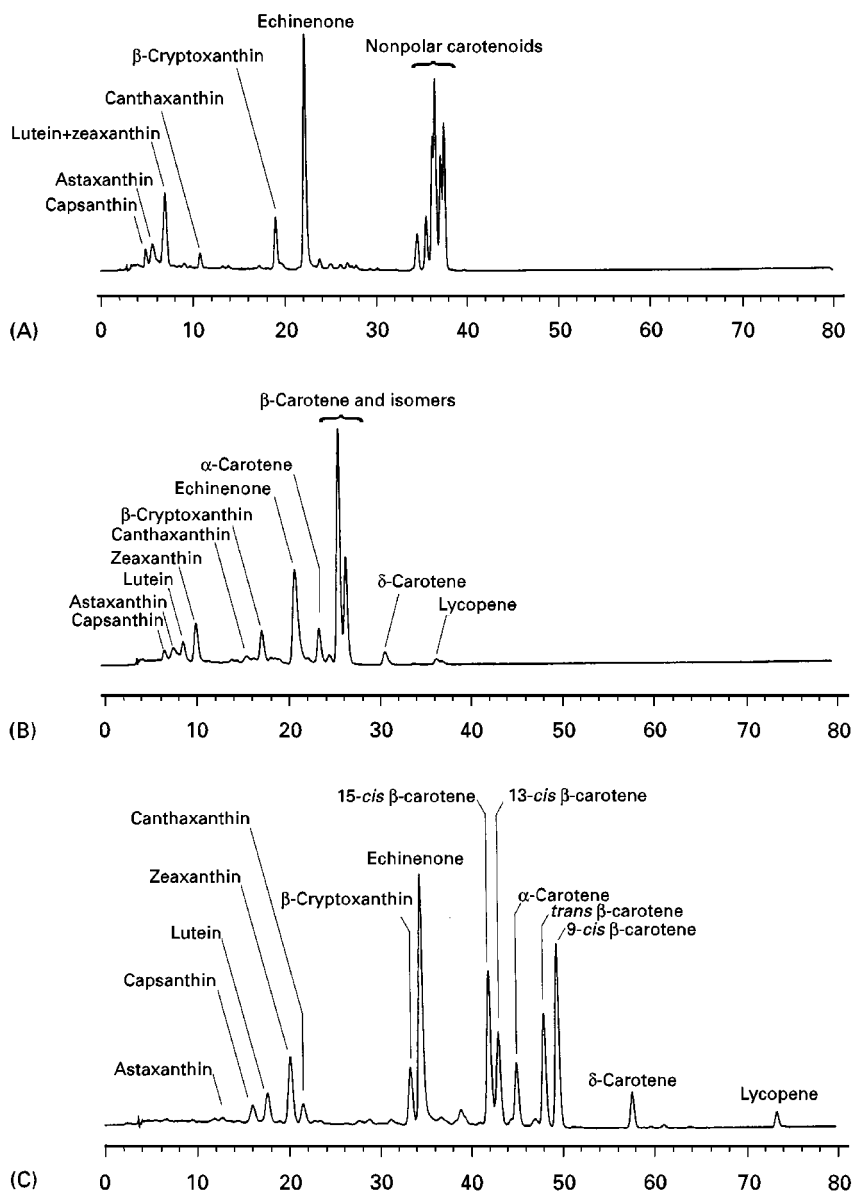


Figure 5 Separations of carotenoid standards on commercial (A) monomeric and (B) polymeric C_{18} columns, as well as (C) the polymeric C_{30} column. Separation conditions: 81 : 15 : 4 to 6 : 90 : 4 methanol-methyl-*tert*-butyl ether-water over 90 min; 1 mL min⁻¹. Temperature 20°C. (Reproduced with permission from Sander LC, Sharpless KE, Craft NE and Wise SA (1994) Development of engineered stationary phases for the separation of carotenoid isomers. *Analytical Chemistry* 66: 1667-1674.)

elution mode. Initial conditions often include 80–90% methanol buffered with ammonium acetate, followed by 90% acetonitrile. Ethyl acetate or acetone is commonly used as the third solvent to elute the less polar pigments such as the pheophytins. The newer methods use the same solvents, except that an organic modifier is added to the methanol/acetonitrile eluent. Various five-carbon amino compounds have been tested as ion pair reagents, with aqueous pyridine showing the best results with the Vydac 201 TP column. Again, temperature control is essential when using these columns.

Detection

Detection of compounds eluting from HPLC columns is normally done by recording the absorbance (chlorophylls and carotenoids) or the fluorescence (chlorophylls) of algal pigments. Three types of detectors are commonly used for absorbance: fixed wavelength, variable wavelength and full spectrum absorbance detector. The fixed wavelength models are the most sensitive, but the least informative of the three. Full spectrum instruments are now a general requirement of any HPLC set-up for pigment analysis. They

include photodiode array detectors and rapid scanning instruments. Both allow the full absorbance spectrum of each peak to be collected without stopping the flow, facilitating identification of peaks, to the detriment, however, of sensitivity. Instruments with a lamp that has high output in the visible range (e.g. tungsten) are preferred for pigment analysis because of their increased sensitivity.

Fluorescence detectors are either of the filter type, with a band pass excitation filter and a long pass emission filter, or dual monochromator instruments. The filter type is often sufficient for most uses, especially if used in conjunction with an absorbance detector. The use of fluorescence detection along with absorbance detection allows confirmation of the identity of chlorophyll-type compounds since only these fluoresce. Fluorescence detection is also often preferred for quantitative use because of its great sensitivity.

Standards

Few pigment standards were available commercially, until recently (Table 3). However, the high cost of these standards, and the unavailability of a number of them, has prompted researchers to prepare in-house standards, using well-defined algal cultures. Guidelines for the preparation of standards can be found in the specialized literature, and summarized in the recent SCOR UNESCO monograph on algal pigments in oceanography.

Applications

The analysis of photosynthetic pigments is instrumental in numerous studies of the photosynthetic system of bacteria, plants and algae. It is also used in the fields of agriculture and food chemistry, in studies of food processing, and in the use of natural food-colouring agents. In aquatic sciences, algal pigments are used as an index of algal biomass and as biomarkers of different taxonomic groups of algae, particularly when HPLC analysis is applied. This information can then serve in the monitoring of red tides (toxic algal blooms), in studies of aquatic food webs in relation to harvestable resources or in the study of water masses in oceanography. The recent development of satellite remote-sensing of the colour of the oceans, related to their pigment composition and concentration, allows a synoptic perspective previously unobtainable from ship studies. Present studies are developing algorithms that can estimate primary production over wide areas of the oceans from remotely sensed (e.g. sea-viewing wide field-of-view sensor (SeaWiFS)) chlorophyll data.

Table 3 Pigment standards available commercially

<i>Pigment</i>	<i>Company</i>	<i>Location</i>
<i>Chlorophylls</i>		
Chlorophyll <i>a</i>	Sigma Chemical Company Fluka Chemie AG Aldrich Chemical Co. Ltd	St Louis, Missouri, USA Buchs, Switzerland Milwaukee, Wisconsin, USA
Chlorophyll <i>b</i>	Sigma Chemical Company Fluka Chemie AG Aldrich Chemical Co. Ltd	St Louis, Missouri, USA Buchs, Switzerland Milwaukee, Wisconsin, USA
Chlorophyll <i>c</i> ₂	Int. Agency for ¹⁴ C determ.	Hørsholm, Denmark
<i>Carotenoids</i>		
Alloxanthin	Int. Agency for ¹⁴ C determ.	Hørsholm, Denmark
Astaxanthin	Sigma Chemical Company	St Louis, Missouri, USA
19'-Butanoyloxy-fucoanthin	Int. Agency for ¹⁴ C determ.	Hørsholm, Denmark
Canthaxanthin	Fluka Chemie AG Int. Agency for ¹⁴ C determ.	Buchs, Switzerland Hørsholm, Denmark
β,γ -Carotene	Sigma Chemical Company	St Louis, Missouri, USA
β,β -Carotene	Sigma Chemical Company Fluka Chemie AG Aldrich Chemical Co. Ltd	St Louis, Missouri, USA Buchs, Switzerland Milwaukee, Wisconsin, USA
Diadinoxanthin	Int. Agency for ¹⁴ C determ.	Hørsholm, Denmark
Diatoxanthin	Int. Agency for ¹⁴ C determ.	Hørsholm, Denmark
Echinenone	Int. Agency for ¹⁴ C determ.	Hørsholm, Denmark
Fucoanthin	Int. Agency for ¹⁴ C determ.	Hørsholm, Denmark
19'-Hexanoyloxy-fucoanthin	Int. Agency for ¹⁴ C determ.	Hørsholm, Denmark
Lutein	Int. Agency for ¹⁴ C determ.	Hørsholm, Denmark
Lycopene	Sigma Chemical Company	St Louis, Missouri, USA
Myxoxanthophyll	Int. Agency for ¹⁴ C determ.	Hørsholm, Denmark
Neoxanthin	Int. Agency for ¹⁴ C determ.	Hørsholm, Denmark
Peridinin	Int. Agency for ¹⁴ C determ.	Hørsholm, Denmark
Prasinoxanthin	Int. Agency for ¹⁴ C determ.	Hørsholm, Denmark
Violaxanthin	Int. Agency for ¹⁴ C determ.	Hørsholm, Denmark
Zeaxanthin	Int. Agency for ¹⁴ C determ.	Hørsholm, Denmark

Future Developments

Future advances in the field of pigment chromatography can be expected from:

1. development of new RP-HPLC columns, particularly the polymeric ones, and associated testing of the effect of temperature on the separation of pigments with these columns. HPLC equipment will also need to be more closely temperature-controlled to meet this need
2. advances in the field of mass spectrometry, such as electron impact, field desorption and fast atom bombardment, that permit volatilization of small quantities of pigments, and the coupling of mass spectrometry with HPLC (LC-MS) or with supercritical fluid chromatography (SFC-MS). These new methods should be particularly useful in studies dealing with degraded or derived pigments, such as fossil pigments found in sediments or transformation of pigments in food, agricultural, physiological or ecological studies.

See Colour Plate 114.

See also: II/Pigments: Thin-Layer (Planar) Chromatography. Terpenoids: Liquid Chromatography.

Further Reading

- Garrido JL and Zapata M (1996) Ion-pair reversed-phase high-performance liquid chromatography of algal chlorophylls. *Journal of Chromatography A* 738: 285.
- Hodgson DA, Wright SW and Davies N (1997) Mass spectrometry and reverse phase HPLC techniques for the identification of degraded fossil pigments in lake sediments and their application in palaeolimnology. *Journal of Paleolimnology* 18: 335.
- Jeffrey SW, Mantoura RFC and Wright SW (eds) (1997) *Phytoplankton Pigments in Oceanography: Guidelines to Modern Methods*. Paris: UNESCO.
- Mantoura RFC and Llewellyn CA (1983) The rapid determination of algal chlorophyll and carotenoid pigments and their breakdown products in natural waters by reverse-phase high-performance liquid chromatography. *Analytica Chimica Acta* 151: 297.

Millie DF, Paerl HW and Hurley JP (1993) Microalgal pigment assessments using high-performance liquid chromatography: a synopsis of organismal and ecological applications. *Canadian Journal of Fisheries and Aquatic Sciences* 50: 2513.

Roy S (1987) High-performance liquid chromatographic analysis of chloropigments. *Journal of Chromatography* 391: 19.

Šestak Z (1982) Thin layer chromatography of chlorophylls 2. *Photosynthetica* 16: 568.

Van Breemen RB (1996) Innovations in carotenoid analysis. *Analytical Chemistry* 68: 299A.

Van Heukelem L, Lewitus AJ, Kana TM and Craft NE (1994) Improved separations of phytoplankton pigments using temperature-controlled high performance liquid chromatography. *Marine Ecology Progress Series* 114: 303.

Wright SW, Jeffrey SW, Mantoura FRC *et al.* (1991) Improved HPLC method for the analysis of chlorophylls and carotenoids from marine phytoplankton. *Marine Ecology Progress Series* 77: 183.

Thin-Layer (Planar) Chromatography

G. W. Francis, University of Bergen,
Bergen Norway

Copyright © 2000 Academic Press

General Introduction

Colour and Pigments

The colours found in natural organisms are of two types: those which are due to structural effects, and those which result from the presence of pigments. The two types of colouring often occur together. Examples of structural colour are to be found in the scales of fish, the wings of butterflies and the hair of many animals, although structural colour is also to be found in the plant world. The apparent colour depends on the interplay of these effects. It is thus important to realize at the outset that only the colour due to the pigments can be extracted. However, even then the *in vivo* and *in vitro* colours can be vastly different, since the pigments themselves show different colours according to the environment in which they occur – whether in fat globules or aqueous complexes.

Importance

Colour is used by almost all organisms to communicate in one form or another, for example, the defensive colours of insects, the attractive colours of flowers and fruit. The way in which various organisms pro-

duce pigments is genetically determined, and thus related organisms have similar pigment patterns and biologists use pigments to classify organisms at all levels. The commercial value of agricultural and particularly horticultural products is often closely related to their colour.

Natural Pigment Structures

The number of main pigment groups is relatively small. While various pigment groups are of vastly different skeletal types, there is usually little variation of the skeleton within each group and in many cases the possible group of pigments involved can be arrived at based on the observed colour in nature. Thus, while the green colour of chlorophylls is immediately recognizable, the typical flavonoids provide pale yellow colours, and the anthocyanidins, a special group of flavonoid salts, are usually responsible for red-blue colours in plants. The deep yellow to orange red shades resulting from the presence of carotenoids are also readily identified. Variations within a particular group are usually due to two factors: the degree of oxidation and the presence of substituents.

Extraction Methods

The different types of pigment vary greatly in polarity and in their sensitivity to chemical reagents, and thus require different extraction methods. It is best to avoid the use of acids or bases unless necessary, and

as far as possible exposure to air or light. It should be noted that working rapidly and with normal care may sometimes give better results than working with time-consuming rigorous methods, at least at a qualitative level. Normally, a solvent is found that will extract the required pigment type while extracting as little as possible of the remaining components from the substrate. This means essentially that the solvent and pigment type should match as well as possible with respect to polarity. However, even such tailored methods can fail if unusual or unsuspected substituents are present and lead to the identification of artefacts as naturally occurring.

Clean-up and Pretreatment

Even when extracts or individual pigments appear to be pure, the undisclosed presence of colourless impurities should always be investigated. Such impurities are normally readily disclosed by spraying a trial chromatogram with a strong oxidizing agent. This often provides valuable information before final chromatography is undertaken, since the presence of such impurities greatly reduces the efficiency of the plates, in terms of both resolution and capacity. The most common clean-up treatment is the extraction of polar impurities from less polar extracts, or the reverse where waxes are removed either before or after the extraction process. It is important to ensure the removal of residual solvents after such clean-up procedures, or indeed after saponification or hydrolysis, as they will otherwise result in inferior separation. Residual solvents are a common source of problems in chromatography and, in particular, the presence of even minor traces of water (easily removed by azeotropic distillation) can often spoil the separation of hydrophobic pigments.

Chromatography Layers

Chromatography may be carried out on layers coated on plastic or aluminium foils, or glass plates. The type used depends to some extent on whether a quantitative analysis is required since the backing is critical for densitometric methods. Commercial pre-coated plates have the advantage of uniform quality and give more reproducible results than laboratory-coated plates. The procedures given below have all been carried out on commercial plates for this reason. However, it should be noted that only a few adsorbents are available and the plates are expensive if large numbers are required. In addition, some commercial plates contain compounds used in their manufacture which may be extracted if the plates are used preparatively. It is normally possible, with practice, to produce laboratory-made plates that give sim-

ilar results, and in this case there are almost unlimited possibilities for mixing different adsorbents. In the case of larger scale preparative work, it is often easier to work with less dense home-made layers, although care should be taken in handling them to avoid damaging the layer.

Quantification

Densitometry is readily applied to the measurement of pigments, provided the usual precautions are taken to choose suitable wavelength, and drying of the developed plate is carried out in a manner that avoids excessive decomposition. Since pigments are usually worked with on small scales, thin layers are well suited for their preparative or semipreparative separation.

Pigment Groups

The pigment groups treated in more detail below are the main photosynthetic pigments, carotenoids and chlorophylls, and the most widely distributed flavonoid classes, with a separate section for the anthocyanins. Finally, other pigment types are discussed briefly.

Carotenoids

The carotenoids are probably the most widely distributed group of pigments, occurring in all photosynthetic organisms, in most animals and in a wide variety of microorganisms. They normally occur in the free form or as fatty acid esters, although carotenoproteins are common in marine animals and glycosides are found in some microorganisms. They are usually yellow to red in colour, although carotenoproteins are able to provide a full range of colours.

The carotenoids are tetraterpenoids and may be thought of as being made up by a central conjugated chain carrying two end-groups. Some typical carotenoids are shown in **Figure 1**. The number of possible end-group skeletons is quite restricted and structural variation largely derives from the type and position of the functional groups which they contain. The compounds containing only carbon and hydrogen are often called carotenes to differentiate them from their oxygenated analogues, which are then designated as xanthophylls. While all of the compounds in **Figure 1** have 40 carbon atoms, carotenoids containing partial skeletons are known, as are compounds carrying extra isoprenoid units to give skeletons having 45 and 50 carbon atoms.

Extraction methods for carotenoids depend somewhat on the organism being examined. Tissues from higher plants and microorganisms, where carotenoids

are usually present in the free form or as esters, can usually be extracted by hydrocarbon-acetone mixtures. Problems may be encountered with some microorganisms where it is necessary to disrupt the cells before extraction, where compounds may be strongly bound to cell wall material or, less often, where more polar solvents are required to extract glycosidic carotenoids. Animal tissues can contain carotenoproteins and in such cases a choice must be made between extraction with acetone which will free the hopefully unchanged carotenoids from the protein or extraction with suitable buffers of the intact carotenoproteins from which the carotenoids can then be liberated.

The normal procedure for carotenoid analysis is to examine the initial extract to decide whether the compounds are present in the free form or as esters. The esters themselves are much less polar than the free xanthophylls and a check can be made by saponifying an aliquot of the extract. Given a positive result a saponification step can then be applied to the whole extract, although it should be noted that some few carotenoids may suffer changes, e.g. astaxanthin, the main pigment in salmonoids, is changed to the closely related astacene by base treatment. One advantage of saponification of plant extracts is that the chlorophylls, which will otherwise interfere with chromatography, are destroyed and can be easily

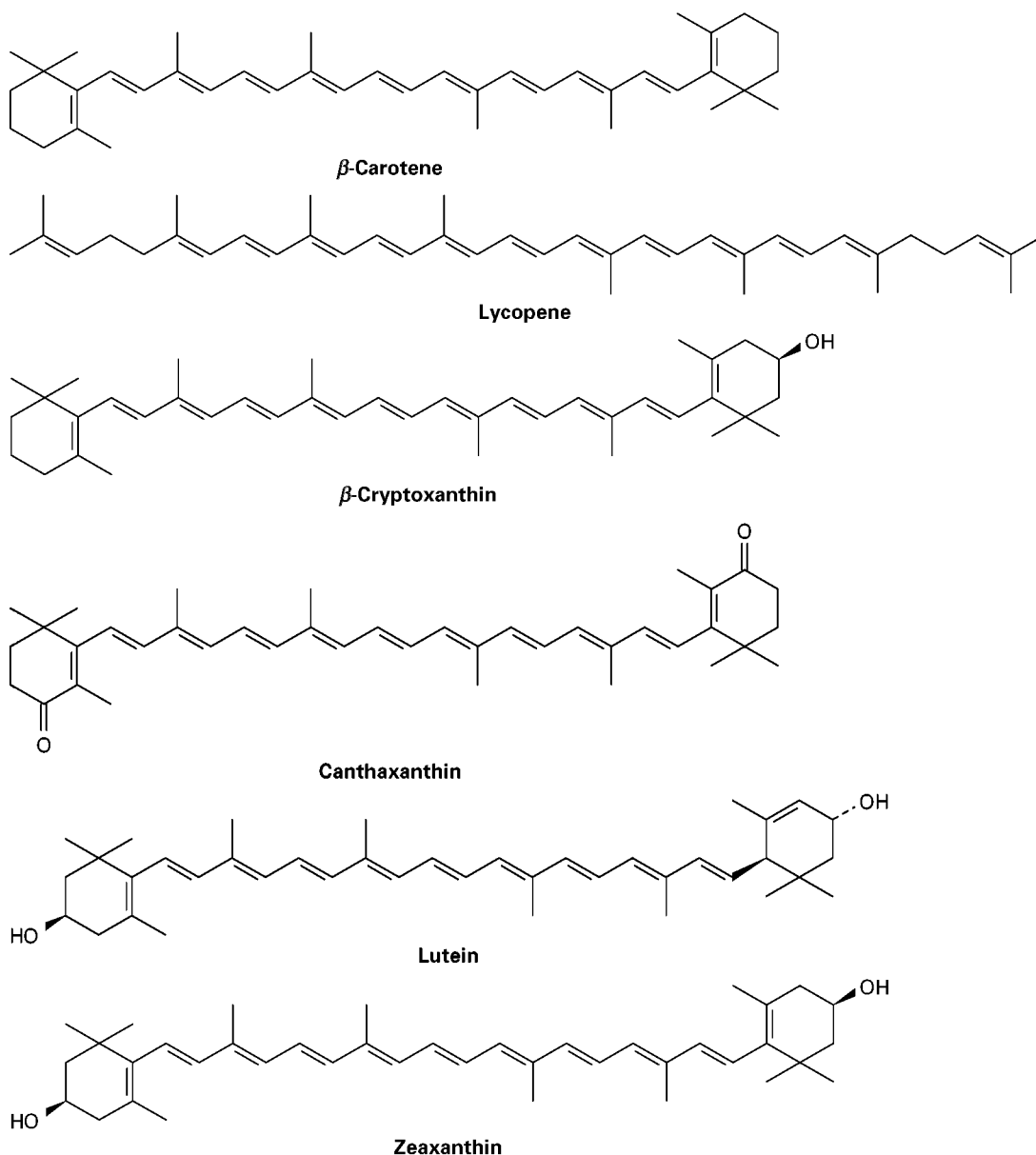
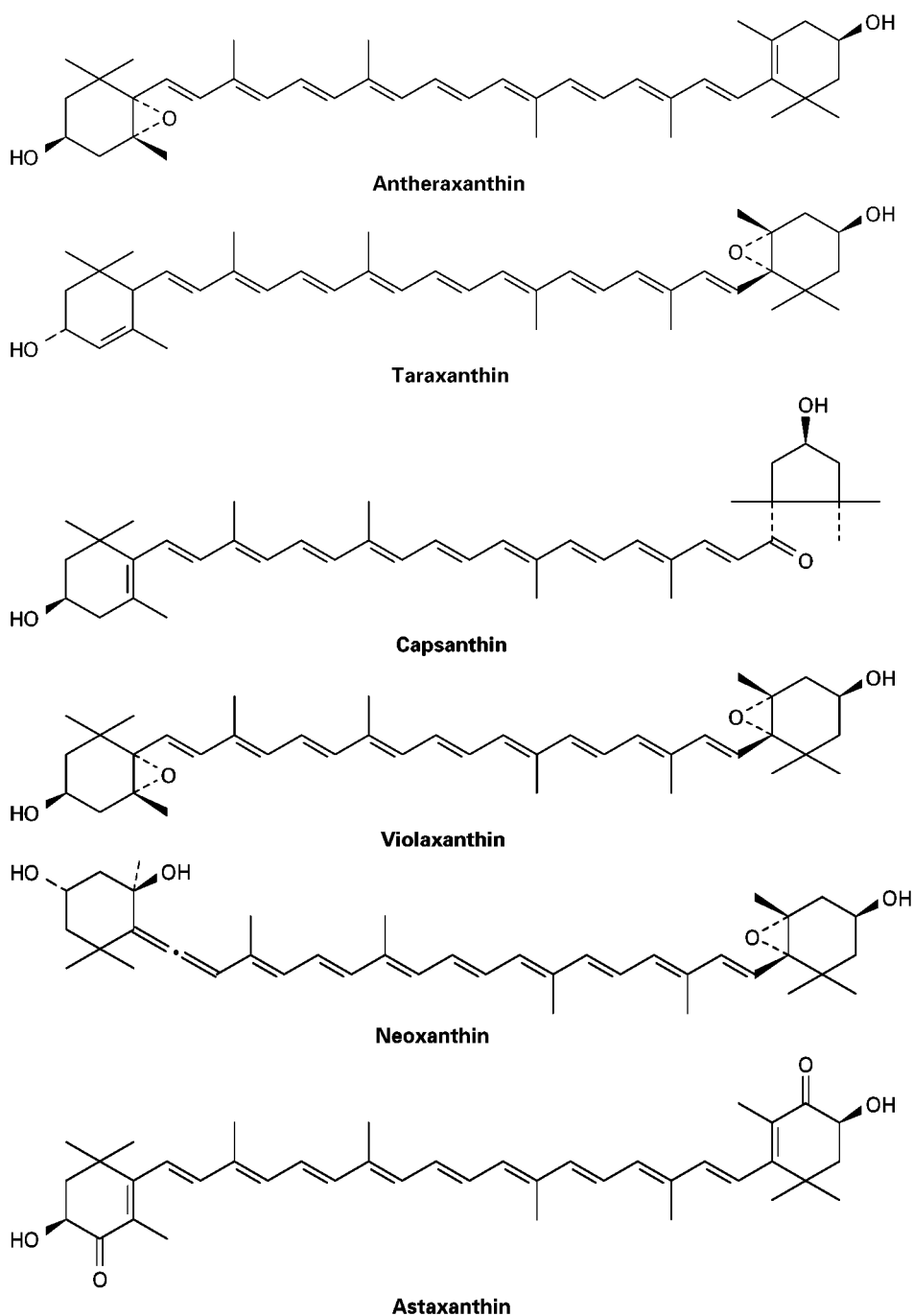


Figure 1 Structures of some typical carotenoids.

**Figure 1** *Continued.*

removed prior to analysis. The effects of saponification can readily be seen in **Figure 2**, which shows a chromatogram of a paprika extract before and after saponification. The unsaponified extract is dominated by the presence of esterified carotenoids, while the esters are totally absent after saponification.

The finished saponified extract should be applied to the plate in a volatile solvent, usually acetone or diethyl ether. While a large number of stationary

phases have been employed, the most reliable are silica gel for normal-phase and octadecylsilylsilica for reversed-phase work, and these suffice to separate the normal range of pigments. If only carotenes are to be analysed, laboratory-coated magnesium oxide plates can be employed. R_F values are given for some common carotenoids in **Table 1**, for both normal-phase and reversed-phase systems. These values show immediately that retention is affected by the number

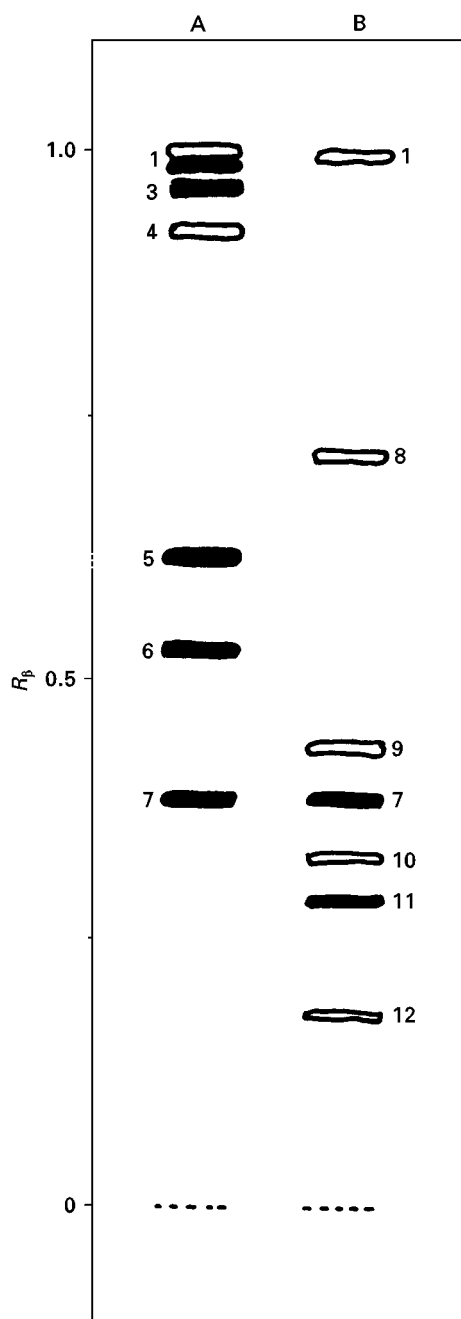


Figure 2 Chromatography of paprika (*Capsicum annuum*). Silica gel 60 (0.25 mm, Merck, Art. 5721) 40% acetone–petroleum ether. (A) Before saponification; (B) after saponification. Identification of zones: 1, β -carotene; 2, capsanthin diesters; 3, capsorubin diesters, 4, zeaxanthin and other diol diesters; 5, capsanthin monoesters; 6, capsorubin monoesters; 7, capsanthin; 8, cryptoxanthin, 9, zeaxanthin; 10, violaxanthin; 11, capsorubin, 12, neoxanthin. Only main zones are shown: filled zones indicate red colour; other zones are yellow.

and nature of functional groups present. Hydroxyl functions have greater effects than carbonyls, which in turn have greater effects than ether groups. Longer chains are more retained than shorter ones in normal-

phase chromatography, while the opposite is true for reversed-phase systems. It should be noted that, while development on silica gel layers with 40% acetone–petroleum ether (40–60°C) gives a generally similar result to that obtained with 20% of *tert*-butanol or *tert*-pentanol, carbonyls have markedly more retention in the latter systems. This difference in behaviour can be utilized when separating complicated mixtures of closely related carotenoids. The choice as to whether to use normal or reversed-phase plates will depend on the compounds present.

Practical procedures All operations with carotenoids should be carried out in dim light, avoiding exposure to air and acids and at temperatures not exceeding 40°C. Carotenoid samples and extracts should be kept in the refrigerator as far as possible.

Extraction The material to be extracted is cut into suitable pieces (1 cm cubes) suspended in three volumes of acetone and subjected to maceration for 2–3 min in a laboratory mixer. The solvent is removed and retained, and the procedure repeated twice. At this stage, much of the water present in the original tissue has been extracted and it is often advantageous to carry out one or two further extractions with acetone–petroleum ether (40–60°C) in a 1 : 1 v/v ratio. Where very polar carotenoids are present, extraction with solvent mixture containing methanol may be required. When the residue is colourless, the extracts are pooled and taken to dryness under reduced pressure. The extract can then be tested for the presence of esters and, in their absence, applied to the thin layers as solutions in diethyl ether or acetone. Otherwise saponification should be performed.

Saponification The dried extract is dissolved in a small amount of diethyl ether or methanol to give a deeply coloured concentrated solution which is then diluted with several volumes of diethyl ether. Saponification is then ensured by adding an equal volume of 10% methanolic sodium hydroxide, replacing the air in the flask with nitrogen, closing firmly, and after brief shaking allowing the mixture to stand at room temperature for 6 h in the dark. After this time the saponification mixture is diluted to three times its volume with 5% aqueous sodium chloride. The carotenoids are then extracted with similar volumes of diethyl ether until the diethyl ether extract is no longer coloured. The combined diethyl ether extracts are then pooled and washed to neutrality with successive portions (normally at least three) of 5% aqueous sodium chloride, before a final wash with

Table 1 Thin-layer chromatography of carotenoids: R_f values (β -carotene = 1.00) for systems 1–4, and R_F values for systems 5 and 6

Carotenoid	Source	Chromatographic system					
		1	2	3	4	5	6
β -Carotene	a	1.00	1.00	1.00	1.00	0.10	0.13
Lycopene	b	1.00	0.97	1.00	1.00	0.17	0.23
β -Cryptoxanthin	a	0.72	0.34	0.78	0.76	0.22	0.31
Canthaxanthin	c	0.71	0.36	0.69	0.66	0.26	0.38
Lutein	d	0.44	0.07	0.56	0.53	0.37	0.55
Zeaxanthin	e	0.44	0.07	0.55	0.50	0.37	0.57
Antheraxanthin	f	0.40		0.40	0.31	0.44	0.60
Taraxanthin	e	0.41		0.43	0.37	0.47	0.62
Capsanthin	g	0.39		0.38	0.28	0.48	0.64
Violaxanthin	d	0.33		0.30	0.19	0.55	0.68
Neoxanthin	d	0.18		0.13	0.08	0.63	0.72
Astaxanthin	h	0.09		0.07		0.85	0.91

System 1: Silica gel 60 (0.25 mm, Merck, Art. 5721) 40% acetone–p.e.; system 2: silica gel 60, 20% acetone–p.e.; system 3: silica gel 60, 20% *tert*-pentanol–p.e.; system 4: silica gel 60, 20% *tert*-pentanol–p.e.; system 5: RP-18 F₂₅₄ (0.25 mm, Merck, art. 15425) p.e.–acetonitrile–methanol (10 : 40 : 50); system 6: RP-18 F₂₅₄, p.e.–acetonitrile–methanol (20 : 40 : 40). Solvent compositions by volume; p.e., petroleum ether (40–60°C). Sources: a, *Sorbus aucuparia* berries; b, *Solanum lycopersicum* fruit; c, commercial; d, *Petroselinum crispum*; e, *Taraxacum officinale* flowers; f, *Lilium x hollandicum* flowers; g, *Capsicum annum* fruit; h, *Salmo salar*.

water. The washed extract is taken to dryness under reduced pressure and dissolved in either acetone or diethyl ether for analysis.

Chromatography The best initial approach to the separation of the carotenoid mixture is to carry out trial runs on silica gel layers using as developers increasing amounts of acetone in petroleum ether (40–60°C), e.g. 0, 5, 10, 20 and 40% v/v. This will immediately give an indication of the polarity of the compounds present and provide guidelines for further work. Where separations are reasonable but there is overlap, a new chromatogram based on the best acetone percentage should be developed with approximately half of that percentage of *tert*-butanol. If normal-phase methods fail or if there is a preponderance of polar compounds, reversed-phase separation should be tried; possible systems are indicated in Table 1. Where single development is insufficient to provide separation, the various zones can usually be scraped off the plate and re-extracted with good recovery rates provided that the process is done quickly and with due care. Separation within the various zones can then be carried out by renewed chromatography with appropriate solvent mixtures, i.e. solvents giving R_F values of about 0.50.

Identification Relatively few carotenoid standards are available commercially, but a large number of natural sources are well documented, and the monographs of Goodwin from 1980 and 1984 are particularly useful sources for this information. Otherwise, many carotenoids can be identified even in small

quantities from their visible light absorption spectra and by microreactions.

Chlorophylls

The chlorophylls are essential for photosynthesis and are thus of universal distribution in photosynthetic organisms. They are tetrapyrroles with a cyclic structure, and in intact tissue occur coordinated to a magnesium (2+) ion. The main pigments, chlorophylls *a* and *b*, differ only in having one methyl substituent in chlorophyll *a*, replaced by a formyl group in chlorophyll *b*. The intact chlorophylls also contain a phytol group which confers a hydrophobic moiety on an otherwise hydrophilic structure (see Figure 3 for structures for chlorophylls *a* and *b*). Chlorophylls *a* and *b*, which absorb light in both blue and red spectral areas, are green in colour, the former being described as blue-green and the latter as yellow-green.

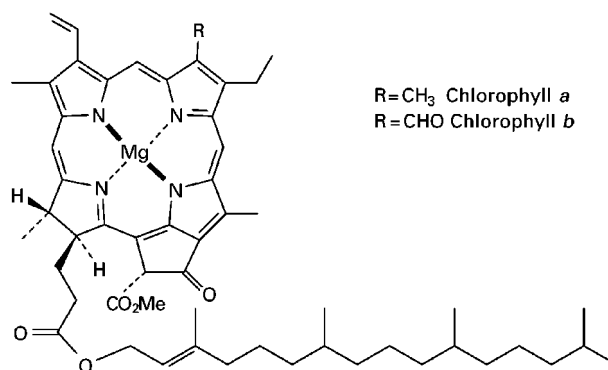
**Figure 3** Structure of chlorophylls.

Table 2 Thin-layer chromatography of chlorophylls and derivatives (R_F values)

Chlorophyll derivative	R	R'	Magnesium	Colour	System 1	System 2
Pheophytin <i>a</i>	CH ₃	Phy	No	Grey	0.93	0.40
Pheophytin <i>b</i>	CHO	Phy	No	Yellow-brown	0.88	0.33
Chlorophyll <i>a'</i>	CH ₃	Phy	Yes	Blue-green	0.80	0.31
Chlorophyll <i>a</i>	CH ₃	Phy	Yes	Blue-green	0.76	0.27
Chlorophyll <i>b'</i>	CHO	Phy	Yes	Yellow-green	0.60	0.25
Chlorophyll <i>b</i>	CHO	Phy	Yes	Yellow-green	0.57	0.22
Pheophorbide <i>a</i>	CH ₃	H	No	Grey	0.36	
Pheophorbide <i>b</i>	CHO	H	No	Yellow-brown	0.18	
Chlorophyllide <i>a</i>	CH ₃	H	Yes	Blue-green	0.08	
Chlorophyllide <i>b</i>	CHO	H	Yes	Yellow-green	0.05	

Structures may be derived from Figure 3 (Phy = phytyl). System 1: cellulose layer (0.1 mm, Merck Art. 5716), light petroleum (40–60°C)–acetone (80 : 20). System 2: silica gel 60 (0.25 mm, Merck Art. 5721), diethyl ether–acetone–isooctane (20 : 20 : 60). All compounds show red fluorescence under UV light.

The relative amounts of chlorophylls *a* and *b* found in higher plants vary according to the species being investigated and prevailing light conditions, a ratio of about 3 : 1 being normal, while the ratio increases in plants growing in sunny situations and decreases in those found in shade. The C-10 epimers, chlorophylls *a'* and *b'*, which co-occur with the main chlorophylls in extracts, are now believed to be present in intact tissue. Other compounds often found in extracts are pheophytins *a* and *b* which differ from the parent chlorophylls only in lacking the magnesium ion, and the pheophorbides where the phytyl chain too has been lost. In addition, the very polar chlorophyllides which are simply derived by hydrolysis of the phytyl ester function in chlorophylls *a* and *b* are often present in small amounts. The pheophytins, pheophorbides and chlorophyllides are regarded as decomposition products produced during extraction.

Water-miscible solvents such as methanol and acetone are normally used for extraction of the chlorophylls which is often carried out in the presence of sodium carbonate to ensure neutralization of acidic impurities. Great care is also required during extraction to avoid undue exposure to heat or light as these lead to increased structural alteration. The extracted pigments are transferred to diethyl ether for concentration and analysis. Chlorophylls can be purified as their readily formed and moderately stable dioxane complexes.

Chlorophylls are normally applied to either cellulose or silica gel thin layers as acetone or diethyl ether solutions. Retention behaviour for illustrative systems may be found in Table 2, where structural parameters are also indicated. A densitometric trace obtained after chromatography of parsley chlorophylls can be found in Figure 4. In all cases the chlorophyll *a* derivative is less retained than the *b* derivative, an expected result of the presence of the

additional aldehyde function in the latter set. While loss of the magnesium ion leads to a reduction in polarity, loss of the phytyl group has the opposite effect. The chlorophyllides which lack the lipophilic phytyl chain remain close to the baseline in these systems.

Extraction The tissue being examined is mixed with 5 volumes of acetone containing small amounts of sodium carbonate, and macerated in a laboratory mixer for 2–3 min. This procedure is repeated until the matrix is colourless. The extracts are combined and concentrated to small volume under reduced pressure, 5% aqueous sodium chloride is added (to increase ionic strength and lessen the solubility of the pigments in the aqueous phase) and the resulting mixture is ex-

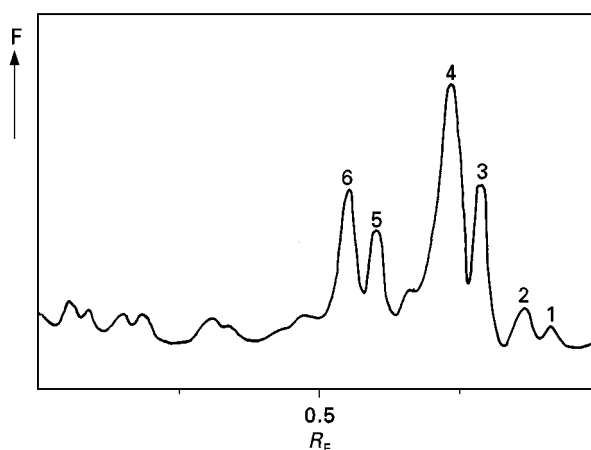


Figure 4 Densitometric trace (fluorescence, excitation at 366 nm, reflectance mode) of a chromatogram of chlorophyll pigments and derivatives obtained from parsley (*Petroselinum crispum*). Cellulose layer (0.1 mm, Merck Art. 5716), light petroleum (40–60°C)–acetone (80 : 20). Identification of zones: 1, pheophytin *a*; 2, pheophytin *b*; 3, chlorophyll *a'*; 4, chlorophyll *a*; 5, chlorophyll *b'*; 6, chlorophyll *b*. Minor zones are not identified.

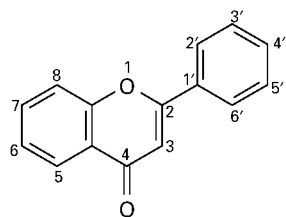


Figure 5 Flavone skeleton showing standard numbering.

tracted repeatedly with similar volumes of diethyl ether. The diethyl ether extracts are combined and taken to dryness under reduced pressure at less than 40°C. The dried material can now be dissolved in fresh diethyl ether for application to the thin-layer plates.

Identification All chlorophyll derivatives show a bright red fluorescence under UV ultraviolet light. Chlorophylls *a* and *b* are commercially available, but can be readily obtained by extraction as described above from spinach. Pheophytins can be prepared by treating diethyl ether solutions of the parent chlorophylls for 2 min with 13% hydrochloric acid. The use of more concentrated acid (30%) leads to the production of the pheophorbides. Chlorophyllides can be obtained if required by enzymatic hydrolysis of the chlorophylls themselves.

Flavonoids

The major classes of the yellow flavonoids are the flavones and flavonols and these will be discussed here. In the next section, the red-blue anthocyanins will be treated. The minor flavonoid classes can in most cases be investigated by similar systems to those described here for flavones and flavonols. The flavonoids are widely distributed in the plant kingdom and are said to occur in all vascular plants. Flavonoids can occur either as the aglycones or more usually as glycosides; the number of known glycosides of quercetin, for example, is in excess of 100.

The flavonoids are made up of two phenyl rings connected by a 3-carbon unit; the various classes are defined by the nature of the bridging unit between the two aromatic systems. The basic flavone structure and the numbering of the skeleton are given in **Figure 5**. Flavonols are regarded as a separate class although they differ from the flavones only in having a 3-hydroxyl group. The normal positions for oxygenation in these compounds are at 5 and 7 in the condensed system (ring A) and at 3', 4' and 5' in ring B.

Flavonoids are readily extracted from plant tissue by maceration in warm methanol and methanol–water mixtures. Where flavonoids are present as glycosides, additional information is to be had by

Table 3 Thin-layer chromatography of flavonoid glycosides (R_F values)

Compound	Source	Position of OH-substituents	R_F
<i>Flavone glycosides</i>			
Apigenin-7-O-glu	c	5,7,4'	0.57
Apigenin-8-C-glu	a	5,7,4'	0.56
Apigenin-7-O-apiosylglu	d	5,7,4'	0.39
Apigenin-6-C-glu-7-O-glu	b	5,7,4'	0.20
Luteolin-7-O-glu	c	5,7,3',4'	0.54
Diosmetin-7-O-rhaglu	e	5,7,3' and 4'-OMe	0.31
<i>Flavonol glycosides</i>			
Kampferol-3-O-rha	f	3,5,7,4'	0.72
Kampferol-3-O-glu	g	3,5,7,4'	0.65
Kampferol-3-O-gal	f	3,5,7,4'	0.59
Quercetin-3-O-rha	h	3,5,7,3',4'	0.69
Quercetin-3-O-glu	i	3,5,7,3',4'	0.53
Quercetin-3-O-gal	h	3,5,7,3',4'	0.51
Quercetin-3-O-rut	j	3,5,7,3',4'	0.30
Isorhamnetin-3-O-glu	k	3,5,7,4' and 3'-OMe	0.58
Isorhamnetin-3-O-rut	k	3,5,7,4' and 3'-OMe	0.36
Myricetin-3-O-rha	l	3,5,7,3',4',5'	0.58
Myricetin-3-O-glu	m	3,5,7,3',4',5'	0.46
Myricetin-3-O-gal	n	3,5,7,3',4',5'	0.45

System: Silica Gel 60 F₂₅₄ (0.25 mm, Merck Art. 5715) with developing solvent: ethyl acetate–formic acid–acetic acid–water (100 : 11 : 11 : 27). Sources: a, *Anthemis nobilis*; b, *Crataegus monogyna*; c, *Petroselinum* spp.; d, *Saponaria officinalis*; e, *Diosma crenulata*; f, *Menyanthes trifoliata*; g, *Astragalus* spp.; h, *Betula* spp.; i, *Equisetum arvense*; j, *Ruta graveolens*; k, *Calendula officinalis*; l, *Myrica rubra*; m, *Primula sinensis*; n, *Camellia sinensis*. glu, glucoside; rut, rutinoside; gal, galactoside; rha, rhamnoside.

subjecting them to acid hydrolysis which only C-glycoside links survive. The products are recovered, dissolved in organic solvent and then subjected to chromatographic analysis.

While a large number of systems can be used to analyse the glycosides, experience suggests that adequate separations can be obtained on silica gel with a solvent systems containing ethyl acetate–formic acid–acetic acid–water in the proportions 100 : 11 : 11 : 27 v/v. Visualization is accomplished by spraying with a 1% diphenylborinic acid ethanolamine ester (Natural Product Reagent A) solution in methanol and thereafter with polyethylene glycol (PEG 4000). The plates are examined under ultraviolet light (366 nm) and the compounds are seen as spots in various yellow-orange-brown-green hues. Table 3 gives the chromatographic behaviour of some flavonoid glycosides with this system. It is apparent that the fact that the flavonols have an extra hydroxyl function does not give an immediately obvious increase in polarity. However, it should be borne in mind that the glycosidic substituent is found on the less exposed 3-position in the flavonols as against more exposed positions in the flavones. However, within each group it is apparent that increasing oxygenation increases polarity somewhat. Much larger

changes in polarity are observed on changing the sugar involved: the rhamnosides are less retained than the glucosides, which in turn are less retained than the galactosides. Unsurprisingly, the biosides and diglycosides are again more retained than the simple monoglycosides.

A wide variety of systems are available for the analysis of free flavonoid aglycones. Examples of such analysis using silica gel, polyamide and reversed-phase (RP 18) layers are given in Table 4. The detection system used is as for the glycosides. Here the trends are more readily seen, with increasing oxygenation, in particular the presence of additional hydroxyls, in general leading to increasing polarity. However, the presence of the 3-OH group in the flavonols opens the possibility of hydrogen bonding to the 4-keto group and thus a corresponding reduction in polarity. Correspondingly, while O-methylation normally reduces polarity, this effect is much reduced when the methylation is of the 3-OH group, since this again frees the keto group from intramolecular hydrogen bonding.

Extraction procedure The intact tissue is cut into small pieces and then macerated with 3 volumes of warm methanol for 2 min, and thereafter stirred for a few

Table 4 Thin-layer chromatography of flavonoid aglycones (R_f values)

Pigment	Colour	Substituents		System		
	(UV)	OH	OMe	1	2	3
<i>Flavones</i>						
Flavone	Blue			0.60	0.86	0.29
5-Hydroxyflavone	Brown	5		0.74	0.88	0.22
7-Hydroxyflavone	Brown	7		0.48	0.51	0.41
Chrysin	Brown	5,7		0.57	0.52	0.33
Apigenin	Green	5,7,4'		0.46	0.18	0.48
Acacetin	G-green	5,7	4'	0.54	0.45	0.30
Apigenin-7',4'-dimethyl ether	G-green	5	7,4'	0.66	0.86	0.14
Luteolin	Yellow	5,7,3',4'		0.38	0.06	0.53
Diosmetin	Green	5,7,3'	4'	0.43	0.41	0.46
<i>Flavonols</i>						
Kaempferol	Y-green	3,5,7,4'		0.48	0.14	0.57
Kaempferid	B-green	3,5,7	4'	0.59	0.38	0.37
Kaempferol-7,4'-dimethyl ether	B-green	3,5	7,4'	0.73	0.74	0.18
Kaempferol-3,7,4'-trimethylether	Green	5	3,7,4'	0.69	0.87	0.19
Quercetin	Brown-o	3,5,7,3',4'		0.41	0.06	0.67
Rhamnetin	Orange	3,5,3',4'	7	0.48	0.24	0.45
Quercetin-3,7-dimethyl ether	Orange	5,3',4'	3,7	0.46	0.47	0.46
Morin	Green	3,5,7,2',4'		0.29	0.02	0.73
Fisetin	Orange	3,7,3',4'		0.36	0.08	0.70
Robinetin	Orange	3,7,3',4',5'		0.22	0.01	0.82

System 1: Silica gel 60 F₂₅₄ (0.25 mm, Merck Art. 5715) toluene–ethyl formate–formic acid (50 : 40 : 10); system 2: polyamide (0.15 mm, Merck Art. 5555/0025), toluene–butanone–methanol (60 : 25 : 15); system 3: RP-18 F₂₅₄ (0.25 mm, Merck Art. 15425) methanol–formic acid–water (58 : 10 : 16). Solvent compositions by volume. Colour observed under 366 nm after spraying with Natural Product Reagent A followed by polyethyleneglycol (PEG-4000): b, blue; o, orange; y, yellow.

minutes while heating to about 60°C. Filtration can be followed by a second extraction with a 1:1 mixture of methanol and water. The extracts are combined, the solvents removed and the pigments redissolved in methanol prior to application to the thin layers for separation.

Hydrolysis The dried extract is dissolved in equal volumes of methanol and 2 mol L⁻¹ hydrochloric acid and refluxed for 1 h. The mixture is then cooled and the aglycones extracted into diethyl ether or ethyl acetate. The resultant solution is taken to dryness under reduced pressure and then redissolved in fresh organic solvent prior to analysis. The sugars freed during this process remain in the water solution and these too may be analysed by thin-layer methods.

Identification A considerable number of flavonoid aglycones and glycosides are available commercially. Pure compounds can be isolated from established sources, many of which can be found in the monographs on flavonoid compounds given in the Further Reading section. In the absence of reference com-

pounds, observed polarities and the colours in ultra-violet light after treatment with diphenylboronic acid ethanolamine ester provide valuable evidence of identity.

Anthocyanins

The glycosidic anthocyanins are closely related to the flavonoid classes discussed above, sharing the same basic skeleton. They lack the 4-keto function and have the heterocyclic ring aromatized and thus occur as salts. They provide red-blue colours depending on the substitution pattern present. Only six aglycone anthocyanidins are usual and the structures of these are to be found in **Figure 6**. Both glycosides and aglycones are found in red to purple plant tissues in plants, and they are responsible for the familiar colours of many deep red fruits and fruit juices and red wine, as well as occurring in the leaves of many red-purple ornamental varieties of trees and bushes.

Since the anthocyanins are salts they must be extracted into acidic media. Methanol containing 1% concentrated hydrochloric acid is well suited, although if milder conditions are required, as for

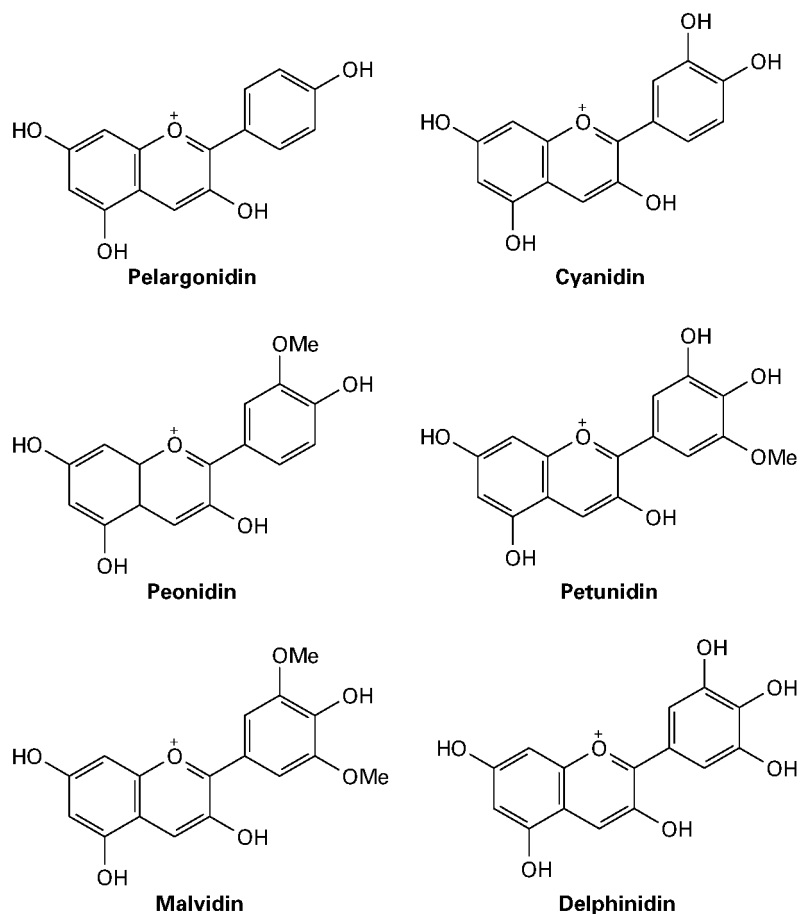


Figure 6 Structures of the most usual anthocyanidins.

Table 5 Thin-layer chromatography of anthocyanidins and anthocyanins (R_F values)

Pigments	Source	Type	System		
			1	2	3
<i>Anthocyanidins</i>					
Delphinidin	a			0.11	0.03
Petunidin	a			0.20	0.05
Cyanidin	a			0.22	0.06
Malvidin	a			0.27	0.07
Peonidin	a			0.31	0.08
Pelargonidin	a			0.35	0.11
<i>Anthocyanins</i>					
Dp-3-glu	b	Mono	0.08	0.38	0.13
Pt-3-glu	c	Mono	0.13	0.49	0.23
Cy-3-glu	b	Mono	0.17	0.51	0.25
Mv-3-glu	c	Mono	0.22	0.64	0.34
Pn-3-glu	c	Mono	0.25	0.64	0.38
Pg-3-glu	d	Mono	0.32	0.65	0.40
Dp-3-rut	b	Bioside	0.24	0.69	0.36
Cy-3-rut	b	Bioside	0.35	0.69	0.49
Pn-3-rut	e	Bioside	0.47	0.76	0.63
Cy-3-sam	f	Bioside	0.47		0.64
Cy-3-sop	f	Bioside	0.62	0.81	0.75
Cy-3,5-diglu	g	di	0.38	0.70	0.52
Pn-3,5-diglu	g	di	0.49	0.81	0.67
Cy-3-glurut	f	tri	0.80	0.86	0.88

Pigment name abbreviations: Dp, Delphinidin; Pt, Petunidin; Cy, Cyanidin; Mv, Malvidin; Pn, Peonidin; Pg, Pelargonidin; glu, glucoside; rut, rutinoside; sam, sambubioside; sop, sophoroside; glurut, (2^o-glucosyl) rutinoside.

Sources: a, hydrolysis product; b, *Ribes nigrum* berry; c, *Vitis vinifera* fruit; d, *Fragaria* spp. berry; e, *Prunus* spp. fruit; f, *Rubus idaeus* berry; g, *Fuchsia* spp. flowers. Glycoside types are indicated as mono (monoglycoside), di (diglycoside), tri (triglycoside) and bioside (glycosylglycoside). R_F values are given for cellulose layers (0.1 mm, Merck Art. 5716), using for development mixtures of concentrated hydrochloric acid, formic acid and water as follows: system 1 (19:19:62), system 2 (7:51:42) and system 3 (25:24:51).

example when the sugar moiety is acylated, this may be replaced by methanol containing 5% acetic acid. After concentration, the solution can be directly subjected to thin-layer chromatography on cellulose.

The individual anthocyanins may be subjected to hydrolysis by refluxing in hydrochloric acid for an hour, after which time the liberated anthocyanidins are extracted into 1-pentanol. The solution is evaporated to dryness under a stream of nitrogen, then redissolved in methanolic hydrochloric acid. This solution can be used directly for chromatography.

Results obtained for the separation of anthocyanins and anthocyanidins on cellulose layers using hydrochloric acid-formic acid-water mixtures as developing solvents are to be found in Table 5. The major trends in the results are immediately obvious.

Looking first at the anthocyanidins it can be seen that polarity increases with the number of hydroxyls present, while the presence of methoxyls has a much smaller effect. Examination of the monoglucosides shows that while a considerable increase in polarity is observed as a result of glucosylation, the effect seen above is carried over to this group of compounds. The same trend is seen in the even more polar biosides where the rutinosides are ordered in the same way and in the diglucosides where cyanidin diglucoside is less polar than the corresponding peonidin derivative. The single triglycoside examined is, as expected, even more polar than the diglycosides. These general findings are well seen in the chromatographic results obtained on separation of the pigments from raspberry and blackcurrant fruits (Figure 7).

Extraction procedure The intact tissue is cut into small pieces and then macerated with 3 volumes methanol containing 1% concentrated hydrochloric acid for 3 min. The extract is decanted and retained, and the procedure repeated twice. The extracts are then collected together and an equal volume of petroleum ether (40–60°C) added. After shaking vigorously for 2 min the layers are separated and the aqueous extract re-extracted in the same way with a further portion of petroleum ether. The defatted extract is then dried under reduced pressure. The pigments are redissolved in methanolic hydrochloric acid for chromatographic analysis.

Hydrolysis The defatted extract is dissolved in equal volumes of methanol and 8 mol L⁻¹ hydrochloric acid and refluxed for 1 h. The mixture is then cooled and the free anthocyanidins extracted by shaking with 1-pentanol. The 1-pentanol layer is separated and the solvent is removed in a stream of nitrogen (35°C). The anthocyanidins are then redissolved in methanol containing 1% concentrated hydrochloric acid. The sugars freed during this process remain in the water solution and these too may be analysed by thin-layer methods.

Identification Anthocyanins are not readily available commercially and are best extracted freshly from established sources. The anthocyanidins are then readily obtained by hydrolysis as described above. The specialized flavonoid monographs suggested for further reading give long lists of suitable sources.

Other Pigments

A large number of other pigment groups occur in nature. Among the less polar and more abundant

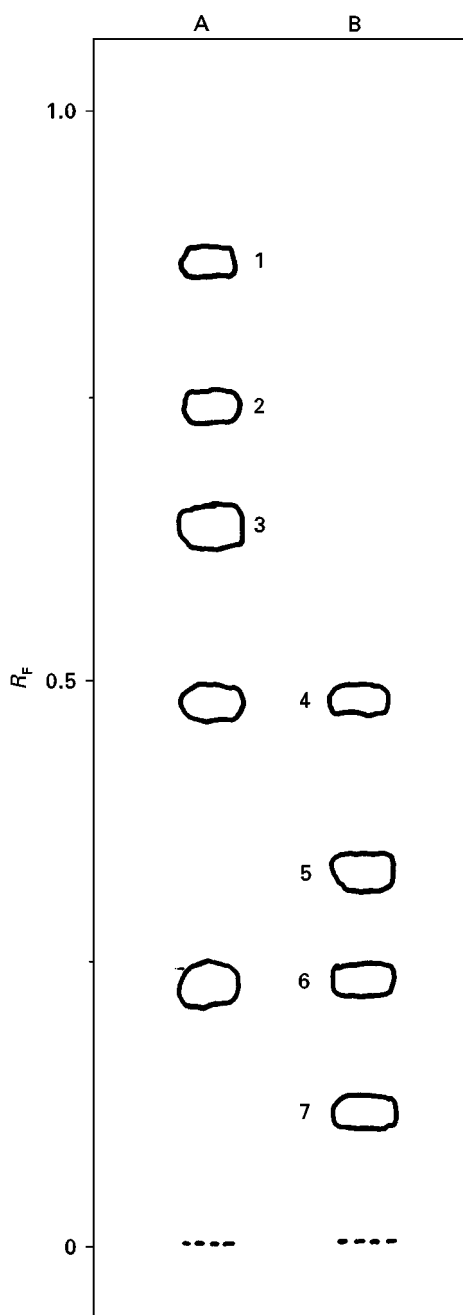


Figure 7 Chromatography of anthocyanins from (A) raspberry (*Rubus idaeus*) and (B) blackcurrant (*Ribes nigrum*). Cellulose layer (0.1 mm, Merck Art. 5716) using for development a mixture of concentrated hydrochloric acid, formic acid and water (25:24:51). Identification of zones: 1, cyanidin-3-(2^G-glucosyl)rutinoside; 2, cyanidin-3-sophoroside; 3, cyanidin-3-sambubioside; 4, cyanidin-3-rutinoside; 5, delphinidin-3-rutinoside; 6, cyanidin-3-glucoside; 7, delphinidin-3-glucoside.

of these are the various quinones, which can be investigated by thin-layer chromatography, although no particular system seems to be useful for more than a small groups of compounds. Other compounds

which should be mentioned are the many groups of tetrapyrrole pigments, both cyclic and acyclic, but these are highly polar and individual chromatographic systems are again required for each type.

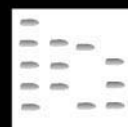
Future Trends

The popularity of thin-layer chromatography for the analysis of pigments seems likely to continue as interest in natural pigments as food colorants increases. The possibility of carrying out some 20 parallel analyses on a single plate in 1 h ensures that the method represents a good alternative to high performance liquid chromatography. The fact that thin-layer chromatographic systems are cheap and easy to use, that the results are immediately observable, and that the method is both rugged and transportable will probably lead to increasing applications in the production side of the food industry. Applications of this type would be expected to lead fairly rapidly to an increase in the relatively small number of specialized spray reagents presently available for work with pigments.

Further Reading

- Andersen ØM and Francis GW (1996) Natural products. In: Sherma J and Fried B (eds) *Handbook of Thin Layer Chromatography*, pp. 715–752. New York: Marcel Dekker.
- Britton G, Liaen-Jensen S and Pfander H (eds) (1995) *Carotenoids*, vol. 1A. *Isolation and Analysis*. Basel: Birkhäuser.
- Goodwin TW (ed.) (1976) *Chemistry and Biochemistry of Plant Pigments*, 2nd edn. London: Academic Press.
- Goodwin TW (1980) *The Biochemistry of the Carotenoids I—Plants*. London: Chapman & Hall.
- Goodwin TW (1984) *The Biochemistry of the Carotenoids II—Animals*. London: Chapman & Hall.
- Gross J (1991) *Pigments in Vegetables*. New York: Van Nostrand Reinhold.
- Harborne JB (1967) *Comparative Biochemistry of the Flavonoids*. London: Academic Press.
- Harborne JB and Mabry TJ (eds) (1982) *The Flavonoids: Advances in Research*. London: Chapman & Hall.
- Harbone JB, Mabry TJ and Mabry H (eds) (1975) *The Flavonoids*. London: Chapman & Hall.
- Markakis P (1982) *Anthocyanins as Food Colours*. London: Academic Press.
- Markham KR (1982) *Techniques of Flavonoid Identification*. London: Academic Press.
- Parker L (ed.) (1992) *Methods in Enzymology*, vol. 213 – *Carotenoids*. San Diego: Academic Press.
- Sesták Z (1982) Thin layer chromatography of chlorophylls 2. *Photosynthetica* 16: 568–617.
- Stahl E (1969) *Thin Layer Chromatography*, 2nd edn. New York: Springer Verlag.

POLYCHLORINATED BIPHENYLS: GAS CHROMATOGRAPHY



D. E. Wells, FRS Marine Laboratory, Aberdeen, UK

Copyright © 2000 Academic Press

Introduction

From the initial detection of polychlorinated biphenyls (PCBs)* in biological tissue in the 1970s by Jensen there has been a continuous development in the analytical chromatographic techniques to determine these chemicals (Table 1). PCBs occur as complex mixtures which have a considerable impact on the cost of a complete analysis. Highly sophisticated techniques are required for the congener separation, and clean-up methods to prepare the samples tend to be labour intensive. Multi-residue methods in which several polyhalogenated hydrocarbons (PHHs) groups such as chlorobornanes (toxaphene), polychlorinated naphthalenes (PCNs), polychlorinated dibenzo-*p*-dioxins (PCDDs), polychlorinated dibenzofurans (PCDFs), polychlorinated diphenyl ethers (PCDEs) and their brominated homologues, can be determined in parallel are available, but this approach can lead to a compromise, resulting in lower recoveries and unresolved peaks in the chromatograms.

The first separation of PCBs was obtained using packed gas chromatographic columns with industrial formulations as calibration standards to quantify a single total value for the PCB. This early technology did not have the resolution to separate the PCBs into individual congeners and the most appropriate method to estimate these contaminants at that time was unquestionably by the summation of the peak heights or areas of the low resolution chromatogram. The continual development of sample preparation, chromatographic separation and the final determination has improved the reliability of the data in many laboratories. This has allowed a more detailed interpretation of the data, including the toxic non-ortho chloro and mono-ortho chlorobiphenyls (CBs).

Of the 209 CBs, 132 have been measured in industrial formulations at or above the 0.05% level. The original selection of CBs, made by the European

Union Community Bureau of Reference in 1982, included CB 28, 52, 101, 118, 138, 153, and 180 and has now been adopted widely in many terrestrial, marine and food monitoring programmes. However this limited number of congeners was insufficient to study the specific toxicological effects and spatial patterns of these contaminants. These congeners, on their own, do not provide data for the TEQ† values needed for legislative or for environmental policy purposes.

The groups of toxic of CBs are:

Non-ortho CBs	CB 77, 81, 126, 169
Mono-ortho CBs (penta)	CB 105, 114, 118, 123
Mono-ortho CBs (hexa)	CB 156, 157, 167
Mono-ortho CBs (hepta)	CB 167

A schematic diagram of the isolation, separation, clean-up, group separation and final detection in environmental matrices in relation to the chromatographic separation of the congeners is given in Figure 1.

Sample Preparation for Gas Chromatography (GC)

The main difficulties for CB analysis are still the separation of these congeners (i) from other co-extractants both at the bulk level, e.g. lipids, (ii) from other trace contaminants, e.g. chlorobornanes (toxaphene) and (iii) from other interfering congeners, e.g. CB 77 and CB 110. With the present methodology it is now possible to measure individual CBs routinely at the pg kg^{-1} and with care at the fg kg^{-1} . Trace amounts of co-extracted materials such as lipids, wax esters and sulfur degrade the analytical chromatographic column which is both expensive and time-consuming to replace. Effective clean-up of the sample extracts is essential prior to GC and liquid chromatography (LC)-GC separation because traces of lipids (0.1 mg) will become significant if the final sample volume is reduced to ca. 100 μL .

Destructive clean-up methods are mainly alkaline treatment (saponification) or oxidative dehydration (sulfuric acid treatment). Alkaline treatment is similar

*The term 'Polychlorinated Biphenyl (PCB)' refers to the technical mixtures found in the formulation and the measurements made on the basis of calibration with these mixtures. *Chlorobiphenyl (CB)* refers to the individual congener named by the Ballschmitter number.

†TEQs refer to the sum of the concentration of the congener equivalent to 2, 3, 7, 8 TCDD obtained by using the toxic equivalence factor for each PCB.

Table 1 Chronological development of chlorobiphenyl analysis

<i>Year</i>	<i>Development</i>
1925	Large scale manufacture of PCB formulations.
1966	First reported measurement of PCBs as 'Avian Peaks'. Packed GC column separation of PCBs. Concentration in samples estimated against industrial formulations and summation of mixed component peaks in the chromatogram.
1969	Development of adsorption column chromatography for clean-up of biological tissue.
1975	Introduction of glass capillary columns. Improved separation of PCBs.
1970's	Development of stable GC evens and electronics to improve reproducibility of retention indices.
1980	Individual chlorobiphenyl congeners identified and systematically numbered. Introduction of fused silica capillary columns. Improved GC column stability.
1984	Retention times of all 209 CBs measured on an SE 54 capillary column.
1985	Reference materials, certified for individual CBs become available. Commercial availability of many of the 209 CBs. Reports of retention times on polar and semi-polar stationary phases. Development of multi-dimensional chromatography.
1988	Focus on the analysis of planar, toxic CBs and the application of toxic equivalence concentrations (TECs) for CBs as well as dioxins.
1989	Separation of CBs on the basis of their spatial configuration. Identification of all congeners present in main commercial formulations.
1989–1993	LC/GC coupled online. Development of multidimensional GC.
1990	Use of pyrenyl-silica HPLC for separation of non- and mono-ortho CBs.
1990's	Development and application of novel extraction techniques including accelerated solvent extraction, microwave assisted extraction, Soxhtec, supercritical fluid extraction.
1992	Expansion of retention data for 5 GC phases of different polarity for all congeners in commercial mixtures (> 0.05%), except CB 69, 75, 96 and 182; series coupled columns.
1993	SFE-GC coupled techniques.
1995	Improvements of pyrenyl-silica HPLC separation through temperature control.
1994/8	Use of pyrenyl-silica column for separation of CBs and PCDD/Fs.
1997/9	Modular multidimensional gas chromatography.

to the saponification used in conjunction with extraction, but is applied sequentially to the solvent extraction instead of applying it to the matrix directly.

Non-destructive methods use solid-phase columns, gel permeation techniques and dialysis. Alumina columns are very effective and probably one of the most frequently used clean-up methods. Silica and florisil columns are alternative adsorbents. Gel Permeation Chromatography (GPC) or size exclusion chromatography (SEC) has also been used for lipid removal and for separation based on molecular size. SX-3 Bio Beads are used in most cases. Dialysis techniques include the use of a polythene film of pore size ca. 50 μm . The CBs migrate from the fat through the polythene tube to the cyclohexane solvent surrounding the tube. Dynamic dialysis inside a Soxhlet gives a recovery of over 95% in 8 h. The rate of dialysis is temperature dependent with the optimum temperature being around 43°C, above which the lipids are also dialysed at an unacceptable rate. Sulfur must be removed from the sample extracts by percolation through an activated copper column, since the element is sufficiently soluble in organic solvents and, in large quantities, can completely saturate the detector signal, particularly the ECD.

Group Separation

Group separation of the CBs is necessary (i) to separate the non-ortho CBs and the mono-ortho CBs that occur at relatively lower concentrations, e.g. CB 105, CB 156 from the other congeners, (ii) to remove other interfering PHHs and (iii) to remove further traces of co-extracted material remaining from the extraction of the bulk matrix.

Silica gel columns containing 1–2 g of adsorbent are frequently used to obtain such a pre-separation. The CBs and chlorobenzenes are eluted with a non-polar solvent (hexane or iso-octane) in the first fraction. Other sorbents such as florisil have also been used.

The isolation of the non-ortho CBs is based primarily on the planarity of the molecule compared with the ortho CBs, and as such these congeners tend to be separated along with other planar PHHs. There are three techniques used to fractionate PCDDs, PCDFs and planar CBs. These methods use gravity carbon columns, HPLC with graphitized carbon columns and HPLC with PYE [2-(1-pyrenyl) ethyl dimethyl silica] columns. Other HPLC column phases have been developed to isolate the planar contaminants from other PHHs including 2,4-dinitrophenyl mer-

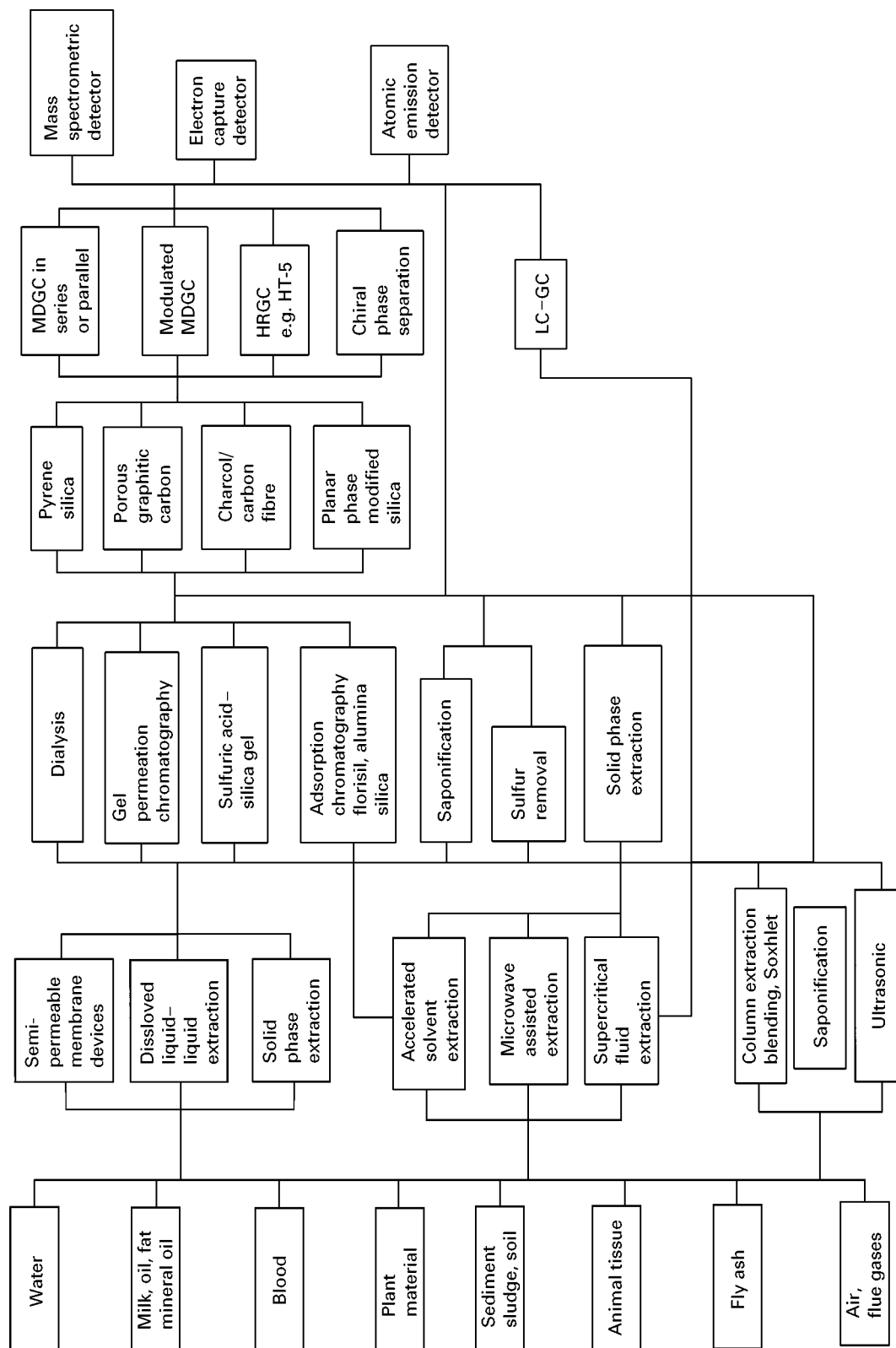


Figure 1 The schematic flow diagram of the analysis of chlorobiphenyls. The connecting routes show the types of environmental samples, the methods of extraction which are currently available, the clean-up techniques, the group separation, high resolution chromatographic separation and the range of detectors used for the final measurement.

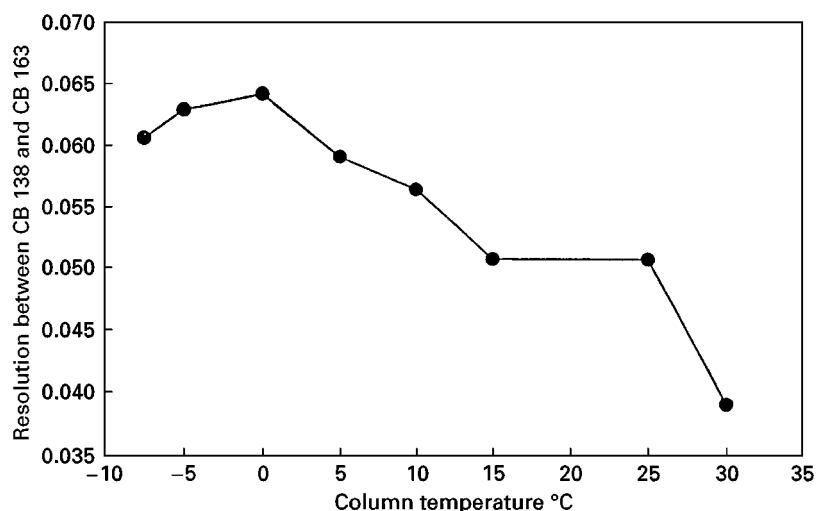


Figure 2 The resolution between CB 138 and CB 163 on a pyrenyl-silica HPLC column, 250 × 0.46 mm. i.d. as a function of the column temperature. The maximum resolution occurs around 0°C. The column cooling was controlled by a solid-state Peltier heat pump.

captroparyl silica (DNMPM), dinitroanilinepropyl silica (DNAP) and tetranitrofluoriminopropyl silica (TENF). When the congeners are finally determined by GC, it is not necessary for them to be resolved from each other by HPLC.

The separation of CBs on the Comosil PYE column is temperature dependent (Figure 2). One of the more difficult separations between CB 138 and CB 163 on most GC columns* is possible on the PYE column providing that the column temperature is reduced to ca. 0°C. The porous graphitic carbon column to separate CB 77 and CB 110 along with the other non-ortho and mono-ortho CBs uses a double forward and reverse constant flow with hexane as an eluant.

LC-GC Combinations

Linking LC with GC aids the development of automated analysis and reduces the likelihood of contamination. There is also a substantial increase in the resolving power of 2D chromatography over a single system, especially where the polarity of the phases is orthogonal. The preferred combination of columns can sometimes be difficult because the polarity of the phases and the solvents used can make the linking difficult. Interfacing the LC to the GC has also been hampered by the relative volumes of the carrier fluids (liquids and gases). Rather than have a continuous flow-through system, we can overcome both difficulties in linking LC with GC by using the modulated approach by cryofocusing the eluate from the first column, removing the first solvent before flushing

onto the second column with an alternative fluid, i.e. a second solvent in the case of LC-LC, or by flash vaporizing into the carrier gas in the case of LC-GC.

Gas Chromatography

The chromatographic separation techniques for different congener groups is given in Table 2.

Sample Injection

There are three main injection techniques used in the analysis of CBs in environmental tissues, the splitless, the programmed temperature vaporizing (PTV), and the on-column injector. The splitless injector is used by most laboratories for CB analysis and must be optimized for splitter time, needle length in relation to the length and volume of the injector, and the type and cleanliness of the injection liner. The advantage of the on-column over the splitless injector is that the optimum conditions are more straightforward and there is less opportunity for mass discrimination over the range of CBs, primarily since all of the sample is injected onto the column. However, the sample must undergo a rigorous clean-up. Insufficiently cleaned samples seriously affect the column performance when using an on-column injector, whereas analyses with a splitless injector are less affected by non-volatile deposits. Only the glass liner requires regular, routine replacement.

Chromatographic Phases

Packed columns used in the 1970s and early 1980s have been replaced initially by glass and then by higher resolution, polyimide coated, fused silica cap-

*The separation between CB 138 and CB 163 can now be achieved using the HT5 stationary phase.

Table 2 Chromatographic separation techniques for different groups of congeners

Congener	Group		
	Major mono-ortho CBs 105, 118, 156	Minor mono-ortho CBs 114, 123, 157, 167, 189	Non-ortho CBs 77, 126, 169
<i>Single techniques</i>			
Single-column GC without pre-separation	Possible with care	Difficult	Currently not possible
LC (with diode-array)	Currently not possible	Currently not possible	Possible with care at relatively high levels
MDGC	Easy	Easy	Difficult
<i>Hyphenated techniques</i>			
LC-GC online	Difficult	Difficult	Difficult
Adsorption charcoal	Easy	Difficult	Difficult
PGC*-HPLC-GC offline	Easy	Easy	Easy
PYE-HPLC-GC offline			
LC-GC offline	Easy	Easy	Easy

* PGC, porous graphitic carbon.

illary columns. Stationary phases of different polarities can be used for the determination of CBs, but non-polar and medium-polar phases generally offer a higher resolution.

A number of stationary phases tailored to the separation of CBs (Table 3) have shown considerable improvement over the more conventional proprietary phases available. These phases have had greater success in separating additional congeners when used in series with more conventional columns. A 1,2-dicarba-*closo*-dodecacarborane polydimethylsiloxane (HT-5) column has been used in series with a CPSil-8 (5% diphenyl polydimethylsiloxane) column with helium as carrier gas to separate 84 congeners using an electron-capture detector (ECD) (and

108 congeners using mass spectrometry detection (MS)). The HT-5 column has an upper temperature limit in excess of 300°C enabling fast temperature programming and analysis in less than 60 min. The HT-5 phase has been further optimized by using a 60 m × 0.25 µm i.d. fused silica column with a film thickness of 0.25 µm able to separate 106 congeners with ECD and 138 congeners with MS. This includes the separation of the critical CB 138/CB 163 pair. A prototype smectic liquid-crystalline polysiloxane column is able to separate some CB mixtures that have been more difficult to separate on more conventional columns such as CB 28/31 and CB 138/163. This phase is also useful to separate the non-ortho and mono-ortho CBs.

Table 3 Co-elution CBS on capillary GC columns with different stationary phases

Congener	HT-5	CPSil 5	CPSil 8	CPSil 19	CPSil 88	CPSil 8/HT-5
28	–	–	–	–	16	–
52	–	–	–	–	–	–
77	149	–	110	–	82/183/187	–
101	60	–	84	–	55	84
105	141	132	132	–	129	–
118	–	–	149	–	200/123	149
126	167/185/202	129	129/178	–	–	–
128	159/174	–	167	–	193/201	167
138	–	160/163	160/163	160/163/158	–	160/163
153	–	–	–	–	–	–
156	172	171	202/171	–	–	202
157	–	202	173/200	180/197	–	–
158	175/178	–	–	163/138	138/160	–
169	–	–	–	203/196	–	–
170	–	–	190	190	–	–
180	193	–	–	197	197	–
194	–	–	–	–	–	–

Multidimensional Gas Chromatography (MDGC)

Currently, all of the ca. 132 congeners detectable in formulations and environmental matrices cannot be separated on a single GC or HPLC column (Table 2). However, the separation power can be substantially increased when columns are coupled either in series or in parallel. The greatest separation is obtained by using different systems and/or phase types to maximize the orthogonality of the separations. Multiple columns such as serially-coupled columns parallel-coupled columns, two-dimensional GC and, recently, comprehensive multidimensional GC (MDGC) have been developed to provide greater resolution of complex mixtures such as CBs.

In two-dimensional GC co-eluting compounds are 'heart-cuts' as they elute from the first capillary column and are transferred to a second capillary column of a different polarity which is able to separate the isolated group of compounds. This technique offers a complete separation of certain groups of unresolved congeners which are 'heart-cut' from the first column. The technique is limited by the number of 'heart-cuts' which can be made in one chromatographic run, since more than three to four lead to peak overlap on the second column. Analysis times of the 'heart-cut' two-dimensional GC are also relatively long. Nevertheless this technique has been applied to the determination of CBs in environmental samples. The mono-ortho CBs 60, 74, 114, 123, 157, 167 and 189 have been determined in Aroclor mixtures and seal tissue using MDGC with ECD combining the Ultra 2 and FFAP columns. This direct method was found to be preferable to the separation of the mono-ortho CBs and the other congeners by HPLC. Either MDGC or off line HPLC separation of the mono-ortho CBs is often necessary to reduce the risk of false positive results from interferences since these congeners occur at relatively lower concentrations compared with the di- and tri-ortho CBs.

Comprehensive, modulation MDGC yields truly three-dimensional chromatograms (2D time base \times concentration). Two capillary columns are connected in series by a retention gap which can be heated very quickly in a reproducible way. The eluants from the first column are cryofocused in the retention gap for a period of ca. 3 min, after which time the retention gap, which has a minimum thermal capacity, is heated quickly to 'inject' the focussed compounds onto the second column of different polarity. The second chromatogram lasts for approximately the same period of time as the period of cryofocusing, so that a time series of 3 min chromatograms are produced to provide a two-dimensional separation (Figure 3). Because peaks collected at the

modulator are very highly focussed before they enter the second column, an extremely high sensitivity can be obtained in combination with a very high selectivity.

Chiral Separation

Of the 209 CBs, 78 display axial chirality due to the steric hindrance to free rotation about the C–C axis of the two aryl rings, and of these 19 possess 3 or 4 chlorine atoms in the ortho position. The CBs 84, 88, 91, **95**, 131, **132**, 136, **149**, 171, **174**, 183, and 196 are present in commercial mixtures; the four in bold type are present above the 2% level. GC separation of the 19 stable atropisomers have been made on the following columns:

- 2,3,6-Tri-O-methyl- β -cyclodextrin
- 2,3-Di-O-methyl-6-O-hexyldimethylsilyl- β -cyclodextrin
- 2-6-Di-methyl-3-O-n-pentyl- γ -cyclodextrin
- 6-O-tert-Butyldimethylsilyl-2,3-di-O-methyl- β -cyclodextrin
- tert-Butyldimethylsilylated- β -cyclodextrin.

The enantiopure CBs have been isolated by chiral HPLC. The (–) CBs 84, 132, 136, and 176 eluted before the (+) enantiomers while the order was reverse for CB 135 and 175. The enantiomers CB 95, CB 132 and CB 149 in Clophen A60 have been separated using MDGC to 'heart-cut' the congeners from the first column (DB-5) onto the second chiral phase, heptakis (2,3,6-tri-O-methyl)- β -cyclodextrin (Chirasil-Dex). However, to date none of the enantiomers have been shown to be specifically toxic or able to induce any observable biological effect.

Detection

The power of the GC separation, especially with the thin (0.1 μ m) film phases, must be matched by the sensitivity and the specificity of the detector to measure concentrations of CBs at the 10^{-12} – 10^{-14} level. These low levels of detection are required for the analysis of samples from relatively clean areas of the environment, for example the polar regions, oceanic and remote atmospheric samples. They are also required for samples obtained from small organs from single animals taken as part of biological effects studies or the investigative analysis of human adipose tissue.

Insufficient chromatographic resolution and incorrect calibration of the detector (Table 3) are still the primary source of error in the determination of CBs by GC. Errors associated with the calibration of the detector can be greatly reduced by implementing the

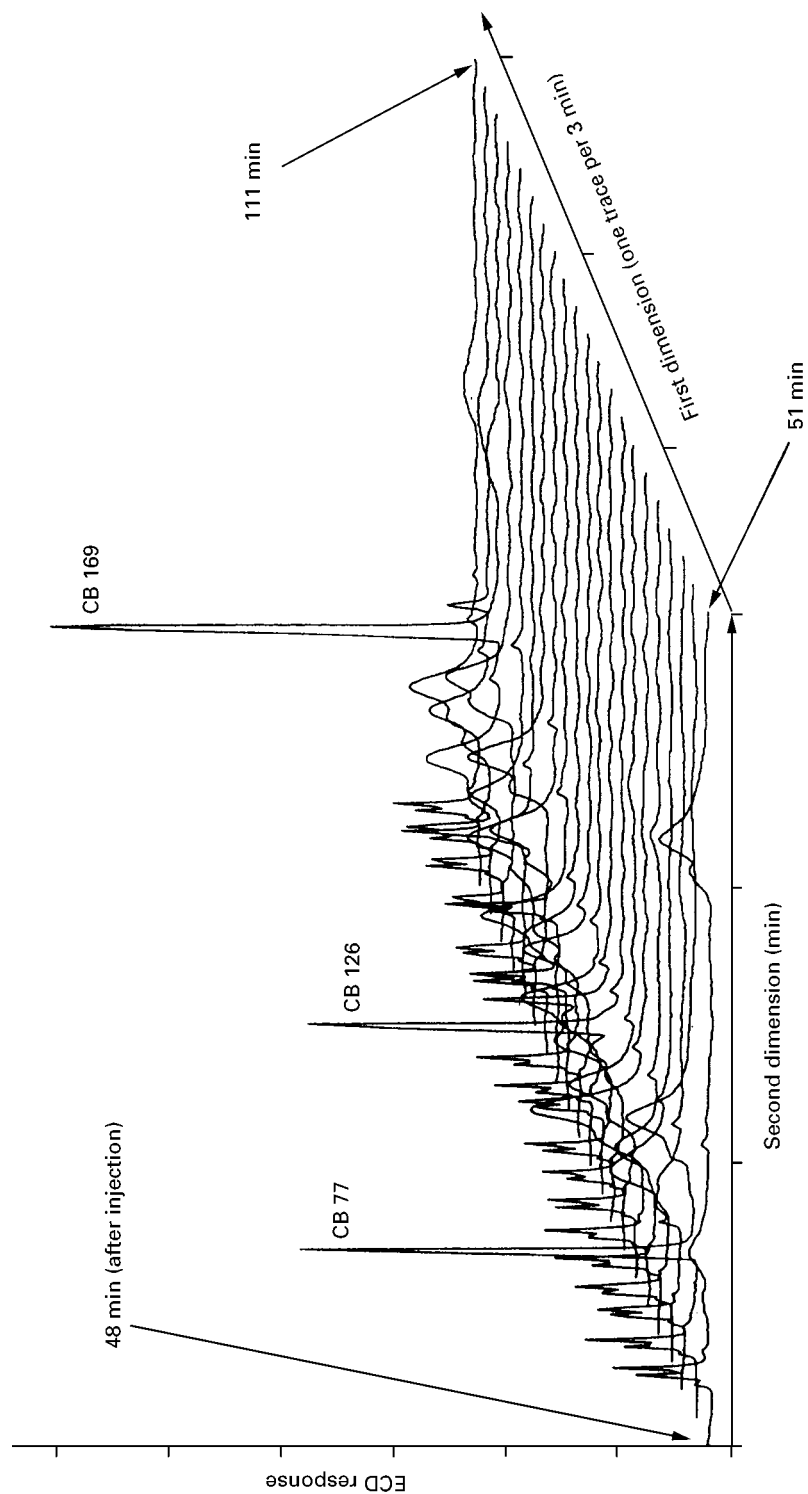


Figure 3 GC-ECD chromatogram of CB 77, CB 126, CB 169 showing the use of the Thermal Desorption Modulator (TDM). The first column was 24 m \times 0.2 mm i.d. 0.15 μ m SB smectic phase, 24 cm 0.1 mm i.d. 0.12 μ m CP Sil 8 TDM and a 5.3 \times 0.2 mm i.d. 0.33 μ m Ultra 2 second column. The TDM was desorbed every 3 min. (Reproduced from Geus H-J de, Boer J de and Brinkman UA (1997) *J. Chromatogr. 767*: 137–151, with permission, from Elsevier Science.)

following guidelines:

- only use certified solids or solutions. These are available for most congeners;
- confirm the identity of the material(s) provided by MS;
- control the preparation dilution and storage of calibrants by weight;
- store ampoule stock and working calibration solutions in a cool dark place. Avoid using screw top containers and do not store screw top containers in the refrigerator;
- confirm the purity of all solvents used by concentrating to ca. $\times 100$ and analysing with an ECD and an FID;
- calibrate the detector with sufficient frequency to ensure the response factor for each congener is ca. $< \pm 5\%$ of the actual response;
- check the frequency of calibration, which is a function of the cleanliness of the GC system;
- check new stock solutions against previous calibration solutions or against independent solutions of known quality.

A summary of the detectors which have been used for the determination of CBs is given in **Tables 4** and **5** along with the relative advantages, disadvantages, relative cost and current detection limits. ECDs were used initially because of their high sensitivity for electronegative compounds, but MS detection has become a routine method for measurement. Modern MS instruments are easy to operate, are more selective than the ECD, and have a better linear range.

Electron-Capture Detection

The most widely used detector for CB analysis is still the ECD. It is inexpensive, easy to use, highly sensitive and selective towards halogenated compounds containing one or more halogen atoms. Unfortunately the detector is not only sensitive to the number of

halogen atoms, but also to the spatial configuration of the molecules and its cross sectional area. This means that the detector response is specific not only to each congener, but also to its enantiomers, if they exist. The detector also has a small linear range, making it effectively non-linear requiring both constant and multi-level calibration, although the small (380 μL) frequency pulsed, constant current detectors have extended the linear range. Recently a micro-ECD with a cell size of ca. 150 μL has been developed to further improve sensitivity and linear dynamic range.

Mass Spectrometry

The mass spectrometric detector (MSD) is fast becoming the preferred alternative to the ECD. The simpler MSD and Ion Trap Detectors (ITDs) have been fully integrated with capillary GC and most instruments now have a fused silica column terminating inside the ion source of the MS. The ITD differs from other MS techniques in that the ions formed by ionisation are trapped electronically and then destabilized according to their mass and transferred to the electron multiplier outside the trap itself. The MSD is now a robust instrument and although it requires more specialist attention than the ECD, it does offer considerably more power in terms of sensitivity, selectivity and confirmatory analysis. The MSD has a much wider linear range than the conventional ECD used for much of the routine CB analysis.

The high resolution MS provides highly specific mass detection with resolution between 6000 and 10 000 provided by accurate mass marking with PFK at m/e 316.9824 to prevent mass drift. This not only offers a high specificity, but also considerably reduces the likely interference with other trace contaminants such as PCDDs and PCDFs.

A further advantage of MS is provided by the increased sensitivity of Negative Ion Chemical Ionization (NICI) with molecules containing more than four chlorine atoms. The sensitivity can be further

Table 4 Summary of methods of calibration

Type	Use/advantage	Misuse/disadvantage
Single point calibration	Semi-quantitative, screening technique, calibrant and sample within ca ± 5 -10% linear detectors	Inaccurate, especially at low concentrations. Not suited to the ECD
Bracketing standards	Small linear range of the ECD. MS detection	Extrapolation beyond the upper and lower limits
Multipoint calibration	Most accurate method for ECD. Requires quadratic or cubic spline type curve fit	Time-consuming in use, maintenance of calibration solutions
Labelled internal standards ^{13}C , ^2H	Mass spectrometric detector, compensates for all recovery losses	Not suitable for ECD. Does not give any information on the intrinsic efficiency of the method.

Table 5 Detectors used for the determination of CBs by gas chromatography

<i>Detector</i>	<i>Advantages</i>	<i>Disadvantages</i>	<i>Detection level</i>	<i>Relative cost</i>
High resolution MS (HRMS)	Very high specificity and sensitivity. Provides spectral identification. Use ^{13}C labelled analogues	Highly specialized operation High capital and maintenance cost	Low ng kg^{-1}	Very high*****
Isotope dilution MS (IDMS)	Very high specificity and sensitivity. Provides spectral identification. Use ^{13}C labelled analogues	Highly specialized operation High capital and maintenance cost	$5 \mu\text{g kg}^{-1}$	Very high**
Low resolution (LRMS) quadrupole and MSD	Used primarily as an GC detector	Specialist operation Moderate capital and maintenance cost	CB 28 PCI $200 \mu\text{g kg}^{-1}$ NCI $700 \mu\text{g kg}^{-1}$ CB 80 PCI $253 \mu\text{g kg}^{-1}$ NCI $2.2 \mu\text{g kg}^{-1}$	High*****
Ion trap detector (ITD)	Used primarily as a GC detector	Specialist operation Low maintenance cost Own ITD MS library	Low $\mu\text{g kg}^{-1}$	Moderate*****
MS-MS	Separation of unresolved compounds in the MS itself	Specialist operation High capital and maintenance cost	Low ng kg^{-1}	Very high*****
Flame ionization detector (FID)	Simple and easy to use. Good linearity. Useful as a check on clean-up efficiency	Poor sensitivity and specificity.	0.5 mg kg^{-1}	Low*
Atomic emission detector (AED)	Response only dependent on elemental composition Robust and stable	Poor sensitivity	0.1 mg kg^{-1}	Moderate***
Electron-capture detector (ECD)	Very sensitive. Inexpensive. Directly coupled to GC	Only selective for electron capturing material like halogenated hydrocarbons Response dependent on molecular structure. Small linear range	$0.1 \mu\text{g kg}^{-1}$	Low*****

***** Very applicable.

* Not very applicable.

enhanced by operating in the selective ion monitoring (SIM) or multiple ion monitoring (MIM) modes as opposed to the total (full scan) ion current mode (TIC). The main disadvantage with using the MS in SIM or MIM is that the confirmatory power of the technique is considerably reduced. In this mode the CBs generate a strong molecular base peak with a limit of detection (LOD) of 40–100 fg. One of the main advantages of MS, in addition to sensitivity and specificity, is the ability to use ^{13}C labelled compounds as internal standards to compensate for losses during sample preparation, especially at the fg level. Using ^{13}C congeners reduces the need for extensive recovery experiments or having to apply recovery corrections in the method validation and improves the overall variance of the data. High resolution cap-

illary GC coupled with tandem MS-MS provide a very powerful separation technique both by the chromatography but also in the mass spectrometer itself. The MS-MS will separate components that are not resolved by a single GC-MS alone.

Atomic Emission Detector (AED)

The AED is a well established and widely used detector for elemental analysis. Although the AED has an excellent sensitivity for most elements, it has a low relative sensitivity for halogens. As a result it has tended to be overlooked as a detector for trace organic contaminants in favour of the ECD and more recently the MSD. The AED is relatively very stable and, in contrast to the ECD, has a common molar response for compounds of equal halogen content.

Commercial AED instrumentation, with a detection limit of ca. 250–400 pg, has been too insensitive for the determination of CBs in all but the most contaminated samples. Recent AED development has used a 350 kHz on-column RF plasma set at 837.6 nm for the CI emission operating at 350°C with He at 10 mL min⁻¹ as make-up gas and O₂ as the plasma dopant. The capillary column is positioned so as to sustain the plasma *inside* the end of the column. This 'on-column' configuration improves the detection limit by $\times 30$ and provides sufficient sensitivity to be compared directly with the ECD in the analysis of real sediment samples.

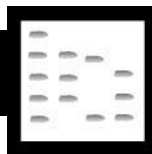
See also: II/Chromatography: Gas: Detectors: Mass Spectrometry; Detectors: Selective; Multidimensional Gas Chromatography; Sampling Systems; **Extraction:** Solid-Phase Extraction. III/Insecticides: Gas Chromatography; **Pesticides:** Gas Chromatography.

Further Reading

- Ahlborg UG, Becking GC, Birnbaum LS *et al.* (1994) Toxic equivalency factors for dioxin-like PCBs. Report on a WHO-ECEH and IPCS consultation. *Chemosphere* 28: 1049–1067.
- Ballschmiter K, Bacher R, Mennel A *et al.* (1992) The determination of the chlorinated biphenyls, chlorinated

- dibenzodioxins and chlorinated dibenzofurans. *Journal of High Resolution Chromatography* 15: 260–270.
- Berg M van den, Birnbaum L, Bosveld ATC *et al.* (1998) *Environ. Health Perspect.* 106: 775–792.
- Erickson MD (1997) *Analytical Chemistry of PCBs* (2nd edn). New York: CRC Press Inc.
- Hess P, de Boer J, Cofino WP *et al.* (1995) Critical review of the analysis of non- and mono-ortho chlorobiphenyls. *Journal of Chromatography A* 703: 417–465.
- Larsen B, Bøwadt S, Tilio R and Facchetti S (1992) Congener specific analysis of 140 chlorobiphenyls in technical mixtures on five narrow-bore GC columns. *International Journal of Environmental Analytical Chemistry* 47: 47–68.
- Mullin M D, Pochini C, McGrindle S *et al.* (1984) High resolution PCB analysis: synthesis and chromatographic properties of all 209 PCB congeners. *Environmental Science and Technology* 18: 468–476.
- Wells DE (1993) Current developments in the analysis of polychlorinated biphenyls (PCBs) including planar and other toxic metabolites. In: Barcelo D (ed.) *Environmental Analysis: Techniques, Application and Quality Assurance*, pp. 113–148. Amsterdam: Elsevier Science Publishers.
- Wells DE and Hess P (1999) Methods for the determination and evaluation of chlorinated biphenyls (CBs) in environmental matrices. In: Barcelo D (ed.) *Environmental Analysis: Techniques, Applications and Quality Assurance*. Amsterdam: Elsevier Science Publishers.

POLYCYCLIC AROMATIC HYDROCARBONS



Gas Chromatography

H. K. Lee, National University of Singapore,
Kent Ridge, Republic of Singapore

Copyright © 2000 Academic Press

Introduction

Polyaromatic hydrocarbons (PAHs) constitute a very extensive and probably the most structurally assorted group of organic compounds. They are ubiquitous to the environment, and may well be the most widely studied class of environmental pollutants. Unfortunately, because of their diverse nature, there is no single nomenclature that describes collectively these compounds to everyone's satisfaction. Thus, one is likely to come across the terms polyaromatic hydrocarbons, polyaromatic compounds, polynuclear aromatic hydrocarbons or polycyclic aromatic hydro-

carbons in the scientific literature, even though all may actually be referring to this same class of chemicals. For the purpose of this article, PAH is used in the broadest sense possible, so that even those compounds that contain atoms other than carbon and hydrogen may be included in the discussion.

PAHs are formed primarily from the combustion of fossil fuels, with major sources being of anthropogenic origin, although bacteria and plants also contribute some PAHs to the environment. Interest in these compounds dates back to 18th-century England when it was suggested that scrotal cancer afflicting chimney sweeps could have been caused by substances present in soot from burning coal. PAHs were still unknown at that time, of course. It was only 150 years later, in the 1930s, that it was finally confirmed that soot contains benzo[*a*]pyrene and dibenz[*a,h*]anthracene, two PAHs with carcinogenic properties. Research into PAHs was given significant impetus by this discovery and, to this day, enormous interest is still focused on these compounds, not only in studies

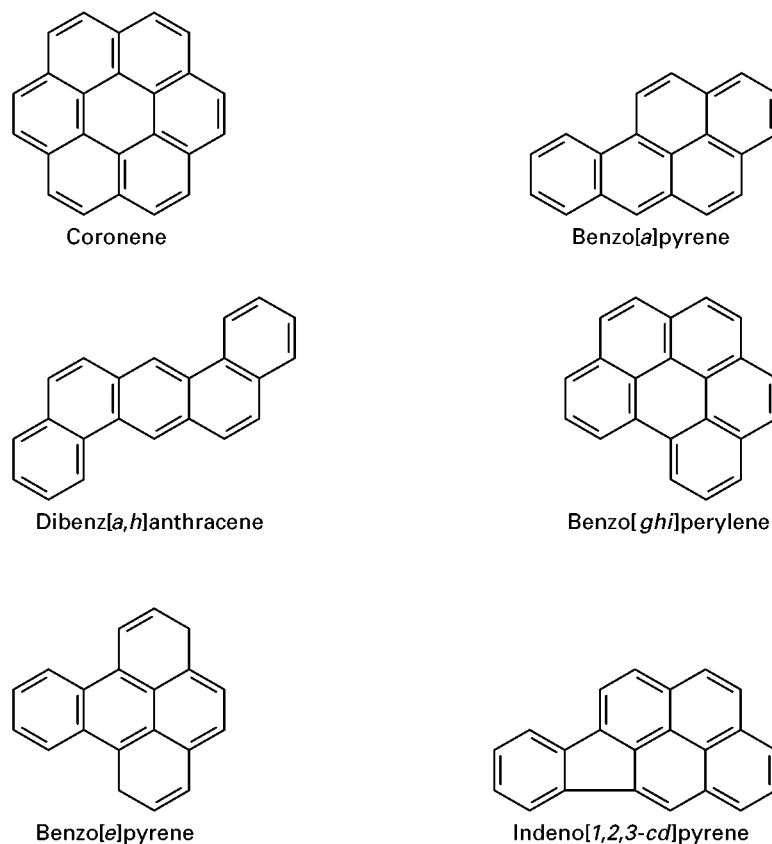


Figure 1 Structures of some common polyaromatic hydrocarbons.

on chemical carcinogenesis, but also in analytical science, for which PAHs have become favoured test analytes. Befitting their status as important pollutants, the US Environmental Protection Agency has designated 16 PAHs as priority pollutants. **Figure 1** shows the structures of some common PAHs.

PAHs are found in a variety of environmental samples (airborne particulates, water, soil) and even in food cooked at high temperatures (grilled meats and fish, for example). Moreover, they are often present as complex mixtures containing dozens of components. It is therefore essential to analyse for PAHs in environmental and other samples to which the human population in particular may be exposed.

Why we need to identify and quantify PAHs in such samples is clear. Since many but not all PAHs are carcinogenic and/or mutagenic, and complex mixtures normally contain both types, the only way to assess the risks posed by those with high carcinogenic potential is to characterize them individually. Additionally, the type and variability of different combustion sources produce PAH profiles (in terms of the composition and quantities of the individual compounds) that are characteristic of their origins. For instance, motor vehicle exhaust fumes contain rela-

tively more benzo[ghi]perylene, coronene and cyclopenta[cd]pyrene than any other sources. Thus, careful examination of such profiles can help to identify the PAH source, and health control steps can be taken to reduce or even eliminate emissions from the particular source. To be able to provide accurate information on individual PAH components in complex mixtures, a technique with good separation capability is imperative. Coupled with its other advantages, such as reasonably fast analysis and sensitivity, gas chromatography is most appropriate for PAH separation. This article focuses on the application of gas chromatography to the separation of PAHs. Attention is placed on the use of capillary columns since analysis by packed columns of such complex mixtures is impractical.

General Considerations

To be separated by gas chromatography, compounds must be volatile and thermally stable within the range of temperature used in the analysis. In this respect, PAHs conform to the requirements, since those containing up to about 24 carbon atoms are amenable to analysis by the procedure. There are exceptions, of

course, since volatilities do vary, even for compounds with the same carbon number.

The value of high resolution gas chromatography for separating complex multicomponent PAH mixtures was first recognized in 1964. This was the first application of capillary column gas chromatography to PAHs. Today, this technique remains the most amenable, and therefore the method of choice, for separating these compounds. Fortunately, it has been ascertained that virtually all of the PAHs that have been found to be carcinogenic or mutagenic are also relatively volatile – thus, gas chromatography is the method of choice to analyse for them, especially if based on considerations of cost and ease of use.

The application of capillary gas chromatography to PAH analysis took a leap forward in the 1970s when several column pretreatment procedures were devised to overcome the problems associated with coating liquid phases on glass column wall surfaces. Columns coated by surface adsorption were not easily reproducible. For high efficiency separations the coating of the liquid phase should be a thin, uniform film; complete coverage of the surface is also essential to counter active sites which compromise chromatographic integrity. One way of achieving satisfactory surface modification was by acid-leaching the Lewis acids present in the glass used to manufacture columns; much improved chromatography was the result.

General improvements in gas chromatography in relation to high efficiency separations have gone hand-in-hand with PAH analysis. Mention was made above of these compounds being commonly used as test substances to evaluate new or improved analytical procedures. This is because of the interest in their carcinogenic properties, their widespread environmental occurrence and their availability as multicomponent standard mixtures.

An early illustration of the power of capillary gas chromatography for separating complex mixtures of PAHs was provided by work published in the mid-1970s. More than 20 PAHs, including sulfur-containing compounds, present in carbon black from petroleum feedstocks were separated on a capillary column coated with SE-52 (5% phenyl methylsilicone gum) stationary phase (Figure 2). Isomers and trace compounds not previously detected could be resolved.

Subsequent work further illustrated the excellent resolution capillary columns could offer when more than 100 PAHs (including alkylated compounds) isolated from airborne particulates were separated. Interestingly, isomers differentiated only by alkyl group positions could be well resolved.

Further improvements in PAH analysis have subsequently come in the form of newer stationary phases, especially those with increased thermal stability. Chemically bonded and cross-linked polymeric phases were introduced in the early 1980s, along with

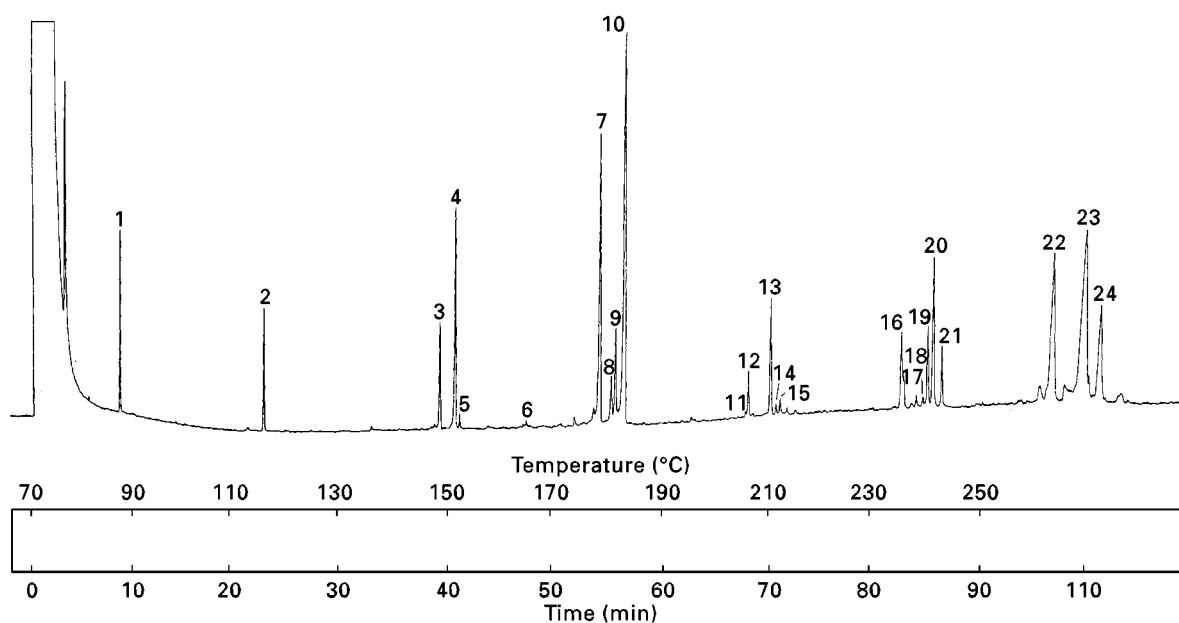


Figure 2 Chromatogram of PAHs, including sulfur-PAHs (peak 9, benzo[def]dibenzothiophene; peak 11, benzo[a]dibenzothiophene) in extract of furnace black from petroleum feedstocks. (Reproduced with permission from Lee ML and Hites RA (1976) Characterization of sulfur-containing polycyclic aromatic compounds in carbon blacks. *Analytical Chemistry* 48: 1890–1893.)

columns made of fused silica. They allow analyses to be performed at elevated temperatures, in contrast to physically coated columns. These phases also have greater wettability characteristics, meaning that, even at high temperatures, their homogeneity is maintained, and they do not collapse into droplets. Chromatographic data are more consistent and reliable as a result of these improvements; this is an important consideration if information about composition and identity is needed from environmentally derived PAH samples.

Methylsilicone stationary phases have been most commonly employed for separating PAHs; these include SE-30, OV-1, OV-101 and SP-2100. Others that provide good performance, like SE-52, referred to above, are based on the same material. Some examples of these are SE-54 (1% vinyl, 5% phenyl methylsilicone), OV-3 (10% phenyl methylsilicone), OV-7 (20% phenyl methylsilicone) and OV-17 (phenylmethylsilicone). Of these, SE-52 and SE-54 have perhaps been the favoured stationary phases of most people working on PAH analysis. Commercial suppliers now list many phases under their own labels that are equivalent or nearly equivalent to those mentioned above and that are optimized for PAH analysis.

Liquid crystalline stationary phases have also played a role in the history of PAH analysis by gas chromatography. They offer the promise of separating closely related PAHs with greater efficiency than conventional stationary phases. The motivation for applying such phases was the complexity of PAH mixtures, especially in relation to isomers which differ significantly in their carcinogenic properties (e.g. benzo[*a*]pyrene which is carcinogenic and benzo[*e*]pyrene which is less so, and benz[*b*], [*j*] and [*k*]-fluoranthenes which possess a range of carcinogenic activities). Liquid crystal phases seemed to be most suited to packed-column gas chromatography since it was the latter (with conventional stationary phases) that lacked the capability to separate closely related components.

The rationale for using liquid crystal packings is that, in comparison to conventional phases they are better able to exploit slight structural differences in isomeric PAHs, thus enabling their resolution. Separation is based on relative permeation of differently shaped PAH between layers of the liquid crystals.

Despite demonstration of some impressive results with liquid crystal phases, the advent of capillary columns, coupled with improvements in conventional stationary phases, column treatment and column coating technologies have led to a slight loss of interest in these phases, not only for separating PAHs but also other analytes. (Such phases have been coated

onto capillary columns and are still sporadically utilized for PAH analysis.) The main disadvantages of these phases are that their properties tend to change over prolonged use, and long equilibrium times are needed between runs, although newer phases have higher thermal stabilities and tolerance. Additionally, PAH retention behaviour appears to be extremely difficult to predict, and expectations based on knowledge of retention of very similar PAHs are often at variance with subsequent experimental observations.

Applications

Some of the more important applications of gas chromatography to PAH analysis have been in atmospheric pollution studies. As heavy traffic densities and industrial pollution are a common feature in major cities of the world, the carcinogenic and mutagenic potential of airborne particulates in urban atmospheres has attracted increasing attention. PAHs are commonly emitted into the atmosphere adsorbed on particulate matter from major combustion sources such as motor vehicle engines via their exhaust systems, uncontrolled natural or deliberate burning of forests, wood and coal, refuse, domestic and industrial power and heat generation. The most convenient method of collecting particulate samples is by drawing contaminated air through a filter. The entrapped particulates are then extracted for their PAH content. Another popular method is to trap PAHs directly on adsorbents (e.g. polyurethane plugs), which are subsequently extracted. Various procedures of extraction include Soxhlet extraction with a suitable organic solvent, followed by additional clean-up steps to isolate the PAH fraction. Other, more rapid extraction methods such as supercritical fluid extraction, accelerated solvent extraction and microwave-assisted solvent extraction have been introduced, the latter in particular has become very popular in recent years.

Although the flame ionization detector (FID) is commonly used for PAH analysis, its universality of response and thus lack of selectivity dictate that after sample extraction careful and sometimes laborious clean-up procedures must be performed to isolate the PAH fraction before gas chromatographic separation. The electron-capture detector (ECD) has also been used for PAH analysis, and ECD-FID response ratios can be calculated and used to differentiate between PAH of similar structures. **Figure 3** shows a chromatogram of PAHs extracted from urban air-borne particulates, generated by the two detectors simultaneously. The FID (lower trace in the figure) and ECD (upper trace) complement each

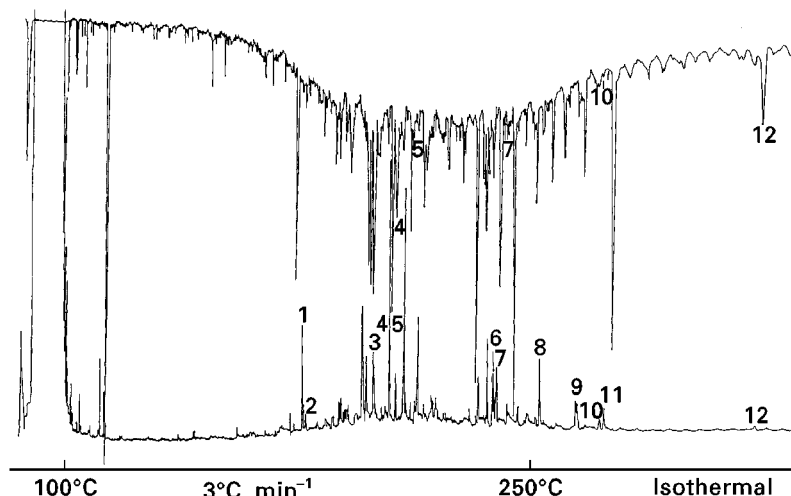


Figure 3 Chromatogram of polyaromatic hydrocarbons from urban particulates generated from simultaneous (bottom) flame ionization and (top) electron-capture detection (FID and ECD). Peak identities: 1, Phenanthrene; 2, anthracene; 3, 3,6-dimethylphenanthrene; 4, fluoranthene; 5, pyrene; 6, benz[*a*]anthracene; 7, chrysene/triphenylene; 8, β , β -binaphthalene; 9, benzo[*j*] and [k]fluoranthene; 10, benzo[*e*]pyrene; 11, benzo[*a*]pyrene; 12, *o*-phenylpyrene. (Reproduced with permission from Bjorseth A and Eklund G (1981) Analysis of polynuclear aromatic hydrocarbons by glass capillary gas chromatography using simultaneous flame ionization and electron capture detection. In: Bertsch W, Jennings WG and Kaiser RE (eds) *Recent Advances in Capillary Gas Chromatography*, pp. 477–490. Heidelberg: Dr Alfred Hüthig Verlag.)

other to provide more positive identification of the PAHs.

Increasingly, mass spectrometry as a gas chromatographic detector is assuming greater importance for most PAH applications because of its greater sensitivity in quantitative analysis (based on its selected ion-monitoring mode in which ions that are characteristic of particular components are monitored) and improved diagnostic power. Using mass spectrometry with less drastic ionization conditions (chemical ionization, negative ion chemical ionization, etc.), similar or isomeric PAHs can be identified with greater certainty, in contrast to electron impact ionization which normally cannot be used to differentiate between such PAH structures since they often give nearly identical mass spectra. In addition to FID, ECD and mass spectrometry, other detectors have been coupled to gas chromatography for PAH analysis. These include the Fourier transform infrared detector, the photoionization detector, the photometric detection and the nitrogen-specific chemiluminescence detector – all of which respond to certain elements or functionalities in compounds, and thus afford a measure of selectivity.

Particulates emitted from vehicles that use diesel fuel have been found to have significant mutagenic potential due to the presence of the nitro-PAHs such as nitropyrenes, nitrofluoranthenes, dinitropyrenes, hydroxynitropyrenes and acetoxynitropyrenes. Some evidence suggests that there may be some other as yet uncharacterized compounds pres-

ent in diesel particulates that are mutagenic but do not belong to the nitropyrene family. Evidence of diesel particulates having greater mutagenicity than other types of particulates normally found in urban atmospheres has also been reported, based on results of a study carried out in a Japanese city. Some previously unknown mutagens were detected and identified; these included PAHs containing NO₂ substituents as well as a nitrogen atom in the ring nucleus. The discovery of these compounds underscores the enormous complexity and diversity represented by the family of PAHs.

In recent years, the size of airborne particulates has become a major issue in the assessment of the health risks posed by these atmospheric pollutants. For example, smaller-sized particles can be transported over greater distances, since they take longer to settle, if at all, increasing their transboundary pollution potential. They are also more easily inhaled, and are therefore more hazardous to health. There has been research to determine the link between particle size with the PAH composition associated with it. If a link can be determined, the health effects of various-sized particles can be better understood and studied. This may allow more effective control of emissions of PAHs to be implemented, by focusing on the emission sources with which particular groups of PAHs are associated. The gas chromatograms of PAHs associated with particulates of sizes < 0.5 μm and > 7.2 μm are shown in Figure 4. It is observed that the two chromatographic profiles are significantly different.

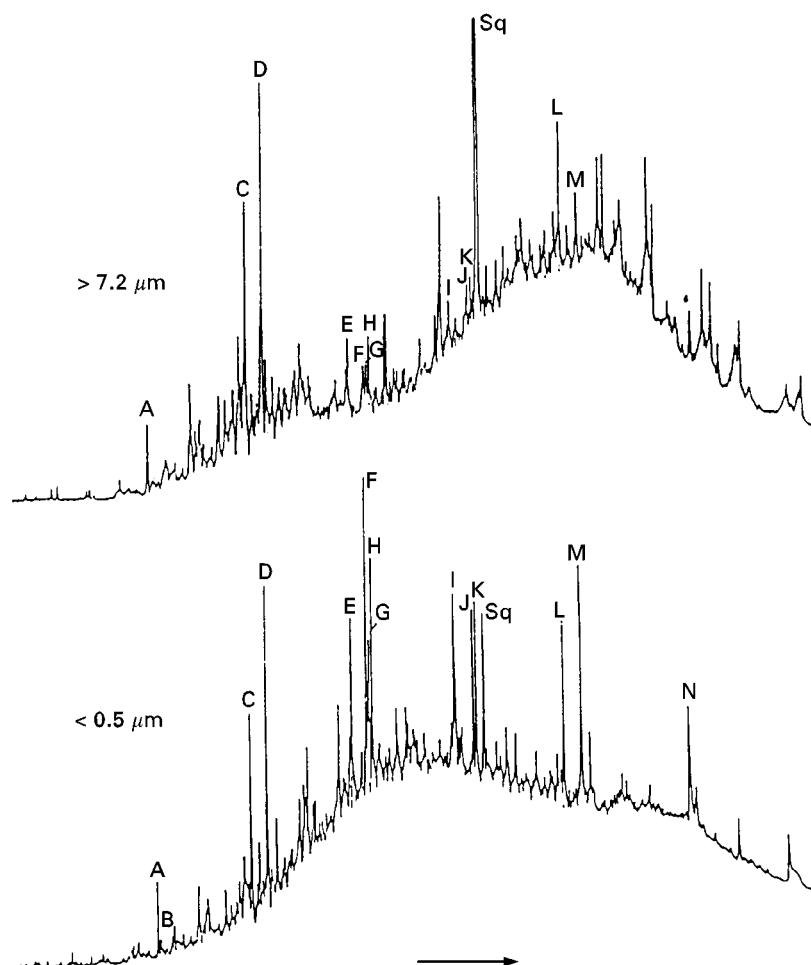


Figure 4 Chromatogram of the aromatic fraction of urban particulates. Top trace: extract from particulates of size $> 7.2 \mu\text{m}$. Bottom trace: extract from particulates of size $< 0.5 \mu\text{m}$. Peak identities: A, Phenanthrene; B, anthracene; C, fluoranthene; D, pyrene; E, benzo[ghi]fluorene; F, 4(H)cyclopenteno[cd]pyrene; G, benz[a]anthracene; H, chrysene/triphenylene; I, benzo[b] and [f]fluoranthene; J, benzo[e]pyrene; K, benzo[a]pyrene; L, indeno[1,2,3-cd]pyrene; M, benzo[ghi]perylene; N, coronene; Sq = squalene. (Reproduced with permission from Aceves M and Grimalt JO (1993) Seasonally dependent size distributions of aliphatic and polycyclic aromatic hydrocarbons in urban aerosols from densely populated areas. *Environmental Science and Technology* 27: 2896–2908.)

The urban atmosphere is only one of the environmental classes in which information on PAH is of interest. Much work has been done, and is continuing, on industrial effluents, and workplace and indoor atmospheres. Interesting insights on indoor PAH pollution have resulted from studies carried out by gas chromatography. Emissions from home appliances such as natural gas space heaters and water heaters have been found to contain PAHs, including the oxygen, nitrogen and sulfur analogues. Such findings are significant because they draw attention to the PAH exposure faced by young children and non-working adults in domestic dwellings. The comment has been made that more attention should perhaps be focused on such indoor pollution by PAH by health authorities than hitherto. **Figure 5** shows a reconstructed total ion mass chromatogram for exhaust emissions

from home appliances using natural gas. Samples were collected on a main filter and a backup filter.

Another form of indoor pollution far removed from urban or suburban settings may also be important. In rural communities, wood, charcoal or coal combustion in open stoves is often used for cooking. In confined dwellings with little or no ventilation, exposure to the combustion products, including PAHs, represents significant risks. Indeed, in a rural commune in China, the women exhibited a high lung cancer mortality rate even though most of them were non-smokers. Using gas chromatography-mass spectrometry, researchers determined PAHs, alkylated PAHs and nitrogen PAHs in particulates collected in commune households during cooking, primarily performed by these women. In many other parts of Asia as well as in Africa, similar lifestyles are followed;

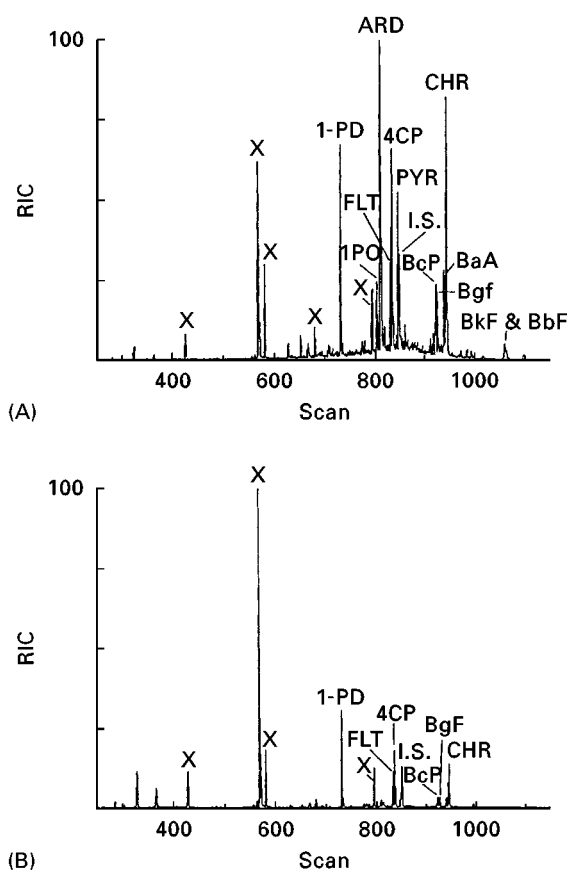


Figure 5 Total reconstructed ion current (RIC) or exhaust emissions from natural gas-fired home appliances: (A) fine particle front filter samples; (B) backup filter samples. Peak identities: I.S., internal standard ($n\text{-C}_{24}\text{D}_{50}$); 1-PD, co-injection standard (1-phenyldodecane); 1PO, 1*H*-phenalen-1-one; FLT, fluoranthene; ARD, cyclopenta[*def*]phenanthren-4-one; PYR, pyrene; BcP, benzo[*c*]phenanthrene; BgF, benzo[*ghi*]fluoranthene; BaA, benzo[*a*]anthracene; CHR, chrysene/triphenylene; BkF, benzo[*k*]fluoranthene; BbF, benzo[*b*]fluoranthene; X, contaminant. (Reproduced with permission from Rogge WF, Hildemann LM, Mazurek MA, Cass GR and Simoneit BRT (1993) Sources of fine organic aerosol, Part 5: natural gas home appliances. *Environmental Science and Technology* 27: 2736–2744.)

thus, indoor PAH pollution is a real threat that needs to be monitored more closely.

Notwithstanding the vast body of literature available on the use of gas chromatography for atmospheric PAH analysis, there has been a tremendous amount of work in other areas where information on these compounds is of interest. Capillary gas chromatography has been the major technique in the identification and determination of PAH mixtures in samples such as cooked foods, coal tar and creosote, soils and sediments, cigarette and marijuana smoke condensates, used engine oils and other oil products, carbon black, natural and contaminated waters in-

cluding rain and snow, marine organisms, petroleum products, asphalt, tyre particles and other rubber products, burnt plastics, coke, shale oils, biological sewage sludge, fly ash from incinerators, and soot from a variety of sources like forest and agricultural fires.

Concluding Remarks

Gas chromatography, particularly when used with capillary columns, has been the mainstay of separation techniques for the analysis of complex mixtures. The analysis of PAHs has virtually been intertwined with the technological progress of gas chromatography over the past few decades. Despite the introduction of other high performance separation methods such as liquid chromatography and supercritical fluid chromatography, gas chromatography has remained the technique of choice for separating PAHs in a large variety of samples. Although gas chromatography can be considered to be a mature technique, it is unlikely that its pre-eminent role in PAH analysis will be seriously challenged in the foreseeable future, even given the past and current tremendous pace of progress in analytical chemistry, particularly in separation science.

See also: III/Flame Ionization Detection: Thin-Layer (Planar) Chromatography; Mass Spectrometry.

Further Reading

- Bjorseth A (ed.) (1983–85) *Handbook of Polycyclic Aromatic Hydrocarbons*. New York: Marcel Dekker.
- Dipple A, Moschel RC and Bigger CAH (1984) Polynuclear aromatic carcinogens. In: Searle CE (ed.) *Chemical Carcinogens*, ACS Monograph 182, 2nd edn, Vol. 1, pp. 41–163. Washington, DC: American Chemical Society.
- Grob RL (ed.) (1995) *Modern Practice of Gas Chromatography*, 3rd edn. New York: Wiley.
- Harvey RG (1996) *Polycyclic Aromatic Hydrocarbons*. New York: Wiley-VCH.
- Jennings W (1980) *Gas Chromatography with Glass Capillary Columns*, 2nd edn. New York: Academic Press.
- Jennings W, Mittlefehldt E and Stremple P (1997) *Analytical Gas Chromatography*. New York: Academic Press.
- Liberti A, Cartoni GP and Cantuti V (1964) Gas chromatographic determination of polynuclear Aromatic Hydrocarbons in dust. *Journal of Chromatography* 15: 141–148.
- Onuska FI and Karasek FW (1984) *Open Tubular Column Gas Chromatography in Environmental Sciences*. New York: Plenum Press.
- Vo-Dinh T (ed.) (1988) *Chemical Analysis of Polycyclic Aromatic Compounds*. New York: John Wiley.

Solid-Phase Extraction

F. Borrell and R. M. Marcé, Universitat Rovira I Virgili, Tarragona, Spain

Copyright © 2000 Academic Press

Polycyclic aromatic hydrocarbons (PAHs) are usually defined as a group of chemicals with two or more fused benzenoid rings. If elements other than carbon and hydrogen are present, the term polycyclic aromatic compounds (PAC) is used. PAHs are natural constituents of crude oil and many other petrochemical products and they are also formed by the incomplete combustion of organic matter. Therefore, they enter the environment from a wide variety of sources such as automobile emissions, industrial processes, waste incineration facilities, domestic heating systems and natural events such as forest fires and volcanic eruptions.

Natural sources of PAH emission have always existed but since the industrial revolution there has been a rapid increase in the loading of the environment with petrochemical PAHs and particularly with PAHs of pyrolytic origin.

The PAHs, both from natural and anthropogenic origins, are released into the atmosphere as vapour or adsorbed on to particles. They are then dispersed and transported long distances by wind before being deposited on the ground or in water, directly or in rain. PAHs are also present in water samples as a result of sewage from industries which use these compounds in their manufacturing processes (e.g. pharmaceuticals, explosives, plastics, synthetic dyes, pesticides and so on).

PAHs are one of the most contaminating groups of pollutants in the environment because of their mutagenic and carcinogenic activity. The activity of each compound depends on its chemical structure. Typically, environmental samples contain a complex mixture of various PAHs, including isomeric structures and both alkylated and nonalkylated PAH forms. **Figure 1** shows the structure of the 16 PAHs considered as priority pollutants by the US Environmental Protection Agency (EPA).

In PAH mixtures of petrochemical origin, two- or three-ring compounds are more abundant than the heavier PAHs, which have four or more rings. On the other hand a typical mixture from a high temperature combustion source contains mainly unsubstituted compounds and PAHs with four or more rings are more abundant than the smaller ones. So, PAHs in natural samples are always encountered as mixtures.

In the environment, PAHs may be eliminated or transformed to even more toxic compounds by chemical reactions such as photooxidation, sulfonation or nitration. For instance, pyrene, which is not mutagenic, can be transformed to nitropyrene, which is highly mutagenic, when nitrogen dioxide is present. In some conditions, traces of nitric acid in the nitrogen dioxide can also transform some PAHs into nitro-PAHs.

Because of their mutagenic and carcinogenic properties, PAHs have been determined in a variety of environmental matrices including air, water, soil, sludge and tissue. The European Community directive (98/83/EC) on the quality of drinking water established the global maximum admissible concentration of four PAHs (benzo(*b*)fluoranthene, benzo(*k*)fluoranthene, benzo(*ghi*)perylene and indeno(1,2,3-*c-d*)pyrene) as $0.10 \mu\text{g L}^{-1}$ and specified an individual value of $0.010 \mu\text{g L}^{-1}$ for benzo(*a*)pyrene. The World Health Organization (WHO) considers only benzo(*a*)pyrene with a reference value of $0.7 \mu\text{g L}^{-1}$.

Determination of PAHs

PAHs can be determined by high performance liquid chromatography (HPLC), gas chromatography (GC), supercritical fluid chromatography (SFC) and capillary electrophoresis (CE), but the preferred method is reversed-phase HPLC.

In GC, the most usual detection systems are flame ionization and mass spectrometry, with the latter becoming increasingly common. However, GC is unable to determine the nonvolatile and high molecular mass PAHs. SFC has also been used; its main advantages are its high separation efficiencies and short analysis times. UV-visible, fluorescence or mass spectrometric detectors can all be used.

Micellar electrokinetic capillary chromatography (MEKC) or cyclodextrin-modified CE are capable of separating all 16 PAHs in under 20 min. Despite the advantages in resolution power, the main drawback of MEKC is its poor concentration sensitivity, but this can be partially solved by using a fluorescence detector.

HPLC with a diode array detector enables the UV-visible spectra to be compared and is quite often used to determine PAHs. Fluorescence detection is the most suitable because of its higher sensitivity, although a few PAHs – for instance, acenaphthylene – do not show fluorescence. Spectrofluorimetric

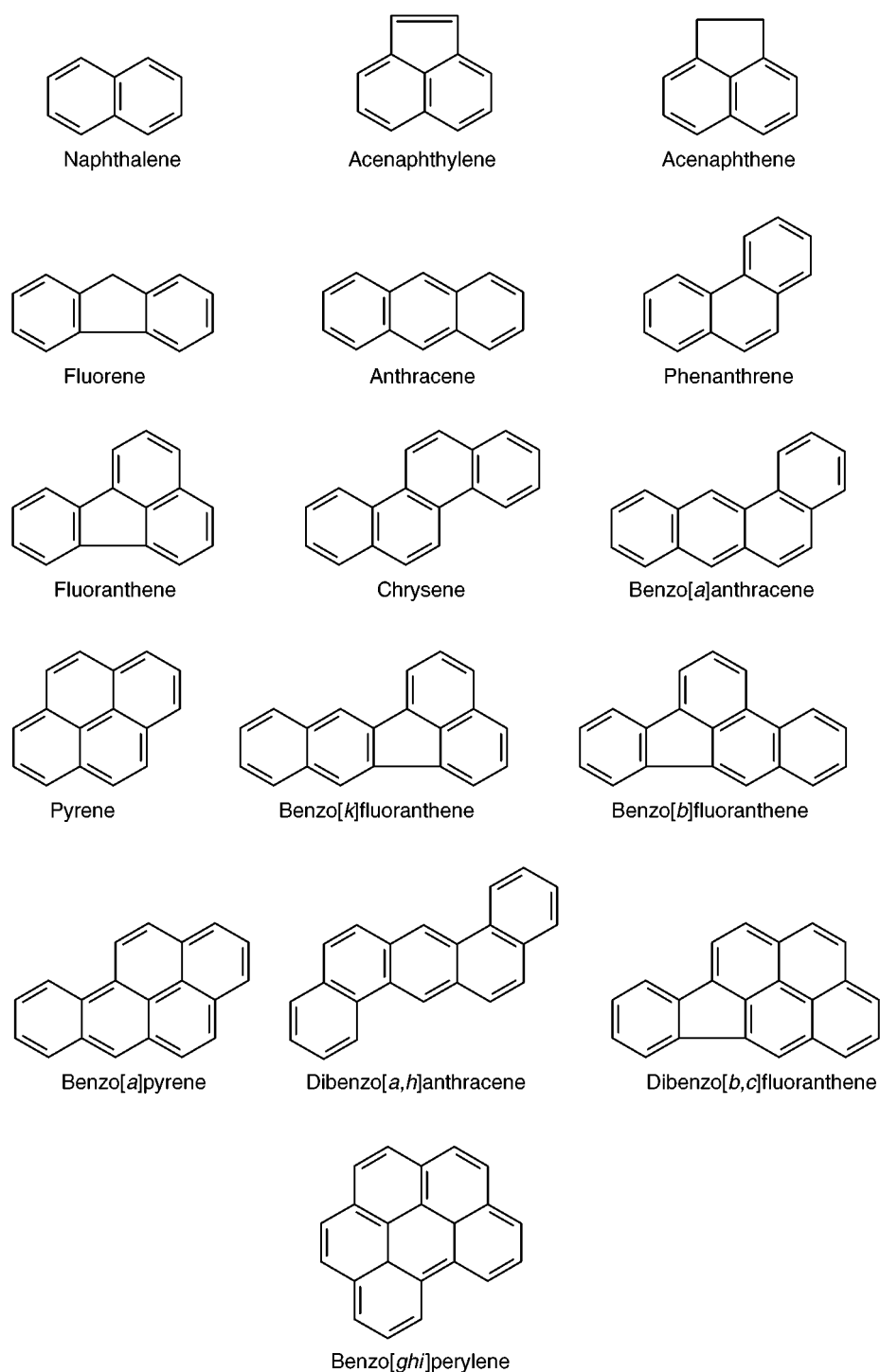


Figure 1 Chemical structure of the 16 PAHs considered to be priority pollutants by the US EPA.

detection and wavelength programming enable each compound to be detected at its maximum emission wavelength and so sensitivity and selectivity can be improved. If a micellar mobile phase is used instead of an aqueous–organic one, lower concentrations can be detected. Other detection techniques, such as amperometry, have also been used and the limits of

detection are lower than those obtained with UV detection.

Sample-handling Techniques

Because of their toxicity and the low levels to be determined, PAHs are determined in various kinds of

samples which usually require treatment before chromatographic determination. For solid samples, such as soils, sludge, sediments and tissues, the classical Soxhlet extraction is still used, but the extraction is tedious and time-consuming. Other newer techniques, such as supercritical fluid extraction, microwave-assisted solvent extraction and ultrasonic extraction, have proved to be suitable for extracting PAHs and the times required are considerably less. Some of these techniques are followed by a clean-up step, usually performed by solid-phase extraction.

For gaseous samples, different kinds of adsorbents are used to retain the PAHs. PAHs associated with particulate matter are usually collected on filters and then vaporized and PAHs in the vapour phase are trapped by a back-up solid sorbent. Samples are desorbed using Soxhlet apparatus, ultrasonication or supercritical fluid extraction. Sample clean-up is usually required and performed by solid-phase extraction.

Liquid-liquid extraction is gradually being replaced as a technique for extracting organic compounds from liquid samples because it uses considerable amounts of toxic solvents. In this respect, solid-phase extraction has been shown to give good results. Other techniques, such as closed-loop stripping or supercritical fluid extraction, alone or after the solid-phase extraction of the aqueous sample, also give good results. For water samples, results are better when supercritical fluid extraction is applied after solid-phase extraction and not when supercritical fluid extraction is applied alone.

Solid-phase Extraction

In the determination of PAHs, solid-phase extraction is mainly applied to liquid samples but, as already mentioned, it is also applied in the clean-up step with gaseous or solid samples after other extraction techniques. The following discussion mainly refers to the analysis of aqueous samples but some references will be made to other kinds of samples.

Several kinds of sorbents in a variety of devices (e.g. cartridges or discs) may be used for the solid-phase extraction of PAHs. Solid-phase extraction is usually carried out in the offline mode but the online mode does have some advantages and recently has been increasingly used. Solid-phase extraction has been coupled to HPLC and also to GC and SFC to determine PAHs.

One of the most recently developed techniques for extracting PAHs is solid-phase microextraction (SPME) where the sorbent is coated on to a fused-silica fibre mounted in a syringe-like device. SPME is

a solvent-free technique, which is its main advantage, but it also has disadvantages compared to SPE.

Addition of Solvent or Micellar Media to Aqueous Samples

The solid-phase extraction of PAHs may seem to be a simple process because of their high hydrophobicity and because there are no expected breakthrough problems. However, the low solubility of the PAHs, which decreases as molecular weight increases, does present a problem. There may also be sorption problems during sampling and storage and to avoid these problems, it is necessary to increase their solubility. Normally this is done by adding organic solvents, such as acetonitrile, methanol and 2-propanol, or surfactants to the sample as solubilizers. The percentage of this solvent in the samples is a critical parameter because if it is low it may not be enough to solubilize the high molecular weight PAHs, whereas if it is high, the breakthrough volume will be low for the low molecular weight PAHs. Therefore, for each kind of sample, solid-phase extraction sorbent and organic solvent, this parameter must be optimized. Typical values are between 10 and 25%, depending on the solvent added and the sorbent used. **Table 1** shows the influence of 2-propanol on the PAH recoveries. The higher the percentage of 2-propanol, the lower the recovery of low molecular weight PAHs, whereas the higher the percentage of 2-propanol, the higher the recoveries of high molecular weight PAHs.

Surfactants have also been used instead of organic solvents. Surfactant molecules are amphiphilic, and have a polar and nonpolar moiety. Because of their amphiphilic nature, surfactant molecules can dissolve in water as monomers, or form a micelle with other surfactant molecules. The concentration at which they start to form micelles is termed the critical micelle concentration (CMC). The CMC depends on factors such as the surfactant itself, temperature, ionic strength and the presence of organic additives. It is the concentration at, or concentration range over which, solution properties like surface tension show an abrupt change in value. To solve the problems arising from the low solubility of PAHs in water and their adsorption on surfaces, surfactants such as sodium dodecyl sulfate (SDS; anionic type, molecular mass 288 and $8.3 \times 10^{-2} \text{ mol L}^{-1}$ CMC), cetyl trimethylammonium chloride (CTACl; cationic type, molecular mass 320 and $8.0 \times 10^{-4} \text{ mol L}^{-1}$ CMC), Brij-35 (neutral type, molecular mass 1182 and $1.0 \times 10^{-4} \text{ mol L}^{-1}$ CMC), have been used, among others. The concentration of surfactant significantly affects the recovery of the PAHs, as shown in **Table 2**, where the influence of the surfactant concentration on PAH recovery is demonstrated.

Table 1 Influence of the percentage of 2-propanol in a sample of PAHs using C₁₈ and SDB membrane extraction. (Results are the mean of three determinations)

Compound	Recovery and RSD (%) in the presence of 2-propanol					
	0%		10%		15%	
	C ₁₈	SDB	C ₁₈	SDB	C ₁₈	SDB
Naphthalene	86 ± 3.1	89 ± 3.0	80 ± 5.2	75 ± 7.6	70 ± 7.2	62 ± 8.7
Acenaphthylene	83 ± 4.3	85 ± 3.1	80 ± 5.5	80 ± 4.5	75 ± 6.1	65 ± 7.6
Acenaphthene	85 ± 3.3	87 ± 3.6	83 ± 4.5	82 ± 4.3	81 ± 5.6	70 ± 6.3
Fluorene	87 ± 3.5	85 ± 4.1	85 ± 3.5	80 ± 5.5	86 ± 5.8	73 ± 6.3
Phenanthrene	84 ± 4.0	88 ± 3.2	92 ± 3.0	90 ± 3.2	95 ± 3.2	78 ± 5.7
Anthracene	79 ± 5.2	81 ± 3.1	85 ± 3.4	75 ± 4.5	93 ± 3.1	78 ± 5.5
Fluoranthene	75 ± 5.0	70 ± 4.9	92 ± 3.1	80 ± 4.8	97 ± 3.0	79 ± 4.8
Pyrene	74 ± 6.1	70 ± 5.2	92 ± 3.2	75 ± 5.6	97 ± 3.3	71 ± 5.8
Benzo(a)anthracene	64 ± 7.5	52 ± 7.6	72 ± 4.6	82 ± 4.7	98 ± 3.4	85 ± 4.3
Chrysene	71 ± 6.8	53 ± 8.2	75 ± 5.2	80 ± 3.5	99 ± 3.2	84 ± 3.8
Benzo(b)fluoranthene	66 ± 7.4	45 ± 8.7	74 ± 6.3	77 ± 4.7	99 ± 3.1	85 ± 4.1
Benzo(k)fluoranthene	74 ± 6.9	50 ± 7.8	85 ± 4.1	78 ± 5.6	95 ± 3.2	88 ± 4.0
Benzo(a)pyrene	54 ± 8.7	44 ± 8.6	75 ± 5.2	69 ± 7.5	95 ± 4.0	85 ± 4.2
Dibenz(a,h)anthracene	59 ± 8.8	39 ± 8.9	77 ± 5.6	73 ± 7.7	97 ± 3.3	72 ± 5.6
Benzo(ghi)perylene	60 ± 8.3	37 ± 10.0	81 ± 4.8	70 ± 8.3	97 ± 3.1	82 ± 4.8
Indeno(1,2,3-cd)pyrene	63 ± 7.9	40 ± 9.4	90 ± 3.3	75 ± 8.0	93 ± 3.1	80 ± 6.2

SDB, styrene-divinylbenzene. RSD, relative standard deviation.

Sorbents

For aqueous samples, C₁₈-bonded silica is mainly applied, although good results can also be obtained with styrene-divinylbenzene (SDB). Some authors claim that results are best when different sorbents are combined. For example, in the analysis of drinking

Table 2 Influence of surfactant concentration on recovery of PAHs, after 10 mL preconcentration on a 10 × 3 mm i.d. Boos silica pre-column

Compound	Analyte recovery (%; n = 2) at Brij-35 concentration (× 10 ⁻⁴ mol L ⁻¹) of				
	0.0	0.5	1.1	3.0	6.0
Naphthalene	18	15	13	12	12
Acenaphthene	55	53	55	39	32
Fluorene	73	75	83	54	38
Phenanthrene	42	37	52	84	75
Anthracene	41	38	55	80	69
Fluoranthene	21	23	48	91	84
Pyrene	17	20	46	99	88
Benzo(a)anthracene	16	20	46	94	64
Chrysene	16	19	45	94	62
Benzo(b)fluoranthene	14	26	49	82	54
Benzo(k)fluoranthene	14	23	48	81	54
Benzo(a)pyrene	14	24	49	81	52
Dibenz(a,h)anthracene	11	30	53	62	31
Benzo(ghi)perylene	7	29	32	50	31
Indeno(1,2,3-cd)pyrene	7	28	32	50	31

Reproduced with permission from Brouwer *et al.* (1994).

water samples, the best results are obtained from combined octadecylsilane (C₁₈)-ammonia (NH₂) solid-phase cartridges, whereas PAHs from soil samples were best extracted with silica (Si)-cyano (CN) or C₁₈-CN combinations.

One group of researchers compared three different bonded silica sorbents, C₁₈, cyano and phenyl, and demonstrated that results are best for C₁₈-bonded silica. Results are shown in Table 3, where CH₃CN and CH₂Cl₂ are used as organic solvents to elute PAHs.

The chromatographic system to be used must also be taken into account. It has been demonstrated that, to determine PAHs by HPLC-fluorescence in lake sediments, C₁₈-bonded silica and silica columns could be used satisfactorily in the clean-up and preconcentration step. However, they could not be used with GC-mass spectrometry (GC-MS) for PAHs greater than chrysene, due to interference from aliphatic waxes.

Another group tested various specific sorbents such as Chromspher II, a diol-treated porous glass chemically modified with a copper phthalocyanine trisulfonic acid derivative (Boos glass), a diol-modified silica with the same copper compound (Boos silica) and a copper phthalocyanine trisulfate-modified polymethacrylamide. It was shown that the second material (Boos silica) was quite useful for the trace enrichment of PAHs containing three or more fused benzene rings but for the smaller PAHs, conventional C₁₈-bonded silica gave better results.

Table 3 Comparison of recoveries for different solid phases with CH_2Cl_2 or CH_3CN

PAH	Octadecyl phase				Cyano phase				Phenyl phase			
	CH_2Cl_2				CH_2Cl_2				CH_2Cl_2			
	%Recovery	%RSD	%Recovery	%RSD	%Recovery	%RSD	%Recovery	%RSD	%Recovery	%RSD	%Recovery	%RSD
1	108	7	71	29	32	14	19	32	72	3	45	22
2	97	3	67	32	57	12	30	27	81	12	68	11
3	112	3	71	39	82	8	34	19	90	11	64	20
4	109	4	68	50	96	7	39	31	90	12	54	21
5	23	6	57	66	94	14	38	54	88	7	35	9
6	85	6	53	73	88	16	36	64	80	6	31	12
7	73	11	46	89	73	35	28	86	105	3	23	8
8	72	13	45	95	73	34	27	90	105	2	22	10
9	51	13	46	57	44	41	38	54	65	11	40	31
10	63	10	54	34	49	40	45	39	66	11	51	19
11	53	12	50	68	46	49	44	46	60	23	48	29
12	27	12	55	53	46	15	42	54	60	16	52	30
13	57	18	47	75	49	27	46	47	60	25	47	54
14	61	13	61	57	58	26	58	39	62	36	60	22
15	53	26	53	60	51	31	51	51	56	45	54	33
16	57	19	56	81	52	33	51	36	59	32	57	36

Volatile PAHs: 1, naphthalene; 2, acenaphthylene; 3, acenaphthene; 4, fluorene; 5, phenanthrene; 6, anthracene; 7, fluoranthene; 8, pyrene. High molecular PAHs: 9, benz(a)anthracene; 10, chrysene; 11, benzo(b)fluoranthene; 12, benzo(k)fluoranthene; 13, benzo(a)pyrene; 14, indeno(1,2,3-cd)pyrene; 15, dibenz(a,h)anthracene; 16, benzo(ghi)perylene. Reproduced with permission from Sargenti and McNair (1998).

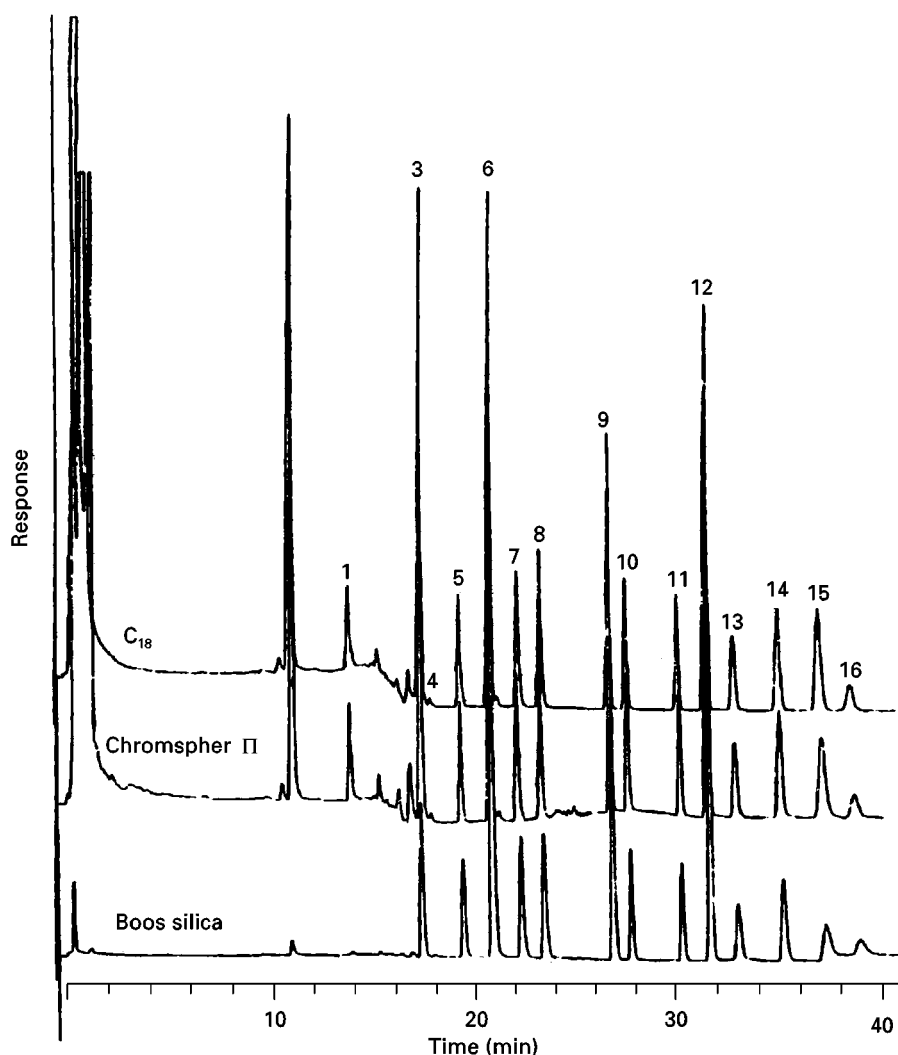


Figure 2 Online trace enrichment LC-fluorescence chromatograms of 10 mL surface water, containing $3 \times 10^{-4} \text{ mol L}^{-1}$ Brij-35, spiked at the 100 ng L^{-1} level with all PAHs, using Boos silica, Chromspher Π or C_{18} -bonded silica pre-columns. Peak assignment: 1, naphthalene; 2, acenaphthene; 3, fluorene; 4, phenanthrene; 5, anthracene; 6, fluoranthene; 7, pyrene; 8, benzo[*a*]anthracene; 9, chrysene; 10, benzo[*b*]fluoranthene; 11, benzo[*k*]fluoranthene; 12, benzo[*a*]pyrene; 13, dibenz[*a,h*]anthracene; 14, benzo[*ghi*]perylene; 15, indeno[1,2,3-*cd*]pyrene. For other conditions, see text. Reproduced with permission from Brouwer *et al.* (1994).)

Figure 2 shows chromatograms obtained in the analysis of 10 mL of surface water spiked with PAHs using Boos silica, Chromspher Π and C_{18} -bonded silica pre-columns. The Boos silica gives the cleanest chromatogram but has lost the two most volatile compounds.

Apart from the sorbents already mentioned, other sorbents such as Florisil (SiO_2 and MgO) can rapidly and efficiently recover PAHs for petroleum and sediment extracts as a clean-up step after another extraction technique.

Solid-phase extraction is widely used after the ultrasonication extraction or microwave extraction of soils and sediments, as a clean-up step before chromatographic determination. In these cases,

Florisil or C_{18} -bonded silica are the sorbents which are most used. SPE is also used before supercritical fluid extraction to analyse aqueous samples and results are better with solid-phase extraction-supercritical fluid extraction than with supercritical fluid extraction alone. Table 4 shows the results obtained when different extraction techniques were applied to determine PAHs in water samples. Much better results can be seen when solid-phase extraction technique is added to the supercritical fluid extraction one.

Most of the sorbents are used as cartridges but membrane discs can also be used to concentrate PAHs; the main advantages of discs are the considerable reduction in extraction time and the higher sur-

Table 4 Comparison of recoveries for different extraction techniques for extraction of 16 PAHs from spiked HPLC-grade water

PAH	SPE		SPE-SFE		SFE ^a		LLE	
	%Recovery	%RSD	%Recovery	%RSD	%Recovery	%RSD	%Recovery	%RSD
1	108	7	91	58	40	30	15	67
2	97	3	65	58	44	28	17	47
3	112	3	76	29	55	23	14	42
4	109	4	82	5	61	21	18	30
5	23	6	87	15	54	11	35	11
6	85	6	82	13	51	10	46	8
7	73	11	204	19	40	5	89	5
8	72	12	188	21	39	7	88	4
9	51	13	59	14	44	14	84	22
10	63	10	75	22	41	11	104	18
11	53	12	59	22	66	21	97	39
12	27	12	65	22	66	25	108	34
13	57	18	63	28	66	28	95	40
14	61	13	65	34	75	22	92	38
15	53	26	67	30	78	27	109	51
16	57	19	70	27	76	20	103	41

SPE, solid-phase extraction; SFE, supercritical fluid extraction; LLE, liquid-liquid extraction. Volatile PAHs: 1, naphthalene; 2, acenaphthylene; 3, acenaphthene; 4, fluorene; 5, phenanthrene; 6, anthracene; 7, fluoranthene; 8, pyrene. High molecular PAHs: 9, benz(a)anthracene; 10, chrysene; 11, benzo(b)fluoranthene; 12, benzo(k)fluoranthene; 13, benzo(a)pyrene; 14, indeno(1,2,3-*cd*)pyrene; 15, dibenz(a,h)anthracene; 16, benzo(ghi)perylene.

^aDirect SFE.

Reproduced with permission from Sargenti and McNair (1998).

face of extraction, which means fewer clogging problems for the sorbent. They also enable larger volumes to be extracted with the same amount of sorbent than when cartridges are used.

Two different membranes, C₁₈-bonded silica and SDB were studied to determine PAHs from surface water. Prior to the extraction procedure, the discs were conditioned to prevent interfering peaks in the chromatogram. In this process, for C₁₈ discs, 20 mL of organic elution solvent (dichloromethane-ethyl acetate-acetonitrile, 50 : 30 : 20 v/v/v) was added to the filtration reservoir and slowly drawn through the discs by applying a slight vacuum. After drawing air through the discs for 5 min, 20 mL of an acetone-water mixture (80 : 20 v/v) was added and slowly drawn through the filtration discs, followed by 10 mL of Milli-Q water. The styrene-divinylbenzene copolymer discs were conditioned with 20 mL of acetone, 20 mL of acetonitrile and 20 mL of dichloromethane. After each addition a vacuum was applied to remove interfering compounds from the discs. Then, 20 mL of Milli-Q water was added and drawn through the disc before sample preconcentration.

Table 1 shows the recovery values obtained when C₁₈-bonded silica and SDB membrane discs were used in the determination of PAHs. In this case, 100 mL of Milli-Q water spiked with 0.5 µg L⁻¹ of 15 PAHs and 29 µg L⁻¹ of acenaphthylene were concentrated and

then eluted twice with 15 mL of organic mixture. In this table the influence of adding 2-propanol to the sample is also shown, as already mentioned.

Another group studied the solid-phase extraction of PAHs in water samples using solid-phase extraction discs with a glass fibre matrix (GFM) and recoveries were good for the six PAHs studied. The main advantage of this GFM sorbent is the high speed of extraction, and the lower amount of solvent required compared with the conventional cartridge. **Figure 3** shows the chromatograms of analysis of seawater and riverwater using this kind of membrane.

Other selective sorbents, immunosorbents, based on antigen-antibody interactions, have also been used for selective isolation of PAHs from complex environmental samples. The extraction of the PAHs from sediments by sonication with dichloro-methane-methanol, subsequent extract dilution with water and extraction with an anti fluorene immunosorbent gave similar results to those obtained with conventional clean-up procedures but selectivity was higher.

Desorption Solvent

After cleaning and conditioning the SPE cartridges or discs, the sample, with an organic solvent or micelle medium added, is applied. Then, organic solvents such as acetonitrile, tetrahydrofurane, acetone, *n*-hexane, methylene chloride, ethyl acetate and ethyl ether or mixtures of them are used to desorb PAHs.

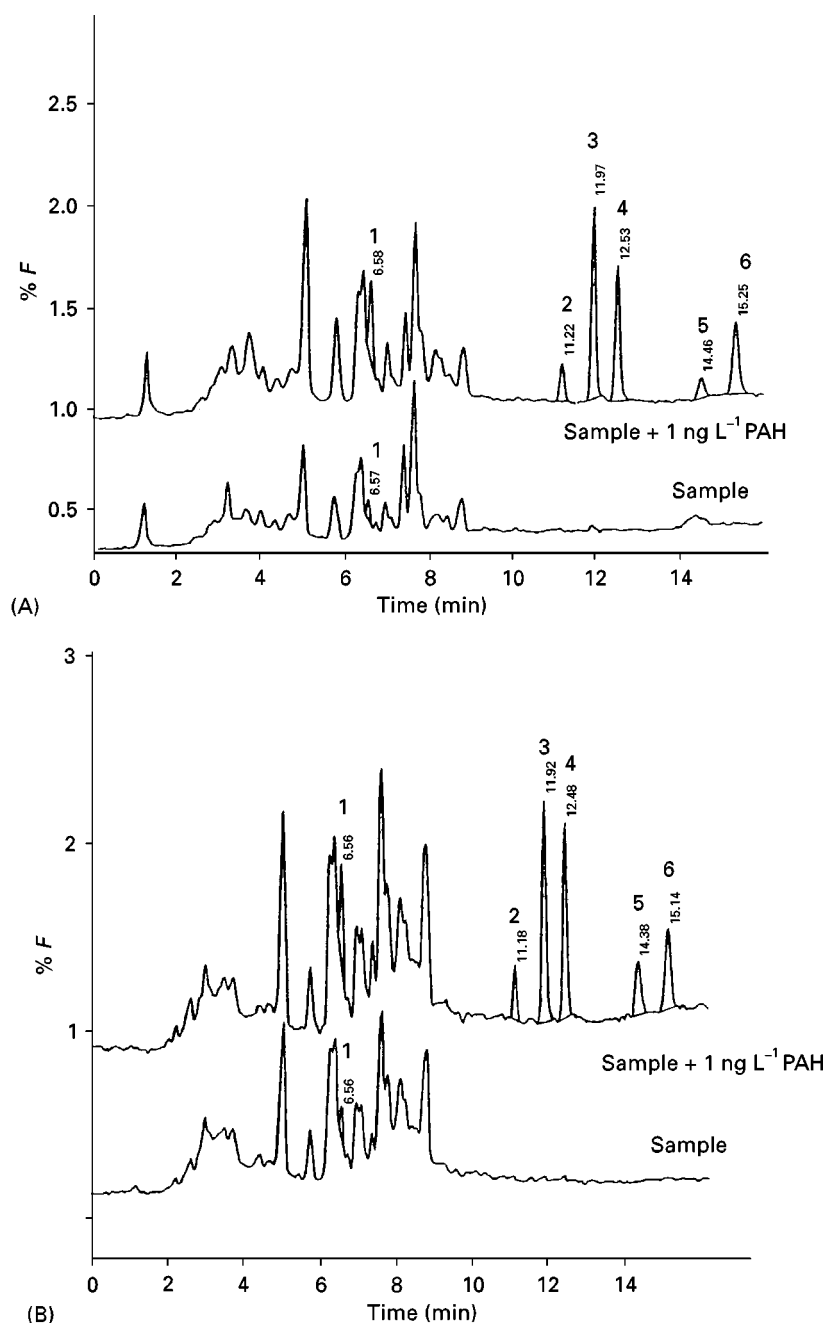


Figure 3 Separation and recovery of PAHs in (A) seawater and (B) riverwater, after being spiked with 1 ng L⁻¹ for each compound, except fluoranthene (10 ng L⁻¹) and indeno[1,2,3-*cd*]pyrene (5 ng L⁻¹) to 1 L of sample. Peak assignment: 1, fluoranthene; 2, benzo[*a*]fluoranthene; 3, benzo[*k*]fluoranthene; 4, benzo[*a*]pyrene; 5, benzo[*ghi*]perylene; 6, indeno[1,2,3-*cd*]pyrene. Reproduced with permission from Urbe and Ruana (1997).

Recoveries of the low molecular weight PAHs are higher with nonvolatile solvents, but the recoveries for most of the PAHs with 4–6 aromatic rings are higher when a nonpolar solvent is used. So, in order to ensure optimum recoveries of all the PAHs, mixtures of solvents are usually recommended.

If the solvent used is compatible with the chromatographic system, concentration of the ex-

tracts is usually required to lower the limit of quantification. If the solvent is not compatible with the HPLC system, the extract obtained is dried with sodium sulfate evaporated at room temperature under a current of nitrogen or with a rotary evaporator and the residue dissolved in the mobile phase. The volume of organic solvent used in the solid-phase extraction membrane system is usually bigger than the volume

used in a cartridge system (between 30 and 50 mL and 1–5 mL, respectively).

Online Solid-Phase Extraction Chromatographic System

The main advantages of online systems are that the samples have to be manipulated less, they reduce analysis time and they consume less organic solvent.

SPE-HPLC is the most straightforward coupling method and therefore the most used. The sample preparation and conditioning steps are similar to those used in the offline but only the mobile phase is required to elute the compounds retained in the pre-column which is connected online to the analytical column.

The most used sorbents are the C₁₈-bonded silicas and SDB, although other specific sorbents can also be used. Depending on the sorbent and the solvent added to the aqueous sample, some interfering peaks can appear in the chromatogram, even when fluorescence detection is used. For instance, MeOH, acetonitrile and 2-propanol were tested as organic modifiers in the analysis of 50 mL of Milli-Q water with 15% of organic solvent by online solid-phase extraction with SDB discs. In this study, when using MeOH, peaks at the same retention time as naphthalene, phenanthrene, fluoranthene and pyrene appeared in the chromatogram. 2-Propanol gave peaks with the same retention time as naphthalene and phenanthrene. When acetonitrile was used, the blank was much cleaner and no interferences appeared in the chromatogram.

Table 5 shows the recoveries obtained when different percentages of acetonitrile are used in the analysis of PAHs by online SPE-HPLC. It can be seen that it is necessary to increase the percentage of acetonitrile to increase the recovery of high molecular weight compounds. However, this distorts the peaks of the low molecular weight compounds and so they could not be quantified. This happened to naphthalene, acenaphthene and fluorene when 25% of acetonitrile was used and, for this reason, 15% acetonitrile is the maximum concentration that can be used. However, at this percentage, the recovery value for the high molecular weight compounds is quite low, so the authors recommend that the PAHs should be analysed in two separate runs with 15% acetonitrile and 20% 2-propanol as modifiers, for the low molecular weight compounds (from naphthalene to pyrene) and the high molecular weight compounds (from benzo[a]anthracene to indeno[1,2,3-cd]pyrene). Figure 4 shows a chromatogram of the analysis of 50 mL tap water using acetonitrile as organic solvent for low molecular weight compounds and IPA for the high molecular weight compounds.

Table 5 Recovery values obtained in the analysis of 50 mL of a standard solution of 0.4 µg L⁻¹ using nine SDB discs at several percentages of ACN and IPA

Compounds	Percentage of ACN				Percentages of IPA		
	10%	15%	25%	35%	10%	20%	30%
Naphthalene	81	77	–	–	85	78	70
Acenaphthene	77	74	–	–	87	81	68
Fluorene	72	84	–	–	82	80	70
Phenanthrene	50	78	74	–	85	83	80
Anthracene	52	72	76	–	80	96	77
Fluoranthene	42	82	85	–	91	87	82
Pyrene	46	86	92	–	80	82	90
Benzo[a]anthracene	45	55	90	98	74	82	92
Chrysene	44	53	87	92	76	85	90
Benzo[b]fluoranthene	32	48	71	82	72	83	92
Benzo[k]fluoranthene	44	57	76	88	74	82	95
Benzo[a]pyrene	42	52	65	85	72	80	90
Dibenzo[a,h]anthracene	31	59	63	82	70	78	85
Benzo[ghi]perylene	28	58	69	78	68	82	89
Indeno[1,2,3-cd]pyrene	25	54	62	72	62	81	82

– Not quantified.

ACN, acetonitrile; IPA; isopropanol.

Using online SPE-HPLC it is possible to detect these compounds at very low ng L⁻¹ levels. Table 6 shows linearity range and limits of detection of PAHs in sea water.

Online coupling of solid-phase extraction to GC or SFC requires an additional step: drying the pre-column before elution with the organic solvent in order to remove the water present when aqueous samples are analysed. An organic solvent added to the samples is also required in order to avoid adsorption of the PAHs. When SPE-GC is used, a small volume of an organic solvent, usually ethyl acetate, is used to pass the retained compounds to the chromatographic column via a loop type or an on-column interface. When SPE-SFC is used, the same mobile phase is used to elute the retained compounds.

Conclusions

PAHs are mainly determined by HPLC fluorescence and detection because of its high sensitivity. To reach the very low levels of concentration required, an extraction concentration technique is necessary. Solid-phase extraction is the preferred technique both for extracting aqueous samples and cleaning up after other extraction techniques.

C₁₈ silica cartridges or discs are the most recommended in online and offline modes.

One of the characteristics of the extraction of PAHs is the need for an organic solvent or a surfactant

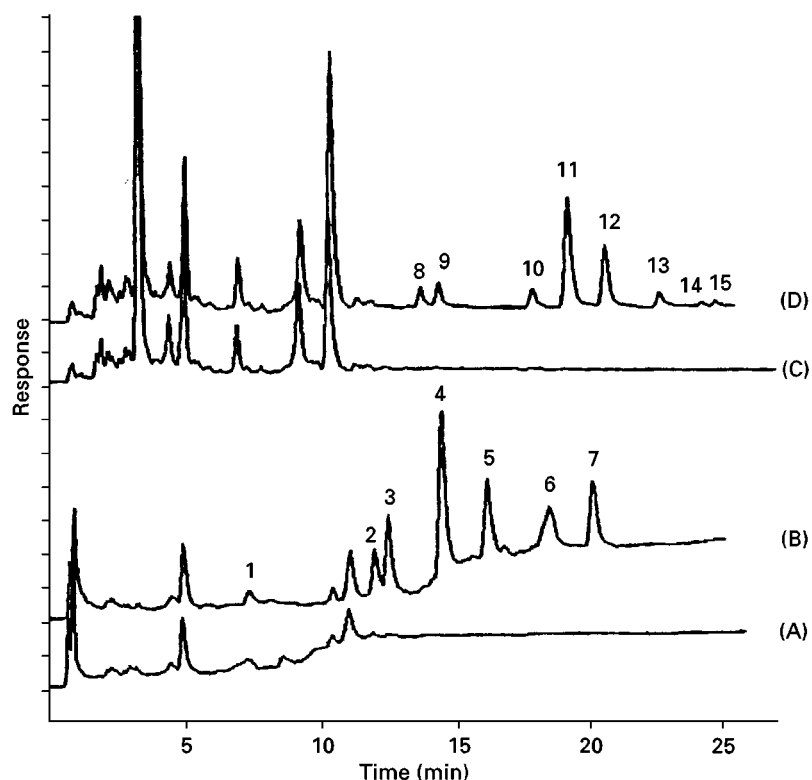


Figure 4 LC chromatogram of the analysis of 50 mL tap water using acetonitrile as organic solvent for low molecular weight compounds and isopropanol for the high molecular weight compounds. Analysis of low molecular weight compounds in tap water with addition of a standard solution of 10 ng L⁻¹ (B) and without any addition (A). Analysis of high molecular weight compounds in tap water in the same conditions (C,D). Peak assignment: 1, naphthalene; 2, acenaphthene; 3, fluorene; 4, phenanthrene; 5, anthracene; 6, fluoranthene; 7, pyrene; 8, benzo[*a*]anthracene; 9, chrysene; 10, benzo[*b*]fluoranthene; 11, benzo[*k*]fluoranthene; 12, benzo[*a*]pyrene; 13, dibenz[*a,h*]anthracene; 14, benzo[*ghi*]perylene; 15, indeno[1,2,3-*cd*]pyrene. (Reproduced with permission from El Harrak *et al.* (1998)).

to be added to the samples, in order to avoid adsorption of these compounds in the system.

The use of solid-phase extraction and HPLC with fluorescence detection enables low levels (at ng L⁻¹ in

water samples) of PAHs to be determined in real samples.

Table 6 Linear range and limits of detection of PAHs in seawater. Volume of sample 50 mL

Compound	Linear range (ng L ⁻¹)	<i>r</i> ²	LOD (ng L ⁻¹)
Naphthalene	400–2.0	0.9994	1.0
Acenaphthene	400–1.0	0.9997	0.5
Fluorene	400–1.0	0.9995	0.5
Phenanthrene	400–0.5	0.9999	0.2
Anthracene	400–1.0	0.9998	0.5
Fluoranthene	400–1.0	0.9997	0.5
Pyrene	400–0.5	0.9998	0.2
Benzo[<i>a</i>]anthracene	200–2.0	0.9997	0.5
Chrysene	200–2.0	0.9999	0.4
Benzo[<i>b</i>]fluoranthene	200–2.0	0.9999	0.3
Benzo[<i>k</i>]fluoranthene	200–0.5	0.9998	0.2
Benzo[<i>a</i>]pyrene	200–2.0	0.9997	0.2
Dibenzo[<i>a,h</i>]anthracene	200–0.5	0.9998	0.2
Benzo[<i>ghi</i>]perylene	200–5.0	0.9996	2.0
Indeno[1,2,3- <i>cd</i>]pyrene	200–5.0	0.9995	2.0

See also: **III/Environmental Applications:** Solid-Phase Microextraction; Supercritical Fluid Extraction. **Immunoaffinity Extraction: Polycyclic Aromatic Hydrocarbons;** Gas Chromatography; Supercritical Fluid Chromatography; Thin-Layer (Planar) Chromatography.

Further Reading

- Brouwer ER, Hermans ANJ, Lingeman H and Brinkman UATh (1994) Determination of polycyclic aromatic hydrocarbons in surface water by common liquid chromatography with fluorescence detection, using on-line micelle-mediated samples preparation. *Journal of Chromatography A* 669: 45–57.
- El Harrak R, Calull M, Marcé RM and Borrull F (1996) Determination of polycyclic aromatic hydrocarbons in water by solid-phase extraction membranes. *International Journal of Environmental Analytical Chemistry* 64: 47–57.
- El Harrak R, Calull M, Marcé RM and Borrull F (1998) Influence of the organic solvent in on-line solid-phase

- extraction for the determination of PAHs by liquid chromatography and fluorescence detection. *Journal of High Resolution Chromatography* 21: 667–670.
- Leeming R and Hamer W (1990) Determination of polycyclic aromatic hydrocarbons in lake sediments. *Organic Geochemistry* 15: 469–476.
- Messer DC and Taylor LT (1995) Method development for the quantitation of trace polyaromatic from water via solid-phase extraction with supercritical fluid elution. *Journal of Chromatographic Science* 33: 290–296.
- Peltonen K and Kuljukka T (1995) Air sampling and analysis of polycyclic hydrocarbons. *Journal of Chromatography A* 710: 93–108.
- Pérez S, Ferrer I, Hennion M-C and Barceló D (1998) Isolation of priority polycyclic aromatic hydrocarbons from natural sediments and sludge reference materials by an anti-fluorene immunosorbent followed by liquid chromatography and diode array detection. *Analytical Chemistry* 70: 4996–5001.
- Sargenti SR and McNair HM (1998) Comparison of solid-phase extraction and supercritical fluid extraction for extraction of polycyclic aromatic hydrocarbons from drinking water. *Journal of Microcolumn Separations* 10: 125–131.
- Thurman EM and Mills MS (1998) *Solid Phase Extraction. Principles and Practice*. New York: John Wiley.
- Urbe I and Ruana J (1997) Application of solid-phase extraction discs with a glass fiber matrix to fast determination of polycyclic aromatic hydrocarbons in water. *Journal of Chromatography A* 778: 337–345.

Supercritical Fluid Chromatography

K. D. Bartle, University of Leeds, UK

Copyright © 2000 Academic Press

Introduction

There is tremendous analytical interest in polycyclic aromatic compounds (PAC) because of their carcinogenic properties and their impact on the environment. PAC mixtures can be very complex and extend over a wide range of molecular masses. They mainly originate from the combustion of fossil fuels and are widespread in the environment.

The most commonly used separation techniques for PAC are gas chromatography (GC), high performance liquid chromatography (HPLC) and supercritical fluid chromatography (SFC). GC is often the technique of choice since it works well for low molecular weight and volatile compounds. It is also preferred because the high diffusivity of solutes in gases results in relatively short analysis times. HPLC employs liquids of high solvating power, high densities and high viscosities but is often time-consuming and has much less resolving power than GC.

Separation of PAC by SFC

Although HPLC and GC are commonly used for the analysis of PAC mixtures, SFC has a number of advantages. SCF have diffusivities that are more gas-like, viscosities lower than liquids and densities that are more liquid-like. The resulting mass transfer coefficients lead to a more rapid analysis in SFC than in HPLC. The diffusion coefficients and viscosities of SCF allow GC-like separations on capillary columns but at much lower temperatures because of the high

solvating power of SCF. The approach in SFC involves the use of columns of the packed LC type, packed capillary (micro-packed) and the open tubular (capillary) GC type columns.

SFC on Packed Columns

Packed columns usually of the commercial HPLC variety were used in nearly all the early work in SFC. The length and internal diameter (i.d.) of SFC packed columns are constrained by (a) the larger pressure drops as compared to open tubular columns and (b) high flow rates, making interfacing to GC detectors more difficult. Often, narrow-bore packed columns with a diameter of 1 to 2 mm are used because they can be installed in a capillary SFC instrument and are compatible with many detectors.

Early work on the separation of polycyclic aromatic hydrocarbon (PAH) standards revealed that reduced particle size led to increased resolution, and that analysis times were reduced in comparison with HPLC; it was also shown that PAH elution order could be varied by changing the operating temperature and/or the pressure. Marked changes in retention and selectivity are brought about by the addition of a modifier to the mobile phase. Detailed studies of the retention characteristics of PAH on a wide range of packed columns showed that retention in SFC with CO₂-based mobile phases correlates most closely with reverse phase HPLC. Very rapid analysis (< 6 minutes) of the sixteen Environmental Protection Agency target PAH was demonstrated on a 15 cm long column packed with a specially bonded C₁₈ silica (Figure 1). Efficient separation of PAH can be achieved by coupling columns of different selectivity. Plate numbers up to 220,000 and separation of up to

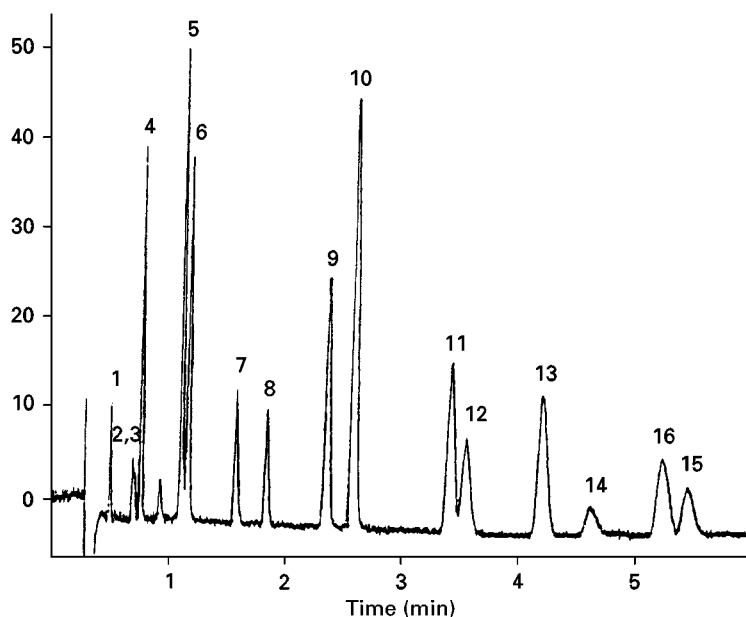


Figure 1 Supercritical fluid chromatography (SFC) of the EPA/PAH mixture. Chromatographic conditions: 5 mL min⁻¹; CO₂/MeOH mobile phase; gradient of 10% MeOH/min from 1% up to 50% then hold at 50%; pressure gradient of 95 bar min⁻¹ from 80 bar up to 200 bar then hold at 200 bar; temperature 40°C for 3 minutes then gradient of 7°C per minute to 60°C. Detection UV absorbance at 254 nm. Peak identification 1 naphthalene; 2 acenaphthylene; 3 acenaphthene; 4 fluorene; 5 phenanthrene; 6 anthracene; 7 fluoranthene; 8 pyrene; 9 benz[*a*]anthracene; 10 chrysene; 11 benzo[*b*]fluoranthene; 12 benzo[*k*]fluoranthene; 13 benzo[*a*]pyrene; 14 dibenz[*a, h*]anthracene; 15 benzo[*ghi*]perylene; 16 indeno[1,2,3-*cd*]pyrene. Reproduced with permission from Heaton *et al.* (1994).

60 PAH can be achieved by coupling up to seven packed (HPLC) columns together.

SFC on Capillary Columns

Capillary column SFC is often preferred to packed column SFC for separation of PAC mixtures because of better resolution (Figure 2). The price paid, however, is much slower analysis and the use of unmodified CO₂ as mobile phase, in which the higher molecular weight PAC are less soluble.

A variety of mobile phases other than CO₂ have been studied in order to increase the selectivity for a wide range of samples and solutes in work which also indicated that the choice of stationary phase for capillary SFC must take into account the solvating power and the reactivity of the supercritical fluid; the stationary phase must be sufficiently immobilized and must not react with the mobile phase to avoid being washed out of the column by the carrier fluid. Supercritical ammonia has been used because of its high polarity and reasonable critical parameters ($T_c = 132.5^\circ\text{C}$, $P_c = 112.5\text{ atm}$).

A similar range of stationary phases has been used in the capillary SFC of PAC as has been applied in capillary GC: 100% methyl and 5% phenyl siloxanes, and the more selective 5% biphenyl and cyanopropyl siloxanes. Very selective SFC separations have been shown on liquid crystalline phases

(Figure 3). Isomers may be resolved on the basis of the length-to-breadth ratio and planarity of PAH since they are compatible with the ordered 'rod-like' structure of the phase.

Detection in SFC of PAC

Flame-ionization (FID) is the most commonly used detector in capillary SFC of PAC, but the UV absorption detector has most often been applied in packed column work because of the presence of modifiers. Photodiode array detection then allows identification of parent PAH. Nitro PAC have been determined by capillary SFC with the use of the thermionic detector (TID); no modification is necessary and the detector is sensitive and stable during density programming. Low concentrations of sulfur-containing PAC have been detected with the aid of the flame photometric detector in capillary SFC. The photoionization detector uses a high-energy UV lamp to ionize the eluted PAH, and offers high sensitivity with some selectivity over non-aromatic compounds.

Spectroscopic detection has often been used in SFC to allow PAC identification. PAC are weak IR absorbers, but may be identified from the FTIR spectra of compact spots deposited by CO₂ mobile phase elimination at the restrictor exit; PAH isomers may be differentiated by their FTIR spectra, e.g. chrysene from

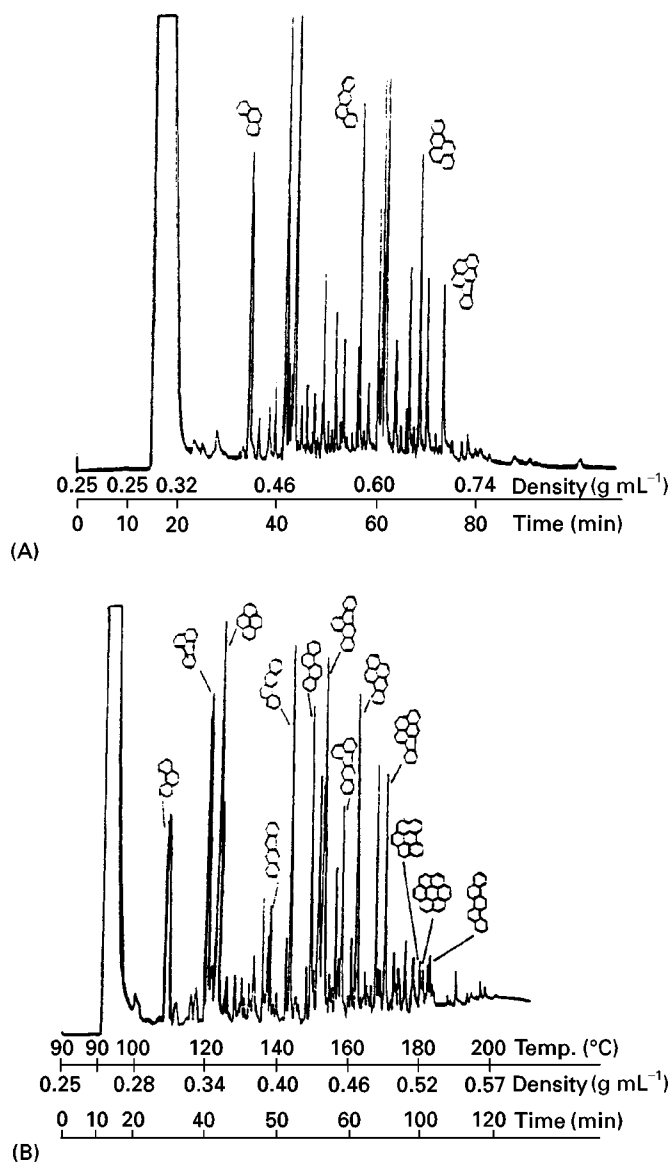


Figure 2 SFC chromatograms of total coal tar polycyclic aromatic hydrocarbons (A) constant temperature 110°C, density program, (B) simultaneous temperature/density program. Chromatographic conditions: (A) constant temperature at 90°C; density ramp rate of 0.007 g mL⁻¹ min⁻¹ up to 0.75 g mL⁻¹; 10-m × 0.50-μm i.d fused silica capillary column coated with biphenyl carboxylate ester liquid crystalline (SB-Smectic); FID at 350°C. Reproduced with permission from Kithinji *et al.* (1990) *Journal of High Resolution Chromatography* 13: 27.

benz[*a*]anthracene. Flow-cell FTIR is less useful in SFC of PAC because of the interference from bands from CO₂ mobile phase. Supercritical xenon is a better solvent than CO₂ for PAH, and does not obscure their FTIR spectra but is extremely expensive.

SFC has been interfaced to mass spectrometry (MS) in a number of analyses of PAC; low flow rates in capillary SFC make it particularly useful. SFC-MS is then employed in the identification of PAC especially from their molecular weights. The fluorescence detector has been used in SFC of PAH mixtures with

pentane mobile phase. Both excitation and emission spectra have been used in high sensitivity analysis of PAH.

Multidimensional Chromatography

PAC mixtures are often too complex for their analysis in a single chromatographic system. Multidimensional chromatography, generating much higher resolution, and improved separation of PAC mixtures, has been demonstrated in coupled SFC-SFC of both

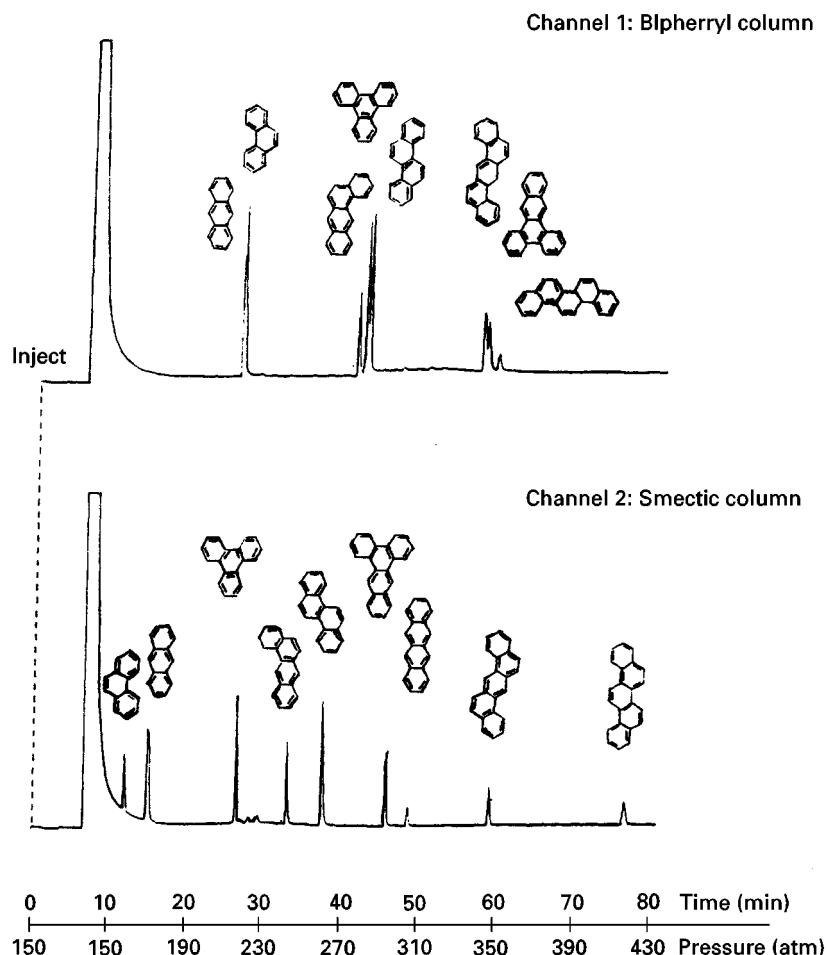


Figure 3 Simultaneous separation of a mixture of 3-, 4- and 5- ring polycyclic aromatic hydrocarbon isomers on biphenyl and smectic columns. Chromatographic conditions: Column 1 – open tubular column coated with a 0.25- μm film of 30% biphenyl-methylpolysiloxane stationary phase (Biphenyl-30); Column 2 – open tubular column coated with a 0.25- μm film of smectic biphenylcarboxylate ester liquid crystalline polysiloxane stationary phase (SB-Smectic-50); CO_2 at 120°C ; pressure program from 150 atm (hold for 10 min) to 450 atm min^{-1} ; FID at 300°C . Reproduced with permission from Raynor *et al.* (1990) *Journal of High Resolution Chromatography* 13:22.

packed column–capillary column and capillary column–capillary column arrangements. The first column can provide chemical class separation, while the second resolves closely related compounds and isomers.

Applications of SFC to PAC Mixtures

SFC is a useful procedure in PAC analysis by providing complementary information to that from GC and HPLC.

Group-type separation by HPLC and open-column chromatograph is unsatisfactory, and SFC methods have proven markedly superior. Packed columns (often silica and silver-salt impregnated silica in tandem) were first used for this application, but certain separations (e.g. saturates from olefins) were often inadequate unless supercritical SF_6 or complex column switching were employed.

Aromatic content of fuels is determined by SFC in an ASTM method on a silica packed column with CO_2 . Separation of aromatic compounds on the basis of ring number has been demonstrated on packed capillary columns, and also by two-dimensional capillary SFC–SFC. FID detection with CO_2 mobile phase allows ready quantitation.

Simulated distillation (SIMDIS) of fuels is often used to replace actual distillation in the determination of boiling point distribution. While GC is often used in SIMDIS, damage to columns and sample degradation resulting from the high temperatures necessary to elute high MW compounds has led to the development of SFC methods in which oven temperatures as low as 150°C are sufficient to elute PAC boiling beyond 750°C because of their greater solubility in supercritical CO_2 mobile phase at densities up to 0.71 g mL^{-1} . A column packed with

C₆ bonded silica was especially useful in correlating SFC retention with boiling point for a variety of PAC types.

PAC from fossil fuel and environmental samples have commonly been analysed by SFC, with an application range beyond that of GC and much improved resolution over HPLC methods. Coal-derived PAH containing as many as twelve rings have been eluted in SFC. Identification and quantitation is straightforward with the aid of FID, UV and MS detectors. Very rapid analysis of environmental mixtures of PAC has been demonstrated on a C₁₈ column with CO₂/methanol mobile phase and simultaneous pressure, temperature and composition programming.

Many nitrogen-containing PAC cannot be analysed by GC because they are thermally labile, and SFC with TID has been especially useful in allowing identification of hydroxynitrofluorenes and nitropyrenequinones.

Further Reading

- Berger TA and Wilson WH (1993) Packed column SFC with 220 000 plates. *Analytical Chemistry* 65: 1451.
- Chang H-CK, Markides KE, Bradshaw JS and Lee ML (1988) Selectivity enhancement for petroleum hydrocarbons using a smectic liquid crystalline stationary phase in SFC. *Journal of Chromatographic Science* 26: 280.
- Heaton DM, Bartle KD, Clifford AA, Myers P and King BW (1994) Rapid separation of PAH by packed column SFC. *Chromatographia* 39: 607.
- Kuei JC, Tarbet BJ, Jackson WP *et al.* (1985) SFC with supercritical ammonia mobile phase. *Chromatographia* 20: 25.
- Lee ML and Markides KE (eds) (1990) *Analytical Supercritical Fluid Chromatography and Extraction*, ch. 7, Chromatography Conferences Inc., Provo, Utah.
- Raynor MW, Davies IL, Bartle KD *et al.* (1988) *J. High Resolution Chromatography* 11: 766.
- Shariff SM, Robson MM and Bartle KD (1997) SFC of polycyclic aromatic compounds: a review. *Polycyclic Aromatic Compounds* 12: 147.

Thin-Layer (Planar) Chromatography

G. Donnevert, University of Applied Sciences, Giessen, Germany

Copyright © 2000 Academic Press

Polycyclic aromatic hydrocarbons (PAH) originate from organic materials (i.e. oil, gasoline, tobacco, garbage, etc.) due to pyrolysis or incomplete combustion. Several hundred different PAH are known, and traces of them can be found nearly everywhere in our environment. In water PAH occur either in solution or adsorbed on to particulate material. As certain PAH are known to be highly carcinogenic, six easily detectable PAH were specified, in order to be used as indicators for the large group of PAH. The structural formulae of these six compounds are given in Table 1. In 1971 the World Health Organization (WHO) set the maximum acceptable level of the sum of these six PAH in potable waters at 200 ng L⁻¹. This standard was adopted by the European Community, who fixed the maximum admissible concentration for the sum of the six reference substances in drinking water to 0.2 µg L⁻¹, calculated as carbon.

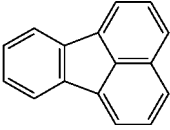
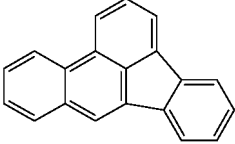
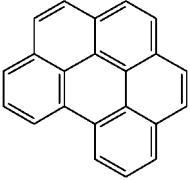
Thin-layer chromatography (TLC) is one analytical method for the determination of these PAH, in addition to other chromatographic techniques. For standard chromatograms, standard solutions containing fluoranthene with five times the level of the other PAH are usually used. This is based on the fact that fluoranthene is present at approximately five times

the level of the other PAH in the majority of water samples. A TLC method using development in two dimensions with two different solvent systems has been known for many years. After separation, the PAH are visualized by irradiation with ultraviolet light, and normally the concentration range of the PAH is visually estimated by comparison with standard chromatograms. In addition to this old semiquantitative TLC method, some modern and more efficient TLC methods have been devised.

The improvement of plate material leading to high performance thin-layer chromatography (HPTLC) allowed the development of efficient procedures for qualitative and quantitative analysis of PAH. A big advantage of the HPTLC methods is the possibility of applying up to 18 samples on to one plate, whereas with the two-dimensional method only one sample could be analysed per plate.

Before the PAH can be separated by TLC, they must be extracted from water samples using, for example, cyclohexane. For a sample volume of 1 L 25 mL of solvent is suitable; larger volumes may be convenient in some cases, e.g. when emulsions form. The solvent extract is concentrated to a small volume and, if necessary, materials interfering in the analysis are removed from the extract using column chromatography with alumina or silica gel. The methods described in the following paragraphs can also be applied to extracts of food, soil, smoke and

Table 1 Names and structures of the six PAH

		Structure		Structure
Name	Fluoranthene		Name	Benzo(a)pyrene
Abbreviation	F		Abbreviation	BaP
Chemical formula	$C_{16}H_{10}$		Chemical formula	$C_{20}H_{12}$
% Carbon	95.0% C		% Carbon	95.2% C
Name	Benzo(b)fluoranthene		Name	Benzo(k)fluoranthene
Abbreviation	BbF		Abbreviation	BkF
Chemical formula	$C_{20}H_{12}$		Chemical formula	$C_{20}H_{12}$
% Carbon	95.2% C		% Carbon	95.2% C
Name	Benzo(ghi)perylene		Name	Indeno(1,2,3-cd)pyrene
Abbreviation	BP		Abbreviation	IP
Chemical formula	$C_{22}H_{12}$		Chemical formula	$C_{22}H_{12}$
% Carbon	95.6% C		% Carbon	95.6% C

other sample material. For some of these samples special, and very time-consuming, clean-up procedures are needed. Therefore TLC is mainly used for the analysis of drinking water.

Thin-Layer Chromatography Method with Development in Two Dimensions

Different adsorbent stationary phases can be used for the separation of PAH. An excellent resolution of the six WHO PAH is obtained on a mixed phase consisting of aluminium oxide G and 40% acetylated cellulose in a 7:3 weight ratio. With these plates fluoranthene can be determined in the range of 10–100 ng per spot and the other PAH in the range of 5–80 ng per spot.

Preparation of the TLC Plates

Plates may be prepared as follows using conventional glass TLC plates and a plate-coating apparatus (the quantities given are sufficient for five plates): 28 g aluminium oxide G and 12 g cellulose 40% acetylated are thoroughly mixed with 5 mL ethanol. Clean glass plates 20 × 20 cm are coated with this mixture at a thickness of 0.25 mm. The coating is air-dried at room temperature for 10–15 min, then activated at 110°C for 30 min. After activation the plates are cooled and stored in a desiccator.

Application of the Sample Extract or Standard Solution

The concentrated extract (0.05–0.1 mL) is spotted in the bottom left corner of the plate, 20 mm from each

edge. Microsyringes or capillaries can be used to apply the sample; the diameter of the spot should be about 4–6 mm. The spotting solvent needs about 2–3 min to evaporate at room temperature.

Standard mixtures of the six PAH are applied in the same manner in order to obtain standard chromatograms for the estimation of the PAH concentration.

Development of the Plates

For the chromatographic separation, tanks which have been allowed to equilibrate with the solvent for at least 15 min are used. The migration distance should be about 18 cm in both directions.

- Solvent system 1: a mixture 9 vol *n*-hexane and 1 vol toluene
- Solvent system 2: a mixture of 4 vol methanol, 4 vol diethyl ether and 1 vol water

After separation in solvent system 1, the plate is removed from the tank and dried at ambient temperature in a fume cupboard for 10–15 min. It is then rotated through 90° anticlockwise from the first direction of development and developed in solvent system 2. Afterwards the plate is again removed from the tank and dried in a fume cupboard at ambient temperature for 10–20 min.

The development times are approximately 30 min for solvent system 1 and 90 min for solvent system 2.

Visual Evaluation of the Chromatograms

The plates are irradiated with 366 nm ultraviolet light to visualize the PAH as a series of fluorescent

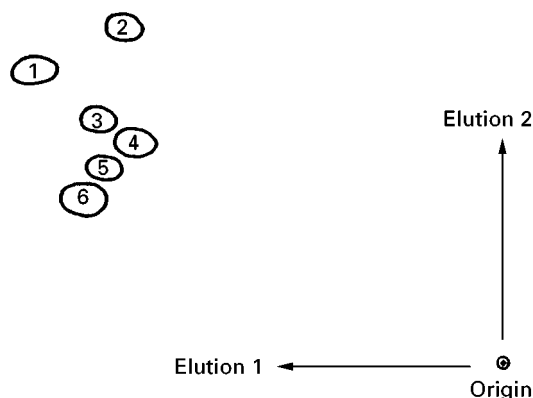


Figure 1 Standard PAH chromatogram viewed under UV light with F (1, turquoise), BP (2, violet), BkF (3, violet), IP (4, yellow), BbF (5, turquoise) and BaP (6, violet).

spots. In a dark cabinet plates with standard chromatograms can be viewed simultaneously with a sample chromatogram to estimate the concentration visually. A typical standard chromatogram is given in **Figure 1**. A chromatogram of a river water sample is shown in **Figure 2**.

Quantification of the Spots using a Scanning Fluorimeter

It is also possible to evaluate the chromatograms using a scanning fluorimeter, but this procedure is very time-consuming and therefore in most cases only semiquantitative evaluation by visual estimation is used.

Table 2 Suitable excitation and emission wavelengths

Compound	Excitation wavelength (nm)	Emission wavelength (nm)
Fluoranthene	365	462
Benzo(b)fluoranthene	302	452
Benzo(k)fluoranthene	302	431
Benzo(a)pyrene	297	405 or 430
Benzo(ghi)perylene	302	419 or 407
Indeno(1,2,3-cd)pyrene	300	500

For the scanning method, first the coordinates defining each spot are recorded using a standard plate. The instrument settings (slit height and width, wavelengths, etc.) required to achieve good curves must be determined individually for the available equipment, because these settings will vary with the type of instrument. For guidance, suitable excitation and emission wavelengths are given in **Table 2**.

The standard and the sample plates are scanned using the same instrument settings. For each spot on the plates the area of the peak is measured. The mass of each individual PAH in the sample can then be calculated by comparison with the standard.

Determination of PAH by HPTLC with Fluorescence Detection

The two methods described below are applicable to the determination of the six selected PAH in drinking

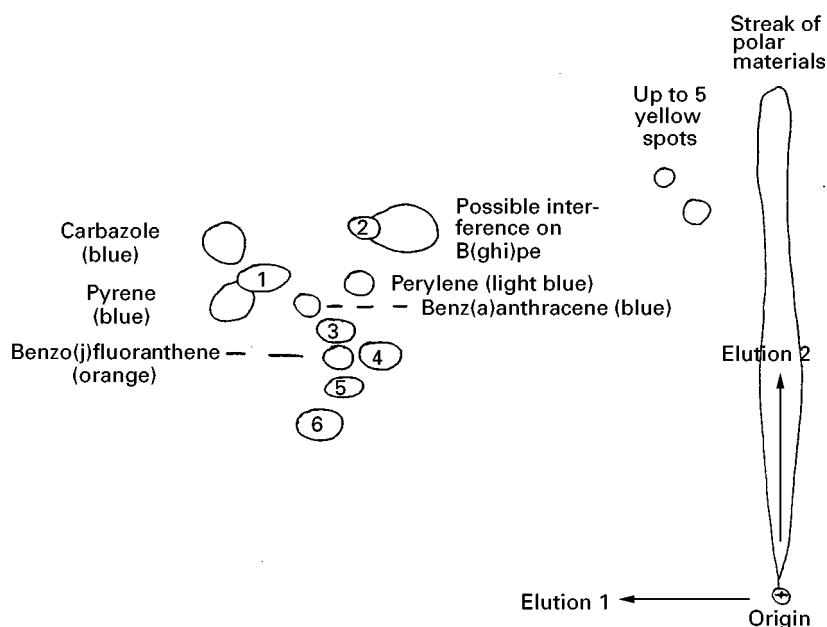


Figure 2 River water chromatogram viewed under UV light with F (1, turquoise), BP (2, violet), BkF (3, violet), IP (4, yellow), BbF (5, turquoise) and BaP (6, violet).

water, ground waters and moderately polluted surface waters. For other samples, containing a lot of interfering substances, specially developed clean-up procedures are necessary.

The first method uses HPTLC RP-18 plates and is a screening method for semiquantitative determination. It can be used to screen for samples with PAH concentrations near or above the limiting value, which then have to be analysed quantitatively.

For the quantitative method, using caffeine-impregnated HPTLC silica gel plates, the chromatograms are evaluated by *in situ* fluorescence measurement at constant or differing wavelength combinations. This method has a working range of 40–240 ng L⁻¹ for the sum of the six PAH.

PAH are extracted from the water sample by liquid-liquid extraction as described above. The extract is evaporated to dryness and the residue taken up in a small defined volume of solvent. An aliquot of this extract is applied on to the HPTLC plate. A more detailed description of the methods is given below.

HPTLC Method with RP-18 Plates

Plate Material

HPTLC-pre-coated RP-18 plates, preferably with fluorescence indicator, are used. Plates with concentrating zones may also be used. RP-18 materials with different degree of coverage (carbon loading) are commercially available and, depending on this, different mobile phases have to be used.

Application of Sample Extracts and Standard Solutions

Several samples may be analysed simultaneously on one HPTLC plate, together with two or more reference solutions of different concentrations. For screening purposes it is also possible to apply sample extracts and reference solutions on both ends of the HPTLC plate, provided the plate is developed in a horizontal development chamber.

Aliquots, e.g. 25%, of the total sample extracts (40–120 µL) are applied either by means of an automated volume-dosing device or by hand as bands or spots. For the application of spots HPTLC RP-18 plates with a concentrating zone are preferred and the volumes should not be more than 10 µL. If using band application, the bands should have a length of 7 mm and the intervals should be 3 mm. For band application the extract should not be too concentrated, and it is advantageous to apply higher volumes, e.g. 30 µL.

Development of the Plates

The development is performed in a development chamber for low consumption of mobile phase, suitable for trace analysis.

Depending on the carbon loading, one of the following mobile phases is used:

- a mixture of acetonitrile, 2-propanol and methanol (1 + 2 + 1) for high carbon loading C₁₈ material
- a mixture of acetonitrile, water and methanol (10 + 2 + 10) for low carbon loading C₁₈ material

The chromatogram is developed at room temperature either vertically in a trough chamber or horizontally in a horizontal development chamber, without chamber saturation. Using a trough chamber, the run time for a migration distance of 6.5 cm is about 20 min. In a horizontal development chamber, the run time for a migration distance of 6 cm is about 20 min, and for 4.5 cm about 15 min.

After development the plate is dried for 2 min in a stream of air at ambient temperature.

Visual Evaluation of the Chromatograms

If the dried plate is viewed under an ultraviolet lamp at 366 nm only three to four fluorescing zones can be recognized. Figure 3 shows two examples: first, a chromatogram of the six PAH on a plate with high carbon load C₁₈ material, with a concentrating zone,

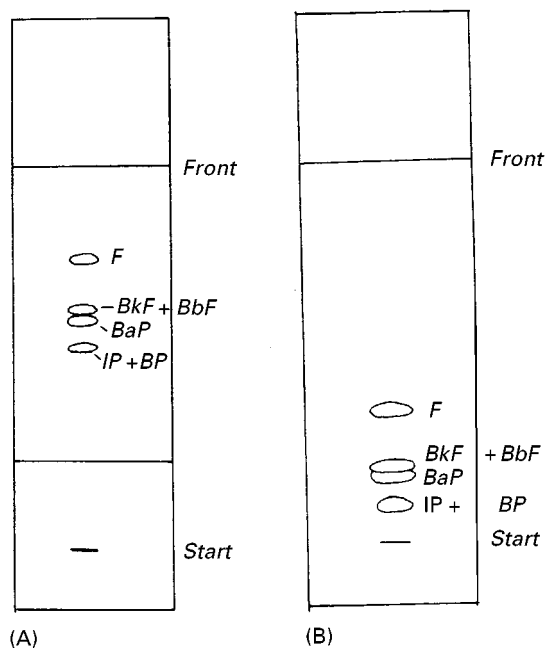


Figure 3 Chromatogram of the six PAH on HPTLC RP-18 plates. (A) high carbon load C₁₈ material, plate with concentrating zone; (B) low carbon load C₁₈ material.

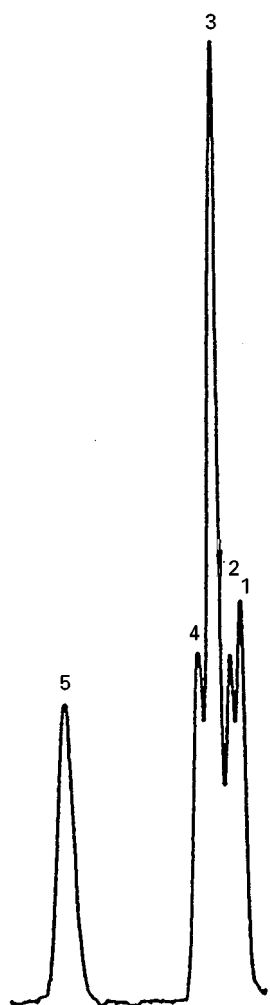


Figure 4 Fluorescence scan of a chromatogram track with 2 ng per spot of BP, IP, BaP, BbF, BkF and 10 ng per spot of F. The separation from the start to the front is IP (1), BP (2), BaP and BkF (3), BbF (4) and F (5).

and second, a chromatogram of the six PAH on a plate with low carbon load C_{18} material.

This separation is sufficient to evaluate the sample chromatograms visually by comparison with standard chromatograms. The individual PAH can be identified by colour, R_F value, and position relative to the reference chromatogram. The colours of the PAH are: F = light blue, BkF = dark blue, BbF = blue, BaP = violet, IP = light yellow and BP = violet. The concentration of the PAH in the sample extracts can be estimated by the fluorescence intensity of the zones. If, as in most drinking and ground waters, the fluorescence intensity is not stronger than the fluorescence of a corresponding standard, the PAH concentration lies below the limiting value, and therefore quantitative measurement is not necessary.

Influence of Temperature

Working at lower temperatures leads to better separation. The six PAH can be separated at -20°C into five fractions. Figure 4 shows the fluorescence scan after chromatographic development on a high carbon load C_{18} material. The separation is still not satisfactory as BaP and BkF are not separated. Due to this, the described separation technique is not suitable for quantitative analysis of the individual compounds.

HPTLC Method with Caffeine-impregnated Silica Gel Plates

The ability of PAH to form charge transfer complexes can be successfully employed when applied to silica gel thin layers impregnated with different electron acceptors, such as caffeine. In the following paragraphs charge transfer chromatography on caffeine-impregnated HPTLC silica gel plates is described. The chromatographic separation at room temperature is an alternative method to the screening method on HPTLC RP-18 plates. If the development is performed at -20°C , the six PAH can be easily separated into six fractions and the chromatograms can be evaluated quantitatively.

Plate Material

Caffeine-impregnated HPTLC silica gel 60 plates are commercially available, but the impregnation can also be carried out in the laboratory.

For caffeine impregnation HPTLC silica gel 60 plates are dipped for 4 s into a solution containing 4 g caffeine in 96 g dichloromethane and then dried at 110°C for 30 min. Prior to use, the plates should be cleaned by running a blank chromatogram to the upper edge, using dichloromethane. This pre-washing step is especially recommended if quantitative determination is intended. Afterwards the plates need to be reactivated by heating at 110°C for 30 min. The activated plates should be stored in a desiccator until use.

Application of the Sample Extracts and Standard Solutions

Aliquots of sample extracts and standard solutions are applied on to the same plate, preferably as bands, using an automated volume-dosing device.

For screening purposes, extracts and standard solutions are applied as bands or spots on both ends of the HPTLC plate, provided the plate is developed in a horizontal development chamber.

For quantitative analysis only band application is recommended. The bands should have a length of 7 mm and the intervals should be 3 mm. The applied volumes should be between 10 and 30 μL .

Development of the Plates at Room Temperature

After application of the samples, the plate is preconditioned for 30 min over water. Then the chromatogram is developed vertically or horizontally in a development chamber without chamber saturation, using a mixture of diisopropyl ether and *n*-hexane (4 + 1) as mobile phase. Using a trough chamber, the run time for a migration distance of 6.5 cm is about 25 min; in a horizontal development chamber, the run time for a migration distance of 6.5 cm is about 15 min, and for 4.5 cm about 10 min. After development the plate is dried for 2 min in a stream of air at ambient temperature. Then, in order to stabilize the fluorescence intensity of the chromatogram zones for more than 1 h, the plate is dipped into a solution of liquid paraffin-*n*-hexane (1 + 2) for 2 s, then dried again for 2 min. This not only leads to stabilization but in addition the fluorescence intensity is doubled for F, BkF, BbF and IP, and enhanced by a factor of 5 for BaP and BP.

Visual Evaluation of the Chromatograms

If the dried plate is viewed under an ultraviolet lamp at 366 nm, five fluorescing zones can be recognized (Figure 5A). The individual PAH can be identified by colour, R_F value and relative position to the reference chromatogram. The concentration of the PAH in the

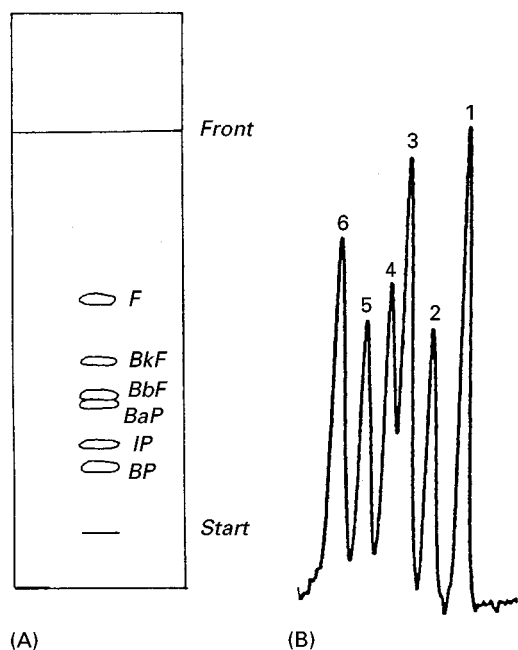


Figure 5 (A) Chromatogram of the six PAH on a caffeine-impregnated HPTLC silica gel plate. Development at room temperature. (B) Fluorescence scan of a chromatogram track with 2 ng per spot BP (1), IP (2), BaP (3), BbF (4) and BkF (5) and 10 ng per spot of F (6). Development at room temperature.

sample extracts can be estimated by the fluorescence intensity of the zones. The fluorescence scan of the chromatogram (Figure 5B) shows that there is no baseline separation between BaP and BbF. Therefore a quantitative evaluation of the chromatograms, developed at room temperature, would not yield reliable results for these substances.

Development of the Plates at -20°C

After sample application, the plate has to be precooled in a freezer cabinet at -20°C for 20 min. Then the chromatogram is developed vertically in a trough chamber without chamber saturation at -20°C with dichloromethane as mobile phase. The chamber has to be kept, for equilibration, at -20°C for at least 60 min before the analysis. The run time for a migration distance of 6.5 cm is about 20 min. Development in a horizontal development chamber does not give reproducible results.

After development the plate is dried for 2 min in a stream of air at ambient temperature. Then, in order to stabilize and increase the fluorescence intensity of the chromatogram zones, the plate is dipped, as described above, into a solution of liquid paraffin-*n*-hexane.

Fluorescence Densitometric Evaluation

Using the separation procedure at -20°C described above, the six PAH can be completely separated. Therefore this procedure is well suited for quantitative determination.

The chromatograms can be evaluated by measuring either the peak height or peak area using a scanner at an excitation wavelength of 366 nm and a fluorescence wavelength of 400 nm (edge filter). Standard chromatograms are evaluated to calculate a calibration function. The fluorescence intensity of the chromatogram zones is linearly related to the amount of PAH applied, up to 12 ng per spot for fluoranthene and up to 2.4 ng per spot for the other five PAH. The precision of the calibration functions is excellent (coefficients of variation between 1.7% and 3.8%).

If applying spots, the slit of the scanner should be broader than the largest zone of the chromatogram in the *x*-direction. If applying bands, the recommended slit width in the *x* direction is 1/2 to 2/3 of the band length. In the *y* direction, the slit should not be smaller than 0.3 mm.

Figure 6A shows the position of the six PAH on the caffeine-impregnated HPTLC silica gel plate. The fluorescence chromatogram (Figure 6B) demonstrates that the described procedure yields nearly baseline separation.

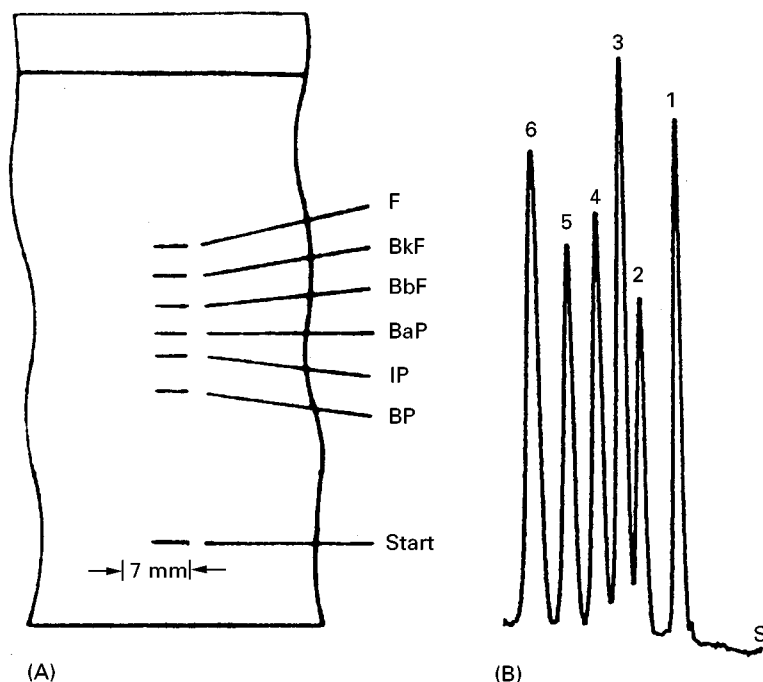


Figure 6 (A) Chromatogram of the six PAH on caffeine-impregnated silica gel plates, developed at -20°C ; (B) Fluorescence chromatogram of a track with 2 ng per spot BP (1), IP (2), BaP (3), BbF (4) and BkF (5) and 10 ng per spot of F (6); development at -20°C .

Figure 7 shows the chromatogram of a ground water sample, in which all six PAH were found, plus one unknown fluorescing substance. This was an ideal sample, but other fluorescing substances may interfere with the determination of the PAH. In such cases the PAH can be selectively detected, using different excitation and emission wavelengths.

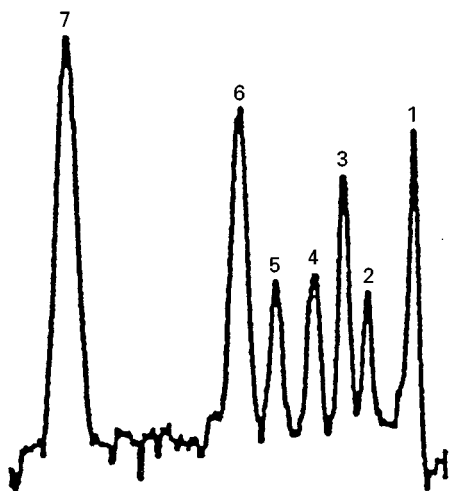


Figure 7 Fluorescence scan of a ground water sample with BP (1), IP (2), BaP (3), BbF (4), BkF (5), F (6) and an unknown substance (7).

Spectroscopic Identification

As the six PAH show different optical properties it is possible to detect them selectively. With HPTLC, which is characterized by offline detection, it is easy to repeat the scanning procedure several times using different easily selectable fluorimetric conditions within a short time period.

For example Figure 8 shows the evaluation of the same chromatogram at different excitation wavelengths and emission filters. By spectroscopic selection it is possible to guarantee the correctness of qualitative and quantitative results.

Conclusion

TLC is an efficient and versatile analytical method. The costs per sample are low and, because many samples can be analysed in one development step, the time to achieve results for a series of samples is comparably short. Although TLC has many advantages, this method is not often used for the analysis of PAH; the equipment for quantitative HPTLC is not widespread in water laboratories and only the screening method to control the observance of the limiting value for drinking water has found greater acceptance. Many laboratories prefer high performance liquid chromatography or gas chromatography for

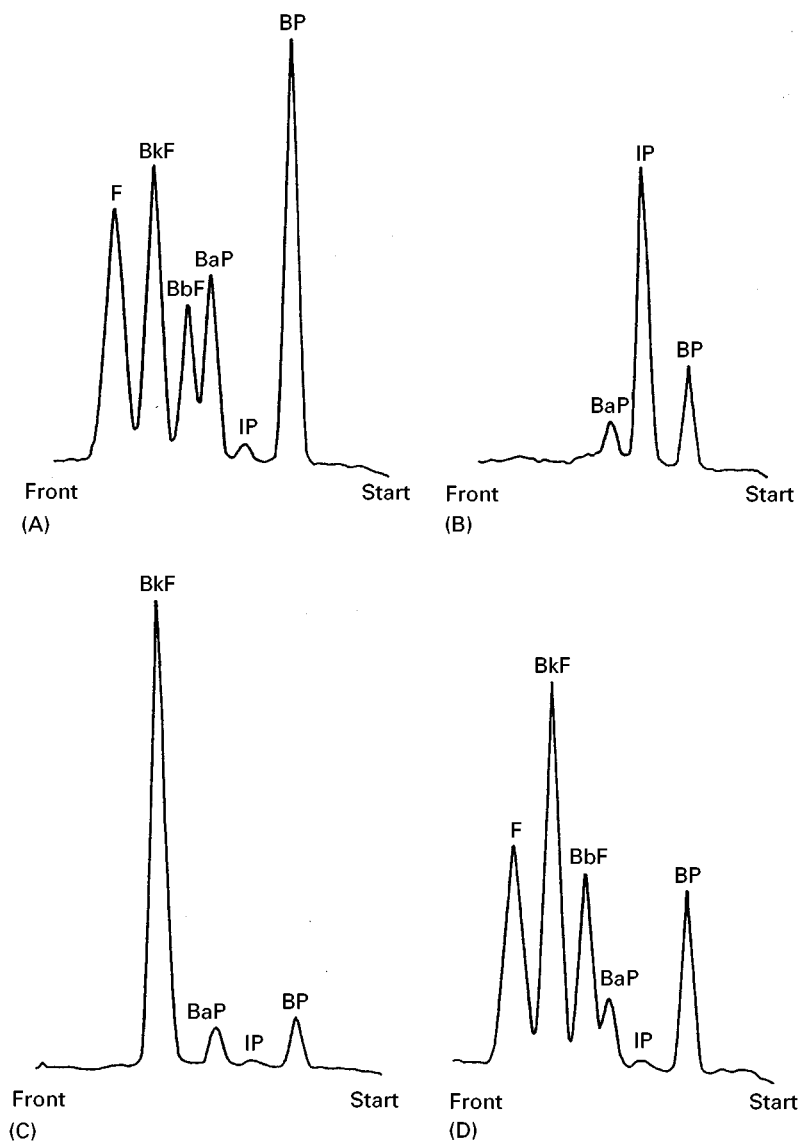


Figure 8 Fluorescence scan of the same chromatogram track. Selective detection using different excitation (λ_{exc}) and fluorescence (λ_{fl}) wavelengths: (A) $\lambda_{\text{exc}} = 365 \text{ nm}$; $\lambda_{\text{fl}} = 436 \text{ nm}$; (B) $\lambda_{\text{exc}} = 436 \text{ nm}$; $\lambda_{\text{fl}} = 578 \text{ nm}$; (C) $\lambda_{\text{exc}} = 405 \text{ nm}$; $\lambda_{\text{fl}} = 436 \text{ nm}$; (D) $\lambda_{\text{exc}} = 334 \text{ nm}$; $\lambda_{\text{fl}} = 436 \text{ nm}$.

the quantitative determination of PAH, because the separation efficiency of these methods is better and they can be automated. Therefore further development in the field of PAH determination with TLC cannot be expected, although modern HPTLC offers a lot of possibilities.

See also: II/Chromatography: Thin-Layer (Planar): Densitometry and Image Analysis; Instrumentation; Layers; Modes of Development: Conventional; Spray Reagents. III/Impregnation Techniques: Thin-Layer (Planar) Chromatography: Polycyclic Aromatic Hydrocarbons: Gas Chromatography; Liquid Chromatography; Supercritical Fluid Chromatography.

Further Reading

- Futoma DJ, Smith SR, Smith TE and Tanaka J (1981) *Polycyclic Aromatic Hydrocarbons in Water Systems*. Boca Raton: CRC Press.
- Geiss F (1987) *Fundamentals of Thin Layer Chromatography (Planar Chromatography)*. Heidelberg: Huethig.
- Harvey RG (1997) *Polycyclic Aromatic Hydrocarbons*. New York: Wiley-VCH.
- Henschel P and Laubereau PG (1989) *Water Pollution Research Report 17-HPTLC Applied to the Analysis of the Aquatic Environment*. Brussels: Commission of the European Communities.
- ISO/TC 147/SC 2/WG 19 (1996) *Water Quality – Determination of Polynuclear Aromatic Hydrocarbons (PAH) – Part 1: Determination of six PAH in Water by*

High Performance Thin Layer Chromatography with Fluorescence Detection. Geneva: DIS 7981-1.

Jork H, Funk W, Fischer W and Wimmer H (1989) *Thin Layer Chromatography – Reagents and Detection Methods. Physical and Chemical Detection Methods: Fundamentals, Reagents I.* Weinheim: Wiley-VCH.

Jork H, Funk W, Fischer W and Wimmer H (1993) *Thin Layer Chromatography – Reagents and Detection Methods. Physical and Chemical Detection Methods:*

Activation Reactions, Reagent Sequences, Reagents II. Weinheim: Wiley-VCH.

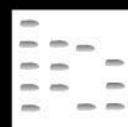
Sherma J (ed.) (1991) *Handbook of Thin Layer Chromatography.* New York: Dekker.

Sherma J and Fried B (1996) *Practical Thin-layer chromatography.* Boca Raton: CRC Press.

Stahl E (ed.) (1969) *Thin Layer Chromatography.* Berlin: Springer.

WHO (1993) *Guidelines for Drinking Water Quality,* 2nd edn. Geneva: WHO.

POLYETHERS: LIQUID CHROMATOGRAPHY



K. Rissler, Ciba Specialty Chemicals,
Basle, Switzerland

Copyright © 2000 Academic Press

Introduction

Before chromatography became an efficient tool for polymer fractionation, classic extraction procedures played a dominant role. These techniques comprise, e.g., dissolution and precipitation, depending on the solvent-non-solvent ratio and M_r , extraction of native polymer or polymer adsorbed onto a solid support with organic solvents of increasing dissolution capability, and partition between two immiscible liquids. In contrast, Baker-Williams and temperature rising elution fractionation (TREF), also used in polymer chemistry, are chromatographic techniques. Although separation of polymers by means of various classic extraction procedures are still in use, chromatographic characterization now plays the dominant role and affords an optimum degree of structural information. In this respect, polyethers of the polyethylene glycol (PEG), polypropylene glycol (PPG) and polybutylene glycol (PBG) family, all extensively used in different fields of chemistry and engineering, have been selected as model compounds for separation of polymers because they differ widely in chemical properties and polarity, ranging from hydrophilic (PEGs) to hydrophobic (PBGs) in either native form or mono-(di-)O-alkyl(arylalkyl) (Figure 1A–C) and amino-terminal derivatives (Figure 1B). For this reason, they comprise a group of polymers accessible to a broad range of chromatographic separation techniques including high performance liquid chromatography (HPLC), size-exclusion chromatography (SEC), thin-layer chromatography (TLC), supercritical fluid chromatography

(SFC) and capillary zone electrophoresis (CZE). Gas chromatography (GC) only provides separation of the low-molecular-weight (M_r) members of polyethers with upper limits of M_r of approximately 600. TLC and SFC are of minor importance and are not considered. Although extensively used for determination of M_r values, SEC is also excluded because it exhibits only moderate resolution and does not permit differentiation of the individual types of polyether on the basis of the underlying chemistry.

This survey gives a short overview of the current state of HPLC technology of polyethers and deriva-

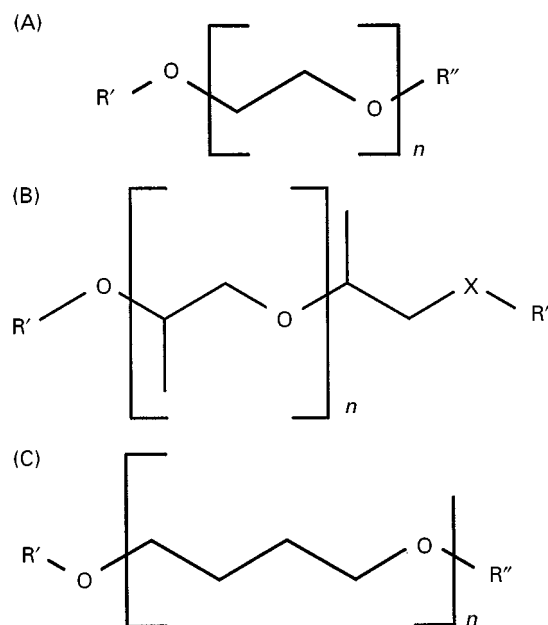


Figure 1 Structures of polymers. (A) R' , $R'' = H$, n -alkyl, alkyl-C=O, aryl(alkyl); $R' = R''$, $R' \neq R''$; (B) $R' = H$, glyceryl, trimethylolpropyl; $R'' = H$ ($X = O$), H_2 ($X = N$); (C) $R' = R'' = H$, alkyl, aryl(aroyl); $R' = R''$, $R' \neq R''$.

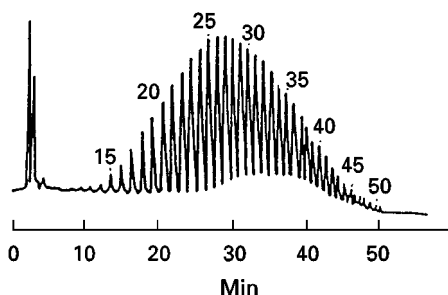


Figure 2 Gradient elution of the oligomers from NPE. Eluent A, n-hexane-2-propanol (40:60, v/v); eluent B, ethanol-water (80:20, v/v). Gradient: 10–95% B in 45 min. (Reproduced from Anghel DF, Balcan M, Voicu A, *et al.* (1994) *Journal of Chromatography*, 668: 375–383, with permission from Elsevier Science.)

tives. For more detailed information on liquid chromatography of this class of substances the reader is referred to recently published review articles (see Further Reading).

Special Features of Chromatographic Separation of Polymer Systems

Chromatographic behaviour of synthetic polymers substantially differs from that of low-molecular-weight analytes for a variety of reasons: (i) small diffusion coefficients of macromolecules in solution, (ii) the size of the macromolecules often being of the same order of magnitude as the pore diameter of the stationary phase, (iii) retention of polymers via trains of numerous repeat units, (iv) flexibility of the polymer chains enabling conformational changes, and (v) limited solubility. Synthetic polymers are usually composed of a large number of identical structural units, which dependent on the experimental conditions, give rise to more or less broad M_r distribution, ranging from some hundreds to millions. The situation is still more complicated when statistical, random and block copolymers are formed. Isocratic HPLC, typically applied for low M_r analytes, is not suited for exhaustive separation of individual oligomers, because of the great number of molecules often differing greatly in M_r . Separation of polymers built up from different chemical units (e.g., copolymers and/or polymers containing different end groups, such as, e.g., non-ionic surfactants) should ideally be effected according to either degree of polymerization expressed by the number of repeat units n and thus, M_r weight distribution, or chemical composition (CCD) and functionality type distribution (FTD). However, unfortunately, only in rare cases are both aims achievable within a single chromatographic run and therefore, so-called two-dimensional chromatography is required.

Furthermore, in a much more pronounced manner than for low-molecular-weight analytes, conformational effects must be considered appropriately taking into account distinct structure-dependent intramolecular interactions invoked by both nonpolar (e.g., hydrophobic = van der Waals) and polar (e.g., hydrogen bonding, dipole–dipole, ionic, etc.) interactions. All these effects are responsible for the often

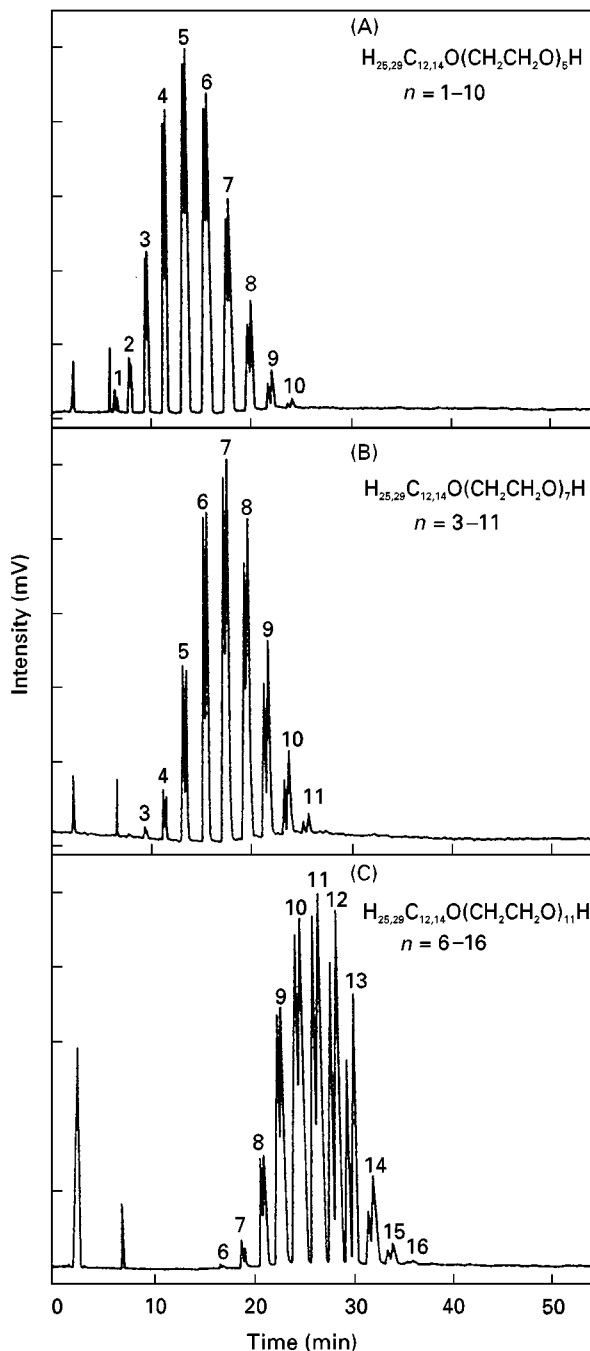


Figure 3 HPLC analysis of linear alkylethoxyalcohol oligomers: (A) AE5; (B) AE7; (C) AE11. (Reproduced from Bear GR (1988) *Journal of Chromatography* 459: 91–107, with permission from Elsevier Science.)

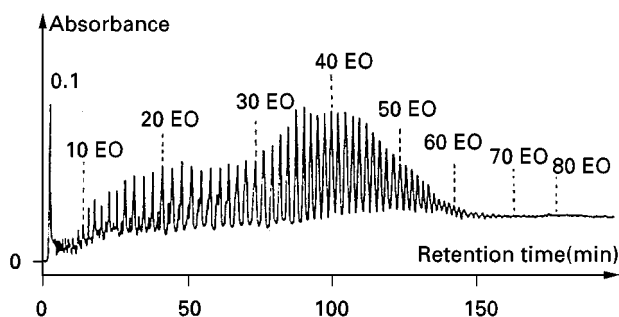


Figure 4 Analysis of a mixture of non-ionic polyoxyethylene (POE) surfactants KM25 (10^4 ppm, w/w) and Cetanol AT (10^4 ppm, w/w) as esters by normal-phase partition chromatography. (Reproduced from Desbène PL and Desmaizères B (1994) *Journal of Chromatography* 661: 207–213, with permission from Elsevier Science.)

unexpected chromatographic properties more or less substantially deviating from the analyte's intrinsic hydrophobicity based on calculation of hydrophobic increments. This behaviour takes into account the phenomenon of multiple attachment of the polymer chain, which means that adsorption onto the stationary phase surface is not effected by participation of the whole macromolecule but attributable to alternating trains of repeat units, whereas a substantial part of the molecule still extends into the surrounding mobile phase. Moreover, the flexibility of the chains easily allows conformational changes, which are further influenced by the gradual change in mobile phase composition during gradient chromatography.

High Performance Liquid Chromatography of Polyethers

Normal-Phase Liquid Chromatography (NP-HPLC)

NP-HPLC is defined as separation on polar stationary phases using pure organic eluents of increasing polarity. For this reason, either bare silica gel or so-called bonded-phase materials, such as 3-cyanopropyl- (CN), 3-aminopropyl- (NH_2) as well as 2,3-dihydroxypropyl (Diol) silica gel are used as solid supports for the separation of fatty alcohol and fatty acid polyethoxylates, the lower M_r members of native PEG and the corresponding octyl- and nonylphenol derivatives. In general, separation occurs with respect to the number of ethoxymers, although side-chain isomerism as well as differences in the length of the alkyl substituent is also observed in some cases yielding substantial splitting of the oligomer peaks. In contrast, polypropylene (PPG) and polybutylene glycols (PBG), possessing a substantially more hydrophobic polymer backbone, are better separated by

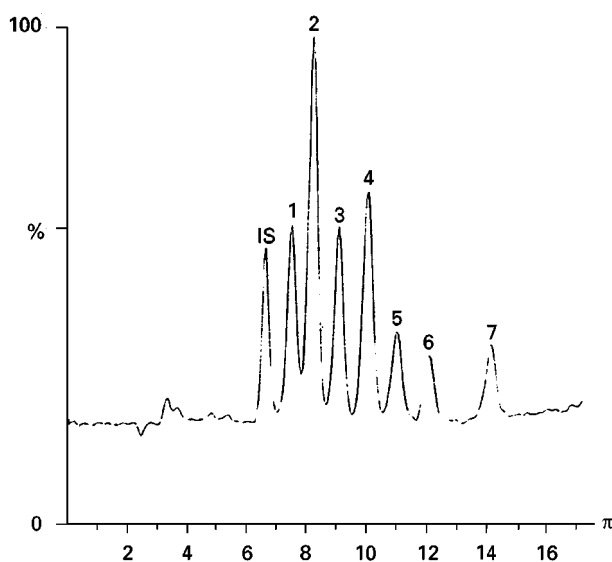


Figure 5 LC/MS chromatogram obtained by injecting the composite working standard solution containing NPEOs and alkylethoxylates (AEOs). The analytes in this synthetic mixture are, in order of elution: 1, NPEOs; 2, C-12 EOs; 3, C-13 EOs; 4, C-14 EOs; 5, C-15 EOs; 6, C-16 EOs; and 7, C-18 EOs. IS (internal standard), C-10 EO₆. (Reproduced from Crescenzi C, Di Corcia A and Samperi R (1995) *Analytical Chemistry* 67: 1797–1804.)

reversed-phase HPLC (RP-HPLC). Whereas combinations of pure organic solvents often containing small amounts of water to accelerate the adsorption-desorption equilibrium are used on bare silica, the NH_2 , CN and Diol materials are also run under typical RP-HPLC conditions with aqueous organic eluents. Although native silica gel is still used for PEG derivatives, it is being replaced more and more by

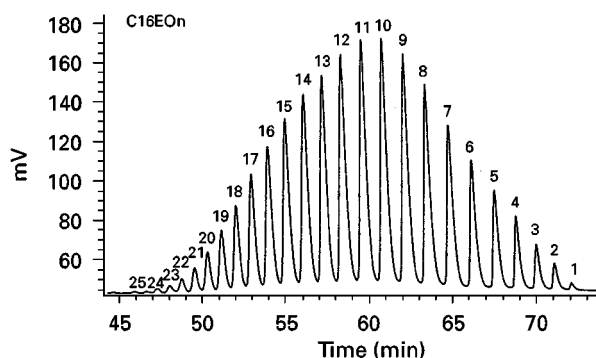


Figure 6 Separation of ethoxylated hexadecanol C16EO (average ethoxylation degree = 10) on reversed phases (stationary phase: Nucleosil 120-3 C18 (250 × 4); mobile phase: A- H_2O , B- CH_3CN , 1 mL min⁻¹. Gradient programme: 46 → 55% B/20 min, 55 → 76% B/30 min, 76 → 90% B/15 min; ELSD-50 mm N₂, 110°C). (Reproduced from Miszkiewicz W and Szymanowski J (1996) *CRC Critical Reviews in Analytical Chemistry* 25: 203–246.)

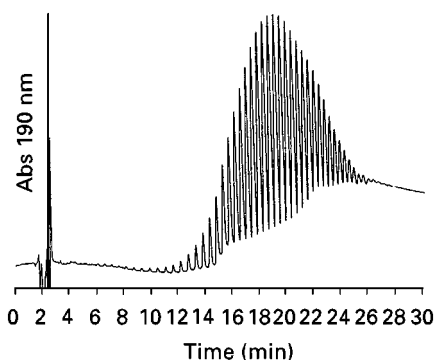


Figure 7 HPLC analysis of PEG with an average molecular weight of 2000 daltons carried out on two ODS columns at 60°C and with a detector sensitivity of 0.2 a.u.f.s. (Reproduced from Escott REA and Mortimer N (1991) *Journal of Chromatography* 553: 423–432, with permission from Elsevier Science.)

CN, NH₂ and Diol matrices, which behave as deactivated silica and thus allow a better fine-tuning of the chromatographic conditions. In addition, PEGs with $M_r > 2000$ are irreversibly retained on bare silica gel matrices and thus should be separated by RP-HPLC. It should be emphasized that the bonded-phase materials are not as sensitive towards traces of water in organic solvents compared with silica gel and retention times and peak shapes exhibit excellent reproducibility making them suitable for long-term application without marked loss of chromatographic performance.

Although isocratic NP-HPLC yields satisfactory resolution of PEGs with lower degree of oligomeriza-

tion, the higher oligomers are often truncated and merge more and more with the baseline. This drawback can easily be overcome by the solvent gradient technique, which is the predominant method for separation of polymers. Usually, chromatography starts with a mobile phase of low polarity, such as, e.g., n-hexane, n-heptane, isooctane, cyclohexane, etc., and methanol, ethanol, acetonitrile, 2-propanol, tetrahydrofuran (THF), dioxane, etc., are used as the polar modifiers. Due to insufficient miscibility when using methanol and acetonitrile in combination with alkanes, a third component affecting solvent compatibility is required and THF, dichloromethane and chloroform have been successfully applied. In contrast, ethanol and 2-propanol being more lipophilic compared to methanol and acetonitrile, dissolve in aliphatic and cycloaliphatic solvents at any volume ratio. In particular when using the most polar silica gel, elution is often started with a significant percentage of solvents with intermediate polarity like dichloromethane, chloroform or diethyl ether instead of pure alkane and thus, no additional compatibility modifier is necessary. Nevertheless, a third eluent is often used for chromatographic fine-tuning.

Excellent oligomer resolution of octylphenyl-(OPEO), nonylphenyl-(NPEO) and alkyl-ethoxylates is achieved on bare silica gel (Figure 2), CN, NH₂ (Figure 3), *p*-nitrophenyl-bonded silica (Figure 4) and Diol matrices.

Sometimes peak-splitting of the signals of the individual NPEO oligomers occurs, revealing structural heterogeneity within the nonyl side chain, which is

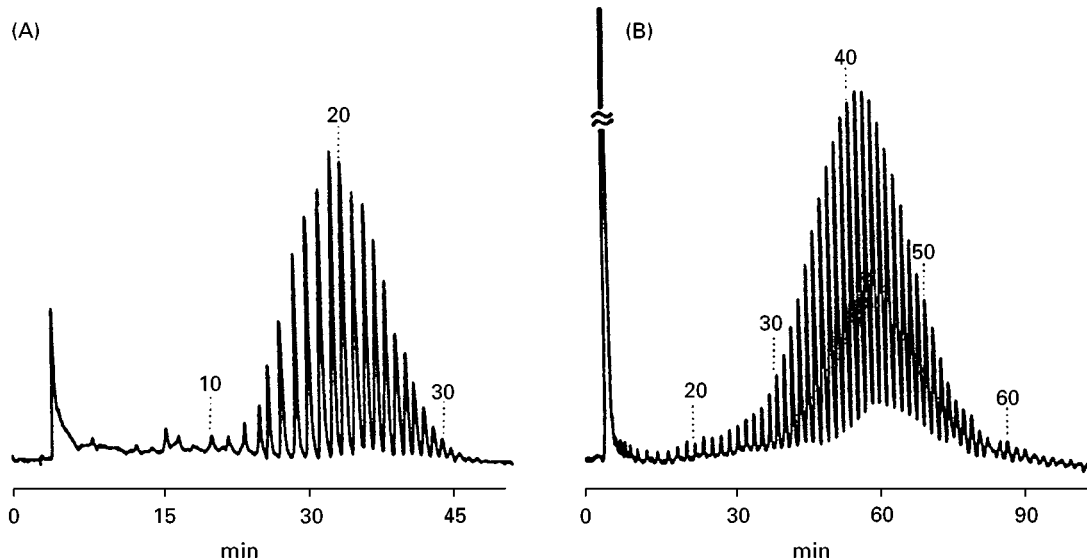


Figure 8 Chromatograms of 3,5-dinitrobenzoyl derivatives of PEGs by HPLC. Conditions: column. 5 μ m Spherisorb NH₂ (250 \times 4.6 mm I.D.); detection, UV at 276 nm (A) PEG 1000, (B) PEG 2000. (Reproduced from Sun C, Baird M and Simpson J (1998) *Journal of Chromatography A* 800: 231–238, with permission from Elsevier Science.)

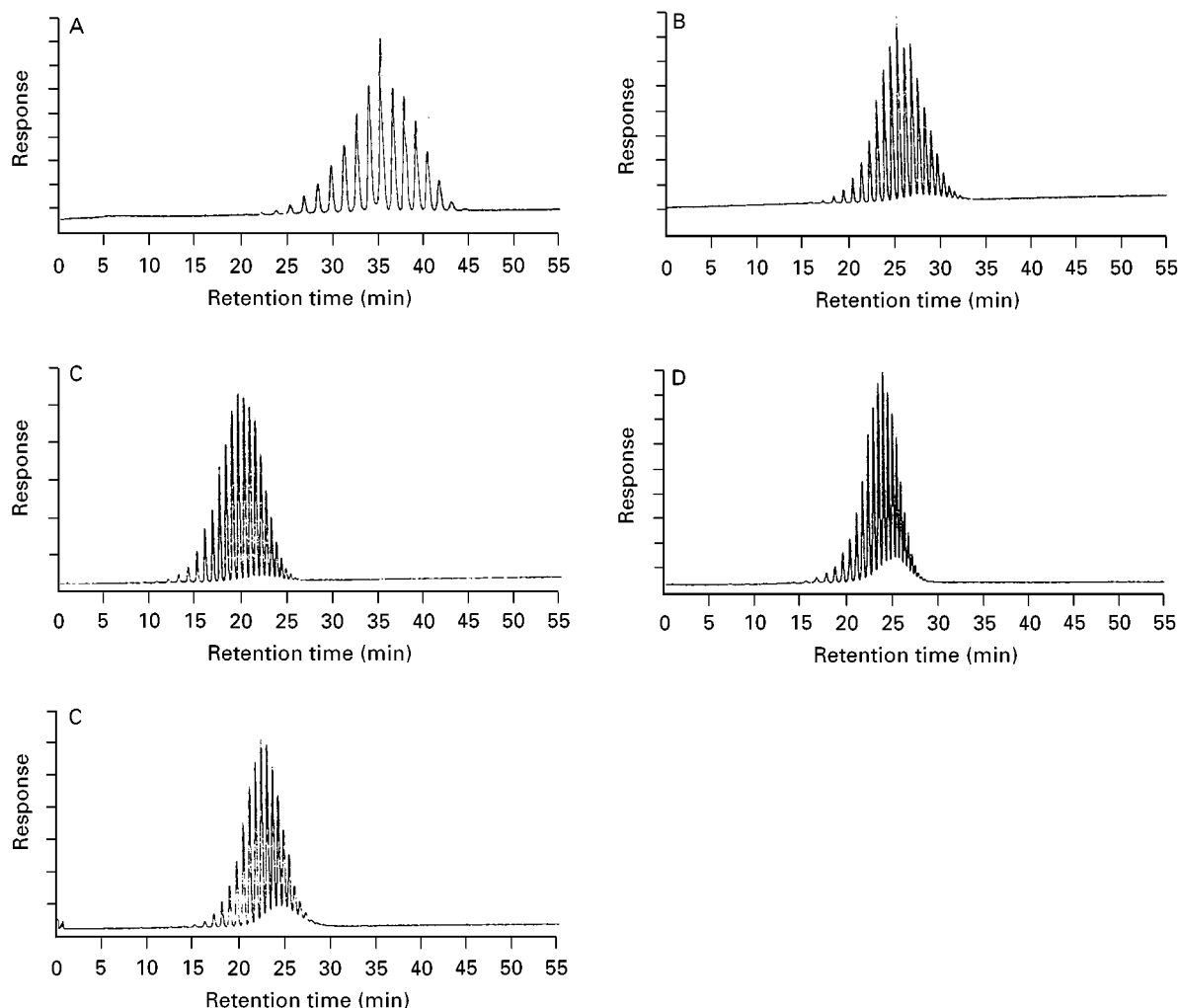


Figure 9 Chromatograms with PPG-1200 and acetonitrile as organic solvent. (A) C_{18} ; (B) C_8 ; (C) C_4 ; (D) C_{phenyl} ; (E) C_1 . (Reproduced from Rissler K, Künzi H-P and Grether H-J (1993) *Journal of Chromatography* 635: 89–101, with permission from Elsevier Science.)

not observed in OPEOs. In the same way separation according to the number of ethoxymers (EO) units as well as the chemical composition of the fatty alcohol chain of nonionic surfactants (NIS) is achieved on an NH_2 stationary phase (Figure 3). Nevertheless, in most cases information with respect to both ethoxymers distribution and chemical composition of the alkyl substituent is unsatisfactory and thus RP-HPLC is required for differentiation of the alkyl end groups. Due to the increasing interactive surface of the PEG derivatives with increasing number n of repeat units, retention time of each oligomer increases with M_r , whereas in contrast, the lipophilic end group plays an only marginal role.

In the case of OPEOs and NPEOs bearing an aromatic moiety, signal monitoring is easily accomplished by both UV and fluorescence detection (FD), whereas evaporative light scattering detection (ELSD) is preferred for the alkylpolyethoxylates (Figure 3).

However, in gradient elution with varying concentration of a modifier more or less absorbing in the lower UV range, such as, e.g., ethyl acetate, THF, etc., it is advisable to use wavelengths ≥ 250 nm to keep the baseline drift as low as possible. Polyether derivatives lacking a chromophore, such as fatty alcohol or fatty acid polyethoxylates, are amenable to UV detection after conversion to their benzoyl, 3,5-dinitrobenzoyl and phenylurethane derivatives, which in general, give high yields. Furthermore, for extremely sensitive measurement, the hydroxy functions of the polyether samples can be reacted with fluorophores providing high quantum yields, like fluorenylmethoxycarbonyl chloride, 1-naphthylisocyanate, 1(2)-naphthoyl chloride, carbazol-9-carbonyl chloride, 1(9)-anthrolycyanide, etc. Whereas derivatizations with isocyanates run uncatalysed at about 60°C within 1–2 h, the acyl chlorides require base catalysis (e.g., pyridine, triethylamine,

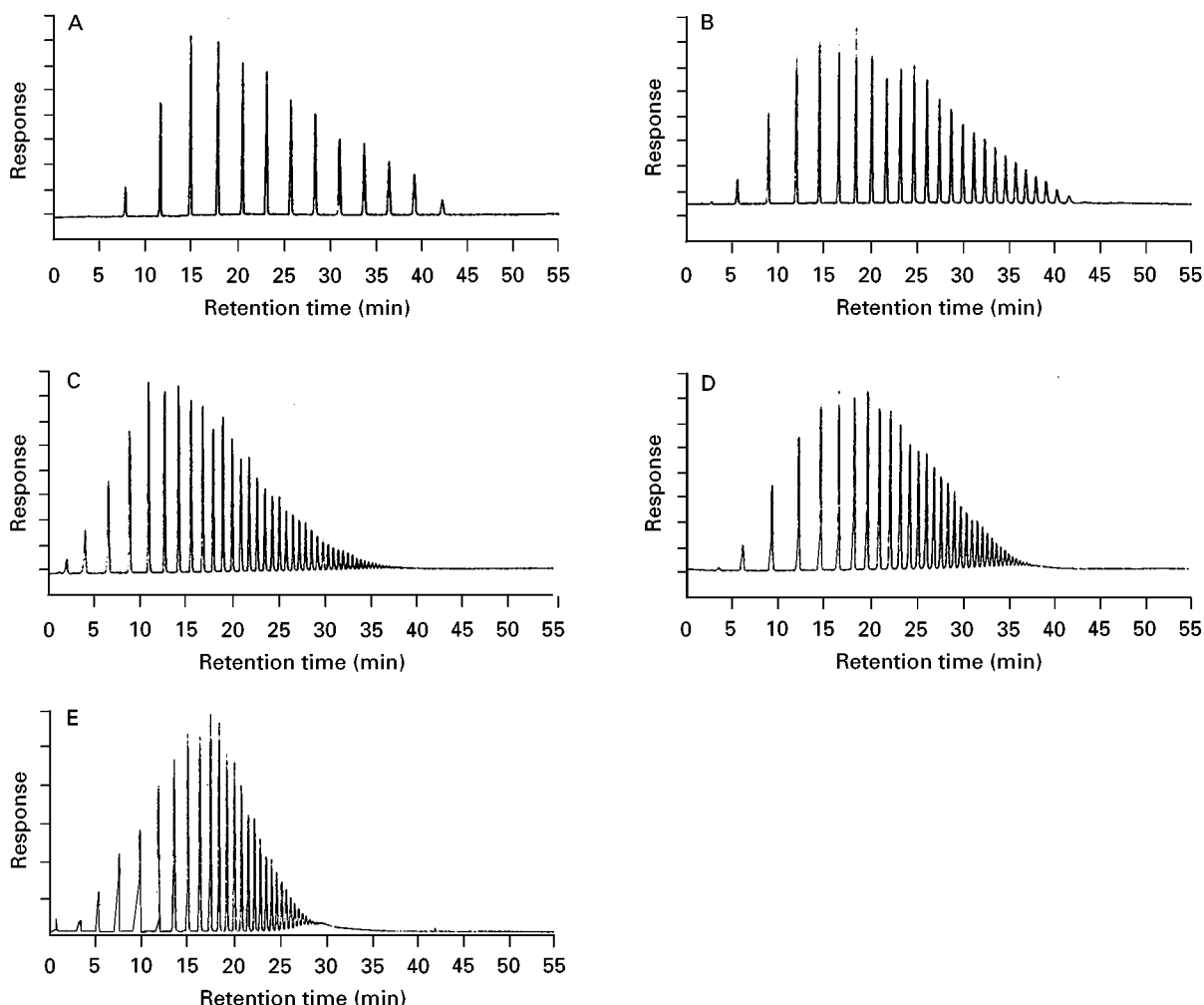


Figure 10 Chromatograms with PBG-1000 and acetonitrile as organic solvent. (A) C_{18} ; (B) C_8 ; (C) C_4 ; (D) C_{phenyl} ; (E) C_1 . (Reproduced from Rissler K, Künzi H-P and Grether H-J (1993) *Journal of Chromatography* 635: 89–101, with permission from Elsevier Science.)

methylimidazole, etc.). In the latter cases either heating for about 0.5–1 h or working at room temperature for about 0.5–2 h generally affords good yields.

Reversed-Phase Liquid Chromatography (RP-HPLC)

RP-HPLC is effected on hydrophobic stationary phases using eluents of decreasing polarity. In general, it is the method of choice for separation of PEG-based nonionic surfactants (NIS) with respect to the chemical structure of the hydrophobic end groups without separation according to the degree of ethoxylation (Figure 5) and also PEGs, PPGs and PBGs. In most applications octadecasilyl silica gel (C_{18}) and/or octylsilyl silica gel (C_8) stationary phases with binary gradients of acetonitrile (methanol)–water are used.

Separation of alkylpolyethoxylates according to the number of ethoxylate units with an acetonitrile

–water gradient on a C_{18} column has also been reported (Figure 6) and retention increases with decreasing number of ethoxymers. Surprisingly, the elution order of oligoethylene glycol phenyl (octylphenyl) ethers is reversed in mobile phases of methanol and water.

Although being significantly less hydrophobic than their corresponding NIS counterparts, satisfactory separation of PEGs is achieved for the species up to $M_r \approx 2000$ using a C_{18} column, whereas in general, PEGs with $M_r \geq 2000$ merge more and more into a common signal envelope. Figure 7 reveals separation of PEG 2000 by use of two C_{18} columns in series.

Despite the fact that separation of PEGs according to the degree of ethoxylation decreases substantially at $M_r > 2000$, PEGs widely differing in M_r ranging from some hundreds to some hundred thousands can be efficiently separated from each

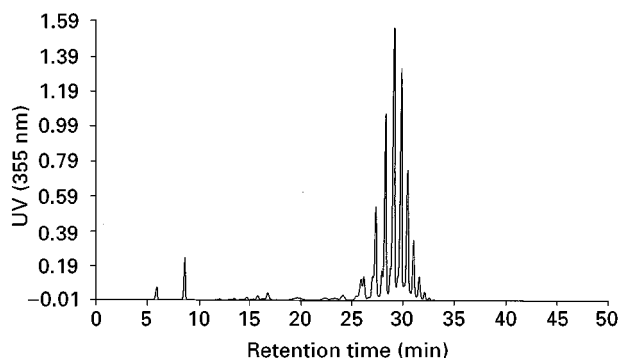


Figure 11 RP-HPLC of Jeffamine D 400™ derivatized with 2,4-dinitrofluorobenzene on a Nucleosil 5C18 column (125 × 4.6 mm; 5 μm) with a gradient from water to 65% acetonitrile–10% THF at 25 min, 80% acetonitrile–20% THF at 40 min, 80% acetonitrile–20% THF for 10 min followed by a drop to the starting conditions and re-equilibration for 14 min at a flow rate 1.5 mL min⁻¹; detection wavelength 355 nm. (Reproduced from Rissler K (1998) unpublished results.)

other as single peaks using binary acetonitrile (methanol)–water gradients and C₁₈ or C₈ stationary phases. In contrast, bonded phases, such as CN and Diol materials, run under RP-HPLC conditions, are less suited for efficient separations of PEGs with $M_r \leq 2000$ into their oligomers. The exception is an NH₂ matrix providing excellent separation of PEGs up to M_r of about 2000 as their 3,5-dinitrobenzoyl derivatives with a binary gradient of acetonitrile and water (Figure 8).

As a consequence of the substantially better interaction of their more hydrophobic backbones with nonpolar stationary phases, PPGs (Figure 9) and PBGs (Figure 10) are much better resolved into individual oligomers and often baseline separation is achieved.

PPGs up to $M_r \approx 2000$ can be sufficiently separated with binary acetonitrile–water gradients, whereas the higher M_r oligomers elute as more or less broad but unresolved signals. At $M_r > 2000$ it becomes more and more difficult to achieve complete elution of either native PPGs or their amino-terminal derivatives from a highly hydrophobic C₁₈ matrix with binary gradients of acetonitrile and water. However, when acetonitrile is replaced by methanol, complete elution of PPGs with higher M_r is accomplished, but the oligomers merge into an unresolved signal envelope. This is attributed to a better solvation of the polyether backbone by methanol compared with acetonitrile due to hydrogen bonding between the ether oxygens and the hydroxy function of methanol and therefore, interactions with the hydrophobic stationary phase are efficiently counterbalanced. The obvious ‘sticking effect’ of high M_r PPG samples onto

a C₁₈ column can also be overcome by stationary phases with lower carbon content, such as, e.g., C₈ and C₄ matrices with acetonitrile as well as methanol as the organic modifier, both showing comparable efficiency. Alternatively, THF can be used as a ‘solubility enhancer’ in combination with acetonitrile for separation of either PPGs or PBGs on C₁₈ stationary phases.

Conversion of the native PPG amines (Figure 1b) into their acetamide or 2,4-dinitrofluorobenzene (DNFB) derivatives (Figure 11) prior to chromatography, which is readily achieved with pyridine–acetic acid anhydride (1 : 1, v/v) or DNFB, respectively, is required to avoid interactions with residual silanols. Alternatively, the unmodified amines can also be separated with trifluoroacetic acid (TFA) as a mobile

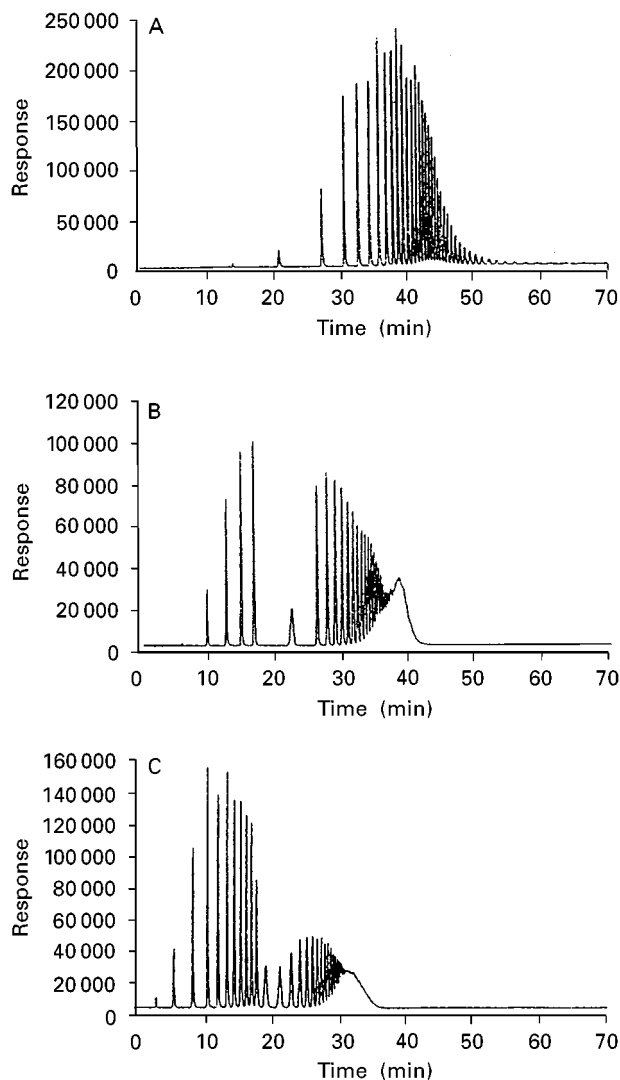


Figure 12 HPLC of PBG 1000 on a C₁₈ column with (A) methanol, (B) ethanol and (C) 2-propanol as the organic modifier. (Reproduced from Rissler K, Fuchslueger U and Grether H-J (1993) *Journal of Chromatography* 654: 309–314, with permission from Elsevier Science.)

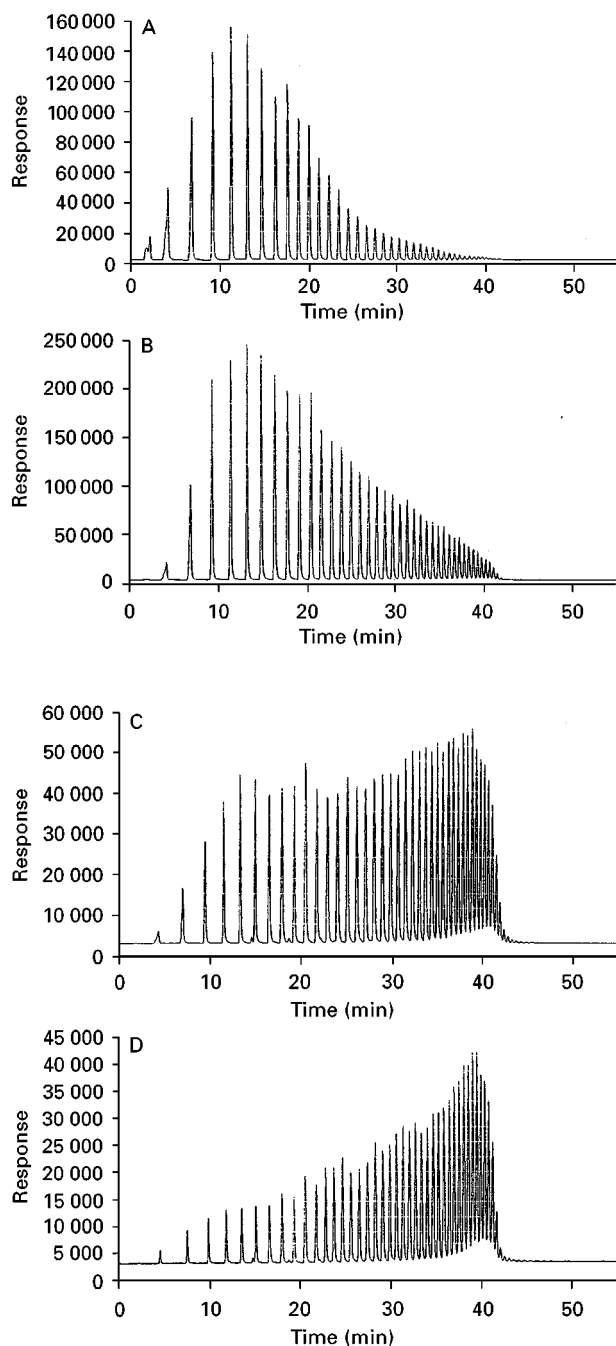


Figure 13 Chromatograms of (A) PBG 650, (B) PBG 1000, (C) PBG 2000 (D) PBG 3000 on a C_4 column and acetonitrile as organic modifier. (Reproduced from Rissler K and Fuchslueger U (1994) *Journal of Liquid Chromatography* 17: 2791–2808.)

phase additive for suppression of silanophilic interactions, but signal resolution is lower compared with the corresponding acetamides and DNFB derivatives.

PBGs exhibit still more pronounced solute–matrix interactions and so PBG 650 (average M_r 650) does not completely elute from a C_{18} matrix with a binary gradient of acetonitrile and water. In contrast, com-

plete elution as well as excellent peak resolution is achieved on a C_{18} column with methanol as the organic modifier, whereas under these conditions, substantial amounts of PBG 1000 still remain on the stationary phase. A further change of organic modifier to ethanol or isopropanol affords complete elution of PPG 1000 (Figure 12), PBG 2000 and PBG 3000, but only the low-to-medium M_r oligomers are sufficiently separated, whereas the higher M_r sample constituents merge into a broad and unresolved signal. Presumably the same solvation effect as postulated for the PPGs also holds true.

Either excellent separation or complete elution is achieved for PBG 650, PBG 1000, PBG 2000 and PBG 3000 on a C_4 matrix with a binary gradient of acetonitrile and water and up to about 60 oligomers are observed (Figure 13). Although a column with markedly lower hydrophobicity compared with C_{18} and C_8 stationary phases is used, interactions of the substantially more hydrophobic PBG samples compared with PPGs are sufficient to give good resolution.

Underivatized PEGs, PPGs and PBGs are eluted in the range of increasing M_r , due to their continuously increasing interactive surface, whereas in the case of PEGs, the converse is true for the corresponding alkyl- and/or arylalkyl-substituted derivatives as a consequence of the dominant role of the lipophilic substituent on solute–stationary phase interactions.

Both signal monitoring by UV and ELSD can be applied and in particular ELSD is the method of choice for the native polyethers when sensitivity is not crucial, because it is at least one order of magnitude less sensitive than UV detection. Therefore, measurement of low amounts of polyethers requires derivatization with a chromophor or fluorophor. However, reaction with aromatic moieties has a dramatic influence on signal resolution of PEGs, which almost completely vanishes, whereas in contrast, PPG (Figure 14) and PBG (Figure 15) oligomers are still well resolved after conversion to their 3,5-dinitrobenzoyl derivatives. PPG amines having been reacted to the corresponding acetamides (DNFB derivatives) can be measured by either UV detection at 210 (355) nm or ELSD.

Unlike a UV detector, where concentration-dependent responses are measured and for this reason, calculation of response factors for the different oligomers is required, ELSD is a typical mass detection system like a refractive index detector. As a consequence, the signal intensities reflect the true mass distribution of oligomers. Moreover, ELSD offers an advantage over UV detection because it allows the use of solvents strongly absorbing in the usual UV range, such as, e.g., acetone and methylethylketone, and

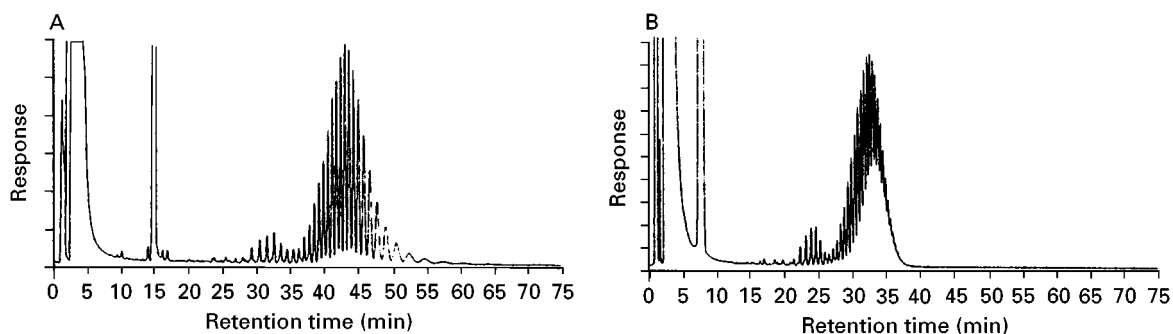


Figure 14 Chromatograms with PPG-1200 after derivatization with DNBCl and acetonitrile as organic solvent. (A) C_{18} ; (B) C_8 . (Reproduced from Rissler K, Künzi H-P and Grether H-J (1993) *Journal of Chromatography* 635: 89–101, with permission from Elsevier Science.)

furthermore, no baseline drift is observed with gradient elution.

Dual detection offers a further powerful tool in polymer separation and measurement of both UV and ELSD responses allow differentiation of, e.g. polyethoxylates containing either aromatic or aliphatic end groups.

During the past few years HPLC-mass spectrometry (LC-MS) has gained increased interest providing exact structural information and opening an additional dimension for polymer characterization. In contrast, matrix-assisted laser desorption ionization time-of-flight mass spectroscopy (MALDI-TOF/MS) is still used off-line and is excellently suited for M_r and end group determination.

'Pseudo Reversed-Phase' Liquid Chromatography (pseudo RP-HPLC)

In contrast to their use in classical NP-HPLC with pure organic solvents of increasing polarity, bare silica gel stationary phases can also be operated with aqueous organic solvents of decreasing polarity, typically encountered in RP-HPLC. This new technique, termed 'pseudo reversed-phase' HPLC, is gaining more and more importance for polyether characterization.

Both native PEGs or their alkyl/arylalkyl derivatives (Figure 16) are efficiently separated according to the number of repeat units and in particular, much better oligomer resolution of the former compounds is achievable compared with RP-HPLC. Exceptions are RP-HPLC on an NH_2 -bonded phase and ion exchange chromatography. However, despite this great advantage, retention rapidly increases with increasing M_r , but PEG 3000 is still separated into the maximum number of oligomers with an eluent system consisting of acetonitrile and water containing THF as the 'solubility modifier', as confirmed by MALDI-TOF/MS after conversion to its α,ω -bis(naphthylurethane) derivative (Figure 17). PEG samples with $M_r > 3000$ are strongly adsorbed onto the polar column matrix and can only be released from it with THF as the mobile phase modifier, but resolution vanishes completely.

Ion-exchange Chromatography (IEC)

Although lacking any ionizable groups, PEGs and their alkyl and/or arylalkyl derivatives can be separated by IEC, which is attributable to the unique properties of the 1,2-dioxoethylene structural units, being able to form five-membered cyclic complexes with alkali metal ions, such as K^+ . Separation of PEG

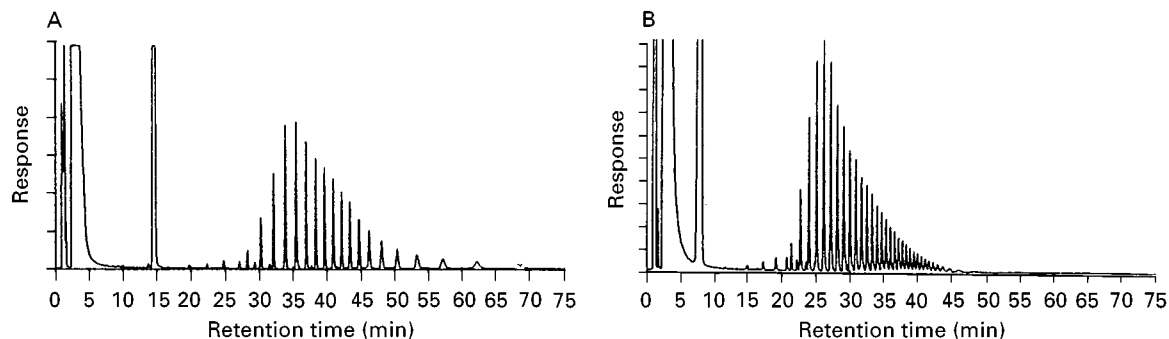


Figure 15 Chromatograms with PBG-1000 after derivatization with DNBCl and acetonitrile as organic solvent. (A) C_{18} ; (B) C_8 . (Reproduced from Rissler K, Künzi H-P and Grether H-J (1993) *Journal of Chromatography* 635: 89–101, with permission from Elsevier Science.)

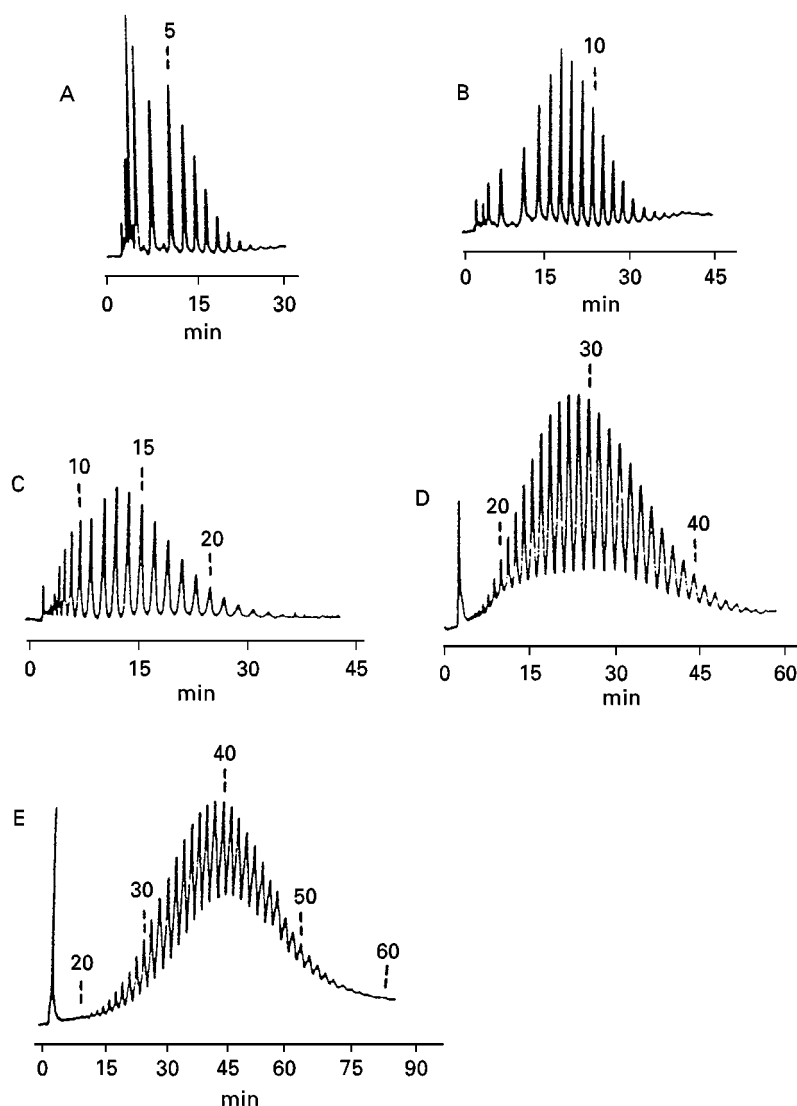


Figure 16 HPLC chromatograms of Synperonic NPs using gradient programme: (A) Synperonic NP6; (B) Synperonic NP10; (C) Synperonic NP15; (D) Synperonic NP30; (E) Synperonic NP40. Conditions: column, 5- μ m Spherisorb NH_2 (250 \times 4.6 mm I.D.). (Reproduced from Sun C, Baird M, Anderson HA and Brydon DL (1996) *Journal of Chromatography A* 731: 161–169, with permission from Elsevier Science.)

is achieved on either typical polymer-based cation exchangers (Figure 18) or on easily ionizable weakly basic stationary phases, such as NH_2 . In the latter case, retention occurs by complexation of PEG at the ammonium sites of the stationary phase, being protonated by use of a slightly acidic mobile phase, and competitive displacement of the solute with increasing concentrations of K^+ ions in the eluent. Optimum results are obtained with potassium perchlorate in methanol and resolution is achieved according to both hydrophobic moiety and number of repeat units. As expected, retention increases with increasing number of ethoxymers, but this effect is so large that already PEGs of $M_r \approx 2000$ are almost irreversibly retained on the column.

Liquid Chromatography under Critical Conditions (LCCC)

LCCC is a typical method used in polymer analysis as the first step of ‘two-dimensional’ chromatography. It is applicable in either normal or reversed-phase LC modes and separates mixtures of polymers according to their different chemical composition. In contrast to HPLC of polymers, requiring gradient conditions for efficient separation of homologues, LCCC is an isocratic technique.

In general, LC of polymers is governed by (i) exclusion, (ii) solubility and (iii) adsorption. Depending on both temperature and composition of the solvents and nonsolvents used all three modes can occur. In

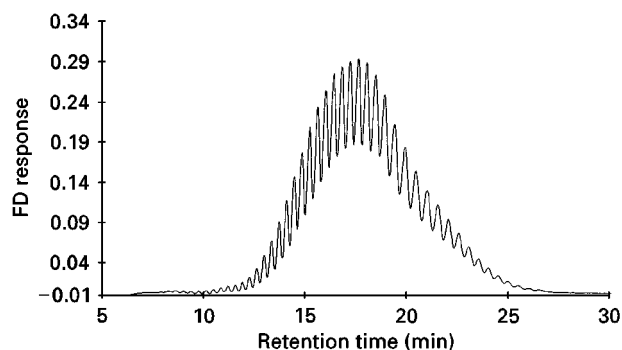


Figure 17 Chromatogram obtained from 100 ppm of the α,ω -bis(1-naphthylurethane) derivative of PEG 3000 dissolved in 10 μ L THF on a Spherisorb Si 80 column (125 \times 4.6 mm, 5 μ m) with a ternary gradient of acetonitrile, water and THF (20% acetonitrile–80% water to 80% acetonitrile–20% THF in 40 min, followed by a drop to the starting conditions within 1 min and re-equilibration for 14 min (Reproduced from Rissler K, Wyttenbach N, Börnsen KO (2000) *Journal of Chromatography A*, in press, with permission from Elsevier Science.)

size exclusion a strong eluent is used, which ideally prevents enthalpic solute–stationary phase interactions affecting elution of sample constituents in the range of decreasing M_r . When the percentage of nonsolvent is raised, retention increases and changes more and more from pure size exclusion to precipitation or adsorption. A further increase of the percentage of nonsolvent affords pronounced solute–stationary phase interactions, resulting in separation of molecules proportional to their M_r . LCCC marks the transition point between size exclusion and adsorption. At this critical point of adsorption, complete compensation of the enthalpic as well as entropic terms of the solute's adsorption occurs. If polymers possessing different end groups differ in molar mass but not in chemical structure of repeat units are separated, a nonsolvent–solvent ratio can be found, at which oligomers merge into a common peak, regardless of their M_r . In this case, separation is

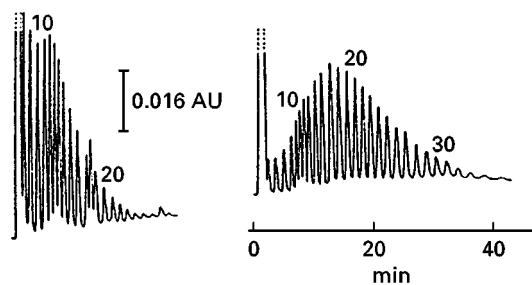


Figure 18 Typical separation in terms of POE chain distribution of POE(10)O (left) and POE(20)O (right). Mobile phase, methanol (0–3 min) to 7.5 mM KCl in methanol (30 min). Other conditions are given in the text. (Reproduced from Okada T (1992) *Journal of Chromatography* 609: 213–218, with permission from Elsevier Science.)

only achieved with respect of end group functionality, whereas molecular weight heterogeneity is not revealed (**Figure 19**). In a subsequent step, all components having identical end groups can be separated according to M_r by SEC.

Future Developments

Owing to its excellent resolving power, capillary zone electrophoresis (CZE) may play an increasing role in polymer separation and recent applications seem to be promising. The chemistry of the inner surface of the capillaries resembles that of open tubular HPLC and therefore, a wide variety of materials ranging

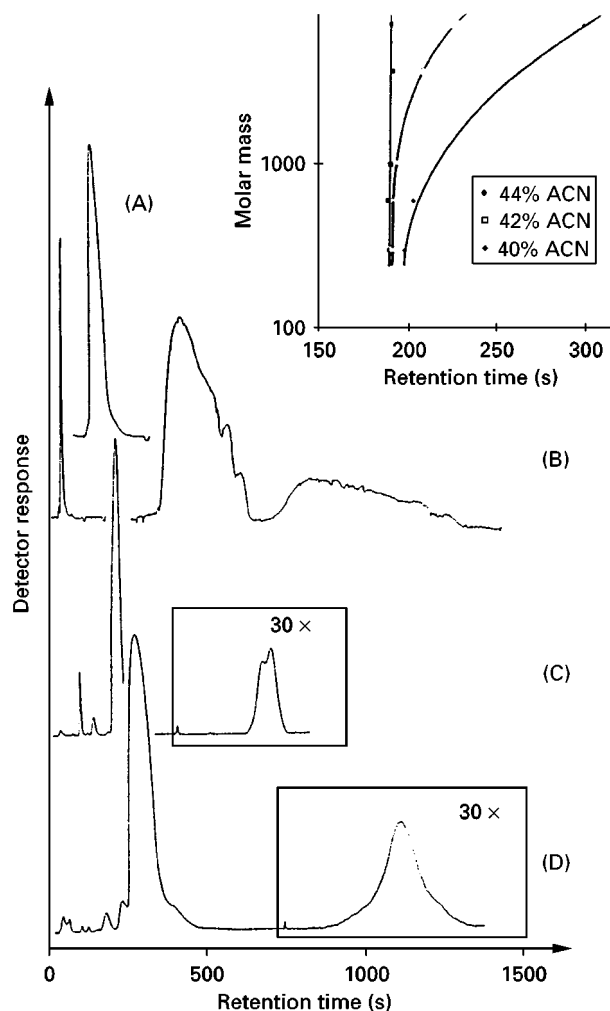


Figure 19 Critical diagram molar mass vs. retention time of polyethylene glycol (inset upper right corner) and chromatograms of functional PEOs at the critical point of adsorption of polyoxyethylene (PEO), stationary phase: Nucleosil RP-8, 60 \times 4 mm I.D., solvent: acetonitrile–water 44:56% by volume, samples: C_{10} -PEO (A), C_{13} , C_{15} -PEO (B), octylphenol-PEO (C), nonylphenol-PEO (D). ACN, acetonitrile. (Reproduced from Pasch H and Zammert I (1994) *Journal of Liquid Chromatography* 17: 3091–3108.)

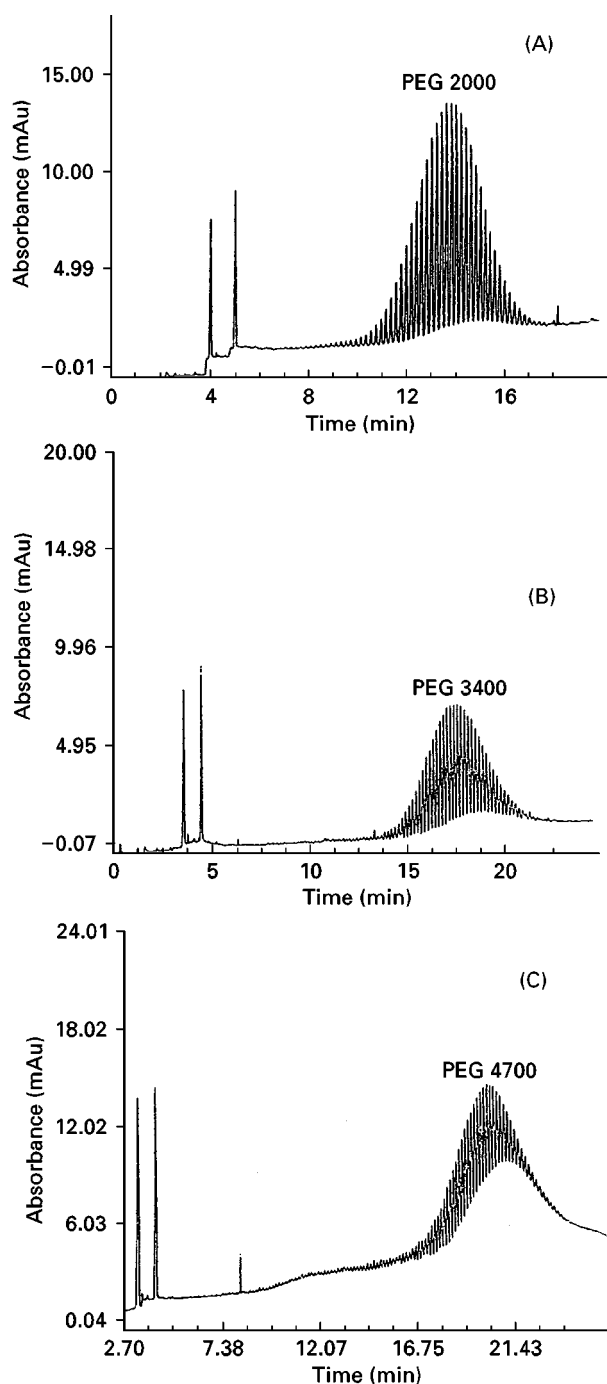


Figure 20 (A) Electropherogram of a PEG 2000 4% dextran solution. (B) Electropherogram of a PEG 3400 3% dextran solution. (C) Electropherogram of a PEG 4700 3% dextran solution. (Reproduced from Barry JP, Radtke DR, Carton WJ *et al.* (1998) *Journal of Chromatography A* 800: 13–19, with permission from Elsevier Science.)

from strongly polar (silica gel coated) to strongly hydrophobic (C_{18} coated) as well as gel-coated (e.g., PAGE) capillaries are available. Whereas CZE of polyethers as well as the NIS-based derivatives require derivatization with, e.g., phthalic anhydride or trimellitic acid anhydride yielding one and two free

carboxy groups, respectively, per hydroxy function, the polyether amines are amenable to classical electrophoresis. Nevertheless, derivatization of neutral analytes with a charge-creating agent is not an ultimate prerequisite, because polymers can also be separated by micellar electrokinetic capillary chromatography (MEKC). Optimum separation efficiency of PEGs is achieved in the capillary gel electrophoretic mode after derivatization with trimellitic acid anhydride and the whole amount of oligomers can be separated up to M_r 5000, as confirmed by MALDI-TOF/MS investigations (Figure 20). As in HPLC, detection is performed by monitoring either UV response in the usual wavelength range down to about 200 nm or FD and depends on the chromophore introduced by derivatization.

At least at the moment, CZE affords separation of PEG oligomers up to $M_r \approx 5000$. However, signal resolution is not unlimited and markedly depends on the ratio $\Delta m/M$ (m = mass of repeat unit, M = total mass of polymer), i.e., the lower the ratio $\Delta m/M$ the lower the differences in the interactive surfaces between polymer $M(n)$ and $M(n+1)$. Fortunately, mass spectrometry, due to its unsurpassable resolution, still yields oligomer differentiation when separation into individual oligomers by chromatographic techniques fails. Nevertheless, prior chromatographic fractionation is essential to obtain clear and well-interpretable mass spectra. In this respect electrospray ionization (ESI) TOF/MS performed on-line and MALDI-TOF/MS carried out off-line with the isolated fractions are the methods of choice. Whereas polar polymers, such as, e.g., polyethers, polyacrylic acid and its esters are easily ionizable, addition of silver salts facilitates ionization of nonpolar analytes, such as, e.g., polystyrene, polybutadiene, bisphenol-A-diglycidylethers or phenol-novolaks.

In conclusion, it is expected that chromatography coupled to MS and therefore affording optimum structural information, will be dominant in future applications.

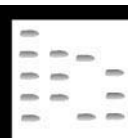
See also: II/Chromatography: Liquid: Enhanced Fluidity Liquid Chromatography; Mechanisms: Size Exclusion Chromatography. III/Gradient Polymer Chromatography: Liquid Chromatography: Synthetic Polymers: Liquid Chromatography.

Further Reading

- Cserhati T and Forgacs E (1997) Separation and quantitative determination of non-ionic surfactants used as pesticide additives. *Journal of Chromatography A* 774: 265–279.
- Engelhardt H, Beck W, Kohr J and Schmitt T (1993) Neue analytische Methoden (44): Kapillarzonenelektrophorese:

- Methoden und Möglichkeiten. *Angewandte Chemie* 105: 659; *Angewandte Chemie*, International Edition English 32: 629.
- Francuskiewicz F (1994) *Polymer Fractionation* (Springer Lab Manual). Heidelberg: Springer Verlag.
- Glöckner G (1987) *Polymer Characterization by Liquid Chromatography*. Amsterdam: Elsevier.
- Glöckner G (1991) Gradient HPLC of copolymers and chromatographic cross fractionation. Berlin: Springer Verlag.
- Marcomini A and Zanette M (1996) Chromatographic determination of non-ionic aliphatic surfactants of the alcohol polyethoxylate type in the environment. *Journal of Chromatography A* 733: 193–206.
- Miszkiewicz W and Szymanowski J (1996) Analysis of nonionic surfactants with polyoxyethylene chains by high performance liquid chromatography. *CRC Critical Reviews in Analytical Chemistry* 25: 203–246.
- Pasch H and Trathnigg B (1997) *HPLC of Polymers*. Berlin: Springer Verlag.
- Rissler K (1996) High performance liquid chromatography and detection of polyethers and their mono (carboxy)alkyl and -arylalkyl substituted derivatives. *Journal of Chromatography A* 7742: 1–54.

POLYMER ADDITIVES: SUPERCRITICAL FLUID CHROMATOGRAPHY



T. P. Hunt, ICI Technology, Middlesbrough, UK

Copyright © 2000 Academic Press

Introduction

Commercial polymers contain small quantities of low molecular weight additives which are evenly dispersed throughout the polymer matrix. They are typically present at concentrations in the order of 0.1–1.0% (w/w) but can be as high as 60% w/w in certain formulations. They make an important contribution to the properties and suitability of particular polymer grades.

The analysis of polymer additives is a two-stage process. The additives are first separated from the polymer by solvent extraction or reprecipitation. The extracted additives are then separated and quantified by a suitable chromatographic technique. This article is concerned with the application of supercritical fluid chromatography (SFC) to this second stage. However this also involves a discussion of coupled supercritical fluid chromatography–supercritical fluid extraction (SFE-SFC) in which both stages are combined into a single analysis.

Polymer Additives

The most common polymer additives are stabilizers, plasticizers, lubricants and flame retardants. Stabilizers are added to prolong the useful life of a polymer formulation by protecting it from thermal and light-assisted oxidation. This process is caused by the formation in the polymer chain of free radical sites which can react with oxygen to form unstable peroxy radicals and ultimately cause polymer chain scission.

Stabilizers are divided into four main classes: UV absorbers, primary antioxidants, secondary antioxidants and quenchers.

UV absorbers such as benzophenones and triazoles screen the polymer from harmful photons by absorbing them and then dissipating the excitation energy as heat so there is no radical formation. Primary antioxidants are typically hindered phenols. They react with free radicals to prevent further propagation. Secondary antioxidants destroy the hydroperoxide sites on the polymer chain which could otherwise be converted to peroxy radicals. They tend to be sulfur- or phosphorus-containing compounds. Quenchers are usually organonickel compounds and their function is to take over the energy absorbed by the chromophores in the polymer and dissipate it as heat.

Lubricants are added to make the polymer easier to process by controlling the melt rheology during thermoplastic moulding. They optimize the properties of the finished article to create smooth and unblemished surfaces and minimize stress fractures. External lubricants are compounds that are added to a polymer blend to control the degree of adhesion and friction between the polymer melt and hot processing equipment. Internal lubricants are added to polymer blends to reduce the melt viscosity to facilitate lower processing temperatures and to improve heat dissipation. Many lubricants possess a combination of internal and external characteristics. Lubricants are typically fatty alcohols, acids and esters and hydrocarbon waxes.

Plasticizers are high-boiling, organic chemicals which are often present at high concentrations, solvating the polymer chains to form stable gels. As a result,

intermolecular forces are reduced and this leads to a lower polymer glass transition temperature. The polymer is consequently less brittle and more easily worked. Typical plasticizers are phthalates, adipates and polychlorinated hydrocarbons. Flame retardants are typically chlorinated organophosphates.

It is evident then that a vast number of chemical species are used as polymer additives. They have widely varying volatilities with molecular weights potentially varying from 200 to 1000 Da. They tend to be of low to medium polarity and many do not have UV chromophores. Polymer formulations contain unique combinations of additives (called additive packages) which often contain 10 or more compounds. Thus the identification and quantitation of these additive packages is a challenging chromatographic problem.

Advantages of SFC for Polymer Additive Analysis

The analysis of extracted polymer additives by means of chromatographic separation has been reviewed by Handley. Gas chromatography (GC) has been used to analyse plasticizers and some stabilizers. It has the advantage of employing the near-universal flame ionization detector (FID) as the standard detector. Many additives, however, are not volatile enough to be efficiently separated by GC and, although high temperature GC has made recent advances, this approach is not suitable for most stabilizers because they tend to be thermally labile. This has led to liquid chromatographic techniques being favoured. Gel permeation chromatography (GPC) and high performance liquid chromatography (HPLC) methods have been developed. GPC has the wider molecular weight range but its use is severely limited by its inferior resolution compared to HPLC. Unfortunately, HPLC separations tend to employ gradient elution and this necessitates the use of UV detectors. This means that conventional HPLC is not applicable to the analysis of additives which lack a UV chromophore.

SFC has been widely applied in the analysis of polymer additives. It is a potentially attractive alternative because it can combine a compatibility with the universal FID detector with a capability to elute high boiling components at lower temperatures than GC. This capability arises from the properties of the supercritical fluid (SF) which is the mobile phase in SFC. This is a dense fluid which is above or near its critical temperature and pressure. It has solvating properties, which are similar to those of a liquid, and transport properties which approach those of a gas. The enhanced solubility of high-boiling polymer ad-

ditives in a SF compared with their solubility in a gas enables them to be eluted at much lower temperatures than is possible for GC. SFC also compares favourably with LC because of the higher binary diffusion coefficients and the lower viscosities of the SF compared to the liquid phase. The higher diffusion coefficients of polymer additives in an SF give enhanced resolution. The lower viscosity results in a lower pressure drop across an analytical column and this means that higher flow rates can be used to give faster separations. SF mobile phases have been used with both packed and capillary columns to achieve polymer additive separations.

Capillary Column Separations

Capillary SFC separations of polymer additives are performed using conventional GC columns with modified polysiloxane-bonded stationary phases. Unmodified carbon dioxide is used as the mobile phase. Reported separations typically use columns of 50 or 100 μm internal diameter (i.d.) with typical film thicknesses varying from 0.05 to 0.5 μm . These narrow-bore columns are required to achieve an equivalent resolution to the 250–320 μm columns, which are used in conventional GC, because the diffusivity range of supercritical carbon dioxide is lower than that of a GC carrier gas. Similarly, the relatively short 10 m column length reflects the higher viscosity of supercritical carbon dioxide.

Capillary columns in SFC tend to be characterized by better resolution than packed columns; however, they also have an inferior sample capacity and produce longer analysis times.

Capillary SFC is carried out using GC analysers which are modified by the addition of a high pressure pump to deliver liquid carbon dioxide to the top of the column. The other end of the column is connected to the FID via a pressure restrictor which accounts for most of the pressure drop in the system. This allows the column pressure to be controlled by increasing the flow rate until the required level is achieved. The earliest restrictors were approximately 10 cm lengths of 5–10 μm fused silica but these have subsequently been replaced by frit and integral restrictors. The limitation of this type of fixed restrictor is that independent control of both flow and pressure is impossible. The pressure is controlled by changing the flow rate and vice versa. Pressure programming is always used for polymer additive separations. Typical flow rates are very low and this means that syringe pumps with their superior performance are routinely used. Capillary SFC is compatible with all GC detectors, including the FID; however, the depressurization of carbon dioxide through the restrictor results in Joule-Thompson cooling of the detector and relative-

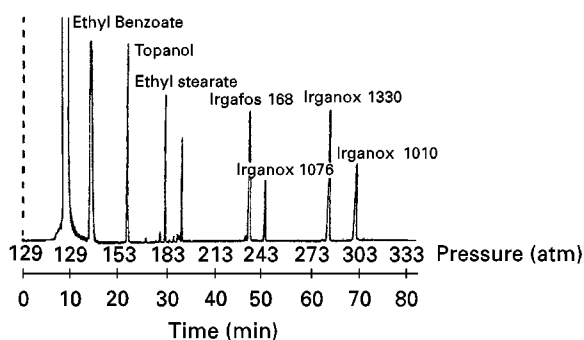


Figure 1 Chromatogram of polymer additive standards on a 10 m \times 50 μ m i.d. Octyl column at 110°C. Mobile phase: carbon dioxide pressure programmed from 129 atm (12 min) to 350 atm at 3 atm min⁻¹. (Reproduced with permission from Moulder *et al.* (1989).)

ly high FID temperatures (300–400°C) are required to compensate for this effect.

Polymer additive separations tend to be performed isothermally at temperatures between 80 and 140°C. The additives are eluted by means of a pressure/density gradient. The column pressure is initially held at a low pressure (8–15 MPa) for 5–10 min to allow the solvent to elute through the system while the less soluble additives are retained at the top of the column. The pressure is then increased at a rate of between 0.25 and 1 MPa min⁻¹ to reach a final pressure of 35–45 MPa. Those additives which have the highest solubility in the mobile phase are solvated at lower pressures and consequently are eluted first. Additives with lower solubilities elute later. Many additive packages are composed of components with similar polarities and their solubilities and hence their retention times are largely determined by their molecular weights, with lighter molecules eluting first. A typical chromatogram is shown in **Figure 1**.

A wide range of additives have separated using polysiloxane phases. These include phenolic antioxidants, benzotriazoles, thioesters, organophosphite and organometal stabilizers; fatty acid, ester and amide lubricants; and organophosphate flame retardants. Methyl, octyl, phenyl and biphenyl substituted stationary phases have been used. Biphenyl columns have been found to give better separations than methyl columns and their use has dominated in later publications.

Packed Column Separations

These are divided into two distinct categories: separations on 1 mm (i.d.) columns of lengths between 10 and 40 cm; and separations on conventional 4.6 mm (i.d.) \times 20–25 cm (length) HPLC columns. The stainless-steel columns are packed in both cases with 5 μ m particles of bonded silica. Packed column SFC

has been used to elute phenolic antioxidants, benzotriazoles, thioesters and organophosphite stabilizers, fatty ester and amide lubricants and phthalate plasticizers.

Separations on 1 mm columns are similar to those on capillary columns. They are performed using capillary SFC instrumentation with the pressure restrictor adjusted to give a higher flow rate range. Unmodified carbon dioxide is used as the mobile phase, the column is operated isothermally at 100–150°C and the additives are eluted with a pressure programme. The pressure is initially held at 10–15 MPa and then increased at 0.5–1.2 MPa min⁻¹ to a final pressure of 35–45 MPa. Nonpolar octadecyl phases are most commonly used for these separations; however, more polar octyl, phenyl and polyethylene glycol phases have also been used. A typical separation is shown in **Figure 2**. Packed columns are more active than capillaries and this can lead to peak tailing for more polar additives. This tailing can be minimized by adding a polar modifier to the carbon dioxide mobile phase at approximately 1% (v/v). Formic acid is commonly used for this purpose it has a low FID response. An alternative approach is to use 250–320 μ m (i.d.) fused silica columns which are packed with bonded silica particles. These packed capillary columns exhibit lower activity than conventional packed columns and they generate flow rates which are more compatible with the FID.

Separations on 4.6 mm columns resemble normal-phase HPLC separations. The column is operated isothermally at the lower temperature range of 40–60°C and isobarically with the pressure set to 10–20 MPa with the flow rate set to 2–4 mL min⁻¹. The additives are eluted by means of a composition

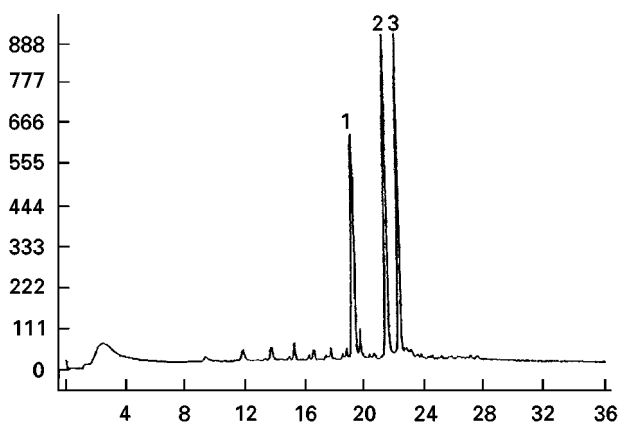


Figure 2 Chromatogram of polyethylene additives on a 25 cm \times 1 mm i.d. C₁₈ column at 150°C. Mobile phase: carbon dioxide pressure programmed from 1500 psi (6 min) to 6000 psi at 200 psi min⁻¹. Peaks: 1, Tinuvin 326; 2, Irgafos 168; 3, Irganox 1076. (Reproduced with permission from Ryan *et al.* (1990).)

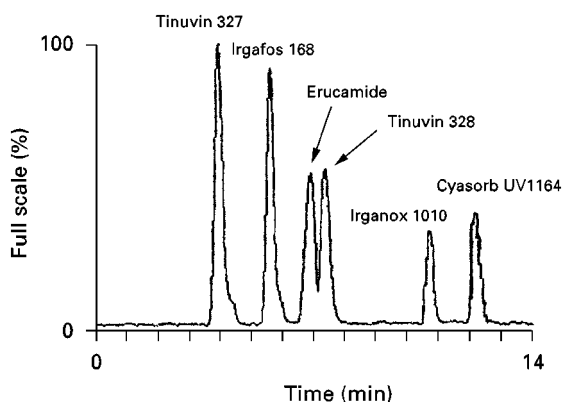


Figure 3 Chromatogram of polymer additives on a 25 cm \times 4.6 mm i.d. C_{18} column. Mobile phase: carbon dioxide/methanol at 200 bar and 2 mL min^{-1} . Methanol concentration programmed from 2% (1 min) to 10% (5 min) at 0.89% min^{-1} . (Reproduced with permission from Carrot *et al.* (1998).)

gradient of a polar modifier (usually methanol) in carbon dioxide. They are sequentially desorbed from the stationary phase as the polarity of the mobile phase increases. The elution order in such separations is determined by the relative adsorption strengths of the additives which in turn are determined by their functional groups and polarities. Hence, the least polar additives elute first and more polar additives elute later. Polar cyano, amino and diol phases are best suited to this mechanism; however, octadecyl columns can also be used due to the presence of residual silanol groups. A typical composition gradient separation is shown in Figure 3.

Composition gradient separations are performed using modified HPLC instrumentation. The high flow rates necessitate the use of binary piston pump systems. The larger system volume allows the use of back-pressure regulators which give independent control of both pressure and flow rate. UV detectors are used because organic modifiers are not compatible with the FID.

Offline Analysis: Sample Injection and Calibration

Sample introduction in SFC is achieved using HPLC-type high pressure injection valves. A fixed-volume injection loop is filled with the additive solution, then switched into the SF flow path and swept on to the column. A 200 nL loop is typically used in capillary SFC; however, even this volume is sufficient to overload a 50 μm column. Hence, flow split and time split techniques are used so that only a fraction of the 200 nL aliquot is introduced into the column.

Time split injection is a convenient procedure for routine analysis. It does not suffer from the problem

of additive molecular weight discrimination, which is associated with flow split injection, but it gives poor additive peak area repeatabilities (10–20%) and the low sample capacity also leads to relatively poor sensitivity. The lower limit of detection (using FID) for a single additive solution, which is injected in time-split mode on to a 50 μL column, is approximately 100 p.p.m. (w/v). For a 5 mL extract of a 5 g polymer sample this is equivalent to 100 p.p.m. (w/w) concentration of the additive in the polymer. This detection limit should be an adequate characterization of most polymer additive packages; however, it is not sufficient for studies on the migration of additives into food simulants where there is a requirement to detect additives in food simulants at p.p.b. levels. Greater sensitivity can be achieved by means of large volume injection/solvent venting techniques.

The sample capacity of a packed column in SFC compares favourably with HPLC and a similar range of sample volumes (5 μL –1 mL) is employed. This means that it is possible with packed column SFC to achieve the p.p.b. (w/v) level limits of detection which are required for additive migration work.

The sample injection repeatability is similar to that obtained in HPLC and this means that multi-level external standards can be used for the additive peak area–concentration calibration. The poor repeatability of capillary SFC injection, conversely, means that in this case an internal standard must be used for calibration.

Online SFE-SFC

Online SFE-SFC has been reviewed by Levy and Ashraf-Khorassani. The polymer is analysed in a single process without any intermediate preparation. It involves the transfer of the whole of the SFE extract on to the SFC analyser and this means that online SFE is more sensitive than equivalent offline procedures where the extract is diluted in an aliquot of solvent for subsequent injection on to an analyser. Hence it is ideally suited for trace analysis or for applications where there is little available sample. However the counterpoint of this argument is that the sample size is limited by the capacity of the interfaced analyser. This can be a disadvantage. Additives should be evenly dispersed throughout a batch of polymer chips. However, in practice, process faults can cause localized variations so that the additives are more concentrated in some chips than in others. In this circumstance it is clearly important for a representative analysis to be able to sample from more than one chip.

The most widely used coupling system is called cryotrapping. This involves feeding the SFE outflow

into a vented collection tee or retention gap which is cooled by adiabatically vaporizing liquid CO_2 through it. The extracted analytes are deposited in the retention gap during the extraction whilst the SF is vented to the atmosphere. When the extraction is complete the vent is closed and deposited analytes are eluted by the SF into the column.

Calibration curves for quantitative analysis can be obtained from online extractions on known amounts of free additive. These are then used to convert the online additive peak areas from the polymer extraction into concentration values. However, the validity of this approach depends on the complete removal of the additives from the polymer during the SFE step. Alternatively, the system can be calibrated using similar polymer samples of known additive concentration. It is not necessary with this procedure completely to extract all of the polymer additives so long as the extraction conditions for the polymer sample and standard are identical.

Identification of Unknown Additives

FID and UV detection are sufficient for the analysis of an additive package of known composition. The order of the eluting peaks is determined in this case by comparing their retention times with those of the pure additives, eluted under identical conditions; however, this procedure is clearly impossible for the identification of a mixture unknown additives. Hence there is a requirement for the SFC separation to be coupled with a spectroscopic technique which records sufficient structural and fingerprinting data on the eluting additive to enable it to be identified either by deduction or by comparison with library records.

Fourier transform infrared (FTIR) spectroscopy can be coupled indirectly to capillary SFC by depositing the additive on to an infrared disc or directly by passing the column outflow through a flow cell. The latter technique is possible because carbon dioxide exhibits just two narrow absorption bands in the near infrared spectrum. Alternatively xenon, which is completely transparent to infrared, can be used as the mobile phase. Both interfaces have been successfully used to identify a wide range of stabilizers; however, they lack sensitivity and quantitative measurements have not been achieved. The poor sensitivity necessitates the use of 100 μm i.d. columns.

Carbon dioxide is a nonprotonated solvent and this makes SFC the ideal chromatographic technique to couple with ^1H nuclear magnetic resonance (NMR). The relatively large dead volume of the NMR probe means that it can only be interfaced with packed column SFC with flow rates $>1\text{ mL min}^{-1}$ and

sample loadings of 20–120 μL . This procedure has been used to analyse phthalate plasticizers. Unfortunately, SFC-NMR signals have been found to be pressure-dependent and exhibit increased spin-lattice relaxation times.

SFC has been most successfully coupled to mass spectroscopy (MS). MS detectors can be used in several modes to give molecular ion data and structural data from fragmentation patterns which can be compared with library records to identify an unknown additive. Total ion chromatograms can also be used for quantitative analysis. Capillary SFC is interfaced directly by feeding the end of the column into the ionization chamber of the MS. The MS signal is not affected by the SFC pressure gradient. This has been used for the identification and quantitation of flame retardants from polyurethane foams. Several interfaces (moving belt, thermospray, particle beam) have been used to couple packed-column SFC and MS. These tend either to inhibit the range of compatible SFC conditions or result in the loss of volatile components. The most promising system is currently atmospheric pressure chemical ionization MS which has been used with a carbon dioxide-methanol composition gradient to identify and quantify benzotriazoles and phenolic stabilizers.

Conclusion

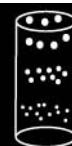
SFC is a useful technique for the analysis of a wide range of polymer additives. It can elute nonvolatile and thermally labile additives which are not suitable for analysis by GC and it gives better resolution and faster separations compared with HPLC. Useful separations are obtained with both packed and capillary columns. Capillary separations generally involve 50 μm i.d. columns and FID detection with unmodified carbon dioxide used as the mobile phase. The additives are eluted with a pressure/density gradient. Packed columns with i.d. $<1\text{ mm}$ can also be operated in this way; however, separations on 4.6 mm i.d. columns employ composition gradients at a fixed temperature and pressure with UV detection. Capillary SFC generally gives separations of superior resolution but with longer analysis times and poor sensitivity.

The flexibility of SFC as a technique for the analysis of polymer additives is further enhanced by the ease with which it is interfaced to other techniques. SFE-SFC enables the detection of trace levels of additives which could not be analysed by offline procedures. SFC-FTIR, SFC-NMR and SFC-MS give the capability to determine the chemical structures of additives from polymer samples of unknown compositions.

Further Reading

- Albert K (1997) Supercritical fluid chromatography–proton magnetic resonance spectroscopy coupling. *Journal of Chromatography A* 785: 65.
- Berg BE, Hegna DR, Orlie N and Geibrokk T (1992) Preliminary study of specific migration of polymer additives from polypropylene to an acid-based food simulant. *Journal of High Resolution Chromatography* 15: 837.
- Berger TA (1995) *Packed Column SFC*. London: Royal Society of Chemistry.
- Carrot MJ, Jones DC and Davidson G (1998) Identification and analysis of polymer additives using packed-column supercritical fluid chromatography with APCI mass spectrometric detection. *Analyst* 123: 1827.
- Combs MT, Ashraf-Khorassani M and Taylor LT (1997) Packed column supercritical fluid chromatography–mass spectroscopy: a review. *Journal of Chromatography A* 785: 85.
- Gächter R and Müller H (1990) *Plastics Additives Handbook*. Munich: Hanser.
- Geibrokk T, Berg BE, Hoffman S *et al.* (1990) Characterisation of polymer additives by capillary supercritical fluid chromatography and by liquid chromatography. *Journal of Chromatography* 505: 283.
- Handley A (1993) *Polymer Characterisation*, Glasgow: Blackie.
- Kithinji JP, Bartle KD, Raynor MW and Clifford AA (1990) Rapid analysis of polyolefin antioxidants and light stabilisers by supercritical fluid chromatography. *Analyst* 115: 125.
- MacKay GA and Smith RM (1993) Supercritical fluid extraction and chromatography–mass spectroscopy of flame retardants from polyurethane foams. *Analyst* 118: 741.
- Moulder R, Kithinji JP, Raynor MW *et al.* (1989) Analysis of chemical additives in polypropylene films using capillary supercritical fluid chromatography. *Journal of High Resolution Chromatography* 12: 688.
- Raynor MW, Bartle KD, Williams A *et al.* (1988) Polymer additive characterisation by capillary supercritical fluid chromatography/fourier transform infrared microspectrometry. *Analytical Chemistry* 60: 427.
- Ryan TW, Yocklovich SG, Watkins JC and Levy EJ (1990) Quantitative analysis of additives in polymers using supercritical fluid extraction–supercritical fluid chromatography. *Journal of Chromatography* 505: 273.
- Smith RM (1988) *Supercritical Fluid Chromatography*. London: Royal Society of Chemistry.
- Wieboldt RC, Kempfert KD and Dalrymple DL (1990) Analysis of polyethylene using supercritical fluid extraction/supercritical fluid chromatography and infrared detection. *Applied Spectroscopy* 44: 1028.

POLYMERS



Field Flow Fractionation

M. E. Schimpf, Boise State University,
Boise, ID, USA

Copyright © 2000 Academic Press

Introduction

Two subtechniques of the field-flow fractionation (FFF) family are used to separate polymers with high resolution on an analytical scale; these are thermal FFF (ThFFF) and flow FFF (FIFFF). For lipophilic polymers, ThFFF excels in the analysis of high-molecular-weight-polymers ($M > 10^6 \text{ g mol}^{-1}$) and gel-containing polymers. ThFFF can also separate polymer blends and copolymers according to chemical composition. For hydrophilic polymers, FIFFF compares well with size-exclusion chromatography (SEC) for the analysis of polymers with $M > 10^3 \text{ g mol}^{-1}$, and like ThFFF, excels when

$M > 10^6 \text{ g mol}^{-1}$. By varying factors that control retention, each FFF application can be optimized, and programming such factors allows highly polydisperse samples to be analysed with unparalleled precision in a single run. FFF channels are more expensive than SEC columns, but with proper maintenance, channel lifetimes are virtually unlimited.

FFF, like liquid chromatography, relies on the differential migration of dissolved or suspended materials as they are flushed through a conduit. Unlike chromatography, however, the FFF separation relies on interactions of the analyte with an applied field rather than a stationary phase. As a result, the FFF separation occurs in a single phase (see **Figure 1**) with minimal exposure to surfaces, and the flowing liquid has a laminar profile. These features make for a gentle separation, so that fragile molecules and molecular complexes can be characterized with little disruption.

FFF instrumentation (**Figure 2**) is similar to that for chromatography, and consists of a pump to drive the carrier liquid, an injection port, the separation channel, and a detector to monitor the channel effluent.

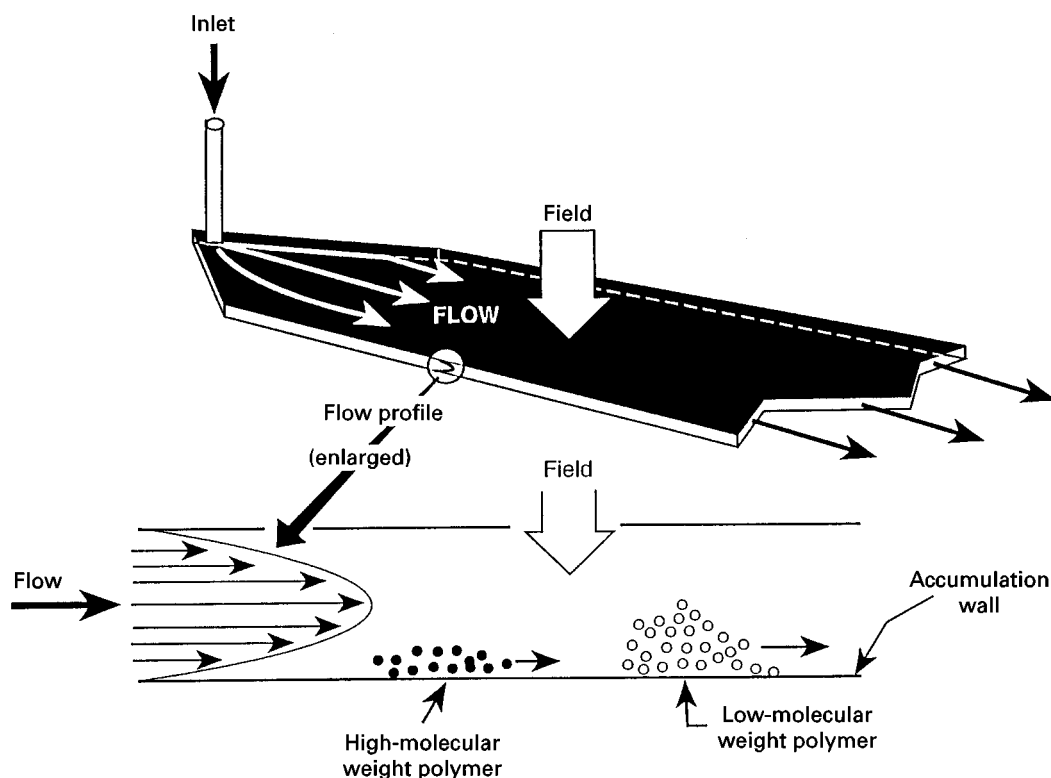


Figure 1 Illustration of the separation mechanism in FFF. The field compresses larger material into a thinner layer against the accumulation wall, where they move more slowly.

A computer is used to control the applied field and to store the detector signal. Samples are injected with a microsyringe, either directly or via an injection valve.

One of the greatest strengths of FFF is its ability to directly measure physicochemical parameters on analyte components using well-defined models of retention. In FIFFF, for example, the diffusion coefficient (D) can be calculated directly from a component's

retention time. From D , the hydrodynamic size can be calculated, and if the intrinsic viscosity is measured independently, the molecular weight can be determined. Molecular weight can also be obtained directly from retention measurements through calibration standards. In ThFFF, D values can also be calculated from measured retention times once an additional parameter for each polymer type is obtained, as discussed below. An additional advantage

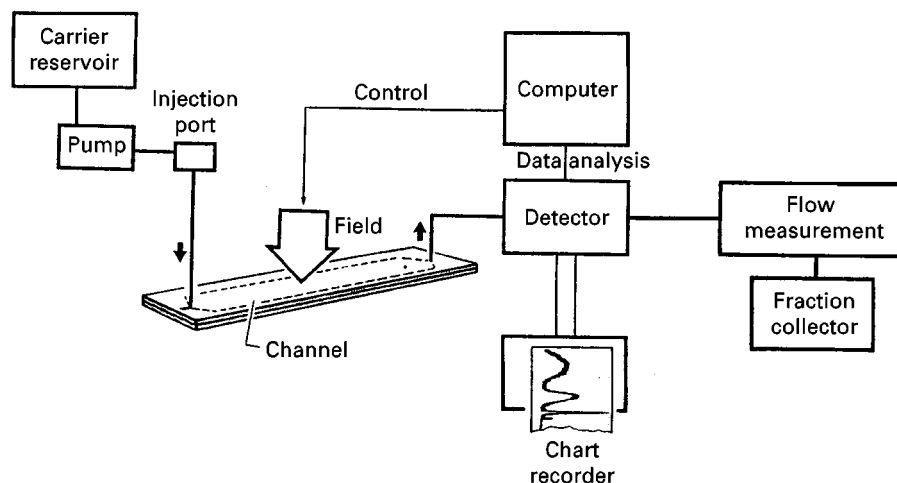


Figure 2 Schematic diagram of the FFF instrument.

of ThFFF is that band broadening is well defined, allowing for the determination of highly precise molecular-weight determinations.

Besides its placid nature and theoretical tractability, another attractive feature of FFF is its applicability to a wide variety of materials and situations. For example, FIFFF has been used to separate materials ranging in size from 10^3 to 10^{18} g mol $^{-1}$. However, flexibility comes with a price, and the user must understand the separation mechanism in order to apply FFF to new and different samples with efficiency. Outlined below are the more common applications of both ThFFF and FIFFF for polymer analysis with comparisons, when appropriate, to SEC.

Principles and Theory of Retention

The FFF channel has the shape of a ribbon (Figure 1), with a length of typically 30–50 cm, a breadth of 1–3 cm, and a typical thickness of 0.05–0.25 mm. A stream of carrier liquid is introduced at one end of the channel and exits at the other end. Since the channel has a high aspect ratio, the flow of carrier liquid is laminar, with a parabolic velocity profile across the thin dimension. A field is applied across the thin dimension, and a mixture to be separated is injected at the inlet end of the channel. As the mixture is transported by carrier liquid to the outlet, interactions with the field compress the sample against one wall, where slower streamlines exist. The concentration of sample at the accumulation wall is opposed by diffusion, and the result is a sample cloud with a concentration that decreases exponentially with distance from the wall. Components that interact differently with the field will form zones of different thickness at the accumulation wall. The dependence of zone thickness l on the force F of the interaction with the field is:

$$l = kT/F \quad [1]$$

where k is Boltzmann's constant and T is temperature. The thickness of the zone determines the extent to which its migration through the channel is reduced.

The extent to which an analyte is retained in FFF can be specified, as in chromatography, by its retention ratio R :

$$R = t^\circ/t_r = V^\circ/V_r \quad [2]$$

where t_r and V_r are the time and volume of carrier liquid, respectively, required to flush a component through the channel; the void time t° and void volume V° are the analogous parameters for a component

that does not interact with the field. The dependence of retention ratio R on zone thickness l is:

$$R = 6\frac{l}{w} \left[\coth\left(\frac{1}{2l/w}\right) - 2\frac{l}{w} \right] \quad [3]$$

The ratio l/w is given the symbol λ , and is referred to as the retention parameter, since it alone describes the relative migration of a component zone. As $\lambda \rightarrow 0$, $R \rightarrow 0$, and the analyte does not move through the channel. As $\lambda \rightarrow \infty$, $R \rightarrow 1$, and the analyte moves at the average velocity of the carrier liquid. As λ is reduced, the bracketed term in eqn [3] approaches unity, so that for many applications the relationship between R and λ is described by the following simple equation:

$$R = 6\lambda \quad [4]$$

The retention ratio of an eluting component can be determined experimentally through eqn [2] and translated into a λ value using eqn [3]. Values of λ , in turn, can be related to physicochemical properties of the analyte, as discussed below.

The properties that govern F (or λ) vary with the nature of the applied field, i.e. with the FFF subtechnique. In all sub-techniques, however, retention varies directly with the magnitude of the applied field. This relationship facilitates tuning the field in order to optimize each application, so that routine analyses can be performed with maximum efficiency. For highly polydisperse samples, the magnitude of the field can even be programmed in order to reduce the separation time of such samples. Field programming is analogous to temperature programming in gas chromatography and gradient elution in liquid chromatography. Figure 3 illustrates the ThFFF separation of seven polymer standards ranging in M from 9000 to 5.5×10^6 g mol $^{-1}$ in a single run.

Thermal FFF

In ThFFF, the applied field is a temperature gradient formed by heating and cooling, respectively, the two walls that define the thin dimension of the channel. A schematic of the ThFFF channel is illustrated in Figure 4. When placed in a temperature gradient, polymers migrate toward the lower temperature. This effect, which is known as thermal diffusion, governs the retention parameter (λ) in the following way:

$$\lambda_{Th} = \frac{D}{D_T \Delta T} \quad [5]$$

Here D_T is the coefficient of thermal diffusion, which relates mass flux to a temperature gradient, and ΔT is

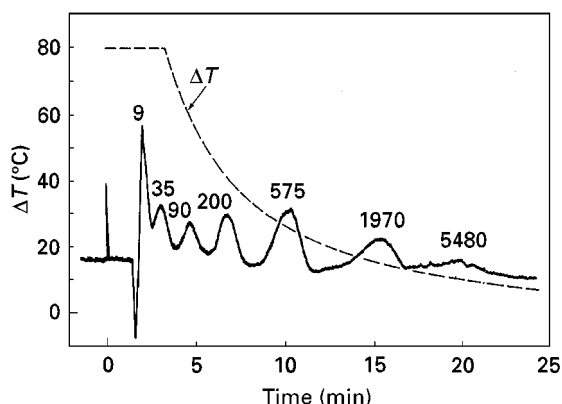


Figure 3 Separation of a seven-component mixture by ThFFF with field programming. Values above peaks are molecular weights expressed as $\times 10^3 \text{ g mol}^{-1}$. Reprinted with permission from J. C. Giddings, V. Kumar, P. S. Williams and M. N. Myers (1990). In: Craver D and Provder T (eds) *Polymer Characterization by Interdisciplinary Methods*, ACS Advances in Chemistry Series No. 227, C. Washington, D.C.: ACS Publications.

the temperature drop across the channel. Equation [5] is actually an approximation because of an assumption that the temperature gradient is constant; this is not strictly true because solvent thermal conductivity changes with temperature across the channel. In fact, eqn [3] is also an approximation for ThFFF because of the temperature dependence of the solvent viscosity, which leads to a skewed velocity

profile. Various approaches have been used to refine eqns [3] and [5] in order to account for such temperature effects (see Martin, 1998), but for routine polymer analysis such refinements are not necessary.

The dependence of λ_{Th} on D/D_T means that neither D nor D_T can be computed by itself, only the ratio D/D_T . Fortunately, D_T is independent of molecular weight and branching configuration for a given polymer-solvent system, at least for random-coil homopolymers. As a result, λ_{Th} is a linear function of D for a given system when ΔT is held constant. Thus, once D_T is determined for a given system, values of D can be calculated directly from measurements of λ_{Th} in that system.

Since D_T is independent of molecular weight M , the separation of polymers by ThFFF is rooted, like SEC, in the dependence of D on M ; that dependence is given by the following expression:

$$D = \frac{kT}{6\pi\eta_0} \left(\frac{10\pi N_A}{3M[\eta]} \right)^{1/3} \quad [6]$$

where η_0 is the viscosity of the solvent, N_A is Avagadro's number, and $[\eta]$ is the intrinsic viscosity of the polymer. The relationship defined by eqn [6] forms the basis for universal calibration in SEC, and is applicable to ThFFF provided D_T is known for each polymer-solvent system to which the universal calibration is applied.

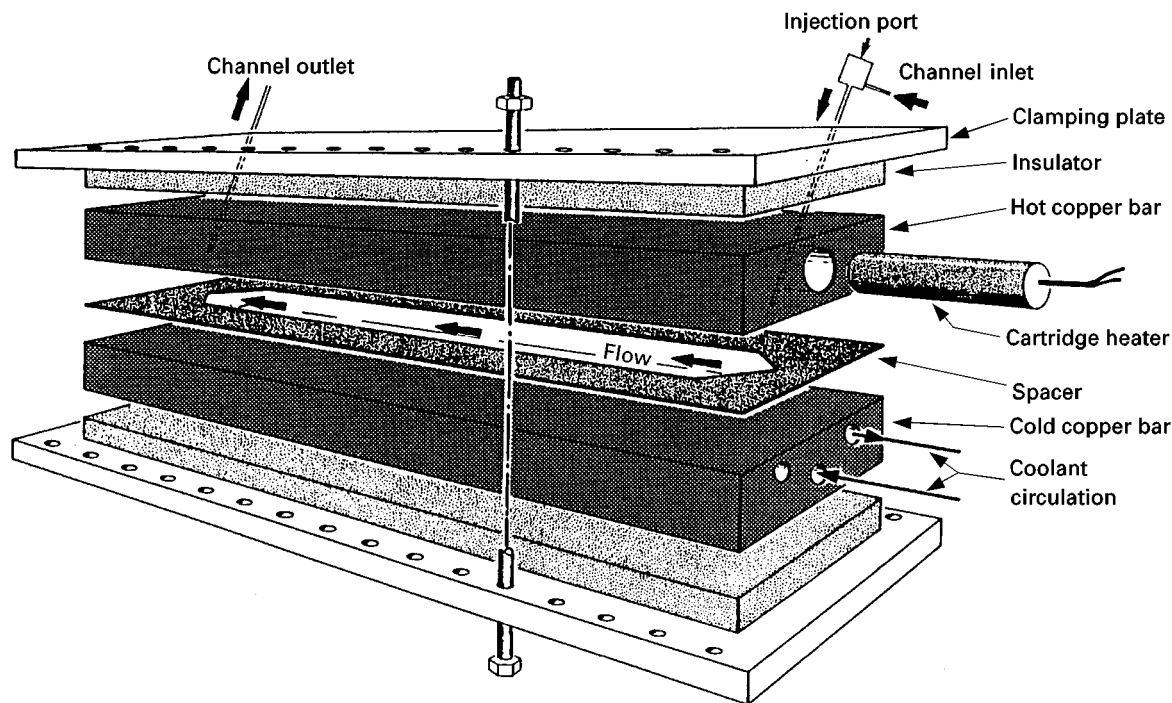


Figure 4 Basic design of the ThFFF channel, which is formed by a spacer sandwiched between two nickel-coated copper bars. One of the bars is heated while the other is cooled.

Flow FFF

In FIFFF, the applied field is a flow of carrier liquid across the thin dimension of the channel. This cross-flow is made possible by constructing one or both channel walls with a fritted material that is permeable to the carrier liquid (Figure 5). As a result, the flowing liquid has two perpendicular vectors. The axial-flow vector lies along the length of the channel, has a parabolic velocity profile across the thin dimension, and carries sample through the channel as in other FFF subtechniques. The cross-flow vector is directed across the channel, has a relatively flat velocity profile, and serves as the applied field by physically transporting material to the accumulation wall. A semipermeable membrane placed against the accumulation wall prevents analyte from penetrating the wall, while allowing the carrier liquid to pass through.

FIFFF employs one of two channel designs.

- In the symmetric design (SyFIFFF), both the accumulation wall and the (opposite) depletion wall are

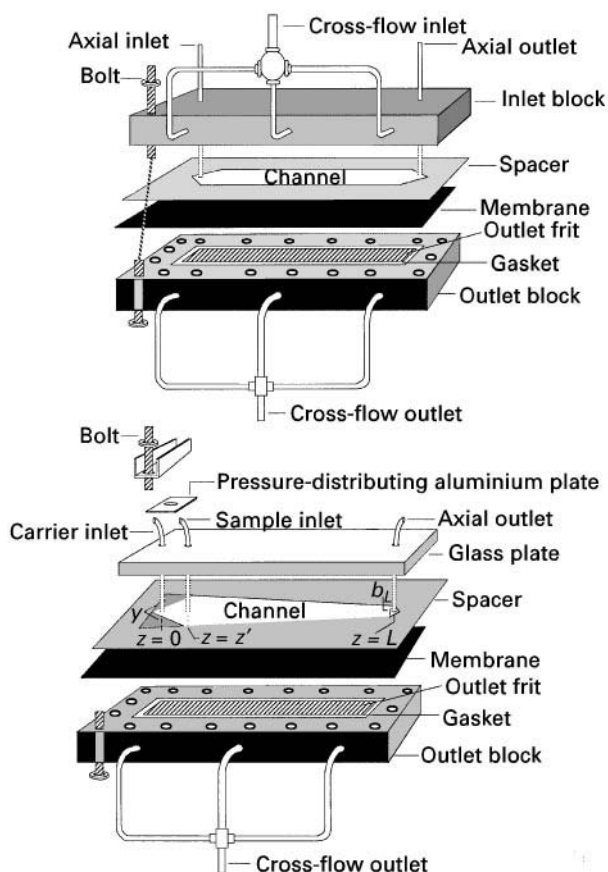


Figure 5 Basic design of the flow FFF channel. In the symmetrical channel (top), the channel spacer is sandwiched between two frits, which allow carrier liquid to flow across the thin dimension of the channel. In the asymmetrical channel (bottom), a solid plate replaces the upper frit, which is transparent in order to see inside the channel during operation.

porous, and the axial flow and cross flow are controlled independently with separate pumps.

- In the asymmetric design (AsFIFFF), the depletion wall is replaced with a glass plate so that a single inlet stream serves as the source for both axial flow and cross flow.

The relative magnitudes of the two flow vectors are controlled by adjusting the relative amount of back-pressure applied at the axial outlet versus the cross-flow outlet. In contrast to the symmetric design, the axial velocity diminishes along the length of an asymmetric channel as fluid is lost through the accumulation wall. To compensate for this effect, the width of the asymmetric channel is tapered from inlet to outlet. However, except for a specific ratio of cross-to-axial flow rates, the axial velocity will still vary along the length of the channel. Therefore, for AsFIFFF, eqn [3] is not valid and must be replaced with:

$$R = \frac{t^\circ}{t_r} = \frac{6}{w} \frac{\int_0^w e^{(-x/l)B(x)} x dx - \frac{1}{w} \int_0^w e^{(-x/l)B(x)} x^2 dx}{\int_0^w e^{(-x/l)B(x)} dx} \quad [7a]$$

Here x is the distance from the accumulation wall:

$$B(x) = 1 - \frac{x^2}{w^2} + \frac{x^3}{2w^3} \quad [7b]$$

and:

$$t^\circ = \frac{V^\circ}{V_C} \ln \left(1 + \frac{V_C}{V_{out}} \left\{ 1 - \frac{w \left[b_o z' - \frac{(b_o - b_L)(z')^2}{2L} - y \right]}{V^\circ} \right\} \right) \quad [7c]$$

where V_C and V_{out} are the volumetric rates of flow thorough the cross-flow and axial-flow outlets, respectively. Parameters b_o and b_L are the breadths of the channel at the sample inlet and outlet, respectively, z' is the distance between the carrier inlet and the focusing position (discussed below), and y is the area reduction of the accumulation wall due to the tapered inlet (see Figure 5).

Asymmetric channels have two primary advantages: (1) they are less costly, and (2) the inside of the channel can be seen through the glass plate. By observing the motion of an injected dye, flow irregularities caused by a poorly sealed channel are easily visualized. On the other hand, the advantages of the

symmetric design are: (1) the axial flow and cross flow can be controlled independently, and (2) the equations relating R to λ are simpler.

In both FIFFF channel designs, the cross flow pushes all components with the same velocity (U) toward the accumulation wall. As a result, only the opposing motion of diffusion governs retention:

$$\lambda_F = \frac{D}{Uw} = \frac{DV^\circ}{V_c w^2} \quad [8]$$

Like ThFFF, the well-established inverse dependence of λ on field strength imparts flexibility and allows field programming, so that the most efficient possible method can be developed for each application.

Application to Polymer

Within the FFF family, the choice between thermal and flow FFF is a simple one for polymer analysis. In general, FIFFF is used for hydrophilic polymers, while ThFFF is best suited to lipophilic polymers. In either case, an advantage that FFF has over SEC is its greater peak capacity. In principle, V_r is unlimited in FFF, although 20 channel volumes represent a practical limit. In SEC, V_r is limited at the high end by the permeation volume (equal to one column volume), and at the low end by the exclusion volume.

Lipophilic Polymers

For lipophilic polymers with $M < 10^4 \text{ g mol}^{-1}$, ThFFF suffers from a lack of resolution, therefore SEC is almost mandatory, and certainly preferred. However, above 10^4 g mol^{-1} , the resolving power of ThFFF increases rapidly, and exceeds that of SEC for $M > 10^5 \text{ g mol}^{-1}$. For ultra-high molecular-weight polymers ($M > 10^6$), SEC becomes increasingly limited by shear-induced fragmentation of the chains as they travel through the packed bed under high pressure, and ThFFF is clearly superior.

Between 10^4 and 10^6 g mol^{-1} , neither SEC nor ThFFF has an overwhelming advantage for the analysis of many polymers. In general, ThFFF is more difficult to implement than SEC because there are more factors under the control of the user that influence retention. While this adds flexibility, only by understanding the separation mechanism and governing equations can one avoid certain pitfalls in choosing the proper parameters for each application.

For analysing certain types of lipophilic polymers, ThFFF has some rather unique advantages. The absence of shear forces, which make ThFFF especially suited to ultra-high molecular-weight polymers, was mentioned above. Using re-injection techniques, and

the absolute measurement of M by light scattering, the integrity of ThFFF analyses on high molecular-weight polymers that degrade in SEC columns has been clearly demonstrated. The open ThFFF channel is also amenable to gel-containing polymers. Since sample filtration is not required, microgels are not lost in the analysis, and an estimate of the gel content can even be obtained. ThFFF is also well suited to polyolefins, which are difficult to separate by SEC because high temperatures ($> 130^\circ\text{C}$) are required for their dissolution. At these temperatures, column packings used in SEC tend to degrade at an elevated rate, while the ThFFF channel is more robust.

Although the thermal diffusion coefficient D_T is independent of molecular weight, it varies with polymer composition. As a result, ThFFF can resolve polymer components that differ chemically even when their diffusion coefficients (or hydrodynamic volumes) are identical. This is in contrast to SEC, where components with similar diffusion coefficients cannot be separated. The dependence of retention on polymer composition can be used to separate copolymers according to composition, and when the dependence of D_T on copolymer composition is known, the chemical composition can be calculated from retention data. Such is the case for random (statistical) copolymers, where D_T is a weighted-average of the D_T values of the homopolymer constituents, with the weighting factors being the mole-fractions of each component in the copolymer. Thus, by measuring the retention of a copolymer of unknown composition, its D/D_T value can be calculated using eqns [3] and [5]. With an independent measure of D , a value for D_T can be calculated, and from D_T the copolymer composition. For block copolymers, a linear dependence of D_T on composition requires the polymers to be dissolved in a non-selective solvent, which is a solvent that is equally good for all copolymer components. Unfortunately, with highly branched block copolymers, even a non-selective solvent will fail to yield a linear dependence.

ThFFF is incapable of resolving the components of certain polymer mixtures. For example, when the composition of a polydisperse copolymer changes with molecular weight, two components that differ in both molecular weight and composition may have the same D/D_T ratio, even though their individual values of D and D_T differ. Such components will co-elute, in which case the combination of SEC and ThFFF is extremely powerful. Components can first be separated according to differences in D using SEC, then fractions from the SEC column, which are homogeneous in D , can be further separated according to D_T by ThFFF. Figure 6 illustrates such a combination applied to a polymer-copolymer mixture that neither

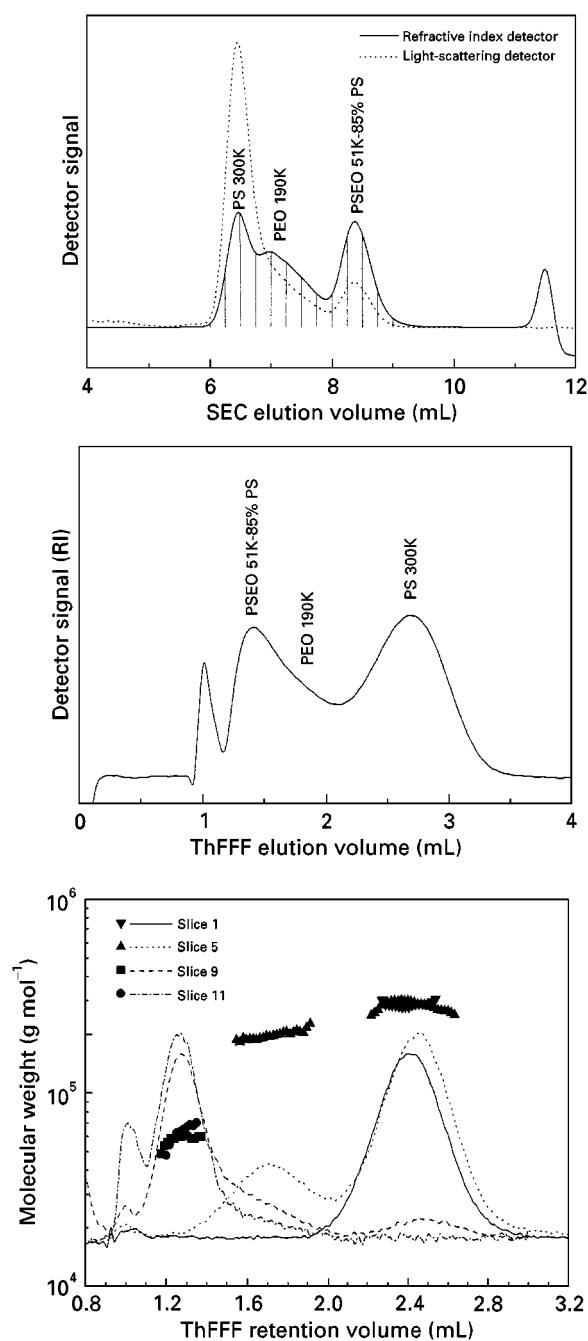


Figure 6 Cross-fractionation of a three-component polymer mixture by SEC and ThFFF. The mixture could not be sufficiently resolved for characterization by either SEC (top) or ThFFF (middle) alone. Cross-fractionation of SEC elution slices (bottom) provided enough resolution to determine the molar mass of each component with a multi-angle light-scattering detector (Dawn DSP, Wyatt Technology, Santa Barbara, CA). The composition of the components were determined from D and D_T values calculated from SEC and ThFFF retention volumes, respectively.

SEC nor ThFFF alone can separate. By cross-fractionating the mixture, the three components were sufficiently resolved to determine both the molecular weight and composition of each component.

Highly precise information on the polydispersity of lipophilic polymers can be obtained with ThFFF because column dispersion is well modelled, and its effect on the elution profile can therefore be removed. For example, plots of plate height H versus flow rate are linear. Such plots can be extrapolated to zero flow rate to yield an intercept term from which the sample polydispersity can be calculated. This method is used to obtain highly precise measurements of the polydispersity ($\mu < 1.005$) of polymers prepared by anionic polymerization. By comparison, the precision of SEC for such measurements is reduced by an order of magnitude because of uncertainties in the contribution of column dispersion to plate height. For a more detailed analysis, a well-defined band-broadening function can be mathematically removed from the elution profile to obtain highly precise molecular-weight distributions. With more polydisperse polymers ($\mu < 1.005$), column dispersion is nearly negligible in ThFFF when typical flow rates are used, so that elution profiles can be converted directly into accurate molecular-weight distributions.

Hydrophilic Polymers

For analysing hydrophilic polymers, FIFFF shares many of the advantages and limitations of ThFFF when compared to SEC. A notable difference is that FIFFF can be extended to lower molecular weights (10^3 g mol^{-1}). Another difference is that the effects of column dispersion cannot be completely removed from a FIFFF elution profile because of factors associated with the accumulation wall membrane.

SEC has been criticized for its lack of consistency in the separation of charged polymers. Part of the problem with SEC is attributed to interactions with the packing material. These interactions are often referred to as 'nonexclusion effects'. Electrolytes can be used to minimize such effects, but the conditions required to avoid both adsorption and repulsion are rather specific to each polymer, and are typically found through trial and error. Verification that an SEC separation is dominated by differences in D or M rather than interactions with the packing material can be a time-consuming process, and still not guarantee the accurate analysis of nonstandard samples. In FFF, the surfaces available for interactions with the sample are greatly reduced by the absence of packing material. Interactions with the accumulation wall can still be a factor, however, since samples are compressed against the wall by the applied field. However, they are less of a problem in FIFFF compared to SEC, and this allows for a wider range of aqueous solutions to be used in the analysis of charged polymers.

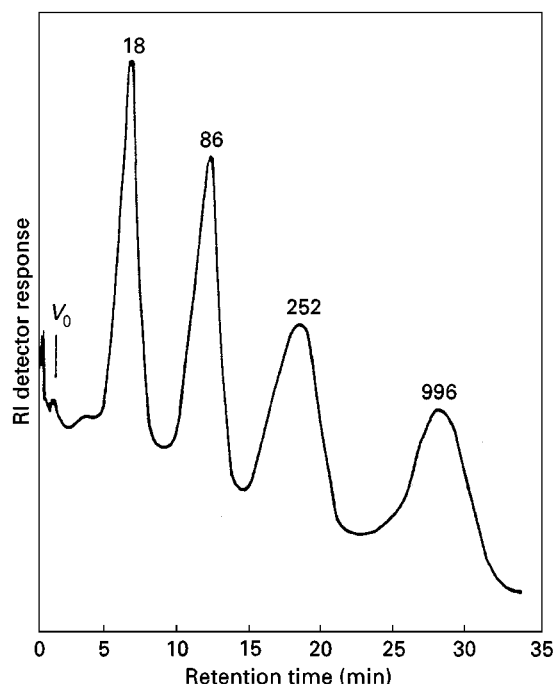


Figure 7 Separation of poly(ethylene oxide) standards by FIFFF. The cross-flow field was programmed to exponentially decay (decay-time constant 8 min) from an initial value of 5.9 mL min^{-1} . Values above peaks are molecular weights expressed as $\times 10^3 \text{ g mol}^{-1}$. Reprinted with permission from Kirkland JJ, Dिल्s CH Jr and Rementer SW (1992) Molecular weight distribution of water-soluble polymers by flow field-flow fractionation. *Analytical Chemistry* 64: 1295–1303. Copyright © 1992 American Chemical Society.

FIFFF has been applied to a wide variety of hydrophilic polymers. **Figure 7** illustrates the separation of poly(ethylene oxide) standards with an asymmetrical FIFFF channel using a programmed field. By decaying the field over time, four components ranging in M from 18 000 to 996 000 g mol^{-1} were resolved in 30 min.

Combined with a multi-angle light scattering (MALS) detector, FIFFF is being used to study the conformational dynamics of hydrophilic polymers in solution. Besides its ability to work within a wider range of solvent conditions, its broad size range is responsible for the unique ability of FIFFF–MALS to characterize the structural properties of such polymers in a partially aggregated state.

FIFFF is also being used to study copolymers. For example, the viscometric and aggregation properties of hydrophilic graft copolymers have been studied, as well as the micelle-forming behaviour of such copolymers. FIFFF has also been used to characterize the size and molecular weight of humic and fulvic acids, as well as to study changes in their conformation and aggregation properties as they occur over time upon alterations in solution properties.

Polysaccharides are another class of polymers that have proven difficult to separate by SEC. These materials have a wide range of industrial applications, from coating and packaging to plasma additives and blood substitutes. The physical, biological, and clinical properties of these materials vary with their molecular-weight distribution, which is generally quite broad. It is difficult to prepare robust SEC packings that are capable of analysing these fragile macromolecules without complications of sample adsorption, shear degradation and clogging of the column. FFF has been used to fractionate a wide variety of polysaccharides according to their molecular weight.

FIFFF is used to separate ultra-high molecular-weight polymers, as well as aggregates of lower molecular-weight polymers. For example, SEC fails to completely separate many dextran samples because of the exclusion boundary. The size and molecular weight of such samples are routinely characterized by FIFFF with MALS detection.

Determination of Molecular-Weight Distributions by FFF

The simplest calibration plots in thermal and flow FFF take the following form:

$$\log(V_r) = A + S_m \log M \quad [9]$$

where A and S_m are calibration constants for a given polymer–solvent system. Parameter S_m is termed the mass-based selectivity. However, at low levels of retention ($R > 0.2$), S_m changes with R . An alternate form of eqn [9] allows for the use of low levels of retention without losing linearity in the calibration plot:

$$\log(V_r - V^\circ) = A + S_m \log M \quad [10]$$

Equation [10] allows retention to be calibrated over a wide range in molecular weight for a given polymer–solvent system without requiring the calculation of retention parameter λ . The problem remains, however, that neither eqn [9] nor eqn [10] allows for an adjustment in field strength, which is one of the great benefits of FFF, as it allows the field to be optimized for each individual sample. In order to have a single calibration equation for different field strengths, one must incorporate the field strength S :

$$\log \lambda S = B + b \log M \quad [11]$$

The field strength S is the magnitude of the temperature drop (ΔT) across the channel in ThFFF, and the

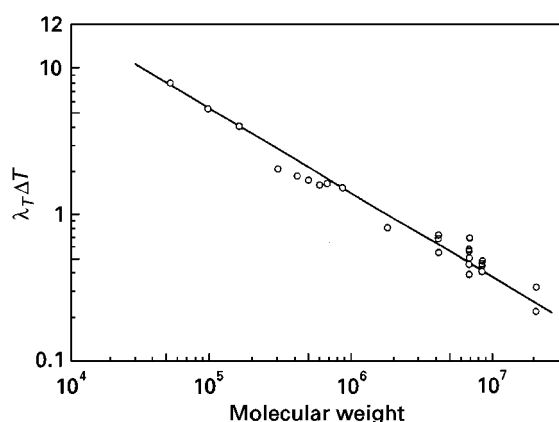


Figure 8 Plot of $\log \lambda_T \Delta T$ versus $\log M$ for polystyrene samples, illustrating the validity of the calibration model expressed by eqn [11]. The cold wall temperature was 15°C and ΔT ranged from 8 to 81°C. The carrier liquids included tetrahydrofuran and ethylbenzene. A single plot can be used for both solvents because they yield a similar dependence of D/D_T on M for polystyrene. Reprinted with permission from Gao YS, Caldwell KD, Myers MN and Giddings JC (1985) Extension of thermal field-flow fractionation of ultra-high molecular weight polystyrenes. *Macromolecules* 18: 1272. Copyright © 1985 American Chemical Society.

rate of cross flow (V_C) in FIFFF. By calibrating FFF channels in terms of $\log \lambda S$ versus $\log M$, the field strength can be changed to optimize the separation of a given sample without the need for re-calibration. Figure 8 illustrates calibration plots in the form of eqn [11] for ThFFF.

Compared to SEC, universal calibration equations in FFF have the potential for being much broader in scope. In SEC, a given column can be ‘universally’ calibrated and applied to several types of polymers of similar conformation, provided the intrinsic viscosity is also measured on all standards and samples. In FIFFF, the same concept can be applied, but D is measured directly, so that calibration is not required at all if viscosity is measured independently. In ThFFF, each polymer–solvent system requires a set of different calibration constants, but once such constants are determined, they are applicable to all ThFFF channels in the ‘universe’. Of course, the temperature can affect calibration constants, as it does in SEC. Therefore, in ThFFF, the cold wall temperature must be the same in all channels that use a given set of calibration constants.

Trends

FFF will continue to be utilized primarily for the characterization of ultra-high molecular-weight polymers, which are difficult to characterize by SEC. One of the fastest-growing areas for FIFFF is the study of hydrophilic systems that undergo complex interac-

tions. Such interactions are often the key to understanding biological activity in protein and nucleic acid complexes, as well as the complex rheological behaviour of polysaccharides. Regarding the application of ThFFF to industrial polymers, two applications will continue to expand. The first of these is the application to copolymers. As our understanding of thermal diffusion increases, the ability to extract compositional information from fractionated copolymer samples will grow. A growing number of scientists are researching this promising aspect of ThFFF technology.

The second area of growth is the application of ThFFF to the separation of colloidal materials. While this type of sample has been historically considered the domain of flow and sedimentation FFF, the unique ability of ThFFF to separate these materials by composition in both organic and aqueous carrier liquids is gaining the attention of several groups in both industry and academia.

The characterization of polymers will continue to benefit from the combination of FFF with informative detectors such as MALS, dynamic light scattering, intrinsic viscosity, and infrared detectors. For the last thirty years, the characterization of materials by FFF has relied on calibration with standards or the use of retention theory to extract analytical information. Calibration is limited by the availability of polymer standards, and while FFF has the unique ability to produce physicochemical parameters directly from retention theory (i.e. without calibration), this too has limitations. Absolute molecular-weight detectors produce molecular-weight values without the need for calibration curves. When a complex sample is first separated by FFF, a light-scattering detector produces a molecular weight value for hundreds or even thousands of relatively monodisperse components of the sample. The result is a highly accurate determination of the entire molecular-weight distribution of the sample. The combination of FFF–MALS has been particularly popular, as evidenced by the fact that greater than 20% of the papers presented at a recent FFF symposium involved MALS detection.

See also: II/Chromatography: Liquid: Mechanisms: Size Exclusion Chromatography. Particle Size Separation: Theory and Instrumentation of Field Flow Fractionation. Field Flow Fractionation: Thermal.

Further Reading

Gunderson JJ and Giddings JC (1986) Comparison of polymer resolution in thermal field-flow fractionation and size exclusion chromatography. *Analytica Chimica Acta* 189: 1–15.

- Jeon SJ and Schimpf ME (1999) Cross-fractionation of copolymers using SEC and thermal FFF for determination of molecular weight and composition. In: Provder T (ed.), *Chromatography of Polymers: Hyphenated and Multi-Dimensional Techniques*, ACS Symposium Series 731, ch. 10, pp. 141–161. Washington, D.C.: ACS Publications.
- Kirkland JJ, Dilks CH and Rementer SW (1992) Molecular weight distributions of water-soluble polymers by flow field-flow fractionation. *Analytical Chemistry* 64: 1295–1303.
- Lee S Determination of molecular weight and size of ultra-high molecular weight polymers using thermal field-flow fractionation and light scattering. In: Provder T, Barth HG and Urban MW (eds), *Chromatographic Characterization of Polymers: Hyphenated and Multidimensional Techniques* (*Advances in Chemistry Series* 247), 93–107. Washington, DC: American Chemical Society.
- Lee S and Molnar A (1995) Determination of molecular weight and gel content of natural rubber using thermal field-flow fractionation. *Macromolecules* 28: 6354–6356.
- Lou J, Myers MN and Giddings JC (1994) Separation of polysaccharides by thermal field-flow fractionation. *Journal of Liquid Chromatography* 17: 3239–3260.
- Martin M (1998) Theory of field-flow fractionation. *Advances in Chromatography* 39: 1–138.
- Pasti L, Roccasalvo S, Dondi F and Reschiglian P (1995) High temperature thermal field-flow fractionation of polyethylene and polystyrene. *Journal of Polymer Science B: Polymer Physics* 33: 1225–1234.
- Schimpf ME, Myers MN and Giddings JC (1987) Determination of polydispersity of ultra-narrow polymer fractions by thermal FFF. *Journal of Applied Polymer Science* 31(1): 117–135.
- Schimpf ME, Caldwell KD and Giddings JC (eds) (2000) *FFF Handbook*, New York: John Wiley.
- Thielking H and Kulicke W-M (1996) Online coupling of flow field-flow fractionation and multiangle laser light scattering for the characterization of macromolecules in aqueous solution as illustrated by sulfonated polystyrene samples. *Analytical Chemistry* 68: 1169–1173.
- Wittgren B, Wahlund KG, Derand H and Wesslen B (1996) Size characterization of a charged amphiphilic copolymer in solutions of different salts and salt concentrations using flow field-flow fractionation. *Langmuir* 12: 5999–6005.

Supercritical Fluid Extraction

H. J. Vandenburg, Express Separations, Roecliffe, North Yorkshire, UK

Copyright © 2000 Academic Press

Introduction

Plastics are a mixture of the polymer itself and many small molecules. Some, such as antioxidants and plasticizers, are added to the polymer to alter the properties. Others, such as residual monomers, processing aids and feedstock contamination are present inadvertently. The levels of these compounds must be accurately known by manufacturers and regulators in order to assess whether the plastic is fit for its intended purpose. There are usually many compounds present in the plastic, which makes analysis of their levels whilst still in the plastic very difficult. Usually, therefore, the compounds must be separated from the bulk polymer before analysis. Conventional methods include liquid/solid extraction and dissolution followed by reprecipitation of the polymer. Conventional solvent extraction methods tend to be very slow, e.g. Soxhlet extraction may require 24 hours to complete, and the dissolution/reprecipitation methods may result in extracts contaminated by oligomeric ‘waxes’, requiring further clean up before

analysis. Methods producing clean, fast extracts are therefore very useful. The techniques of supercritical fluid extraction (SFE), pressurized fluid extraction (PFE) and microwave assisted extraction (MAE) have been shown to decrease extraction times, with lower use of solvents than conventional methods.

The Extraction Process

In SFE and PFE, the matrix is held in a cell, and the solvent is pumped into the cell under pressure. Commonly in SFE, the solvent is pumped continuously past the sample (dynamic extraction), dissolving the analyte molecule and carrying it out of the cell to be collected. In PFE it is more common for the solvent to be pumped until the cell is full, and then left for a period of static extraction. The analyte dissolves in the solvent, which is then flushed by more solvent from the cell to the collecting vial. MAE is carried out in one container, in which sample and solvent are placed. The solvent is heated by microwaves, and the analytes dissolve in the solvent. The vessel must then be allowed to cool before opening, and the extraction liquid can be separated from the extracted polymer by simple filtering. In simple terms, extractions with all methods can be thought of as proceeding in two

steps, movement of the extracting compound from the bulk polymer to the surface by diffusion, and then dissolution in the solvent. The rates of these two steps is influenced by several factors.

Factors Affecting Extraction Rate

Particle size The distance the molecule has to move affects the time it takes to reach the surface. Small particles and thin films are therefore preferred. For spherical particles, the rate of extraction is proportional to $1/(\text{radius})^2$. Thus grinding 3 mm beads to 0.5 mm particles should increase extraction rate 36 times. For complete extraction, it is the size of the largest particles which dictates the extraction time, not the average particle size. Sieving to remove the largest particles can increase extraction rates dramatically. Grinding polymers generates considerable heat, and this can cause loss of analytes by degradation or volatilization. Polymers are usually freeze-ground under liquid nitrogen to prevent loss of analyte. A problem with polymers is that the particles can easily stick together, increasing the effective particle size.

Rate of diffusion Diffusion is driven by the tendency of a material to move from an area of high concentration to low concentration. The rate of diffusion depends on the size of the concentration gradient and the diffusion coefficient, a measure of how easily the diffusing material can move through the matrix. The diffusion coefficient follows the Arrhenius equation:

$$D = D_0 \exp(-E/RT)$$

where D is the diffusion coefficient, E is the activation energy, T is the absolute temperature and R the gas constant. The diffusion coefficient will be greatest when E is small and T is large. Several factors affect the rate of diffusion, as outlined below.

Size of diffusing molecule Smaller molecules can more easily move through the matrix, hence activation energy is lower for smaller molecules and diffusion is faster.

Polymer matrix The more open the matrix, the lower the activation energy, and the faster the diffusion. The 'openness' of the matrix is affected by several factors. For polymers of the same type, the density gives a good indication. Thus diffusion is faster through low density polyethylene than high density polyethylene. The crystallinity of the polymer also has a large influence. The molecules in crystalline parts of a polymer are more highly ordered and

densely packed than the amorphous parts, and hence diffusion is much slower through crystalline than amorphous polymer. An important factor in extraction from polymers is therefore the glass transition temperature, T_g , at which the polymer moves from a glassy to an amorphous state. The diffusion is much faster at temperatures higher than T_g .

Temperature The temperature affects the diffusion directly, by the T term in the Arrhenius equation, and through effects on the polymer. From the Arrhenius equation, the temperature should be as high as possible to maximize D . However, at very high temperatures, the polymer will soften and melt. This will cause the particles to agglomerate, and hence slow down the extraction. High temperatures could also cause the extracting molecule to decompose or react. The extraction temperature should always be above T_g for the polymer, but below the softening point.

Solubility If the concentration of the material at the surface is higher than the solubility, the amount extracted will be limited to that which can dissolve in the solvent. This will in turn slow down the rate at which the material diffuses to the surface, as the concentration gradient will be smaller. In solubility limited extractions, the extraction rate can be increased by increasing the solvating power of the solvent. In SFE, this can be either by increasing the pressure or adding a modifier. Increasing the flow rate will dissolve more material in unit time, and, therefore, has a similar effect to increasing the solubility.

Models of Extraction

Mathematical models have been developed to describe the extraction process, using equations for diffusion and solubility. Two terms are defined, a diffusion term, D/a^2 , and a term proportional to solubility, ha , where a is the radius of the particles. The proportion of the total extracted (m/m_0 , where m is the amount remaining and m_0 the amount at time = 0) can then be defined in terms of these variables. Plotting $\ln(m/m_0)$ against time produces a characteristic shaped line, shown in **Figure 1(A)**. The amount remaining in the polymer falls rapidly at first, as the surface analyte is extracted. The plot then becomes linear, as the surface concentration falls and the extraction is controlled by the diffusion rate. The stages occurring during extraction can be illustrated by the concentration of analyte across a particle. **Figure 2(A)** shows a completely diffusion limited case, where ha is infinite. The concentration at the surface rapidly falls to zero, and the extraction is then

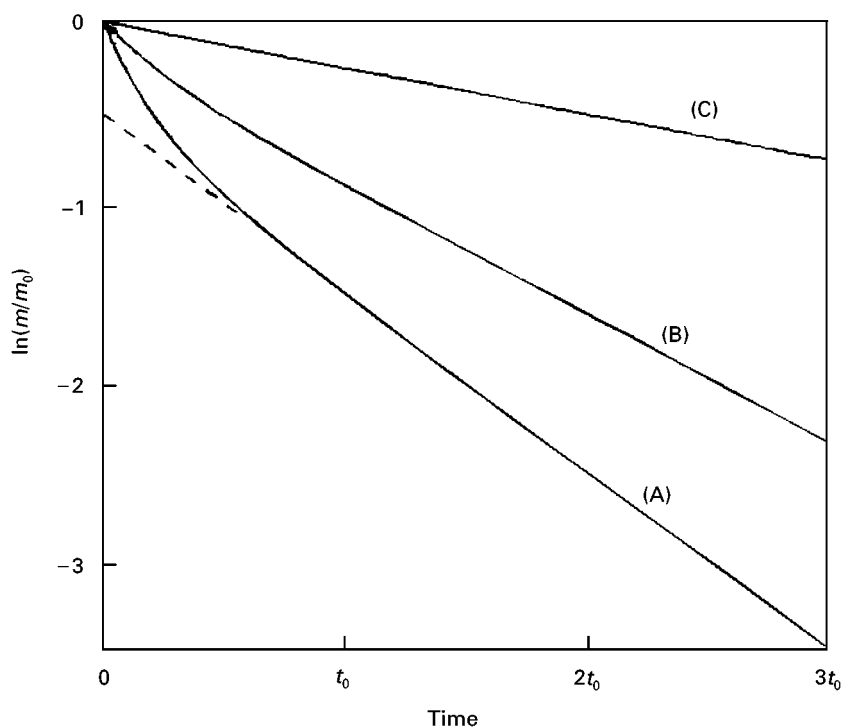


Figure 1 Plots of $\ln(m/m_0)$ for extractions with different solubilities. (A) = diffusion-limited extraction ('hot ball' model). (B) = intermediate solubility. (C) = solubility-limited extraction.

limited only by the rate at which analyte diffuses to the surface. This diffusion limited extreme is the 'hot ball' model, so called because it used modified equations describing the cooling of a hot sphere. The

opposite extreme is shown in **Figure 2(C)**, where, the diffusion is much faster than the ability of the solvent to remove analyte from the surface. The concentration gradient remains flat as the material is dissolved. The intermediate case shows the position where both solubility and diffusion play a significant part in the extraction. In each case, the initial step is the formation of the smooth concentration profile across the particle. This occurs during the sharply falling part of the $\ln(m/m_0)$ plot. After this, the profile retains the same shape, but reduces in size during the linear (exponential) part of the $\ln(m/m_0)$ plot.

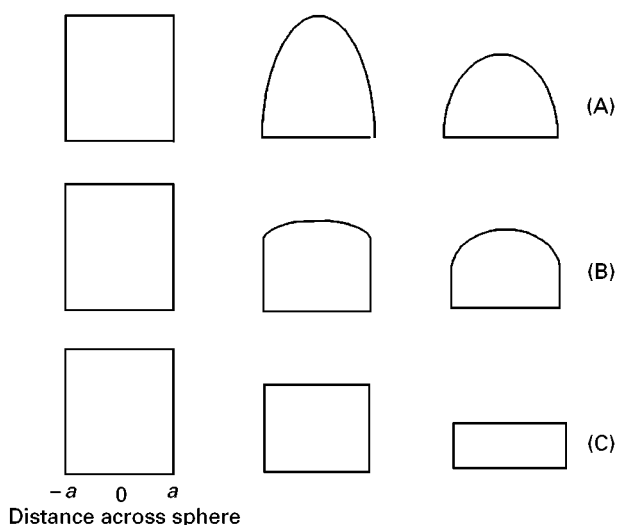


Figure 2 Concentration profiles during extraction for different values of solubility. (A) $ha = \infty$. Corresponds to Figure 1(A), the 'hot ball' model, extraction completely diffusion-limited. (B) ha intermediate. Corresponds to Figure 1(B), solubility and diffusion both contribute to extraction rate. (C) $ha = 1$. Corresponds to Figure 1(C). Solubility-limited extraction.

Diffusion- or Solubility-limited?

The strategies required to optimize an extraction often depend on the limiting factor, solubility or diffusion. Often, both will play a significant part in determining the extraction rate, but the dominance of one factor over the other can lead to short cuts in the optimization process. If diffusion is limiting (hot ball model), then greater swelling and higher temperatures will accelerate extraction. Increasing the flow rate or solubility will not help. In the case of solubility-limited extraction, greater swelling of the polymer will not help, and raising the temperature is likely to slow down SFE as the density of the solvent diminishes.

There are different methods for identifying the limiting factor in an extraction. A plot of $\ln(m/m_0)$ may show the classic 'hot ball' shape, indicating significant diffusion control (Figure 1(A)). If the line is straight, intersecting the origin, then this indicates solubility-limited behaviour (Figure 1(C)). A problem with these methods is that nonspherical particles, nonuniform initial distribution of analyte in the particle or a mixture of particle sizes can easily distort the shape of the curve. An alternative method is to measure extraction rates at different flow rates. If the extraction is diffusion-limited, then increasing the flow rate will have little effect. However, increasing the flow rate of a solubility-limited extraction will increase the extraction rate. Figure 2 shows concentration profiles during extraction for different values of solubility.

Effect of CO₂ on Polymers

CO₂ dissolves in polymers, swelling, softening and plasticizing them. Material will diffuse much faster through the swollen polymer, and diffusion rates can be increased by several orders of magnitude. The T_g and softening points are also lowered. The extent of this lowering depends on the pressure and the nature of the polymer. CO₂ is mainly soluble in the amorphous part of a polymer, so the greater the amorphous content, the larger the effect of the CO₂. Increasing the pressure also causes more CO₂ to enter the polymer. The result is a complex interaction, with CO₂ lowering T_g , which increases the amorphous content, allowing more CO₂ to enter. This means that the softening point is not easy to predict from the usual softening point. In most cases, higher pressure of CO₂ will increase extraction rates in SFE from polymers, as this will enhance both solubility and diffusion, by increased swelling of the polymer. For highly amorphous or rubbery polymers, a maximum can be reached in the extraction rate with increasing pressure. This is because the softening point is lowered by the extra CO₂ dissolving in the polymer as the pressure increases. If it is lowered below the extraction temperature, the particles will agglomerate and slow the extraction. In these cases careful optimization of pressure and temperature is required for maximum extraction rates. Addition of a solvent as a modifier to the CO₂ can also swell the polymer, as well as increase the solubility of the analytes. A solvent known to swell the polymer at room temperature will have the greatest swelling effect.

SFE from Polymers

As indicated above, the optimization of SFE from polymers is not straightforward. Generally, the

optimum conditions are likely to be at as high a temperature as possible, just below that at which the polymer melts, with as high a pressure of CO₂ as possible. The addition of a small amount (10%) of a cosolvent or modifier which is known to swell the solvent will accelerate extraction. There are many examples of polymer extractions with SFE, and extraction times are usually much shorter than conventional extraction times.

Pressurized Fluid Extraction

PFE is similar to SFE. The sample is held in a cell and the solvent is passed over it at elevated temperature and pressure. The commercial Accelerated Solvent Extraction (ASETM) is a trademark of Dionex Corp., and uses static extraction. Modified SFE equipment has also been used, and can use static or dynamic extraction. The solubility of polymer additives in liquid solvents at the high temperatures used in PFE is likely to be high enough that extractions are largely diffusion-limited. This is illustrated in Figure 3 for the extraction of Irganox 1010 from polypropylene. The curve has been fitted assuming ba is infinite, i.e. completely diffusion limited (hot ball model). The fit is reasonably good, indicating that the assumption is valid. Pressure has much less effect on liquids than supercritical fluids. Liquids are almost incompressible, and therefore the pressure applied only has the effect of keeping the solvent liquid above its atmospheric boiling point.

The most difficult part of method development for PFE of polymers is selecting the solvent. Solvents used for atmospheric pressure extractions have usually been selected to swell the polymer, hence speeding up the extraction. However, when these solvents are used at high temperatures, the polymer dissolves. As the solvent cools in the transfer lines of the equipment, the polymer drops out of solution, causing blockages. Partially dissolved or melted polymer also agglomerates, increasing particle size and slowing down extraction rates. Solvents conventionally used for polymer extractions therefore cannot be used for PFE. The interaction between the solvent and polymer can be considered as a continuum, from no interaction (no swelling) through increasing swelling until eventually dissolution occurs which can be thought of as infinite swelling. The degree of interaction generally increases with temperature for a given solvent, and therefore, a solvent will just dissolve a polymer at a particular temperature, called the 'theta temperature'. We can assume that the extent of swelling is similar for each solvent at just below the theta temperature. The criteria for the best PFE extractions from polymers are

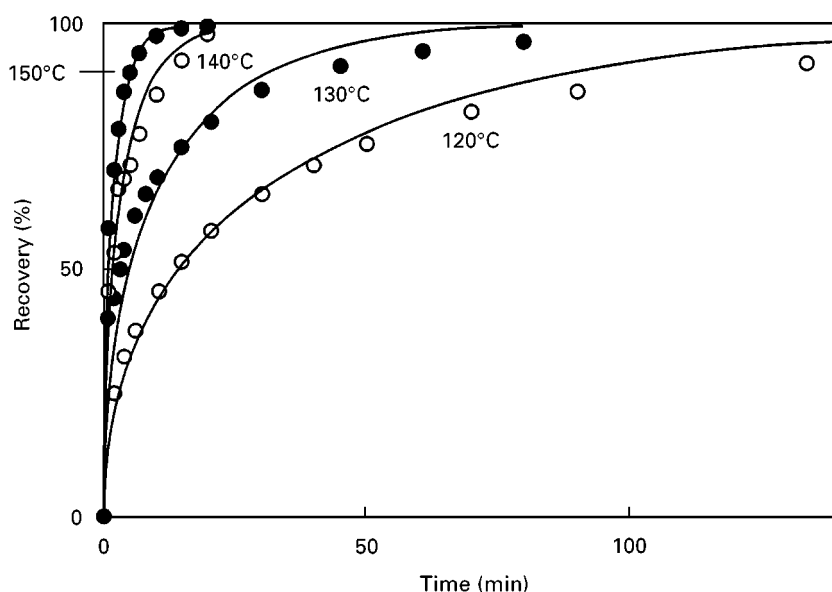


Figure 3 Extraction of Irganox 1010 from polypropylene by PFE. Symbols = experimental results, solid lines = fitted curve using the 'hot ball' model. (Reproduced with permission from Vandenburg, Clifford, Bartle *et al.* (1998) *Analytical Chemistry*, 70: 1943–1948).

as follows:

1. The temperature should be as high as possible to make D as large as possible. For a given 'openness' of the polymer structure, the higher the temperature, the faster the extraction. There will be an upper limit to the temperature, set either by the melting point of the polymer or the stability of the extracted analyte, which we can call T_{\max} .
2. The polymer structure should be as 'open' as possible. This effectively means that the polymer should be swelled as much as possible without dissolution or agglomeration of particles.

By combining the requirements of 1 and 2 above, what is required from the best extraction solvent is that the theta temperature is just above T_{\max} . The diffusion will then be maximized through both the highest temperature possible and the most open polymer structure. No other combination will give faster extraction.

Solvent Selection

Hildebrand Solubility Parameter

How can we select the best solvent? The use of solubility parameters is a good starting point. The Hildebrand solubility parameter is defined as the internal energy of vaporization divided by the molar volume. It is also called the cohesive energy density, and gives an indication of how strongly the material is held together. The principle of 'like dissolves like' applies, and solvents will dissolve polymers with a similar

solubility parameter. The theta temperature tends to be higher the greater the difference in solubility parameter between solvent and solute. There are several more sophisticated measures of solubility in polymers, which take into account polar and hydrogen bonding interactions, but are not as simple as the Hildebrand parameter, which sums up the solubility behaviour as a single number. Hildebrand parameters are also widely available for polymers and solvents. Examples of common solvents and polymers is given in Table 1. However, the simplicity of the parameter also means that exact numeric accuracy is sometimes lost, and specific numerical predictions are difficult to make from this parameter alone.

Table 1 Solubility parameters of selected solvents and polymers

Material	Solubility parameter ($\text{MPa}^{1/2}$)
Hexane	14.9
Cyclohexane	16.8
Ethyl acetate	18.6
Chloroform	19.0
Dichloromethane	19.8
Acetone	20.3
2-Propanol	23.8
Ethanol	26.0
Methanol	29.7
Polypropylene	16.6
PVC	19.5
PET	20.5
Nylon 66	28
PMMA	19.0

Use of Binary Mixtures

A suggested scheme for PFE solvent selection is to use the solubility parameter as a guide for initial solvent selection of a binary mixture. The exact proportions of the solvents can then be determined with a few simple experiments. The two solvents should be a 'good' solvent, which has a solubility parameter close to that of the polymer, and a 'poor' solvent, with a solubility parameter distant from the polymer. Initially, T_{\max} is determined by extracting with pure poor solvent for a set time at increasing temperatures. Initially, the amount extracted will increase with temperature as swelling and diffusion rate are increased. Eventually a maximum will be reached, representing either the melting of the polymer or the decomposition of the analyte. The maximum swelling at this temperature is then determined by a series of extractions with increasing amounts of the good solvent, again until a maximum is reached when the polymer begins to dissolve and agglomerate. If required, the proportions and temperature can be fine tuned to further maximize extraction rates. Often the initial values will be sufficient, and further marginal improvements not worth the extra effort. Once these conditions are identified, the time for the extraction can be determined by a series of extractions on the same sample until no further analyte is detected.

Examples of the best solvent mixtures suggested to date for some polymers are indicated in Table 2.

An advantage of this system of selection is that the solvents can be selected from any with a close and distant solubility parameter. The criteria may be cost, environmental considerations or simply those easily available. Equally good extractions could be obtained from a variety of different solvent mixtures. The extraction time for ground polymers is likely to be minutes rather than hours. Using the conditions in Table 2, the extraction times for polypropylene, nylon and PVC were all under 20 min. This is much faster than extractions using conventional extraction techniques.

Microwave Assisted Extraction

MAE can be either 'open focused', where the vessel is at atmospheric pressure, or 'closed vessel', where the solvent is kept liquid above the usual boiling point in a sealed, pressure resistant vessel. The effects of microwaves on extraction can be either purely thermal or through some other interaction of the microwaves with the matrix or analyte. For extraction from polymers, nonthermal effects have not yet been satisfactorily demonstrated, and the benefits for extraction may be primarily thermal. There are two components to the enhanced extraction rates for MAE:

1. Microwaves heat the solvent directly, resulting in much faster heating than conventional oven heating.
2. The closed pressure vessels allow heating above the atmospheric pressure boiling point of the solvent.

In MAE the extraction is always static. The solvent and polymer are placed in a vessel and heated by microwaves. The analyte dissolves in the solvent. Typical vessel sizes are 100 mL (e.g. MES 1000 by CEM Corp., USA).

In order to be heated by microwaves, the solvent must have a significant dielectric constant (relative permittivity). Some examples for common solvents and their dielectric constant are given in Table 3.

Optimization of extraction conditions with MAE is similar to that in PFE. Solvents and temperatures which are effective for PFE are also likely to be good for MAE, and extraction conditions can be worked out in a similar way. An extra requirement is that a major component of the solvent must have a significant dielectric constant, which does restrict the choice of solvents.

An alternative possible with MAE is the dissolution/precipitation approach. MAE does not have the problems of blocked transfer lines associated with PFE, and therefore it is not a problem if the polymer dissolves. The issue is whether the dissolution occurs faster than the extraction without dissolution. If the particles of polymer can be prevented from softening

Table 2 Suggested extraction conditions for PFE from some polymers

<i>Polymer</i>	<i>Poor solvent (%)</i>	<i>Strong solvent (%)</i>	<i>Extraction temperature (°C)</i>
Polypropylene	Propan-2-ol (97.5)	Cyclohexane (2.5)	140
PVC (plasticized with di-octylphthalate)	Hexane (60)	Ethyl acetate (40)	170
PET	Ethyl acetate (100)		190
Nylon 66	Hexane (60)	Ethanol (40)	170
PMMA	Hexane (70)	Ethyl acetate (30)	150

Table 3 Dielectric constant of solvents at 25°C

Solvent	Dielectric constant
Water	78
Nitrobenzene	35
Methanol	33
Ethanol	24
Ammonia	17
Hydrogen sulfide	9 (at – 85°C)
Benzene	2
Carbon tetrachloride	2
Cyclohexane	2

and agglomerating before dissolving, then it is likely that the dissolution will be fast. This is an area which requires further investigation.

MAE extractions of polymers have not been reported as much as SFE and PFE extractions, but those that have indicate very rapid extractions. In some cases, the most time-consuming part is the cooling of the vessels before opening. The advantages over PFE are more rapid heating and no possibility of blocking the transfer lines. The disadvantages are a more limited choice of solvents and longer cooling down times. SFE, PFE and MAE offer distinct advantages over conventional extraction methods, but at higher initial cost. The particular method chosen will depend on the exact requirements for extractions in the individual laboratory.

See also: II/Extraction: Microwave-Assisted Extraction; Supercritical Fluid Extraction. III/Microwave-Assisted

Extraction: Environmental Applications. Pressurised Fluid Extraction: Non-Environmental Applications.

Further Reading

- Barton AFM (1983) *Handbook of Solubility Parameters and Other Cohesion Parameters*. Boca Raton: CRC Press.
- Barton AFM (1990) *Handbook of Polymer-Liquid Interaction Parameters and Solubility Parameters*. Boca Raton: CRC Press.
- Clifford AA (1999) *Fundamentals of Supercritical Fluids*. Oxford: OUP.
- Dean JR (1993) *Applications of Supercritical Fluids in Industrial Analysis*. Boca Raton: Chapman and Hall.
- McHugh MA and Krukonis VJ (1994) *Supercritical Fluid Extraction, Principles and Practice*, 2nd edn. Stoneham: Butterworth Heinmann.
- Taylor LT (1996) *Supercritical Fluid Extraction*. New York: John Wiley and Sons.
- Vandenburg HJ and Clifford AA (1999) Polymers and polymer additives. In: Handley AJ (ed.) *Extraction Methods in Organic Analysis*. Sheffield: Sheffield Academic Press.
- Vandenburg HJ, Clifford AA, Bartle KD *et al.* (1997) Analytical extraction of additives from polymers. *Analyst* 122: R101–R115.
- Wenclawiak B (1992) *Analysis with Supercritical Fluids: Extraction and Chromatography*. Berlin: Springer-Verlag.
- Westwood SA (1993) *Supercritical Fluid Extraction and its use in Chromatographic Sample Preparation*. Boca Raton: Chapman and Hall.

POLYSACCHARIDES



Centrifugation

S. E. Harding, University of Nottingham, Leicestershire, UK

Copyright © 2000 Academic Press

Polysaccharides are, as their name implies, polymers of saccharide residues. The general formula of saccharide or carbohydrate residues is often quoted as $(\text{CH}_2\text{O})_n$, although this is an oversimplification which needs to be modified in many cases to take into account, e.g. amino, sulfate and phosphate groups. Most saccharide residues are five or six membered

ring structures with one member of the ring being oxygen.

Polysaccharides are becoming increasingly important in biomedical, pharmaceutical food and health products. The role of preparative centrifugation in polysaccharide development has not been significant compared to other classes of compounds such as nucleic acid and proteins. In part, this may be due to the considerable heterogeneity of polysaccharides, and techniques such as chromatography and precipitation-based methods have been more commonly applied. However, *analytical* centrifugation techniques are becoming increasingly used as a means of characterizing the size and shape of polysaccharides in solution as well as for investigating their interaction with each other and with other biopolymers such as pro-

teins. Analytical centrifugation is also being used as an alternative to rheological methods for investigating the structure of polysaccharide gels. Analytical centrifugation is well suited for the analysis of polydisperse materials and (apart from density gradient methods) does not involve another separation medium.

The aim of this article is threefold:

1. to survey briefly the types of information that can be obtained about polysaccharide systems by analytical centrifugation;
2. to describe those aspects of the equipment that are of particular relevance for obtaining this information;
3. to describe the types of experiments used to obtain this information.

The centrifugation methods applied to macromolecules are termed *ultracentrifugation*, because of the high rotor speeds (up to 60 000 rpm) required to produce sedimentation or a measurable concentration redistribution. At these high speeds the rotor needs to be in a vacuum chamber to avoid friction-heating effects. An analytical ultracentrifuge is an ultracentrifuge equipped with a special optical system for monitoring the sedimentation process.

Despite the fact that Svedberg, who won the Nobel Prize in 1926 for inventing the analytical ultracentrifuge, and his PhD student Gralen both conducted extensive work on the ultracentrifugation of polysaccharides, it is only relatively recently that the technique has been more widely utilized for the study of these substances.

Measurable Parameters

Molecular Weights and Heterogeneity

One of the most fundamental pieces of information describing a macromolecule is its molecular weight, M . M values for polypeptides can usually be evaluated without difficulty from chemical sequence information. For polysaccharides this is not the case, primarily because of their heterogeneity due to polydispersity and also, in some cases, self-association phenomena. An average molecular weight, usually the weight average, M_w , is normally specified. M_w is usually available to better than $\pm 10\%$ from sedimentation equilibrium in the ultracentrifuge, and M_z to somewhat less precision depending on the optical detection system employed. In some circumstances M_n can also be measured, although osmotic pressure is a more appropriate technique. The ratios of the z average molecular weight, M_z to M_w or M_w to the number-average, M_n are used as indices for poly-

dispersity, popular with commercial manufacturers of polysaccharides as a measure of the narrowness of a molecular weight distribution.

Direct molecular weight distributions are more difficult to obtain with centrifugation procedures and depend on assumed models (Gaussian, log-normal etc.): nowadays size exclusion chromatography systems coupled online to multi-angle light-scattering systems, or SEC-MALLS are much more common, but the ultracentrifuge still provides a valuable check on the M_w or M_z .

A good indication of chemical heterogeneity (e.g. purity) of a saccharide system can be provided by analytical isopycnic density gradient ultracentrifugation.

Molecular Shape or Gross Conformation

In general two levels of information are sought:

1. Delineation between the conformation type or zone of a polysaccharide, as represented by the Zonal diagram of **Figure 1**: extra rigid rod, rigid rod, semi-flexible coil, random coil and globular/highly branched.
2. Having established the conformation type, more quantitative information can be sought. For example, for approximately rigid structures this can be given in terms of the triaxial dimensions or shape of the molecule: for more flexible chain-like structures the chain diameter, d , contour length L and the flexibility can be described in terms of the persistence length, L_p (**Figure 2**).

Water Binding or Hydration

The sedimentation coefficient from sedimentation velocity experiments in the ultracentrifuge depends not only on molecular conformation but also the extent of solvent binding (chemical interactions via, for example, hydrogen bonds or just physical entrainment). Water binding is an important functional property of polysaccharides (for example, in foods, or as hydrogel drug delivery forms). Unfortunately, the conformation has to be known or assumed to obtain the extent of swelling through water binding: conversely, assumptions of water binding extent are often required to obtain quantitative conformation information.

Analytical Ultracentrifuges and Polysaccharides

Analytical ultracentrifuges have already been described by Lewis elsewhere in this encyclopedia. The traditional ultracentrifuges, such as the classical Model E analytical ultracentrifuge from Beckman

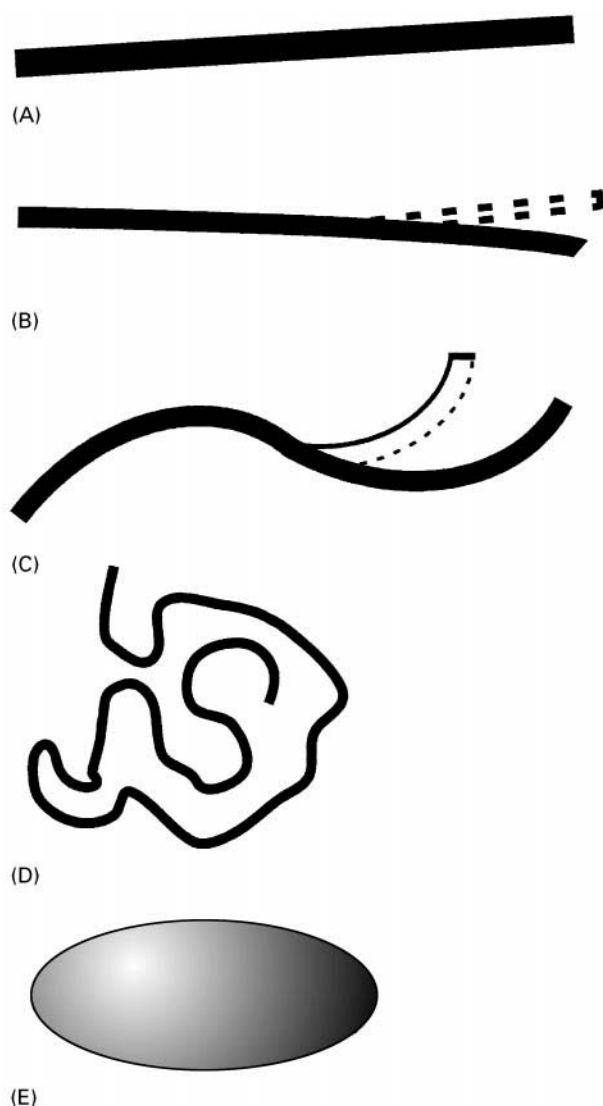


Figure 1 Conformation zoning of polysaccharides: (A) extra rigid rod; (B) rigid rod; (C) semi-flexible coil; (D) random coil; (E) globular or highly branched. (Reproduced from Pavlov GM, Rowe AJ and Harding SE (1997) Conformation zoning of large molecules using the analytical ultracentrifuge. *Trends in Analytical Chemistry* 16: 401, with permission from Elsevier Science.)

Instruments (Palo Alto, USA), have now largely been replaced by the new generation Optima XL-A and XL-I, also from Beckman. Both have full online computer data capture and analysis facilities.

Optima XL-A Ultracentrifuge

This model appeared in *c.* 1990 and is equipped with a UV/visible absorption optical detection system. Unfortunately, polysaccharides are generally transparent in the visible and also, unlike proteins and nucleic acids, in the near UV (wavelength $\lambda > 240$ nm). In the far UV (200–220 nm), they absorb and can therefore

in principle be detected. Unfortunately other materials such as buffer salts also absorb strongly in this region and hence for many applications an absorbing chromophore must be attached to the polysaccharide. Some success has been achieved with this latter approach, although possible alterations to the structure and molecular weight (e.g. a state of self-association) caused by the incorporation of the chromophore can result in measurement errors. Other polysaccharides, such as xylans and pectins, have some inherent absorbance at ~ 240 – 260 nm and this can be taken advantage of.

Optima XL-I Ultracentrifuge

This model appeared in *c.* 1996 and, in addition to the UV/visible absorption optics of the XL-A, has a refractometric optical system known as Rayleigh interference optics. This optical system can be applied to proteins, nucleic acids and polysaccharides. One drawback for sedimentation equilibrium (molecular weight) work is that, because of the upper limit of ~ 12 mm of the optical path length of the centrifuge cell, the lower limit for the concentration of the polysaccharide solution loaded into the cell is ~ 0.8 mg mL⁻¹. This is a major limitation for polysaccharides since low concentrations are necessary to minimize the effects of the large thermodynamic nonideality of these substances, compared to proteins.

Model E Ultracentrifuge

These have not been commercially available for 20 years but there are a number still in active use, although only a few are being applied to the study of polysaccharides. Besides Rayleigh interference, they also have another type of optical system, not current-

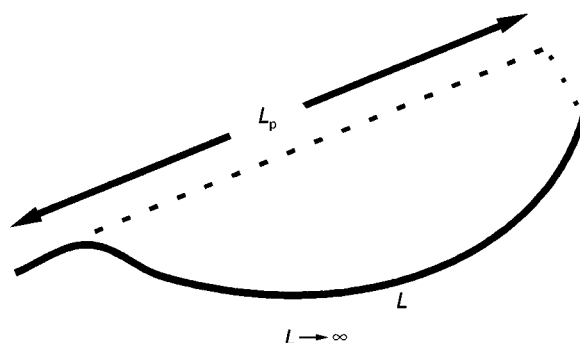


Figure 2 More detailed conformation representations of polysaccharides in solution: length and flexibility parameters for a linear polysaccharide: L , Contour length; L_p , persistence length, defined as the projection length along the initial direction of chain of length L and in the limit of $L \rightarrow$ infinity. (Reproduced with permission from Tombs and Harding 1998.)

ly available on the Optima machines, the Schlieren or refractive index gradient system, permitting high concentrations and facilitating gel work. For molecular weight analysis, Rayleigh optics give primarily M_w , whereas Schlieren optics yield M_z . Thus the model E is ideal for obtaining polydispersity indices (M_z/M_w , see above). However, because of the lack of availability of this instrument, people requiring this type of measurement need to consult the handful of laboratories still running these instruments.

Types of Ultracentrifuge Experiment for Polysaccharide Analysis

The principal types of measurement using the analytical ultracentrifuge on solutions of polysaccharide are:

- Sedimentation equilibrium: for obtaining the weight average molecular weight, M_w , and the z average molecular weight, M_z . Molecular weights are conventionally expressed in daltons or in molar mass units (g mol^{-1}). The thermodynamic second virial coefficient, B ($\text{mL mol}^{-1} \text{g}^{-2}$) can also be measured.
- Sedimentation velocity: for obtaining the sedimentation coefficient, s (measured in seconds (s) or svedbergs (S), where $1 \text{ S} = 10^{-13} \text{ s}$) and the concentration dependence or Gralen parameter k_s (mL g^{-1}) of the sedimentation coefficient. Both s and k_s can be used to obtain conformation, water binding and molecular weight information.
- Boundary spreading experiments: for obtaining the translational diffusion coefficient, D ($\text{cm}^2 \text{s}^{-1}$) and its concentration dependence parameter, k_D (mL g^{-1}). The polydispersity of polysaccharides is however a major complicating factor.
- Analytical isopycnic density gradient ultracentrifugation: primarily used for assaying the purity of a polysaccharide preparation on the basis of density.

In addition, sedimentation velocity and equilibrium can be used to probe the structure of gels, primarily through measurement of the swelling pressure of the gel, and also the mobility/diffusion of molecules through gels or incompatible mixed-phase systems.

Sedimentation Equilibrium of Polysaccharide Solutions

In this method the ultracentrifuge is spun at a speed sufficiently low (for example, $\sim 10\,000$ rpm for a pectin polysaccharide of $M_w \sim 200$ kDa) that the centrifugal force is comparable to the back-force due to diffusion. The distribution of the polysaccharide in the centrifuge cell is recorded using Rayleigh optics

and equilibrium is typically established between 24 and 48 h. Attainment of equilibrium is assessed by comparing optical records taken at 4–8 h intervals. The time required to attain equilibrium depends on the polysaccharide and the length of solution column in the centrifuge cell: a 3 mm column requires ~ 0.1 mL for a 12 mm optical path length cell (XL-I or Model E) or ~ 0.25 mL for a 30 mm cell (Model E only). Shorter columns take less time but yield less precise information. The length of time of an experiment can be compensated for by running samples in multiples using multi-hole centrifuge rotors and/or multi-channel centrifuge cells.

Molecular Weight Determination

The simplest interpretation of the optical records from a sedimentation equilibrium experiment is obtained from the average slope of a plot of the log of the concentration, $C(r)$ in the cell versus the square of the radial displacement, r , from the rotor centre: such a slope yields the apparent weight-average molecular weight, $M_{w,app}$. In evaluating the average slope, care must be taken to include as much of the distribution in the centrifuge cell as possible (from meniscus to cell base). Fortunately, software (MSTAR) is available to assist with this task. Rayleigh optics only record concentration of solute relative to the meniscus, thus requiring the concentration at the meniscus to be determined in order to convert relative concentrations to $C(r)$. After these factors have been taken into account, extrapolation of $1/M_{w,app}$ to $C = 0$ (where C is the cell loading concentration) yields the reciprocal of the weight average M_w from the intercept and, also the second thermodynamic virial coefficient, B , or as an alternative notation A_2 from the limiting slope. (This term also appears in osmotic pressure or static light-scattering measurements.) Correct to first order in concentration, this extrapolation is described by:

$$1/M_{w,app} = (1/M_w) \cdot (1 + 2BM_w C) \quad [1]$$

Herein lies a difference between proteins and polysaccharides. The nonideality term $2BM_w C$, which can often be neglected at low concentration for proteins, is usually significant even at low concentration for polysaccharides because of their much greater nonideality: indeed, the term $1 + 2BM_w C$ represents the factor by which measurement of $M_{w,app}$ at a finite concentration C underestimates the true molecular weight (Table 1). This nonideality derives from the large exclusion volumes of these substances and from the fact that many are polyelectrolytes (highly negatively charged, such as pectins, alginates, xanthan, carrageenan, or highly positively charged, such as chitosans). However, although these polyelectrolyte

Table 1 Comparative molecular weights and nonidealities of polysaccharides from sedimentation equilibrium measurements

	$10^{-6} \times M_w$ ($g\ mol^{-1}$)	$10^4 \times B$ ($mL\ mol^{-1}\ g^{-2}$)	BM_w ($mL\ g^{-1}$)	$1 + 2BM_wC^a$
Pullulan P5	0.0053	10.3	5.5	1.002
Pullulan P50	0.047	5.5	25.9	1.010
Xanthan (fraction)	0.36	2.4	86	1.035
β -glucan	0.17	6.1	104	1.042
Dextran T500	0.42	3.4	143	1.057
Pullulan P800	0.76	2.3	175	1.070
Chitosan (Protan 203)	0.44	5.1	224	1.090
Pullulan P1200	1.24	2.2	273	1.109
Pectin (citrus, fraction)	0.045	50.0	450	1.180
Scleroglucan	5.7	0.50	570	1.228
Alginate	0.35	29.0	1015	1.406

^aBased on the lowest possible loading concentration ($\sim 0.2\ mg\ mL^{-1}$ in a cell with a 30 mm path length centrepiece).

effects can be largely suppressed by the inclusion of a low molecular weight electrolyte to increase the ionic strength of the solution, eqn [1] is usually only valid for dilute solutions of polysaccharides and at higher concentrations, extra terms (in C^2 or C^3) are necessary. In such cases direct nonlinear, extrapolation of $M_{w,app}$ to $C = 0$ usually gives a better estimate of M_w than the reciprocal ($1/M_{w,app}$) extrapolation procedures. The other big difference between proteins and polysaccharides is that the latter are usually very polydisperse.

It is also possible from a single experiment to obtain local or point average $M_{w,app}(r)$ at radial positions r , as a function of $C(r)$. Extrapolation of $M_{w,app}(r)$ to $C(r) = 0$ provides a further estimate for M_w , although because of redistribution of solute in the centrifuge cell this can yield and underestimate for M_w . From further manipulations, including concentration extrapolations to the radial positions of the solution meniscus and bottom of the centrifuge cell, the (apparent) z average molecular weight $M_{z,app}$ can be obtained. Similar corrections to $C = 0$ are required to obtain M_z (although the factor in eqn [1] is 4, not 2). A more precise estimate for $M_{z,app}$ can be obtained if Schlieren optics are used instead of Rayleigh optics: this is because Schlieren optics record the concentration gradient, $dC(r)/dr$ (as opposed to $C(r)$) versus radial displacement, r .

In cases where there may be reversible self-association phenomena, the B term in eqn [1] must be modified to incorporate an association term.

Sedimentation Velocity of Polysaccharide Solutions

At higher speeds than used for sedimentation equilibrium, sedimentation forces become well in excess

of diffusion forces and a macromolecular species will sediment. The sedimentation coefficient, s , of a macromolecular component is its sedimentation rate per unit centrifugal field. It will be a function of the size, shape and degree of water association or hydration of the biopolymer. Like the apparent molecular weight, $M_{w,app}$, it will be affected by the nonideality of the system, and will need correcting for these effects by measuring at a series of concentrations and extrapolating to zero concentration to yield the ideal or infinite dilution value s^0 . For polysaccharides this is best accomplished with a reciprocal plot:

$$1/s_{20,w} = (1/s_{20,w}^0) \cdot (1 + k_s C) \quad [2]$$

where C is the sedimenting concentration and k_s is the concentration dependence or Gralen parameter. The subscripts 20,w mean that, by convention, sedimentation coefficients measured at a given temperature are corrected using simple formulae to standard conditions of solvent viscosity and density: that of water at 20°C.

As with eqn [1] for M_w , eqn [2] for $s_{20,w}^0$ is generally only applicable for dilute solutions of polysaccharides: for higher concentrations, and even for dilute solutions of certain extremely nonideal polysaccharides like alginate and xanthan, higher order terms in C are needed to describe adequately the concentration dependence. As with M_w , where such higher terms are necessary, direct extrapolation of $s_{20,w}$ to $C = 0$ rather than $1/s_{20,w}$ is generally a more reliable procedure for estimating $s_{20,w}^0$. Both $s_{20,w}^0$ and k_s can be used for conformation and hydration analysis, and also as a less direct alternative to sedimentation equilibrium for molecular weight estimation.

Besides the use of higher rotor speeds (for example, $\sim 50\ 000\ rpm$ for a pectin polysaccharide of $s_{20,w}^0 \sim 2\ S$), longer solution column lengths are gener-

ally used (~ 1 cm corresponding to ~ 0.4 mL of solution in a 12 mm path length Optima XL-I centrifuge cell), compared with sedimentation equilibrium experiments.

General Conformation Analysis of Polysaccharides

The Wales-van Holde ratio A useful guide to the gross conformation is the Wales-van Holde ratio. The Wales-van Holde ratio is defined as the ratio of the Gralen parameter k_s to the intrinsic viscosity $[\eta]$. The intrinsic viscosity can be measured relatively simply by viscometric or rheological methods, and both parameters are expressed in units of mL g^{-1} . It is known that this ratio has values of about 1.6 for random coils and spherical conformations and reduces to a limiting value of approximately 0.2 for rigid rod-shaped molecules. A proviso for the use of k_s in this way is that, for highly charged macromolecules, charge effects must be suppressed by using (aqueous) solvents of sufficient ionic strength (Table 2).

The Mark-Houwink-Kuhn-Sakurada Representation The Wales-van Holde ratio can be used to distinguish rods from either spheroidal or random coil conformations but cannot be used to distinguish between the latter two. However, advantage can be taken of the polydispersity of polysaccharides in that if the sedimentation coefficient and molecular weights are measured for a series of fractions (separated by column chromatographic procedures) of a polysaccharide preparation, then the exponent in the relation between $s_{20,w}^0$ and M weight or volume-average can be used to distinguish random coils from rods and spheroidal conformation types:

$$s_{20,w}^0 = K'' M^b \quad [3]$$

Table 2 Values of the Wales-van Holde ratio $k_s/[\eta]$ and the Mark-Houwink-Kuhn-Sakurada b coefficient for some polysaccharides

	$k_s/[\eta]$	b	Conformation
Dextran fractions		0.44	Random coil
DIT-dextran		0.56	Semi-flexible coil
Pullulans	1.4	0.45	Random coil
Yeast mannan	1.3	0.43	Random coil
β -glucans	0.4		Extended
Alginates	0.6		Extended
Pectins (low methoxy)	0.2	0.17	Rigid rod
Xanthan (keltrol)	0.28		Rigid rod
Amylopectin*	1.45		Spheroidal/heavily branched

DIT, di-iodotyrosine dextran. All in aqueous solvent except* (90% dimethyl sulfoxide).

Eqn [3] is known as a Mark-Houwink-Kuhn-Sakurada (MHKS) or just Mark-Houwink relation. Other MHKS relations exist between intrinsic viscosity and M (exponent a or α), radius of gyration and M (exponent c or ν) and the diffusion coefficient and M (exponent $-e$). The exponent b (sometimes given as $1-b$), measured from double logarithmic plots of $s_{20,w}^0$ versus M , has characteristic values depending on the conformation type: these are 0.67, 0.4–0.5 and 0.15 for spheres, random coils and rigid/extra rigid rods respectively (Table 2).

If K'' and b have been measured for a series of polysaccharide fractions, the molecular weights of subsequent preparations of that polysaccharide can then be estimated from measurement of $s_{20,w}^0$.

Conformation zoning from combination of $s_{20,w}^0$, k_s and the mass per unit length An even better guide to the overall conformation type or zone (Figure 1) can be obtained by combining $s_{20,w}^0$, k_s and the mass per unit length, M_L . The latter parameter must be measured using a separate technique, but a number of M_L values for polysaccharides have been published on the basis of electron microscopy or X-ray diffraction studies. The concept of zoning in this manner was conceived in terms of empirical data of polysaccharides of known conformation (Figure 3A), supported by the theoretically known limits for spheres and extra-rigid rods, to produce the characteristic diagnostic plot of Figure 3B.

For a polysaccharide whose conformation type or zone is unknown, from measurement of $s_{20,w}^0$ and k_s from a sedimentation velocity experiment and knowledge of, or an assumption concerning, M_L , the conformation zone can be read directly from Figure 3B.

More Detailed Conformation Analysis of Polysaccharides

Once the conformation type or zone has been established, more detailed information about conformation can be sought. It is worth stressing that, because of the inherent polydispersity of polysaccharides, much of the information obtained can only represent average properties: claims of parameter measurements to a high precision should be treated with some caution.

$s_{20,w}^0$ - M relations: worm-like coil modelling The simple MHKS dependence of $s_{20,w}^0$ on M described above has been extended for linear polymers (zone A–D molecules of Figure 1), including DNA and polysaccharides to include terms containing the mass per unit length M_L (or molecular weight M and the

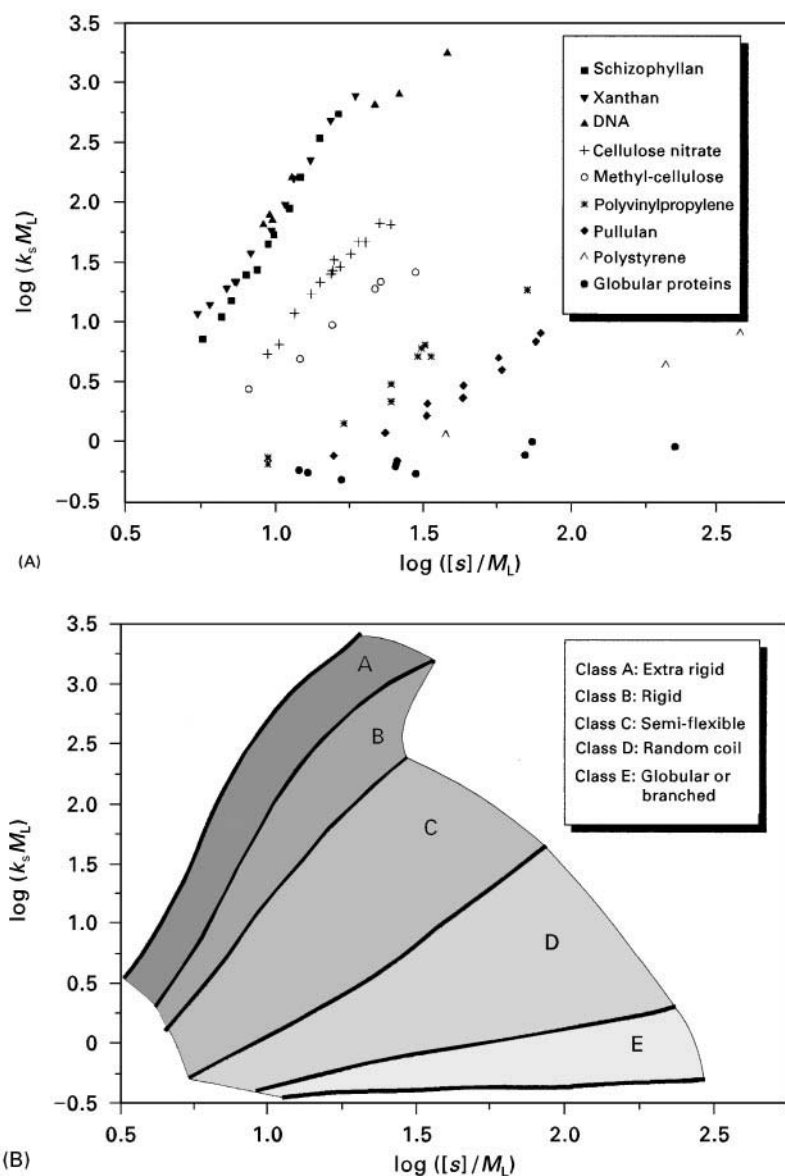


Figure 3 Sedimentation conformation zoning of polysaccharides. (A) Dependence of $\log(k_s M_L)$ versus $\log [s]/M_L$ for 82 macromolecules of known conformation type. (B) Corresponding diagnostic plot: for a measured $[s]$, k_s and M_L , the conformation of a given polysaccharide can be zoned. $[s] = s_{20,w}^0 \eta_0 / (1 - \bar{v} \rho_0)$ where η_0 and ρ_0 are the viscosity of water at 20°C and \bar{v} the partial specific volume. $[s]$ can also be defined for other solvents, although k_s must then correspond to that solvent. (Reproduced from Pavlov GM, Rowe AJ and Harding SE (1997) Conformation zoning of large molecules using the analytical ultracentrifuge. *Trends in Analytical Chemistry* 16: 401, with permission from Elsevier Science.)

contour length, L), the chain diameter, d , and the persistence length, L_p . As with MHKS, worm-like coil modelling has not only been worked out for the sedimentation coefficient, but also for other hydrodynamic parameters.

The Wales–van Holde ratio, $k_s/[\eta]$, for rigid structures It has already been noted how this ratio can help to distinguish rod-shape polysaccharides from the more randomly coiled and spheroidal materials.

For approximately rigid structures, more precise information about the molecular conformation, in terms of average ellipsoidal axial ratios, can be obtained without the complication of having to take into account molecular hydration, since this is essentially eliminated in the ratio. Detailed relations are available between $k_s/[\eta]$ (referred to for simplicity by the parameter R) and the axial ratio for ellipsoids of revolution, or the two axial ratios for general triaxial ellipsoids. We stress the phrase approximately rigid

structures. For polysaccharides this procedure would not be applicable to flexible coils, but may be applicable to rod-shaped or highly branched structures (zones A, B or E molecules of Figure 1): k_s has however been mainly applied in this way to protein systems, and not polysaccharides.

$s_{20,w}^0$ and the frictional ratio In addition to $k_s/[\eta]$, the sedimentation coefficient $s_{20,w}^0$ can also be used directly to extract the axial ratios of a quasi-rigid structure. Knowledge of $s_{20,w}^0$, together with the molecular weight and other parameters (density ρ_0 and viscosity η_0 of water at 20.0°C) yields the particle frictional parameter known as the translational frictional ratio f/f_0 . This in turn can be related to a shape parameter known as the Perrin function, P , and swelling ratio, S_w , defined as the ratio of the volume of a macromolecule swollen through hydration to that of the anhydrous macromolecule:

$$f/f_0 = P \cdot S_w^{1/3} \quad [4]$$

Thus, if S_w is known or assumed, the shape parameter P can be found and from this the axial ratios from rigorous hydrodynamic relations. Besides complications through molecular flexibility, the stumbling block is S_w . Whereas for proteins, S_w will be moderate (~ 1 – 2) and predictable to a certain degree, for polysaccharides this will not be so. In fact, eqn [4] is more useful from a polysaccharide context for predicting S_w , since, despite the presence of the cube root term, f/f_0 is still essentially a more sensitive function of swelling than shape.

Measurement of Water Binding or Swelling Ratios S_w

It has been shown how measurement of the frictional ratio (via $s_{20,w}^0$) can be used to estimate S_w , the swelling ratio. For a rigid structure, if the shape is established from measurement of $k_s/[\eta]$, then P can be defined and hence S_w found from eqn [4].

For more general structures, another route that has been suggested, applicable to both rigid and flexible structures, is to use the ratio of the concentration dependence term for viscosity (k_η) to k_s :

$$S_w \sim k_\eta/k_s \quad [5]$$

k_η (mL g⁻¹) comes from the analogous relation of eqn [2] for viscosity:

$$\eta_{\text{red}} = [\eta](1 + k_\eta \cdot C)$$

where η_{red} (mL g⁻¹) is the reduced viscosity at concentration C .

Diffusion Measurements

One of the classical ways of measuring translational diffusion coefficients, D , is to use the optical system on the ultracentrifuge to follow the time-dependent spreading of a layered boundary between a macromolecular solution and its solvent: if a rotor speed is employed, large enough to stabilize the system but low enough so as to minimize appreciable sedimentation, measurement of boundary height and width changes with time can be used to measure D . The diffusion coefficient itself can be corrected to standard conditions of temperature and solvent viscosity (water at 20.0°C) to give $D_{20,w}$, and extrapolated to zero concentration to give $D_{20,w}^0$ and the concentration dependence parameter k_d (mL g⁻¹). $D_{20,w}^0$ combined with $s_{20,w}^0$ in the Svedberg equation can be used to estimate the molecular weight. Alternatively $D_{20,w}^0$ provides a different route to $s_{20,w}^0$ for obtaining the frictional ratio f/f_0 .

Although measurement of $D_{20,w}^0$ in this way is highly reliable for many protein systems, there are problems with polysaccharides, again deriving from polydispersity: indeed, this application of the ultracentrifuge has now largely been superseded by dynamic light-scattering methodology.

Analytical Density Gradient Centrifugation

Density Gradient Sedimentation Equilibrium

By dispersing the polysaccharides in a dense salt solution, a density gradient can be created in an ultracentrifuge cell. For a mixed macromolecular solute a particular macromolecular species will move or band at that region in the density gradient which corresponds to its own density: this procedure is known as density gradient or isopycnic (isodensity) sedimentation equilibrium. Normally, caesium salts are used to provide this gradient for polysaccharides. Since most polysaccharides have similar densities (or partial specific volumes), this is not very good for separating mixed polysaccharide systems, but is, however, useful for separating polysaccharides from glycoproteins or proteins. It has, for example, been recently used to assay the purity of xylans from other molecular contaminants. The method assumes no significant interaction between the caesium salts and the polysaccharide.

Density Gradient Sedimentation Velocity

A less dense solute may be used (e.g. sucrose) to retard the sedimentation rate in sedimentation velocity (enhancing resolution) as opposed to inducing banding in sedimentation equilibrium. The method

assumes no interaction between the solute and the macromolecule. However, since the sedimentation coefficients are usually very small (often between 1 and 2 S) – because of their large frictional ratios – and because of potential interactions with the separating medium, this method has not found major use for polysaccharide analysis or separation.

Polysaccharide Gels: Swelling Pressure

Sedimentation Equilibrium

If a gel is subjected to a centrifugal field, low enough to avoid sedimentation of the gel itself (typically < 10 000 rpm), a concentration gradient will be established as in a conventional sedimentation equilibrium experiment on a solution. The gradient indicates the locally dependent de-swelling of the gel, which is caused by the swelling pressure generated by the centrifugal field. The concentration gradient will depend on the structure of the gel (number and strength of the cross-links) and whether the gel is reversible or not.

Sedimentation Velocity

At sufficiently high rotor speed (> 10 000 rpm), the polymer concentration may drop to a sufficiently low level near the meniscus that a sol phase will appear: a conventional sedimentation velocity experiment can be performed, monitoring the movement of the boundary between gel and sol.

Data from sedimentation equilibrium and sedimentation velocity can be used to obtain the thermodynamic, elastic and structural parameters of the gel, complementing data from classical rheological approaches. Although gelatin has been the main focus of attention with this technique, several polysacchar-

ide gels have been successfully characterized, such as carrageenan, pectin and alginate.

See also: II/Particle Size Separation: Theory and Instrumentation of Field Flow Fractionation. III/Polysaccharides: Liquid Chromatography.

Further Reading

- Cölfen H (1998) Analytical ultracentrifuge technologies for the characterization of biopolymer gels and microgels. *Biotechnology and Genetic Engineering Reviews* 16: 87–140.
- Harding SE (1995) Some recent developments in the size and shape analysis of industrial polysaccharides in solution using sedimentation analysis in the analytical ultracentrifuge. *Carbohydrate Polymers* 28: 227–237.
- Harding SE, Rowe AJ and Horton JC (eds) (1992) *Analytical Ultracentrifugation in Biochemistry and Polymer Science*. Cambridge: Royal Society of Chemistry.
- Lavrenko PN, Linow KJ and Görnitz E (1992) The concentration dependence of the sedimentation coefficient of some polysaccharides in very dilute solution. In: Harding SE, Rowe AJ and Horton JC (eds) *Analytical Ultracentrifugation in Biochemistry and Polymer Science*, pp. 517–548. Royal Society of Chemistry. Cambridge.
- Pavlov GM (1997) The concentration dependence of sedimentation for polysaccharides. *European Biophysical Journal* 25: 385–397.
- Rowe AJ (1992) The concentration dependence of sedimentation. In: Harding SE, Rowe AJ and Horton JC (eds) *Analytical Ultracentrifugation in Biochemistry and Polymer Science*, pp. 394–406. Cambridge: Royal Society of Chemistry.
- Schachman HK (1959) *Ultracentrifugation in Biochemistry*. New York: Academic Press.
- Svedberg T and Pederson O (1940) *The Ultracentrifuge*. Oxford: Oxford University Press.
- Tombs MP and Harding SE (1998) *Introduction to Polysaccharide Biotechnology*. London: Taylor and Francis.

Liquid Chromatography

J. M. Matés and C. Pérez-Gómez, University of Málaga, Málaga, Spain

Copyright © 2000 Academic Press

Introduction

Separation, analysis and molecular weight distribution are very important for the characterization of polysaccharides in biochemistry, microbiology, agriculture and the food industry. During biosynthesis, a large range of components of different molecular

weight are formed. Gas chromatography (GC) can be used for the analysis of very complex polysaccharide mixtures whereas high performance liquid chromatography (HPLC) is preferred for simple polysaccharide mixtures and for purification.

High Performance Liquid Chromatography

HPLC was introduced into the field of carbohydrate chemistry for the separation of mono- to tetrasaccharides of neutral sugars found in natural products

Table 1 Pre-column derivatization of carbohydrates for use in HPLC

Reagent	Column	Mobile phase
2-Aminoacridone	C18 reverse or normal-phase	Ammonium acetate-acetonitrile
2-Aminopyridine	C18 reverse or normal-phase	Acetonitrile-citrate buffer
Dansyl chloride	Spherisorb ODS2	Acetonitrile-water
Dansyl hydrazine	C18 reversed-phase	Acetonitrile-water
Phenylisocyanate	C18 reversed-phase	Acetonitrile-phosphate buffer
Benzoyl chloride	Silica	Ethyl acetate-hexane
<i>o</i> -Phthalaldehyde	C18 reversed-phase	Acetonitrile-methanol-water

of interest to the food industry. However, more recent applications have included the analysis and purification of oligo- and polysaccharides containing neutral and acetamido sugars and sialylated, sulphated and phosphorylated oligosaccharides.

Several different HPLC packing materials and solvent systems have been investigated for carbohydrate separation including native and derivatized oligosaccharides chromatographed on bare silica, bonded silica (NH₂-silica), silica modified with soluble amines *in situ*, reversed phase (RP), anion- and cation-exchangers and size-exclusion chromatography (Table 1). In several instances, a combination of different chromatographic modes is required for the complete separation of all isomers present in mixtures of polysaccharides obtained from biological sources.

Experimental Approach

There are a number of different HPLC processes for separating carbohydrates that depend on different chemical and physical properties for resolution. These analyses can be divided into ion-exchange processes at high temperature ($\geq 60^\circ\text{C}$) and adsorption (partition) processes at lower (room) temperatures. The most commonly used ion-exchange process involves the separation of borate complexes on quaternary ammonium anion-exchange resins (Figure 1). Borate forms complexes with most carbohydrates. The stability of these is influenced by the spatial arrangement of the alcohol groups involved, *cis* hydroxyl groups forming the most stable compounds. The columns may be run isocratically using borate buffers or by the use of gradient or stepwise elution using borate buffers of increasing molarity or containing increasing salt concentrations. The resolution obtained with this process normally increases with increasing temperature as long as the ion-exchange resin is stable.

Polysaccharides may be separated in all these processes using aqueous acetonitrile solvents. The variation of elution times of all the components with the separation parameters (e.g. temperature, acetonitrile concentration, buffer pH) must be determined by computer analysis or by visual inspection of the curves. Microbial growth inhibitor should be present in all aqueous phases.

Techniques for Carbohydrate Chromatography

By using different approaches to synthesis, stationary phases for almost any known type of chromatographic interaction can be provided. Continuous porous polymer rods can, for example, be produced *in situ* by thermal or photopolymerization on suitable monomers. These stationary phases can be transformed to adapt them for ion exchange or hydrophobic interaction chromatography. A more specific interaction can be introduced by 'imprinting' the polymers during synthesis with the future analyte (enantioselective/affinity stationary phases). In a different approach, a sol-gel technique can be used to produce stationary phases on a silica basis. These phases are mechanically more stable and were, for instance, used to separate polyaromatic carbohydrates and sugars within minutes.

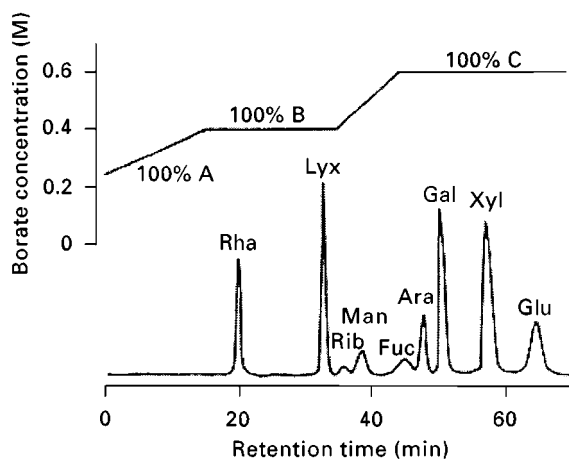


Figure 1 Analysis of an equimolar mixture of aldoses. A mixture of 15–60 nmol of L-rhamnose (Rha), D-lyxose (Lyx), D-ribose (Rib), D-mannose (Man), L-fucose (Fuc), L-arabinose (Ara), D-galactose (Gal), D-xylose (Xyl) and D-glucose (Glu) was dissolved in 100 μL of water and applied to a Hitachi No. 2633 resin column (8 mm i.d. \times 8 cm). The packing is a quaternary ammonium resin with an average bead diameter of 11 μm . The borate gradient (1 mL min⁻¹) was used to elute the carbohydrates using buffers A (0.25 mol L⁻¹, pH 8.2), B (0.4 mol L⁻¹, pH 7.4) and C (0.6 mol L⁻¹, pH 9.3). Post-column detection was by fluorimetry after reaction with 2-cyanoacetamide-borate. (Reproduced with permission from Chaplin MF and Kennedy JF (eds) (1994) *Carbohydrate Analysis: A Practical Approach*, 2nd edn, p. 17. Copyright IRL Press Limited.)

Adsorption chromatography Adsorption, or normal phase, chromatography relies on the surface hydroxyl groups of silica (and to a lesser extent alumina) which can interact with solutes and effect a separation on account of the different strengths of interaction. The separation of neutral oligosaccharides cannot be carried out conveniently by this method although limited separations can be achieved in water or by using aqueous-organic mixtures. The method is well suited to the analysis of derivatives of oligosaccharides of low degree of polymerization using non-aqueous eluents. The use of high concentrations of organic solvents in an aqueous eluent gives rise to problems of solubility of polysaccharides.

Bonded-phase chromatography By far the most frequently used systems for separation of oligosaccharides are those using chemically bonded phases that fractionate materials on the basis of their relative affinities for the mobile phase and the bonded phase. The two most important types of column are those containing the aminopropyl-bonded phase and a hybrid phase containing cyanopropyl- and aminopropylsiloxane-bonded ligands.

Separation of series of oligosaccharides from, for example, hydrolysed starch can readily be achieved with up to a degree of polymerization of 10 in 15–20 min using acetonitrile–water eluents containing 35–40% water (Figure 2). Increasing the water content to 45% can increase the number of detectable oligosaccharides up to about 15 units. However very high-molecular-weight materials cannot be analysed due to excessive retention and solubility problems in acetonitrile–water eluents. For a full analysis, separation by gel permeation or ion exchange is also required.

Instead of using a bonded silica aminopropylsiloxane-bonded phase, an alkyldiamine or polyalkylamine can be added to the eluent forming a dynamic equilibrium between an amine-containing phase coating the silica and that in the eluent. Separations are similar to those obtained using chemically bonded aminopropyl sorbents with separations of up to 20–25 units in 45 min with eluents containing 50% water in acetonitrile (Figure 3).

Ion-exchange chromatography Anion-exchange resins of styrene-divinylbenzene matrices in the sulfate form have been reported for the separation of the simple disaccharides using eluents of 80–90% ethanol in water. Rapid and efficient separation of simple and complex carbohydrates by high performance anion-exchange chromatography is obtained using a quarternized alkylamine sorbent made of

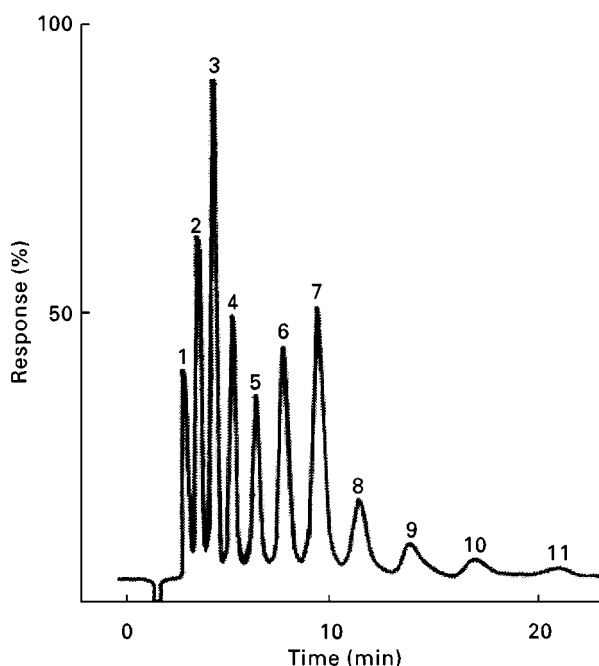


Figure 2 Separation of starch-derived oligosaccharides on a Spherisorb S5 NH₂ column (1, 2, 3, etc., refer to the degree of polymerization of the oligosaccharide). (Reproduced with permission from Chaplin MF and Kennedy JF (eds) (1994) *Carbohydrate Analysis: A Practical Approach*, 2nd edn, p. 48. Copyright IRL Press Limited.)

chemically modified nonporous and monodisperse highly cross-linked styrene copolymer particles having a diameter of 2.5 μm and a surface area of 3 $\text{m}^2 \text{g}^{-1}$. In this technique there are many advantages of using short columns instead of those currently used in high performance anion-exchange chromatography in terms of separation time.

On the other hand, cation resins in the lithium form have been used for similar analyses using 90% ethanol in water eluents. The use of 4 and 8% cross-linked cation-exchange resins in the calcium or silver form have been used to provide a rapid separation of oligosaccharides. It is possible to obtain a total analysis of material applied to the column and the use of water as the only eluent (Figure 4).

An early approach to reduce stationary phase mass transfer resistance was to form thin ion-exchange shells on the surface of an impervious core, e.g. glass beads to give 'pellicular' materials. The major application of pellicular anion exchangers is in the chromatography of carbohydrates at $>\text{pH } 12$, where most carbohydrates become anionic and can be separated on a column packed with a strong anion exchanger. Because carbohydrates undergo chemical changes on prolonged exposure to strong alkali, the separation time must be short.

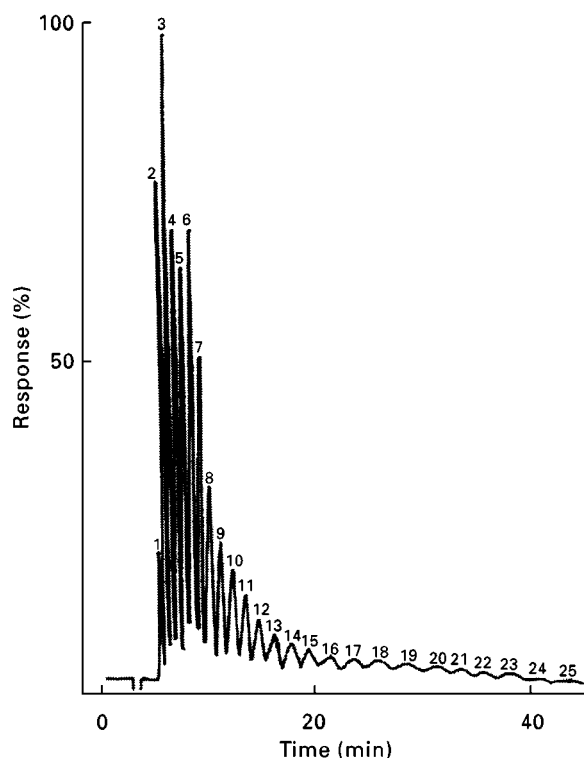


Figure 3 Separation of starch-derived oligosaccharides on an *in situ*-modified silica column using 1,4-diaminobutane (0.01% v/v) as modifier. Numbers refer to the degree of polymerization of the oligosaccharide. (Reproduced with permission from Chaplin MF and Kennedy JF (eds) (1994) *Carbohydrate Analysis: A Practical Approach*, 2nd edn, p. 49. Copyright IRL Press Limited.)

Gel permeation chromatography There has been no direct replacement for the cross-linked polysaccharide or polyacrylamide materials used for traditional gel permeation analysis of oligosaccharides. Some advances have been made with the development of silica matrices deactivated by chemical bonding of an organic ether stationary phase to provide a hydrophilic surface.

Fractionation ranges extended down to 10–12 units whilst bare silica can extend the fractionation range down to 5–6 units. Even with the modified materials, adsorption effects are present and elution with ionic buffers is recommended within the pH range 2–7.

Water-compatible hydroxylated polyether-based matrices have been developed which overcome some of the disadvantages of silica-based materials and have fractionation ranges which are comparable to the cross-linked polysaccharide and polyacrylamide gels. In spite of their lower selectivity compared to silica-based matrices, such materials have a very high stability towards alkaline pH (up to pH 12). Separation times are of the order of one-third to one-tenth

that of traditional low-pressure gel permeation analysis, but they are inferior to those currently obtained by ion-exchange chromatography. Consequently, less emphasis is placed on high performance gel permeation chromatography for oligosaccharide fractionation.

Detection Systems

Detection of oligosaccharides eluting from HPLC columns is the biggest challenge and weakest link in the analysis of polysaccharides. When sensitivity in the submicrogram range is required the only method readily available is the use of pre-column derivatization with separation via adsorption chromatography and detection via UV monitoring or pulsed electrochemical detection at noble metal electrodes. Attempts to use strong cation-exchange resins to hydrolyse the glycosidic bonds in polysaccharides to give complete conversion to monosaccharides and lower oligosaccharides after chromatographic separation has been reported with the resulting saccharides being detected as reducing compounds.

Direct Detection

UV absorbance Carbohydrates do not absorb light in the UV or visible range and have no fluorescence. Polysaccharides, however, do absorb at wavelengths in the far UV. The higher absorbance is at about 188 nm but, due to noise in the detection signal below 190 nm, detection is normally performed at wavelengths between 192 and 200 nm. The response, depending largely on the freedom of the carbonyl

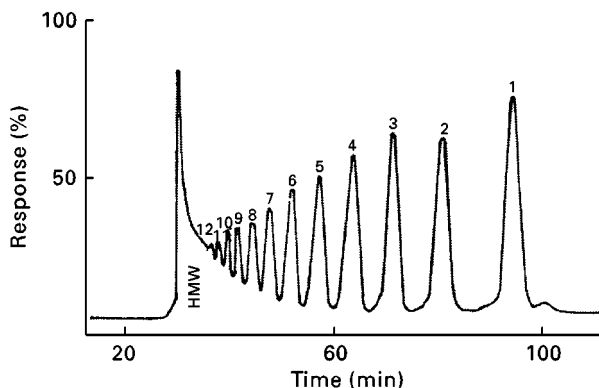


Figure 4 Separation of starch-derived oligosaccharides by high performance ion-exchange chromatography using 4% cross-linked cation-exchange resin with silver counterions (1, 2, 3, etc., refer to the degree of polymerization of the oligosaccharide; HMW, high-molecular-weight material above). (Reproduced with permission from Chaplin MF and Kennedy JF (eds) (1994) *Carbohydrate Analysis: A Practical Approach*, 2nd edn, p. 50. Copyright IRL Press Limited.)

group, differs between the polysaccharides. Analyses are restricted to solvents such as acetonitrile–water mixtures that do not absorb significantly at these wavelengths. Oligosaccharides containing acetamido groups or sialic acids can be detected by absorbance in the range 180–220 nm with a detection limit of approximately 1 nmol. The best signal-to-noise ratio for a range of carbohydrates is found between 195 and 210 nm.

For preparative separations, a higher wavelength can be used. The sensitivity decreases by 10- and 100-fold by increasing the wavelength of detection from 208 to 218 and 228 nm. Polysaccharides having unsaturated monosaccharides formed by enzymic digestion of sulfated glycosaminoglycans have an absorption maximum at 232 nm. The sensitivity of detection of these oligosaccharides at 232 nm is less than 1 nmol.

The sensitivity can be further improved (down to 1 pmol) by introducing a strongly UV-absorbing group such as benzoyl or phenylisocyanate into the molecules. Diode array detection is a technique widely used in combination with reversed-phase HPLC for the separation and quantitative determination of polysaccharides. The detection limit obtained by this method is about 5 pmol. In the determination of the degree of polymerization of agar-type polysaccharides, samples are prepared adding 1 g of starch to 10 mL of 0.2 mol L⁻¹ trifluoroacetic acid, heating at 100°C for one hour, then adding 90 mL of absolute ethanol and storing at -70°C to allow precipitated saccharides to settle. It is also necessary to remove all remaining traces of ethanol by evaporation under nitrogen since ethanol interferes with retention of the larger oligomers. Finally, the dried residue is redissolved and filtered in deionized water prior to injection.

The simplest and ideal methods of detection are those that do not require chemical derivatization of the sugars but in order to increase the sensitivity of detection, they may be derivatized to give light-absorbing or fluorescent compounds before or after LC separation. This approach may be very useful, especially if it allows the use of efficient chemically bonded or underivatized silica columns.

The sensitivity of carbohydrate detection can be greatly increased by introducing a radioactive label, either by reduction with sodium boro[³H]hydride or de-*N*-acetylation and re-*N*-acetylation with [¹⁴C]acetic anhydride. Oligosaccharides isolated from biological sources are often obtained in reduced and/or de-*N*-acetylated form. Analysis of reduced oligosaccharides has an additional advantage in that reduction destroys the anomeration at the reducing end, thus simplifying chromatography and subsequent structural analysis.

The separation of anomers is also given by HPLC after pre-column derivatization of reducing oligosaccharides with acetyl, benzoyl and phenylisocyanate groups. Therefore, reduction is usually performed routinely as part of these derivatization procedures. The sensitivity of detection of the latter two derivatives by UV would usually obviate the need to introduce a radioactive label.

Several online radioactive detection systems are available with both solid scintillant cells and the possibility of addition of liquid scintillant, for example, from Berthold, Beckman and Nuclear Enterprises. For ³H-labelled oligosaccharides, approximately 10⁴ and 10² cpm are required for detection by the two types of measuring technique. The sensitivity of detection of ¹⁴C is of order of 10³ cpm.

Early post-column derivatization methods for carbohydrate detection employed strong acids and thus required acid-resistant equipment. For example, the use of orcinol–concentrated sulfuric acid reagent required an elaborate carbohydrate analyser to be set up for direct post-column detection. Similar methods, such as the phenol–sulfuric acid assay, have proved useful for separate, off-column hexose determination. The sensitivity of detection for these methods is approximately 20 nmol hexose which is slightly less than by UV detection of native oligosaccharides containing hexose and hexosacetamido sugars, but represents a greatly improved sensitivity for detection of oligosaccharides containing neutral sugars alone.

More recent post-column derivatization methods have used noncorrosive reagents, particularly for detection of reducing sugars after borate-complex ion-exchange chromatography. The copper complexes of 2,2'-bicinchoninate, ethanolamine–boric acid and 2-cyanoacetamide, for example, have been used to detect 1 nmol oligosaccharide. Detection of less than 1 nmol oligosaccharide has been reported using tetrazolium blue reagent (3,3'-[3,3'-dimethoxy-1,1'-biphenyl-4,4'-diyl]bis[2,5-diphenyl-2H-tetrazolium] dichloride) which has the additional advantage of achieving this sensitivity in the absence of borate buffer and at a lower reaction temperature of 85°C. The method is suitable for both reduced and reducing oligosaccharides.

The ammoniacal cupric sulphate assay is sensitive but simple and avoids the corrosive reagents and complex heating/mixing protocols of some other post-column detection methods. It is of general application to substances that react with cuprammonium, for example, carbohydrate derivatives and glycols, and is not sensitive to changes in the solvent composition. Monosaccharides do not seriously interfere in this assay if the periodate oxidation reaction

takes place below 40°C and they are not present in an overwhelming excess. They can be detected if the periodate oxidation is allowed to take place at a higher temperature (e.g. 100°C). Periodate oxidation alone may be used for post-column detection of cyclitols, aldoses, alditols and ketoses by monitoring the absorbance at 260 nm. Assay with cyanoacetamide uses noncorrosive reagents, shows good linearity and is highly sensitive for aldoses, hexosamines and alduronic acids. The fluorescence is quenched by acetonitrile, if present in the eluate, but the absorbance is unaffected.

Refractive index and light-scattering detection A detection method of general applicability makes use of changes in refractivity. It is at least ten times less sensitive than UV detection due to high background noise caused by temperature fluctuations and pump pulsations.

Many of the early HPLC studies on carbohydrates used a differential refractive index detector because these studies were carried out on oligosaccharides containing neutral sugars only, which absorb weakly in the UV region. The disadvantages of using a refractometer are that only isocratic elution is possible and the sensitivity is relatively low, 10–100 nmol being required for detection.

Light scattering (LS) can be used for measuring the molar mass of polysaccharides. Several polysaccharides have been routinely characterized by LS for the determination of the molecular weight distribution. The molecular weight distribution can be used to determine the polydispersity (M_w/M_n) and the heterogeneity in a sample.

Electrochemical detection of polysaccharides Nanomolar detection of both reducing and reduced neutral oligosaccharides and polysaccharide hydrolysates has been reported using pulsed amperometric detection (PAD) employing a gold electrode. This method is stated to have the advantage of increased detector durability compared with potentiometric and single potential detectors. Detection of carbohydrates in the presence of a high concentration of potentially interfering salts is also possible. An increased sensitivity for detection of reducing sugars (down to 1 pmol) has been reported using amperometric detection of polysaccharides chromatographed in sodium phosphate buffer after post-column reaction with copper bis(phenanthroline) in alkaline solution at 96°C.

PAD, in conjunction with high-pH anion-exchange chromatography, has also become the method of choice for analysing sugars. Their direct electrochemistry on noble metal electrodes suffers from electrode

fouling due to absorption of oxidized species on the electrode surface. PAD overcomes this problem by using a triple-step potential waveform. In the first step (data recording), the gold electrode is held at a potential suitable for oxidation of the analyte. The second step raises the potential to some higher value, where absorbed oxidation products are oxidized further into mobile phase-soluble products, thereby cleaning the electrode. Finally, the electrode generates a new gold oxide surface. Using this technique, closely related saccharides can be separated and detected in the 10 to 100 pmol range.

Analysis of Complex Mixtures

HPLC of glycopeptides is not widely developed because of peptide interferences. In fact, a given glycan located in a given peptide sequence of the protein generally gives rise to a mixture of glycopeptides due to the random nature of proteolytic action. Chemical or enzymatic removal of glycans from such complex mixtures solves this problem and allows the use of HPLC. It is possible to use different HPLC techniques such as:

- anion-exchange chromatography of sialyloligosaccharides (Figure 5A);
- partition chromatography of neutral and acidic oligosaccharides on primary amine-bonded silica or alkyl diol-bonded silica (Figure 5B);
- reversed-phase chromatography of neutral oligosaccharides on C_2 and C_{18} -bonded silica (Figure 5C).

Conjugation of two fluorescent ortho-substituted aniline derivatives, 2-aminobenzamide (2-AB) and 2-anthranilic acid (2-AA), to *N*- and *O*-glycans have been recently investigated. Conjugation conditions for attaching 2-AB and 2-AA to core-fucosylated and nonfucosylated glycans have been developed using complex *N*-glycans radiolabelled at the nonreducing terminus with [3H]C₆-galactose.

Most glycolipid separations have involved derivatizing the glycolipids to allow UV detection. The derivatives are usually benzoyl or *p*-nitrobenzoyl esters and the columns are based on silica gel. For instance, ceramides (0.1–1.0 mg) are dissolved in 20% benzoyl chloride in 0.6 mL of dry pyridine and heated at 60°C for 1 h. The solvent is evaporated to dryness in a stream of N₂ and taken up in a small volume of hexane for injection into the liquid chromatograph. The mobile phase is a linear gradient system of 0.20% methanol to 0.75% methanol in hexane. The detector operates at 254 nm and the minimum detection is about 10 pmol of each glycolipid.

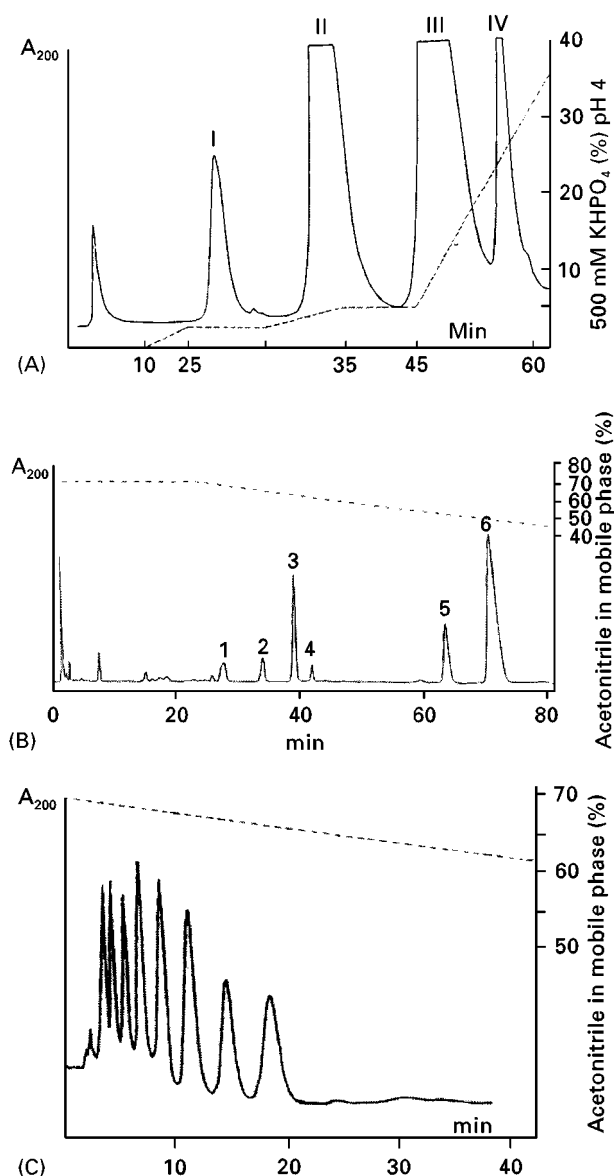


Figure 5 (A) HPLC on 10 μ m Micropak AX-10 column of sialoglycans liberated by hydrazinolysis of α_1 -acid glycoprotein. I, II, III, IV: mono-, di-, tri- and tetrasialylated glycans. The recovery was 91%. (B) HPLC on 5 μ m of glycan-alditols liberated by β -elimination from Cad erythrocyte membrane glycoporphin. 1: NeuAc(α 2-3)Gal(β 1-3)GalNAc-ol; 3: NeuAc(α 2-3)GalNAc(β 1-4)Gal(β 1-3)GalNAc-ol; 5: NeuAc(α 2-3)Gal(β 1-3)[NeuAc(α 2-6)]GalNAc-ol; 6: NeuAc(α 2-3)[GalNAc(β 1-4)]Gal(β 1-3)[NeuAc(α 2-6)]GalNAc-ol. (C) HPLC on alkyl diol-bonded silica of oligomannoside-alditols from the urine of a patient with a mannosidosis. M₂G-ol to M₉G-ol: oligomannoside-alditols containing from 2 to 9 mannose residues. (Reproduced with permission from Chaplin MF and Kennedy JF (eds) (1994) *Carbohydrate Analysis: A Practical Approach*, 2nd edn, pp. 155, 157 and 158. Copyright IRL Press Limited.)

The *p*-nitrobenzoyl derivatives are more sensitive to UV detection than the benzoyl derivatives but the benzoyl derivatives are better separated than the

p-nitrobenzoyl derivatives. A problem exists for regenerating the native glycolipide. It is not too difficult to remove *O*-benzoyl groups but the *N*-benzoyl group on amino sugars and in the ceramide fragment are far more difficult to remove. The use of a catalyst such as 4-dimethylaminopyridine in the benzoylation reaction with benzoic anhydride produces only *O*-benzoyl substitution.

Determination of the Position of Glycosidic Linkages. Combined HPLC and Mass Spectrometry (HPLC-MS)

Oligosaccharides released from human transferrin have been derivatized with 2-aminoacridone (2-AMAC) prior to analysis by either reversed- or normal-phase HPLC. Collected fractions of 2-AMAC-derivatized glycans have been analysed by matrix-assisted laser desorption/ionization time-of-flight mass spectrometry, before and after desialylation (Figure 6).

A procedure for analysis of a mixture of neutral and acidic sugars in bacterial whole-cell hydrolysates using high performance anion-exchange liquid chromatography-electrospray ionization-tandem mass spectrometry (HPAEC-ESI-MS-MS) has been described. HPAEC is well established as a high-resolution chromatographic technique, in conjunction with pulsed amperometric detection. Alternatively, for more selective detection, sugars (as $M-H^-$ ions) are monitored using ESI-MS. Sugar identification is achieved by MS-MS using ESI.

Another simple, sensitive method for the structural characterization of oligosaccharides by fast atom bombardment-mass spectrometry (FAB-MS) has been designed. Oligosaccharides are labelled with a UV chromophore (which also serves as a charge-stabilizing group) and with a hydrophobic alkyl tail. The chromophore, a 2,4-dinitrophenyl group, aids UV detection and stabilizes negative ion species formed during analysis by FAB-MS. The hydrophobic tail, provided by an octyl group, enhances the surface activity of the analytes and makes them amenable to separation on a C18-bonded phase. This method has been applied to the structural analysis of the components of a mixture of starch maltodextrins with a degree of polymerization 1-16, to the analysis of the structure of pure maltohexose, and to a previously characterized oligosaccharide from *Rhizobium* capsular polysaccharide.

HPLC technology has been developed that is capable of resolving subpicomolar quantities of mixtures of fluorescent-labelled neutral and acidic

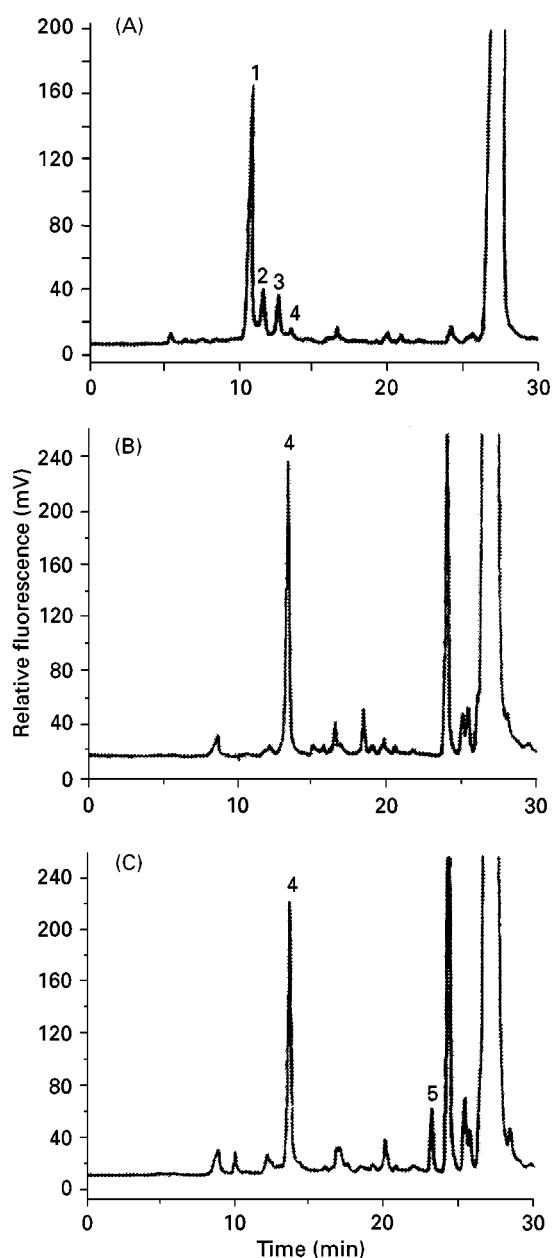


Figure 6 Reversed-phase HPLC analysis of glycan mixture from transferrin: (A) untreated; (B and C) digested with sialidase and a mixture of sialidase and fucosidase, respectively, prior to derivatization with 2-aminoacridone. (Reproduced with permission from Charlwood J, Birrell H, Tolson D and Camilleri P (1998) *Analytical Chemistry* 70: 2531. Copyright American Chemical Society.)

glycans simultaneously and in their correct molar proportions. The reproducibility of the separation system, the predictability of glucose unit values, and the quantitative response of the detection system for individual fluorescently labelled glycans allows automation for the analysis of neutral sugars using a combination of enzymes as in the reagent array analysis method (RAAM). In addition, the simultaneous

resolution of both acidic (sialylated) and neutral products from the RAAM digestion allowed direct analysis of sialylated glycans, eliminating the previous need to remove sialic acid residues in a preliminary step.

Future Developments

As shown above, the greatest advances in the detection and characterization of polysaccharides will evolve from advances in mass spectrometry. The current ability to identify, with little ambiguity, virtually any high-molecular-weight biopolymer via the electrospray interface between HPLC and MS will continue to improve, in terms of ease of use, lower sample requirements and higher molecular-weight ranges. Advances will use detection techniques incorporating the strengths of each technique in sequential detection schemes. UV detection prior to MS is already common. Improvements will also come about with regard to the mapping of carbohydrates and polysaccharides.

The emphasis for the future does not appear to reside in reaction detection for HPLC of polysaccharides, but rather in more sophisticated instrumental methods of detection. Electrochemistry seems to hold much appeal, and yet it has not realized its full potential. Pulsed amperometric detection methods are maturing; chemically modified electrodes can be much more selective and sensitive than glassy carbon or Au/Hg-type electrodes. Multiple-array detectors, perhaps with chemically modified electrodes or different noble metal electrodes (Ni, CuO), may also provide more information of a qualitative nature. Current detection methods such as UV-visible, fluorescence and light scattering will always be useful for qualitative information, identification of the chromatographic performance of a peak, and for absolute quantitation, but they may never provide 100% specific information about the structure. On the other hand, the use of circular dichroism or optical rotary dispersion for detection of the conformation of polysaccharides can be equally used.

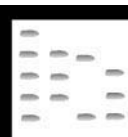
See also: II/**Chromatography: Liquid:** Derivatization; Detectors: Fluorescence Detection; Detectors: Ultraviolet and Visible Detection; Mechanisms: Ion Chromatography; Mechanisms: Size Exclusion Chromatography. III/**Carbohydrates:** Gas Chromatography and Gas Chromatography-Mass Spectrometry; Liquid Chromatography. Ion-Exclusion Chromatography: **Liquid Chromatography.**

Further Reading

Altmann F (1992) Determination of amino sugars and amino acids in glycoconjugates using precolumn de-

- rivatization with *o*-phthalaldehyde. *Analytical Biochemistry* 204: 215–219.
- Chaplin MF and Kennedy JF (eds) (1994) *Carbohydrate Analysis: A Practical Approach*, 2nd edn, pp. 15, 41, 66, 152, 209. Oxford: IRL Press.
- Charlwood J, Birrell H, Tolson D and Camilleri P (1998) Two-dimensional chromatography in the analysis of complex glycans from transferrin. *Analytical Chemistry* 70: 2530–2535.
- Guille GR, Rudd PM, Wing DR, Prime SB and Dwek RA (1996) A rapid high-resolution high-performance liquid chromatographic method for separating glycan mixtures and analyzing oligosaccharide profiles. *Analytical Biochemistry* 240: 210–226.
- Karger BL and Hancock WS (ed.) (1996) *Methods in Enzymology* 270: 67, 119, 190.
- Lim CK (ed.) (1986) *HPLC of Small Molecules: A Practical Approach*, pp. 49. Oxford: IRL Press.
- Ohsuga H (1996) The carbohydrate moiety of the bermuda grass antigen BG60. New oligosaccharides of plant origin. *Journal of Biological Chemistry* 271: 26653–26658.
- Robles MD, Matés JM and Niell X (1995) Determination of the degree of polymerization of agar-type polysaccharides by a high-performance liquid chromatography method. *Journal of Liquid Chromatography* 18: 3175–3178.
- Wunschel D, Fox KF, Fox A *et al.* (1997) Quantitative analysis of neutral and acidic sugars in the whole bacterial cell hydrolysates using high-performance anion-exchange liquid chromatography-electrospray ionization tandem mass. *Journal of Chromatography* 776: 205–219.
- Zhang Y, Cedergren RA, Nieuwenhuis TJ and Hollingsworth RI (1993) *N,N*-(2,4-dinitrophenyl)octylamine derivatives for the isolation, purification, and mass spectrometric characterization of oligosaccharides. *Analytical Biochemistry* 208: 363–371.

POROUS GRAPHITIC CARBON: LIQUID CHROMATOGRAPHY



M.-C. Hennion, Laboratoire Environnement et Chimie Analytique, Paris, France

Copyright © 2000 Academic Press

Introduction

Various carbonaceous sorbents have been used successfully since the early days of gas chromatography (GC), but for many years their application to liquid chromatography (LC) was unsuccessful. Active carbons with high specific surface areas were shown to be microporous and to contain polar groups at their surface, which provided poor LC performance. Graphitized carbon blacks (GCBs) lacked sufficient mechanical strength to withstand high LC pressures, in addition to having polar surface groups. In the 1970s, bonded silicas were extensively developed, but they had some disadvantages including solubility in the eluents, hydrolysis of the bonded chain at low or high pH, and the effects of the unavoidable unreacted silanol groups. Several attempts were made to prepare graphite-based sorbents that would not suffer from the disadvantages of bonded silica sorbents, but it was not until 1979 that Knox and Gilbert patented a method for making a robust porous carbon that possessed the required properties for use in LC. An improved version of this material became commercially available in 1988 under the tradename Hypercarb®. Although one or two other carbons made by

Japanese workers are sometimes mentioned, most of the studies and applications described in the literature utilize the porous graphitized carbon (PGC) Hypercarb®.

The properties of PGC come from its highly ordered crystalline structure composed of large flat layers of carbon atoms. It has proven to be unique, behaving as a stronger reversed-phase sorbent than any other existing reversed-phase packing or as a normal-phase sorbent. Separations of both nonpolar and highly polar mixtures can be performed that are impossible with other sorbents. Resolution of anionic and cationic analytes can be achieved in one run. These properties are partly explained by a retention mechanism that is quite different from that of other LC stationary phases. The properties of PGC are discussed here together with some selected applications.

Structure and Characteristics of PGC

PGC is obtained by impregnating a porous silica with a phenol–formaldehyde mixture. This mixture is polymerized within the pores of the silica gel and carbonized at 1000°C. The silica is then removed by dissolution in a concentrated (5 mol L⁻¹) sodium hydroxide solution. Graphitization is performed in the temperature range 2000–2800°C to remove the micropores. The resulting macroporous material has a flat crystalline surface.

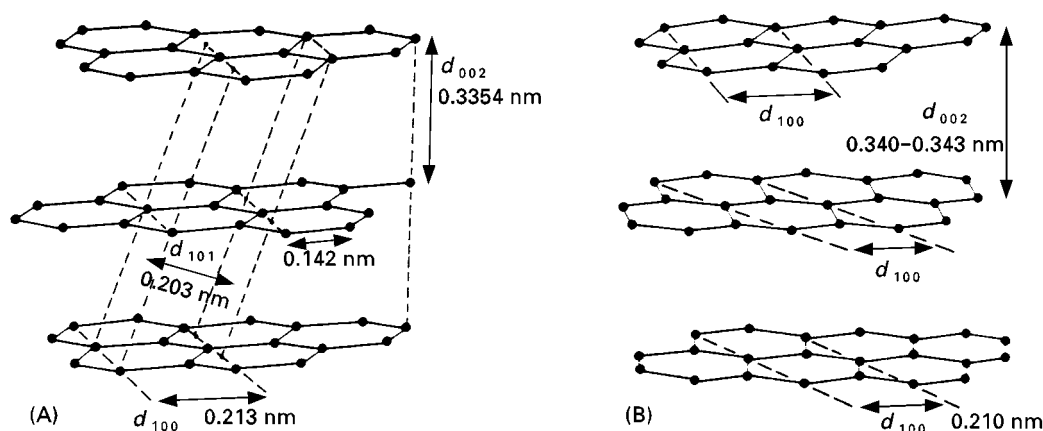


Figure 1 Structure of (A) 3D graphite and (B) 2D porous graphitic carbon.

PGC does not have the true graphite structure, in which layers are well organized in three dimensions, as shown in **Figure 1A**. Rather it has a two-dimensional (2D) graphite structure composed of layers of hexagonally arranged carbon atoms in the sp^2 hybridization. The close intertwining of the graphitic sheets provides the rigidity and mechanical stability. The layer spacing is slightly larger than in 3D graphite, as shown in **Figure 1B**.

PGC meets the required properties for a good LC sorbent. It is available in a narrow particle-size distribution with mean particle diameter of 5 or 7 μm , it has an average specific surface area of $120 \text{ m}^2 \text{ g}^{-1}$, a uniform pore structure with mean pore diameter of 25 nm, and a porosity of 75%. Designed to withstand pressures of more than 400 bar, PGC is geometrically stable and free from any swelling or shrinking. It is inert to the common organic eluents and to extremes of pH. In the early stage of commercialization, some columns packed with the 7 μm material lacked efficiency, but significant improvements have been made and the 5 μm packing now available has a guaranteed efficiency of $60\,000 \text{ plates m}^{-1}$ and offers batch-to-batch reproducibility.

The flat homogeneous surface of PGC is responsible for its unique selectivity to geometrical isomers. The extensive layers of carbon atoms containing delocalized π electrons and the high polarizability are responsible for its unique retention mechanism.

Retention Mechanism

Mobile-Phase Effects: Reversed-Phase Behaviour for Polar and Nonpolar Analytes

The reversed-phase behaviour of PGC towards nonpolar and polar analytes has been observed in many

applications. **Figure 2** shows plots of the logarithm of the retention factor of phenol, 1,3-dihydroxybenzene (resorcinol) and 1,3,5-trihydroxybenzene (phloroglucinol) against the methanol volume fraction (ϕ) in a water/methanol mobile phase for PGC and two other reversed phases, C_{18} silica and the styrene-divinylbenzene porous copolymer PRP-1. Two important features of PGC are highlighted in this figure. First, the addition of methanol to the mobile phase results in a similar decrease in retention for all three sorbents, thus showing a classical reversed-phase dependence. However the retention values, and in particular the retention order, indicate that the behaviour of PGC is different from that of the other two materials for the analytes considered in this figure.

Retention of Nonpolar Analytes: A Strong Hydrophobic Sorbent

Since PGC was produced with the objective of being an improved reversed-phase material compared with the widely used C_{18} silicas, the first applications were made with nonpolar analytes, and PGC is described as a stronger hydrophobic sorbent than C_{18} silica. A common way of comparing the hydrophobicity of sorbents is to measure the effect of the addition of a methylene group in an homologous series. The methylene increment is 4.5 and 3.8 for the n -alkanols on PGC and C_{18} silica, respectively, with pure water as mobile phase. Kriz and co-workers compared the retention of 52 aromatic hydrocarbons, mostly alkylbenzenes, on PGC, C_{18} silica, phenylsilica, silica and alumina. **Figure 3** shows the variation of the retention factor on PGC according to the number of carbon atoms for both the series of n -alkylbenzenes and the series of methylbenzenes. The methylene increment measured for the n -alkylbenzenes was 0.22 using PGC with pure methanol, compared with

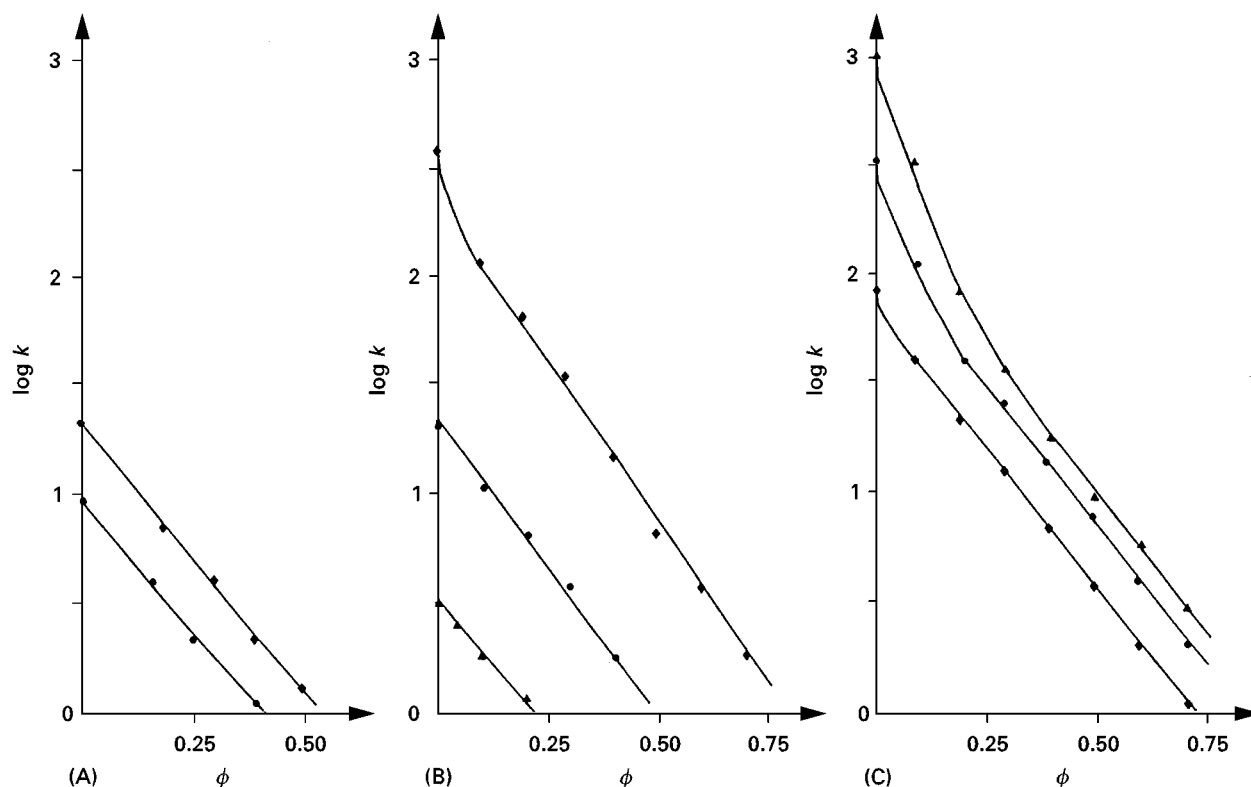


Figure 2 Variation of the retention factors ($\log k$) with the mobile phase composition obtained on (A) LiChrosorb RP-18, (B) PRP-1 and (C) PGC. Solutes: \blacklozenge , phenol; \bullet , resorcinol; \blacktriangle , phloroglucinol. ϕ is the volume fraction of the mobile phase. (Reprinted from Coquart V and Hennion M-C (1992) Trace-level determination of polar phenolic compounds in aqueous samples by HPLC and on-line preconcentration on porous carbon. *Journal of Chromatography* 600: 195–201. Copyright (1992) with permission from Elsevier Science.)

values of 0.17 and 0.10 with C_{18} silica and phenyl-silica using a methanol/water mobile phase (80 : 20 v/v). Another important feature that can be seen from Figure 3 is the possibility given by PGC for discriminating between the two series. In the same study it was shown that C_{18} silica is unable to differentiate between the addition of a methylene group to an alkyl chain and the addition of methyl group to the benzene ring. A very slight difference could be observed on phenylsilica. Silica and alumina with pentane as mobile phase could discriminate between the two series, but with a methylene increment close to zero for the n -alkylbenzene series. This study illustrates well with the higher hydrophobicity of PGC over C_{18} silica as a reversed-phase sorbent for these nonpolar analytes, as well as its superior selectivity towards isomeric compounds.

Retention of Very Polar Analytes: Comparison with a Hydrophobic Reversed-Phase Mechanism

Several studies have shown that PGC does not behave as a perfect reversed-phase sorbent. Figure 2 shows that the same order is observed for C_{18} silica and

PRP-1 and that the retention factor decreases with the analyte's polarity from phenol to resorcinol and phloroglucinol. Plots of phloroglucinol for C_{18} silica have not been reported because this analyte is too polar to be retained with a methanol-rich mobile phase; it has been proposed as an experimental probe for the determination of the void volume of C_{18} columns. This corresponds to a retention mechanism based on hydrophobic interactions. The higher retention observed with PRP-1 is explained by additional π - π interactions between these aromatic analytes and the styrene-divinylbenzene matrix of the PRP-1 sorbent.

On PGC, the retention increases with the number of hydroxy groups. There is a great difference in retention for phloroglucinol with retention factors in water, k_w , of 1050 with PGC, 3 with PRP-1 and 0.3 with C_{18} silicas. Values of $\log k_w$ have been extrapolated from the variation of the retention factors in water/methanol mixtures from curves similar to those in Figure 1. These values, which allow comparison with C_{18} silicas and the apolar copolymer PRP-1, are reported in Table 1 for some mono-, di- and tri-substituted benzene derivatives.

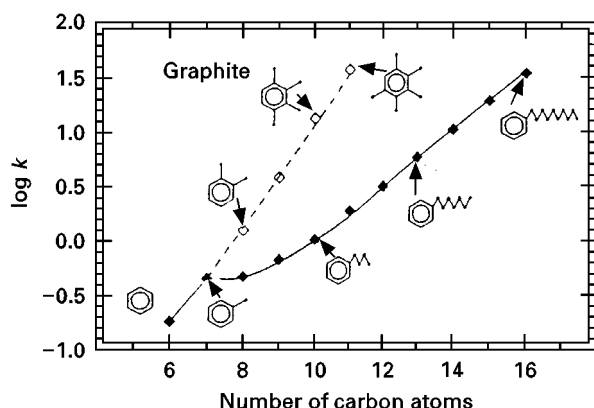


Figure 3 Dependence of $\log k$ values for polymethylbenzenes and n -alkylbenzenes on carbon numbers. Packing material: graphite; eluent: methanol; temperature 20°C. Broken line drawn through points for the polymethylbenzenes; full line drawn through points for n -alkylbenzenes. (Reprinted from Kriz J, Adancova E, Knox JH and Hora J (1994) Characterization of adsorbents using aromatic hydrocarbons. Porous graphite and its comparison with silica gel, alumina, octadecylsilica and phenylsilica. *Journal of Chromatography A* 663: 151–161. Copyright (1994) with permission from Elsevier Science.)

First, when comparing values for monosubstituted benzenes, compounds are more retained by PRP-1 than they are by PGC or C_{18} silica. The comparison between C_{18} silica and PGC indicates that some solutes are less retained and some more retained by PGC than they are by C_{18} . The di- and tri-substituted benzenes listed in Table 1 are rather polar compounds and are either not, or only slightly, retained by C_{18} silicas, which explains why the $\log k_w$ values have not been reported. The comparison between the retentions on PRP-1 and on PGC are informative.

Table 1 Comparison of reversed-phase sorbents using extrapolated $\log k_w$ values obtained with C_{18} silica, PRP-1 and PGC

Solute	C_{18}	PRP-1	PGC
<i>Monosubstituted</i>			
Benzene	2.2	3.5	1.45
Aniline	1.08	2.5	1.35
Phenol	1.55	2.4	1.8
Benzoic acid	1.9	3.2	2.4
Nitrobenzene	2.05	3.6	2.45
<i>Di- and tri-substituted</i>			
4-Aminophenol		1.1	2.05
1,4-Diaminobenzene		1.2	2.4
4-Aminobenzoic acid		2	2.85
4-Hydroxybenzoic acid		2.3	2.7
3,5-Dihydroxybenzoic acid		1.35	3
1,3-Dihydroxybenzene		1.35	2.35
1,4-Dihydroxybenzene		0.83	2.15
1,3,5-Trihydroxybenzene		0.5	2.7

With PRP-1, the $\log k_w$ values obtained with two polar substituents are always lower than those measured for each corresponding monosubstituted benzene, whereas the opposite is observed with PGC. For example, $\log k_w$ of aminophenol is 1.1 with PRP-1 and is lower than both $\log k_w$ of phenol (2.4) and aniline (2.5). With PGC, $\log k_w$ of aminophenol is 2.05 and is higher than $\log k_w$ of both phenol (1.8) and aniline (1.35). Since on C_{18} silicas and PRP-1, the retention order is correlated with the polarity of the molecules, but not on PGC, the retention mechanisms must, therefore, be very different.

Many studies have been carried out on the retention mechanism on C_{18} silica, which has been shown to be primarily governed by hydrophobic interactions between the analytes and the carbonaceous moieties of the alkyl chain bonded at the silica surface. The octanol–water partition coefficient (K_{OW}) has been shown to be a good measure of the hydrophobicity of compounds. To a first approximation, the retention order is linked to this octanol–water partition coefficient as shown in Table 2, which lists the $\log k_w$ values obtained for the three reversed-phase materials and the $\log K_{OW}$ values for the very polar degradation products of triazines. The $\log k_w$ values decrease with $\log K_{OW}$ values for both C_{18} silicas and PRP-1 and analytes are no longer retained when compounds become very polar and more soluble in water than in octanol, as shown by negative $\log K_{OW}$ values. On PGC, the $\log k_w$ values also decrease with $\log K_{OW}$, but only slightly and they are still very high for the water-soluble analytes.

An extensive study has measured or estimated $\log k_w$ values for 46 polar benzene derivatives. The correlation between $\log K_{OW}$ and $\log k_w$ is shown in Figure 4. The relationship is good on C_{18} silica. With PRP-1, $\log k_w$ values are more scattered but the relationship is still acceptable. On PGC, there is no relationship at all except for n -alkylbenzenes, and a high retention is observed for very polar compounds with $\log K_{OW}$ values between 0 and 1.5.

The high retention of very polar analytes, particularly those in an ionized form, is a key property that has been explored for extraction purposes. The trace analysis of water-soluble pollutants requires an extraction step before analysis, the parameters of which can be predicted from LC data, especially $\log k_w$ values. PGC is the only sorbent able to extract from water very polar degradation products, such as those reported in Table 2.

The delocalization of the π electrons in the large graphitic bonds and the high polarizability of the carbon are responsible for strong induction interactions in addition to solvophobic interactions. The result is that the presence of hydrophilic groups in the

Table 2 Relationship between the retention factor obtained for triazines and some very polar degradation products on reversed-phase materials and the corresponding octanol–water partition coefficient

Compound	$\log K_{OW}$	$\log k_W^a$		
		C_{18}	PRP-1	PGC
Atrazine	2.7	3.4 ± 0.2	> 4	> 4
Simazine	2.3	3.0 ± 0.2	> 4	> 4
Deethylatrazine	1.6	2.6 ± 0.1	3.5 ± 0.3	3.2 ± 0.2
Hydroxyatrazine	1.4	2.5 ± 0.1	3.0 ± 0.2	3.4 ± 0.2
Deisopropylatrazine	1.2	2.1 ± 0.1	3.1 ± 0.2	> 3.5
Hydroxydeethylatrazine	0.2	1.5 ± 0.1	1.8 ± 0.1	2.8 ± 0.2
Deethyldeisopropylatrazine	0	1.3 ± 0.1	1.2 ± 0.1	2.8 ± 0.2
Hydroxydeisopropylatrazine	-0.1	1.0 ± 0.1	1.0 ± 0.1	3.0 ± 0.2
Cyanuric acid (2,4,6-trihydroxy-1,3,5-triazine)	-0.2	< 0.5	< 0.5	2.6 ± 0.1
Ammelide (2-amino-4,6-dihydroxy-1,3,5-triazine)	-0.7	< 0.5	< 0.5	2.5 ± 0.1
Ammeline (2,4-diamino-6-hydroxy-1,3,5-triazine)	-1.2	< 0.5	< 0.5	2.4 ± 0.1

^a The values of $\log k_W$ are experimental or extrapolated from measurements in water/methanol mobile phases.

solute molecule does not cause as great a retention decrease on carbon as on C_{18} silica. Any molecular mass increase in the solute, be it in hydrophobic or dipolar moieties, tends to cause a retention increase.

The term ‘hydrophobic adsorption’ was introduced to characterize the positive interaction between the PGC and the solute, as opposed to the ‘hydrophobic partitioning’ observed with C_{18} silica. When polar

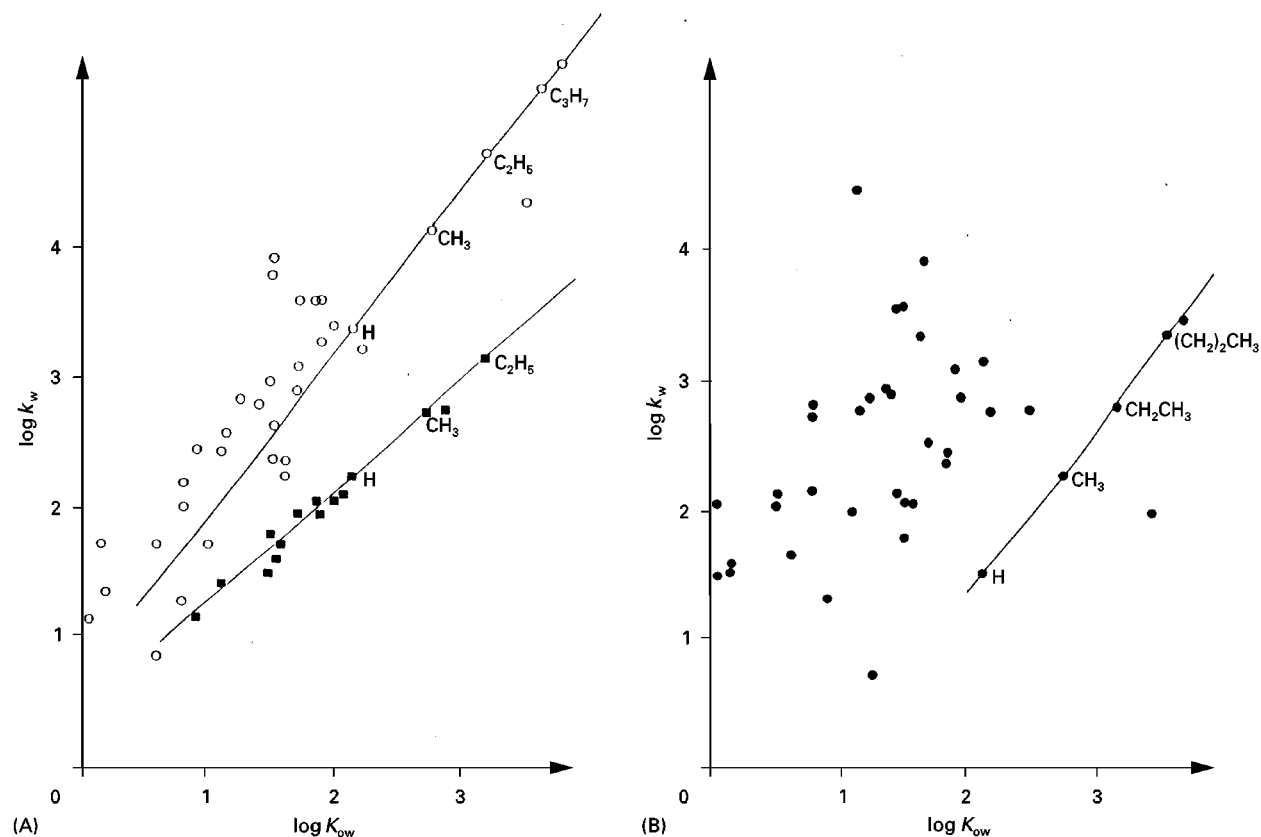


Figure 4 Relationship between $\log k_W$ obtained for various mono-, di- and tri-substituted benzene derivatives and $\log K_{OW}$. (A) $\log k_W$ obtained on (■) C_{18} silica and (○) PRP-1 copolymer; (B) $\log k_W$ values on PGC. (Reprinted from Hennion M-C, Coquart V, Guenu S and Sella C (1995) Retention behaviour of polar compounds using porous graphitic carbon with water-rich mobile phases. *Journal of Chromatography A* 712: 287–301. Copyright (1995) with permission from Elsevier Science.)

analytes are of interest, the electronic interactions have been shown to be more important than the hydrophobic interactions in the retention mechanism. The exploitation of data shown in Figure 4 has demonstrated that the relative position of the substituents on the ring is important and that retention on PGC is very sensitive to the electronic density of the solute molecule. The effect of the polarity of the solutes, taking into account field and resonance effects, has been studied using local dipolar moments and the overall electron excess charge density. The analyte retention factors of polar analytes can be predicted through correlation between $\log k_w$ and the electron excess charge density.

Selection of the Mobile Phase: Solvent Strength

Few attempts have been made to establish the eluotropic strengths (ϵ^0) of commonly used organic solvents with PGC. Using the Snyder equation, the results indicate that the range of solvent strengths for any eluent is small compared with that of silica base sorbents (about 0.2 unit compared with 1 unit). There is no PGC eluotropic series similar to that of silica or alumina. Another result is that the ϵ^0 value for any eluent may depend upon the solutes or the group of solutes used to determine it. However, the evidence confirms that water is undoubtedly the weakest solvent. Methanol and acetonitrile are shown to be of equivalent weakness, while dioxan, tetrahydrofuran (THF) and dichloromethane have the strongest elution strengths. The elution strength of hexane has been shown to depend strongly on the polarity of the analytes, but is generally intermediate between methanol or acetonitrile and THF.

The retention factors of some pesticides and other organic pollutants measured using a PGC column eluted with methanol, THF and methylene chloride are reported in Table 3. The results show that retention can be very high with methanol and that THF and methylene chloride are stronger eluents. Measurements performed with acetonitrile indicate that the retention factors are similar to those obtained with methanol. Once more, there is no apparent relationship between polarity and retention of compounds. A polar pesticide such as metatritron is highly retained in pure methanol, and to a less extent by THF and methylene chloride.

It is important to realize that methanol or acetonitrile are similar weak solvents and compounds that will not elute with methanol will not elute with acetonitrile. Unlike C_{18} silica, the PGC column should not be washed with acetonitrile, and a stronger solvent such as dioxan or THF is required. If the retention of polar, ionizable analytes is too low, then ion-pairing agents can be used in the same way as in

Table 3 Retention factors of various analytes measured in pure organic solvent (methanol, tetrahydrofuran and methylene chloride)

Compound	$\log k_{ow}$	$\log K$		
		MeOH	THF	CH_2Cl_2
Oxamyl	-0.4	-0.51	-1.42	-1.22
Methomyl	1.2	0.04	-0.92	-1.01
Metatritron	0.8	> 1.4	0.23	0.26
Fenuron	1.0	0.28	-0.56	-0.66
Deisopropylatrazine (DIA)	1.1	0.57	-0.71	-0.28
Deethylatrazine (DEA)	1.5	0.22	-1.01	-1.04
Metoxuron	1.6	1.28	0.05	-0.02
Metribuzin	1.6	-0.35	-1.42	-1.04
Aminocarb	1.7	-0.25	-1.35	-1.01
Carbendazim	1.5	1.4	0.79	nd
Chloridazon	1.2	0.96	-0.13	-0.05
Simazine	2.3	0.97	-0.49	-0.39
Atrazine	2.5	0.62	-0.82	-0.85
Diuron	2.8	> 1.4	0.17	nd
Linuron	2.8	1.38	-0.10	-0.16
3,5-Dichlorophenol	3.6	0.52	-0.73	-0.51
2,4,5-Trichlorophenol	4.1	0.99	-0.12	0.20
Anthracene	4.7	> 1.66	1.21	nd
Pentachlorophenol	5	> 1.4	0.81	nd

nd, not determined.

reversed-phase LC to increase the retention. When compounds are strongly retained, the PGC surface can be modified by adsorption of various molecules such as trifluoroacetic acid (TFA) in order to reduce the retention of polar analytes. When looking at some of the values in Table 3, the high retention of phenanthrene in pure THF indicates that nonpolar analytes can be totally retained. The addition of a surfactant such as Tween 80 has been shown to reduce the retention of hydrophobic molecules by 15–20%.

Selected Applications

Geometrical Isomers and Diastereoisomers

PGC allows unique selectivity for geometrical and diastereoisomers owing to its flat structure. A typical example is the separation of phenol and *o*-, *m*- and *p*-cresol which can be achieved in less than 10 min, whereas it is impossible to separate *m*- and *p*-cresol on C_{18} silica. Other examples include the isomers of xylene, some ionizable isomers such as anisidic, toluic, bromobenzoic and nitrobenzoic acids, and the isomers of the corresponding basic forms (anisidine, toluidine, etc.).

Another interesting application from the environmental field is the pre-separation of the less toxic

PCBs from the more toxic non-*ortho* PCBs using hexane/dichloromethane (70 : 30 v/v) as an extraction solvent. A 50 × 4.6 mm column has been specifically developed for the purpose.

Enantiomers

PGC is not a chiral phase but it can be used as a support to separate enantiomers by the addition of chiral discriminators in the mobile phase. The advantages over silica-based sorbents is that the surface of PGC is homogeneous, which allows rapid equilibration. The separation of the enantiomers of a benzodiazepine can be achieved by the addition of β -cyclodextrin to the mobile phase. Another chiral discriminator, carbobenzoxyglycyl-L-proline, was used for the separation of the optical isomers of hydrophilic amino alcohols strongly retained on silica-based materials. The enantiomers were eluted in 5 min on PGC. Another advantage is that the range of chiral compounds can be extended to the whole pH range.

Instead of adding the chiral modifier to the mobile phase, Knox and Wan have coated the PGC with a near-monolayer of an adsorbed enantiomeric modifier (*L*- or *D*-isomers of *N*-(2-naphthalenesulfonyl)phenylalanine), which then acts as an adsorbed stationary phase. Separations of the enantiomers of amino- and hydroxy acids were obtained in this way.

Basic and Acidic Compounds

Because of their inertness, PGC columns can be used over the entire pH range without deterioration of column efficiency and are therefore well suited to the separation of basic or acid compounds. Separation of basic compounds on C_{18} silicas is sometimes difficult and often poor peak shapes are observed, owing to strong secondary ionic interactions between residual silanol groups and the basic analytes. Figure 5 illustrates the difference that was observed for the separation of monochloroanilines and hydroxychloro- or methylchloroanilines. On C_{18} silica (Figure 5A), the more polar 2-hydroxy-5-chloroaniline is eluted first and separation of the monochloroanilines requires a mobile phase containing 33% acetonitrile. On PGC (Figure 5B), monochloroanilines are eluted before 2-hydroxy-5-chloroaniline and the initial mobile phase contains 68% methanol. Little tailing is observed on PGC as compared to C_{18} silica. This has also been observed for the separation of aromatic amines and pyridine.

The use of extreme pH is illustrated by the separation of aromatic amino acids with a mobile phase at pH 1, or the separation of benzodiazepines carried out at pH 10.6. Another example is the separation of

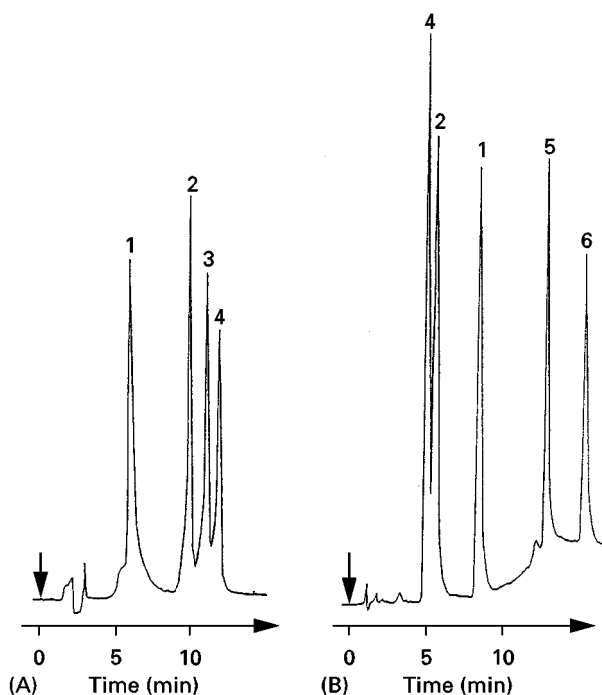


Figure 5 Separation of aniline derivatives (A) using a C_{18} column and (B) using a PGC column.

(A) Spherisorb ODS, 25 cm × 0.46 cm i.d.; mobile phase, 33% acetonitrile with 67% of a 0.05 mol L⁻¹ sodium acetate/acetic acid solution at pH 4.6. (B) Hypercarb column, 10 cm × 0.46 cm i.d. packed with 7 μ m particles; mobile phase, 68% methanol with 32% of a 0.05 mol L⁻¹ sodium acetate/acetic acid solution at pH 4.6 from 0 to 6 min and then gradient up to 91% methanol at 9 min.

Analytes: 1, 2-hydroxy-5-chloroaniline; 2, 2-chloroaniline; 3, 3-chloroaniline; 4, 3-chloroaniline; 5, 5-chloro-2-methylaniline; 6, 2,3-dichloroaniline. UV detection at 240 nm.

water-soluble sugars, which can be ionized at high pH and retained by PGC through the use of ion pairing.

Ionic Compounds

In most cases, ions can be retained on PGC without the help of ion-pairing agents. Remarkable separations of small ionizable compounds of biomedical interest have been published by Lim *et al.* The retention of anionic compounds is explained by electronic interactions occurring between the lone pair electrons of the anionic analyte and the delocalized π bonds of the PGC. Examples include the determination of oxalic acid in human urine; this analyte is totally ionized in water and its separation from the other organic compounds in urine cannot be achieved using a C_{18} silica column. The combination of a sample preparation step using a C_{18} pre-column, which retains hydrophobic interferences but not oxalic acid, and a separation step with a PGC column, allows

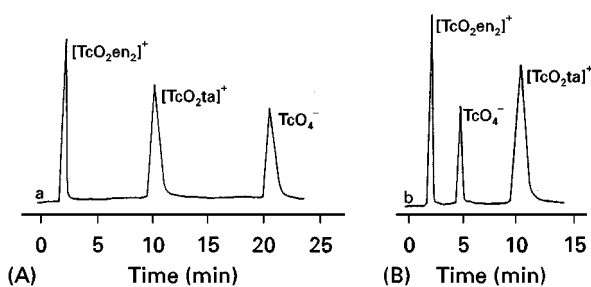


Figure 6 Separation of pertechnetate (TcO_4^-), dioxo(bis-ethylenediamino)technetium, $[\text{TcO}_2\text{en}_2]^+$, and dioxo(1,5,8,12-tetraazadodecane)technetium, $[\text{TcO}_2\text{ta}]^+$, on PGCs (A) with 2% (v/v) acetonitrile in 0.1% TFA as eluent; (B) with 2% acetonitrile in 1% TFA as eluent; flow rate, 1 mL min^{-1} ; detector, radiometric. (Reprinted from Gu G and Lim CK (1990) Separation of anionic and cationic compounds of biomedical interest by HPLC on porous graphitic carbon. *Journal of Chromatography* 515: 183–192. Copyright (1990) with permission from Elsevier Science.)

oxalic acid to be separated from other polar compounds using a mobile phase containing 0.08% TFA. Creatine and creatinine can also be determined in urine and in serum within 8 min using 3% (v/v) acetonitrile and 0.1% TFA.

Anionic and cationic compounds can be separated simultaneously with a mobile phase containing an electronic modifier such as TFA and an organic modifier (e.g. acetonitrile). PGC has been used to separate pertechnetate anions (TcO_4^-) from other mono-cationic amine complexes as shown in Figure 6A with a mobile phase containing 2% (v/v) acetonitrile in 0.1% TFA. TcO_4^- is retained exclusively by electronic interactions while the cationic complexes are retained by hydrophobic reversed-phase interaction. The separation can be controlled precisely according to the nature of the interactions. Increase in the concentration of TFA had a significant effect on the retention time of TcO_4^- , as shown in Figure 6B. The TFA acts as an 'electronic modifier'. Modifying the acetonitrile content affected the retention of the two cationic complexes, but not that of the anionic TcO_4^- .

Ion exchange chromatography can be achieved by modifying the surface of the PGC polyethyleneimine, which is rendered insoluble by flushing the column with a phosphate buffer. This column provides good separation of simple anions and it has been verified that retention is by a simple ion exchange mechanism.

Highly Polar and Water-Soluble Analytes

The use of PGC for the separation of very polar analytes is an important area that is far from being fully explored. Some pertinent examples include the analysis of highly water-soluble carbohydrates, drug metabolites and polar pesticides and their degrada-

tion or transformation products. Many of the separations that have been performed in this area are not possible with other reversed-phase materials.

Monosaccharides can be directly eluted with water from PGC and disaccharides with water containing either 15% methanol or 4% acetonitrile, each peak being split into anomers. A range of alditols containing up to five monosaccharides has been separated using an acetonitrile gradient with 0.05% TFA by Davies *et al.* These workers concluded from the order of retention that the retention mechanism involved interaction of the polar segments of the carbohydrate with the delocalized electrons of the PGC layers. Other examples have been presented for the separation of mono- and disaccharides, sugar acids and sugar amines using mobile phases at pH up to 13.

Figure 7 shows an example of the separation of highly polar pesticides using an acetonitrile/water gradient with an initial content of 10% acetonitrile.

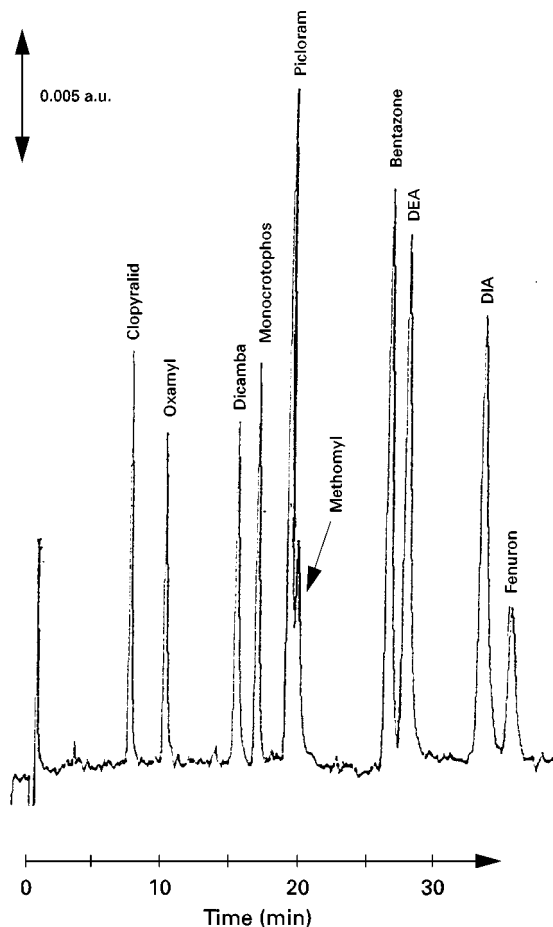


Figure 7 Analytical separation of polar pesticides using $10 \text{ cm} \times 0.46 \text{ cm}$ i.d. Hypercarb column packed with $5 \mu\text{m}$ particles; mobile phase: 0.005 mol L^{-1} phosphate buffer at pH 7 and acetonitrile, gradient from 10% acetonitrile to 15% from 0 to 5 min and up to 40% and 40 min. UV detection at 220 nm.

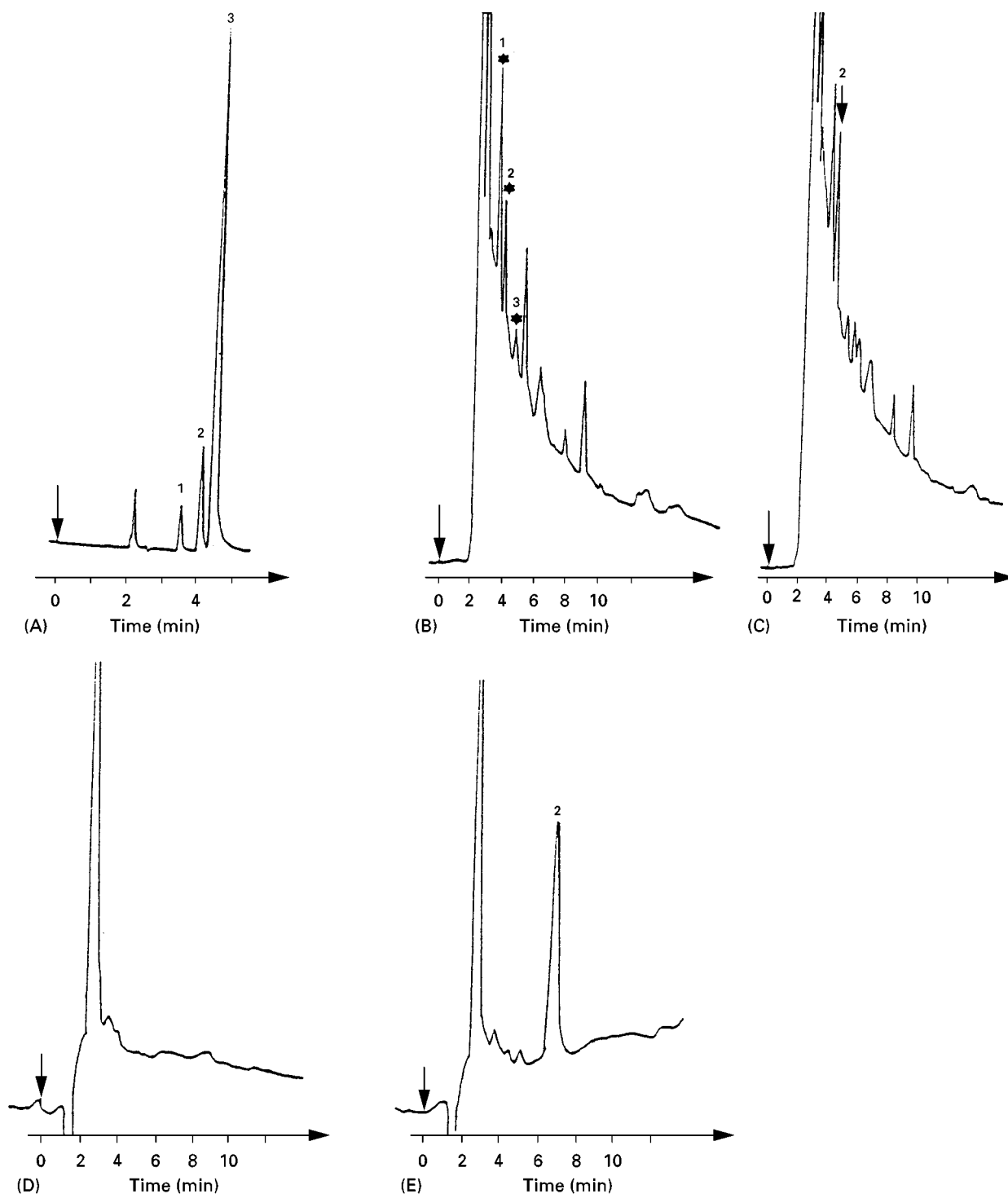


Figure 8 (A) Separation of (1) ammeline, (2) cyanuric acid and (3) ammelide using a 25 cm \times 0.46 cm i.d. C_{18} column (Spherisorb ODS) eluted with a 10^{-3} mol L^{-1} perchloric acid solution. (B) Analysis of a water extract from 250 mL of drinking water not spiked and (C) spiked with $5 \mu g L^{-1}$ of cyanuric acid. (D) and (E) Analysis of the same samples as in (B) and (C) using a Hypercarb analytical column eluted with methanol/0.05 mol L^{-1} phosphate buffer at pH 7 (30 : 70 v/v). UV detection at 220 nm. Extract from water obtained using a commercial solid-phase extraction cartridge packed with PGC.

With a similar gradient applied to a C_{18} column, the retention order is different and oxamyl and deisopropylatrazine (DIA) are only slightly retained. An-

other example is the separation of the polar degradation products of atrazine. Ammeline, ammelide and cyanuric acid (see Table 2) can be separated with an

aqueous mobile phase but with retentions close to the void volume of the column, as shown in **Figure 8A**. Therefore, when these analytes are to be determined in real water at trace levels, the extraction and concentration step generates many interfering compounds that hinder the detection of early eluted analytes, as shown in **Figure 8B** where peaks marked with the stars may correspond to the three analytes. **Figure 8C** corresponds to the extract spiked with cyanuric acid, but no sound conclusion can be made. It was verified that the water did not contain cyanuric acid because, using a PGC column, cyanuric acid is eluted within 8 min with a mobile phase containing 30% methanol. With this column and eluent there is no problem with the separation between the analyte of interest and the interfering coextracted analytes, which are eluted in the peak close to the void volume of the column with such a mobile phase (**Figure 8D** and **E**).

Future Trends

Designed to be the 'perfect reversed-phase material', PGC has been shown to possess a unique chromatographic behaviour, different from other reversed-phase materials. It makes possible the separation of many solutes over a wide range of polarities and is well suited for the separation of positional isomers. Its inert structure allows a complete pH range of eluents to be used, permitting a greater exploitation of the functionality of analytes. The possibility for modification of its surface has opened new areas of applications.

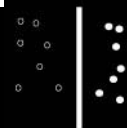
Its unusual retentive behaviour for polar analytes has led to separations that cannot be achieved with other available stationary phases. More work is undoubtedly necessary to achieve a better understanding of the unique behaviour of PGC.

Further Reading

Forgacs E and Cserhati T (1995) Retention strength and selectivity of a porous graphitized carbon column: theoretical aspects and practical applications. *Trends in Analytical Chemistry* 14: 23–29.

- Gu G and Lim CK (1990) Separation of anionic and cationic compounds of biomedical interest by HPLC on porous graphitic carbon. *Journal of Chromatography* 515: 183–192.
- Guenu S and Hennion M-C (1994) On-line sample handling of water-soluble organic pollutants in aqueous samples using porous graphitic carbon. *Journal of Chromatography A* 665: 243–251.
- Hennion M-C, Coquart V, Guenu S and Sella C (1995) Retention behaviour of polar compounds using porous graphitic carbon with water-rich mobile phases. *Journal of Chromatography A* 721: 287–301.
- Knox JH and Ross P (1997) Carbon-based packing materials for liquid chromatography, structure, performance and retention mechanism. In: Brown PR and Grushka E (eds) *Advances in Chromatography*, vol. 37, pp. 74–119. New York: Marcel Dekker.
- Knox JH and Wan QH (1995) Chiral chromatography of amino- and hydroxy-acids on surface modified porous graphite. *Chromatographia* 40: 9–14.
- Kriz J, Adamcova E, Knox JH and Hora J (1994) Characterization of adsorbents by HPLC using aromatic hydrocarbons: porous graphite and its comparison with silica gel, alumina, octadecylsilica and phenylsilica. *Journal of Chromatography A* 663: 151–161.
- Pichon V, Chen I, Guenu S and Hennion MC (1995) Comparison of sorbents for the solid-phase extraction of the highly polar degradation products of atrazine (including ammelide, ammelide and cyanuric acid). *Journal of Chromatography A* 711: 257–267.
- Ross P and Knox JH (1997) Carbon-based packing materials for liquid chromatography: applications. In: Brown PR and Grushka E (eds) *Advances in Chromatography*, vol. 37, pp. 122–162. New York: Marcel Dekker.
- Tanaka N, Tanigawa T, Kimata K, Hosoya K and Araki T (1991) Selectivity of carbon packing materials in comparison with octadecylsilyl- and pyrenylethylsilylsilica gels in reversed-phase liquid chromatography. *Journal of Chromatography* 549: 29–41.
- Wan QH, Davie MC, Shaw PN and Barrett DA (1995) Chromatographic behaviour of positional isomers on porous graphitic carbon. *Journal of Chromatography A* 697: 218–227.
- Wan QH, Davie MC, Shaw PN and Barrett DA (1996) Retention behaviour of ionizable isomers in reversed-phase liquid chromatography: a comparative study of porous graphitic carbon and octadecyl bonded silica. *Analytical Chemistry* 68: 437–446.

POROUS POLYMER COMPLEXES FOR GAS SEPARATIONS: MEMBRANE SEPARATIONS



H. Asanuma, The University of Tokyo, Tokyo, Japan
N. Toshima, Science University of Tokyo
 in Yamaguchi, Yamaguchi, Japan

Copyright © 2000 Academic Press

The Polymer–Metal Complex as a Gas Adsorbent

Solid adsorbents are promising materials for gas separation. A separation is achieved by selectively adsorbing one of the components of a gas mixture onto the surface of a solid adsorbent. To achieve an efficient separation, high selectivity towards the targeted gas against others is necessary. Some metal complexes are quite useful for this purpose. For example, gaseous molecules with non-bonding electrons or π -electrons such as carbon monoxide (CO), ethylene (C_2H_4), and nitrogen monoxide (NO) are co-ordinated reversibly on transition metals (Cu(I), Fe(II), Ag(I), and so on). Thus, solid adsorbents for these gases can be prepared conveniently by immobilizing the corresponding metal complexes on a polymeric resin. The polymer–metal complexes thus formed have good selectivity for the gaseous molecules. However, the polymer used as a support for the metal complex can significantly affect the adsorption properties. For instance, polymer–metal complexes acquire fairly high durability against undesirable molecules compared with the metal complexes without polymer support due to the polymer effect. Another important property of the polymer support is its *porosity*, which regulates the efficiency of the gas separation.

Importance of Porosity for the Efficient Gas Separation

Generally, porous structures are required for useful solid adsorbents. For example, metal complexes supported on a non-porous (gel-type) polymeric resin do not show rapid adsorption, although the metal complex itself binds smoothly to the target molecule. The same phenomenon is observed in conventional physical adsorption processes. The high adsorption capacity of active carbon is mainly attributed to the extremely large surface area of this material ($S \cong 1000 \text{ m}^2 \text{ g}^{-1}$). Similarly, a porous structure is also essential for polystyrene resins which are applied industrially for separation processes. The same ma-

terials formed as round solid beads without physical pores are useless as adsorbents. The significance of the porous structure is well understood by the following simple calculation. In the case of a spherical polystyrene resin *without* porous structure, only the outer surface contributes to the surface area. The specific surface area per unit weight ($\text{m}^2 \text{ g}^{-1}$) is expressed in the following equation as a function of the radius (r nm) of the resin:

$$S = 3 \times 10^3 / (d \cdot r) \quad [1]$$

where d is the density of the polystyrene resin (in this case, d is 1.04 g cm^{-3}). To provide $100 \text{ m}^2 \text{ g}^{-1}$ of S to the polystyrene resin, r would be as small as 29 nm which corresponds to the size of colloidal particles. A nano-sized polystyrene powder is practically useless as an adsorbent so that the technology to provide porous structure is of critical importance.

Preparation of Porous Polymer Complex Adsorbent

Crosslinked polystyrene resin (Pst) is normally used as a starting material of the porous polymer–metal complex. Ways for preparing porous polymer complexes from this resin are illustrated schematically in Figure 1. Primarily, polystyrene resin itself needs to have a porous structure as a matrix. Porous polystyrene resin can be synthesized through special polymerization techniques which are demonstrated below (step 1 in Figure 1). Certain metal ions can form complexes with aromatic hydrocarbons so that the obtained resin is also available as a support without further chemical modification. Complexation of metal ions with polystyrene resin provides the porous polymer–complex adsorbent.

Various organic ligands for the complexation with target metal ions can be also chemically introduced into the porous polystyrene resin (step 2). In this method the porous polymer–complex is obtained by simple complexation of the chelate resin with metal ions. However, porosity can then be further enhanced through complexation of multivalent metal ions and treatment with an organic solvent (step 3). In the following sections, steps 1 and 3 in Figure 1, which are very important processes to prepare porous polymer complex adsorbents, are described in detail.

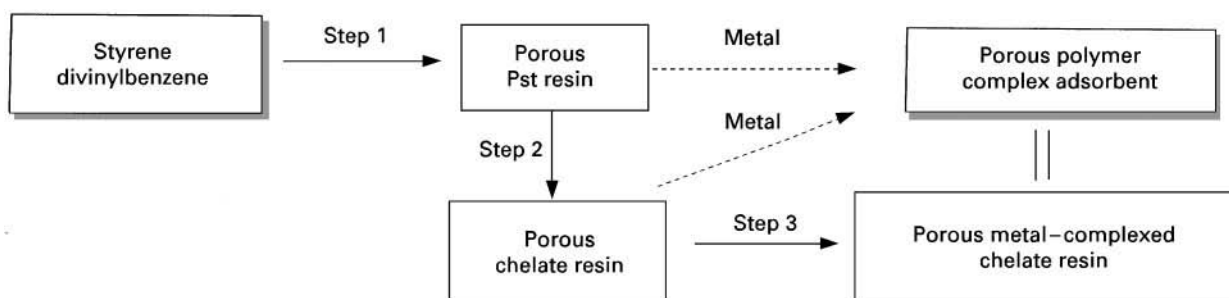


Figure 1 Processes for the preparation of porous polymer metal complexes.

Preparation of Porous Polymeric Resin

As mentioned in the previous section, the polymeric resin itself needs to have a porous structure to prepare porous polymer-metal complexes. Typically, high porosity is provided by the polymerization in the presence of a *porogen*. Generally, there are two methods for the preparation of porous polymers.

Addition of a precipitating solvent as a porogen

This method is based on polymerization in the presence of a *precipitating solvent* (porogen) which solubilizes styrene but not polystyrene. Typical precipitating solvents include heptane, *tert*-amyl alcohol (2-methyl-2-butanol), 2-butanol, and isooctane (2,2,4-trimethylpentane). When polymerization is carried out in the presence of these solvents, nano-sized microgels (polystyrene gel) are separated during the polymerization from the system as illustrated schematically in **Figure 2(A)**. These microgels are connected with each other during the copolymerization and form the three-dimensional network of the polymer beads. The resin obtained is an opaque white colour due to the physical pores formed in the beads.

In contrast, polystyrene resin prepared in the absence of the precipitating solvent is transparent. The nature of the beads (pore size distribution, specific surface area, and so on) can be regulated by the kind of porogen used, and various proportions of divinylbenzene and styrene.

Addition of a soluble linear polymer In this case, a molecular imprinting technique is applied for the pore generation. A soluble linear polymer (polystyrene) added as a template in the copolymerization system is incorporated into the resin. This linear polymer is finally eluted by the subsequent treatment of the resin with an appropriate solvent leaving a hole as illustrated in **Figure 2(B)**. Instead of a linear polymer, a reverse micelle composed of a surfactant (such as sodium bis(2-ethylhexyl)sulfosuccinate) can also be used as a porogen. Pore size distribution, surface area and total pore volume can be elegantly controlled by the size of reverse micelle formed in the copolymerization system.

Formation of metal complex with porous polystyrene resin These porous polystyrene resins themselves

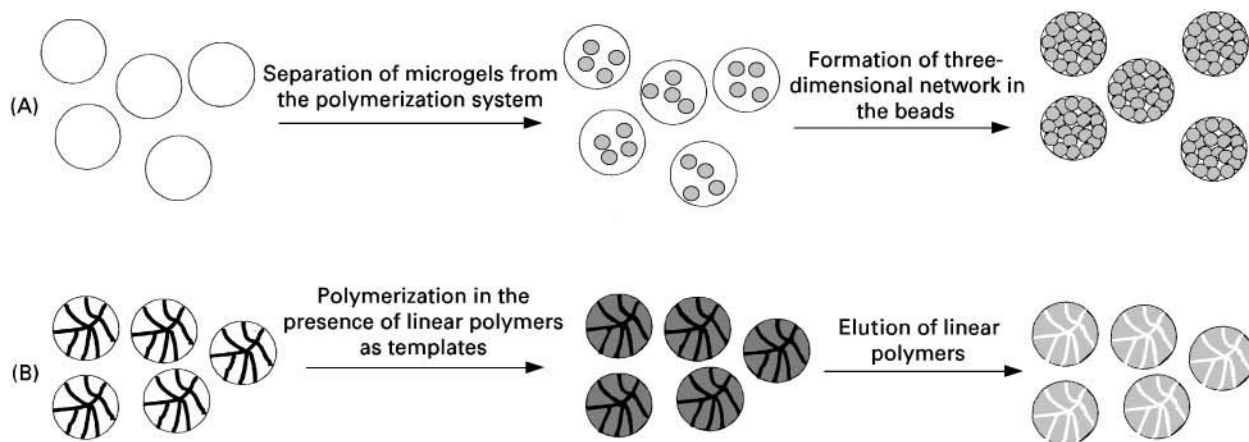


Figure 2 Schematic illustration of the procedures for the preparation of porous crosslinked polystyrene resin. (A) Addition of a precipitating solvent as a porogen. (B) Addition of a soluble linear polymer.

(without chemical modification) are excellent supports of the metal complexes when benzene moieties function as ligands. Double salts such as AlCuCl_4 and AgAlCl_4 are easily immobilized on the polystyrene beads because they preferentially form complexes with π -ligands such as benzene and toluene. For instance, a porous polymer-metal complex of AlCuCl_4 can be prepared by the treatment of AlCuCl_4 and porous polystyrene resin in dry carbon disulfide followed by the evaporation of the solvent. Although a toluene solution of AlCuCl_4 is very unstable to water, the polymer-metal complex has high water-resistivity due to the protection of the polystyrene matrices. This polystyrene resin-immobilized AlCuCl_4 complex functions as an excellent adsorbent of CO (*vide infra*).

Complexation of Porous Polymer to Improve Porosity

The second technique (step 3 in Figure 1) to provide high porosity is based first on complexation with metal ions and secondly subsequent treatment with an organic solvent. The porosity of the styrene-divinylbenzene copolymer having iminodiacetic acid (IDA) moieties (chelate resin; CR, see Figure 5A) can be regulated by complex formation with metal ions, followed by treatment with organic solvents. Maximum porosity is achieved by complex formation of Fe(III) with chelate resin in water and subsequent washing with methanol ($S = 329.2 \text{ m}^2 \text{ g}^{-1}$), whereas no measurable pores are observed without this technique (specific surface area of the original sodium type of the resin is below $0.1 \text{ m}^2 \text{ g}^{-1}$). In the following sections, this technique is described in detail.

Treatment with an organic solvent The network of the polymer is not too rigid, but rather flexible when a small amount of crosslinking agent (divinylbenzene for polystyrene resin) is used. Therefore, the porosity of the resin can be altered by solvent treatment before desiccation. Generally, the porosity decreases when the resin swollen with a good solvent (a solvent which has high affinity with the resin) is desiccated whereas it increases by desiccation after treating the swollen resin with a less-swelling solvent. In the case of polystyrene resin, the porosity decreases by the desiccation from toluene; a good swelling solvent. High porosity is obtained when the resin swollen with toluene is desiccated after having been washed with methanol or acetone in which polystyrene resin cannot swell. The same is true for chelate resin-immobilized metal complex (CR-Me). The chelate resin swells in water due to the hydrophilic IDA moieties so that chelate resin dried from water does not exhibit high porosity. A porous polymer-metal complex can

be obtained by desiccation after having been washed with organic solvent such as methanol in which CR-Me cannot swell. For example, the specific surface area of CR-Fe(II) complex dried after treatment with methanol is $43.1 \text{ m}^2 \text{ g}^{-1}$ whereas that dried from water is as low as $3.2 \text{ m}^2 \text{ g}^{-1}$.

The increase in surface area on washing with an organic solvent is attributed to the suppression of shrinkage caused by the desiccation as illustrated in Figure 3. The CR-Me complex swollen in water keeps a rubberlike state (state A in Figure 3). When the solvent (water) in the resin is exchanged with an organic solvent miscible with water, many microgels are generated by a similar phenomenon to the 're-precipitation' of the polymer (state B). During exchange of the solvent, the resin complex is transformed from the rubberlike state into a glassy state because of the poor swelling in the organic solvent. In this glassy state, the shrinkage of the resin complex by desiccation is suppressed due to the low mobility of the polymer (state C). Consequently, surface area increases because pores produced in the resin complex remain. On the contrary, the resin complex swollen in water shrinks during the evaporation of water because the polymer chains have a high mobility in the rubberlike state (state D).

Efficient exchange of water in the resin with an organic solvent promotes the generation of microgels. Therefore, a solvent of high miscibility with water provides high porosity. The specific surface area of the CR-Fe(II) complex increases monotonously with increase in the solubility parameter δ as shown in Figure 4. Solvents with close δ values are very miscible with each other so that a large δ provides large porosity (note that δ of water is 47.9). Maximum porosity ($= 43.1 \text{ m}^2 \text{ g}^{-1}$ for CR-Fe(II) complex) is obtained from methanol which has the closest δ value ($= 29.7$) to that of water.

Complexation with metal ions of high valency The porosity of the CR-Me complex is also affected by the metal ions bound on IDA moieties as shown in Table 1. Metal ions with high valency are quite effective for providing a large surface area. The CR-Fe(III) complex prepared by desiccation from methanol has a maximum porosity ($S = 329.2 \text{ m}^2 \text{ g}^{-1}$), which is about 10 000 times larger than that of the original CR-Na(I) resin dried from water.

Metal ions (divalent and trivalent cations) are immobilized on CR through complex formation with IDA moieties, producing a 1 : 1 complex as shown in Figure 5(A). In addition to the solvent treatment, the electrostatic repulsion among the metal ions on IDA moieties also contributes to the suppression of the

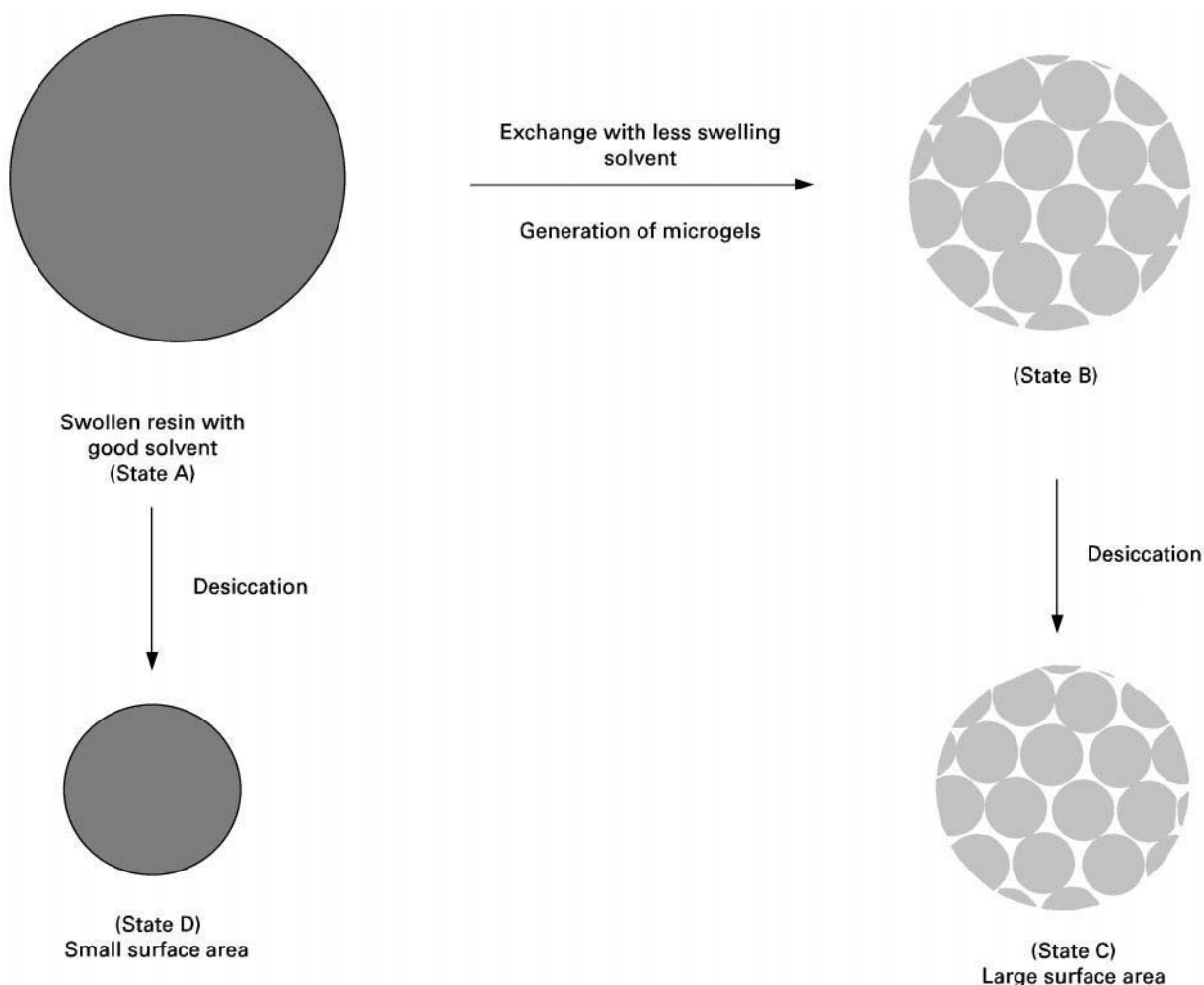


Figure 3 Effect of solvent treatment of the swollen resin on the porosity.

shrinkage, which provides much higher porosity. Since interaction on a molecular level creates these pores, the size of pores generated by this method is smaller than 2.5 nm.

This phenomenon is characteristic of a chelate resin with IDA moieties. The reverse tendency is observed on crosslinked polystyrene sulfonate or polyacrylate. The porosities of these resins is decreased by high valent metal ions because anionic residues are cross-linked by the metal ions through electrostatic interaction as illustrated in Figure 5(B), which promotes shrinkage of the resin.

Gas Separation by Porous Polymer-Metal Complexes

Porous polymer-metal complexes prepared as above are available for efficient gas separation. High porosity directly contributes to the rapid adsorption of target gaseous molecules. In addition, the polymer matrix provides the adsorbent with durability against

contamination compared with the corresponding monomeric system. In the following subsections, separations of CO, ethylene, and NO are demonstrated in detail.

Adsorption of CO and C₂H₄ by Porous Polystyrene-Immobilized Metal Complex

A toluene solution of AlCuCl₄ reversibly absorbs gaseous CO molecules through co-ordination on Cu(I). Thus, immobilization of AlCuCl₄ on polystyrene resin provides an excellent solid adsorbent of CO. The adsorbent composed of porous crosslinked polystyrene beads (Bio-Beads SM-2, surface area 300 m² g⁻¹) and AlCuCl₄ rapidly adsorbs an equimolar amount of CO to the charged Cu(I) within 10 min at 20°C as shown by the solid circles in Figure 6. In contrast, it takes more than a day to reach equilibrium when a gel-type resin (Bio-Beads S-X1) is used as a support (open circles).

Since AlCuCl₄ complex reversibly coordinates C₂H₄, the same polystyrene-immobilized AlCuCl₄

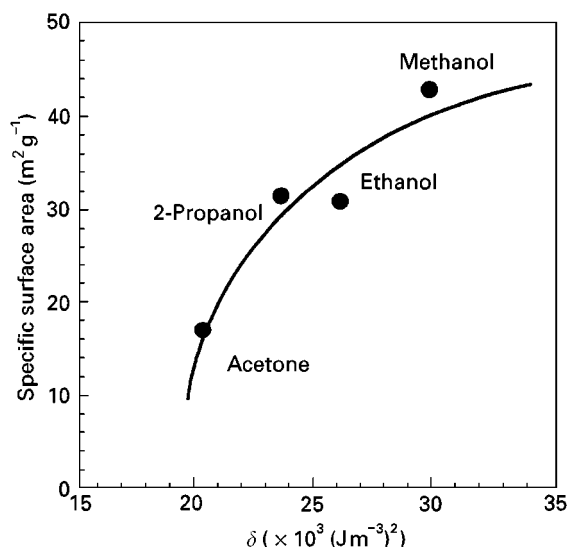


Figure 4 Relationship between the specific surface area and the solubility parameter (δ) of the solvent used for washing the water-swollen CR-Fe(II) complex. The parameter δ corresponds to the square root of the cohesive energy density $(E/V)^{1/2}$, where E and V are the cohesive energy (energy of vaporization) and volume of unit weight of the solvent, respectively. If the δ solubility parameters of the two solvents are close to each other, it indicates that they have high mutual miscibility. Note that the δ value of water is 47.9. (Reproduced with permission from Toshima N, Asanuma H and Hirai H, *Bulletin of the Chemical Society of Japan* 62: 893–902 (1989), p. 901 by courtesy of the Chemical Society of Japan.)

complex also functions as a solid adsorbent of C_2H_4 . The same porous solid adsorbent binds 1.40 times as much C_2H_4 as the charged Cu(I) under the identical conditions of CO adsorption described above. Since a double salt of $AgAlCl_4$ binds C_2H_4 reversibly, porous polystyrene-immobilized $AgAlCl_4$ prepared in a same manner as $AlCuCl_4$ system also functions as a solid adsorbent of C_2H_4 . In this case, selective adsorption towards C_2H_4 against CO is achieved because it does not show binding activity to CO. Both $AlCuCl_4$ and $AgAlCl_4$ are so water-sensitive that toluene solutions of these double salts lose 70% of gas-binding activity by contact with 9000 ppm of water vapour for 10 min. In contrast, polystyrene-immobilized double salts maintain their initial gas-binding activities after contact with water vapour, due to the protection of the metal complex by the hydrophobic polystyrene.

Adsorption of NO by Porous Chelate Resin-Immobilized Fe(II) Complex

CR-Fe(II) complex The complex of Fe(II) and a polyamine *N*-carboxylate [ethylenediaminetetraacetate acid (EDTA), nitrilotriacetate acid (NTA), and IDA]

can bind NO through complex formation. Their aqueous solutions themselves are promising candidates for the absorption of NO because of their high capacity. A solid adsorbent of NO can be prepared by immobilization of above ligand on a polymer chain. For this purpose, the chelate resin involving IDA moieties is available. The porous polymer beads of the chelate resin-Fe(II) complexes which have been demonstrated in the previous section are quite useful as an adsorbent for NO.

Porous chelate resin-immobilized Fe(II) (CR-Fe(II)) complexes are prepared by desiccation of the complex after washing with methanol ($S = 43.1 \text{ m}^2 \text{ g}^{-1}$). The CR-Fe(II) complex shows such high NO adsorption capacity that almost all the NO is removed from 6 dm^3 of nitrogen containing 1000 ppm of NO within 25 min, as shown by the solid circles in Figure 7. On the other hand, the CR-Fe(II) complex prepared by washing with water ($S = 3.2 \text{ m}^2 \text{ g}^{-1}$) does not exhibit such a high adsorbing capability (open circles). The adsorption rate of NO linearly increases with an increase in the specific surface area of CR-Fe(II) complex. This fact clearly demonstrates that the improvement of the porosity contributes directly to rapid adsorption of NO. The adsorbent is completely regenerated by desorption treatment such as keeping the CR-Fe(II)-NO at 90°C under 3 mmHg for 3 h. The CR-Fe(II) complex can be repeatedly used for NO adsorption without significant deterioration.

Nitrogen monoxide is co-ordinated on the Fe(II) ion through 1 : 1 complex formation so that the following Langmuir adsorption isotherm can be applied for the detailed analysis of adsorption properties:



$$1/K = (P/[\text{CR-Fe(II)-NO}])[\text{CR-Fe(II)}] - P \quad [3]$$

where P is the partial pressure of NO (atm) and $[\text{CR-Fe(II)-NO}]$ is the amount of the NO adsorbed at equilibrium (mmol). From the linear plots of P against $P/[\text{CR-Fe(II)-NO}]$, the effective Fe(II) and the dissociation constant ($1/K$; atm) can be calculated from the slope and the intercept of the ordinate, respectively. Table 2 shows the results of Langmuir analyses of CR-Fe(II) complexes with different washing solvents (i.e. different surface area). The K values of each CR-Fe(II) complex is around $8 \times 10^3 \text{ atm}^{-1}$, which does not depend on the washing solvents. The equilibrium constant (K) is even larger than that of an aqueous solution of the Fe(II)-EDTA complex ($5.6 \times 10^3 \text{ atm}^{-1}$). By contrast, the amount of effective Fe(II) ion increases proportionally with the speci-

Table 1 Specific surface area of various chelate resin-immobilized metal complex

Metal	Specific surface area* ($\text{m}^2 \text{g}^{-1}$)		Molar ratio of immobilized metal ion to IDA moieties
	Water [†]	Methanol [†]	
Li(I)	1.1	6.8	2.0
Na(I)	< 0.1	3.3	2.0
K(I)	< 0.1	1.6	2.0
Mg(II)	2.5	22.6	1.0
Ca(II)	3.6	33.3	0.94
Sr(II)	3.2	25.1	1.0
Ba(II)	3.5	19.0	1.0
Al(III)	4.7	54.1	0.77
Fe(III)	5.9	329.2	1.0

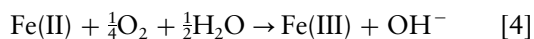
*BET surface area per 1 g of the chelate resin in the sodium form.

[†]Solvent used for washing the resin-immobilized metal complex. (Reproduced with permission from Toshima N and Asanuma H, *Polymers for Gas Separation*, p. 157 by the courtesy of VCH Publishers.)

fic surface area caused by washing with an organic solvent. Thus, wash-treatment does not raise the complex formation constant K , but raises the amount of effective Fe(II) ions through an increase in the surface area.

Immobilization of Fe(II) complex on the polymeric resin has another advantage compared with the aqueous Fe(II) complex. As mentioned at the beginning of

this section, the complexes of Fe(II) and polyamine N-carboxylates (for example, IDA) themselves are promising candidates for the absorption of NO. But an aqueous solution of Fe(II)-IDA, a monomeric model of the CR-Fe(II) complex, readily deteriorates with oxygen through oxidation of Fe(II) to Fe(III) which does not absorb NO. In contrast, the CR-Fe(II) complex has some durability in the presence of oxygen. Both CR-Fe(II) complex and Fe(II)-IDA (each has 16.2 mmol of Fe(II)) can remove more than 90% of NO from 6 dm³ of nitrogen containing 1000 ppm of NO at room temperature before contact with air. In the case of Fe(II)-IDA complex, however, the amount of adsorbed NO decreases below 20% after contact of the complex with air for 60 min. About 80% of Fe(II) ions are oxidized by this treatment. In contrast, a decrease in the amount of adsorbed NO with the CR-Fe(II) complex is scarcely observed, and more than 50% of initially immobilized Fe(II) ions remain without oxidation. This distinct durability of CR-Fe(II) complex to oxygen is mainly attributed to the absence of water. The oxidation of Fe(II) is accelerated by the presence of water according to the following equation:



In the case of Fe(II)-IDA complex, water is inevitably required as a solvent so that oxidation of Fe(II) ions

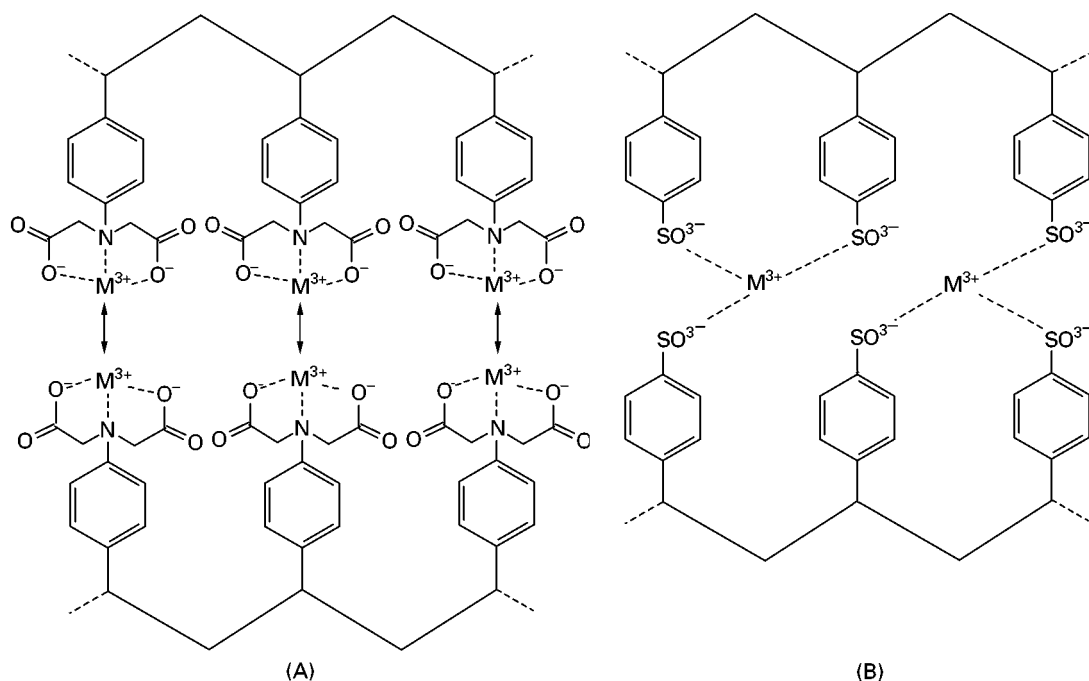


Figure 5 Schematic illustration of the resin-immobilized trivalent metal complex. (A) Chelate resin-immobilized trivalent metal complex. Metal ions are bound to IDA moieties through 1 : 1 complex formation. (B) Polystyrene sulfonate resin-immobilized trivalent metal complex. Ionic moieties are crosslinked by trivalent metal ions through electrostatic interaction. (Reproduced with permission from Toshima N and Asanuma H, *Polymers for Gas Separation*, p. 159 by the courtesy of VCH Publishers.)

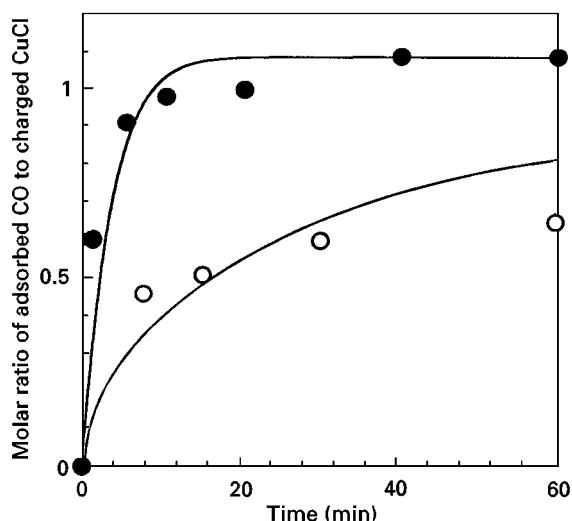


Figure 6 Adsorption of CO by the AlCuCl_4 complex supported on the porous polystyrene resin (●) and gel-type polystyrene resin (○) under 1 atm of CO at 20°C. (Reproduced with permission from Toshima N and Asanuma H, *Polymers for Gas Separation*, p. 152 by the courtesy of VCH Publishers.)

proceeds rapidly. The polymer-metal complexes do not need solvents since metal complexes are dispersed on polymeric matrices. This is one of the advantages of polymer-metal complexes. Furthermore, oxida-

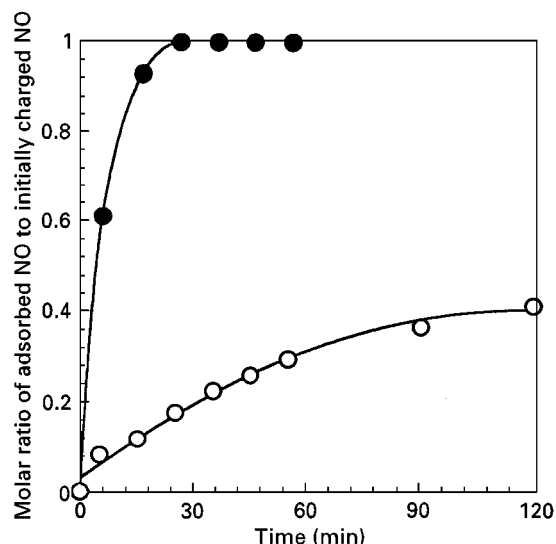


Figure 7 Adsorption curves for NO by the CR-Fe(II) complex prepared by drying after washing with methanol (●) and water (○). These CR-Fe(II) complexes are composed of 8.0 g of chelate resin (involving 21.0 mmol of IDA moieties) and 16.2 mmol of Fe(II) ions. The adsorption experiments are carried out by circulating 6 dm³ of nitrogen containing 1000 ppm of NO at room temperature at the rate of 1.6 dm³ min⁻¹. (Reproduced with permission from Toshima N, Asanuma H and Hirai H, *Journal of Polymer Science, Part A Polymer Chemistry* 28: 907-922 (1990), p. 912 by the courtesy of John Wiley.)

Table 2 Effect of the washing solvent on the complex formation constant (K) at room temperature and the effective amount of Fe(II) ions

Solvent	Effective Fe(II) (mmol g ⁻¹)	Surface area (m ² g ⁻¹)	K^* (10 ³ atm ⁻¹)
Methanol	0.282	43.1	8.33
Ethanol	0.197	31.1	8.33
Acetone	0.144	17.1	6.67

*Binding constant CR-Fe(II)-NO complex formation as determined from Langmuir plots based on eq. [3]. (Reproduced with permission from Toshima N and Asanuma H, *Journal of Polymer Science, Part A Polymer Chemistry* 28: 907-922 (1990), p. 918 by courtesy of John Wiley.)

tion of Fe(II) ions in CR-Fe(II) is suppressed even in the presence of water, probably due to the protection of the metal complex by the polymer matrix.

Highly porous CR complex with mixed valences of Fe(II) and Fe(III) The CR-Fe(II) complex efficiently adsorbs NO, however, the ratio of the effective amount of Fe(II) ions with respect to total immobilized ions is only 0.14, indicating that the CR-Fe(II) complex does not fully exhibit its potential adsorbing capacity. To obtain the potential ability of CR-Fe(II), further enhancement of porosity is effective. Thus, Fe(III) is incorporated into the CR-Fe(II) complex in order to make the complex more porous. The chelate resin-mixed valence iron complex can be prepared by immobilizing both Fe(II) and Fe(III) ions simultaneously. Immobilization of a large amount of Fe(III) ions is preferable for high porosity. The mixed valence complex composed of 1.27 mmol of Fe(III) and 0.44 mmol of Fe(II) (per 1 g of the chelate resin involving 2.6 mmol of IDA moieties) adsorbs NO much more rapidly as expected. Specific surface area of the mixed valence complex is as large as 128.0 m² g⁻¹. Without Fe(III) ions (with 0.62 mmol of Fe(II) ions per 1 g of CR), rapid adsorption is not achieved due to the small porosity ($S = 5.3$ m² g⁻¹). Langmuir analysis (see Table 3) clearly demonstrates the role of each iron ion. Since the binding constant K of NO adsorption by the mixed valence complex is almost the same as that of the CR-Fe(II) complex, the active centre for NO adsorption of the mixed valence complex is identical with that of CR-Fe(II). The amounts of the effective Fe(II) ions for the mixed valence complex and CR-Fe(II) (determined from Langmuir plot) are 0.12 and 0.28 mmol, respectively as listed in Table 3. The value of the efficiency, R , of Fe(II) ions can be estimated from the ratio of the amount of effective Fe(II) to the amount of immobilized Fe(II). The efficiency R of the mixed valence iron complex is larger than that of the CR-Fe(II) complex due to an

Table 3 Amount of effective Fe(II) ions on CR-Fe(II) and mixed valence complex

Complex	Immobilized ion		Surface area (m ² g ⁻¹)	K* (10 ³ atm ⁻¹)	Effective Fe(II) (mmol g ⁻¹)	R [†]
	Fe(III) (mmol g ⁻¹)	Fe(II) (mmol g ⁻¹)				
CR-Fe(II)	0	2.01	43.1	8.33	0.28	0.14
CR-Fe(II), Fe(III)	1.27	0.44	128.1	10.0	0.12	0.26

*Binding constant of CR-Fe(II)-NO complex formation as determined from Langmuir plots based on eqn [3].

†Efficiency of Fe(II) immobilized on chelate resin determined as the ratio of effective Fe(II) to the amount of immobilized Fe(II). (Toshima N and Asanuma H, *Journal of the Chemical Society, Chemical Communications* 1989: 1075-1076, p. 1076 by the courtesy of Royal Society of Chemistry.)

increase in the surface area, demonstrating that the Fe(III) ions work by making the resin porous. The use of these two metal ions enables efficient NO adsorption.

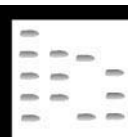
The polymeric resin as well as the metal complex itself greatly affects the adsorbing ability for the target gas molecules as described in the case of CO, C₂H₄, and NO adsorption. It has been demonstrated clearly that large surface area directly contributes to the rapid adsorption of gaseous molecules. In some cases, the nature of the support dominates the whole adsorption property of the polymer-metal complex rather than the nature of the metal complex. Therefore, further regulation of porosity (e.g. pore size distribution) is quite significant in order to achieve efficient separation of the target gas. Metal complexes are promising compounds for reversible coord-

ination of gaseous molecules so that metal complexes immobilized on polymeric supports with properly regulated porosity will provide further useful materials for efficient gas separation.

Further Reading

- Hojo N (ed.) (1976) *Chelate Resin and Ion Exchange Resin*. Tokyo: Kodansha.
- Ruthven DM (1984) *Principles of Adsorption and Adsorption Process*. New York: John Wiley.
- Toshima N (ed.) (1992) *Polymers for Gas Separation*. New York: VCH.
- Toshima N, Endo T and Yamamoto T (1998) *Chemistry of Functional Polymeric Materials*. Tokyo, Asakura.
- Unger KK, Rouquerol J, Sing KSW and Kral H (eds) (1988) *Characterization of Porous Solids*. Amsterdam: Elsevier.

POROUS POLYMERS: LIQUID CHROMATOGRAPHY



A. Coffey, Polymer Laboratories Ltd,
Shropshire, UK

Copyright © 2000 Academic Press

Introduction

Polymers have been used as stationary phases in liquid chromatography (LC) for nearly 40 years. Initially they were used for size exclusion chromatography (SEC), a noninteractive means of separating molecules based on their size. This technique was originally applied to water-soluble macromolecules and is often referred to as gel filtration chromatography (GFC). Gel filtration describes the process particularly well: the stationary phase originally described

was a lightly cross-linked agarose in bead form, although other polysaccharides and also acrylamide-based materials are still employed today.

Characteristically such microporous gels are extremely soft and can easily be crushed. They do not possess a fixed pore structure and analytes can diffuse in and out of the aqueous swollen polymer particles. As a consequence column pressures must be minimized; reduced liquid flow rates and wide-bore columns are a necessity, resulting in extremely long run times. By 1964 a new polymeric stationary phase had been introduced based on cross-linked polystyrene. This material had sufficient cross-linker (in this case divinylbenzene) to ensure a high degree of physical strength when compared with earlier microporous

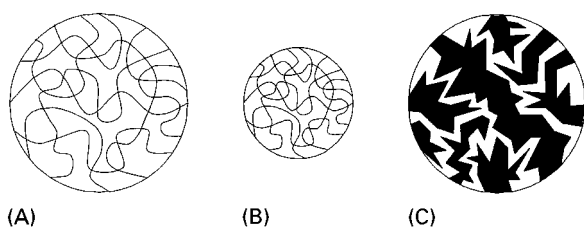


Figure 1 Representation of (A) solvated and (B) nonsolvated microporous beads and (C) a macroporous bead.

particles. The new polymer particles were also made in such a way that the network of pores within the beads was permanent and unaffected by the solvent used. Such particles, which are described as macroporous (**Figure 1**), immediately became useful for the size exclusion separation of organic-soluble macromolecules (or gel permeation chromatography, GPC, as it is commonly known).

Today many types of polymer are employed as stationary phases in chromatography, in both macroporous and microporous forms (**Table 1**). Their use is not restricted to SEC but also covers many aspects of adsorption-based chromatography.

Manufacture of Polymeric Particles

Most polymer-based stationary phases are manufactured as spherical particles, commonly using a suspension polymerization technique. Polystyrene, cross-linked with divinylbenzene (**Figure 2**), is perhaps the commonest form of synthetic polymer used in chromatography at the present time.

The manufacture of poly(styrene-*co*-divinylbenzene) particles, or PS/DVB, involves dispersing a mixture of the monomers including cross-linker and a suitable initiator, all dissolved in an appropriate solvent, into a larger volume of immiscible liquid, known as the continuous phase. Rapid stirring is used to produce the appropriate droplet size, at which point polymerization is triggered; in the case of an organic peroxide or persulfate this is achieved by heating, causing thermal decomposition of the initiator.

Table 1 Comparison between microporous and macroporous particles

<i>Microporous</i>	<i>Macroporous</i>
Low cross-link (< 12%)	High cross-link (> 20%)
High swell	Low swell
Variable pore size	Fixed pore size
Poor physical stability	Good physical stability
Low flow/low pressure applications	High flow/high pressure applications
Wide column diameters	Narrow column diameters

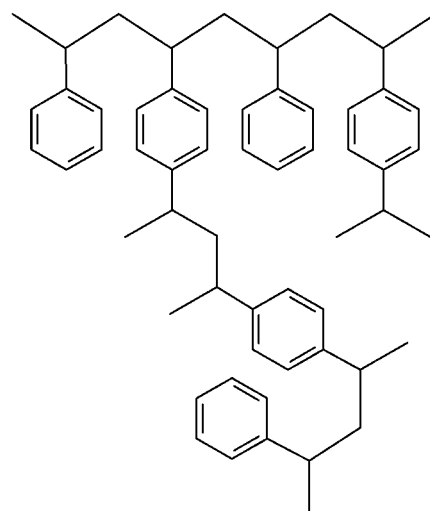


Figure 2 Chemical structure of poly(styrene-*co*-divinylbenzene).

Restricting the amount of cross-linker to less than 12% (by weight) produces a soft microporous particle, whereas using much higher levels of cross-linker (> 20%) produces a rigid particle. In order to introduce the pore structure, the solvent used to dissolve monomers and cross-linker must be a porogen. A porogen acts as a good solvent for the monomers but a poor solvent for the resulting polymer. Once polymerization commences, the growing polymer chain starts to precipitate into small globules, causing phase separation. The globules partially coalesce until all the monomers have been consumed, resulting in polymeric particles containing porogen-filled pores (**Figure 3**).

The particles are then thoroughly washed to remove all traces of porogen and any surface active agents that may also have been used during the manufacturing process. The resultant macroporous particles do not generally have the correct particle size distribution, particularly for high performance applications, and require further refinement by sieving or classification.

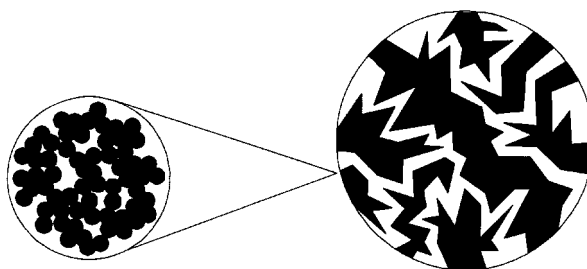


Figure 3 Representation of microspheres formed during suspension polymerization of a macroporous particle.

Size Exclusion Chromatography

The principle of SEC relies on the fact that smaller analytes can penetrate further into the bead, whether they are microporous or macroporous. This increases their residence time so that they elute later from the column. Large macromolecules may be excluded from the pore structure completely, whereas small molecules will totally permeate the accessible pore structure of the beads.

In the manufacture of macroporous particles the choice of porogen and the quantity used enables careful control of the resulting pore size and pore volume. It is thus possible to produce an extensive variety of different products for the analysis of various compounds covering a wide range of molecular weight distributions. Often it is not possible to find an individual column suitable for the analysis of a particular polymer and several different columns employed in series may be required. The actual selection process relies on the accurate calibration of individual columns with highly characterized polymer standards with narrow polydispersity (Figure 4).

The development of such techniques has progressed as equipment has been improved and packing materials have evolved. Modern highly efficient stationary phases tend to have a small particle diameter and are packed into relatively narrow bore columns (6–8 mm i.d.) in lengths of 20–60 cm. This has allowed SEC separations to be performed in minutes rather than hours.

Another recent development has been the use of mixed bed columns (Figure 5). It was discovered by Yau *et al.* in 1978 that by combining two or more packing materials with different individual pore sizes into the same column it was possible to extend the separation range of such a column, thus greatly simplifying the selection process.

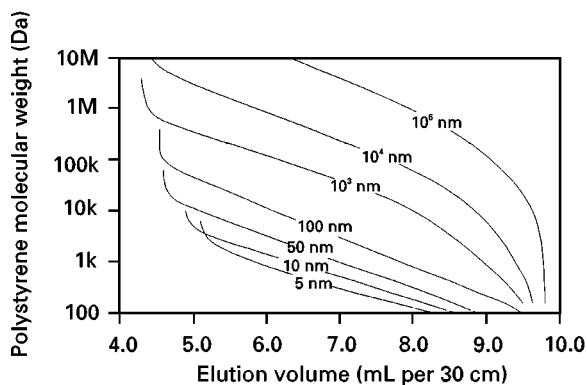


Figure 4 Calibration curves for individual pore sized GPC columns. Column: PLgel, 300 × 7.5 mm, pore size as indicated; eluent: tetrahydrofuran; flow rate: 1.0 mL min⁻¹; detector: refractive index (RI).

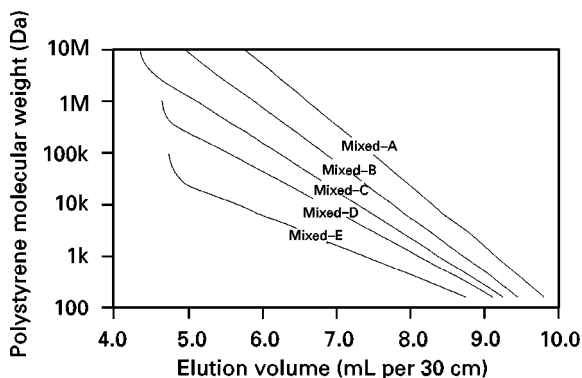


Figure 5 Calibration curves for mixed-bed GPC columns. Conditions as for Figure 4.

While macroporous PS/DVB particles are ideally suited to GPC with organic solvents, such materials are extremely hydrophobic and are not satisfactory for use in SEC separations in an aqueous medium. To eliminate unwanted secondary interactions between the analyte and the stationary phase it becomes necessary either to coat PS/DVB particles with a hydrophilic layer or to move to a completely different polymer system that is inherently aqueous-compatible. Materials produced by both techniques are commercially available, as well as those from silica-based matrices. A polyhydroxyl coating, when applied to PS/DVB particles, can be immobilized by cross-linking it into place utilizing any remaining vinyl groups on the internal and external surfaces of the beads arising from unreacted divinylbenzene. A common alternative polymer system based on methacrylate monomers is also used to produce a range of hydrophilic macroporous particles suitable for GFC.

Reversed-Phase Chromatography

The macroporous polystyrene-based supports used for GPC have also been adapted to reversed-phase chromatography (RPC) applications. The PS/DVB matrix is sufficiently hydrophobic and, coupled with an extremely high internal surface area, this means that analytes partition between the mobile phase and the support in a similar manner to alkyl-bonded silica stationary phases (Figure 6).

Some small molecules may still be able to permeate the polymer structure itself despite the extensive cross-linking and so a stronger organic phase may be required. For example, using methanol as an organic phase can lead to excessive retention times unless it is used in the presence of a small amount of a stronger organic eluent such as tetrahydrofuran. Conversely acetonitrile rarely, if ever, presents any problems.

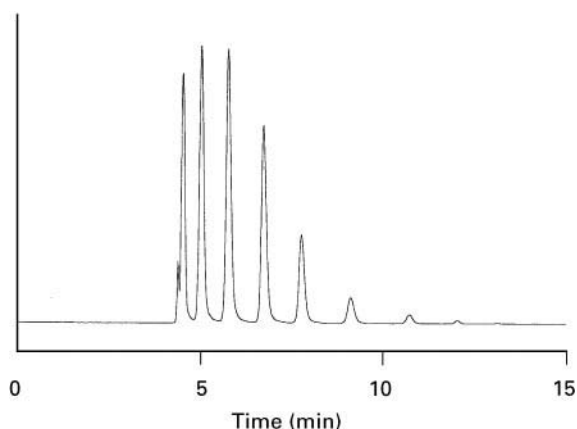


Figure 6 Reversed-phase separation of polyethylene glycol. Column: PLRP-S 10 nm 5 μm , 150 \times 4.6 mm; eluent: 40% acetonitrile; flow rate: 0.5 mL min⁻¹; detector: PL-EMD 960 evaporative light-scattering detector.

Given the aromatic electron-rich ring structure of the PS/DVB matrix, it is perhaps unsurprising that π - π interactions are sometimes observed, leading to longer than expected retention times for some compounds. This is in contrast with the acidic nature of silica-based material. Even high density coverage and extensive end-capping cannot completely eliminate residual silanol groups. These are frequently the source of band broadening of basic analytes, usually observed as a severe tailing of the peak.

The absence of any surface functionality or the need to modify the surface of PS/DVB with alkyl ligands results in an extremely inert stationary phase. This property can be exploited, allowing separations to be performed at pH 9 or above where even the most technologically advanced base-deactivated silica matrices will begin to degrade rapidly. In addition it allows sodium hydroxide solution to be used for clean-up and depyrogenation purposes, which is a significant benefit in preparative purification of pharmaceutical products. The properties of silica-based and polymeric reversed-phase materials are compared in Table 2.

PS/DVB stationary phases prove amenable to all aspects of conventional RPC including ion pair and ion suppression techniques. Figure 7 shows the separation of six proteins by reversed-phase ion pair chromatography.

For other forms of RPC, such as hydrophobic interaction chromatography (HIC), PS/DVB particles are too hydrophobic. The technique is principally applied to protein separations and relies on gradient elution profiles that run from high salt concentrations to low salt concentrations. At high salt concentration proteins are forced to interact with hydrophobic sites on the resin and are retained. As the salt concentration is

Table 2 Comparison between silica-based and polymeric reversed-phase materials

Alkyl-bonded silica	PS/DVB
pH 2–9	pH 1–14
Dissolution of Si matrix	Matrix not soluble
Loss of alkyl ligand	No bonded phase
Leaching of heavy metal contaminants	No contaminants
Packed bed density $\sim 0.6 \text{ g mL}^{-1}$	Packed bed density $\sim 0.3 \text{ g mL}^{-1}$

decreased the proteins elute from the column. Polymeric materials suited to this type of application are hydrophilic matrices that have been modified to make them weakly hydrophobic by inclusion of a relatively low level of short chain alkyl groups or phenyl rings.

Ion Exchange

Ion exchange materials are frequently derived from polymers owing to the relative ease with which the appropriate ionic functionality can be introduced. Both strong and weak anion and cation exchangers can be formed on polystyrene supports and find use in a wide variety of application areas (Table 3).

One difficulty that can occur is due to nonspecific interactions arising from the hydrophobic nature of the PS/DVB backbone. This ‘feature’ has been exploited in related applications such as ion chromatography and ion exclusion chromatography, but for protein separations this property is less desirable. One solution is to coat the hydrophobic macroporous PS/DVB particle with a hydrophilic layer, in much the same way as for aqueous size exclusion applications described above, prior to introduction of the ionic functionality.

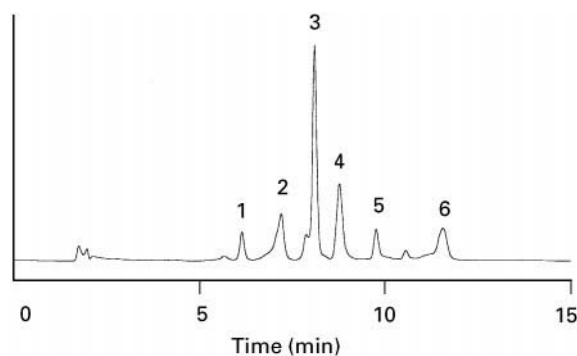


Figure 7 Reversed phase ion pair separation of six proteins. Column: PLRP-S 100 nm 8 μm , 150 \times 4.6 mm; eluent: 20–50% aq. acetonitrile with 0.1% trifluoroacetic acid, 0–20 min; flow rate: 1.0 mL min⁻¹; detector: UV, 254 nm. Key: 1, ribonuclease A; 2, cytochrome c; 3, lysozyme; 4, bovine serum albumin; 5, myoglobin; 6, ovalbumin.

Table 3 Useful ion exchange functionalities

Type	Functional group	pH range
Strong cation exchanger	$-\text{SO}_3^-$	> 3
Weak cation exchanger	$-\text{CO}_2^-$	> 8
Weak anion exchanger	$-\text{NH}_3^+$	< 6
Strong anion exchanger	$-\text{NR}_3^+$	< 9

When applying a coating technique the risk of pore in-filling remains, which would reduce both the accessibility and ionic capacity towards large biomolecules such as proteins. A very thin uniform layer is required but problems can arise if small areas of polystyrene remain exposed. These will interfere with the separation mechanism and so strict quality control procedures are required to detect such weaknesses. An alternative approach to increase the surface density of the ionic functionality has been to apply a thin layer of microspheres to the surface of the particle, thus significantly increasing the surface area.

Ion Chromatography

Ion chromatography is a particularly important analysis technique, often used for analysis of inorganic ions in water. It covers an enormous range of application areas and may be considered independently from ion-exchange chromatography. Stationary phases for ion chromatography usually possess a very low level of ionic functionality, perhaps 1% that of conventional ion exchange resins. This is so that a very dilute buffer solution can be used as eluent together with a conductivity or similar electrochemical detector in order to achieve the degree of sensitivity required. Even so, several commercial systems require the use of a suppressor column to reduce the background conductivity of the eluent further and so increase detection sensitivity. Indirect UV detection has also been used but can cause difficulties.

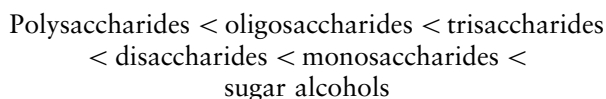
Ion Exclusion and Ligand Exchange

Ion exclusion and ligand exchange chromatography are specialized forms of ion exchange, but where many of the columns used are based on low cross-linked microporous PS/DVB gels. The principal application areas for the two column types are the analysis of organic acids and carbohydrates, respectively. Ion exclusion resins are sulfonated polystyrene particles with a cross-link content of around 4–8%. A very high level of sulfonation is used during manufacture, which renders the PS/DVB matrix hydrophilic. Dilute sulfuric acid is commonly used as the eluent in ion exclusion in order to ensure that the organic acids exist in the fully protonated, neutral

form. The separation mechanism has some size exclusion properties owing to the soft nature of the resin, but the principal mode of interaction is through hydrogen bonding and ionic interactions. Some reversed-phase-type of hydrophobic interactions may also remain. The separation of organic acids by ion exclusion chromatography is illustrated in Figure 8.

Since the stationary phase has such a low level of crosslinker it is usually packed into columns of 7–8 mm i.d. in lengths of up to 30 cm. Even so, the flow rate that can be passed through such columns without generating excessive back-pressure is very low, in the order of 0.5–0.6 mL min⁻¹. The viscosity of water or dilute sulfuric acid is such that the separation is normally carried out at elevated temperature (40–60°C). Some care is needed when performing separations involving certain types of carboxylic acid as it is possible to cause inter- or intramolecular reactions where carboxylic acid groups and hydroxyl groups are both present – dehydration can occur, generating anhydrides and generally interfering with the separation mechanism.

This type of sulfonated polystyrene resin can be further modified to produce media for ligand exchange separations of polysaccharides. By introducing a heavy metal counterion – commonly calcium, lead or sodium – it is possible to introduce a new type of interaction mechanism. The resins still possess size exclusion properties and so the elution order of simple carbohydrates is:



The separation of disaccharides, such as maltose and sucrose, and monosaccharides, such as glucose

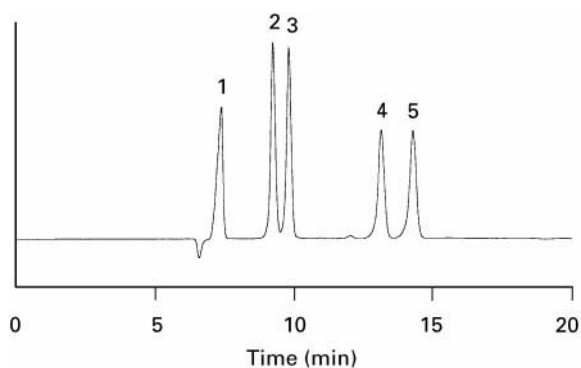


Figure 8 Ion exclusion separation of organic acids. Column: PL Hi-Plex H, 300 × 7.7 mm; eluent: 0.005 mol L⁻¹ H₂SO₄; temperature: 55°C; flow rate: 0.6 mL/min; detector: UV, 210 nm. Key: 1, oxalic acid; 2, citric acid; 3, tartaric acid; 4, succinic acid; 5, lactic acid.

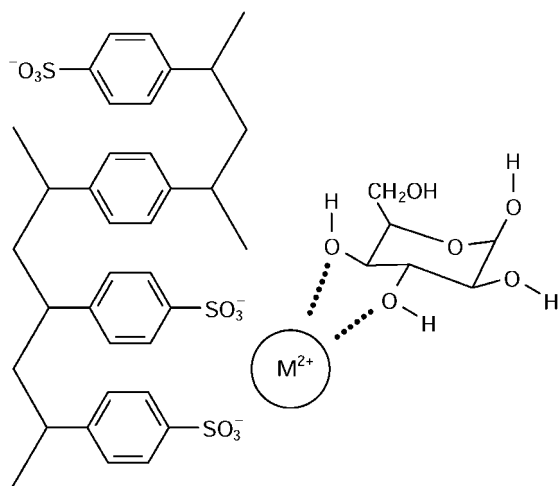


Figure 9 Mechanism of interaction for ligand exchange separation of saccharides.

and fructose, is influenced by the degree of interaction of the numerous hydroxyl groups on the sugar molecules with the metal counterion. Each saccharide molecule has a unique arrangement of axial and equatorial hydroxyl groups, which are able to interact through hydrogen bonding to a greater or lesser extent. The interaction mechanism is illustrated in Figure 9.

The separation is further confused by the ability of sugar molecules to exist in an equilibrium state between two anomeric forms (and briefly as the linear molecule). Sugar alcohols are linear and they are able to adopt a flexible conformation, greatly increasing the degree of interaction, and hence retention time, on such columns. Figure 10 shows the separation of carbohydrates by ligand exchange.

Unlike with ion exclusion materials, it is not possible to use sulfuric acid as an eluent otherwise the heavy metal counterion would be stripped and re-

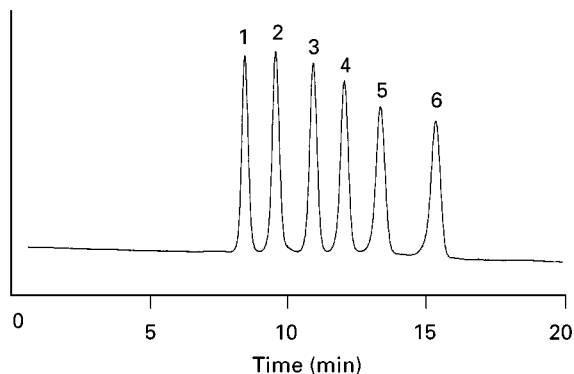


Figure 10 Ligand exchange separation of carbohydrates. Column: PL Hi-Plex Ca, 300 × 7.7 mm; eluent: water; temperature: 85°C; flow rate: 0.6 mL min⁻¹; detector: RI. Key: 1, raffinose; 2, lactose; 3, glucose; 4, galactose; 5, fructose; 6, erythritol.

placed. It is also important to avoid fouling of individual column types with dissimilar heavy metal ions. The same restrictions on flow rate apply to these column types as to their ion exclusion counterparts but, because the risk of side reactions is removed, the temperature for such analyses can be further increased up to 85°C.

Affinity Chromatography

Affinity chromatography relies on the introduction of a suitable ligand onto the surface of the resin. Frequently residual hydroxyl functionality is used to react with epichlorohydrin. This generates epoxide groups on the surface of the stationary phase, which can then be used to react with amines on the ligand molecule where appropriate.

As with other separations performed in predominantly aqueous media, it is important to eliminate nonspecific binding. For this reason PS/DVB materials are not particularly suitable unless coated with a hydrophilic film. Methacrylate resins (as described above) can be manufactured incorporating the epoxide functionality *in situ*; otherwise agarose-type materials are perhaps the most common.

Other Unusual Polymeric Supports

A number of unique polymer-based materials have been introduced in recent years to enable unusual separations to be performed. Many of these materials are covered more extensively elsewhere in this encyclopedia and so are not covered in detail here.

Chiral separations can be considered to be a form of affinity chromatography – the ligand chosen is often chiral itself or otherwise possesses an unusual affinity for another chiral molecule. A further development of this process has been to incorporate a ligand as a template molecule into the monomer mixture during the polymerization process. The ligand is removed during washing and clean-up of polymer particle but a molecular imprint remains that can increase the retention time for these molecules during actual analyses.

Pirkle supports are unusual in the respect that the outer surface of the bead contains a different functionality to the inner surface of the macropores. This is usually achieved by modifying the chemistry of the bead as a whole, but then the outer surface of the bead is further modified using a polymeric reagent or enzyme that is excluded from the pore structure. For very large molecules such as plasmids or DNA, which may be unable to penetrate even the largest pores of polymeric media, separations are still possible by using solid particles. The surface area in comparison

to a macroporous molecule is fractional but by using very small particle diameters it can be increased somewhat to enable a separation to take place. The small particle size results in an extremely high back-pressure, and so column lengths are greatly reduced.

In a move away from particles it has become possible to polymerize the monomer/porogen mixture within the column itself, generating the pore structure in much the same way as particles but resulting in a monolith structure – a rigid polymeric cylinder containing through pores as well as diffusive pores. Columns containing such structures are now commercially available.

See also: II/Chromatography: Liquid: Mechanisms: Ion Chromatography; Mechanisms: Reversed Phases; Mechanisms: Size Exclusion Chromatography. III/Carbohydrates: Liquid Chromatography.

Further Reading

Hashimoto T (1991) Macroporous synthetic hydrophilic resin-based packings for the separation of biopolymers. *Journal of Chromatography* 544: 249–255.

Lloyd LL (1991) Rigid macroporous copolymers as stationary phases in high-performance liquid chromatography. *Journal of Chromatography* 544: 201–277.

Meehan E (1995) Semirigid polymer gels for size exclusion. In: Chi-san Wu (ed.) *Handbook of Size Exclusion Chromatography*, p. 25–46. New York: Marcel Dekker.

Moore JC (1964) Gel permeation chromatography. 1. A new method for molecular weight distribution of high polymers. *Journal of Polymer Science A* 2: 835–843.

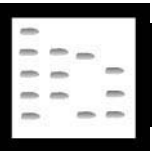
Porath J and Flodin P (1959) Gel filtration: a method for desalting and group separation. *Nature* 183: 1657–1659.

Yang Y-B and Regnier FE (1991) Coated hydrophilic polystyrene-based packing materials. *Journal of Chromatography* 544: 233–247.

Yau WW, Ginnard CR and Kirkland JJ (1978) Broad-range linear calibration in high-performance size-exclusion chromatography using column packings with bimodal pores. *Journal of Chromatography* 149: 465–487.

Yau WW, Kirkland JJ and Bly DD (1979) Bimodal pore-size separations: optimum linearity and range. In: *Modern Size Exclusion Chromatography*, p. 267. New York: Wiley.

PORPHYRINS: LIQUID CHROMATOGRAPHY



C. K. Lim, MRC Toxicology Units, Leicester, UK

Copyright © 2000 Academic Press

Introduction

Porphyrins are cyclic tetrapyrrolic compounds (Figure 1) occurring widely in nature. They are, except for protoporphyrin, the oxidized by-product of the porphyrinogens (hexahydroporphyrins) which are the intermediates in the pathways of haem and chlorophyll biosynthesis.

The analysis and separation of porphyrins not only is important in the fields of chemistry and biochemistry of this important group of tetrapyrrolic pigments but is also valuable in the biochemical diagnosis of human porphyrias, a group of diseases associated with abnormal haem biosynthesis and consequently the overproduction of haem precursors. Since some of the enzymes of the haem pathway are sensitive to certain toxic chemicals, analysis of porphyrin excretion patterns may provide a sensitive indicator of exposure to these toxic chemicals which often results in characteristic and diagnostic metabolic alterations of the pathway.

Figure 2 shows the structures of some of the most commonly analysed naturally occurring porphyrins. High performance liquid chromatography (HPLC) is the best technique for the separation of these and other porphyrins. The resolution achieved by HPLC is far superior to other methods, including thin-layer chromatography and capillary electrophoresis (CE).

The HPLC separation of porphyrins, their important metal complexes and hexahydroporphyrins (por-

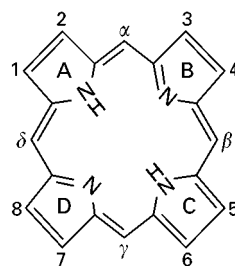


Figure 1 Structure of porphyrin macrocycle (Fischer's numbering system). The four pyrrole rings are designated A, B, C and D. The β -positions, which are usually substituted with acetic acid (Ac), propionic acid (Pr), methyl (Me), ethyl (Et) and vinyl (V) groups, are numbered 1–8. The four methine bridges or meso-positions are denoted α , β , γ and δ .

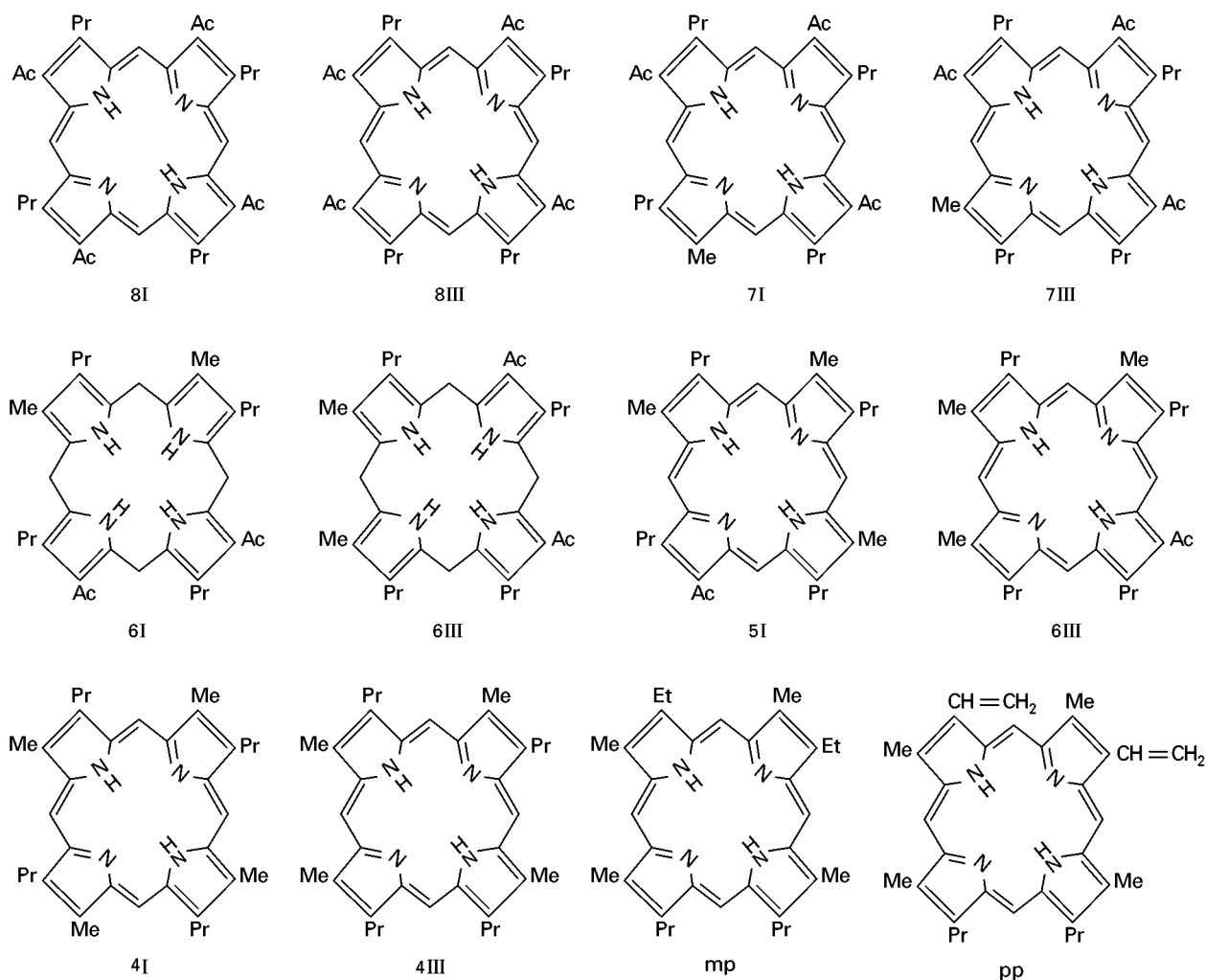


Figure 2 Structures of some commonly analysed naturally occurring porphyrins. 8I, Uroporphyrin I; 8III, uroporphyrin III; 7I, heptacarboxyl porphyrin I; 7III, heptacarboxyl porphyrin III; 6I, hexacarboxyl porphyrin I; 6III, hexacarboxyl porphyrin III; 5I, pentacarboxyl porphyrin I; 5III, pentacarboxyl porphyrin III; 4I, coproporphyrin I; 4III, coproporphyrin III; mp, mesoporphyrin; pp, protoporphyrin.

pyrinogens) are described below with particular reference to the choice of columns, mobile phases and methods of detection.

Separation of Porphyrin Methyl Esters

Porphyrins may be separated as the underivatized free acids or as their methyl esters following esterification of the carboxylic acid groups. The choice often depends on the application and the sample matrix in which the porphyrins are extracted.

Although many of the methods reported for the separation of porphyrin methyl esters are by normal-phase chromatography on silica, they are better separated by reversed-phase HPLC. Reversed-phase HPLC provides better resolution and is able to separate the type-I and type-III isomers of hexacarboxyl porphyrin hexamethyl ester, pentacarboxyl porphyrin pentamethyl ester and coproporphyrin tet-

ramethyl ester. Furthermore, the polar porphyrins (e.g. hydroxylated uroporphyrins) which are difficult to elute from normal-phase columns are easily eluted before uroporphyrin from the reversed-phase column because the elution order is the opposite of that encountered in normal-phase chromatography.

Figure 3 shows the separation of a mixture of porphyrin methyl esters by normal phase (A) and reversed-phase HPLC (B). The superiority of the latter is clearly demonstrated. The resolution of normal-phase separation could be improved by using 3- μ m particle size silica, but is still insufficient compared with RP-HPLC.

Separation of Porphyrin Free Acids

Choice of Column

Porphyrin free acids are best chromatographed on a reversed-phase column. Chemically bonded silica

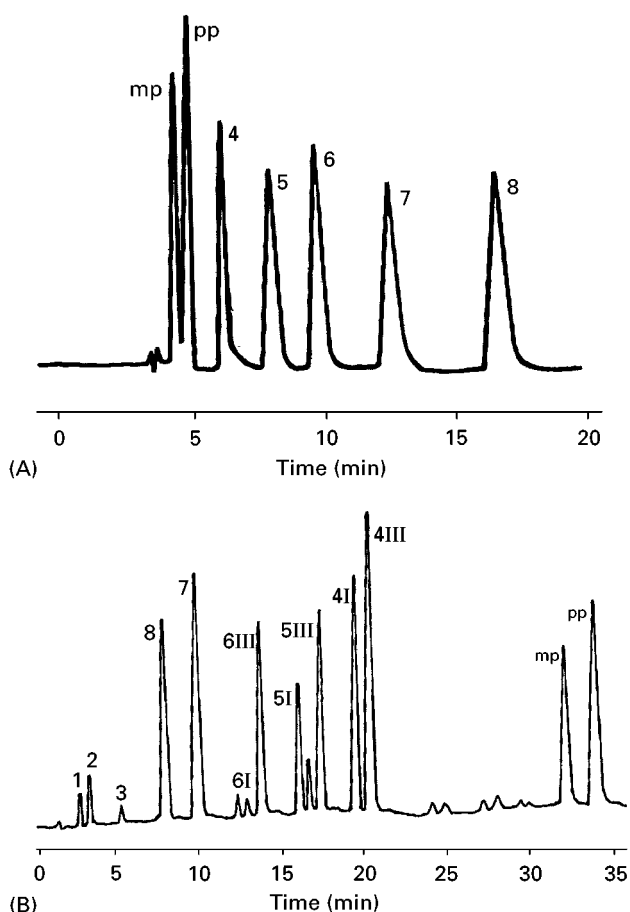


Figure 3 HPLC separation of porphyrin methyl esters. (A) Normal phase (μ Porasil, 300×4 mm, $10\text{-}\mu\text{m}$ particle size); eluent, *n*-heptane–methyl acetate (3 : 2, v/v); flow rate, 1.5 mL min^{-1} . (B) Reversed-phase (Hypersil ODS, 250×4.6 mm, $5\text{-}\mu\text{m}$ particle size); eluent, linear gradient elution from 70% acetonitrile in water to 100% acetonitrile in 30 min; flow rate, 1 mL min^{-1} . Peaks: 1, 2 and 3 = hydroxylated porphyrins; 4, 5, 6, 7 and 8 refer, respectively, to tetra- (copro), penta-, hexa-, hepta-, and octa- (uro) carboxyl porphyrin; I and III denote type-I and type-III isomers; mp = mesoporphyrin; pp = protoporphyrin.

with different hydrocarbon chain lengths, from C_1 (trimethylsilyl groups) to C_{18} (octadecylsilyl groups) have all been successfully used for the separation of porphyrins. A C_{18} column is preferred because it is more stable towards aqueous buffer than a C_1 column. The wide range of base-deactivated C_{18} column packings (e.g. Hypersil-BDS) further improves the efficiency of porphyrin separations and is the column of choice.

Choice of Mobile Phase

The porphyrins derived from the haem biosynthetic pathway are amphoteric compounds ionizable and soluble in both acids and bases. They are therefore

ideal for separation by RP-HPLC in the presence of an ion-pairing agent (e.g. tetrabutylammonium phosphate) or by ionization control with an acid (e.g. trifluoroacetic acid), a base (e.g. triethylamine) or a buffer solution (e.g. ammonium acetate buffer).

The choice of a correct mobile phase is obviously important for achieving an optimal separation. With the increasing use of online HPLC–mass spectrometry (LC–MS), the chosen mobile phase ideally should also be fully compatible with mass spectrometry. The introduction of hybrid electrospray quadrupole/time-of-flight MS allows sensitive and specific analysis of porphyrin free acids by LC–MS. To exploit this capability a mobile phase that is sufficiently volatile and is able to separate the whole range of porphyrins, including the complex type-isomers, is highly desirable. This rules out reversed-phase ion pair chromatography and the use of phosphate buffer. Simple acidic eluent such as 0.1% trifluoroacetic acid–acetonitrile mixtures can be used for the separation of porphyrins. However, resolution of the type-isomers of uro- and hepta-carboxyl porphyrins was not achieved although type-isomers of porphyrins with 6, 5, and 4 carboxyl groups were well separated.

To date, mobile phases containing ammonium acetate buffer provide excellent resolution and column efficiency as well as being fully compatible with

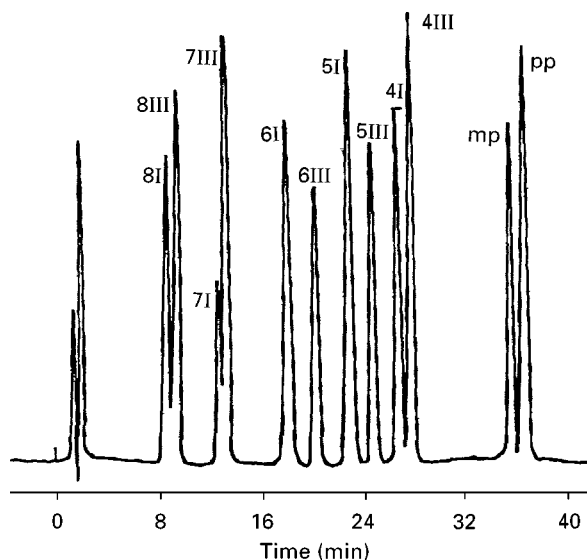


Figure 4 Separation of a standard mixture of porphyrins. Column, Hypersil-SAS (150×5 mm, $5\text{-}\mu\text{m}$ particle size); solvent A, 10% (v/v) acetonitrile in 1 M ammonium acetate buffer, pH 5.16; solvent B, 10% (v/v) acetonitrile in methanol; elution, 30 min linear gradient from 0% B to 65% B followed by isocratic elution at 65% B for a further 10 min; flow rate, 1 mL min^{-1} ; detection, 404 nm. Peaks: 8, 7, 6, 5 and 4 refer, respectively, to octa- (uro), hepta-, hexa-, penta- and tetra- (copro) carboxyl porphyrin; I and III denote type-I and type-III isomers; mp = mesoporphyrin; pp = protoporphyrin.

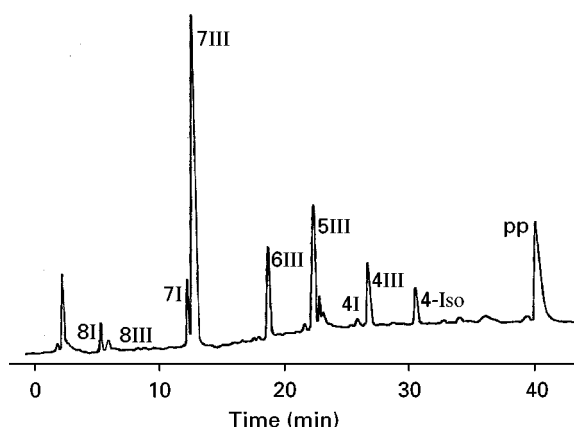


Figure 5 Separation of porphyrins in the faecal extract of a patient with porphyria cutanea tarda (PCT). Column, Hypersil-ODS (250×4.6 mm, $5\text{-}\mu\text{m}$ particle size); solvent A, 10% acetonitrile in 1 M ammonium acetate buffer (pH 5.16); solvent B, 10% acetonitrile in methanol; elution, linear gradient at 1 mL min^{-1} from 10% to 90% solvent B in 30 min, followed by isocratic elution at 90% B for a further 10 min; detection, 404 nm. Peaks: 4-Iso = isocoproporphyrin; pp = protoporphyrin; other peaks are identified as in Figures 3 and 4.

LC-MS operation. This buffer has been studied for the separation of porphyrins in detail and the following conclusions have been drawn:

1. The molar concentration of ammonium acetate buffer in the mobile phase significantly affected the retention and resolution. The optimum buffer concentration is 1 M. Below 0.5 M, excessive retention and peak broadening results, particularly in isocratic elution. At above 1.5 M, rapid elution with the consequent loss of resolution was observed.
2. The retention and resolution of the porphyrins are greatly influenced by the pH of the ammonium acetate buffer. Increasing the pH decreased the retention with loss of resolution. The optimum pH range is between 5.1 and 5.2, although this is column dependent. This pH range is, however, suitable for most reversed-phase columns.

In earlier studies it was shown that the isocratic elution of uroporphyrin I and III from reversed-phase columns was organic modifier specific and, with methanol as the organic modifier and 1 M ammonium acetate (pH 5.16) as the aqueous buffer, excessive retention and peak broadening was observed. The methanol adsorbed on the hydrocarbonaceous stationary phase surface is able to form extensive hydrogen bonds with the eight carboxyl groups of uroporphyrin, thus resulting in long retention and peak broadening. This effect is less significant in the separation of porphyrins with fewer

carboxyl groups. Nevertheless it is best to avoid using methanol as the sole organic modifier in porphyrin separations, especially when uroporphyrin is one of the components to be separated.

Replacing methanol with acetonitrile results in excellent resolution of uroporphyrin isomers within convenient retention times. Acetonitrile, however, is immiscible with 1 M ammonium acetate when its proportion is above 35% in the mobile phase. While acetonitrile–1 M ammonium acetate buffer mobile phase systems are excellent for the separation of porphyrins that can be eluted at up to 30% acetonitrile content (8-, 7-, 6-, 5- and 4-carboxyl porphyrins), they are not suitable for the separation of porphyrins that required a higher proportion of acetonitrile for elution, such as the dicarboxyl mesoporphyrin and protoporphyrin. In order to achieve simultaneous separation of all the porphyrins, therefore, a mixture of acetonitrile and methanol as the organic modifier is required. 1 M ammonium acetate buffer is completely miscible with methanol. A mixture consisting of 9–10% (v/v) acetonitrile in methanol as the organic modifier thus overcomes the hydrogen bonding effect caused by methanol and the solubility problem of 1 M ammonium acetate in acetonitrile. In practice, gradient

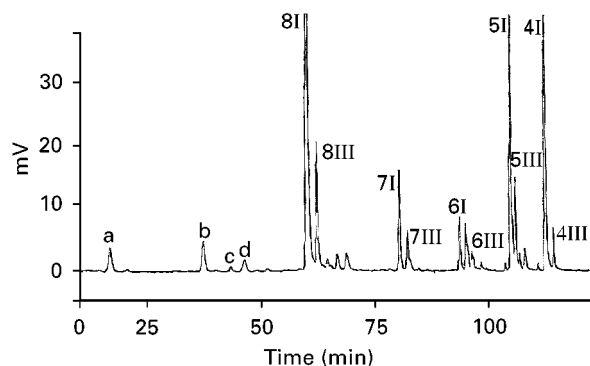


Figure 6 Separation of porphyrins in the urine of a patient with congenital erythropoietic porphyria (CEP). Column, Hypersil-BDS C_{18} (250×4.6 mm, $5\text{-}\mu\text{m}$ particle size); solvent A, 10% (v/v) acetonitrile in 1 M ammonium acetate buffer, pH 5.16; solvent B, 10% acetonitrile in methanol. The elution programme was: 0 to 20 min, isocratic elution at 100% A; 20 to 36 min, linear gradient from 0% B (100% A) to 8% B; 36 to 46 min, isocratic elution at 8% B; 46 to 56 min, linear gradient from 8% B to 16% B; 56 to 66 min, isocratic elution at 16% B; 66 to 86 min, linear gradient from 16% B to 30% B; 86 to 95 min, linear gradient from 30% B to 38% B; 95 to 108 min, linear gradient from 38% B to 42% B; 108 to 118 min, linear gradient from 42% B to 66% B; 118 to 128 min, linear gradient from 66% B to 75% B; 128 to 138 min, linear gradient from 75% B to 90% B; 138 to 145 min, isocratic elution at 90% B. The flow rate was 1 mL min^{-1} throughout. Detection, 404 nm. Peaks: a = meso-hydroxyuroporphyrin I; b = β -hydroxy propionic acid uroporphyrin I; c = hydroxyacetic acid uroporphyrin I; d = peroxyacetic acid uroporphyrin I. The other peaks are identified as in Figures 3 and 4.

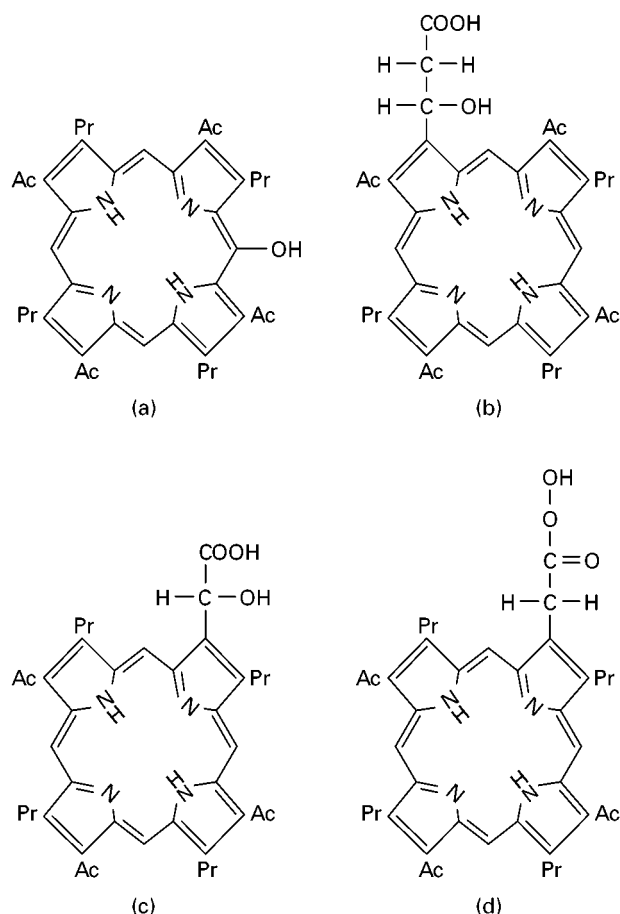


Figure 7 Structures of meso-hydroxyuroporphyrin I (A), β -hydroxypropionic acid uroporphyrin I (B), hydroxyacetic acid uroporphyrin I (C) and peroxyacetic acid uroporphyrin I (D).

elution is carried out by inclusion of 10% (v/v) acetonitrile in each of the gradient solvents, i.e. 1 M ammonium acetate (pH 5.16) and methanol.

Separation of Porphyrin Mixtures by Gradient Elution

The separation of a standard mixture of porphyrins on a C_{18} -bonded RP Column (Hypersil-SAS) with the optimized gradient mixtures of 10% acetonitrile in 1 M ammonium acetate, pH 5.16 (solvent A) and 10% acetonitrile in methanol (solvent B) is shown in Figure 4. The complete resolution of uro-, heptacarboxyl-, hexacarboxyl-, pentacarboxyl- and coproporphyrin isomers and the dicarboxyl meso- and proto-porphyrins required just 38 min.

Figure 5 shows the separation of porphyrins on a Hypersil-ODS column, extracted from the faeces of a patient with porphyria cutanea tarda (PCT). It clearly demonstrates the applicability of the system to biomedical analysis.

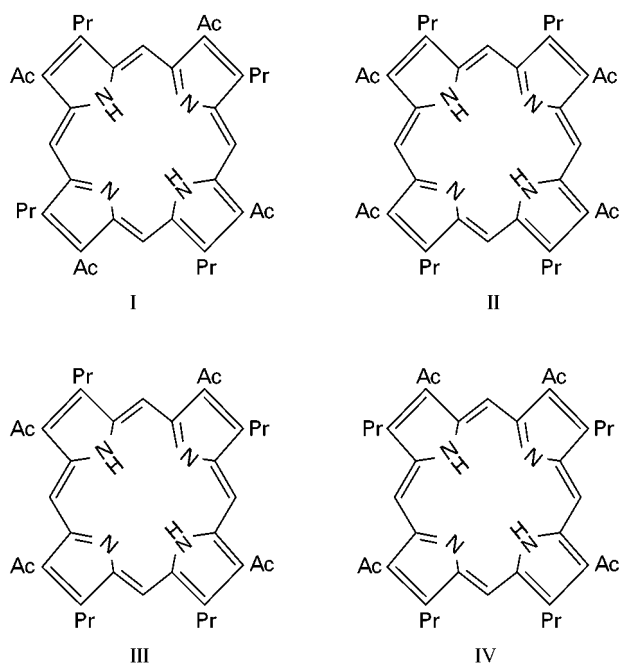


Figure 8 Structures of the four type-isomers of uroporphyrin.

The gradient system can be easily modified if the separation of polar hydroxylated porphyrins is needed. The separation of porphyrins, including hy-

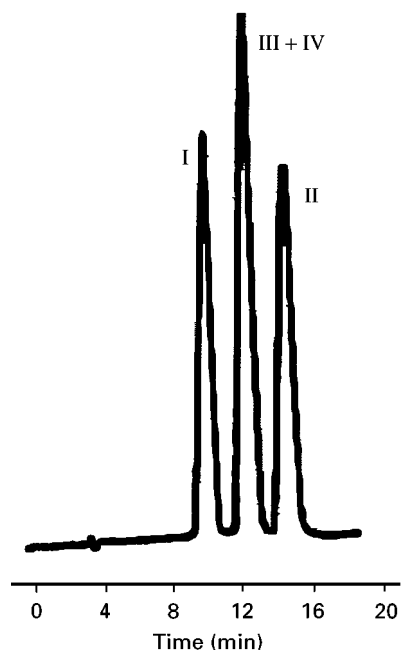


Figure 9 Separation of uroporphyrin type-isomers. Column, Hypersil-ODS (250 \times 4.6 mm, 5- μ m particle size); eluent, 13% (v/v) acetonitrile in 1 M ammonium acetate buffer, pH 5.16; flow rate, 1 mL min⁻¹; detection, 404 nm.

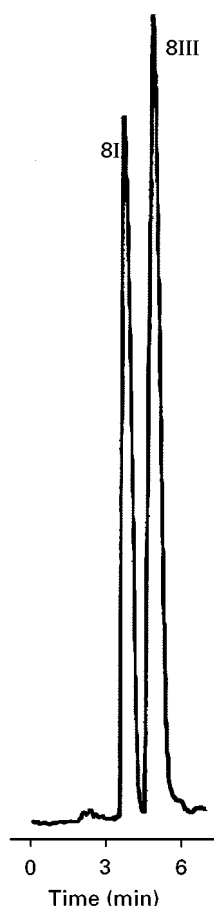


Figure 10 Separation of uroporphyrin I and III isomers. Column, Hypersil-BDS C_{18} (250×4.6 mm, $5\text{-}\mu\text{m}$ particle size); eluent, 9% (v/v) acetonitrile in 1 M ammonium acetate buffer, pH 5.55; flow rate, 1 mL min^{-1} ; detection, 404 nm.

droxy- and peroxyacid-porphyrins, in the urine of a patient with congenital erythropoietic porphyria (CEP) on a Hypersil-BDS (C_{18}) column with an extended elution programme is shown in Figure 6. The structures of the hydroxy- and peroxyacid-porphyrins are shown in Figure 7.

Separation of 8-, 7-, 6-, 5- and 4-Carboxylporphyrin Isomers

The separation of the type-isomers, especially type-I and type-III isomers, is of diagnostic value. The separation of isomers of porphyrins resulted from the decarboxylation of uroporphyrinogen I and III is important for understanding the biochemistry of this part of the haem biosynthetic pathway. Individual porphyrin isomers are best separated by isocratic elution with an appropriate amount of acetonitrile or acetonitrile and methanol in 1 M ammonium acetate buffer, pH 5.16, as eluent.

Uroporphyrins (Eight COOH)

There are four type-isomers of uroporphyrin, denoted I, II, III and IV by Fischer to show the four ways in which the acetic acid groups (Ac) and propionic acid groups (Pr) arranged around the eight β -positions of the porphyrin macrocycle (Figure 8). The naturally occurring type-I and type-III isomers can be easily separated on an ODS column with 13% (v/v) acetonitrile in 1 M ammonium acetate, pH 5.16, as eluent. The system resolved uroporphyrin I from the III + IV and II isomers but could not separate the III and IV isomers (Figure 9). Alternatively, a base-deactivated ODS column (e.g. Hypersil-BDS C_{18}) is used with 9% acetonitrile in 1 M ammonium acetate, pH 5.55, as eluent (Figure 10), which provides a more rapid separation of the I and III isomers.

Heptacarboxyl Porphyrins (Seven COOH)

There are five heptacarboxyl porphyrins that can be formed by the decarboxylation of uroporphyrin I and III. Heptacarboxyl porphyrin I (7I; Figure 11) is derived from the symmetrical uroporphyrin I and the four type-III heptacarboxyl porphyrins (7a, 7b, 7c and 7d; Figure 11) are formed by the random decarboxylation of one of the four acetic acid groups of the asymmetrical uroporphyrin III.

The complete separation of the four type-III heptacarboxyl porphyrins has not been achieved, although the type-I isomer was easily separated from the type-III isomers. With 28% acetonitrile-methanol (1 : 9 v/v) in 1 M ammonium acetate (pH 5.16) as eluent on a Hypersil-BDS column, the four type-III isomers were resolved into three peaks in the elution order 7c, 7d and 7a + 7b (Figure 12). The four type-III isomers could, however, be completely separated following conversion to the corresponding heptacarboxyl porphyrinogens by reduction (see section on Reversed-Phase Chromatography of Porphyrinogens).

Hexacarboxyl Porphyrins (Six COOH)

The structures of the two type-I (6Iab and 6Iac) and six type-III (6ab, 6ac, 6ad, 6bc, 6bd and 6cd) hexacarboxyl porphyrin isomers are shown in Figure 13. On an ODS column (Hypersil-ODS) with 16% (v/v) acetonitrile in 1 M ammonium acetate, pH 5.16 as mobile phase, the two type-I isomers were well resolved from the most abundant naturally occurring 6ad, but complete separation of the other isomers was not achieved (Figure 14).

Pentacarboxyl Porphyrins (Five COOH)

There are four type-III (5bcd, 5acd, 5abc and 5abd) and one type-I (5I) pentacarboxyl porphyrins (Figure 15). These five isomers have been separated on

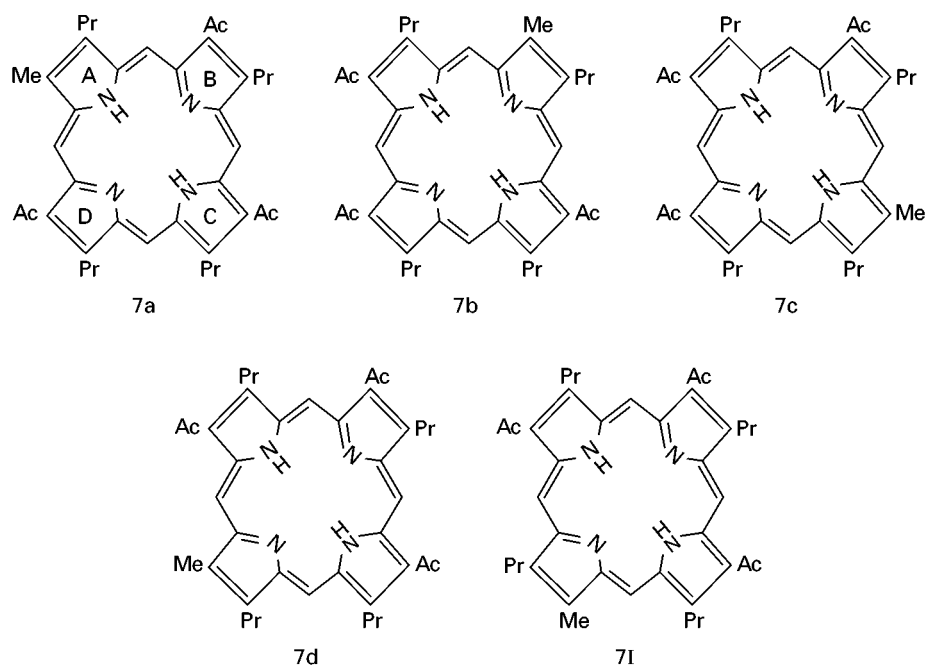


Figure 11 Structures of heptacarboxyl porphyrin isomers. Isomer 7I is heptacarboxyl porphyrin I. Isomers 7a, 7b, 7c and 7d are type-III isomers. The letters a, b, c and d denote the position of methyl group (Me), i.e. the position in which an acetic acid group (Ac) has been decarboxylated. Pr represents a propionic acid group.

a Hypersil-BDS column with acetonitrile–methanol–1 M ammonium acetate buffer (4.5 : 40.5 : 55, by volume), pH 5.16, as eluent (Figure 16). The elution order was 5I, 5bcd, 5abc, 5acd, and 5abd.

Coproporphyrins (Four COOH)

The structures of the four type-isomers (I, II, III and IV) of coproporphyrin are shown in Figure 17. All

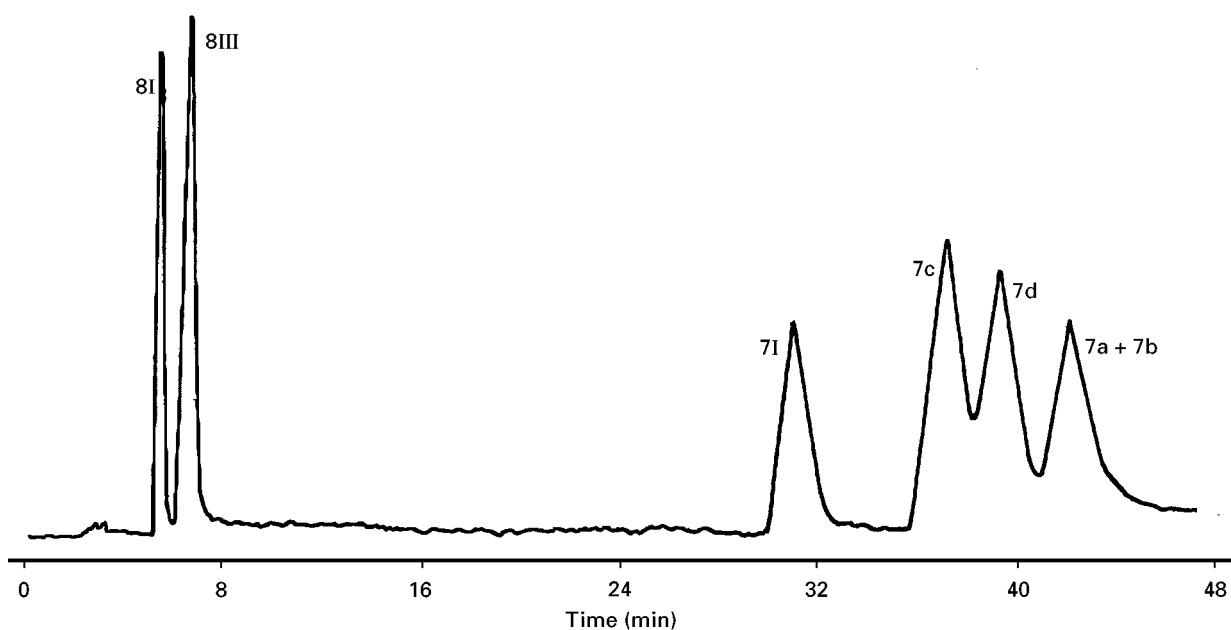


Figure 12 Separation of heptacarboxyl porphyrin isomers. Column, Hypersil-ODS (250 × 4.6 mm, 5-μm particle size); eluent, 28% (v/v) acetonitrile–methanol (1 : 9) in 1 M ammonium acetate buffer, pH 5.16; flow rate, 1 mL min⁻¹; detection, 404 nm. See Figure 11 for structures and peak identification.

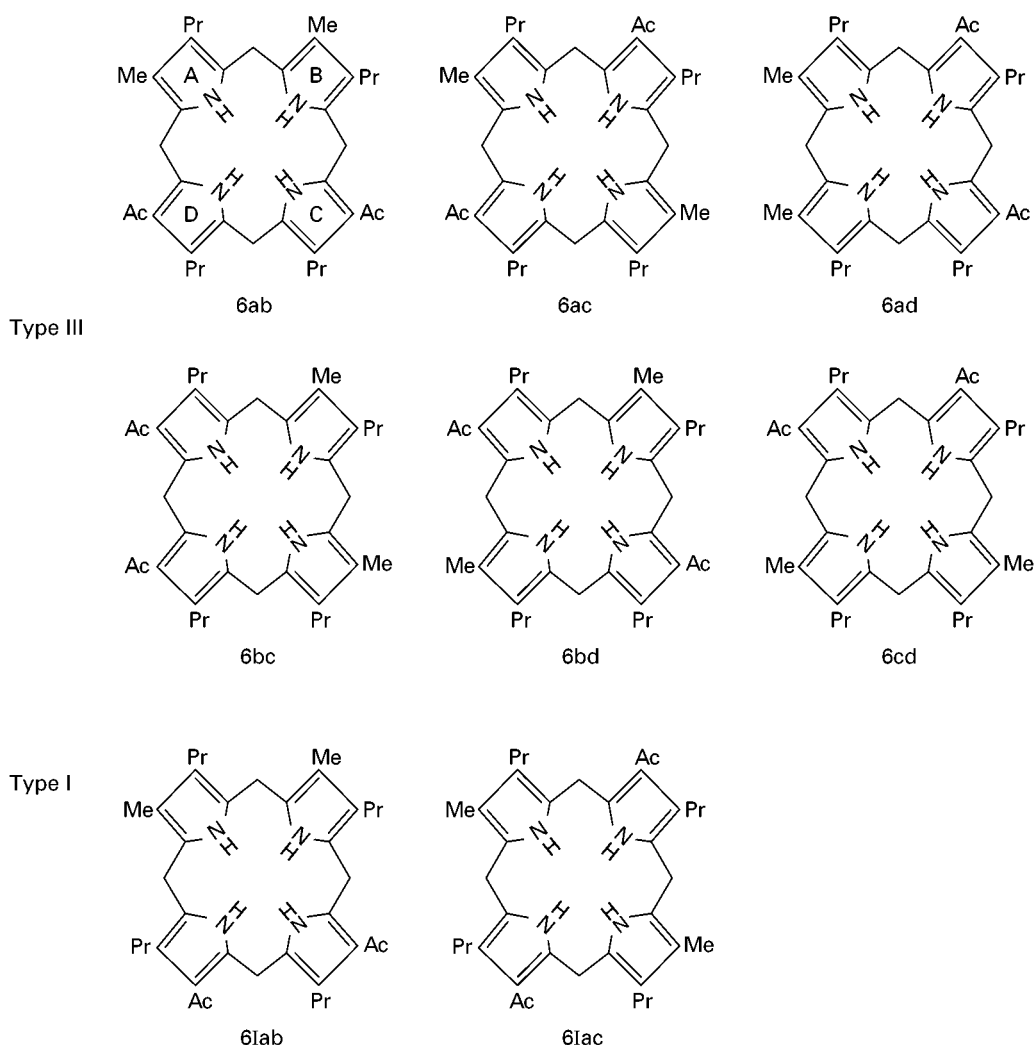


Figure 13 Structures of hexacarboxyl porphyrin isomers. 6lab and 6lac are type-I and 6ab, 6ac, 6ad, 6bc, 6bd and 6cd are type-III isomers. The letters a, b, c and d denote the position of methyl groups.

four isomers were easily separated by reversed-phase HPLC on an ODS column with 26% (v/v) acetonitrile in 1 M ammonium acetate buffer (pH 5.16) as eluent (Figure 18). Rapid separation of coproporphyrin I and III isomers could be achieved by using a mobile phase of 30% acetonitrile in 1 M ammonium acetate buffer (pH 5.16) or employing a Hypersil-BDS column which is less retentive but still maintains the resolution.

Retention Mechanism of Porphyrins in Reversed-Phase Chromatography

The dominant retention mechanism is hydrophobic interaction between the porphyrin side-chain substituents and the non-polar hydrocarbonaceous functions of the stationary phase surface. The relative hydrophobicity of the side-chain β -substituents

of the porphyrins is $\text{CH}=\text{CH}_2 > \text{CH}_2\text{CH}_3 > \text{CH}_3 > \text{CH}_2\text{CH}_2\text{COOH} > \text{CH}_2\text{COOH}$. The relative retention of the porphyrins is therefore dependent on the relative number of hydrophobic substituents available for interaction and is thus dominated by the number of alkyl (particularly methyl) groups present in the molecule. The retention increases with increasing number of alkyl substituents, and the following elution order was observed; uroporphyrin (8COOH), heptacarboxyl porphyrin (7COOH, 1CH₃), hexacarboxyl porphyrin (6COOH, 2CH₃), pentacarboxyl porphyrin (5COOH, 3CH₃), coproporphyrin (4COOH, 4CH₃), mesoporphyrin (2COOH, 4CH₃, 2CH₂CH₃) and protoporphyrin (2COOH, 4CH₃, 2CH=CH₂).

This retention mechanism is also applicable to the separation of type-isomers. For example, the elution order (I, III, IV, II) of coproporphyrin isomers could be explained as follows.

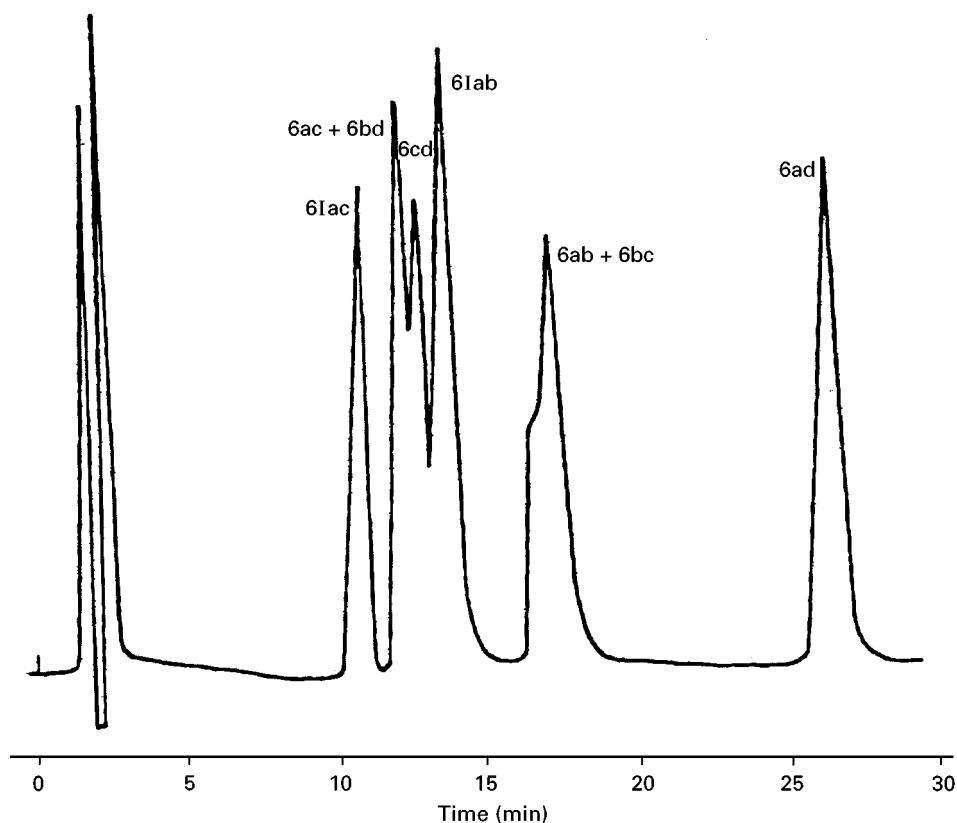


Figure 14 Separation of hexacarboxyl porphyrin isomers. Column, Hypersil-ODS (250 × 4.6 mm, 5- μ m particle size); eluent, 16% (v/v) acetonitrile in 1 M ammonium acetate buffer, pH 5.16; flow rate, 1 mL min⁻¹; detection, 404 nm. See Figure 13 for structures and peak identification. (Reproduced from Lim *et al.* (1983) *Journal of Chromatography* 282: 629–641, with permission from Elsevier Science.)

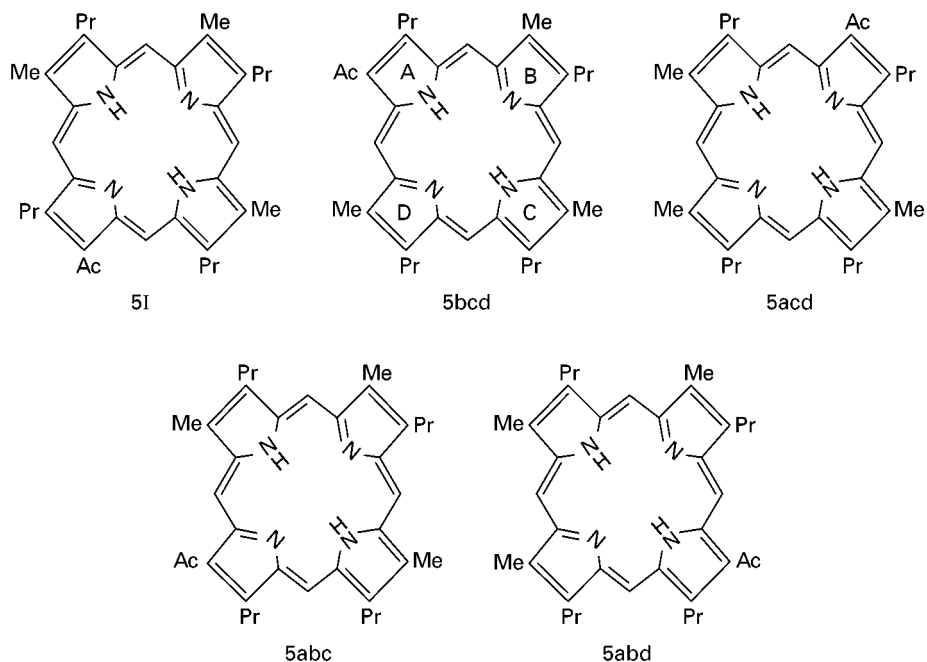


Figure 15 Structures of pentacarboxyl porphyrin isomers. 5I is type-I pentacarboxyl porphyrin. Isomers 5bcd, 5acd, 5abc and 5abd are type-III isomers. The letters a, b, c and d denote the position of methyl groups.

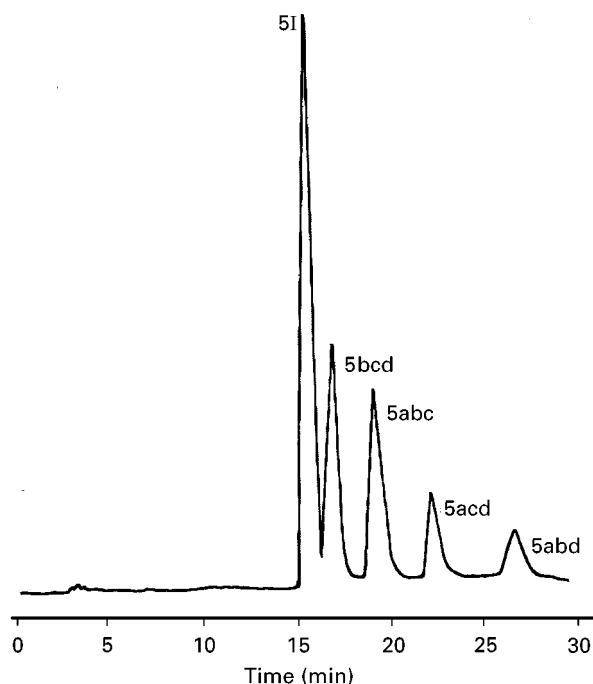


Figure 16 Separation of pentacarboxyl porphyrin isomers. Column, Hypersil-BDS C_{18} (250×4.6 mm, $5\text{-}\mu\text{m}$ particle size); eluent, acetonitrile-methanol-1 M ammonium acetate buffer (4.5 : 40.5 : 55, by volume), pH 5.16; flow rate, 1 mL min^{-1} ; detection, 404 nm. See Figure 15 for structures and peak identification.

Coproporphyrin II is the longest retained compound because it has two pairs of adjacent CH_3 groups (Figure 17) which provides the largest hydro-

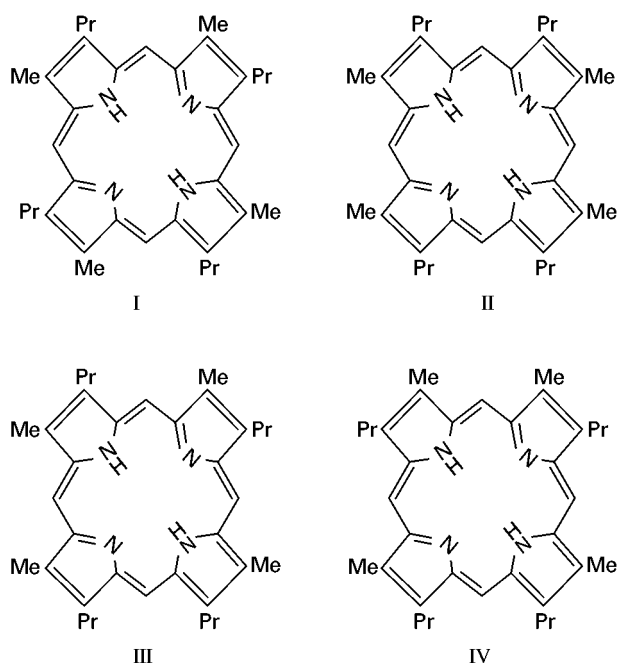


Figure 17 Structures of type-I, II, III and IV isomers of coproporphyrin.

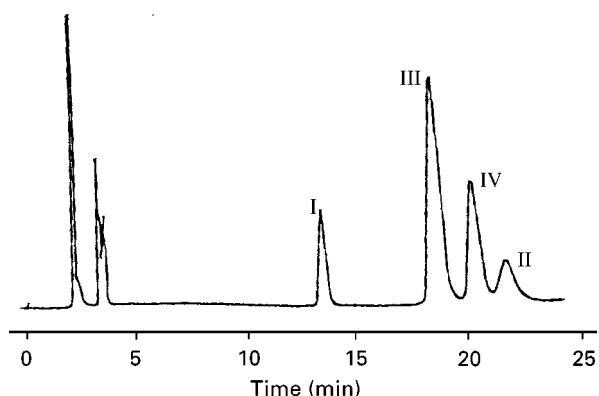


Figure 18 Separation of type-I, II, III and IV isomers of coproporphyrin. Column, Hypersil-ODS (250×4.6 mm, $5\text{-}\mu\text{m}$ particle size); eluent, 26% (v/v) acetonitrile in 1 M ammonium acetate buffer, pH 5.16; flow rate, 2 mL min^{-1} ; detection, 404 nm.

phobic surface area available for interaction. The symmetrical coproporphyrin I has no adjacent CH_3 groups and is the least hydrophobic. It is the fastest eluting isomer. Coproporphyrin III and IV each have a pair of adjacent CH_3 groups. In this situation the relative distance between the adjacent CH_3 pair and the remaining two non-adjacent CH_3 groups becomes an important factor in determining the relative hydrophobicity. In coproporphyrin IV, each of the adjacent CH_3 groups is five bonds away from the nearest

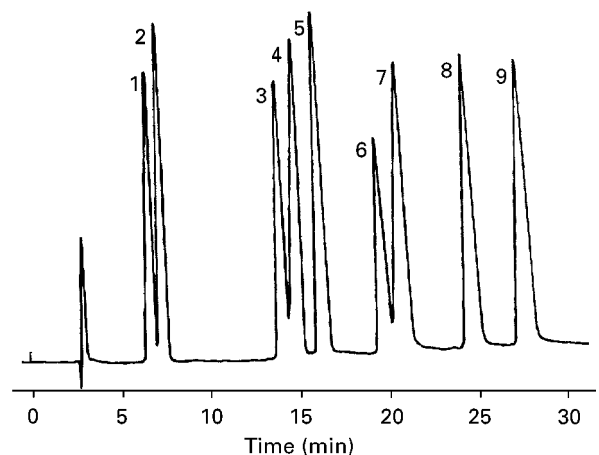


Figure 19 Separation of dicarboxylic porphyrins and metalloporphyrins. Column, Hypersil-SAS (C_1 , 250×4.6 mm, $5\text{-}\mu\text{m}$ particle size); eluent, methanol (solvent A) and 1 M ammonium acetate buffer, pH 4.6 (solvent B); elution, 62% A isocratically for 6 min, then linear gradient to 70% A from 6.1 to 13 min followed by isocratic elution at 75% A; flow rate, 1 mL min^{-1} ; detection, 404 nm. Peaks: 1 = Co(proto-porphyrin); 2 = Co(mesoporphyrin); 3 = Fe(proto); 4 = Fe(meso); 5 = deuteroporphyrin; 6 = Zn(meso); 7 = Zn(proto); 8 = mesoporphyrin; 9 = protoporphyrin. (Reproduced with permission from Lim *et al.* (1984) *Journal of Chromatography* 317: 333-341.)

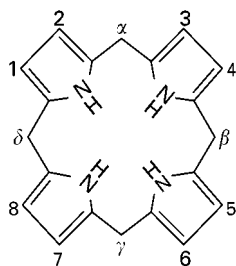


Figure 20 Structure of porphyrinogen (hexahydroporphyrin) macrocycle.

non-adjacent CH_3 group. In coproporphyrin III these are five and six bonds apart, respectively. The slightly longer distance (one bond-distance) between one of the adjacent CH_3 groups and its nearest non-adjacent CH_3 group (six instead of five bonds apart) is sufficient to make coproporphyrin III less hydrophobic than and therefore eluted before coproporphyrin IV (Figure 18).

The elution order of the penta- and hexa-carboxyl porphyrin isomers could be similarly predicted. This also explains why it was difficult to resolve the type-III heptacarboxyl porphyrin isomers since the single CH_3 group present in these molecules makes them very similar in hydrophobic surface area. The study of retention behaviour is useful in elucidating the nature of side-chain substituents present in unknown porphyrins.

Reversed-Phase Chromatography of Metalloporphyrins

The most important naturally occurring metalloporphyrins are the Mg, Fe, Cu, Zn and Co complexes of dicarboxyl porphyrins. Iron complexes form the prosthetic groups of the various haemoproteins, Mg complexes are found in the chlorophylls and Co complex in vitamin B_{12} . In heavy metal poisoning, particularly lead intoxication, erythrocyte Zn-protoporphyrin is elevated.

The mobile phases developed for the separation of porphyrins have been modified for the separation of dicarboxyl porphyrins and metalloporphyrins. These highly hydrophobic porphyrins are best separated on the least hydrophobic C_1 -bonded column. Methanol is the preferred organic modifier since the dicarboxyl porphyrins and their metal complexes do not form extensive hydrogen bonds with the methanol extracted into the stationary phase, as with uroporphyrin. Methanol gave better resolution of dicarboxyl porphyrins and their metal complexes and is totally miscible with the 1 M ammonium acetate buffer (pH 4.6) used in the mobile phase. The separation of

a mixture of dicarboxyl porphyrins and metalloporphyrin is shown in Figure 19.

The insertion of a metal ion which completely occupies the centre of the porphyrin hole significantly alters the electronic environment around the central nitrogen atoms. The retention of the metalloporphyrin is therefore dependent on the ability of the inserted metal ion to accept axial ligands from the mobile phase. Co and Fe complexes are good axial ligand acceptors and may add two extra ligands; Zn complex can add one extra ligand, while further coordination of the Cu complex is only possible under special conditions. The addition of polar axial ligands leads to a decrease in the overall hydrophobicity of a molecule and therefore its retention. Thus, the elution order of Co, Fe, Zn and Cu complexes, was observed for both meso- and proto-porphyrins.

The elution order of the Zn and Cu complexes of meso- and proto-porphyrins is the same as that for meso- and proto-porphyrins with the former eluted before the latter. These metalloporphyrins do not accept axial ligands readily and their relative reten-

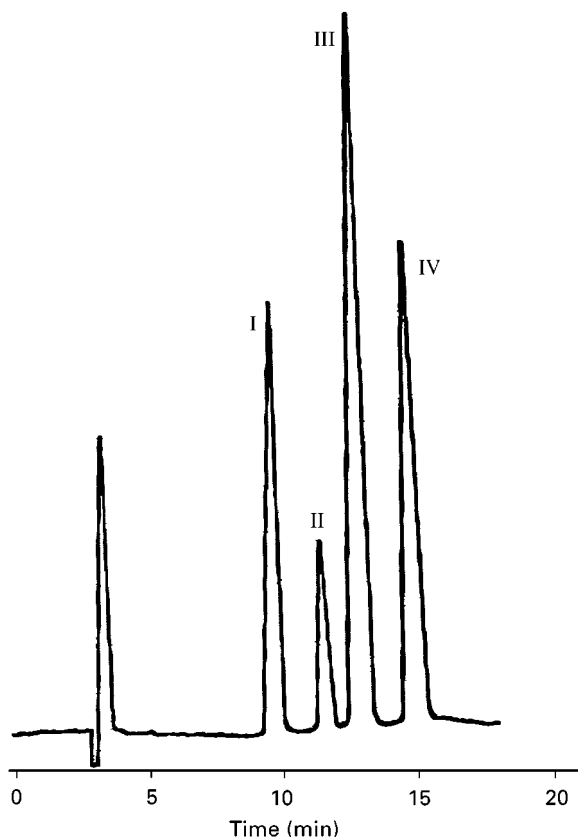


Figure 21 Separation of coproporphyrinogen I, II, III and IV isomers. Column, Hypersil-ODS (250×4.6 mm, $5\text{-}\mu\text{m}$ particle size); eluent, 25% (v/v) acetonitrile in 1 M ammonium acetate buffer, pH 5.16; flow rate, 1 mL min^{-1} ; detection, amperometric at $+0.75\text{ V}$. (Reproduced with permission from Lim *et al.* (1986) *Biochemistry Journal* 234: 629–633.)

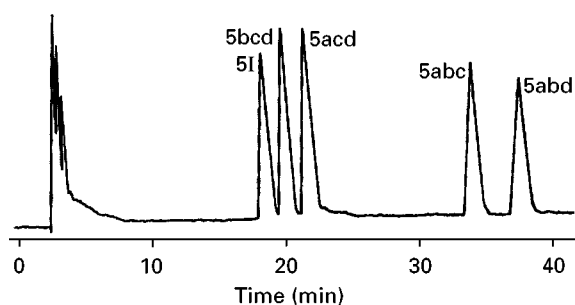


Figure 22 Separation of pentacarboxyl porphyrinogen isomers. Column, Hypersil-ODS (250×4.6 mm, $5\text{-}\mu\text{m}$ particle size); eluent, 40% (v/v) methanol in 1 M ammonium acetate buffer, pH 5.16; flow rate, 1 mL min^{-1} ; detection, amperometric at $+0.70$ V.

tion is still governed by the relative hydrophobicity of the side-chain substituents.

The elution order of the Co and Fe complexes of meso- and proto-porphyrins is the reverse of that observed for Zn and Cu complexes. Co and Fe complexes are excellent axial ligand acceptors. The decrease in electron density at the pyrrolic nitrogens in metalloprotoporphyrins due to the vinyl groups of protoporphyrin is reflected in the chelated metals, leading to increased affinity for the donor electrons of the extra axial ligands. This leads to a decrease in the hydrophobicity of Co- and Fe-protoporphyrins.

Reversed-Phase Chromatography of Porphyrinogens

The porphyrinogens are hexahydroporphyrins (Figure 20). They are the true intermediates in the bio-

synthesis of haem, chlorophylls and vitamin B₁₂. Porphyrinogens are not often separated because they are easily oxidized to the corresponding porphyrins by air and it is mainly the porphyrins which are present in body fluids and excreta. Studies have shown that isomers of porphyrinogens are better resolved than the corresponding porphyrins. The separation of porphyrinogen isomers is therefore important in situation where the separation of porphyrin isomers is incomplete or could not be achieved.

Coproporphyrinogen, Penta-, Hexa-, Hepta-carbonyl Porphyrinogens and Uroporphyrinogen Isomers

The complete separation of coproporphyrinogen I, II, III and IV isomers could be achieved in 15 min on an ODS column with 25% (v/v) acetonitrile in 1 M ammonium acetate buffer (pH 5.16) as mobile phase (Figure 21). Porphyrinogens are more flexible compounds than the rigid porphyrin macrocycles. In the flexible coproporphyrinogen molecules, the small CH₃ substituents in each isomers may be subjected to varying degrees of steric hindrance or shielding by the larger propionic acid groups, depending on the adopted conformation. This alters the expected available surface area for hydrophobic interaction and makes prediction of elution order based on hydrophobic interaction by the methyl group difficult. The conformation of porphyrinogens under reversed-phase conditions have not been studied.

The superior separation of porphyrinogens compared with porphyrins was similarly observed for penta-, hexa- and hepta-carboxyl porphyrinogens

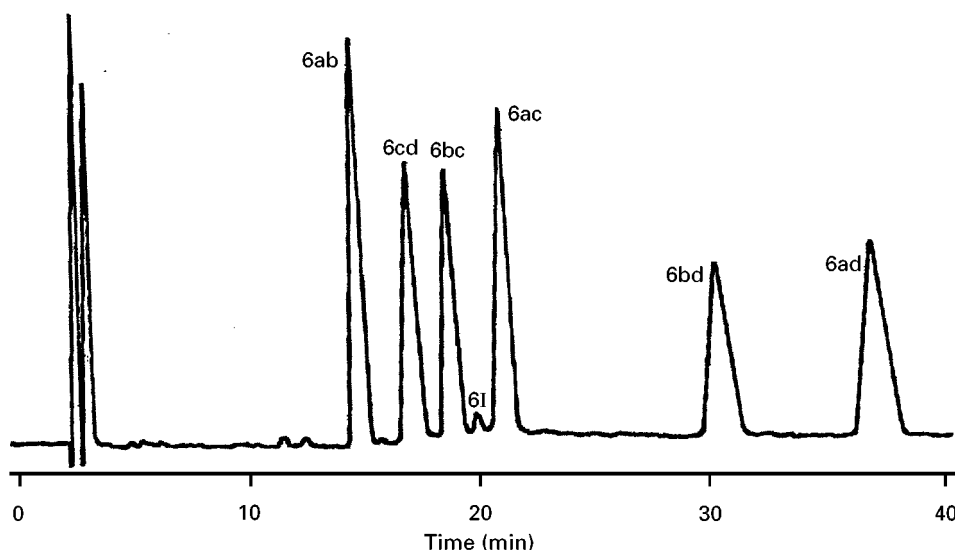


Figure 23 Separation of hexacarboxyl porphyrinogen isomers. Column, Hypersil-ODS (250×4.6 mm, $5\text{-}\mu\text{m}$ particle size); eluent, acetonitrile-methanol-1 M ammonium acetate (8 : 12 : 80, by volume); pH 5.16; flow rate, 1 mL min^{-1} ; detection, amperometric at $+0.70$ V.

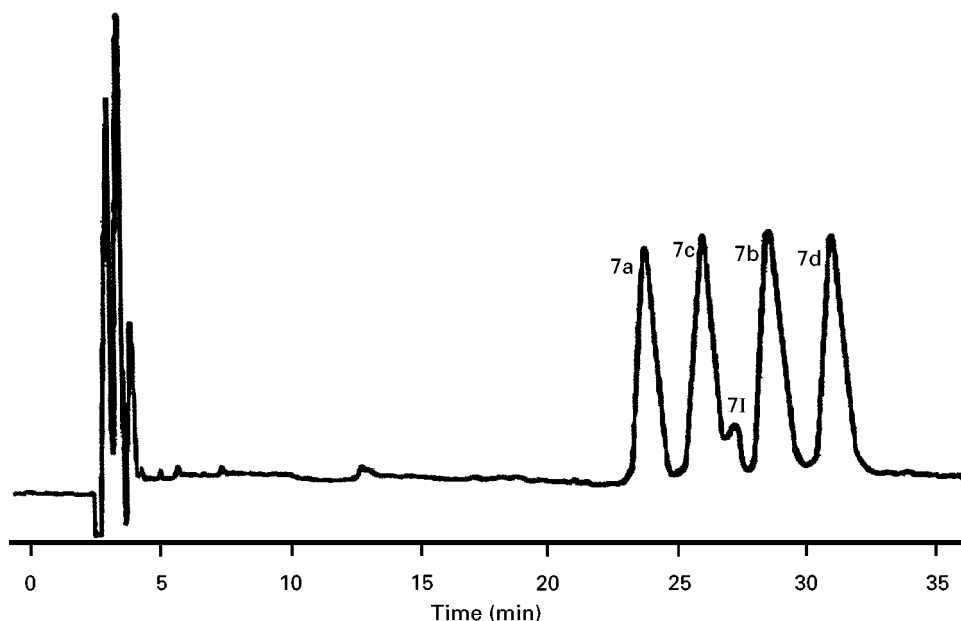


Figure 24 Separation of heptacarboxyl porphyrinogen isomers. Column, Hypersil-ODS (250×4.6 mm, $5\text{-}\mu\text{m}$ particle size); eluent, acetonitrile–methanol–1 M ammonium acetate, (7 : 3 : 90, by volume) pH 5.16; flow rate, 1 mL min^{-1} ; detection, amperometric at $+0.70\text{ V}$. (Reproduced with permission from Lim *et al.* (1987) *Biochemistry Journal* 247: 229–232.)

(Figures 22, 23 and 24, respectively). The improvement for the heptacarboxyl porphyrinogens was such that all four type-III isomers could be easily resolved (Figure 24).

For the uroporphyrinogens, there was no improvement in resolution over the porphyrins and a reversal of elution order was observed for the type-I and type-III isomers (Figure 25).

Detectors for Porphyrins and Porphyrinogens

Porphyrins have intense red fluorescence and are therefore easily detected with great sensitivity and specificity with a fluorescence detector set at excitation wavelengths of 400–420 nm and emission wavelengths of 600–620 nm.

Porphyrins have an intense absorption band at about 400 nm (Soret band) with molar extinction coefficients often around 400 000. Detection at the Soret band region with a UV-visible detector also provides excellent detectability.

Porphyrinogens are colourless compounds devoid of fluorescence and with only weak UV absorptions at the 220 nm region. They are best detected electrochemically by the oxidation mode because of the ease of oxidation of these compounds.

In terms of sensitivity and specificity, the mass spectrometer is the ‘detector’ of choice. Online LC–MS, especially with electrospray quadrupole

time-of-flight MS–MS, allows porphyrins, metalloporphyrins and porphyrinogens to be detected and characterized with ease.

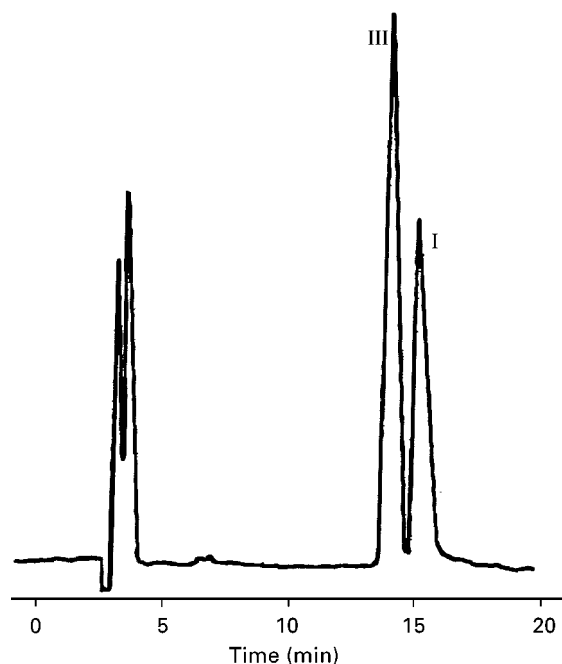


Figure 25 Separation of uroporphyrinogen I and III isomers. Column, Hypersil-ODS (250×4.6 mm, $5\text{-}\mu\text{m}$ particle size); eluent, 6% (v/v) acetonitrile in 1 M ammonium acetate buffer, pH 5.16; flow rate, 1 mL min^{-1} ; detection, amperometric at $+0.70\text{ V}$.

Future Developments

There are two areas in porphyrin separation which are expected to develop further in the future. The first is in column technology. The improvement achieved by the introduction of base-deactivated reversed-phase is expected to continue and better columns with improved resolution and reproducibility can be expected. The second is in online LC-MS-MS operation. With the introduction of high sensitivity and resolution mass spectrometers, analysis of porphyrins will be a lot easier in the future.

See also: II/Chromatography: Liquid: Detectors: Mass Spectrometry.

Further Reading

Dolphin D (ed.) (1978) *The Porphyrins*, vol. 1. New York: Academic Press.

Jordan PM (ed.) (1991) *Biosynthesis of Tetrapyrroles*. London: Elsevier.

Li F, Lim CK and Peters TJ (1987) HPLC of porphyrinogens with electrochemical detection. *Chromatographia* 24: 421-422.

Lim CK, Rideout JM and Peters TJ (1984) High-performance liquid chromatography of dicarboxylic porphyrins and metalloporphyrins: retention behaviour and biomedical applications. *Journal of Chromatography* 317: 333-341.

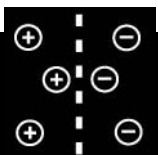
Lim CK, Li F and Peters TJ (1988) High-performance liquid chromatography of porphyrins. *Journal of Chromatography, Biomedical Applications* 429: 123-153.

Luo J and Lim CK (1995) Isolation and characterization of new porphyrin metabolites in human porphyria cutanea tarda and in rats treated with hexachlorobenzene by HPTLC, HPLC and liquid secondary ion mass spectrometry. *Biomedical Chromatography* 9: 113-122.

Moss GP (1987) Nomenclature of tetrapyrroles. *Pure and Applied Chemistry* 59: 779-832.

Smith KM (ed.) (1974) *Porphyrins and Metalloporphyrins*. Amsterdam: Elsevier.

POWDERED RESINS: CONTINUOUS ION EXCHANGE



P. A. Yarnell, Graver Technologies, Glasgow, DE, USA

Copyright © 2000 Academic Press

process incorporated ion exchange and filtration into one unit operation.

Introduction

The use of finely divided (powdered) forms of ion exchange resins began in the early 1960s. Prior to that, synthetic ion exchange resins were manufactured as granules, or preferably spherical beads. The ion exchange granules and beads were used in packed beds to treat liquids, most commonly water. The Graver Water Conditioning Company pioneered the use of the powdered ion exchange resins made by grinding ion exchange resin beads or granules into powders. They discovered that a thin layer of powdered resin offered a dramatic improvement in ion exchange reaction rate versus a conventional packed bed of resin. In 1966 Joseph A. Levendusky of Graver Water Conditioning patented a powdered resin system (named Powdex®) that has been the basis for most practical applications of this technology. This process utilized a pre-coat of powdered ion exchange resins applied to a septum or filter. Thus, the pre-coat

Basic Principles

The original pre-coats were made by combining powdered anion exchange resin with powdered cation exchange resin in a water slurry. Both types of resin were ground moist (40-60% moisture content) into powders using grinding equipment such as hammer mills. This grinding process resulted in a distribution of particle sizes, typically from 1 to 200 µm in diameter. These distributions were centred in the 35-70 µm range. Thus, the powdered ion exchange particles are roughly two orders of magnitude smaller than conventional ion exchange resins (Figure 1). The grinding process also results in a tremendous increase in surface area and, consequently, a higher surface area to weight ratio.

Particle size of powdered ion exchange resins is the most important factor in determining performance of pre-coats. In these applications, resin particle size influences ion exchange capacity utilization, filtration efficiency, filtration capacity and pre-coat characteristics (integrity, uniformity, lifetime). In their classic paper, Frisch and Kunin elucidated the effects of



Figure 1 Powdered ion exchange resins.

particle size on kinetics (the rate of reaction) and, hence, utilization of capacity for ion exchange resins. Specifically, both exchange rate and utilization are inversely proportional to particle diameter. **Figure 2** illustrates the relationship between particle size and ion exchange kinetics for standard-sized bead, small-sized bead and powdered strongly basic anion resin. Because of their inherently better kinetics, powdered resins typically exhibit equal, or higher, operating capacities to those of bead resin counterparts.

When mixed in water, powdered resin particles of opposite charge flocculate to form a larger, well-defined agglomerate. This agglomerate particle is commonly called a floc. The size of the floc formed

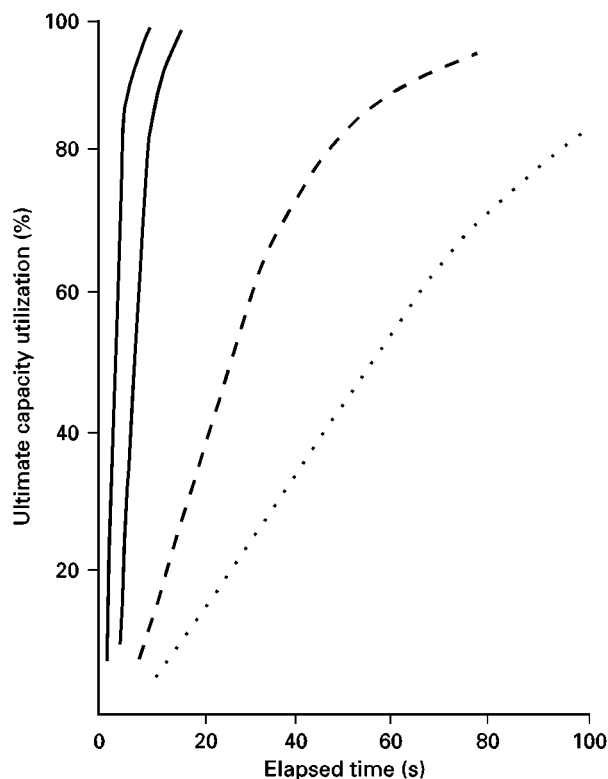


Figure 2 Ion exchange kinetics as a function of particle size. Continuous lines, powdered resin; dashed line, 50-100 mesh; dotted line, 16-40 mesh.

Table 1 Surface charges of powdered resins

Resin type	Ionic form	Zeta potential (mV)
Strongly acidic cation	Hydrogen	-42
Strongly acidic cation	Sodium	-40
Strongly acidic cation	Ammonium	-30
Strongly basic anion	Hydroxide	+48

depends on the surface area and the surface charge of the particles prior to flocculation. The increased surface area resulting from the grinding process explains why powdered resin particles flocculate to a much greater extent than corresponding standard-size resin particles. Electrical charges on the surface of powdered resin particles are measured using zeta potentials. **Table 1** summarizes the zeta potentials for specific ionic forms of common powdered ion exchange resins used in pre-coats.

The flocculated mixture of cation and anion resins has a volume up to 20 times that of the unmixed components in water. As the floc forms, void volume between particles increases dramatically, resulting in this increased bulk volume. Factors, such as the ratio of the two resin components, the ionic forms of the components, the resin slurry concentration, the ionic strength of the solution, the temperature of the slurry and particle sizes of the components and determine the bulk volume of the flocculated mixture.

In addition to their ion exchange capabilities, pre-coats offer excellent filtration. This filtration results from a combination of fine particles (high surface area per unit weight) and significant porosity within the pre-coat. The presence of charged ion exchange sites further enhances the filtration performance. In this regard, the new and freshly regenerated powdered resins found in pre-coats optimize filtration efficiency.

Pre-coat Formulations

The original pre-coat formulations, such as those used in the Powdex® process, were made from just two powdered ion exchange components: a strongly basic anion resin and a strongly acidic cation resin. Typically, these resin components were supplied in the regenerated (ionic) form (H^+ for the cation and OH^- for the anion). These powdered components were added to water and stirred to form a slurry. The bulk volume of the resultant slurry could be controlled by addition of an innocuous organic material, such as dilute polyacrylic acid, which reduces clumping. This organic material binds tightly to the surface of one of the components, typically the anion resin, thus effectively reducing the surface charge of that

component. Use of individual components allows the pre-coat user to adjust the cation to anion ratio according to the requirements of the application. As the technology has evolved, pre-coat manufacturers have offered alternative ionic forms (ammonium, sodium, morpholinium and chloride) and alternative resin chemistry components (weak electrolytes, macroporous exchangers and Type II strongly basic anions) for specific applications.

Premix pre-coats are formulated and tested before shipment to a customer. In contrast to the ultimate flexibility associated with component pre-coats, premixing by the manufacturer guarantees a specific ratio of components and a uniformly mixed material.

In 1976 the first premix incorporating fibre along with the anion and cation resin components was introduced; the corresponding patent was granted 4 years later. Chopped alpha-cellulose fibre was used in this premix and still is the most common fibre constituent in pre-coats. Cellulose fibres are hydrophilic and contain carboxylic groups whose charge facilitates flocculation with resin components. The tendency for fibre flocculation with resin components can be further enhanced by charging the fibre with an ionic polymer with a significant zeta potential. Inclusion of the fibre increases filtration efficiency and minimizes pre-coat cracking caused by the adsorption of colloids on the surface of the anion resin particles. The fibre adds bulk volume and porosity; the amount of bulk depends on the length and rigidity of the fibre: longer and more rigid fibres produce bulky pre-coats and vice versa. A variety of noncellulosic fibres have been used in premixes. Both polyacrylonitrile (PAN) and composite polystyrene/polyethylene fibres are used in current commercial formulations. In the latter case, the polystyrene fibres are functionalized with ion exchange sites, typically sulfonic acid type, to form an ion exchange resin fibre. Fibre can also be incorporated in standard pre-coats via addition as a separate component. Moreover, the fibre can be utilized separately either as an underlay pre-coated prior to the resin components, or conversely, as an overlay pre-coated after the resin components.

Commercial premixes currently popular are available in a variety of component ratios, as shown in Table 2. Pre-coats are formulated on a dry weight basis. Many fibres have virtually no moisture content, while most ion exchange resins contain 40–60% water unless dried. The premixes listed in Table 2 are available with either hydrogen form or ammonium form cation resin. The 4:5 cation-to-anion ratio common to fibre-containing premixes yields a roughly stoichiometric mix of cation and anion exchange sites.

Table 2 Common premix pre-coat compositions

<i>Resin content (dry weight ratio)</i>		<i>Mix content (dry weight ratio)</i>	
<i>Cation resin</i>	<i>Anion resin</i>	<i>Fibre</i>	<i>Resin</i>
1	1	0	1
2	1	0	1
3	1	0	1
4	5	1	1
4	5	1	2
4	5	1	9

Pre-coat Properties

Typically, three properties characterize pre-coats and premixes: moisture content, settling volume and supernate turbidity. Premixes are made from a slurry of the components. The slurry is dewatered by means of centrifugation or a similar mechanical process. The dewatered premix retains water associated with the ion exchange resin sites. Moisture content, or water retention as it is sometimes called, is a measure of the amount of water relative to the solids content of the premix. Typically, moisture contents vary between 50 and 70%. The settling volume measures flocculation of a pre-coat under standardized conditions. The measurements are done in a graduated cylinder with a specific volume and specific concentration of pre-coat slurry. Slurry volume is measured initially and after a specific settling time (t) and calculated according to the following equation:

$$\text{Settling volume } [V/V](\%) = 100 \times (V_t/V_0)$$

Settling volumes typically vary from 40–70%. High settling volumes are indicative of increased pore volume and, consequently, bulky pre-coats, while low settling volumes are indicative of ‘tight’ pre-coats. As the settling volume increases, depth filtration improves, but ion exchange efficiency tends to decline. Turbidity is measured on the supernatant at the conclusion of the settling volume test. Turbidity is recorded in nephelometric units (NTU): values below 10–15 NTU are considered acceptable. Low turbidity values are indicative of full incorporation of pre-coat components. Typically, anion resins generate more very small particles than cation resins during the grinding process. These fine anion resin particles, in turn, are the least likely to be fully flocculated in the pre-coat and consequently cause turbidity. Fibres are another potential source of turbidity. Fibre particles have weaker charges than resin particles and thus prove harder to flocculate fully in a pre-coat. Fortunately, the addition of the correct amount of the properly charged dilute polyelectrolyte (e.g. polyacrylic acid or polyacrylamide) usually flocculates these

unincorporated particles and dramatically improves turbidity. Thus, turbidity measurements assist manufacturers in formulating premixes and users in preparing pre-coats satisfactorily from components.

The American Society for Testing and Materials (ASTM) has published validated test methods for measuring properties of the powdered ion exchange resins used in pre-coat materials. Specifically, Standard D 4266-83 covers measurement of the operating capacity for both powdered cation exchange resins (either hydrogen or ammonium form) and powdered anion exchange resins (hydroxide form). Similarly, Standard D 4456-85 encompasses determination of particle size distributions and solids content for powdered ion exchange resins (see Further Reading).

Pre-coat Equipment

Before the introduction of powdered ion exchange resins, materials such as diatomaceous earth and cellulose fibres were coated on to leaf filter elements or wire screen septa. While both these materials and this type of equipment are still used in pre-coat operations, the use of powdered ion exchange resins in

pre-coats has led to equipment modifications and improvements.

The basic equipment used for pre-coating with powdered ion exchange resins is fairly simple: a tank for mixing powdered components into a slurry and a filter or septum suitable for retaining the slurry solids. In addition to these basic components, pumps, piping, valves and instrumentation are used in virtually all pre-coat systems. **Figure 3** is a schematic drawing of a typical system used in commercial applications. Vessels used for pre-coating operations generally contain an array of tubular filter elements or septa. These arrays fall into two major designs: top tube sheet and bottom tube sheet. **Figures 4** and **5**, respectively, are schematic drawings of these two designs. The term 'tube sheet' refers to the support structure to which the individual elements are attached. Top tube sheet elements originally were designed to use stainless steel wire cloth or well screen elements. These metal elements have relatively large diameter (0.075–0.150 mm) openings. Bottom tube sheet elements typically use continuously wound yarn elements with much smaller openings (nominal ratings of 0.001–0.010 mm). These filter elements come

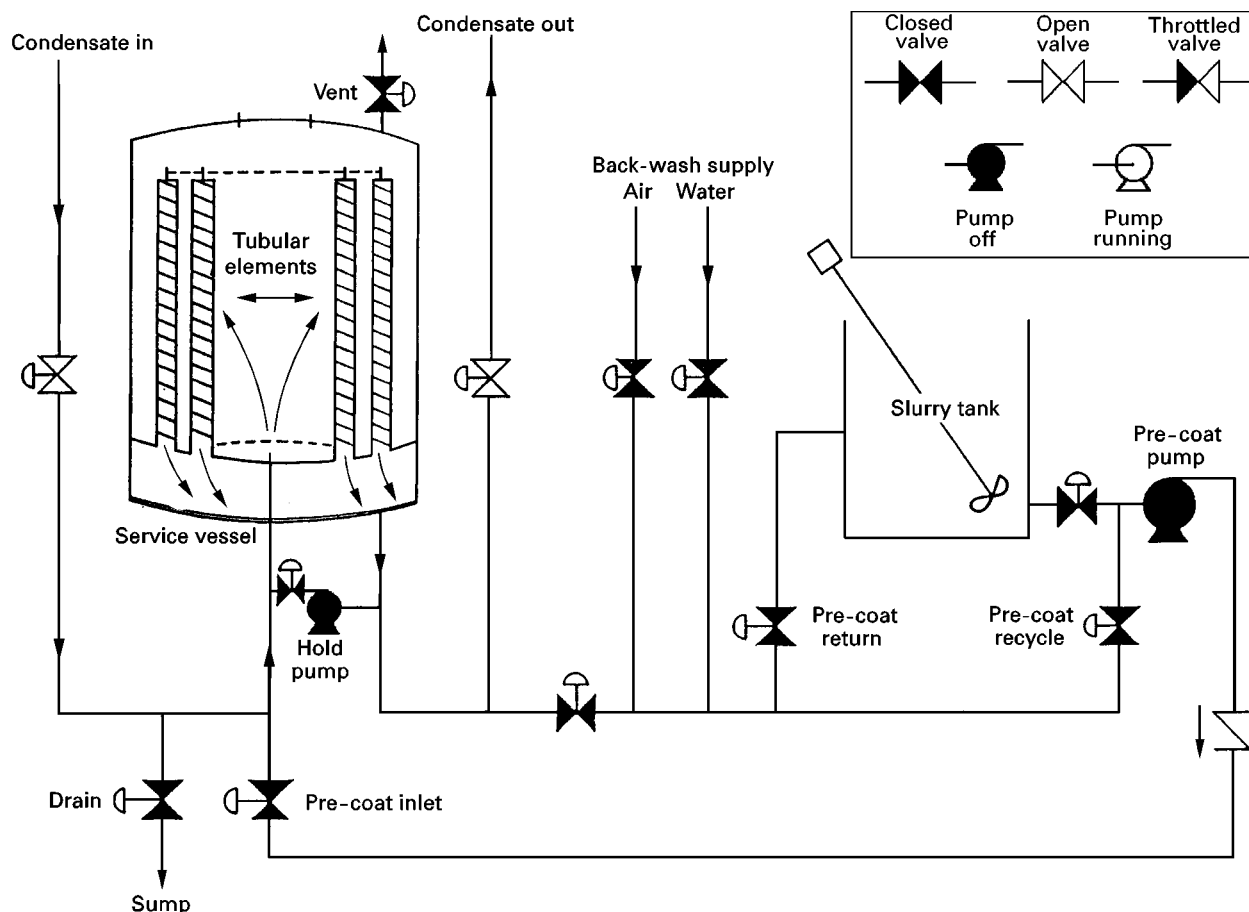


Figure 3 Typical pre-coat system schematic.

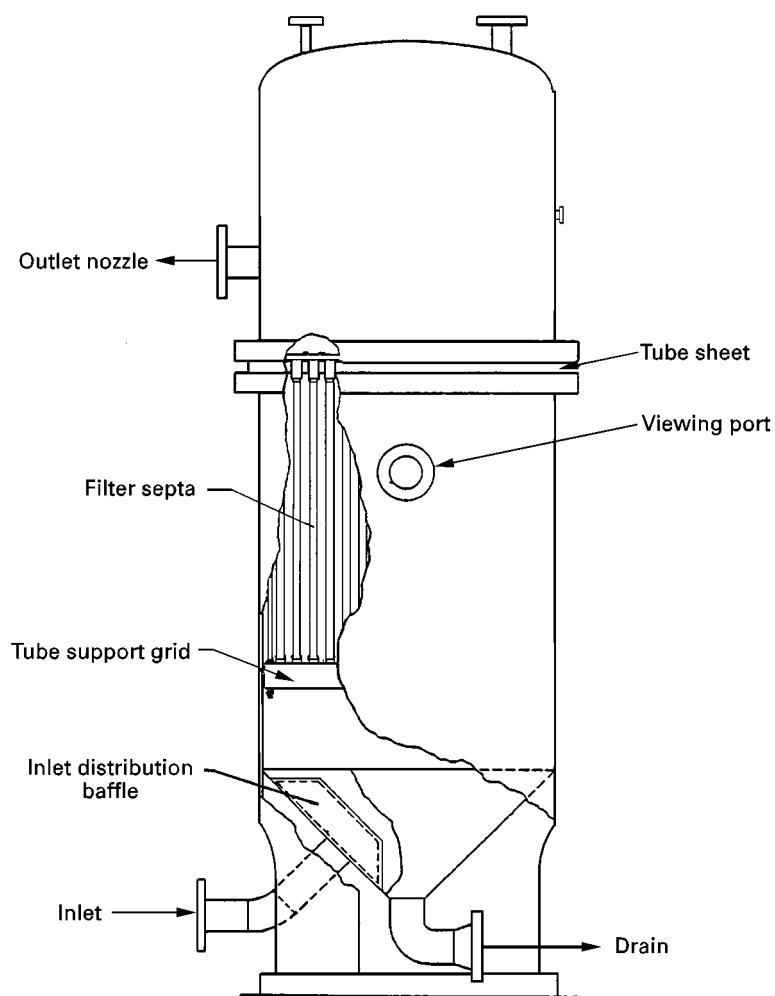


Figure 4 Pre-coat system design: top tube sheet.

in a variety of diameters and lengths; large vessels accommodate 127–203 cm elements. A variety of fibres, including polyester, polypropylene, nylon and carbon, are used for the yarn winding, depending on the application.

It should be noted that powdered resin pre-coats can be applied to traditional septa such as leaf filters or plate and frame filter presses. Resin pre-coats can also be used in beds in columns similar to bead resins. This type of usage is typically limited to small bed depths due to hydraulic considerations (pressure drop across the bed).

Operation

The slurry tank is filled with water, preferably de-ionized. Individual powdered components or a premixture of the same are weighed out, added to the water and mixed using a mechanical stirrer. Generally, dosage rates of the pre-coat vary from 0.73 to

1.46 dry kg pre-coat per square metre of surface area on the septum. This dosage will result in a pre-coat of 0.63–1.27 cm depth. Recently, thin-layer pre-coats have become popular with dosage rates of 0.24–0.49 dry kg m⁻². Overlays and underlays are often pre-coated at even lower dosage rates of 0.10–0.24 dry kg m⁻².

The pre-coat is applied to the filter or septum as a slurry via the pre-coat pump at an area flow rate of 0.68–1.70 L s⁻¹ m⁻². The slurry concentration as it enters the pre-coat vessel is critical. A concentration of 0.05% is ideal, though not always attainable. The pre-coat recycle loop shown in Figure 3 is used to optimize slurry concentration entering the pre-coat vessel through dilution. The objective is to lay down a uniform pre-coat across the length of each and every filter element. A low slurry concentration will translate into small floc size. The small floc, in turn, can be carried to the upper portion of the vessel despite low flow in that region. Alternatively, larger floc particles

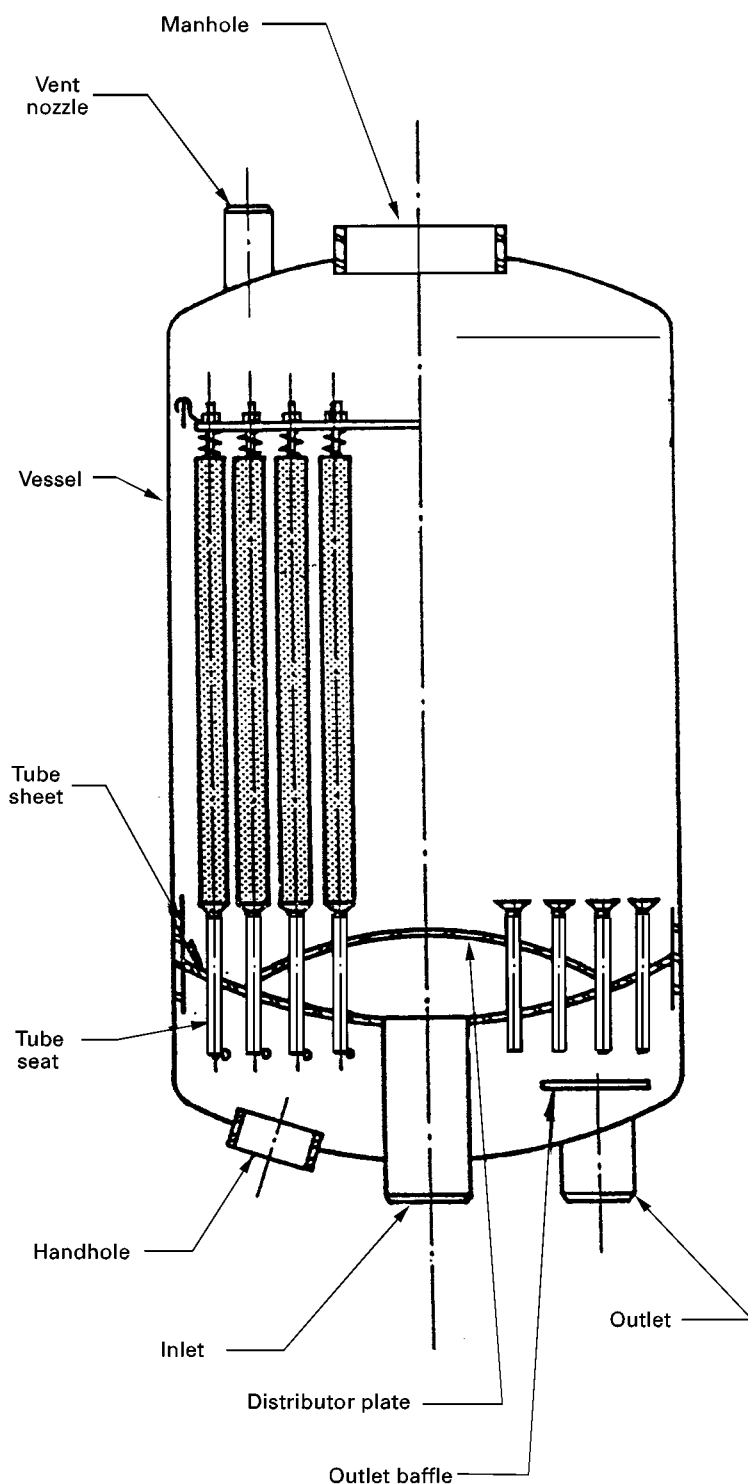


Figure 5 Pre-coat system design: bottom tube sheet.

can reach a point where the flow carrying them upward is balanced by gravity. The consequence of this condition is reflocculation where floc grows in size, then falls towards the bottom. Even if the refloc eventually pre-coats the filter, its large particle size

creates an uneven surface. Pre-coating, along with recirculation, continues until all powdered material is deposited on the surface of the filter elements. This process takes 10–90 min, after which additional recirculation allows the system to clear (residual turbid-

ity in water dissipates). At this point, the pre-coat is ready for standby or service. If the standby option is chosen, the hold pump maintains sufficient flow across the pre-coat to prevent it from falling off the filter element. In some instances, application of additional pre-coat material – a technique known as body feed – during the service cycle greatly enhances system performance.

During the service cycle, the pre-coat removes contaminants from the feed solution via ion exchange, adsorption and filtration mechanisms. The purified solution passes through the pre-coat and the filter element and emerges as product. Water quality, usually measured by conductivity and/or ionic content, and pressure drop across the pre-coat are monitored throughout the service cycle. During the service cycle, the pre-coat contracts and tightens as it is loaded with ions, organics and colloids. The area flow rate during the service cycle is $2.0\text{--}2.7\text{ L s}^{-1}\text{ m}^{-2}$. Deterioration of one of the measurement parameters determines the end point of the service cycle (e.g. differential pressure drop across the pre-coat increases by 0.70 kg cm^{-2}). At this point, the expended pre-coat is removed from the filter via back-wash. During back-washing flow across the pre-coat is reversed and the solids are slurried to waste. With the evolution of pre-coat technology, back-washing has also changed from simple surges of water or air to combinations of high pressure air and water. The scrubbing properties of the air and water combination are further enhanced by repeated applications, each with a different level of water in the pre-coat vessel. The greatest effect occurs on the element in the immediate vicinity of the air–water interface in the vessel. These elaborate processes are designed to remove pre-coat particles embedded in the filter element as well as the bulk pre-coat on the surface. At the conclusion of the back-washing steps, the system is ready for the next pre-coat.

Over the years, mechanical innovations have improved upon the original pre-coating process. Metering tanks feed the resin slurry into the mix tank at a specific rate, thus offering excellent control over slurry concentration. Draft tubes installed in the pre-coat vessel carry pre-coat particles directly from the inlet at the bottom of the vessel to the top of the vessel. With the draft tube design, slurry flow is split and the filter elements are exposed to pre-coat flow both top-down and bottom-up. The result is a more even pre-coat deposition on the element.

Applications

Powdered pre-coats have been useful in a wide variety of applications. Among the most common are polish-

ing steam condensates; treatment of low activity radioactive wastes; decolorization, decalcification and clarification of sugar juices, sugar syrups and polyhydric alcohols; clarification of fluids containing electrolytes and colloids; purification of antibiotics, vitamins and other pharmaceuticals; removal of toxic and noxious organics from potable and industrial waters; recovery of precious metals; pretreatment of high purity water systems; recovery of catalyst residues from reaction mixtures; and removal of traces of acids, bases and salts from polar solvents. Most pre-coat applications involve removal of impurities present in low concentrations.

Powdered ion exchange resin pre-coats were first utilized in electric power plants. Originally, bead-form ion exchange resins were used to remove (polish) soluble ionic contaminants from condensate prior to recycle to the steam generators. Powdered resin pre-coats combined this ion exchange polishing capability with filtration of colloidal and particulate materials such as a mixture of transition metal oxides (Fe, Cu, Co, etc.) present in steam condensate due to erosion or corrosion. Pre-coat technology was applied in both nuclear and fossil steam-generating plants. This technology proved particularly valuable in the boiling water reactor (BWR)-type nuclear plants. Unlike their bead counterparts, powdered pre-coats generate no liquid waste regenerants since they are designed to be nonregenerable and disposable solids. Issues such as short run lengths due to the high level of suspended solids in BWR condensate led to the development of pre-coats incorporating fibre in addition to powdered resins. The use of powdered resins in nuclear condensate polishing is so prevalent that operational guidelines have been issued by the US industry (see Further Reading).

In addition to condensate polishing, powdered pre-coats are used in reactor water clean-up (RWCU), elevated temperature heater drain and fuel pool purification applications in nuclear power plants. Powdered pre-coats have also been widely adopted in nuclear power plants for radioactive waste systems. In these systems, the powdered resin materials are pre-coated directly on to existing filters replacing diatomaceous earth or cellulose fibres. They offer both efficient ion exchange capacity and corrosion product filtration. These pre-coat materials have been tailored to remove specific troublesome radionuclides with a long half-life such as ^{60}Co , ^{90}Sr , ^{134}Cs and ^{137}Cs . In addition to synthetic organic ion exchange resins, both natural and synthetic zeolites are utilized in selective radioactive waste applications. Similarly, alternative resin types such as ammonium form or morpholinium form strongly acidic cation and weakly acidic cation components

are commercially available to customers from public utilities.

Blaine and Down first described the application of powdered ion exchange resin technology for decolorizing sugar syrups. Colour bodies in sugar syrups are high molecular weight entities which anion exchange resins typically selectively remove. Blaine and Down reasoned that reaction kinetics, as controlled by particle diffusion, are much slower in viscous liquids such as sugar syrups than typically found in water applications. Consequently, finely divided powdered resins decolorize much more rapidly than their larger bead counterparts. Moreover, the powdered resins are used as disposable, non-regenerable filter pre-coats, thus eliminating the need for chemical regenerants for the ion exchange resin. These pre-coats offer increased operating capacity for colour removal without generating unacceptably high pressure drop across the pre-coat. The high decolorization capacities also result in lowered sugar losses from dilution during the sweetening-off and sweetening-on steps. Sugar pre-coats offer clarification through filtration in addition to decolorization.

The initial sugar decolorization pre-coats contained mixtures of anion and cation exchange resins. Over the years, commercial formulations have expanded to include mixtures of selective anion exchange resins, powdered activated carbons and/or chopped fibres depending on the specific application. These formulations are tailored for the clarification and decolorization of sugar syrups (cane, corn and beet), fruit juices (grape, apple) and polyhydric alcohols (glycerine, sorbitol). The decolorization performance of these pre-coats compares favourably with traditional technologies (bone char, granulated activated carbon and regenerable ion exchange resins), especially as a final polishing step. In addition, tailored pre-coats remove species that cause undesirable taste and odour in the product. Pre-coats also offer limited de-ashing (deionizing) capacity in sugar syrups. De-ashing is limited by the number of ion exchange sites, not to mention the competition from colour bodies for the anion exchange sites. Low capital investment, limited space requirements and reduced energy costs are cited as advantages for the pre-coat technology in sugar applications.

Future Directions

Powdered pre-coat usage has been declining in recent years, especially in utility applications. Few new power generation plants are designed and built with pre-coat systems. In nuclear power plants, the cost of

radioactive resin disposal continues to rise dramatically. Thus, utilities have minimized the use of ion exchange resins, including powdered pre-coats, in these facilities. The introduction of thin-layer pre-coat technology has further accelerated this trend. Because of the risk of leaching after burial, concerns are increasing over the ultimate fate of formulations containing biodegradable fibres such as cellulose. Fortunately, alternative fibres such as PAN, nylon, polyethylene and polyester fibres can be substituted for the cellulosic fibre in pre-coat formulations. The PAN fibre formulations offer the added advantage of extended run length to a given differential pressure drop end point. Pleated filter elements have replaced yarn wound filter elements in many plants. The pleated elements offer excellent iron removal without using a powdered pre-coat.

Premix pre-coats are increasingly popular, replacing traditional powdered component pre-coats. Premixes offer the convenience of a one-step operation and do not necessitate operator adjustments during pre-coating. Of course, the flexibility of adjusting powdered component ratios on each cycle depending on influent conditions is lost with premixes. As available human resources (operators) shrink, the popularity of premixes will continue to grow. Customers demand and receive ultrahigh purity powdered pre-coats. Specification limits on residual contaminants such as iron, copper, aluminium, silica, sodium, potassium, calcium and magnesium for powdered pre-coats are typically set at 50 p.p.m., 25 p.p.m. or even 10 p.p.m. by dry weight. These stringent specifications apply to both resin components and pre-coat formulations. Increasingly, selective ion exchange media, including zeolites, are being incorporated into pre-coat formulations. Radioactive waste applications, discussed above, are a perfect example of this trend. Custom-designed powdered pre-coats of all types are growing in popularity.

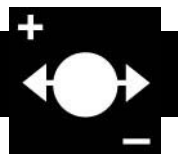
See also: II/Ion Exchange: Historical Development; Organic Ion Exchangers; Theory of Ion Exchange.

Further Reading

- Storer RA (ed.) (1997) *Annual Book of ASTM Standards, Water II*, Vol. 11.02. West Conshohocken, Pennsylvania: American Society for Testing and Materials.
- D' Angelo P (ed.) (1993) *Condensate Polishing Guidelines for PWR and BWR Plants*. Palo Alto, California: Electric Power Research Institute.
- Frisch NW and Kunin R (1960) Kinetics of mixed-bed deionization: I. *American Institute of Chemical Engineers Journal* 6: 640.

- Halbfoster CJ (1980) US Patent no. 4, 190, 532. *Charged Filter Aid Material and Ion Exchange Bed*.
- Helferich F (1962) *Ion Exchange*. New York: McGraw-Hill.
- Kunin R (1958) *Ion Exchange Resins*, 2nd edn. Malabar, Florida: Robert E. Krieger.
- Kunin R, Tavares A, Forman R and Wilber G (1984) In: Naden D and Streat M (eds) *Ion Exchange Technology*. pp. 563–578. Chichester, UK: Ellis Horwood.
- Levendusky JA (1966) US Patent no. 3,250,702. *Process for Purifying Liquid and Particulate Ion Exchange Material Used Thereof*.
- Salem E (1994) US Patent no. 5,376,278. *Improved Filter and a Method for Separating Particles from a Liquid Stream*.
- Yoshioka T and Shimamura M (1983) *Bulletin of the Chemistry Society of Japan* 56: 3726.

PREPARATIVE ELECTROPHORESIS



R. M. C. Sutton and A. M. Stalcup,
University of Cincinnati, Cincinnati, OH, USA

Copyright © 2000 Academic Press

Introduction

The development of electrophoresis in the early part of the 20th century proved to be an extremely important tool for the separation of biologically important molecules such as amino acids, peptides, proteins and DNA. There are four main types of electrophoresis, known as zone electrophoresis, step-field electrophoresis, isoelectric focusing and isotachopheresis. This review discusses the development of zone electrophoresis and step-field electrophoresis for preparative applications.

Electrophoresis instruments use mobility differences in the presence of an electric field to separate mixtures into individual components. The mobility differences between individual species are proportional to the net charge to size ratios of the species. Therefore, separations are most effective for solutes with large differences in this ratio. Additional separation mechanisms, such as molecular sieving using gels, have since been incorporated in the modes of electrophoresis to increase the range of applicability. At present, there are a wide range of electrophoresis instruments and methods which are used routinely in the biotechnology industry for analytical measurements. In contrast, the use of preparative electrophoresis is far less extensive.

The major distinction between analytical and preparative electrophoresis lies in the size and processing of samples. In the case of preparative electrophoresis, sample sizes are generally much larger (mg to g) in comparison with analytical electrophoresis (ng to µg) depending on the availability of the species of inter-

est. Such large samples must not be too crude because irreversible adsorption of some unwanted species can render the system inoperable. The samples also require the collection of fractions after separation, which is often not the case with analytical separations. Thus, after separation, it is essential that the solutes can be easily removed from the buffer solution if they are to be prepared as pure compounds. The constitutions of buffer solutions must therefore be carefully chosen, preferably with volatile components, which facilitate collection of the species of interest.

Preparative electrophoresis systems require scaling up from the respective analytical systems and modifications to the instrumentation have been made which attempt to contend with complications arising from the scale-up. For instance, an inherent problem with electrophoresis is thermal convection caused by the flow of ions in the presence of an applied electric field. As electrophoresis systems are scaled up for preparative applications, convection problems and heat dissipation in the system become more significant owing to the decrease in the relative surface area. Anticonvective media such as filter paper, agarose, starch, glass powder or polyacrylamide have been used to limit these convection processes. The use of anticonvective media, however, has led to other problems, such as adsorption, endosmosis and diffusion. These combined factors have therefore prompted the development of a number of different designs of preparative electrophoresis systems that are suitable for continuous or batch-wise separations of multicomponent mixtures. Two basic strategies have evolved which are collectively termed preparative free-flowing electrophoresis or preparative gel electrophoresis. Both strategies exploit the same basic electrophoresis process for the separation, although both approaches have been used in a variety of configurations.

Preparative Free-flowing Electrophoresis

In the case of free-flowing electrophoresis, there is no anticonvective medium. Separation of samples therefore occurs in free solution and sample zone broadening, as a result of convection, tends to be more pronounced than in the analogous gel method. A support, such as paper, may be used for the buffer to flow across and is cooled to maintain maximum thermal stability in the system. One method of reducing convection processes in the system is to perform the investigations in a cool room (e.g. at 5°C). Such temperatures also ensure that there is no degradation of heat-sensitive samples.

Early reports of free-flowing electrophoresis were first made by Barrolier who devised a continuous separation process. A system was developed in which an electric field was applied perpendicularly to the direction of the buffer flow. Sample was introduced as a constant stream into the top of the system which travelled in the same direction as the buffer. As in the case of other electrophoresis systems, differences in the charge to size ratios of the solutes caused mobility differences in the presence of an electric field. This, in turn, brought about movement of the solutes perpendicularly to the pumped buffer flow, leading to a lateral separation between the two electrodes. Separators at the end of the support facilitated collection of the sample streams into pure fractions (Figure 1). The system was found to be suitable for a series of highly mobile dyes, but convection in the system made it more difficult to separate more complex samples.

A more drastic approach to suppress thermally induced density gradients contributing to convection has been to perform electrophoresis experiments in space. The microgravitational fields in orbiting spacecraft provide a suitable environment for reduced convection in electrophoretic processes.

An alternative design for free-flowing electrophoresis apparatus was developed by Dobry and Finn: this utilized upward movement of the buffer and samples. In this apparatus, electrodes were separated from the system by means of semipermeable membranes placed perpendicularly to the cylindrical electrophoresis chamber. This caused differences in the direction of migration of the solutes, perpendicular to the direction of the buffer flow, and a range of dyes was successfully separated. On separation of the solutes, a series of outlet ducts at the top of the apparatus enabled collection of the purified species. Unfortunately, this early apparatus also appeared to have problems with convection because an effective cooling system was absent. This inferred the occurrence of a temperature gradient within the system, which would affect slower-moving protein mixtures more significantly.

It was not until recently, however, that the approach of reducing convective processes in free-flowing electrophoresis has been made simpler and more effective. This new approach has been labelled capillary free-flow electrophoresis. A coolant solution is continuously passed through a number of evenly spaced Teflon capillary tubes within the separation chambers and has been found considerably to reduce convection processes in the electrophoresis system

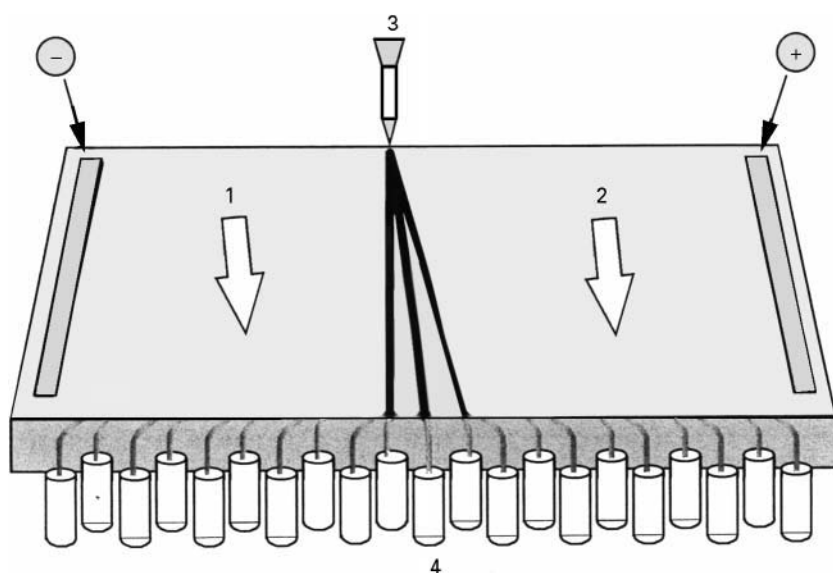


Figure 1 A free-flow electrophoresis system. The direction of buffer flow is indicated by 1 and 2. Sample enters continuously at 3 and purified solutes are collected at the vials at position 4.

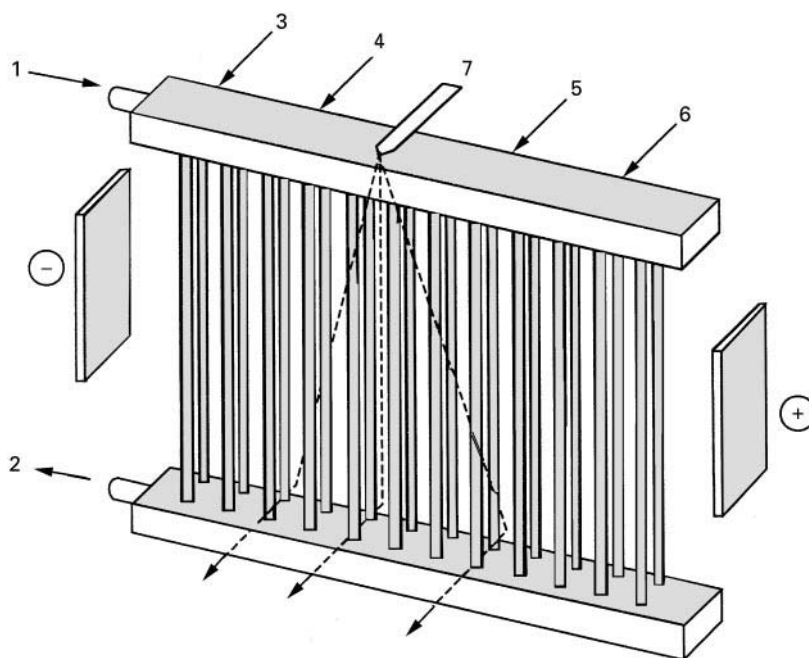


Figure 2 Design of capillary free-flow electrophoresis system. Cooling water enters at 1, passes through a series of parallel Teflon tubes (number reduced for simplification) and exits at 2. Buffer enters at ports 3–6 and sample stream enters at 7.

(Figure 2). The coolant tubes have not been found to affect the quality of separations adversely. As in the case of previous free-flow systems, the sample is continuously introduced into the system. Therefore the potential for the purification of large quantities of solutes is available (e.g. 1 g h^{-1}).

A more complex-free flowing electrophoresis instrument was designed by Hjertén to address the problem of convection. An apparatus was constructed in which the buffer flowed through a straight horizontal tube, which was rotated axially at constant velocity. The rotating tube alleviated the effects of gravitational convection and sedimentation. Although this system appeared suitable for analytical separations, convection was still a problem with regard to the quantities used for preparative use. The addition of anticonvective media, such as a density gradient, formed using sugar solutions, or the use of a gel was still required. This instrument was in fact the precursor of the capillary electrophoresis instrument.

Another unique approach to free-flow electrophoresis utilized a fluid endless belt. This design is analogous to a small conveyor belt in the vertical position. Movement of the solutes around the belt reduces convection and sedimentation processes occurring in the system. The sample is introduced as a continuous stream close to the electrode from which the solutes are repelled and are collected from the other side of the system, close to the electrode to which they are

attracted. All solutes must, however, be attracted to the same electrode. The solutes travel around the belt several times during the electrophoresis process, moving approximately perpendicularly to the electric field. Solute with the highest mobilities travel farthest across the belt and the separated solutes are collected at the outlets.

Preparative Gel Electrophoresis

The incorporation of gels as a solid support assists in the prevention of convective distortion of the analyte zones. Another advantage of using gels is that there may be an additional effect of molecular sieving which can be exploited to enhance the separation of solutes such as proteins. As a result of these considerations, a number of different gel types have been developed for preparative electrophoresis systems.

One of the first designs of a preparative gel apparatus developed by Hjertén used a starch gel in the form of a horizontal slab. One of the main differences between this system and the free-flowing systems was that sample introduction was not continuous. Using this system, separation of milligram quantities of lysozyme and β -lactoglobulin was achieved over periods of about 40 h.

Another type of gel that has been used with success is agarose. Agarose has been found to be a better support than agar, owing to its purity, and displays very little electroendosmosis. Agarose also displays

little adsorption of proteins and therefore migration of solutes is similar to that in free solution.

The greatest number of investigations using preparative gel electrophoresis, however, has been with polyacrylamide-based gels. A significant advantage of using polyacrylamide gels is that pore radii (between 0.5 and 3.0 nm) can be easily controlled by adjusting the acrylamide concentration and the concentration of the cross-linking agent. As with analytical procedures, gel buffer pH and ionic strength as well as electrode buffer pH and ionic strength must be considered before separation.

A popular method of preparative separation is to use polyacrylamide with detergent in the buffer. Ryan *et al.* modified a preparative polyacrylamide gel for use with systems containing the anionic detergent sodium dodecyl sulfate (SDS). As in analytical gel electrophoresis, addition of the SDS allows separation based on the molecular weight of the solutes. The preparative gel method used was essentially that of Laemmli. This type of system has been found to be suitable for a large number of applications listed in the literature.

Early development in the use of polyacrylamide gels for preparative electrophoresis was stimulated by the development of discontinuous or disc electrophoresis by Ornstein and Davis. Disc electrophoresis enables sharpening of sample zones by using variable conditions within the electrophoresis system. Discontinuities in the separation system are achieved by incorporating different buffer compositions or the same buffer composition at different pH throughout the gel and/or by using voltage gradients during electrophoresis. One of the main features of disc electrophoresis is a concentrating step, which ensures that the sample is compressed into an extremely thin band before electrophoretic separation of the solutes. This type of gel usually consists of three components. The largest portion is the separating gel, which is preceded by a spacer gel and then a small mixture of the sample, in either gel or viscous solution. Lewis and Clark described such a system for the preparative separation of components from rat pituitary glands.

Another variant of disc electrophoresis employs the sequential use of two buffer systems at different pH. A pH close to the isoelectric point of one species is chosen to effect separation initially. This enables migration of one species whilst the other species moves very little. After separation of the two species, the pH of the buffer solution is changed, which causes a rapid increase in the mobilities of both species. Both species are continuously eluted from the gel where they can be detected followed by suitable fraction collection. This approach was found to resolve two forms of phosphoproteins successfully.

Gel Configurations

Since the initial introduction of preparative gel electrophoresis systems in the early 1960s, a range of different instrument designs have also been developed to incorporate gels. Some systems have used glass and others have used LuciteTM (Perspex) for mechanical support of the gel. An advantage using glass is that it has higher thermal conductivity than Perspex, but it has been found that, as the walls become narrower, surface effects from glass become enhanced. In contrast to free-flowing electrophoresis, the use of anticonvective media in these systems allows for magnetic stirrers to be used in the buffer reservoirs. These maintain uniform concentration of buffer components and also prevent bubble trapping. The units have mainly been either cylindrical or slab-like and electrophoresis has been performed in either a vertical or horizontal orientation. In the case of cylindrical gels, gel column heights are important and mainly depend on the diameter of the column used and the sample loading. Improvements in the vertical column cylindrical gel systems have been made by addition of direct cooling. Convection processes have also been reduced by forming the gel around a central cooling capillary. In these cases, elution buffer can be utilized to carry samples to a UV detector before fraction collection and also to cool down the gel as it passes through the central capillary.

A preparative gel apparatus developed by Hediger used a completely sealed system. External buffer reservoirs were used for the electrode and elution buffer. The gel was placed between two adapters in a vertical cylinder. The upper adapter, which was easily movable since it was motor-driven, had a gel-pouring device, which enabled easy preparation of both gradient and nongradient gels.

Slab gels can be run in a vertical or a horizontal position and were initially designed in order to increase the amounts of sample that could be handled in one electrophoretic run. It is not clear whether slab gels offer improved separations over cylindrical gels, owing to the problems associated with cooling and fraction collection in comparison with the column gels.

Hjertén developed a large-scale system that involved a vertical slab gel. This apparatus enables the separation of up to 1 g of material. After elution from the separation chamber, the solutes enter a granular bed of agarose spheres. They are then displaced from the granular bed by a buffer flow, which transfers them to a fraction collector. The system has been used effectively for the separation of a series of proteinases.

The development of an annular-shaped electrophoresis apparatus by Southern enabled a larger

surface area of the gel to be utilized when compared to gels of conventional geometry. The outer electrode is wrapped around the gel and the inner electrode runs on a bobbin on the inside. A rapid flow of buffer passes between a semipermeable membrane and the central electrode to facilitate cooling of the gel. Sample is introduced into a small slot that runs around the periphery of the gel annulus. The material moves from the outside of the gel in concentric circles towards the centre, where it is eluted. Solutes are therefore moving from a large area to a much smaller area, which enables the use of high sample loads. In this case, the fraction volume was kept to a minimum by employing discontinuous elution. The electronics for this system were later modified so that, after electrophoresis was stopped, the current was reversed for a short period of time to remove solutes adsorbed on to the semipermeable membrane surrounding the electrode, before eluting the purified samples from the gel.

Sample Recovery using Preparative Gels

In contrast to free-flow electrophoresis, where sample collection is performed during electrophoresis, preparative gel electrophoresis allows samples to be collected after electrophoresis. Also, most preparative gel electrophoresis is performed as a batch process. There are two methods for recovering the purified samples when using preparative gel systems. Solutes can either be recovered from the gel after the electrophoretic separation, or eluted from the gel during electrophoresis and collected sequentially. In the first case, solutes can be recovered from the gel mechanically (analogous to thin-layer chromatography) or by using electro dialysis. In one example, using polyacrylamide gel columns, samples were cut from the gel using a jig. This method enabled sections to be cut reproducibly from subsequent gels.

The second recovery mode involves electrophoretic migration of analytes from a cylindrical gel using a continuous elution system. As electrophoresis proceeds, the end of the gel is continually flushed with a buffer solution and solutes are transported from the gel. This enables samples to be detected as they leave the system using some form of online detection. After detection, a fraction collector can be used to establish the integrity of the purified samples. An important part of the design of the continuous elution system is a dialysis membrane which is usually placed between the end of the separation gel and the bottom buffer solution. This membrane prevents migration of the solutes into the main buffer solution. For continuous elution systems, elution buffer pH and ionic strength must also be considered.

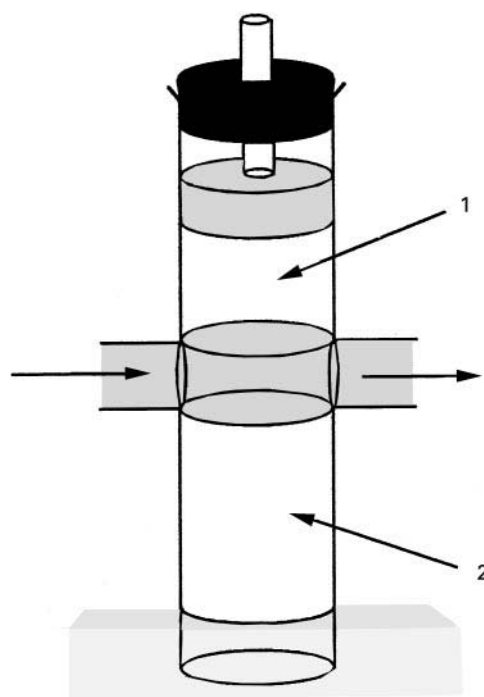


Figure 3 Side-arm apparatus. The top gel is 1 and the bottom gel is 2. The arrows indicate the elution buffer flow collecting solutes.

A variant of the continuous elution recovery system employs continuous elution from between two gel column halves. A dialysis membrane, placed on top of the bottom gel, ensures complete elution of the solutes as they reach the end of the separating gel. The assembly consists of a 2 cm outer diameter glass tube with two side arms through which buffer is pumped (Figure 3). A system of this type was effective for the separation of a series of bean leaf proteins.

Another method of collecting solutes, after electrophoresis, has been developed and is known as discontinuous elution. Electrophoresis is stopped for short periods of time whilst solutes which have passed through the gel are collected from a cup at the bottom of the gel. This method is believed to reduce dilution of the samples in comparison with continuous elution systems. After removing the solutes and buffer solution from the cup, the cup is refilled with fresh buffer solution and electrophoresis is reinitiated.

Discontinuous sample collection may be fairly time-consuming owing to the intermittent sample collection process. This was one of the reasons that led to the development of automated preparative gel electrophoresis systems. One such system was designed by Hodson and Latner. After a period of time, electrophoresis in the system is stopped and buffer, containing solutes which have passed through the gel, is collected and the buffer chamber refilled. Up to

300 mg of protein mixtures may be separated using the system, with the potential for further scale-up.

Another discontinuous sample collection system, for use with slab gels, has been developed by Polsky *et al.* An electronic timer was used which controlled the collection of samples and refilling of buffer in the elution chamber. Electrophoresis was terminated during collection of the samples. Polyacrylamide slab gels were found to have much higher sample capacities than agarose gels. Two practical considerations concerning the buffer solution were made during this work because of run times exceeding 100 h. Chloride-free buffers were used to prevent build-up of chlorine gas and sterile solutions were used: these inhibit growth of bacteria in the system. The system was effective in resolving and collecting fragments of genomic DNA.

Buffer Types

In accordance with analytical electrophoresis, a wide range of buffers is also available for preparative electrophoresis. Essentially, the type of buffer used in the system depends on the type of sample to be separated and on the type of separation system used. High ionic strength buffers can cause significant Joule heating in a system, whereas low ionic strength buffers may cause protein aggregation.

Detection

One of the main differences between analytical and preparative electrophoresis is that quantitative detec-

tion of solutes is not as critical. This enables cruder detection methods to be used in preparative work. These detection systems can be used in real time with online detection or, in the case of some noncontinuous elution systems, after the separation has finished.

In continuous elution systems, factors which are important in terms of sample detection are the elution buffer flow rate and the elution buffer fraction volume. High elution buffer rates can cause the solutes to become too dilute for the method of detection. Slow buffer rates may cause loss of resolution between the solutes owing to diffusion. One of the most popular forms of online detection is ultraviolet-visible spectrophotometry. Not all solutes absorb or fluoresce in this region of the spectrum, but detection can be achieved in some cases using dye-staining methods. Offline detection includes light scattering, radiography, densitometry, analytical gel electrophoresis and mass spectrometry.

Commercially Available Systems

A number of preparative electrophoresis systems were available in the early 1960s but, owing to lack of demand, are no longer available. This is probably a result of increased competition from other preparative methods such as high performance liquid chromatography.

A large preparative free-flow electrophoresis system was developed at the Harwell Laboratory of the UK Atomic Energy Authority, known as the Bio-stream separator. This was a large apparatus in which

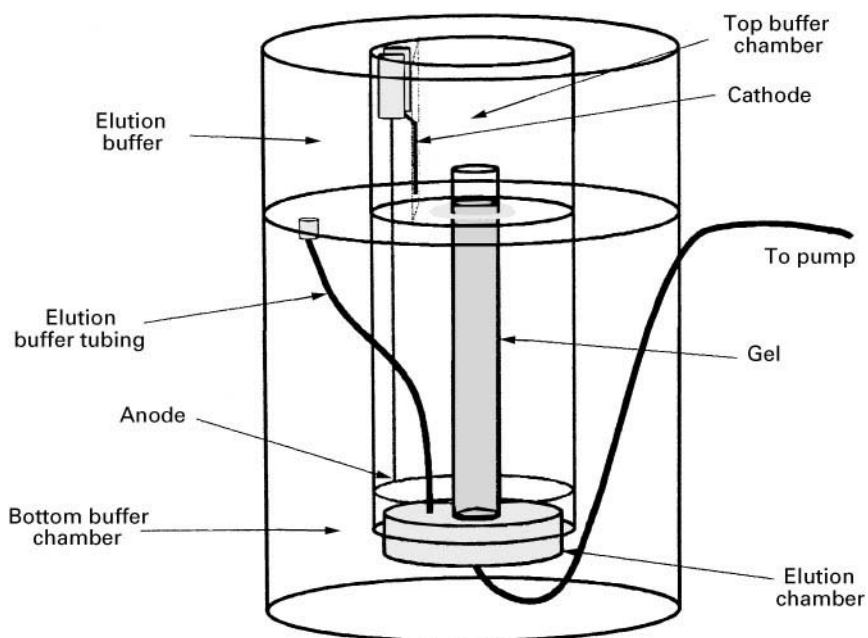


Figure 4 Bio-Rad Mini Prep-Cell.

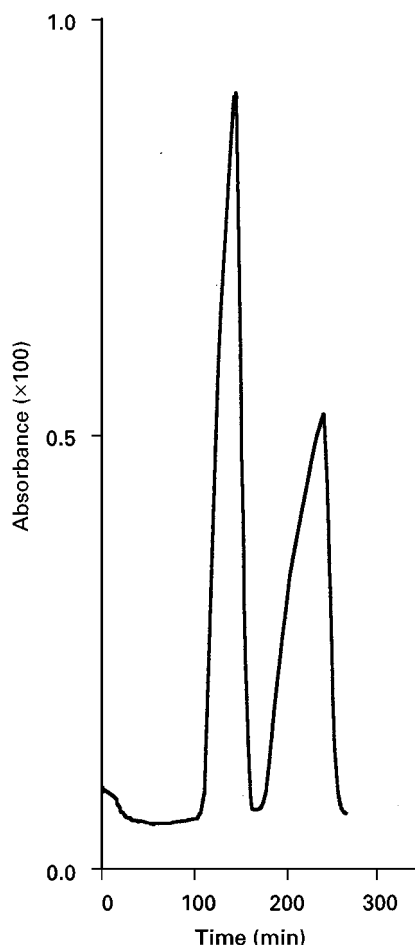


Figure 5 Separation of piperoxan enantiomers using the Mini-Prep Cell.

laminar flow conditions were maintained by rotation of the outer wall of the annulus. Although allegedly being capable of preparing 100 g h^{-1} of protein, it never became readily available on the commercial market.

Bio-Rad Laboratories (Hercules, CA) currently have several preparative gel electrophoresis systems for use with gels (**Figure 4**). These are continuous elution devices based on vertical column gels. One of the larger systems has a ceramic core that is used for cooling the gel.

A capillary free-flow electrophoresis system has been patented by R&S Technologies. The device is believed to be considerably better than previously produced free-flowing electrophoresis systems owing to reduced convection in the system from the capillary cooling.

Applications

As in the case of many of the systems described previously, the main applications for preparative gel

electrophoresis systems are large biomolecules such as nucleic acids, enzymes and antigens. Recent developments in preparative gel electrophoresis, however, have extended its applicability to the preparation of enantiomerically pure pharmaceuticals (**Figure 5**). This has been achieved by the addition of a sulfated β -cyclodextrin chiral additive to the buffer of a system employing a vertical column agarose gel in the apparatus shown in **Figure 4**.

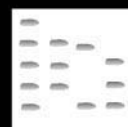
Future Developments

The continued development of analytical and preparative instruments can only lead to further improvements in some of the systems previously mentioned. Limitations in design and development of these devices are reducing significantly as engineering and electrical methodologies improve. In contrast to the continuing development, and more widespread use of preparative gel electrophoresis, continuous free-flow electrophoresis instruments offer an interesting prospect for development now that the problems of convection have been more fully addressed by the use of capillary cooling.

Further Reading

- Catsimpoalas N (ed.) (1978) *Electrophoresis '78*, vol. 2. New York: Elsevier.
- Chrambach A, Dunn MJ and Radola BJ (1987) *Advances in Electrophoresis*, vol. 1. New York: Weinheim.
- Duesberg PH and Rueckert RR (1965) Preparative zone electrophoresis of proteins on polyacrylamide gels. *Analytical Biochemistry* 11: 342–361.
- Grafin DE (1995) *Electrophoretic Methods*. New York: Academic Press.
- Hediger MA (1984) Apparatus and method for preparative gel electrophoresis. *Analytical Biochemistry* 142: 445–454.
- Ketterer ME, Kozerski GE, Ritacco R and Painuly P (1997) Investigation of capillary free-flow electrophoresis for separation of Co, Cr and As species in aqueous solution. *Separation Science and Technology* 32: 641–654.
- Lewis UJ and Clark MO (1963) Preparative methods for disk electrophoresis with special reference to the isolation of pituitary hormones. *Analytical Biochemistry* 6: 303–315.
- Maurer HR (1971) *Disc Electrophoresis*, 2nd edn. New York: Walter de Gruyter.
- Polsky F, Edgall MH, Seidman JG and Leder P (1978) High capacity gel preparative electrophoresis for purification of fragments of genomic DNA. *Analytical Biochemistry* 87: 397–410.
- Roman MC and Brown PR (1994) Free flow electrophoresis. *Analytical Chemistry* 66: 86A.
- Ryan TE, Woods DM, Kirkpatrick FH and Shamoo AE (1975) Modification of the Shandon southern apparatus MKII for SDS preparative polyacrylamide gel electrophoresis. *Analytical Biochemistry* 72: 359–365.

PREPARATIVE SUPERCRITICAL FLUID CHROMATOGRAPHY



J. R. Williams, Sultan Qaboos University,
Al-Khod, Sultanate of Oman, UK

R. Dmoch, University of Leeds, Leeds, UK

Copyright © 2000 Academic Press

Introduction

Supercritical fluid chromatography (SFC) on a preparative scale is of interest because of its advantages over high performance liquid chromatography (HPLC). The high diffusivity and low viscosity of supercritical fluids allow rapid separation. The solvent strength can easily be controlled by changing pressure and/or temperature, so that mobile phases with a fixed composition can be used to separate many types of solute. Furthermore, many supercritical fluids are volatile or gaseous under normal ambient conditions, so that solutes can easily be recovered from the collected fractions by depressurization.

Preparative-scale SFC is now being used to separate high-value materials where preparative HPLC can be difficult to use. Peaks are narrower in SFC and for these difficult separations, very little overloading can be done to take advantage of this. Consequently, the maximum amount of material obtained in a run is of the order of 100 mg in preparative SFC, compared with the much larger amounts which are sometimes obtainable in preparative HPLC. Large-scale SFC systems can either be built in the laboratory or purchased commercially.

The unique physicochemical properties of supercritical fluids have convinced many workers that preparative SFC might be useful and relatively simple compared with preparative gas chromatography (GC), which is unsuitable for involatile and thermolabile compounds, and preparative liquid chromatography (LC), in which fraction-eluent separation can be problematic.

Preparative SFC is based on the following steps: periodic injection of the feed into a continuous flow of eluent, chromatographic separation due to selective interactions of the components of the sample with both the eluent and the stationary phase, detection at the column outlet, fraction collection, separation of the fractionated compounds from the eluent, further purification of the compounds and, optionally, recycling the eluent (Figure 1).

Preparative-scale SFC can be divided into two types: small-scale and large-scale. Small-scale can be

defined as the isolation of milligrams to a gram of pure product for, say, structure analysis. Bench-scale equipment derived from common analytical apparatus can be used with the adoption of nondestructive detection, fraction collection and eluent removal. However, for industrial-scale production (1 g h^{-1} to 1 kg h^{-1}), large-scale equipment has to be used, posing different problems, even if the same concept is applied. In preparative SFC, most studies have been devoted to the former aspect.

History and Development

Preparative-scale SFC was first suggested in 1962 by Klesper *et al.* and an appropriate collection apparatus was constructed 10 years later by Jentoft and Gouw (Table 1). However, it was not until 1982, 20 years after it was first suggested, that a patent appeared on the technique from Perrut. Two years later, Chapelet-Letourneux and Perrut were the authors of a meeting abstract on preparative SFC. In 1986, the first papers were published by Ecknig and Polster, followed months later by an article from Jusforgues *et al.*

In the 1980s, predictably, reports of preparative SFC were small in number. However, during the 1990s, the total amount of material published on

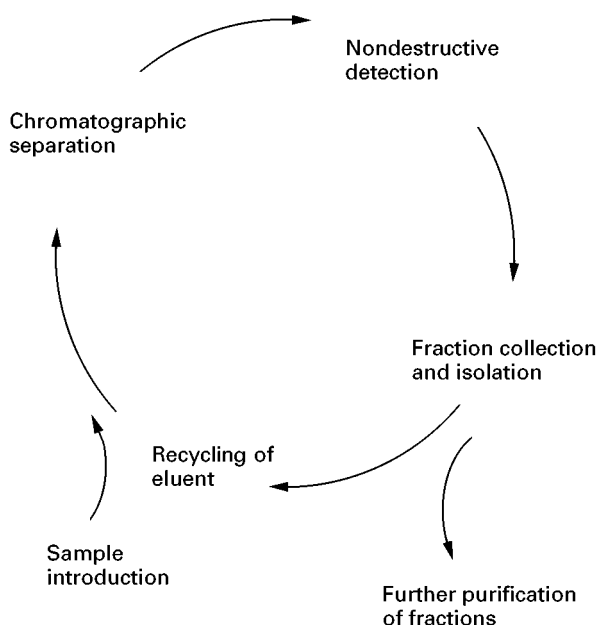


Figure 1 Flow diagram of the basic steps of preparative SFC.

Table 1 Historical perspective of preparative-scale supercritical fluid chromatography (SFC)

Year	Development
1962	SFC was suggested as a preparative tool
1972	Preparative SFC collection apparatus constructed
1982	First patent on preparative SFC published
1984	First meeting abstract on preparative SFC appeared
1986	First papers on industrial-scale preparative SFC published
1988	Jasco produce first commercial semipreparative SFE-SFC system
1990	First commercial process-scale SFC system by Prochrom

SFE, supercritical fluid extraction.

preparative-scale SFC has slowly increased; recently, publications have remained steady at three or four per year (Figure 2).

The early work was performed on SFC systems built in the laboratory. At the end of the 1980s, commercial equipment became available from Jasco and Prochrom.

During the development of preparative-scale SFC, it was used for the separation of relatively simple, low-cost test substances, such as paraffins. Once the technique had been refined, it was applied to high-value complex samples, such as pharmaceuticals.

Instrumentation

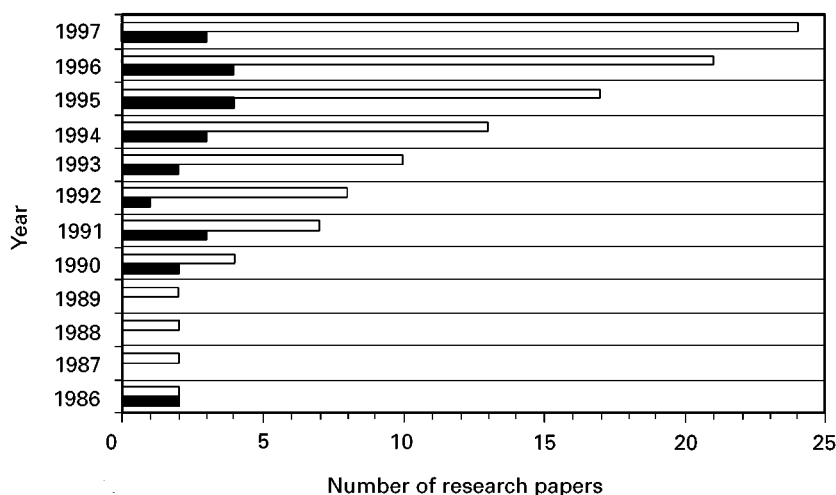
A general preparative-scale SFC consists of a pumping system, a core chromatographic section (an injection loop, a column and a detector) followed by the

back-pressure regulator (BPR) and fraction collection system. Depending on the type used, the collection system may be located either before or after the BPR (Figure 3). The discussion in this section will be limited to the example in Figure 3, with further examples being explored later.

Pumping System

The pumping system must be capable of delivering the mobile phase (e.g. carbon dioxide modified with methanol) at a total flow rate of above 30 mL min^{-1} and at a pressure of up to 400 bar. Such a system requires judicious choice of pump with an efficient cooling system to ensure that the carbon dioxide is pumped as a liquid. The carbon dioxide pump, the modifier pump and the mixer may be integrated into one pumping system or may be separate components (as in Figure 3). An accurate method of delivering modified carbon dioxide must be used for reproducible results. The use of a single and dual pumping system has been investigated. Many methods have been developed to allow the addition of a modifier to a premixed mobile phase. The former can deliver an accurate flow of modifier while the composition of a premixed mobile phase can vary with use. A flow-splitting method has been used where a fraction of the carbon dioxide displaces the modifier, after which the flows are recombined. The dual pumping systems allow one pump to control the carbon dioxide flow while the other controls modifier flow.

Syringe pumps have been used, but with the high flow rate required on larger preparative systems, their relatively small capacity limits their use. Thus, a reciprocating dual pumping system is becoming the

**Figure 2** Growth in the number of research papers published on preparative SFC. The numbers quoted do not include review articles, poster presentations or meeting abstracts. Open boxes, cumulative, filled boxes, annual.

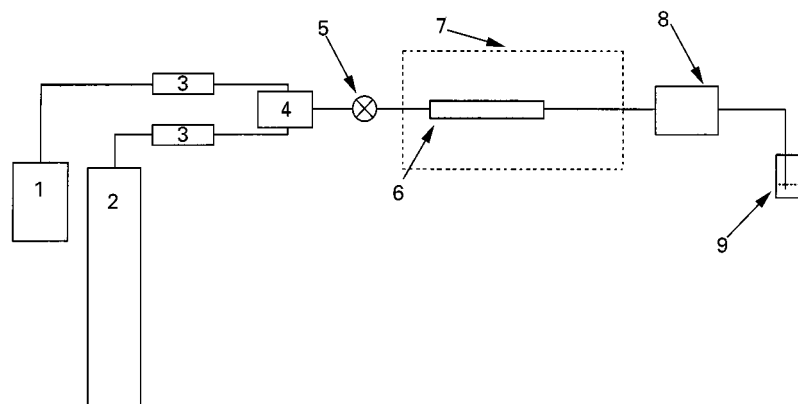


Figure 3 Schematic diagram of a preparative SFC system. 1, Modifier; 2, CO₂ cylinder; 3, pump; 4, mixer; 5, injector; 6, column; 7, oven; 8, detector; 9, collection vessel.

most common because it is able to deliver a continuous stable flow.

Injection System

The injection system may be located inside the column oven to allow injection into a supercritical fluid or outside, as in Figure 3. The injection system most commonly used is as in HPLC, but much work is being applied to the development of novel injection methods for preparative SFC. It has been noted that large-volume injections, such as those required in preparative separations, may cause phase separations of the mobile phase and the injection solvent. Although not always so, this may have detrimental effects on the efficiency of separation. To overcome this, much work has been successfully focused on the development of a solventless injection system, where the injection solvent is removed prior to introduction to the column. The sample can then be focused on a pre-column, thus eliminating any band broadening.

Columns

The most common columns used in preparative SFC are standard HPLC columns. For small-scale preparative work, analytical columns can be used. However, for larger-scale separations, preparative columns are necessary. A wide range of packing is available; the most common type is octadecylsilane bonded phases.

Detection

Preparative SFC is compatible with the detection methods available in both GC and HPLC. The most common detector for preparative SFC is the ultraviolet-visible (UV/Vis) detector. Although more sensi-

tive, the flame ionization detector (FID) is not often used because of restrictor plugging, which occurs when the highly concentrated effluent is introduced. In addition, most organic modifiers cannot be used with the FID. However, less sensitive refractive index detectors or an evaporative light-scattering sensor can be used as a universal detector if necessary. To enhance and allow many separations in SFC, a polar modifier must be used as carbon dioxide alone does not have sufficient polarity. The use of a modifier thus reduces the number of detection methods available, unless specific modifiers are chosen, for example, an FID can still be used with carbon dioxide modifier with formic acid or formamide.

Back-pressure Regulators

The BPR is used to maintain SFC system pressure above the critical pressure of the mobile phase. The BPR can be a simple restrictor like a capillary tube of either fused silica or stainless steel having appropriate dimensions for the required back-pressure and flow rate. However, in order to change the back-pressure using the same piece of restrictor, one needs to change the flow rate because the back-pressure is only produced by flow resistance. Although fused silica restrictors are the most common and cheapest BPR, they can be blocked by certain solutes or samples during use, and they can break when some organic solvents are used, or if scratched.

Another type of back-pressure device is a mechanical or electrical feedback regulator. This is a complex regulator which consists of a pressure-sensing device and a needle valve. The regulator can control the back-pressure irrespective of the mass flow rate of the fluid. Although more expensive than a restrictor, it is much less likely to become blocked. The supercritical fluid depressurizes in the BPR and emerges at atmos-

pheric pressure as a gas (carbon dioxide) and as a liquid (modifier), and it is then that the separated material is deposited into or on a collector.

Collection Methods

Many trapping methods have been tested and developed in preparative SFC. The mobile-phase modifier can be used as a trapping fluid. This was demonstrated by Heaton and co-workers who fractionated polycarboxylic acid mixtures. They found that purities were close to 100%. In-line trapping methods have proved to be just as efficient. Many different collection methods have been investigated using pressurized pre-BPR and depressurized post-BPR traps. Comparison of four depressurized collection methods showed that a collection solvent and/or cooling of the collection vessels was required to achieve good recoveries. Without these measures, recoveries fell dramatically. Collection into pressurized vessels was compared with deposition on to semipreparative thin-layer chromatography (TLC) plates and the latter gave poorer recoveries.

Principles of Separation

The principles of preparative SFC can be illustrated by taking a mixture of two compounds present in equal proportions. Providing their peaks are well resolved, a graph of purity against the fraction of material collected in total will look like curve 1 in Figure 4. The first half recovered will be a pure fraction of one of the compounds. The second half, collected separately, will contain the other compound. This is the ideal situation. For a poorer separation, curve 2 is encountered. Here, the second compound begins to elute before all the first has been collected. In the worst case, illustrated by curve 3, both compounds elute together.

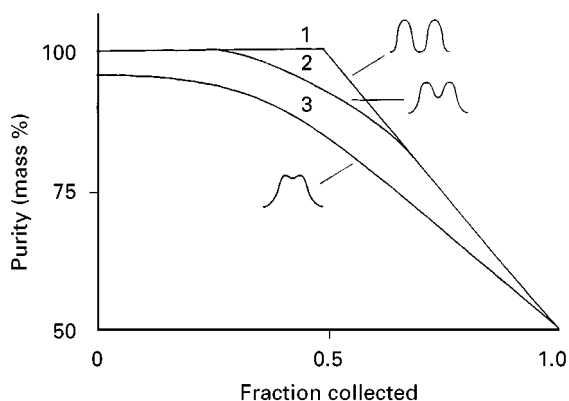


Figure 4 Plot of purity versus fraction collected for different degrees of separation.

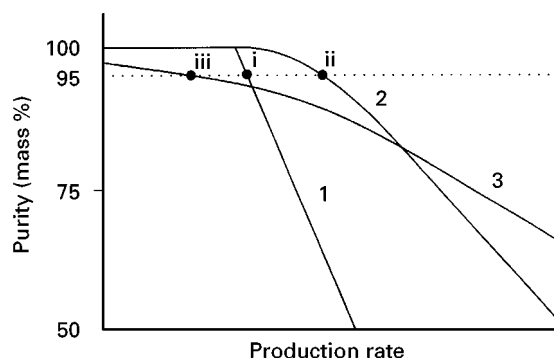


Figure 5 Plot of purity versus production rate for different degrees of separation.

Optimization

The variables to be optimized include the type of column, the concentration of modifier (if any), pressure, temperature, flow rate and loading.

Usually, optimization of column type, pressure, temperature and modifier concentration is conducted on an analytical scale. Initially, the chromatograms from experiments without trapping are scrutinized to help choose the best conditions.

However, for the optimization of flow rate and loading conditions, trapping experiments can be performed to obtain plots of purity against production rate for different conditions. The rate of production of the eluent from the end of the column can be improved by increasing flow rate or loading, for a given set of conditions. However, this can have a deleterious effect on separation. Consequently, if purity is presented versus rate of production, the curves 1, 2 and 3 (Figure 4) will become extended (Figure 5). The horizontal dotted line in Figure 5 signified 95% purity and it dissects the curves 1, 2 and 3 at i, ii and iii, respectively. These points can also be shown as a graph of production rate against loading or flow rate for a purity of 95% (Figure 6). Consequently, it can be seen how an optimum loading or flow rate can be chosen for a given purity.

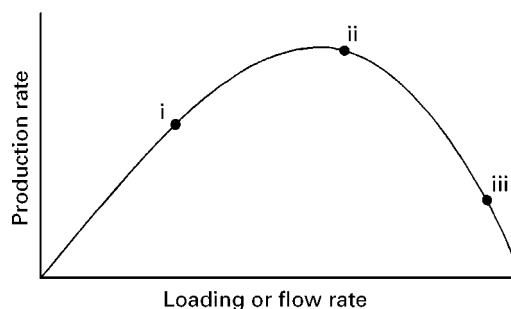


Figure 6 Plot of production rate versus loading or flow rate for a given required purity.

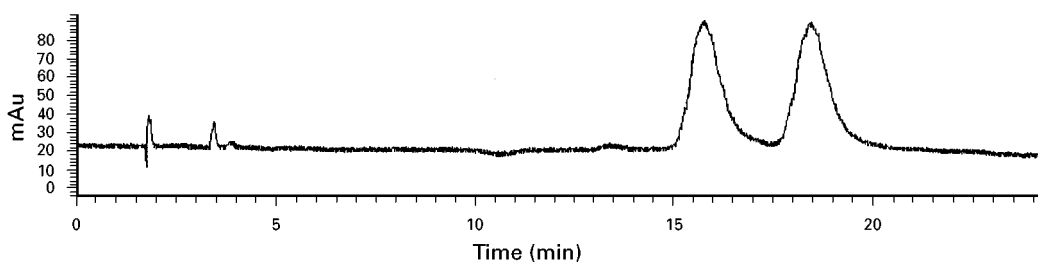


Figure 7 Chromatogram of the separation of a chiral benzimidazole.

For purities less than 100%, the purity versus production rate curves can be fitted to a quadratic. The resultant equations can be exploited to calculate values of production rate at a given purity for the various loadings. Plots can then be produced of production rate against loading. Consequently, an optimum loading can be obtained for a required purity.

Applications

The relatively low throughput of preparative SFC dictates that the technique is only economically viable for high-value substances, such as natural products, polymers and pharmaceuticals.

Probably the most promising area for preparative SFC is in chiral separations where several applications have been reported. The racemates of important biological compounds have been isolated into their optically pure forms. Shorter analysis times have also been observed when performing chiral separations of β -blockers, benzodiazepines, non-steroidal anti-inflammatory agents and β -agonists. An example of the separation of a chiral benzimidazole and 2,2,2-trifluoro-1-(9-anthryl)ethanol achieved using SFC is shown in Figures 7 and 8.

Preparative SFC has been applied successfully to polymers. Highly isotactic (*-it*) and highly syndiotactic (*-st*) fractions of poly(methyl methacrylates) (PMMA), where the degree of polymerization (DP) ranges from 25 to 50, have been isolated by Ute *et al.* (1993). This represents an improvement on earlier work where the same authors preparatively separated

PMMA with DP ranging from 19 to 29. An example of separation of a PMMA is shown in Figure 9.

Preparative-scale separations using supercritical fluids have been coupled to reaction systems to separate products of synthesis reaction. Jacobson *et al.* designed a supercritical fluid synthesis system with on-line preparative SFC using supercritical ammonia. ^{14}C -labelled anisole, L-methionine and 4-methoxyphenylguanidine were isolated and found to have a radiochemical purity of >98%.

Several compounds of pharmaceutical and biological interest have been isolated by preparative SFC and it has been reported that the supercritical technique was faster and more efficient than preparative HPLC.

Large-scale preparative SFC is a promising method for producing valuable fractions free from solvent and, at first glance, it is surprising that there have been so few reports on semi-industrial preparative SFC separations. In practice, however, problems have been reported with mobile-phase recycling, mobile-phase product separation, sample injection, fraction collection and columns, all of which are more crucial than on a smaller scale.

Conclusions

Preparative SFC is still applied to only a minority of compounds and is underutilized, although the number of applications for which it has been used is increasing. As SFC is used on a wider variety of compounds, many of these applications will undoubtedly be transferred to the preparative scale.

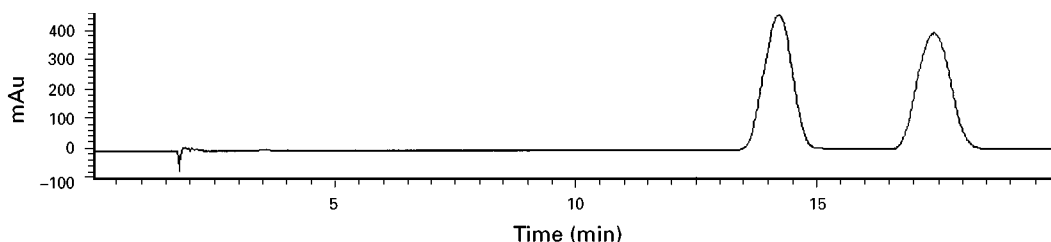


Figure 8 Chromatogram of the separation of 2,2,2-trifluoro-1-(9-anthryl)-ethanol.

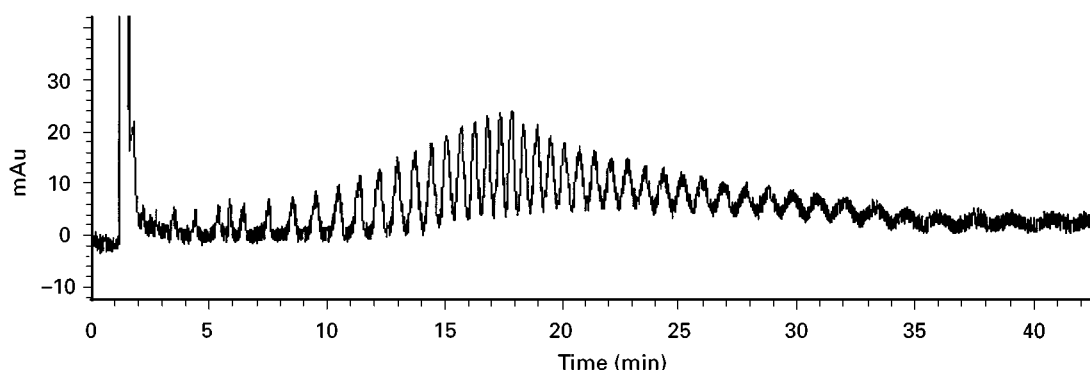


Figure 9 Chromatogram of the separation of a poly(methyl methacrylate).

The main disadvantages associated with using HPLC as a preparative separation technique are not experienced with SFC, namely the removal of the collected sample from the mobile phase and subsequent disposal of the mobile phase.

Further Reading

- Bartle KD, Bevan CD, Clifford AA *et al.* (1995) Preparative-scale supercritical fluid chromatography. *Journal of Chromatography A* 697: 579–585.
- Blum AM, Lynam KG and Nicolas EC (1994) Use of a new Pirkle-type chiral stationary phase in analytical and preparative subcritical fluid chromatography of pharmaceutical compounds. *Chirality* 6: 302–313.
- Ecknig W and Polster HJ (1986) Supercritical chromatography of paraffins on a molecular-sieve – analytical and preparative scale. *Separation Science and Technology* 21: 139–156.
- Heaton DM, Bartle KD, Myers P and Clifford AA (1996) Use of modifier as trapping fluid in preparative supercritical fluid chromatography. *Journal of Chromatography A* 753: 306–311.
- Hirata Y, Kawaguchi Y and Funada Y (1996) Refractive index detection using an ultraviolet detector with a capillary flow cell in preparative SFC. *Journal of Chromatographic Science* 34: 58–62.
- Jacobson GB, Markides KE and Langstrom B (1997) Supercritical fluid synthesis and on-line preparative supercritical fluid chromatography of ^{11}C -labelled compounds in supercritical ammonia. *Acta Chemica Scandinavica* 51: 418–425.
- Jusforgues P, Berger C and Perrut M (1987) New separation process – preparative supercritical fluid chromatography. *Chemie Ingenieur Technik* 59: 139–156.
- Ute K, Miyatake N, Osugi Y and Hatada K (1993) Isotactic and syndiotactic pentacontamers (50mer) of methyl methacrylate obtained by fractionation with preparative SFC: the GPC analysis of the 50mers and their stereocomplexes. *Polymer Journal* 25: 1153–1160.
- Ute K, Miyatake N, Asada T and Hatada K (1992) Stereoregular oligomers of methyl methacrylate 6. Isolation of isotactic and syndiotactic MMA oligomers from 19-mer to 29-mer by preparative supercritical fluid chromatography and their thermal analysis. *Polymer Bulletin* 28: 561–568.
- Via J and Taylor LT (1994) Experimental determination of changes in methanol modifier in premixed carbon-dioxide cylinders. *Analytical Chemistry* 66: 1459–1461.
- Whatley J (1995) Enantiomeric separation by packed-column chiral supercritical fluid chromatography. *Journal of Chromatography* 697: 251–255.

PRESSURIZED FLUID EXTRACTION: NON-ENVIRONMENTAL APPLICATIONS



J. L. Ezzell, Dionex Corporation, Salt Lake City
Technical Center, Salt Lake City, UT, USA

Copyright © 2000 Academic Press

Introduction

Pressurized fluid extraction (PFE), also referred to as accelerated solvent extraction (ASE), is a liquid

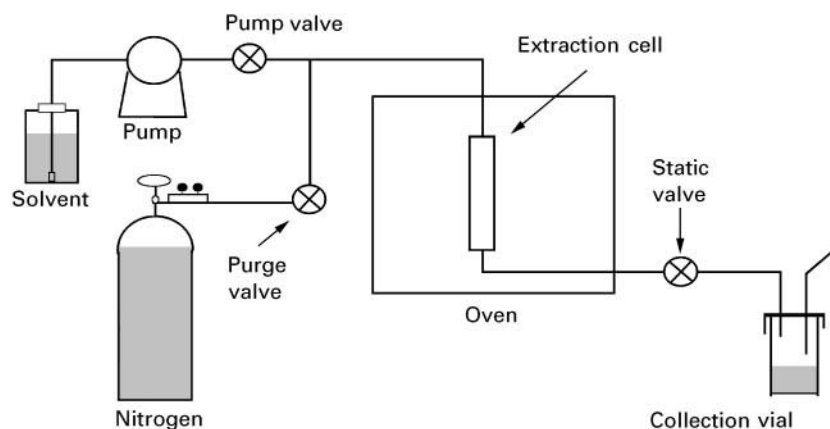


Figure 1 Schematic diagram of a pressurized fluid extraction (PFE) system.

solvent extraction technique developed and introduced by Dionex Corporation in 1995. While the initial applications focus of this technique was the environmental area, the versatility and ease of use of the approach has proven useful for laboratories performing extractions in the food and polymer industries, as well as in the pharmaceutical and consumer products areas.

Traditional reflux based extraction techniques such as Soxhlet extraction can take anywhere from 8 to 48 h to perform, with 24-h extractions common. Other liquid solvent based extraction techniques such as wrist shaker, hot-plate boiling and sonication require copious amounts of solvent and often involve labour-extensive steps such as filtering or concentration prior to extract analysis. One thing that they all have in common is operation at ambient pressure. An increase in temperature beyond the boiling point of the solvent is not possible owing to solvent evaporation.

Pressurized fluid extraction is performed by using the same solvents as in the traditional approaches, but at higher temperatures than is possible in these techniques. This increase in temperature improves the kinetics of the process, resulting in more efficient extractions (faster and using less solvent) compared with traditional approaches. The solvents are used under pressure so that their liquid state is maintained at the heated conditions. For example, solvents such as water, methanol, acetone or hexane are routinely used in PFE at 75–150°C. The solvents are maintained as liquids under pressure, normally at 10.4 MPa (1500 psi). PFE is therefore performed using very hot liquids to expedite the extraction process.

The flow-through design of the technique results in extracts which do not require the extended work of filtration as a means of separating the sample matrix

from the extracted analytes. In further contrast to traditional extraction approaches, all of the basic steps of PFE are amenable to automation, freeing the analyst from the labour-intensive nature of most sample preparation protocols. Automated PFE systems can extract up to 24 sample cells, and have the necessary safety considerations for unattended operation built in.

Instrumentation

A schematic diagram of a PFE system is shown in **Figure 1**. The PFE extraction procedure consists of a combination of dynamic and static flow of solvent through a heated extraction cell containing the sample. These cells must be capable of safely withstanding the pressure requirements of the system, and are normally constructed of stainless steel, with frits in the end caps to allow the passage of solvent while retaining the solid sample. Disposable cellulose or glass fibre filters may be used in the cell outlets to avoid compaction of fine particles on the frit surface, which may impede the solvent flow. Solvent pressure is regulated via a high-performance liquid chromatography (HPLC) type pump and outlet valves control the flow of solvent from the cell to the collection vial. Compressed nitrogen is used to purge all of the liquid from the cell into the vial at the completion of the extraction.

Sample Preparation

Proper sample preparation is essential in order to obtain efficient and reproducible extractions. The ideal sample for extraction is a dry, finely divided solid, in which the extraction solvent can easily and thoroughly penetrate the sample matrix. Whatever can be done, within reason, to make samples ap-

proach this definition will be beneficial to the extraction process. Generally, samples should be prepared for PFE extraction in the same manner as traditional techniques. Samples with large particle size (> 1 mm) should be ground so as to increase the surface contact of the matrix and solvent. Wet or sticky samples should be mixed with drying agents such as sodium sulfate or Hydromatrix (pelleted diatomaceous earth), or with dispersing agents such as Ottawa sand prior to extraction. Typical sample sizes used in PFE are 1–30 g of solid or semi-solid material.

Sample Extraction Parameters

Extraction Solvent

As extraction parameters, solvent choice and temperature will have the greatest impact on extraction efficiency with PFE. An extraction solvent should be chosen which will solubilize the target analyte(s), but leave the majority of the sample matrix intact. This is normally done by matching the polarity of the solvent and analyte. PFE extraction can be performed with the entire range of aqueous and organic solvents, with the exception of strong mineral acids (hydrochloric, nitric, sulfuric) which will attack the stainless steel flow-path of the system. In those cases where an acidic pH is required, small amounts (1–5%) of acetic, phosphoric or other weak acids can be used. The choice of solvent should also be considered in the light of the post-extraction analysis technique. Solvents such as methanol and acetonitrile are suitable for direct HPLC injection, while solvents such as hexane, methylene chloride or acetone are more suitable for concentration and gas chromatography (GC) analysis. If the target compounds are easily oxidized, solvents should be degassed prior to use. It has been observed that solvents which perform only marginally well at ambient temperature often perform quite well at elevated temperature. This increases the range of solvent choices available to the analyst considering PFE, as more than one solvent may give good recoveries of target analytes. The selection of the appropriate solvent can then be made based on selectivity of extraction, solvent cost, safety and exposure factors, and compatibility with post-extraction processing steps. Solvent mixtures should also be considered in cases where minor adjustments to polarity are desired.

Extraction Temperature

PFE extraction can be performed from ambient temperature to 200°C. Increased temperature will increase the efficiency of the extraction process, and this should be optimized short of the point at which

analyte degradation or excessive co-extraction of matrix components occurs. Many PFE applications are performed in the 75–150°C range, with 100°C as the recommended starting point for new methods development. In this temperature range, significant increases in extraction efficiency are observed without the breakdown of target compounds. If an extraction is to be performed on a compound with a known degradation point, then the PFE method should be developed to operate below that point. Extractions performed at low (40–70°C) or ambient temperatures may be sufficient for analytes which are weakly or only surface bound to the sample matrix. The extracts generated using PFE will be similar in composition to those produced by other techniques using the same solvents. If a post-extraction clean-up step is required following a Soxhlet extraction, the same process will most likely need to be performed following PFE.

Extraction Pressure

Although essential to the process, pressure is not generally considered a critical parameter in PFE. Normal operating pressures of 10.3–13.8 MPa (1500–2000 psi) are well above the threshold pressures required to maintain the solvents in their liquid states at PFE operating temperatures. The main purpose of using pressures in the ranges indicated is to provide rapid filling and flushing of the extraction cells. Typical PFE extractions are performed in 12–20 min, although this time can be extended for difficult samples. In addition, multiple static cycles can be used periodically to introduce aliquots of fresh solvent during the extraction process.

Method Development

When developing a method for PFE the following approach has proven useful. A representative sample should be prepared as outlined above; select an extraction cell size which most closely matches the desired sample size. The extraction cells do not need to be filled completely, but a full cell will use less solvent in the extraction process than a partly filled one. Select the extraction solvent using the considerations listed above, although normally the same solvent or solvent mixture used in a traditional liquid extraction method is used. Extract the sample starting with the standard PFE conditions: pressure = 0.3 MPa (1500 psi), temperature = 100°C, heat time = 5 min, static time = 5 min, flush volume = 60% of cell volume, purge time = 60 s, static cycles = 1.

Extract the same sample multiple times in order to assess the efficiency of the method. If there is significant analyte present in the second or third extracts,

adjust the following parameters (one at a time), and repeat the validation process:

1. Increase the temperature (use 20°C steps).
2. Add a second or third static cycle.
3. Increase the static time (use 5-min increments).

If these steps do not result in a complete extraction, re-examine the sample preparation steps and/or the choice of extraction solvent.

Applications: Food

PFE extraction in the food industry is used for both the analysis of natural components such as fat, and to detect the presence of contaminants such as residual pesticides. New labelling requirements require food manufacturers to describe more accurately the total fat content of their products. This requires adequate monitoring of both raw and processed food samples. Pesticide residue analysis in foods has been, and will continue to be, a persistent and necessary analytical challenge. Proper selection of extraction solvent with food matrices can limit the high level of co-extractables typical with these sample types.

Fat Extraction

The determination of total fat in powdered infant formula is performed using a solvent mixture of hexane–acetone (4:1) at 100 or 125°C. Three 5-min static cycles are used in the method. Milk-based formulas are prepared by mixing 1 g of sample with 3 g of hydromatrix prior to cell loading and extraction at 125°C. Soy-based and hydrolysed milk-based formulas are mixed with wet hydromatrix (3 g + 0.4 g water) and extracted at 100°C. PFE extraction of these samples can be performed without the aggressive alkaline pretreatments required by some methods. Extraction results were compared directly with results obtained using alkaline pretreatment followed by Majonnier extraction with a mixture of petroleum ether, diethyl ether and ethanol (AOAC Method 932.06). The results obtained for the PFE extracts averaged 99.7% of the Mojonnier results for six different formula types, including a certified reference material (SRM 1846) available from the National Institute of Standards and Testing (NIST). The fat content was determined gravimetrically, and verified by fatty acid methyl ester (FAME) analysis.

Fat extraction from a variety of meat samples is performed by mixing 3–4 g of a homogenous meat sample with 6 g of hydromatrix. Moisture can be removed from the samples by drying in a microwave oven prior to extraction. Up to five samples can be dried at once in an 800 W oven at full power for

Table 1 Pressurized fluid extraction (PFE) and Soxhlet results for the extraction of fat from a variety of high fat processed meat samples

Sample	% Fat by PFE	Standard deviation (n = 3)	% Fat by Soxhlet
Beef	40.74	1.12	40.85
Pepperoni	42.66	0.28	43.15
Chorizo	27.98	0.22	27.84
Bacon	46.66	0.82	46.83
Sausage	33.80	0.28	33.54

3 min. Samples are then extracted using either petroleum ether or hexane at 125°C, with two, 2-min static cycles. Extraction results were compared with a 4-hour soxhlet extraction with petroleum ether (AOAC Method 90.39). The results for a variety of samples are shown in Table 1. The PFE method used here was shown to be useful for both low and high fat meat samples and results in a considerable time savings compared with the traditional approach.

Pesticide Residues

Using methods originally designed for soil samples, pesticide residues can be efficiently extracted from food samples including raw grains and fruits and vegetables. Wet samples should be mixed with sodium sulfate or hydromatrix prior to extraction. Extraction of organochlorine pesticides is performed using a solvent mixture of 10% acetone in hexane at 100°C. This solvent mixture limits the amount of co-extractables which are present in extracts produced with higher percentage acetone mixtures. Organophosphorus pesticides can be recovered with acetonitrile, ethyl acetate, methanol or acetone/methylene chloride mixtures, at temperatures ranging from 60 to 100°C. The more polar pesticides and herbicides, such as the sulfonyl ureas, can be efficiently extracted with a mixture of acetone and 0.1 M ammonium carbonate aqueous solution (20:80) at ambient temperature.

Applications: Polymers

PFE extraction in the polymer area has focused on additive analysis and general product structure characterization. For quantitative extraction of polymer matrices, samples should be ground prior to analysis. This can be accomplished with a liquid nitrogen grinder (cryo-grinder) as opposed to conventional laboratory grinders. Another major consideration in PFE extraction of polymers is the choice of extraction solvent. In other application areas the solvents used in existing methods are generally transferred and used in the PFE method. Traditional polymer methods,

however, swell and/or dissolve the sample matrix by boiling in a nonpolar solvent, followed by cooling and precipitation of the polymer. In PFE extraction, the goal is to separate the target additives of components from the sample matrix. The use of nonpolar solvents in this application will simply dissolve the entire sample and move it to the collection vial, or worse, it will precipitate in the transfer lines and plug the system flow path. The strategy developed for PFE extraction of polymers is to select a relatively polar solvent, which will solubilize the target analytes while leaving the majority of the sample matrix intact. Temperature is used to soften the matrix and a small amount of nonpolar solvent is added to increase penetration of the matrix. Cellulose thimbles are often used inside the PFE extraction cells to facilitate loading of the ground sample (normally 0.5–1.0 g) and prevent softened polymer from sticking to the sides of the vessel. Since small amounts of polymer matrix may be present in the extracts, samples are normally passed through a syringe filter prior to HPLC or GC analysis.

Additives from Polypropylene and Polyethylene

UV stabilizers, antioxidants and antislip agents are routinely added to polymer formulations to modify their properties for specific applications. Extraction and analysis of these compounds is essential in order to monitor that formulation levels are within specification. The antioxidant products (Irganox®, Irgafos® (Ciba Inc.), Erucamide, etc.) are a group of compounds commonly used in both low and high density polyethylene (LDPE and HDPE, respectively) preparations. Extraction of these compounds is performed at 140°C, using a solvent mixture of 2.5% cyclohexane in isopropyl alcohol. Three, 3-min static cycles are used to produce optimum results. Using these conditions, values equivalent to the results from reflux based extraction methods can be obtained. Chimassorb®944 (Ciba Inc.) is extracted from polypropylene (PP) using acetonitrile at 150°C. PFE can also be used to monitor the loss of Irganox 1076 which occurs after γ -irradiation.

Plasticizers in PVC

Traditional extraction of plasticizer content from polyvinyl chloride (PVC) is performed according to ASTM D 2124 recommendations. This method uses 120 mL petroleum ether in a 6-h Soxhlet extraction. The PFE method developed for this application uses petroleum ether at 100°C, with three, 1-min static cycles. The method does not require post-extraction filtering. GC analysis of the compounds extracted – dioctyl adipate (DOA), trioctyl phosphate (TOP),

Table 2 Extraction of plasticizers from polyvinyl chloride (PVC) by pressurized fluid extraction (PFE) and Soxhlet

Compound	PFE %	Soxhlet %
DOA	9.81	9.56
TOP	9.50	9.28
DOP	9.42	9.35
TOTM	9.17	9.05

dioctyl phthalate (DOP) and trioctyl mellitate (TOTM) – showed average recovery of 101.7% relative to the reflux method (Table 2).

Total Extractables from Styrene-butadiene Rubber

Styrene-butadiene rubber (SBR) is used in the manufacturing process of many consumer products including automobile tyres. The total extractable content of the rubber consists of oils and organic acids, and is usually measured gravimetrically. The PFE method developed for this application uses 2-propanol at 150°C, with three, 3-min static cycles. The results shown in Table 3 indicate an average recovery of 99.9% relative to the target value.

Structure Characterization

The extraction of monomers and oligomers from formed polymers is used as an indicator to assess the completeness of the polymerization reaction. The extraction of monomer (caprolactam) from nylon-6 and oligomers (dimer, trimer) from 1,4-butylene terephthalate (PBT) was performed at 170°C with hexane-ethanol (60:40). Results indicate that recoveries equivalent to Soxhlet were obtained.

Applications: Pharmaceuticals

PFE extraction is used in the pharmaceutical industry both in the quality control of finished products and in the characterization of raw materials and product candidates. Extractions are normally performed on 1–10 g samples at temperatures ranging from ambient to 100°C, using polar solvents such as water,

Table 3 Total extractables from styrenebutadiene rubber (SBR) by pressurized fluid extraction (PFE)

Sample	PFE %	Standard deviation (n = 3)	% Recovery
1	32.66	0.17	100.2
2	32.77	0.04	100.5
3	33.89	0.19	100.1
4	34.44	0.31	98.9

methanol, ethanol and acetonitrile. Tablets, plants and other samples of large size should be ground prior to extraction.

Natural Products

The extraction of capsaicinoids from cayenne fruit, Hypericin from St John's Wort and alkaloids from goldenseal root is performed using ethanol, methanol or acetonitrile as extraction solvents at 100°C. St John's Wort extracts were analysed by UV/VIS absorbance at 516 nm following alumina cartridge clean-up to remove co-extracted chlorophylls. Hypericin content (measured as total dianthrone) was determined to be 0.44% with a %RSD = 4.1 ($n = 4$). This was consistent with a label claim of a minimum 0.3% hypericin. Goldenseal root was extracted according to the same conditions and analysed for total berberine content. HPLC analysis showed a total berberine content of 1.44% with a %RSD of 2.8 ($n = 4$). Water was also investigated as a potential solvent but was shown to extract too much of the samples matrix, which complicated the final analysis. In other studies, PFE extraction was compared with Soxhlet, reflux and steam distillation techniques for the extraction of St John's Wort, horse chestnut seed, milk thistle fruit, tumeric rhizome and thyme herb. Using methanol and temperatures ranging from 50 to 100°C, results comparable to or better than those obtained following USP method guidelines were obtained.

Animal Feeds

Extraction of an animal feed containing spiked levels of an anti-schizophrenic drug being tested in rats was performed at 100°C with methanol. Cattle feed containing the veterinary medicinal lasalocid (coccidiostat) was extracted using methanol containing 0.3% acetic acid at 80°C. Both extracts were analysed by HPLC and produced results comparable (96–105%) to the existing wrist-shaker techniques.

Transdermal Patches

Extraction of finished product is an essential part of the pharmaceutical quality control process. Transdermal patches containing nitroglycerin were extracted using ethanol at ambient temperature. The backing was peeled off of the patch and the sticky side was pressed onto sand in order to prevent the patch from sticking to itself. The patch, either 10 or 20 cm², was then curled into the extraction cell and Ottawa sand added as inert filler. The results shown in Table 4 indicate a recovery of the active compound at 96–99% of the result obtained from the standard method, which involved extended shaking and extract filtering prior to analysis.

Table 4 Recovery of nitroglycerin from transdermal patches using pressurized fluid extraction (PFE) and wrist shaker methods

Sample	PFE (mg)	SD ($n = 10$)	Wrist shaker (mg)	SD ($n = 10$)
10 cm ² patch	31.4	0.44	31.7	0.48
20 cm ² patch	62.0	2.4	64.6	0.71

Ocular Inserts

Extraction of diclofenac sodium (anti-inflammatory) from an ocular insert used following cataract surgery was performed using methanol at 100°C. The polymeric tube containing the drug was cut into pieces prior to loading into the extraction cell. Results showed a recovery of 99.1% with a %RSD of 2.5 ($n = 8$). The PFE method replaces a 16-h Soxhlet extraction requiring 200 mL of solvent per sample.

Tablets

Extraction of felodipine (anti-hypertensive) in tablets was performed using acetonitrile at 100°C. Quantitative recovery (98%) from a single tablet was obtained by wrapping the tablet in a filter paper and crushing it. The crushed tablet and filter paper were then added to the extraction cell. Extraction of whole, uncrushed tablets resulted in less than adequate recovery.

Applications: Consumer Products

Tobacco

PFE extraction of tobacco is currently used to assess the total content of nicotine and other active and marker compounds, as well as flavour characterization and carbohydrate and sugar analysis. The extraction of raw and processed tobacco is performed with a variety of polarity solvents and at temperatures ranging from 50 to 100°C, depending on the types of compounds being targeted.

Detergents

Extraction of the organic constituents of granular and liquid detergents is performed using ethanol at 150°C. The conventional reflux extraction method used to determine total alcohol extractables is a multi-step process requiring 700 mL of solvent and 4 h to complete. The PFE extraction method for this sample is complete in 12–18 min and uses 15 mL of solvent per sample. Liquid detergent samples are mixed with an equal weight of hydromatrix prior to loading into the extraction cell. The results summarized in Table 5 show an average recovery of

Table 5 Recovery of organic extractables from granular and liquid detergents using pressurized fluid extraction (PFE) and reflux extraction methods

Sample	PFE %	Reflux %
Granular 1	22.40	22.16
Granular 2	33.49	34.10
Granular 3	39.22	38.50
Granular 4	22.76	21.80
Granular 5	30.69	30.10
Liquid 1	45.35	44.35
Liquid 2	55.87	55.25

101.6% obtained with PFE compared with the conventional method, with a threefold improvement in reproducibility.

Textiles

The total extractable content of sized warp yarns is typically performed using AATCC Method 97-1995. This method is a series of three extractions using water, enzyme (bacterial amylase) and trichloroethane (TCE). Cotton and cotton/polyester yarns are extracted using PFE with water at 180°C, followed by extraction with TCE at 50°C (no enzyme was used). This method yields results slightly greater than those obtained with the standard method for total extractables by gravimetric determination and iodine spot test for polyvinyl alcohol and starch removal.

Paper

Total extractables from paper pulp is performed using methylene chloride at 125–150°C. Samples are prepared by cutting or shearing into small strips prior to cell loading. Three, 3-min static cycles are used to generate results of 101% of the standard reflux extraction method (analysis performed gravimetrically).

Summary

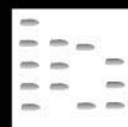
Conventional extraction times range from 4 to 48 h whereas PFE extractions are normally performed in 12–20 min. While the decrease in extraction time is favourable for most laboratories in general, it can be critical for those industries where laboratory data is used in feedback control of production cycles and manufacturing quality control. The volume of solvents used in PFE can be as much as 10–20 times less

than traditional extraction methods. When factors such as safety and analyst exposure, as well as solvent purchase and disposal costs are considered, the benefits of PFE can be quite substantial for most laboratories. When compared directly with traditional extraction techniques, the recoveries generated by PFE normally equal or slightly exceed the comparative method. The ability of PFE to use the same liquid solvents used in traditional methods allows for rapid conversion to this technique, without much effort involved in methods development. Once a PFE method has been developed for a class of compounds, that same method can be successfully applied to a variety of matrix types without adjustment to extraction parameters. This lack of matrix dependency has allowed a very small set of standard methods to be applied to a large number of sample types.

Further Reading

- Ezzell JL (1999) In: Handley AJ (ed.), *Extraction Methods in Organic Analysis: Pressurised Fluid Extraction (PFE) in Organic Analysis*, pp. 146–164. Sheffield: Sheffield Academic Press.
- Hamburger M, Benthin B and Danz H (1999) Pressurized liquid extraction of medicinal plants. *Journal of Chromatography A* 837: 211–219.
- Obana H, Kikuchi K, Okihashi M and Hori S (1997) Determination of organophosphorus pesticides in foods using an accelerated solvent extraction system. *Analyst* 122: 217–220.
- Richter BE (1999) The extraction of analytes from solid samples using accelerated solvent extraction. *LC/GC* 17: 6S, S32.
- Richter BE, Jones BA, Ezzell JL, Porter NL, Avdalovic N and Pohl C (1996) Accelerated solvent extraction: a technique for sample preparation. *Analytical Chemistry* 68: 1033–1039.
- Schäfer K (1998) Accelerated solvent extraction of lipids for determining the fatty acid composition of biological material. *Analitica Chimica Acta* 358: 69–77.
- Vandenburg HJ and Clifford AA (1999) In: Handley AJ (ed.), *Extraction Methods in Organic Analysis: Polymers and Polymer Additives*, pp. 221–240. Sheffield: Sheffield Academic Press.
- Vandenburg HJ, Clifford AA, Bartle KD, Zhu SA, Carroll J, Newton ID and Garden LM (1998) Factors affecting high-pressure solvent extraction (accelerated solvent extraction) of additives from polymers. *Analytical Chemistry* 70: 1943–1948.

PROSTAGLANDINS: GAS CHROMATOGRAPHY



J. Nourooz-Zadeh and C. C. T. Smith,
University College London, London, UK

Copyright © 2000 Academic Press

Introduction

Metabolism of free (nonesterified) arachidonic acid (5,8,11,14-*cis*-eicosatetraenoic acid) via the cyclooxygenase (COX) pathway produces a cascade of biologically active compounds collectively known as prostaglandins (PGs). These include prostaglandin D₂ (PGD₂), prostaglandin E₂ (PGE₂), prostaglandin F₂ (PGF₂), prostacyclin (PGI₂) and thromboxane A₂ (TXA₂) (Figure 1). The analysis of PGs and related compounds in isolated cells and organs has proved relatively easy. By contrast, measurement of PGs in plasma presents a more challenging analytical task. This is because: (1) a more complex mixture of chemically related compounds exists in plasma; (2) PGs exert their effects locally, i.e. within a short distance of their site of production, and are consequently rapidly metabolized; and (3) *ex vivo* generation of PGs may occur. PG metabolites are generally present in biological fluids, including plasma and urine, in higher concentrations than their precursors. These metabolites are not formed during processing and therefore the problem of generating artefactual results does not arise. It has been suggested that the measurement of PG metabolites in urine may represent a more reliable approach for assessing *in vivo* generation of PGs than does quantification of primary products in plasma.

Recently, it has been shown that free-radical peroxidation of polyunsaturated fatty acids (PUFAs) by a mechanism independent of the COX-pathway also produces novel families of PGF-like compounds. In contrast to the COX-derived products, COX-independent products are present mainly esterified to phospholipids and with the side chains across the cyclopentane ring in the *cis* orientation. Figure 2 illustrates the structural differences between COX-dependent and COX-independent 9 α ,11 α -PGF_{2 α} . COX-independently derived PGF-like compounds are collectively known as isoprostanes. The measurement of isoprostanes has received considerable attention because they have proved to be a reliable marker of oxidative stress. Determination of the different families of isoprostanes also allows the assessment of the peroxidation of individual PUFAs. Accumulating data indicate that the metabolic fate of

non-COX-derived PGF-like compounds is similar to that of the COX-derived products.

PGs and related compounds can be assessed by several methods including bioassay, radioimmunoassay (RIA), high performance liquid chromatography (HPLC) linked to RIA or UV or mass spectrometric (MS) detection and gas chromatography-mass spectrometry (GC-MS). GC-MS is the preferred method for the quantification and structural validation of PGs, combining the high resolution of GC separation employing fused silica capillary columns with the specificity and sensitivity of mass spectrometry.

Analysis of PGs by GC-MS

The analytical procedures for the isolation and determination of PGs in plasma and urine involve a number of steps.

Selection of an Internal Standard

The use of an internal standard is vital for accurate and precise assay of PGs and related compounds by GC-MS. An ideal internal standard should have similar physicochemical properties to the compound being analysed, and should be taken through the entire analytical procedure, i.e. extraction, enrichment and derivatization. Stable isotope-labelled internal standards are generally used for the assay of PGs and related compounds. These are prepared by replacing sufficient atoms of ¹H or ¹⁶O by the corresponding stable isotopes ²H and ¹⁸O. Many tetradeuterated [²H₄] PGs are commercially available. By contrast, carboxylic ¹⁸O-labelled PGs have to be synthesized. The following precautions should be considered during sample processing: (1) the amount of the internal standard should be at least of the same order as that expected for the compound being analysed; (2) the possibility of back-exchange of ²H by ¹H from water during alkaline hydrolysis or following catalytic hydrogenation should be considered; and similarly (3) back-exchange of carboxylic ¹⁸O by ¹⁶O in an esterase-rich environment such as plasma.

Isolation from Biological Samples

The strategies for the routine isolation of PGs and related compounds from biological samples involve

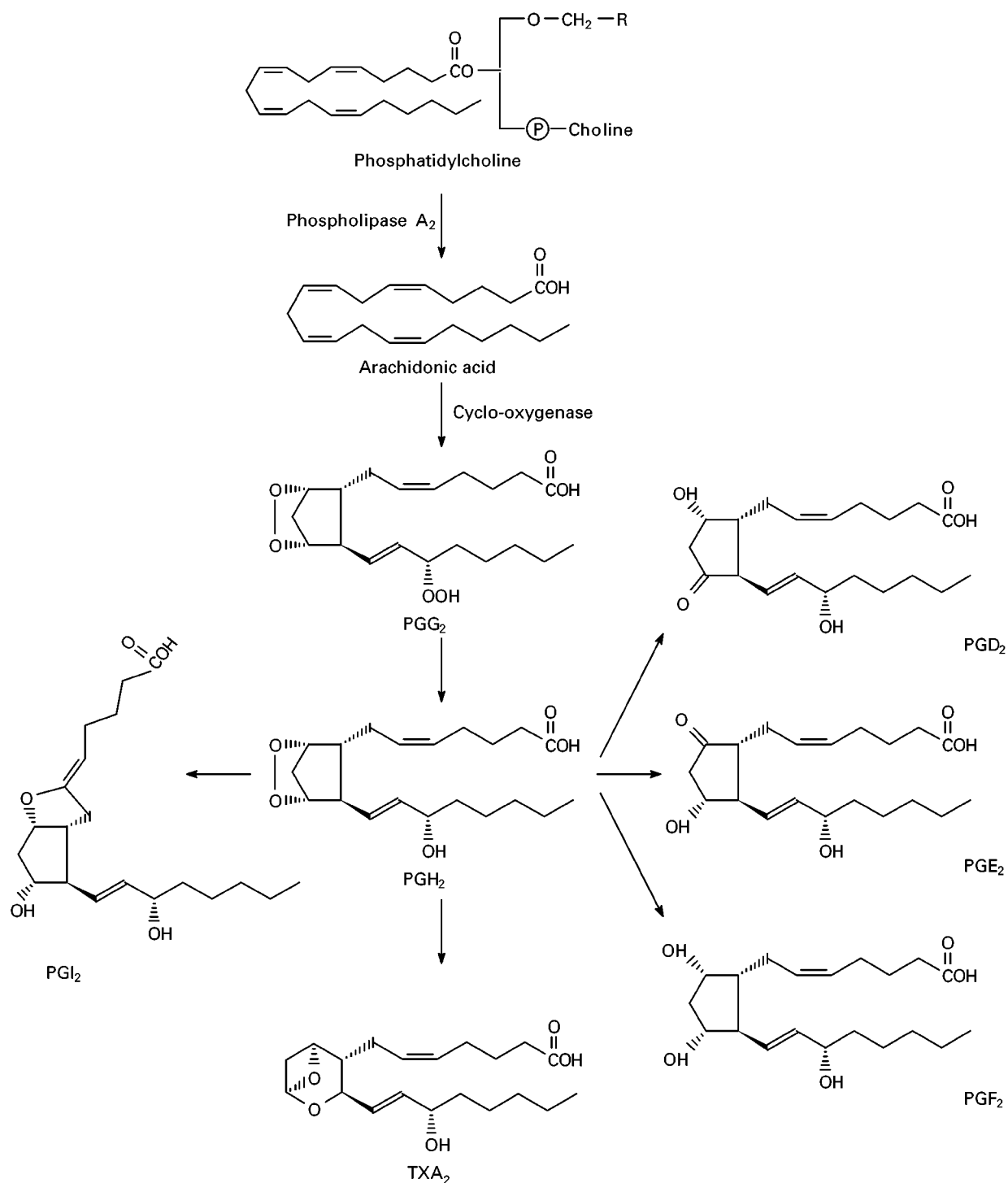


Figure 1 The release of arachidonic acid by phospholipase A₂ and its metabolism by the cyclooxygenase enzymes.

conventional solvent extraction and/or chromatographic separation involving solid-phase extraction (SPE) and thin-layer chromatography (TLC). In both situations, the samples are acidified to pH 2 to minimize ionization of the carboxylic groups of PGs. The solvent of choice for partitioning of PGs and related

compounds from biological samples is ethyl acetate. SPE entails passing the sample through a disposable octadecylsilica (C₁₈) cartridge. Lipophilic compounds are retained on the column while salts and polar compounds are removed by washing the column with water or water/acetonitrile. PGs are eluted from the

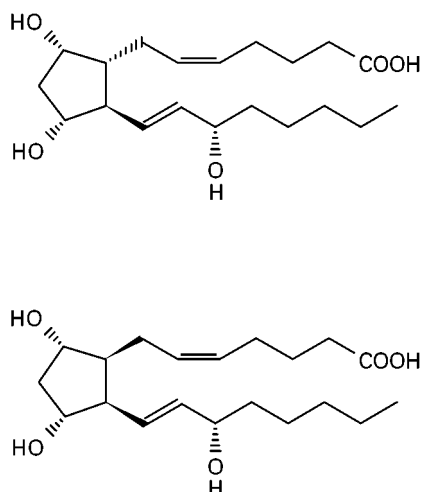


Figure 2 Structural differences between (A) COX-dependent 9 α ,11 α -PGF_{2 α} and (B) COX-independent 9 α ,11 α -(8-*epi*)-PGF_{2 α} .

column using a combination of organic solvents such as hexane, ethyl acetate and isopropanol. The final step in the purification of PGs and related compounds involves thin-layer chromatography (TLC); one-step TLC for plasma and two-step for urine. Replacement of the C₁₈ and TLC procedures with an aminopropyl-silica cartridge substantially increases the recovery of PGF-like compounds and reduces analysis time. Immunoaffinity chromatography has also been used for the purification of PGs from biological fluids. The advantages of this method over multistep procedures are: (1) its simplicity and shorter analysis times; (2) the addition of a further degree of specificity to the analysis. Unfortunately, its implementation has been limited to leading laboratories in the field because the column materials are not commercially available.

Exploiting a unique chemical property of a prostaglandin such as 2,3-dinor-6-oxo-PGF_{1 α} is another approach for the isolation of structurally related products (Figure 3). 2,3-dinor-6-oxo-PGF_{1 α} can exist in different isomeric forms depending on pH. At acid pH, the 2,3-dinor-6-oxo-PGF_{1 α} is converted to a lactone. This property allows isolation of 2,3-dinor-6-oxo-PGF_{1 α} from other polar compounds such as free fatty acids. Quantitative recovery of 2,3-dinor-6-oxo-PGF_{1 α} is achieved by hydrolysis in a mild aqueous base.

Plasma isoprostanes are mainly present esterified to phospholipids and therefore have to be hydrolysed prior to SPE and/or TLC processing. Briefly, plasma (1 mL) is incubated with 1 mol L⁻¹ aqueous potassium hydroxide at 45°C for 1 h to release esterified isoprostanes. The pH is then adjusted to 2 using HCl. The internal standard is added and the isoprostanes isolated as described above. For the analysis

of isoprostanes in tissue samples, homogenates (50–100 mg tissue mL⁻¹) are hydrolysed with 1 mol L⁻¹ potassium hydroxide at 45°C for 1 h. The pH is then adjusted to 2 and total lipids extracted with 10 volumes of ethyl acetate. Isoprostanes are then isolated by a single chromatography step on an aminopropyl cartridge.

Derivatization

Chemically untreated PGs are not suitable for GC analysis. Therefore, protection of functional moieties in PGs is carried out first to increase their volatility, improve chromatographic separation and to enhance assay sensitivity and specificity. The most common derivatization reactions used for PGs are: (1) esterifi-

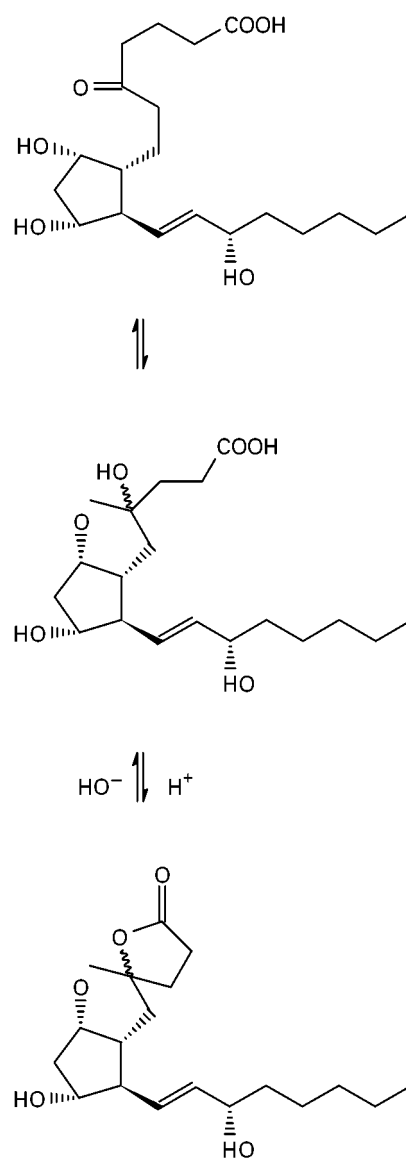


Figure 3 Equilibrium between the ketone and lactone forms of 2,3-dinor-6-oxo-PGF_{1 α} .

cation of the carboxylic moieties; (2) etherification of hydroxy moieties; (3) methoximation of keto moieties; and (4) boronation of hydroxy moieties.

For the purposes of PG quantification by gas chromatography/negative ion chemical ionization (GC-MS/NICI), pentafluorobenzyl (PFB) ester derivatives of the monocarboxylic forms of PG are prepared. The reaction is carried out by incubating the final lipid extract in the presence of the catalyst *N,N*-diisopropylethylamine (DIPEA) at 45°C for 1 h. Methyl ester derivatives of PGs are prepared using diazomethane in ether solution. Methyl esters can also be prepared using methanolic solutions of hydrogen chloride or hydrochloric acid.

Hydroxy moieties are converted to trimethylsilyl (TMS) ether derivatives. Bis(trimethylsilyl)trifluoroacetamide (BSTFA) is the most frequently used derivatization agent. A quantitative conversion to trimethylsilyl ether is achieved by incubating standards or the final lipid extract at 60°C for 1 h or overnight at 4°C in the presence of DIPEA. *t*-butyl(dimethylsilyl) (BDMS) ether derivatives are occasionally prepared as an alternative to TMS because they produce fragments of higher relative molecular mass during mass spectrometric analysis. The main disadvantages of the BDMS derivatives are: (1) bulkiness that results in incomplete derivatization of stearic-hindered hydroxy moieties; and (2) relatively long retention times.

Hydroxy groups may also be converted to alkylboronate derivatives. Alkylboronate derivatives are prepared by incubating PGs and related compounds with *n*-butylboronic acid under anhydrous conditions. These derivatives are mainly employed to determine the stereochemistry of the hydroxy moieties in the prostaglandin F (PGF)-series. Alkylboronate derivatives can only be formed if both hydroxy groups on the cyclopentane ring of a PGF molecule are *cis* orientated.

Keto moieties of PGs and related compounds are converted to *O*-alkyloximes by incubating authentic standard or buffered urine with a saturated methoxyamine hydrochloride solution in pyridine. It is important to remove the derivatization reagent completely because it causes deterioration of the chromatographic column. Chromatography on a short column of Sephadex LH-20 is therefore advisable.

Hence, derivatization is carried out in the order: methoximation, esterification, boronation and finally silylation to minimize side reactions.

Injector

The most common techniques for introducing high boiling point compounds such as PGs into the GC are programmed-temperature vaporization (PTV) and

splitless injection. The PTV is designed to allow rapid heating and cooling of the injector. Briefly, sample (2 μ L in iso-octane) is introduced into a temperature-controlled injector that is initially maintained at 75°C and is then raised to 85°C immediately after injection. Since iso-octane has a boiling point of 98–99°C the temperature will be sufficient to evaporate the majority of the solvent and simultaneously concentrate the sample onto the surface of the injector, which is lined with inert glass. After allowing sufficient time for removal of excess solvent, the injector temperature is rapidly raised to 275°C. This ensures that volatilization of high boiling point components occurs and permits a quantitative refocusing of the analyte at the head of the column.

The alternative method for introducing PGs into the GC, i.e. using a splitless injector, relies on cold trapping and/or a solvent effect to refocus the analyte on the head of the capillary column. Sample (2 μ L in hexane) is usually introduced over a period of 30–60 s onto the column.

Column Heating

GC is performed using an oven temperature program that starts at an initial temperature of 80–100°C. The rates at which oven temperatures are increased range from 20°C min⁻¹ to 30°C min⁻¹. The final temperature will be 280°C or higher, depending upon the upper limit specified for the column being employed. The time over which the column is maintained at maximum temperature (e.g. 280°C) depends upon the elution time of the compound being analysed.

Detectors

Mass spectrometry is used to detect PGs as they emerge from a GC. This approach has proved to be a flexible, sensitive and selective technique. The most popular modes of ionization employed by prostanoid researchers are described below.

Electron impact (EI) The electrons used for the ionization have an average energy of 70 eV. Initial ionization energies for most organic molecules are between 8 and 15 eV. When a molecule enters the ionization chamber the high energy causes fragmentation of the parent compound. This mode of ionization provides information on the relative molecular mass and molecular structure of the compound. Methyl ester derivatives are mainly used for GC-MS/EI. Quantitative analysis is performed by selected ion monitoring (SIM) of fragments characteristic of the compound being analysed. The concentration of a particular component in the sample is calculated by determining the ratio of intensity of a certain ion in

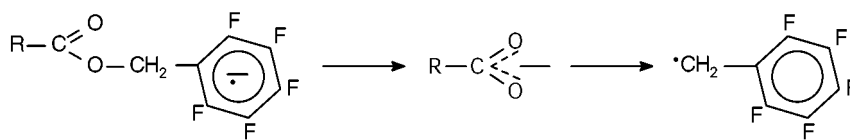


Figure 4 Formation of a carboxylated anion corresponding to the intact molecule [M-PFB]⁻ or [M-181]⁻ during final analysis of PFB-esters by NICI.

the sample to that of the internal standard. The detection limit for GC-MS/EI is 200 pg injected onto the column.

Positive ion chemical ionization (PICI) PICI is a softer ionization technique than EI and therefore molecules are less likely to undergo fragmentation. This leads to an abundance of protonated molecular ions. The detection limit for GC-MS/PICI is a few nanograms.

Negative ion chemical ionization (NICI) PGs and related compounds are not good electron-capturing substances. However, they contain at least one terminal carboxylic moiety that can be esterified with electron-capturing groups such as pentafluorobenzyl (PFB) esters. As illustrated in **Figure 4**, the PFB ester forms a molecular ion after initial electron capture. This leads to the loss of the PFB radical and the formation of a stabilized carboxylated anion corresponding to the intact molecule [M-PFB]⁻ or [M-181]⁻. For most PFB esters, the carboxylate anion constitutes > 60% of the total ion. This makes NICI a highly efficient ionization process. The combined sensitivity and selectivity of NICI has made it the method of choice for quantitative analysis of PGs. Quantitative analysis is performed using selected ion monitoring (SIM) of the carboxylate anion [M-181]⁻. The detection limit for SIM is from 200 fg to 5 pg.

Gas chromatographic separation The most widely used stationary phase for fused silica capillary columns for the separation of PGs and related compounds is 100% dimethylsilicone commercially known as DB1, Rtx-1, SE-30, Sil-5 CB or Ultra 1. This phase has a CP-value of 5, CP-being an index that predicts selectivity and polarity for a given stationary phase. CP-values range between zero for a nonpolar stationary phase and 100 for the most polar. Other investigators have used an intermediate polarity stationary phase (CP = 19), typical commercial names being DB-1701, Rtx-1701 and Sil-19 CB. These stationary phases consist of a mixture of 86% dimethylsilicone, 7% phenylsilicone and 7% cyanopropylsilicone.

There have been problems with regard to the separation of 9 α ,11 α -PGF_{2 α} , 9 α ,11 β -PGF_{2 α} and 9 β ,11 α -PGF_{2 α} using both low- and medium polar stationary phases. Clear separation of all three PGF-ring isomers is of interest with regard to clinical conditions linked to increased production of 9 β ,11 α -PGF_{2 α} such as asthma and anaphylaxis. We have found that SPB-1701 (80% dimethylsilicone, 5% phenylsilicone, 15% cyanopropylsilicone), which is considered a medium polar stationary phase with a CP-value of 20, is superior to DB-1701 for the separation of PGF₂ isomers. The improved separation of the PGF₂ isomers using the SP-1701 may be explained by the dipole moment introduced by the cyanopropyl functionality. **Figure 5** shows a baseline separation of PGF₂ isomers including 9 β ,11 α -PGF_{2 α} , 9 α ,11 α -(8-*epi*)-PGF_{2 α} , 9 α ,11 β -PGF_{2 α} and 9 α ,11 α -PGF_{2 α} . The signal monitored at *m/z* 569 represents the carboxylated anion of the PGF₂ isomers as PFB ester/TMS ether whereas that at *m/z* 573 represents the tetradeuterated 9 α ,11 α -PGF_{2 α} internal standard.

Figure 6 shows a typical example of a SIM chromatogram obtained with simultaneous monitoring of 6-oxo-PGF_{1 α} , 2,3-dino-6-oxo-PGF_{1 α} , TXB₂, 2,3-dinor-TXB₂ and 11-dehydro-TXB₂ in human urine using a DB1 column. PGs and related compounds were purified by immunoaffinity chromatography and the final lipid extract was sequentially converted to PFB ester, methyloxime and TMS ether derivatives prior to analysis by GC-MS/NICI.

Figure 7 shows a baseline separation of *syn* and *anti* isomers of urinary PGD metabolites as PFB ester/methyloxime/TMS ether derivatives using a DB-1701 column. The peaks labelled I and II (*m/z* 514) represent the *syn* and *anti* isomers of urinary PGD metabolite. The signal monitored at *m/z* 522 is the tetraoxygen-¹⁸O-labelled PGD metabolite internal standard. The peaks labelled III and IV represent a COX-independent urinary PGD-metabolite. As can be seen, *syn* and *anti* isomers derived from PGD are fully resolved by capillary gas chromatography.

There is less agreement on the best GC conditions for the separation of C₂₀-isoprostanes. C₂₀-isoprostanes are a series of PGF₂-like compounds derived from peroxidation of arachidonic acid by a mechanism independent of the COX pathway. Peroxidation

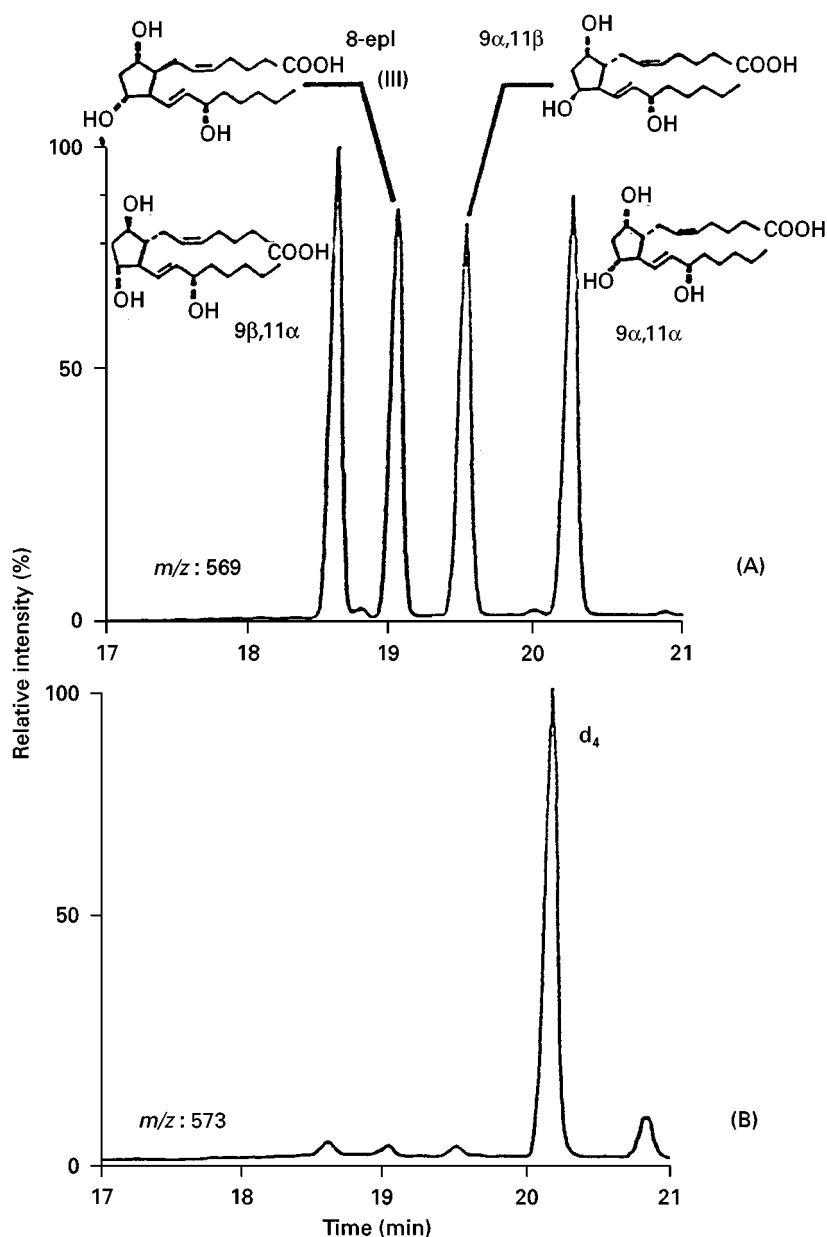


Figure 5 Gas chromatographic separation of the PGF₂-isomer as PFB ester/TMS ether derivatives using an SP-1701 column (30 m; 0.25 i.d.; film thickness 0.25 μ m). (A) PGF₂-isomers; (B) tetradeuterated PGF_{2 α} as the internal standard. (Reproduced from Nourooz-Zadeh *et al.*, 1995, with permission from Elsevier Science.)

of arachidonic acid at positions C₇, C₁₀ and C₁₃ would produce four families of PGF₂-like compounds. Each sub-family would have 16 diastereoisomers, since the hydroxy groups on the prostanoic skeleton can be arranged in the 2³ configuration. Theoretically, 64 C₂₀-isoprostane isomers can be formed during the peroxidation of arachidonic acid. Of these, 9 α ,11 α -(8-epi)-PGF_{2 α} , has received considerable attention because it is commercially available and has been shown to be biologically active. Both DB1 and DB1701 stationary phases have been used to assay C₂₀-iso-

prostanes in biological samples. A comparison of typical GC-MS/NICI chromatograms for 9 α ,11 α -(8-epi)-PGF_{2 α} in human plasma using DB-1701 and SP-1701 is shown in Figure 8. Once again, the SP-1701 phase is superior to the DB-1701 phase in separating the *R* and *S* isomers of 9 α ,11 α -(8-epi)-PGF_{2 α} . To the best of our knowledge, no chromatograms have been published for the analysis of C₂₀-isoprostanes as PFB esters/BDMS in human plasma.

The SP-1701 stationary phase is also useful for the separation of C₂₀- and C₂₂-isoprostanes (PGF₃ and

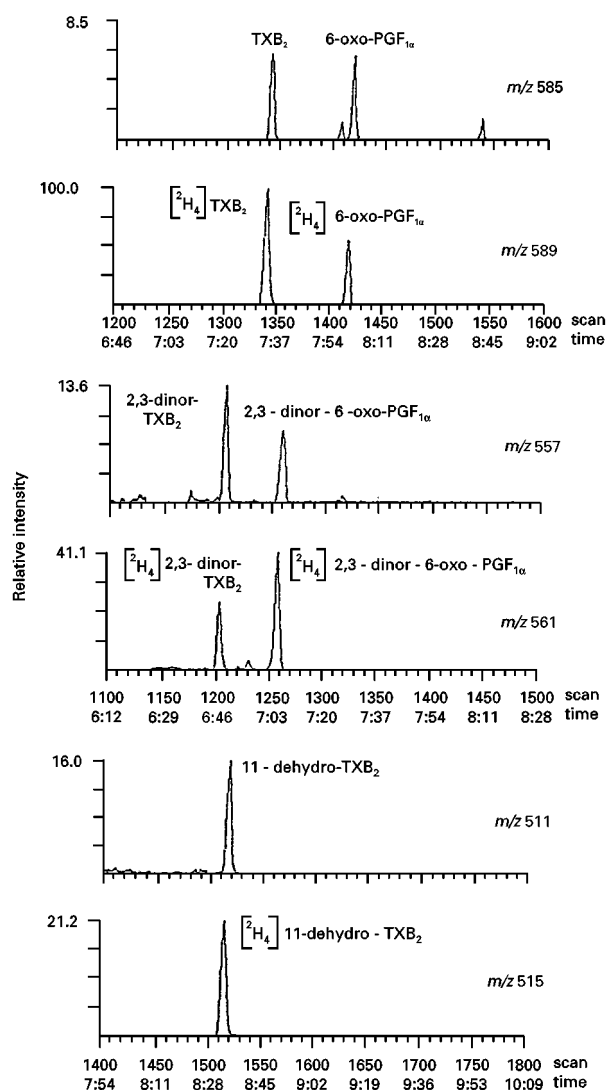


Figure 6 Selected ion monitoring chromatograms of simultaneous analysis of urinary 6-oxo-PGF_{1α}, 2,3-dinor-6-oxo-PGF_{1α}, TXB₂, 2,3-dinor TXB₂ and 11-dehydro-TXB₂ using a DB1 column (30 m; 0.25 i.d.; film thickness 0.25 μm). (Reproduced with permission from Barrow *et al.* (1989) *Biochimica Biophysica Acta* 993: 121-127.)

PGF₄-like compounds, respectively) in biological samples. The order of elution for the isoprostanes is C₂₀-PGF₂ followed by C₂₀-PGF₃ followed by C₂₂-PGF₄, with clear separation between the different species. Therefore, this unique property of the SP-1701 phase facilitates the parallel determination of all three classes of PGF-like compounds in a single sample. A typical GC-MS/NICI chromatogram for the separation of PGF₂- and PGF₄-like compounds in human brain tissue is shown in **Figure 9**. The upper spectrum monitored at *m/z* 569 represents C₂₀-PGF₂-like compounds. The middle at *m/z* 593 represents

C₂₂-PGF₄-like compounds, while the lower spectrum at *m/z* 573 is the internal standard.

Identification of Compounds Based on their Retention Times

Reproducibility of chromatographic separation is important for the identification of a given compound in biological samples. For routine purposes, identification of a particular component is based on its retention time relative to that of an isotope-labelled internal standard. During GC separation on capillary columns, ²H-labelled internal standard elutes 1–2 s earlier than the corresponding unlabelled compound. Carboxylic ¹⁸O-labelled internal standard appears at the same retention time as the corresponding unlabelled PGs or their metabolites. Co-injection of a mixture of the samples of interest with an appropriate amount of external standard also adds a degree of confidence to the identification of the compounds based on their relative retention times.

Preparation of a Standard Curve for Quantification

A calibration curve for a given compound is prepared by plotting the peak height ratio of the unlabelled prostanoid/labelled analogue against the concentration of the compound being analysed. Such plots are generated using least-squares linear regression analysis and provide a gradient and intercept for the determination of the concentration of the corresponding unlabelled component in the sample.

Inter- and Intra-Assay Coefficients of Variation

These are determined by adding a known amount of an external standard to a sample that contains the compound of interest at a low concentration. At least four samples are required to provide an intra-assay coefficient of variation (COV). To establish the inter-assay COV, a minimum of four samples should be prepared on at least four occasions with different calibration curves.

Conclusions

The use of multistep chromatographic procedures in combination with GC separation on a medium polar capillary column and electron capture detection is the best approach for the analysis of PG and related compounds in biological samples. The method can be used for a wide range of lipid peroxidation products formed by mechanisms dependent or independent of the COX pathway. This is particularly important in

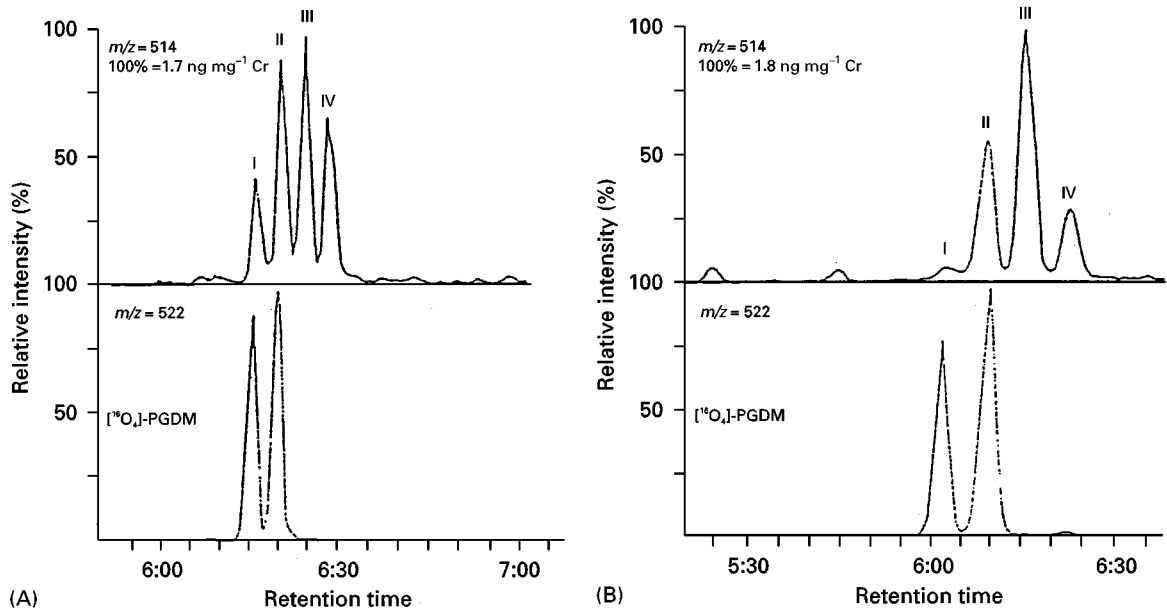


Figure 7 Selected ion monitoring chromatograms of analysis of urinary PGD metabolites using a DB1701 column (15 m; 0.25 inner diameter; film thickness 0.25 μ m). (Reproduced with permission from Morrow JD *et al.* (1991) *Analytical Biochemistry* 193: 142–148).

the measurement of urinary isoprostanes and their precursors because nonenzymatic peroxidation of individual PUFAs produces an array of PGF-like com-

pounds. The sensitivity and specificity of the assay can be improved by using GC-MS/MS or GC-tandem MS.

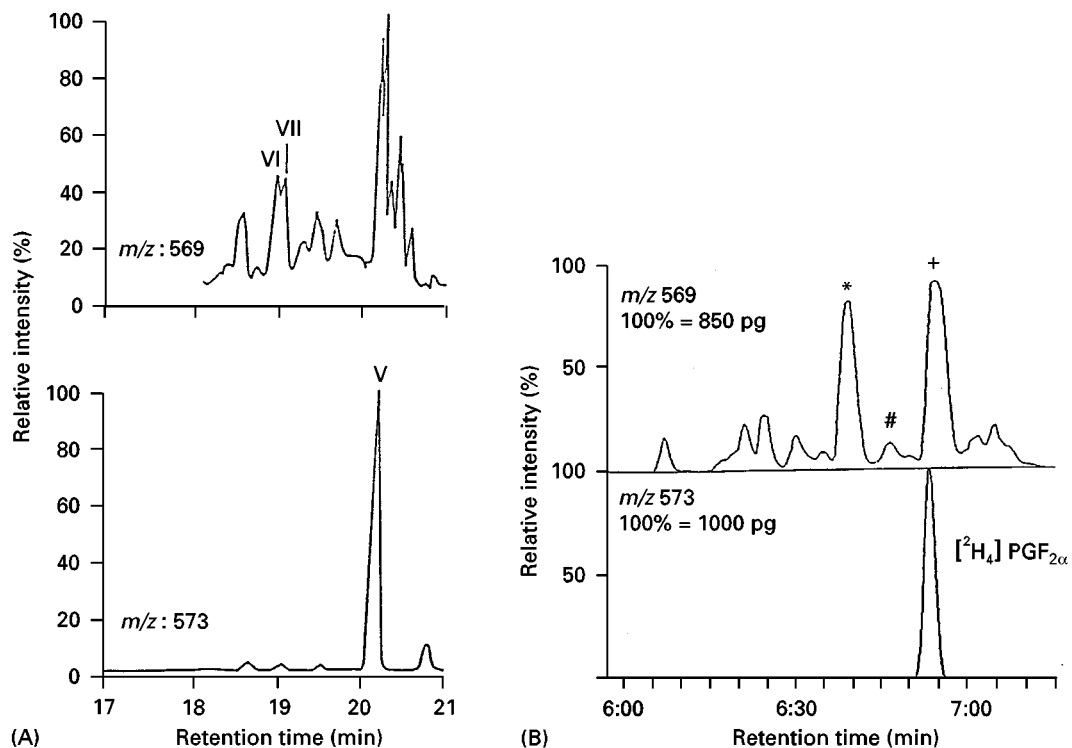


Figure 8 Comparison of chromatographic profiles of C_{20} -PGF₂-isoprostanes in human plasma using DB-1701 and SP-1701 stationary phases. (Part (A) reproduced with permission from Nourooz-Zadeh J (1999) *Methods in Enzymology* 300: 13–17; part (B) reproduced with permission from Morrow JD *et al.* (1994) *Methods in Enzymology* 233: 163–174).

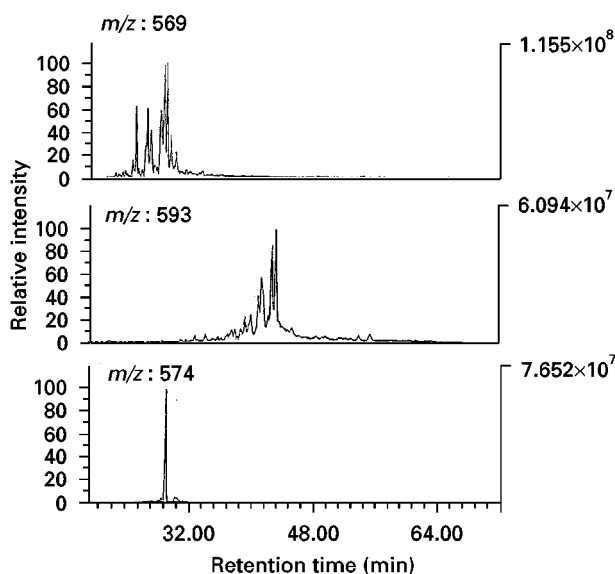


Figure 9 Selected ion monitoring chromatograms of simultaneous analysis of C_{20} -PGF₂- and C_{22} -PGF₄-isoprostanes in human brain.

See Colour Plate 115.

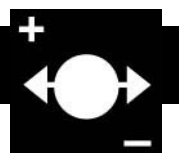
See also: **II/Chromatography: Gas:** Column Technology; Derivatization; Detectors: Mass Spectrometry. **Extraction:** Solid-Phase Extraction. **Appendix: 2/Essential**

Guides to Method Development in Gas Chromatography. Essential Guides to Method Development in Solid-Phase Extraction.

Further Reading

- Baily JM (ed.) (1991) *Prostaglandins, Leukotrienes, Lipoxins and PAF*. New York: Plenum Press.
- Benedetto C, McDonald-Gibson RG, Nigam S and Slater TF (eds) (1987) *Prostaglandins and Related Substances: A Practical Approach*. Washington, DC: IRL Press.
- Gross ML and Seyama Y (eds) (1994) *Biological Mass Spectrometry: Present and Future*. New York: John Wiley.
- Morrow JD and Roberts LJ (1997) The isoprostanes: unique bioactive products of lipid peroxidation. *Progress in Lipid Research* 36: 1–21.
- Nourooz-Zadeh J, Gopaul NK, Barrow S, Mallet A and Ånggård EE (1995) Analysis of F₂-isoprostanes as indicators of non-enzymatic lipid peroxidation in vivo by GC-MS/NICI. *Journal of Chromatography B* 667: 199–208.
- Rokach J, Khanapure SP, Hwang SW *et al.* (1997) The isoprostanes: a perspective. *Prostaglandins* 54: 823–851.
- Tsikak D (1998) Application of gas-chromatography-tandem mass spectrometry to assess *in vivo* synthesis of prostaglandins, thromboxane, leukotrienes, isoprostanes and related compounds in humans. *Journal of Chromatography B* 717: 201–245.

PROTEINS



Capillary Electrophoresis

S. P. Radko, National Institutes of Health, Bethesda, MD, USA

Copyright © 2000 Academic Press

Electrophoresis, mostly in the slab gel format, and high performance liquid chromatography (HPLC) are the two techniques commonly employed for protein separation during the past decades. After emerging in the early 1980s, capillary electrophoresis (CE) has been recognized as a new tool for protein analysis and characterization: it combines a number of aspects of both electrophoresis and HPLC. Based on differences in charge-to-size ratio or isoelectric point (pI) of protein macroions, the separations in CE are inherently electrophoretic. However, online detection producing quantitative information in the form of peak area or height, single sample analysis in a serial fashion, and the possibility of performing separation in the presence of flow (generated by electroosmotic current) are features of CE similar to those of HPLC. These features lend CE to easy automation, in contrast to the labour-intensive methods of conventional (gel) electrophoresis. Since heat dissipation by convection is effectively suppressed in capillaries of less than 0.2 mm i.d., the separation can be performed in free solutions without a gel. The high heat dissipation properties of thin fused silica capillaries also enable one to apply field strengths of several hundred volts per centimetre, thus greatly reducing the time of separation.

To date, CE techniques analogous to a number of conventional electrophoretic methods such as zone electrophoresis, isoelectric focusing and sieving (size-dependent) separations have been developed and numerous applications of CE to separation and characterization of proteins have been demonstrated. In the particular mode of CE as capillary zone electrophoresis, short separation times (often a few minutes) combined with relatively large diffusion constants of proteins were expected to provide separation efficiencies exceeding a million theoretical plates. However, such potential efficiency has never been practically achieved, and this mostly appears to be due to the interactions of proteins with the capillary walls.

The approaches to reducing protein interactions with the capillary walls and the modes of CE applied to protein analysis are briefly considered below.

Approaches to Reducing Protein–Silica Surface Interactions

The high surface activity of fused silica at neutral pH, combined with the high surface-to-volume ratio of thin capillaries is a major problem in applying CE to protein separation. In general, the protein–silica surface interactions give rise to peak broadening and asymmetry, compromising the resolution. In bare fused silica capillaries, these interactions often result in uncontrolled alterations of the electroosmotic flow (EOF) and irreproducible migration times, low mass recovery of proteins or even their irreversible adsorption with loss of sample. Over the last 10 years, great efforts have been made to develop conditions for protein analysis under which the protein–capillary wall interactions are minimized and the EOF is either suppressed or stabilized.

In the pH range of 3–10, the charge density of the capillary inner surface is known to increase progressively due to the ionization of weakly acidic silanol groups. The charge density on the wall is near zero at pH < 3 (silanol groups become fully protonated) and saturated above pH 10 (silanol groups are fully dissociated). Thus, protein species possessing a pI higher than the pH of the electrophoretic buffer will experience an electrostatic attraction to the negatively charged silanols. Beside silanol groups, fused silica bears a variety of other active sites such as inert siloxane bridges and hydrogen-bonding sites. These active sites can join in the protein immobilization on the inner surface of the capillary, by interacting with the hydrogen-bonding and hydrophobic regions of the protein.

The electrostatic attraction between protein molecules with a net positive charge at a given pH and ionized silica is believed to play a key role in the protein–capillary wall interactions. Thus, operating at extremes of pH (at pH < 3 where silanol ionization is very low or at pH > 11 where proteins carry a net negative charge) appears to be the simplest approach to their minimization. Though such an approach has been demonstrated to be successful in a number of applications, operation at pH extremes in general reduces charge diversity, diminishing the separation selectivity. The pH extremes also tend to

denature proteins and induce formation of multiple conformers. The electrostatic attraction between proteins and the silica surface may be reduced by increasing the ionic strength of electrolyte solutions (100 mmol L⁻¹ or greater). However, the high ionic strength limits the applied voltage, consequently decreasing efficiency and increasing the analysis time. Deactivation of silanol groups may also be achieved by derivatizing them with organosilanes but the carbon moieties of organosilanes make the capillary wall highly hydrophobic.

Two approaches appear to be the most successful in rendering CE suitable for routine protein separations: first, incorporation of appropriate additives into the electrolyte solution to mask or compete for either the silanol groups or the basic amino acid residues of the protein which are exposed to the solution; and second, use of capillaries with an inner surface modified by an adsorbed or covalently attached polymeric coating. A large variety of chemicals and modification procedures currently exist which can effectively reduce protein-wall interactions and control the EOF so that a separation efficiency of several hundred thousands of theoretical plates has become practically achievable. Several types of coated capillaries are commercially available, and are described below.

The incorporation of buffer additives permitting successful protein separations in bare fused silica capillaries has the advantage of simplicity. Ideally, the buffer additive should not compromise the selectivity of separation by interacting with the analyte, alter the buffer pH or increase the operating current, and should in general exhibit low UV absorbance. Organic compounds of different kinds have been extensively examined as the buffer additives. Since mostly they interact with the silica surface in a dynamic fashion, the method of modifying the capillary walls by using buffer additives is known as dynamic coating.

A large database of organic compounds and buffer components suitable for improving CE performance in protein separations has been established. This database includes zwitterionic salts (methylglycine and trimethylglycine, trimethylammoniumpropyl and butyl sulfonates), an extensive number of mono-, di- and polyamines, surfactants (ionic and zwitterionic fluorosurfactants as well as nonionic surfactants of the Brij and Tween series) and neutral polymers (cellulose derivatives, dextran, polyvinyl alcohol, polyethylene glycol). However, the effectiveness of dynamic coatings is mostly evaluated with standard mixtures containing a small number of proteins or with variants of a single protein. Therefore, it is not possible to predict how a particular additive

will act in conjunction with complex biological samples. Such samples may consist of a broad spectrum of proteins ranging widely in their degree of hydrophobicity, pI values and molecular weight. Despite this limitation, the present database of buffer additives known to improve protein separations may be very useful in developing methods for a targeted component analysis like the purity control of recombinant proteins, food analysis, or electrophoretic analysis of haemoglobins, serum or urine proteins.

Though the main mechanism by which the buffer additives improve protein separation appears to be their interaction with the silica surface, they can play an additional role – binding to the protein. In a number of cases, the additives have been shown to modulate selectivity by enhancing differences in electrophoretic mobility (e.g. some surfactants upon complexation to proteins, or alkyl diamines and their derivatives upon binding to protein glycoforms).

The incorporation of diaminealkanes, polyamines and fluorinated cationic and zwitterionic surfactants in the electrophoretic buffer effectively controls both the magnitude and direction of EOF.

Adsorbed coating differs from dynamic coating by the degree of permanence, but the demarcation line between them is arbitrary. In the case of an adsorbed coating, the coating agent should not be present in the electrophoretic buffer during a run. As a rule, polymeric species are used for adsorbed coating. Permanence can result from the high binding affinity of the coating agent to the silica surface (polymeric amines, polyethylene oxide) and may be enhanced by subsequently cross-linking the adsorbed species into a continuous, permanent film (e.g. polyethyleneimines treated with diepoxide after adsorption to capillary walls). The permanence can also result from the ability of the coating agent to form, upon a particular treatment, polymeric films physically covering the silica surface (cellulose acetate and polyvinyl alcohol films are examples). The polymers may be adsorbed not directly to the silica surface but to a hydrophobic layer formed by moieties of a surfactant covalently attached to the capillary inner walls (hybrid coating). Hybrid coating appears to be the most flexible, since the polymeric layer can easily be removed by rinsing the capillary with an organic solvent and polymeric species of other types may be adsorbed, depending on the separation goal. An example of protein separation in a capillary with the hybrid coating is presented in **Figure 1**.

The covalently attached polymeric coating is usually carried out by grafting polymers to a silica surface derivatized with organosilanes. In the subsequent step, polymer chains may be cross-linked to help stabilize the coating. Several neutral (cellulose

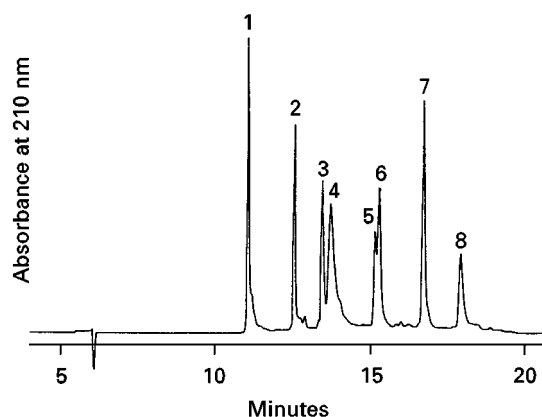


Figure 1 Electropherogram of some acidic and basic proteins in a capillary with hybrid coating (after derivatizing with the organosilane, the capillary was coated with epoxybutane-modified hydroxypropylcellulose). Other conditions: 0.05 mol L⁻¹ NaH₂PO₄, pH 3.0; detection at 210 nm, + 21 kV, 30 mA. Capillary total length, 85 cm; effective length, 50 cm, 50 μ m i.d. Peak assignment: 1, cytochrome c, pI 10.2; 2, lysozyme, pI 11.0; 3, β -lactoglobulin A, pI 5.1; 4, conalbumin, pI 6.0; 5, haemoglobin, pI 5.6; ribonuclease A, pI 9.3; 7, α -chymotrypsinogen A, pI 9.2; 8, trypsin inhibitor, pI 4.2. Reproduced with permission from Yang C and El Rassi Z (1998) Capillary zone electrophoresis of proteins with fused-silica capillaries having polymers and surfactants adsorbed onto surfactant moieties previously covalently bound to the capillary column surface. *Electrophoresis* 19: 2278–84. Copyright: Wiley-VCM.

derivatives, epoxy polymers, dextran) and cationic (polyvinylimidazole, polyethyleneimine derivatives) polymers have been employed for the covalently attached coating. The most popular polymer used for the polymeric coating is polyacrylamide. This coating is mostly performed with polyacrylamide chains polymerized *in situ*.

It should be noted that, despite the variety of materials and procedures used to prepare the coated capillaries, they do not appear to vary markedly in separation properties. The diversity of chemistries underlying the capillary coating is likely to reflect the continuous search for a 'magic' coating and inadequacy of any single approach to provide satisfactory results for all applications. A particular problem arises due to difficulties in optimizing the coating process. The quality of coating appears to depend on the quality of the fused silica surface, which may vary between different sources of capillaries and even between different batches of silica; this requires a corresponding adjustment in capillary pretreatment and coupling chemistries.

Modes of Capillary Electrophoresis Applied to Protein Analysis

Capillary zone electrophoresis (CZE), capillary isoelectric focusing and sieving capillary electrophoresis

in polymeric media are the modes of CE most widely used for separating and characterizing proteins. A number of commercial kits for capillary isoelectric focusing and sieving separations are now available. Capillary isotachopheresis has in rare cases been employed for protein analysis. Micellar electrokinetic chromatography has generally exhibited a poor selectivity in separating proteins. This is probably due to the inability of relatively large protein molecules to partition into the detergent micelle.

Capillary Zone Electrophoresis

CZE is the simplest of the CE modes and straightforward to perform (Figure 1 depicts a typical example of a CZE separation). When employing CZE for protein separation, the choice of capillary (uncoated or with the particular type of coating) and buffer additives should be made carefully depending on sample composition. The uncoated capillaries generally require a prior conditioning step. Detection based on either UV adsorption or laser-induced fluorescence (LIF) is most often employed in the CZE of proteins. Depending on the detection mode, a sample pretreatment may be necessary.

The sensitivity of the detection by UV absorbance is limited since both the optical length (= capillary internal diameter) and sample volumes (typically, a few nanolitres) are very small in CZE. Though the sensitivity can be greatly increased by detecting proteins in the wavelength range of 200–220 nm, UV detection still requires a relatively high concentration of analyte in a sample. That is not always the case and a preconcentration of the sample, often of a volume of a few microlitres, is needed. Several online and offline preconcentration techniques can be employed in CZE. The first and simplest approach to online sample preconcentration is zone sharpening by stacking. Proteins dissolved in a buffer with a conductivity lower than that of the run buffer (commonly, the diluted run buffer) become concentrated at the interface between the sample and the run buffer due to a high voltage drop in the sample zone. Preliminary sample desalting is often necessary for this approach and special methods have been developed for desalting (and concentrating) microlitre volumes of protein samples, using small pore polyacrylamide gels.

Isotachopheresis is the other popular technique to concentrate samples. The preconcentration may be performed either online or in a coupled column, and in the presence of salts. The gain in detection limit is 10- to 100-fold and can be increased up to 1000-fold when a hydrodynamic counterflow is employed. Another efficient method of protein preconcentration is selective accumulation of the proteins on

a solid-phase affinity support. This method has been used in both online and offline modes, with several hundred-fold concentration.

After derivatization with a fluorophore, proteins may be detected online by LIF. A number of fluorescent dyes capable of covalently binding to protein molecules (e.g. fluorescein, naphthalenedicarboxaldehyde and fluorescamine) have been used, providing mass detection limits in the attomole range (initial sample concentrations of 10^{-8} to 10^{-10} mol L $^{-1}$). However, covalent binding of the dyes frequently results in a broadening of protein peaks or even in the formation of multiple peaks due to multiple derivatization.

Capillary Isoelectric Focusing

Like conventional isoelectric focusing (IEF), capillary isoelectric focusing (cIEF) is based on differences in isoelectric points (pIs) of proteins. In cIEF, a stabilizing gel is not required and, due to the high field strength, the focusing process usually takes only 5–15 min. The cIEF can provide resolution of up to 0.01 pH units, comparable with that of the most successful applications of conventional IEF.

Sensitivity of detection based on UV absorbance (at 280 nm) is generally satisfactory for cIEF, due to the concentration of proteins from a relatively large injected volume into a small volume of the focused zone. Capillaries with a hydrolytically stable coating effectively preventing protein adsorption and changes in the EOF are required for successful cIEF separations. As in conventional IEF, protein precipitation due to the high protein concentration at the isoelectric point is a potential problem in cIEF and is addressed in the same way: using strong solubilizing agents, such as urea and nonionic detergents, in the ampholyte mixture.

Size-dependent Separation of Proteins by Capillary Electrophoresis

Although the use of narrow bore capillaries abolishes the need for gel media to suppress convection, another important feature of gels – their capability to provide size-dependent separation of macromolecules – is clearly beneficial for protein analysis. Efforts to adopt gels to the capillary format were made in the early days of CE. However, technical difficulties, such as bubble formation and the fast deterioration of polyacrylamide gels during serial runs, limit the use of gel-filled capillaries. These difficulties have been overcome by using replaceable sieving media such as solutions of entangled polymers. While gels are polymerized *in situ*, polymer solutions are usually prepared by dissolving commercially available polymers in the run buffer and are pumped into the capillary before each run. Solutions of dextran,

polyethylene oxide, polyvinyl alcohol and linear polyacrylamide have been demonstrated to be suitable for protein analysis. Though the use of coated capillaries is generally recommended, uncoated capillaries may also be employed if a polymer solution produces sufficient viscosity (typically >100 cP). The main drawback of polymer solutions is that resolution is not as high as that obtained with gel-filled capillaries.

Size-dependent separation by CE of protein–sodium dodecyl sulfate (SDS) complexes provides information similar to that obtained from conventional SDS-polyacrylamide gel electrophoresis (SDS-PAGE), as illustrated in **Figure 2**. The limits of UV detection are comparable to those obtained in SDS-PAGE with Coomassie blue staining, whereas total analysis time for multiple samples is even shorter for CE than that for, e.g. a 16-channel slab gel. Size-based analysis by CE in sieving media under native conditions has been demonstrated for proteins. Usually, such analysis employs constructing a Ferguson plot (the logarithm of protein mobility vs. polymer (gel) concentration). Such construction is extremely time-consuming in traditional PAGE but becomes practical by using CE in replaceable sieving media. The Ferguson plot-based analysis may also be useful in estimating the molecular weight of proteins whose binding with SDS is anomalous (e.g. membrane proteins, glycoproteins, highly basic proteins) and that of aggregates and complexes of proteins.

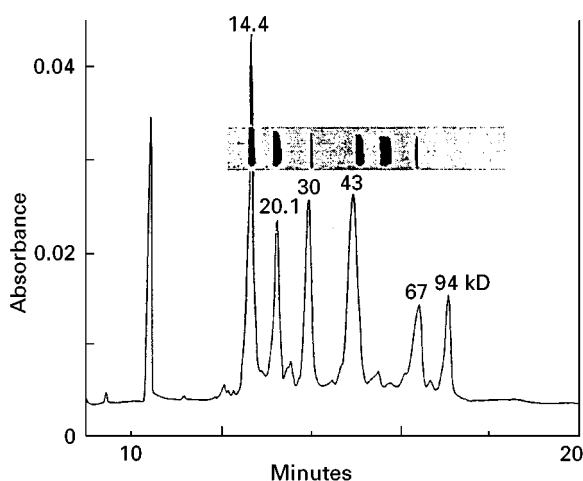


Figure 2 Capillary electrophoresis sieving separation of a standard SDS–protein mixture. Sieving matrix, 3% solution of polyethylene oxide. Inset shows the SDS-PAGE trace of the same mixture. Numbers above the peaks correspond to protein molecular weight. Buffer: 100 mmol L $^{-1}$ Tris-CHES, pH 8.8, 0.1% SDS. Condition: 300 V cm $^{-1}$, 20°C. Detection at 214 nm. Reproduced with permission from Guttman A (1996) Capillary sodium dodecyl sulfate-gel electrophoresis of proteins. *Electrophoresis* 17: 1333–41. Copyright: Wiley-VCM.

Protein Characterization by Capillary Electrophoresis

In addition to the targeted component analysis and sample profiling, CE has been employed in a number of specific electrophoresis-based approaches aiming at the characterization of protein–ligand interactions, protein functional activity and structure.

Affinity capillary electrophoresis (ACE) has been applied to the study of protein interactions with drugs, carbohydrates, nucleic acids and other proteins. In a typical ACE experiment, the receptor is subjected to electrophoresis in a capillary containing free ligand at different concentrations. The receptor–ligand binding (K_{on}) and dissociation (K_{off}) constants are estimated by Scatchard analysis of shifts in the receptor's mobility in response to ligand concentrations. The analysis of peak broadening has been shown to be useful for estimating K_{on} and K_{off} constants, if the characteristic times of receptor–ligand interactions are comparable with migration time of the analyte. The receptor–ligand complex equilibrium and separation process can be affected by capillary wall effects and/or the use of buffer additives. These limitations must be addressed when developing an ACE method.

The potential of CE in analysing antibody–antigen complexes has been extensively studied over the last few years in order to develop CE-based immunoassays (IA). The CE-based IA offers advantages of high speed of a single analysis, detection of antigen at trace concentrations (10^{-10} mol L⁻¹ if the LIF detection and fluorescently derivatized antibodies are employed) and the potential for automation. Despite some successful examples, CE has generally exhibited the inability to perform direct IA due to the lack of separation between bound and free antibodies. Though this drawback has been overcome in the competitive CE-based IA, the sensitivity of the competitive IA does not meet the detection levels required for many important clinical tests.

A CZE-based approach to microassaying enzyme activity has recently been developed. In this 'in-tube' approach, the enzyme and substrate are electrophoretically mixed inside the capillary under conditions where their mobilities differ. Another new application of CZE to protein characterization is studying protein folding/unfolding transitions. Due to recent advances in capillary coating and the inherent ability to perform electrophoresis in short time intervals, CZE appears capable of reliably distinguishing different forms of protein conformations, providing a new instrumental approach to the quantitative analysis of the conformational equilibrium of proteins.

Coupling Capillary Electrophoresis to Other Techniques for Protein Analysis

Several multidimensional separation systems for protein analysis, incorporating CE, have been proposed over the last decade. Two-dimensional (2-D) techniques such as CE-CE (using CE separations with two different carrier systems), HPLC-CZE, size exclusion chromatography (SEC)-CZE, and even a 3-D technique combining SEC-HPLC-CZE have been reported. The multidimensional systems possess tremendous resolving power and may be extremely useful in analysing complex biological samples, but there are drawbacks. Separation times are generally long and can last 2–12 h. Beside the technical difficulties of interfacing different separation systems, the compatibility of mobile-phase and run buffers as well as maintaining the detection sensitivity adequate for trace analysis in the sequential separations are the most significant problems.

By coupling CE with mass spectrometry (MS), the molecular weight of separated proteins can easily be determined. It is also possible, using MS, to detect proteolysis and deamidation, find glycosylation variants, and, with peptide mapping, confirm the primary structure of proteins. Though online interfacing of CE with MS has progressed substantially in recent years, the successful online combination of CE and MS is still a challenging instrumental problem. In addition to the interface design issue, practical considerations concerning the compatibility between the run buffer and the sheath liquid as well as differences in their flow rates at the interface must be addressed when dealing with CE-MS coupling.

Conclusions

After an initial period of fast technical progress, over the last decade CE has been increasingly focused on developing practical methods for protein separation and characterization. To date, due to advances in capillary coating, CE may be viewed as a practical tool for rapid, sensitive and quantitative analysis of minute amounts of protein samples, with great utility in targeted component analysis. For many applications, it can replace HPLC and conventional gel electrophoresis but more often it should be used in conjunction with other separation techniques, providing different selectivity or automated analysis. Since the acceptance of CE in the clinical laboratory for routine protein-based diagnostics depends considerably on meeting adequate throughput, attempts to develop high throughput CE systems are likely to be intensified. With a decrease in the real cost and improvement in sensitivity and resolving power of

MS detection, the increasing use of a combined CE-MS technique can be expected.

To be more widely accepted in the area of biomedical research, CE-based protein separations must demonstrate a number of features that match the success of conventional (gel) electrophoretic systems. Besides profiling complex protein samples, these systems allow for immunological and enzymatic assaying of separated proteins as well as for simultaneous transfer of sample components into another separation dimension without altering the separation in the first one. All of these are achieved with minimal disturbance of zone integrity. Thus, the major efforts will probably be made in developing both multidimensional separation systems involving CE and CE-based separation systems permitting post- or on-column enzymatic and immunological analysis of the separated components of complex biological samples. Incorporating immobilized enzymes or antibodies into CE-MS systems will revolutionize the analysis of protein structure and, especially, glycoprotein analysis.

Further Reading

Camilleri P (ed.) (1998) *Capillary Electrophoresis: Theory and Practice*, 2nd edn. Boca Raton: CRC Press.

El Rassi Z (ed.) (1997) *Electrophoresis* 18: No. 12/13. Special Issue on Capillary Electrophoresis and Electrochromatography.

Hjerten S (1996) Capillary electrophoretic separation in open and coated tubes with special reference to proteins. *Methods in Enzymology* 270: 296.

Karger BL, Chu YH and Foret F (1995) Capillary electrophoresis of proteins and nucleic acids. *Annual Review of Biophysics and Biomolecular Structure* 24: 579.

Khaledi MG (ed.) (1998) *High-performance Capillary Electrophoresis: Theory, Techniques, and Applications*. New York: Wiley.

Landers JP (ed.) (1997) *Handbook of Capillary Electrophoresis*, 2nd edn. Boca Raton: CRC Press.

Lunte SM and Radzik DM (eds) (1996) *Pharmaceutical and Biomedical Applications of Capillary Electrophoresis*. Oxford: Pergamon.

Righetti PG (ed.) (1996) *Capillary Electrophoresis in Analytical Biotechnology*. Boca Raton: CRC Press.

Righetti PG and Deyl Z (eds) (1997) *Journal of Chromatography B* 699, Special Volume: Proteins: Advanced Separation Technologies.

Wehr T, Rodriguez-Diaz R and Zhu M (1999) *Capillary Electrophoresis of Proteins*. New York: Marcel Dekker.

Centrifugation

A. Yamazaki, Kresge Eye Institute, Wayne State University, Detroit, MI, USA

Copyright © 2000 Academic Press

Introduction

Modern technological developments have made centrifugation one of the most important and widely applied techniques in experimental research. In biological studies centrifugation is used for the extraction and isolation of biological materials and for the measurement of physical properties of macromolecules. Indeed, biological materials have been extracted and isolated for more than a thousand years using centrifugal forces. In the 1920s, Svedberg and other researchers developed motor-driven centrifuges which had an optical system to observe sedimentation of macromolecules during centrifugation, and used these instruments for the measurement of physical properties of macromolecules, especially proteins. The molecular mass of most proteins was determined using these analytical centrifuges until 1970, but they

have not been recently used for that purpose because much easier methods for the measurement of molecular mass, such as size exclusion chromatography and sodium dodecyl sulfate (SDS)-gel electrophoresis, have been developed. More recently, centrifugation has become an indispensable tool for the isolation of proteins, nucleic acids and subcellular particles. The use of centrifuges has also been revived for the measurement of physical properties of proteins, especially for the characterization of protein associations and protein-protein interactions. In this section, important points of theory and practice for the separation and isolation of proteins by centrifugation are summarized.

Theoretical Basis of Centrifugation

Although a rigorous understanding of sedimentation theory is not required for the separation and isolation of proteins, a review of some basic principles will be helpful for understanding the establishment of conditions and the interpretation of experimental results obtained. Because of their random thermal motion,

macromolecular particles in a solution do not show any perceptible sedimentation in a uniform gravitational field. However, these macromolecular particles do sediment under a centrifugal force. If the effect of diffusion is neglected, in a solution (density ρ) the motion of a particle (mass m and volume V_p) that is located a distance r from the axis revolving with angular velocity ω can be expressed by the following equation:

$$vf = m\omega^2 r - \rho\omega^2 r V_p \quad [1]$$

where v is the velocity of the sedimenting particle, f its frictional coefficient; $m\omega^2 r$ the centrifugal force and $\rho\omega^2 r V_p$ the buoyant force. This equation may be rearranged to give:

$$v = dr/dt = s\omega^2 r \quad [2]$$

where:

$$s = \frac{m - \rho V_p}{f}$$

This is the well-known sedimentation equation in which s is the sedimenting coefficient and has dimensions of time. For most biological macromolecules, the magnitude of s is about 10^{-13} s. Therefore, the unit of sedimentation, the Svedberg (S), has been defined as being equal to 10^{-13} s. The standard sedimentation coefficient ($S_{20,w}$) is defined as that equivalent to sedimentation in water at 20°C. The sedimentation coefficients ($S_{20,w}$) of some proteins are shown in Table 1.

The sedimentation coefficient s may be transformed to a more practical form. The mass of 1 mole of particles, M , is

$$M = mN_o \quad [3]$$

where N_o is Avogadro's number. Thus, a particle's volume, V_p , may be expressed in terms of its molar mass:

$$V_p = mv = vM/N_o \quad [4]$$

where v is the particle's partial specific volume.

Eqns [1], [3] and [4] may be combined to give:

$$vf = \frac{M(1 - v\rho)\omega^2 r}{N_o} \quad [5]$$

When eqns [2] and [5] are combined, s may be expressed as:

$$s = \frac{v}{\omega^2 r} = \frac{M(1 - v\rho)}{N_o f} \quad [6]$$

Since the particle's partial volume, v , may be expressed by the reciprocal of the buoyant density of the particles, ρ_p , as $v = 1/\rho_p$, s may also be expressed as:

$$s = \frac{v}{\omega^2 r} = \frac{M(1 - \rho/\rho_p)}{N_o f} \quad [7]$$

Since $f = 6\pi\eta r_p$, where η is the viscosity of the liquid medium and r_p is the radius of unsolvated spherical particle, these equations indicate that the sedimentation velocity, v , is related to the sedimentation coefficient s , which is mostly a function of particle size, density of the particle ρ_p , density of the medium ρ and the viscosity of the liquid medium, η . In other words, for a given particle, sedimentation is directly related to particle size, particle density and the centrifugal field, and inversely to the viscosity and density of the liquid medium.

Centrifugation for Protein Separation

Centrifuges may be classified on the basis of the maximum speed, namely, low speed, high speed and ultracentrifuges. Each of these can be used in the various steps of protein separation and isolation from biological materials. Low speed centrifuges are used routinely for the initial processing of biological samples. This type of centrifuge can be mainly used to isolate cells and organelles that contain target proteins by pelleting these materials. High speed centrifuges, with maximum speeds of 8000–25 000 rpm, are mainly used for the preparation of subcellular fractions. These centrifuges can generate about 60 000 g, which is enough to separate proteins from debris of cells and organelles. In order to isolate proteins from other proteins, ultracentrifuges are

Table 1 Sedimentation coefficients of some proteins

Protein	$S_{20,w}$
Cytochrome C (bovine heart)	1.71
Egg-white lysozyme	1.9
Insulin	1.95
Ribonuclease A (bovine pancreases)	2.00
Myoglobin (horse heart)	2.04
α -Chymotrypsin (bovine pancreases)	2.40
Pepsin	2.8
g-Actin	3.7
Lactate dehydrogenase (pig heart)	6.93
Catalase (horse liver)	11.2
Glutamate dehydrogenase (bovine liver)	26.6
Fibrinogen (human)	7.63
Haemocyanine (octopus)	58.7
Haemocyanine (snail)	100

required. Modern ultracentrifuges can generate approaching 1 000 000 g, which is sufficient to pellet even small proteins. Ultracentrifuges can be divided into two types: analytical and preparative. Analytical ultracentrifuges have a device by which the sedimentation rate of molecules can be optically measured during centrifugation and can be used to obtain data on the sedimentation properties of particles. The masses of most proteins were determined by these ultracentrifuges before development of simpler molecular mass determination methods. Eqn [4] indicates that the particle's mass $m = M/N_0$ can be determined from its sedimentation coefficient s , if its frictional coefficient f , is known, as indicated in eqn [6].

Preparative ultracentrifuges are designed for sample preparation. This kind of ultracentrifuge is also commonly used for quantitative estimations of sedimentation coefficients of particles in a density gradient, although the data obtained are not as accurate as those obtained using analytical ultracentrifuges. Preparative ultracentrifugation can be divided into two methods, namely differential ultracentrifugation and density gradient centrifugation. Differential centrifugation is based on the differences in the sedimentation rates of particles in samples. If a suspension of particles is centrifuged in a tube without a density gradient, each particle will move toward the bottom of a tube. In this case, the rate of sedimentation, v , is dependent upon s (eqn [2]). Since s is mostly a function of particle size, the rate of sedimentation is proportional to particle size. In the course of the ultracentrifugation, two fractions can be obtained from a solution of particles: a pellet containing sedimented particles and a supernatant solution of the unsedimented fraction. A given particle in the solution may sediment to the pellet or near the bottom, as illustrated in Figure 1. As might be expected, this centrifugation will first sediment the largest particles in the sample solution to the bottom of the tube. The only particle that is in purified form is the most slowly sedimenting one, but the yield is very low. The major problem with differential centrifugation is that the centrifugal force necessary to pellet the larger particles is also often sufficient to pellet the smaller particles initially near the bottom of the tube (Figure 1). To separate one particle from another effectively, a 10-fold difference in mass is usually required. Thus, this centrifugation is recommended for the separation of proteins from large particles such as cells or organelles. However, it cannot be used for the isolation of one protein from another because the partial specific volume, v_p , of most proteins (in eqn [6]) is not sufficiently different.

Eqn [6] assumes that centrifugation is performed in a homogeneous medium. However, centrifugation

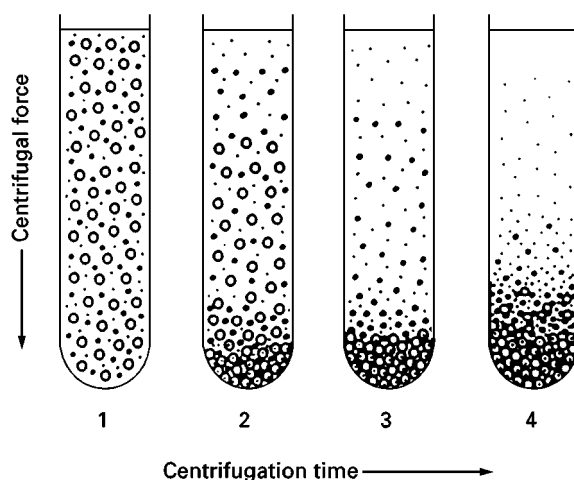


Figure 1 Fractionation of particles by differential centrifugation. Reproduced with permission from Griffith (1979).

can be carried out in a solution of an inert substance in which the concentration increases from the top to the bottom of the centrifuge tube, i.e. density increases from top to bottom. In such density gradient centrifugation of a mixture of particles with different sizes or buoyant densities, a particle will become stationary when $(1 - v\rho)$ in eqn [6] is zero. Thus, various components will separate according to size or buoyant densities, and form bands or zones of particles with similar densities. Thus, the use of such density gradients greatly enhances the resolving power.

There are two types of density gradient ultracentrifugation: isopycnic and rate-zonal ultracentrifugation. In isopycnic centrifugation, separation is based on the centrifugation of particles in a density gradient through which the particles move until their densities are the same as those of the surrounding medium, i.e. in eqn [7], $\rho_p = \rho$ (Figure 2). The sample is mixed with a relatively concentrated solution of a low molecular mass substance, such as CsCl, and is centrifuged until the solution achieves equilibrium under the high centrifugal field. The low molecular mass substance forms a steep density gradient. It is not obligatory to load the sample on top of the gradient. In the centrifugation, particle size only affects the rate at which particles reach their isopycnic position. Since variations in amino acid composition give proteins with only slightly different densities, isopycnic centrifugation can be used only when proteins are associated with nonprotein components such as lipids or polysaccharides, and their density differences are sufficient for the separation. Various gradient media can be used for the separation of these proteins because proteins form a band at low density in most gradient media. For example, in addition to CsCl,

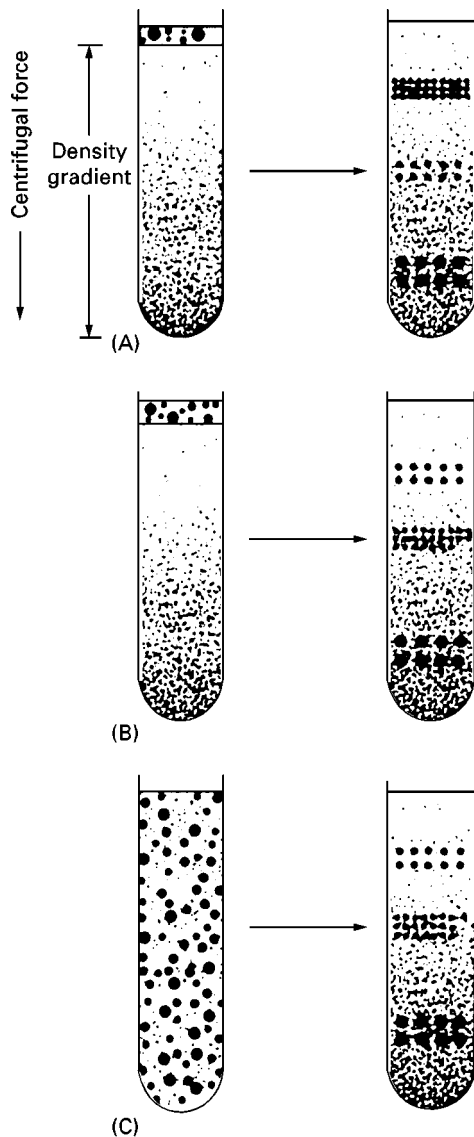


Figure 2 Types of density gradient centrifugation. (A) Rate-zonal centrifugation. (B) Isopycnic centrifugation using a preformed density gradient. (C) Isopycnic centrifugation using a self-forming gradient. Reproduced with permission from Rickwood (1992) by permission of Oxford University Press.

RbCl, NaBr or KBr can also be used to form shallower gradients for better resolution of these proteins.

Rate-zonal centrifugation is ideal for particles of defined size such as protein and RNA. In the rate-zonal ultracentrifugation, a mixture containing particles is layered on top of a density gradient. Loading the concentrated samples to the top of the gradient increases the eventual resolution of recovered particles. Sucrose is commonly used to form a density gradient. During centrifugation, particles move through the gradient at their characteristic sedimentation rates, forming zones that can be recovered at the end of the run (Figure 2). Because the

sedimentation rate is more affected by molecular size, the rate-zonal ultracentrifugation separates similarly shaped macromolecules largely on the basis of their molecular masses. It should be noted that particles separated by the rate-zonal centrifugation may not be homogeneous because particles with similar mass, even proteins, are sometimes heterogeneous.

Practical Aspects for Protein Separation by Centrifugation

Since rate-zonal centrifugation is commonly used for the separation of proteins, the following discussion will focus on a practical approach for this technique.

Types of Rotor

Preparative centrifuge rotors can be classified into four types: fixed angle, swinging-bucket, vertical and zonal. In fixed-angle rotors, the tubes are positioned at a fixed angle. These rotors are often used for differential ultracentrifugation and are very efficient for the separation of proteins from cells and organelles. Typically, a sample is loaded atop a gradient which reorients as the rotor is spun (Figure 3). During centrifugation, the larger particles are first sedimented across the tube, hit the wall of the tube, and slide down to form a pellet at the bottom.

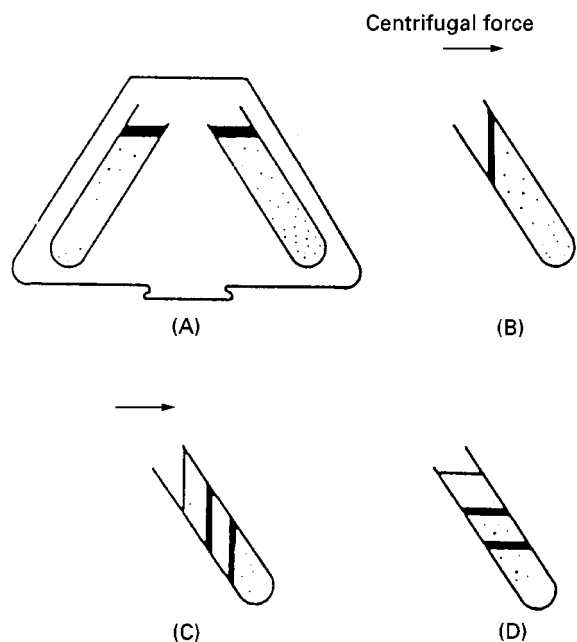


Figure 3 Operation of fixed-angle rotors. (A) The gradient is prepared, the sample is loaded and the centrifuge tubes are placed into the rotor. (B) Both sample and gradient reorient during acceleration. (C) Bands form as particles sediment. (D) Bands and gradient are both reoriented when the rotor is at rest. Reproduced with permission from Rickwood (1992) by permission of Oxford University Press.

Efficiency for the pelleting of particles is high due to the short sedimentation path. However, fixed-angle rotors are not common for protein separation because the pelleting process also disrupts sample zones as particles sediment through the gradient. Thus, fixed-angle rotors are mainly used for the pelleting of materials.

For the separation of proteins from other proteins, especially for small scale separation, the swinging-bucket rotor is widely used for rate-zonal centrifugation. This type of rotor is also used for the estimation of sedimentation coefficients of proteins. As shown in **Figure 4**, in the swinging-bucket rotor, the sample tubes are loaded into individual buckets which hang vertically while the rotor is at rest. When the rotor begins to rotate, the buckets swing out perpendicular to the axis of rotation. In these rotors, resolution of particles is high because particles sediment with a relatively long path length. For the same reason, run times are generally longer. Many types of swinging-bucket rotors are commercially available. The centrifuge tube should be as long as possible if high resolution is the objective. For large volume samples, swinging-bucket rotors with wider tubes should be used because the sample can be loaded in a narrow zone while still reducing particle interactions during sedimentation.

Vertical rotors are suitable for isopycnic as well as for rate-zonal separations. However, this type of rotor is not practical for the separation of proteins. As a result of diffusion and reorientation during

centrifugation, sample bands will be significantly broader than analogous bands in swinging-bucket rotors. In addition, if the sample contains pellets or floats, these materials will distribute along the length of the tube and can subsequently contaminate the supernatant during reorientation at the end of run.

Choice of Density Gradient

A density gradient is essential for rate-zonal centrifugation to support the zones of particles as they sediment. In addition, the sample can be loaded on to the top of the gradient as a narrow zone and the increasing density from the top to the bottom of the density gradient suppresses mechanical disturbances. Moreover, the presence of a gradient of increasing viscosity serves to sharpen the sample zones during centrifugation. The density gradient material for protein separation requires the following properties.

1. The materials should be sufficiently soluble in water to produce the range of densities needed.
2. Solutions of the gradient materials should be adjustable to a pH and ionic strength that are not harmful to proteins in the sample.
3. The materials should not interfere with methods of analysis of the target protein.

Sucrose has most often been used as a gradient material. Sucrose is inexpensive and extremely soluble in aqueous media and can be used to produce density gradients ranging up to 1.35 g mL^{-1} . Thus, it is suitable for separation of almost all proteins in cells. Although concentrated solutions of sucrose have high osmotic potential that cause shrinkage of certain cells and organelles, the high osmotic pressure has relatively less effect on the biological properties of proteins. Generally, sucrose is relatively inert to proteins, although contaminants in many commercial sources of sucrose may interact with proteins. Such impurities can be removed by treatment with activated charcoal. However, it is best to purchase specially purified sucrose for density gradient work. To sterilize sucrose solutions, autoclaving (100°C or above) of the solution should be avoided and treatment with 0.1% diethylpyrocarbonate is recommended. As described above, isopycnic centrifugation can be used for the separation of different types of proteins. However, it should be noted that the density of sucrose, even of a saturated solution, is too low for the separation. For this purpose, RbCl , NaBr or KBr can be used to form shallower gradients for better resolution.

Glycerol is used to stabilize some proteins, especially membrane-bound proteins, and provides gradient densities ranging up to 1.26 g mL^{-1} . Thus, glycerol gradients are widely used for the separation

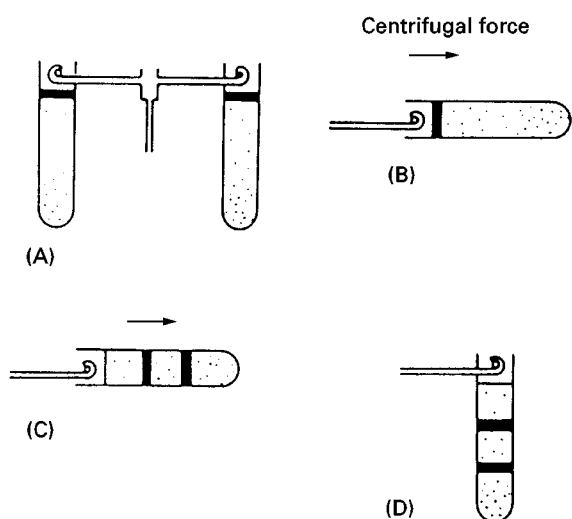


Figure 4 Operation of swinging-bucket rotors. (A) The gradient is performed and the sample is loaded on the top of the gradient. (B) Centrifuge bucket reorients as rotor accelerates to lie perpendicular to the axis of rotation. (C) Bands form as the particle sediment. (D) Rotor decelerates. Centrifuge bucket comes to rest in its original vertical position. Reproduced with permission from Rickwood (1992) by permission of Oxford University Press.

of proteins by rate-zonal separations. However, it should be noted that the high viscosity of glycerol reduces the effective density range and glycerol appears to inhibit some enzyme activities.

Preparation of Gradients

Density gradients can be divided into two types: continuous and discontinuous. For protein separation, continuous gradients are usually used in rate-zonal centrifugation. The most common continuous gradient for protein separation is a linear gradient in swinging-bucket tubes. A linear gradient is a gradient in which the density increases linearly in a tube of constant cross-sectional area with increasing distance from the centre of rotation. Thus, in this configuration the linear gradient can be defined as one where the density increases linearly with volume.

When designing a linear gradient in swinging-bucket rotors, several points should be emphasized. The density at the top of the gradient must be sufficient to support the sample while the density of the bottom of the gradient must not exceed the density of proteins to be separated. In general, the greater the slope of the gradient, the better the resolution obtained because the viscous drag rises rapidly as the sucrose concentration increases. Usually, as a first attempt, a 5–30% or 10–40% sucrose gradient should be used. It should be emphasized that the sample volume is related to the slope of the gradient because a given slope of gradient can only tolerate a limited amount of sample before gradient inversion occurs. Poor resolution during rate-zonal centrifugation almost always results from overloading.

Linear gradients are prepared using gradient makers. Many configurations of gradient maker are available. The simplest gradient makers consist of two vessels of equal cross-sectional area joined by a connecting channel with a stopcock. One chamber is a reservoir and the other chamber has a mixing device and an exit connected to the centrifuge tube. There are two methods for preparing linear gradients:

1. The reservoir contains the less dense solution, the mixing chamber contains the denser solution, and the gradient is routed to the wall of the centrifuge tube at the top. This method is readily applicable to centrifuge tubes made of hydrophilic materials such as cellulose nitrate and cellulose acetate butyrate.
2. The reservoir contains the denser solution, the mixing chamber contains the less dense solution, and the gradient is routed to the bottom of the centrifuge tube. This method can be applied to any type of centrifuge tube and it is much easier to prepare the gradient without disturbance.

The gradient should be prepared and maintained at 4°C.

Preparation of Sample

The sample should be ready for loading before the gradient is prepared and should be kept cold for many preparations. The sample is usually prepared in the same buffer as the gradient. In addition, several points are important in sample preparation:

1. The sample solution must have a density less than that of the gradient.
2. Gradients should be centrifuged as soon as possible after the sample has been loaded to prevent so-called droplet sedimentation.
3. For optimal resolution in rate-zonal centrifugation, the sample must be loaded on to the top of gradient and the sample volume should not exceed 2–3% of the gradient volume.

Loading of the sample on to the density gradient is one of the most crucial steps in rate-zonal centrifugation. The simplest method is to use a pipette to load the sample directly to the meniscus at the tube wall.

Conditions During Centrifugation

Smooth acceleration and deceleration are important for all gradient work. In addition, control of the temperature of the sample and gradient are important for reliable and reproducible sedimentation. Fortunately, most modern ultracentrifuges are equipped with programmed acceleration and deceleration modes which minimize the disturbance of gradient and temperature control. It should be emphasized that, during the gradient reorientation phase of a run using a swinging-bucket rotor, the rotor should be accelerated as slowly as possible up to 1000 rpm, and the brake switch should be off below 1000 rpm during deceleration.

Recovery of Fractions from the Gradient

After centrifugation, gradients are fractionated to recover protein bands. Great care must be taken at this stage to avoid loss of resolution. Several points should be emphasized.

1. All operations should be designed to minimize disturbance of the gradient.
2. The volume of the tubing from the gradient to the fraction collector should be minimized.
3. Care must be taken to avoid contamination of the recovered fractions by pelleted materials.
4. The gradient should be fractionated at a slow flow rate, particularly if viscous materials are used for the gradient.

In order to collect the entire gradient in a series of fractions, several methods may be applied. The simplest is to pierce the bottom of the tube with a needle, and collect the gradient as it drops out. Another method is to pump the gradient from the bottom of the tube with a narrow capillary tube. However, this method is not recommended because of the potential to disturb the gradient and resulting loss of resolution.

See also: III/Proteins: Capillary Electrophoresis; Crystallization; Electrophoresis; Field Flow Fractionation; High-Speed Countercurrent Chromatography; Ion Exchange.

Further Reading

Griffith OM (1979) *Ultracentrifuge Rotors: A Guide to Their Selection*. Palo Alto, Beckman Instruments.

Hsu HW (1981) *Separation by Centrifugal Phenomena*. New York: John Wiley.

Laskin AI and Last JA (eds) (1974) *Subcellular Particles, Structures, and Organelles*. New York: Marcel Dekker.

Neurath N and Hill RL (eds) (1975) *The Proteins*, 3rd edn. New York: Academic Press.

Price CA (1982) *Centrifugation in Density Gradient*. New York: Academic Press.

Rickwood D (ed.) (1983) *Iodinated Density Gradient Media: A Practical Approach*. Oxford: IRL Press.

Rickwood D (ed.) (1984) *Centrifugation*, 2nd edn, *A Practical Approach*. Oxford: IRL Press.

Rickwood D (ed.) (1992) *Preparative Centrifugation, A Practical Approach*. Oxford: Oxford University Press.

Schachman HK (1959) *Ultracentrifugation in Biochemistry*. New York: Academic Press.

Sheeler P (1981) *Centrifugation in Biology and Medical Science*. New York: John Wiley.

Crystallization

M. Y. Gamarnik, Nanoscale Phases Research, Bensalem, PA, USA

Copyright © 2000 Academic Press

Introduction

The first protein crystals described in the literature were obtained by Hünefeld in 1840. Hünefeld observed hemoglobin crystals after slow drying of blood pressed between two slides of glass. It is remarkable that this first result demonstrated the basic principle used today, that protein crystals similar to inorganic crystals may be produced by concentration of a protein in solution through slow dehydration. Throughout the history of protein crystal growth, the rationale for protein crystallization has been, firstly, separation of proteins from complex extracts, and then, starting in the 1930s, as purification as determination of the three-dimensional structure of protein molecules.

Knowledge about the three-dimensional structure is necessary to better understand the functions of protein molecules in living systems and plants. Three-dimensional structure can be determined by X-ray diffraction. For X-ray diffraction, good quality protein crystals of appropriate sizes are required. Crystal sizes in each direction should be at least 0.1 mm, if using a strong beam of synchrotron radiation, or at least 0.3 mm for conventional sources of X-rays.

Protein molecules in the crystalline state are more stable than in solution. Therefore, crystallized pro-

teins are more stable against denaturation and may be preserved for a significantly longer period of time than in solution. That is the reason that protein crystallization is often directed as much on preservation as on separation and purification.

This article comprises a brief description of general principles of protein crystal growth and a description of various techniques of protein crystallization with the emphasis on methods using a small amount of a crystallizing solution, from about 1 to 20 μL . The consumption of small amounts of protein is of value, since screening and optimization tests of determination of crystallization conditions typically require many portions of protein solution.

General Principles of Protein Crystallization

Intermolecular Interaction

To crystallize a protein it should be first of all dissolved to give a solution where the protein molecules become close one to another to create a nucleus that grows into a crystal.

An essential feature of protein solutions, associated with the complex structure and large size of protein molecules, is that the molecules may be charged by electric charges, of the same polarity, resulting in long-range electrostatic repulsion. This peculiarity is mediated by the ability of macromolecules to acquire protons from a solution or give up protons into the solution depending on the pH. The charge value of

protein molecules increases with the difference between pH of the solution and pH in the isoelectric point, pI , of the solution. At $pH = pI$, molecules become neutral, and accordingly, the long-range repulsion is absent. For most proteins pI is in the range 4.5–6.0.

At short distances van der Waals forces of attraction act between molecules. Competition between repulsion and attraction determines the state of protein molecules in solution. If the repulsion dominates, molecules remain apart in solution, protein is dissolved and no clusters or crystals are created. If attractive forces dominate, the molecules gather into clusters, that may form nuclei to yield crystals. For creation of well-ordered nuclei the attractive forces should be strong enough to provide slow clusterization but not so strong as to impair the formation of the crystal structure.

The Coulombic repulsive forces are affected usually by an addition to the protein solution of buffers, salts, precipitants and other additives. Buffers influence acidity; the pH of the solution alters the difference between pH and pI . This in turn changes charge values of protein molecules and accordingly the long-range repulsion. There are various buffers providing different pH: 0.1 M sodium acetate, pH = 4.6, 0.1 M trisodium citrate dehydrate, pH = 5.6, 0.1 M sodium cacodylate, pH = 6.5, 0.1 M HEPES, pH = 7.5, 0.1 M tris hydrochloride, pH = 8.5, etc.

Salts added to a protein solution may screen the repulsive interaction between the molecules. For instance, a 0.1–0.2 M aqueous solution of sodium chloride essentially shields the repulsive electrostatic forces. Precipitants such as polyethylene glycol (PEG) of various molecular weights, isopropanol and sodium formate, decrease the solubility of protein, initiating creation of clusters or nuclei.

Nucleation

Nucleation is initiated by fluctuation of density in a system of atoms or molecules. Crystallization in protein solutions is initiated by protein concentration fluctuation in a solvent. In regions of higher concentration, molecules are associated in clusters because of smaller intermolecular distances thus increasing attractive forces. Generally, clusters may be stable or metastable.

Reduction of repulsive interaction between protein molecules is a necessary condition of nucleation peculiar to proteins and other macromolecular substances. But it is still not enough to create a stable nucleus which becomes a seed for crystal growth. The mutual position of protein molecules should correspond to a minimal energy to form thermodynamically stable nuclei.

Thermodynamic free energy of a cluster in solution consists of two parts: volume energy, ΔG_v , and surface energy, ΔG_s . The volume energy is negative, so that it stabilizes the cluster, but surface energy is positive tending to make the cluster unstable. Competition between these two parts of the overall free energy determines the stability of clusters. The total free energy of a cluster, $\Delta G = \Delta G_v + \Delta G_s$, depends on its size, r , so that $\Delta G = \Delta G(r)$. This dependence reveals a maximum at a critical size, $r = r_c$. At sizes larger than r_c clusters become a stable nucleus capable to grow as a crystal. At sizes less than the critical size, clusters tend to dissolve, since they are energetically unstable.

The critical nucleus size, r_c , decreases with an increase of the supersaturation of protein solution $\beta = c/c_{\text{sat}}$, since $\Delta G_v \sim -\ln \beta$ and accordingly $r_c \sim 1/\ln \beta$. Here c is the concentration of protein in solution and c_{sat} is the concentration of the protein in saturated solution. In other words, c_{sat} is the solubility of the protein. Consequently, nucleation may occur only at $\beta > 1$, i.e. at protein concentration, c larger than the concentration of saturated solution, c_{sat} . This condition indicates also that the chemical potential of a cluster is lower than the chemical potential of the solution, and accordingly the volume energy ΔG_v is negative. An increase of the supersaturation, β also reduces the maximum of the total free energy, $\Delta G(r_c)$, which should be overcome to create a stable nucleus, because $\Delta G(r_c) \sim 1/(\ln \beta)^2$.

Nucleation is affected by many other parameters, such as relative specific surface energy of protein crystals in solutions, temperature, mobility and substructure of protein molecules, impurities, rate of supersaturation, etc. That is the reason that nucleation of proteins is an important step in protein crystallization, which often requires many screening experiments.

Crystal Growth

A zone of lower concentration is formed around a nucleus after it starts to grow, consuming surrounding molecules. The difference between the protein concentration in the bulk of the solution and in the depletion zone becomes a driving force, transporting the protein molecules from solution to the growing crystal. This mass transport is realized generally by diffusion and convection due to gradients of protein concentration. Slow transport of the molecules is required to yield good quality crystals. This is achieved at low supersaturation and low rate of dewatering of the protein solution and by crystallization at lower temperatures, ~ 4 – 6°C .

Mechanisms of attachment of protein molecules to the lattice of growing crystals have been investigated

intensively in recent years with the atomic force microscope. It was demonstrated by Malkin *et al.* with several proteins, lysozyme, thaumatin, canavalin, catalase and apoferritin, that macromolecules grow by all surface integration mechanisms involved in the crystallization of small molecules. The protein crystals reveal growth on screw dislocations and by two- and three-dimensional nucleation.

A screw dislocation generates steps that propagate along the crystal surface. The steps contain kinks at the crystal surface into which molecules are incorporated, building crystal layers in a spiral fashion around the dislocation core. This mechanism is realized basically at lower supersaturations, about 1–1.5. At higher supersaturations, protein crystals grow typically by two-dimensional nuclei formed on the surfaces. Absorption of three-dimensional nuclei have also been detected. The three-dimensional clusters are developed into multilayer stacks or microcrystals.

Absorption of impurities may cause a cessation of growth of macromolecular crystals. Dubrin and Feher revealed parallel step trains on lysozyme crystal surface accounted for by impurities, impeding the subsequent crystal growth. Malkin *et al.* have detected surfaces of lysozyme crystals completely covered by impurity absorption layers resulting in the cessation of growth.

Methods of Crystallization

Proteins may initially contain a large amount of impurities, such as salts, other classes of macromolecules, denaturated molecules, solid particles and other contaminants impeding crystallization. Therefore, proteins should be purified for crystallization tests. The same applies to buffers, salts and

precipitants used in crystallizing solutions. Descriptions of preparation and handling of proteins for crystallization and methods of characterization of macromolecules can be found in Further Reading.

There are many methods, techniques and apparatus for protein crystal growth depending on configuration of experiment – hanging drop, sitting drop or crystallization in a capillary. The method used also depends on the way the solution is supersaturated: by vapour diffusion, liquid–liquid diffusion, dialysis, mixing with a precipitant, change of temperature, etc. Other factors include gravity conditions and mass transport in solution, crystal growth in microgravity, gel method, crystallization in drops and suspended in heavy liquids.

Hanging and Sitting Drop

A hanging or sitting drop comprising a solute protein, to be crystallized, with a crystallizing agent, is equilibrated against a reservoir solution containing the crystallizing agent at higher concentration than in the drop (Figure 1). The reservoir, a glass vessel, is closed by a glass cover slip and sealed by grease to prevent the liquids evaporating. The drop volume is usually from 1 to 10 μL , the volume of reservoir solution is $\sim 0.5\text{--}1\text{ mL}$. An increase of concentration of crystallizing agent in the drop leads to a supersaturation of protein solution necessary for crystallization. Equilibration is achieved by vapour diffusion of water or other volatile components and continued until vapour pressures in the drop and in the reservoir become equal.

The crystallizing agent may comprise a buffer, such as sodium acetate, tris hydrochloride, HEPES or sodium cacodylate, a precipitant, such as polyethylene glycol, isopropanol or sodium formate, and a salt.

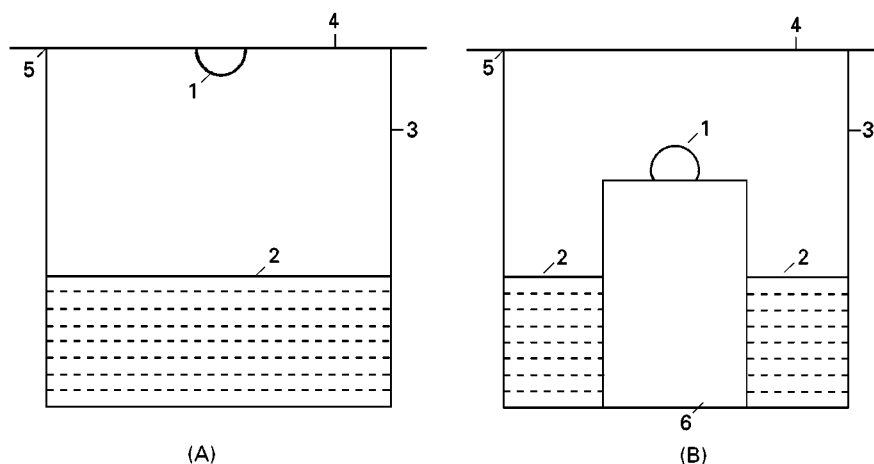


Figure 1 Schematic presentation of hanging- and sitting-drop techniques. (A) Hanging drop; (B) sitting drop. (1) Drop of protein solution, (2) reservoir solution, (3) glass vessel, (4) coverslip, (5) sealing rim, (6) inverted glass pot. (From Ducruix and Giedge (1992) by permission of Oxford University Press.)

If there are no volatile components except water, diffusion of water occurs from the drop to the reservoir solution. This decreases the drop volume and accordingly increases the concentration of all the components. In the presence of a volatile species, such as isopropanol, in the crystallizing agent, diffusion proceeds in two directions, from the reservoir to the drop, and in the opposite way, from the drop to reservoir, of water. Equilibrium is achieved after the saturated partial vapour pressures of evaporating components become equal in the drop and in the reservoir. In this case, the drop may decrease or increase in volume or remain the same.

The often used ratio between concentrations of the crystallizing agent in the reservoir and the drop is 2. This is obtained by mixing equal volumes of protein solution and the reservoir solution. It may be, for instance, a mixture of 2 μL of the reservoir and 2 μL of the protein solution in the hanging or sitting drop. If only water diffusion takes place in the absence of other volatile species, at equilibrium the final volume of the drop will be half the original volume. Accordingly, concentration of all components in the drop, protein, buffer, salt and precipitant double.

Nucleation and crystal growth in a drop are affected essentially by rate of equilibration. The rate depends on the difference between vapour pressures in the drop and reservoir, which in turn depends on the content of the crystallizing agent, temperature, and the size and shape of the drop. Significantly lower equilibration rates with polyethylene glycol rather than ammonium sulfate as a precipitant have been demonstrated. A decrease of equilibrium rate with increase in drop size and with decrease of temperature has also been revealed. The time for $\sim 90\%$ equilibration varies from a day to about one month.

In the hanging-drop technique, crystals are basically created at the bottom of the drop, near the surface. This may be caused by forming a layer of supersaturated protein solution near the surface during evaporation of water. The subsequent distribution of protein concentration over the whole drop is diffusion limited.

The contribution of convection is small, since the supersaturated layer is of higher density and located at the bottom of the drop. Such inhomogeneity applies to nucleation as much as to crystal growth.

In the sitting-drop, distribution of protein concentration is different. Evaporation forms initially a layer of higher concentration near the surface at the top. This excessive concentration is then distributed quickly over the drop by convection. Accordingly, nucleation and the start of crystal growth occur practically at the same protein supersaturation. This is a disadvantage in comparison with the hanging-drop

technique, since crystals grow at higher supersaturation. From another point of view, however, the sitting-drop method is energetically more favourable and heterogeneous nucleation on various substrates, including minerals can take place.

For screening and optimization tests, multichamber plates are utilized, containing many wells of the type shown in Figure 1. Plastic Linbro boxes, normally used for tissue culture, are convenient for hanging-drop tests. Each such box contains 24 wells. To prepare tests, about 0.7–1.0 mL of crystallizing agent is put in each reservoir. A drop comprising a mixture of protein solution and reservoir solution is placed on the glass coverslip. Then, the coverslip with the drop is gently turned over and set on the vessel rim covered with a thin layer of grease. In a similar way, the sitting-drop tests are prepared, with the difference that the drop is placed on an inverted glass pot (Figure 1).

Method for Crystal Growth in a Capillary

A vapour diffusion method for growing crystals inside capillary tubes, invented by M. Y. Gamarnik and U. R. Alvarado, is illustrated in Figure 2. The crystallizing unit comprises a capillary tube containing a column made up of three layers. The first layer is a protein solution to be crystallized, which may contain a buffer, salt, precipitant and other additives. The second layer is an absorbent, which is typically a liquid, such as glycerol or a highly concentrated salt solution. In the preparation of the crystallizing unit, the protein solution and absorbent are placed in the capillary tube so that they are segmented by an air section. The ends of the capillary tube are sealed by end-caps. The liquids are placed sequentially in the capillary tube by a syringe. The lengths of the protein solution, absorbent and air layer segments are selected by experimenter, but the usual lengths are from 2 to 20 mm.

The internal diameter of the capillary tube is selected so that the capillary forces, acting on the liquids, held within the sealed tube, are sufficient to prevent direct contact between the liquids during handling or transportation. The internal diameter is usually less than 3 mm, but for crystallization tests from about 1–10 μL of protein solution the diameter should be about 0.6–1.5 mm.

The vapour of the solvent, which is normally water, diffuses from the protein solution through the air layer to the absorbent because of the difference in the water vapour pressures in the protein solution and absorbent. Evaporation of water from crystallizing solution results in an increase of concentration of protein and other components – buffer, salt and

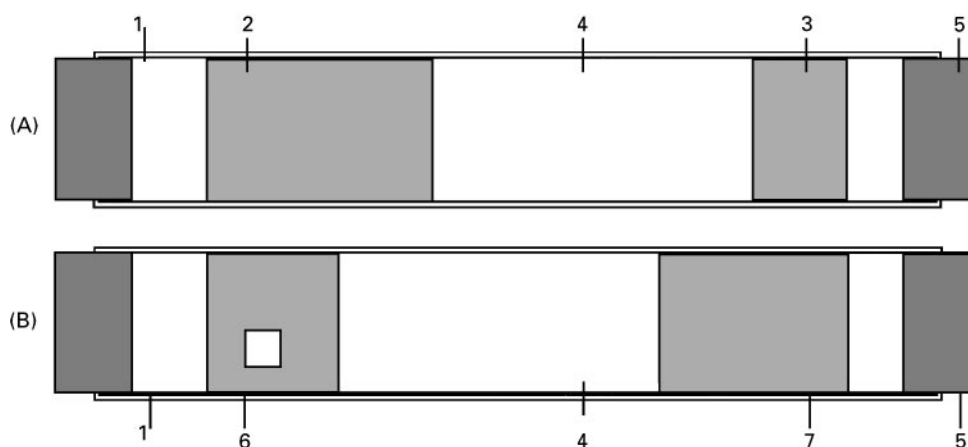


Figure 2 Schematic presentation of vapour diffusion method for crystal growth inside a capillary tube. (A) Initial configuration, (B) final configuration. (1) Capillary tube, (2) protein solution, (3) absorbent, (4) air layer, (5) end-caps, (6) protein solution with grown crystal, (7) absorbent containing absorbed water.

precipitant – which were initially present. Nucleation and growth of a protein crystal occur within the crystallizing solution after it reaches the appropriate supersaturation.

During the vapour transport, the length of the air layer remains approximately constant but shifts toward the crystallizing solution. The length of the protein solution layer decreases. Accordingly, the length of the absorbent, containing absorbed water, increases (Figure 2B). At any time during crystal growth, it is possible to calculate the concentration of protein and other additives in the protein solution by the relative change of its length.

A desired rate profile of water evaporation can be set by appropriate choice of concentration and volume of the protein solution and absorbent, the length of the air layer and the temperature. Often it is desirable to set a relatively rapid rate of evaporation during the initial phase of the growth process leading to nucleation, followed by a lower rate of evaporation during the crystal growth process. To accomplish this profile, the air layer length should be small, about 3–5 mm, and the absorbent layer length should be also small, in comparison with the length of protein solution layer. The short air layer establishes a relatively fast dewatering followed by a rapid increase of concentration of protein solution, while the small volume of absorbent allows a relatively rapid decrease in the rate of evaporation after the initial phase of evaporation, due to dilution of the absorbent by the absorbed water. This profile, initiating nucleation with subsequent slow crystal growth, usually yields a single crystal or a few crystals in each portion of the protein solution. This is beneficial since the dissolved protein feeds only one or a few crystals during the growth, resulting in their larger size.

Liquid–Liquid Diffusion Techniques

Interface diffusion In the interface-diffusion method for protein crystal growth two liquids – a protein solution and a solution of the crystallizing agent – make contact and are separated at an interface. Equilibration is achieved by diffusion of the crystallizing agent and protein across the liquid–liquid interface. Diffusion leads to a slow increase in the concentration of the crystallizing agent in the protein solution near the interface. Nucleation occurs in the interface region after sufficient supersaturation. Subsequent slow crystal growth is provided by the relatively small interface region of the higher protein supersaturation.

A basic difficulty in this technique is bringing the liquids into contact without convection, i.e. without rapid mixing. Convection may be reduced if the less dense solution is gently placed on the more dense solution. Crystallization experiments conducted under microgravity conditions in space avoided convection during solution contact when the interface-diffusion technique was used.

To use only a small amount of protein solution, about 2–20 μL , the liquids may be brought into contact in a capillary tube of diameter in the range ~ 1 –2 mm.

Dialysis In the dialysis technique, the protein solution and crystallizing-agent solution are separated by means of a molecular membrane. Both solutions are in contact with the membrane, which allows diffusion of small molecules, but prevents macromolecules passing. The maximum molecular weight of molecules able to diffuse through the membrane pores is determined by the molecular weight cutoff (MWCO).

The MWCO of contemporary dialysis membranes is in the range from 100 to 300 000 Da.

During equilibration, molecules of buffer, salt, precipitant or water may diffuse through the membrane from the crystallizing agent to the protein solution and also in the opposite direction, resulting in crystallization. For micro-quantities of protein solution, capillaries of small internal diameters, about 1–2 mm are used. The protein solution is placed in a capillary, the end of which is capped by the membrane. The membrane end of the capillary is then put into an appropriate agent solution for crystallization.

Batch technique Microbatch techniques include crystallization under oil, with droplets of about 1–10 μL of crystallizing solution. It was demonstrated that application of paraffin and silicone oils affect the rate of equilibrium, resulting in a better quality of crystals. A containerless method has been developed, where the crystallizing solution drop is suspended between two oil layers of different density, preventing the undesirable contact of the protein solution with walls of a vessel.

A drawback of the batch method is that, typically, many nuclei are formed resulting in the growth of many crystals, and it takes much effort to find the conditions for growing just one or a few crystals in a single batch.

Gel Method

In the gel method, crystallization in a gel results in the protein solution being trapped by a loose network which is stretched over the whole volume of the solution. The gel comprises macropores, of about 100 nm in size, filled with the crystallizing solution. The macropores are interconnected, by a dense system of micropores, of about 10 nm in size.

Entrapping of the crystallizing solution by the gel network prevents natural convection and sedimentation. Accordingly, equilibration between the protein solution and the crystallizing agent is mediated by diffusion only, through the gel pores. This results in slow crystal growth, improving the quality of the produced crystals if no gel structure is incorporated in the crystal lattice, as is often the case. Various crystal growth techniques can be used with a gel, such as hanging-drop technique, liquid–liquid diffusion and dialysis. Silica gel and agarose gel are most often used for protein crystallization.

Crystallization in Microgravity

Protein crystal growth has been studied under microgravity conditions conducted in space (satellites and

space shuttles). Space-grown crystals are frequently of better quality than the same protein crystals grown on the earth. Under microgravity conditions, convection and sedimentation are suppressed. Accordingly, transport of molecules, supersaturating the protein solution, is mediated by diffusion only, providing slow crystal growth. Typically, crystals are suspended and grow freely in different crystallographic directions, forming a well-ordered structure and equilibrium shape.

Various methods have been used for crystal growth experiments in space, including interface-diffusion, dialysis and vapour diffusion. Most methods have a device or a means to connect or disconnect interaction between the protein solution and crystallizing agent so that mixing only takes place under zero gravity. Typically, two wells, one of which is filled with protein solution and a second one filled with crystallizing agent, are brought into contact in orbit through a connecting valve or by a relative movement of the wells.

Concluding Remarks

Experiments, directed at crystallization of proteins require an understanding of the main principles of nucleation and growth and need much testing. Some tests are associated with a decrease in critical supersaturation, necessary for nucleation, through selection of appropriate buffers, salts and precipitants or by exploration of substrates for heterogeneous nucleation. Other methods follow the development and use of crystallization cells, consuming small amounts of protein solution, through decreasing the internal diameter of capillaries (in the capillary method) or the size of droplets in microbatch and hanging-drop experiments.

Small volume crystallization cells will be adapted for microgravity experiments to reduce space requirements on satellites and shuttles, accordingly reducing their cost. This may be realized by modification of the capillary technique, shown in Figure 2. For instance, two air layers may be used instead of one, separated from each other by a water barrier layer. The water barrier layer delays absorption of the vapour from the protein solution until the barrier layer is eliminated by absorption into the absorbent. The necessary delay is typically one or two days, from preparation of the tests until the spacecraft carrying the crystal growth device has attained microgravity conditions.

Development of crystallization methods at lower critical supersaturation seems to be supported by a broadening of our knowledge of the main principles governing nucleation and growth of macromolecular crystals.

See also: II/Crystallization: Additives; Molecular Design; Control of Crystallizers and Dynamic Behaviour; Polymorphism. III/Supercritical Fluid Crystallization.

Further Reading

- Chernov AA (1984) *Modern Crystallography. III. Crystal Growth*. Berlin: Springer-Verlag.
- Darby NJ (1993) *Protein Structure*. Oxford: IRL Press, Oxford University Press.
- Ducruix A and Giedge R (1992) Methods of crystallization. In: Ducruix A and Giedge R (eds) *Crystallization of Nucleic Acids and Proteins. A Practical Approach*. Oxford: IRL Press, Oxford University Press.
- Fehér G and Kam Z (1985) Nucleation and growth of protein crystals: general principles and assays. *Methods in Enzymology* 114: 77–111.
- Lorber B and Giedge R (1992) Preparation and handling of biological macromolecules for crystallization. In: Ducruix A and Giedge R (eds) *Crystallization of Nucleic Acids and Proteins. A Practical Approach*. Oxford: IRL Press, Oxford University Press.
- McPherson A (1982) *Preparation and Analysis of Protein Crystals*. New York: John Wiley.
- McPherson A (1991) A brief history of protein crystal growth. *Journal of Crystal Growth* 110: 1–10.
- McPherson A (1997) Recent advances in the microgravity crystallization of biological macromolecules. *Trends in Biotechnology* 15: 197–200.
- Robert MC, Provost K and Lefaucheur F (1992) Crystallization in gels and related methods. In: Ducruix A and Giedge R (eds) *Crystallization of Nucleic Acids and Proteins. A Practical Approach*. Oxford: IRL Press, Oxford University Press.
- Rosenberger F, Vekilov PG, Muschol M and Thomas BR (1996) Nucleation and crystallization of globular proteins – what we know and what is missing. *Journal of Crystal Growth* 168: 1–27.
- Scopes RK (1987) *Protein Purification. Principle and Practice*. New York: Springer-Verlag.

Electrophoresis

M. J. Schmerr, National Animal Disease Center, Ames, IA, USA

Copyright © 2000 Academic Press

Transmissible spongiform encephalopathies are neurodegenerative diseases found in both humans and animals. The oldest known member of this family of diseases is scrapie in sheep and goats and the most infamous member is bovine spongiform encephalopathy or 'mad cow disease'. These diseases are fatal for the individuals who become infected. As a result, there is a considerable amount of interest in developing methods to detect early infection. This would enable removal of animals from food chains and by-products used for cosmetic and health care. For humans, an early diagnosis may make it possible to treat infected individuals with drugs to arrest the course of the disease.

A feature of these diseases is the accumulation of rod-shaped fibrils in the brain that form from an aggregated protein. This abnormal protein is a protease-resistant form of a normal host cell glycoprotein (prion protein). When the aggregated protein is denatured in sodium dodecyl sulphate (SDS) and β -mercaptoethanol, a monomer form of $M_r \sim 27$ kDa is observed. This abnormal prion protein is used as a marker for infection with a transmissible spongiform encephalopathy.

The abnormal prion protein is insoluble in most biological buffers, whereas the normal prion protein is soluble. In natural infections, the abnormal prion protein is found in very low concentrations. It is found in higher amounts in rodent-adapted strains of the disease. These properties of insolubility and low concentrations present quite a challenge for the development of analytical methods to detect this protein.

Most of the methods used to detect the prion protein are based on histological techniques and are used postmortem. Immunoassays can be used to measure the prion protein. Most of the antibodies that have been produced to the abnormal prion protein have been made to the denatured form. Removing these denaturants is a major problem in the development of immunoassays. Western blot can be used to detect the prion protein but cannot be easily automated. Some new approaches using chemiluminescence and time-resolved fluorescence in plate assays have been developed. The amount of prion protein detected by these assays is in the range of picomoles or > 500 fmol. To improve sensitivity, we have approached this problem using capillary electrophoresis with laser-induced fluorescence. Fluorescent-labelled peptides from immunogenic epitopes of the prion protein can be detected in the attomole range using this technique. A competition immunoassay using fluorescein-labelled peptides was developed which is

able to detect the abnormal prion protein in the low picogram range; this method can quantitate the amount of prion protein. This assay was based on the separation of the free peptide from the immunocomplexed peptide. Unlike most immunoassays which measure only the antibody-bound ligand, both the free and the bound peptide can be measured.

Method Development

Preparation of Tissues

Scrapie-infected tissues including brain, lymph node and buffy coats were obtained from sheep confirmed positive for abnormal prion protein by Western blot. Normal tissues were obtained from sheep from a scrapie-free flock and were confirmed negative by the above tests. Briefly, the tissues were weighed, and ground to a fine powder in liquid nitrogen. Buffy coats were prepared from blood and placed in 2 mL of 20 mmol L⁻¹ phosphate pH 7.0, 0.15 mol L⁻¹ NaCl, and frozen at -70°C until they were processed as the tissues. After grinding, the tissues were placed in 20 mmol L⁻¹ Tris pH 7.4, 0.15 mol L⁻¹ NaCl, 0.005 mol L⁻¹ MgCl₂ (10% w/v) and incubated at 37°C for 1 h in 50 µg mL⁻¹ DNase. After incubation with DNase the tissue homogenates were treated with proteinase K (50 µg mL⁻¹) for 1 h at 37°C and held overnight at 4°C. Sodium *N*-lauroyl-sarcosine was added to the homogenate to make the solution 10% in the detergent. The homogenate was incubated for 1 h at 37°C and then was centrifuged at 10 000 g for 20 min to remove particulates. The resultant supernatant fluid was centrifuged at 230 000 g for 1 h. The pellet was resuspended in 10 mmol L⁻¹ Tris pH 7.4 (250 µL g⁻¹ of the initial brain sample). The sample was solubilized in 0.01 mmol L⁻¹ Tris HCl, pH 8 containing 2 mmol L⁻¹ ethylenediamine-tetraacetic acid 5% SDS and 10% hexafluoro-2-propanol at 100°C for 10 min.

Chromatography

To remove the SDS, the sample was applied to a poly-HYDROXYETHYL A (PolyLC, Inc., Columbia, MD, USA) high performance liquid chromatography column (200 × 4.6 mm) in 95% acetonitrile, 5% water containing 0.1% trifluoroacetic acid and 50 mmol L⁻¹ hexafluoro-2-propanol (buffer A). The flow rate was 0.5 mL min⁻¹. The conditions for eluting abnormal prion protein were buffer A for 8 min and then a linear gradient to 100% water containing 0.1% trifluoroacetic acid and 50 mmol L⁻¹ hexafluoro-2-propanol (buffer B) in 15 min, 100% buffer B for 10 min. Peak fractions were collected and dried in a vacuum centrifuge. Fractions were resuspended

in 10 µL of dH₂O and tested for abnormal prion protein in the capillary electrophoresis assay.

Peptide Synthesis and Antibody Preparation

Four peptides from the prion protein were synthesized. The peptide sequences were CGQGGGTHNQWNKPSL (spanning amino acid positions 89–103), CNDWED-RYYRENMYR (142–154), (CRYPNQVYYRPVDRYSNQNNFVHD (155–177) and RESQAYYQRGASVIL (218–232) (Multiple Peptide Systems, San Diego, CA, USA). The peptides were labelled with fluorescein through a γ -butyric acid linkage on the N-terminus during synthesis. The peptide 218–232 is used here as a representative sample.

Rabbits were immunized with each peptide and specific antibodies were produced for each peptide. These antisera reacted with scrapie-infected brain but not with normal brain on Western blot analysis. Rabbit IgG was prepared by passing each antiserum over an affinity column. Briefly, 10 mg of a peptide was coupled to agarose resin modified with an *N*-hydroxyl succinimide ester in 1.0 mL dimethyl formamide at room temperature for 20 min. After coupling, the resin was washed with 5 mL of 0.1 mol L⁻¹ 3-(*N*-morpholino)propanesulfonic acid (MOPS) pH 7.5 (column wash buffer). Unreacted ester groups were deactivated with 0.1 mol L⁻¹ *N*-(2-hydroxyethyl)piperazine-*N'*-(4-butanedisulfonic acid) (HEPES) pH 8.0 and 0.1 mol L⁻¹ NH₄Cl for 15 min. Before antibodies were applied to the peptide column they were purified using protein G chromatography. After diluting 1 : 2 in column wash buffer, the antibodies were then applied to the affinity column and recycled over the column for several cycles. The column was washed with column wash buffer and the antibodies eluted with 0.1 mol L⁻¹ NaH₂PO₄, pH 2.5 into tubes containing 50 µL of 1 mol L⁻¹ HEPES, pH 8.5. The absorbance was measured at 280 nm. Fractions with absorption at 280 nm were pooled, aliquoted and frozen at -20°C.

Immunocomplex Formation

Fifteen microlitres containing ~0.2–20 pmol of the fluorescent-labelled peptide were mixed with varying amounts (0.5–5 µg) of purified rabbit IgG to determine the antibody concentration that forms ~50% of the total immune complex formation. The final volume of the sample was adjusted to 20 µL with capillary running buffer. After mixing the components, the samples were incubated at 25°C for ~10 min and at 4°C overnight. The height of the immune complex peak was measured and replicate samples of the peaks varied less than 1%. Slight changes in the antibody reactivity, temperature and

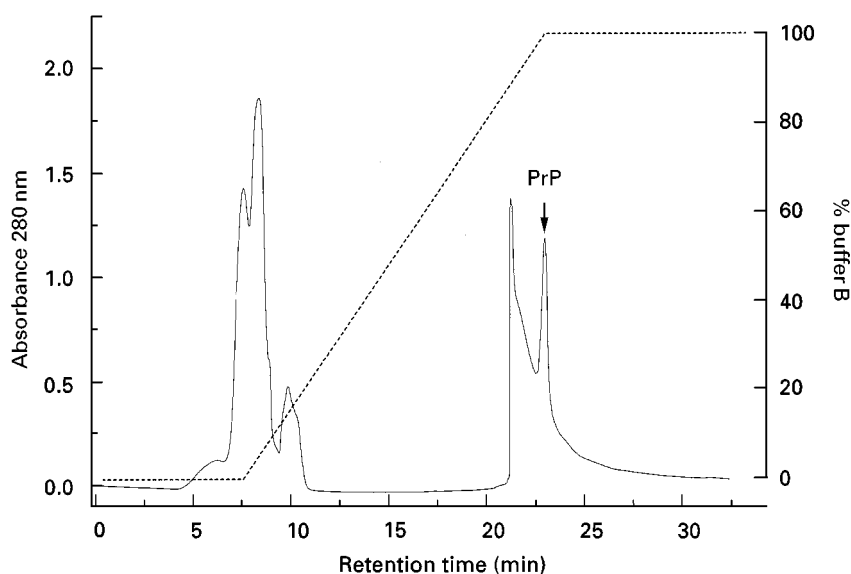


Figure 1 A chromatogram showing hydrophilic interaction chromatography on poly-HYDROXETHYL A. The peak that was positive for abnormal prion protein (PrP) is indicated. The gradient conditions for running the column are shown by the dashed line.

preparation of the running buffer caused small variations in the height of the immunocomplex peak from day to day. Known concentrations of unlabelled peptides corresponding to the fluorescent-labelled peptides were used to generate standard curves.

Free Zone Capillary Electrophoresis

Free zone capillary electrophoresis was performed on a Beckman P/ACE 5500 controlled by P/ACE Station software. Laser-induced fluorescence detection was

done using an air-cooled argon laser with excitation at 488 nm and emission at 520 nm. An unmodified capillary 20 cm (length to the detector) \times 20 μ m i.d., total length 27 cm capillary was used with a 200 mmol L⁻¹ Tricine buffer that was adjusted to pH 8.0 by 6 mol L⁻¹ NaOH. This buffer was selected after studying the effect of higher pHs and other concentrations of the buffer on the separation, immunocomplex formation and fluorescence. To prevent the abnormal prion protein from adhering to the

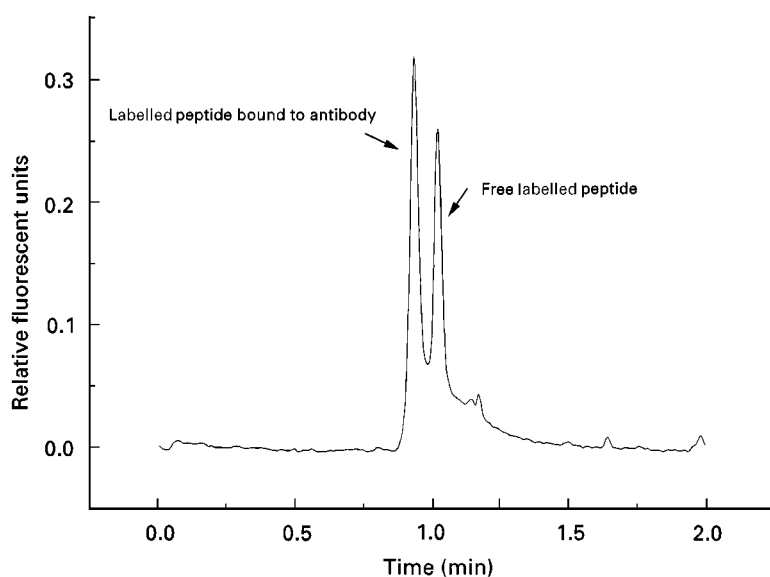


Figure 2 An electropherogram showing the immunocomplex peak for the fluorescein-labelled peptide 218-232 and the free peptide peak.

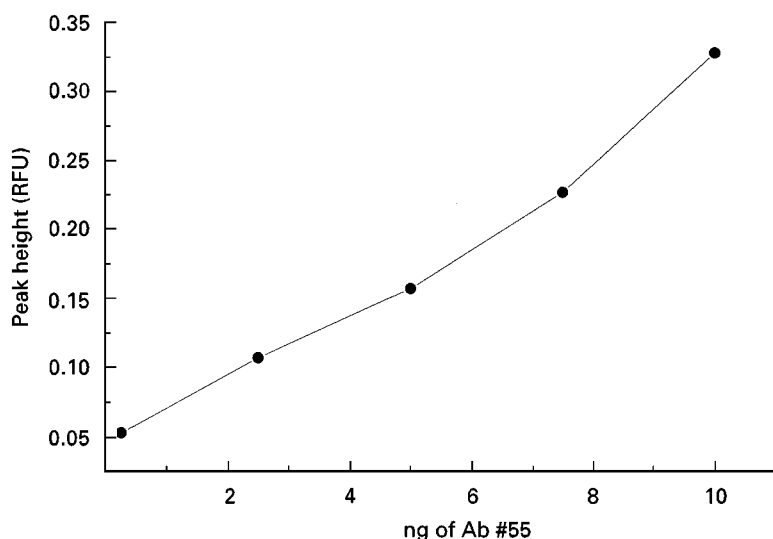


Figure 3 A plot of the peak height of the immunocomplex peak versus the amount of antibody added to the assay.

capillary walls, 0.1% *n*-octylglucoside (Boehringer Mannheim, Indianapolis, IN, USA) and 0.1% bovine serum albumin (Sigma Chemical Co., St. Louis, MO, USA) were added to the buffer. In preparation for separation, the capillary was rinsed for 1 min with 0.25 mol L⁻¹ NaOH, rinsed for 2 min with water and then rinsed for 2 min with buffer. The separating conditions were 30 kV for 3 min at 20°C with a current of ~20 μ A. The sample was injected for 15 s followed by a 5 s injection of running buffer. The sample volume was ~0.95 nL. Rinses were carried out under high pressure and sample injection carried out under low pressure.

Results

Hydrophilic Interaction Chromatography

Figure 1 shows a chromatogram of the results of hydrophilic interaction chromatography. This chromatography removes the SDS and other interfering compound so that the reproducibility of the assay is improved.

Capillary Electrophoresis Immunoassay

By the addition of fluorescein at the amino terminal during synthesis, the sensitivity of this assay is enhanced 100-fold relative to the chemical addition of

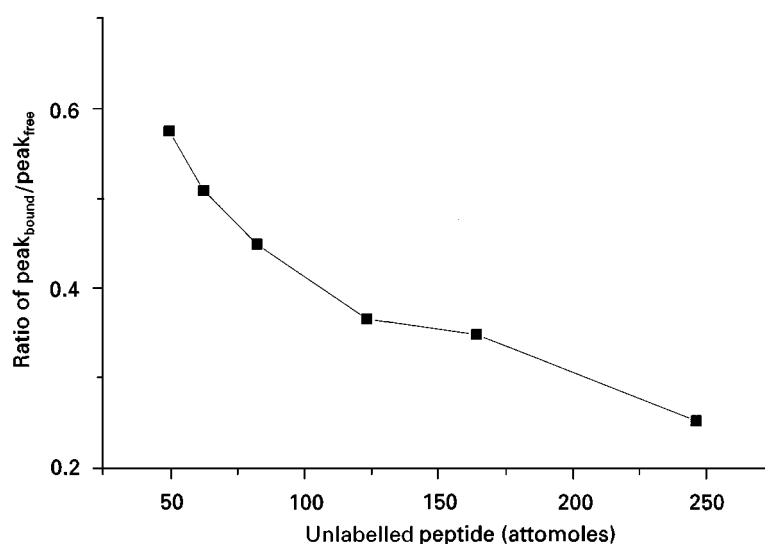


Figure 4 Plot of the ratio of the height of the immunocomplex peak/height of the free peptide peak versus the amount of unlabelled peptide added to the assay.

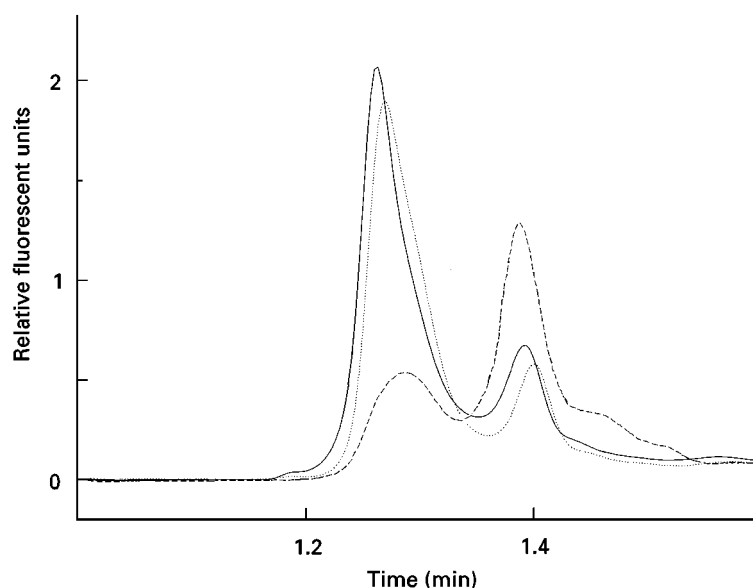


Figure 5 Representative electropherograms of antibody control (continuous line), normal brain sample (dotted line) and scrapie-infected brain sample (dashed line).

fluorescein after synthesis of the peptide. An electropherogram showing the peptide and the immunocomplex peak when antibody is added to the assay is shown in **Figure 2**. A titration curve of antibody amount versus the height of the immunocomplex peak is shown in **Figure 3**. The amount of antibody that binds ~50% of the fluorescein-labelled peptide was chosen as the amount to be used in the competition assays of the abnormal prion protein with the labelled peptide for binding sites on the specific antibody. Competition is determined by measuring the ratio of

the height of the immunocomplex peak and of the free peptide peak. A standard curve was determined by adding known amounts of unlabelled peptide into the assay. This curve is shown in **Figure 4**. Electropherograms representing the immunocomplex peak, a preparation from a normal sheep and a preparation from a scrapie-infected sheep are shown in **Figure 5** (peptide 218–232). An electropherogram representing a sample from a lymph node of an infected sheep is shown in **Figure 6**. **Figure 7** depicts three electropherograms showing the antibody control,

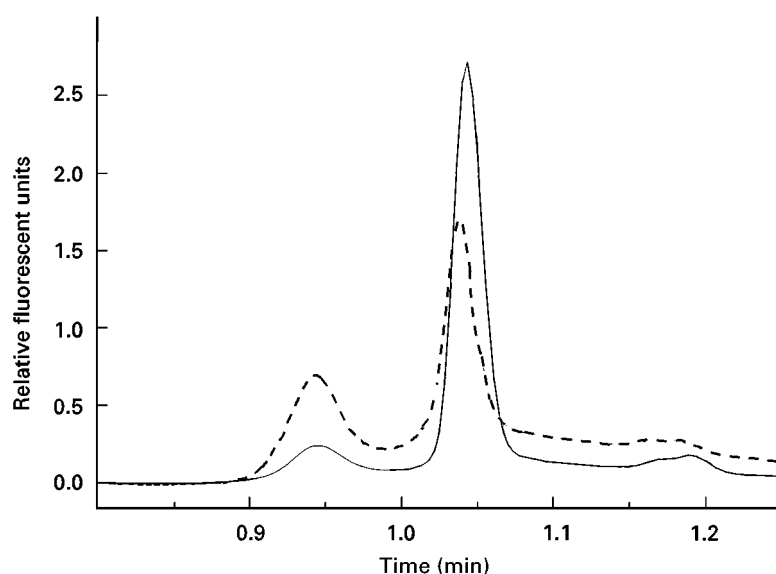


Figure 6 Representative electropherograms of antibody control (dashed line) and a sample from an infected lymph node (continuous line).

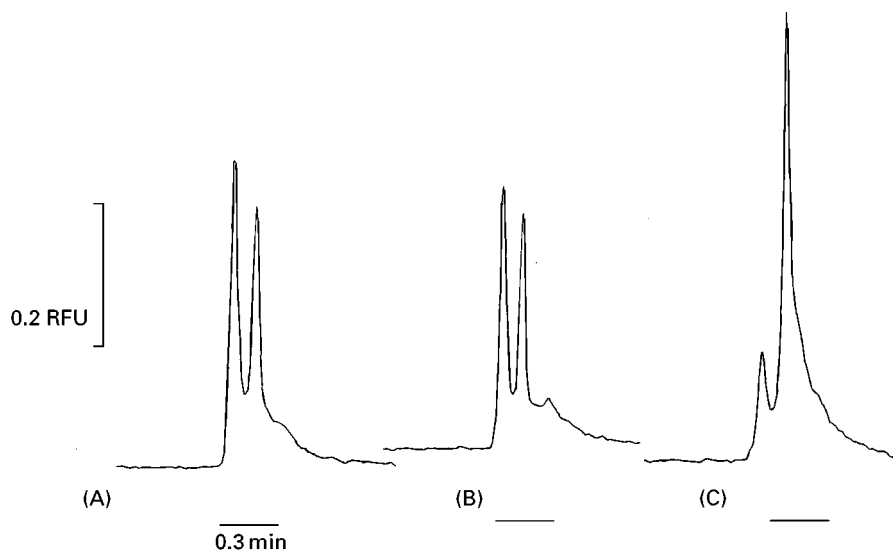


Figure 7 Representative electropherograms of (A) antibody control; (B) buffy coat from a scrapie-negative sheep; (C) buffy coat from a scrapie-positive sheep.

samples extracted from buffy coats of a normal sheep and from a buffy coat of a scrapie-infected sheep.

Concluding Remarks

The capillary electrophoresis assay described in this study is reproducible, more sensitive and faster than other analytical tests. The samples used in the capillary electrophoresis assay were obtained from brain and the lymphoid system of the animals. The sensitivity of this assay made it possible to test samples from other tissues that contain much less abnormal prion protein than brain samples. This assay has the potential to use tissues and fluids from live animals and diagnose animals prior to the onset of clinical signs of disease. Automation of this test could lead to more economical and efficient methods for testing for abnormal prion protein.

Further Reading

Altria KD (ed.) (1996) *Capillary Electrophoresis Guidebook: Principles, Operation and Applications*. Totowa, New Jersey: Humana Press.

Landers JP (ed.) (1997) *Handbook of Capillary Electrophoresis*, 2nd ed. London: CRC Press.

Prusiner SB (ed.) (1996) Prions, Prions, Prions. *Current Top. Microbiol. Immunol.* vol. 207. Berlin: Springer.

Prusiner SB (1996) Prion biology and diseases—laughing cannibals, mad cows, and scientific heresy. *Medical Research Review* 16: 487–505.

Prusiner SB (1997) Prion diseases and the BSE crisis. *Science* 278: 245–251.

Schmerr MJ and Jenny AL (1998) A diagnostic test for scrapie-infected sheep using a capillary electrophoresis immunoassay with fluorescent-labelled peptides, *Electrophoresis* 19: 409–414.

Schmerr MJ *et al.* (1999) Use of capillary electrophoresis and fluorescent labeled peptides to detect the abnormal prion protein in the blood of animals that are infected with a transmissible spongiform encephalopathy. *Journal of Chromatography A* 853: 207–214.

Weissmann C (1996) The ninth Datta lecture. Molecular biology of transmissible spongiform encephalopathies. *FEBS Letters* 289: 3–11.

Field Flow Fractionation

R. Hecker and H. Cölfen, Max-Planck-Institut für Kolloid und Grenzflächenforschung (Kolloidchemie), Am Mühlenberg, Golm, Germany

Copyright © 2000 Academic Press

Introduction

This review focuses on the use of field-flow fractionation (FFF) for the characterization of proteins and protein assemblies such as protein aggregates, DNA

and viruses. FFF is based on the differential transport rates of solutes in a ribbon-like channel when interacting with an applied field. The type of field may be chosen from a wide range, for example an electrical potential, sedimentation, a hydrodynamic cross-flow, a thermal gradient and so forth. A schematic of this is shown in **Figure 1**. The solute will therefore occupy a region above the sample wall, with a mean position determined by the balance between the solute's diffusion and the sample-applied field interaction. Although there exist further complications for solutes greater than $\sim 0.5 \mu\text{m}$ diameter, they are not relevant given the small hydrodynamic diameter of proteins. Positioned at the outlet of the channel is a sample detector of some sort, typically a traditional high-performance liquid chromatography (HPLC) spectrophotometric detector, although a significant development has been with the application of a number of detectors providing complementary information about the sample. Such detectors include spectrophotometric and refractive index types, and more recently light scattering for molecular mass, electrospray-mass spectrometry, and inductively coupled plasma, although the last two have not yet been applied to protein studies.

There are a number of advantages offered by the FFF methods over other contemporary protein analysis methods. FFF is often more rapid than analytical

ultracentrifugation, and the range of fields available provide FFF with greater versatility. In comparison with gel-permeation chromatography, FFF is not impeded by a size exclusion limit, the low exposed surface area limits sample loss through adsorption on to the exposed surface, and the availability of field programming allows a wide range of materials to be analysed in a single channel. The open channel geometry usually allows FFF to characterize samples without need for pretreatment, such as filtration, and provides a very high upper limit to the protein size range. Similarly, the open channel allows the theoretical basis of FFF to provide direct access to fundamental physical constants of proteins, often without the need for calibration. Finally, both FFF and gel electrophoresis may separate a protein mixture, but sample collection is simpler in FFF.

Flow FFF

The 'universal' nature of (cross)-flow FFF (Fl-FFF) has led to its wide use for protein characterization. The free choice of carrier liquid, whether a buffer or a simulated native environment, avoids denaturing the protein. Flow FFF has two configurations, the original symmetric form and the newer asymmetric method, differing only how the field is generated in the fractionation cell and sample-loading protocols.

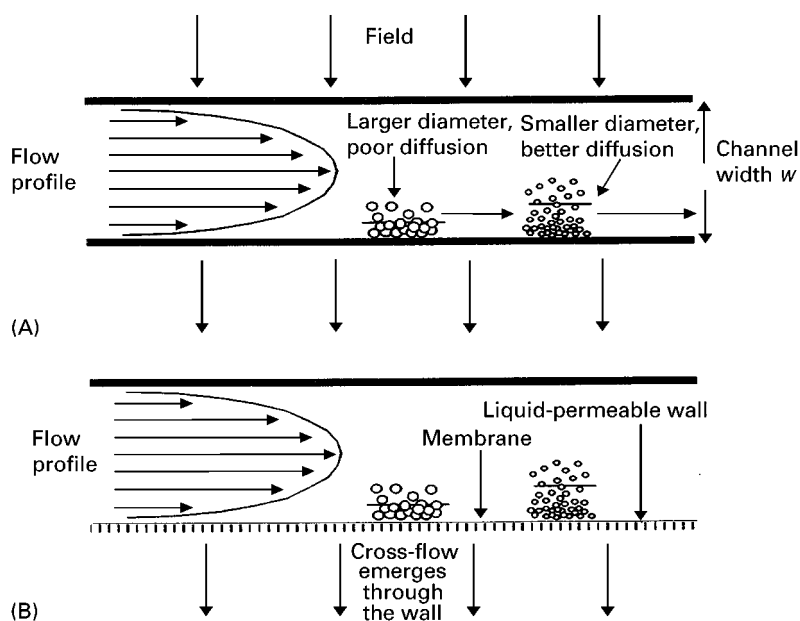


Figure 1 (A) Schematic of the mechanism of FFF separation of proteins. The smaller protein, with greater diffusivity, competes more successfully with the applied field and occupies a mean position further from the accumulation wall. Samples occupying the higher mean position is subject to more rapid flow laminae, and elutes earlier. The particle sizes represented, the channel thickness and the extent of back-diffusion are not to scale. (B) For the subtechnique flow FFF, the accumulation wall is a liquid-permeable porous material, typically ceramic. A membrane exists over the accumulation wall to prevent the samples from leaving the cell through this wall. The upper wall may or may not be porous as well, depending whether the symmetrical or asymmetrical variant is used.

Table 1 Compilation of flow FFF physicochemical data relevant for selected common proteins and with comparison to commercial polystyrene latexes

Sample	Molecular mass (Da)	Diffusion coefficient ($\times 10^{11} \text{ m}^2 \text{ s}^{-1}$, $\times 10^7 \text{ cm}^2 \text{ s}^{-1}$)
Cytochrome c (bovine heart)	13 400	11.4
Ovalbumin (chicken egg)	45 000	8.71
Bovine serum albumin	64 000	6.89
Catalase (horse liver)	221 000	4.30
Apo ferritin	450 000	3.84
Urease	483 000	3.46
Ferritin	622 000	2.91
Tobacco mosaic virus	$\approx 40\,000\,000$	0.46
Polystyrene latex, \varnothing 0.090 μm		0.45
Polystyrene latex, \varnothing 0.311 μm		0.22

In both cases, the separation is a direct function of the diffusion coefficient, where the most highly diffusive components are the least retained. A compilation of common biological samples and their diffusion coefficients are provided in **Table 1**.

FI-FFF is capable of separating proteins with only a 15% size difference within 3–10 min. Reported results for animal proteins and biopolymers include albumins (human and bovine serum, egg), globulins (γ -globulin, haemoglobin, thyroglobulin), ferritin, apoferritin, lysozyme, casein, blood products (human and rat blood plasmas, lipoproteins) and nucleic acids. Proteins from an industrial perspective are represented by a growing body of work emerging on the characterization of proteins from flours used for bread-making purposes.

In all of the above cases, no sample treatment is needed prior to injection, such as exhaustive dialysis or filtration. This is to be expected, as the permeable membrane acts as a dialysis cell, and the open channel will not become clogged and require a filter. Since the sample is not manipulated beforehand, the presence of aggregate structures remains unaltered. **Figure 2** shows baseline resolution of a biological mixture. Protein dimers elute as satellite peaks at ~ 1.4 retention times of the monomer, followed similarly by the higher aggregates eluting later. Most significantly, the entire separation takes place in only four minutes.

The asymmetric flow FFF variant does not inject the sample directly into the inlet line. Rather, a sample pump introduces the sample into the cell and opposing flows from both ends of the cell hydrodynamically focus the sample into a narrow band across the channel before elution. This allows for remarkably well-resolved and efficient protein separations. **Figure 3** illustrates the sensitivity of the technique. Two plasmid fragments were injected at low concentration ($0.1 \mu\text{g } \mu\text{L}^{-1}$) and volume ($1 \mu\text{L}$) while exhibiting both baseline resolution and elution in less

than 15 min. One further advantage of the focusing method is the immobilization of the sample prior to elution. For a very dilute sample, multiple injections subject to these opposing flows produce an on-channel concentrating effect, where the protein is retained on the membrane at the focus point.

During any form of chromatography, sample dilution is inevitable. For small quantities of proteins this may challenge the limits of the detectors used. FFF offers an advantage over other methods through the ability to skim off the atmosphere of carrier liquid and greatly reduce sample dilution before detection. Sample enhancement was first mentioned in the literature in the early 1990s and now enjoys routine use in

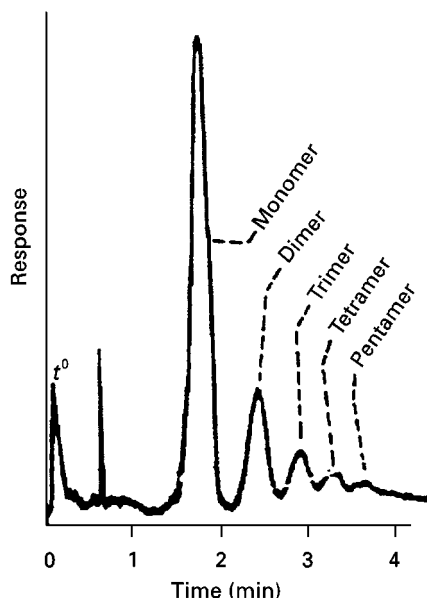


Figure 2 Separation of a monoclonal antibody from its higher clusters showing separable peaks up to pentamer aggregation. (Reproduced with permission from Giddings (1993) *Science* 260: 1456, Copyright the American Association for the Advancement of Science.)

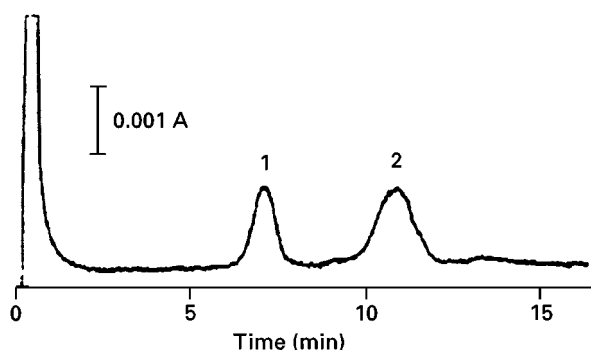


Figure 3 Separation of (1) 2390 bp and (2) 4320 bp plasmids by asymmetrical FFF. (Reproduced with permission from Litzén A and Wahlund KG (1989) *Journal of Chromatography* 476: 413 Copyright Elsevier Science BV.)

contemporary practice. Both symmetrical and asymmetrical variants have been successfully applied to proteins. Of special interest is the frit inlet–frit outlet modification. These methods in tandem enhance detectability and aid fractionation stability. The combination of frit inlet and outlet has been reported as recently as 1999, for the automation of wheat protein fractionation.

One rarely discussed drawback to the FI-FFF method is the requirement of a membrane for sample retention. For adhesive protein samples, this demands compatibility between the sample, membrane and the carrier solution. Biopolymers can strongly adsorb on to particular membranes and at modest ionic strengths may be completely adsorbed. The simplest method to test this is to inject samples over a range of concentrations and/or volumes and ensure there is

proportionality between detected signal size and the amount of sample. A partial, reversible adsorption leads to an increased retention and this would indicate that the sample is erroneously large, or induce a number of fractionation profile artefacts. Clearly the chemistry of the system, between the sample, membrane and carrier, must be known before any statements may be made.

The membrane's physical characteristics may also be significant. Firstly, membrane compressibility and protrusion into the channel reduce the channel thickness and elution is more rapid, although this is easily detected by measuring the channel void volume with an unretained probe. More subtle effects include surface roughness and membrane pore size, as demonstrated by **Figure 4**. Although the experimental arrangement, carrier sample chemistry and flow rates are the same for both experiments, the effect of the membrane is clear. The molecular mass of cytochrome c is only just greater than the membrane size cut-off (12 500 versus 10 000), and the delayed retention from the poor membrane may be attributed to a partial physical entrapment in the pores. For the poor membrane the pore size distribution may be particularly wide, leading to a greater proportion of the sample suffering excessive retention. The mean size and size distribution of the pores of the membrane are clearly an issue of importance. A simple solution is to choose a much finer membrane, for example a cut-off at 3000 or 5000 is appropriate for cytochrome c, but the pressure drop across the channel may be incompatible with high field flow rates needed for sufficient retention of small species. The

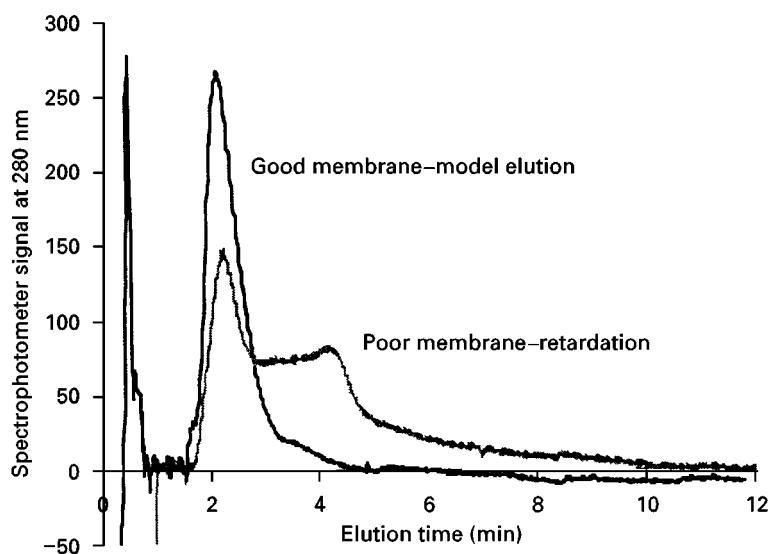


Figure 4 Superposition of two elution profiles for cytochrome c (0.82 mg mL^{-1} , $25 \text{ }\mu\text{L}$) in 0.05 mol L^{-1} 2-[N-morpholino]propanesulfonic acid ('mops') buffer at pH 6.2. The membranes are both regenerated cellulose, with cited 10 000 molecular weight nominal pore sizes from different suppliers. From Hecker, unpublished results.

presence of the membrane therefore determines the smallest-sized species capable of being retained in a FI-FFF channel.

Such membrane effects have been used to advantage, however. Proteins have been characterized with a separation based on both standard FFF principles and enhanced retention for some species by sample-membrane interactions. This offers a remarkably wide scope for characterizing systems with subtle differences in physical sizes but dissimilar chemistries, but assigning peaks in the fractionation profile calls for a number of pure standards and calibration processes.

Of particular interest to protein science is the observation and quantification of protein-ligand or protein-protein interactions. Such an example is provided in **Figure 5** for the interaction between immunoglobulin IgG and an interacting ligand, polyglutamic acid, with the conjugate peak showing a small amount of free ligand. Quantifying such an interaction to measure the binding constant is a more difficult task. It is necessary to be able to produce fractionation profiles of the components as a function of concentration, implying that sample loss on to the membrane must be prevented. Furthermore, at least two from the protein, ligand or complex peaks must be well separated for quantification if the stoichiometry is known prior to the experiment, otherwise all three must be resolved. This precludes

many simple systems, for example bovine serum albumin (BSA)/anti-BSA, or ovalbumin/concavalin A, where the hydrodynamic sizes of these species are too similar for reliable quantification.

The application for protein interaction studies is limited to processes in which the interaction time is insignificant compared to the transport time, effectively making protein studies with a kinetic barrier to interaction difficult. Further, the use of FFF to investigate sample-sample interactions has been criticized, in that during transport dilution will occur so equilibrium in the FFF channel will be different to that of the mixing conditions. These limitations are clearly not relevant for rapid, near-irreversible interactions.

The opportunity for the study of protein shape by FI-FFF is possible. Like other hydrodynamic methods, the information available from these methods renders them primarily as complementary methods to high resolution crystallography or magnetic resonance. Nevertheless, both theory and practice, discussed by Cölfen and Pauck, demonstrate that retention is a function of molecular shape (**Figure 6**), with the retention decreasing with the degree of asymmetry.

All these examples show that FI-FFF is a powerful technique for protein characterization, as it is both very rapid and requires only microgram or smaller amounts of sample. Future potential can be seen in the quantification of interactions between proteins. However, potential factors affecting the results and possibly producing artefacts, such as membrane-sample interaction or sample shape, must be considered when interpreting the results.

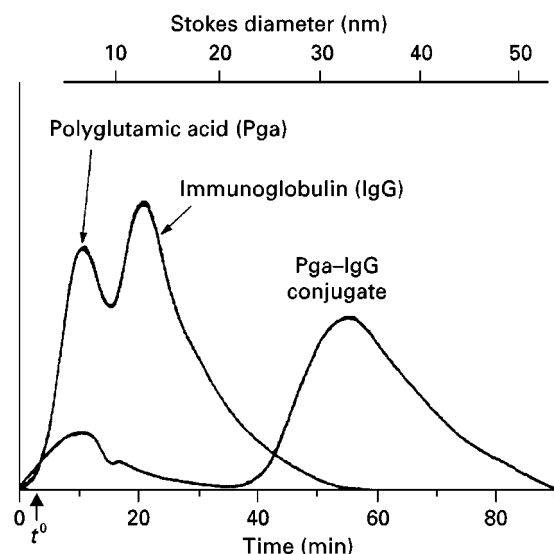


Figure 5 Elution profiles of the components of a protein-polymer ligand mixture, immunoglobulin IgG and polyglutamic acid, and their covalent conjugate. The fractionation of the conjugate suggests that a quantity of the polyglutamic acid remains unbound, and offers a method of determining the binding constants of such mixtures. (Reproduced with permission from Giddings JC *et al.* (1992) *Journal of Liquid Chromatography* 15: 1729 Copyright Marcel Dekker.)

Sedimentation FFF

The technique of sedimentation FFF balances the back-diffusion of the sample against sedimenting forces, a function of the sample's hydrodynamic diameter, density difference and the rotation rate applied. Sedimentation FFF offers significantly greater size-based sensitivity over FI-FFF, with a corresponding greater resolution. The method is also free of the complications arising from the membrane required by FI-FFF, although the possibility of electrostatic effects between the sample and cell cannot be ruled out. Unfortunately for protein applications, where the hydrodynamic diameters are of the order of a few nanometers and sample density is close to that of the buffering liquid, the rotation rate of the channel, and thereby the applied force field, must be high. None the less, successful application of the sedimentation FFF method to the characterization of biopolymers has been reported. The samples of interest tend to be among the larger biopolymers, and

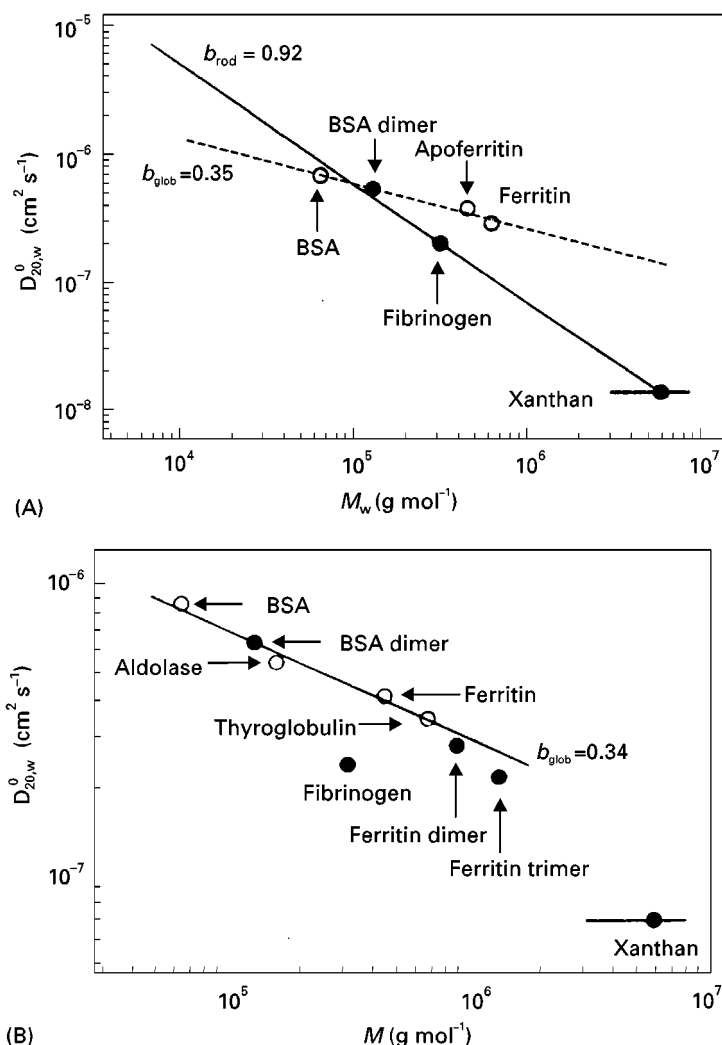


Figure 6 Temperature-corrected diffusion coefficients for a variety of proteins, using both analytical ultracentrifugation (A) and asymmetric FFF (B). The molecular weight–diffusion coefficient relationship is linear for the globular proteins, represented as open circles. Less spherical samples (filled circles) show a deviation from the linearity, with increasing deviation with eccentricity. (Reproduced with permission from Pauck T and Cölfen H (1998) *Analytical Chemistry* 70: 3886 Copyright the American Chemical Society.)

reported examples include DNA, proteoglycans, fibrinogen and myohemerythrin.

Thermal FFF

Thermal FFF, employing the Soret effect, is also suitable for the separation of biomolecules. Unfortunately, the thermodiffusion effect is extremely poor in water. The use of organic solvents restricts statements about the native state in aqueous-based buffer, and furthermore extensive conformational changes and even denaturation may occur which significantly restrict the range of applicable samples. Reported uses of thermal FFF for biological samples have been limited to the polysaccharides, dextrans, ficolls, pululans and cellulose, and the starch polymers amylose

and amylopectin, in dimethylsulfoxide as carrier liquid. Partially aqueous carriers have been investigated but it is the fraction in organic solvent that explicitly determines retention.

Electrical and Magnetic FFF

Electrical FFF is a subtechnique devoted to the fractionation of proteins, as reflected in the number of examples with protein applications. The narrow channel leads to high electrophoretic gradients across the cell, so samples with similar electrophoretic mobilities and differences in diffusion may be separated. As such, electrical FFF exists as a complement to electrophoresis. As early as 1972, a paper by Caldwell *et al.* first demonstrated the possibilities of

electrical FFF for the separation of albumin, lysozyme, haemoglobin and γ -globulin in buffer solutions at different pH.

Later, the performance of an electrical FFF channel with flexible membranes, a channel with rigid membranes and a circular channel for the separation of proteins was described. In these studies, human and bovine serum albumin, bovine γ -globulin, cytochrome *c*, egg white lysozyme and soluble ribonucleic acid (t-RNA) as well as denatured proteins were successfully separated. Unfortunately, the electrical field induces charge polarization of carrier liquid species, such that they migrated adjacent to the electrodes and then screen the electrical field. These early experi-

mental configurations of electrical FFF utilized ion-permeable membranes separating the channel volume from the electrode compartments. These conditions led to difficulties in forming a homogeneous electric field, and from the late 1970s the technique entered a period of quiescence. Results published in the early to mid 1990s using conductive, rigid walls of either graphite or gold-plated glass, have allowed reproducible separations, while the addition of a redox couple in the carrier liquid, such as quinone-hydroquinone, reduced the polarization effects. Due to these delays in experimental development, electrical FFF is less mature than other FFF techniques.

Electrical FFF is also well suited to measuring protein adsorption on to surfaces. The thin layer provides only subtle differences to the hydrodynamic size and net density, making flow or sedimentation FFF analysis difficult. However, the adsorption dramatically influences the surface charge and thereby influences both sample-field interaction and retention, as shown in Figure 7.

Although not formally FFF, dielectrophoresis in combination with fluid flow through an open chamber with interdigitated sinusoidally corrugated electrodes has been used for the separation of proteins and DNA.

A minor method, magnetic FFF, has been applied to study the retention behaviour of BSA in the presence and absence of nickel nitrate. In the presence of nickel ions, the retention time of the BSA sample was 6% higher with the magnetic field than it was without the field. Retention times reported for BSA samples both with and without a magnetic field did not differ in the absence of Ni (II). However, the application range of magnetic FFF for protein separations is very limited, and the method can only be applied in exceptional conditions.

Micropreparative FFF Applications

A variant of the FFF apparatus, the split-flow thin cell (SPLITT) permits continuous separation of milli- or even gram quantities of material. The apparatus is similar to a FFF cell equipped with both frit inlets and outlets. Initial configurations fed a mixture of large particles into the upper wall and carrier liquid into the base, while at the other end of the cell the liquid flowed out of two opposing exits. The ratio between the flows produces a hydrodynamic 'splitting plane' in the cell. During passage the larger particles could sediment sufficiently to exit at the other end of the SPLITT cell through the base, while smaller, less dense particles did not pass the splitting plane and eluted through the top. For protein applications, an electrical potential applied across such a cell in a range of buffers allows proteins with greater

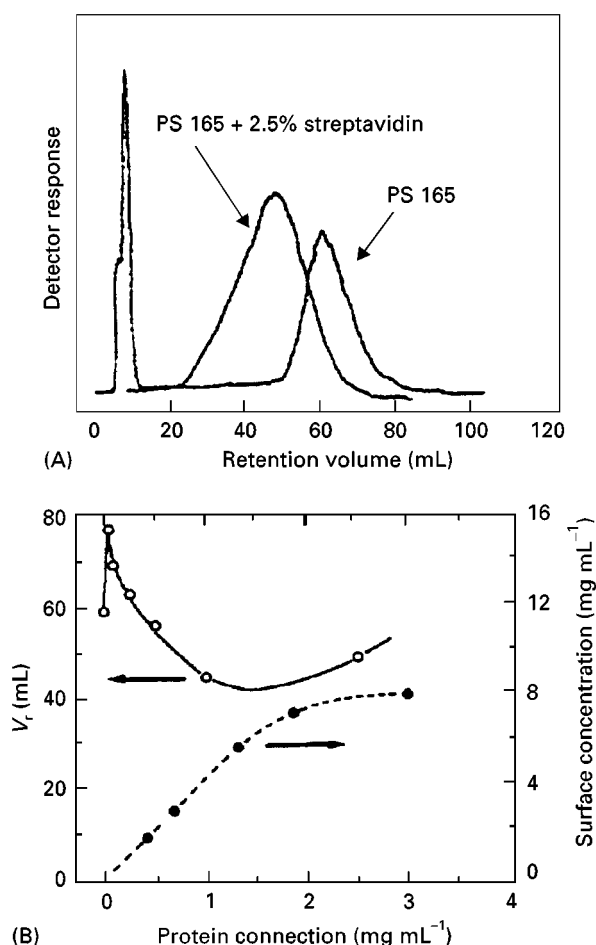


Figure 7 The coating of streptavidin on to a standard 165 nm diameter polystyrene (PS) latex bead affects the elution of the latex substrate by electrical FFF. Under pH 7.2 fractionation conditions the latex has a negative surface charge while the protein is isoelectric. The lower net surface potential is reflected in the poorer retention of the coated bead (A). The magnitude of this peak shift quantifies the degree of surface coating, as shown by the correlation in retention with the protein adsorption isotherm (B). (Reproduced with permission from Schimpf and Caldwell (1995) *American Laboratory* 27: 64–68.)

electrophoretic mobility to pass the splitting plane. The separation of a mixture of model proteins by such a method has been reported. The relatively high throughput reported (15 mg h^{-1}) makes this an interesting development for routine purification, but it requires a difference in protein pI of about two units as a necessary precondition for separation.

Miniaturization of FFF

There is a drive to produce the equivalent of hand-held devices for sample analysis based on the FFF principles, the chip laboratory. Advantages of such methods include the ability to analyse freshly sampled, or to undertake a number of simultaneous parallel analyses. For such miniaturized devices the injection volume is a significant proportion of the channel volume, with commensurate band-broadening problems, while theory predicts that some quantities, such as retention ratio and plate height, degrade with decreasing size. None the less, the reported developments for microfabricated electrical and dielectrophoretic FFF show healthy progression.

Concluding Remarks

The early development of FFF was hindered by the experimental complexity of the method and a focus on theory over practice. Over the last ten years, a number of simplifying experimental features such as the frit inlet-outlet system, and a fuller understanding of the theoretical background have led to a dramatic worldwide rise in the number of applications. It seems unlikely that more novel fields will be introduced into this family of techniques, but the subtlety of application is increasing. Methods and procedures are developing, from the analysis of simple proteins and mixtures, to protein aggregates,

proteins in complex matrices and increasingly fragile samples such as liposomes, where the open channel has few, if any, real analytical competitors.

The other exciting branch of development is increased commercial application, where the FFF method becomes a 'black box' technique. Leading the way is the FI-FFF method, but with the recent innovations in electrical FFF, the dominance of gel electrophoresis for protein analysis may be passing.

See also: III/Proteins: Centrifugation.

Further Reading

- Cölfen H and Antionetti M (2000) Field-flow-fractionation techniques for polymer and colloid analysis. *Advances in Polymer Science* 150: 67–187.
- Giddings JC (1991) *Unified Separation Science*. New York: John Wiley.
- Giddings JC (1993) Field-flow fractionation: analysis of macromolecular, colloidal, and particulate materials. *Science* 260: 1456–1465.
- Janca J (1988) *Field-Flow Fractionation*. Chromatographic Science Series vol. 39. New York: Marcel Dekker.
- Liu MK, Li P and Giddings JC (1993) Rapid protein separation and diffusion coefficient measurement by frit inlet flow field-flow fractionation. *Protein Science* 2: 1520–1531.
- Martin M (1998) Theory of field-flow fractionation. *Advances in Chromatography* 39: 1–138.
- Myers MN (1997) Overview of field-flow fractionation. *Journal of Microcolumn Separations* 9(3): 151–162.
- Schimpf ME and Caldwell KD (1995) Electrical field-flow fractionation for colloid and particle analysis. *American Laboratory* 27(6): 64–68.
- Wahlund K-G and Litzén A (1989) Application of an asymmetric flow field-flow fractionation channel to the separation and characterisation of proteins, plasmids, plasmid fragments, polysaccharides, and unicellular algae. *Journal of Chromatography* 461: 73–87.

Glycoproteins: Liquid Chromatography

See III/GLYCOPROTEINS: LIQUID CHROMATOGRAPHY

High-Speed Countercurrent Chromatography

Y. Shibuswa, Tokyo University of Pharmacy and Life Science, Tokyo, Japan

Y. Ito, National Institutes of Health, Bethesda, MD, USA

Copyright © 2000 Academic Press

Introduction

Countercurrent chromatography (CCC) is essentially a form of liquid–liquid partition chromatography. Its unique feature among other chromatographic systems is derived from the fact that the method uses no solid support and the stationary phase is retained in the column with the aid of gravity or centrifugal force. The method has been termed after two classic partition techniques – countercurrent distribution and liquid chromatography.

A great advance in the CCC technology was made with the discovery of a new hydrodynamic phenomenon in a rotating coiled tube, which provided the basis for developing a highly efficient CCC system called high-speed CCC (HSCCC). In the last decade, types XL, XLL, XLLL and L cross-axis coil planet centrifuges (CPCs) have been developed to perform CCC with highly viscous polar solvent systems, such as polyethylene glycol (PEG) potassium phosphate, PEG dextran aqueous–aqueous two-phase systems. The absence of a solid support eliminates various complications that might arise from this in conventional chromatographic systems and the CCC has the ability to preserve the functional and enzymatic activity of proteins.

Apparatus

The cross-axis coil CPCs, which include types X and L and their hybrids (see Figure 3 in the article on Countercurrent chromatography), are used for protein separation. These modified versions of the

HSCCC centrifuge have a unique feature among the CPC systems in that the system provides reliable retention of the stationary phase for viscous polymer-phase systems. Figure 1 shows five different types of cross-axis CPCs. A series of studies has shown that the stationary-phase retention is enhanced by laterally shifting the position of the coil holder along the holder shaft, apparently due to the asymmetry of the laterally acting force field between the upper and the lower halves of the rotating coil. The degree of the lateral shift of the coil holder is conventionally expressed by L/R , where L is the distance from the middle point of the rotary shaft to the coil holder and R is the distance from the centrifuge axis to the holder axis. Types XL, XLL, XLLL and L have been effectively used for protein separations with various polymer-phase systems. For example, the polymer-phase system composed of PEG and potassium phosphate has a relatively large difference in density between the two phases, so it can be retained in XL–XLL column positions which provide efficient mixing of the two phases. On the other hand, the viscous polymer-phase system composed of PEG and dextran has an extremely low interfacial tension and small density differences between the two phases so that they tend to emulsify under vigorous mixing. Therefore, the type XLLL or L column position, that provides less efficient mixing under a strong centrifugal force field, is required to achieve satisfactory retention of the stationary phase for this polymer-phase system.

Figure 2 shows the XLLL cross-axis CPC ($L/R = 3.5$) equipped with a pair of multilayer coil separation columns. Each column consists of 2.6 mm i.d. polytetrafluoroethylene (PTFE) tubing wound on to a coil holder hub, forming multiple layers of left-handed coils. Table 1 lists various CPC models that have been used for the preparative separation of proteins, together with various parameters, including the

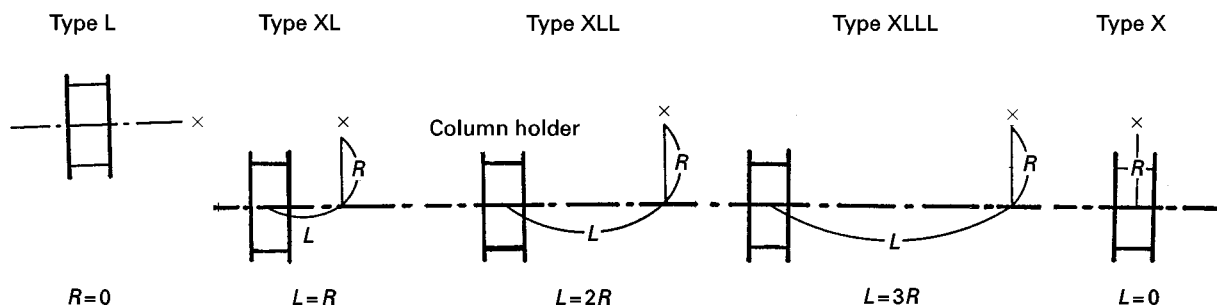


Figure 1 Orientation of the column holder on the axis of rotation in five different types of the cross-axis coil planet centrifuges. \times , axis of revolution; dashed line, axis of rotation; L , lateral shift; R , revolution radius.

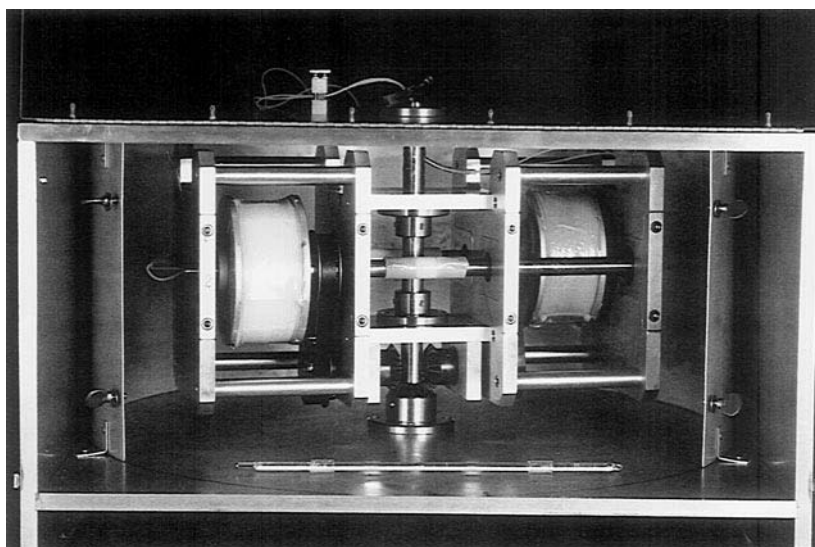


Figure 2 Type XLLL cross-axis CPC equipped with a pair of multilayer coils connected in series.

dimensions of columns and column holders, and β values of multilayer coils.

Polymer-phase Systems for Preparative Separation of Proteins

CCC utilizes a pair of immiscible solvent phases pre-equilibrated in a separatory funnel where one phase is used as the stationary phase and the other as the mobile phase. There are two typical polymer-phase systems available for protein separation: PEG dextran and PEG potassium phosphate systems.

PEG Dextran Systems

The polymer-phase system composed of PEG and dextran has a characteristic feature: small molecules are partitioned fairly evenly between the two phases,

whereas macromolecules such as DNA and polynucleic acids are distributed unilaterally in one phase or the other, depending on the pH of the solvent system. Consequently, the system can be used effectively for separation of these macromolecules using pH gradient elution. The PEG dextran system forms two layers without addition of high salt concentration, which tends to be precipitated in PEG phosphate systems (see below) at high salt concentrations. On the other hand, the PEG dextran system has a serious drawback in its CCC application. At high dextran concentrations the viscosity of the lower phase increases, and the similar polarity of the two polymers reduces interfacial tension between the two phases, resulting in a high probability of emulsification. A typical PEG dextran polymer system contains 4.4% (w/w) PEG 8000, 7% (w/w) dextran T500 and 10 mmol L^{-1}

Table 1 Type of apparatus and dimensions of columns used for protein separation

<i>x</i> -axis CPC	$(L/R)^a$	Coil holder		Columns				
		Diameter (cm)	Width (cm)	i.d. (mm)	Length (m)	Layers	Capacity (mL)	β Values ^b
Type XL	(1.25)	10.0	5.0	2.6	31	3	165	0.50–0.60
		15.2	5.0	2.6	11	1	60	0.76
		15.2	5.0	2.6	64	4	340	0.76–0.90
Type XLL	(2.0)	3.8	5.0	2.6	47	8	250	0.25–0.60
		7.6	5.0	2.6	53	6	280	0.50–1.00
Type XLLL	(3.5)	3.8	5.0	2.6	57	9	300	0.50–1.30
		3.4	5.0	2.6	83	12	440	0.45–1.50
Type L	(infinity)	3.6	5.0	2.6	25	5	130	0.16–0.27 ^c

^a L = Distance from the centre of the holder shaft to the coil holder; R = distance from the centrifuge axis to the holder shaft.

^b $\beta = r/R$.

^c $\beta = r/L$, where r is the distance from the holder axis to the coil.

Table 2 Preparation of polymer two-phase solvent systems

	Concentration (% w/w)			pH
	PEG 1000	K ₂ HPO ₄	KH ₂ PO ₄	
1	12.5	12.5	0	9.0
2	12.5	9.375	3.125	7.7
3	12.5	8.33	4.17	7.3
4	16.0	12.5	0	9.2
5	16.0	10.4	2.1	8.0
6	16.0	8.33	4.17	7.3
7	16.0	6.25	6.25	6.8

potassium phosphate buffer at proper pH. This two-phase system consists of a PEG-rich upper phase and a dextran-rich lower phase.

PEG Potassium Phosphate Systems

The PEG potassium phosphate system is complementary to the PEG dextran system in that it tends to distribute low-molecular-weight compounds unilaterally in either the upper or lower phase while macromolecules such as proteins are more evenly distributed between phases. Consequently, once a suitable partition coefficient for the target protein is obtained, the system yields high-purity fractions al-

most free from contamination by low-molecular-weight impurities that either elute immediately after the mobile phase front or remain almost permanently in the column.

Table 2 shows the composition of seven different PEG 1000 potassium phosphate systems. The ratio of the monobasic and dibasic potassium phosphate determines the pH of the solvent system and the partition coefficient of the protein samples. In all these solvent systems, the upper layer is rich in PEG and the lower layer is rich in phosphate.

Profilin-actin Complex Purification from Crude *Acanthamoeba* Extract

Using the type L cross-axis CPC equipped with a pair of multilayer coils (130 mL capacity), profilin-actin complex has been purified directly from an *Acanthamoeba* extract with a polymer-phase system composed of 4.4% (w/w) PEG 8000, 7% (w/w) dextran T500 at pH 6.8. The lower dextran-rich phase was used as the stationary phase. The sample solution was prepared by adding the correct amounts of PEG 8000 and dextran T500 to 12.5 g of the *Acanthamoeba* crude extract to adjust the two-phase composition to that of the solvent phases used for separation. The separation was carried out by pumping the PEG-rich

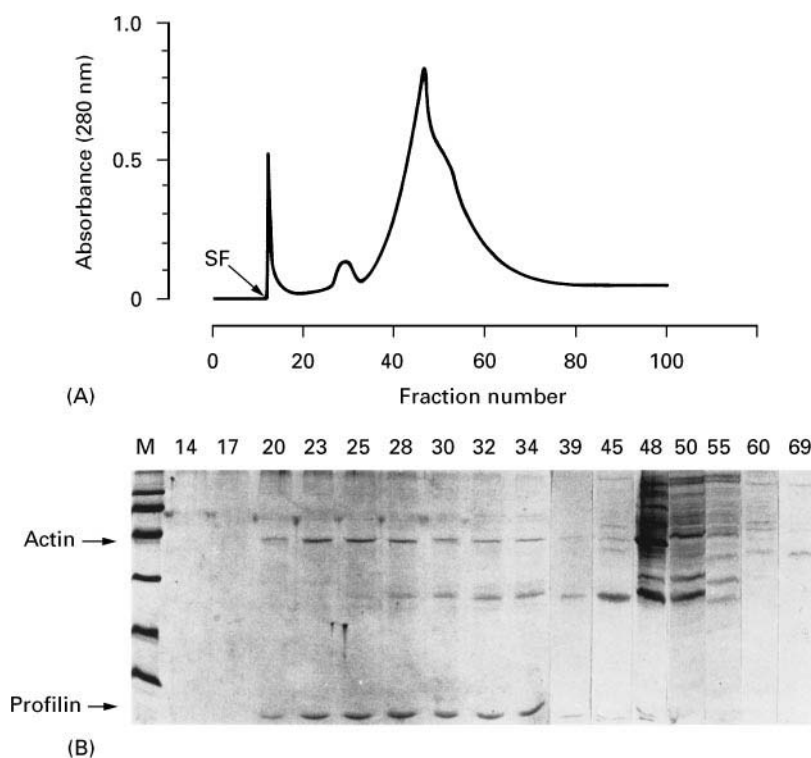


Figure 3 Purification of profilin-actin complex from *Acanthamoeba* soluble extract. Experimental conditions: column is a 2.6 mm i.d. PTFE multilayer coil $\times 2$, $\beta = 0.16$ – 0.27 ; 130 mL capacity; sample consists of 12.5 g *Acanthamoeba* soluble extract; solvent system is 4.4% (w/w) PEG 8000, 7% (w/w) dextran T500 in a 10 mmol L^{-1} potassium phosphate buffer at pH 6.8; mobile phase is the upper phase; flow rate: 0.5 mL min^{-1} ; revolution: 900 rpm; SF, solvent front.

upper phase into the head of the column at 0.5 mL min^{-1} under a high-revolution speed of 1000 rpm. The results are shown in Figure 3A. The solvent front emerged at the 14th fraction (3 mL per fraction) whereas the profilin-actin complex was eluted in fractions 20 to 28, well separated from other components. The impurities were mostly eluted later with a retention volume close to the total column capacity (around fractions 33–60), while some were also found near the solvent front (fraction 15). Identification of the profilin-actin complex was made by 12% sodium dodecyl sulfate-polyacrylamide gel electrophoresis (SDS-PAGE), as illustrated in Figure 3B. The retention of the lower stationary phase was 69% of the total column capacity.

Countercurrent Chromatographic Fractionation of Lipoproteins from Human Serum

The performance of the XLL cross-axis CPC has been evaluated by the direct separation of high- and low-density lipoproteins (HDLs and LDLs) from human serum. The effects of the molecular weight of the PEG was studied with a polymer-phase system composed

of 16% (w/w) PEG, 12.5% (w/w) potassium phosphate. Figure 4 shows the chromatograms of human serum (4 mL) obtained from four solvent systems containing different molecular weight PEGs (600, 1000, 2000 and 4000).

In each experiment, the CCC column was first entirely filled with the PEG-rich upper stationary phase, and the sample solution (a mixture of 4 mL human serum and 2 mL each of upper and lower phases, to which the required amounts of PEG and potassium phosphate were added to adjust the two-phase composition) was injected through the sample port. Then, the potassium phosphate-rich lower mobile phase was eluted through the column at a flow rate of 2 mL min^{-1} while the apparatus was rotated at 500 rpm. The lipoprotein fractions obtained in the CCC were characterized using polyacrylamide gel disc electrophoresis (disc PAGE). Serum proteins in the CCC fractions were also characterized by SDS-PAGE.

In the PEG 600 system (Figure 4A), all proteins including HDLs, LDLs and serum proteins were strongly retained in the PEG-rich stationary phase and eluted together when the column was eluted in

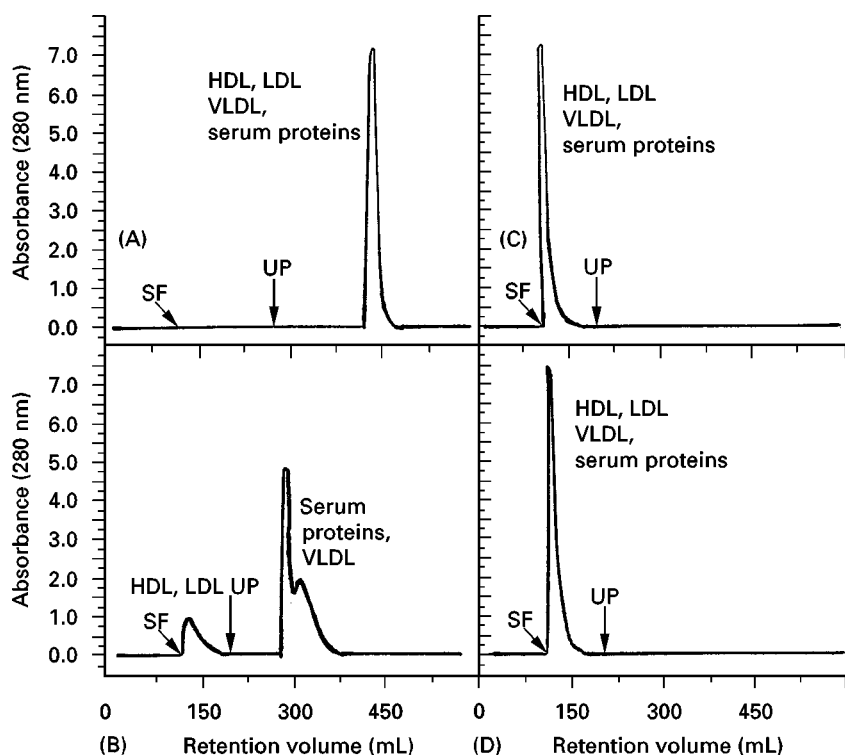


Figure 4 Countercurrent chromatographic fractionation of HDL-LDL and VLDL-serum protein fractions from human serum with four different aqueous polymer-phase systems containing (A) PEG 600; (B) PEG 1000; (C) PEG 2000; (D) PEG 4000. Experimental conditions: column is a 2.6 mm i.d. PTFE multilayer coil \times 2, $\beta = 0.76$ –0.90, 340 mL capacity; sample is a mixture of 4 mL volume of human serum, 2 mL of the upper and the lower phases, to which the required amounts of PEG and potassium phosphate were added to adjust the two-phase composition; solvent system consists of 16% (w/w) PEG 1000, 12.5% (w/w) K_2HPO_4 (pH 9.2); mobile phase is the lower phase; flow rate: 2.0 mL min^{-1} revolution: 500 rpm; SF, solvent front; UP, starting point of the reversed elution mode with the upper phase mobile.

a reversed elution mode with the PEG-rich upper phase. Similarly, when PEGs with molecular weights higher than 2000 were used in the solvent system, all proteins including HDLs, LDLs and serum proteins were mostly distributed to the potassium phosphate-rich lower phase and eluted together at the solvent front (Figure 4C and D). Successful separation of the combined HDL and LDL fraction was achieved with the 16% (w/w) PEG 1000, 12.5% (w/w) potassium phosphate solvent system at pH 9.2, where both HDLs and LDLs were eluted together near the solvent front, while other proteins, including very-low-density lipoproteins (VLDLs) and serum proteins were retained in the column for much longer. The separation time of these two lipoproteins was 3 h. The VLDLs were eluted by the PEG-rich upper phase in the second peak or its shoulder (Figure 4B).

These results show that both HDL-LDL and VLDL-serum protein fractions were fractionated within 3 h by CCC with a polymer-phase system composed of 16% (w/w) PEG 1000 and 12.5% (w/w) dibasic potassium phosphate at a relatively high flow rate of 2 mL min^{-1} .

Purification of HDLs, LDLs and VLDLs from Human Serum by Combined Use of CCC and Hydroxyapatite Chromatography

In the previous section, two lipoprotein fractions (HDL-LDL and VLDL-serum proteins) were obtained from human serum using a polymer-phase system by the type XL cross-axis CPC equipped with a large-capacity column (340 mL). A small-capacity column (60 mL) mounted on the same apparatus can be employed to shorten the separation time. Figure 5 shows a chromatogram of human serum (4 mL) obtained with the cross-axis CPC using 16% (w/w) PEG 1000, 12.5% (w/w) dibasic potassium phosphate (pH 9.2). The separation was performed at 500 rpm and at a flow rate of 0.5 mL min^{-1} using the lower phase as the mobile phase. Both HDLs and LDLs were eluted together near the solvent front, while other proteins were retained in the column much longer. After collecting the HDL-LDL fraction (CCC-fr. 1), VLDLs were eluted together with serum proteins (CCC-fr. 2) by pumping the upper phase in the reverse direction. The separation was completed within 4.5 h. The lipoproteins in each peak were confirmed by agarose gel electrophoresis with Oil Red 7B staining, and the serum proteins were also detected by 10% SDS-PAGE with Coomassie Brilliant Blue protein staining.

The CCC fractions 1 (HDL-LDL) and 2 (VLDL-serum proteins) were each separately dialysed against distilled water until the concentration of the potassium phosphate was reduced to that in the starting

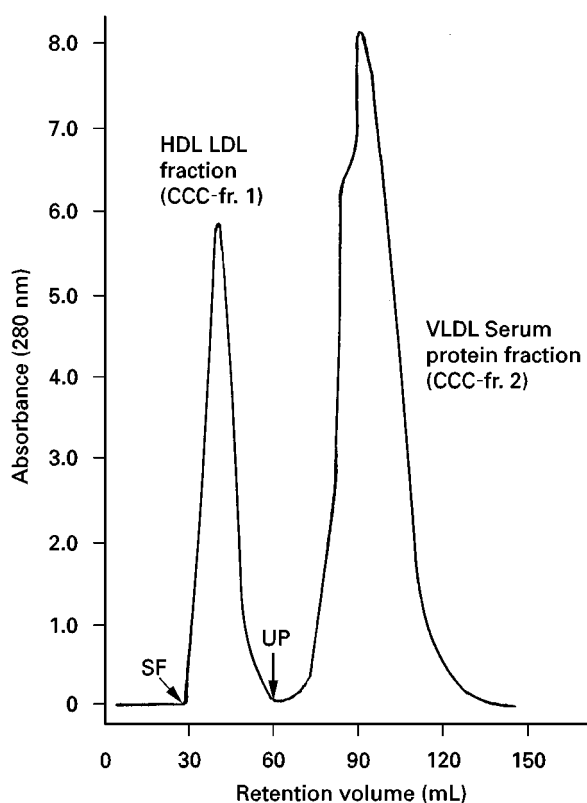


Figure 5 Countercurrent chromatographic separation of HDL-LDL and VLDL-serum protein fractions from human serum by small-capacity columns. Experimental conditions: column is a 2.6 mm i.d. PTFE multilayer coil $\times 2$, $\beta = 0.76$, 60 mL capacity; sample is a 4 mL volume of human serum containing 0.9 g PEG 1000 and 0.7 g dibasic potassium phosphate; solvent system consists of 16% (w/w) PEG 1000, 12.5% (w/w) K_2HPO_4 (pH 9.2); mobile phase is the lower phase; flow rate: 0.5 mL min^{-1} ; revolution: 500 rpm; SF, solvent front; UP, starting point of the reversed elution mode with the upper phase mobile.

buffer used for hydroxyapatite chromatography. The concentrates of both fractions were chromatographed separately on the hydroxyapatite column. Figure 6 shows the elution profile on hydroxyapatite obtained from CCC-fr. 1. A 1.4 mL volume of the concentrate was loaded on the Bio-Gel HTP DNA-grade column ($5.0 \times 2.5 \text{ cm i.d.}$) and eluted at 1.0 mL min^{-1} with 75 and 290 mmol L^{-1} potassium phosphate buffer at pH 7.4. Two lipoprotein peaks were eluted: the first peak (HA-fr. 1) contained HDLs and the second peak (HA-fr. 2) contained LDLs.

The concentrate (1.5 mL) of CCC-fr. 2 was similarly chromatographed (Figure 7). The separation was performed with two-step elution with 290 and 650 mmol L^{-1} potassium phosphate buffers at pH 7.4. Most of the serum proteins, including albumin and globulins, were eluted with 290 mmol L^{-1} potassium phosphate buffer (HA-fr. 3) at pH 7.4. The VLDLs, on the other hand, were retained in the

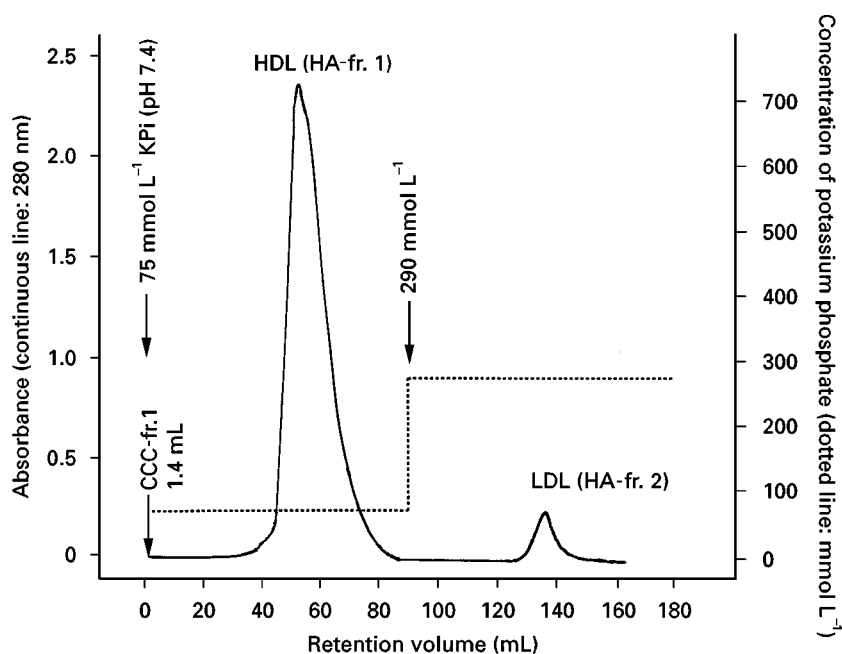


Figure 6 Stepwise elution profile of HDLs and LDLs of the CCC fractions by hydroxyapatite chromatography. Experimental conditions: column is Bio-Gel HTP DNA-grade hydroxyapatite (5.0×2.5 cm i.d.); eluents are 75 and 290 mmol L⁻¹ potassium phosphate buffers at pH 7.4; flow rate: 1.0 mL min⁻¹ sample is the 1.4 mL concentrate of HDL-LDL CCC fraction containing 13.9 mg total proteins (CCC-fr. 1).

column for much longer and were eluted with 650 mmol L⁻¹ potassium phosphate buffer (HA-fr. 4). Lipoproteins in the hydroxyapatite chromatographic

fractions were confirmed by agarose gel electrophoresis. The results of agarose gel electrophoresis indicated that HDLs, LDLs and VLDLs were present

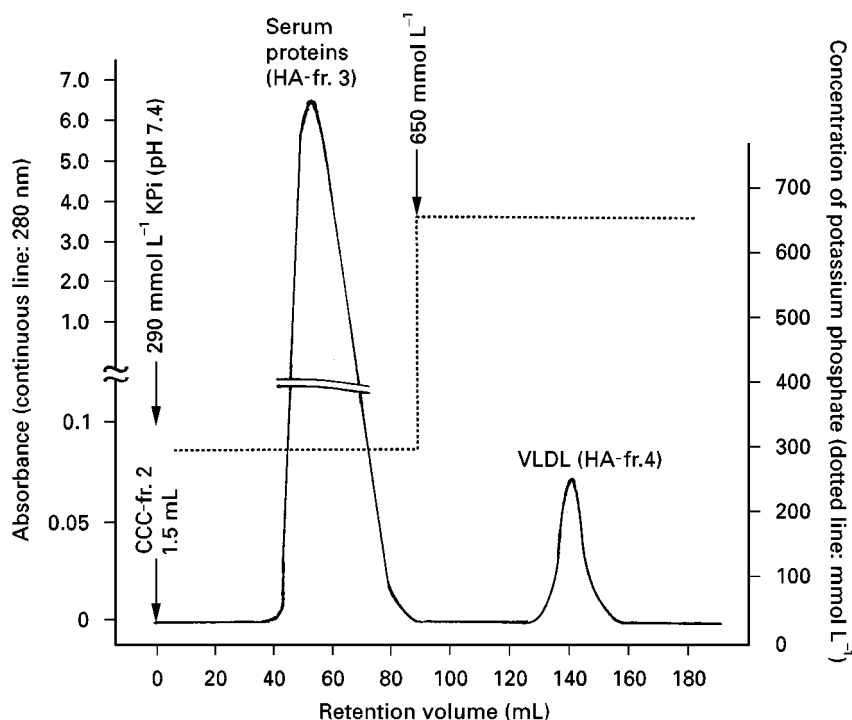


Figure 7 Stepwise elution profile of VLDL-serum proteins fraction of the CCC fractions by hydroxyapatite chromatography. Experimental conditions: column is Bio-Gel HTP DNA-grade hydroxyapatite (5.0×2.5 cm i.d.); eluents are 290 and 650 mmol L⁻¹ potassium phosphate buffers at pH 7.4; flow rate: 1.0 mL min⁻¹; sample is the 1.5 mL concentrate of serum protein-VLDL CCC fraction containing 41.8 mg of total proteins (CCC-fr. 2).

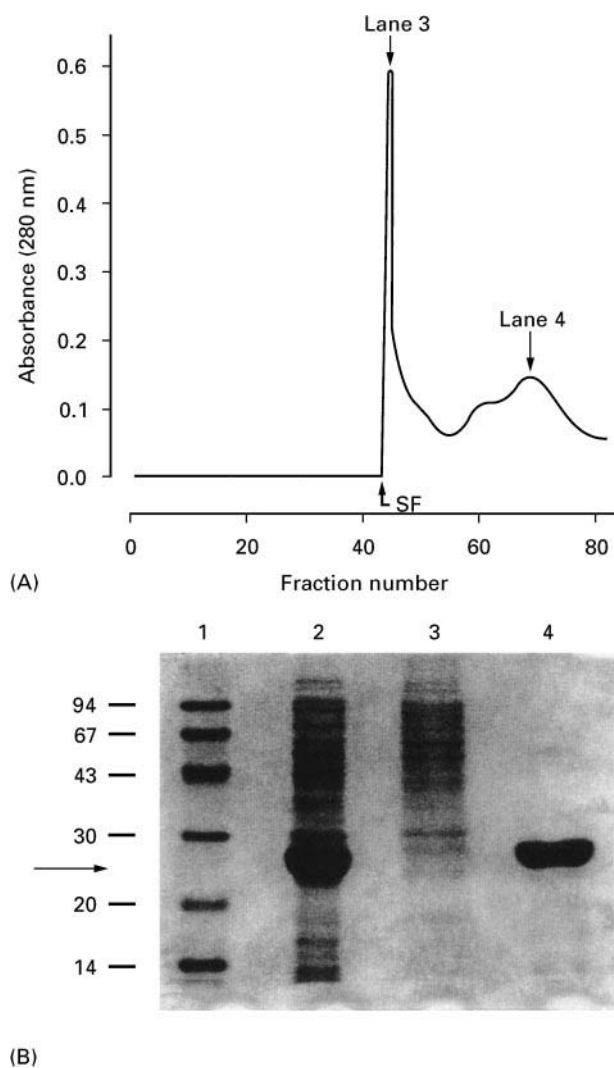


Figure 8 Countercurrent chromatographic purification of purine nucleoside phosphorylase (PNP) from crude extract of *Escherichia coli* (A) and SDS gel electrophoresis profile of CCC fractions (B). Experimental conditions: column is a 2.6 mm i.d. PTFE multilayer coil $\times 2$, $\beta = 0.25$ – 0.60 , 250 mL capacity; sample consists of crude PNP in 10 mL solvent; solvent system consists of 16% (w/w) PEG 1000, 6.25% (w/w) K_2HPO_4 , 6.25% (w/w) KH_2PO_4 (pH 6.8); mobile phase is the upper phase; flow rate: 0.5 mL min^{-1} ; revolution: 750 rpm; SF, solvent front. Lane 1, molecular weights markers; Lane 2, crude extract; Lane 3, HSCCC fraction 46 (solvent front); Lane 4, HSCCC fraction 71 (213 mL).

in HA-fr. 1, HA-fr. 2 and HA-fr. 4, respectively. From the results of SDS-PAGE of the hydroxyapatite fractions, HA-frs. 1, 2 and 4 are free from serum proteins and HA-fr. 3 contained only serum proteins.

Purification of Recombinant Enzymes from Crude *Escherichia coli* Lysate

The capability of the XLL cross-axis CPC was further examined in the purification of some recombinant enzymes from a crude extract of *Escherichia coli* lysate. The polymer-phase system used was 16%

(w/w) PEG 1000, 6.25% (w/w) monobasic and 6.25% (w/w) dibasic potassium phosphate (pH 6.8). The phosphate-rich lower phase was used as the stationary phase. About 1.0 mL of crude lysate containing purine nucleoside phosphorylase (PNP) in 10 mL of the above solvent system was loaded into the multilayer coil and eluted with the PEG-rich upper phase at a flow rate of 0.5 mL min^{-1} . **Figure 8A** shows the chromatogram of crude PNP lysate obtained. A 3 mL volume was collected in each fraction. The solvent front emerged at the 46th fraction (138 mL retention volume) and purified PNP was obtained from fractions 65–80 (195–240 mL). **Figure 8B** shows the 12% SDS gel electrophoresis patterns of the CCC fractions obtained from the crude PNP lysate. Gel electrophoresis clearly demonstrates that PNP in the crude *E. coli* lysate was highly purified by CCC via a single pass through the column.

Purification of recombinant uridine phosphorylase (UrdPase) from *E. coli* lysate has been performed similarly, as shown in **Figure 9**. The polymer phase system was the same as that used for the purification of recombinant PNP described above. About 2.0 mL of the crude lysate in 4 mL of the solvent, 1 mL of upper phase and 3 mL of lower phase containing 16% PEG 1000 and 12.5% potassium phosphate, was loaded on the column and eluted with the PEG-rich upper phase at 0.5 mL min^{-1} . In **Figure 9**, protein concentration in the eluted fractions (solid line) is plotted against the retention volume. The chromatogram shows four protein peaks. Most of the protein mass was eluted immediately after the solvent front in fractions 35–55 (105–165 mL), whereas the enzyme activity of the UrdPase coincides with the fourth protein peak corresponding to fractions 75–95 (230–285 mL). These results indicate that recombinant UrdPase can be highly purified from the crude *E. coli* lysate in a one-step operation within 10 h by the XLL cross-axis CPC.

Purification of Lactic Acid Dehydrogenase from Bovine Heart Crude Extract

CCC has been applied to the purification of lactic acid dehydrogenase (LDH) from a crude bovine heart filtrate using the XL cross-axis CPC. The separation was performed with a polymer-phase system, composed of 16% (w/w) PEG 1000, 12.5% (w/w) potassium phosphate at pH 7.3.

Figure 10A shows chromatograms of the bovine heart crude extract obtained, where the PEG-rich upper phase was used as the stationary phase. The separation was performed at 500 rpm at a flow rate of 1.0 mL min^{-1} using the phosphate-rich lower phase as the mobile phase. The enzymatic activity of LDH was detected between the second and third

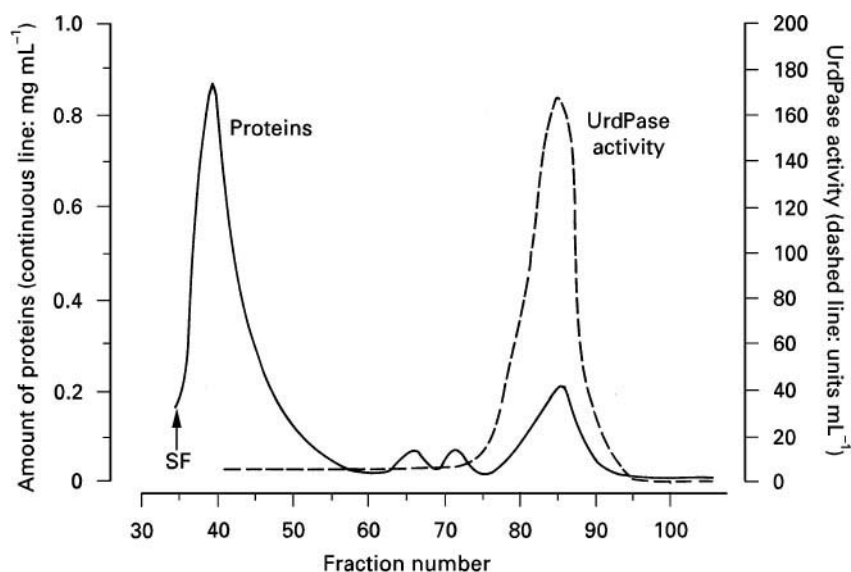


Figure 9 Countercurrent chromatographic purification of uridine phosphorylase (UrdPase) from crude *Escherichia coli* lysate. Experimental conditions: column is a 2.6 mm i.d. PTFE multilayer coil $\times 2$, $\beta = 0.25$ – 0.60 , 250 mL capacity; sample consists of 2 mL crude UrdPase in 4 mL solvent; solvent system consists of 16% (w/w) PEG 1000, 6.25% (w/w) K_2HPO_4 and 6.25% (w/w) KH_2PO_4 (pH 6.8); mobile phase is the lower phase; flow rate: 0.5 mL min^{-1} ; revolution: 750 rpm; SF, solvent front.

peaks. These fractions were analysed by 12% (w/v) SDS-PAGE with Coomassie Brilliant Blue staining (Figure 10B), indicating that the LDH is actually contained in 30 mL of eluent (fractions 140–170 mL) without detectable contamination from other proteins. The traditional techniques used for purification of LDH require several steps, including precipitation with ammonium sulfate, centrifugation and dialysis;

hence they are very tedious and time-consuming. By combined use of the XL cross-axis CPC and the aqueous polymer-phase system described above, LDH is purified within 3 h.

These results show that, with relatively simple manipulation of several parameters (buffer, polymer molecular mass, rotation speed), CCC is well suited to the rapid purification of enzymes from very crude

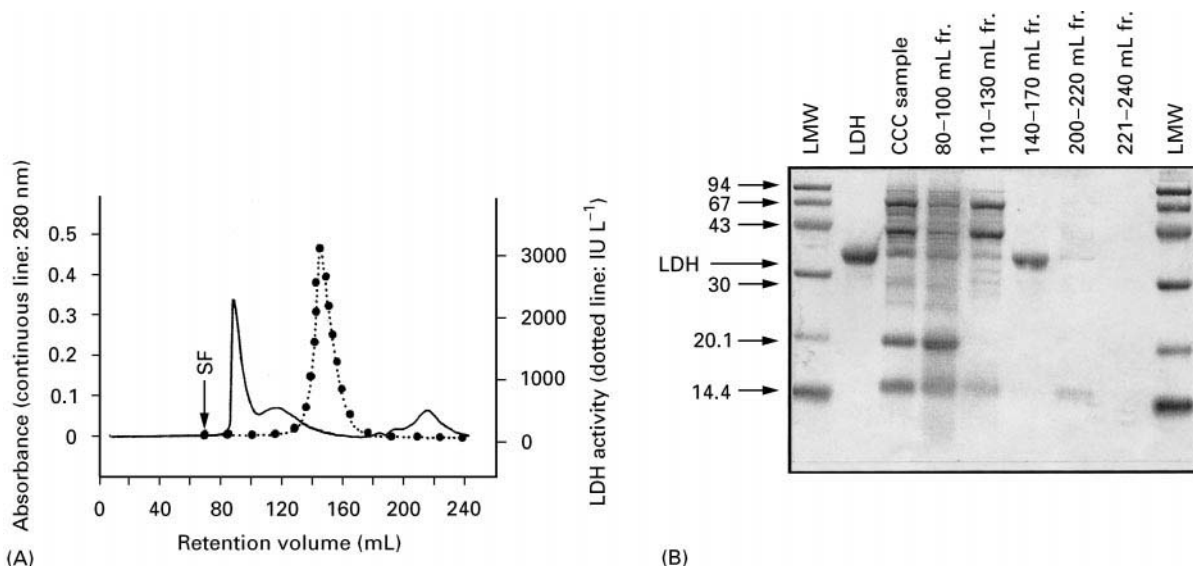


Figure 10 (See Colour Plate 116) (A) Countercurrent chromatography of bovine heart homogenate and (B) SDS-PAGE profile of the fractions. Experimental conditions: column is a 2.6 mm i.d. PTFE multilayer coil $\times 2$, $\beta = 0.50$ – 0.60 , 165 mL capacity; sample is a mixture of 3 mL bovine heart crude extract, 3 mL solvent system (1.5 mL each phase); solvent system consists of 16% (w/w) PEG 1000 12.5% (w/w) potassium phosphate (pH 7.3); mobile phase is the lower phase; flow rate: 2.0 mL min^{-1} ; revolution: 500 rpm; SF, solvent front. LMW, low molecular weight protein markers.

tissue extracts. Because of the protective effect of a high concentration of polymers and potassium phosphate, the native structure of the proteins is preserved at room temperature during separation, and the support-free partitioning eliminates sample loss and deactivation of enzymes which is often caused by using the solid support in conventional chromatography. We expect that these merits of the method will apply in the purification of other enzymes.

Conclusion

The capability of the cross-axis CPCs for performing CCC has been demonstrated in the separation and purification of proteins. The unique feature of the apparatus is that it provides sufficient retention of the stationary phase for viscous, low interfacial tension polar solvent systems, such as aqueous-aqueous polymer phase systems. Consequently, the method can be utilized for the fractionation of a wide variety of proteins without adsorptive sample loss and denaturation of proteins caused by the solid support. The CCC method may be further extended to the purification and fractionation of other biopolymers.

See Colour Plate 116.

See also: **II/Chromatography:** Countercurrent Chromatography and High-Speed Countercurrent Chromatography: Instrumentation. **Chromatography: Liquid:** Countercurrent Liquid Chromatography. **Appendix 1: Essential**

Guides for Isolation/Purification of Enzymes and Proteins; Essential Guides for Isolation/Purification of Immunoglobulins.

Further Reading

- Albertsson P-Å (1986) *Partition of Cell Particles and Macromolecules*, 3rd edn, New York: Wiley Interscience.
- Conway WD (1990) *Countercurrent Chromatography, Apparatus, Theory and Applications*. New York: VCH.
- Shibusawa Y (1996) Separation of proteins by high-speed countercurrent chromatography. In: Ito Y and Conway WD (eds) *High-Speed Countercurrent Chromatography*, ch. 16, pp. 385–414. New York: Wiley Interscience.
- Shibusawa Y, Chiba T, Matsumoto U and Ito Y (1995) Countercurrent chromatographic isolation of high- and low-density lipoprotein fractions from human serum. In: Conway WD and Petroski RJ (eds) *Modern Countercurrent Chromatography (ACS Monographs)*, ch. 11, pp. 119–128. Washington, DC: American Chemical Society.
- Shibusawa Y, Mugiyama M, Matsumoto U and Ito Y (1995) Complementary use of countercurrent chromatography and hydroxyapatite chromatography for the separation of three main classes of lipoproteins from human serum. *Journal of Chromatography, Biomedical Applications* 664: 295–301.
- Shibusawa Y, Eriguchi Y and Ito Y (1997) Lactic acid dehydrogenase purification from bovine heart crude extract by counter-current chromatography. *Journal of Chromatography, Biomedical Applications* 696: 25–31.

Ion Exchange

P. R. Levison, Whatman International Ltd,
Maidstone, Kent, UK

Copyright © 2000 Academic Press

Introduction

Proteins are polymers of amino acids, the so-called 'building blocks of nature' and are found in all living matter be it of animal, microbial or vegetable origin. By their very structure proteins have an electrical charge and can therefore be fractionated by ion exchange processes. This paper briefly reviews the principles underlying protein purification by ion exchange and addresses some of the process issues associated with their purification.

Proteins

As living cells reproduce, genetic material is passed from parent cells to daughter cells in the form of DNA. DNA is a template coding for the various proteins required for the developing organism. As the organism grows, cells differentiate to form the various organs of the mature organism. Each cell has the capability to express every single protein of the organism, but in life only a small fraction of proteins are expressed. For example muscle cells produce actin and myosin to facilitate movement, the pancreas produces chymotrypsinogen and trypsinogen to facilitate digestion and lymphocytes are responsible for the expression of immunoglobulins which provide immunity from infection and disease.

Because of their functional and structural roles in nature, proteins have significant commercial potential in many areas including food and beverage, biological detergents, diagnostic enzymes, veterinary, agricultural and pharmaceutical applications. However, because of their diversity, the challenges of their purification are immense and their isolation from a particular tissue or organ, regardless of host, may be regarded as 'searching for a needle in a haystack'.

Protein Structure

Proteins are polymers of amino acids bonded together through amide linkages. There exist 20 common amino acids in nature ranging in molecular mass from 75 to just over 200 Da. Proteins range in molecular mass from around 10 000 up to > 1 000 000 Da, and consequently their amino acid sequence or primary sequence may be hundreds of residues in length. Of the 20 amino acids, several have positively or negatively charged side chains, while others have neutral side chains, which may have hydrophilic or hydrophobic properties. The primary sequence of a protein results in a zwitterion with the positively charged N terminus balancing the negatively charged C terminus. However, the charges of the side chains of the charged amino acids and the pK_a values of their functional groups give, at least in principle, an overall positive or negative charge at a given pH. However, proteins are not simple structures and certain sequences of amino acids fold to give secondary structures such as helices and pleated sheets. This secondary structure scrambles up to give a three-dimensional tertiary structure. Some proteins exist as an assembly of subunits giving a quaternary structure. Many proteins are glycosylated to aid with molecular recognition *in vivo* and this influences their shape and surface properties.

The net effect of the three-dimensional structure of proteins is that their theoretical charge or hydrophobicity based on a primary sequence bears little relation to the actual properties of the molecule in its native state. If, for example, all the charged groups are buried inside a pocket in the molecule, then its response to an ion exchanger may be quite weak. The three-dimensional structure of a protein is associated with function and for the purified protein to have intrinsic value, its three-dimensional structure should be retained. This presents practical difficulties in terms of purification, because a denatured protein may not readily, if at all, refold back to its native state. For mammalian systems, typical physiological conditions are pH 7.4 and 0.15 M NaCl and most proteins would be stable and active under these conditions. However, deviations in operating pH and, to

a lesser extent, ionic strength, may irreversibly denature the protein of interest, which can severely restrict the mode of purification available to the chromatographer.

Methods of Protein Purification

Prior to carrying out any practical studies, the protein chemist is provided with a range of chromatographic techniques, the use of which should enable effective purification to be achieved. Those techniques suitable for low pressure operation include those listed in Table 1. While all of these techniques are suitable for laboratory-scale use, those typically scaled-up include ion exchange, hydrophobic interaction, affinity and size exclusion. These techniques each exploit differing physicochemical properties of the protein molecules as manifest by their three-dimensional structure. Ion exchange chromatography and hydrophobic interaction chromatography rely on electrostatic interactions between a charged stationary phase and charged surfaces of the protein or hydrophobic interactions between a hydrophobic stationary phase and hydrophobic surfaces of the protein respectively. Affinity separations rely on a biospecific interaction, for example the interaction of an enzyme with its immobilized substrate or an immunoglobulin with its immobilized antigen. Size exclusion chromatography is a molecular sieving effected by the three-dimensional size and shape of the protein. One or more of these techniques should be suitable for protein purification with their choice influenced by the selectivity requirements of the process in terms of both the target and contaminants.

Ionic Properties of Proteins

For the reasons described above, all proteins will have ionic properties, and their three-dimensional structure imparts a subtle uniqueness to their ionic charge, which is available for exploitation by ion exchange chromatography during their purification. In a similar manner to small molecules, such as organic acids, which vary their charge with pH, as prescribed by their pK_a , proteins have an isoelectric point or pI . The

Table 1 Techniques available for low pressure chromatography of proteins

Salt precipitation
Ion exchange
Size exclusion
Hydrophobic interaction
Thiophilic interaction
Affinity
Chiral

pI of a protein is the pH where it has a net charge of zero.

When the pH is greater than the pI , the protein will have a net negative charge and may bind to an anion exchanger, provided that the pH is less than the pK_a of the functional group. If the pH is less than the pI the protein will have a net positive charge and may bind to a cation exchanger, provided the pH is greater than the pK_a of the functional group. As a rough guide most proteins have a pI of less than 7, ranging typically from 4.5 to 6.5. The major exceptions are the immunoglobulins which typically have a pI of greater than 7.

Ion Exchange Chromatography of Proteins

Principles

On the basis of the physicochemical issues discussed above, it might appear that by following a few simple rules, centred around pH , an ion exchange separation can be designed. The first barrier to overcome is to find out the pI of the protein. Unless the protein is well characterized, this may not be documented, and although it can be readily determined by techniques such as isoelectric focusing, this presupposes that it can be obtained in a relatively pure state. A second barrier is the pH and ionic strength stability ranges of the protein. This can be determined readily by a parametric study, centred around a robust assay for the protein, typically linked to its biological function. A third, and often underestimated barrier, is the influence of the other contaminants within the feedstream and how they may impact on the efficiency of the ion exchange separation. For example, competitive adsorption of an unwanted contaminant to the adsorbent can significantly hamper the selectivity of the separation and the process economics. Other key considerations include the mobile phase composition as defined by the preceding chromatographic step and its impact on an ion exchange separation and the eluent composition and its impact on the subsequent downstream step.

Method Scouting

In the light of the issues highlighted above, the chromatographer can start to develop the ion exchange process. A broad strategy for ion exchange is represented in **Figure 1**. Intuitively, it would seem reasonable to expect ion exchange steps to be of the positive form, whereby the target is retained by the exchanger, and assuming elution volume is less than feedstock volume, has the potential to effect product concentration. Such an approach may be preferable if

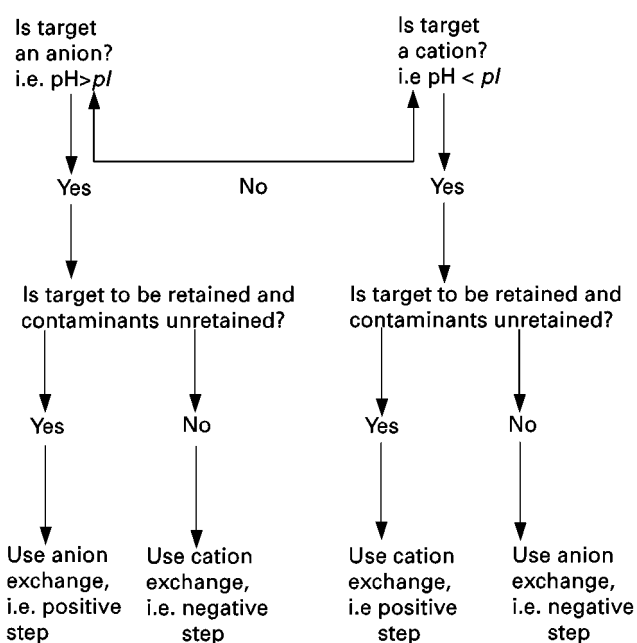


Figure 1 Approaches to development of an ion exchange chromatographic process. Copyright © 1998 Whatman International Ltd., reproduced with permission.

the target binds more strongly to the exchanger than the contaminants, so they are displaced by the target during loading. The isolation of ovalbumin from hen egg-white by anion exchange chromatography is one such example (**Figure 2**), where we have shown ovalbumin to displace the less anionic conalbumin component during adsorption. However, the desorbed protein product is typically in a mobile phase containing up to 1 M NaCl and this may be unsuitable for adsorption in a subsequent step, for example an affinity interaction. If this is the case then another unit process, such as diafiltration, needs to be introduced which may be costly, time-consuming and could result in additional yield/activity loss.

An approach which may often be dismissed, but in fact can be highly efficient is the negative step. In this case the contaminants bind to the adsorbent and the target passes unretained during loading. Since there is no volume reduction, product concentration remains constant, but purity increases. If the target is present in excess, then a modest adsorbent volume may suffice, which has an impact on cost, but perhaps as important, the mobile phase composition remains unchanged, which may facilitate the subsequent chromatographic step. Negative steps are routinely employed during immunoglobulin isolation from serum or plasma, where the anionic albumin contaminants adsorb to an anion exchanger at neutral pH , while the cationic immunoglobulin fraction passes unretained through the exchanger, as represented in **Figure 3**.

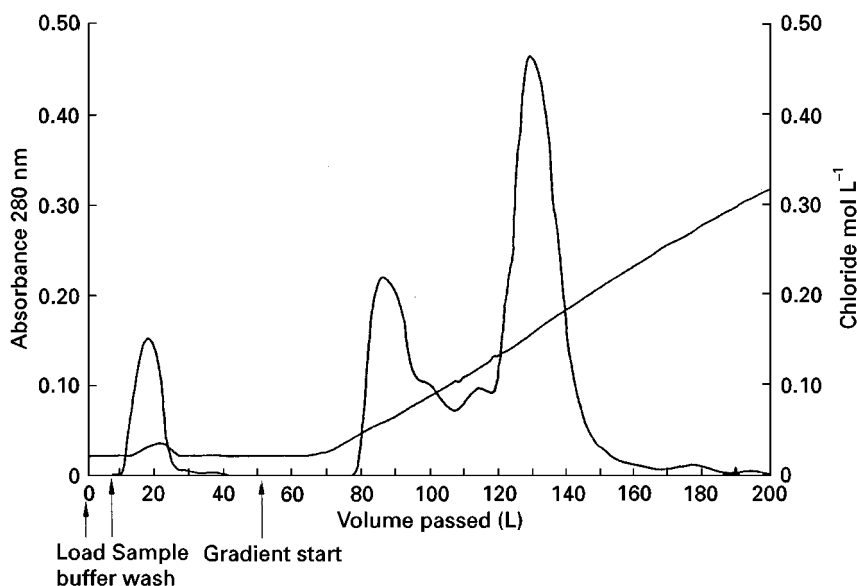


Figure 2 Chromatography of hen egg-white proteins on Whatman DE52 using 0.025 M Tris/HCl buffer, pH 7.5 in a column (45 cm i.d. \times 16 cm) at a flow rate of 1 L min⁻¹. Copyright © 1998 Whatman International Ltd., reproduced with permission.

These are some of the fundamental considerations during method scouting and are based on two questions. Firstly, at a given pH will the target bind to an anion exchanger or a cation exchanger? Secondly, is this what is wanted?

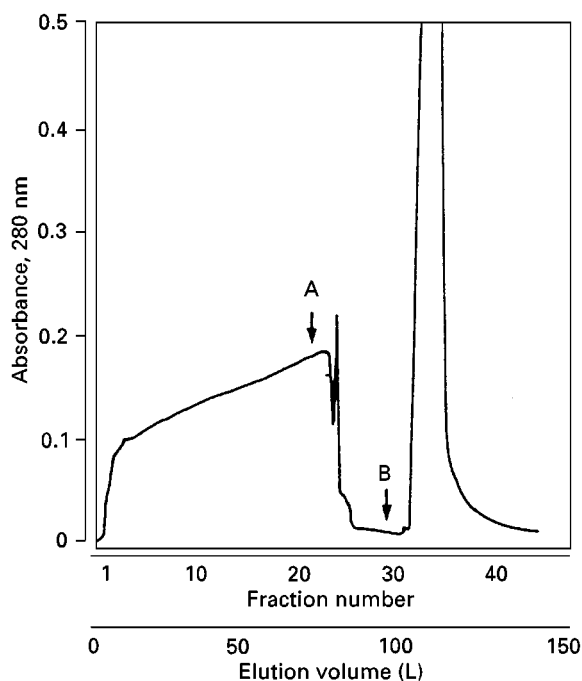


Figure 3 Chromatography of a goat serum preparation on Whatman QA52 using 0.02 M Tris/HCl buffer, pH 7.5 in a column (32.5 cm i.d. \times 12 cm). A, denotes a wash in loading buffer; B, denotes a wash using loading buffer containing 0.5 M NaCl. Copyright © 1998 Whatman International Ltd., reproduced with permission.

Given that the mobile phase of the feedstock is determined by the upstream process and any significant adjustments add cost and complexity, the chromatographer can now start to address these two questions. Due to the nature of proteins and the influences of protein : protein interactions which may occur in the feedstream, it is difficult, if not impossible, to predict the optimal chromatographic conditions without practical study. It is therefore common practice to carry out a parametric study, investigating the influence of pH and ionic strength with different ion exchangers. This is potentially a time-consuming process, but one that will aid in process optimization. This traditionally was performed manually, but more recently automated workstations have become commercially available which can be programmed to carry out multivariable parametric studies automatically.

Media Selection

A key consideration during method scouting is which ion exchanger to use. The protein chromatographer is offered a range of strong or weak anion or cation exchangers, from several suppliers. The functional groups are broadly similar across the range, but the base matrices range from polysaccharides including agarose, cellulose and dextran to polymeric supports and advanced composites. Given that each manufacturer has proprietary chemical processes, the offerings available are quite diverse. In order to assess the impact of media selection on method scouting and development, we screened 70 different commercially

available anion and cation exchangers, which may be considered for process-scale protein separations. Each medium was screened under identical conditions. Perhaps not surprisingly, our data demonstrated that 70 different media had 70 different properties. Our data, descriptive rather than prescriptive, suggest that media effectiveness is process dependent rather than supplier dependent and the thought process of 'it worked last time' is not an appropriate rationale for developing a second process using the same adsorbent.

Method Development

When an appropriate ion exchanger and mobile phase system have been identified, it must then be decided whether to conduct the separation in either a column contactor or a batch stirred tank system. The former technique, being contained, lends itself to automation and control, but the latter technique, albeit classical, should not be dismissed. If, for example, the feedstream/adsorbent volume ratio is high, perhaps $> 20:1$, then the time to pump the feedstream through a packed bed of adsorbent would be several hours. A batch stirred tank adsorption including medium collection by centrifugation should take less than 1 h. Similarly in a large scale process where several hundreds of kilograms of ion exchanger are used, columns are costly and often cumbersome to use, so a large batch system may be preferred due to its simplicity.

For highly selective separations where desorption and elution conditions are critical then a column-based technique would be appropriate, typically using gradient elution.

As stated earlier, proteins are large molecules with a size up to hundreds of angstroms and consequently diffusion into and out of the pores of an ion exchanger is the rate limiting step both in terms of capture efficiency during adsorption and selectivity during desorption and elution. In order to enhance each of these parameters, one needs to maximize residence time of the adsorbate with the adsorbent to increase the capture efficiency of the target protein and in order to maximize selectivity, one needs to provide adequate time for the desorbed protein to diffuse into the bulk liquid phase, so it elutes as a sharp peak. Flow rate is clearly the critical factor to regulate these adsorption/desorption rates and this equates with process-time. Unlike ion exchange of small ions, where pore diffusion rates while limiting have minimal criticality, they are crucial for effective ion exchange chromatography of proteins and must be considered during methods development. Typical linear flow rates for polysaccharide-based ion exchangers would be $30\text{--}300\text{ cm h}^{-1}$ and for advanced

polymeric-based media, a further 10-fold increase in flow may be possible. However, it should be noted that the maximum flow rate specification of the ion exchanger and an operational flow rate for effective protein binding and elution may be widely different, and will likely to be determined by the nature of the protein separation itself.

Scale-down Studies

Having defined the ion exchanger, the mobile phases and the mode of operation, a series of small scale studies will be carried out at the laboratory bench to assess process economics and perhaps to carry out sensitivity analysis and validation support studies.

Scaled-down studies are very valuable and enable a substantial amount of data to be generated and collated in a cost-effective manner, although the time-scale may be similar to that required for large scale work. The key feature of a small scale study is that the contactor is a scaled-down version of the process system. For a batch process the aspect ratio of the tank and tip speed of the agitator, etc., would be the same for both scales of operation. The ratio of feedstock volume to mass of ion exchanger would be constant as would the contact times for adsorption, washing and elution. For a column separation, column bed height would be identical at both scales of operation and linear flow rate would be maintained throughout the process. Provided that all mobile phase volumes used were in proportion to the amount of ion exchanger used, and that feedstock and buffer compositions remain unaltered, a small scale study should be a good model of the large scale process separation. In the anion exchange chromatography of hen egg-white proteins, for example, we have reported the 1000-fold scale-up of a column process from a 25 mL column to a 25 L column.

Process validation is a critical area in the isolation of therapeutic proteins. In these applications it is crucial that for multiple uses of the adsorbent, the eluting fraction containing the target protein has a consistent composition from run to run and that it meets a specification in terms of microbial bioburden, endotoxin levels, pyrogenicity and viral contamination. These aspects of process validation have been adequately reviewed by Sofer and Nystrom.

A widely used mobile phase for regeneration of ion exchangers following protein chromatography is sodium hydroxide. It is well established that exposure of a column of ion exchanger to $0.5\text{--}2.0\text{ M NaOH}$ for up to 12 h is an effective means of regenerating the medium. Importantly, these conditions are also acknowledged to be effective at sanitization of the ion exchange system, and we have confirmed this to be

the case following gross microbial contamination of columns of both anion and cation exchangers.

A key element of process validation is the chemical stability of the ion exchanger to the cleaning/sanitizing reagent systems. We have developed protocols for monitoring hydrolysis of functional groups, referred to as ligand leakage, and also matrix dissolution, in order to address these concerns.

These process validation studies are typically conducted in scale-down mode, and confirmatory checks made subsequently at process scale.

Process Scale Ion Exchange Chromatography of Proteins

Having defined the feedstock and mobile phases, selected the ion exchanger and selected a batch or column mode of operation, the chromatographer should find himself or herself in a position to scale-up the process.

It is difficult to predict cost information on process scale ion exchange separations since much depends on the upstream and downstream process requirements and reusability of the ion exchanger, etc. We have reported a cost estimate for single usage of 25 kg of DE52 in batch and column operation (see Ganetsos and Barker), but this is exemplary only. Unfortunately information of this type, while in existence, is proprietary and therefore withheld.

Industry has carried out large scale ion exchange chromatography of proteins for the last few decades

and with the established principles described above, there is no reason to assume that things will change significantly over the short to medium term. In the longer term, developments in fluidized/expanded beds and membrane adsorbers may offer new opportunities in this area of chromatography.

See also: II/Affinity Separation: Rational Design, Synthesis and Evaluation: Affinity Ligands. III/Proteins: Centrifugation; Electrophoresis; High-Speed Countercurrent Chromatography.

Further Reading

- Ganetsos G and Barker PE (eds) (1993) *Preparative and Production Scale Chromatography*. New York: Marcel Dekker.
- Levison PR, Mumford C, Streater M, Brandt-Nielsen A, Pathirana ND and Badger SE (1997) Performance comparison of low-pressure ion-exchange chromatography media for protein separation. *Journal of Chromatography A* 760: 151.
- Shillenn JK (ed.) (1996) *Validation Practices for Biotechnology Products*. West Conshohocken: ASTM.
- Sofer GK and Nystrom L-E (1991) *Process Chromatography. A Guide to Validation*. London: Academic Press.
- Stryer L (1981) *Biochemistry*, 2nd edn. San Francisco: Freeman.
- Subramanian G (ed.) (1991) *Process-scale Liquid Chromatography*. Weinheim: VCH.
- Verrall MS (ed.) (1996) *Downstream Processing of Natural Products*. Chichester: John Wiley.

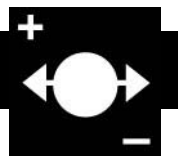
Metalloproteins: Chromatography

See III/METALLOPROTEINS: CHROMATOGRAPHY

Thin-Layer (Planar) Chromatography

See III/PEPTIDES AND PROTEINS: Thin-Layer (Planar) Chromatography

PROTEOMICS: ELECTROPHORESIS



M. J. Dunn, National Heart and Lung Institute, Imperial College of Science, Technology and Medicine, Harefield Hospital, Middlesex, UK

Copyright © 2000 Academic Press

Introduction

The first complete genome sequence, that of *Haemophilus influenzae*, was published in 1995. Intense effort over the last three years has resulted in the completion of the genomes for a further 12 micro-organisms

ranging in complexity from *Mycoplasma genitalium*, with a genome size of only 0.58 Mb encoding less than 500 proteins, to *Escherichia coli*, with a genome size of 4.6 Mb encoding more than 4000 proteins (Table 1). The complexity of the eukaryotic genomes has resulted in slower progress, with only one organism, the yeast *Saccharomyces cerevisiae*, having been completed (Table 1). However, significant progress is being made for a variety of other species, with the estimated date for the completion of the human genome currently being 2001 (Table 1).

The vast amount of information being generated by the various genome sequencing programmes has the potential to contribute significantly to our understanding of how an organism functions and its evolutionary relationships with other life forms. However, it has already become clear that genomics alone will not provide all of the answers. For those organisms whose genomes have been completed, typically around 30% of the genes can be assigned definite functions with up to a further 30% being attributed functions on the basis of homology with other genes of known function. The remaining 40% of the structural genes can often not even be attributed putative

functions. A further limitation of the genomic approach is that it does not provide any insights into the ways an organism may modify its pattern of gene expression in response to different conditions.

Analysis of Gene Expression

These problems can only be solved by direct investigation of gene expression, which can be achieved at either the level of messenger RNA (mRNA) or protein. A variety of techniques such as cDNA microarrays and serial analysis of gene expression (SAGE) make it possible to undertake mass screening of mRNA expression and establish which particular mRNAs are expressed in an organism under any given condition. However, recent studies have highlighted an important limitation of this approach in that *there is not always a direct correlation between RNA abundance and the amount of the corresponding functional protein within the cell*.

A further major limitation of studies at the level of mRNA is that they are unable to provide any information of processes of co- and post-translational modification of proteins. The modification of proteins by processes such as phosphorylation, glycosylation, sulfation, hydroxylation, N-methylation, acylation, prenylation and N-myristoylation, can result in significant modulation of their functional properties. Knowledge of these processes is therefore important for a complete understanding of gene expression.

Table 1 Some organisms whose genomes have been completely sequenced and others which are the subject of active genome sequencing programmes

Organism	Size (Mb)	ORFs	Year completed
Microorganisms			
<i>Mycoplasma genitalium</i>	0.58	470	1995
<i>Ureaplasma urealyticum</i>	0.75	640	
<i>Mycoplasma pneumoniae</i>	0.81	679	1996
<i>Treponema pallidum</i>	1.14	1000	
<i>Borrelia burgdorferi</i>	1.44	843	1997
<i>Aquifex aeolicus</i>	1.50	1512	1998
<i>Helicobacter pylori</i>	1.66	1590	1997
<i>Methanococcus jannaschii</i>	1.66	1738	1996
<i>M. thermoautotrophicum</i>	1.75	1855	1997
<i>Haemophilus influenzae</i>	1.83	1743	1995
<i>Streptococcus pyogenes</i>	1.98	1900	
<i>Archaeoglobus fulgidus</i>	2.18	2436	1997
<i>Nisseria gonorrhoeae</i>	2.2	2100	
<i>Pyrobaculum aerophilum</i>	2.22	1900	
<i>Synechocystis</i> PCC6803	3.57	3168	1996
<i>Bacillus subtilis</i>	4.20	4100	1997
<i>Mycobacterium tuberculosis</i>	4.41	3924	1998
<i>Escherichia coli</i>	4.60	4288	1997
Eukaryotes			
<i>Saccharomyces cerevisiae</i>	13.0	5885	1996
<i>Dictyostelium discoideum</i>	70	12500	
<i>Arabidopsis thaliana</i>	70	14000	
<i>Caenorhabditis elegans</i>	80	17800	
<i>Drosophila melanogaster</i>	170	30000	
<i>Homo sapiens</i>	2900	50000	

ORFs = open reading frames.

Proteome Analysis

The realization that these problems can only be addressed through studies at the level of protein expression has resulted in increasing interest in the area which has become known as 'proteome analysis'. The term 'proteome' was first coined by a collaborative team of scientists at Macquarie and Sydney Universities in 1995 and is defined as the **protein complement of the genome** of an organism. Increasing genomic complexity together with the potential for co- and post-translational modifications make proteome analysis a difficult task for higher organisms. As a consequence, active proteome programmes are currently restricted to some of the simpler organisms such as mollicutes (*M. genitalium*, *Spiroplasma melliferum*), prokaryotes (*E. coli*, *Chlamydia trachomatis*) and yeast (*S. cerevisiae*).

The complexity of eukaryotic proteomes has resulted in the term 'proteomics' or 'proteome analysis' being used in a narrower context in which it is used to characterize patterns of protein (and thereby gene) expression in particular cell type and tissues. This

approach can provide new insights into a variety of biological processes such as development, apoptosis and the cell cycle and add to our knowledge of the mechanisms that control gene expression. There is also considerable interest in applying proteomics to the study of diseases, where it promises further understanding of these processes at the molecular level and may lead to the discovery of new diagnostic markers and novel therapeutic targets. The pharmaceutical industry is also expressing considerable interest in the potential of proteomics in the process of drug discovery, as well as for analysis of the pharmaceutical and toxicological effects of existing therapeutics.

Need for Protein Separation

The five main steps of proteome analysis are shown in **Figure 1**. The primary requirement is that we must be able to separate the very complex protein mixtures present in lysates of cells, tissues and organisms. It is generally accepted that the best method currently available is two-dimensional polyacrylamide gel electrophoresis (2D electrophoresis). While there are several possibilities for combination of electrophoretic procedures, the most effective approach is a combination of a first-dimension separation by isoelectric focusing (IEF) under denaturing conditions with a second-dimension separation by sodium dodecyl sulfate-polyacrylamide gel electrophoresis (SDS-PAGE). This results in the sample proteins being separated according to their charge properties (i.e. isoelectric point, pI) in the first dimension followed

by a size-based (molecular weight) separation in the second dimension. As the charge and size properties of proteins are essentially independent parameters, this results in the sample proteins being distributed across the whole area of the 2D separation (**Figure 2**).

O'Farrell Method of 2D Electrophoresis

The method of 2D electrophoresis (2DE) described by O'Farrell in 1975 has formed the basis of almost all subsequent developments in 2-DE. This method used a combination of IEF in cylindrical gels (cast in capillary tubes) containing 8 M urea and 2% of the nonionic detergent, Nonidet P-40 (NP-40), with the SDS-PAGE system of Laemmli. However, for effective use in proteome analysis, 2DE must be capable of consistently reproducible high resolution protein separations. This proved to be problematic largely due to the nature of the synthetic carrier ampholytes (SCA) used to generate the pH gradients for IEF. SCA are small molecules which are freely mobile within the IEF gel, and the electroendosmotic flow of water which occurs during IEF results in their migration towards the cathode. This process is known as cathodic drift and results in pH gradient instability, with loss of the more basic proteins from the final 2D gel pattern.

2DE using IPG IEF

This problem has been largely overcome with the development of the Immobiline reagents (Amersham Pharmacia Biotech) for the generation of immobilized pH gradients (IPG) for IEF. The Immobiline reagents are acrylamide derivatives which give a series of buffers with different pK_a values distributed across the range pH 3–10. The appropriate Immobiline reagents, calculated from the extensive series of published recipes, are added to the mixture used for gel polymerization, resulting in the buffering groups which will form the pH gradient being covalently attached via vinyl bonds to the polyacrylamide backbone. This immobilization of the pH gradient renders it immune to the effects of electroendosmosis, resulting in highly stable IEF separations.

Despite early problems which were encountered in the application of IPG IEF to 2DE separations, this method has now become the method of choice for the first dimension of 2DE. The procedure which is now used is largely based on the work of Görg and her colleagues (see Further Reading). Briefly, IPG IEF is performed in individual gel strips, 3–5 mm wide, cast on plastic supports. After IEF, the gel strips are equilibrated to allow the separated proteins to interact with SDS, and then applied either to the

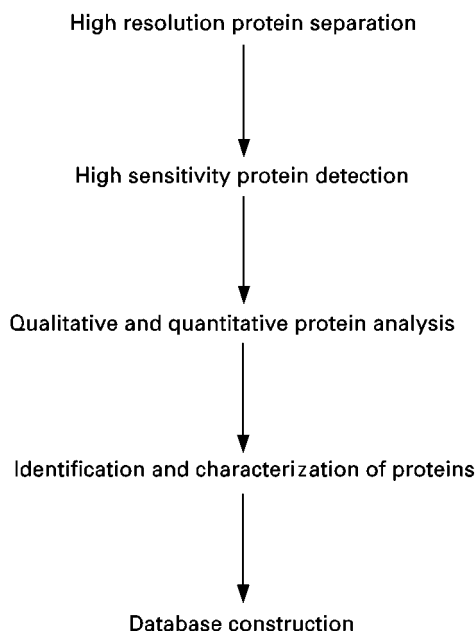


Figure 1 The five main steps in proteome analysis.

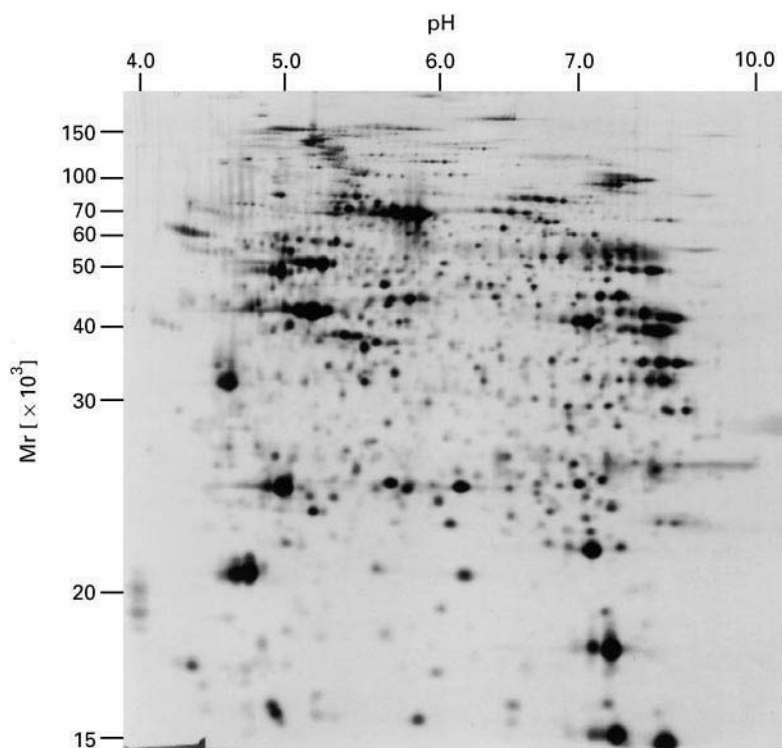


Figure 2 A 2DE separation of 100 μg of human heart using a nonlinear pH 3.5–10 IPG IEF gel was used in the first dimension and 12% SDS-PAGE in the second dimension. The separated proteins were visualized by silver staining.

surface of a horizontal SDS-PAGE gel to the top of a vertical. Interlaboratory studies of heart, barley and yeast proteins have unequivocally demonstrated the excellent reproducibility of both protein spot position and quantity that can be achieved with this method.

Separation Capacity of 2DE

The ability of 2DE to resolve complex mixtures of proteins is dependent on the gel area used for the separation. Thus, the 'standard' combination of 18 cm IPG strips with 20 cm SDS-PAGE gels is capable of routinely separating 2000 proteins from lysates of whole cells and tissues. It has been shown that very large gel formats (up to 30 cm in each dimension) are capable of separating up to 10 000 proteins from such samples, but this is achieved at the expense of the ease of gel handling and processing. In contrast, only a few hundred proteins can be separated using mini-format 2DE, but this approach has the advantage of rapid separations for screening purposes.

IPG IEF also provides great flexibility in the choice of pH gradient used for the separation, providing an additional approach to maximize the efficiency of separation of the particular protein mixture under investigation. Thus, IPG IEF gels spanning the range pH 3.5–10 are ideal for examining the diversity of protein

in a sample (Figure 2). Optimal resolution of proteins in a particular pH range can be achieved using narrower pH gradients (Figure 3).

A further advantage of IPG IEF is that it has a very high capacity for micropreparative 2DE protein separations, particularly using a recently described method in which IPG strips are reswollen directly in a solution containing up to several mg of the protein sample to be analysed.

Protein Detection

The next requirement for effective proteome analysis is detection of the separated proteins at high sensitivity. The Coomassie brilliant blue dyes have been the most commonly used reagents for detecting protein zones separated by gel electrophoresis, but their limited sensitivity (around 0.5 μg per protein spot) necessitates the use of relatively high sample loadings (> 500 μg). Much higher sensitivity of detection (0.1 ng per protein spot) can be achieved by silver staining (Figures 2 and 3), but there can be problems in using this method as a quantitative procedure as it is known to be non-stoichiometric. Silver staining intensity is linear over the range from 0.04 to 2 ng protein/ mm^2 , but above this limit the stain becomes nonlinear, resulting in saturation and even negative staining effects.

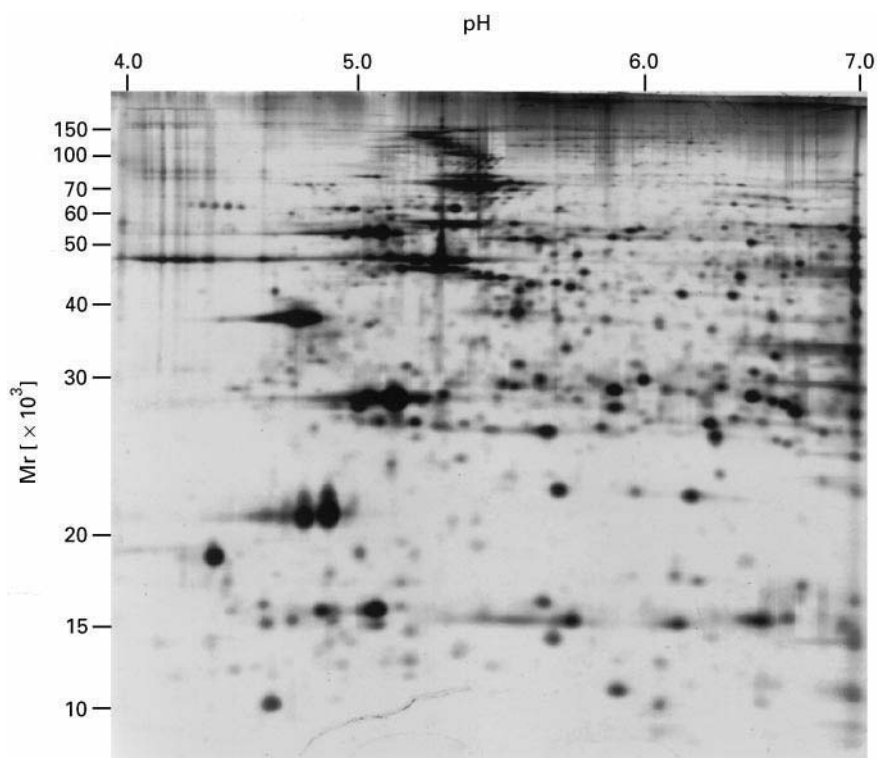


Figure 3 A 2DE separation of 100 μ g of human heart using a linear pH 4–7 IPG IEF gel was used in the first dimension and 12% SDS-PAGE in the second dimension. The separated proteins were visualized by silver staining.

Many of these problems can be overcome using detection methods based on the use of fluorescent compounds. Such methods are highly sensitive and generally exhibit excellent linearity and a high dynamic range, making it possible to achieve excellent quantitative analysis if a suitable imaging device is used. A variety of fluorescent compounds are available for labelling proteins prior to electrophoresis. However, such pre-electrophoretic staining often results in charge modification, resulting in alterations in spot positions during 2DE. Recently, compounds which react with cysteine or lysine residues have been used successfully for 2DE. The cysteine-reactive reagent, monobromobimane was found to have a sensitivity of 1 pg protein per spot when imaged using a cooled CCD camera. The amine-reactive cyanine dyes, propyl Cy3 and methyl Cy5, have been used to label *E. coli* proteins. These dyes are claimed to have an inherent positive charge, thereby preserving the overall charge of the proteins after coupling. Due to their spectral properties, the two dyes can be distinguished when present together, allowing two different samples each labelled with one of the dyes to be mixed together and separated on the same 2DE gel. This method, which has been termed difference gel electrophoresis (DIGE), has great potential for improving the efficiency of detection of differ-

ences in 2DE protein patterns between different samples.

One approach to overcoming the problems associated with charge modification during the IEF dimension is to label the proteins while present in the first dimension gel after IEF, prior to the second dimension separation by SDS-PAGE. The fluorescent compound 2-methoxy-2,4-diphenyl-3(2H)-furanone (MDPF) and a fluorescent maleimide derivative have been used in this way. The alternative approach is to label the proteins after the 2DE separation has been completed. Recently, two post-electrophoretic fluorescent staining reagents, SYPRO orange and red have been described. These stains have a very high sensitivity (2 ng protein per spot) and excellent linearity with a high dynamic range.

Metabolic labelling of proteins with a radiolabelled amino acid prior to their separation by 2DE provides a very sensitive method for protein detection. This approach is most commonly used with *in vitro* cell culture systems, but it is also possible to radiolabel synthetically the proteins in small pieces of fresh tissue. While proteins can be readily radiolabelled postsynthetically by methods such as radioiodination with [125 I] or reductive methylation with [3 H]-sodium borohydride, these result in significant charge modifications precluding their use in proteome analysis.

Qualitative and Quantitative Analysis

The first step in the analysis of 2DE protein profiles is to produce a digitized image. Stained gels can be digitized using a flat-bed scanning laser densitometer or a suitably modified document scanner. Autoradiographic film images of 2DE separations of radiolabelled proteins can also be imaged in this way, but more accurate quantitation can be achieved using a phosphorimaging scanner. Fluorescently labelled protein separation patterns can be visualized using either a dedicated scanning laser densitometer (fluorimeter) or a camera system fitted with cooled CCD array. Several commercial software systems for the analysis of 2DE gels are now available running on desktop workstations (Unix, PC, Mac). These systems make it possible to extract quantitative and qualitative information from individual 2DE gels, to match protein patterns from large collections of 2DE gels, and thereby establish comprehensive databases which can be used to investigate quantitative protein expression in cells, tissues and organisms.

Protein Identification and Characterization

It is clear from the foregoing that 2DE provides information on the *pI*, molecular weight and relative abundance of the separated proteins. However, it provides no direct clues to their identities or functions. The *pI* and molecular weight information can be used to search sequence databases for proteins with similar properties, for example using the TagIdent tool (<http://www.expasy.ch/www/guess->

[prot.html](http://www.expasy.ch/www/guess-prot.html)), but the uncertainty of molecular weight estimation by SDS-PAGE (typically around $\pm 10\%$) makes this process unreliable. Recently, mass spectrometry (MS) has been used to measure directly the mass of proteins separated by 2DE. In this approach the proteins are transferred by Western blotting onto the surface of a nitrocellulose or PVDF membrane which is then treated with a matrix required for MS. The protein spot of interest is excised, mounted directly into a matrix-associated laser desorption/ionization mass spectrometer (MALDI-MS) and the mass of the intact protein measured (Figure 4). We have found that this method is very accurate, usually within 1% of the predicted mass, but requires a MALDI-MS fitted with an infrared laser. While such mass data can be invaluable in characterizing post-translational modifications of proteins, it is unlikely on its own to result in unequivocal protein identification. Fortunately, over the last few years, several methods have been developed which make it possible to identify and characterize proteins separated by 2DE (Figure 5).

Western Blotting

The first major advance in the characterization of proteins separated by gel electrophoresis was the development of Western blotting. In this technique, the separated proteins are transferred ('blotted') from the restrictive gel matrix, usually by application of an electric field perpendicular to the plane of the gel ('electroblotting'), onto the surface of a suitable membrane support such as nitrocellulose or PVDF. The proteins can then be probed with a variety of ligands,

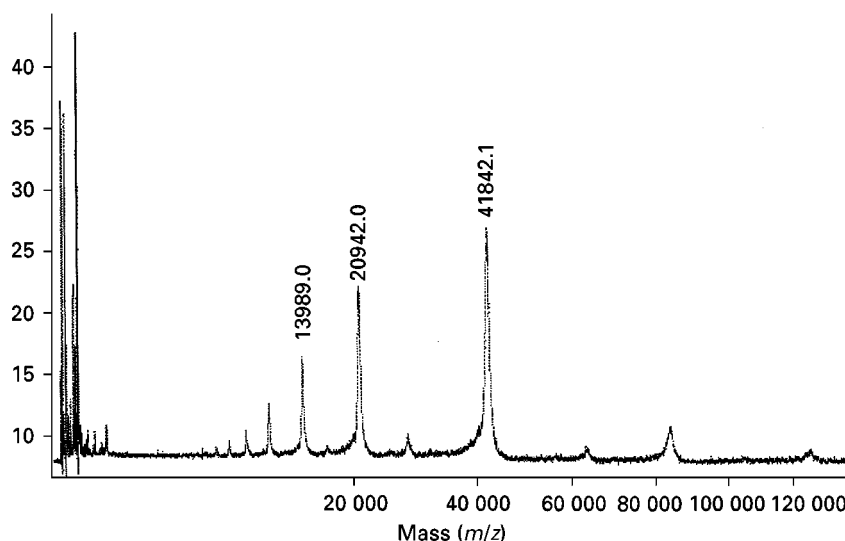


Figure 4 IR-MALDI mass spectrum of a protein spot from a 2D gel electroblotted onto a PVDF membrane. Mass peaks indicated are multiply charged or dimers of the molecular ion. The protein spot is known to be cardiac α -actin. The measured mass of the molecular ion (41842.1) is very close to the theoretical value determined from its amino acid sequence (41784.6).

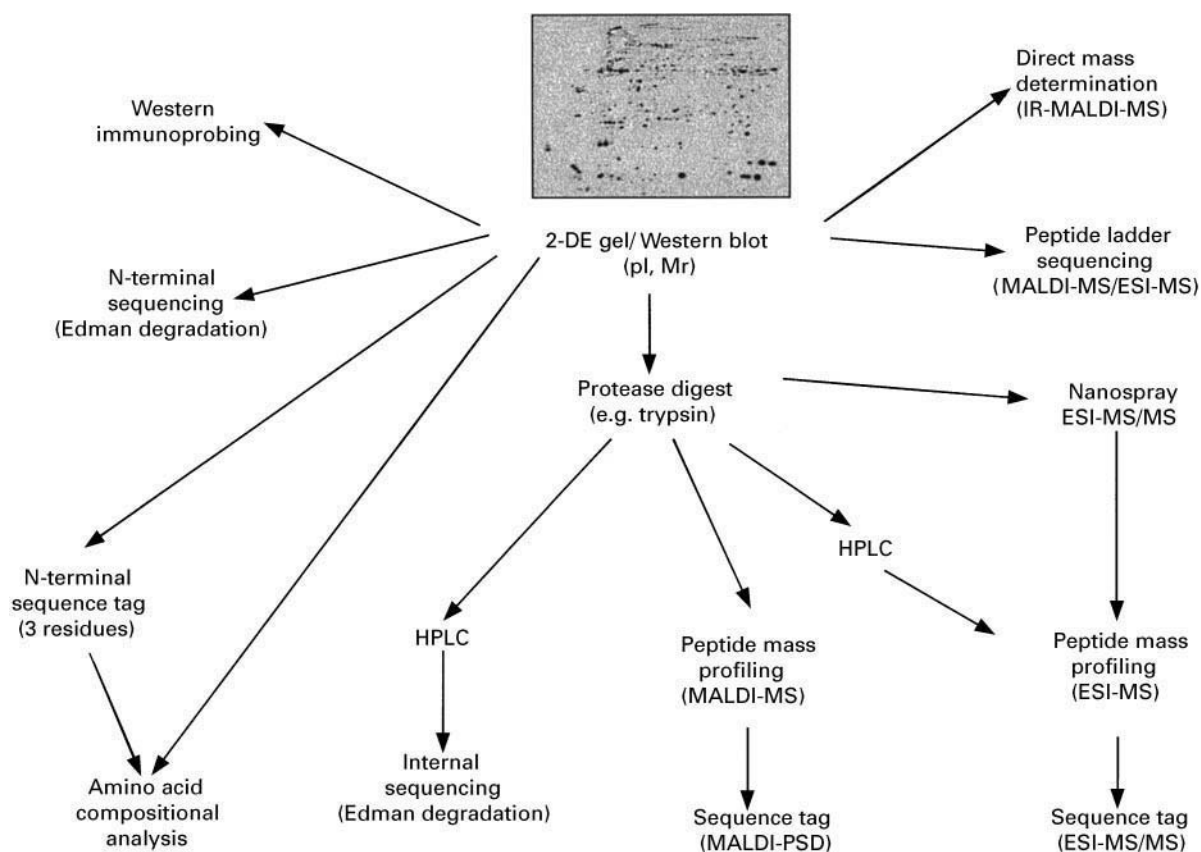


Figure 5 Methods currently used for the identification and characterization of proteins separated by 2DE.

particularly poly- and monoclonal antibodies. This approach has been used quite extensively for the identification of known proteins separated by 2DE, but is a very time-consuming process that is dependent on the availability of a suitable panel of specific antibodies reactive with the denatured proteins in 2DE gels.

Amino Acid Sequence Determination by Edman Degradation

Amino acid sequence, even if this is only a few residues in length, is the most specific method of protein identification. The chemical sequencing of proteins has been possible for half a century since the development of the method known as Edman degradation in 1949. This remained a laborious manual procedure until the development of the first automated protein sequenators, with the first commercial 'spinning cup' instrument becoming available in 1971. This instrument was relatively insensitive, requiring at least 10 nmol of sample (equivalent to 500 µg for a 50 kDa protein). However, progress in sequenator technology has resulted in the current generation of gas-liquid sequenators which are capable of generat-

ing N-terminal sequence information from low picomole quantities of protein (1 pmol is equivalent to 0.05 µg for a 50 kDa protein). This level of sensitivity is compatible with the amount represented by many of the spots present on micropreparative 2DE gels and this method remains the method of choice if extended runs of N-terminal protein sequence are required. This is a particularly important consideration for the analysis of apparently 'novel' proteins, i.e. sequences not present in protein and nucleotide databases. Although chemical protein sequencing is a sensitive and informative method of protein identification, throughput is very low, typically one or two samples per day. Thus, there is a need for alternative approaches which allow rapid and sensitive screening of gel proteins separated by 2DE, so that only those which cannot be identified unequivocally or appear to be novel require further detailed characterization.

Problem of N-Terminal Blockage

A major problem with protein sequencing by Edman degradation is that many proteins lack a free α -amino group, due to co- or post-translational modification.

Such N-terminal blockage occurs typically in up to 50% of eukaryotic proteins and results in no sequence being obtained. This problem can be overcome by subjecting the separated protein, either *in situ* within the gel matrix or after Western blot transfer onto a nitrocellulose or PVDF membrane, to chemical (e.g. CNBr) or enzymatic (e.g. trypsin) cleavage to generate shorter peptides which can be isolated and sequenced. The cleavage products are then usually separated by RP-HPLC, and selected peptide fractions directly applied to the protein sequenator. This procedure is highly efficient, but the determination of multiple stretches of sequence usually requires two to three times more protein than does N-terminal protein sequence analysis.

Amino Acid Compositional Analysis

Amino acid compositional analysis (AAA) is the best method for the absolute measurement of protein abundance. Current methods for the analysis of fluorescently derivatized amino acids have sub-pmole sensitivity and so can be applied directly to proteins separated by 2DE. An individual proteins have more or less unique amino acid compositions, AAA can be an excellent method for the rapid identification of proteins separated by 2DE, in which the experimental amino acid composition is compared with amino acid sequences generated *in silico* from protein and nucleotide sequence databases. The major drawback of this approach is that the output is a ranked list of possible protein identities (Figure 6) and the 'correct' protein does not necessarily occur as the first ranked entry. This method is better used in conjunction with another rapid method of protein identification such as peptide mass profiling (see later) and this orthogonal approach has been found to be useful for identifying proteins even across the species barrier. Another approach to improving protein identification by AAA is to generate a short N-terminal protein 'sequence tag' by Edman degradation and to use this in combination with the AAA data for protein identification.

Peptide Mass Profiling

It has long been realized that the peptides generated by chemical (e.g. CNBr) or enzymic (e.g. trypsin) digestion of a protein are characteristic of that protein and such peptide fingerprints or maps analysed by chromatography or electrophoresis have been used for investigating the relatedness of proteins. The advent of MS methods for the analysis of peptides has made this into a much more powerful approach for protein identification. In this method the peptide

masses obtained by MS of a protein digest are used to interrogate databases of peptide masses generated *in silico* from protein and nucleotide sequence databases. As in the case of AAA, this technique of peptide mass profiling or fingerprinting produces a list of possible protein identities ranked in order of probability (Figure 7). The reliability of this method can be increased by combining peptide mass profiling data from two or more separate digests (e.g. trypsin, Lys-C) or by adopting an orthogonal approach in combination with AAA (see above).

The enzymatic cleavage of the 2DE protein spot can be carried out either *in situ* within the gel matrix or after electroblotting to a suitable membrane (nitrocellulose or PVDF). After recovery, the unfractionated peptide can be readily analysed by MALDI-MS (Figure 7). Alternatively, the peptide mixture can be fractionated by high performance liquid chromatography (HPLC), with the fractions being analysed either offline by MALDI-MS or online by electrospray ionization (ESI)-MS using a quadrupole or ion-trap instrument.

Amino Acid Sequence Determination by Mass Spectrometry

Recently alternative techniques for the determination of the primary sequence of peptides and proteins have been developed based on the use of mass spectrometry (MS). This can be achieved by peptide fragmentation within the spectrometer or by a method termed 'ladder sequencing'. In the latter approach, Edman chemistry or enzymic degradation with aminopeptidase or carboxypeptidase is used under limiting conditions to produce an overlapping series of truncated peptides. These differ in size according to the number of amino acid residues which have been removed from their N- or C-terminus, allowing the sequence to be deduced by measurement of the peptide masses by MALDI-MS. A high mass accuracy is required and it is not possible to distinguish between leucine and isoleucine as these residues have an identical mass.

The alternative approach is to take advantage of the ability of two-stage mass spectrometers, either MALDI-MS with post-source decay (PSD) or ESI-MS/MS triple-quadrupole or ion-trap instruments, to induce fragmentation of peptide bonds. It is possible to use this approach to generate extended *de novo* amino acid sequence information, but it requires considerable expertise to interpret the complex spectra that are obtained. However, partial sequence data is an extremely powerful adjunct to the identification of proteins by peptide mass profiling.

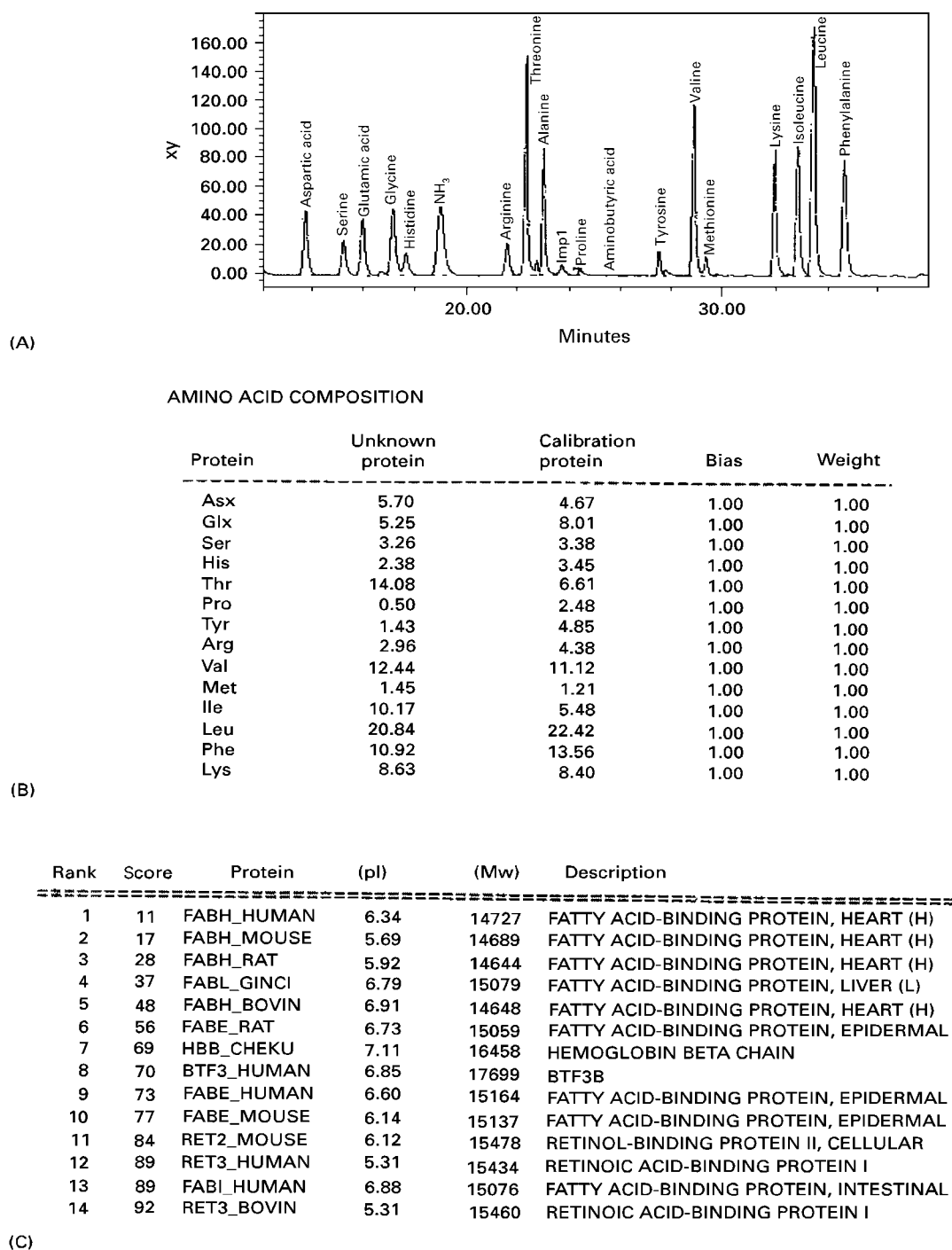


Figure 6 The identification of a protein spot from a 2DE separation by amino acid compositional analysis. (A) HPLC analysis of pre-column derivatized amino acids resulting from hydrolysis of the protein spot. (B) Amino acid composition determined from the HPLC analysis. (C) Result of the amino acid composition database search indicating that the protein is cardiac fatty acid binding protein.

The method known as 'peptide sequences tagging' is based on interpretation of a portion of the ESI-MS/MS or PSD-MALDI-MS fragmentation data to generate a short partial sequence or 'tag', which is used in combination with the mass of the intact parent peptide ion, and provides a significant amount of additional information for the homology search.

A powerful extension of this approach has been the development of a nano-electrospray ion source that allows spraying times of more than 30 min from about 1 μ L of sample. The sensitivity of this method is in the low femtomole range and silver stained 2DE protein spots containing as little as 5 ng protein have been successfully sequenced. Moreover, using this

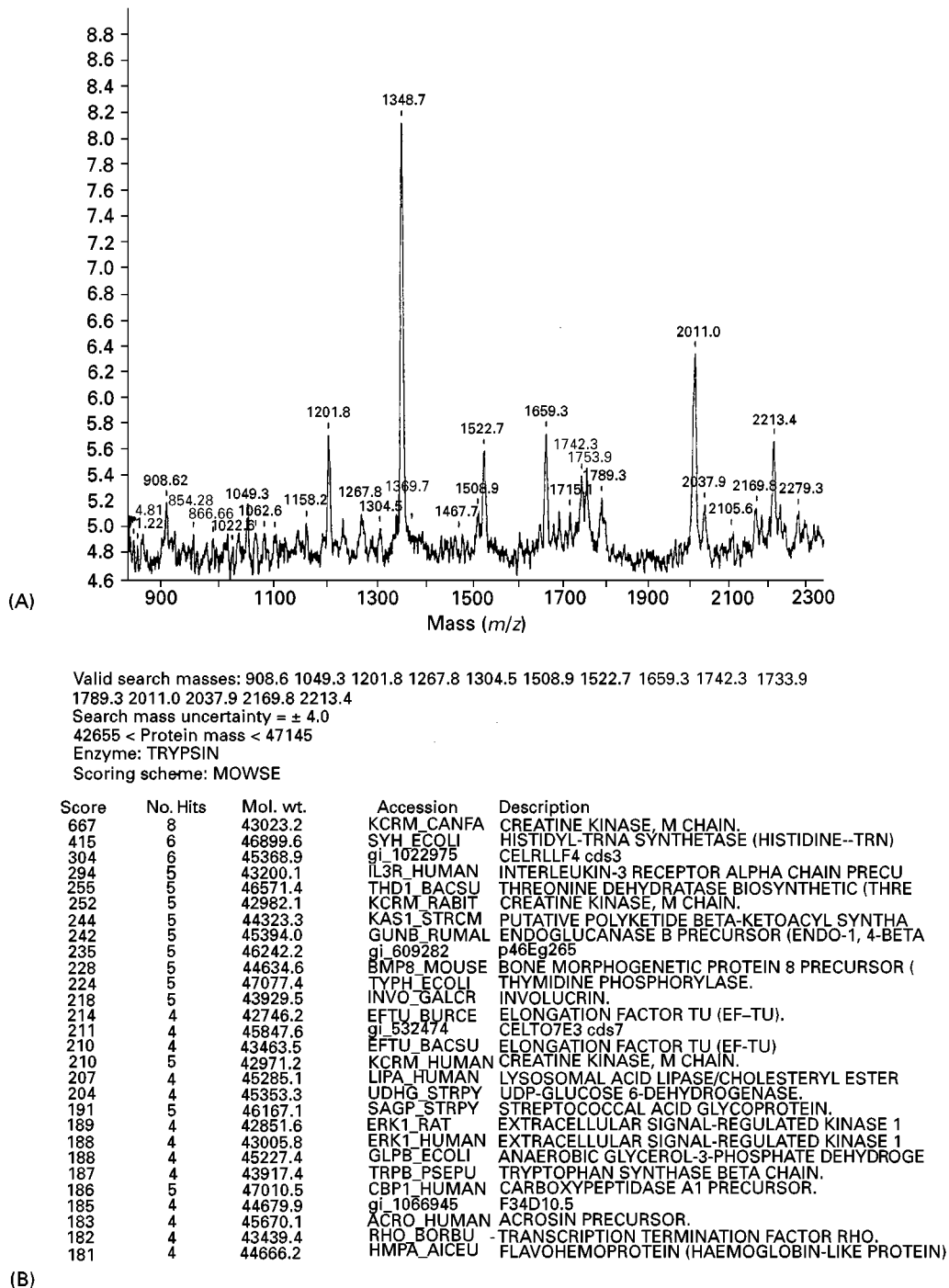


Figure 7 The identification of a protein spot from a 2DE separation by peptide mass fingerprinting. (A) MALDI-MS spectrum of the tryptic digest of the protein spot. (B) Result of the peptide mass database search indicating that the protein is the M-chain of creatine kinase.

method it is possible to sequence multiple peptides from a digest without the need for their prior separation by RP-HPLC.

An alternative approach is based on the automated interpretation of ESI-MS/MS fragmentation data which is used to directly search sequence databases. In the first step in this process all those peptides that

can be generated from proteins in the sequence databases and whose masses match those of the measured peptide ion are identified. The fragment ions expected for each of the candidate peptides are then calculated and the experimentally determined MS/MS spectrum is then compared with the predicted spectra using cluster analysis algorithms. This

method has been fully automated and sensitivity is at the low femtomole level.

Database Construction

The final requirement for proteome analysis is the construction of databases to store the data generated and to make this readily available within the laboratory and, where possible, accessible to other scientists worldwide. The best approach to this is currently offered by the World Wide Web (WWW) on the Internet. There is currently no international standard for the construction of such databases, but in order that there should be good connectivity between them it has been suggested that they are constructed according to a set of fundamental rules. Databases conforming to these rules are said to be 'Federated 2D Databases' and a list of these can be viewed at WORLD-2DPAGE (<http://www.expasy.ch/ch2d/2d-index.html>).

Conclusions

From the foregoing discussion it can be seen that proteomics provides an interface with genomics which can provide information on protein expression in biological systems. This information will aid our understanding of complex cellular processes and the way in which they react to varying conditions. Proteomics will also provide insights into processes of disease at the molecular level and should result in the development of novel diagnostics and therapeutics.

Further Reading

- Dunn MJ (1987) Two-dimensional polyacrylamide gel electrophoresis. In: Chrambach A, Dunn MJ and Radola BJ (eds) *Advances in Electrophoresis*, vol. I, pp. 1–109. Weinheim: VCH.
- Görg A, Boguth G, Obermaier C, Posch A and Weiss W (1995) Two-dimensional polyacrylamide gel electrophoresis with immobilized pH gradients in the first dimension (IPG-Dalt): The state of the art and the

- controversy of vertical versus horizontal systems. *Electrophoresis* 16: 1079–1086.
- Humphery-Smith I, Cordwell SJ and Blackstock WP (1997) Proteome research: Complementarity and limitations with respect to the RNA and DNA worlds. *Electrophoresis* 18: 1217–1242.
- Lamond AI and Mann M (1997) Cell biology and the genome projects: A concerted strategy for characterizing multiprotein complexes by using mass spectrometry. *Trends in Cell Biology* 7: 139–142.
- Patterson SD (1994) From electrophoretically separated protein to identification: Strategies for sequence and mass analysis. *Analytical Biochemistry* 221: 1–15.
- Patterson SD and Aebersold R (1995) Mass spectrometric approaches for the identification of gel-separated proteins. *Electrophoresis* 16: 1791–1814.
- Pennington SR, Wilkins MR, Hochstrasser DF and Dunn MJ (1997) Proteome analysis: From protein characterization to biological function. *Trends in Cell Biology* 7: 168–173.
- Sutton CW, Wheeler CH, U S, Corbett JM, Cottrell JS and Dunn MJ (1997) The analysis of myocardial proteins by infrared and ultraviolet laser desorption mass spectrometry. *Electrophoresis* 18: 424–431.
- Wan JS, Sharp SJ, Poirer GM *et al.* (1996) Cloning differentially expressed mRNAs. *Nature Biotechnology* 14: 1685–1691.
- Wasinger VC, Cordwell SJ, Cerpa-Poljak A *et al.* (1995) Progress with gene-product mapping of the Mollicutes: *Mycoplasma genitalium*. *Electrophoresis* 16: 1090–1094.
- Wheeler CH, Berry SL, Wilkins MR *et al.* (1996) Characterisation of proteins from two-dimensional electrophoresis gels by matrix-assisted laser desorption mass spectrometry and amino acid compositional analysis. *Electrophoresis* 17: 580–587.
- Wilkins MR, Pasquali C, Appel RD *et al.* (1996) From proteins to proteomes: Large scale protein identification by two-dimensional electrophoresis and amino acid analysis. *Biotechnology* 14: 61–65.
- Wilkins MR, Williams KL, Appel RD and Hochstrasser DF (1997) *Proteome Research: New Frontiers in Functional Genomics*. Berlin: Springer.
- Wilm M, Shevchenko A, Houthaeve T *et al.* (1996) Femtomole sequencing of proteins from polyacrylamide gels by nanoelectrospray mass spectrometry. *Nature* 379: 466–469.
- Yates JR (1998) Database searching using mass spectrometry data. *Electrophoresis* 19: 893–900.

PURGE-AND-TRAP: GAS CHROMATOGRAPHY

See III/VOLATILE ORGANIC COMPOUNDS IN WATER: GAS CHROMATOGRAPHY

PYROLYSIS: GAS CHROMATOGRAPHY

See II/CHROMATOGRAPHY: GAS / Pyrolysis Gas Chromatography

QUANTITATIVE STRUCTURE-RETENTION RELATIONSHIPS (QSRR) IN CHROMATOGRAPHY



R. Kaliszan, Medical University of Gdańsk,
Gdańsk, Poland

Copyright © 2000 Academic Press

Introduction

To relate structure and chromatographic retention an approach is needed that lacks the rigour of thermodynamics but which provides otherwise inaccessible information. Such an approach is a combination of detailed models with certain thermodynamic concepts.

Linear free-energy relationships (LFER) may be regarded as linear relationships between the logarithms of the rate or equilibria constants for one reaction series and those for a second reaction series subjected to the same variation in reactant structure or reaction conditions. Retention parameters can be assumed to reflect the free-energy changes associated with the chromatographic distribution process. Accordingly, a chromatographic column can be treated as a 'free-energy transducer', translating differences in chemical potentials of analytes, arising from differences in their structure, into quantitative differences in retention parameters.

Assuming LFER it is possible to determine relative inputs of individual structural groups, fragments or features, to a property measured for a series of compounds in various chemical, physical, physicochemical and biological experiments. Such structural parameters (descriptors) can then be related to retention parameters.

The existence of LFER is normally proved statistically. The basic methodology of employing LFER to predict differences in pharmacological activity within a series of related agents was proposed in 1964 by Hansch and Fujita (QSAR, quantitative structure-activity relationships). Multiple regression analysis was applied in 1977 to chromatographic data (QSRR, quantitative structure-retention relationships). Other chemometric methods of data analysis have since been introduced to QSRR. QSRR are now one of the most extensively studied manifestations of LFER and, at the same time, the most common application of chemometrics.

Methodology and Goals of QSRR Analysis

To undertake QSRR studies two kinds of input data are needed (Figure 1). One is a set of quantitatively comparable retention data (dependent variable) for a sufficiently large (for statistical reason) set of analytes. The other is a set of quantities (independent variables) assumed to account for structural differences among the analytes being studied. Through the use of chemometric computational techniques, retention parameters are characterized in terms of various descriptors of analytes (and/or their combinations) or in terms of systematic knowledge extracted (learnt) from these descriptors.

To obtain statistically significant and physically meaningful QSRR, reliable input data are required and stringent mathematical analysis must be carried out. If this is not done, formally valid correlations may be developed for chemically invalid principles.

Once good QSRR have been obtained, one can exploit them for:

1. prediction of retention of a new analyte;
2. identification of the most informative structural descriptors possessing the highest retention prediction potency;
3. insight into the molecular mechanism of separation operating in individual chromatographic systems;
4. evaluation of physicochemical properties of analytes, e.g. their hydrophobicity (lipophilicity);
5. prediction of relative biological (pharmacological) activities within a set of drugs and other xenobiotics.

Retention Parameters for QSRR

The great advantage of the QSRR analysis over other quantitative structure-property relationship studies is that chromatography can readily produce a large amount of relatively precise and reproducible data. In a chromatographic process all conditions may be kept constant and hence the structure of an analyte becomes the single independent variable in the system.

The most commonly used retention parameter in gas chromatography is the Kováts retention index. When the adjusted retention times are used to calculate retention indices, parameters are obtained that

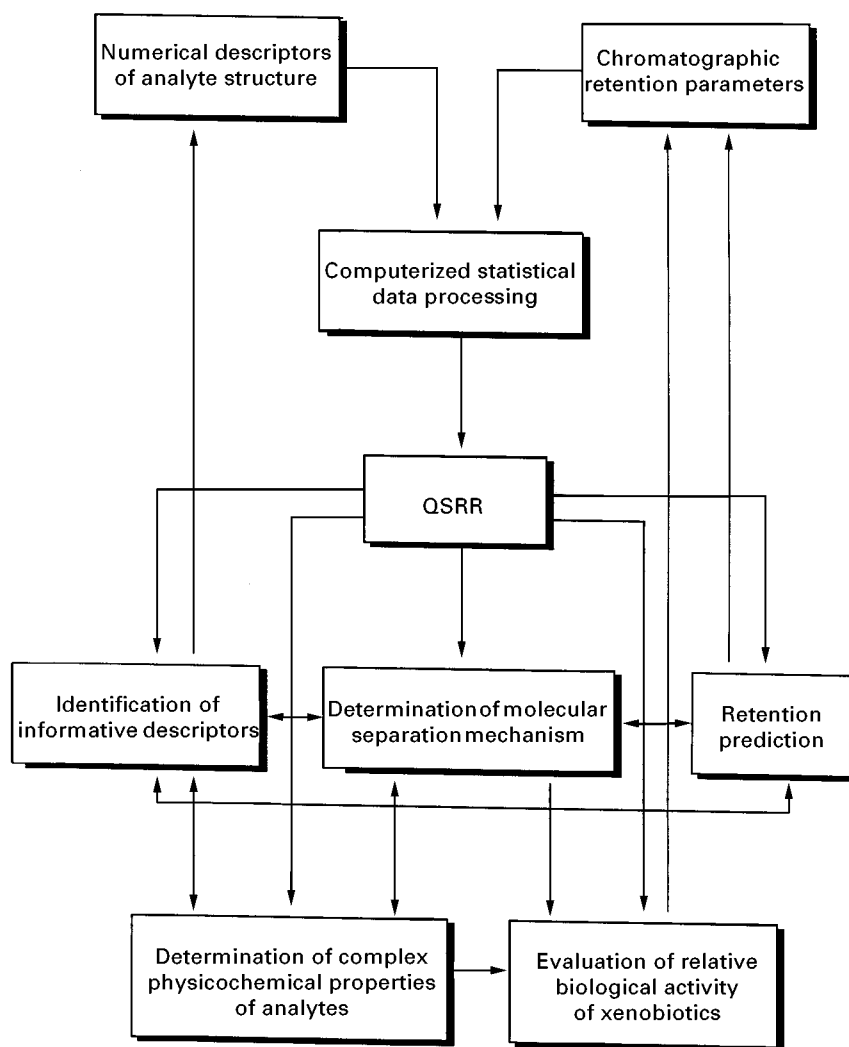


Figure 1 Methodology and goals of studies of quantitative structure-retention relationships (QSRR). (Adapted with permission from Kaliszan R (1992) Quantitative structure-retention relationships. *Analytical Chemistry* 64: 619A-631A. Copyright 1992 American Chemical Society.)

depend only on the column temperature and the stationary phase used. Kováts retention indices are highly reproducible; with a well-designed experimental technique, an interlaboratory reproducibility of one unit is possible. Sometimes in QSRR studies the logarithms of retention volumes of solutes are used instead of Kováts indices.

Classical thin-layer chromatographic (TLC) retention parameters are of rather limited reproducibility. The use of well-defined small-diameter stationary phase particles and a better knowledge of the parameters that determine the efficiency of chromatographic systems have led to the development of high performance TLC (HPTLC). An advantage of TLC over column chromatography, from the point of view of QSRR studies, is that tens of analytes can be simultaneously chromatographed on the same plate.

The retention parameter from TLC (and also from paper chromatography) that is normally used in QSRR is the R_M value. The R_M value is defined as $\log((1/R_F) - 1)$, where R_F is the distance migrated by the sample from the origin compared with the distance migrated by the solvent front from the origin.

The LFER-based retention parameter in high performance liquid chromatography (HPLC) is the logarithm of the retention factor k . The retention factor is defined as in eqn [1].

$$k = (t_R - t_M)/t_M = (V_R - V_M)/V_M \quad [1]$$

where t_R and V_R are the retention time and the retention volume of the analyte. The quantities t_M and V_M denote the elution time and the elution volume of an unretained compound.

HPLC retention data for QSRR analysis are usually obtained by measuring $\log k$ at several fixed eluent compositions (isocratic conditions) and then by extrapolating the dependence of $\log k$ on a binary eluent composition to a common mobile phase composition based on the Soczewiński-Snyder model:

$$\log k = \log k_w - S\varphi \quad [2]$$

In eqn [2] S is a constant for a given analyte and a given HPLC system and φ is the volume fraction of one of the mobile phase components. In the case of reversed-phase HPLC, k_w is a hypothetical retention factor expected for pure water (buffer) mobile phase ($\varphi = 0$).

The curvature often observed in plots of $\log k$ versus φ leads to a quadratic relationship:

$$\ln k = A\varphi^2 + B\varphi + C \quad [3]$$

where A , B and C are constants for a given analyte and a given chromatographic system. The $\ln k$ value calculated from eqn [3] by assuming $\varphi = 0$ is only occasionally used in QSRR analysis.

In spite of considerable effort, the relationships between retention and mobile phase composition are approximate. Often the values of $\log k_w$ extrapolated from a number of isocratic measurements in water/organic modifier eluents of varying compositions to a pure water eluent (the intercepts in eqn [2]) are different from those determined experimentally (when this is possible). Reversed-phase HPLC $\log k_w$ data are also usually different when derived from aqueous systems modified with different organic solvents. Still, the determination of $\log k_w$ appears to be the most reliable means of normalizing the retention parameters for QSRR analysis.

It should be noted here that some workers advocate using as the dependent variable the parameter S from eqn [2] or its ratio to $\log k_w$.

The electrophoretic mobility, μ_{el} , of spherical particles is described by a simple equation:

$$\mu_{el} = (z\Phi)/(6\pi\eta aN) \quad [4]$$

where z is the effective charge, Φ is the charge per mole of protons, η is the viscosity of the medium, a is the radius of the charged species and N is the Avogadro number.

A parameter normally measured in capillary electrophoresis (CE) is migration time, t . In a given CE system this parameter is inversely proportional to the electrophoretic mobility, μ . A normalized parameter, μ ($\text{cm}^3 \text{V}^{-1}$) allows comparison of data obtained in different CE systems. If a series of analytes is analysed

under the same conditions, then $1/t$ and μ are equivalent.

Chemometric Procedures in QSRR

Assuming LFER, a given chromatographic retention parameter may be described (statistically) by a set of analyte structural descriptors:

$$\text{Retention parameter} = f(a_1x_1, \dots, a_nx_n) \quad [5]$$

The coefficients a_1 – a_n for individual n descriptors are calculated by multiple regression. There are computer programs available commercially that are able to derive regression coefficients and to evaluate a statistical value of the regression model assumed.

Whether or not any of the possible models are statistically significant is judged on the basis of several statistical significance parameters. Among them are: the correlation coefficient (R); the standard error of estimate (S_E); the value of the F-test of the overall significance (F); the values of t -test of significance of individual regressors (t); and the cross-correlation coefficients between the independent variables in the regression QSRR equation. Even if the values of these statistical parameters are within the acceptable range, one cannot exclude a chance correlation. This may result when too many variables are surveyed to correlate too few retention data.

Multivariate methods of data analysis, like discriminant analysis, factor analysis and principle component analysis, are often employed in chemometrics if multiple regression methods fail. The most popular chemometric method in QSRR is principle component analysis (PCA). By PCA one reduces the number of variables in a data set by finding linear combinations of those variables that explain most of the variability.

Commercially available software packages tabulate the component weights and the values of individual principal components. Plots of component weights for each variable (structural descriptor) are useful in QSRR analysis. Analogously, scatterplots for the first two principal components illustrate the distribution of objects (analytes) according to their inputs to the principal components.

There is an approach in QSRR in which principal components extracted from analysis of a large table of structural descriptors of analytes are regressed against the retention data in a multiple regression, i.e. principal component regression (PCR). The partial least squares (PLS) approach with cross-validation also finds application in QSRR.

Neural networks (NN) is a method of data analysis that emulates the brain's way of working. NNs are considered powerful tools and techniques for carrying out signal processing, modelling, forecasting and pattern recognition. A NN has its input neurons that load the system with descriptor values. Next, there are the hidden layers that weight and mix the incoming signals, and an output layer with neurons predicting the calibrated response values. The advantage of NNs lies in nonlinear transformations of signals occurring at every neuron. The NNs are trained to respond properly using a representative set of structural data and the corresponding retention parameters. The well-trained (but not an overtrained) NN predicts retention based on input information of an analyte.

Selection of Structural Descriptors

The translation of molecular structures into numerical descriptors is important not only in QSRR but also to many subdisciplines of chemistry and pharmacology.

A popular strategy for identifying structural parameters in QSRR analysis is to start from the accepted theories of chromatographic separation. Such structural parameters should quantify the abilities of analytes to take part in the postulated intermolecular interactions that determine chromatographic separations. Empirical or semiempirical structural parameters of analytes based on the solvatochromic comparison method and on linear solvation energy relationships (LSER) belong to that category of structural descriptors. Also, reliable predictions of retention have been demonstrated using the LFER-based experimental substituent or fragmental constants.

The structural descriptors that are commonly used in QSRR analysis are classified in **Table 1**.

The structural descriptors related to molecular size may be related to the ability of an analyte to take part in nonspecific intermolecular interactions (dispersive interactions or London interactions) with the components of a chromatographic system. They are the factors most often found significant in QSRR analysis. The bulkiness parameters are decisive in the description of separations of closely congeneric analytes. For example, carbon number normally suffices to differentiate the members of a homologous series. On the other hand, when dealing with the set of analytes of the same size (e.g. isomers), they may appear not to be significant in QSRR analysis. This does not mean that dispersive interactions are meaningless for separation of congeners but just that they are closely similar, and hence the respective term in

Table 1 Structural descriptors in QSRR

<i>Classification</i>	<i>Descriptors</i>
Molecular bulkiness descriptors	Carbon number Molecular mass Refractivity Polarizability Van der Waals volume and area Solvent-accessible volume and area Total energy
Molecular geometry descriptors	Length-to-breadth ratio Moments of inertia Shadow area parameters
Physicochemical empirical and semiempirical parameters	Hammett constants Hansch constants Taft steric constants Hydrophobic fragmental parameters Solubility parameters Linear solvation energy relationship (LSER) parameters Partition coefficients Boiling temperatures p <i>K</i> _a values
Molecular polarity descriptors	Dipole moments Atomic and fragmental electron excess charges Orbital energies of HOMO and LUMO Partially charged areas Local dipoles Submolecular polarity parameters
Molecular topological descriptors	Molecular connectivity indices Kappa indices Information content indices Topological electronic index
Indicator variables	Zero-one indices
<i>Ad hoc</i> designed descriptors	

the QSRR equation apparently loses statistical significance.

What is more or less intuitively understood as molecular polarity of an analyte is difficult to quantify unequivocally. The descriptors of polarity are expected to account for differences among analytes regarding their dipole-dipole, dipole-induced dipole, hydrogen bonding and electron pair donor-electron pair acceptor (EPD-EPA) interactions. To find a good descriptor of these chemically specific interactions is difficult; the more so since changes in the polarity of an analyte also change its ability to take part in size-related interactions and affect analyte geometry.

Obviously, geometry-related or molecular shape parameters are difficult to quantify one-dimensionally. Single numbers reflecting molecular shape

differences are adequate only in the case of rigid and planar solutes. They become significant in QSRR equations if the range of analytes considered comprises compounds of similar size and polarity.

Physical meaning of the molecular graph-derived descriptors is never clear *a priori*. It is rather that good QSRR allow for assigning physical meaning to individual topological indices.

The empirical physicochemical parameters have good informative value for determining the mechanism of retention operating in a given chromatographic system. The problem is, however, the lack of such descriptors for the analytes of interest in actual QSRR studies.

Indicator values ('dummy variables') 0–1 are assigned depending on the presence or absence of a given structural feature in an analyte molecule. They serve to improve statistics but help occasionally to identify a structural descriptor of real physical significance.

The established structural descriptors listed in Table 1 seldom suffice to derive QSRR for the actual chromatographic data and often *ad hoc* descriptors have to be designed and included. QSRR analysis helps to test the predictive potency of the proposed structural descriptors, which may also appear suitable for deriving other kinds of structure–property relationships.

Prediction of Retention

Prediction of retention within homologous series is feasible owing to the linear relationships that are normally observed between retention parameters, $\log k$, and carbon numbers of analytes, n (Figure 2). The slopes of lines, B , for various homologous series chromatographed under the same conditions are very similar, whereas the intercepts, A , may vary:

$$\log k = A + Bn \quad [6]$$

Occasionally linear correlations are observed between retention parameters and molecular bulkiness descriptors of analytes that are not homologues. A good prediction of retention within a series of related nonpolar analytes, such as polyaromatic hydrocarbons (PAH) or alkylbenzenes, can be obtained using van der Waals volume as the structural descriptor.

The bulkiness descriptors can account for separation of analytes when dispersive interactions (London interactions) are the only interactions effective in a given chromatographic system, or when differences in polar interactions among analytes are not significant.

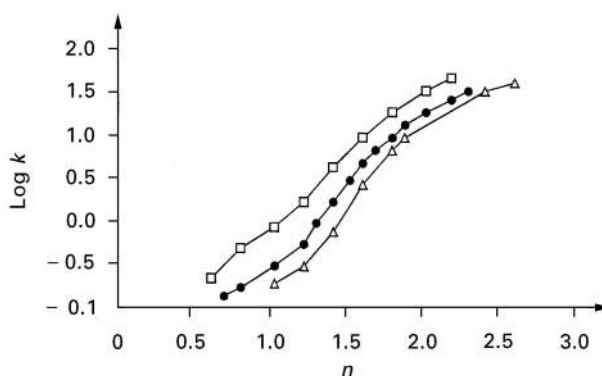


Figure 2 Plots of $\log k$ versus carbon number, n , of analyte for HPLC on a polyfunctional C_{18} -bonded silica with pure methanol eluent at 25°C: *n*-alkanes (\square), methyl-*n*-alkanoates (\bullet) and *n*-alkanols (\circ). (Reprinted from Tchaplal A, Herson S, Lessellier E and Colin H (1993) General view of molecular interaction mechanisms in reversed-phase liquid chromatography. *Journal of Chromatography A* 656: 81–112, with permission of Elsevier Science.)

The ability of an analyte to take part in polar interactions is difficult to characterize by means of a single descriptor. Hence simple QSRR involving analyte polarity descriptors, e.g. dipole moments, are rare.

Normally in chromatography (excepting affinity chromatography) molecular shape effects on retention are of minor importance in comparison with the effects of molecular size and molecular polarity. In the case of planar/nonpolar PAH isomers, retention is linearly related to a shape descriptor (the degree of elongation of the analyte molecule).

There are numerous reports on good performance of the molecular connectivity index (Randić index) and its modifications in predicting retention of congeneric analytes, including isomers. The correlations are good when retention is on nonpolar stationary phases, but not when polar phases are involved. Whereas on the nonpolar phases the nonspecific dispersive interactions determine differences in retention among the analytes, the more specific polar interactions become discriminative in the case of polar phases (and polar analytes).

Using substituent electronic constants to derive simple QSRR with a real retention prediction ability has seldom succeeded. A wider application in that respect is found in Hansch substituent hydrophobic constants, π , and Rekker or Hansch–Leo fragmental hydrophobic constants, f . The sums of these constants (plus corrections due to intramolecular interactions) account well for retention in reversed-phase liquid chromatographic systems.

Regarding the latter systems, even better predictions are provided by an empirical parameter – the

logarithm of the *n*-octanol–water partition coefficient, $\log P$. Another useful empirical retention predictor appears occasionally to be boiling point, T_b , for example the boiling point of isomeric hydrocarbons in the gas chromatography.

Prediction of retention of variously substituted derivatives of parent compounds in a given separation system can be based on the Martin rule:

$$\log k_s = \log k_p + \sum_{i=1}^n \tau_i \quad [7]$$

In eqn [7] k_p is the retention parameter of a parent compound, k_s is the corresponding value for the derivative carrying *n* substituents and the summation represents the retention increments due to individual substituents τ_i . Having appropriate values for functional groups of interest, one needs only to determine retention of the parent structure to be able to calculate retention of a derivative. To get reliable predictions, correction factors are introduced in eqn [7] to account for mutual interactions between substituents (electronic, steric, hydrogen bonding). However, in the case of polyfunctional analytes, interactions between substituents make retention predictions of rather limited value.

A semiempirical description of reversed-phase HPLC systems, allowing for the prediction of the relative retention and selectivity within a series of analytes, has been developed by Jandera. The approach consists of determining the interaction indices and the structural lipophilic and polar indices. A suitable set of standard reference analytes is necessary to calibrate the retention (or selectivity) scale.

The multiparameter QSRR based on linear solvation energy relationships (LSER) possess a high predictive power regarding reversed-phase HPLC retention. The model developed by Abraham and co-workers to predict the *n*-octanol–water partition coefficient, $\log P$, appears to be useful also in the case of $\log k$ from reversed-phase liquid chromatography:

$$\log k = c_0 + c_1 V_x + c_2 \pi_2^H + c_3 \sum \alpha_2^H + c_4 \sum \beta_2^H + c_5 R_2 \quad [8]$$

In eqn [8] V_x is the so-called McGowan's characteristic volume, which can be calculated simply from molecular structure; π_2^H is the dipolarity/polarizability of the analyte, which can be determined through gas-chromatographic and other measurements; $\sum \alpha_2^H$ is the effective or summation hydrogen bond acidity; $\sum \beta_2^H$ is the effective or summation hydrogen bond basicity; and R_2 is an excess molar refraction, which

can be obtained from refractive index measurements and is an additive quantity. The LSER-based structural descriptors are available for a large number of compounds.

Experimentally determined ionic radius, I_r , and energy of ionization, E_i , accompanied by atomic mass, A_m , produce a three-parameter regression equation predicting capillary electrophoretic mobility of metal cations. The QSRR equation indicates that atomic mass approximates to the retardation factors (negative input to mobility) whereas the ionic radius is an approximate measure of the effective charge on the analyte. Energy of ionization can play the role of a secondary, but significant, correction factor to the effective charge. Unfortunately, there are no good QSRR to predict the CE retention of organic analytes.

A typical multiparameter approach to predicting retention of an unknown compound based on structural features and chromatographic properties of other representative compounds consists of generating a multitude of analyte descriptors that are next regressed against retention data. The structural descriptors are usually derived by computational chemistry methods for the energy-optimized conformations. Software systems have been developed that produce and process hundreds of quantum chemical, molecular modelling, topological and semiempirical additive–constitutive descriptors after sketching the molecule on the computer. Observing all the rules and recommendations for meaningful statistics, the minimum number of descriptors (uncorrelated) is selected that are needed to produce a QSRR equation with a good predictive ability. The descriptors that eventually serve to predict retention of new analytes are sometimes of obscure physical meaning. For example, it is difficult to ascribe definite physical sense to such descriptors reported in predictive QSRR as 'the surface area of the positively charged portion of the molecule divided by the total surface area' or 'total entropy of the molecule at 300 K divided by the number of atoms'. Nevertheless, for several groups of compounds, prediction of retention by means of QSRR is reliable enough for identification purposes, especially when there is no better alternative. Exemplary predictive QSRR are for polychlorinated dibenzofurans and biphenyls, anabolic steroids, stimulants and narcotics used as doping agents, barbituric acid derivatives, polyaromatic and nitrated polyaromatic hydrocarbons, etc.

There are QSRR of useful predictive potency that comprise only physically interpretable terms. Reversed-phase HPLC retention of simple aromatic solutes on typical octadecyl silica columns has been related to a molecular bulkiness descriptor (total energy), a polarity descriptor (local dipole) and the energy of the

highest occupied molecular orbital of analytes. Good prediction of liquid chromatographic retention of about 50 aromatic acids was realized using as regressors the calculated theoretical logarithm of the *n*-octanol–water partition coefficient ($\log P$), the dipole moment, the principal ellipsoid axes, the sum of the charges on the oxygen and nitrogen atoms, the energy of the highest occupied molecular orbital (HOMO) and the electrophilic superdelocalizability for the aromatic carbon atom.

In Figure 3 is illustrated the predictive performance of QSRR for 216 HPLC retention data points. The points are for 36 analytes chromatographed in six eluents on a diol stationary phase. The eluents were heptane containing 0.5% of tetrahydrofuran, dioxane, ethanol, propanol, octanol and dimethylformamide. In Figure 3 the $\log k$ data experimentally measured are plotted against the values predicted by eqn [9]:

$$\begin{aligned} \log k = & 0.100 \text{ polarizability (analyte)} \\ & - 0.400 \log P \text{ (analyte)} \\ & - 0.330 E_{\text{HOMO}} \text{ (analyte)} \\ & + 1.106 E_{\text{HOMO}} \text{ (eluent)} \\ & + 0.401 E_{\text{LUMO}} \text{ (eluent)} \end{aligned} \quad [9]$$

with the values $n = 216$, $R = 0.97$, $s = 0.097$ and $F = 655$. In this equation n is the number of data points used to derive regression equation, R is the multiple correlation coefficient, s is the standard error of estimate and F is the value of F-test of significance; E_{LUMO} denotes energy of the lowest unoccupied mo-

lecular orbital and E_{HOMO} is energy of the highest occupied molecular orbital.

Figure 3 reflects realistically the actual predictive power of QSRR. The predictive QSRR equations normally hold within the family of analytes for which they were derived and may be used for tentative identification of chromatographic peaks.

In recent years a three-dimensional quantitative structure–biological activity relationship method known as comparative molecular field analysis (CoMFA) has been applied to construct a 3D-QSRR model for prediction of retention data. The CoMFA 3D-QSRR model is obtained by systematically sampling the steric and electrostatic fields surrounding a set of analyte molecules and then correlates the differences in these fields to the corresponding differences in retention.

Several reports have recently appeared on predictions of retention data from structural descriptors by means of neural networks (NN). By now the predictions provided by NN are of similar reliability to those obtained from regression models.

QSRR and Molecular Mechanisms of Retention

The QSRR equations that comprise physically interpretable structural descriptors can be discussed in terms of the molecular mechanisms involved in the chromatographic process. There is evidence that different structural parameters of analytes account for retention differences in GC on polar versus nonpolar stationary phases. Also, the structural descriptors in

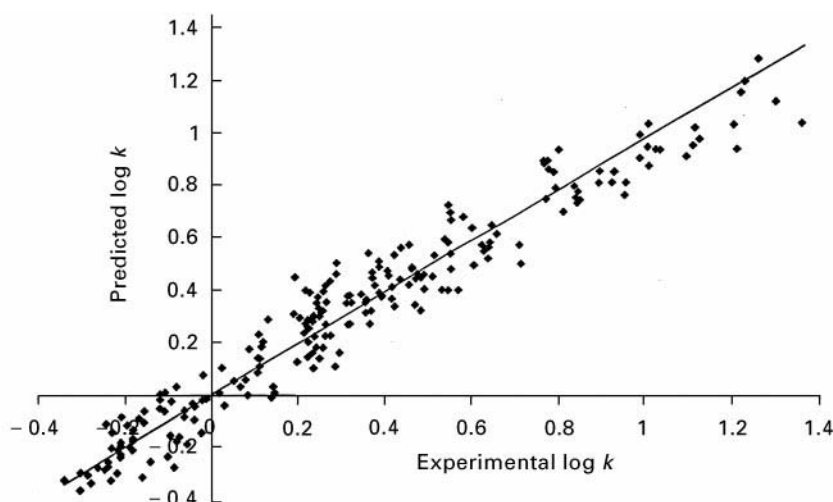


Figure 3 Plot of $\log k$ predicted by eqn [9] against experimental data determined on a diol column for 36 chalcone derivatives with heptane eluent containing 0.5% tetrahydrofuran, dioxane, ethanol, propanol, octanol or dimethylformamide. (Reprinted with permission from Azzaoui K and Morin-Alloy L (1996) Comparison and quantification of chromatographic retention mechanisms on three stationary phases using structure–retention relationships. *Chromatographia* 42: 389–395. Copyright Friedrich Vieweg & Sohn.)

QSRR equations that are valid for normal and for reversed-phase HPLC systems are different. In the case of apparently similar chromatographic systems, the differences in retentive properties of stationary phases may be reflected by the magnitude of the regression coefficients for analogous descriptors. Comparative QSRR studies are especially valuable when new chromatographic phases are introduced.

A general rule is that QSRR equations are characterized by two kinds of structural descriptors: one that accounts for the bulkiness or size of an analyte and one that encodes its polar properties. Size descriptors are always significant in GC on nonpolar phases and in reversed-phase HPLC, whereas the significance of polar descriptors increases as polarity of both the stationary phases and the analytes increases.

Publications give evidence that in GC on polar phases and in normal-phase (adsorption) liquid chromatography (HPLC and TLC) the chemically specific, molecular size-independent intermolecular interactions are assumed to play the main retention-determining role. For example, the HPLC retention parameters determined for substituted benzenes on porous graphitic carbon are described by QSRR equations comprising polarity descriptors but no bulk descriptors. Because, in general, it is difficult to quantify polarity properties precisely, the QSRR for GC on polar phases and for normal-phase HPLC are usually of lower quality than for GC on nonpolar phases and in reversed-phase liquid chromatography.

QSRR differentiate in a quantitative (statistical) manner stationary phase materials of different chemical nature. However, when the stationary phases that belong to the same chemical class are compared, such as hydrocarbon-bound silicas for reversed-phase HPLC, the results obtained are ambiguous.

The proper QSRR strategy aimed at objective characterization of differences in retentive potency of individual chromatographic systems should employ a well-designed set of test analytes. The analytes should be selected in such a way that, within the test set, the intercorrelations are minimized among the individual analyte structural descriptors. At the same time, the selection of test analytes should provide a wide range and even distribution of individual structural descriptor values. In addition, the series of analytes should be large enough to assure statistical significance of the QSRR equations but not too large so as to remain experimentally manageable.

Often the retention parameters of test analytes are first linearly regressed against the reference $\log P$ values from the *n*-octanol–water partition system. Good correlations obtained are usually interpreted as evidence of a partition mechanism operating in the chromatographic system under study.

Several QSRR studies aimed at comparison of retention mechanisms on individual alkyl silica reversed-phase materials for HPLC have employed LSER-based analyte parameters. It was observed generally that the most important analyte parameters that influence retention are bulkiness-related (molar volume, molar refraction) and hydrogen bonding basicity, but not hydrogen bonding acidity. The analyte dipolarity/polarizability appeared to be a minor but often significant factor. However, on poly(styrene-divinylbenzene) stationary phases the dipolarity/polarizability term provides an important positive input to QSRR.

The results of QSRR studies in which eqn [8] was applied to the retention parameters, $\log k_w$, from measurement on alkyl silica phases with methanol–water and acetonitrile–water eluents are instructive. The most significant parameters appeared to be hydrogen bond basicity (β_2^H) and McGowan volume (V_x) of analytes. The third significant parameter in QSRR equations is either dipolarity/polarizability (π_2^H) in the case of methanolic eluents or hydrogen bond acidity (α_2^H) in the case of acetonitrile-modified mobile phases.

The rationalization of these results might be as follows. The dispersive interactions of analytes (characterized by V_x) and hydrogen bonding interactions in which an analyte molecule is a hydrogen-bond acceptor (characterized by $\sum \beta_2^H$) significantly affect the retention of analytes in both water–methanol/stationary phase and water–acetonitrile/stationary phase equilibrium systems. However, in methanolic systems the third significant factor determining equilibrium is the ability of an analyte molecule to be preferentially attracted by polar molecules of methanol owing to the dipole–dipole and dipole-induced dipole interactions (characterized by π_2^H). In the systems containing acetonitrile, the π_2^H descriptor becomes insignificant in QSRR equations. Instead, the ability of the analyte to be preferentially attracted by the eluent owing to hydrogen bonding in which the analyte serves as a hydrogen bond donor (characterized by $\sum \alpha_2^H$) becomes more significant. The well-known hydrogen bond acceptor properties of acetonitrile manifest themselves in eqn [8] as a retention-decreasing term $k_4 \sum \alpha_2^H$ with a negative value of the k_4 regression coefficient.

Most readily interpretable would appear to be the molecular mechanism of retention in terms of QSRR equations comprising the parameters of analytes obtained from molecular modelling. One can easily assign physical meaning to van der Waals surface area or solvent-accessible molecular surface area (SAS) as differentiating the strength of dispersive interactions between the analyte and the molecules forming

chromatographic systems. Dipole moment (μ) should also account for differences among analytes regarding their dipole-dipole or dipole-induced dipole interactions. Energies of the lowest unoccupied molecular orbital (E_{LUMO}) and the highest occupied molecular orbital (E_{HOMO}) should explain the differences in the tendency of analytes to take part in the charge transfer interactions. Yet reliable QSRR employing these structural descriptors are rare and hold only for selected sets of analytes.

In QSRR concerning reversed-phase HPLC retention parameters, the net positive effects on retention are due to the analyte bulkiness descriptors. The dispersive attractions of an analyte are stronger with the bulky hydrocarbon ligand of the stationary phase than with the small molecules of aqueous eluent. The net effect on retention provided by dipole moment (or its square) is negative. This is because the dipole-dipole and dipole-induced dipole attractions are stronger between the polar (polarized) analyte and polar molecules of eluent than between the same analyte and the nonpolar hydrocarbon ligand of the stationary phase. Unfortunately, these types of QSRR are not precise enough to differentiate individual alkyl silica stationary phase materials in a quantitative, statistically significant manner. They are significant enough, however, to reflect the differences in retention mechanism operating in the reversed-phase and in the normal-phase HPLC systems or in GC on nonpolar and polar phases.

Factorial methods of data analysis (principal component analysis, correspondence factor analysis, spectral mapping analysis) provide classification of stationary phases based on retention data determined for short series of test analytes. Among the commercially available materials for HPLC those can be selected that possess closely similar retention properties. Also, a stationary phase with clearly distinctive properties can be identified, which can be useful for specific method development.

Chromatographic Methods of Determination of Hydrophobicity

Hydrophobicity or lipophilicity is understood to be a measure of the relative tendency of an analyte 'to prefer' a nonaqueous over an aqueous environment. The partition coefficients of the substances may differ if determined in different organic-water solvent systems but their logarithms are often linearly related. Octanol-water is a reference system that provides the most commonly recognized hydrophobicity measure: the logarithm of the partition coefficient, $\log P$. The standard 'shake-flask' method for determining partition coefficients in liquid-liquid

systems has several disadvantages. Having appropriate QSRR, the chromatographic data can be used to predict $\log P$. Many good correlations of reversed-phase liquid chromatographic (HPLC or TLC) parameters with $\log P$ have been reported for individual chemical families of analytes and chromatographic methods for assessing the hydrophobicity of drugs and environmentally important substances have officially been acknowledged and included in the *OECD Guidelines for Testing Chemicals*.

On the other hand, the partition chromatographic systems are not identical with the *n*-octanol-water partition system. Each chromatographic system produces an individual scale of hydrophobicity. Hence attempts to reproduce $\log P$ by means of liquid chromatography are only partially successful. Centrifugal countercurrent chromatography (CCCC) provides a better chance of mimicking $\log P$ but the inconvenience of this method and the need for special equipment hinder its wider application.

The versatility of chromatographic methods of hydrophobicity assessment can be attributed to the use of organic modifiers in aqueous eluents. Normally, the retention parameters determined at various organic modifier-water (buffer) compositions are extrapolated to zero organic modifier content. The extrapolated parameters ($\log k_w$ from HPLC and R_M^0 from TLC) depend on the organic modifier used.

Alkyl silica stationary phases and methanol-water eluent are most often used in hydrophobicity studies. The problem with these phases is that the hydrophobicity of nonionized forms of organic bases cannot be determined because of the chemical instability of silica-based materials at higher pHs (above about pH 8). Also, specific interactions of analytes with the free silanols of alkyl silicas disturb partition processes.

The limitations of standard reversed-phase materials have been partially overcome by introducing modern specially deactivated hydrocarbon-bonded phases, immobilized on alumina or zirconia supports and on polymeric materials. Using the latter two types of stationary phase materials one can determine HPLC retention factors under acidic, neutral and alkaline conditions. That way a universal, continuous chromatographic hydrophobicity scale can be constructed, as is the standard $\log P$ scale.

Hydrophobic properties of xenobiotics are assumed to affect their passive diffusion through biological membranes and binding to pharmacological receptors. If the hydrophobicity measuring system is to model a given biological phenomenon, then similarity of the component entities is a prerequisite.

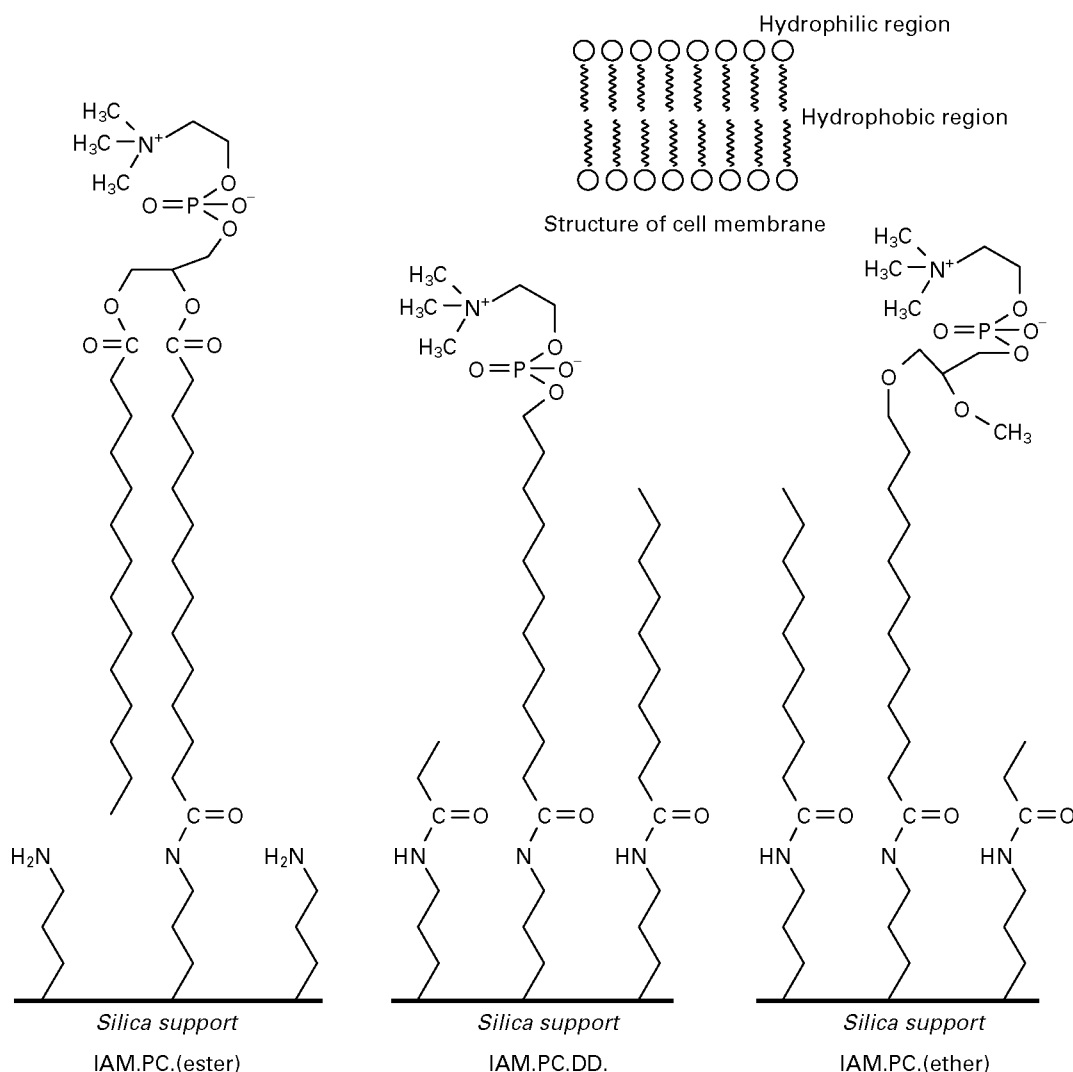


Figure 4 Chemical structures of ligands of three types of immobilized artificial membrane (IAM) columns of Pidgeon (Liu H, Ong S, Glunz L and Pidgeon C (1995) Predicting drug-membrane interactions by HPLC: structural requirements of chromatographic surfaces. *Analytical Chemistry* 67: 3550-3557. Copyright 1995 American Chemical Society.) and a schematic model of a biological membrane.

Hence the partition system to model the transport through biological membranes should be composed of an aqueous phase and an organized phospholipid layer. The immobilized artificial membranes (IAM) introduced by Pidgeon as a packing material for HPLC (Figure 4) appear to be reliable and convenient models of natural membranes.

Correlations between $\log k$ data determined on IAM-type columns and $\log P$ values are generally not high nor are the correlations between $\log k$ from IAM columns and $\log k_w$ determined by liquid chromatography employing standard stationary phase materials. This means that retention data determined on IAM columns contain information on the properties of analytes that is distinct from that provided by the *n*-octanol-water system and by the hydrocarbon-

silica reversed-phase columns. There is evidence that the hydrophobicity characteristics provided by IAM columns are better suited for modelling the pharmacokinetics of drug processes.

Retention Parameters in Predicting Bioactivity of Analytes

Biological processes of drug absorption, distribution, excretion and drug-receptor interaction are dynamic in nature as are the analyte's distribution processes in chromatography. The same fundamental intermolecular interactions determine the behaviour of chemical compounds in both biological and chromatographic environments. Modern techniques and procedures of HPLC and CE allow for inclusion

of biomolecules as active components of separation systems and QSRR processing of appropriate sets of chromatographic data can reveal systematic information regarding the xenobiotics studied. This information can be used to elucidate molecular mechanisms of pharmacological action and to facilitate rational drug design.

It is often sufficient to identify and employ a specific chromatographic system yielding hydrophobicity values of analytes best conforming to $\log P$ data. Normally, chromatographic systems that produce retention parameters less correlated to $\log P$ are discarded but information extracted from diversified retention data may be more appropriate for prediction of pharmacological properties of analytes than information based on an individual hydrophobicity scale. To extract meaningful information from diversified (yet often highly mutually intercorrelated) sets of data, multivariate chemometric methods of data analysis are employed. Large matrices of retention data determined for test series of analytes in many chromatographic systems differing in type of stationary and/or mobile phases, are processed by factorial methods, usually by principal component analysis (PCA). If two to three extracted abstract factors (principal components) account for most of the variability in a large set of retention data then the distribution of test analytes can be presented graphically. Clustering of analytes owing to similarity of their chromatographic behaviour in diverse separation systems is usually observed. If that clustering agrees with the pharmacological classification of the test agents, then recalculations are done after including the retention data for drug candidates. Indications on potential pharmacological activity of new analytes can be obtained even before biological experiments. This approach can facilitate preselection of drug candidates, especially among a multitude of compounds produced by combinatorial chemistry. The challenge is to design and select the chromatographic systems yielding retention data of sufficient classification potential.

Figure 5 shows the distribution of drugs belonging to several pharmacological classes on the plane determined by the first two principal components, which together account for 81.5% of the variance in the retention data measured in eight HPLC systems. The HPLC systems employed different stationary phases (standard and specially deactivated hydrocarbon bonded silicas, polybutadiene-coated alumina, immobilized artificial membranes and immobilized α_1 -acid glycoprotein). Methanol-buffer eluents of varying composition and pH were used. The clustering of analytes is consistent with their established pharmacological classification. Also, the partial overlap of

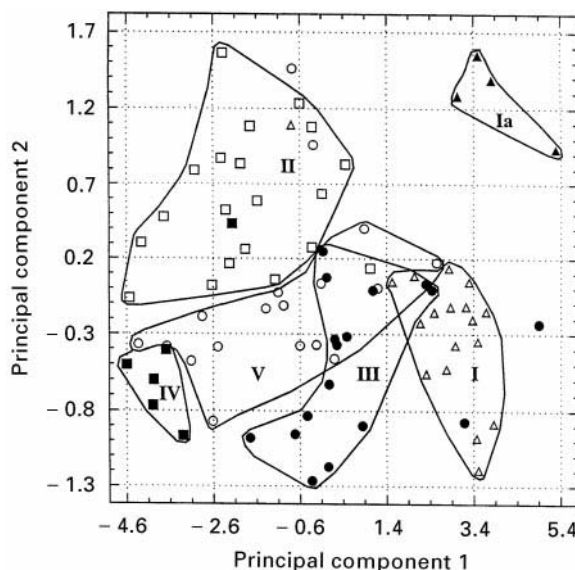


Figure 5 Pharmacologically consistent distribution scatterplot of drug classes on the plane determined by two first principal components extracted from a 8×83 (drugs \times HPLC systems) matrix of diversified retention data. Roman numbers denote: I, psychotropic drugs; Ia, inactive phenothiazines; II, β -adrenolytics; III, histamine H_1 receptor antagonists; IV, histamine H_2 receptor antagonists; V, drugs binding to α -adrenoceptors. (Reprinted from Nasal A, Buciński A, Bober L and Kaliszan R (1997) Prediction of pharmacological classification by means of chromatographic parameters processed by principal component analysis. *International Journal of Pharmaceutics* 159: 43–55, with permission of Elsevier Science.)

individual clusters is interpretable in terms of partially overlapping pharmacological properties of individual drugs.

There are individual processes of drug action that are satisfactorily modelled by HPLC on immobilized artificial membrane (IAM) columns. QSRR equations have been reported predicting several pharmacokinetic parameter of β -adrenolytic drugs from their $\log k$ parameters determined on IAM columns. Good predictions by means of $\log k_{IAM}$ have also been reported regarding antithaemolytic activity of phenothiazine neuroleptics. The human skin permeation of steroids also correlates better with $\log k_{IAM}$ than with $\log P$.

The $\log k_{IAM}$ alone will not suffice to predict binding of basic drugs to the serum protein, α_1 -acid glycoprotein (AGP). However, combining that parameter with atomic excess charge on aliphatic nitrogen, N_{ch} , and a size parameters, S_T , in a multiple regression equation results in a good prediction of AGP binding. The S_T parameter is the area of a triangle having one vertex on the aliphatic nitrogen and the two remaining vertices on the extremely positioned atoms in the drug molecule (Figure 6). The QSRR equation has

the form:

$$\begin{aligned} \log k_{\text{AGP}} = & 0.6577 (\pm 0.0402) \log k_{\text{IAM}} \\ & + 3.342 (\pm 0.841) N_{\text{ch}} \\ & - 0.0081 (\pm 0.0030) S_{\text{T}} \\ & + 1.688 (\pm 0.245) \end{aligned} \quad [10]$$

with the values $n = 49$, $R = 0.929$, $s = 0.163$, $F = 92$ and $p < 10^{-5}$.

Equation [10] may be useful as a first approximation to the relative binding of a drug to AGP without the need to perform biochemical experiments. It can help to identify structural features of the binding site of basic drugs on AGP (Figure 6). The site can be modelled as a conical pocket. Its internal surface contains hydrophobic regions at the base of the cone and an anionic region close to the apex of the cone. Protonated aliphatic nitrogen guides drug molecules towards the anionic region. Hydrophobic hydrocarbon fragments of the interacting drugs provide anchoring in the hydrophobic regions of the binding site. There is a steric restriction for the molecule to plunge into the binding site.

QSRR analysis of HPLC data determined on an immobilized human serum albumin (HSA) column helps to suggest the topography of two binding sites of different affinity to benzodiazepine enantiomers. Also, the mechanism of interaction of phenothiazine neuroleptics with melanin can be rationalized by means of QSRR analysis of HPLC retention data. Another QSRR study concerns interactions of drugs with immobilized keratin and collagen.

In general, QSRR analysis of retention parameters determined on immobilized biomacromolecules can yield reliable predictions of activity and identification of the required binding structural properties of

drugs and drug candidates. The approach appears especially promising now that biotechnologically produced pharmacological receptors are becoming available.

Concluding Remarks

In 1991 Giddings wrote 'Because pure theory is impractical, progress in understanding and describing molecular equilibrium between phases requires a combination of careful experimental measurements and correlations by means of empirical equations and approximate theories'. This has been realized in a systematic manner over a period of 20 years through QSRR analysis. During that time a consistent research strategy has been developed and established within the area. Easy access to computers equipped with advanced statistics and molecular modelling software has ensured rapid progress and engendered a wide interest in QSRR among chromatographers and other specialists.

QSRR are employed by analytical chemists to help identify unknown members of individual classes of analytes of pharmacological, toxicological, environmental or chemical interest. At the same time, QSRR of good retention prediction capability help to identify structural descriptors for analytes that provide acceptable estimates of properties other than chromatographic ones. In this way, chromatographic systems allowing for fast and convenient evaluation of analyte hydrophobicity can be identified. Also, QSRR confirm the suitability of the LSER-based descriptors for property predictions.

Well-designed QSRR studies are helpful in identifying the structural features within a family of analytes that affect retention in a given separation system. In this way molecular mechanisms of retention may be explained. With a designed test series of analytes the QSRR derived for retention data determined in individual separation systems provide objective, numerical characteristics for these separation systems. This is especially useful for quantitatively comparing retention properties of various stationary phase materials.

Chromatographic retention data can be employed to predict pharmacological properties of analytes. By employing chromatographic systems comprising biomacromolecules, large amounts of data can be obtained that reflect differences among analytes with regard to their interactions with given biomacromolecules. These data can be used to derive QSRR explaining the mechanism of drug-biomacromolecule interactions. In effect, the topography of binding sites for drugs on individual biomacromolecules can be characterized. By employing

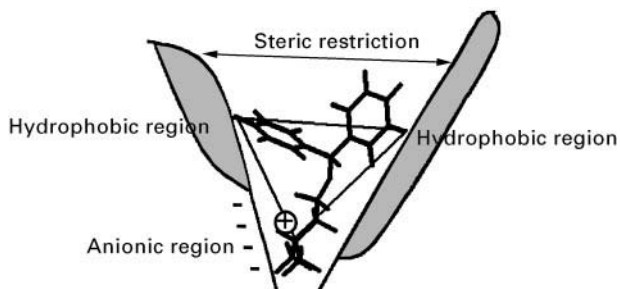


Figure 6 Mode of binding of the organic base drugs derived from QSRR analysis of HPLC data determined on an immobilized α_1 -acid glycoprotein column. (Adapted with permission from Kaliszan R, Nasal A and Turowski M (1995) Binding site for basic drugs on α_1 -acid glycoprotein as revealed by chemometric analysis of biochromatographic data. *Biomedical Chromatography* 9: 211–215. Copyright John Wiley & Sons Limited.)

biotechnologically acquired pharmacological receptor proteins to generate drug-receptor interaction data and by applying QSRR analysis, the preselection of drug candidates can be facilitated and experiments on animals reduced.

See also: **II/Chromatography: Liquid: Mechanisms: Reversed Phases.**

Further Reading

Carr PW, Martire DE and Snyder LR (eds) (1993) The retention process in reversed-phase liquid chromatography. *Special Volume of Journal of Chromatography A* 656: 1–618.

Forgács E and Cserhádi T (1997) *Molecular Bases of Chromatographic Separations*. Boca Raton, FL: CRC Press.

Giddings JC (1991) *Unified Separation Science*. New York: Wiley.

Jinno K (ed.) (1997) *Chromatographic Separations Based on Molecular Recognition*. New York: Wiley-VCH.

Jurs PC (1996) *Computer Software Applications in Chemistry*, 2nd edn. New York: Wiley.

Kalisan R (1987) *Quantitative Structure–Chromatographic Retention Relationships*. New York: Wiley.

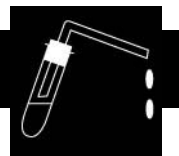
Kalisan R (1997) *Structure and Retention in Chromatography. A Chemometric Approach*. Amsterdam: Harwood Academic Publishers.

Kier LB and Hall LH (1986) *Molecular Connectivity in Structure–Activity Analysis*. Letchworth: Research Study Press.

Pliška V, Testa B and van de Waterbend H (eds) (1996) *Lipophilicity in Drug Action and Toxicology*. Weinheim: VCH.

Smith RM (1995) *Retention and Selectivity in Liquid Chromatography*. Amsterdam: Elsevier.

REACTIVE DISTILLATION



S. M. Mahajani, Monash University, Clayton, Victoria, Australia

S. P. Chopade, Michigan State University, East Lansing, MI, USA

Copyright © 2000 Academic Press

Introduction

Reactive distillation is a combination of separation and reaction in a single process. Commercial reactive distillation processes for the manufacture of methyl *t*-butyl ether (MTBE) and methyl acetate were successfully commissioned in 1981 and 1983, respectively. These processes have a distinct edge over their conventional predecessors. The reactive distillation process is particularly advantageous in the case of reversible reactions where the conversion is limited by thermodynamic equilibrium. Some of the important benefits of reactive distillation are: reduced capital cost; employment of low mole ratios of reactants; energy saving owing to utilization of the heat of reaction; and automatic temperature control and elimination of hot spots. The commercial process of MTBE manufacture has shown that heterogeneous catalysts such as ion exchange resins can be advantageously used in reactive distillation columns. Innovative techniques of confining the small size resin particles (0.3–2 mm) in the column, allowing efficient solid–liquid contact and high void fraction, have been

developed by CDTech, Sulzer, Koch Engineering and BASF. An alternative approach is to prepare a catalyst in the form of conventional column packing and pack it directly into the reactive distillation column.

Recognizing the potential of reactive distillation for a particular process is a difficult task, as not all the reactions can be conducted effectively in this way. Once its potential has been identified, the next step is to design the reactive distillation column for the required task. The simultaneous existence of multiple processes such as mixing, mass transfer and reaction are involved, and the design method requires thorough knowledge of both chemical and physical equilibria as well as the reaction kinetics. Graphical representations of liquid phase compositions, called residue curve maps or distillation maps, are commonly used to analyse the reactive distillation process. Though some efforts have been made to study the underlying theory of the design method, the work is still at its preliminary stage. Another approach to understanding the behaviour of this process is to perform computer simulations and predict the performance of a column of known configuration.

In this article the important aspects of commercial reactive distillation processes of MTBE and methyl acetate manufacture are described in detail. Recent trends in the experimental and theoretical investigations in this area are also outlined. The potential importance of reactive distillation in some industrial

processes such as hydrolysis of methyl acetate and recovery of chemicals from aqueous streams is discussed.

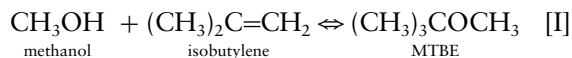
MTBE Production

The area of particular interest where reactive distillation can be used is the production of fuel ethers such as MTBE. Gasoline reformulation using these ethers as environmentally benign octane boosters has been driven by various Clean Air Acts, which have boosted MTBE production to a new level. By 2001 the production of MTBE is expected to be 25×10^6 tonnes per annum worldwide. *t*-Amyl methyl ether (TAME) and ethyl *t*-butyl ether (ETBE) are also emerging as promising fuel additives. In addition to its property as an antiknock agent to enhance the octane number of the fuel, MTBE improves the water tolerance limit of the fuel and has a higher calorific value than that of other additives such as methanol.

Another important aspect of carrying out the etherification to near complete conversion is its efficient use in separating the *iso*-olefins from the refinery stream containing both normal and secondary butenes (C_4 or C_5), which are otherwise very difficult to isolate. A reactive distillation column can handle the mixed olefins quite effectively and exploits the presence of inert butenes to improve performance. This separation is necessary because *n*-butenes are required in the pure form for homopolymerization and as a feed for the oxidative production of butadiene.

Reaction Details

MTBE is a product of the liquid-phase reaction of isobutylene and methanol, catalysed by a strong acidic macroreticular ion exchange resin. The reaction is highly selective, so that methanol reacts only with isobutylene in the presence of other C_4 olefins [1].



$$\Delta H_{298}^0 = -37.7 \text{ kJ mol}^{-1}$$

The favourable temperature and pressure ranges for the reaction to occur are 323–373 K and 5–15 atm, respectively. The useful side reactions are the dimerization and oligomerization of isobutylene and butadiene as well as the formation of codimers. Since, until recently, only butadiene-extracted C_4 refinery streams were used for MTBE production, the only important by-product is diisobutylene, which consists of the isomers 2,4,4-trimethyl-1-pentene and 2,4,4-

trimethyl-2-pentene. The other side reactions, which are of less importance, are formation of *t*-butanol by reaction of isobutylene with water present as a feed impurity, the formation of traces of dimethyl ether by methanol condensation, and the double bond isomerization of 1-butene. Amberlyst 15®, a macroporous cation exchange resin, is widely used as a catalyst for this reaction. Numerous investigations on the kinetics of this reaction system have been reported in the literature. A model based on systematic studies of reaction kinetics (eqn [1]) and equilibrium of this system incorporating the activities of the compounds has been developed and is used by many investigators for column simulation studies.

$$r = m_{\text{cat}} q_{\text{acid}} k_f \left(\frac{a_{\text{IB}}}{a_{\text{MeOH}}} - \frac{1}{K_{\text{eq}}} \frac{a_{\text{MTBE}}}{a_{\text{MeOH}}^2} \right) \quad [1]$$

In eqn [1], m_{cat} is the catalyst loading, q_{acid} is the ion exchange capacity and a_i is the activity coefficient of the corresponding component (IB, isobutylene, MeOH, methanol). The forward reaction rate constant k_f and the equilibrium constant K_{eq} have been fitted experimentally. As a result of the high polarity of methanol, the reaction mixture is highly nonideal and involves formation of two binary azeotropes and one ternary reactive azeotrope. The activities of the components can sometimes be up to 20 times their mole fractions.

Commercial Process

Conventional processes for the manufacture of MTBE (see Figure 1) use a catalytic reactor with a slight excess of methanol (methanol/isobutylene = 1.05–2). The products correspond to the near-equilibrium conversion of about 90–95%. The reaction mixture is separated using distillation, but suffers from complications resulting from the formation of binary azeotropes methanol–MTBE and isobutylene–methanol. The unreacted isobutylene is also difficult to separate from other volatile C_4 products. With the reactive distillation process, almost complete conversion of isobutylene is obtained, thereby eliminating the separation and recycle problems. Figure 2 provides a schematic representation of this process. A fixed-bed pre-reactor is used to achieve near-equilibrium conversion. The product stream equivalent to the equilibrium conversion is fed to the reactive distillation column, wherein, the residual amount of isobutylene is reacted with methanol. The reactive distillation column is composed of three sections, the middle of which is a reactive zone packed with a solid catalyst. The top nonreactive rectifying section performs the separation of inert gases and

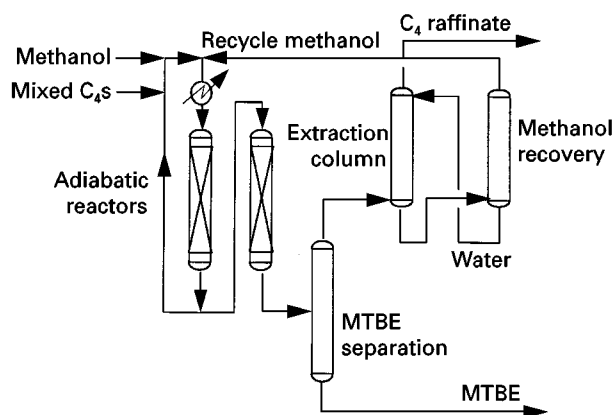


Figure 1 Conventional process for MTBE manufacture.

excess methanol, while the bottom section separates out MTBE in pure form. The boiling points of MTBE and methanol are 328 K and 337.5 K, respectively. This may seem surprising, as MTBE is the bottom product while unreacted high boiling methanol is collected through the distillate. The behaviour is caused by the formation of an MTBE-methanol low boiling azeotrope, which lifts methanol from the stripping section of the column.

The pioneering work to commercialize this technology was performed by Smith from Chemical Research and Licensing Company, who has been awarded several patents for different catalyst structures, column internals design and flow schemes. Some patents have also been assigned to researchers from ELF who claim to have used alternating catalytic and noncatalytic zones successfully to carry out the etherification. The efforts in these studies were directed towards minimizing the pressure drop in the catalyst bed and providing maximum residence time

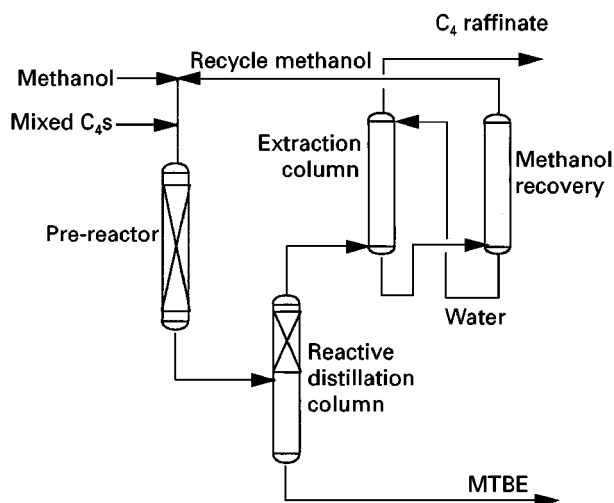


Figure 2 Reactive distillation process for MTBE manufacture.

for the liquid in the catalytic zone. This was achieved by providing separate free passage to the up flowing vapour stream either by packing the catalyst in the downcomers or by providing annular space in the catalyst bed, thereby isolating reaction and distillation zones in a single column. UOP, Koch Engineering and Hüls AG have jointly developed the Ethermax process for producing ethers by reactive distillation. The process uses Koch Engineering's Katamax packing, where a solid acid catalyst is confined in screen envelopes.

Simulation Studies

Following the successful commercialization of the MTBE process, numerous studies simulating a catalytic distillation column have appeared in the literature. The basic idea behind simulation studies is to predict the overall conversion of either isobutylene or methanol, and examine the product purity at a steady state for a known column configuration and feed composition. Various software packages such as ASPEN PLUS, SPEEDUP, etc, have been used effectively for this purpose.

The interesting discovery of multiple steady states for a column operated under identical conditions has attracted the attention of many researchers in the recent past. Several studies examining the reasons for the existence of these steady states have been reported. Experimental findings confirmed this fact and showed that the same column configuration operated under similar conditions can give rise to two different conversions. Simulation studies using an ASPEN PLUS flowsheet simulator for a column with a total of 17 reactive and nonreactive stages, operated at 11 atm with two different feed streams of methanol and butenes, result in either 36% or 99% isobutylene conversion when methanol is fed to the 10th stage. The methanol feed plate was varied by following either top-to-bottom or bottom-to-top sequence and it was found that only at certain feed plates (9–12) were multiple conversions realized (see Figure 3). The steady-state conversion in this multiplicity region depends upon which sequence is followed to simulate the column. In the upgoing sequence low conversions are obtained, while the downgoing sequence is associated with high conversions. Subsequent efforts on column simulation have confirmed this finding. Installation of the methanol feed at more than one location has been suggested to avoid the unwanted steady state caused by column misoperation.

A mechanistic explanation has been provided as to why MTBE production by reactive distillation may yield multiple solutions. It was found that the initial estimates for temperature and composition profiles

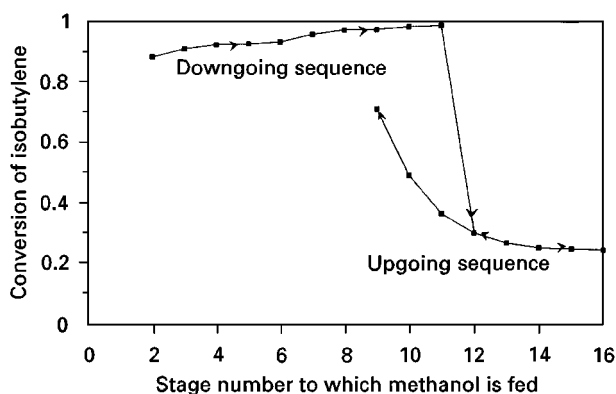


Figure 3 Steady-state multiplicity behaviour of the MTBE process.

decide whether a steady-state simulation would converge to a high conversion or a low conversion solution. In order to obtain a high conversion solution, the lower section of the column must contain sufficient MTBE to lift the entire amount of methanol to the reactive zone. Second, in the reactive zone, the reaction mixture must be diluted to avoid a substantial amount of MTBE decomposition. Initial estimates of the composition at the lowest stage in the reactive zone are crucial in deciding the nature of the steady state. This is expected to be due to the inherent coupling between 'lift' and 'dilution' effects that takes place on this stage.

Recent simulation studies on reactive distillation of MTBE and TAME indicate two types of multiple steady states. The first, discussed above, arises out of the interaction between reaction and vapour-liquid equilibrium. The second multiple steady state is related exclusively to the chemical reaction and arises because of the highly nonlinear concentration dependence of methanol activity at low operating pressures. The only experimental evidence of multiple steady states reported so far comes from work on etherification for TAME synthesis in a pilot plant of Nestle Oy. It is therefore necessary to perform dynamic simulations during the first steps of the design process in order to avoid dynamic surprises.

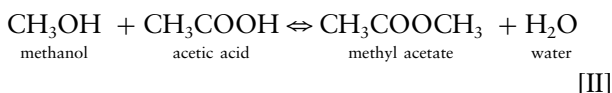
Another interesting finding of MTBE simulation studies is the oscillatory behaviour of the reactive distillation column. Sustained oscillations of boiling temperature and reflux have been reported in experimental studies on reactive distillation. It has been proved that the nonreactive and nonideal interactions

Methyl Acetate Production

Methyl acetate is another high volume commodity chemical that is manufactured commercially using reactive distillation. It finds applications as an intermediate in the manufacture of a variety of polyesters such as photographic film base, cellulose acetate, Tenite cellulosic plastics and Estron acetate.

Reaction Details

The reaction of methanol and acetic acid to give methyl acetate (reaction [III]) has equilibrium limitations.



$$\Delta H_{298}^0 = -8.0 \text{ kJ mol}^{-1}$$

$$K_{\text{eq}} = \frac{a_{\text{MeOAc}}a_{\text{H}_2\text{O}}}{a_{\text{AcOH}}a_{\text{MeOH}}} = 5.2 \quad [2]$$

Equation [2] gives the equilibrium constant K_{eq} as a function of the activity coefficients a_{MeOAc} (methyl acetate), $a_{\text{H}_2\text{O}}$ (water), and a_{AcOH} (acetic acid).

Thus the reaction product will contain all four components even if one of the reactants is used in excess. The reaction can be conducted in the temperature range 310–393 K and at a pressure of 1 atm. The only important side reaction is the formation of dimethyl ether by the condensation of methanol. This reaction is predominant at high temperatures.

Though the reaction has been commercialized in a reactive distillation column, it is surprising that a systematic study on the kinetics of this reaction in the presence of sulfuric acid as catalyst is not evident in the open literature. As in the MTBE system, the rate expression in the form of activities is strongly preferred because the high polarity of water and methanol compared to that of methyl acetate leads to strongly nonideal solution behaviour. Because of the commercial success of reactive distillation and the proven potential of the ion exchange resins, some efforts have been made to propose a rate expression for an ion exchange resin-catalysed reaction. The expression for the rate, r , based on kinetic data generated over a range of molar feed ratios more typical of reactive distillation conditions, is given by:

$$r = \frac{k(a_{\text{HOAc}}a_{\text{MeOH}} - a_{\text{MeOAc}}a_{\text{H}_2\text{O}}/K_{\text{eq}})}{(1 + K_{\text{HOAc}}a_{\text{HOAc}} + K_{\text{MeOH}}a_{\text{MeOH}} + K_{\text{MeOAc}}a_{\text{MeOAc}} + K_{\text{H}_2\text{O}}a_{\text{H}_2\text{O}})} \quad [3]$$

between methanol and isobutylene are responsible for these effects.

where k is the rate constant, K_{eq} is the equilibrium constant and the K_i s are the adsorption coefficients

involved in the Langmuir–Hinshelwood/Hougen–Watson model (HOAc, methyl acetate, MeOH, methanol; MeOAc, methyl acetate, H₂O, water). The expression has been successfully used to verify the experimentally observed residue curve maps of this system. The residue curve maps shows no distillation boundaries and hence, ultrahigh purity methyl acetate and water can be obtained through a proper design of reactive distillation column.

Commercial Process

Conventional processes before the 1980s used multiple reactors with a large excess of one of the reactants to achieve high conversion of the other. The product is difficult to purify because of the formation of methyl acetate–methanol and methyl acetate–water azeotropes. Different means to break the methyl acetate–methanol azeotrope were employed, such as use of several atmospheric and vacuum distillation columns or extractive distillation. A typical process contained two reactors and eight distillation columns, making it complex and capital intensive.

Eastman Kodak has developed a reactive distillation process for the manufacture of high purity and ultrahigh purity methyl acetate. The remarkable factor is that, in spite of the reaction having unfavourable equilibrium limitation, high purity product is obtained using a near-stoichiometric mole ratio of methanol and acetic acid. The reactive distillation column used in the process is shown in **Figure 4**. In order to explain the process, the column can be divided in four stages starting from the top as: (1) methyl acetate enrichment; (2) water extraction; (3) reaction; and (4) methanol stripping. The reaction occurs in the middle section (section 3) in a series of countercurrent flashing stages with sulfuric acid as the catalyst. In section 2, acetic acid acts as an extracting agent and extracts water (breaking the methyl acetate–water azeotrope) and some methanol. Acetic acid and methyl acetate are separated above the acetic acid feed, in the methyl acetate-enriching section (section 1), allowing pure methyl acetate to be recovered as the overhead product. Methanol is stripped from water in the bottom section (section 4) and water is the bottom product. Some intermediate boiling compounds are formed because of the impurities present in feed. Hence, a small stream is withdrawn just above the catalyst feed point and treated separately in an impurity-removal system. The impurities are stripped and concentrated, and the methanol + methyl acetate stream is recycled to the reaction zone. The reactive distillation column has been successfully operated at a near-stoichiometric mole ratio of acetic acid and methanol, yielding high

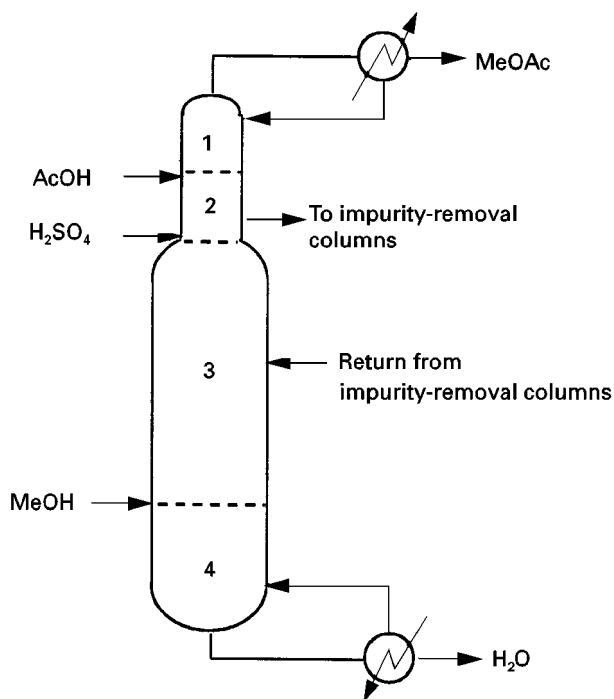


Figure 4 Reactive distillation process for methyl acetate manufacture.

purity methyl acetate as the product. The whole process is integrated in a single column, eliminating the need for a complex distillation column system and recycle of the methanol–methyl acetate azeotrope. A single reactive distillation column at Eastman Kodak's Tennessee plant produces 180 000 metric tons per year of high purity methyl acetate. The composition profile of the column shown in **Figure 5** demonstrates that the methyl acetate can be manufactured in a single column without need for additional purification steps.

Hydrolysis of Methyl Acetate

Methyl acetate–water mixture is produced in large quantities from purified terephthalic acid (PTA) plants. The manufacture of poly(vinyl alcohol) (PVA) also produces large quantities of methyl acetate (1.68 kg per kg PVA). Since methyl acetate is a comparatively low value solvent, it has to be sold at a lower price; hence it would be a better idea to hydrolyse it economically and recover methanol and acetic acid for reuse in the process.

Conventional processes for the hydrolysis of methyl acetate use a fixed-bed reactor followed by a complex arrangement of several distillation/extraction columns. The conversion is limited by unfavourable equilibrium (equilibrium constant 0.14–0.2) and a large amount of unconverted methyl

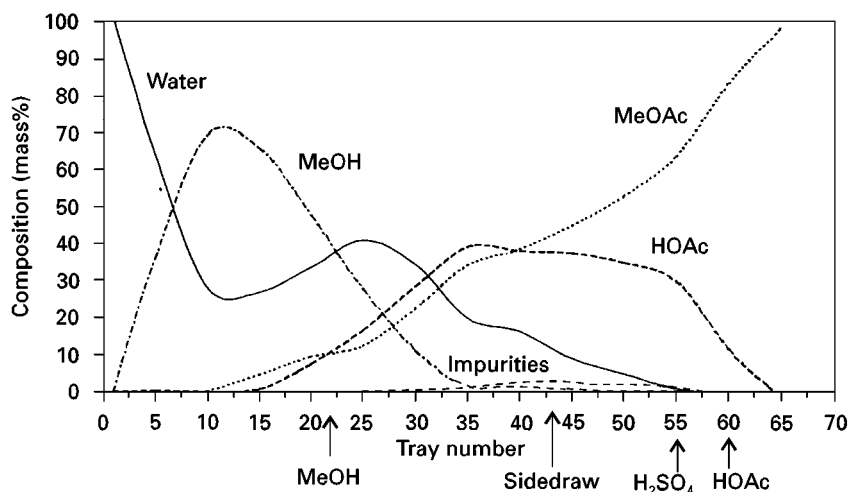


Figure 5 Composition profile in methyl acetate reactive distillation column.

acetate has to be separated and recycled. A schematic diagram of a typical conventional process is given in **Figure 6**. The reaction is carried out in a fixed-bed reactor and the product stream contains all four components. Four additional columns are required to separate methanol and acetic acid streams and recycle unconverted methyl acetate, along with methanol, to the reactor.

The above has shown how reactive distillation simplifies the process in the case of the manufacture of methyl acetate. A similar concept can be applied to the hydrolysis reaction. A reactive distillation process has been developed on a laboratory scale for the hydrolysis of methyl acetate using an ion exchange resin catalyst in a special form. Converting the process from conventional to reactive distillation offers the possibility of eliminating many complicated steps. The use of solid acid catalysts obviates the need for recovery of the spent acid and the use of exotic

construction materials. Resin was moulded into 7 mm × 7 mm pellets using polyethylene powder. The distillation column was directly packed with these pellets, which played the role of both catalyst and packing.

A schematic diagram of the proposed reactive distillation process is shown in **Figure 7**. Water is fed at the top of the reactive section and methyl acetate is introduced at the bottom of the reactive section. The column is operated under total reflux of methyl acetate-methanol azeotrope. The stripping section strips all the methyl acetate and the bottom product is essentially free of methyl acetate. The bottom product, which now contains only methanol, water and acetic acid, can be easily separated using two distillation columns in series giving methanol and acetic acid as products. Thus, this process eliminates two main pieces of equipment from the conventional process: (1) a water wash column for the separation of methanol from methyl acetate, and (2) a methanol-enriching

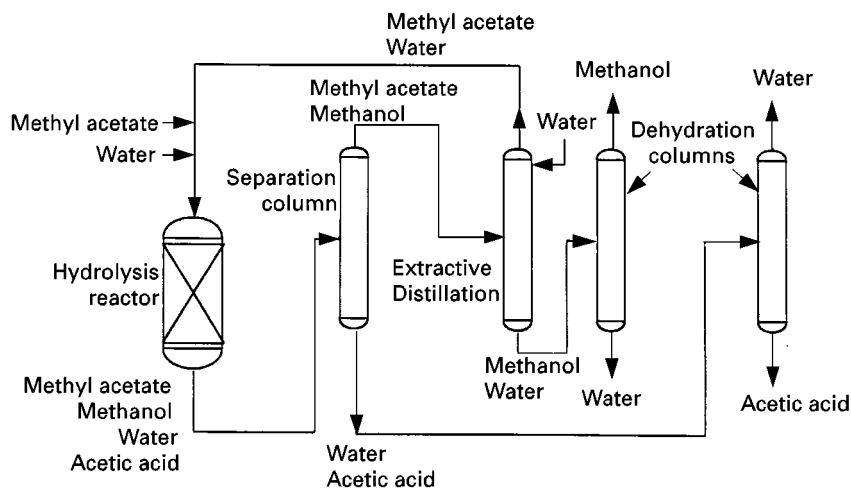


Figure 6 Conventional process for hydrolysis of methyl acetate.

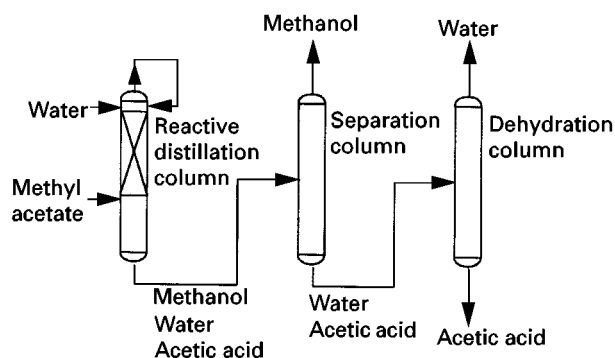


Figure 7 Reactive distillation process for hydrolysis of methyl acetate.

column for recovery of water-diluted methanol. Conversions to the tune of 99% are achieved in this process. The estimated heat savings are 50% that of the conventional process.

Recovery and Purification of Chemicals

The esterification reaction has also been successfully employed for the recovery of acetic acid from aqueous streams. Dilute acetic acid is produced in large quantities in many processes, such as the manufacture of cellulose esters, terephthalic acid and dimethyl terephthalate; and also in reactions such as acetylation and nitration. The recovery of acetic acid from these streams is a daunting problem. The conventional methods for recovery are azeotropic distillation, simple distillation and liquid-liquid extraction. With the advent of reactive distillation processes, esterification of acetic acid with methanol seems an attractive alternative. Laboratory experiments have been carried out to recover acetic acid in a reactive distillation column. The column contained commercially available ion exchange resin along with Rashig rings. The use of a solid acid catalyst offers noncorrosive conditions so that a less expensive construction material can be used. Up to 84% recovery of acetic acid as methyl acetate was achieved. Hoechst Celanese Corporation has recently described a reactive distillation process for the recovery of acetic acid from aqueous solutions as methyl acetate. With the use of acidic ion exchange resin as catalyst, more than 90% recovery from 5–30% aqueous acetic acid is claimed. They also suggest the use of Koch Engineering's Katamax packing as catalyst.

Reactive distillation can be applied for the recovery of many other chemicals from dilute streams. The polymer industry is often faced with the challenge of treatment of aqueous formaldehyde solutions, as it is a nuisance to the environment and it is difficult to

remove trace quantities of formaldehyde. Reactive distillation with methanol, ethanol or ethylene glycol not only brings down the formaldehyde concentration to the ppm level, but also yields useful acetal products. Similarly, nonboiling chemicals such as glyoxal and glyoxylic acid can be recovered from their aqueous solutions through the formation of their corresponding acetals or esters, which can be separated by distillation. CDTech has recently developed a reactive distillation process for hydrodesulfurization, called the CDHDS process, which is aimed at producing low sulfur fuels to meet stringent future environmental regulations at the lowest cost.

Reactive distillation has reportedly been employed for the purification of bisphenol A of polycarbonate grade, where impurities in the form of carbonyl compounds such as acetone, mesityl oxide, hydrotopraldehyde, etc., have to be reduced from about 3000 ppm to <10 ppm. A continuous reactive distillation column has been claimed to be a versatile method to achieve this objective.

Concluding Remarks

Reactive distillation offers several benefits over conventional processes for MTBE and methyl acetate manufacture. The commercial success of MTBE manufacture by reactive distillation has led to numerous investigations in the recent past on almost every aspect of this process. The generation of kinetic and equilibrium data at boiling temperatures, simulation and design studies, control strategies and identification of new reactions as candidates for reactive distillation, are some of the areas being investigated. Simulation studies of catalytic distillation for etherification have highlighted the important aspects of steady state multiplicity. This concept carries a special significance and plays an important role in design methods. Future work on simulation will see other reactions displaying this unusual phenomenon. Eastman Kodak has demonstrated the feasibility and advantages of reactive distillation at the commercial scale for methyl acetate manufacture. The process has scope for improvement in the sense that solid acid catalyst can be employed instead of sulfuric acid. Different techniques of confining the small beads of ion exchange resin in fibre glass cloth, wire mesh or structured packing have been developed. These catalysts offer very good vapour-liquid contact and activity but replacing the deactivated catalyst would be labour-intensive and time-consuming. The future focus should be on development of a catalyst in the form of a conventional column packing, such as Raschig rings, which would have good mechanical strength, activity and stability under the reaction conditions. Reactive

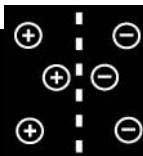
distillation may find a place in many other processes such as hydrolysis of methyl acetate, recovery of carboxylic acid from their aqueous solutions, hydrosulfurization and purification of phenols.

See also: II/Distillation: Energy Management; Historical Development; Instrumentation and Control Systems; Theory of Distillation.

Further Reading

- Agreda VH, Partin LR and Heise WH (1990) High purity methyl acetate via reactive distillation. *Chemical Engineering Progress* 86(2): 40–46.
- Ancillotti F, Pescarollo E, Szatmari E and Lazar L (1987) MTBE from butadiene-rich C_4 s. *Hydrocarbon Processing* 66: 50–53.
- Bravo JL, Pyhalahiti A and Jarvelin H (1993) Investigations in a catalytic distillation pilot plant: vapour/liquid equilibrium, kinetics, and mass transfer issues. *Industrial and Engineering Chemistry Research* 32: 2220–2225.
- Chopade SP and Sharma MM (1997) Reaction of ethanol and formaldehyde: use of versatile cation exchange resins as catalysts in batch reactors and reactive distillation columns. *Reactive and Functional Polymers* 32(1): 53–65.
- Chopade SP and Sharma MM (1997) Acetalization of ethylene glycol with formaldehyde using cation exchange resins as catalysts: batch versus reactive distillation. *Reactive and Functional Polymers* 34(1): 37–45.
- DeGarmo JL, Parulekar VN and Pinjala V (1992) Consider reactive distillation. *Chemical Engineering Progress* 88(3): 43–50.
- Fuchigami Y (1990) Hydrolysis of methyl acetate in distillation column packed with reactive packing of ion exchange resin. *Journal of Chemical Engineering of Japan* 23: 354–359.
- Hauan S, Hertzberg T and Lein KM (1995) Why methyl *tert*-butyl ether production by reactive distillation may yield multiple solutions. *Industrial and Engineering Chemistry Research* 34: 987–991.
- Jacobs R and Krishna R (1993) Multiple solutions in reactive distillation for methyl *tert*-butyl ether synthesis. *Industrial and Engineering Chemistry Research* 32: 1706–1709.
- Kolah AK, Mahajani SM and Sharma MM (1996) Acetalization of formaldehyde with methanol in batch and continuous reactive distillation columns. *Industrial and Engineering Chemistry Research* 35(10): 3707–3720.
- Mohl KD, Kienle A, Gilles ED, Rapmund P, Sundmacher K and Hoffman U (1997) Nonlinear dynamics of reactive distillation processes for the production of fuel ethers. *Computers and Chemical Engineering* 21: S989–S994.
- Neumann R and Sasson Y (1984) Recovery of acetic acid by esterification in a packed chemorectification column. *Industrial and Engineering Chemistry Process Design and Development* 23: 654–659.
- Nijhuis SA, Kerkhof FPJM and Mak ANS (1993) Multiple steady states during reactive distillation of methyl *tert*-butyl ether. *Industrial and Engineering Chemistry Research* 32: 2767–2774.
- Nocca JL, Leonard J, Gaillard JF and Amigues P (1989) Process for manufacturing a tertiary alkyl ether by reactive distillation. US Patent 4 847 431.
- Rehfinger A and Hoffman U (1990) Kinetics of methyl tertiary butyl ether liquid phase synthesis catalysed by ion exchange resin – I. Intrinsic rate expression in liquid phase activities. *Chemical Engineering Science* 45(6): 1605–1617.
- Scates MO, Parker SE, Lacy JB and Gibbs RK (1997) Recovery of acetic acid from dilute aqueous streams formed during a carbonylation process. US Patent 5 599 976.
- Sharma MM (1995) Some novel aspects of cationic exchange resins as catalysts. *Reactive and Functional Polymers* 26: 3–23.
- Smith LA (1980) Catalyst system for separating isobutene from C_4 streams. US Patent 4 215 011.
- Smith LA (1981) Catalytic distillation process. US Patent 4 307 254.
- Song W, Venimadhavan G, Manning JM, Malone MF and Doherty MF (1998) Measurement of residue curve maps and heterogeneous kinetics in methyl acetate system. *Industrial and Engineering Chemistry Research* 37: 1917–1928.
- Sundmacher K and Hoffmann U (1995) Oscillatory vapour–liquid transport phenomena in a packed reactive distillation column for fuel ether production. *Chemical Engineering Journal and the Biochemical Engineering Journal* 57: 219–228.

RESINS AS BIOSORBENTS: ION EXCHANGE



S. Belfer, The Institutes for Applied Research,
Ben-Gurion University of the Negev, Beersheva,
Israel

Copyright © 2000 Academic Press

Introduction

The term biosorbent is usually applied to solid polymeric media employed in the purification, separation or isolation of biotechnological products. To assure

efficient sorption, these materials must meet certain requirements: they must have a high sorption capacity combined with ease of regeneration, good kinetic properties and mechanical stability over many sorption-regeneration cycles. Both ion exchange resins and their precursors, the inert polymer matrices, are extensively used to isolate fermentation products, including low molecular weight compounds, such as acetic acid, and high molecular weight compounds, such as enzymes and proteins.

Ion exchange resins have been traditionally used in water treatment technologies, for example for desalination and softening and for wastewater treatment. Their first application to pharmaceuticals may be dated to the 1950s and 1960s, although the greatest surge in interest in terms of papers and patents published occurred in the period 1960–75.

Pharmaceuticals

Of the various pharmaceutical products processed by ion exchange technologies, antibiotics are probably the most important. Because antibiotics mostly consist of charged molecules, they lend themselves readily to isolation with ion exchange resins, and with cation exchangers in particular. In January 1945, Van Dolah, Christenson and Shelton filed a US patent application claiming the use of organic cation exchangers for the purification of streptomycin and streptothricin. First to be used for this purpose were the phenol-sulfonic acid-type cation exchangers (Amberlite IR-100, Ionac C-200, Dowex 30). These were followed by high capacity carboxylic acid exchangers for commercial applications (Amberlite IRC-50). Both groups are characterized by a gel structure. They have no open pores in the dry state, but when placed in contact with aqueous solutions they undergo swelling and acquire the ability to uptake large ions.

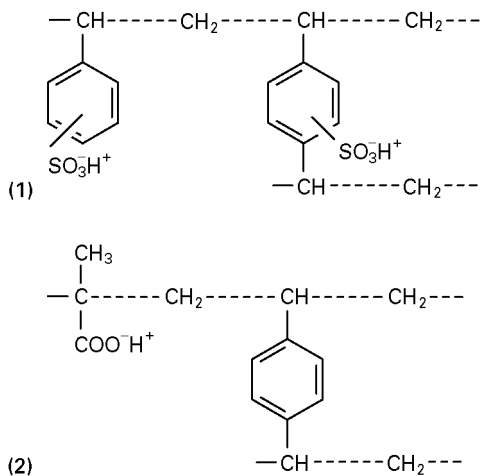
Commercialization of the macroporous sorbents of the Amberlite XAD series by Rohm and Haas in the 1960s was a revolutionary step in ion exchange technology and opened up new possibilities for the isolation of antibiotics. Macroporous sorbents had the necessary mechanical strength, provided large surface areas for sorption, and had appropriate pore sizes for rapid transport. Macroporous resin sorbents such as the polyaromatics Amberlite XAD-4, -16 and -1180, Diaion HP20, media consisting of aliphatic esters (Amberlite XAD-7) and nitrated aromatics (nitrated Amberlite XAD-16) were recommended for large scale application for antibiotics.

Vitamins constitute another class of pharmaceuticals that are purified by ion exchange resins. Vitamin B₁₂, for example, is produced by microbial fermentation and can be separated from the broth using a carboxylic acid exchanger.

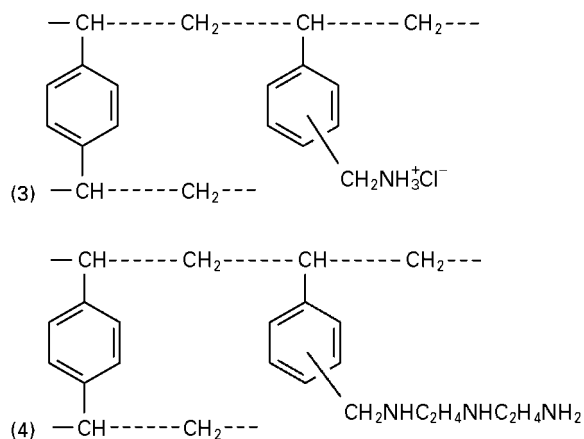
Proteins are based on copolymers of amino acids and may thus be regarded as polyionic materials. At a given pH they bear either a positive or a negative charge depending on their isoelectric point. Proteins are therefore eminently suitable for isolation by ion exchange technology. Exchangers based on matrices consisting of cross-linked polyacrylic and phenol-formaldehyde polymers have been used for large scale protein purification. However, the traditional ion exchangers are generally unsuitable for the adsorption of proteins due to their hydrophobicity, high charge density and high degree of cross-linking, which result in low protein capacities and a tendency towards denaturation of sorbed molecules. After the introduction in 1956 of the first ion exchanger specifically designed for proteins, a number of highly hydrophilic polysaccharide matrices have been proposed, all of them less rigid and more hydrophilic than the polystyrene type of biosorbents.

Synthesis of Resins

Today's ion exchange technology is based on organic polymer matrices. The typical spherical ion exchange beads are made by suspension polymerization of styrene with divinylbenzene to form an insoluble polymer gel. The mixture of monomers to which an initiator of radical polymerization has been added is stirred into an aqueous suspension under conditions designed to give the desired droplet size. This mixture is heated for several hours to yield solid spherical beads, which are then treated with concentrated sulfuric acid at about 80°C to obtain cation exchange resin. The final product is a sulfonated cross-linked polystyrene – the strong-acid cation exchanger most widely used commercially. It has a capacity of 5.25 mmol g⁻¹ calculated for oven-dried resin. The structural formula of the resin is given below (Structure 1), together with the formula of a weak-acid cation exchanger based on acrylic acid copolymerized with DVB (Structure 2).



Anion exchange resins are produced by a two-step process. First, chloromethylation is applied to introduce chloromethyl groups. The second step is amination. When a tertiary amine such as trimethylamine is used, the product is a strong-base quaternary ammonium compound (Structure 3). This resin is the anionic equivalent of the sulfonic cation exchange materials. The capacity of a typical strong-base resin is 3.9–4.2 mmol g⁻¹ of dry resin. The use of a secondary amine, such as dimethylamine or other multifunctional amine, gives various weakly basic resins, for example the one shown in Structure 4.



The resins mentioned above are among those most commonly used as ion exchangers. However, a wide range of resins tailored for specific needs is available; further information may be found in commercial catalogues as well as in relevant monographs. For

illustration, a list of synthetic resins manufactured by Mitsubishi and designed for protein separation is given in Table 1, together with the relevant recommendations.

As an alternative to the highly hydrophobic organic polymeric matrices, ion exchange materials for biological compounds have also been developed from cross-linked dextran, agarose and beaded crystalline cellulose polymers. The functional groups typically added to such matrices are shown below.

Anionic functional groups

Aminoethyl (AE)	$\text{---OCH}_2\text{CH}_2\text{NH}_3^+$
Diethylaminoethyl (DEAE)	$\text{---CH}_2\text{CH}_2\text{N}(\text{CH}_2\text{CH}_3)_2$
Quaternary aminoethyl (QAE)	$\text{---OCH}_2\text{CH}_2\text{N}^+(\text{C}_2\text{H}_5)_2\text{---CH}_2\text{CH}(\text{OH})\text{CH}_3$

Cationic functional groups

Carboxymethyl (CM)	$\text{---OCH}_2\text{COO}^-$
Phospho	$\text{---PO}_4\text{H}_2^-$
Sulfopropyl (SP)	$\text{---CH}_2\text{CH}_2\text{CH}_2\text{SO}_3^-$

DEAE-cellulose, an anion exchanger containing diethylaminoethyl groups attached to the cellulose, is applied extensively. An exchanger of this type having a content of basic groups of only 1 mmol g⁻¹ adsorbs three-quarters of its own weight of bovine plasma albumin from 0.2% solution in 0.01 mol L⁻¹ sodium phosphate at pH 7.0. CM-cellulose, a cation exchanger, which contains carboxymethyl groups, adsorbs its own weight of horse carbon monoxide haemoglobin from 0.2% solution in 0.01 mol L⁻¹ sodium phosphate at pH 6.0. Cellulose ion exchangers with improved characteristics are now available, and numerous studies on their use in

Table 1 Sepabeads FP series product list^a

Grade	Functional group	Pore size ^b			Chromatography mode				
		Small	Medium	Large	GFC	CEC	AEC	HIC	AFC
FP-HG	OH	FP-HG20	FP-HG13	FP-HG05	⊙				
FP-CM	CH ₂ COOH		FO-CM13			⊙			
FP-QA	N ⁺ (CH ₃) ₂ C ₂ H ₄ OH		FP-QA13				⊙		
FP-DA	N(C ₂ H ₅) ₂	FP-DA20	FP-DA12 FP-DA13	FP-DA05			⊙ ⊙		
FP-HA	NH(CH ₂) ₆ NH ₂	FP-HA20	FP-HA13					⊙	
FP-BU	O(CH ₂) ₃ CH ₃		FP-BU13	FP-BU05				⊙	
FP-OT	O(CH ₂) ₇ CH ₃		FP-OT13					⊙	
FP-PH	OC ₆ H ₅		FP-PH13			⊙	⊙		
FP-CL	N(CH ₂ COOH) ₂		FP-CL13						⊙
FP-BL	Cibacron blue 3G-A		FP-BL13						⊙

^aAverage particle size approximately 120 μm.

^bThe second digit in the product name refers to the pore size. GFC, gel filtration chromatography; CEC, cation exchange chromatography; AEC, anion exchange chromatography; HIC, hydrophobic interaction chromatography; AFC, affinity chromatography. From Paion, Manual of Ion-Exchange Resins and Synthetic Absorbents.

the separation of biologicals have been reported in the last 5 years.

Characteristics of Resins

Selection of the exchange resin for a given application is a process of compromise based on examination of many factors, such as the polar nature of the sorbate, the size of the sorbate, resin capacity, equilibrium relationships, elution properties and flow characteristics.

Adsorption Isotherm

In order to design a purification process based on an ion exchange technique, it is essential to know something about the capacity of the exchanger. Equilibrium sorption capacity is commonly determined with the help of the sorption isotherm, which gives the sorption uptake (q) and the final equilibrium concentration of the residual solute in solution (c). Sorption isotherms are measured by placing solutions with different concentrations of solute in contact with a known weight of the resin at a constant temperature until equilibrium is attained. Calculation of the difference between the concentration of product before and after equilibrium, c^* , gives the sorbed protein mass q^* . Plotting q^* versus c^* yields the equilibrium sorption isotherm. Assuming that single-site interaction occurs between bioproduct and sorbent, and also that nonspecific interactions are absent, the apparent constant K_A and the maximum product-binding capacity q_m may be evaluated by fitting the experimental data to the well-known Langmuir model:

$$q^* = \frac{q_m \cdot K_A \cdot c^*}{1 + K_A \cdot c^*}$$

Non-Langmuirian behaviour may point to multiple interaction sites. In such cases, appropriate models may be worked out to fit the experimental data and used to determine whether this behaviour may be due to additional nonspecific interaction sites from the sorbent's surface, or to product-product interactions with the first adsorption layer.

Kinetics of Adsorption

Another important factor of sorption performance is the kinetics of the adsorption/desorption reactions. The rates of these reactions dictate the length of time that has to be allowed to attain equilibrium. For example, the adsorption of protein on to packed beds involves three processes.

First, the protein is transported from the bulk fluid to the outer surface of the adsorbent particles by film mass transport. Second, intraparticle transport occurs

by diffusion. Finally, the protein binds to ligand attached to the inner surface of the particle. It is important to determine which of these processes is the rate-limiting step.

Process Design

Isolation of bioproducts by ion exchange processes can be carried out either batchwise or by traditional packed-bed techniques. In the former, the exchanger is added to the product solution in a vessel which is mixed until sorption has occurred.

Packed-Bed Column

In a packed-bed column the movement of liquid through the bed approximates to plug flow, resulting in a maximum number of theoretical equilibrium stages within the column and hence good adsorption and chromatographic performance. The overall flow performance is strongly related to the length and shape of the ion exchange zone evolving during sorption and regeneration. This zone appears between the section of column saturated with product and the section that still contains fresh sorbent. As loading or regeneration progresses, the zone moves along the column in the direction of the liquid flow. Breakthrough occurs when the zone approaches the end of the column and the concentration in the outlet stream increases sharply. Breakthrough profiles provide a measure of the performance of different ion exchangers in packed-bed operations. A sharp breakthrough profile is desirable in order to achieve efficient use of sorbent. Figure 1 shows breakthrough profiles for two hypothetical adsorbents with identical equilibrium capacities. It can be seen that a greater proportion of bed capacity is used in the case of sharp breakthrough.

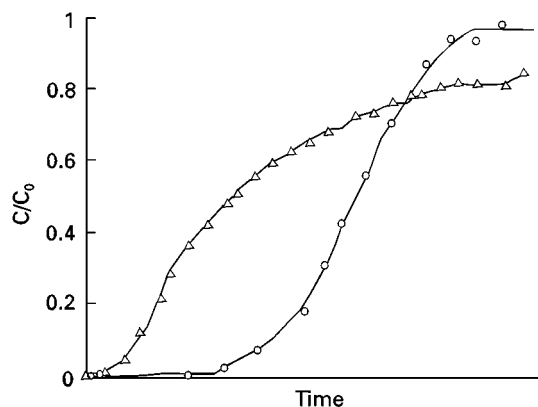


Figure 1 Hypothetical breakthrough curves for two sorbents. The unfavourable breakthrough curve (triangles) is flat and trailing, while the favourable breakthrough curve (circles) is sharp and steep.

Fluidized Bed Column

In a fluidized bed, liquid upflow through the column causes the resin particles to become separated from each other. This technology has attracted attention for biochemical separation processes because it enables direct treatment of crude feedstocks from fermentation reactors. There are two important criteria that must be met before fluidized bed sorption can be considered a viable method for separating products from unfiltered fermentation broths. First, broth solids must have a lower terminal settling velocity than the resin, and the terminal velocity of the resin must be sufficient to achieve reasonable time cycles. Terminal velocity is defined as the upflow velocity at which particles will not remain in the column. Second, the dynamic adsorptive capacity of the resin for the product must be of such a magnitude that optimal yield, purity and cycle time can be achieved.

Determining optimum resin terminal velocity and dynamic sorptive capacity for a specific product is a complex process. The breakthrough curves are usually obtained for a variety of design and operating conditions (column size, distributor, bed type, bed height, flow rate and number of stages). It is also essential to find an appropriate mathematical model for simulation and optimization of the processes. An extensive literature exists describing the mode of operation of fluidized beds with reference to bioproduct

separation. A schematic representation of fluidized bed separation is given in Figure 2.

New Developments

Although ion exchangers remain the most frequently used media for separation of biological mixtures, some novel approaches have emerged. Perfusion chromatography is one of them. This method exploits the fact that particle resins have very large pores (600–800 nm) that permit convective flow. A high surface area for sorption is provided by the presence of numerous small diffusive pores. Thus, convection rather than diffusion dominates the mass transport of the sample molecules. This makes the process 10 times faster than the usual separation process without much loss in capacity or resolution.

Another approach which has emerged as a powerful separation tool is immobilized metal affinity chromatography (IMAC). In this method, immobilized ligands, like iminodiacetic acid, produce chelates with transition metal ions (such as Ca^{2+} , Zn^{2+} and Fe^{3+}) which, when exposed to a protein, form a ternary complex on the protein surface. Further isolation is then accomplished with ease.

In conclusion, the latest developments in sorption media and separation technology provide a broad and varied basis for identification of appropriate sorbents and selection of contact mode between feedstock and sorbent.

See also: II/Chromatography: Protein Separation. Ion Exchange: Organic Ion Exchangers.

Further Reading

- Calmon C and Kressman TRE (1957) *Ion-exchangers in Organic and Biochemistry*. New York: Interscience.
- Chase HA (1994) Purification of proteins by adsorption chromatography in expanded beds. *TIBTECH* 12: 296.
- Cowan GH, Gosling IS and Sweetenham WP (1987) Modelling for scale-up and optimization of packed-bed columns in adsorption and chromatography. In: Kerral MS and Hudson MJ (eds) *Separations for Biotechnology*, p. 152. Chichester: Ellis Horwood.
- Draeger N and Chase HH (1990) Modelling of protein adsorption in liquid fluidized bed. In: Pyle DC (ed.) *Separations for Biotechnology*, p. 325. London/New York: Elsevier.
- Gailliot FP, Cleason C, Wilson JJ and Zwarick J (1990) Fluidized bed adsorption for whole broth extraction. *Biotechnology Progress* 6: 370–375.
- Garcia AA (1991) Strategies for the recovery of chemicals from fermentation: A review of the use of polymeric adsorbents. *Biotechnology Progress* 7: 33–42.

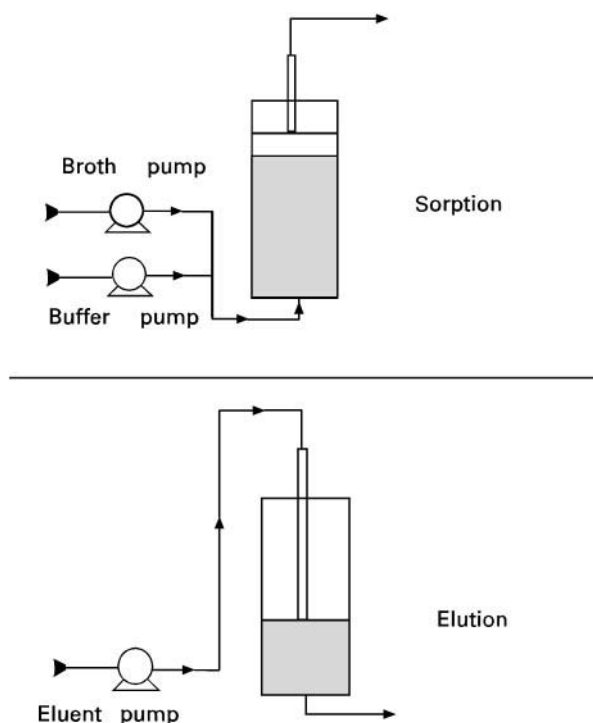


Figure 2 Schematic representation of fluidized bed separation.

- Gelfferich F (1962) *Ion-exchange*. New York: McGraw-Hill.
- Graf H, Rabaud JN and Egly UM (1994) Ion-exchange resins for the purification of monoclonal antibodies from animal cell culture. *Bioseparation* 4: 7–20.
- Greig JA (ed.) (1996) *Ion-exchange Developments and Applications*. Proceedings of IEX '96. Cambridge: Royal Society of Chemistry.
- Levison PR (1993) Process scale liquid chromatography. In: Kennedy JF, Philips GO and Williams PA (eds) *Cellulose: Materials for Selective Separation and Other Technologies*. Chichester: Ellis-Horwood.
- Pirotta M (1991) Ion-exchangers in pharmacy, medicine and biochemistry. In: Dorfner K (ed.) *Ion Exchangers*. New York.
- Rossomando EF (1990) Ion-exchange chromatography. In: Deutscher MP (ed.) *Methods in Enzymology*, vol. 182, *Guide to Protein Purification*, pp. 309, 409. New York: Academic Press.
- Streat M and Cloete FLD (1987) Ion exchange. In: Rousseau RW (ed.) *Handbook of Separation Process Technology*. New York: Wiley.

RESTRICTED-ACCESS MEDIA: SOLID-PHASE EXTRACTION



J. Haginaka, Mukogawa Women's University,
Nishinomiya, Japan

Copyright © 2000 Academic Press

Introduction

For the determination of drugs and their metabolites in serum or plasma by high performance liquid chromatography (HPLC), tedious and time-consuming pretreatment procedures such as liquid-liquid extraction, solid-phase extraction (SPE) or membrane-based extraction are often required. Among those pretreatment procedures, SPE is the most widely used for extraction of target compounds in biological fluids. However, direct injection of serum or plasma samples onto HPLC or SPE materials causes protein denaturation with accumulation of materials on the sorbent, resulting in undesired loss in the capacity and selectivity of the sorbent. Thus, it is essential to remove serum or plasma proteins before loading the samples onto the HPLC or SPE sorbents. Recently, restricted access media (RAM) materials were introduced for direct injection of proteinaceous samples onto the HPLC or SPE materials. With RAM materials large molecules such as proteins are eluted in the void volume without destructive accumulation because of restricted access to some surfaces, while allowing small molecules such as drugs and their metabolites to reach the hydrophobic, ion-exchange or affinity sites and be separated. One approach uses an internal-surface reversed-phase (ISRP) material, produced from porous silica gels, which has hydrophobic interior and hydrophilic exterior surfaces, as shown in Figure 1. The ISRP-GFF material (GFF = glycine-L-phenylalanine-L-phenylalanine) was prepared from covalently modified glyceryl-

propyl (i.e. diol) phases by attachment of the tripeptide GFF, bonded via the amino groups to the glycerylpropyl groups. The phenylalanine moieties were then cleaved from the external surface of the silica with carboxypeptidase A, which is too large to enter the small pores. After this enzymatic treatment, the glycerylpropyl moieties and glycine residues remain on the external surface. Because the ISRP concept was innovative for drug determinations in serum, many RAM materials were subsequently developed. Another RAM material based on silica gels is shielded hydrophobic phase (SHP), which consists of a

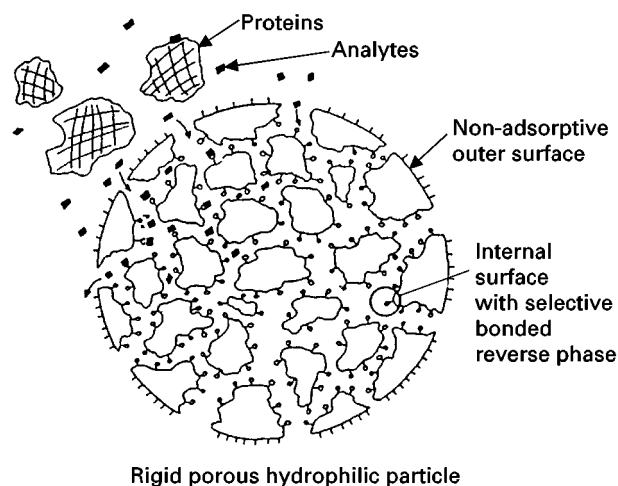


Figure 1 Schematic representation of an internal-surface reversed-phase (ISRP) material. Proteins do not adsorb on the hydrophilic exterior surfaces and do not penetrate into the hydrophobic interior surfaces, while analytes can reach the interior surfaces and be separated. (Reproduced with permission from Perry JA (1991) The internal surface reversed phase. Concept and applications. *Journal of Liquid Chromatography* 13: 1047–1074.)

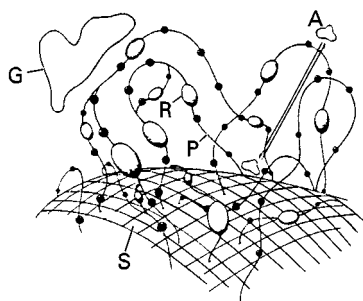


Figure 2 Schematic representation of a shielded hydrophobic phase (SHP) material. S = silica gel matrix; R = hydrophobic pocket; P = hydrophilic network; G = large unretained protein; A = small retained analyte. (Reproduced with permission from Gisch DJ, Hunter BT and Feibush B (1988) Shielded hydrophobic phase: a new concept for direct injection analysis of biological fluids by high-performance liquid chromatography. *Journal of Chromatography* 433: 264–268.)

hydrophilic polyoxyethylene network embedded with phenyl groups, bonded to both the external and internal surfaces of the particles (Figure 2). Other RAM materials based on silica gels include semipermeable surface, dual zone and mixed function phase materials.

RAM materials based on polymer beads have also been developed. For example, one polymer-based RAM material was prepared from porous uniformly sized poly(glycidyl methacrylate-co-ethylene dimethacrylate) beads. Hydrolysis of the epoxide groups to diols can be carried out exclusively within the large pores of the medium through the use of a polymeric catalyst, polystyrenesulfonic acid (average molecular weight, 141 000 Da). The epoxide groups remaining in the small pores after hydrophilization of the large pores were then reacted with either hydrophobic

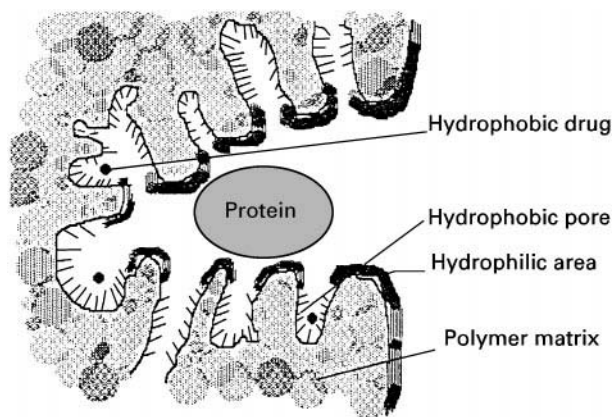


Figure 3 Schematic representation of a polymer-based RAM material modified in pore-size selective fashion using a polymer catalyst. (Reproduced with permission from Smigol V, Svec F and Fréchet JMJ (1994) Novel uniformly sized polymeric stationary phase with hydrophilized large pores for direct injection HPLC determination of drugs in biological fluids. *Journal of Liquid Chromatography* 17: 891–911.)

C₁₈ or phenyl groups, or more polar diethylamino groups. The pore-size selective modification of porous materials provided the RAM materials as shown in Figure 3.

RAM materials could be used for direct serum injection assays of drugs as HPLC or SPE materials. The former materials have been designed and used preferentially as packings for large-size (150 × 4.6 mm i.d.), i.e. analytical columns. In this case the extraction and separation of analytes take place simultaneously. For SPE RAM, sorbents were packed into a small (typically 5–30 mm × 3–4.6 mm i.d.) precolumns connected to an analytical column via a six-port valve, i.e. switching valve. In the coupled-column mode this is a sequential process. The two approaches for the extraction and analysis of the target compounds in biological fluids by HPLC are compared in Table 1.

Single-column Mode

When using the RAM materials, the ionic strength and pH of an eluent, and the content of organic modifier are limited in order to prevent precipitation of serum proteins. For the ISRP–GFF materials, the recommended eluent pH range was 6.0–7.5. The recovery of serum proteins was low at acidic pH. This is due to the electrostatic attractions of the serum proteins having a net positive charge (isoelectric point, *pI* of serum albumin, 4.7) and the external glycine residues having a negative charge. Taking into account the *pK_a* values of the bound glycine (between 2.3 and 3.0), the recovery of serum proteins might be higher with an eluent pH below 2. However, chemically bonded columns cannot be used for long periods at this pH because of the hydrolysis of the bonded phase. However, for RAM materials such as SHP, whose external surface has no charges, there is no eluent pH limitation. These materials can be used at any pH suitable for siloxane-bonded silicas (pH 2–8). These results demonstrated that external uncharged surfaces should be suitable for the external layers of RAM materials. With regard to the eluent, an ionic strength of 0.05–0.2 was used. The preferred organic modifiers are acetonitrile, 2-propanol, tetrahydrofuran and methanol because they can afford a wide selectivity in controlling solute retention on the accessible hydrophobic surfaces. The content of the organic modifier should be < 20%.

Direct serum injection assays of drugs were carried out on the ISRP–GFF materials. The chromatograms of plasma spiked with probenecid or lidocaine at clinical levels (50 µg mL⁻¹ for probenecid, 5.94 µg mL⁻¹ for lidocaine) are shown in Figures 4 and 5, respectively, together with those for methanolic solutions of the

Table 1 On line sample extraction and analysis: comparison of single-column and coupled-column modes. (Reproduced with permission from Boos K-S and Grim C-H (1999) High-performance liquid chromatography integrated solid-phase extraction in bioanalysis using restricted access precolumn packings. *Trends in Analytical Chemistry* 18: 175–180)

Parameter	Single-column mode	Coupled-column mode
Matrix elimination and analyte separation	Simultaneous	Sequential
Peak capacity	Low	High
Selectivity	Low	High
Incidence of interferences	High	Low
Sample volume	< 100 μL	>>100 μL
Analyte enrichment	No	Yes
Limit of quantification	Increased	Decreased
Mobile-phase composition	Restricted (pH, additives)	Variable
Detection	UV > 240 nm Fluorescence detection – yes Electrochemical detection – no	No limitation
Column lifetime	Short	Long
Cost/analysis	High	Low

same concentration. The recovery was calculated from the peak-area ratio of a given concentration of the drug dissolved in plasma and methanol. Despite the differences in the bound fractions (83–94% for probenecid and 65–77% for lidocaine), both drugs were almost completely recovered from plasma samples. The large difference in the intensities of the background peaks in these chromatograms is due to

the difference in the detection wavelengths. Naturally, the shorter wavelength (220 nm for lidocaine) reveals more matrix peaks at a higher intensity than the longer wavelength (254 nm for probenecid). In

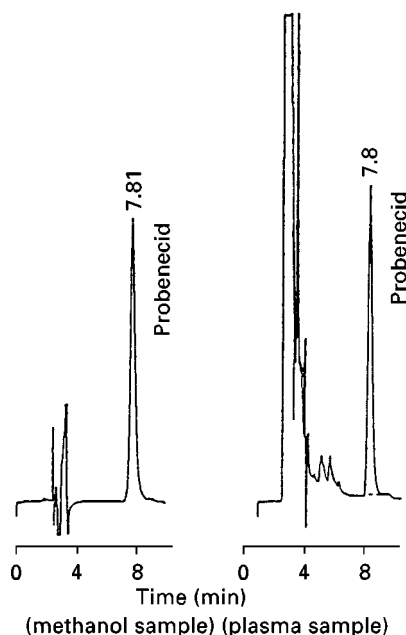


Figure 4 Separation of probenecid from human plasma. Mobile phase, 0.1 M potassium phosphate buffer–tetrahydrofuran (95:5), pH 7.0; flow rate, 1.0 mL min⁻¹; stationary phase, ISRP–GFF column, 150 mm × 4.6 mm i.d.; detection, UV (254 nm); injection volume, 10 μL . (Reproduced with permission from Nakagawa T, Shibukawa A, Shimono N *et al.* (1987) Retention properties of internal-surface reversed-phase silica packing and recovery of drugs from human plasma. *Journal of Chromatography* 420: 297–311.)

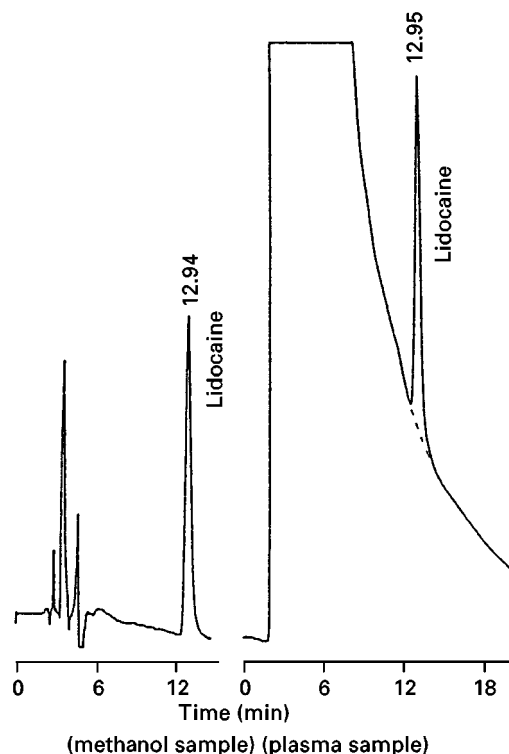


Figure 5 Separation of lidocaine from human plasma. Mobile phase, 0.1 M potassium phosphate buffer–tetrahydrofuran (9:1), pH 7.2; flow rate, 0.8 mL min⁻¹; stationary phase, ISRP–GFF column, 150 mm × 4.6 mm i.d.; detection, UV (220 nm); injection volume, 10 μL . (Reproduced with permission from Nakagawa T, Shibukawa A, Shimono N *et al.* (1987) Retention properties of internal-surface reversed-phase silica packing and recovery of drugs from human plasma. *Journal of Chromatography* 420: 297–311.)

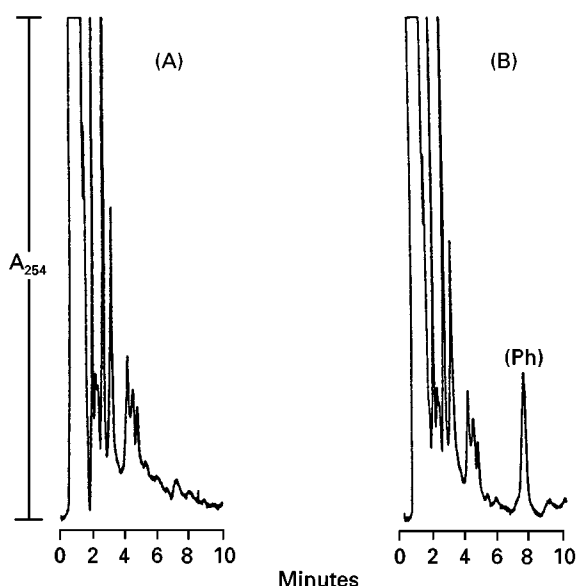


Figure 6 Chromatograms of fetal bovine serum (A) and phenytoin (Ph)-spiked fetal bovine serum (B) at pH 2.5. Chromatographic conditions: column, SHP column (150 mm \times 4.6 mm i.d.); mobile phase, acetonitrile – 50 mM KH_2PO_4 (pH 2.5) (15 : 85); flow rate, 2.0 mL min^{-1} ; temperature, ambient; detection, UV at 254 nm, 0.008 a.u.; injection volume, 25 μL . (Reproduced with permission from Gisch DJ, Feibush B, Hunter BT *et al.* (1989) A new HPLC concept for direct analysis of drugs in biological matrices: shielded hydrophobic phase. *BioChromatography* 4: 206–215.)

both cases the eluent pH was about 7. However, phenytoin was not eluted under the neutral conditions on the SHP materials, but when the eluent pH was adjusted to 2.5, it was eluted and resolved from serum matrix components (Figure 6). Because of the presence of secondary amines on phenytoin, the retention factor of phenytoin was decreased by reducing the eluent pH. Since the SHP materials had no charged groups on the external surface as described above, they could be used at eluent pH 2.5.

In the above applications, less than 100 μL of serum sample was injected. At higher sample volumes, analyte peaks were broadened and a plateau peak was observed. The plateau peak is dependent on the unbound fraction of analyte. Whether the broadened or plateau peak appears; that is, when the unbound drug fraction is higher, we can inject a larger sample volume for direct serum injection assays of the drug without peak-broadening.

On the other hand, both free and total drug concentrations could be simultaneously determined by injecting such a larger sample volume that the plateau peak of a drug appears. Figure 7 shows the chromatogram of 8.00 $\mu\text{g mL}^{-1}$ carbamazepine (CBZ) in human plasma. CBZ was well separated from the blank peak and gave a clear and wide plateau. The CBZ concentration calculated from this plateau height was

1.97 $\mu\text{g mL}^{-1}$, which agreed with the free CBZ concentration determined by means of ultrafiltration (2.08 $\mu\text{g mL}^{-1}$). Furthermore, it is interesting that the CBZ concentration calculated from the area of this plateau was 8.06 $\mu\text{g mL}^{-1}$, in agreement with the total CBZ concentration of this plasma sample. This implies that both free and total drug concentrations can be determined simultaneously by a single analysis based on the height and area of the drug plateau, respectively. However, it is required to inject a large sample volume (in this case, 1.8 mL plasma sample) in order to observe the plateau peak. Further, the plateau peak cannot always be separated from blank peak, dependent on the drug separated.

Coupled-column Mode

As shown in Table 1, the advantages of a coupled-column mode include separation selectivity (ability to couple precolumns and analytical columns of different selectivity), detection sensitivity (analyte enrichment due to larger sample volumes and reduced number of interfering peaks), and higher variability of mobile phases and detection modes. In recent times RAM materials have mainly been used in the coupled-column mode.

Figure 8 shows a representative chromatogram obtained after the direct injection of an untreated human serum sample onto a RAM precolumn. The injection was followed by fully automated online extraction and subsequent separation of antiepileptic

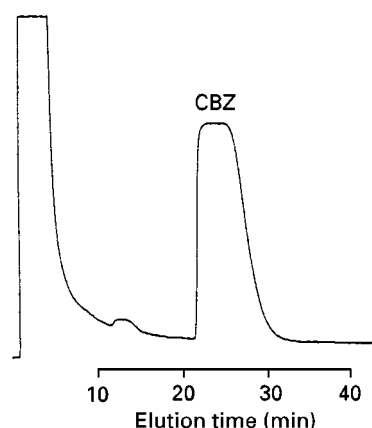


Figure 7 Determination of unbound and bound concentrations of carbamazepine (CBZ) in human plasma. Total concentration of CBZ is 8 $\mu\text{g mL}^{-1}$. Stationary phase: ISRP–GFF column (150 mm \times 4.6 mm i.d.). Mobile phase: potassium phosphate buffer (pH 7.4, $I = 0.17$). Flow rate: 1.2 mL min^{-1} . Detection: UV 300 nm. Column temperature: 37°C. Injection volume: 1.8 mL. (Reproduced with permission from Shibukawa A, Nakagawa T, Nishimura N *et al.* (1989) Determination of free drug in protein binding equilibrium by high-performance frontal analysis using internal-surface reversed-phase silica support. *Chemical & Pharmaceutical Bulletin* 37: 702–706.)

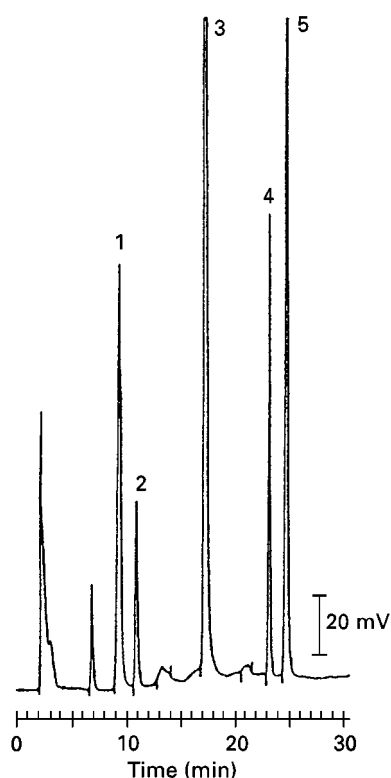


Figure 8 Coupled-column analysis of antiepileptic drugs in serum. Precolumn: 25 mm \times 4 mm i.d., LiChrospher RP-18 ADS (particle size, 25 μ m); analytical column: 250 mm \times 4 mm i.d., LiChrospher 60 RP-Select B (particle size, 5 μ m); loading mobile phase: 0.5 M monobasic sodium phosphate (pH 4.0) for 0 min at 0.5 mL min⁻¹; transfer mobile phase: 5:95 (v/v) acetonitrile–water for 5 min at 0.5 mL min⁻¹; separation mobile phase: acetonitrile–water with a linear acetonitrile gradient from 5% to 34% in 34 min at 0.5 mL min⁻¹; detection: UV absorbance at 205 nm; sample: 100 μ L of analyte-spiked serum. Peaks: 1 = ethosuximide (10.3 nmol), 2 = primidone (1.8 nmol), 3 = phenobarbital (6.6 nmol), 4 = carbamazepine (1.3 nmol), 5 = phenytoin (2.5 nmol). (Reproduced with permission from Boos K-S and Rudolphi A (1997) The use of restricted-access media in HPLC. Part I. Classification and review. *LC-GC* 15: 602–611.)

drugs on a conventional analytical reversed-phase HPLC column. The precolumn (25 mm \times 4 mm i.d.) packed with one of ISRP materials (particle size, 25 μ m) can tolerate 2000 injections or more of 50 μ L of human plasma.

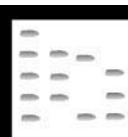
Future Trends

Since the invention of the ISRP–GFF materials, various RAM materials have been developed for direct serum injection assays of drugs with single- and coupled-column modes. However, they are lacking in selectivity because hydrophobic or ion-exchange ligands are used as the analyte binding ligands. In the future, more selective ligands such as immunoaffinity or chemoaffinity ligands or molecularly imprinted polymers have the potential to further improve selectivity and sensitivity in bioanalysis.

Further Reading

- Boos K-S and Grim C-H (1999) High-performance liquid chromatography integrated solid-phase extraction in bioanalysis using restricted access precolumn packings. *Trends in Analytical Chemistry* 18: 175–180.
- Boos K-S and Rudolphi A (1997) The use of restricted-access media in HPLC. Part I. Classification and review. *LC-GC* 15: 602–611.
- Haginaka J (1991) Drug determination in serum by liquid chromatography with restricted access stationary phases. *Trends in Analytical Chemistry* 10: 17–22.
- Rudolphi A and Boos K-S (1997) The use of restricted-access media in HPLC. Part II. Applications. *LC-GC* 15: 814–823.
- Shibukawa A, Kuroda Y and Nakagawa T (1999) High-performance frontal analysis for drug–protein binding study. *Journal of Pharmaceutical and Biomedical Analysis* 18: 1047–1055.
- Thurman EM and Mills MS (1998) *Solid-phase Extraction: Principles and Practice*. New York: Wiley-Interscience.

REVERSED-FLOW GAS CHROMATOGRAPHY



N. A. Katsanos, University of Patras, Patras, Greece
F. Roubani-Kalantzopoulou, National Technical University of Athens, Zografou, Greece

Copyright © 2000 Academic Press

Introduction

Gas chromatography (GC) is a technique that is used not only to separate substances from each other, but also to ‘separate’ physicochemical quantities by

measuring the value of one in the presence of another, e.g. the rate of a chemical reaction in the presence of diffusion phenomena. Several books, reviews and original papers have been published dealing with physicochemical measurements by GC. Some of the properties measured pertain to the moving gas phase, e.g. diffusion coefficients of solutes into the carrier gas, and the emphasis is on determining the properties of the solutes. However, the majority of physicochemical properties studied by GC relate to the stationary phase and its interaction with well-known probe solutes, e.g. the catalytic properties of the solid stationary phase for reactions between gases. This is termed inverse gas chromatography and has the stationary phase of the system as the main object of investigation. The procedures employed are the same as those used in direct GC, but the results are used to derive properties of the stationary phase. The main source of information obtained experimentally is the broadening of the chromatographic elution peaks, mainly due to nonfulfilment of the assumptions under which the central chromatographic equation is derived, namely: (1) negligible axial diffusion of the solute gas in the chromatographic column; (2) linearity of the distribution isotherm; and (3) instantaneous equilibration of the solute between the mobile and the stationary phase. Classical chromatographic systems are not usually in true equilibrium during the retention period, so that extrapolation to infinite dilution and zero carrier gas flow rate is required to approximate true equilibrium parameters.

Another approach to extracting information about the physicochemical properties of the stationary phase from the elution peaks is based on the analysis of the statistical moments of the peaks. Both of these approaches, i.e. measurement of the broadening of the peaks and analysis of their statistical moments,

are dynamic measurements because of the convective movement of the carrier gas inside the chromatographic column. In many cases achieving an acceptable precision for the quantities determined is a difficult, if not impossible, task. The reversed-flow gas chromatography (RF-GC) technique offers an additional route from experimental measurements to the properties of the stationary phase, as described below.

Physical Description and Experimental Arrangement of the System

Although there would be no GC without a mobile gas phase, i.e. a carrier gas, in most studies its flow rate remains constant throughout a single experiment. The magnitude of the flow rate is usually treated as an adjustable parameter. There are, however, two flow rate perturbation methods, the *stopped-flow* and the *reversed-flow* techniques. Both are very simple to apply and consist of either *stopping* the carrier gas flow for short time intervals, or *reversing* the direction of its flow from time to time. Experimentally, this is easily done by using shut-off valves in the first technique and a four-port valve in the second, as shown in Figure 1. By switching the valve from the position shown by the solid lines to that indicated by the broken lines, the carrier gas, flowing initially from end D_1 to D_2 of the sampling column, now flows in the opposite direction, i.e. from D_2 to D_1 . The sampling column is a usual 1/4 in (6.35 mm) stainless-steel or glass chromatographic tube of total length $l' + l$ ranging from 40 + 40 cm to 100 + 100 cm, either straight or bent and empty of any solid or liquid material.

The system also contains two other columns: a separation column and a diffusion column.

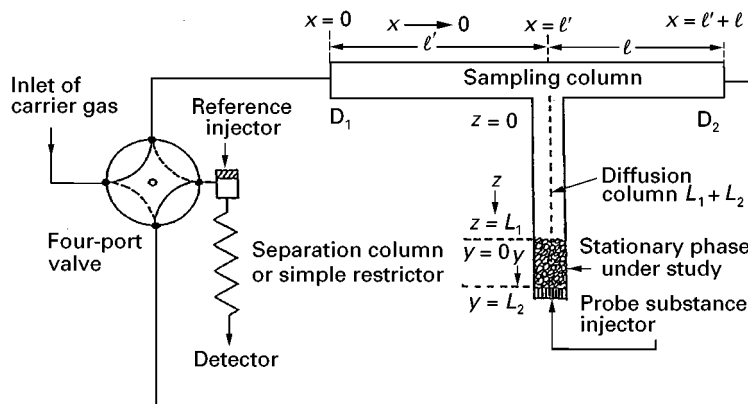


Figure 1 Schematic representation of columns and gas connections showing the principle of RF-GC. Reprinted from *Journal of Chromatography A* 775; 1997, 211–224, with permission from Elsevier Science.

A separation column of any suitable diameter and length is placed before the detector. The carrier gas flows normally in one direction through this column without any reversal, as shown by the gas connections of the valve. The separation column is filled with ordinary stationary-phase material and is used to effect the separation of two or more substances reaching the valve from the sampling column. A reference injector at the inlet end of the separation column is used for identification purposes. If only one substance reaches the detector, a simple restrictor suffices.

A diffusion column of the same diameter as the sampling column and length 30–100 cm is connected perpendicularly at about the middle of the sampling column; it is closed at the other end, and therefore no carrier gas flows through it.

The whole system of the three columns described above is placed within the oven of an ordinary gas chromatograph, with the columns and the connection tubes properly bent. The question naturally arising is: what happens when the direction of the carrier gas flowing through the sampling column is reversed, if it is not reversed in the separation column and there is no flow at all through the diffusion column? If the diffusion column does not contain any stationary phase, but only stagnant carrier gas, nothing would happen. If a probe gas is introduced through the injector into the empty diffusion column, the repeated flow reversals of duration 10–100 s would create narrow and symmetrical peaks like those shown in **Figure 2** (*sample peaks*). From the height H of these peaks in arbitrary units, measured as a function of time, t , that elapses between the injection of probe substance and the respective flow reversal, the diffusion coefficient of the substance into carrier gas can be calculated. Finally, if a certain length L_2 (3–12 cm) of the diffusion column is filled with a stationary phase, the *diffusion band* obtained by plotting H or $\ln H$ against t is different from before, owing to the interactions of this phase with the gaseous probe. This is a way of separating the pure chromatographic process from the rate or equilibrium processes involving the stationary phase.

The RF-GC method was first introduced in 1982, after preliminary studies on heterogeneous catalysis. It was later developed for measuring various physicochemical quantities pertaining to both, substances contained in the moving gas phase and stationary-phase behaviour. The technique was reviewed in 1988 and again more recently. It does not have any of the disadvantages connected with the carrier gas flow and the instrumental spreading of the chromatographic bands, because the phenomena being studied take place inside the diffusion column $L_1 + L_2$ (cf. Figure 1), with no carrier gas flowing

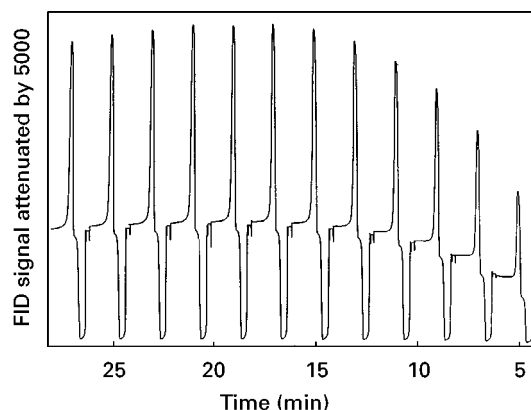


Figure 2 Sample peaks of propene in nitrogen carrier gas, with section L_2 (9.6 cm) containing 0.67 g TiO_2 , at 323.2 K. FID, flame ionization detector.

through it. The flow reversals are used merely as a means for repeated sampling of the concentrations at the point $x = l'$, i.e. at the exit of the section L_1 . This sample is transported to the separation column (containing another stationary phase for separation purposes only), and then to the chromatographic detector, without measuring the elution velocity of the sample peaks or the carrier gas flow rate, provided it is steady. An obvious difference between conventional elution gas chromatography and RF-GC is that in the former longitudinal gaseous diffusion currents are parallel to the chromatographic current, while in the second method diffusion is, from the outset, physically separated from the chromatography by placing the diffusion process perpendicular to the chromatographic process.

Mathematical Models

Inverse gas chromatography has been used for studying many properties of solids, such as the glass transition of polymers, their crystallinity and melting point, and the thermodynamics of their solutions. The RF-GC technique is a useful tool for inverse chromatographic studies, particularly when gas–solid interfaces are involved. Several such studies have been published. Here a short outline of its possibilities is given using some characteristic examples. Take for instance the determination of diffusion parameters, adsorption–desorption rate constants and isotherms, and catalytic rate constants of some gaseous probes on typical solid catalysts, supported or not. All these physicochemical properties can be determined simultaneously in a single gas chromatographic experiment lasting a few hours. The experiment resembles those conducted with a plug flow reactor, but without a gas flowing through it, as Figure 1 shows. It is only gaseous diffusion of the reactant(s) and product(s) that

causes the movement of these substances through the solid bed along the length coordinate y , and then along length coordinate z to the junction $x = l'$ of the sampling column. Two diffusion coefficients of the probe molecules are involved in these movements: D_1 in section L_1 and another D_2 in section L_2 influenced by the bed obstruction factor γ . These are taken care of implicitly in the mathematical analysis, without using the actual values of D_1 and D_2 from the literature.

The mass balance equation of the probe reactant A in the region y (cf. Figure 1) filled with the stationary phase under study is:

$$\frac{\partial c_y}{\partial t} = D_2 \frac{\partial^2 c_y}{\partial y^2} - k_{-1} \frac{a_s}{a_y} (c_s^* - c_s) \quad [1]$$

where c_y is the gaseous concentration of the probe A in region y ; t is the time measured from the moment of injection of A as an instantaneous pulse (delta function, δ) onto the solid bed, at $y = L_2$; k_{-1} is the rate constant for desorption of A from the bulk solid; a_s is the amount of stationary phase per unit length of solid bed; a_y is the cross-sectional area of the void space in region y ; and c_s , c_s^* are the concentrations of A adsorbed on the solid at time t and at equilibrium, respectively.

An analogous mass balance equation is valid for the gaseous concentration c_z of A in diffusion column z :

$$\frac{\partial c_z}{\partial t} = D_1 \frac{\partial^2 c_z}{\partial z^2} \quad [2]$$

It is noteworthy that the usual convective terms $-\nu(\partial c_y/\partial y)$ and $-\nu(\partial c_z/\partial z)$ of gas chromatographic mass balances (ν being the average linear velocity of the carrier gas) are missing from both the above equations, since no carrier gas flows through column sections y and z . This makes the solution of differential eqns [1] and [2] much easier, and all disadvantages connected with the carrier gas flow mentioned before disappear. No 'competition' between ν and rate processes on the gas-solid interface takes place. No corrections of ν are required, not even the measurement of its approximate value is needed, except only to calculate a calibration factor g which is needed in the isotherm determinations. Both eqns [1] and [2] have the form of Fick's second law for diffusion in one dimension, the first equation being modified only by inclusion of the far right-hand side term describing the overall rate of adsorption of the probe gas A onto the surface of the stationary phase.

The system of partial differential equations, eqns [1] and [2], is complemented by:

1. the rate of change of the adsorbed concentration c_s :

$$\frac{\partial c_s}{\partial t} = k_{-1}(c_s^* - c_s) - k_2 c_s \quad [3]$$

now including a rate constant k_2 of a possible first- or pseudofirst-order surface reaction of the adsorbed substance A; and

2. a local experimental adsorption isotherm:

$$c_s^* = \frac{n_s}{a_s} \delta(y - L_2) + \frac{a_y}{a_s} k_1 \int_0^t c_y(\tau) d\tau \quad [4]$$

where n_s is the initially adsorbed amount of A, k_1 is a dynamic adsorption rate constant, and τ is a dummy variable for the time t . The adsorption equilibrium is local and instantaneous, the adsorption parameter k_1 transforming the area under the c_y versus t curve into c_s^* .

Equation [4] describes the actual experimental isotherm, not necessarily a linear one, without the help of an *a priori* isotherm equation (Langmuir, BET, etc.). The graphical experimental isotherm can be constructed in detail if desired, but this is not necessary. Only the basic definition by eqn [4] suffices to incorporate the exact isotherm into the mathematical calculations. The nonlinearity in general is automatically taken into account.

The use of a dummy variable τ for the time t simply facilitates the notation in the integral of eqn [4] without any special meaning attached to τ .

The system of eqns [1]–[4] is solved under the initial conditions:

$$c_z(0, z) = 0, \quad c_y(0, y) = \frac{n_A}{a_y} \delta(y - L_2)$$

and:

$$c_s(0, y) = 0 \quad [5]$$

where n_A is the total amount of A injected. The solution is effected by using double Laplace transforms of all terms with respect to time and length coordinates, under the given initial conditions and the isotherm eqn [4], and subject to the appropriate boundary conditions at $z = 0$, $z = L_1$ and $y = L_2$. By means of various approximations this leads to the expression:

$$H^{1/M} = g c_z(0, t) = A_1 \exp(B_1 t) + A_2 \exp(B_2 t) + A_3 \exp(B_3 t) + A_4 \exp(B_4 t) \quad [6]$$

where H is the height (in arbitrary units, say cm) of sample peaks measured from the ending baseline of the chromatogram, like that of Figure 2, M is the response factor of the detector ($M = 1$ for the FID), and g is a calibration constant for the detector, transforming cm of H to mol cm^{-3} of the concentration $c_z(0, t)$ of probe substance A at $z = 0$ and time t .

A steady-state approximation for c_s in eqn [3], $dc_s/dt = 0$, leads to:

$$H^{1/M} = gc_z(0, t) = A_5 \exp(B_5 t) + A_6 \exp(B_6 t) + A_7 \exp(B_7 t) \quad [7]$$

instead of eqn [6].

The detailed assumptions on which the derivation of eqns [6] and [7] was based have been published (see Further Reading).

It is seen from eqns [6] and [7] that $c_z(0, t)$, i.e. the gaseous concentration of the probe A at the point $z = 0$ of the diffusion column (cf. Figure 1), as measured by H , should be fitted to the sum of four or three exponential functions of time. This can be achieved by a nonlinear least-squares PC program in the *Journal of Chromatography A* (1998) papers listed in the Further Reading, by entering the pairs H (peak height), t (time of reversal) in the DATA lines. The exponential coefficients of time B_1, B_2, B_3 and B_4 of eqn [6] and B_5, B_6 and B_7 of eqn [7], are calculated, together with the respective pre-exponential factors A_1, A_2, A_3 and A_4 of eqn [6], and A_5, A_6 and A_7 of eqn [7]. This PC program is based on the so-called exponential stripping method of Sedman and Wagner. The calculation of the B_i and A_i values ($i = 1, 2, \dots, 7$) is guided by the overall goodness of fit expressed by the square of the correlation coefficient r^2 . This universally accepted criterion, calculated and printed, is in the range 0.990–0.999 in most cases, showing a remarkable goodness of fit for a nonlinear regression analysis. A 't' test of significance for the smallest r^2 usually found shows that it is highly significant, with a probability smaller than 0.05% of being exceeded. The program also prints, together with the B values, their standard errors, which are usually reasonable for physicochemical measurements.

The question naturally arises as to the meaning and physical content of the parameters A_i and B_i so determined. These are given directly and explicitly by the solution of the system of eqns [1]–[5] that led to eqns [6] and [7]. They are written below:

$$\alpha_2(1 + V_1) + k_{-1} + k_2 = -(B_1 + B_2 + B_3 + B_4) = X \quad [8]$$

$$\begin{aligned} \alpha_2(1 + V_1)(k_{-1} + k_2) + \alpha_1\alpha_2 + k_1k_{-1} \\ = B_1B_2 + B_1B_3 + B_1B_4 + B_2B_3 + B_2B_4 + B_3B_4 = Y \end{aligned} \quad [9]$$

$$\begin{aligned} \alpha_1\alpha_2(k_{-1} + k_2) + \alpha_2V_1k_1k_{-1} + k_1k_{-1}k_2 \\ = -(B_1B_2B_3 + B_1B_2B_4 + B_1B_3B_4 + B_2B_3B_4) = Z \end{aligned} \quad [10]$$

$$\alpha_2V_1k_1k_{-1}k_2 = B_1B_2B_3B_4 = W \quad [11]$$

$$\alpha_2(1 + V_1) = -(B_5 + B_6 + B_7) = X_1 \quad [12]$$

$$\alpha_1\alpha_2 + \frac{k_1k_{-1}k_2}{k_{-1} + k_2} = B_5B_6 + B_5B_7 + B_6B_7 = Y_1 \quad [13]$$

$$\frac{\alpha_2V_1k_1k_{-1}k_2}{k_{-1} + k_2} = -(B_5B_6B_7) = Z_1 \quad [14]$$

$$\alpha_1 = 2D_1/L_1^2, \quad \alpha_2 = 2D_2/L_2^2,$$

$$V_1 = 2V_G(\text{empty})\varepsilon/V_G + L_2^2/L_1^2 \quad [15]$$

where V_G and V'_G are the gaseous volumes of the void spaces in regions z and y , respectively and ε the external porosity of the solid bed. The X, Y, Z, W, X_1, Y_1 and Z_1 are just auxiliary parameters to facilitate the calculation of the primary kinetic parameters k_1, k_{-1} and k_2 from B_i . This is done as follows: the sum $k_{-1} + k_2$ is obtained from the difference $X - X_1$, from the ratio W/Z_1 , or as a mean value of these two. Subtraction of $k_{-1} + k_2$ from X gives the value of $\alpha_2(1 + V_1)$. From this, α_2V_1 is easily computed since V_1 is given by the relation [15]. The calculation of k_1k_{-1} follows from the relation:

$$\begin{aligned} k_1k_{-1} = \left\{ Y - \alpha_2(1 + V_1)(k_{-1} + k_2) - \frac{Z}{k_{-1} + k_2} \right. \\ \left. + \frac{W}{\alpha_2V_1(k_{-1} + k_2)} \right\} / \left(1 - \frac{\alpha_2V_1}{k_{-1} + k_2} \right) \end{aligned} \quad [16]$$

Then, dividing W by α_2V_1 and by k_1k_{-1} gives the value of k_2 . The value of k_{-1} follows from the difference $(k_{-1} + k_2) - k_2$, and that of k_1 from the ratio k_1k_{-1}/k_{-1} .

The pre-exponential factors A_1, A_2, A_3 and A_4 of eqn [6] and A_5, A_6 and A_7 of eqn [7] are explicit functions of $gm\alpha_1\alpha_2/\dot{V}$, where \dot{V} is the volumetric flow rate of the carrier gas, and of $B_1, B_2, B_3, B_4, k_{-1}, k_2, m$ and m_s , but the analytical form of this dependence is not required in the calculations.

It is well known that the values of the three rate constants k_1, k_{-1} and k_2 , especially determined at various temperatures, are of primary importance in characterizing solid adsorbents and catalysts. The experimental data, i.e. the H, t pairs from the chromatogram, can be analysed by using a linear adsorption isotherm, instead of the real experimental isotherm (eqn [4]) without bothering whether it is linear or nonlinear. Both methods lead to the

simultaneous determination of three primary kinetic parameters, namely, k_1 , k_{-1} and k_2 . From these primary rate constants, the method based on the linear isotherm calculates the overall mass transfer coefficients K_G and K_S for the gaseous and the solid phases, respectively, while the real isotherm method computes also the deposition velocity V_d and the overall reaction probability γ of the solute with the stationary phase, by means of the relations:

$$V_d = \frac{k_1 V_G(\text{empty}) \varepsilon}{A_s} \times \frac{k_2}{k_{-1} + k_2} \quad [17]$$

$$\frac{1}{\gamma} = \left(\frac{R_g T}{2\pi M_B} \right)^{1/2} \times \frac{1}{V_d} + \frac{1}{2} \quad [18]$$

where R_g is the ideal gas constant, T the absolute temperature, A_s the total surface area of the solid, and M_B the molar mass of the probe gas. The original definition of V_d was the flux of gas to the solid surface divided by the concentration difference between the bulk gas-phase and the surface. The values of k_1 , k_{-1} , k_2 , V_d and γ are calculated and printed directly by running the PC program mentioned before.

It is clear from the definitions of V_d and γ that both parameters are independent of molecular diffusion,

being related only to the local adsorption isotherm (k_1), the desorption rate constant (k_{-1}) and the surface reaction rate constant (k_2).

The only physicochemical assumptions made concerning the gas-solid interactions are that all parameters measured directly or calculated indirectly refer to elementary steps at equilibrium. Thus the ratio k_1/k_{-1} represents the equilibrium distribution constant K , according to the principle of microscopic reversibility. Note that it is not easy to measure simultaneously rate constants of adsorption (k_1) and desorption (k_{-1}) at a dynamic equilibrium state like that justified experimentally in the experiments described here.

Finally, the explicit calculation of the isotherms has been described in the literature. However, eqn [6] provides an easy route to the calculation of the distribution of surface adsorption energies, ε , the local monolayer capacities, i.e. the maximum adsorbed concentrations, c_{\max}^* , of the probe substance on each kind i of adsorption sites, and the local adsorption isotherms $\theta_i(p, T, \varepsilon)$ on heterogeneous surfaces of solids. Many papers and books have recently been published on this subject. From c_{\max}^* , in mol per g of adsorbent, multiplying by the Avogadro number N_A and the cross-sectional area of the probe molecules in m^2 , one can find the specific surface area of the stationary phase in $\text{m}^2 \text{g}^{-1}$.

Table 1 Adsorption, desorption and surface reaction parameters for various hydrocarbons on four metal oxides, at 323.2 K, based on a linear and a nonlinear isotherm model

C_xH_y	$k_1 (10^{-4} \text{ s}^{-1})$		$k_{-1} (10^{-4} \text{ s}^{-1})$		$k_2 (10^{-4} \text{ s}^{-1})$		$K_G (10^{-9} \text{ cm s}^{-1}) V_d (10^{-9} \text{ cm s}^{-1})$		$\gamma (10^{-13})$
	Linear	Nonlinear	Linear	Nonlinear	Linear	Nonlinear	Linear	Nonlinear	Nonlinear
<i>Metal oxide: Fe₂O₃</i>									
C ₂ H ₂	1.56	16.0	3.51	47.8	6.17	21.6	16.4	16.3	12.7
C ₂ H ₄	131	0.0182	1.26	397	3.41	444	1380	0.561	0.454
C ₂ H ₆	92.0	13.4	4.99	11.3	3.25	20.3	969	28.3	23.7
C ₃ H ₆	1.47	0.0094	3.16	521	4.13	560	15.4	0.448	0.444
1-C ₄ H ₈	2.64	527	2.94	0.0821	2.67	0.338	27.8	2280	2610
<i>Metal oxide: Cr₂O₃</i>									
C ₂ H ₂	6.76	15.5	2.69	99.9	0.340	0.383	0.196	0.132	0.151
C ₂ H ₄	7.55	14.2	2.38	167	0.270	0.385	0.219	0.0733	0.0839
C ₂ H ₆	6.06	9.4	3.04	81.5	0.211	0.429	0.176	0.110	0.126
C ₃ H ₆	3.94	9.02	2.20	62.5	0.016	0.133	0.114	0.0428	0.0490
1-C ₄ H ₈	4.91	2.63	1.08	33.4	0.218	0.805	0.142	0.138	0.158
<i>Metal oxide: ZnO</i>									
C ₂ H ₂	11.8	6.90	3.52	54.3	0.211	0.936	0.440	0.374	0.291
C ₂ H ₆	7.76	7.80	2.85	124	0.370	0.695	0.295	0.137	0.114
<i>Metal oxide: PbO</i>									
C ₂ H ₂	0.180	5739	0.280	0.0322	4.52	28.9	21.2	244800	190900
C ₂ H ₆	45.3	10.0	11.9	64.5	3.18	15.9	5250	84.5	70.8
C ₃ H ₆	0.510	6.37	7.61	35.2	3.33	14.9	58.5	81.0	80.3
1-C ₄ H ₈	1.51	5.11	3.59	5.75	2.13	23.6	138	289	331

Some Representative Results

Applying the previous theoretical analysis for the characterization of some metal oxides used as solid catalysts gave the values of the physicochemical parameters k_1 , k_{-1} , k_2 , K_G , V_d and γ for five probe hydrocarbons. These are given in Table 1, calculated for both the linear and nonlinear isotherm models. It is seen that the values of some physicochemical parameters are significantly different for the two models; it is clear that for an inorganic solid of the kind used as a catalyst the linear isotherm model is inadequate, due to the nonuniformity of the surface. The two physicochemical parameters k_1 and k_{-1} characterize any newly prepared catalyst. These constants can be measured easily and accurately and their values supply a reliable catalyst characterization.

An *a priori* acceptance of an adsorption isotherm equation is not needed, which is preferred to the Langmuir or the BET isotherms for this purpose. Any new catalyst sample can be tested by measuring adsorption and desorption rate constants before utilization. From Table 1, it can be seen that many values obtained from the nonlinear isotherm model are 1–4 orders of magnitude different from those corresponding to the linear model. All physicochemical quantities based on the nonlinear model are intended to characterize newly prepared catalysts, on the basis of accurately defined physicochemical concepts.

In some cases in Table 1 the ratios of the same parameters determined with linear and nonlinear isotherms are inverted in going from one gas–solid system to another. This is probably due to the fact that solid surfaces are very heterogeneous as regards adsorption energy distribution and this heterogeneity may differ greatly from one solid to another for the same hydrocarbon, and from one hydrocarbon to another for the same solid. The local adsorption isotherm of eqn [4] is very sensitive to the energy distribution function on the surface, whereas simple overall linear isotherms are not.

Of course, it is not possible from the measurements at one temperature to conclude whether the gas–solid interactions represent physical adsorption or chemisorption. Experiments at various temperatures, however, will give heats of adsorption and activation energies, from which it may be possible to draw conclusions about the nature of the adsorption processes.

Conclusion

The RF-GC technique is a useful tool in inverse GC studies. It has also some advantages for adsorption isotherm determinations in that: (1) the gaseous diffusion and resistance to mass transfer are not neglected, (2) the sorption effect in dynamic chromatographic systems is nonexistent, (3) the pressure gradient is negligible along the solid bed, and (4) the experimental isotherm can be determined in the presence of a surface reaction of the adsorbate. This is very important when dealing with catalysts, when many determinations based on chemisorption must follow every catalyst preparation.

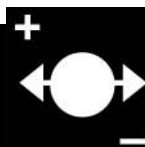
The method briefly outlined here has been used for several published physicochemical measurements. Results have also been obtained for deposition parameters of air pollutants on solid surfaces with a simultaneous determination of the apparent rate constant of gaseous reactions above the solid, and also for the measurement of various rate coefficients and equilibrium constant by utilizing the solid phase as an internal wall coating of denuder tubes in place of the diffusion column.

See also: **II/Chromatography: Gas:** Theory of Gas Chromatography.

Further Reading

- Abatzoglou Ch, Iliopoulou E, Katsanos NA, Roubani-Kalantzopoulou F and Kalantzopoulos A (1997) *Journal of Chromatography A* 775: 211–224.
- Gilbert SG (1984) *Advances in Chromatography* 23: 199–228.
- Katsanos NA (1982) *Journal of the Chemical Society, Faraday Transactions* 178: 1051–1063.
- Katsanos NA (1988) *Flow Perturbation Gas Chromatography*. New York: Marcel Dekker.
- Katsanos NA and Roubani-Kalantzopoulou F (1995) *Journal of Chromatography A* 710: 191–228.
- Katsanos NA, Thede R and Roubani-Kalantzopoulou F (1998) *Journal of Chromatography A* 795: 133–184.
- Rudzinski W and Everett DH (1992) *Adsorption of Gases on Heterogeneous Surfaces*. New York: Academic Press.
- Sedman AJ and Wagner JG (1976) *Journal of Pharmaceutical Sciences* 65: 1006–1010.
- Sotiropoulou V, Vassilev GP, Katsanos NA, Metaxa H and Roubani-Kalantzopoulou F (1995) *Journal of the Chemical Society, Faraday Transactions* 91: 485–492.
- Vassilakos Ch, Katsanos NA and Niotis A (1992) *Atmospheric and Environment* 26A: 219–223.

RIBONUCLEIC ACIDS: CAPILLARY ELECTROPHORESIS



J. Skeidsvoll, University of Bergen, Bergen, Norway

Copyright © 2000 Academic Press

Introduction

With the introduction of capillary electrophoresis (CE), a new generation of electrophoretic techniques has seen the light of day. The scientific literature today describes a large number of applications of this powerful analytical technique in the analysis of nucleic acids. For nucleic acids, as for most other analytes, CE offers significant advantages over many of the conventional electrophoretic techniques. In general, CE is characterized by short analysis time, high resolution, accuracy and reproducibility, quantitative online detection and automation. The small sample volumes required and the extreme sensitivity CE offers, represent a large analytical potential for samples of biological origin. The fundamental analytical and operational parameters for the separation of nucleic acids by CE were identified around 1990. A decade later, CE is considered a fully developed technology for the analysis of DNA. The rapid development of this application of CE seems to have been driven by the many practical applications of electrophoretic separation and detection of DNA in both basic and applied science.

The first reported analysis of RNA by CE was published in 1993 by Reyes-Engel *et al.* and describes the separation and quantification of a specific messenger RNA by capillary zone electrophoresis. To date, only a limited number of articles have been published which focus on the application of CE in the analysis of RNA. The reason for this is not obvious, considering the widespread use of conventional gel electrophoresis of RNA throughout the biomedical scientific field. The fact that RNA, in many respects, displays similar characteristics as DNA, should constitute the basis for significant efforts in the development of RNA analyses based on CE. However, the scientific literature holds promise for a substantial increase in the use of CE in RNA analyses. The following sections intend to give a basic introduction to CE of RNA, with emphasis on important analytical and operational parameters in the analyses. Finally, examples from a diverse group of applications are presented.

Capillary Electrophoresis of RNA

In general, electrophoretic separation of RNA is based on the differences in electrophoretic mobilities of the analytes. As in conventional electrophoresis, the rate of migration of a RNA molecule in CE depends on the mass and the dimensions of the molecule, the charge carried, the applied current and the resistance of the medium. In an electric field, at moderate pH, negatively charged RNA migrates toward the anode. A number of parameters affect the separation of RNA in CE (see below). CE of RNA can be divided into two separate categories based on the principle by which the molecules are separated: capillary zone electrophoresis (CZE) and capillary gel electrophoresis (CGE). In CZE, the RNA molecules are mainly separated by their charge to mass ratio. From the fact that nucleic acids larger than a few nucleotide units have approximately identical charge to mass ratio, CZE provides little or no separation power. Consequently, only single RNA species can be identified by this technique, unless multiple labelling is being used. In CGE, the RNA molecules are separated mainly by their molecular dimensions, i.e., the ability of the different analytes to migrate through a gel matrix. CGE is by far the most common technique for RNA analyses. A description of CGE of RNA is given in the following section.

Capillary Gel Electrophoresis of RNA

Analytical parameters of significance for the separation of DNA by CGE, including gel polymer concentration, electrical field strength and temperature, have been investigated and optimized for the analysis of RNA molecules ranging from oligomers (10 to 40 bases) to several kilobases (Figure 1).

RNA Migration in Capillary Gel Electrophoresis

In conventional gel electrophoresis, the migration of a RNA molecule is inversely related to the \log_{10} molecular mass. However, base composition (primary structure) and secondary structure can affect this relationship. In CGE, separation is achieved because large molecules move more slowly through the gel than small molecules. Separation within a given RNA molecular range is obtained by selecting a gel of

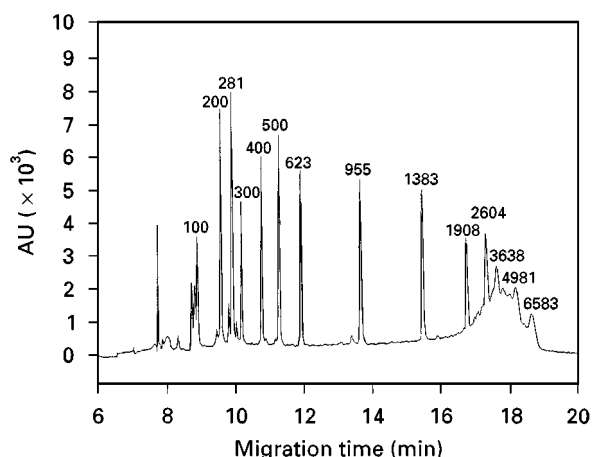


Figure 1 Electropherogram of RNA molecular-mass marker. The sample was denatured, injected at 300 V cm^{-1} for 10 s and subjected to CGE at 200 V cm^{-1} in $1 \times \text{TBE}/8 \text{ mol L}^{-1}$ urea containing 0.3% HPMC. AU, arbitrary units. (Reprinted from Skeidsvoll J and Ueland PM (1996) Analysis of RNA by capillary electrophoresis. *Electrophoresis* 17: 1512–1517. Copyright 1996, with permission from Wiley-VCH Verlag GmbH.)

appropriate pore size. Experiments have demonstrated that CGE of higher molecular mass RNA (in the range from 100 bases to more than 6 kb) to a large extent resembles CGE of single-stranded DNA. An interesting finding is that RNA

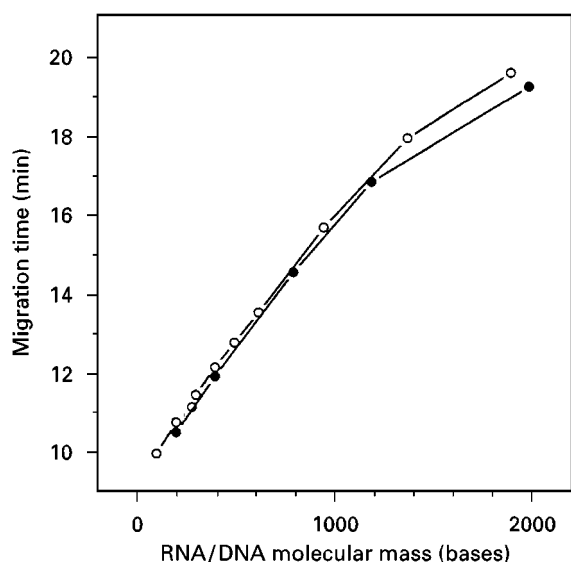


Figure 2 Comparison of migration of RNA and single-stranded DNA. A molecular-mass marker containing RNA and DNA components was denatured by pre-incubation at 95°C for 3 min in the presence of 80% formamide and subjected to electrophoresis in a separation buffer containing 8 mol L^{-1} urea and 0.3% HPMC. Migration time is plotted versus molecular mass for RNA (\circ) and DNA (\bullet). (Reprinted from Skeidsvoll J and Ueland PM (1996) Analysis of RNA by capillary electrophoresis. *Electrophoresis* 17: 1512–1517. Copyright 1996, with permission from Wiley-VCH Verlag GmbH.)

and single-stranded DNA of identical length display different migration when co-analysed under completely denaturing conditions, DNA having a slightly higher migration rate than RNA (Figure 2). The shift in migration for DNA vs. RNA is found constant for molecules ranging from 100 to approximately 1000 bases. The phenomenon is explained by the higher charge to mass ratio of single-stranded DNA.

An inherent property of the (single-stranded) RNA molecule is the potential to form secondary structures or intramolecular and intermolecular hydrogen bonds. To what extent the reaction takes place is primarily a function of the RNA sequence. The predictable determination of RNA molecular mass is essential in most RNA techniques based on electrophoretic separation. Consequently, in order to prevent unpredictable migration of RNA due to the formation of secondary structures, CE should be carried out under completely denaturing conditions. Such conditions can be accomplished through optimization of physical and/or chemical parameters. For example, heating the sample in the presence of a denaturant prior to electrophoresis and addition of a denaturant in the electrophoresis and separation buffers combined with high temperature during electrophoresis should have a strong denaturing effect. Denaturants are chemical compounds that disrupt hydrogen bonds. The most commonly used denaturant, urea, is often added to the separation buffer in very high concentrations (up to 8 mol L^{-1}). Despite an extensive use of buffer additives, data from both conventional RNA gel electrophoresis and CE of RNA indicate that even the presence of 8 mol L^{-1} urea in the separation buffer is not sufficient to completely disrupt intramolecular or intermolecular hydrogen bonds. Addition of the stronger denaturant formamide in concentrations up to 30% (in addition to 3.5 mol L^{-1} urea) and performing CE at 60°C has been necessary to disrupt extensive secondary structures in a hammerhead ribozyme (37 nucleotides) and to provide appropriate separation from its substrate (17 nucleotides). In addition, a decrease in ionic (cationic) strength and an increase in pH are known to have a denaturing effect on RNA. Common problems related to inefficient separation, detection and identification of RNA in CE, probably result from incomplete denaturation of RNA.

Important Analytical and Operational Parameters

From the comprehensive scientific literature describing CE of nucleic acids, it is obvious that operational parameters like capillary dimensions (m) electrical field

strength (E , $V\text{ cm}^{-1}$) and temperature (t , $^{\circ}\text{C}$) have to be chosen carefully to optimize the separation of RNA.

In most applications of CE in RNA analyses, the electroosmotic flow is eliminated through the use of surface-modified (coated) capillaries. This considerably simplifies the experimental design and leaves the scientist with a limited number of variable analytical and operational parameters.

Buffer Composition

In general, all buffer systems that are used for CZE can also be used for CGE. The most common buffers are the Tris-borate buffers (i.e., TBE) with a pH range of 7.5–9.0. Buffer additives like methanol and acetonitrile are used in separation buffers optimized for low-molecular-mass RNA. Urea and formamide are mainly added as denaturants. Moreover, the addition of urea to the separation buffer has been found to increase the resolution of RNA (except for oligoribonucleotides less than 5 bases).

Gel-forming Polymers

A number of different gel-forming polymers have successfully been used in both DNA and RNA separations by CE. The separation matrices comprise both cross-linked gel polymers like polyacrylamide and noncross-linked gel polymers like linear polyacrylamide and cellulose derivatives. Through the optimization of composition and concentration, noncross-linked polymers have now taken over as the predominant separation matrices for most RNA analyses. These materials have demonstrated significant advantages over cross-linked polymers, including ease of preparation and use, physical stability and uncomplicated washing and refilling procedures between analyses. The resolving power of these gels mainly depends on the concentration of the dissolved polymer – dilute gels are used for high-molecular-mass RNA molecules and more concentrated gels for low-molecular-mass RNA.

A systematic study of the electrophoretic separation of RNA at different concentrations of a noncross-linked polymer gel demonstrated that high concentrations ($>0.3\%$) hydroxypropylmethylcellulose (HPMC) were optimal for the separation of RNA less than 1000 bases and low concentrations were optimal for the separation of higher molecular-mass RNA. The results are consistent with data from the separation of DNA by CE.

A number of separation matrices, optimized for different ranges of RNA molecular mass, are commercially available. Additionally, matrices are available which contain denaturants.

Electrical Field Strength

Electrical field strength is recognized as an important operational parameter in CE of RNA. An increase in electrical field strength is found to result in a logarithmic decline in migration times. Efficiency, N (number of theoretical plates) and resolution, R_s , are found to have a more complex relation to the electrical field strength, although a clear tendency towards a decline in both parameters with increased electrical field strength has been demonstrated. In general, low electrical field strengths are preferable for the optimal separation of RNA molecules larger than 100 bases. With the increase in electrical field strength, an increased current will result in the production of heat (Joule heating), which, if excessive, adversely affects the separation by causing broadening of the migrating zones.

Temperature

Temperature, an important analytical and operational parameter, influences both total analysis time and system efficiency. The effect is mainly mediated by a decrease in the separation buffer viscosity. A linear decrease in migration time for RNA molecules ranging from 200 to 2000 bases has been observed for temperatures ranging from 20 to 50°C . The separation efficiency and resolution were found essentially constant over the temperature range. In addition, temperature is a parameter of significant importance in the CE of RNA due to its denaturing effect on intra- and intermolecular hydrogen bonds.

Quantitative Aspects

For a general description of the quantitative aspects of injection in CE, see 'DNA: Capillary Electrophoresis'. Electrokinetic injection is the most common injection mode for RNA in CE. In order to obtain quantitative data, an external reference should be added to or co-injected with the RNA sample. Ideally, the external reference should resemble the sample of interest, but be readily identifiable. Hydrodynamic injection is often used in experiments for the determination of reaction kinetics or in studies of enzymatic activity. Hydrodynamic injection provides representative samples for analysis.

UV absorbance is the most common detection principle for RNA in CE. Despite its general usefulness, the technique suffers from low sensitivity as compared to other detection principles (e.g., laser-induced fluorescence) and represents a limiting factor in some RNA analyses. Detection of RNA based on (laser-induced) fluorescence confers the selectivity

and sensitivity required for a number of analyses where the concentration of analytes is low. However, this detection principle normally requires the covalent attachment of fluorophores to target molecule(s) or fluorogenic buffer additives.

Applications

The application of CE to RNA includes a diverse group of analyses, which often includes one or a combination of the following elements:

- Characterization of RNA molecular dimensions (mass or spatial structure).
- Characterization of RNA sequence.
- Characterization of RNA reaction kinetics.
- Characterization of RNA-binding constants.

An example of a group of CE-based RNA analyses that combines more than one of these elements is the hybridization techniques, which both rely on molecular mass determination and sequence-specific detection of the RNA of interest. In the applications described, RNA samples originate either from chemical synthesis (oligoribonucleotides) or are extracted from biological material. The last group comprise RNA of eukaryotic, prokaryotic and viral origin.

Characterization of RNA Molecular Dimensions (Mass or Spatial Structure)

Capillary electrophoresis analysis of synthetic short-chain oligoribonucleotides (Figure 3) Thirty synthetic oligoribonucleotides, ranging from 3 to 18 nucleotides were analysed by CE in a nondenaturing noncross-linked gel polymer. An equation was developed, based on the experimental data which, under fixed conditions, accounts for the influence of charge to mass ratio (i.e., net charge and base composition) on migration time. High resolution (1 nucleotide unit) was

obtained for homologous series of oligoribonucleotides, and, to some extent, for groups of oligoribonucleotides of identical length, but different sequence.

CGE is often used to determine the quality of chemically synthesized oligoribonucleotides and can be used in conjunction with HPLC to develop an effective method for the purification of crude oligonucleotide solutions.

Low-molecular-mass RNA fingerprinting of bacteria by capillary electrophoresis RNA profiling provides a direct genotypic fingerprint technique for the identification and classification of bacteria by generating an electropherogram including three groups of molecules of taxonomic significance, small tRNAs, large tRNAs, and 5S rRNA (ranging from 70 to 135 nucleotides). The technique is of particular importance for molecular ecology and taxonomic studies, and can also be applied directly to analyses of environmental samples. CGE using both noncross-linked polymer gels (HPMC) and cross-linked polyacrylamide gels have been investigated and optimized for their applicability in the separation of this class of RNA molecules. Good resolution was obtained only for small tRNAs up to approximately 80 nucleotides using cross-linked gels, larger tRNAs and 5S rRNA could not be resolved with this experimental set-up. The use of noncross-linked polymer gels resolved tRNAs and 5S rRNA under nondenaturing conditions, even when they possessed only different secondary structure or small differences in length (1–5 nucleotides). CE using HPMC in the separation buffer resulted in both good peak resolution and reproducibility and was suitable for routine fingerprinting of bacterial low-molecular-mass RNA.

Investigation of intracellular metabolism of a stabilized ribozyme by CGE after uptake by transfection or as free ribozyme CGE has been used to investigate

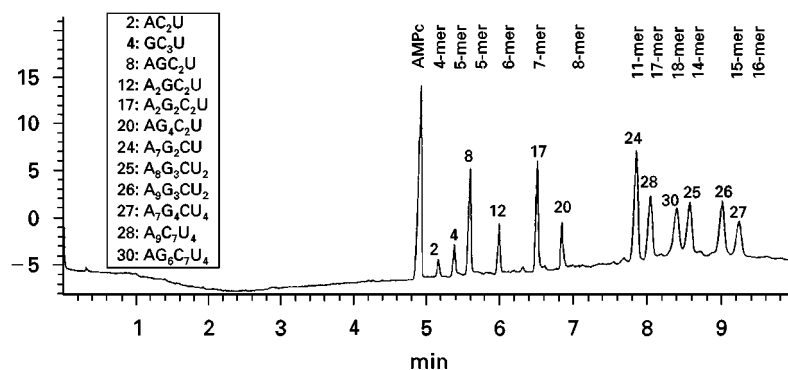


Figure 3 CGE analysis of a mixture of 12 oligoribonucleotides from 4 to 18 units under nondenaturing conditions. (Reprinted from Kolesar JM, Allen PG and Doran CM (1997) Direct quantification of HIV-1 RNA by capillary electrophoresis with laser-induced fluorescence. *Electrophoresis* 697: 189–194. Copyright 1997, with permission from Elsevier Science.)

cellular uptake and degradation of a fluorescein labeled chemically stabilized ribozyme (37-mer). After internalization by transfection or uptake of free ribozyme, electrophoretic peaks of intact ribozyme and different degradation products were easily resolved and the amount of intracellular intact ribozyme quantified. Using laser-induced fluorescence for detection, the method offered extreme sensitivity with estimated limit of detection: 10 and 200 pmol L⁻¹ ribozyme from cell extracts and cell medium, respectively.

A third example include the direct quantification (by UV absorbance measurements) of HIV-1 RNA in human plasma by CZE.

Characterization of RNA Sequence

An important and diverse group of analytical RNA techniques is based on sequence-specific hybridization between two single-stranded nucleic acids and the electrophoretic separation, detection and quantification of the intermolecular reaction product (hybrid). Consequently, the analyses involves characterization of RNA in two dimensions, size and sequence. The Northern (RNA) blotting technique, the nuclease- (S1 or RNase) protection assays and other RNA-hybridization techniques play an important role in the qualitative and quantitative analysis of all classes of RNA in biological systems. The techniques often involve use of radioisotope labels in detection.

CE-based hybridization analyses of RNA has been successfully demonstrated for a number of applications. In general, the hybridization reactions are carried out pre-column (in solution) and the separation and detection of the hybrids on-column. It is demanding to transfer the conventional hybridization techniques to the capillary format and important challenges are related to the development of selective and compatible conditions for both the pre-column and on-column elements of the analyses. Additionally, the low sample volumes injected in CE represent significant analytical and instrumental challenges.

Direct quantification of a specific messenger RNA by capillary zone electrophoresis Total RNA was isolated from whole blood and hybridized with a biotinylated oligonucleotide specific for a receptor mRNA (angiotensin II). The hybrid was first captured on streptavidin-conjugated magnetic beads, then eluted and finally quantified by UV absorbance in CZE. Using this procedure, quantification of the expression of low expressed genes is easy and fast and subject to two limiting factors: the specificity of the capturing oligonucleotide or probe selected and the amount of total RNA. The procedure represents an nonradioactive alternative to conventional RNA ana-

lyses like Northern blotting, RT-PCR or the nuclease- (S1 or RNase) protection assays.

Direct quantification of HIV-1 RNA by capillary electrophoresis with laser-induced fluorescence (LIF) detection (Figure 4) A hybridization method using a HIV-specific probe with analysis by CE-LIF was developed. Plasma samples from HIV-seropositive patients were lysed to obtain RNA, hybridized with a fluorescein-labelled HIV-specific DNA probe, digested by a specific RNase to remove nonhybridized RNA and analysed by CE-LIF in presence of the fluorescent intercalator thiazole orange (TO). 19 fg (corresponding to 1710 copies per mL of starting plasma) of HIV RNA was quantitatively detected. The technique, analogous to the conventional RNase protection assay, takes advantage of signal amplification by using the RNA-binding fluorescent intercalator TO. Calibration is done through the analysis of a fluorescein-labelled RNA marker. The actual approach appears to be an efficient, sensitive and reliable method to specifically and quantitatively analyse RNA from a variety of sources.

Detection of oligonucleotide N3'-P5' phosphoramidate/RNA duplexes with capillary gel electrophoresis The DNA analogues N3'-P5' phosphoramidates (3'-phosphoramidates) has demonstrated favourable properties as hybridization probes, including high melting temperature of duplexes with RNA and high reaction rate at low ionic strengths. The RNA hybridization technique takes advantage of the 3'-phosphoramidate oligomer properties as hybridization probes through duplex formation with short complementary strands of RNA of identical length (9 nucleotides). Hybrids were found to have unique relative mobilities in CGE, compared to the reactants. The ability of CGE to detect the presence of, and to discriminate between, perfect duplexes and duplexes that contained a base mismatch were demonstrated under routine electrophoretic running conditions. In conclusion, the study indicates that 3'-phosphoramidate oligonucleotides may have application in nucleic acid based diagnostics.

Characterization of RNA Reaction Kinetics

Current commercial CE instrumentation offers the scientist operational functions like thermostated sample compartments, automatic sampling and thermostated analyses. These functions increase the potential of CE technique developments, compared with most conventional gel electrophoresis systems, and are especially useful in studies of reaction kinetics, for the determination of association and dissociation constants and in enzymatic assays.

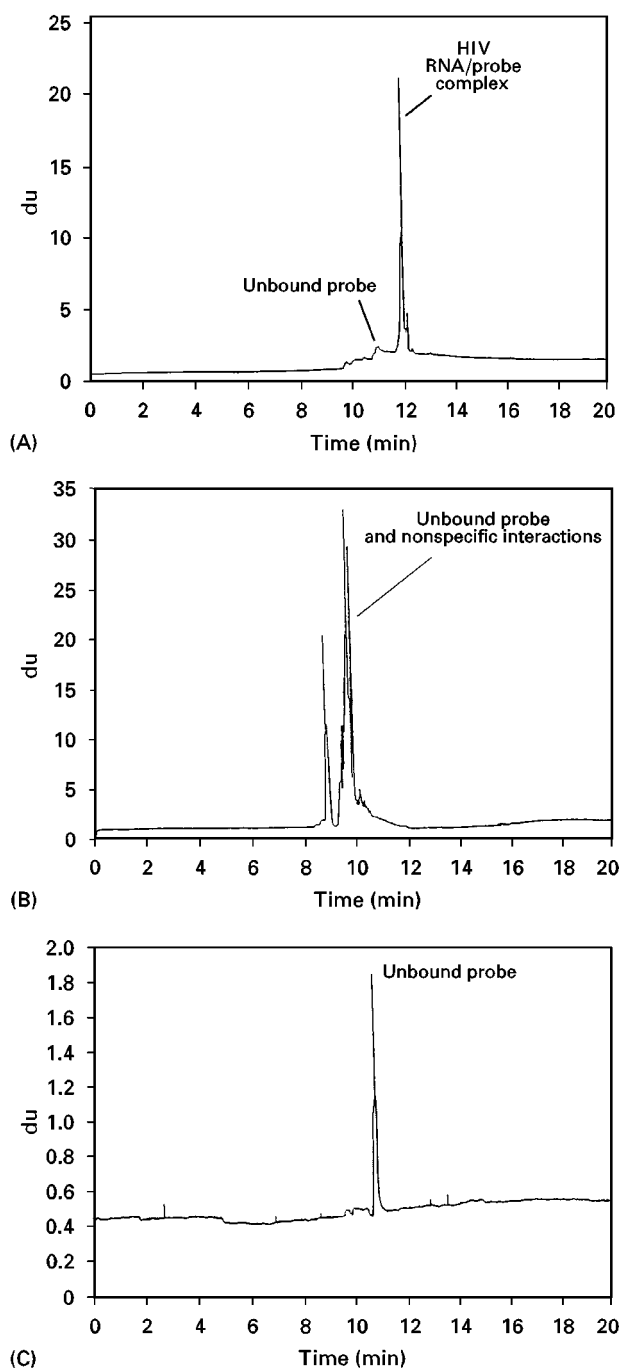


Figure 4 Electropherogram from a hybridization experiment. RNA samples obtained from a HIV-seropositive patient and a seronegative volunteer were hybridized with a HIV-specific probe and analysed by CGE: (A) HIV RNA/probe complex (HIV-positive patient); (B) seronegative volunteer; (C) negative control containing all reaction components except RNA. (Reprinted from Kolesar JM, Allen PG and Doran CM (1997) Direct quantification of HIV-1 RNA by capillary electrophoresis with laser-induced fluorescence, *Journal of Chromatography B* 697: 189–194. Copyright 1997, with permission from Elsevier Science.)

A thermostated and closed sample vial and a computer-controlled injection system is equivalent to a chemical reaction chamber and an automatic

sampling operation, respectively. CE has developed into an effective technique, for example, determination of apparent equilibrium constants for molecular association in solution. Examples of CE being used in the characterization of RNA reaction kinetics are described below.

Determination of the catalytic activity of a hammerhead ribozyme (Figure 5) Ribozymes are sequences of catalytic RNA. The catalytic activity of a synthetic hammerhead ribozyme (37-mer), i.e., the hydrolysis of its RNA substrate (17-mer), has been determined by regular injection from the reaction vial. Kinetic parameters like k_m and k_{cat} were calculated from the integrated area of the decreasing substrate peak. Experimental conditions compatible with both ribozyme activity and CE separation of ribozyme and substrate were determined by careful optimization of the reaction mixture (sample) and the separation buffer. A combination of thermal and chemical denaturation was necessary to separate the oligoribonucleotides. Kinetic analyses were performed in the range where

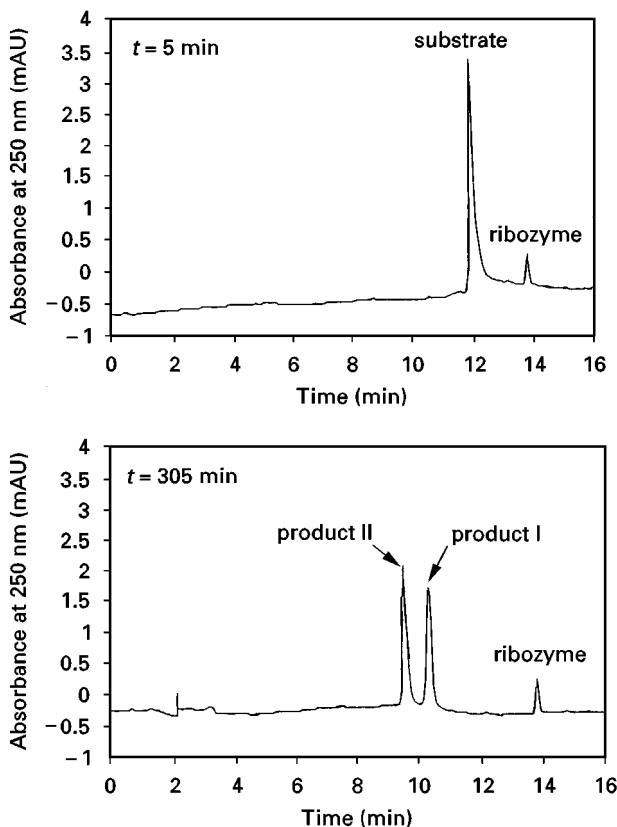


Figure 5 Typical electropherograms demonstrating different stages in a ribozyme-mediated catalytic breakdown of a RNA oligonucleotides substrate. (Reprinted from Saevens J, Schepdael AV and Hoogmartens J (1999) Capillary electrophoresis of RNA oligonucleotides: catalytic activity of a hammerhead ribozyme. *Analytical Biochemistry* 266: 93–101. Copyright 1999, with permission from Academic Press.)

the substrate exhibited linear detector response. RNA detection by UV absorbance was found to be a limiting factor in the Michaelis–Menten analysis.

Characterization of pre-tRNA maturation by RNase using capillary gel electrophoresis A CGE-based technique has been developed in order to characterize the reaction kinetics and mechanism for maturation of a set of pre-tRNA^{fMet} mutants. At all steps of the study of RNase P, including the preparation of the pre-tRNA (quality), the kinetic analysis and the control and yield of the purification steps, CGE was found appropriate and reliable.

Analysis of a ribonuclease H digestion of N3'–P5' phosphoramidate–RNA duplexes by capillary gel electrophoresis The activity of a ribonuclease H (RNase H)-mediated RNA hydrolysis of duplexes formed by oligodeoxyribonucleotides or their analogue, N3'–P5' phosphoramidates and complementary RNA strands, have been investigated. The enzymatic assay conditions were carefully optimized enabling sampling directly from the reaction mixture. CGE electropherograms revealed that RNA–N3'–P5' phosphoramidates duplexes remained intact and therefore did not appear to be a substrate for RNase H.

Conclusion

Today, CE of nucleic acids has become an important analytical technique for biochemists and molecular

biologists and the scientific studies described here clearly illustrate the applicability of CE in the analysis of RNA. Through efficient separations of RNA molecules ranging from a few bases to several kilobases, the specific and sensitive detection of RNA sequences and the study of RNA reaction kinetics, scientists have taken advantage of the prominent characteristics of CE. Compared to the analysis of DNA, additional challenges exist in the analysis of RNA, challenges mainly related to RNA stability and conformation. However, efforts should be made to overcome problems related to inefficient separation, identification and detection of RNA in CE. Extended insight into these phenomena will realize the inherent potential of CE for a diversity of RNA analyses.

Further Reading

- Cellai L, Onori AM, Desiderio C and Fanali S (1998) *Electrophoresis* 19: 3160–3165.
- Dedonisio L, Raible AM and Gryaznov SM (1998) *Electrophoresis* 19: 1265–1269.
- Katsivela E and Höfle MG (1995) *Journal of Chromatography A* 717: 91–103.
- Kolesar JM, Allen PG and Doran CM (1997) *Journal of Chromatography B* 697: 189–194.
- Saevels J, Schepdael AV and Hoogmartens J (1999) *Journal of Analytical Biochemistry* 266: 93–101.
- Skeidsvoll J and Ueland PM (1996) *Electrophoresis* 17: 1512–1517.

RNA

See III/DEOXYRIBONUCLEIC ACID PROFILING: Capillary Electrophoresis

SELECTIVITY OF IMPRINTED POLYMERS: AFFINITY SEPARATION



O. Ramström, ISIS – Université Louis Pasteur, Strasbourg, France

Copyright © 2000 Academic Press

Ever since the discovery of antibodies and receptors, and their remarkable selectivities for almost any given chemical structure, scientists have been intrigued by the quest of mimicking their properties in synthetic or

semisynthetic systems. A material carrying a selective preference for one ligand in comparison with other structurally similar compounds would be of outstanding use in a wide variety of situations, extending from molecular transportation, via analysis, to catalysis and synthesis. A multitude of sophisticated approaches have also been developed over the years, with the objective of controlling ligand binding to an artificial receptor.

Molecular imprinting technology (MIT) is an emerging concept that meets the objective of creating substrate selective materials in a fairly simple, yet efficient, manner. This technique is based on the formation of binding sites, or 'imprints', in a macromolecular matrix, or other suitable molecular support, by a molecular casting procedure. The ligand of interest is thus acting as an active guide, positioning the formation of the binding site, and the outcome is a two- or three-dimensional network embracing the template. Using dynamic interactions between the ligand (or its substitute) and selected building blocks, materials carrying a memory of the ligand structure can be formed. Once the formation of the network is established, the ligand can be removed, thus exposing the binding sites, which are subsequently accessible for repeated binding. A more general description of the molecular imprinting concept is presented elsewhere in this Encyclopedia.

The ligand affinities that can be obtained by this concept are quite remarkable and are often very similar to what can be achieved by the natural systems they are mimicking. Binding constants in the nanomolar range have been reported. Likewise, the selectivities they display are conspicuous, such that very small differences in ligand structure can be distinguished. Thus, the dynamic arrangement of interacting groups in the binding site, moulded in place by the imprinting process, can result in very specific interactions between the imprinted material and the targeted ligand. In this section, the selectivity of molecular imprinted polymers and other matrices will be discussed, focusing on their use in affinity separation.

Molecularly Imprinted Materials

Of all areas where molecularly imprinted materials have found applications, such as diagnostic assays,

drug delivery, sensor technology, and catalytic protocols, by far the most explored field is their use in separation science. Such materials have been developed for use in liquid chromatography (molecular imprinting chromatography, MIC), solid-phase extraction (SPE), capillary electrophoresis, membrane technology and library screening protocols. Especially, chiral discrimination has been heavily investigated, and a large number of impressive chiral separations have been performed. More detailed overviews with respect to chiral separation, as well as to SPE, by these materials can be found elsewhere in this Encyclopedia.

Affinity Separation

As is the case with all types of affinity-based separation techniques, imprint-based protocols can be considered as a mixed-type separation process. The recognition between the analytes and the matrix relies on both affinity-type interactions, exerted by the ensemble of interactions between the analyte and the matrix in the recognition site, and less selective processes, such as general ion exchange, metal coordination and hydrophobic interactions. Although this mixed-type separation can sometimes be advantageous in as much as it offers a means for the analytical chemist to control the retention, most often it is a drawback, and attempts have been made to mask unwanted recognition contributions. For example, the nonselective ion exchange contribution of charged moieties in the matrix can be chemically blocked, resulting in a material where only the charged groups in the sites are active (Figure 1).

The phenomenon of nonspecific binding can sometimes be difficult to distinguish from the affinity process, since a comparison between a material that has been imprinted to a nonimprinted blank can result in differences for compounds that should not be recognized. Since the physical properties of the material

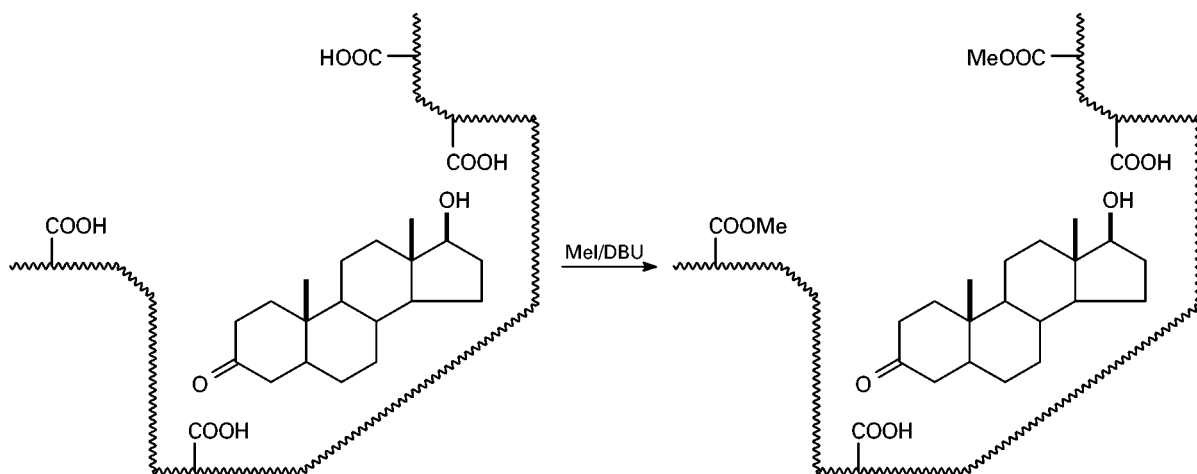


Figure 1 Reduction of nonspecific binding by chemical blocking.

will inevitably change upon imprinting, a change in retention will also be found for compounds not selectively recognized by the material. For example, if a material is prepared using methacrylic acid as functional monomer, the resulting imprinted material may show more pronounced retention than its nonimprinted counterpart. This phenomenon can in part be attributed to the formation of carboxylate dimers in the blank material, thus displaying fewer carboxylate groups free to interact with the analytes. On the other hand, in the imprinted material the carboxylate groups take part in the recognition process and are more exposed to the analytes. Thus, in order to estimate the selectivity of imprinted materials, an estimate of the behaviour of both imprinted and nonimprinted matrices needs to be made. For a full investigation, the behaviour of two or more imprinted matrices is also a very useful comparison. The nonimprinted matrix will address nonselective contributions for a chosen eluent. A set of imprinted matrices will provide information on both the selectivity accomplished and the physical change introduced by the imprinting process. Of course, when chiral separations are targeted, the chiral discrimination in itself is proof of the accomplished selectivity, since a nonimprinted matrix will normally never show enantioselectivity (unless chiral building blocks are used).

Selectivity

As mentioned above, the selectivities that can be accomplished with molecularly imprinted materials are often on a par with natural binders such as antibodies and biological receptors. In most cases, however, this can only be achieved by careful consideration of the system chosen, with respect to the ligand and the building block functionalities. Although much of the beauty and attraction of the entire concept lies in its seemingly compliant facility, design is none the less imperative for the outcome of an efficient imprinting process. It is only after judicious control of all system parameters that highly selective materials can be produced. Rational design is thus involved in using interactions as specific as possible from the very start. Most of the bond types used are chosen in order to acquire a desired selectivity directly from the resulting interaction with its corresponding counterpart, and this selectivity can subsequently be further accentuated by the imprinting process.

Molecular Imprinting Protocols

The characteristics of the imprinting process depend very much on the strength of the bonds used between the ligand and the functional building blocks, ranging



Figure 2 The higher the bond energy used for point interactions, the higher the compliance of the positioning of the groups in the site, but the lower the applicability of the concept. For this reason, most protocols are based on noncovalent systems.

from strong, albeit reversible, covalent bonds to weak, noncovalent interactions. What can be gained from an increased strength between the ligand and the functional building blocks during the imprinting process is often a drawback during the utilization of the resulting materials, and vice versa if noncovalent bond types are used. If too strong bonds are used, such as carboxylic amides and esters, the ease with which the extraction/rebinding process can procure is strongly limited, requiring exceedingly harsh conditions. Thus, weaker bond types have to be employed (Figure 2). Amongst reversible covalent bond types that have been used are boronic esters, imines and disulfides, all easily reversible under reasonably mild conditions. However, only boronic acid esters have been successfully used in chromatographic systems, due to their faster exchange kinetics, which is a reflection of their very low bond strength in aqueous environments ($\Delta G \sim 12 \text{ kJ mol}^{-1}$ for the interaction between phenylboronic acid and glucose).

The special characteristics of metal coordination make these very useful for molecular imprinting. The binding strengths lie between covalent and noncovalent, and can be easily varied by exchange of the metal ion used. The bond energy for a commonly used building block, iminodiacetate (IDA) complexed with Cu^{2+} and imidazole, amounts to $\sim 20 \text{ kJ mol}^{-1}$ at room temperature in aqueous solution.

Although the use of reversible covalent bonds, as well as metal coordination, meets the prerequisite of strong interactions prior to fixation, these systems suffer from one serious drawback – only a limited number of ligands can be targeted using these bond types. Noncovalent interactions on the other hand permit a broader utility range that can be covered, largely making them more advantageous. This is in accordance with biological systems, where molecular complexes are often formed by a plethora of noncovalent interactions such as hydrogen bonds and ion pairing. Although these interactions, when considered individually, are weak compared to covalent bonds, the concerted action of several of these bond types often leads to complexes with very high stability. The high degree of specificity that can be achieved, in combination with the dynamic properties of the interactions, makes these bond types a prerequisite for many biological processes, and has also

been the preferred choice in many imprinting protocols.

Attempts to overcome the drawbacks from the respective protocols, but still be able to benefit from their advantages, can be made by combining the two extremes. Thus, protocols based on covalent binding during the fixation process, but switching to noncovalent interactions afterwards, have been designed, for example, successful protocols based on cleavage of esters, carbonates and amides.

Origin of Selectivity

The complex, normally macromolecular nature of molecularly imprinted materials has precluded a full understanding of the recognition mechanism between the analyte and the matrix. Physical methods, such as solid-state nuclear magnetic resonance, Fourier transform infrared, atomic force microscopy (AFM) and electron spin resonance (ESR), have revealed some of the characteristics of the materials, but a more detailed account of the site architecture remains to be resolved. In contrast, the complexes between the functional building blocks and the print species, formed in solution prior to any imprinting process, can be studied more easily. Obviously, the use of covalent interactions, and often metal coordination interactions, results in structures that can be well characterized by common physical organic methods. In noncovalent systems the situation is more complex, but the use of solution-phase methods has allowed a picture of the interactions to be drawn. Although imprinting of these complexes/adducts may change their structures considerably, the information that can be retrieved from such studies is nevertheless valuable.

The recognition of events taking place in encounters between ligands and receptors is highly dependent on the additive effect of a number of binding forces. An optimal combination of the potential binding forces may lead to strong binding. Thus, in order to achieve proficient complexation between the host molecule and the guest species, several factors such as shape complementarity, functional complementarity and contributions from the surrounding pool of solvent have to be considered.

In all imprinting protocols, be they based upon covalent or noncovalent interactions, the most important factor governing the substrate selectivity is the quality and number of point interactions used to form bonds in solution prior to fixation, gelation or polymerization. In self-assembly systems using noncovalent interactions, the main factors responsible for selective rebinding of ligands to the imprinted sites have been shown to be strong noncovalent bonds such as charge-charge interactions and hydrogen bonding.

Other types of interactions, such as π - π stacking and dipole interactions, may take part as well, but normally to a lesser extent. The three-dimensional arrangement of these interaction points, a reflection of the solution-phase situation set in place by the polymerization step, leads to an inherent specificity of the formed sites. Likewise, in metal coordination systems, the major points of interaction occur between the immobilized metal ions and the coordination sites of the analyte, and the reversible covalent interactions between the functional moieties of the matrix and their counterparts of the analyte make up the major interaction in covalent systems.

In addition to these point interactions, the architecture of the surrounding matrix determines the steric limits of the site, thus providing a more or less efficient van der Waals surface to the analyte. Although the arrangement of the functional moieties in the matrix accounts for most of the selectivity, the shape of the site also plays an important role. The configuration of the surrounding matrix backbone, as cast in place around the print molecule, contributes to the overall ligand specificity (Figure 3). This effect is sometimes less pronounced and substantial freedom in ligand structure can be observed, but often the effect is considerable and minute differences in size can be distinguished. In several cases, the position of a single methyl group is crucial for recognition. In this perspective, the shape effect of the site is particularly pronounced for parts of an imprinted molecule in close proximity to the point interactions. For structural features of the analyte more distal from such bonds, the shape is less important.

Forms of Selectivity

The topic of chemical selectivity can be categorized into three main groups:

1. chemoselectivity, i.e. differentiation among various functional groups in a polyfunctional molecule

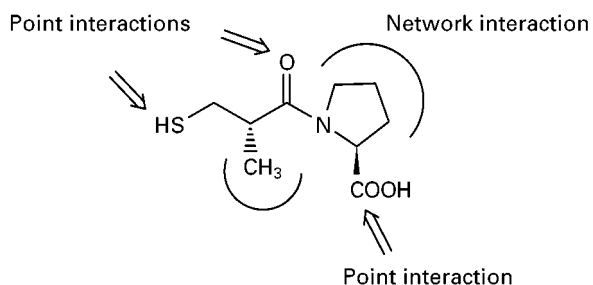


Figure 3 Schematic representation of interactions between a chosen ligand (here captopril) and a molecularly imprinted material. In addition to possible point interactions, whether covalent (disulfide, acetal, ester) or noncovalent (hydrogen bonds, coulombic electrostatic), the backbone of the imprinted network may also contribute to overall selectivity.

2. regioselectivity, referring to orientational control of the interaction
3. stereoselectivity, specifying the control of stereochemistry in the recognition site

Sometimes the last group is further subdivided with reference to the control of relative stereochemistry (diastereoselectivity) and absolute stereochemistry (enantioselectivity). A further physical type of selectivity is the discrimination of molecular size – an issue that may be of substantial importance when dealing with macromolecules and solid matrices.

Chemoselectivity In imprinting protocols based upon reversible covalent bonds, such as boronate esters, disulfides and imines, the chemoselectivity is principally a consequence of the properties of the covalent bond type chosen. Thus, for boronate esters, *vic*-diols are preferred as they give more stable esters than, e.g., mono-alcohols or *gem*-diols, and disulfides are formed exclusively from thiols. Other bond types of a slightly more general character, e.g. acetals, selective for carbonyl groups/alcohols, and imines, selective for carbonyl/amino moieties, are however potentially useful in recognizing a wider variety of ligands.

In metal coordination systems, the coordination properties of the ligand-metal ion pair govern most of the chemoselectivity that can be expected. This programmed selectivity can easily be changed, simply by changing the metal ion. If such a molecularly imprinted material is charged with different metal ions, the coordination properties can be fine-tuned. Such a bait-and-switch strategy has been used for changing the binding strength from high affinity during the imprinting process to low affinity in the rebinding/separation process. For example, Cu(II) can be changed for Zn(II), since the latter displays a weaker

affinity for imidazole groups. When the ion itself is the target species (ligand), coordinating building blocks are normally chosen to occupy less than or equal to half of the coordinating bonds of the ion, allowing for adaptation during the imprinting process (Figure 4). The ionic recognition that can be achieved with such systems is often remarkable, and systems that are able selectively to distinguish small differences in ionic size and coordination pattern have been designed.

In noncovalent systems, the chemoselectivity is much less obvious in the design of the interactions. If a print molecule contains charges or hydrogen-bonding moieties, and functional monomers are chosen accordingly, the inherent chemoselectivity in the complexes formed is less strong, and other ligands can compete for the interactions as well. In addition, the functional building blocks, as well as the ligands, may self-interact to some extent. Nevertheless, a dramatic chemoselectivity can be accomplished when the strength of the noncovalent interaction is altered, for example, by introducing substituents which change the electronic density of a compound, or substituting a hydrogen taking part in a hydrogen bond. For example, caffeine (**1b**) binds very poorly to a molecularly imprinted material prepared against theophylline (**1a**), only differing in the exchange of a hydrogen for a methyl group, and the exchange of a hydroxyl group for a keto group in cortisol/cortisone (**2a/2b**) results in a remarkable loss in binding (Figure 5).

More elaborate systems, which can recognize certain motives in a given ligand, can however be designed. For example (Figure 6), the barbiturate structure (**3**), displaying two acceptor–donor–acceptor hydrogen bonding motifs, can be very selectively recognized in solution by a corresponding amidopyridine (**4**) displaying a donor–acceptor–donor counterpart. In comparison with monovalent functional mono-

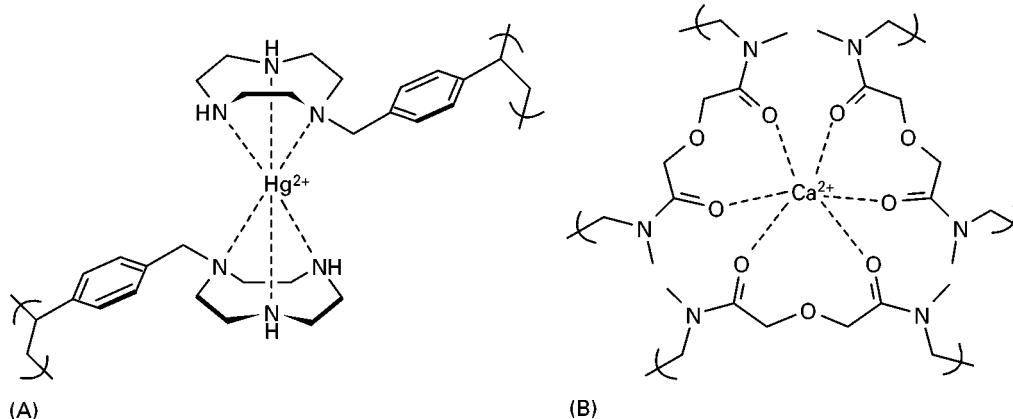


Figure 4 Metal ions can be very selectively recognized by imprinted matrices. For example, Hg(II) can be distinguished from Cd(II), Pb(II) and Cu(II) by the imprinted structure (A). Similarly, material (B) could selectively separate Ca(II) and Mg(II).

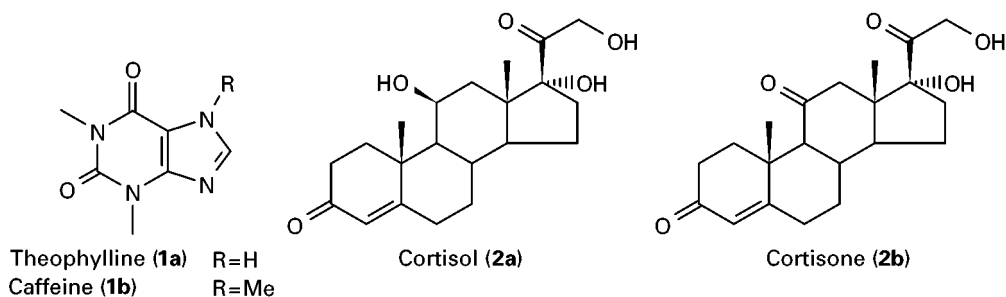


Figure 5 Examples of high chemoselectivity in noncovalent systems. Caffeine (**1b**) and theophylline (**1a**) differ only in one methyl group. Nevertheless, caffeine does not bind to matrices prepared against theophylline. Similarly, cortisone (**2b**) binds poorly to an anticortisol (**2a**) polymer.

mers, a high chemoselectivity can be designed for a chosen structure prior to the imprinting process. On the other hand, if a carefully designed multipoint system does not allow for dynamic adjustment, not much is gained from the imprinting process. In this example, the general structure (**3**) is well recognized, irrespective of R and R' .

In all these cases, however, the chemoselectivity that is more or less rationally designed upon examination of the target print species can be radically enhanced by the imprinting process. This is particularly the case when dealing with less specific noncovalent interactions. The positioning of the functional groups in the three-dimensional network of the matrix, together with the formation of the site or imprint, often results in a tremendous increase in specificity.

Regioselectivity Regioselectivity can often be nicely demonstrated by molecularly imprinted materials using all types of imprinting protocols. In this case, the imprinting process *per se*, rather than the bond type, endows high regioselectivity. It is mainly due to proper three-dimensional (or two-dimensional) positioning of the functional building blocks in the finally produced matrix that high selectivity can be accomplished. Sometimes, however, the selectivity is also

a consequence of the architecture of the surrounding backbone of the imprinted matrix in addition to organized point interactions. Obviously, this works concertedly, such that the build-up of the matrix backbone may force the originally noninteracting parts of the functional building blocks to accommodate a position, resulting in steric hindrance of different analytes.

A number of systems have been designed where *bis*-functional compounds displaying a difference in distance between the point interactions can be efficiently distinguished by the produced matrix. For example, a range of either *bis*-aldehydes (**5a/5b**) or diketones (**6a/6b**) could be selectively discriminated by matrices produced using imine- and acetal-formations, respectively (**Figure 7**).

Another example is the imprinting of *bis*-imidazole structures using Cu(II) coordination. A selectivity between the structures could be recorded, largely dependent upon the positioning of the Cu ions in the material. In these examples, the distance between the point interactions can be considered as being of major importance for recognition.

Similar studies have been pursued using noncovalent interactions, e.g. the interactions of *bis*-pyridyl and *bis*-aniline compounds with carboxylic acids, which show high distance selectivities also.

Although investigations of such *bis*-compounds can be considered as interesting model studies, proving the utility of the imprinting concept, many examples of compounds of more practical interest, e.g. food additives or drugs, have been examined. Steroids, for instance, are a class of compounds that lends itself to being both interesting model systems as well as commercially important, and several impressive steroid separations have been demonstrated. For example, β -11-OH-progesterone (**7a**) can be most selectively separated from β -17-OH-progesterone (**7b**) (**Figure 8**), in part due to the reasonably rigid steroid framework, which helps to lower the entropy loss upon steroid binding compared to a more flexible molecule.

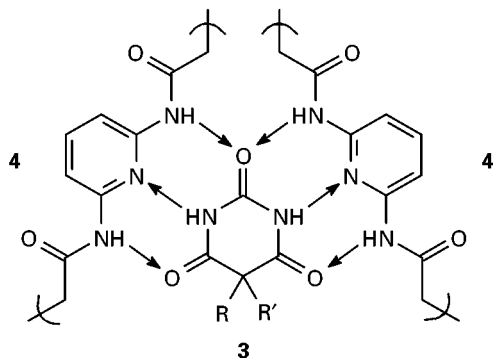


Figure 6 Multiple hydrogen bonding between cyclobarbital (**3**) and *bis*-amidopyridines (**4**).

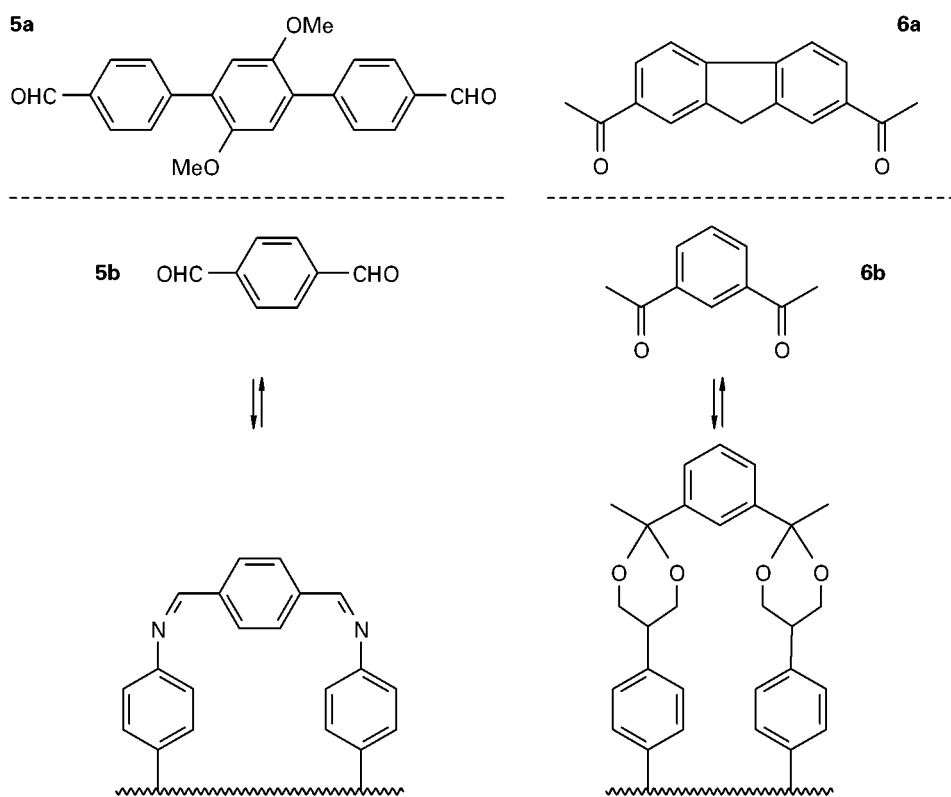


Figure 7 Distance selectivity in reversible covalent systems. Bis-aldehydes **5a/5b**, and bis-ketones **6a/6b** could be distinguished by matrices prepared against one of the structures using imine and ketal formation, respectively.

Stereoselectivity The physical properties of enantiomers, i.e. identical properties in a symmetrical environment, render them ideal substrates for the study of imprinting specificity. This is one of the reasons why this aspect has been the most extensively studied in MIT in general, and in MIC in particular. Indeed, this quality offers the clearest evidence for the outcome of a successful imprinting process. Obviously, if chiral discrimination can be introduced in a matrix through an imprinting process, based upon exclusively achiral building blocks, an indisputable demonstration of the concept is obtained.

A large number of investigations concerning chiral separations by molecularly imprinted materials have been performed, and hardly any type of compound has been neglected from examination. Thus, compounds such as amino acids, carbohydrates, nucleic acids and pharmaceuticals have all been applied in various imprinting protocols. The stereoselectivity that can be achieved is also quite extraordinary, and differences in binding of single hydroxyl groups (*R*- and *S*-timolol), and even single methyl groups can sometimes be observed (*R*- and *S*-naproxen). The interested reader can find a more detailed overview of chiral separations using molecularly imprinted materials elsewhere in this Encyclopedia (Kempe M,

Chiral Separation: Molecular Imprints as Stationary Phases).

Conclusions and Future Prospects

MIT is a technique that has substantially improved over the last few years. Many of the drawbacks initially encountered have gradually been overcome, and intense research is ongoing to resolve some of the remaining challenges. As has been pointed out, the technique is already competent at recognizing very small structural differences, and the ultimate venture that prevails in this respect is the separation of isotopes. Another task that needs further attention, although some steps have already been taken in this direction, is the selective recognition/separation of biological macromolecules, and even whole cells.

For affinity separation, however, high affinities may not always be the ultimate goal. High affinities sometimes lead to situations where elution from the affinity matrix requires harsh condition. For this reason, a material providing a lower affinity can sometimes be advantageous, and the process of binding/elution can be accomplished using mild conditions. Likewise, a high selectivity is not always a goal in itself, and materials with lower selectivity

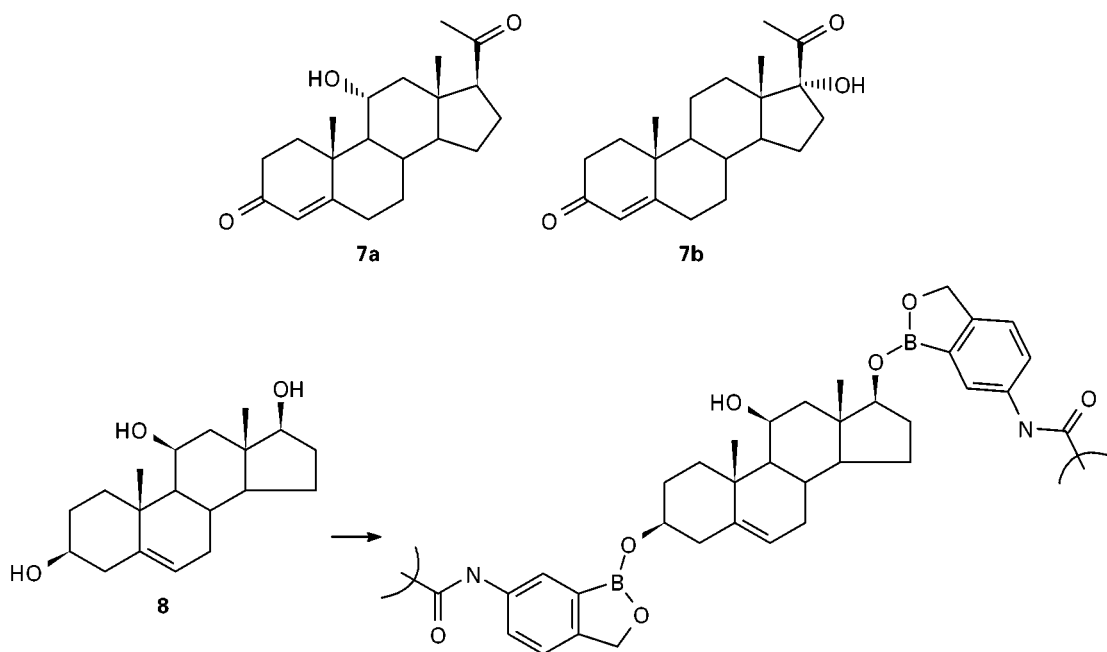


Figure 8 Examples of the high regioselectivity that can be achieved by matrices produced against steroids. β-11-OH-progesterone (**7a**) and β-17-OH-progesterone (**7b**) were efficiently separated by a molecularly imprinted chromatographic stationary phase. The androstene-triol (**8**) could be selectively acetylated in the 11-position upon protection/binding to the matrix.

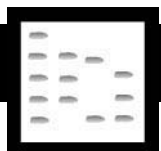
can also be preferable. This is the case when performing separations of groups of molecules rather than a single species, such as the recognition of the β-lactam group as a whole, rather than individual penicillins. Using materials that are apt at recognizing a ‘molecular chord’, rather than single ‘molecular notes’, can sometimes be beneficial.

See also: I/Affinity Separation. II/Affinity Separation: Immunoaffinity Chromatography; Imprint Polymers. III/Chiral Separations: Molecular Imprints as Stationary Phases. Immunoaffinity Extraction. Molecular Imprints for Solid-Phase Extraction. Selectivity of Imprinted Polymers: Affinity Separation.

Further Reading

- Andersson LI (1998) Molecular imprinting as an aid to drug bioanalysis. In: Reid E, Hill H and Wilson I (eds) *Drug Development Assay Approaches, Including Molecular Imprinting and Biomarkers*, pp. 2–12. Royal Society of Chemistry.
- Bartsch RA and Maeda M (eds) (1998) Molecular and ionic recognition with imprinted polymers. ACS Symposium Series 703.
- Mosbach K (1994) Molecular imprinting. *Trends in Biochemical Science* 19: 9–14.
- Ramström O and Ansell RJ (1998) Molecular imprinting technology: challenges and prospects for the future. *Chirality* 10: 195–209.
- Remcho VT and Tan ZJ (1999) MIPs as chromatographic stationary phases for molecular recognition. *Analytical Chemistry* 71: A248–A255.
- Sellergren B (1997) Noncovalent molecular imprinting: antibody-like molecular recognition in polymeric network materials. *Trends in Analytical Chemistry* 16: 310–320.
- Shea KJ (1994) Molecular imprinting of synthetic network polymers: the *de novo* synthesis of macromolecular binding and catalytic sites. *Trends in Polymer Science* 2: 166–173.
- Vidyasankar S and Arnold FH (1995) Molecular imprinting: selective materials for separations, sensors and catalysis. *Current Opinion in Biotechnology* 6: 218–224.
- Whitcombe MJ, Alexander C and Vulfson EN (1997) Smart polymers for the food industry. *Trends in Food Science and Technology* 8: 140–145.
- Wulff G (1995) Molecular imprinting in cross-linked materials with the aid of molecular templates – a way towards artificial antibodies. *Angew. Chem. Int. Ed. Engl.* 34: 1812.
- Yano K and Karube I (1999) Molecularly imprinted polymers for biosensor applications. *Trends in Analytical Chemistry* 18: 199–204.

SILVER ION



Liquid Chromatography

W. W. Christie, Scottish Crop Research Institute,
Dundee, Scotland

Copyright © 2000 Academic Press

The Nature of the Technique

The technique of silver ion chromatography, which is sometimes termed 'argentation chromatography', was first introduced for the separation of fatty acid derivatives in two papers which appeared almost simultaneously in *Chemistry* and *Industry* in 1962. In its earliest manifestations, it was adapted to thin-layer chromatography (TLC) and to low pressure column chromatography. The former is still in widespread use today, but high performance liquid chromatography (HPLC) has more recently been adapted to the purpose and may be expected to slowly supplant TLC. Gas chromatography with stationary phases containing silver ions has been used to separate mixtures of hydrocarbons containing low molecular weight olefins, but is not practical for analytes of higher molecular weight. While lipid chemists, especially those concerned with fatty acid derivatives, have made most use of silver ion chromatography, it has also been used for a wide range of aliphatic and alicyclic compounds, including terpenes, sterols, carotenoids, insect pheromones, etc. However, applications only to separation of more conventional lipids will be described here as examples of what can be accomplished. A number of review articles have appeared, that by Morris (1966) covering the early literature and those by Nikolova-Damyanova and colleagues (Nikolova-Damyanova, 1992; Dobson *et al.*, 1995) bringing the topic up to date. Details of practical methods are given in a book by Christie (1989).

Silver ion chromatography is based on a distinctive property of unsaturated organic compounds, that is the capacity to complex with transition metals in general, and with silver ions in particular. The complexes are of the charge-transfer type in which the unsaturated compound acts as an electron donor and the silver ion as an electron acceptor. In the accepted model, it is believed that there is formation of a σ -type bond between the occupied 2p orbitals of an olefinic double bond and the free 5s and 5p orbitals of

the silver ion, and a (probably weaker) π -acceptor backbond between the occupied 4d orbitals of the silver ion and the free antibonding 2p π^* orbitals of the olefinic bond. In chromatographic systems, complexes are only formed transiently and are in kinetic equilibrium with the free olefin. The coordination forces are weak, and IR spectra show very little shift in frequencies from those of free double bonds, for example. Stable silver ion-olefin complexes have been isolated in some circumstances, and then X-ray crystallography has demonstrated that each silver ion can interact with two double bonds simultaneously. Other metals can form such complexes but none other than silver has the correct combination of properties for general chromatographic use.

Until recently, the technique was very much an *ad hoc* one that worked, but without a sound theoretical basis. Silver ion TLC cannot be used to generate reproducible chromatographic data, for example. However, some useful qualitative data are available from studies with simple model compounds and in particular it is apparent that:

- Unsaturated aliphatic and alicyclic compounds form more stable complexes than do aromatics.
- The stability decreases with increasing chain length of the aliphatic substrate.
- The stability decreases with increasing numbers of substituents of a double bond in the order $RCH=CH_2 > R_2C=CH_2 > cis\ RCH=CHR > trans\ RCH=CHR > R_2C=CHR > R_2C=CR_2$. The greater stability of the *cis*-isomer may be due either to the relief of strain when the complex is formed or to steric hindrance by the two alkyl moieties when they are in a transposition to each other.
- Conjugated polyenes form less stable complexes than do those with methylene-interrupted double bonds, and the greatest stability is when two methylene groups separate double bonds, perhaps because a chelate complex can then be formed.
- The stability of a silver ion complex increases when a hydrogen atom from a molecule of the $RCH=CHR$ type, for example, is replaced with deuterium or tritium.
- Monoenes form stronger complexes than monoynes (one acetylenic bond).
- The strength of complexation increases as the temperature is lowered.

As far as has been ascertained, these rules also apply to larger molecules such as simply fatty acid

derivatives, and to all forms of silver ion chromatography. However, there are few quantitative experimental or theoretical data on the mechanism of complex formation between silver ions and complicated unsaturated molecules like glycerolipids, which have up to three unsaturated fatty acids per molecule, although again, there is a substantial body of qualitative information.

A complicating factor, when considering silver ion complexation in the context of a chromatographic system, is the role of the support material. The most widely used support for TLC, silica gel, possesses appreciable polarity and absorptive activity. Therefore, the elution order of lipids cannot always be ascribed to the complexation reaction with silver ions and double bonds only, although this is usually the most important factor. A separate but related problem is the topology of silver ions on the surface of the adsorbent. For example, in silver ion TLC it is apparent that part of the silver nitrate remained in crystalline form filling the pores of the silica gel while a further proportion remains dissolved in the water which is always bound to silica gel. The aqueous silver nitrate is assumed to be responsible for complex formation, and some experience seems to confirm this observation. For example, Nikolova-Damyanova considers that there is no need for incorporation of excessive amounts of silver nitrate ($> 1\text{--}2\%$) into TLC systems.

When discussing mixed retention mechanisms in chromatography, it is also necessary to consider the mobile phase. A proper choice of solvents determines the selectivity of a separation to an appreciable extent. Again, there are no systematic data available, but it has often been noted that better resolution is achieved by using chlorinated solvents as major components of the mobile phase in silver ion chromatography.

The more recent marriage of silver ion chromatography with HPLC has given us a better understanding of the mechanism of silver ion chromatography and this is discussed below.

Silver Ion Thin-Layer Chromatography

Silver ion TLC uses simple equipment and can afford excellent results in practice. Precoated TLC plates are available commercially, although it is not difficult to prepare one's own (but wear gloves!). Thus, silver nitrate is simply incorporated into the aqueous slurry used to suspend the silica gel and the plates are spread and activated in the usual way, though some care is necessary to minimize exposure to light. Sometimes 10–20% of silver nitrate relative to silica gel is recommended by authors, but 1–2% is generally sufficient.

Alternatively, plates can be impregnated with silver nitrate by careful immersion in a bath of a solution of silver nitrate in methanol or acetonitrile, and this option is often favoured with precoated TLC plates. After the plates have been activated, they should be stored in a desiccator in the dark.

Lipids are spotted on to the TLC plate and this is usually developed in a closed tank (in the dark) containing an appropriate mobile phase. However, Nikolova-Damyanova recommends using open tanks and carefully regulated volumes of solvent. Chromatography is most often carried out at ambient temperature, although temperatures as low as -20°C have on occasion been recommended to increase the strength of complexation and improve the separation. When the mobile phase nears the top of the plate, the latter is removed from the tank, and dried in a stream of air or nitrogen.

Various methods of detection and quantification are available. For example, one popular method consists in spraying the plate with concentrated sulfuric acid, and heating it at 180°C in an oven. The separated components are charred (converted to carbon) and can be quantified directly by scanning densitometry. A procedure of this kind is of course destructive to the sample, and has to be carried out with great care to avoid hazard to the operator.

Alternatively, the developed plate can be sprayed with a solution of 2',7'-dichlorofluorescein in methanol (0.1% w/v). After evaporation of the solvent, the plate is viewed under a UV lamp; lipids appear as yellow spots against a dark purple background. The lipid/silica gel spots are scraped from the plate, and lipids are recovered by extraction with an appropriate solvent, though the extracts may have to be washed with a solution of dilute buffer (pH 9) to eliminate any silver nitrate and dye that co-elute. Commonly components are identified and quantified by gas chromatography of the fatty acid methyl esters, following transesterification, in the presence of an added internal standard, such as an odd-chain fatty acid.

As an example, **Figure 1** illustrates the separation of fatty acid methyl esters by silver ion TLC. Saturated fatty acids do not form complexes with silver ions, so migrate ahead of the other components on the plate. *Trans*-monoenes form less stable complexes than *cis*-monoenes, so the former migrate faster. Dienoic fatty acids come next followed by polyenes, which under these conditions remain near the origin. A separation of this kind is the standard method for reliable quantification of fatty acids with *trans* double bonds. If the polarity of the mobile phase is increased, polyenoic fatty acid derivatives can be resolved into fractions with three, four, five and six double bonds, but saturated, and mono- and

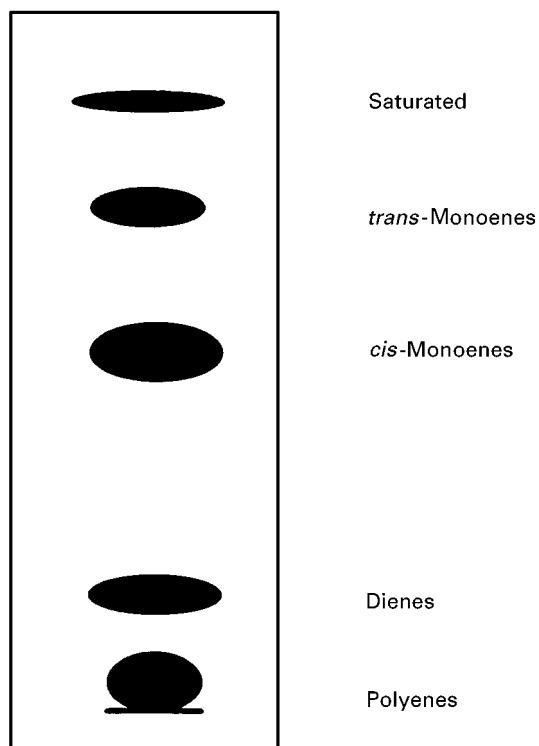


Figure 1 Silver ion TLC (Kieselgel GTM containing 2% silver nitrate) of fatty acid methyl esters, with hexane/diethyl ether (9 : 1, v/v) as mobile phase.

dienoic fatty acids will then run together near the solvent front.

Figure 2 is a schematic representation of a silver ion TLC separation of triacylglycerols (which can include all the common oils and fats of commerce), which contain three fatty acids per molecule. In this instance, trisaturated species elute first followed by disaturated monoenoic; the latter separating into two fractions (more or less completely) according to whether the unsaturated fatty acid is on position 2 of the glycerol moiety or in one of the outer positions. Then, the monosaturated dimonoenoic species is eluted followed by a fraction containing one dienoic fatty acid with two saturated, i.e. a dienoic fatty acid is retained more strongly than two monoenes, and so on.

Phospholipid molecular species have been resolved in this way also, both in intact form (technically difficult) or after enzymatic conversion to non-polar diacylglycerol derivatives.

Although the equipment is simple and inexpensive, there are many drawbacks to silver ion TLC procedures, not least that silver ions are eluted from TLC plates and contaminate fractions in preparative applications, as do silica gel and dyes used for detection purposes. Silver nitrate leaves indelible stains on

benches, equipment and the fingers of the analysts. HPLC methods do not suffer from these difficulties.

Preparative Scale Column Chromatography

By analogy with silver ion TLC it has proved possible to impregnate silica adsorbents (or better, acid-washed FlorisilTM) with silver nitrate and pack into columns to enable separation of fatty acids by degree of unsaturation. However, the technique suffers from many of the problems associated with silver ion TLC.

As an alternative, macroreticular sulfonic acid ion exchange resins have been utilized as adsorbents for silver ion column chromatography. The resin is loaded with silver ions by passing an aqueous solution of silver nitrate through a column of resin until excess silver ions start to elute. The column is then washed with water and methanol, and methanol is used further as the mobile phase. Recently, Amberlyst XE 284TM has been shown to give the best results, but the separations improved significantly only when the mobile phase of methanol was modified with

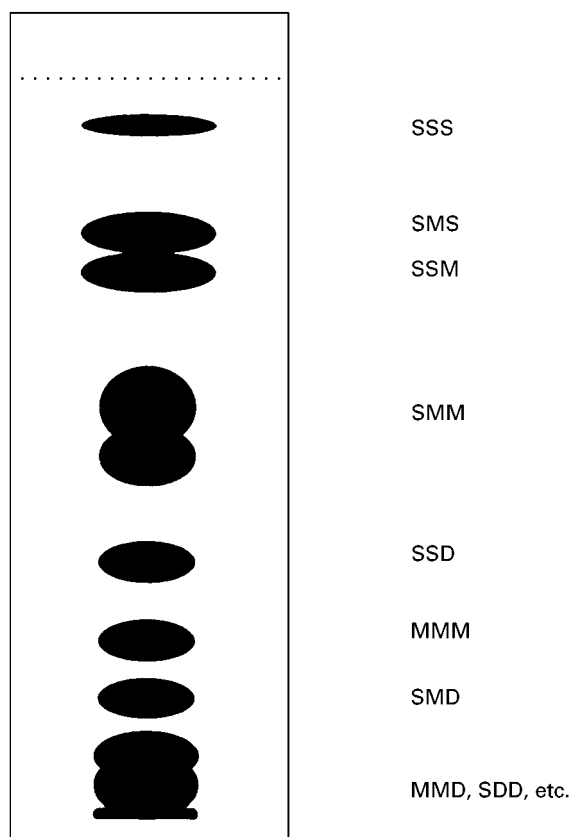


Figure 2 Silver ion TLC (Kieselgel GTM containing 10% silver nitrate) of triacylglycerols, with chloroform/methanol (99 : 1 v/v) as mobile phase. Abbreviations: S = saturated, M = *cis*-monoenoic and D = dienoic fatty acyl residues.

acetonitrile, which enabled a good resolution of monoenes, dienes, trienes and tetraenes (DeJarlais *et al.*, 1983). Further improvements were obtained by grinding the resins first to 270–350 mesh.

This technique permits fractionation of mixtures of unsaturated fatty acids by degree of unsaturation on the 10 to 20 gram scale. As the silver ions are held by ionic bonds, they are not leached from the column and clean fractions are obtained. However, the range of mobile phases that can be employed is limited, otherwise swelling and compaction of the resin will occur.

Silver Ion High Performance Liquid Chromatography

The approach to silver ion HPLC adopted by Christie (1987) is to load a silica-based ion exchange medium (chemically bonded phenyl sulfonic acid groups) with silver ions. Again, the silver ions are held by ionic bonds and are not leached from the column, while rigidity of the silica matrix prevents compaction of the packing material during gradient elution. Preparation of the column involves merely taking a standard prepacked column with the appropriate stationary phase (Nucleosil™ 5SA) and introducing the silver ions via an injector while pumping water through the column. Finally, the aqueous phase is replaced with organic solvents. Only 50 to 80 mg of silver ions are bound to the stationary phase, but this is quite sufficient for very many useful separations.

Lipids lack chromophores that facilitate UV detection, although it is possible to use UV detection with appropriate fatty acid derivatives. Therefore, for much of the work with silver ion HPLC columns, evaporative light-scattering detectors have been employed as they permit the use of complex gradients and mobile phases containing such solvents as dichloromethane and acetone. Although the detector is destructive in that the sample is lost in the current of air, it is possible to insert a stream splitter between the end of the HPLC column and the detector to divert much of the sample for collection.

Chlorinated solvents, such as dichloromethane or dichloroethane, form the basis of the more useful mobile phases, and the polarity can be increased to elute highly unsaturated components by adding acetone or especially acetonitrile, which has a high affinity for silver ions. Presumably the high dielectric constant of the chlorinated solvents facilitates the interaction between silver ions and the double bonds. However, acceptable results can also be obtained with hexane as the main component of the mobile phase if a little acetonitrile is present.

Methyl esters are the most widely used fatty acid derivative for chromatography, because of the ease of preparation and their relatively low molecular weight. One useful application of silver ion HPLC is the separation of such derivatives from animal or fish lipids, into fractions with zero to six double bonds. Simplification of complex mixtures by this means makes the task of identification by other chromatographic means or by mass spectrometry much easier.

However, by an appropriate choice of solvents, it is possible to separate positional and geometrical isomers of unsaturated fatty acids on a micro-preparative scale, a feat not readily achieved by other chromatographic procedures. For example, the separation obtained with phenacyl esters of the three main naturally occurring octadecenoic acid isomers is illustrated in **Figure 3**; all are clearly resolved to baseline. It has become evident that the distance of the double bond from the carboxyl group is more important in governing the separation of positional isomers than is the terminal region of the molecule. Phenacyl derivatives of fatty acids were prepared at first so that quantification with UV detection was possible, but fortuitously, it has now become apparent that such derivatives give especially favourable separations (and this is also true for silver ion TLC). This technique can be used with equal facility for the separation of simple fatty acid derivatives with *trans* double bonds, and will undoubtedly supplant TLC for the purpose. Positional isomers of polyunsaturated fatty acid derivatives can be resolved similarly by increasing the polarity of the mobile phase.

Silver ion HPLC is also of great value for separation of molecular species of triacylglycerols. The simplest elution scheme is a gradient of acetone into dichloroethane–dichloromethane, which serves for fats with low levels of linoleic acid, such as sheep adipose tissue or bovine milk fat. This

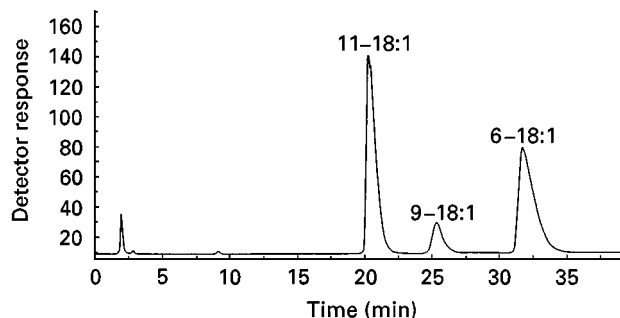


Figure 3 Separation of phenacyl esters of the isomeric octadecenoic acids, petroselinic (6-18:1), oleic (9-18:1) and vaccenic (11-18:1), by HPLC on a Nucleosil™ 5SA column in the silver ion form eluted with dichloromethane/dichloroethane/acetonitrile (50:50:0.25 by volume), with evaporative light-scattering detection.

gives resolution of the main components with zero to three double bonds in total in the fatty acyl chains, including separation of fractions with *trans*- from those with *cis*-monoenoic residues. Most triacylglycerol samples are likely to contain appreciable proportions of linoleic acid, and resolution into molecular species is then accomplished by ternary gradient elution, simply by introducing acetonitrile into acetone after the first fractions are recovered. Such a separation of adipose tissue triacylglycerols is illustrated in Figure 4. One dienoic acyl moiety is retained more than twice as strongly as a monoene, and one triene (18 : 3 (*n*-3)) is retained by the same amount as two dienoic residues in a molecule, so there is some overlap of dienoic and trienoic species when α -linolenic acid is present in a sample. Otherwise, the basis of the separation is similar to that described earlier for TLC applications, in that trisaturated species elute first, followed by disaturated monoenoic and so forth.

Such highly unsaturated triacylglycerols as linseed oil and fish oils have been resolved satisfactorily. With the former, trilinolenin is the most abundant single fraction, and a simple progression of fractions with increasing numbers of double bonds are eluted until this species is reached. When the more saturated molecules of fish oils are eluted, resolution is excellent and it is perhaps surprising to find appreciable amounts of trisaturated and disaturated monoene species. Baseline resolution is no longer possible when molecules containing polyunsaturated fatty acids begin to elute, because the wide range of positional isomers causes similar components to overlap. Nevertheless, valuable separations of species contain-

ing two saturated and/or monoenoic fatty acids and one polyenoic fatty acid especially can be achieved.

In silver ion chromatography, the order of elution of triacylglycerol species is easily understood because only one property of the molecules is involved, i.e. degree of unsaturation. The alternative technique used for molecular species separations is reversed-phase chromatography, with octadecylsilyl phases, which effects separation both by chain length and degree of unsaturation, each double bond reducing the effective chain length by the equivalent of about two methylene groups. When used in sequence the two techniques make a much more powerful tool. Fish oils give highly complex chromatograms with reversed-phase HPLC, for example, and identification of individual components is impossible. On the other hand, when fractions from silver ion HPLC are collected and then subjected to reversed-phase HPLC, separation is then, in effect, by chain length only and the main peaks are easily identified. Each HPLC fraction can be examined in turn in this way, and much more information obtained in comparison to the use of either technique on its own.

Some Mechanistic Considerations

In silver ion HPLC, we have a reasonable understanding of how the silver ions are bound to the stationary phase via the phenylsulfonic acid groups. There may be some residual silanol groups on the surface of the silica matrix, but these should not influence separations greatly when relatively polar chlorinated solvents are used in the mobile phase. Also in HPLC, we can control both the composition and flow rate of the mobile phase with a high degree of accuracy. Finally, we can control the temperature of the column, an important factor in the complexation reaction between silver ions and double bonds. Accurate chromatographic retention data can thereby be obtained for a variety of lipid analytes of known structure.

It is known that silver ions can interact with two double bonds in a fatty acyl residue at the same time, but can they also react with one double bond and the unpaired electrons on the carboxyl moiety as shown schematically in Figure 5? This might explain how different positional isomers of fatty acids are separable by this technique. For example, electron-rich esters, such as the phenacyl derivatives illustrated, are held much more strongly than are methyl esters when the double bond is within about eight carbons of the carboxyl group, and the elution patterns of series of isomers are very different. From a 9-18 : 1 fatty acid derivative onwards, when the possibility of such a simultaneous interaction would seem to be less likely, there is no significant difference between methyl and phenacyl

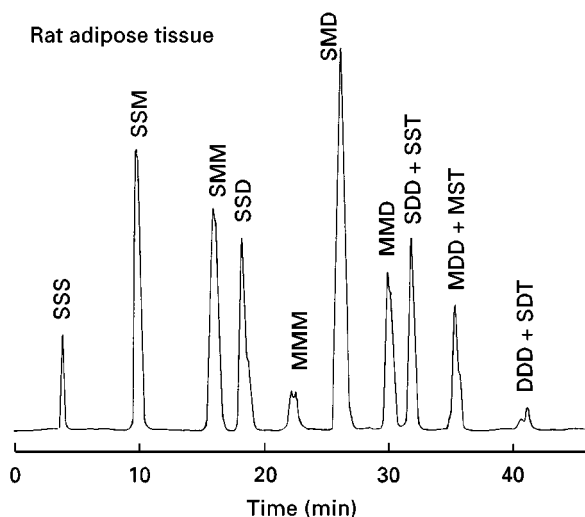


Figure 4 Separation of triacylglycerols from rat adipose tissue by HPLC on a Nucleosil™ 5SA column in the silver ion form, with evaporative light-scattering detection. Abbreviations: S, saturated; M, monoenoic; D, dienoic; T, trienoic fatty acyl residues. (Adapted from Christie, 1988.)

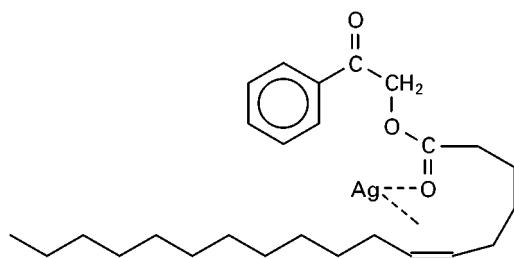


Figure 5 Schematic representation of the interaction of a silver ion with the phenacyl ester derivative of petroselinic acid.

esters. Experiments with esters with a variety of different electron-donating and electron-withdrawing substituents now provide firm evidence for this hypothesis.

An interaction between one silver ion and two double bonds at the same time may explain the chromatographic behaviour of fatty derivatives with two or more double bonds in the acyl chain in silver ion HPLC. When the distance between the double bonds is optimum, i.e. with a 1,5-*cis,cis*-diene system, fatty acids are very strongly retained, and the effect diminishes as the number of methylene groups between the double bonds is varied. If the double bonds interacted singly with silver ions, it might have been anticipated that the kinetics of the system would be such that retention would be comparable in magnitude to the sum of the individual parts, but this is clearly not so. This theory of complexation between silver ions and bis-double bond systems could potentially be applied to polyenoic fatty acid derivatives. It would predict that a triene would be held twice as strongly as a diene, a tetraene three times as strongly and so forth. Such a simple relationship is not found in practice (the degree of complex formation is even greater than anticipated), possibly because interactions with the ester moiety have to be taken into consideration and because the conformations of polyenes may permit some interactions between silver ions and double bonds that are remote from each other, via the formation of pseudo-cyclic structures.

Analogous physicochemical studies of the behaviour of triacylglycerols on silver ion chromatography suggests that a dual interaction is important in this instance also. For example, it has been shown that highly unsaturated triacylglycerols are retained especially

strongly; a species with nine double bonds is held 10 000 times as strongly as one with a single double bond. It is the strength of this interaction rather than the efficiency of the column *per se* that is responsible for the quality of the separations. However, here further work is certainly necessary to confirm the mechanism.

See also: III/Lipids: Liquid Chromatography; Thin-Layer (Planar) Chromatography. Oils, Fats and Waxes: Super-critical Fluid Chromatography. Silver Ion: Thin-Layer (Planar) Chromatography.

Further Reading

- Christie WW (1987) A stable silver-loaded column for the separation of lipids by high-performance liquid chromatography. *Journal of High Resolution Chromatography; Chromatography Communications* 10: 148.
- Christie WW (1988) Separation of molecular species of triacylglycerols by high-performance liquid chromatography with a silver ion column. *Journal of Chromatography* 454: 273.
- Christie WW (1989) *Gas Chromatography and Lipids. A Practical Guide*. Dundee: The Oily Press.
- DeJarlais WJ, Adlof RO and Emken EA (1983) Acetonitrile as eluent in silver resin chromatography. *Journal of the American Oil Chemists' Society* 60: 975.
- Dobson G, Christie WW and Nikolova-Damyanova B (1995) Silver ion chromatography of lipids and fatty acids. *Journal of Chromatography B* 671: 197.
- Laakso P and Christie WW (1991) Combination of silver ion and reversed-phase high-performance liquid chromatography in the fractionation of herring oil triacylglycerols. *Journal of the American Oil Chemists' Society* 68: 213–223.
- Morris LJ (1966) Separation of lipids by silver ion chromatography. *Journal of Lipid Research* 7: 717.
- Nikolova-Damyanova B (1992) Silver ion chromatography and lipids. In: Christie WW (ed.) *Advances in Lipid Methodology – One*, pp. 181–237. Dundee: The Oily Press.
- Nikolova-Damyanova B, Christie WW and Herslöf BG (1995) Retention properties of triacylglycerols on silver ion high-performance liquid chromatography. *Journal of Chromatography A* 694: 375.
- Nikolova-Damyanova B, Christie WW and Herslöf BG (1996) Mechanistic aspects of fatty acid retention in silver ion chromatography. *Journal of Chromatography A* 749: 47.

Thin-Layer (Planar) Chromatography

B. Nikolova-Damyanova, Bulgarian Academy of Sciences, Sofia, Bulgaria

Copyright © 2000 Academic Press

Introduction

Silver ions (Ag^+), like the ions of many other transition metals, interact specifically with

Table 1 List of compounds subjected to Ag-TLC

Class	Compounds
Lipids	Fatty acid mixtures
	Isomeric octadecenoic and octadecadienoic fatty acids
	Furanoid fatty acids
	Cyclopropene fatty acids
	Oxygenated unsaturated acids
	Triacylglycerol mixtures of natural fats and oils of terrestrial and marine origin
	Phospholipids
Terpenes	Sterol esters
	C ₁₀ , C ₁₅ , C ₂₀ terpenes
	Terpene alcohols
Hydrocarbons	Monoterpenes
	Acyclic olefines
	Alkylbenzenes
	Alkylphenylsulfides
Miscellaneous	Steroids
	Sterols
	Sterol acetates
	Derivatized unsaturated aldehydes and ketones
	Prostaglandins
	Hydroxyprogesterones
	Estrogens
	Mineral oils

unsaturated compounds to form complexes with olefinic double bonds. In 1938 Winsten and Lukas and in 1952 Nichols demonstrated that the interaction between Ag^+ and double bonds might be of interest for chemical analysis. By applying a liquid-liquid distribution system with Ag^+ present in the aqueous phase it was possible to separate easily unsaturated from saturated compounds and *E*- from *Z*-monounsaturated olefins. The great potential of this interaction for separation of unsaturated compounds was fully recognized when gas-liquid chromatography (GLC) and thin-layer chromatography (TLC) developed into routine analytical techniques.

The chromatographic technique that utilizes the interaction between Ag^+ and an olefinic bond to conduct the separation process is now called argentation (silver ion) chromatography. Argentation chromatography was first developed as a GLC technique. However, argentation TLC (Ag-TLC) soon became a basic separation method for the analysis of different types of unsaturated compounds. For many years it has been a most valuable method in lipid analysis, providing essential information about the lipid structure and composition.

Compounds that have been most frequently examined by Ag-TLC are listed in Table 1.

Silver Ion Complexation with Double Bonds

The model now considered to represent correctly the bonding between Ag^+ and a double bond was suggested by Dewar in 1951. It supposes the formation of a σ -type bond between the occupied $2p\pi$ orbitals of an olefinic double bond and the free $5s$ and $5p$ orbitals of the Ag^+ , and a (probably weaker) π -acceptor backbond between the occupied $4d$ orbitals of the silver ion and the free antibonding $2p\pi^*$ orbitals of the olefinic bond (Figure 1).

It is suggested that a silver ion interacts with one mono-olefin molecule to give a planar complex with a triangular structure. However, there is evidence that a silver ion may interact with two ethylenic molecules. X-ray studies of crystalline silver ion complexes with some short chain aliphatic diolefins show that the Ag^+ is coordinated with two double bonds from different olefinic molecules.

The stability of the silver ion-double bond complex is influenced by the spatial arrangement of the overlapping orbitals, the basicity of and electronic effects in the olefinic molecule, and by solvent effects. Quantitative data (for example equilibrium constants) exist only for a number of short chain mono-olefins, diolefins with accumulated, conjugated and separated methylene-interrupted double bonds, and for some cyclopenta- and cyclooctadienes. Most of these data, as well as the estimation of the relative strength of other complexes, are based on chromatographic measurements.

The general conclusions about complex formation reached so far are as follows:

1. Unsaturated acyclic and carbocyclic compounds form more stable complexes than do aromatics.
2. Carbocyclic compounds with a single exocyclic double bond form stronger complexes than do carbocyclic compounds with a single internal double bond. Cyclopenta- and cyclooctadienes

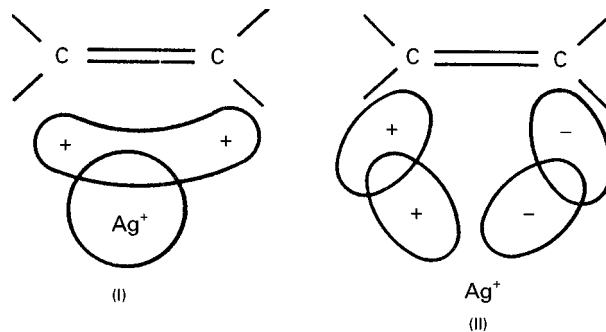


Figure 1 Schematic presentation of the interaction between a silver ion and a double bond.

form very stable complexes, especially when having a 1,5-diene system.

3. For acyclic compounds it has been found that:
 - the stability decreases with the increasing chain length;
 - the stability decreases with an increasing number of substituents at the double bond in the order $\text{RCH=CH}_2 > \text{R}_2\text{C=CH}_2 > \text{R}_2\text{C=CHR} > \text{R}_2\text{C=CR}_2$;
 - the stability increases when a hydrogen atom from a molecule of the RCH=CHR type is replaced with deuterium or tritium atom. The effect has been ascribed to greater electron release from a C–D than from a C–H bond, i.e. to the higher basicity of the deuterated molecule;
 - *cis* (*Z*)-isomers form stronger complex than do *trans* (*E*)-isomers. The greater stability of the *cis*-isomer is ascribed either to the relief of strain when the complex is formed or, more probably, to the steric hindrance of the double bond in *trans*-isomers;
 - diolefins form more stable complexes than do mono-olefins, but conjugated dienes form less stable complexes than do those with methylene-interrupted double bonds;
 - the stability increases with increasing distance between the double bonds. The most stable diene complexes are formed by the 1,5-diene system, perhaps because a chelate complex can be formed in the latter case.

Generally, the rate of complex formation for most acyclic compounds is very rapid. The complexes are usually unstable and exist in equilibrium with the free form of the olefin. The coordination forces seem to be very weak. The IR spectrum, for example, shows very little shift in frequencies from those of free double bonds. These particular properties of complexation between a double bond and a silver ion are favourable for use in chromatography.

The Technique of Ag-TLC

The Layer

Argentation TLC is utilized in two modifications: analytical and preparative. Both home-made and precoated plates (glass only) are used. Plate dimensions may vary from 5 cm × 20 cm to 20 cm × 20 cm. High performance TLC plates (HPTLC) have recently been found to be useful. Home-made layers, despite their messy preparation, are more versatile and often provide better separations than commercially prepared ones. Common adsorbents are listed in Table 2.

The thickness of the adsorbent layer ranges from 0.2 to 0.3 mm for analytical plates and from 0.5 to 1.0 mm for preparative plates. Fully automated spreaders for home-made layers are commercially available but simple spreaders are equally effective. However, some practice is needed for layer preparation and precoated plates are now mostly preferred.

The Incorporation of Silver Ions

There are two general ways to perform silver ion TLC of which by far the most common is to use a layer of adsorbent impregnated with a silver salt. It is possible as an alternative to add a silver salt to the mobile phase when a reversed-phase TLC separation is performed. This approach has found limited use only. Although the influence of the salt anion has not been studied systematically, there is evidence that its nature may affect the resolution. A list of silver salts used and their supposed effect is shown in Table 3.

Impregnation can be performed by incorporating the silver salt into the slurry of adsorbent used to make the layer. Also, the prepared plate can be immersed in a methanol, acetone or acetonitrile solution of the silver salt or sprayed with one of these solutions. Only the first approach affords proper control of the silver content of the layer. However, it is inconvenient and messy and is now rarely used. Since

Table 2 Adsorbents, frequently used with Ag-TLC

Adsorbent	Compounds to be separated	Comments
Silica gel G (binder is calcium sulfate)	Fatty acids	Fatty acids should be first converted into methyl esters.
	Triacylglycerols	Components are separated as intact compounds.
	Diacylglycerols	Compounds are separated after conversion into acetates.
	Polar lipids	Polar lipids should be converted into less polar derivatives, either by removing or by derivatizing the polar head.
	Terpenes	Compounds are usually separated as intact compounds.
Silica gel H (no binder)	Polar lipids	It is possible to separate polar lipids as intact compounds on this layer.
Alumina	Fatty acids	Species are separated as free fatty acids and as methyl esters. Alumina as adsorbent should be used with care since it is known to react with some analytes and solvents.

Table 3 List of silver salts used in Ag-TLC

<i>Salts</i>	<i>Components to be separated</i>	<i>Comments</i>
Silver nitrate	Fatty acids derivatives Triacylglycerols Polar lipids Terpenes	The most frequently used silver salt with very broad application for various separations. Silver salts other than silver nitrate are supposed to improve the separation.
Ammonia solution of silver nitrate	Fatty acid methyl esters	
Silver sulfamate	Fatty acid methyl esters	
Silver benzenesulfonate	Fatty acid methyl esters	
Silver iodate	Terpenes	
Silver perchlorate	Terpenes	

it appears that the content of silver ions in the layer may not, in fact, be critical, immersion procedures are mostly used. They can be standardized sufficiently well to provide repeatable results. Spraying procedures are less easily controlled. Spraying may have to be repeated from two to six times until the adsorbent layer is properly wetted. Sufficient spraying of the layer is somewhat arbitrary and depends on personal skill and on the samples to be examined. Immersion or spraying are only applicable to precoated plates. These plates should be immersed in a silver salt solution (methanol or acetonitrile) for not less than 15–20 min. A dynamic impregnation technique has also been proposed. The plate is developed with a 10–20% solution of silver nitrate in acetonitrile. It has been claimed that in this way a gradient of silver ions is formed in the development direction. The gradient is claimed to improve the separation of triacylglycerols. The approach has not found wide application and its advantages cannot be estimated.

The silver content of the adsorbent layer varies between rather broad limits and differs for analytical and preparative plates (Table 4). Layers containing a high percentage of silver nitrate were considered necessary to achieve good analytical resolution. This high percentage is, however, very inconvenient. The plates are very sensitive to light and this can greatly hamper detection and quantification. Impregnation by immersion in 0.5% methanolic silver nitrate provides excellent results in the

resolution of lipids, for example, without this disadvantage.

Treatment of the Plates and Precautions

Plates should be used immediately after being dried in air (for 1 h). Many workers activate the plates before use by heating at 110°C for about 1 h. However, good results have been reported after activation for only 5 min. Thus, it seems that the necessity for activation is questionable, and the analyst must trust to his or her own experience and the nature of the samples that are being handled. Activation has been found to be very important for silica gel H plates and temperatures higher than 110°C for periods of much longer than 1 h have been recommended.

Atmospheric humidity has an appreciable effect on separation, especially of highly unsaturated species. It is recommended that activated TLC plates be kept in a desiccator over drying agents (ideally in the dark). However, it is not easy to control humidity in practice. This may be one of the reasons for the relatively poor overall reproducibility of migration and resolution in separations performed by Ag-TLC.

Sample Preparation

Terpenes and triacylglycerols are applied as solutions of appropriate concentration in suitable solvents. Preliminary fractionation and purification from accompanying compounds is required. Fatty acids should be converted into less polar derivatives, usually into methyl esters. Recently, aromatic derivatives of fatty acids have proved to provide much better separation of difficult-to-resolve mixtures. Ag-TLC has not been very successful in separating intact complex lipids. Most of the reported procedures employ preliminary fractionation into specified classes and conversion of the latter into less polar derivatives.

Sample size is an important factor since overload greatly worsens the resolution. Analytical Ag-TLC on 0.2 mm thick layers requires samples of a maximum

Table 4 Concentration of the silver nitrate solutions and methods for impregnation of a TLC layer

<i>AgNO₃ (%)</i>		<i>Impregnation</i>
<i>Analytical plates</i>	<i>Preparative plates</i>	
0.5–2	1–5	Immersion Incorporation Spraying
5–30	5–20	
10–40	40	

of 30 µg. For preparative separation (0.5–1.0 mm layer thickness) the sample size can be scaled up to 80–100 mg, depending on the sample composition, the quantitative ratio between components and the required resolution.

Development

Most separation protocols recommend ascending development in covered tanks in which the atmosphere has been saturated with the vapour of the mobile phase. The saturation is considered to shorten the duration of development and often to improve the reproducibility. There are no firm data to support this conclusion and it might depend on the nature of the analyte. Poor separation and tailing of zones have also been reported under these conditions. Excellent separations of fatty acids and triacylglycerols are obtained without saturation of the atmosphere, or even in an open container. The geometry and volume of the developing container can also affect the separation. Narrow rectangular tanks and a moderate volume of the developing solvent provide better resolution.

Ag-TLC plates are normally developed at ambient temperature, but some improved resolution of fatty acid isomers requires a temperature of -20°C . It is assumed that resolution improves because the stability of the Ag^+ complexes increase when the temperature decreases. This might be true, but the properties of the sorbent and mobile phase also change at low temperatures. The action of all three factors is probably responsible for the better separations.

Various solvents are used to give two or three component mobile phases. Some of those most frequently used for separation of fatty acids and triacyl-

glycerols are listed in Table 5. Plates are often developed more than once to improve resolution. The separation should start with the most polar phase and proceed, after drying between runs, with mobile phases of gradually decreasing polarity. In this way, highly unsaturated components are resolved first and do not move further with subsequent developments when the more saturated components are separated. Obviously, the separation will improve substantially if a continuous development can be applied. In a simple approach, which has been used for the analysis of fatty acids and triacylglycerols, the development proceeds in an open cylindrical tank where a fixed volume (4–15 mL) of the mobile phase has been added. As the mobile phase is eluted through the plate, it is permitted to evaporate from the upper edge. Resolution was very effective and excellent results have been reported including the separation of positional isomers of triacylglycerols. This open system is quite sensitive towards the laboratory environment but operates very well in skilled hands.

Detection

All detection reagents that are suitable for visualizing compounds separated on plain silica plates are, in principle, suitable for use with Ag-TLC, particularly when the percentage of silver ions in the layer is below 2%. Destructive procedures are used for location, for identification and, to some extent, for quantification purposes. The reagent can be introduced by spraying, by treatment of the plates with its vapours or by incorporating into the layer. Some of the most commonly used detecting reagents for lipids are listed in Table 6. Solutions of chlorosulfonic acid in acetic acid, ethanolic phosphomolibdic acid and antimony

Table 5 Examples of mobile phases used to separate fatty acids and triacylglycerols by Ag-TLC

Compound	Mobile phase composition, by volume	Development
Fatty acids with 0–3 double bonds	Hexane–diethyl ether, 90 : 10 or 80 : 20 Hexane–acetone, 100 : 4	One-fold development in closed tanks. One-stage development in open cylindrical tanks. <i>E</i> - and <i>Z</i> -monounsaturated fatty acids are clearly separated.
Fatty acids with 0–6 double bonds	First plate: hexane–diethyl ether, 90 : 10 Second plate: hexane–diethyl ether, 60 : 40	Fatty acids are separated on two different plates. Species with 0–3 double bonds are separated on the first plate. Polyunsaturated species are separated on the second plate.
Triacylglycerols with 0–6 double bonds	Hexane–diethyl ether–acetic acid, 94 : 4 : 2 Benzene–ethyl acetate, 9 : 1 Benzene–diethyl ether, 85 : 15 Hexane–diethyl ether, 80 : 20 Chloroform–methanol, 96 : 4 Hexane–acetone, different proportions	All components are separated on a single plate by one-stage development. These mobile phases are used for both analytical and preparative separations in closed tanks. Development in open tanks with specified volume of the mobile phase, see the example in Figure 4.

Table 6 List of frequently used staining reagents for detecting lipids in Ag-TLC

<i>Reagent</i>	<i>Comments</i>
25–70% sulfuric acid	A destructive reagent, usually applied by spraying as solution in ethanol. Spraying must be very thorough and even, especially if the plate is considered for densitometric quantification. Spots are detected by heating the plate at temperatures of 150–200°C.
3% aqueous solution of copper acetate in phosphomolybdic acid	Advantageous in that precoated plates can be immersed in the solution, thus providing an even staining. Spots are visualized by heating.
Sulfuryl chloride	A highly volatile destructive reagent that allows convenient treatment of the plate in a closed container. This treatment provides even staining when the plate is heated. Suitable for densitometric quantification of lipids.
Rodamin 6G, 2,7-dichlorofluorescein	Nondestructive reagents used for preparative isolation of material for further examination. Plates are sprayed with diluted (>1%) solutions of the reagents in acetone. Spots are detected by viewing under UV light. The isolated material is purified from the detecting reagent by elution through a small silica gel column.

perchlorate in chloroform have been used to detect terpenes separated by Ag-TLC.

Spraying is a rapid but inconvenient and quite hazardous operation and should be avoided if and when possible and replaced by treatment with vapours. Incorporation of the charring reagents into the layer should be performed with circumspection, since it may change the nature of the resolution.

For preparative purposes, after detection, the separated zones are carefully scraped from the plate and the compounds are extracted from the sorbent with suitable polar solvents. As such material is likely to be subjected to further analysis, the extracts should be purified first. For example, in lipid analysis, excess silver ions and 2,7-dichlorofluorescein can be removed by passing the extract through small silica columns or by washing with bicarbonate, ammonia or sodium chloride solutions.

Identification

An advantage of Ag-TLC is the easy identification of the separated components with a substantial degree of certainty. A reference compound, or reference mixture of compounds, is usually applied beside the sample. The reference and the sample are developed simultaneously and this allows the migration distances (the R_F values) to be compared. Fatty acids and triacylglycerols form, for example, mixed zones with the matching reference components. In case of ambiguity, preparative Ag-TLC is applied to isolate and collect the component(s) in question for subsequent spectral analysis.

Quantification

As in all TLC techniques indirect and direct approaches for quantification have been employed. The most widely used procedure involves scraping off the detected zone and eluting the component(s) with suitable solvent. Then any of the available chromatographic or spectral techniques for quantification can be applied. Scanning densitometry can be used to measure the quantities of the separated compounds after a carefully chosen staining procedure. Staining is required since even UV-absorbing or UV-tagged compounds have either a very weak, or even no, signal in the presence of Ag^+ in the layer. Procedures have been reported for reliable densitometric quantification of fatty acids and triacylglycerols without the need for calibration graphs and correction coefficients, for example. **Figure 2** presents the densitometric profile of a triacylglycerol mixture separated by Ag-TLC.

Interactions in Argentation TLC

The rules of complex formation, presented above, have been found to be generally valid in the majority of separations performed by Ag-TLC. In many cases it is possible to predict the migration order. Interaction of Ag^+ with compounds that have more than two double bonds, however, seems to be less well understood. This primarily concerns lipids. A mixture of fatty acids, for example, may comprise components of different chain length (from 12 up to 22 carbon atoms) and of zero to six double bonds in the

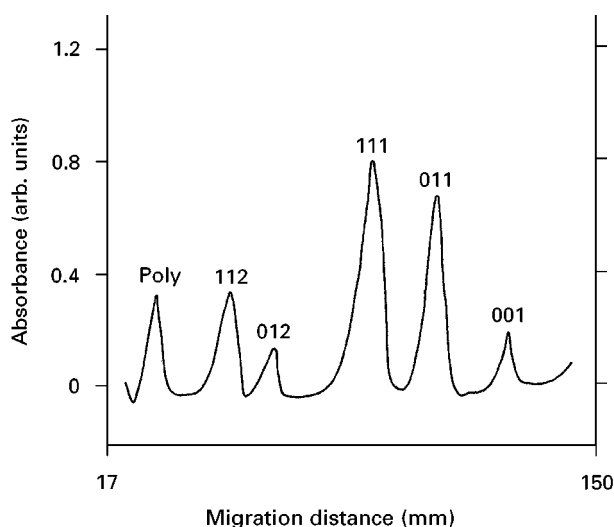


Figure 2 Densitogram of olive oil triacylglycerols separated by Ag-TLC. Conditions: laboratory-made 5 cm \times 20 cm glass plate, 0.2 mm thick silica gel layer impregnated with 0.5% methanolic silver nitrate (by dipping); sample size: 20 μ g; mobile phase: 6 mL light petroleum–acetone–ethyl acetate, 100 : 3 : 2 (by volume); one-stage development in an open cylindrical tank; detection: successive treatment with bromine (30 min) and sulfuryl chloride (30 min) vapours followed by carbonization by heating at 180–200°C on a temperature-controlled hot plate; scanning: Shimadzu CS-930 densitometer in zigzag mode; beam dimensions: 1.2 mm \times 1.2 mm; working wavelength: 450 nm. Peak identity: Poly, minor components, containing octadecatrienoic fatty acid; the figures indicate the number of double bonds in the acyl residues but not their position in the glycerol backbone.

chain. Double bonds can be either *cis* (*Z*) or *trans* (*E*) or both and can have different position in the chain. Triacylglycerols and glycerophospholipids are complex mixtures of species that differ in the type and position of the acyl residues. So far, there are no theoretical or experimental studies on the mechanism of complex formation between Ag^+ and complicated unsaturated molecules. Almost nothing appears to be known about the electronic and steric effects in these molecules and their possible influence on complexation.

Attempts have been made to present the complexation of lipids in Ag-TLC in quantitative terms. Estimation has been made on the basis of the chromatographic retention of different molecular types. For example, arbitrary values of 0, 1, 2 + 2*a* and 4 + 4*a*, where $a < 1$, have been proposed for the complexing power of stearic, oleic, linoleic and linolenic fatty acids (with 0, 1, 2 and 3 double bonds, respectively). Evidently, the increase in the complexing power values is greater than the increase in the number of double bonds. More accurate equations have been proposed but, in general, the values are

close to those determined earlier and confirm the above conclusion. It has also been assumed that the respective values for the tri- or diacylglycerols can be expressed as a simple sum of the values for the fatty acyl residues. The assumption considers that the contribution of a fatty acid in a complex lipid molecule is not affected by the strength and properties of the silver ion complexes with neighbouring fatty acids in the same molecule. Such models are too simple and do not take account of the steric factors that may especially affect the complexation of a triacylglycerol molecule.

The role of the support material must be also taken into account. The most widely used support, silica gel, possesses appreciable polarity and absorption activity. Therefore, the retention of unsaturated compounds cannot be ascribed to the complexation reaction with Ag^+ and double bonds only, although clearly that is a major factor. The retention of an unsaturated molecule in any such system is the result of a mixed retention mechanism. For example, an unsaturated fatty acid methyl ester has been assumed to complex with the silver ions through its double bond(s) and to interact with the silanol moieties through its methyl ester group. Depending on the position of the double bond, the molecules will have different conformations. Those molecules may be held more strongly when the distance between the double bond and the ester group has a better fit with the distance between the silver ion and the silanol moiety. These two interactions have been suggested in explanation of the specific migration patterns of positionally isomeric fatty acid methyl esters. A mixed retention mechanism should be taken into account in the case of unsaturated compounds with other polar functional groups which are subjected to Ag-TLC.

A separate but related problem is the topology of silver ions on the adsorbent surface. For example, it was found that part of the silver nitrate remained in crystalline form, filling the pores of the silica gel after drying the plate to make the layer active. However, a proportion of the silver nitrate remained dissolved in the water, which is always bound to silica gel. The aqueous silver nitrate was assumed to be responsible for complex formation. Saturation of the silica layer with water before separation has even been proposed in order to obtain a pure complexation reaction. If the excess silver nitrate does indeed remain in a crystalline form and does not take part in complexation, impregnation of the layer with a highly concentrated solution of silver nitrate is of no practical value. Some of the results obtained with Ag-TLC seem to confirm this observation.

Retention and Resolution of Unsaturated Compounds in Ag-TLC: Examples

In general terms, acyclic unsaturated compounds migrate and can be resolved by Ag-TLC depending on the number, configuration and, occasionally, on the position of the double bond in the molecule, the number of the double bonds being the governing feature. The separation of fatty acids and triacylglycerols illustrates very well the resolution ability of Ag-TLC.

The migration pattern of fatty acids with zero to six double bonds is presented in Figure 3. For qualitative purposes it is possible to resolve fatty acids with unsaturation in the above interval on a single 5 cm × 20 cm plate using two solvent systems in sequence. Migration cannot always be predicted in the case of a mixture of fatty acids of different chain lengths. According to the general rules, when chain length increases, stability of the complex with silver ions decreases. This means that longer chain fatty acids will migrate ahead of shorter chain species of the same unsaturation (note the place of docosatetraenoic, 4a, and of octadecatetraenoic, 4b, fatty acids on Figure 3). The migration order of triacylglycerols follows the same rules, i.e. species with up to nine double bonds and acyl residue chains of 16–18 carbon atoms are ordered according to the increasing retention: 000, 001, 011, 002, 111, 012, 112, 003, 112, 013, 113, 222, 023, 123, 223, 133, 233, 333 (the figures indicate the number of double bonds in the acyl moiety but not their position in the molecule). It should be noted that of two species with an equal number of double bonds that in which all (or most) of the double bonds are concentrated into one fatty acyl moiety is held more firmly (011 and 002, for example). The separation of natural triacylglycerol mixtures depends strongly on the quantitative proportions between the components. For example, a mixture of components with relative high saturation can be resolved on a single TLC plate by the successive use of two mobile phases of decreasing polarity as illustrated in Figure 4. For satisfactory resolution of plant triacylglycerols with up to nine double bonds three different plates and two-stage development of each plate with mobile phases of different polarity is required. The approach provides accurate identification and densitometric quantification of the separated species.

E- and *Z*-isomers are normally easy to distinguish. An example of the separation of a fatty acid mixture is shown in Figure 5. Argentation TLC is may be the easiest and cheapest way to determine *trans*-monoenes in dietary fats.

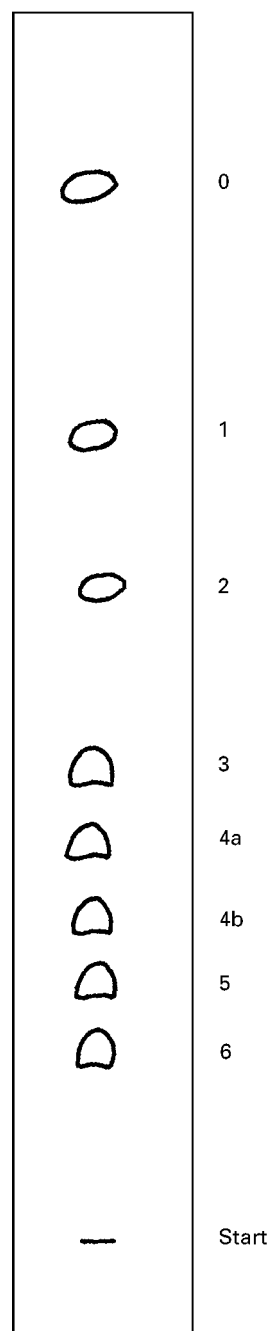


Figure 3 Migration pattern of fatty acid methyl esters with zero to six double bonds in Ag-TLC. Conditions: laboratory-made 5 cm × 20 cm glass plate, 0.2 mm thick silica gel layer impregnated with 0.5% methanolic silver nitrate (by dipping); mobile phase: 5 mL light petroleum–acetone–formic acid, 97 : 2 : 1 (by volume); one-stage development in an open cylindrical tank; detection: as in Figure 2. Spot identity: the figures indicate the number of double bonds; 4a, methyl docosatetraenoate; 4b, methyl octadecatetraenoate.

Under specified conditions Ag-TLC differentiates between mono- or diunsaturated fatty acids with different position of the double bond(s) in the carbon chain. In 1970 Gunstone and colleagues supposed

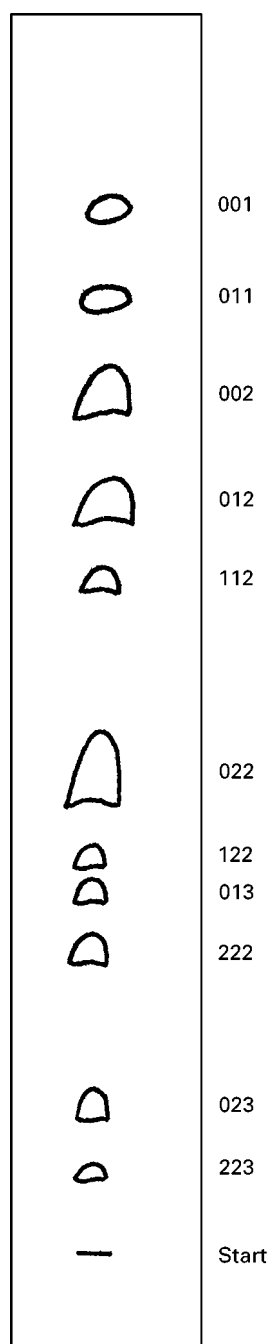


Figure 4 Migration pattern of coffee triacylglycerols. Conditions: laboratory-made 5 cm × 20 cm glass plate, 0.2 mm thick silica gel layer impregnated with 0.5% methanolic silver nitrate (by dipping); sample size 50 µg; two-stage development with 4 mL light petroleum–acetone, 100 : 4 (by volume) followed by 15 mL light petroleum–acetone, 100 : 4 (by volume); detection: as in Figure 2. Spot identity: the figures indicate the number of double bonds in the acyl residues but not their position in the glycerol backbone.

that this is due to the participation of the fatty acid molecule in additional reaction(s) with either the silver ions or with the adsorbent. Reliable resolution was achieved in isolated cases only. The approach

was therefore of hardly any practical value until recently, when it was shown that separation depends strongly on the nature of the ester moiety. The effect is demonstrated in Figure 6 and has been assigned to the participation of the ester group and the double bond in simultaneous complexation with a silver ion to give a chelate-type complex.

Of practical value is the resolution of triacylglycerols that differ by the position of the unsaturated fatty acid residue in the triacylglycerol molecule (Figure 7). Since the position of acyl residues is strictly specific in natural triacylglycerol mixtures, Ag-TLC provides an easy way to distinguish between natural and modified edible fats and oils and the approach is of value to the food industry.

Conclusion

Ag-TLC is a valuable qualitative and quantitative method for the separation of unsaturated compounds, lipids in particular. Ag-TLC has the advantages of rapidity, simplicity and versatility and does not require expensive instrumentation. The information obtained reflects the whole sample, thus helping the analyst to make rapid, correct and efficient judgements. It is widely used as a preliminary step in combination with other chromatographic techniques such as GC and HPLC. Sufficiently pure

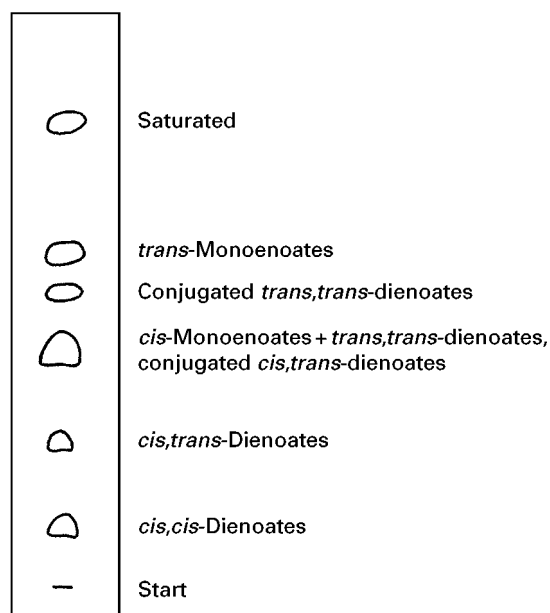


Figure 5 Migration pattern of *E*-, *Z*-fatty acid methyl esters. Conditions: laboratory-made 5 cm × 20 cm glass plate, 0.2 mm thick silica gel layer impregnated with 0.5% methanolic silver nitrate (by dipping); two-stage development with 2 mL light petroleum–acetone, 100 : 2 (by volume) followed by 3 mL light petroleum–acetone, 100 : 0.7 (by volume); detection: as in Figure 2.

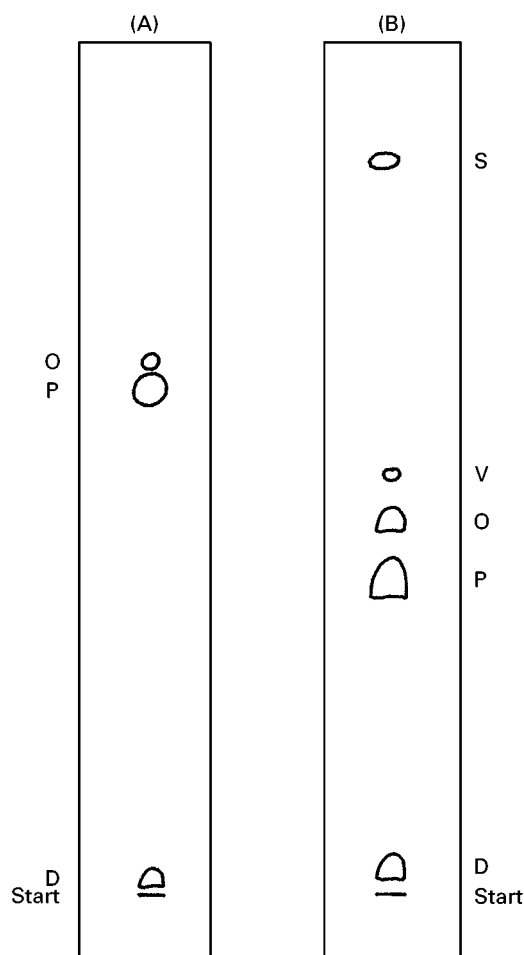


Figure 6 Migration pattern of mono-unsaturated octadecenoic fatty acids differing in the position of the double bond in the carbon chain. Sample: aniseed oil. Conditions: laboratory-made 5 cm × 20 cm glass plate, 0.2 mm thick silica gel layer; detection: as in Figure 2. (A) Separation of the fatty acid as methyl esters. The layer is impregnated with 1% methanolic silver nitrate (by dipping); development is in an open cylindrical tank with light petroleum-acetone, 100 : 5 (by volume) at -20°C . (B) Separation of the fatty acids as phenacyl esters by two-stage development in a closed cylindrical tank (no preliminary saturation of the atmosphere) with a mobile phase of chloroform-acetone, 100 : 0.25 (by volume) at ambient temperature. Note the improved resolution achieved after conversion of the fatty acids into phenacyl esters. Spot identity: S, saturated fatty acids, V, vaccenic acid, 11-18 : 1; O, oleic acid, 9-18 : 1; P, petroselinic acid, 6-18 : 1; D, linoleic acid, 9, 12-18 : 2 (position of double bond-number of carbon atoms : number of double bonds).

components can be collected for further structural elucidation by spectral methods. Combined with scanning densitometry, Ag-TLC meets all requirements of a reliable quantitative method for determination of positional and configurational fatty acid isomers and of triacylglycerols in natural samples.

The resolution power of Ag-TLC will undoubtedly increase if and when an automatically controlled

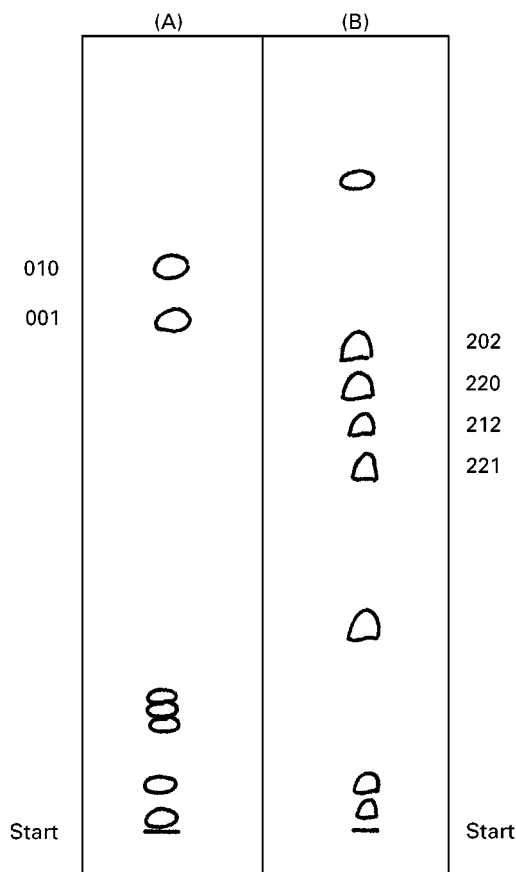


Figure 7 Migration pattern of positionally isomeric triacylglycerols by Ag-TLC. Conditions: laboratory-made 5 cm × 20 cm glass plate, 0.2 mm thick silica gel layer. (A) Sample: randomized lard; layer impregnated with 1% methanolic silver nitrate; one-stage development in an open cylindrical tank with 12 mL chloroform-methanol, 95.5 : 0.5 (by volume). (B) Sample: randomized sunflower oil; layer impregnated with 2% methanolic silver nitrate; one-stage development in an open cylindrical tank with chloroform-methanol, 97.5 : 2.5 (by volume). Spot identity: the figures indicate the number of the double bonds and the position of the acyl residue in the glycerol backbone.

system for continuous development with a sequence of different mobile phases becomes available.

See also: II/Chromatography: Thin-Layer (Planar): Instrumentation; Layers; Modes of Development: Conventional; Modes of Development: Forced Flow, Overpressured Layer Chromatography and Centrifugal; Spray Reagents. III/Impregnation Techniques: Thin-Layer (Planar) Chromatography. Lipids: Gas Chromatography; Liquid Chromatography; Thin-Layer (Planar) Chromatography. Silver Ion: Liquid Chromatography.

Further Reading

Ackman RG (1991) Application of thin layer chromatography to lipid separation: neutral lipids. In: Perkins EG (ed.) *Analysis of Fats, Oils and Lipoproteins*, pp. 60-82. Champaign, IL: American Oil Chemists' Society.

- Cagniant D (ed.) (1992) *Complexation Chromatography*. New York: Marcel Dekker.
- Christie WW (1987) *High Performance Liquid Chromatography and Lipids*. Oxford: Pergamon.
- Christie WW (1982) *Lipid Analysis*, 2nd edn. Oxford: Pergamon.
- De Ligny CL (1976) *Advances in Chromatography* 14: 265–304.
- Fried B and Sherma J (1996) *Practical Thin-Layer Chromatography – A Multidisciplinary Approach*. Boca Raton, FL: CRC.
- Fried B and Sherma J (1998) *Thin-Layer Chromatography – Techniques and Application*, 4th edn. New York: Marcel Dekker.
- Gmelin Handbuch der Anorganischen Chemie (1975) *Silver*, vol. 61, TI.B5. Berlin: Springer-Verlag.
- Morris LJ (1966) Separation of lipids by silver ion chromatography. *Journal of Lipid Research* 7: 717–732.
- Morris LJ and Nichols BW (1972) Argentation thin layer chromatography of lipids. In: Niedewieser A (ed.) *Progress in Thin Layer Chromatography and Related Methods*, vol. 1, pp. 74–93. Ann-Arbor, MI: Ann-Arbor-Humphrey Science Publishers.
- Nikolova-Damyanova B (1992) Silver ion chromatography and lipids. In: Christie WW (ed.) *Advances in Lipid Methodology – One*, pp. 181–237. Ayr: The Oily Press.

SODIUM CHLORIDE: CRYSTALLIZATION



R. M. Geertman, Akzo Nobel Chemicals Research, Arnhem, The Netherlands

Copyright © 2000 Academic Press

Introduction

Salt has been a part of human existence since time immemorial. It was used for cooking wheat and barley as early as 5000 BC. The first salt was gathered from shallow lagoons where seawater could evaporate. Later rock salt was mined, and in the Alps, for instance, rock salt is known to have been mined as early as 1400 BC. Because of its importance to human life, salt has had an influence on economy, history and culture. Many sayings and words are derived from the use of salt: e.g. ‘to be worth one’s salt’ is a compliment, the Bible speaks of ‘the salt of the earth’ and soldier is derived from the Latin ‘*sal dare*’ which means to give salt.

Indeed, in ancient times salt had a much greater value than it has nowadays. It was traded weight by weight with gold, and the salt trade was very profitable. The Hanseatic League started by trading in salt. Taxes on salt were very common, and in that sense salt has played a role in many important historic events. The French Revolution was partly in protest against salt taxes. Gandhi’s campaign of civil disobedience, which eventually led to the independence of India, started when he evaded the British salt monopoly by producing salt himself.

Uses of Salt

Before the industrial revolution and the discovery of the electrolysis process, the uses of salt were limited.

The main uses were for the cooking, preserving and pickling of food and the tanning of hides. These uses are still very important, as salt is essential for the human body. With the development of chemical processes the uses of salt have diversified enormously. Apart from uses in the food industry, salt is, for instance, used in dyeing, paper production, highway de-icing, oil well drilling and the production of soda ash. Electrolysis of salt is the major source of chlorine and sodium hydroxide for the chemical industry. Chlorine is essential for the production of a number of plastics, insecticides and pharmaceutical compounds. Either directly, or in the form of derivatives, salt finds application in more than 14 000 ways. This multitude of applications can be divided into three major categories: chemical uses, highway de-icing, and food-related uses. In the industrialized nations the chemical industry accounts for approximately 50% of the salt consumption, and highway de-icing for about 30% while food applications make up the remainder. In developing countries most of the salt produced is used in food.

Production of Salt

As salt is the most abundant nonmetallic mineral, most countries have the ability to produce salt. It is so abundant that it is hard to estimate salt reserves. In the United States alone, reserves are estimated at 55 trillion tonnes. In 1996, 192 million tonnes of salt were produced, approximately 55% in the industrialized nations and about 45% in developing countries. Details are given **Table 1**.

Table 1 World production of salt in 1996

Country	Amount produced (in millions of metric tons)
United States	42.9
Peoples' Republic of China	28.9
Canada	12.3
Germany	10.9
India	9.5
Mexico	8.5
Australia	7.9
Other	71.8
Total	192.0

Salt is a cheap commodity. At a 1997 price level of US \$60 per tonne for chemical grade, merchant-delivered salt and US \$10 per tonne for captive use, salt is cheaper than any other refined chemical. Because of the low price of salt relative to the transportation costs, most salt production plants are in the vicinity of salt users. Producing an acceptable grade of purity at the lowest deliverable costs is the most important consideration for salt producers throughout the world.

How the salt is produced depends very much on the form in which the salt is available. In subtropic, arid regions salt is mostly produced by evaporating seawater. Large production facilities for so-called solar salt can be found in India, Australia and Mexico. In temperate regions, where the climate is less favourable for the evaporation of seawater, rock salt is mined. This can be done in two ways. Provided the salt deposit is close to the surface, it can be mined in the classical roof and pillar method. The rock salt is crushed, sorted and sold as a low grade quality. For more demanding applications further purification is needed. If the salt deposits are more deeply located, the solution mining technique is used. This involves pumping water down through a borehole to dissolve the salt, and recovering the resulting brine. The brine is then purified to remove foreign ions, and evaporated. The salt produced in this way is known as vacuum salt.

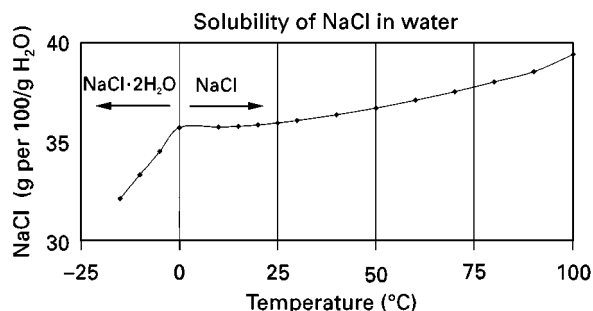
Fundamentals of Salt Crystallization

Salt or sodium chloride can occur in two forms. The first and best known form is the anhydrous form, NaCl. The second form is the dihydrate which is formed in a pure brine at temperatures below 0.1°C. The solubility of the dihydrate form is weakly temperature dependent, whereas the solubility of the anhydrous form is nearly temperature independent. The temperature dependence of the solubility of salt in water is given in Figure 1.

The anhydrous form, NaCl·0H₂O, crystallizes in the *Fm3m* space group in which each sodium ion is octahedrally coordinated by six chloride ions, and vice versa. The {1 0 0} faces are the slowest growing faces, resulting in the typical cube shape of salt crystals. By adding additives the {1 1 1} faces can be retarded, thus yielding octahedral shapes. Additives such as Fe (CN)₆⁴⁻ or NTAA (nitrosyl triacetamide) poison the {1 0 0} surfaces, resulting in preferential growth along edges and on corners. These shapes are given in Figure 2, together with a number of intermediate shapes where both cubic and octahedral faces are visible.

As mentioned before, salt is very soluble in water, so the growth rate of salt crystals is diffusion controlled. Like many other very soluble salts, the driving force needed to obtain acceptable growth rates (in the order of 10⁻⁸ m s⁻¹) is low, typically of the order of 0.1% or lower. Salt crystals produced in a forced circulation crystallizer (the most common type used for salt crystallization) typically have a mean size of 350–400 µm. In draft tube baffled (DTB) type crystallizers salt crystals can become larger, in the order of 500–1000 µm. Apart from the influence on the mean crystal size, the low driving force for crystallization also strongly reduces agglomeration. Agglomerated salt can only be obtained using techniques such as antisolvent crystallization where high driving forces are involved. There are three mechanisms for the incorporation of impurities in the final crystalline product. The first is direct incorporation of the impurity in the crystal lattice, the second is the formation of inclusions and the third is insufficient washing of the crystals.

In contrast to organic crystals, and to a lesser extent hydrated salt crystals, the ions are densely packed in the crystal lattice. This effectively prevents the incorporation of larger molecules in the crystal lattice as the lattice strain and the enthalpies involved are extremely unfavourable. This applies to many ions that have marked differences in ionic radius or charge from either the chlorine or sodium ion. The

**Figure 1** Solubility of NaCl in water.

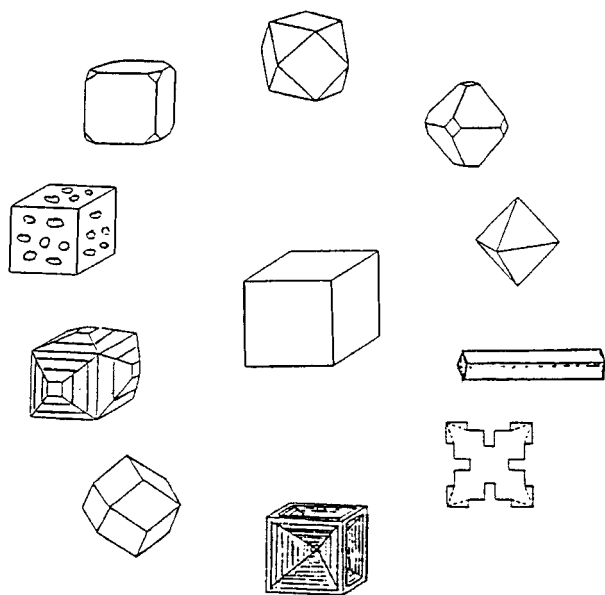


Figure 2 Different crystal forms observed during the crystallization of common salt. Reproduced with permission from Elsevier Science.

tendency of salt to form solid solutions is therefore very limited. The only notable exception is with the incorporation of bromide, which is therefore very hard to remove as an impurity, once incorporated.

The second mechanism, the formation of inclusions, is much more common. In industrial crystallization the solid fraction in the slurry is high and therefore collisions between crystals are frequent. If the energy involved in a collision event is high enough the corners of the cubic salt crystals will be damaged and the crystals will be strained. Regrowth of these damaged corners is often imperfect and inclusions are formed. An effective method of reducing the impurity uptake through this mechanism, though at the cost of production capacity, is to lower the solids fraction of the slurry. It should be noted that this mechanism only occurs when large crystals are produced. If the crystals are small the kinetic energy involved in the collisions is not high enough to damage the crystals.

Good washing of the crystalline product is very important for the final purity. By evaporating water not only is salt produced, but the impurities are also concentrated. Any mother liquor that remains will therefore have a profound detrimental effect on the product purity. More impure mother liquors require better washing. This is more important for solar salt than for vacuum salt. Vacuum salt is produced from purified brine that contains, apart from NaCl, few very soluble salts, so despite incomplete washing the amount of impurities will still be relatively low. Concentrated seawater, in contrast, also contains high concentrations of very soluble salts, especially mag-

nesium salts. Insufficient washing therefore has much more influence on the product purity. Another important aspect when washing solar salt is the agglomeration.

A striking example of the influence of agglomeration on the final product purity is provided by the antisolvent crystallization of NaCl. Though the crystals are crystallized from a mother liquor containing as much as 50% weight antisolvent (on a solvent basis) the uptake of the antisolvent is as low as 30 ppm. Diluting the antisolvent stream with water, which reduces the driving force for crystallization, should result in a decrease in the impurity concentration. However this effect is offset by the increased agglomeration of the system, so instead of the expected lowering of concentration the concentration of antisolvent is increased to 100 ppm.

Irrespective of the method by which salt is produced, seawater is the source of salt (salt deposits are the result of natural solar salt production). The impurities present in brine or rock salt are therefore the same. These impurities are mainly Ca^{2+} , Mg^{2+} , Sr^{2+} , Br^- and SO_4^{2-} . All these impurities have undesirable effects on the electrolysis of sodium chloride and need to be removed during the production process. During electrolysis calcium, strontium and magnesium are deposited as hydroxides on the electrodes, which is of course not desired. The presence of Br^- leads to the formation of ClBr , which is also unwanted. Finally the presence of sulfate increases the cell potential needed for electrolysis, thus increasing production costs. A further impurity is iron, which is not only present in the salt, but is also added in the form of ferrocyanide, an anticaking agent. Though needed for proper salt handling, the presence of iron interferes with the membrane electrolysis. The ferrocyanide must therefore be decomposed and the iron precipitated as the hydroxide salt prior to electrolysis of the sodium chloride solution.

The strategy for removing these impurities depends on the production method. For solar salt production fractional crystallization combined with careful washing is employed, whereas in vacuum salt production the brine is purified prior to crystallization of the sodium chloride. In the rock salt production various recrystallization methods are used.

Solar Salt

Crystallization sequence Seawater contains nearly all elements of the periodic system in varying amounts. The composition of seawater is given in Table 2. When seawater is evaporated many different salts will be formed, at different stages during the evaporation. In that sense production of pure sodium chloride from seawater somewhat resembles

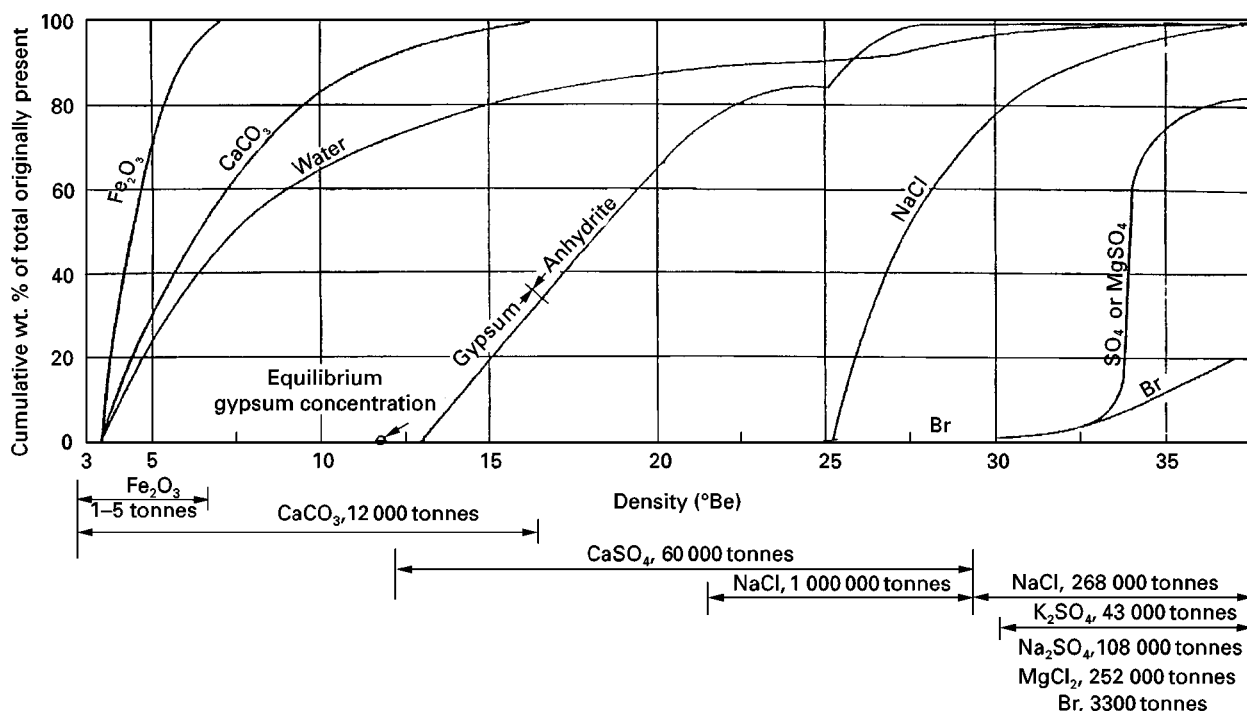
Table 2 Composition of seawater

Component	Amount present (g per 1000 g seawater)
Ca	0.408
SO ₄	2.643
Mg	1.265
Cl	18.95
K	0.380
Na	10.48
Br	0.065
Total	34.19

the distillation of crude oil, where one is interested in obtaining well defined fractions. When seawater is concentrated gradually iron oxide and calcium carbonate start to crystallize first, but the amount of iron oxide produced is negligible. Then calcium sulfate precipitates. It is important to note that when sodium chloride is subsequently crystallized, the mother liquor is concentrated with respect to both of the salts mentioned. After crystallizing about 75% of the available sodium chloride (at which stage 97% percent of the water has been evaporated), sodium bromide will start to crystallize as a solid solution with sodium chloride, and the so-called bitterns will also crystallize. The term bitterns is used for a collection of magnesium, potassium, sulfate and chloride salts, such as KCl, MgCl₂, MgSO₄ and double salts. It

is derived from the bitter taste of these salts. The whole sequence is depicted graphically in Figure 3. This figure shows the relationship between the density of the brine expressed as degrees Baume ($^{\circ}\text{Be} = 145 - (145/\text{specific density at } 15.6^{\circ}\text{C})$) and the crystallization of the various salts. The concentration factor can be deduced from the cumulative amount of water evaporated, which is also given in the figure.

Plant layout To produce pure salt, the crystallization of iron oxide, calcium carbonate and calcium sulfate must be physically separated from the sodium chloride crystallization. This is achieved in solar salt works by having two kinds of ponds: concentration ponds and crystallizer ponds. Approximately 90% of the water must be evaporated before salt starts to crystallize, so the concentration ponds are much larger than the crystallizer ponds. Though the water is not completely evaporated in the crystallization section (the brine is discharged before the bitterns start to crystallize), the concentration pond/crystallizing pond area ratio is usually around 10 to 1. Evaporation is a slow process, so solar plants must occupy a large area. The solar salt plants in Australia and Mexico, which supply the chemical industries in Japan and the United States, are tens of square kilometres in size. The seawater needs to be concentrated in stages so most solar salt plants have 5–10

**Figure 3** Deposition of salts during the evaporation of sea water at 25°C.

concentration ponds in series. These ponds are shallow to obtain the best surface area/volume ratio, with the depth usually between 50 and 80 cm. Small, low levees separate the different ponds. The crystallizer ponds are smaller, ranging from several hundred square metres in the case of manual harvesting to several acres in the case of mechanical harvesting. After harvesting the salt is transported to the washing plant. An example of the layout of a solar salt plant is given in Figure 4.

Solar salt production The need for large shallow ponds in the vicinity of the sea determines where solar salt plants can be operated. Small plants can be found in all coastal areas near the tropics, large plants only in India, Australia and Mexico. Such plants are operated all year round. Further north than the tropics, in arid areas as far north as western France, the operation is seasonal; the salt is harvested before the winter rains dissolve the salt produced.

Production of solar salt is started by taking in seawater. The seawater is concentrated by evaporation and the brine is reduced to about 60% of its original volume. After the first concentration stage the brine is transferred to another area where calcium carbonate starts to precipitate. Here a further 15% of the original volume is evaporated and the brine is

transferred to a third type of pond, the gypsum precipitation pond. The brine is concentrated to the point at which sodium chloride nearly starts to crystallize before it is transferred to the pickling pond where the brine, now saturated with sodium chloride, is kept before being transferred to the crystallizer pond. This pond is needed to reduce the gypsum supersaturation in the brine. At this point about 90% of the water has been evaporated. In the crystallizers, depending on the required purity, 70–75% of the available sodium chloride is crystallized before the remaining bitterns are discharged. Production of high quality solar salt is very much a question of knowing when to start producing halite and when to stop.

A major concern is the sealing of the ponds to prevent losses. It is impossible to treat the bottom of the ponds because of their large size, so the ponds must have a base such as clay, which is (fairly) impervious to water. The precipitated calcium carbonate (and also gypsum) will improve the sealing during operation so the losses will go down with time. By regularly changing the brine flow through the plant, all concentration ponds will be used as calcium carbonate and gypsum precipitation ponds, thus ensuring minimum brine losses (provided of course that the ponds are equal in size). Note that this is only possible in small plants.

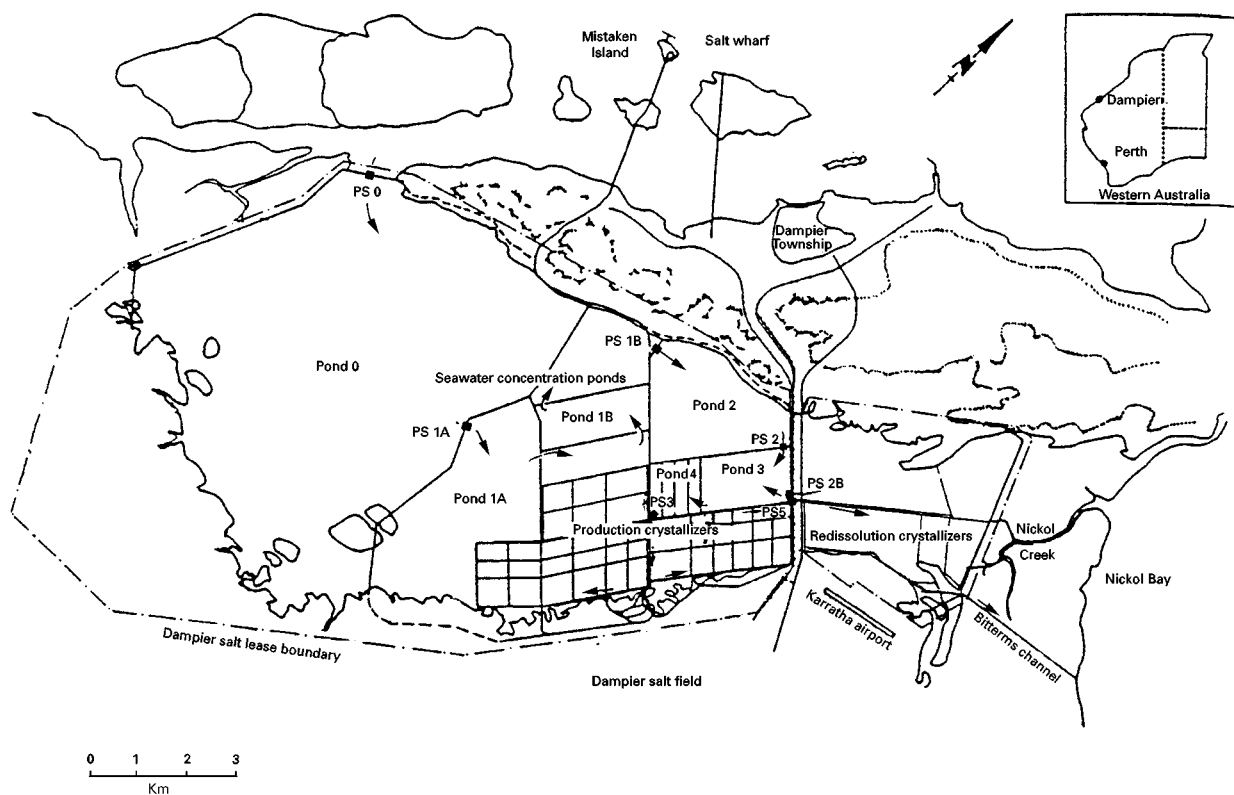


Figure 4 Schematic diagram of Dampier salt field layout and location map of Western Australia. Reprinted from Garrett DE, with kind permission from Elsevier Science Ltd.

The transmission of solar light in the brine is high, which reduces the evaporation rate. To enhance sunlight absorption dyes are added. The most common practice nowadays is to add algae which reduce the light transmission from 96% to 55–70%. An additional advantage is that the algae mats will also plug the pond bottom. Care must be taken not to increase the viscosity too much through abundant algae growth, or other organisms have to be introduced to keep the algae concentration within limits. Red halophilic bacteria are added to the crystallizing ponds for the same purposes.

The rate at which water evaporates depends on the climate. The amount of sunshine, the mean temperature, the relative humidity, the wind velocity and the average amount of precipitation determine the net evaporation rate. Accurate figures for the net evaporation are needed both for design purposes and for process control (read brine management). For design purposes climate data (incorporating amount of sunshine, air temperature and humidity and wind velocity) and brine data are taken into account. The gross evaporation rate can then be calculated by multiplying the difference in vapour pressure between air and brine by a mass transfer coefficient. In this mass transfer coefficient factors such as temperature, net gain of radiant energy and the heat transfer coefficient are taken into account.

For production purposes another model is generally used. The evaporation of water from a fresh water pan, situated on the site, is measured. This figure is then corrected for the salinity, the size of the pan and the rainfall.

$$\begin{aligned} \text{Evaporation (pond)} = & (\text{evaporation (pan)} \\ & \times k_{\text{scale}} \times k_{\text{salinity}} - \text{rainfall}) \\ & \times \text{area} \times \rho_w \end{aligned}$$

Here k_{scale} and k_{salinity} the scale factors and ρ_w is the density of water. Using this method it is possible to estimate how much has been evaporated from each pond, to decide when to pump brine from one pond to another, to take in sea water, etc.

In the crystallizer ponds a salt floor is formed during the crystallization of sodium chloride. The salt is harvested by completely removing the salt floor (in seasonal operations) or scraping the top layer (in year round operations). When the salt is mechanically harvested great care should be taken that the floor is strong enough to accommodate heavy equipment. Usually salt floors for mechanical harvesting are at least half a metre thick.

After harvesting the salt is washed by mixing the crystals with fresh saturated brine, and transferred to

a mesh conveyor where the brine is drained off. Generally sea water sprays are then used to finish the washing process. Provided the washing is carried out very thoroughly, and the crystals are crushed to remove the mother liquor contained in cavities, solar salt can reasonably pure, though not as pure as vacuum salt. In most cases solar salt contains significantly more magnesium (300–500 ppm), calcium (200–300 ppm) and sulfate (1000–1500 ppm) than vacuum salt.

The salt can be upgraded using the Salex[®] process. This process utilizes the difference in density and morphology between sodium chloride and other minerals. The salt crystals containing the impurity crystals are countercurrently washed with a saturated brine. The salt crystals settle, and the impurity (mainly gypsum) crystals are carried away with the brine and left to settle in a separate tank. The clarified brine can then be reused. By leaving the produced salt piles exposed to rain, impurities will preferentially dissolve, thus improving the salt quality. This is called the rain wash method.

Rock Salt

Provided the rock salt deposits are close to the surface, rock salt can be mined in the classical way. First a vertical shaft is dug until the salt bearing deposit has been reached. Then horizontal shafts are blasted and the salt thus produced is transported to the surface. For de-icing use the salt is only crushed and sorted by size. For chemical applications the rock salt must be upgraded. This can be achieved in several ways. First of all, the rock salt can be completely dissolved. The resulting brine is then treated in the same manner as brine obtained by solution mining. As this process is more expensive than solution mining it is hardly ever used. The second option is to recrystallize the brine by making use of the fact that sodium chloride also has a hydrated solid phase.

This process works as follows. First small, crushed salt crystals are suspended in a brine at a temperature of 5°C. The brine is then cooled to a temperature lower than 0°C. At this temperature NaCl is more soluble than the hydrated phase, NaCl·2H₂O. The anhydrous sodium chloride crystals will dissolve and sodium chloride dihydrate crystals will be formed. When the slurry now containing the dihydrate crystals is heated, the process is reversed. The dihydrate crystals will dissolve and anhydrous crystals will be formed. During the two consecutive crystallization steps the impurities present in the dissolving crystals will remain to a large extent in the brine, instead of ending up in the new crystals formed. Using this method, the purity of the salt can be markedly improved without having to evaporate the brine. After the recrystallization steps the now purified

crystals are separated from the brine and the brine is reused after treatment.

Vacuum Salt

Brine purification Vacuum salt is the name given to salt produced by evaporative crystallization. Water is injected into a salt deposit through a borehole, and dissolves the salt so the resulting brine can be recovered. This brine is then purified before salt is produced by evaporative crystallization. The deposits used for this kind of salt production lie at depths between a few hundred and three thousand metres. Two pipes are used, one bearing fresh water to the cavern, the other transporting brine to the surface. Because of surface subsidence and ground movements, the caverns cannot get too large. Normally the size is smaller than 100 m in width. Furthermore, above the cavern a layer of a few metres of salt must be maintained to protect the overlying strata from brine penetration. Once the cavern has reached its maximum allowable size, solution mining is stopped and a new borehole is drilled.

It is interesting to note that the salt mined in such a way has already been crystallized once. All salt deposits are remains from earlier lakes and seas, which have been evaporated. Thus the salt is already separated from the calcium sulfate and bitterns originally present in the seawater.

Though already purer than the saturated brine produced by seawater evaporation, the brine produced still contains significant amounts of calcium, magnesium, sulfate and bromide ions. Most of these ions are removed in the brine purification process. First the sulfate is removed by adding calcium oxide, which leads to the precipitation of gypsum. The oxide increases the pH of the brine, which induces the precipitation of magnesium hydroxide. Thus in the first stage sulfate and magnesium are removed. To reduce production costs this process is carried out using very simple equipment. Calcium oxide is simply mixed with the brine in a very large tank. To decrease the

supersaturation further tanks are used. The solids are removed by draining the tanks and emptying them.

A drawback to this procedure is the increased calcium level in the brine. To reduce this level gases from an on-site power plant are usually used. The carbon dioxide yields carbonate, due to the high pH of the brine, which together with calcium forms the almost insoluble calcium carbonate. Because of the high salt concentration and high temperature, vaterite is formed rather than the usual calcite. This is an advantage because strontium, which is also present in the brine, is also effectively removed as strontium carbonate forms a solid solution with vaterite.

Crystallization After purification the water is evaporated and salt is crystallized. To conserve energy this is done in several stages. Each stage is operated under a lower pressure so the brine boils at a lower temperature. The vapour produced by the previous stage condenses in a heat exchanger and as this steam was formed at a higher temperature, the brine starts to boil. In this way the steam used in the primary stage can be reused several times. This principle is shown in Figure 5. Thus the total amount of energy involved in the production of vacuum salt is greatly reduced. In a typical four-effect installation (see Table 3) the first effect operates at slightly elevated pressures while the other effects operate under reduced pressure, hence the name vacuum salt.

Generally salt crystallizers are of the forced circulation type with external heat exchangers. For a production of 1 million tonnes per year, a total crystallizer capacity of 800–1000 m³ is needed. The separate crystallizers can be operated in different modes. The salt produced can be separated from the mother liquor separately for each crystallizer, or the slurry can be transported from one effect to the other, thus increasing the solids content of the slurry in each successive stage. This has important implications for the purity. In the first case the salt produced in the first crystallizer is the purest. Little water has (yet)

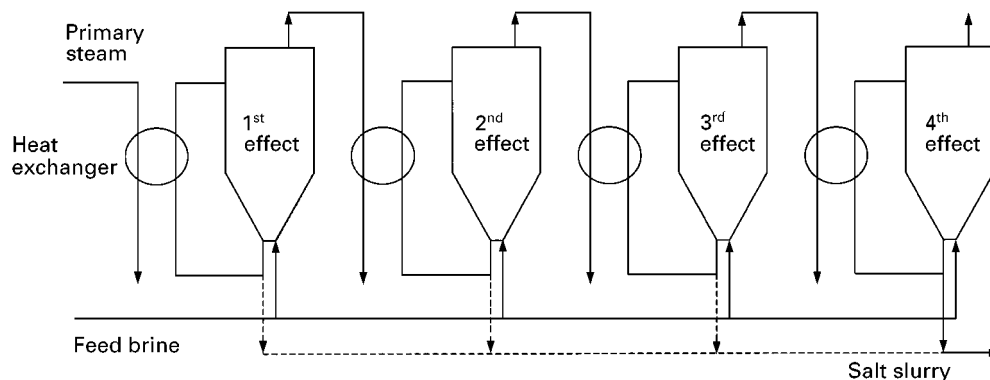


Figure 5 Scheme of a four effect evaporative crystallization plant.

Table 3 Temperatures and pressures in a four-effect evaporative crystallization plant

Effect	1	2	3	4
Pressure (bar)	2.0	0.89	0.34	0.18
Temperature (°C)	120	96	72	58

been evaporated and the impurity concentration is low. In the successive crystallizers the impurities are gradually concentrated, which has a detrimental effect on the purity. Thus different grades of salt are produced.

When the slurry is transported from one effect to the other, only one grade of salt is produced, which represents the mean purity when compared with the other method. There will be local differences in purity, the centres of the 'oldest' crystals being the purest, whereas the newer crystals and the collision prone corners of the larger crystals will contain more impurities.

Brine recovery As with the production of solar salt, the amount of impurities determines when the crystallization is stopped. Again bromide is important in that respect, as it is very difficult to remove. One is then left with a brine containing valuable salt that unfortunately it is difficult to recover because of the high impurity content. Several procedures have been devised to cope with this problem. The first process, used by Akzo Nobel, is the Bromin process. In this process the remaining sulfate- and bromine-rich mother liquor is further evaporated in a separate crystallizer, where sodium sulfate is crystallized in addition to sodium chloride. The remaining, greatly reduced amount of mother liquor, now very rich in bromine, is discharged in a nonproductive borehole. Sodium chloride and sodium sulfate are added to the raw brine entering the brine purification. Sodium sulfate dissolves and the sulfate precipitates as calcium sulfate.

At the Salinen Austria GmbH production facility nearly the same procedure is used, but instead of crystallization of anhydrous sodium sulfate and sodium chloride, the company claims that sodium chloride and glaserite ($\text{Na}_2\text{SO}_4 \cdot 3\text{K}_2\text{SO}_4$) are formed. After washing with raw brine, the glaserite is dissolved and the sulfate serves to precipitate calcium while the sodium chloride remains behind.

Another method involves cooling the remaining brine, thus producing Glauber salt, $\text{Na}_2\text{SO}_4 \cdot 10\text{H}_2\text{O}$. Subsequent evaporation of the mother liquor yields sodium chloride. The remaining brine is then discarded.

See Colour Plate 117.

Further Reading

- Burnard E (1993) The use of computer models in solar salt field process control. *Seventh Symposium on Salt*, vol. I, pp. 499–505. Amsterdam: Elsevier Science Publishers.
- Flachberger H and Krenn K (1999) Zum Stand der Technik im Bereich der Aufbereitung von Salzmineralien. *Berg- und hüttenmännischen Monatshefte* 144(6): 234.
- Garrett DE (1969) Factors in the design and layout of solar salt plants. Part I. Pond layout and construction. *Proceedings of the Third International Symposium on Salt*, pp. 63–69. Northern Ohio Geological Society, Cleveland, Ohio, USA.
- Jongema P (1983) Optimization of the fuel consumption of an evaporation plant with the aid of the exergy concept. *Sixth International Symposium on Salt*, pp. 463–496. Salt Institute, Alexandria, Virginia, USA.
- McArthur JN (1980) An approach to process and quality control relevant to solar salt field operations in the northwest of Western Australia. *Proceedings of the Fifth International Symposium on Salt*, pp. 325–338. Northern Ohio Geological Society, Cleveland, Ohio, USA.
- Mersmann A (1995) *Crystallization Technology Handbook*. New York: Marcel Dekker Inc.
- Nielsen AE (1984) Electrolyte crystal growth mechanisms. *Journal of Crystal Growth* 67: 289–310.
- Ninane L, Craido Cl and Thomas L (2000) Purification of rocksalt by a new process at low temperature. *Proceedings of the Eighth International Symposium on Salt*, pp. 451–458. Amsterdam: Elsevier Science Ltd.
- Sedivy VM (1996) Purification of salt for chemical and human consumption, Krebs Swiss, Zurich, Switzerland, in *Industrial Minerals*, April.
- Surdyk J, Leder AE and Ishikawa-Yamaki M (1998) CEH Product Review – Sodium Chloride. *Chemicals Economics Handbook 1998*. SRI International, Menlo Park, CA 94025-3477, USA.
- US Geologic Survey (1996) U.S. Geologic Survey Minerals Information 983 National Center, Reston, VA 20192, USA.
- Venkatesh Mannar MG and Bradley HL (1984) *Guidelines for the Establishment of Solar Salt Facilities from Seawater, Underground Brines and Salted Lakes*. Industrial and Technological Information Bank, Industrial Information Section, United Nations Industrial Development Organization, New York.
- Venkatesh Mannar MG and Dunn JT (eds) Consumption and uses of salt. In: *Salt Iodization for the Elimination of Iodine Deficiency*. International Council for Control of Iodine Deficiency Disorders.

SOLID-PHASE EXTRACTION OF DRUGS

See III/BIOANALYTICAL APPLICATIONS: SOLID-PHASE EXTRACTION

SOLID-PHASE EXTRACTION WITH CARTRIDGES



D. A. Wells, Sample Prep Solutions Company,
Maplewood, MN, USA

Copyright © 2000 Academic Press

Introduction

Sample preparation is an important component of an analytical method. It is used to concentrate an analyte to improve its limits of detection, as well as to isolate an analyte from unwanted matrix components that can cause interferences upon analysis. Solid-phase extraction (SPE), as a tool for this sample concentration and isolation, has gained acceptance since its commercial introduction circa two decades ago. SPE is performed using commercial packed cartridges (containing approximately 50–500 mg packing material) as well as discs (containing from 4–500 mg). Many formats, chemistries and sizes of SPE products are available to meet a range of separation needs.

Solid-phase extraction is preferred to other types of sample preparation techniques, such as liquid-liquid extraction (LLE), for many reasons. SPE is an efficient technique, often achieving higher recovery of analyte than other methods of sample preparation because of its selectivity. The chemistry of attraction between an analyte and the solid sorbent can be exploited by pH and solvent considerations to allow interaction yet exclude interferences. SPE is a less time-consuming and labour-intensive technique. Extraction typically involves adding different liquids through SPE columns in parallel and collecting the eluate at the final step. Emulsion formation is eliminated – in LLE an emulsion sometimes forms between the aqueous and organic layers preventing phase separation. Organic solvent consumption is far less using SPE than typical LLE techniques, saving money in terms of both purchase costs of solvents and costs to dispose of these regulated solvents. Reduced exposure of the analyst to organic solvents also improves safety in the laboratory. Unlike LLE the SPE procedure using columns can be automated. There are several hardware choices available commercially that transform SPE from a manual procedure into a fully automated one, allowing the analyst to perform other tasks in the laboratory. Batch procedures of automation are available in which a number of samples are extracted to yield the same number of eluates ready for analysis.

On-line serial automation is common, in which a sample is extracted then injected by the instrument and, while analysis is ongoing, the next sample is extracted. Miniaturization of SPE allows the convenient use of smaller sample sizes and the ability to physically work with eluates as small as 50 µL when using the disc format.

The SPE technique has been shown to be useful for a variety of sample matrices, including (but not limited to): drinking water and river water, air, biological fluids (e.g., blood, serum, plasma, urine), tissues, peptides, drug formulations, microbial broths, animal feed, beverages, fruits and vegetables, and soil. Thus, the number of applications for this sample preparation technique in the literature is extensive and can be found spanning the last 25 years. It is the goal of this chapter to highlight many of the applications of SPE for a variety of sample matrices and demonstrate the versatility and usefulness of this sample preparation technique (Table 1).

Table 1 Examples of classical analytical applications using solid-phase extraction

<i>Market</i>	<i>Application</i>
Environmental	Trace enrichment of organic pollutants from water
	Organic acids, detergents and surfactants from water
	Insecticides and pesticides from soil
	Explosives residues in groundwater
	Oil and grease analysis
Food	Pesticides in fruits and vegetables
	Sodium benzoate in colas and fruit juice
	Plant growth regulators in spinach juice
	Toxic fungal metabolites in rodent feed
	Vitamins in food
	Cholesterol oxidation products in milkfat
	Caffeine in beverages
Biotechnology	β-Agonists and antibiotics in meat products
	Purification and fractionation of proteins and peptides
	Desalting of peptides
	Purification of DNA from microbial broths
Pharmaceutical	Antibiotic content in ointments
	Aspirin content in tablets
	Drugs in serum, plasma and urine
Clinical	Catecholamines in plasma and urine
	Lipids in serum
	Drugs in tissues
	Vitamins and steroids in serum
	Cyclosporin in blood

Environmental Applications

Trace Enrichment from Environmental Samples

The gas and liquid chromatographic analyses of polar pollutants in waters (e.g. for drinking, river and effluent) require a concentration step before analysis to determine part-per-million levels and lower, as regulations specify. Solid-phase extraction is the most widely used technique for trace enrichment of polar environmental pollutants since it uses low volumes of hazardous organic solvent, can be automated using cartridges and discs, and the analysis can be done either off-line in batches or on-line with the chromatographic system.

Typically, 1 L volumes of water samples are required for analysis in the United States, as mandated by the Environmental Protection Agency (EPA). Hydrophobic C18 and C8 sorbents are commonly used for the majority of trace enrichment needs; the analyte structure dictates the optimal sorbent chemistry. Practical considerations for passing 1 L of water through a SPE cartridge favour the use of larger diameter (47 or 90 mm) discs (e.g. glass fibre and PTFE-based) for these applications. While both discs and cartridges can be automated, discs are preferred for their much larger cross-sectional surface area. Using discs, liquid can be passed through at high flow rates without loss of analyte, thus reducing the extraction time to about 10–15 min instead of about 1 h for narrower cartridges.

Aqueous samples (100 mL to 1 L) containing organochlorine pesticides (e.g. lindane, methoxychlor, or endosulfan) can be concentrated from water, made acidic by using C18 bonded silica in 47 mm discs. Elution from the sorbent is accomplished using 3–5 mL aliquots of ethyl acetate, from which water is removed in a separate step using anhydrous sodium sulfate, it is then concentrated before analysis using gas chromatography (GC) with electron capture detection (ECD). Polyaromatic hydrocarbons (e.g. phenanthrene, pyrene, anthracene), organophosphorous pesticides (e.g. diazinon, methyl parathion), and herbicides (e.g. atrazine, alachlor) may be analysed in a similar manner using C18 sorbent and ethyl acetate elution from discs prior to GC analysis.

Phenols and chlorinated phenols are moderately polar compounds that can display ionic character at pH values above 7. Another group of polar compounds displaying ionic character is the acid herbicides (e.g. 2,4-dichlorophenoxyacetic acid, 2,4,5-trichlorophenoxyacetic acid and dicamba). Rather than C18 bonded silica, a more efficient sorbent for extraction of these types of compounds is polystyrene divinylbenzene (SDB), an organic polymer. SDB has

a slightly different selectivity than C18, owing to its aromaticity, that allows it to extend its range of attraction to include more polar species such as phenols. Other advantages of SDB are that it is totally organic, is stable across the entire pH range, and has greater capacity per gram than comparable reversed-phase bonded silica sorbents. Extraction of these phenols is performed with a SDB disc (or cartridge). Elution from the sorbent is accomplished using 3–5 mL aliquots of acetonitrile (methanol or acetone may be substituted) before analysis.

Diquat and paraquat are examples of polar compounds that are quaternary amines, thus always positively charged. These analytes are found only in very small concentrations in water, since they more readily attract to soils and plants via their cationic functionality. They can be concentrated from water on a cyano sorbent or some types of C8 sorbent, those that have a high degree of residual silanols available for attraction of cationic species. The extraction method for C8 includes an ion-pairing agent, to which paraquat and diquat bind. Elution with 5 mL methanol containing acid and diethylamine disrupts this binding; analysis is by HPLC. Table 2 lists examples of USA EPA methods employing disc solid-phase extraction.

On-Line Techniques

While SPE is a successful technique performed in batch mode before the analysis step, there can be drawbacks such as loss of sensitivity (only an aliquot of the total mass isolated is used), losses due to evaporation or during transfer and contamination from external sources. Instrumentation has now advanced to allow for on-line trace enrichment, where the sample eluent is injected onto a high-pressure liquid chromatography (HPLC) apparatus. The sample can be isolated on a guard column while the HPLC is running the previous sample, so time is not lost between isolation and analysis. The cartridge performing the extraction on-line, coupled to a liquid chromatographic system, can be commercially bought, such as the PROSPEKT system (Spark Holland) or constructed by hand using Empore® (3M Company) membrane extraction discs placed into a holder (4.6 mm internal diameter). Multi-residue methods that extract a variety of pesticides (acidic, neutral and basic) from waters are commonly used. In order to preconcentrate all these compounds simultaneously, it is necessary in most cases to acidify the sample and use a C18 bonded silica or polymer-based SDB sorbent in series with a cation exchanger. In order to avoid rapidly overloading the cation exchanger with samples of high ionic strength, calcium ions are first precipitated

Table 2 United States Environmental Protection Agency EPA methods allowing the use of solid-phase extraction for sample preparation

<i>Method number</i>	<i>Analytes</i>	<i>Sorbent</i>	<i>Analysis technique^a</i>
506	Phthalate and adipate esters in drinking water	C18	GC/PID
507	Nitrogen and phosphorous containing pesticides in water	C18	GC/NPD
508	Chlorinated herbicides and organochlorine pesticides in water	C18	GC/ECD
513	TCDD (2,3,7,8-tetrachlorodibenzo- <i>p</i> -dioxin) in drinking water	C18	GC/MS
515.2	Chlorinated acids in water	SDB	GC/ECD
525.1	Organic compounds in drinking water	C18	GC/MS
548.1	Endothall	Strong anion exchange	GC/MS
549.1	Diquat and paraquat in drinking water	C18, C8 or strong cation exchange	HPLC/UV
550.1	Polycyclic aromatic hydrocarbons (PAH) in drinking water	C18	HPLC/UV and fluorescence
552.1	Haloacetic acids and dalapon in drinking water	Strong anion exchange	GC/ECD
553	Benzidines and nitrogen containing pesticides in water	C18	HPLC/MS
554	Ozonation disinfection by-products (carbonyl compounds)	C18	HPLC
1613 Revision B	Tetra- to octa-chlorinated dioxins and furans	C18	HRGC/HRMS
1664	Oil and grease	C18	Gravimetric and infrared
3535 (SW846)	Organochlorine pesticides and phthalate esters from groundwater, wastewater and TCLP leachates	C18, SDB	Various GC/ECD techniques

^aAbbreviations: GC, gas chromatography; PID, photoionization detector; ECD, electron-capture detector; MS, mass spectrometry; HPLC, high-performance liquid chromatography; UV, ultraviolet, HRMS, high resolution mass spectrometry.

with oxalic acid and heavy metals are complexed with ethylenediaminetetraacetic acid (EDTA) prior to SPE. SPE cartridges on-line are sometimes preloaded with sodium dodecyl sulfate (SDS) to improve retention of basic pollutants at low pH.

Organic Acids Found in the Environment

The trace determination of EDTA in environmental water samples is an example of an analytical challenge – one in which the analyte readily chelates with metals, is very water soluble and is an organic acid. EDTA is commonly used in the clean-up of radioactivity and heavy metal wastes, and is also found in the environment as a detergent and water softening agent. Chelation of EDTA with toxic metals facilitates the migration of these hazardous materials from ground dumps into a water-soluble state where they can be transported into lakes, rivers and streams. The sample preparation technique of choice for EDTA is SPE since it improves detection limits compared with other techniques and can be fully automated. The lowest detection limits ($0.15 \mu\text{g L}^{-1}$, five times lower than previously reported methods using GC-mass spectrometry (MS) and HPLC) have been obtained using capillary electrophoresis (CE) with ion-spray

tandem mass spectrometry (MS-MS) for selective detection.

The sample preparation of EDTA from water samples (5 mL) involves conversion of all free and chelated EDTA present into the nickel EDTA chelate by adding $100 \mu\text{L Ni}(\text{NO}_3)_2$ at a pH from 7–9. The pH is then adjusted to about 3.0 using about $12 \mu\text{L}$ of 9% formic acid. This sample is added to preconditioned strong anion exchange solid-phase extraction cartridges (SPEC® (Ansys Diagnostics glass fibre disc cartridges). Wash solvents used (in order) are water (adjusted to pH 3.0 with formic acid), water (neutral pH), and methanol. Finally, the NiEDTA is eluted using a solution of 50 mM trifluoroacetic acid, 1 mM bromothymol blue and 5% methanol. The eluate is evaporated to dryness, reconstituted in 0.1% ammonium hydroxide, evaporated to dryness again, and then reconstituted in $30 \mu\text{L}$ water for analysis. This extract is then analysed by CE-MS. The strongly acidic elution solvent dissociates the NiEDTA complex, while bromothymol blue displaces the remaining NiEDTA from the disc. Reconstitution in ammonium hydroxide facilitates the re-complexation of the NiEDTA.

Food Applications

Pesticides in Food

Food applications using SPE present complexities that are not encountered in water extractions. Substances such as apples, lettuce, tomatoes and strawberries have tissue components that must be removed before extraction, and the analytes within the tissue fluids must be made available for extraction or removal prior to analysis. Multiple pesticides are commonly analysed in food crops. One popular multi-residue screening technique is the Luke II method, in which a crop sample (100 g) is homogenized with a water-miscible solvent (acetone). However, other crop materials that have solubility in acetone are also extracted. The solvent and water from the crop are then filtered and the filtrate subjected to a series of liquid-liquid partitioning extractions. The resulting mixture is subjected to two or more SPE packed cartridge (or disc) clean-up steps using sorbents with varying selectivity to remove co-extracted materials while pesticides pass through. Use of SPE techniques within this method allows for reduced solvent use and improved throughput.

A variation of this approach described uses SPE discs with reversed-phase sorbents (SDB-RPS disc stacked on top of a carbon disc; 3M Company) to capture the pesticides, rather than the co-extracted substances that often use normal-phase sorbents. This disc procedure is as follows. A 100 g sample of each crop material is mechanically blended with 100 mL acetone. The puree is filtered through a glass fibre filter and three 10-mL aliquots (10 g crop equivalent, wet weight) of each filtrate are transferred to centrifuge tubes, and the volume is reduced under nitrogen to about 5 mL. Water is added to adjust volume to 15 mL. SPE discs are conditioned with acetone, followed (in order) by ethyl acetate, methanol, then water. Samples are filtered through each disc. When the entire sample has been extracted, the discs are removed and inverted, so that SDB-RPS is on the bottom and carbon on the top. Elution is accomplished with 2 mL acetone, followed by two successive 5-mL aliquots of ethyl acetate. The eluent is dried using anhydrous sodium sulfate, then concentrated by evaporation to 5 mL volume, and analysed by GC-ECD. The combination of SDB-RPS and carbon sorbent chemistries for the extraction is superior to reversed-phase bonded silica sorbents to extend the range of attraction to the more polar pesticides with high water solubility, namely dimethoate, *o*-methoate and methamidophos. SDB-RPS contains the SDB chemistry but because of the nature of sulfonic acid groups bonded on the SDB surface it captures cationic moieties also. Carbon is used to capture

analytes not retaining on SDB-RPS. By reversing the order of sorbents for elution, the pesticides never come in contact with the carbon and are quantitatively recovered.

β -Agonists in Cattle Meat

β_2 -Agonists (e.g. clenbuterol, brombuterol, mabuterol and mapenterol), originally developed for treatment of chronic obstructive pulmonary diseases in humans, have been misused as a repartitioning agent in the fattening of cattle. When cattle are treated, residues may remain in the meat and liver. In order to monitor regulatory bans on use of these drugs in cattle, samples are removed at slaughterhouses and analysed for the presence of these illegal growth promoters. Urine is the matrix most commonly used for the analysis of these β -agonist drugs. Solid-phase extraction has been shown to be an effective technique for these drugs, using reversed-phase or mixed-mode sorbents (containing both reversed phase and cation exchange functionalities). The SPE procedure adds 1 mL 0.5 M potassium phosphate buffer pH 4.0 to 5 mL urine, followed by centrifugation. A mixed-mode sorbent bed is conditioned with methanol, water, then 0.1 M potassium phosphate buffer pH 4.0. The sample is loaded onto the cartridge, followed by a wash solvent of 70% methanol in water. After drying the cartridge, elution is accomplished with ethanol-*n*-hexane-ammonium hydroxide (70 : 25 : 5, v/v/v) in two sequential portions. Solvent is evaporated under nitrogen and heat and reconstituted in 25% acetonitrile in water for HPLC analysis.

Biotechnology Applications

Purification and Fractionation of Proteins and Peptides

Proteins are significant components of most physiological samples. It is often important to measure very low concentrations of specific peptides in biological fluids for diagnosis of disease states and to investigate physiological roles of certain peptides. Examples include examining the role of atrial natriuretic peptide in cardiovascular disease, studying β -endorphins involved in the neurochemistry of the brain, and isolating lymphokines to monitor their effect on immune system regulation. The quantification of a peptide such as casein in milk products is an application in the food area requiring isolation and purification. Solid-phase extraction is commonly used as a preliminary purification step to remove cross-reacting or interfering materials in sample matrices before analysis.

One common approach to purifying hydrophilic proteins or peptides is to fractionate crude proteinaceous extracts and remove hydrophobic proteins. Proteins above 15–20 000 molecular weight are usually too large and cannot easily enter the pores of typical 60–100 Å bonded silica particles. Thus, these large proteins pass unretained through reversed-phase sorbents and can be effectively eliminated from the analyte in this manner. The procedure is as follows. The sample is loaded onto the SPE column in an aqueous buffer, then washed with dilute aqueous acid (e.g. 0.1% trifluoroacetic acid, TFA) to remove salts and low molecular weight contaminants. Peptide analytes of interest are eluted with a mixture of organic solvent (acetonitrile or propanol) in water containing 0.1% TFA. The SPE sorbents useful for peptide retention, in increasing order of hydrophobicity, can generally be stated as cyano < C2 < phenyl < cyclohexyl < C8 < C18. Very polar peptides should be isolated using sorbents with a high retention ability such as C8 or C18. Very hydrophobic peptides could be isolated with a less retentive sorbent such as cyano or C2. Medium and highly hydrophobic peptides could be efficiently isolated and fractionated with phenyl and cyclohexyl sorbents.

SPE based on ionic interaction of proteins can efficiently fractionate peptide mixtures into neutral, acidic and basic pools. In ion exchange chromatography, adsorption of proteins depends on the protein's isoelectric point relative to the column pH. Proteins with a high isoelectric point will bind tightly to a cation exchange column in the presence of a low pH and a low salt concentration. Proteins with a high isoelectric point will bind tightly to a cation exchange column in the presence of a low pH and a low salt concentration. Proteins with a low isoelectric point will bind tightly to an anion exchange column in the presence of a high pH and a low salt concentration. Hydrophobic interaction chromatography uses a high salt concentration to induce an interaction between hydrophobic regions of a protein and a weakly hydrophobic column packing. In all three cases, elution of the bound proteins can be achieved using a salt gradient.

On-Line Preconcentration using SPE

The techniques of CE and on-line CE-MS have been widely documented for the analysis of therapeutically important peptides of diverse nature. A limitation of CE is that it works best for small sample volumes (typically < 50 nL for a 50 µm internal diameter capillary). This volume restriction leads to a poor concentration limit of detection (CLOD) when compared with typical HPLC and

LC-MS systems. The incorporation of a membrane preconcentration cartridge (containing SPE in a membrane format) in-line with the CE capillary has allowed the introduction of much larger sample volumes (e.g. 100 µL), lowering the CLOD. Typical materials used for the preconcentration are reversed-phase sorbents, such as SDB and C18 bonded silica. This technique has allowed the analysis of biomolecules present in complex matrices, such as proteins in aqueous humour.

Pharmaceutical Applications

Bacitracin Extraction from a Pharmaceutical Ointment

Bacitracin ointment, an oily pharmaceutical formulation, is a mixture of at least nine antibiotic polypeptide complexes. These peptides are very polar and soluble in water and ethanol, but not in acetone or hexane. They can be separated from the ointment base by adding chloroform to the sample matrix, and the polar peptide antibiotics are adsorbed to a polar diol SPE column. Upon addition of the matrix to the column, the nonpolar solvent and ointment products pass through. A wash of chloroform removes potentially interfering components of the formulation. Antibiotics are removed from the sorbent using 0.1N HCl; protons from the acid displace the drugs from the hydroxyl groups on bonded silica surface. This technique can be useful for other drug substances by optimizing the SPE conditions for the properties of the drug and excipients, and selecting the appropriate sorbent and eluent systems.

Analysis of Aspirin Content in Tablets

Aspirin can be analysed for content in tablets by using a mixed mode sorbent containing both anion exchange and reversed-phase characteristics. Polysorb MP-2 (Interaction) polymer is a cross-linked vinylpyridine. At low pH the polymer is protonated and exhibits anion exchange and reversed-phase properties. At high pH, the polymer is neutralized and exhibits only reversed-phase properties. The sorbent is conditioned with acid/organic 10/90 (v/v) to induce polymer ionization. After sample loading, the sorbent is washed with 20–50% acetonitrile/water to neutralize the sorbent bed prior to elution of bound aspirin. Elution is accomplished with acetonitrile 30% NH₄OH–30 mM diammonium sulfate monohydrate (6 : 2 : 1, v/v/v). The polymer becomes neutral at this basic pH > 12.9 and aspirin remains ionized, disrupting its interaction with the sorbent and eluting. Salt acts as counteranion to further assist in the elution of aspirin.

Clinical Applications

Catecholamines from Plasma and Urine

Catecholamines (e.g. dopamine, epinephrine and norepinephrine) are of clinical interest for their role in neurochemistry as diagnostic indicators of pheochromocytoma. These dihydroxylated amines are commonly analysed by HPLC with electrochemical detection. Many different SPE sorbents have been reported for their sample preparation. Alumina particles (about 50 mg) are added to plasma and buffer in a suspension, followed by centrifugation and subsequent elution from alumina. Reversed-phase C18 has also been used, as well as phenylboronic acid and strong cation exchange (SCX). The urine analysis of catecholamines examines metabolites such as vanillylmandelic acid and homovanillic acid. Typically, solid-phase extraction (SPE) uses SCX sorbent to provide cleaner chromatograms, either alone or in addition to alumina or phenylboronic acid.

Lipids

The extraction of lipids, including phospholipids, fatty acids, cholesterol, cholesteryl ester, and triglycerides in serum has been accomplished using polar SPE sorbents such as silica and aminopropyl. The sample matrix is extracted with a nonpolar solvent such as chloroform, and this extract is passed through a preconditioned polar aminopropyl sorbent for attraction of analytes by hydrogen bonding and weak ion exchange mechanisms. Neutral lipids are eluted with chloroform–propanol (2:1, v/v), fatty acids are eluted with 2% acetic acid in diethyl ether, and phospholipids are eluted with methanol. The neutral lipid fraction is evaporated and reconstituted in hexane. The hexane mixture is then passed through a second amino SPE column. The cholesteryl esters are eluted with hexane, with the second column in series with the first column to trap cholesterol, which elutes with triglycerides. Triglycerides are eluted with hexane–diethyl ether–methylene chloride (89 : 1 : 11, v/v). The two amino columns are separated and cholesterol is eluted from both – di- and mono-glycerides elute from the upper amino column. Cholesterol is eluted with 5% ethyl acetate in hexane, diglycerides are eluted with 15% ethyl acetate in hexane and monoglycerides are eluted with chloroform–methanol (2 : 1, v/v).

Drugs in Tissues

The majority of reported methods for drug extraction involve plasma, serum, urine or other polar fluids that can easily pass through SPE cartridges. However, blood and tissue extraction applications have not

been reported with much frequency in the published literature. The extraction of drugs from tissues, such as liver, kidney, intestine, brain, muscle and adipose tissue is important for the forensic toxicologist, in particular, since urine and blood are not available in post-mortem cases. Concentrations of drugs in tissues are also of great interest to researchers investigating the deposition of drugs in certain tissues (e.g. ophthalmic drug delivery into the eye and delivery of antidepressant drugs into the brain).

Drug extraction from tissues involves first homogenization of the tissue with aqueous solution. After homogenization, an enzyme digestion (e.g. Carlsberg subtilisin, lipase or protease) step and/or protein precipitation can be used, followed by centrifugation. Sometimes a small percentage (10–20%) of organic solvent (e.g. methanol) is added to the water or buffer for homogenization, and the solution is passed through an SPE cartridge. Alternatively, 100% methanol or acetonitrile can be used and, after centrifugation, the solvent is evaporated, reconstituted in aqueous solution or buffer, and passed through an SPE cartridge. In addition to typical SPE sorbents, diatomaceous earth is another choice for the analyst; it facilitates a liquid–liquid extraction by attracting analytes to the particles to increase surface area available for extraction when an organic solvent is passed through the diatomaceous earth column. The use of ‘high-flow’ SPE columns is now a reality owing to larger particle-size sorbents in columns, typically 100–120 µm particle sizes instead of 40–60 µm.

Conclusion

Solid-phase extraction has been demonstrated to be a reliable and cost-effective technique for the selective isolation and concentration of a wide range of analytes and sample matrices, and offers many improvements over traditional techniques such as liquid–liquid extraction. Some of the classic applications for SPE include environmental trace enrichment of organic pollutants, extraction of pesticides and growth promoters from foods, purification of peptides, drug analysis in pharmaceutical dosage forms and clinical applications for drugs in physiological matrices. Its ability to solve sample preparation problems has been well documented in the literature over the past two decades. There is a wide choice of sorbents for SPE, including nonpolar, polar, ion exchange and mixed mode chemistries, providing the analyst with the selectivity necessary to obtain clean extracts for analysis. SPE can be used either manually or with greater throughput using automated workstations. The introduction of new sorbents with more selective modes of attraction, novel product formats

such as the SPE disc, and the proliferation of automated techniques for performing the extractions, ensure that SPE will continue to be a preferred technique for sample preparation in many different analytical disciplines.

See also: II/Extraction: Solid-Phase Extraction. III/Solid-Phase Extraction with Discs.

Further Reading

- Berrueta LA, Gallo B and Vicente F (1995) A review of solid-phase extraction: basic principles and new developments. *Chromatographia* 40(7/8): 474–483.
- Guzman NA, Park SS, Schaufelberger D *et al.* (1997) Review: new approaches in clinical chemistry: on-line analyte concentration and microreaction capillary electrophoresis for the determination of drugs, metabolic

- intermediates and biopolymers in biological fluids. *Journal of Chromatography B* 697: 37–66.
- Hurst WJ (1996) Bonded solid-phase extraction for the sample preparation of food materials. *Seminars in Food Analysis* 1(1): 3–9.
- Koester CJ and Clement RE (1993) Analysis of drinking water for trace organics. *Critical Reviews in Analytical Chemistry* 24(4): 263–316.
- Krishnan TR and Ibrahim I (1994) Solid phase extraction technique for the analysis of biological samples. *Journal of Pharmaceutical and Biomedical Analysis* 12(3): 287–294.
- Scheurer J and Moore CM (1992) Solid-phase extraction of drugs from biological tissues – a review. *Journal of Analytical Toxicology* 16: 264–269.
- Thurman EM and Mills MS (1998) *Solid-Phase Extraction: Principles in Practice*, pp. 161–195. New York: John Wiley & Sons.

SOLID-PHASE EXTRACTION WITH DISCS



C. F. Poole, Wayne State University, Detroit, MI, USA

Copyright © 2000 Academic Press

Introduction

Solid-phase extraction is a well-established technique for the isolation, concentration and matrix simplification of analytes in samples with unfavorable properties for direct analysis by the best available approach. Extraction is achieved using a particulate sorbent packed into columns of short length (sometimes called ‘cartridges’) or immobilized in the form of a thin disc, referred to generically as ‘disc technology’. Since the same sorbent chemistry is used for the extraction step and liquid desorption for the elution step in both approaches, the two techniques differ only in format. On an evolutionary scale, solid-phase extraction using short columns was introduced as a laboratory-scale technique in the late 1970s and came to prominence in the 1980s. Disc technology, by comparison, was first introduced in 1989, and is still evolving as a competitive technique to short packed columns. Simply stated, disc technology should be viewed as an alternative approach to performing solid-phase extraction with additional benefits and capabilities derived from the difference in format. Whereas packed columns are easily prepared in the laboratory for evaluating new sorbent chemistries and evaluating sampling properties, discs, so far,

have only been produced in a manufacturing setting. Consequently, sorbent selection and device optimization have been restricted by market-driven considerations. As a consequence, the main applications of disc technology are generally narrowly focused on the needs of large volume users more so than is the case for conventional short packed columns.

Disc Formats

Solid-phase extraction discs are available in different styles and sizes. Particle-loaded membranes (Empore™ discs) contain 8–12 µm sorbent particles homogeneously distributed in a web of short poly(tetrafluoroethylene) (PTFE) fibrils. These are formed into 0.5-mm thick discs with diameters from 4 to 96 mm. They are flexible and superficially resemble filter paper discs. They are used with some supporting structure such as a fritted glass filter or porous plastic support. The discs contain about 90% by weight of sorbent with the balance being the PTFE microfibrils. Some characteristic physical properties are indicated in Table 1. Particle-loaded membranes are also available in a syringe barrel format similar to conventional short packed column-sampling devices. In this case, the sorbent bed contains particles of a larger diameter, about 50 µm, in thicker discs, about 1.0 mm, sealed into the base of a 4 mm (1 mL), 7 mm (3 mL), 10 mm (6 mL) and 20 mm diameter (40 mL) open syringe barrel. These discs have an integral prefilter consisting of a graded density of poly(propylene)

Table 1 Rough guide to the physical properties of solid-phase extraction disc according to disc diameter

Property	4 mm	7 mm	10 mm	25 mm	47 mm	90 mm
Surface area (cm ²)	0.13	0.38	0.80	4.9	17	64
Bed mass (mg) ^a	4	10	25	140	500	1850
Flow rate (mL min ⁻¹)	0.5	1.5	3	20	60	250
Elution volume (mL)	0.15	0.25	0.5	3	10	35
Typical sample volume (mL)	< 1	< 5	< 25	< 250	< 1000	< 5000

^aSilica-based sorbents.

microfibrils on the top sampling surface. They are recommended as a replacement for short packed column-sampling devices as well as for processing small volumes of viscous biological fluids. Particle-embedded glass fibre discs (SPECTM discs) contain particles of a narrow size distribution, about 10–30- μ m diameter, woven into a glass fibre-supporting matrix. The smaller diameter discs are rigid and self-supporting but large-diameter discs require a supporting structure similar to the particle-loaded membranes. Particle-embedded glass fibre discs are also available with a depth filter region of 0.1–0.2 mm combined with a sorbent extraction region of 0.8–0.9-mm thickness. Laminar discs (SpeedisksTM) contain 10 μ m sorbent particles in a consolidated 0.5- or 1-mm thick bed (usually) retained by two glass-fibre filters held in place by screens and a retaining ring in a preassembled cartridge with a 50-mm diameter sampling area. This configuration is designed to provide high sample flow rates for extracting large volumes of water.

Solid-phase extraction discs are available as loose discs for use in filtration-style apparatus for large volume samples and in open syringe barrels and cartridges for extracting intermediate and small sample volumes. These forms are compatible with sample processing using suction, positive pressure, syringe filtration and centrifugation. Common sorbents include octadecylsiloxane- and octylsiloxane-bonded silica particles, styrene-divinylbenzene porous polymers, porous polymer and silica-based cation and anion exchangers, mixed mode sorbents, activated carbon and immobilized crown ether sorbents. Other sorbents could easily be produced in a disc format if a sufficient market to support their production could be identified. Solid-phase extraction discs have been used primarily for sample preparation prior to chromatographic analysis. The disc format supports other, if minor applications at present, such as *in situ* detection using radioactivity counting, phosphorescence, and matrix-induced laser desorption mass spectrometry, etc. SPECTM discs can be inserted directly into a hole in a glass fibre thin-layer sheet and developed in a conventional manner combining recovery and separation into a single step. This ap-

proach is commonly used for toxicological screening of biological fluids.

Advantages of Disc Technology

The change in format from a short packed column to a disc has some attendant advantages for solid-phase extraction. These can be briefly summarized as follows. The larger cross-sectional area of discs and decreased pressure drop compared to conventional column-like sampling devices results in shorter sample processing times and decreased plugging by suspended particle matter. This is important in environmental surveillance programmes, such as the analysis of surface waters for persistent or toxic substances, where large sample sizes are common to obtain adequate detection limits and samples are often burdened by suspended particle matter. The large surface area per unit bed mass of the discs facilitates passive sampling approaches to solid-phase extraction and related uses as an indirect monitor of bioconcentration (discussed later).

The use of smaller diameter sorbent particles and the greater stability of the sorbent bed results in improved kinetic performance and reduced channeling. This allows the use of a smaller bed mass for extraction and results in less variation between sampling devices. The reduced bed mass provides cleaner sample backgrounds and lower interferences by minimizing nonspecific matrix adsorption. Smaller bed masses allow miniaturization of sampling devices for convenient handling of small sample sizes together with smaller elution volumes for analyte recovery. They also facilitate novel sampling approaches such as in-vial elution and on-disc derivatization (discussed later).

Kinetic Characteristics

Forced-flow planar chromatography has been used to study the kinetic properties of octadecylsiloxane-bonded silica particle-loaded membranes and particle-embedded glass fibre discs (Table 2). The total porosity of the discs is about 0.50, comprised mainly of interparticle porosity (about 0.40) with a large

Table 2 Kinetic properties of octadecylsiloxane-bonded silica solid-phase extraction discs

Property	Particle-loaded membranes	Particle-embedded glass fibre discs
Total porosity	0.52–0.54	0.51
Interparticle porosity	0.37–0.48	0.47
Intraparticle porosity	0.06–0.15	0.04
Specific permeability (10^{-14} m^{-2})	2.2–2.5	8.4
Flow resistance parameter	1000–1250	900–1000
Apparent particle size (μm)	5.8–7.7	15.3
Nominal pore diameter (nm)	6	8
Minimum plate height (μm)	56	
Optimum mobile phase velocity (mm s^{-1})	0.13	
<i>Coefficients for Knox equation</i>		
A	3.75 (0.5–1.5 for columns)	
B	1.72 (1.0–4.0 for columns)	
C	1.54 (0.05–0.7 for columns)	

fraction of the particle pore volume inaccessible to the mobile phase. This is not unusual for porous silica sorbents with a high loading of bonded phase restricting access to the pore volume. It is also compatible with the desire for a high sorption capacity and is not necessarily an undesirable feature. The specific permeability and flow resistance parameter support the hypothesis that the disc structure is homogeneous and devoid of through pores (holes), an essential requirement for a thin sampling medium. The apparent particle size for the particle-loaded membranes, about $7 \mu\text{m}$, and particle-embedded glass fibre discs, about $15 \mu\text{m}$, are in reasonable agreement with the manufacturers' claims given the assumptions used in calculations for converting the pressure–flow relationships to particle size values. The particle-loaded membrane provides an optimum plate height of $56 \mu\text{m}$ at a linear velocity of 0.13 mm s^{-1} . A 0.5-mm disc of 47-mm diameter will provide between 4 and 9 theoretical plates over the flow rate range of $5\text{--}100 \text{ mL min}^{-1}$ with a maximum value at 13 mL min^{-1} . Compared to typical slurry-packed columns, the contribution of both flow anisotropy and resistance to mass transfer to the plate height are unusually large for the particle-loaded membranes, and while the bed may have an homogeneous structure, it does not have an ideal kinetic structure. Fortunately, large plate numbers are not required for efficient extraction.

Disc Selection

The parameters of interest in selecting a disc for a particular application are size, sorbent chemistry and sample capacity. Referring to Table 2, large-diameter discs are used for processing large sample volumes to improve sample throughput. Small-diameter discs are used for processing small sample volumes and to recover analytes in a small solvent volume to eliminate the need for solvent evaporation

prior to analysis. Small-diameter discs are frequently used in clinical, forensic and pharmaceutical analysis and large-diameter discs in environmental analysis. The same sorbents used for conventional solid-phase extraction are generally used for disc extraction, but since discs are used for a narrower range of applications at present, the number of frequently used sorbent types is smaller (Table 3). The majority of applications proposed to date involve sampling of aqueous solutions. Octadecylsiloxane-bonded silica, poly(styrene-divinylbenzene) and activated carbon sorbents are used for general reversed-phase sampling; porous polymer and silica-based cation and anion exchangers are used for isolating ionizable and ionic compounds; and chelating ligands for the selective isolation of metals (particularly precious metals and radionuclides). Discs with different sorbent chemistries can be stacked on top of each other and analytes recovered in a single elution or as groups after physically separating the discs. Stacked discs of the same or varied sorbent chemistry are useful for extracting complex samples containing compounds that differ significantly in polarity or ionization, for achieving larger breakthrough volumes, and as an approach for reducing interferences by the selective sorption of the matrix by one disc and the analytes by the other. Stacked discs of a reversed-phase and cation exchange type are a suitable alternative to mixed-mode sorbents for isolating drugs and their metabolites from biological fluids. Discs containing porous polymer sorbents have been proposed for air sampling, particularly as a replacement for poly(urethane) foams, but have not been widely adopted.

In recent years, disc-based solid-phase extraction has become a popular technique for sample cleanup in ion chromatography and capillary electrophoresis. The interfering ions, often at relatively high concentrations, can mask, broaden or change the migration time of the ions of interest. The Novo-CleanTM discs

Table 3 Sorbent selection for disc applications

<i>Sorbent</i>	<i>General applications</i>
Octadecylsiloxane- and octylsiloxane-bonded silica	Octadecylsiloxane-bonded sorbents are widely used for reversed-phase sampling by non-specific sorption (and are more widely used than octylsiloxane-bonded sorbents). There are many applications to the extraction of non-polar and moderately polar pesticides (all classes), herbicides, phthalate and adipate esters, polycyclic aromatic compounds, food additives, pharmaceutical compounds, hydrocarbons and grease, etc. from aqueous solution. A large number of approved methods for water analysis.
Poly(styrene-divinylbenzene)	Used for compounds poorly extracted by octadecylsiloxane-bonded silica sorbents because of high water solubility such as polar pesticides, herbicides, phenols and pharmaceutical compounds. Lightly sulfonated, acylated and hydroxymethylated polymers claimed to provide higher recovery of neutral polar compounds because of better surface compatibility with aqueous samples.
Activated carbon	Applications similar to poly(styrene-divinylbenzene) but less frequently used. Methods proposed for triazine herbicides, some polar pesticides and <i>N</i> -nitrosodialkylamines.
Mixed mode	Usually co-bonded octadecylsiloxane and benzenesulfonic acid groups (or sorbent mixtures) used predominantly in clinical toxicology and pharmaceutical analysis for the simultaneous isolation of drugs and their metabolites. A number of established methods for drugs of abuse (marijuana and cocaine metabolites, amphetamines, phencyclidine and opiates) in biological fluids.
Sulphonic acid and quaternary amine ion exchangers	Selective isolation of ionic and easily ionizable compounds. Many methods for acidic herbicides and pesticides in water and basic drugs in biological fluids. Porous polymer sorbents are stable over the whole pH range. Sulphonated cation exchange polymers in the hydrogen, silver or barium forms used for cleanup of samples analysed by ion chromatography and capillary electrophoresis.
Crown ethers	Silica or other support with tethered mixed oxygen–nitrogen donor cryptands used for the selective isolation of metals by molecular recognition mechanisms. Commonly used for the isolation of precious metals (Pd, Pt, Rh) and radionuclides (Cs, Sr, Pb) from high concentrations of other metals to determine environmental burden and for dating geochemistry samples. Other applications include the removal of base metal impurities (Bi, Sb, Fe, Pb, Bi, Cu, Hg) from refinery streams, plating baths, etc.

contain a sulfonic acid-functionalized resin in the hydrogen, silver or barium forms housed in a cartridge adapted for syringe filtration. The hydrogen form is used to remove hydroxide and carbonate ions from samples by neutralization. The silver form is used to remove excess halide ions from samples by formation of insoluble silver halide salts that precipitate in the disc matrix. **Figure 1** shows an example of the detection of nitrate, fluoride and phosphate in a hydrochloric acid digest of a paper coating by capillary electrophoresis. The barium form is used to remove sulfate through the formation of insoluble barium sulfate.

Sample Processing

A generic outline for processing aqueous samples using disc technology is presented in **Table 4**. This

can be rescaled for different disc and sample sizes using the data in Table 1. The sampling process begins with decontamination of the disc by rinsing with organic solvent to remove impurities followed by solvent conditioning to facilitate effective and reproducible sorption of the analytes. Before the sample is added to the disc the conditioning solvent is rinsed from the disc with water to avoid premature breakthrough of analytes. For large sample volumes, a small amount of organic solvent (1–5% v/v) is added to aqueous samples to maintain a constant sample velocity. This usually has little influence on the breakthrough volumes except for porous polymer sorbents with a low degree of crosslinking. The selective adsorption of organic solvent by the polymer changes the sorbent volume and selectivity, resulting in changes in the breakthrough volume of up to an order of magnitude when either methanol,

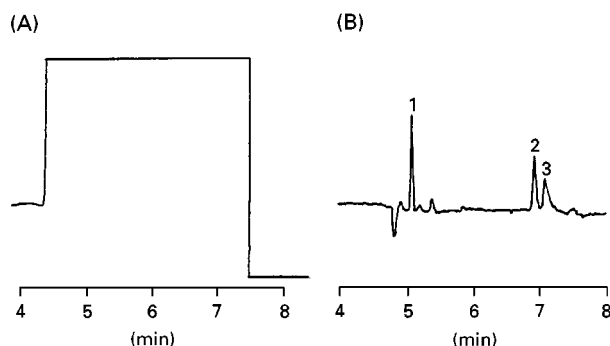


Figure 1 Separation of trace concentrations of nitrate (1), fluoride (2) and phosphate (3) anions (1–10 p.p.m.) from a hydrochloric acid digest of a paper coating without treatment (A) and after disc cleanup using a Novo-Clean IC-Ag disc (B) by capillary electrophoresis. (Reproduced with permission from Saari-Nordhaus R and Anderson JM (1995) Membrane-based solid-phase extraction as a sample clean-up technique for anion analysis by capillary electrophoresis. *Journal of Chromatography A* 706: 563–569. Copyright Elsevier Science.)

2-propanol, acetonitrile or tetrahydrofuran are used as sample processing solvents (Table 5). These results are not in any way artifactual and are adequately predicted by the solvation parameter model for the breakthrough volumes. A sample processing solvent is not usually required for small sample volumes. Viscous samples may be easier to handle if diluted with either water or an organic solvent to increase their sample-processing rate. Samples containing a significant amount of particulate matter should be either prefiltered, processed with a filter aid (cover the surface of the disc with 1 cm of 40- μ m glass beads), processed by using a combination of a disc with an integral depth filter, or processed after adjusting the pH to dissolve soluble particles. Weak acids and bases are extracted by ion exchange or by ion suppression reversed-phase sampling at a suitable pH.

Increasing the ionic strength of the sample (e.g. adding sodium chloride) may improve the extraction of neutral compounds in reversed-phase extractions. The drying stage is important because water retained by the disc (and the disc support structure) contaminates the elution solvent and may cause difficulty if the solvent is to be reduced in volume or the analytes analysed by gas chromatography. Water may also reduce the efficiency of the elution step, particularly for elution solvents only partially miscible with water. Discs are usually dried by suction, but other possibilities include freeze-drying or desiccation over a drying agent with or without vacuum. For silica-based sorbents, a masking agent such as triethylamine (1% v/v) is sometimes added to the eluting solvent to increase the recovery of basic compounds strongly retained by interaction with silanol groups. Supercritical fluid extraction with carbon dioxide has been used to recover analytes isolated by disc extraction from water. In this case, the discs were used for preconcentration and media exchange since supercritical fluid carbon dioxide provides a poor extraction medium for aqueous solutions.

Passive Sampling and Bioconcentration

Passive sampling involves the extraction of organic compounds by immersion of the sampling disc in aqueous samples as opposed to filtering samples through the extraction disc. This process is convenient but little explored. One reason is the slow equilibrium of the extraction process even for stirred solutions. The uptake of organic compounds in a stirred solution depends on the size of the disc, time and the degree of mixing. Uptake by the disc may never be complete in a reasonable time but greater than 80%

Table 4 Generic guide for sample processing using solid-phase extraction discs. In this example, a 47-mm disc and a 1-litre water sample are used for illustration

Decontamination	With disc installed in filtration apparatus (or cartridge) rinse with 10 mL of solvent (acetonitrile) by allowing the solvent to soak into the membrane for a few minutes and then remove by suction.
Condition	As above but using 10 mL of methanol. Before the last drop of methanol has been sucked through the disc, add 10 mL of deionized water. The disc should not be allowed to suck dry until after the sample has been processed. It may be necessary to break the vacuum for ease of manipulating solutions.
Sample	The sample containing 1% (v/v) methanol is passed through the disc with a suitable reservoir in place. Filter aid or a prefilter may be required for samples with a heavy burden of particulate matter. The sample is processed at a flow rate between about 50 and 100 mL min ⁻¹ using a vacuum of about 10–20 mmHg.
Drying	Bulk water is removed from the disc and sampling apparatus by sucking air through the disc under full vacuum for about 3 min. Volatile compounds may be lost.
Recovery	The analytes are recovered by passing two 5-mL volumes of acetonitrile through the disc. The first volume of acetonitrile is allowed to soak into the disc for a few minutes and then gently sucked through the disc. Without letting the disc run dry, the second volume of solvent is added to the disc and sucked through the disc. The disc is then allowed to suck dry.

Table 5 Breakthrough volumes (cm³) of some organic compounds on porous polymer particle-loaded membrane discs with 1% (v/v) organic solvent in water

Compound	Acetonitrile	Tetrahydrofuran	2-Propanol	Methanol
Anisole	575	300	1750	1300
Acetanilide	95	25	100	75
2-Phenylethanol	150	25	100	200
Heptan-1-ol	2700	300	2700	1000
Propyl propanoate	1400	200	1250	750

extraction of pesticides in an agitated 500 mL sample using a 47-mm diameter particle-loaded membrane in 24 h was reported. Octadecylsiloxane-bonded silica discs have been explored as surrogate models for bioconcentration. This process is referred to as 'biomimetic extraction' and is used to estimate the selective uptake of organic compounds by aquatic species. Biomimetic extraction results in the preferential concentration of the more hydrophobic compounds from water and is theorized to provide a more realistic approach to assessing environmental effects of soluble organic compounds than results obtained by total extraction techniques. Measurements are made using passive disc sampling under conditions that avoid sample depletion to emulate the sorption of organic compounds by aquatic species. This is a relatively new approach to toxicity assessment and requires further work to establish a satisfactory relationship between the sorption properties of the disc and those of target aquatic species.

In-Vial Elution and Derivatization

The in-vial elution method reduces the amount of organic solvent used for recovery and eliminates tedious sample-preparation steps compared to conventional methods. This technique is an equilibrium-based approach for the recovery of extracted analytes. After extraction, the dried disc is placed in an autosampler vial and covered with a few mL of solvent. Recovery depends on the selection of the solvent, temperature and equilibration time. An equilibration time of 4 h, or overnight, at room temperature is sufficient in many cases to provide acceptable recovery (> 90%) and method precision as well as being compatible with automated sample analysis in gas and liquid chromatography. Addition of a derivatizing reagent to the solvent used for desorption allows both steps to be performed simultaneously in the same vial without removal of the disc. The vial can be sealed and heated to enhance the rate of derivatization. Common reactions employed so far include trimethylsilylation and alkylation for gas chromatographic analysis but other reagents should be equally applicable. It was demonstrated that ion

exchange discs catalyse the rate of alkylation of acid herbicides, surfactants and pesticides using a solution of an alkyl iodide as the derivatizing reagent. An example is shown in Figure 2.

Preservation and Storage

Samples or their extracts frequently have to be stored between sampling and analysis. Compounds differ in their stability to various storage conditions. The degradation or loss of pesticides and other organic compounds stored in water is mainly due to hydrolysis, biodegradation, photolysis and evaporation. Solid-phase extraction discs provide a convenient storage medium for compounds recovered from natural waters. General results indicate that discs provide equivalent or greater stability to the storage of pesticides in water at 4°C containing inhibitors to reduce

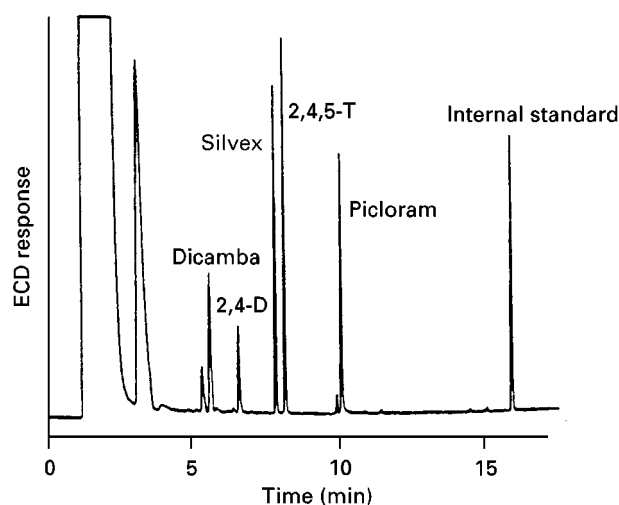


Figure 2 Use of in-vial elution and derivatization for the determination of chlorinated acid herbicides in an extract from a spiked (< 10 µg L⁻¹ each) river water sample by gas chromatography. A 500-mL sample was processed through a 25-mm strong anion-exchange disc, the disc dried by suction, sealed in an autosampler vial with 1 mL of acetonitrile and 0.2 mL of methyl iodide and heated at 80°C for 1 h, and excess methyl iodide removed by evaporation. (Reproduced with permission from Field JA and Monohan K (1996) Chlorinated acid herbicides in water by strong anion-exchange disc extraction and in-vial elution and derivatization. *Journal of Chromatography A* 741: 85–90. Copyright Elsevier Science.)

biodegradation. One of the primary mechanisms of disc degradation was identified as hydrolysis resulting from contact with water remaining in the disc after drying by suction. Stability was increased by desiccation of the discs. Stability has to be judged on an individual compound basis but discs provide a more efficient and convenient medium for extract preservation. Their low weight and small size make them a useful medium for shipping.

Automation and Multi-Well Formats

The introduction of solid-phase extraction discs occurred at a time when the automation of common laboratory process was very much in vogue for improving the quality of laboratory information and to reduce operating costs. Most disc extraction processes can be automated. Series-coupled filtration devices are popular for parallel processing of environmental water samples. Disc sampling devices in cartridge format are compatible with the automated and robotic workstations in use for automated sample preparation using conventional packed column formats. Multi-well microtitre plates have been adapted to disc extraction by incorporating the disc in the bottom of the well and using automated liquid-handling systems for high throughput extractions. This is achieved by a combination of automated parallel processing and eluent collection without volume reduction in a matching multi-well plate compatible with standard autoinjection devices. This approach meets the high sample throughputs demanded of current applications in bioanalysis and combinatorial chemistry for drug discovery. Short precolumns containing several discs stacked in series or packed with a spiral of particle-loaded membrane have been used for online extraction combined with liquid chromatography for pesticide monitoring of drinking and surface water samples. This is not an area that extraction discs dominate, and although useful and successful, clear advantages over short packed columns have not been demonstrated.

Future Developments

Most developments in disc technology are recent enough that they are still to some extent regarded as novel rather than routine laboratory tools. They are expected to continue to replace conventional short packed columns in those applications where the disc format has specific advantages. In addition, disc technology has already defined new opportunities for expansion of solid-phase extraction in passive sampling, storage and preservation of extracts, field sampling, and as an indirect indicator of bioconcentration.

Since discs are not laboratory-made products, the variety of disc chemistries available is linked to the identification of a viable market for a commercial product. For the present, this has tended to decouple efforts to promote disc technology from modern research on sorbent chemistry for the next generation of solid-phase extraction products.

See also: II/Extraction: Solid-Phase Extraction. III/Sorbent Selection for Solid-Phase Extraction.

Further Reading

- Barcelo D and Alpendurada MF (1996) A review of storage and preservation of polar pesticides in water samples. *Chromatographia* 42: 704–712.
- Beals DM, Britt WG, Bibler JP and Brooks DA (1998) Radionuclide analysis using solid-phase extraction discs. *Journal of Radioanalytical and Nuclear Chemistry* 236: 187–191.
- Degel F (1996) Comparison of new solid-phase extraction methods for chromatographic identification of drugs in clinical toxicological analysis. *Clinical Biochemistry* 29: 529–540.
- Fernando WPN, Larrivee ML and Poole CF (1993) Investigation of the kinetic properties of particle-loaded membranes for solid-phase extraction by forced flow planar chromatography. *Analytical Chemistry* 65: 588–595.
- Izatt RM, Bradshaw JS and Bruening RL (1996) Accomplishment of difficult chemical separations using solid phase extraction. *Pure and Applied Chemistry* 68: 1237–1241.
- Lingeman H and Hoekstra-Oussoren SJF (1997) Particle-loaded membranes for sample concentration and/or clean-up in bioanalysis. *Journal of Chromatography B* 689: 221–237.
- Mayer ML, Poole CF and Henry MP (1995) Sampling characteristics of octadecylsiloxane-bonded silica particle-embedded glass fibre discs for solid-phase extraction. *Journal of Chromatography A* 695: 267–277.
- Michor G, Carron J, Bruce S and Cancilla DA (1996) Analysis of 23 polynuclear aromatic hydrocarbons from natural water at the sub-ng L⁻¹ level using solid-phase extraction and mass-selective detection. *Journal of Chromatography A* 732: 85–99.
- Pichon V, Charpak M and Hennion M.-C (1998) Multi-residue analysis of pesticides using new laminar extraction discs and liquid chromatography and application to the French Priority List. *Journal of Chromatography A* 795: 83–92.
- Plumb RS, Gray RDM and Jones CM (1997) Use of reduced sorbent bed mass and disc membrane solid-phase extraction for the analysis of pharmaceutical compounds in biological fluids, with application in the 96-well format. *Journal of Chromatography B* 694: 123–133.
- Poole SK and Poole CF (1996) Influence of solvent effects on the breakthrough volume in solid-phase extraction

using porous polymer particle-loaded membranes. *Analyt* 120: 1733–1738.

Tomkins BA and Griest WH (1996) Determination of N-nitrosodimethylamine at part-per-trillion concentration in contaminated ground and drinking waters featuring carbon-based membrane extraction discs. *Analytical Chemistry* 68: 2533–2540.

Verbruggen EMJ, Van Loon WMGM, Tonkes M, Van Duijn P, Seinen W and Hermens JLM (1999) Biomimetic extraction as a tool to identify chemicals with high bioconcentration potential: an illustration by two fragrances in sewage treatment plant effluents and surface waters. *Environmental Science and Technology* 33: 801–806.

SOLID-PHASE EXTRACTION: SORBENT SELECTION

See III/SORBENT SELECTION FOR SOLID-PHASE EXTRACTION

SOLID-PHASE MATRIX DISPERSION: EXTRACTION



S. A. Barker, Louisiana State University,
Baton Rouge, LA, USA

Introduction

Matrix solid-phase dispersion (MSPD) is a patented analytical process for the preparation, extraction and fractionation of solid and/or viscous biological samples prior to instrumental or other forms of analysis. MSPD involves the direct mechanical blending of samples with standard solid-phase extraction (SPE) bonded-phase solid support materials. In this process, the bonded-phase support acts as both an abrasive to produce disruption of sample architecture and as a 'bound' solvent that assists in accomplishing sample disruption. The sample is dispersed over the surface of the bonded-phase support material, producing a unique mixed-character phase for conducting target analyte isolation. This process has been applied to the isolation of a wide range of drugs, pollutants and other compound classes from a variety of sample matrices. The factors affecting the use of MSPD and its applications for sample preparation, extraction and fractionation are addressed.

Development of MSPD

The classical application of all forms of liquid chromatography requires that the sample be applied in a liquid state to the head of the column. Thus, in order to accommodate the use of solid-phase extraction (SPE) columns and discs in the development of an analytical procedure, methodology must also be

developed to render the sample and target analytes contained therein into a liquid, relatively non-viscous, particulate-free and homogeneous condition. While some biological fluids are readily obtained in this form, most biological samples do not start out being directly applicable to SPE. This presents the analyst with some rather unique opportunities to apply or develop the best process for rendering a sample into a form compatible with liquid chromatography. Indeed, the most difficult and complex samples to analyse are the solids and semi-solids that are derived from a biological origin. Such samples may be obtained from animal or vegetable material and consist of a non-homogeneous array of fat and/or other tissues, fibre, pulp, etc.

For these and other reasons, the preparation of biological samples for SPE requires an initial disruption of the gross architecture of the sample. This step in the process assures access to all of the components of a sample and initiates the necessary homogeneity required for analysis. Disruption and homogenization also provide a larger overall surface area, generating greater access to solvents and reagents used for analyte isolation, which is the next step in the process. Samples that are by their nature already reasonably homogeneous, such as milk, fruit juices, plasma, etc., are less complicated in this regard but may be too viscous or contain particulates that could hinder rapid SPE extraction and fractionation. For such samples, dilution, filtration and/or centrifugation often solve these problems.

Classical processes for solid or semi-solid sample disruption usually involve one or various combinations

of the following: mincing, shredding, grinding, pulverizing and/or pressurizing of the sample. All of these approaches accomplish the basic requirement of disrupting sample architecture. This initial disruption may be followed or accompanied by the addition of solvents, acids, bases, buffers, abrasives, salts, detergents, chelators, etc., in an effort to more completely disrupt cellular and architectural composition and initiate the extraction and fractionation of various sample components from the analyte(s) of choice. Unfortunately, the creation of often intractable emulsions is often a consequence of these actions and repeated centrifugation, re-extraction and sample manipulation may be required to render the sample suitable for application to an SPE column. Application of this entire process strives to obtain the analyte(s) in solution, free from solids, emulsions or suspensions, reducing the solid sample to a homogenous liquid extract.

In 1989, a technique that remedied many of the complications of dealing with solid samples in their subsequent extraction using solid-phase materials was developed. This was accomplished by literally combining the sample directly with the bonded-phase solid support. This process, designated as matrix solid-phase dispersion (MSPD), was observed to simultaneously accomplish several steps in the more classical approach to sample preparation and SPE extraction/fractionation. A sample (tissue, fruit, etc.) is placed in a glass mortar containing a bonded-phase solid support material, such as octadecylsilyl silica (C_{18}). The solid support and sample are manually blended together using a glass pestle. In this process, the irregularly shaped silica-based solid support serves as an abrasive that promotes disruption of the sample's general architecture, and also acts as a bound solvent which appears to further disrupt the sample by inducing lysis of cell membranes. The blended material is packed into a column suitable for conducting sequential elution with solvents and the blended sample components, and their distribution in the bonded-phase support provides a new phase that exhibits a unique character for performing sample fractionation (Figure 1).

Examination of blended tissues by scanning electron microscopy (SEM) showed that sample architecture had been completely disrupted and that sample matrix components had apparently been evenly distributed over the surface of the bonded phase/support, forming an observable layer. The thickness of this 'new phase' of dispersed matrix is approximately 100 μm , similar to that of some micelle or membrane bilayers. Indeed, it appears that this is what occurs in the MSPD process. The sample is distributed over the surface of the bonded phase as a function of interac-

tions with the support and the bonded phase. The tissue matrix components themselves, form a layered phase consisting of support/lipophilic bonded-phase/sample lipids and a further distribution of sample-associated compounds arranged in and on this new phase based on their own relative polarities.

MSPD Versus Other Forms of Chromatography

MSPD is physically and functionally different from classical SPE in the following ways: (1) MSPD is a process that accomplishes sample disruption and dispersal onto particles of very small size, providing an enhanced surface area for subsequent extraction, whereas sample disruption must be conducted as a separate step in preparing samples for SPE; (2) SPE samples must be in a liquid form, relatively free of solids and of moderate viscosity before addition to the column, while MSPD directly handles solid or viscous liquid samples; and (3) The physical and chemical interactions of the components of the system are greater in MSPD and different, in some respects, from those seen in classical SPE or other forms of liquid chromatography.

In applying the MSPD process to a sample, the interactions observed between the individual components and the target analyte(s) involve (1) the sample components with the solid support, (2) the sample components with the bonded phase, (3) the analyte with the solid support, (4) the analyte with the bonded phase, (5) the analyte with the dispersed sample components, (6) all of the above interacting with the elution solvent(s) and their sequence of addition, and (7) the dynamic interactions of all of the above occurring simultaneously. Nonetheless, general chemical principles involved in conducting SPE and other forms of chromatography are also operable in applying MSPD. Thus, the chemical composition and characteristics of the solid support and bonded-phase are expected to affect the retention and elution of the analytes. These same properties will also apply to the dispersed sample components and the unique phase that is created.

Factors Affecting MSPD Extraction and Fractionation of Samples

To date, only the use of silica-based support materials has been reported for MSPD. The use and effect of synthetic polymer-based solid supports is a subject for further study, particularly supports that possess unique surface and pore chemistries, such as

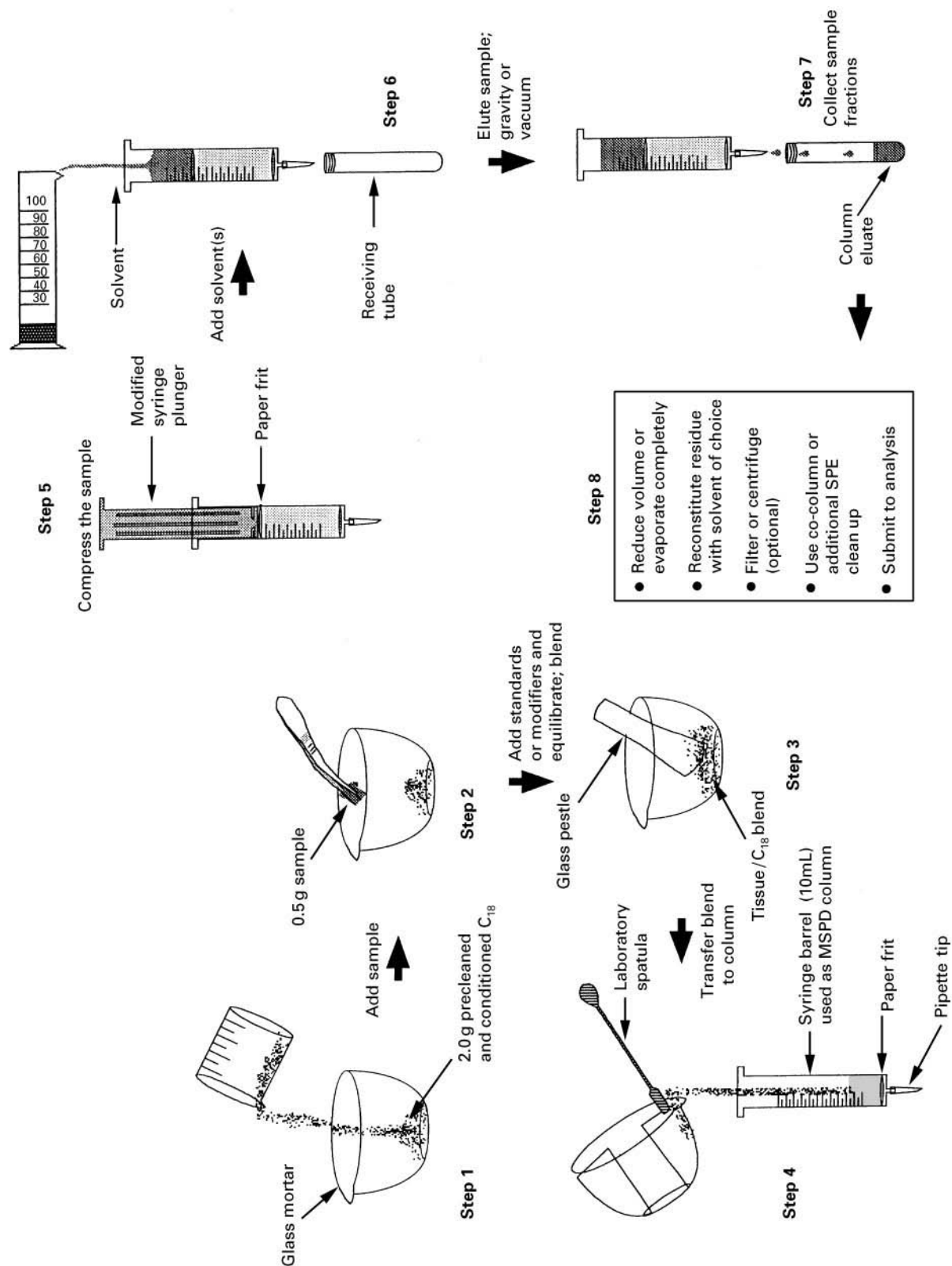


Figure 1 A schematic representation of a MSPD procedure.

hydrophobic interaction supports. For silica-based materials, however, studies have shown that the pore size is of minor importance in MSPD. This effect could vary with the sample and should be considered, however.

The effect of average particle-size diameter has also been examined. As may well be expected, the use of very small particle sizes (3–10 μm) leads to extended solvent elution times for a MSPD column, requiring excessive pressures to obtain adequate flow. However, 40- μm particle size materials (60 Å average pore diameter) have been used most frequently and quite successfully. It has been reported that a blend of silicas possessing a range of particle sizes (40–100 μm) also work quite well, and such materials also tend to be less expensive.

Depending on the application, non-encapped materials or materials having a range of carbon loading (8–18%) may also be used. It is a simple matter to examine these variables for a given application and should be considered for obtaining the best extraction efficiency and the cleanest sample.

The bonded phase will, of course, play a pivotal role. Depending on the polarity of the phase chosen, rather dramatic effects on the results may be observed and a range of available phases should be examined for each application. It has been reported that in applications requiring a lipophilic bonded phase, C_{18} and C_8 can be used interchangeably and that the best ratio of sample to bonded-phase material is 1 to 4. Most applications have employed lipophilic bonded-phase (C_{18}) materials, blending 2.0 g of solid support with 0.5 g of sample. The best ratio is, of course, dependent on the application and should be examined as a variable during method development. Ratios of bonded-phase to sample less than 4 : 1 have been used successfully and samples have been scaled up to 2 g from the typical 0.5 g used in most MSPD procedures, blended with a proportionately greater amount of solid support.

In general, it has been observed that the isolation of more polar analytes from biological samples is assisted by the use of polar phases (cyanopropyl, for example) and less polar analytes by less polar phases. This would be expected based on retention characteristics of compounds from classical SPE.

Preconditioning of the materials used for MSPD greatly enhances analyte recovery, as has been established with SPE. However, in MSPD it also appears to speed the process of sample blending and dispersal by breaking the surface tension differences that may exist between the sample and bonded-phase solid support. As with SPE, washing or rinsing the solid support materials prior to use also eliminates contaminants from the final eluates obtained for analysis.

MSPD column character may also be altered by modifying the matrix prior to or during the blending step. Several extraction studies designed to isolate a variety of different drugs have shown that addition of chelating agents, acids, bases, etc. at the time of blending affects the distribution and elution of target analytes from the sample. The elution profile of matrix components is likewise affected. This effect can be predicted from basic chemistry and applied in MSPD during sample blending and/or by alteration of the elution solvent composition. This effort to increase or suppress ionization of analytes and sample components greatly affects interactions of specific analytes with the blended phase and the eluting solvent(s). Thus, the use of matrix modification should be considered, as in SPE, as a possible variable to be controlled for attaining reproducible and efficient MSPD extraction.

The correct choice of elution solvents and the sequence of their application to a column is of utmost importance to the success of MSPD or SPE fractionation of samples. Elution solvent sequence and composition can be varied to obtain the best analytical results, when attempting to isolate the analyte or further clean the column of interfering substances with each solvent step. The nature of MSPD columns and the enhanced degree of interaction permit isolation of different polarity analytes or entire chemical classes of compounds in a single solvent or in differing polarity solvents passed through the column. This characteristic makes MSPD amenable to conducting multiresidue isolation and analysis on a single sample. In this regard, true gradient elution of a MSPD column has not been reported to date but should, nonetheless, prove applicable to the complete fractionation of samples.

It has been observed that, in an 8-mL elution of a 2-g C_{18} column blended with 0.5 g of sample, most of the target analytes eluted in the first 4 mL, or in approximately one column volume. This will, of course, vary with each application and with appropriate solvent selection but should be examined to reduce the use of solvent and the elution of other potentially interfering components.

The solid support, bonded phase and solvent elution sequence are all critical in performing MSPD, as they are in SPE. However, they may prove less influential overall than the effect of the sample matrix itself. It should be kept in mind that in MSPD the sample itself is dispersed throughout the column. In contrast, much of the sample is retained only in the first few millimeters of the column bed in SPE. In MSPD, the sample matrix components cover much of the bonded-phase support surface, creating a new phase that is dependent on their interactions with the

solid support and bonded phase, interactions that give the MSPD column its character. This new phase, in association with the analyte's distribution and own interactions with it, are perhaps the most important controlling factors.

This matrix effect has been seen by anyone who conducts chromatography, particularly on large numbers of samples that are less than pristine. Repeated sample injection can create a build-up of non-volatilized or non-eluting sample components at the head of a gas chromatography (GC) or liquid chromatography (LC) column, introducing a new 'phase'. This new phase may subsequently affect the stability, elution and retention character of target analytes as they come into contact with it. The discontinuity of phases within the analytical column may lead to peak tailing, the formation of shoulders or multiple peaks for a single analyte. It can lead, over time, to complete loss of analytes that interact strongly with the new phase. This 'matrix effect', or deposition of sample components as an additional phase, is incorporated throughout the column in MSPD. The dispersion of components establishes a new level of, and consistency in, equilibrium distribution of analytes that is fundamentally different from that seen from limited or discontinuous phases.

Another interesting aspect of this effect is that the analytes tend to co-elute in fractions that are not wholly consistent with predicted solubility behaviour. This observation may underscore a further unique property of MSPD. Elution of a sample is designed to remove the target analyte(s) but, even in SPE, one simultaneously fractionates and co-elutes some of the sample components. In MSPD the total amount of sample components present is much greater. In performing mass-balance experiments, it has been observed that the entire sample, minus a few per cent of what appeared to be denatured macromolecules and connective tissues, can be eluted from an MSPD column. Thus, sequential elution of liver tissue blended with C₁₈ recovers 98% of sample triglycerides in hexane and 98% of phospholipids and steroids in dichloromethane. Sugars and polyols are found in the acetonitrile fraction and phosphorylated sugars in water. The presence and concentration of eluted proteins follows the sequence methanol > water > acetonitrile > ethyl acetate. Approximately 7% of the total mass of the sample remains on the column, consisting of connective tissues and denatured macromolecules, including DNA and related nucleotide polymers. Thus, the MSPD process has been used to disrupt otherwise rugged and difficult-to-lyse bacteria, and to simultaneously perform fractionation of the sample for subsequent analysis to identify unique cellular components. These results

point to the fact that many of the unique elution properties of MSPD are due, not only to interactions of target analytes with the dispersed matrix but, also, an association of the matrix with the target analyte as specific classes of matrix components are eluted. Therefore, co-elution of target analyte in association with a particular class of matrix component, which is simultaneously interacting with the other materials remaining on the column, seems to be an important factor in the overall chromatographic character of the MSPD process.

The eluates obtained from an MSPD column are often amenable to immediate instrumental analysis, being adequately clean for direct injection. This is, of course, dependent on the sensitivity of the method and whether concentration is required before the analysis. However, in the majority of cases additional steps are required to address the removal of the co-eluting matrix components described above. In a number of cases this additional clean up of the sample has been accomplished by the use of secondary solid-phase materials. For example, bonded-phase material of the same polarity or even of different character than that used in blending can be packed at the bottom of the MSPD column (co-column). Alternatively, the MSPD column may be eluted directly onto a standard SPE column or disc material for the purposes of conducting further sample clean up and/or analyte concentration. Similarly, the eluate may be evaporated and reconstituted for application to another form of chromatography, analysis by immunoassay, etc. Other techniques employed to conduct MSPD eluate clean up have involved the use of classical liquid-liquid extraction, conducted on a small scale, prior to analysis.

While the process of preparing a MSPD column is currently a manual one, the steps of elution, collection and concentration of fractions, etc. are amenable to automation.

Conclusions

A list of MSPD applications for the isolation of a range of compounds from a variety of matrices is shown in Table 1. This list illustrates the rather generic character of MSPD for performing the extraction of a variety of matrices for a number of compounds. In most cases, MSPD has been found to provide equivalent results to older official methods conducted by more classical countercurrent and/or SPE techniques. Further, it has been rather consistently observed that MSPD requires 95% less solvent and can be performed in 90% of the time of such classical methods. The use of smaller sample sizes, combined with lower solvent consumption, purchase and disposal, make MSPD competitive

Table 1 Applications of MSPD to the analysis of residues in various matrices

Analyte(s)	Matrix
Aminoglycosides	Bovine kidney
Benzimidazoles	Beef liver
Benzimidazoles	Swine muscle
Beta-agonists	Bovine liver
Carbofuran	Corn
Chloramphenicol	Milk
Chlorsulfuron	Milk
Chlorsulon	Milk
Clenbuterol	Bovine liver
Furazolidone	Chicken muscle
Furazolidone	Milk
Furazolidone	Swine muscle
Ivermectin	Fish muscle
Ivermectin	Milk
Ivermectin	Bovine liver
Moxidectin	Bovine tissues
Nicarbazin	Animal tissues
Oxolinic acid	Catfish
Oxytetracycline	Catfish muscle
PCBs	Fish
Pesticides	Beef fat
Pesticides	Catfish muscle
Pesticides	Crayfish
Pesticides	Fish
Pesticides	Fruit, vegetables
Pesticides	Milk
Pesticides	Oysters
Sulfa drugs	Chicken tissues
Sulfadimethoxine	Catfish muscle
Sulfadimethoxine	Catfish, plasma
Sulfonamides	Infant formula
Sulfonamides	Milk
Sulfonamides	Salmon muscle
Sulfonamides	Swine muscle
Sulfonamides	Eggs
Tetracyclines	Milk

with such methods on several levels and should be considered as an alternative when pursuing new analytical methodology. This is especially the case for solid or semi-solid biological materials.

See also: II/Extraction: Solid-Phase Extraction; Solvent Based Separation. III/Solid-Phase Extraction with Cartridges. Sorbent Selection for Solid-Phase Extraction.

Further Reading

- Barker SA (1992) Application of matrix solid-phase dispersion (MSPD) to the extraction and subsequent analysis of drug residues in animal tissues. In: Agarwal VK (ed.) *Analysis of Antibiotic Residues in Food Products of Animal Origin*, pp. 119–132. New York: Plenum Press.
- Barker SA and Floyd ZE (1996) Matrix solid-phase dispersion (MSPD): implications for the design of new bonded-phase surface chemistries. In: Pesek JJ, Matyska MT and Abuelafiya RR (eds) *Chemically Modified Surfaces: Recent Developments*, pp. 66–71. Cambridge, UK: Royal Society of Chemistry.
- Barker SA and Long AR (1992) Tissue drug residue extraction and monitoring by matrix solid-phase dispersion (MSPD)-HPLC analysis. *Journal of Liquid Chromatography* 15: 2071–2089.
- Barker SA, Long AR and Hines ME (1993) The disruption and fractionation of biological materials by matrix solid-phase dispersion. *Journal of Chromatography* 629: 23–34.
- Barker SA, Long AR and Short CR (1989) Isolation of drug residues from tissues by solid-phase dispersion. *Journal of Chromatography* 475: 353–361.
- Crouch MC and Barker SA (1997) Analysis of toxic wastes in tissues from aquatic species: applications of matrix solid-phase dispersion. *Journal of Chromatography* 774: 287–309.
- US Patent # 5 272 094. Issued 21 December (1993) A bonded-phase matrix dispersion and extraction process. Isolation of drugs, and drug residues, from biological specimens, and tissues (Dr Steven A Barker; co-patent applicant, Dr Austin R Long, Louisiana State University).

SOLID-PHASE MICROEXTRACTION



Biomedical Applications

H. Kataoka, Okayama University, Tsushima, Okayama, Japan

H. L. Lord and J. Pawliszyn, University of Waterloo, Ontario, Canada

Copyright © 2000 Academic Press

Analysis of drugs in biological samples is growing in importance owing to the need to understand the therapeutic and toxic effects of drugs and to continue the development of more selective and effective drugs. Furthermore, the screening and confirmation of abused drugs in body fluids is important for the detection of potential users of drugs and the control of drug addicts following withdrawal therapy. Simultaneous analysis of these drugs in biological samples

is required in many circumstances, such as clinical control for diagnosis and treatment of diseases, doping control, forensic analysis and toxicology. Although high efficiency instruments have been developed, most analytical instruments cannot handle the sample matrix directly. Therefore, sample preparation is very important to achieve a practical and reliable method for the analysis of complex matrices such as biological samples. In general, over 80% of analysis time is spent on sampling and sample preparation steps such as extraction, concentration and isolation of analytes. However, previous sample preparation techniques, such as liquid-liquid extraction and solid-phase extraction, have their problems. These techniques are generally time-consuming and require large volumes of samples and solvents. For example, a long sample preparation time limits the number of samples that can be analysed, and multi-step procedures are prone to loss of analytes. Furthermore, the use of a large amount of solvent influences trace analysis, and also causes environmental pollution and health concerns. Ideally, sample preparation techniques should be fast, easy to use, inexpensive and compatible with a range of analytical instruments.

Solid-phase microextraction (SPME), developed by Pawliszyn and co-workers in 1990, is a new sample preparation technique using a fused-silica fibre that is coated on the outside with an appropriate stationary phase. The analyte in the sample is directly extracted onto the fibre coating. The method saves preparation time, solvent purchase and disposal costs, and can improve the detection limits. It has been used routinely in combination with gas chromatography (GC) and GC/mass spectrometry (GC/MS), and successfully applied to a wide variety of compounds, especially for the extraction of volatile and semi-volatile organic pollutants from water samples. SPME was also introduced for direct coupling with high performance liquid chromatography (HPLC) and LC/MS in order to analyse weakly volatile or thermally labile compounds not amenable to GC or GC/MS. The SPME/HPLC interface, equipped with a special desorption chamber, is utilized for solvent desorption prior to HPLC analysis, instead of thermal desorption in the injection port of the GC. Moreover, a new SPME/HPLC system known as in-tube SPME, was recently developed using an open-tubular fused-silica capillary column as the SPME device in place of the SPME fibre. In-tube SPME is suitable for automation, and automated sample handling procedures not only shorten the total analysis time, but also usually provide better accuracy and precision relative to manual techniques.

In this article, we review SPME techniques coupled with various analytical instruments and the

applications of these techniques to drug analysis. The review consists of two main parts. In the first part, general aspects of SPME techniques are surveyed for fibre and in-tube SPME methods coupled with various instruments. In the second part, applications of the SPME methods in drug analysis are considered according to the drug type.

SPME Techniques Coupled with Various Analytical Instruments

Fibre SPME

The fibre SPME device consists of a fibre holder and fibre assembly with built-in fibre inside the needle. In fibre SPME, analytes are extracted directly from the sample onto a polymeric stationary phase coated on the fibre. When the fibre is inserted into the sample, the target analytes partition from the sample matrix into the stationary phase until equilibrium is reached. Two types of fibre SPME techniques can be used to extract analytes: headspace SPME and immersion SPME. In headspace SPME, the fibre is exposed in the headspace of gaseous, liquid or solid samples. In immersion SPME, the fibre is directly immersed in liquid samples. The fibre with concentrated analytes is then transferred to an instrument for desorption, followed by separation and quantification. Headspace and immersion SPME techniques can be used in combination with any GC, GC/MS, HPLC and LC/MS system. The process of the fibre SPME/GC method is shown in Figure 1.

In fibre SPME, the amount of analyte extracted onto the fibre depends on the polarity and thickness of the stationary phase coating on the fibre, extraction time, and the concentration of analyte in a sample. In general, volatile compounds require a thick polymer coat and a thin coat is effective for semi-volatile compounds. Extraction of analytes is also typically improved by agitation, addition of salt to the sample, changing the pH, and temperature. Although full equilibration is not necessary for accurate and precise analysis by SPME, consistent extraction time and other SPME parameters are essential. Furthermore, it is important to keep a consistent vial size and sample volume. In general, immersion SPME is more sensitive than headspace SPME for analytes predominantly present in the liquid. On the other hand, headspace SPME is suitable for the extraction of more volatile compounds. Extractions from biological samples by headspace SPME exhibit lower background than extractions obtained by immersion SPME. Because the headspace and immersion SPME techniques differ in kinetics, both approaches should be evaluated to optimize fibre SPME conditions for

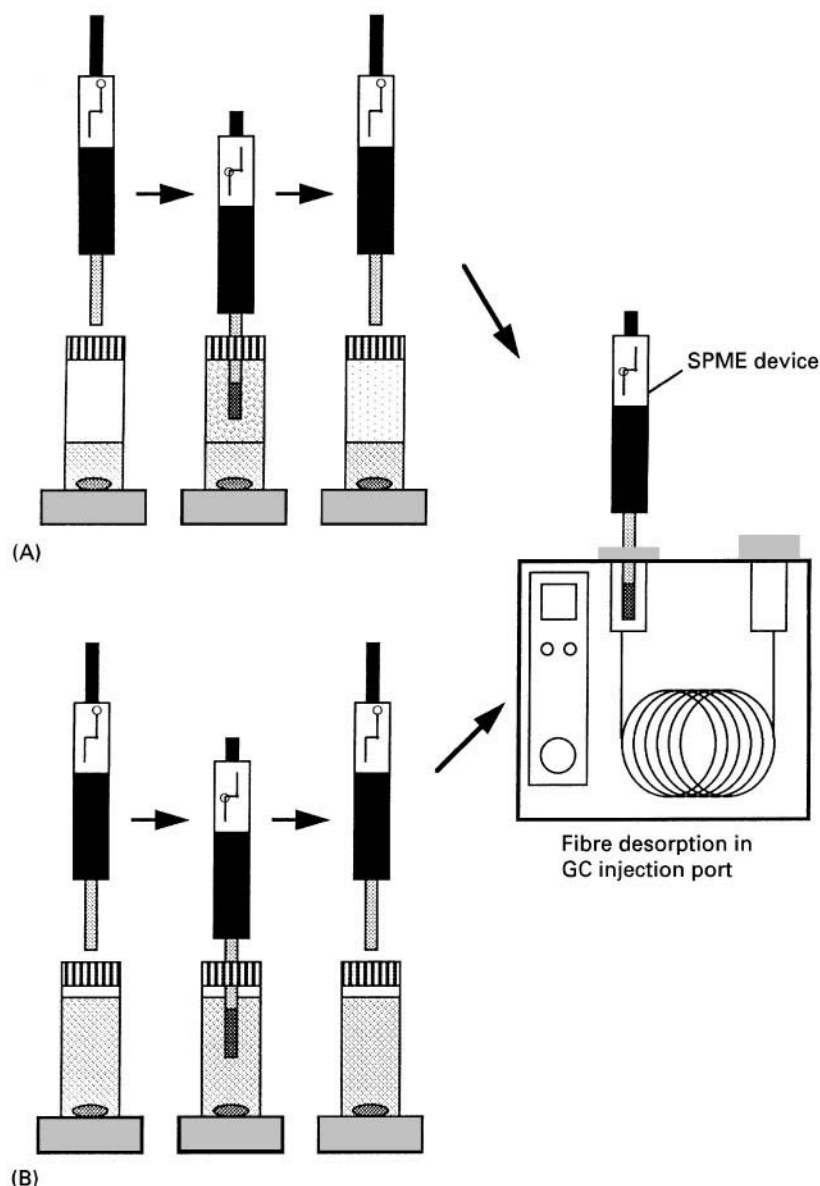


Figure 1 Schematic illustration of headspace and immersion SPME/GC methods. (A) Headspace SPME; (B) direct immersion SPME.

analytes. Fibre SPME techniques in combination with GC or GC/MS are unsuitable for the extraction of less volatile or thermally labile compounds. Thus derivatization approaches are frequently used to extract polar compounds from biological samples. Four types of derivatization techniques in combination with SPME are implemented. Direct derivatization in the sample matrix is similar to well-established approaches used in solvent extraction. Analytes are extracted by SPME after derivatization in the vial. For in-coating derivatization with the fibre-doping method, simultaneous derivatization and extraction are directly performed in the fibre coating by a two-step process: (1) dope fibre with derivatization agent and (2) expose doped

fibre to sample for extraction. This technique can be used for polar volatile compounds. Another in-coating derivatization technique is performed by the following two-step process: (1) dope fibre to sample for extraction and (2) expose doped fibre in the headspace of derivatizing agent. For derivatization in the injection port, the analyte extracted by SPME is desorbed in a GC injection port and then derivatized with additional reagent.

The desorption of analyte from the fibre coating is performed by heating the fibre in the injection port of a GC or GC/MS, or by loading solvent into the desorption chamber of the SPME/HPLC interface. Efficient thermal desorption of an analyte in a GC

injection port is dependent on the injection depth, injector temperature, and exposure time. A narrow-bore GC injector insert is required to ensure high linear flow and the fibre needs to be exposed immediately after the needle is introduced into the insert. Needle exposure depth should be adjusted to place the fibre in the centre of the hot injector zone. Desorption time is determined by the injector temperature and the linear flow rate around the fibre. The HPLC interface, on the other hand, consists of a six-port injection valve and a special desorption chamber, and requires solvent desorption of the analyte prior to HPLC or LC/MS analysis. A typical SPME/HPLC interface is shown in Figure 2. The desorption chamber is placed in the position of the injection loop. After sample extraction, the fibre is inserted into the desorption chamber at the 'load' position under ambient pressure. When the injector is changed to the 'inject' position, mobile phase contacts the fibre, desorbs the analytes, and delivers them to the HPLC column for separation. Two desorption techniques can be used to remove the analytes from the fibre: dynamic desorption and static desorption. In dynamic desorption, the analytes can be removed by a moving stream of mobile phase. When the analytes

are more strongly adsorbed to the fibre, the fibre can be soaked in mobile phase or other strong solvent for a specified time by static desorption before injection onto the HPLC column. In each desorption technique, rapid and complete desorption of analytes using minimal solvent is important for optimizing the SPME/HPLC or SPME/LC/MS methods.

In-tube SPME

In-tube SPME using an open-tubular capillary column as the SPME device was developed for coupling with HPLC or LC/MS. It is suitable for automation, and can continuously perform extraction, desorption and injection using a standard autosampler. With the in-tube SPME technique, organic compounds in aqueous samples are directly extracted from the sample into the internally coated stationary phase of a capillary column, and then desorbed by introducing a moving stream of mobile phase or static desorption solvent when the analytes are more strongly absorbed to the capillary coating. A schematic diagram of the automated in-tube SPME/LC/MS system is shown in Figure 3. The capillaries selected have coatings similar to those of commercially available SPME fibres. The capillary column is placed between the

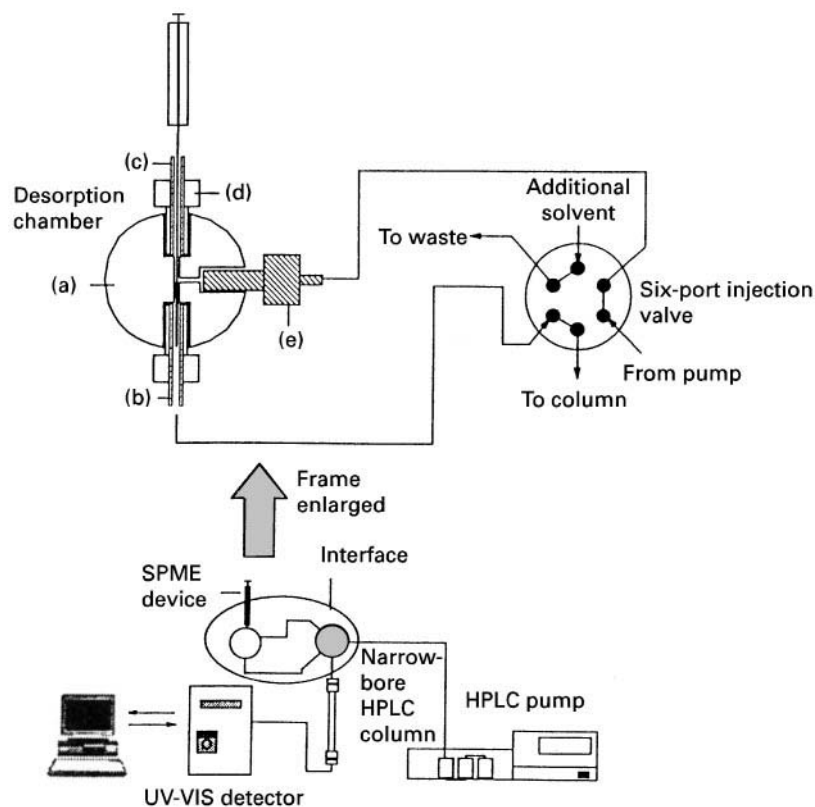


Figure 2 Schematic of the SPME-HPLC system. (a) Stainless steel (SS) 1/16 inch tee joint; (b) 1/16 inch o.d., 0.02 inch i.d., SS tubing; (c) 1/16 inch o.d. poly(ether ether ketone) (PEEK) tubing (0.02 inch i.d.); (d) two-piece finger-tight PEEK union; (e) PEEK tubing (0.005 inch i.d.) with a one-piece PEEK union. (Reproduced with permission from Pawliszyn J (1997) *Solid Phase Microextraction: Theory and Practice*. Translated by permission of John Wiley & Sons, Inc. All rights reserved.)

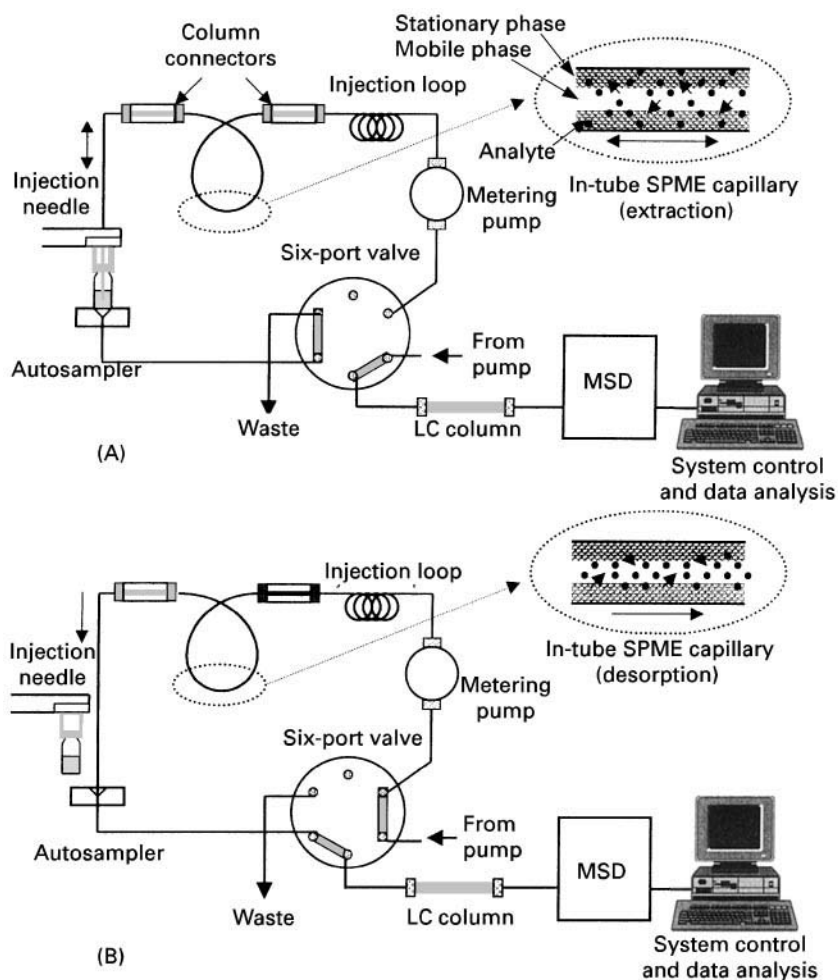


Figure 3 Schematic of the in-tube SPME/LC/MS system. (A) Load position (extraction phase); (B) injection position (desorption phase). (Reproduced with permission from Kataoka H, Narimatsu S, Lord HL and Pawliszyn J (1999) *Analytical Chemistry* 71: 4237. Copyright American Chemical Society.)

injection loop and the injection needle of the HPLC autosampler. While the injection syringe repeatedly draws and ejects sample from the vial under computer control, the analytes partition from the sample matrix into the stationary phase until equilibrium is reached. Subsequently, the extracted analytes are directly desorbed from the capillary coating by mobile phase flow or by aspirating a desorption solvent. The desorbed analytes are transported to the HPLC column for separation, and then detected with UV or a mass selective detector (MSD).

In in-tube SPME, the amount of analyte extracted by the stationary phase of the capillary column depends on the polarity of capillary coating, number and volume of draw/eject cycles and the sample pH. A capillary column 50–60 cm long is optimal for extraction. Below this level, extraction efficiency is reduced, and above this level, peak broadening is observed. In general, complete equilibrium extraction is not obtained for any of the analytes, because the analytes are partially desorbed into the mobile phase

during each eject step. The target analytes with higher K -values need longer equilibration times. Although an increase in number and volume of draw/eject cycles can enhance the extraction efficiency, peak broadening is often observed in this case. The optimal flow rate of draw/eject cycles is $50\text{--}100\ \mu\text{L min}^{-1}$. Below this level, extraction requires an inconveniently long time, and above this level, bubbles form on the inside of the capillary and extraction efficiency is reduced. The in-tube SPME technique does not need a special SPME/HPLC interface for desorption of analytes. The analytes extracted onto the capillary coating can be easily desorbed by a moving stream of mobile phase or desorption solvent when the analytes are more strongly adsorbed to the capillary coating. Carryover in the in-tube SPME method is lower or eliminated in comparison with the fibre-SPME method.

Although the theories of fibre and in-tube SPME methods are similar, the significant difference between these methods is that the extraction of analytes

is performed on the outer surface of the fibre for fibre-SPME and on the inner surface of the capillary column for in-tube SPME. Therefore, with the in-tube SPME method, it is necessary to prevent plugging of the capillary column and flow lines during extraction, and typically particles must be removed from samples by filtration before extraction. On the other hand, with the fibre-SPME method, it is not necessary to remove particles before extraction because they are removed by washing the fibre with water before insertion into the desorption chamber of the SPME/HPLC interface. Another significant difference between in-tube SPME and manual fibre-SPME/HPLC is the possible decoupling of desorption and injection with the in-tube SPME method. In the fibre-SPME method, analytes are desorbed during injection as the mobile phase passes over the fibre. On the other hand, in the in-tube SPME method, analytes are desorbed by mobile phase or by aspirating a desorption solvent from a second vial, and then transferred to the HPLC column by mobile-phase flow. The fibre-SPME/HPLC method also has the advantage of eliminating the solvent peak from the chromatogram, but peak broadening is sometimes observed because analytes can be slow to desorb from the fibre. With the in-tube SPME method, peak broadening is not observed because analytes are completely desorbed before injection.

Biomedical Applications: Drug Analysis

SPME methods applied to the analysis of various abused and therapeutic drugs in biological samples are listed in Table 1, according to the drug type, sample type, extraction device, extraction mode, and analytical technique. The SPME methods using 100- μm polydimethylsiloxane (PDMS) fibres in combination with GC or GC/MS are widely used for the analysis of various drugs. The SPME methods coupled with HPLC or LC/MS are used for the analysis of less volatile or thermally labile drugs. For recent reviews of some of these methods for drug analysis see Pawliszyn, Lord and Pawliszyn, Namera *et al.*, Junting *et al.*, Kataoka *et al.* and Sporkert and Pragst in the Further Reading section.

Amphetamines and Related Compounds

Yashiki and co-workers developed a simple and rapid method for analysing amphetamine (AM) and methamphetamine (MA) in urine and blood samples by headspace SPME and GC/MS-selected ion monitoring (SIM). In order to move the analytes into the headspace, the sample was heated at 80°C for 20 min under K_2CO_3 or NaOH alkaline conditions. Sub-

sequently, a 100- μm PDMS fibre was exposed to the headspace for 5 min, and then inserted into the injection port of GC/MS for desorption. The method was twenty times more sensitive than the conventional headspace method. Lord and Pawliszyn optimized several extraction parameters for the analysis of AM and MA in urine samples by headspace SPME/GC-flame ionization detection (FID). Centini *et al.* and Battu *et al.* reported simultaneous analysis of amphetamines and their analogues, such as 3,4-methylenedioxyamphetamine (MDA), 3,4-methylenedioxymethamphetamine (MDMA) and 3,4-methylenedioxyethylamphetamine (MDEA), in urine samples by headspace SPME using a 100- μm PDMS fibre. As shown in Figure 4, a clean total-ion chromatogram is obtained from a urine sample spiked with 100 ng mL⁻¹ of each of the 21 central nervous system stimulants and extracted by the headspace SPME method. Koide *et al.* applied this technique to the analysis of amphetamines in hair samples.

Degel, Penton, Ishii *et al.*, Makino *et al.* and Myung *et al.* used the direct immersion technique in order to improve the extraction efficiency and sensitivity. The extraction recoveries of AM and MA by the immersion SPME method are several times higher than those by the headspace SPME method. Ugland *et al.* reported an SPME technique in combination with derivatization. After derivatization with alkylchloroformate, amphetamines and their methylenedioxy analogues were analysed by immersion-fibre SPME/GC-nitrogen-phosphorus detection (NPD) or GC/MS.

Kataoka *et al.* developed an in-tube SPME/LC/MS method for the analysis of amphetamines and their methylenedioxy analogues using Omegawax (Supelco, Bellefonte, PA, USA) capillary as the extraction device. As shown in Figure 5, these drugs spiked into urine samples were selectively analysed without interference peaks by SIM-mode detection.

Anaesthetics

Kumazawa *et al.* developed headspace and direct-immersion-SPME methods for the analysis of ten local anaesthetics in blood samples. These drugs were extracted with 100- μm PDMS fibres after deproteinization of the sample with perchloric acid. Heating in a NaOH and $(\text{NH}_4)_2\text{SO}_4$ solution during headspace SPME gave the best recoveries of the drugs and the cleanest backgrounds. The recoveries for all drugs in the sample mixture at neutral pH in the presence of NaCl were greater than for that of a sample at the same pH without NaCl (see Figure 6). Although a small amount of background noise appeared in the direct immersion-SPME method, the advantage of using immersion-SPME is that recovery is much better than that of headspace-SPME.

Table 1 SPME methods for the analysis of drugs in biological samples

Drugs	Specimen	Extraction device	Extraction mode ^a	Hyphenated analysis	Reference
<i>Amphetamines and related compounds</i>					
AM, MA	Urine	100- μ m PDMS fibre	HS	GC/MS	<i>Forensic Sci. Int.</i> (1995) 76: 169.
AM, MA	Blood	100- μ m PDMS fibre	HS	GC/MS	<i>Forensic Sci. Int.</i> (1996) 78: 95.
AM, MA, MDMA, MDEA	Urine	100- μ m PDMS fibre	HS	GC/MS	<i>Forensic Sci. Int.</i> (1996) 83: 161.
AM, MA	Urine	100- μ m PDMS fibre	DI	GC/MS	<i>Clin. Biochem.</i> (1996) 29: 529.
AM, MA	Urine	100- μ m PDMS fibre	DI	GC/FID	<i>Can. Soc. Forensic Sci. J.</i> (1996) 29: 43.
AM, MA	Urine	65- μ m PDMS/DVB fibre	DI	GC/NPD	<i>Jpn. J. Forensic Toxicol.</i> (1996) 14: 228.
AM, MA	Urine	100- μ m PDMS fibre	HS	GC/FID	<i>Anal. Chem.</i> (1997) 69: 3899.
AM, MA	Urine	100- μ m PDMS fibre	D + DI	GC/NPD	<i>J. Chromatogr. B</i> (1997) 701: 29.
MA	Urine	100- μ m PDMS fibre	DI	GC/MS	<i>Chromatography</i> (1997) 18: 185.
AM, MA, MDA, MDMA, MDEA etc.	Urine	100- μ m PDMS fibre	HS	GC/MS	<i>J. Chromatogr. Sci.</i> (1998) 36: 1.
AM, MA	Hair	100- μ m PDMS fibre	HS	GC/NPD	<i>J. Chromatogr. B</i> (1998) 707: 99.
AM, MA, MDMA	Urine	100- μ m PDMS fibre	DI	GC/MS	<i>J. Chromatogr. B</i> (1998) 716: 359.
AM, MA, MDA, MDMA, MDEA	Urine	100- μ m PDMS fibre	D + DI	GC/NPD	<i>J. Pharm. Biomed. Anal.</i> (1999) 19: 463.
AM, MA, MDA, MDMA, MDEA	Urine	Omegawax 250 capillary	IT	GC/MS	<i>J. Chromatogr. B</i> (submitted).
<i>Anaesthetics</i>					
Lidocaine etc.	Blood	100- μ m PDMS fibre	HS	GC/FID	<i>Jpn. J. Forensic Toxicol.</i> (1995) 13: 182.
Lidocaine etc.	Blood	100- μ m PDMS fibre	DI	GC/FID	<i>Chromatographia</i> (1996) 43: 59.
Phencyclidine	Urine, blood	100- μ m PDMS fibre	HS	GC/SID	<i>Chromatographia</i> (1996) 43: 331.
Lidocaine etc.	Blood	100- μ m PDMS fibre	HS	GC/MS	<i>J. Chromatogr. B</i> (1998) 709: 225.
Lidocaine	Urine	100- μ m PDMS fibre	DI	GC/FID	<i>Chromatographia</i> (1998) 47: 678.
<i>Anorectics</i>					
Fenfluramine	Urine	30- μ m PDMS fibre	DI	GC/MS	<i>J. Microcolumn Sep.</i> (1997) 9: 249.
<i>Antidepressants</i>					
Amitriptyline, imipramine etc.	Urine	100- μ m PDMS fibre	HS	GC/FID	<i>Jpn. J. Forensic Toxicol.</i> (1995) 13: 25.
Amitriptyline	Urine	100- μ m PDMS fibre	DI	GC/MS	<i>Clin. Biochem.</i> (1996) 29: 529.
Amitriptyline, imipramine etc.	Plasma	100- μ m PDMS fibre	DI	GC/NPD	<i>J. Chromatogr. B</i> (1997) 696: 217.
Amitriptyline, imipramine etc.	Blood	100- μ m PDMS fibre	HS	GC/FID	<i>J. Chromatogr. Sci.</i> (1997) 35: 302.
Maprotiline, mianseline, selipitline	Blood	100- μ m PDMS fibre	HS	GC/MS	<i>J. Anal. Toxicol.</i> (1998) 22: 396.
<i>Antiepileptics</i>					
Valproic acid	Plasma	100- μ m PDMS fibre	DI	GC/FID	<i>J. Chromatogr. B</i> (1995) 673: 299.

Table 1 Continued

Drugs	Specimen	Extraction device	Extraction mode ^a	Hyphenated analysis	Reference
Antihistaminics					
Diphenhydramine etc. Ranitidine	Urine, blood Urine	100- μ m PDMS fibre Omegawax 250 capillary	HS IT	GC/FID LC/MS	<i>J. Chromatogr. Sci.</i> (1997) 35: 275. <i>J. Chromatogr. B</i> (1999) 731: 353.
Antihypertensives					
Propranolol etc.	Urine, serum	Omegawax 250 capillary	IT	LC/MS	<i>Anal. Chem.</i> (1999) 71: 4237.
Antipsychotics					
Promazine etc.	Urine, blood	100- μ m PDMS fibre	HS	GC/FID	<i>Jpn. J. Forensic Toxicol.</i> (1996) 14: 30.
Barbiturates					
Barbital etc.	Urine	65- μ m Carbowax/DVB fibre	DI	GC/MS	<i>J. Chromatogr. A</i> (1997) 777: 275.
Benzodiazepines					
Diazepam	Urine	100- μ m PDMS fibre	DI	GC/MS	<i>Clin. Biochem.</i> (1996) 29: 529.
Diazepam	Plasma	Solvent-modified 85- μ m PA fibre	DI	GC/NPD	<i>J. Chromatogr. B</i> (1997) 689: 357.
Diazepam etc.	Urine	65- μ m PDMS/DVB fibre	DI	GC/FID	<i>Jpn. J. Forensic Toxicol.</i> (1997) 15: 16.
Diazepam etc.	Urine	85- μ m PA fibre	DI	HPLC/UV	<i>Chromatography</i> (1997) 18: 244.
Diazepam etc.	Urine, serum	65- μ m Carbowax/DVB fibre	DI	GC/FID	<i>J. Microcolumn Sep.</i> (1998) 10: 193.
Benzodiazepine metabolites	Urine	100- μ m PDMS, 85- μ m PD fibre	DI	GC/MS GC/ECD	<i>J. Anal. Toxicol.</i> (1999) 23: 54.
Narcotics and other illicit drugs					
Cocaine	Urine	100- μ m PDMS fibre	DI	GC/NPD	<i>Jpn. J. Forensic Toxicol.</i> (1995) 13: 207.
Meperidine	Urine, blood	100- μ m PDMS fibre	HS	GC/FID	<i>Jpn. J. Forensic Toxicol.</i> (1995) 13: 211.
Cocaine	Urine	100- μ m PDMS fibre	DI	GC/NPD	<i>Chromatography</i> (1997) 18: 185.
Morphine, heroin etc.	Urine	65- μ m PDMS/DVB 100- μ m PDMS fibre	HS DI	GC/MS GC/FID	<i>Anal. Chem.</i> (1997) 69: 3899.
Cannabinoids	Saliva	100- μ m PDMS fibre	DI	GC/MS	<i>Anal. Chem.</i> (1998) 70: 1788.
Cannabinoids	Hair	30- μ m PDMS fibre	DI	GC/MS	<i>J. Anal. Toxicol.</i> (1999) 23: 7.
Nicotine					
Nicotine, Cotine	Urine	100- μ m PDMS fibre	HS	GC/MS	<i>Jpn. J. Forensic Toxicol.</i> (1995) 13: 17.
Nicotine, Cotinine	Urine	100- μ m PDMS fibre	DI	GC/FID	<i>Clin. Biochem.</i> (1996) 29: 529.
Steroids					
Estrone, estradiol etc. Corticosteroids	Serum Urine	85- μ m PA fibre 65- μ m Carbowax/ DVB fibre	DI + D DI	GC/MS LC/MS	<i>J. High Resolut. Chromatogr.</i> (1997) 20: 171. <i>Rapid Commun. Mass Spectrom.</i> (1997) 11: 1926.

^aHS: headspace; DI: direct immersion; IT: in-tube; D: derivatization.

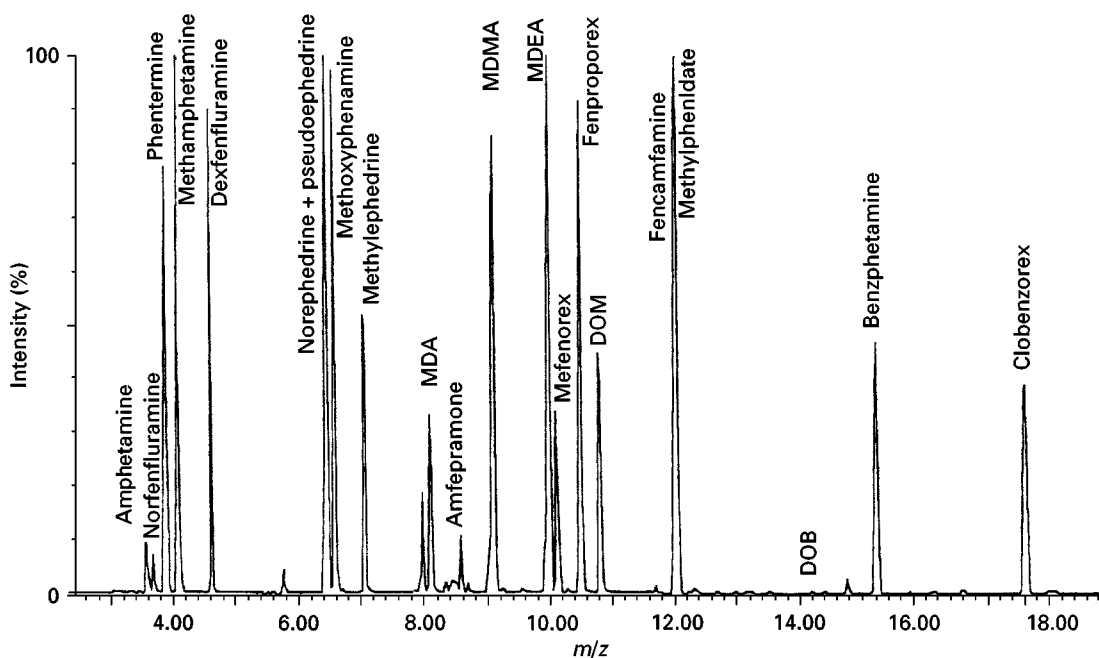


Figure 4 Total-ion chromatogram of a urine sample extract spiked with 21 central nervous system stimulants at $1000 \mu\text{g L}^{-1}$. SPME conditions: fibre, $100 \mu\text{m}$ PDMS; extraction, at 80°C headspace for 10 min with stirring; desorption, exposure for 10 min in GC injection port. GC/MS conditions: column, PTA-5 ($30 \text{ m} \times 0.32 \text{ mm i.d.}$, $0.5 \mu\text{m}$ film thickness); injector, splitless mode at 200°C ; split opening time, 2 min; oven temperature, programme from 60 to 120°C at $30^\circ\text{C min}^{-1}$, then to 210°C at 5°C min^{-1} , and finally to 280°C at $30^\circ\text{C min}^{-1}$ and hold at 280°C for 5 min; transfer line and detector temperature, 280°C ; helium flow-rate, 1.3 mL min^{-1} ; ionization, 70 eV . (Reproduced with permission from Battu C, Marquet P, Fauconnet AL, Lacassie E and Lachâtre G (1998) *Journal of Chromatographic Science* 36: 1, by permission of Preston Publications, A Division of Preston Industries, Inc.)

Furthermore, Kumazawa *et al.* reported a method for analysis of phencyclidine in urine and whole blood by headspace-SPME and GC with a surface ionization detector (SID). Watanabe *et al.* developed a simple method for analysis of five local anaesthetics in blood samples by headspace SPME using a $100\text{-}\mu\text{m}$ PDMS fibre and GC/MS-SIM. Koster *et al.* reported direct immersion-SPME methods coupled with GC-FID and HPLC-UV for the determination of lidocaine in urine samples. Desorption of the PDMS fibre in HPLC is more complicated than the desorption in GC, because it is dependent on the composition of the mobile phase or the desorption solvent.

Antidepressants

Kumazawa *et al.* developed a simple headspace-SPME method for the analysis of four tricyclic antidepressants in urine and whole-blood samples. These drugs were extracted with a $100\text{-}\mu\text{m}$ PDMS fibre after heating at 100°C in the presence of a NaOH solution. Namera *et al.* reported a headspace-SPME/GC-MS method for the analysis of three tetracyclic antidepressants in whole-blood samples, and its application to a medicolegal case of setipitiline intoxication. Ulrich and Martens developed a direct immersion-SPME method for the simultaneous analysis of ten antidepressant drugs and metabolites in plasma sam-

ples, and applied the method to toxicological analysis after the accidental or suicidal intake of higher doses. The sample was extracted with a $100\text{-}\mu\text{m}$ PDMS fibre for 10 min and the fibre was exposed in the GC injection port at 260°C for 1 min after washing in 50% methanol and subsequent drying at room temperature. As shown in Figure 7, these drugs in plasma samples were selectively analysed by NPD without interference peaks. However, the recoveries of antidepressants from plasma samples were very low due to the high protein binding of these drugs. The limits of quantification for these drugs in plasma samples were $90\text{--}200 \text{ ng mL}^{-1}$. The sensitivity can be considerably improved by increasing the extraction time and dilution of plasma samples with water.

Benzodiazepines

Krogh *et al.* developed a direct immersion-SPME method in combination with GC-NPD for the analysis of diazepam in plasma samples. The polyacrylate (PA) fibre doped with 1-octanol was used to extract diazepam from the samples. The solvent-modified PA fibre was found to be more efficient in the extraction of diazepam than the untreated PA and PDMS fibres. This technique offers sufficient enrichment for bioanalysis, high selectivity, and short sample preparation time. However, the potential of the

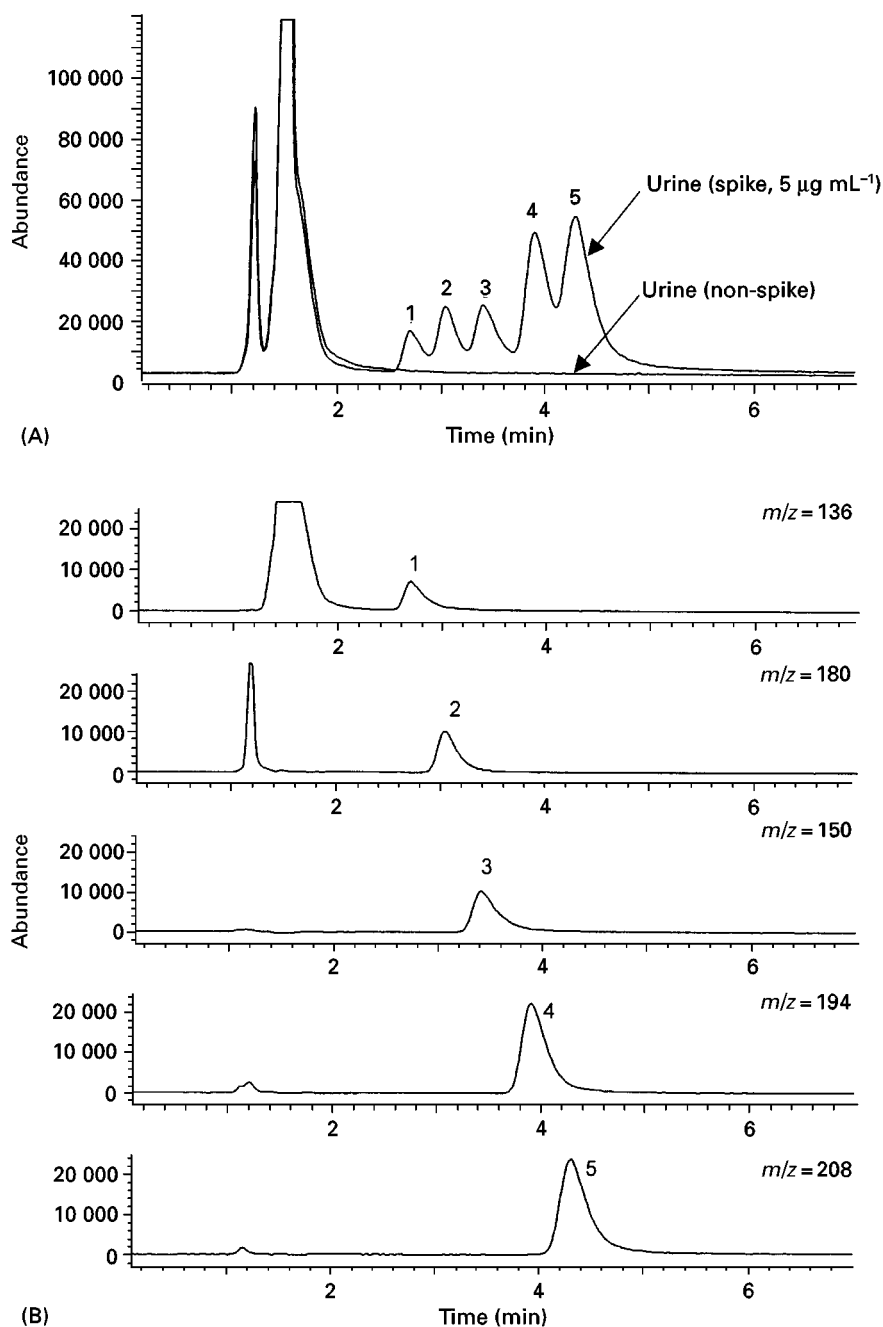


Figure 5 Total ion and SIM chromatograms obtained from urine samples spiked with amphetamines by in-tube SPME/LC/MS. (A) Total ion chromatograms obtained from urine and spiked urine samples; (B) SIM chromatograms obtained from spiked urine sample. Urine sample ($10 \mu\text{L}$) was diluted ten times with water and used for analysis after filtration. Stimulants were spiked at a concentration of 5 mg mL^{-1} urine. LC/MS conditions: column, Supelcosil LC-CN ($3.3 \text{ cm} \times 4.6 \text{ mm i.d.}$, $3 \mu\text{m}$ particle size); column temperature, 25°C ; mobile phase, acetonitrile/ 50 mM ammonium acetate ($15:85$); flow-rate, 0.4 mL min^{-1} ; fragmentor voltage, 40 V ; ionization mode, positive ESI; SIM ion, $m/z = 136$ (AM), 150 (MA), 180 (MDA), 194 (MDMA) and 208 (MDEA). In-tube SPME conditions: capillary, Omegawax 250 ($60 \text{ cm} \times 0.25 \text{ mm i.d.}$, $0.25 \mu\text{m}$ film thickness); sample pH, 8.5 ; draw/eject cycles, 15 ; draw/eject volume, $35 \mu\text{L}$; draw/eject flow-rate, $100 \mu\text{L min}^{-1}$; desorption solvent, mobile phase. Peaks: 1, AM; 2, MDA; 3, MA; 4, MDMA; and 5, MDEA. (Reproduced with permission from Kataoka H, Lord HL and Pawliszyn J (2000) *Journal of Analytical Toxicology* 24: 263, by permission of Preston Publications, A Division of Preston Industries, Inc.)

solvent-modified SPME technique is limited by the incompatibility of the SPME coatings with most organic solvents. Luo *et al.* developed a direct immersion-SPME method for the simultaneous analysis of

five benzodiazepines in urine and serum samples. These drugs were efficiently extracted from these samples with a $65\text{-}\mu\text{m}$ Carbowax/divinylbenzene (DVB) fibre under conditions of saturated salt with

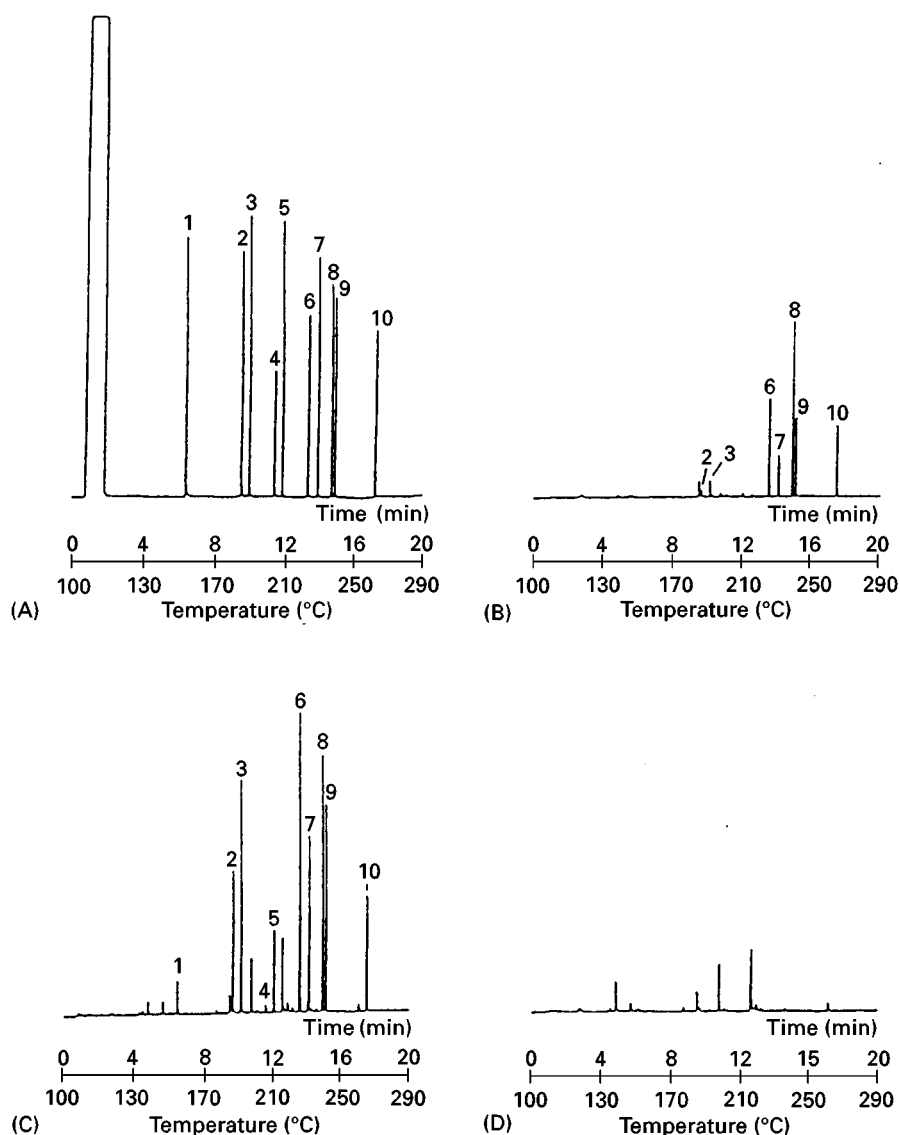


Figure 6 Capillary GC of ten local anaesthetics extracted from human whole blood by use of direct immersion-SPME. (A) The authentic drugs (50 ng each on column); (B) a drug extract at pH 7 without salt; (C) a drug extract at pH 7 in the presence of 0.5 g NaCl; (D) a blank extract at pH 7 in the presence of 0.5 g NaCl. The mixture of ten drugs (5 µg each) was added to 1 mL of human whole blood. SPME conditions: fibre, 100 µm PDMS; extraction, at room temperature for 40 min with stirring; desorption, 1 min exposure in GC injection port. GC conditions: column, DB-17 (30 m × 0.25 mm i.d., 0.25 µm film thickness); column temperature, initially hold at 100°C for 1 min and increase to 290°C at 10°C min⁻¹; injector and detector temperatures, 250°C; He carrier gas flow-rate, 3 mL min⁻¹; injection, splitless; detector, FID. Peaks: 1, ethyl aminobenzoate; 2, prilocaine; 3, lidocaine; 4, procaine; 5, mepivacaine; 6, tetracaine; 7, bupivacaine; 8, *p*-(butylamino)benzoic acid-2-(diethylamino)ethyl ester; 9, benoximate; and 10, dibucaine. (Reproduced with permission from Kumazawa T, Sato K, Seno H, Ishii A and Suzuki O (1996) *Chromatographia* 43: 59.)

pH 7 and sampling at 45°C with agitation, and analysed by GC-MS.

Guan *et al.* analysed the metabolites of benzodiazepines from acid-hydrolysed urine samples using a direct immersion-SPME method in combination with GC-electron capture detection (ECD). The detection limits were 2–20 ng mL⁻¹ for most drugs tested. Jinno and Taniguchi, however, developed an SPME method coupled with HPLC for the analysis of six benzodiazepines in human urine samples. Sensitiv-

ity may be increased by the combination of saturated salt and weakly alkaline conditions in the extraction matrix. As shown in Figure 8, a 65-µm PA fibre was found to be more efficient in the extraction of benzodiazepines than a 100-µm PDMS fibre.

Narcotics and Other Illicit Drugs

Kumazawa *et al.* and Makino *et al.* developed direct immersion SPME methods in combination with GC-NPD for the rapid analysis of cocaine in urine

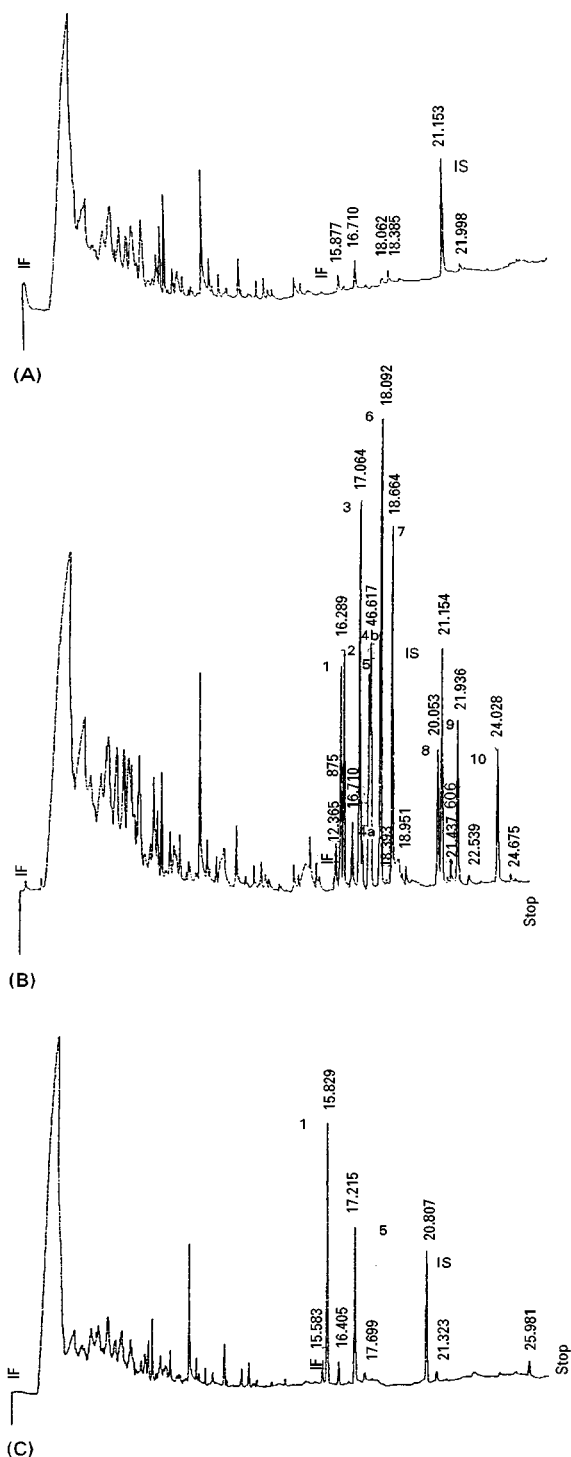


Figure 7 Typical SPME-GLC-NPD chromatograms obtained from (A) blank plasma with internal standard, (B) plasma spiked with ten antidepressant drugs and metabolites, each 375 ng mL^{-1} , and (C) a sample of a patient after suicidal intoxication with amitriptyline (amitriptyline, 766 ng mL^{-1} ; nortriptyline, 489 ng mL^{-1}). SPME conditions: fibre, $100\text{-}\mu\text{m}$ PDMS; extraction, shaking at 700 rpm for 10 min at 22°C ; desorption, 1 min exposure in GC injection port. GC conditions: column, DB-1 ($30 \text{ m} \times 0.32 \text{ mm i.d.}$, $0.25 \text{ }\mu\text{m}$ film thickness); column temperature, programme from 140°C to 220°C at $20^\circ\text{C min}^{-1}$ and from 220°C to 270°C at 2°C min^{-1} ; injector and detector temperatures, 260°C and 300°C , respectively; N_2 carrier gas flow-rate, 0.7 mL min^{-1} ; injection, splitless; detector, NPD. Peaks: 1, amitriptyline; 2, trimipramine; 3, imipramine; 4a, *cis*-doxepine; 4b, *trans*-doxepine; 5, nortriptyline; 6, mianserine; 7, desipramine; 8, maprotiline; 9, clomipramine; and 10, desmethylclomipramine. IS, internal standard (chloramitriptyline). (Reproduced with permission from Ulrich S and Martens J (1997) *Journal of Chromatography B* 696: 217. Copyright Elsevier Science.)

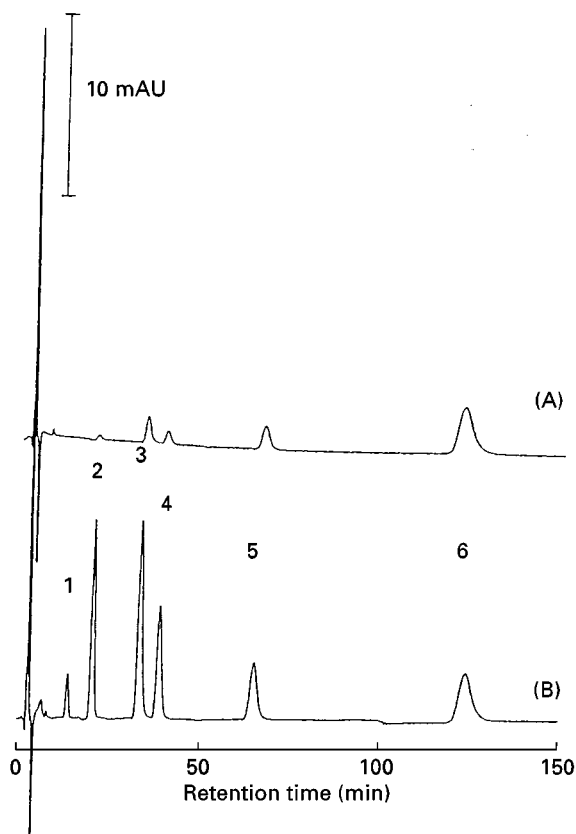


Figure 8 Chromatograms of extracted drugs with (A) 100- μm PDMS and (B) 85- μm PA. SPME conditions: extraction, stirring at 840 rpm for 3 h at 60°C; desorption, 30 min exposure in desorption chamber. HPLC conditions: column, Siperiorex ODS (250 mm \times 1.5 mm i.d.); mobile phase, acetonitrile/water; flow-rate, 100 $\mu\text{L min}^{-1}$; detection, UV at 220 nm. Peaks: 1, nitrazepam; 2, flunitrazepam; 3, fludiazepam; 4, diazepam; 5, clotiazepam; and 6, medazepam. (Reproduced with permission from Jinno K and Taniguchi M (1997) *Chromatography* 18: 244.)

samples. Recovery of cocaine by this technique using a 100- μm PDMS fibre was 20%, and the detection limit was about 12 ng mL $^{-1}$. Lord and Pawliszyn applied the SPME/GC-FID method developed for amphetamines to the analysis of meperidine, codeine, methadone, morphine and heroin in spiked urine samples. Furthermore, Hall *et al.* applied an immersion SPME technique to the analysis of four cannabinoids in human saliva. These drugs were extracted with a 100- μm PDMS fibre and analysed in the range from 5 to 500 ng mL $^{-1}$ by GC/MS. Using this method, Δ^9 -tetrahydrocannabinol (Δ^9 -THA) was detected in a saliva sample collected 30 min after the subject had smoked marijuana (Figure 9).

Strano-Rossi and Chiarotti reported an immersion SPME method using a 30- μm PDMS fibre in combination with GC/MS for the analysis of cannabinoids in alkaline hydrolysed hair samples. The method is also applied to the analysis of other drugs such as methadone, cocaine and cocaethylene in hair samples.

Other Drugs

Yashiki *et al.* developed a simple and rapid method for the analysis of nicotine and its principal metabolite, cotinine, in urine samples using headspace SPME and GC/MS-SIM. Krogh *et al.* applied a direct immersion SPME technique to the analysis of the antiepileptic drug valproic acid in plasma samples. The drug was extracted with a 100- μm PDMS fibre after dialysis of plasma samples, and then analysed by GC-FID. Seno *et al.* developed headspace SPME methods for the simple analysis of five phenothiazine drugs and thirteen diphenylmethane antihistaminic drugs and their analogues in urine and whole blood samples. A 100- μm PDMS fibre was exposed in the headspace of the sample vial after preheating of the sample in the presence of NaOH, and the drugs extracted in the fibre were analysed by GC-FID. The recoveries from blood extracts were lower than those from urine extracts for all drugs. Hall and Brodbelt reported a direct immersion SPME method coupled with ion-trap GC/MS for the analysis of eight barbiturates in

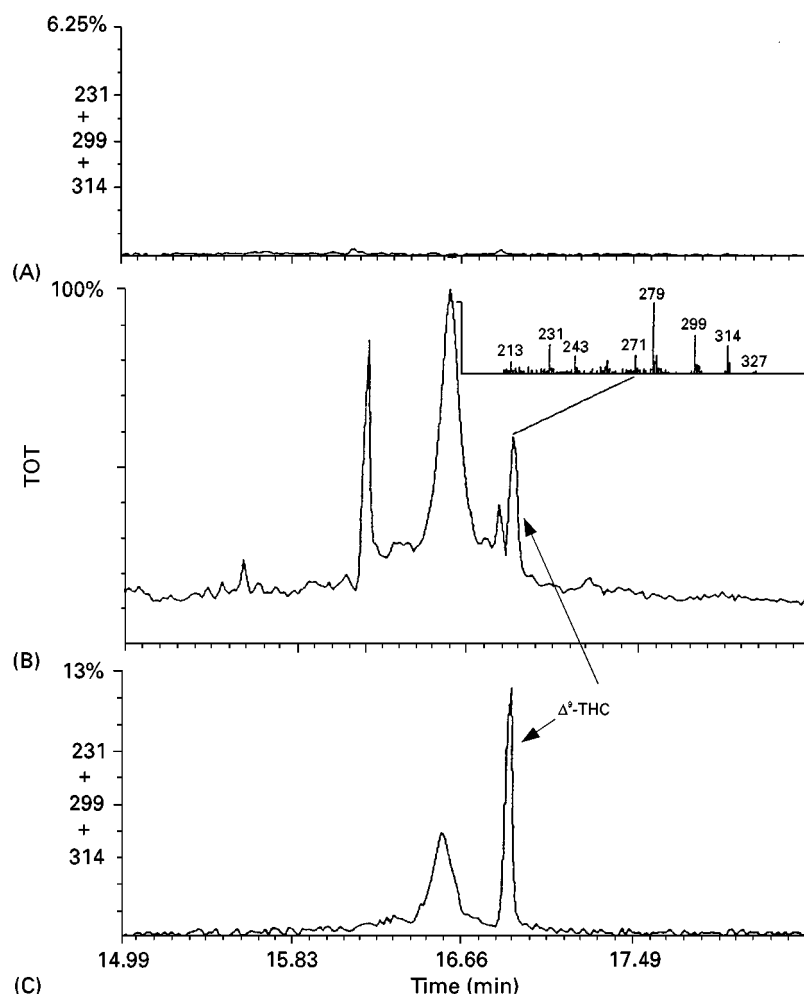


Figure 9 Chromatograms after performing SPME on human saliva samples prior to and after marijuana smoking. (A) SIM chromatogram of saliva sample before marijuana smoking; (B) total ion chromatogram of saliva sample after marijuana smoking; (C) SIM chromatogram of saliva sample after marijuana smoking. SPME conditions: fibre, 100 μm PDMS; extraction, immersion for 10 min with stirring; desorption, exposure for 12 min in GC injection port. GC/MS conditions: column, DB-5ms (30 m \times 0.25 mm i.d., 0.5 μm film thickness); oven temperature, initially hold at 50°C for 0.2 min and increase to 280°C at 15°C min⁻¹, and finally hold at 280°C for 2 min; transfer line temperature, 280°C; detection, ion trap (electron ionization mode); SIM ion, Δ^9 -THC (m/z = 231, 299, 314). (Reproduced with permission from Hall BJ, Satterfield-Doerr M, Parikh AR and Brodbelt JS (1998) *Analytical Chemistry* 70: 1788. Copyright American Chemical Society.)

urine samples. A 65- μm Carbowax/DVB fibre was suitable for the extraction of these drugs. The detection limits reached 1 ng mL⁻¹. Okeyo *et al.* developed a straightforward method for performing derivatizing reactions of five steroids *in situ* in SPME fibres. After extraction of drugs from serum samples by direct immersion SPME, the drugs extracted on 85- μm PA fibre were derivatized in the headspace of the silylating reagent bis(trimethylsilyl)trifluoro-acetamide, and then analysed by GC/MS. With derivatization, SPME and GC analysis can be easily extended to the analysis of semi- and non-volatile compounds.

Volmer and Hui developed a SPME/LC/MS method for isolating and analysing eleven corticosteroids and two steroid conjugates from urine samples. After extraction in the vial by direct

immersion SPME using 65- μm Carbowax/DVB fibre, the drugs extracted in the fibre were desorbed in the desorption chamber of the SPME/HPLC interface, and then analysed by electrospray LC/MS. As shown in **Figure 10**, several corticosteroids and steroid sulfates spiked in urine samples were selectively analysed, although a minor peak was observed in the blank control urine in the SIM trace for cortisone.

Furthermore, Kataoka *et al.* developed an automated in-tube SPME/LC/MS method for the determination of the histamine H₂-receptor antagonist ranitidine in urine samples. The ranitidine in urine samples was directly extracted into Omegawax 250 capillary by 10 draw/eject cycles of 30 μL of sample at pH 8.5, desorbed from the capillary with

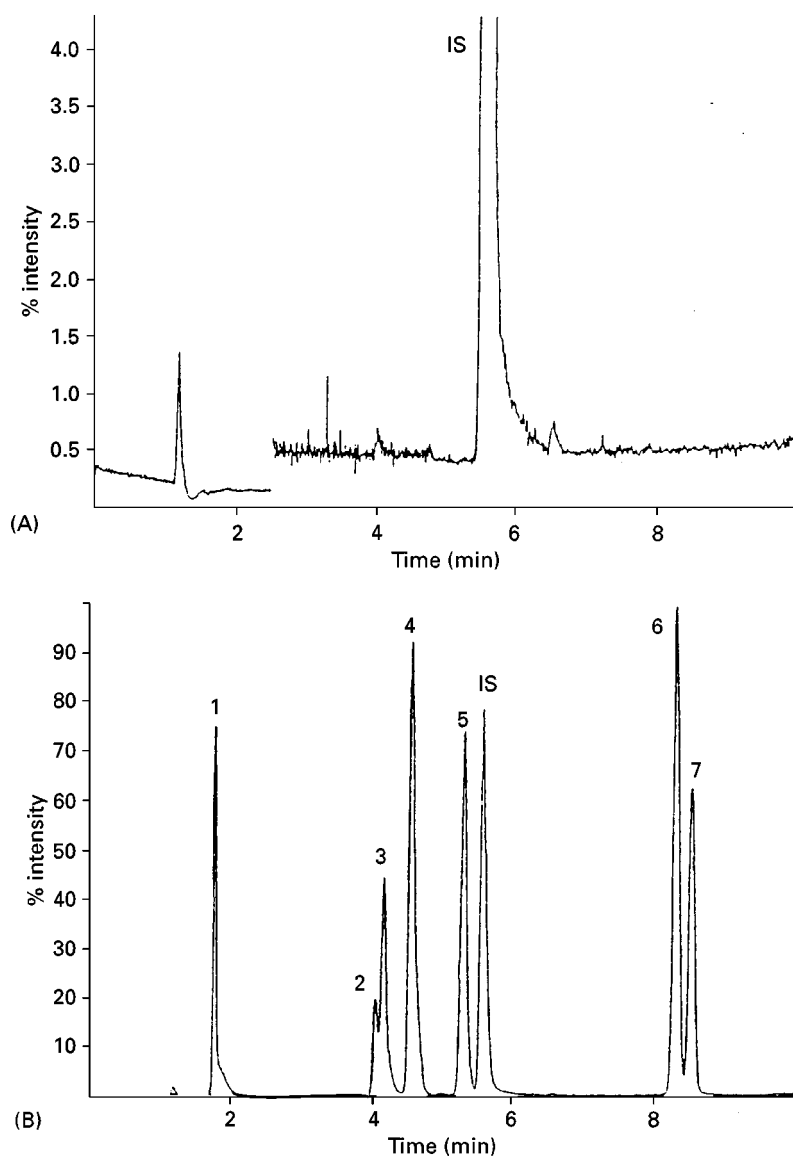


Figure 10 SPME/LC/MS analysis of several corticosteroids and steroid conjugates by time-scheduled SIM. The original urine sample was spiked at the 20 mg mL^{-1} level. (A) Blank control urine; (B) spiked urine. LC/MS conditions: column, YMC ODS-AQ ($50 \text{ mm} \times 4.0 \text{ mm i.d.}$, $3 \mu\text{m}$ particle size); column temperature, 25°C ; mobile phase, A = 100 mM ammonium acetate and B = acetonitrile/methanol ($50 : 50$; + 100 mM ammonium acetate), A : B was gradient programmed from $60 : 40$ to $20 : 80$ in 10 min ; flow-rate, 1 mL min^{-1} ; fragmentor voltage, 40 V ; ionization mode, negative ESI. SPME conditions: fibre, $65 \mu\text{m}$ carbowax/DVB; sample pH, 8.5 ; extraction, immersion for 15 min with stirring; desorption, methanol/water ($50 : 50$) for 5 min . Peaks: 1, estriol-3-sulfate; 2, cortisone; 3, fludrocortisone; 4, estrone-3-sulfate; 5, 6-methylprednisolone; 6, budesonide (epimer B); 7, budesonide (epimer A); IS = internal standard (niflumic acid) at $20 \mu\text{g mL}^{-1}$. (Reproduced with permission from Volmer DA and Hui JPM (1997) *Rapid Communications in Mass Spectrometry* 11: 1926. Copyright John Wiley & Sons Limited.)

methanol, and then analysed by electrospray LC/MS. Using this technique, nine beta-blockers and metabolites in urine and serum samples were also analysed. These methods were simple, rapid, selective and sensitive, and directly applied to urine samples and serum samples after ultrafiltration. Propranolol (PL) and its metabolites were successfully detected in the serum sample of a patient administered PL (see Figure 11).

Prospective of SPME in Biomedical Analysis

The main advantages of SPME are simplicity, rapidity, solvent elimination, high sensitivity, small sample volume, lower cost and simple automation. Since 1995, a number of SPME methods have been developed to extract drugs from various biological samples such as urine, serum, plasma, whole blood, saliva

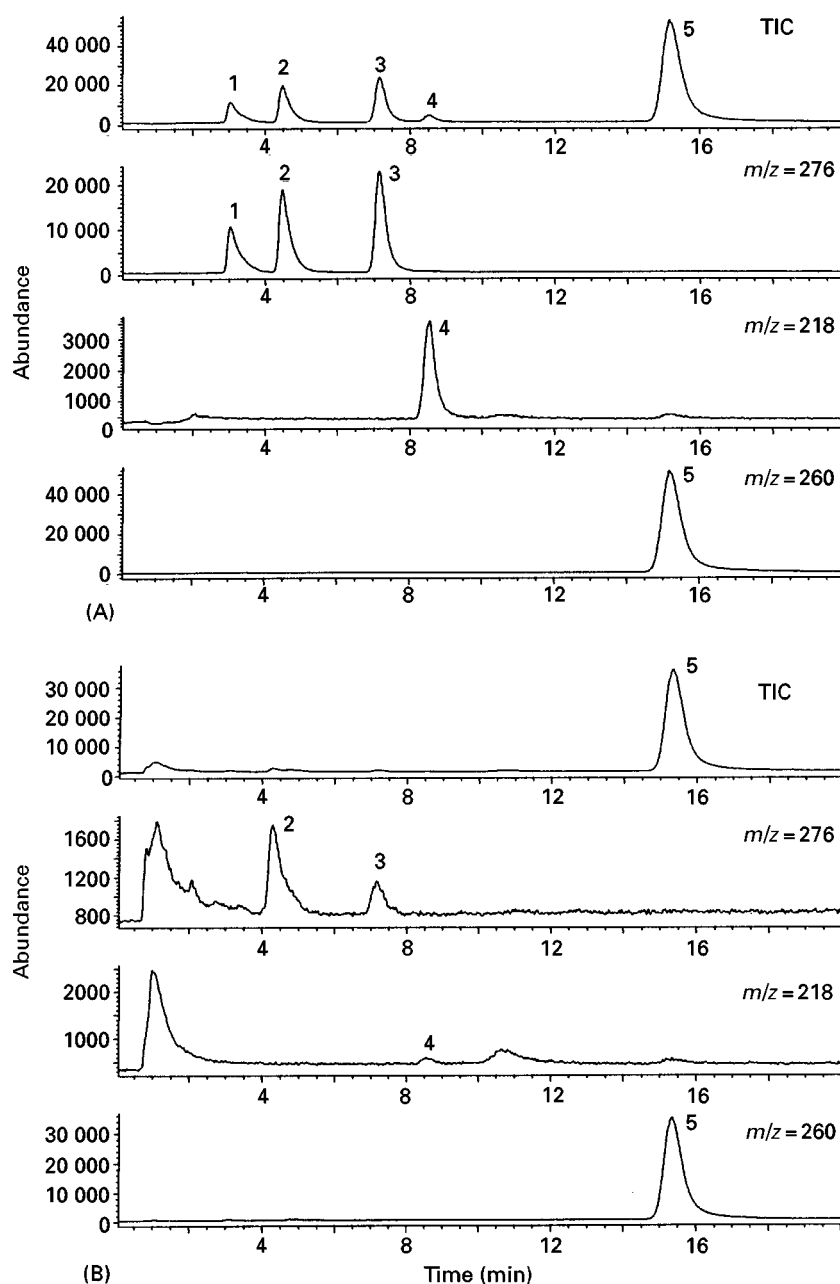


Figure 11 Total ion and SIM chromatograms obtained from standard propanolol and its metabolites, and a clinical serum sample by in-tube SPME/LC/MS. (A) Standard solution containing 200 ng mL^{-1} propanolol (PL), 50 ng mL^{-1} 4-hydroxypropanolol (4-OH-PL) and 7-hydroxypropanolol (7-OH-PL), 20 ng mL^{-1} 5-hydroxypropanolol (5-OH-PL) and *N*-desisopropylpropanolol (NDP). (B) Clinical serum sample ($100 \mu\text{L}$). Serum sample was diluted five times with 1% acetic acid and used for analysis after ultrafiltration. LC/MS conditions: column, Hypersil BDS C_{18} ($5.0 \text{ cm} \times 2.1 \text{ mm i.d.}$, $3 \mu\text{m}$ particle size); column temperature, 25°C ; mobile phase, acetonitrile/methanol/water/acetic acid (15 : 15 : 70 : 1); flow-rate, programme from 0.25 to 0.45 mL min^{-1} for 20 min run; fragmentor voltage, 70 V ; ionization mode, positive ESI; SIM ion, $m/z = 218$ (NDP), 276 (hydroxypropanolols) and 260 (PL). In-tube SPME conditions: capillary, Omegawax 250 ($60 \text{ cm} \times 0.25 \text{ mm i.d.}$, $0.25 \mu\text{m}$ film thickness); sample pH, 8.5; draw/eject cycles, 15; draw/eject volume, $35 \mu\text{L}$; draw/eject flow-rate, $100 \mu\text{L min}^{-1}$; desorption solvent, mobile phase. Peaks: 1, 5-OH-PL; 2, 4-OH-PL; 3, 7-OH-PL; 4, NDP; and 5, PL. (Reproduced with permission from Kataoka H, Narimatsu S, Lord HL and Pawliszyn J (1999) *Journal of Analytical Chemistry* 71: 4237. Copyright American Chemical Society.)

and hair. The affinity of the fibre coating for an analyte is the most important factor in SPME. As shown in Table 1, fibre coatings of different polarity and thickness were selected for each drug. Most drugs

in biological samples were extracted with $100\text{-}\mu\text{m}$ PDMS for nonpolar drugs and $85\text{-}\mu\text{m}$ PA for polar drugs. A solvent-modified fibre can improve selectivity and shorten extraction time. Although the theories

of fibre and in-tube SPME methods are similar, there are significant differences between these methods. The extraction of analytes is performed on the outer surface of the fibre for fibre SPME and in the inner surface of the capillary for in-tube SPME. Commercially available SPME fibres for drug analysis are limited, by GC capillary columns with a vast array of stationary phases are commercially available for in-tube SPME. Headspace fibre SPME is suitable for the extraction of drugs in gaseous, liquid and solid samples, because of the avoidance of contact with an aggressive matrix incompatible with the fibre. Direct immersion fibre SPME can be used to extract drugs from clear and cloudy liquid samples, however, in-tube SPME is limited to the extraction of clear liquid samples. The headspace SPME technique, therefore, is suitable for direct extraction from whole blood samples, while immersion fibre SPME or in-tube SPME methods require deproteinization or ultrafiltration of these samples prior to extraction. As mentioned above, the extraction efficiency of fibre SPME depends on extraction time, agitation, heating, sample pH and salt concentration. For in-tube SPME, number, volume and speed of draw/eject cycles, and sample pH are important factors for efficient extraction. On the other hand, the desorption of analyte from a fibre or capillary coating depends on the temperature of the injection port and exposure time in combination with GC or GC/MS, or component and volume of solvent when used in combination with HPLC or LC/MS. Therefore, these SPME parameters should be optimized when developing a new SPME method for drug analysis.

With further development of new coating materials, such as affinity coatings for target drugs and chiral coatings for optically active drugs, the further development of derivatization methods, further coupling with different analytical instruments, such as capillary electrophoresis, and improvement of the extraction and desorption conditions, the SPME technique is expected to be widely applied in the future for highly efficient extraction of drugs from various biological samples.

See also: II/Chromatography: Gas: Derivatization. Extraction: Solid-Phase Microextraction.

Further Reading

Battu C, Marquet P, Fanconnet AL, Lacassie E and Lachatre G (1998) Screening procedure of 21 amphetamine-related compounds in urine using solid-phase microextraction and gas chromatography-mass spectrometry. *Journal of Chromatographic Science* 36: 1-7.

mine-related compounds in urine using solid-phase microextraction and gas chromatography-mass spectrometry. *Journal of Chromatographic Science* 36: 1-7.

Degal F (1996) Comparison of new solid-phase extraction methods for chromatographic identification of drugs in clinical toxicological analysis. *Clinical Biochemistry* 29: 529-540.

Eisert R and Levsen K (1996) Solid-phase microextraction coupled to gas chromatography: a new method for the analysis of organics in water. *Journal of Chromatography A* 733: 143-157.

Junting L, Peng C and Suzuki O (1998) Solid-phase microextraction (SPME) of drugs and poisons from biological samples. *Forensic Science International* 97: 93-100.

Kataoka H, Narimatsu S, Lord HL and Pawliszyn J (1999) Development of on-line in-tube solid-phase microextraction/LC/MS system. *Chromatography* 20: 237-246.

Kroll C and Borchert HH (1998) Solid phase microextraction (SPME) for sample preparation during drug metabolism studies. *Pharmazie* 53: 172-177.

Lord HL and Pawliszyn J (1998) Recent advances in solid-phase microextraction. *LC-GC* S41-S46.

Namera A, Yashiki M, Kojima T and Fukunaga N (1998) Solid phase microextraction in forensic toxicology. *Japanese Journal of Forensic Toxicology* 16: 1-15.

Pawliszyn J (1995) New directions in sample preparation for analysis of organic compounds. *Trends in Analytical Chemistry* 14: 113-122.

Pawliszyn J (1997) *Solid Phase Microextraction: Theory and Practice*. New York: John Wiley.

Pawliszyn J (1999) *Applications of Solid Phase Microextraction*. Cambridge, UK: The Royal Society of Chemistry.

Penton ZE (1997) Sample preparation for gas chromatography with solid-phase extraction and solid-phase microextraction. *Advances in Chromatography* 37: 205-236.

Sporkert F and Pragst F (2000) Use of headspace solid-phase microextraction (HS-SPME) in hair analysis for organic compounds. *Forensic Science International* 107: 129-148.

Ulrich S and Martens J (1997) Solid-phase microextraction with capillary gas-liquid chromatography and nitrogen-phosphorus selective detection for the assay of antidepressant drugs in human plasma. *Journal of Chromatography B: Biomedical Applications* 69: 217-234.

Volmer DA and Hui JPM (1997) Rapid determination of corticosteroids in urine by combined solid-phase microextraction/liquid chromatography/mass spectrometry. *Rapid Communications in Mass Spectrometry* 11: 1926-1934.

Zhang Z, Yang MJ and Pawliszyn J (1994) Solid phase microextraction: a new solvent-free alternative for sample preparation. *Analytical Chemistry* 66: 844A-853A.

Environmental Applications

A. Andrews, Ohio University, Athens, OH, USA

Copyright © 2000 Academic Press

Introduction

Solid-phase microextraction (SPME) was first described by Pawliszyn and co-workers from the University of Waterloo in 1989 and has rapidly become a popular extraction method in research.

Briefly, SPME uses an immobilized liquid polymer phase coated on the outside of a fused silica fibre. By dipping this fibre into either a liquid (usually aqueous) sample, or the headspace above a liquid sample, absorption of the analytes from the matrix into the polymer layer occurs. Analyte desorption occurs in either the heated inlet port of a gas chromatograph or a specially constructed inlet loop in the case of liquid chromatographic analysis.

Adjustment of the sample pH or ionic strength can be used to enhance the analyte partitioning into the fibre coating. The adjustment of ionic strength is commonly carried out by the addition of an inorganic salt such as sodium chloride. To reduce the time taken for equilibrium between the fibre coating and the sample agitation is used. This is usually achieved with a magnetic stir bar system.

SPME has the advantage that it is a solvent-free technique, which reduces both environmental pollution and sample preparation time, as no additional concentration step is required. There is no packed cartridge bed, as with solid-phase extraction (SPE), and so SPME does not suffer from plugging and is complete in two stages. This minimizes the chance of analyte loss or operator error.

There are now many examples of the extraction of analytes of environmental interest. This article will cover the more recent examples from each class of environmental pollutants. Articles listed in the Further Reading cover these areas in more depth than is possible here.

Volatile Organic Chemicals

One of the most common environmental applications of SPME is the analysis of volatile organic compounds. The chemicals frequently used as representative of this class are benzene, toluene, ethylbenzene and the xylene isomers (BTEX).

Most BTEX extractions have been carried out using polydimethylsiloxane (PDMS) as the polymer

coating on the fibre. Whilst PDMS works well for the extraction of the BTEX compounds, the recoveries from the sample are typically in the 0.1–10% range. With such a low recovery, the limits of detection (LOD) are often higher than those achieved with conventional purge-and-trap analysis.

An interesting way to reduce LODs without resorting to more expensive detectors is to use a fibre freshly coated with PDMS that is then dipped in extra-fine powdered activated charcoal. The total thickness of this coating is approximately 100 μm , which is similar to the thickness of a commercially available fibre.

Using the PDMS/charcoal-coated fibre, recoveries of greater than 90% are achieved in about 15 min extraction time at 25°C, or in under 10 min at 75°C using headspace analysis and salting out of the sample, as illustrated in **Figure 1**. These high recoveries give LODs of $\leq 21 \text{ pg mL}^{-1}$ with GC analysis using a flame ionization detector (FID). This is over an order of magnitude better than the LODs for the US Environmental Protection Agency method 524.2, and two orders better than conventional PDMS SPME with gas chromatography (GC)-FID analysis.

Surfactants

Alkylphenol surfactants are becoming of increasing concern due to their possible role as endocrine disrupters. SPME analysis of this class of surfactants eliminates the need for the concentration step frequently required with conventional liquid–liquid extraction or SPE.

As alkylphenol ethoxylate surfactants are not amenable to GC analysis without derivatization, and SPME with derivatization is a much less well-developed technique than classical SPME, analysis of the surfactants has been accomplished by normal-phase gradient high performance liquid chromatography (HPLC) with UV detection.

This requires a specific interface for desorbing the surfactants from the fibre after adsorption (**Figure 2**). The fibre desorption chamber is a three-way tee in which two outlets are connected to the injection valve and the third houses the SPME device. Flow to the tee is via stainless steel tubing (d) and back to the injection port is via poly(ether ether ketone) (PEEK) tubing (e) connected via a finger-tight PEEK union (f). The SPME device (g) is positioned in the top part of the tee. One of the problems initially encountered with this device was stripping of the fibre coating by

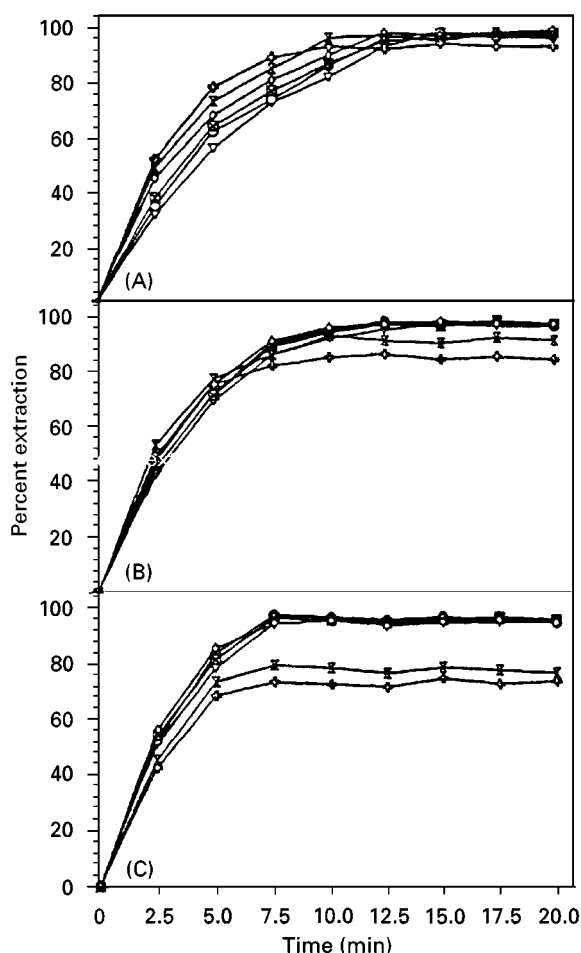


Figure 1 Dependence of extraction efficiency on exposure time and temperature. BTEX concentration, 500 pg mL^{-1} of each compound; stirring speed, 50% of maximum; amount of NaCl, 15 g. (A) $T = 25^\circ\text{C}$; (B) $T = 50^\circ\text{C}$; (C) $T = 75^\circ\text{C}$. Open circles, benzene; open squares, toluene; filled circles, ethylbenzene; filled squares, *p*-xylene; open triangles, *m*-xylene; filled triangles, *o*-xylene. Reproduced with permission from Djozan DJ and Assadi J (1997). Copyright Elsevier Science.

the narrow internal diameter stainless steel tubing (d). This was because of swelling of the coating, which occurred in the desorption solvents used. Increasing the diameter of the tubing to account for this swelling solved this problem. In order to be able to withstand the high pressures used in HPLC, a slip-free supercritical fluid extraction connector (i) was used to provide a strong seal. A large diameter Teflon tube (h) and a regular ferrule (j) complete the desorption device.

When analysing for surfactants, it is important that the extraction method does not discriminate against any of the oligomers present in the sample. A Carbowax/template resin-coated SPME fibre was found to show good extraction of the various chain length surfactants. To ensure that the extracted ethoxamer

distribution was the same as the original sample, salting out of the sample was carried out; without this, a bias towards shorter chain ethoxamers is obtained.

The final analysis method has been successfully applied to the determination of a number of surfactants, as shown in Figure 3. LODs for the individual alkylphenol ethoxamers are in the low p.p.b. range.

Hetero-organic Pollutants

Compounds with nitrogen, sulfur or oxygen (NSO) in the aromatic ring system are frequently encountered as pollutants in groundwater. These hetero-organic pollutants are often the result of creosote contamination. For NSO groundwater analysis, LODs in the ng L^{-1} range are required. Currently this is only achievable with liquid-liquid extraction using a concentration step.

For SPME analysis of NSOs, out of three fibre coatings investigated, PDMS, polyacrylate (PA) and Carbowax, only the PA coating successfully extracted all of the 15 NSO compounds investigated. However, the amount extracted at equilibrium is small, ranging from 0.4% for pyrrole to 57% for dibenzofuran. Although pH over the range of 7–10 does not affect the amount extracted, higher pH values degrade the fibre coating. Adjusting the sample ionic strength by adding sodium chloride increases the amount extracted.

The LODs obtained, distribution coefficients and aqueous solubility of the NSO compounds investigated are shown in Table 1. In comparison to a conventional analysis this SPME method showed improved performance for water soluble and semivolatile NSOs, but poorer performance for the volatile NSOs. Carryover from one sample to the next was also a problem and necessitated a 10 min offline fibre cleaning process between samples. Fibres were found to degrade slowly with use, and were discarded after 50 analyses.

Pesticides and Herbicides

The monitoring of groundwater for pesticide and herbicide contamination is a common environmental analysis. Accordingly, there have been a number of reports on the use of SPME for pesticide extraction. Many different classes of pesticides have been studied, including the organochlorine and organophosphorus pesticides.

With organophosphorus pesticides, the best fibre coating is an XAD polymer (polystyrene-divinylbenzene)

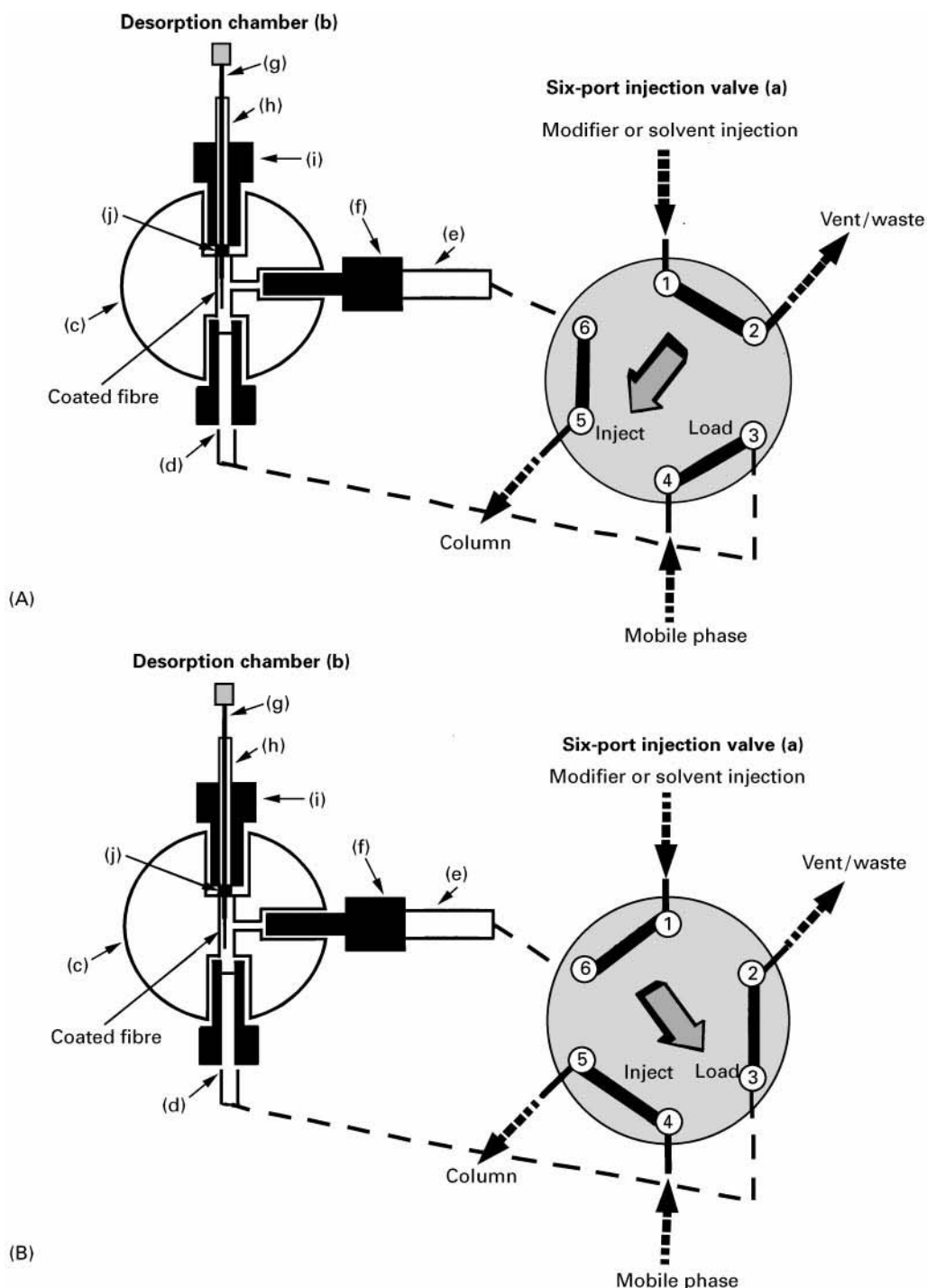


Figure 2 Modified SPME-LC interface in (A) the fibre desorption and (B) insertion modes. Arrows indicate flow direction. Reproduced with permission from Boyd-Boland and Pawliszyn (1996). Copyright American Chemical Society.

phase. The aromatic character of this material provides superior extraction for many of the organophosphorus pesticides in comparison to a PDMS phase. This class of pesticides is one group of compounds where salting out has no beneficial effect. The limitation of the SPME extraction was that the

relative standard deviation (RSD) values seen were very large – up to 80% in some cases. In addition, some carryover from run to run was experienced. Until these problems can be solved, the method is more suitable for screening than for routine analysis.

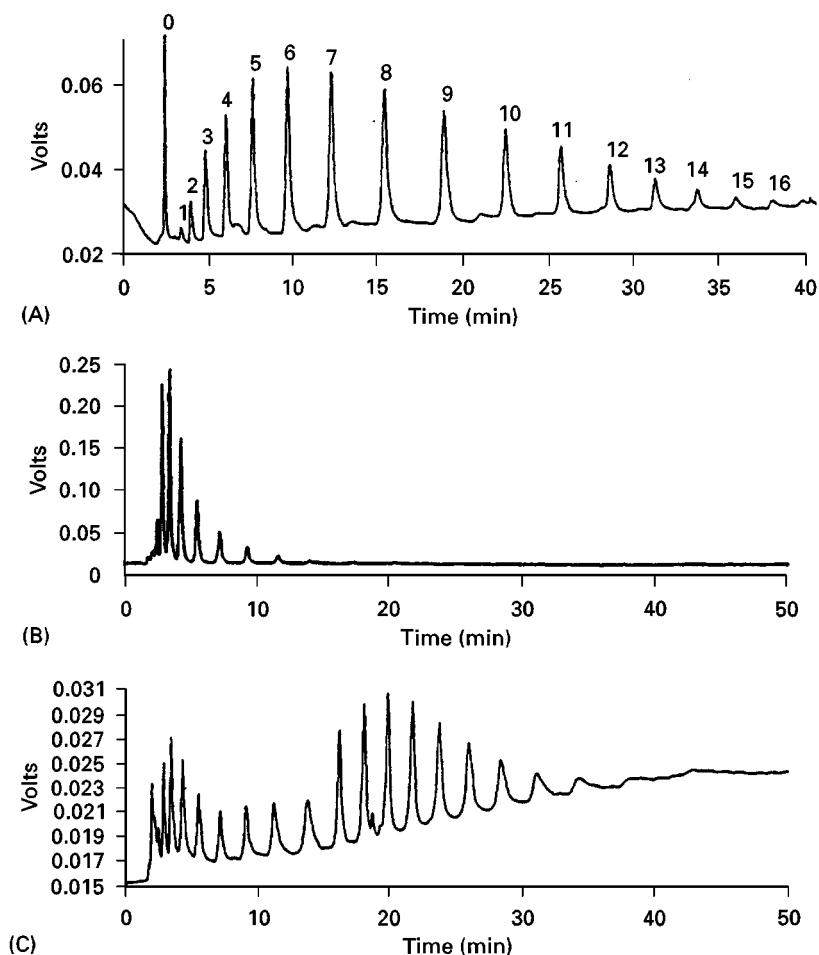


Figure 3 LC chromatograms of the extracted alkylphenol ethoxylates: (A) Triton X-100; (B) Rexol 25/4; (C) Rexol 25/5. Peak assignment in (A) refers to the number of units in the ethoxylate chain. Reproduced with permission from Boyd-Boland and Pawliszyn (1996). Copyright American Chemical Society.

One of the great areas of potential for SPME is automated analysis. This has been partially demonstrated in the field of pesticide analysis by coupling SPME extraction from a flow cell with GC-FID. The online flow-through cell used is shown in **Figure 4**. The extraction is performed whilst pumping the sample in a closed loop for 30 min. Changing the flow rate from 0.1 to 10 mL min⁻¹ did not affect the precision of the extraction, presumably because flow inside the extraction chamber where the fibre is positioned is turbulent across this entire range. Method precision was found to compare well with other sample agitation methods, such as fibre vibration or magnetic stirring.

This method has been applied to the analysis of the S-triazines (herbicides) and, although not fully automated, as operator intervention was required to transfer the SPME fibre from the extraction cell to the GC, it is clearly a step in that direction.

Polycyclic Aromatic Hydrocarbons and Polychlorinated Biphenyls

Many of the samples analysed for environmental contamination are solids, in particular soils and sludges. These present a challenge to SPME, particularly in the case of semivolatiles, such as polycyclic aromatic hydrocarbons (PAHs) and polychlorinated biphenyls (PCBs), where heating and headspace extraction cannot be used.

A solution to this problem is first to extract the analytes of interest with subcritical water and then extract the resulting subcritical water solution via SPME. In this way, no hazardous solvents of any kind are used during the extraction procedure.

Extractions are carried out in a heavy-duty stainless steel pipe partially filled with solid sample and approximately 3.5 mL of HPLC-grade water. Care should be taken to avoid samples which might react with water leading to pressures higher than expected.

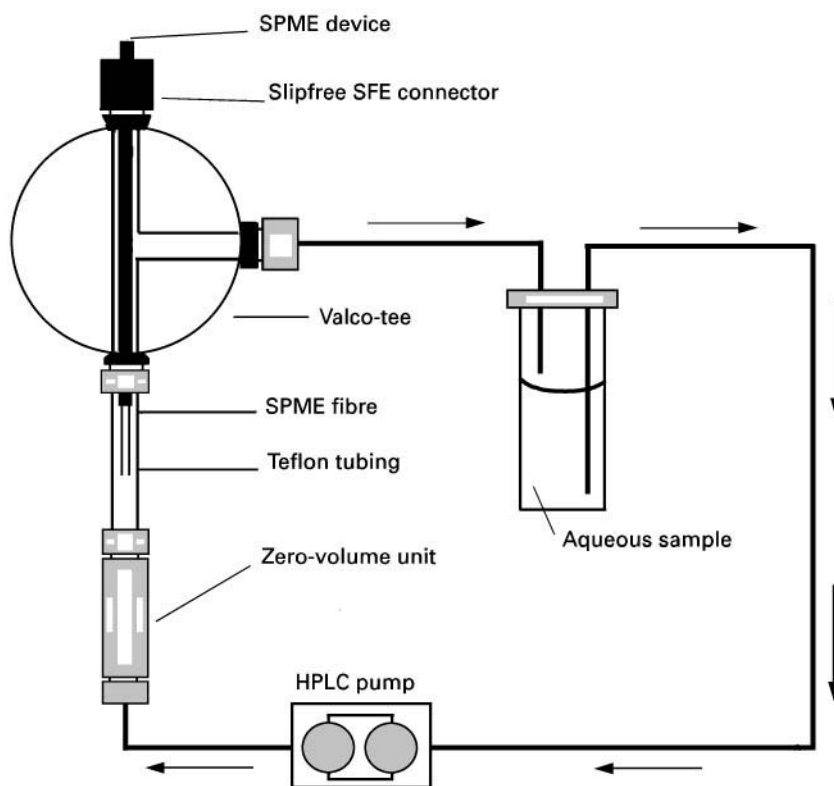
Table 1 The measured distribution constants between polyacrylate fibre and water, the octanol–water partition coefficients ($\log K_{ow}$), aqueous solubility (mg L^{-1}), limit of detection of NSO by SPME-GC-FID and SPME-GC-ITMS in $\mu\text{g L}^{-1}$ and %RSD

Compound	K	$\log K_{ow}$	S_w (mg L^{-1})	LOD-FID ($\mu\text{g L}^{-1}$)	LOD-MS ($\mu\text{g L}^{-1}$)	% RSD ITMS ($\mu\text{g L}^{-1}$)
Thiophene	0.34	1.81	3600	nd.	1.0	14
1-Methylpyrrole	0.04	—	Soluble	nd.	2.5	13
Pyrrole	0.10	0.75	58 000	nd.	10	12
2-Methylpyridine	0.02	1.06	Soluble	nd.	(10)	5.9
2,4-Dimethylpyridine	0.09	—	Soluble	nd.	(10)	14
Benzofuran	3.1	2.67	—	3	0.03	4.2
Benzothiophene	7.9	3.12	130	2	0.02	5.8
Quinoline	0.46	2.03	6500	15	0.3	10
Indole	3.2	2.00	1850	2	0.02	6.9
2-Methylquinoline	0.53	2.23	—	10	0.2	3.3
Dibenzofuran	22	4.12	6.6	2	0.03	10
Dibenzothiophene	27	5.45	1.0	2	0.02	11
Acridine	7.7	3.50	46	0.5	0.02	9.2
Carbazole	29	3.71	1.2	0.5	0.02	10
DBT-sulfone	4.9	—	—	0.5	0.04	9.1

— Unknown; n.d., not detected; LOD, determined by $100 \mu\text{g L}^{-1}$ standard solutions. Reproduced with permission from Johansen and Pawliszyn (1996) Copyright John Wiley & Sons, Inc.

The sealed pipe is then heated in a GC oven for an initial extraction time period. After cooling, conventional SPME extraction using a $100 \mu\text{m}$ PDMS-coated fibre of 1.8 mL of the resulting supernatant liquid is carried out in a 2 mL vial.

Increasing the temperature of the water extraction to 250°C improved the extraction of PAHs but further increases in temperature did not improve the results. Increasing the water extraction time from 15 to 60 minutes also increased the amount of PAHs

**Figure 4** Instrumental set-up for the online flow-through cell. The SPME fibre hosts in a Valco-tee unit sealed by a vespel ferrule. The aqueous sample is pumped by a HPLC pump from the sample vial through the extraction cell and back to the reservoir (closed loop). Reproduced with permission from Eisart and Pawliszyn (1997). Copyright Elsevier Science.

extracted, but not by enough to justify the increased time taken for the extraction procedure. One point of note was the unusual conversion of d_{10} -anthracene to d_8 -anthracene during the extraction. This was unexpected, as the hot liquid water used is regarded as being relatively unreactive and other deuterated standards did not show the same effect.

Partitioning of the higher molecular weight PAHs back on to the soil during cooling of the water extract was found to be a problem that affected quantification, unless deuterated standards for each compound were added.

PCBs are another ubiquitous environmental pollutant that have been determined by using SPME extraction in a variety of water samples. Conventional 100 μm PDMS fibres were found to give sufficient extraction of PCBs from water samples in 15 min to have a LOD of around 5 pg mL^{-1} for each congener with GC and electron-capture detection. This would allow reasonably fast screening of samples for the presence of PCBs.

Carryover was found to be present on not only the SPME fibres, but also the Teflon coated stir-bars, which were used to agitate the solution for more efficient extraction. New stir bars were required for each sample to avoid this problem. Eliminating fibre carryover was more difficult but offline desorption, coupled with running blanks between every sample, minimized the problem.

Old fibres (used more than 30 times) were found to show more severe carryover than new fibres. This

degradation in use meant that even with the off-line desorption, carryover could still be present, and would necessitate regular changing of the fibre.

In contrast to many other SPME studies, it was found that no direct correlation existed between the octanol-water partitioning coefficient (K_{ow}) and the fibre-water coefficient (K_{SPME}). The deviations begin to occur with analytes of molecular mass greater than 200 and, hence, for these compounds, K_{ow} cannot be used to estimate K_{SPME} .

Suspended solids in real water matrices were found to reduce the aqueous PCB concentration by up to 50% after spiking within 24 h. This partitioning on to suspended solids is similar to that seen for PAHs.

Chlorobenzenes

Chlorobenzenes are classified as priority pollutants in both the US and the European Union. SPME has been evaluated in both the headspace sampling and direct sampling modes for the determination of chlorobenzenes in soil samples. One of the problems of using SPME with soil samples is that quantification problems occur with soil samples that have a high organic content when using the external calibration method. This has necessitated the use of the standard addition method for reliable quantitation.

Another problem with heavily contaminated soils is the overloading of the detector beyond the linear dynamic range by the large amount of analyte extracted. This is a particular problem with detectors such

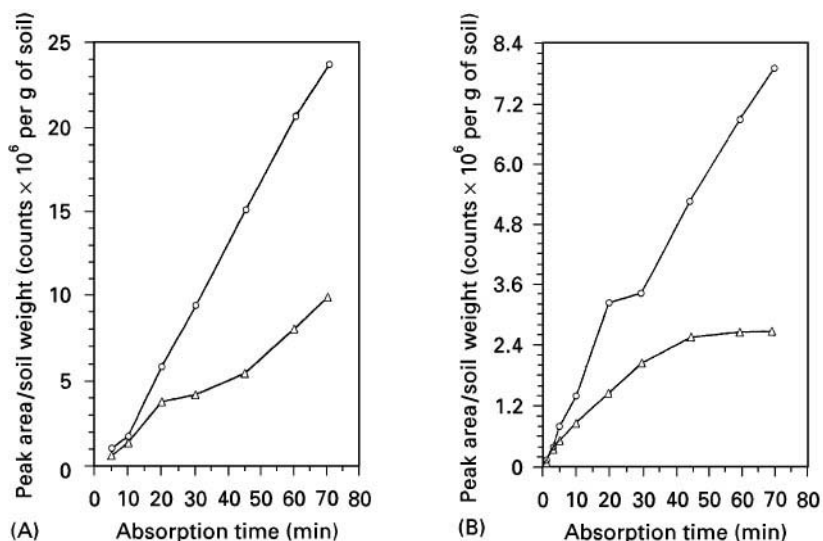


Figure 5 Effect of (A) (circles; 10%; triangles, 30%) methanol and (B) (circles, 20%; triangles, 30%) acetone on the absorption time profile of pentachlorobenzene by direct SPME-GC-ITMS using a 100 μm PDMS fibre with 0.030 g of soil, 40 mL of water-organic solvent; stirring speed 1000 rpm, sampling temperature 30°C, exposure time 25 min; splitless injection mode. Reproduced with permission from Sarrión *et al.* (1998). Copyright Elsevier Science.

as the ion trap mass spectrometer (ITMS). The addition of a water-miscible solvent, such as acetone (up to 30% v/v), to the water, which has previously been added to the soil sample, reduces the amount extracted into the fibre to within the linear dynamic range of the ITMS. The organic solvent also reduces the time required to reach equilibrium and allows shorter extraction times to be used. This is illustrated in Figure 5.

Using a 100 μm PDMS fibre, there was no significant difference seen in RSD values between headspace and direct sampling. A 7 μm PDMS fibre did show higher RSD values than the 100 μm PDMS fibre for headspace sampling. Using GC-ITMS analysis, the LODs were between 30 and 100 pg g^{-1} for the 100 μm fibre and headspace sampling. Headspace sampling gave a cleaner extract and resulted in a longer fibre life than the direct sampling method.

Comparison of SPME results obtained on a reference soil (CRM-530 or industrially contaminated clay soil) with results from other laboratories, mostly using Soxhlet extraction, showed good agreement for the mean values of the analytes.

Organometallics

Most SPME applications in the environmental field have been with organic pollutants. With the use of derivatization SPME, this has recently been extended to include some organometallic pollutants.

For heavy metals there is a strong dependence of the toxicity with the chemical form and the speciation of an element in a sample.

Sodium tetraethylborate (NaBEt_4) is a useful derivatizing agent for a number of organometallic compounds, including those of lead, mercury, cadmium,

Table 2 Reproducibility and limits of detection for tin using SPME-GC-ICPMS

Component	RSD ($n = 10$) (%)	LOD ($3 s$, $n = 10$) (ng L^{-1} as metal)
Monobutyltin	5.2	0.34
Dibutyltin	8.9	2.1
Tributyltin	14	1.1
Methyl mercury	11	4.3
Trimethyl lead	8.2	0.19

Reproduced with permission from Moens *et al.* (1997). Copyright American Chemical Society.

tin and selenium. Using this reagent, derivatization can be performed in aqueous solution simultaneously with the extraction.

Optimal derivatization conditions were obtained at a pH of 5.3 using 1 mL of a 1% NaBEt_4 solution with 25 mL of sample. The rate-limiting step was the extraction into the fibre coating in the headspace extraction mode and not the derivatization.

Compromise extraction conditions were used of 10 min extraction time at 25°C. Longer extraction times increase the amount extracted, but 90% is extracted within the first 10 min. Increasing the extraction temperature increased the amount extracted for some compounds, but decreased the amount for others. As a result, 25°C was chosen, as it avoids the need for sample heating.

Using GC with inductively coupled plasma-mass spectrometry (ICP-MS) detection, LODs in the low parts per trillion were obtained, as shown in Table 2. The method has been applied to a standard reference material (NRC PACS-1, a marine sediment) to determine organotin content. A clean extract was obtained, as can be seen in Figure 6. The results for the dibutyl- and tributyltin showed good agreement with

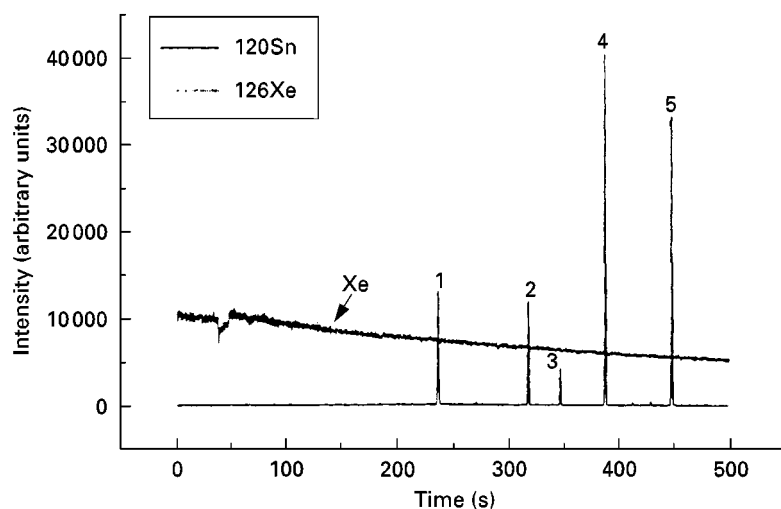


Figure 6 LC chromatogram of the PACS-1 reference material. Identification of peaks, 1, tetraethyltin; 2, monobutyltin; 3, tripropyltin; 4, dibutyltin; 5, tributyltin. Reproduced with permission from Moens *et al.* (1997). Copyright American Chemical Society.

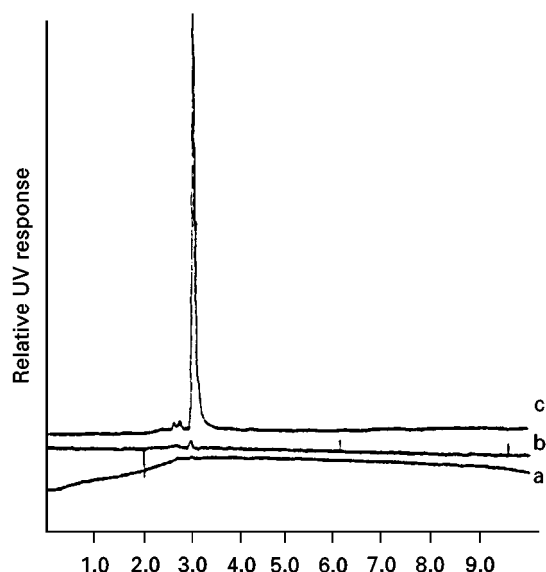


Figure 7 LC chromatogram for SPME injection with UV detection at 275 nm. (a) Fibre blank for microporous hollow fibre without dipping with DBC and HgCl_2 solution. (b) DBC blank microporous hollow fibre only dipping with 0.02 mol L^{-1} DBC solution for 5 min. (c) Microporous hollow fibre dipping with DBC solution for 5 min, then dipping with 0.02 mol L^{-1} HgCl_2 aqueous solution for 5 min. Reproduced with permission from Jia *et al.* (1998). Copyright John Wiley & Sons, Inc.

the certified values and the values obtained via a classical liquid-liquid extraction.

The values for monobutyltin were significantly higher than the certified values. This has been reported as being a problem with the derivatization using NaBEt_4 for monobutyltin and is not attributed to any problems with the SPME part of the analysis.

Metal Ions

Inorganic metal ion analysis has also been achieved with SPME. In order to extract metal ions from aqueous solution, an unusual fibre constructed of a hydrophobic microporous polypropylene material was used. This fibre had a film thickness of $30 \mu\text{m}$ and 30% of the surface area was covered with pores of dimensions $0.05 \times 0.15 \mu\text{m}$. In order to extract mercury(II) ions from aqueous solution, dibenzo-18-crown-6 (DBC) was absorbed from solution into this hollow fibre and then this DBC-filled fibre was used for the extraction.

Separation of uncomplexed DBC from the DBC-mercury(II) complex was achieved by normal-phase HPLC with UV detection. The extraction equilibrium between the fibre and the solution with DBC was reached in under 30 s. This is a very rapid equilibrium for SPME. The time to reach equilibrium for the mercury(II) ions between the treated fibre and aqueous

solution was significantly longer; equilibrium was not reached after 1 h. In order to keep extraction time closer to the HPLC analysis time, 10 min extraction was used. With this extraction time and UV detection, the LOD for mercury(II) ions was around 500 p.p.b. The use of a more sensitive detection technique should significantly reduce this LOD.

The effectiveness of the extraction can be seen in Figure 7. No reports on the selectivity of this technique for metal ions have been published and this remains a key area for the future.

Future Developments

SPME is currently poised to become one of the major sample preparation methods for aqueous environmental samples in the future. The advantages that it offers, such as ease of use, no solvent and no plugging, make it a potential replacement for many of the liquid-liquid and SPE methods currently used. The expansion of SPME to the analysis of other analytes which are currently difficult to partition into the fibre coatings is another expected trend. This may be achieved by the development of new fibre coatings or by coupling existing coatings with derivatization or complexation reactions.

The future for SPME in the analysis of solids is less certain. Unless more robust SPME methods than those currently described are found, the replacement of Soxhlet extraction by SPME seems unlikely. Additionally, the problem of carryover is a cause for concern with the analysis of higher molecular weight analytes. Currently the cost of SPME fibres does not allow them to be used as single-use devices. This may, of course, change in the future and single-use fibres are the surest way to ensure that there is no carryover.

See also: **II/Extraction:** Analytical Extractions; Solid-Phase Microextraction; Solid-Phase Extraction. **III/Carbamate Insecticides in Foodstuffs: Chromatography & Immunoassay.** **Surfactants:** Liquid Chromatography. **Inclusion Complexation: Liquid Chromatography.** **Pesticides:** Extraction from Water. **Polychlorinated Biphenyls: Gas Chromatography.** **Superheated Water Mobile Phases: Liquid Chromatography.**

Further Reading

Boyd-Boland AA and Pawliszyn JB (1996) Solid-phase microextraction coupled with high-performance liquid chromatography for the determination of alkylphenol ethoxylate surfactants in water. *Analytical Chemistry* 68: 1521–1529.

- Dean JR (1998) Solid phase microextraction. In: *Extraction Methods for Environmental Analysis*, ch. 5. New York: John Wiley.
- Djozan DJ and Assadi J (1997) A new porous-layer activated-charcoal-coated fused silica fiber: application for determination of BTEX compounds in water samples using headspace solid-phase microextraction and capillary gas chromatography. *Chromatographia* 45: 183–189.
- Eisart R and Levsen K (1996) Solid-phase microextraction coupled to gas chromatography: new method for the analysis of organics in water. *Journal of Chromatography A* 733: 143–157.
- Eisart R and Pawliszyn J (1997) Design of automated solid-phase microextraction for trace analysis of organic compounds in aqueous samples. *Journal of Chromatography A* 776: 293–303.
- Hageman KJ, Mazeas L, Grabanski CB *et al.* Coupled subcritical water extraction with solid phase microextraction for determining semivolatile organics in environmental solids. *Analytical Chemistry* 68: 3892–3898.
- Jia C, Luo Y and Pawliszyn J (1998) Solid phase microextraction combined with HPLC for determination of metal ions using crown ether as selective extracting reagent. *Journal of Microcolumn Separations* 10: 167–173.
- Johansen SS and Pawliszyn J (1996) Trace analysis of hetero aromatic compounds (NSO) in water and polluted groundwater by solid-phase microextraction (SPME). *Journal of High Resolution Chromatography* 19: 627–632.
- Moens L, De Smaele T, Dams R *et al.* (1997) Sensitive, simultaneous determination of organomercury, -lead and -tin compounds with headspace solid phase microextraction capillary gas chromatography combined with inductively coupled plasma mass spectrometry. *Analytical Chemistry* 69: 1604–1611.
- Pawliszyn J (1997) *Solid Phase Microextraction: Theory and Practice*. New York: Wiley-VCH.
- Sarrion MN, Santos FJ and Galceran MT (1998) Strategies for the analysis of chlorobenzenes in soils using solid-phase microextraction coupled with gas chromatography-ion trap mass spectrometry. *Journal of Chromatography A* 819: 197–209.
- Yang Y, Miller DJ and Hawthorne SB (1998) Solid-phase microextraction of polychlorinated biphenyls. *Journal of Chromatography A* 800: 257–266.

Food Technology Applications

R. Marsili, Dean Foods Technical Center,
Rockford, IL, USA

Copyright © 2000 Academic Press

Introduction

The chemicals responsible for off-flavours, malodours and taints in foods and beverages can originate from incidental contamination from environmental (outside) sources (e.g. air, water, packaging material, a contaminated ingredient) and from chemical reactions occurring within the food material itself (e.g. lipid oxidation, enzymatic action, microbial metabolic reactions). In addition, imbalance off-flavours can occur when certain ingredient components that are normally present and often essential to the product are present in abnormally high or low concentrations.

When significant off-flavour problems occur, one of the first priorities of the food chemist is to identify any volatile or semivolatile organic chemicals that may be responsible. Once the identity of the off-flavour chemical(s) has been established, it is possible to speculate on its mechanism of formation and then decide on what corrective actions to implement to eliminate recurrence of the problem in the future.

Analytical Strategy for Studying Off-Flavours

The following steps are commonly used when trying to determine which chemicals in a particular food or beverage sample are the most important contributors to off-flavours:

- Extraction of volatiles/semivolatiles. The chemicals responsible for the food taint must be extracted and usually concentrated from the food matrix. This sample preparation step is critical to success. To isolate and evaluate potential chemical components that are responsible for the food taint, analytes must be separated from interfering chemicals in the food matrix.
- Injection into the gas chromatograph (GC: with or without cryofocusing).
- Separation of extracted volatiles on a GC capillary column with a suitable liquid phase. It is not uncommon to miss important polar compounds because the chemicals do not chromatograph well on nonpolar phases. Often the extraction technique is blamed, but the problem could simply be that an inappropriate analytical capillary column was used for the separation. One example is not detecting volatile fatty acids because separation was attempted on a nonpolar column.

- Determination of peak odour by olfactometry. It is often advantageous to sniff peaks as they elute from the GC column. The odour characteristics and intensities of the eluting peaks can help the analyst determine if the chemical is a likely contributor to the malodour or off-flavour. A variety of olfactometry detectors are commercially available; olfactometry detectors with heated transfer lines are highly recommended.
- Determination of which volatiles/semivolatiles are the most potent contributors to the product's odour. Gas chromatography-olfactometry (GCO) analysis has evolved over time to include dilution techniques (Aroma Extraction Dilution Analysis, AEDA and CharmAnalysis), cross-modal matching (Osme) and maximum perceived intensity. Of these three GCO modifications, extract dilution techniques and cross-modal matching have become the most common techniques used in analytical work on food flavours. Further discussion of the various GCO techniques is beyond the scope of this article.

Perhaps the most critical and challenging step in the process of characterizing the flavour of foods is the sample preparation technique used to isolate/concentrate the flavour compounds from the food matrix. Since it is not uncommon for the chemicals responsible for food malodours to be present at p.p.b. and even p.p.t. levels, the extraction technique must collect as many molecules of off-flavour chemicals as possible for GCO analysis. If the goal is to identify the chemicals responsible for an off-flavour, the sample preparation method selected should extract a representative profile of as many organic volatiles/semivolatiles from the sample as possible. On the other hand, it is also important that the extraction technique does not introduce or create volatiles that are not in the food product. For example, sample preparation techniques that involve heating the sample (e.g. steam distillation) can generate artifact peaks in sample chromatograms, and these odiferous artifacts may be misinterpreted as the cause of the malodour/off-flavour problem.

This article will discuss why solid-phase microextraction (SPME) is such an excellent extraction/concentration technique for the study of food off-flavours and taints.

Advantages of SPME as an Extraction Technique

Chemicals responsible for off-flavours can be polar, semipolar and nonpolar and cover a wide range of functional groups, boiling points and molecular

Table 1 General comparison of common analyte extraction techniques for studying food aromas (actual parameters vary depending on sample matrix, analyte, type of GC detector)

	Sample matrix	Sample size (g)	Detection limit	Range of volatiles analysed			Sample automation	Sample prep time (min)
				Gases	Volatile	Semivolatile		
Static headspace (SH)	G/L/S	0.1–10	p.p.m.				Yes	5–30
Dynamic headspace (DH)/Tenax	L/S	1–1000	p.p.b.–p.p.t.				Yes	10–30
Solid-phase microextraction (SPME)	G/L/S	0.1–10	p.p.b.–p.p.t.				Yes	5–60
Solvent extraction (SE)	L/S	0.1–10	p.p.b.				No	> 30
Supercritical fluid extraction (SFE)	S ^a	0.1–10	p.p.b.				Yes	10–60
Direct thermal desorption (DTD)	S	0.001–0.10	p.p.b.				No	5–10
				Boiling point (°C)				
				– 100 0 100 200 300 400				

G, Gas; L, liquid; S, solid; p.p.t., parts per trillion; p.p.b., parts per billion; p.p.m., parts per million.

^aCapable of analysing liquids, but usually requires binding of liquid portion of sample with an inert matrix material.

weights. As a result, no one analytical extraction/sample preparation method works in all cases. It is not uncommon that multiple sample preparation methods are required to identify the chemicals responsible for off-flavours and malodours in a particular sample.

Each sample preparation technique has advantages and disadvantages. The choice of a suitable sample preparation technique depends on several factors, including number of samples to be tested, how quickly results are needed, type of sample (matrix effects), the nature of the analytes of interest (i.e. functional group, molecular weight, boiling point, thermal stability, etc.), desired detection limits and required accuracy.

Table 1 compares a few popular extraction techniques used prior to GC analysis. Considering the wide range of sample sizes that can be analysed by

SPME, the low detection limits, the wide range of analyte boiling points that can be analysed, the fact that SPME can be automated and the short sample preparation time, it is no surprise that SPME is rapidly growing in popularity. The low cost of SPME equipment is also an advantage.

One often overlooked benefit of SPME is its high precision and accuracy compared to other GC sampling techniques. Studies comparing the precision and accuracy of SPME to other GC sampling techniques show that analytical results based on SPME extraction are often more precise and accurate than results based on other sample preparation techniques.

Several polar and nonpolar fibres with varying affinities for specific classes of compounds are now available. As a result, SPME fibre type can be selected in order to optimize results for a particular analyte class. Compounds that interfere with the

Table 2 SPME fibre selection guide

Analyte class	Fibre type	Linear range
Acids (C ₂ –C ₈)	Carboxen-PDMS	10 p.p.b.–1 p.p.m.
Acids (C ₂ –C ₁₅)	CW-DVB	50 p.p.b.–50 p.p.m.
Alcohols (C ₁ –C ₈)	Carboxen-PDMS	10 p.p.b.–1 p.p.m.
Alcohols (C ₁ –C ₁₈)	CW-DVB	50 p.p.b.–75 p.p.m.
	Polyacrylate	100 p.p.b.–100 p.p.m.
Aldehydes (C ₂ –C ₈)	Carboxen-PDMS	1 p.p.b.–500 p.p.b.
Aldehydes (C ₃ –C ₁₄)	100 µm PDMS	50 p.p.b.–50 p.p.m.
Amines	PDMS-DVB	50 p.p.b.–50 p.p.m.
Amphetamines	100 µm PDMS	100 p.p.b.–100 p.p.m.
	PDMS-DVB	50 p.p.b.–50 p.p.m.
Aromatic amines	PDMS-DVB	5 p.p.b.–1 p.p.m.
Barbiturates	PDMS-DVB	500 p.p.b.–100 p.p.m.
Benzidines	CW-DVB	5 p.p.b.–500 p.p.b.
Benzodiazepines	PDMS-DVB	100 p.p.b.–50 p.p.m.
Esters (C ₃ –C ₁₅)	100 µm PDMS	5 p.p.b.–10 p.p.m.
Esters (C ₆ –C ₁₈)	30 µm PDMS	5 p.p.b.–1 p.p.m.
Esters (C ₁₂ –C ₃₀)	7 µm PDMS	5 p.p.b.–1 p.p.m.
Ethers (C ₄ –C ₁₂)	Carboxen-PDMS	1 p.p.b.–500 p.p.m.
Explosives (nitroaromatics)	PDMS-DVB	1 p.p.b.–1 p.p.m.
Hydrocarbons (C ₂ –C ₁₀)	Carboxen-PDMS	10 p.p.b.–10 p.p.m.
Hydrocarbons (C ₅ –C ₂₀)	100 µm PDMS	500 p.p.t.–1 p.p.m.
Hydrocarbons (C ₁₀ –C ₃₀)	30 µm PDMS	100 p.p.t.–500 p.p.b.
Hydrocarbons (C ₂₀ –C ₄₀₊)	7 µm PDMS	5 p.p.b.–500 p.p.b.
Ketones (C ₃ –C ₉)	Carboxen-PDMS	5 p.p.b.–1 p.p.m.
Ketones (C ₅ –C ₁₂)	100 µm PDMS	5 p.p.b.–10 p.p.m.
Nitrosamines	PDMS-DVB	1 p.p.b.–200 p.p.b.
Polyaromatic hydrocarbons	100 µm PDMS	500 p.p.t.–1 p.p.m.
	30 µm PDMS	100 p.p.t.–500 p.p.b.
	7 µm PDMS	500 p.p.t.–500 p.p.b.
Polychlorinated biphenyls	30 µm PDMS	50 p.p.t.–500 p.p.b.
Pesticides, chlorinated	100 µm PDMS	50 p.p.t.–500 p.p.b.
	30 µm PDMS	25 p.p.b.–500 p.p.b.
Pesticides, nitrogen	Polyacrylate	50 p.p.t.–500 p.p.b.
Pesticides, phosphorus	100 µm PDMS	100 p.p.t.–1 p.p.m.
	Polyacrylate	100 p.p.t.–500 p.p.b.
Phenols	Polyacrylate	5 p.p.b.–500 p.p.b.
Surfactants	CW-TPR	1 p.p.m.–100 p.p.m.
Sulfur gases	Carboxen-PDMS	10 p.p.b.–10 p.p.m.
Terpenes	100 µm PDMS	1 p.p.b.–10 p.p.m.
Volatile organic chemicals	Carboxen-PDMS	100 p.p.t.–500 p.p.b.
	100 µm PDMS	20 p.p.b.–50 p.p.m.
	30 µm PDMS	100 p.p.b.–50 p.p.m.

chromatography when the food extract is analysed by GC can be eliminated or at least minimized. If lipid oxidation is being studied, for example, the analyst could choose a Carboxen-PDMS fibre to measure aldehydes in the 1–500 p.p.b. range. If concentrations of aldehydes above 500 p.p.b. are present, the Carboxen-PDMS fibre will become saturated and a 100 μm PDMS fibre would be a better choice. A SPME fibre selection guide is shown in Table 2.

For some applications, the portability of SPME is an important advantage. After analytes are adsorbed on an SPME fibre, they can be maintained on the fibre for an extended period of time by sealing the end of the fibre with a septum. This allows for convenient field sampling. Perfumers have used this technique, for example, to extract aroma chemicals from flowers in greenhouses, as well as the fragrant chemicals from exotic flowers found in the canopy of tropical rainforests. Another example is a food chemist who is trying to determine if a malodour in a particular food product is being absorbed by the product because it has been stored near odiferous foods (e.g. spices) or perhaps industrial solvents. The food chemist can extract volatiles from the air in a warehouse or walk-in cooler with SPME, transport the SPME device with the trapped volatiles to the laboratory for GC analysis, and see if the GC profile matches the profile of a problem sample.

Retention characteristics are highly dependent on the fibre used and the volatility of the adsorbed analytes. Studies have shown that even highly volatile compounds can be stored on Carboxen-PDMS fibres for 3 days at room temperature without loss. The pore dynamics of Carboxen 1006 make it a true adsorbent. Retention of volatiles on 100 μm PDMS fibres, however, is not nearly as good. Even when fibres are stored at -4°C , only the least volatile analytes will be retained.

Specific Applications of SPME for Resolving Food Taints

The examples and case studies that follow illustrate the advantages of SPME as a sample preparation tool for the study of off-flavours and malodours in foods and beverages.

Light-Induced Off-Flavours in Milk: SPME vs. Headspace Analysis

Two types of light-induced oxidation reactions occur in milk and dairy products. Initially, a burnt, oxidized flavour develops and predominates for approximately 2–3 days. Dairy technologists refer to this off-flavour note as light-activated flavour (LAF). Degradation of sulfur-containing amino acids of the serum (whey)

proteins is probably responsible for this reaction. The exact reaction products for LAF have not been clearly elucidated. Methional [(3-methylthio)propanal], however, has been implicated as a possible contributor. Understanding the true impact that methional has on LAF is difficult to determine because it is relatively unstable and breaks down into more stable components, including mercaptans, sulfides and disulfides. Recently, researchers have postulated an alternative mechanism for the formation of dimethyl disulfide by singlet oxygen oxidation of methionine.

In addition to the poorly understood LAF off-flavour, a second type of light-induced off-flavour occurs in milk and is attributed to lipid oxidation. This off-flavour, often characterized as metallic or cardboard-like, usually develops after 2 days and does not dissipate. Aldehydes (especially pentanal and hexanal) and, to a lesser degree, ketones (e.g. 1-hexen-3-one and 1-nonen-3-one), alcohols and hydrocarbons have been observed to form in milk as a result of light-induced lipid oxidation reactions. When milk is exposed to light, various carbonyl compounds form from the reaction of light and oxygen with unsaturated fatty acids in the milk fat triglycerides and other milk fat components. Autoxidation of unsaturated fatty acids involves a free radical reaction, forming fat hydroperoxides that degrade to various malodorous compounds (e.g. hexanal, the predominant lipid reaction by-product in light-exposed milk in the case of linoleic acid).

In one recent study to quantitate pentanal and hexanal in light-abused milk (skim milk and 2% fat milk), a comparison was made using two different sample preparation techniques: dynamic headspace (DH) with a Tenax trap and SPME with a Carboxen-PDMS fibre. Results, which are summarized in Table 3, show that standard calibrations with SPME were more linear for both analytes in both types of milk samples than with DH. (Calibration was based on the method of additions technique using an internal standard of 4-methyl-2-pentanone.) Furthermore, the SPME method had about the same detection limit as the DH method. To test the precision of each method, four replicates spiked with 2 ng mL^{-1} of each aldehyde were compared for both types of milk samples. When coefficients of variations were calculated for this study, SPME proved to be more precise than DH.

For these particular samples and these particular analytes, SPME consistently demonstrated better precision without a sacrifice in sensitivity. Furthermore, none of the problems with carryover, background or artifact peaks that sometimes occur with DH systems were observed with the SPME experiments. No carryover peaks were detected in milk samples, even

Table 3 Comparison of the principal analytical parameters for pentanal and hexanal analysed by DH/GC-MS and SPME/GC-MS

Compound	Sample	Analytical technique	Detection limit (ng mL ⁻¹)	Repeatability of four replicates at 2 ng mL ⁻¹ (coefficient of variation, %)	Linear least-squares correlation coefficients ^a
Pentanal	Skim	DH	0.1	8.0	0.966
		SPME	0.1	1.9	0.990
Hexanal	Skim	DH	0.3	21.1	0.910
		SPME	0.5	7.1	0.995
Pentanal	2% Milk	DH	0.3	7.6	0.996
		SPME	0.3	2.1	0.999
Hexanal	2% Milk	DH	0.8	8.3	0.982
		SPME	0.8	4.9	0.993

^aFor calibration curve of five standards ranging from 0.0 to 30.0 ng mL⁻¹.

when injecting the SPME fibre immediately after it was used to analyse a milk sample spiked with high levels (500 ng mL⁻¹) of each of the following aldehydes: butanal, isopentanal, pentanal, hexanal, heptanal and octanal.

Because so many different parameters need to be optimized when performing DH and SPME experiments, care must be taken when comparing SPME and DH for precision, accuracy and sensitivity, and it is probably an over-simplification to say that one method is better than another. None the less, this work shows that SPME is a viable extraction technique for measuring oxidation products in milk and dairy products.

Highly Volatile Malodorous Chemicals

Highly volatile compounds can be responsible for off-flavours and malodours and can be difficult to trap and isolate. DH techniques with Tenax trapping often fail to trap and detect low molecular weight polar compounds. Static headspace works well for highly volatile chemicals but may not be sensitive enough for some applications.

SPME is an ideal extraction tool for highly volatile analytes. Consider, for example, the analysis of acetaldehyde in buttermilk. Acetaldehyde has a boiling point of 21°C.

Acetaldehyde in buttermilk The delicate flavour associated with high quality cultured buttermilk is contributed by several bacterial metabolites, including lactic acid, traces of acetic and formic acids, ethanol, diacetyl and carbon dioxide. Two different types of bacteria are used in buttermilk starter cultures: the acid-producing types (usually strains of *Streptococcus lactis* or *S. cremoris*) and the aroma bacteria (usually *Leuconostoc citravorum*). Diacetyl, the major flavour component of buttermilk, is produced by the fermentation of citric acid by the aroma-producing bacteria.

One common type of off-flavour in buttermilk is called the green flavour defect. It is caused by the loss of diacetyl (by conversion to acetyl methylcarbinol by diacetyl reductase enzyme in the culture bacteria) and an increase in acetaldehyde production. Measuring the acetaldehyde to diacetyl ratio is a good way to monitor this flavour defect.

As shown in **Figure 1**, SPME (e.g. Carboxen-PDMS) is an excellent way to extract acetaldehyde, diacetyl, acetic acid and other flavour-important metabolites from buttermilk. Even with SPME, however, it is necessary to use cryofocusing (typically at -100°C) after thermal desorption from the SPME fibre and prior to injection into the GC capillary column. With cryofocusing, sharp GC peaks are obtained for acetaldehyde; without cryofocusing, the acetaldehyde peak may not be detected at all.

1,3-Pentadiene from sorbate degradation Testing for 1,3-pentadiene in foods and beverages is another example of how SPME can be used to quantitate a highly volatile malodorous compound. Sorbic acid (2,4-hexadienoic acid) and its water-soluble potassium salt are commonly used as food preservatives to prevent yeast and mould growth. Foods in which sorbate has commercially useful antimicrobial activity include baked goods, cheeses and other dairy products, confectionery products, dried fruits, fish products, fruit juices, jellies (with artificial sweeteners), syrup, vegetables and wine.

One problem with potassium sorbate is that some moulds in the genus *Penicillium* can grow in the presence of up to (approximately) 1.2% potassium sorbate. Furthermore, some of these moulds have the ability to decarboxylate sorbic acid, producing 1,3-pentadiene, a highly volatile compound with an extremely strong hydrocarbon-like odour (typically kerosene-like).

As in the case of testing for acetaldehyde in buttermilk, using SPME with a Carboxen-PDMS fibre and

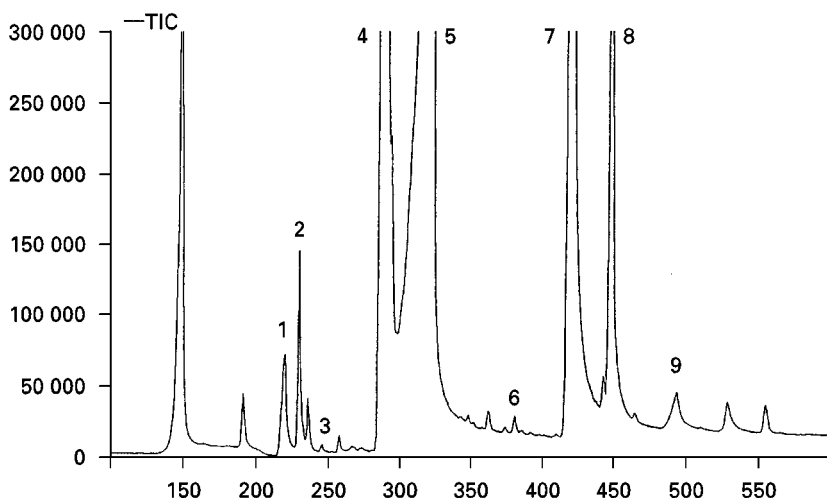


Figure 1 Volatiles in buttermilk by SPME (Carboxen-PDMS) extraction followed by GC-MS. Sample preparation: 2 mL of buttermilk, 7 μ L of internal standard solution (54 p.p.m. 4-methyl-2-pentanone), and a small magnetic stirring bar were added to a 4 mL GC vial and sealed. Headspace volatiles were extracted by SPME for 20 min at 50°C. Peak identities: 1, acetaldehyde; 2, acetone; 3, dimethyl sulfide; 4, diacetyl; 5, acetic acid; 6, 2-pentanone; 7, ethyl acetate; 8, internal standard; 9, butyric acid.

cryofocusing prior to release into the analytical column works well for measuring 1,3-pentadiene in foods and beverages. A chromatogram showing 1,3-pentadiene in a ready-to-drink refrigerated tea product is shown in **Figure 2**. A consumer complained that this particular tea sample had a kerosene odour.

High Boiling Point Compounds with Musty Odours

While extremely volatile compounds can be challenging to extract and isolate, so too are high boiling point semivolatile chemicals. Sometimes it is necessary to use combinations of sample preparation techniques to extract and isolate sufficient quantities of this type of malodorous compound from foods to achieve meaningful analytical results.

Algae, fungi, bacteria and *Actinomyces* are known to produce geosmin (GSM) and 2-methylisoborneol (MIB). These semivolatile, lipophilic compounds have a muddy, musty odour perceived as disagreeable to consumers. Both compounds are rapidly absorbed from water into the lipid tissue of fish and other aquatic organisms. When either compound is present in tissue at concentrations exceeding 0.7 μ g kg⁻¹, they render fish unfit for retail sale.

Current methods for quantifying the concentrations of MIB and GSM in catfish include: purge-and-trap-solvent extraction (P&T-SE); microwave distillation-solvent extraction (MD-SE) and microwave distillation-solid phase extraction (MD-SPE). These methods are time-consuming, labour-intensive and require the use of small quantities of flammable and/or toxic solvents or expensive microwave equipment. A faster and less expensive method could find broad application in catfish flavour research, the cat-

fish-processing industry and other aquaculture industries plagued by this problem.

Lloyd and Grimm, USDA research chemists, have developed a rapid and simple analytical procedure for quantitating low levels of GSM and MIB in catfish tissue. Their method combines microwave distillation (MD) with SPME. MD transfers lipophilic volatile analytes from the lipid-rich matrix of catfish tissue into an aqueous matrix, and SPME is then used to extract and concentrate the volatile organic compounds from the aqueous solution. The technique is a prime example of how combinations of two or more sample preparation techniques can be a potent strategy for resolving analytical problems that are inadequately addressed by a single sample preparation technique.

While SPME has been shown to be a sensitive, reproducible, quantitative sample preparation tool, the direct analysis of p.p.b. levels of GSM and MIB in fish tissue is not possible with SPME. Due to their lipophilic nature, MIB and GSM partition from fish tissue into the headspace in such low concentrations that direct SPME is ineffective. Combining MD with SPME yields a rapid, extremely sensitive technique for the analysis of thermally stable volatile and semivolatile compounds in complex matrixes. **Figure 3** is a schematic diagram of a typical MD-SPME apparatus for analysing MIB and GSM in fish tissue.

Mouldy/Musty Chemicals in Wine and Corks

Cork from *Quercus suber* has been used as a closure for wine bottles since the 17th century. Cork offers unique physical properties as a closure, including

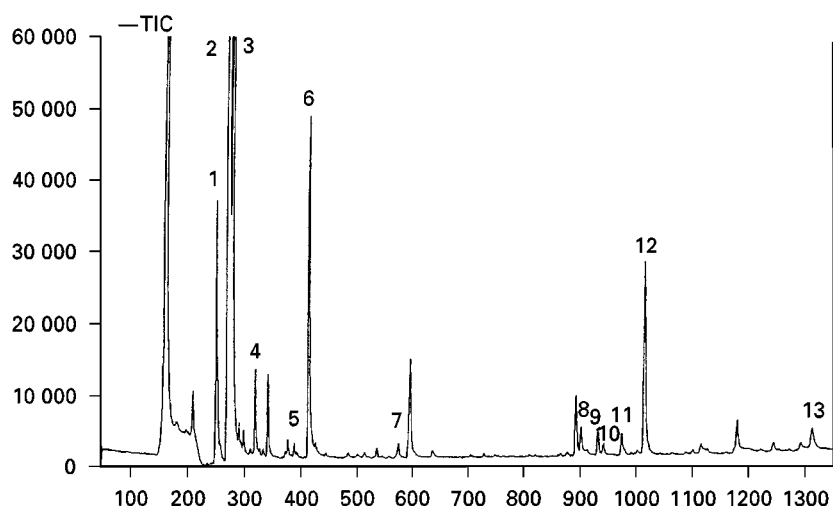


Figure 2 Volatiles in tea with a kerosene-like off-flavour by SPME (Carboxen-PDMS) extraction followed by GC-MS. Sample preparation: 2 mL of tea and a small magnetic stirring bar were added to a 4 mL GC vial and sealed. Headspace volatiles were extracted by SPME for 20 min at 50°C. Peak identities: 1, acetone; 2 and 3, 1,3-pentadiene isomers; 4, 2-butanone; 5, pentanal; 6, 2-pentanone; 7, hexanal; 8, 4-methyl-6-hepten-3-one; 9, 2,3-dehydro-1,8-cineole; 10, hexyl acetate; 11, 1,4-cineole; 12, 1,8-cineole; 13, α -terpineol.

long-lasting flexibility, hydrophobicity and gas impermeability. Over the last two decades, the incidence of mouldy and musty off-flavours in cork-sealed wines has increased significantly. 2,4,6-Trichloroanisole (TCA) has been identified as the primary chemical responsible for cork taint. The human olfactometry threshold for TCA is 4–10 ng L⁻¹ in white wine and 50 ng L⁻¹ in red wine. In the case of wine, a worldwide loss of roughly US\$1 billion per year is attributed to cork taint.

The use of SPME fibres to extract TCA from the headspace over an agitated wine and moistened cork matrix is a short, inexpensive and solvent-free method to determine TCA. Due to the efficient adsorption properties of PDMS SPME fibres and the high sensitivity of GC-MS, the limit of detection of

2.9 ng L⁻¹ TCA is low enough to detect problem wine and cork samples that exceed the olfactory threshold range in wine of 4–50 ng L⁻¹.

Immersion of the SPME fibre into the wine was found to give poorer sensitivity and can increase contamination of the injector system and shorten the lifetime of the SPME fibre and analytical GC column.

Free Fatty Acids by Headspace and Immersion Techniques

Free fatty acids (FFAs), even at relatively low concentrations, are critical to both desirable and undesirable flavours in many types of food systems. Low levels of FFAs are difficult to detect in cheese and other food samples by dynamic or static headspace methods. SPME offers two alternative approaches to determine

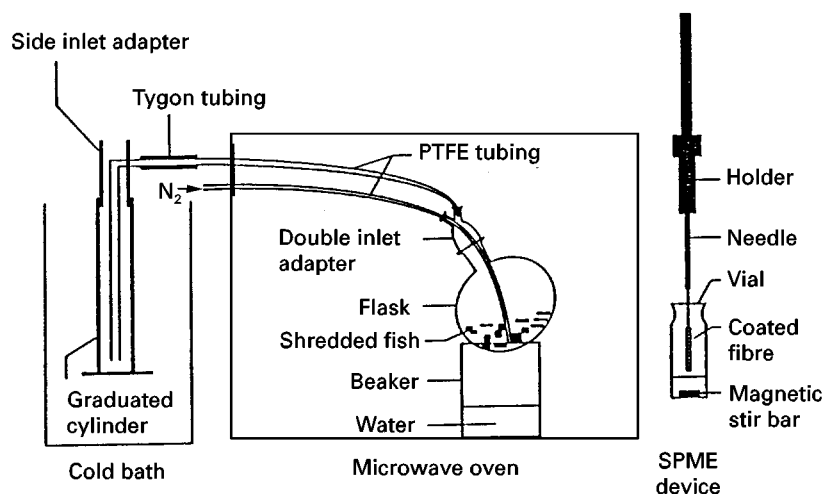


Figure 3 MD-SPME apparatus for analysing 2-methylisoborneol and geosmin in fish tissue.

Table 4 Linearity of responses for free fatty acids using immersion SPME (50 p.p.b.–25 p.p.m.)

<i>Acid</i>	<i>% RSD of response factor</i>
Acetic	140
Propionic	16.1
Isobutyric	14.4
Butyric	18.9
Isovaleric	12.1
Valeric	14.2
Hexanoic	9.1

Courtesy of Dr Robert Shirey, Supelco Inc., Bellefonte, PA.

these compounds in cheese: the solid sample can be warmed for headspace sampling, or the sample can be liquefied for sampling by immersion SPME. Shirey, Supelco's SPME applications chemist, investigated both approaches for monitoring FFAs in cheeses using varied extraction conditions.

The headspace SPME approach offered the greatest sensitivity for these analytes, but immersion of the fibre into the liquefied samples produced the widest range of linear responses. Under all conditions, acetic acid was particularly difficult to quantify (Table 4).

The following conditions were used for the analysis of Parmesan cheese for FFAs: sample: 100 mg cheese in 40 mL vial; SPME fibre: 65 μ m Carbowax®/divinylbenzene StableFlex™; extraction method: headspace for 15 min at 65°C; desorption: 1 min at 250°C.

Sanitizer Contamination in Milk

The food and beverage industry is now less dependent on chlorine-based sanitizers for disinfecting processing equipment. Because application does not lead to toxic halogenated organic compounds, peroxyacetic acid (PAA)-based sanitizers are now widely used for disinfection in cleaning-in-place (CIP) systems in breweries and dairies. One problem with PAA-based sanitizers, however, is that even small amounts of PAA contamination can lead to severe off-flavours in milk. This problem can occur if sanitizers are not completely rinsed from processing lines prior to processing the next load of milk.

PAA, which can be quantitated in milk by HPLC after derivatization with methyl *p*-tolylsulfide, has a half-life in milk of approximately 20 min. As a result, PAA concentrations normally fall below threshold taste limits after only a few hours, even in milk contaminated with relatively large quantities of PAA. Once milk is contaminated with PAA, however, there is a significant off-flavour that fails to dissipate over time. The PAA-induced reactions that lead to this off-flavour defect are not well understood but probably involve oxidation of the milk proteins by PAA and/or hydrogen peroxide. To determine if an

off-flavour in milk has occurred because of PAA contamination, one approach is to check acetic acid levels, since PAA degrades to water and acetic acid. Headspace SPME with a Carboxen-PDMS or a Carbowax-divinylbenzene StableFlex fibre is capable of detecting p.p.b. levels of acetic acid in milk.

One popular sanitizer used by some dairies is Matrixx™ (Ecolab, St Paul, MN). Matrixx has the following composition (approximate): 4.4% PAA, 6.9% hydrogen peroxide and 3.4% octanoic acid. Figure 4 shows chromatograms of a control milk sample (no off-flavour) and a sample with a severe off-flavour that was suspected to be caused by contamination with Matrixx. Peaks for acetic and octanoic acids are indicators that the sample is contaminated with Matrixx sanitizer. The following conditions were used for the analysis: sample: 2 mL of low fat milk + 1 mL 0.1-N phosphoric acid + 1 g salt in a 9 mL vial; SPME fibre: 65 μ m Carboxen-PDMS; extraction method: headspace (with stirring) for 12 min at 40°C; desorption: 2 min at 250°C. The analytical capillary column was FFAP™ (Free Fatty Acid Phase).

Off-Flavours from Packaging Materials

Ironically, packaging materials, which are designed to preserve the freshness and flavour of foods and beverages, can be directly responsible for causing off-flavour defects. Although plastic packaging material consists primarily of nonvolatile high molecular weight polymers, volatile low molecular weight compounds are often added to improve functional properties of the materials: plasticizers to improve flexibility, antioxidants to prevent oxidation of the plastic polymers and the food inside the packaging and UV blockers to prevent yellowing of polymeric material when it is exposed to light. Additional additives include polymerization accelerators, cross-linking agents, antistatic chemicals and lubricants.

Occasionally, packaging materials are not adequately cured before they are used. As a result, a small amount of solvent associated with the manufacturing of the packaging materials or from the inks and dyes used on packaging graphics remains and is absorbed by the food material inside the package.

Screening packaging material for undesirable residual solvents is a simple task with SPME. Figure 5 shows volatiles extracted from the headspace of a closed, new (unused) cottage cheese carton (680 g fill weight). The lidstock is a linear low density polyethylene (Dow 2503 resin), and the container body is polypropylene (Montell copolymer). The volatiles were sampled simply by poking a pinhole through the top of the closed container and inserting an SPME fibre (Carboxen-PDMS) through the hole. A small magnetic stirring bar was placed inside the carton to

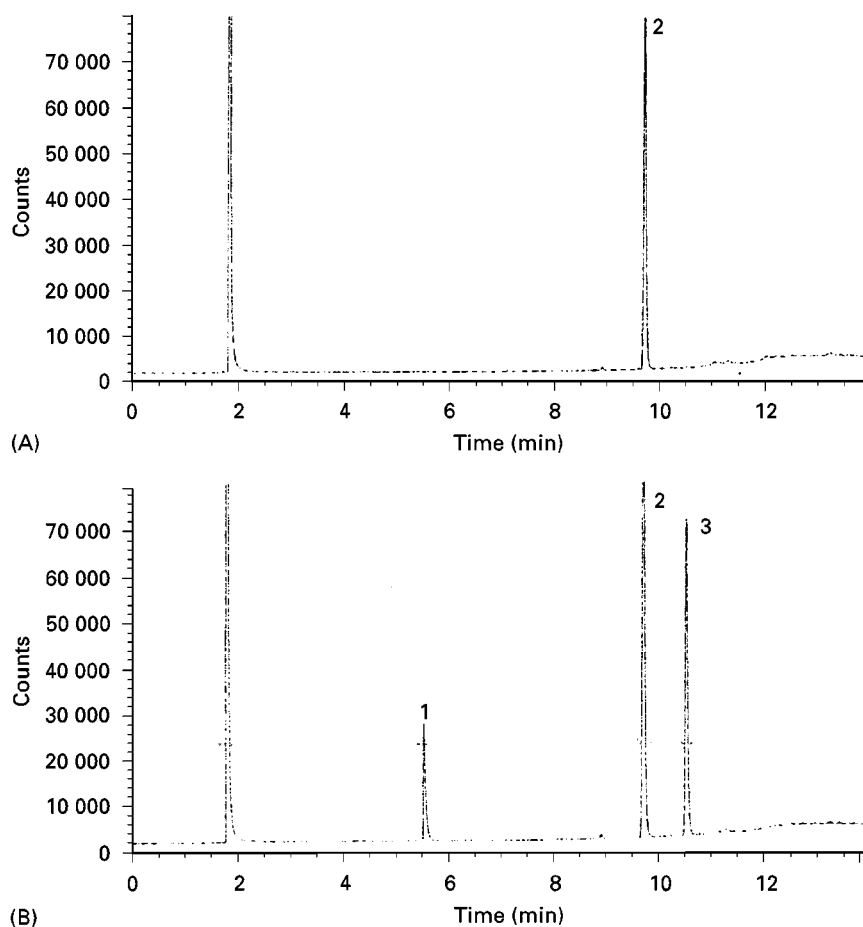


Figure 4 (A) Low fat milk control and (B) complaint low fat milk with off-flavour. Peak identities are as follows: 1, acetic acid; 2, internal standard (2-ethylhexanoic acid); 3, octanoic acid. Complaint sample is contaminated with 0.11% Matrixx sanitizer. Concentration of octanoic acid is 37 p.p.m. See text for details of method.

facilitate air movement over the fibre. The fibre was exposed to the atmosphere in the carton for 30 min at room temperature. A large number of volatiles was

detected. Nearly all peaks detected were hydrocarbons of various chain lengths. However, a significant amount of trichloroethylene was also detected.

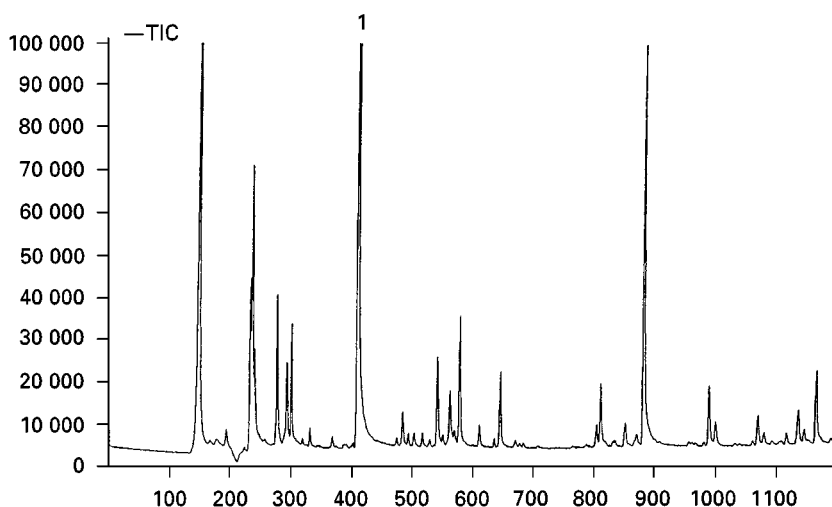


Figure 5 Volatiles extracted from the headspace of a closed, new (unused) cottage cheese carton (680 g fill weight) by SPME. Peak no. 1 is trichloroethylene; most of the other chromatographic peaks are alkanes. See text for details of method.

A few types of malodorous packaging solvents that have been found to cause off-flavours in foods include styrene, ethylstyrene, trimethylbenzene isomers and propyl acetate.

Pesticides in Wine

Not all food taints involve odiferous chemicals that contribute to off-flavours. Contamination of foods with pesticides is another type of food taint of critical concern. Wine is one type of beverage that can be contaminated with pesticides.

Procymidone fungicide Procymidone is a fungicide which is widely used against *Botrytis cinerea* on wine grapes. If improperly applied, undesirable residues at concentrations ranging from a few p.p.b. to several hundred p.p.b. can be found in wine after fermentation and even in old bottles because of its well-known persistence. The standard analytical sample preparation method for testing procymidone in wine is based on time-consuming liquid-liquid extraction or solid-phase extraction (SPE) using polymeric bonded silica cartridges.

Urruty and co-workers at the Université de Bordeaux (Périgueux, France) found that SPME (100 μ m PDMS) results for procymidone in white and red wine correlated very well to ELISA test results. SPME was as fast as ELISA and offered slightly better precision.

Methyl isothiocyanate soil fumigant Another chemical of concern to wine makers is methyl isothiocyanate (MITC). It is used as a soil fumigant for nematodes, fungi and other diseases in vegetables and fruits. MITC is illegally employed as an antifermentative substance in wines. The addition of antifermentative agents in wines is controlled by EC and non-EC regulations. In particular, the Italian legal system does not allow the use of MITC in wines and requires the control of all exported wines. Solvent-solvent extraction is the traditional sample preparation method for measuring MITC in wines.

Grandini and Riguzzi (Bologna, Italy) compared SPME with the official Italian method. The SPME fibre used was Carbowax-divinylbenzene (65 μ m). For SPME, headspace sampling of 5 mL of wine in a 10 mL vial was conducted for 30 min; 1.25 g of sodium chloride was added to the sample.

The lengthy standard sample preparation for MITC in wine was as follows: a 100 mL sample of wine was spiked with 100 μ L 4-ethylpyridine (internal standard). The pH of the wine was adjusted to 7 with sodium hydroxide. The sample was then extracted three times with 15 mL of pentane. Anhydrous sodium sulfate was added to the solvent, which was then concentrated to 0.3 mL with a rotary

evaporator at 40°C. No vacuum was applied, in order to minimize MITC loss.

SPME-GC with a nitrogen-phosphorus detector (NPD) gave a minimum detectable limit of 1 p.p.b. and a linear detector response in the 1–200 p.p.b. range. Although many methods use the NPD, including the official method, they are not able to obtain minimum detectable limits of less than 10 p.p.b. Compared to the official method, SPME offered the following advantages: low minimum detection limits, wide linearity range, short analysis time and low costs. Furthermore, sample pretreatment is eliminated and solvents are not used.

Quality Control (QC) Applications: SPME-MS-MVA as an Electronic Nose

The combination of SPME with GC and mass spectrometry-olfactometry detection is a potent tool for understanding the causes of food off-flavours, malodours and taints. However, the complexities involved in performing capillary GC testing, as well as the difficulties associated with the interpretation of results, require highly trained chemists. Furthermore, the technique is time-consuming and not amenable to the rapid product evaluation and decision-making that is often required in quality control situations. Even with assistance from peak recognition software that matches corresponding peaks in different chromatograms, the large number of GC peak data associated with flavour/off-flavour studies of food systems is time-consuming and prone to errors. As a result, SPME-GC-MS-OD is essentially a tool for research and development chemists and chromatographers.

Advantages of SPME-MS-MVA for QC Applications

There is, however, a relatively new SPME-based technique that has proved useful for food quality control applications. The technique has been referred to as SPME-MS-MVA (solid-phase microextraction-mass spectrometry-multivariate analysis). Essentially, the analytical system is an electronic nose (e-nose) in which a mass spectrometer replaces the typical chemical sensor array, and SPME replaces static or dynamic headspace sampling as the extraction technique to introduce volatiles/semivolatiles to the detector. The GC is used, with the only modification being the substitution of the typical 30 m coated capillary column with a 1 m uncoated fused silica column.

The speed, simplicity, sensitivity, portability and relatively low cost of SPME make it an ideal extraction technique for introducing volatiles and semivolatiles to the e-nose detector. With multiple manual SPME set-ups, it could be possible to analyse

one sample every 3 min using the same GC-MS system. Another advantage of using SPME as a way of introducing volatiles into the e-nose detector is that different fibres can be selected for different applications (see Table 2).

Using a mass spectrometer as a chemical sensor is advantageous because it is sensitive and robust, does not suffer from memory effects, and is not poisoned by low levels of moisture injected from SPME extractions. Furthermore, unlike typical commercial e-nose chemical sensors based on conducting polymers, metal oxides, surface acoustic wave (SAW) devices, quartz crystal microbalances (QCMs), or combinations of these devices, reliable easy-to-use benchtop MS detectors have been in routine use for decades and have a proven track record.

Another advantage of SPME-MS-MVA is that it can easily be converted to SPME-GC-MS simply by replacing the 1 m uncoated fused silica transfer line with an appropriate 30 m coated capillary GC column. Researchers can then perform more detailed traditional analyses, including identification and quantitation of specific odour-active GC peaks. This approach can be extremely helpful in determining what masses to monitor (as well as what masses to exclude) for specific e-nose application using MS as the chemical sensor.

Specific SPME-MS-MVA QC Applications

With SPME-MS-MVA, the ability to identify individual chemical components is lost. However, the trade-off is the gain in speed and simplicity of interpretation of results. The technique is rapid and generally gives comparative rather than quantitative information. It is ideally suited for quick quality assurance (QA)/QC screening.

SPME-MS-MVA generates mass intensity tables for each sample tested. The mass intensity data used to prepare the principal component analysis (PCA) scores plots in Figures 6 and 7 were obtained in the following manner:

1. Sample volatiles were extracted using SPME (65 μ m Carboxen-PDMS) and desorbed from the SPME fibre by the heated GC injection port (250°C) into a 1 m deactivated fused silica transfer line heated to 50°C.
2. Data acquisition (from m/z 50 to m/z 150) was discontinued after 2 min.
3. The masses of the single resulting chromatographic peak generated by the ion fragments from headspace volatiles of the sample were averaged from 8 to 80 s, while masses from 0 to 7 s and from 81 to 100 s were subtracted as background.

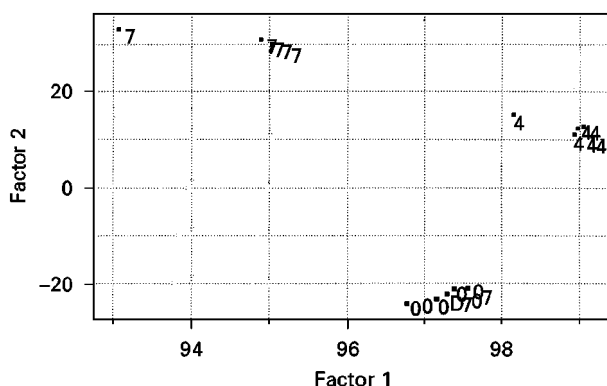


Figure 6 Principal component analysis scores plot of mass intensity data for control and light-abused soybean oils as determined by SPME-MS-MVA. Soybean oil: days of fluorescent light exposure (200 FC). 0, 0 days; 4, 4 days; 7, 7 days; D7, 7 days in the dark.

4. The resulting mass intensity list provided the data used for PCA.

Two QA/QC examples of SPME-MS-MVA are provided below.

Off-flavour development in soybean oil exposed to light Deodorized commercial soybean oil was exposed to fluorescent light for different time periods and analysed by SPME-MS-MVA. Prior to extraction, the soybean oil was placed in a 50 mL Nessler tube and exposed to 200 foot candles (FC) of fluorescent light. Four different types of samples were analysed: control soybean oil (fresh oil, normal taste, no light exposure); control oil exposed to light for 4 days; control oil exposed to light for 7 days; and a Nessler tube filled with control oil, wrapped in aluminium foil, and stored alongside the

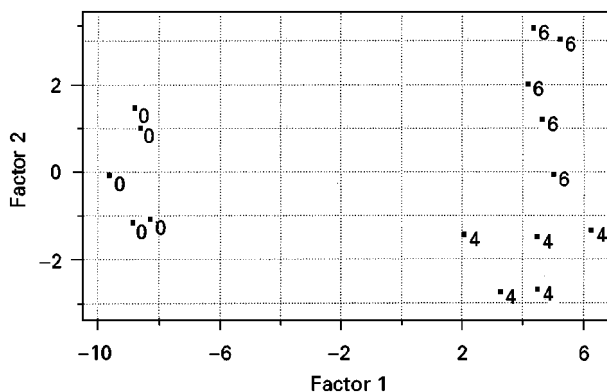


Figure 7 Principal component analysis scores plot of mass intensity data for fresh boiled beef and boiled beef refrigerated for 4 days and 6 days and then reheated. Results generated by SPME-MS-MVA technique. 0, 0 days (freshly boiled); 4, 4 days storage at 4°C; 6, 6 days storage at 4°C.

light-exposed oils for 7 days. All Nessler tubes were sealed with Parafilm® and stored at 22°C. Six samples of each type were prepared and analysed, except for the 7-day-old sample stored in the dark (i.e. wrapped in foil); only three samples of this treatment were analysed.

SPME procedure 2 g soybean oil was added to a 9 mL glass GC vial and capped with a polytetrafluoroethylene septum closure. Samples were heated to 45°C in a water bath and stirred vigorously with a small stirring bar while the SPME fibre was exposed to the headspace vapours in the vial for 12 min.

Results The PCA scores plot for this set of samples appears in Figure 6, which shows that SPME-MS-MVA is capable of grouping together samples of soybean oil that have been exposed to similar levels of light abuse.

Warmed-over flavour (WOF) in boiled beef A beef sample (500 g of chuck roast) was boiled for 60 min in a water bath. The internal temperature of the beef reached 92°C. Immediately after boiling, the hot meat was ground in a meat grinder, split into six separate samples and analysed by SPME-MS-MVA. After storage at 4°C for 4 days, the samples were reheated to 50°C in a convection oven for 30 min. Organoleptic evaluation of the samples showed that their flavour had changed from a typical beef flavour to an off-flavour characterized as tallowy, green and metallic. Samples were again refrigerated, stored for an additional 48 h, and re-analysed after warming to 50°C.

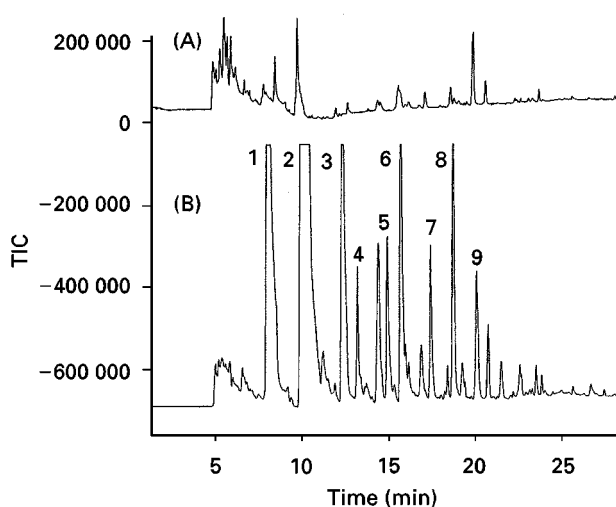


Figure 8 Development of warmed-over flavour in cooked beef. SPME-GC-MS chromatogram of boiled beef (A) at 0 days and (B) after 6 days of storage and then reheated to 50°C. Peak identities: 1, pentanal; 2, hexanal; 3, heptanal; 4, 2,4-nonadienal; 5, octanal; 6, 2,3-octanedione; 7, nonanal; 8, 1-octen-3-ol; 9, 2-heptenal.

Samples after 6 days of storage developed even stronger WOF notes.

SPME procedure 0.5 g boiled beef (ground) plus 2.5 mL water were added to a 9 mL glass GC vial. All other conditions were the same as the soybean oil SPME procedure given above.

Results The PCA scores plot for this set of samples appears in Figure 7. SPME-MS-MVA is capable of identifying groups of samples with similar levels of WOF.

To ensure that SPME was measuring volatiles that are known to contribute to WOF (e.g. aliphatic aldehydes, 2,4-nonadienal, etc.), a fresh boiled beef sample (0 days) and a 6-day sample were analysed by SPME-GC-MS. The resulting chromatograms, shown in Figure 8, prove that SPME is extracting compounds that have been identified as the source of WOF by other researchers. The chromatogram was generated using the identical method used for SPME-MS-MVA, with the exception that the 1 m transfer line was replaced with a 30 m FFAP capillary column.

Conclusion

As the numerous examples in this article illustrate, SPME is one of the most potent extraction, isolation and concentration techniques available for studying off-flavour chemicals in foods and beverages. Improvements in SPME technology will probably be made in the near future, making the technique even more useful to flavour chemists. Important recent developments in fibre technology include:

1. StableFlex™ fibres (which exhibit greater flexibility and increased strength compared to previous fibres);
2. a highly cross-linked PDMS fibre coating to minimize bleed and improve thermal stability;
3. coatings containing micro-adsorbent beads for retention and selectivity for many polar and volatile analytes;
4. dual-coated fibres that have the ability to efficiently extract low levels of both polar and nonpolar analytes in the same sample.

See also: II/Chromatography: Gas: Headspace Gas Chromatography. **Extraction:** Solid-Phase Microextraction. III/Airborne Samples: Solid Phase Extraction. **Fragrances:** Gas Chromatography.

Further Reading

Charalambous G (ed.) (1978) *Analysis of Foods and Beverages*. New York, NY: Academic Press.

- Charalambous G (ed.) (1992) *Off-Flavors in Foods and Beverages*. Amsterdam: Elsevier Science.
- Contis ET, Ho C-T, Mussinan CJ, Parliament TH, Shahidi F and Spanier AM (eds) (1998) *Food Flavors: Formation, Analysis and Packaging Influences*. Amsterdam: Elsevier Science.
- Elmore JS, Mehmet AE and Muttram DS (1997) Comparison of dynamic headspace concentration of tenax with solid phase microextraction for the analysis of aroma volatiles. *Journal of Agriculture and Food Chemistry* 45: 2638–2641.
- Heath HB and Reineccius G (eds) (1986) *Flavor Chemistry and Technology*. New York: Van Nostrand Reinhold.
- Ho C-T and Manley CH (eds) (1993) *Flavor Measurement*. New York: Marcel Dekker.
- Marsili RT (ed.) (1997) *Techniques for Analyzing Food Aromas*, pp. 237–289. New York: Marcel Dekker.
- Marsili RT (1999) Comparison of solid phase microextraction and dynamic headspace method for the GC-MS analysis of light-induced lipid oxidation products in milk. *Journal of Chromatography Science* 37: 17–23.
- Marsili RT (1999) SPME-MS-MVA as an electronic nose for the study of off-flavors in milk. *Journal of Agriculture and Food Chemistry* 47: 548–654.
- Scheppers-Wercinski SA (ed.) (1999) *Solid Phase Microextraction: A Practical Approach*. New York: Marcel Dekker.

Overview

J. R. Dean, University of Northumbria at Newcastle, Newcastle upon Tyne, UK

Copyright © 2000 Academic Press

Introduction

Solid phase microextraction (SPME) has been applied to a diverse range of analytes and sample types. The growth in the application of SPME, since its inception in 1990, can be seen in **Figure 1** (information from the *Science Citation Index*, February 1999). SPME is used as both a method of preconcentration and as a sampling device for (predominantly) chromatographic analysis. SPME has been used in conjunction with a range of other techniques, such as, ultraviolet and infrared spectroscopy, Raman spectroscopy and mass spectrometry, but it is its use in chromatographic analysis which is the focus of this article. SPME has most commonly been coupled to gas chro-

matography (GC), although some applications have coupled it to high-performance liquid chromatography (HPLC) (**Figure 2**). The following discussion will concentrate primarily on the use of SPME coupled with GC.

The SPME device consists of a fused silica fibre, coated with a stationary phase (**Table 1**) and mounted in a syringe-type holder (**Figure 3**). The SPME holder has two functions: to provide protection for the fibre and allow insertion into the hot environment of the GC injector using a needle. As samples and standards are normally introduced into a GC via a syringe the use of this device offers no additional complexity.

At rest the fused silica-coated fibre is retracted within the protective needle of the SPME holder. In operation however, the fibre is exposed to the analyte within its matrix (air, water, solid) for a predetermined amount of time. The active length of the fibre is typically 1 cm. Two common approaches for sample extraction are employed; direct and headspace (**Figure 4**). The first involves direct contact between the coated fibre and the sample matrix; in this way analytes within the sample are able to be transported to the fibre coating. This transportation can be achieved by several means. In the case of liquid (or solid samples that have been mixed with an aqueous solution, i.e. a slurry), transportation is achieved by agitation of the sample vial, agitation of the fibre, stirring or sonication of the sample solution. For gaseous samples, natural convection is usually sufficient. In the headspace mode, the process relies on the release of volatile compounds from the sample matrix. This may be achieved by heat, chemical modification or the inherent volatility of the analyte.

After sampling, the fibre is retracted within its holder for protection until inserted in the hot injector

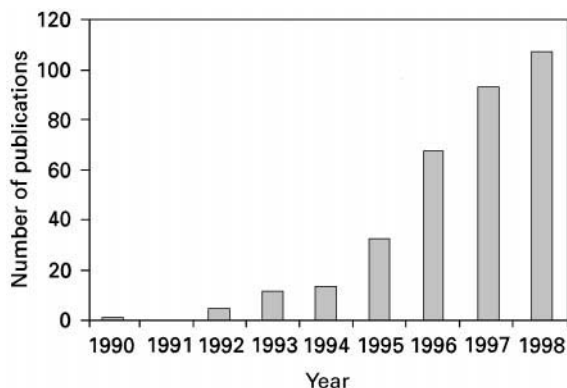


Figure 1 Frequency of SPME publications per year (information from the *Science Citation Index*, February 1999, Copyright International Scientific Communications, Inc.).

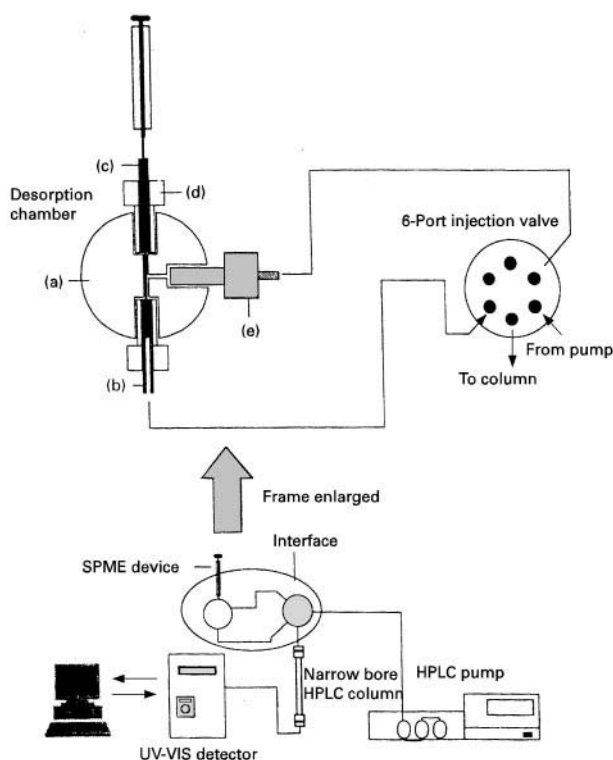


Figure 2 Solid phase microextraction-high-performance liquid chromatography interface (reproduced with permission, from *Analytical Chemistry* 67: 2530, 1995, Copyright American Chemical Society).

of the GC or mobile phase of the HPLC; desorption of analytes occurs due to the influence of temperature (GC) or organic solvent (HPLC). In either case the fibre is exposed for a particular time to allow for effective desorption of the analytes. As the coating on the fibre is selective towards the analyte, it is common to find that no solvent peaks are present in the subsequent chromatograms. As the fibre coating is selective towards the target analytes it is important to select the most appropriate fibre coating for the sampling process. **Figure 5** compares the influence of three fibre coatings, i.e. polystyrene-divinylbenzene (XAD), polyacrylate, and polydimethylsiloxane (PDMS) for the extraction of 49 organophosphorus pesticides from a water sample. The selectivity of each fibre coating is evident from the chromatograms (Figure 5).

It is important to note that the fibre can equally adsorb analytes from the atmosphere as well as the sample (in some cases the atmosphere may be the sample). Extreme caution should be taken first of all to clean the fibre. This can be done, for example, by exposing the fibre to the hot injector of the GC before sampling. Also, it is important to minimize the time between the sorption step and the subsequent desorption and analysis step.

Table 1 Commercially available fibre coatings

•	7 μm Polydimethylsiloxane (bonded)
•	30 μm Polydimethylsiloxane (non-bonded)
•	100 μm Polydimethylsiloxane (non-bonded)
•	85 μm Polyacrylate (partially crosslinked)
•	60 μm Polydimethylsiloxane/divinylbenzene (partially crosslinked)
•	65 μm Polydimethylsiloxane/divinylbenzene (partially crosslinked)
•	75 μm Polydimethylsiloxane/Carboxen (partially crosslinked)
•	65 μm Carbowax/divinylbenzene (partially crosslinked)
•	50 μm Carbowax/Template resin (partially crosslinked)

Quantitation in SPME is achievable in much the same way as for any other sample analysis. For example, in GC a series of standard solutions are prepared in organic solvent over the appropriate concentration range for the analytes under investigation. From the results obtained a calibration graph can be constructed [a plot of signal intensity (area or peak height) versus concentration]. Then, an organic solvent extract of the unknown is injected into the GC and its response compared to the calibration graph. In the same manner for SPME, a series of standard solutions need to be prepared in aqueous solution or soil slurry form. The fibre is then exposed to the solution (or soil slurry) for a prespecified time and then introduced into the hot injector of the GC. In

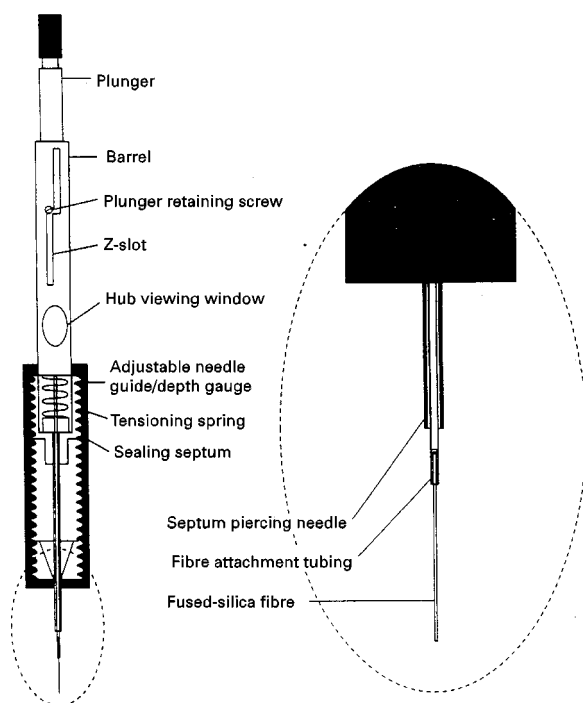


Figure 3 Solid phase microextraction device (reproduced with permission from *Analytical Chemistry* 66: 844A, 1994, Copyright American Chemical Society).

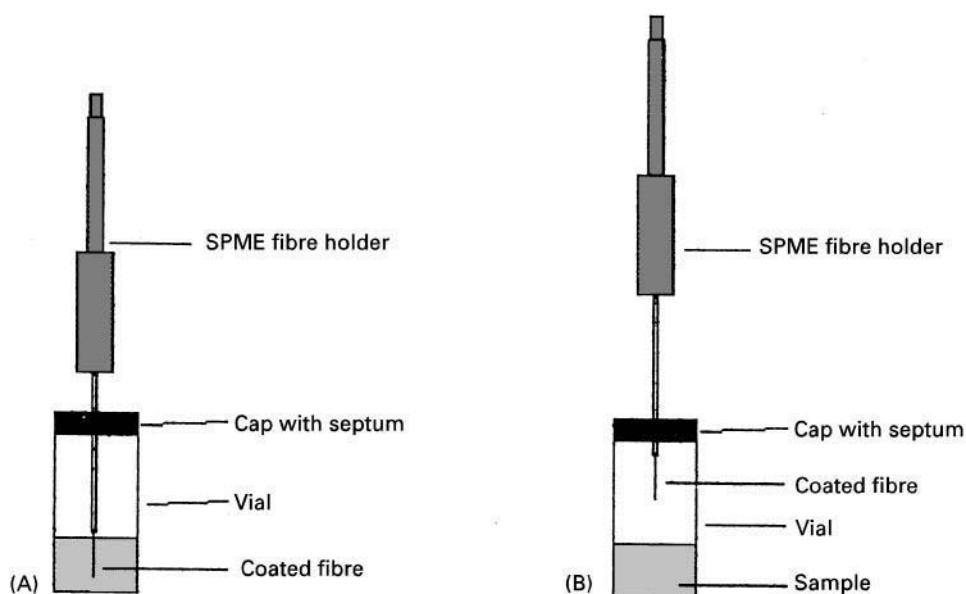


Figure 4 Common approaches for SPME. (A) Direct SPME and (B) headspace SPME.

this manner a calibration graph can be constructed. Similarly, an aqueous SPME extract (or slurry extract) of an unknown sample is injected in the GC and its signal response compared with the calibration graph. Calibration is also done in this manner for headspace SPME, the difference being that the fibre is exposed to the headspace above the sample only and not placed in the solution or soil slurry itself. It is common practice to utilize an internal standard for all quantitative analysis. Calibration is also possible using the method of standard additions. For further information on quantitative headspace methods see the book by Kolb and Ettre listed in the Further Reading section.

The diversity of applications of SPME is continually expanding, limited only by people's ingenuity, so it is not unfamiliar to find applications of SPME in such diverse areas as environmental and clinical, food and pharmaceutical, forensic and military use. However, the most popular application area is environmental analysis (water and soil). In order to provide examples of the diversity of applications, selected areas have been considered. For further information, the reader is recommended to consult the Further Reading Section or the current scientific literature.

Extraction of Analytes from Aqueous Matrices

Analysis of polar and labile analytes in aqueous matrices usually involves extraction and preconcentration. This has traditionally been based on

liquid-liquid extraction (LLE). In this context, a small volume of organic solvent is added to a larger volume of the aqueous sample and shaken (it may be necessary to 'salt-out' the analytes, this is done by saturating the aqueous sample with an inorganic salt). The organic phase containing the analytes is then analysed. [Note: additional preconcentration may be required using evaporation in a stream of inert gas (manual or automated) or vacuum evaporation.] However, if the analytes are sufficiently volatile they can be purged from an aqueous sample using a gas, such as nitrogen, preconcentrated by trapping on a suitable sorbent, e.g. Tenax, at low temperature and eluted by rapidly heating the trap. The analytes are then directly transferred into a gas chromatograph for separation and detection. This procedure, known as dynamic headspace or 'purge and trap' sampling is an effective procedure for volatile analytes. An alternative to the requirements for extraction and preconcentration of non-volatiles is solid phase extraction (SPE).

SPE uses a stationary phase, such as C_{18} -silica, to adsorb analytes from a large volume of sample solution. Elution of analytes is then achieved by using a small volume of organic solvent. In this manner, effective extraction and preconcentration is achieved. The use of SPME takes this method a stage further in miniaturization.

Effective extraction and preconcentration of analytes in aqueous matrices can be achieved using SPME. Two approaches are commonly used. In the first approach, the fibre is inserted directly into an aqueous sample for a prespecified time, with or

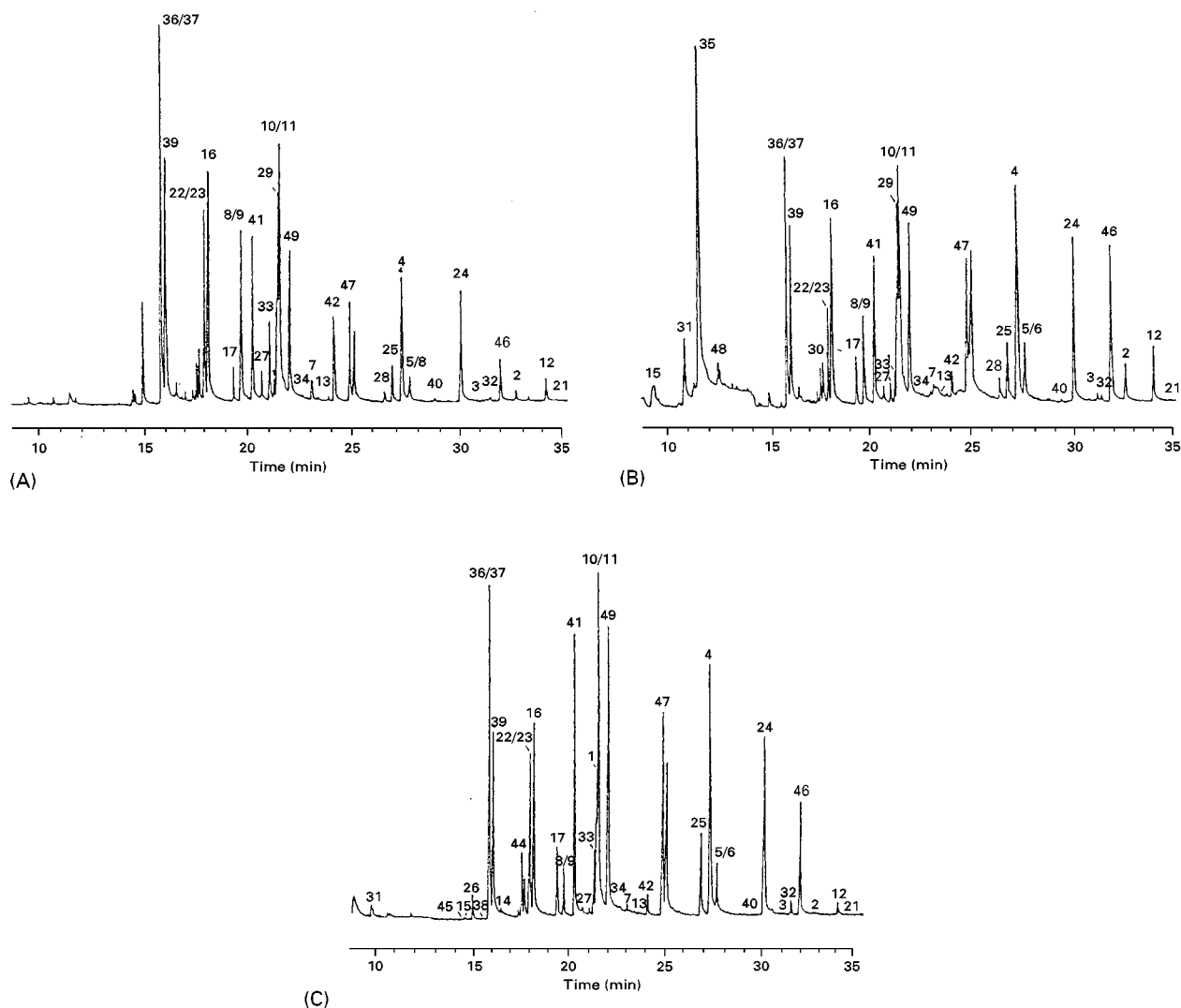


Figure 5 SPME of $3 \mu\text{g L}^{-1}$ organophosphorus pesticides. (A) $15 \mu\text{m}$ XAD polystyrene-divinylbenzene-coated fibre, (B) $85 \mu\text{m}$ polyacrylate-coated fibre, and (C) $30 \mu\text{m}$ polydimethylsiloxane-coated fibre. (Reproduced with permission from *Journal of High Resolution Chromatography* 20: 487, 1997, Copyright John Wiley & Sons Limited.) GC conditions: column 30 m length $\times 0.25 \text{ mm}$ internal diameter $\times 0.25 \mu\text{m}$ film PTE-5 fused silica open tubular; temperature programme 60°C (4 min hold) to 150°C at $30^\circ\text{C min}^{-1}$ and from 150 to 300°C at 5°C min^{-1} (hold for 3 min). SPME conditions: $15 \mu\text{m}$ XAD coated fibre; adsorption time, 30 min; desorption time, 20 min at 270°C . Eighty-five μm polyacrylate coated fibre; adsorption time, 30 min; desorption time, 20 min at 280°C . Thirty μm polydimethylsiloxane coated fibre; adsorption time, 30 min; desorption time, 20 min at 300°C . Spiking level was $3 \mu\text{g L}^{-1}$ per compound; sample volume was 1.5 mL . **Peak identification:** 1 = aspon; 2 = azinphos-ethyl; 3 = azinphos-methyl; 4 = bolstar; 5/6 = carbophenothion/famphur; 7 = chlorfenvinphos; 8/9 = chlorpyrifos-methyl/parathion-methyl; 10/11 = chlorpyrifos/parathion-ethyl; 12 = coumaphos; 13 = crotoxyphos; 14 = demeton-O; 15 = demeton-S; 16 = diazinon; 17 = dichlorfenthion; 18 = dichlorvos; 19 = dicrotophos; 20 = dimethoate; 21 = dioxathion; 22/23 = disulfoton/phosphamidon; 24 = *O*-ethyl-*O*-(4-nitrophenyl)phenylphosphono-thioate (EPN); 25 = ethion; 26 = ethoprop; 27 = fenitrothion; 28 = fensulfothion; 29 = fenthion; 30 = fonophos; 31 = hexamethylphosphoramide (HMPA); 32 = leptophos; 33 = malathion; 34 = merphos; 35 = mevinphos; 36/37 = monocrotophos/sulfotepp; 38 = naled; 39 = phorate; 40 = phosmet; 41 = ronnel; 42 = stiropfos; 43 = tetraethylpyrophosphate (TEPP); 44 = terbufos; 45 = thionazin; 46 = tri-*O*-cresylphosphate; 47 = tokuthion; 48 = trichlorfon; and 49 = trichloronate.

without stirring and with or without the addition of salt. The fibre is then retracted into its protective holder and the adsorbed analytes desorbed in either the hot injector of the GC or in the mobile phase of an HPLC system. This approach is to be favoured for the more non-volatile, labile type of analytes. The alternative approach is to place a small volume of the

liquid sample in a sealed vial and to insert the fibre into the headspace above the sample for a prespecified time. Again, stirring may be beneficial as well as the addition of salt. In addition, warming the sample vial may prove to be beneficial by increasing the concentration of volatile analytes in the headspace above the sample.

Table 2 Limits of detection (ng L^{-1}) for selected pesticides from water using a $95\ \mu\text{m}$ polyacrylate coated fibre

Compound	FID ^a	NPD ^b	MS ^c	MS ^d
EPTC	2000	50	0.8	16
Butylate	1000	20	0.1	1
Vernolate	1000	20	0.5	2
Pebulate	1000	20	1	19
Molinate	2000	60	0.3	12
Propachlor	6000	800	15	16
Cycloate	800	20	0.05	1
Trifluralin	400	30	0.02	1
Benfluralin	300	30	0.4	1
Simazine	1000	70	1	15
Atrazine	7000	40	3	11
Propazine	10 000	50	0.3	6
Profluralin	200	30	0.1	1
Terbacil	15 000	200	1	9
Metribuzin	14 000	200	3	19
Bromacil	19 000	400	0.1	8
Metolachlor	1000	200	0.01	8
Isopropalin	300	10	0.1	1
Pendimethalin	200	20	0.1	1
Oxadiazon	300	30	0.01	1
Oxyfluorfen	200	300	6	1
Hexazinone	2000	6000	1	15

^a Determined from $100\ \mu\text{g L}^{-1}$ solutions.^b Determined from $10\ \mu\text{g L}^{-1}$ solutions.^c Determined from $0.01\ \mu\text{g L}^{-1}$ solutions.^d Calculated for the line of best fit with a zero intercept, over the range $0.1\text{--}100\ \mu\text{g L}^{-1}$ ($n = 3$). Values (a)–(c) are from Boyd-Boland AA and Pawliszyn J (1995) *Journal of Chromatography* 704: 163. Values for (d) are from Boyd-Boland AA *et al.* (1996) *Analyst* 121: 929.

Direct Extraction

Examples of the direct approach have allowed multiple analytes, e.g. pesticides, to be determined in aqueous samples. For example, limits of detection for the determination of pesticides in water by GC with flame ionization detector (FID), nitrogen-phosphorous detector (NPD) or mass spectrometer (MS), using a $95\ \mu\text{m}$ polyacrylate-coated fibre, are shown in Table 2. Other SPME conditions are as follows: a 50 min equilibration time with stirring at room temperature; and desorption by inserting the fibre into the hot GC injector (250°C) for 5 min. Similarly, selected detection limits for a $100\ \mu\text{m}$ polydimethylsiloxane fibre are shown in Table 3. A typical SPME–GC–NPD chromatograph for the analysis of drinking water spiked with 36 pesticides (EPA Method 507) at the $10\ \mu\text{g L}^{-1}$ is shown in Figure 6. In addition, to evaluating the sensitivity of SPME by determining detection limits, an alternative approach is to evaluate the performance of SPME against a traditional aqueous extraction procedure (liquid–liquid extraction). Results for the extraction

of 20 organochlorine pesticides extracted from a groundwater sample by both SPME and LLE are shown in Figure 7. In the case of SPME, a $30\ \mu\text{m}$ polydimethylsiloxane fibre was inserted in a sample volume of $1.5\ \text{mL}$ for 20 min. Desorption was achieved by insertion into the GC injector for 10 min at 260°C . The spiking level was $1\ \mu\text{g L}^{-1}$. For LLE a $100\ \text{mL}$ sample spiked at the $0.5\ \mu\text{g L}^{-1}$ level was extracted with $20\ \text{mL}$, then $10\ \text{mL}$ of hexane. The combined extracts were dried with anhydrous sodium sulfate and concentrated to $1\ \text{mL}$ using a stream of nitrogen prior to analysis. In most cases similar results were obtained by SPME and LLE. Anomalous results for endosulfan I and II were reported.

Examples of the direct approach for non-volatile compounds, using SPME–HPLC, are shown in Figures 8 and 9. In Figure 8, a comparison is made between SPME and a $1\ \mu\text{L}$ loop injection for the analysis of polycyclic aromatic hydrocarbons (PAHs) using reversed phase HPLC. Using the SPME–HPLC interface, as shown in Figure 2, thirteen PAHs have been analysed after sampling for 30 min using a $7\ \mu\text{m}$ PDMS-coated fibre. Some differences, in terms of peak height, are noted (Figure 8) for peaks 1–4 when SPME is compared with direct injection. These differences are attributable to the selectivity of sampling associated with SPME. The versatility of the SPME–HPLC approach is further highlighted in Figure 9. In this case, an alkylphenol ethoxylate (Triton X-100) in the aqueous phase is sampled for 60 min with stirring

Table 3 Limits of detection (ng L^{-1}) for selected pesticides from water using a $100\ \mu\text{m}$ polydimethylsiloxane-coated fibre

Compound	NPD ^a	MS ^a	MS ^b
Dichlorvos	1500	80	30
EPTC	20	10	2
Butylate	50	20	1
Vernolate	100	20	1
Pebulate	40	10	14
Molinate	110	20	4
Cycloate	130	30	1
Simazine	360	10	18
Atrazine	110	30	23
Propazine	40	10	5
Diazinon	60	10	1
Disulfoton	40	10	0.7
Metolachlor	220	20	9

^a Determined from $100\ \mu\text{g L}^{-1}$ solutions. Other SPME conditions: 20 min equilibration time from a saturated sodium chloride solution at room temperature and pH 7. From Choudhury TK *et al.* (1996) *Environmental Science Technology* 30: 3259.^b Calculated for the line of best fit with a zero intercept, over the range $0.1\text{--}100\ \mu\text{g L}^{-1}$ ($n = 3$). Other SPME conditions: 50 min equilibration time with stirring at room temperature. From Boyd-Boland AA *et al.* (1996) *Analyst* 121: 929.

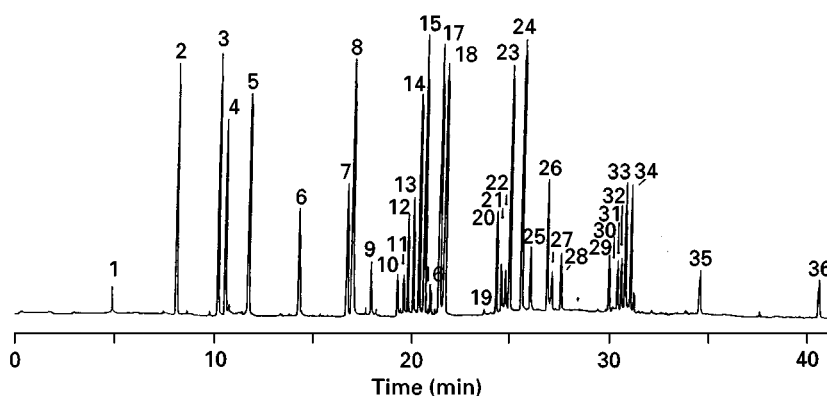


Figure 6 SPME-GC-NPD analysis of drinking water spiked with $10 \mu\text{g L}^{-1}$ each pesticide (36). (Reproduced with permission from *American Chemical Society, Environmental Science and Technology*, 30(11): 3259, 1996.) SPME conditions: $100 \mu\text{m}$ polydimethylsiloxane fibre; adsorption time, 20 min; desorption time, 5 min at 220°C . Samples were extracted with stirring at ambient temperature, at pH 7.0 and with a final 4.0 mL saturated sodium chloride solution. GC conditions: 30 m length \times 0.32 mm internal diameter \times 0.25 mm film 5% phenyl/95% dimethylsilicone fused silica open tubular column; temperature programme 100°C to 300°C at 4°C min^{-1} . 1 = dichlorvos, 2 = EPTC, 3 = butylate, 4 = vernolate, 5 = pebulate, 6 = molinate, 7 = cycloate, 8 = ethoprop, 9 = chlorpropham, 10 = simazine, 11 = atraton, 12 = prometon, 13 = atrazine, 14 = propazine, 15 = terbufos, 16 = pronamide, 17 = diazinon, 18 = disulfoton, 19 = disulfoton sulfone, 20 = simetryn, 21 = alachlor, 22 = ametryn, 23 = prometryn, 24 = terbutryn, 25 = metolachlor, 26 = triademeton, 27 = MGK 264, 28 = diphenamid, 29 = butachlor, 30 = carboxin, 31 = stirofos, 32 = fenamiphos, 33 = napropamide, 34 = merphos, 35 = norflurazon and 36 = fenarimol.

and at room temperature. Desorption is achieved by exposing the fibre for 1 min to the mobile phase. Separation is achieved using normal phase HPLC.

Headspace SPME from Water

In headspace SPME, the fibre is exposed to the air above an aqueous sample, which is in equilibrium with

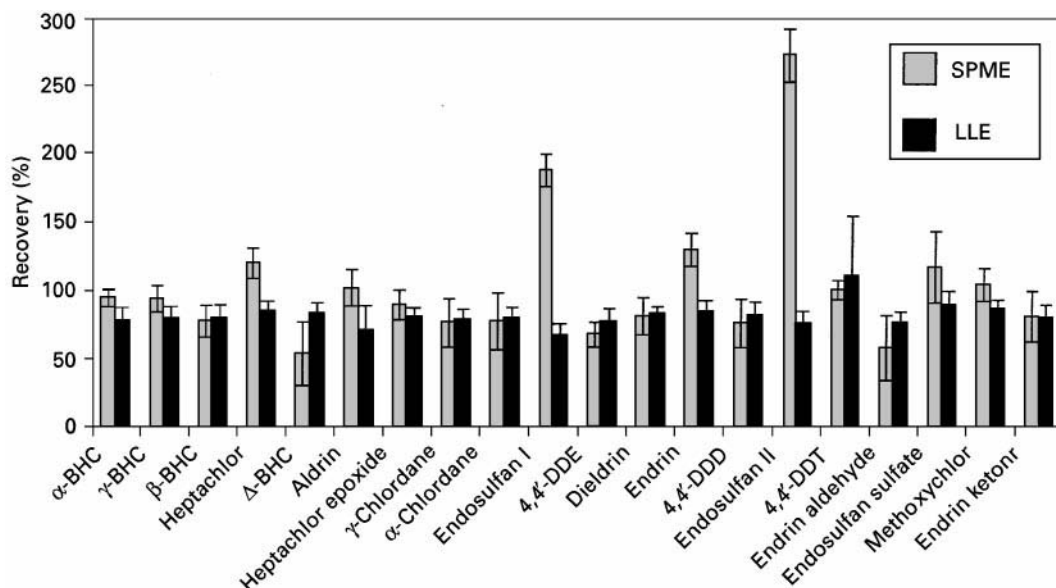


Figure 7 Extraction of 20 organochlorine pesticides from groundwater: Comparison between SPME and LLE. (Adapted from *Journal of High Resolution Chromatography* 19: 247, 1996.) SPME conditions: $30 \mu\text{m}$ polydimethylsiloxane fibre; adsorption time, 20 min; desorption time, 10 min at 260°C . Spiking level was 1 g L^{-1} . Sample volume was 1.5 mL. There were three determinations. GC conditions: 30 m length \times 0.25 mm internal diameter \times 0.25 mm film SPB-608 fused silica open tubular column; temperature programme 100°C (4 min hold) to 150°C at $30^\circ\text{C min}^{-1}$ then to 300°C (8.6 min hold) at 8°C min^{-1} . LLE conditions: 100 mL sample extracted with 20 mL, then 10 mL hexane. Extracts were then combined, dried with anhydrous sodium sulfate and concentrated to 1 mL under a stream of nitrogen. Spiking level was 0.5 g L^{-1} . There were three determinations. GC conditions: 15 m length \times 0.53 mm internal diameter \times 0.88 mm film HP-5 fused silica open tubular column; temperature programme 150°C (0.5 min hold) to 275°C (5 min hold) at 5°C min^{-1} .

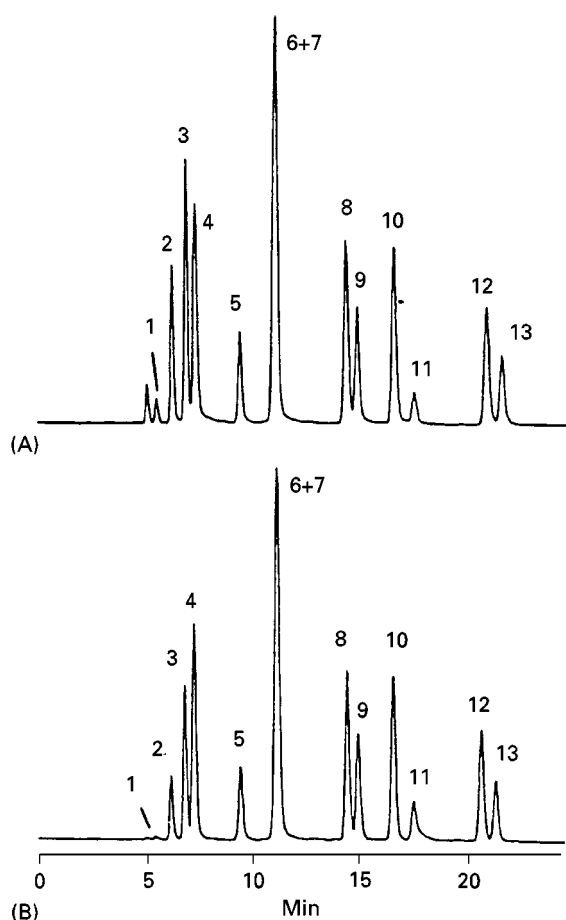


Figure 8 Separation of polycyclic aromatic hydrocarbons by (A) 1 μ L loop injection, and (B) SPME using a 7 μ m PDMS-coated fibre for 30 min from 100 ppb of each compound spiked into water. (*American Chemical Society, Analytical Chemistry*, 67: 2530, 1995.) HPLC conditions: column, 25 cm \times 2.1 mm internal diameter, 5 μ m ODS; flow rate, 0.2 mL min⁻¹; (detection, UV 254 nm; solvent programme, acetonitrile–water (80 : 20, v/v) linear gradient to 100% acetonitrile in 15 min. SPME conditions: 7 μ m polydimethylsiloxane fibre; adsorption time, 30 min with stirring. Spiking level was 100 ppb. Peak identification: 1 = acenaphthylene, 2 = fluorene, 3 = phenanthrene, 4 = anthracene, 5 = pyrene, 6 = benz[a]anthracene, 7 = chrysene, 8 = benzo[b]-fluoranthene, 9 = benzo[k]fluoranthene, 10 = benzo[a]pyrene, 11 = dibenzo[ah]anthracene, 12 = indeno[1,2,3-cd]pyrene, and 13 = benzo[ghi]perylene.

the aqueous phase. For this approach to be useful the analytes of interest must partition favourably into the vapour phase. Therefore, the approach is useful for volatile organic compounds in aqueous samples. Most work has been done with the BTEX compounds, i.e. benzene, toluene, ethylbenzene and the xylene isomers.

Samples and standards are introduced into glass vials, e.g. 40 mL volume, with Teflon-lined septa. It is beneficial for the speed of extraction to add a (Teflon-coated) stirring bar and/or salt for 'salting-out' to

improve sensitivity. Then, each vial is capped. The septum is then pierced and the SPME device inserted. The exposed coated-silica fibre is positioned approximately 1 cm above the surface of the aqueous sample. The entire assembly is mounted on a magnetic stirring plate. Care is required during the stirring process that the vortex generated is not so vigorous so that the aqueous sample comes into contact with the exposed fibre (a vortex of depth 1 cm is adequate). In addition, the sample vial may be heated, by placing it in a temperature controlled water bath at temperatures in the range 40–80°C. The extraction time can be varied between 5 and 50 min, as desired. After a suitable exposure time, the fibre is retracted into its holder, withdrawn from the vial and immediately inserted into the hot injector of the GC for subsequent separation and detection. The typical performance of this type of headspace SPME is summarized in Table 4. The results in Table 4 compare the statistical detection limits obtained by both the headspace SPME and purge and trap approaches. In both cases, the statistical detection limits were approximately an order of magnitude higher than those required for the analysis of drinking water (US EPA Method 524.2). The use of a more sensitive detector, for instance an ion trap mass spectrometer, could lower the detection limits achievable.

Extraction of Analytes from Solid Matrices

Traditional approaches for the extraction of analytes include Soxhlet extraction (and its variants), shake flask extraction and sonication. Soxhlet extraction is frequently referred to as the benchmark technique, so it is not surprising to find that results obtained with newer extraction techniques are compared to data obtained by Soxhlet extraction. While Soxhlet is used as the method of choice for many people for extracting analytes from solid matrices, it is a time-consuming process and uses relatively large volumes of organic solvent. Alternatives have therefore been sought to produce analytical data more rapidly and that use smaller amounts of organic solvent (or none at all). In this context, alternatives that have been proposed include supercritical fluid extraction, microwave-assisted extraction and pressurized fluid extraction. However, the high capital cost of all these alternatives and in some cases the level of expertise required to operate the instruments effectively has precluded their wide acceptance. In this context, the use of SPME has been proposed. However, in order for SPME to be of any use, the analytes must be released from the solid matrix and enter either a liquid phase or the gaseous phase. Variants on these themes for SPME are now considered.

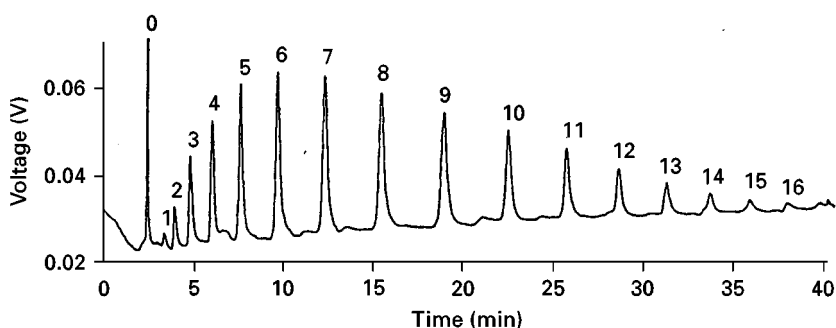


Figure 9 Normal phase HPLC chromatogram of extracted Triton X-100. Peak assignment refers to the number of units in the ethoxylate chain. (*American Chemical Society, Analytical Chemistry* 68: 1521, 1996.) HPLC conditions: column, 25 cm \times 4.6 mm internal diameter, 5 μ m Supelcosil LC-NH₂; flow rate, 1.5 mL min⁻¹; detection, UV 220 nm; solvent programme, 3–53%B, where A is 90 : 10, v/v hexane–2-propanol and B is 90 : 10, v/v 2-propanol–water. SPME conditions: carbowax/template resin fibre; adsorption time, 60 min with stirring at room temperature; desorption time, 1 min. Spiking level was 100 ppm. Sample volume was 4 mL.

Several approaches can be adopted for the extraction of analytes from solid matrices using SPME. These include direct extraction of the analytes from a soil–water suspension or slurry; extraction of the analyte from the sample matrix using hot water; or, headspace extraction. In the first two approaches, it is assumed that the analytes are highly soluble in water and that water is a suitable solvent to liberate the analyte from its matrix. The latter scenario assumes that the analytes of interest are volatile or semi-volatile so that they are available in the headspace above the sample.

Table 4 Analysis of BTEX compounds from aqueous samples: determination of statistical method detection limits (μ g L⁻¹)^a

Compound	Headspace SPME ^b	Purge and trap ^c	EPA 524.2 ^d
Benzene	0.70	0.38	0.03
Toluene	0.30	0.37	0.05
Ethylbenzene	0.35	0.43	0.03
m-/p-xylene	0.23	0.72	0.05
o-xylene	0.19	0.30	0.06

^aData from MacGillivray B *et al.* (1994) *Journal of Chromatographic Sciences* 32: 317.

^bHeadspace SPME conditions: 100 μ m polydimethylsiloxane fibre was used to extract BTEX compounds from a 25 mL of water containing 10.0 g of NaCl. The sample was stirred and the temperature maintained at 40°C. The extraction time was 50 min. The fibre was desorbed for 2 min at 180°C. Analysis was by GC-FID.

^cPurge and trap conditions: 5 mL samples were purged for 10 min using a helium flow rate of 40 mL min⁻¹ and a sample temperature of 40°C. The compounds were trapped on a Tenax-charcoal trap. Analysis was by GC-MSD in the full scan mode.

^dUS Environmental Protection Agency guidelines for BTEX in drinking water (method 524.2). Reference: Measurement of Purgeable Organic Compounds in Water by Capillary Column Gas Chromatography/Mass Spectrometry, Revision 3.0, US EPA Office of Research and Development, Cincinnati, OH, 1989, EPA Document EPA/600/4-88/039.

Direct (Slurry) SPME

For slurry extraction, a known quantity of sample, e.g. 10 mg to 1 g of soil, is mixed with a solvent (water) and stirred. It may be necessary to adjust the pH of the solution (to convert all compounds to a non-ionized form) and add salt to improve the extraction efficiency. The SPME fibre is then exposed directly to the resultant suspension or slurry for a prespecified time (1–60 min) and then analysed. In addition, it also assumes that the matrix itself will not interfere with the extraction process. If this is the case, the SPME fibre can be placed inside a protective membrane in the slurry. The major limitation of this approach is that the membrane itself does not preclude any of the analytes of interest. However, this approach has not yet been fully tested and further evaluation is necessary. Typical results for the analysis of chlorophenols from a contaminated land site are shown in Table 5 using the slurry SPME approach and two methods of quantitation (direct calibration using an internal standard and the method of standard addition). The results are compared with those obtained by Soxhlet extraction. A typical SPME–GC–MS chromatogram of the soil sample is shown in Figure 10.

Combined Hot Water Extraction–SPME

An alternative to the slurry method is to extract the solid sample with hot water and then isolate the analytes from the water using SPME prior to chromatographic separation and detection. This is a relatively new approach with few relevant publications to date. The basis of the approach, however, is that hot, pressurized water can selectively leach analytes from the solid matrix. Early work has suggested that the water temperature needs to be above 200°C and a pressure of 50 atm for effective

Table 5 Slurry analysis using SPME of a soil sample: comparison with Soxhlet extraction^a

Compound	SPME/internal standard ($\mu\text{g g}^{-1}$) ^b	SPME/standard addition ($\mu\text{g g}^{-1}$) ^b	Soxhlet extraction ($\mu\text{g g}^{-1}$) ^c
2,4-Dichlorophenol	0.9	1.9	2.0
2,4,6-Trichlorophenol	2.4	3.7	4.4
2,3,4,6-Tetrachlorophenol	7.6	8.4	12.8
Pentachlorophenol	533.8	562.2	642.4

^a Data from Lee MR *et al.* (1998) *Journal of Chromatography* 806: 317.

^b SPME: 40 mg of soil in 12.5 mL of a $20 \mu\text{g L}^{-1}$ internal standard (2,4,6-tribromophenol) solution and, then solution was diluted to 50 mL with pH 1 buffer solution and 5 M KCl added.

^c Soxhlet: 2 g soil extracted with 150 mL of n-hexane-acetone (1 : 1) for 8 h. Analysis using GC-SIM-MS.

extraction of semi-volatile compounds of environmental interest including polycyclic aromatic hydrocarbons (PAHs). It is also important in this type of work to be vigilant for analyte degradation, which obviously might result in lower recoveries than expected (but also not to neglect the possibilities of formation of compounds of interest). The dynamic extraction of organic pollutants from solid matrices

using water is possible using apparatus designed for supercritical fluid extraction (Figure 11A). By placing the soil sample in the extraction cell of the SFE apparatus, effective extraction using water can be accomplished at elevated temperature ($> 200^\circ\text{C}$) and pressure (50 atm). Quantitation is then achieved using SPME by inserting the fibre in the water extract (Figure 11B) followed by chromatographic analysis.

Preliminary results using this type of approach are shown in Table 6.

Headspace-SPME

Instead of using SPME to extract from the aqueous extract or slurried sample an alternative strategy uses headspace-SPME. In this approach SPME is used to extract volatile or semi-volatile analytes from the headspace above a solid sample. A soil sample (10 mg to 1 g) is placed in a headspace vial and the vial is

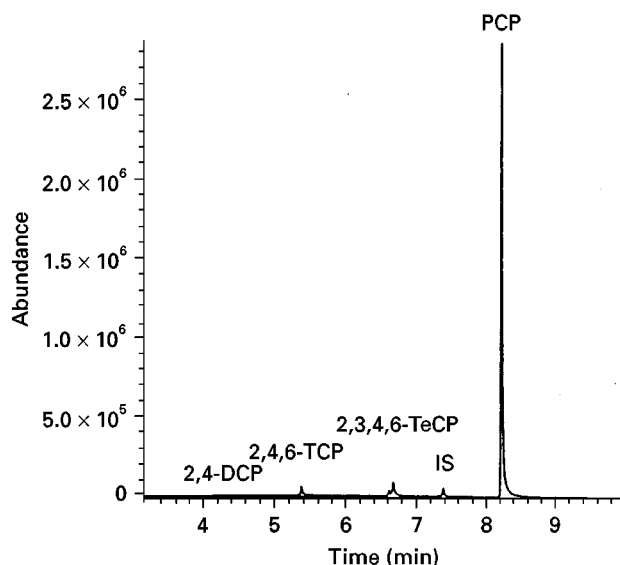
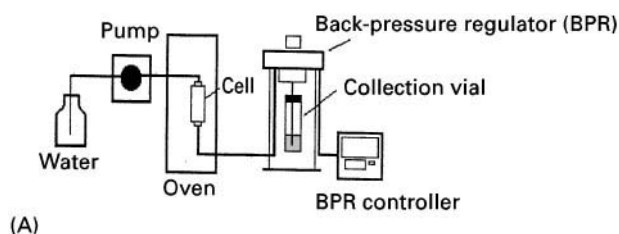
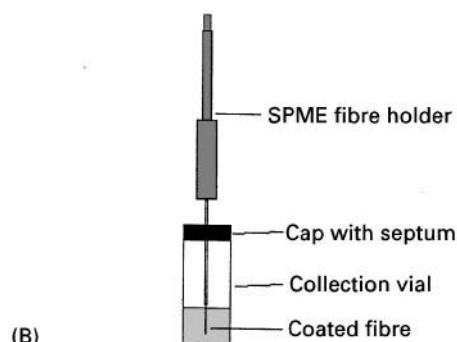


Figure 10 SPME-GC-MS chromatogram of a real soil sample contaminated with chlorophenols. (*Journal of Chromatography A*, 806: 317, 1998, Copyright Elsevier Science.) GC conditions: column, 30 m length \times 0.25 mm internal diameter \times 0.5 μm film DB-5.625 fused silica; injection, splitless mode with an injector temperature of 290°C , and a splitless time of 1 min; temperature programme $60\text{--}190^\circ\text{C}$ at $30^\circ\text{C min}^{-1}$ and from 190 to 310°C at $10^\circ\text{C min}^{-1}$. Slurry preparation: 40 mg of sieved soil (mesh size 1.981 mm and 2.000 mm) was prepared in 12.5 mL, of $20 \mu\text{g mL}^{-1}$ internal standard solution and, then, the solution was diluted to 50 mL with pH 1 buffer solution and 5 M KCl added. SPME conditions: 85 μm polyacrylate coated fibre; adsorption time, 40 min with stirring at 1000 rpm; desorption time, 2 min at 290°C . Peak identification: 2,4-DCP = 2,4-dichlorophenol; 2,4,6-TCP = 2,4,6-trichlorophenol; 2,3,4,6-TeCP = 2,3,4,6-tetrachlorophenol; IS = 2,4,6-tribromophenol; PCP = pentachlorophenol.



(A)



(B)

Figure 11 Combined hot water extraction-SPME: (A) Apparatus for hot water extraction and (B) quantitation using SPME.

Table 6 Dynamic high temperature water extraction of selected polycyclic aromatic hydrocarbons from an urban air particulate reference material (NIST 1649)^a

Compound	Certified concentration $\mu\text{g g}^{-1}$ (%RSD)	Estimated concentration as % of certified concentration (%RSD) ($n = 3$) ^b
Fluoranthene	7.0 (7)	134.0 (16)
Pyrene	7.2 (7)	87.5 (15)
Benzo[a]pyrene	2.9 (17)	72.0 (29)

^a Reference: Daimon H and Pawliszyn J (1996) *Analytical Communications* 33: 421.^b High temperature water extraction: 250°C and 50 atm.

sealed by crimping with an appropriate cap, e.g. an open-centred aluminium cap containing a PTFE/grey-butyl moulded septum. In order to promote the release of volatiles a small quantity of water (10–30%) may be added to the soil sample. In addition, the volatility of an analyte can be increased by heating the sample. This can simply be done by placing the sealed sample vial in a thermostatically-controlled water bath. It has been suggested that at ambient temperature this headspace SPME approach can be effective for three ring PAH compounds or more volatile compounds.

Conclusion

While SPME has been applied to a wide range of application areas, it is those with an environmental theme that have been mainly used to date. The main focus of this article is on the method of operation for a range of sample types. Specific examples have been provided as to the application of SPME for extraction of analytes from aqueous and solid

matrices. In addition, the different forms of analysis from aqueous samples are considered, i.e. direct and headspace sampling while for solid samples, the use of a slurry technique, prior to hot water extraction and headspace SPME is considered. The experimental data provided should act only as a guide to the potential and diverse applications of SPME.

See also: **II/Chromatography: Gas:** Headspace Gas Chromatography. **III/Environmental Applications:** Soxhlet Extraction.

Further Reading

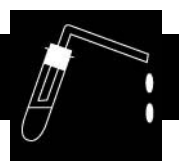
Dean JR (1998) *Extraction Methods for Environmental Analysis*. Chichester: John Wiley.

Kolb B and Ettre LS (1997) *Static Headspace-Gas Chromatography. Theory and Practice*. New York: Wiley-Interscience.

Pawliszyn J (1997) *Solid-Phase Microextraction. Theory and Practice*. New York: John Wiley.

Pawliszyn J (ed.) (1999) *Applications of Solid-Phase Microextraction*. Cambridge: Royal Society of Chemistry.

SOLVENTS: DISTILLATION



B. Buszewski, Nicholas Copernicus University, Torun, Poland

This article is reproduced from Encyclopedia of Analytical Science, Copyright © 1995 Academic Press

Introduction

In modern chemical analysis various physicochemical methods are used to achieve high detection sensitivity. In trace analysis, reported detection levels are often measured in $\mu\text{g mL}^{-1}$ (ppm) ng mL^{-1} (ppb), as well as in pg mL^{-1} (ppt). Achievement of such low detection levels has been made possible by the use of modern analytical instruments equipped with new types of detectors and by improved sample prepara-

tion methods. Both factors are closely related to the purity of the solvents used as the mobile phases in different variants of liquid chromatography (LC), capillary zone electrophoresis (CZE), liquid-liquid (LLE) and solid-phase (SPE) extraction, filtration and flotation. Moreover, high-purity solvents are also employed to dilute samples investigated using chromatography, spectral and electrochemical analysis. Thus, solvents used in chemical analysis must fulfil many physicochemical requirements.

High-purity solvents, for example for liquid chromatography (LC) and/or for spectroscopy, are produced by many manufacturers. However, purification and quality testing of solvents are often necessary before use, particularly in the above-mentioned techniques

applicable to multicomponent systems. For instance, the mobile phases in LC, CZE and SPE are often modified by different organic and/or inorganic salts.

In this article the most important physicochemical properties of commonly used solvents are briefly reviewed, including methods of their purification, recovery and quality testing.

Solvents: Properties and their Usage

In many cases the purity of the solvents used has a great influence on whether the molecular processes occurring in a multicomponent system proceed in the desired manner. The quality of measured data can often be improved by using high-purity solvents. For chromatography or spectroscopy a good solvent is characterized by high purity, and in consequence, by low values characterizing the transparency (cut-off) and refraction (refractive index). Parameters such as reactivity and good miscibility are also important criteria for solvent selection. In LC investigations, multicomponent solvents which have low boiling points (between 20 and 60°C) and low viscosity ($\eta < 50$ cP) are preferred. A good solvent should be able to dissolve the sample, although this is seldom a problem in analytical separations when the mobile phase has the correct strength.

The important physical parameters characterizing the most commonly used solvents in many analytical techniques are listed in Table 1. On the basis of this table it can be seen that LC is the most frequently applied technique and consequently it consumes a large amount of the various solvents. A high usage of solvents in LC results from the various separation modes of this technique.

In normal-phase (adsorption) liquid chromatography (NPLC) aliphatic hydrocarbons (e.g. *n*-hexane, *n*-heptane) are usually used as the mobile phase. The elution strength of these solvents is often modified by other organic compounds. A fundamental problem with NPLC eluents is the presence of dissolved water and trace amounts of the higher-fraction olefines. These contaminations can cause changes in the cut-off values (UV detection, spectrophotometry), baseline perturbation and poor reproducibility of retention data. Halogenated solvents such as dichloromethane can react with other reactive organic solvents (e.g. acetonitrile) and form crystalline products.

In reversed-phase liquid chromatography (RP-LC) aqueous solutions of methanol, acetonitrile, tetrahydrofuran and dioxane are used as eluents. In this mode of LC the most serious problem, besides the purity of the organic modifiers in the mobile phase, is the

Table 1 Properties of solvents used in various analytical techniques

<i>Solvent</i>	<i>UV-cut-off (nm)</i>	<i>Refractive index (25°C)</i>	<i>Boiling point (°C)</i>	<i>η (25°C) (cP)</i>	<i>ϵ (20°C)</i>
Acetone	330	1.356	56	0.30	20.70
Acetonitrile	190	1.341	82	0.34	37.50
Benzene	280	1.498	80	0.60	2.30
<i>n</i> -Butanol	210	1.397	118	2.60	17.52
Carbon tetrachloride	265	1.457	77	0.90	2.24
Chloroform	245	1.443	61	0.53	4.80
Cyclohexane	200	1.423	81	0.90	2.02
Cyclopentane	200	1.404	78	0.42	1.97
Diethyl ether	218	1.350	35	0.24	4.30
Dimethylformamide	268	1.428	153	0.80	36.73
Dimethylsulfoxide	268	1.477	189	2.00	4.70
Dioxane	215	1.420	101	1.22	2.21
Ethanol	210	1.359	78	1.08	24.60
<i>n</i> -Heptane	195	1.385	98	0.40	1.92
<i>n</i> -Hexane	190	1.372	69	0.30	1.88
Isooctane	197	1.389	99	0.47	1.94
Methanol	205	1.326	65	0.54	32.71
Methylene chloride	233	1.421	40	0.41	8.93
<i>n</i> -Octanol	205	1.427	195	7.31	10.30
<i>n</i> -Pentane	195	1.355	36	0.22	1.84
<i>i</i> -Propanol	205	1.384	84	1.90	20.30
<i>n</i> -Propanol	240	1.385	97	1.90	20.30
Tetrahydrofuran	212	1.405	66	0.46	7.56
Toluene	285	1.494	110	0.55	2.40
Water		1.333	100	0.89	80.00

η , viscosity; ϵ , dielectric constant.

purity of the water, which may contain trace impurities of phenols, hydrocarbons, etc. Tetrahydrofuran is frequently used as the solvent in gel permeation chromatography (GPC). It must be stabilized by butylate hydroxytoluene (BHT), which is used as an antioxidant. However, in ion suppression and ion pair RP-LC the mobile phases are often modified by the addition of compounds which can change the dissociation constants of analytes, such as inorganic and organic acids or ionic substances (e.g. ammonium chloride, cetyl chloride). All these components may contain inconvenient impurities which can also crystallize, causing some perturbation in detection during the elution process. As a result of these impurities extra peaks may appear in the chromatograms, making identification of the substances analysed more difficult. The impurities may interfere with the analyte's retention even if a UV-transparent mobile phase (e.g. methanol–water, acetonitrile–water and/or ethanol–water) is used.

Figure 1 shows the peak heights of different compositions of solvent gradually decreasing from their cut-off limits to become very low or almost negligible at wavelengths larger than 320 nm.

Another factor which influences the separation process and which may result from solvent impurities during chromatographic elution is peak tailing and/or peak splitting. In solid-phase extraction (SPE) irreversible sorption of solvent impurities on active sites of packing materials (e.g. surface silanols or chemically bounded ligands with polar groups such as $-OH$, $-NH_2$, $-CN$, etc.) can be manifested by relatively high differences in reproducibility of recoveries.

Therefore, before chromatographic or spectroscopic measurements are made, a special preparation

(e.g. isolation, purification and preconcentration) of the sample is recommended. For this purpose techniques such as LLE, SPE, filtration and membrane separation are used. It should be mentioned that high-purity solvents are required to prepare analytical samples.

Methods of Solvent Purification

There are many methods of solvent purification, but the most common are simple distillation, fractional distillation and steam distillation. A recent method of solvent purification using solid-state packing materials is becoming more popular. It can be carried out by LC, SPE, filtration, and ultrafiltration utilizing membranes.

Distillation

Distillation is the oldest and simplest procedure for solvent purification, and it is also inexpensive. It is based on Raoult's law, which states that the partial vapour pressure of a solvent is proportional to its mole fraction. The physical foundations of separation by distillation depend on the distribution of constituents between the liquid and the vapour phases being at equilibrium. In general, the composition of the vapour is different from the composition of the distillate. Only azeotropic mixtures distill without a change in their composition. However, during distillation of a normal mixture the principal component with the lowest boiling point distills first, followed by compounds with higher boiling points. The effectiveness of distillation depends on the physical properties of the components in the mixture, the equipment used and the method chosen.

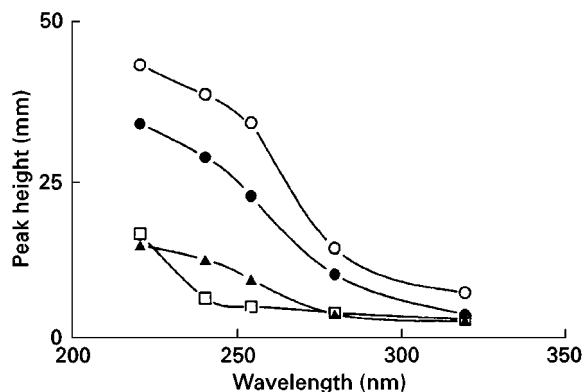


Figure 1 Plot of peak heights versus wavelength of radiation in the UV spectrophotometer for the mobile phase methanol (analytical grade) – water (home purified) at compositions 30 : 70% (v/v) (○), 50 : 50% (v/v) (●) and 70 : 30% (v/v) (▲), and composition 50 : 50% (v/v) (□) prepared from LC-grade solvents (J. T. Baker, Deventer, The Netherlands). (Reproduced with permission from Buszewski, Bleha and Berek (1985).)

Simple distillation Simple distillation refers to the process in which molecules transferred from the liquid phase to the vapour phase are not subjected to partial condensation or contact with the condensed liquid prior to reaching the condenser. The composition of the vapour near the liquid phase does not change as it moves toward the condenser. In this technique, equipment requirements are minimal; usually a flask fitted with a condenser and a product receiver are sufficient.

Fractional distillation Fractional distillation is used when a more efficient separation process than simple distillation is required. This type of distillation is an equilibrium process in which the composition of the distillate is constantly changing as the distillation proceeds. The main element of the apparatus is the distillation column, which consists of a series of

plates placed one above the other in a suitable tube. The column is placed under the receiver. Liquid evaporating from one (lower) plate condenses on the next (higher) plate, where it again evaporates. On each plate an equilibrium between the liquid and the vapour is established. Vapour enriched in more volatile components flows upwards, whereas vapour enriched in less volatile components flows downwards. The performance of the column increases with an increasing number of plates.

Steam distillation Steam distillation is a simple distillation procedure in which evaporation of the mixture is achieved either by continuously blowing steam through the mixture or by boiling water and the sample together. If the sample contains both hydrophobic and hydrophilic components, two layers of distillate develop. In typical steam distillation two layers can be recovered individually. Aqueous distillation seems to provide the best compromise between time, cost and effort.

In many cases satisfactory results are achieved by using distillation for solvent purification. Water used in LC investigations should normally not be purchased, but should be prepared by the user. An inexpensive and easy laboratory procedure for water purification is as follows: deionized water with added alkaline solution of KMnO_4 is left for a few days, and then the solution is distilled twice in an apparatus made of hard glass. The conductivity of water purified in this fashion is 10^{-6} S m^{-1} .

In Figure 2, plots of absorbance for three combinations of water and methanol mixtures of various purities are shown. The main source of UV absorption by the binary mobile phase was evidently impurities in the methanol. A comparison of the two bottom curves shown in Figure 2 proves the effectiveness of water purification by distillation.

Other solvents, such as aliphatic and aromatic hydrocarbons, alcohols, ethers, tetrahydrofuran and halogenated solvents, can also be purified using distillation methods. However, in many cases the solvent impurities, e.g. water in aliphatic hydrocarbons or halogenated solvents, can make distillation less efficient. In these cases it is necessary to use more effective methods for solvent purification.

Adsorption Methods

In adsorption chromatography (NPLC), control of the water content in the solvents is important. In some cases it is preferred to mix known amounts of dry and water-saturated solvents together in order to know the percentage of water saturation. Generally, analytical grade purity solvents should not contain

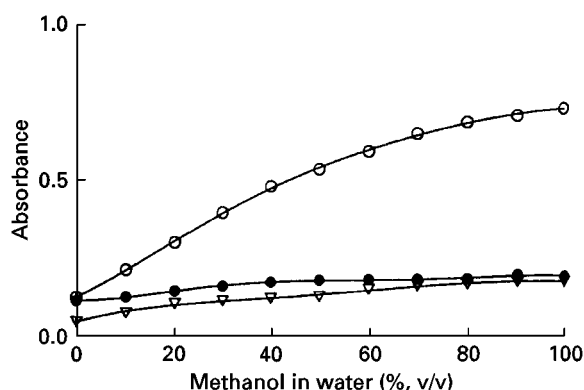


Figure 2 Plot of absorbance for mixtures of water and methanol at 254 nm versus the composition of the solution obtained on the basis of spectrophotometric data using a 3 cm quartz cuvette. Key: ∇ , methanol (analytical grade) and water (home purified); \bullet , methanol (LC grade, J. T. Baker, Deventer, The Netherlands) and water (home purified); and \circ , water and methanol (LC grade, J. T. Baker). (Reproduced with permission from Buszewski, Bleha and Berek (1985).)

impurities. On the other hand, the addition of activated molecular sieve beads (0.4 or 0.5 nm in diameter) to the flask with the solvents clearly improves their purity and reduces the water content. Various impurities, in addition to water, can be often removed by adsorption methods, particularly frontal analysis, which is often utilized in LC.

In this method a glass column packed with small adsorbant particles (0.15–0.2 mm in diameter), usually dried silica gel or alumina oxide, is used (Figure 3). Before solvent purification the column is heated at 473 K for 8 h under vacuum conditions (10^{-3} Torr) to remove physically adsorbed water. After this operation, unpurified solvent is injected into the column using a syphon-type injector. The purified solvent is collected in a solvent receiver equipped with a moisture trap.

During LC investigations purification and stabilization of the mobile phase is frequently carried out on precolumns. These columns are located between the solvent reservoir and the injector valve. SPE, in conjunction with frontal analysis, is also used for solvent clear-up. It is mainly used for purifying small amounts of solvents, particularly for sample dilution.

Filtration and Membrane Techniques

A reliable and easy laboratory technique for solvent purification is filtration. The mobile phase containing added buffers or reagents may be filtered through a filter (0.5 μm mesh or smaller) to remove particulate matter which can damage the system. The equipment for filtration is very simple, generally consisting of an Erlenmeyer flask connected to vacuum and

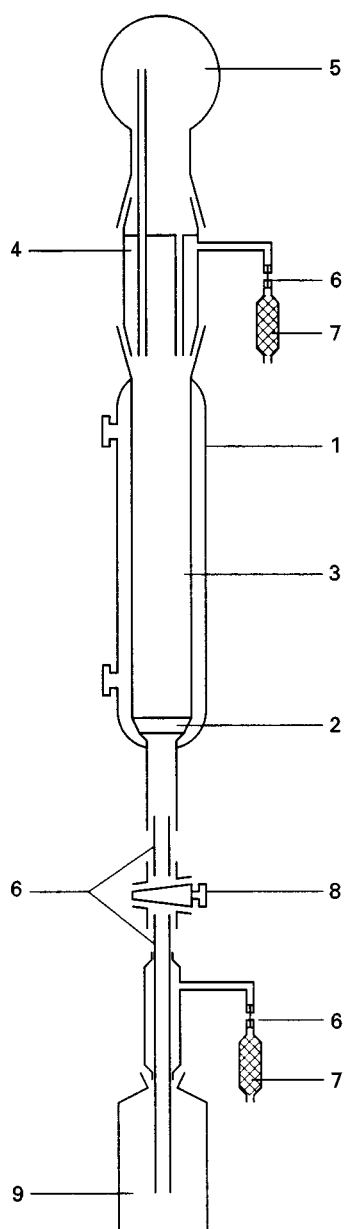


Figure 3 Apparatus for solvent purification. 1, glass column with cooling jacket; 2, glass sinter; 3, silica gel or alumina adsorbent; 4, syphon-type injector; 5, container for unpurified solvent; 6, PTFE tube; 7, moisture trap; 8, valve; 9, receiver for purified solvent. (Reproduced with permission from Buszewski, Lodkowski and Trocewicz (1987).)

a reservoir, in which a porous filter disc or membrane is placed. The porous discs are usually made from nonporous spherical glass beads (1–2 μm in diameter) and/or PTFE. Membranes are usually made from PTFE, cellulose or nylon. To improve the efficiency of the separation process, the surface of the filter discs or membrane is often modified chemically, as are the packing materials, with chemically bonded phases in RP-LC and/or SPE. In this case the surface properties

(hydrophobic or hydrophilic) of filters and/or membranes determine the degree of purification.

Water may be purified satisfactorily using a compact water purification system that combines filtration, deionization and charcoal treatment in a convenient, high-volume unit.

Ultrafiltration Ultrafiltration is the other alternative to filtration, where large molecules are separated from solution by using membranes. Membranes are commercially available for separation molecules with relative molecular masses in the range 10^3 – 10^6 . Ultrafiltration is primarily used for the isolation of low- or high-molecular mass substances from different solvents. **Figure 4** shows a comparison of the efficiency of acetonitrile purification utilizing frontal analysis combined with ultrafiltration.

Reverse osmosis Reverse osmosis is similar to ultrafiltration except that membranes of a much smaller pore diameter are employed and the operating pressure is much higher. The operating pressure must exceed the natural osmotic pressure. This technique has been successfully applied to the purification of water and organic solvents.

Dialysis In dialysis, solvents are purified by differential diffusion through membranes under a concentration gradient. The overall efficiency of this process is controlled by the ratio of the flow rates and the properties of membrane, fluid channel and local fluid velocity.

Recovery and Quality Control

After the purification process or before using solvents in various analytical techniques, quality control is necessary. For this reason, many different analytical

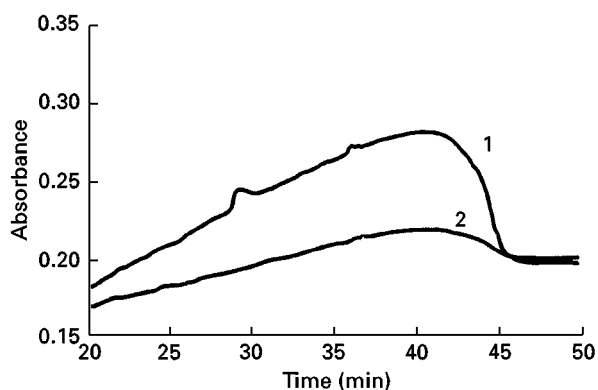


Figure 4 Liquid chromatograms with UV detection using acetonitrile as the mobile phase purified through (1) frontal analysis and (2) ultrafiltration.

Table 2 Concentration of water and difference in absorbance for cut-off (ΔA) of solvents before (C_b) and after (C_a) purification

Solvent	ΔA (% v/v)	C_b (mg L ⁻¹)	C_a (mg L ⁻¹)
Acetonitrile A	69.7	2216.0	167.0
Acetonitrile B	10.2	297.0	143.0
Benzene	24.6	308.0	27.5
Cyclohexane	16.8	49.0	4.5
n-Heptane	21.3	18.8	7.7
n-Hexane	17.2	19.6	8.6
Methanol A	77.05	650.0	134.0
Methanol B	3.6	120.0	114.0
Tetrahydrofuran	61.3	1081.0	32.6
Toluene	23.1	167.0	10.0

Reproduced with permission from Buszewski, Lodkowski and Trocewicz (1987).

methods have been utilized for measuring the characteristic parameters. Generally, chromatographic techniques such as gas chromatography (GC), LC, thin-layer chromatography (TLC) have been used, but ultraviolet (UV), infra-red (IR) and nuclear magnetic resonance (NMR) spectroscopy can also be applied. Water in many organic solvents is usually determined by Karl Fischer titration. On the basis of experimental data obtained before and after purification the efficiency of the clean-up procedure is determined. In general, the efficiency of purification process, e.g. the recovery, is expressed by the coefficient R . This parameter is defined as the ratio of the volume or concentration of removed impurities to the volume or concentration of solvent before purification:

$$R \pm \sigma = (V_a \pm \sigma_a)(V_b \pm \sigma_b) \times 100\% \text{ (v/v)} \quad [1]$$

or:

$$R \pm \sigma = (C_a \pm \sigma_a)(C_b \pm \sigma_b) \times 100\% \text{ (v/v)} \quad [2]$$

where V_a , C_a and V_b , C_b denote volume or concentration of the removed impurities and solvent samples, respectively, and σ , σ_a , σ_b are individual standard deviations.

Table 2 summarizes the results of solvent purification by frontal analysis. In each case, purification of the solvent improves its absorbance at the cut-off point (ΔA).

The small improvement found in the case of the LC grade methanol B is as expected for this high-purity solvent. The high impurity (absorbance difference, $\Delta A = 77.5\%$) of analytical grade methanol A precludes its use in LC investigations. Similarly, toluene, benzene, tetrahydrofuran and acetonitrile A cannot be used in LC measurements without prior purification.

Recovery values for the purification of water, acetonitrile, alcohols, ketones, aliphatic and aromatic hydrocarbons obtained in distillation methods are usually in the range 85–95% (v/v). In the case of halogenated solvents this range is narrower, i.e. 75–80% (v/v). Utilizing membrane techniques for solvent clear-up, it is possible to obtain recovery in the range 90–97% (v/v).

See also: II/Distillation: Laboratory Scale Distillation. Membrane Separations: Filtration. III/Flash Chromatography.

Further Reading

- Brock TD (1983) *Membrane Filtration*. Madison: Science Technology.
- Buszewski B, Bleha T and Berek D (1985) UV detection of solvent peaks in liquid chromatography with mixed eluents. *Journal of High Resolution Chromatography and Chromatography Communications* 8: 860–862.
- Buszewski B, Lodkowski R and Trocewicz J (1987) Purification of solvents for liquid chromatography. *Journal of High Resolution Chromatography and Chromatography Communications* 10: 527–528.
- Hampel CA and Hawley GG (eds) (1973/74) *Handbook of Chemistry and Physics*, 54th edn. Cleveland: CRC Press.
- Minear RA and Keith LH (eds) (1984) *Water Analysis*, vol. III. Orlando: Academic Press.
- Poole CF and Poole SK (1991) *Chromatography Today*. Amsterdam: Elsevier.
- Riddick JA and Bunger WB (1970) *Organic Solvents*, 3rd edn. New York: Wiley Interscience.

SORBENT SELECTION FOR SOLID-PHASE EXTRACTION



E. M. Thurman, US Geological Survey, Lawrence, KS, USA

Copyright © 2000 Academic Press

Solid-phase extraction (SPE) is a method of sample preparation that concentrates and purifies analytes from solution by sorption onto a disposable solid-phase cartridge, followed by elution of the analyte

with a solvent appropriate for instrumental analysis. The mechanisms of retention include reversed phase, normal phase, size exclusion, and ion exchange. Solid-phase extraction was invented in the mid 1970s as an alternative approach to liquid-liquid extraction for sample preparation.

Initially, SPE was based on the use of polymeric sorbents, such as XAD resins, which were packed in small disposable columns for use on drug analysis. The early environmental applications consisted of both XAD resins and bonded-phase sorbents, such as C₁₈. These precolumns were used for sample trace enrichment prior to liquid chromatography and were often done on line, which means at the same time as liquid chromatography. However, these first, steel, on-line precolumns were quickly replaced with an off-line column made of plastic, in order to be both inexpensive and disposable. Eventually, the term solid-phase extraction was coined for these low-pressure extraction columns.

SPE columns are now typically constructed of polypropylene or polyethylene and filled with 40- μ m packing material with different functional groups. A 20- μ m polypropylene frit is used to contain from 50 mg to 10 g of packing material. A liquid sample is passed through the column and analytes are concentrated and purified. The sample volume that can be applied ranges from 1 mL to over 1 L. The sample may be applied to the column by positive pressure or by vacuum manifold. After quantitative sorption of the analyte, it is removed with an appropriate elution solvent.

Therefore, SPE is a form of 'digital' liquid chromatography that removes the solute onto a solid-phase sorbent by various sorption mechanisms. The term 'digital' refers to the on/off mechanism of sorption and desorption. The goal of SPE is to quantitatively remove the analyte from solution and completely recover it in an appropriate solvent. Purification consists of removing the analyte from interfering compounds and concentrating the analyte in a small volume of solvent. For example, pesticides are concentrated from a water sample by SPE into a small volume of organic solvent for analysis by gas chromatography/mass spectrometry. Interfering substances, such as humic and fulvic acids, ionic metabolites and salts are removed.

Typically, SPE replaces liquid-liquid extraction as a sample preparation tool and provides a method that is simple and safe to use. The benefits of SPE include: high recoveries of analytes; purified extracts; ease of automation; compatibility with chromatographic analysis; and reduction in the consumption of organic solvents. As a result of the flexibility that SPE offers, it has found application in the preparation of environ-

mental, clinical, and pharmaceutical samples. The simplicity of the SPE procedure and the use of disposable SPE supplies have encouraged the design of automated sample preparation stations, which decrease the time and cost of sample preparation. Finally, recent advances in on-line methods of SPE allow automation of sample preparation directly to both liquid and gas chromatography.

How to do SPE

Figure 1 illustrates the four-step process of SPE. First the solid-phase sorbent is conditioned (step 1). This simply means that a solvent is passed through the sorbent to wet the packing material and to solvate the functional groups of the sorbent. Furthermore, the air that is present in the column is removed and the void spaces are filled with solvent. Typically, the conditioning solvent is methanol, which is then followed with water or an aqueous buffer. The methanol followed by water or buffer activates the column in order for the sorption mechanism to work properly for aqueous samples. Care must be taken not to allow the bonded-silica packing or the polymeric sorbent to go dry. In fact, if the sorbent dries for more than several minutes under vacuum, the sorbent *must* be reconditioned. If it is not reconditioned the mechanism of sorption will not work effectively and recoveries will be poor for the analyte.

Another cleaning step of the sorbent may also be added during conditioning, if necessary. Simply, the eluting solvent is passed through the column after the methanol wetting step to remove any impurities that may be present in the packing material. This cleaning step would then be followed by methanol and aqueous buffer, which prepares the column for sample addition.

Next, the sample and analyte are applied to the column (step 2, Figure 1). This is the retention or loading step. Depending on the type of sample, from 1 mL to 1 L of sample may be applied to the column either by gravity feed, pumping, aspirated by vacuum, or by an automated system. It is important that the mechanism of retention holds the analyte on the column while the sample is added. The mechanisms of retention include Van der Waals (also called non-polar, hydrophobic, partitioning, or reversed-phase) interaction, hydrogen bonding, dipole-dipole forces, size exclusion, and cation and anion exchange. During this retention step, the analyte is concentrated on the sorbent. Some of the matrix components may also be retained and others may pass through, which gives some purification of the analyte.

Step 3 (Figure 1) is to rinse the column of interferences and to retain the analyte. This rinse will

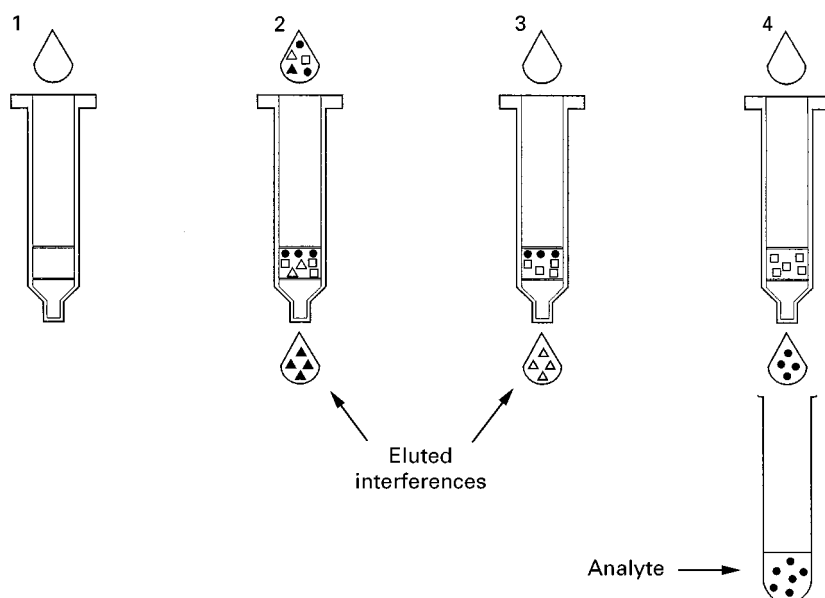


Figure 1 The four-step process of solid-phase extraction. Step 1, condition sorbent; step 2, apply sample and analyte; step 3, wash; step 4, analyte elution. (Reprinted from Thurman and Mills (1998) Copyright John Wiley & Sons, Inc.)

remove the sample matrix from the interstitial spaces of the column, while retaining the analyte. If the sample matrix is aqueous, an aqueous buffer or a water/organic-solvent mixture may be used. If the sample is dissolved in an organic solvent, the rinse solvent could be the same solvent.

Finally, in step 4 an appropriate solvent is used that is specifically chosen to disrupt the analyte-sorbent interaction, resulting in elution of the analyte from the sorbent. The eluting solvent should remove as little as possible of the other substances sorbed on the column. This is the basic method of solid-phase extraction.

Columns and Apparatus for SPE

The sorbents used for SPE are packaged in three basic formats. There are discs, cartridges, and syringe barrels. **Figure 2** shows the different types of presentation of SPE products. The discs are available in different diameters from 4 to 90 mm, the 'standard' disc size being 47 mm. Cartridges vary from as little as 100 mg to 1 g or more. Syringe barrels are available in different volumes and with different masses of packing material. Syringe barrels range in size from 1 to 25 mL and packing weights from 50 mg to 10 g. These various sorbents allow for the effective treat-

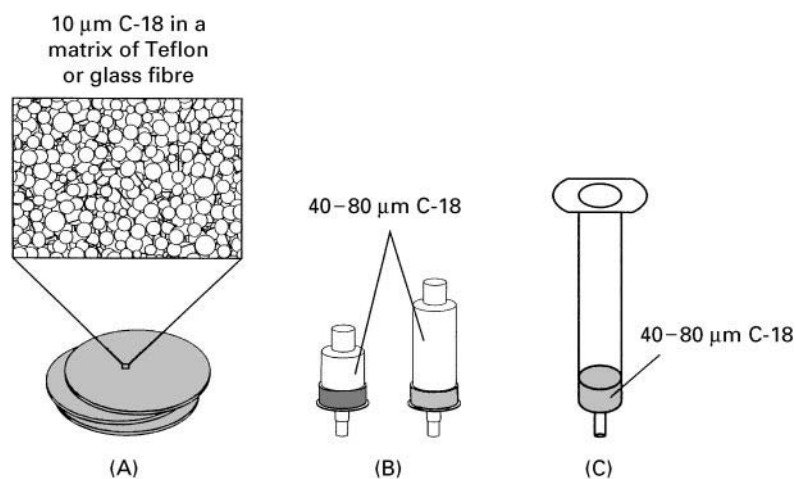


Figure 2 The three formats of SPE: (A) discs; (B) cartridges; and (C) syringe barrels. (Reprinted from Thurman and Mills (1998) Copyright John Wiley & Sons, Inc.)

ment of different types of sample and different sample volumes.

Currently, the most commonly used format for SPE consists of a syringe barrel that contains 40- μm sorbent material, with a 20- μm polypropylene frit at the bottom and a 20- μm polypropylene frit at the top of the syringe. The syringe barrel is typically polypropylene with a male Luer-tip fitting and is disposable. Some vendors do make glass syringe barrels and Teflon frits, but these configurations are used less frequently. The glass and Teflon system is used when one is interested in the analysis of plasticizers or is concerned with the potential sorption of specific analytes onto the polyethylene tube.

Solvent reservoirs may be used to increase the volume of the syringe barrel. Reservoirs are typically 50–100 mL in volume. Coupling fittings are used to join the reservoirs and syringe barrels between the Luer fitting and the opening of the syringe barrel (Figure 3).

The barrel of the syringe terminates in a male Luer tip. The male Luer tip is the standard fitting on SPE cartridges, so that they are interchangeable with different SPE vacuum manifolds. The vacuum manifold is used to draw the sample and eluting solvents through the syringe barrel under negative pressure by applying a vacuum to the manifold. Figure 4A shows a typical vacuum-manifold system, which is fitted with a small vacuum pump and a waste receiver. Stopcock valves are available to control the vacuum applied to each column. Other types of sample processing that may be used include centrifugation (Figure 4C) and positive pressure (Figure 4D), which forces the sample through the syringe barrel from above. Simple gravity flow through the syringe barrel or cartridge may also be used (Figure 4B).

A typical solid-phase extraction cartridge (see Figure 2) consists of a polyethylene body with both a female and male Luer tip for positive pressure from a syringe, or negative pressure from a vacuum manifold. Polyethylene frits measuring 20 μm are placed at either end of the cartridge to hold the packing material in place. The packing material is packed and compressed to improve or optimize flow characteristics.

The third type of SPE format is the disc, which is available in several styles by different manufacturers. One of the most popular extraction discs is the Empore® extraction disc, which consists of 8–12 μm particles of packing material embedded in an inert matrix of polytetrafluoroethylene (PTFE) fibrils. Because the particles are suspended in PTFE, no binder is required to give structure to the disc and the matrix is essentially inert. The discs are not coated with PTFE so that they can interact with the solvent and sample during extraction. The discs are available in

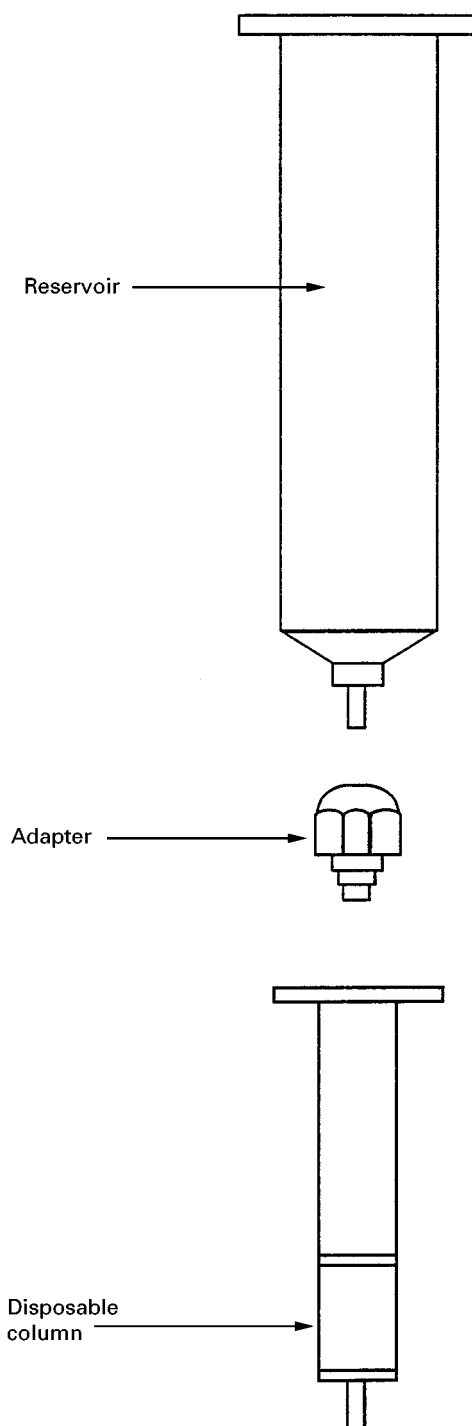


Figure 3 Disposable column and reservoir. (Reprinted from Thurman and Mills (1998) Copyright John Wiley & Sons, Inc.)

a membrane format as loose discs, or are placed in a syringe-barrel format called an extraction disc cartridge. The syringe-barrel format consists of a standard polyethylene syringe that is fitted with a 20- μm Teflon frit, an Empore® disc, and a prefilter of glass fibre. This arrangement allows for micro-scale work using the disc. Discs are conditioned and used in

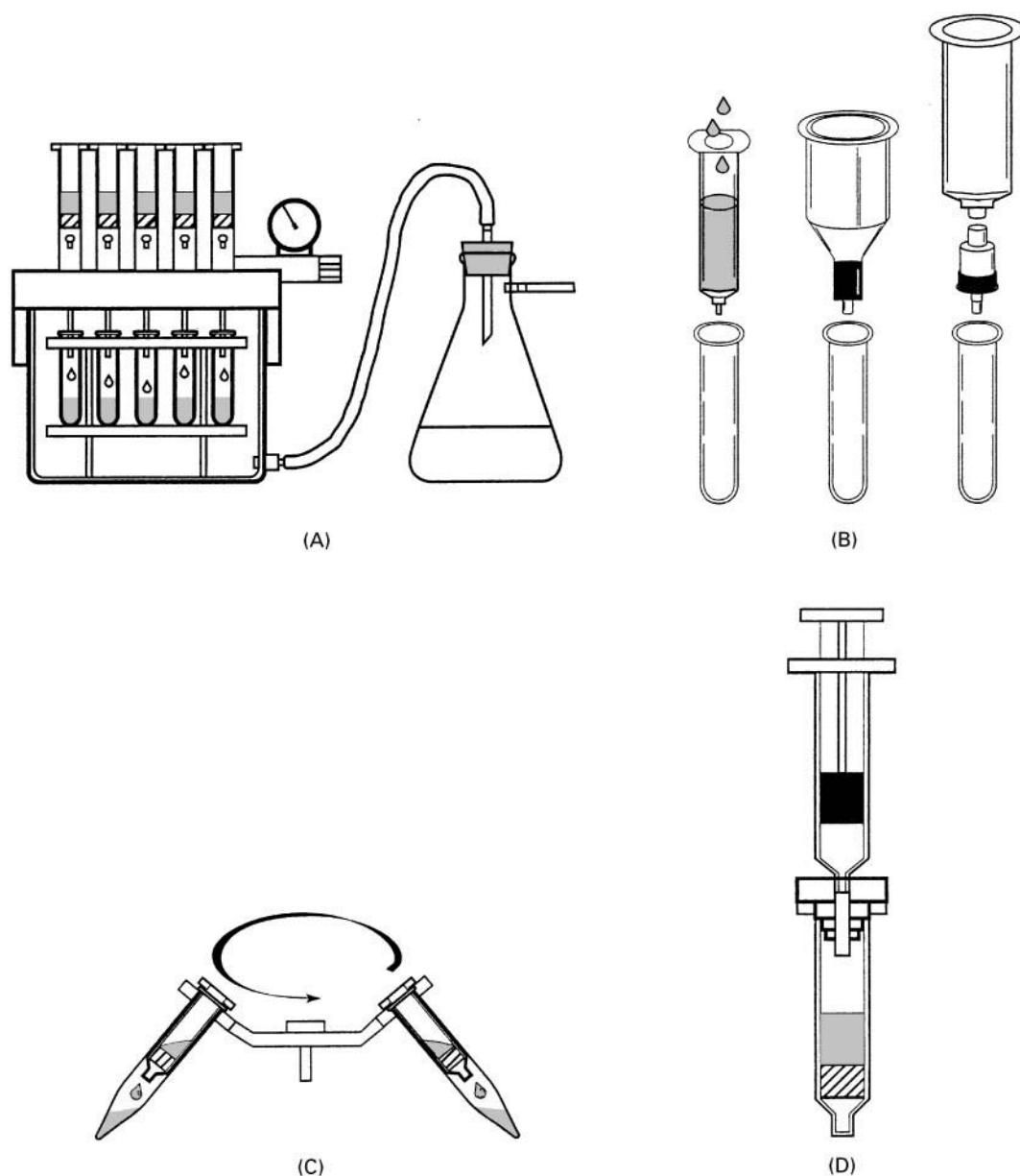


Figure 4 Techniques for processing SPE cartridges: (A) vacuum manifold; (B) gravity; (C) centrifugation; and (D) positive pressure. (Reprinted from Thurman and Mills (1998) Copyright John Wiley & Sons, Inc.)

a similar fashion to the packed columns, with flow of sample by negative pressure by vacuum.

A major advantage of the disc format is rapid mass transfer because of the greater surface area of the 8–12 μm particles, which results in high flow rates for large volume samples. This rapid flow rate is especially useful for environmental samples where 1 L of water may be processed in as little as 15 min. Rapid mass transfer owing to embedding of small particles into the disc also means that channelling is reduced and small volumes of conditioning and elution solvents may be used. For example, a 4-mm disc in syringe format (extraction disk cartridge) requires

only 100 μL of elution solvent, and a 7-mm disc uses only 250 μL . This volume is small compared with the millilitre amounts applied to a 3–5-mL syringe barrel that contains loose packing.

Another type of disc called SPEC[®] manufactured by Ansys, Inc., uses a glass-fibre matrix rather than Teflon to hold the sorbent particles. This disc has a somewhat more rapid flow rate and is more rigid and thicker than the Teflon disc. There is another disc called the Speedisk[®] manufactured by J. T. Baker, which consists of 10- μm packing material that is sandwiched between two glass-fibre filters without any type of Teflon binder.

Sorbents and Modes of Interaction

The sorbents used for SPE are similar to those used in liquid chromatography, including normal phase, reversed phase, size exclusion, and ion exchange. Normal-phase sorbents consist of a stationary phase that is more polar than the solvent or sample matrix that is applied to the SPE sorbent. This means that water is not usually a solvent in normal-phase SPE because it is too polar. Normal-phase sorbents, therefore, are used in SPE when the sample is an organic solvent containing an analyte of interest. Polar interactions, such as hydrogen bonding and dipole–dipole interactions, are the primary mechanisms for solute retention.

Reversed-phase sorbents are packing materials that are more hydrophobic than the sample. Reversed-phase sorbents are commonly used in SPE when aqueous samples are involved. The mechanism of interaction is Van der Waals forces (also called non-polar, hydrophobic, or reversed-phase interactions) and occasionally secondary interactions such as hydrogen bonding and dipole–dipole interactions. Size-exclusion sorbents utilize a separation mechanism based on the molecular size of the analyte. It is a method only recently being used in SPE, usually in conjunction with reversed phase or ion exchange. Ion-exchange sorbents isolate analytes based on the ionic state of the molecule, either cationic or anionic,

where the charged analyte exchanges for another charged analyte that is already sorbed to the ion-exchange resin. SPE applications in this case are essentially identical to classical ion exchange.

Thus, the mechanisms of interaction include: hydrogen bonding and dipole–dipole forces (polar interactions); Van der Waals forces (non-polar or hydrophobic interactions); size exclusion; and cation and anion exchange. Some sorbents combine several interactions for greater selectivity. The extensive line of sorbent chemical structures facilitates one of the most powerful aspects of SPE, which is selectivity. Selectivity is the degree to which an extraction technique can separate the analyte from interferences in the original sample. The number of possible interactions between the analyte and the solid phase facilitates this selectivity.

Table 1 lists the common sorbents that are available for SPE and their mode of action (i.e. reversed phase, normal phase, ion exchange, and size exclusion). Typically the sorbents consist of 40- μm silica gel with approximately 60- \AA -pore diameters. Chemically bonded to the silica gel are the phases for each mode of action. For reversed-phase sorbents, an octadecyl (C_{18}), octyl (C_8), ethyl (C_2), cyclohexyl, and phenyl functional groups are bonded to the silica. Typical loading of reversed-phase sorbents varies from approximately 5% for the C_2 phase to as much as 17% for the C_{18} phase. The per cent loading is the

Table 1 Common sorbents available for SPE

<i>Sorbent</i>	<i>Structure</i>	<i>Typical loading</i>
Reversed phase		
Octadecyl (C_{18})	$-(\text{CH}_2)_{17}\text{CH}_3$	17% C
Octyl (C_8)	$-(\text{CH}_2)_7\text{CH}_3$	14% C
Ethyl (C_2)	$-\text{CH}_2\text{CH}_3$	4.8% C
Cyclohexyl	$-\text{CH}_2\text{CH}_2\text{-cyclohexyl}$	12% C
Phenyl	$-\text{CH}_2\text{CH}_2\text{CH}_2\text{-phenyl}$	10.6% C
Graphitized carbon	Aromatic carbon throughout	
Copolymers	Styrene divinylbenzene	
Normal phase		
Cyano (CN)	$-(\text{CH}_2)_3\text{CN}$	10.5% C, 2.4% N
Amino (NH_2)	$-(\text{CH}_2)_3\text{NH}_2$	6.4% C, 2.2% N
Diol (COHCOH)	$-(\text{CH}_2)_3\text{OCH}_2\text{CH}(\text{OH})\text{CH}_2(\text{OH})$	8.6% C
Silica gel	$-\text{SiOH}$	—
Florisil	Mg_2SiO_3	—
Alumina	Al_2O_3	—
Ion exchangers		
Amino (NH_2)	$-(\text{CH}_2)_3\text{NH}_2$	1.6 meq g^{-1}
Quaternary amine	$-(\text{CH}_2)_3\text{N}^+(\text{CH}_3)_3$	0.7 meq g^{-1}
Carboxylic acid	$-(\text{CH}_2)_2\text{COOH}$	0.4 meq g^{-1}
Aromatic sulfonic acid	$-(\text{CH}_2)_3\text{-phenyl-SO}_3\text{H}$	1.0 meq g^{-1}
Size exclusion		
Wide-pore hydrophobic (butyl)	$-(\text{CH}_2)_3\text{CH}_3$	5.9% C
Wide-pore ion exchangers—COOH		12.2% C

amount of C_2 or C_{18} phase that is present by weight of carbon. The capacity of the sorbent in mg g^{-1} of analyte that may be sorbed is related to both the chemistry of the phase and the loading weight of carbon. Polymeric sorbents, such as styrene divinylbenzene and carbon, also are used for reversed-phase SPE. These sorbents were some of the classical reversed-phase sorbents introduced in the 1960s. They are currently produced in purified form and are useful for the isolation of more polar solutes that have low capacities on the C_{18} reversed-phase sorbents.

For normal-phase SPE, cyanopropyl (CN), aminopropyl (NH_2), and diol functional groups are chemically bonded to the silica gel. The loading on the cyano, amino, and diol columns are sufficiently large (~ 6 – 10% as carbon) in that they may sometimes be used for reversed-phase applications, especially for the removal of hydrophobic solutes from water or other polar solvents. These hydrophobic solutes would otherwise sorb too strongly to a more hydrophobic C_8 or C_{18} sorbent and would be difficult to elute. Straight silica gel is also used for normal-phase SPE along with Florisil (magnesium silicate) and alumina (aluminum oxide in neutral, basic, and acidic forms).

Ion-exchange sorbents usually contain both weak and strong cation and anion functional groups bonded to the silica gel (Table 1). Strong cation-exchange sorbents contain ion-exchange sites consisting of sulfonic acid groups, and weak cation-exchange sorbents contain sites consisting of carboxylic acid groups. Strong anion-exchange sites are quaternary amines, and weak anion-exchange sites are primary, secondary, and tertiary amines. Strong and weak refers to the fact that strong sites are always present as ion-exchange sites at any pH, while weak sites are only ion-exchange sites at pH values greater or less than the pK_a , which determines whether a site contains a proton or not. The typical loading for an ion-exchange sorbent is expressed in meq g^{-1} of sorbent, which is called the exchange capacity of the sorbent. The values vary from $\sim 0.5 \text{ meq g}^{-1}$ to 1.5 meq g^{-1} . These exchange capacities are somewhat less than a typical ion-exchange resin, which will have from 2 to 5 meq g^{-1} because of a higher density of ion-exchange sites. Also these SPE ion-exchange sorbents are not as rugged as the polymeric ion-exchange resins because of the silica matrix of the SPE sorbent, which is susceptible to dissolution by strong acid or base. The typical ion-exchange resin, however, consists of a cross-linked styrene-divinylbenzene polymer.

Size-exclusion sorbents, called wide-pore sorbents (Table 1), use a silica-gel matrix with a large pore size (approximately 275 – 300 \AA) rather than the 60-\AA

pores of most bonded-phase silicas. The advantage of the larger pore size is that molecules of larger molecular weight (> 2000 daltons) may enter the pore of the sorbent and sorb by hydrophobic, polar, or ion exchange interactions. Two examples are shown in Table 1. One is a hydrophobic sorbent of C_4 (butyl) with a carbon loading of almost 6% , and the other is a weak cation sorbent using the carboxyl exchange site.

Another packing material, which is not listed in Table 1, was recently introduced for drug analysis. It is a mixed-mode resin. This packing material contains both a bonded reversed-phase group (typically a C_8) and a cation-exchange group on a silica gel or a polymeric matrix. The combination of bonded groups is used so that both types of mechanisms retain the analyte at different times, or simultaneously, in the clean up of complex samples of urine and blood. The principle of the mixed-mode resin is that different wash solvents may be used to remove interferences, but that the solute is always retained by one or both of the interactions.

Applications of SPE

Table 2 shows a general application guide for the use of SPE sorbents. The C_{18} reversed-phase sorbent has historically been the most popular packing material and has been used most frequently. The surface of the sorbent is one of the most hydrophobic and has a large capacity. Capacity is the amount of analyte sorbed (usually expressed in mg g^{-1}) before breakthrough occurs. Applications of C_{18} reversed phase include: isolation of hydrophobic species from aqueous solutions, such as drugs and metabolites from urine, serum, plasma, and other biological fluids; desalting of peptides and oligonucleotides; isolation of pigments from wine and beverages; and trace enrichment of pesticides from water for analysis by gas chromatography/mass spectrometry or high pressure liquid chromatography.

Graphitized carbon and reversed-phase polymeric sorbents are also frequently used in environmental applications, such as trace enrichment, for soluble molecules that are not isolated by reversed-phase sorbents, such as C_{18} . Water soluble analytes require a more hydrophobic sorbent with greater surface area per gram for complete retention. Carbon and polymeric sorbents may also be used for polar metabolites of drugs and pharmaceuticals that are poorly retained on C_{18} . Another advantage of the aromatic sorbents is their selective interaction with the aromatic rings of analytes. Because both the graphitized carbon and the styrene divinylbenzene structures contain aromatic rings, they have the ability to sorb analytes by a

Table 2 Selected application guide for SPE

<i>Sorbent</i>	<i>Application</i>
C ₁₈	Reversed phase application one of the most hydrophobic phases Drugs in serum, plasma, and urine Organic acids in wine Pesticides in water by trace enrichment
Graphitized carbon polymeric sorbents (styrene divinylbenzene)	Reversed phase application one of the most hydrophobic phases Trace enrichment of polar pesticides from water Isolation of polar drug metabolites
C ₈	Reversed phase application—hydrophobic phase Drugs from serum, urine, and plasma Peptides in serum and plasma
Silica	Normal phase application—polar neutral phase Isolation of low to moderate polarity species from non-aqueous solution Lipid classification
Florisil	Normal phase application—polar slightly basic phase Isolation of low to moderate polarity species from non-aqueous solution Pesticides in food and feeds Polychlorinated biphenyls in transformer oil
Alumina A	Normal phase application—acidic polar phase Isolation of hydrophilic species in non-aqueous solution Low capacity cation exchange
Cation exchange	Cation exchange phase Isolation of cationic analytes in aqueous or non-aqueous solutions Fractionation of weakly basic proteins and enzymes
Anion exchange	Anion exchange phase Isolation of anionic analytes in aqueous or non-aqueous solutions Extraction of acidic and weakly acidic proteins and enzymes
Mixed mode	Reverse phase (C ₈) and cation exchange phase Isolation of basic and amphoteric drugs from serum, plasma, and urine
Aminopropyl NH ₂	Normal phase, reverse phase, and weak cation exchange Low capacity weak anion exchanger Drugs and metabolites from body fluids Petroleum and oil fractionation
Cyanopropyl CN	Normal phase and reversed phase Analytes in aqueous or organic solvents Drugs and metabolites in physiological fluids
Diol OH	Normal phase and reversed phase Analytes in aqueous or organic solvents Drugs and metabolites in physiological fluids

specific pi-pi interaction. This sorption mechanism may selectively isolate aromatic compounds.

The C₈ reversed-phase sorbents (Table 2) are often the most popular sorbent for drug analysis because of a shorter hydrocarbon chain than a C₁₈ sorbent. The shorter chain length makes it much more easy for secondary interactions between the analyte and the silica gel which enhances retention of the analyte. This added interaction is useful in the purification of drugs and metabolites from blood and urine because

they contain basic nitrogen atoms that may hydrogen bond to the silica gel.

Normal-phase sorbents such as silica and Florisil are used to isolate low to moderate polarity species from non-aqueous solutions. Examples of applications include lipid classification, plant-pigment separations, and separations of fat-soluble vitamins from lipid extracts, as well as the clean up of organic solvent concentrates obtained from a previous SPE method or liquid-liquid extraction. Alumina is

used to remove polar species from non-aqueous solutions. Examples include vitamins in feeds and food, and antibiotics and other additives from feed. Normal-phase chromatography has been used for a number of years and most applications for normal-phase column chromatography may be easily transferred over to normal-phase SPE.

Cation and anion exchange is used to isolate ionic compounds from either aqueous or non-aqueous solutions. Examples of applications are: isolation of weakly basic proteins; removal of acidic pigments from wines and fruit juices; and the removal of organic acids from water. Many of the applications of classical ion exchange may be used in ion-exchange SPE; however, care must be exercised in the use of strong acids and bases with SPE ion-exchange sorbents that are based on a silica matrix. Furthermore, care must be taken not to exceed the ion-exchange capacity of the sorbent.

Finally, sorbents such as aminopropyl, cyanopropyl, and diol can be used for both reversed-phase and normal-phase separations. Many manufacturers supply their sorbents in variety packs, which may be used for methods development. Also quality assurance reports are commonly available for the various sorbents, which is a good indication of their reproducibility.

Automation of SPE

Automation of a manual SPE method can provide many benefits, which include safety, improved results, and cost savings. Because automated workstations are mechanical they can operate in environments that are hostile, for example, noisy production locations or a refrigerated room. The use of automation results in improved precision because of reduced operator errors compared with manual methods of SPE. For these reasons automation provides for better utilization of resources.

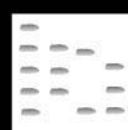
There are many types of automation equipment for SPE. They include semi-automated instruments, workstations that carry out the entire SPE operation without intervention, and robotic systems that carry out many activities besides SPE and are specially customized for the user. Finally, there are on-line SPE-HPLC systems that allow the user to merely add the sample to the autosampler and analyse the sample directly. The concept of on-line SPE is that a sample is pumped and processed onto the SPE cartridge while the liquid chromatograph or gas chromatograph is processing the preceding sample.

See also: II/**Chromatography: Liquid:** Column Technology. **Extraction:** Solid-Phase Extraction. III/**Solid-Phase Extraction with Cartridges. Solid-Phase Extraction with Discs.**

Further Reading

- Fritz JS (1999) *Analytical Solid-Phase Extraction*. New York: John Wiley.
- Hennion M and Pichon V (1994) Solid-phase extraction of polar organic pollutants from water. *Environmental Science and Technology* 28: 576A–583A.
- Horack J and Majors RE (1993) Perspectives from the leading edge in solid-phase extraction. *LC-GC* 11: 74–90.
- McDonald PD and Bouvier ESP (1995) *Solid Phase Extraction Applications Guide and Bibliography, a Resource for Sample Preparation Methods Development, 6th Edition*. Milford, Massachusetts: Waters.
- Poole SK, Dean TA, Oudesma JW and Poole CF (1990) Sample preparation for chromatographic separations and overview. *Analytical Chimica Acta* 236: 3–42.
- Simpson N and Van Horne KC (1993) *Sorbent Extraction Technology Handbook*. Harbor City, CA: Varian.
- Thurman EM and Mills MS (1998) *Solid-Phase Extraction: Principles and Practice*. New York: John Wiley.
- Varian Sample Preparation Products (1992) *Applications Bibliography*. Harbor City, CA: Varian.
- Zief M and Kiser R (1988) *Sorbent Extraction for Sample Preparation*. Phillipsburg, NJ: J. T. Baker.

SPACE EXPLORATION: GAS CHROMATOGRAPHY



R. Sternberg and F. Raulin,
Universités Paris 12 et 7, CNRS UMR 7583,
Créteil cedex, France
C. Vidal-Madjar, CNRS UMR 7581,
Thiais, France

Copyright © 2000 Academic Press

The development in the past 40 years of space exploration has brought important information about the formation and evolution of the solar system and has opened a broad study of organic matter and its continuous chemical evolution which led to the appearance of life.

The study of the physics and chemistry of planetary environments (Table 1) has provided important information about the origin of Earth's early atmosphere and comparative planetology gives a better understanding of our own planet. Titan, the largest satellite of Saturn, because of the composition and density of its atmosphere, is of particular interest for the understanding of the prebiotic chemistry on primitive Earth. Comets are also of interest since they contain very large amounts of organic material and they are considered as the most primitive objects in the solar system, retaining traces of its early evolution.

Since the beginning of space exploration, most of the many probes which have been sent to explore other planetary atmospheres and surfaces have carried analytical instruments to determine the elemental, isotopic and molecular (inorganic and organic) compositions of extraterrestrial environments. Severe constraints are required in space instrumentation such as low weight and small size, low power consumption, high mechanical strength and resistance to deep space conditions. Gas chromatography (GC) fulfils these requirements and is one of the most frequently used technique for *in situ* analysis in space missions.

Chemical sensors based on GC and mass spectrometry (MS) instrumentation have already been used in atmospheric probes or surface landings for analysing extraterrestrial environments, including the analysis of surface materials from Venus and Mars. Until recently, the equipment was only packed column GC with mainly magnetic, then quadrupole mass spectrometers (MS).

Since the Titan atmospheric probe of the Cassini-Huygens mission, launched in 1997 to reach the vicinity of Saturn in 2004, highly sensitive pyrolysis-GC-MS instruments have been developed using capillary columns.

The Rosetta comet exploratory mission, to be launched in 2003, will use, in two GC-based experiments, miniature thermal conductivity detectors (TCDs) and

a new design of time of flight mass spectrometer (TOF), based on a specific geometry of the MS allowing analysis of low mass compounds and good resolution.

This article reviews the different chromatographic instruments used in previous missions to Mars, Venus and Titan as well as those which are being developed, in particular for the forthcoming cometary mission.

Missions to Mars

Mars is presently the most likely planet on which there is a possibility of finding past, or even present extraterrestrial life. The average atmospheric pressure on its surface is extremely low, about 7 mbar. The primary atmospheric constituent, CO₂, produces a small warming of the surface above radiation temperature (Table 1).

One of the main objectives of the Viking mission to Mars was the search for Martian life. The US National Aeronautics Space Administration (NASA) sent two identical spacecraft to Mars in 1976. Each Viking lander, carrying scientific instruments, was successfully placed on the surface of Mars. Biemann was responsible for the MS instrument designed mainly for the detection of organic compounds in the GC-MS mode, but also used to determine independently the composition of the minor constituents of the lower atmosphere. In addition, biological investigations were carried out on board the landers. Oyama and Berdahl used GC in a gas exchange experiment (GEX) to determine the gas composition changes above a soil sample humidified or incubated in the presence of an aqueous nutrient.

Viking GC-MS Experiments

The GC-MS system (Table 2) was designed to analyse the organic compounds released from a heated surface sample. It consists of different sub-systems: (1) three sample ovens mounted in a sample holder, (2) a GC, (3) an effluent divider to protect the MS, (4) a carrier gas separator and (5) the MS itself.

Table 1 Extraterrestrial environments already analysed or planned to be analysed by gas chromatography

	Distance to sun (AU)	Surface temperature (°C)	Surface pressure (bar)	Atmosphere	
				Major constituents	Organic compounds
Venus	0.7	460	90	CO ₂ , N ₂	None
Earth	1	22	1	N ₂ , O ₂	Many
Mars	1.5	– 70 to 20	0.007	CO ₂ , N ₂	Not detected
Titan	9.6	– 180	1.5	N ₂ , CH ₄	Several hydrocarbons and nitriles
Comets	1.1–5.1	– 200	< 0.001	H ₂ O, CO, CO ₂ , H ₂ CO, CH ₃ OH	Many

Table 2 An overview of gas chromatography instruments of *in situ* planetary missions

<i>Mission</i>	<i>Launch arrival</i>	<i>Experiment sample size</i>	<i>Analytical columns</i>	<i>Temperature carrier gas</i>	<i>Detectors</i>
NASA Viking–Mars	1975/1976	GEX 0.1 cm ³ (gas)	One pair of Porapak Q (7.6 m × 1 mm)	24°C, He	1 Thermistor TCD (32°C)
		GC–MS 0.06 cm ³ (soil)	One Tenax coated with polymetaphenoxylene (2 m × 0.76 mm)	50°C (12min) + linear prog. to 200°C, H ₂	MS
NASA Pioneer–Venus–Venus	1978/1978	LGC 0.35 cm ³ (gas)	In parallel: one pair of Porapak N (15.85 m × 1.1 mm); one pair of PDVB (2.13 m × 1.1 mm)	18°C, He 62°C, He	In parallel: two thermistor TCDs
USSR Venera12–Venus	1978/1978	SIGMA GC (gas)	In series: one Polysorb (2 m) 1 molecular sieve (2.5 m); one reduced manganese	70°C, Ne	In series: three Ne ionization
USSR Vega–Venus	1984/1985	SIGMA-3 GC (gas and aerosol)	In parallel: one Porapak QS + N; one Porapak QS + N; one Porapak T	70°C, He, N ₂ , N ₂	He ionization + TCD; ECD; ECD
NASA/ESA Cassini–Huygens–Titan	1997/2004	GC–MS (gas and aerosol)	In parallel: one carbon molecular sieve (2 m × 0.75 mm); one glassy carbon WCOT (14 m × 1.8 mm); 1 CPP–DMPS WCOT (10 m × 1.8 mm)	H ₂ isothermal 30–60°C	Five MS sources (three connected to each column)
ESA Rosetta–comet P/Wirtanen	2003/2011	COSAC/GC–MS (nucleus)	In parallel: six WCOT capillaries; two PLOT capillaries	He 30–60°C	One MS, eight nano TCDs
		PTOLEMY/GC–MS (nucleus)	Two WCOT capillary; one He chemical trap; one cold trap		One MS

For both instruments on the Viking Lander-1 (VL-1) and Viking Lander-2 (VL-2), one sample oven could not operate and the analyses were limited to four samples from the Martian surface. Two were from the Chryse Planitia region (VL-1) and other two from Utopia Planitia (VL-2). For each sample, a number of analyses were performed with various GC oven temperature (50, 200, 350 or 500°C). The GC–MS operated successfully, as contaminant peaks (methyl chloride, fluorocarbon) were detected. The analysis of Martian soil samples demonstrated the absence of organic compounds above the detection limit of the GC–MS instrument (a few ppb for the more volatile organic compounds).

Viking Gas Exchange Experiments (GEX)

The biology instrument system had three different experiments integrated in the same package: the pyrolytic release, the label release and the gas exchange

(GEX) experiments. In the GEX experiments Martian soil samples were introduced, and a GC, with thermal conductivity detection (TCD), measured ppm concentrations of metabolic gases such as methane. An incubation gas (a mixture of CO₂, He and Kr) was introduced into the test cell and the biological activity was stimulated either by humidifying the soil or by adding a nutrient solution in the incubation chamber (temperature between 5 and 27°C). The changes in the composition of the incubation gas were measured periodically with a miniaturized GC.

The GC instrument (Table 2) was designed to analyse light gases such as N₂, O₂, CH₄, Kr, Ne and CO₂ at detection limits ranging from 20 to 60 ppm. Ar and CO were co-eluted on the Porapak Q column used. The composition of the Martian atmosphere was determined by GC at both landing sites (four analyses). The mean abundances were: CO₂ 96.2%, N₂ 2.3%, O₂ < 2.3% and Ar 1.5%, assuming that Ar abundance is an order of magnitude larger than for CO.

The gas changes that occurred in the incubation chamber of the GEX have raised much debate. The decrease of CO₂ just after wetting the sample material has been explained by pH changes. The significant amount of O₂ and its increase by humidifying the sample could be due to the decomposition of inorganic oxidants in the Martian soil.

Missions to Venus

Extreme temperatures (up to 460°C) and pressures (up to 90 atm) are encountered during the descent, with many reactive materials in a mainly CO₂ atmosphere (Table 1). The clouds of the lower atmosphere are composed of droplets of sulfuric acid. In a number of experiments, the very short time of descent of the probe through the Venusian atmosphere limited the time available for GC analysis.

Pioneer Venus Gas Chromatograph

The GC on board the sounder probe of the NASA Pioneer Venus mission was designed by Oyama and co-workers for the *in situ* measurement of the composition of the lower atmosphere of Venus. It is a modified version of the GC used in the Viking GEX (Table 2). The separation was performed on the two different analytical columns, each connected to a TCD. The analysis of light gases (mainly Ne and CO) was performed at 16°C, using a long column packed with Porapak N. The short column packed with a polydivinyl benzene (PDVB) porous polymer was used for separating gases from CO₂ to SO₂ at 62°C.

The Pioneer Venus probe entered the Venusian atmosphere on December 1978. During the time for the probe to reach the surface (54 min), the GC analysed three atmospheric samples at 52, 42 and 22 km altitudes. Chlorofluorocarbons were added to the third sample in order to calibrate the instrument. Table 3 gives the Venus atmospheric composition at

different altitudes from the Pioneer Venus GC measurements. The water result is consistent with the value of the vapour pressure in presence of sulfuric acid solutions.

For Ar, the lower abundance, as published in an earlier paper, was due to an incorrect identification (Ar was identified as O₂ and CO as Ar) as the assignment of the peaks was made on the basis of absolute retention times. Later, a correction accounting for flow rate variations and relying on retentions relative to those of Freon internal standards was published.

Venera 12 Gas Chromatograph

In December 1978 the *in situ* analysis of the chemical composition of the Venusian atmosphere was performed by Gelman and co-workers with a GC on board the USSR Venera 12 lander. The SIGMA instrument (Table 2) consists of three GC units arranged in series, each with a column connected to a pure neon ionization detector operating in the current-saturation mode with β -sources of different activities.

A column packed with a modified sorbent was used to separate H₂S, COS, SO₂ and H₂O, in the presence of CO₂. The low boiling point gases (O₂, N₂, Kr, CH₄ and CO) were analysed with a column packed with molecular sieves. The third column (a chemical reactor packed with reduced manganese) was used to obtain the Ar content. The columns and detectors were thermostatted at 70°C.

Since the ionization detectors are sensitive to carrier gas (neon) contamination, the whole GC system was pressurized during storage and flight. Eight samples were analysed from a 42 km altitude to the surface, with 18 chromatograms for the separation of sulfur compounds (first detector) and 27 for light gases (second detector). The GC of the Venera mission could not analyse for Ne, as this was used as the carrier gas. The Ar abundance (Table 3) was determined from its response as a negative peak. This

Table 3 Gas chromatography measurements of the lower atmospheric composition of Venus

	Mission				
	Pioneer-Venus			Venera 12	Vega
Altitude (km)	52	42	22	0–42	60–55
CO ₂ (% by volume)	95.4	95.9	96.4 ± 0.1		
N ₂ (% by volume)	4.60 ± 0.14	3.54 ± 0.04	3.41 ± 0.01	2.5 ± 0.5	
H ₂ O (% by volume)	<0.06	0.52 ± 0.07	0.135 ± 0.015	<0.01	
Ne (ppm by volume)	<8	11	4.3 ± 0.7		
O ₂ (ppm by volume)	44 ± 25	16 ± 7		<20	
Ar (ppm by volume)	60.5	63.8 ± 13.6	67.2 ± 2.3	40 ± 20	
CO (ppm by volume)	32	30 ± 18	19.9 ± 3.1	28 ± 14	
SO ₂ (ppm by volume)	<600	176	185 ± 43	130 ± 60	<100
H ₂ SO ₄ (mg m ⁻³) aerosol					~1

behaviour enabled estimation of the O₂ mixing ratio (<2.10–3.00% by volume) as the GC of Venera instrument did not directly measure O₂ concentration (O₂ coelutes with Ar). The values of Ar and O₂ mixing ratios lie in the same range of experimental error as the revised data of the Pioneer Venus GC.

Measuring atmospheric composition with different instruments is clearly advantageous, allowing cross-checks and preventing measurement errors. The quite good agreement of the data in Table 3 validates the results and gives a reasonable basis for models of Venusian atmospheric chemistry.

Vega GC Experiments

The two spacecraft of the Vega mission reached Venus in June 1985. The atmospheric probes (Vega 1 and 2) used a balloon to allow an hour's duration for the descent into the Venusian atmosphere. The SIGMA-3 GC on board each probe was designed by Mukhin and co-workers for the analysis of the gases and aerosols of the Venus cloud layer (60–55 km altitude). Three GC sub-units were arranged in parallel, each having a column connected to a different detector. Three different detectors were used: a helium ionization detector, a TCD and an electron-capture detector (ECD). The carrier gas was helium except for the sub-unit employing the ECD (carrier gas: ultrapure N₂). The separation of H₂S, COS and SO₂ in the presence of CO₂ and water vapour was performed at 70°C, with a column packed with a mixture of Porapak QS and Porapak N.

In the gas analysis mode, the sample was heated at 80°C and directly injected on to the column. At the sampling altitude (60–55 km) the experiment demonstrated the absence of H₂S, COS and SO₂ down to the detection limit of the GC instrument (10–100 ppm, depending on the substance). In the pyrolytic mode, the cell containing a carbonized fibre-glass filter was heated at 350°C. At this temperature H₂SO₄ is broken down into CO₂, H₂O and SO₂. The comparison of flight experiments with simulation data enabled estimation of the concentration of H₂SO₄ in the Venusian atmosphere to be about 1 mg m⁻³ for the 60–55 km altitude range.

Missions to Titan

Titan, a giant satellite of Saturn, has a dense atmosphere (Table 1). As with the Earth's atmosphere the main constituent is N₂. CH₄ is present at a low percentage. Traces of other organic compounds were revealed by Voyager's infrared spectrometer. The presence of these compounds was also predicted by Raulin and co-workers from the results of laboratory simulations. In addition, the atmosphere contains

aerosols and cloud droplets that obscure the surface of the satellite.

One of most important goals of the Cassini-Huygens mission to Titan is the *in situ* analysis of the composition of Titan's atmosphere. Successfully launched on October 1997, the NASA spacecraft (Cassini) carries a probe (Huygens) provided by the European Space Agency (ESA). After release from the orbiter in November 2004, the probe will slowly descend to Titan by deploying three parachutes. The six scientific experiments on the probe are designed to determine the physical and chemical properties of the atmosphere and the surface of Titan. Among these instruments are the GC-MS and the aerosol collector and pyrolyser (ACP).

Huygens GC-MS Experiments

The main objective of the GC-MS designed by Niemann and co-workers is to measure the chemical composition of the stratosphere and troposphere (from 170 km to the surface) during the 2.5 h descent. The GC-MS connected to the ACP will determine the nature and the abundance of the organic and inorganic compounds present in the atmosphere, both in the gaseous phase and in the aerosols themselves.

Three columns operating in parallel will be used to separate the expected species of Titan's atmosphere (Table 2). The identification and detection are achieved by connecting each column to an independent MS ion source. The MS (quadrupole, range 2–150 amu) will operate in two modes, either coupled to the GC or independently, by direct sample injection (Figure 1). For many substances (noble gases and many organics) mixing ratios as low as 0.1 ppb will be detected.

Capillary columns will be used for the first time for the *in situ* analysis of an extraterrestrial planetary atmosphere. Sternberg and co-workers selected the columns of the Cassini-Huygens mission for their compatibility with the severe constraints imposed by the experiment: fast analysis time, stability of the stationary phase (vacuum, cosmic rays, high energy electronic bombardment, inlet carrier gas pressure, 1.4–1.9 bar, outlet flow-rate of <1 mL min⁻¹, isothermal analysis in the range of 30–60°C. The first column, a carbon molecular sieve micro-packed column, will be used to separate light gases such as N₂ to CH₄. The second, a wall-coated open-tubular (WCOT) capillary column of glassy carbon will be used to separate low molecular mass hydrocarbons (C₁–C₃). The analysis of the saturated and unsaturated hydrocarbons (C₄–C₈) and the nitriles (up to C₄) will be achieved using a silicosteel WCOT capillary column having a slightly polar

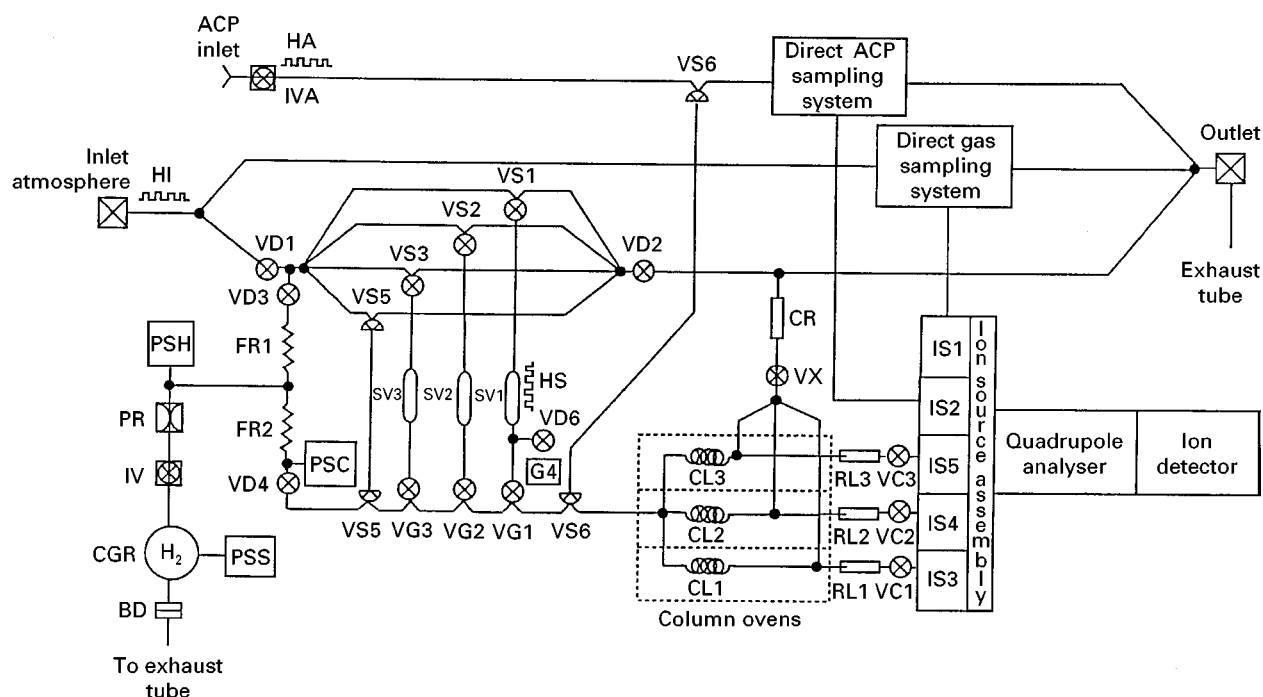


Figure 1 Schematic diagram of the GC-MS instrument on board Huygens. Abbreviations: ACP, aerosol collector pyrolyser; BD, burst diaphragm; CL, column; CR, column restrictor; CGR, carrier gas reservoir; FR, flow restrictor; G, getter pump; HA, heater (inlet ACP); HI, heater (inlet atmosphere); HS, heater (sample volume); IV, isolation valve (H_2 system); IVA, isolation valve (inlet ACP); PR, pressure reducer; PSH, pressure sensor (H_2 tank); PSC, pressure sensor (column); RL, restrictor leak; SV, sample volume; VC, valve (column); VD descent/analysis control valve; VG, sample/carrier gas valve; VS, sample valve. (Reproduced from Sternberg R, Szopa C, Coscia D, Zubrzycki S, Raulin F, Vidal-Madjar C, Niemann H and Israel G (1999) Gas chromatography in space exploration. Capillary and micropacked columns for in-situ analysis of Titan's atmosphere. *Journal of Chromatography A* 846: 307 with permission of Elsevier Science.)

stationary phase: cyanopropyl phenyl (CPP) dimethylpolysiloxane (DMPS) (Figure 2).

Aerosol Collector and Pyrolyser (ACP) Instrument

The ACP instrument was designed by Israel and co-workers to sample and collect the aerosols of Titan's atmosphere, and then to transfer the products from evaporation or pyrolysis to the Huygens GC-MS, for analysis. The aerosols are collected on a multilayered stainless filter by direct impaction for the first sampling (135–80 km). A pump is used at lower altitudes (80–32.5 km) and (22–17 km) to draw the atmosphere through the filters for the two other samplings. The filter is moved to an oven and heated at 250° or 600°C. Labelled nitrogen is used to transfer the gas and pyrolytic products to the GC-MS.

Each sample will be analysed using the direct MS mode. The GC-MS analysis will be performed once with the 600°C pyrolysis sequence. The tests for validating the ACP-GC-MS experiment were made by analysing the products synthesized by Raulin, Coll and co-workers when the photolytic and radiolytic processes expected in Titan's atmosphere were simulated (Figure 3).

Mission to Comets

It is generally believed that cometary nuclei, due to their formation in the outer solar system at very low temperatures, should retain the composition of the solar nebula and thus the average composition of the solar system. Considered as the most primitive bodies of the solar system, comets are believed to have seeded Earth with organic matter and water (Table 1) through numerous impacts on the surface of the primitive Earth. Therefore, cometary exploration is of primary importance for a better understanding of the solar system, as well as the origin of life on Earth. Following several cometary fly-by missions (e.g. Giotto, Vega) which provided the first images of a cometary nucleus and *in situ* measurements of the composition of gas and dust released from the surface, the ESA Rosetta mission will explore the nucleus of P/Wirtanen comet. The ESA Rosetta mission will be launched in 2003 and after two gravity-assisted fly-bys of Earth and Mars, it will reach the comet in 2011. The Rosetta mission will include a spacecraft and a landing probe for the *in situ* analysis of the cometary nucleus and its environment. The scientific

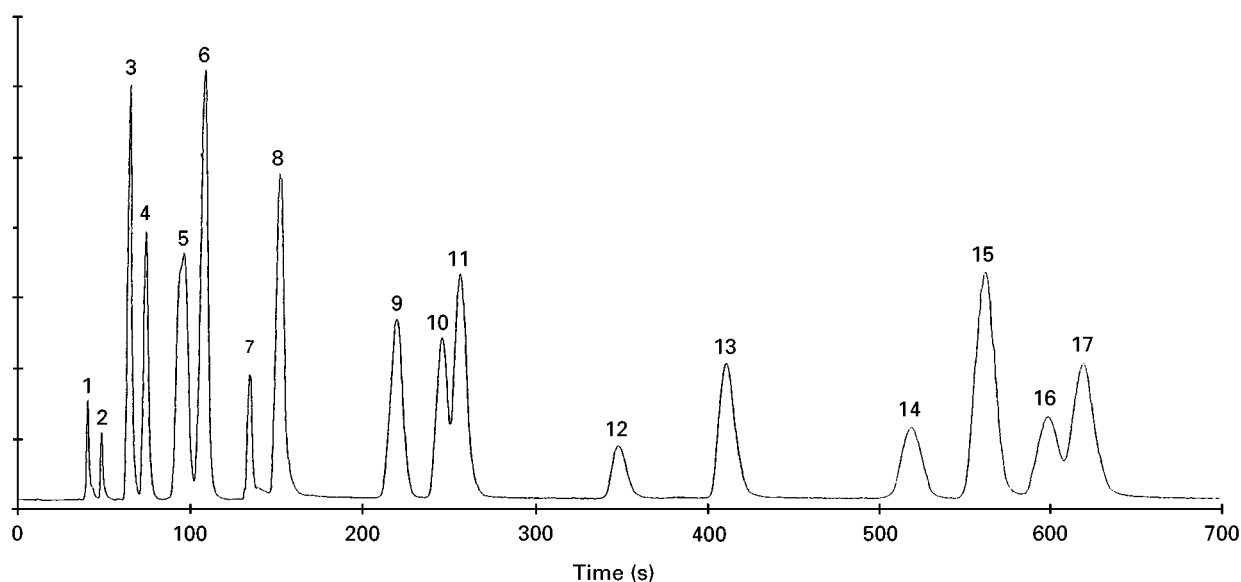


Figure 2 Chromatogram of a mixture of hydrocarbons and nitriles with the CPP-DMPS (14 : 86) WCOT capillary column for *in situ* analysis of Titan's atmosphere. Capillary column MXT 1701 (10 m \times 0.18 mm). Carrier gas, He; temperature, 30°C, pressure drop, 0.3 bar. (1) Methane, (2) 1-butene, (3) n-pentane + 1-pentene, (4) 2-methyl-2-butene, (5) cyclopentane + 3-methylpentane, (6) n-hexane + 1-hexene, (7) acetonitrile, (8) acrylonitrile, (9) n-heptane + cyclohexene, (10) benzene + methacrylonitrile, (11) propionitrile, (12) iso-butyronitrile, (13) *cis*- or *trans*-crotonitrile, (14) n-octane, (15) butyronitrile, (16) toluene, (17) *cis*- or *trans*-crotonitrile. (Reproduced from Sternberg R, Szopa C, Coscia D, Zubrzycki S, Raulin F, Vidal-Madjar C, Niemann H and Israel G (1999) Gas chromatography in space exploration. Capillary and micropacked columns for *in situ* analysis of Titan's atmosphere. *Journal of Chromatography A* 846: 307 with permission from Elsevier Science.)

payload of the cometary lander includes two instruments for chemically analysing the surface.

The first experiment, named COSAC (cometary sampling and composition experiment), has been built by Rosenbauer and co-workers at the Max-Planck-Institut für Aeronomie (Lindau, Germany) and the second, Modulus (method of determining and

understanding light elements from unequivocal stable isotope compositions), has been built by Pillinger and co-workers at the Planetary Science Research Institute, Open University (Milton Keynes, UK). These two instruments will use state-of-the-art GC techniques, involving pyrolysis and MS.

Cometary Sampling and Composition (COSAC) Experiments

The COSAC experiments by Py-GC-MS are designed to analyse gases either sampled directly from the atmosphere around the nucleus, or provided by the heating of nucleus material collected by the lander's sampler which can drill to a depth of at least 20 cm.

The pyrolyser consists of micro-ovens, mounted on a carousel, which allow vaporization by stepwise heating of the cometary solid sample. The GC subsystem contains eight capillary columns divided into two packages of four sharing a common injector. Up to four columns, which can be selected individually, can be operated in parallel in the temperature range 0–200°C. GC detection is performed by miniature solid-state thermal conductivity detectors. COSAC can be used as a stand-alone instrument or can be coupled to the time-of-flight (TOF) MS. Five of the GC columns are WCOT and PLOT columns dedicated to general chemical composition analysis. In term of speed, efficiency, weight and carrier

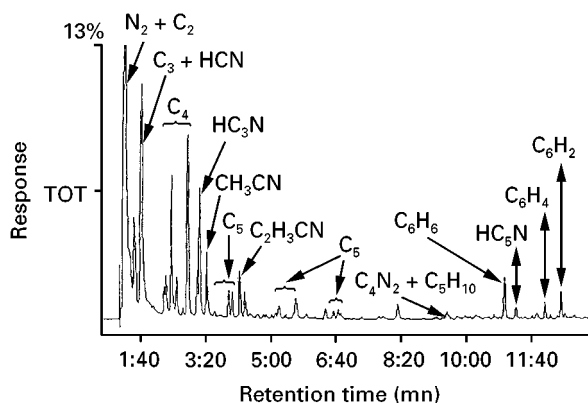


Figure 3 GC-MS analysis of a gaseous sample obtained after irradiation (5 h spark discharge) of a gas mixture of N_2 (800 mbar) and CH_4 (13 mbar) at 100–150 K. Capillary column CP-Sil-5CB (25 m \times 0.15 mm). Carrier gas, He; temperature, 20°C, then programmed at low temperature (< 150°C). (Adapted from Coll P, Guillemin JC, Gazeau MC and Raulin F (1999) Report and implications of the first observation of C_4N_2 in laboratory simulations of Titan's atmosphere. *Planetary Space Science* 47: 1433–1440.)

gas flow-rate, these PLOT capillary columns will advantageously replace packed columns. The three other columns will be dedicated to the measure of chirality. Using chiral stationary phases they will be able to separate enantiomers, and thus determine the eventual presence of an enantiomeric excess.

Due to the large fraction (50%) of water vapour which is expected in the cometary sample, a single chemical water trap will be placed ahead of the columns. The mass of the COSAC experiment is constrained to 4.38 kg and the average power consumption during operation should not exceed 15 W.

The Modulus GC-MS Experiments

The Modulus experiments will determine the abundance and isotopic composition of major, minor and trace constituents of the cometary nucleus. It uses several analytical trains in parallel, each set composed of: chemical reactors to quantitatively chemically transform the cometary samples into very light volatile compounds, GC columns to purify and separate the resulting gases and detectors, including an ion trap MS, to quantitatively analyse these gases.

By converting the elements of interest into specific gases of low molecular weight such as O₂, CO₂, N₂ and CH₄, the Modulus experiment only requires a MS of low mass range with limited resolution. Thus, it uses an ion trap MS with a mass of 10–20 g (not including its power supply). The entire experiment could require less than 3 kg weight and 5 W of power. Two WCOT capillary columns, one of which has a ceramic coating stationary phase, will be used. Highly specific to volatiles (including permanent gases and water) this stationary phase is robust and withstands space constraints. It has to be noted that a variant of this experiment will equip the Orbiter craft to enable a comparative study between the chemical composition of the coma and the nucleus to be carried out.

Future Developments

Mars is the most interesting planet to study because it may once have had an atmosphere similar to that of the primitive Earth. In the next decade, an extensive space programme will be devoted to the exploration of the planet with the purpose of comparing its evolution with that of the Earth. The most consistent explanation for the Viking failure to detect organic molecules lies in photochemically produced oxidants (such as H₂O₂) which originated in the atmosphere and diffused into the soil, and are potential sources of degradation of organic compounds. Missions, such as the Mars Sample Return (to be launched in 2007) are now being planned with a landing probe

including an experiment for exobiological characterization of the Martian surface material. The objectives of these missions, in the frame of a large international programme involving NASA, ESA, CNES and other national space agencies, are to search for subsurface water as well as for traces of life (past and present), organic compounds and oxidants. Several instruments on board the lander, among them a Py-GC-MS, will perform an *in situ* analysis of the subsurface, at depths where the effects of ultraviolet radiation and oxidizing agents are negligible.

Space instrumentation, because of its many constraints, has brought about several technological developments in the field of chromatography and has opened the way for the chemical analysis of more complex compounds in extraterrestrial environments. But there is a need of new instrumentation for the analysis of non-volatile and/or thermally fragile organic compounds, such as amino acids, incompatible with pyrolysis techniques. The adaptation of high-performance liquid chromatography (HPLC) and supercritical fluid chromatography (SFC) to space conditions seems difficult. Chemical derivatization coupled to GC (CD-GC) might be the solution. The development of an automated chemical derivatization process is under investigation and could be used for the *in situ* analysis of the Martian soil in forthcoming missions to Mars.

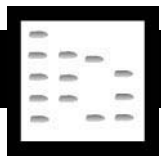
See also: II/Chromatography: Gas: Detectors: General (Flame Ionization Detectors and Thermal Conductivity Detectors); Detectors: Mass Spectrometry; Detectors: Selective; Pyrolysis Gas Chromatography; Sampling Systems. III/Atmospheric Analysis: Gas Chromatography. Chiral Separations: Gas Chromatography. Gas Analysis: Gas Chromatography.

Further Reading

- Biemann K, Oro J, Toulmin III P, Orgel LE, Nier AO, Anderson DM, Simmonds PG, Flory D, Diaz AV, Rushneck DR, Biller JE and Lafleur AL (1977) The search for organic substances and inorganic volatile compounds in the surface of Mars. *Journal of Geophysical Research* 82: 4641.
- Coll P, Guillemin JC, Gazeau MC and Raulin F (1999) Report and implications of the first observation of C₄N₂ in laboratory simulations of Titan's atmosphere. *Planetary Space Science* 47: 1433–1440.
- Gelmen BG, Zolotukhin VG, Lamonov NI, Levchuk BV, Mukhin LM, Nenarokov DF, Okhotnikov BP, Rotin VA and Lipatov AI (1979) Venera 12 analysis of Venus atmospheric composition by gas chromatography. *Pris'ma v Astronomicheskii Zhurnal* 5: 217.
- Israel G, Cabane M, Coll P, Coscia D, Raulin and Niemann H (1999) The Cassini-Huygens ACP experiment and exobiological implications. *Advances in Space Research* 23: 319.

- Mahaffy PR, A'Hearn MF, Atreya SK, Bar-Nun A, Bruston P, Cabane M, Carignan GR, Coll P, Crifo JF, Ehrenfreund P, Harpold D, Gorevan S, Israel G, Kasprzak W, Mumma MJ, Niemann HB, Owen T, Raulin F, Riedler W, Schutte W, Sternberg R and Strazzulla G (1999) The Champollion cometary molecular analysis experiment. *Advances in Space Research* 23: 349.
- Mukhin LM, Nenarokov DF, Porschnev NV, Bondarev VB, Gelman BG, Israel G, Raulin G, Runavot J and Thomas R (1987) Preliminary calibration results of Vega 1 and 2 SIGMA-3 gas chromatograph. *Advances in Space Research* 7: 329–335.
- Niemann H, Atreya S, Bauer SJ, Biemann K, Block B, Carignan G, Donahue T, Frost S, Gautier D, Harpold D, Hunten D, Israel G, Lunine J, Mauersberger K, Owen T, Raulin F, Richards J and Way S (1997) The gas chromatograph mass spectrometer aboard Huygens. *European Space Agency (ESA)-SP-1177*: 85–107.
- Oyama VI and Berdahl BJ (1977) The Viking gas exchange experiment results from Chryse and Utopia surface samples. *Journal of Geophysical Research* 82: 4669.
- Oyama VI, Carle GC, Woeller F, Pollack JB, Reynolds RT and Craig RA (1980) Pioneer Venus gas chromatography of the lower atmosphere of Venus. *Journal of Geophysical Research* 85: 7891.
- Rosenbauer H, Fuselier SA, Ghielmetti A, Greenberg JM, Gosemann F, Ulamec S, Israel G, Livi S, MacDermott JA, Matsuo T, Pillinger CT, Raulin F, Roll R and Thiemann W (1999) The COSAC experiment on the lander of the ROSETTA mission. *Advances in Space Research* 23: 333–340.
- Sternberg R, Szopa C, Coscia D, Zubrzycki S, Raulin F, Vidal-Madjar C, Niemann H and Israel G (1999) Gas chromatography in space exploration. Capillary and micropacked columns for in-situ analysis of Titan's atmosphere. *Journal of Chromatography A* 846: 307–315.
- Wright IP and Pillinger CT (1998) Modulus – an experiment to measure precise stable isotope ratios on cometary materials. *Advances in Space Research* 21: 1537–1545.

STEROIDS



Gas Chromatography

H. L. J. Makin, St Bartholomew's and the Royal London School of Medicine and Dentistry, London, UK

Copyright © 2000 Academic Press

Introduction

This review aims to summarize the application of gas chromatography (GC) to the analysis of steroids. The review concentrates mainly on hyphenated GC–mass spectrometry technology as the use of GC linked to detectors other than mass spectrometry (MS) is now decreasing. A survey of literature using MEDLINE indicated that in the period 1990 to date, more than 90% of around 400 references used GC–MS, as might be expected as the mass spectrometer is now the most effective detector for GC and simple, cheap and sensitive bench-top GC–MS systems are now widely available. Use of MS can often compensate for poor GC resolution or peak shape, but use of GC–MS still requires that attention is paid to optimization of both GC and MS behaviour, if maximum sensitivity is required. The MS, of course, has the added advantage that it can provide structural data and can be used to confirm that a GC peak is indeed a steroid. By com-

paring the mass spectrum obtained with those in a library can often identify the steroid. Retention time data, on their own, are not a satisfactory criterion for identification but can be considerable value when combined with MS data.

Steroids range from the C_{18} oestrogens to C_{27} sterols such as cholecalciferol (vitamin D) and include androgens, progestagens, corticosteroids and bile acids as well as a large number of synthetic steroids, some of which may be used therapeutically. The formulae of some of these steroid types are illustrated in Figure 1 in III/STEROIDS/Liquid Chromatography and Thin-Layer (Planar) Chromatography. Alternatively readers can consult the *Dictionary of Steroids*, which lists some 10 000 steroids together with their formulae, trivial and systematic names and other useful information.

Derivatization

Most steroids have melting points in excess of 150°C (estradiol-17 β , the female sex hormone, for example, has a melting point of 176°C). It is therefore often necessary to derivatize steroids of interest in order to optimize their GC performance. Derivatization improves volatility, a necessary characteristic as the analyte in GC must be in the vapour phase. High injection (around 350–400°C) and column temperatures (up to 350°C) may also be necessary to achieve

separation, especially of higher molecular weight steroids and their derivatives. The raised temperature necessary to achieve satisfactory separation, also brings with it the problem of analyte decomposition, although decomposition should not be taken to mean destruction. It is, for example, possible to separate oestrogens and androgens and some progestagens without derivatization, but 17-hydroxylated C_{21} steroids (such as cortisol) undergo thermal side-chain cleavage and cholecalciferol (vitamin D_3) and its metabolites all undergo B-ring closures, giving rise to two isomers, even when derivatized. Such characteristic reactions may often have useful diagnostic features. It is also possible to enhance particular thermal reactions such as dehydration by the use of catalysts in order to obtain quantitative conversion in the injection port to dehydration products, which may have improved MS characteristics. 25-Hydroxyvitamin D_3 can be analysed in this way using aluminium powder in the injection port and the dehydration product has intense high mass ions which improve sensitivity of MS detection and of course time-consuming derivatization is avoided. Figure 1 illustrates this particular example.

Derivatization also improves GC peak shape as the presence of hydroxyls increases adsorption during chromatography and at very low concentrations this adsorption may give rise to a nonlinear response. In addition, if GC-MS is to be used, the appropriate choice of derivative may also have a profound influence on sensitivity and/or specificity of detection. An example of this is given in Figure 2, where the mass spectrum of the 3,17 β -di(trimethylsilyl) ether of 19-nor-androsterone is compared with the spectrum from the 17 β -trimethylsilyl (TMS) ether. In this example (this is the urinary metabolite which is measured in order to confirm abuse of the anabolic steroid nandrolone), it can be seen that the intensity of the two high mass ions in the di-TMS ether (which is a 3-enol ether) are considerably greater than those for the mono-TMS ether, allowing greater sensitivity and specificity of measurement. Table 1 lists some of the common methods of derivatization, which protect against adsorption and decomposition and at the same time improve MS characteristics. Negative-ion chemical ionization (CI) techniques, which use soft ionization and yield predominately the molecular or pseudo-molecular ion, can provide very sensitive assay methods but require the presence of electron-capturing moieties. Most steroids do not possess these and derivatization is often used in this context to provide steroid derivatives containing the necessary chlorine, iodine or bromine atoms (e.g. perfluoroacyl or chloro- or iodomethyldimethylsilyl ether derivatives). For the higher energy electron im-

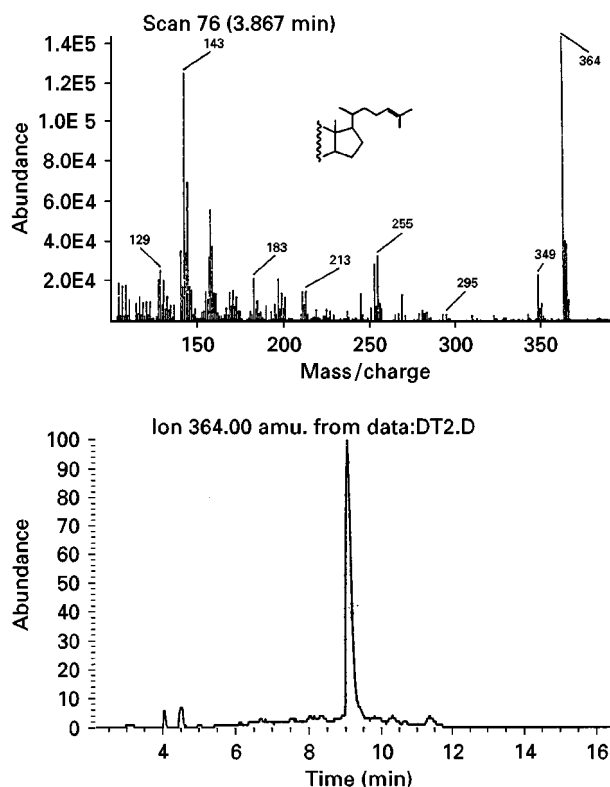


Figure 1 On-column quantitative dehydration of underivatized 25-hydroxyvitamin D_3 using aluminium powder in the injection liner. (Upper panel) EI(+) mass spectrum of the dehydration product(s) – there are at least two dehydration products, which do not separate, but only one is illustrated. Note the greatly increased intensity of the molecular ion – m/z 364. (Lower panel) Single ion monitoring of m/z 364, indicates only a single peak. (From G Jones *et al.* In: *Modern Chromatographic Analysis of Vitamins* (eds A DeLeenheer, WE Lambert and HJ Nellis), 2nd edn. New York: Marcel Dekker, 1992, with permission of authors and publisher.)

pact ionization (EI), halogenated derivatives are not necessary and hydroxyl groups are usually derivatized as TMS ethers and oxo groups as O-methyloximes (or enolized to give enol-TMS ethers). Mixed derivatives are also used (e.g. O-methyloxime-TMS derivatives) and in this example the oxime is formed first and protects the oxo group against subsequent enolization by the silylating reagent.

17-Hydroxylated C_{21} steroids are thermostable when derivatized as 17-TMS-ethers-20-oximes and can thus be analysed without degradation. Steroid carboxylic acids (e.g. bile acids) will not run in GC systems except as aliphatic esters (usually this means formation of methyl esters as otherwise molecular weight and thus retention time increases). Other esters have, however, been used for GC of faecal extracts to separate the bile acids from the neutral sterols, which are insufficiently resolved as methyl-TMS ethers. Use of *n*-butyl-TMS ethers increases the

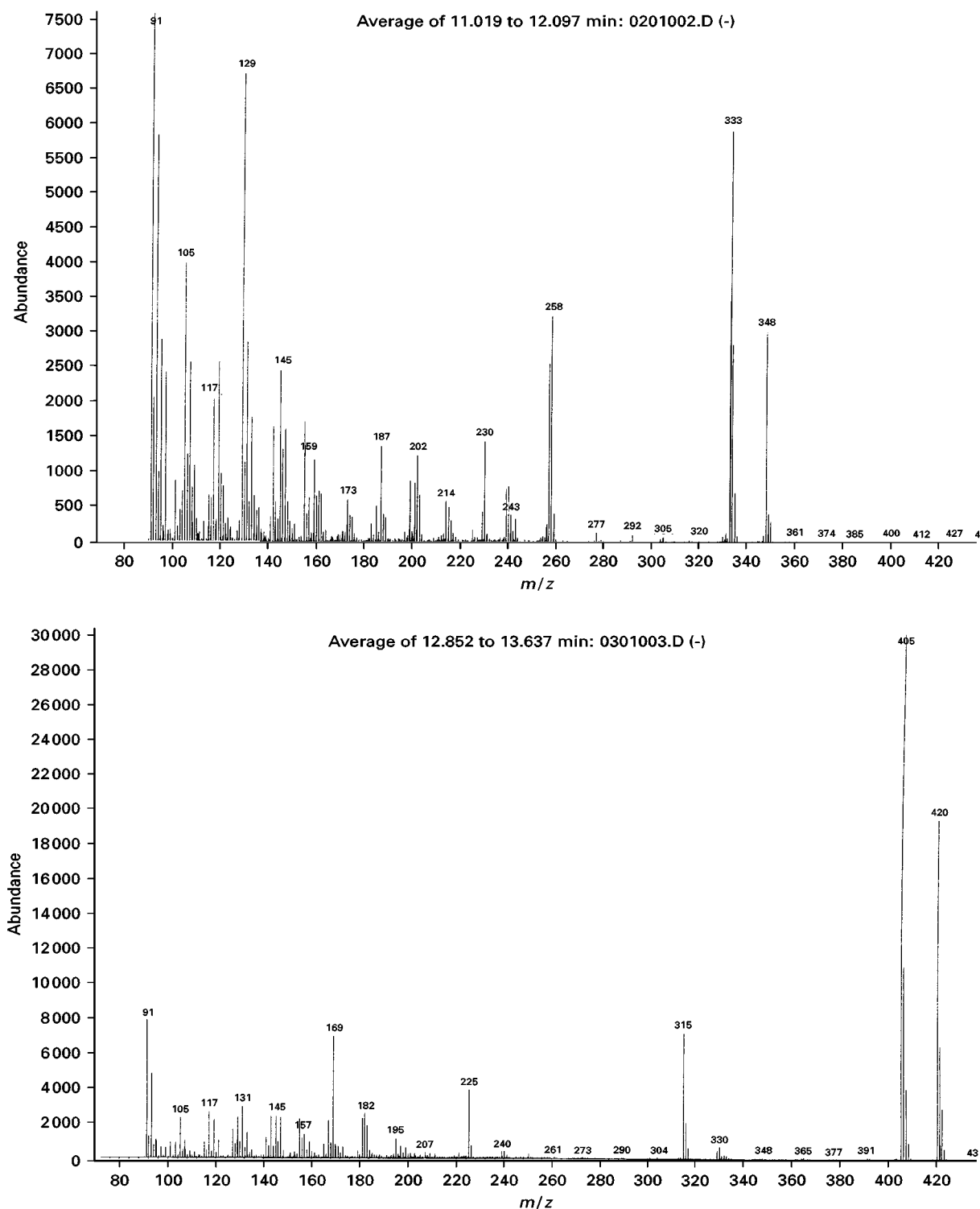


Figure 2 Enhanced sensitivity of detection of the anabolic steroid, nandrolone, by formation of different derivatives. (Top) EI(+) mass spectrum of the 17 β -trimethylsilyl ether and (bottom) EI(+) mass spectrum of the 3-enol, 17 β -di(trimethylsilyl) ether. It can easily be seen that the two ions at m/z 405 and m/z 420 of the di-TMSI carry more of the total ion current than the corresponding ions (m/z 333 and m/z 348) of the mono-TMS. These mass spectra were produced using equal amounts of nandrolone and the ion at m/z 91 offers a useful index for comparison. (With permission of Mrs J Nolan.)

retention time of the bile acids sufficiently to separate them from the sterol-TMS ethers. This is illustrated in Figure 3. Other derivatives have also been used which

are selective for particular parts of the steroid structure, such as formation of cyclic boronates across vicinal hydroxyls. Such derivatives being selective

Table 1 Some derivatization procedures used for the GC and GC-MS analysis of steroids. This list is not comprehensive but includes the majority of the most popular derivatives

<i>Steroid group</i>	<i>Derivative</i>	<i>Formula*</i>
Hydroxyl	Trimethylsilyl ether (TMS)	$(\text{CH}_3)_3\text{Si-O-St}$
	<i>t</i> -Butyldimethylsilyl ether (TBDMS)	$(\text{CH}_3)(\text{CH}_3)_2\text{Si-O-St}$
	Chloromethyldimethylsilyl ether	$(\text{CH}_2\text{Cl})(\text{CH}_3)_2\text{Si-O-St}$
	Dimethylethylsilyl ether	$(\text{CH}_3\text{CH}_2)(\text{CH}_3)_2\text{Si-O-St}$
	Pentafluorophenyldimethylsilyl ether	$(\text{C}_6\text{F}_5)(\text{CH}_3)_2\text{Si-O-St}$
	Acetate ester	$\text{CH}_3\text{CO-O-St}$
	Formate ester	HCO-O-St
	Hepta- and pentafluorobutyrate ester	$\text{CF}_3\text{CF}_2\text{CH}_2\text{CO-O-St}$ $\text{CF}_3\text{CF}_2\text{CF}_2\text{CO-O-St}$
	Dimethylisopropylsilyl ether	$(\text{CH}_3)_2(\text{CH}_3\text{CHCH}_3)\text{Si-O-St}$
Vicinal hydroxyls	<i>n</i> -Butylboronate ester	$\text{CH}_3(\text{CH}_2)_3\text{B-(O)}_2\text{-St}$
Oxo groups	O-Methyloxime	$(\text{St-C})=\text{N-O-CH}_3$
	Enol-TMS ether	$(\text{St-C}=\text{C})\text{-O-Si}(\text{CH}_3)_3$
	O-perfluorobenzoyloxime	$(\text{St-C})=\text{N-O-C}_6\text{F}_5$
Carboxylic acids	Methyl ester	$(\text{St-CO})\text{OCH}_3$
	Isobutyl ester	$(\text{St-CO})\text{O}(\text{CH}_2)_2\text{CH}(\text{CH}_3)_2$
	<i>n</i> -Butyl ester	$(\text{St-CO})\text{O}(\text{CH}_2)_3\text{CH}_3$

*St = steroid.

are diagnostic of structure and may also have the advantage of improving sensitivity and specificity of measurement.

Column Performance

For good GC performance, the intention is to obtain symmetrical peaks with retention times as short as necessary to achieve the desired separation. In the past considerable attention was paid to the development of different stationary phases in order to optimize resolution but the advent of capillary column and their linkage to MS systems has reduced the need for new stationary phases. Although capillary columns with a variety of bonded stationary phases are available, most GC-MS systems for steroids use non-selective (nonpolar) methylsilicone phases (e.g. HP1 columns from Hewlett-Packard), although more polar phases may be necessary for particular separations (i.e. C_{20} steroid carboxylic acids). Columns are usually around 15–30-m long (i.d. 0.2–0.4 mm with film thickness from around 0.1 μm upwards) and carrier gas flow rates are 1–2 mL min^{-1} , allowing direct insertion of the column exit into the ion source of the mass spectrometer. There are numerous means of sample injection but we have found the easiest to be direct on-column splitless injection using a syringe. For optimum chromatographic performance, we have found that the injection temperature is best kept at 400°C and that the choice of solvent can also have influence. This high temperature causes considerable

problems in that most injection port septa are not suitable and breakdown products cause interference. This has been overcome by use of a septumless injection system (JADE injector) in which the syringe needle injects onto the column through two stainless-steel ball-bearings, which form the back-pressure seal. Other injection procedures have found favour in the steroids field, all of which strive to inject as much of the extract as possible. These systems include a dropping glass needle in which the sample is loaded into small glass capillaries which can be automatically loaded sequentially into the heated zone of the injector. Cold trapping splitless injection has also proved useful in that it allows for the on-column injection of relatively large volumes of solvent into silanized glass liners. Injection systems which load the whole of the extract onto the top of the column necessarily shorten column life and for quantitative work, column deterioration must be monitored to achieve consistent and high sensitivity. When deterioration is detected, the column can be regenerated by removal of the top 10 cm or so but this may lead to alteration in retention characteristics of steroid derivatives.

Prior to GC analysis, steroids must be extracted and purified, the degree of purification depending upon the specificity of the detector system employed. Specific GC-MS systems require less pre-purification but the possible contamination of the MS ion source must always be considered. Extended column life and increased periods between ion source cleaning are

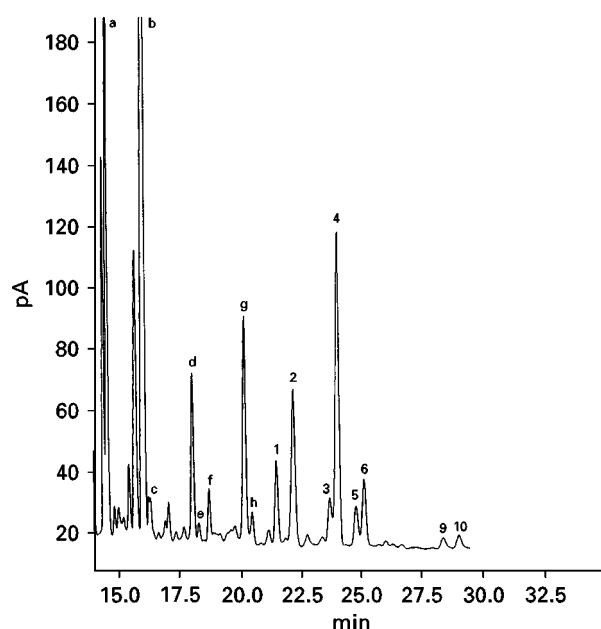


Figure 3 GC chromatogram of sterols and bile acids present in stool from a healthy control. 10 mg of freeze-dried stool containing 20 μ g nor-cholic acid was subjected to derivatization. After dissolving in 200 μ L hexane, 1 μ L was injected into the GC column. Chromatographic and derivatization details can be found by consulting the original paper. Peak identification: 1, nor-cholic acid; 2, lithocholic acid; 3, iso-deoxycholic acid; 4, deoxycholic acid; 5, chenodeoxycholic acid; 6, cholic acid; 9, 3-oxo,12 α -hydroxy-5 β -cholanoic acid; 10, 12-oxo-lithocholic acid; a, coprostanol; b, cholesterol; c, 24-methyl-coprostanol; d, campesterol; e, 24-ethylcoprostanol; f, stigmasterol; g, sitosterol; h, sitostanol. (From AK Batta *et al* (1999) *Journal of Lipid Research* 40: 1148–1154, with permission of authors and FASEB.)

obtained if attention is paid to pre-column purification. Silylating reagents should also be removed prior to injection by use of small Lipidex 5000 columns, unless they are sufficiently volatile not to cause a problem. Trimethylsilylimidazole, a valuable reagent for the formation of TMS ethers on sterically hindered hydroxyls (e.g. at positions C11 β , C17 α , C25), must be removed before GC–MS, whereas N-methyl-N-trimethylsilyltrifluoroacetamide (MSTFA) can be injected directly. Steroid glucuronides and sulfates must be hydrolysed prior to GC as they do not run in GC systems unless special derivatization methods are adopted. While we have found trimethylsilyl ethers to be stable, others have not. It is advisable therefore to store and inject steroid TMS ethers in MSTFA.

Mass Spectrometry and Other Detectors

The GC of steroids can be carried out with a variety of detectors, flame ionization (FID) being the most

widely used today. Electron-capture detectors (ECD) which were commonly used in the past to improve sensitivity of detection, have now largely been replaced with negative ion chemical ionization (CI) mass spectrometry. Selective detection of steroid oximes can be accomplished using nitrogen-phosphorus detectors. Today, however, the mass spectrometer in various forms offers the most versatile detection system for GC, providing improved selectivity and sensitivity in comparison to other detectors. Because of the successful development of immunoassays for most of the clinically important steroids, GC has not in recent times found much application for individual steroid analysis, although occasional publications can still be found. However, the advent of capillary columns with immense resolving power suggested the possibility of utilizing GC as a means of examining in a quick and simple way, the complex patterns of steroids in human urine and how they change in disease states. In the late 1970s Shackleton, utilizing the pioneering work of Gardiner and Horning of ten years before, introduced the concept of urinary steroid profiling. Urinary steroid extracts (with or without β -glucuronidase hydrolysis) were derivatized to form steroid O-methyloxime-TMS ether derivatives and analysed using capillary open-tubular columns monitoring the analytes by flame ionization detection. Use of two internal standards allowed the quantification of 23 different steroids in children with various steroid abnormalities. These robust techniques are still in use today and provide valuable information to assist clinical diagnosis and monitoring of treatment and modern data handling technology has greatly eased the task of interpreting these complex profiles. The urinary profiling technique also allows identification of unknown peaks in the extract, when the original flame ionization detector is replaced with a mass spectrometer. An example of this methodology is illustrated in **Figure 4**. Further information about this valuable approach to urinary steroid analysis by GC–MS and its application in the diagnosis of steroid related disorders can be found in Shackleton's article in the Further Reading section.

The necessary process of purification and derivatization means that for quantitative work, suitable internal standards must be used. For GC–MS the best internal standards are of course stable isotope (deuterium or carbon-13) labelled analogues of the analyte. In these situation at least three isotopic atoms must be incorporated and the percentage of the triply labelled standard (i.e. in the case of deuterium labelled, d_3) should be greater than 99%. Deuterium labels are usually introduced by acid-catalysed deuterium exchange and thus the label may not be

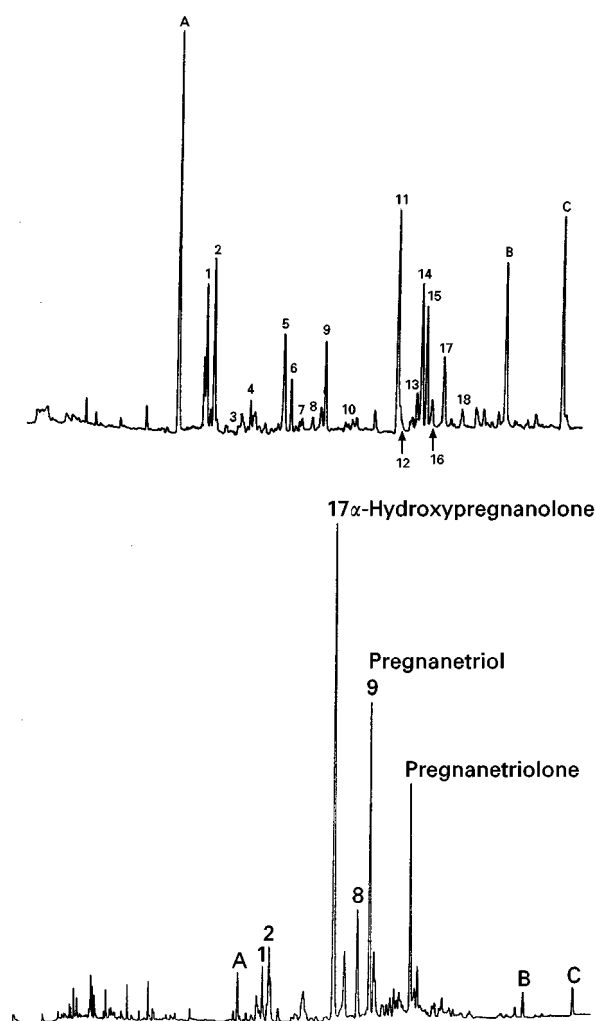


Figure 4 Steroid profiles by gas-liquid chromatography obtained from urine samples from (upper trace) a normal adult and (lower trace) a 16-year-old male with congenital adrenal hyperplasia (21-hydroxylase deficiency). Steroids were extracted with Sep-Pak C18 cartridges and after hydrolysis of glucuronide and sulfate conjugates, re-extracted and O-methyloxime-trimethylsilyl ether derivatives were formed. These were analysed by GLC using an OV1 capillary column. The major metabolites of 17-hydroxyprogesterone (the substrate of the 21-hydroxylase enzyme) are named in the lower trace. Other peaks are as follows: A, B and C: internal standards, androstanediol, stigmasterol and cholesteryl butyrate; 1: androsterone; 2: aetiocholanolone; 3: dehydroepiandrosterone (DHEA); 4: 11-oxo-androsterone; 5: 11 β -hydroxy-androsterone; 6: 11 β -hydroxy-aetiocholanolone; 7: 16 α -hydroxy-DHEA; 8: pregnanediol; 9: pregnanetriol; 10: androstenetriol; 11: tetrahydrocortisone; 12: tetrahydro-11-dehydrocorticosterone; 13: tetrahydrocorticosterone; 14: *allo*-tetrahydrocorticosterone; 15: *allo*-tetrahydrocortisol; 16: α -cortolone; 17: β -cortolone + β -cortol; 18: α -cortol. (Kindly provided by Dr Norman Taylor, King's College School of Medicine and Dentistry.)

stable in acid conditions. Ideally ^{13}C -labelled standards are to be preferred but this requires incorporation into the nucleus of the steroid which can only be achieved by extensive synthetic chemistry. All ster-

oids are analysed by GC-MS in the same way and the criteria used to ensure specificity/accuracy are those adopted by the Substance Abuse and Mental Health Services Administration (SAMHSA) for drug confirmation in employee drug-screening programmes – two, but preferably three, specific ions (with as high a mass : charge ratio as possible) must be monitored and the results derived from each ion must not deviate by more than 10% from the mean. **Figure 5** illustrates the chromatograms obtained by multiple ion detection, monitoring two of the relevant ions of the analyte (25-hydroxyvitamin D_3) and the equivalent two ions from the hexadeuterated internal standard present in a plasma sample extract. In this example the standard curve relating peak height ratio (analyte : internal standard against mass of standard analyte) was linear and the intercept was not significantly different from zero.

Isotope dilution GC-MS is widely acknowledged as the gold standard of steroid analysis and is used as a means of providing target values for external quality-assurance schemes and for the confirmation of immunoassay screening procedures for drugs of abuse. **Table 2** gives brief details of the application of this methodology to the analysis of steroids in body fluids, which are taken from papers in the literature published between 1998–1999 and use both stable isotope-labelled and unlabelled internal standards. The availability of accurate and precise methods of steroid analysis by GC-MS is becoming of increasing public interest as the number of sportsmen and women in whose urine metabolites of anabolic steroids are found, continues to increase. It is clear that it is important for steroid (and other) drug testing that proper methodology for both qualitative detection and quantitation is available and this methodology can withstand public scrutiny. GC-MS provides precisely this. Excellent and up to date reviews of the application of GC and GC-MS to the analysis of steroids can be found in the Further Reading.

Mass Spectrometry for Structural Analysis

The other important aspect of GC-MS, apart from providing a high specificity method of steroid assay, is the role of MS as a means of identifying both known and unknown steroids. The use of the GC in this context is simply a means of delivering a relatively purified steroid derivative to the MS. The present author and his colleagues have successfully used GC-MS as a means of studying the metabolism of calcitriol analogues in target tissues and while the illustrations given are derived from these studies, they have wider application and the methodology used can

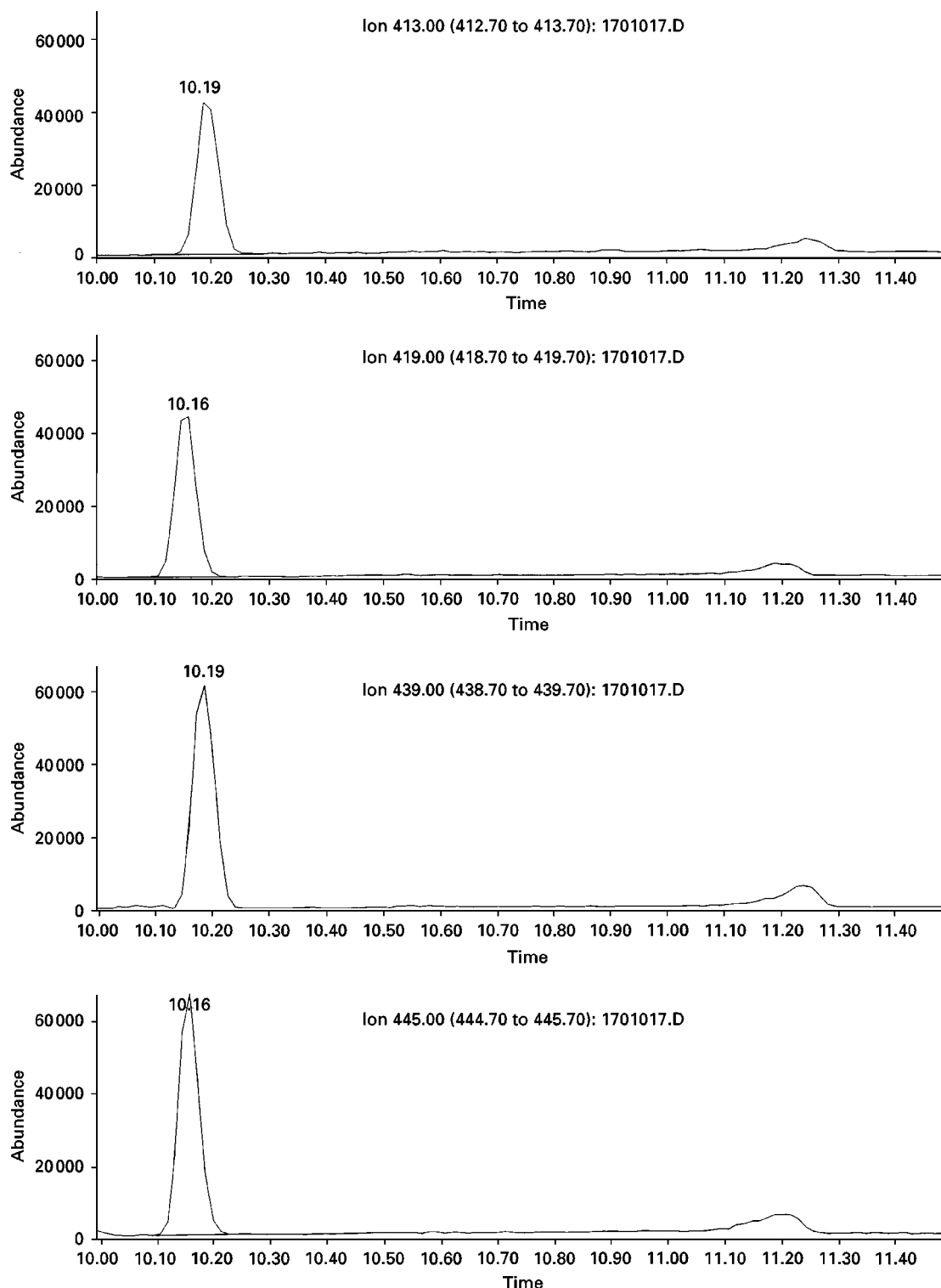


Figure 5 Isotope dilution mass fragmentography of 25-hydroxyvitamin D₃. GC was carried out after formation of per-trimethylsilyl ether derivatives using a non-selective OV1 column. An internal standard, [25,26-²H₆]25-hydroxyvitamin D₃, was added to the plasma sample prior to extraction and purification. The GC column was inserted into the ion source of the mass spectrometer and four ions were monitored (m/z 413 and 439 from the analyte and the corresponding ions, m/z 419 and m/z 445, from the internal standard). It will be noted that the hexadeuterated internal standard runs slightly earlier than the non-deuterated analyte. In this case the ratio of peak areas of analyte to internal standard gave a straight-line response which went through zero. Only two ions were monitored in this example whereas increased specificity can be obtained if three are monitored. The major peaks, the pyro-isomer and the isopyro-isomer, can be seen at approximately 11.20 min. Both peaks have a cyclized B-ring.

Table 2 Some examples of methods for the measurement of steroids by gas-liquid chromatography, published in 1998–1999

<i>Subject</i>	<i>Column details</i>	<i>Derivatives used</i>	<i>Internal standard</i>	<i>Detection</i>
Urinary steroid metabolite analysis	Non-selective methylsiloxane and 5% phenylmethylsiloxane 17 and 25 m × 0.2 mm	O-methyloxime-trimethylsilyl ethers	Androstanediol, stigmasterol and cholesteryl butyrate	Flame ionization detection* or mass spectrometry (EI+)
Ovarian steroids in the catfish	15 m DB1 column	O-methyloxime-trimethylsilyl ethers	None given	Mass spectrometry (EI+)
3 α -Reduced neuroactive steroids in human plasma	30 m × 0.25 mm with 0.2 μ m film thickness – HP5	O-methyloxime-heptafluorobutyrate esters	None given	Mass spectrometry (EI+)
Anabolic steroid metabolites in urine	30 m × 0.2 mm with 0.33 μ m film thickness. 5% phenylmethylsiloxane (ultra-2)	Pentafluoropropionates	[1,2- ² H ₂]-Testosterone	Mass spectrometry (CI–) using methane as reagent gas)
Detection of exogenous testosterone administration	DB7 (50% phenylmethylsiloxane). 30 m × 0.25 mm with 0.15 μ m film thickness	Acetates	Not relevant as only ¹³ C/ ¹² C ratios being measured	Mass spectrometry – combustion isotope ratio
Endogenous 19-nor-androsterone and aeticholanolone in human urine	HP1 30 m × 0.25 mm with 0.25 μ m and HP5 (5% phenylmethylsiloxane) 25 m × 0.2 mm with 0.33 μ m	Trimethylsilyl ethers (enols) and t-butyl-dimethylsilyl ethers	Trideuterated 19-nor-aeticholanolone	Mass spectrometry (EI+)
Serum DHA and DHA sulfate	DB5 30 m × 0.25 mm with 0.25 μ m film thickness	No derivatization	Androst-5-en-3 β -ol-16-one methyl ester	Ion trap mass spectrometry (EI+)
Testosterone: epitestosterone in equine urine	17 m × 0.2 mm with 0.11 μ m film thickness (5% phenyl-methylsiloxane)	3-Trimethylsilyl ether-17-pentafluorophenyldimethylsilyl ether	Not applicable as ratio being measured	Mass spectrometry (EI+)
Testosterone in hair	Optima 1 25 m × 0.2 mm with 0.1 μ m film thickness	Heptafluorobutyrate	Trideuterated testosterone	Mass spectrometry (EI+)
Urinary 3-oxo- Δ^4 -bile acids	30 m × 0.2 mm methylsiloxane	Carboxylic acid methyl ester-dimethylethylsilyl ether and O-methyloximes	3 α ,7 α -Dihydroxy-24-nor-5 β -cholanolic acid	Mass spectrometry (EI+)
Biliary elimination of endogenous 19-nortestosterone	None given	Heptafluorobutyrate	Trideuterated 19-nortestosterone	High-resolution mass spectrometry (EI+)

*See Figure 4 which illustrates the application of GC–FID for urinary steroid analyses.

DHA, dehydroepiandrosterone.

be applied to all steroids and their metabolites. Figure 6 shows the GC trace of calcitriol (1,25-dihydroxyvitamin D₃) as the per-trimethylsilyl derivative. Two peaks are always seen, as B-ring cyclization which occurs at the high temperature of the injection port quantitatively produces pyro- and isopyro-isomers which are always formed in the same ratio. Thus for every vitamin D-like compound, two GC peaks are observed. It is the pyro-peak which predominates and Figure 6 also shows the EI(+) mass spectrum derived at the apex of the pyro-peak after background subtraction. For the purpose of structural analysis, EI(+) spectra are preferable to CI spectra as CI is a much softer technique giving less

useful fragmentation – a similar objection applies to LC–MS, which also uses soft ionization. It is of course also possible to obtain a spectrum of the un-derivatized, albeit cyclized, calcitriol by ignoring the GC and inserting the calcitriol into the ion source of the MS by direct probe. This gives a molecular ion (M⁺) of 416. Examination of the mass spectrum of the per-TMS derivative shown in Figure 6 indicates a molecular ion of 732. Knowing that each TMS formed increases the molecular weight by 72 amu, it is possible to calculate the number of hydroxyl groups in an unknown compound (632 – 416 = 216 and 216/72 = 3). Metabolism of calcitriol and its analogues usually involves cytochrome P450-catalysed

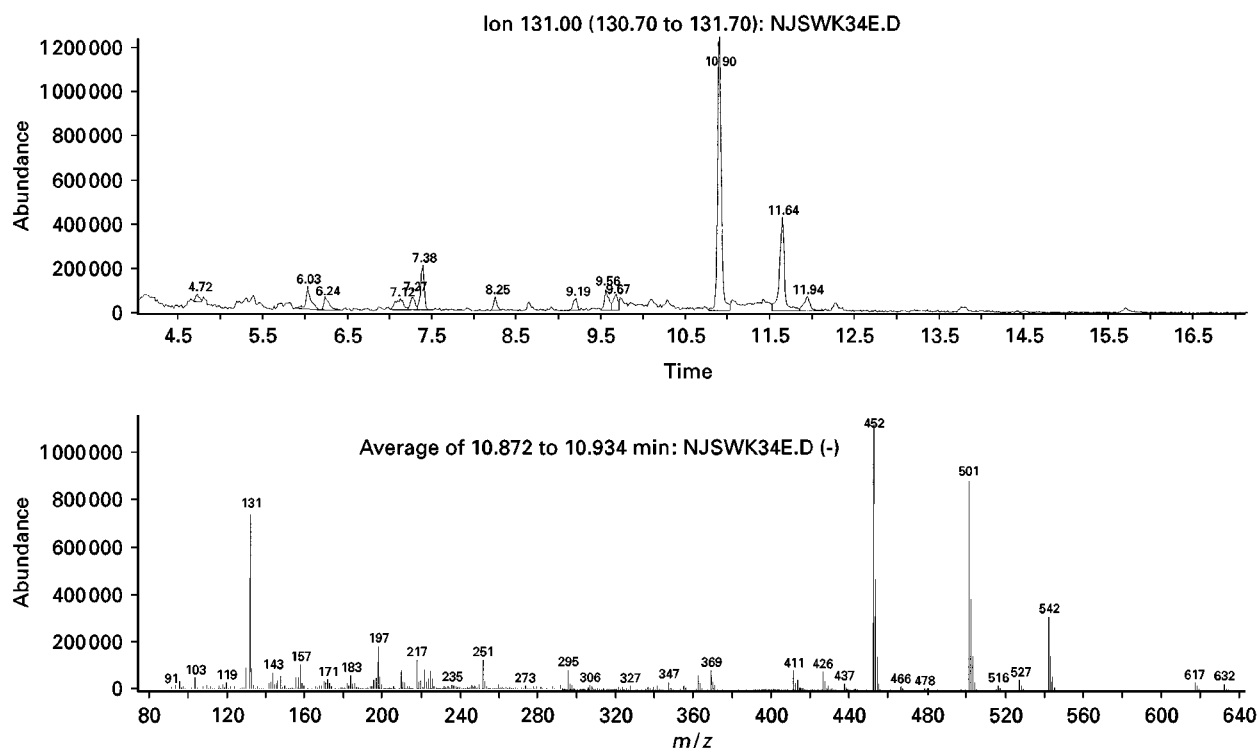


Figure 6 EI(+) mass spectrum of 1,25-dihydroxyvitamin D₃. The total ion current is shown in the upper panel indicating the two cyclized isomers (pyro- at 10.90 min and isopyro- at 11.64 min) which are formed. In the lower panel is the mass spectrum of the per-trimethylsilyl ether of the pyro-isomer.

hydroxylation(s). The number of hydroxylations can be determined by the same procedure described above and if the MS of the per-TMS of the substrate is known, direct probe MS is not necessary. However further interpretation of the MS becomes necessary in order to decide where on the steroid molecule the hydroxylation has occurred. It is clearly also possible to deduce the presence of an oxo group as this increases the molecular ion of the substrate by 14 amu but again knowledge of the presence of this group does not determine its position. To carry out these calculations, it is necessary to be able to determine the molecular ion value. It is not always possible to do this directly as the mass spectra of the steroids usually have very low intensity molecular ions. However, as can be seen in Figure 6, all these cyclized steroid-TMS ethers have a prominent (M-131)⁺ ion, which is usually derived from A-ring cleavage, as well as (M-90)⁺ ions, derived by successive loss of silanols. It is therefore possible even in the absence of discernible M⁺ ions in the spectrum, to determine the *m/z* value of the molecular ion.

For the identification of the position of extra hydroxyls and oxo groups or even truncation, where cytochrome P450 lyases have cleaved the side chain, GC retention time data can prove extremely useful. Hydroxylation increases retention time but the fur-

ther out along the side chain (distal) the hydroxylation is, the longer the retention time. Truncation, by reducing molecular weight, clearly decreases retention time. Retention time, although useful is not sufficient on its own and further study of the fragmentation data has to be made. Further examples can be obtained by consultation of the texts listed in the Further Reading section. Consideration should also be given to the use of chemical reactions which modify the molecule under investigation. Reduction of oxo groups with sodium borohydride and subsequent derivatization as TMS ethers and GC-MS provides further evidence of structure. Cleavage of carbon-carbon bonds between vicinal hydroxyl groups with periodate can also provide valuable information about the site of hydroxylation if the reaction product is subsequently derivatized and subjected to GC-MS.

A very good example of the interpretation of mass spectra obtained from GC-MS of per-TMS derivatives is given in Figure 7. The metabolites illustrated here are all mono-hydroxylated metabolites of 1 α -hydroxyvitamin D₃ and thus give the same value of 632 amu for their molecular ion. All four metabolites show the characteristic (M-131)⁺ ion at *m/z* 501 as well as (M-90)⁺, 542 and (M-90-90)⁺, 452. The abundance of the M⁺ ion is, as usual, very low but it can easily be confirmed as being the ion at *m/z* 632 by

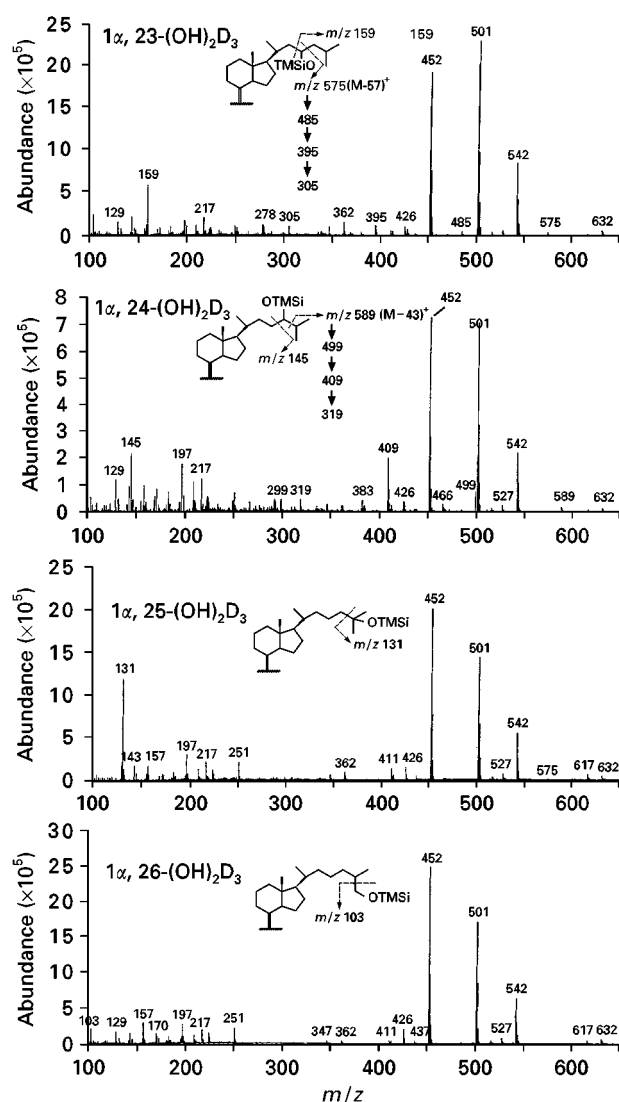


Figure 7 The EI(+) mass spectra of metabolites of 1 α -hydroxyvitamin D₃ (1 α -OHD₃). GC-MS was carried out after derivatization to form the per-trimethylsilyl ethers. Both pyro- and isopyro-isomers of each metabolite were observed but the mass spectrum of the pyro-isomer (the major peak) is shown in each case. The major ions (m/z 632 (M^+), m/z 542, 432 and 362 (not highlighted) (M^+ losing successive silanols) and m/z 501 (M^+ losing 131 by A-ring cleavage) are the same in all the spectra. m/z 217 is the characteristic ion always seen in these 1,25-dihydroxylated steroids and m/z 251 (not highlighted) arises by side-chain cleavage and subsequent loss of three silanols. It is however possible to distinguish each isomer from the characteristic fragmentation patterns illustrated for each above the appropriate spectrum. (From G Jones and HLJ Makin (2000) In: *Modern Chromatographic Analysis of Vitamins* (eds A DeLeenheer, WE Lambert and HJ Nellis), 3rd edn. New York, Marcel Dekker, to be published, with permission of authors and publisher.)

consideration of the origin of the more abundant ions. Although not shown here, the retention times increase as the hydroxylation position moves distally along the side chain. It is the presence of other less abundant ions of lower m/z value, which are diagnos-

tic for the position of the hydroxyl on the side chain and the derivation of these ions is shown in the fragmentation patterns illustrated in Figure 7. Many other examples of this sort of elucidation of seco-steroid structure can be given, all of which rely on the same sort of approach.

Routine steroid analysis at ng mL⁻¹ concentrations by GC-MS utilizes low-resolution mass spectrometry but there are occasions when increased sensitivity is required for the detection/measurement of steroids at concentrations in the pg mL⁻¹ range. This can be achieved by using high-resolution (double-focusing)

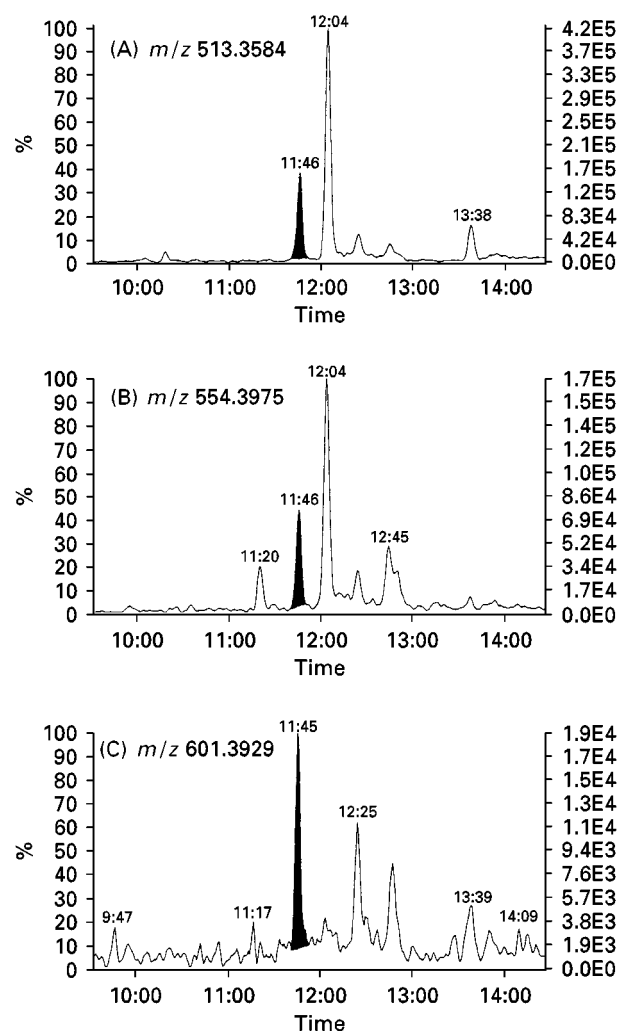


Figure 8 High-resolution mass fragmentography of an extract of serum from a patient taking vitamin D₂, showing ion chromatograms of per-trimethylsilylated (TMS) ether of putative 1 α ,24-(OH)₂D₂, monitoring three separate ions, m/z 513.3584 (A), m/z 554.3975 (B), and m/z 601.3929 (C), showing the trace between 9 and 14 min. The peaks from the pyro-isomer of 1 α ,24-(OH)₂D₂-TMS are shaded. The ion ratios in this extract are the same as those in the mass spectrum of the authentic compound. (From EB Mawer *et al.* (1998) *Journal of Clinical Endocrinology and Metabolism* 83: 2156-2166, with permission of authors and publisher.)

instruments which, although they increase specificity, reduce overall sensitivity but paradoxically allow increased sensitivity of measurement by increasing the signal : noise ratio. GC-HRMS has successfully been used for the measurement of a calcitriol analogue, hexafluorocalcitril, with a minimum detectable limit of 2 pg mL^{-1} , which gives this assay the sensitivity to measure plasma calcitriol itself, which circulates at concentrations around 30 pg mL^{-1} . This principle is, of course, generally applicable and most steroids can be detected at lower concentrations by the use of GC-HRMS. This technique has been used mainly by laboratories interested in the detection of anabolic steroids in athletes' urine (e.g. metandienone, stanozolol and clostebol) as a means of detection of drug abuse in sport but also as a means of detecting illicit steroid administration to cattle (4-chlorotestosterone). It has occasionally been suggested, as in the case of nandrolone, that metabolites observed have arisen *de novo* by *in vivo* metabolism from other steroids rather than from exogenous sources. Use of GC-combustion-MS (isotope ratio mass spectrometry) has been shown, by measuring the $^{12}\text{C} : ^{13}\text{C}$ ratios, to have considerable potential as a means of distinguishing between exogenous and endogenous sources. Figure 8 gives a further example of the sensitivity of GC-HRMS which was used to demonstrate the presence of $1\alpha,24$ -dihydroxyvitamin D_2 in human plasma by focusing on three specific ions and demonstrating that they had a retention time the same as the standard and were present in the same ratio and as they were in the MS of the pure standard. Similar studies with low-resolution MS detection were unable to demonstrate the presence of this steroid.

Conclusion

GC-FID of steroids is today primarily confined to the analysis of urinary steroid profiles, a technique introduced in the 1980s but, as a brief examination of the recent literature will show, still produces valuable

clinical information today. Much improved data are obtained when the GC is interfaced with the a mass spectrometer, allowing greater sensitivity and specificity of detection with the added benefit of structural information about unknown steroids. It is interesting to note that C_{21} steroids are usually analysed by immunoassay or LC-MS whereas GC-MS is still widely used for the specific analysis of oestrogens and androgens, particularly in the sports area where the definitive detection of anabolic steroids is required. GC-MS, particularly when high-resolution MS is used, is still more sensitive than LC-MS for steroid assay and EI(+) ionization methodology provides more useful structural information than can be achieved with LC-MS or even LC-MS-MS. It will be interesting to see whether GC-MS will hold its own against LC-MS over the next ten years.

See also: II/Chromatography: Gas: Derivatization; Detectors: Mass Spectrometry; High Temperature Gas Chromatography. *III/Steroids:* Liquid Chromatography and Thin-Layer (Planar) Chromatography; Supercritical Fluid Chromatography.

Further Reading

- Hill RA, Kirk DN, Makin HLJ and Murphy GM (eds) (1991) *Dictionary of Steroids*. London: Chapman and Hall.
- Makin HLJ, Gower DB, and Kirk DN (eds) (1995) *Steroid Analysis*. London and Glasgow: Blackie Academic and Professional.
- Makin HLJ, Trafford DJH and Nolan J (1998) *Mass Spectra and GC Data of Steroids: Androgens and Estrogens*. Weinheim: Wiley-VCH.
- Shackleton CHL (1993) Mass spectrometry in the diagnosis of steroid-related disorders and hypertension research. *Journal of Steroid Biochemistry* 45: 127-140.
- Wolthers BG and Kraan GPB (1999) Clinical applications of gas chromatography and gas chromatography-mass spectrometry of steroids. *Journal of Chromatography A* 843: 247-274.

Liquid Chromatography and Thin-Layer (Planar) Chromatography

H. L. J. Makin, St Bartholomew's and the Royal London School of Medicine and Dentistry, London, UK

Copyright © 2000 Academic Press

Introduction

This review aims to summarize the application of liquid chromatography (LC) in all its forms, including thin-layer chromatography (TLC), for the analysis of

steroids. As LC relies on either adsorption or partition, extraction of the analyte from the matrix, a similar process, has been considered, as has the necessary final step of LC-quantitation. Readers who seek further information are encouraged to use the texts given in the Further Reading section, which are valuable sources of information from which original research references can be obtained as well as information about alternative means of steroid analysis.

Steroids comprise a large group of compounds which occur naturally in both plants and animals. Their structures are all based upon the cyclopentanoperhydrophenanthrene nucleus and all the naturally occurring steroid hormones are synthesized in humans *in vivo* from cholesterol. Some steroid hormones – those derived from vitamin D₃ which are derived from cholesterol precursors – have a broken B-ring and are described as secosteroids. Various

chemical modifications of the nucleus can be made by increasing the size of the rings or modifying them in some way to produce large numbers of synthetic steroids. As an illustration of the wide variety of steroids which are available today, the *Dictionary of Steroids* lists around 10 000 compounds. Steroids have a wide spectrum of therapeutic uses and this has encouraged the synthesis of large numbers of synthetic steroids in an attempt to enhance or depress

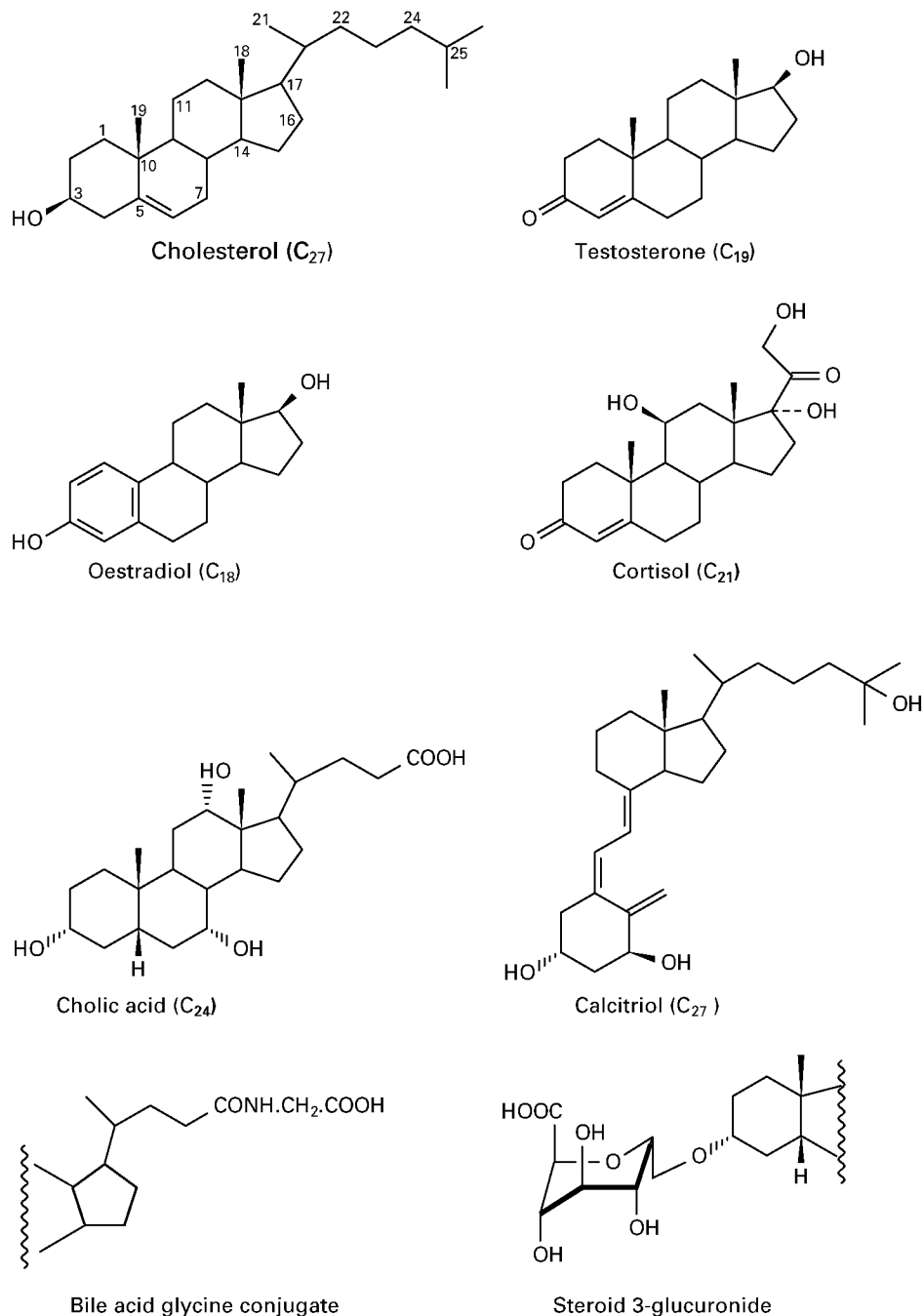


Figure 1 Formulae of some naturally occurring steroids. The numbering system used to identify the individual carbon atoms in the steroid skeleton is also illustrated.

particular physiological responses. From the point of view of a person working in a biomedical environment, the naturally occurring steroids are of particular interest and these include the gluco- and mineralo-corticoids secreted by the adrenal cortex, the sex hormones produced in the gonads, progesterone synthesized in the placenta and the bile acids which aid the digestion of fats. The parent compound of all these naturally occurring human steroids, cholesterol, is an integral part of the structure of cell membranes. The nomenclature of steroids is complicated by the fact that trivial names of many important steroids (see, for example, cortisol and testosterone in Figure 1) are still widely used. There are agreed IUPAC rules for the nomenclature of steroids but application of these rules gives rise to long and cumbersome names. Readers who are unfamiliar with steroid nomenclature are referred to the *Dictionary of Steroids* which contains a very useful summary. Figure 1 also illustrates the numbering of some of the important carbons in the steroid nucleus.

It has been estimated that, of the armoury of therapeutic drugs available for prescription in the UK, around 25% either are or contain steroids in their formulation. Because of the physiological and therapeutic importance of steroids and the huge number of different steroids which one may encounter, they represent a considerable analytical challenge. In this short summary of the liquid chromatographic methods for the separation of steroids, attention will be devoted in the main to the separation and quantitation of the naturally occurring steroid hormones and bile acids. Figure 1 gives the structures of some of the important steroids which are found in human serum and examples of their conjugates. Readers who wish to learn more about the infinite variety of steroids are referred to the classic organic chemistry text by Fieser and Fieser and the *Dictionary of Steroids*. A text on the Biochemistry of Steroid Hormones is given in the section on Further Reading.

Steroids are in the main hydrophobic, a property conferred by the nucleus, and this hydrophobicity is modified by hydroxyls and oxo groups on the periphery of the nucleus. Steroids are often conjugated with glucuronic and sulfuric acids, particularly through the hydroxyl at carbon 3. These conjugates are of course more water-soluble than the unconjugated steroid. The side chain attached to carbon 17 of the nucleus in cholesterol contains a further 10 carbons and this side chain is *in vivo* enzymatically cleaved between C₂₄ and C₂₅ to produce the C₂₄ bile acids and between C₂₀ and C₂₂ to produce steroid hormones. The C₂₄ carboxyl can also be conjugated with glycine and taurine which again increase the water-solubility of these molecules. There is therefore quite a wide

variation in hydrophobicity between different classes of steroids and within these classes, which can be further modified by conjugation. Most steroids are neutral but the phenolic A ring of the oestrogens and the C₂₄-carboxyl in the bile acids render them acidic and this property can be used for the differential extraction of these two classes of steroids.

In any analytical system there are three interdependent steps: extraction (removal of the analyte from the matrix), separation of the analyte from other compounds, which may interfere in the final step – quantitation. Separation and quantitation are clearly very closely linked in that a quantitation procedure of high specificity may well not require such intensive separation as would be required with a low specificity quantitation. Because of the chemical similarity of the many steroids with each other and, in general, the lack of highly specific quantitation procedures, separation of steroids prior to quantitation is still extremely important. Each of these three stages will be dealt with individually but it must be remembered that, when an analytical procedure is being put together, one stage cannot be viewed in isolation from the others.

Extraction

Unconjugated steroids are hydrophobic and are relatively easy to extract from the aqueous matrices in which they are often found. The apparent dichotomy of hydrophobicity and the presence of unconjugated steroid hormones in human plasma is resolved when one recognizes the presence of specific binding globulins. The main glucocorticoid, cortisol, has a specific binding globulin (transcortin) and the sex hormones also have a specific globulin which transport these steroids in human blood. To extract steroids therefore from serum or plasma, it is necessary to disrupt the steroid–protein binding. Some steroids, such as cholesterol or vitamin D₃, are particularly difficult to extract and it is thought that this occurs because they become involved in lipoprotein structure. It is possible to overcome this difficulty by extracting with ethanol–ammonium sulfate or pentylamine. Most steroids however can be extracted from plasma/serum or incubation medium with a simple Bligh & Dyer extraction which utilizes methanol–chloroform (2 : 1, v/v). A simple wash of the organic extract with alkaline buffer will remove fatty acids which are also extracted but may interfere in subsequent analysis. However, washing with alkaline buffer may also remove substantial quantities of acidic steroids such as bile acids and oestrogens. In the past, ether was a common solvent for steroid extraction as it is less dense than water and the

aqueous layer can be frozen with solid CO₂ and the organic extract poured off. However, in more safety-conscious times, the flammability of ether has reduced its use.

The extraction of steroids using solvents is discussed in more detail in texts cited in the Further Reading section. Such procedures should not be viewed solely as a means of extraction as judicious choice of solvents can give a surprising degree of selectivity and particular steroid groups can be preferentially extracted. Steroid conjugates, which are more difficult to remove from aqueous media, can also be extracted from, for example, human urine using ether-isopropanol after saturation of the urine with ammonium sulfate—so-called forced extraction. The conjugates can then be hydrolysed using enzymes (β -glucuronidase or sulfatase) or, in the case of sulfate, acid solvolysis can be utilized. The need for hydrolysis of steroid conjugates depends upon the subsequent separation and quantitation techniques. Clearly hydrolysis of conjugates loses information which may or may not be of importance. As will be seen later, modern methods of analysis using LC-mass spectrometry (LC-MS) allow for the separation and quantitation of intact conjugates and it may therefore be unnecessary to hydrolyse before proceeding to the separation or steps.

Solvent extraction leads to the generation of relatively large volumes of potentially hazardous solvents which need to be removed, usually using a rotary evaporator or simply blowing nitrogen onto the solvent while heating it not higher than about 40°C. Solvents which have high boiling points or solvent mixtures containing water are particularly difficult to remove. Because of these problems, other methods of extraction have been investigated and, in the case of steroids, major advances have been made, particularly in the field of solid-phase and immunoaffinity extraction. As examples of solid-phase extraction (SPE), one can consider the use of microparticulate silica for the extraction of steroids and vitamin D metabolites. There are a wide variety of such materials which are all based upon microparticulate silica, modified by derivatizing the polar groups with silanes (i.e. octadecylsilane (ODS) C₁₈, is widely used). Structures and performance of the solid-phase materials can most readily be obtained by looking at the catalogues of manufacturers of these materials. In the UK a very useful source of information is the catalogue of International Sorbent Technology, a major supplier of such materials (e.g. Bond-Elut). Sep-Pak is another useful proprietary brand, manufactured and marketed by Waters. As an example of the use of these materials, vitamin D₃ metabolites in plasma, although not vitamin D₃ itself, can be extrac-

ted with acetonitrile, which disrupts the protein binding. After centrifugation to remove the precipitated protein, the extract is then poured through an ODS-silica column or cartridge (Sep-Pak C₁₈ or Bond-Elut C₁₈) and the metabolites of interest can be eluted, after washing, with methanol. A similar procedure can be used for other steroids in plasma or urine and often their conjugates as well.

SPE techniques for steroid extraction, although not specific, are increasingly used in preference to solvent extraction. The SPE material can often be reused many times, if satisfactory washing procedures are applied between each use. Highly specific extraction can be achieved using immunoaffinity columns where antibodies to specific steroids or groups of steroids are immobilized by linking to Sepharose. Aqueous mixtures of steroids can then be passed down the column: steroids of interest are bound to the antibody and after the unwanted steroids have passed through the column the steroid antibody binding can be disrupted and the steroid(s) of interest eluted. In ideal cases using highly specific antibodies and a relatively specific quantitation, it may not be necessary to carry out any further separation procedures. Sometimes simple procedures can be extremely effective. As an example, the binding of some plasma steroids to specific globulins can allow selective extraction as ammonium sulfate can sometimes be used to precipitate the specific globulin, which brings the steroid of interest with it.

Separation

Today high performance liquid chromatography (HPLC) is widely used for steroid separation because this technique can be directly linked to quantitation. This is, however, not to imply that other methods of separation may not find use in particular applications. Open-column chromatography (either adsorption or partition) is still used with advantage on occasions. A major and very useful separatory technique is TLC and, if microparticulate material is used, it becomes high performance TLC (HPTLC). TLC is particularly advantageous in that numbers of separations can be carried out at the same time and the apparatus required is inexpensive. For these reasons and because TLC is relatively easy to carry out, it is still quite widely used and scrutiny of recent papers on steroid separation confirms this. It is however true to say that very little development of TLC systems has occurred in the last 20 years and most systems are based upon methods described prior to 1980. TLC can also be used as a preliminary means of investigating new solvent systems for the separation of steroids by HPLC.

Column Chromatography

This procedure utilizes adsorbent materials such as alumina, Florisil (magnesium silicate) or silica. Steroids are adsorbed to these materials and are eluted by solvents of increasing polarity. The order of elution depends upon the solvent and the differing polarity of the steroids under consideration. Clearly, the more polar a steroid (in general, this means the more hydroxyls it contains), the more hydrophilic the steroid becomes and the longer it takes to be eluted. These adsorbent materials are usually packed into small columns (for example, Pasteur pipettes can be used) and exquisite separations can now be achieved by the use of microparticulate silica. These columns are simple to use, provide rapid separations and have the advantage that after washing they can be reused many times. Classical steroid separations using columns can be achieved by partition chromatography using biphasic solvent systems. The stationary aqueous phase is mixed with celite (a diatomaceous earth) and this material is packed into the column; the steroid mixture is applied and eluted with the organic mobile phase. This is rather a cumbersome procedure but does offer a considerable degree of separation. It is not widely used today, although examples of partition chromatography used in this way can still be found. An example of this technique for the separation of some progesterone metabolites is illustrated in Figure 2.

Modified cross-linked dextran columns (i.e. Lipidex) have been used to provide steroid separations and can find more mundane uses such as the removal of excess trimethylsilylimidazole reagent when forming steroid trimethylsilyl ethers. A similar material, Sephadex LH-20, has also been used to fractionate steroids into free steroids, glucuronides, mono- and disulfates. Sephadex can also be modified by linking it to form, for example, diethylaminoethyl-substituted material which can act as an ion exchanger as well as a size exclusion material. These ion exchange/gel filtration columns are particularly useful for the separation of steroid conjugates; for example, bile acids can be separated by the use of another modified Sephadex, PHP-LH20. Figure 3 shows such a system for the separation of steroids and their conjugates from human urine prior to gas chromatography-MS (GC-MS).

Thin-Layer Chromatography

TLC is in effect very similar to column chromatography and is based on the same principles. A thin layer of adsorbent or inert material is spread on a glass, plastic, or aluminium sheet. For the separation of steroids using organic solvents, the use of thin layers on plastic sheets is not recommended and either glass or aluminium should be used. After separation, steroids may be recovered from the plate by scraping off the thin layer and eluting the steroid of interest.

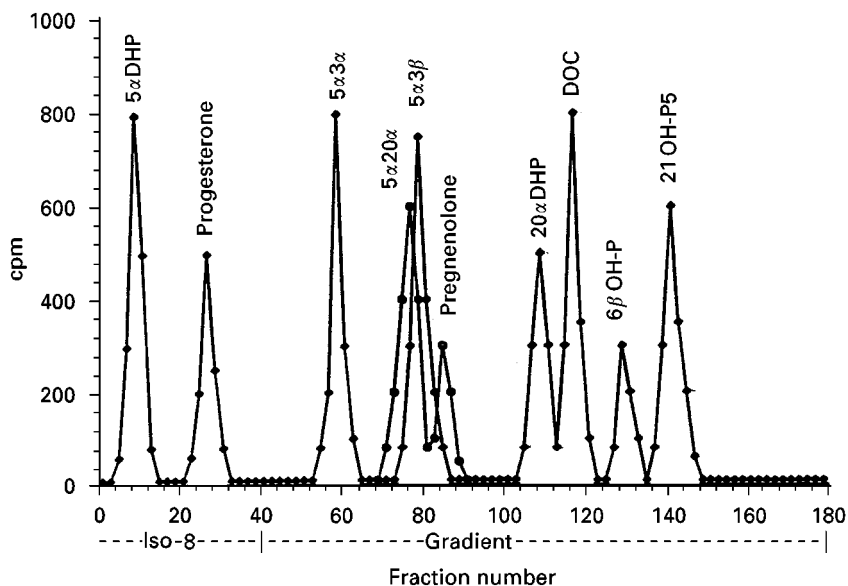


Figure 2 Chromatogram of selected C_{21} steroids in urine. Radiolabelled and nonradiolabelled authentic steroid standards were applied to a 40 g column of celite-propylene glycol and eluted with iso-octane (e.g. Iso-8, 40 fractions) and thence a linear gradient of iso-octane-ethyl acetate (e.g. Iso-8, 140 fractions). Steroids are identified as follows: 5α DHP, 5α -pregnane-3,20-dione; $5\alpha3\alpha$, 5α -pregnan-3 α -ol-20-one; $5\alpha20\alpha$, 5α -pregnan-20 α -ol-3-one; $5\alpha3\beta$, 5α -pregnan-3 β -ol-20-one; 20α DHP, Δ^4 -pregnen-20 α -ol-3,20-dione; DOC, Δ^4 -pregnen-21-ol-3,20-dione; 6β OH-P, Δ^4 -pregnen-6 β -ol-3,20-dione; 21 OH-P5, Δ^5 -pregnen-3 β ,21-diol-20-one. (Reproduced with permission from Dombroski RA, Casey ML and MacDonald PC (1997) *Journal of Steroid Biochemistry* 63: 155-163.)

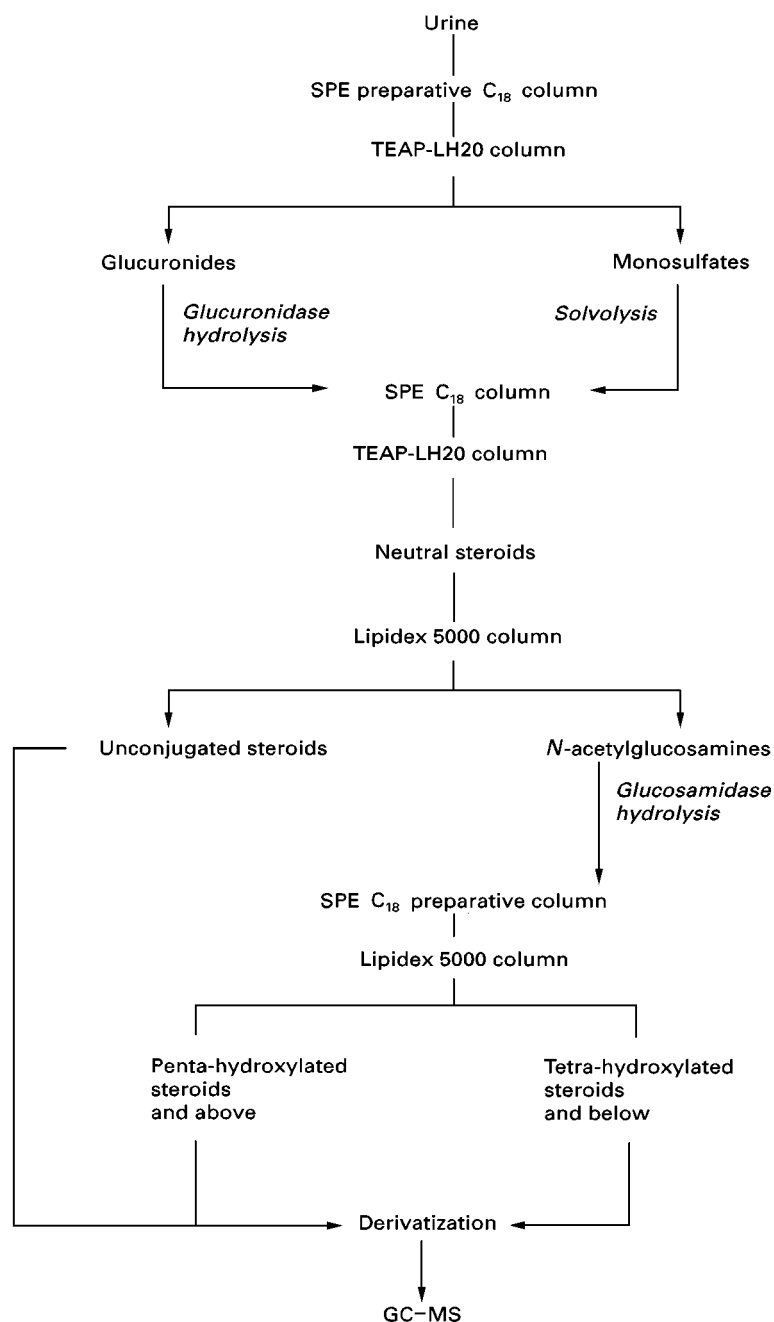


Figure 3 Use of solid-phase extraction and Sephadex-based packing materials for the extraction and separation of steroids and their glucuronide, sulfate and *N*-acetylglucosaminide conjugates from human pregnancy urine prior to analysis by gas chromatography–mass spectrometry (GC-MS). (Reproduced with permission from Meng LJ, Griffiths WJ and Sjövall J (1996) *Journal of Steroid Biochemistry and Molecular Biology* 58: 585–598.)

The advantage of thin layers on aluminium foil is that the area of interest can be cut out and the whole area of the plate can be eluted without removing the adsorbent.

The commonest forms of TLC for the separation of steroids use adsorbent thin layers of either alumina or silica gel, although there are descriptions of reversed-

phase partition TLC. Use of microparticulate silica (HPTLC) confers a slightly enhanced selectivity in separation but HPTLC is not widely used. The steroid extract of interest is applied to the bottom of the plate and eluted with various solvents. Because of the ability of such separation systems to deal with a number of separations at once, they are still quite widely used

today. The vast majority of separation systems use silica gel but alumina has been used to separate C₁₉ androgens. The resolution is achieved by judicious choice of solvents as the number of adsorbents available is limited.

Very little development of this separation technique for steroids has been carried out over the last 20 years as attention has been diverted towards the development of HPLC. Recent TLC systems using silica gel and eluting with ethyl acetate: petroleum ether have enabled hydroxylated metabolites of progesterone to be resolved and again using silica gel with benzene–heptane–ethyl acetate or chloroform–ethyl acetate has enabled resolution of catechol oestrogens. In many instances, however, suitable solvents can no longer be used as they pose unacceptable risks of flammability or toxicity (e.g. benzene). A study of papers published in the last 10 years involving the use of TLC for the separation of steroid metabolites indicates that most procedures were published many years ago, although the recent use of cyclo-

dextrin in the TLC of bile acids (cyclodextrin in the mobile phase) and steroidal drugs (cyclodextrin polymer-coated silica) has been an interesting innovation.

Table 1 lists some examples of the recent use of TLC for the separation of steroids and clearly illustrates the increasing reliance on silica gel as the adsorbent, using the differing polarity of the elution solvent mixture for resolution. Most of the development systems are modifications of previously published solvent mixtures. Table 1 also illustrates the use of two-dimensional TLC and multiple development in the same direction. It is also possible to utilize one solvent mixture for de-fatting, followed by another to separate the steroids of interest or sequential solvent systems, separating first one group of steroids followed by a second solvent mixture to separate another steroid group.

The problem associated with the use of TLC for the separation of steroids is to locate the position of the steroids after chromatography and some methods

Table 1 Some examples of recent use of TLC for steroid separation

<i>Steroids</i>	<i>Adsorbent</i>	<i>Development solvent</i>	<i>Detection</i>
Side chain cleavage products of ¹⁴ C-cholesterol	Silica gel G	Di-isopropyl ether–hexane–acetic acid (70 : 30 : 2)	Radioactivity by autoradiography
Metabolites of 7 α -OH-androstene-3,17-dione	Silica gel	Ethyl acetate–hexane (3 : 7)	
7-Hydroxylated DHEA	Silica gel F254	Ethyl acetate	UV absorption
Oestrogens	Keisegel 60 F254	Toulene–acetone (4 : 1)	UV absorption and iodine vapour
³ H corticosteroids	Silica gel 60 F254	Choloroform–acetone (23 : 2)	Autoradiography
³ H testosterone metabolites	Polygram SIL G	Methylene chloride–diethyl ether (4 : 1)	Autoradiography
Oestrogens	Whatman LK6DF Silica gel 60	Ether–chloroform (6 : 4) Chloroform–ethyl acetate (4 : 1)	Iodine vapour
Corticosteroids	Silica gel	Ethyl acetate–isooctane (7 : 3)	
Corticosteroid sulfates	Silica gel	Chloroform–methanol–NH ₄ OH (65 : 25 : 0.1) Ethyl acetate–methanol–NH ₄ OH (75 : 25 : 2)	
Progesterone metabolites	Fisherbrand F254	Two-dimensional TLC \times 2 with chloroform–ether (10 : 3) then \times 2 in hexane–ethyl acetate (5 : 2)	Iodine vapour and UV absorption
Androst-16-ene biosynthesis	PE-SIL-G Silica gel	Chloroform–acetone (9 : 1) and hexane–ethyl acetate (5 : 3.5) Run \times 2	Iodine vapour and UV absorption
Metabolites of ³ H-progesterone, -pregnenolone and -DHA	Fisher silica gel 60 F254	Two-dimensional TLC firstly to de-fat in cyclohexane–ethyl acetate (95 : 5) \times 5–7. Then toluene–acetone (8 : 2) \times 2, finally \times 2 in first direction with cyclohexane–ethyl acetate (1 : 1)	Autoradiography

used for this purpose are also summarized in Table 1. For steroids containing UV-absorbing groups, such as the δ -4-3-oxo group in the A-ring of most active steroid hormones and the aromatic ring in the oestrogens, visualization can be achieved by examining the plate under UV light. To improve the detection of steroids absorbing at around 240 nm, most commercially available TLC plates have a fluorescent material incorporated which improves detection of the absorption of UV light at around 254 nm. Other techniques are often destructive and require reagents to be sprayed on to the plate. Thus, to avoid destroying the steroid of interest, it is necessary to have standards run on the same plate at the side so that the position of the steroids of interest can be gauged. There are other nondestructive means of visualization, such as the use of iodine vapour but these are not always satisfactory, particularly at low concentrations. One advantage of TLC is in the separation of radiolabelled steroids which can be visualized by autoradiography.

High Performance Liquid Chromatography

The application of HPLC to the separation of steroids has been extensively studied over the last 20 years. A detailed and comprehensive review of the HPLC of steroid hormones was published in 1988 and updated in 1995 (see Further Reading). HPLC is in essence no different to the column and thin-layer systems discussed above, although the resolving power of modern HPLC columns is significantly greater: some reversed-phase columns achieving 60 000–80 000 theoretical plates per metre. New solvent systems for normal-phase HPLC can be investigated using TLC. Columns, because of the high resolving power which can now be achieved, are usually quite short (100–300 mm long with an internal diameter of 4.6 mm). Microbore columns (< 2 mm in diameter) can be used to reduce mobile phase consumption but may present practical problems because of the limitation in sample capacity. However, microbore columns may have considerable application in LC-MS, because of the low solvent flow rates. Silica contains free OH groups and these can be modified, replacing the OH for example with cyanopropyl (CN, used for the separation of corticosteroids) or aminopropyl (NH_2 , used for the separation of oestrogens). Improved resolution of particular steroids can sometimes be achieved using these modified silicas and, for example, silica-CN gives selective retention of steroids containing oxo groups, and has been particularly useful in the separation of the 25-hydroxyvitamin D_3 -23,26-lactone which is difficult to resolve from 24,25-dihydroxyvitamin D_3 in conventional normal-phase HPLC systems. Reversed-phase HPLC is usu-

ally based on silica modified with silanes of various chain lengths – C_{18} (ODS) silica is the most widely used material for this purpose. Column packings based on synthetic material are now being made available and may in the future replace silica. Considerable advances in the production and quality of these packing materials have been made over the past 10 years and thus reproducibility of separations has improved.

Most steroid separations today use reversed-phase systems with C_{18} or C_8 silica, although an exception to this general rule is the separation of metabolites of vitamin D which use normal-phase systems eluting with hexane–isopropanol–methanol or hexane–methanol–chloroform. Binary hexane–isopropanol systems give significant tailing and resolution problems which are improved by the use of ternary solvent mixtures. These normal-phase systems give excellent resolution of the metabolites of vitamins D_2 and D_3 but do not separate the vitamins themselves (Figure 4), which can be achieved using reversed-phase ODS–silica eluting with methanol–water. If steroids are to be recovered from the eluting solvent, it is clearly advantageous if normal-phase systems with sufficient resolving power can be developed as the removal of aqueous solvents used in

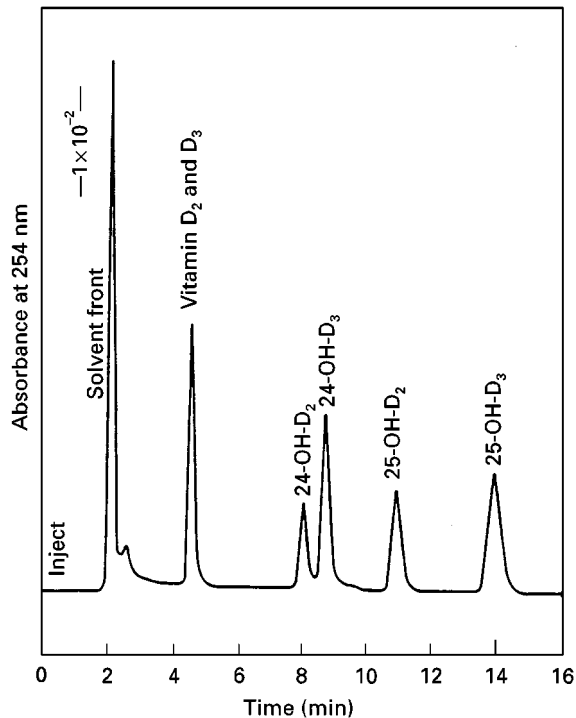


Figure 4 LC separation of vitamins D_2 and D_3 , 24-OH- D_2 , 24-OH- D_3 , 25-OH- D_2 and 25-OH- D_3 , using Zorbax-SIL and eluting with 2.5% isopropanol in hexane. (Reproduced with permission from Jones G and DeLuca HF (1975) *Journal of Lipid Research* 16: 448–453. Copyright 1975 FASEB.)

Table 2 Examples of some recent HPLC systems for the separation of steroid hormones and bile acids

<i>Steroid group</i>	<i>Carbon atoms</i>	<i>Stationary phase</i>	<i>Mobile phase</i>	<i>Comments</i>
Vitamin D	C ₂₇ (D ₃ series)	Zorbax ODS	MeOH (MeCN)-H ₂ O (acid)	Separation of D ₃ and D ₂
Secosteroids	C ₂₈ (D ₂ series)	Zorbax CN Zorbax SIL	Hx-IPA-MeOH Hx-IPA-MeOH	Retards metabolites containing oxo groups Usual system for metabolite resolution
Bile acids	C ₂₄	YMC GEL C8 Bile Pak II	MeCN-H ₂ O + cyclodextrin Gradient with MeCN-MeOH-PO ₄ buffer	Bile acids and their conjugates as bromopyrenacyl esters Bile acid conjugates using post-column immobilized 3 α OHSDH and fluorescence detection
Corticosteroids	C ₂₁	Cosmosil C ₁₈ Novapak C ₁₈ Nucleosil C ₈	MeOH-H ₂ O gradients MeOH-buffer MeCN-H ₂ O + HCOOH	Corticosterone and DOC Electrospray-MS of DHE and DHF Dexamethasone metabolites
Progesterone metabolites	C ₂₁	Finepak SIL-C ₁₈	Tetrahydrofuran or MeCN-imidazole buffer	Pregnane- and pregnene-diols
Androgens	C ₁₉	NovaPak C ₁₈ Hypersil BDS-C ₈ Hibar Lichrosorb-DIOL	Gradient of MeCN-H ₂ O Gradient of 7.5 mmol L ⁻¹ NH ₄ Ac-MeOH Hx-IPA	DHEA and 7-OH-DHA in newborn foal's blood LC-MS of testo. and epi-testo. glucuronides/sulfates Metabolites of DHT and androstanediol
Oestrogens	C ₁₈	Wakosil C ₁₈ Beckman ODS	MeOH-H ₂ O MeCN-H ₂ O + cyclodextrin	Plasma oestrogens-pre-column derivatization as benzimidazoles Urinary oestrogens

reversed-phase separations causes considerable difficulties. Corticosteroids have been successfully separated using normal-phase systems based on DIOL-silica sorbents (-Si-2,3-dihydroxypropoxypropyl) and ion exchange HPLC has also been used for the separation of polar oestrogens. Some recent examples of typical HPLC systems used for the separation of steroids are given in Table 2, which illustrates the fact that most methods in use today are reversed-phase systems using ODS/C₁₈ packings.

All steroids are susceptible to permanent absorption and/or chemical destruction or modification by unsilanized glass surfaces, exposed metal and by non-inert supports and, for quantitative HPLC, great care must be taken to remove or reduce such materials. Sorbents containing accessible hydroxyl groups should not be used for the separation of 18-hydroxylated steroids as chemical modification of these steroids may occur during chromatography. Although not relevant to HPLC, it should be pointed out that partially end-capped ODS-silica can still be used with advantage in particular situations for rapid separations after SPE. As an example, the use of Bond-Elut C₁₈-OH allowed both extraction and subsequent separation on the same cartridge in a method for the assay of calcitriol (1,25-dihydroxyvitamin D₃).

One particular advantage of HPLC is that it is not destructive and can thus be used for the separation and quantitation of intact steroid conjugates. These

polar molecules are not susceptible to analysis by GC as the high temperature necessary to maintain steroids in the vapour phase causes hydrolysis of the conjugate. Examples of the application of HPLC to the separation of androgen and oestrogen glucuronides and the application of LC-MS(MS) to the separation of intact conjugates and steroid fatty acid esters are given in the Further Reading section. An example of such a separation is given in Figure 5. Until the advent of HPLC, steroid conjugates had to be hydrolysed prior to resolution and important information was thus lost. The use of LC, particularly when coupled to MS(MS), has allowed resolution and quantitation of intact conjugates together with structural information. HPLC systems for steroid conjugates are usually but not exclusively reversed-phase primarily based on ODS-silica eluting with methanol-, tetrahydrofuran-, acetonitrile-water or buffer solvent systems. The conjugates can be detected in the same way as nonconjugated steroids and this is discussed below.

Detection/Quantitation

This is the final and perhaps most important step and there are a variety of methods which can be used for the detection or quantitation of steroids. These methods are usually considered only in conjunction with HPLC as they are usually insufficiently specific

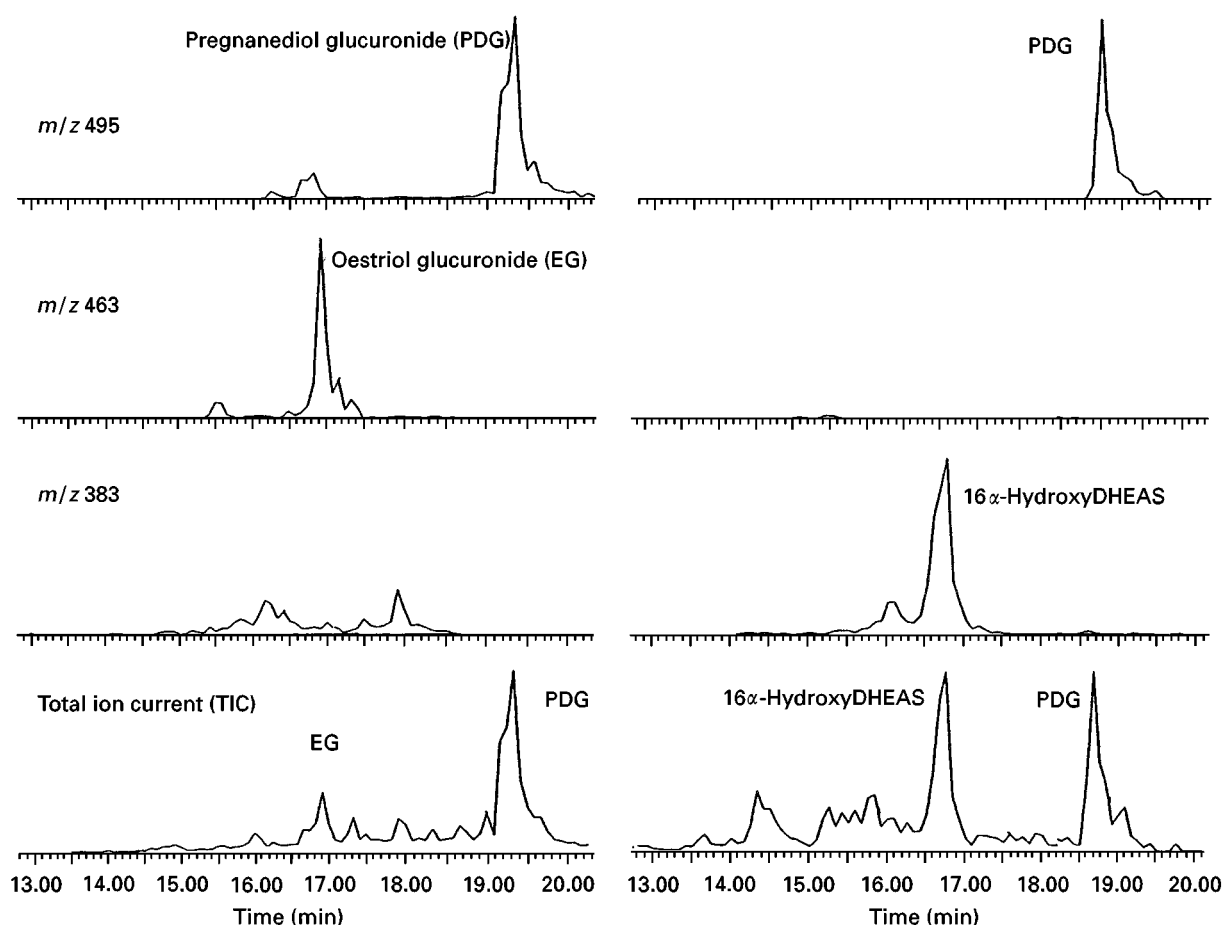
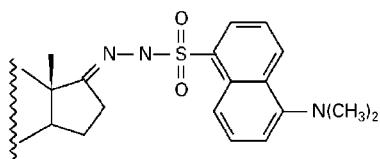


Figure 5 Analysis of maternal urine for the detection of placental sulfatase deficiency (PSD). The microbore HPLC-ES-MS chromatograms represent selected ions for detection of pregnanediol glucuronide, oestriol glucuronide and 16 α -hydroxy-DHEA sulfate. The selected-ion chromatograms on the left of the figure are from a normal individual and those on the right are from a patient with PSD. Oestriol and its glucuronide cannot be synthesized by women with PSD, and the precursor 16 α -hydroxy-DHEA sulfate is a dominant steroid in urine. The amount injected into the microbore column was equivalent to 25 μ L of urine, the eluate being split 10 : 1 prior to the mass spectrometer. The column used was a Reliasil number 9, 1 \times 100 mm. Solvent A was 98% 10 mmol L⁻¹ ammonium acetate in H₂O, 2% acetonitrile; solvent B was 100% acetonitrile. The gradient was 2% B to 30% over 20 min, and a flow rate of 40 μ L min⁻¹ was used. From Makin HLJ, Gower DB and Kirk DN (eds) *Steroid Analysis* (1995) Reproduced with permission from Kluwer Academic Publishers.

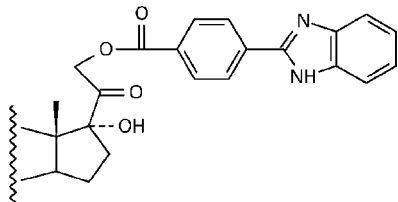
to be used without rigorous prior separation of interfering steroids – the exception to this being immunoassay which can, depending upon the antibody, be sufficiently selective and sensitive for use directly on plasma/serum without extraction or prior purification. There are a number of such assays available today but their uncritical use can lead to problems. An example of this is an immunoassay for 17-hydroxyprogesterone, developed for use with adults. This was applied to the diagnosis of a genetic defect in cortisol biosynthesis, congenital adrenal hyperplasia. The possible interference in this assay by 17-hydroxypregnenolone sulfate which is normally produced in very young children was not appreciated. A simple solvent extraction procedure overcame this problem once it was detected.

It is often the case that one or other of the simple purification procedures, such as selective solvent extraction, use of mini-columns or even TLC on small plates can greatly enhance specificity and there are many examples of this in the literature. It is often unnecessary to use expensive HPLC systems to resolve these steroid analytical problems and consideration of the physicochemical properties of the steroid of interest may often suggest a simple non-HPLC solution. Immunoassay is however one of the most sensitive methods of steroid quantitation and, coupled with HPLC, even with a relatively non-specific antibody, can provide a system with both high specificity and sensitivity. It does however require collection of the eluent – so called offline detection.

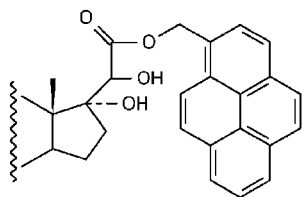
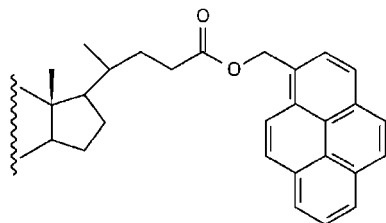
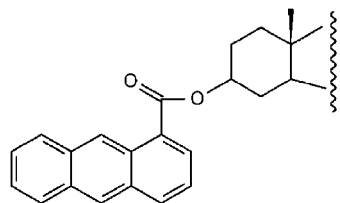
1. Dansyl hydrazones of 17-oxosteroids



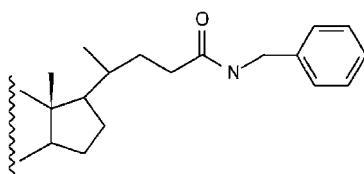
2. 2(4-carboxyphenyl)-5,6-dimethylbenzimidazole esters of corticosteroids



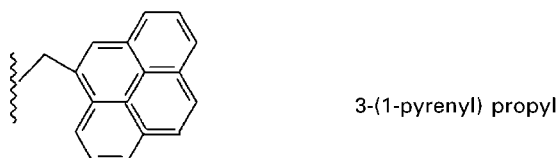
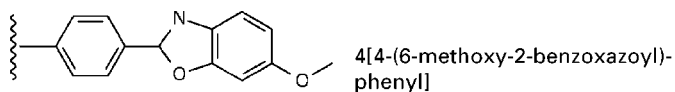
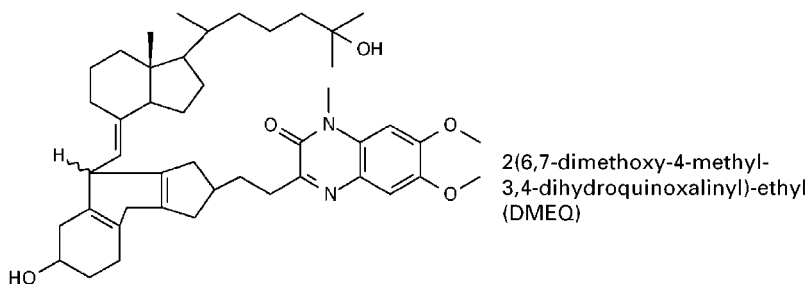
3. 3(1-anthroyl) and 1-pyrenylmethyl esters of bile acids and corticosteroids



4. N-benzylamides of bile acids



5. Substituted 1,2,4-triazoline-3,5,3,5-dione (TAD) adducts of vitamin D metabolites

**Figure 6** HPLC of steroids with fluorescent detection – some examples of pre-column derivatives.

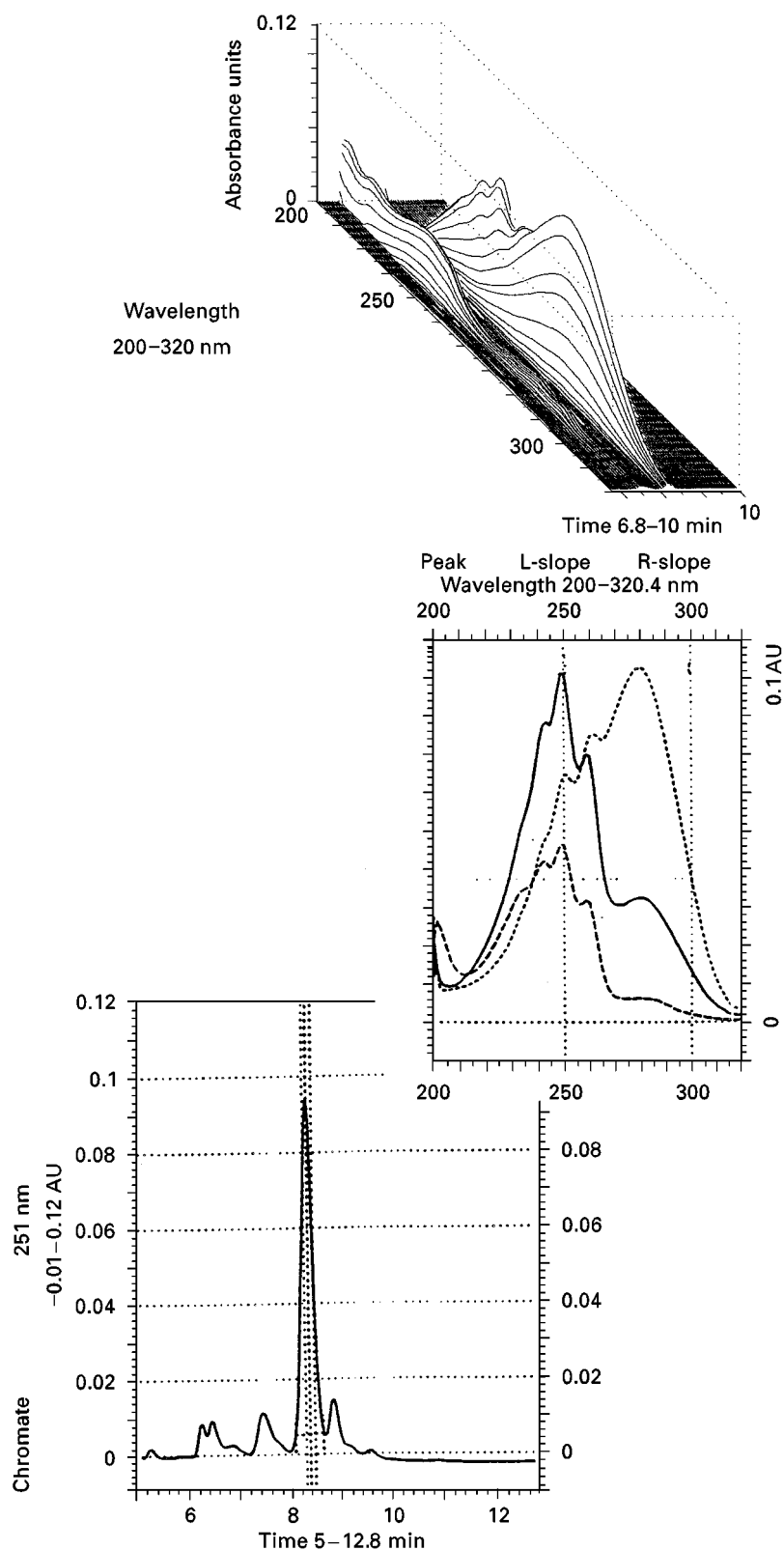


Figure 7 Use of photodiode array detection in HPLC separation of metabolites of 25-hydroxydihydrocholesterol₃. Monitoring the eluent at 251 nm indicates what appears to be a single homogeneous peak. Examination of the UV spectra at the leading edge, the apex and the trailing edge clearly demonstrates the presence of a contaminant. From Makin HLJ, Gower DB and Kirk DN (eds) *Steroid Analysis* (1995). With permission from Kluwer Academic Publishers.

Other detection methods can be used, such as UV absorption with or without derivatization, fluorimetry after chemical modification or derivatization or electrochemical detection. These detection/ quantitation methods can usually be carried out online – that is to say, that the HPLC eluent can be directly and continuously monitored. When chemical derivatization is required, this can be carried out prior to HPLC (pre-column derivatization) but this may reduce resolution. In such cases it is also possible to carry out the derivatization after the HPLC separation (post-column derivatization). Some examples of pre-column derivatization used for fluorescent detection are illustrated in Figure 6.

One particular method of UV monitoring of eluents from HPLC separations is the photodiode array detector. With this detector the absorption of the eluent is continuously monitored over a range of wavelengths and the data stored in a computer. Reconstructed chromatograms can be obtained at a later date, as can three-dimensional reconstructions (showing time versus absorbance versus wavelength). An example of photodiode array detection is illustrated in Figure 7, which demonstrates that what appears to be a single peak when monitored at 251 nm is in fact composed of two unresolved compounds and this can be demonstrated by comparing the UV spectra obtained at the leading edge, the apex and the trailing edge of the peak. This lack of resolution is also seen in the three-dimensional picture. This particular separation was obtained when examining the metabolites of a chemical analogue of 25-hydroxyvitamin D.

HPLC can also be linked to mass spectrometry and, increasingly, techniques are becoming available for the direct linking of the column to the mass spectrometer. In the past, mass spectrometry of HPLC eluents had, like immunoassay, required that eluents be collected and prepared for mass spectrometry. The availability of ionization techniques (such as atmospheric pressure ionization, electrospray, etc.) now allow the HPLC eluent to go directly to the mass spectrometer. Many steroids are susceptible to ionization in such systems but others require derivatization to achieve satisfactory ionization. In these systems the elution solvents should contain water or salts, which implies the use of reversed-phase separation. This is not a particular problem with most steroids but for particular steroid groups (e.g. metabolites of vitamin D) it may require the development of new solvent systems. Such ionization procedures are inevitably low energy and fragmentation is limited. The advantage of this low energy ionization is that intact steroid conjugates can be examined. However, low energy ionization is inefficient, limits the sensitivity of detec-

tion and does not yield information about structure. To some degree this structural limitation can be resolved by utilizing LC-MS-MS where the first mass spectrometer allows only the major ion obtained to pass through to a collision cell. Here the ion is subjected to higher energy ionization or bombardment, producing further fragments which can then be analysed by a second mass spectrometer, yielding structural information. Such systems are expensive but are immensely valuable. Unfortunately, LC-MS and LC-MS-MS are not as sensitive as GC-MS, which has been widely used for the measurement of many steroids present at low concentrations in human body fluids. High resolution GC-MS can of course increase sensitivity of detection even further.

Conclusion

The advent of simpler and cheaper mass spectrometers which allow direct coupling of the LC column has meant that less attention needs to be paid to resolution and the development of solvent systems and column packings to achieve improved resolution is no longer as important. Attention has therefore shifted towards increasing sensitivity by the use of microbore columns with the low flow rates required for maximum ionization in the MS and the use of nanospray ESI. Today excellent mass spectra can be obtained using such systems with femtomole concentrations of analyte. There is considerable scope for further enhancement of sensitivity and selectivity by improved MS design of both hardware and software.

Acknowledgements

Readers are encouraged to seek further information from the texts quoted below which are fully referenced and allow entry to the extensive research literature on this topic. In preparing this review, I acknowledge the debt I owe to all the researchers in this area whose results I have used but whose work I have not been able to acknowledge directly.

See also: II/Chromatography: Liquid: Mechanisms: Normal Phase; Mechanisms: Reversed Phases. III/Steroids: Thin-Layer (Planar) Chromatography.

Further Reading

- Fieser LF and Fieser M (1959) *Steroids*. New York: Van Nostrand Reinhold.
- Heftmann E (ed.) (1983) *Chromatography: Fundamentals and Applications of Chromatographic and Electrophoretic Methods. Part B: Applications*. Amsterdam: Elsevier.

- Hill RA, Kirk DN, Makin HLJ and Murphy GM (eds) *Dictionary of Steroids*. London: Chapman & Hall.
- Kautsky MP (ed.) (1981) *Steroid Analysis by HPLC: Recent Applications*. New York: Marcel Dekker.
- Makin HLJ (ed.) (1984) *Biochemistry of Steroid Hormones*, 2nd edn. Oxford: Blackwell Scientific Publications.
- Makin HLJ and Newton R (eds) (1988) *High Performance Liquid Chromatography in Endocrinology*. Berlin: Springer Verlag.
- Makin HLJ, Gower DB and Kirk DN (eds) (1995) *Steroid Analysis*. London: Blackie.

Supercritical Fluid Chromatography

**K. Yaku, K. Aoe, N. Nishimura and
T. Sato**, Tanabe Seiyaku, Osaka, Japan
F. Morishita, Kyoto University, Kyoto, Japan

Copyright © 2000 Academic Press

Supercritical fluid chromatography (SFC) has been recognized as a powerful separation technique complementing gas chromatography (GC) and high performance liquid chromatography (HPLC). Klesper *et al.* published results of the use of supercritical dichlorodifluoromethane and monochlorodifluoromethane to separate involatile nickel porphyrin in 1961. The development of the technique was limited by instrumental and experimental difficulties due to the high temperatures and pressures required to maintain the mobile phase in a supercritical state. Novotny and Lee, however, developed SFC with a capillary column (cSFC) in 1981, which led to significant advances in the technique. In 1982 Gere *et al.* developed an instrument for packed-column SFC (pSFC) based on modification of an HPLC. They demonstrated, using polycyclic aromatic hydrocarbons as probe molecules, that the resolution per unit time in pSFC was 5–10 times better than in HPLC with the same columns, due to more favourable diffusivity in supercritical fluids.

The advantages of SFC have been described elsewhere in this *Encyclopedia*. Pure carbon dioxide fluid is a solvent of inadequate polarity. For the analysis of polar compounds by SFC, alcohol is generally added to a mobile-phase fluid as a modifier. Small amounts of polar modifiers significantly increase the solvent strength of the mobile phase and make it possible to elute polar compounds. In particular, pSFC has been applied to various kinds of polar compounds such as drugs, and shown to be superior to HPLC with respect to analysis time, efficiency and selectivity.

The nonpolar steroids cholesterol and ketosteroids are easily eluted by either cSFC or pSFC with pure carbon dioxide. Synthetic corticosteroids, which are widely used therapeutically for the suppression of

adrenocortical functions, inflammatory and allergic diseases, have multiple hydroxyl functional groups in the structures. In order to modify the efficacy and suppress adverse reactions, many corticosteroids have been synthesized. Thin-layer, normal and reversed-phase chromatography have been used for the analysis of these compounds. For a number of the synthetic corticosteroids used in therapy, very little work has been carried out by pSFC. These polar steroids are probably difficult to elute with pure carbon dioxide due to its poor solvent strength.

In this article, the pSFC retention behaviour of synthetic corticosteroids, possessing one to four hydroxyl groups, are focused on. The effect of several parameters (stationary phase, modifiers, pressure and temperature) on retention and efficiency are considered. The chemical structures of corticosteroids are shown in **Figure 1**. They were chromatographed using a pSFC instrument modified from a commercial HPLC system. The addition of methanol to carbon dioxide and adoption of an aminopropyl stationary phase produced both good resolution and symmetric peak shapes. Both plate number and resolution indicated that the maxima were around the critical temperature (40–50°C) of the binary fluid. The selectivity and separation of the analytes in pSFC are superior to those in existing normal and reversed-phase HPLC. Seven polar corticosteroids, possessing one to four hydroxyl groups, showed baseline separation within 6.5 min with a modifier gradient method.

Instrumentation of pSFC

Most studies have been done using commercial pSFC instruments. However, a pSFC with the same performance as a commercial instrument can easily be constructed. The HPLC for pSFC operation requires some simple adaptations to allow use of supercritical carbon dioxide as a mobile phase. The pSFC system constructed by the authors by modifying a Shimadzu HPLC is shown in **Figure 2**.

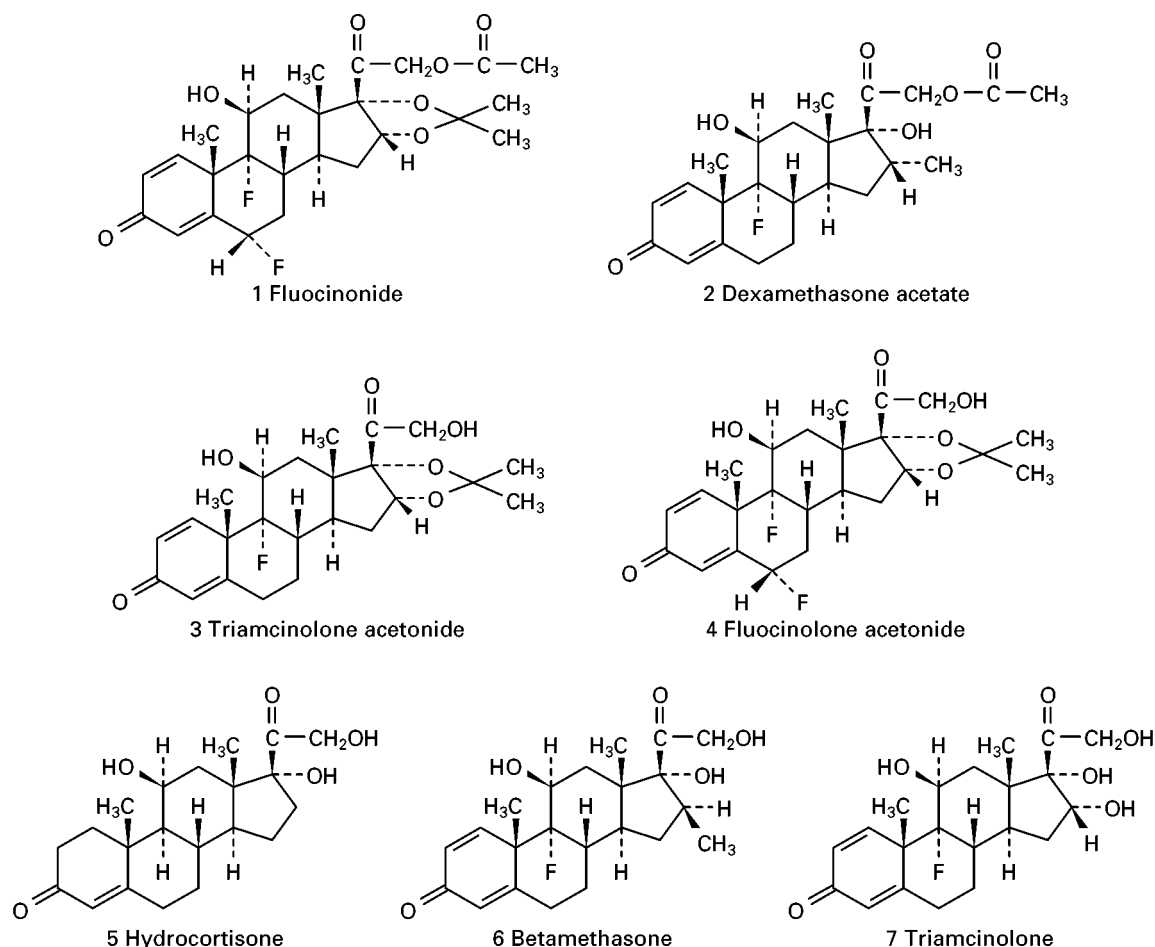


Figure 1 Structures and symbols of synthetic corticosteroids.

Effect of Analytical Parameters

Stationary Phase

Peak shapes of polar solutes on a packed column are often poor when pure carbon dioxide is used as the mobile phase. The separation of steroids has been performed using columns with phenyl, nitrophenyl, diol, aminopropyl, octadecyl and cyanopropyl-modified silica and pure silica as packing materials. It is likely that only polar modifiers used with polar stationary phases produce both good resolution and symmetrical peaks. As shown in **Figure 3**, an aminopropyl column exhibited the best selectivity and peak shape with a reasonable retention time in comparison with the others. Octadecyl and phenyl columns showed poor separation: the former did not retain any solutes and the latter did not separate under the operating conditions used. On the silica support, the solutes showed appropriate retention but poor separation and peak shape. Although the retention times of triamcinolone acetonide, fluocinolone acetonide, hydrocortisone and betamethasone were almost the

same as those on the aminopropyl column, the separation factor, α , of the two pairs – steroids possessing two hydroxyl groups, and steroids possessing three hydroxyl groups – decreased remarkably on silica. A reversed elution order, however, was observed on the silica, which showed that it is possible to change selectivity by selecting the stationary phase.

Modifier

In pSFC, the addition of a modifier to a mobile phase should be considered from the viewpoint of its effect on either the stationary phase or on the mobile phase. Berger *et al.* have studied the effect of column and mobile-phase polarity using steroids. They concluded that polar modifiers tended to decrease the intensity of the solute–silanol interaction, and more polar stationary phases produced greater retention, requiring the use of modifiers to obtain reasonable retention times. Blilie and Greibrokk indicated that the modifiers functioned as deactivation agents by direct interactions with residual silanol groups, and also as modifiers of the eluting power of the mobile phase.

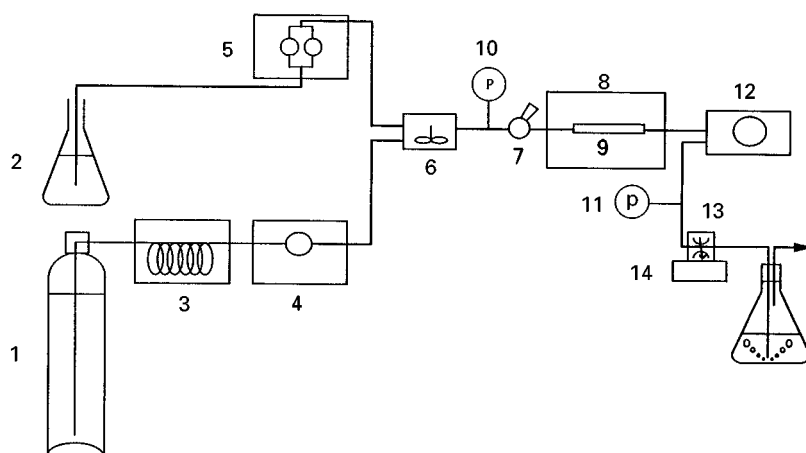


Figure 2 Schematic diagram of packed-column supercritical fluid chromatography. 1, Carbon dioxide cylinder; 2, modifier; 3, cooling bath; 4, LC-6A pump; 5, LC-9A pump; 6, dynamic mixer; 7, injector; 8, oven; 9, packed column; 10 and 11, pressure monitor; 12, detector; 13, back-pressure regulator; 14, dry thermo unit.

No corticosteroids were eluted from the column packed with Cosmosil 5NH₂ with pure carbon dioxide as the mobile phase and a modifier had to be added. The effect of modifiers with different polarities on the retention of corticosteroids is shown in **Figure 4**. The addition of 11.8% (v/v) methanol to carbon dioxide gives the best resolution and symmetrical peak shapes within 14 min. In comparison, the addition of the same amount of 99.5% ethanol, and of 95% ethanol reduced resolution but remarkably improved the peak shape of the most polar compound, triamcinolone, in the corticosteroids. This should be attributed to deactivation of the active sites on the silica support by the water in the 95% ethanol.

Janssen *et al.* confirmed that the effect of a few per cent of modifier in pSFC is largely due to deactivation

of residual silanol groups on the silica support, and the accessibility to the active sites depends strongly on the size and structure of the modifier molecules. According to Janssen *et al.*, the same volume percentage of tetrahydrofuran (THF) and methanol was needed to cover 95% of the surface, but since no corticosteroid was eluted under these conditions when methanol was replaced with THF, the effect of the modifier on retention of corticosteroids consists in the enhancement of the solvent strength of the mobile phase rather than deactivation of the active sites on the silica support.

The capacity factor of every corticosteroid decreased two- to fourfold with a 1.8-fold increase in methanol concentrations over the range 9.1–16.7% v/v. All solutes were eluted within 5 min using carbon

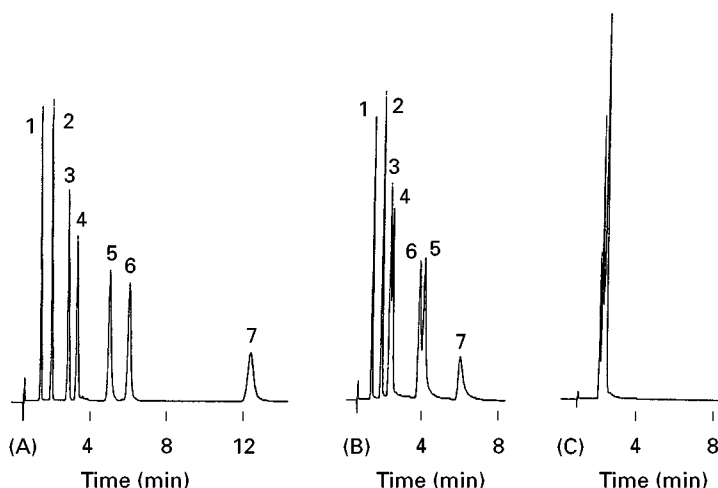


Figure 3 Effect of column on retention of corticosteroids. (A) Cosmosil NH₂; (B) Ultron VX-SIL; (C) Zorbax phenyl. Operating conditions: mean pressure 213 kg cm⁻², flow rate of CO₂ 3 mL min⁻¹, flow rate of methanol 0.4 mL min⁻¹, temperature 40°C. Peaks: as in Figure 1.

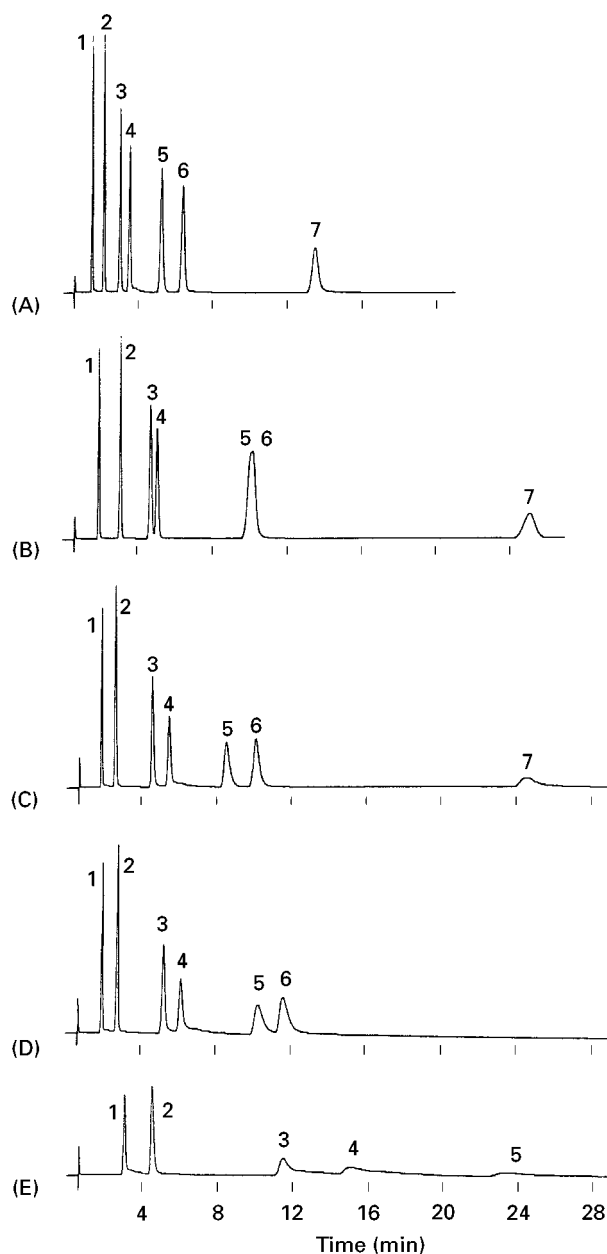


Figure 4 Effect of modifiers on retention of corticosteroids. (A) Methanol; (B) ethanol (95%); (C) ethanol (99.5%); (D) 1-propanol; (E) 2-propanol. Operating conditions: column Cosmosil 5NH₂, inlet pressure 224 kg cm⁻², outlet pressure 191 kg cm⁻², flow rate of CO₂ 3 mL min⁻¹, flow rate of modifier 0.4 mL min⁻¹, temperature 40°C. Peaks: as in Figure 1.

dioxide modified with 16.7% (v/v), and the resolutions among them were more than 1.6.

Calculated relative standard deviations (RSD) of 0.35–0.70% for t_R , 0.82–1.47% for k and 0.50–1.34% for peak area are shown in Table 1, indicate that the pSFC modified from a commercial HPLC system has a good performance and is useful for a routine analysis.

Pressure

In a study of seven corticosteroids, the capacity factor of each solute decreased by a factor of two with an increase in the range of 107–223 kg cm⁻². A few researchers have measured the densities of modified supercritical fluids experimentally. Berger measured the density of binary fluids using a U tube densitometer and drew the constant density lines in plots of the pressure against the composition for methanol–carbon dioxide system at three temperatures. The densities of CO₂–methanol (12%, v/v) at different pressures can be calculated by extrapolating the lines in the pressure range 105–180 bar. The plots of $\ln k$ against the binary fluid density revealed that there is a linear relationship between them in SFC, as expected.

Except for fluocinonide, theoretical plate numbers (N) reached maximum values at 126 and 144 kg cm⁻², as shown in Figure 5. The maximum N values were *c.* 4700–9800. Corresponding to the behaviour of the N values, the resolutions between the adjacent solutes also showed a maximum at 126–162 kg cm⁻². Since the mass flow rate was kept constant, the linear velocity varied with pressure. The minimum plate height was obtained in this pressure range. These results reveal that pressure is one of the significant parameters for optimizing the operating conditions.

Temperature

The retention of corticosteroids increases with an increase in the temperature (decrease in the density). The N values of each solute also increase with temperature as shown in Figure 6, and reach maximum values at 39 or 49°C, with the exception of hydrocortisone. The maximum N value for triamcinolone is *c.* 8400 at 39°C but only *c.* 3200 at 58°C, corresponding to about a 60% decrease. Although little variation in the separation factor (α) of any pair of neighbouring solutes was observed over the wide range of temperature measured, resolution reached maximum values at 39–49°C, corresponding to the behaviour of the N values. The critical temperature and pressure

Table 1 Repeatability (RSD%, $n = 6$)

Corticosteroids	t_R (min)	k	Peak area
Fluocinonide	0.37	1.15	1.01
Dexamethasone acetate	0.35	1.10	0.75
Triamcinolone acetonide	0.49	1.39	1.08
Fluocinolone acetonide	0.60	1.47	1.34
Hydrocortisone	0.64	1.39	0.67
Betamethasone	0.70	1.39	1.09
Triamcinolone	0.45	0.82	0.50

Operating conditions as in Figure 3.

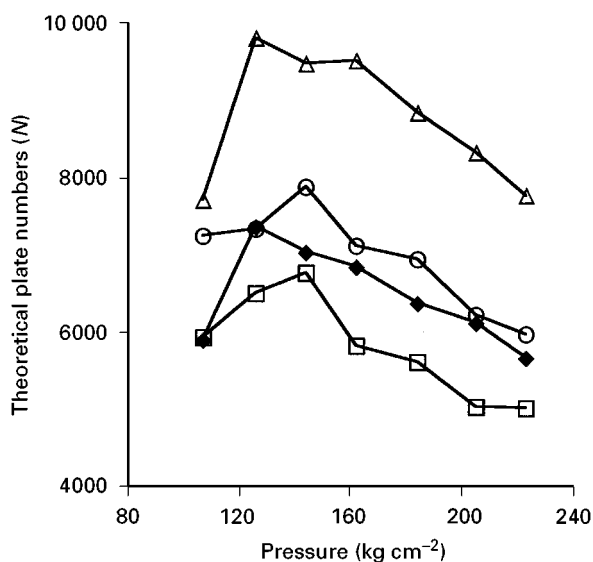


Figure 5 Relationship between theoretical plate numbers and pressure. Operating conditions: mean pressure 107, 126, 144, 162, 184, 205 and 223 kg cm⁻²; other conditions as in Figure 4. Symbols: squares, hydrocortisone; diamonds, fluocinolone acetate; circles, betamethasone; triangles, triamcinolone.

were reported to be 36.85°C and 80 bar and 50°C and 95 bar for 2% methanol and 16% methanol in carbon dioxide, respectively. So, the critical temperature for 12% methanol in carbon dioxide, which we used as the mobile phase, can be assumed to be in the range of 40–50°C: the maximum

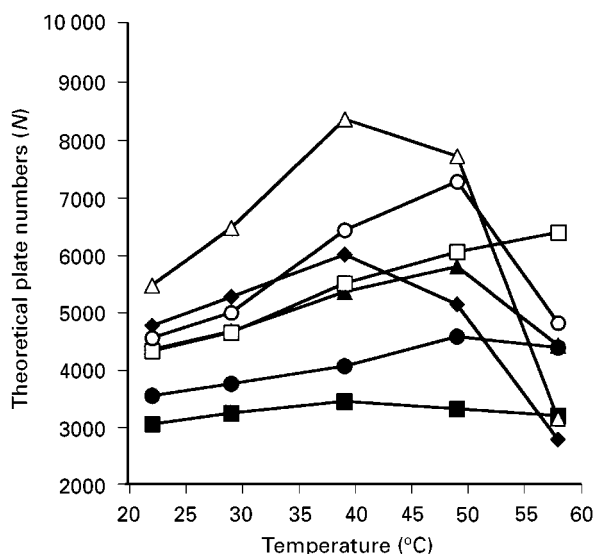


Figure 6 Relationship between theoretical plate numbers and temperature. Operating conditions: temperature 22, 29, 39, 49 and 58°C, mean pressure 213 kg cm⁻², other conditions as in Figure 4. Symbols: filled squares, fluocinolone; filled circles, dexamethasone acetate; filled triangles, triamcinolone acetate; diamonds, fluocinolone acetate; open squares, hydrocortisone; open circles, betamethasone; open triangles, triamcinolone.

N and resolution were obtained around the critical temperature.

Separation with Modifier Gradient

A wide range of polar corticosteroids has been separated in a modifier gradient elution mode. As shown in Figure 7, all solutes were eluted within 6.5 min by increasing the methanol content from 11.8% (v/v) to 17.0% (v/v) at 0.52% (v/v) per min, and keeping the CO₂ flow rate constant. Good peak shapes, completely baseline separated, were observed. The stable baseline without drift and noise is considered to be due to the good mixing process of the binary fluid. In pSFC, a modifier gradient is one of the most effective techniques for the analysis of polar steroids.

Comparison with HPLC

The retention of a wide range of corticosteroids by pSFC using an aminopropyl silica column has been compared with that in normal and reversed-phase

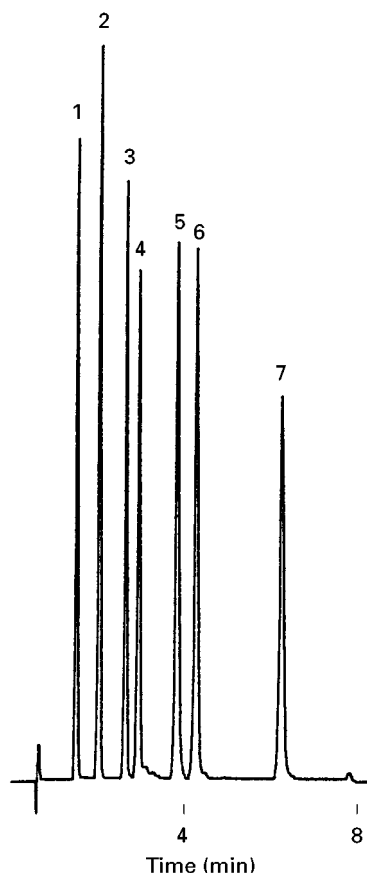


Figure 7 Gradient elution of corticosteroids. Operating conditions: column Cosmosil 5NH₂, flow rate of CO₂ 3 mL min⁻¹, methanol gradient 11.8–17.0% (v/v) at 0.52% (v/v) per min, mean pressure 206 kg cm⁻², temperature 40°C. Peaks: as in Figure 1.

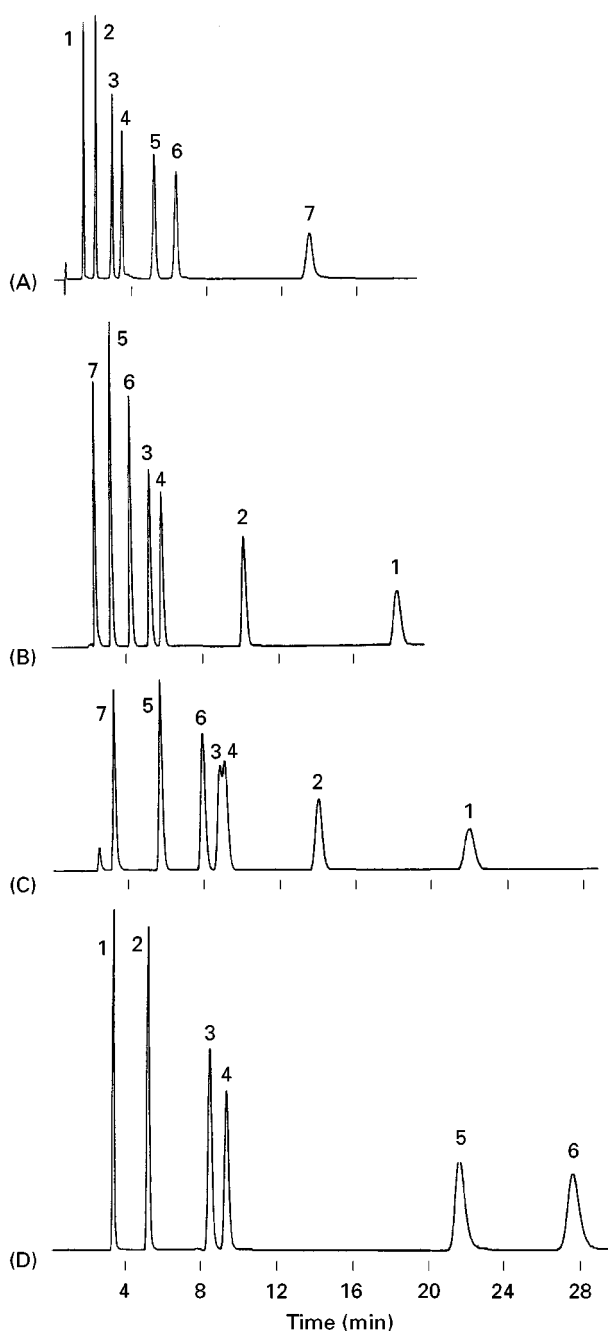


Figure 8 Chromatograms of corticosteroids. (A) Packed-column SFC; operating conditions as in Figure 3; (B) reversed-phase-HPLC (40% acetonitrile); (C) reversed-phase-HPLC (55% methanol); (D) normal-phase-HPLC. Peaks: as in Figure 1.

HPLC. The observed chromatograms are shown in Figure 8. Since the most polar corticosteroid among the analytes, triamcinolone, was not dissolved in the mobile phase, it could not be eluted in the normal-phase mode. The elution order of corticosteroids in pSFC is the same as that in normal-phase HPLC and is mainly determined by the number of hydroxyl groups present in the compound: firstly, fluocinonide with a single OH

group; dexamethasone acetate, triamcinolone acetonide and fluocinolone acetonide with two OH groups; then hydrocortisone and betamethasone with three OH groups; and finally triamcinolone, with four OH groups. Corticosteroids are eluted almost in reversed order in reversed-phase HPLC, but it is noteworthy that the pairs of triamcinolone acetonide and fluocinolone acetonide, and hydrocortisone and betamethasone are eluted in the same order as in pSFC.

The elution order of these compounds with the same number of OH groups seems to be closely related to their dipole moment. The estimated dipole moments were 1.19 and 2.04 debye for triamcinolone acetonide and fluocinolone acetonide, and 0.52 and 2.24 debye for hydrocortisone and betamethasone.

A similar range of *N* values was obtained in each chromatographic mode, i.e. *c.* 3600–8000 in pSFC, *c.* 4800–8700 in normal-phase HPLC and *c.* 2300–11 000 in reversed-phase HPLC. The separation of triamcinolone acetonide and fluocinolone acetonide, which show the lowest resolution and the same elution order in the normal- and reversed-phase systems, are comparable. The resolution of these solutes is 2.73 by pSFC, 2.04 by normal-phase HPLC, 0.53 by reversed-phase HPLC with a methanol mixture, mobile phase, and 2.20 by reversed-phase HPLC with an acetonitrile mixture, mobile phase. The elution time of all solutes in pSFC is about four times faster than in normal-phase HPLC and about 1.5 times faster than in reversed-phase HPLC.

These results suggest that the pSFC conditions used give a higher selectivity and better separation efficiency than normal-phase and reversed-phase HPLC for the analysis of corticosteroids which possess one to four hydroxyl groups.

Conclusion

PSFC is useful for the analysis of polar steroids, and its application as a rapid method for quality control and routine analysis can be expected in the future.

Acknowledgements

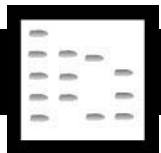
This article was adapted from Yaku K, Aoe K, Nishimura N, Sato T and Morishita F (1997) Retention behavior of synthetic corticosteroids in packed-column supercritical fluid chromatography. *Journal of Chromatography A* 773: 277–284. Copyright 1997, with kind permission from Elsevier Science.

Further Reading

Anton K and Berger C (eds) (1998) *Supercritical Fluid Chromatography with Packed Columns – Techniques*

- and Applications. Chromatographic Science Series, vol. 75. New York: Marcel Dekker.
- Charpentier BA and Sevenants MR (eds) (1988) *Supercritical Fluid Extraction and Chromatography – Techniques and Applications*. ACS Symposium Series 366. Washington, DC: American Chemical Society.
- Chester TL, Pinkston JD and Raynie DE (1994) Supercritical fluid chromatography and extraction. *Analytical Chemistry* 66: 106R.
- Gere DR (1983) Supercritical fluid chromatography. *Science* 222: 253.
- Smith RM (ed.) (1988) *Supercritical Fluid Chromatography*. RSC Chromatography Monographs Series. London: Royal Society of Chemistry.
- Smith RM and Hawthorne SB (eds) (1997) Supercritical fluids in chromatography and extraction (complete in one issue). *Journal of Chromatography A* 785.

STEROLS



Supercritical Fluid Chromatography

F. J. Señoráns, Universidad Autónoma de Madrid, Spain

K. E. Markides, Uppsala University, Uppsala, Sweden

Copyright © 2000 Academic Press

Introduction

In supercritical fluid chromatography (SFC) the mobile phase is a fluid subjected to pressures and temperatures near or above its critical point. This fact determines the mobile phase properties (e.g. diffusivity, density, viscosity, etc.) that are intermediate between those of gases and liquids and can be varied and controlled by small changes in the pressure or temperature. The most common fluid used in SFC is carbon dioxide, which has a critical temperature of 31°C, allowing the separation of thermally labile compounds under mild conditions. SFC can be carried out with open tubular and packed columns, with differences in selectivity, detection and need of modifier addition to the carbon dioxide. Both types have been employed in the separation of sterols in a wide variety of samples. Supercritical carbon dioxide has an adequate solvating power for sterol separation with both column types without the need of modifier addition. It is therefore possible to separate sterols in complex samples at lower temperatures than gas chromatography and in shorter times than liquid chromatography.

Importance of the Analysis of Sterols

The analysis of sterols is of great significance from the health point of view and for the quality control of numerous food products.

With respect to quality control of food and nutrition studies, the sterols of vegetable origin (phyto-

sterols) are found in complex mixtures in numerous plants, with the mixture containing some major sterols and a great variety of minor compounds (Figure 1). Thus, the sterol profile can be indicative of the origin, or species or variety of food from vascular plants, as well as from fungi or marine organisms. Additionally, these compounds are fundamental in the study of several metabolic pathways.

In the animal world, the variety of sterols is not so broad, and the main constituents are cholesterol and derivative esters. For that reason, supercritical carbon dioxide has been employed for the selective extraction of cholesterol from meat products and edible animal fats, to obtain healthier food for human intake.

On the other hand, some sterol oxides (oxysterols) are known for their toxicity, mutagenicity or carcinogenic properties, a fact that makes the determination of their concentrations in natural matrices very necessary, especially in studies of food quality and physiology.

Characteristics of the Separation of Sterols Using Supercritical Fluids

The main properties of supercritical fluid chromatography which affect sterol separation are related to the high solvating power of supercritical fluids and a low viscosity, which yields a high resolving power and rapid throughput. In addition to its other advantages, the ability of SFC to resolve complex mixtures of low volatility compounds allows the direct injection of samples that contain sterols with no or little pretreatment.

Some sterols can be degraded or lost during exposure to light, heat or extreme values of pH. In the SFC of sterols, all these factors can be avoided, providing a separation under mild conditions that preserves the integrity of the sample.

Finally, the relatively good solubility of compounds with intermediate polarity and volatility such as the sterols has also frequently been utilized in

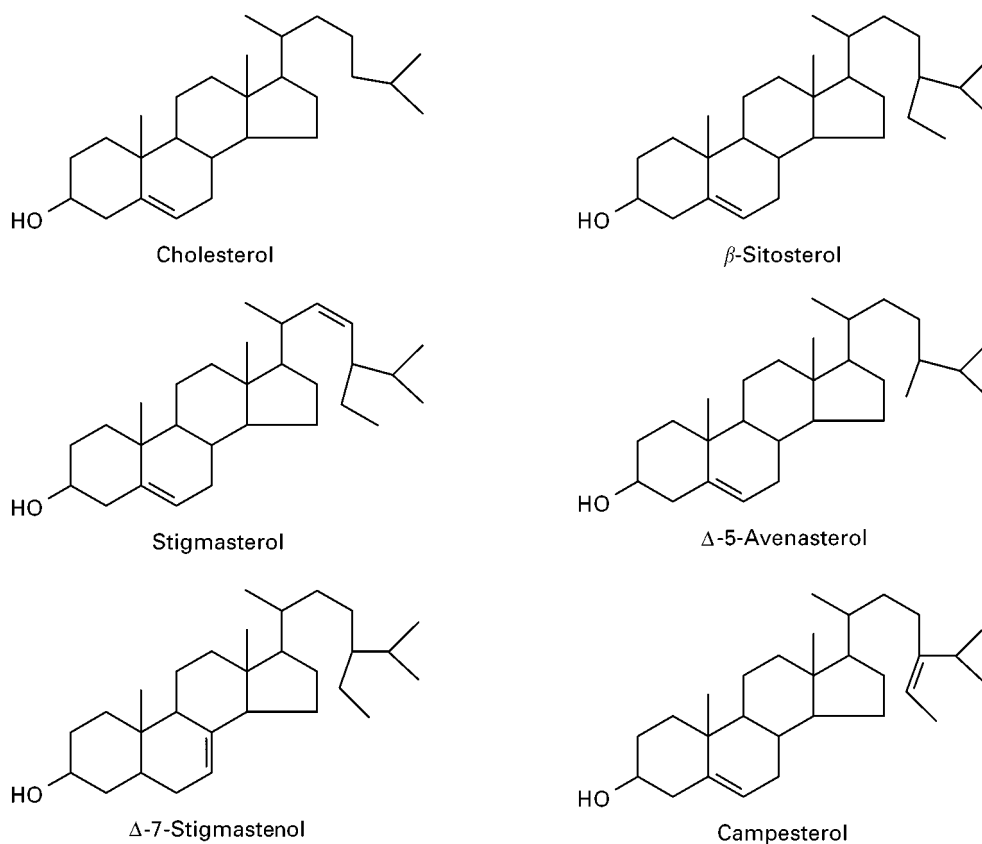


Figure 1 Structures of the main sterols analysed by SFC.

supercritical fluid extraction (SFE) for sample fractionation of the sterols from complex matrices, creating new possibilities for the use of supercritical fluids in multidimensional systems. The solubilities and chromatographic data of the main sterols in supercritical carbon dioxide are well known, and can be found in various books and review articles (see Further Reading).

Isolation of Sterol Subclasses and Sample Preparation

The determination of the sterol fraction in complex matrices such as food provides valuable information on the quality of the product, as well as its purity, origin and plant variety. This analysis presents some difficulties owing to the complexity of the matrix and the relatively low concentration of the sterols in these samples. The most widely used method includes a solvent extraction of the lipid material and isolation of the sterolic fraction, usually after removing the triglycerides through saponification of the lipids and subsequent extraction of the unsaponifiable matter with an organic solvent.

This unsaponifiable fraction contains the sterols and other minor components, such as tocopherols,

terpenic alcohols, and hydrocarbons, and therefore often needs to be fractionated. This is conventionally performed by thin-layer chromatography or by solid-phase extraction, prior to high resolution chromatographic analysis.

When the objective is to separate many individual sterols, there is an additional fractionation of the unsaponifiable components after the extraction and sample pretreatment, to isolate the main sterol subclasses (i.e. 4,4-dimethylsterols, 4-methylsterols and 4,4-desmethylsterols, and their esters, oxides and other derivatives), and before the separation of the individual sterols of the subclass of interest. This last fractionation is usually carried out by open column liquid chromatography, thin-layer chromatography, high performance liquid chromatography or more recently supercritical fluid chromatography, after which the sterols can be injected in a gas chromatograph, with or without derivatization.

This whole procedure including saponification, extraction and fractionation is not only time consuming and error prone, and may degrade labile sterols creating artefacts. Consequently, new approaches have been developed in the last few years that avoid several or all these steps by using multidimensional systems or even direct injection into a SFC column.

SFC in Multidimensional Systems

Multidimensional systems take advantages of two different chromatographic separations with complementary characteristics, e.g. one extraction stage and one chromatographic stage. The first step is aimed at producing a clean and undiluted sample containing the fraction of interest, and the second provides a high resolution separation of the target analytes.

It is often the case in chromatography that the largest source of error in the quantitative analysis of sterols and the most time-consuming part of the analytical method is the sample preparation and extraction stage. The main advantages of online systems is that they provide a fast and easily automated sample preparation procedure which reduces or avoids many of the errors of manual extraction. Also, less solvent consumption gives reduced exposure, toxic hazards and lower disposal cost.

The online methods applied to sterol analysis have conventionally consisted in the direct coupling of normal or reversed phase liquid chromatography with capillary gas chromatography (LC-GC), which allows the isolation of the sterolic fraction by LC, followed by online transfer to the gaseous separation in a fast and effective way. An alternative approach is to use packed columns to isolate the sterolic fraction by SFC, as shown recently by Medvedovici *et al.* in 1997, who used a conventional packed column (20 cm \times 4.6 mm) with aminopropylsilica gel as stationary phase, for further analysis by capillary gas chromatography-mass spectrometry. This approach can replace the classical preparation methods, yielding a much shorter time with good reproducibility, and it can be automated.

A more interesting approach is the online coupling of SFE and SFC, that allows the transfer of the solutes from the solid matrix to the chromatograph, reducing solvent usage and the need for sample clean-up. This technique has been applied to the separation in open tubular columns of cholesterol in food, and may prove to be of great importance in the future, with the use of packed column SFC; such columns have a large sample capacity and shorter analysis time.

The use of SFC in multidimensional chromatographic systems has a number of advantages. The most common multidimensional system to date, LC-GC, is limited to the determination of thermally stable and volatile solutes, but SFC can replace either the first step (fractionation), or the second step (high resolution chromatography), or even both. In the case of SFE-SFC, the transfer is performed without changes in the mobile phase providing less risk of loss of analytes.

Direct Introduction in SFC

While the analysis of sterol esters does not present difficulties by gas chromatography, a sample preparation step is needed however to remove the fatty material, in order to minimize interferences and protect the GC system. In many cases, the advantage of SFC is that the untreated sample can be injected directly onto a packed column allowing estimation of several lipid fractions at the same time.

Another approach consists in the use of SFC either for fractionation of the oil or for direct selective analysis of the sterol composition of the sample, without previous treatment. This direct injection is a particularly promising technique, and has been applied to the analysis of oils from marine sources to obtain fingerprints of different oil compositions, taking advantage of the very simple sample preparation requirements of SFC.

Separation of Individual Sterols

For the determination of individual sterols, SFC provides the same resolution as gas chromatography and short run times, at temperatures as low as 50–80°C in packed column SFC.

A particular problem is the detection system. Simultaneous detection of many sterols is difficult with ultraviolet detection, as some of the sterols do not possess high absorptivity. Hence this detection mode must often be combined with others to provide a comprehensive detection capability. For this reason, the most usual detection systems for sterol determination are flame ionization detector (FID) or mass spectrometry, which can easily be used with either gas chromatography or SFC.

Separations of sterols have been performed by open tubular column SFC, in samples such as soybean oil derivatives or commercial antioxidant mixtures. Other compounds of interest such as tocopherols, squalene, or even di- and triglycerides can be determined simultaneously (see Table 1). (Note that Table 1 is not intended to be a comprehensive review, but aims to provide general information on selected applications.)

Although the most common method for the SFC of free sterols is to employ open tubular columns, separations of sterol-related compounds have also been achieved with columns having different packing materials, ranging from pure silica, to phenyl-, diol-, amino-, or octadecyl-modified silica. For packed columns, the peak symmetry is improved and the retention times of the sterols are shortened when a modifier is added to the mobile phase. This moderates the influence of the free silanol groups of the silica and is analogous to the end-capping of an HPLC silica-based

Table 1 Determination of individual sterols by supercritical fluid chromatography

Column type	Sample	Identified compounds	Detector	Reference
Open tubular 10 m × 50 µm i.d. SB methyl 100	Hamster faeces	Free sterols Sterol esters	FID	Pinkston <i>et al.</i> (1991) <i>Journal of High Resolution Chromatography</i> 14: 401–406
Open tubular 10 m × 100 µm i.d. SB-octyl-50	Soybean oil deodorizer distillate	Free sterols	FID MS/EI	Synder <i>et al.</i> (1993) <i>Journal of the American Oil Chemists Society</i> 70: 349–354
Open tubular 10 m × 50 µm i.d. SB phenyl 5, 0.25 µm film	Soybean oil condensate	Four sterols, Three tocopherols	FID	Galuba and Gogolewski (1997) <i>Chemia Analityczna</i> 42: 245–248

EI, electron impact; MS, mass spectrometer.

stationary phase. In general, the separation of the sterols in SFC is affected by parameters such as the number, location, nature and conformation of the functional groups present in the molecules.

One special case is the determination of cholesterol, which is very often performed on samples with few or no other sterols and where the main objective is to separate this analyte from other non-sterolic

lipids and minimize the sample preparation, as will be discussed below.

Determination of Cholesterol and Cholesteryl Esters

In the last few years, the relationship between plasma cholesterol levels and the risk of atherosclerosis and

Table 2 Determination of cholesterol by supercritical fluid chromatography

Column type	Sample	Studied analytes	Detector	Reference
Packed column 250 mm × 4.6 mm i.d. particle size 5 µm Kaseisorb ODS-300-5	Human serum	Cholesterol Cholesteryl esters	UV and FID	Nomura <i>et al.</i> (1993) <i>Analytical Chemistry</i> 65: 1994–1997
Open tubular 10 m × 50 µm i.d. SB-octyl-50, 0.25 µm film	Human serum	Cholesterol Cholesteryl esters	FID	Kim <i>et al.</i> (1994) <i>Journal of Chromatography B</i> 655: 1–8
Open tubular 20 m × 50 µm i.d. SB phenyl 5	Milk fat	Cholesterol	FID	Huber <i>et al.</i> (1995) <i>Journal of Chromatography A</i> 715: 333–336
Open tubular 20 m × 100 µm i.d. DB-5	Fish oils	Cholesterol Other lipids	FID	Staby <i>et al.</i> (1994) <i>Journal of the American Oil Chemists Society</i> 71: 355–359
Open tubular 20 m × 100 µm i.d. DB-5, 0.4 µm film	Marine oils	Cholesterol Cholesteryl esters	FID	Staby <i>et al.</i> (1994) <i>Chromatographia</i> 39: 697–705
Open tubular 25 m × 100 µm i.d. DB-5, 0.1 µm film	Fish and shark oils	Cholesterol Cholesteryl esters Other lipids	FID	Borch-Jensen and Mollerup (1996) <i>Chromatographia</i> 42: 252–258
Open tubular 20 m × 100 µm i.d. DB-5, 0.1 µm film	Shark liver oils	Cholesterol Cholesteryl esters Other lipids	FID	Borch-Jensen <i>et al.</i> (1997) <i>Journal of the American Oil Chemists Society</i> 74: 497–503

coronary heart disease has been confirmed, resulting in an increase in concern about dietary and blood cholesterol levels. As a consequence, the determination of serum cholesterol is one of the most frequent clinical diagnostic measurements currently undertaken. It is usually performed after hydrolysis, quantifying the total cholesterol by routine enzymatic or colorimetric methods. In many cases, it would be more useful to separately determine free sterols and cholesteryl esters in serum to provide more complete clinical information. This analysis can be carried out by SFC at low temperature, without saponification or derivatization (see Table 2). (Again, Table 2 is not a comprehensive review but aims to provide general information on selected applications.) The determination of individual cholesteryl esters cannot be performed by the enzymatic methods available, while gas chromatography requires high temperature to elute the high-molecular-mass unsaturated esters, causing thermal decomposition. Moreover, the detection of cholesterol and related compounds is not very sensitive in HPLC with ultraviolet detection, since free sterols generally have low absorption coefficients. These problems are avoided with SFC in com-

bination with the highly sensitive FID or with mass spectrometry.

Cholesterol Analysis in Human Serum

The analysis of cholesterol in human serum has been performed with both open tubular and packed column SFC, at temperatures of 65 and 45°C, respectively. With open tubular columns, it is possible to determine quantitatively free, total and individual esterified cholesterol with a simple liquid-liquid extraction without derivatization. The use of FID gives detection limits of 4–6 pg. The quantitative results for the analysis of total cholesterol in reference sera and real samples show good agreement between the SFC, GC (with derivatization), and enzymatic methods.

With columns packed with inert octadecylsilica, there is no need to add any modifier to the carbon dioxide, allowing the simultaneous use of ultraviolet and FID. In addition, the use of carbon dioxide as the supercritical fluid allows ultraviolet detection at wavelengths as low as 190 nm, which are usually below the practical limit with HPLC because of the general absorption of most solvents at this

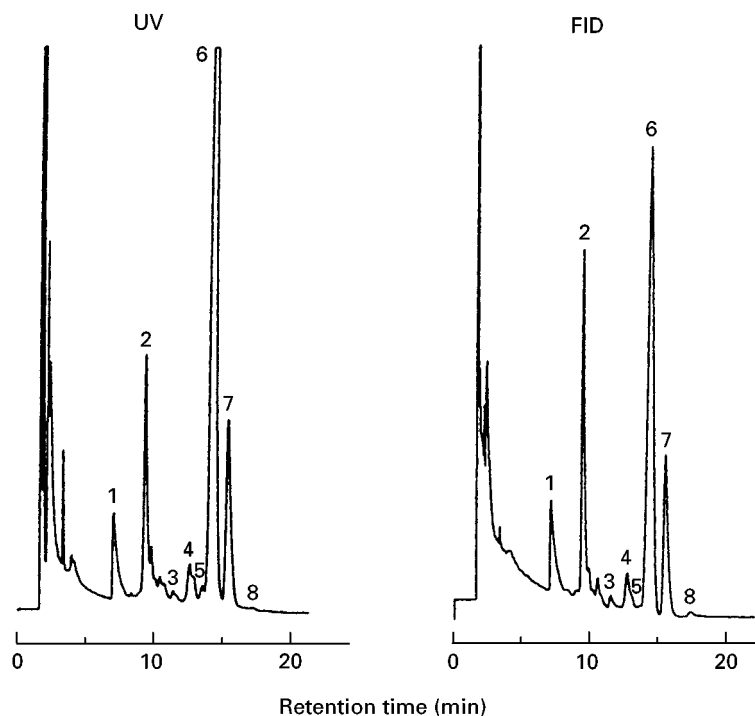


Figure 2 Chromatograms of cholesterol and cholesteryl esters from human serum reference material with ultraviolet (UV) (wavelength 190 nm) and flame ionization detection (FID). Peak identification: (1) cholesterol, (2) cholesteryl laurate (internal standard), (3) cholesteryl myristate, (4) cholesteryl palmitoleate, (5) cholesteryl linolenate, (6) cholesteryl palmitate + cholesteryl linoleate + cholesteryl arachidonate, (7) cholesteryl oleate, (8) cholesteryl stearate. Chromatographic conditions: reversed-phase HPLC column (250 mm × 4.6 mm i.d.; particle size, 5 μm), column temperature 45°C, CO₂ pressure 200 atm, CO₂ flow rate 750 mL min⁻¹ at room temperature under 760 mmHg. (Reproduced from Nomura *et al.* (1993) *Analytical Chemistry* 65: 1994–1997, with kind permission from the authors and the publisher. Copyright 1993 American Chemical Society.)

wavelength. Use of lower wavelengths in ultraviolet detection results in a greater sensitivity than higher wavelengths for all cholesterol and cholesteryl esters. Both ultraviolet and FID showed good agreement in a study of cholesterol and their esters, with a detection limit of 20 ng for cholesterol and cholesteryl palmitate, though better reproducibility was obtained with UV detection (Figure 2).

Supercritical fluid chromatography can be a useful tool in studies on cholesterol and cholesteryl ester metabolism in serum and biological fluids in general, though some improvements in the selectivity are still needed to properly resolve some difficult pairs of sterol esters.

Cholesterol Analysis in Edible Oils

There are numerous applications of SFC with capillary columns for the determination of components of oils of marine animals especially from Møllerup's group at the Technical University of Denmark (see Table 2). In these samples, numerous lipids have been analysed including cholesterol and its esters, together with vitamin E, squalene, and di- and triglycerides. Open tubular column SFC is therefore very convenient for these complex samples owing to its high resolution and relatively low analysis temperature (150–170°C versus 250–300°C for GC). For example, the analysis of cholesterol and cholesteryl esters in seafood, shark liver, seal and other fish oils has been accomplished with open tubular column SFC both with direct injection of the diluted oil and with previous saponification and fractionation by thin-layer chromatography (see Table 2). The latter purification avoids the overloading of the open tubular columns (100 µm internal diameter) by the squalene that is present in high concentrations in these samples. Saponification followed by fractionation is, however, time consuming and the recovery of minor components can be difficult. With direct injection in SFC, simultaneous determination of cholesterol, triglycerides and other lipids has been achieved, with enhanced separation power compared with HPLC, while gas chromatography always requires sample pretreatment of these oils to ensure chemical stability at high temperatures.

In other solid and more heterogeneous foods, sample preparation is the most time-consuming step in the routine determination of, for instance, cholesterol levels in daily diet and remains the largest source of error in the quantitative analysis of sterols.

Future Trends

Current developments in new types of columns, equipment and detectors for SFC show that this technique is still developing and expanding and will

achieve greater use in the future, particularly with the advent of new chromatographs for packed capillary columns and with automation of modifier addition, which will be very valuable in the determination of more polar sterols and their oxides in samples where high resolution and mild conditions are imperative.

Another important development is the more frequent use of solvents under subcritical conditions which, in practice, is eliminating the rather artificial boundary between SFC and liquid chromatography.

One of the main advantages of using packed capillary columns over conventional packed columns is the improved performance when this separation is coupled to mass spectrometry, thus providing structural determination of the sterols. This is expected to be especially important in the coming years owing to the development of new commercial equipment for SFC-MS.

Another potential source of improvement is the use of new detectors with higher sensitivity than ultraviolet but compatible with the use of modifiers in packed capillary column SFC. The amperometric detector is a good example.

These anticipated developments in SFC technology will be important in the field of sterol analysis, though an automated SFE-SFC without tedious sample preparation and large solvent consumption would be one of the most valuable future developments for sterol analysis.

Further Reading

- Berg BE, Lund HS and Greibrokk T (1997) Separation and quantification of components of edible fat utilizing open tubular column in SFC. Sample introduction by direct injection and SFE coupled on-line to SFC. *Chromatographia* 44: 399–404.
- Chester TL (1996) Supercritical fluid chromatography for the analysis of oleochemicals. In: King JW and List GR (eds) *Supercritical Fluid Technology in Oil and Lipid Chemistry*. Champaign, Illinois: AOCS Press.
- Heupel RC (1989) Isolation and primary characterization of sterols. In: Nes WD and Parish EJ (eds) *Analysis of Sterols and Other Biologically Significant Steroids*. San Diego, California: Academic Press.
- Hoving EB (1995) Review. Chromatographic methods in the analysis of cholesterol and related lipids. *Journal of Chromatography B* 671: 341–362.
- Jinno K (ed.) (1992) *Hyphenated Techniques in Supercritical Fluid Chromatography and Extraction*. Amsterdam: Elsevier.
- Lee ML and Markides KE (eds) (1990) *Analytical Supercritical Fluid Chromatography and Extraction*. Provo, Utah: Chromatography Conferences.
- Medvedovici A, David F and Sandra P (1997) Analysis of sterols in vegetable oils using off-line SFC/capillary GC-MS. *Chromatographia* 44: 37–42.

Staby A and Mollerup J (1993) Separation of constituents of fish oil using supercritical fluids: a review of experimental solubility, extraction and chromatographic data. *Fluid Phase Equilibria* 91: 349–396.

Xie LQ, Markides KE, Lee ML, Hollenberg NK, Williams GH and Graves SW (1993) Bioanalytical application of multidimensional open tubular column supercritical fluid chromatography. *Chromatographia* 35: 363–371.

Thin-Layer (Planar) Chromatography

J. Novaković, PRO.MED.CS, Prague,
Czech Republic

K. Nesměrál, Charles University, Prague,
Czech Republic

Copyright © 2000 Academic Press

Sterols are steroid compounds widely distributed in various biological materials, e.g. variety plant and animal lipids, medications, food and dietary supplements. They are basic metabolites in living organisms and they are also precursors of a variety of bile acids, provitamins and steroid hormones. Therefore the analysis of sterols is important in biochemistry, medicine and pharmacy. There is considerable interest in the study of the relationship of plasma cholesterol concentrations to the risk of developing coronary artery disease. Determination of phytosterols and cholesterol is important for the diagnosis of phytosterolaemia and in dietary treatment of hypercholesterolaemia.

The collective name for sterols has been adopted for all naturally occurring crystalline unsaponifiable steroid alcohols. The basic sterol is 5 α -cholestane, and the structure numbering system for sterols are given in **Figure 1**. In general, these compounds are 3-monohydroxysteroids, having 27, 28 or 29 carbon atoms and nearly all have one or more double bonds. The double bond is most commonly found at position 5, with double bonds at C₇ and C₂₂ also being prevalent. Sterols are classified into five groups: cholesterol and its companions, zoosterols, phytosterols, mycosterols and vitamin D. Examples of sterols from each group are given in **Table 1**.

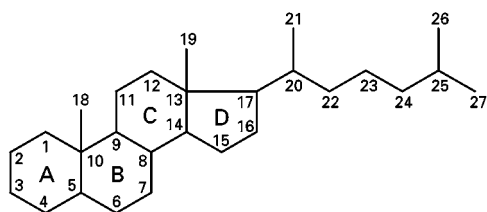


Figure 1 5 α -Cholestane skeleton and numbering system for sterols.

There are four principal methodologies used in sterol chromatography: gravity flow column liquid chromatography (GCC), high performance liquid chromatography (HPLC), gas chromatography (GC) and thin-layer chromatography (TLC). For its selectivity, sensitivity and efficiency, TLC is one of the most frequently employed procedures for the separation of sterols, both for their characterization and for their quantitative analysis.

Preparation of Sample

Since sterols are present in different materials, sample preparation is a very important part of their analysis.

The first step is an extraction procedure which is performed either directly on the previously deproteinized sample or after cleavage of any conjugates present. Diethyl ether, dichloromethane, ethyl acetate, chloroform and other medium polarity organic solvents can be used for extraction.

The next step is purification of the extract or, more exactly, separation of sterols from other lipids, usually by TLC on a silica gel G plate using an *n*-heptane–diethyl ether–acetic acid (85 : 15 : 1) mixture as the mobile phase. Under these conditions the cholesterol and phytosterols are concentrated in one band. Separation and quantitative analysis of individual sterols are performed after elution from the plate by GC, TLC or some other technique.

Some sterols (e.g. vitamin D) are sensitive to atmospheric oxygen, traces of acids and bases, light and heat. Therefore, all steps should be carried out in a cool place, protected from exposure to direct light, and only highly purified solvents should be used.

Stationary Phases and Solvent Systems

Generally, the chromatographic separation of individual sterols is difficult due to the large number of epimers and unsaturated isomers. Various forms of silica gel are most frequently used in the TLC of

Table 1 Examples of sterols

Number of carbon atoms	Trivial name	Systematic name	Group of sterols ^a
27	Vitamin D ₃ (cholecalciferol)	$\Delta^{5,7}$ -Cholestadiene-3 β -ol with open B-ring	5
	Cholesterol	Δ^5 -Cholestene-3 β -ol	1
	7-Dehydrocholesterol (provitamin D ₃)	$\Delta^{5,7}$ -Cholestadiene-3 β -ol	1
	Desmosterol	$\Delta^{5,24}$ -Cholestadiene-3 β -ol	2
28	Dihydrocholesterol	5 α -Cholestane-3 β -ol	1
	Brassicasterol	24- β -Methyl- $\Delta^{5,22}$ -cholestadiene-3 β -ol	3
	Campesterol	24- α -Methyl- Δ^5 -cholestene-3 β -ol	3
	Ergosterol (provitamin D ₂)	24- β -Methyl- $\Delta^{5,7,22}$ -cholestatriene-3 β -ol	3
	Fungisterol	24- β -Methyl- Δ^7 -5 α -cholestene-3 β -ol	4
	Vitamin D ₂ (ergocalciferol)	24- β -Methyl- $\Delta^{5,7,22}$ -cholestatriene-3 β -ol, with open B-ring	5
29	Dihydro- β -sitosterol	24- β -Ethyl-5 α -cholestane-3 β -ol	3
	β -Sitosterol	24- β -Ethyl- Δ^5 -cholestene-3 β -ol	3
	Stigmasterol	24- β -Ethyl- $\Delta^{5,22}$ -cholestadiene-3 β -ol	3
30	Lanosterol	4,4,14-Trimethyl- $\Delta^{8,24}$ -cholestadiene-3 β -ol	1

^aGroup of sterols: 1, cholesterol and its companions; 2, zoosterols; 3, phytosterols; 4, mycosterols; 5, vitamin D.

sterols; separation can be classified, according to the type of stationary phase, into four main groups: silica gel, silver nitrate silica gel, reversed-phase and bromine-system TLC.

Silica Gel TLC

The separation of individual sterols by adsorption chromatography on silica gel pre-coated plates is relatively easy when there are differences in the type, number, position or configuration of polar groups, but it is difficult in the absence of such differences.

The chromatographic properties of sterols on silica gel G plates using two solvent systems, benzene–diethyl ether (9 : 1) and benzene–diethyl ether (85 : 15) have been studied. The resulting R_F values are listed in Table 2. However, the separation of sterols with these systems is incomplete.

Table 2 Relative retentions of some sterols on silica gel G

Sterol	R_F value	
	System I	System II
Cholesterol	0.20	0.47
7-Dehydrocholesterol	0.19	
Desmosterol	0.20	0.46
Brassicasterol	0.20	
Ergosterol	0.19	0.43
Vitamin D ₂	0.19	
β -Sitosterol	0.20	
Stigmasterol	0.20	
Lanosterol	0.31	0.62

Stationary phase: silica gel G; mobile phase: (I) benzene–diethyl ether (9 : 1); (II) benzene–diethyl ether (85 : 15); visualization: sulfuric acid.

Date from Xu *et al.* (1988).

The separation of cholesterol and cholesterol esters from other lipid fractions on silica gel pre-coated plates using the following solvent systems: first, chloroform–methanol–water (65 : 25 : 4), second, *n*-hexane–acetone (100 : 1) and third, *n*-hexane–acetone (100 : 3) has also been reported. The plates are developed with the first solvent system to 8 cm from the origin. After drying, the plates are developed to 18 cm above the origin with either of the other solvent systems. Cholesterol and four cholesterol ester subfractions are separated from other lipid fractions.

Silica gel GF plates have been used to separate cholesterol, cholesteryl propionate and low molecular weight cholesteryl esters by one-stage one-dimensional TLC. This work employed four solvent systems, the best separation among cholesteryl formate, cholesteryl acetate and cholesteryl propionate was achieved using chloroform–diethyl ether–acetic acid–1-propionic acid (92 : 1.5 : 1 : 5 : 0.5).

The solvent systems used for the separation of eight 3 β -sterols of considerable biological interest, which differ only in ring B and/or in the side chain, on silica gel G pre-coated plates has also been investigated. The separation was performed using first, cyclohexane–ethyl acetate–water (600 : 400 : 1); second, cyclohexane–heptane (1 : 1), third, cyclohexane–ethyl acetate–water (1560 : 440 : 1), and fourth, isooctane–carbon tetrachloride (19 : 1). Differences in resolving power between polar and nonpolar systems were observed. Resolution of the pairs with saturated and unsaturated side chain β -sitosterol–stigmasterol and cholesterol–desmosterol was finally effected by a mixture of saturated hydrocarbons.

Separation of vitamin D from its close structural analogues, including provitamin D, irradiation

products of provitamin D and decomposition products, has been carried out on nonimpregnated layers of silica gel G with the solvent system cyclohexane–dichloroethane–diethyl ether (5 : 3 : 2). TLC has also been used for pre-purification of saponified samples before GC analysis as well as for their *in situ* quantitative analysis. Determination of the maximum permissible limit of concentration of ergosterol in ergocalciferol using silica gel G as the stationary phase with a cyclohexane–peroxide-free ether (1 : 1) mixture containing 0.1 g L⁻¹ butylhydroxytoluene is an official method in the European Pharmacopoeia 1997.

In general, monosaturated sterols like cholesterol, provitamin D (e.g. ergosterol) and vitamins D are separable, but closely related sterols like cholesterol, stigmasterol and β -sitosterol are not resolved on silica gel.

Silver Nitrate TLC (Argentation Chromatography)

Several methods have been published for separation of structurally related sterols. A procedure utilizing π -complex formation between Ag(I) ions and the double bonds occurring in various locations in the sterol molecules has been frequently applied. Argentation TLC is a method for separating compounds based on differences in number and position of double bonds in the molecule. In this case, silica gel is suspended in an aqueous solution of silver nitrate before spreading on the plate. Silver nitrate can also be sprayed on to a pre-prepared layer.

Argentation TLC of sterols has been thoroughly investigated. The R_s values (relative retention relating to cholesterol) of selected sterols and sterol acetates separated on silica gel G–silver nitrate pre-coated plates using the solvent systems chloroform–diethyl ether–acetic acid (97 : 2.3 : 0.5) and chloroform–light petroleum (b.p. 60–80°C)–acetic acid (25 : 75 : 0.5) are listed in Table 3.

Sterols that differ in the number and position of double bonds are clearly separated by means of silver nitrate TLC, but separation of cholesterol from the phytosterols was not achieved.

Reversed-phase TLC

One of the pioneer works on reversed-phase TLC (RP-TLC) used silica gel impregnated with paraffin oil as the stationary phase and methyl ethyl ketone as the mobile phase for the separation of lipids, including cholesterol esters. Kieselguhr G has been used following impregnation with undecane as the stationary phase with the solvent systems acetic acid–water (90 : 10) and acetic acid–water (92 : 8) for the separation of sterols and sterol acetates, respectively. R_s values of some sterols and sterol acetates obtained by RP-TLC are given in Table 4.

Table 3 Separation of sterols and sterol acetates on silica gel G–silver nitrate layers

Sterol	R_s value	
	System I (sterols)	System II (sterol acetates)
Cholesterol	\equiv 1.00	\equiv 1.00
7-Dehydrocholesterol	0.44	0.43 ^a
Dihydrocholesterol	1.14	1.25
Brassicasterol	0.98	0.68
Vitamin D ₂	0.64	
Dihydro- β -sitosterol	1.14	1.30
β -Sitosterol	1.00	1.00
Stigmasterol	0.98	0.87
Lanosterol	1.70	0.78

^aAfter two developments.

Stationary phase: silica gel G–silver nitrate. Mobile phase: (I) chloroform–diethyl ether–acetic acid (97 : 2.3 : 0.5); (II) chloroform–light petroleum (b.p. 60–80°C)–acetic acid (25 : 75 : 0.5). Visualization: dibromofluorescein.

Data from Copius-Peereboom and Beekes (1965).

The critical pair cholesterol–brassicasterol was not separated in these RP systems and RP-TLC separation according to the degree of unsaturation using the so-called bromine system was suggested (see below).

A good separation of the pairs vitamin D₂/D₃ and pre-vitamin D₂/D₃ on silica gel and Kieselguhr G impregnated with silicone oil eluted with acetone–water mixture has been achieved.

The Bromine System TLC

The separation of unsaturated sterols from their saturated analogues can be substantially improved by

Table 4 R_s values of some sterols and sterol acetates obtained in RP-TLC

Sterol	R_s value	
	System I (sterols)	System II (sterol acetates)
Cholesterol	\equiv 1.00	\equiv 1.00
7-Dehydrocholesterol	1.12	1.26
Dihydrocholesterol	0.90	0.89
Brassicasterol	1.00	1.00
β -Sitosterol	0.86	0.83
Stigmasterol	0.93	0.91
Lanosterol	0.84	0.97

Stationary phase: Kieselguhr G impregnated with undecane; mobile phase: (I) acetic acid–water (90 : 10); (II) acetic acid–water (92 : 8), visualization: phosphomolybdic acid.

Data from Copius-Peereboom JW and Beekes HW (1962). The analysis of mixtures of animal and vegetable fats. III. Separation of some sterols and sterol acetates by thin-layer chromatography. *Journal of Chromatography* 9: 316.

Table 5 R_s values of some sterols acetates in the bromine system TLC

<i>Sterol acetates</i>	R_s
Cholesterol	$\equiv 1.00$
7-Dehydrocholesterol	Front
Dihydrocholesterol	0.85
Brassicasterol	1.13
β -Sitosterol	0.82
Stigmasterol	1.06
Lanosterol	Front

Stationary phase: Kieselguhr G impregnated with undecane; mobile phase: acetic acid–acetonitrile (1 : 3) + 0.5% of bromine, visualization: antimony trichloride.

Data from Copius-Peereboom and Beekes (1965).

bromination. After spotting the sterol sample at the starting zone, some drops of bromine are spotted on the same place. The plate is then developed with a benzene–ethyl acetate mixture (2 : 1), by means of which the spots of cholesterol and dihydrocholesterol are separated. Thus, sterol acetates have been separated

on Kieselguhr G impregnated with undecane using solvent system acetic acid–acetonitrile (1 : 3) + 0.5% bromine. R_s values of some sterol acetates are given in Table 5.

Bromination of the double bonds before or during chromatography completely changes the mobilities of the unsaturated compounds, promoting their separation from the saturated derivatives. In this way the critical pair cholesterol–brassicasterol can be clearly separated.

Detection and Quantitation

Detection

Sterols that have UV absorbance can be detected at 254 nm (providing that TLC separation is performed on a layer with a fluorescent indicator). Since a number of sterols do not have UV absorbance suitable for detection, most applications still involve visualization based on chemical reactions. Visualization procedures used to detect and characterize sterols are well

Table 6 Detection procedures based on chemical reactions used in TLC analysis of sterols

<i>Detection reagent</i>	<i>Visualization procedure</i>	<i>Sterols</i>
<i>Acids</i>		
Perchloric acid (70%)	Spray	Vitamin D ₂
Phosphomolybdic acid (15% ethanolic solution)	Spray, heat at 110°C for 10 min	Various sterols
Sulfuric acid (conc. or 50%)	Spray, heat at 110°C for 15 min, observe in day and UV light before and after heating	C ₂₇ sterols, cholestane and lanostane series, ergosterol
<i>Metal salts</i>		
Antimony pentachloride (30% in chloroform)	Spray, heat at 120°C for 5 min	Various sterols
Antimony trichloride (50% in conc. acetic acid)	Spray, heat at 100°C for 10 min	Brominated sterols
Cadmium chloride (50% in 50% ethanol)	Spray, heat at 90°C for 15 min, observe in UV light	Brominated sterols, cholesteryl esters
Copper sulfate		Saturated species
Cupric acetate (3% in 8% phosphoric acid)	Spray, heat at 150°C for 30 min	Unsaturated species
<i>Aldehydes</i>		
<i>p</i> -Anisaldehyde (1% in acetic acid–sulfuric acid (98 : 2) mixture)	Spray, heat at 90°C for 10 min	Sterol and sterol acetates
Salicylaldehyde	Spray with pure salicylaldehyde, heat at 80°C for 5 min, spray with 0.5 mol L ⁻¹ sulfuric acid, heat again at 90°C for 10 min	Sterol and sterol acetates
Vanillin (0.5% in sulfuric acid–ethanol (4 : 1) mixture)	Spray, heat at 100°C for 5 min	Cholestanols and cholestanones
<i>Ketone reagents</i>		
2,4-Dinitrophenylhydrazine (5% in methanol)	Spray and spray again with conc. sulfuric acid	Ketonic sterols

established. Detection reagents can be classified into four groups: acids, metal salts, aldehydes and ketone reagents. The most frequently used detection procedures are listed in Table 6.

TLC coupled with flame ionization detection (TLC-FID) has been used to detect sterols. The separation is performed on specially prepared thin quartz rods coated with adsorbent sintered on to the surface of thin rods. The adsorbent is usually silica gel and the solvent system is basically the same as in classical TLC.

TLC-FID is a useful technique for the separation of cholesterol and its esters from other lipid classes. Separation of individual sterols, especially phytosterols (e.g. β -sitosterol, campesterol, brassicasterol, stigmasterol, etc.) using TLC-FID is not possible. On the other hand, groups of sterols differing in the number of methyl groups in position 4 (i.e. 4-demethylsterols, 4-methylsterols and 4,4-dimethylsterols) can easily be separated by TLC-FID.

The TLC separation of sterols is often used for preparative purposes. After elution from the plate, the sterols can be analysed by some other technique (spectrophotometry, fluorimetry, GC, GC-MS, HPLC), which is why it is sometimes necessary to visualize them using nondestructive reagents such as iodine vapour, water spray or fluorescent reagents (e.g. fluorescein, Rhodamine B). Fluorescent reagents can be incorporated in the slurry, during the preparation of the layer. An example of a nondestructive detection using radiolabelled [4- 14 C] cholesterol and cholesteryl [14 C]oleate added as internal standards has also been reported where desmosterol in monkey spermatozoa was separated on silica gel G. The free sterol band containing both cholesterol and desmosterol was detected, extracted from the plate and after, derivatization, analysed by GC.

Quantitative *in situ* Analysis

Due to progress in plate technology and instrumentation, modern TLC has become a comparable method to other chromatographic techniques in terms of accuracy, precision, reliability and repeatability. In modern TLC, the main steps are automated, including the sample application on the plate – the step considered the most critical for quantitative evaluation. Several examples of direct quantitation of sterols on TLC plate are discussed below.

Cholesterol ester mapping of human serum by high performance TLC (HPTLC) has been performed. Quantitative analysis was carried out at 546 nm after postchromatographic derivatization with phosphomolybdic acid. The densitogram of a standard mixture containing cholesterol esters is given in Figure 2.

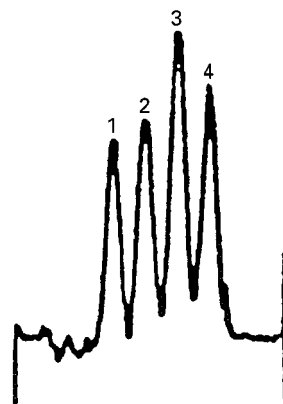


Figure 2 Densitogram of a standard mixture containing 33 ng of each cholesterol ester. 1, Cholesterol palmitate; 2, cholesterol oleate; 3, cholesterol linolate; 4, cholesterol linoleate. Separation was performed on HPTLC Kieselgel 60 F₂₅₄ (Merck) in carbon tetrachloride solvent system. (Reproduced with permission from Kovács *et al.*, 1989. Copyright 1989 American Association for the Advancement of Science.)

HPTLC silica gel plates and a dual solvent system, consisting of a run with isopropyl ether–acetic acid (96 : 4) followed by a run in the same direction with petroleum ether (b.p. 60–70°C)–diethyl ether–acetic acid (90 : 10 : 1) has been to determine cholesterol in egg yolk as well as in butter and cream samples. Cholesterol was detected with cupric acetate reagent, lipid zones were quantified by densitometry.

Quantitative measurement of free cholesterol in serum on a silica gel/sodium carboxymethylcellulose plate has also been reported. The solvent system was petroleum ether–ethyl acetate–glacial acetic acid (80 : 20 : 1). Spraying with vanillin was used for visualization. The colour of the cholesterol spot was stable for *c.* 20 min. *In situ* measurement was done by densitometry at 525 nm with a detection limit of 40 ng per spot. The peak area was linearly related to the amount of cholesterol over the range 80–700 ng per spot.

Cholesterol, cholesteryl esters and other neutral lipids have been analysed in plasma by TLC-FID. Separation was performed on Chromarods S with hexane–diethyl ether–formic acid (52 : 8 : 0.1).

Quantitative *in situ* analysis of vitamin D in cod liver oil has been demonstrated by measuring absorbance at 268 nm on silica gel layers after dual development (first with *n*-hexane, then with cyclohexane–diethyl ether (1 : 1) mixture). Vitamin D was also determined in foods and in human milk by *in situ* reflectance measurement.

TLC and Characterization of Sterols

The chromatographic behaviour of each compound depends on the stereochemistry and location of polar

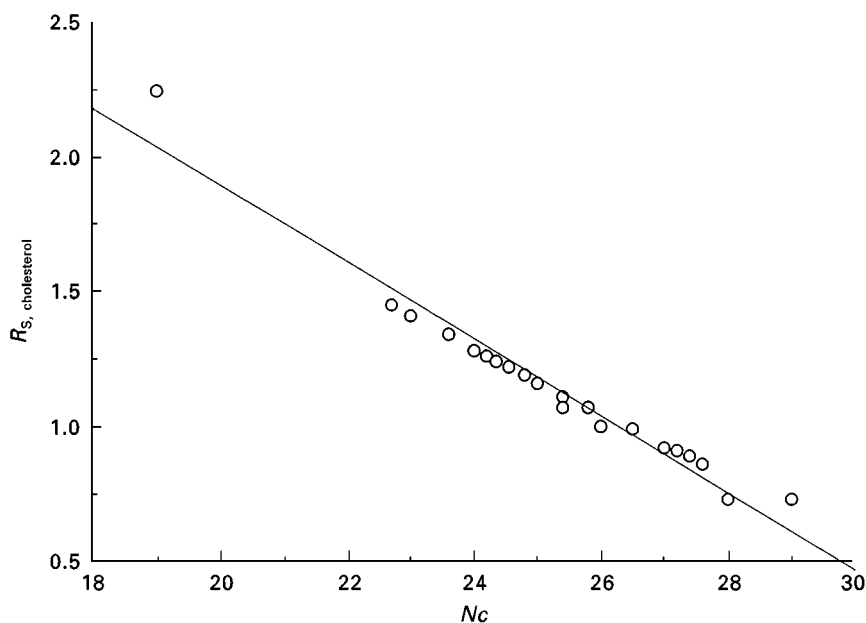


Figure 3 Relationship between R_S values and the carbon numbers for sterol acetates in RP-TLC; coefficient of linear correlation, $R = 0.9793$. Stationary phase: Kieselguhr G impregnated with undecane; mobile phase: acetic acid–acetonitrile (1 : 3). Nc = number of carbon atoms – number of double bonds. (Data from Copius-Peerboom and Beekes, 1965.)

substituents, the solubility, partition coefficients and equilibrium constants of the compound in the solvent system, the size and shape of the molecule and the degree of hydration. The quantitative structure–chromatographic retention relationship study between sterols, TLC mobilities and their structures has been investigated by several authors.

A separation of steroids according to the degree of unsaturation has been investigated. In structural analysis, argentation TLC and the bromine system can give information about the number and position of double bonds in a molecule. A linear relationship between the R_S value and carbon numbers (Nc = number of carbon atoms – number of double bonds) in the system undecane/acetic acid–acetonitrile (1 : 3) for saturated and Δ^5 -unsaturated sterols has been found. This linear relationship is shown in Figure 3.

Adsorption TLC is not only a method of sample purification, but the R_F value also provides a clue to the compound's structure. The structural feature that mostly contributes to the chromatographic behaviour of sterols in adsorption TLC is the presence of a free 3β -OH group. Converting the 3β -OH to an acetoxy, methoxy, keto, or 3α -OH results in a steroid with a less polar R_F value relative to the R_F value obtained for cholesterol.

Separation of individual cholesterol ester subfractions according to the sum of the carbon atoms and numbers of double bonds in their fatty acid moieties has been performed.

The elution order of vitamin D photoisomers can be correlated with the increasing planarity of the molecules. R_F values of vitamin D photoisomers on silica gel with solvent system cyclohexane–dichloroethane–diethyl ether (5 : 3 : 2) were 0.18 (pro-vitamin D_3), 0.23 (tachysterol₃), 0.27 (lumisterol₃) and 0.31 (pre-vitamin D_3).

A visualization procedure can give additional information about sterol structure, since different reagents produce different colours with individual sterols. Some reagents are specific for individual functional group (e.g. 2,4-dinitrophenylhydrazine for keto group).

Future Developments

A general tendency in modern TLC is separation on HPTLC stationary phases, online coupling with other separation techniques (e.g. HPLC-TLC), as well as online coupling with spectroscopic methods. *In situ* recording of UV-visible spectra is most commonly used. However, the recording of Fourier transform infrared, Raman or mass spectra is more informative. Although these combinations have frequently been reported in the literature, there is still no example of their application in the field of sterol analysis. Due to the great variety of chemically closely related sterols, online combination of TLC and spectroscopic methods can be considered a powerful tool for their isolation and *in situ* characterization.

See also: II/Chromatography: Thin-Layer (Planar): Densitometry and Image Analysis; Spray Reagents. III/Flame Ionization Detection: Thin-Layer (Planar) Chromatography. Impregnation Techniques: Thin-Layer (Planar) Chromatography. Silver Ion: Thin-Layer (Planar) Chromatography. Sterols: Supercritical Fluid Chromatography.

Further Reading

- Bennett RD and Heftmann E (1962) Thin-layer chromatography of sterols. *Journal of Chromatography* 9: 359.
- Copius-Peereboom JW and Beekes HW (1965) The analysis of mixtures of animal and vegetable fats. V. Separation of sterol acetates by thin-layer chromatography in reversed-phase systems and on silica gel G-silver nitrate layers. *Journal of Chromatography* 17: 99.
- Hung GWC and Harris AZ (1989) Separation of low-molecular-weight cholesteryl esters by thin-layer chromatography. *Microchemical Journal* 40: 208.

- Kovács L, Martos É, Pick J and Pucsok J (1989) Cholesterol ester mapping of human serum by HPTLC. *Journal of Planar Chromatography* 2: 155.
- Lisboa BP (1969) Chromatography of sterols and steroids. In: Marinetti GV (ed.) *Lipid Chromatographic Analysis*, vol. 2, pp. 57-147. New York: Marcel Dekker.
- Ranny M (1987) *Thin-layer Chromatography with Flame Ionization Detection*. Prague: Academia.
- Sherma J and Fried B (eds) (1996) *Handbook of Thin-layer Chromatography*, 2nd edn. New York: Marcel Dekker.
- Tvrzická E and Votruba M (1994) Thin-layer chromatography with flame-ionization detection. In: Shibamoto T (ed.) *Lipid Chromatographic Analysis*, pp. 51-73. New York: Marcel Dekker.
- Xu S, Norton RA, Crumley FG and Nes WD (1988) Comparison of the chromatographic properties of sterols, select additional steroids and triterpenoids: gravity-flow column liquid chromatography, thin-layer chromatography, gas-liquid chromatography and high-performance liquid chromatography. *Journal of Chromatography* 452: 377.

STRONTIUM FROM NUCLEAR WASTES: ION EXCHANGE



P. Sylvester, Texas A & M University, College Station, TX, USA

Copyright © 2000 Academic Press

Introduction

The development of new inorganic ion exchange materials for the selective removal of strontium and other radionuclides from nuclear waste has progressed rapidly in recent years. ^{90}Sr is an important component of many nuclear wastes and is a high yield fission product of ^{235}U . It is relatively short-lived with a half-life of 28.8 years and, along with ^{137}Cs , is the source of a large percentage of the initial radioactivity and heat generation of spent nuclear fuel. During the reprocessing of nuclear fuel, irradiated uranium fuel rods are dissolved in nitric acid and uranium and plutonium are separated from the fission products and other actinides by means of the Purex process. Tributylphosphate (TBP) dissolved in an organic phase, such as odourless kerosene, is contacted with the nitric acid solution, and plutonium and uranium nitrates are selectively complexed by the TBP and extracted into the organic

phase. The majority of fission products, including ^{90}Sr , remain in the aqueous acidic phase, which can then be concentrated by means of evaporation and stored prior to permanent disposal. In addition to the acidic high level waste stream, numerous other streams are generated during reprocessing operations as a result of washing, decontamination and scrubbing operations. Details of some specific streams generated by the nuclear industry from which ^{90}Sr needs to be selectively removed from large excesses of inert ions will be given later in this article.

A convenient method of selectively removing contaminant species from higher concentrations of inert ions is by ion exchange. Organic ion exchange resins are used in many industries for the selective removal of ions from aqueous streams. These materials consist of a polymeric backbone (commonly polystyrene) to which has been attached functional groups such as carboxylic or sulfonic acids to produce cation exchangers, or tertiary or quaternary amines to produce anion exchange resins. However, the use of organic resins in the nuclear industry is limited for a number of reasons. These include:

- low resistance to damage by ionizing radiation, thus limiting operational life;
- low thermal stability;
- limited chemical stability;
- low selectivity in comparison to inorganic ion exchange materials;
- incompatibility with grout or cement, making the final disposal of spent resins a problem.

Inorganic ion exchangers offer a number of advantages over conventional organic resins including greater selectivity and both chemical and radiolytic stability. Additionally, they are compatible with current waste encapsulation techniques and are stable enough that they can be used as a final waste form for long-term storage. The major drawback to the use of inorganic ion exchangers is that they are typically synthesized as fine powders, which are unsuitable for use in column operations. However, there are now a number of techniques available to allow these powders to be produced as pellets or particles suitable for column operations, while still retaining fast ion exchange kinetics and the ion selectivity of the original material. A number of reviews of available materials and their ion exchange selectivities have been written, and as new materials and methods of manufacture are being developed, the use of inorganic materials both in the nuclear industry and elsewhere will undoubtedly expand. Some of the major classes of materials that are currently being used (or are under evaluation) for the selective removal of ^{90}Sr from nuclear wastes are described in the following sections.

Zeolites

Zeolites are hydrated aluminosilicates with open framework structures. These consist of building blocks of $\{\text{SiO}_4\}$ and $\{\text{AlO}_4\}$ tetrahedra which can be interlinked to give a wide range of different materials with regular tunnels and cavities. The presence of trivalent aluminium in the framework results in a net negative charge that is neutralized by the absorption of cations. Specific zeolites exhibit high selectivities for strontium and caesium over other alkali and alkaline earth cations. This has led to their use in the treatment of some nuclear waste streams. Details of zeolite synthesis, structures, applications and information on their ion exchange properties can be found in the literature and will not be detailed in this article.

Clinoptilolite is a common natural zeolite with the ideal formula $\text{Na}_6\text{Al}_6\text{Si}_{30}\text{O}_{72} \cdot 24\text{H}_2\text{O}$, though due to interactions with natural groundwaters, some of the Na^+ ions will have been replaced by K^+ , Mg^{2+} and Ca^{2+} ions. It is currently used on a large scale both in the UK and the USA for the treatment of nuclear

waste solutions such as cooling pond water. This is one of the largest waste streams in terms of the volume of liquid, and consists of water used to cool and shield irradiated uranium fuel rods prior to their disposal or reprocessing. For example, spent pressurized water reactor (PWR) fuel is generally stored under water for up to 5 years to allow short-lived radioisotopes, such as ^{131}I ($T_{1/2} = 8.06$ days) and ^{106}Ru ($T_{1/2} = 367$ days), to decay away, and thus make the fuel rods easier to handle. Storage is often accompanied by the release of tiny amounts of radioactivity, primarily ^{137}Cs and ^{90}Sr , from the fuel rods into the cooling water thus necessitating removal of the radioactivity before the water can be discharged to the environment. Modern fuel is typically clad in zircalloy or stainless steel and the release of radioisotopes is minimal. However, older fuel types such as the UK's Magnox fuel and fuel stored at the Hanford site in Washington State, USA, do release significant radioactivity.

Fuel storage pond waters are relatively pure and contain minimal dissolved cations that can compete with the ^{90}Sr and ^{137}Cs for the available ion exchange sites. Compositions of a fuel pond simulant from the Hanford site and the composition of an average pond water from the British Nuclear Fuels plc. (BNFL) Sellafield, UK site are given below in **Table 1**.

At the Sellafield plant, BNFL employs two 9.6 m^3 beds of clinoptilolite in the site ion exchange effluent plant (SIXEP) to decontaminate the pond water used for storage of Magnox fuel before controlled discharge to the sea. This clinoptilolite originates from the Mud Hills deposit in the Mojave Desert, California, and has been crushed and sieved to give a particle size of 0.4–0.8 mm in diameter. A schematic of the SIXEP plant is given in **Figure 1**.

Table 1 Composition of two fuel cooling ponds

Component	Hanford N-basin (ppm)	Sellafield (ppm)
Al	0.78	0.3
B	28.4	nd
Ba	3.1	0
Ca	33.4	1.7
Cs	6.47×10^{-5}	3217 Bq mL^{-1a}
K	2.5	3.6
Mg	0.70	0.3
Na	37.2	48.5
Sr	0.39	287 Bq mL^{-1a}
pH	8.2	11.4

^a The activities of ^{90}Sr and ^{137}Cs correspond to pondwater concentrations of 5.38×10^{-5} ppm and 8.69×10^{-4} ppm, respectively. There is unlikely to be significant nonactive caesium present; however, the amount of nonactive strontium is likely to be significantly greater than the ^{90}Sr concentration. nd, not determined.

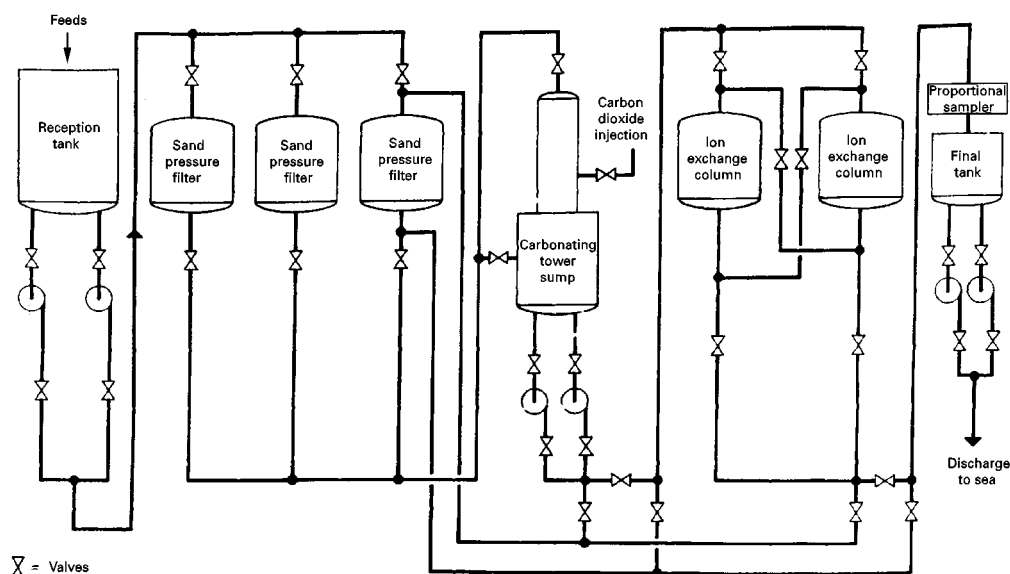


Figure 1 Schematic of BNFL's site ion exchange effluent plant (SIXEP). (Reproduced with the permission of BNFL.)

The feed is pumped through a sand filter to remove any particulates and is then treated with carbon dioxide to decrease the pH to approximately 7. The feed passes through two beds of clinoptilolite in series before being sampled and discharged to the Irish Sea. On average, approximately 3000 m³ of effluent per day pass through the plant, which corresponds to a contact time of only 4.6 minutes per ion exchange bed. The clinoptilolite is very effective and typically removes 98.7% of the strontium and over 99.7% of the caesium from the stream prior to its discharge, and each bed lasts for approximately 6 months online.

Another area in which zeolites can be used for the removal of radioactive strontium is in groundwater remediation. Groundwaters have relatively low ionic strengths similar to pond waters, but differ in that the predominant inactive ions in solution are magnesium and calcium rather than sodium. There is also natural, nonradioactive strontium present, typically in the order of a few tenths of a part per million, which will also be removed along with the radioactive ⁹⁰Sr. Since Mg²⁺ and Ca²⁺ compete strongly with Sr²⁺ for the available ion exchange sites on the zeolites, the observed distribution coefficients (K_{ds}) for Sr tend to be considerably lower than in pond waters, and the higher concentration of strontium results in a shorter ion exchange bed life. However, the low cost of natural zeolites (less than US \$0.5 per lb for clinoptilolite) means that they are economically viable.

Sodium Nonatitanate

Sodium nonatitanate (NaTi), Na₄Ti₉O₂₀ · xH₂O, displays a very high selectivity for strontium in basic

media. The synthetic procedure is relatively simple and has been scaled up to allow the titanate to be produced on an industrial scale. A soluble source of titanium, such as titanium isopropoxide, is added to a 50% sodium hydroxide solution, resulting in the immediate formation of a white precipitate. The mixture is then heated in a hydrothermal bomb for approximately 21 h at a temperature of 200°C. The product is filtered, washed to remove excess NaOH, and dried to produce a white powder. The final material has a low crystallinity and consequently it has not been possible to determine the crystal structure. However, the titanate is believed to consist of layers of TiO₆ octahedra separated by exchangeable sodium ions and water molecules. At room temperature, the interlayer space is approximately 10 Å, but the distance can vary considerably depending upon the drying temperature, and hence the number of water molecules in the interlayer space. This material is now available from Allied Signal Inc. (Des Plaines, Illinois, USA) and similar products can also be obtained from Selion Inc. (Merden, Connecticut, USA) and Boulder Scientific Company (Mead, Colorado, USA).

Sodium nonatitanate exhibits a very high selectivity for strontium over alkali and other alkaline earth metals in basic media. In acidic media, the material has a high affinity for protons, so strontium selectivity is negligible. Consequently, this allows the nonatitanate to be stripped of absorbed strontium using dilute acid and reused. Sodium nonatitanate readily hydrolyses in water, exchanging protons for sodium ions; this results in a considerable increase in the solution pH. Consequently its use for treating groundwaters contaminated with ⁹⁰Sr is limited. However, its stability in highly

alkaline conditions makes it ideally suited for the treatment of alkaline nuclear wastes. This aspect will be discussed later.

Titanosilicates

Two separate classes of titanosilicate ion exchange materials have been developed for the selective extraction of strontium from nuclear wastes. Both classes are composed of a titanosilicate framework, but the crystal structures and the Ti:Si ratios are different and hence so are the ion exchange properties.

The first class of materials is exemplified by sodium titanosilicate (NaTS), with the ideal formula $\text{Na}_2\text{Ti}_2\text{O}_3\text{SiO}_4 \cdot 2\text{H}_2\text{O}$. This can be synthesized in a crystalline form which has allowed its structure to be determined using X-ray powder methods. The titanosilicate was found to have a tetragonal unit cell with $a = b = 7.8082(2) \text{ \AA}$ and $c = 11.9735(4) \text{ \AA}$. Edge-sharing TiO_6 clusters reside in all eight corners of the unit cell and silicate tetrahedra are located midway between the clusters and link them together. This arrangement produces tunnels parallel to the c -axis where the exchangeable sodium ions and the water molecules reside. The remaining sodium ions are located in the framework, bonded by silicate oxygens and are thus not exchangeable. Due to steric repulsions and space limitations, some of the sodium ions in the tunnels are replaced by protons, leading to an actual formula of $\text{Na}_{1.64}\text{H}_{0.36}\text{Ti}_2\text{O}_3\text{SiO}_4 \cdot 1.84\text{H}_2\text{O}$. This exchanger is synthesized by hydrothermally heating a titanium silicate gel of appropriate stoichiometry in $6 \text{ mol L}^{-1} \text{ NaOH}$ at 170°C for 2 days.

This material has been shown to have a high selectivity for Cs^+ ions in both acid and alkaline pH and a high selectivity for strontium in alkaline media. Caesium ions exchanged onto the titanosilicate are strongly held in the tunnels, as shown in Figure 2, and are not readily leached off, thus the material is not regenerable. Strontium is readily removed by washing with dilute acid. A related material is currently marketed by UOP as a crystalline silicotitanate (CST) under the tradename IE-910 for the powder, and IE-911 for an engineered form suitable for use in column operations. The CST has shown excellent selectivity for ppm levels of caesium ions in the presence of $7 \text{ mol L}^{-1} \text{ Na}^+$ ions and is currently being considered for use removing ^{137}Cs and ^{90}Sr from alkaline nuclear wastes in the USA.

The second class of titanosilicate materials has the crystal structure of the natural mineral pharmacosiderite. Pharmacosiderite has the ideal formula $\text{KFe}_4(\text{AsO}_4)_3(\text{OH})_4$ and crystallizes in the cubic

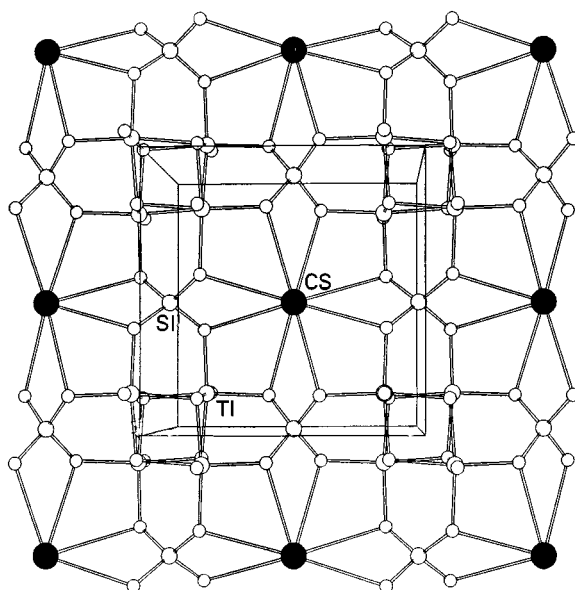


Figure 2 The structure of the caesium-exchanged titanosilicate showing Cs^+ ion in the centre of the tunnel.

system. Titanosilicates with the general formula $\text{M}_3\text{H}(\text{AO})_4(\text{BO}_4)_3 \cdot 4\text{--}6\text{H}_2\text{O}$ ($\text{M} = \text{H, K, Na, etc.}$; $\text{A} = \text{Ti, Ge}$; $\text{B} = \text{Si, Ge}$) have been prepared using hydrothermal techniques. A homogeneous gel of appropriate stoichiometry was hydrothermally treated in an excess of either KOH or CsOH at 200°C for 1–3 days. Sodium and proton forms were then prepared by exhaustively ion exchanging the material with either HCl or NaCl . The best studied of these materials is the potassium pharmacosiderite, $\text{K}_3\text{H}(\text{TiO})_4(\text{SiO}_4)_3 \cdot 4\text{H}_2\text{O}$ (KTS-Ph), in which $a = b = c = 7.7644(3) \text{ \AA}$. Each unit cell consists of

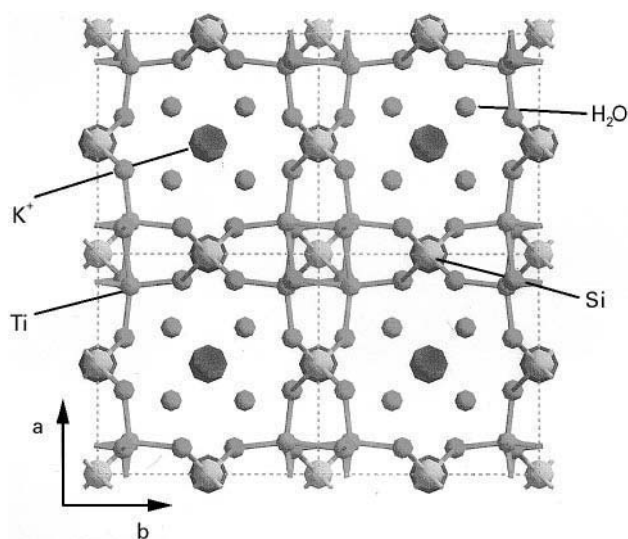


Figure 3 The structure of potassium pharmacosiderite $\text{HK}_3(\text{TiO})_4(\text{SiO}_4)_3 \cdot 4\text{H}_2\text{O}$ with the K^+ ion located in the centre of the tunnels. $a = b = c = 7.7644(3) \text{ \AA}$.

clusters of four titania octahedra linked to each other by silicate groups, as shown in Figure 3. This produces a series of intersecting tunnels parallel to the *a*, *b* and *c* axes with the exchangeable ions residing close to the face-centres of the unit cell.

It has proved possible to substitute Ge for both Si and Ti in the pharmacosiderite framework, thus allowing the size of the tunnels to be carefully tailored. These materials have shown selectivity towards both Cs^+ and Sr^{2+} but are not as effective as the sodium titanosilicate, NaTS, described previously. However, the caesium ion can be eluted from the exchanger, so unlike NaTS, the pharmacosiderites are regenerable making them more cost-effective.

Removal of Strontium from High Ionic Strength Wastes

In the USA, there are over 100 million gallons of radioactive mixed waste stored in 332 tanks distributed over a number of Department of Energy (DOE) sites. Much of this tank waste is highly alkaline and is typically over 7 mol L^{-1} in Na^+ . The majority of this waste is found at the Hanford site in Washington State, where there is approximately 65 million gallons of high-level waste stored in 177 tanks. All of the Hanford tanks are highly alkaline and were generated as by-products of the production of ^{239}Pu for nuclear weapons manufacture. Initially, the waste was in a nitric acid matrix, but to minimize corrosion of the steel tanks, sodium hydroxide was added to neutralize the wastes and to precipitate much of the radioactivity. The composition of each tank is different, but in general, the wastes consist of three distinct phases. At the bottom of the tank is a metal hydroxide sludge, at the top is a salt cake, predominantly made up of nitrate salts, and between these layers is an alkaline supernate. ^{90}Sr is found in all three layers, but tends to predominate in the sludge layer. However, in cases where there are significant amounts of complexing agents, considerably greater ^{90}Sr activity is found in the supernate. The composition of two supernate simulants developed at Pacific Northwest National Laboratory (PNNL) to mimic the tank wastes are given in Table 2.

Both waste simulants represent dilution of actual tank wastes, which is envisaged to be necessary to allow ease of handling without excessive precipitation of salts occurring. NCAW represents tank 241-AZ-102, and 101-SY represents tank 241-SY-101, both diluted to approximately 5 mol L^{-1} in Na^+ . This latter tank contains significant amounts of complexants such as ethylenediaminetetraacetic acid (EDTA) and citric acid. Zeolites are unsuitable for the treatment of these tank wastes because they lack sufficient selectiv-

ity for strontium in the presence of high sodium concentrations, and they are also unstable in highly alkaline conditions. However, the titanate and the titanosilicates are synthesized in strongly alkaline media and thus exhibit a high stability in these tank wastes. In addition, all of the exchangers exhibit good radiation stability, thermal stability and excellent resistance to extreme chemical environments.

The sodium nonatitanate and the titanosilicate ion exchange materials were evaluated in preliminary batch experiments using ^{89}Sr as a surrogate for ^{90}Sr . Here, 0.05 g of exchanger was contacted with 10 mL of waste simulant spiked with ^{89}Sr , giving a volume to mass ratio of 200 : 1, for 18 h using a rotary shaker. The mixtures were then filtered through a $0.2 \mu\text{m}$ filter and the activity of the aqueous phase determined using liquid scintillation counting. K_d values for strontium were then calculated according to eqn [1] below:

$$K_d = (A_i - A_f)/A_f \times v/m \quad [1]$$

where A_i is the initial activity of solution (counts per minute mL^{-1}); A_f is the final activity of solution (counts per minute mL^{-1}); v is the volume of solution (mL); and m is the mass of exchanger (g).

Table 2 The composition of two Hanford tank waste simulants

Species	NCAW (mol L^{-1})	101-SY (mol L^{-1})
Al	0.43	0.42
Ca	0	4.20×10^{-3}
Cs	5.00×10^{-4}	4.19×10^{-5}
Fe	0	1.96×10^{-4}
K	0.12	0.034
Mo	0	4.20×10^{-4}
Na	4.99	5.1
Ni	0	2.50×10^{-4}
Rb	5.00×10^{-5}	4.20×10^{-6}
Sr	2.70×10^{-7}	4.10×10^{-6}
Zn	0	5.00×10^{-4}
Carbonate	0.23	0.038
Fluoride	0.09	0.092
Hydroxide	3.4	3.78
Hydroxide (free)	1.68	2.11
Nitrate	1.67	1.29
Nitrite	0.43	1.09
Sulfate	0.15	4.75×10^{-3}
Phosphate	0.025	0.02
Citric acid	0	5.00×10^{-3}
Na_4EDTA	0	5.00×10^{-3}
HEDTA	0	3.75×10^{-3}
Iminodiacetic acid	0	0.031
Na_3 nitrilotriacetate	0	2.50×10^{-4}
Sodium gluconate	0	0.013
pH	14.5	14.4

Na_4EDTA , ethylenediaminetetraacetic acid, tetra sodium salt.
HEDTA, *N*-(2-hydroxyethyl)ethylenediaminetriacetic acid.

Table 3 The removal of strontium from Hanford tank waste simulants by inorganic ion exchange materials

<i>Ion exchanger</i>	<i>NCAW, K_d (mL g⁻¹)</i>	<i>% Sr removed</i>	<i>101-SY, K_d (mL g⁻¹)</i>	<i>% Sr removed</i>
Clinoptilolite	48	19.35	Not tested	–
NaTi	235 000	99.93	295	61.1
NaTS	270 000	99.93	231	54.7
KTS-Ph	20 200	99.55	31	13.2

The results obtained for the three ion exchangers are displayed in Table 3. For comparative purposes, the strontium K_d for the Mud Hills clinoptilolite was also included, although this number should be viewed with caution because clinoptilolite is not stable in highly alkaline media and will have undergone substantial decomposition.

It can be seen that all of the synthetic ion exchange materials exhibited a very high selectivity for strontium from NCAW with K_d values in the tens or hundreds of thousands. Clinoptilolite performed very poorly, with a K_d of only 48 mL g⁻¹ compared with the best material, the sodium titanosilicate, which had a K_d of 270 000 mL g⁻¹. By contrast, the K_d values from the 101-SY simulant were very low for all of the materials, indicating that the presence of relatively high concentrations of EDTA, citric acid and other complexants has resulted in the strontium being strongly chelated and thus not readily extractable by ion exchange. However, recent studies have indicated that this problem can be overcome by the addition of Ca²⁺ or other ions to the waste in sufficient quantity to saturate all of the EDTA and other complexants present, and thus release the strontium into solution where it can be removed by strontium-selective ion exchangers. Alternatively, the complexants can be destroyed using an appropriate chemical oxidation technique and the strontium removed by ion exchange.

Column Experiments

Column experiments using ⁸⁹Sr-spiked NCAW were performed to further evaluate the efficiency of the sodium nonatitanate, the sodium titanosilicate and the potassium pharmacosiderite at removing Sr under dynamic conditions. This necessitated pelletizing the ion exchange materials using approximately 15% by weight of a hydrous titania binder. Hydrous titania also shows some affinity for strontium in alkaline media, but tests proved that the K_d values were insignificant in comparison to the ion exchange materials.

Approximately 1 mL of material was slurried into a column and NCAW, spiked with ⁸⁹Sr to give a total strontium concentration of 2.7×10^{-7} mol L⁻¹, was then passed through at a flow rate of approximately 20 bed volumes per hour (BV h⁻¹). The ⁸⁹Sr activity

in the solution exiting the column was then analysed using liquid scintillation counting. Percentage breakthrough was calculated according to eqn [2]:

$$\% \text{Breakthrough} = (A_f/A_i) \times 100 \quad [2]$$

where A_f is the ⁸⁹Sr activity exiting the column and A_i is the ⁸⁹Sr activity entering the column.

The breakthrough curves obtained for the materials are given in Figure 4. Also included is the breakthrough curve for the commercially available IE-911 determined under the same operating conditions. The nature and percentage binder present in the IE-911 is unknown, but in simple batch equilibrium experiments Sr K_d values in excess of 25 000 mL g⁻¹ were obtained for ⁸⁹Sr in NCAW. Figure 4 shows that breakthrough of ⁸⁹Sr from the IE-911 bed is almost instantaneous, indicating very poor kinetics of exchange. By contrast, all three of the other exchangers show < 5% ⁸⁹Sr breakthrough for over 1500 bed volumes. Breakthrough was first obtained for the potassium pharmacosiderite and was followed by the sodium titanate and had reached approximately 25% and 17% respectively after 3000 bed volumes had been passed. By contrast, the breakthrough for the titanosilicate was still only around 5% when the experiment was terminated after the passage of 3500 bed volumes. This indicates rapid kinetics for all of the materials except the IE-911 and also an appreciable capacity for

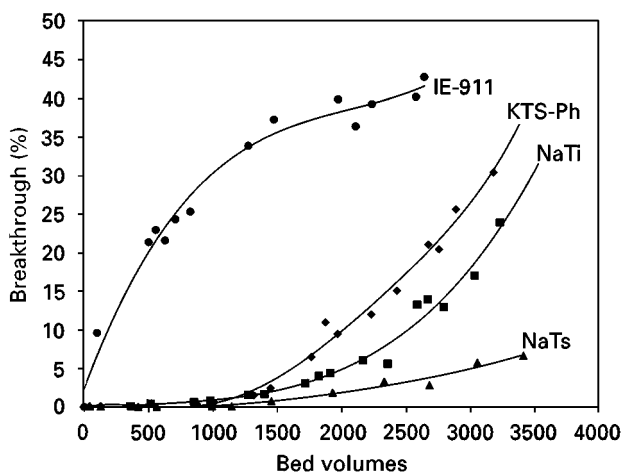


Figure 4 ⁸⁹Sr breakthrough curves for IE-911, NaTi, NaTS and KTS-Ph for NCAW at a flow rate of 20 BV h⁻¹.

strontium. Thus, all of the materials, particularly the sodium titanasilicate, have good potential for the decontamination of high-salt, alkaline nuclear wastes.

Conclusions

Inorganic ion exchangers have a wide number of applications within the nuclear industry and are preferred over conventional organic resins. Zeolites are ideal for the treatment of dilute wastes, provided that the pH is not too extreme, and their relatively low costs make their use highly economical. For more extreme wastes like those encountered in the Hanford storage tanks, new titanium-based materials have been developed that are able to withstand the high alkalinity and have sufficiently high selectivity to remove trace levels of strontium in the presence of molar quantities of other ions. Although these synthetic exchangers cost hundreds of US dollars per kilogram, their extreme selectivity and ability to be regenerated makes them viable options for the treatment of these extremely complex wastes.

Acknowledgements

I would particularly like to acknowledge Professor Abraham Clearfield, Dr. Elizabeth Bluhm and Gina Graziano at Texas A&M University, who worked with me on the titanate and titanasilicate ion exchange materials.

See also: I/Ion Exchange. II/Ion Exchange: Catalysis: Organic Ion Exchangers; Historical Development;

Inorganic Ion Exchangers; Novel Layered Materials: Non-Phosphates; Novel Layered Materials: Phosphates; Organic Ion Exchangers; Surface Complexation Theory: Multispecies Ion Exchange Equilibria; Theory of Ion Exchange.

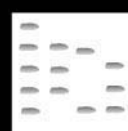
Further Reading

- Amphlett CB (1964) *Inorganic Ion Exchangers*. Amsterdam: Elsevier.
- Barrer RM (1982) *Hydrothermal Synthesis of Zeolites*. London: Academic Press.
- Breck DW (1984) Malabar, FL: Robert E. Krieger.
- Clearfield A (ed.) (1982) *Inorganic Ion Exchange Materials*. Boca Raton, FL: CRC Press.
- Clearfield A (1988) The role of ion exchange in solid state chemistry. *Chemical Reviews* 88: 125–148.
- Clearfield A (1995) Inorganic ion exchangers: a technology ripe for development. *Industrial Engineering and Chemistry Research* 34(8): 2865–2872.
- Dyer A (1988) *An Introduction to Zeolite Molecular Sieves*. Chichester: J. Wiley & Sons.
- Dyer A, Hudson MJ and Williams PA (eds) (1993) *Ion Exchange Processes: Advances and Applications*. Cambridge: The Royal Society of Chemistry.
- Helfferrich F (1962) *Ion Exchange*. New York: McGraw Hill.
- Lombardo NJ and Schulz WW (eds) (1998) *Science and Technology for the Disposal of Radioactive Tank Wastes*. New York: Plenum.
- Streat M (ed.) (1988) *Ion Exchange for Industry*. Chichester: SCI/Ellis Horwood Ltd.
- Williams PA and Hudson MJ (eds) (1990) *Recent Developments in Ion Exchange* 2. Barking: Elsevier.

SUB-CRITICAL WATER: EXTRACTION

See III / SUPERCRITICAL FLUID EXTRACTION-SUPERCRITICAL FLUID CHROMATOGRAPHY

SUGAR DERIVATIVES: CHROMATOGRAPHY



S. C. Churms, University of Cape Town, South Africa
Copyright © 2000 Academic Press

Because sugar derivatives are generally present as complex mixtures, chromatographic techniques are crucial in their analysis. The spectrophotometric methods, and other methods mentioned in this article, serve primarily as chromatographic detection

systems, and spectroscopic methods are frequently used in conjunction with chromatography.

Detection Reagents for Planar Chromatography and for Qualitative and Spot Tests

Detection reagents that are specific for particular derivatives, or can distinguish certain classes from

others, are listed in Table 1, which also shows the colours produced in each case and, where known, the detection limit. These reagents are used in spot tests and as detection reagents in planar chromatography, those not containing corrosive acids being applicable to both paper and thin-layer chromatography.

Gas Chromatography

Some sugar derivatives are sufficiently volatile to be analysed by gas chromatography (GC) without further derivatization; this particularly applies to the partially methylated methyl glycosides and methyl glycoside methyl esters produced by methanolysis of methylated polysaccharides. Multiple peaks, corresponding to α and β anomers of pyranoside and furanoside forms, are given by each glycoside, a factor that complicates analysis but can aid the identification of the individual components of simple, well-resolved mixtures. Unsubstituted methyl glycosides require derivatization for analysis by GC; they are successfully analysed as either trimethylsilyl (TMS) ethers or trifluoroacetyl (TFA) esters. Here again the characteristic patterns of multiple peaks produced can facilitate identification. However, for analysis of complex mixtures it is desirable to simplify the chromatogram by elimination of the anomeric centre.

The mixtures of partially methylated sugars obtained in methylation analysis of polysaccharides are usually submitted to GC as the acetylated alditol derivatives, for which a large body of mass spectrometry (MS) data is available. However, for some carbohydrates, notably amino- and acetamidodeoxy sugars, the GC retention times of the derived alditol acetates are excessively long. For aminodeoxyhexoses this problem can be overcome by nitrous acid deamination of the amino sugars before reduction and acetylation, or by *N*-methylation of the aminodeoxyalditols prior to acetylation. The most satisfactory procedure in the analysis of the mixtures of sugars obtained on hydrolysis of bacterial cell wall polysaccharides or glycoconjugates is derivatization to *O*-methyloximes, followed by acetylation or trimethylsilylation. No more than two peaks are produced by each component of the mixture and simultaneous analysis of neutral and amino sugars, as well as *N*-acetylneuraminic acid, muramic acid and its *N*-acetyl derivative and 3-deoxy-*D*-manno-2-octulosonic acid (KDO), within 40 min is possible by capillary GC as the acetylated *O*-methyloximes.

GC analysis of uronic acids also requires derivatization by specific methods if the multiple peaks given by methyl glycoside methyl esters or TMS ethers are to be avoided. Conversion to the oxime is an option in this case too, or the acids may be reduced to

aldonic acids (by sodium borohydride reduction of the alduronates) and analysed as the TMS derivatives of the aldono-lactones or the acetylated derivatives of the *N*-alkylaldonamides produced on reaction of the aldono-lactones with a *L*-alkylamine in pyridine. Both methods of derivatization proceeding via the aldonic acids result in the production of a single GC peak for each uronic acid present. The latter method has the advantage that simultaneous analysis of aldoses, as the alditol acetates, is possible – the alditol acetates have much shorter retention times than the *N*-alkylaldonamide acetates. Complete analysis of neutral and acidic sugars within 20 min is possible by capillary GC of these derivatives.

Oligosaccharide-alditols, up to tetrasaccharide level, can be analysed by GC as their permethylated derivatives. The volatility of those containing acetamidodeoxyhexose residues can be increased by *N*-trifluoroacetylation of these residues (through transamidation by trifluoroacetylation under carefully controlled conditions) prior to methylation. This procedure permits GC analysis of oligosaccharide-alditols containing up to seven sugar residues and also allows the use of the electron capture detector, with a hundredfold increase in sensitivity.

Recommended conditions for GC analysis of various sugar derivatives are listed in Table 2. Comprehensive retention data are available in the literature.

Liquid Chromatography

Carbohydrate derivatives can be analysed by liquid chromatography (LC) in various modes, depending on the polarity of the molecule and whether acidic or basic groups are present. Nonpolar compounds, or those rendered nonpolar by derivatization to increase the sensitivity of analysis, are amenable to reversed-phase LC or adsorption chromatography on silica. For hydroxylic compounds such as alditols, several options are available, including normal-phase LC on bonded amino phases or amine-modified silica (the column packing being modified *in situ* by addition of a polyfunctional amine to the mobile phase); LC on a cation exchange resin in the Ca^{2+} form (ion-moderated partitioning) or, as borate complexes, on an anion exchange resin; and ion chromatography, with pulsed amperometric detection. Recently, cyclodextrin-bonded silica has also proved effective.

The oligosaccharide-alditols obtained in degradative structural studies of glycoproteins can also be analysed by LC in various ways; normal-phase LC, ion exchange, ion chromatography and size exclusion chromatography. Amino- and acetamidodeoxyhexoses and the hexitols derived from them can be analysed by normal-phase LC; ion-moderated

Table 1 Reagents used in qualitative analysis for detection of sugar derivatives

<i>Derivatives</i>	<i>Reagent mixture</i>	<i>Procedure</i>	<i>Colour produced</i>
Alditols and cyclitols	<p>Fluor's reagent:</p> <p>(a) HgO (5%, m/v) in HNO₃ (5%, m/v), diluted 1 : 1 before use</p> <p>(b) Barium acetate (10%, m/v) mixed 1 : 10 with glacial acetic acid</p> <p>Periodate-<i>p</i>-anisidine:</p> <p>(a) <i>p</i>-Anisidine (1%, m/v) in ethanol (70%, v/v)</p> <p>(b) NaIO₄ (0.1 mol L⁻¹ aqueous solution) mixed 1 : 10 with acetone</p> <p>Vanillin-perchloric acid:</p> <p>(a) Vanillin (1%, m/v) in ethanol</p> <p>(b) HClO₄ (3% aqueous solution). Mixed 1 : 1 with (a) before use</p>	<p>Spray with (a); heat at 90–100°C for 10 min; spray with (b); heat at 100°C for 10–30 min</p> <p>Spray with (a); heat at 105°C for 5–10 min; dip in (b)</p> <p>Spray; heat at 85°C for 5–10 min</p>	<p>Specific for polyols; cyclitols give orange spots (detection limit 5–10 µg inositol); alditols and other polyols grey to black</p> <p>Polyols and aldonic acids give white spots on brown background; distinguished from aminodeoxy sugars, uronic acids and neutral sugars (see below)</p> <p>Polyols give pale blue to lilac spots (detection limit 20–30 µg); cyclitols and most aldoses do not react; ketoses give grey-green spots, rhamnose brick-red</p>
Aldonic acids and aldonolactones	<p>Periodate-<i>p</i>-anisidine: see above</p> <p>Hydroxylamine-iron (III) chloride</p> <p>(a) Hydroxylamine hydrochloride (1 mol L⁻¹) in methanol</p> <p>(b) KOH (1.1 mol L⁻¹) in methanol</p> <p>(c) FeCl₃ (2%, m/v) in HCl (1% aqueous solution)</p>	<p>See above</p> <p>Spray with 1 : 1 mixture of (a) and (b); dry at room temperature for 10 min; spray with (c)</p>	<p>Aldonic acids give white spots on brown background (see above)</p> <p>Aldonolactones revealed as purple spots; other lactones and esters also react</p>
Amino- and acetamidodeoxy sugars	<p>Elson-Morgan reagent</p> <p>(a) KOH (25%, m/v) in aqueous ethanol (80%, v/v)</p> <p>(b) Pentane-2,4-dione (acetone), redistilled (1%, v/v) in 95% ethanol, fresh solution</p> <p>(c) <i>N,N</i>-Dimethyl-<i>p</i>-aminobenzaldehyde (10%, m/v) in conc. HCl</p> <p>(d) Ethanol (95%)</p> <p>Fluorescamine</p> <p>(a) Triethylamine (10%, v/v) in dichloromethane</p> <p>(b) Fluorescamine (0.05%, m/v) in acetone</p> <p>Ninhydrin</p> <p>0.1% (m/v) solution in 1-butanol</p> <p>Periodate-<i>p</i>-anisidine</p> <p>See above</p>	<p>Dip through mixture of (a) and (b) (1 : 10); heat at 110°C for 5 min; dip through mixture of (c) and (d) (1 : 1); dry in stream of cold air</p> <p>Spray with (a); dry in air; spray with (b); dry in air; spray again with (a)</p> <p>Spray, heat at 105–110°C for 10 min</p> <p>See above</p> <p>See above</p>	<p>Specific for amino- and acetamidodeoxyhexoses. Transient purple spots at room temperature; heating to 80°C gives permanent red spots for free aminodeoxy sugars, purple-violet for acetamidodeoxy sugars</p> <p>Specific for amino- and acetamidodeoxy sugars. Fluorimetric scanning (excitation 390 nm, emission 475 nm) detects amino sugars (detection limit 100 pmol)</p> <p>Specific reagent; purple spots produced</p> <p>Yellow spots on brown background</p> <p>Purple spots</p>
Esters and lactones	<p>Hydroxylamine-iron (III) chloride</p> <p>See above</p>	<p>See above</p>	<p>Purple spots</p>
Ketals	<p>2,4-Dinitrophenylhydrazine</p> <p>0.4% (m/v) solution in 2 mol L⁻¹ HCl</p>	<p>Spray; heat at 105°C for 5 min</p>	<p>Specific for keto group; ketoses and ketals (e.g. pyruvate) give orange spots on light yellow background</p>

Table 1 Continued

Derivatives	Reagent mixture	Procedure	Colour produced
Methyl ethers and methyl esters	<i>p</i> -Anisidine hydrochloride 3% (m/v) solution in 1-butanol	Spray; heat at 110°C for 10 min	Methyl ethers give highly characteristic pink, red or brown spots, some fluorescent under UV. Methyl esters of methylated uronic acids give bright pink colour
Neuraminic acids	Resorcinol-HCl-Cu(II) (a) Resorcinol (0.2%, m/v) in 4 mol L ⁻¹ HCl (b) Aqueous solution of CuSO ₄ · 5H ₂ O (0.1 mol L ⁻¹). Mix (a) and (b) (40 : 1) at least 4 h before use Periodate-thiobarbiturate (a) NaIO ₄ (0.5 mol L ⁻¹) in 0.025 mol L ⁻¹ H ₂ SO ₄ (b) Ethylene glycol-aetone-conc. H ₂ SO ₄ (50 : 50 : 0.3 v/v/v) (c) Sodium 2-thiobarbiturate, 6% (m/v) in H ₂ O	Spray; heat at 110–120°C for about 20 min Spray with (a); leave at room temperature for 15 min; dry thoroughly in stream of air; spray with (b); dry similarly. If odour of formaldehyde persists spray again with (b). Finally, spray with (c); heat at 100°C for 10 min	Neuraminic acids give blue spots; ketoses also react Only neuraminic acids give red spots (detection limit about 3 µg)
Phosphates	Ammonium molybdate 10% (m/v) aqueous solution (20 mL) added to conc. HCl (3 mL) with shaking; NH ₄ Cl (5 g) added	Spray	Phosphorylated derivatives give immediate yellow colour of ammonium phosphomolybdate
Uronic acids	<i>p</i> -Anisidine hydrochloride See above Periodate- <i>p</i> -anisidine See above Mixed indicators Thymol blue (0.025%, m/v) and bromothymol blue (0.06%, m/v) in 95% ethanol; 1 mol L ⁻¹ NaOH added until blue-green colour reached	See above See above Spray	Red spots; do not fluoresce under UV Red spots on brown background; do not fluoresce (distinction from spots given by neutral sugars) Uronic acids and oligomers (e.g. oligogalacturonic acids) give red spots on green background

Table 2 Conditions recommended for GC analysis of sugar derivatives

Compounds	Derivatives for GC	Column type	Phase	Temperature (°C)	Gas; flow rate (mL min ⁻¹)
Acetals, isopropylidene	Run as such	Packed	(1) OV-225, 3% on Supelcoport (100–120 mesh) (2) ECNSS-M, 3% on Gas-Chrom Q (100–120 mesh); 1 and 2 mixed 7 : 4	90 → 190°C at 4°C min ⁻¹	N ₂ ; 20
Alditols	Acetates	Packed	OV-225, 3% on Chromosorb W-HP (80–100 mesh) OV-225	210	He; 40
Aminodeoxyhexoses	Alditol acetates, deaminated	Capillary	Silar 10C	100 → 250°C at 4°C min ⁻¹	He; 1
	Trifluoroacetates	Capillary		190°C (4 min); 190 → 230°C at 4°C min ⁻¹ ; 230°C (8 min)	H ₂ ; 9
		Packed	OV-101, 5% on Chromosorb W AW DMCS (60–80 mesh) OV-225	120	N ₂ ; 50
		Capillary		70°C (2 min); 70 → 180°C at 5°C min ⁻¹ ; 180°C (15 min)	N ₂ ; 1.5
Aldonic and aldonic acids	TMS ethers	Packed	OV-1 or OV-17, 0.5% on Chromosorb G (100–120 mesh) OV-101	160	N ₂ ; 30
		Capillary		100°C (2 min); 100 → 200°C at 20°C min ⁻¹ ; 200°C (5 min)	H ₂ ; 2
Aldonolactones	TMS ethers	Packed	OV-1 or OV-17, 0.5% on Chromosorb G (100–120 mesh) SP-2340, 3% on Supelcoport (100–120 mesh) SP-2330	160	N ₂ ; 30
	Acetylated <i>N</i> -alkylaldonamides (1-propyl or 1-hexyl usual alkyl substituents)	Capillary	DB-1701 (bonded phase)	190 → 260°C at 5°C min ⁻¹ 200°C (2 min); 200 → 235°C at 3°C min ⁻¹ ; 235°C (5 min) 220 → 270°C at 1°C min ⁻¹	He; 20 He; 10 He; 12
Aminodeoxyhexoses	Alditol acetates, <i>N</i> -methylated	Packed	EGSS-X, 2% on Chromosorb W AW DMCS (60–80 mesh) SP-2340, 3% on Supelcoport (100–120 mesh) Silar 10C	195	N ₂ ; 45
	Alditol acetates, deaminated	Capillary		150 → 220°C at 2°C min ⁻¹ 190°C (4 min); 190 → 230°C at 4°C min ⁻¹ ; 230°C (8 min)	N ₂ ; 40 H ₂ ; 9
	Alditols, trifluoroacetylated	Packed	OV-101, 5% on Chromosorb WAW DMCS (60–80 mesh)	120	N ₂ ; 50

Table 2 Continued

Compounds	Derivatives for GC	Column type	Phase	Temperature (°C)	Gas; flow rate (mL min ⁻¹)
Amino- and acetamidodeoxy-hexoses	Methyl glycosides, trifluoroacetylated	Capillary	OV-210	120 → 210°C at 1°C min ⁻¹	Ar; 1
			SE-30	90°C (4 min); 90 → 250°C at 8°C min ⁻¹	He; 1.5
	Methyl glycosides, trimethylsilylated	Packed	SE-30, 3% on Chromosorb W-HP (100–120 mesh)	80 → 250°C at 2°C min ⁻¹	N ₂ ; 25
		Capillary (fused silica)	CP-Sil 5	140°C (2 min); 140 → 260°C at 8°C min ⁻¹	He; 1
	O-Methyloximes, acetylated	Capillary	OV-1	175°C (4 min); 175 → 260°C at 4°C min ⁻¹ ; 260°C (5 min)	He; 0.5
Anhydroalditols	O-Methyloximes, trimethylsilylated	Capillary (fused silica)	SP-2100	180	He; 1
		Capillary (fused silica)	CP-Sil 5	130 → 220°C at 2°C min ⁻¹	N ₂ ; 1.5
	TMS ethers	Capillary (fused silica)			
Cyclitols	Trifluoroacetates	Packed	Dexsil 410, 3% on Chromosorb W-HP (80–100 mesh)	100°C (1.5 min); 100 → 310°C at 3.5°C min ⁻¹ (3.5 min), 6°C min ⁻¹ (5 min), 15°C min ⁻¹ (5 min); 25°C min ⁻¹ (4 min); 310°C (6 min)	N ₂ ; 20
		Packed	SE-30, 3% on Gas-Chrom Q (80–100 mesh)	130 → 190°C at 2°C min ⁻¹	N ₂ ; 25
Methyl ethers	Alditol acetates	Packed	OV-225, 3% on Chromosorb W-HP (80–100 mesh)	175	He; 40
		Capillary (fused silica)	DB-225 (bonded phase)	195	He; 1
		Capillary	OV-275	165 → 215°C at 2°C min ⁻¹ ; 215°C (15 min)	He; 1.5
		Capillary (fused silica)	OV-275 (bonded phase)	150 → 250°C at 4°C min ⁻¹ ; 250°C (10 min)	He; 0.8
		Capillary	SE-30	90°C (4 min); 90 → 250°C at 8°C min ⁻¹	He; 1.5
Methyl glycosides	Trifluoroacetates	Packed	SE-30, 3% on Chromosorb W-HP (100–120 mesh)	80 → 250°C at 2°C min ⁻¹	N ₂ ; 25
		Capillary (fused silica)	CP-Sil 5	140°C (2 min); 140 → 160°C at 8°C min ⁻¹	He; 1
	TMS ethers	Capillary (fused silica)	DB-5 (bonded phase)	150 → 220°C at 2°C min ⁻¹	N ₂ ; 1

Table 2 Continued

Compounds	Derivatives for GC	Column type	Phase	Temperature (°C)	Gas; flow rate (mL min ⁻¹)
Methyl glycosides, methylated	Run as such	Packed	Ethylene glycol succinate, polyester, 14% on Chromosorb W (80–100 mesh)	155	He; 40
Muramic acid, KDO and neuraminic acid derivatives	O-Methylloximes, acetylated	Capillary	OV-1	175°C (4 min); 175 → 260°C at 4°C min ⁻¹ ; 260°C (5 min)	He; 0.5
Oligosaccharide-alditols	Permethylated	Packed	Dexsil 300, 1% on Supelcoport (100–120 mesh)	150 → 320°C at 4°C min ⁻¹	He; 40
	Permethylated, N-trifluoroacetylated	Capillary	OV-101	200°C (2 min); 200 → 350°C at 4°C min ⁻¹	He; 0.8
Uronic acids	Methyl glycoside methyl esters, trimethylsilylated	Capillary (fused silica)	CP-Sil 5	140°C (2 min); 140 → 260°C at 8°C min ⁻¹	He; 1
	O-Methylloximes, trimethylsilylated	Capillary (fused silica)	DB-5 (bonded phase)	150 → 220°C at 2°C min ⁻¹	N ₂ ; 1
	Aldonolactones, trimethylsilylated	Capillary (fused silica)	SP-2100	180	He; 1
	N-Alkylaldonamides, acetylated	Packed	OV-1 or OV-17, 0.5% on Chromosorb G (100–120 mesh)	160	N ₂ ; 30
		Capillary	SP-2340, 3% on Supelcoport (100–120 mesh)	190 → 260°C at 5°C min ⁻¹	He; 20
		Capillary	SP-2330	200°C (2 min); 200 → 235°C at 3°C min ⁻¹ ; 235°C (5 min)	He; 10
		Capillary (fused silica)	DB-1701 (bonded phase)	220 → 270°C at 1°C min ⁻¹	He; 12

partitioning on a cation exchange resin with an aqueous-organic solvent system as eluent; cation exchange chromatography; or ion chromatography. Uronic acids, on the other hand, are best analysed by anion exchange chromatography or ion-moderated partitioning on a cation exchange resin in the H^+ form. The same applies to aldonic acids and aldolactones. Oligogalacturonic acids are similarly analysed, but ion chromatography and ion pair chromatography (with the tetrabutylammonium cation in the mobile phase) are further options in this case. The ion pair method has been applied to both normal oligogalacturonic acids and the unsaturated products (with 4,5-unsaturated residues at their non-reducing termini) given on digestion of pectic acid with *endo*-polygalacturonic acid lyase. The unsaturated acids obtained on lyase digestion of glycosaminoglycuronans can also be analysed by this method, as well as by anion exchange chromatography and ion-moderated partitioning on a cation exchange resin with an aqueous-organic solvent system.

The various LC systems applicable to analysis of carbohydrate derivatives are listed in Table 3. Retention data have been published elsewhere.

Electrochemical Methods Linked to LC

The pulsed amperometric detector, in which analytes are oxidized at the surface of a gold electrode, a selected potential being applied between this and a silver/silver chloride reference electrode, with a glassy carbon counterelectrode maintaining the potential without excessive drain on the reference electrode, has proved highly successful when applied in ion chromatography of carbohydrates at high pH (≥ 12). Not only neutral sugars but also alditols, amino- and acetamidodeoxyhexoses, neuraminic acid derivatives and uronic acids can be analysed in this way. If the concentration of NaOH in the eluent is too low for optimal response of the detector, post-column addition of NaOH at higher concentration is required; an example of this is the analysis of amino- and acetamidodeoxyhexoses, which are best resolved with eluents containing 10–15 mmol L^{-1} sodium hydroxide, but are only detected satisfactorily after addition of 0.3 mol L^{-1} sodium hydroxide to the column effluent. The method is applicable to oligosaccharides, including the complex series, neutral, sialylated or phosphorylated, derived from glycoconjugates, and is now extensively used in analysis of such oligosaccharides.

It is only readily oxidizable compounds that can be analysed by oxidation at the surface of a glassy carbon electrode, and this permits the determination of L-ascorbic acid in the presence of other carbohydrates

that are not electroactive with this electrode. Examples include the analysis of algal extracts for L-ascorbic acid and its C5 diastereoisomer, D-erythorbic acid, at nanogram levels, after LC on a microparticulate cation exchange resin (H^+ form), eluted with 0.1 mol L^{-1} formic acid; co-eluting reducing sugars and lactones do not interfere when the carbon electrode is used as a detector. The use of this electrochemical detector has also proved invaluable in the determination of L-ascorbic acid in beers, to which it is added as an antioxidant; in a recommended procedure the glassy carbon electrode is used as a detector in LC of the beer samples on C_{18} -silica, eluted with a citrate buffer (pH 4.4) containing N-methyldodecylamine (1 mmol L^{-1}) as an ion-pairing reagent. The detection limit for ascorbic acid is about 1 ng.

Conductivity detectors can be used in the analysis of charged molecules. An example is afforded by the simultaneous determination of inositol phosphates, sugar phosphates and aliphatic organic anions such as pyruvate, lactate and citrate in physiological samples (rat brain and liver) by ion chromatography with conductivity detection. A post-column micromembrane suppressor, continually regenerated with dilute sulfuric acid, replaces the sodium ions in the eluent ($NaHCO_3$ – Na_2CO_3 ; see Table 3) with hydrogen ions, thus removing the eluent anions by conversion to carbon dioxide and water. This method permits detection of phosphates in the range 20–100 pmol.

Supercritical Fluid Chromatography

Carbon dioxide, widely regarded as the most useful mobile phase for supercritical fluid chromatography (SFC) is a poor solvent for polar solutes and those having high molecular mass. For this reason such solutes require derivatization to nonpolar products before analysis by SFC is possible. In the carbohydrate field the main successes of the method have been its application to series of homologous oligosaccharides, such as the maltodextrins, as their permethylated or trimethylsilylated derivatives, and to permethylated glycoconjugates. Coupled to chemical ionization mass spectrometry (CI-MS), SFC affords a sensitive analytical method (with detection limits at the picomole level) in such applications as monitoring of degradation of polysaccharides (e.g. starch) and profiling of glycoconjugates. With ammonia as the reactant gas for CI-MS, selected-ion monitoring of the $[M + NH_4]^+$ ions as the analytes emerge from the SFC column permits sensitive detection of derivatized glucooligosaccharides to a degree of polymerization (DP) of 15 and above; for the glycoconjugate derivatives the molecular mass limit is not in

Table 3 LC systems applicable to analysis of carbohydrate derivatives

Compounds	Column packing	Mobile phase	Temperature (°C)	Detection system
Acetates	Silica	<i>n</i> -Hexane-acetone (10 : 1) or <i>n</i> -hexane-ethyl acetate (1 : 1)	RT	RI or UV
Acetylated oligosaccharides (to DP 30–35)	C ₁₈ -silica	Acetonitrile–water, linear gradient, 10 → 70% acetonitrile (80 min)	65	UV
Alditols	NH ₂ -silica	Acetonitrile–water (4 : 1)	RT	RI
	Amine-modified silica (impregnated with tetraethylenepentamine)	Acetonitrile–water (3 : 1), containing tetraethylenepentamine (0.02%)	RT	RI
	Cyclodextrin-bonded silica	Acetonitrile–water (4 : 1)	RT	RI
	Cation exchange resin (Ca ²⁺ form)	Water	65	RI
	Cation exchange resin (Pb ²⁺ form)	Ethanol–water (1 : 4)	80	RI
	Anion exchange resin (quaternary ammonium type)	0.50 mol L ⁻¹ borate buffer, pH 7.1 (35 min) 0.35 mol L ⁻¹ borate buffer, pH 8.1 (30 min) 0.50 mol L ⁻¹ borate buffer, pH 10.5 (25 min)	65	Photometric or fluorimetric automated periodate–petane-2,4-dione method
	Pellicular anion exchanger used in ion chromatography	0.15 mol L ⁻¹ NaOH	RT	Pulsed amperometric
Aldonic and aldaric acids	Cation exchange resin (H ⁺ form)	4.5 mmol L ⁻¹ H ₂ SO ₄	25	UV
	Anion exchange resin (quaternary ammonium type)	0.2 mol L ⁻¹ ammonium formate, pH 3.2 For aldaric acids: 0.16 mol L ⁻¹ NaCl containing MgCl ₂ (20 mmol L ⁻¹)	45 85	UV UV
Amino and acetamidodeoxy-hexoses and -hexitols	NH ₂ -silica	Acetonitrile–0.15 mmol L ⁻¹ phosphate buffer, pH 5.2 (4 : 1)	RT	UV
	Cation exchange resin (H ⁺ form)	Acetonitrile–water (23 : 2)	30	UV, automated 2-cyanoacetamide method
	Cation exchange resin (Na ⁺ form) used in amino acid analyser	0.1 mol L ⁻¹ sodium citrate, pH 7.2 20 mmol L ⁻¹ Na ₂ B ₄ O ₇ , pH 8.0	40 (15 min); 63 (45 min) 60	Photometric, automated ninhydrin method Fluorimetric, automated <i>o</i> -phthalaldehyde method
	Pellicular anion exchanger used in ion chromatography	10 mmol L ⁻¹ NaOH; post-column addition of 0.3 mol L ⁻¹ NaOH to raise pH to optimum for detection method	RT	Pulsed amperometric detector
As benzoylated hexitols	Silica	<i>n</i> -Hexane-dioxane-dichloromethane, linear gradient, 22 : 2 : 1 → 4 : 2 : 1 (80 min)	RT	UV
As pyridylamino derivatives	C ₁₈ -silica	0.25 mol L ⁻¹ sodium citrate buffer, pH 4.0, containing acetonitrile (1.0%)	RT	Fluorimetric

Table 3 Continued

Compounds	Column packing	Mobile phase	Temperature (°C)	Detection system
Ascorbic acid	Cation exchange resin (H ⁺ form)	4.5 mmol L ⁻¹ H ₂ SO ₄ or 0.1 mol L ⁻¹ HCOOH	25	UV
	C ₁₈ -silica	25 mmol L ⁻¹ sodium citrate buffer, pH 4.4, containing <i>N</i> -methyldecylamine (1 mmol L ⁻¹)	30 RT	Amperometric (glassy carbon electrode) Amperometric, as above
Cyclitols	Amine-modified silica (impregnated with tetraethylenepentamine) Cation exchange resin (Ca ²⁺ form)	Acetonitrile–water (3 : 1), containing tetraethylenepentamine (0.02%) Water	RT 85	RI RI
Gangliosides	NH ₂ -silica	(A) Acetonitrile–5 mmol L ⁻¹ phosphate buffer, pH 5.6 (83 : 17) (B) Acetonitrile–20 mmol L ⁻¹ phosphate buffer, pH 5.6 (1 : 1) Gradient elution: Solution A (7 min); A → A + B (33 : 17) in 53 min; → A + B (9 : 16) in 20 min	RT	UV
Benzoylated	Silica	<i>n</i> -Hexane–dioxane, linear gradient, 7 → 23% dioxane (18 min)	RT	UV
Glycolipids, benzoylated	Silica	<i>n</i> -Hexane–dioxane, linear gradient, 2.5 → 25% dioxane (13 min); isocratic (5 min)	RT	UV
Glycosides, methyl	Silica C ₁₈ -silica Cation exchange resin (Ca ²⁺ form)	Acetonitrile–water (9 : 1) Water Water	RT RT 1.5	RI RI RI
Benzoylated	C ₁₈ -silica	Acetonitrile–water, linear gradient, 35 → 90% acetonitrile (65 min)	RT	UV
Glycosides, other Acetylated	Silica	Benzene–ethyl acetate (9 : 1) For aryl glycosides: Chloroform–carbon tetrachloride (3 : 2) Methanol–water (13 : 7)	RT	UV
Benzoylated	C ₁₈ -silica Silica	Benzene–ethyl acetate (99 : 1)	RT	UV
Lactones	Cation exchange resin (H ⁺ form)	4.5 mmol L ⁻¹ H ₂ SO ₄	25	UV
Methyl ethers, as alditols	C ₁₈ -silica	Water–acetonitrile (99 : 1)	RT	RI

Table 3 Continued

Compounds	Column packing	Mobile phase	Temperature (°C)	Detection system
Neuraminic acid derivatives, KDO and derivatives	Anion exchange resin (quaternary ammonium type)	0.75 mmol L ⁻¹ Na ₂ SO ₄ For KDO disaccharides: 10 mmol L ⁻¹ Na ₂ SO ₄	RT	UV
Neuraminic acids, DDB derivatives	C ₁₈ -silica	Water-methanol-acetonitrile (77 : 15 : 8)	RT	Fluorimetric
Oligogalacturonic acids, to DP 10	Cation exchange resin (H ⁺ form)	5 mmol L ⁻¹ H ₂ SO ₄	85	RI
DP 5-20	Pellicular anion exchanger used in ion chromatography	0.15 mol L ⁻¹ NaOH, with sodium acetate, gradient: 0.40 mol L ⁻¹ (2 min); 0.40 → 0.90 mol L ⁻¹ (43 min)	RT	Pulsed amperometric
Oligosaccharides, chitin, to DP 5	NH ₂ -silica	Acetonitrile-water (7 : 3)	25	RI
Oligosaccharides, from glycoproteins	NH ₂ -silica	Acetonitrile-15 mmol L ⁻¹ phosphate buffer, pH 5.2 (4 : 1); isocratic (30 min); buffer 20 → 45% (50 min)	RT	UV
		For higher oligosaccharides : (8-12 sugar residues): Linear gradient: buffer 20 → 44% (80 min)		
	Pellicular anion exchanger used in ion chromatography	For neutral oligosaccharides: (2-11 sugar residues): (A) 0.10 mol L ⁻¹ NaOH (B) 0.10 mol L ⁻¹ NaOH containing sodium acetate (0.15 mol L ⁻¹)	RT	Pulsed amperometric
		Gradient elution: A (10 min) A → A + B (1 : 4) in 60 min Post-column addition of 0.3 mol L ⁻¹ NaOH to raise pH for detection method For sialylated oligosaccharides (3-8 sugar residues): 50 mmol L ⁻¹ NaOH containing 100 mmol L ⁻¹ sodium acetate		
Oligosaccharides (2-8 residues), from hyaluronic acid	NH ₂ -silica	0.1 mol L ⁻¹ KH ₂ PO ₄ , pH 4.75	RT	UV
Oligosaccharide-alditols, from glycoproteins, 2-7 residues	NH ₂ -silica	Acetonitrile-1 mmol L ⁻¹ KH ₂ PO ₄ , pH 5.4 (3 : 2)	RT	UV
2-20 residues	Size exclusion chromatography packing	Water	55	RI or scintillation counting after labelling with ³ H

Table 3 Continued

Compounds	Column packing	Mobile phase	Temperature (°C)	Detection system
Oligosaccharide-alditols, ethylated and methylated (2–6 residues)	C ₁₈ -silica	Acetonitrile–water, various proportions from 1 : 1 to 3 : 2, or linear gradient, 50 → 65% acetonitrile (45 min)	RT	RI, MS
Oligosaccharides, pyridylamino derivatives (2–20 residues)	Two-dimensional mapping: (1) C ₁₈ -silica (2) NH ₂ -silica	For column 1: (A) 10 mmol L ⁻¹ phosphate buffer, pH 3.8; (B) A containing 1-butanol (0.5%) Linear gradient, 20 → 50% B (60 min) For column 2: (C) Acetonitrile–3% acetic acid in water containing triethylamine, pH 7.3 (13 : 7) (D) As C, but proportions 1 : 1 Linear gradient, C → D (50 min)	55 40	Fluorimetric Fluorimetric
Phosphates	Pellicular anion exchanger used in ion chromatography C ₁₈ -silica	2.4 mmol L ⁻¹ NaHCO ₃ –1.92 mmol L ⁻¹ Na ₂ CO ₃ For monophosphates: 20 mmol L ⁻¹ HCOOH, containing tetrabutylammonium hydroxide (8 mmol L ⁻¹) as ion-pairing reagent and Eu complex (0.02 mmol L ⁻¹) as detection reagent For diphosphates: 20 mmol L ⁻¹ HCOOH–20 mmol L ⁻¹ HCl–40 mmol L ⁻¹ NaCl; concentration of tetrabutylammonium hydroxide increased to 30 mmol L ⁻¹ , that of Eu complex unchanged	RT 38	Conductivity anion micromembrane suppressor UV photometry of adduct with Eu complex
Phosphorylated oligosaccharides (2–5 sugar residues)	Pellicular anion exchanger used in ion chromatography	0.1 mol L ⁻¹ NaOH (5 min); linear acetate gradient, 0 → 0.6 mol L ⁻¹ sodium acetate in 0.1 mol L ⁻¹ NaOH (67 min); isocratic (5 min)	RT	Pulsed amperometric
Unsaturated oligosaccharides (2–7 residues), from lyase digestion of:				
Alginate	C ₁₈ -silica	Acetonitrile–0.1 mol L ⁻¹ phosphate buffer, pH 6.5 (1 : 9), containing tetrabutylammonium hydroxide (10 mmol L ⁻¹)	RT	UV

Table 3 Continued

Compounds	Column packing	Mobile phase	Temperature (°C)	Detection system
Pectic acid	C ₁₈ -silica	Methanol-0.05 mol L ⁻¹ phosphate buffer, pH 7.0 (3 : 7), containing tetrabutylammonium bromide (25 mmol L ⁻¹)	40	UV
	Anion exchanger (quaternary ammonium) bonded to silica	0.4 mol L ⁻¹ sodium acetate buffer, pH 5.4	40	UV
Hyaluronic acid	C ₁₈ -silica	(A) Acetonitrile-8 mmol L ⁻¹ H ₃ PO ₄ (1 : 4), pH of mixture 7.6; contains tetrabutylammonium hydroxide (10 mmol L ⁻¹) (B) Acetonitrile-6 mmol L ⁻¹ H ₃ PO ₄ (3 : 2), pH of mixture 7.5; concentration of ion-pairing reagent as in A	RT	UV
		Linear gradient, A → A + B (19 : 1) in 18 min	RT	UV
Unsaturated sulfated oligosaccharides, from lyase digestion of glycosamino-glyronans	Anion exchanger (quaternary ammonium) bonded to silica	For oligosaccharides to hexasaccharide: Linear gradient, 0.2 → 0.8 mol L ⁻¹ NaCl, pH 3.5 (50 min)	RT	UV
	NH ₂ -silica	Disaccharides only: 10 mmol L ⁻¹ Na ₂ SO ₄ -1 mmol L ⁻¹ CH ₃ COOH	50	UV
	Cation exchange resin (Na ⁺ form)	Disaccharides only: Acetonitrile-methanol-0.8 mol L ⁻¹ ammonium formate buffer, pH 4.5 (13 : 3 : 4)	70	UV
Uronic acids	Cation exchange resin (H ⁺ form)	4.5 mmol L ⁻¹ H ₂ SO ₄	25	UV
	Anion exchanger (quaternary ammonium) bonded to silica	5 mmol L ⁻¹ KH ₂ PO ₄ (pH 4.6) containing methanol (5%)	RT	UV
		0.7 mol L ⁻¹ CH ₃ COOH	40	RI

RT, Room temperature; RI, refractive index.

Table 4 Solvent systems useful in TLC and paper chromatography of sugar derivatives

<i>Derivatives</i>	<i>Stationary phase</i>	<i>Solvent system^a</i>
Acetals and ketals	Silica gel	Benzene-ethanol (2 : 1) Benzene-acetic acid-ethanol (2 : 2 : 1) For pyruvate: Ethyl acetate-acetic acid-formic acid-water (12 : 3 : 1 : 4) (threefold development) Acetonitrile-water (9 : 1)
Acetates	HPTLC plates with bonded aminopropyl phase, impregnated with NaH ₂ PO ₄ (0.2 mol L ⁻¹) Silica gel	 Benzene-ethyl acetate (7 : 3) Benzene-methanol (9 : 1)
Alditols	Paper Paper impregnated with tungstate (0.15 mol L ⁻¹) CMC paper (La ³⁺ , Ca ²⁺ or Ba ²⁺ forms) Cellulose plates impregnated with tungstate (0.15 mol L ⁻¹) Silica gel impregnated with NaH ₂ PO ₄ (0.5 mol L ⁻¹)	1-Butanol-ethanol-water (4 : 1 : 5), upper layer 2-Butanone-acetic acid-saturated aqueous solution of H ₃ BO ₃ (9 : 1 : 1) Acetone-1-butanol-water (5 : 3 : 2) 1-Butanol-ethanol-water (10 : 1 : 2) Acetone-1-butanol-water (5 : 3 : 2) 2-Propanol-acetone-0.2 mol L ⁻¹ lactic acid (6 : 3 : 1)
Aldonic acids and aldonolactones	Cellulose plates Silica gel, HPTLC	1-Butanol-acetic acid-water (6 : 1 : 2) Ethyl acetate-pyridine-acetic acid-tetrahydrofuran-water (50 : 22 : 4 : 15 : 15)
Amino- and acetamidodeoxyhexoses	Paper Cellulose plates	Ethyl acetate-pyridine-acetic acid-water (5 : 5 : 1 : 3) 1-Butanol-pyridine-benzene-water (5 : 3 : 1 : 3) 1-Butanol-pyridine-0.1 mol L ⁻¹ HCl (5 : 3 : 2) Two-dimensional development: (1) 2-Propanol-90% HCOOH-water (20 : 1 : 5); (2) Lutidine-water (13 : 7) 1-Propanol-water (7 : 1)
Dansyl derivatives	Silica gel	Cyclohexane-ethyl acetate-ethanol (6 : 4 : 3)
Anhydroalditols	Silica gel	1-Butanol-acetone-water (5 : 4 : 1)
Anhydro sugars	Silica gel, HPTLC, impregnated with borate (0.1 mol L ⁻¹) HPTLC plates with bonded aminopropyl phase, impregnated with NaH ₂ PO ₄ (0.2 mol L ⁻¹)	Acetonitrile-water (9 : 1)
Branched-chain sugars (apiose, hamamelose and derivatives)	Paper	1-Butanol-pyridine-acetic acid-water (60 : 40 : 3 : 30) 1-Butanol-ethyl acetate-acetic acid-water (8 : 6 : 5 : 8)
Cyclitols	Paper	Acetone-water (4 : 1)
Gangliosides	Silica gel, HPTLC	Methyl acetate-2-propanol-33 mmol L ⁻¹ KCl (9 : 6 : 4) Acetonitrile-2-propanol-50 mmol L ⁻¹ KCl (10 : 67 : 23)
Glycosides, aryl, acetylated	Silica gel	Acetonitrile-2-propanol-2.5 mol L ⁻¹ aqueous ammonia (2 : 13 : 5) 2-Butanone-light petroleum (1 : 3)

Table 4 Continued

Derivatives	Stationary phase	Solvent system ^a
Glycosides, methyl	Paper	t-Pentanol–1-propanol–water (8 : 2 : 3)
	Cellulose plates	Ethyl acetate–pyridine–acetic acid–water (5 : 5 : 1 : 3)
Methylated	Silica gel	1-Butanol–acetic acid–water (3 : 1 : 1)
		Benzene–ethanol–water (170 : 47 : 15), upper layer
Methyl ethers	Paper	1-Butanol–ethanol–water (4 : 1 : 5), upper layer
		2-Butanone–water azeotrope (85 : 7)
	Cellulose plates	2-Butanone–saturated with water
	Silica gel	2-Butanone–water azeotrope
		Benzene–ethanol–water–aqueous ammonia (200 : 47 : 15 : 1), upper layer
	Silica gel impregnated with H ₃ BO ₃ (0.1 mol L ⁻¹)	1-Butanol–acetone–water (4 : 5 : 1)
Muramic acid (separated from aminodeoxyhexoses)	Cellulose plates	Two-dimensional development : (1) 2-Propanol–90% HCOOH–water (20 : 1 : 5), (2) Lutidine–water (13 : 7) Acetonitrile–ethanol–acetic acid–water (13 : 2 : 1 : 4)
	Silica gel	Methanol–water (5 : 2)
Neuraminic acids, N-acetyl and N-glycolyl	Silica gel	Ethyl acetate–acetic acid–water (2 : 1 : 2), twofold development
Oligogalacturonic acids (to DP 9)	Cellulose plates	Ethanol–25 mmol L ⁻¹ CH ₃ COOH (21 : 29), 35°C
	Silica gel, HPTLC	Acetonitrile–water (18 : 7)
Oligosaccharides, chitin (to DP 6)	HPTLC plates with bonded aminopropyl phase, impregnated with NaH ₂ PO ₄ (0.2 mol L ⁻¹)	
Oligosaccharides, from hyaluronic acid (2–8 residues)	Silica gel	2-Propanol–water (33 : 17), containing NaCl (50 mmol L ⁻¹)
Phosphates	Paper	Methanol–90% HCOOH–water (16 : 3 : 1), containing tetrasodium salt of EDTA (0.05%, m/v)
Unsaturated disaccharides, from lyase digestion of glycosaminoglycuronans, run as dansylhydrazones	Silica gel	1-Propanol–2-propanol–1-butanol–water (6 : 9 : 1 : 4), containing NaCl (40 mmol L ⁻¹) and ammonia (10 mmol L ⁻¹)
Uronic acids and alduronolactones	Paper	1-Butanol–acetic acid–water (2 : 1 : 1)
		Ethyl acetate–acetic acid–formic acid–water (18 : 3 : 1 : 4)
		Ethyl acetate–acetic acid–pyridine–water (10 : 3 : 3 : 2)
		Ethyl acetate–acetic acid–water (3 : 1 : 1)
	DEAE-cellulose paper	1-Butanol–acetic acid–water (6 : 1 : 2)
	Cellulose plates	1-Butanol–ethanol–0.1 mol L ⁻¹ H ₃ PO ₄ (1 : 10 : 5)
	Silica gel impregnated with NaH ₂ PO ₄ (0.3 mol L ⁻¹)	

^aAll proportions are by volume.

Table 5 Lectins used in affinity chromatography of oligosaccharides

Lectin	Specificity
Concanavalin A (Con A)	α -D-Man, terminal or substituted only at O2; terminal β -D-GlcNAc at O2 promotes binding
<i>Datura stramonium</i> agglutinin (DSA)	$[\beta$ -D-Gal (1 \rightarrow 4) β -D-GlcNAc (1 \rightarrow 3)] _n , i.e. poly (<i>N</i> -acetylglucosamine); binds tri- and tetraantennary oligosaccharides lacking this sequence if outer Man residue is substituted at O2 and O6 by <i>N</i> -acetylglucosamine
<i>Griffonia simplicifolia</i>	Terminal α -D-Gal
<i>Helix pomatia</i> (HP)	Terminal α -D-GalNAc
<i>Lens culinaris</i> (lentil)	Terminal α -D-Man: outer Man residue substituted at O2 and O6 by GlcNAc
Phytohaemagglutinin, erythroagglutinating (E ₄ -PHA)	Bisecting GlcNAc at O4 of inner Man residue and sequence β -D-Gal (1 \rightarrow 4) β -D-GlcNAc (1 \rightarrow 2) α -D-Man in outer chains
Phytohaemagglutinin, leukoagglutinating (L ₄ -PHA)	Tri- and tetraantennary oligosaccharides with outer Man residue substituted at O2 and O6 by <i>N</i> -acetylglucosamine
<i>Pisum sativum</i> (pea)	Terminal α -D-Man; α -L-Fuc at O6 of 4-linked GlcNAc in inner core of <i>N</i> -linked oligosaccharide
<i>Ricinus communis</i> agglutinin (RCA-I)	Terminal β -D-Gal
<i>Sambucus nigra</i>	α -NeuAc (2 \rightarrow 6) Gal \gg α -NeuAc (2 \rightarrow 3) Gal
<i>Wisteria floribunda</i>	β -D-GalNAc (1 \rightarrow 4) Gal $>$ α -D-GalNAc (1 \rightarrow 3) Gal and α -D-GalNAc (1 \rightarrow 3) GalNAc: substitution of 4-linked Gal by NeuAc at O3, or of 3-linked Gal by α -L-Fuc at O2 weakens binding

excess of 5000. For these the addition of methanol to the carbon dioxide mobile phase has proved advantageous. Fused-silica microbore capillary columns, with a bonded methylpolysiloxane stationary phase (DB-1 and, especially, DB-5 are very effective), are used at temperatures ranging from 90 to 120°C and with pressure programming over the range 10–40 MPa (100–400 bar) at about 0.5 MPa min⁻¹ (5 bar min⁻¹). Under these conditions there is resolution of α and β anomers (more pronounced with the TMS derivatives) and fine structure is discernible in glycoconjugates.

Thin-Layer Chromatography (TLC) and Paper Chromatography

While nonpolar derivatives can be separated by thin-layer chromatography (TLC) on unmodified silica plates, resolution of polar molecules is generally poor unless the silica gel layer is impregnated beforehand with an inorganic salt capable of interacting with carbohydrates. Borate or phosphate buffers are most

often used for this purpose; tungstate can also prove effective, especially in TLC of alditols. The same applies to TLC on high performance (HP) TLC plates, particularly those carrying a bonded aminopropyl phase, which is liable to react covalently with sugars and derivatives containing hydroxyl groups. Some separations, particularly those of aminodeoxy sugars, that are not well resolved on impregnated silica gel plates, are better on unmodified silica plates. Cellulose plates also give satisfactory resolution of these derivatives, and of neutral sugars and uronic acids, but two-dimensional development is often required. Impregnation of these plates with tungstate greatly improves their resolving power for alditols.

Although paper chromatography has largely been superseded by TLC, there are groups of sugar derivatives that are far better resolved on paper than by TLC methods. The mixtures of partially methylated sugars obtained in methylation analysis of polysaccharides afford a prime example: resolution on cellulose plates is better than that on silica plates but

paper chromatography remains the most effective method. As in the case of TLC, separation of alditols on paper is improved by impregnation of the paper with tungstate. Papers having ion exchange properties can also be used to good effect in separations of some sugar derivatives: uronic acids and aldobiouronic acids are well resolved on DEAE-cellulose paper (anion exchanger), while carboxymethylcellulose paper, converted beforehand to the La^{3+} , Ca^{2+} or Ba^{2+} forms, gives excellent resolution of alditols.

Some solvent systems that have proved effective in TLC and paper chromatography of sugar derivatives are listed in Table 4.

Affinity and Enzyme Methods

Affinity Chromatography

Lectin affinity chromatography is a valuable technique in analyses of glycoconjugates, as the isolation and identification of glycopeptides and the various oligosaccharides obtained on removal of the carbohydrate side chains from the protein or lipid moieties are greatly facilitated by chromatography on a series of short columns, each containing a different lectin covalently coupled to agarose gel. The lectins are selected according to their specificity towards carbohydrates having certain of the main structural features found in the oligosaccharides, and in this way the complex mixture of oligosaccharides can be fractionated according to structure. Some of the lectins that have proved useful in such studies are listed in Table 5, together with their carbohydrate-binding specificities.

The oligosaccharides are usually applied to the lectin columns in phosphate-buffered saline (PBS), pH 7.2, Tris-buffered saline (TBS), pH 8.0, or 10 mmol L^{-1} Tris-HCl buffer, pH 7.5; sodium azide (0.02%, m/v) is added as a preservative and small amounts of calcium, magnesium and manganese chlorides (1 mmol L^{-1}) are essential to the binding action of some lectins, notably concanavalin A. Oligosaccharides that are not bound or are only retarded on the lectin column are eluted with these buffers, but those that are strongly bound require the addition of a competing hapten to the eluent. Haptens applicable to the lectins listed above include methyl α -D-mannopyranoside, lactose, GalNAc, GlcNAc and N,N'-diacetylchitobiose.

A recent development in affinity chromatography is the use of monoclonal antibodies as ligands; these are highly specific but less strongly reactive than lectins, and the dissociation constants of the complexes formed with bound solutes are sufficiently low to permit rapid fractionation, the oligosaccharides reacting

with the ligand being merely retarded on the column, not totally immobilized. An example of the use of this technique is afforded by the complete separation of two of the oligosaccharides of human milk, α -NeuAc(2 \rightarrow 3) β -D-Gal(1 \rightarrow 3) β -D-GlcNAc(1 \rightarrow 3) β -D-Gal(1 \rightarrow 4)Glc (lactosialyltetrasaccharide, LSTa) and that designated sialyl Le^a, which carries α -L-Fuc at O4 of GlcNAc. On a short column containing monoclonal antibody 19.9 coupled to agarose gel, with 10 mmol L^{-1} Tris-HCl buffer, pH 7.5, as eluent, the two oligosaccharides are rapidly separated, the fucosylated sialyl Le^a being the more retarded. The active oligosaccharides of blood group A are similarly fractionated according to chain lengths and degree of fucosylation by chromatography on immobilized IgM antibody, with TBS as eluent. Use of columns in which such antibodies are coupled to microparticulate silica makes possible very rapid separations of oligosaccharides (in 20 min or less). This new technique of high performance liquid affinity chromatography (HPLAC) has great potential in applications such as clinical analysis, for which methods that are highly specific but also efficient are required.

Enzyme Methods

Enzyme methods are particularly useful in analyses of glycoconjugates, for the release of mono- or oligosaccharides that are not easily liberated by acid hydrolysis or are acid-labile, and in the determination of some constituents. The determination of neuraminic acid derivatives in glycoproteins or glycolipids is a striking example of this use of enzymes. The sample (~ 200 μg), dissolved in 60 mmol L^{-1} phosphate buffer (pH 7.0, 800 μL), is incubated at 37°C for 1 h with *Clostridium perfringens* neuraminidase (EC 3.2.1.18) and N-acylneuraminate pyruvate-lyase (EC 4.1.3.3). The former (0.5 U) liberates the neuraminic acid derivatives from glycosidic linkages and the latter (0.3 U) cleaves the molecules to produce N-acyl-mannosamines and pyruvate. The mannosamine derivatives are well separated from GlcNAc, GalNAc and neutral sugar components of glycoconjugates by LC (H^+ form cation exchange resin, 92% acetonitrile in water; see Table 3) and may be determined in this way. Alternatively (or in addition), the proportion of neuraminic acids may be found by determining the pyruvate released, using the definitive lactate dehydrogenase method.

For release of N-linked oligosaccharides from glycoproteins, digestion with N-oligosaccharide glycopeptidase (EC 3.5.1.52) offers a milder alternative to the standard hydrazinolysis procedure. After pepsin digestion of the protein moiety, the product, dissolved in 0.1 mmol L^{-1} citrate-phosphate buffer,

is digested with the glycopeptidase (1 mU per 1000 nmol of oligosaccharides) at 37°C for 15 h. For sequencing purposes, smaller oligosaccharides may be obtained by subsequent digestion with various exoglycosidases, such as α -L-fucosidase (EC 3.2.1.51), β -D-galactosidase (EC 3.2.1.23) and β -N-acetylglucosaminidase (EC 3.2.1.30). The mixtures of oligosaccharides are separated by LC (see Table 3).

Enzyme methods are also important in the analysis of glycosaminoglycuronans, which are very resistant to acid hydrolysis. Hyaluronidase (EC 3.2.1.35) randomly cleaves the (1 \rightarrow 4) bonds linking the acetamidodeoxyhexose residues to glucuronic acid in both hyaluronic acid and the chondroitin sulfates, to yield the disaccharide repeating unit and oligomers. An exception to this is leech hyaluronidase (EC 3.2.1.36), which specifically cleaves the β -D-GlcA (1 \rightarrow 3) β -D-GlcNAc linkages in hyaluronic acid, yielding a different series of oligomers. All of these, including some with odd numbers of sugar residues, obtained by removal of the nonreducing GlcA end-groups with β -glucuronidase (EC 3.2.1.31) or of nonreducing GlcNAc end-groups with β -N-acetylglucosaminidase, are well separated by LC (see Table 3).

A sensitive analytical method for glycosaminoglycuronans is afforded by LC of the unsaturated oligosaccharides produced on digestion with enzymes having lyase activity, which give disaccharides or, in the case of hyaluronic acid, tetra- and hexasaccharides with 4,5-unsaturated residues (4-deoxy-L-threo-hex-4-enopyranosyluronic acid from D-glucuronic acid or L-iduronic acid) at their nonreducing ends. Chondroitinase ABC (EC 4.2.2.4) digests chondroitin 4- and 6-sulfate and dermatan sulfate, whereas chondroitinase AC (EC 4.2.2.5) does not act upon dermatan sulfate, and LC analysis (Table 3) of the mixtures of unsaturated, sulfated disaccharides produced by each enzyme permits quantification of the respective parent glycosaminoglycuronans. Typically, the proteoglycan (1–1000 μ g) is digested at 37°C for 16 h with the enzyme (0.05 U) in Tris buffer (pH 6.0). Hyaluronic acid can be determined specifically by LC analysis of the unsaturated tetra- and hexasaccharide produced on digestion with the lyase from *Streptomyces hyalurolyticus* (H-1136), which cleaves this polymer selectively. Recently the LC profiles of the products of digestion of heparin with heparin lyase (EC 4.2.2.7), from *Flavobacterium heparinum*, have been suggested as a means of characterizing this polydisperse glycosaminoglycuronan: di-, tetra- and hexasaccharides, differing in degree of sulfation and proportion of iduronic acid, are produced, their proportions in the mixture varying with the source of the heparin.

Structural analysis of alginates, which contain blocks of mannuronic acid and guluronic acid residues, all (1 \rightarrow 4) linked, is facilitated by the use of enzymes acting exclusively on one of these acids, leaving intact blocks of the other. These enzymes are lyases, producing unsaturated oligosaccharides from the portions of the polymer that they attack. For example, a β -D-mannuronase has been isolated from actively growing tissues of the seaweed *Sargassum fluitans* and an α -L-gulonase from the bacterium *Klebsiella aerogenes* type 27. Digestion may be monitored by LC analysis of the unsaturated oligosaccharides (Table 3). This applies also to digestion of pectic acid with *endo*-polygalacturonic acid lyase (EC 4.2.2.10). The saturated oligogalacturonic acids produced on digestion of this polymer with *endo*-polygalacturonase (pectinase: EC 3.2.1.15) are also analysed by LC.

Specific Problems: Analysis of Acidic Derivatives

Whereas the enzyme methods discussed above are used in the degradation of glycoproteins and glycolipids, which contain sugar derivatives – such as the neuraminic acid derivatives – that are unstable when heated in acid, and of glycosaminoglycuronans and polyuronans, which are strongly resistant to acid hydrolysis, it is the latter technique that is most widely used to liberate the constituent monosaccharides from other heteropolysaccharides. For those containing aldobiouronic acid linkages, which are far less readily hydrolysed than are glycosidic linkages between neutral sugars, slow release and low yields of both hexuronic acids and the contiguous (interior) sugar residues make quantification difficult. The use of vigorous conditions or prolonged exposure to acid in attempting to improve the yields of these constituents is liable to cause both decarboxylation of the acid and decomposition of some of the neutral sugars already liberated (pentoses being especially vulnerable). For quantitative GC analysis, the difficulty can be obviated by prior reduction of the carboxyl groups in the uronic acid compounds. This is best effected by treatment with a carbodiimide at pH 4.75, followed by reduction with sodium borohydride or borodeuteride at pH 7.0; if the latter is used, the hexoses produced from the hexuronic acids are labelled with deuterium and thus readily identifiable by GC-MS of the derived alditol acetates.

In methylation analysis, the problems posed by resistance to acid hydrolysis of linkages involving methylated uronic acid residues (present as methyl esters) are similar. In this case the recommended procedure is reduction of the carboxylate ester groups

with lithium aluminium deuteride in dry oxolane (tetrahydrofuran) at 70°C for 16 h. The ester residue is then converted to a 6,6-dideuteriohexose residue, the O-methyl ethers of which are easily distinguishable by GC-MS of the derived alditol acetates.

An alternative to acid hydrolysis that is applicable to most polysaccharides and glycoconjugates, including those containing acid-labile residues or glycosidic linkages resistant to hydrolysis, is afforded by methanolysis, in which the sample is heated in methanolic HCl, the conditions employed depending upon the nature of the sugar residues present. After suitable derivatization, all components of methanolysates, now present as methyl glycosides or, in the case of hexuronic acids, methyl glycoside methyl esters, can be analysed simultaneously, either by GC (Table 2) or by LC (Table 3). The procedure is also applicable to methylation analysis, the methylated methyl glycosides and methyl glycoside methyl esters being amenable to GC without further derivatization (Table 2).

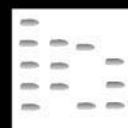
See Colour Plate 118.

See also: **II/Chromatography:** Paper Chromatography. **Chromatography: Gas:** Derivatization; Detectors: Mass Spectrometry. **Chromatography: Liquid:** Derivatization. **Chromatography: Thin-Layer (Planar):** Spray Reagents. **III/Impregnation Techniques: Thin-Layer (Planar) Chromatography.** **Polysaccharides:** Centrifugation; Liquid Chromatography.

Further Reading

- Churms SC (1982) *CRC Handbook of Chromatography: Carbohydrates*, vol. I. Boca Raton, FL: CRC Press.
- Churms SC (1991) *CRC Handbook of Chromatography: Carbohydrates*, vol. II. Boca Raton, FL: CRC Press.
- Churms SC (1996) Recent progress in carbohydrate separation by high-performance liquid chromatography based on hydrophilic interaction. *Journal of Chromatography A* 720: 75–91.
- Dey PM (ed.) (1990) *Methods in Plant Biochemistry*, vol. 2, *Carbohydrates*. London: Academic Press.
- El Rassi Z (ed.) (1995) *Carbohydrate Analysis. High Performance Liquid Chromatography and Capillary Electrophoresis*. Amsterdam: Elsevier Science.
- Ginsburg V (ed.) (1987) Lectin affinity chromatography of glycopeptides. *Methods in Enzymology* 138: 232–259.
- Ginsburg V (ed.) (1989) Analysis of complex oligosaccharides from glycoconjugates by affinity chromatography and high-performance anion-exchange chromatography. *Methods in Enzymology* 179: 30–82.
- Reinhold VN, Sheeley DM, Kuei J and Her GR (1988) Analysis of high molecular weight samples on a double-focusing magnetic sector instrument by supercritical fluid chromatography/mass spectrometry. *Analytical Chemistry* 60: 2719–2722.
- Whistler RL, Wolfrom ML, BeMiller JN and Shafizadeh F (eds) (1962) *Methods in Carbohydrate Chemistry*, vol. I. New York: Academic Press.
- Whistler RL and BeMiller JN (eds) (1976) *Methods in Carbohydrate Chemistry*, vol. VII. New York: Academic Press.

SULFUR COMPOUNDS: GAS CHROMATOGRAPHY



W. Wardencki, Technical University of Gdańsk, Gdańsk, Poland

Copyright © 2000 Academic Press

Introduction

Sulfur compounds, of both biogenic and anthropogenic origin, constitute a large group of compounds, ranging from simple gases up to complex polycyclic aromatics. These compounds can be present in various, usually complex matrices, such as air (gaseous), water systems (aqueous), various petroleum fractions (gaseous, liquid and solid), in beverages and food-stuffs and in pharmaceutical formulations.

Environmentalists believe that these compounds are responsible for the damage of our environment through acid deposition, rapid acidification of lakes,

the loss of forests, the corrosion of metal structures and historical monuments. The interest in biogeochemistry results from the role some sulfur compounds play in global chemical cycles. Dimethyl sulfide (DMS) in sea water, produced in the oceans, is believed to play a critical role in the global sulfur cycle and the radiation balance of the Earth. Also, other sulfur compounds may contribute significantly to the sulfur flux in the atmosphere. In foods, beverages and in water, trace levels of sulfur-containing compounds are responsible for taste and odour problems. They are also the source of malodorous conditions in municipal sewage systems. Refiners worldwide give particular attention to these compounds because in petrochemical and chemical applications even trace levels of sulfur impurities may cause concern. They can poison the catalysts, impart

undesirable properties to final products or produce general air pollution when fuel is burnt.

For these reasons sulfur-containing compounds are of constant concern in many fields. Gas chromatography, due to combination of separation capability and sensitive detection is still a prime technique for the analysis of these compounds in various matrices.

General Problems of the Determination of Sulfur Compounds by Gas Chromatography

The analysis of sulfur compounds in different environmental matrices is still a big challenge for the analytical chemist. The main difficulties in their determinations are related to the two main obstacles.

The first is common with general problems encountered in trace analysis. Most of these compounds are present at low concentrations, frequently at the low parts per trillion (ppt) level. They may be encountered in very complex matrices and in a broad range of concentrations (often several orders of magnitude). Complex mixtures can cause interference problems between major and minor constituents.

The second difficulty is due to the highly reactive nature of sulfur compounds. It is well known that these compounds have absorptive, adsorptive, photo-oxidative and metal catalytic oxidative features. This can lead to irreversible adsorption, reaction with each other, catalytic reactions, rearrangements catalysed by different materials and reactions with substances they come into contact with. Because of these reasons special precautions should be undertaken during all steps of their analysis, e.g., during sample treatment (sampling, storage, pre-concentration and isolation) as well as during the gas chromatographic analysis.

When sulfur content is relatively high (up to percentage level) and the matrix is very complex, like crude oil, direct GC analysis can be frequently done, reducing the analysis time and eliminating the possibility of analyte losses. Such samples, due to possible interference problems, require very effective separation systems and very selective (specific) detectors. The choice of a detector with high selectivity for sulfur over hydrocarbon is crucial.

Due to the diversity of the matrices in which sulfur compounds can be present it is convenient to discuss each type of sample separately.

Atmospheric Sulfur Gases

Sulfur gases are released into the atmosphere from various natural and anthropogenic sources. The most abundant atmospheric sulfur compounds are: hydro-

gen sulfide (H_2S), carbonyl sulfide (COS), dimethyl sulfide (DMS), dimethyldisulfide (DMDS), carbon disulfide (CS_2) and methanethiol (methyl mercaptan – MeSH). These compounds have received a great deal of attention because of the suggestion that the emission of natural compounds may be substantial even compared to anthropogenic sources of sulfur dioxide (SO_2). Frequently, all these compounds are called ‘reduced sulfur compounds’, S(-II), abbreviated to RSCs. These compounds, together with other sulfur species with boiling points up to ca. 200°C , are usually termed ‘volatile sulfur compounds’ (VSCs). Considering VSCs the emphasis is especially put on DMS, which is the predominant form of volatile sulfur compounds in the oceans.

Sampling

Sampling vessels (glass bottles, bulbs, canisters and polymeric bags) for sulfur gases should be as inert as possible in order to minimize adsorption losses and to avoid possible reactions during sampling. For these reasons, all materials in sampling vessels, tubing and unions in contact with the sample should be carefully chosen. The conditioning or covering of surfaces with inert materials or application of surface deactivation procedures such as silanization is usually necessary.

Glass sampling bottles or bulbs are commonly used for collecting and transporting gas samples or to blend calibration gas mixtures. Stainless steel canisters and Teflon bottles are very convenient. Frequently, the canisters are conditioned by heating under vacuum before use. Sampling bags made of Tedlar film which is a polyvinyl fluoride (PVF) are chosen because of their inertness. To prevent losses of sulfur compounds, sampling vessels and connections may be covered with aluminium foil to avoid photo-chemical reactions.

Preconcentration

Due to the low concentration of sulfur species in air (ppb or ppt level) different preconcentration techniques have been applied before the gas chromatographic analysis proper. The most frequently used methods for these purposes are sorption on certain metals, sorption on solid sorbents and cryogenic trapping.

Sorption on metals This pre-concentration method is based on the ability of certain metals (mainly gold, palladium and platinum) to chemisorb sulfur gases. Glass or quartz tubes filled with gold wool, gold-coated glass beads, gold-plated sand or metal foils are used for this purpose. The sample may be passed through a Teflon tube containing a thin metal foil of

palladium (Pd), platinum (Pt) or gold (Au). Custom-fabricated Pd on Pt has the advantage of the analytical collection efficiency of Pd and an increased durability and lifetime. Rapid desorption of the sulfur compounds is achieved by passing a current through the foil. Such a technique (metal foil collection/flash desorption and flame photometric detection) has demonstrated a detection limit for total sulfur concentration of around 10 pptv (10^{-11}).

Sorption on solid sorbents Adsorption on solid sorbents is one of the simplest and most efficient methods of concentration of volatile compounds. Adsorbent trapping is very popular, especially when traps are kept at low temperatures. Ambient temperature trapping may frequently give poor recoveries due to poor collection efficiency.

Many sorbents, such as activated charcoal, silica gel, aluminium oxide, graphitized carbon black, molecular sieves and porous polymers have been applied to collect volatile sulfur species. The use of porous polymers is the most widespread since the collected substances can be desorbed from porous polymers more easily, compared to desorption from charcoal. Furthermore, collection efficiency on porous polymers is less sensitive to water vapour in the sampling atmosphere. The trapped compounds are usually released by thermal desorption and injected into a GC column. Before this operation, they may be subjected to cryothermal focussing in a capillary in order to obtain a narrow injection band.

Among the porous sorbents, Tenax has the highest popularity. Tenax has a low affinity for water, and breakthrough volume is relatively independent of humidity. It is well suited for thermal desorption techniques as it exhibits high thermal stability (375°C) and can be subjected to repeated temperature cycling without deterioration. The determination of several sulfur gases can be easily conducted, even though Tenax has a relatively low specific surface area (ca. $19\text{ m}^2/\text{g}$) which consequently limits the sampling volume. In practice, Tenax GC or TA is used together with Chromosorb 106 and Sphercarb as backup adsorbents. In order to retain the low boiling organic sulfur compounds that are present in many samples, cooling the trap with liquid nitrogen may be necessary but this creates a problem when excessive amounts of methane are present. Cooling with solid carbon dioxide is suitable for trapping of VOS compounds under these circumstances. Carbosieve adsorption tubes can be used for collecting CS_2 after purging it from seawater samples.

For moist air samples (96% relative humidity) acceptable recoveries have been observed for the following sorbents: silica gel (recovery for MeSH

> 95%), molecular sieve (recovery for MeSH 73.9% for COS 75%) and Carbosieve III S (recovery for COS 71.7%) used with calcium chloride as a drying agent. For methanethiol, recovery values showed no significant changes during 36 h storage or using different flow rates in the range of $10\text{--}80\text{ mL min}^{-1}$.

Cryogenic trapping Cryogenic trapping is the technique of choice for collecting VSCs from air samples but is not always practical due to transportation and storage difficulties at remote locations.

Cryogenic trapping is very popular after purging VSCs from various water samples and therefore is also discussed in the next section.

Analysis of VSCs in air is complicated by the oxygen, SO_2 and NO_2 which can cause variable and often severe sampling losses by oxidation of these compounds. Scrubbers for oxidant removal include Teflon and Tygon shavings, and various substrates (glass fibre filters, Chromosorb, Anakrom, and glass beads) coated with Na_2CO_3 or manganous oxide, MnO .

Sulfur Compounds in Aqueous Matrices

Sampling

Aqueous samples for the analysis of VSCs are usually collected in glass or polymer bottles. Glass vessels are frequently silanized in order to minimize losses due to adsorption on the walls. Brown glass is used to stop biological and chemical processes which can occur under the influence of light. Teflon and polyethylene are frequently used. During sampling the vessels should be filled to the top to exclude air and minimize head space losses.

Isolation and/or Preconcentration

Because direct analysis of sulfur compounds in water matrices is often impossible, various preconcentration or isolation procedures are applied before the analysis proper. Solvent extraction and static and dynamic headspace techniques are most popular.

Liquid extraction Solvent extraction is not as frequently applied as formerly because this technique has several disadvantages, i.e., handling toxic solvents, the trapped substances become diluted, automation is difficult and the procedures are time consuming. The most popular solvents for the VSCs are diethyl ether, hexane or mixtures of these solvents.

Static gas extraction methods Headspace-gas chromatography (HS-GC) analysis can be applied

successfully for the analysis of VSCs in different liquid matrices. It can be also applied in physical chemistry studies of these compounds, being a valuable tool for acquiring data on gas–solid and gas–liquid systems. For example, it was used for the determination of distribution coefficients, K , of selected organosulfur compounds in air–water systems as well as their temperature, ionic strength and concentration dependencies.

Generally, the detection limit of the static headspace technique is 10 to 100 times poorer than that of the dynamic technique, i.e., purge and trap (PT).

Dynamic gas extraction methods Purge and trap assemblies can be used for isolation and preconcentration of volatile sulfur species in water samples. The extraction efficiency varies with the gas considered and the extraction facilities employed such as the dimensions of the purge vessel, bubble size distribution, sample volume and temperature, purge gas flow rate and sparge time. All these parameters should be carefully considered before applying the technique for a particular purpose.

Due to the low detection limits which can be obtained with the PT technique, it is extensively used to determine VSCs in water. Several PT procedures have been developed especially for the most important natural sulfur compound – dimethyl sulfide (DMS) – a climatically active trace gas.

Recently, there has been an interest in dimethyl sulfoxide (DMSO) determination. DMSO is also an environmentally significant compound because of its potential role in the biogeochemical cycle of DMS. Direct injection and separation of aqueous DMSO offers a simple and fast application, but exhibits limited sensitivity due to limitation on injection volumes. More frequently, DMSO reduction and subsequent analysis of the evolved DMS by purge-and-trap preconcentration has been used.

The P&T technique can also be applied for the determination of sulfur species in sediments.

Sulfur Compounds of Fossil Fuel-Origin

Trace level sulfur speciation and detection in crude oil and in different petroleum products is traditionally difficult due to the complex hydrocarbon matrix. Additionally, the fact that sulfur compounds are polar and the hydrocarbons matrices are non-polar favours the loss of sulfur compounds to active sites in analytical instruments and sample vessels. The development of sulfur-specific detectors for gas chromatography has added impetus to use of this technique for the analysis of petroleum fractions. For

example, selectivity of the sulfur chemiluminescence detector (SCD) allows the determination of sub-ppm level of sulfur compounds in the presence of percent levels of co-eluting hydrocarbons.

The usual approach for characterization of the very complex nature of different individual sulfur compounds in a crude oil is to fractionate the oil into narrow boiling range cuts (prefractionation) and to analyse each fraction, which simplifies the analysis. Sample preparation/cleanup is needed, especially for analysis of high boiling fractions (coal-derived liquids, shale oil), before GC, Solid phase extraction (SPE), using various cartridges with different solvent mixtures, followed by normal-phase liquid chromatography has been applied for separation of polycyclic aromatic sulfur heterocyclic compounds (PASHs) from polycyclic aromatic hydrocarbons (PAHs). PASHs can be found not only in fossil fuels, but also in sediments, mussels, fish and airborne particulate matter. The separation and determination of individual alkyl-substituted PASHs isomers in environmental matrices is difficult because of the isomeric structures of these species due to asymmetry imposed by the sulfur atom. Relatively good resolution of many PASHs isomers has been obtained on a smectic liquid crystal column (**Figure 1**).

In research and in everyday practice, one frequently encounters situations where not only the concentrations of both sulfur and non-sulfur compounds but also both percentage levels and low concentrations (ppm and ppb levels) of sulfur species have to be determined. In such cases two parallel detectors can be used. For example, coupling of sulfur chemiluminescence (SCD) and thermal conductivity detectors (TCD) enables the determination of concentration of both sulfur-containing (from percentage to ppb levels) and other gaseous compounds through simultaneous sampling, separation, and detection. Also simultaneous SCD and FID detection can be useful in many cases.

The sulfur-selective detectors, mainly SCD and atomic emission detector (AED), can be interfaced to simulated distillation (SimDis) systems to measure the boiling point range distribution of heteroatoms (S and N) in various petroleum fractions. Such an approach is applied for process control, quality assurance and product specification purposes. Very good sulfur SimDis chromatograms have been obtained considering the fact that typical sulfur levels in refinery streams are several orders of magnitude lower than the hydrocarbon levels.

The sulfur-selective detectors have been used for oil spill identification by finger-printing of various crude oils. The specific identification of different dibenzothiophenes by GC–high resolution MS has

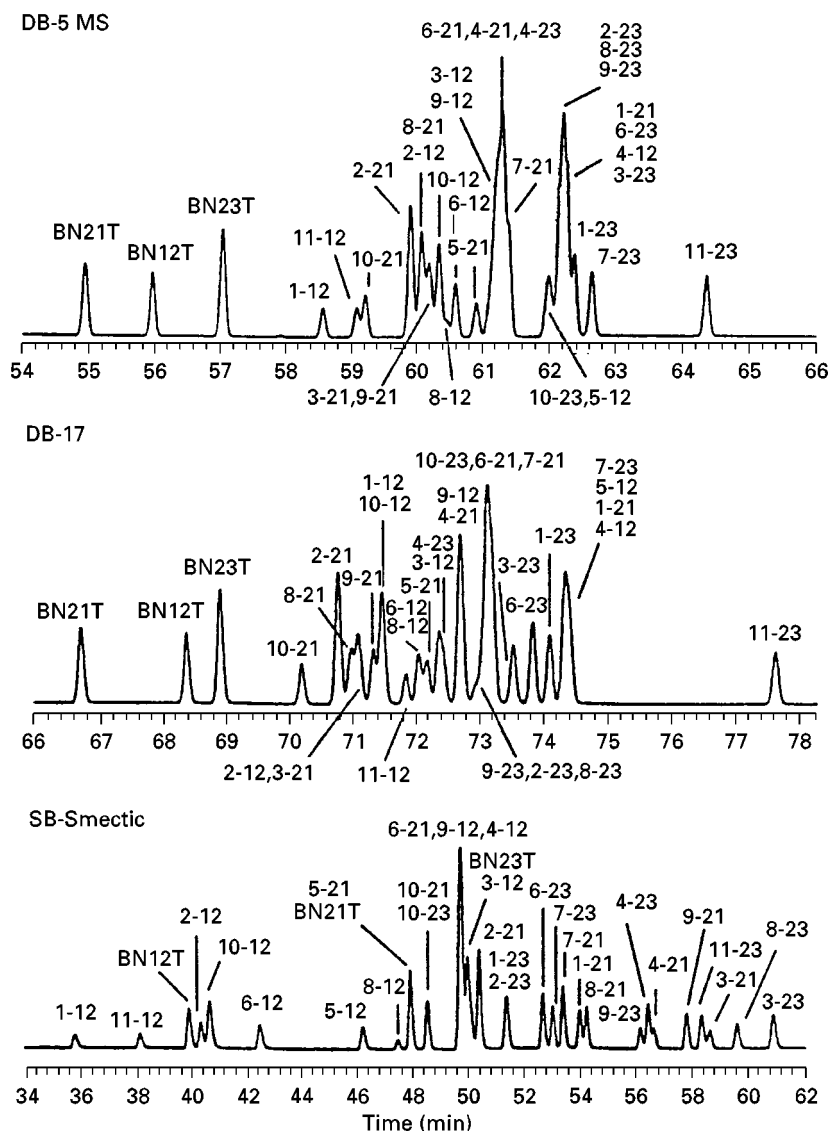


Figure 1 GC-MS separation of 3 benzo[*b*]naphthothiophene (BNT) (m/z 234) isomers and 30 methylbenzo[*b*]naphthothiophene (MeBNT) isomers (m/z 248) on different stationary phases: DB-5MS, DB-17 and SB-Smectic. BN12T = benzo[*b*]naphtho[1,2-*d*]thiophene, BN21T = benzo[*b*]naphtho[2,1-*d*]thiophene, and BN23T = benzo[*b*]naphtho[2,3-*d*]thiophene. Numbers identify the specific methylbenzo[*b*]naphthothiophene isomers, e.g., 1-12 = 1-methylbenzo[*b*]naphtho[1,2-*d*]thiophene, 8-21 = 8-methylbenzo[*b*]naphtho[2,1-*d*]thiophene, 11-23 = 11-methylbenzo[*b*]naphtho[2,3-*d*]thiophene, etc.

permitted differentiation of very similar crude oils, even from the same field.

The ability to speciate the sulfur compounds is an advantage of GC method over elemental analysis, but total sulfur can also be determined by GC by summation of all the sulfur-containing peaks.

Sulfur Compounds in Beverages and Foodstuffs

Volatile sulfur compounds have been detected in wine, beer (Figure 2), dairy products, coffee, fish, garlic and tobacco smoke. In food chemistry

these compounds contribute significantly to odour and flavour because they often possess characteristic smells and sensory thresholds (ca. $1 \mu\text{g kg}^{-1}$ for DMS).

For isolation of sulfur compounds from different food matrices, headspace sampling (HS) is the best method. For example, HS-GC has been used for the determination of VSCs in water-alcohol solutions and brandies. It was found that headspace concentrations of sulfur, H_2S , MeSH , EtSH , DMS, CS_2 , DES, thiophene, DMDS and DEDS increased with increasing ratio between the gas and liquid phase volumes and was proportional to the temperature. However, it

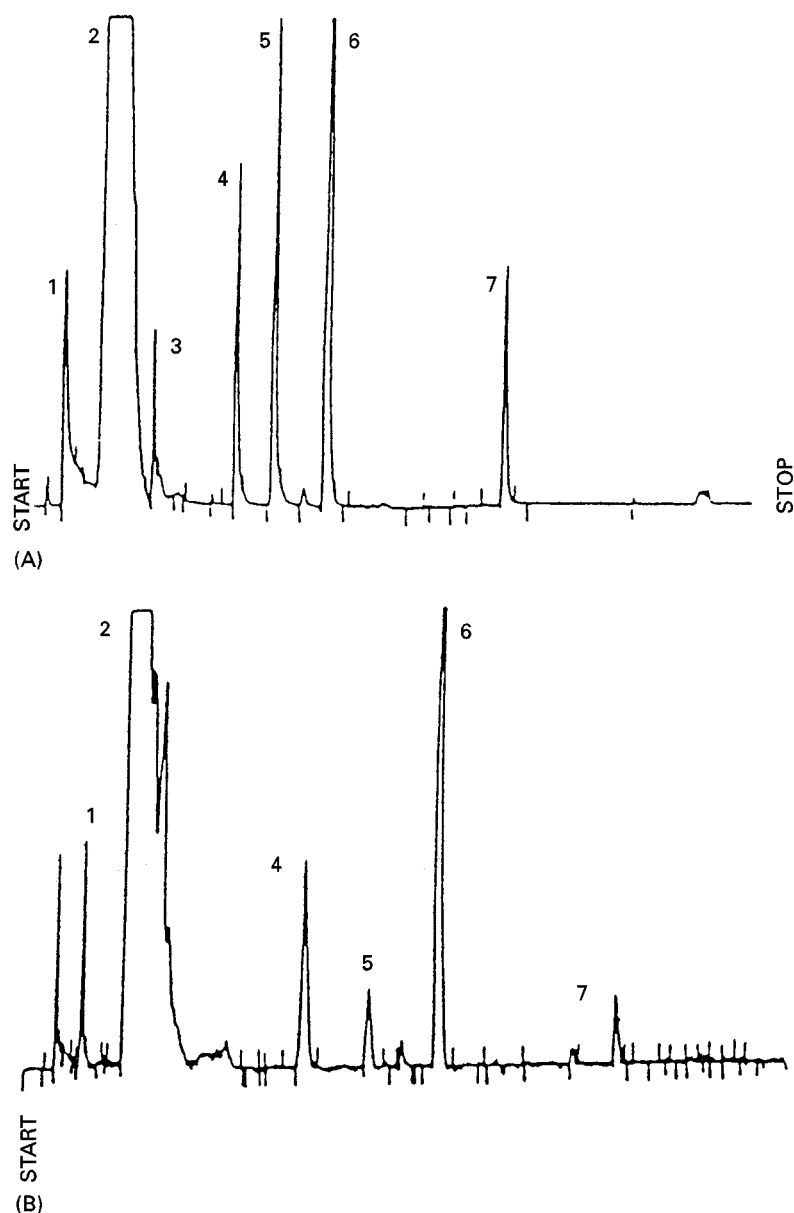


Figure 2 GC-SCD chromatograms of (A) a beer with a sulfury character and (B) a non-sulfury beer. GC conditions: column: DB-5, 30 m, 0.53 mm I.D., 1.5 μ m film thickness; injector temperature: 150°C; column temperature programme: 20–50°C at 5°C min⁻¹, 50–180°C at 8°C min⁻¹, 10 : 1 split injection. Peaks: (1) methanethiol; (2) dimethyl sulfide; (3) ethylene sulfide; (4) diethyl disulfide; (5) dimethyl disulfide; (6) isopropyl sulfide (internal standard) and (7) dimethyl trisulfide.

diminished with increasing ethanol content and was insensitive to the liquid phase salt concentration. HS sampling has also provided qualitative and quantitative data of sulfur species in dairy products.

Storage Stability of Samples

In order to avoid losses or possible transformations of sulfur compounds, samples should be analysed as soon as possible. Keeping the samples at sub-ambient temperature can improve the stability of sulfur compounds. Sulfur concentrations in an air sample

collected cryogenically and stored in a freezer were found not to change over a 2 week period. A Tenax trap containing VSCs collected from air was stored for at least 1 week at 196°C in liquid nitrogen without any loss of sulfur compounds.

For sulfur gases the most convenient method of storage seems to be in Tedlar bags. The concentrations of the five sulfur gases (COS, CS₂, MeSH and EtSH) in such bags were stable for two weeks even at the ppb concentration. Tedlar bags are not suitable for SO₂ and H₂S. In these cases, SO₂ concentration decreased from 22 ppb to less than 1 ppb in 2 h and

H₂S lost half of its original concentration of 70 ppb in about 10 days. The stability of sulfur gases in glass sampling bulbs is influenced by the gas matrix (nitrogen and air) and moisture. Reduced sulfur gases collected in glass bulbs can remain in the bulbs for approximately 24 h without major changes in gas concentrations if the sample is dry and does not contain oxygen (concentration decreased less than 5%) but dried air samples should be analysed within 3 h. Glass bulbs are not useful for collecting sulfur gases if the sample in the bulbs contains moisture (significant decrease in H₂S and MeSH concentrations was observed).

The stability of freshwater samples is strongly affected by the temperature at which it is stored. For example, it was reported that the stability of DMS in freshwater is shorter than the 48 h found in seawater samples.

Because the presence of reduced sulfur compounds in seawater is closely related to biological activity, the stability of samples may depend on the depth of sampling. When a sample was taken from the Baltic Sea at 4 m depth and was stored at 5°C in the dark, the concentration of DMS first rose dramatically after 4 days (nearly 10 times) and later decreased. Concentration of sample taken from 50 m depth did not change over a 2 week period. Samples can most probably be stored longer if the cold trap is maintained in liquid nitrogen.

To suppress microbial activity, compounds such as phenols, mercuric chloride, sodium azide and HCl can be added to water samples.

When immediate analysis is not possible, refrigeration of sample for analysis of sulfur compounds in aqueous solutions is recommended as the best way to maintain sample integrity at least for periods up to 48 h.

Separation Systems

Column packing for chromatographic determination should be chosen not only with respect to the complete separation of a given mixture but should also be selected with respect to minimize losses due to adsorption and catalytic reactions and rearrangements. These are particularly important when packed metal and glass column are used.

The most common material used for packed columns in the analysis of VSCs is Teflon. Supelpack S (specially treated Porapak QS), different Chromosorbs, Porapak Q, N or QS, Triton X 305, Chromosil 310 or 330 (specially treated silica gel), Carbopack B or BHT 100 and 3% polyphenyl ether and 1% phosphoric acid on Chromosorb T have all been reported for VSCs analysis.

Good separation of many gaseous sulfur compounds can be obtained on Chromosil 310 and 330 and Supelpack (Figure 3). The latter can resolve the

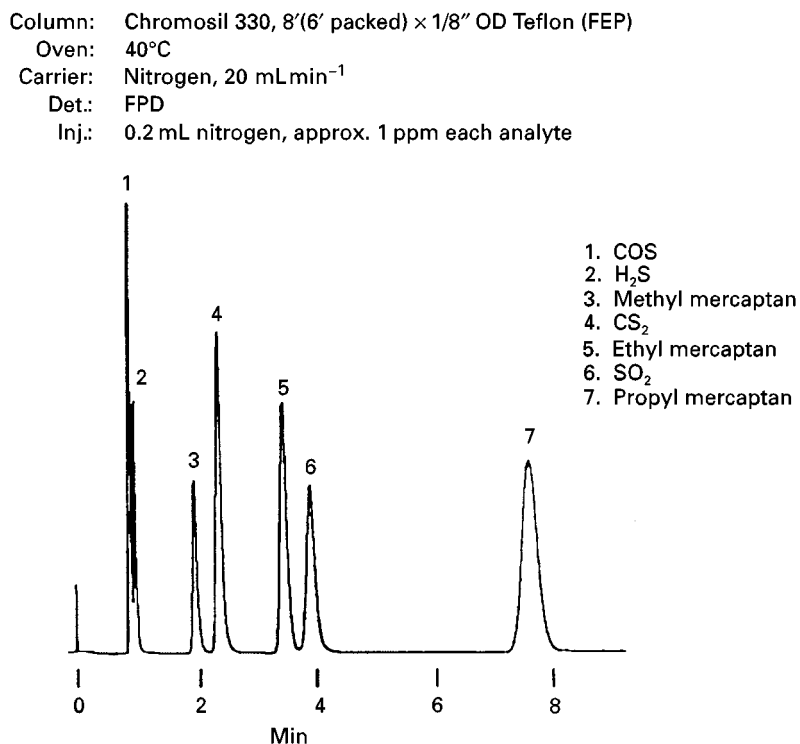


Figure 3 Trace light sulfur gases and C1–C3 mercaptans. (From Supelco Bulletin 722, reprinted with permission of Supelco, Bellefonte, PA 16823, USA.)

large peak of CO_2 (evolved from acidified seawater) from the much smaller and neighbouring H_2S and COS peaks.

Development of fused silica capillary columns has provided more inert surfaces for trace sulfur analysis. As with most analysis, no single capillary column can assure the combination of sample capacity, good resolution and reasonable analysis time for the wide range of sulfur species in different sample matrices. The analysis of VSCs has been achieved with methyl silicone phases like BD1 or Rtx1 with thick films (4–5 μm). Generally, columns with thicker films provide increased separation of volatile sulfur compounds and are better suited for analysis of low level volatile sulfur compounds in gases (Figure 4). On such non-polar columns retention times are governed primarily by boiling points and the retention sequence can be predicted from boiling-point data.

Thick films separate most VSCs in programmed temperature analysis with an initial temperature of 40–50°C. For the separation of H_2S , COS and SO_2 sub-ambient column temperatures must be used (Figure 5).

Recently, porous layer open tubular (PLOT) columns have become commercially available. The usefulness of such columns has been demonstrated for analysis of sulfur compounds such as COS, H_2S and DMS.

Smectic liquid crystalline columns may offer unique selectivity for isomeric polyaromatic sulfur compound (PASHs) mixtures that are not possible with other columns. Unfortunately, extensive use of the SB-smectic column at the upper temperature limit (250°C isothermal, 270°C during temperature programmed) can reduce the useful lifetime and column selectivity often changes dramatically with use.

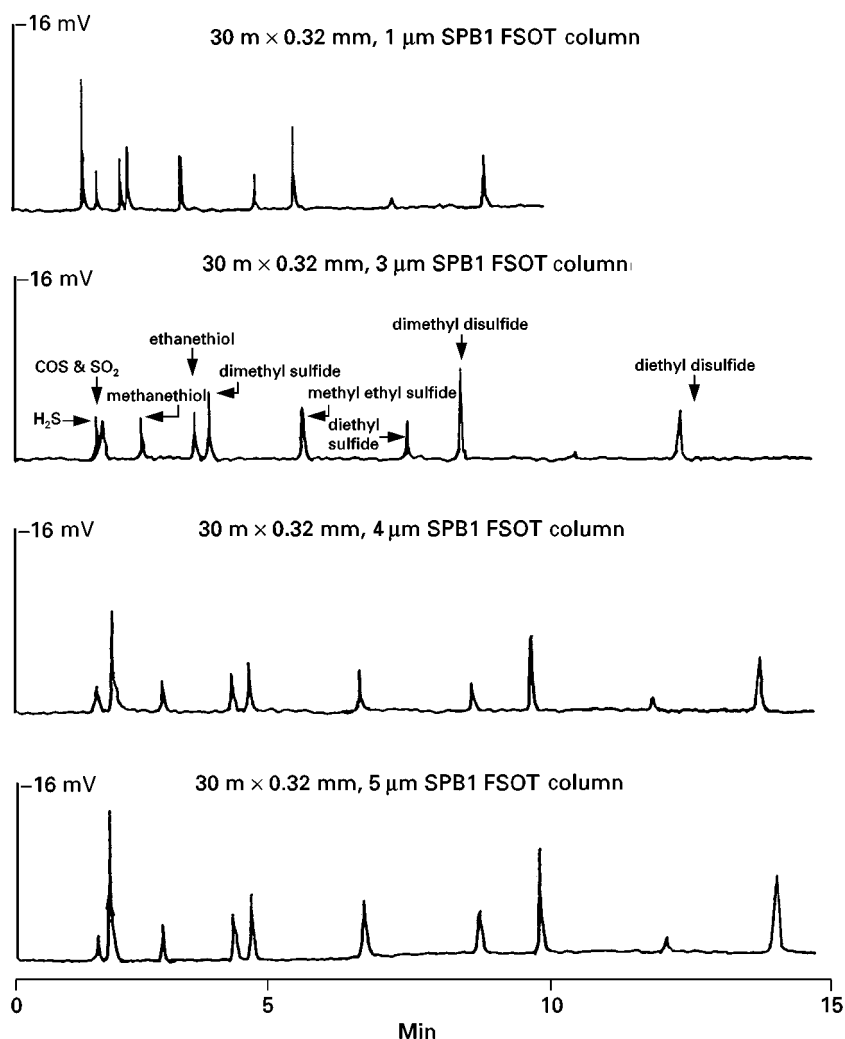


Figure 4 Effect of stationary film thickness on the separation of sulfur-containing compounds. Sample: gas phase standard of 10 component mixture of sulfur compounds: 1 mL split injection (split ratio 10 : 1), SCD, temperature programme 1 min at 35°C, 35–200°C at 10 min. Reproduced with permission from Hutte (1990).

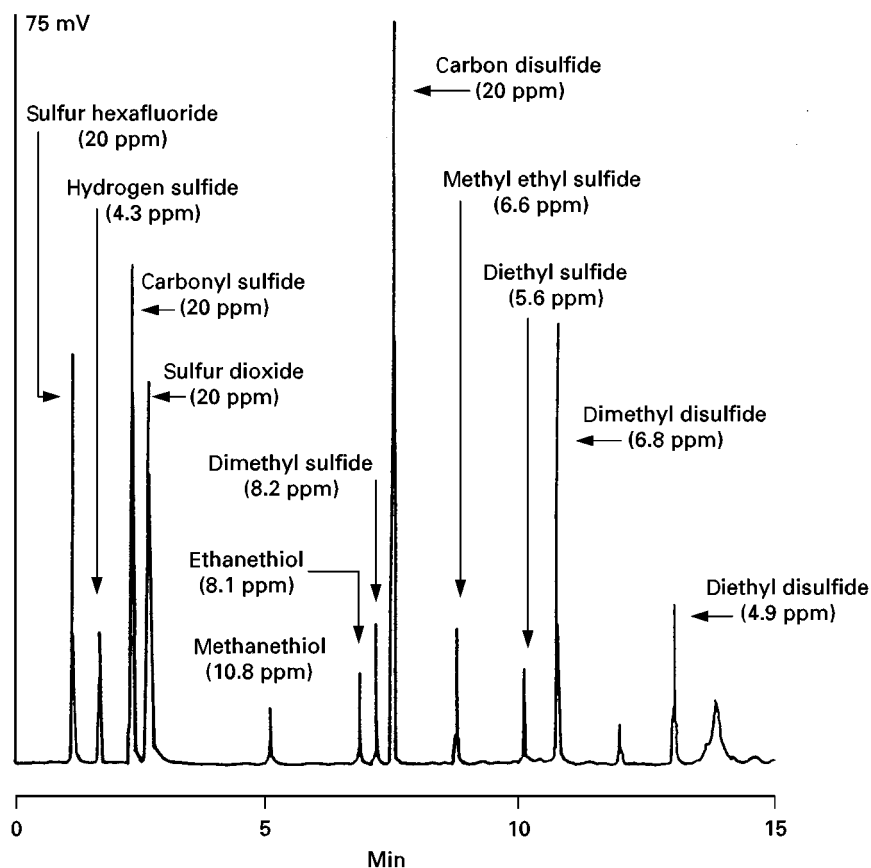


Figure 5 Sub-ambient column temperature separation of sulfur gas standard: GC conditions: 1 mL split injection (split ratio 10 : 1), injection port at 250°C, FID temperature 300°C. Column temperature programme: 2 min at -30°C, -30-200°C at 20° min⁻¹. Detector conditions: SCD integration time 0.03 s. Reproduced with permission from Hutte (1990).

Detection Systems

The value of GC for sulfur compounds analysis is found in the availability of selective and sensitive detectors. These detectors are especially useful because matrices requiring sulfur analysis are often very complex. Such detectors can reduce the analysis time by eliminating laborious and time-consuming procedures of sample preparation, which can also often cause contamination or loss of analytes. Selective detectors have found extensive application in the determination of sulfur compounds in various matrices because of these reasons.

Table 1 lists the basic characteristics of the most frequently used sulfur-selective detectors.

The flame photometric detector (FPD) is still the most widely used sulfur selective detector. The FPD exhibits a non-linear (exponential) response to sulfur compounds and response factors may be compound-dependent but it is relatively inexpensive, robust and adequate for many applications. The major advantage of the FPD is its application to gases and fuels. However, major co-eluting hydrocarbons pres-

ent in liquid fuels have a quenching effect on the sulfur response. Also the injection of aqueous samples directly into a GC-FPD system is not recommended because the injected water can extinguish the detector flame and non-volatile material contained in the sample can contaminate the injection port and column. An increase of the detector temperature prevents the flame from being extinguished but working at temperatures higher than 250°C may produce a poor baseline. An improved FPD called a pulsed flame photometer detector (PFPD) employs a pulsed flame and time-resolved emission detection with gated electronics. The improvements include one to two orders of magnitude sensitivity enhancement, about an order of magnitude of increased selectivity and reduced quenching effects.

A more recent alternative to the FPD is the sulfur chemiluminescence detector (SCD). Recent applications of this detector have shown that it gives good performance in terms of detectability, selectivity, linearity and a nearly equimolar response to sulfur. It does not suffer significantly from quenching or interferences. The combination of fused silica capillary

Table 1 Basic characteristics of gas chromatographic sulfur-sensitive detectors

<i>Detector</i>	<i>Detection limit [gS/s]</i>	<i>Selectivity [S/C]</i>	<i>Linear concentration range (decades)</i>	<i>Ease of operation</i>	<i>General characteristics</i>
FPD	10^{-11}	10^{-3} – 10^5	3 ^a	Moderate	Exponential and compound-dependent response, susceptible to flame-out and quenching effects
PFPD*	10^{-13}	10^6	3 ^a	Moderate	Less quenching than for the regular FPD
ECD	Variable up to 10^{-15}	Variable	4	Simple	Strongly compounds-dependent response, very high sensitivity to SF ₆ itself or post-column converted sulfur compounds
SCD** (flame version)	10^{-12}	$> 10^6$	4–5	Moderate	Linear and nearly equimolar response, non-susceptible to quenching or interferences, very convenient for petroleum applications
SCD (non-flame version)	10^{-13}	$> 10^7$	4–5	Simple	
AED***	10^{-12}	10^4	3–4	Difficult	Small susceptibility to quenching or interferences, possibility of elemental composition confirmation
HECD ⁺	10^{-11}	10^4 – 10^6	3–5	Complicated	Possible interferences of other organic compounds
PID ⁺⁺	10^{-12}	Poor	6	Moderate	Many factors influence the detector response
MS	10^{-11}	Specific	5	Complicated	Convenient for identification of complex mixture, new membrane techniques assure lower detection limit
FT-IR	10^{-12}	Specific	4	Complicated	Applied only for highly complex mixture. Strongly compound-dependent

^aAfter linearization.

*Pulsed flame photometric detector.

**Sulfur chemiluminescence detector.

***Atomic emission detector.

⁺ Hall electrolytic conductivity detector.⁺⁺ Photoionization detector.

columns and the SCD provides a powerful tool for the measurements of trace levels of sulfur containing compounds in complex matrices (Figure 6). The performance of the SCD can be improved by changing the means of sulfur-chemiluminescent-species production from a hydrogen flame (commonly referred to as a flame SCD) to a closed hydrogen/air burner (a flameless SCD). The flameless SCD is typically an order of magnitude more sensitive than the flame version. An extremely low detection limit of 25 fgS/s has been reported but most authors have observed a limit between 0.1 and 1 pgS/s.

The atomic emission detector (AED) has a good combination of specificity and sensitivity for the analysis of volatile sulfur-containing compounds. The AED is better than the FPD because it does not exhibit as many problems with interferences, quenching, and compound-dependent responses. The AED can be used to confirm the elemental composition of

a compound by its ability to monitor several atomic lines simultaneously. The response of the AED to sulfur at 180.7 nm is reported to have linear range of 2×10^4 , and sensitivity of 1.7 pgS/s and a selectivity over carbon of 1.5×10^3 .

The electrolytic conductivity detector (HECD or Hall detector) has found limited applications in analysis of VSCs probably because it requires regular attention. The electrolyte must be kept extremely clean and sulfur specificity is limited by high concentrations of co-trapped carbon dioxide. Despite these problems, the HECD performs well in the sulfur detection mode. The detector response is linear up to 50 ng sulfur, selectivity of sulfur to carbon is typically better than 10^4 , and the limit of detection is 1 pgS/s.

The electron-capture detector (ECD) can also be used for determination of a variety of sulfur containing compounds, e.g., SO₂, H₂S, thiols and organic

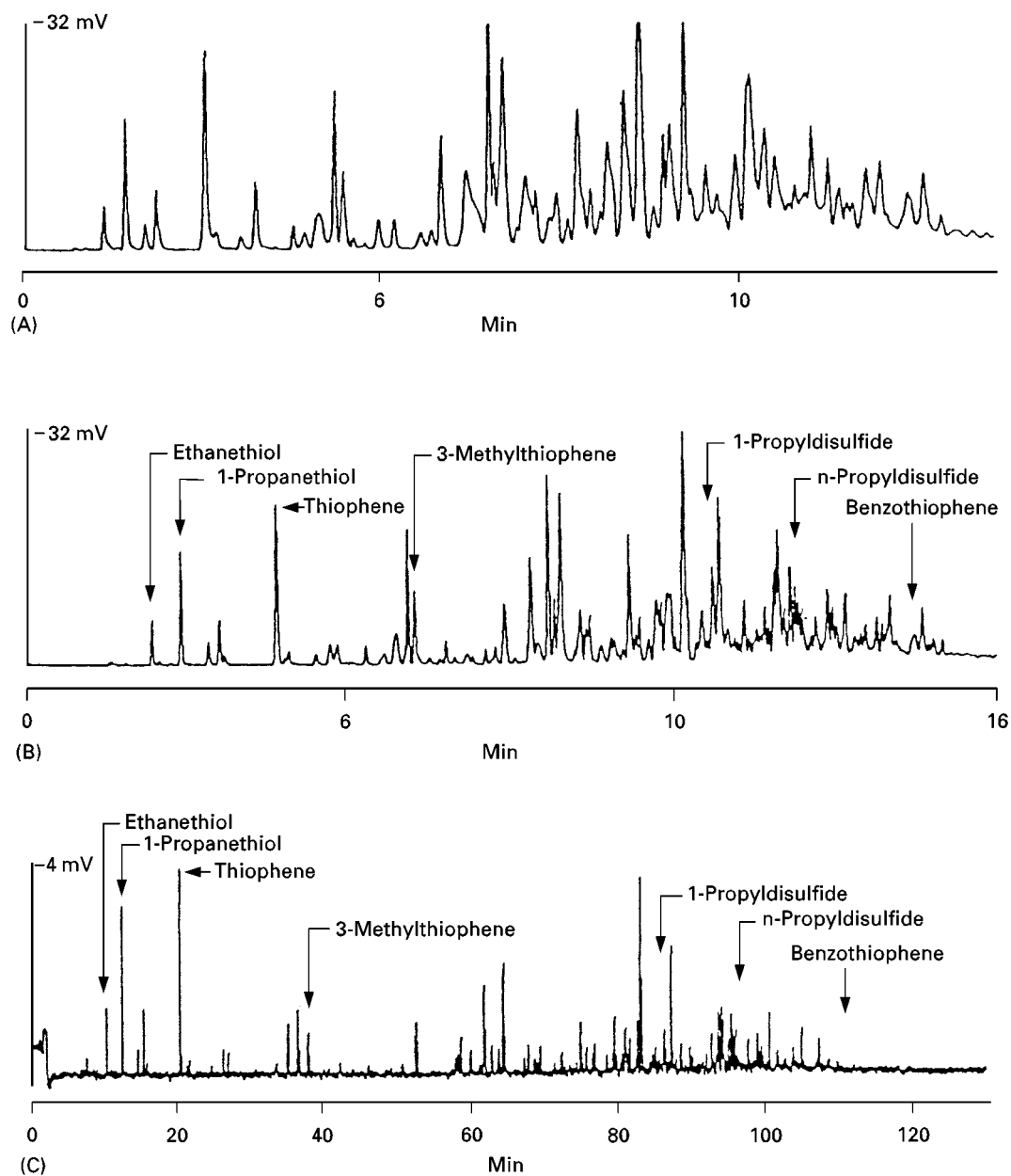


Figure 6 Comparison of column resolution for the analysis of sulfur components of raw naphtha feedstock (SCD). Capillary columns: A: 15 m \times 0.53 mm i.d. DB-1 (1.5 μ m film thickness); B: 30 m \times 0.32 mm i.d. SPB-1 (1 μ m film thickness); C: 100 m \times 0.25 mm i.d. SPB-1 (0.5 μ m film thickness). GC conditions: 1 μ L direct injection for column A, 1 μ L split injection for column B (split ratio 10 : 1) and column C (split ratio 100 : 1). Injection port temperature 250°C. Column temperature programme: column A: 1 min at 35°C 35–200°C at 8°C min⁻¹; column B: 1 min at 35°C, 35–200°C at 10°C min⁻¹; column C: 13 min at 35°C, 35–45°C at 10°C min⁻¹, 15 min at 45°C, 45–60°C at 1°C min⁻¹, 60–300°C at 2°C min⁻¹. Reproduced with permission from Hutte (1990).

mono- and di- and trisulfides. Although the ECD is only moderately sensitive to SO₂ and H₂S, both are detected in the concentration range 0.1–1 μ g g⁻¹ in a 1 mL air sample. For COS, CS₂, MeSH, H₂S and DMDS the detector displays a sensitivity comparable to the FPD but is much less sensitive towards DMS and thiophene. SF₆ can be detected at extremely low levels with minimum detectable peaks lower than 0.2 fmol. The inertness and extremely low detectabil-

ity of SF₆ has led to the development of a method in which the original sulfur compounds are fluorinated and then detected as SF₆.

The application of GC-MS systems is becoming more popular in the analysis of various sulfur compounds. Determination of sulfur compounds in underground reservoirs of natural gas and town gas (RSH, RSR and RSSR type compounds) by GC-MS has been carried out using the ion CH₂ = S⁺H

Table 2 Representative examples of sulfur gas determination by gas chromatography

Matrix	Analysed compounds	Sample preparation	Column		Dimension	Temperature conditions	Detector	Detection limit
			Material	Packing				
Atmospheric sulfur gases	COS, MeSH, CS ₂ , DMS, SF ₆	Chemisorption on gold wool + cryotrapping or only direct cryotrapping	Fused silica	BP-1	30 m × 0.32 mm × 1 µm	Isothermally, 35°C	AED	0.1 nmol m ⁻³
Air from a petroleum plant	H ₂ S, C ₁ –C ₇ thiols, DMS	Trapping on Tenax TA, placed in PTV injector, cryotrapping on column	Fused silica	GS-Q	30 m × 0.53 mm	1 min at 100°C, 100–240°C at 8°C min ⁻¹ , 30 min at 240°C	FPD	pgS
Gases from sweetening process	H ₂ S, COS, CS ₂ , thiophene, MeSH, (ppm level) in CH ₄ , CO ₂ , C ₂ H ₄ (% level)	Direct injection	Fused silica	CP-Sil 5CB	50 m × 0.32 mm × 0.5 µm	3 min at 75°C; 75–120°C at 20°C min ⁻¹	SCD TCD	ppb level
Gases from workplace environment	DMS, DES	Trapping on Tenax TA, cryofocusing (–150°C)	Stainless steel	Porapak Q	4 m × 3.2 mm o.d.	10 min at 120°C		
			Fused silica	DB-1	15 m × 0.52 mm × 1.5 µm	2 min at 60°C; 60–100°C at 10°C min ⁻¹ , 1 min at 100°C; 100–250°C at 30°C min ⁻¹	FPD + FID	µg m ⁻³
Atmospheric gas	DMS, DMDS in presence of volatile organic compounds	Cryogenic trapping on Tenax (Peltier effect)	Fused silica	Paraplot Q	10 m × 0.32 mm	7 min at 55°C; 55–216°C at 12°C min ⁻¹	MS	ppt level
Tropospheric airborne gases	COS, H ₂ S, CS ₂ , DMS	Trapping in Teflon trap (liquid argon) After separation fluorination to SF ₆					FPD MS ECD	ppt level
Atmospheric sulfur gases	H ₂ S, COS, SO ₂ , DMS MeSH, CS ₂ , DMDS EtSH, iPr SH	Cryogenic trapping in Teflon trap or in FSOT retention gap	Fused silica	DB-1/DB-Wax	30 m × 0.53 mm × 5 µm/ 3 m × 0.53 mm × 1 µm	1.2 min at 30°C; 30–140°C at 30°C min ⁻¹ , 2 min at 30°C; 30–140°C at 15°C min ⁻¹	FPD MS	50 pgS 5 pgS
Antarctic atmosphere	SF ₆	Sorption on Porapak Q (–77°C)	Stainless steel	Molecular sieve 5A	30 cm pre-column + 3 m	Isothermally, 65°C (back flushed when SF ₆ reaches main column)	ECD	ppt level

Table 3 Representative examples of sulfur compound determinations in aqueous matrices by gas chromatography

Matrix	Analysed compounds	Sample preparation	Column			Temperature conditions	Detector	Detection limit
			Material	Packing	Dimension			
Antarctic marine waters	H ₂ S, COS, SO ₂ , MeSH, DMS	Purging, preconcentration on Tenax TA (ambient temperature), thermal desorption	Teflon	Carbopack B/1.5% XE 60/1% H ₃ PO ₄	3 m × 0.25 mm	40–140°C–temperature programming	FPD	6–160 ng L ⁻¹
Atlantic surface water	DMS, DMDS, CS ₂ , dimethyl selenide, dimethyl iodide	Purging, trapping in cold trap	Fused silica	SE-54	50 m × 0.32 mm × 5 µm	3 min at 70°C, 70–180°C at 3°C min ⁻¹	AED or ECD	0.5–0.8 ppm
Aqueous matrices (distilled water, tap water, kraft mill condensate)	H ₂ S, MeSH, DMS, DMDS	Filtration with glass fibre filters, direct injection split mode (10 : 1)	Fused silica	DB Wax	30 m × 0.53 mm × 1 µm	5 min at 40°C; 40–160°C at 30°C min ⁻¹ , 3 min at 160°C, 160–200°C at 40°C min ⁻¹	FPD	0.3 mg L ⁻¹
Heavily polluted water	H ₂ S, COS, MeSH, DMS, CS ₂ , DMDS	Purging, cryogenic trapping (–80°C)	Teflon	Carbopack BHT-100	1.4 m × 3 cm	1 min at 5°C; 5–50°C at 30°C min ⁻¹ , 2 min at 50°C; 50–100°C at 30°C min ⁻¹ , 7 min at 100°C	FPD	ng S
Water samples, sediments	H ₂ S, COS, MeSH, DMS, CS ₂ , DMDS	Purging, cryocondensation secondary cryofocusing	Teflon	Carbopack BHT-100	1.4 m × 3.2 cm	–5–100°C at 30°C min ⁻¹ , 8 min at 100°C	FPD	pg S
Surface and potable water, industrial effluents, sediments	21 organosulfur compounds (thiophenes, sulfides, sulfones, benzothiazole)	Purging, trapping on Tenax, extraction with hexane or methylene chloride	Fused silica	DB-5	25 m × 0.25 mm × 0.33 µm	4 min at –50°C, –50–200°C at 16°C min ⁻¹ , 8 min at 200°C; 200–220°C at 16°C min ⁻¹	MS	ppb level
Anoxic-lake water	H ₂ S, COS, MeSH, CS ₂ , EtSH, DMS	Purging, cryotrapping on Tenax TA (solid CO ₂), heating with hot air (200°C)	Glass	UCON 50 HB 5100	25 m and 50 m	0°C–45°C at 3°C min ⁻¹	FPD, MS	ng L ⁻¹

Table 4 Representative examples of sulfur compounds determination in beverages and food stuff by a gas chromatography

Matrix	Analysed compounds	Sample preparation	Column		Temperature conditions		Detector	Detection limit
			Material	Packing	Dimension			
Garlic samples (whole non-peeled, peeled cloves, crushed cloves, juices)	15 sulfides, disulfides and trisulfides	Head space (5 and 45 min)	Fused silica	HP-5	25 m × 0.31 mm × 0.53 μm	2 min at 40°C, 40–70°C at 3°C min ^{−1} , 70–205°C at 7.5°C min ^{−1} , 205–250°C at 25°C min ^{−1}	AED and MS	
			Fused silica	HP-1	25 m × 0.32 mm × 0.17 μm	1 min at −20°C, −20 to −10°C at 10°C min ^{−1} , −10 to −40°C at 30°C min ^{−1} , 40–150°C at 70°C min ^{−1}	MIP-AED	from 0.4 ng L ^{−1} for EtSH to 0.9 ng L ^{−1} for DMS
Grape juice	COS, CS ₂ , DMS	Head space	Glass	Porapak QS		5 min at 80°C; 80–120°C at 12°C min ^{−1}	FPD	
Alcoholic beverages	H ₂ S, MeSH, EtSH, DMS, CS ₂ , ethyl-methyl sulfide, DES, DMDS, DEDS	Head space	Fused silica	SPB-1-Sulfur	30 m × 0.32 mm × 4 μm	1 min at 35°C; 35–55°C at 10°C min ^{−1} , 55–250°C at 25°C min ^{−1}	SCD	10 μg L ^{−1}
Packaged food (wine, orange juice)	SO ₂ in presence of CO ₂ and H ₂ O	Head space	Teflon	Chromosorb 108	1.2 m × 2 mm	90°C and 120°C	HECD	0.81 ng L ^{−1}

Table 5 Representative examples of sulfur compounds determination in fossil fuel related samples by gas chromatography

Matrix	Analysed compounds	Sample preparation	Column		Packing	Dimension	Temperature conditions	Detector	Detection limit
			Material						
Gases from plasma reactors (also atmosphere from microelectronic processes and polluted air)	H ₂ S, COS, SO ₂ , CS ₂ , thiols, sulfides in the presence of C ₁ –C ₅ hydrocarbons (HC)	Vacuum extraction from reaction tube or direct injection from pressurized cylinders and syringes	Teflon	Chromosorb 105	80 cm × 2 mm	1 min at 60°C, 60–180°C at 20°C min ^{–1} , 2 min at 180°C	FID and FPD	10 ^{–10} gS/s 10 ^{–12} gHC/s	
			Fused silica	SPB-1 Sulfur	30 m × 0.32 mm × 4 μm	3 min at 10°C, 10–300°C at 10°C min ^{–1}	SCD and FID		
Natural gas	H ₂ S, SO ₂ , CS ₂ , C ₁ –C ₄ thiols, DMS, DMDS, DEDS, methylethylsulfide, 2-ethylthiophene	Direct injection, split mode, 10 : 1	Fused silica	DB-1	60 m × 0.25 mm × 0.25 μm	35–100°C at 10°C min ^{–1} , 100–225°C at 2°C min ^{–1} , 20 min at 225°C	SCD and FID	0.01% (w/w) of total S	
Light petroleum fractions (cracked gasolines, diesels)	Thiophene, benzothiophene, dibenzothiophene and their alkyl substituted homologues	Direct injection, split mode, 1 : 100	Fused silica	SPB-1	30 m × 0.32 mm × 4 μm	35–125°C at 30°C min ^{–1} , 125–260°C at 5°C min ^{–1}	AED	H ₂ S-single ppm thiols-total S-hundreds ppm	
Commercial diesel fuels	Thiophene, benzothiophene, dibenzothiophene, thiols	Direct injection after dilution with n-hexane (1 : 100), on-column mode	Fused silica	HP-5	25 m × 0.32 mm × 0.52 μm	50–110°C at 30°C min ^{–1} , 110–210°C at 2.5°C min ^{–1} , 210–280°C at 2°C min ^{–1} , 5 min at 280°C	FPD		
Fossil fuels (coal tar, crude oil)	80 polycyclic aromatic sulfur heterocyclic compounds (3–5 rings)	Prefractionation solid-phase extraction, LC clean-up	Fused silica	DB-5MS	60 m × 0.25 mm × 0.25 μm	1 min at 60°C, 60–150°C at 45°C min ^{–1} , 2 min at 150°C, 150–300°C at 2°C min ^{–1} , 25 min at 300°C	MS	Only for retention indexes determination	
				DB-17		1 min at 60°C, 60–90°C at 35°C min ^{–1} , 1 min at 190°C, 190–320°C at 1°C min ^{–1}			
				Liquid crystalline polysiloxane (SB-Smectic)		1 min at 60°C, 60–190°C at 35°C min ^{–1} , 1 min at 190°C, 190–266°C at 1°C min ^{–1}			

with m/z 47. The ion with m/z 45 is more intense in some sulfur compounds, but is often found in oxygen compounds ($C_2^+H_4OH$) as well. Twenty-one organosulfur compounds (DMS and DMDS among others) were detected in the approximate concentration range 0.1 to 2000 ppb in water, industrial effluent, sediment and fish samples using an automated GC-MS system. A GC-MS method for DMS and SO_2 determination in air in real time at the sub parts per trillion level with a high pressure selected-ion chemical ionization flow reactor has been developed. The use of isotope dilution GC-MS with perdeuterated DMS for DMS determination in sea water gives better than 2% precision. By using the ratio of the MS response at m/z 62 and m/z 68, compensation can be made for instrumental drift as well any losses in sampling ambient air. Another significant advantage is the ability to determine DMS concentration by stripping only a small fraction of DMS from solution, resulting in artefact-free DMS concentration. In addition, larger volumes of water can be sampled by eliminating the need for long sampling periods required to remove DMS quantitatively from solution. Highly sensitive and specific continuous measurement of DMS in air, using triple quadrupole mass spectrometry with atmospheric pressure chemical ionization, has been demonstrated. Detection limits in continuous direct monitoring were determined for DMS (24 pptv), H_2S (1 ppbv), for MeSH, COS and CS_2 (about 10 ppbv).

Calibration

The preparation of reliable standard mixtures is an important step in analysis. The simplest way to calibrate a GC system for gas analysis is by injecting a suitable volume of a standard gas. Low concentration standards, usually needed in trace analysis, can be obtained by applying the exponential dilution flask technique or with permeation tubes. To minimize non-linear response problems (as for flame photometric detector) the calibration curves should cover the anticipated concentration range. For calibration, the gases from diffusion tubes are diluted with an inert gas and frequently led through a glass loop injected onto the column with appropriate valves. A new concept for the generation of standard mixture of thiols, based on thermal decomposition of a substance chemically bonded to the surface of silica gel, has been developed. The method enables preparation of a standard mixture containing volatile, malodorous, unstable and toxic compounds. For example, standard mixture of MeSH and PrSH have been generated by heating silica gel with anchored dithiocarbamate groups.

In analysis of liquids, primary standards are usually prepared in an appropriate solvent which should not interfere with the determined compounds. All standard solutions should be stored in vials with headspace volume as small as possible and kept at low temperature ($\leq 4^\circ C$).

Examples of Applications

Due to the diversity of sulfur compounds and various matrices in which they can be present, the chromatographer is faced with a difficult task when separation, identification and quantification of specific sulfur species are desired. The approach needed for the analysis of these compounds depends on several factors. In choosing the appropriate procedure, the analyst should consider the form of sulfur compounds to be determined, their levels of concentrations, the physical state and the complexity of the matrix. Tables 2–5 present representative examples of sulfur compounds determination in various matrices using gas chromatography. The examples include sample preparation techniques, columns with chromatographic conditions, and detectors.

Conclusions

Gas chromatography, especially high resolution gas chromatography, perhaps more than other methods, fulfils the requirements needed for the analysis and structure elucidation of multicomponent environmental mixtures in which different sulfur species can be present in nanogram or picogram amounts. It should be noted that, besides selective high resolution columns and sensitive sulfur-specific detectors, most qualitative and quantitative determination of sulfur-containing compounds requires efficient sample enrichment techniques and quantitative desorption from traps. The applied procedure should also minimize adsorption losses of the sulfur compounds in the whole analytical system and reduce possible rearrangements of sulfur analytes. Significant progress is still being made in all steps of sulfur analysis in various environmental matrices but such procedures are not still routinely applied in many laboratories. Future developments should be focused on procedures that can be used during long research expeditions, directly aboard ships, or in situ for real-time measurements.

See Colour Plate 119.

See also: II/Chromatography: Gas: Detectors: General (Flame Ionization Detectors and Thermal Conductivity Detectors); Detectors: Mass Spectrometry; Detectors: Selective; Gas-Solid Gas Chromatography; Headspace Gas Chromatography; Multidimensional Gas Chromatography;

Sampling Systems. **III/Flavours: Gas Chromatography. Appendix 2: Essential Guides to Method Development in Gas Chromatography.**

Further Reading

- Hutte RS (1995) The sulfur chemiluminescence detector. In Adlard ER (ed.) *Chromatography in Petroleum Industry*, Amsterdam: Elsevier.
- Hutte RS, Johansen NG and Legier MF (1990) Column selection and optimization for sulfur compounds analysis by gas chromatography. *Journal of High Resolution Chromatography* 13: 421–426.
- Karchmer JH (1970) *The Analytical Chemistry of Sulphur and its Compounds, Part I*. New York: John Wiley & Sons Inc.
- Karchmer JH (1972) *The Analytical Chemistry of Sulphur and its Compounds, Part II*. New York: John Wiley & Sons Inc.
- Mössner SG, Lopez de Alda MJ, Sander LC, Lee ML and Wise SA (1999) Gas chromatographic retention behaviour of polycyclic aromatic sulfur heterocyclic compounds (dibenzothiophenes, naphtho[b]thiophenes, benzo[b]naphthiophenes and alkyl-substituted derivatives) on different derivatives of different selectivity. *Journal of Chromatography* 841: 207–228.
- Saltzman ES and Cooper WJ (1989) *Biogenic Sulphur in the Environment*. Washington: American Chemical Society.
- Simo R (1998) Trace chromatographic analysis of dimethyl sulphoxide and related methylated sulfur compounds in natural waters. *Journal of Chromatography A* 807: 151–164.
- Thompson M and Stanisavujevic M (1980) Gas chromatography and gas chromatography–mass spectrometry of organosulphur compounds and other labile compounds. *Talanta* 27: 477–493.
- Tibbets PJC and Large R (1988) Improvements in oil fingerprinting: GC/HR MS of sulfur heterocycles. *Petroanalysis '87: Dev. Anal. Chem. Pet. Ind.*, pp. 45–57. Chichester: John Wiley and Sons.
- Wardencki W (1998) Problems with the determination of environmental sulphur compounds by gas chromatography. *Journal of Chromatography A* 793: 1–19.
- Wardencki W and Zygmunt B (1991) Gas chromatographic sulphur-sensitive detectors in environmental analysis. *Analytica Chimica Acta* 225, 1–13.

SUPERCRITICAL FLUID CRYSTALLIZATION



A. S. Teja and T. Furuya, Georgia Institute of Technology, Atlanta, GA, USA

Copyright © 2000 Academic Press

Introduction

Supercritical crystallization processes use the special properties of supercritical fluids that make these fluids particularly suitable as solvents or antisolvents. In both cases, an expansion of a solution is used to create supersaturation, which is the driving force for nucleation and growth of the solute.

A supercritical fluid (SCF) is a fluid above its critical temperature and pressure. It is characterized by physical properties (such as viscosity and diffusivity) that can be continuously varied between those of liquids and gases. The liquid-like density of a SCF is associated with its ability to dissolve solutes, and hence its solvent power. Since this density can be changed significantly by changing the pressure and temperature in the critical region, the solvent properties of a supercritical fluid can be tailored for specific applications. **Figure 1** shows the relationship between pressure and density of carbon dioxide. The region above the critical pressure and temperature

(7.38 MPa, 302.3 K) is commonly referred to as the supercritical region of carbon dioxide. It is important to note that the largest changes in the fluid density with changes in temperature and/or pressure in the single-phase region occur near the critical point. Therefore, large changes of solvent power can be achieved with small changes in pressure or temperature in the critical region. It should be added here that a supercritical crystallization process involves mixtures of solute and solvent; however, these mixtures are generally dilute so that their critical points are close to the critical point of the solvent. The behaviour depicted in **Figure 1** may therefore be considered to be representative of the behaviour of dilute mixtures of constant composition.

If a supercritical fluid loaded with solute is expanded, then the resulting change in density may lead to precipitation of the solute. If these changes in density are made to occur rapidly, then the process is known as the rapid expansion of supercritical solutions, or RESS. Very high supersaturations may be achieved in RESS processes over a very short period of time. This generally favours the deposition of small crystals and narrow size distributions. Also, the crys-

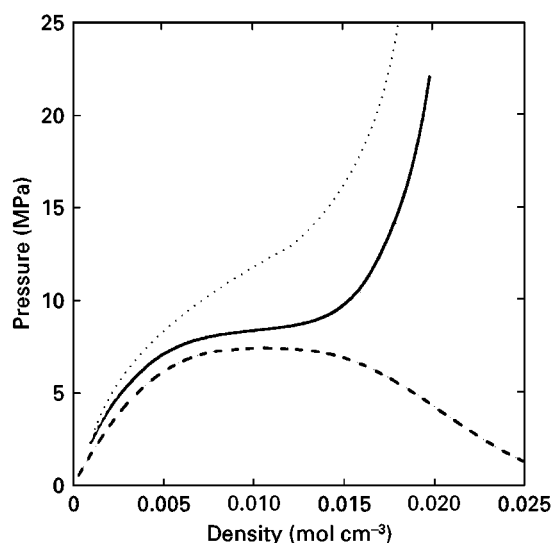


Figure 1 Pressure-density behaviour of CO_2, 330 K; —, 310 K; ----, phase boundary.

tals are generally free of solvent inclusions because the solvent is likely to be in the gaseous state at the end of the expansion.

Introduction of a supercritical fluid into an organic solvent can also result in expansion of the liquid phase, and hence, in large changes in density. If a solution containing a desired solute is expanded sufficiently by the supercritical fluid, then the liquid phase will no longer be a good solvent for the solute and nucleation will occur. In this case, the supercritical fluid acts as an antisolvent, and the crystallization process is known as the supercritical antisolvent (SAS) process, or by a variety of other names that are discussed below. Changes in the pressure, temperature, or rate of supercritical fluid addition provide an opportunity for tailoring the SAS crystallization process for specific applications.

Crystallization by the Rapid Expansion of a Supercritical Solution (RESS)

The rapid expansion of a supercritical solution (RESS) by decompression can lead to very large changes in density and, hence, in the solubility of a solute in the supercritical solvent. This can result in very high supersaturation when supercritical solutions are depressurized, leading to the formation of a large number of nuclei. A typical RESS apparatus is shown in Figure 2. Solvent is pressurized in a pump until a pressure above its critical pressure is attained. The supercritical state is achieved by passing the pressurized solvent through a heat exchanger maintained at a temperature above the critical temperature of the solvent in a constant-temperature bath. The super-

critical fluid is then passed through a bed of solute where it becomes saturated with the solute. The loaded solution is then heated to a designed pre-expansion temperature, and finally expanded quickly through an expansion device, such as a nozzle or a capillary, into a collection vessel. The expansion device is generally heated to prevent resublimation or solvent condensation. The collection vessel is maintained at a constant temperature and pressure or vacuum, and the products are collected on a suitable substrate placed in the path of the expansion jet. The pressure in the collection vessel is ambient, but may sometimes be higher in order to control the particle size; or it may be below atmospheric to prevent condensation of any solvent that is a liquid at ambient conditions. Variations of this equipment are possible, particularly if the solvent is to be recycled. Also, a dual RESS or DURESS process has been proposed whereby two RESS expansions are carried out in a concentric expansion device and yield, for example, a solid solute coated with a polymer.

The RESS process is applicable to any material that can be dissolved in a supercritical solvent and is particularly useful for materials of low volatility. A few examples of crystallized materials using the RESS process are shown in Table 1. Scanning electron microscopy (SEM) micrographs of crystals obtained by RESS processes are shown in Figure 3. RESS expansions result in essentially homogeneous nucleation of the solute. The morphology of the product is determined by a number of factors, including the solute and its concentration, the device used for the expansion, the pre-expansion temperature, the flow rate, and the pressure drop on expansion. High concentrations of solute tend to produce powders, whereas low concentrations generally produce thin layers or films. The particle size has been found to increase with solute concentration prior to expansion. Also, processing conditions may be chosen such that the solvent is a gas at exit conditions and can be easily separated from the deposited solute. If conditions are chosen so that a two-phase mixture is

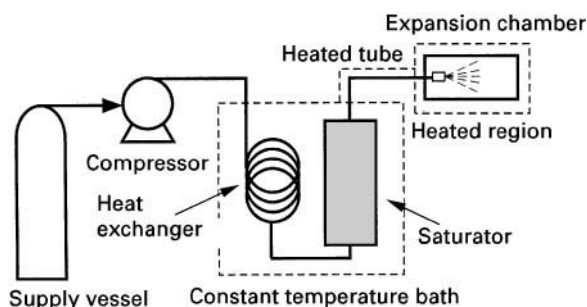


Figure 2 Experimental apparatus for a RESS process.

Table 1 Substances processed using RESS

<i>Materials</i>	<i>Supercritical fluid</i>	<i>Morphologies, particle size (μm)</i>
<i>Inorganics</i>		
$\alpha\text{-Al}_2\text{O}_3$	Water	Films, ~ 0.08 thickness
SiO_2	Water	Spheres, 0.1–0.5
		Films, > 1.0 thickness
GeO_2	Water	Spheres, 0.5–1.3
$\text{ZrO}(\text{NO}_3)_2$	Ethanol	Particles, ~ 0.1
Polycarbosilane	Pentane	Fibres, 1 diameter
		Particles, < 0.1
<i>Organics</i>		
Benzoic acid	CO_2	Particles, 3–8
β -Carotene	Ethylene	Particles, 1–2
Cellulose acetate	Pentane	Fibres, 0.8 diameter
Naphthalene	CO_2	Particles, 2–50
<i>n</i> -Octacosane	CO_2	Particles, 2–6
Phenacetin	CO_2	Particles, ~ 10
Phenanthrene	Trifluoromethane	Particles, ~ 3
	CO_2	Particles, 1.6–6.6
Stigmasterol	CO_2	Fibres, ~ 0.2 diameter
<i>Polymers</i>		
Poly-1-butene	CO_2	Spheres, < 5
Poly(carbosilane)	Pentane	Particles, < 0.1
		Fibres, 1 diameter
Polycaprolactone	CO_2	Spheres, < 5
	CDFM ^a	Spheres, 1–5
		Fibres, 2–7
Polyethylene succinate	CO_2	Spheres, < 5
Polyethylene methacrylate	CDFM	Particle/fibre blend
Poly(glycolic acid)	CO_2	Particles, 10–20
Poly(L+)-lactic acid	CO_2	Particles, 10–120
	CDFM	Particles, 0.2–0.6
Poly(DL)-lactic acid	CO_2	Particles, 10–20
Polymethyl methacrylate	Propane	Particles, 0.5–1.0
		Fibres, 1 diameter
	CDFM	Particles/fibres
Polyphenylsulfone	Propane	Spheres, ~ 0.5
Polypropylene	Propylene	Fibres, ~ 2.5 diameter
	Pentane	Fibres, 1 diameter
Polystyrene	Pentane	Spheres, 20
		Fibres, 0.8–2.5 diameter

^aCDFM, chlorodifluoromethane.

formed during the expansion, solid may condense to yield a thin solid film.

There is a possibility of fibre formation from supercritical solutions when an organic polymer is the solute. The polymer may form either a liquid or solid after decompression, depending on the polymer melting temperature relative to the post-expansion temperature. Fibres are generally formed when the expansion is carried out in a capillary nozzle and the post-expansion temperature is close to the melting temperature of the polymer so that the polymer deposits as a liquid on the nozzle walls. RESS expansion of polymers yields powders when the temperature is not close to the melting temperature of the polymer. The extremely short times of product formation in

the expansion of supercritical solutions also makes it possible to produce multicomponent mixtures of powders with uniform distribution of the components. Such powders have tremendous commercial potential in the ceramic industry.

The pressure, temperature, and supersaturation profiles in and outside the expansion device determine the size of the crystals produced in the RESS process and the crystal size distribution. The pressure and temperature profiles in the expansion device can be modelled by solving the mass, energy, and momentum conservation equations for the adiabatic expansion of the supercritical fluid. Typical profiles for a capillary nozzle are shown in **Figure 4**. The free-jet expansion after the fluid exits

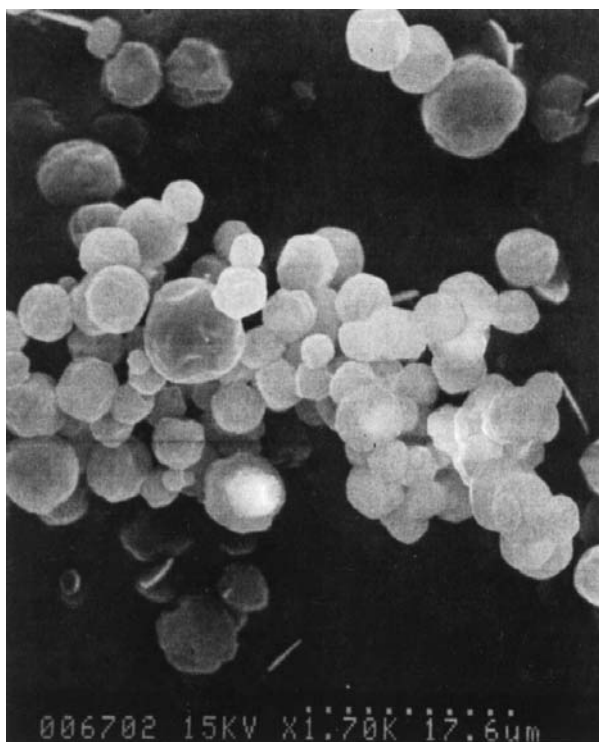


Figure 3 SEM micrographs of *n*-octacosane crystals obtained in RESS expansion of a CO₂ solution.

the device can also be modelled and is shown schematically in **Figure 5**. Calculations have shown that a Mach disc is formed a few nozzle diameters downstream from the nozzle exit and that the pressure and temperature are very low in the region between the exit and the Mach disc. High supersaturations may therefore be obtained before, in, or after the fluid exits the nozzle and the exact profile must be known

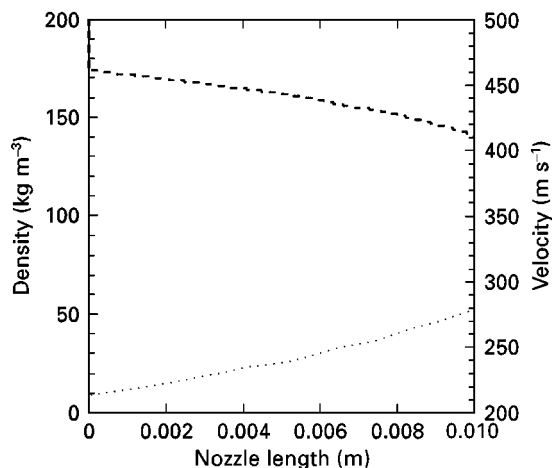


Figure 4 Density and velocity profiles in a RESS expansion of CO₂ through a capillary nozzle at 443 K and 17.39 MPa. ..., Velocity; ----, density.

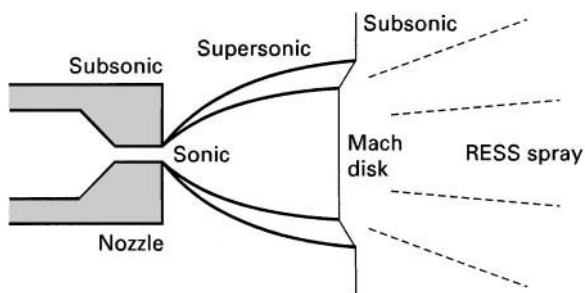


Figure 5 Free jet expansion of a supercritical fluid solution from a capillary.

if control of the crystal size and crystal size distribution is desired.

Crystallization by the Addition of a Supercritical Antisolvent (SAS)

In the supercritical antisolvent (SAS) process, a pressurized fluid is used as an antisolvent for precipitating a solid that is dissolved in a liquid solvent. The supersaturation of the solid is created by the volumetric expansion of the liquid solution. After crystallization of the solute, it is possible to remove the antisolvent completely by pressure reduction. Control of the particle size distribution is also possible by manipulation of the process variables.

Many organic solvents show at least partial miscibility with gases and supercritical fluids at moderate to high pressures. Introduction of the SCF antisolvent into such organic solvents will result in dissolution of the antisolvent and an expansion of the liquid phase. This expansion can be quite significant, as shown for ethyl acetate–carbon dioxide mixtures in **Figure 6**. In

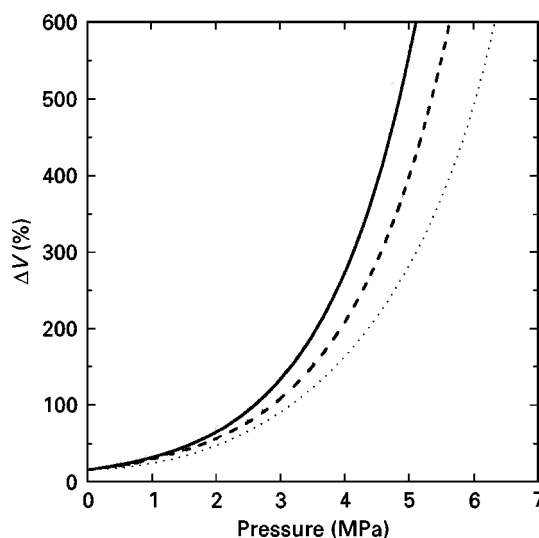


Figure 6 Volumetric expansion of an ethyl acetate with CO₂. —, 25°C; ----, 30°C; ···, 40°C.

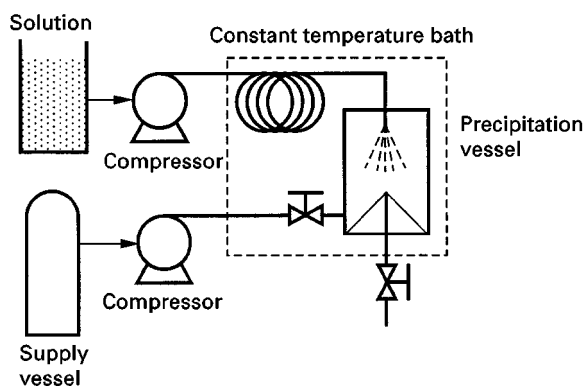


Figure 7 Experimental apparatus for a batch SAS process.

this figure, $\Delta V(\%)$ is defined as follows:

$$\Delta V(\%) = 100\{V(p, T) - V_0\}/V_0 \quad [1]$$

where $V(p, T)$ is the volume of the liquid phase when loaded with antisolvent, and V_0 is the volume of the pure liquid phase at atmospheric conditions. This expansion is large near the critical temperature of the antisolvent.

The following requirements must be satisfied for a successful SAS process: the solute must be soluble in the organic solvent at ambient temperatures and insoluble (or sparingly soluble) in the SCF antisolvent. The organic solvent must be at least partially miscible with the SCF antisolvent as described above. Many organic solids satisfy these requirements, although this is not true of inorganic compounds. Inorganic compounds are generally soluble in water or acids such as sulfuric acid, but these solvents do not expand appreciably when contacted with simple gases such as

CO₂ or light hydrocarbons. However, many cobalt, nickel iron and chromium salts are soluble in acetone, cyclohexane or *N*-methylpyrrolidone, and these solvents have been used to develop SAS recrystallization processes.

The SAS process may involve antisolvent injection into a liquid phase (gas injection) or liquid solution injection into a SCF antisolvent (liquid injection) operation. Both these processes can be operated continuously or in batch mode.

A typical experimental apparatus for batch operations is shown in **Figure 7**. In the case of gas injection, a vessel is loaded with a known quantity of liquid solution containing the dissolved solute, and then the SCF antisolvent is added to the solution from the top or bottom of the vessel. This causes the liquid phase to expand and the solute to precipitate. The rate of antisolvent addition is an important parameter for the control of morphology and size of the solid particles obtained in this process. Rapid addition of the antisolvent generally leads to smaller and more uniform particles. Slower addition of the SCF can result in a range of particle sizes. The morphology of the particles can also be controlled by the rate of antisolvent addition, and by the organic solvent used to dissolve the solute. Examples of particles precipitated in gas injection operations are summarized in **Table 2**.

In the case of liquid injection, the precipitation vessel is pressurized by the addition of the SCF and then the liquid solution is injected into the vessel. The injected liquid solution is expanded by the dissolving SCF causing the solids to precipitate. In one variation of this type of operation, the liquid solution and the SCF antisolvent are continuously delivered to a

Table 2 Substances processed using SAS with gas injection

<i>Compounds</i>	<i>Solvent^a</i>	<i>Antisolvent</i>	<i>Morphologies, particle size (μm)</i>
<i>Explosives and propellants</i>			
Nitroguanidine	DMF, cyclohexane	CO ₂	Crystals: spheres, snow-balls, starbursts, 1–100
Cyclonite, homocyclonite	Acetone, γ-butyrolactone	CO ₂	Crystals, > 200
Cyclonite	Acetone, cyclohexanone	CO ₂	Crystals, < 5
Homocyclonite	Acetone	CO ₂	Crystals, 2–5
<i>Polymers</i>			
Aramids	DMF	CO ₂	Crystalline spherulites, 1–10 long fibres
Polyhyaluronic acid methyl ester	DMSO	CO ₂	Spheres, 0.3
<i>Pharmaceuticals</i>			
Abecarnil	Isopropyl acetate	CO ₂	Crystals, 10–50
<i>Inorganics</i>			
Cobalt chloride	Acetone	CO ₂	Crystals

^aDMF, Dimethylformamide; DMSO, Dimethyl sulfoxide.

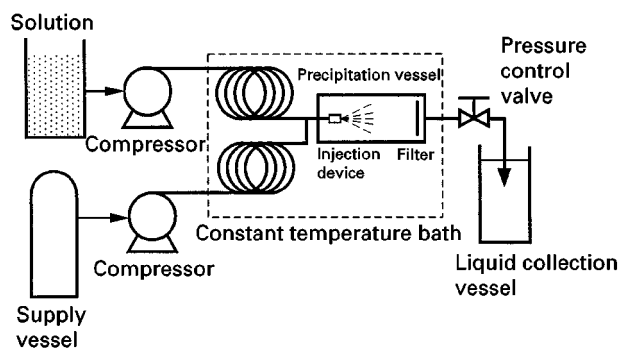


Figure 8 Experimental apparatus for a continuous liquid injection SAS process.

precipitation vessel in an apparatus similar to that shown in **Figure 8**. In this operation, solids precipitate continuously in the vessel, as the gas phase (SCF) leaves through a pressure-control valve. The valve also maintains the pressure inside the vessel constant. The ratio of the two flow rates (flow rate of the liquid solution and that of the SCF antisolvent), and the type of contact (co-current or countercurrent) can be important in the evolution of the precipitation process. Continuous precipitation using liquid injection has been given various acronyms such as precipitation by compressed antisolvent (PCA), aerosol solvent extraction system (ASES) and solution en-

hanced dispersion by supercritical (SEDS) fluid process. These processes have been carried out using slightly different precipitation procedures and in slightly different apparatus. At the end of the precipitation procedure, the vessel is washed with antisolvent to remove the liquid. This washing procedure is necessary because any liquid solvent remaining after depressurization could redissolve the solute.

Examples of solutes precipitated using liquid injection are summarized in **Table 3**. These examples include polymer microspheres, where the temperature of the precipitation vessel and the concentration of polymer in the solution play an important role in determining the morphology. There is a tendency for the polymer particles to agglomerate when the temperature is higher than the glass transition temperature of the polymer. Also, a high polymer concentration in solution produces fibres. On the other hand, micron-sized particles with a narrow size distribution can be obtained by adjusting the conditions of co-solvent and injection devices.

The liquid solution injection device plays a key role in SAS operations. The injector is designed to produce very small liquid droplets that expand in the precipitation vessel. Various geometries have been proposed to achieve this, including nozzles, capillaries, vibrating orifices and co-axial capillaries. The precipitation vessel must be designed to mix two phases and to

Table 3 Substances processed using SAS with liquid injection

<i>Compounds</i>	<i>Solvent^a</i>	<i>Antisolvent</i>	<i>Morphologies, particle size (μm)</i>
<i>Polymers and biopolymers</i>			
Poly (L-lactide)	CH ₂ Cl ₂	CO ₂	Spheres, 1–10
Polystyrene	Toluene	CO ₂	Spheres, 0.1–20 Microballoons
Polyacrylonitrile	DMF	CO ₂	Microfibrils, hollow fibres
<i>Pharmaceuticals</i>			
Insulin, catalase, trypsin, lysozyme	DMSO, DMF	CO ₂	Spheres, 1–5
Methylprednisolone acetate	THF	Ethane	Crystals, 2.5–8.5
Hydrocortisone acetate	DMF	CO ₂	Crystals, 2.5–8.5
Salmeterol xinafoate	Acetone	CO ₂	Crystalline modification, 1–10
Sodium cromoglycate	Methanol	CO ₂	Spheres, 0.1–20
Tetracycline	NMP	CO ₂	Spheres, 0.15–0.6
Salbutamol	DMSO	CO ₂	Long rods, 1–3 length
<i>Catalysts, inorganics</i>			
Red lake C, pigment yellow 1, pigment Blue 15	Acetone	CO ₂	Spheres, > 0.6
Barium acetate, copper acetate	DMSO	CO ₂	Spheres, 0.1–0.4
Yttrium acetate	DMSO	CO ₂	Spheres, 0.1–0.3
Samarium acetate, neodymium acetate	DMSO	CO ₂	Spheres, 0.1–0.3
Zinc acetate	DMSO	CO ₂	Spheres, 0.05–0.02

^aDMF, dimethylformamide; DMSO, dimethyl sulfoxide; THF, tetrahydrofuran; NMP, *N*-methyl-2-pyrrolidone.

provide heating/cooling. Filtration of the particles at high pressures also requires special equipment.

In summary, both RESS crystallization and SAS crystallization appear to be promising methods for generating supersaturation and therefore represent alternatives to conventional crystallization. Such alternatives may prove attractive in applications such as polymer and pharmaceutical processing, or in particle design for drug delivery. It is possible to obtain a variety of morphologies and particle sizes in these processes by proper choice of conditions and expansion devices. However, *a priori* design of supercritical crystallization processes is not yet possible because the interaction between phase equilibria, expansion paths, and crystallization kinetics in these processes is not yet well understood.

See also: II/Crystallization: Control of Crystallizers and Dynamic Behaviour; Polymorphism.

Further Reading

Berends EM, Bruinsma OSL and van Rosmalen GM (1993) Nucleation and growth of fine crystals from supercritical carbon dioxide. *Journal of Crystal Growth* 128: 50–56.

Dixon DJ, Johnston KP and Bodmeir RA (1993) Polymeric materials formed by precipitation with a compressed fluid antisolvent. *AIChE Journal* 39: 127–139.

Gallagher PM, Coffey MP, Krukoni VJ and Klasutis N (1989) Gas anti-solvent recrystallization: new process to recrystallize compounds insoluble in supercritical fluids. In: Johnston KP and Penninger JML (eds) *Supercritical Fluid Science and Technology*, ACS Symposium Series 406, pp. 334–354. Washington DC: American Chemical Society.

Griscik GJ, Rousseau RW and Teja AS (1995) Crystallization of *n*-octacosane by the rapid expansion of supercritical solutions. *Journal of Crystal Growth* 155: 112–119.

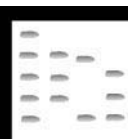
McHugh MA and Krukoni VJ (1994) *Supercritical Fluid Extraction: Principles and Practice*, 2nd edn. Boston: Butterworth-Heinemann.

Palakodaty S, York P and Pritchard J (1998) Supercritical fluid processing of materials from aqueous solution: the application of SEDS to lactose as a model substance. *Pharmaceutical Research* 15: 1835–1843.

Reverchon E (1999) Supercritical antisolvent precipitation of micro- and nano-particles. *Journal of Supercritical Fluids* 15: 1–21.

Tom JW and Debenedetti PB (1991) Particle formation with supercritical fluids – a review. *Journal of Aerosol Science* 22(5): 555–584.

SUPERCritical FLUID EXTRACTION–SUPERCRITICAL FLUID CHROMATOGRAPHY



H. J. Vandenburg, Express Separations Ltd.,
Roecliffe, N. Yorkshire, UK

Copyright © 2000 Academic Press

Introduction

The transfer of extracted analytes to a chromatography column can be either offline or online. In offline analysis, the extracted analytes are collected and then an aliquot is manually transferred to the chromatography system. Online analysis is where the extracted analytes are automatically transferred to the analytical column. The intrinsic problems with offline collection are that sample loss and contamination are possible, the process is difficult to automate and the sample must be diluted with solvent to allow transfer, resulting in higher detection limits. Coupling extraction and chromatography minimizes many of these problems. Supercritical fluid extraction (SFE) and supercritical fluid chromatography (SFC) are ideally suited for coupling together as the most

frequently used solvent, carbon dioxide (CO₂), is the same for both techniques. In the case where pure CO₂ is used, the extracted analytes can be deposited at the start of the analytical column simply by reducing the pressure, and chromatography started by increasing the pressure again. Capillary SFC (cSFC) benefits particularly from online methods. The columns are small and easily overloaded, particularly with injection solvent. For example, a 1-μL injection occupies 0.5 m of a 50-μm i.d. column. Larger injections can easily cause band broadening and peak splitting. The limitation of injection size increases the detection limit. A logical method of solving the intrinsic problems of offline collection and cSFC is to link them online.

Samples for which SFE–SFC is Applicable

The main alternatives to SFC are GC and HPLC. Online coupling of SFE and HPLC is difficult, as the presence of gaseous CO₂ is incompatible with HPLC

analysis. If the analytes are thermally stable and volatile GC is the best separation technique to use. Many flavour and fragrance compounds in complex food samples should therefore be analysed by SFE-GC. The same is true of polychlorinated biphenyls (PCBs), pesticides and polyaromatic hydrocarbons (PAHs) in environmental samples.

When the sample contains thermally labile or reactive compounds, SFE-SFC is recommended. The procedure is excellent for thermally unstable polymer additives in commercial plastics or for fatty acids and triglycerides in food, etc. which cannot be analysed by GC very easily without derivatization. Natural products such as those containing terpene compounds or hops which contain highly reactive bitter compounds such as humulone and lupulone must also be analysed by SFC or HPLC as rearrangement can easily occur at elevated temperatures. Speciation studies on organotin, an important environmental pollutant, are difficult using GC or HPLC as derivatizations are required to increase volatility or provide a chromophore. Other application areas specific to SFC include the analysis of explosives and certain steroids, vitamins and other drug residues in biological samples. SFE-SFC finds important applications in environmental science. The analysis of pollutants in matrices such as soil and sediments, and extraction of sorbents on which pollutants in air or water have been selectively adsorbed have been analysed with this technique.

Capillary and Packed Column SFC

There are two broad categories of SFC, capillary and packed column. Capillary SFC was developed from capillary GC, and packed column SFC is more akin to HPLC. There are advantages to each. cSFC uses open tubular capillaries with bonded stationary phases. Compounds with differing solubilities in CO₂ are eluted using pressure programming, where the pressure, and hence density and solvent strength of the mobile phase is increased during the separation. This is the equivalent of temperature programming in GC. Use of modifiers is rare, partly due to difficulties of mixing at very low flow rates and partly because the 'universal' FID cannot be used with modifiers present. Open tubular capillaries offer little resistance to the flow of the fluid and columns can be long. A major problem with capillary SFC is the low sample capacity. The capillary columns are easily overloaded and very small injections are required, reducing sensitivity. Packed column SFC uses columns packed with HPLC packing materials. Small particles offer a high resistance to the fluid flow, and hence there is a pressure drop across the column. This results in a reverse

density gradient along the column, in which the fluid has the lowest solvent strength at the elution end of the column. This gradient is working against any pressure gradient applied, and can lead to precipitation of solutes. Elution in packed column SFC is now often controlled by addition of a modifier such as methanol rather than pressure programming. Use of modifiers means that the FID cannot be used, and detection for packed column SFC is more usually by UV absorbance detectors. However, modifiers allow more polar stationary phases to be used, which have much greater interaction with polar molecules. When CO₂ alone is used, the stationary phase must also be nonpolar, otherwise the solvent strength is not sufficient to elute polar compounds. The analyte interacts only poorly with both stationary and mobile phases, resulting in poor peak shape. The poor results with polar compounds on packed SFC columns has also been attributed to polar active sites (residual silanols) present on the silica. These are thought to be better shielded in coated capillaries. The solvent strength of modified CO₂ can be varied from similar to pentane for pure CO₂ to similar to acetonitrile with addition of 40% methanol.

The different natures of capillary and packed column SFC also lead to differences in instrumentation. The flow rates in cSFC are very low, and pressure is usually controlled by restrictors. These can be linear capillaries whose diameter and length can be adjusted to provide the required pressure. Adjustable, heated needle valves have also been used. The problem with whichever system is used is that the restrictor is a passive device, limiting mass flow at the pressure set by the pumps. Blockages can occur, and the flow rate is not well controlled. Flow rates in packed column SFC are much higher, which allows the use of manual or automatic back pressure regulators, which control the pressure independently of flow rate. Pressure, flow rate and solvent composition can, therefore, be much better controlled in packed column SFC. In reality, packed column and capillary SFC are very different techniques, with different areas of application.

SFE-SFC Interface

The analytes extracted during the SFE step can be introduced onto the analytical column in two main ways. The SFE extract can be passed through a sample loop and an aliquot directed to the SFC column, or the analytes can be trapped after the SFE and introduced onto the column in one go.

Aliquot Sampling

The simplest of interface for SFE-SFC is by aliquot sampling. A part of the extract is sampled by passing

it through an injection loop of the SFC system. A closed- or an open-loop system may be used. Closed-loop static SFE-cSFC involves the sample being sealed in an extraction cell for a period of static extraction. The extraction cell is connected to the sample loop of an injection valve. The analytes diffuse to the loop, and after equilibrium is reached the valve is actuated and an aliquot is injected into the SFC column.

The major advantage of this procedure is that small aliquots of the extract can be taken for consecutive analysis with virtually no difference in the extraction profile. However, a major disadvantage is that the solute containing extraction fluid has to reach equilibrium and diffuse out of the cell and into the injection valve before sampling is made. This can take many hours before complete equilibrium is attained. Recirculating pumps could be used to reach equilibrium in a shorter time, but these can easily become contaminated.

The system can be sampled more rapidly by allowing a portion of the extraction solution to pass through the loop to atmosphere, to flush the loop with fresh solution. A low-flow restrictor is connected to a valve inline after the injector, as shown in **Figure 1**. Static extraction can be carried out with the high-pressure valve closed. Opening this valve to the restrictor allows dynamic extract and filling of the sample loop. Actuation of the rotary valve passes the contents of the loop to the analytical column, and either static or dynamic extraction can be continued. This is known as open-loop SFE, and with this configuration one also has the opportunity of passing the sample through a detector (UV or FID). At periodic

intervals aliquots of the extract can be injected into the SFC column for analysis.

Aliquot sampling diverts only a small portion of the extract to the SFC column, and is therefore not suitable for quantitative SFC analysis. SFE-SFC with aliquot sampling is a good technique for basic qualitative investigation and for measuring fundamental parameters such as partition coefficients of solutes in supercritical fluids. However, it is limited in that it is not usually suited to quantitative or trace analysis where analytes in the whole extract must be accumulated prior to chromatographic analysis.

Trapping of Analytes

In contrast to static extraction with aliquot sampling, dynamic SFE-SFC operates principally by continuously exposing the analytes to a fresh stream of supercritical fluid. Extracted components are accumulated from this stream in a trap of some kind. Only after extraction is complete are the trapped analytes transferred to the SFC column for analysis. The major advantages of dynamic SFE-SFC are that it is much more rapid than static SFE-SFC and that trace analysis can be performed. The whole of the extracted material is passed to the SFC column, therefore the sensitivity is much greater than for offline analysis. **Figure 2** shows a schematic of a simple online SFE-SFC system. A high-pressure syringe pump supplies the extraction cell with fluid. The outlet of the cell is connected to a capillary flow restrictor which is connected to an accumulating trapping system. During extraction the depressurized gas from the restrictor passes through the trap and is then vented to the atmosphere through valve 1. The extracted analytes

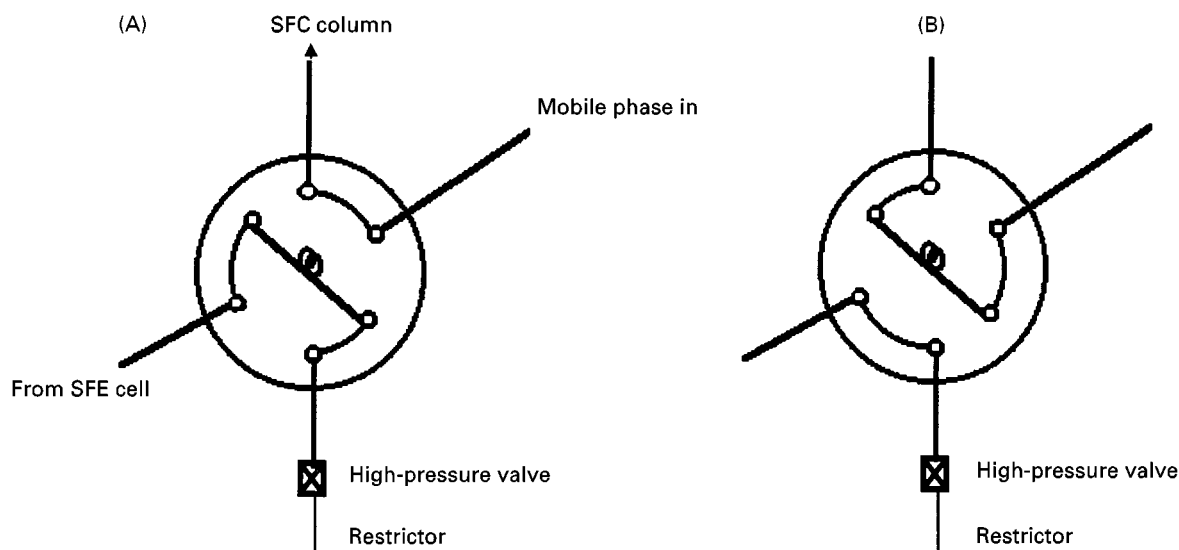


Figure 1 Schematic of open-loop aliquot sampling system (A) Filling loop, dynamic extraction mode. (B) Injecting to column.

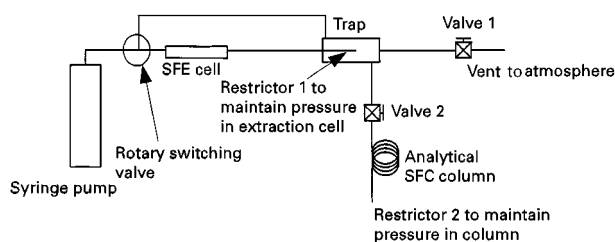


Figure 2 Schematic of SFE-SFC system.

are concentrated within the trap. After extraction is completed, valve 1 closes and valve 2 opens, switching the CO_2 onto the SFC column. The rotary valve switches the flow to the trap to avoid the cell and associated restrictor. This raises the pressure within the trap and the CO_2 becomes a supercritical fluid and capable of dissolving the trapped analytes and carrying them to the column.

If uncoated fused silica tubing is used to connect the trap to the analytical column (the retention gap), the analytes will, in theory, be unretained during the transfer. The pressure of CO_2 needed to effect the transfer need only be enough to provide some solubility of the analytes. Once they reach the stationary phase film of the SFC column they become concentrated as a narrow band, as the relatively low density solvent is not strong enough to elute the compounds from the stationary phase. After trapping is complete, the chromatography can be initiated using a pressure programme. If such phase ratio focusing occurs successfully, then good chromatographic efficiency is observed during the separation. If this process works well, the length and internal diameter of the retention gap do not significantly affect the resolution.

Other more complicated systems have been reported using on-off and multiport switching valves to allow continuous extraction or to permit the extraction cell to be vented during simultaneous chromatographic analysis. The 'plumbing' of such a system can be constructed to any specific requirement.

Since analytical SFE is most often performed with fluids that decompress to gases at ambient conditions (such as CO_2 , 1 mL min^{-1} of which produces a gas flow of approximately 500 mL min^{-1}), the success of trapping depends on the success of recovering the analytes from the expanded gas. Fast flow rates tend to elute volatile analytes from the trap, thus, for quantitative results, recovery of extracted components should be performed at lower flow rates. The problem of loss of volatile analytes is often not severe in SFE-SFC, as these are likely to be analysed by SFE-GC. Therefore SFE-SFC traps generally need be more concerned with trapping less volatile materials.

Trapping procedures

There are several methods of trapping extracted components from dynamic SFE in preparation for online SFC analysis. The requirements are to efficiently trap all the material from the gas or low-pressure stream from the extractor, and then to release all the components when the flow is switched to the analytical column. Two methods are used for this:

- cryogenic trapping; and
- trapping on an adsorbent stationary phase; the stationary phase can be either on particles packed into the trap, or coated onto a fused silica capillary.

Cryogenic trapping

Trapping on uncoated fused silica retention gaps A length of uncoated fused silica capillary can be cooled by expanding CO_2 . Solutes passing through the capillary in the depressurized gas stream from the SFE will be trapped in the cooled section. The cooling can then be switched off, and the section pressurized with CO_2 to redissolve the analytes. **Figure 3** shows an arrangement for a cryogenically cooled fused silica trap. In this arrangement the expanded mobile phase from the extraction cell is released from a different outlet than the incoming CO_2 for the SFC. This minimizes contamination of the system from previous analyses. The extracted analytes are in contact only with deactivated fused silica after leaving the extraction cell, which reduces loss of polar analytes by adsorption on metal surfaces.

The flow rate of the expanding extraction fluid and the temperature at which analytes are trapped markedly affect the recoveries obtained when uncoated fused silica tubing is used. In many systems, linear extraction restrictors are used, since they provide the correct flow rate range for online coupling with capillary SFC. They also tend not to plug as quickly as other restrictors when used for SFE. The length and internal diameter of the capillary restrictor tubing

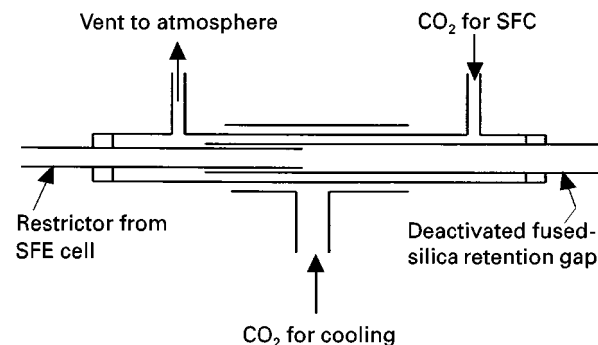


Figure 3 Cryogenically cooled trap.

and the pressure at which the extraction is performed should therefore be considered to obtain suitable flow rates.

Restrictors with internal diameters greater than 30 μm result in higher extraction efficiencies, but lower recoveries and significant band broadening of more volatile components. However, restrictors with internal diameters less than 15 μm do not allow sufficient flow for efficient extractions over a short period of time, but yield good chromatographic peak shapes. As a rough guide, the gaseous flow rates from 15-cm lengths of 15-, 20-, 25- and 30- μm restrictors at a pump pressure of 300 atm are, approximately, 80, 150, 240 and 300 mL min^{-1} , respectively. A good compromise therefore is to use a restrictor with a flow rate of 100–200 mL min^{-1} . Lengths of capillary tubing of 20 or 25 μm i.d. are suitable for most needs.

The trapping efficiency is also strongly dependent on the trapping temperature. The higher the temperature, the more volatile components will be lost from the trap. Cooling in the region of -40°C to -60°C will allow trapping of C_{10} hydrocarbons with reasonable efficiency. The trap should only be cooled to a sufficient temperature to trap the analytes of interest, as too low a cryofocusing temperature may result in restrictor plugging, or components, such as water, freezing in the restrictor. This reduces the rate of extraction and makes it difficult to reproduce analyses. An alternative arrangement for trapping volatile substances is to keep the restrictor hot and deposit the analytes in the transfer line held in a cryogenically cooled oven as shown in Figure 4.

The use of micropacked columns has also been reported. In this case the restrictor can be vented onto the head of the analytical column. The cooling of the expanding gas cools the column and the analytes are deposited on the packing at the start of the column.

Trapping on coated fused silica retaining pre-columns
An alternative to the cryotrapping method is the use

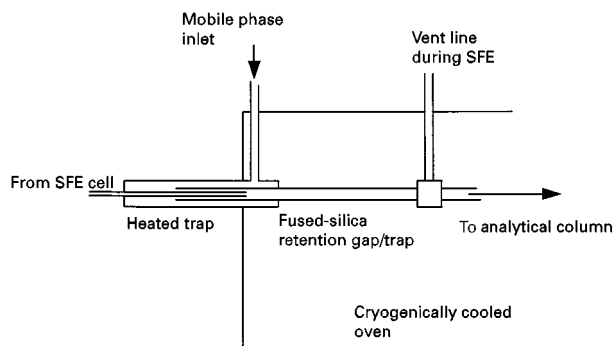


Figure 4 Arrangement for keeping restrictor hot and trapping in cryogenically cooled oven.

of a coated fused-silica retaining pre-column for concentrating extracted solutes. Compared to uncoated fused silica, coated columns such as GC columns are much more effective at trapping. The key is to trap effectively, but allow the mobile phase to elute the trapped materials during the pressure programme. It is likely that a column coated with a similar material to the analytical column will be effective. The phase thickness on the column is also important, thicker phases having a greater trapping power. This method allows the trapping at room temperature using widely available bonded-phase GC columns.

Trapping on sorbent traps Sorbents may also be used as an effective method of trapping. This entails the use of short traps (usually 2 cm in length) packed with organic sorbents such as Tenax-GC, Carbotrap or with HPLC packing materials. Bonded silica and polymeric stationary phases designed for solid-phase extraction (SPE) are available with a wide variety of functionality, and would make ideal packing material for this application. These materials will effectively trap the analytes from the low-pressure gas stream, and can then be desorbed by high-pressure supercritical CO_2 . The considerations are similar to those when using coated silica columns. It is important when using such a system that breakthrough of the analytes from the sorbent does not occur and also that the desorption behaviour is suitable for online chromatographic analysis. Desorption is performed by increasing the trap temperature or by using the supercritical fluid to desorb the sample. The process is effectively the same as SPE, with supercritical CO_2 as the desorbing solvent. The stationary phase should be selected to have a strong enough affinity to trap the analytes from the gas stream, but to be desorbed by supercritical CO_2 . Supercritical CO_2 is essentially non-polar, and it is unlikely that polar compounds could be eluted from polar stationary phases. It is not always possible to elute all the trapped analytes with CO_2 , and supercritical nitrous oxide has been found to be more effective than supercritical carbon dioxide in removing solutes from adsorbents. However, the oxidizing nature of this material has resulted in explosions, and is not recommended. It is therefore more important to select the most appropriate stationary phase which will trap the analytes, and then be desorbed by the mobile phase.

Use of Modifiers and Solvent Venting

Although CO_2 is a versatile extraction solvent, sometimes modifiers are needed to solvate particular analytes or overcome analyte–matrix interactions.

This presents a problem in SFE-SFC. With cryogenically cooled traps, the modifier will be trapped and block the restrictor, or flood the column when the flow is switched to the analytical column. If the modifier becomes liquid after depressurization, it will dissolve the analytes and elute them from coated traps. Coated capillaries can be used to trap the analytes, provided the modifier is present at a sufficiently low concentration to remain as a vapour in the CO₂ gas stream. Therefore the upper limit for the modifier addition is that at which CO₂ is saturated at atmospheric pressure and the trapping temperature. For methanol the maximum addition at 25°C is 14%. It is important that the pressure in the trap does not rise, as this may cause the modifier to liquefy. Wide-bore coated capillaries may be needed for the trap to reduce back pressure, and a second, narrow-bore column will catch any breakthrough from the wide-bore trap. A short gas purge will remove any residual modifier, and the analytes can then be transferred to the analytical column dissolved by supercritical CO₂. It may be necessary to introduce a refocusing trap, which will focus the analytes from the supercritical CO₂, as the trap volumes may be quite large, which would otherwise lead to band broadening.

Apart from use of modifiers, other situations occur when large amounts of solvent are trapped with the analyte. Co-extraction of low-molecular-weight solvents or reactants along with the desired analytes is one example. Provided the co-extractant is sufficiently volatile and the analyte involatile, then the unwanted material can be removed from the intermediate trap by gas purge. The analytes can then be transferred to the analytical column with supercritical CO₂.

SFE as a Sample-Introduction Technique

As stated previously, one of the problems of cSFC is sample introduction without flooding the column with solvent. Aqueous samples are a problem for capillary and packed-column SFC, as water is only slightly soluble in CO₂. SFE can be used as a solventless sample introduction technique to avoid this problem. One method to achieve this is to inject the sample onto a pre-column fitted with a restrictor. The solvent will flood the column for some distance. The solvent can be removed by gas purging, leaving the less volatile analytes behind. The entire pre-column is then pressurized with supercritical CO₂ to dissolve the analytes and carry them to the analytical column. In effect, the pre-column is acting as an SFE cell. Samples dissolved in aqueous media can be concentrated and transferred to packed or capillary columns

while maintaining high efficiency. The use of solid sorbents has proved very useful in sample introduction to SFC. The dissolved analytes are injected onto a sorbent, the solvent can then be removed by evaporation and the analytes transferred to the analytical column using SFE-SFC. The whole process has been called SPE-SFE-SFC. This method is particularly applicable to biological samples where the analyte has no chromophore. These are often thermally labile, and therefore analysis by GC or HPLC is problematical. Direct sample introduction to SFC is also a problem due to the aqueous nature of the samples. Use of an intermediate trap and solvent purging to remove the water and introduce the analytes to the SFC column allows much larger samples to be introduced, improving sensitivity by a factor of 100 or more. In environmental analysis, samples of several hundred millilitres can be passed through a solid-phase extraction cartridge to concentrate impurities. The cartridge can then be eluted with CO₂ to the analytical column. This system could also be used as an HPLC-SFC interface.

Optimization of Conditions for SFE-cSFC

A number of parameters must be optimized for successful analysis by coupled SFE-cSFC. Principal among these are the conditions for quantitative extraction. This should begin with a determination of the supercritical fluid extractability of the analyte(s) from the non-sorptive matrices (filter paper, etc.) to assess the appropriate solvent, density and temperature conditions. Trial runs on spiked samples then allow investigations of matrix-solute interactions; if necessary these may be overcome by a period of static extraction. The kinetics of extraction must then be determined in order to define the required extraction time.

Factors affecting the efficiency of intermediate trapping must then be addressed. The nature of the analyte is crucial, while the possible presence of co-extracted, interfering compounds demands either selectivity during extraction, or the trapping on an adsorbent from which selective desorption into the SFC column is possible. The sample size must be carefully chosen so that the capacity of the SFC column is not exceeded, and the extracting supercritical solvent must be of sufficient purity to avoid introduction of extraneous material into the column. Finally, the conditions for efficient SFC analysis must be optimized, preferably offline. Correct choice of column, temperature and pressure/density programme are vital. Compromises may be inevitable if the extracted analytes have a range of polarities.

Conclusion

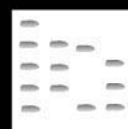
Coupled SFE-SFC has shown itself to be a very useful technique for those samples for which it is applicable. The ability to transfer all the extract to the analytical column without manipulation increases sensitivity, reduces contamination and sample handling. The overloading of capillary columns is avoided. Now that methods for using modifiers in the extraction solvent and SFE sample injection methods have been developed, there is every likelihood that SFE-SFC will become a more widely used technique.

See also: II/Chromatography: Supercritical Fluid: Fourier Transform Infrared Spectrometry Detection; Historical Development; Instrumentation; Large-Scale Supercritical Fluid Chromatography; Theory of Supercritical Fluid Chromatography.

Further Reading

- Anton K and Berger C (eds) (1998) *Supercritical Fluid Chromatography with Packed Columns*. New York: Marcel Dekker.
- Berger TA (1995) *Packed column SFC*. RSC Chromatography Monographs. Cambridge: The Royal Society of Chemistry.
- Clifford T (1999) *Fundamentals of Supercritical Fluids*. Oxford: Oxford University Press.
- Ramsey ED (ed.) (1998) *Analytical Supercritical Fluid Extraction Techniques*. Dordrecht: Kluwer Academic Publishers.
- Wenclawiak B (ed.) (1992) *Analysis with Supercritical Fluids: Extraction and Chromatography*. Berlin: Springer-Verlag.
- Westwood SA (1993) *Supercritical Fluid Extraction and its Use in Chromatographic Sample Preparation*. London: Chapman and Hall.

SUPERHEATED WATER MOBILE PHASES: LIQUID CHROMATOGRAPHY



R. M. Smith, Loughborough University,
Loughborough, Leics, UK

Copyright © 2000 Academic Press

At room temperature, water on its own is an unattractive solvent in liquid chromatography. In reversed-phase chromatography, water is a weak eluent and is often regarded as an inert component of the mobile phase. It is mainly used to dilute a stronger organic component and thus control the overall eluent strength. In contrast, in normal-phase chromatography, water is a powerful eluent and interacts strongly with the stationary phase, often deactivating it. Even trace amounts in a nonpolar eluent (or even in a sample) will markedly alter the retention properties of a silica surface. In separation methods aqueous eluents are used primarily for ion exchange chromatography or for the size exclusion separation of biological molecules.

However, this represents the situation at room temperature and atmospheric pressure. When liquid water is heated under pressure, its dielectric constant, viscosity and surface tension all decrease. These changes in the properties of water are well known but have largely remained the province of the physical chemist and chemical engineer. They have been widely studied because of the importance of water as a heat transfer agent and they play their part in the design and construction of steam power generation

plant and in related areas. Above 374°C under a pressure of 221 bar, a single supercritical phase is obtained. Although these conditions seem extreme for the laboratory, they occur in nature in the ocean depths at the spreading points in the earth's crust where water issues from fumeroles at 350–400°C and 250 bar.

In recent years organic chemists have been attracted by the possibility of using superheated or supercritical water to achieve clean solvent-free conditions and to generate novel reaction conditions which are not available at room temperature. It has also been employed as a solvent for the high temperature oxidation for waste remediation or for the destruction of hazardous materials such as nerve gases and explosives as an alternative to high temperature incineration. In inorganic chemistry, supercritical water has been used as a solvent to enable high temperature reactions to be carried out without the inconvenience of using molten salts.

However, the analytical chemist has made little use of water under pressure, although the potential of supercritical water as a fluid solvent for chromatography was recognized by Lovelock in 1958. Some work has exploited steam as a mobile phase in gas chromatography, but the condensed phase has largely been ignored. Although liquid chromatographers have used elevated temperatures to improve separations or efficiencies, in almost every case the composition of the organic-aqueous eluent was kept

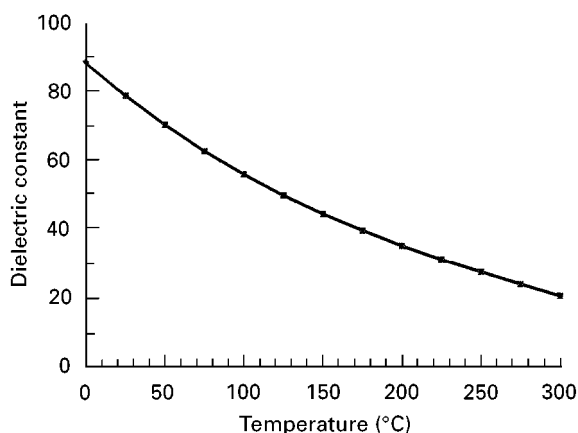


Figure 1 Change in dielectric constant of water with temperature.

constant and only the effect of the temperature was studied, typically up to 70–80°C.

Recently, the changes in the properties of liquid water above 100°C have attracted the interest of the analytical chemists, who have recognized that these low polarities might provide an environmentally clean solvent for extraction. Subsequently, the use of superheated water has also been applied to liquid chromatography. Some of the published papers have referred to this region of the phase diagram as subcritical water but this could imply any temperature less than 374°C. This review will instead employ the expression superheated water, which is defined as water held as a liquid under pressure between 100°C and the critical point.

Properties of Superheated Water

As the temperature of water is raised under a sufficiently high pressure for it to remain in the liquid state

there is a steady decrease in its dielectric constant (Figure 1) from about 80 at room temperature to less than 25 at 300°C. These changes represent a marked change in the solvent polarity of the water. By 250°C the dielectric constant of water is about 30, which is less than that of methanol at room temperature, so that even under conditions well below its critical point, water will resemble the polarity of common organic solvents used as eluents in reversed-phase liquid chromatography. There is also a decrease in the viscosity of water from 1.0 cp at room temperature to 0.28 cp at 100°C, as well as in the surface tension.

The pressure conditions usually needed to carry out supercritical fluid chromatography (SFC) with carbon dioxide can be as high as 300–500 bar in order to achieve a sufficiently high density to provide a reasonable solvent strength. However, the vapour pressure of water (Figure 2) is modest and even by 200°C only reaches 15 bar, so that only moderate pressures are required to maintain a liquid state. In addition, the density of hot liquid water changes by only a small amount with changes in the applied pressure. The solvation properties are thus effectively independent of pressure. This is in marked contrast to supercritical carbon dioxide where pressure control is critical because of its marked effect on density.

Application in Analytical Extractions

The first serious analytical chemistry interest in the potential of water under pressure above 100°C came in 1994, when Hawthorne and colleagues investigated the extraction of organic pollutants from environmental solids with supercritical and subcritical water. They had been prompted by reports that the solubility of benzo[*a*]pyrene increases from 4 ng mL⁻¹ under ambient conditions to approximately 10% by weight

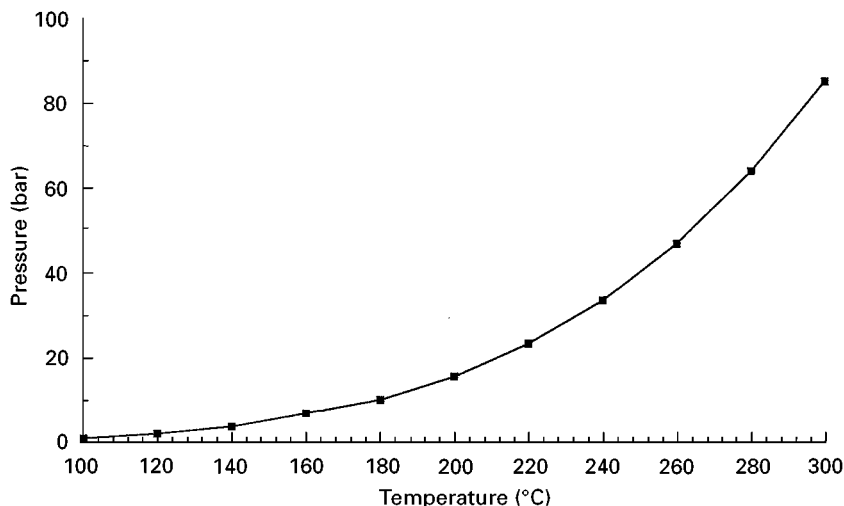


Figure 2 Change in vapour pressure of water with temperature.

at 350°C and 100 bar. This represents an increase in solubility of about 25 million. They found considerable solubility for polar analytes, such as chlorinated phenols, and even a significant solubility for nonpolar analytes, such as naphthalene at 50°C. Raising the temperature resulted in an increased solubility for polynuclear aromatic hydrocarbons (PAHs) and by 250°C all their test compounds except the *n*-alkanes had been completely extracted. The alkanes required supercritical conditions and were completely extracted at 400°C. These results confirmed that superheated water had a sufficiently high solubilizing power to be used as a solvent for even nonpolar analytes. They then demonstrated that subcritical conditions of 250°C and 50 bar would also efficiently extract PAHs from soil samples. In addition, good recoveries were obtained from air particulates. These results also showed that pressure was not an important factor, in marked contrast to the pressure dependence of supercritical fluid extraction with carbon dioxide.

Subsequently they studied the extractions further and showed that polychlorinated biphenyls (PCBs) could be extracted from soils and sediments with subcritical water. At 300°C and 50 bar, complete extraction could be achieved in pure water. Other workers have found that water can be used for the extraction of PCBs from a range of matrices in good yield. In a similar study, the pesticides Dacthal and acid metabolites have been extracted from soil with superheated water.

Chromatography using Superheated Water as the Mobile Phase

It was realized that if superheated water could extract PAHs from soils and dissolve PCBs, then it

was behaving as a less polar solvent than the methanol–water and acetonitrile–water mixtures conventionally used as mobile phases in reversed-phase liquid chromatography. It should therefore be possible to use superheated water as a mobile phase and achieve typical reversed-phase liquid chromatographic separations. Many studies have examined the effect of increasing the temperature on separations and have shown that there is a consistent drop in retention with an inverse relationship to the absolute temperature (k varies as $1/T$ K). However, most of this work has either looked at temperature effects using constant eluent composition or has been limited to 80–90°C by the volatility of the organic components of the mobile phase.

In 1996, Smith and Burgess demonstrated that under a modest pressure it was possible to carry out the reversed-phase separation of phenols using superheated water at 160°C on a polystyrene-divinylbenzene (PS-DVB) column. The equipment was a combination of high performance liquid chromatography (HPLC) and gas chromatography (GC) systems (Figure 3) with some components from a packed-column SFC system. The water mobile phase was pumped using a single reciprocating pump but, unlike SFC, there was no need to cool the pump heads to condense the mobile phase. As the mobile-phase polarity can be controlled by temperature, no modifier pump was needed. The column was heated in a GC column oven which enabled the temperature to be controlled up to 350°C. To maintain the pressure a SFC back-pressure regulator was used. A detector fitted with a high pressure flow cell was originally employed but, because the back-pressures required are relatively low, in later studies standard HPLC spectroscopic flow cells were used for fluorescence

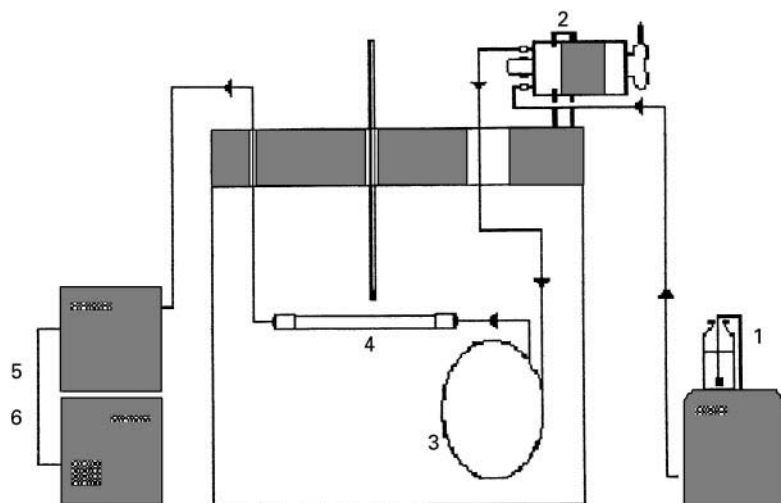


Figure 3 Superheated water chromatograph. Components: 1, pump; 2, injection valve; 3, preheating coil; 4, column; 5, detector; 6, back-pressure regulator.

and ultraviolet-visible spectroscopy. It is also possible to replace the back-pressure regulator with a length of narrow-bore PEEK tubing.

A PS-DVB packed column was used in the first studies because this material can be used without problems in size exclusion chromatography at 160°C and is thermally stable at this temperature. Phenols were examined with a methanol–water eluent and then the methanol content was reduced while raising the temperature in steps. With each increase in temperature the retention times decreased. By 180°C in the absence of methanol, the samples had similar retention times to those in 20 : 80 acetonitrile–water at room temperature.

The relative retention of a wide range of analytes from phenols, amides, esters to simple aromatic compounds demonstrated that the retention followed a similar pattern to conventional reversed-phase liquid chromatography. The separation followed the hydrophobicities of the analytes and the homologous parabens eluted in order of increasing chain length. They were also stable, showing neither hydrolysis nor oxidation. The separations, as expected, were insensitive to the back-pressure applied to the column.

It was also realized that programming the temperature of the column during the separation would systematically reduce the eluent polarity. This produced an effect similar to gradient elution, and would speed up and focus later peaks. Inorganic buffers could also be added to control the pH without causing any problems.

Stationary Phases for Superheated Water Chromatography

Most of the work that has been reported has employed PS-DVB columns which have shown reasonable temperature stability. They can be used up to about 220°C before softening appears to reduce their lifetime. As in ordinary HPLC, these columns show a marked difference in the retention of nonpolar and hydrogen-bonding analytes. The latter, including alcohols and phenols, have markedly lower retentions than nonpolar analytes such as alkylbenzenes and nitrobenzene. These latter compounds cannot be easily eluted even at 230°C.

Porous graphite carbon (Hypercarb) has been examined as an alternative thermally stable stationary phase. No instability was observed and the separations of mixtures of phenols, anilines and aryl amides were similar to those obtained at room temperature with conventional eluents (Figure 4).

There is particular interest in octadecylsilica (ODS)-bonded silica phases because of their widespread use in conventional liquid chromatography.

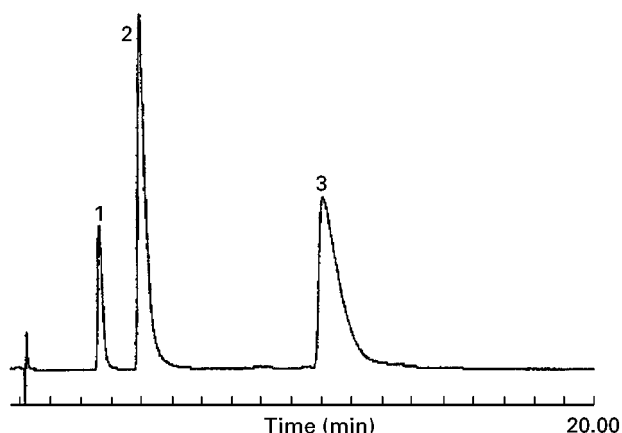


Figure 4 Separation of amides on porous graphitic carbon column at 190°C. Analytes: 1, benzenesulfonamide; 2, benzamide; 3, *m*-toluamide.

However, although a number of different silica-based bonded-phase materials have been examined, they all show quite rapid degradation at temperatures greater than 100°C. Even though they have a lower retention capacity than the PS-DVB columns and do not require such high temperatures to obtain elution, it appears that this matrix is insufficiently stable for routine use.

A second problem was that, when highly end-capped ODS-bonded materials were examined with 100% water as the eluent, the octadecyl chains collapsed on to the silica surface on cooling the column to room temperature. As a result, the retention capacity of the column dropped markedly and this was not restored by heating. Instead, the column had to be treated with methanol–water mixtures. Similar problems have been reported in reversed-phase liquid chromatography at room temperature when the mobile phase contains less than 2% methanol.

A promising alternative stationary phase is polybutadiene-coated zirconia, a relatively new material, which is reported to be stable in water at 200°C. It gives good separations and peak shapes. The order of elution is similar to that on ODS phases in conventional reversed-phase liquid chromatography.

The elevated temperatures would be expected to reduce mass transfer effects in the mobile phase because of higher diffusion rates and this would result in improved separation efficiencies. Van Deemter curves of column plate heights against mobile-phase flow rate of water at elevated temperature determined for the PS-DVB and Hypercarb columns have been compared with acetonitrile–water separations at room temperature. In both cases, at the optimum flow rates the height equivalent to one theoretical plate (HETP) values are similar, but in superheated water the efficiency decreases rapidly at lower flow rates. This

effect can be ascribed to a higher diffusion rate in the mobile phase at the higher temperature.

Detection in Superheated Water Chromatography

One of the advantages of superheated water chromatography is that it increases the possible number of detection methods that can be employed compared to liquid chromatographic methods using an organic solvent. However, with some detectors the mobile phase had to be cooled to room temperature to avoid baseline instability due to refractive index effects. So far no problems have been experienced due to the analytes coming out of solution between the column and detector, probably because the concentrations are generally low and the transfer time to the detector is brief.

Because usually only low back-pressures (less than 50 bar) are required to maintain the liquid state in the column, standard liquid chromatography flow cells can frequently be employed for ultraviolet-visible and fluorescence spectroscopic detection. Alternatively, high pressure ultraviolet-visible flow cells designed for SFC application can be used. In both methods of detection, one advantage of water as an eluent is that it is transparent down to 190 nm. This enables low wavelength detection of unconjugated double-bond chromophores without solvent interference. However, some fluorescence detection is reduced compared to organic solvents because of quenching by the polar aqueous solvent.

The absence of an organic modifier raised the possibility that the eluent could be passed to a flame ionization detector. This could provide a simple method of universal detection for liquid chromatography, which previously has only been obtainable using mass spectrometry. This possibility was realized by Miller and Hawthorne, who demonstrated the use of the FID in 1997 to detect alkanols, phenols and amino acids, and confirmed by others.

Another detector that has problems in conventional liquid chromatography, because of mobile phase interference, is on-line nuclear magnetic resonance spectroscopy (LC-NMR). Many of the problems can be overcome by employing superheated heavy water (deuterium oxide) as the mobile phase. Compared to deuterated organic modifiers, deuterium oxide is relatively cheap and unlike supercritical fluid chromatography the flow cell can be at room temperature and pressure. This makes stop-flow detection easier and characteristic proton-NMR spectra have been obtained for a range of compounds, including barbiturates, sulfonamides and a number of pharmaceuticals and natural products.

It has also been demonstrated that superheated water chromatography can be linked to mass spectrometry using a standard LC-interface to give a superheated water LC-NMR-MS system. These separations using superheated deuterium oxide have also provided some interesting exchange reactions which are more selective and specific than those reported with supercritical deuterium oxide.

Application of Superheated Water Chromatography

A wide range of analytes (Table 1) has been examined by superheated water chromatography. They have generally been moderately polar and could be characterized as analytes where conventional liquid chromatography would employ a mobile phase with 60% or less organic modifier. Less polar analytes, such as alkylbenzenes, can currently cause problems because they require a mobile-phase temperature above the limit of the polymeric stationary phases primarily used so far.

The principal groups of compounds examined so far have been phenols (Figure 5), alcohols, amino acids, esters, pharmaceuticals, water-soluble vitamins and lactone natural products. The method is still relatively new and further applications are constantly being developed. Although there was concern that the separation conditions might cause sample oxidation, hydrolysis or degradation, so far few compounds have caused problems. Not surprisingly, aspirin is hydrolysed but this occurs readily even at room temperature. Nitrobenzene appears to degrade and there is some suggestion that other nitro-compounds are also thermally unstable in hot water. In contrast, compounds such as the parabens (4-hydroxybenzoate

Table 1 Typical compounds which have been separated by superheated water chromatography

Aryl aldehydes
Amino acids
Aryl alkyl ketones
Aryl amides
Aryl amines
Arylsulfonamides
Parabens
Pharmaceuticals, including:
Barbiturates
Caffeine
Paracetamol
Phenacetin
Sulfonamides
Phenols, including:
Cresols
Guaiacol
Methoxyphenols
Phenol
1,2,3-Trihydroxybenzene

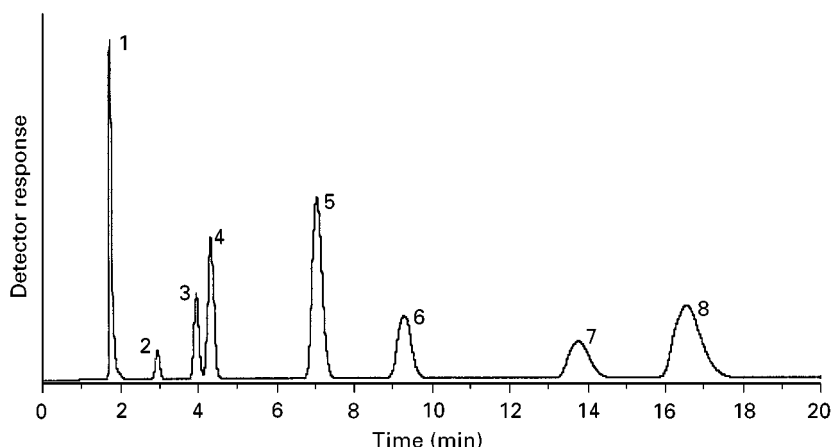


Figure 5 Functional group selectivity of PS-DVB column. Conditions: column, PLRP-S; temperature, 200°C. Solutes: 1, hydroquinone; 2, *p*-cyanophenol; 3, phenol; 4, *p*-methoxyphenol; 5, *p*-cresol; 6, *p*-bromophenol; 7, 3,5-xyleneol; 8, 2,4-xyleneol.

esters) which might be thought to be susceptible both to oxidation and to hydrolysis, have been separated without difficulty. One reason may be that, as the temperature is raised and the water becomes less polar, it also becomes a weaker hydrolysis agent.

See also: II/Chromatography: Liquid: Mechanisms: Reversed Phases; Nuclear Magnetic Resonance Detectors. **Extraction:** Supercritical Fluid Extraction. III/Environmental Applications: Pressurized Fluid Extraction. Porous Polymers: Liquid Chromatography.

Further Reading

Chienthavorn O and Smith RM (1999) Buffered superheated water as an eluent for reversed-phase high performance liquid chromatography. *Chromatographia* 50: 485–489.
Hawthorne SB, Yang Y and Miller DJ (1994) Extraction of organic pollutants from environmental solids with sub- and supercritical water. *Analytical Chemistry* 66: 2912.

Kuhlmann B, Arnett EM and Siskin M (1994) Classical organic reaction in pure superheated water. *Journal of Organic Chemistry* 59: 3098.

Miller DJ and Hawthorne SB (1997) Subcritical water chromatography with flame ionisation detection. *Analytical Chemistry* 69: 623.

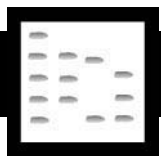
Smith RM and Burgess RJ (1996) Superheated water – a clean eluent for reversed-phase high-performance liquid chromatography. *Analytical Communications* 33: 327.

Smith RM and Burgess RJ (1997) Superheated water as an eluent for reversed-phase high-performance liquid chromatography. *Journal of Chromatography* 785: 49.

Smith RM, Chienthavorn O, Wilson ID, Wright B and Taylor SD (1999) Superheated heavy water as the eluent for HPLC-NMR and HPLC-NMR-MS. *Analytical Chemistry* 71: 4493–4497.

Yang Y, Bøwdt S, Hawthorne SB and Miller DJ (1995) Subcritical water extraction of polychlorinated biphenyls from soil and sediment. *Analytical Chemistry* 67: 4571.

SURFACTANTS



Chromatography

J. G. Lawrence, Unilever Research
Bebington, Merseyside, UK

Copyright © 2000 Academic Press

Introduction

‘Surfactant’ is a contraction of ‘surface active agent’. It has come to be used interchangeably with

detergent, particularly when applied to cleaning products such as fabric washing powders, soaps, hard-surface cleaners and the many other products used for cleaning in and around the home. Solutions of surfactants exhibit one or more of the properties of detergency, foaming, wetting, emulsifying, solubilizing and dispersing.

This article will deal with the main classes of surfactants used as commercial detergents, which are not single compounds but mixtures of compounds of the same general structure but having a range of alkyl chain lengths. Surfactants have the follow-

ing general properties:

- They are molecules composed of groups of opposing solubilities, typically an oil-soluble hydrocarbon chain and a water-soluble ionic group.
- They are soluble in at least one phase of a liquid system.
- They form oriented monolayers at phase interfaces.
- They form micelles (aggregates of molecules or ions) above a limiting concentration in solution.

Chromatographic separations are important in surfactant analysis for a number of reasons. The most important of these is based on their ability to separate both molecules of different, though similar, structures and molecules from within a structural family on the basis of carbon chain length, chain branching or positional isomer distribution. Many procedures for surfactant analysis give average values for the property determined. Two quite different examples are titrimetric determination of the active level of a surfactant which requires a value for the mean molecular weight of the surfactant to calculate the weight percent of active material and determination of the degree of ethoxylation of an alcohol or alkylphenol ethoxylate by proton nuclear magnetic resonance, which gives a value for the average degree of ethoxylation but no information on the ethoxamer distribution. Chromatographic techniques can supply the mean molecular weight to use with the titration and both the detailed ethoxamer and alkyl chain length distribution of the ethoxylate. Such detailed knowledge of molecular composition is required for full understanding of surfactants and their properties.

Other areas of surfactant analysis in which chromatographic techniques are used are determination of levels and composition of surfactants in products and in the environment, particularly in studying decomposition, and in studying the detailed composition of the surfactant itself including low levels of impurities or contaminants which may result from the manufacturing process. Legislative and consumer pressures for cleaner, safer, more environmentally friendly raw materials and products are resulting in such analyses becoming increasingly common.

In the following sections, the most common surfactants in the detergents and related industries and the chromatographic techniques (gas-liquid chromatography, high performance liquid chromatography, supercritical fluid chromatography, thin-layer chromatography, capillary electrophoresis) used in their analysis will be described. The examples have been chosen to illustrate the variety of sample preparation, separation and detection procedures which can be used.

Anionic Surfactants

Alkylbenzenesulfonates

Alkylbenzenesulfonates are the most common of the commercial anionic surfactants. Their general structure is *p*-alkylbenzenesulfonic acid, sodium salt (**Figure 1**) where the alkyl chain may range from C9 to C14 with the benzenesulfonate moiety attached in different proportions at each carbon atom from C2 to the central carbon of the chain. The carbon chain is essentially linear to permit biodegradation, though there is a minor usage of branched alkylbenzenesulfonates for specific applications.

Gas chromatography Gas chromatography (GC) of alkylbenzenesulfonates requires some pretreatment of the molecule to enable it to be volatilized. The most common pretreatments are desulfonation and derivatization. The following examples demonstrate a number of sample preparation and detection options:

- Desulfonation of alkylbenzenesulfonate with phosphoric acid to the corresponding linear alkylbenzene (LAB) followed by separation on a fused silica capillary column (**Figure 2**). This procedure enables both the alkyl chain lengths and the attachment points of the benzene ring along the chain to be determined.
- Desulfonated linear alkylbenzenesulfonate (LAS) or LAB can be prefractionated from complex detergent and environmental samples using argentation thin-layer chromatography (TLC), in which the TLC plate is coated with silver nitrate to modify the separation process. The separated spots are recovered from the plate and analysed using similar conditions to those in **Figure 1**. Electron impact mass spectrometry (EIMS) detection is used to give component identification.
- LAS and dialkyltetralinsulfonates are converted to their sulfonyl chlorides by reaction with phosphorus pentachloride and then to their trifluoroethyl derivatives by reaction with trifluoroethanol. These derivatives are separated using similar conditions to those described in **Figure 2**.

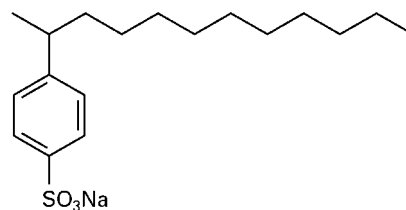


Figure 1 C12 2-phenylalkylbenzenesulfonate, sodium salt. Courtesy of RSC.

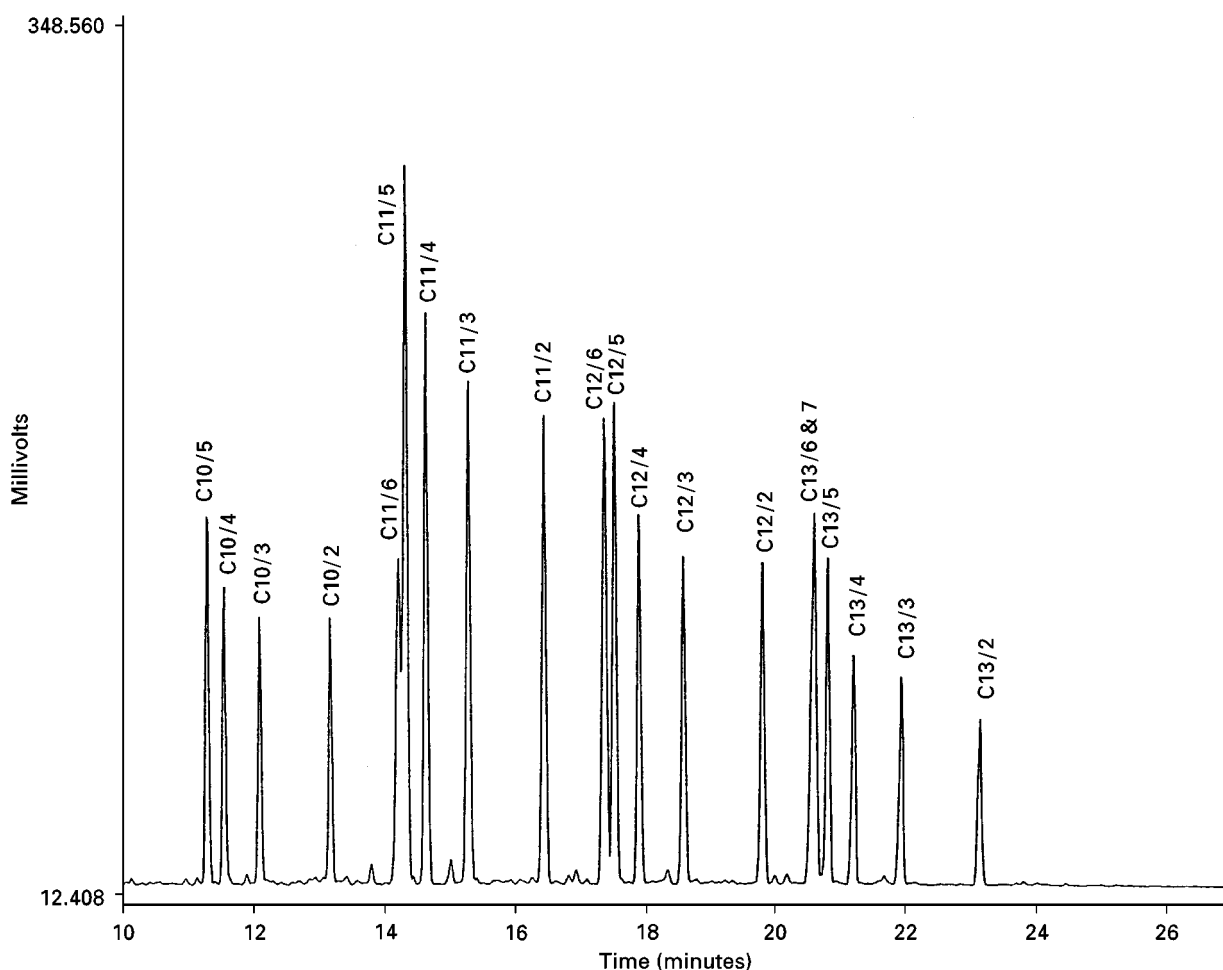


Figure 2 C10–C13 linear alkylbenzene. Column 25 m \times 0.2 mm i.d. fused silica capillary of HP1 (0.33 μ m film) programmed from 120°C to 240°C at 3°C per minute, final temperature held for 20 min, injector and detector at 275°C, FID, carrier helium at 1 mL min⁻¹, splitless injection. Courtesy of RSC.

- Aqueous solutions of LAS are shaken with tetrabutylammonium hydrogensulfate to form ion pairs. Injection of the ion-pair solution into a GC injection port at 300°C forms the butylsulfonate derivatives of the LAS which are separated on a HP-5 column (20 m \times 0.2 mm i.d., 0.33 μ m film) programmed from 110°C to 220°C at 10°C per minute then 300°C at 6°C per minute with a final 3-minute hold. Detection is by EIMS to give full spectral information.
- LAS is rapidly and efficiently converted to its methylsulfonate ester by derivatization with trimethoxyorthoacetate at room temperature and separated as in Figure 3.

High performance liquid chromatography The advantage of high performance liquid chromatography (HPLC) for the separation of LAS is that, in contrast to GC, sample preparation specifically to make the

LAS compatible with HPLC is unnecessary. LAS can be determined by HPLC by a number of procedures of which examples to demonstrate different separation and detection conditions are given below.

The chain-length distribution of LAS can be determined on a column (300 \times 3.9 mm) of μ -Bondapak C18 (10 μ m) using a linear gradient from 70 : 30 acetonitrile–0.15 mol L⁻¹ sodium perchlorate solution to 90 : 30 of the two solutions. UV photometric detection is at 230 nm. Peaks are eluted in order of increasing alkyl chain length.

The positional isomer distribution is determined using a column (250 \times 4 mm i.d.) of Spherisorb ODS II (3 μ m) with an isopropanol–water–acetonitrile gradient with 0.02 mol L⁻¹ sodium perchlorate added and UV detection at 225 nm.

Both chain length and positional isomer distribution can be obtained using a Zorbax ODS column (250 \times 4.6 mm i.d.) with a gradient from acetonitrile–water

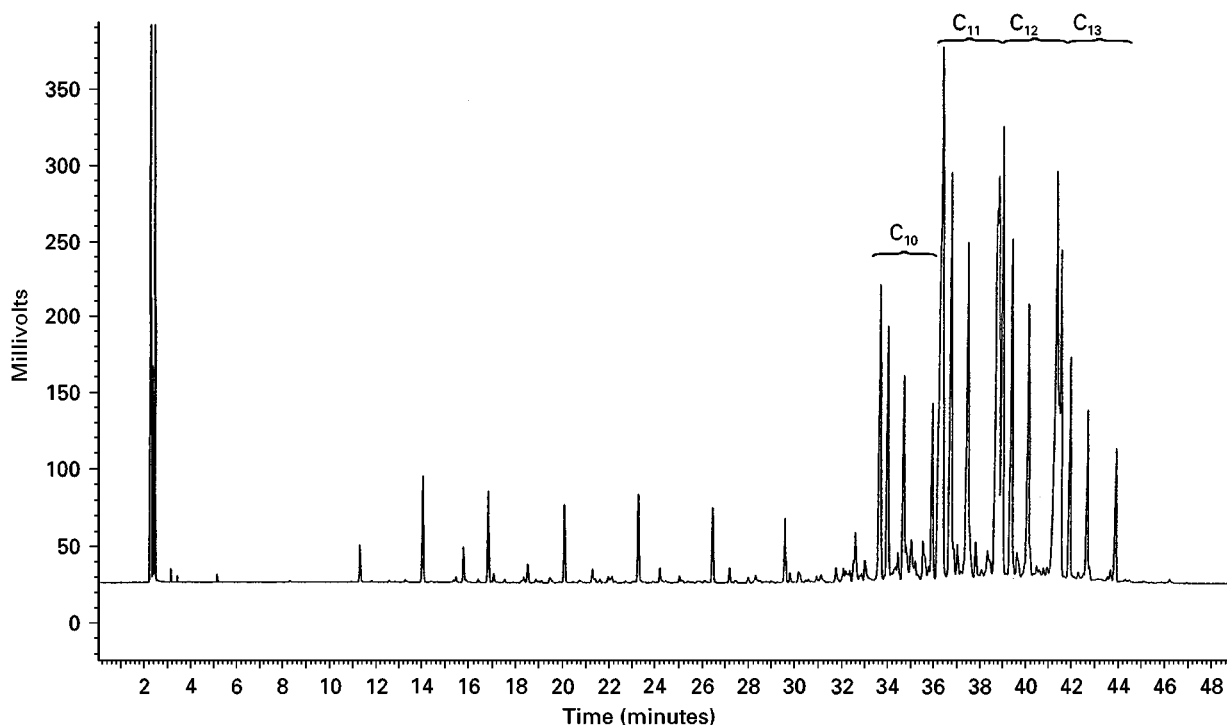


Figure 3 Chromatogram of methyl esters of C10–C13 linear alkylbenzene. Column 25 m \times 0.2 mm i.d. fused silica capillary of HP1 (0.33 μ m film) programmed from 120°C to 240°C at 3°C per minute, final temperature held 20 min, injector and detector at 275°C, FID, carrier helium at 1 mL min⁻¹, splitless injection. Courtesy of RSC.

(40 : 60) + 100 mmol L⁻¹ sodium chloride to acetonitrile–water (60 : 40) with UV photometric detection at 225 nm.

Other separation techniques The analysis of LAS using a silica gel G layer (a standard TLC silica) impregnated with 10% ammonium sulfate and 2-methyl-4-pentanone–propyl alcohol–0.1 mol L⁻¹ acetic acid–acetonitrile (20 : 6 : 1.6 : 1, v/v/v/v) and visualization by spraying with phosphomolybdic acid in ethanol followed by charring by heating has been described.

Supercritical fluid chromatography has been used for analysis of alkylbenzenesulfonates on a fused silica open tubular column (10 m \times 0.53 or 0.25 mm i.d.) coated with a 0.1 or 0.2 μ m film of SE54 with carbon dioxide as mobile phase and FID detection. The LAS is derivatized before analysis.

Capillary electrophoresis can be used for the separation of LAS by alkyl chain length. Conditions are a fused silica capillary (60 cm \times 50 μ m i.d., 40 cm to detector) with a buffer of acetonitrile–water (40 : 60), 3.0 mmol L⁻¹ magnesium ion, pH 6.0, 10 mmol L⁻¹ sodium acetate. Applied voltage is 30 kV and detection is by UV at 220 nm.

Alkyl Sulfates

Alkyl sulfates normally exist as a group of compounds with a range of alkyl chain lengths (Figure 4).

They can be readily determined by GC following acid hydrolysis, recovery of the parent alcohols, and separation either as the alcohols or after conversion of the alcohols to their trimethylsilyl ether derivatives. Typical conditions are a 10 m \times 0.53 mm i.d. column of methylsilicone phase programmed from 70°C to 240°C at 5°C per minute with helium as carrier and FID. The HPLC separation of alkyl sulfates by carbon chain length uses a column 25 cm \times 4.6 mm i.d. ODS material with gradient elution from 60 to 30% aqueous acetonitrile containing 0.01 mol L⁻¹ disodium hydrogenphosphate and 0.01 mol L⁻¹ sodium nitrate. Detection is at 242 nm. This is an example of inverse photometric detection where nitrate in the mobile phase absorbs a constant level of radiation apart from when the level of nitrate is reduced by the presence of the non-absorbing alkyl sulfate anion. It is the reduced absorbance which is monitored.

Alkyl sulfates can be separated on a synthesized cross-linked amine-fluorocarbon polymer on silica column with 0.2 mmol L⁻¹ naphthalenedisulfonate–35% acetonitrile mobile phase. Both indirect conductivity and indirect photometric detection can be used.

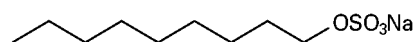


Figure 4 Sodium decyl sulfate. Courtesy of RSC.

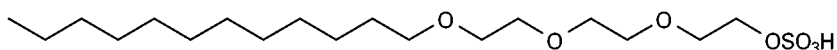


Figure 5 C12 alkyl 3-ethoxysulfate. Reproduced with permission from the American Chemical Society.

TLC separation of alkyl sulfates and alkyl ether sulfates using a silica gel layer with acetone–tetrahydrofuran (9 : 1, v/v) and visualization with Pina-cryptol Yellow has been described.

Alkylethoxy Sulfates

Alkylethoxy sulfates (AES) have the general formula $\text{CH}_3(\text{CH}_2)_n(\text{OCH}_2\text{CH}_2)_m\text{SO}_4\text{Na}$ where n is commonly in the range 9 to 17 and mean values of m are in the range 2 to 20 (Figure 5). They are formed by reaction of alcohols with ethylene oxide to give a desired molar ratio of ethoxylate though in practice they are a broad distribution of ethoxylate ratios peaking at the desired mole ratio. The alcohol ethoxylate is subsequently sulfated.

The hydrophobe (alkyl chain) distribution of alkylethoxylated sulfates can be obtained through GC by reaction of the AES with 30% HBr in glacial acetic acid at 90°C overnight to give alkyl bromides followed by separation on a column (6 ft \times $\frac{1}{8}$ in o.d.) of 10% OV-17 on Chromosorb W with temperature programming from 100°C to 250°C at 8°C per minute with helium as carrier gas and FID. AES can be analysed by HPLC on a 2.5 cm \times 2 mm i.d. column of C18 reversed-phase material with a water–tetrahydrofuran gradient system. The detector is the evaporative light-scattering detector as the molecules being separated have no strong chromophore. There are a number of alternative gradient systems.

To obtain more detailed distributions by either GC or HPLC, the molecule can be desulfated and analysed as described below for ethoxylated alcohols.

Sulfonates

As for alkyl sulfates, alkylsulfonates exist in a range of alkyl chain lengths with the added complication that they can be primary, secondary or α -olefinsulfonates and also mono- and disulfonates with hydroxy and -ene substitution (Figure 6).

Alkylsulfonates are separated by HPLC on a synthesized cross-linked amine-fluorocarbon polymer or silica column with 0.2 mmol L⁻¹ naphthalenedisulfonate–35% acetonitrile mobile phase. Both indirect conductivity and indirect photometric detection can be used.

Separation of positional isomers of alkylmonosulfonates is obtained using Hypersil ODS I phase with

acetonitrile–water gradient and *N*-methylpyridinium chloride as visualization reagent for indirect photometric detection. Baseline separations are obtained.

As for LAS, aqueous solutions of secondary alkanesulfonates (SAS) can be shaken with tetrabutylammonium hydrogensulfate to form ion pairs. Injection of the ion-pair solution into a GC injection port at 300°C forms the butylsulfonate derivatives of the SAS which are separated using on an HP-5 column (20 m \times 0.2 mm i.d., 0.33 μ m film) programmed from 110°C to 220°C at 10°C per minute then 300°C at 6°C per minute with a final 3-minute hold. Detection is by EIMS to give full spectral information.

The separation of α -olefinsulfonates (AOS) into their hydroxy, alkene, and disulfonate isomers together with chain length information is achieved using a column (25 cm \times 4.6 mm) of Zorbax TMS with a mobile phase of methanol–water (75 : 25, v/v) and refractive index detection. This separation has also been demonstrated at an operating temperature of 55°C.

An alternative column for separation of AOS by carbon chain and isomer is a Novapak Phenyl column (150 \times 2 mm) with a mobile phase of 70 : 20 : 10 10 mmol L⁻¹ ammonium acetate–acetonitrile–tetrahydrofuran (THF) at 0.2 mL min⁻¹ with full-scan MS detection to confirm peak identification. Supercritical fluid chromatography has been used for analysis of alkylsulfonates on a fused silica open tubular column (10 m \times 0.53 or 0.25 mm i.d.) coated with 0.1 or 0.2 μ m SE54 with carbon dioxide as mobile phase and FID detection. The sulfonates are derivatized as described above for LAS before analysis. Capillary electrophoresis can be used to separate C4 to C12 alkanesulfonates by alkyl chain length. Conditions are a fused silica capillary (60 cm \times 50 μ m i.d., 40 cm to detector) with a buffer of aqueous pH 7.0, 1.0 mmol L⁻¹ magnesium ion, 5.0 mmol L⁻¹ phosphate, 5.0 mmol L⁻¹ salicylate solution. Applied voltage is 30 kV, and indirect photometric detection is at 230 nm.

Other Anionics

Sodium salts of alkyl (C10–C14) sulfosuccinates are separated on a 250 \times 4.6 mm i.d. column of 10 μ m Nucleosil C8 with aqueous 0.01 mol L⁻¹ tetrabutylammonium hydrogensulfate–methanol (23 : 77) at pH 3 as mobile phase with refractive index detection.

The separation of sodium isethionate from its alkyl isethionate ester on a Vydac 302 IC column with

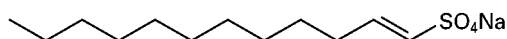


Figure 6 C13 α -olefin sulfonate, sodium salt.

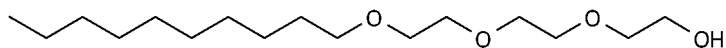


Figure 7 C10 alkyl 3-ethoxylate.

methanol–20 mol L⁻¹ phthalic acid–water (3 : 5 : 12) and conductivity detection has been described.

Nonionic Surfactants

The two most common nonionic surfactants are ethoxylated alcohols and ethoxylated alkylphenols (Figure 7). Synthesis of alkyl ethoxylates is described above under AES. Alkylphenyl ethoxylates are synthesized similarly but with the added structural feature that the phenyl ring is attached at different carbon atoms along the alkyl chain. The alkyl chain is commonly nine carbon atoms.

Ethoxylated alcohols and alkylphenols can be separated by GC on a fused silica capillary column (30 m × 0.25 mm; 0.25 μm film) of SE-54 using helium as carrier gas and EI or CI (chemical ionization) (methane) MS detection. Temperature programming is from 70°C (1 min) to 300°C (10 min hold) at 3°C per minute. Ethoxylates up to 6 EO units are detected.

Separation of alkylphenyl ethoxylates and alkyl ethoxylates on an aluminium-clad fused silica column

(10 m × 0.53 mm i.d.) of OV-1 with helium as carrier gas, FID, and temperature programming to 325°C has been demonstrated. The hydrophobe distribution can be obtained via reaction to alkyl bromides as described above for AES.

Silylation of alcohol ethoxylates to their trimethylsilyl ether derivatives, when combined with temperature-programmed GC using a non-polar methylsilicone column, gives an extremely complex pattern of peaks (Figure 8).

HPLC analysis of alkyl ethoxylates is made complicated by the lack of a strong UV chromophore. Derivatization to introduce a chromophore is an option. Reaction to form phenyl isocyanate derivatives which can then be detected by UV after separation on a μ-Bondapak C18 column according to alkyl chain length or on a μ-Bondapak amine column according to degree of ethoxylation. The evaporative light-scattering detector reduces the need for derivatization for HPLC. Separation by ethoxamer is shown in Figure 9.

Alkylphenol ethoxylates can be readily detected by UV. Columns and separation conditions are similar

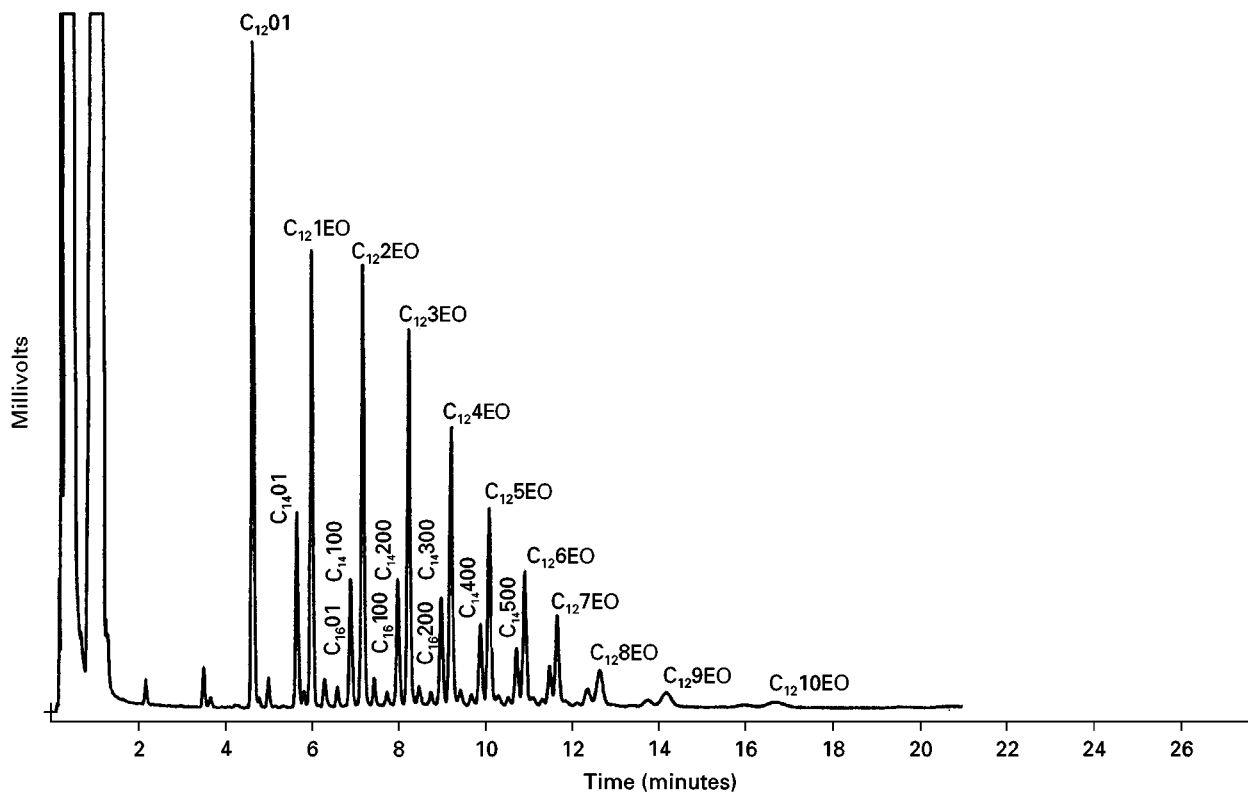


Figure 8 Separation of C12/C14/C16 3 EO alkyl ethoxylate as trimethylsilyl ethers. Column 10 m × 0.53 mm i.d. methylsilicone (1.0 μm film) programmed from 70°C to 240°C at 10°C minute, injector and detector 270°C, carrier helium at 15 mL min⁻¹, FID.

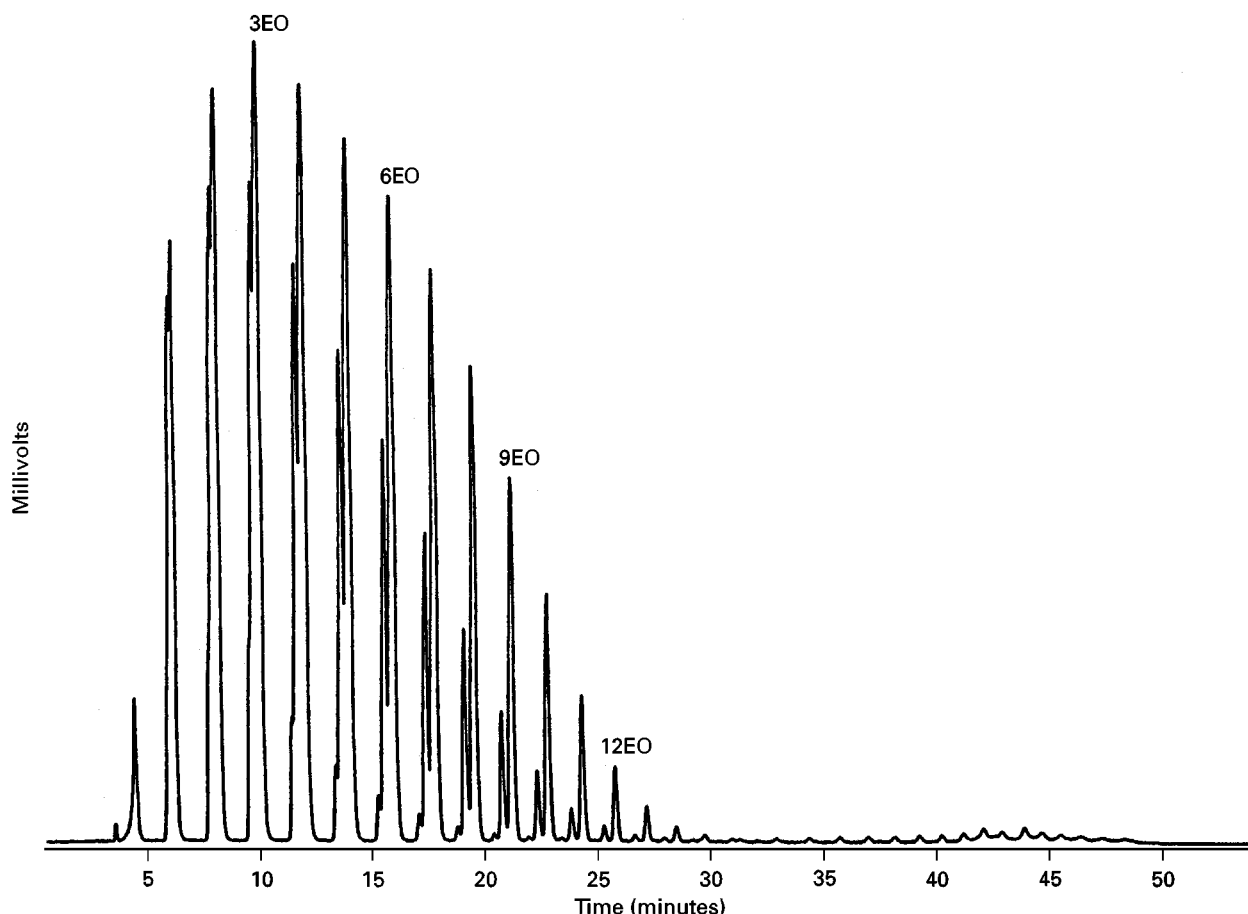


Figure 9 HPLC of C12/C14/C16 alkyl 3 EO ethoxylate. Column 250×4 mm i.d. Nucleosil 50 silica. Linear gradient: ethyl acetate–water (99 : 1, v/v) to acetone–water (90 : 10, v/v) over 60 min. Evaporative light-scattering detector.

to those for alcohol ethoxylates. Ethoxamer distribution can be determined on a LiChrosorb amine column (250×4.6 mm i.d.) with a hexane–isopropanol to aqueous isopropanol gradient system and UV detection at 277 nm.

Separation of ethoxylated fatty acids is obtained using a column (250×4.6 mm i.d.) of Nucleosil DIOL with hexane–isopropanol–water–acetic acid (105 : 95 : 10 : 1, v/v).

TLC can also be used for the determination of nonionic surfactants using a silanized silica gel GF254 layer with aqueous 80% methanol as developing solvent and a scanning densitometer at 525 nm for detection.

Alkylphenyl ethoxylates may be analysed using a Kieselgel F60 layer with chloroform–methanol as developing solvent. IR detection is feasible with such systems.

Supercritical fluid chromatography (SFC) has been extensively applied to analysis of alcohol ethoxylates. Examples are separation of ethoxylated alcohols on a 20 m×0.1 mm i.d. column of poly(dimethylsiloxane) with density programmed carbon dioxide at

100°C as mobile phase and FID. Response factor corrections are required for quantitative analysis. SFC can be used to determine alkyl chain distributions of ethoxylated alcohols after reaction with 50% HBr in glacial acetic acid to give their alkyl bromides.

An alternative to FID detection for SFC analysis of these molecules is evaporative light-scattering detection.

Cationic Surfactants

Cationic surfactants are generally based on a quaternary ammonium structure with a number of long (>C10) alkyl chains attached either directly to the nitrogen atom or through an ester linkage (Figure 10).

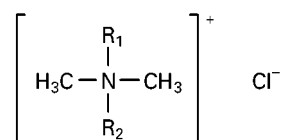


Figure 10 Dialkyldimethylammonium chloride. R_1 and R_2 are typically based on hardened tallow.

As cationics are nonvolatile, the contribution which GC can make to their analysis is in determination of their alkyl substitution. This is achieved by a degradation reaction. Alkyltrimethylammonium and dialkyldimethylammonium cationics are converted by Hoffmann degradation to their alk-1-enes by heating on a water bath for 30 min with potassium *t*-butoxide in benzene–DMSO (4 : 1). After extraction and clean-up, the alkenes are separated on a glass column (2 m \times 3 mm i.d.) of 5% SE-30 on Chromosorb W AW-DMCS (80–100 mesh) temperature programmed from 160°C to 270°C at 6°C per minute with nitrogen as carrier gas and FID.

Alkyl chain distribution can also be obtained by thermal decomposition in the chromatograph injection port followed by separation on a 1 m \times 2 mm i.d. column packed with 8% Carbowax 20M (KOH treated) on acid-washed Chromosorb W (80–100 mesh) and programmed from 70°C to 210°C at 8°C per minute with nitrogen as carrier gas and FID.

The chain-length distribution for cationics containing ester linkages is obtained by alkaline hydrolysis followed by extraction of the resulting fatty acids and conversion of the acids to their methyl esters. (See below for separation conditions.)

Cationic surfactants are more amenable to HPLC than to GC analysis as HPLC can analyse the intact molecule. The separation of mono-, di-, and trialkyl methylammonium quaternaries uses a column 250 \times 4.6 mm of 5 μ m RSil Polyphenol with guard column, a mobile phase gradient from 90 hexane–10 THF–methanol to 10 : 90, both solvents containing 5 mmol L⁻¹ trifluoroacetic acid, and evaporative light-scattering detection.

Cationics of the structure alkylamidopropyl-*N*-(2,3-dihydroxy)-*N,N*-dimethylammonium chloride have been analysed on a column (150 \times 4 mm i.d.) of μ -Bondapak CN with water–acetonitrile–THF (57 : 42 : 1, v/v) containing 0.1% trifluoroacetic acid as mobile phase and differential refractive index detection. Quantification is with an external standard and the method has also been applied to cosmetic as well as detergent products. Cationics of the structure difatty acid ester of 2,3-dihydroxypropyltrimethylammonium chloride can be separated into mono- and di-esters on a Partisil PAC column 250 \times 4.6 mm i.d. with chloroform–methanol–acetic acid (94 : 6 : 0.1, v/v) as mobile phase and refractive index detection.

The separation of imidazoline type cationics on a column (150 \times 4.6 mm i.d.) of 3 μ m Develosil ODS-3 with 0.1 mol L⁻¹ sodium perchlorate in methanol–acetonitrile–deionized water (60 : 60 : 5, v/v) as mobile phase and UV detection at 240 nm has been demonstrated. This procedure gives separation of different chain-length alkyl substitution.

A final example of separation of dialkyldimethylammonium quaternaries on a column of 5 μ m PLRP-S with a mobile phase of 5 mmol L⁻¹ methanesulfonic acid in 70% acetonitrile uses post-column ion suppression and atmospheric pressure ionization mass spectrometry for component identification. TLC can be used to separate and compare cationics of the dialkyldimethylammonium, fatty acid esters of 2,3-dihydroxypropyltrimethylammonium, and fatty acid esters based on methyltriethanolamine quaternaries on a single plate. Separations are by numbers of substituent groups and the different structures are also separated. Conditions are Merck HPTLC Silica HF₂₅₄ with a developing solvent chloroform–methanol–acetic acid–water (72 : 20 : 5 : 3, v/v). Visualization can be with iodoplatinate spray reagent.

Soap

Soap, the sodium salt of fatty acids in the chain length range C10 to C18 (Figure 11) is analysed by protonation of the salts to their acids and derivatization of the acids with boron trifluoride–methanol to give fatty acid methyl esters. A wide range of stationary phases and conditions have been used for the separation (Figure 12). The fatty acids obtained from soap can be analysed by HPLC without derivatization using a column (150 \times 4 mm i.d.) of 5 μ m Hitachi Gel 3056 at 50°C with methanol–5 mmol L⁻¹ tetrabutylammonium phosphate (3 : 1, v/v) at pH 7.5 with conductivity detection.

Betaines

Betaines are amphoterics. The two most common types are alkylbetaines and alkylamidopropylbetaines. The alkyl moiety of the latter is generally based on coconut fatty acids.

Separation by chain length of both types of betaine is obtained on a cation-exchange column, Nucleosil 100-5 SA, 5 μ m, 250 \times 4 mm i.d., with a mobile phase of 70% acetonitrile–30% 0.05 mol L⁻¹ lithium hydroxide in water adjusted to pH 1.6 with phosphoric acid (v/v). A column temperature of 40°C is used together with diode array detection at 210 nm.

Contaminants

Common contaminants in commercial surfactants are ethylene oxide, 1,4-dioxane, sultones and dialkyltetralins.

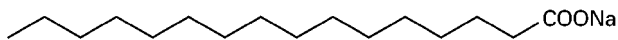


Figure 11 Sodium salt of palmitic acid.

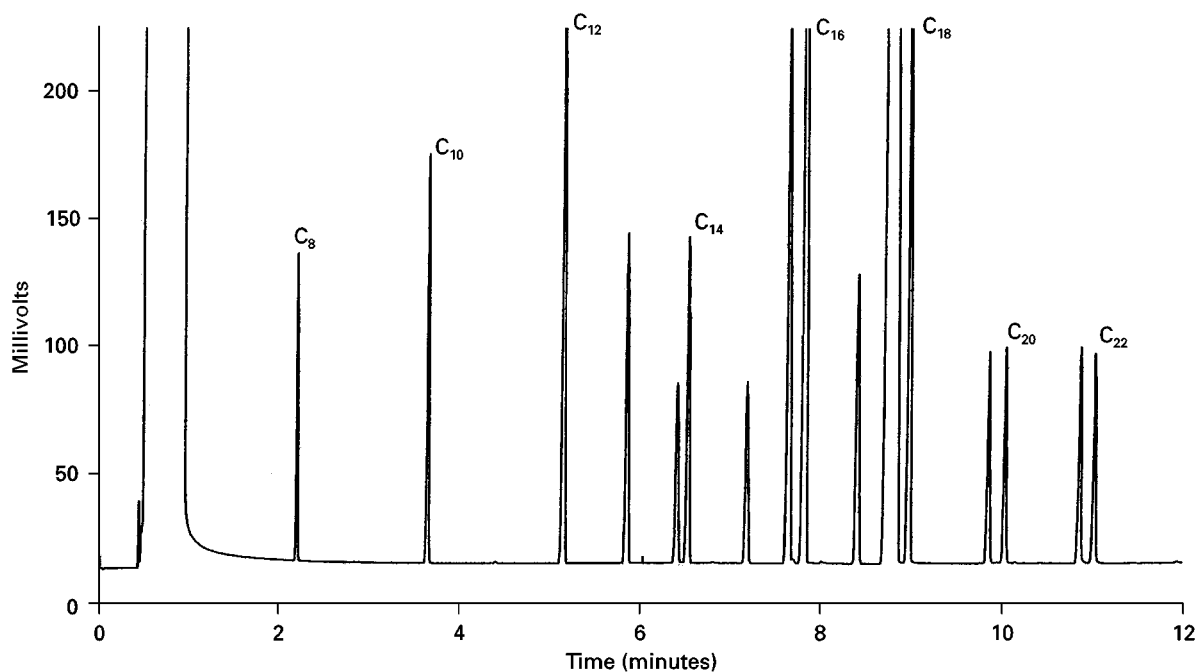


Figure 12 C8 to C22 fatty acid methyl esters. Column: Chrompack CPSIL5, 10 m \times 0.32 mm i.d., film 0.12 μ m, temperature programme 50°C to 200°C at 15°C per minute. Carrier helium at 1.5 mL per minute, FID, cool-on-column injection.

Ethylene oxide is used for ethoxylation of alcohols and alkylphenols. Levels of unreacted ethylene oxide are defined and must not be exceeded in the finished raw material.

Ethylene oxide in alcohol ethoxylates is determined by equilibrium headspace analysis. An aliquot of the vapour is analysed on a column (8 ft \times 0.125 in) of Chromosorb 102 (80–100 mesh) (a gas–solid phase) programmed from 120°C (5 min) to 190°C (10 min) at 8°C per minute, with helium as carrier gas and FID. A detection limit of 1 μ g g⁻¹ is achieved. An alternative column, also used for ethylene oxide in AES, is 3 m \times 1.8 mm i.d. 0.8% THEED/Carbopack C (80–100 mesh).

For improved quantification, both methods can be adapted to a method of standard additions.

1,4-Dioxane is a by-product of the sulfation of alcohol ethoxylates. The industry standard method is equilibrium headspace GC and involves sample preparation using the method of standard additions for quantification. There is some flexibility as to whether capillary or packed columns are used and the actual phase required.

An alternative approach describes the use of a totally deuterated 1,4-dioxane analogue with isotope dilution and MS detection to minimize matrix effects. The separation is carried out on a 60 m \times 0.32 mm i.d. column of Supelcowax 10, temperature programmed from 50°C (2 min) to 100°C at 5°C per minute.

An HPLC approach for 1,4-dioxane in alkylether sulfates is a column (250 \times 4.6 mm i.d.) of 5 μ m LiChrospher C-8 with an aqueous acetonitrile gradient and UV detection at 200 nm. An external calibration curve is used for quantification.

1,3- and other sultones occur as by-products of the formation of α -olefin sulfonates. Certain sultones are potent sensitizers and must be controlled. 1,3-Sultones are determined in α -olefin sulfonates by extraction with diethyl ether, trapping from a silica column, and GC on a column (1 m \times 3 mm) of 2% DEGS on Chromosorb W AW-DMCS (60–80 mesh) at 220°C with helium as carrier and flame photometric (sulfur mode) detection.

Alternatively, detection limits down to 0.2 ng g⁻¹ can be obtained with negative chemical ionization MS with methane as reagent gas. 1,3-Sultones can also be determined by HPLC following extraction from α -olefin sulfonate and separation on a column (200 \times 4.6 mm i.d.) of 5 μ m CPS Hypersil with hexane–ethyl acetate (90 : 10, v/v) as mobile phase and differential refractive index detection. Quantification is by external standard.

Dialkyltetralins occur in linear alkyl benzene, the precursor of LAS. Again, there are set limits as to permissible levels. They are determined on a column (250 \times 4 mm i.d.) of 5 μ m Lichrosorb Si60 with dry iso-octane as mobile phase and UV detection at 254 nm. A reference standard is available from ECO-SOL to calibrate the method.

Future Developments

As has been described above, there are many alternative approaches to the chromatographic analysis of commercial surfactants. The approach to be used for any analysis may be determined by a number of factors, the information required, the equipment available, the time available to carry out the analysis. As we move into the twenty-first century, there will be a trend towards faster analysis and analysis requiring less sample handling. Automation will increase, requiring less and less skilful human input. Data handling will become faster and more intelligent in order to deal with greater volumes of data generated in shorter times. Use of new separation techniques will be investigated, particularly electro-driven techniques and some will replace existing techniques for certain analyses. Overall, separation systems will become smaller with advantages of lower solvent and carrier gas use, less use of laboratory space, and with

increased portability to permit use away from the laboratory.

See also: **II/Chromatography: Gas:** Detectors: Selective. **Chromatography: Liquid:** Derivatization; Detectors: Evaporative Light Scattering; Ion Pair Liquid Chromatography. **Chromatography: Thin-Layer (Planar):** Densitometry and Image Analysis; Layers. **III/Detergent Formulations: Ion Exchange. Surfactants:** Liquid Chromatography. **Thin-Layer Chromatography-Vibration Spectroscopy.**

Further Reading

- Cullum DC (ed.) (1994) *Introduction to Surfactant Analysis*. Glasgow: Blackie A & P.
 Kirk-Othmer (1997) *Encyclopedia of Chemical Technology. Surfactants*, 4th edn. New York: John Wiley.
 Spitz L (ed.) (1996) *Soaps and Detergents. A Theoretical and Practical Review*. AOCS Press.

Liquid Chromatography

T. M. Schmitt, BASF Corporation, Wyandotte, MI, USA
 Copyright © 2000 Academic Press

Introduction

Liquid chromatography (LC) is very useful for the characterization of individual surfactants. Most commercial surfactants are mixtures of members of homologous series, and LC is capable of defining these mixtures according to their homologue distribution, indicating, for example, alkyl chain length or degree of polymerization. LC is also the preferred technique for the quantitative determination of many surfactants, especially ionic surfactants in mixtures. The utility of LC stems from the properties of surfactants – these compounds have good solubility in the usual LC mobile phases and possess diverse chemical functionality, but at the same time they are not volatile enough for ready analysis by alternative technologies such as gas chromatography (GC) or simple mass spectrometry (MS). The structures of common surfactants are given in **Table 1**.

Surfactants are usually analysed in LC systems containing a substantial percentage of organic solvent so as to inhibit micelle formation. The presence of micelles will confound LC analysis.

Formulations and Mixtures of Surfactants

LC is used for quality control of formulations such as cleaning compounds and pharmaceutical prepara-

tions. LC is often the easiest and most specific method for determining surfactant concentration in a well-understood mixture. On the other hand, LC is not often useful for analysis of unknown formulations unless MS detection is available. This is because of the limited separation range of any single LC system.

Sometimes, especially in quality control where there are no unknown components, no preliminary sample work-up is necessary. This is particularly true of ionic surfactants. More often, especially for non-ionics, a gross separation of the surfactants from the matrix is required. This can be accomplished by solvent extraction of the dried solids or by liquid-liquid extraction or solid-phase extraction (SPE) of an aqueous solution.

Alkylarylsulfonates and alkylphenol ethoxylates can be determined with a minimum of sample work-up because of the availability of a specific detection method, fluorescence, to distinguish them from other surfactant and nonsurfactant compounds that may also be present. For the very common mixtures of anionic and nonionic surfactants, ion exchange chromatography systems result in nonionic surfactants eluting prior to anionics, while reversed-phase systems result in the nonionics being retained longer than anionics.

Environmental Analysis

LC is widely applied in environmental analysis, but it is not used for routine monitoring of effluents, except by industry for the analysis of specific process streams

Table 1 Structures of common surfactants

Surfactant	Structure
<i>Cationic surfactants</i>	
Quaternary amines	$RR'R''N^+Cl^-$ $R, R', R'', R''' = H \text{ or } C_1-C_{18} \text{ alkyl or } C_6H_5CH_2$
<i>Anionic surfactants</i>	
Linear alkylbenzene sulfonates	$4-RC_6H_4SO_3^-Na^+$ $R = C_{10}H_{21}-C_{14}H_{29}$
Alkyl sulfates	$ROSO_3^-Na^+$ $R = C_8H_{17}-C_{18}H_{37}$
Alkanesulfonates	$RSO_3^-Na^+$ $R = C_8H_{17}-C_{18}H_{37}$
Ether sulfates	$4-RC_6H_4O(CH_2CH_2O)_xSO_3^-Na^+$ or $R'O(CH_2CH_2O)_xSO_3^-Na^+$ $R = C_9H_{19}; R' = C_{12}H_{25}-C_{18}H_{37}; x = 2-10$
α -Olefin sulfonates (mixtures of alkenesulfonates and hydroxyalkanesulfonates)	$RSO_3^-Na^+$ $R = C_{11}H_{21}-C_{20}H_{39} \text{ or } C_{11}H_{22}OH-C_{18}H_{36}OH$
Ether carboxylates	$RO(CH_2CH_2O)_xCH_2COO^-Na^+$ $R = C_{12}H_{25}-C_{18}H_{37}; x = 5-25$
Sulfosuccinate esters	$ROOCHSO_3CH_2COOR^-Na^+$ or $HOOCCHSO_3CH_2COOR^-Na^+$ $R = C_8H_{17}$
α -Sulfofatty acid methyl esters	$RCH(SO_3^-)COOCH_3Na^+$ and $RCH(SO_3^-)COO^-2Na^+$ $R = C_{12}H_{25}-C_{16}H_{33}$
<i>Nonionic surfactants</i>	
Alkylphenol ethoxylates	$4-RC_6H_4O(CH_2CH_2O)_xH$ $R = C_8H_{17}, C_9H_{19} \text{ or } C_{12}H_{25}; x = 3-50$
Alcohol ethoxylates	$RO(CH_2CH_2O)_xH$ $R = C_{12}H_{25}-C_{18}H_{37}; x = 5-60$
Acid ethoxylates	$RCOO(CH_2CH_2O)_xH$ $R = C_{11}H_{23}-C_{17}H_{35}; x = 5-20$
EO/PO copolymers	$HO(CH_2CH_2O)_y(CH(CH_3)CH_2O)_x(CH_2CH_2O)_yH$ $x = 16-70; y = 1-100$
Esters	$\begin{array}{c} \text{O} \\ \parallel \\ \text{CH}_2\text{CHOHCHOORCHCH}_2\text{OHCH}_2\text{OOR} \end{array}$ $R = C_{16}/C_{18} \text{ alkyl}$

where the composition is uniform and well understood. The standard wastewater methods, for example those based on colorimetric tests, give a gross value for total surfactant concentration and are most suitable for routine environmental monitoring.

LC is used, however, in special investigations of environmental impact to give information on the concentration and degradability of specific surfactants in particular environmental areas, relying on the ability of LC methods to precisely characterize surfactant homologues. A preliminary separation or preconcentration is always necessary. The most common pretreatment method nowadays is SPE, especially when low levels of surfactant must be determined. C_{18} media are most often applied, in the form of SPE cartridges or extraction discs. Nonpolar resin of the poly(styrene/divinylbenzene) type is also used. A secondary separation of the surfactants into nonionic, cationic and anionic fractions can be performed on ion exchange media.

LC is the method of choice for determining anionic surfactants in the environment. It is also preferred for the determination of the anionic degradation products of these surfactants. LC is the best method for the determination of nonionics (especially when coupled with MS), if detail on homologue distribution is needed. LC is less often applied to environmental determination of cationics, since interference is not as serious a problem with the standard methods for determining cationics in wastewater as it is for other surfactants.

Analysis of Individual Surfactants

Anionic Surfactants

LC analysis of anionic surfactants is a mature technology. Detection is a simple matter, either by direct UV absorption of aromatic surfactants or by inverse photometric detection of the aliphatic compounds.

Alkylarylsulfonates The commercial product, linear alkylbenzenesulfonate (LAS) is a mixture containing a range of alkyl chain lengths, typically C_{10} – C_{14} . Reversed-phase LC with a C_4 or C_8 column effectively separates LAS according to the length of the alkyl chain (Figure 1). A C_{18} packing gives a more complex chromatogram because the individual compounds of discrete alkyl chain length are themselves partially resolved into isomers; in many cases this resolution is not needed or desired (Figure 2). In any case, GC analysis after desulfonation is a better method for determining isomers. Aqueous mixtures of acetonitrile, methanol and tetrahydrofuran (THF) are appropriate mobile phases, generally containing a salt such as 0.1 mol L^{-1} sodium perchlorate. Detection is by UV absorbance at 225 nm or fluorescence with excitation at 225 nm and emission at 290 nm. Fluorescence detection is advantageous for trace analysis.

Alkyl sulfates Alkyl sulfates with chain lengths in the surfactant range (C_{10} and higher) are readily separated according to increasing alkyl chain length in a reversed-phase system with methanol/water mobile phase containing a salt such as sodium perchlorate. The pH is often adjusted to 2.5 or 3.0. Gradient programming is impractical if detection is by direct low wavelength UV, differential refractive index (DRI) or conductivity. Gradients are successful with detection by indirect UV (typically, methylpyridinium chloride is added to the eluent) or evaporative light scattering (ELS). If anion exchange chromatography is used, elution is in order of decreasing alkyl chain length.

Alkanesulfonates These are generally separated with the same systems used for alkyl sulfates. In a mixture, the peaks of the alkyl sulfates and alkanesulfonates are interspersed, with the alkyl sulfates more strongly retained on reversed-phase column packings than alkanesulfonates of the same chain length. Separation from anionic surfactants of other types is usually straightforward. Interference from alkyl sulfates can be eliminated by subjecting the sample to acid hydrolysis to convert them to the corresponding alcohols and sulfuric acid; sulfonates are not affected by this treatment.

Ether sulfates Alkylphenol ether sulfates and alcohol ether sulfates can be resolved by reversed-phase chromatography with elution in the order of both increasing alkyl chain length and increasing (or decreasing) ethoxy chain length (Figure 3). An alkylamine ion-pairing agent may be added to increase retention time. Unsulfated alcohol or alkylphenol ethoxylate impurities elute first under paired-ion con-

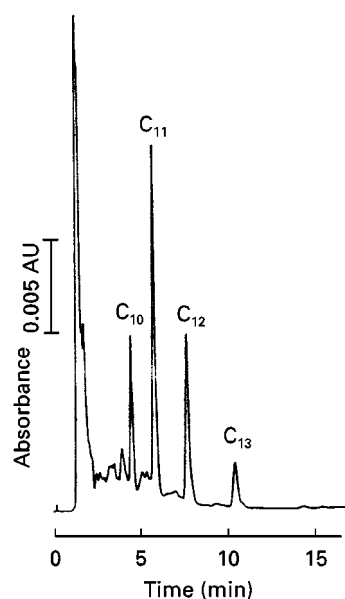


Figure 1 LAS isolated from river water and analysed isocratically using a C_4 reversed-phase column. Labels indicate alkyl chain length. Column: Wakosil 5C4, $4.6 \times 150 \text{ mm}$. Mobile phase: 0.1 mol L^{-1} sodium perchlorate in 50 : 50 $\text{CH}_3\text{CN}/\text{H}_2\text{O}$. Detection: UV, 220 nm. (Reproduced with permission from Yokoyama Y and Sato H (1991) Reversed-phase HPLC determination of linear alkylbenzenesulphonates in river water by precolumn concentration. *Journal of Chromatography* 555: 155–162. Copyright (1991) Elsevier Science.)

ditions. A single peak for easy quantification can sometimes be obtained by using a very short reversed-phase column and a step gradient.

Normal-phase systems are also used for analysis of ether sulfates, with stationary phases of bare silica or

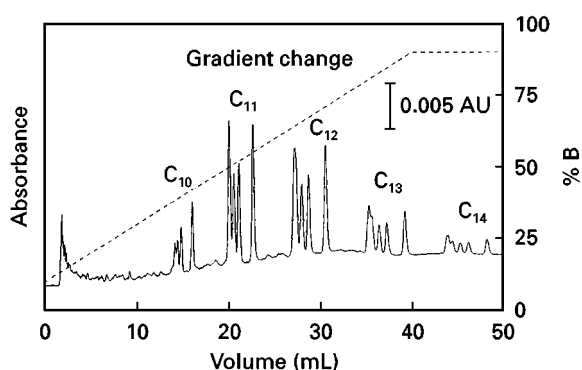


Figure 2 Chromatogram of commercial LAS mixture analysed using a reversed-phase column and gradient elution. Labels indicate groups of isomers for various alkyl chain lengths. Column: Zorbax ODS, $4.6 \times 250 \text{ mm}$. Mobile phase: $\text{CH}_3\text{CN}/\text{H}_2\text{O}$ gradient with increasing concentration of NaCl. Detection: UV, 225 nm. (Reproduced with permission from Chen S and Pietrzyk DJ (1994) Reversed-phase LC separation of linear alkylbenzenesulphonates. Effect of mobile phase ionic strength. *Journal of Chromatography A* 671: 73–82. Copyright (1994) Elsevier Science.)

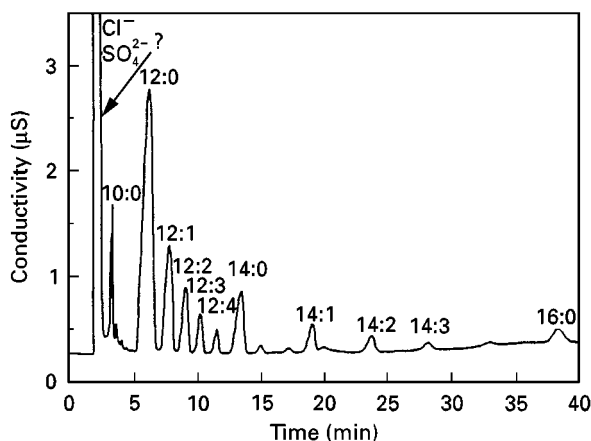


Figure 3 Chromatogram of a lauryl ether sulfate isolated from shampoo. Labels indicate alkyl chain length and number of moles of ethylene oxide. Column: Alltech Surfactant C₈, 4.6 × 250 mm. Mobile phase: MeOH/H₂O, 45 : 55, 0.00023 mol L⁻¹ in NH₄OAc. Detection: conductivity. (Reproduced with permission from Stemp A, Boriraj VA, Walling P and Neill P (1995) Ion chromatographic characterization of ethoxylated anionic surfactants. *Journal of the American Oil Chemists' Society* 72: 17–21.)

amino- or cyanopropyl-silica. In this case, the nonionic material elutes first, followed by the anionic material, each in order of increasing ethoxylation. An ion-pairing agent such as cetyltrimethylammonium chloride may be added to give more rapid elution of anionic material. A relatively hydrophilic mobile phase is often used in conjunction with the ion-pairing agent.

α-Olefin sulfonates These compounds give complex chromatograms that reflect the complexity of their composition. The commercial product is formed of approximately equal portions of alkenesulfonates and hydroxyalkane sulfonates, each carrying the chain length distribution of the alkene feedstock. Disulfonates may also be present. α-Olefin sulfonates are analysed by reversed-phase LC with methanol/water and added salt. DRI or low wavelength UV detection is suitable. Elution is in order of increasing chain length, with hydroxyalkanesulfonates eluting prior to the corresponding alkenesulfonates and with all disulfonates eluting prior to all monosulfonates (Figure 4). Complete resolution is not obtained if the starting α-olefin was a mixture of many chain lengths, as is usually the case with commercial products.

Petroleum sulfonates and alkylnaphthalenesulfonates These are frequently separated on anion exchange packings with elution according to increasing degree of sulfonation. Reversed-phase systems have also been used. Resolution by alkyl chain length is

sometimes attained, but, more often, the practitioners are content with a single peak for the active agent.

Ether carboxylates Only reversed-phase systems have been demonstrated for separation of these products, generally with acetonitrile/water mobile phase. Elution is always according to increasing chain length of the alkyl or alkylphenol moiety. Depending on the system, there may be an overtone of separation according to increasing or decreasing ethoxy chain length. As with ether sulfates, separation from nonionic impurities is straightforward. Alkylphenolether carboxylates are easily detected in the UV (225 or 254 nm), while the alkylether carboxylates require low wavelength UV, DRI or ELS detection.

Sulfosuccinate esters These are analysed most readily by reversed-phase LC in the presence of an ion-pairing agent. If not monodisperse as to alkyl chain length, they are eluted in order of increasing alkyl length. Separation from other anionic surfactants can usually also be accomplished by reversed-phase chromatography.

α-Sulfofatty acid methyl esters These also are easily separated according to alkyl chain length by reversed-phase methods. Ion-pairing agents are rarely used.

Soap Fatty acids are separated according to increasing alkyl chain length on a C₁₈ column with methanol/water mobile phase and refractive index

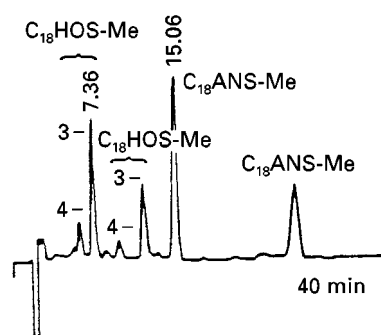


Figure 4 Chromatogram of α-olefin sulfonate after hydrogenation and formation of methyl esters. Peak identification: 4- and 3-hydroxyhexadecylsulfonate, methyl ester; 4- and 3-hydroxyoctadecylsulfonate, methyl ester; hexadecylsulfonate, methyl ester; octadecylsulfonate, methyl ester. Column: Inertsil C₁₈, 4.6 × 250 mm. Mobile phase: MeOH/H₂O, 85 : 15. Detection: refractive index. (Reproduced with permission from Matsutani S and Endo Y (1991) Separation and determination of sulfonate type anionic surfactants including 2-sulfonatofatty acid methyl ester by methyl ester derivatization and HPLC analysis. *Yukagaku* 40: 566–573.)

detection. Ionic strength and pH must be controlled. Analysis is either at low pH without an ion-pairing agent or at high pH with ion-pairing. It should be noted that most practitioners prefer GC for analysis of fatty acids (as methyl esters).

Cationic Surfactants

LC is the most generally useful method for determination of cationic surfactants. All commercial cationic surfactants are salts of quaternary amines (quats). Most of these, like the long-chain alkyltrimethylammonium salts, have good water solubility and are readily analysed by reversed-phase LC. Control of pH and ionic strength is necessary and inverse spectrophotometric detection gives the best results for quats without an aryl moiety; toluenesulfonate or xylenesulfonate are used as counterions for detection. Retention times are influenced by the hydrophobicity of the counterion. Conductivity detection is also applicable, especially if ion chromatography instrumentation is used with a nonpolar stationary phase (this configuration is sometimes called 'mobile-phase ion chromatography'). Of course, UV detection can be used for compounds with pyridyl or benzyl substituents. Since quats exhibit long retention times on C_{18} stationary phases, reversed-phase LC is most often performed on cyano columns, usually with methanol/water or acetonitrile/water mobile phase.

Quats are sometimes analysed using cation exchange packings. While the separating ability of the ion exchange systems is not as great as that attained with normal- or reversed-phase systems, ion exchange is sometimes preferred for formulation analysis because interference is minimized in that only the cationic materials are seen.

The quats used as fabric softeners for household laundry contain two long alkyl chains and have poor water solubility. For reasons of solubility, these are most easily analysed by normal-phase chromatography. Bare silica stationary phases are never used, but rather cyanoamino, amino, DIOL or polyphenol phases. Chloroform/methanol mobile phases work well, usually with a little added acetic acid. Conductivity and ELS are suitable for detection.

Common fabric softener quats, including ester quats, can be characterized by normal-phase chromatography on a polyphenol column with a hexane/methanol/THF gradient and added trifluoroacetic acid. Elution is in order of decreasing alkyl length, with the quats well resolved from unquaternized amine impurities.

For trace analysis, detection is sometimes accomplished by paired-ion extraction of the HPLC effluent with a fluorescent anion, followed by phase separation and fluorescence detection.

Nonionic Surfactants

Ethoxylated nonionics are most easily characterized by normal-phase chromatography. This permits the separation of the compounds according to the length of the ethoxy chain, with the longer chain homologues eluting later. Amino-bonded stationary phases are often used along with the usual nonpolar mobile phases such as hexane.

Separation of homologues can also be accomplished by reversed-phase chromatography. Reversed-phase LC is usually applied to higher ethoxylates because normal-phase LC resolution deteriorates with higher molecular weight. Solvent systems of methanol/water or acetonitrile/water are usual. Order of elution can be according to increasing or decreasing order of ethoxylation, depending on the particular reversed-phase media and solvents used, the particular nonionic surfactant and whether it has been derivatized. The order of elution even depends on the molecular weight: elution is sometimes according to reverse order of ethoxylation for lower members of a series and according to increasing order of ethoxylation for higher members of the same series.

Reversed-phase HPLC is effective for separation of ethoxylated surfactants according to the identity or chain length of the hydrophobic moiety. Caution is required, since under various reversed-phase conditions separation according to degree of ethoxylation will also occur, as mentioned above. Unless MS detection is available, this two-dimensional separation makes quantification difficult, so the system is usually optimized to minimize the influence of hydrophilic homogeneity. If MS detection is used, then the separation by hydrophobe is sufficient for complete characterization of the surfactant, with the MS detector giving the information on ethoxy homologue distribution. The sensitivity of the MS detector is not identical for all homologues. For precise work, calibration must be performed over the entire range of composition.

Size exclusion chromatography (SEC) is sometimes applied to the analysis of nonionic surfactants, particularly higher molecular weight surfactants like the ethylene oxide/propylene oxide (EO/PO) copolymers. Nonaqueous systems are most useful for this analysis for two reasons. First, formation of micelles is discouraged. Micelle formation is a function of concentration, so SEC can show different values for molecular weight depending on sample concentration. Second, aqueous SEC column packings often have a silica backbone. Polyethoxy compounds are strongly adsorbed to silica, resulting in mixed-mode separation rather than separation only according to molecular size.

Polyethylene glycol (PEG) impurity is determined in most ethoxylated surfactants by reversed-phase separation with 95 : 5 methanol/water and DRI or ELS detection. PEG elutes as a single peak prior to the surfactants.

The refractive index of nonionic surfactants is a function of degree of ethoxylation. Thus, the response of a differential refractive index detector varies for homologues, with the variation being most significant at low degrees of ethoxylation.

Alcohol ethoxylates (AE) Commercial products are mixtures of homologues containing a distribution of alkyl chain length and ethoxy chain length. Conventional LC analysis fails to give a single peak for alcohol ethoxylate. Rather it yields a series of peaks more-or-less resolved corresponding to the alkyl or ethoxy distribution. This limitation is only overcome by using backflush techniques.

Derivatives may be formed to improve detectability of AE. Derivatization also influences retention time, so that a gradient system optimized for underivatized AE must be modified for chromatography of the derivatives. Typical derivatizing agents are phenyl isocyanate, naphthyl isocyanate and 3,5-dinitrobenzoyl chloride. Fluorescence detection is sometimes used in environmental analysis with fluorescent derivatizing agents such as 1- and 2-naphthoyl chloride and naphthyl isocyanate.

Normal-phase chromatography, preferably on aminopropyl- or cyanopropyl-bonded silica, will give the ethoxy distribution (Figure 5). Reversed-phase chromatography on C_{18} media serves to separate by alkyl chain length. In either case, solvent programming is usually required for complete resolution of a commercial product, so either an ELS detector is used or the surfactant is first derivatized to permit use of a UV detector. If reversed-phase solvents are not optimized, a separation by ethoxy chain length is superimposed on the separation by alkyl chain length.

Alkylphenol ethoxylates (APE) Almost all commercial products are based upon a monodisperse hydrophobe, usually nonylphenol. Therefore, quantification is usually performed by reversed-phase chromatography on C_{18} media using an isocratic methanol/water or acetonitrile/water eluent and UV detection, resulting in a single peak. Octylphenol ethoxylates are easily separated from nonylphenol ethoxylates by such systems.

As with alcohol ethoxylates, separation by degree of ethoxylation is easily performed with any of the usual normal-phase stationary phases, with the cyano packings most popular. Amino and bare silica media are also used (Figure 6). Reversed-phase LC is also applied, especially for higher degrees of ethoxylation.

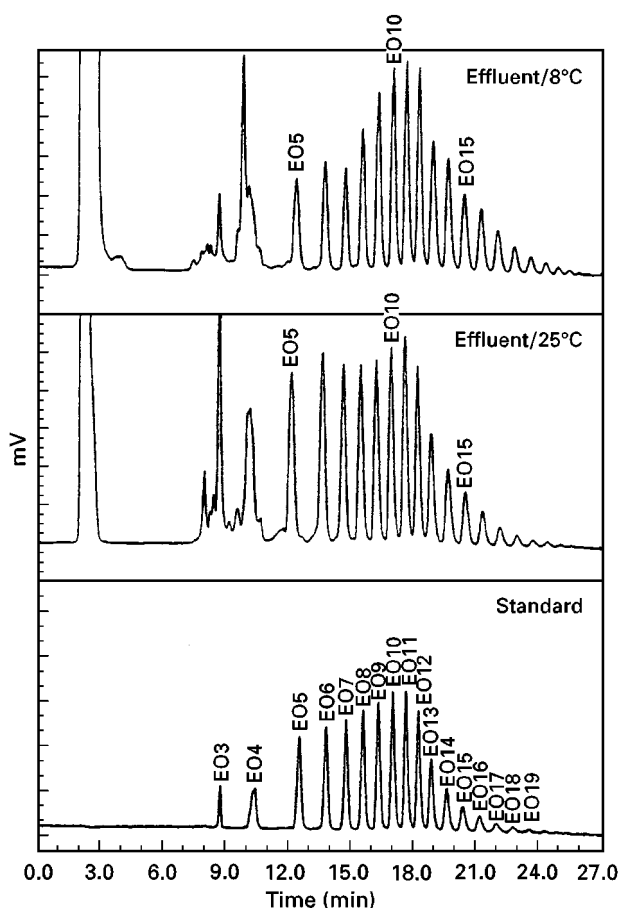


Figure 5 Chromatogram of C_{13} alcohol ethoxylate from a biotreatment study. Analysis using a CN normal phase column with gradient programming and evaporative light scattering detection. Labels indicate ethoxy chain length. Column: Rainin Microsorb CN, 4.6×250 mm, 45°C . Mobile phase: gradient, hexane/THF/(90 : 10 2-PrOH/ H_2O); from 100 : 0 : 0 to 80 : 20 : 0 in 5 min, then to 52 : 30 : 18 in 15 min, then to 40 : 40 : 20 in 5 min. Detection: ELS (Reproduced with permission from Dubey ST, Kravetz L and Salanitro JP (1995) Analysis of nonionic surfactants in bench-scale biotreater samples. *Journal of the American Oil Chemists' Society* 72: 23–30.)

UV detection (225 or 275 nm) is always used since it gives a uniform molar response to the homologues. For trace analysis, fluorescence detection is applicable since APEs have native fluorescence.

Ethoxylated acids These compounds can be considered as esters of PEG and fatty acids, with the commercial products also containing diester, residual fatty acid and free PEG. Reversed-phase chromatography with methanol/water separates the ethoxylated acid, PEG diester, free PEG and free fatty acid, and usually also serves to separate the compounds from other surfactants. As with other ethoxylates, normal-phase chromatography gives resolution by ethoxy chain length. SEC is often useful to resolve the

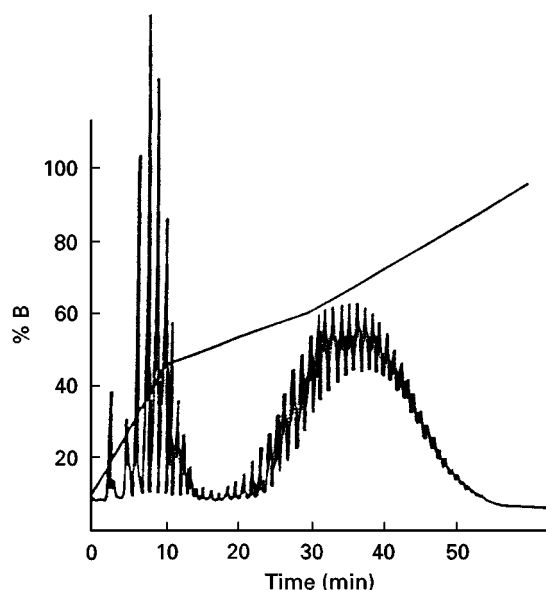


Figure 6 Chromatogram of a mixture of two commercial products, nominal 4-mole and 30-mole ethoxylates of nonylphenol, analysed by normal-phase HPLC. Column: Hewlett-Packard Si-100, 4.6×200 mm, 30°C . Mobile phase: gradient; A = 80/20 *n*-hexane/ethyl ether; B = 40:30:20:10:1:0.5 dioxane/ethyl ether/*n*-hexane/2-PrOH/ H_2O /HOAc; 5 to 95% B in 45 min. Detection: UV, 280 nm. (Reproduced with permission from Anghel DF, Balcan M, Voicu A and Elian M (1994) *Journal of Chromatography A* 668: 375–383. Copyright (1994) Elsevier Science.)

mono- and diesters. DRI and ELS detectors are most applicable. Low wavelength UV detection must be used with caution because of the disproportionate response from unsaturated fatty acid moieties.

Esters Esters of fatty acids with glycerol and sugars are separated according to degree of acyl character by either normal-phase or reversed-phase chromatography. Reversed-phase elution is according to increasing acyl character, while normal-phase elution is in order of decreasing acyl character (i.e. according to both the chain length of the acyl groups and their number). Normal-phase LC is usually performed with a DIOL stationary phase and propanol/water mobile phases. The ELS detector is most applicable, although historically many applications have been developed using DRI or UV at wavelengths of 220 nm or less.

EO/PO block copolymers In the absence of interfering compounds, polymers of the poloxamer type can sometimes be determined by reversed-phase HPLC with methanol, but the most common separation technique is SEC. The copolymers useful for detergents and pharmaceuticals are higher in molecular weight than most other synthetic surfactants, so SEC can be used for both qualitative and quantitative

analysis. If conventional LC is used, depending on the specific product, a reversed-phase system with acetonitrile/water can be optimized to be indifferent to EO chain length, separating the surfactant according to length of the PO chain. DRI detection is generally used for the block copolymers.

Alkanolamides These compounds, for example the C_{10} – C_{18} fatty acid monoethanolamides, are eluted according to increasing acyl chain length by reversed-phase chromatography with methanol/water solvents. These systems may also be used for formulation analysis. Detection is a challenge: DRI and low wavelength UV are most common, and ELS and nitrogen-specific detectors have been applied in more recent times. *N*-Methylglucosamides are analysed in the same way.

Alkyl polyglycosides Reversed-phase LC with methanol/water will separate these compounds, with elution according to increasing chain length of the acyl constituents. For compounds of the same acyl chain length, polyglycosides elute prior to monoglycosides. ELS detection is typically used.

Amphoteric Surfactants

Amphoteric surfactants are almost always separated on C_{18} columns with methanol/water mobile phase. The pH is often held as low as the column will tolerate and a salt such as sodium perchlorate is added. Under such conditions, the amphoteric surfactant behaves much like a cationic surfactant and the same detection methods are used as discussed above for cationics.

Betaines These compounds can be separated, with elution by increasing alkyl chain length by reversed-phase LC or by decreasing chain length using cation exchange chromatography. DRI detection is most often chosen, although low wavelength UV and ELS are sometimes applied.

Phosphatides These compounds must be discussed separately from other amphoteric. They are constituents of the natural surfactant, lecithin, but they also have great biochemical importance. Normal-phase LC serves to separate the main constituents of commercial lecithin: phosphatidylethanolamine, phosphatidylcholine, phosphatidylinositol, phosphatidylserine and phosphatidic acid. (Each of these consists of a number of individual compounds containing various acyl groups.) The normal-phase separation is traditionally performed on a bare silica column with low wavelength UV detection. Since it is mainly double

bonds that give the detector response, and since each of the individual components contains acyl chains of varying unsaturation, quantification by UV is only approximate. The ELS detector is rapidly becoming standard for this analysis. Since this detector is tolerant of solvent gradients, other normal-phase columns, notably the DIOL column, may be used instead of bare silica. These give better reproducibility but do not have sufficient resolving power for lecithin analysis in the absence of gradient programming.

Separation by acyl chain length is accomplished by reversed-phase LC of fractions separated by the normal-phase methods. LC-MS is an obvious way to simplify the characterization of unknowns. Precise phosphatide analysis is very much an activity of specialists and the field is advancing rapidly.

Conclusions

LC is the only practical method to characterize many surfactants according to their oligomer or homologue distribution. It is also the best way to determine quantitatively many surfactants, particularly ionic surfactants.

However, in spite of improvements in instrumentation and in stationary phases, LC is not easy. It demands more time and training of the operator than most analytical techniques. Preliminary sample preparation is very often necessary for mixtures and environmental samples, making an LC analysis an expensive analysis.

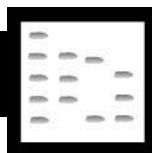
Continued development in the areas of detection (especially in element-selective detectors, detectors specific for chemical functionality, and LC-MS interfaces) will make LC even more useful in the future. For example, the ELS detector, even though suffering from problems in linearity in its present incarnation, has already greatly expanded the utility of LC for analysis of lecithin and ethoxylates.

See also: II/Chromatography: Liquid: Mechanisms: Ion Chromatography; Ion Pair Liquid Chromatography; Mechanisms: Reversed Phases. **Extraction:** Solid-Phase Extraction.

Further Reading

- Balazs PE, Schmit PL and Szuhaj BF (1996) HPLC of soy phospholipids. *Journal of the American Oil Chemists' Society* 73: 193–197.
- Cross J (ed.) (1998) *Anionic Surfactants: Analytical Chemistry*, 2nd edn. New York: Marcel Dekker.
- Cross J and Singer EJ (eds) (1994) *Cationic Surfactants: Analytical and Biological Evaluation*. New York: Marcel Dekker.
- Di Corcia A (1998) Characterization of surfactants and their biointermediates by liquid chromatography-mass spectrometry. *Journal of Chromatography A* 794: 165–185.
- Evans KA, Dubey ST, Kravetz L *et al.* (1997) Quantitation of alcohol ethoxylate surfactants in environmental samples by electrospray mass spectrometry. *Journal of the American Oil Chemists' Society* 74: 765–773.
- Garti N, Kaufman VR and Aserin A (1983) Analysis of nonionic surfactants by HPLC. *Separation and Purification Methods* 12: 49–116.
- Miszkiewicz W and Szymanowski J (1996) Analysis of nonionic surfactants with polyoxyethylene chains by HPLC. *Critical Reviews in Analytical Chemistry* 25: 203–246.
- Rissler K (1996) HPLC and detection of polyethers and their mono(carboxy)alkyl and arylalkyl substituted derivatives. *Journal of Chromatography A* 742: 1–54.
- Schmitt TM (1992) *Analysis of Surfactants*. New York: Marcel Dekker.
- Stache HW (ed.) (1996) *Anionic Surfactants: Organic Chemistry*. New York: Marcel Dekker.
- Thiele B, Günther K and Schwuger MJ (1997) Alkylphenol ethoxylates: trace analysis and environmental behavior. *Chemical Review* 97: 3247–3272.
- Wilkes AJ, Walraven G and Talbot GM (1992) HPLC analysis of quaternary ammonium salts with the evaporative light scattering detector. *Journal of the American Oil Chemists' Society* 69: 609–613.

SYNTHETIC POLYMERS



Gas Chromatography

J. K. Haken, The University of New South Wales, Sydney, NSW, Australia

Copyright © 2000 Academic Press

Introduction

Successful gas chromatography (GC) requires that the sample be volatile at the operating temperature. The majority of synthetic polymers are of substantial molecular weight, i.e. in excess of 20 kDa, and not amenable to direct chromatographic examination.

Figure 1 shows the molecular weight limitations of compounds suitable for gas and liquid chromatography. Monomers with molecular weights in the range 50–100 Da are particularly suitable for direct GC.

Performance-enhancing or compounding additives in polymers are also usually amenable to direct examination. The major difficulty with these materials is separation or extraction from the polymer matrix, which generally accounts for over 90% of the product. Plasticizers form a major part of many polymer compounds and monomeric plasticizers may frequently be examined directly or after extraction. Polymeric plasticizers, and polymeric additives after separation, require examination by pyrolysis or by spectrometric tools. The finely divided polymer is subjected to thermal desorption or extraction or digestion with solvents. Extraction with supercritical fluids is finding greater use and has the advantage that the removal of extraction solvent is simplified.

To increase the volatility of polymers, a reduction in molecular weight must be achieved. This is most commonly carried out by pyrolysis or thermal degradation in the absence of oxygen, or to a lesser extent by chemical degradation, which is applicable to most condensation polymers. Both techniques are indirect methods of analysis where the polymer is characterized by analysis of the volatile products of the degradation. A recently developed technique, known as pyrolytic methylation, effectively combines both methods and is applicable to condensation polymers. To date this new technique has found its major application in forensic science.

Pyrolysis

Pyrolysis techniques possess several advantages. The sample preparation is negligible, while the time for

analysis is relatively short in comparison with that needed for other instrumental techniques. In addition the sample required for pyrolysis is small.

Pyrolysis was originally carried out separate from the GC instrument, but *in situ* pyrolysis in a device directly attached to the GC was soon universally employed. The pyrolysers available are of two basic types:

- (1) Furnace type. The polymer sample is introduced into a heated microfurnace attached to the injection port of the chromatograph and the volatile pyrolysis products are rapidly swept into the column by the carrier gas.
- (2) Pulse mode type. The polymer is attached to the pyrolysis element, which is rapidly heated to a predetermined temperature. The volatile pyrolysis products are rapidly swept into the chromatograph as before. The pyrolysis element may be either a filament or ribbon device that is resistively heated or a Curie point device. With Curie point heating the polymer is deposited on a wire of ferromagnetic material. The wire is rapidly heated to its Curie point using induction. A range of wires with Curie points from 358°C for a nickel wire to 980°C for a wire consisting of 50 : 50 iron and cobalt are available. Ribbon and filament pyrolysers normally use materials of high resistance that are inert in nature, such as platinum or other noble metals; this reduces the possibility of reactions occurring with the degraded sample.

Both types of pyrolysers are used, each type having both advantages and disadvantages, but the two pulse mode instruments are most widely utilized.

The first application of pyrolysis and gas chromatography was in 1954, when vinyl polymers

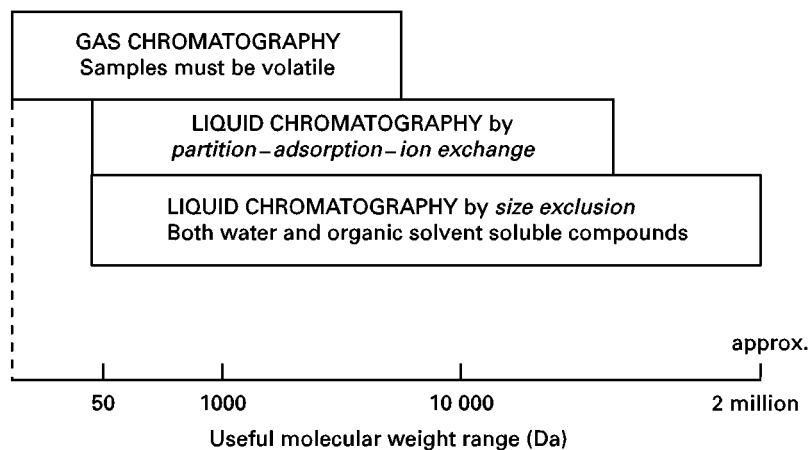


Figure 1 Approximate useful ranges of common chromatographic procedures. (Reproduced from Haken JK (1990) *Trends in Analytical Chemistry* 8:14 with permission of Elsevier Science Publishers.)

and copolymers were heated at 650°C in a stream of nitrogen. The volatile products were condensed and subjected to gas chromatography. *In situ* pyrolysis quickly followed with the use of a filament device, which was little different to that which has subsequently found extensive usage with almost every conceivable type of polymer.

Early workers used large samples, which resulted in poor heat transfer, the occurrence of combination reactions of the volatile fragments and the production of nonreproducible results. Bibliographies of papers and compilations of pyrolysis results, both as pyrograms and bar charts, date from the 1960s, but the early literature is of limited value as the reproducibility is often poor, and the techniques used do not always represent current practice. Libraries of pyrograms have appeared in texts, but the experimental conditions are frequently omitted and it is difficult to reproduce the results.

It has long been recognized that small samples, typically much less than 1 mg, good heat transfer, rapid heating of the pyrolysis element and rapid removal of the degradation products from the heated zone are essential in achieving reproducible results.

Packed chromatographic columns were widely used in the early work, but capillary columns that offer enhanced separation are now almost universally employed. The detection limits of the flame ionization detector, the mass spectrometer and the Fourier transform infrared detectors in current use are orders of magnitude better than that required by the smallest possible pyrolysis sample. In the 1980s a sample of 800 ng of acrylic polymer would produce a mass spectrum of about 30 compounds when pyrolysed. More recently samples of 1 µg have been used for forensic casework, while sample sizes of 2 µg have been generally used, the major difficulty being in handling and weighing these small samples. With such quantities a chromatogram containing dozens of peaks can be obtained and a mass spectrometer attached to the GC will provide a mass spectrum of each peak. The spectra may be interpreted offline or in many cases may be identified by simultaneous online matching with an inbuilt computer containing a library of spectra, which shows the degree of probability of the match.

Pyrolysis Temperature and Heating Time

The temperatures used for pyrolysis are variable and depend to some extent on the nature of the polymer. Polymers of high thermal stability or which are highly crosslinked obviously require a higher temperature than a simple thermoplastic. The bond strengths of the constituent atoms and the association of atoms influence both the ease and type of degradation that

occurs, as rupture of the weakest bonds will predominate. The formation of stable free radicals generally occurs. Little pyrolysis of polymers occurs with the lowest available Curie point wire, i.e. 358°C and temperatures of 500–600°C might be considered as lower limits. The optimum temperature is considered to be near 800°C. An excessively high pyrolysis temperature is to be avoided, as with increasing temperature fragmentation of the pyrolysis products occurs, with an increased amount of very low molecular weight gaseous products being formed. These products are not helpful in achieving identification as they are typical of organic compounds generally rather than of a particular polymer.

The heating time, while variable, is short and may range from seconds to a fraction of a second. With Curie point pyrolysis the heating period is usually less than with filament or ribbon types. In either case the time to achieve the final temperature must be short. Pyrolysis under the conditions selected must be essentially complete, a situation that is readily checked by reheating the element after pyrolysis and determining if further pyrolysis products are separated. The flow rate of the carrier gas that passes through the pyrolyser should be such that the pyrolysis products are readily swept from the heated pyrolysis zone into the column, minimizing the recombination of reaction products. Such secondary products may be more characteristic of the apparatus than of the polymer. The unreactive carrier gases normally used can be conveniently employed. Gases that react with the reaction products are used in special circumstances, the most common being oxygen for use in oxidation studies or hydrogen with a suitable catalyst for hydrogenation.

An advantage of the resistively heated pyrolyser is that stepwise pyrolysis, where the same sample is pyrolysed at increasing temperatures, may be carried out. This technique has been used with low temperatures to remove the majority of additives and monomeric plasticizers, and also with higher temperatures to study the ease of polymer degradation. A disadvantage of resistively heated pyrolysers is that the resistance of the heating element may vary over time owing to corrosion and thinning of the wire. With a variation in the resistance of the wire, the nominal temperature is not achieved when the same current is applied and the pyrolysis results are variable.

Enclosed Curie point pyrolysis (ECP) has been described where the sample is deposited on the Curie point element and sealed in a capillary tube, with pyrolysis taking place in the tube. The tube is subsequently broken in the carrier gas flow. The method has been used for the study of the oxidation of polyisobutylene. A comparison with conventional resistive pyrolysis and ECP shows that a method for

distinguishing gas phase versus melt phase secondary reaction is possible.

Polymer Degradation

Degradation may occur by a variety of mechanisms, or combination of these. The common mechanisms are described below.

Most addition polymers incorporate a carbon-carbon backbone. With a polyolefin such as polyethylene, the bonds are equivalent and the rupture is random. The strength of the C-C bond is approximately 349 kJ mol^{-1} (83 kcal mol^{-1}) and that of the C-H bond is approximately 393 kJ mol^{-1} (94 kcal mol^{-1}), so that rupture of the former bond occurs. In these circumstances a large number of fragments result and the mechanism is termed random scission. The hydrocarbons with terminal free radical ends require to be stabilized. The fragment with a free radical end may extract a hydrogen atom from an adjacent fragment and become a saturated end. In extraction a free radical is created on the adjacent fragment. This fragment commonly stabilizes by β -scission, where the induced free radical site becomes an unsaturated molecule end. This process continues and produces a sequence of three hydrocarbons, the first saturated, the next with a double bond at one end, and the third with a double bond at both ends, a series of n -alkanes, α -olefins and α,ω -diolefins being formed from methane to hydrocarbons of near 40 carbon atoms.

Where the carbon atoms are not equivalent, such as in polyvinyl chloride where the bond strength of the C-Cl bond is 305 kJ mol^{-1} (73 kcal mol^{-1}), random scission does not occur – rather aromatic compounds are formed. Hydrogen chloride is eliminated and the free radicals on the adjacent sites form a sequence of double bonds to make an unsaturated backbone. This then fragments to form a series of aromatic compounds.

A third mechanism that occurs with a few polymers containing α -methyl substitution, i.e. polymethyl methacrylate and polymethyl methacrylamide, is unzipping or reformation of monomer. Here fragmentation of the C-C backbone occurs with the free radical fragments formed undergoing β -scission with the elimination of a molecule of monomer and formation of a new free radical fragment. Repeated β -scission leads to the formation of more monomer, which is frequently in excess of 95% of the original monomer concentration. The yields of monomer vary greatly with the polymer. The lower polyalkyl methacrylates yield essentially all monomer, but as the substituent alkyl chain becomes larger the monomer yield decreases. With polylauryl methacrylate the monomer yield is approximately 70%, as some degradation of the alkyl chain occurs.

Polystyrene degrades by a combination of mechanisms, and the monomer yield is approximately 40%. Unzipping reactions are of little importance in the degradation of polyacrylates, where the monomer yield is in the order of 5%.

Microstructure

Pyrolysis GC of polymers allows determination of the microstructure in addition to the chemical composition. The polymer of simplest chemical composition, polyethylene, is prepared by polymerization under different conditions and with a variety of catalysts to produce products with greatly differing physical properties, dependent on the microstructure. Short- and long-chain branching occurs, as does stereoregularity.

First to be analysed were polymers produced by high pressure processes. These contain a significantly branched structure with both short-chain branching (C1-C6) and long-chain branching, as illustrated in Figure 2A. The introduction of low pressure processes using metal alkyl catalysts has allowed the production of products with structures as shown in Figure 2B and 2C.

The low density polymer produced by high pressure processes undergoes random scission and produces a strong sequence of triplet peaks corresponding to α,ω -diolefins, α -olefins and n -alkanes of each carbon number, with weak multiple peaks of isoalkanes, isoalkenes and isoalkadienes between the triplets.

A technique that has been used in polyolefin pyrolysis for decades is *in situ* simultaneous hydrogenation of the pyrolysis products, hydrogen being used as the carrier gas with a pre-column containing

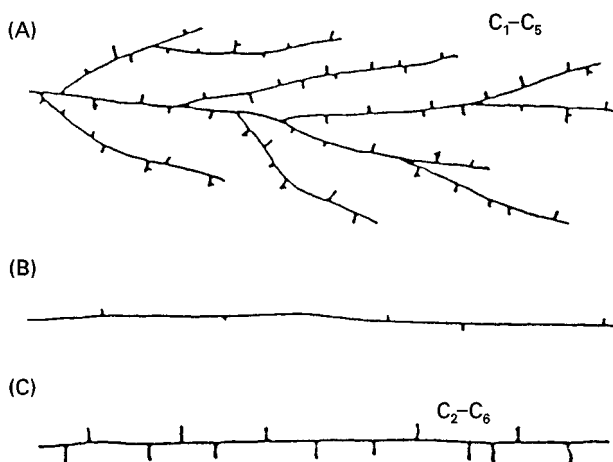


Figure 2 Structures of various polyethylenes. (A) Low density polyethylene (LDPE); (B) high density polyethylene (HDPE); (C) linear low density polyethylene (LLDPE). (Reproduced from Wampler TP (1995) *Applied Pyrolysis Handbook*, p. 81 with permission of Marcel Dekker.)

a hydrogenation catalyst inserted between the pyrolyser and the injection port. With this technique the triplets become single peaks of the *n*-alkane and the intermediate peaks are reduced in number and increased in intensity, with iso compounds of comparable structure forming single isoalkane peaks.

While ethylene is symmetric, propylene and other olefins are not, and the possibility of head to tail, head to head and tail to tail combinations exists; such differences are evident in pyrograms. With copolymers of polyethylene and polypropylene, pyrograms containing peaks associated with each monomer are observed; however, with different catalysts the intensity of the individual peaks vary. This is used as a measure of the sequence distribution of monomer units along the chain. Sequence distribution determination is not restricted to polyolefins, but has also been reported with many other important polymer systems.

The tacticity of various polymers, including polystyrene, has been determined by pyrolysis gas chromatography. With polystyrene, fragments characteristic of the polystyrene chain, ranging from monomer to pentamer, were observed in the pyrogram. The relative intensities of the tetramer and pentamer peaks reflect the original tacticity.

Minor and subtle differences in the end groups of a particular polymer system frequently cause significant alterations of the properties of the polymer, particularly concerning thermal stability and transparency. It is well known in gas chromatography that the polysiloxane materials frequently used as stationary phases possess high thermal stability when appropriate end termination is employed. Details of end termination are also of value in determining polymerization mechanisms. The identification and determination of end groups is difficult owing to their low concentration. Pyrolysis-GC has been used to characterize many polymer systems. Examples are polymethyl methacrylate radically polymerized in toluene solution with benzoyl peroxide initiation under varying conditions. The peak intensities of some products characteristic of the end groups present have been interpreted in terms of polymerization temperature and solvent/monomer in the feed.

Methacrylate end groups in polystyrene samples have been determined by reaction with tetramethylammonium hydroxide where methyl methacrylate was split out and determined. The initiator used was *s*- or *n*-butyl lithium and on pyrolysis the main product was styrene monomer together with a considerable amount of dimers and trimers. Various minor fragments clearly showed the presence of *n*-butyl end groups. Similar analyses of end groups in other polymers have been reported, including end groups in polycarbonates.

Chemical Degradation

Alkyd resin constituents have been determined for decades, the method used being chemical cleavage followed by estimation by gravimetry, colorimetric or spectrophotometric means. The analysis of alkyd resins was revolutionized in the 1960s by US Government workers who determined the reaction products by GC.

The Zeisel reaction has also been extended by the use of GC; traditionally all alkoxy groups were estimated as methoxy groups. With GC, the alkoxy groups are converted to the corresponding alkyl halides by reaction with hydriodic acid in phenol prior to chromatographic separation of the individual halides.

Gas chromatography was early applied to the estimation of the hydrolysis products of polyurethanes, polyethers, polysiloxanes and polyamides.

In situ Chemical Degradation

The degradative analysis of many polymers with *in situ* GC was developed by scientists working on determination of the volatile degradation products in the 1970s. They conducted vigorous hydrolytic cleavage in a reactor constructed from a furnace pyrolyser attached to the injection port of a gas chromatograph. A 30 mol% excess of a prefused mixture of potassium hydroxide (85% KOH approximating to the hemihydrate) and 1–10% sodium acetate as flux was heated for 0.5–1.0 h at temperatures within the range 200–350°C. Volatile reaction products were examined by GC while the reaction products that formed alkanoate soaps remained in the reactor.

All the alkali metal hydroxides have been used for alkali fusion, although potassium hydroxide is preferred as its melting point is suitable and organic compounds have greater solubility in a potassium hydroxide melt than in a sodium hydroxide melt. **Table 1** shows the melting points of the common alkali metal hydroxides in both the anhydrous and hydrated forms.

Most acids, both organic and inorganic, have been used to effect hydrolysis and to achieve cleavage of ethers. They include phosphoric, hydrochloric, sulfuric, hydrobromic, hydroiodic and *p*-toluenesulfonic acids. Mixed anhydrides of *p*-toluenesulfonic and acetic acid or trifluoroacetic anhydride or trifluoroacetic acids have also been used. Some of the acids, particularly sulfuric acid and hydrochloric acid, produce by-products, while phosphoric and hydrobromic acids have often been used successfully. The ether groups in alkylene oxide polymers have been cleaved using a mixed anhydride of *p*-toluenesulfonic acid and acetic anhydride. The reaction is

usually conducted by heating in a microflask with an appropriate condenser. The polymer may be converted to compounds suitable for GC or the reaction products may be worked up as derivatives.

External Chemical Degradation

The work described above has been extended, by employing external fusion, to allow all of the reaction products to be identified as volatile products or as derivatives amenable to GC. Hydrolytic reactions using alkaline or acidic catalysts are achieved, as is acidic cleavage of ether groups. In several cases polymers have been examined using simultaneous hydrolysis and alkylation.

The advantages of external fusion are listed below:

1. Fusion is more rapid, efficient and more readily controlled than *in situ* degradation as the water necessary for the reaction remains in the reaction environment rather than tending to be swept into the cold trap.
2. Multiple fusions can be carried out in an external heater without restricting the use of a gas chromatograph, or, more importantly, restricting examination to GC alone.
3. Materials that would ordinarily be retained in the reactor as soaps or other material of low volatility can be examined after appropriate chemical reaction and/or derivatization.
4. Hydrolytic degradation and cleavage of ether groups can be conducted simultaneously or separately.
5. Other analytical techniques can be used as appropriate.
6. All of the components of a polymer can be analysed rather than simply those sufficiently volatile for direct GC.

The quantitative nature of both acid and alkaline fusion reactions has been reported and a number of polymers have been studied with acceptable results.

Table 1 Melting points of alkali metal hydroxides

Alkali metal hydroxide	Melting point	
	Anhydrous	Hydrate
Potassium hydroxide	360	125 ^a
Sodium hydroxide	318	64.3 ^b
Lithium hydroxide	417	— ^{b,c}

^aCommercial potassium hydroxide contains 15% water and is present as the hemihydrate.

^bPresent as the monohydrate.

^cDecomposes to form lithium hydroxide and water.

Nitrogenous polymers Nitrogenous polymers have been widely studied. These include: polyamides such as the simple nylon materials; the condensation products of dicarboxylic acids and diamines and the condensation products of α,ω -aminoalkanoic acids; the dimer polyamids (using the C₃₆ dimer dicarboxylic acids prepared from vegetable oils); the aramid fibres (using an aromatic diamine and a dicarboxylic aromatic acid); and the polyhydrazides produced using hydrazine. Polyimides produced by the polymerization of benzene tetracarboxylic acids and aromatic diamines and copolymers of amides and imides have also been analysed using alkali fusion.

Polyesters External chemical degradation has been used to analyse polyesters, both containing oils and oil-free, as well as silicone alkyds and crosslinked systems of polyesters with various aminoplasts. In a crosslinked system the aminoplast butylated ureaformaldehyde is itself cleaved, while with other aminoplasts only the butylated groups are removed.

Simple fibreglass-reinforced plastic (FRP) and vinyl ester laminates are cleaved by this method. With the laminates and silicone polyesters, the siliceous fibreglass (normally E-glass, a very low alkali borosilicate glass containing approximately 50% silica and 10% boron trioxide) or organic silicone is converted into an organic derivative amenable to GC examination. A chromatogram showing the trimethylsilyl (TMS) derivatives of the polyols, dicarboxylic acids and organic siloxane moiety produced from a silicone polyester is shown in **Figure 3**. Other reinforcement materials that are used in aerospace and other specialized applications include polyester or polyamide (NomexTM) reinforcements, both of which are amenable to hydrolytic cleavage.

Polyurethanes Polyurethanes are conventionally the reaction products of an isocyanate with an ether or ester and terminated with hydroxyl groups. While these materials are relatively resistant to hydrolysis, they can be readily cleaved by vigorous hydrolytic reactions. The polyurethane ether materials are more resistant to simple solution hydrolysis than are the polyurethane esters. Many polyurethane compounds have been studied using both alkaline and acidic hydrolysis. The simple condensation products – chain-extended materials produced using a short-chain polyol or an amine; polyether polyurethanes used in medicine; transparent polyurethanes that use polycaprolactone diols; isocyanate-based copolyamide resins; and a urethane crosslinking agent used in reversion-sensitive natural rubber – have all been examined using vigorous hydrolysis reactions. Determination of the tertiary amino groups allows the

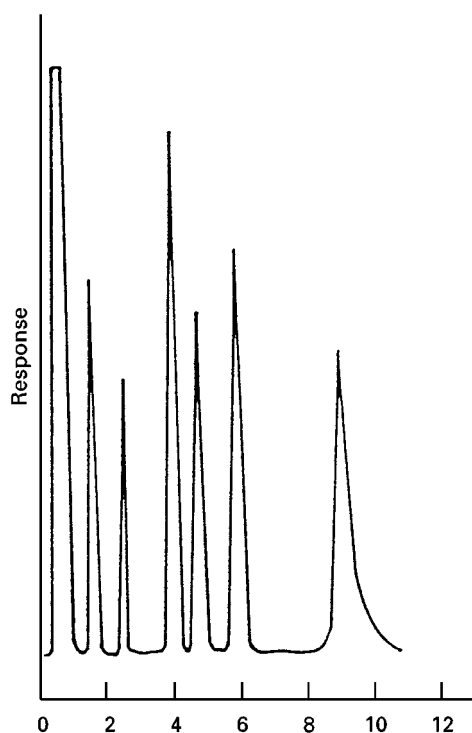


Figure 3 Gas chromatogram showing simultaneous separation polyols, dicarboxylic acids and silicate TMS derivatives of: 1, solvent peak; 2, neopentyl glycol; 3, silicate; 4, trimethylol ethane; 5, trimethylol propane; 6, adipic acid; 7, isophthalic acid. (Reproduced from Haken JK *et al.* (1985) *Journal of Chromatography* 441: 207–212 with permission of Elsevier Science Publishers.)

number of secondary amino groups in polyurethanes to be determined, and an estimate of the degree of crosslinking to be made.

Epoxy resins Only simple epoxy systems, either as the ether or crosslinked with amine compounds, can be cleaved by fusion. The majority of epoxy systems are complex networks that are sterically hindered and resistant to cleavage.

Polysulfones The aliphatic polysulfones are readily cleaved by vigorous hydrolysis. However, the aromatic polysulfones that find application as high temperature polymers, either alone or frequently as copolymers with polyethers, are resistant to hydrolytic cleavage.

Liquid crystal polyesters Liquid crystal polyesters based on *p*-hydroxybenzoic acid, *p,p*-biphenol, terephthalic acid and 2-hydroxy-6-naphthoic acid, which are also used as high temperature polymers, are readily cleaved by vigorous hydrolysis.

Summary

Systems that have been successfully subjected to chemical cleavage include polyacrylates, polyamides,

polyimides, polyurethanes, polysiloxanes, polyurethanes, polyesters (containing vegetable oil and vegetable oil-free), liquid crystal polyesters, polyhydrazides and silicone polyesters. **Table 2** shows polymers and additives that have been examined using both *in situ* and external pyrolysis. Copolymers that include more than one functional class have been examined; these include polycarbonate–polydimethylsiloxane block copolymers and isocyanate-based copolyamides.

With a completely unknown sample alkali fusion is recommended, followed if necessary by acid reaction. This ensures that some reactants, such as polyethers, are not cleaved into such small fragments that their initial composition is not apparent. For some purposes acid reaction is more rapid. For routine purposes some of the extraction steps, which simply serve to separate functional classes, may be eliminated. The reduction or elimination of extraction steps increases the quantitative nature of the analyses. It has been shown that the cleavage reactions are essentially quantitative and that errors are introduced by the extraction steps.

Pyrolytic Methylation

The term pyrolytic methylation was first used in 1979 to describe the coinjection of tetramethylammonium hydroxide with free carboxylic acids and phenols into the injection port of a gas chromatograph, resulting in the formation of methyl derivatives. The application to polymers did not occur until a decade later. Simultaneous pyrolysis and alkylation was conducted by the use of tetramethylammonium hydroxide or tetrabutylammonium hydroxide mixed with the polymer in a pyrolyser. Typically a 5 µg sample of polymer and 2 µL of the derivatizing reagent is subjected to Curie point pyrolysis at 770°C. Separation is by capillary GC with confirmation using mass spectrometric detection.

The reaction mechanism has been discussed and the evidence suggests that reactions occur by the following mechanism. When intimately mixed with tetramethylammonium hydroxide and heated to temperatures above 400°C, the polymer undergoes hydrolysis with the strongly basic agent forming salts of the hydrolysed products. These then undergo thermal fragmentation to the methyl derivatives. The term SPM, or simultaneous pyrolysis methylation, has been acknowledged to be something of a misnomer and the process has been renamed ‘thermally assisted hydrolysis and methylation’, with the abbreviation THM.

Applications

Alkyd and polyester resins The use of THM has largely been directed towards polymers that find

Table 2 Polymers and additives examined using *in situ* and external pyrolysis

Material	Product/s of reaction	Unidentified products
<i>In situ</i> pyrolysis		
Nylons	Diamine	Alkali metal soap of acid
Phthalate esters	Corresponding alcohol	Alkali metal soap of acid
Polyacrylamide	Ammonia	^a
Polyacrylonitrile	Ammonia	^a
Polyamides	Diamine	Alkali metal soap of acid
Poly(amides-imides)	Diamine	Alkali metal soap of acid
Polycarbonesiloxanes	Amine and diamine	Nil
Polychloroacrylate esters	Corresponding alcohol	Alkali metal soap of acid
Polyimides	Diamine	Alkali metal soap of acid
Polymethacrylate esters	Corresponding alcohol	Alkali metal soap of acid
Polysiloxanes	Aliphatic or aromatic hydrocarbon	^a
Polyurethanes	Diamine	Alkali metal soap of acid
External pyrolysis		
Alkyd resins	Acids and polyols as derivatives	Nil
Alkyd resins, crosslinked	Acids and polyols as derivatives	^b
Butylated urea formaldehyde	Carbon dioxide and <i>n</i> -butyl trifluoroacetate	Nil
Epoxy resins	Diamines and acetate derivatives	^b
Nylons	Diamines and diacids as derivatives	Nil
Phthalate esters	Alcohols and acids as derivatives	Nil
Polyacronitrile	Ammonia	^a
Polyacrylamide	Ammonia	^a
Polyamides	Diamine and acids as derivatives	Nil
Polyhydrazides	Hydrazine and diacids	Nil
Polyamides	Diamines and acids as derivatives	Nil
Polysiloxanes	Hydrocarbons and silica derivatives	Nil
Polyurethanes	Diamines and ester or ether derivatives	Nil
Silicone polyesters	Silicone, acid and diol derivatives	Nil

^aReaction with pendant groups.^bLimited application.

application in surface coatings. Pyrolysis and methylation of alkyd resins gives methyl esters of the constituent acids and methyl ethers of the polyols. A soyabean oil-pentaerythritol-orthophthalic alkyd resin produced C₈-C₁₆ methyl alkylanoates from the vegetable oil; tri- and tetramethyl ethers of pentaerythritol, dimethyl orthophthalate and methyl benzoate from the benzoic acid used as the chain regulator; and cyclopentanone from scission of C-O bonds of adipic acid, dimethyl isophthalate and methyl benzoate.

The fibre polyester, polyethylene terephthalate, gave benzene, a degradation product obtained on pyrolysis, dimethyl terephthalate and methyl benzoate as a combination product. It was evident in the analysis that no product attributable to the ethylene portion of the polymer was reported. This result is different from that obtained by hydrolytic degradation and chromatography, where a component peak attributable to the ethylene or butylene chains was identified.

The partial structure of alkyd resins may be elucidated; in addition to identification of the carboxylic acids and polyhydric alcohols as the appropriate

esters and ethers, the drying oil type, degree of cure, the oil length and modification with rosin and epoxy resins may be determined. The most common polyhydric alcohols used in alkyd resins are glycerol and pentaerythritol, resulting in the formation of the di- and trimethyl esters and the tri- and tetramethyl esters, respectively. All three of the isomeric phthalic acids are readily separated on the low polarity capillary column used. Methyl benzoate is observed, which is a problem as some of this compound is due to decarboxylation of some of the phthalic acid and differentiation of the use of benzoic acid as a chain terminator is not possible. All types of oils, both vegetable and the more highly unsaturated marine types, are readily characterized before autoxidative polymerization. However, after 'drying' or autoxidative polymerization, little unsaturation remains. The relative proportion of unsaturated to saturated fatty acid methyl esters gives an indication of the cure or age of the alkyd resin. A simple alkyd resin based on linseed oil-pentaerythritol-orthophthalic acid was examined over 5 months. The following conclusions were made:

1. Before autoxidative polymerization the ratio of linolenic acid (9,12,15-octadecatrienoic acid) to palmitic acid (hexadecanoic acid) was significant but the unsaturation rapidly decreased such that after 2 days all the linolenic acid had been removed by crosslinking.
2. After 2 weeks the ratio of oleic acid (9-octadecadienoic acid) to stearic acid (octadecanoic acid) slowly began to reduce with time. After 4 months the concentration of oleic acid had been reduced by approximately two-thirds of its initial concentration.
3. Nonanedioic acid began to appear after 3 days and increased to a maximum in 1 month. The oil length of an alkyd resin is the percentage of fatty acid acylglycerols present in the total resin solids. By considering the ratio of products from the drying oil to the aromatic compounds from the phthalic acids, an approximation of the oil length may be obtained. Some decarboxylation occurs however, and the value of the estimate is reduced. Naturally occurring modifiers, i.e. rosin (as methyl dehydroabietate), have been determined, as have epoxy resins.

Epoxy resins A simple epoxy ether, i.e. a bisphenol A epichlorohydrin condensate, on pyrolysis produced three component peaks – phenol, isopropenyl phenol and bisphenol A. However, on pyrolytic methylation a variety of components was produced including phenol, isopropenyl phenol, the monomethyl ethers of these compounds and bisphenol A. The diether of bisphenol A was also formed.

Polyvinyl acetate Pyrolysis butylation has been used with low molecular weight products such as vinyl acetate-containing polymers where the vinyl acetate formed by pyrolysis is advantageously examined as vinyl butyrate, the disadvantage being that by-products, i.e. *n*-butanol and tributylamine, are formed.

Polymethyl acrylates Pyrolytic butylation of a methacrylic copolymer produced *n*-butyl methacrylate. *n*-Butyl acetate and *n*-butyl butyrate were produced from a cellulosic acetate-butyrate copolymer and *n*-butyl cyanoacrylate was produced from a commercial cyanoacrylate adhesive.

Rosin adducts The rosin-based resins have been extensively studied. While these are natural polymers, they are used in many modified forms. Abietic acid is the principal acid and it contains both a conjugated diene and a carboxylic acid, both of which are readily reacted on a commercial scale. Wood rosins contain a high proportion of diterpentine and mixtures of

seven organic acids. Pyrolytic methylation has allowed the identification of (1) fumaric acid, (2) sandaraco-fumaric acid, (3) pallstic acid, (4) isofumaric acid, (5) dehydroabietic acid, (6) abietic acid and (7) neoabietic acid.

Para-substituted alkylphenol resins or modifications with rosin or its esters produce characteristic pyrograms when subjected to pyrolytic methylation. Tertiary butylphenol and *p*-nonylphenol are the tonnage phenols used. Traces of the free phenols result from both phenol modifications and methyl- and dimethyl-substituted phenols. Pentaerythritol rosin esters produce peaks due to the methyl esters of dehydroabietic acid and abietic acid in addition to the tri- and tetramethyl ethers of pentaerythritol. Modification of rosin with fumaric or maleic acids produce dimethyl fumarate. Rosin and reaction products with fumaric acid have been detected as a size on paper at the 1% level.

Polycarbonates Polycarbonates have been cleaved using alkaline reaction. Various phenolic compounds are formed by C–C bond cleavage as well as by cleavage of carbonate linkages. Almost quantitative degradation of the main chain occurs through reactive pyrolysis at the carbonate linkages to yield the dimethyl derivatives of the constituents.

Liquid crystal polyesters As in chemical degradation, reaction occurs with liquid crystalline polyesters, partial reaction occurring with products based on *p*-hydroxybenzoic acid and 2-hydroxy, 6-naphthoic acid. Quantitative results were achieved by varying the reaction conditions. Similar liquid crystalline polyesters based on 4-hydroxybenzoic acid, terephthalic acid and 4,4-biphenol produced almost quantitative results.

Conclusion

The application of GC to synthetic polymers has been outlined using three types of methods – pyrolysis, chemical degradation and pyrolytic alkylation. In all cases a considerable reduction in molecular weight is achieved before GC. Pyrolysis is applicable to both addition and condensation polymers and occurs by thermal degradation of the constituent chemical bonds. Chemical degradation and pyrolytic alkylation are applicable to condensation polymers with degradation at the location of constituent functional groups. Pyrolysis in some cases produces quantitative results, while chemical degradation usually produces quantitative results. Pyrolytic alkylation has to date been used only for qualitative analysis.

See also: II/Chromatography: Gas: Derivatization; Detectors: Mass Spectrometry; Pyrolysis Gas Chromatography. Extraction: Supercritical Fluid Extraction.

Further Reading

- Challinor JM (1991) The scope of pyrolytic methylation reactions. *Journal of Analytical and Applied Pyrolysis* 20: 15–24.
- Crompton TR (1989) *Analysis of Polymers, An Introduction*. London: Pergamon.
- Cross J (1987) *Non Ionic Detergents – Chemical Analysis*. New York: Marcel Dekker.
- Haken JK (1993) Fusion reaction chromatography: a powerful analytical technique for condensation polymers. *Advances in Chromatography* 33: 177–231.

- Haken JK (1996) Degradative polymer analysis by chromatography. *Journal of Chromatography* A756: 1–20.
- Haken JK (1998) Pyrolysis gas chromatography of synthetic polymers. A bibliography. *Journal of Chromatography A* 825: 171–187.
- Mitchell J Jr (ed.) (1991) *Applied Polymer Analysis and Characterization*, vols 1 and 2. Munich: C. Hanser-Verlag.
- Taguchi VY (1990) Derivatization reactions. In: Clements RE (ed.) *Gas Chromatography, Biochemical, Biomedical and Chemical Applications*, pp. 129–177. New York: Wiley.
- Wampler TP (1995) *Applied Pyrolysis Handbook*. New York: Marcel Dekker.
- Whitlock LR and Siggia S (1974) Fusion reaction gas chromatography. *Separations and Purification Methods* 3: 299–337.

Liquid Chromatography

C. H. Lochmüller, Duke University, Durham, NC, USA

Copyright © 2000 Academic Press

Introduction

The goals in the use of liquid chromatography for the separation of polymers and polymer oligomers include the determination of purity, the production of pure/purer polymer mixtures and for obtaining quality control data for polymer intermediates. There are fundamentally two partition mechanism options for such separations: size exclusion or sorption in the sense of surface adsorption or dissolution into a stationary phase. Size exclusion involves the partition of the molecules of interest from the mobile phase into the stationary mobile phase contained in the various pores of the solid support. The extent to which the stationary liquid is explored by the polymer molecules is determined by their Stokes' radius (dynamic size) and the volume of mobile phase in pores of a diameter large enough for penetration to be possible. Adsorption onto or sorption into a phase coated or grafted as a thin film on the surface of a solid support is dominated by solubility in the mobile phase and the chemical potential for sorption of the polymer molecules in a given mobile phase in contact with a given stationary phase. Because stationary phase supports used in modern liquid chromatography are themselves porous, mixtures of size exclusion in the presence of sorption and *vice versa* are known.

Size Exclusion

Historically, size exclusion has been the method most often used for polymer separation, purification and molecular weight determinations. The technique developed in parallel in the 'organic' polymer area and the biological polymer area. When used in organic polymer work, the term 'gel permeation' is used. In water soluble biopolymer work, it is called 'gel filtration'. There is no fundamental difference in the principles involved and both are size exclusion based. In liquid chromatography molecules move in the direction of development because of mobile phase flow. Most gel electrophoresis methods are, in reality, size exclusion based separations and that includes the gel methods used for sequencing of nucleotide fragments. There the driving force is electromigration of molecules with essentially identical ionic mobility which reptate through a porous polymer medium at rates proportional to size.

Sorption

Despite the potential attractiveness of a method which could introduce chemical selectivity in to the separation of polymers, sorption methods have seen little practical application until more recent times. The sole exception is the ion exchange purification of polyelectrolytes such as proteins. The history of the development of polymer high-performance liquid chromatography (HPLC) is an interesting one and is detailed in subsequent paragraphs. The reader should keep the following introduction in mind when

considering various models for retention of polymers in sorption techniques.

The liquid chromatography of small molecules is dominated by solubility of the molecule[s] of interest in the moving or mobile phase. This is in stark contrast to gas chromatography where the stationary phase contribution dominates. One controls retention and the large fraction of selectivity (differential migration) in liquid chromatography by mixing various solvents to obtain differential solubility sufficient for the task of separation. That is not to suggest that the stationary phase is not important. It is, but generally as a secondary effect.

The rate of change of retention volume (or time at constant flow) for small molecules (m.w. < 2 kD) is not steep compared to polymers. Thus the strategy for small molecule separations is to use combinations of solvents in which one solvent is a good solvent and the other is more hostile or 'poorer' in terms of solubility of the molecules of interest. Polymers, on the other hand can have very rapid transitions from soluble to insoluble over narrow ranges of good/poor solvent mole fraction.

It is also common practice to inject samples of small molecules in a solvent which is good compared to the mobile phase. This technique can have awkward effects in polymer chromatography. If the mobile phase is one in which the solubility is already very small or near zero, the injected plug of good solvent moves with the leading and trailing edge of the plug being depleted of solute. The net effect is to coat the column with polymer with the excess eluting at the void volume. Columns are well-designed packed beds and, as such, are very poor mixers. The solution is to dissolve the polymer in the mobile phase and to mix the sample solution with the mobile phase before column contact.

There has been much interest in methods for the fractionation of macromolecules using reversed-phase, high-performance liquid chromatography (RPLC). Reversed-phase methods are those that have a relatively polar mobile phase and relatively non-polar stationary phase, e.g. water and paraffin oil. If it were possible to achieve both isocratic and gradient elution of polymer oligomers and isomers, then these separation techniques could provide vastly more insight and control than is currently the case in a majority of the applications where size exclusion alone dominates.

Certainly debates over the validity of models are an important scholarly aspect of the current dialogue. Successful models based on sound physico-chemical principles could guide the development of practical applications. The short-term solution is likely to be a combination of models if the historical case for the application of HPLC to small molecules applies here.

Although there are many reported successful examples of polymer separations and several models have been suggested, the retention mechanism of polymers in RPLC remains unclear. Glöckner suggests a 'precipitation-redissolution' model for the gradient elution of polymers. In this model, polymer molecules repeatedly precipitate onto the stationary phase and redissolve into the mobile phase until finally eluting at a mobile phase composition at which the polymer is totally soluble. Retention depends solely on the mobile phase with the column playing a passive role providing only a large surface area as support for the precipitate. Armstrong, Martire, Boehm and Bui proposed a model for critical solvent composition behaviour found by some in the isocratic elution of polymers. This model is often called BMAB theory or critical solution theory. This theory was developed from a statistical treatment of the equilibrium distribution of infinitely dilute polymer molecules between a mobile phase and a stationary phase based on the Flory-Huggins theory. According to the model, the range of the mobile phase composition within which finite retention factor (k) values can be observed under isocratic elution conditions is very narrow for high molecular weight polymers. Plots of $\log k$ versus the mobile phase composition show slopes that mean that polymer molecules are either infinitely retained or not retained at all. Therefore, isocratic retention should be impossible. It can be concluded from this model that the separation is strictly mobile-phase controlled and has little to do with the column length. If either of these models are correct in every detail, isocratic elution is impossible because, under isocratic elution, the polymer molecules either flow through the column without any retention or strongly adhere to the stationary phase without ever eluting.

In contrast, Snyder and coworkers assert that no special model is needed for the polymer retention and the traditional models can be used in interpreting the retention behaviour of polymers.

After numerous failures in attempts to reproduce the published work of others, Lochmüller and McGranaghan were the first to consider the likely fate of the injected polymer sample in the mobile phase prior to its contact with the column. They found that traditional retention behaviour was obtained only when the sample was adequately mixed with the mobile phase using a low dispersion, crocheted capillary tube placed between the sampling device and the column. They reported that polystyrenes of molecular weight ranging from 2000–2 800 000 Da could be separated under isocratic elution conditions with binary mobile phases of tetrahydrofuran/H₂O and dichloromethane/acetonitrile. Finite, non-zero k values

and linear relationships of $\log k$ versus the volume percentage of tetrahydrofuran and dichloromethane were observed. Alhedai, Boehm and Matire subsequently reported the isocratic elution behaviour of polystyrene homopolymers.

In polymer RPLC, separations are achieved by using a mixture of 'good' and 'poor' solvents as the mobile phase. A good solvent is one that is thermodynamically favourable for polymer solution and a poor solvent is thermodynamically unfavourable. Since polymers have low solubility in poor solvents, polymer samples are often dissolved in a good solvent for chromatography. The result is that the injected sample plug is a better solvent than the actual mobile phase. For hydrophobic polymers, the good solvent usually is a strong solvent in RPLC. Often sample preparation is followed by injection without any further treatment of the sample. Because chromatographic columns are, by their very design, poor mixing devices and the equilibration between the polymer sample and the mobile phase may be slow on the chromatographic time scale, the polymer sample can remain well solvated from its interior in the injection solvent and isolated from the mobile phase and stationary phase effects. Under the worst conditions, the mobile phase can be so hostile to the polymer that the polymer sample will co-elute with the injected plug of the good solvent. This 'solvent effect' could explain why normal chromatographic retention behaviour was not observed in some of the previous studies. In addition, polymer molecules can undergo various conformational changes in the chromatographic process due to the difference between the injection solvent and the mobile phase. These conformational changes can complicate separations and make reproducible, meaningful results difficult to obtain. The use of a pre-column mixer and an initial binary solvent whose composition is close to the mobile phase composition affords equilibration between the polymer and the mobile phase and also affords a more uniform elution condition.

There are, of course, significant differences in the properties that distinguish different polymer types from each other that must be taken into account in guiding method development. In the special case of some biological polymers such as proteins and polypeptides, a contribution of size exclusion and ion exchange is possible and careful manipulation of the ion exchange effect can provide resolution of genetically different isoenzymes. In other cases where the polymer has groups with little acid-base difference, as in the case in gene sequencing, it is possible to cleave the macromolecule at specific sequence events and to tag these fragments. The resulting fragments are then separated through size exclusion in a gel

matrix using electrokinetic driving force through the gel space. Current applications of HPLC are more limited and most of the literature examples of protein resolution are carried out with molecules differing by thousands of Daltons and are limited to 'analytical' purposes through the use of denaturing conditions where narrow peak shape is more important than retention of native structure.

Many, if not most, common organic polymers are either non-electrolytes or strong polyelectrolytes. In the latter case, the most common situation is one in which the ionized or ionizable function is the same for each repeating unit and/or the groups have nearly identical pK_a values. Ion exchange is, thus of little use in the resolution of oligomers. In the case of non-ionizable polymers, such as the polystyrenes, the methacrylates, acrylates, polyesters and ethers, the use of RPLC offers the possibility of selectivity by both solvent effect and stationary phase interaction. If ordinary chromatography is possible, then it could be possible to resolve oligomers, to resolve copolymer variations by chemical selectivity and thus improve the quantitation as well as the isolation of such materials.

There are two solutions to the steep gradient in $d \ln k / d \text{Vol}\%$. The first is to find a second at a solvent less hostile to the polymer under investigation. The second is provided by modern instrumentation and that is that a gradient mixer will mix mixtures. This second option involves running a gradient where the A solvent or poor solvent is already a mixture and the same for B. In principle, a gradient can be run from 60% A to 58% A in a way reproducible to 1% by volume A in B. In this manner, the steep gradient in $d \ln k / d \text{Vol}\%$ is slowly traversed in the gradient mixing process. The results can be dramatic and it is possible to resolve individual polystyrene oligomers at an average molecular weight of 100 kD.

Figure 1 shows a separation of two polymethylmethacrylate samples, one a synthetic sample containing lower molecular weight oligomers after gel permeation separation, and the other a nominally monodisperse 75 kD standard. Figure 2 is the linear dependence of retention as a function of tetrahydrofuran vol% in water for a wide range of polyethylene glycol monodisperse standards. Note how the slope steepens with increasing molecular weight. Figure 3 is a similar plot for poly-L-, poly-D- and poly-D,L-tryptophans. Note the linearity of response but also that the lines for all poly-L and the poly-D,L are not parallel despite the molecular weight being the same (~ 5.5 kD).

There are many good reasons to want to use a single component, isocratic elution method. The first is the cost per sample run. The second is that

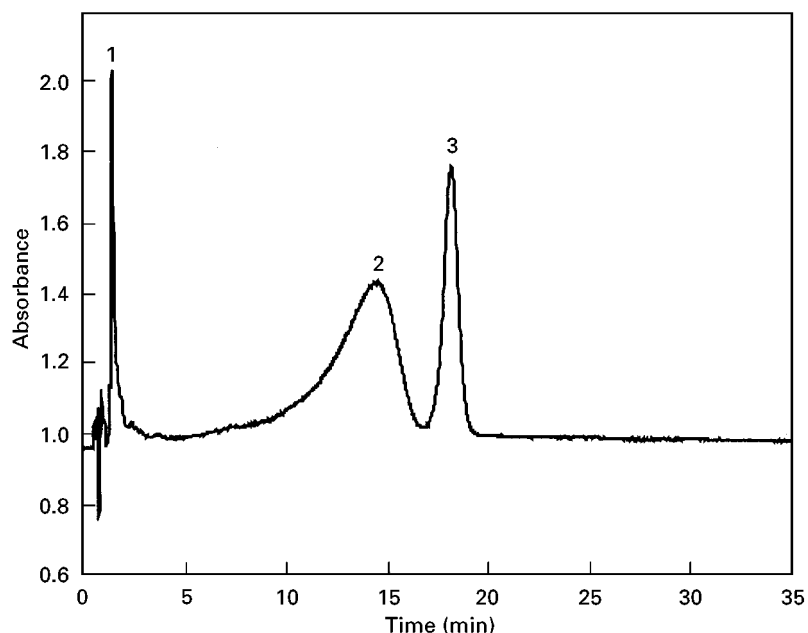


Figure 1 Separation of a mixture of PMMA 33.5-kD (2) and PMMA 75-kD (3) in gradient mode with mobile phase THF/water from 68/32 to 80/20 in 20 min on a Hypersil® 20 cm \times 2 mm C18 column. (Reproduced, in part, from the author's work with permission of the *Journal of Chromatography Science* and Preston Publications.)

only one solvent need be removed from the collected polymer sample. The potential of modern liquid chromatography is to produce samples which are truly monodisperse. The fewer separation solvents the better. A possible route is the use of a single solvent and the temperature dependence of k . Of course, the magnitude of the temperature effect on retention is in direct proportion to the solubility dependence. The temperature gradient can be applied as it is in gas chromatography, i.e. as a gradient over

time. Another is a gradient over space, the column length. The first example of a spatial gradient was in the separation of polyethylene glycols. These polyethers have a decreasing solubility in water with increasing temperature. Thus a column kept at high temperature will show large retention volumes for polyethylene glycols and a gradient run from hot to cold is an option. A column kept relatively hot at the inlet and cold at the outlet will show a reduced rate of development for polyethylene glycols at the

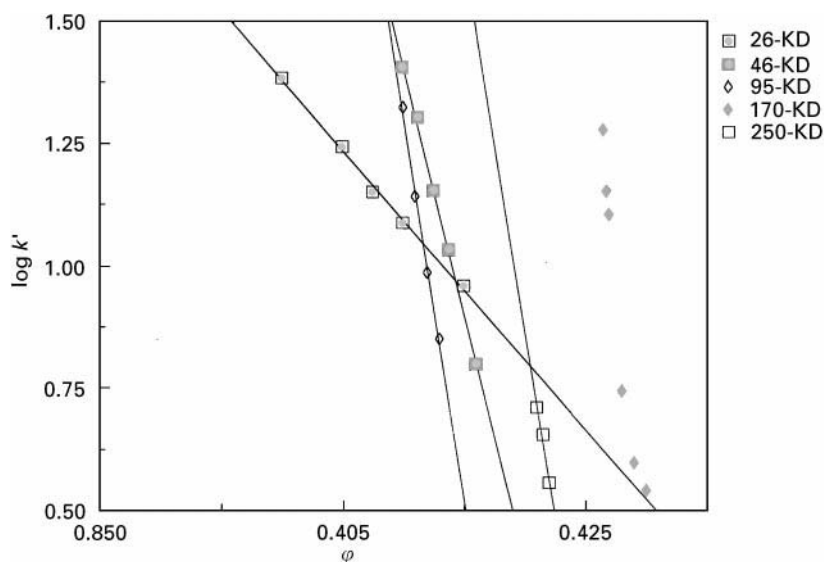


Figure 2 Linear plots of $\log k'$ (retention factor) vs. volume fraction of THF in water for PEG samples. (Reproduced, in part, from the author's work with permission of the *Journal of Chromatography Science* and Preston Publications.)

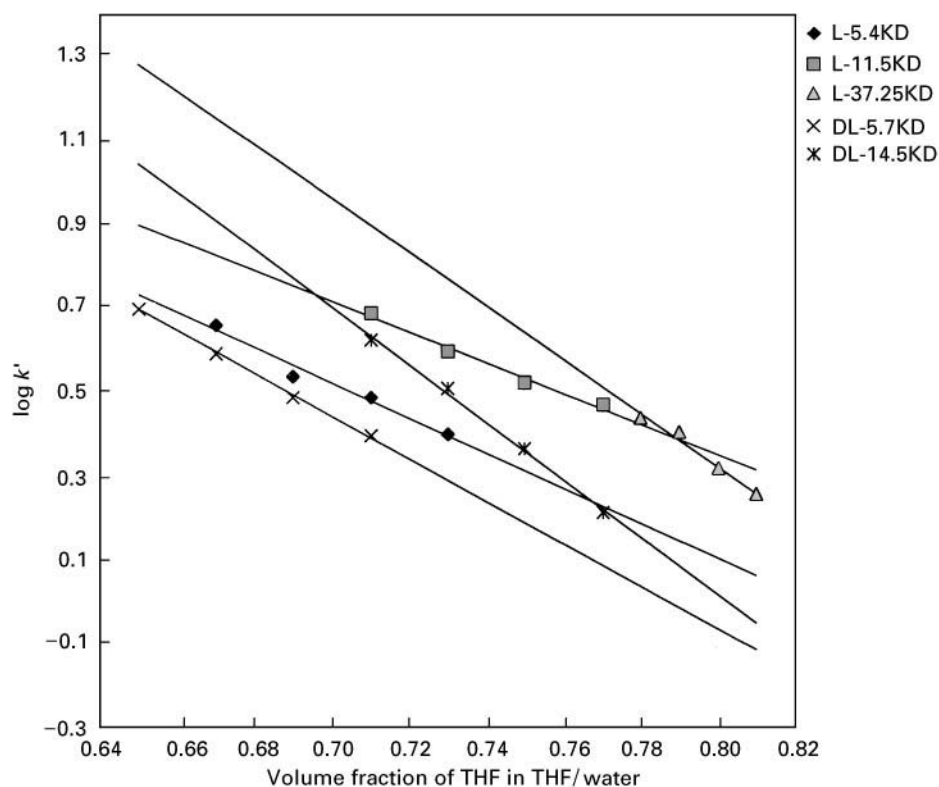


Figure 3 Dependence of $\log k'$ versus volume fraction of THF poly(L-tryptophan)s and poly(DL-tryptophan)s. (Data taken in part from work reported in Lochmüller and Chun Jiang (1994) *Journal of Liquid Chromatography* 17: 3179–3189.)

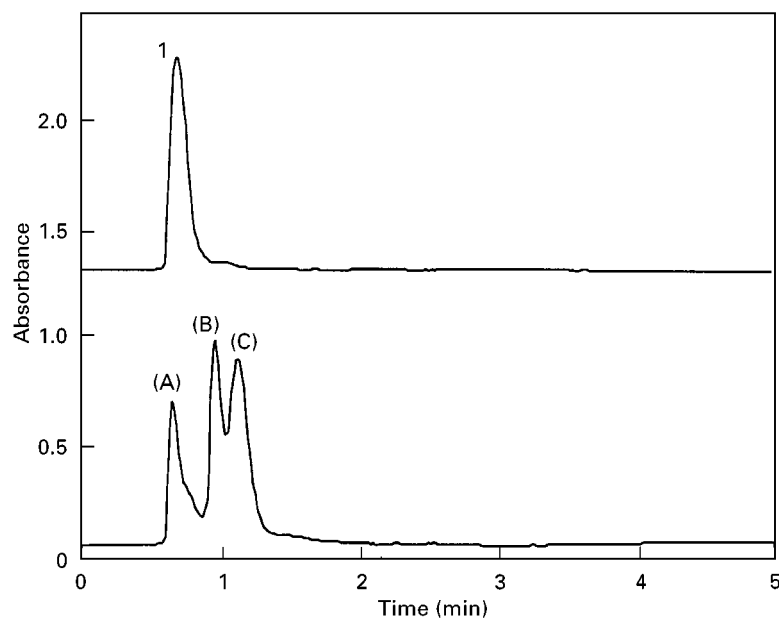


Figure 4 Chromatograms of mixture (1) of PEG 26-KD (A), 46-KD (B) and 95-KD (C) (ACN/H₂O 42/58; Top, $t = 23^\circ\text{C}$; the thermal gradient was $-0.05^\circ\text{C min}^{-1}$ started from 28°C . Bottom, $t_{\text{inlet}} = 40^\circ\text{C}$, $t_{\text{outlet}} = 23^\circ\text{C}$, the gradient was $0.7^\circ\text{C cm}^{-1}$ along the 10 cm column. (Reproduced, in part, from the author's work with permission of the *Journal of Chromatography Science* and Preston Publications.)

inlet and higher at the outlet. The effect is a function of molecular size within the polymer class. Figure 4 is an example of both approaches.

See also: **II/Chromatography: Liquid:** Mechanisms: Reversed Phases; Mechanisms: Size Exclusion Chromatography; **III/Gradient Polymer Chromatography: Liquid Chromatography. Peptides and Proteins:** Liquid Chromatography.

Further Reading

Armstrong DW and Bohem RE (1984) *Journal of Chromatographic Science* 22: 378.
Barth HG and Janca J (1991) Polymer analysis and characterization. *Journal of Polymer Science* 1991.

Barth HG and Mays JW (1991) *Modern Methods of Polymer Characterization*. New York: Wiley and Sons.
Bohem RE and Matire DE, Armstrong DW and Bui KH (1984) *Macromolecules* 17(3): 400.
de Gennes R (1979) *Scaling Concepts in Polymer Physics*. Ithaca: Cornell University Press.
Glöckner G (1987) *Polymer Characterization by Liquid Chromatography*. Elsevier.
Lochmüller CH and Chun Jiang (1994) *Journal of Liquid Chromatography* 17: 3179–3189.
Lochmüller CH and Chun Jiang (1995) *Journal of Chromatographic Science* 561–567.
Lochmüller CH, Qicai Liu and Chun Jiang (1996) *Journal of Chromatographic Science* 34: 69–76.
Shalliker RA, Kavanagh PE, Russell IM and Hawthorne DG (1992) *Chromatographia* 33: 427–433.
Snyder LR, Stadalius MA and Quarry MA (1983) *Analytical Chemistry* 55: 1412A.

Thin-Layer (Planar) Chromatography

L. S. Litvinova, Institute of Macromolecular Compounds of Russian Academy of Sciences, Petersburg, Russia

Copyright © 2000 Academic Press

The use of thin-layer chromatography (TLC) in polymer analysis was first mentioned in 1968. Belenkii and Inagaki with their co-workers described separations according to the composition of random styrene-methyl methacrylate and styrene-methyl acrylate copolymers with molecular weights varying from 40 to 200 kDa. Since then polymer TLC has been developed intensively and other researchers have also begun to work actively in this field.

The mechanisms of polymer TLC have been investigated and the methods for the determination of molecular weight (MW) and molecular weight distribution (MWD) of homopolymers, such as polystyrene (PS), poly(ethylene oxide) (PEO) and poly(methyl methacrylate) (PMMA), have been developed. Impressive results were obtained for separations in accordance with different features of the polymer architecture. This investigation of structural heterogeneity of styrene-methyl methacrylate (S-MMA) copolymers have made it possible to separate random, block and alternating copolymers as well as two- and three-block copolymers. The stereoregular heterogeneity of PMMA and polybutadiene (PB) has also been determined. Styrene (S) and butadiene (BD) block copolymers have been studied and deuterated and hydrogenous PS separated.

In the vast majority of studies silica gel has been employed as a sorbent with the occasional use of

alumina. In 1976 Belenkii and co-workers reported that critical conditions exist on passing from size-exclusion to adsorption chromatography of polymers. The first reviews on polymer TLC appeared in 1977. In 1980 Glöckner demonstrated the importance of gradient elution for polymer separations, and in 1982 Armstrong and co-workers used reversed-phase plates to separate homopolymers according to MW. More recent reviews have been by Glöckner (1987) with the most comprehensive review presented by Gankina and Belenkii in 1991.

Here the behaviour of macromolecules and small molecules are compared and the mechanism of chromatographic processes and the analysis of different types of polymer heterogeneity considered.

Behaviour of Macromolecules under TLC Conditions

TLC is one of the most efficient methods used for the fractionation of polymers and the analysis of their heterogeneity. The chromatographic behaviour of polymers differs from that of low MW compounds in many ways that can be revealed even in the analysis of narrow-dispersity homopolymers. Unlike low MW compounds, polymers are characterized by physical heterogeneity, i.e. they are a mixture of macromolecules with different degrees of polymerization (polymer homologues). The concept of 'molecular weight' is replaced by the expression 'average MW', which is a statistical average value. In addition to physical heterogeneity characterized by molecular weight distribution (MWD), chromatographic

methods of analysis also enable the determination of chemical, functional, structural, stereoregular and topological polymer heterogeneity.

Macromolecules are characterized by low diffusion coefficients in solution and by even lower coefficients in pores. This adversely affects the kinetics of entrance and exit of macromolecules in and out of sorbent pores. Macromolecules consisting of many repeat units are, moreover, characterized by multi-centre adsorption, which makes the sorption-desorption process slower and more complex. Both these factors hinder interphase mass transfer and, hence, chromatographic zones become broader in the longitudinal direction. At the limit, tails and tracks appear on chromatograms in both adsorption and adsorptionless chromatography (Figures 1 and 2). In TLC both these factors become apparent as the mobile phase velocity is increased as a result of the increase of sorbent particle size. Hence, it must be borne in mind that in polymer analysis the eluent velocity is subject to greater limitations than in the analysis of low MW substances. To avoid the appearance of false zones and tails in polymer analysis, sorbents with a particle size of 5–8 μm must be used.

Specific properties of polymers are a consequence of the large size of their molecules. According to current concepts, a long flexible chain molecule in a dilute solution is coiled. The coil size is comparable to that of the pores. In the absence of adsorption the molecules enter the pore when the coil size is smaller than that of pores. When the coil size is too large, the molecule is excluded from the pore.

Even dilute polymer solutions are characterized by considerable viscosity, this viscosity increases with concentration and MW. The chromatographic zone forms a region with high viscosity, past which the mobile phase flows. This leads to an increase in the

size of chromatographic zones in the longitudinal direction (in the direction of mobile phase motion). Moreover, the longitudinal size of the zone increases both with concentration of the polymer in the zone and with increase in MW (Figure 2). Therefore, the shape of the polymer chromatographic zones is usually elongated in the direction of mobile phase motion, not only because of heterogeneity in MW and spreading as a result of slow interphase mass transfer, but also because of the viscous effect.

Polymers dissolve much more slowly than low MW compounds and their dissolution is preceded by swelling. Since, in TLC, dissolution precedes chromatography, the slower dissolution rate of polymers with high MW in the starting zone is manifested as tails on a plate at high eluent velocity (particle size 20 μm). Moreover, polymer solubility depends on MW, and the polymers usually become less soluble as MW increases.

The coil size (hydrodynamic volume) at a fixed MW is not constant. It depends on the thermodynamic quality of the solvent (thermodynamic quality expresses the measure of thermodynamic affinity of the solvent for the polymer) and also varies on passing from the mobile to the stationary phase.

There are several points of view about the mechanism of macromolecule adsorption. One view is that during adsorption the macromolecule diffuses from the solution into the sorbent pore, more or less retaining its globular shape. Another hypothesis states that in adsorption on the pore surface the molecule is uncoiled and lies flat on this surface. This becomes possible as a result of enthalpy gain when the chain segments interact with active centres on the sorbent surface. This gain exceeds the increase in the free energy because of entropy decrease. This process is accompanied by a considerable decrease in the

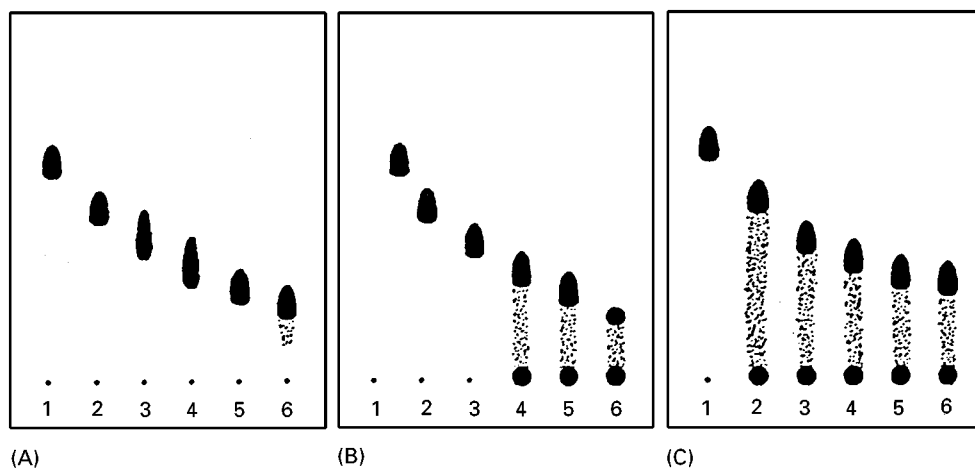


Figure 1 TLC of PS with MW (kDa) of (1) 20, (2) 111, (3) 200, (4) 498, (5) 865 and (6) 2610 on plates coated with silica gel KSKG with d_p (μm) of (A) 9.3, (B) 12.8 and (C) 19. Eluent: cyclohexane-benzene-acetone (12 : 1 : 1).

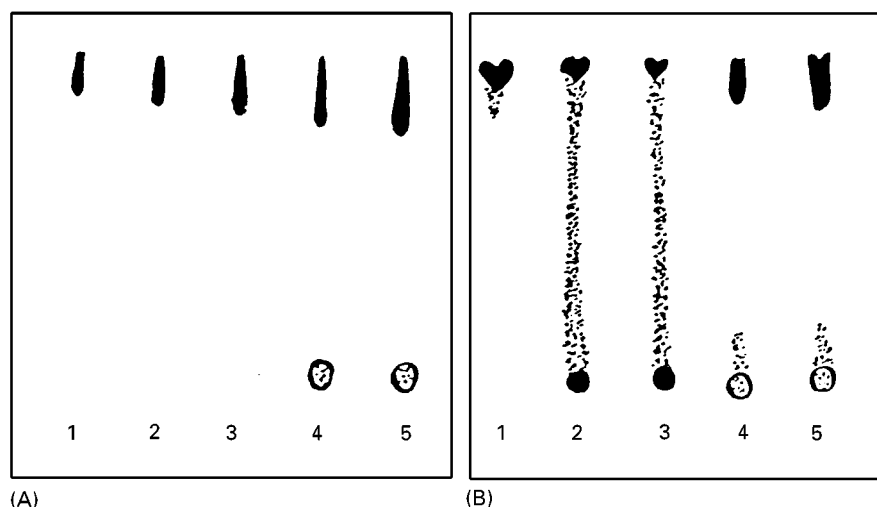


Figure 2 Adsorptionless TLC of PS with MW (kDa) of (1) 20, (2) 111, (3) 200, (4) 498 and (5) 867 on silica gel plates with sorbent particle size d_p (μm) of (A) 6.5 and (B) 19.0. Mobile phase: toluene.

volume occupied by the macromolecule, i.e. by an increase in density. As a result, the macromolecules are adsorbed on the surface of small pores inaccessible to them in a size-exclusion regime. Consequently, the change in free energy ΔG , when a macromolecule enters a pore is the sum of the change in entropy ΔS and enthalpy ΔH of the system ($\Delta G = \Delta H - T\Delta S$). The entropy change is caused by a decrease in the number of conformations of the macromolecule inside the pore over that in solution. The value of ΔH is due to the interaction of chain units with the pore walls.

It has been established experimentally, and confirmed theoretically, that in polymer chromatography the adsorption region and the molecular-sieve region are separated by a critical point at which the change in the conformational free energy of the macromolecule on passing from the mobile into the stationary phase is equal to zero. At this point the macromolecules undergo first-order phase transition. Under critical conditions homopolymers are not separated according to molecular weight; the pore structure of the sorbent and its specific area do not influence the behaviour of macromolecules. Hence, the number of separation mechanisms for polymers is greater than that for low MW compounds: besides adsorption chromatography ($-\Delta G > 0$, $k_d > 1$) at least two other chromatographic regimes are possible:

- $-\Delta G < 0$, $k_d < 1$ – size-exclusion chromatography (SEC);
- $-\Delta G = 0$, $k_d = 1$ – adsorption chromatography under the critical conditions (ACCC), where k_d is the distribution coefficient.

It is possible to pass from adsorption regime to size exclusion and vice-versa by varying temperature and

eluent composition or by modifying the adsorbent. These facts experimentally confirm a single mechanism of the liquid chromatography of polymers.

Chromatographic Regimes Applied to the TLC of Polymers

Adsorption–Exclusion Regimes

Adsorption TLC Adsorption TLC (ATLC) is used more extensively in polymer analysis. Enthalpy change is the dominant factor in the mechanism of adsorption separation of macromolecules. By selecting appropriate chromatographic conditions, adsorption activity of macromolecules can increase with increasing MW or the fraction of adsorption-active polar groups (for copolymers or homopolymers with functional groups).

ATLC is used to separate homopolymers according to their MW, functional groups and stereoregularity. It can also be used for the separation of copolymers according to composition and for the analysis of the MWD of oligomers with complete separation into oligomer homologues.

The most complex problem in ATLC is mobile phase selection. It is solved for the separation of homopolymers according to MW. In this case, the eluent for corresponding oligomer homologues is selected first (using, for example, the ‘Prizma’ model). Subsequently, a small amount of the adsorption-active component, the displacer, is added.

Exclusion TLC Entropy change is the dominant factor in the mechanisms of exclusion separation of macromolecules (ETLC). The chromatographic mo-

bility of macromolecules is determined by the ratio of the size of macromolecules to pore size and increases with the increasing hydrodynamic volume of the macromolecules. The exclusion effect is seen in TLC when two conditions are obeyed: the adsorption activity of the sorbent is suppressed and its pores are filled with the solvent. The interparticle volume should remain free. Pore filling can be accomplished either by pre-elution with subsequent removal of the solvent from the interparticle volume: the solvent passes along the plate before sample spotting; or else capillary condensation takes place during preliminary plate saturation with solvent vapour in a saturated chromatographic chamber. In the latter case the samples are spotted before saturation (or pore filling). Solvents or their mixtures in which analytes migrate along a dry sorbent layer with the front are used as eluents. The pore size distribution of the sorbent is of great importance and resolution in ETLC is lower than that in ATLC.

Adsorptionless TLC Adsorptionless (or viscometric) TLC is a type of exclusion TLC. It is carried out when the mobile phase moves along the dry sorbent layer. In this case the polymer is concentrated near the eluent front because the pores of the sorbent are accessible to it.

Moreover, a viscous polymer solution in the chromatographic zone plays the role of a kind of plug along which the solvent flows. Hence, the chromatographic zone acquires a droplike elongated shape and distinct boundaries. The zone length increases with both polymer concentration and its MW. For a fixed polymer quantity, the length of the chromatographic zone (L) is a function of intrinsic viscosity ($[\eta]$, at

infinite dilution). This dependence is obeyed for polymers of different nature, i.e. it is of universal character and can be obtained with the aid of any type of polymer standards (Figure 3). To determine $[\eta]$, it is necessary to plot the calibration dependence $L = f([\eta])$ by using four or five polymer standards in the required MW range at $C = \text{const}$. Subsequently, the length of the chromatographic zone is determined under the same conditions. Viscosity average MW value can be easily determined according to the Mark-Kuhn-Houwink equation with the aid of its coefficients available from reference books.

Adsorption TLC under critical conditions In adsorption TLC under critical conditions (ATLC), the changes in enthalpy during polymer interaction with the sorbent surface are compensated for by increasing entropy of the macromolecule when it enters the pore: $-\Delta H = T\Delta S$. ATLC under critical conditions is used to analyse heteropolymers: polymers and oligomers containing functional groups, block copolymers (AB and ABA types) and graft comb-like copolymers. Using ATLC it is possible to separate linear, cyclic and branched structures. In this regime one of the components of the copolymer undergoes chromatography under critical conditions and remains 'invisible' – having no effect on separation. Another component of the copolymer, the characteristics of which should be determined, takes part in the chromatographic process according to an adsorption or a size-exclusion mechanism. Critical conditions can be implemented either by using an adsorbent, the pores of which are filled with the eluent (analogously to ETLC) or by eluent migration along a dry sorbent layer. In the former case critical conditions are indicated by the absence of a separation according to MW for homopolymers with the same chemical composition as that component of the copolymer which should become 'invisible'. In the latter case the indication of critical conditions is the absence of separation (R_F values are equal) of homopolymers differing in MW but containing the same functional groups (Figure 4).

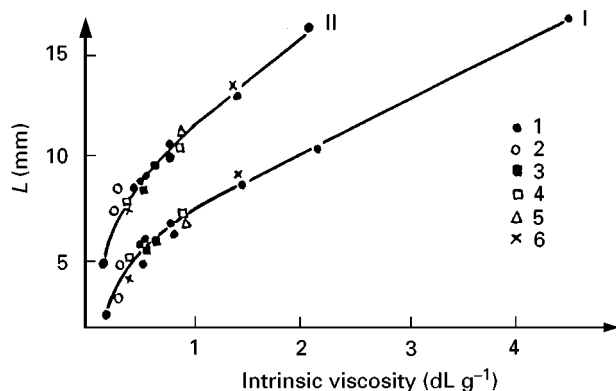


Figure 3 Dependence of zone length (L) on intrinsic viscosity for (1) PS, (2) PMMA, (3) polycarbonate, (4) polyisoprene (PI), (5) poly(vinyl chloride) and (6) poly(α -methyl styrene) with MW (kDa) of 20.8, 111, 200, 498, 867, and 2610 (1); 60.6 and 75 (2); 36.4 and 50.2 (3); 32.5 and 109 (4); 75 (5); and 97 and 610 (6) at a fixed polymer quantity (μg) of (I) 4 and (II) 10. Binder: gypsum; layer thickness, 500 μm .

Precipitation–Extraction Regimes

Precipitation TLC Precipitation TLC (PTLC) was first suggested and its mechanism investigated by Kamiyama and Inagaki in 1971. The classical examples are the separation of PMMA according to MW using a chloroform–methanol (29 : 71) mixture as the mobile phase.

In PTLC mixtures of polymer, solvent and adsorption-active precipitant (a thermodynamically poor solvent) are used as the mobile phase. Separation

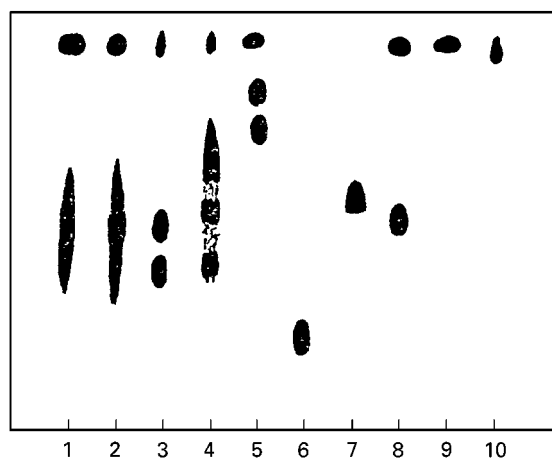


Figure 4 ATLC of reaction mixtures, obtained by the reaction of PSLi with (1–4) methyl acetate, and (5) methyl benzoate; of tertiary alcohols (6) $(C_8H_{17})_2C(OH)CH_3$ and (7) $(C_8H_{17})_2C(OH)C_6H_5$, of (8) polymer ketone $PS-CH_2-C(C_6H_5)_2-COCH_3$ and its PS precursor with MW 0.4 kDa and PS standards with MW (kDa): (9) 0.4 and (10) 40. Reaction mixtures (1–5) contain: PS precursors with MW (kDa): (1, 5) 0.4, (2) 0.6, (3) 6.4 and (4) 13.5, polymer ketone $PS-CO-R$ with the same MW as that of PS precursors, and tertiary polymer alcohol $(PS)_2C(OH)-R$ with double MW, where R is $-CH_3$ or $-C_6H_5$. Conditions are close to the critical point for PS: adsorbent is silica gel KSKG; mobile phase is toluene- CCl_4 (1 : 4) mixture.

occurs as a result of changes in the dissolution properties of the mobile phase along the chromatographic plate, for instance, as a result of partial evaporation of mobile phase components demixing during chromatography. The dissolution properties of the mobile phase can also be changed by delivering it with a changing composition to the plate. The initial mobile phase should contain the adsorption-active component at a concentration completely preventing polymer adsorption.

During PTLC when the individual polymer species with different MW pass along the plate they undergo a continuous series of precipitations and extractions. The elementary PTLC process is the separation of a polymer solution into the dilute phase, which is transported with the solvent flow, and the concentrated gel phase which is precipitated on the surface of sorbent particles.

PTLC is used to separate homopolymers and random copolymers by MW and to separate a block copolymer from the corresponding homopolymers. The analysis of oligomers with the aid of PTLC is not effective. The working range of MW exceeds 10 kDa.

Extraction TLC The action of extraction TLC is opposite to that of precipitation TLC. Extraction TLC is based on selective dissolution and desorption of the polymer in the starting zone region. Desorbed

polymer fractions are displaced to the eluent front. Eluent migration length is not significant. Polymer zones move along the plate in size-exclusion mode. Since the eluent moves along a dry sorbent layer, separation according to MW does not take place. In this method a single component mobile phase or binary solvent mixtures are used most often; gradient column chromatography is the closest analogue. Under conditions of extraction TLC the gradient is replaced by stepwise elution.

Using extraction TLC it is possible to separate compounds differing essentially in solubility or adsorption activity: isotactic and atactic polystyrene, isotactic and atactic PMMA, poly-1,4 trans- and 1,2-butadiene and to separate the S-MMA block copolymer from PS and PMMA.

Some Problems in Polymer Analysis

Determination of MW and MWD TLC, like other chromatographic methods, is not an absolute method. Therefore, in order to determine physical or chemical heterogeneity, polymer standards with known characteristics are necessary. Belenkii and Gankina state that in order to determine the MWD, it is necessary first to establish the dependence of R_F on MW with the aid of narrow-disperse standards, secondly to obtain a densitogram of the chromatographic zone, thirdly to establish the dependence of the recorded signal (I) on polymer mass (P) for different R_F s and to determine $(dP/dI)_{R_F}$, fourthly to determine the distribution of polymer mass in the zone $P(R_F)$, and finally to calculate MWD according to the following equation:

$$P(M) = P(R_F) \left(\frac{dM}{dR_F} \right)_{R_F}$$

If the distribution, $P(M)$ is known, it is also possible to obtain the expressions for weight-average MW

$$\bar{M}_w = \frac{\int_0^\infty M^2 P(M) dM}{\int_0^\infty M P(M) dM}$$

number average MW:

$$\bar{M}_n = \frac{\int_0^\infty M P(M) dM}{\int_0^\infty P(M) dM}$$

and heterogeneity:

$$H = \frac{\bar{M}_w}{\bar{M}_n}$$

An important point increasing the precision of MWD determination is the correction for instrumental broadening in SEC. This is attained with the aid of

two-dimensional chromatography. In the first direction the chromatographic zone is separated according to MW and also undergoes chromatographic spreading. In the second direction the separation according to MW may be neglected. The dispersion of chromatographic spreading is equal to the difference between zone dispersion after the second and the first elution in the direction of the second elution. For correction, the calculated dispersion of chromatographic spreading is subtracted from the total dispersion of the polymer zone after the first elution in the direction of mobile phase migration.

Analysis of Copolymers

As polymer molecules very often contain functional groups or consist of chains differing in chemical nature, polymers are characterized by a mixed separation mechanism. The analysis of copolymers exhibiting chemical and structural heterogeneity requires more complex elution procedures: for example, stepwise, two-dimensional, gradient and continuous TLC. In most cases TLC is combined with column chromatography or pyrolysis-gas chromatography (GC), as well as with spectroscopic methods.

In the analysis of block and graft copolymers or branched homopolymers, the following problems should be solved:

- the diagnosis of a copolymer or a branched homopolymer;
- the determination of linear homopolymer present in the copolymer; and
- the investigation of MW and MWD of copolymers.

The first two problems can be solved by comparing the chromatographic mobility of the polymer being analysed with that of the corresponding linear homopolymers in appropriate solvents using ATLC or PTLC. An indispensable condition of separation is the difference in adsorption activity or solubility of A and B homopolymers. Difficulties can appear if their properties are similar and also when block copolymer complexes with one of the homopolymers are formed.

Additional proofs of copolymer presence can be obtained by double detection of the chromatographic spots, for example, by using reagents specifically staining homopolymers of different types and by spectroscopic methods *in situ*, or after elution of the polymer zone from the plate.

To evaluate the MW of block-copolymer components, one can use ATLC under critical conditions.

Oligomers

Oligomers are built from the same monomer units as polymers, but their chain is much shorter

(MW < 10 kDa). Polymers in dilute solutions are characterized by the following types of interactions: solvent-solvent, solvent-polymer segment, polymer segment-segment, solvent-surface, and polymer segment-surface, whereas for oligomer segment-segment interaction and local entropy effects are small. Oligomers without end groups are readily separated into oligomer homologues on polar adsorbents by adsorption chromatography. It is also easy to separate according to MW, oligomers with end groups for which the energies of interaction with adsorbent for the central (ϵ_c) and end (ϵ_e) units are similar. If the energy of interaction with silica gel is much lower for the central chain unit than for the end groups ($\epsilon_c < \epsilon_e$), separation according to the types of functionality will take place. Therefore, to separate according to MW it is necessary to use silica gel modified either chemically (for example, RP₁₈) or dynamically (for example, the separation of PEO oligomers in a pyridine-water mixture, 0.1 : 10).

Two-component mobile phases are known to separate some oligomers according to MW on silica gel: PS, PI, poly(propylene glycol), PEO and its various derivatives, oligoacrylates, etc. If the MW of one of the members of the homologous series on the chromatogram is known, corresponding standards are not necessary to calculate MWD.

For oligomers used in the production of synthetic polymers, the distribution according to the types of functionality (FTD) is very important. It characterizes the relative content of macromolecules with different functionalities in the oligomer. The functionality type of chemical compounds is determined by the number and nature of functional group. For macromolecular compounds the concept 'functionality' just as the concept 'molecular weight' has a statistical significance. In order to characterize distribution width according to functionality types the values of number-average (\bar{f}_n) and weight-average (\bar{f}_w) functionality are used:

$$\bar{f}_n = \sum n_i f_i / \sum n_i$$

$$\bar{f}_w = \sum n_i f_i^2 / \sum n_i f_i$$

where $n_i = p_i / MW_i$ (is the number of moles of macromolecules i with molecular weight MW_i , functionality f_i and weight p_i).

Oligomers are separated according to the number and nature of functional groups by adsorption chromatography under the critical conditions or under conditions close to critical. An example of this separation is shown in Figure 4. A scanning densitometer or a videodensitometer can be used for quantitative FTD determination.

Future Developments

TLC of polymers is more complex than that of small molecules for the following reasons: the size of sorbent pores and that of macromolecules are similar and co-operative effects exist which are characteristic of macromolecules as multcentred formations. For the same reasons, TLC of polymers is a very useful technique to investigate chromatographic mechanisms. The open sorbent layer in TLC makes it much easier to detect and investigate chromatographic artefacts than by column chromatography. The versatility of this method, the absence of restrictions with respect to solvents, and high sensitivity to functional groups (ATLC) make it possible to analyse effectively the compositional and structural heterogeneity of polymers.

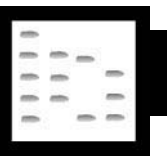
Further development of this method involves investigations of mechanisms of adsorption and chromatography of macromolecules, more extensive use of chemically modified sorbents, more extensive application of quantitative methods of analysis and such promising methods as overpressured-layer chromatography (OPLC). The investigation of macromolecules with complex architecture and of reaction mixtures is not possible without perfecting complex methods of investigation. The combination of ATLC and column chromatography in different regimes and the combination of TLC with spectroscopic methods, especially with MALDI-TOF-MS are very promising.

See also: **II/Chromatography:** Size Exclusion Chromatography of Polymers. **III/Polymers:** Field Flow Fractionation; Supercritical Fluid Extraction.

Further Reading

- Alger MSM (1989) *Polymer Science Dictionary*. London: Elsevier Applied Science.
- Armstrong DW and Bui KH (1982) Nonaqueous reversed-phase liquid chromatographic fractionation of polystyrene. *Analytical Chemistry* 54: 706–708.
- Bui KH and Armstrong DW (1984) Determination of polymer molecular weight and molecular weight distribution by reverse phase thin layer chromatography. *Journal of Liquid Chromatography* 7: 45–58.
- Belenkii BG and Gankina ES (1977) Thin-layer chromatography of polymers. *Journal of Chromatography (Chromatographic Review)* 141: 13–90.
- Belenkii BG and Vilenchik LZ (1983) Thin-layer chromatography of polymers. *Modern Liquid Chromatography of Macromolecules*, pp. 361–411. Amsterdam: Elsevier Science.
- Gankina ES and Belenkii BG (1991) Polymers and oligomers. In: Sherma J and Fried B (eds) *Handbook of Thin-layer Chromatography*. Chromatographic Science Series, vol. 55, 807–862. New York: Marcel Dekker.
- Glöckner G (1987) Thin layer chromatography. *Polymer Characterization by Liquid Chromatography*. Journal of Chromatography Library, vol. 34, pp. 476–507. Amsterdam: Elsevier Science.
- Inagaki H (1977) Thin layer chromatography. In: Tung LH (ed.) *Fractionation of Synthetic Polymers*, pp. 23–29. New York: Marcel Dekker.
- Litvinova LS (1998) Practical aspects of adsorption chromatography of synthetic polymers. *Journal of Planar Chromatography – Modern TLC* 11: 114–118.
- Litvinova LS, Belenkii BG and Gankina ES (1991) Quantitative analysis of polymers on the basis of the lengths of chromatographic zones in adsorptionless TLC. *Journal of Planar Chromatography – Modern TLC* 4: 304–308.

TERPENOIDS: LIQUID CHROMATOGRAPHY



P. K. Inamdar,* Hoechst Marion Roussel India Limited Research Centre, Mumbai 400080, India
Sugata Chatterjee, Merck Development Centre Limited, MIDC, Talaja, India

Copyright © 2000 Academic Press

Introduction

Essential oils are secondary metabolites of plant origin and are complex mixtures of fragrance and

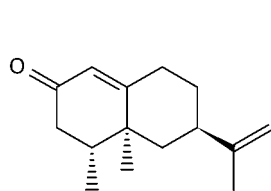
flavour substances. They originate in roughly one-third of known plant families and are isolated from plant bodies by extraction or distillation procedures. The composition of the constituents are dependent on the isolation method used, the part of the plant body from which they are isolated and also on their thermal, pH and intrinsic chemical stability. Most essential oils are currently separated from nonvolatile materials by steam distillation. As for other classes of natural products, a fully satisfactory definition of essential oils is difficult to put into words. Although they are volatile plant materials, they do not leave a grease stain on paper.

* Retired. Present address: Camlin Limited, Pharmaceutical Division, Camlin House, J. B. Nagar, Andheri (E), Mumbai 400 059, India.

Terpenoids in Essential Oils

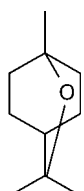
The majority of the essential oils of commercial interest are mixtures of mono- and sesquiterpenoids, containing only minor amounts of compounds belonging to other classes. The second largest group of essential oils consists of aromatic compounds including phenolic ones. The terpenoid components occur admixed with the corresponding terpene hydrocarbons, which generally contribute less to the aroma component. Among the popular essential oils are bergamot, grapefruit, lemon, lime, mandarin, orange, petitgrain and neroli oils belonging to the citrus class of oils. These oils contain varying proportions of different types of monoterpenoids, e.g. linalyl acetate, linalool, citrals (geranial and neral), corresponding acetates, and nootkatone. Lime oil, one of the most important distilled citrus oils contains 1,4- and 1,8-cineole, terpinen-4-ol and α -terpineol, along with aromatic p-cymene, which is probably derived from limonene by oxidation. Another important class of essential oils is cedar oils, which are characterized by the sesquiterpenoids cedrol, cedryl acetate, cedrene, thujone, thujopsene, *trans*- α -atlantone and the monoterpenoids pinenes and delta-3-carene along with 2-*trans*-4-*cis*-decadienyl isovalerate. A major class of essential oils derived from the plant class *Eucalyptus* has about 500 species. Monoterpenoids such as citronellal, citronellol, isopulegol, piperitone and β -phellandrene are the important constituents apart from geraniol and nerol. See [I]–[VII] for structures of some of these components of essential oils.

Other important essential oils are grass oils, e.g. lemon grass oil containing citral, geraniol, etc. Vetiver oil has high sesquiterpene content of α and β vetivone.



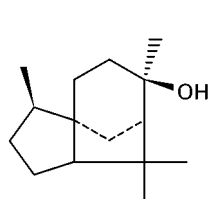
(+)-nootkatone

Structure [I]



1,8-cineole

Structure [II]



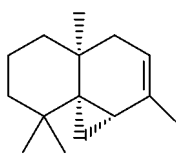
(+)-cedrol

Structure [III]



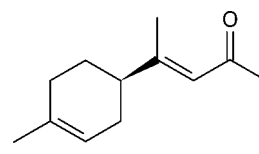
(-)-thujone

Structure [IV]



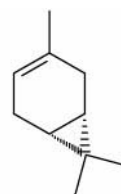
thujopsene

Structure [V]



trans- α -atlantone

Structure [VI]



Δ -carene

Structure [VII]

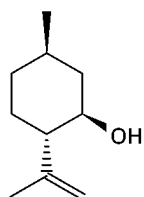
Lavandula oils contain linalool and linalyl acetate in the lavender oil variety whereas lavandin oil contains camphor and 1,8-cineole. Essential oils of the mentha variety are characterized by the presence of menthol, menthone and menthyl acetate. Spearmint oil of the mentha variety contains carvone, dihydrocarveol, menthone and limonene. Pulegone is also found in the mentha variety of oils. Balsam and wood terpentine oils contain bornyl acetate along with pinenes, limonene, p-menthadienes, whereas the Sage oils class of essential oils contain sclareol and α - and β -thujones.

There are other varieties of essential oil containing terpenoids, e.g. ambrette seed oil; amyris oil containing sesquiterpenoids, e.g. elemol, eudesmols and α -agarofurans. Buchu leaf oils contain menthone, isomenthone, pulgione and bifunctional diosphenols also known as 'buchu camphors' and some sulfur-containing terpenoids, e.g. p-menthane-8-thiol-3-one and its thioacetate. The plethora of essential oils containing mono- and sesquiterpenoids occurring in nature is extremely large and a description of the principal constituents in them is beyond the scope of this chapter. Among the oils having importance in the perfumery industry, rose oil contains damascenone, *cis*-rose oxide and verbenone in various species; sandalwood oil contains the santalols; rosemary oil contains verbenone; patchouli oil has patchoulol and norpatchoulol; orris root oil contains neoiso- α -irone; jasmin oil contains *cis*-jasmone and methyl jasmonate; guaiac wood oil contains guaiol; and costus root oil contains costol and dehydrocostuslactone.

Among the essential oils used as food flavouring, ginger oil contains the zingiberenes, *ar*-curcumen and β -sesquiphellandrol, copaiba (balsam) oil con-

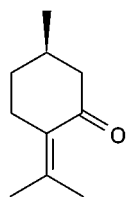
tains caryophyllene, celery seed oil contains β -selinene, cardamom oil has 1,8-cineole and α -terpinyl acetate. Some tea aroma components are presumed to be derived partly from the ionone series of compounds (probably derived from carotene besides other terpenoids such as methyl jasmonates, which give the sweet taste to Oolong tea leaves.

Essential oils also have therapeutic significance, e.g. in antiseptics and antibacterials, analgesics (clove, peppermint, lavender, birch oils), anti-fungals (tea tree, thyme), anti-inflammatories (German chamomile, lavender), anti-toxics (chamomile oil), anti-virals (*Melissa officinalis*, *Eucalyptus smithii*, *Ravensara aromatica*, *Niaouli*), diuretics (juniper oil), balancers, deodorants, digestives (anise, caraway, peppermint, lavender), spasmolytics (basil, majoram, German chamomile, cypress, laurel), mucolytics and expectorants (*Eucalyptus globulus*, pine, anise, thyme). They are also used as insecticides and insect repellents (citronella, cinnamon, geranium). See structures [VIII]–[XXIV] for some components of therapeutic essential oils.



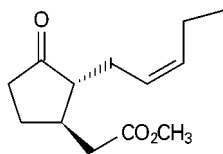
(-)-isopulegol

Structure [VIII]



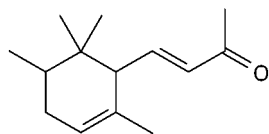
(+)-pulegone

Structure [IX]



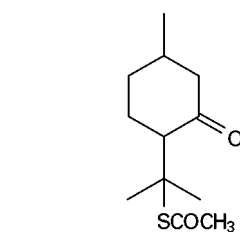
methyl jasmonate

Structure [X]



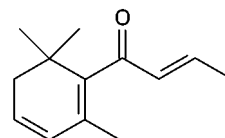
neoiso- α -irone

Structure [XI]



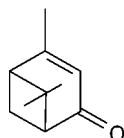
p-menthene-3-one-8-thiolacetate

Structure [XIV]



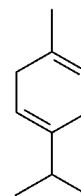
β -damascenone

Structure [XV]



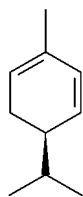
verbenone

Structure [XVI]



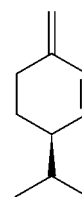
1,4-*p*-menthadiene

Structure [XVII]



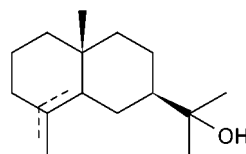
1,5-*p*-menthadiene

Structure [XVIII]



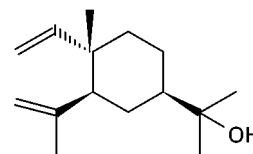
1(7),2-*p*-menthadiene

Structure [XIX]



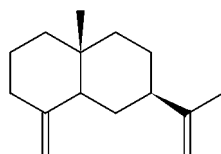
(+)- β - or (+)- γ -eudesmol

Structure [XX]



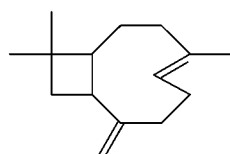
(-)-elemol

Structure [XXI]



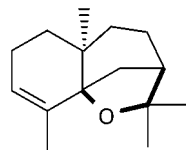
(+)- β -selinene

Structure [XII]



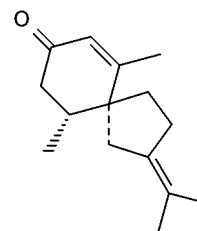
Caryophyllene

Structure [XIII]



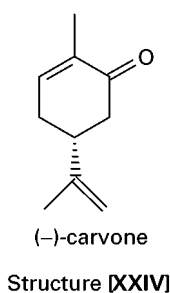
(+)- α -agarofuran

Structure [XXII]



β -vetivone

Structure [XXIII]



Analysis of Essential Oils

The economic importance resulting from their fragrance and aroma which is used extensively in the perfume and food flavour industries as well as the therapeutic applications requires that reliable analytical methods are available for qualitative and quantitative analysis of the individual ingredients as well as methods for their preparative separation from the complex mixtures they exist in. In fact, most varieties of essential oils are so complicated that resolution and analysis of any single component of interest is a formidable task. Although liquid and gas chromatographic separations on analytical and preparative scales have been used, such techniques are plagued with the problems of weak UV absorbance, volatility and thermal instability of many of the ingredients. Most of the essential oils contain only very minor amounts of the active principles and large amounts of undesired components that obscure the separation and reduce the sensitivity. The important developments that have taken place in liquid chromatographic analysis of essential oils over the years are

discussed later. Before attempting any liquid chromatography (LC) or gas chromatography (GC) analysis, the terpene hydrocarbons are usually removed by distillation because of their considerably lower odour and aroma values. Furthermore, these olefins polymerize and are poorly soluble in lotions.

Thin-Layer Chromatography

Thin-layer chromatography (TLC) is an inexpensive technique and was the earliest LC method used to provide information on the complexity of essential oils. TLC studies of thymus essential oil on SiO_2 plates using various developing solvent systems and detection by spray reagents, e.g. H_2SO_4 charring, could identify thymol and carvacrol as the essential components by comparison with standard substances. This TLC method has been further employed to quantify these components by scanning densitometry. Additionally, quantification of geraniol, citral, terpinen-4-ol, cineole and gamma-terpinol have been carried out on thymus essential oil. Coscia described various reagents used to quantify mono-, sesqui- and other terpenoids (also polyphenols) such as carotenoids, tocopherols, retinoids, etc. in analysis of essential oils by TLC.

HPLC Analysis of Essential Oils

Almost 90% of the components present in essential oils that are responsible for fragrance and flavour are in the boiling range of 150–300°C and possess ideal vapour pressure to be successfully analysed by gas chromatography. The molecular weights of these

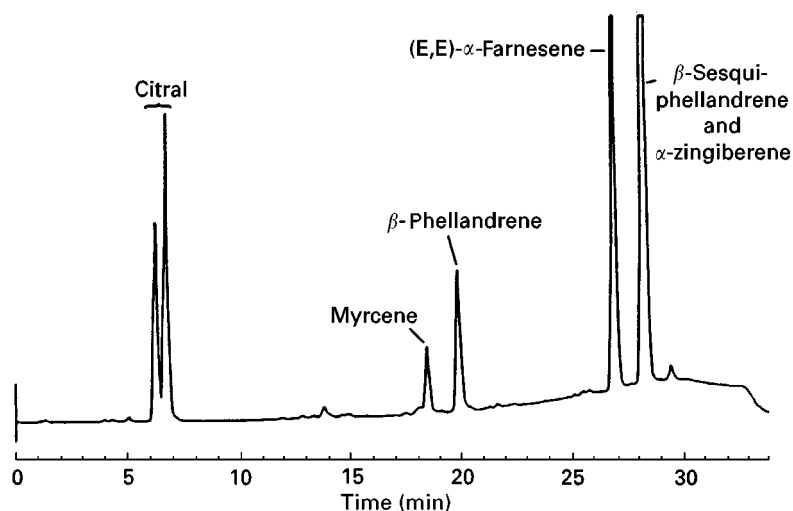


Figure 1 Typical analytical HPLC separation of citrus essential oil mixture. Analytical HPLC of a citral-type ginger oil. Experimental conditions: 15 × 0.46 cm. Column filled with Microsorb 5 μm C-18 silica gel, solvent MeCN; H_2O = 6 : 1 to MeCN; H_2O = 95 : 5 in 30 min, 1 mL min⁻¹, detection 236 nm. (Courtesy Springer-Verlag GmbH & Co.)

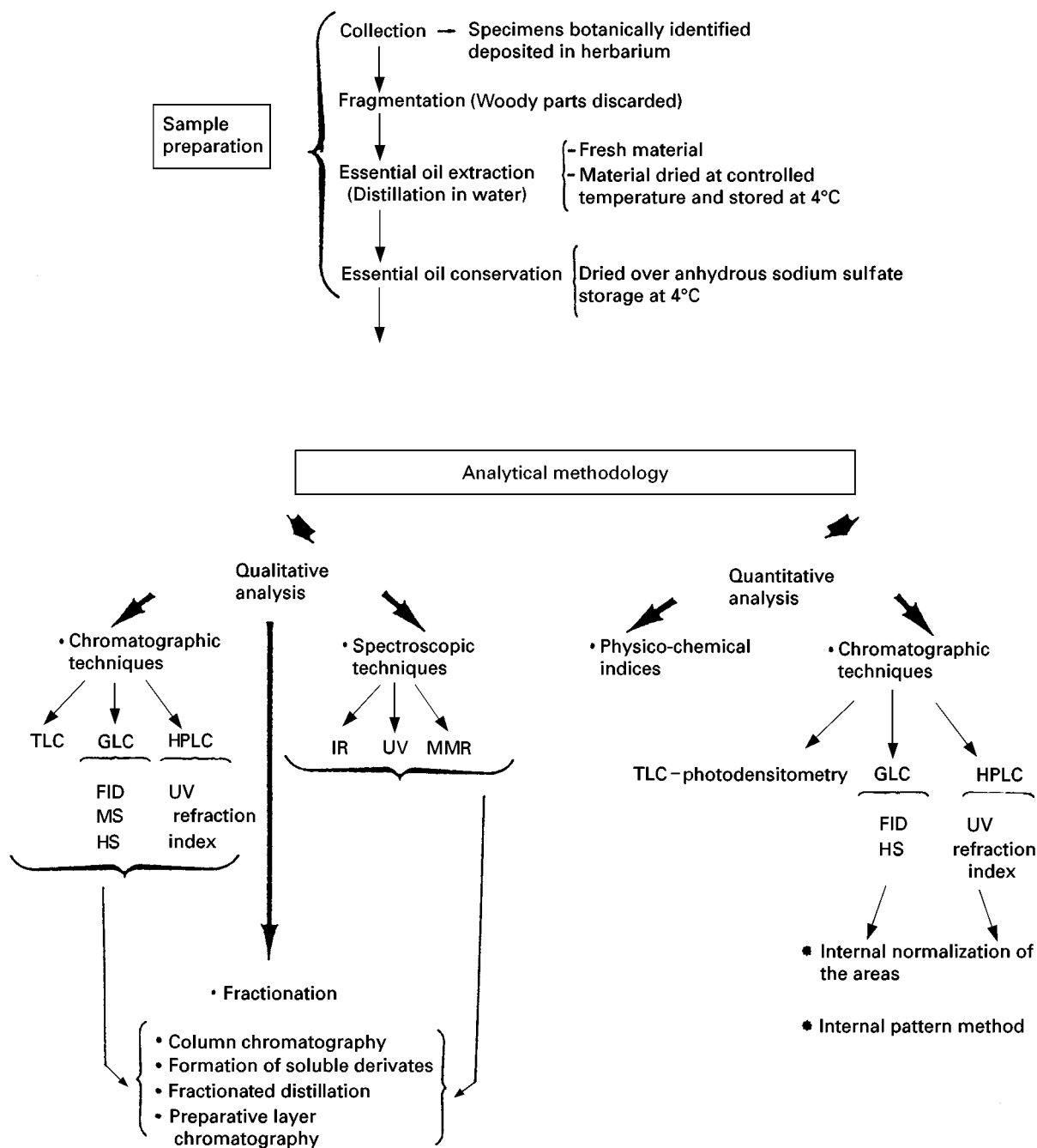


Figure 2 General protocol recommended for the identification and quantification of essential oil components. (Courtesy, Springer-Verlag GmbH and Co.)

compounds are mainly in the range up to 300 amu, thus making GC-MS an ideal technique for analysis and identification. However HPLC is being used increasingly to analyse essential oils (Figures 1–4) and in fact HPLC shows certain significant advantages over currently used open tubular column GC methods, such as minimal exposure to air, the avoidance of high temperature degradation, ease of separ-

ation of nonvolatile components and higher sample recovery. Furthermore, although as mentioned earlier, a majority of the terpenoids are weakly absorbing in the ultraviolet (UV) region due to the lack of a chromophore, the availability of highly sensitive online ultraviolet-visible (UV/Vis) detectors has expanded the utility of high performance liquid chromatography (HPLC) applications in essential oil

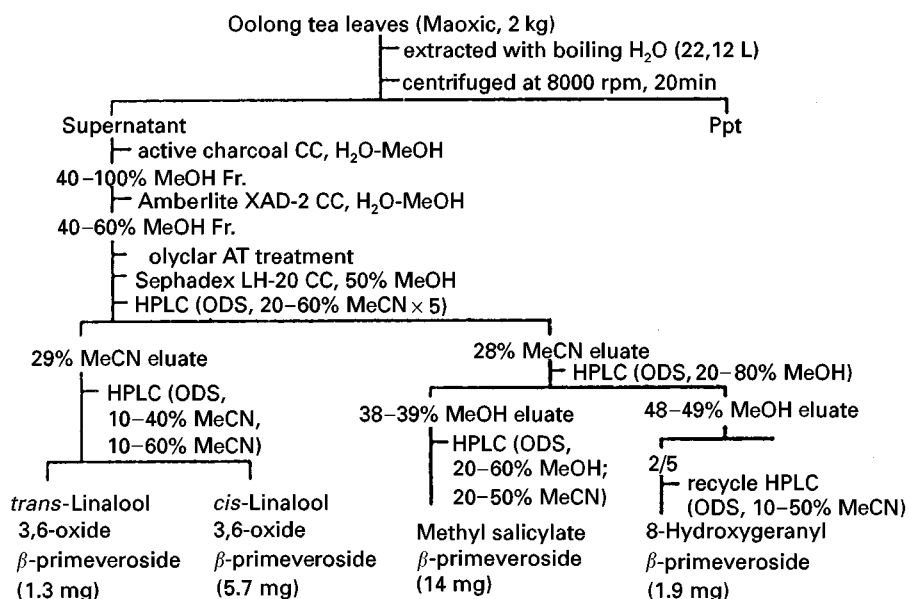


Figure 3 Isolation procedure of aroma constituents from Oolong tea.

analysis. The problem of UV detection on normal phase columns using eluents that are strongly UV absorbing has been largely alleviated by using reversed-phase columns which permit the use of solvents

like methanol and acetonitrile, and detection by end absorption, i.e. between 200–220 nm. Although differential refractive index (RI) and polarimetric detectors have been used, they suffer from poor sensitivity. Polarimetric detection is however claimed to have better selectivity. Pulsed electrochemical detectors have been used for flavour-active alcohols by Le Fur. Primary terpenols are detectable at ppb level with others at ppm level. Primary and secondary alcohols can be quantified with good repeatability and sensitivity.

Since essential oils are highly complex mixtures; HPLC is of great assistance for both the separation of the components into classes and of such a class into its components. Such pre-fractionation is followed by subsequent high-resolution GC (HRGC) analysis of the fractions. Multiple LC separations have been frequently carried out in tandem in order to obtain adequate pre-fractionation before subjecting each fraction to GC analysis. Thus the labile sesquiterpene germacrene B has been isolated by Clark from lime peel oil as an important flavour impact component. Various types of HPLC columns have been used, e.g. normal phase, diol-bonded silica and reversed phase, e.g. C2, C4, C8 and C18. In one example strawberry jam was previously gel filtered through Sephadex LH-20 to remove fatty acids. The resulting material was subjected to gradient HPLC using a diol-bonded silica column and gradient elution using pentane-diethyl ether resulting in two major fractions, the first containing hydrocarbons, esters, aldehydes and ketones and the second fraction consisting of polar

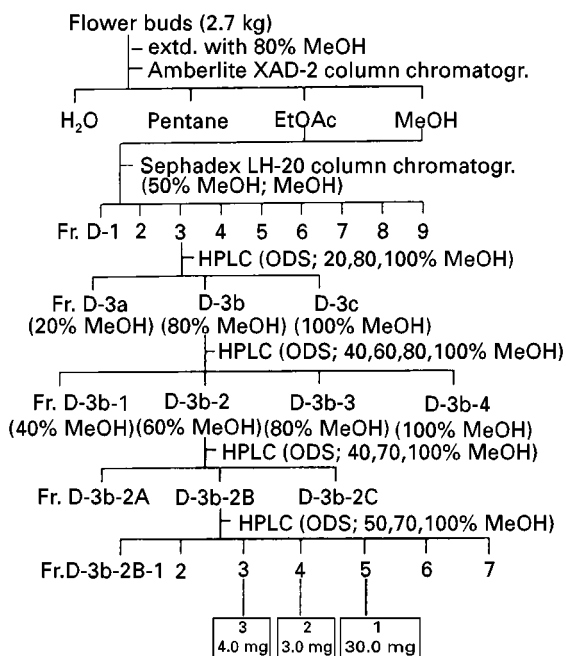


Figure 4 Isolation procedure of linalyl β-vicianoside, bornyl β-primeveroside, and 2'-phenylephenylthyl β-primeveroside from *Gardenia jasminoides*. (Figures 3 and 4 – Reproduced from *The International Congress of Flavours, Fragrances and Essential Oils*.)

compounds such as alcohols, hydroxy esters and lactones. GC-MS analysis of these fractions identified 150 compounds as compared to only 60 in the absence of HPLC pre-fractionation. Computer-controlled online HPLC-HRGC has thus emerged as a powerful method for essential oil analysis. Munari used a fully automated HPLC-GC instrument for HPLC pre-separation of citrus oil into four major fractions – hydrocarbons, aldehydes, esters and alcohols – using gradient elution, and the fractions were automatically transferred to the GC. HPLC pre-separation with multiple GC transfer from a single HPLC injection combined with other identification techniques, e.g. mass spectrometry (MS), Fourier transform infrared (FT-IR) spectrometry gives additional advantage of online identification. The most widely used among such techniques is high performance liquid chromatography-gas chromatography-mass spectrometry (HPLC-GC-MS). This technique has been used in a fully automated form by Mondello for the analysis of several essential oils: bergmot, lemon, clementine, sweet orange, bitter orange, grapefruit and Mexican lime. The information was more accurate than that obtained by only GC-MS analysis of the essential oil. Using chiral GC columns Giovanni determined the enantiomeric distribution of the monoterpene alcohols in citrus essential oils. In the same vein it can be envisaged that such multidimensional techniques as microbore HPLC-electrospray ionization/MS-MS holds great potential in essential oil analysis since in addition to improved column efficiency, the second mass analyser permits mixture analysis by interpretation of the collision activated dissociation (CAD) spectrum obtained.

Separation of Enantiomeric Components

The terpenoids present in essential oils are chiral molecules occurring in enantiomerically pure form. HPLC analysis using chiral columns and co-elution with authentic optically pure compounds furnish information on the chirality of the constituents. HPLC separation of enantiomeric mixture of α -pinene, β -pinene, camphene and limonene were carried out by Moeder on a C4 column with UV detection at 210 nm and a mobile phase containing 5–20 mM of α -cyclodextrin, or 0.01–0.8 mM of β -cyclodextrin (90:10 mixture of MeOH and 0.1% phosphoric acid). Equations were derived for the apparent formation constants of the diastereoisomeric complexes of the solute with cyclodextrin and their stoichiometry estimated. It was observed that efficient separation was achieved with only α -cyclodextrin for these bicyclic terpenes. Chiral discrimination of enantiomeric

derivatives of α -pinene has been achieved using amylose *tris*(3,5-dimethylphenyl)carbamate as the chromatographic stationary phase. The major contributing factor to achieve such separation is H-bonding of the analytes with the carbamated amylose.

Supercritical Fluid Chromatography

Supercritical fluid chromatography (SFC) has also been used for the separation of terpenoid compo-

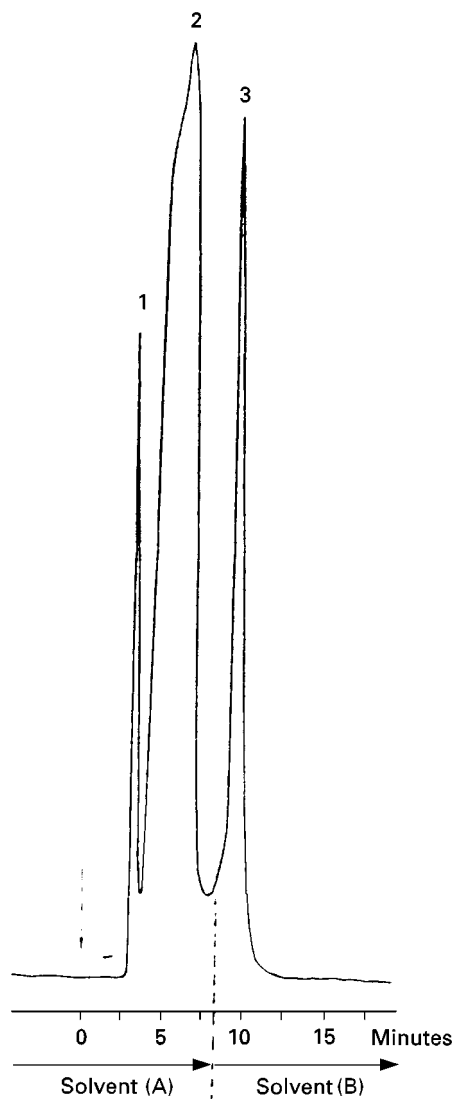


Figure 5 Enrichment of essential oil fractions by semi-preparative HPLC. HPLC fractionation of an essential oil at a flow rate of 8 mL min^{-1} . Conditions: column, $24 \text{ cm} \times 10 \text{ mm i.d.}$ LiChroprep RP 18 ($40 \mu\text{m}$), mobile phases. (A) methanol–water 82.5 : 17.5 (v/v), (B) methanol, flow rate 8 mL min^{-1} , detector, UV 220 nm. 1 = oxygen-containing compounds, 2 = monoterpene hydrocarbons, 3 = sesquiterpene hydrocarbons. (Courtesy Kluwer Academic Publishers, The Netherlands.)

nents. The advantage of SFC lies in the fact that it has features of both GC and LC. Both GC and LC columns can be used and various detectors like flame ionization detector (FID), UV and MS can be used making it a nearly universal technique. To illustrate the application of SFC 2-Z- and 3-E-nerolidols, R/S-geranyliol, α -bisabolol and 2E,6E-fernesol were separated in 10 min on a column packed with 5 μ m Zorbax Z215 silica equipped with a guard column of the same material operated at 40°C with CO₂ containing 0.5% MeOH as the mobile phase and monitoring the components at 220 nm. In another example eight terpene components of cinnamon oil were separated on a delta-bond SiO₂ column at 125°C using a gradient elution of 100% CO₂ to 7% EtOH in CO₂. The detection limits were typically 1.0 μ g mL⁻¹ for the terpenes with a linear response over four decades.

Preparative Liquid Chromatography

Isolation of individual essential oils is a formidable task because of their complexity. Open column chromatography, droplet countercurrent chromatography (DCCC), rotation locular countercurrent chromatography (RLCCC) and gel permeation chromatography are some of the techniques which

have found considerable use. However each of these techniques has its weaknesses. Multiple separations on either normal- or reversed-phase packing materials (40–70 μ M) using low to medium pressure (10–40 bar) accomplishes substantial enrichment of the components in terms of their functional group type and/or polarity. Using step or gradient elution techniques the complex mixtures of terpene hydrocarbons, carbonyl compounds, alcohols, esters, etc. can be cut into fractions. Online UV detection and automatic fraction cutting considerably enhances the utility of such medium pressure liquid chromatography–low pressure liquid chromatography (MPLC–LPLC) techniques. The fractions can then be subjected to preparative HPLC using columns of inner diameter >10 mm to furnish the semipure components. Even preparative HPLC may have to be repeated several times before adequate resolution is achieved. The pooled fractions are then subjected to semi-preparative HPLC (column i.d. <10 mm) followed by peak collection from analytical columns to yield the pure terpenoids. The level of purity desired depends on the use for which the component materials are required. Some representative HPLC traces for the separation of essential oil components are shown in Figures 5–7. In several cases where the terpenoids exist as glycosides or some such deriva-

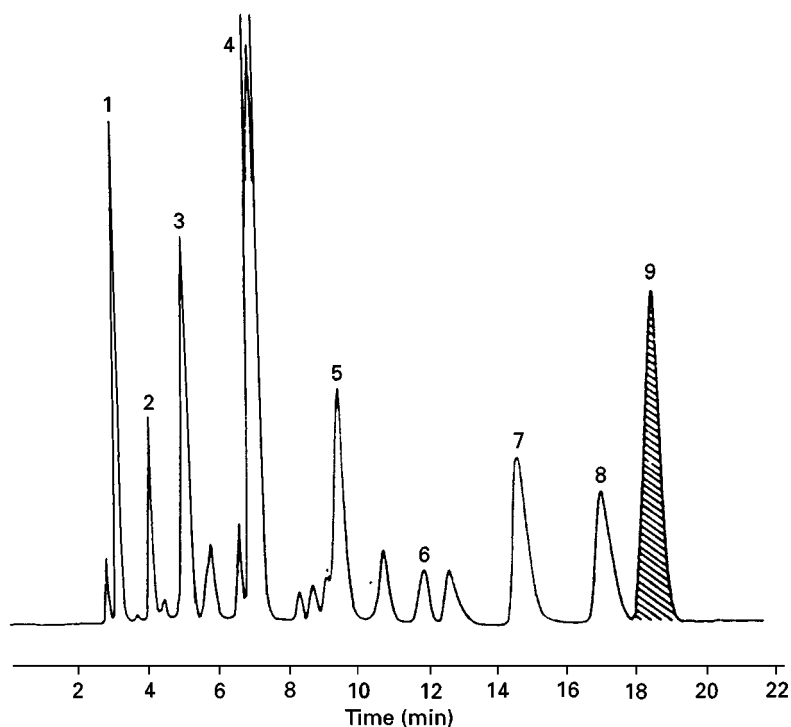


Figure 6 HPLC separation of sesquiterpene hydrocarbons. Conditions: 300 \times 4 mm i.d. Lichroprep Si 60 (7 μ m) column with 48% water. Eluent: n-pentane. 1 = α -copaene, 2 = δ -elemene, 3 = β -elemene. 4 = β -caryophyllene, 5 = α -bergamotene. 6 = β -bisabolene, 7 = α -humulene. 8 = δ -cadinene, 9 = standard. (Courtesy Kluwer Academic Publishers, The Netherlands.)

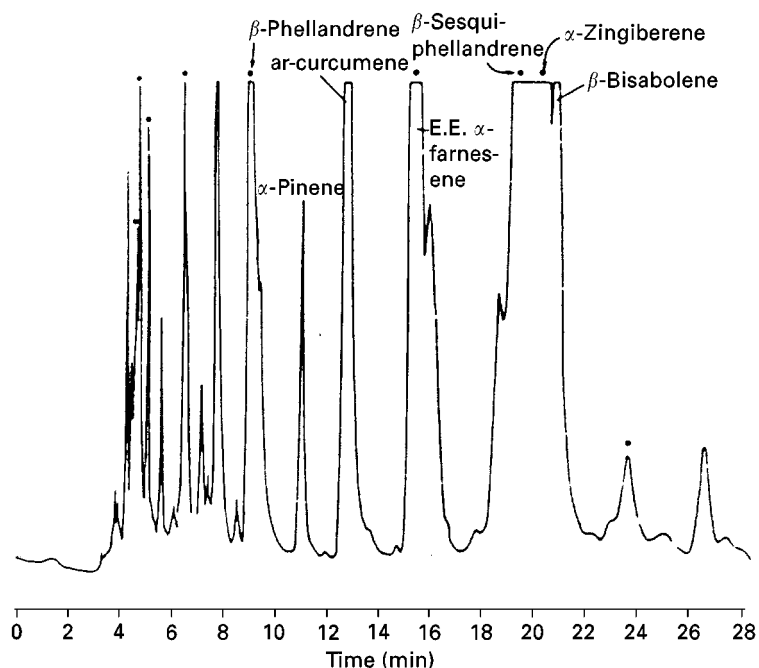


Figure 7 Semi-preparative HPLC of ginger oil. Experimental conditions: load 4 mL oil dissolved in 4 μ L EtOH, column 25 \times 1 cm. Filled with Microsorb 5 u C-18 silica gel, solvent MeCN-H₂O = 9 : 1. 4 mL min⁻¹, detection UV 215 nm. (Courtesy Springer-Verlag, GmbH and Co.) • indicates UV absorption at 245 nm.

tives, pre-purification using other forms of liquid chromatography like hydrophobic interaction chromatography on HP or XAD types of resins is done followed by separation of individual compounds on a reversed-phase HPLC column. Two such examples are the separation of linalyl β -vicianoside, bornyl β -primeveroside and 2-phenylethyl β -primeveroside from *Gardenia jasminoides*. Separation of *cis*-linalool 3,7-oxide-6-O- β -D-apiofuranosyl- β -D-glucopyranoside from oolong tea leaves was achieved using similar methodology.

Conclusion

In view of the importance of essential oils in the perfume, food and flavour industries as well as their therapeutic applications, it is imperative that research in their analysis and isolation continues. The crux of the problems associated with such endeavours lies basically in the fact that the constituents of essential oils most often occur in very minor amounts. Therefore the aim of further analytical research has to be directed to the achievement of the highest possible sensitivity and resolution. HPLC analysis using micro

columns containing either normal- or reversed-phase silica as packing material coupled to detectors like the electrospray ionization mass spectrometer with ion-trap detectors permitting MSⁿ analysis holds good potential. Electroanalytical techniques like capillary electrophoresis can go a long way in both qualitative and quantitative analysis of essential oil constituents. Capillary electrophoresis interfaced with MS and/or a photodiode array detector is likely to solve the problems of separation complexity of essential oil components.

See also: **II/Chromatography:** Liquid Chromatography-Gas Chromatography. **III/Essential Oils:** Gas chromatography; Thin-Layer (Planar) Chromatography. **Medium-Pressure Liquid Chromatography.** **Natural Products:** Supercritical Fluid Chromatography.

Further Reading

- Bauer K and Garbe D (1993) *Common Fragrance and Flavour Materials*. VCH Verlagsgesellschaft, mbh.
- Hostettmann M and Hostettmann A (1986) *Preparative Chromatographic Techniques (Applications in Natural Products Isolation)*. Berlin: Springer-Verlag.

Linskens HF and Jackson JF (1991) *Essential Oils & Waxes*. Berlin: Springer-Verlag.
Recent Trends in Flavour Evaluation of Spices Newer Trends in Essential Oils and Flavours (1991) New Delhi, India: Tata MacGraw-Hill Publishing Co.

Svendsen and Scheffer (1985) *Essential Oils and Aromatic Plants*. Dordrecht, The Netherlands: Junk Publishers.
 Sweig G and Sherma J (1984) *CRC Handbook of Chromatography, Terpenoids*, vol. 1. Boca Raton, Florida: CRC Press Inc.

THERMALLY-COUPLED COLUMNS: DISTILLATION



R. Smith, Centre for Process Integration, UMIST, Manchester, UK

Copyright © 2000 Academic Press

Introduction

A considerable amount of energy is used in distillation operations. Energy integration has proven to be successful in reducing energy costs for conventional distillation arrangements. However, the scope for energy integration of conventional distillation columns into an overall process is often limited. Also, practical constraints often prevent integration of distillation columns with the rest of the process.

If the column cannot be integrated with the rest of the process or, if the potential for heat integration is limited by the heat flows in the background process, then we must turn our attention back to the distillation operation itself and look at unconventional arrangements.

Figure 1 shows two conventional arrangements for the separation of a three-component mixture. The sequence shown in Figure 1A is the so-called direct sequence, in which the lightest component is taken overhead in each column. The indirect sequence shown in Figure 1B takes the heaviest component as bottom product in each column.

One of the most significant unconventional arrangements involves thermal coupling. Figure 2 shows a number of unconventional arrangements that use thermal coupling. In thermal coupling part of the heat transfer necessary for the separation is provided by direct contact via material flows. Figure 2A shows a side-rectifier arrangement and Figure 2B a side-stripper arrangement. Arrangements similar to that in Figure 2B are widely used in petroleum refining. The fully thermally coupled arrangement in Figure 2C (sometimes known as the Petlyuk column) has been known for over 50 years. Various studies have shown that thermally coupled arrangements can

save up to 30% of energy costs when compared with conventional arrangements.

Simple Versus Complex Columns

Consider first the design of distillation systems comprising only simple columns. These simple columns employ:

- one feed split into two products;
- key components which are adjacent in volatility;
- a reboiler and a condenser.

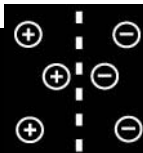
For a three-component mixture in which simple columns are employed, the decision is between the two sequences illustrated in Figure 1.

Consider the first characteristic of simple columns, which involves a single feed being split into two products. As a first option to two simple columns, the possibilities shown in Figure 3 can be considered, in which three products are taken from one column. The designs can be both feasible and cost-effective when compared with simple arrangements, but only for certain conditions. If the feed is dominated by the middle product (typically more than 50% of the feed) and the heaviest product is present in small quantities (typically less than 5%) then the arrangement shown in Figure 3A can be an attractive option. If a pure middle product is required, then it is usually only possible if there is a large volatility difference between components B and C, with the middle product taken as a vapour to assist the separation. The heavy product must find its way down the column past the side-stream. Unless the heavy product has a small flow and the middle product a high flow, a reasonably pure middle product cannot be achieved.

If the feed is dominated by the middle product (typically more than 50%) and the lightest product is present in small quantities (typically less than 5%), then the arrangement shown in Figure 3B can be an attractive option. This time the light product must find its way up the column past the side-stream. If

- Alberti G and Bein T (eds) (1996) *Solid State Supramolecular Chemistry: two and three dimensional inorganic networks*, Vol. 7 in Atwood JL, Davies JED, Macnicol F and Vögtle F (eds) *Comprehensive Supramolecular Chemistry*. Amsterdam: Elsevier.
- Aranda P and Ruiz-Hitzky W (1992) Poly(ethylene oxide)-silicate intercalation materials. *Chemistry of Materials* 4: 1395-1403.
- Beck JS, Vartuli JC, Roth WJ *et al.* (1992) A new family of mesoporous molecular sieves prepared with liquid crystal templates. *Journal of the American Chemical Society* 114: 10834-10843.
- Clearfield A (ed.) (1982) *Inorganic Ion Exchange Materials*. Boca Raton, FL: CRC Press.
- Galarneau A, Borodawalla A and Pinnavaia TJ (1995) Porous clay heterostructures formed by gallery-templated synthesis. *Nature* 374: 529.
- Garcia ME, Naffin JL, Deng N and Mallouk TE (1995) Preparative scale separation of enantiomers using intercalated α -zirconium phosphate. *Chemistry of Materials* 7: 1968-1973.
- Giannelis EP (1996) Polymer layered silicate nanocomposites. *Advanced Materials* 8: 29-35.
- Jones DJ, El Mejjad R and Rozière J (1992) Intercalation and polymerization of aniline in layered protonic conductors. In: Bein T (ed.) *Supramolecular Architecture, Synthetic Control in Thin Films and Solids*, ACS Symposium Series 499, pp. 220-230. Washington, DC: American Chemical Society.
- Nazar LF, Zhang Z and Zinkweg D (1992) Insertion of poly(*para*-phenylenevinylene) in layered MoO_3 . *Journal of the American Chemical Society* 114: 6239-6240.
- Ohtsuka K (1997) Preparation and properties of two-dimensional microporous pillared interlayered solids. *Chemistry of Materials* 9: 2039-2050.
- Olivera-Pastor P, Maireles-Torres P, Rodríguez-Castellón E *et al.* (1996) Nanostructured inorganically pillared layered metal(IV) phosphates. *Chemistry of Materials* 8: 1758-1769.
- Rouxel J (1992) Design and chemical reactivity of low-dimensional solids: some soft chemistry routes to new solids. In: Bein T (ed.) *Supramolecular Architecture, Synthetic Control in Thin Films and Solids*, ACS Symposium Series 499, pp. 88-113. Washington, DC: American Chemical Society.
- Schöllhorn R (1996) Intercalation systems as nanostructured functional materials. *Chemistry of Materials* 8: 1747-1757.
- Wang L, Schindler J, Kannewurf CR and Kanatzidis MG (1997) Lamellar polymer- Li_xMoO_3 nanocomposites via encapsulative precipitation. *Journal of Materials Chemistry* 7: 1277-1283.

THE NUCLEAR INDUSTRY: ION EXCHANGE



J. Lehto, University of Helsinki, Helsinki, Finland

Copyright © 2000 Academic Press

Introduction

Ion exchange is used in nearly all phases of the nuclear fuel cycle beginning in the early stages of uranium ore treatment where ion exchange is one of the major processes used: uranium is removed from ore leach liquors using anion exchange resins.

At nuclear power plants, ordinary organic ion exchange resins are mainly used for the removal of ionic and particulate contaminants from the primary circuit, condensate and fuel storage pond waters. Ion exchange resins are also used for the solidification of low- and medium-activity nuclear waste solutions. The number of applications of selective inorganic ion exchangers in the separation of radionuclides from nuclear waste solutions has been increasing since the mid-1980s.

In nuclear fuel reprocessing plants, the main separation method is solvent extraction. Ion ex-

change is, however, used for the solidification of low- and medium-activity waste solutions, as well as for the partitioning of radioactive elements for further use.

This article reviews all the most important areas of the utilization of ion exchangers in the nuclear power industry. Special attention is paid to ion exchange processes, which involve radionuclide removal functions, and to new developments in selective ion exchange materials.

Ion Exchange Materials Used in the Nuclear Industry

Nuclear Grade Ion Exchange Resins

Organic ion exchangers used at nuclear power plants are based on conventional poly(styrene-divinylbenzene) resins with sulfonic acid ($-\text{SO}_3^-$) and quaternary ammonium ($-\text{N}(\text{CH}_3)_3^+$) functional groups for cations and anions, respectively. Nuclear grade resins,

however, have to meet higher quality requirements than those used in most other industries.

First of all, the purity levels of nuclear grade resins have to be very high and, in particular, leachable corrosive impurities such as chloride and sulfate in anion exchange resins should be avoided. Second, nuclear grade resins should have high levels of the desired ionic form. For example, cation exchange resins in the hydrogen form, used in mixed beds for demineralization, should not contain a high proportion of sodium ions because they become activated in the neutron flux of the primary circuit and increase the radiation field. The content of heavy metals should also be very low. Thus, nuclear grade cation exchange resins are usually a minimum of 99% purity in the hydrogen form and typically the sodium and iron contents are below 0.01% and the contents of other metals even lower. ^7Li -form resins, used in some pressurized water reactors, have a 99% minimum purity in the lithium form. Nuclear grade anion exchange resins have a 95% minimum in the OH^- form, the rest being mainly in the CO_3^{2-} form. The contents of chloride and sulphate in anion exchange resins are typically very low, less than 0.1% and 0.3%, respectively. In addition to a high purity and a high level of desired ionic form, nuclear grade resins are more uniform in particle size compared with conventional resins and the amount of fines is very low.

Organic ion exchange resins are used in nuclear plants in two ways (Figure 1). First, as deep beds, i.e. columns packed with bead form resins. The volume of a bed is typically $1\text{--}2\text{ m}^3$ and the bead size 20–50 mesh. Their second use is as pre-coat filters, i.e. inert filters coated with a layer of crushed anion-cation resin mixture; the layer thickness is typically 5 mm and the particle size 200–400 mesh. Pre-coat filter systems are mainly used in the purification of solutions that contain high proportions of solid matter.

Inorganic Ion Exchangers

Use of inorganic ion exchangers at nuclear plants has been increasing since the mid-1980s. Utilization has been limited in nuclear waste management processes where the main advantage of inorganic ion exchangers over organic exchangers has been their superior selectivities to certain radionuclides. Other advantages are their resistance to radiation and high temperatures. The main problems which have hindered installation of inorganic ion exchange materials have been that they have not been available in stable grains or granules suitable for use in packed bed columns and that many of them are not chemically stable in high or even moderate acidities and alkalinities. As will be seen below, some of these problems have been overcome in the last 10 years.

Ion Exchange in the Processing of Uranium Ores

Uranium ores are first ground into submillimetre particles and uranium is leached out with sulfuric acid. If the ore contains a large quantity of acid-consuming CaCO_3 , leaching is carried out with sodium or ammonium carbonate solution. In sulfuric acid and carbonate solutions, uranium forms soluble sulfate and carbonate complexes, predominantly $\text{UO}_2(\text{SO}_4)_3^{4-}$ and $\text{UO}_2(\text{CO}_3)_3^{4-}$. These anionic complexes are removed from leach liquor with strongly basic anion exchange resins. For further processing, uranium sulfate is eluted from resin with dilute ($0.1\text{--}1.0\text{ mol L}^{-1}$) acid solutions. In the case of carbonate leaching, elution from the resin is carried out with dilute sodium chloride or ammonium nitrate solutions instead of acid to prevent formation of carbon dioxide in the column.

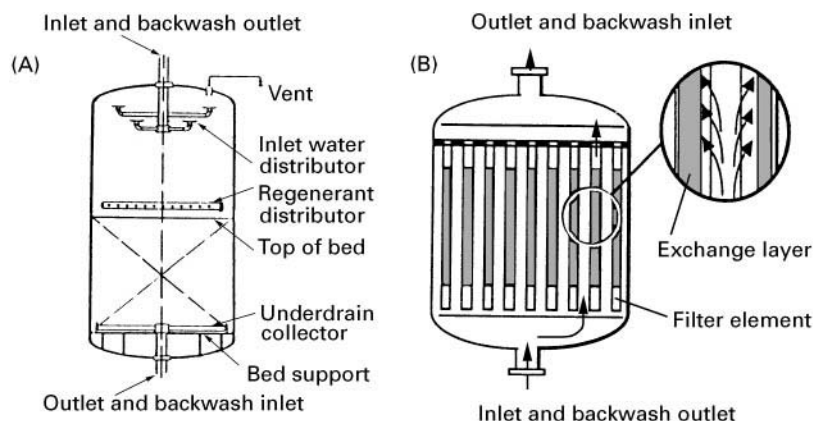


Figure 1 Typical deep bed (A) and pre-coat filter (B) units used at nuclear power plants.

Ion Exchange Processes at Nuclear Power Plants

Ion exchangers are utilized for many purposes at nuclear power plants (NPP):

- Purification of primary coolant water
- Control of primary coolant water chemistry
- Polishing of steam condensate
- Production of make-up water
- Purification of spent fuel storage pond water
- Treatment of waste solutions.

Most of these processes are used in all types of nuclear power plants. Purification of the primary coolant by ion exchange is, of course, not necessary in gas cooled reactors. Control of primary coolant chemistry applies only to some pressurized water reactors (PWR), using both light and heavy water as a moderator/coolant. Polishing of steam condensates is important in all reactor types but only in boiling water reactors (BWR) does it play an important role in removing radioactive contaminants. The two Finnish nuclear power plants, Olkiluoto NPP and Loviisa NPP, are given below as examples of installations using typical ion exchange systems for boiling water and pressurized water reactors. Loviisa NPP uses some 15 tonnes of ion exchange resins per annum and Olkiluoto NPP 22 tonnes.

Purification of Primary Coolant Water

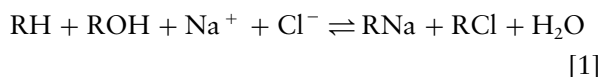
In nuclear power reactors the primary coolant water is circulated from the reactor vessel to the steam generator (PWR)/turbine (BWR) and back. In BWRs the primary coolant is pure water but in PWRs it also contains boric acid, which is used as a moderator to slow down the neutrons and LiOH or KOH to adjust the pH. Primary coolant water contains radioactive components in ionic and particulate form and these have to be removed to prevent the build-up of excessive radiation fields. There are two types of radioactive contaminants in the primary circuit: fission products originating from leakages from the fuel elements, the most important of these nuclides being ^{137}Cs , and activated corrosion products from reactor materials, of which ^{60}Co and ^{63}Ni are usually the most important (^{51}Cr , ^{54}Mn , ^{58}Co and ^{65}Zn can be found as well). Caesium exists in solution in ionic form and the corrosion products are mainly in the form of particles. In the removal of these radioactive contaminants, ion exchange resins work both as ion exchangers and as mechanical filters.

The exhaustion of the ion exchangers in all the processes at nuclear power plants is determined by one of the following parameters:

- Increased conductivity in the effluent
- Increased radioactivity in the effluent
- Increased pressure drop.

Especially in the processes where large amounts of solid fines are to be removed, increased pressure drop is the dominant parameter.

At the Olkiluoto NPP, which has two 710 megawatt (MW) BWRs, primary circuits are purified with two parallel deep bed units each of 1.5 m³ volume. The beds consist of equal quantities of cation and anion exchange resins. The function of the ion exchange purification system is to remove all ionic contaminants. The resins are initially in the H⁺ and OH⁻ forms and they demineralize water as shown in eqn [1].



where R is the resin matrix. The temperature of the water (270°C) has to be lowered to 60°C before conveying it into the ion exchanger bypass. The flow through each unit is about 2% of the total flow. Resins are replaced twice a year and solidified, without regeneration, with bitumen in the ratio of about 1:1 for final disposal.

At the Loviisa NPP, which has two 440 MW PWRs, the primary circuits are purified by two independent ion exchange systems. The first one is a deep bed having 1 m³ of equal amounts of cation and anion resins. The second system consists of two beds, of 1 m³ each, one being a cation exchanger and the other an anion exchanger. In both systems the exchangers are initially loaded in H⁺ and OH⁻ forms but in the early stages of the run they reach equilibrium with ions in the coolant water. The cation exchanger is converted into the H⁺/K⁺/NH₄⁺/Li⁺ form and the anion exchanger into the BO₃³⁻ form. Potassium originates from KOH used to adjust the pH to 7.0–7.3, NH₄⁺ from the addition of ammonia and lithium from the neutron-induced nuclear reaction, $^{10}\text{B}(n, \alpha)^7\text{Li}$. The flow through both these systems is 20 m³ h⁻¹, which is about 10% of the total volume of the primary circuit water. Resins in the beds are replaced approximately once a year. Spent ion exchangers are stored in stainless steel tanks and will in the future be solidified for final disposal, possibly by direct incorporation in concrete.

Deep beds containing ion exchange resins in the bead form remove both ions and particles. Removal of ^{137}Cs is practically 100%. In eight Swedish BWR plants the removal efficiency for corrosion prod-

ucts has been found to be about 95% for copper and chromium, 85–95% for cobalt and zinc and 80–90% for iron and nickel.

Polishing of Steam Condensate

In BWRs, the primary circuit water is boiling and the steam goes directly to turbines, after which it is condensed back to water and recirculated in the reactor vessel. This condensate is cleaned with ion exchanger filters. At the Olkiluoto NPP the condensate (60°C) goes through seven parallel filter units. Each unit has 25 L polypropylene pre-coat filter elements, which are coated with powdered anion and cation resins in a ratio of 1 : 2 or 1 : 3. The amount of resins in the seven units totals about 150–200 kg. Ion exchangers on the filters are replaced every 40–60 days. The primary purpose of the clean-up system is to remove ionic and particulate contaminants from the condensate. The removal efficiency for ionic radioactive species is higher than 90% and for particulate corrosion products 40–95%. In cases of leakages in the condenser, the clean-up system should also be able to remove ionic contaminants from the condenser coolant, which, in the case of the Olkiluoto NPP, is sea water.

In PWRs, condensate polishing is not important in removing radioactive contaminants because the condenser is located in the secondary circuit. The need for radioactivity removal from the condensate arises only if there is a leakage in the steam generator. The purpose of the condensate polishing, therefore, is usually the removal of corrosion products and corrosive agents.

Purification of Spent Fuel Storage Pond Water

Spent nuclear fuel is stored in water-filled ponds for several years after removal from the reactor. The water becomes contaminated because there is a large amount of particulate matter on the surface of fuel elements and because there are leakages of fission products through the fuel element cladding. In order to remove these contaminants, as well as the corrosive agents, the pond water is circulated through ion exchange filters. At the Olkiluoto NPP, fuel pond waters are purified with pre-coat filters in which the filter elements have been coated with H^+ - and OH^- -form resins in the ratio of 3 : 1. The flow through the filters is $180\text{ m}^3\text{ h}^{-1}$. At the Loviisa NPP there are separate 2 m^3 cation and anion exchanger beds in H^+ and BO_3^{3-} forms, respectively, and the particle removal is accomplished with mechanical filters. The flow rate is $18\text{--}40\text{ m}^3\text{ h}^{-1}$.

Treatment of Radioactive Waste Solutions

Low- and medium-activity waste solutions, originating from various sources such as leakages from

primary circuit, drainage waters, decontamination solutions, laundries, etc., are usually concentrated by evaporation or solidified by precipitation or by ion exchange. The most important radionuclides in power plant waste solutions are usually ^{137}Cs and ^{60}Co . At the Olkiluoto NPP most waste solutions are solidified with ordinary ion exchange resins, and both deep beds and pre-coat filters are used. After removal of radioactivity by the resins, they are dried and mixed with bitumen in the ratio of 1 : 1, and finally cast into 200 L steel drums for final disposal.

The number of novel ion exchange applications in nuclear waste management has been increasing since the late 1980s. Evaporators have been replaced by ion exchange processes and more selective ion exchangers, especially zeolites, have been introduced into separation processes. There are two main advantages in using selective ion exchange materials: firstly, reduction in final waste volumes and thus in waste disposal costs; and, secondly, reduction in environmental discharges of radioactivity. In 1986–87 Duratek Co., for example, replaced evaporators at four PWRs in the USA with ion exchange units. In these units there are five 0.85 m^3 columns in series, packed with both conventional ion exchange resins and novel ion-selective materials. The burial volume reduction, obtained with these new systems, was 94–95% and costs decreased by 33–77%. The decontamination factors, however, were only moderate being 15–20 for caesium and 4–24 for cobalt. Decontamination factor (DF) is the ratio of initial solution activity to the activity of purified solution.

At the Catawba NPP, USA, organic resins were replaced in 1987 with a natural zeolite, clinoptilolite, in the treatment of low-level nuclear waste solutions. Clinoptilolite is an aluminium silicate mineral with the ideal composition of $(\text{Na}_2\text{K}_2)\text{O} \cdot \text{Al}_2\text{O}_3 \cdot 10\text{SiO}_2 \cdot 8\text{H}_2\text{O}$, where sodium and potassium ions are exchangeable for caesium. In column operation with 0.7 m^3 beds, caesium breakthrough typically occurs at 6000 bed volumes, compared to 1300 bed volumes obtained earlier with organic resins. In the laboratory studies, which were made to select the best ion exchange material, it was found that chabazite and mordenite zeolites worked as effectively as clinoptilolite, but the latter was chosen because of its lower price. Zeolites are used also at other NPPs in the USA for the removal of caesium for low-activity waste solutions.

Zeolites were also used at the Three Mile Island NPP, USA, for the decontamination of highly active waste solution from the reactor accident in 1979. 2780 m^3 of waste solution, which had ^{137}Cs and ^{90}Sr as major radioactive contaminants, were processed with an ion exchange system having four 230 L

zeolite columns in series. The columns contained two zeolites, IONSIV IE-96 and IONSIV A-51 (UOP, USA), in the ratio of 3 : 2. IE-96 has a Si/Al ratio of 2 : 3, typical for zeolite Y, and was selected because of its selectivity to caesium; A-51 has a Si/Al ratio of 1 : 1, typical for zeolites A and X, and was found to be selective for strontium. In total 10 columns containing some 60 000 Ci of caesium and strontium, were obtained from the process. The zeolites were vitrified for final disposal by adding glass-forming agents and heating at 1050°C.

In the 1990s a new, extremely selective ion exchange material for caesium separation, a transition metal hexacyanoferrate product CsTreat® (Selion, Finland), has been used at nuclear power plants. The general formula of transition metal hexacyanoferrates is $A_x[M_2Fe(CN)_6] \cdot xH_2O$, where M is a transition metal, such as cobalt, nickel or zinc, and A is the exchangeable alkali metal (Na, K). Transition metal hexacyanoferrates have long been known as superior ion exchangers for caesium compared with organic resins and zeolites. The first application, however, using granular hexacyanoferrate in packed bed columns, was commenced in 1992 at the Loviisa NPP, Finland. The solutions treated are evaporator concentrates, which are highly alkaline and contain very high concentrations of inactive salts, typically sodium at 3 mol L⁻¹ and potassium at one-tenth of this value. These types of solutions would cause instant breakthrough of caesium from zeolite and organic resin beds. In the first full-scale run, one 8 L hexacyanoferrate column processed 182 m³ of waste solution with a decontamination factor of 2000. Thus the volume reduction obtained by this method was 23 000. Another application of CsTreat® is the removal of caesium from dilute salt solutions (Na 100–300 ppm, K 10–20 ppm, Ca 20–60 ppm) at Callaway NPP, USA, where it replaces an evaporator system. Since there are also other waste components to be removed the system contains, in addition to a 250 L CsTreat® bed, mechanical filters, a charcoal bed and a mixed resin bed. During the first eight months the system purified 1800 m³ (7000 bed volumes) of waste effluents. The ¹³⁷Cs level in the purified solution was most of the time below the detection limit or at least below the target limit of 2 Bq L⁻¹ (5×10^{-7} µCi mL⁻¹). The expected additional lifetime of the bed is as long as 7 years.

Successes comparable to those with cesium removal have not been obtained for cobalt. Most waste solutions containing ⁶⁰Co are neutral or alkaline and usually the cobalt does not exist only in the divalent cation form. The forms in which the radioactive cobalt does exist are not exactly known but it is thought

to be present, in addition to divalent cations, as colloids, hydrolysis products and complexes. The most widely and successfully used separation materials for cobalt have been activated carbons. The uptake mechanism is rather complex and varies from product to product but probably activated carbons act as multifunctional materials, including ion exchange, complexation and adsorption.

For the more effective separation of activation/corrosion products ⁶⁰Co and ⁶⁵Zn, a new organic resin Diphonix has been employed at Millstone NPP, USA, since 1995. Diphonix (Eichrom Industries, USA) has a poly(styrene-divinylbenzene) matrix but the functional groups are chelating diphosphonic groups ($-(PO_3)_2^{2-}$). In addition there are sulfonic acid groups which improve the kinetics of ion exchange. In tests prior to installation of full-scale Diphonix beds at Millstone, decontamination factors (DF) for ⁶⁰Co and ⁶⁵Zn were 100 and below when a Diphonix was used alone. Combining an anion exchange resin bed with Diphonix bed increased the DF up to 1000. The processing capacity of the Diphonix bed for ⁶⁰Co and ⁶⁵Zn was at least 6000 bed volumes, which is at least 3–10 times higher than that obtained with the previously used ordinary mixed bed system.

Ion Exchange Processes at Nuclear Fuel Reprocessing Plants

Spent nuclear fuel contains about 96% uranium, 3% fission products, 1% plutonium and less than 0.1% other transuranium elements. In reprocessing the fissile material, uranium and plutonium are separated from fission products and from other actinides and recycled for the production of nuclear fuel for reactors. The main separation process utilizes solvent extraction and most reprocessing plants use the Purex process. As the first organic ion exchange resins became available in the 1940s, reprocessing schemes using ion exchange in the main process were designed but were never used due to the poor decontamination factors achieved. Today, ion exchange is used at reprocessing plants only in the secondary waste effluent treatment and separation streams.

Separation Processes

The most important use of ion exchange in the separation processes is the purification of plutonium solutions, which can be carried out with both cation and anion exchangers. Anion exchange processes, however, yield better decontamination from impurities. At high nitric acid concentrations plutonium forms the hexanitro complex anion $Pu(NO_3)_6^{2-}$, which can

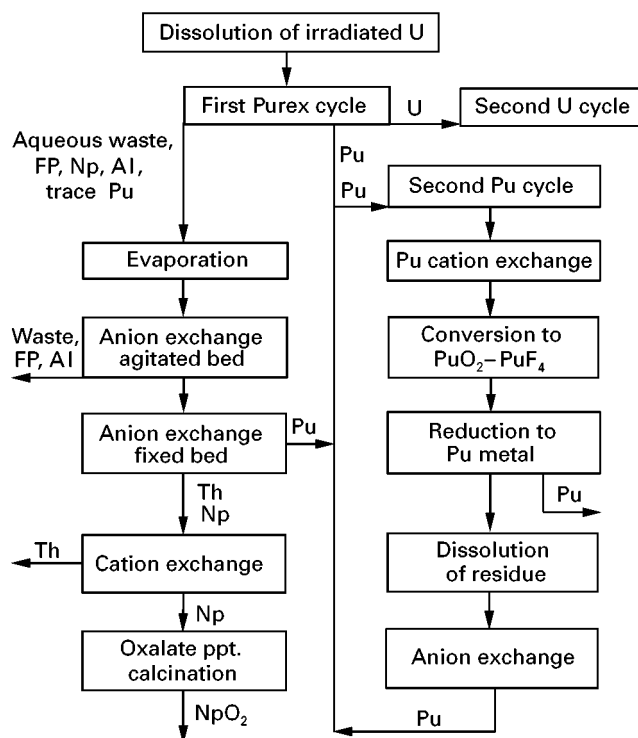
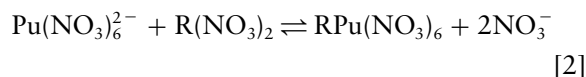


Figure 2 Ion exchange processes in the reprocessing of spent uranium fuel at the Savannah River Plant, USA.

be sorbed on an anion exchange resin in the following way:



The optimum nitric acid concentration is 7 mol L⁻¹. Plutonium can be eluted from the resin with diluted nitric acid (0.35 mol L⁻¹) as the hexanitro complex is destroyed. The decontamination factor for all other elements but neptunium is very good. Plutonium can be purified from neptunium by eluting with 5.5 mol L⁻¹ HNO₃ containing iron(II) sulfamate and hydrazine, instead of 0.35 mol L⁻¹ HNO₃. Plutonium is reduced to Pu(III) and elutes from the column, while Np(IV) remains.

Anion and cation exchange processes can also be used for the separation of plutonium and neptunium from the high-level waste solutions of the Purex process (Figure 2). Plutonium is recycled to the Purex process and neptunium turned into NpO₂ to be used as irradiation targets.

Treatment of Radioactive Waste Solutions

The high activity waste effluents from civilian reprocessing plants are usually calcined and vitrified for final disposal. In the 1970s and 1980s studies

were carried out on the use of inorganic ion exchangers, zeolites and sodium titanate, in the solidification of highly active waste solutions but no such processes are currently employed. In the late 1980s a zeolite IONSIV IE-96 was, however, used at West Valley reprocessing plant in New York for the removal of ¹³⁷Cs in 2100 m³ of highly active neutralized Purex-process-derived waste solution. In total about 30 columns of 1.7 m³ volume were obtained, the volume reduction thus being about 40-fold. The decontamination factor was higher than 10 000. Zeolite, together with the sludge from the tank bottom, was vitrified for final disposal.

Starting in 1997, the Japan Atomic Energy Research Institute (JAERI) inaugurated the first use at reprocessing plants of highly selective inorganic ion exchange materials in packed bed columns for the removal of ¹³⁷Cs and ⁹⁰Sr from reprocessing waste effluents and the process has worked successfully. In this pilot-scale process 2 L columns are packed in the ratio of 1 : 1 with the hexacyanoferrate product CsTreat® and a sodium titanate product SrTreat® (Selion, Finland) which is a highly selective ion exchanger for strontium in alkaline media and efficiently takes up other multivalent radionuclides. In laboratory tests with JAERI simulant (pH 10, 2.4 mol L⁻¹ NaNO₃) the average decontamination factor of SrTreat® for strontium was 8400 at 1500

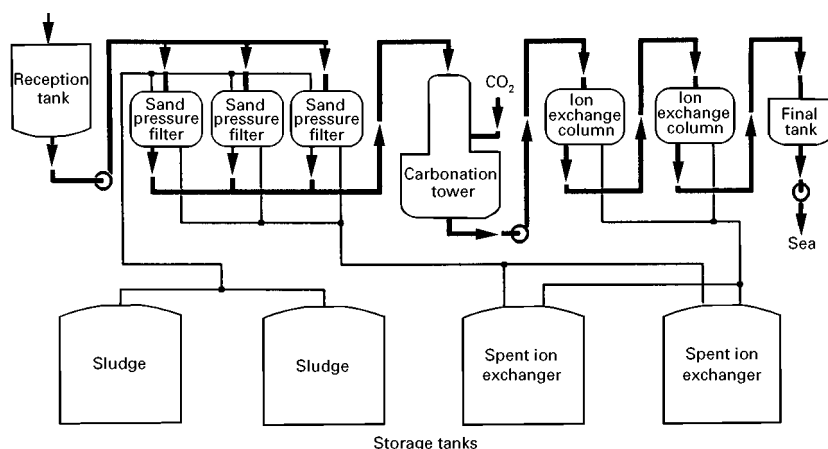


Figure 3 Simplified process flow diagram for the Site Ion Exchange Effluent Plant (SIXEP) at Sellafield, UK.

bed volumes. In other tests SrTreat® has also been shown to take up strontium most efficiently from military waste effluents (see below) which represent the most severe conditions where ion exchange can be considered for use in waste management.

In 1985 the Site Ion Exchange Effluent Plant (SIXEP), using the natural clinoptilolite zeolite for the removal of caesium and strontium from spent fuel pond waters, was put into operation at the BNFL Sellafield reprocessing plant in the UK. Spent fuel to be reprocessed is stored in water-filled storage ponds and some 3600 m³ of the pond water have to be purged every day to keep the radiation in the ponds at an acceptable level. From this water, containing radioactive caesium and strontium, as well as activated corrosion products, particulate matter is first removed in sand filters and the pH is lowered with CO₂ from 11.5 to 8.0 to avoid the dissolution of the zeolite exchanger. Finally, the solution is passed through two beds in series, both columns filled with 10 m³ of zeolite (Figure 3). The plant annually processes 700 000 m³ of pond water, containing 17 000 Ci activity. The decontamination factors are typically 2000 and 500 for caesium and strontium, respectively, and the plant treats 20 000 bed volumes per change of zeolite. The yearly consumption of zeolite is 40 m³.

At the Sellafield plant there is also another major waste treatment process utilizing ion exchange, the Enhanced Actinide Removal Plant (EARP), commissioned in 1994. From the mainly medium activity solutions the alpha nuclides are removed by increasing the pH to 10–11, which causes the precipitation of iron hydroxides and subsequently practically all actinides. Solid/liquid separation is accomplished with cross-flow filtration through ceramic mem-

branes. The removal of caesium is carried out by addition of preformed nickel hexacyanoferrate sludge, which removes caesium by ion exchange and yields moderate decontamination factors of 10–50. This way of using selective ion exchangers, called seeded ultrafiltration, is well suited to combination with coprecipitation with ferric floc, but in general it is much less efficient when compared with the use of exchangers in packed bed columns, taking into account both decontamination factors and processing capacities.

Decontamination of Military Waste Effluents

Especially in the USA and Russia there are huge amounts of highly active waste effluents, originating from nuclear weapons programmes, stored in tanks, a large number of which are leaking or expected to leak. The US Department of Energy has launched a long-term programme to treat and solidify tank wastes, which consist of salt cakes and sludges in the tank bottoms and supernatants above. In total, there are 300 000 m³ of tank wastes, especially at the Hanford and Savannah River sites. Supernatants are highly alkaline, their pH being above 14, and the concentration of salts is very high, for example that of sodium is as high as 7 mol L⁻¹. The objective is to separate the main soluble radionuclides, ¹³⁷Cs, ⁹⁰Sr and ⁹⁹Tc, to minimize the volume of highly active waste to be disposed of. It is expected that ion exchange will be the main process used to do this. The extreme conditions in the solutions impose the most stringent requirements on the exchangers, considering both selectivity and chemical stability. Development of materials for tank waste remediation is discussed in the next section.

New Developments in Ion Exchange Materials

In the development of nuclear grade ion exchange resins, used in primary coolant and condensate purification, the main effort has been to decrease the fractions of leachables, both resin fragments and ionic leachables. In the development of ion exchange materials for waste treatment, where ordinary organic resins are mostly ruled out due to their low selectivities, the most important objectives have been:

1. To obtain highly selective exchanger materials for certain radionuclides.
2. To obtain ion exchange materials stable and capable of ion exchange in highly acidic or highly alkaline media.
3. To obtain ion exchangers in granular or bead forms suitable for packed bed column operations.

The highest selectivities have been found with inorganic ion exchangers. The biggest effort in developing novel ion exchange materials for radionuclide removal has been devoted to caesium-selective exchangers. In the mid-1980s zeolites were the first generation of caesium-selective exchangers. Thereafter, a wide variety of exchangers have been studied for this purpose; transition metal hexacyanoferrates, such as CsTreat[®] discussed earlier, have the highest selectivity for caesium (Table 1).

Utilization of zeolites and CsTreat[®] has been discussed above. Crystalline silicotitanate CST (UOP, USA) has been developed during the 1990s by optimizing the Si/Ti ratio in the exchanger and using additional metals ions, such as niobium, in the structure of the layered material. The most important possible utilization of CST is the remediation of US tank wastes, since CST has been reported to be stable in their extremely alkaline environments and to be efficient for the uptake of both caesium and strontium from the supernatants. Many other inorganic ion exchangers, especially mixed oxides, have been developed and commercialized by Allied Signal, USA.

Table 1 Selectivity coefficients of Cs/Na exchange in commercial Cs-selective ion exchange materials

<i>Ion exchanger</i>	<i>Selectivity coefficient</i>
Sulfonic acid resin	< 10
Mordenite (zeolite)	450
Resorcinol formaldehyde resin (SRL)	11 400
Silicotitanate (CST)	18 000
Hexacyanoferrate (CsTreat [®])	1 500 000

A wide variety of chelating resins have been developed and tested for the separation of transition metal ions from solution. Of these, only a few resins, particularly iminodiacetic acid [R-N-(CH₂-COOH)₂] and aminophosphonate (R-NH-CH₂-PO₃H₂), are manufactured commercially but no applications in the nuclear industry have been reported. The only exception is the Diphonix resin discussed above. The company manufacturing Diphonix, Eichrom Industries, also produces several other radionuclide-selective resins. These 'extraction chromatographic resins' are mainly based on the incorporation of complexing agents, known to be efficient in solvent extraction processes, into the solid resin matrix so that they can be used in packed bed columns. An example of these resins is the SrResin which contains a strontium-selective crown ether in the resin matrix. The high prices of these chromatographic resins are likely to limit their use to analytical applications.

⁹⁹Tc is an important radionuclide in high activity waste effluents due to its very long half-life. Technetium is mainly present as a pertechnetate anion TcO₄⁻ and is difficult to remove. No really selective ion exchanger has so far been developed for the effective separation of technetium from waste effluents. However, the capability of ordinary anion resins to take up technetium has been improved by modifying the side chains in the functional groups -R-N(C_xH_y)₃⁺ of strongly basic anion exchange resins. For example, compared with a commercial resin containing ethyl groups as C₂H₅, a test resin containing both hexyl and propyl groups removed TcO₄⁻ from ground water much more efficiently, the processing capacity being more than × 30 higher.

Further Reading

- Bibler JP (1990) Ion exchange in the nuclear industry. In: Williams PA and Hudson MJ (eds) *Recent Developments in Ion Exchange* (vol. 2) p. 121. Barking, UK: Elsevier Applied Science.
- Campbell DO and Burch WD (1990) The chemistry of fuel processing: present practices, future trends. *Journal of Radioanalytical Nuclear Chemistry Articles* 142: 303.
- Carley-Macaulay KW (1985) Survey of solvent extraction and ion exchange in radioactive waste processing. In: Logsdail DH and Mills AL (eds) *Solvent Extraction and Ion Exchange in the Nuclear Fuel Cycle*, p. 127. Southampton, UK: Ellis Horwood.
- International Atomic Energy Agency (1984) *Treatment of Low- and Intermediate-Level Liquid Radioactive Wastes*. Technical Reports Series No. 236, IAEA, Vienna.
- Kühne G (1991) Ion exchangers in nuclear technology. In: Dorfner K (ed.) *Ion Exchangers*, p. 873. Berlin, New York: Walter de Gruyter.

- Lehto J (1993) Ion exchange in the nuclear power industry. In: Dyer A, Hudson HG and Williams PA (eds) *Ion Exchange Processes: Advances and Applications*, p. 39. Cambridge, UK: The Royal Society of Chemistry.
- Lehto J and Harjula R (1997) Selective separation of radionuclides from nuclear waste solutions with inorganic ion exchangers, *React Funct Polym* (in press).
- Navratil JD (1989) Ion exchange technology in spent fuel reprocessing. *Journal of Nuclear Sciences and Technology*, 26: 735.
- Shultz WW, Wheelwright EJ, Godbee H, Mallory CW, Burney GA and Wallace RM (1984) Ion exchange and adsorption in nuclear chemical engineering. In: *AIChE Symposium Series* 80(233): 96.

NUCLEIC ACIDS



Centrifugation

A. Marziali, University of British Columbia, Vancouver, Canada

Copyright © 2000 Academic Press

Introduction

Centrifugation has been applied to nucleic acid isolation and purification through numerous protocols which, at some level, contain elements of one or more of three basic techniques: isopycnic or density equilibrium separation, phenol-chloroform extraction, and differential precipitation. Even if we consider only the protocols that are in current use, numerous variations on these appear in the literature. These variations result from the intended use of the product, the required purity from specific contaminants, the cost and throughput goals of the technique, and often the author's personal preferences. This article will make no attempt to cover all variations but will instead illustrate by example the basic forms of centrifuge-based techniques for nucleic acid separation as they are presently used. A rough guide to these three basic techniques and their applications is contained in Table 1. Each of these will subsequently be described separately.

Recent demands imposed on nucleic acid purifications by large scale DNA sequencing operations have led to the development, and increased use of filtration-based purification methods for high throughput separations. Though the cost of the filter membranes required for these separations is much higher than the cost of centrifugation, the throughput and ease of automation of the membrane based methods make them preferable in many situations. Recent developments in automation of centrifugation, discussed in the last section of this article, may reverse this trend.

Isopycnic Separations

General Principle

Isopycnic separations rely on the balancing of the buoyant and centrifugal forces acting on a submerged sample during centrifugation. When a sample of density ρ_s and effective volume V is placed in a medium of density ρ_m in the presence of a centrifugal field a , the sample feels an upward buoyant force $F_b = \rho_m Va$, and an opposing centrifugal force $F_c = \rho_s Va$. Consequently, the sample will move 'up' toward the rotation axis if $\rho_s < \rho_m$ and 'down' if $\rho_s > \rho_m$. This motion terminates when the sample reaches the boundary of the medium or when it enters a region of the medium where $\rho_s = \rho_m$. Based on this principle, if a sample container is filled with a medium whose density increases gradually in the downward direction, a sample injected in this medium will migrate to the region of the medium that matches the sample density (provided such a region exists). This location is known as the isopycnic point of the sample.

Samples may therefore be separated based on their densities provided a medium is found that can be formed into a density gradient and whose density range includes that of the sample. One of the criteria in the selection of separation media for a specific sample is to ensure that this condition is met.

After a substantial migration period (often over a day), the sample fractions of different densities can be observed as bands within the medium. Extraction of these bands is performed by puncturing the centrifuge tube with a hypodermic needle and withdrawing the desired band. The resolution provided by this method is a function of the separation medium and the relative density difference in the fractions to be separated.

In the case of nucleic acids, RNA and DNA exhibit very different densities in aqueous solutions and therefore can be separated. Cesium salt solutions are typically used as the separation medium since in

Linskens HF and Jackson JF (1991) *Essential Oils & Waxes*. Berlin: Springer-Verlag.
Recent Trends in Flavour Evaluation of Spices Newer Trends in Essential Oils and Flavours (1991) New Delhi, India: Tata MacGraw-Hill Publishing Co.

Svendsen and Scheffer (1985) *Essential Oils and Aromatic Plants*. Dordrecht, The Netherlands: Junk Publishers.
 Sweig G and Sherma J (1984) *CRC Handbook of Chromatography, Terpenoids*, vol. 1. Boca Raton, Florida: CRC Press Inc.

THERMALLY-COUPLED COLUMNS: DISTILLATION



R. Smith, Centre for Process Integration, UMIST, Manchester, UK

Copyright © 2000 Academic Press

Introduction

A considerable amount of energy is used in distillation operations. Energy integration has proven to be successful in reducing energy costs for conventional distillation arrangements. However, the scope for energy integration of conventional distillation columns into an overall process is often limited. Also, practical constraints often prevent integration of distillation columns with the rest of the process.

If the column cannot be integrated with the rest of the process or, if the potential for heat integration is limited by the heat flows in the background process, then we must turn our attention back to the distillation operation itself and look at unconventional arrangements.

Figure 1 shows two conventional arrangements for the separation of a three-component mixture. The sequence shown in Figure 1A is the so-called direct sequence, in which the lightest component is taken overhead in each column. The indirect sequence shown in Figure 1B takes the heaviest component as bottom product in each column.

One of the most significant unconventional arrangements involves thermal coupling. Figure 2 shows a number of unconventional arrangements that use thermal coupling. In thermal coupling part of the heat transfer necessary for the separation is provided by direct contact via material flows. Figure 2A shows a side-rectifier arrangement and Figure 2B a side-stripper arrangement. Arrangements similar to that in Figure 2B are widely used in petroleum refining. The fully thermally coupled arrangement in Figure 2C (sometimes known as the Petlyuk column) has been known for over 50 years. Various studies have shown that thermally coupled arrangements can

save up to 30% of energy costs when compared with conventional arrangements.

Simple Versus Complex Columns

Consider first the design of distillation systems comprising only simple columns. These simple columns employ:

- one feed split into two products;
- key components which are adjacent in volatility;
- a reboiler and a condenser.

For a three-component mixture in which simple columns are employed, the decision is between the two sequences illustrated in Figure 1.

Consider the first characteristic of simple columns, which involves a single feed being split into two products. As a first option to two simple columns, the possibilities shown in Figure 3 can be considered, in which three products are taken from one column. The designs can be both feasible and cost-effective when compared with simple arrangements, but only for certain conditions. If the feed is dominated by the middle product (typically more than 50% of the feed) and the heaviest product is present in small quantities (typically less than 5%) then the arrangement shown in Figure 3A can be an attractive option. If a pure middle product is required, then it is usually only possible if there is a large volatility difference between components B and C, with the middle product taken as a vapour to assist the separation. The heavy product must find its way down the column past the side-stream. Unless the heavy product has a small flow and the middle product a high flow, a reasonably pure middle product cannot be achieved.

If the feed is dominated by the middle product (typically more than 50%) and the lightest product is present in small quantities (typically less than 5%), then the arrangement shown in Figure 3B can be an attractive option. This time the light product must find its way up the column past the side-stream. If

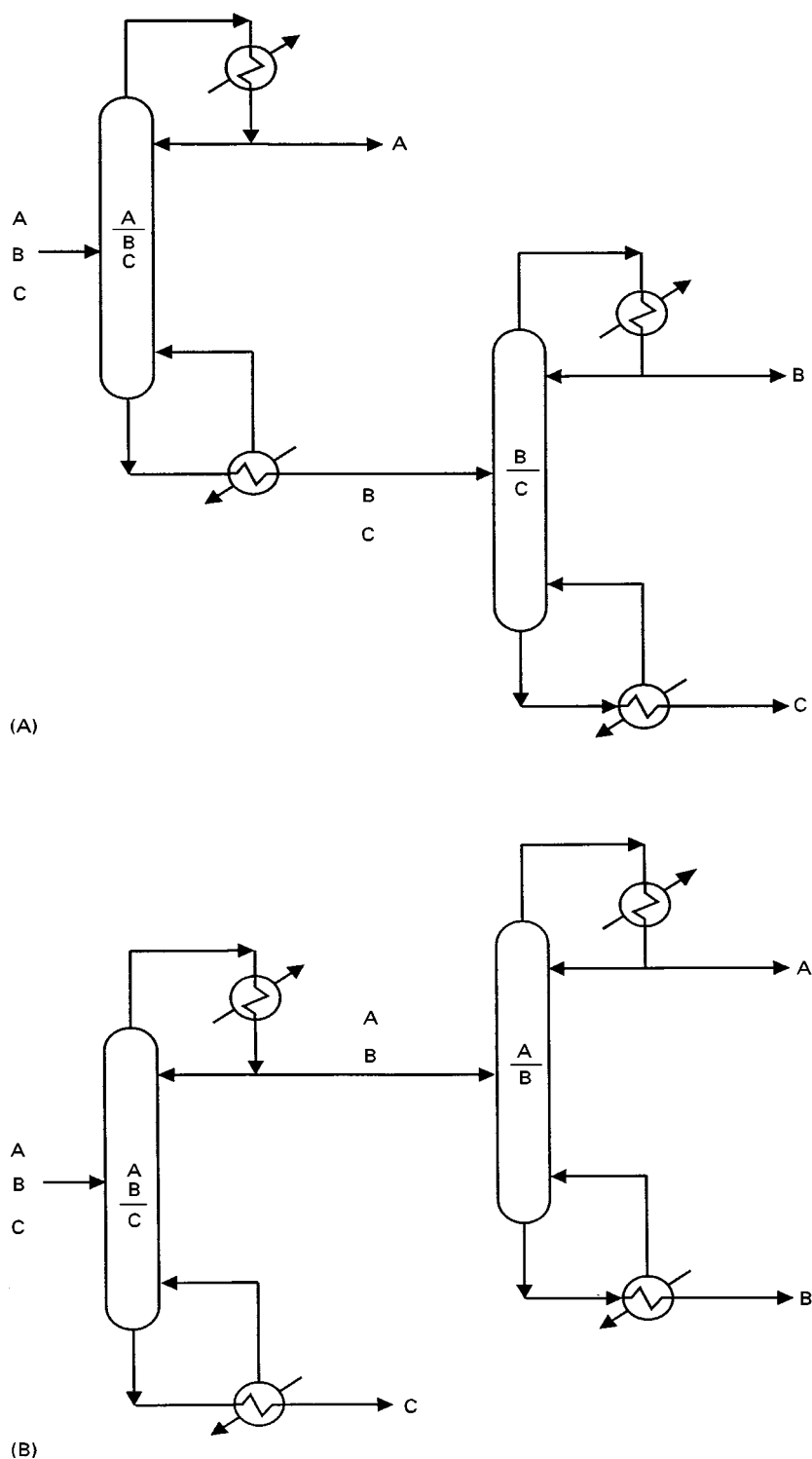


Figure 1 The (A) direct and (B) indirect sequences of simple distillation columns for a three-component separation. (Reproduced with permission from Triantafyllou and Smith (1992) *Transactions of the Institution of Chemical Engineers, Part A* 70: 1992.)

a pure middle product is required, then it is usually only possible if there is a large volatility difference between components A and B, with the middle product taken as a liquid to assist the separation.

In summary, single-column side-stream arrangements can be attractive when the middle product is in excess and one of the other components is present in only minor quantities. Thus, the side-stream column

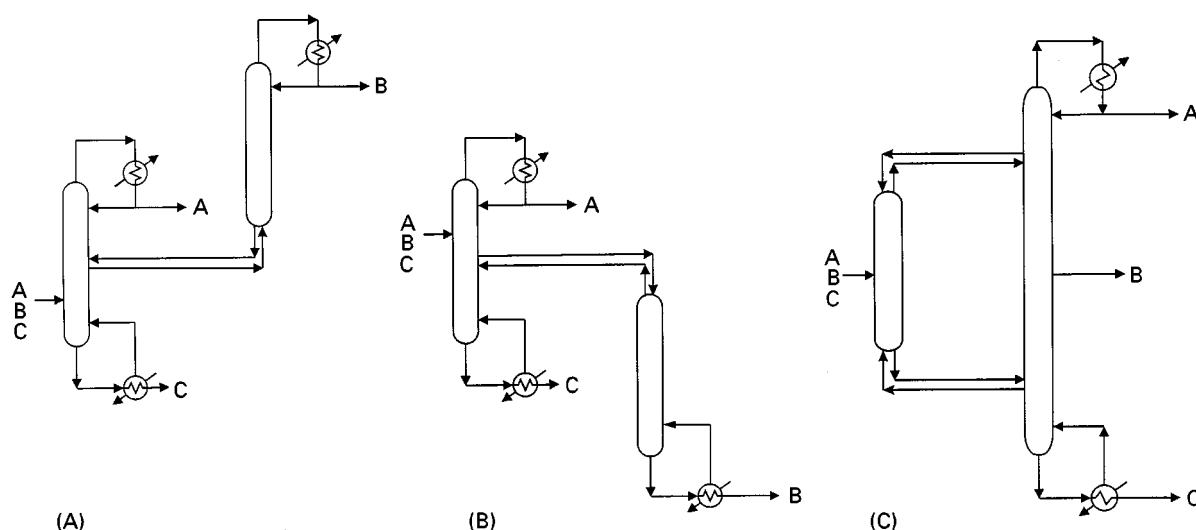


Figure 2 Thermally coupled columns. (A) Side-rectifier; (B) side-stripper; (C) fully thermally coupled column. (Reproduced with permission from Triantafyllou and Smith (1992) *Transactions of the Institution of Chemical Engineers, Part A* 70, 118.)

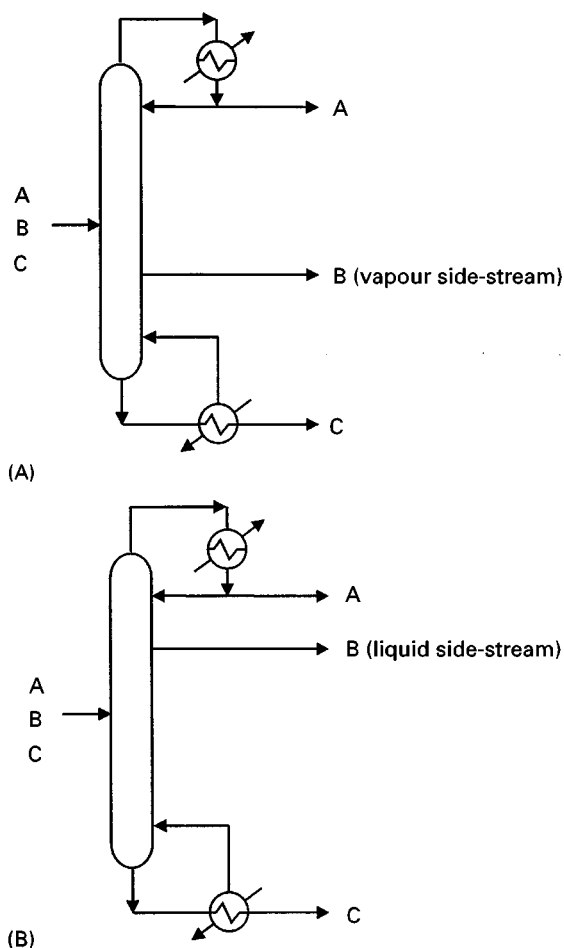


Figure 3 Distillation columns with three products. (A) More than 50% middle component and less than 5% heaviest component; (B) more than 50% middle component and less than 5% lightest component. (From Smith and Linnhoff (1988) *Chemical Engineering Research and Design*, 66, 195, reproduced with permission from the Institution of Chemical Engineers.)

only applies to special feed compositions. More generally applicable arrangements are possible by relaxing the restriction that separations must be between adjacent key components.

Consider a three-product separation as shown in Figure 4A in which the lightest and heaviest components are chosen to be the key separation in the first column. In such a case, two further columns are required to produce pure products. However, note that the bottoms and overheads of the second and third columns in Figure 4A are both pure B. Hence the second and third columns could simply be connected and product B taken as a side-stream, as shown in Figure 4B. The arrangement in Figure 4B is known as a prefractionator arrangement. Note that the first column in Figure 4B, the prefractionator, has a partial condenser to reduce the overall energy consumption. The prefractionator arrangement in Figure 4B typically requires 30% less energy than conventional arrangements for the same separation duty. The extent of the energy saving depends on the feed composition and the relative volatility of the components being separated. The energy saving results from the fact that the prefractionator arrangement is thermodynamically more efficient than a simple arrangement.

To understand why this is the case, consider the sequence of simple columns shown in Figure 5. In the direct sequence shown in Figure 5, the composition of component B in the first column increases below the feed as the more volatile component A decreases. However, moving further down the column, the composition of B decreases again as the composition of the less volatile component C increases. Thus, the composition of B reaches a peak, only to be remixed.

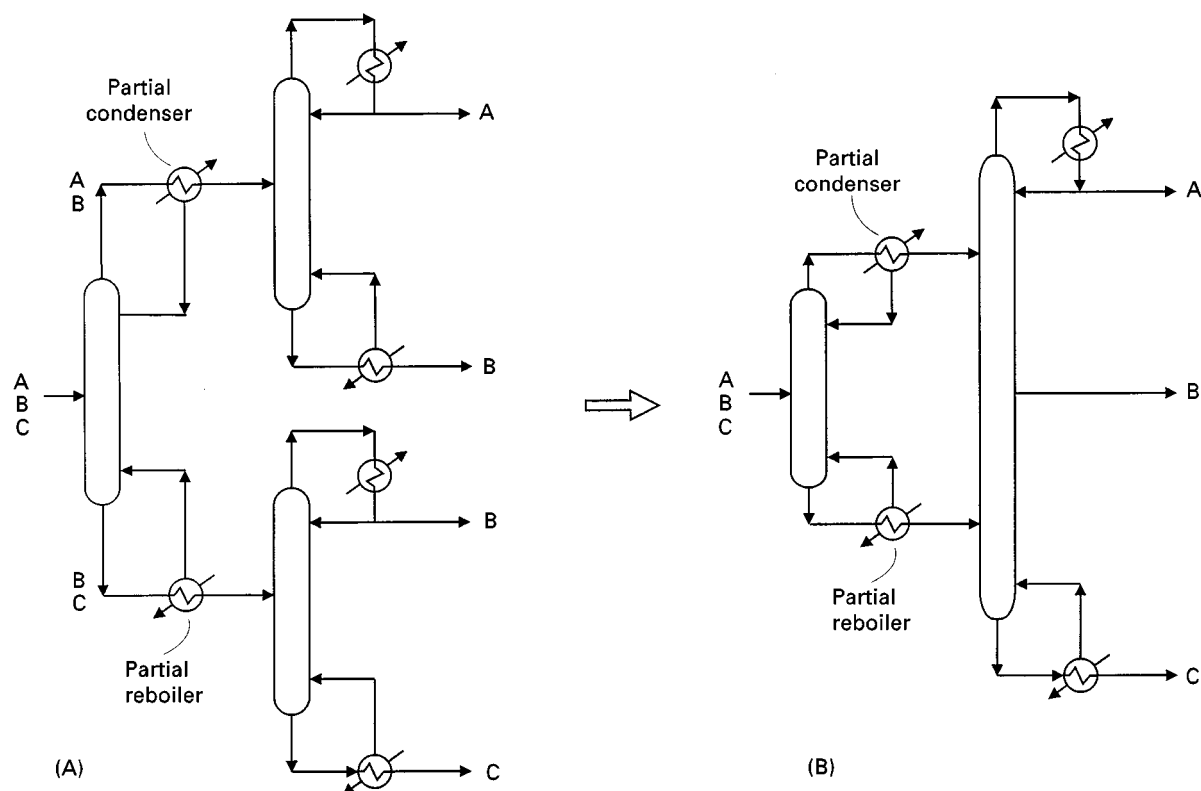


Figure 4 Choosing nonadjacent keys leads to the prefractionator arrangement. (A) Sequence for three product separation using nonadjacent keys; (B) prefractionator arrangement. (Reproduced with permission from Smith (1995) *Chemical Process Design*, McGraw-Hill.)

Similarly, with the first column in the indirect sequence, the composition of B first increases above the feed and reaches a maximum only to decrease as

the more volatile component A increases. Again, the composition of B reaches a peak, only to be removed.

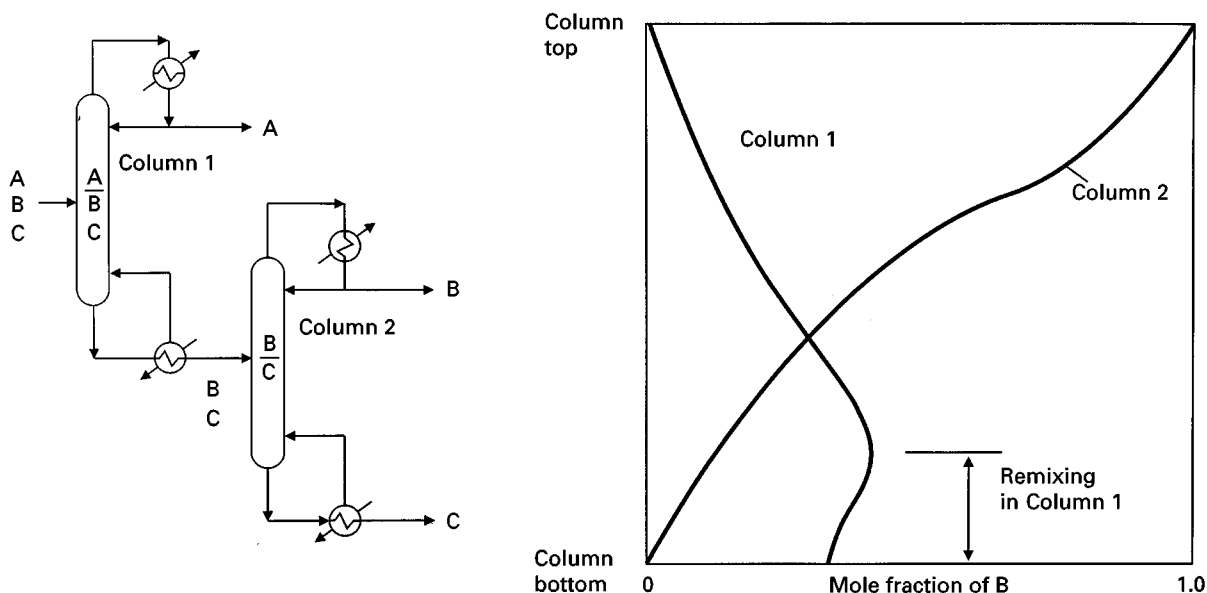


Figure 5 Composition profiles for the middle product in the columns of the direct sequence show remixing effects. (From Triantafyllou and Smith (1992) *Transactions of the Institution of Chemical Engineers, Part A* 70, 118, reproduced by permission of the Institution of Chemical Engineers.)

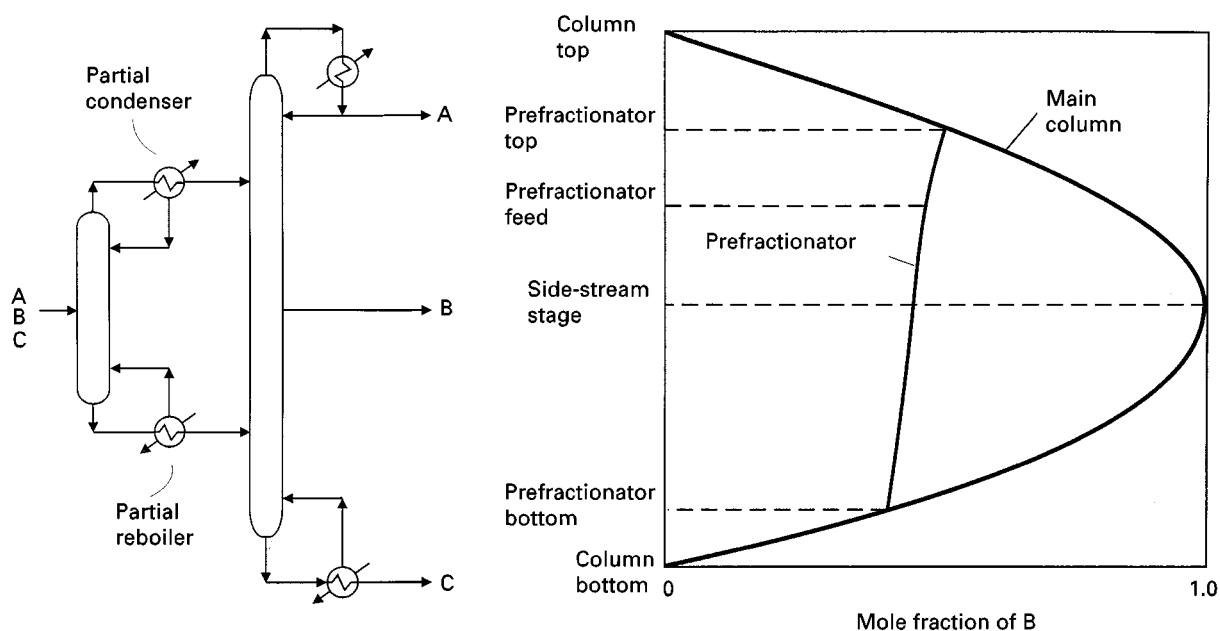


Figure 6 Composition profiles for the middle product in the prefractionator arrangement show that there are no remixing effects. (From Triantafyllou and Smith (1992) *Transactions of the Institution of Chemical Engineers, Part A* 70, 118, reproduced by permission of the Institution of Chemical Engineers.)

This remixing which occurs in both sequences of simple distillation columns is a source of inefficiency in the separation. By contrast, consider the prefractionator arrangement shown in **Figure 6**. In the prefractionator, a crude split is performed so that component B is distributed between the top and bottom of the column. The upper section of the prefractionator separates AB from C, whilst the lower section separates BC from A. Thus, both sections remove only one component from the product of that column section and this is also true for all sections of the main column. In this way, the remixing effects which are a feature of both simple column sequences are avoided.

In addition, one other feature of the prefractionator arrangement is important in reducing mixing effects. Losses occur in distillation operations due to mismatches between the composition of the column feed and the composition on the feed tray. Because the prefractionator distributes B between top and bottom, this allows greater freedom to match the feed composition with one of the trays in the column to reduce mixing losses at the feed tray.

Distillation Using Thermal Coupling

Rather than each column having a reboiler and condenser, it is possible to use material flows to provide some of the necessary heat transfer by direct-contact thermal coupling.

First consider thermal coupling of the simple sequences from **Figure 1**. **Figure 7A** shows a thermally coupled direct sequence in which the reboiler of the first column is replaced by thermal coupling. Liquid from the bottom of the first column is transferred to the second as before, but now the reboiler of the second column supplies the vapour required by the first column. The four column sections marked as 1, 2, 3 and 4 in **Figure 7A** can be rearranged to form a side-rectifier arrangement, as shown in **Figure 7B**.

Similarly, **Figure 8A** shows a thermally coupled indirect sequence in which the condenser of the first column is replaced by thermal coupling. The four column sections marked as 1, 2, 3 and 4 in **Figure 8A** can again be rearranged, but this time forming a side-stripper arrangement.

Both the side-rectifier and side-stripper arrangements have been shown to reduce the energy consumption compared with simple two-column arrangements. This results from reduced mixing losses in the first (main) column. As with the first column of the simple sequence, a peak in composition occurs with the middle product, but now advantage of the peak is taken by transferring material to the side-rectifier or side-stripper.

Side-stripper arrangements are commonly used in petroleum refinery separations. **Figure 9A** shows a typical arrangement for distillation of crude oil. The main column is fed with the pre-heated crude oil feed. Products are taken from various points from the main

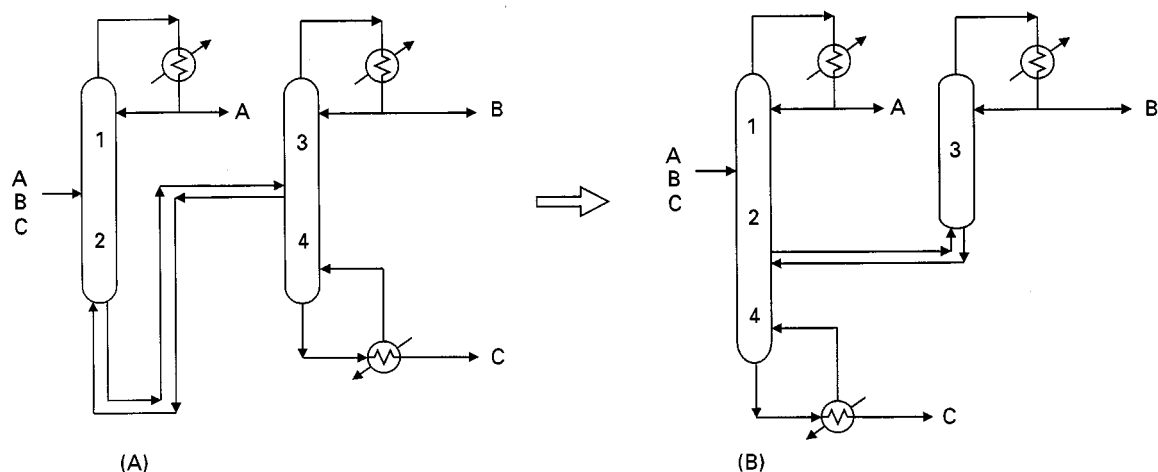


Figure 7 Thermal coupling of the direct sequence. (A) Thermally coupled direct sequence; (B) side-rectifier arrangement. (Reproduced with permission from Smith (1995) *Chemical Process Design*, McGraw-Hill.)

column via side-stripper columns. Heat is also removed at various points through the main column via pumparounds. Pumparounds take liquid from the column, cool it and return it to the column at a higher point, effectively acting as intermediate condensers. Heat to the side-strippers is supplied from either reboilers or live steam injection. The arrangement shown in Figure 9A is equivalent to a sequence of simple columns in the indirect sequence, as shown in Figure 9B.

Consider now thermal coupling of the prefractionator arrangement from Figure 10A. Figure 10B shows the equivalent thermally coupled prefractionator arrangement, sometimes known as the Petlyuk column. To make the two arrangements in Figure 10 equivalent, the thermally coupled prefractionator requires extra plates to substitute for the prefractionator condenser and reboiler.

Various studies have shown that the thermally coupled arrangement in Figure 10B requires typically 30% less energy than a conventional arrangement using simple columns. The saving depends on the feed mixture. In most cases the fully thermally coupled column in Figure 10B requires less energy than the side-rectifier and side-stripper arrangements, for the same separation. The prefractionator arrangement in Figure 10A and the thermally coupled prefractionator (Petlyuk column) in Figure 10B are similar in terms of total heating and cooling duties, but there are differences in the temperatures at which the heat is supplied and rejected.

Figure 11 shows the evolution from the prefractionator in Figure 11A to the thermally coupled prefractionator in Figure 11B. Finally, in Figure 11C, the thermally coupled prefractionator uses a single shell with a vertical baffle dividing the central section

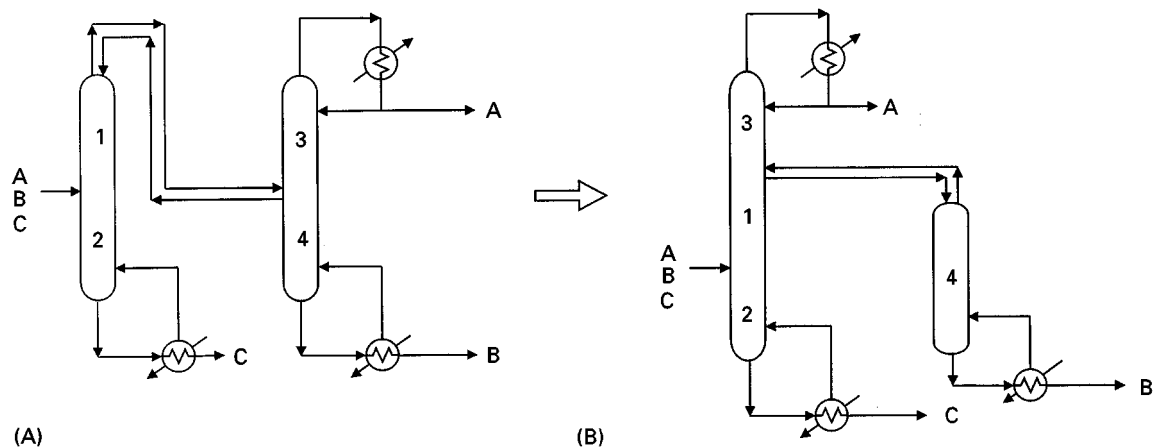


Figure 8 Thermal coupling of the indirect sequence. (A) Thermally coupled indirect sequence; (B) side-stripper arrangement. (Reproduced with permission from Smith (1995) *Chemical Process Design*, McGraw-Hill.)

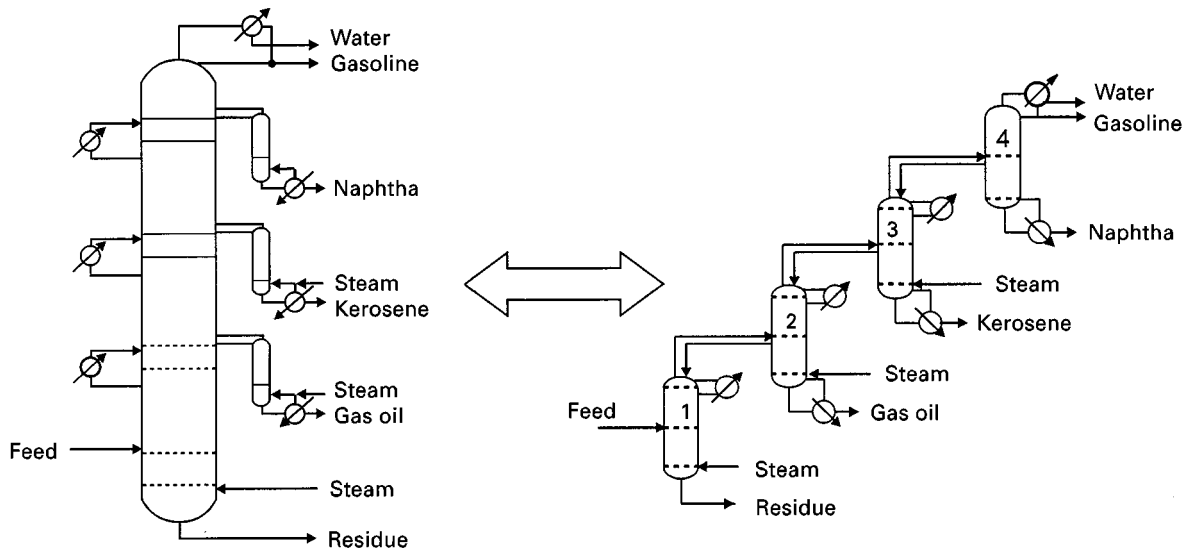


Figure 9 The typical crude oil distillation column decomposes to a sequence of simple columns in the indirect sequence.

of the shell into two parts, known as the dividing wall column or partition column. The arrangements in Figure 11 require almost the same energy consumption, which typically is 30% less than a conventional arrangement. However, in the case of the prefractionator in Figure 11A, the heat load is supplied at two points and rejected from two points. In addition, the dividing wall column in Figure 11C requires

typically 30% less capital cost than a two-column arrangement of simple columns.

Dividing Wall Columns

Dividing wall columns, as shown in Figure 11C, have been known for over 50 years and yet it is only recently that they have been applied in practice. It is

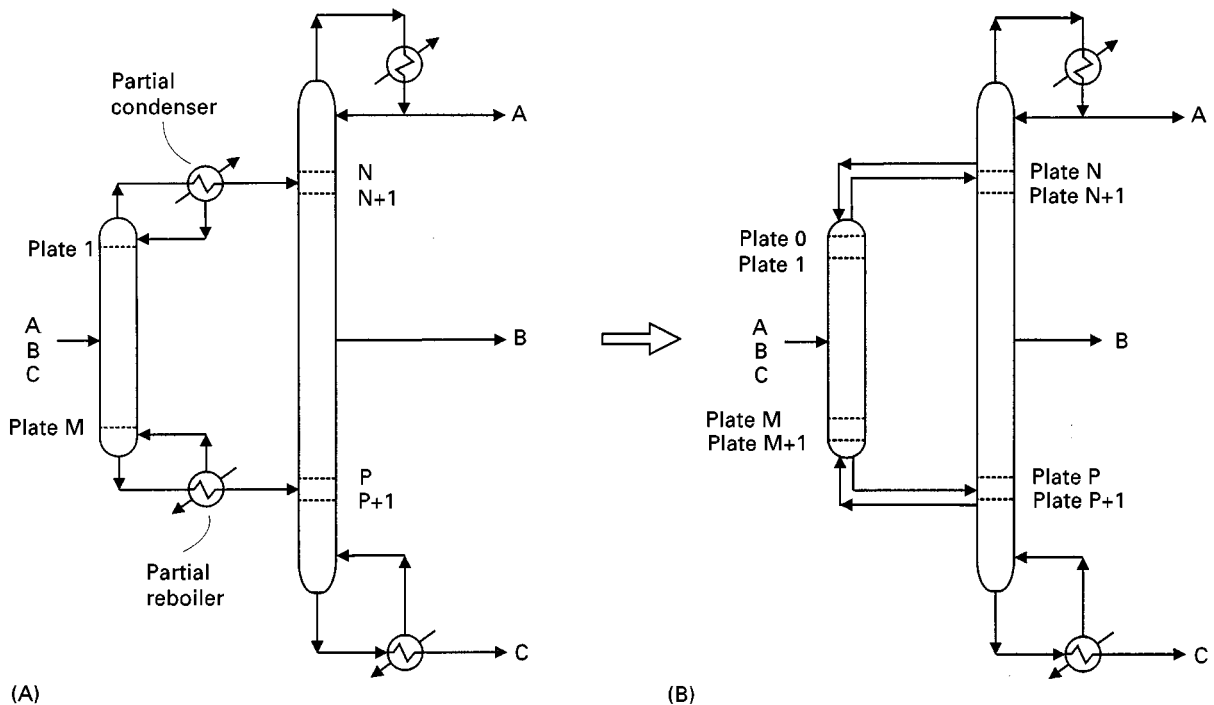


Figure 10 Thermal coupling of the prefractionator arrangement. (A) Prefractionator; (B) thermally coupled prefractionator. (Reproduced with permission from Smith (1995) *Chemical Process Design*, McGraw-Hill.)

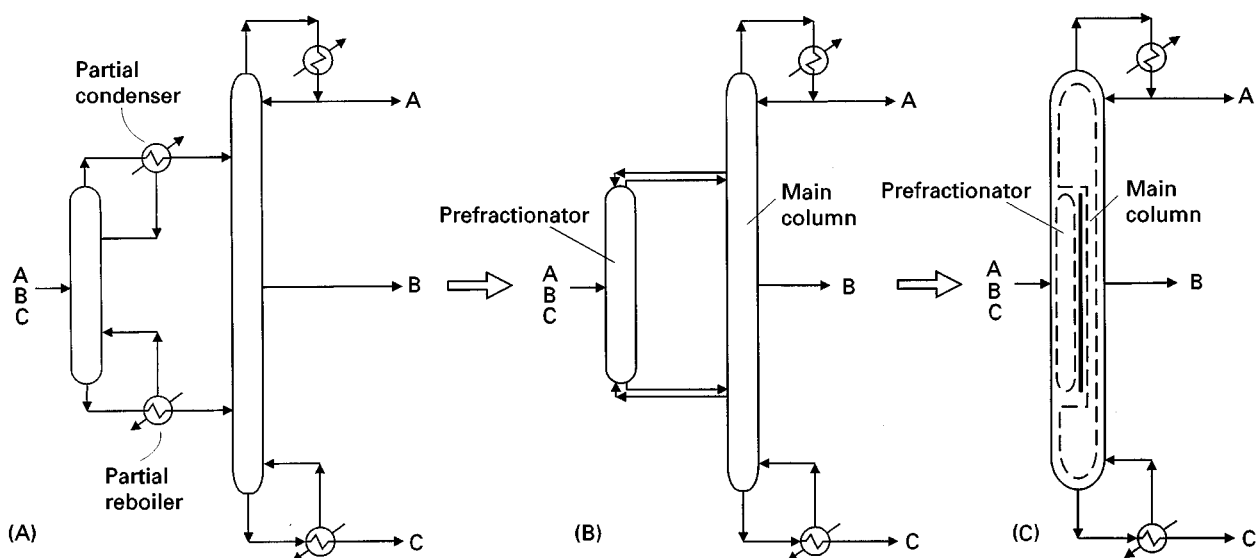


Figure 11 The thermally coupled prefractionator can be arranged in a single shell. (A) Prefractionator arrangement; (B) thermally coupled prefractionator (Petlyuk column); (C) dividing wall column. (Reproduced with permission from Smith (1995) *Chemical Process Design*, McGraw-Hill.)

true that the basic design is more problematic than a single conventional column, because there are more degrees of freedom in the design. However, methods have been developed to initialize the degrees of freedom prior to detailed simulation. Detailed simulation of the dividing wall column is carried out by modeling it as a Petlyuk arrangement, as shown in Figure 10B. Control of the column has also been

a concern. However, such concern is misplaced, as the control is straightforward, being effectively the same as control of a side-stream column. Standard temperature and composition control configuration schemes can be employed. The hardware and column internals for the dividing wall column are also standard, despite the presence of the dividing wall. However, it should be noted that the column performance

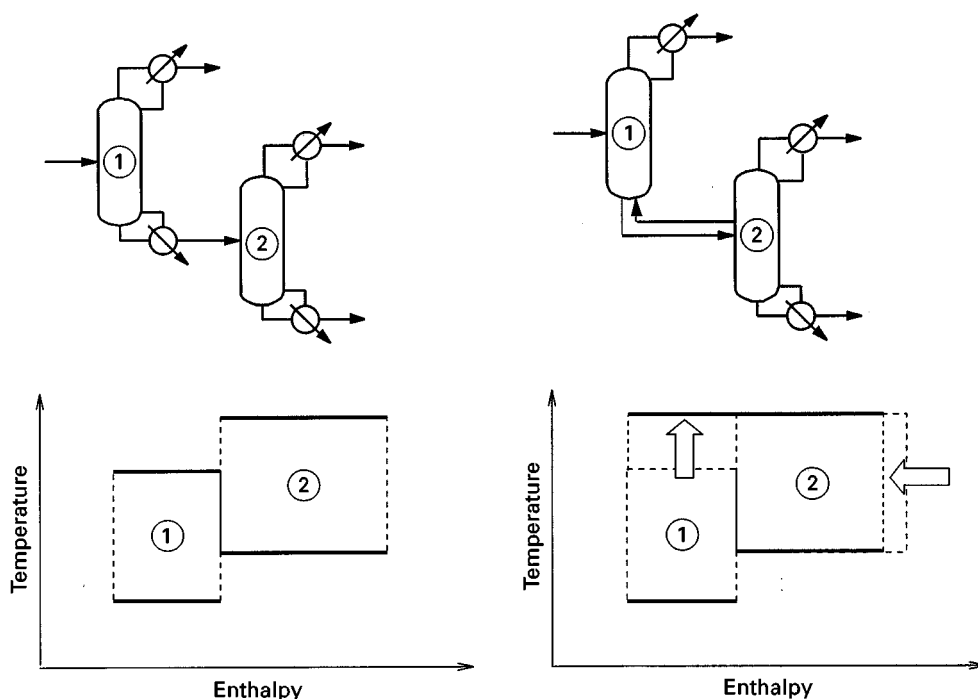


Figure 12 Thermal coupling reduces the quantity of energy required but makes temperatures more extreme.

suffers if the dividing wall is not insulated in some way. This can be done in practice by using two plates separated by a layer of insulation.

Temperature of Heat Supply and Rejection

So far the benefits of thermal coupling have been discussed in terms of the reduced energy required. Let us now consider the temperature at which the heat needs to be supplied and rejected if thermal coupling is used. It is always preferable to add the heat to the reboiler at the lowest temperature possible and to reject heat from the condenser at the highest temperature possible. In the first instance, this allows cheaper hot and cold utilities. In addition, if heat integration of the reboiler and condenser is to be considered, heat integration will also always benefit from lower reboiler temperatures and higher condenser temperatures.

Figure 12 compares a conventional and a thermally coupled arrangement in terms of temperature and enthalpy. In the conventional arrangement there is freedom to choose the pressures of the two columns independently, and thus the temperatures of the two condensers or the two reboilers can be varied independently. In the case of the thermally coupled arrangement no such freedom exists. Although the thermally coupled arrangement requires a smaller heat load than the conventional arrangement, more of the duties are at extreme levels. The smaller duties work to the benefit of utility costs and heat integration but the more extreme levels work against them.

Summary

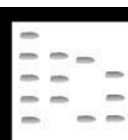
Thermally coupled distillation columns offer considerable benefits in terms of operating costs. Side-stripper, side-rectifier and fully thermally coupled arrangements such as the Petlyuk column can save typically 30% of the energy consumption compared with sequences of simple columns. The magnitude of the saving depends on the feed composition and relative volatility of the components being separated. The dividing wall column also offers large potential savings in capital cost. Apart from the use of side-stripper arrangements in the petroleum refinery industry there has been reluctance on the part of process designers to exploit the full potential of thermal coupling. Control of thermally coupled arrangements does not present any particularly difficult problems.

See also: II/Distillation: Energy Management; Modeling and Simulation; Theory of Distillation.

Further Reading

- Biegler LT, Grossmann IE and Westerberg AW (1997) *Systematic Methods of Chemical Process Design*. New Jersey: Prentice Hall.
- Douglas JM (1988) *Conceptual Design of Chemical Processes*. New York: McGraw Hill.
- King CJ (1980) *Separation Processes*. New York: McGraw Hill.
- Smith R (1995) *Chemical Process Design*. New York: McGraw Hill.

THIN-LAYER CHROMATOGRAPHY – VIBRATION SPECTROSCOPY



E. Koglin, Research Center Juelich,
Juelich, Germany

Copyright © 2000 Academic Press

Introduction

The utility of vibrational spectroscopy in chemical structure elucidation of separated thin layer chromatography (TLC) spots has been recognized for many years. Although the traditional method has been infrared spectroscopy (Fourier transform infrared spectrometry (FTIR)) a number of com-

peting techniques now exist including normal Raman scattering (RS), Raman microspectroscopy (Micro-Raman), Fourier transform Raman (FT-Raman) and surface-enhanced Raman scattering (SERS). Since each type of spectra provide essential vibrational profile of analytes from the TLC plate, the different disciplines are natural partners in a general spectroscopic analysis. All methods involve the vibrational energy of the molecule and thus provide molecular and structural information about the separated sample. However, since infrared (IR) absorption, Raman scattering and SERS have different selection rules – what is frequently strong in

a Raman spectrum is weak in an IR spectrum and vice versa. For this reason, a combined IR and Raman system offers the flexibility of working with almost any sample, as well as complete vibrational information from numerous compounds.

Up to now the combination of TLC separation and IR spectroscopy has been approached in roughly two ways. The classical approach for recording IR spectra is to elute the separated TLC zones from the layer onto an IR-transparent pellet or powder (sample transfer TLC-FTIR). Numerous workers have attempted to record diffuse reflectance Fourier transform infrared (DRIFT) spectra directly on TLC plates (*in situ* TLC-FTIR). A small number of research groups have studied the applicability of near-infrared spectroscopy (NIR) in the reflectance mode as an *in situ* detection tool in TLC.

Although IR spectroscopy still yields the largest number of publications in the field of TLC vibrational analysis many serious attempts are now being made to explore the analytic potential of Raman spectroscopy in new and challenging areas of TLC spot identification. The use of Raman scattering eliminates moisture and background absorption problems which may be present in the infrared-based techniques. Therefore, a number of important advantages to this Raman technique exist: (1) most common TLC matrices can be used with little interference, (2) spectra can be taken *in situ* from wet or dry plates, (3) the well-known advantages of NIR excitation ($\lambda_{\text{ex}} = 1064 \text{ nm}$) in FT-Raman (avoidance of fluorescence and photo-induced sample damage), (4) the use of Raman microspectroscopy which allowed unambiguous placement of the laser focus on the TLC plate with spatial resolution of the order of $1 \mu\text{m}$.

One of the significant limitations of the application of Raman spectroscopy in the field of TLC chromatogram spot characterization is the lack of sensitivity. An important step forward was made by SERS. Raman scattering intensities from adsorbed substances on nano-metal particles (Ag, Au, Cu) are increased by a factor of 10^5 – 10^6 compared to those of the nonadsorbed compounds at equal concentration. For TLC this SERS effect is accomplished by spraying chromatograms with colloidal silver solution or silver coating in a vacuum chamber (post-chromatographic SERS activation in TLC). By using SERS microprobe techniques (laser spots down to $1 \mu\text{m}$ in size) and high performance thinlayer chromatography (HPTLC) plates it is possible to achieve low picogram detection limits for HPTLC spots.

Fourier Transform Infrared Spectroscopy (FTIR)

Sample Transfer TLC-FTIR

The classic approach and most frequently used method for recording infrared spectra of substances separated by TLC or HPTLC involves removal of the sample zone from the plate, usually followed by extracting the analytes via a solvent to an IR-transparent pellet or powder. This technique makes it possible to measure full IR spectra at a reasonable sensitivity using conventional FTIR transmission or DRIFT detection. Commercial accessories are available for a simple and convenient procedure for the transfer of the analyte spots to cups containing IR-transparent substrates. The use of this method has been illustrated by the analysis of dyes, quinones, coal extracts and biochemical substances. Reasonable IR spectra with full spectral features can be obtained from 1 to $0.01 \mu\text{g}$ of sample per spot. The main reason for using transfer in TLC-FTIR is to avoid the strong absorption bands in the mid-IR (400 – 4000 cm^{-1}) from the TLC stationary phase. Over the years, numerous other transfer methods for the combination of TLC or HPTLC and FTIR detection have been described in the literature. The normal method involves removal of zones (scraping off), elution of the spot analyte, deposition on the material transparent to IR and the measurement by FTIR. However, the removal of zones from the plate increases the risk of contamination and can result in further reactions. The "wick-stick" technique consists of pressing KBr micro pyramids onto the TLC plate at locations corresponding to the analyte spot. With a development perpendicular to the first development, the analytes are eluted into the pyramids, which are then dried and pressed into pellets. The Eulochrom system involves the elution of analyte zones from silica-gel TLC plates by means of small amounts of methanol, then solvent evaporation and pellet preparation. A simple and convenient procedure in conjunction with TLC sheets with a liquid-permeable support such as the Empore TLC sheet is the transfer of separated spots to a powder layer of potassium bromide. After ordinary TLC development, the sheet is put in a sheet holder chamber and a thin layer of KBr powder is applied on the upper side of the Empore TLC sheet. After this KBr coating, zones are eluted from the sheet by means of a wetted fritted glass unit and thus moved into the powder layer.

Thermal desorption FTIR analysis can be used to avoid the interference from TLC stationary phases with analyte because strong interaction between the analyte and the stationary phase causes significant

band shift. Therefore, vapour-phase spectrum libraries can be used directly for sample identification. This method can be applied to thermally stable substances which can be desorbed from thermally stable TLC stationary phases. The separated TLC spot is scraped off and loaded onto the sample pan of a thermogravimetric analyser (TGA/FTIR). Spectra are easily identified for samples present at a level of 10 µg per TLC zone. A detection limit of 0.8 µg is found for analysis of methyl benzoate.

Over the years, research and practical applications have shown that sample transfer TLC-FTIR technique (offline coupling for TLC and FTIR) can be effective and useful as a reliable TLC spot identification method.

***In situ* TLC-FTIR**

IR spectral identification of a TLC spot by means of sample transfer TLC-FTIR methods is usually time consuming and problematic. Alternatively, IR spectroscopic information about TLC-separated materials can be obtained *in situ* by means of a variety of FTIR techniques. Monitoring the TLC zones by direct DRIFT measurements, transmission spectroscopy, infrared microspectroscopic detection and photoacoustic FTIR (PA-FTIR) enables both qualitative and quantitative characterization of separated spots. To acquire useful IR spectra the *in situ* TLC spot method requires the background measurement of the adsorbent free of any sample. The final IR spectrum is obtained by either ratioing sample and background measurements or subtracting the background spectrum from the sample spectrum. This part of the *in situ* TLC-FTIR detection method is very important for the quality of the resulting analyte IR spectrum. Depending on the nature of the isolated TLC spots and the goal of the analysis, the choice of IR measurement can be either DRIFT or transmission.

Today online coupling of TLC(HPTLC) and DRIFT spectroscopy can be carried out using commercially available equipment. By combination a computer-controlled x-y stage with a specially constructed DRIFT unit and an FTIR spectrometer it is possible to obtain direct IR chromatograms of TLC spots. The chromatograms can be generated both frequency-dependent as spectral windows of a certain range and frequency-independent as a Gram-Schmidt trace. Depending on the infrared absorptivity of the TLC analyte and the distance run in the chromatogram, the limits of identification, the validated detection limits, and the limits of quantification lie between 10 ng and 2.5 µg.

In general, use of automated multiple development (AMD) for TLC separation can improve the online

DRIFT identification limit by one-third compared to conventional TLC separation techniques.

The *in situ* FTIR detection of spots on a plate by means of IR transmission measurements requires an IR transparent support, e.g. silica gel coated on AgCl plates. A thin adsorbent coating and IR transparency of the silver chloride support permits enough energy throughput to acquire analyte species at 0.1–10 µg of material. The detection limit of this technique in conjunction with programmed multiple development and special postcoatings can be improved to the nanogram level. This technique is limited to noncommercially available AgCl speciality plates.

The development of microchannel TLC spot identification with diffuse reflectance infrared microspectroscopic detection is also a method for specific practical applications. In this case a zirconia stationary phase is used instead of silica or alumina. Zirconia shows significantly higher reflectivity than silica or alumina resulting in only moderate background interferences. The detection limit for this specially prepared plate is about 1–10 ng.

Photoacoustic FTIR has been suggested as the technique of choice over DRIFT analysis of high IR-absorbing sample matrices. Photoacoustic spectrometry (PAS) is based on the phenomenon that light impinging on the solid TLC plate, can produce an acoustic signal. PAS involves therefore the measurement of oscillating pressure variations of a confined inert gas situated above the TLC plate. In combination with a PAS cell an FTIR spectrometer can yield photoacoustic IR spectra, which can be applied for TLC zone identification purposes. PA-FTIR does not require sample preparation and avoids the effects of light scattering and reflection.

TLC-NIR

Both mid-infrared (mid-IR) and NIR spectroscopy are important techniques for TLC or HPTLC spot analysis because of their sensitivity and versatility. The main difference between mid-IR and NIR is that bands in the mid-IR are primarily due to molecular fundamental vibrations, and absorption in the NIR region, 800–2500 nm, is primarily due to overtone and combination bands of, O-H, N-H, S-H and C-H functionalities. In the NIR region absorption is rather weak and TLC adsorbents such as silica gel have no strong absorption bands in these NIR regions, so background interferences are very small. Also, nearly all analytes of interest absorb in the NIR region.

Direct, *in situ* diffuse transmission FT-NIR microspectroscopic detection of separated HPTLC spots of different kinds of phospholipids give typical results

from which the usefulness of the TLC-NIR method can be evaluated. The limit of detection with a narrow NIR beam of light (0.4 mm^2) is under $1 \mu\text{g}$, and the correlation coefficient of the calibration curve is about 0.98 for phospholipid amounts from 1.25 to $10 \mu\text{g}$. Detection limits of less than $1 \mu\text{g}$ of selected sugar samples on developed TLC plates have been demonstrated with the use of NIR detection with a diffuse-transmittance geometry.

Raman Spectroscopy

TLC/Normal RS

In contrast to FTIR spectroscopy, where we have been concerned with the absorption of infrared light, RS depends on the frequency of the laser light scattered by molecules as they undergo rotation and vibration and in this respect it is similar to infrared spectroscopy. Since the selection rules are different, the information obtained from the laser Raman spectrum often complements that obtained from FTIR studies and provides valuable structural information. The intensity of Raman scattering is directly proportional to the laser excitation intensity and to the concentration of the TLC sample. This is important in quantitative studies. Therefore, laser RS can be considered as a tool for *in situ* analysis of TLC or HPTLC spots, since materials such as silica gel matrices give weak Raman spectra and minimal interference with the spectra of the adsorbed species on the TLC plate.

Using an argon-ion laser for visible excitation (488 or 514 nm) and dispersive Raman units, detection limits for different separated nonresonant substances are in the μg region. In the past *in situ* Raman microspectroscopic investigations on different TLC plates have shown that the detection limit by means of this Raman method could be improved up to the ng region. As an example, nonresonant Raman spectroscopy of representative explosive samples separated on silica gel plates have shown that visible conventional macro-sampling RS can be used nondestructively to detect and identify this substance class down to a few micrograms. The same investigations by means of visible Raman microprobe spectroscopy (scanning laser diameter of $8 \mu\text{m}$) gave improved detection of these explosive substances (the detection limit of TNT is $0.5 \mu\text{g}$).

TLC/Resonance RS

As the laser exciting frequency in the Raman experiment approaches an allowed electronic transition in the molecule being investigated, those normal modes that are vibronically active in the electronic transition

exhibit a pronounced enhancement in their Raman intensities. Most examples of resonance-enhanced RS involve the enhancement of totally symmetric modes. The resonant Raman effect can enhance Raman intensities by factors of the order of 10^5 . This means that corresponding lower concentrations of scattering molecules on the TLC spot can be used, therefore improving the detection limit. An example of the enhanced intensity from the resonance Raman effect is the investigation of silica gel TLC zones of metalloporphyrins. Using 514.5 nm excitation and an optical multichannel analyser, nanogram levels of the strong absorbing analytes (Ni-uroporphyrin, Ni-protoporphyrin) in the visible spectral range have been obtained.

TLC/FT Raman

The past few years have seen pronounced growth in the use of dispersive and interferometric RS in the field of TLC spot identification, largely attributable to increased awareness of the technique's potential as well as the new methodology and hardware. These developments include, in particular, near infrared Fourier transform Raman spectroscopy (NIR FT-Raman). Since the development of NIR lasers, both fluorescence and photodecomposition problems have been reduced or avoided in most cases. In particular, the Nd:YAG lasers emitting at 1064 nm have proven advantageous due to their long wavelength λ , high power, and stable intensity. Absorption of the TLC plates from the silica coating and the glass substrate are avoided and the full Raman spectral range may be collected without interference. Commercially available X-Y-Z stages for TLC plates can be placed directly in FT-Raman instruments and the measurement of the TLC spot taken *in situ*. One further advantage arises from the use of newly developed HPTLC plates for Raman spectroscopy (Merck, HPTLC aluminium sheet Si 60 F254s Raman). The potential and benefit of this *in situ* hyphenation of HPTLC and Raman spectroscopy in its broad spectral range, no interference by the silica matrix, identical spectra with standard Raman spectra, high sensitivity of detection and about 10-fold intensity of signal/noise compared to conventional HPTLC plates.

The feasibility of measuring the Raman spectra of chlorinated hydrocarbon pesticides on TLC adsorbents was initially studied using high concentrations (about $100 \mu\text{g cm}^{-2}$) of separated pesticides on normal silica gel TLC plates. In the case of N-heterocyclic pesticides the detection limit on normal HPTLC plates could be reduced to low $\mu\text{-gram}$ region. As an example, **Figure 1** shows the FT-Raman investigations of the MPP(1-methy-4-phenylpyridi-

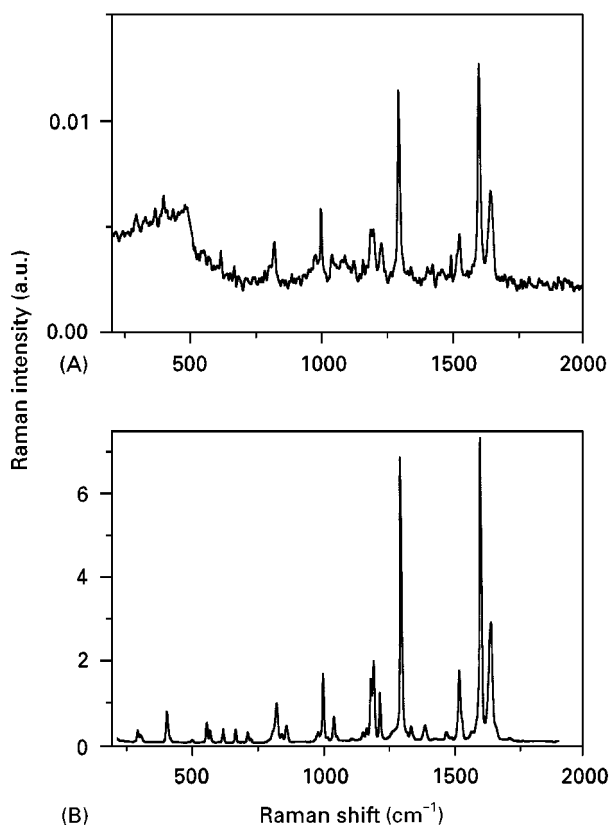


Figure 1 FT-Raman spectra of the pesticide 1-methy-4-phenylpyridiniumiodine (MPP). (A) 500 ng of MPP spotted on a HPTLC silica gel 60 plate and (B) as the pure crystalline powder. Bruker: NIR FT-Raman spectrometer RFS 100; $\lambda_{\text{ex}} = 1064 \text{ nm}$, laser power 630 mW, 4 cm^{-1} resolution.

niuniodine) pesticide on a silica gel HPTLC plate and the corresponding pure material. In comparing the two spectra, no significant band shifts were observed but all bands in the spectrum of the HPTLC spot were broader than in the spectra of the polycrystalline pure substance.

In some basic experiments, the feasibility was demonstrated of obtaining artifact- and fluorescence-free spectra by *in situ* FT-Raman spectroscopy of paracetamol, fluorene and rhodamine B on silica gel TLC plates. For the strong Raman scatterer fluorene, the detection limit was found to be 500 ng for a 3 mm diameter TLC spot.

Several pharmaceutical test compounds have also been investigated and together with the use of FT-Raman spectral libraries for identification of TLC spectra and different search algorithms have been compared.

At present further work is in progress to investigate factors which could improve the *in situ* spot analysis of TLC, HPTLC and Raman-HPTLC plates by means of FT-Raman spectroscopy.

SERS Spectroscopy

The discovery that Raman vibrational signals from molecules adsorbed on nanometer scale metal particle structures are enhanced by 10^6 to 10^9 has caused extraordinary interest and excitement. This Raman technique, known as SERS offers new possibilities as a spectroscopic probe in the field of TLC separation science. It was shown that excellent Raman spectra could be obtained for low nanogram to picogram amounts of nonresonant and fluorescent substances on filter paper, paper chromatographic supports, and TLC or HPTLC plates using SERS spectroscopy.

The Raman scattering cross-section of an adsorbed molecule on nanometal structures can be further increased by utilizing a laser excitation frequency which is in resonance with an electronic transition in that molecule. This molecular resonance Raman scattering and the SERS effect can combine to give surface-enhanced resonance Raman scattering (SERRS) so that the limit of detection is further increased. Therefore, by detecting resonant molecules on TLC (HPTLC) plates in conjunction with the SERRS effect, very low concentrations have been achieved in many fields of research. Another striking feature of SERRS spectroscopy is that the fluorescence of the analyte on TLC plates can be completely quenched by the presence of a nanometal surface. Therefore, the SERRS quenching effect generates a high-quality surface Raman spectrum.

For TLC (HPTLC) this SERS or SERRS effect is accomplished by spraying chromatograms with colloidal silver solutions (reduction of AgNO_3 with NaBH_4 or citrate). In order to further improve the sensitivity of the TLC-SERS method experiments have been carried out in the field of well-defined vacuum-deposited silver films onto the separated and developed TLC plates. The TLC plates were mounted on a holder inside a vacuum chamber where silver is thermally evaporated onto the plate. The evaporation rate and the silver thickness are controlled in order to find out the most intense SERS signals. Such SERS-activated TLC plates are stable for many weeks and can therefore be considered as an 'analytical diskette' for Raman spectroscopy. In addition to these post-activation methods, two other possibilities for SERS activation can be identified: (1) the simultaneous activation of the plate with spotting of the sample, e.g. by dissolving the sample in Ag colloidal solution, (2) pre-activation of TLC plates via *in situ* decomposition of silver carboxylates.

In order to reveal the optimal conditions in TLC-SERS spectroscopy, atomic force microscopy (AFM) was applied to investigate the surface morphology of the Ag labelled TLC substance spots (colloid

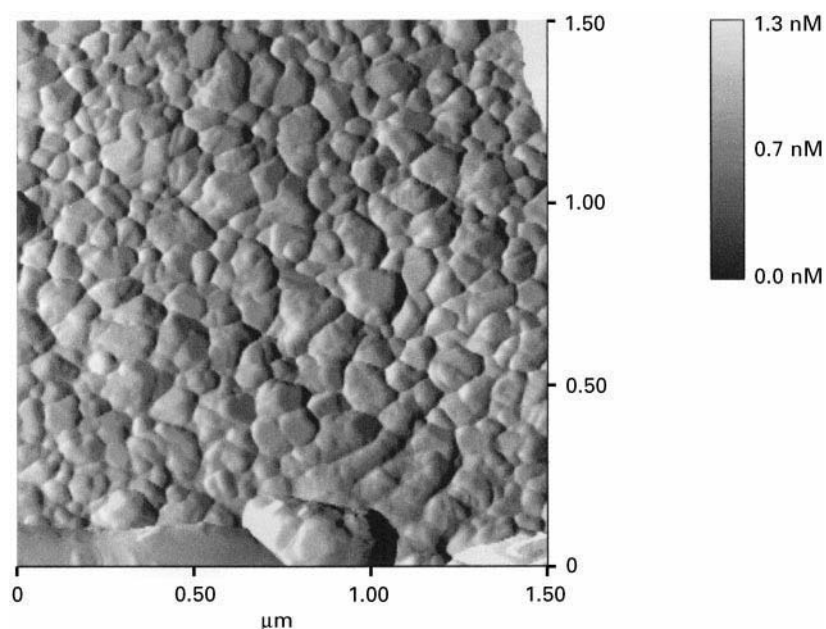


Figure 2 (See Colour Plate 120) AFM photograph of a silver-coated HPTLC silica gel KG60 plate (post-overlayer SERS activation). NanoScope III; tapping mode.

TLC-SERS and overlayer TLC-SERS). **Figure 2** shows an example of the AFM picture of a post-activated silver-coated HPTLC silica gel plate in the μm scale (post-overlayer SERS activation).

TLC/VIS-SERS

The first report on the combination of planar chromatography and SERS with colourless (non-resonance Raman scatterer) analyte spots was the direct analysis of HPTLC spots of nucleic purine derivatives in 1987. After separation and drying, HPTLC plates were sprayed to wetness with colloidal silver solution by a spray atomizer. The chromatogram zones were analysed at room temperature by a computer-controlled double beam monochromator and the excitation wavelength was the 514.5 nm line of an argon ion laser. Limits of detection were estimated to be less than 5 ng/spot. Comparison of these HPTLC/VIS-SERS spectra with normal Raman spectra of molecules in aqueous solution reveals significant differences: (1) the relative band intensities are changed due to vibration-dependent surface-enhanced scattering mechanism, (2) band shifts can occur (e.g. shift of ring breathing mode of adenine from 724 to 736 cm^{-1}), (3) band broadenings were observed in the HPTLC/VIS-SERS spectra.

In clinical chemistry, immunoassay methods in conjunction with TLC play an important role in the routine determination of active substances in body fluids. For instance it is possible to separate theophylline without difficulty from its positional isomers

and from other xanthine derivatives. *In situ* identification of these compounds using online HPTLC/VIS-SERS can be performed in the ng region.

Examples of TLC/VIS-SERS measurements from many research groups have been selected to illustrate the high sensitivity, molecular specificity, accuracy, easy SERS sample preparation, and the significant manifold application.

The result of all these investigations is that the TLC/VIS-SERS detection appears to depend on different factors which must be considered before any normal application. Close approach to, or direct contact with, silver colloids of investigated analytes are a prerequisite of Raman scattering enhancement. Furthermore the size, shape, dimension and electrical charge density of the silver colloids are very important. Control and optimization of all these parameters would increase the feasibility of TLC/VIS-SERS *in situ* detection to a maximum number of chemical compounds separated on TLC(HPTLC) plates.

TLC/SERRS

The surface-enhanced resonance Raman effect in the field of chromatogram spot identification, first reported in 1984 by Tran (see Further Reading), has led to the study of a variety of separated dye molecules with different chromatographic techniques. Three structurally similar dyes, crystal violet, malachite green and basic fuchsin were chosen in order to show the potential of SERRS for the direct identifica-

tion of chromatogram spots separated by means of paper chromatography. The detailed vibration spectra allowed identification and the limit of detection was 2 ng cm^{-2} .

After this work, different types of dyes, TLC (HPTLC) plates, the role of the supporting matrix and sol preparation protocols were investigated and examined for their influence on the SERRS signal. The investigations of all these effects and the construction of a remote sensing Raman spectrometer to investigate the model compound pararosaniline resulted in the maximum SERRS intensity yielding a detection limit of about 108 femtomol (33 pg) of this pararosaniline dye.

Another very interesting application is the incorporation of SERRS as a detector for a liquid chromatography (LC)-coupled TLC system. In this SERRS/LC/TLC system, effluent from the LC system was deposited onto the TLC plate and an activated Ag sol was added to the plate. Optical fibres carried the 514.5 laser light to the TLC plate and the scattering radiation to the Raman spectrometer. The dye molecule, pararosaniline acetate, was found to give a linear SERRS signal over the concentration of 1×10^{-5} to $1 \times 10^{-7} \text{ M}$ range and the limit of detection was 750 fmol.

The measurements of other highly fluorescent molecules such as acridine orange, rhodamine, Glu-P2 as well as N-containing PAHs separated on HPTLC plates have shown that the sensitivity is so high that *in situ* vibrational investigations are possible with low picogram amounts of material.

Today, it is clear that TLC/SERRS spectroscopy can be widely applied to obtaining structural information about very small amounts of coloured substances (dyes, pigments) separated by TLC or HPTLC.

TLC/Micro-SERS

Following the rule that 'an optimized Raman scattering sample is a micro sample' Raman microspectrometers have been designed for investigation of small particles in the μm range. Although there is earlier work in the coupling of a microscope and a Raman spectrometer, by far the largest amount of work has been carried out in the past 10 years. The new generation of Raman microprobe spectrometers comprise modern monochromators with notch filter systems, charged coupled device (CCD) detectors and confocal optics. This type of laser confocal Raman microspectrometer permits the acquisition of Raman spectra from TLC(HPTLC) spots down to $1 \mu\text{m}$ in size and allows the unambiguous placement of the laser focus at the chromatogram with a spatial resolution of $1 \mu\text{m}$.

In the first study on HPTLC/Micro-SERS, a Raman microspectrometer consisting of an argon ion laser, a microscope, a triple monochromator and a multi-channel detector was used. With this system it was possible to acquire VIS-SERS spectra of silica gel HPTLC spots of DNA bases and dibenzofuran at the low picogram level. Considering the fact that the laser focus is about $1 \mu\text{m}$, the irradiated spot mass is only a few femtograms. Combining this microsurface-enhanced Raman scattering and HPTLC has also enabled *in situ* analysis of chromatogram spots of cationic surfactants in amounts down to subnanogram levels.

Micro-Raman equipment and the SERRS effect have been used for selective detection of structurally similar aminotriphenylmethane dyes separated by HPTLC. *In situ* SERRS spectra were recorded after the application of aqueous Lee-Meisel hydrosol solution (reduction of silver nitrate with sodium citrate) to the analyte spot. The limits of identification of the dyes are of the order of 5 ng (applied amount).

Recently the optical detection and spectroscopy of single molecules and single nanoparticles was achieved with the use of SERRS spectroscopy for rhodamine 6G adsorbed on selected silver nanoparticles. This was the first application of Raman spectroscopy in the field of 'probing single molecules by means of Raman vibration spectroscopy'.

As a result of the dramatic improvement of the sensitivity in the coupling of TLC and SERRS microspectroscopy, it is possible to probe low numbers of molecules on TLC plates. Figure 3 shows the high sensitivity of TLC/Micro-SERRS spectroscopy by demonstrating the identification of rhodamine 6G on a HPTLC plate at a concentration as low as $1 \mu\text{L}$ of 10^{-10} M solution applied on the plate. Considering the fact that the 488 nm laser spot is only $1 \mu\text{m}$ in diameter, the number of R6G molecules in the analysed area are substantial between 400 and 600.

Figure 4 shows the topography of a selected area from the silver colloidal SERS activated silica gel (KG60) HPTLC spot of R6G. This AFM picture clearly shows the Ag nanoparticle adsorbed on the silica gel particles of the HPTLC plate. Depending on the colloid aggregation on the substance/silica zone, the diameter of the Ag particles is in the region between 10 and 60 nm.

According to the short range sensitivity of SERRS (about 1 nm from the surface) the spectra obtained from the HPTLC spot are attributed to molecules which have a direct contact to the surface of the colloids.

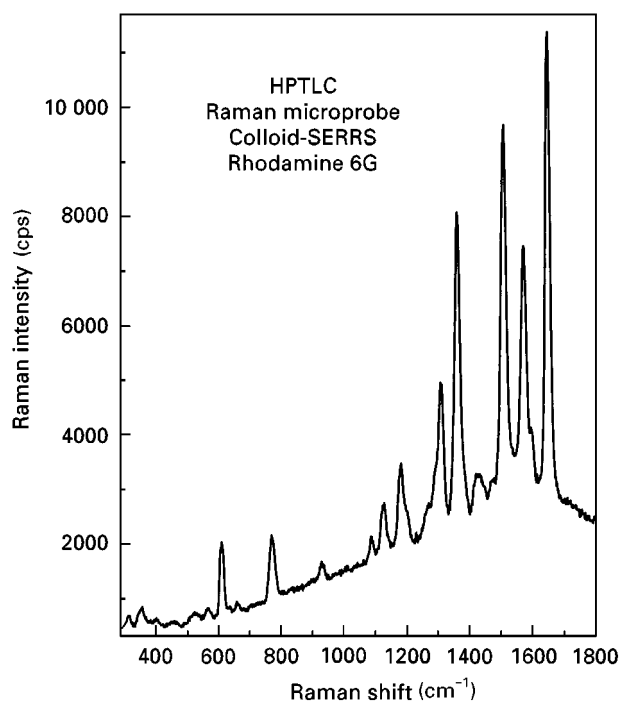


Figure 3 HPTLC/SERRS microprobe analysis of rhodamine 6G. 1 μL of 10^{-10} M R6G applied on the silica gel (KG60) HPTLC plate. 1 μm selected with the focused laser beam. Laser excitation line, 488 nm; laser power at the spot, 8 mW; integration time, 3 s; number of reads, 80. Number of molecules in the scattering volume 400–600 R6G molecules.

TLC/FT-SERS

Some years ago, NIR FT-SERS spectroscopy was suggested as an alternative experimental method to conventional dispersive Raman spectroscopy in TLC/SERS. Because of the NIR excitation at 1064 nm and the fluorescence-quenching effect of the SERS effect, TLC plates containing indicator could be used without any problem. In the first TLC/FT-SERS experiments, good-quality FT-SERS spectra of a spot of 40 ng rhodamine B was recorded after spraying with a silver colloid solution. These preliminary results have shown that the SERS effect also works on TLC plate spots in the NIR spectral range. In general, it was also found that the enhancement factor at 1064 nm excitation was increased by one or two orders of magnitude as compared with the 514.5 laser excitation.

Direct analysis of sub-femtogram quantities of carotenoids on different types of TLC plates has been made possible by associating FT-Raman micro spectroscopy with the SERS effect. In this HPTLC/micro-FT-SERS experiment, detection of 10^{-5} M crocetin corresponded to a deposited mass of 1.65×10^{-8} g, thus in the 8 μm laser spot an analysed mass of 0.02 fg. These postactivation SERS investigations have also shown that SERS intensity is not dramatically influenced from the TLC layer thickness, particle size distribution, mean particle size and presence or absence of a fluorescence indicator.

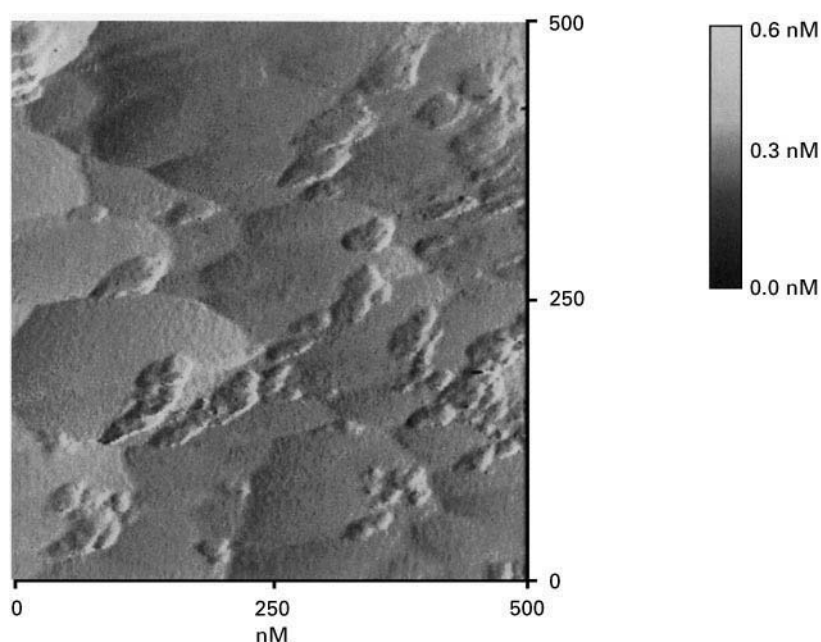


Figure 4 (See Colour Plate 121) AFM (tapping mode) surface plot of a silver colloidal SERRS activated silica gel plate (KG60, Merck). A selected $X = Y = 500$ nm spot area of a 1 μL of 10^{-10} M rhodamine 6G spotted on the plate. The silver hydrosol marker has a diameter of between 10 and 60 nm.

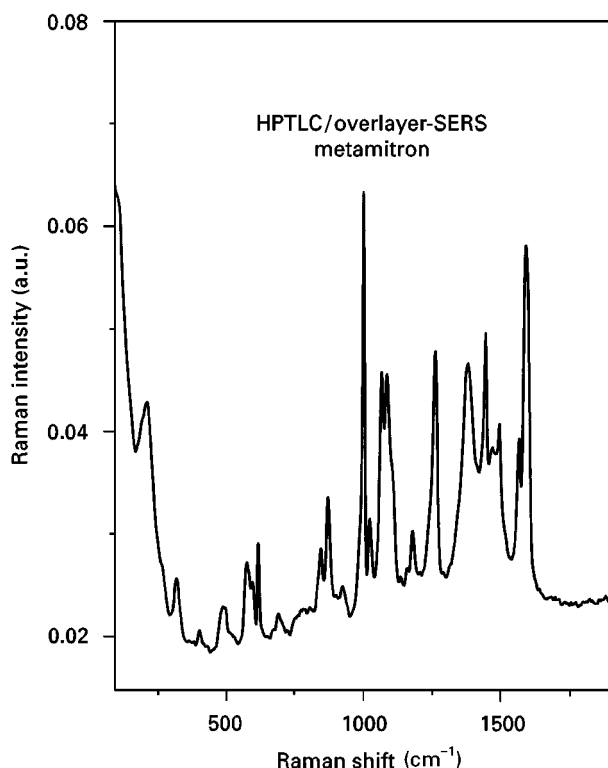


Figure 5 HPTLC/FT-SERS analysis of metamitron on a KG60 plate with a silver-coated layer of 20 nm thickness. 1 μ L of 10^{-5} M metamitron spotted on the KG60 plate. Bruker: NIR FT-Raman spectrometer RFS 100 S; $\lambda_{\text{ex}} = 1064$ nm, laser power 400 mW, 4 cm^{-1} resolution.

The possibility of TLC/FT-SERS pre-activation of TLC plates has been demonstrated for heterocyclic and aromatic species (pyrene, anthracene fluoranthene, biphenyle and benzoquinoline). The pyrolysis of pre-deposited silver oxalate forms FT-SERS system based on TLC plate. This thermal decomposition of silver oxalate represents a new, simple method of pre-activation in TLC/FT-SERS spectroscopy. The disadvantage is that R_F values on these pre-activated TLC plates are strongly influenced by the Ag clusters on the plate. Therefore, in this case one has new separation conditions on the TLC plate.

The most useful and effective method for TLC/FT-SERS spectroscopy is the postchromatographic silver coating of the TLC plate inside a vacuum evaporator (overlay TLC/FT-SERS). As an example to demonstrate this new technique, a HPTLC/FT-SERS spectrum of metamitron (1 μ L of 10^{-5} M metamitron spotted on HPTLC-KG60 plate) which was coated with a 20 nm thick layer of silver, is shown in **Figure 5**. Therefore this overlay TLC/FT-SERS spectroscopy is very suitable for the investigation of separated pesticide spots on TLC plates.

As a consequence of their advantages the combination of TLC/FT-SERS techniques with silver coating of the TLC plate inside a vacuum evaporator will extend the use of surface-enhanced Raman spectroscopy to a much greater range of samples than examined so far.

Conclusion

The examples of the coupling of TLC and vibration spectroscopy in the separation technique reviewed in this article have been selected to illustrate the sensitivity, molecular specificity of separated substance zones, accuracy, ease of sample preparation, and the many significant applications of FT-IR, Raman analysis and SERS spectroscopy for substances in the adsorbed state on TLC (HPTLC) plates. The sensitivity and rich spectral information that FT-IR, Raman and SERS provide have spurred the rapid development of technology for using vibration spectroscopy as an analytical detection method of separated TLC spots. With the extremely high enhancement of the Raman scattering signals on SERS-activated TLC plates it is possible to identify *in situ* separated TLC spots at the pico- and femtogram level. Further work is in progress to investigate factors which could improve the utility of vibrational spectroscopy in chemical structure elucidation of separated TLC zones.

See Colour Plates 120, 121.

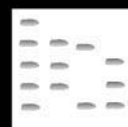
See also: **II/Chromatography: Thin-Layer (Planar):** Modes of Development: Conventional. **III/Dyes:** Thin-Layer (Planar) Chromatography. **Pesticides:** Thin-Layer (Planar) Chromatography. **Pigments:** Thin-Layer (Planar) Chromatography.

Further Reading

- Garrel LG (1989) Surface-enhanced Raman scattering. *Analytical Chemistry* 61: 401A–411A.
- Gocan S and Cimpan G (1997) Compound identification in thin layer chromatography using spectrometric methods. *Reviews of Analytical Chemistry* 16: 1.
- Koglin E, Kreisig SM and Copitzky T (1998) Adsorption of organic molecules on metal nanostructures: State of the art in SERS spectroscopy. *Prog Colloid Polym Science* 109: 232.
- Mustillo DM and Ciurczak EW (1992) The development and role of near-infrared detection in thin-layer chromatography. *Applied Spectroscopy Reviews* 27: 125.
- Petty C and Cahoon N (1993) The analysis of thin-layer chromatography plates by near-infrared FT-Raman. *Spectrochimica Acta* 49A: 645–655.
- Somsen GW, Morden W and Wilson ID (1995) Planar chromatography coupled with spectroscopic techniques. *Journal of Chromatography A* 703: 613–665.

- Somson GW, Riet P, Gooijer C, Velthorst NH and Brinkman, UAT (1997) Characterization of aminotriphenylmethane dyes by TLC coupled with surface-enhanced resonance Raman spectroscopy. *Journal of Planar Chromatography* 10: 10–17.
- Soper SA, Ratzlaff KL and Kuwana T (1990) Surface-enhanced resonance Raman spectroscopy of liquid chromatographic analytes on thin-layer chromatographic plates. *Analytical Chemistry* 62: 1438–1444.
- Stahlmann S and Kovar KA (1998) Analysis of impurities by high-performance thin-layer chromatography with FTIR and UV absorbance detection *in situ* measurements: chlorodiazepoxide in bulk powder and in tablets. *Journal of Chromatography A* 813: 145–152.
- Tran CD (1984) Subnanogram Detection of Dyes on Filter Paper by Surface-Enhanced Raman Scattering Spectroscopy. *Analytical Chemistry* 56: 824–826.

TOBACCO VOLATILES: GAS CHROMATOGRAPHY



W. M. Coleman, R. J. Reynolds Tobacco Company,
Winston-Salem, NC, USA

Copyright © 2000 Academic Press

Introduction

The leaves of tobacco plants, *Nicotiana tabacum*, have been shown by Tso and Stedman to consist of a wide array of organic and inorganic compounds. For general classification, the components of the leaf can be described as volatile, semivolatile and non-volatile. The nature of the compounds making up the components of the leaf range from nonpolar constituents such as hydrocarbons to very polar compounds such as carboxylic acids and amines. The structural identity of these components has been determined in many laboratories, including those of DeMole and Lloyd, through the use of classical wet chemical separation techniques coupled with end determinations involving, in some cases, further separations by gas chromatography (GC). In some cases, headspace volatiles have been trapped on Tenax or charcoal then either thermally or solvent desorbed. Supercritical carbon dioxide has also been used for extraction. In some of the earlier work, the separations were performed on packed glass GC columns and somewhat later on coated glass columns.

With the advent of multidimensional GC (MDGC), the labour-intensive sample preparation techniques associated with wet chemical separations of selected fractions were for the most part eliminated. With the MDGC approach, a concentrated solution of a tobacco essential oil in a volatile organic solvent can be directly injected on to a fused silica capillary pre-column, followed by heart-cutting on to another column. The phase of the pre-column of the MDGC system essentially serves as a replacement for the wet chemical separation approach. In this way, as many

as 80 new compounds were tentatively identified in a flue-cured tobacco essential oil. Detection and identification of the volatile components of the essential oils were possible through the use of mass selective detectors and matrix isolation Fourier transform infrared spectroscopy.

Another approach for the lower molecular weight volatiles employed automated purge-and-trap (P & T)-GC with flame ionization (FID) and mass selective detection (MSD). A relatively nonpolar DB-5 ((5% phenyl)methylpolysiloxane) column was employed for the separation of the volatiles. In further advances on the P & T method, the influences of ionic strength and pH on the yield of volatile materials have been reported. By employing a cryofocusing approach coupled with a DB-1701 ((14% cyanopropyl-phenyl)methylpolysiloxane) fused silica column of intermediate polarity, and an internal standard, semiquantitative analytical data were provided on the volatiles from a variety of natural products.

Through the use of multiple fused silica GC columns of different bonded phases, a universal commonality describing the nature of the volatile materials from a wide range of natural products has been developed. The types and profiles of volatile low molecular weight compounds found in the headspace above tobacco leaves has been shown to bear remarkable similarities to the profiles from a diverse array of heat-treated natural products such as coffee, peanuts and soybeans. The common thread linking all of the products has been ascribed to the presence of specific reactions between amino acids and other nitrogen sources with sugar molecules to yield volatile components such as pyrazines and aldehydes. For details of the work outlined in this section, see the papers by Coleman *et al.* in the Further Reading section.

This article describes the current GC approaches to the analysis of volatiles from tobacco. Results are described on approaches involving dynamic headspace-GC-MSD, as well as automated solid-phase microextraction (SPME)-GC-MSD.

Experimental

Dynamic Headspace P & T-GC-FID-MSD

Solid samples Representative samples of dry cured tobacco leaves were finely ground in a coffee grinder prior to analysis. After grinding, the moisture content of the tobacco leaves was adjusted to 20% by weight and the samples were allowed to age overnight at room temperature ($\sim 23^{\circ}\text{C}$). Finely ground moisture-adjusted tobacco leaves (3–5 g) were placed in a 25 mL sampling tube and affixed to the sampling port of a Tekmar LSC 2016/LSC 2000 P & T unit. Six replicates were run to obtain adequate statistical analyses. Average % relative standard deviation values for the total FID area counts for the solid samples were approximately $\pm 10\%$. After reaching the desired temperature, the contents of the 25 mL sampling tube were swept with helium, at a known flow rate for a specified length of time. The volatiles in the gas stream were efficiently trapped on a Tenax column (12 in \times 1/8 in i.d. SS tube) held within the Tekmar LSC 2000 unit. After sweeping the sample, the contents of the Tenax trap were thermally desorbed and transferred via a heated, aluminium-clad, deactivated, 0.53 mm i.d. fused silica transfer line to the injection port of a Hewlett Packard (HP) 5880 GC set at 250°C . Liquid nitrogen was employed to cool the GC oven to 0°C during the transfer of the volatiles. Upon completion of the transfer, the GC oven was temperature-programmed up to 250°C . The effluent from the DB-1701 column was split via an SGE low dead-volume splitter to the FID and MSD detectors at a ratio of 20 : 80. An HP 5970 Mass Selective Detector operation at 70 eV in the electron impact mode served as the MSD. The analyses were automated by means of basic programming of the HP 5880 GC terminal. The parameters employed in the analysis of the volatiles from solid tobacco leaves are listed in Table 1.

The volatile constituents were identified with the aid of GC retention indices as well as results of library mass spectral searches of Wiley, NBS and internal mass spectral databases.

Aqueous liquids and suspensions To a 5 mL sparge tube was added 1 mL of the tobacco liquid extract or suspension. The sparge tube was affixed to the Tekmar LSC 2016. Analysis then proceeded as described in the preceding section.

Table 1 Instrumental parameters for P & T-GC-MSD-FID analyses

Sample volatilization temperature	70°C
Sample volatilization time	20 min
Trapping material	Tenax
Trap desorption temperature	175°C
Trap desorption time	10 min
GC oven initial temperature	0°C
GC oven first programme rate	$2^{\circ}\text{C min}^{-1}$
GC oven final value	47°C
GC oven second programme rate	$10^{\circ}\text{C min}^{-1}$
GC oven final value	250°C
GC oven final time	10 min
GC column	DB-1701
GC column length	30 m
GC column i.d.	0.32 mm
GC column film thickness	1 μm

Automated SPME-GC-MSD

Aqueous liquids and suspensions A Varian 8200 CX AutoSampler with SPME II Sample Agitation was mounted on top of an HP 5890 Series II Plus GC equipped with a HP 5972 MSD operating either in the electron impact mode at 70 eV or in the selected ion monitoring (SIM) mode. This GC was fitted with a relatively polar DB-Wax (polyethylene glycol (PEG)) fused silica column (30 m \times 0.25 mm i.d., 0.5 μm film thickness, J & W Scientific). The MSD interface and GC injection port temperatures were 250°C . The GC oven was temperature-programmed from 40 to 140°C at $5^{\circ}\text{C min}^{-1}$, then to 220°C at $10^{\circ}\text{C min}^{-1}$ and held there for 4 min. Splitless injections were made and the split was opened after 1 min. The fibre was automatically submerged in the solution, vibrated for 0.75 min, removed, injected, and held in the injection port for 30 min, employing parameters set via operating software.

SPME fibres for automated injections were obtained from Supelco and employed strictly following the manufacturer's instructions for use and activation.

Prior to analysis by automated SPME, the aqueous heat-treated tobacco suspensions were manually filtered through a Whatman Autovial equipped with a 0.45 μm polyvinylidene fluoride filter and designed for use with aqueous solutions. Then, to a 1.8 mL vial equipped with Teflon-lined septum, was added, via a Rainin EDP Plus Motorized Microliter Pipet, 1.7 mL of the filtered solution. Strict attention to consistency in the addition of 1.7 mL was necessary to obtain reproducible results. The charged vials were loaded on the sample carousel and automatically sampled employing the instrumentation software provided by Varian and HP. In some cases it was necessary to dilute the heat-treated suspensions to obtain reproducible

fibre performance. Fresh samples were used for every injection.

SIM was used for the quantitative determination of selected pyrazines in the heat-treated suspensions. The selected compounds and accompanying selected ions (m/z) are listed as follows: methylpyrazine, 94, 95, 96; C2 pyrazines, 107, 108, 109, 110; C3 pyrazine, 121, 122, 123, 124 and C4 pyrazines, 135, 136, 137 and 150. The C2, C3 and C4 notations are used to denote a class of pyrazines. For example, C2 pyrazines would include all of the dimethylpyrazines as well as ethylpyrazine. Identical arguments are used for the C3 and C4 terms.

Discussion of Results

The distinct aromas associated with such materials as cured tobacco, roasted peanuts, roasted coffee and baked bread are familiar to most people. The identity of a large majority of these volatile aromatic components has been published recently. Within the tobacco industry, skilled individuals can easily distinguish between the types of tobacco employed in American blended cigarettes. This is not surprising in light of the unique patterns of the headspace volatiles found for these tobaccos (**Figure 1**). In a number of cases, some of the volatiles found in the headspace above the tobaccos are common to all of them and the main difference lies in the relative amounts of these common volatiles. For example, 2-butanone was common to three tobacco samples; however, the relative amounts were significantly different. In 1996 Coleman *et al.* demonstrated that this quantitative difference in the amount of specific headspace volatiles is common to a diverse array of natural products.

Use of the DB-1701 column with intermediate polarity served very well in providing sufficient resolution to assist in identifying the vast majority of compounds. Some of these compounds are listed in **Table 2** with numbers which correspond to peak identities throughout the entire manuscript. Each of the components listed in **Table 2** has been previously identified by Tso and Stedman in tobaccos. Thus, P & T-GC-MSD is a viable approach for the identification and segregation of tobacco types.

Roasting of natural products has often been associated with the production of pleasant aromas and tastes. In some cases these pleasant sensory responses have been attributed to the presence of low concentrations of volatile pyrazines and aldehydes. The presence of these compounds has been linked to the reaction of nitrogen sources such as amino acids with carbon sources such as sugars. Toasting of burley

tobacco leaves at approximately 150°C for 5 min produces an aroma associated with toasted natural products. Analysis of the headspace above the toasted burley tobacco reveals the presence of low molecular weight compounds also found in other heated natural products (**Figure 2**).

Increased levels of the Strecker aldehydes, 2-methylpropanal, 3-methylbutanal and 2-methylbutanal, relative to the starting tobacco are leading indicators of the sugar–nitrogen reactions. The reaction to form Strecker aldehydes is one of a series of complex reactions, collectively referred to as the Maillard reaction, occurring simultaneously between nitrogen sources such as amino acids and sugars during the heat treatment of natural products. When valine, leucine, isoleucine, phenylglycine and phenylalanine react with, for example, fructose at elevated temperatures, the following Strecker aldehydes are produced: 2-methylpropanal; 3-methylbutanal; 2-methylbutanal; benzaldehyde; and benzeneacetaldehyde. Thus, the presence of these compounds in the headspace above heat-treated natural products serves as an excellent indicator of amino acid–sugar reactions. In addition, an increased amount of volatile pyrazines in the headspace above heated natural products serves as a witness to the reaction between nitrogen sources and sugars. Further changes can be noted in the profile of the toasted burley relative to the starting material. Substantial increases in the relative amounts of solanone, neophytadiene and damascenone, all known burley constituents, can be found in the toasted material (**Figure 3**).

As before, the intermediate polarity of the DB-1701 column served well in providing sufficient chromatographic resolution of the volatile components.

Cooking natural products to produce edible materials with positive sensory attributes in some instances occurs in what can be viewed as an aqueous suspension. Boiling rice, beans or cooking a roast under pressure are simple examples. It has been shown that heat treatment of an aqueous suspension of burley tobacco, at 170°C for 30 min, produces some similar volatile materials (**Figure 4**) as are found in the headspace, for example, above a heat-treated peanut suspension. The headspace of both samples is dominated by the presence of Strecker aldehydes, sugar thermal degradation products and pyrazines. On a relative basis, the volatile materials detected in the heat-treated suspension were not detectable in the starting tobacco. The volatile components in the heat-treated aqueous burley tobacco suspension were also indicative of the sugar–nitrogen chemistries known to produce Strecker aldehydes and volatile pyrazines when heating tobacco alone.

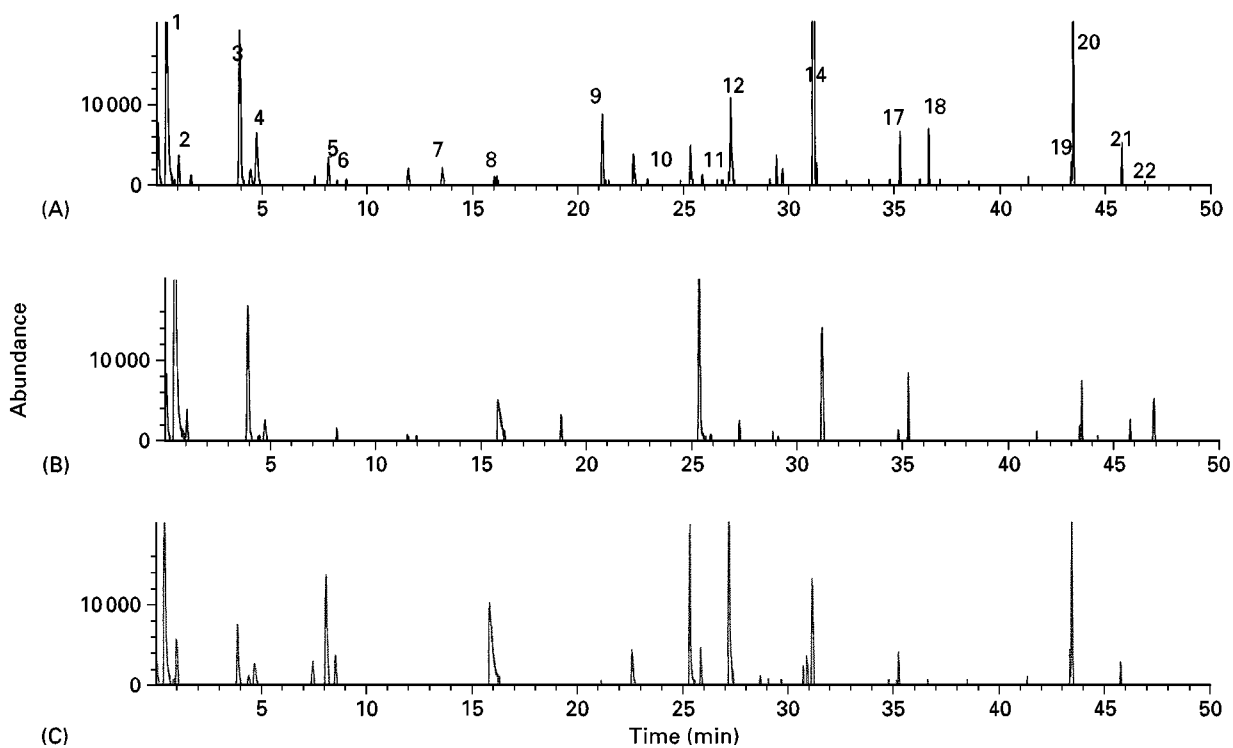


Figure 1 Headspace volatiles from dynamic headspace analysis of selected tobaccos. (A) Turkish; (B) flue-cured; (C) burley.

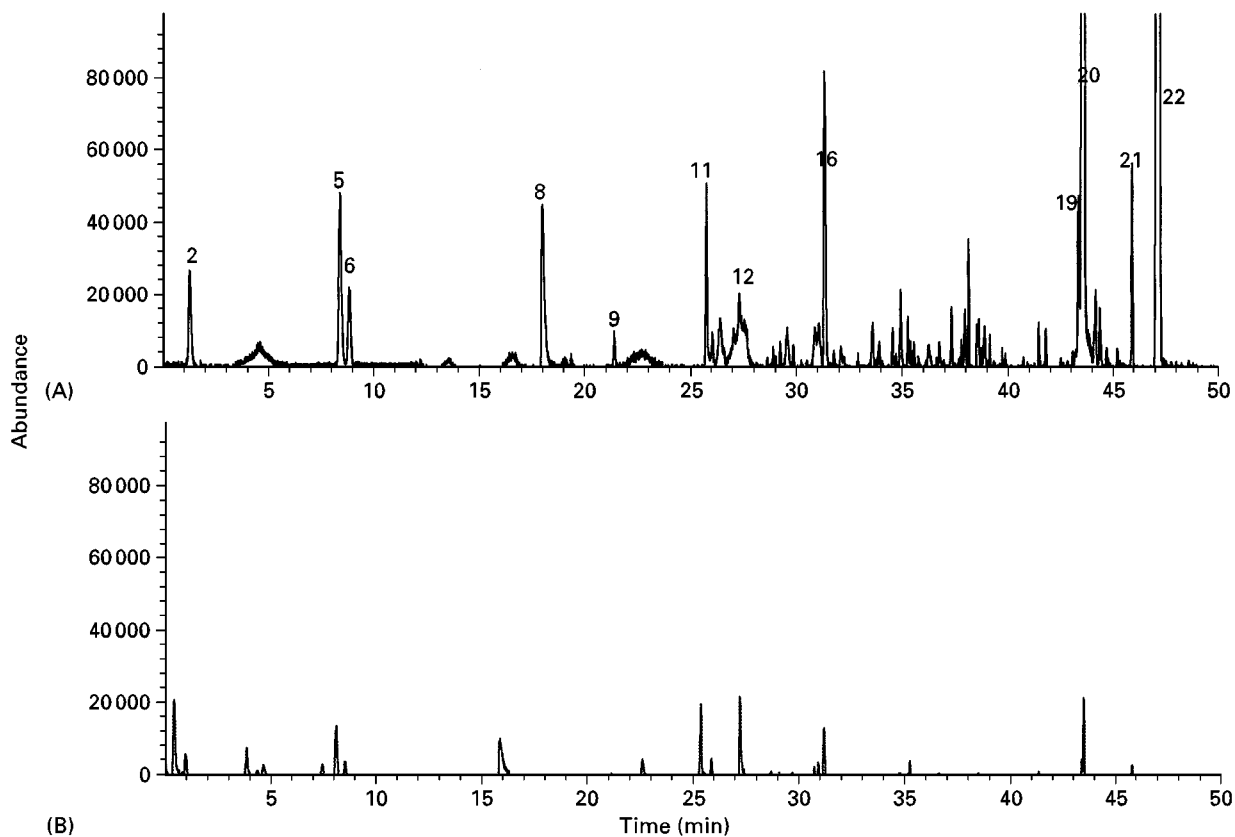


Figure 2 Headspace volatiles from dynamic headspace analysis of (A) toasted burley and (B) burley tobacco.

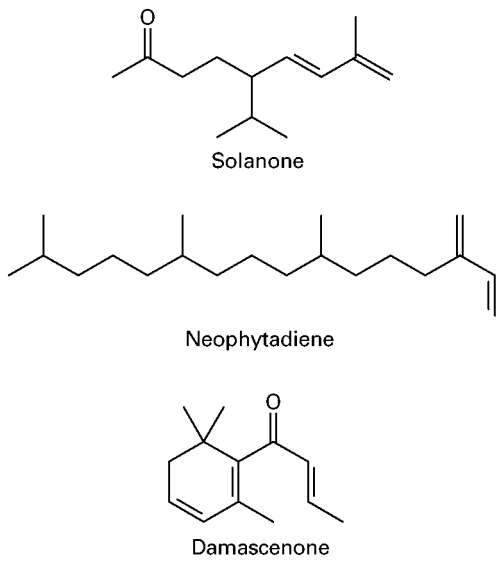


Figure 3 Structures of some compounds present in heat-treated tobaccos.

Certain amino acids have been postulated in model systems by Waller and Feather to be directly involved in the production of pyrazines and selected aldehydes by means of the Strecker degradation mechanism. That is, upon reaction with selected sugars, certain

Table 2 Compounds identified and numbered in selected figures

Compound number	Identification
1	Acetone
2	2-Methylpropanal
3	2-Butanone
4	2,3-Butanedione
5	3-Methylbutanal
6	2-Methylbutanal
7	2,3-Pentanedione
8	Acetic acid
9	Hexanal
10	Methylpyrazine
11	Furfural
12	C2 Pyrazines ^a
13	Acetylfuran
14	6-Methyl-5-hepten-2-one
15	C3 Pyrazines ^b
16	Benzaldehyde
17	C14 Hydrocarbon
18	C15 Hydrocarbon
19	Nicotine
20	Solanone
21	β -Damascenone
22	Neophytadiene

^aPyrazines such as dimethylpyrazine and ethylpyrazine.

^bPyrazines such as methylethyl pyrazines.

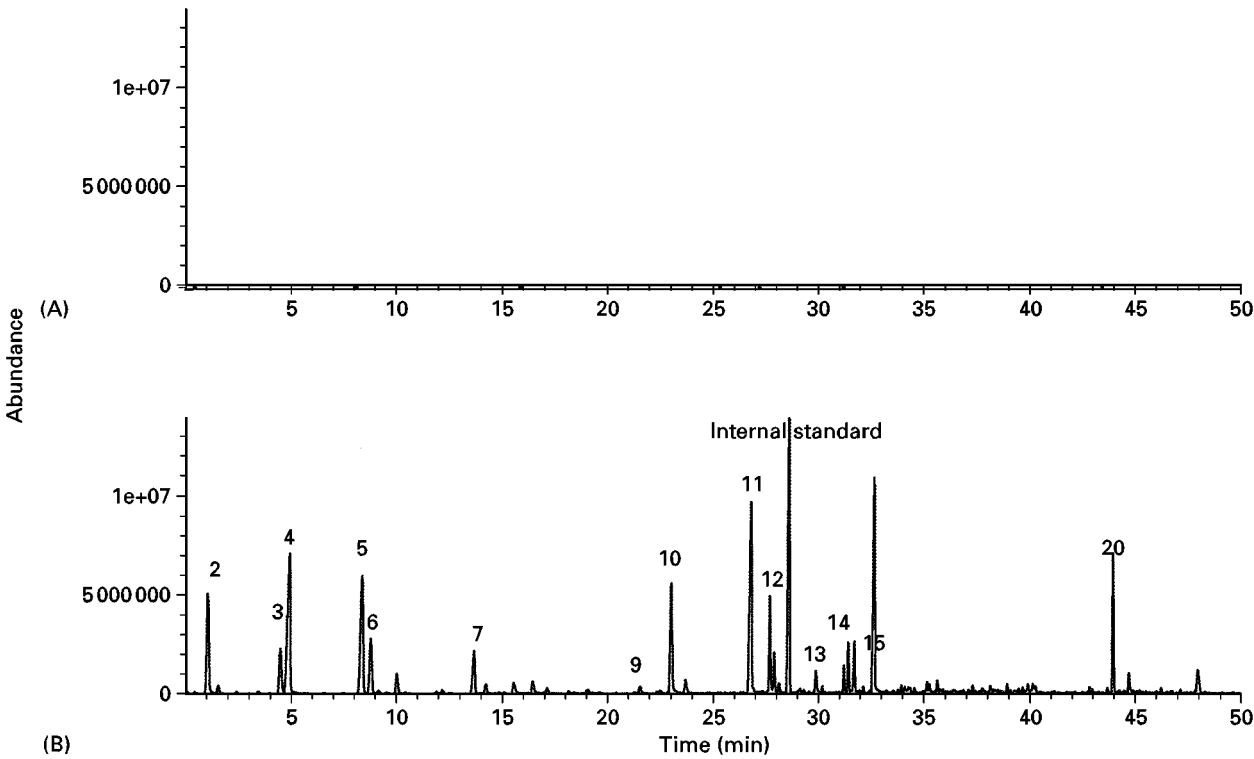


Figure 4 Headspace volatiles from dynamic headspace analysis of (A) burley tobacco and (B) a heat-treated burley tobacco suspension.

amino acids will yield volatile aldehydes corresponding in large part to the structure of the parent amino acid backbone. Specifically, for example, phenylalanine upon reaction with sugars yields as a volatile aldehyde benzaldehyde, while valine will yield 2-methylpropanal. Dynamic headspace analysis of aqueous suspensions of burley tobacco with mmole quantities of added phenylalanine and valine show elevated levels of benzaldehyde and 2-methylpropanal (Figures 5 and 6) respectively. These results provide the first evidence implicating the Maillard and Strecker reactions within a tobacco matrix. Again, the DB-1701 GC column provides the necessary resolution.

Recently, manual SPME-GC-MSD has been shown to be an excellent analytical approach for the quantitative determination of volatile components associated with heat-treated natural products. Specifically, the quantitative analysis of pyrazines, furfurals, thiazoles and pyridines has been demonstrated in aqueous media. With the introduction of an automated injection system analytical precision has improved. Application of automated SPME (AutoSPME)-GC-MSD to the analysis of a heat-treated tobacco suspension revealed some of the first insights

into a variety of reaction mechanisms occurring during the heating process (Figure 7). The origin of pyridine, myosmine, β -nicotyrine and pyrrole-2-carboxaldehyde can probably be directly linked to the decomposition of the alkaloid, nicotine. The origin of the pyrazines is no doubt related to sugar-nitrogen reactions (see above), and the furans can be attributed to the thermal decomposition of sugars. Searches for the appropriate SPME fibre resulted in the selection of a carboxenpolydimethylsiloxane fibre. This particular fibre is suited to the analysis of relatively polar compounds in aqueous solutions. The best column for the analysis was found to be a relatively polar DB-Wax, which provided the most information concerning the reaction mechanisms.

Further application of AutoSPME-GC-MSD in the SIM mode has provided additional insights into the formation of volatile pyrazines during the heat treatment of aqueous tobacco suspensions. Model studies indicate the formation of pyrazines through the coupling of two molecules (Figure 8). Thus, should the source of the N in the two molecules be ^{15}N , then the possibility of changes in the m/z values for pyrazines could be either one or two. For example, the m/z for methylpyrazine could be changes from

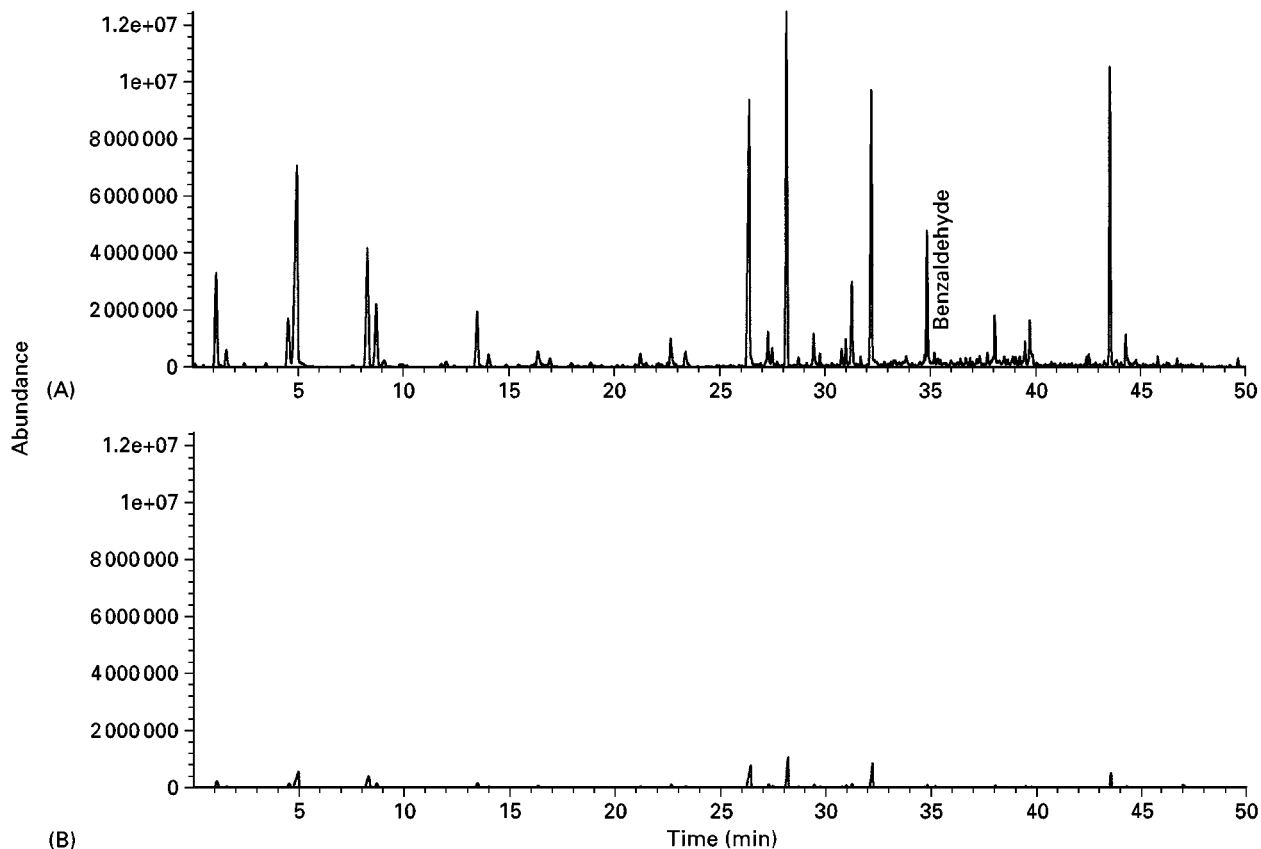


Figure 5 Headspace volatiles from dynamic headspace analysis of two tobacco dusts: (A) tobacco dust plus phenylalanine; (B) tobacco dust.

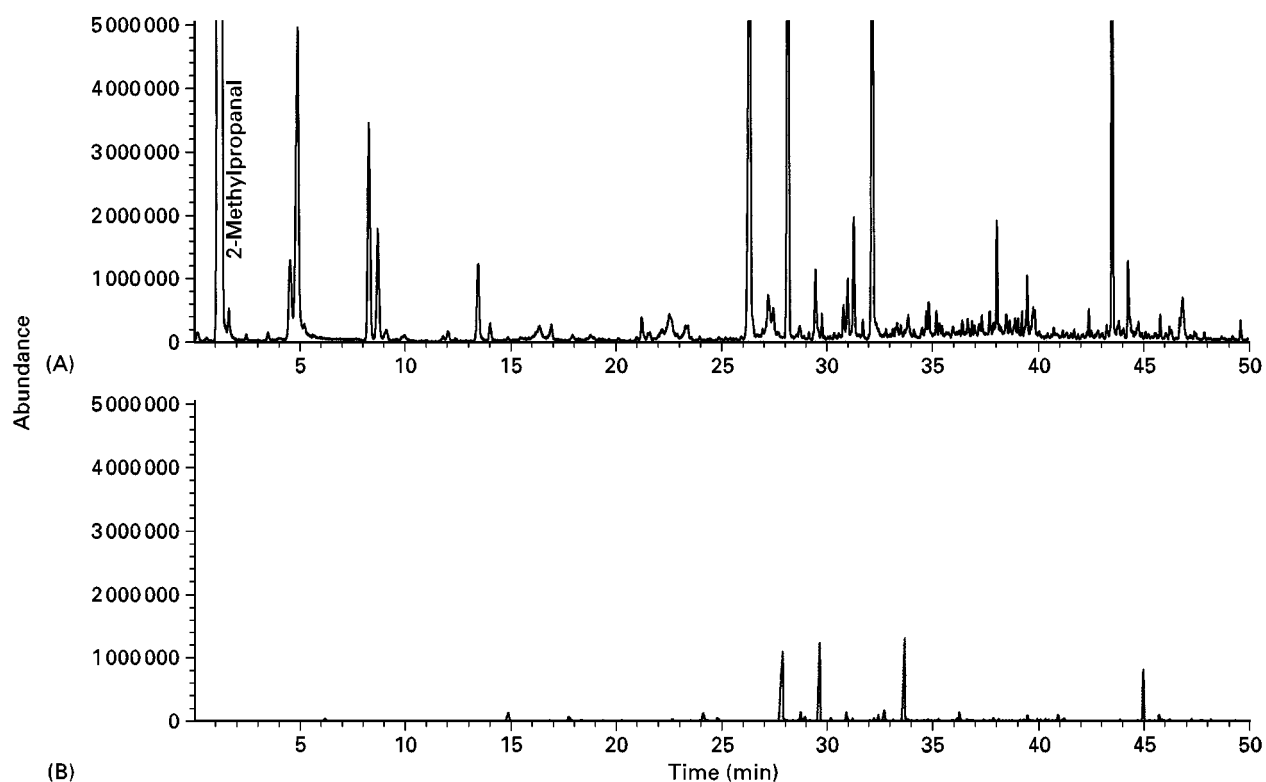


Figure 6 Headspace volatiles from dynamic headspace analysis of tobacco dust suspensions. (A) Tobacco dust plus valine; (B) tobacco dust.

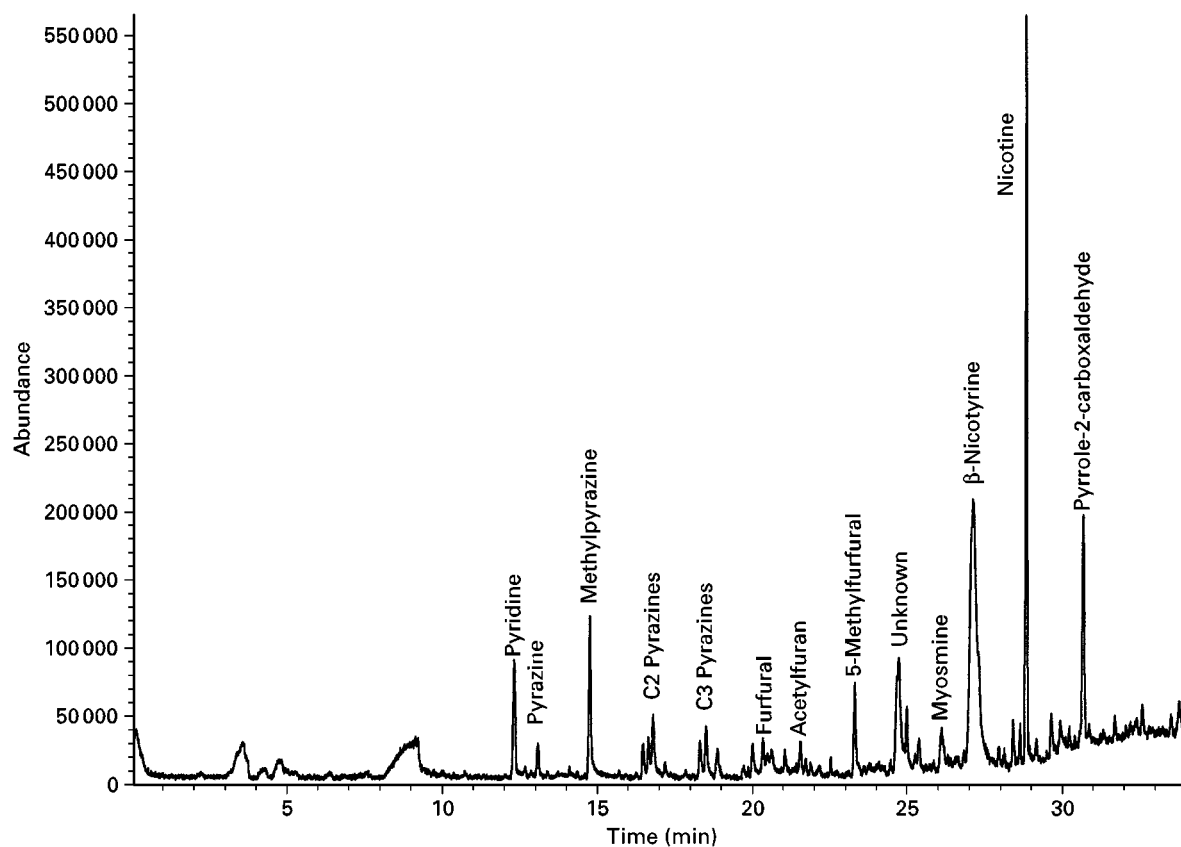


Figure 7 Total ion chromatogram from AutoSPME of aqueous heat-treated tobacco suspension using a carboxen polydimethylsiloxane SPME fibre.

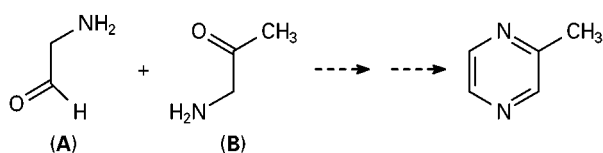


Figure 8 Formation of methylpyrazine from two molecules.

a molecular ion of 94 to molecular ions of either 95 or 96. In other words, the distribution of the ions $m/z = 94, 95, 96$, would substantially change if ^{15}N were incorporated into the methylpyrazine molecule. Model studies have also indicated that a possible source of nitrogen for the formation of pyrazines is the ammonium ion. Labelling the ammonium ion with ^{15}N would seem to be a viable approach for determining one of the possible mechanisms associated with pyrazine formation in a heat-treated tobacco matrix.

Thus, to an aqueous tobacco dust suspension was added a mmole quantity of $^{15}\text{NH}_4\text{OAc}$. A control reaction was also performed with no additive. After heat treatment at 170°C for 30 min in a sealed reactor, AutoSPME-GC-MSD-SIM was performed on the

filtrate (Figure 9), with the focus on methylpyrazine. Alteration of the m/z pattern observed for the methylpyrazine produced in the control experiment was definitely evident. The shift in abundance toward the ions $m/z = 95$ and 96 directly implicated the inclusion of both one and two ^{15}N atoms into the methylpyrazine molecule, obviously from the added $^{15}\text{NH}_4\text{OAc}$. Thus, for the first time, by employing AutoSPME-GC-MSD-SIM, a direct link between the presence of naturally occurring reagents such as ammonium ions and the production of volatile aromatic compounds such as pyrazines has been clearly demonstrated.

Conclusion

GC in combination with such sample preparation techniques as automated dynamic headspace and SPME has been demonstrated to be an effective analytical tool for the qualitative and quantitative examination of tobacco volatiles. Through the use of an MS detector in the SIM mode, understanding has been acquired of the formation of the volatiles on a molecular basis.

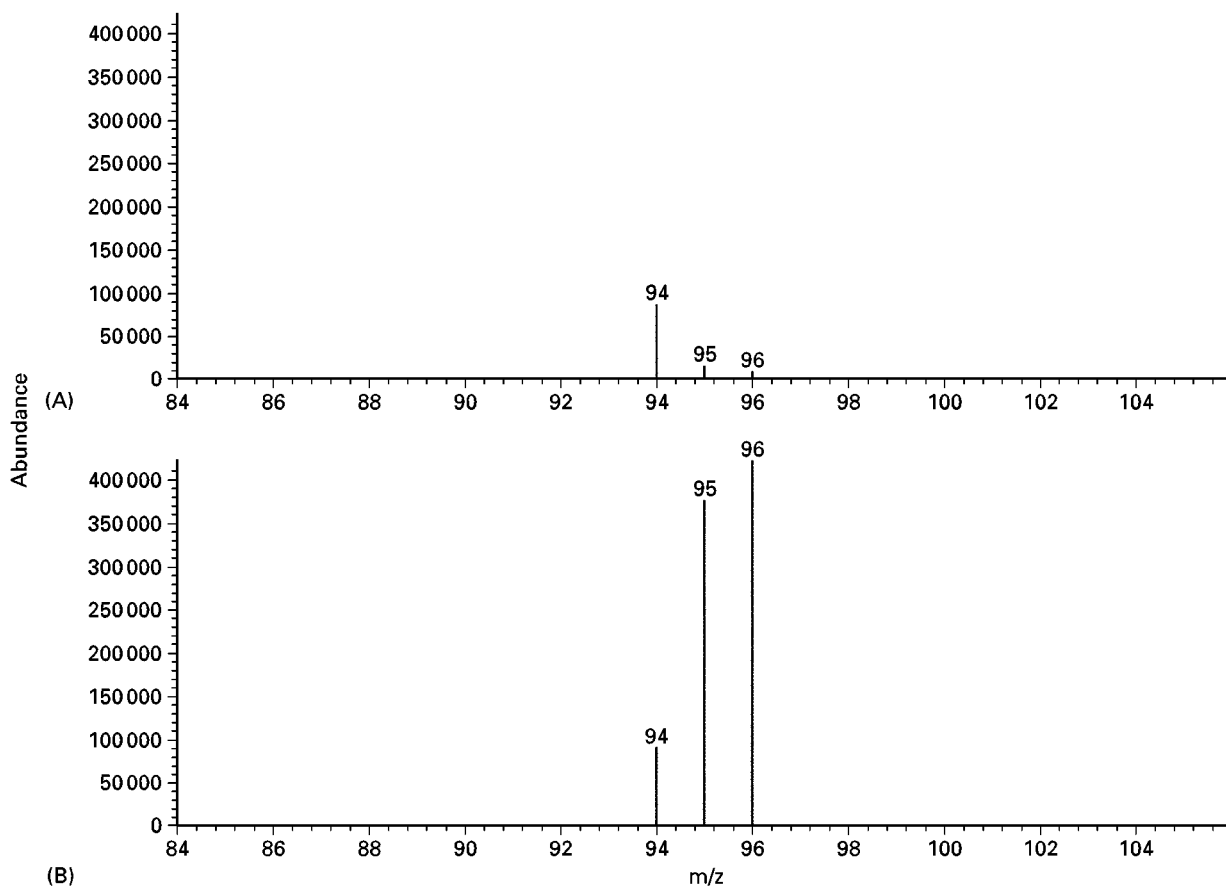


Figure 9 Selected ion-monitoring mass spectra of methylpyrazine produced in heat-treated tobacco suspensions (A) without additive; (B) with added $^{15}\text{NH}_4\text{OAc}$.

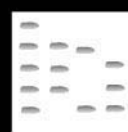
See Colour Plate 122.

See also: **II/Chromatography: Gas:** Column Technology; Detectors: Mass Spectrometry; Headspace Gas Chromatography; Historical Development; Theory of Gas Chromatography. **Extraction:** Solid-Phase Extraction; Solid-Phase Microextraction.

Further Reading

- Coleman WM III (1992a) The volatile and semivolatile components of supercritical fluid and methylene chloride extracts of selected tobaccos. *Journal of Essential Oil Research* 4: 113.
- Coleman WM III (1992b) Automated purge-and-trap-gas chromatography analysis of headspace volatiles from natural products. *Journal of Chromatographic Science* 30: 159.
- Coleman WM III (1996) A chromatographic study of the influence of ion concentrations and pH on the yield of volatile materials from heat-treated natural product extracts. *Journal of Chromatographic Science* 34: 1.
- Coleman WM III (1997) A study of the behavior of polar and nonpolar solid-phase microextraction fibers for the extraction of Maillard reaction products. *Journal of Chromatographic Science* 35: 245.
- Coleman WM III and Gordon BM (1994) *Advances in Chromatography*, vol. 34, Ch. 2, p. 57. New York: Marcel Dekker.
- Coleman WM III, White JL and Perfetti TA (1994) A hyphenated GC-based quantitative analysis of volatile materials from natural products. *Journal of Chromatographic Science* 32: 323.
- Coleman WM III, White JL and Perfetti TA (1996) Investigation of a unique commonality from a wide range of natural materials as viewed from the Maillard reaction perspective. *Journal of Science of Food Agriculture* 70: 404.
- DeMole E and Berthet D (1972) A chemical study of burley tobacco flavour (*Nicotiana tabacum* L.) I. Volatile to medium-volatile constituents (b.p. $\leq 84^\circ/0.001$ Torr). *Helvetica Chimica Acta* 55: 1866.
- Gordon BM, Uhrig MS and Borgerding MF *et al.* (1988) Analysis of flue-cured tobacco essential oil by hyphenated analytical techniques. *Journal of Chromatographic Science* 26: 174.
- Lloyd RA, Miller CW and Roberts DL *et al.* (1976) Flue-cured tobacco flavor I. Essence and essential oil components. *Tobacco Science* 20: 43.
- Sakaki K, Niino K, Sakuma H and Sugawara S (1984) Analysis of the headspace volatiles of tobacco using an ether trap. *Agriculture Biological Chemistry* 48: 3121.
- Stedman RL (1968) The chemical composition of tobacco and tobacco smoke. *Chemical Reviews* 68: 153.
- Tso TC (1990) *Production, Physiology and Biochemistry of Tobacco Plant*. Beltsville, MD: Ideals.
- Waller WR and Feather MS (eds) (1983) *The Maillard Reaction in Foods and Nutrition*. ACS Symposium Series 215. Washington, DC: American Chemical Society.

TOXICOLOGICAL ANALYSIS: LIQUID CHROMATOGRAPHY



A. P. De Leenheer, W. Lambert and J. Van Bocxlaer,
University of Gent, Gent, Belgium

Copyright © 2000 Academic Press

Introduction

With the introduction of high performance liquid chromatography (HPLC) coupled to detection systems providing spectral information (e.g. photodiode array detection and mass spectrometric detection, HPLC-DAD and LC-MS) the development of HPLC methods for broad-spectrum drug screening has attracted great interest in forensic laboratories. The information obtained by these methods is two-fold, i.e. retention data and spectral information, creating a powerful identification system. The growing literature describing HPLC as a broad-spectrum technique demonstrates its unique and essential position in toxicological investigations.

A number of important parameters in toxicological screening by HPLC include column packing material, column dimensions, detection, standardization and peak purity assessment. These topics will be treated while the applicability will be demonstrated by presentation of selected examples of general screening and specific detection of a limited number of compounds.

Column Packing Materials**Underivatized Silica**

Unmodified silica can retain drugs by a weak cation exchange mechanism and was used for broad-spectrum drug screening as early as 1975. The main problem, however, with the use of underivatized silica is the substantial variability of this material. Different brands of silica and even different batches

of the same brand of silica packing material often result in different retention of selected basic drugs. As a consequence, chromatographic conditions (same batch of same brand of packing, eluent composition, temperature control) need to be exactly defined and strictly followed before reproducible retention times or *retention factors* (k) can be obtained in one laboratory or in different laboratories (the latter being even more difficult). The impact of all these parameters on retention is more substantial in an adsorption system than under reversed-phase conditions. Due to these difficulties, the use of underivatized silica in the application of adsorption chromatography to systematic toxicological analysis (STA) remains rather limited.

Bonded-phase Packing Material

Bonded-phase chromatography, and more especially reversed-phase chromatography on octyl- or octadecylsilica, is by far the most popular liquid chromatographic technique used in STA. In the early 1980s valuable methods for basic drugs on modified silica began to appear. Also practical solutions to the tailing problem were established and refinements were under investigation. Free silanol functions are known to have a marked influence on retention behaviour of different drugs. These silanol effects can be reduced by changing the pH of the eluent or by addition of competing aliphatic bases (amine modifiers) as surface masking agents. Various manufacturers have launched specially prepared columns claimed to be free of silanol effects and providing more reproducible retention times. This is mainly achieved by deactivation of the free silanols by various endcapping procedures and by elimination of the trace metals from the silica support.

Alternatively, polymeric stationary phases have also been introduced. However, although the ability to run these packing materials at pH values even higher than 9 permits the analysis of basic drugs as un-ionized compounds without tailing, these polymeric phases have only a limited application in systematic toxicological analysis.

Recently, again in an effort to eliminate chromatographic problems due to residual silanol groups and to prevent the incorporation of buffer salts in the eluent, an alumina-based packing material coated with polybutadiene has also been used for broad-spectrum drug screening purposes. The inherent absence of silanol functions on this packing material simplifies the retention mechanism, eliminates the need for addition of amine modifiers and prevents irreversible adsorption of co-extracted impurities. In addition, aluminum oxide as well

as the polybutadiene coating are stable in the pH range of 2 to 12. This polybutadiene coating has hydrophobic properties comparable to reversed-phase packing materials. Consequently the same solvent mixtures can be used as in reversed-phase chromatography. By incorporation of NaOH in the eluent ($0.0125 \text{ mol L}^{-1}$), basic drugs can be chromatographed without tailing. Of course, this high pH results in poor retention of phenolic compounds (e.g. morphine) or carboxylic acids (e.g. benzoylecgonine). The latter compounds need to be chromatographed on a second and classical reversed-phase packing material. This approach of using two different and complementary packing materials is certainly not unique in systematic toxicological analysis.

Chromatographic Conditions

Due to the large differences in polarity of the compounds encountered in broad-spectrum screening and in view of simultaneous chromatography of parent drugs and metabolites in nearly all reversed-phase chromatographic systems, gradient elution is used. The few systems based on adsorption chromatography apply isocratic elution.

In LC-MS the choice of the solvent composition is limited. The use of nonvolatile mobile phase constituents (e.g. phosphate buffers) is absolutely prohibited. This limits the practical use of LC-MS by excluding techniques like ion pair and ion exchange liquid chromatography.

Offline sample preparation procedures based on liquid-liquid extraction or solid-phase extraction are not really the subject of this article. However, automation of solid-phase extraction coupled directly with injection and chromatographic analysis and on-line enrichment based on the use of two or more high pressure columns or cartridges (column switching) are already commercialized for broad-spectrum screening in toxicological analyses and therefore worthy of mention.

Detection Systems

Besides retention data, spectral information is essential for the positive identification of an unknown substance. Therefore, detection systems not providing spectral information (e.g. fixed wavelength UV detection, electrochemical detection) have found only limited application in toxicological laboratories such as for repetitive analysis of a small group of structurally similar compounds (e.g. epinephrine, norepinephrine in the case of electrochemical detection).

Photodiode Array Detection

The introduction of diode array and fast-scanning absorption detectors allowed the acquisition of UV (and visible) spectral data during the chromatographic process. This combination of the discriminatory power of the chromatographic retention parameters (which is lower for HPLC than GC) with that of the UV spectral data increased the overall reliability of an HPLC analysis in the area of toxicology. Standard reference spectra can be stored in a database tagged with parameters of retention in order to restrict the search into a window around each retention parameter.

The major problem in the identification of unknown compounds by a UV spectral match is the lack of fine structure in the UV spectrum of many compounds. The identification of metabolites is also difficult because biotransformations do not always result in a drastic change of the UV spectrum. Several studies from the area of chemometrics have provided models for UV spectral matching methods used for toxicological drug analysis. Peak maxima, calculation of differences between normalized spectra and between first-derivative spectra are thereby essential data for estimations of similarity or dissimilarity.

Ideally, each toxicological laboratory should build up its own library of UV spectra recorded under stringent chromatographic conditions. Analysis of unknown samples and recording unknown UV spectra should then be performed under exactly the same chromatographic conditions (column, eluent composition, gradient, pH, etc.) because at least the last three of these parameters can affect the observed absorbance. Another source of library variability is detector-to-detector variation. Because different photodiode array detectors use different numbers of diodes, a UV library development on one system may not be able to meet the same criteria on another instrument.

Co-elution of drugs with other drugs or with endogenous co-extracted substances remains one of the major causes of errors in HPLC analysis. Erroneous conclusions can be drawn if a co-eluting compound mimics the UV spectrum of a known compound or when the co-elution of two compounds results in a spectrum that does not match any library spectrum. Therefore, before running a library search, peak purity assessment is essential. This can be done either manually by comparison of the spectrum at different positions of the emerging peak, or alternatively some computer programs automatically indicate the peak purity under each peak in the chromatogram. The software of the more sophisticated systems even allows peak deconvolution of two co-eluting compounds, resulting in the specific UV spectrum and

quantitative contribution of each compound. Other software systems claim to be able to determine the individual drugs from a UV spectrum even if this is a result of up to six compounds eluting at the same retention time. However, it should be notified that in the latter case previous information on the probable co-eluting drugs is essential. This can be obtained from other chromatographic techniques.

Mass Spectrometric Detection

The combination of liquid chromatography and mass spectrometry (LC-MS) offers a major improvement regarding drug identification compared with the above-mentioned HPLC-DAD combination.

The improved resolution and the higher separation efficiency together with the desire to interface HPLC with mass spectrometric detection have been the major driving forces behind the development of capillary LC. Unlike GC, interfacing problems between LC and MS are still a challenge for researchers. Since the early 1970s interfaces have been constructed each applying a different technique to eliminate the chromatographic eluent, which of course cannot be introduced directly into the high vacuum region of a mass spectrometer. At least seven major interfacing techniques exist, i.e. moving belt (MB), particle beam (PB), direct liquid introduction (DLI), fast atom bombardment (FAB), thermospray (TS), electrospray (ES) and atmospheric pressure chemical ionization (APCI).

It is beyond the scope of this contribution to give an extensive overview of these different techniques. However, the respective advantages and/or disadvantages of a number of these techniques, especially in view of their application to broad-spectrum screening, will be presented. Both the DLI and the MB techniques have only historical interest and have virtually disappeared from the area of toxicological analysis. Particle beam and FAB proved to be valuable for specific applications such as the detection of steroids (PB) or the detection of compounds with high molecular mass (FAB). However, in other applications sensitivity is often a problem for these two techniques. Of primary interest for toxicological analysis are the three remaining techniques: thermospray, electrospray and atmospheric pressure chemical ionization. Because TS is able to handle flow rates of conventional HPLC systems ($1\text{--}2\text{ mL min}^{-1}$) it became the first popular HPLC-MS interface to be used in many fields with a high sensitivity. Because the ion production in this technique is dependent on the solvent composition, the application of TS with gradient elution can result in difficulties.

Electrospray operates without heat in the spray ionization step which makes this technique suitable

for thermolabile compounds, such as sulfate conjugates of drugs.

Both ES and APCI have found a wider use during the last decade with APCI having an excellent sensitivity especially for hydrophobic compounds. Electrospray has the advantage of being applicable to a wide range of analyte polarity.

Looking to the number of applications and keeping in mind that ES and APCI have not yet been exploited to their full potential, these two techniques together with TS are the most interesting techniques for toxicological analysis. The three techniques are based on a relatively soft ionization process so the mass spectra obtained sometimes lack the fragment ions necessary for confirmation of the identity of an unknown compound.

Quadrupole mass spectrometers are used most frequently because of their ruggedness, however, ion trap instruments are becoming more and more common in STA. Coupling to an ion trap spectrometer is interesting for a variety of reasons, e.g. economical aspects, sensitivity and the ability to run MS-MS experiments. Other techniques, such as collision-induced dissociation in tandem mass spectrometric configurations are also becoming available.

Reliability of Retention

As already mentioned, the efficiency of a HPLC system is considerably less than that of a capillary GC set-up so the risk of co-elution is greater. In addition, the retention behaviour of a compound (together with the spectral information, a pivotal criterion for identification of an unknown substance) is often imprecise. Batch-to-batch variation and variation of

packing materials between different manufacturers result in inconsistent retention data. In addition, coating of the active sites by irreversible adsorption and loss of the bonded-phase by ageing of the column can also contribute to changes in retention. Of course this problem can be overcome by injection of the authentic standard directly after the tentative identification of a compound. This procedure, however, is time consuming and presupposes prior identification even without a perfect match of the retention time and the availability of a pure standard. Several studies have evaluated the use of homologous hydrocarbon series, multiple drug reference standards and nitroalkanes to minimize the effect of irreproducible HPLC retention data. Although these relative retention procedures improve the reproducibility, it is difficult to obtain linear relative retention scales by using a homologous series of compounds during gradient elution, the latter being the most popular technique for liquid chromatographic toxicological screening purposes. The use of multiple drug standards instead of non-drug compounds such as nitroalkanes results in a more effective correction for retention shifts. Both principles can also be combined by calculation of retention indices of compounds from their retention times by linear interpolation between standard drugs, whose retention indices have been previously determined on a nitroalkane scale.

Applications

A number of recently developed broad-spectrum screening procedures based on HPLC-DAD are brought together in Table 1. They all use

Table 1 Operating conditions of HPLC-DAD in toxicological broad-spectrum screening

Column	Eluent	Flow rate (mL min ⁻¹)	Standardization	Number of compounds	Year
Superspher 100 RP18 4 µm; 125 × 4 mm	Acetonitrile : triethylamine phosphate; gradient	1	1-Nitroalkanes 18 standard drugs	383	1994
Symmetry C8 5 µm; 250 × 4.6 mm	Phosphate buffer (pH 3.8) : acetonitrile; gradient	1 to 1.5	None	600	1997
Supelcosil LC-DP 5 µm; 250 × 4.6 mm	Acetonitrile : phosphoric acid : triethylamine; isocratic	0.6	None	272	1995
Lichrospher 100 RP8 5 µm; 250 × 4 mm	Acetonitrile : phosphoric acid : triethylamine; isocratic	0.6	None	280	1995
Hypersil C18 5 µm; 150 × 4.6 mm	Acetonitrile : phosphate buffer (pH 3.0) : sodium octyl sulfate : triethylamine; gradient	1	None	>300	1997
Aluspher RP-select B 5 µm; 125 × 4 mm	Methanol : water containing 0.0125 mol L ⁻¹ NaOH; gradient	1	None	>150	1995
Spherisorb S5 ODS-2 5 µm; 150 × 3.8 mm	Acetonitrile : phosphate buffer (pH 3.1); gradient	1	<i>p</i> -Methylphenyl- phenylhydantoin	130	1993

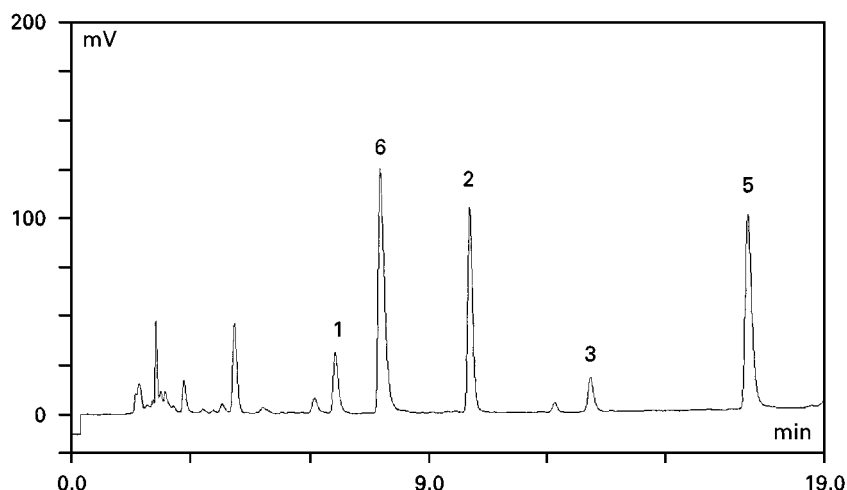


Figure 1 Chromatogram of a real postmortem whole blood sample. Peaks: (1) benzoylecgonine; (2) 2'-methylbenzoylecgonine; (3) cocaine; (5) 2'-methylcocaine; (6) 3,4-methylenedioxy-*N*-ethylamphetamine. Levels: (1) 0.1; (2) 0.65; (3) 0.1; (5) 0.65; and (6) 1.3 $\mu\text{g mL}^{-1}$. (Reproduced with permission from Clauwaert *et al.*, 1997.)

reversed-phase packings on either a silica or an alumina matrix. All except two procedures apply gradient elution and standardization of the retention is rather an exception (two procedures out of seven). The authors present lists of a large number of drugs and toxicologically relevant compounds (ranging from 130 to 600) and state that this is not a limitation but that other compounds can also be added to these lists.

It is not possible to give a similar table showing the operating conditions of LC-MS applied to broad-spectrum screening in forensic sciences. Screening the literature rapidly demonstrates that to date LC-MS has only been applied to selected compounds or groups of compounds such as steroids, thiourea pesticides, mycotoxins, tricyclic antidepressants and 10 illicit drugs (all by TS), diuretics, non-steroidal anti-inflammatory drugs, carbamate pesticides (by ES) and β -agonists, carbamate pesticides and alkaloids by APCI. For detailed information on the operating conditions of these various applications we refer to the specialized literature in this field.

Application

The applicability of HPLC coupled to photodiode array detection as well as to mass spectrometric detection in the field of forensic sciences will be demonstrated by the analysis of cocaine and some of its metabolites by both techniques. Cocaine, benzoylecgonine and cocaethylene have been determined by HPLC-DAD using 2 mL of blood, serum or urine under reversed-phase gradient conditions. The quantitative limit, defined as that concentration that can be

determined with an acceptable reproducibility ($\leq 6\%$), is 50 ng mL^{-1} for benzoylecgonine and cocaine and 25 ng mL^{-1} for cocaethylene (using 2 mL of body fluid) (Figure 1).

On the other hand, cocaine, benzoylecgonine, ecgonine methylester, ecgonine and norcocaine have been quantified in urine (1 mL) with an LC-MS system based on step-gradient elution of a large (250×7.6 mm) steric exclusion column followed by atmospheric pressure chemical ionization-mass spectrometry. The detection limits (signal-to-noise ratio = 3) under selected ion monitoring (SIM) mode conditions were 320, 200, 200, 20 and 60 ng mL^{-1} for ecgonine, benzoylecgonine, ecgonine methyl ester, cocaine and norcocaine, respectively. Unfortunately, quantitative limits were not reported for this method (Figure 2).

Both systems used solid-phase extraction for sample preparation. Due to their non-UV-absorbing properties ecgonine and ecgonine methyl ester were not detected in the HPLC-DAD system. This system was, however, able to detect and to chromatograph other toxicologically relevant compounds while for the LC-MS system this is not mentioned.

Conclusion and Perspectives

Besides further optimization of both the liquid chromatographic and the spectrometric parts of the described configurations, a great challenge for the future is the automation of those systems. Complete automation of an analytical procedure including online sample pretreatment is always advantageous

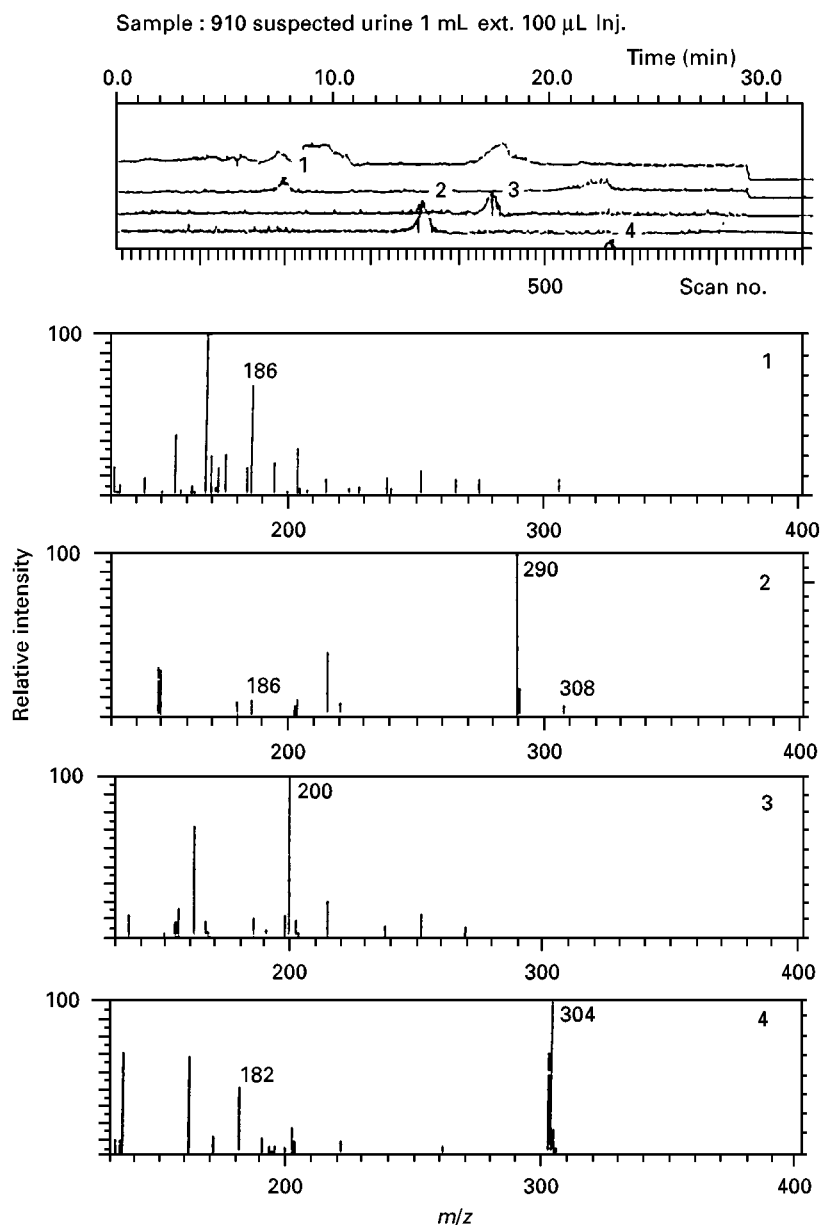


Figure 2 Mass chromatograms and mass spectra of extracts obtained from suspected urine. Peaks. (1) ecgonine; (2) benzoylecgonine; (3) ecgonine methyl ester; (4) cocaine. Levels: (1) 3.2; (2) 4.8; (3) 3.6; and (4) 0.8 $\mu\text{g mL}^{-1}$, respectively. (Reproduced with permission from Nishikawa *et al.*, 1994.)

in STA. Because the optimum performance of HPLC-DAD and more especially of LC-MS are determined by the simultaneous optimization of a large number of interrelated parameters (flow, pressure, temperature, voltage ...), expert systems should be optimized allowing fully automated tuning and control.

The different detection principles as well as the comparable sensitivity demonstrate the complementary character of both HPLC-DAD and LC-MS. In the future, both techniques will undoubtedly gain in

interest and will play an essential function in forensic sciences.

Further Reading

- Binder SR (1996) Analysis of drugs of abuse in biological fluids by liquid chromatography. *Advances in Chromatography* 36: 201–271.
- Bogusz M and Erkens M (1994) Reversed-phase high-performance liquid chromatographic database of retention

- indices and UV spectra of toxicologically relevant substances and its interlaboratory use. *Journal of Chromatography A* 674: 97–126.
- Clauwaert KM, Van Bocxlaer JF, Lambert WE and De Leenheer AP (1997) Liquid chromatographic determination of cocaine, benzoylecgonine, and cocaethylene in whole blood and serum samples with diode-array detection. *Journal of Chromatographic Science* 35: 321–328.
- Gaillard Y and Pépin G (1997) Use of high-performance liquid chromatography with photodiode-array UV detection for the creation of a 600-compound library. Application to forensic toxicology. *Journal of Chromatography A* 763: 149–163.
- Hoja H, Marquet P, Verneuil B, Lotfi H, Pénicaud B and Lachâtre G (1997) Applications of liquid chromatography-mass spectrometry in analytical toxicology: a review. *Journal of Analytical Toxicology* 21: 116–126.
- Koves EM (1995) Use of high-performance liquid chromatography-diode array detection in forensic toxicology. *Journal of Chromatography A* 692: 103–119.
- Lai C-K, Lee T, Au K-M and Chan AY-W (1997) Uniform solid-phase extraction procedure for toxicological drug screening in serum and urine by HPLC with photodiode-array detection. *Clinical Chemistry* 43: 312–325.
- Lambert WE, Meyer E and De Leenheer AP (1995) Systematic toxicological analysis of basic drugs by gradient elution on an alumina-based HPLC packing material under alkaline conditions. *Journal of Analytical Toxicology* 19: 73–78.
- Nishikawa M, Nakajima K, Tatsuno M, Kasuya F, Igarashi K, Fukui M and Tsuchihashi H (1994) The analysis of cocaine and its metabolites by liquid chromatography/atmospheric pressure chemical ionization-mass spectrometry (LC/APCI-MS). *Forensic Science International* 66: 149–158.
- Sato K, Kumazawa T and Katsumata Y (1994) On-line high-performance liquid chromatography-fast atom bombardment mass spectrometry in forensic analysis. *Journal of Chromatography A* 674: 127–145.

TOXINS: CHROMATOGRAPHY

See III/MARINE TOXINS: CHROMATOGRAPHY; NEUROTOXINS: CHROMATOGRAPHY

TRACE ELEMENTS BY COPRECIPITATION: EXTRACTION



K. Terada, Kanazawa University, Kanazawa, Japan

Copyright © 2000 Academic Press

In separation by precipitation, contamination with other elements by coprecipitation is undesirable. However, since the publication by Bonner and Kahn of a summary on the separation of carrier-free radioactive tracers by coprecipitation in 1951, this technique has found wider application to the separation and preconcentration of trace elements in various kinds of samples, such as natural water, treated wastewater, high purity metals and geological and biological materials.

In modern textbooks, coprecipitation is recommended for separation and preconcentration of a single trace element or a group of trace elements when the concentration is too low to be directly precipitated or the amount is too small to be handled. In general,

coprecipitation of trace elements is carried out with inorganic and organic precipitants attaining high degrees of concentration, so that subsequent determinations can be performed by using the precipitate itself.

Mechanism

Depending on the nature of the solid phase produced in a solution and the experimental conditions, coprecipitation occurs by different mechanisms. Although the various types of coprecipitation cannot be distinguished clearly, they may be classified according to the following mechanisms: (i) the formation of mixed crystals and mixed chemical compounds, (ii) surface adsorption and the occlusion and (iii) mechanical inclusion of trace components into the other compounds during crystal formation. However, these processes often proceed concurrently, making the precipitation process quite complicated.

Isomorphous Mixed-Crystal Formation

The processes of coprecipitation by isomorphous mixed-crystal formation have been well studied, and the distribution of trace elements is found to be governed by either the Berthelot–Nernst or the Doerner–Hoskins law.

Berthelot–Nernst distribution law (homogeneous distribution). If digestion is continued throughout the precipitation process, equilibrium will be established between the trace elements in the interior of the crystals and the solution, resulting in homogeneous distribution of the trace element in the precipitate. Then, the following equation applies:

$$\frac{(\text{Trace element})_{\text{ppt}}}{(\text{Carrier})_{\text{ppt}}} = D \frac{(\text{Trace element})_{\text{soln}}}{(\text{Carrier})_{\text{soln}}}$$

The higher the value of D , the higher the enrichment of trace elements.

Doerner–Hoskins law (logarithmic distribution)

When the ions cannot reach the interior of the crystals, equilibrium will be established between the trace elements in the solution and those on an extremely thin surface layer of the crystals. This results in logarithmic distribution of the impurities, and the following equation is applicable:

$$\log \frac{T_o}{T_s} = \lambda \cdot \log \frac{C_o}{C_s}$$

where T and C represent trace element and carrier, subscript o and s denote the concentration in the solution before and after the precipitation, respectively.

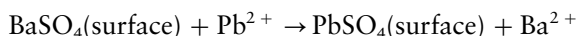
In practice, coprecipitation of the trace elements may occur between the above two limiting distribution laws.

Surface Adsorption

The surface of a precipitate is particularly reactive. Ions at the surface of a crystal are incompletely coordinated and hence are free to attract other ions of opposite charge from the solution. The surface adsorption of ions on ionic precipitates has been described by the Paneth–Fajans–Hahn rule which demonstrates that adsorption generally increases with the growing surface area of the crystal and with the decrease in solubility of the compounds of the trace elements which the elements form with oppositely charged ions of the crystal. However, there are many exceptions to this rule. For example, in spite of the low solubility of PbCl_2 or PbI_2 , they do not coprecipitate with HgCl_2 or HgI_2 .

Two other factors, the dissociation constant of the adsorbed compounds and the deformation ability of the ions, are important for adsorption. The smaller the dissociation of the adsorbed electrolyte, the larger the adsorptivity. The adsorptivity also increases with increased deformability of the adsorbed electrolyte. The deformability usually increases with the size of the ion.

Another mechanism of adsorption presented by Pauling is an ion exchange process. When the radius of an ion in the solution is similar to an ion on the surface of the crystal, they are exchangeable with each other. This is more effective when an ion in the solution forms slightly soluble compounds with an ion of opposite charge in the crystals. Thus, lead (II) ions can be adsorbed on the surface of a barium sulfate precipitate even in the absence of excess sulfate ion in the solution, according to the following exchange reactions:



Occlusion and Mechanical Inclusion

When an ion adsorbed on a crystal surface from the solution is trapped by subsequent crystal layers, the ion will be occluded in the interior of the precipitate. This situation can be prevented with colloidal precipitates rather than with crystal ones, especially in a rapid precipitation process. For example, freshly precipitated hydroxides or sulfides contain a certain amount of impurities, most of which are released upon ageing of the precipitates. Thus, coprecipitation by occlusion generally gives a poorly reproducible yield of the trace elements to be coprecipitated.

Coprecipitation with Inorganic Precipitants

Coprecipitation of trace elements with inorganic precipitants is usually carried out using colloidal precipitates with a large surface area such as metal hydroxides and sulfides. Among various hydrated oxides, coprecipitation with those of iron(III) and manganese(IV) have been commonly used and are the most studied, but many other hydroxides, such as $\text{Al}(\text{OH})_3$, $\text{Be}(\text{OH})_2$, $\text{La}(\text{OH})_3$, $\text{Th}(\text{OH})_4$ and $\text{Zr}(\text{OH})_4$, and mixtures of metal hydroxides, such as $\text{Fe}(\text{OH})_3$ and $\text{Ti}(\text{OH})_4$, have also been employed.

Coprecipitation techniques are commonly used to separate and concentrate trace elements from very dilute solutions, such as natural water. Since the solubilities of the metal hydroxides or sulfides are mainly governed by the pH value of the solution,

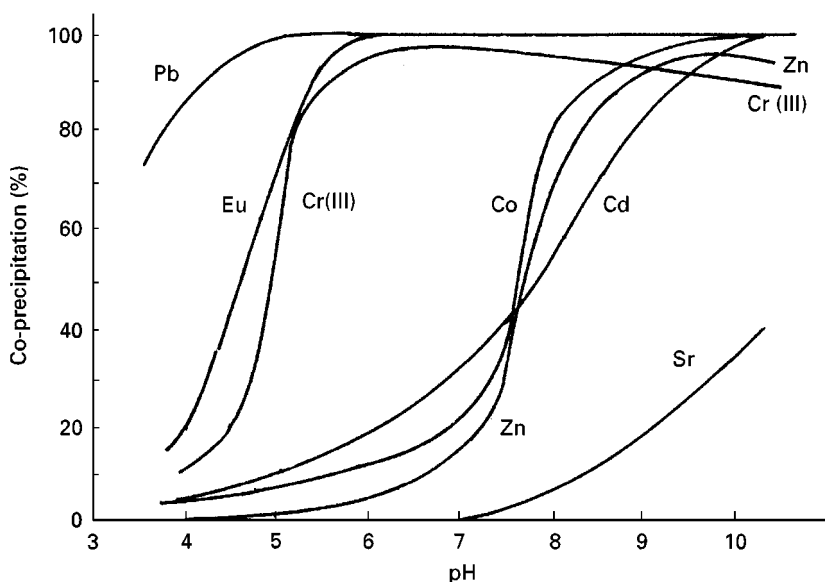
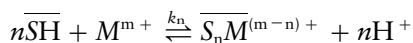


Figure 1 Relation between co-precipitation recoveries of metals with iron(III) hydroxide and pH of the solution.

control of pH is essential for an effective coprecipitation of trace metals. **Figure 1** shows coprecipitation yields of some metal ions with iron(III) hydroxide. It can be seen that removal of many metal ions from a solution may be possible at pH 9–10. However, it should be noted that the coprecipitation yield is also affected by the amounts of precipitants used, the coexisting salts and the ageing time of precipitation. Since most metals form sparingly soluble hydroxides, coprecipitation by hydrated metal oxides is usually of low selectivity, so that different trace metals are likely to be coprecipitated simultaneously.

Three possible mechanisms relating to the adsorption of the trace metal ion on the hydrated metal oxide surface prior to coprecipitation have been suggested.

The first involves ion exchange between adsorbed hydrogen on the hydrated oxide surface and the trace metal ion M in solution according to the equation:



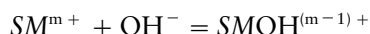
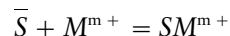
where n is the number of molecules of the hydrated metal oxide and the surface area per molecule is S . M represents the metal cation of charge m . Then the distribution coefficient D is given by:

$$D = \frac{[M]_{\text{surface}} (\text{mol kg}^{-1})}{[M]_{\text{solution}} (\text{mol dm}^{-3})} = \frac{K_n \overline{S_nH^n}}{(H^+)^n}$$

By taking logarithms the equation becomes:

$$\log_{10} D = npH + \log_{10}(K_n) + n\log_{10}(SH).$$

The second postulated mechanism involves the chemical sorption of the trace metal ion M^{m+} on the surface of the hydrated metal oxide, followed by the adsorption of hydroxyl ions:



The third possible mechanism requires the adsorption of hydrolytic complexes of the trace metal ion, rather than the metal ion itself, on the surface of the hydrated metal oxide:

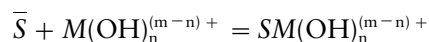
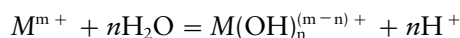


Table 1 shows examples of preconcentration of trace elements by coprecipitation with inorganic precipitants.

Coprecipitation with Organic Collectors

Organic collectors are mainly complexing agents which are sparingly soluble in aqueous solution and form complex compounds with the desired metal ions. The mechanisms of coprecipitation of trace elements with organic collectors have been described by Minczewski *et al.* According to them:

Table 1 Coprecipitation of trace elements with inorganic precipitants

<i>Precipitants</i>	<i>Trace elements</i>	<i>Sample, experimental conditions, comments</i>
Hydroxides		
Al(III)	Cr(III), (VI), Mo, W	Natural waters. Quantitative precipitation: Cr(III) (pH 5–9), Mo (pH 4–5), W (pH 6–8), Cr (VI) (pH 5–6, but it is not quantitative)
	Ce, Eu, La, Lu, Nd, Sm, Tb, Th, Tm, Yb, U	Hot spring and crater waters. 10 mg Al to 2 dm ³ sample. Al precipitation is carried out at near boiling temperature with 14% NH ₃ solution to reach pH 6.5–7.5
	Th, U	Hot spring and crater lake waters. Al ₂ (SO ₄) ₃ (25 mg) is added to 1 dm ³ sample. pH is adjusted to 7–8 with 14% NH ₃ solution
	Li	Geothermal waters: pH should be high (>12.5–13) and a long mixing time is required. The recovery yield is increased by removal of Ca ions and polymerized silica
Be(II)	As	High purity iron steel. Sample (1 g) is digested with HNO ₃ . 5 cm ³ BeSO ₄ (1 mg Be/cm ³) is added in the presence of EDTA (mask matrix elements). As coprecipitates as BeNH ₄ AsO ₄ with Be(OH) ₂ . Perfect recovery is obtained between 1.0 and 3.5 mol L ⁻¹ HCl with relative standard deviation (RSD) of c. 13% for 1.0 µg g ⁻¹ As. Detection limit is 0.3 µg g ⁻¹ of solid sample
	P	High purity iron steel. Same procedure as As. Coprecipitation recovery is 98.7%. Arsenic is removed from the solution as AsBr ₃ for Mo-blue spectrophotometry of P
Bi(III) + In(III)	Co, Cu, Fe, Mg, Ni	High purity Ti metal. 0.5 g sample is dissolved in 6 mol L ⁻¹ HCl (20 cm ³) + HF (0.5 cm ³). Bi(III) and In(III) are added (10 mg and 20 mg, respectively). After addition of 4 cm ³ of H ₂ O ₂ , pH is adjusted to 9.5 with 7.5 mol L ⁻¹ NaOH (pH > 11 for Mg). Ageing time 30–60 min. Perfect recoveries are obtained for all metals. RSD: 0.22%, 0.28%, 2.8%, 0.05% and 0.84%. Detection limit: 0.10, 0.5, 1.8, 0.08, 0.36 µg g ⁻¹ for Co, Cu, Fe, Mg, Ni, respectively
Fe(III)	Cd, Co, Eu	Seawater. Coprecipitation yield in the radionuclide levels: Cd (85% at pH 9.0, Fe 35 mg dm ⁻³), Co (95% at pH 9.0, Fe 35 mg dm ⁻³), Eu (c. 100% at pH 9.0 Fe 10 mg dm ⁻³ , at pH 6.0–9.0, Fe 35 mg dm ⁻³)
	Mo	Seawater. To 500 cm ³ sample, 9 mol L ⁻¹ H ₂ SO ₄ (1.0 cm ³) and 0.1 mol L ⁻¹ FeCl ₃ (3.0 cm ³) are added. c. 96.5% coprecipitation yield of Mo is obtained at pH 4.0; it decreases with increasing pH value
	Cr(III), (VI)	Urine. Cr(III) is found to be precipitated at pH 10, while Cr(VI) remains in the solution. Cr(VI) is only coprecipitated at 4–7
	Cr(III)	Seawater. 4 cm ³ of 2 mol L ⁻¹ HCl, 4 mg Fe(III) are added to 2 dm ³ sample, heat to 50–60°C, 60 cm ³ borate buffer (19.07 g borate + 4 g NaOH in 1 dm ³) is added to solution to pH c. 7.5. Recovery for Cr > 99% at concentration 0.4 µg dm ⁻³ . Precision is ± 0.02 µg dm ⁻³
	As, Cr, Ge, P, Sb, Se, Te, W	Water sample. Optimum pH ranges are 5–7 for Sb and Se, 5–8 for As and W, 5–10 for Cr, Ge and Te, 6–7 for P. Preconcentration factor is 50 for all except Se, where it is only 5
	Cu, Mn, Ni, Pb, Zn	Natural waters. 2 mg Fe(III) is added to 200 cm ³ sample; pH adjusted to 9 (NaOH). Detection limit is c. 1 µg dm ⁻³ . ICP-AES is employed
	Se	Seawater, silicates, marine organisms. 20 mg Fe(III) is added to 5 dm ³ seawater, pH is adjusted to 5–6. After 2 h standing, another 20 mg Fe(III) is added to solution, pH to 4–6 with aq. NH ₃ . RSD is 6.0% for 0.5 µg Se dm ⁻³
	V	Seawater, natural water, biological materials, sediments, rocks. 15 cm ³ 1.0 mol L ⁻¹ HCl and 30 mg Fe(III) are added to 3 dm ³ seawater; pH is adjusted to 5–6 with aq. NH ₃ . Precipitate is dissolved in 10–20 cm ³ 2 mol L ⁻¹ HCl. Coefficients of variation are 2.8% for seawater, 1.3% for silicate rocks, 2.5% for marine plants. Quantitative recovery is attained for 1.8 µg V dm ⁻³
	Ag, Cd, Ce, Cr, Cs, Er, Eu, Gd, La, Mn, Rb, Sr, Yb	Low level waste solution. Effect of pH was studied. Sorption of Cs ⁺ and Rb ⁺ is not strongly pH-dependent, but coprecipitation is low (20%)
	Zn	Quantitative recoveries are obtained for Ag (pH > 8), Cd, Mn, Zn (pH ~ 10), Cr(III) (pH 9–10), Ce, Er, Eu, Gd, La, Yb (pH ~ 10). Sr (pH 11–11.5, 65%). Freshly precipitated Fe(OH) ₃ can be used for the decontamination of radionuclides
	Te	Hair. Sample (2–4 g) is digested with a mixture of HCl + HClO ₄ , heated to evolving fumes, then boiled with 20% HCl to reduce Te to Te(IV). 5 mg Fe(III) is added, pH is adjusted to 9, and centrifuged. Precipitate is dissolved with 3.3 cm ³ conc. HCl, then diluted to 10 cm ³ . Recovery is 96.2 ± 2.4% for 0.2 µg Te

(Continued)

Table 1 *Continued*

<i>Precipitants</i>	<i>Trace elements</i>	<i>Sample, experimental conditions, comments</i>
Hydroxides		
Ga(III)	Al, As, Cd, Co, Cr, Cu, Fe, La, Mn, Ni, Pb, Ti, Y, Zn	Seawater. 5 mg Ga is slowly added to 1 dm ³ seawater. pH is adjusted to 9.0 (NaOH), ageing for 24 h. Precipitate is washed with H ₂ O (remove Na, Mg, K, Ca), dissolved with 2.5 cm ³ 1 mol L ⁻¹ HCl, diluted to 5 cm ³ . 200-fold concentration is achieved. Quantitative recoveries are attained at pH 9.0 for Al, Co, Cr, Cu, Fe, La, Mn, Ni, Ti, Y, Zn. As(III), Cd, Pb (<90%, pH 10)
In(III)	Cu, Fe, Ni	Ti alloy. Sample (0.2 g) is dissolved in HCl, 3 cm ³ H ₂ O ₂ is added to mask Ti. 10 mg In(III) is added, pH is adjusted to 9.0 (NaOH). 100% recoveries at pH 8.5–9.0. Detection limit: Cu 0.8, Fe 8.1, Ni 1.4 µg g ⁻¹ alloy
	Cd, Co, Cr, Cu, Fe, Mn, Ni, Pb	Natural waters. 10 mg In(III) to 100 cm ³ sample. pH to 9.5. Precipitate is separated by centrifuge, dissolved in 1 cm ³ 2.5 mol L ⁻¹ HBr. All are quantitatively coprecipitated. Determination limits for GF-AAS are Cd 0.003, Cu 0.02 µg dm ⁻³
La(III)	As, Bi, Sb, Se, Te	Mo metal. 1 g Mo is dissolved in a mixture of 2 cm ³ conc. HNO ₃ + 6 cm ³ conc. HCl. 50 mg La and small amount filter paper pulp to solution. pH is adjusted to 10.0 (NaOH). After filtration, precipitate is dissolved four times with 2 cm ³ , boiling 6 mol L ⁻¹ HCl. Coprecipitation and dissolution are repeated. Recoveries at pH 10.0, As 96.8, Bi 112.0, Sb 92.4, Se 100.1, Te 106.0% for each 5 µg
	Co, Fe, Mn, Ni, Zn	Seawater. 5 mg La to 1 dm ³ sample, pH adjusted to 9.8 with 1 mol L ⁻¹ Na ₂ CO ₃ . Precipitation at 80°C for 30 min and later aged for several hours
Mn(IV)	Bi, Pb, Sb, Sn	Ni matrix. Ni is dissolved with 25 cm ³ (1 + 1) HNO ₃ , pH adjusted to 2–3 with (1 + 1) aq. NH ₃ . Volume is made up to 200 cm ³ by adding 0.008 mol L ⁻¹ HNO ₃ . MnO ₂ is formed from MnSO ₄ + KMnO ₄ in the presence of acids with 2-min boiling followed by standing for 30 min. Precipitate is treated with 50 cm ³ 10 mol L ⁻¹ HCl. 100% coprecipitation for Bi, Sb, Sn in 6.5 mg Mn precipitated, while Pb in 30 mg Mn, each in 1–100 µg dm ⁻³
	Mo	Seawater, silicates, biological materials. 1.0 dm ³ water is pH adjusted to 2 with dil. HCl. Each 2 cm ³ ethanol and 1 mol L ⁻¹ KMnO ₄ is added and stands overnight. Precipitate is dissolved in saturated aqueous solution of SO ₂ . Quantitative coprecipitation is in the range of pH 1.3–5.5 for Mo level < 5 µg dm ⁻³ seawater
	Ga	Aqueous solution. Coprecipitation conditions are studied. To 200 cm ³ solutions containing Ga (0.5–1000 µg) 5 cm ³ 5% MnSO ₄ is added and adjusted pH to 1.5–1.6 with HCl or H ₂ SO ₄ , to boiling and slowly added 2.5 cm ³ 1.25 mol L ⁻¹ KMnO ₄ , then stands for 5–7 min. Precipitate is dissolved in 10 cm ³ 5% HCl containing 8–10 drops 3% H ₂ O ₂ . Ga is perfectly recovered
	As	Cu, Fe, Ni metals. Sample (0.1–2.0 g) is dissolved in 20–30 cm ³ HNO ₃ (1 + 1). pH to 1.0–2.0 with aq. NH ₃ (except for Fe). As is coprecipitated by adding 60 mg KMnO ₄ + 10 mg Mn(II). Precipitate is dissolved in mixture (HNO ₃ + H ₂ O ₂). Detection limit: 20 ng cm ⁻³
Te(IV)	Se	High salt waste water. After boiling 100 cm ³ of sample (1 mol L ⁻¹ HCl) for 30 min in the presence of 5 g hydrazinium sulfate p.p.b. level Se(IV,VI) is quantitatively coprecipitated with 25–500 µg Te(IV) and completely collected on nitrocellulose membrane filter (pore size 0.2 µm). Heavy metals (high level) do not interfere
	Ag, Au, Pd, Pt, Rh	Cu, Fe, Ni-ores. 1 g sample is dissolved with aqua regia (10 cm ³) at 180°C for 5 h and diluted to 100 cm ³ . 10 cm ³ is evaporated, leached with 0.5 mol L ⁻¹ HCl, Ag is trapped on Dowex 50 w × 8 column and eluted with 0.5 mol L ⁻¹ HCl. Au, Pd, Pt, Rh in 2 mol L ⁻¹ HCl are coprecipitated by adding 5 mg Te (TeCl ₃) and SnCl ₂ (28%)
Th(IV)	Mo	Seawater. To 500 cm ³ seawater (1 cm ³ 9 mol L ⁻¹ H ₂ SO ₄) is added 3–4 cm ³ 0.1 mol L ⁻¹ Th(NO ₃) ₃ , adjusting pH to 6.0 (aq. NH ₃) and standing for 30 min. Precipitate is collected on millipore filter, dissolved in HCl. Precipitation yields: 99.5 (pH 6.0), 81.5 (pH 7.5), 61.6 (pH 8.5)
Zr(IV)	Bi	Sea-, spring-, river waters. To sample ZrOCl ₂ is added, pH to 9.0 with aq. NH ₃ . Precipitate is dissolved in 4 mol L ⁻¹ HCl. Quantitative recovery is obtained at Zr > 10 mg in the pH range 8.8–9.2. > 0.5 mg Al, As(III), Cu, Sn interfere
	Cd, Cu, In, Pb	Sediments. To sample solution containing 0.04 g sediment, 1 cm ³ ZrOCl ₂ is added and pH is adjusted to 8.8. Precipitate is dissolved in 25 cm ³ 4 mol L ⁻¹ HCl. 0.01 µg g ⁻¹ In in sample solution is quantitatively recovered with > 5 mg Zr at pH 8.4–8.8. Cu and Pb are quantitatively collected at pH 8.25–9.0. 0.05 mg As, Bi interfere with Cu determination; 0.05 mg Sn(II), 0.1 mg As(III), Ti(I) interfere with Pb determination. Optimum pH for Cd is 9.0

(Continued)

Table 1 Continued

Precipitants	Trace elements	Sample, experimental conditions, comments
Hydroxides		
	Sb	Seawater, algae, silicates. 1 dm ³ water is added 3 cm ³ 6 mol L ⁻¹ HCl and 300–400 mg K ₂ Cr ₂ O ₇ , heating to 75–85°C for 1 h. After cooling, 150 mg ZrCl ₄ completes dissolution; pH is adjusted to 5.0 ± 0.3, ageing at least 90 min. Recoveries of Sb 99.2% (pH 3.0), 99.1% (pH 5.0), 93.7% (pH 7.5). Standard deviation: 0.003–0.009 µg dm ⁻³ for 0.08–0.42 µg dm ⁻³ Sb
Sulfides		
Bi(III)	As, Sb, Se	Water samples. Coprecipitation is carried out in 1.2 mol L ⁻¹ HCl solution. Minimum amounts: As(III) 10 ng, Sb(III) 50 ng, Se 20 ng
Cd(II)	Cr, Cu, Fe, Mn, Pb, V	BaCl ₂ solution. Coprecipitation conditions are studied for 1 µg of Cr, Fe, Mn, Pb, V, 0.1 µg of Cu. CdS is precipitated from Cd(CH ₃ COO) ₂ with Na ₂ S. Optimum conditions: pH 7–8, BaCl ₂ 15%
In(III)	Co, Cr, Cu, Mn, Zn	Calcite. 0.3 g sample is dissolved with HF, HNO ₃ and HClO ₄ , diluted to 200 cm ³ . 30 mg In is added; pH adjusted to 9.0. In ₂ S ₃ is precipitated by adding 0.1 g thioacetamide. Coprecipitation recoveries: Co 89.4%, Cr 94.5%, Cu 88.8%, Mn 94.9%, Zn 89.1% for each concentration of 25 p.p.m.
Pb(II)	Cu	Tap water, iron and steel. 30 cm ³ tap water is acidified with 0.5 cm ³ 6 mol L ⁻¹ HCl. After adding 1.0 mg Pb, PbS precipitates by passing H ₂ S. Precipitate is dissolved in conc. HCl (1 cm ³). RSD: 0.7% for 5 µg dm ⁻³
Sulfates, phosphates		
Pb(II)	Cr(III)(VI)	Seawater. Na ₂ SO ₄ (0.2 mol L ⁻¹ 8 cm ³) added to 800 cm ³ sample; pH adjusted to 3; 8 cm ³ Pb(NO ₃) ₂ added dropwise. Precipitate filtered on Nuclepore. Cr(VI) only coprecipitates with PbSO ₄ at pH 3. To another 800 cm ³ sample 3 cm ³ 0.2 mol L ⁻¹ Pb(NO ₃) ₂ and 0.2 cm ³ 1 mol L ⁻¹ NH ₄ H ₂ PO ₄ , pH adjusted to > 6 with aq. NH ₃ . Both Cr(III), Cr(VI) are quantitatively coprecipitated with Pb ₃ (PO ₄) ₂ . In seawater, molar ratio of Pb to PO ₄ ³⁻ is kept at 3 for perfect recovery of Cr (VI). 0.08 µg dm ⁻³ Cr is detectable
Bi(III)	Am, Cm, Np, Pu	Sequential separation by coprecipitation with BiPO ₄ , by using suitable oxidizing and reducing agents. Cm(III) is separated from Am, Np, Pu, U in their (VI) valency states by adding K ₂ S ₂ O ₈ -Ag ⁺ before coprecipitation. Next, Am(III) is separated from Np, Pu, U by adding C ₂ H ₅ OH. Pu(IV) is separated from Np and U by adding NaNO ₂ . Last, Np(IV) is coprecipitated by addition of H ₂ O ₂ . Recoveries: Cm (98.5%), Am (97.6%), Pu (94.7%) and Np (96.0%)
Fluorides		
Ca(II)	Cu, Fe	Surface adsorption was shown to be the main cause for coprecipitation. Cu(II) is coprecipitated as counter ion to excess F ⁻ , whereas Fe(III) coprecipitates as FeF ₆ ³⁻ in competition with matrix fluoride
	U	Aqueous solution. To sample 5 cm ³ 1 mol L ⁻¹ Ca(NO ₃) ₂ , 30 cm ³ 0.3 mol L ⁻¹ NH ₄ F solutions are added dropwise. Applicable to coprecipitation of 0.01 ng dm ⁻³ U
	Th	Uranium ore. 1 g sample is digested in 50 cm ³ of mixture (8 mol L ⁻¹ HCl + 0.01 mol L ⁻¹ (NH ₄) ₂ SiF ₆) by heating for 4 h. To solution 10 mg La carrier, HF is added to precipitate LaF ₃ . Precipitate is dissolved with 16 mol L ⁻¹ HNO ₃ . Recovery of ²³⁴ Th tracer is 85% with RSD of ± 12% for 1 p.p.m. level
Oxalates		
Ca(II)	La, Lu, Tb	Biological materials. Substoichiometric precipitation of rare earth elements was studied. To 8 cm ³ of solution containing 0.0125 mol L ⁻¹ Ca(II), 2.0 × 10 ⁻⁷ –6.0 × 10 ⁻⁵ mol L ⁻¹ radioactive RE(III) and 1.25 × 10 ⁻³ mol L ⁻¹ CCl ₃ COOH–0.1 mol L ⁻¹ oxalic acid. At pH 2–5 complete coprecipitation is attained
	Ce, Pm, Sr, Y	Urine. 500 cm ³ is wet-ashed. Resulting salt is treated with 30% H ₂ O ₂ , dissolved in H ₂ O, pH is adjusted to 3.0 (aq. NH ₃). Oxalate is removed by dissolving precipitate in hot HNO ₃ , heating in the presence of 70% HClO ₄ . Residue is treated with H ₂ O ₂ to reduce Ce(IV) to Ce(III) followed by dissolution with H ₂ O. Recoveries: Ce 87%, Pm 89%, Sr 100%, Y 64%

(Continued)

Table 1 *Continued*

<i>Precipitants</i>	<i>Trace elements</i>	<i>Sample, experimental conditions, comments</i>
Salts and metals		
AgCN	Pd	Pure metals. Highly selective for Pd in 10^7 – 10^9 fold excess of Ag, Al, Bi, Cd, Co, Cu, Fe, Mn, Ni, Pb, Sn, Th, Ti, U, Zn. Coprecipitation of Pd is not influenced. Pd is coprecipitated with AgCN. RSD 4–16%; detection limit: $10^{-7}\%$ Pd
As	Se, Te	Geological and biological samples. After digestion of samples by mineral acids ($\text{HNO}_3 + \text{HClO}_4$). Na_3AsO_3 (c. 1.5 mg As) is added. As(III) is reduced to elemental As by phosphorous acid at 80°C for 15 min. Ageing at room temperature for at least 8 h to complete flocculation. Detection limit is 0.1 p.p.m. of Se and Te

1. The sparingly soluble organic compound, such as a bulky organic cation, forms an ion pair with the anionic complex.
2. An insoluble salt formed between the organic anion and the metal cation is coprecipitated together with the excess of the reagent, e.g. metal-8-quinolate in excess of 8-hydroxyquinoline.
3. A soluble chelate compound of a trace metal can be coprecipitated with the precipitate formed between the excess of the reagent and a bulky different organic reagent cation.
4. An inner complex of the metal ion to be separated is coprecipitated with a large excess of the organic reagent such as 1-(2-pyridylazo)-2-naphthol.

Table 2 Coprecipitation of trace elements with organic collectors

<i>Collectors</i>	<i>Trace elements</i>	<i>Samples, experimental conditions, comments</i>
Organic carriers		
α -Benzildioxime (α -BD)	Ni	Seawater. 500 cm ³ samples, 1 mg α -BD, pH \sim 9.5. Ageing time can be minimal. Even 0.2 p.p.b. Ni can be determined
DDTCA (diethyldithiocarbamic acid)	As, Cd, Cu, Fe, Mn, Ni, Pb, Se, Zn	Water samples. Ni, Cu are completely precipitated between pH 1 and 11. Cd, Fe(III), Pb, Zn begin to precipitate at pH 1–2 but complete precipitation is only obtained above pH 4 (pH 5 was used). Complete recovery of As is only obtained at pH 5.0–5.5. For very pure water, metal carrier should be used. Citrate is a powerful masking agent for Fe
	Co, Eu, Mn, Zn	Natural water samples. To 250 cm ³ sample, 20 cm ³ 2% (w/v) NaDDTC solution and 5 cm ³ buffer solution (pH 5) are added. Coprecipitation capacity: 900 $\mu\text{mol L}^{-1}$. Recoveries: Co 97–98%, Eu 88–100%, Mn 85–98%, Zn 82–100%
	Cu, Fe, Hg, Zn	Saline water. To 250 cm ³ sample, 400 mg freshly prepared NaDDTC is added at pH 4.0
DDTCA + dibenzylidene-D-sorbitol (DBS)	As, Cd, Cr, Cu, Fe, Mn, Pb, Sb, Zn	Industrial wastewater, river water. Concentration range 1–50 μg . pH 5.0–5.5 (acetate buffer). 100 mg NaDDTC, 17 mg DBS as flocculant. 94–100% recovery for Mn
Diethylammonium <i>N,N'</i> -DDTC	Cd, Cr, Cu, Hg, Ni, Pb	Drinking, wastewaters. To 500 cm ³ sample is adjusted pH to 5.0–5.5 (acetate buffer), then diethylammonium <i>N,N'</i> -DDTC is added to make 2%. Recovery ranges: Cd 84–94%, Cr 86–102%, Cu 94–106%, Hg 100–108%, Ni 99–110%, Pb 88–92%
DBDTCA (dibenzylthiocarbamic acid)	As(III),(V), Cd, Fe, Zn	Fresh water. pH 2. 100 cm ³ samples, 10 mg of Na-salt of DBDTCA in methanol added. As(III) coprecipitates but not As(V) which precipitates after reduction to As(III) with KI + $\text{Na}_2\text{S}_2\text{O}_3$. Recovery of As(III) 100% in pH range 1–3 but drops drastically for higher pH. 2–3 mg of DBDTCA is sufficient. High recoveries are obtained for Cd, Fe and quite high (87.5%) for Zn
DBDTCA + phenolphthalein	Se(IV)	Fresh water and seawater. 500 cm ³ sample is adjusted to pH 2. 10 mg of Na-salt of DBDTCA and 100 mg phenolphthalein in methanol are added. Without phenolphthalein, recovery is 97% but decreases with ageing time. pH should be < 4 . In the presence of phenolphthalein ageing does not reduce the yield
Dithizone	Ag, Bi, Cd, Cu, Hg, Pb, Pd, Zn	Dilute HCl and HNO_3 solutions. After adjusting acid concentration, 0.1 g ascorbic acid added to reduce Fe(III), finally dithizone is added. Recoveries depend on the acid concentration. (HCl, M, recovery, %) Bi (10^{-2} – 5×10^{-2} , 95), Cd (< 0.002 , 95), Cu (< 2 , 95), Hg (< 1.5 , 95), Pb (< 0.001 , 95), Pd (< 1 , 95), Zn (3×10^{-4} , ~ 40)

(Continued)

Table 2 *Continued*

Collectors	Trace elements	Samples, experimental conditions, comments
Dithizone + phenolphthalein	Ag, Co	Surface water. 4 dm ³ water to be made 0.5 mol L ⁻¹ H ₂ SO ₄ solution; About 28 mg dithizone and 300 mg phenolphthalein are added. Phenolphthalein helps in collecting the precipitate. At pH 1 only Ag is coprecipitated. Co is recovered quantitatively at pH 6.5–8. Dithizone in glacial CH ₃ COOH, phenolphthalein in ethyl alcohol
2-Mercaptobenzimidazole (MBI)	Ag, Au, Hg, Sn, Ta	Seawater. Recoveries were studied at pH 1, 3, 5. To 20 dm ³ seawater (pH 1) 5 g MBI in 100 cm ³ ethanol were added and aged for 2 days (0–5°C). High recoveries are obtained at the following pH ranges: Ag (1–5), Au(1), Hg(1–5) Sn(5), Ta(1–3)
Nioxime (1,2-cyclohexane-diondioxime)	Ni	Aqueous solution. Selective precipitation of Ni at µg level at pH 7.0–9.5. Large amounts of Co, Cu, Fe are masked with Na-tartrate and Ca-EDTA. 32 mg nioxime is used
Oxine (8-hydroxyquinolinol)	Ce, Fe, Pr, Pu	Aqueous solution. Fe was co-crystallized with oxine produced <i>in situ</i> by hydrolysis of 8-acetoxyquinoline. Ce, Pr, Pu also quantitatively recovered
	Cd, Cu, Mn, Pb, Zn	Seawater. The metal ions are quantitatively precipitated in pH range 7.0–8.5 with oxine alone (5 cm ³ of 2% solution) kept at 70°C for 3 h. Detection limits (ng dm ⁻³): Cd 1.4, Cu 10, Mn 5, Pb 10, Zn 6. Recoveries > 98%
	Al	Aqueous solutions. 100 cm ³ sample, pH 6.8–6.9 (0.07 mol L ⁻¹ phosphate buffer). Slow addition of 160 mg oxine. Ageing 1 h. Sensitivity 0.1–0.02 p.p.m.
PAN (1-(2-pyridylazo)-2-naphthol))	Cr(III), Cu, Hg, Mn, Ni, Zn	Seawater. 0.5–4 dm ³ , metal ions are precipitated by adding 20 mg of PAN ethanol solution and heating at 70–80°C for 10 min at pH 6.5–10 for Cu, Ni, Zn; high pH ~10 for Cr(III), Mn. It is preferred that pH should be ~9 in order to decrease coprecipitation of Ca. Alkali and alkaline earth metal ions do not interfere
Organic carriers		
	U	Seawater, tap water, digestate of biological samples. Coprecipitation is most effective at pH 4.5–6.5 with recovery of 85–94%. In the presence of 1,2-cyclohexylenedinitrilo tetra acetic acid (CyDTA) as a masking agent. The method is highly selective for U. Detection limit: 3–4 ng dm ⁻³ for 500 cm ³ samples and 5 µg kg ⁻¹ for 0.5 g biological samples
Thionalide (2-mercapto-N-2-naphthylacetamide) + Oxine	As(III), Cu, Sb(III)(V)	Seawater. 0.005–0.25 mol L ⁻¹ H ₂ SO ₄ . As is only precipitated quantitatively at H ₂ SO ₄ > 0.2 mol L ⁻¹ As(V) is reduced to As(III) by ascorbic acid. 0.015 mol L ⁻¹ H ₂ SO ₄ is used for total As precipitation. 8 cm ³ 2% thionalide in acetone is used. Sb and Cu are coprecipitated with oxine at pH 6–9 while As is not coprecipitated at all
TPAC (tetra-phenylarsonium chloride)	⁹⁶ TcO ₄ ⁻	Aqueous perchlorate solution. Recovery is constant at pH in the range 0.5–13. Precipitation yield is highly affected by TPAC and ClO ₄ ⁻ concentrations. At 25°C, > 90% yields are obtained at TPAC > 0.02 mol L ⁻¹ . Coprecipitation of Tc(IV) is very low
Metal + organic carriers		
Fe (DBDTC) ₃	U	Natural waters. To 500 cm ³ sample. 20 µg Fe(III) and 2 cm ³ 0.1 mol L ⁻¹ KH ₂ PO ₄ (pH 4) are added prior to pH adjustment to 4.0 ± 0.02. DBDTC (1%, 1 cm ³) is added, stirring (15 min), ageing (15 min). Detection limit is 0.4 p.p.b.
Fe (TMDTC) ₃ (tetra-methylenedithiocarbamate)	Cd, Co, Cu, Ni, Pb	Mineral water. 0.5 mg Fe(III) to 200–250 cm ³ sample, pH to 2–3, CO ₂ is boiled out, 50 mg TMDTC is added. The choice of Fe(III) is due to its high concentration in mineral water. High recoveries are obtained > 95%
Co(PDC) ₃ (pyrrolidine dithiocarbamate)	Cd, Cu, Ni	Seawater. 100 cm ³ samples are adjusted to pH 2 (6 mol L ⁻¹ HCl). 50 µg Co (as CoCl ₂), 10 mg APDC are added and aged for 5 min. Precipitate is dissolved in acetone
Pb(PDC) ₂	Co, Cu, Hg	Dead Sea surface water. To 1 dm ³ sample 2.5 mg Pb is added, pH to 3.6, and 20 mg APDC is added. Determination by X-ray fluorescence
Al-oxinate or In-oxinate	Co, Cu, Mo	Agricultural sample digestate. Al-oxinate perfectly recovers Co, Mo, but not Cu. Addition of thionalide or tannic acid or both leads to quantitative recovery for both Al- and In-oxinates. To a 500 cm ³ sample 15 mg Al, 500 mg oxine are added; pH to 4.5; 200 mg tannic acid, 20 mg thionalide
Mg-oxinate	Al, Cd, Co, Cu, Mn, Ni, Pb, Zn Cr(III), Mo, V	Aqueous solutions. To 100 cm ³ solution, 20 mg Mg ²⁺ , 100–200 mg oxine are added at pH 9. Ageing at 70°C for 1 h. Recoveries: 100% except for Cr (83%), Mo (64%), V (70%). Cr recovered at 98% at pH 10.5

5. A chelate of the trace metal is adsorbed and coprecipitated with a water-insoluble organic compound. Several metal dithizonates can be coprecipitated with phenolphthalein.
6. The metal ions are coprecipitated by means of colloidal-chemical sorption on a mixture of insoluble organic reagents.

Typical examples of the coprecipitation of trace metals with organic collectors are listed in **Table 2**.

See also: **II/Extraction:** Analytical Extractions; Analytical Inorganic Extractions.

Further Reading

Alfassi ZB (ed.) (1994) *Determination of Trace Elements*. Weinheim: VCH Verlagsgesellschaft.

Alfassi ZB and Wai CM (eds) (1992) *Preconcentration Techniques for Trace Elements*. Boca Raton, FL: CRC Press.

Bonner NA and Kahn M (1951) *Radioactivity Applied to Chemistry*. New York: John Wiley.

Kolthoff IM, Sandell EB and Meehan EJ (1969) *Quantitative Chemical Analysis*, 4th edn. New York: Macmillan.

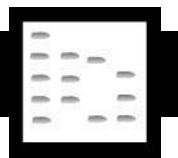
Minczewski J, Chwastowska J and Dybczynski R (1982) *Separation and Preconcentration Methods in Inorganic Trace Analysis*. Chichester: Ellis Horwood.

Mizuike A (1983) *Enrichment Techniques for Inorganic Trace Analysis*. Berlin: Springer-Verlag.

Walton AG (1967) *The Formation and Properties of Precipitates*. New York: Interscience.

Zolotov YA and Kuz'min NM (1990) *Preconcentration of Trace Elements*. Amsterdam: Elsevier.

TRIGLYCERIDES



Liquid Chromatography

V. Ruiz-Gutierrez and J. S. Perona,
Instituto de la Grasa (CSIC), Seville, Spain

Copyright © 2000 Academic Press

Synopsis

High performance liquid chromatography (HPLC) has become a useful tool for the analysis of triglycerides from all sources. This article reviews developments for the analysis of molecular species of triglycerides, including stationary phases, mobile phases, sample solvents, detection and identification. It also points out the advantages of silver-ion HPLC and emphasizes the need for stereospecific analysis in the complete determination of triglyceride molecular species because currently this is not possible by reversed-phase HPLC. Finally, the application of HPLC to triglycerides from fats and oils is described.

Introduction

The goal of chromatographic analyses of lipids is the resolution of all classes and molecular species for the purpose of a complete identification and characterization of all the components of a fat or an oil. This characterization is not complete without the

determination of their triglyceride (TG) molecular species profile. Once the fatty acid composition of a determined fat or oil is clear, the knowledge of how these fatty acids are distributed within the glycerol molecule is of major interest.

Fractionation of TGs has been carried out by different chromatographic techniques. Argentation thin-layer chromatography (Ag-TLC) has been employed to separate TG fractions, with subsequent analysis of their fatty acid methyl esters. Direct gas chromatography, using fused-silica capillary columns coated with high-temperature polar stationary phases has also been used for this purpose with rather poor results.

The introduction of chemically bonded phases and high performance liquid chromatography (HPLC) increased the usefulness of liquid chromatography for the separation of TGs. The first paper dealing with the HPLC of triacylglycerols (TGs) was published in 1975 by Pei *et al.* Simple TGs of medium-chain length were separated on a reversed-phase column. Other workers then began to use HPLC for the analysis of long-chain TGs, on silicic acid columns, reversed-phase columns, or both. The first fractionation of natural TGs by HPLC on reversed-phase columns was performed independently in 1977 by Plattner *et al.* and Wada *et al.* The later authors were the first to establish a parameter, termed the partition number (PN; $PN = CN - 2ND$, where CN is the total number of carbons and ND is the number of double bonds in the fatty acids constituting the TG molecule) for

characterizing TG molecules. They found that TGs on reversed-phase columns eluted in increasing order of PN. Today, reversed-phase high performance liquid chromatography (RP-HPLC) is the most frequently employed technique for separating complex mixtures of TGs, as it allows a good resolution of mixtures into molecular species, based on properties such as molecular weight, degree of unsaturation, polarity and molecular configuration. Nevertheless, despite notable success, the progress in RP-HPLC has not been easy, due to difficulties encountered in the process of separation, detection and identification.

One of the main difficulties in the HPLC analysis of TGs is the formation of the so-called 'critical pairs', that is, molecules found to have close behaviour on reversed-phase columns in spite of the difference in chain lengths, number of double bonds and geometrical configuration. Critical pairs, therefore, have been defined as those structures, with the same PN. This problem has not been solved in natural fat analysis yet. However, a long time ago standards of critical pairs of TGs were separated. El-Hamdy and Perkins were able to separate two geometrical isomers: triolein (54 : 3 ccc) from trielaidin (54 : 3 tt), which differ only by the configuration of the double bonds.

The second difficulty is the establishment of a chromatographic system capable of simultaneously resolving TGs with large differences in carbon chain lengths. The separation of short-chain, medium-chain and long-chain TGs in the same chromatogram, involves the utilization of elution gradients and sometimes yields different responses in different parts of the chromatogram.

The third difficulty is the detection of molecules at the column outlet. Refractive index and ultraviolet detectors have been employed, but the analysis of complex mixtures of TGs requires specific detectors. The emergence of the evaporative light-scattering detector (ELSD) and the application of mass spectrometry (MS) to HPLC has been decisive for the analysis of TGs.

The last major problem is the identification of chromatographic peaks. As very few pure standards are commercially available and as many critical pairs remain unresolved, this is one of the most difficult aims to attain. Again, HPLC-MS looks like a useful tool for this purpose, although several authors have developed other systems for TG identification.

Nomenclature

The proposal of Hirshmann has now been universally adopted for structural assignments. An 'sn-' prefix is included in the names of all glycerols. Each fatty acid in the glycerol molecule is identified by listing the sn-1, sn-2 and sn-3 position in order. A 'rac' prefix

indicates that the middle fatty acid in the abbreviation is attached at the sn-2 position, while the remaining two acids are equally divided between the sn-1 and sn-3 positions, yielding a racemic mixture of two enantiomers. A 'β' prefix indicates that the middle fatty acid esterifies the β- or sn-2 position.

Mobile Phase

The selection of the mobile phase is one of the most important factors regarding TG liquid chromatographic analysis. Plattner *et al.* briefly examined the effect of solvent composition upon triglyceride separations. Later, Pauls compared seven binary solvent mixtures for the analysis of olive oil triglycerides. They achieved the best critical pair separation with the use of acetonitrile as weak solvent. *n*-Propionitrile has also been proposed as an eluent but disadvantages include high cost and toxicity. Recently, Hirano and Takahasi have established three factors for the selection of mobile phase solvents in order to obtain optimum column efficiency. Solvents should be low in molecular weight and viscosity but high in solubility of TGs. These factors must be balanced to ensure high column efficiency.

The function of the organic modifier is to improve the solubility of the compounds in the mobile phase, so as to provide changes in their polarity, and thus increase peak selectivity. An increase in the solvent strength of the mobile phase is directly related to an increase in both retention time and resolution of TGs, including critical pairs. Among the organic modifiers tried, Pauls *et al.* showed that chloroform and tetrahydrofuran had the greatest solvent strength for the elution of the critical pair POO-OOO (52 : 2-54 : 3, PN = 48), while the best resolution for the pair LOO-LPO (54 : 4-52 : 3, PN = 46) was achieved with dichloromethane. The dependence of resolution upon solvent composition is a function of the extent to which a solvent can shift retention per double bond compared to the extent to which it shifts retention per carbon unit. The most commonly employed binary solvent mixture for TG analysis is acetone in acetonitrile as the weak solvent. However, acetone is incompatible with UV detectors as it absorbs at the same wavelengths as TGs.

The analysis of TGs by RP-HPLC has been performed for a long time with isocratic elution, due to the general use of refractive index (RI) detection. This system has provided good results for simple oils, but the analysis of complex fat mixtures, i.e. animal fats, requires gradient elution conditions. The goal is to achieve a good resolution for poorly retained TGs (saturated molecular species with short-chain fatty acids) and, at the same time, to elute, in a reasonable

separation time, the most retained TGs (saturated molecular species with long-chain fatty acids). This permits the resolution of complex mixtures of TGs, such as those from fish oils, containing long-chain polyunsaturated fatty acids, and from milk fats, with a broad range of PN values.

Acetone, *n*-propanol, methyl tert-butyl-ether or dichloromethane, give good results when used in gradient conditions with acetonitrile. The gradient systems can be linear or nonlinear. Nonlinear gradients, and step gradients have shown better separations of critical pairs.

Sample Solvent

The sample solvent is of great importance when the sample is a complex mixture of TGs with a wide range of polarity, because it is enormously difficult to find an appropriate solvent for all the TGs. Moreover, the selected solvent must permit an appropriate contact between the solute and the stationary phase for chromatographic separations. Tsimidou and McRae studied the influence of the injection solvent on the RP-HPLC of TGs. They found that chloroform produced inferior resolution under all conditions, which was accentuated by the injection of large vol-

umes. Acetone was recommended, but it is not suitable for high-molecular-weight saturated TGs. Mobile phase has also been suggested as an ideal solvent, but others have employed hexane obtaining better results.

Stationary Phase

Reversed-phase columns are used for separating homologous series of compounds, such as TGs. Previous studies have shown that octadecylsilane (ODS) stationary phases on spherical particles have the best selectivity for TGs, with little variation among the columns of different manufacturers. Columns with a particle size of 3 μm have the highest intrinsic efficiency; however, until recently, their use was restricted because of the high operating pressure needed.

Most RP-HPLC analyses are carried out without column thermostating. However, various workers have shown that an increase in temperature affects retention and selectivity, yielding poorer separations. Although lower temperatures give better separations, elution times are increased significantly. Moreover, highly saturated TGs may precipitate out of the mobile phase. For these reasons, the choice of column temperature must represent a compromise

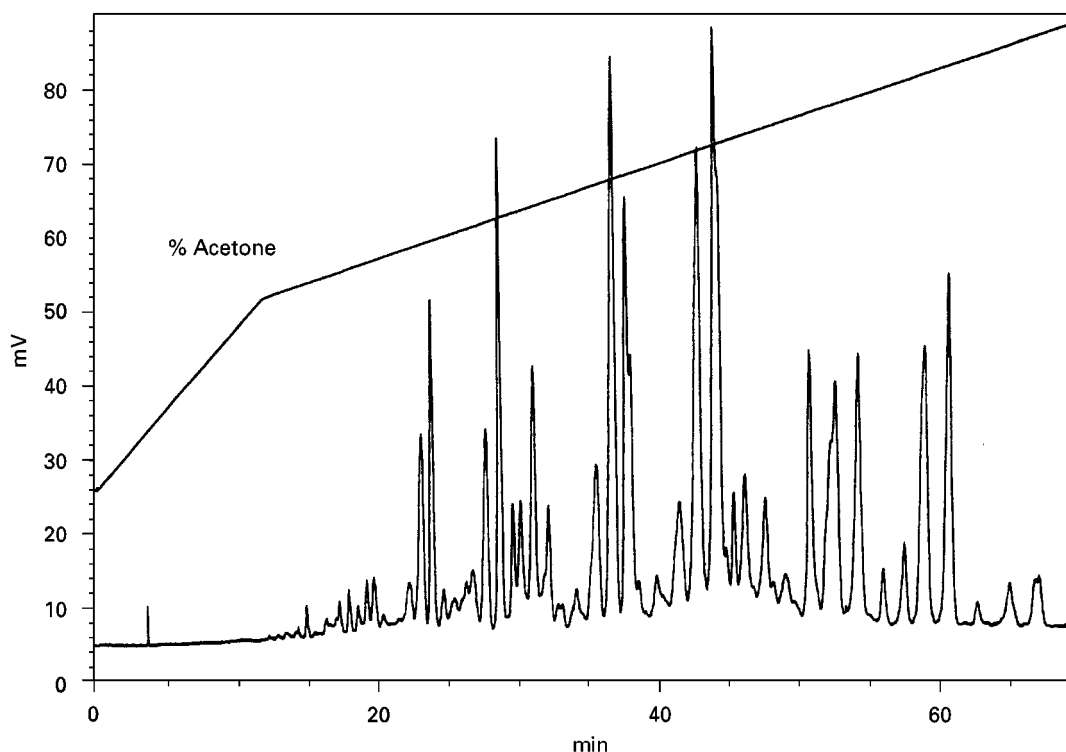


Figure 1 RP-HPLC of fish oil triglycerides. HPLC conditions: Waters 2690 liquid chromatograph equipped with a Spherisorb ODS-2 column (250 \times 4.6 mm), coupled to a Eurosep DDL-31 light-scattering detector; solvent, a two-step gradient of 20–80% acetone in acetonitrile at flow rate 1 mL min⁻¹.

between good solubility of saturated TGs concomitant with good selectivity of critical pairs.

In 1996, Hirano and Takahashi discussed the theoretical aspects of improving resolution of TG molecular species via RP-HPLC when working at low temperatures. They analysed fish oils (Figure 1), with a low melting point, establishing a critical temperature (-15°C), below which there is no improvement in resolution. Similar results had been obtained before, through lowering temperature only to 15°C .

Detectors

When most separations were made by isocratic elution systems. Refraction index (RI) detection was extensively employed, but complex mixtures of TGs require gradient elution, making RI detection impossible. Moreover, it had low sensitivity and different responses for saturated and highly unsaturated TGs.

The UV detector is compatible with gradient elution and has been used for HPLC analyses of TGs. The absorption region from 200 to 230 nm (ester bond) is used to detect TGs. However, many solvents also absorb at these wavelengths, causing baseline drift with gradient elution systems. In addition, different TGs have nonuniform molar extinction coefficients, and consequently calculation of their response factors with standards is needed for quantitative analysis. Other workers have used flame ionization detection (FID) and attained good sensitivity and baseline stability with elution gradient. Nurmela and Satama tested FID for TGs. They found a variable response for different TGs, although the variation was smaller than with UV detectors. In addition, a nonlinear response of the detector was observed for injections $<5\text{ }\mu\text{g}$. This may be a shortcoming, because only a small portion of the solvent eluted from the column can be introduced into the FID.

The introduction of the mass or evaporative light-scattering detector (ELSD) has brought a major advance in the detection of lipid classes upon HPLC separation. ELSD, being sensitive only to the mass of vaporized analyte, is not limited by the absorption characteristics of the individual components and/or the nature of the eluents. For this reason, it is compatible with gradient elution and volatile solvents do not give baseline drift, as they are removed before detection of the analyte by evaporation. The only requirement is that the compounds to be detected must be much less volatile than the solvent.

ELSD was described for the first time at the end of the 1970s. In 1984, Robinson and Macrae, compared ELSD with UV and RI detectors for the analysis of butter TGs (Figure 2). ELSD provided better

chromatograms, and unlike UV, allowed utilization of acetone. Subsequently, the influence of nebulizer gas pressure, temperature, mobile phase composition and flow rate on the response of the detector was investigated. Regardless of the exponential response of the detector, which depends on solute concentration, nowadays ELSD is the most commonly

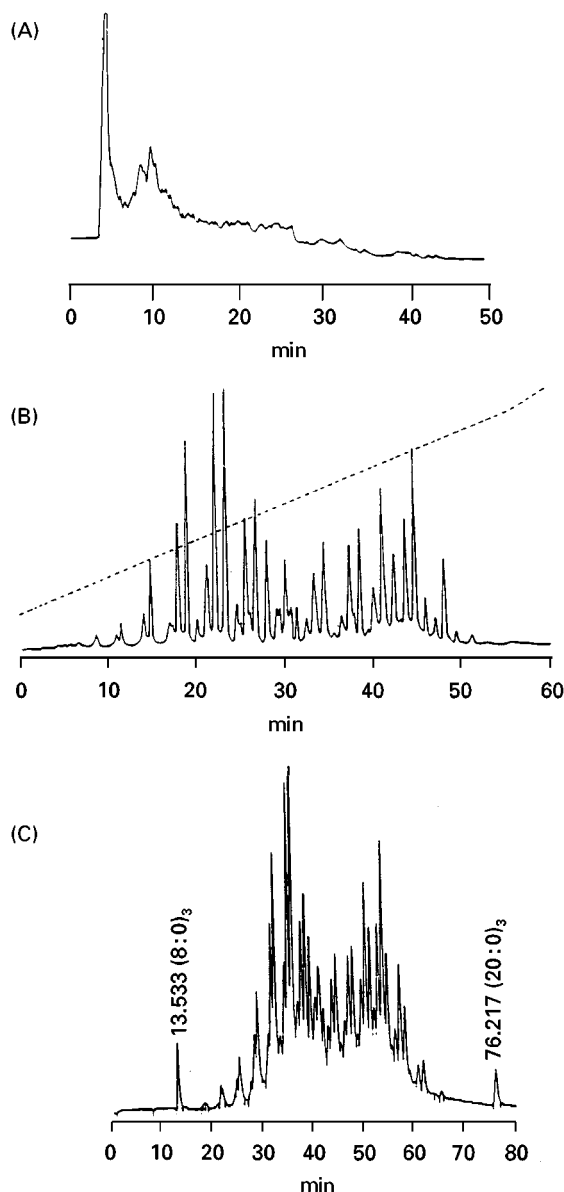


Figure 2 RP-HPLC of butter triglycerides. (A) Refractive index detection; Spherisorb-5-ODS-2 and isocratic elution of acetone in acetonitrile. (B) Light-scattering detection: same conditions as (A). (Reproduced with permission from Robinson JL, Tsimidou M and Macrae R (1984) *Journal of Chromatography* 303: 386. Copyright Elsevier Science). (C) Ultraviolet detection; two Lichrospher 100 CH-18/2 columns and isocratic elution of acetone in acetonitrile; tricaprylin (8 : 0)₃, and triarachidin (20 : 0) are internal standards. (Reproduced with permission from Nurmela KVV and Satama LT (1988) *Journal of Chromatography* 435: 139. Copyright Elsevier Science.)

employed detector for TG molecular species determination.

Identification of Molecular Species

In spite of their usefulness, all detectors described above have the shortcoming of poor limited structural identification. Mass spectrometry (MS) has become necessary for a complete identification of TG species.

Several methods for mass spectrometry of TGs have been proposed but some drawbacks have been found. Electron impact ionization methods generally result in spectra containing low molecular weight fragments, with no quasimolecular ions present. Electrospray ionization (ESI) provides only quasimolecular ions with no fragmentation. Unfortunately, this lack of fragmentation can result in ambiguity in structural assignments for TGs with identical molecular weight. Information on both the molecular weights and the fatty acyl residues of TGs have been achieved by combination of RP-HPLC and atmospheric pressure chemical ionization MS. Desorption chemical ionization (DCI) and positive ion chemical ionization (PICI) have also been successfully used for TG structural characterization.

When MS is not possible, some authors have used the equivalent carbon number (ECN) for the tentative identification of TGs. The ECN of each TG in the sample is the ECN of the hypothetical saturated TG having the same retention time. When carbon numbers (CNs) are plotted against ECN, straight parallel lines are found for different unsaturated TGs. Thus a theoretical prediction can be achieved, which has become a useful tool for TG identification.

The linear relationship between the retention factor (k) and PN values of the TG, was first established by Wada *et al.* in 1977. Then Herslöf *et al.* estimated theoretically the ECN for unsaturated TGs, on the basis of their relative retention times, from an experimental linear relationship between relative retention time and carbon number. This ECN is analogous to PN ($\text{ECN} = \text{CN} - a'\text{ND}$), with the difference that in this case the value of a' depends on the chromatographic system used for measurements. However, a' generally takes values close to 2 and when $a' = 2$, the values for the ECN and NP are equal. Takahashi *et al.* calculated the value for a' from the relationship between $\log k'$, CN and ND ($\log a' = q + b'\text{CN} + c'\text{ND}$). The value of a' is the quotient between the constants b' and c' . These equations are calculated under isocratic conditions, and are not appropriate for gradient-elution systems. For this reason, some workers have developed new relationships based on the same

parameters, as the equivalent chain length (L) or the theoretical carbon number (TCN).

The chromatographic behaviour of TG molecules in RP-HPLC depends not only on CN and ND but also on the number of unsaturated fatty acids within the molecules (NUFA), because TGs with the same ECN are eluted in the order of the increasing constituent saturated fatty acids. This leads to the equation for ECN ($\text{ECN} = \text{CN} + a_1\text{ND} + a_2\text{NUFA}$).

The TG prediction process becomes increasingly complex when the fat contains a great number of different fatty acids, since the number of possible combinations can be extremely high. Therefore, and as a second part of the prediction process from the ECN, some authors have proposed the application of the equations developed by Takahashi *et al.* These workers developed a matrix model with CN and ND as variables for each fatty acid esterifying the glycerol molecule.

Silver-ion Chromatography

Silver-ion HPLC can be performed on a reversed-phase column (silver ions in the mobile phase), on a silver-loaded, cation-exchange column, or on a silver-loaded silica column. Silver-ion chromatography separates TGs according to their degree of unsaturation, the distribution of double bonds between the fatty acyl residues within a single molecule, the configuration and position of double bonds within each fatty acid and the stereospecific position in which fatty acids are esterified. The mechanism of separation is based on the ability of the π -electrons in the double bonds of the fatty acids to interact with the silver ions of the stationary phase.

Silver ions are incorporated into columns in two different ways: by impregnating the silica-gel support with a silver salt or by bonding silver ions to the phase by means of an ion-exchange phase. The impregnation of columns with silver ions is generally made with silver nitrate in concentrations from 5% to 10%. The problem of short column life is avoided with cation-exchange supports, such as macroreticular sulfonic acid resins or silica-gel supports with chemically bonded methylsulfonic acid groups.

The mobile phase is an important factor affecting the separation of TGs by silver-ion HPLC. However, the nature of the interactions between the silver ions, unsaturated solutes and solvents in the mobile phase has not been fully elucidated. Some workers have suggested using elution gradients combining chlorinated hydrocarbons with acetone and acetonitrile.

Components separated by silver-ion HPLC are commonly detected by evaporative light-scattering detectors (ELSD) or FID, because they place fewer

limitations on the choice of solvents for the mobile phase, but these detectors do not provide structural information on molecular composition. For this reason, mass spectrometry has recently been employed for this purpose.

Christie *et al.* have made the greatest progress in developing silver-ion chromatographic systems. Subsequently, other authors have applied their method for separation of TGs from different natural sources. More useful information of the TG composition of natural fats may be achieved by combining this technique with RP-HPLC. Silver-ion HPLC allows separation of TGs with the same degree of unsaturation; the fractions obtained can then be analysed by RP-HPLC with chain length as a factor for separation.

Stereospecific Analysis

For the complete TG characterization of a fat it is necessary to know not only the fatty acids that constitute a TG molecule but also the positions of attachment. This is of importance because physicochemical properties change depending on the position in which a fatty acid is attached.

However, the stereospecific analysis of a fat is one of the most difficult tasks to undertake, since these molecules are similar in physical and chemical properties. When positions *sn*-1 and *sn*-3 are occupied by distinct acyl groups, the TG molecule will be asymmetric and will have optical activity. However, when the same fatty acid is allocated at both positions, diastereomer forms are outlined. This is not rare, since the main biosynthetic route in animal and plant tissues is the *sn*-glycerol-3-phosphate pathway, and enzymatic systems in this pathway can be specific to certain fatty acids or to certain fatty acid combinations.

Vander Wall and Coleman and Fulton independently developed a theory of fatty acid distribution in the glycerol molecule. They postulated that fatty acids are distributed randomly in the *sn*-2 position and randomly, but independently from *sn*-2, in the *sn*-1 and *sn*-3 positions. They demonstrated that it is possible to know the fatty acid distribution from data obtained on the stereospecific fatty acid composition of the distinct fractions collected after hydrolysis. However, hydrolysis has revealed that fatty acids do not follow a random distribution in TG molecules. In fact, vegetable oils have C₁₈ polyunsaturated fatty acids at the *sn*-2 position, with saturated and C₂₀ and C₂₂ polyunsaturated fatty acids at *sn*-1 and *sn*-3. Oleic acid (C_{18:1}) is distributed at the three positions. Among animal tissues, ample differences can be found. The majority of animal fats have saturated fatty acids at the *sn*-1 position; however, there are

fats like pig adipose tissue, with palmitic acid at *sn*-2, or milk fat, with long-chain saturated fatty acids at the *sn*-1 and *sn*-2 positions.

HPLC analysis, which gives the stereospecific distribution of TGs, uses as substrate mono- and diacylglycerols, obtained after hydrolysis of TGs in the first step of the process. This hydrolysis is usually made through a Grignard reaction with magnesium ethyl bromide. Mono- and diacylglycerols are separated by thin-layer chromatography (TLC) or by solid-phase extraction (SPE). The products obtained may be analysed by liquid-solid chromatography, reversed-phase liquid chromatography or chiral-phase liquid chromatography. By liquid-solid chromatography 1,2-, 1,3- and 2,3-diacylglycerols are separated through formation of (S)-(+)-1-(1-naphthyl)ethyl urethane diastereoisomeric derivatives. The combination of the total fatty acid composition obtained by gas chromatography and liquid-solid chromatography permits calculation of the stereospecific composition of the fatty acids in the TGs of a natural fat.

Reversed-phase chromatography (RP-HPLC) has been less widely employed for this purpose. Sempore and Bezard achieved separations of 3,5-dinitrophenyl urethane (DNFU) derivatives of 1,2- and 2,3-diacylglycerols with a octadecylsiloxane-bonded silica (ODS) column and a mobile phase composed of acetonitrile and acetone. By RP-HPLC Redden *et al.* separated fractions containing all the molecular species of 1,2-, 1,3- and 2,3-diacylglycerol.

Finally, greater success has been achieved using chiral-phase HPLC. Acceptable separations have been obtained for both DNFU derivatives of monoacylglycerols and diacylglycerols employing chiral phases of (S)-2(4-chlorophenyl)isovaleroyl-D-phenylglycine or N-(R)-1-(1-naphthyl)ethylaminocarbonyl-(S)-valine chemically attached to an aminopropylsilane support. However, drawbacks include high retention times and poor resolution. Recently, new chiral stationary phases have been proposed, with (R)-(+)-1-(naphthyl)ethylamine. These phases provide improved resolution and reduction of separation times by using shorter columns. By this method 1,2- and 2,3-diacylglycerols are separated into fractions, which are subsequently analysed by gas chromatography in order to determine their fatty acid composition.

Applications of Triglyceride Analyses by HPLC

Knowledge of the TG profile could be a more appropriate tool to characterize oils and fats, avoiding the

use of saponification and formation of methyl esters. HPLC has become as routine as gas chromatography (GC), providing more complete information about TG composition of fats and oils.

At a research and development level, detailed TG structural information might facilitate understanding of TG biosynthesis in plant and animal cell metabolism, where the activity of acyltransferases are involved. In this regard, knowledge of the TG molecular species of a dietary fat, as well as the TG composition of organs and tissues, can provide significant information for nutritional purposes.

Vegetable Oils

Virgin olive oil presents a characteristic and unique pattern of TGs, which may be used to determine origin and to detect adulteration. Due to its relative simplicity in TG composition and its relevance in human nutrition, HPLC was soon employed in the study of olive oil. In this work, isocratic mobile phases and refractive index detectors were employed. With these conditions, up to 10 TG molecular species could be detected. Triolein (OOO) was found to be the main TG, with the important presence of dioleoyl-linoleoyl-glycerol (LOO) and dioleoyl-palmitoyl-glycerol (POO). Later studies, carried out by RP-HPLC with ELSD, showed that approximately one-half of the total content of TGs corresponds to OOO, while the corresponding percentage of POO is close to 20% and LOO close to 10%. In spite of the improvement achieved, with the utilization of gradient elution systems and ELSD, some critical pairs still remain unresolved.

TG analysis has been extensively employed for the characterization of edible oils. El-Hamdy and Perkins determined the TG composition of olive and soybean oils. The latter oil contained mainly trilinolein (LLL) and dilinoleoyl-oleoyl-glycerol (LLO). Similar results were reported by other authors using isocratic conditions. In the first analysis of soybean oil using gradient elution and ELSD, 19 chromatographic peaks were detected, but could not be identified. A similar number of chromatographic peaks were resolved by Barron *et al.* and Hierro *et al.* using gradients and ELSD. Unexpectedly, LLO was not as abundant as was originally determined; in both studies, LLL was the main TG, followed by LnLO and then LLO. However, Rezanka *et al.* found significant amounts of LLO and low amounts of LLnO by RP-HPLC with MS. These differences might be due to different gradients and mobile phases.

Several other oils of interest have been characterized by HPLC. Perrin and Prevot determined the TG composition of various vegetable oils by gradient

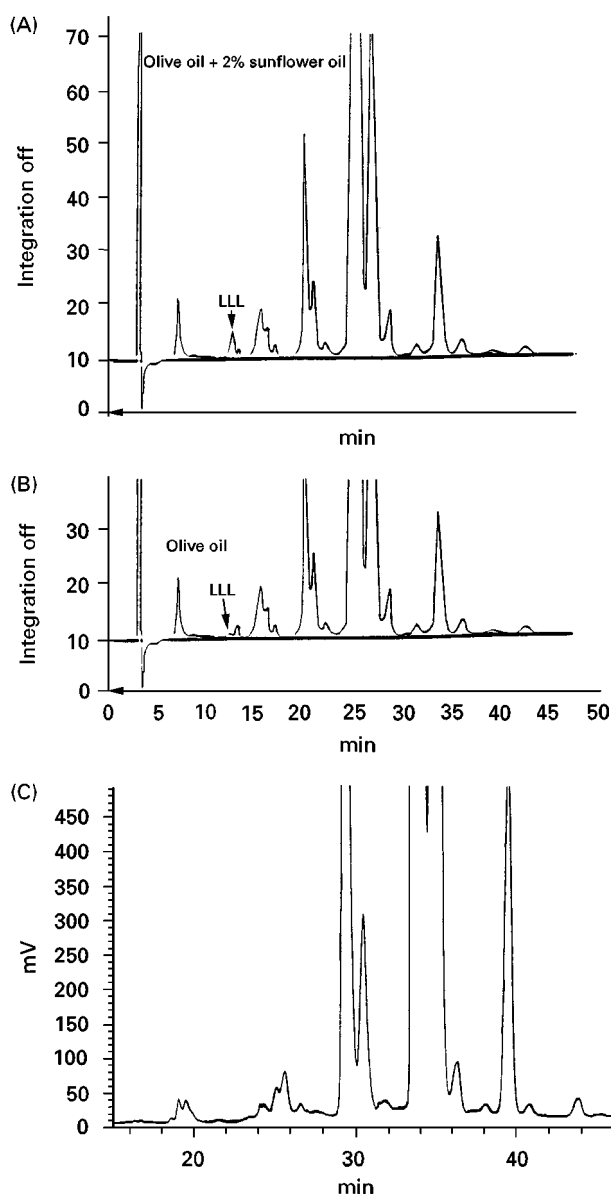


Figure 3 RP-HPLC of virgin olive oil triglycerides. (A) Refractive index detection. Hewlett-Packard HP-1050 liquid chromatograph equipped with a RP-18 column (250 × 4.6 mm), coupled to a Hewlett-Packard HP-1047A refractive index detector; solvent, 50 : 50% acetone in acetonitrile at a flow rate of 0.9 mL min⁻¹. (B) Virgin olive oil with 2% sunflower oil. Same conditions as (A). (C) Light-scattering detection. Waters 2690 liquid chromatograph equipped with a Novapak column (150 × 3.9 mm), coupled to a Eurosep DDL-31 light scattering detector; solvent, linear gradient of 50 : 50% acetone in acetonitrile at flow rate 1 mL min⁻¹.

elution RP-HPLC with a light-scattering detector (Figure 3). They analysed oils rich in oleic acid, such as olive and rapeseed oils, oils rich in linoleic acid (soybean and sunflower oils), oils rich in both oleic and linoleic acids (peanut oil) and oil rich in saturated fatty acids (palm oil). They also developed analyses of lard and tallow with great success, identifying more

than 11 chromatographic peaks for each oil or fat. More recently, a newly introduced oleic-rich oil, high oleic sunflower oil, as well as two oils with similar fatty acid composition, borage and primrose oil, have been analysed, each showing a different TG distribution.

Animal Fats

Characterization of animal fats Animal fats are more complex than vegetable oils. The great difference in the fatty acids contained in these fats causes two basic problems. The first one is the difference in chain length and degree of unsaturation, which makes it difficult to achieve a good resolution for all TGs. The second problem is that there is a great number of different fatty acids in animal fats, thus a greater number of TGs appear in the chromatograms, and there are more critical pairs.

Animal fats are employed for industrial purposes. The prediction of the melting behaviour of a fat is difficult due to the complexity of the constituent TGs.

Although the amount of stearic or linoleic acids has been proposed as a good predictor of the consistency of a fat, determination of the TG species provides more information, since not only the fatty acid composition but also the positions in which those fatty acids are esterified, are responsible for its physical behaviour.

Lard is the cheapest animal fat, and commercial shortenings, providing improved physical properties, are usually prepared by its interesterification. Al-Rasheed *et al.* analysed pig lard by RP-HPLC with RI detection to characterize it before and after randomization. Lard has been analysed many times before. Other interest has been focused on pig fat TG characterization to determine the conditions used in pig husbandry.

Because of its complexity, the structural elucidation of milk and butter fat TGs is a formidable task. The large number of fatty acids it contains has made milk fat a particular challenge in terms of TG separation and identification. Until the introduction of ELSD, no satisfactory results had been obtained. The

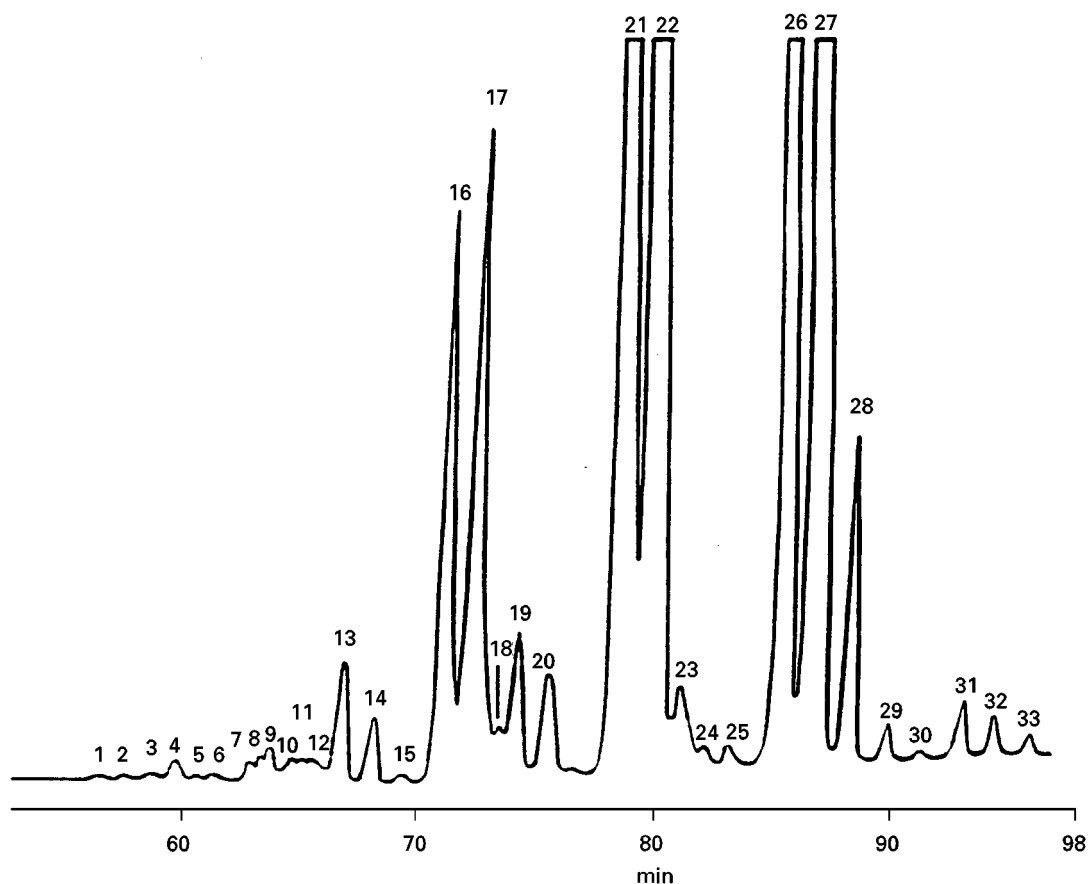


Figure 4 RP-HPLC of rat liver triglycerides. Two columns (Spherisorb ODS-2 3 μm) connected in series with a nonlinear elution gradient of 20–100% (v/v) acetone in acetonitrile were developed at a rate flow of 1.0 mL min⁻¹. (Reproduced with permission of Perona JS and Ruiz-Gutierrez V. *Journal of Liquid Chromatography and Related Technologies*, in press. Copyright Marcel Dekker.)

first to analyse butter fat by HPLC with ELSD were Robinson and Macrae in 1984; they also compared the chromatograms obtained with those of other detectors, such as UV and RI. As milk fat needs gradient-elution systems, the latter detectors offered poor resolution. FID, with linear and non-linear gradients of acetone in acetonitrile has also been used to give 62 peaks. Resolution was enhanced when ELSD was applied, almost always with acetone in the elution system. Using this method, up to 111 peaks were separated with a nonlinear gradient of acetone–acetonitrile as mobile phase.

Nutritional interest Not only industry is interested in the evaluation of the TG content of foods. Medical and nutritional benefits can be achieved through determination of molecular species of TGs.

Human milk, as well as cow or ewe milk fat, have been subjected to analysis for both industrial and nutritional purposes. The objective is to achieve the substitution of the oils employed at present in milk formulas for infants (coconut oil, corn oil) with others closer in composition to human milk. The TG structure seems to be an important factor for the bioavailability and absorption process of fats in the first weeks of life. It has been suggested that unsaturation of TG fatty acids does not affect pancreatic lipase levels, whereas the chain length of the constituent fatty acids does appear to exert an effect. The distribution of fatty acids within the glycerol molecule might also effect absorption, as it has been shown to regulate TG hydrolysis to 2-monoacylglycerol and fatty acids.

The physiological effects of TG structure and composition of the diet are more relevant in the intestine and liver, the most actively involved tissues in TG synthesis and secretion. The specificity of lipolytic enzymes for fatty acids acylated at the *sn*-1 position of the glycerol molecule affects the re-synthesis of TGs either in enterocytes or hepatocytes. After this re-synthesis, TGs are transported via lipoproteins, to peripheral tissues so that their constituent fatty acids are incorporated into the cellular lipid metabolism. However, until recently little has been done on TG from these tissues or lipoproteins.

Thirty-one molecular species of TG from rat liver have been identified by RP-HPLC with an ELSD by Perona *et al.* (Figure 4). Oleic, linoleic or palmitic acids formed the main TGs in the rat liver. Rat liver had also been investigated for TG molecular species by other workers using ELSD, resolving a lower number of TGs. Yang *et al.* observed that the fatty acid composition and the major molecular species of TG

in the rat liver were very similar to those of TG in very low density lipoproteins (Figure 5). Parreño *et al.* studied plasma TG composition of a Catalonian population by HPLC.

Adipose tissue is the most important extrahepatic tissue in regulating lipid metabolism. Although it contains up to 97% of TGs, little work has been done to study its composition of TG molecular species. Huang *et al.* have reported 18 molecular species of TGs in rat adipose tissue using HPLC with UV detection (Figure 6).

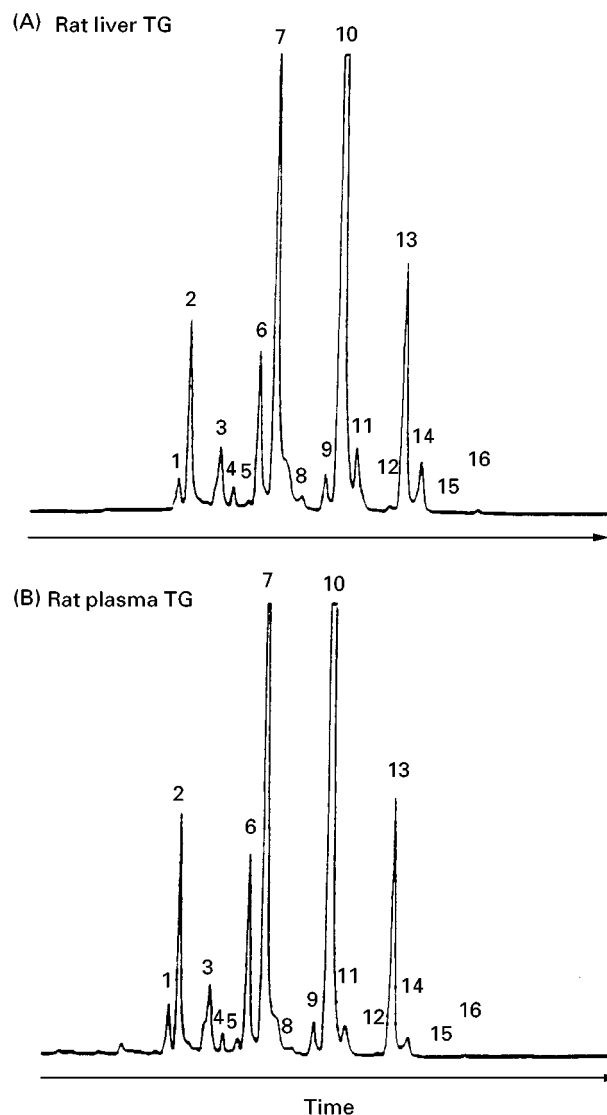


Figure 5 RP-HPLC of rat liver (A) and very low density lipoprotein (B) triglycerides. Supelcosil LC-18 column (250 × 4.6 mm), coupled to a Varex ELSD II light-scattering detector; solvent, linear gradient of 10–90% isopropanol in acetonitrile at flow rate 1 mL min⁻¹. (Reproduced with permission from Yang LY, Kuksis A, Myher JJ and Steiner G (1995) *Journal of Lipid Research* 36: 125. Copyright Journal of Lipid Research.)

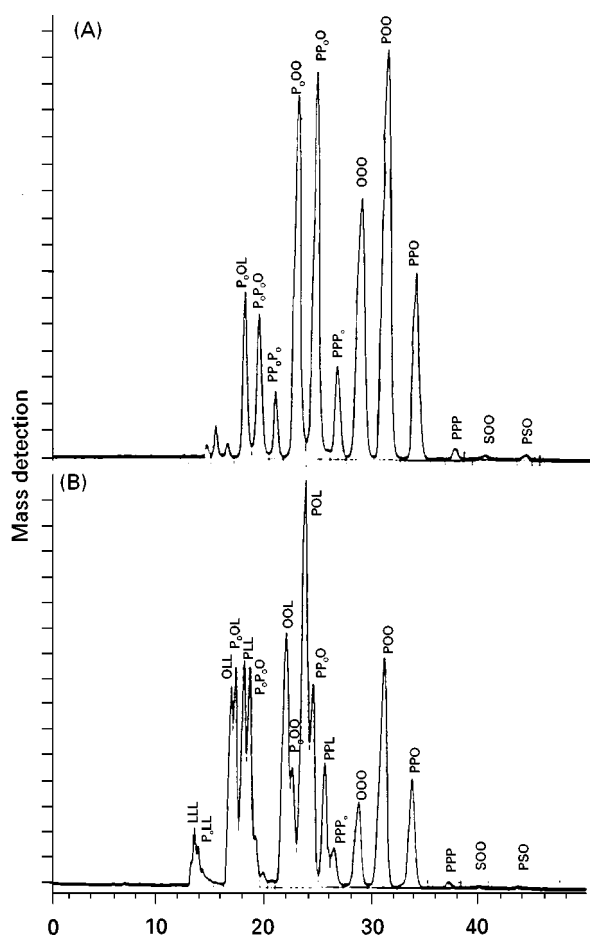


Figure 6 RP-HPLC of rat adipose tissue triglycerides. Two Supelcosil LC-18 (250 × 4.6 mm) columns in series, with UV detector; solvent, 35 : 65% isopropanol in acetonitrile at a flow rate of 2 mL min⁻¹. Rats were fed a diet containing linoleic acid at a level of (a) 0.01 g kg⁻¹, (b) 24 g kg⁻¹. (Reproduced with permission from Huang YS, Lin X, Sminth RS *et al.* (1992) *Lipids* 27: 711. Copyright AOCS Press.)

Conclusion

The chromatographic analysis of TGs has undergone great advances in the last few years. Among other factors, the advent of reversed-phase HPLC and the emergence of the evaporative light-scattering detector (ELSD) allow the resolution of many TG applications in vegetable and animal samples. Nevertheless, the

shortcomings of TG identification need to be improved. Mass spectrometry (MS) is a helpful tool for this purpose. However, it is still difficult for many researchers to incorporate such a technique in their laboratories. The drawback of the incomplete resolution of critical pairs of TGs with the same ECN and the stereo specific analysis of TGs are the two challenges which investigations will have to address in the near future.

See Colour Plate 123.

See also: II/Chromatography: Liquid: Detectors: Ultra-violet and Visible Detection; Mechanisms: Normal Phase; Mechanisms: Reversed Phases. III/Lipids: Gas Chromatography; Thin-Layer (Planar) Chromatography. Oils, Fats and Waxes: Supercritical Fluid Chromatography. Silver Ion: Liquid Chromatography; Thin-Layer (Planar) Chromatography.

Further Reading

- Aitzetmuller K (1997) Recent developments in the analysis of food lipids and other lipids. *Ol. Corps Gras, Lipides* 4(1): 8–19.
- Beare-Rogers JL (1983) *Advances in Nutrition Research*, vol. 5. London: Plenum Press.
- Breckenridge WC (1978) In: Kuksis A (ed.) *Handbook of Lipid Research*, vol. I. New York: Plenum Press.
- Christie WW (1987) *High-Performance Liquid Chromatography and Lipids: A Practical Guide*. Oxford: Pergamon Press.
- Geeraert E and Sandra P (1987) In: Kuksis A (ed.) *Chromatography of Lipids in Biomedical Research and Clinical Diagnosis*. Amsterdam: Elsevier Science Publishers.
- Hammond EW (1982) In: Macrae R (ed.) *HPLC in Food Analysis*. London: Academic Press.
- Hammond EW (1993) In: Hammond EW (ed.) *Chromatography for the Analysis of Lipids*. Florida: CRC.
- Litchfield C (1972) *Analysis of Triglycerides*. New York: Academic Press.
- Marini D (1992) In: Nollet LML (ed.) *Food Analysis by HPLC*. New York: Marcel Dekker.
- Nikolova-Damyanova B (1997) In: Christie WW (ed.) *Advances in Lipid Methodology*. 4. Dundee: The Oily Press.
- Ruiz-Gutiérrez V and Barrón LJR (1995). Methods for the analysis of triacylglycerols. *Journal of Chromatography B* 671: 133–168.

Thin-Layer (Planar) Chromatography

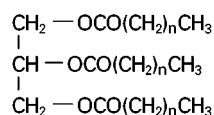
P. E. Wall, Merck Ltd, Poole, Dorset, UK

Copyright © 2000 Academic Press

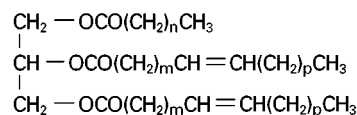
Introduction

Triglycerides (TGs) belong to the larger group of natural products called 'lipids'. A lipid is one of a wide range of natural materials that are generally based on fatty acids or closely related compounds, are insoluble in water, but soluble in organic solvents. Lipids that are solid at ambient temperature are termed 'fats' whilst those that are liquids are described as 'oils'. Lipids can be split into two groups; neutral lipids, which include acylglycerols, fatty acids, alcohols and waxes, and polar lipids, which include phospholipids and glycolipids.

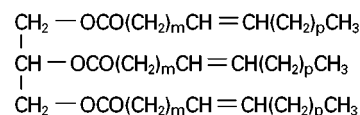
TGs make up a major part of the group of neutral lipids and are found in an extensive range of animal and vegetable fats, seed and plant oils. Lipids are present in body organs and fluids. They also find their way into many other food products, e.g. frying oils, salad dressings, margarine, butter, and various other types of spreads.



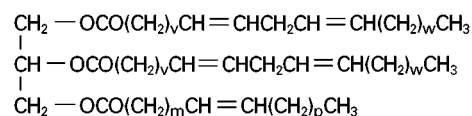
Fully saturated triacylglyceride. (*n* is usually 16 or 18)



Triacylglyceride with one 'arm' saturated and the other two unsaturated. (Values for *m* and *p* can vary, but is most commonly 7)



Triacylglyceride with all three 'arms' unsaturated



Unsaturated triacylglyceride with two 'arms' di-unsaturated and one mono-unsaturated. (*v* and *w* can vary but usually *p* = 7 and *w* = 4)

Figure 1 Structures of different types of underivatized triacylglycerides.

TGs are fully acylated derivatives of the trihydric alcohol, glycerol. Hence more accurately they should be described 'triacylglycerides', but quite often they are commonly called 'triglycerols' or 'triacylglycerols'. The structure of this group of lipids is shown in **Figure 1**. Each 'arm' of the glyceride is an ester of a fatty acid. This chain can be fully saturated or it can vary in unsaturation. Some natural triacylglycerides have the same three ester groups, e.g. tristearin (18:0), tripalmitin (16:0), triolein (18:1), trilinolein (18:2), and trilinolenin (18:3). More usually the fatty acid esters are different on each glycerol 'backbone' leading to many variations dependent on the number of fatty acids available and on the degree of unsaturation.

Degradation

Triacylglycerides are susceptible to hydrolysis with the resulting products being free fatty acids (FFAs), diacylglycerides (DGs), and monoacylglycerides (MGs). If the fatty acid esters are formed from unsaturated fatty acids, then the susceptibility to oxidation and hydrolytic degradation is increased. Unsaturated triacylglycerides undergo oxidative breakdown involving the formation of free radicals. This process can occur just in the presence of atmospheric oxygen at ambient temperature, although the process will be accelerated by increase in temperature. The primary products are initially allylic hydroperoxides that then undergo a series of complex reactions to form volatile compounds including aldehydes, ketones, alcohols, esters, and short chain fatty acids (see **Figure 2**).

Hydrolytic breakdown normally occurs at elevated temperatures and is often catalysed by enzymes; e.g. lipases. This degradation results in di- and monoacylglycerides and long chain fatty acids (see **Figure 3**).

Thin-Layer Chromatography

Without doubt thin-layer chromatography (TLC) is one of the simplest and most widely employed techniques in the analysis of lipids. Over the past 30 years, planar chromatography on a silica gel matrix has proved to be the most practical method of distinguishing between lipid classes including glycolipids, acylglycerols, phospholipids, sphingolipids, and ether lipids. The continued interest in improving the separation capabilities for lipids using TLC is reflected in the recently published literature.

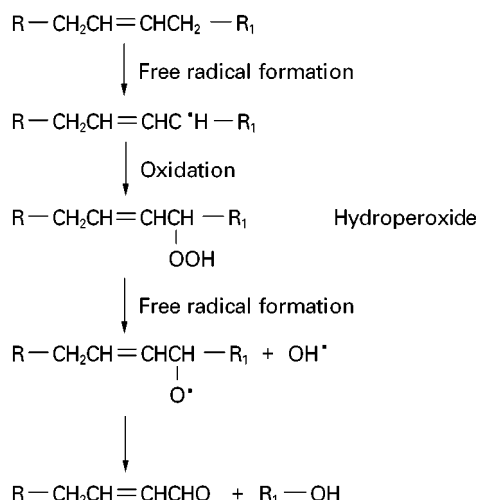


Figure 2 One possible route for autooxidation of unsaturated lipids. R = carbon chain length linked to the glycerol backbone via a COO linkage, R₁ = a saturated carbon chain. Other degradation routes can occur and result in mixtures of aldehydes, ketones, alcohols, esters, and acids. A route to aldehydes and alcohols is shown.

Normal Phase Separations

Of all the stationary phase adsorbents available, silica gel 60 has proved to be the adsorbent of choice for the rapid separation of triacylglycerides and their

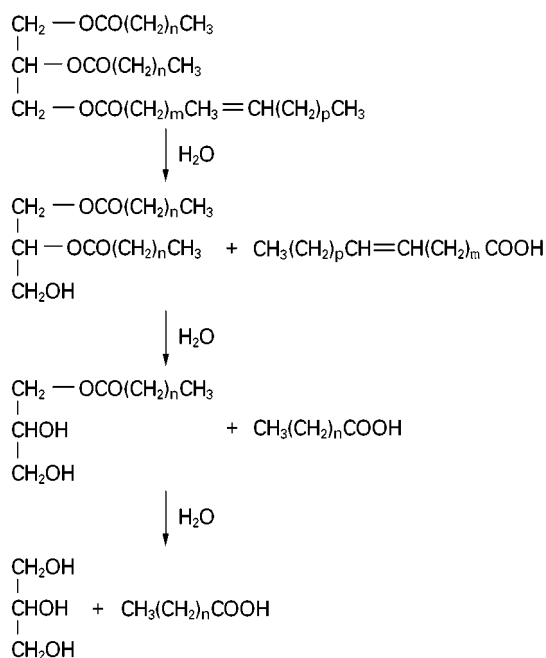


Figure 3 Hydrolytic reaction of a typical triacylglyceride. The reaction is usually catalysed by the presence of lipase. The values of n, m, and p are variable depending on the particular triacylglyceride. In the majority of cases, n = 14 (palmitic) or 16 (oleic), and m and p are 4 and 7, respectively (linoleic).

Table 1 Separation of acylglyceride classes on normal phase silica gel. Mobile phase: n-hexane-diethyl ether-acetic acid (70:30:1, v/v)

Glyceride	R _F value (approx.)
TG	0.70
FFA	0.45
1,2-DG	0.26
1,3-DG	0.23
MG	0.05

hydrolysis products, including any hydrolytic damage that may have occurred as a result of lipolysis. Normal phase separations enable the resolution of neutral lipids into TGs, DGs, MGs and FFA. The solvent used is normally a mixture of diethyl ether and hexane, pentane or a low boiling petroleum spirit. The ratio is in the range of 15–30% v/v diethyl ether in the saturated hydrocarbon. A modification with a small amount of formic or acetic acid (about 1%, v/v) helps to improve resolution and is necessary where any organic acids (fatty or otherwise) are suspected as being present in the sample. This aids in suppressing ionization of any FFA. The order of retention on the chromatographic layer of sample components tends to follow the expected adsorption/partition type mechanisms. The triacylglycerides, being the least polar, exhibit the least retention and hence migrate well up towards the solvent front with any sterol esters that may be present in the sample. Perhaps surprisingly these are closely followed by the fatty acids. DGs migrate much more slowly and monoglycerides show only the minimal movement from the origin. One of the interesting features of the normal phase separation of TG is the ability to clearly resolve the 1,3 and 1,2 isomers of DGs that may be present (see Table 1). In order to attain adequate migration of the MG from the origin, the TLC plate can be developed twice with diethyl ether to a solvent distance of 20–30 mm with intermediate drying. This enables sufficient migration of the MG from any more polar lipids on or near the origin. Following this separation step, the standard development can be carried out as before. Sometimes the TG zone on the chromatogram may appear somewhat elongated and even a partial resolution of components may be observed. This is due to the variation in the saturation and fatty acid ester chain length of the TG present.

For densitometric evaluation, silica gel 60 high performance thin-layer chromatography (HPTLC) plates can be used and samples applied using an automated band applicator. After development and detection with an appropriate reagent the chromato-

Table 2 Separation of acylglyceride classes on normal phase silica gel impregnated with 5% w/v sodium carbonate. Mobile phase: diethyl ether–n-hexane–methanol (65:35:3, v/v)

<i>Glyceride</i>	<i>R_F value (approx.)</i>
FFA	0.00
MG	0.18
1,3-DG	0.79
1,2-DG	0.85
TG	0.98

graphic tracks can be scanned at set wavelengths using a spectrodensitometer. Using external standards on the layer, accurate quantification of the separated components can be obtained.

To a limited extent the enzymic hydrolysis of TG in food products can be followed. Sodium carbonate-impregnated (5%, w/v) silica gel plates are used. Before the sample is applied to the layer, the enzymatic action is terminated by the addition of sodium dodecyl sulfate (SDS). The chromatogram is developed for a very short period (about 1 minute) with diethyl ether–methanol (97:3, v/v), which results in all the acylglycerides migrating with the solvent front and the fatty acids remaining at the origin. A modification to this solvent system; diethyl ether–n-hexane–methanol (65:35:3, v/v) results in a separation of all the various acylglycerides from the fatty acids (see **Table 2**).

Variations on the above mobile phases have been developed depending on the type of separation required and the origin of the sample. **Table 3** lists a number of solvent mixtures that have proved successful for various types of TG separations.

When lipid mixtures prove to be complex, two-dimensional systems can be helpful in resolving the large number of components. Although seldom used, there are instances where two-dimensional TLC has enabled the separation of mixed acylglycerides from steryl esters, methyl esters and fatty acids. Sample components can be resolved using a first development

with n-hexane–diethyl ether (80:20, v/v). This is followed by plate drying and development in the second dimension at 90° to the first using a solvent mixture composed of n-hexane–diethyl ether–methanol (70:20:10, v/v). If more polar lipid components are present, then an alkaline-based solvent mixture is recommended for the development in the first dimension (chloroform–methanol–0.88 ammonia solution–water [65:30:2:2, v/v]) followed by an acid-based one in the second dimension (chloroform–methanol–acetic acid–water [100:15:15:3.5, v/v]).

Other Modifications to Normal Phase Separations

Orthoboric acid Orthoboric acid-impregnated silica gel layers are used in the TLC of TG to prevent acyl migration from the 2 to the 1 or 3 position on the glycerol backbone. The speed of migration is dependent on the acyl moiety. It is therefore important that this effect is prevented from occurring in an analysis of DG and MG. Orthoboric acid does this by weak interaction and complex formation with the free hydroxyl groups on the acylglycerides.

Precoated TLC plates can be impregnated with orthoboric acid (15% w/v) dissolved in water–methanol (25:75, v/v). Either dipping or spraying the plate in the solution gives satisfactory results. The plates are dried after impregnation for 30 minutes at 110°C. Separations can then be performed with methanol–chloroform (3:97, v/v) as solvent.

Silver nitrate Silver nitrate or argentation TLC has been used extensively for the analysis of triacylglycerides. The reason for its popularity is that silver nitrate has a retarding effect on acylglycerides that contain unsaturated fatty acid ester moieties. The silver nitrate forms complexes with varying strength of bonding by interaction with the π double bonds. The more double bonds present, the greater the complexation and the less accessible the double bonds, the less the complexation. Hence, polyunsaturated glycerides and FFA will be more retained than their oligo-

Table 3 Solvent mixtures recommended for the separation of acylglycerides on normal phase silica gel

<i>Acylglycerides</i>	<i>Adsorbent</i>	<i>Mobile phase</i>
TG, DG, MG, FFA (as classes)	Silica gel 60	Diethyl ether–n-hexane–acetic acid (80:19:1, v/v)
TG, DG, MG, FFA from plasma	Silica gel 60	Toluene–diethyl ether–ethyl acetate–acetic acid (8:1:1:20, v/v)
Human aortic lipids including unsaturated TG	HPTLC silica gel	n-Hexane–diethyl ether–acetic acid (65:35:1, v/v)
TG, FFA, amides and cholesterol	Silica gel	Toluene–diethyl ether–ethyl acetate–acetic acid (75:10:13:1.2, v/v)
TG containing oxygenated fatty acid methyl esters	Silica gel 60	n-Hexane–diethyl ether (30:70, v/v)
TG containing epoxy and hydroxyl fatty acids	Silica gel 60	n-Hexane–diethyl ether (1:1, v/v)

Table 4 Solvent mixtures that have proved satisfactory for the separation of acylglycerides on silica gel impregnated with silver nitrate

Sample containing acylglycerides	Mobile phase
Soybean and fish oils	Diethyl ether–n-hexane (8 : 92, v/v)
Palm oil, lard, beef tallow, cocoa butter and groundnut oil	Chloroform–cyclohexane (1 : 1, v/v)
Lard and cocoa butter	Chloroform–benzene–diethyl ether (70 : 30 : 1.5, v/v)
Triacylglyceride standards	Benzene–diethyl ether (85 : 15, v/v)
Positional isomers of triacylglycerides, lard, and sunflower oil	Chloroform–methanol (99 : 1, v/v)
Orange seed oil	Petroleum ether (40–60°C)–acetone (100 : 7, v/v)

unsaturated counterparts whilst any saturated components remain unaffected. As accessibility of the double bonds also has a bearing on the degree of complexation, *cis* and *trans* isomers can be separated and acylglycerides of fatty acids that only differ in the positional location of the double bond can often be resolved.

Impregnation of silica gel 60 plates can be achieved with silver nitrate (10% w/v) dissolved in water–methanol (15:85 v/v). Precoated TLC and HPTLC plates are dipped in the silver nitrate solution for 10–20 s. After draining, the plates are dried in air under fume extraction and then heated for activation at 80°C for 20 minutes.

Argentation TLC has proved to be of immense importance in a number of research areas including plant-derived oils and confectionery fats. In fact, the technique has been proposed as a method for the determination of 2-oleo-1,3-disaturated triacylglycerides in cocoa butter as a part of the necessary analysis in the manufacture of chocolate. As expected, the separation of triacylglycerides follows the order of the number of double bonds with the least unsaturated being the least retained. However, if the unsaturation is in the 2-position, then there is some hindrance to the formation of the silver complex and some differentiation in the separation between the 2- and 1- or 3-position can be observed. As an example of this, it is possible to separate 2-oleo-1,3-distearin (SOS) and 3-oleo-1,2-distearin (SSO). As the interaction of the silver ion with the 2-position isomer is more sterically hindered, this is the one which is less retained on the layer and hence has the slightly higher R_F value. Of course, not only do TG vary in the amount and position of unsaturation, but also both *cis* and *trans* isomers of the same fatty acid esters occur. Examples of this are *cis*-9-octadecanoic acid (oleic acid) and *trans*-9-octadecanoic acid (elaidic acid). If any *trans* isomers are present, these are less retained than the *cis* isomers. Structurally this would be expected as the *cis* double bond is more accessible to the large silver ion, and hence complexes more readily. The general order of separation starting from the least retained and representing the fatty acid

chains of the TG as 0, 1, 2, or 3 depending on the number of double bonds is: 000, 001, 011, 002, 111, 012, 112, 022, 003, 122, 013, 222, 113, 023, 123, 223, 033, 133, 233, 333.

For the common C_{18} chain, the fatty acid chains would be stearic acid (18:0), oleic acid (18:1), linoleic acid (18:2), and linolenic acid (18:3). Whilst C_{18} represents one of the most common chain lengths, shorter and longer chain lengths do occur and this increases the complexity of the problem. Palmitic acid (16:0) occurs more, widely naturally than stearic acid (18:0), being present in almost all vegetable fats, fish oils and milk fats. Fortunately for the analyst, the unsaturated versions of the C_{16} chain such as palmitoleic acid (16:1) are only minor components of seed oils and animal fats and only take on significant proportions in fish oils. Typical solvent mixtures used for the development of silver nitrate chromatograms are given in **Table 4**.

Both symmetrical and unsymmetrical TG are present in lard and cocoa butter and these can be separated effectively with two-dimensional argentation TLC. Unsymmetrical TG occur where the carbon chain on position 1-, 2- or 3- on the glycerol backbone vary in length. Examples of this are: POS (palmitin (16:0), olein (18:1), and stearin (18:0) or PPO (palmitin (16:0), palmitin (16:0), and olein (18:1). The separation is carried out on a dual stationary phase plate. One section of the plate is coated with a thin strip of reversed-phase silica gel, and the rest is coated with a normal phase silica gel. The sample is applied to the reversed-phase strip and the chromatogram developed using acetonitrile–acetone (80:20, v/v) as mobile phase. The normal-phase silica gel portion of the plate is impregnated with silver nitrate and the second dimension development then proceeds with a mobile phase composed of chloroform–benzene–diethyl ether (70:30:1.5, v/v).

Reversed-phase Separations

The resolution of TG on reversed-phase layers is usually noticeably better than that on normal-phase TLC. Although separation of acylglycerides, and FFA

Table 5 Stationary and mobile phase conditions for the separation of acylglycerides and free fatty acids on reversed-phase silica gel plates

Sample containing acylglycerides	Stationary phase	Mobile phase
Most seed oils (e.g. sunflower, olive, rapeseed oils)	HPTLC-silica gel RP18 glass plates	Dichloromethane–acetic acid–acetone (1) (20 : 40 : 50, v/v)
Most seed oils	HPTLC silica gel RP18 glass plates	Chloroform–acetonitrile–acetone (2) (20 : 40 : 50, v/v)
Most seeds oils, DG, MG, and FFA	HPTLC silica gel RP18 glass plates	Dichloromethane–ethyl acetate–methanol–acetic acid (3) (27 : 22 : 38 : 12, v/v)

into respective groups is possible using normal-phase silica gel, reversed-phase layers will resolve individual members of these groups into sharp, often well-defined, zones. However, it is only possible to detect unsaturated acylglycerides and fatty acids on reversed-phase layers. This may initially be viewed as a limiting feature of the technique, but as the separation number even with HPTLC layers in one dimension is rarely more than 20, there is always only a finite length of chromatographic layer available in which the separation can occur. Hence, as the saturated lipids are undetectable, there is more separation capacity available for unsaturated compounds.

The reversed-phase separation of TG has resulted in a method for the identification of fatty oils. The protocol is given in the BP98 appendix XN and the EP97 (2.3.2) and shows a typical chromatogram obtained on HPTLC RP18 layers for a number of seed

oils. The test method acts as an identification for a wide range of oils as each has a TLC ‘fingerprint’ of unsaturated acylglycerides unique to itself. Solvent mixtures that give good separation reproducibility for reversed-phase are given in **Table 5**. Solvent mixtures 1 and 2 are comparable, but solvent mixture 3 gives similar resolution for the TG at lower R_F values and also good resolution for many of the DGs, MGs and FFAs. This solvent mixture therefore has been used effectively for investigations into the deterioration of frying oils. **Figure 4** shows a typical chromatogram of a blended frying oil.

As the separation has occurred almost purely by partition, it is possible to relate the positions on the chromatogram of the acylglycerides to the degree and the position of the unsaturation in the molecule. This then enables the prediction of the position of acylglycerides on the chromatogram and aids in the

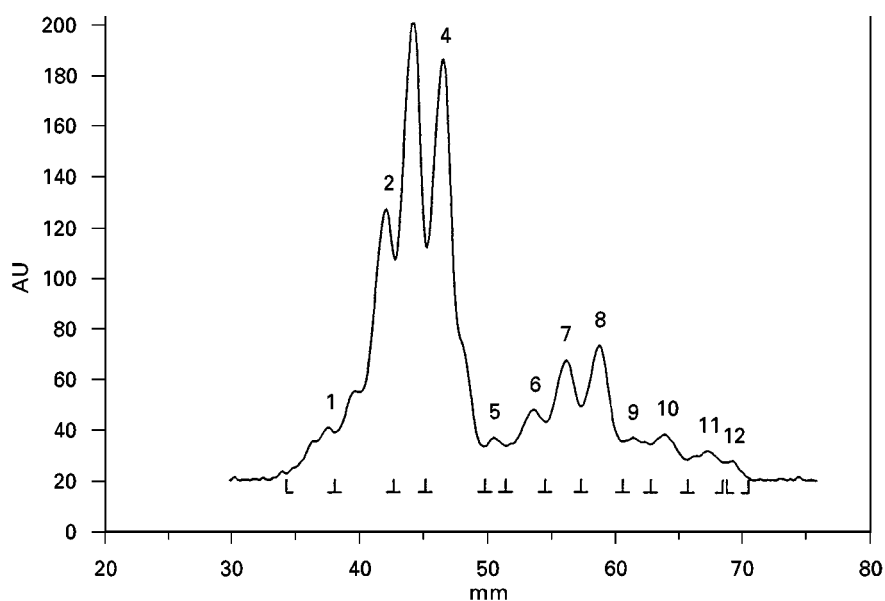


Figure 4 Separation of unsaturated acylglycerides and FFA on HPTLC silica gel RP18 glass plates. Mobile phase: dichloromethane–ethyl acetate–methanol–acetic acid (27 : 22 : 38 : 12, v/v). Detection with 1% w/v phosphomolybdic acid in ethanol. Plate heated to 100°C for 5 minutes. Scanned at 700 nm with a spectrodensitometer. Sample: degraded blended frying oil. Peaks 1–5 are triacylglycerides, peaks 6–8 are diacylglycerides, peak 10 is a free fatty acid and peaks 11 and 12 are monoacylglycerides.

identification of unknowns. The acylglycerides are separated according to the equivalent carbon number (ECN). This is defined as:

$$ECN = CN - 2n$$

where CN = carbon number, n = number of double bonds.

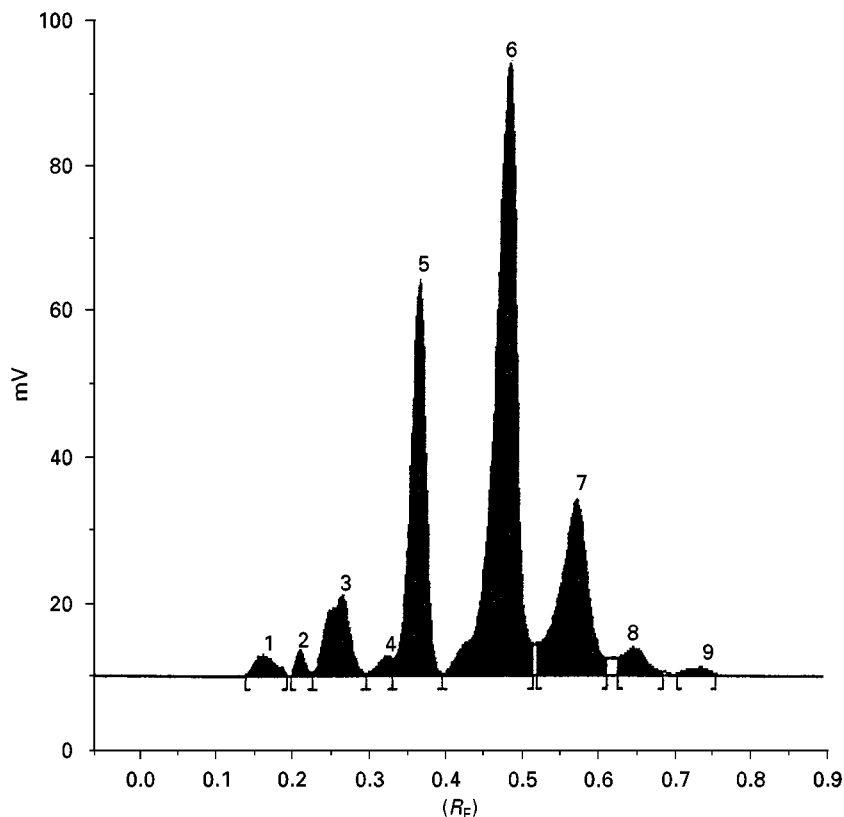
However, this does not take into consideration the position of the double bonds. For this reason

in HPLC an adjustment has been made to this equation:

$$ECN = CN - d_1n_1 - d_2n_2 - d_3n_3$$

where n_1 , n_2 , and n_3 are the number of double bonds attributable to oleic, linoleic and linolenic acids, respectively.

The values d_1 , d_2 and d_3 are calculated by means of reference triacylglycerides. They are: $d_1 = 2.60$, $d_2 = 2.35$ and $d_3 = 2.17$.



Wavelength: 700 nm

Peak No.	R_F value	%
1	0.16	1.52
2	0.20	1.87
3	0.26	5.85
4	0.32	1.42
5	0.36	28.98
6	0.48	44.93
7	0.57	12.84
8	0.64	2.01
9	0.74	0.58

Figure 5 Separation of unsaturated triacylglycerides on an HPTLC silica gel RP18 layer impregnated with silver nitrate (5% w/v solution). Mobile phase: dichloromethane–ethyl acetate–methanol–water–acetic acid (25 : 20 : 35 : 6 : 6, v/v). Detection with 1% phosphomolybdic acid in ethanol. Plate heated to 130°C for 10 minutes. Scanned at 700 nm with a spectrodensitometer. Sample: Fresh blended frying oil. Peaks 3 and 6 are triolein and trilinolein respectively. Other peaks are other unsaturated triglycerides, sterols, and antioxidants unidentified.

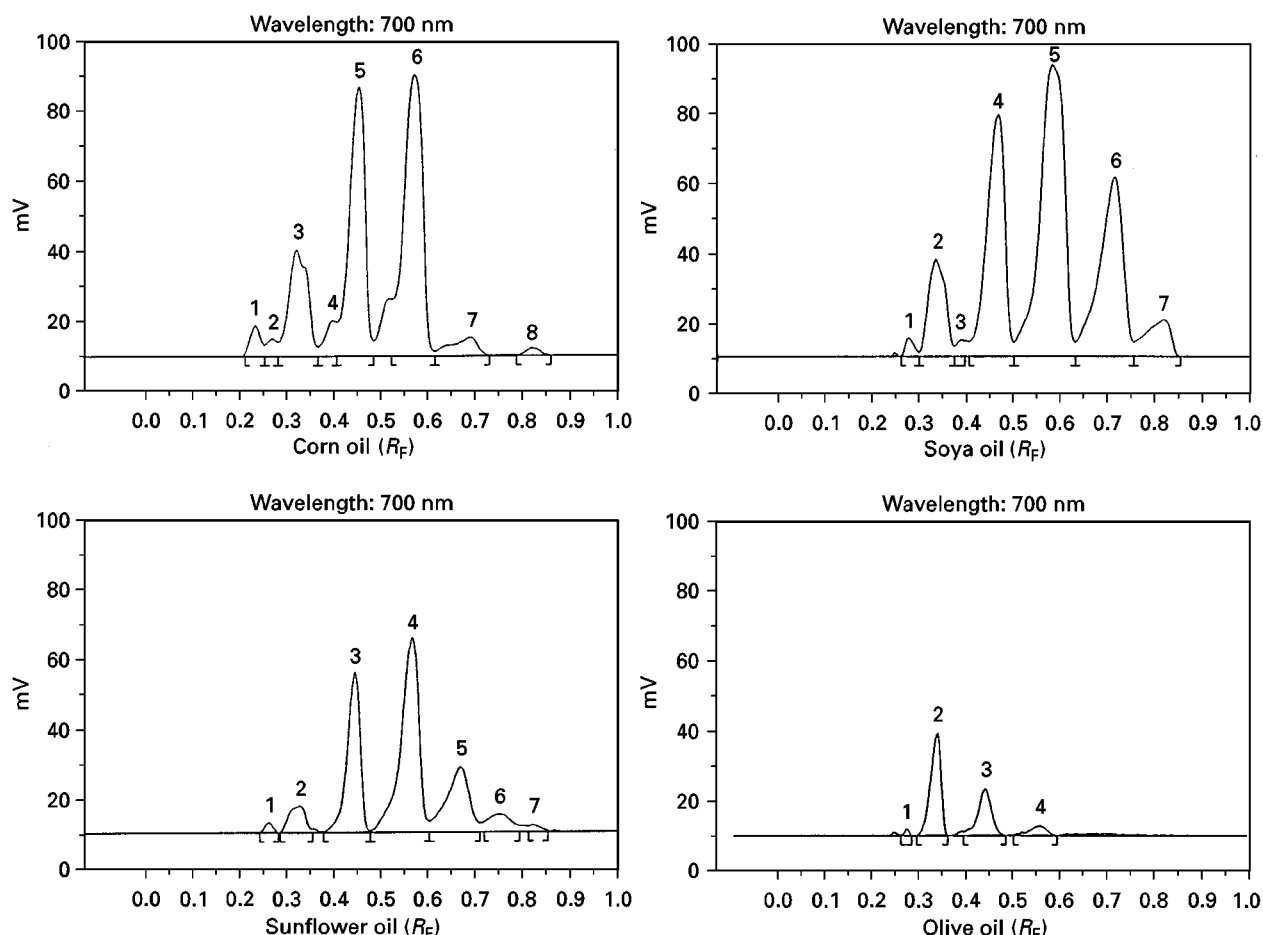


Figure 6 Separation of unsaturated triacylglycerides on an HPTLC silica gel RP18 layer impregnated with silver nitrate (5% w/v solution). Separation conditions as in Figure 5. (Corn oil) Peaks 3 and 6 are triolein and trilinolein respectively. Other peaks not identified. (Soya oil) Peaks 2 and 5 are triolein and trilinolein respectively. Other peaks not identified. (Sunflower oil) Peaks 2 and 4 are triolein and trilinolein respectively. Other peaks not identified. (Olive oil) Peaks 2 and 4 are triolein and trilinolein respectively. Other peaks not identified.

Silver nitrate As with normal phase silica gel, it is possible to modify reversed phase silica gel with silver nitrate. Pre-coated reversed phase silica gel layers can either be impregnated or, where applicable, silver nitrate can be added to the mobile phase. A suitable impregnating reagent can be prepared with silver nitrate (5% w/v) dissolved in water-methanol (10:90, v/v). The separations obtained indicate a much stronger though limited resolving capability than is possible with unmodified reversed-phase layers (see Figure 5). The triacylglycerides are separated over a much wider R_F range enabling more marked differences to be observed in the chromatograms for a number of plant seed oils. A comparison of these is shown in Figure 6. However, as mentioned previously the technique does have limitations. DGs, MGs, and FFAs will all be found at or near the solvent front if the mobile phase has been adjusted to

give maximum resolution for the triacylglycerides. Detection is also not as sensitive as for the corresponding reversed-phase layers (about a four-fold reduction).

Detection Methods

Detection of acylglycerides relies upon the use of chemical reagents as any UV absorbance is weak and none of these neutral lipids show any natural fluorescence (either in the visible or UV spectrum). Most chemical methods rely on reduction or charring techniques for acylglycerides. However, these can still be quite sensitive with the limit of detection usually being in the nanogram range. FFAs are much more reactive and hence a much wider range of detection reagents are available. The same applies to any degradation products due to oxidation where aldehydes, ketones or esters may have formed.

Detection on Normal Phase Layers

Visualization of both saturated and unsaturated acylglycerides is easily achieved on normal phase silica gel layers. However, it should be borne in mind that if the detection reagent is a charring one, then care must be taken when commercial pre-coated plates or sheets are used, particularly with sulfuric acid or chlorosulfonic acid. This is because in order to obtain good reproducibility and abrasive resistance, the pre-coated layers contain a small percentage of a polymeric organic binder. Unfortunately this can also char along with the sample components limiting the contrast between chromatographic zones and the background. However, if the temperature and duration of heating are carefully controlled, good results can be obtained.

Iodine vapour gives very good sensitivity, giving yellow-brown zones on a pale yellow background. The unsaturated compounds are stable for a much longer period of time than the saturated ones. The interaction with the π double bonds forms an iodine complex that is much more stable than the adsorption of iodine by the saturated compounds, which is reversible. These results can be made much more permanent by spraying the plate with soluble starch solution that forms dark blue complexes on the zones where iodine has been adsorbed.

Phosphomolybdic acid reagent (1–5%, w/v solution in ethanol) is probably the most popular reagent for lipid detection and gives a limit of sensitivity of 50–200 ng, depending on the glyceride. Zones appear after heating as blue-grey on a yellow background.

This yellow background can be destained by exposure to ammonia vapour.

Other reagents that have been used to good effect are listed along with the above in Table 6.

Detection on Reversed-phase Layers

Of all the reagents listed in Table 6, the first four can also be used on reversed-phase layers. However, they can only be used to detect unsaturated acylglycerides and FFAs. Sensitivity, however, is on a par with normal phase layers with both iodine vapour and phosphomolybdic acid giving the best results. Charring reagents are best avoided as the background easily chars as well due to the fact that it is bonded with an aliphatic carbon chain.

Detection on Argentation-modified Phases

On commercial pre-coated layers, phosphomolybdic acid gives results comparable with those obtained on normal or reversed-phase plates. There is usually a lack of background staining which improves the contrast. The use of ammonia vapour though is not to be recommended as this reacts with the excess silver nitrate and a brown speckled background appears. For the reversed-phase plates, heating is required at a higher temperature (150°C for 10 minutes) to detect the unsaturated zones.

Some charring techniques have been used for 'home made' normal phase silver nitrate modified layers but these involve the use of very aggressive chemical reagents.

Table 6 Detection reagents suitable for the visualization of acylglycerides and free fatty acids on normal silica gel layers (non-commercial)

<i>Detection reagent</i>	<i>Acylglyceride detected</i>	<i>Observation</i>
Iodine vapour	Both saturated and unsaturated	Yellow/brown zones
Phosphomolybdic acid spray or dip followed by heating at 100–120°C for 10 minutes	Both saturated and unsaturated and FFA	Blue-grey zones on yellow background
Manganese (II) chloride/sulfuric acid [(0.2 g manganese chloride in water (30 mL) – methanol (30 mL) plus sulfuric acid (2 mL)] Heat at 100–120°C for 10 minutes	All acylglycerides and FFA	Brown zones on white background
Copper (II) acetate/sulfuric acid (copper acetate (3% w/v) in phosphoric acid (10% v/v)) Heat at 100–120°C for 10 minutes	All acylglycerides and FFA	Brown-grey zones on a white background
Sulfuric acid (10–20% v/v) Heat at 120–150°C for 15 minutes	Both saturated and unsaturated and FFA	Black or grey zones
Berberine solution (10 mg/100 mL ethanol)	All acylglycerides	Yellow fluorescent zones under UV at 360 nm

Future Developments

It seems unlikely that major developments will occur in the future with improvement of the separation method of acylglycerides on normal and silver nitrate impregnated silica gel. However, the use of the newer commercially available smaller particle size ($\sim 4 \mu\text{m}$) and spherically shaped particles will result in an improvement in resolution, sensitivity and scanned peak shape of chromatographic zones. Automated multiple development (AMD) has already proved to be an excellent analytical tool for focusing zones in lipid separations but is still very much in its infancy with a big potential available for acylglyceride separations.

There is no doubt that reversed-phase HPTLC provides a reliable method for following the breakdown of oils and fats in use. The commercial possibilities here have yet to be fully exploited. There is still much work to be done in developing reliable, but simple, and rapid methods of analysis for triacylglyceride breakdown. Presently available HPTLC procedures not only have the potential to analyse and quantify the total FFA, but also to separate these and determine them individually. Some quantitative work on acylglycerides has already been accomplished, but in the future it should be possible to quantify far more. One of the present drawbacks has been the lack of availability of pure standards, particularly for many of the unsaturated acylglycerides. This is not altogether surprising as many are unstable and need to be kept deep frozen to avoid degradation.

The use of TLC for the analysis of triacylglycerides has further potential in the quantification of other organic species that may be present in oils and fats. Some oils naturally contain tocopherol, which acts as an antioxidant, and other oils may have this, or other antioxidants, added to extend their life. Sterols can also be present. As TLC requires little sample preparation before application to the chromatographic layer, the technique is usually quite easy (and many samples can be analysed at the same time). Many of these other compounds can be separated and determined quantitatively. The future of TLC for the analysis of triacylglycerides shows considerable potential.

See also: II/Chromatography: Thin-Layer (Planar): Densitometry and Image Analysis; Layers; Spray Re-

agents. III/Impregnation Techniques: Thin-Layer (Planar) Chromatography. Lipids: Gas Chromatography; Liquid Chromatography; Thin-Layer (Planar) Chromatography. Oils, Fats and Waxes: Supercritical Fluid Chromatography. Silver Ion: Liquid Chromatography; Thin-Layer (Planar) Chromatography. Triglycerides: Liquid Chromatography. Appendix 17: Thin-Layer (Planar) Chromatography: Detection.

Further Reading

- Dobson G, Christie WW and Nikolova-Damyanova B (1995) Silver ion chromatography of lipids and fatty acids. *Journal of Chromatography B* 671: 197–222.
- Gunstone F (1996) *Fatty Acid and Lipid Chemistry*. London: Blackie Academic and Professional.
- Hammond EW (1993) *Chromatography for the Analysis of Lipids*. London: CRC Press.
- McSavage J and Wall PE (1998) Optimization of a mobile phase in reversed-phase HPTLC for the separation of unsaturated lipids in vegetable oils degraded during frying. *Journal of Planar Chromatography* 214–221.
- Myher JJ and Kuksis A (1995) General strategies in chromatographic analysis of lipids. *Journal of Chromatography B* 671: 3–33.
- Nikolova-Damyanova B and Amidzhin B (1991) Densitometric quantification of triglycerides. *Journal of Planar Chromatography* 397–401.
- Olsson NU (1992) Advances in planar chromatography for the separation of food lipids. *Journal of Chromatography* 624: 11–19.
- Ritchie AS and Lee MH (1987) A note on: Triglyceride analysis using silver nitrate and 2-phase 2-dimensional thin-layer chromatography. *Recent Advances in Thin-layer Chromatography*. London: Plenum Press.
- Ruiz-Gutiérrez V and Barron LJR (1995) Methods for the analysis of triacylglycerols. *Journal of Chromatography B* 671: 133–168.
- Salia SK and Das SK (1996) A simple densitometric method for the estimation of polar and non-polar lipids by thin layer chromatography with iodine vapour, visualization. *Journal of Liquid Chromatography and Related Technologies* 19: 3125–3134.
- Touchstone JC (1995) Thin-layer chromatographic procedures for lipid separation. *Journal of Chromatography B* 671: 169–195.
- Traitler H, Jacolet C and Winter H (1990) Triacylglycerol structure elucidation planar chromatographic separation of randomly formed diacylglycerols. *Journal of Planar Chromatography* 177–180.

ULTRASOUND-ASSISTED METAL EXTRACTIONS



C. Bendicho and I. Lavilla, Universidad de Vigo, Vigo, Spain

Copyright © 2000 Academic Press

Introduction

Ultrasonic energy has been used for a wide variety of applications in industry, medicine and science. In the analytical chemistry field, most applications lie in the ability of ultrasound to extract compounds from the solid matrix. Solid-liquid extraction with the use of ultrasonic energy (i.e. ultrasound-assisted extraction) has been successfully applied for many years as a sample pretreatment method to extract organic compounds from matrices to which they are weakly bound (e.g. environmental samples). Sonication methods have been compared to other methods for pretreatment of solid samples (e.g. Soxhlet extraction, accelerated solvent extraction and supercritical fluid extraction), being competitive to them owing to its simplicity, efficiency and ease of use. Moreover, sonication methods do not involve the use of high temperatures, pressures or concentrated and harmful chemicals. Usually, ultrasound has been applied to the sample with the use of ultrasonic cleaning baths. Ultrasonic cleaning baths are readily available, large numbers of samples can be simultaneously treated and low-cost instrumentation is involved, but they lack the capability of transmitting sufficient ultrasonic power to produce the desired effects on the sample.

More recently, ultrasound-assisted extraction has been applied to the separation of inorganic compounds and metal ions from the matrix, to facilitate their analytical determination, and to avoid traditional sample pretreatment methods such as dry or wet ashing, which involve tedious and time-consuming treatments with corrosive reagents.

Other application areas of ultrasound-assisted extraction include the selective extraction of different physicochemical forms of elements for speciation. In this case, advantage is taken of the nondestructive character of ultrasound treatments which, under suitable conditions, maintain the integrity of the extracted species.

Finally, ultrasound can accelerate many sequential extraction schemes which are traditionally applied for metal partitioning in environmental samples such as soils, sludges and sediments.

Ultrasound-Assisted Extraction for Metal Determination

Intensive sample pretreatment of biological, environmental and industrial samples is frequently a necessary requirement for elemental analysis, so that ideally a matrix-free solution is obtained. Typically, dry ashing or wet ashing methods involve the use of high temperatures or corrosive reagents, usually under pressure, which demands very stringent safety conditions. However, a simple analyte separation without matrix decomposition is enough for many analytical techniques. Thus, atomic absorption spectrometry (mainly with the use of electrothermal atomization) allows analytical determinations to be carried out with minimum sample pretreatment owing to the low dependence of the analytical signal on the accompanying matrix as compared with other techniques for elemental analysis.

Thus, in the authors' laboratory, a number of elements have been quantitatively extracted from a large variety of matrices when probe-type sonicators operated under optimized conditions are employed. Toxic metals such as Cd and Pb can be easily extracted from mussel tissue and other biological samples, the exact extraction conditions depending on the metal. Cadmium could be quantitatively extracted from a sample mass of 10 mg slurried in a 1.5 mL volume. The sample has to be previously ground, the particle size being a critical parameter in the case of Pb since extraction efficiency diminishes for a particle size large than 150 μm . For Cu and Cd, extraction can be achieved for a particle size larger than 200 μm . The presence of an acidic medium is an essential requirement for quantitative extraction to be attained. For analytical techniques such as electrothermal atomic absorption spectrometry (ETAAS), nitric acid is recommended since unlike hydrochloric acid it does not form volatile compounds with analytes, which are the origin of interferences. In addition, nitric acid combined with the ultrasonic action promotes matrix oxidation so that analyte extraction is facilitated. Minimum acid concentration used for quantitative extraction depends again on the analyte to be extracted. A nitric acid concentration as low as 0.05% v/v is sufficient for quantitative extraction of Cd, whereas Pb requires at least 1% v/v nitric acid. Additional parameters controlling the amount of ultrasonic power delivered to the sample such as sonication time

and vibrational amplitude of the probe (expressed as a percentage of the nominal power) should be optimized for best performance. Metals which are easy to extract, such as Cd, require very short sonication times, typically less than 1 min while stronger bound metals such as Pb require 3–5 min. When using a 100 W probe sonicator, at least a 10% amplitude is necessary for extraction of Cd, while a 60% amplitude is required for Pb. Sample mass is also an important variable; extraction is usually quantitative for a mass of less than 20 mg suspended in 1.5 mL volume. Although the preparation of suspensions in larger volumes with larger amounts of ground material is also feasible, preparation of suspensions in autosampler cups is a more convenient way for ETAAS when sample homogeneity is not a limiting factor. An experimental design applied to the extraction process of Cd and Pb confirmed that soft sonication conditions (minimum sonication time and amplitude) along with maximum particle size (e.g., >200 μm) could be used for quantitative solid-liquid extraction of Cd provided that maximum acid concentration was used (e.g., 3% v/v). On the other hand, Pb needed maximum sonication time, amplitude and acid concentration together with minimum particle size. The concentration of nitric acid proved to be the most critical factor for achieving quantitative extraction.

A study carried out with Pb as target analyte and certified reference materials has shown the importance of using the appropriate ultrasonic processor so that quantitative extraction is attained. Thus, an ultrasonic cleaning bath is not suitable since only a fraction of the analyte is brought into solution even using long sonication times (e.g., 60 min). When comparing two probe-type sonicators (50 versus 100 W), quantitative extraction was observed with the 100 W sonicator for all biological materials attempted. The explanation for the above results could lie in the greater ability of probe-type sonicators to cause cavitation in the liquid medium, which results in a more efficient disruption of solid particles, so facilitating metal extraction.

Incomplete extraction was observed for Pb and Cd from sediments, thereby indicating that matrix-analyte binding plays an important role in the solid-liquid extraction process. This may be due to particle disruption being more difficult with hard materials such as sediments, so that unless the analyte is adsorbed on the surface the fraction of analyte occluded inside the solid particles will not be brought into solution, hence resulting in incomplete extraction.

Usually, the ultrasonic action will cause the matrix to be partly extracted into the liquid medium, but

Table 1 Percentage of metal extracted from certified reference materials using ultrasound irradiated with a probe ultrasonic processor

Certified sample	% Extraction			
	Cd ^a	Cu ^b	Cr ^c	Pb ^c
BCR 278 Mussel tissue	101.8	82.4	42.0	94.2
NRCC DORM-2 Dogfish muscle	93.0	93.2	2.7	–
NRCC DOLT-2 Dogfish liver	91.6	–	32.9	–
BCR 60 Aquatic plant	101.4	102.4	30.2	101.2
BCR 145 R Sewage sludge	56.3	–	46.6	104
BCR 320 River sediment	75.4	–	15.0	69.0
NRCC TORT-2 Lobster hepatopancreas	–	–	69.3	–
BCR 482 Lichen	–	–	23.7	–
GBW07605 Tea leaves	–	–	–	95.5

^aCapelo JL, Lavilla I and Bendicho C (1998) *Journal of Analytical Atomic Spectrometry* 13: 1285–1290.

^bCapelo JL, Filgueiras AV, Lavilla I and Bendicho C (1999) *Talanta* 50: 905–911.

^cCapelo JL, Lavilla I and Bendicho C (1999) *Journal of Analytical Atomic Spectrometry* 14: 1221–1226.

background absorbance caused by the small amount of matrix released can be easily handled by the background correction system (Table 1).

The use of other analytical techniques for detection after ultrasound-assisted extraction has also been reported. For instance, Ashley has studied the extraction of Pb from several standard reference materials (SRMs) such as lead-based paint, urban particulate and river sediment followed by anodic stripping voltammetry (ASV). Analytical results were satisfactory after ultrasonic extraction for 30 min using a 10% v/v nitric acid solution. ASV has been also used for determination of Pb in workplace air samples collected in the field using cellulose ester membrane filters. The filters were subjected to ultrasound under the conditions given above for SRMs. An advantage of ultrasound-assisted extraction methods over methods involving matrix decomposition (e.g., microwave-assisted digestion) is the ability to use them in the field, hence facilitating on-site analysis with portable instruments.

The use of diluted acids for extraction can also offer a simplified methodology for determination of metals by flame atomic absorption spectrometry (FAAS). In a comparison of five methods for pretreatment of plant samples, Matejovic and Durackova found that extraction of metals could be accomplished with 1 M hydrochloric acid in an ultrasonic bath. After sonication the extracts were filtered so that no particulate material could clog the nebulizer. In this case, the use of a nonoxidizing and complexing

acid such as hydrochloric acid is perhaps more convenient than other acids, since it avoids a final evaporation step to remove the excess of acid as is necessary when concentrated acids are used for mineralization in conventional digestion procedures. Incomplete release of P bound into organic compounds and Fe was observed with this procedure.

Leaching of heavy metals from aquatic plants used as environmental biomonitors has been performed by ultrasound-assisted extraction with a 1% w/w HCl + 15% w/w HNO₃ mixture. In this case, two consecutive extractions were needed to quantitatively extract Mn, Cu and Zn, the recovery of Cu being only about 75%, with RSDs lower than 2.5%. In order to obtain good analytical performance when applying ultrasound-assisted extraction, all the variables influencing the process should be borne in mind: concentration of the suspension (i.e. sample mass and extraction volume), particle size, sonication time, sonication amplitude, type of acid and its concentration, and temperature. This last variable is seldom considered for its influence on ultrasonic extractions. Since most ultrasonic cleaning baths warm up slowly during operation, many applications reported with these devices for extraction use a pre-heated liquid so that temperature is constant, hence improving reproducibility. On the other hand, acoustic cavitation is diminished on increasing the temperature above 50°C, and consequently extraction efficiency is also diminished. Thus, some workers have found only partial extraction for some elements when using a pre-heated ultrasonic bath or allowing the bath to warm up during operation to a temperature higher than 50°C. Other workers have reported quantitative extraction of metals such as Cd, Cu, Pb and Mn from powdered biological samples when sonication is carried out at 40°C. Other extractants successfully employed for solid-liquid extraction with an ultrasonic cleaning bath include dilute HCl, HNO₃ and H₂O₂. Some procedures employing ultrasonic baths for sample pretreatment were aimed at complete digestion of the sample by the use of concentrated acids, and therefore cannot be regarded as extraction procedures.

Applications of Ultrasound-Assisted Extraction for Element Speciation

Ultrasound extraction shows advantageous features for element speciation. Organometallic species can be extracted without changes in their integrity under suitable extraction conditions. Both organic and aqueous extraction media have been used for separation of organometallic and inorganic species from

the solid matrix, most applications using ultrasonic cleaning baths for extraction.

A recent application of ultrasound-assisted extraction with the use of a probe-type sonicator has been reported for mercury speciation in combination with flow injection-cold vapour-atomic absorption spectrometry (FI-CVAAS) for detection. In this case, a 400 mg portion of sample and 1–7 mL of 0.5–7 M acid were placed in a centrifuge tube and sonicated at a fixed ultrasound amplitude for 1–5 min. Selective extraction of methylmercury required less than 5 mL of 2 M HCl, the extraction being quantitative (>95%) when the HCl volume was higher than 2 mL. The extraction could be accomplished using ultrasound amplitude in the range 20–70% for 2–5 min. The optimization procedure was addressed to selectively extract methylmercury from slurried biological samples such as mussel tissue; inorganic mercury extraction required higher HCl concentrations. Both mercury species could be extracted with 5 mL of 5 M HCl and sonicating at 20–70% amplitude for 3–5 min. Methylmercury was determined using sodium tetrahydroborate(III) as reducing agent whereas inorganic mercury was determined by selective reduction with stannous chloride in the extracts containing both species. The limits of detection were 11 and 5 ng g⁻¹ for methylmercury and inorganic mercury, respectively. The repeatability (between-batch precision), was in the range 5–10% for both mercury species.

In a study on As extraction, similar distributions of arsenicals (e.g., arsenobetaine, arsenocholine and dimethylarsinic acid) were found in a comparison between accelerated solvent extraction and sonication. Nonpolar As is extracted with acetone whereas polar As is extracted with 50% w/w methanol.

Cr(VI) has been extracted from industrial hygiene samples with an ultrasonic cleaning bath at 40–50°C for 1 h using alkaline solutions containing 0.05 M (NH₄)₂SO₄–0.05 M NH₃. The Cr(VI) was separated from other cations present in the extract by retention with an anion-exchange resin. Elution of Cr(VI) from the resin was performed with a buffer solution at pH 8. The eluate was acidified with HCl and the complex between Cr(VI) and 1,5-diphenylcarbazide was measured by flow injection-UV/VIS detection. Determination of total Cr following ultrasonic extraction was also feasible using a prior oxidation step with Ce(IV) so that Cr(III) is converted into Cr(VI). This simple and effective preparation method compared favourably with other methods employing intensive treatments leading to matrix decomposition (e.g., acid digestion) for determination of total Cr in fly ash, paint chips, etc.

Sequential Extraction of Metals from Environmental Samples

The bioavailability and mobility of trace metallic and metalloid elements in the environment depend on the chemical form of the element and the type of binding to the matrix. Sequential extraction schemes, although far from being perfect, have the ability to extract elemental species from particular solid phases in sediments, soils and sewage sludge. However, application of these schemes entails a difficult experimental task owing to the large number of slow and tedious stages. For instance, the Tessier scheme apportions metal distribution in four different stages: (1) exchangeable, (2) associated to carbonates, (3) associated to Fe and Mn oxides and (4) associated to organic matter and sulfides. For dissolving a particular solid phase, chemical extractants are applied successively to the solid sample, each follow-up treatment being more drastic in chemical action or different in nature from the previous one. Thus, for

the phases mentioned above, an MgCl_2 solution, an NaOAc solution, an $\text{NH}_2\text{OH}\cdot\text{HCl}$ solution, and an $\text{HNO}_3 + \text{H}_2\text{O}_2$ solution are used sequentially. The Tessier scheme requires an overall operation time of about 18 h. Ultrasonic energy from a probe-type sonicator has been employed for acceleration of the sequential chemical extraction of Cu, Cr, Ni, Pb and Zn from sediment and sewage sludge samples. Conventional and ultrasound-accelerated Tessier extraction schemes offered similar partitioning patterns for the two first fractions (i.e., exchangeable and carbonate-bound) when applied to a sewage sludge sample. However, significant differences in metal extractability were observed for some metals when applying the ultrasound-accelerated Tessier scheme to river sediments. On the other hand, a good agreement for the total extractable contents (i.e., sum of metal contents found in each stage) was seen for Ni, Pb and Zn in sewage sludge and Cr, Ni, Pb and Zn in river sediment, meaning that the ultrasound methodology could be useful for fast screening of extractable

Table 2 Analytical results obtained by applying the conventional and the modified Tessier sequential extraction schemes for metal partitioning in a river sediment and a sewage sludge

Fraction	Element	River sediment ^a			Sewage sludge ^b		
		Conventional method ($X \pm \text{SD}$) ^c	Ultrasound method ($X \pm \text{SD}$) ^c	Recovery ^d (%)	Conventional method ($X \pm \text{SD}$) ^c	Ultrasound method ($X \pm \text{SD}$) ^c	Recovery ^d (%)
Exchangeable	Cu	2.17 ± 0.05	1.90 ± 0.1	87.6	18.4 ± 0.18	18.2 ± 0.12	98.9
	Cr	ND	ND	–	ND	ND	–
	Ni	12.2 ± 0.3	12.1 ± 0.4	99.3	9.51 ± 0.18	9.24 ± 0.23	97.2
	Pb	9.83 ± 0.16	9.73 ± 0.34	99.0	10.9 ± 0.26	10.7 ± 0.26	97.6
	Zn	14.2 ± 0.3	14.0 ± 0.4	98.6	96.7 ± 2.1	96.2 ± 3.7	99.5
Carbonate-bound	Cu	15.5 ± 0.47	4.21 ± 0.27	27.2	8.16 ± 0.11	8.1 ± 0.12	98.7
	Cr	ND	ND	–	ND	ND	–
	Ni	14.1 ± 0.57	14.0 ± 0.21	99.3	6.35 ± 0.09	6.16 ± 0.25	97.0
	Pb	41.1 ± 0.37	40.6 ± 0.83	98.9	13.7 ± 0.24	13.6 ± 0.19	99.8
	Zn	70.8 ± 1.34	69.2 ± 1.43	97.7	80.0 ± 1.1	78.6 ± 1.6	98.2
Fe–Mn oxide-bound	Cu	7.71 ± 0.35	18.7 ± 0.28	242	10.3 ± 0.16	26.1 ± 0.27	253
	Cr	7.06 ± 0.11	2.85 ± 0.1	40.4	ND	ND	–
	Ni	6.0 ± 0.23	6.0 ± 0.3	100	4.58 ± 0.30	4.42 ± 0.14	96.3
	Pb	165.4 ± 3.7	134 ± 1	81.2	19.7 ± 0.71	19.2 ± 0.16	97.7
	Zn	130 ± 3	106 ± 1	81.3	397 ± 3	393 ± 3	99.1
Organic matter-bound	Cu	152 ± 2	149 ± 4	98.3	165 ± 3	46.3 ± 0.43	28.0
	Cr	3.92 ± 0.04	ND	0.0	8.31 ± 0.23	ND	0.0
	Ni	ND	ND	–	6.00 ± 0.12	5.97 ± 0.32	99.5
	Pb	5.60 ± 0.36	34.6 ± 0.63	618	16.0 ± 0.46	15.6 ± 0.47	97.4
	Zn	15.4 ± 0.24	32.2 ± 1.0	210	90.0 ± 2.0	58.4 ± 2.0	64.9

^aPérez-Cid B, Lavilla I and Bendicho C (1999) *International Journal of Environmental Analytical Chemistry* 73: 79.

^bPérez-Cid B, Lavilla I and Bendicho C (1999) *Fresenius Journal of Analytical Chemistry* 363: 667.

^cAverage of three determinations (expressed as $\mu\text{g g}^{-1}$) \pm standard deviation.

^dThe recovery was calculated in the following way: [metal leached using the accelerated method/metal leached using the conventional method] \times 100.

ND, non detected.

metals in solid environmental samples. The operation time per sample was 20 and 28 min for sewage sludge and river sediment, respectively, when ultrasound was used for the Tessier scheme (Table 2).

The sequential extraction scheme, proposed by the Community Bureau of Reference (BCR), now the Standards, Measurement and Testing Programme, consists of three stages: acid-soluble, reducible and oxidizable. The reagents employed are a HOAc solution, an $\text{NH}_2\text{OH}\cdot\text{HCl}$ solution and an H_2O_2 solution, respectively. Despite using a stage less than the Tessier scheme, its operation time is much longer (about 51 h per sample). Application of the BCR scheme to sewage sludge showed that a drastic shortening in time from 51 h to about 22 min per sample could be achieved by the use of ultrasonication. In this case, a much better agreement between the conventional and the ultrasound-accelerated BCR schemes was found in all fractions, so that information concerning extractable metal contents from sewage sludge was virtually the same.

Conclusions

Ultrasound-assisted extraction can be used as an alternative to traditional sample preparation methods for elemental analysis and speciation where matrix separation rather than complete matrix elimination is performed. Sonication methods usually involve mild treatments which meet an important requirement for speciation, i.e., extraction of the species of interest without changes in their integrity. As a result of the decreased amount of matrix released during sonication treatments, matrix interferences can also be reduced. Additionally, ultrasonic treatments provide a significant speeding up of those methods requiring long and tedious extractions (e.g., sequential extraction of metals from solid environmental samples). So far, analytical results obtained on applying ultrasound for sample preparation are very promising, and new developments are expected on the topics addressed in the present work. On-line solid-liquid extraction with the use of ultrasound will require specially designed ultrasonic cells to further simplify sample treatment.

See also: II/Extraction: Analytical Inorganic Extractions. III/Microwave-Assisted Extraction: Environmental Applications.

Further Reading

Amoedo L, Capelo JL, Lavilla I and Bendicho C (1999) Ultrasound-assisted extraction of lead from solid samples: a new perspective on the slurry-based sample prep-

aration methods for electrothermal atomic absorption spectrometry. *Journal of Analytical Atomic Spectrometry* 14: 1221–1226.

Ashley K (1998) Ultrasonic extraction of heavy metals from environmental and industrial hygiene samples for their subsequent determination. *Trends in Analytical Chemistry* 17: 366–372.

Capelo JL, Lavilla I and Bendicho C (1998) Ultrasound-assisted extraction of cadmium from slurried biological samples for electrothermal atomic absorption spectrometry. *Journal of Analytical Atomic Spectrometry* 13: 1285–1290.

El Azouzi H, Cervera ML and de la Guardia M (1998) Multi-elemental analysis of mussel samples by atomic absorption spectrometry after room temperature sonication. *Journal of Analytical Atomic Spectrometry* 13: 533–538.

Lavilla I, Capelo JL and Bendicho C (1998) Determination of cadmium and lead in mussels by electrothermal atomic absorption spectrometry using an ultrasound-assisted extraction method optimized by factorial design. *Fresenius Journal of Analytical Chemistry* 363: 283–288.

Lavilla I, Pérez-Cid B and Bendicho C (1998) Leaching of heavy metals from an aquatic plant (*Lagarosiphon major*) used as environmental biomonitor by ultrasonic extraction. *International Journal of Environmental Analytical Chemistry* 72: 47–57.

Luque de Castro MD and da Silva MP (1997) Strategies for solid sample treatment. *Trends in Analytical Chemistry* 16: 16–23.

Mamba S and Kratochvil B (1995) Application of ultrasound to dissolution of environmental samples for elemental analysis. *International Journal of Environmental Analytical Chemistry* 60: 295–302.

Matejovic I and Durackova A (1994) Comparison of microwave digestion, wet and dry mineralization, and solubilization of plant sample for determination of calcium, magnesium, potassium, phosphorus, sodium, iron, zinc, copper and manganese. *Communications in Soil Science and Plant Analysis* 25: 1277–1288.

McKiernan JW, Creed JT, Brockhoff CA, Caruso JA and Lorenzana RM (1999) A comparison of automated and traditional methods for the extraction of arsenicals from fish. *Journal of Analytical Atomic Spectrometry* 14: 607–613.

Minami H, Honjo T and Atsuya I (1996) A new solid-liquid extraction sampling technique for direct determination of trace elements in biological materials by graphite furnace atomic absorption spectrometry. *Spectrochimica Acta, Part B* 51: 211–220.

Pérez-Cid B, Lavilla I and Bendicho C (1998) Speeding up of a three-stage sequential extraction method for metal speciation using focused ultrasound. *Analytica Chimica Acta* 360: 35–41.

Pérez-Cid B, Lavilla I and Bendicho C (1999) Analytical assessment of two sequential extraction schemes for metal partitioning in sewage sludge. *Analyst* 121: 1479–1484.

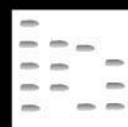
Rio-Segade S and Bendicho C (1999) Selective reduction method for separate determination of inorganic and total mercury in mussel tissue by flow-injection cold vapor technique. *Ecotoxicology and Environmental Safety* 42: 245–252.

Rio-Segade S and Bendicho C (1999) Ultrasound-assisted extraction for mercury speciation by the flow-injection–cold vapor technique. *Journal of Analytical Atomic Spectrometry* 14: 263–268.

VENOMS: CHROMATOGRAPHY

See III/NEUROTOXINS: CHROMATOGRAPHY

VETERINARY DRUGS: LIQUID CHROMATOGRAPHY



H. F. De Brabander and K. De Wasch, University of Ghent, Merelbeke, Belgium

Copyright © 2000 Academic Press

For the analysis of residues of veterinary drugs, liquid chromatography (LC) is of increasing importance: some of these molecules are polar, heat-sensitive and/or difficult to analyse by gas chromatography–mass spectrometry (GC-MS). Moreover, LC is the method of choice for components of high molecular mass. Since the introduction of benchtop LC-MS instruments, there has been an increasing number of publications on the application of this technique in the field of residue analysis.

Equipment

In LC a large variety of packed columns are in use but most residue separations are carried out with some kind of reversed-phase material based on modified silicas (RP-18, RP-8, etc.). Hitherto, in our laboratory, a particle size of 5 µm with column dimensions 150 × 2.1 mm has been commonly used. For a laboratory involved in residue analysis under accreditation, the daily reproducibility of the chromatogram from column to column is very important (see section on quality criteria, below). In the future, column material of smaller particle sizes (3 µm) may be used routinely, allowing faster separation, higher sample throughput and better limits of detection.

The nature of the mobile phase depends on the column used. In most cases a mixture of water and an organic solvent such as methanol or acetonitrile is used. Special LC grades of solvents are necessary. For analysis of residues, gradient elution is a must. In

most cases the column has to be cleaned from interfering components after each run by a gradient. As well as organic solvents, a number of chemicals may be added to the mobile phase (buffers and chelating agents) but the compatibility of these products with the detector should be checked. For LC-MS only volatile components (e.g. trifluoroacetic acid) can be used and this limitation sometimes hinders the transformation of an LC into an LC-MSⁿ method.

Autoinjection is a must for the routine analysis of residues of veterinary drugs, not only for higher sample throughput but also for reproducibility in the validation of the results. However, particular attention should be drawn to the danger of cross-contamination with such injectors, especially in combination with LC-MS which has low detection limits.

Detectors

For screening purposes universal detectors such as UV and light-scattering detectors are used. However, for the confirmation of suspect samples more is required than just retention time and detector response. Since the results of laboratory analysis may have a serious impact on individuals and companies, false positives must be avoided at any price. For example, a sample of poultry feed, analysed by ion chromatography, was suspected to contain KSCN (a thyreostatic drug). Both the retention time and co-chromatography met the quality criteria. However, the presence of KSCN was so unlikely that the effluent was collected and mixed with Fe³⁺ (to give a red colour with SCN). This test was negative. Later on, it was found that the sample contained acetylsalicylic acid, which is often used in poultry rearing, and that the two molecules are not separated in the chromatographic system used.

More analytical evidence could be gathered by using a diode array detector (DAD). However, at low concentrations of the analyte and/or dirty samples, interferences are very likely. With a fluorescence detector more specific analysis at lower detection limits can be performed but in most cases some kind of derivatization of the analyte is needed.

The mass spectrometric detector is very important in residue analysis: the most common interfaces are electrospray (ES) and atmospheric pressure interface (API).

Quantification

Quantitative analysis is necessary for residues of legal veterinary drugs having a maximum residue limit (MRL). The method used must have limit of quantification of (at least) half the MRL. The validation of quantitative method is very time-consuming and expensive. Therefore, qualitative LC is often used for analysis of residues of illegal substances (with a so-called zero tolerance). However, quantitative methods always have a qualitative aspect (a value for the correct substance) while qualitative methods always contain a quantitative background (e.g. the estimation of peak intensities). This quantitative aspect is reflected in the so-called action limits: levels of residues which an efficient laboratory should be able to reach (e.g. 2 p.p.b. for anabolics). In our laboratory, qualitative data (residue present or not) are transferred into quantitative data as follows: a large number of samples (e.g. 50 urines of different origin) are spiked with several anabolics at a certain level (e.g. the action limit) and analysed. The percentages 'detected spikes' are calculated. A 95% detection levels is statistically accepted. So, it could be stated to the inspection services: 'if a sample contains the spiked level, the residue will be detected with a 95% probability'. Higher or lower levels will be detected with higher or lower probabilities. It should also be mentioned that quantification of one signal (e.g. a UV

absorbance) is easier than quantification of a complex signal (e.g. a mass spectrum). However, complex signals give much more information. Internal standards play an important role in quantification in residue analyses. For LC-MS the availability of deuterated standards is often a limiting factor.

Generally, it is important to convince customers (e.g. inspection services) that very reliable quantitative analysis of many samples with low detection limits in a short time for a very low price is not possible.

Special Features of LC

LC-MSⁿ

The first benchtop LC-MS-MS machine based on a modification of an ion trap was introduced in 1996. In tandem MS an ion (e.g. the molecular ion) may be chosen as parent ion, isolated and concentrated in the trap, while all other ions are ejected. Afterwards the speed of the ion is increased: the ion collides with He present in the trap and fragments. The fragment ions (daughter ions) are measured. The daughter ions are theoretically derived from the parent ion only, but in practice some interference is still present (**Figure 1**).

With quadrupoles, MS-MS is normally the end of the story. In an ion trap one daughter ion may be concentrated and fragmented over and over again. In theory, MSⁿ opens the way to a significant reduction of the clean-up of the sample. However, fewer and fewer ions of the analyte are present and the signal-to-noise ratio competes with the ability of the apparatus to detect ions. In practice MS² is only needed for analysis of most residues with LC-MS.

LC as Clean-up in Residue Analysis

Some hyphenated techniques are claimed to be so specific that they only need minimum sample clean-up. In our experience this is not yet true for the analyses of all residues (e.g. anabolics in complex

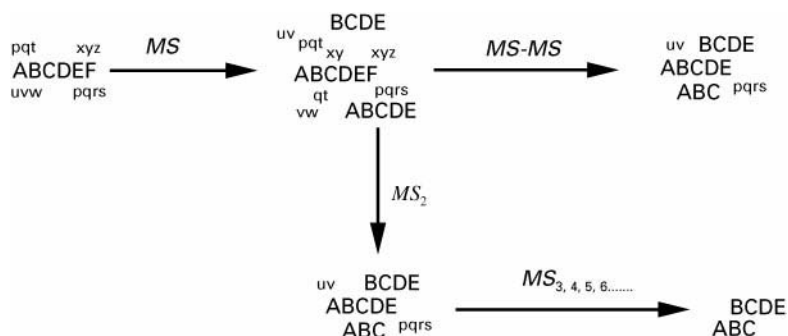


Figure 1 MS (ABCDEF, analyte; pqt, xyz, uvw and pqrs, interferences); MS-MS on ABCDEF; MSⁿ: formation of granddaughter and grandgranddaughter ions.

matrices at the p.p.b. ($\mu\text{g kg}^{-1}$) level). The clean-up of the primary extract needs special attention. LC purification adds a considerable value to the specificity of the method and influences the reliability of the results in a positive sense. By fraction collection, very clean extracts are obtained and the limit of detection is substantially decreased.

Immunological methods can also be coupled to LC to eliminate interfering substances.

Quality Criteria for the Use of LC in Residue Analysis

Minimum quality criteria for the identification of residues using different analytical techniques have been published in the European Commission (EC) directive 93/256. For LC the EC has specified the following quality criteria for methods of analysis which may be used for confirmatory purposes:

1. The analyte should elute at the retention time which is typical for the corresponding standard analyte under the same experimental conditions.
2. The nearest peak maximum in the chromatogram should be separated from the designated analyte peak by at least one full peak width at 10% of the maximum height.
3. The absorption maximum in the spectrum of the analyte should be at the same wavelength as those of the standard analyte within a margin determined by the resolution of the detection system. For diode array detection this is typically within ± 2 nm.
4. The spectrum of the analyte above 220 nm should not be visually different from the spectrum of the standard analyte for those parts of the two spectra with a relative absorbance $\geq 10\%$. This criterion is met when the same maxima are present and no observed point in the difference between the two spectra is more than 10% of the absorbance of the standard analyte.
5. For confirmatory purpose, if the method is not used in combination with other methods, then co-chromatography in the LC step is mandatory.

Discussion of the Quality Criteria

1. Quality criterion 1 is same for any chromatographic procedure: the retention times of the two peaks, formed by the analyte and the standard, should correspond. Otherwise the analyte clearly differs from the standard. A window of 3% is a reasonable quality criterion. Where a great deviation occurs, co-chromatography may be used (see point 5).

2. Criterion 2 requires a resolution of one between two peaks. However, this quality criterion is not clearly described in the EC document. Here the question might be put whether the criterion should only be required for peaks with the same maximum wavelength. For example, an analyte with maximum absorbance of 430 nm may in practice be readily distinguished from an interfering compound with a maximum of 310 nm, even if they partly co-elute. In LC-MSⁿ, this criterion will theoretically not be valid if deuterated standards, which nearly co-elute, are used.
- 3 and 4. These criteria match only LC-DAD. For LC-MSⁿ criteria have not yet been described.
5. In criterion 5, co-chromatography is required for proper identification of an analyte. The usefulness of co-chromatography may be questioned: co-chromatography may prove that the peak in question is not the analyte but not that the peak is without any doubt the analyte. Moreover, it is important that the concentration of standard analyte added is of the same magnitude as that of the sample.

Examples of LC Methods in Residue Analysis

In this section some examples of LC and LC-MSⁿ methods for residues of some illegal growth promoters, legal drugs and feed additives are discussed. More extensive information can be found in the Further Reading section.

LC Methods for Illegal Growth Promoters

Thyrestatic drugs The use of these drugs in cattle results in a spectacular weight gain, arising mainly from an increased filling of the gastrointestinal tract and an augmented water retention. In our laboratory a specific thin-layer chromatography (TLC) method for the determination of thiouracil and analogous compounds has been established. For additional confirmation, the final extract of the TLC method could also be analysed by LC-MSⁿ yielding specific MS² and MS³ spectra (Figure 2).

Anabolic steroids The use of anabolic steroids as growth promoters in the fattening of animals is prohibited in all EU member states. GC-MS is the method of choice for a large number of these components. But some compounds such as stanozolol and its most important metabolite in cattle (16 β -hydroxystanozolol; Figure 3) are difficult.

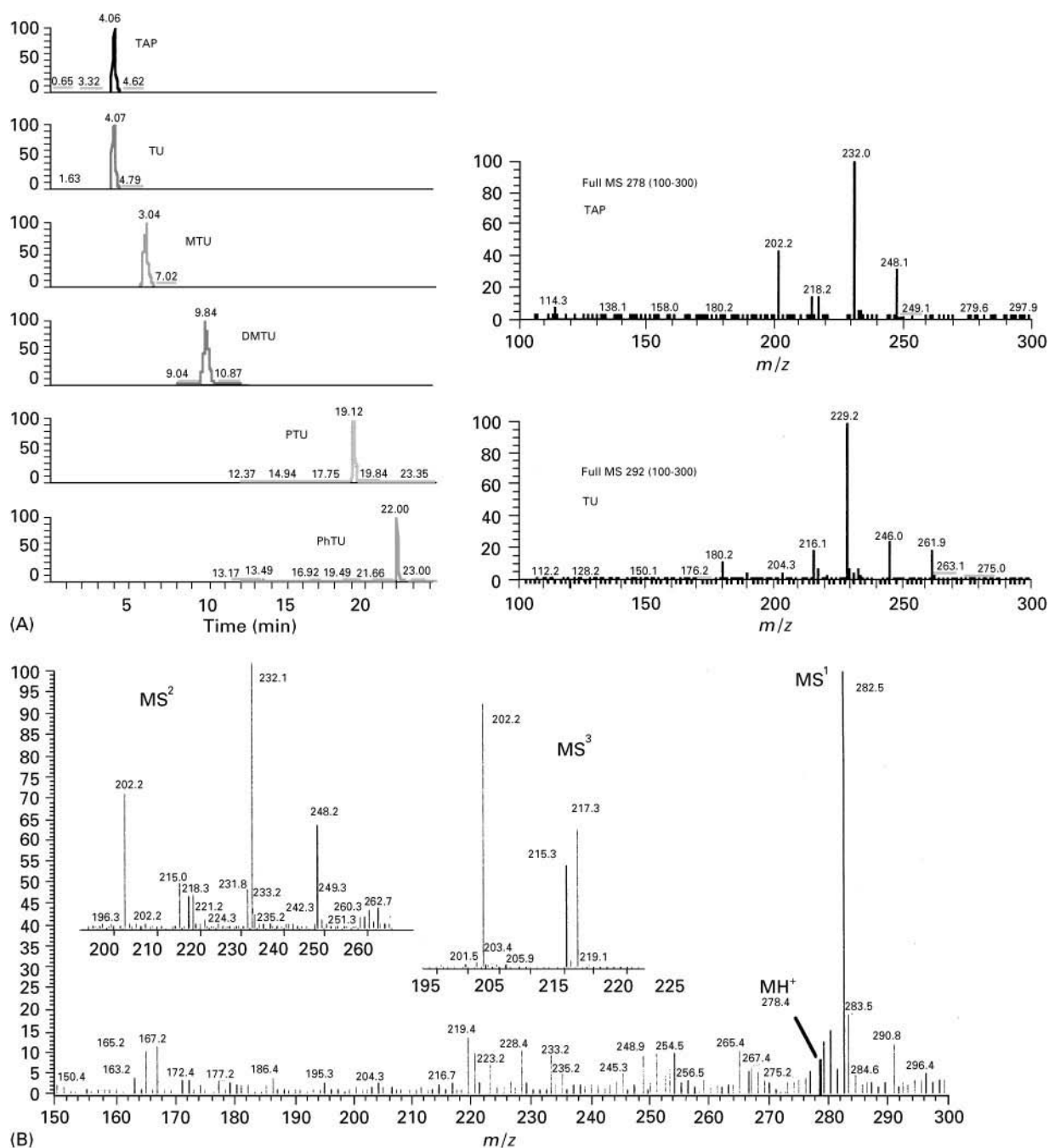


Figure 2 (A) Chromatogram and MS² spectra of some thyreostats. Thyreostats: 4(6)-R-thiouracil (R = H (TU); methyl (MTU); n-propyl (PTU); phenyl (PhTU)); TAP, 1-methyl-2-mercaptoimidazole (tapazole); DMTU, (4(5,6)-dimethyl-2-thiouracil). (B) MS¹, MS² and MS³ spectrum of the thyreostat tapazole.

Recently, GC-MS, LC-MS, MS-MS and MSⁿ methods for this metabolite have been described and compared, in a collaborative study between three Belgian and three Dutch laboratories. It was observed that the spectra obtained on different types of LC-MS systems are clearly different: from one diagnostic ion (in a single quadrupole) to a lot of diagnostic ions

with LC-MSⁿ. This illustrates the difficulty of working out quality criteria for LC-MSⁿ analysis.

β-Agonists During the 1980s the β-agonists found illegal application in animal breeding (extra weight gain together with a repartition between muscle and fatty tissue). An LC method with post-column

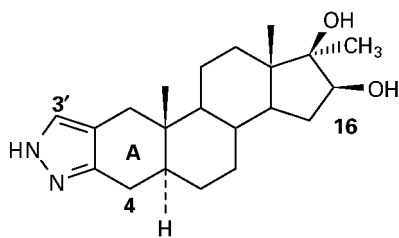


Figure 3 16 β -Hydroxystanozolol: the most important metabolite of stanozolol in cattle.

derivatization (with a diazotization mixture) for the determination of clenbuterol and analogues has been described. Later, the very specific detection for anilines was replaced by MSⁿ detection: it is easier to switch from one analyte to another with an LC-MS system than with a post-column derivatization detector. Moreover, deuterated clenbuterol can be used for quantification. In **Figure 4** a chromatogram of some β -agonists (not all are represented here) and an example of an MS² spectrum (tulobuterol) are given.

Corticosteroids Corticosteroids are also abused in cattle fattening. The weight gain is probably due to secondary effects of the corticosteroids, such as water retention. For the analysis of residues of corticosteroids, GC-MS with negative ion chemical ionization (NCI) detection is still the method of choice. However, for the identification of newly used corticosteroids in injection sites, LC-MSⁿ offers more

identification power than GC-MS (no derivatization; different MSⁿ spectra).

Anti-infection Agents

This broad range of chemicals is used for both therapeutic and/or growth-promoting reasons. Screening for residues of antibacterials in slaughtered animals is carried out in most states by microbial inhibition tests on kidney tissue. In the case of a positive test, the identity and (in the case of legal drugs) the concentration of the substance should be determined. It is in this aspect that LC and LC-MS methods are mostly used.

Sulfonamides Several LC methods for the determination of sulfonamides have been described. In our laboratory an LC method from the literature was quickly transformed into an LC-MSⁿ method. In **Figure 5** a chromatogram and MS² spectra of some sulfonamides are given. Currently, six sulfonamides are monitored in one run.

Antibiotics For antibiotics such as penicillins, cephalosporins, quinolones, macrolides and tetracyclines a lot of LC and some LC-MS methods have been described. For tetracyclines, for example, ligands (e.g. oxalic acid) have to be added to the mobile phase to prevent extreme tailing. Post-column derivatization (e.g. with ZrCl₄) followed by fluorescence detection is

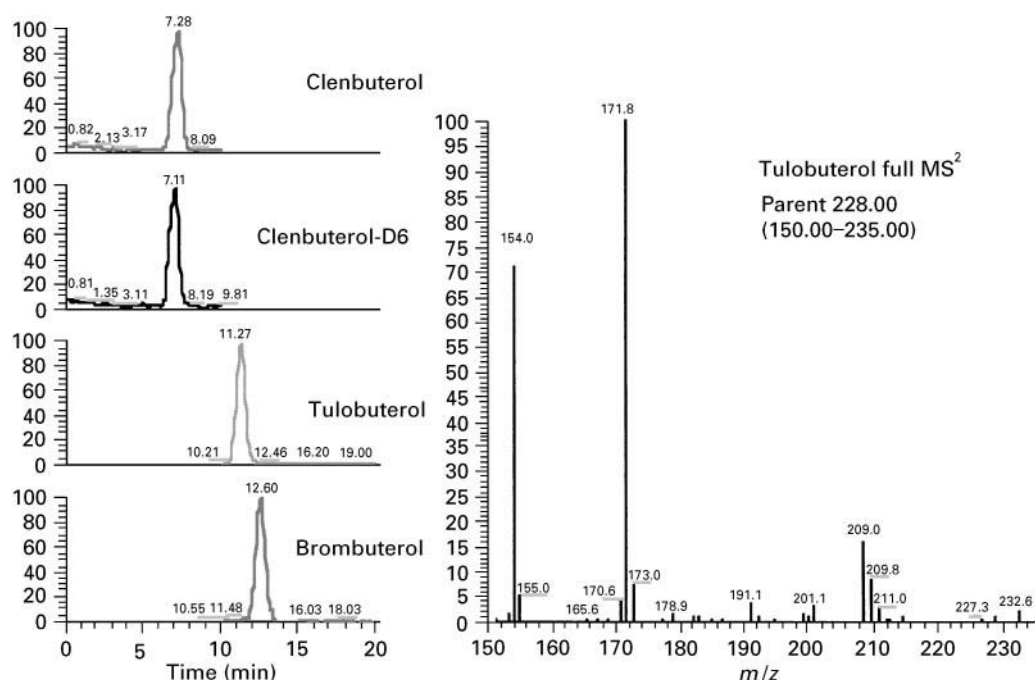


Figure 4 Chromatogram of some β -agonists and MS² spectrum of tulobuterol.

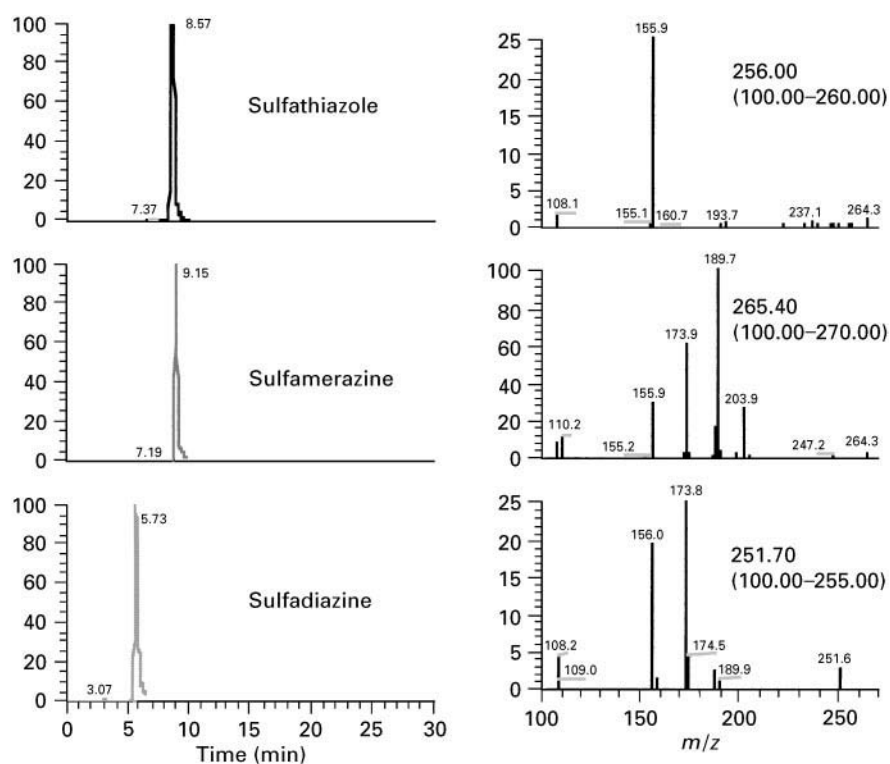


Figure 5 Chromatogram and MS² mass spectra of some sulfonamides.

very specific for these molecules yielding very low limits of detection: 0.5–1.5 $\mu\text{g kg}^{-1}$ in comparison with 2–5 $\mu\text{g kg}^{-1}$ with LC-MS.

Antiparasitic Agents

An example of a potent antiparasitic veterinary drug is ivermectine (a macrocyclic lactone disaccharide).

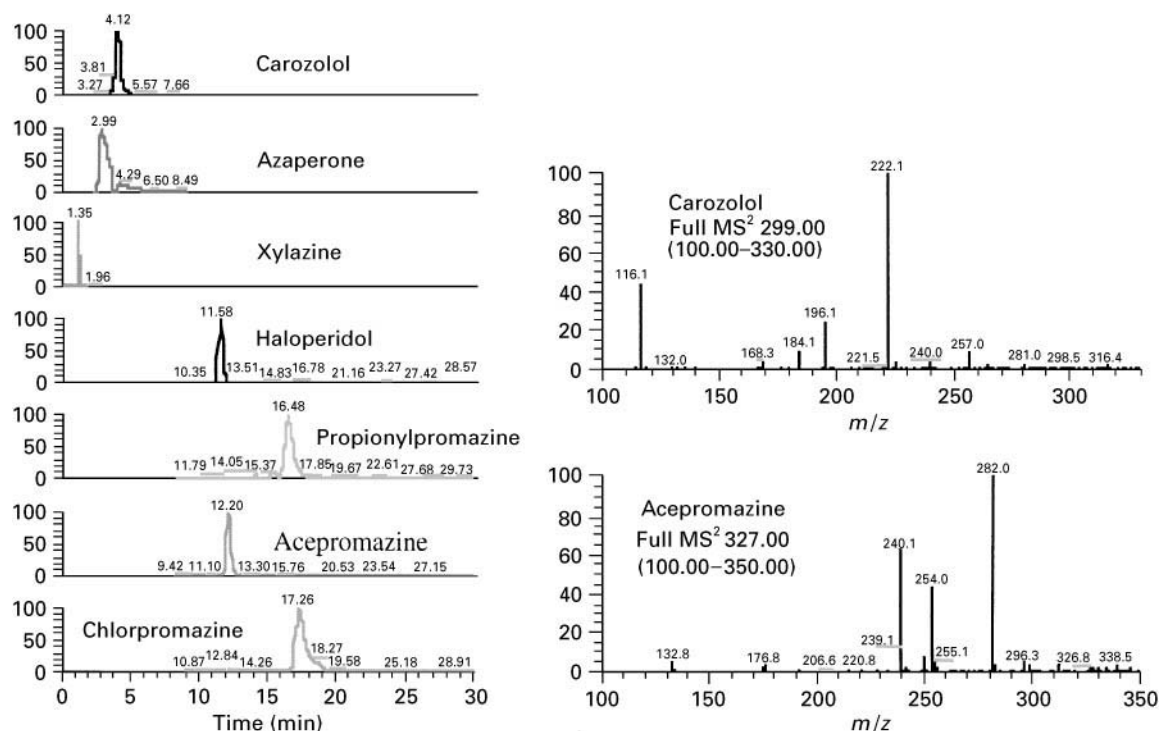


Figure 6 Chromatogram and MS² mass spectra of some tranquilizers.

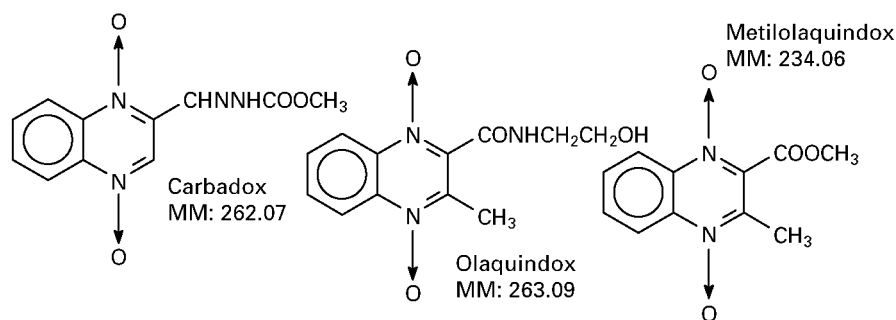


Figure 7 Formulas of carbadox, olaquinox and metilolaquinox.

The drug is effective in low dosages and therefore requires methods with low detection limits (MRL: $15 \mu\text{g kg}^{-1}$ in porcine liver). Since the molecule has a high molecular mass, LC is the method of choice. HPLC-UV methods for screening of ivermectine residues in animal tissues and milk have been described. For confirmation the molecule can be derivatized (with methylimidazole-acetic anhydride) and analysed by LC with a fluorescence detector.

Tranquillizers

Tranquillizers may be used illegally to prevent stress during the transport of pigs and bulls to the abattoir. A large number of LC methods have been published for the determination of residues of these components. In our laboratory one method was transferred into an LC-MSⁿ method with which seven tranquillizers could be determined in a short time. In **Figure 6** mass chromatograms and the MS² spectra of these components are given. The data, given in Figures 4–6 were obtained with the same apparatus. This is an illustration of the ease of switching from one analyte to another.

Feed Additives

Some components are not considered as veterinary drugs but as feed additives. Examples are the quinoxalines, carbadox and olaquinox. However, residues of these components may be present in edible tissue as well. Also nonregistered equivalents of these components could be used: as an example, the presence of metilolaquinox was suspected in animal feed: this was possibly a modification of olaquinox with a methyl group. LC analysis gave a chromatogram containing a large peak different from carbadox and olaquinox. However, LC-MS analysis gave a molecular mass less than carbadox and olaquinox. By combining MS with NMR a structure for this molecule was proposed (**Figure 7**). This example illustrates the important of MS in residue analysis.

Conclusion

The demands for specificity, reliability, speed and turnover in residue analysis of veterinary drugs are continuously increasing. LC, especially with MS detection, is a reliable analytical technique which should be able to cope with these stringent demands. In comparison with GC and GC-MS, a large range of analytes can be covered and in most cases there is no need for derivatization. It is also easy to switch an LC-MS system from one analyte to another. The lower yield of the LC-MS interfaces and the poorer separation power of LC columns in comparison with GC may be regarded as points to be improved.

The use of illegal alternatives to registered drugs or feed additives poses two important problems for routine inspection: first of all there is no target component. The situation is comparable with the search for a unknown needle in an unknown haystack. Secondly, no analytical standards of the molecule are available. MS (and MSⁿ) is able to give more information about a suspect peak. The future of LC in residue analysis will depend largely on the possibilities of identification of illegal substances abused and qualitative and quantitative analysis of legal veterinary drugs with LC-MSⁿ.

See Colour Plate 124.

See also: II/Chromatography: Liquid: Detectors: Mass Spectrometry; Detectors: Ultraviolet and Visible Detection; Mechanisms: Reversed Phases. **III/Forensic Sciences:** Liquid Chromatography.

Further Reading

- Crosby NT (1998) *Determination of Veterinary Residues in Food*. Lancaster: Technomic.
- Heitzman RJ (ed.) (1994) *Veterinary Drug Residues*. Oxford: Blackwell Scientific.
- March RE and Hughes RJ (eds) (1992) *Quadrupole Storage Mass Spectrometry*. New York: Wiley Interscience.
- Nollet L (ed.) (1992) *Food Analysis by HPLC*. New York: Marcel Dekker.

Oka H, Nakazawa H, Harada K-I and MacNeil JD (eds) (1995) *Chemical Analysis for Antibiotics Used in Agriculture*. Arlington: AOAC International.

O'Keeffe M (ed.) (2000) *Residue Analysis in Food – Principles and Applications*. Amsterdam: Harwood Academic Publishers.

Proceedings of the International Symposium on Analysis of Anabolizing and Doping Agents. I: Ghent, 1988:

J. Chromatogr. 489 (1989). II: Ghent, 1990: J. Chromatogr. 564 (1991). Ghent, Belgium.

Proceedings of the International Symposium of Hormone and Veterinary Drug Analysis. I: Ghent, 1992: *Anal. Chim Acta* 275 (1993). II: Bruges, 1994: *The Analyst* 119 (1994). III: Bruges, 1998: *The Analyst* 123, 12 (1998).

VIRUSES: CENTRIFUGATION



L. L. Bondoc Jr., BioPort Corporation, Lansing, MI, USA

Copyright © 2000 Academic Press

Viruses have proved to be detrimental as well as beneficial. They are notoriously infectious agents that are at the root of several major diseases in man, domesticated animals, and agricultural crops. However, their attenuated or noninfectious forms have been used as vaccines, enabling the development of immunity against particularly devastating diseases. Recently, replication-deficient viruses have been used as agents for gene delivery and as potential vaccine carriers, as they have evolved efficient mechanisms of infectivity.

Viruses are particulate in nature and are made up essentially of DNA or RNA, wrapped in a predominantly protein coat. They range in size from 20 to 2000 nm (0.02–2 μm) and in molecular weight from 4×10^6 to 2×10^9 Da. Many viruses possess an envelope that is typically derived from the host cellular membrane.

Initial isolation of viruses usually involves centrifugation, particularly density gradient centrifugation (DGC). For almost half a century DGC has been regarded as the most rapid, and reliable preparative procedure for the isolation of highly purified and concentrated virus preparations for subsequent physicochemical and biological characterization. As such, it is used as a benchmark against which alternative methods can be evaluated. To date the technique has permitted the isolation and subsequent characterization of a plethora of viruses belonging to at least 39 major families.

Centrifugal Separations

Although significant improvements in centrifugation hardware have led to increased operational efficien-

cies, the theory behind centrifugation and the variations of the technique as applied to viruses are well characterized. In a suspension of particles, the rate at which particles sediment when subjected to a centrifugal force depends on the nature of the particles, the nature of the medium, and the magnitude of the centrifugal force. For spherical particles, the sedimentation rate or velocity of the particle depends on a variety of factors as indicated in eqn [1], one of the many forms of the Svedberg equation:

$$dr/dt = [2r_p^2(\rho_p - \rho_m)\omega^2 r]/9\eta \quad [1]$$

where dr/dt is the velocity of the particle; r_p is the radius of the spherical particle; ρ_p is the density of the particle; ρ_m is the density of the medium; ω is the angular velocity; r is the radial distance of the particle from the axis of rotation; the product $\omega^2 r$ is proportional to the centrifugal force; and η is the viscosity of the medium. It is possible to define a particle in terms of its behaviour in a centrifugal field by manipulation of eqn [1] to yield a simplified version of the Svedberg equation (eqn [2]) that uses the sedimentation coefficient, s , where:

$$s = (dr/dt)/\omega^2 r \quad [2]$$

For most biological macromolecules, the magnitude of s is about 10^{-13} s, so this value is used as the unit of sedimentation, the Svedberg (S). The sedimentation coefficient for viruses varies between 40 and 4500 S, while for globular proteins it is 2–5 S.

Types of Separations

For a particular viral preparation, the most effective centrifugal separation procedure is one that yields a concentrate with significant recovery of bioactivity

and high quality based on several measures of purity. There are three types of centrifugal separations available for viruses: (1) differential centrifugation; (2) rate-zonal centrifugation; and (3) DGC or isopycnic centrifugation. Differential centrifugation separates particles according to size as well as density (from eqn [1]), since denser particles will form pellets at a faster rate than less dense particles of the same mass. By choosing an appropriate centrifugal force and centrifugation time, it is possible to clarify a viral suspension from contaminating fermentation debris by first pelleting the contaminants at a given g force and leaving the virus in suspension, then pelleting the virus at a higher g force. Viruses that are unstable when pelleted can be sedimented on a cushion or plug of material (e.g. caesium chloride, sucrose, potassium tartrate, Nycodenz (Nyegaard & Co.), and glycerol) that has a density higher than that of the viral particles. The major problems with this mode of separation are the low yields and low resolution from contaminants. Differential pelleting is often used for the initial processing of heterogeneous mixtures, to obtain fractions that are enriched in the virus particles of interest prior to further purification.

In rate-zonal centrifugation particles move at different rates depending upon their mass. To avoid the co-sedimentation of particles of different sizes, samples are typically layered as a narrow zone on top of a density gradient. The gradient is used to facilitate the layering of the sample and to minimize convection currents in the liquid column during centrifugation that would otherwise disrupt the particle zones as they move down the tube. Rate-zonal separations are ideal for particles of uniform size but not for particles of the same type that are heterogeneous in size. Furthermore, even though separation conditions can be optimized, it is not yet possible to recover the separated fractions as fractionated species. For viral preparations this mode of centrifugation is primarily used for characterizations, such as molecular weight determination and the determination of possible interactions with other molecules.

The most common method of centrifugal separation for viruses is DGC, or isopycnic centrifugation. In this process the particles move until their density is the same as that of the surrounding medium. The particles are separated purely on the basis of their density, and their size only affects the rate at which they reach their isopycnic positions. Because the separation is an equilibrium process, run times are generally much longer than for rate-zonal or differential centrifugation. Prolonged centrifugation does not affect the separation as long as the gradient remains stable and the activity and integrity of the particles

are not adversely affected by centrifugation. Materials are typically spun at 25 000–200 000 g for up to 20 h. Samples are loaded either on a pre-formed gradient or on self-forming gradient media.

Centrifugation Media

For isopycnic separations, the choice of media is important. There are several desirable characteristics for a medium, the most important being that the maximum density of the gradient is greater than that of the particles to be separated. In general viruses have buoyant densities in the range 1.1–1.5 g cm^{-3} . However, as a result of different levels of hydration of viral particles in different media, the densities of the particles can vary depending on the medium being used. The physico-chemical properties of the solutions of the gradient medium should be known, and it should be possible to determine the precise concentration of the medium using one or more of these properties (e.g. refractive index or densitometry). The medium should be inert and safe to use, and should not interfere with monitoring of the zones of fractionated material within the gradient (e.g. by ultraviolet or visible absorbance, radioactivity counting, protein determination, etc.). It should be easy to separate the sample material from the gradient medium (by dialysis, ultrafiltration, or centrifugation) without loss of the sample or sample activity. Ideally the medium should also form solutions of low ionic strength with low viscosity and be iso-osmotic with the virus.

Gradient media for DGC are either ionic or nonionic. Commonly used ionic media include caesium salts (e.g. caesium chloride), potassium salts, rubidium salts and sodium salts (e.g. sodium chloride). These materials are used to form solutions with maximum buoyant densities of 1.4–2.6 g mL^{-1} . Gradients of caesium salts, especially caesium chloride, are used almost exclusively for virus purification. They can be pre-formed using any of the standard techniques or they can be formed *in situ* by centrifugation. Solutions containing caesium salts are highly ionic, and while they are nonviscous, they all have high osmolarities. Gradients formed from these salts, differ with respect to their solubility, maximum density, activity and steepness, all of which can affect the banding of materials.

Nonionic gradient media can be subdivided into carbohydrates, iodinated gradient solutes, colloidal silica suspensions and proteins. Sucrose, a disaccharide, has been widely used for the isopycnic fractionation of viruses. Its popularity is due to its inertness towards biological materials, ready availability, low cost, and stability. The main disadvantages of sucrose

include its high osmotic strength, high viscosity, hypertonicity for solutions more concentrated than 9% (w/v) and rather low buoyant density of 1.03 g mL^{-1} . Sucrose gradients must be pre-formed for isopycnic fractionations.

To circumvent the problems that arise from fractionating osmotically sensitive particles in high osmotic strength sucrose solutions, several polysaccharides have been used as gradient media. These include glycogen, dextrans, and Ficoll (Pharmacia). Ficoll is produced by the chemical copolymerization of sucrose molecules with epichlorohydrin to give a polymer with a molecular weight of 400 kDa. Ficoll solutions below 20% (w/v), equivalent to a buoyant density of 1.07 g cm^{-3} , have a relatively low osmolarity, although at higher concentrations the osmolarity rises sharply. Gradients of Ficoll, which have a higher viscosity and better stability than sucrose gradients, must be prepared using a gradient mixer.

Most iodinated gradient media used in the separation of viruses are derivatives of triiodobenzoic acid to which hydrophilic groups have been attached to increase water solubility. The ionic forms of these compounds include the sodium or *N*-methylglucamine salts of metrizoate, diatrizoate, and iothalamate, and the nonionic forms include metrizamide and Nycodenz. These materials form stable solutions at buoyant densities up to 1.45 g cm^{-3} . Iodinated compounds have several advantages, including much lower osmolarities and viscosities than sucrose at all densities. Gradients of these media can be pre-formed or generated in place.

Colloidal silica gradients have been used for several years, but only one preparation, namely Percoll (Pharmacia), has been developed for centrifugation. In this particular preparation the silica particles are coated with polyvinylpyrrolidone, which minimizes their interaction with biological material and also stabilizes the colloid against freezing and thawing and the presence of salts. Its solutions are isoosmotic and its low viscosity facilitates the rapid banding of viruses. However, Percoll is precipitated at low pH and solutions of high ionic strength destabilize the colloidal suspension. Gradients of Percoll readily self-form, or can be pre-formed using a simple mixer. Percoll forms suspensions at buoyant densities up to 1.13 g cm^{-3} . The removal of Percoll from virus solutions can be problematic because Percoll particles (17–30 nm in diameter) are very close in size of some viruses.

Proteins have a hydrated buoyant density of approximately 1.27 g cm^{-3} and can be used as gradient media, but no applications to viruses have been reported.

Types of Gradients

Pre-formed gradients for DGC of viruses can be continuous or discontinuous. Continuous gradients may be linear, convex, or concave and are usually prepared using a dedicated gradient former. Discontinuous or step gradients are prepared by successively layering solutions of different density. Pre-formed gradients must be handled very carefully prior to centrifugation to avoid gradient disruptions caused by vibration or temperature variations. The virus sample itself, which must have a density less than that of the top of the gradient, is gently layered onto the gradient before centrifugation is started. To minimize changes in the density profile at the top of the gradient, the sample volume should be small compared with the gradient volume.

For self-forming gradients the initial sample volume is not a concern, as the sample is either mixed with a concentrated solution of the gradient solute or solid gradient solute is added to give the correct initial density. The duration of centrifugation for self-forming gradients is longer than that for pre-formed gradients since time is required to form the gradient.

Rotors

DGC can be carried out in all the available types of rotors. Preparative centrifuge rotors are classified into four main types, namely swing-out (swinging bucket), fixed angle, vertical, and zonal. In swing-out or horizontal rotors, the tubes of sample solutions are placed in individual buckets that move out perpendicular to the axis of rotation as the rotor rotates. This creates a long migration path to separate viruses along the density gradient and requires a long period to achieve significant separation. Horizontal rotors can be spun to attain maximum speeds corresponding to 100 000 g or more.

In fixed angle rotors the tubes are at a fixed angle (varying from 14° to 40°) to the axis of rotation, and when the rotor rotates the solution reorients in the tubes. This reorientation enhances the loading capacity of the isopycnic gradients. Rotors with shallow angles are more efficient at pelleting because the sedimentation pathlength is shorter. Fixed angle rotors are designed to operate up to very high centrifugal forces ($>600\,000 \text{ g}$).

As the name suggests, in vertical rotors the tubes are held in a vertical position, and centrifugal forces similar to those for fixed angle rotors can be achieved. When the vertical rotor turns, the solution begins to reorient through 90° . Vertical rotors thus have short sedimentation pathlengths, so the diameter of the

tube and the capacities of the gradients in these rotors are higher than in horizontal and fixed angle rotors.

Zonal rotors are often used for gradient separation. Although the sample is pumped into a hollow rotor chamber, the working principle of these rotors is similar to that for vertical rotors, as it is the gradient solution that reorients during the run, before the sample is introduced under centrifugation. There are two types of zonal rotors, namely batch and continuous flow, that differ based on the volume of sample they can be used to process. Batch type centrifugation is typically used for 10–200 mL samples while for larger sample volumes of 100 L or more, continuous flow centrifugation is required. For volumes 200 mL to 100 L, vertical rotors can be used.

Recovery

Recovery of viral particles from DGC is performed either manually or automatically. After centrifugation density gradients can be recovered or unloaded from the bottom, middle or the top of the tube. The methods for unloading gradients from the bottom of the tube include bottom puncture of the tube or withdrawal using a narrow tube inserted through the gradient to the bottom. Targeted bands from within the gradient can also be unloaded by puncturing the tube at the appropriate position. The methods for unloading gradients from the top of the tube include direct unloading from the top or collection by upward displacement of the gradient by introducing a dense, preferably immiscible liquid at the bottom of the centrifuge tube. Automated collection systems with flow-arrest or volumetric monitoring are available commercially. Automated recovery systems require a heavy displacement solution such as 65% sucrose or Maxidens (Nyegaard & Co.), an inert, nonviscous organic liquid immiscible with aqueous gradients. Great care must be taken in fractionating gradients after centrifugation since resolution is easily lost at this stage. All operations should be designed to minimize disturbance of the gradient.

Conclusion and Future Developments

DGC is still the method of choice for the initial, relatively quick isolation of novel viral particles. The gradient medium, gradient shape, type of rotor, and mode of recovery are determined empirically,

for a particular viral preparation, to yield the highest possible recovery of bioactive purified virus and permit subsequent characterization and use.

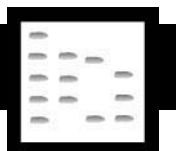
The advent of gene therapy using viruses for gene delivery or as vaccine carriers has encouraged the development of scaleable procedures for virus isolation and purification based on centrifugation. With this impetus gradient media, rotor designs, and modes of recovery continue to be improved.

See also: II/Centrifugation: Theory of Centrifugation.

Further Reading

- Bondoc LL Jr and Fitzpatrick S (1998) Size distribution analysis of recombinant adenovirus using disc centrifugation. *Journal of Industrial Microbiology & Biotechnology* 20: 317–322.
- Brakke MK (1951) Density gradient centrifugation: a new separation technique. *Journal of the American Chemical Society* 73: 1847–1848.
- Cantor CR and Schimmel PR (1980) *Biophysical Chemistry. Part II: Techniques for the Study of Biological Structure and Function*. San Francisco: W.H. Freeman and Company.
- Croyle MA, Anderson DJ, Roessler BJ and Amidon GL (1998) Development of a highly efficient purification process for recombinant adenoviral vectors for oral gene delivery. *Pharmaceutical Development and Technology* 3: 365–372.
- Foster GD and Taylor SC, eds (1998) *Plant Virology Protocols*. Totowa: Humana Press.
- Griffith OM (1986) *Techniques of Preparative, Zonal, and Continuous Flow Ultracentrifugation*, 5th edn. Palo Alto: Beckman Instruments.
- Mushahwar DC, Erker JC, Muerhoff AS *et al.* (1999) Molecular and biophysical characterization of TT virus: evidence for a new virus family infecting humans. *Proceedings of the National Academy of Sciences U.S.A.* 96: 3177–3182.
- Myers TM, Smallwood S and Moyer SA (1999) Identification of nucleocapsid protein residues required for Sendai virus nucleocapsid formation and genome replication. *Journal of General Virology* 80: 1383–1391.
- Payment P and Trudel M (1993) *Methods and Techniques in Virology*. New York: Marcel Dekker Inc.
- Rickwood D, ed. (1984) *Centrifugation: A Practical Approach*, 2nd edn. Oxford: IRL Press Limited.
- Soeda E, Krauzewicz N, Cox C *et al.* (1998) Enhancement by polylysine of treatment of transient, but not stable, expression of genes carried into cells by polyoma VP1 pseudocapsids. *Gene Therapy* 5: 1410–1419.

VITAMINS



Fat-Soluble: Thin-Layer (Planar) Chromatography

W. E. Lambert and A. P. De Leenheer,
Universiteit Gent, Gent, Belgium

Copyright © 2000 Academic Press

Introduction

Thin-layer chromatography (TLC) is a very widely used chromatographic technique allowing the separation of simple mixtures followed by a qualitative identification or a semiquantitative visual analysis of the samples. All this can be performed in an inexpensive and simple way without requiring highly sophisticated instrumentation.

On the other hand, high performance thin-layer chromatography (HPTLC) is a highly instrumental technique allowing fast and very efficient separations with quantitative results of accuracy and precision rivalling those obtained by the far more popular techniques such as high performance liquid chromatography (HPLC) and gas chromatography (GC). The small particle size (5 μm) and the more uniform layer of the stationary phase of the commercially pre-coated HPTLC plates are responsible for this increased efficiency and sensitivity.

This article focuses on the specific separation of fat-soluble vitamins by TLC. Strategies from sample preparation, stationary phases, mobile phases and detection modes will be discussed for each vitamin separately. However, from the recent reviews published biennially in *Analytical Chemistry* it can be seen that the number of new applications of TLC to the analysis of fat-soluble vitamins is diminishing all the time.

The chemistry (stability) of the different compounds, will be treated because of its importance in TLC analyses.

Vitamin A

The structures of vitamin A and of some related compounds are presented in Figure 1. The parent compound, all-*trans*-retinol or vitamin A, is an isoprenoid structure with five conjugated double bonds resulting in an absorption maximum at 325 nm (in *n*-hexane or ethanol), in a high molar extinction coefficient and in a sensitivity of the compound towards isomer formation and/or oxidation. The formation of isomers is catalysed by light and iodine while the relative amount of the isomers depends on the wavelength and on the solvent used. The four exocyclic double bonds can theoretically result in the formation of 16 isomers. All have been characterized. An increase in the number of *cis* bonds generally results in a lower absorption maximum as well as a decrease of the molar extinction coefficient relative to the all-*trans* isomer. Vitamin A and the Vitamin A-related compounds are also sensitive towards oxidation and peroxidation by contact with air. The presence of transition group metals is known to catalyse this reaction.

To prevent degradation it is imperative to take special precautions when working with vitamin A-related compounds, for example, storing the samples at very low temperature, working under subdued light, avoiding drastic reagents and contact with air or peroxide-containing organic solvents.

The lability of these compounds makes research in the vitamin A field a real analytical challenge. Especially during the TLC process, special precautions are necessary, as will be described below.

Chromatographic Conditions

TLC on polar inorganic nonmodified sorbents such as alumina and silica remains very popular. Silica plates can be activated by heating at 120°C for 1 h in an attempt to enhance resolution, while spraying the plates with a solution of an antioxidant has been reported to prevent degradation of the compounds on the plates.

As with what is known from liquid chromatography, chromatographic systems based on silica plates with eluents of hexane, petroleum ether or cyclohexane, with a variable amount of a more polar solvent such as 8% diethyl ether, 50% diethyl ether or 20% ethyl acetate, offer the best separation of the geometric isomers of vitamin A compounds. In a similar way, high performance silica gel thin-layer

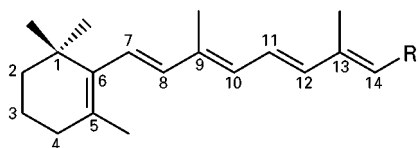


Figure 1 Structure of vitamin A. Related compounds include retinol ($\text{R}=\text{CH}_2\text{OH}$), retinal ($\text{R}=\text{CHO}$), retinoic acid ($\text{R}=\text{COOH}$) and retinyl palmitate ($\text{R}=\text{CH}_2\text{OCO}(\text{CH}_2)_{14}\text{CH}_3$).

Table 1 Representative R_F values of geometric isomers of vitamin A compounds

Compound	a	b	c	d
<i>Retinol</i>				
All- <i>trans</i>	0.09	0.14	0.21	
9- <i>cis</i>		0.17	0.23	
13- <i>cis</i>		0.23	0.28	
11- <i>cis</i>	0.12	0.28	0.28	
<i>Retinal</i>				
All- <i>trans</i>	0.27	0.47	0.46	
9- <i>cis</i>		0.52	0.50	
11- <i>cis</i>	0.47	0.58	0.53	
13- <i>cis</i>		0.60	0.55	
<i>Retinoic acid</i>				
All- <i>trans</i>				0.34
13- <i>cis</i>				0.39

a, Silica gel: hexane-ether (92:8, by vol.); b, silica gel: hexane-ether (50:50, by vol.); c, silica gel: cyclohexane-toluene-ethylacetate (50:30:20, by vol.); d, silica gel: diethyl ether-cyclohexane-acetone-glacial acetic acid (40:60:2:1, by vol.).

plates eluted with diethyl ether-cyclohexane-acetone-glacial acetic acid allows the separation of all-*trans*- and 13-*cis*-retinoic acid in gel formulations (Table 1). Separation of vitamin A from the lipophilic vitamins is also possible on silica plates eluted with mixtures of benzene-petroleum ether-acetic acid. Under these conditions the water-soluble vitamins remain at the origin. Very often, classical TLC on silica plates serves as a kind of clean-up step before offline quantification, e.g. for the quantification of vitamin A in fruits and vegetables. With the introduction of the smaller HPTLC plates, more efficient separations together with shorter development times are possible. This has allowed the quantitative determination of retinol and of α -tocopherol in plasma with tocopheryl acetate as an internal standard.

In isolated cases kieselguhr plates or talc, starch or cellulose thin layers have been impregnated with 10% paraffin oil in cyclohexane. This was applied to a study of the hydrophobicity of a number of vitamin A-related compounds and for a separation of vitamin A-acetate from vitamin A-palmitate. For these studies the impregnated plates were eluted with mixtures of methanol-water (95:5, by vol.) and of acetone-concentrated acetic acid (30:20, by vol.).

Both the elution order of the compounds under investigation and the composition of the elution solvents clearly demonstrate a reversed-phase type of retention under these conditions.

Reversed-phase stationary phases such as RP-2 or C₁₈ are also used in the analysis of vitamin A-related compounds. The separation on the RP-2 phase, how-

ever, is less efficient than that obtained on paraffin oil-impregnated kieselguhr. Separation on a C₁₈ phase and on a silica phase (on one single plate) has been used in a two-phase two-dimensional TLC determination of all-*trans*- and 13-*cis*-retinoic acid in cream samples. The reversed-phase step served to separate the retinoic acid isomers from the cream excipients, while the silica sorbent was ideally suited for the separation of the two isomers from each other. Generally, on reversed-phase TLC plates, methanol or acetonitrile can separate retinol from retinyl acetate while dichloroethane with acetonitrile can separate the long chain retinyl esters.

Detection

Quenching the fluorescence of the indicator fixed on the thin-layer plate itself (F_{254}) is a very common and nondestructive way to localize spots on a TLC plate. Of course, this can also be applied to vitamin A compounds. Retinol and retinyl esters on the other hand can be identified by the yellow-green fluorescence they exhibit under 366 nm UV light. Other techniques to visualize vitamin A compounds include absorption of iodine vapours (with the formation of brown spots) or destructive procedures such as spraying with sulfuric acid.

Other spray reagents include SbCl₃ or SbCl₅ solutions in chloroform, a 5% solution of phosphomolybdic acid in ethanol and a mixture of equal volumes of a 1% aqueous solution of potassium permanganate and a 5% aqueous solution of sodium carbonate. After heating the plate coloured spots appear for vitamin A. The same reagents are often applied to visualize vitamins D and E.

As an alternative a large array of dyes has been evaluated as visualizing agents for fat-soluble vitamins, including vitamin A. The different dyes (aniline blue, alkaline blue, brilliant green, neutral red, bromocresol green, bromothymol blue, thymol blue, phenol red, helasol green, brilliant cresyl blue and bromophenol blue) are used as a solution of 50 mg of the dye either in 100 mL of water or in 100 mL of a 2% aqueous sodium hydroxide solution. Evaluation of the plates is then performed 20 min after spraying or after acceleration of the reaction by heating the plates at 110°C for 15 min.

For quantitative measurements, densitometric evaluation can be applied to vitamin A compounds. In this way, absorbance can be measured by diffuse reflectance at 290 nm using a mercury lamp, while UV spectra can be recorded between 200 and 400 nm with a deuterium lamp. Detection limits for retinol using this technique are around 160 ng mL⁻¹ using 200 μ L plasma. By using tocopheryl acetate as an

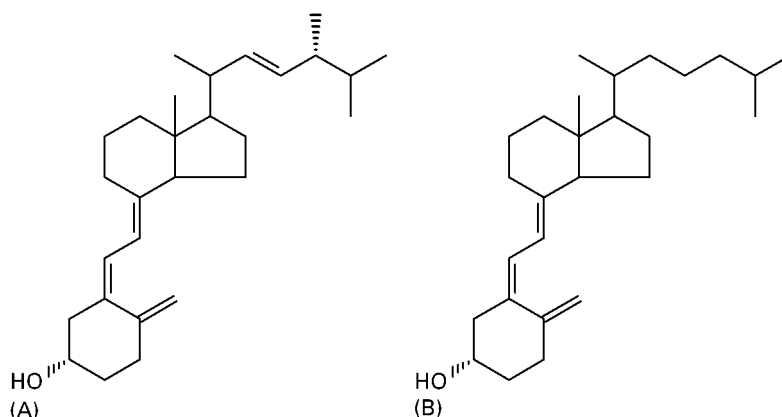


Figure 2 Structure of (A) vitamin D₂ (ergocalciferol) and (B) vitamin D₃ (cholecalciferol).

internal standard, the coefficient of variance (inter plate and intra plate) can be kept below 12.5%.

Using the dyes as a visualizing agent, the highest sensitivity on a silica plate can be obtained with bromophenol blue (in 2% aqueous sodium hydroxide) without heating the plate. Under these conditions 3 µg can be visualized. The same reagent applied on a partition-type TLC plate (silica gel impregnated with a 5% solution of paraffin oil in chloroform) resulted in a fivefold decrease in sensitivity towards vitamin A.

Vitamin D

Vitamin D and its structural analogues are a group of 9,10-seco-steroids: their basic structures are shown in **Figure 2**. The D₂ series (ergocalciferol) is of vegetable origin and has a side chain derived from ergosterol containing an additional C₂₂₋₂₃ double bond and a C₂₄ methyl group, whereas vitamin D₃ (cholecalciferol) is formed in the skin of humans and animals and has a side chain derived from cholesterol. The conjugated system of three bonds results in a molar extinction coefficient of 18 300 L mol⁻¹ cm⁻¹ with a λ_{max} at 264 nm. Both analogues are derived photochemically from their respective precursor (provitamin D). Indeed, irradiation of this provitamin D results in various photolysis products such as tachysterol, lumisterol and pre-vitamin D. Pre-vitamin D then undergoes spontaneous rearrangement to vitamin D. In the human body vitamin D₃ is extensively metabolized. The liver converts it to 25-hydroxy vitamin D₃ while further hydroxylation in the kidney yields, among others, 1,25-dihydroxy vitamin D₃. As with vitamin A, protection from light and from air is of great importance for the analysis of vitamin D by TLC.

TLC and, recently, HPTLC have found several applications in vitamin D analysis, including differen-

tiation of vitamin D analogues, separation of vitamin D from other lipids (e.g. sterols, other fat-soluble vitamins), determination of the purity of radiolabelled vitamin D derivatives and analysis of vitamin D metabolites as a part of radioligand assays.

Chromatographic Conditions

Polar inorganic sorbents such as silica gel or, occasionally, alumina have been applied to the separation of vitamin D analogues. In this way, provitamin D₃, tachysterol₃, lumisterol₃ and pre-vitamin D₃ were separated on silica gel and the eluting order of the compounds could be correlated with the increasing planarity of the compounds. Vitamins D₂ and D₃ can be separated on their basis of their hydrophobicity; the double bond in the hydrocarbon chain of vitamin D₂ results in lower hydrophobicity compared with vitamin D₃. This was proven by comparing the R_F values of the two compounds both in an adsorption system (silica gel eluted with benzene-methanol, 9:1) and in a partition system. For the latter experiment, kieselguhr plates impregnated with a 10% solution of paraffin oil in benzene were eluted with different mixtures of methanol-water or acetonitrile-water. In spite of the extra methyl function in the side chain of D₂ the double bond makes this compound more polar than D₃, as demonstrated by their R_F values in the latter system (**Table 2**).

For the separation of vitamin D from other lipids, e.g. in foods, in most cases silica gel plates are applied. In cases where vitamin D has to be separated from sterols (cholesterol, β -sitosterol, stigmasterol or lanosterol), however, alumina may be the preferred stationary phase because silica gel can show too high an adsorption strength towards free sterols.

In particular cases, multiple development of the plates may be necessary, e.g. when vitamin D has to be determined in cod liver oil. Despite the availability of column chromatographic procedures or, more

Table 2 Representative R_F values of vitamins D_2 and D_3^a

Eluent	Compound	
	D_2	D_3
<i>Methanol-water (v/v)</i>		
100:0	0.78	0.74
95:5	0.56	0.48
90:10	0.36	0.33
85:15	0.18	0.15
80:20	0.05	0.04
<i>Acetonitrile-water (v/v)</i>		
100:0	0.60	0.55
95:5	0.50	0.41
90:10	0.38	0.29
85:15	0.29	0.25
80:20	0.23	0.17
75:25	0.12	0.09

^aKieselguhr impregnated with 10% paraffin oil in benzene.

recently, of HPLC, TLC is still used in the clean-up of extracts of lipid-rich matrices such as foods, tissues, oils or multivitamin preparations. The same even holds true for applications of TLC in the sample preparation step for separation of the different metabolites of vitamin D. Of course, in biological matrices the content of the vitamin D metabolites is too low to allow visualization by spray reagents. Typically, the areas corresponding to the compounds of interest are then scraped off and wetted with a small volume of solvent to make it directly amenable to a quantitative radioligand determination.

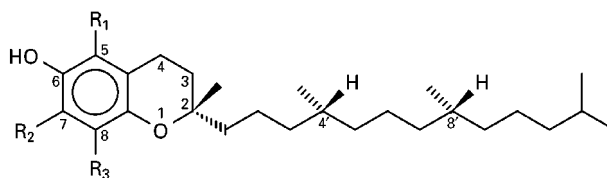
Silica gel and silica gel impregnated with silver nitrate have also been used to monitor the purity of radiolabelled vitamin D. The advantage of the application of TLC for this type of study is based on the fact that TLC offers a total picture of all impurities, whereas in liquid chromatography it can never be totally excluded that some impurities are not eluted.

Polar organic sorbents (e.g. cellulose) or nonpolar bonded phases are infrequently used in vitamin D analysis by TLC. However, separation on kieselguhr plates impregnated with paraffin oil, described above, clearly demonstrates that nonpolar bonded phases are worth evaluation for the separation of D_2 from D_3 .

Detection

Although not very sensitive, UV absorbance or fluorescence quenching (the latter on plates containing a fluorescence indicator) are universal procedures that are valid for the detection of vitamin D.

Iodine vapours, 0.005% aqueous solution of fuchsin or a 0.05% aqueous solution of bromocresol



Compound	R_1	R_2	R_3
α -Tocopherol	CH_3	CH_3	CH_3
β -Tocopherol	CH_3	H	CH_3
γ -Tocopherol	H	CH_3	CH_3
δ -Tocopherol	H	H	CH_3

Figure 3 Structure of tocopherols.

green, can also be used to visualize vitamin D-related compounds.

As already mentioned, for quantification purposes of vitamin D-related compounds, TLC is often incorporated as a clean-up step before offline measurement either by gas chromatography-mass spectrometry (GC-MS) or radioimmunoassay (RIA). This clean-up function offers a certain future for TLC and HPTLC, especially for laboratories specializing in RIA and lacking HPLC equipment.

Vitamin E

Vitamin E is a collective term for tocopherols and tocotrienols, a series of potent antioxidants derived from 6-chromanol by substitution with a saturated (tocopherols) or partially unsaturated (tocotrienols) isoprenoid side chain and one to three methyl functions (Figure 3). The principal form is α -tocopherol (5,7,8-trimethyltolcol) which in nature occurs in the 2*R*, 4'*R*, 8'*R* configuration. Tocol can be regarded as the unsubstituted parent molecule, while α -, β - and γ - and δ -tocopherol form a homologue series of tri-, di- and monosubstituted tocols, respectively. The dimethyltolcols (β - and γ -tocopherol) are positional isomers.

All vitamin E derivatives have strong reducing properties, with α -tocopherol being the most biologically active homologue. By scavenging free radicals and other oxidative species, α -tocopherol is known to protect membrane lipids from peroxidation. Other functions described for vitamin E remain more controversial. In the absence of air, vitamin E derivatives are quite stable to heat and alkali. However, in the presence of air they are rapidly oxidized by alkali and metal ions. Vitamin E derivatives absorb light in the UV region (λ_{max} 292–295 nm; ϵ 3530 L mol⁻¹ cm⁻¹) and they are natively fluorescent (λ_{ex} 205 and 295 nm; λ_{em} 330 nm).

Table 3 TLC conditions for vitamin E-related compounds^a

Compounds	Mobile phase	Visualization	Comments
α -Tocopherol in rat liver	1D: Benzene-ethanol (99:1, v/v) 2D: Hexane-ethanol (9:1, v/v)	20 h at 110–120°C	
α -, γ -, δ -Tocopherol in feeds, oils	Petr.ether-diethyl ether-acetic acid (90:10:1, v/v)	0.004% 2,7-dichlorofluorescein	β -Tocopherol and γ -tocopherol co-migrate
α -Tocopherol in pig organs	1D: Benzene-ethanol (99:1, v/v) 2D: Hexane-ethanol (9:1, v/v)	Ethanol bathophenanthroline-FeCl ₃	
α -, β -, δ -Tocopherol and α -Tocopherol ₃ in algal lipids	Hexane-isopropylether (85:15, v/v)	15 min at 100°C 10% copper(II) sulfate phosphoric acid 10 min at 190°C	β -Tocopherol and γ -tocopherol co-migrate
α -, β -, γ -, δ -Tocopherol and α -, β -, γ -, δ -tocopherol ₃ in cereals and plant oils	1D: Chloroform 2D: Hexane-isopropylether (80:20, v/v)		γ -Tocopherol and β -tocopherol ₃ co-migrate

^aAll separations were done on silica plates.

Chromatographic Conditions

For TLC separation of vitamin E derivatives, silica gel plates have been widely used. Within the group of tocopherols migration is correlated with the degree of ring methylation. However, for the separation of β - from γ -tocopherol (two dimethyl tocols), often two-dimensional TLC is necessary with an eluent based on petroleum ether and diisopropyl ether for the second TLC run (Table 3).

Resolution of the naturally occurring tocopherols and tocotrienols also requires two-dimensional TLC. The separation between β -tocotrienol and γ -tocopherol, in particular, remains an analytical challenge. Both capillary GC and HPLC have now replaced TLC approaches, but the solvents used in HPLC often rely on solvent systems applied in earlier TLC separations.

Traditionally, TLC on silica gel or on alumina has also played an important role in the clean-up of extracts of biological materials for the spectrophotometric analysis of tocopherols/tocotrienols in the presence of a large excess of interfering lipids. The whole procedure, however, often included saponification, extraction, column chromatography and two successive TLC runs before the final spectrophotometric measurement.

Both silica gel and alumina lend themselves to separation of tocopherols from their decomposition products (α -tocopherylquinone, α -tocopherylhydroquinone) from other fat-soluble vitamins or from other lipophilic antioxidants such as butylated hydroxytoluene, butylated hydroxyanisole, ethoxyquin, gallate esters and ascorbyl palmitate.

More recently, reversed-phase chromatographic conditions have been evaluated for the separation of α -, β -, γ - and δ -tocopherol. Kieselguhr G plates impregnated with a 10% solution of paraffin oil in benzene and eluted with methanol-water (9:1, by

volume) offer the best separation. Of the four tocopherols considered, the difference between the R_F values of β - and γ -tocopherol was small.

Alternatively, reversed-phase C₁₈ plates have also been applied to the separation of α -tocopherol from other antioxidants or from the other tocopherols. A new and interesting trend consists of the separation of D and L enantiomers of tocopherol on chiral plates (stationary phase, chiral plate solvent: propanol-water-methanol (8.5:1.0:0.5, by volume) activated by heating at 100°C for 15 min). Because of the different biological activities of both enantiomers, this type of separation should be further investigated.

Detection

The commonest mode of detecting tocopherols and tocotrienols on TLC plates is based on quenching the fluorescence of supports impregnated with a fluorescent indicator. Alternatively, tocopherols and tocotrienols can be visualized by nonspecific procedures such as charring preceded by spraying with sulfuric acid, perchloric acid, nitric acid or 10% copper(II) sulfate in 8% phosphoric acid. More specific visualization procedures are based on the reducing properties of the vitamin E-related compounds. In this way, ferric ions are reduced to ferrous ions which react with α , α' -dipyridine or bathophenanthroline to form a red-coloured complex (Emmerie-Engel reaction). Phosphomolybdic acid and a 20% antimony pentachloride solution in chloroform both produce characteristic colour reactions allowing β -tocopherol to be distinguished from γ -tocopherol, or all four tocopherols from each other. Quantification of vitamin E-related compounds after TLC separation can be performed either off-plate or on-plate. Off-plate methods include scraping the areas of interest from the plate and eluting the compounds with an organic solvent, followed either by a colorimetric measurement or

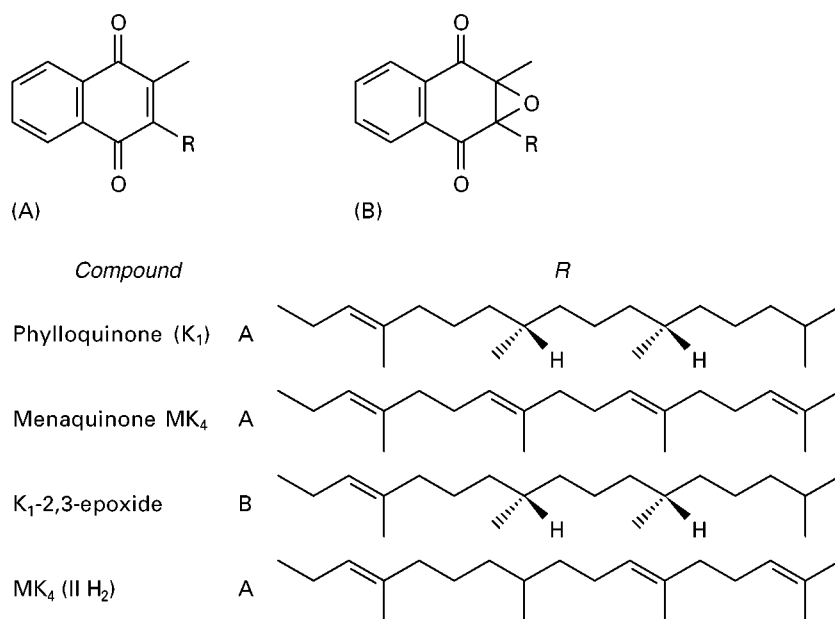


Figure 4 Structure of vitamin K and related compounds.

by GC determination. On-plate quantification is based on densitometry of the coloured spots obtained with chromogenic spray reagents, on the native UV absorbance or on the native fluorescence properties of the compounds of interest.

Vitamin K

All K-vitamins are derivatives of the same 2-methyl-1,4-naphthoquinone nucleus. The number of isoprene units or the number of carbon atoms in the side chain can be used to characterize the molecules. Accordingly, MK_4 contains four isoprene units, or $K_{1(20)}$ has 20 carbon atoms in the side chain (Figure 4). Three molecules, each representative of a particular group of K-vitamins, are of special importance:

1. Phylloquinone (Vitamin $K_{1(20)}$) is synthesized by green plants and is found in chloroplasts of photosynthetic plants. Epoxidation of the double bond between carbons 2 and 3 of the naphthoquinone nucleus results in $K_{1(20)}$ -epoxide
2. Menaquinone- n , also called MK_n , is characterized by a propenyl side chain often containing a large number of isoprene units (up to 13), with n indicating the number of units. Menaquinones (ranging from MK_4 to MK_{13}) are synthesized by bacteria (e.g. *Escherichia coli* and *Staphylococcus aureus*)
3. Synthetic vitamin K_3 (menadione or MK_0) does not occur in nature. In the body, menadione exhibits vitamin K activity by virtue of its *in vivo*

conversion to menaquinones, chiefly MK_4 , by microorganisms or by alkylating enzymes.

Phylloquinone and the other K-vitamins are destroyed in alkaline media and are sensitive to daylight (isomer formation). The K-vitamins are easily reduced but are fairly stable towards oxidizing conditions and heat. Both vitamin $K_{1(20)}$ and MK_n show a characteristic UV absorption spectrum with maxima at 244, 249, 263, 270 and 331 nm (in methanol). Their molar extinction coefficient at 249 nm is of the order of $20\,000\text{ L mol}^{-1}\text{ cm}^{-1}$.

Chromatographic Conditions

TLC procedures for vitamin K can be divided into three main types:

1. adsorption chromatography on silica plates for the separation of *cis-trans* isomers
2. argentation chromatography (also on silica layers) to separate saturated and unsaturated homologues of vitamin K
3. reversed-phase chromatography for the separation of methylated and demethylated K-vitamins

These three systems are complementary and will be treated below.

One major advantage of TLC on silica gel is that silica gel has little or no tendency to catalyse the degradation of vitamin K. This is in contrast to alumina-based separations. Separations on silica are mainly based on differences in polarity, which makes the procedure the method of choice for the isolation

of vitamin K from other lipids. In this way, TLC on silica plates developed with light petroleum ether–diethyl ether (85:15, by volume) is included in the sample preparation for the determination of vitamin K in lipid-rich animal tissues. Although no recent publications have been found, TLC on silica plates is especially suited for the separation of geometric isomers (*cis-trans* isomers).

Silica plates have been impregnated with 5–20% silver nitrate. Under these conditions lipids containing unconjugated double bonds in their side chain form complexes with the silver ions and show a higher retention than the saturated counterparts. Consequently, separation between saturated ($K_{1(20)}$), partly saturated [MK-*n* (H_n)] and fully unsaturated homologues (MK-*n*) becomes possible. On the other hand, in argentation chromatography the resolution between *cis* and *trans* isomers is completely lost. Silver ions are not destructive for vitamin K, so samples can be eluted from the silica afterwards. However, for high molecular weight menaquinones, irreversible adsorption to argentation TLC plates has been reported.

Unlike in argentation TLC, where retention is correlated to the degree of unsaturation, in reversed-phase TLC the retention is based on the length of the side chain. Both techniques are thus perfectly complementary for the separation of menaquinones.

In addition to silica plates and argentation TLC, reversed-phase TLC has been applied to vitamin K-related compounds. Typical eluents consist of water and an organic solvent such as methanol, acetonitrile or tetrahydrofuran. However, because of wettability problems with aqueous solvents, often nonaqueous reversed-phase conditions are used with dichloromethane and methanol (70:30, by vol.) as eluting solvent.

Detection

As with the other fat-soluble vitamins, fluorescence quenching can be applied to localize the position of vitamin K-related compounds on a TLC plate. More sensitive but often destructive for the compounds of interest include spray reagents such as 70% perchloric acid (5–10 min at 105°C), a 0.05% solution

of rhodamine B in ethanol, a 0.2% anilinonaphthalene sulfonic acid solution in methanol and a 10% solution of phosphomolybdic acid in ethanol.

Again densitometry (based on reflectance, transmission) has completely replaced visual inspection as well as the offline quantification after elution of the bands. Densitometry allows internal standardization and results in a higher degree of sensitivity and speed of analysis.

General Conclusions

From the above overview it should be clear that TLC is no longer the method of choice for the analysis of fat-soluble vitamins. The major reason for this lies in the great progress made in HPLC. Newer trends such as HPTLC and densitometric scanning may give TLC a new momentum but never to the extent that it will again supersede HPLC as a routine technique for the determination of fat-soluble vitamins in foods or biological materials. Undoubtedly, however, modern instrumental TLC can offer automation, improved repeatability and more accurate quantification compared to classical TLC.

See also: II/Chromatography: Thin-Layer (Planar): Spray Reagents. III/Vitamins: Liquid Chromatography.

Further Reading

- De Leenheer AP, Lambert WE and Nelis HJ (1992) *Modern Chromatographic Analysis of Vitamins*. New York: Marcel Dekker.
- De Leenheer AP and Lambert WE (1996) Lipophilic vitamins. In: Sherma J and Fried B (eds) *Handbook of Thin-layer Chromatography*, 2nd edn, pp. 1055–1077. New York: Marcel Dekker.
- Friedrich W (1988) *Vitamins*. Berlin: Walter de Gruyter.
- Poole CF and Poole SK (1994) Instrumental thin-layer chromatography. *Analytical Chemistry* 66: 27A–37A.
- Sherma J (1994a) Modern high performance thin-layer chromatography. *Journal of AOAC International* 77: 297–306.
- Weins C and Hauck HE (1996) Advances and developments in thin layer chromatography. *LC-GC International* 9: 710–717.

Liquid Chromatography

M. H. Bui, Swiss Vitamin Institute,
University of Lausanne, Lausanne, Switzerland

Copyright © 2000 Academic Press

Introduction

Vitamins are a group of organic compounds essential to life in very low concentrations. They are either

insufficiently produced by the body or not at all. Inadequate vitamin intake causes deficiency disorders in both humans and animals. The various vitamins are not related to each other chemically and have quite different properties. Two main groups, the fat-soluble and the water-soluble vitamins, may be distinguished.

Increased interest in vitamin research, together with the requirements of food and pharmaceutical quality control, have led to a proliferation of methods for vitamin assay, especially by liquid chromatography (LC). Bioassay methods are no longer used, but microbiological methods, physicochemical methods and chromatographic procedures (thin-layer chromatography, gas chromatography and liquid chromatography) are commonly employed. Classical open-column liquid chromatography is occasionally used, but modern high performance liquid chromatography (HPLC) is by far the technique of choice for vitamin analysis and is the subject of this article.

Vitamin analysis is performed to establish the vitamin status of humans or animals, to determine the potency of foods and feeds, and to monitor the storage stability of vitamin-containing pharmaceutical preparations. Information on the physicochemical and biochemical aspects of vitamins and vitamin intake is widely available in the literature (see Further Reading).

Sample Preparation

Vitamin A, the carotenoids, and vitamins E, D and K belong to the group of fat-soluble vitamins, which are soluble in organic solvents. The water-soluble vitamins B₁, B₂, B₆, B₁₂, C, biotin, folic acid, pantothenic acid, niacin, choline and inositol are soluble in water (Table 1). The structures of some fat-soluble and water-soluble vitamins are shown in Figures 1 and 2.

Sample preparation prior to the final chromatographic analysis is highly dependent upon the nature of the matrix. Minimal preparation is necessary for the analysis of concentrated solutions. For complex biological matrices more elaborate sample preparation procedures may be necessary. A 'recovery test' is highly recommended. This consists of adding a known amount of pure vitamin, approximatively equal to the estimated value in the sample, and processing the fortified sample in the same way as the sample itself. Loss of vitamin during analysis should not exceed 6%.

Fat-Soluble Vitamins

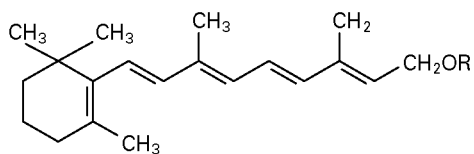
For fat-soluble vitamin assays all manipulations must be carried out in subdued light, in dark glass vessels, and in a nitrogen atmosphere to avoid isomerization and oxidation.

In foodstuffs, major interferences in assays for vitamin A, carotenoids, and vitamins E, D and K are caused by the large excess of other lipids. The vitamin A, carotenoids, and vitamins E and D contents are measured generally after alkaline hydrolysis with ethanolic KOH under a nitrogen stream at 60–80°C for 20–30 min in the presence of an antioxidant. Pyrogallol, hydroquinone, ascorbic acid (vitamin C) and butylated hydroxytoluene (BHT) are the most common antioxidants used during this manipulation. After saponification the free retinol, carotenoids, vitamin E and vitamin D are extracted into *n*-hexane or petroleum ether and evaporated to dryness. Vitamin A, carotenoids and vitamin E are redissolved in an organic solvent compatible with the chromatographic method to be employed. Vitamin K needs milder conditions for extraction from protein. Both vitamins D and K may require further purification before chromatography.

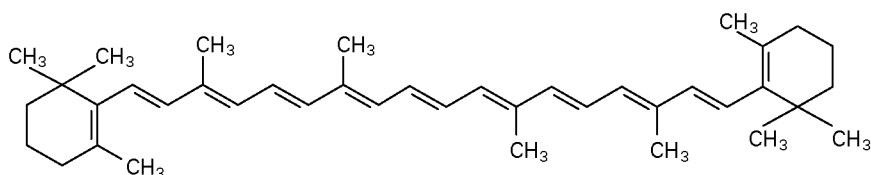
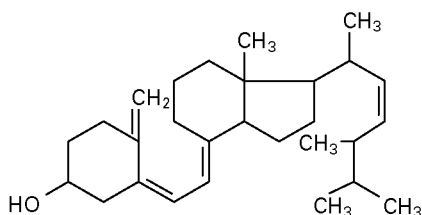
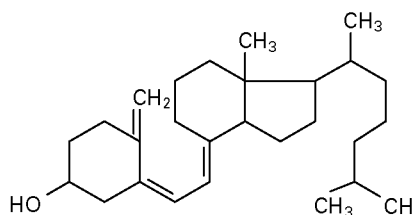
In the analysis of serum, vitamin A or retinol is liberated from its binding protein by denaturation with acetonitrile, ethanol or methanol. An internal

Table 1 Different kinds of vitamins

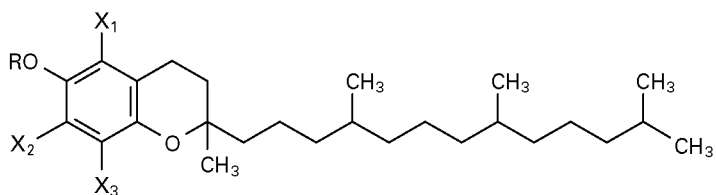
<i>Fat-soluble vitamins</i>	<i>Water-soluble vitamins</i>
Vitamin A (retinol)	Vitamin B ₁ (aneurin, thiamin)
Carotenoids	Vitamin B ₂ (riboflavin)
Vitamin D (ergocalciferol, vitamin D ₂ ; cholecalciferol, vitamin D ₃)	Vitamin B ₆ (pyridoxine, pyridoxal, pyridoxine, pyridoxol)
	Vitamin B ₁₂ (cyanocobalamin)
Vitamin E (α -, β -, γ -tocopherols plus tocotrienols)	Vitamin C (ascorbic acid dehydroascorbic acid)
Vitamin K (phyloquinone, vitamin K ₁ ; menadione, vitamin K ₃)	Biotin
	Folic acid (vitamin B ₉)
	Pantothenic acid (vitamin B ₅ , panthenol)
	Niacin (nicotinamide, vitamin PP)
	Choline
	Inositol (<i>myo</i> -inositol)

Vitamin A

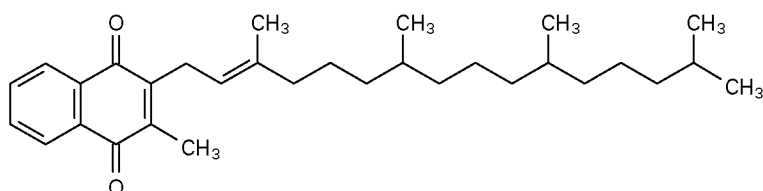
Retinol R = H
 Retinylacetate R = CO · CH₃
 Retinylpalmitate R = CO · (CH₂)₁₄ · CH₃

Provitamin A*β*-Carotene**Vitamin D****Vitamin D₂**
Ergocalciferol**Vitamin D₃**
Cholecalciferol**Vitamin E**

Tocopherol



	X ₁	X ₂	X ₃	R
α-Tocopherol	CH ₃	CH ₃	CH ₃	H
β-Tocopherol	CH ₃	H	CH ₃	H
γ-Tocopherol	H	CH ₃	CH ₃	H
δ-Tocopherol	H	H	CH ₃	H
α-Tocopherol acetate	CH ₃	CH ₃	CH ₃	CO · CH ₃

Vitamin K**Figure 1** Chemical structures of some fat-soluble vitamins.

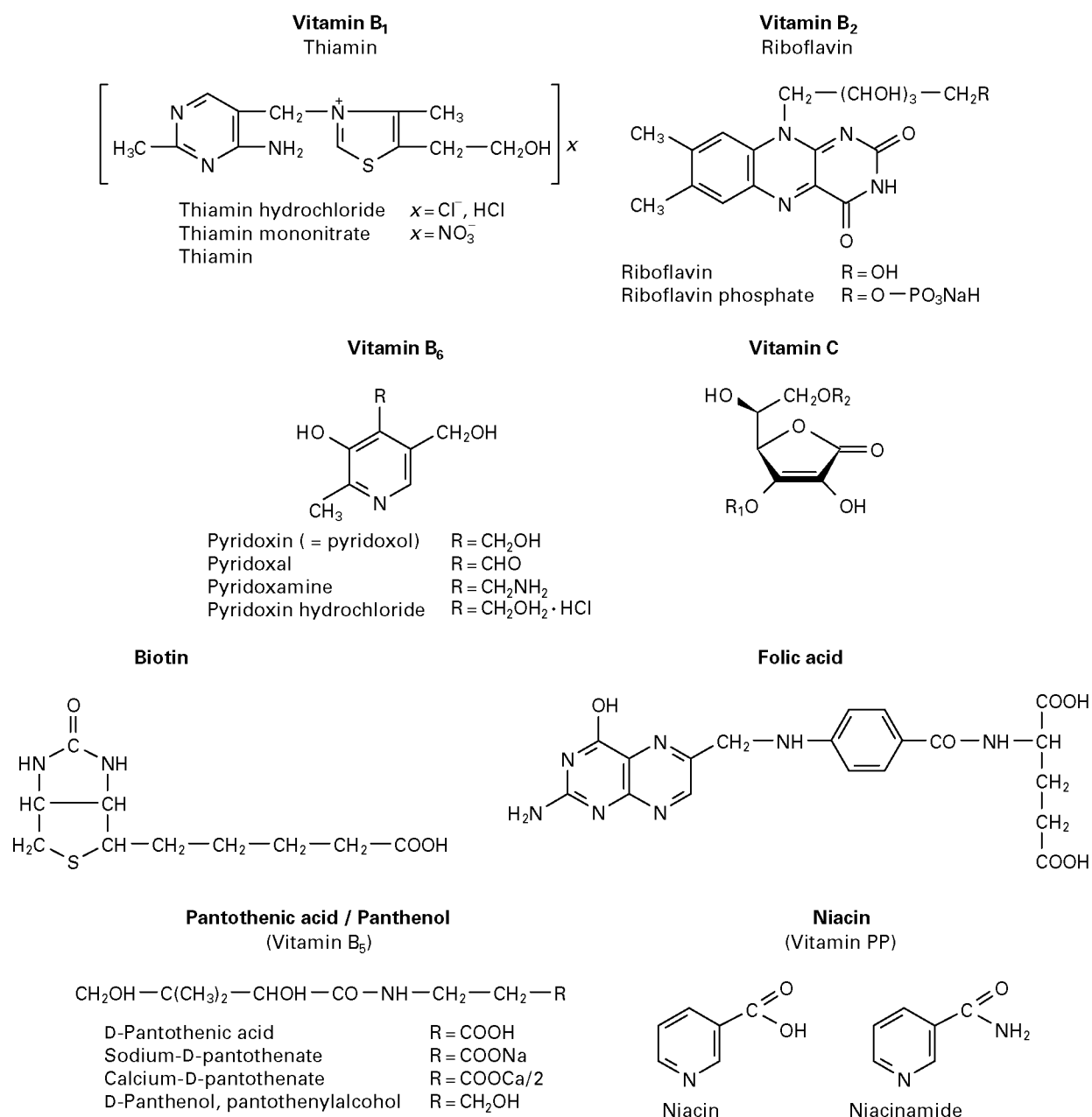


Figure 2 Chemical structures of some water-soluble vitamins.

standard, e.g. either retinyl acetate or tocol, is generally added for quantitation purposes. After protein precipitation the free retinol is extracted with 1% BHT in *n*-hexane solution, evaporated to dryness under nitrogen and subjected to chromatographic separation as above. Vitamin E and carotenoids are extracted in the same manner. Vitamins A, E and carotenoids can be simultaneously injected for LC separation. The analysis of vitamin D and trace quantities of vitamin D metabolites, e.g. 1,25-dihydroxycholecalciferol and 25-hydroxycholecalciferol, and

also the analysis of vitamin K in human plasma, require an additional step for prepurification using column extraction or a semipreparative LC system prior to the final HPLC separation.

Water-Soluble Vitamins

Water-soluble vitamins are in general more stable than fat-soluble vitamins, although vitamin B₂ and to a lesser extent vitamin B₁₂ (folic acid) are light sensitive. All manipulations should therefore be performed in subdued light. No special treatment of samples in

pharmaceutical preparations is required before chromatography. In biological fluids or foodstuffs pre-purification and/or derivatization of the compounds are necessary before LC separation. The methods include acid extraction followed by enzymatic hydrolysis with takadiastase, papain or acid phosphatase, sometimes with pre-column or post-column chromatography. Trichloroacetic, perchloric and metaphosphoric acids are usually preferred for acid extraction. Depending on the aim of the investigation, vitamins can be determined in their free forms or in both free and phosphorylated forms. In the latter case the enzymatic hydrolysis step is omitted.

In blood, plasma and food, vitamin B₁ in protein-free extract is oxidized by agents such as [Fe(CN)₆]³⁻, cyanogen bromide or mercuric chloride to thiochrome in a pre- or post-column chromatography reactor. For pre-column chromatography two different procedures are used. In the first, the thiochrome extract is neutralized by concentrated phosphoric acid to ensure a pH level compatible with the C₁₈ column used for the separation and to eliminate possible pH-dependent alkaline degradation of thiochrome to its disulfide. It is then centrifuged and the supernatant injected into the HPLC. In the second procedure, isobutyl alcohol is used to extract thiochrome after alkaline oxidation. Aliquots of the extracts are then chromatographed.

After acid extraction vitamin B₂ is readily detected owing to its intense fluorescence.

Since vitamin B₆ is present in six chemical forms, there are methods for the simultaneous separation of the three free forms and the three phosphorylated forms as well as methods for determining the sum of all the forms. Pyridoxamine is transformed into pyridoxal by reaction with glyoxylic acid in the presence of Fe²⁺ as catalyst. The pyridoxal is then reduced to vitamin B₆ pyridoxol by the action of sodium borohydride in an alkaline medium before LC separation. Semicarbazide is also used for post-column derivatization of vitamin B₆.

In multivitamin-multimineral preparations, vitamin B₁₂ or cyanocobalamin is extracted with a mixture of dimethyl sulfoxide (DMSO) and water, or ammonium pyrrolidine dithiocarbamate and citric acid in DMSO and water. The extract is centrifuged and the supernatant is diluted with water before concentration and clean-up by solid-phase extraction using a quaternary amine and a phenyl column in series before LC separation. There are few LC methods for the determination of vitamin B₁₂ in human plasma and food.

In biological fluids and foodstuffs a treatment for removing protein is a major requirement for vitamin C assay. Protein precipitation may be done by organic

reagents (methanol or acetonitrile) or mineral acids (perchloric, metaphosphoric acid, etc.). Aqueous solutions of vitamin C are rapidly oxidized on exposure to air. Stabilizers such as hydrogen sulfide and 1,4-dithio-DL-threitol have also been employed. The deproteinization may be followed by an enzymatic oxidation of ascorbic acid to dehydroascorbic acid, which is transformed with 1,2-phenylenediamine to its quinoxaline derivative for final separation.

Biotin, or vitamin H, is very stable. However, the limitation of HPLC lies in the lack of a suitable detection system. There are applications of LC to pharmaceutical products containing at least 300 µg biotin per tablet. In pharmaceutical products and feed premix, biotin is extracted from the matrix with buffer, followed by purification and concentration by solid-phase extraction and separation by LC. However, there are few LC methods for the estimation of biotin in biological samples.

Folic acid (pteroylglutamic acid; also called vitamin M) and its derivatives are stable substances. Folic acid may be determined simultaneously with other water-soluble vitamins in pharmaceutical preparations. In food products folates are extracted from the matrix with buffer and enzymes (e.g. hog kidney and chicken pancreas, or rat plasma conjugase, α -amylase and protease together), followed by purification and concentration by solid-phase extraction or with affinity chromatography before final separation.

In pharmaceutical preparations panthenol, pantothenic and its salt (vitamin B₅) are extracted with a phosphate solution. The extract is centrifuged, filtered and separated by LC. There are few methods for the determination of pantothenic acid and its salt in food products and biological fluids.

Niacin (or nicotinic acid) and nicotinamide are the two different forms of vitamin PP (so called for its pellagra-preventive factor). Nicotinamide is the form of the vitamin generally found in human plasma. Plasma is deproteinated with acetone/chloroform, the organic layer evaporated to dryness, and the methanolic extract of the residue separated by a reversed-phase HPLC. Isonicotinic acid is used as an internal standard. Urine is purified by extraction with chloroform, the aqueous phase evaporated, and taken for separation by LC. In foods vitamin PP is present mostly in its phosphorylated forms. Hydrolysis is necessary to break the ester bonds, releasing the total vitamin PP content of the food for assay. In food products niacin is extracted with buffer and enzyme. The sample extracts are purified through an ion exchange column (e.g. Dowex 1-X8 resin) before HPLC.

In multivitamin preparations 0.1 mol L⁻¹ hydrochloric acid is used to extract the vitamins and

DMSO containing anhydrous citric acid is used to disperse the multivitamin-multimineral preparation, since vitamin B₆ is not completely extracted by either 0.1 mol L⁻¹ hydrochloric acid or DMSO owing to adsorption of the vitamin to the minerals. The extraction of nicotinamide is not impaired by the addition of citric acid to DMSO.

Choline in plant material is extracted with isopropanol containing internal standards and *p*-nitrobenzylhydroxylamine hydrochloride for the formation of *p*-nitrobenzyl oximes. The extract is purified by solid-phase extraction (C₁₈ and ion exchange), after which the choline fraction is benzoylated to yield UV-absorbing derivatives. In biological samples choline is extracted with formic acid in acetone containing an internal standard. After purification the sample is separated by LC.

For the analysis of inositol mono- and diphosphate isomers in foods the method involves extraction of samples with hydrochloric acid and separation of inositol phosphates by anion exchange chromatography.

Liquid Chromatography

Liquid chromatography is an extremely valuable method for separation, identification and quantitation of the different vitamins. Excellent separations can be achieved in a reasonable time for routine analysis.

Fat-Soluble Vitamins

For fat-soluble vitamins normal-phase and reversed-phase chromatography are used.

In the normal-phase modes, silica and nonpolar mobile phases containing *n*-hexane or petroleum ether with a small percentage of a more polar solvent are used. Addition of a small amount of water or alcohol (e.g. ethanol) regulates the sorbent activity, reduces peak tailing and gives better reproducibility of retention times. Silica is the adsorbent of choice for the separation of *cis/trans* isomers and diastereoisomers. Selectivity on silica is determined by the number and the nature of the functional groups as well as the overall steric configuration (position of the double bonds) of the molecule (Figure 3).

In the reversed-phase mode, hydrophobic column packings (C₁₈, C₈, etc., bonded to a silica surface) are used together with an aqueous buffered mobile phase and a water-miscible organic solvent (i.e. methanol, acetonitrile).

Retinol analysis in biological fluids and foods is performed using both normal-phase and reversed-phase chromatography. For normal-phase (or liquid-solid) chromatography there is compatibility

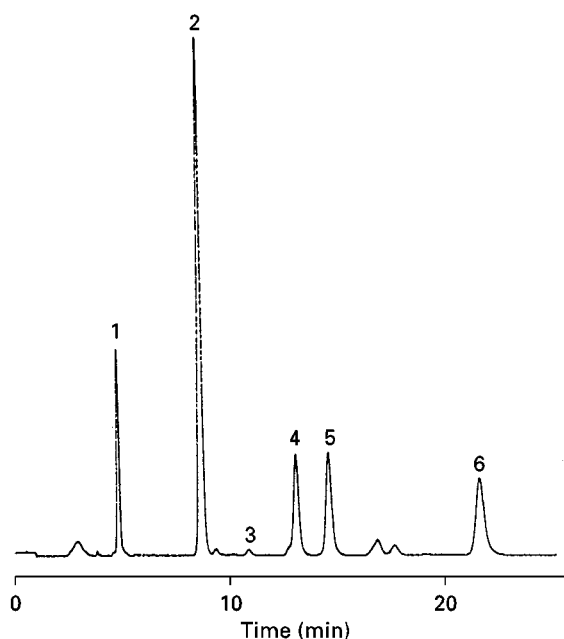


Figure 3 Example of an HPLC separation of α -, β -, γ - and δ -tocopherol from a wheat germ oil sample with α -tocopherolacetate added. Peaks: 1, α -tocopherolacetate; 2, α -tocopherol; 3, α -tocotrienol; 4, β -tocopherol; 5, γ -tocopherol; 6, δ -tocopherol.

Experimental conditions: stationary phase, Lichrosorb Si 60, 7 μ m; column dimension, 250 \times 4.6 mm; mobile phase, *n*-hexane/dioxane (97 : 3 v/v); flow rate, 1.0 mL min⁻¹; injection volume, 20 μ L; detection, fluorimetric with excitation at 295 nm and emission at 330 nm. (Reproduced with permission from Federal Office of Public Health, 1989.)

between the sample extraction solvent and the LC mobile phase; this avoids peak artefacts, especially for lipid extracts. Geometrical isomers such as 11-*cis*, 13-*cis*, 9-*cis* and all-*trans* retinol are well resolved. Retinol serum determination by reversed-phase chromatography allows the use of retinol acetate as internal standard which is well separated from retinol, unlike the case for liquid-solid chromatography. Meanwhile there is an additional step of evaporation of the extraction solvent in the sample preparation procedure before LC.

The most appropriate systems for the separation of polar and nonpolar carotenoids include the use of polymeric C₁₈ or C₃₀ bonded phases without end-capping in conjunction with a moderate pore-size packing column and a methanol-based mobile phase (to obtain a good recovery). *Cis*-isomers of β -carotene are largely resolved from each other and from other carotenes. Separation of lutein and zeaxanthine is also obtained with this system. Better separations of the xanthophylls are also observed. Accurate carotenoid measurements require the right selection of column and mobile phase and, due to the large degree of variability in the purity of commercial carotenoid

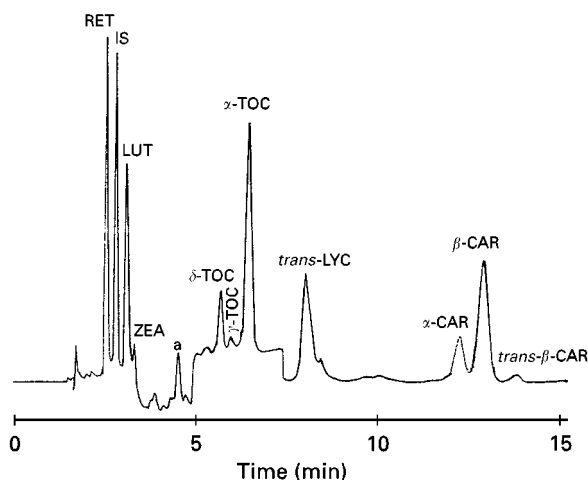


Figure 4 Chromatogram of a human serum sample. Peaks: RET, retinol; IS, retinol acetate (internal standard); LUT, lutein; ZEA, zeaxanthin; δ -TOC, δ -tocopherol; γ -TOC, γ -tocopherol; α -TOC, α -tocopherol; LYC, lycopene; α -CAR, α -carotene; β -CAR, β -carotene; *trans*-CAR, *trans*- β -carotene; a, unidentified carotenoid.

Experimental conditions: stationary phase, Lichrosorb RP-18, 7 μm ; column dimension, 250 \times 4.6 mm and 15 \times 3.2 mm guard column; mobile phase, acetonitrile/tetrahydrofuran/methanol (68 : 22 : 7 v/v/v) adjusted to 100% with ammonium acetate; flow rate, 1.5 mL min⁻¹; injection volume, 15 μL ; detection, programmable and variable-wavelength UV/Vis, 325 nm from 0 to 3.0 min, 450 nm from 3.0 to 4.9 min, 290 nm from 4.9 to 7.4 min, 470 nm from 7.4 to 12.0 min and 450 nm from 12.0 to 15.0 min. (Reproduced with permission from Bui, 1994.)

preparations, special precautions must be taken during calibration. Simultaneous determination of carotenoids, retinoids and tocopherols in serum and foods is performed on a C₁₈ column using wavelength-programmable UV-visible (**Figure 4**), fluorescence or electrochemical detection.

The same separation conditions are used for the separation of α -tocopherol and retinol in biological fluids and foods. α -, β -, γ - and δ -Tocopherol as well as α -, β -, γ - and δ -tocotrienol are well resolved only by normal-phase chromatography. On an RP-18 column α -, β - and δ -tocopherol isomers are all separated, but not β - and γ -tocopherols. Tocol as internal standard is also used for vitamin E determination in serum.

Retinol and α -tocopherol in biological fluids, foods and pharmaceutical preparations can be separated simultaneously by normal- or reversed-phase HPLC.

In biological fluids analyses of vitamin D and its metabolites are performed using solid-phase extraction (SPE) cartridge coupled to semipreparative HPLC on a silica column and analytical HPLC on an octadecyl (C_{18}) column with UV or electrochemical detection (**Figure 5**). They can also be purified by one or two preparative HPLC steps on silica and quantified

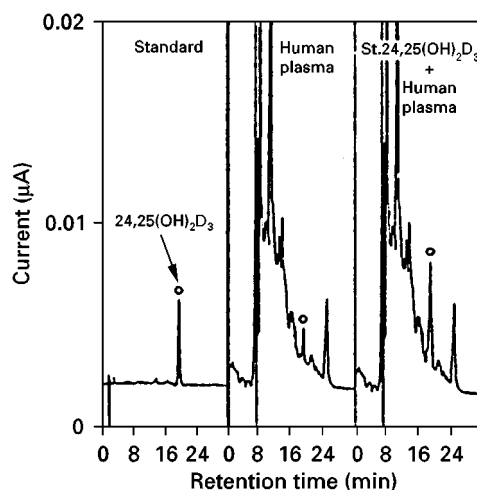


Figure 5 Chromatogram of HPLC-ECD for 24,25-dihydroxycholecalciferol (24,25-(OH)₂D₃).

Experimental conditions: stationary phase, Nucleosil C₁₈, 5 µm; column dimension, 300 × 7.5 mm; mobile phase, 5% (v/v) methanol in acetonitrile with 0.025 mol L⁻¹ HClO₄; flow rate, 1.2 mL min⁻¹; injection volume, 50 µL; detection, dual-electrode electrochemical detection: detector 1 (+0.20 V); detector 2 (+0.60 V). (Reproduced with permission from Masuda *et al.*, 1997.)

by HPLC on a C₁₈ column with UV detection. Vitamin D₂ or D₃ may be used as internal standard (Figure 6).

The analysis of vitamin K (phyloquinone, menaquinone and epoxides), like vitamin D, uses normal-phase semipreparative LC followed by an analytical reversed-phase column with UV or electrochemical detection (**Figure 7**). Water-soluble menadione sodium bisulfite or vitamin K₃ in animal feeds is determined by reversed-phase HPLC with UV detection. To improve vitamin K₃ detection limits, post-column reaction fluorimetric detection is used. Menadione is hydrogenated by sodium borohydride to 2-methyl-1,4-dihydroxynaphthalene, which is detected fluorimetrically.

Water-Soluble Vitamins

Water-soluble vitamins are separated using ion exchange (IEC), normal-phase or reversed-phase chromatography.

Ion exchange chromatography is the preferred method of separation for the analysis of strongly ionic compounds. The chromatographic separation may be optimized by altering the pH or ionic strength of the mobile phase. Reversed-phase chromatography is the method of choice for water-soluble vitamins. Reversed-phase columns such as C₁₈ and mobile phase NH₂ have been employed. The mobile phase is a mixture of methanol or acetonitrile with an acetate or phosphate buffer. For ionic compounds the reversed-phase ion pair mode is generally used. Unlike conventional

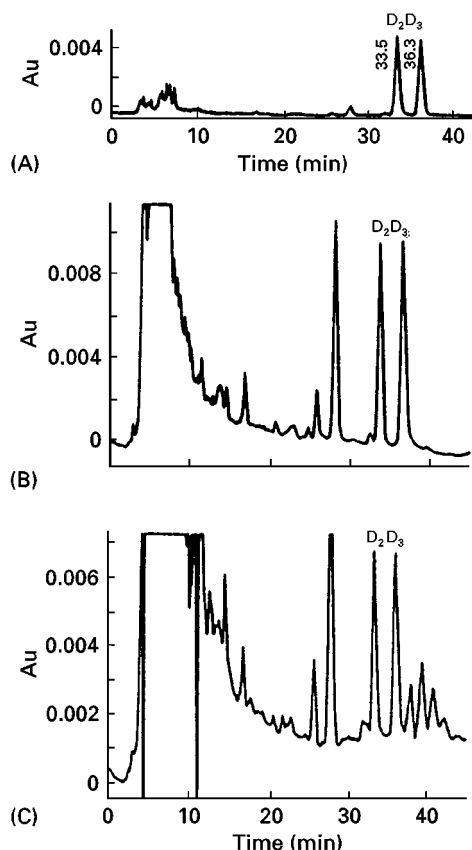


Figure 6 Analytical HPLC chromatograms of (A) standard mixture of ergocalciferol (D₂) and cholecalciferol (D₃); (B) D₂ (internal standard, IS) and D₃ in chicken sample; and (C) D₂ (IS) and D₃ in pork liver.

Experimental conditions: stationary phase, Zorbax ODS + Vydac 201 TP 54 5 μm ; column dimension, 250 \times 4.6 mm; mobile phase, 4% water in methanol; flow rate, 1.0 mL min⁻¹; injection volume, 50 μL ; detection, UV at 264 nm. (Reprinted from Horvath CsG (ed.) (1980) *High Performance Liquid Chromatography*, New York: Academic Press. Copyright © 1980 by Academic Press.)

IEC, this technique can separate nonionic and ionic compounds simultaneously. The chromatographic separation may be optimized by altering the ion pair reagent, pH and ionic strength of the mobile phase.

Water-soluble vitamins (vitamin B₁, thiamin, B₂, riboflavin or riboflavin 5-monophosphate; B₆, pyridoxine and nicotinamide) in commercial vitamin preparations can be separated using either strong cation exchange resins or reversed-phase chromatography using an ion pair reagent (e.g. sodium alkane-sulfonate, dioctyl sodium sulfosuccinate, tetrabutyl ammonium phosphate) in the eluent with UV detection.

Similar LC methods are used for the separation of thiamin in foods and biological fluids, usually with fluorescence detection. In pre-column procedures, silica, C₁₈, NH₂ and poly(styrene-divinyl benzene) phases are used. Since the intensity of thiochrome fluorescence depends on pH and reaches a steady

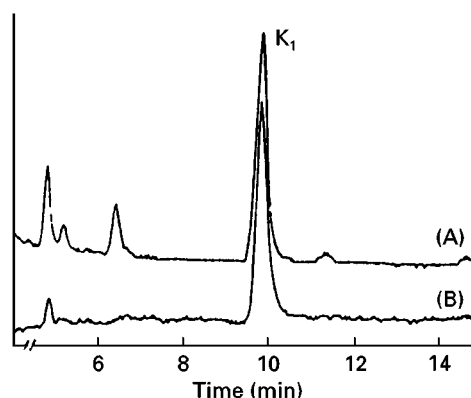


Figure 7 Analytical HPLC chromatogram of a kiwi fruit (A) without purification and (B) with purification with semipreparative HPLC.

Experimental conditions: stationary phase, Vydac 201 TP 548 5 μm ; column dimension, 250 \times 4.6 mm; mobile phase, 96% methanol/0.05 mol of sodium acetate buffer (pH 3); flow rate, 1.5 mL min⁻¹; injection volume, 30 μL ; detection, dual-electrode electrochemical detection: upstream electrode (-1.1 V); downstream electrode (0 V). (Reproduced with permission from Koivu *et al.*, 1997.)

level at pH > 8, the mobile phase should contain a buffer. Polymeric C₁₈ packings are more suitable for these high pH conditions (Figure 8).

C₁₈ columns are used for the determination of riboflavin and its derivatives, flavin mononucleotide (FMN) and flavin-adenine dinucleotide (FAD). The compounds are separated isocratically with a mixture

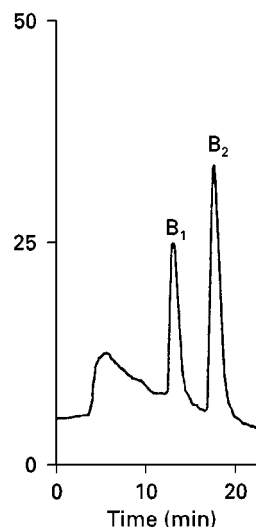


Figure 8 Chromatogram of thiamin (thiochrome) and riboflavin in a skimmed milk sample using fluorescence detection.

Experimental conditions stationary phase, Ultrasphere ODS 5 μm ; column dimension, 250 \times 4.6 mm; mobile phase, methanol/water (20 + 80) containing 0.005 mol L⁻¹ tetrabutylammonium phosphate pH 7.5; detection, fluorimetric with excitation at 360 nm and emission 425 nm. (Reproduced with permission from Augustin, 1984.)

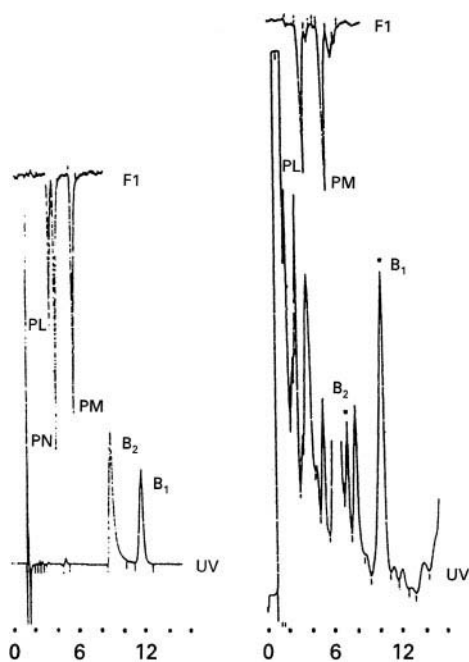


Figure 9 Chromatograms of B₁, B₂ and B₆ vitamers in standard and in whole blood.

Experimental conditions: stationary phase, Nova Pack C₁₈ 5 μ m; column dimension, 125 \times 4.6 mm; mobile phase, 20% methanol in ion pair solution (at least 70 μ L of di-*N*-butylamine solution per litre of the eluent); flow rate, 1.0 mL min⁻¹; detection, UV at 254 nm for B₁; fluorimetric with excitation at 290 nm and emission at 395 nm for B₂. (Reprinted from Setrell WH Jr and Harris RS (eds) (1967) *The Vitamins*, 2nd edn. New York/London: Academic Press. Copyright © 1967 by Academic Press.)

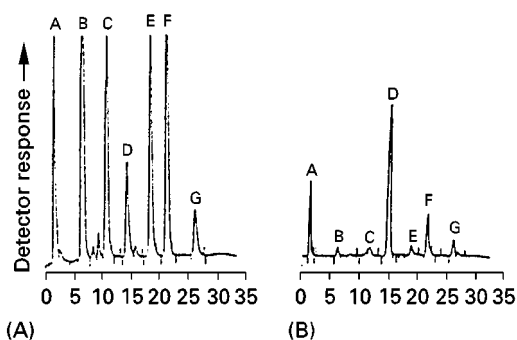


Figure 10 (A) Representative chromatogram of standard vitamin B₆ vitamers, 4-deoxypyridoxine (dPN) and 4-pyridoxic acid (4-PA). Peaks: A, pyridoxal phosphate PLP (8 pmol); B, 4-PA (10 pmol); C, pyridoxamine phosphate PMP (5.5 pmol); D, pyridoxal PL (10 pmol); E, pyridoxine PN (10 pmol); F, dPN (12 pmol); G, pyridoxamine PM (6 pmol). (B) Vitamin B₆ vitamers profile of human plasma.

Experimental conditions: stationary phase, Ultramex C₁₈ guard column (30 \times 4.6 mm) 3 μ m and Ultramex C₁₈ column (150 \times 4.6 mm) 3 μ m; mobile phase, (A) 0.033 mol L⁻¹ phosphoric acid containing 0.01 mol L⁻¹ 1-octanesulfonic acid adjusted to pH 2.2 with 6 mol L⁻¹ potassium hydroxide; (B) 0.33 mol L⁻¹ phosphoric acid in 10% (v/v) 2-propanol adjusted to pH 2.2 with 6 mol L⁻¹ potassium hydroxide; flow rate, 1.2 mL min⁻¹; injection volume, 25 μ L; detection, fluorimetric with excitation at 328 nm and emission at 393 nm. (Reprinted from Setrell WH Jr and Harris RS (eds) (1968) *The Vitamins*, 2nd edn. New York/London: Academic Press. Copyright © 1967 by Academic Press.)

of methanol and water (or buffer solution) using fluorimetric detection (Figure 9).

Simultaneous determination of the six chemical forms of vitamin B₆ in foods and biological samples is performed by IEC or reversed-phase chromatography,

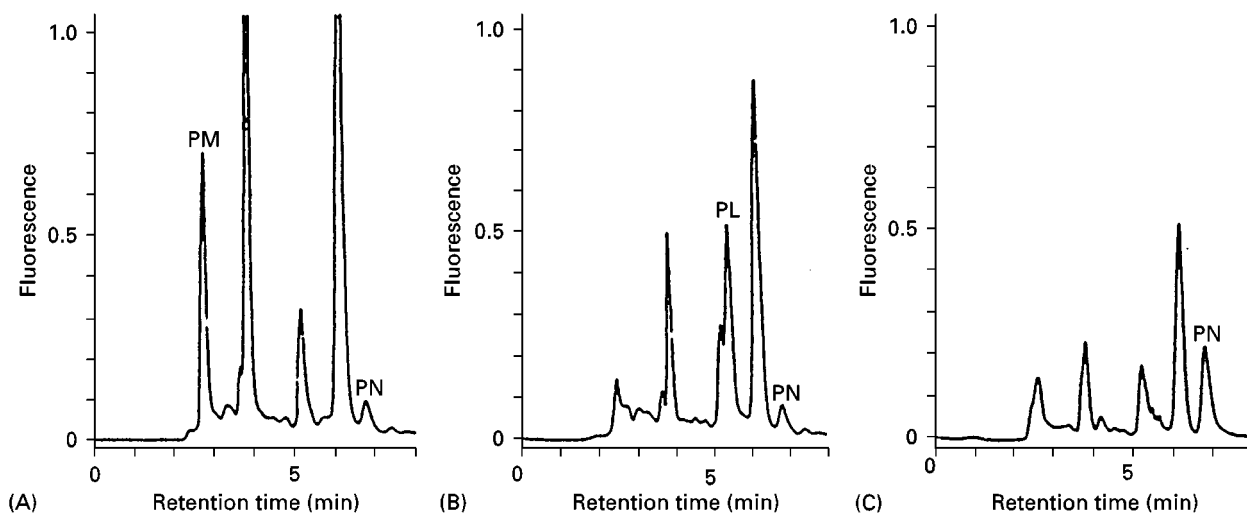


Figure 11 Chromatographic separation of vitamin B₆ vitamers in yeast. (A) With deletion of the deamination and reduction steps; (B) with deletion of the reduction step; (C) without deletion of either step.

Experimental conditions: stationary phase, Lichrospher 60 RP Select B octylsilyl 5 μ m; column dimension, 250 \times 5 mm; mobile phase, acetonitrile/0.05 mol L⁻¹ potassium dihydrogen phosphate (4 : 96) containing 0.5 \times 10⁻³ mol L⁻¹ sodium heptanesulfonate adjusted to pH 2.5 with phosphoric acid; flow rate, 1.0 mL min⁻¹; injection volume, 20 μ L; detection, fluorimetric with excitation at 290 nm and emission at 395 nm. (Reprinted from Setrell WH Jr and Harris RS (eds) (1972) *The Vitamins*, 2nd edn. New York/London: Academic Press. Copyright © 1972 by Academic Press.)

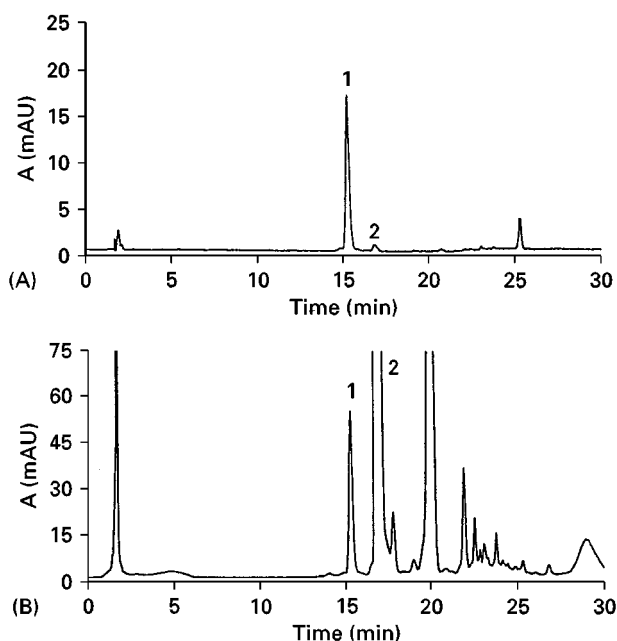


Figure 12 Chromatogram of multivitamin-multimineral tablets at (A) 50 nm and (B) 360 nm after preconcentration and clean-up by solid-phase extraction. Peaks: 1, vitamin B₁₂; 2, vitamin B₂.

Experimental conditions: stationary phase, Bondapak C₁₈ 10 μ m; column dimension, 150 \times 39 mm; mobile phase, (A) methanol/water (10 : 90); (B) methanol/water (90 : 10); gradient elution, linear gradient to 50% B for the first 15 min, followed by 100% B for the next 2 min and maintained isocratically for 10 min; flow rate, 1.0 mL min⁻¹; injection volume, 200 μ L; detection, UV at 550 nm. (Reproduced with permission from Dalbacke and Dahlquist, 1991.)

with or without ion pair reagents; detection is by fluorimetry (Figure 10). The vitamin B₆ content of foods can also be determined by ion pair HPLC after

pre-column derivatization of the free and phosphorylated vitamin into pyridoxol (Figure 11).

Vitamin B₁₂ is separated from other water-soluble vitamins in pharmaceutical preparations by reversed-phase using a methanol/water gradient with detection at 550 nm (Figure 12).

Reversed-phase chromatography is mostly used for ascorbic acid determination. In foods total vitamin C (ascorbic acid and its oxidized form, dehydroascorbic acid) are determined using ion pair chromatography with UV detection. In biological fluids and foods total vitamin C, as its quinoxaline derivative, is separated on a C₁₈ column with fluorescence detection. The determination of ascorbic acid in plasma can also be achieved using a C₁₈ column and electrochemical detection. Another procedure for vitamin C determination consists of first measuring the ascorbic acid present, then reducing the dehydroascorbic acid, at neutral pH, with dithiothreitol, and finally measuring the total ascorbic acid. The dehydroascorbic acid is determined by difference. The separation is on a C₁₈ column with electrochemical detection.

After a clean-up procedure, biotin in pharmaceutical products is assayed using a C₁₈ column with methanol/water as the mobile phase and UV detection. Extracts of folates (folate monoglutamates and folic acid) in food and biological samples after purification are separated by gradient elution and UV or fluorescence detection (Figure 13).

Pantothenic acid is separated from other water-soluble vitamins with an isocratic system on an aminopropyl bonded phase using a mixture of acetonitrile/phosphate buffer as mobile phase and UV detection (Figure 14). Panthenol in multivitamin

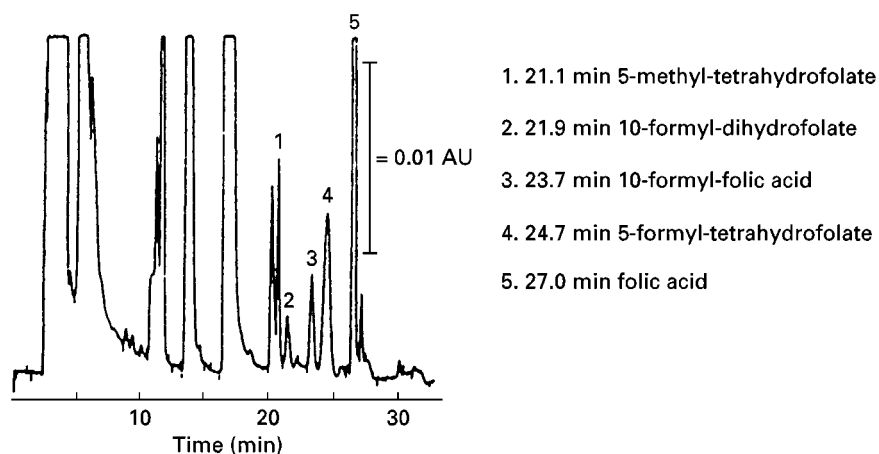


Figure 13 Chromatogram of the main folate forms found in fortified white bread.

Experimental conditions: stationary phase, Phenomenex Ultramex C₁₈ 5 μ m; column dimension, 250 \times 4.6 mm; mobile phase, 33 mmol L⁻¹ phosphoric acid, pH 2.3 with increasing acetonitrile; gradient elution, 5% (v/v) acetonitrile maintained isocratically for the first 8 min, linear gradient to 17.5% (v/v) within 25 min; flow rate, 1.0 mL min⁻¹; detection, UV at 280 nm. (Reproduced with permission from Pfeiffer *et al.*, 1997.)

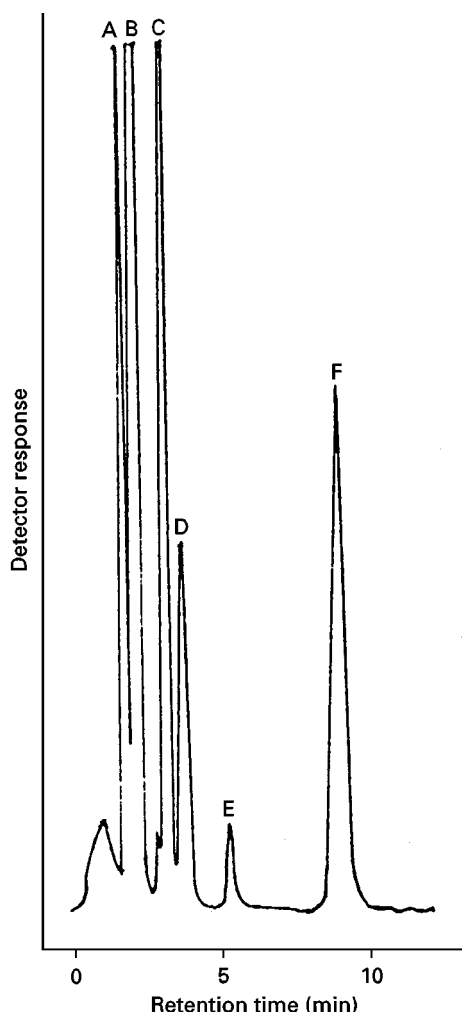


Figure 14 Chromatogram of a high potency B complex tablet extract. Peaks: A, niacinamide; B, vitamin B₆; C, vitamin B₂; D, vitamin B₁₂; E, unknown; F, pantothenic acid.

Experimental conditions: stationary phase, Hibar II Lichrosorb NH₂ 10 μ m; column dimension, 250 \times 4.6 mm; mobile phase, 0.005 mol L⁻¹ monobasic potassium phosphate (pH 4.5)/acetonitrile (13 : 87 v/v) 0.01 mol L⁻¹ 1-octanesulfonic acid; flow rate, 2.0 mL min⁻¹; injection volume, 10 μ L; detection, UV at 210 nm. (Reproduced with permission from Hudson and Allen, 1984.)

preparations is determined on a C₁₈ column with a gradient system using an ion pair reagent (e.g. sodium hexanesulfonate) and UV detection. Niacin and nicotinamide are also separated on a C₁₈ column using an ion pair reagent with UV detection. Isonicotinic acid is used as an internal standard.

Cation exchange chromatography has been used to determine with UV or electrochemical detection. Separations of inositol mono- and diphosphate isomers in foods is performed on an anion exchange column using a sodium acetate in sodium hydroxide gradient with electrochemical detection.

Future Developments

Liquid chromatography is the method of choice for vitamin analysis in pharmaceutical products, foods, feeds and especially in biological fluids. In biological sample analysis LC affords separation of the vitamins, their related compounds and various metabolites for nutrition research. The main problem encountered in biological materials is the detection limit, particularly for water-soluble vitamins. There are two main areas where developments are necessary for future vitamin LC. First, automatic sample preparation techniques involving vitamin purification and enrichment, e.g. automating solid-phase extraction, need to be improved. Second, the coupling LC and mass spectrometric (MS) detection needs to be further developed. These techniques may become leading methods in vitamin analysis in the future.

See also: II/Chromatography: Liquid: Mechanisms: Normal Phase; Mechanisms: Reversed Phases. III/Carotenoid Pigments: Supercritical Fluid Chromatography. Food Technology: Supercritical Fluid Chromatography. Vitamins: Fat-Soluble: Thin-Layer (Planar) Chromatography; Water-Soluble: Thin-Layer (Planar) Chromatography.

Further Reading

- Augustin J (1984) Simultaneous determination of thiamine and riboflavin by liquid chromatography. *Journal of the Association of Official Analytical Chemists* 67(5): 1012–1015.
- Ball GFM (ed.) (1988) *Fat-Soluble Vitamin Assays in Food Analysis*. London and New York: Elsevier Applied Science.
- Ball GFM (ed.) (1994) *Water-Soluble Vitamin Assays in Human Nutrition*. London: Chapman & Hall.
- Böttcher B and Böttcher D (1987) A new HPLC-method for the simultaneous determination of B₁-, B₂- and B₆-vitamins in serum and whole blood. *International Journal for Vitamin and Nutrition Research* 57: 273–278.
- Bui MH (1994) Simple determination of retinol, α -tocopherol and carotenoids (lutein, all-*trans*-lycopene, α - and β -carotene) in human plasma by isocratic liquid chromatography. *Journal of Chromatography B* 654: 129–133.
- Dalbacke J and Dahlquist I (1991) Determination of vitamin B₁₂ in multivitamin-multimineral tablets by high-performance liquid chromatography after solid-phase extraction. *Journal of Chromatography* 541: 382–394.
- De Leenheer AP, Lambert WE and Nelis HJ (eds) (1992) *Modern Chromatographic Analysis of Vitamins*, 2nd edn. New York: Marcel Dekker.
- Federal Office of Public Health (1989) *Vitaminbestimmung in Lebensmitteln und Kosmetika Kapitel 62*. Bern, Switzerland: The Federal Office of Public Health.

- Gaby SK, Bendich A, Singh VN and Machlin LJ (eds) (1991) *Vitamin Intake and Health*. New York: Marcel Dekker.
- Hudson TJ and Allen RJ (1984) Determination of pantothenic acid in multivitamin pharmaceutical preparations by reversed-phase high performance liquid chromatography. *Journal of Pharmaceutical Sciences* 73: 113–115.
- Koivu TJ, Piironen VI, Henttonen SK and Mattila PH (1997) Determination of phyloquinone in vegetables, fruits and berries by high performance liquid chromatography with electrochemical detection. *Journal of Agricultural and Food Chemistry* 45: 4644–4649.
- Masuda S, Okano T, Kamao M, Kanedai Y and Kobayashi T (1997) A novel high-performance liquid chromatographic assay for vitamin D metabolites using a coulometric electrochemical detector. *Journal of Pharmaceutical and Biomedical Analysis* 15 (9–10): 1497–1502.
- Mattila PH, Piironen VI, Uusi-Rauva EJ and Koivistoinen PE (1995) Contents of cholecalciferol, ergocalciferol, and their 25-hydroxylated metabolites in milk products and raw meat and liver as determined by HPLC. *Journal of Agricultural and Food Chemistry* 43: 2394–2399.
- Packer L and Fuchs J (eds) (1993) *Vitamin E in Health and Disease*. New York: Marcel Dekker.
- Pfeiffer CM, Rogers LM and Gregory III JF (1997) Determination of folate in cereal-grain food products using trienzyme extraction and combined affinity and reversed-phase liquid chromatography. *Journal of Agricultural and Food Chemistry* 45: 407–413.
- Reitzer-Bergaentzle M, Marchioni E and Hasselmann C (1993) HPLC determination of vitamin B₆ in foods after pre-column derivatization of free and phosphorylated vitamers into pyridoxol. *Food Chemistry* 48: 321–324.
- Sebrell WH Jr and Harris RS (eds) (1972) *The Vitamins*, 2nd edn. New York/London: Academic Press.
- Sharma SK and Dakshinamurti K (1992) Determination of vitamin B₆ vitamers and pyridoxic acid in biological samples. *Journal of Chromatography* 578: 45–51.

Water-Soluble: Thin-Layer (Planar) Chromatography

J. C. Linnell, Royal Free and University College Medical School, London, UK

Copyright © 2000 Academic Press

As a tool, chromatography has long been important for the separation of vitamins from complex mixtures and their initial isolation and identification would have been greatly hampered without the use of paper, column or thin-layer chromatography (TLC). While more sophisticated chromatographic techniques are now widely available, TLC has great advantages in terms of its simplicity and flexibility of use.

The vitamins classified as water-soluble are all compounds important in human metabolism either as coenzymes or their precursors which the body cannot make for itself (Figure 1). The recommended daily allowance (RDA) of each vitamin ranges from hundreds of milligrams to just a few micrograms a day (Table 1). These compounds have few properties in common apart from their water-solubility, but this fact alone makes TLC an excellent technique for their separation, particularly in pharmaceutical preparations and food products. Even at physiological concentrations, TLC is widely used after extraction of the vitamins from tissues or body fluids. This generally needs to be under acid conditions. Since most of these compounds are unstable at high pH. Some are in addition very light-sensitive. Following TLC separation, special methods of detection may also be required, since tissue levels of most water-soluble vitamins are low or very low.

Thiamin (Vitamin B₁)

Thiamin occurs in plant and animal tissues and the richest sources are seeds and nuts, peas and beans, cereals and yeast. Fish and meat, notably pork, are also good sources. Thiamin is commonly available as its monohydrochloride, but it also forms acid salts and esters with nitric and phosphoric acids. Metabolically, thiamin is required as the coenzyme thiamin pyrophosphate for the mitochondrial metabolism of glucose and pyruvate.

Thiamin may be extracted from tissues, foodstuffs or pharmaceutical preparations with aqueous alcohol mixtures at a pH of 4–6 and separated from closely related compounds and metabolites by TLC on cellulose or silica gel. Various mobile phases have been successfully used, including isopropanol–water–trichloroacetic acid–ammonia (71 : 9 : 20 : 0.3) and butan-1-ol–acetic acid–water (40 : 10 : 50). Thiamin may be separated from its hydrolysis and oxidation products by TLC/densitometry and other chromatographic techniques have been reviewed. Sandwich-type chambers afford rapid separation of thiamin from other water-soluble vitamins by TLC on silica gel GF254 and the spots then located under UV light. An alternative technique for the quantitation of thiamin in pharmaceutical products involves the use of high performance TLC (HPTLC) and post-separation derivatization with a hexacyanoferrate (III)-sodium hydroxide reagent and fluorodensitometry, sensitive down to 500 pg per spot. Other modifications include the use of a fibreoptic probe

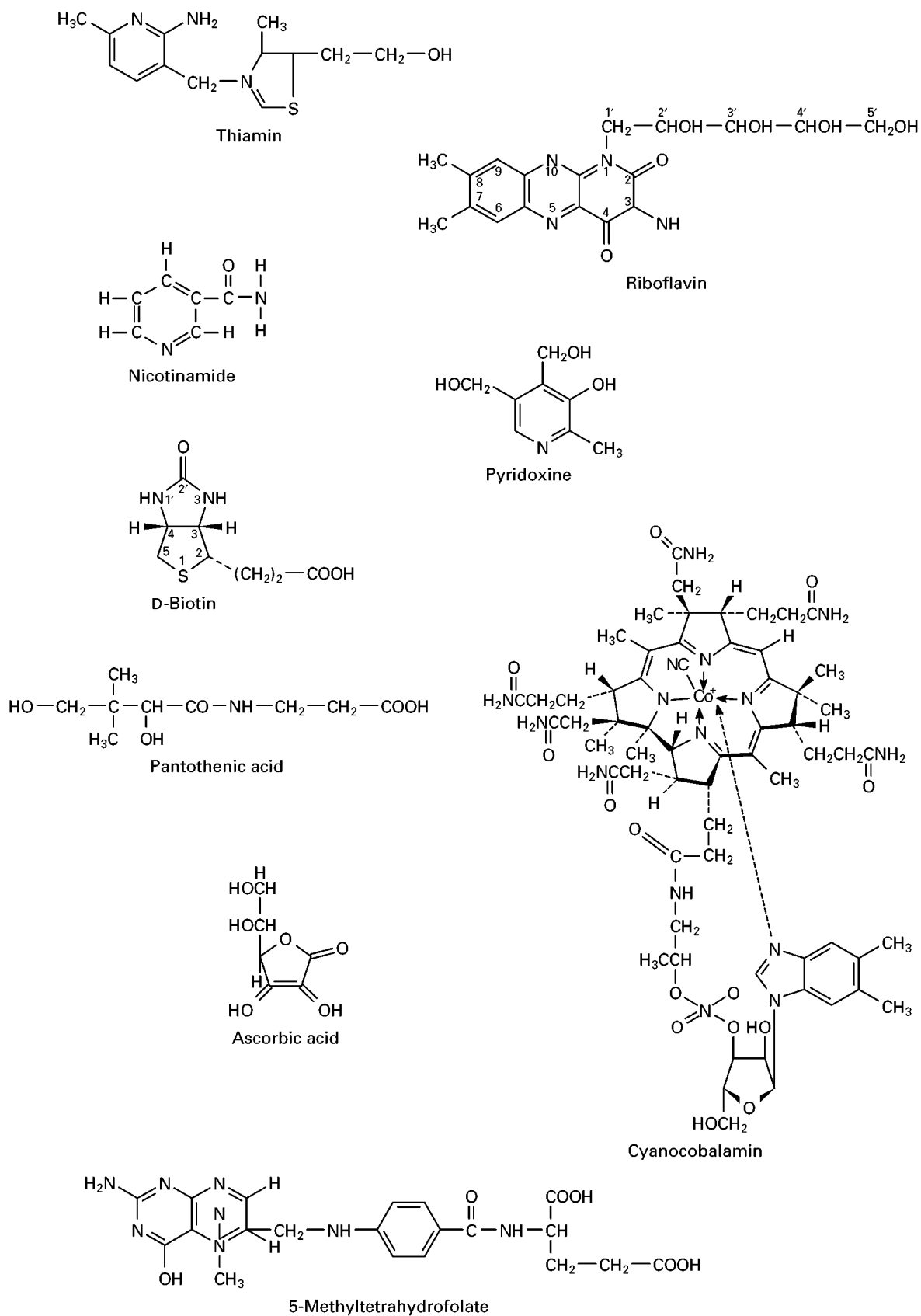


Figure 1 Structural formulae of water-soluble vitamins.

Table 1 Recommended daily allowances^a water-soluble vitamins

<i>Vitamin</i>	<i>RDA</i>
Ascorbic acid	30–75 mg
Nicotinic acid	15–20 mg
Pyridoxine	1–3 mg
Riboflavin	1.5–2.0 mg
Thiamin	1–2 mg
Folic acid	300 µg
Cobalamin	1–2 µg

^aThere is no quoted RDA for biotin or pantothenic acid.

to improve measurement of thiamin in the nanogram range.

Riboflavin (Vitamin B₂)

Riboflavin and other flavinoids occur in dairy produce, meat and to a lesser extent in cereals. Flavins are stable to heat and acid but are destroyed by exposure to light. Ultraviolet irradiation of riboflavin in acid or neutral solution gives rise to the fluorescent compound lumichrome, whereas in alkaline solutions irradiation produces lumiflavin. Flavins are required in the body as their coenzymes flavin mononucleotide and flavin adenine dinucleotide, which are involved in redox reactions involving one- and two-electron transfers and linked to many energy-dependent processes in the body.

Pharmaceutical preparations containing riboflavin may be analysed by applying concentrated ethanolic extracts to silica gel TLC plates developed in butanol–benzene–acetic acid–water (8 : 7 : 5 : 3) or butanol–acetic acid–water (9 : 4 : 5). Foods, tissue samples and urine each require particular methods of sample preparation and these methods and the solvent systems successfully employed have been reviewed elsewhere. A dark room is required for sample preparation and chromatography of flavins to prevent photolytic degradation. The fluorescent property of flavins provides a convenient means of detection and spots may be located under radiation at 254 and 366 nm. HPTLC followed by fibreoptic fluorimetry has been used to measure riboflavin in vitamin mixtures and can detect 48–320 ng. Separation is also effective on mixed-layer plates of GDX-102 and silica gel G (1 : 1) pre-coated with hexadecyltrimethylammonium bromide, developed in 60–70% ethanol.

Nicotinic Acid (Vitamin B₃)

Nicotinic acid (niacin) and various nicotinamides are sources of the coenzyme nicotinamide adenine dinucleotide, synthesized in the mitochondria and vital for

oxidative energy production in many metabolic reactions. Niacin is normally acquired from a balanced diet of meat, fish, whole cereals and yeast. Peas, beans, nuts, fruit and vegetables are also good sources of this vitamin.

Analysis of powdered preparations containing nicotinic acid has been achieved on silica gel plates impregnated with zinc acetate, developed in butanol–benzene–acetic acid–water (8 : 7 : 5 : 3) or butanol–acetic acid–water (9 : 4 : 5) to provide a self-indicating system. An overpressure chromatographic procedure using HPTLC silica gel plates and a mobile phase of butan-1-ol–pyridine–water (50 : 35 : 15) is also effective. This method uses photodensitometric detection to separate nicotinamide from other vitamins and the method is fast, accurate and specific. Other methods based on HPTLC and fibreoptic fluorometric quantitation have been described in which nicotinic acid is converted to a fluorescent derivative before chromatography. After separation, the plate is scanned by a bifurcated fibre-optic which transmits the excitation radiation and collects the signal emitted from the plate. Good calibration curves have been obtained in the range 10–100 ng nicotinic acid.

Pantothenic Acid (Vitamin B₅)

Pantothenic acid is required in the formation of acetyl coenzyme A which holds a key position in many metabolic pathways. Only the natural dextrorotatory form is active. Pantothenic acid is found in most foods of plant and animal origin and good sources include liver, kidney, wheat germ, royal jelly, peanuts, spinach, cheese and peas. There is no quoted RDA, though most diets provide at least 10 mg per day.

Panthenol and pantothenic acid have been identified and quantified in pharmaceutical preparations by extraction with ethanol or benzyl alcohol and separated by TLC on silica gel plates developed in propan-2-ol–water (85 : 15). Spots are measured by spectrodensitometry. Postaire has applied the over-pressure derivatization technique following separation of calcium pantothenate from other hydrophilic vitamins on silica gel HPTLC layers developed in butan-1-ol–pyridine–water (50 : 35 : 15).

Pyridoxine (Vitamin B₆)

Pyridoxine is found chiefly in animal tissues; pyridoxal and pyridoxamine occur in plant tissues. Together these three forms of the vitamin are of vital importance in the body for the synthesis of pyridoxal 5-phosphate which acts as coenzyme to amino

transferases, facilitating more than 60 amino group transfers and other reactions, including formation of neurotransmitters. The RDA is 1–3 mg but may increase on a high protein diet. Good sources are yeast, liver, peanuts, bananas, grapes and pears, beef and fish.

Chromatographic analysis of the vitamin B₆ complex, including sample preparation and pre-TLC extraction, have been well reviewed. Separation of pyridoxine from other water-soluble vitamins in pharmaceutical preparations can be improved by impregnating silica gel plates with zinc acetate to provide a self-indicating system after separation. Impregnation of plates with hexadecyltrimethylammonium bromide has similarly been used to improve the TLC analysis of vitamin B₆ in foods. Postaire has reported better separation and resolution of B₆ from other compounds using the overpressure layer technique than by HPTLC.

Cobalamin (Vitamin B₁₂)

Vitamin B₁₂ is the generic name for a group of vitamins known as cobalamins. The basic molecule consists of a corrin ring enclosing a central cobalt atom subtending axial ligands which determine the form and function of each individual cobalamin. Cyanocobalamin (CNCbl) was the first form of the vitamin isolated in 1948, independently by two groups. Both relied heavily on chromatography for the final separation and purification of CNCbl. Its complex three-dimensional structure was elucidated in 1956 by Dorothy Hodgkin using elegant X-ray crystallographic techniques.

The cobalamin molecule can only be synthesized by microorganisms, but all mammalian cells are equipped to covert the vitamin into its coenzymes. Cobalamin is without known function in plants and, if present, is only associated with the metabolic activity of microorganisms. Hence, unlike folate, dietary sources of the vitamin are exclusively animal in origin and include fish, meat – particularly liver and kidney – eggs and milk. Cobalamin is acid- and heat-stable but, like other hydrophilic vitamins, is destroyed by exposure to high pH. Notable features of cobalamin are that it is a much larger molecule (mol wt of OHCbl is 1346) than any other B-group vitamin and tissue levels are lower than any other, with total amounts in the body amounting to only a few milligrams. The low RDA of 1–2 µg is a reflection of the efficient means employed by the body to retain the vitamin. The low tissue levels of cobalamins naturally cause analytical problems and this has led to the development of enhanced methods of detection, discussed below.

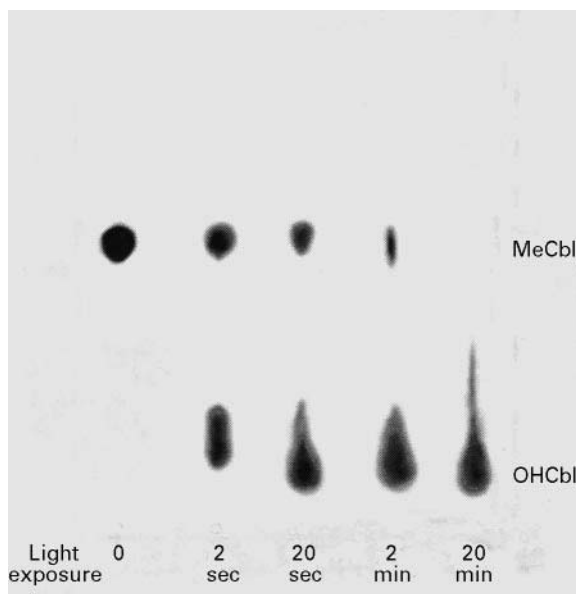


Figure 2 Photolysis of methylcobalamin (MeCbl) in extracts of normal human plasma exposed to daylight. Most of the MeCbl was converted to hydroxocobalamin (OHCbl) in 2 min.

In humans, the two coenzyme forms of vitamin B₁₂ are adenosylcobalamin (AdoCbl) and methylcobalamin (MeCbl) and each is required in specific reactions involving, respectively, isomerization and transmethylation. Both coenzymes are very light-sensitive and are readily converted to hydroxocobalamin (OHCbl) by exposure to white light, as may be demonstrated (Figure 2). MeCbl was first synthesized in the laboratory by Lester Smith and detected in human plasma by Lindstrand in 1963 as an unidentified zone on paper chromatograms. Using large quantities of liver, this compound was isolated using chromatographic methods and characterized as MeCbl.

The bulk of cobalamin in the body occurs as AdoCbl in cells and MeCbl in plasma, but other forms detected include OHCbl, CNCbl and suphitocobalamin, which may be a breakdown product of glutathionylcobalamin, possibly an important metabolic intermediate. A variety of adsorbents may be used for cobalamin TLC but none has been found to better a mixed layer of Whatman CC41 microgranular cellulose and silica gel G (Figure 3). A sensitive two-dimensional TLC method has been developed which allows small blood and tissue samples to be used (Figure 4) to investigate cobalamin metabolism in health and a wide range of diseases, including cobalamin deficiencies and genetic errors of B₁₂ metabolism. The sensitivity of the method relies on the bioautography organism which is a selected strain of *Escherichia coli*, which has a cobalamin growth response down to 1–2 pg. Growth zones are

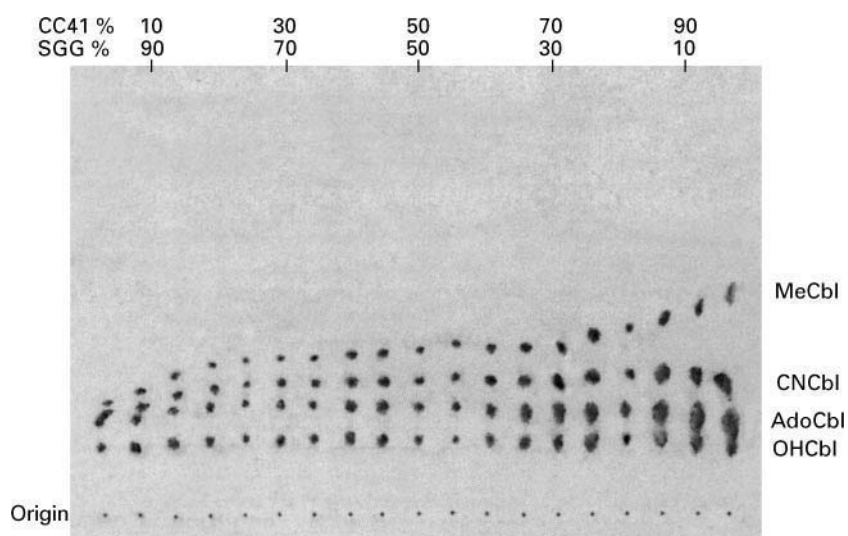


Figure 3 Separation of an aqueous mixture of four cobalamins by TLC on a gradient layer of cellulose (CC41) and silica gel (SGG), showing the influence of varying adsorbent mixtures on separation of the cobalamins. The mobile phase was butan-2-ol-water-0.880 ammonia (75 : 25 : 2).

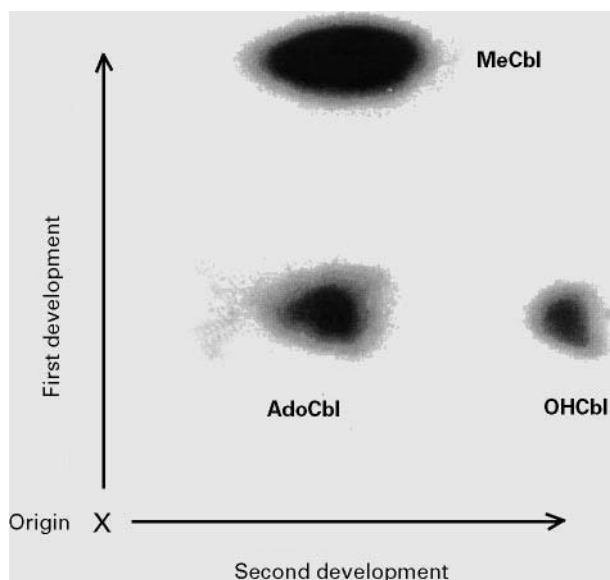


Figure 4 Separation of cobalamins extracted from normal human plasma. The adsorbent was cellulose CC41-silica gel G (3 : 1) developed first in butan-2-ol-water-0.880 ammonia (75 : 25 : 2) and second, in water saturated with benzyl alcohol. The second development was at right angles to the first, after air-drying the plate. Extraction and chromatography were in darkness or by red light. Cobalamin zones were detected bioautographically by over-layering the chromatogram with agar seeded with a cobalamin-sensitive *Escherichia coli* mutant and a tetrazolium growth indicator. The 'sandwich' was incubated at 35°C for 18 h. Methylcobalamin (MeCbl) is the main form present in healthy subjects, with smaller amounts of adenosylcobalamin (AdoCbl) and hydroxocobalamin (OHCbl).

enhanced by inclusion of 2,3,5-triphenyltetrazolium chloride in the agar medium which is converted to the red dye fomazan during growth of the organism. The red zones corresponding to cobalamins separated on the TLC plate are then scanned by densitometer or computer and quantitated. A 10–100-fold increase in sensitivity is gained if radiolabelled cobalamins are separated and the bioautogram growth zones excised and their radioactivity measured.

Folic Acid

Folic acid (pteroylglutamic acid) and related compounds are present at high concentrations in liver, but spinach, broccoli, peanuts and fresh fruit are also good dietary sources. Foliates are important for the synthesis of tetrahydrofolate, which is important with cobalamin for a series of 1-carbon transfer reactions leading to DNA synthesis, failure of which leads to megaloblastic anaemia.

Chromatographic analysis of folate compounds including methotrexate and other antifolates has been reviewed. Process impurities in the reduced folate compound leucovorin calcium may be monitored using a TLC method with fluorescence detection. An overpressure layer TLC procedure (OPLC) has been used to improve the separation of folic acid from other water-soluble vitamins with good recovery and resolution. The method uses silica gel layers developed in butan-1-ol-pyridine-water (50 : 35 : 15) at a rate of 0.25 mL min⁻¹ for baseline separation. Quantitation is achieved without derivatization.

Biotin

Good sources of biotin are liver, pork, nuts, chocolate, pulses, cereals and royal jelly; biotin is widely distributed among all types of food and dietary deficiency is rare. However, biotin is inactivated by avidin, which is present in raw egg white, and severe eczema has been reported from this type of deficiency. This does not arise if cooked eggs are included in the diet, since heat deactivates avidin. Biotin acts as coenzyme to carboxylase enzymes, for example in the catabolism of propionate to methylmalonate. Biotin is stable in acid and neutral solutions and hence may be extracted at low pH before chromatography.

Biotin is separable from other water-soluble vitamins by TLC on silica gel or cellulose layers developed in neutral or acidic butanol–water mixtures. Various detection reagents have been used for biotin, including iodine vapour, 1% potassium permanganate, 1% dimethylaminobenzaldehyde in hydrochloric acid and *p*-dimethylaminocinnamaldehyde in a mixture of methanol and sulfuric acid, which is specific for biotin, yielding intense orange zones with an absorbance maximum at 533 nm. More recently, TLC, HPTLC and OPLC techniques have been compared, using five different mobile phases. Biotin tends to be resolved poorly from pantothenic acid by HPTLC but this is improved by OPLC, although in the systems investigated this led to less than perfect separation of biotin and folic acid.

Ascorbic Acid (Vitamin C)

Ascorbic acid occurs abundantly in fresh fruit, especially blackcurrants, citrus fruit and strawberries, and in most fresh vegetables; good sources are broccoli and peppers. It is destroyed by heat and is not well stored in the body. Ascorbic acid is a good reducing agent and facilitates many metabolic reactions and repair processes.

In pharmaceutical preparations and fruit juices, ascorbic acid is readily separated from other compounds by TLC on silica gel and quantitated directly by absorption at 254 nm. Serum and plasma may be deproteinized with twice the volume of methanol or ethanol. Various ascorbic acid compounds in plant extracts and foods have been separated on cellulose layers and detected by spraying with 2,5-dichlorophenol indophenol. Heulandite, a natural zeolite (particle size 45 µm) has successfully been employed as an adsorbent and ascorbic acid and other hydrophilic vitamins have

separated within 5 cm by ascending chromatography in dimethylformamide. HPTLC and OPLC methods have been developed to improve the separation of ascorbic acid from other water-soluble vitamins, with some success.

Conclusion

TLC is a flexible and well-established technique for the separation of water-soluble vitamins, limited only by the stability of the compounds to be separated, the resolving power of the TLC system and the sensitivity of the detection method. In complex biological systems these factors assume greater importance as vitamin concentrations are lower and metabolites may interfere with the separation. A preliminary extraction step or use of a short clean-up column can help remove salts and other interfering substances and may increase the concentration of vitamins to be chromatographed. Recovery experiments will monitor any selective losses at this stage.

The introduction of HPTLC and OPLC with optimized solvent systems has undoubtedly increased the resolving power for a number of vitamins. Gradient or two-dimensional TLC can increase this still further. Ultimately, it is the means of detection which determines the sensitivity of the system. Fluorimetry has become the method of choice for those vitamins forming fluorescent derivatives, but there are alternatives. One is to overlay the chromatogram with an agar medium seeded with a microorganism whose growth is sensitive to the vitamin. This can detect as little as a few pg of the vitamin. Even higher sensitivity can be achieved using radioactive vitamins detected autographically or with phosphorimagers. In future, the development of an immunoassay technique similar to Western blotting is likely to allow the most sensitive quantitation of vitamins separated by HPTLC.

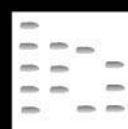
See also: II/Chromatography: Thin-Layer (Planar): Densitometry and Image Analysis; Instrumentation; Modes of Development: Forced Flow, Overpressured Layer Chromatography and Centrifugal; Spray Reagents. III/Vitamins: Liquid Chromatography.

Further Reading

Argekar AP and Kunjir SS (1996) Simultaneous determination of isoniazid and pyridoxine hydrochloride in pharmaceutical preparations by high-performance thin-layer chromatography. *Journal of Planar Chromatography* 9: 390–394.

- Bates CJ (1997) Vitamin analysis. *Annals of Clinical Biochemistry* 6: 599–626.
- Bhushan R and Ali I (1987) TLC resolution of constituents of the vitamin B complex. *Archives of Pharmacology* 320: 1186–1187.
- DeLeenheer WL and DeRuyter G (1985) *Modern Chromatographic Analysis of the Vitamins*. New York: Marcel Dekker.
- Diaz A, Paniagua A and Sanchez F (1993) Thin-layer chromatography and fiberoptic fluorometric quantitation of thiamine, riboflavin and niacin. *Journal of Chromatography A* 655: 39–43.
- Linnell JC, Hussein HA-A and Matthews DM (1970) A two-dimensional chromato-bioautographic method for complete separation of individual plasma cobalamins. *Journal of Clinical Pathology* 23: 820–821.
- Linnell JC and Bhatt H (1995) Inherited errors of cobalamin metabolism and their management. In: Wickramasinghe S (ed.) *Megaloblastic Anaemia: Baillière's Clinical Haematology-International Practice and Research*, pp. 567–601. London: Baillière Tindall.
- Postaire E, Cisse M, Le Hoang M and Pradeau D (1991) Simultaneous determination of water-soluble vitamins by over-pressure layer chromatography and photodensitometric detection. *Journal of Pharmacology Science* 80: 368–370.
- Quadros EV, Hamilton A, Matthews DM and Linnell JC (1978) Isolation of ^{57}Co -cobalamin coenzymes at high specific activity from *Streptomyces griseus*. *Journal of Chromatography* 160: 101–108.
- Sherma J and Fried B (1996) *Handbook of Thin-layer Chromatography*. New York: Marcel Dekker Inc.
- Stahl E (1969) *Thin Layer Chromatography: a Laboratory Handbook*. New York: Springer-Verlag.
- Surmeian M, Ciohodaru G, Ionescu MS and Cosofret VV (1995) Derivative UV-spectrophotometric determination of binary mixtures of procaine hydrochloride with benzoic acid, pyridoxine hydrochloride and 4-aminobenzoic acid from pharmaceutical preparations. *Revue Roumaine de Chimie* 40: 111–117.
- Tseng M-C, Tsai M-J and Wen K-C (1996) Quantitative analysis of acetaminophen, ethoxybenzamide, piroxicam, hydrochlorthiazide, caffeine, chlorzoxasone and nicotinamide, illegally adulterated in Chinese medicinal pills. *Journal of Food and Drug Analysis* 4: 49–56.
- Zempleni J, McCormick DB and Mock DM (1997) Identification of biotin sulfone, bisnorbiotin methyl ketone and tetranorbiotin-1-sulfone in human urine. 65: 508–511.

VOLATILE ORGANIC COMPOUNDS IN WATER: GAS CHROMATOGRAPHY



M. C. Tombs, North West Water Limited,
Warrington, UK

Copyright © 2000 Academic Press

Introduction

An important class of substances for which it is increasingly necessary to analyse in environmental waters comprises a wide range of volatile organic compounds (VOC). These include aromatics such as methylbenzene (toluene) and the dimethylbenzenes (xylenes), and the environmentally persistent halogenated solvents such as tetrachloromethane and trichloroethene. Many of these compounds are finding their way onto national and international lists of proscribed or regulated compounds, and as a result there is a requirement for robust methods of analysis to monitor both the

environment itself and potential sources of discharge to it.

In the aqueous environment, there are a number of sample types that an analyst may be required to examine, each presenting their own problems and challenges and requiring slightly different analytical solutions. Drinking waters, for example, are a relatively straightforward matrix, often with a clearly defined quality standard imposed, such as the requirements of the European Union Drinking Water Directive (see Further Reading). River waters and marine waters may also be required to meet exacting environmental quality standards (EQS), which are frequently much lower than those set for drinking waters where the presence of haloforms, for example, is an accepted by-product of the disinfection process. Monitoring of wastewater effluents is fundamental to environmental quality management, since these are

a major source of VOCs in the environment. Such effluents are frequently complex mixtures of many different compounds present in a wide range of concentrations, and as such offer special challenges to the analyst.

Quantitative analytical methods must therefore offer good precision and accuracy and be able to withstand the rigorous inspection required by the legislative environment, in order to demonstrate satisfactory compliance with the regulations.

This article discusses some of the methods available for the analysis of VOCs in these matrices and is illustrated with examples taken from routine drinking water and wastewater quality analysis. The chromatograms are reproduced here by courtesy of North West Water Laboratory Services.

Sampling Techniques

The first stage of any analysis, whether carried out in the field or remotely in the laboratory, is the collection of a representative sample and the preservation of that sample intact until it reaches the analyst. Without doubt the best approach is to sample straight into the container to be used for the analysis, but this may present logistical problems with handling either very small containers or carrying out precise measurements of volume. It is easy enough to do this in a clean, well-equipped laboratory, but it becomes a much more challenging task on a cold, wet river bank or windswept beach!

The problem is that with the analytes being so volatile, their concentration in the matrix can change significantly between sampling and analysis if the sample is not correctly taken. One method widely used with good results is to use a pre-cleaned screw-cap septum vial, made from borosilicate glass and of around 20 or 40 mL capacity. The vial is rinsed several times with the sample before being filled so that the meniscus stands proud of the brim. A thick septum faced with polytetrafluoroethylene (PTFE) is then slipped sideways over the top of the vial, ensuring that no air bubble remains trapped within, and the septum cap is then firmly screwed down, sealing the sample in the vial. A vial with a leaking seal will obviously cause sample to be lost, but will also allow preferential evaporation of VOCs. Similarly, a vial containing an air bubble will also damage sample integrity by allowing dissolved VOCs to equilibrate between the aqueous and vapour phases. Any subsequent sample taken from the vial for analysis will therefore contain a *lower* concentration of VOCs than the original.

Use of a septum will allow the withdrawal of a subsample from the vial, using a syringe and an air bleed

Table 1 Common options for the analysis of VOCs

<i>Introduction</i>	<i>Separation</i>	<i>Detection</i>
Solvent extraction	GC	FID
Direct aqueous injection		ECD
Headspace		MS
Purge-and-trap		ELCD PID

Note: FID, flame ionization detector; ECD, electron-capture detector; MS, mass spectrometry; ELCD, electrolytic conductivity detector; PID, photoionization detector.

needle, without opening it and risking the possible loss of volatiles. Similarly, a suitable extraction solvent may be added by a displacement technique. Some laboratories use these approaches; others will open the vial and rapidly transfer the required volume to another closed container. Either way, taking further subsamples should be avoided, as the concentration of VOC in the sample will already have begun to change. Further information on sample collection is to be found in a 1987 HMSO publication.

Methods of Analysis

Modern capillary gas chromatography (GC) lends itself particularly well to the low-level analysis of VOCs, offering a good separation of the analytes and high sensitivity. There is a variety of sample introduction techniques in common use and a wide choice of columns is available to the analyst. Several different detector systems can be used, dependent on the analytes and the sensitivity and specificity required.

The actual method of analysis chosen will depend on several factors. These include the analytes themselves, the sample matrix, the resources available to the analyst and the level of confidence required in the results. For example, an analyst interested in a rough-and-ready assessment of the presence of aromatic solvents at levels in excess of 1 mg L⁻¹ might choose to use direct aqueous injection (DAI) with a flame ionization detector (FID) as the simplest way of obtaining the information required. Conversely, an analyst investigating a complex industrial wastewater and providing evidence for prosecuting an illegal discharge may prefer the precision of a headspace sample introduction technique and the confirmatory information which may be obtained by using a mass spectrometer (MS) as a detector. The commonest options are set out in Table 1.

Sample Introduction Techniques 1: Solvent Extraction

Solvent extraction is a useful technique for dealing with relatively clean samples, such as drinking waters

Table 2 Solvent extraction performance data for selected compounds

Compound	Recovery (%)	RSD (%)	LOD ($\mu\text{g L}^{-1}$)
Trichloromethane ^a	85	6.1	0.19
Tetrachloromethane ^a	79	11.7	0.009
Tetrachloroethene ^a	104	3.1	0.012
Benzene ^b	105	nd	1.58
Methylbenzene ^b	99	nd	0.13

^aChlorinated compounds determined at a concentration of $2.5 \mu\text{g L}^{-1}$ (tetrachloroethene $5 \mu\text{g L}^{-1}$) with four degrees of freedom. 20 mL sample extracted with 2.5 mL petroleum ether 30–40°C. Analysis by packed column GC-ECD. From HMSO (1987).

^bAromatic compounds determined at a concentration of $10 \mu\text{g L}^{-1}$. 1 L sample extracted with 10 mL pentane, cleaned up with florisil and concentrated to 1 mL. Analysis by $50 \text{ m} \times 0.2 \text{ mm}$ OV-1 capillary column with FID. From HMSO (1987). RSD, relative standard deviation; LOD, limit of detection; nd, not determined.

or high-quality river waters. The pentane or hexane extraction solvent may be added to the sample vial by displacement, as described above, and the vial is then shaken or rolled for up to 30 min. A sample of the solvent may then be withdrawn – again without opening the vial – and analysed by GC using conventional sample inlet techniques such as split/splitless or on-column injection. Typical sample/solvent ratios of between 5:1 and 20:1 give some sample pre-concentration, but the injection volume of around 1–2 μL restricts ultimate sensitivity.

The technique is well-suited to the analysis of chlorinated hydrocarbons, using an electron-capture detector (ECD), but may also be used in conjunction with most other types of detector, including mass spectrometers. Its main drawback is the time and effort required to carry out the extraction. Some performance data are listed in Table 2.

Sample Introduction Techniques 2: Direct Aqueous Injection

Perhaps the simplest of all sample introduction techniques, direct aqueous injection has been the subject of several papers. It has a number of advantages, not the least of which is convenience: samples collected in the manner described above require no further handling between collection and final analysis. As the name of the technique suggests, a 1 μL aliquot of sample is taken from the vial and injected directly into the instrument, using either an on-column or split/splitless injector.

This technique has been applied to the analysis of trihalomethanes and is said to be reliable and offers good precision and recoveries. Recoveries of 100% and peak area standard deviations of between

1.9 and 5.2% with approximately 14 degrees of freedom at the $10\text{--}100 \mu\text{g L}^{-1}$ level for the four chlorine- and bromine-containing trihalomethanes have been quoted. This compares with recoveries of between 60 and 90% for pentane extraction. The technique has been shown to be applicable to other chlorinated hydrocarbons, including 1,1,1-trichloroethane and tetrachloromethane.

The technique certainly works well with small numbers of samples, but experience in a laboratory handling upwards of 30 analyses daily suggests that the robustness of the analytical system becomes an important factor. Passing relatively large quantities of water vapour through an ECD shortens its useful life, and therefore the alternative inlet techniques described here are to be preferred where large numbers of samples are involved.

Another potential problem with the technique is that there is no initial clean-up of the sample and it is therefore only appropriate for relatively clean samples such as drinking waters. With other sample matrices there is a risk that significant quantities of nonvolatiles (including inorganic salts) can build up at the front of the column, reducing its life; similarly, the presence of less-volatile contaminants remaining on the column may interfere with subsequent analyses.

Despite this, DAI may be used successfully where a minimum effort, rough screening method is required, e.g. for an industrial wastewater. The use of an FID allows other, nonhalogenated compounds such as aromatics to be detected and estimated at milligram per litre levels. This analysis may be sufficient to meet some needs, but could also be used as a pre-screening technique to identify appropriate dilution factors for headspace or purge-and-trap analysis. An example of a chromatogram of a standard solution of aromatic compounds in water is shown in Figure 1.

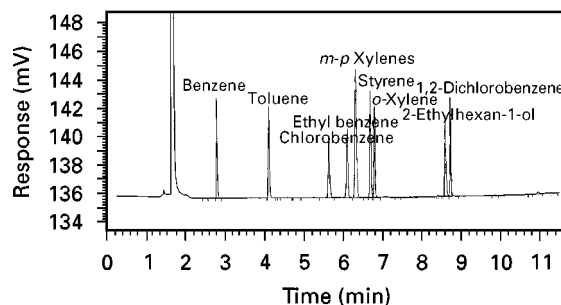


Figure 1 Aromatic compounds in water by DAI. Conditions: 1 μL injection; injector temperature 230°C ; $30 \text{ m} \times 0.25 \text{ mm}$ DB-1 column; temperature program 70°C , hold 2 min $\rightarrow 90^\circ\text{C}$ at $20^\circ\text{C min}^{-1} \rightarrow 260^\circ\text{C}$ at $35^\circ\text{C min}^{-1}$, hold 5 min; FID temperature 280°C . Chromatogram shown is from a standard solution in water containing 10 mg L^{-1} each compound.

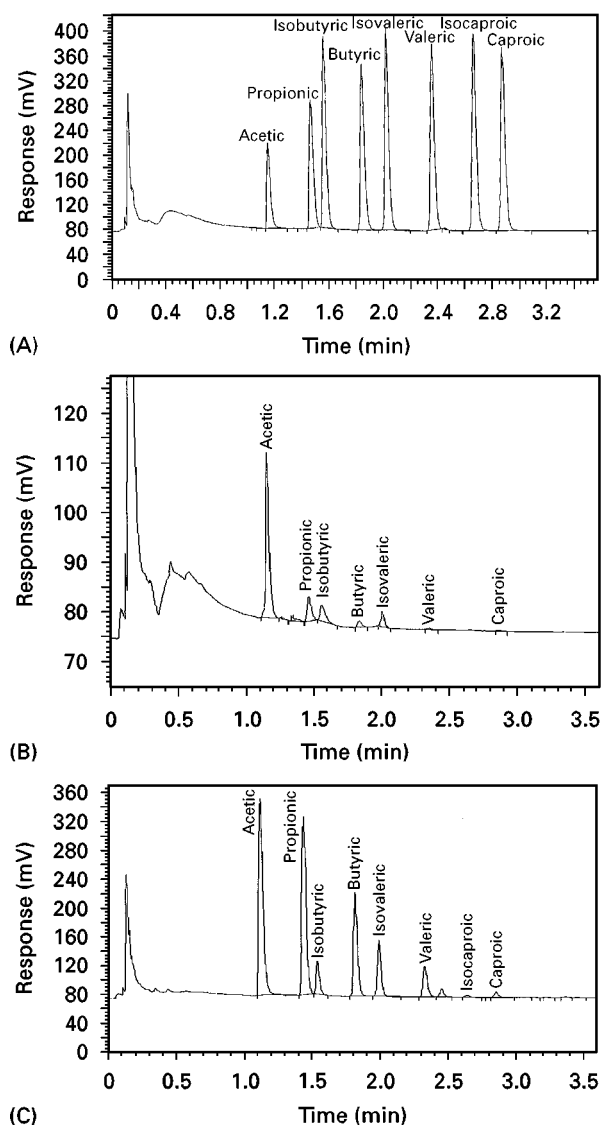


Figure 2 Analysis of VFA in sewage sludge supernatant water by DAI. Conditions: 1 μL 20 : 1 split injection; injector temperature 250°C; 12 m \times 0.53 mm BP-21 column; temperature program 60°C \rightarrow 250°C at 20°C min⁻¹, hold 3 min; carrier gas, nitrogen 3 mL min⁻¹; FID temperature 300°C. (A) Chromatogram shown is from a standard solution in water containing approximately 800 mg L⁻¹ each compound. (B) VFA in digested sludge. Acetic acid concentration 100 mg L⁻¹; others < 10 mg L⁻¹. (C) VFA in a partially digested sludge. Acetic acid concentration approximately 800 mg L⁻¹.

Difficult-to-extract analytes such as alcohols, ketones or volatile fatty acids (VFA) may also be estimated by this technique (Figure 2). A specific application is the analysis of VFA in sewage sludge, the results of which are used to monitor the performance of sludge digesters in wastewater treatment plants. Samples of sludge are centrifuged and the supernatant water filtered through a 1 μm membrane, in order to prevent particulate matter blocking either the injection

syringe needle or the capillary column itself. Acidified with phosphoric or formic acid, the samples are then analysed by direct aqueous injection GC-FID. The analytical range required of the application is typically 1–1000 mg L⁻¹ for each compound, although ethanoic (acetic) acid will predominate in samples from a stable digester.

A simple packed column application of direct aqueous injection is the analysis of methane in water. A 1 μL sample is injected directly onto a 1 m ChromosorbTM 101 column for isothermal analysis at 70°C, with an FID. Calibration is normally carried out using a standard gas mixture.

Sample Introduction Techniques 3: Headspace Analysis

Headspace analysis is a clean, reliable method of introducing volatile analytes to a GC column, and is especially useful where complicated matrices such as industrial wastewaters containing many other contaminants must be analysed. Involving the analysis of just the *vapour* above a sample of water, the method provides instant clean-up by ensuring that only volatile materials are introduced into the GC sample inlet, resulting in a clean chromatogram and enhanced column life.

The technique is a practical application of Henry's law, which states that 'the vapour pressure of a solute is proportional to the amount of solute present in a solution at equilibrium with its vapour'. Thus if the concentration of an analyte in the vapour phase can be measured, it can be correlated by a suitable calibration with its concentration in the sample.

The two methods of introducing samples to the GC are known as *static* and *dynamic* headspace. In the former, the vapour in equilibrium with the sample in a vial is analysed, usually at an elevated temperature; in the latter the vapour is first enriched by actively purging the sample with an inert gas.

Given that the solubility of gases decreases with increasing temperature, raising the temperature of the sample will favour the vaporization of the analytes, enriching the headspace, and this effect is used to enhance analyte recovery. It does mean, however, that temperature must be rigorously controlled both during analysis and from sample to sample, if reproducibility is to be assured.

Static headspace Samples may be collected for this analysis in two ways. A vial can be filled as described previously, or a fixed amount (typically 5–10 mL) of sample may be accurately measured and sealed – with an internal standard, if one is to be used – in a vial of about 20–25 mL capacity, which is to be used for the

analysis. The latter option would allow the sample to be presented to the instrument unopened, minimizing the requirement for sample preparation in the laboratory, but practical considerations in the field mean that the former is often preferred.

Sealed in its headspace vial, the sample is placed in a thermostatted heater and allowed to equilibrate with the air space above it. Some headspace sampling devices will also agitate the sample to accelerate this equilibration. Once equilibrium is established, the vial is pressurized with carrier gas passing through a sampling needle penetrating the septum. On reaching the required pressure, the flow is reversed, carrying sample vapour to the GC inlet. The volume transferred is controlled either by reversing the flow for a fixed time or by the use of a sample loop. The liquid sample therefore does not come into contact with any part of the GC itself.

Calibration of the system is carried out by preparing standard solutions of the analytes of interest in water, and treating them in exactly the same way as samples, sealing the same volume in a vial and subjecting them to the whole procedure described above. Key to the process is consistency: each sample and standard must be treated exactly alike, and automated headspace samplers facilitate this. In order to achieve reproducible results, it is not even necessary for the samples to achieve equilibrium; providing they are consistently treated, i.e. by equilibrating at exactly the same temperature and for the same length of time, reproducibility is assured.

A suitable internal standard can be added to the headspace vial before sealing and then used either directly to calibrate the individual analysis or to aid an external calibration process.

The technique has a good linear range and sensitivity and provides a robust and reliable method of introducing both clean and dirty water samples to a GC with very little sample preparation (Table 3). As might be expected, attainable recoveries measured against standard solutions are close to 100% and

Table 3 Headspace performance data for selected compounds

Compound	Recovery (%)	RSD (%)	LOD ($\mu\text{g L}^{-1}$)
Trichloromethane	99.95	3.4	1.42
Tetrachloromethane	98.30	4.18	0.04
Tetrachloroethene	96.84	4.43	0.44

Data determined at a concentration of $122 \mu\text{g L}^{-1}$ (trichloromethane); $3 \mu\text{g L}^{-1}$ (tetrachloromethane); and $10 \mu\text{g L}^{-1}$ (tetrachloroethene) with approximately 17 degrees of freedom. 5 mL sample equilibrated for 5 min at 80°C . Analysis by $30 \text{ m} \times 0.53 \text{ mm}$ DB-624 capillary column GC-ECD. Data provided by North West Water Laboratory Services.

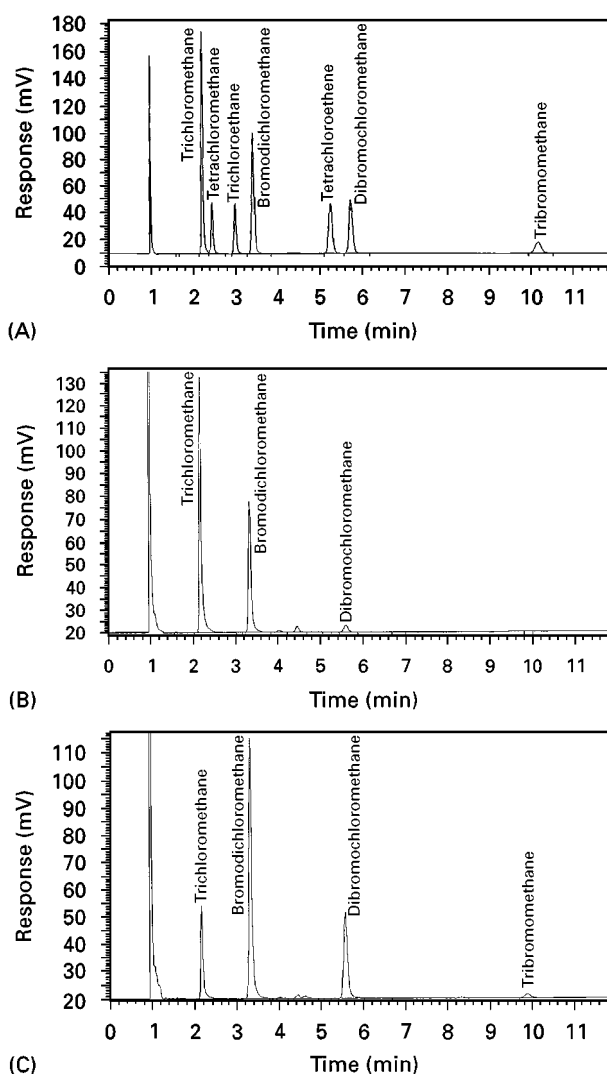


Figure 3 Analysis of trihalomethanes and chlorinated hydrocarbons in drinking water by headspace GC-ECD. Conditions: 5 mL sample, equilibrated for 10 min; $30 \text{ m} \times 0.53 \text{ mm}$ DB-624 column; isothermal at 80°C . ECD temperature 250°C ; carrier gas: nitrogen 7.5 mL min^{-1} . (A) Chromatogram shown is from a standard solution in water containing $91.5 \mu\text{g L}^{-1}$ trichloromethane (highest concentration component) and $2 \mu\text{g L}^{-1}$ tetrachloromethane (lowest). (B) Trihalomethanes in drinking water derived from a surface source. Concentrations: trichloromethane $63 \mu\text{g L}^{-1}$; bromodichloromethane $7 \mu\text{g L}^{-1}$; dibromochloromethane $1 \mu\text{g L}^{-1}$. Note the almost total absence of other chlorinated hydrocarbons. (C) Trihalomethanes in blended drinking water derived from surface and underground sources. Concentrations: trichloromethane $18 \mu\text{g L}^{-1}$; bromodichloromethane $12 \mu\text{g L}^{-1}$; dibromochloromethane $2 \mu\text{g L}^{-1}$; tribromomethane $< 2 \mu\text{g L}^{-1}$. Note the reduced concentration of chlorinated compounds and the increase in brominated compounds.

interferences and column degradation are minimized. It may be used with any detector type, including mass spectrometers. An example of the analysis of trihalomethanes and chlorinated hydrocarbons in drinking water is shown in Figure 3.

Absolute recoveries are dependent on equilibration time and temperature. Increasing the equilibration time to the point where the sample and its vapour are fully equilibrated will maximize recovery; raising the temperature will increase the partial pressure of volatile compounds in the headspace. Systems typically operate at temperatures of up to 80°C: any higher and the increased vapour pressure of the water matrix itself interferes, negating the benefits.

One drawback is the inability to reanalyse samples, because once a vial has been subsampled, the integrity of the sample itself is destroyed and equilibration with the new headspace will alter the composition of the sample. This means that a subsequent repeat analysis cannot be carried out if confirmation of a result is required: a fresh sample must be collected. Although this may present a problem to the environmental analyst, a technique known as 'multiple headspace extraction' (MHE) has been described (see Further Reading) where a sample is equilibrated with successive volumes of gas. Analysis of each successive headspace volume will allow the distribution of the analytes to be determined, providing a measure of an important physical property. Headspace analysis has been used for this purpose almost since it was first developed.

The extrapolation of MHE data to the 'zero equilibration' level provides a measure of the original concentration of an analyte. This may be particularly useful in situations where for some reason it is not possible to calibrate the analytical system with either the analyte or matrix of interest, or where an 'absolute' recovery must be determined.

Dynamic headspace Dynamic headspace or purge-and-trap sampling is an effective way of achieving high sensitivity in the analysis of VOC. This is particularly important in the analysis of environmental samples for comparison with stringent EQS, which frequently test the limits of analytical methodology.

Unlike static headspace, where the sample is simply allowed to equilibrate, in purge-and-trap the sample is purged with an inert gas (usually helium) in order to drive the volatiles out into the vapour phase. The vapour is then caught in a cold trap or adsorbed on an appropriate support before being thermally desorbed and passed to the GC inlet. The method retains the advantage of the headspace technique in terms of presenting a clean sample to the GC, but potentially offers much greater sensitivity (Table 4).

Whilst the technique has the ability to improve sensitivity, the overall range of an analysis may not be increased, since this is dependent on the dynamic range of the detector. This means that with the general tendency to analyse suites of compounds to-

Table 4 Purge-and-trap performance data for selected compounds

Compound	Recovery (%)	RSD (%)	LOD ($\mu\text{g L}^{-1}$)
Trichloromethane	94.10	3.80	0.002
Tetrachloromethane	nd	nd	0.004
Tetrachloroethene	98.80	1.30	0.005
1,2-Dichlorobenzene	77.70	8.50	0.020
Methylbenzene	99.11	0.77	0.001
1,2-Dimethylbenzene	98.38	1.46	0.004

Recovery and RSD data determined at a concentration of $4 \mu\text{g L}^{-1}$ with approximately two degrees of freedom. 25 mL sample purged at 35°C with helium, 50 mL min^{-1} for 10 min. Analysis by packed column GC-FID. From Driss and Bouguerra (1991). LOD, limit of detection. 5 mL sample purged with helium, 40 mL min^{-1} for 2 min. Analysis by $60 \text{ m} \times 0.53 \text{ mm}$ DB-624 capillary column GC with electrolytic conductivity detector and photo-ionization detector. From Mehran, Nickelsen, Golkar and Cooper (1990) *Journal of High Resolution Chromatography* 13: 429–433.

gether, those compounds for which low limits of detection are required can be analysed satisfactorily, but those present in higher concentrations in the same sample may well exceed the range of the detector! For example, purge-and-trap GC-MS analysis of some drinking waters easily achieves the required limit of detection of $0.3 \mu\text{g L}^{-1}$ for tetrachloromethane, but exceeds the linear range of the detector for the trichloromethane present in a much higher concentration.

The optimization of a purge-and-trap method has been examined and both purge gas volume and temperature have a significant effect on analyte recovery. Keeping the purge gas flow rate constant, but extending the purge time from 10 to 20 min, greatly enhanced the recoveries of all the analytes examined, although the recoveries of compounds with a higher solubility in water (e.g. tribromomethane) were still poor. Difficulties have been reported with the use of very short purge times: 1 min gave rise to reproducibility problems due to the mode of operation of the equipment, whereas 2 min resulted in an acceptable performance and a much faster method. Extended purge times may risk compromising recoveries of highly volatile compounds, since these can be purged efficiently in a short time. Recovery is then dependent on the efficacy of the trap in retaining them until the chromatographic separation is ready to begin.

Elevated temperatures also speed recovery. Results obtained from purging for 20 min at 25°C have been found to be comparable with those from a 10-min purge at 40°C. The disadvantage of using a higher temperature is that more water vapour is carried over into the analytical system. Without effective control

Table 5 Effect of purge time and temperature on recovery of selected compounds

Compound	Recovery (%)			
	10 min purge	20 min purge	30°C	40°C
Trichloromethane	78.06	91.81	82.01	87.63
1,2-Dichloroethane	60.55	88.10	62.48	64.75
Tetrachloroethene	98.03	99.10	97.94	100
1,2-Dichlorobenzene	59.86	66.82	60.94	65.41
Methylbenzene	85.73	93.12	88.63	94.05
1,2-Dimethylbenzene	81.86	84.28	84.99	89.66

Data determined at a concentration of $4 \mu\text{g L}^{-1}$ with approximately two degrees of freedom. 25 mL sample purged with helium, 50 mL min^{-1} 10/20-min purge data determined at 25°C . Temperature data determined with a purge time of 10 min. Analysis by packed column GC-FID. From Driss and Bouguerra (1991).

this will interfere with the analysis – particularly with moisture-sensitive equipment such as ECD or mass spectrometers. For this reason, purge temperatures significantly greater than 40°C are not widely used. Table 5 shows the effect of purge time and temperature on the recovery of selected compounds.

Waters containing detergents or other foaming agents may prove difficult to analyse effectively by this technique. It is, however, suitable for use with most types of detector.

Matrix Modification

The use of matrix modifiers is common practice in water analysis, and they are often used to enhance the performance of some methods for the analysis of VOC – in particular the headspace and purge-and-trap methods. The addition of modifiers such as sodium chloride or sodium sulfate to samples prior to analysis will – by modifying the activity coefficient of the VOC solutes and the vapour pressure of the solvent – enhance the relative concentration of the analyte in the headspace above the sample. This effect is most noticeable for the less soluble or less volatile compounds such as the dimethylbenzenes or the dichlorobenzenes, although it may be of limited use with other compounds, such as trichloromethane, where

recoveries may readily be optimized by temperature control.

Although the effect may be used to improve the performance of a method, it is important to remember that the samples themselves may be subject to some variability. Table 6 provides the evidence to show why a seawater sample could not be analysed using a method set up and calibrated for use with drinking water, or vice versa: the performance of the method will differ significantly between the two matrices. For the same reason, it is important that the ionic strength of both samples and standards is consistent. If there is any doubt then an excess of salt (e.g. around 2 g mL^{-1}) should be added to all samples and standards to ensure consistency.

Analytical Columns

Today, most applications for VOC analysis use capillary columns, the length and film thickness of which will depend on the complexity of the analysis. Up to about 20 compounds can be satisfactorily resolved by a 25–30 m column in about 10 min, whereas a 50–60 m column is more appropriate for samples containing 60 or more analytes, taking 30 min to 1 h to achieve an acceptable separation.

Although the superior resolution of the capillary column means that most separations can be achieved using ‘standard’ nonpolar or moderately polar phases such as DB-1 from J & W or BP-5 from SGE, there is an increasing number of columns tailored for specific analyses. These include J & W’s DB-624 phase, designed to substitute for the packed column specified in US Environmental Protection Agency (US EPA) method 624, for purgeable organic compounds. Such columns are designed to optimize the separation and the time required for the analysis of the compounds of interest.

The direct aqueous injection technique requires the use of bonded-phase columns to ensure that the water passing through it does not destroy the column.

Table 6 Effect of ionic strength on recovery of selected compounds

Compound	Purging efficiency		
	0% NaCl	10% NaCl	20% NaCl
Trichloromethane	83.63	93.98	98.52
1,2-Dichloroethane	63.2	67.97	76.17
Benzene	90.12	97.22	99.50
1,3-Dichlorobenzene	72.45	81.59	91.5
1,2-Dimethylbenzene	86.43	96.72	98.91

Purge-and-trap recovery data determined at a temperature of 35°C . From Driss and Bouguerra (1991).

Detectors

Perhaps the commonest detectors used for VOC analysis in the environmental industry are the ECD and the mass spectrometer, primarily because of the keen interest in levels of organochlorine compounds in the environment. However, the FID also finds application in the analysis of hydrocarbons – including aromatics – providing reliable detection and sensitivity down to around $100 \mu\text{g L}^{-1}$ without sample pre-concentration. It may also be used with mixtures of hydrocarbons and some chlorinated solvents, and although limits of detection for the latter are relatively high, the robustness of the detector may make it an appropriate choice for the analysis of an industrial wastewater, for example. As previously described, the FID can be used for the analysis of relatively high concentrations of VOCs by the direct aqueous injection technique.

Where low levels of halogenated solvents are to be determined, by far the best option is to use an ECD, which has a high specificity and sensitivity for many halogenated compounds. This will work with all of the sample introduction techniques previously described, although complex industrial wastewaters may contain compounds that contaminate the detector. In such cases, selective introduction techniques such as headspace or purge-and-trap are to be preferred, as these will eliminate or substantially reduce the contaminants introduced to the system.

When a wide-ranging screen coupled with specificity and reasonable sensitivity is required, then a mass spectrometer may be used. Small bench-top instruments are increasingly found in environmental laboratories, and many are employed in just this kind of activity, coupled to headspace GC systems. Such a configuration provides a good response to a variety of compound classes, is robust enough to handle samples of badly contaminated industrial wastewaters, and yet has sufficient sensitivity to analyse clean river waters to the levels required by most EQS. Additionally, the ability to produce a recognizable mass spectrum lends confidence to the identification of analytes. This is of particular importance when collecting evidence for the prosecution of an illegal discharge. Examples of analysis of chlorinated and aromatic hydrocarbons by headspace GC-MS are shown in Figure 4.

Other detector types in use, particularly in the USA, include the electrolytic conductivity detector (ELCD) and the photoionization detector (PID) specified in some EPA methods. The latter can be up to a hundred times more sensitive than a FID when used for the analysis of some aromatic compounds, but in contrast to both the ECD and ELCD it will not detect the lighter haloalkanes such as those found in drink-

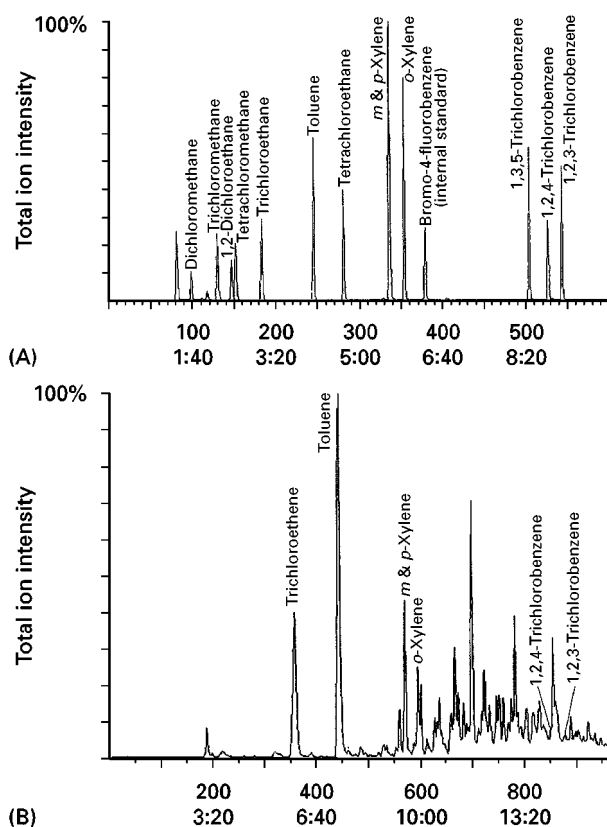


Figure 4 Analysis of VOCs by headspace GC-MS. Conditions: 5 mL sample, equilibrated for 10 min; 30 m \times 0.25 mm DB-5MS column; temperature program 40°C , hold 5 min \rightarrow 200°C at $15^\circ\text{C min}^{-1}$ \rightarrow 250°C at $50^\circ\text{C min}^{-1}$; carrier gas: helium 3 mL min^{-1} ; Ion TrapTM detection, EI mode, 1 s scan, mass range 45–220 amu. (A) Chromatogram shown is from a $100 \mu\text{g L}^{-1}$ standard solution in water. (B) VOCs in trade effluent from a road haulier's premises. Conditions as above except carrier gas approximately 1.5 mL min^{-1} . Approximate concentrations: trichloroethene $1150 \mu\text{g L}^{-1}$; toluene $1700 \mu\text{g L}^{-1}$; *m*- and *p*-xylenes $500 \mu\text{g L}^{-1}$; *o*-xylene $250 \mu\text{g L}^{-1}$; 1,2,4-trichlorobenzene $20 \mu\text{g L}^{-1}$; 1,2,3-trichlorobenzene $40 \mu\text{g L}^{-1}$. Other compounds, including the internal standard, are also present, but cannot be seen on this scale.

ing water. The convenience the ECD offers over the ELCD coupled with the greater specificity and sensitivity of the PID relative to the FID means that a useful application for the detectors in tandem is the analysis of both halogenated and aromatic compounds in the same sample.

Of course, providing the sample introduction technique is compatible (as indeed the headspace methods inevitably will be), any detector type can be used to meet the specific requirements of the analysis.

Conclusion

This article has summarized the main methods of analysing for VOC in common use today and

has briefly described some of the advantages and disadvantages of each. It is hoped that the data illustrating the performance of the methods will assist readers in selecting an appropriate technique for their own application.

It is difficult to see where VOC analysis will go in the future, although possible developments include the more widespread application of automation to the dynamic headspace technique, enabling the unattended analysis of large batches of samples. Continued development of membrane and other direct inlet techniques for mass spectrometry and the shrinking size and price of MS-MS instruments may ultimately render the time-consuming chromatographic separation itself superfluous, offering the prospect of analysis in seconds rather than tens of minutes. However, for the time being the availability of suitable membranes permitting the migration of VOC restricts the application of this technique.

The increasing sensitivity of detection systems could well prove to be of little benefit to the analyst, as it may only serve to encourage the setting of even lower quality standards!

Whatever happens with the equipment and methodology that is employed, it is clear that continued growth in legislation controlling these substances in the environment will lead to an ever-increasing workload for the analytical laboratory.

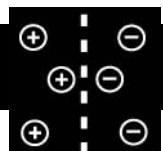
See also: II/Chromatography: Gas: Column Technology; Detectors: General (Flame Ionization Detectors and Thermal Conductivity Detectors); Detectors: Mass Spectrometry; Detectors: Selective; Gas-Solid Gas Chromatography; Multidimensional Gas Chromatography; Sampling Systems; Theory of Gas Chromatography. **Extraction:** Analytical Extractions; Solid-Phase Extraction; Solid-Phase Microextraction. **III/Gas Analysis: Gas Chromatography.**

Further Reading

Carmichael D and Holmes W (1990) Screening of trihalomethanes by direct aqueous injection using electron capture detection. *Journal of High Resolution Chromatography* 13: 267-269.

- Driss MR and Bouguerra ML (1991) Analysis of volatile organic compounds in water by purge-and-trap and gas chromatography techniques. *International Journal of Environmental Analytical Chemistry* 45: 193-204.
- EC (1980) European Community Directive 80/778/EEC relating to the *Quality of Water Intended for Human Consumption*. Brussels: EC.
- Grob K (1984) Further development of direct aqueous injection with electron-capture detection in gas chromatography. *Journal of Chromatography* 299: 1-11.
- Grob K and Habich A (1983) Trace analysis of halocarbons in water; direct aqueous injection with electron-capture detection. *Journal of High Resolution Chromatography and Chromatographic Communications* 6: 11-15.
- HMSO (1980) *Determination of Volatile Fatty Acids in Sewage Sludge* 1979. London: HMSO.
- HMSO (1987) *Determination of Very Low Concentrations of Hydrocarbons and Halogenated Hydrocarbons in Water* 1984-5. London: HMSO.
- HMSO (1988) *The Determination of Methane and Other Hydrocarbon Gases in Water* 1988. London: HMSO.
- Kolb B and Ettre LS (1991) Theory and practice of multiple headspace extraction. *Chromatographia* 32: 505-513.
- Kolb B and Ettre LS (1997) *Static Headspace-Gas Chromatography Theory and Practice*. New York: Wiley-VCH.
- Mehran MF, Nickelsen MG, Golkar N and Cooper WJ (1990) Improvement of the purge-and-trap technique for the rapid analysis of volatile organic pollutants in water. *Journal of High Resolution Chromatography* 13: 492-433.
- Shinohara A, Sato A, Ishii H and Onda N (1991) Capillary headspace-gas chromatography for the characterization of the flavour of fresh vegetables. *Chromatographia* 32: 357-364.
- Temmerman I and Quaghebeur D (1990) Analysis of trihalomethanes by direct aqueous injection (THM-DAI). *Journal of High Resolution Chromatography* 13: 379-381.
- Umbrett GR (1977) Trace analysis by gas chromatography. In: Grob RL (ed.) *Modern Practice of Gas Chromatography*, pp. 365-420. New York: Wiley.
- US EPA (1984) Method 624: Purgeables. *Methods for the Chemical Analysis of Waters and Wastes*, EPA-600 series, vol. 49, no. 209. Cincinnati: US Environmental Protection Agency Environmental Monitoring and Support Laboratory.

WATER TREATMENT



Overview: Ion Exchange

J. Irving, Purolite International Limited, Pontyclun,
Mid Glamorgan, Wales, UK

Copyright © 2000 Academic Press

Introduction

Ion exchange resins are used for many water treatment applications. Of these applications, in terms of the volume of resins used, water softening and demineralization of water are the most significant. Water softening has been practiced commercially for a century or more, making use of a wide range of natural and synthetic products. As the variety of uses for purified water has increased, so has the need to soften and demineralize water. Demineralization has only been practiced since the discovery of synthetic anion exchange resins in the 1920s. Their usefulness increased greatly with the invention of strongly basic anion exchange resins, which can remove weakly acidic compounds such as silica and carbon dioxide, as well as mineral acids. This process of ion exchange can be used as a simple method to produce water of very high purity. In general, as industrial and domestic requirements have grown, specifica-

tions for water quality have become progressively more stringent, and regulations to enforce these have become more strict. Hence the choice of resin types for a particular application becomes increasingly complex.

Applications of Ion Exchange in Water Treatment

A wide variety of new water treatment applications employ ion exchange resins in limited volume and there is limited use in niche areas for many special resin types. However, reverse osmosis (RO) is increasingly being used instead of ion exchange where treated water quality requirements are not particularly high. The use of RO followed by an ion exchange polishing process is often used for the production of high purity water, for example in the manufacture of silicon chips for the computer industry. **Table 1** lists the major water treatment processes in which ion exchange resins are used.

Principles of Ion Exchange Applicable to Water Softening

The properties and theoretical principles of ion exchange resins are fully covered elsewhere. This article

Table 1 Major water treatment processes

<i>Process</i>	<i>Resins used</i>	<i>Significant property</i>	<i>Application areas</i>
Softening	SAC	Hardness selectivity	Domestic, industrial processes, food processing, etc.
Partial softening Dealkalization	WAC WAC	Temporary hardness removal and alkalinity removal	Potable water, beverage industry, industrial processes, laundry, glass washing
Demineralization	WAC, SAC WBA, SBA	Removal of cations Removal of anions	Industrial water processes Steam generation, food processing industry, process water for pharmaceutical use, etc.
Nitrate removal	SBA	Nitrate selectivity	Potable water, food and beverage processing
Metals removal	WAC chelate resins	Selectivity for heavy metals	Wastewater treatment
Sorption	Macronets WBA, SBA	Selectivity for organics	Organic scavenging

Key: WAC, weak acid cation resin; WBA, weak base anion resin; SAC, strong acid cation resin; SBA, strong base anion resin; chelate, chelating ion exchange resin; macronet, special resin with adsorption properties.

discusses only those principles that directly relate to operating performance of the ion exchange resins that are currently used in water treatment.

Ion Exchange Equilibria

Water softening is a very efficient process. Water containing hardness ions (calcium and magnesium) is passed through a cation exchange resin in the sodium form. In dilute solution, the hardness ions are selectively held:

$$K_{Na}^{Ca} = ([Ca_R]/[Na_R^2]) \times ([Na_S^2]/[Ca_S]) \times C_S/C_R \quad [1]$$

where K is a simplified selectivity coefficient describing the equilibrium. $[Ca]$ is the calcium concentration, $[Na]$ is the sodium concentration, and C is the overall ionic concentration. Subscripts R and S represent resin and solution phase, respectively. This equation takes no account of activity coefficients, but nevertheless can be used, certainly for comparative purposes, and usually gives fairly accurate predictions. Clearly the larger the value of K_{Na}^{Ca} , the greater the fraction of calcium residing in the resin phase. Tables of selectivity coefficients have been compiled for a wide variety of cations and anions.

Selectivity for Hardness in Softening and Resin Regeneration

The more dilute the ionic concentration, the higher the calcium (and magnesium) fraction in the resin phase, and the less calcium is needed in the solution phase to satisfy the equation. However, when considering regeneration, the ionic concentration in solution is much higher, so as C_S/C_R tends to a value greater than 1, so less calcium is needed in the resin phase to satisfy the equation. The poorer selectivity of the resin sites for calcium present in high ionic concentrations ensures that the regeneration stage is very efficient. The principle of this equation applies to all comparisons between monovalent ions such as sodium and divalent ions such as calcium. Since magnesium, the other main contributor to total hardness, is also divalent, the principles described apply equally to magnesium. In order that the regeneration process is reasonably efficient, there must be an excess of sodium ions.

Reverse Osmosis

One of the advantages of RO is that no regenerant chemicals are required. The disadvantages of RO is that capital costs are higher and pumping costs can also be high. In addition, the volume of the reject waste can be large, even though the ionic concentration within the reject is quite low. There is also a risk

of membrane fouling. Generally when the total dissolved solids (TDS) in the treated water are high, RO is preferred. However, as both processes are constantly changing in efficiency, the commercial breakeven cost point is constantly changing.

Water Quality and Regeneration Efficiency

Clearly the use of smaller quantities of regenerant would make the ion exchange softening process more efficient and competitive. It has been demonstrated that the ion exchange process must be carried out in a column if the efficiency is to be optimized. For example, regenerating calcium from a resin with sodium chloride solution simply by adding the regenerant to the resin while stirring in a beaker is very inefficient. It suffers from the disadvantage that all the calcium displaced from the ion exchange resin has the opportunity to re-enter the resin and re-occupy the ion exchange sites. On the other hand, in a column operation, the displaced ion is carried away, and cannot return to the same beads at the regeneration entry point. As more fresh regenerant is added this same principle applies to the exchange process further down the column. It has been shown that, as the regenerant contact time in the column was increased to 24 h or more, the efficiency of regeneration decreased to the point where some 25–30% fewer sites were regenerated with the same quantity of regenerant. The final lower value tended asymptotically to that obtained under batch equilibrium conditions.

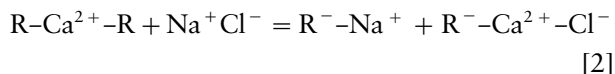
Counterflow and Co-flow Regeneration

A second advantage of column operation is that those beads situated at the point of entry of the regenerant will come in contact with a vast excess of pure regenerant. This ensures that almost all of the hardness ions loaded in the previous cycle are carried away from that part of the resin bed. In a stirred batch system, the ratio of regenerant ions to hardness ions would be approximately equal in every bead, depending on the quantity and concentration of regenerant used. It follows that since the water being treated is in counterflow to that of the regeneration, this allows the treated water to pass the most highly regenerated and rinsed resin at the point of exit, thus ensuring near zero leakage of hardness. Of course, the resin bed must not be disturbed for this advantage to apply. In co-flow regeneration, any regenerant at the treated water outlet has previously been in contact with the ions to be removed, hence this part of the column is least efficiently regenerated. In the following exhaustion cycle the sodium in the water at the outlet can 'back-exchange' for the hardness residual at the column outlet. This results in a significant hardness leak-

age. To optimize the operating efficiency, the use of regenerant chemical should be cut to a minimum. This has the added advantage that less excess regenerant will pollute the environment. From the above arguments, it is easy to see why counterflow regeneration is more efficient.

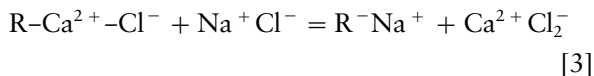
Diffusion in the Regeneration Stage

Returning to eqn [1], it can be shown that reduction of the regenerant quantity to a minimum can create significant disadvantages in the softening process. When the regenerant enters the column, it will inevitably suffer some dilution with the water it displaces. As has already been explained, the lower the ionic concentration in solution, the higher the selectivity for the divalent hardness ions, so any dilution will reduce the efficiency of the regeneration process. However, this dilution at the start of the regeneration process is not a significant disadvantage, because the regenerant is in contact with resin heavily loaded with hardness ions and thus some of these ions are easy to remove. However, as the regeneration proceeds, the concentration of regenerant increases and the beads are increasingly invaded by sodium chloride. This is termed 'Donnan invasion'. In fact, the first molecule of sodium chloride is not effective in achieving any regeneration of divalent hardness because only one of the two hardness bonds is released. The positive charge of the single displaced calcium ion is satisfied with the negatively charged chloride ion.



where R is the matrix and functional group of the strong acid cation (SAC) resin.

A second molecule of sodium chloride is clearly needed to free the hardness (calcium) ion and so allow it to start the diffusion process towards the outside of the beads.



The general direction of the regenerant is towards the centre of the beads as the diffusion of the regenerant proceeds from the solution surrounding the beads. Any hardness ion has to move against the regenerant current to leave a particular bead. Once the regenerant has completed its diffusion path to the centre of each bead, then the outward diffusion of the regenerated hardness can presumably proceed more rapidly.

As the regeneration draws to a close, the regenerant is followed by the displacement rinse. Dilution of the regenerant by the displacement water will cause selec-

tivity reversal, thus any hardness ion still situated inside the beads, and travelling towards the outside, will promptly displace two regenerated sodium sites. If the regenerant quantity is cut to a minimum, then the release of the calcium will be slower (see eqn [2]) and the proportion of diluted regenerant to concentrated regenerant will be greater. It follows that the shorter diffusion path offers a more effective regeneration resulting from improved column efficiency.

The use of beads of a narrow size range and core shell beads with a limited diffusion path offers a superior performance; this has already been seen.

Resin Kinetics

Beads of narrow size range can also present a larger surface area of exchange to the water being treated, and therefore the kinetics of exchange may be improved. Larger beads with a shell core formation also provide ease of access to each individual ion exchange site. These features can be important where high flow rates are used. Other significant factors such as resin bed depth, operating temperature, efficient distribution and collection of the water being treated are also important.

Principles of Ion Exchange Applied to Demineralization

The principles applicable to the softening process also apply to demineralization. It is useful to discuss some of these in more detail.

Resin Selectivity

Demineralization requires an ion exchange process of at least two stages. In the first essential stage, the cations in the water to be treated are replaced with hydrogen by passing the water through strong acid cation (SAC) resin in the hydrogen form. When the resin becomes exhausted to the extent that the water is not treated to the required quality, it must be regenerated with acid.

The first stage of the demineralization process may be improved to combine the use of both a SAC resin and a weak acid cation (WAC) resin. The latter is positioned upstream. This is one of the many ways in which the efficiency of this regeneration process can be varied. Returning to the properties of SAC resins, the process is unlike softening in that there are no advantages from changes in ionic concentration when regenerating sodium. The selectivity for sodium, as compared with hydrogen, may be simplified by the following equation.

$$K_H^{Na} = ([Na_R]/[H_R]) \times ([H_S]/[Na_S]) \quad [4]$$

where H is the hydrogen ion; all other symbols as for eqn [1].

It has been reported that K_H^{Na} varies according to the cross-linking of the SAC resin.

Counterflow Regeneration

The advantages to be obtained in water quality from operation in the counterflow mode are, perhaps, even more important than for softening. The difference between the selectivity of sodium and hydrogen is very small (in fact the coefficient lies between 1 and 2). Hence any residual sodium located near the outlet of the bed is easily displaced. Low sodium leakage is clearly an essential parameter where high water purity is required. It follows that either the whole resin bed must be highly regenerated, or the resin bed has to be operated in the counterflow mode. This ensures that the treated water at the bed outlet is in contact with highly regenerated resin containing only minute traces of sodium.

Mixed Bed

The use of a mixture of SAC resins and strong base anion (SBA) resins, regenerated separately before mixing, has generally been considered the best way to achieve treated water of the highest purity. The passage of water alternately via cation and anion resins affords the more or less continuous neutralization of acids and bases produced by contact with the previous bead of opposite charge. The disadvantage is that the component resins have to be separated before regeneration. Incomplete separation will cause the offending beads to be regenerated with the wrong regenerant, resulting in a significant deterioration in treated water quality. Techniques of rinse recycle and efficient counterflow regeneration are now producing water qualities close to that of mixed bed polishing.

Effects of Sodium Leakage

One further problem occurs if the sodium leakage is high. The treated water from the cation resin outlet (decationized water) passes through the anion resin, regenerated to the hydroxide form. In general, this is a very efficient reaction, because the process is one of neutralization of acids, so the exchange reaction is essentially non-reversible, and the only by-product of the neutralization reaction is water. However, any sodium leakage from the cation resin must be accompanied by an anion to preserve electroneutrality. At the start of the cycle, when the anion resin is freshly regenerated, the anion that accompanies sodium will usually be hydroxide. This is not particularly desirable, but is easily removed by the following mixed bed resins. However, as the resin bed exhausts, the

least selective anion, in exhaustion, will accompany the sodium. This anion is usually silica. Silica can cause deposits in superheaters, boilers, turbines and condensers, so accelerating corrosion. Thus it is clear that sodium leakage carries a two-fold danger.

Anion Leakage

The very high selectivity of the anions of mineral acids for ion exchange resins usually prevents high mineral anion leakage, even though regeneration to remove all of these is rarely complete. As with softening, the efficiency of regeneration is crucial if good capacity and low leakage are required. The use of narrow size range resins can shorten the diffusion path in the regeneration process.

Regeneration Efficiency

The regeneration efficiency of cation resins has already been discussed. In the demineralization process, the regeneration efficiency of anion resins is of even more importance.

- During the actual water treatment process, the removal of anions is essentially an acid-base neutralization. Hence it is driven rapidly more or less to completion. However, the regeneration stage involves the exchange of the loaded ions for the hydroxide ion. Hence this stage is a true ion exchange process where the ions being removed are in competition with the ion being fixed on the resin. It follows that the extent of regeneration is the limiting step, dictating the operating capacity of the resin. In fact, when operating SBA resins at recommended flow rates the operation capacity is normally only 5–10% below the available regenerated capacity. In other words, the chromatographic profile is extremely sharp.
- Type I SBA resins do not regenerate easily. In fact the selectivity coefficient K_{OH}^{Cl} is approximately 15–20 for gel Type I SBA resins, and even higher for equivalent macroporous types.
- Type II and acrylic SBA resins are more easily regenerated, but have the disadvantage that they remove silica less efficiently (especially the Type II); both types have poor thermal stability.
- Recently strong base resin types have been compared in their operating performance and related properties. A Type III resin has been developed that is comparable with Type II or acrylic resins in its ease of regeneration, while having thermal stability and silica removal similar to that of a Type I resin.
- Weak base anion (WBA) resins regenerate quite easily, and can be used in conjunction with SBA resins to improve overall regeneration efficiency. However,

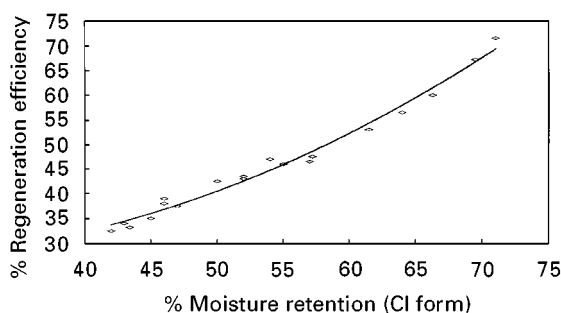


Figure 1 Regeneration efficiency of chloride form SBA Type I clear gel anion at 65 g L^{-1} NaOH.

they do not remove silica or carbon dioxide, so the proportion of WBA to SBA must be controlled to balance the needs of the process. Also the fresh regenerant must be used to regenerate the resins in the order $\text{SBA} \rightarrow \text{WBA}$, otherwise the advantage is lost.

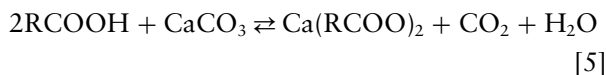
The mechanisms for regenerability of anion resins have been discussed in the literature. Briefly, the high selectivity for chloride, sulfate, and nitrate arises from the fact that these ions are less hydrated than is the hydroxide ion. Hence the hydroxide ion prefers to remain in the aqueous phase. As **Figure 1** shows, the lower the moisture retention of the resin, the more difficult is the regeneration process.

These mechanisms also offer good explanations for the variation in thermal stability between resin types. It has been shown that nucleophilic attack on the nitrogen of the active group by the hydroxide ion is responsible for the thermal degradation. It follows that the more hydrated the hydroxide ion, the lower the electron charge density and the lower the rate of degradation. This is confirmed by experimental data. This subject is further complicated by the differences in selectivity of chloride and sulfate ion in the regeneration process.

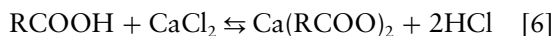
Principles of Dealkalization

The removal of alkalinity is a less common process than softening or demineralization, hence it will only be dealt with briefly. It has long been recognized that hardness associated with bicarbonates (termed temporary hardness) is more of a problem than that associated with mineral acids (permanent hardness). When water is heated the bicarbonate decomposes to carbon dioxide and insoluble calcium carbonate. This forms the scale that is found in the equipment used to heat or transport water. The removal of scale may be achieved by using a weak acid cation resin regenerated to the hydrogen form.

The reaction:



proceeds quite easily, while the reaction



does not, because the ionized acid produced inhibits further reaction.

The WAC resin is easily regenerated with a stoichiometric amount of acid. This makes the process chemically efficient but it is kinetically slow. It also has the advantage that the total dissolved solids are reduced by the removal of the hardness. The volatile carbon dioxide can be removed by deaeration. The main disadvantage is that acid is needed for regeneration.

An alternative process uses a SBA resin in the chloride form. Here the bicarbonate is exchanged for chloride directly. Thus the offending temporary hardness is exchanged for permanent hardness. There is no reduction in total dissolved solids and the operating capacity is lower, but the advantage is that the SBA resin may be regenerated with common salt.

Principles of Nitrate Removal

The World Health Organization (WHO) limit for potable water is 50 ppm of nitrate. Many water sources have higher levels, partly because of the use of nitrate-based fertilizers to boost crop yields. Although this practice has been curtailed in recent years, the problem will remain for many years to come. Ion exchange resins, regenerated with sodium chloride, selectively remove nitrate in preference to bicarbonate, but not in preference to sulfate. This means that the sulfate in the water is also needlessly removed. The exchange of both nitrate and sulfate can result in the chloride level increasing above WHO limits. Where sulfate levels in the water are significant, the use of a specially developed nitrate-selective (over sulfate) resin can give increased capacity and better overall water quality.

Physical Stability of Ion Exchange Resins

Ion exchange resins have to be physically strong to last for the expected life span of 4–6 years, depending upon the resin type, temperature of operation and regeneration, ability to resist irreversible fouling from trace contaminants in the water to be treated, and adherence to the recommended operating conditions.

This means that they have to be mechanically strong and also able to withstand rapid changes in swelling/shrinking arising from changes in ionic form and changes in ionic concentration. It is most important that the ion exchange plant is designed to accommodate the anticipated changes in bed depth, and resins should be free to adjust to the volume changes occurring naturally through the process. Tests have been developed to evaluate osmotic shock resistance; these are mentioned in other articles.

The elimination of the larger beads in the resin bed will reduce the chances of breakdown resulting from osmotic shock, because the build-up of differential stress with changes in ionic concentration is less in smaller beads. Up to now partially activated beads, which have the advantages of a smaller diffusion path described above, have not been physically stable because of the stresses developing between the swelling and shrinking of the activated part of the resin, compared with the properties of the inert core. There are indications that this difficulty is now being overcome.

Plant Design

Water analyses vary considerably, depending on the source of the water supply and the geographical area. Thus it has been impossible over the years to standardize on one type of plant or on which are the most suitable resins. **Table 2** gives an example of the water analysis information needed to design a treatment plant. Changes in total concentration of dissolved salts, the proportion of sodium and silica (as already discussed), the temperature of the water, the ratio of alkalinity to total anions, and the proportion of sulfates, chlorides and nitrates, all have an influence on the operating capacity and treated water quality.

The presence of iron can severely affect the performance of softeners. Iron can slowly accumulate and cause irreversible fouling. It also acts as a catalyst, promoting oxidation of resins that causes an increase in moisture retention and swelling of the resin. This in turn can cause stress within the resin bed, not only on the resin itself, but also on the internal collectors and distributors. The performance of demineralizers can also be affected, especially if only sulfuric acid is available for resin regeneration and resin cleaning.

Natural organic matter can vary both in quantity and quality from area to area, hence the choice of resins and preferred cycle times, the quantity of sodium hydroxide used for regeneration and its temperature as well as cleaning regimes, can vary from region to region.

Basic Principles

Developments in ion exchange resins since the 1940s have been accompanied by developments in engineering equipment and processes, from the invention of styrene-divinyl benzene resins to advances in techniques for TOC removal. The latter is now of utmost importance for the production of ultrapure water.

The basic principles of sizing an ion exchange vessel are quite simple. Let us suppose that it is necessary to treat $F \text{ m}^3$ of water per hour, and it is required to remove $C \text{ eq m}^{-3}$. Then the load per hour is $FC \text{ mol}$, and FCb is the total load presented for an exhaustion cycle of $b \text{ h}$. It is therefore possible to calculate the volume of resin needed, provided the operating capacity ($O \text{ eq m}^{-3}$) for the particular resin is known for the specified operating conditions. If we have $V \text{ m}^3$ of resin, then for the resin plant to treat the

Table 2 Typical water analysis information

<i>Influent water specification</i>					
Origin	Mains water				
Pretreatments	None				
Temperature	8°C				
Organic matter	20.000 mg L ⁻¹ KMnO ₄				
<i>Cation</i>	<i>Concentration (meq L⁻¹)</i>	<i>Anion</i>	<i>Concentration (meq L⁻¹)</i>	<i>Other</i>	<i>Concentration (meq L⁻¹)</i>
Ca	0.900	HCO ₃	0.580	CO ₂	0.010
Mg	0.140	CO ₃	0.000	SiO ₂	0.060
Na	0.300	Cl	0.450		
K		SO ₄	0.310		
Fe		NO ₃	0.000		
TC	1.340	TA	1.340		

TC, total cation concentration; TA, total anion concentration. Note that TC should equal TA. In general if there is a difference the analysis is probably incorrect. If the pH is not neutral, the hydrogen and hydroxide ions should be included in the balance.

water efficiently, the following equation must be satisfied.

$$FCh = OV$$

where h is the time in hours between successive regenerations.

Many factors can affect the operating capacity in a particular situation. This must always be lower than the total volume capacity of the resin. The most important of these factors are the regeneration level and the particular analysis of the water being treated. In certain cases other factors such as flow rate or cycle time, operating and regenerant temperature, treated water quality and cycle end point, and resin bed depth may also need to be taken into account. Furthermore, the plant itself will need to treat some extra water in order to operate successfully. This extra load needs to be allowed for in the design. The more concentrated the feed water the more extra load is placed on the resin beds. Indeed, the water may contain such a high level of dissolved salts that treatment may not be economic. In such cases RO often provides a satisfactory alternative, or as a pretreatment. When all these factors are carefully considered, the optimization of the plant becomes quite complicated, especially when taking into account the various process options and the possible choices of resin types and their various combinations. Such an exercise requires a vast experience of water treatment. To help design engineers and water treatment plant operators to make suitable design plans, computer programs

are now available. In certain cases they are suitable both for new plant and to revamp or modify existing plant. They may also be used to check the current performance of a particular ion exchange line in operation, and to evaluate possible changes in operating parameters. These programs or computer printouts can be obtained from various resin manufacturers and from original engineering manufacturers to help experts in these calculations. They can also serve as useful training for those engineers learning their trade, and for water treatment chemists who need to understand the operations of a particular plant in which they have an interest.

Table 3 gives an example of data provided by a plant design computer program on the design requirements for a specified flow rate and treated water quality. Table 4 gives an example of the engineering data provided by a computer program. Its use can save many hours in calculation time and allow exploration of the many options available before making a final choice.

Choice of Resins

The optimization of any given process requires considerable skill on the part of the design engineer. It is important to understand the strengths and weaknesses of each resin type so that the correct type and particle size are chosen. The design program is extremely useful to balance and match the conditions of regeneration to produce the correct quality and quantity of treated water. The combined experience of the customer and the engineer, together with the expertise and support of resin specialists, is generally regarded as the best approach to determining the optimized conditions of operation and choice of the correct equipment.

Resin Life

Provided that the design has been optimized, in all but the most difficult cases the resin life should be in the range of 4–6 years, depending on the type of resin. In fact SAC resins have been known to last very much longer, provided they are used at the optimum temperature and are kept free of contaminants and potential oxidizing agents. There must also be the provision that regenerate quantities, concentrations and flow rates are designed to avoid stress on the resins. In many cases regular checks on the state of resins can be beneficial. This will prevent build-up of chemical contaminants and highlight any maloperation before real damage is done.

See Colour Plates 125, 126.

See also: I/Ion Exchange.

Table 3 Design requirements

<i>Operating conditions</i>			
Flow rate per line	2.1 m ³ h ⁻¹		
Running time	9.8 h		
Net run	21 m ³		
<i>Treated water quality</i>			
	<i>Achieved</i>	<i>Specified</i>	<i>End point</i>
Conductivity (μS cm ⁻¹)	0.70	1.00	2.00
Silica leakage (ppb)	16	20	500
Sodium leakage (ppm)	0.038		
Residual CO ₂ after SAC filter	0.59 meq L ⁻¹		
<i>Process options</i>			
Ion exchange process	Demineralization		
Plant layout	SAC → SBA		
No. of lines	(as required)		
Resins chosen	SAC SBA		

Table 4 Calculation of full plant design details for an ion exchange plant

		Filter	
		SAC	SBA
<i>Ion exchange load</i>			
Gross run	(m ³)	21	21
Ionic load	(eq)	28	30
<i>Resin data</i>			
Resin type		SAC	SBA
Resin grade		—	—
Theoretical capacity	(eq L ⁻¹ R)	1.15	0.62
Operational capacity	(eq L ⁻¹ R)	0.48	0.56
Resin volume	(L)	58	53
Flow rate	(BV h ⁻¹)	36.9	40.2
Organic load	(g L ⁻¹ KMnO ₄)		7.880
<i>Regeneration data</i>			
Regeneration mode		CTF:FB	CTF:FB
Regenerant		HCl	NaOH
Concentration	%	5.0	4.0
% of Theory		345	180
Level	(g L ⁻¹ R)	61.0	40.0
Total	(kg 100%)	4	2
Excess	(eq)	69	24
Temperature	(°C)		25
Dilution water	(m ³)	0.1	0.0
Slow rinse	(m ³)	0.1	0.2
Fast rinse	(m ³)	Recycling	Recycling
<i>Plant size data</i>			
Bed depth (changing from supplied form as shown)			
Supplied form	(mm)	586	538
Exhausted form	(mm)	562	
Regenerated form	(mm)	609	634
Vessel diameter	(mm)	365	365
Cross-section	(m ²)	0.10	0.10
Cylindrical height	(mm)	Per design	Per design
<i>Hydraulic data</i>			
Linear velocity	(m h ⁻¹)	21.2	21.2
Pressure drop	(kPa)	19.0	14.8
<i>Design factor</i> (Limitations caused by flow rate)		0.42	0.90

Note: BV, bed volume; R, resin.

Further Reading

- Abrams MI and Benezra L (1967) *Encyclopedia of Polymer Science and Technology*, pp. 692–742. Chichester: John Wiley & Sons.
- Chu B, Whitney DC and Diamond RM (1962) *Journal of Inorganic Nuclear Chemistry* 24: 1405–1415.
- Dale J and Irving J (1992) Comparison of strong base resin types. In: Slater MJ (ed.) *Ion Exchange Advances*, pp. 33–40. London: Elsevier Applied Science.
- Diamond RM and Whitney DC (1966) Resin selectivity in dilute to concentrated aqueous solutions. In: Marinsky JA (ed.) *Ion Exchange*, vol. 1, pp. 277–349. New York: Marcel Dekker.
- Dorfner K (1991) Introduction to ion exchange and ion exchangers. In: Dorfner K (ed.) *Ion Exchangers*. Berlin and New York: Walter de Gruyter.
- Harland CE (1994) Some engineering notes. In: *Ion Exchange: Theory and Practice*, 2nd edn, pp. 261–276. Cambridge: Royal Society of Chemistry.
- Helfferich F (1962) Ion exchange equilibria. In: *Ion Exchange*, pp. 151–248. New York: McGraw-Hill.

Newell PA, Wrigley SP, Sehn P and Whipple SS (1996) An economic comparison of reverse osmosis and ion exchange in Europe. In: Greig JA (ed.) *Ion Exchange Development and Applications*, pp. 58–66. Cambridge: Royal Society of Chemistry.

Nolan J and Irving J (1984) The effect on the capacity of strong base anion exchange resins of the ratio of chloride to sulphate in the feed water. In: Naden D and Streat M (eds) *Ion Exchange Technology*, pp. 160–168. Chichester: Ellis Horwood.

Anion Exchangers: Ion Exchange

W. H. Höll, Karlsruhe Nuclear Research Center,
Karlsruhe, Germany

Copyright © 2000 Academic Press

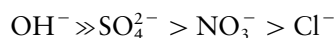
Introduction

Anion exchange resins consist of a polymeric matrix to which different functional groups are attached. Most weakly basic anion exchangers contain tertiary amino groups; in a few cases primary and secondary groups are also encountered. In many cases weakly basic anion exchangers are not monofunctional but possess a variety of amino groups. Strongly basic resins contain quaternary ammonium groups. Standard commercially available exchangers contain either $-N^+(CH_3)_3$ groups (type 1 resins) or $-N^+(CH_3)_2C_2H_4OH$ groups (type 2 resins). Both weakly and strongly basic exchange resins are available in gel-type or macroporous modifications.

Properties and fields of application mainly depend on the dissociation properties of the functional groups in which dissociation plays the most important role. By means of the mass action law, dissociation constants of the protonated amino and ammonium groups can be estimated. The respective numerical values are in the range of $pK_a > 13$ for strongly basic resins and 5–8 for weakly basic resins. Therefore, strongly basic resins are protonated over the entire pH range but weakly basic exchangers are protonated at pH values below 5–8, depending on the type. As a consequence, strongly basic resins will exchange anions in both acid and alkaline solutions. In addition, these exchangers can adsorb weak acids and even ionize very weakly dissociated acids. Weakly basic resins, however, can operate only in acidic media and are unable to convert neutral salts to the respective hydroxides (e.g. NaCl to NaOH). Furthermore, they cannot normally adsorb weak acids.

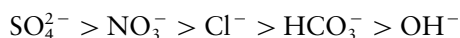
The uptake of anions by resins is subject to specific interactions between counterions and co-ions and the distribution of exchangeable ions depends on the properties of both the exchanger and the ions. Consequently, a favoured sorption of certain types of anions occurs. The sequence of affinities is given either qualitatively by the selectivity series or quantitatively by, for example, separation factors. For weakly basic anion exchangers the sequence of most common anions in fresh water is:

actively by, for example, separation factors. For weakly basic anion exchangers the sequence of most common anions in fresh water is:



Due to the dissociation properties of the functional groups, hydroxyl ions are strongly preferred. This is important for the conversion of these resins to the hydroxyl (or free base) form in the regeneration step, in which only slightly more than the stoichiometric amount of OH^- bearing solutions is required.

For strongly basic anion exchangers the selectivity series is:



For these resins hydroxyl ions are the least preferred among the standard anions. Conversion of the resins to the hydroxyl form therefore requires comparatively large excess amounts of sodium hydroxide.

For elimination of nitrate anions from drinking water the preferred sorption of sulfate ions causes considerable disadvantages. Extensive research during the 1980s has shown that this drawback can be overcome by introducing functional groups which are more hydrophobic and bulkier. By these means, the ability to adsorb sulfate ions is considerably decreased. The so-called nitrate-selective resins which are now commercially available contain triethyl instead of trimethyl groups and, therefore, exhibit a reversed preference for nitrate and sulfate ions.

The rate of exchange depends mainly on the internal interdiffusion of exchanging ions. On the completely ionized strong base resins this diffusion is rather quick and the overall rate of exchange mainly depends on the particle size distribution. With weakly basic exchangers, however, the poor dissociation and further specific interactions between functional sites and diffusing ions considerably slow the rate of exchange. For these resins, both the uptake of acids and conversion to the free base form by means of sodium hydroxide strongly depend on the concentration of the liquid phases.

Strongly basic anion exchangers in the hydroxyl form are subject to considerable degradation of

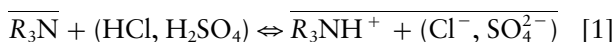
functional groups at temperatures above 40°C, leading to a loss of strongly basic functionality. Weakly basic exchangers are very stable.

Applications

Water Demineralization

The most important application of anion exchangers in water treatment has been in demineralization processes. Demineralization consists of the subsequent cation exchange for hydrogen ions as the first step and either adsorption of acids by a weakly basic exchanger or real anion exchange for hydroxyl ions on a strongly basic exchanger as the second step. As a result, demineralized water is produced: this may be used for various purposes, such as boiler feed water.

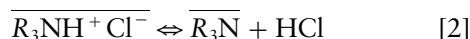
The effluent from the preceding cation exchange step consists of a mixture of strong mineral acids and carbonic acid; this is equivalent to the cations originally dissolved. Furthermore it contains silica and dissolved organic compounds, neither of which are retained by the cation exchangers. If no silica removal is needed, weakly basic anion exchangers in their free base form are used to remove strong mineral acids. This process develops as the uptake of acids:



(Parantheses are used to express the stoichiometry of the exchange; R_3 denotes the matrix of the weakly basic exchanger.) In technical filter columns the uptake of sulfuric and hydrochloric acid results in the development of zones with different predominant loadings: firstly, a sulfate-rich zone close to the inlet; secondly, a chloride zone; and finally, a zone in which the resin is still in the free base form. During the filter run the sulfate and chloride zones become larger and the boundaries between the zones are shifted towards the column outlet. Consequently, chloride ions are the first to appear in the column effluent.

Theoretically, the strong acids should be completely eliminated. In practical installations, however, the leakage of sodium from the strongly acidic cation exchanger cannot be avoided and it is in the range of 2–50 $\mu\text{g L}^{-1}$, depending on the level of regeneration. By this means, the feed solution for the anion exchanger contains some neutral salt which cannot be eliminated. Consequently, an equivalent amount of chloride ions remains in the effluent. Apart from this sodium leakage-caused ‘slip’, the presence of chloride

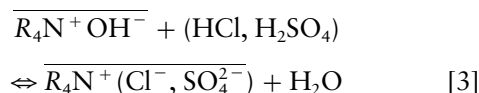
ions may also be due to the hydrolysis of the hydrochloride form of weak base resins:



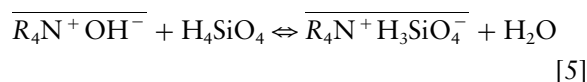
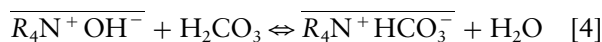
Weak acids like carbonic acid are only adsorbed to a small extent and hydrogen carbonate ions are rapidly replaced by anions of strong acids. Carbonic acid or CO_2 is therefore eliminated either by physical degassing or by means of a strongly basic exchanger. Since the capacity of weakly basic resin increases with increasing total ionic concentration (to which carbonic acid contributes), degassing of CO_2 is often placed after the weakly basic exchanger filter.

Regeneration of weakly basic anion exchangers is usually carried out by means of sodium hydroxide, although other chemicals like $\text{Ca}(\text{OH})_2$ or ammonium hydroxide have also been proposed. To avoid the precipitation of calcium sulfate, the regenerant solutions of anion exchangers generally require calcium-free water. Since the strong acids are easily neutralized, regeneration is efficient. The operating capacity depends on the composition of the raw water and the resulting loading of the anion exchanger. If equal amounts of caustic are applied in the regeneration step, the effective capacity decreases by about 10% if the raw water contains exclusively sulfate instead of only chloride ions.

Unlike with weakly basic resins, the removal of acids by a strongly basic resin develops as a neutralization reaction:



(R_4 denotes the matrix of the strong base resin.) Because of the high pH value in the resin phase, strongly basic exchangers can ionize and adsorb ions from carbonic acid and even from silica:



For boiler feed water, for example, the removal of both carbonic acid and silica is of great interest. Usually, most of the carbonic acid is removed by physically degassing. By this means a large part of the capacity of the strongly basic anion exchanger is saved and the resin has to eliminate only the remaining traces of carbonic acid. The removal of silica is far more complicated than shown in eqn [5] above.

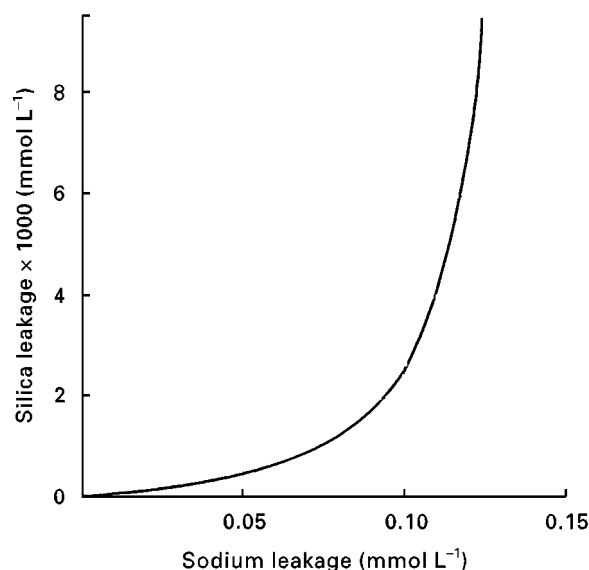


Figure 1 Interdependence of sodium and silica leakage.

During the accumulation in the resin phase, silica starts to polymerize. This is favoured by long cycles as well as by high concentrations in the feed water. Regeneration using NaOH may, therefore, become a dissolution rather than a true ion exchange process. Warm solutions (approximately 50°C) are considerably more effective than solutions at ambient temperature. In addition, regeneration may be adversely influenced by the mode of regeneration and the possible displacement of hydrogen carbonate ions. The leakage of silica is closely related to the leakage of sodium in the preceding cation exchanger (**Figure 1**).

Regeneration of strongly basic resins is generally carried out by means of NaOH at concentrations between 1 and 5%. As with weakly basic exchangers, the resulting operating capacity depends on the composition of the feed water, the relative amount of NaOH, temperature and, to a certain extent, the rate of filtration during regeneration. The relative quantity of NaOH required is considerably higher than for weak base resins and lies between 150 and 250% of the stoichiometric amount. For the slightly weaker basic resins of type 2, the operating capacities are higher than for type 1 resins.

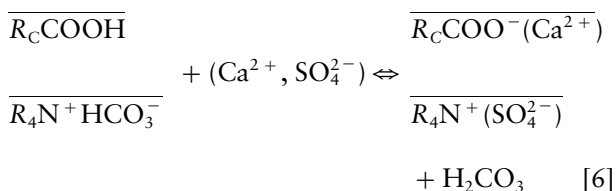
There can therefore be savings in chemicals and cost if the anion exchange step is split into two stages. In the first stage a weakly basic resin is applied for the elimination of strong acids. After physical degassing to remove carbon dioxide, the strongly basic exchanger is exclusively used to eliminate the remainder of the carbonic acid and silica. Both resins are regenerated together: the NaOH solution first passes through the strongly basic resin which requires a concentrated regenerant without impurities. The effluent

then passes the weakly basic resin. Due to the strong preference for hydroxyl ions, considerable levels of impurities can be tolerated.

Demineralization of water by subsequent or simultaneous cation/anion exchange has been realized in countless installations for both fresh and waste water treatment. It has become extremely important for boiler feed water and for ultrapure water for the electronics and pharmaceutical industries. Typical conditions to be met are conductivities below 0.2 $\mu\text{S cm}^{-1}$ and silica concentrations $< 5 \text{ mg L}^{-1}$.

Partial Demineralization of Drinking Water

In Europe numerous water supplies distribute drinking water with elevated total hardness caused by the presence of sulfate and calcium ions. Treatment of such water, therefore, requires the elimination of sulfate ions parallel to diminishing hardness. In such applications complete demineralization is not required. Consequently, considerable leakage of the ion exchangers can be tolerated. The condition of simultaneously diminishing the concentrations of alkaline earth and sulfate ions is met by the carbon dioxide regenerated ion exchange (CARIX) process. This process uses a mixed bed consisting of a weakly acidic resin in the free acid form and a strongly basic resin in the hydrogen carbonate form. In contact with calcium- and sulfate-bearing raw water, both kinds of ions are replaced by carbonic acid:



The advantage of this process is its reversibility: for regeneration, carbon dioxide is dissolved in untreated raw water under a pressure of typically 0.4–0.5 MPa. The carbonic acid solution is pumped across the mixed bed and simultaneously regenerates both resins. Although carbon dioxide is applied in large excess, this does not contribute to the salt content of the waste water which exclusively contains the ions removed during the service cycle. Carbonic acid is a weakly effective regenerant for both resins and generates an effective capacity of $\approx 50\%$ of the total capacity on the cation exchanger and only 20% on the anion exchanger. As a consequence, complete demineralization is not possible and considerable leakage is observed. The possible throughput between two regenerations is small. Within certain limits the

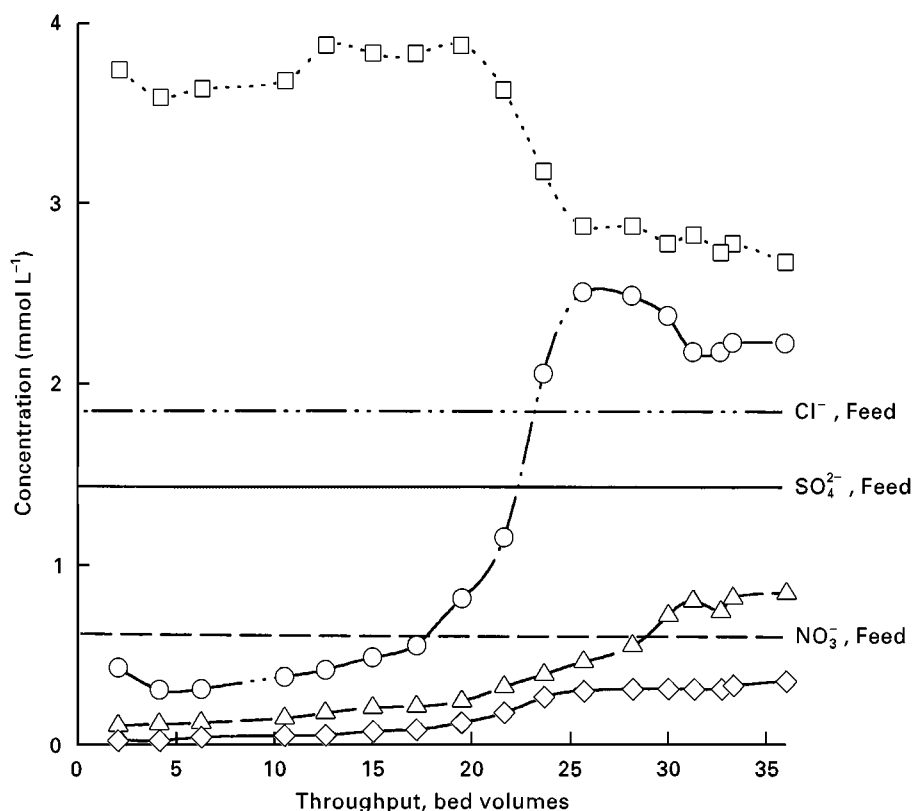


Figure 2 Concentration histories of chloride, nitrate and sulfate in the Carix process. Feed alkalinity (HCO_3^-): 6.5 mmol L^{-1} . Circles, Cl^- ; triangles, NO_3^- ; diamonds, SO_4^{2-} ; squares, HCO_3^- .

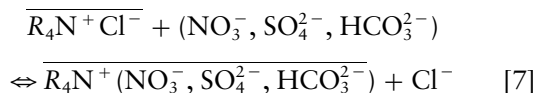
CARIX process can be adapted to the objective of treatment by adjusting the volume ratio $V_{\text{anion}} : V_{\text{cation}}$ of the two resins in the range of 3 : 1 to 1 : 3. With respect to both the removal of sulfate and regeneration by means of carbonic acid, type 2 and acrylic anion exchangers show the best results.

So far, the process has been realized in three full-scale plants in water works in Germany. Each of these plants consists of one or two sets of three filters which operate in a merry-go-round mode. The total throughput for each filter between two regenerations is 35–50 bed volumes. After half of the total throughput, a second filter starts its service cycle. After the full throughput, the filter is regenerated and waits for the next service cycle while the third one is started. The product water is the mixed effluent of the two operating filters. Typically, about 10% of the raw water is needed for regeneration. From the waste water, 90% of the unspent carbon dioxide is recovered. Thus, the consumption of CO_2 amounts to $0.4\text{--}0.45 \text{ kg m}^{-3}$.

Figure 2 shows a typical breakthrough history for standard anions. Average product water concentrations are listed in Table 1.

Nitrate Removal

For many drinking water supplies the presence of nitrate in ground and surface water at elevated concentrations has become a serious problem because of its health effects. As the simplest possibility, nitrate can be eliminated from water by means of strong base anion exchangers in the chloride form:



Using conventional strong-base anion exchangers, the main difficulty of this method arises from the

Table 1 Partial demineralization by means of the CARIX process

Parameter	Raw water	Product water
Total hardness	5.4 mmol L^{-1}	2.3 mmol L^{-1}
Hydrogen carbonate	6.6 mmol L^{-1}	3.4 mmol L^{-1}
Sulfate	1.6 mmol L^{-1}	0.35 mmol L^{-1}
Nitrate	0.6 mmol L^{-1}	0.45 mmol L^{-1}
Chloride	1.5 mmol L^{-1}	1.3 mmol L^{-1}
Conductivity	$930 \mu\text{S cm}^{-1}$	$470 \mu\text{S cm}^{-1}$
pH Value	7.30	7.80

preferred uptake of sulfate ions. Consequently, the nitrate uptake capacity strongly depends on the sulfate/nitrate concentration ratio in the raw water. As an example, for a type 2 resin the nitrate uptake capacity decreases by 60% if the sulfate concentration in the feed increases from 50 to 220 mg L⁻¹.

During the uptake of sulfate, nitrate and hydrogen carbonate by a chloride-loaded conventional anion exchanger, loading zones develop in the filter column: a sulfate-rich zone, a nitrate-rich section and a mixed chloride/hydrogen carbonate zone followed by the resin in its original chloride form.

Due to the development of the zones and the displacement of less preferred anions, continuous change occurs in the effluent composition. When the hydrogen carbonate-rich zone has reached the outlet there is still removal of nitrate species, but an increase in the concentration of hydrogen carbonate and a corresponding increase in the pH in the effluent occur. The column run has to be stopped when the nitrate-rich zone reaches the filter outlet.

Regeneration is carried out using brine solutions of 2–10% NaCl:



The total quantity of NaCl used depends on the tolerable nitrate leakage in the service cycle. To achieve effluent concentrations ≤ 2 mg L⁻¹, the required amount is ≥ 200 g L⁻¹ resin. With smaller quantities the leakage becomes larger.

The operating capacity of conventional anion exchangers depends on both the nitrate and sulfate concentrations of the feed water. Figure 3 shows the respective interdependence for a commercially available type 2 resin.

The objective of treatment normally does not consist of the complete elimination of nitrate but only of its reduction below the maximum permitted concentration. A tolerable nitrate concentration in the product water can therefore be achieved by two different methods: the first uses an exchanger which has been regenerated with a large amount of NaCl. Since the leakage of the column is small, only part of the water has to be treated and can be blended with a by-pass of untreated water.

This kind of nitrate removal process was first realized in 1975 in Long Island in a pseudo-continuous installation. This plant consisted of a closed-loop tube including sections for back-washing, regeneration

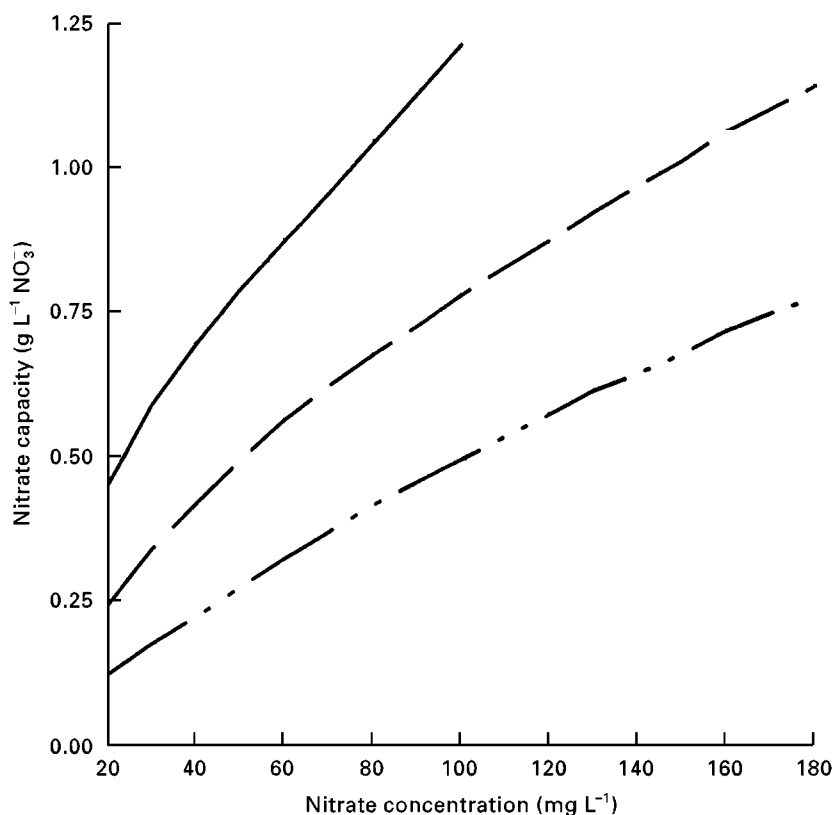


Figure 3 Operating capacity of a type 2 strongly basic anion exchanger depending on the concentrations of nitrate and sulfate in the raw water. Continuous line, 0.36 mmol L⁻¹; dashed line, 0.72 mmol L⁻¹; dotted and dashed line, 2.1 mmol L⁻¹. Resin: Lewatit M600.

Table 2 Data of operation of Ecodenit plant

Parameter	Feed water concentration (mg L ⁻¹)	Product water concentration (mg L ⁻¹)	Waste water concentration (g L ⁻¹)
Nitrate	70	25	25
Sulfate	50	10	10
Hydrogen carbonate	65	55	55
Chloride	50	120	120

and rinsing of the exhausted resin. After exhaustion the resin material in the contacting section is pulsed into the back-wash part, whereas regenerated and rinsed resin material enters the contacting section. The plant was designed for a maximum throughput of 277 m³ h⁻¹. The nitrate concentration was diminished from 100 to 43 mg L⁻¹ as the tolerable maximum.

In the second possibility the amount of NaCl required during regeneration is smaller. As a consequence, the regeneration is less efficient and the nitrate leakage becomes larger. Thus, all the water has to be treated. This principle is shown in the Ecodenit process developed in France. This process operates with NaCl quantities of ≤ 100 g L⁻¹ of resin and uses co-flow regeneration. The first full-scale plant for the treatment of 160 m³ h⁻¹ is in service in northern France. This plant consists of three filters operating in a merry-go-round mode. Each filter contains 8 m³ of a strongly basic resin. Results of the operation of the full-scale plant are summarized in Table 2.

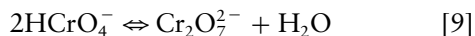
Both principles are combined in a third modification. Such a plant went into service in 1983 in California. The plant was to treat 115 m³ h⁻¹ blended with 45 m³ h⁻¹ raw water. It consists of three columns which are also operated in a merry-go-round mode. For each filter the throughput between two regenerations amounts to 250 bed volumes. The nitrate concentration is decreased from 71 to 11.5 mg L⁻¹ in the mixed effluent of the service filters and to 27–36.5 mg L⁻¹ in the blended product water. Since 1983, numerous nitrate elimination plants have come into service: most apply nitrate-selective exchangers.

Chromate Removal

Chromic acid and chromates are widely used in many applications. Anion exchange offers an ideal opportunity for the removal and recovery of chromates. Both strongly and weakly base resins can be applied.

In aqueous solutions chromate ions exist in different ionic forms. The speciation mainly depends on the pH value. In the acidic region ($1 < \text{pH} < 6.5$) and for

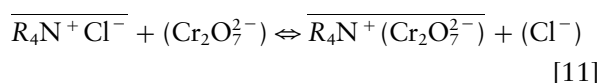
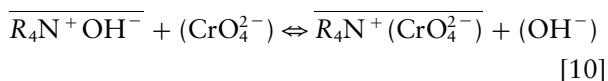
dilute solutions, HCrO₄⁻ is the predominant species. Above pH 6.5 mostly CrO₄²⁻ is found. With respect to ion exchange processes it is important that dimerization occurs at elevated concentrations:



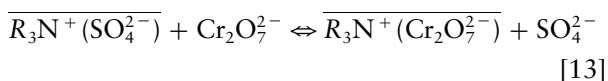
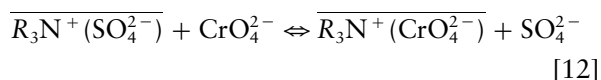
The respective pH conditions may exist in the anion exchanger phase. Therefore, the resins can be considered to be at least partly loaded with Cr₂O₇²⁻ species.

Chromate species are strongly preferred over chloride and sulfate ions under normal conditions. However, at acidic pH this preference vanishes for both weakly and strongly basic anion exchangers when chromate is the trace component. Consequently, fixed-bed experiments using standard acidic chromate-bearing waste waters exhibit a gradual increase in the effluent concentration. An increase in the concentration of competing sulfate ions yields only a negligible decrease in chromate capacity. In contrast to this, an increase in the chloride concentration leads to a considerable decrease in chromate capacity for a given liquid-phase concentration. For weakly basic resins the chromate capacity decreases with increasing pH because of the deprotonation of the functional groups. Below pH 5 the capacity is constant and depends only on the background composition of the solution.

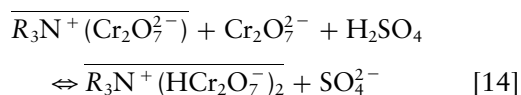
Using strongly basic exchangers chromate can be removed by the following exchange processes:



Weak base anion exchangers are applied, for example in the sulfate form:



Acidification of the feed solution leads to the formation of hydrogen dichromate species, which doubles the capacity of the resins, e.g.:



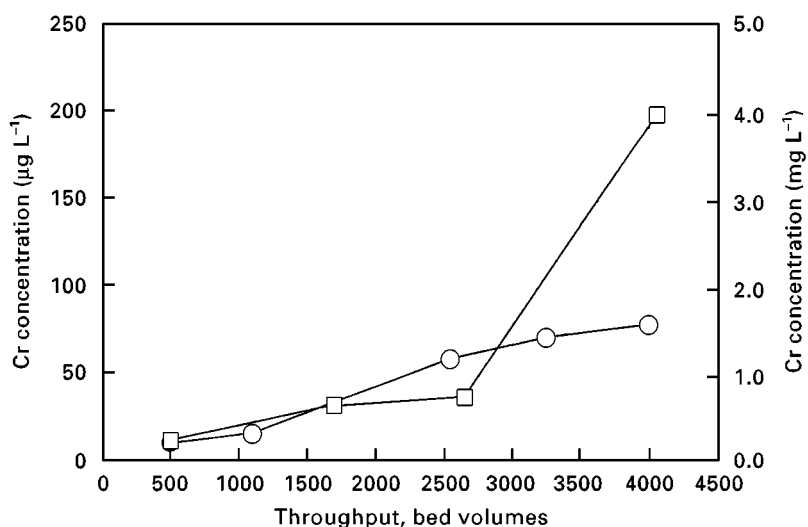
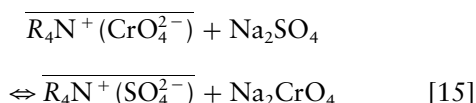
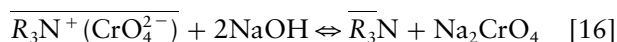


Figure 4 Elimination of Cr(VI) from cooling tower blowdown. Effluent concentration histories of loading (circles) and polishing (squares) columns. Feed water composition: Cl^- (500 mg L^{-1}), SO_4^{2-} (200 mg L^{-1}), Cr(VI) (10 mg L^{-1}), HCO_3^- (100 mg L^{-1}), $\text{Ca}^{2+} + \text{Mg}^{2+}$ (5.5 mmol L^{-1}), Na^+ (250 mg L^{-1}). Resin: Amberlite IRA 94.

After exhaustion, treatment with NaOH will convert hydrogen dichromates to chromates and, subsequently, yield half of the chromate loading on elution. Removal of the remainder of the chromate from the strongly basic exchanger requires concentrated sodium sulfate solutions:



In contrast to strongly basic exchangers, weakly basic ones can be completely regenerated by means of NaOH. However, before the following service cycle, the resins have to be reconverted to the sulfuric acid form:



Chromate species elimination from cooling tower blowdown has been achieved by application of a styrene weakly basic resin in a merry-go-round system with three columns. In the plant, column 1 serves as the crude loading column which eliminates most of the chromate. The relatively low effluent concentrations are further decreased by the second (polisher) column. The third column is regenerated/conditioned or waits for service. When the maximum tolerable effluent concentration of the polisher column is exceeded, the sequence is switched

so that the polisher column now acts as the loading column and the freshly regenerated filter is applied for polishing. The previous loading column is regenerated and conditioned. A typical example is given in Figure 4.

Removal of Organic Substances

Natural organic substances normally have an anionic nature at pH values above neutral. Apart from their elimination in a suitable pretreatment step, they can be adsorbed by both weakly and strongly basic anion exchangers. Uptake of organic substances is due to both ionic and van der Waals forces. They may present a problem for anion exchangers because of a possibly irreversible adsorption by styrene-based gel-type resins.

Both types of exchangers, therefore, can act as scavengers for the removal of organic compounds prior to further ion exchange steps. In general, strongly basic exchangers exhibit a better elimination of humic substances. For demineralization of industrial water they are applied in the chloride form as scavenger units at the head of the deionization train. The basic problems associated with the application of anion exchangers as scavengers in demineralization plants are the additional exchanger unit and the exchange of the organics and hydrogen carbonate ions for chloride. Thus, the effluent composition may be less favourable for the application of weakly acidic exchange resins.

Depending on the total concentration of organic matter in the feed water and to the desired level in the effluent, different resin types are recommended. The combined application of weakly and strongly basic

resins has been successfully applied in the Stratabed® concept, in which two layers of the respective resins, both of the polystyrene type, are used. The application of this concept requires the use of exchange resins with a particle size distribution which allows the maintenance of the stratified bed in each column. Since regeneration is carried out using warm NaOH solution, precipitation of silica is avoided. Favourable conditions are met: waters of poor alkalinity and chloride and sulfate are the major part of the anions present. Acrylic anion exchangers allow a reversible uptake of humic acids. Although the capacity of acrylic resins for organics is poorer, they are highly effective. They can be used in all applications except in condensate polishing with extremely high flow rates. Under these conditions the elastic properties of these resins exclude their use.

At low levels of organic matter in the feed water the application of macroporous weakly basic resins in their free base form in the de-ionization train allows an efficient removal. Furthermore, these resins are less susceptible to irreversible fouling.

In drinking water treatment, macroporous styrene-based strong base resins were employed in Hanover in Germany as a single treatment step for the removal of organic matter from ground water. Dissolved organic carbon was to be reduced from 6.5 to about 3 mg L⁻¹. After 5000 bed volumes, the resin was regenerated by means of an alkaline NaCl solution which could be reused seven times. The plant was shut down in 1995.

Apart from the elimination of natural organic matter, anion exchangers may also be applied to the removal of organics from different types of waste water. Weakly basic resins have been used for the removal of phenol. Sorption is carried out at rather low flow rates of 2–8 BV h⁻¹. NaOH or organic solvents are used for regeneration. Macroporous weakly basic resins in the sulfuric acid form are applied for decolorization of kraft bleach liquors. After exhaustion they are regenerated using NaOH and conditioned by means of sulfuric acid.

See also: I/Ion Exchange. III/Water Treatment: Overview: Ion Exchange. Resins as Biosorbents: Ion Exchange.

Further Reading

- Bayer AG (1974) *Lewatit-Lewasorb Manual*. Leverkusen: Bayer.
- Bolto BA and Pawlowski L (1987) *Wastewater Treatment by Ion Exchange*. London: E. & F. Spon.
- Dorfner K (1991) *Ion Exchangers*. Berlin: Walter de Gruyter.
- Harland CE (1994) *Ion Exchange, Theory and Practice*. Bath: Bath Press.
- Kunin R (1996) *Amber-*hi*-lights*. Littleton, CO: Tall Oaks.
- Mitsubishi Chemical. *Diaion Manual of Ion Exchange Resins and Synthetic Adsorbents*. Mitsubishi Chemical.
- SenGupta AK (ed.) (1995) *Ion Exchange Technology*. Lancaster and Basel: Technomic.

WATER-SOLUBLE VITAMINS: THIN- LAYER (PLANAR) CHROMATOGRAPHY

See **III/VITAMINS/WATER-SOLUBLE: THIN-LAYER (PLANAR) CHROMATOGRAPHY**

WAXES: SUPERCRITICAL FLUID CHROMATOGRAPHY

See **III/OILS, FATS AND WAXES: SUPERCRITICAL FLUID CHROMATOGRAPHY**

WHISKY: DISTILLATION



D. S. Pickerell, Maker's Mark Distillery,
Loretto, KY, USA

Copyright © 2000 Academic Press

Introduction

Grain fermentation yields a water-based liquid mixture commonly referred to as distiller's beer. This beer will typically contain between 5 and 9% by weight ethyl alcohol, 6–8% by weight residual grain solids, and a very small quantity of other compounds known as fusel oils. These fusel oils, also known as congeners, are primarily higher alcohols that are soluble in ethyl alcohol but only partially soluble in water. The congeners contribute to the taste and aroma of whisky and are not typically removed in a single-column distillation.

All separation technologies exploit some difference between items in a mixture or solution in order to cause them to separate. These differences may be physical, chemical or electrical in nature. In particular, distillation takes advantage of the difference in boiling points to separate soluble liquids from one another. Not all liquid solutions may be economically separable by distillation for a variety of reasons. For example, one or more of the liquid components may not appreciably volatilize, or the change in the concentrations of the components between the gas phase and the liquid phase may be so small that the process becomes impractical. It may even happen that there is no change in the composition whatsoever.

In general, during distillation of completely miscible liquids, the component with the higher boiling point moves toward the bottom of the still while the component with the lower boiling point moves toward the top. In whisky production, water boils at a higher temperature while ethyl alcohol boils at a lower temperature. As a result, distillation has an added benefit as the separation technique of choice, because the grain residue is naturally carried to the bottom of the still along with the water. If the still is properly designed, the concentration of alcohol in the still bottoms should be negligible and the discharge from the bottom of the still will contain all of the unwanted grain residues and the excess water.

Vapour–Liquid Equilibrium

In order to understand what happens during the distillation process, we need to address the topic of vapour–liquid equilibrium. For the purpose of this discussion, we will consider the case of distilling a mixture of water and ethyl alcohol at a constant pressure of 1 atm. **Figure 1** shows the vapour–liquid equilibrium curves for this mixture. It should be noted that the concept of a single boiling point is invalid for this type of solution. The lower line is referred to as the bubble point line. At a given concentration of ethyl alcohol in a liquid mixture of ethanol and water, the bubble point line indicates the temperature at which the first bubble of vapour forms as the solution is heated. The upper line is called the dew point line. At a given concentration of ethanol in a vapour mixture of ethanol and water, the dew point line indicates the temperature at which the first drop of condensate is formed as the mixture is cooled.

In order to explain the distillation process, a rather simplistic approach is employed by assuming an absolutely ideal system with no inefficiencies. For actual distillation system design, a much more thorough analysis would need to be done. For illustrative purposes, let us assume we have a liquid solution consisting of 40% by weight ethanol and 60% by weight water in a pot at 82°C. **Figure 2** shows the vapour–liquid equilibrium of this solution, which is currently at point A. Let us further assume that we will add heat to this pot in an effort to bring the temperature up to 99°C, as represented by point B (**Figure 3**). The solution will heat up until the

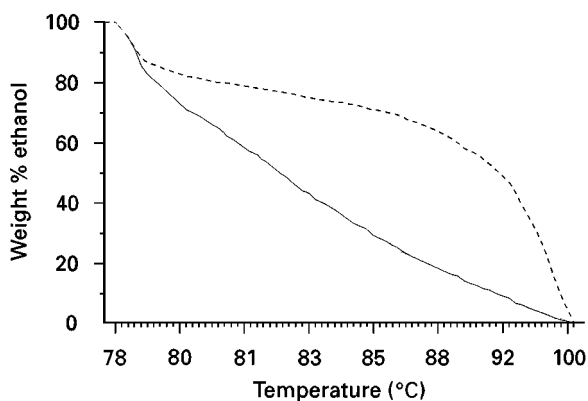


Figure 1 Vapour–liquid equilibrium: ethanol–water, 760 mmHg. Continuous line, bubble point line; dashed line, dew point line.

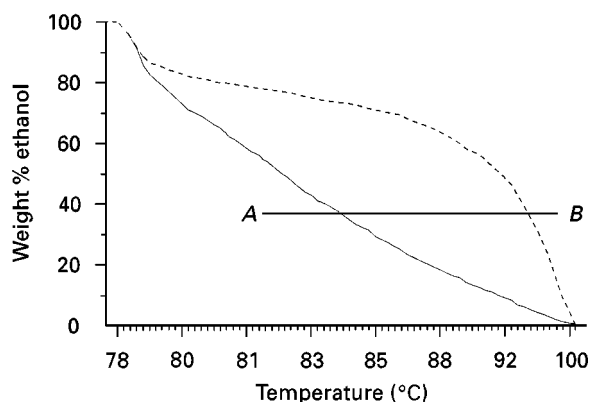


Figure 2 Vapour-liquid equilibrium: ethanol-water, 760 mmHg. Continuous line, bubble point line; dashed line, dew point line.

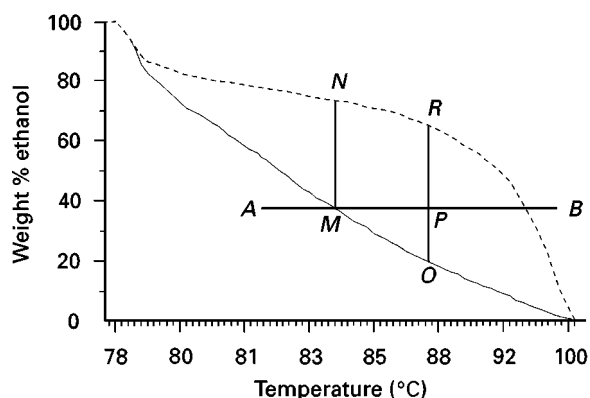


Figure 4 Vapour-liquid equilibrium: ethanol-water, 760 mmHg. Continuous line, bubble point line; dashed line, dew point line.

temperature reaches about 83°C where the heating line intersects the bubble point line at point M. At this point, the first bubble of vapour forms, but because the ethanol vaporizes more easily than the water at this point, the vapour phase is enriched in ethanol. The concentration of ethanol in this first bubble of vapour is found at point N, about 75% ethanol by weight (Figure 4). As the mixture continues to heat up, eventually point P is reached at about 87°C. At this point, the mixture is boiling. The liquid still in the pot has a concentration of about 17%, as indicated by point O, while the total vapour concentration is represented by point R at about 64% ethanol (Figure 5). The solution can continue to be heated until the heating line intersects with the dew point line at point T. At this point there is only one drop of liquid left in the pot and its concentration is found at point S to be about 2% ethanol by weight. If all of the vapour from this experiment was collected, its concentration would be found at point T – approximately 40% by weight ethanol – right back where we

started from, only hotter. The vapour could then be superheated to 99°C at point B, but no further changes in ethanol concentration would occur.

It should be noted that, during the distillation process, once the bubble line is reached, the concentration of ethanol in the liquid phase moves along the bubble point line from left to right, constantly decreasing until the supply of liquid is exhausted. Similarly, the concentration of ethanol in the vapour phase also decreases, along the dew point line, as the liquid in the pot is exhausted. As a result, if we were going to distill ethanol from water in a batch process with a lower limit of acceptable proof, we would have to stop the process before all the ethanol could be recovered. Ideally, we would like to be able to recover all of the ethanol from the solution at some specified constant proof. If point N is the target, we could devise a process where we continually replenish the liquid in the pot at 40% ethanol and a rate equal to the rate that product is taken off by condensation.

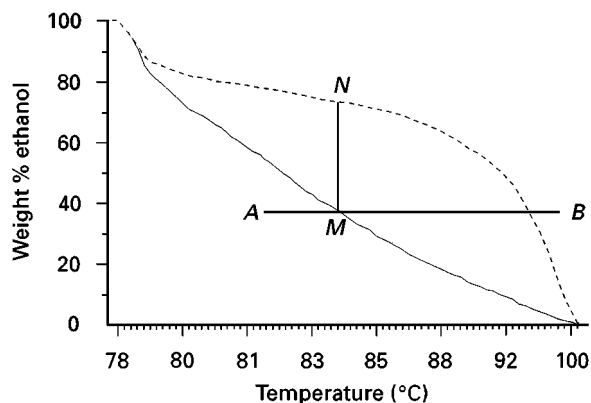


Figure 3 Vapour-liquid equilibrium: ethanol-water, 760 mmHg. Continuous line, bubble point line; dashed line, dew point line.

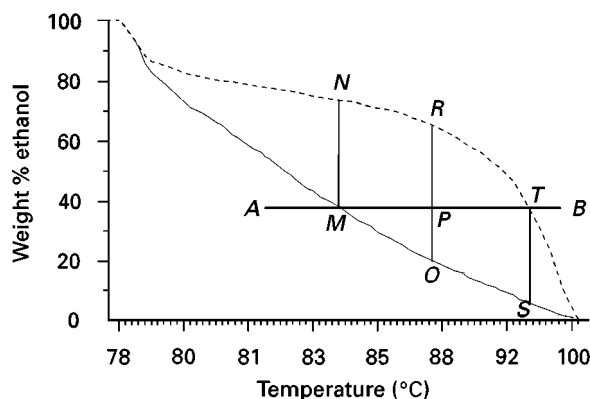


Figure 5 Vapour-liquid equilibrium: ethanol-water, 760 mmHg. Continuous line, bubble point line; dashed line, dew point line.

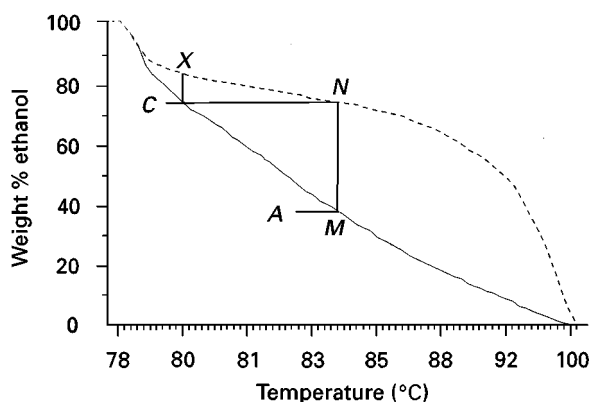


Figure 6 Vapour-liquid equilibrium: ethanol-water, 760 mmHg. Continuous line, bubble point line; dashed line, dew point line.

If a concentration greater than that represented by point N is desired, a single pot cannot accomplish the task (**Figure 6**). Suppose, however, that we set up an apparatus whereby we constantly feed the first pot as described earlier, but now we condense the product vapour and put it in another pot where it can be distilled a second time. The concentration of the vapour from the second pot is represented by point X, about 82% by weight ethanol. It can be seen that adding more pots to this scheme would result in higher and higher concentrations of ethanol in the product. There is, however, a limit to this approach. As the bubble point and dew point lines get closer together, the increase in ethanol concentration per added pot decreases. Eventually, these two lines touch. The point at which these lines touch is called an azeotrope. Azeotrope is a Greek word meaning 'to boil together'. Literally, at this point additional separation by conventional two-phase distillation is impossible because the liquid- and vapour-phase concentrations are identical. In fact, even getting close to the azeotrope requires more advanced distillation practices than those commonly used in whisky production.

By analogy, it can be seen that the problem of recovering the residual ethanol from the still bottoms can also be accomplished through the use of additional distillation stages. In practice, however, the distillation column is a more efficient method of accomplishing these distillation tasks than multiple pot stills. Single malt Scotch whisky makes use of multiple pot stills in the production of their final distillate in a manner similar to that described above.

The Continuous Beer Still

The first distillation element in a multicomponent whisky distillation system is commonly referred to as

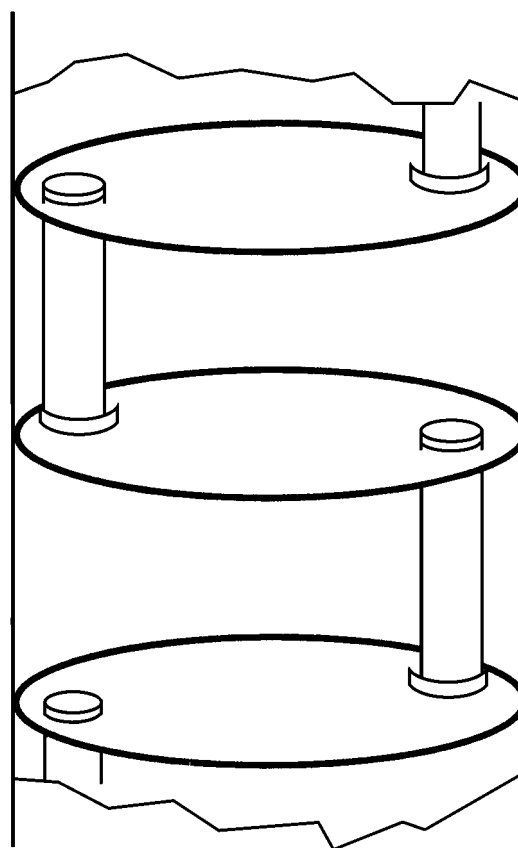


Figure 7 Cut-away of typical distillation column.

the beer still. The beer still consists of a cylindrical shell and number of evenly spaced trays connected by pipes called downcomers. **Figure 7** shows a cut-away view of the inside of a typical beer still. The liquid in the still moves across the trays and down the downcomers. The vapour in the still moves up the column through holes in the tray and through the liquid. The pressure of the vapour under each tray must be great enough to allow the vapour to pass through the holes and through the liquid to the next level up the tray without allowing the liquid to drip through the holes (**Figure 8**). Each time the vapour passes through the liquid, the vapour gains ethanol concentration while the liquid loses ethanol concentration. One tray is roughly equal to one distillation in a pot similar to that discussed earlier. Technically, the vapour condenses in the liquid of the tray above it, and gives off its heat of vaporization. This heat of vaporization in turn revaporizes a corresponding volume of vapour which is richer in ethanol.

The still is conceptually divided into two sections, the stripping section and the rectifying section. The stripping section is the part of the still that is on and below the feed-tray level. This section is referred to as

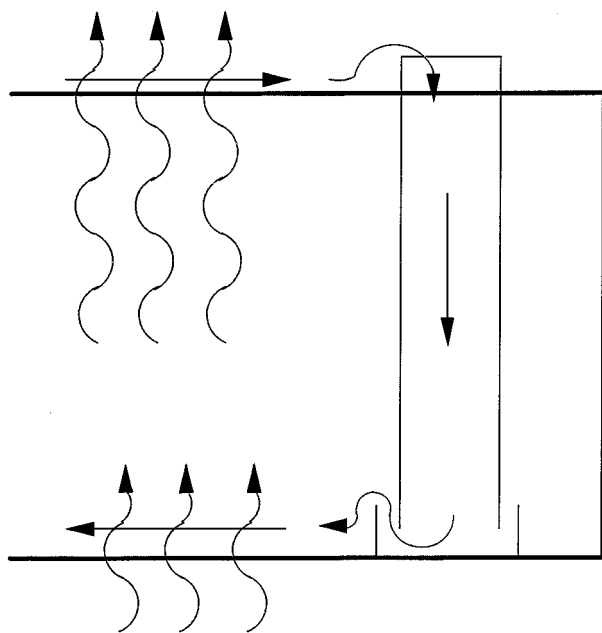


Figure 8 Typical plate flow detail.

the stripping section, because here the residual alcohol is essentially stripped from the feed stream so that the still bottoms have a negligible presence of ethanol. The still must be designed not only to produce a spirit of the desired proof, but also to limit base losses. Typically, the stripping section has about 16–20 plates. The plates in this section must be designed to minimize the likelihood of fouling due to the grain residue being present here. Almost exclusively, sieve trays are used for this purpose because they have larger, less complex vapour openings and wider tolerances to help prevent plugging with grain particles. The space between the trays must also be sufficiently wide to prevent foam and other entrained liquid on one tray from influencing the tray above it.

It is possible for grain particles in the feed to be entrained in and carried upwards by the vapour passing through the feed tray. This can happen on any tray in the stripping section, but it is most critical on the feed tray. Various approaches have been utilized to minimize this problem; almost all are mechanical alterations to the still itself. The most common de-entrainment device is the use of one additional sieve tray immediately above the feed tray.

The rectifying section of the still is the part that is above the feed tray. In this section, the alcohol is concentrated to the desired product proof. Typically, the rectifying section has between two and five plates. The plates in this section are designed to cause more efficient commingling of the vapour with the liquid as the vapour passes through the plate. Since solids are no longer an issue, the contacting mechanisms can be

more intricate and tolerances closer in this section. The plates in this section may also be more closely spaced because foaming and entrainment are much less of a problem here than in the stripping section.

The Beer Heater

As a rule of thumb, the conditions of the feed stream to the still should match, as closely as possible, the conditions on the tray to which the feed is introduced. It has already been noted that the ethanol concentration of the feed stream is generally between 5 and 9% by weight. The concentration can be closely predicted from heat and material balance calculations where no empirical data exist for a given feed stream. It has also been noted that the feed tray is generally near the 18th plate. The feed tray location can also be predicted from detailed will design calculations. The only problem that remains, then, is the feed temperature. When fermentation is complete, the beer temperature is generally about 34°C. The feed tray liquid temperature should be about 93°C. Since the vapour from the still generally has to be cooled and condensed, it provides a convenient source of heat to pre-heat the beer. Usually, the beer feed is passed through a shell and tube-type heat exchanger with large diameter tubes to help alleviate plugging. The vapours from the still are on the shell side of the exchanger.

The condensate from the beer heater is generally returned to the still as reflux. Reflux is the liquid returned to the top of the still. It alters the number of trays required to perform the desired degree of separation as well as the tower cross-sectional area and the heating and cooling loads required for vaporization and condensation. Reflux is generally referred to as a ratio of the liquid returned to the still versus product collected. As the reflux ratio goes up, the number of trays required to perform the separation goes down, but the requisite heating and cooling loads go up. At infinite reflux, the minimum number of trays is achieved, but the maximum heating and cooling loads are required. At minimum reflux, an infinite number of trays is required for the separation, but minimum energy requirements are achieved. An optimum reflux ratio can be calculated and the beer heater can be designed to provide that reflux.

A general rule of thumb for still design would require that the reflux be introduced to the still on the top plate because of its temperature and composition. However, many distillers have made the decision to enter the reflux lower down the column near the beer feed plate for quality reasons. Additionally, the final distillation proof in whisky production is only partly determined by economic considerations. Depending

on the type of whisky being produced, there are generally governmentally prescribed maximum ethanol concentrations which may be permitted during the distillation process. In the case of bourbon, the US Bureau of Alcohol, Tobacco, and Firearms prescribes that the distillate may be taken from the still at no higher than 160 proof (80% ethanol by volume). Of utmost importance, however, are the organoleptic considerations which go into the production parameters for the whisky. Product taken off at a lower proof retains more of the grain character, while product taken off at a higher proof tends to have less of the grain flavour constituents.

The Doubler

Many distillers utilize a doubler in their whisky distillation process. The doubler is basically a pot still, like the one discussed earlier. The doubler acts as one additional distillation stage. It is used in practice for final proof adjustment and for product quality enhancement. There are two fundamentally different ways of operating the doubler. The first is called true double distillation. In true double distillation, the still vapours generally pass through the beer heater first, and then one or more condensers, so that the product is completely condensed back to a liquid form. This liquid is then charged to the doubler where it is heated with steam coils and re-vaporized. The vapour from the doubler is then condensed again and taken off as product.

The doubler can also be operated as a thumper. In this case, the doubler is fitted with a large sparger. The doubler is charged with liquid to a level just above the sparger. The liquid is typically demineralized water or the low proof tails cut from a previous distillation. The vapour from the still first passes through the beer heater then through the sparger in the doubler where it bubbles through the liquid. As the vapour passes through the liquid in the doubler, it flash condenses and gives off its heat of vaporization which, in turn, revaporizes a corresponding volume of vapour which is richer in ethanol. The thumper gets its name from the sound made as the vapour condenses while passing through the liquid. Finally, the ethanol-enriched vapour passes through one or more condensers and is taken off as product.

Reboilers

Most beer stills are heated by direct steam injection from a low pressure steam sparger located in the base of the still. A reboiler is a type of heat exchanger which permits the use of higher pressure steam than a steam sparger will allow. There are several advantages

to using a reboiler. First, it acts as one theoretical plate in the distillation column. Second, it saves on the amount of waste to be disposed of from the still bottoms because it adds no water to the system. However, reboilers are not generally used in whisky production because they have a great tendency to scorch the grain in the bottoms and, hence, degrade the product quality. In other stills with no grain residue, reboilers have been used quite successfully.

Process Control

Control of the continuous beer still is generally accomplished by means of three interrelated control loops. These loops regulate the level of the liquid in the bottom of the still, the flow of steam into the bottom of the still and the flow of the beer feed near the top of the still.

Typically, the liquid level in the bottom of the still is sensed by a level transmitter which, in turn, regulates a control valve on the discharge of a continuously running base level pump. Alternatively, in certain configurations, the base level can be regulated very simply by means of a float valve set at a certain level. This requires that the discharge be capable of gravity flow away from the still bottom. Additionally, newer technology has made it possible to dispense with the control valve on the base level pump. The level transmitter can provide a signal to a frequency inverter which controls the frequency of the electrical current running the pump. This frequency shift will cause the pump to speed up or slow down in relation to the signal from the level transmitter.

In a similar manner, the steam flow to the still is generally held at a constant base pressure or a constant flow rate. Base pressure control is the most common means of steam control. A pressure transmitter in the base of the still above the liquid level provides a control signal to a control valve which, in turn, regulates the flow of low pressure steam into the steam sparger in the bottom of the still. If steam flow control is desired, an orifice plate or vortex flow meter is inserted into the steam line. The flow-sensing device provides the control signal to regulate the control valve. In the past, some distillers have used the still top temperature as a means of regulating the steam flow, while holding the beer feed constant. While this means is effective, it tends to be less reliable due to the relatively large amount of process response lag time.

The beer feed is generally regulated by means of sensing the still top temperature, which is directly related to the proof of the distillate. A temperature transmitter generally provides a control signal to

a process control valve in the beer feed line, which is fed by a constantly running feed pump. More recent technology has made it possible to control the proof more directly by using the temperature-corrected density function of a mass flow meter, which can be correlated to the proof of the discharge from the still. The only downside to the use of a mass flow meter is the process lag time that results from having to measure the proof of the distillate after condensation. Additionally, the control valve can be eliminated from this loop by using a frequency inverter, as described above. Some distillers employ a more sophisticated means of controlling the beer feed to the still by use of a cascaded control loop. Typically, a magnetic flow meter is used to measure the flow of beer to the still and control the operation of the control valve. The still top temperature transmitter provides a signal which is used to manipulate the control settings for this flow control loop.

In addition to the above controls, one or more condensers must also be controlled. Generally, a control valve on the inlet cooling water line is used to control this process. The control signal typically comes from a temperature transmitter which can either be located on the discharge water line or the discharge product line. Due to the relatively quick flow rate of the cooling water with respect to the product flow rate, process control response is generally much better if the temperature transmitter is located on the cooling water discharge line.

Finally, if the product is double-distilled in a true doubler, one additional control loop is required. The steam flow to the steam coils inside the doubler must be regulated. Almost without exception, this loop consists of a steam control valve and a temperature transmitter on the vapour discharge from the doubler. In a manner similar to the still top control,

new technology has made it possible to control the discharge proof more directly using a mass flow meter.

Conclusion

A sign at the Stitzel-Weller distillery in Louisville, Kentucky sums up the traditional view of the impact of science on the beverage alcohol industry:

No Chemist Allowed

Nature and the oldtime know-how of the master distiller get the job done here. Because traditional Kentucky whisky is a natural product, we disdain synthetics, scientist, and their accompanying apparatus. This is a distillery, not a whisky factory.

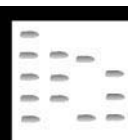
Pappy Van Winkle

Tradition handed down through the generations is the predominant means of whisky production. There are numerous stories of a distiller who had to replace his still because it had worn out. When the new still was being installed, the distiller would make sure that it was identical to the one it was replacing, right down to the dent in the side of the still, which was generally reapplied by the master distiller himself. As a result, technological change is slow to be adopted in an industry where any change in the process may result in a changed taste. Technology is gaining a foothold in the area of process control, where new and better final control elements, transmitters and control systems are always being applied. This traditional approach has also resulted in an almost complete lack of published literature on the topic of whisky distillation, which at best is viewed by the industry as only part science and part art.

See Colour Plate 127.

See also: III/Wine: Gas and Liquid Chromatography.

WINE: GAS AND LIQUID CHROMATOGRAPHY



J. Guasch and O. Busto, Universitat Rovira i Virgili, Tarragona, Spain

Copyright © 2000 Academic Press

Introduction

From the chemical point of view, wines are aqueous alcoholic solutions containing more than 1000 components that can be present at high concentrations (g L^{-1}), but also at trace levels (ng L^{-1}). Some of

these components determine the organoleptic properties of wines, while others are significant for classifying their origin and/or for checking whether some adulteration has taken place. Concentration levels of these compounds vary according to the variety of vine, the climatic conditions under which the grapes were grown, and the conditions under which vinification and ageing processes have been developed.

The quality of wines is established by sensory analysis, which is clearly correlated to their chemical

composition. To assure and control this quality, some essential parameters and characteristic compounds are determined by physical and chemical analyses, which are established principally by the *Office International de la Vigne et du Vin* (OIV). Other constituents whose determination is included in these methods are those associated with the toxicity of wines or which are allowed to be present to some maximum permissible levels.

Until recently, the techniques used in the analysis of this broad variety of properties and compounds have been based on classical methods (mainly gravimetric, titrimetric and colorimetric), which allow an adequate control of the vinification in the wineries. Although chromatographic techniques are not widely used in the OIV methods, the complexity of wine composition has pointed to the use of chromatography in many oenological laboratories, and the improvement in the analysis of wines is undeniably bound up with the development of chromatography.

Almost all the chemical compounds present in wines can be analysed by chromatography, either by direct injection or by prior derivatization. For volatile, thermally stable compounds, gas chromatography (GC) is the most used technique, while for the analysis of nonvolatile and thermally unstable compounds, high performance liquid chromatography (HPLC) is preferred. These techniques are considered in more detail below.

Gas Chromatography

Gas chromatography has been responsible for the most important advances in the knowledge of the volatile fraction of wines. Although the non-volatile fraction can also be analysed by GC after derivatization of the analytes, HPLC methods are simpler and therefore they are preferred for these compounds.

The main application of GC to wine analysis is the study, characterization and determination of the aroma of wines, which originates from their volatile components. Aroma compounds are usually classified according to their chemical functionality, the most important being esters, alcohols, acids, lactones, carbonyl compounds, volatile phenols and sulfur- and nitrogen-containing volatiles. With the exception of ethanol and glycerol, the concentrations of the individual aroma compounds range from 100 mg L^{-1} to 0.1 ng L^{-1} . The human sensory organs are extremely sensitive to certain aroma substances, which can show sensory thresholds much lower than their concentrations in wine. The analysis of wine aroma must, therefore, be optimized in order to determine all these compounds. To perform this kind of analysis, two

different steps must be considered: sample preparation and gas chromatographic separation.

Sample Preparation

The sample pretreatments are conditioned by the wine matrix and the character and the concentration of the analytes to be determined. Wines can be directly injected, but it is more common to inject the extract obtained after the application of pretreatment techniques.

Direct injection is applied to the analysis of the volatiles whose concentration is close to the mg L^{-1} level, so they are easily detected by GC detectors. When injecting wine in this way, the nonvolatile fraction remains in the injector and may be thermally degraded, giving rise to potential interfering substances (artefacts) and unstable baselines. Distillation of the volatile fraction or filtration, after addition of a water-miscible solvent to reduce the polarity of the wine matrix, helps to minimize this problem.

Injection after clean-up and concentration treatments is usually applied to the analysis of trace compounds ($\mu\text{g L}^{-1}$ to ng L^{-1}) to enhance their detectability. At the same time, interfering substances are removed during the isolation procedure. The main problems with these techniques are the occasional quantitative and qualitative changes of the analytes, the formation of artefacts by chemical reactions or thermal decomposition, and the introduction of impurities. For these reasons, the suitability of the isolation and concentration methods for a particular analyte has to be carefully evaluated.

Distillation is normally used to isolate the wine volatiles from the nonvolatiles. It can be carried out at atmospheric or reduced pressure in different distillation modes (direct, steam and fractional). By working at reduced pressure and low temperature chemical reactions or thermal decomposition can be minimized. The most important disadvantage is that the isolates obtained are diluted and it is necessary to combine the distillation with other methods that concentrate the volatile fraction.

Solvent extraction is used to simultaneously isolate and concentrate the volatiles. It is carried out in batch mode (simple or multiple) or continuous mode (by using continuous liquid-liquid extractors). The choice of the solvent is conditioned by the high concentration of ethanol (10–15%) in wines. Owing to their low boiling points and very low polarities, pentane, dichloromethane and their azeotropic mixtures are commonly used because they discriminate against ethanol. Other solvents used are diethyl ether and ethyl acetate. Fluorocarbons were widely used because of their extraction efficiency and very low boiling points, but nowadays they are environmentally

unacceptable. One of the disadvantages of solvent extraction is the use of large volumes of solvents (normally not free of contaminants) and the large amount of time spent in the extraction. Whenever possible, the use of minimum solvent/sample volume ratios enhances the concentration and minimizes contamination problems. At the same time, the efficiency of the extraction can be raised appreciably by salting-out the solution with sodium chloride.

The low boiling points of these solvents allow the concentration of the extracted volatiles by distilling off the solvent. By using a Kuderna–Danish concentrator the loss of volatiles is minimized. Furthermore, a gas stream is used to remove the solvent excess from the extract. This procedure is very effective, but may lead to the introduction of contaminants from the gas and to losses of the most volatile compounds.

Simultaneous distillation–extraction, using the apparatus originally described by Likens and Nikerson, has not been commonly applied to wine analysis. Supercritical fluid extraction is not common, but it is becoming increasingly accepted.

Solid-phase extraction (SPE) has also been used for the isolation of wine aroma compounds. The most common adsorbents are charcoal, silica gel and porous polymers (ChromosorbTM, PorapakTM, Amberlite XADTM and TenaxTM). The volatile compounds retained are usually eluted and/or fractionated by pentane, diethyl ether, dichloromethane, ethyl acetate or their mixtures. This technique is preferred for the analysis of a specific group of volatiles, since the adsorbent used is normally selective. Large volumes of adsorbents and solvents are used in order to assure the whole recovery of analytes, so dilute solutions are obtained. A final step including solvent evaporation is therefore needed.

Headspace techniques are widely used in wine aroma determinations because they enable the direct analysis of the headspace gas above the heated samples, where the compounds responsible for the aroma detected by the human nose are transferred. The static headspace technique is suitable for the analysis of the aromatic compounds of highest concentration, but for the analysis of trace levels it is necessary to use dynamic headspace (purge and trap) techniques. The retention of the volatiles is usually achieved by using either cryo or sorbent traps. Sorbent traps are normally preferred because the retention of water and ethanol is minimized, using the same adsorbents mentioned for SPE. The trapped volatiles are recovered by extraction with small volumes of solvent or by thermal desorption, which can be carried out in the chromatographic injector, enabling the overall sample to be analysed in a single step. On the

other hand, the volatiles obtained by solvent extraction are more dilute, but the sample can be fractionated and therefore injected in several chromatographic runs.

Solid-phase microextraction (SPME) is a single-step solvent-free extraction technique that combines the advantages of both SPE and headspace techniques. It has been increasingly applied to the isolation of flavour compounds. The adsorbent (usually polydimethylsiloxane-, divinylbenzene- or polyacrylate-coated fused silica fibres) is fixed in the needle of a specially designed chromatographic syringe and exposed either to the liquid sample or to the headspace above it. After exposure of the fibre to the sample, absorbed analytes are recovered from the fibre by thermal desorption in a conventional GC injection port.

Chromatographic Separation

The chromatographic separation is normally carried out in a gas chromatograph equipped with a split/splitless injector and a flame ionization detector (FID). On-column injectors with retention gaps are very useful for the analysis of traces because they enable the injection of large volumes of wine extracts and the concentration of the volatile fraction at the head of the chromatographic column. Programmed temperature vaporizer (PTV) injection is also suitable for the direct desorption of volatile compounds trapped on injector glass liners filled with adsorbents.

The detection of the analytes is usually carried out with a FID or a mass spectrometer detector (MSD). Other detectors are used only to detect more specific compounds. The flame photometric detector (FPD) and, more recently, the sulfur chemiluminescence detector (SCD), are widely used for detection of sulfur-containing compounds, mainly thiols, sulfides, disulfides and heterocyclic compounds. The electron-capture detector (ECD) is used to detect halogenated substances, such as chlorophenols and chloroanisoles, which are associated with cork taint off-flavours. The ECD and the nitrogen phosphorus detector (NPD) are widely used for the analysis of pesticide residues and some specific additives.

To characterize the wine flavour, gas chromatography–olfactometry (GCO) has been coupled with different methods that determine the relative aroma intensity. The smell of the different components of the wine aroma is assessed by sniffing the effluent of the chromatographic column in parallel with FID detection.

All kinds of chromatographic columns can be used to separate the volatile analytes of wines, but fused silica capillary columns with different stationary phases are the most common. Polyethylene glycol

phases are preferred for the evaluation of the global wine aroma, while less polar phases (such as methylsiloxane and methylphenylsiloxane phases) are needed for assessing the identification of individual compounds. Chiral phases are used for the separation of the enantiomers of volatile compounds, which exhibit very different sensory properties. Multi-dimensional gas chromatography is used for the analysis of volatiles that are not well separated with a single column.

Selected Applications

Many of the sources listed in the Further Reading section deal with the analysis of wines by GC. The following methods are usually performed in oenological laboratories for routine control and research studies.

According to the OIV method, the determination of methanol and ethyl acetate in wines is carried out by GC-FID. Wine distillates are injected in the split injection mode on a polyethylene glycol column under isothermal conditions. This method enables the simultaneous determination of other compounds present in the distillate, such as acetaldehyde, 1-propanol, 2-methylpropanol, 1-butanol, 2- and 3-methylbutanol, 1-pentanol, 1-hexanol, 2-phenylethanol, ethyl lactate, ethyl succinate, 3-methylbutyl acetate, acetic acid, some polyalcohols and so on. In routine analysis, this procedure is usually simplified when wines are directly injected. **Figure 1** shows an example of the chromatogram obtained under these conditions.

The main aroma compounds of wine distillates are analysed by direct split injection of samples with

a temperature programme that optimizes the separation of the different substances. The compounds determined in wine distillates by this OIV method are methanol, acetaldehyde, acetals, higher alcohols, ethyl esters of fatty acids, acetates of the main alcohols and volatile fatty acids. There are other aroma compounds that can be detected by splitless injection of the extract obtained with a batch extraction using ether/hexane (1 : 1) and magnetic stirring. **Figure 2** shows an example of the chromatogram obtained when a methylene chloride wine extract is injected.

In research work, the isolation of the global aroma of wine is usually performed by continuous solvent extraction using different ratios of pentane-dichloromethane and different times of extraction. The extract is dried over anhydrous sodium sulfate and concentrated either in a Kuderna-Danish device or with a gas stream. The concentrate is injected into the GC-FID, working in splitless mode and with a programmed column temperature. Purge and trap methods are suitable alternatives to this procedure and, more recently, SPME has also found some applications in the determination of the ethyl esters of spirit beverages and in the analysis of the main aroma of fruit juices.

Currently, many other volatile compounds are investigated by GC for their sensory contribution. The most important are terpenes, lactones (solerone, sotolone and oak lactones), carbonyl compounds (hexenals, β -damascenone and α - and β -ionone), volatile phenols (alkylphenols and alkylguaiacols), thiols, sulfides, disulfides, pyrazines and vitispiranes. The particular methods of analysis for these compounds are fully described in publications listed in Further

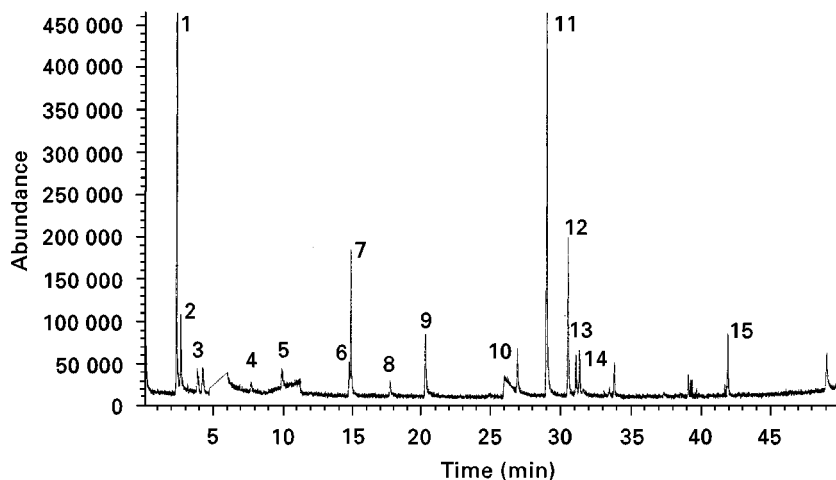


Figure 1 Chromatogram from direct injection of a wine sample (GC-MS). Key: 1, carbon dioxide; 2, acetaldehyde; 3, ethyl acetate; 4, 1-propanol; 5, 2-methyl-1-propanol; 6, 2-methyl-1-butanol; 7, 3-methyl-1-butanol; 8, acetone; 9, ethyl lactate; 10, acetic acid; 11, (D)-2,3-butanediol; 12, *meso*-2,3-butanediol; 13, 1,2-propanediol; 14, 3-ethoxy-1-propanol; 15, 2-phenylethanol.

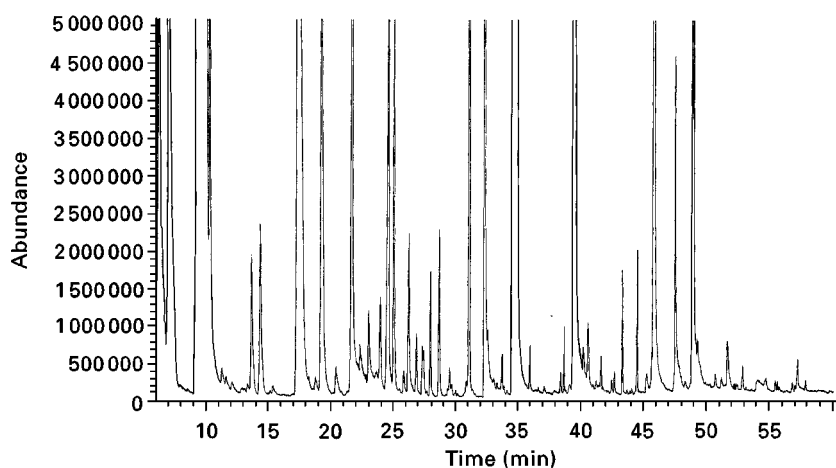


Figure 2 Chromatogram of the injection of a concentrated wine extract obtained by methylene chloride extraction (GC-MS).

Reading. Two examples of chromatograms obtained from the analysis of sulfur compounds (**Figure 3**) and pyrazines (**Figure 4**) are shown.

High Performance Liquid Chromatography (HPLC)

The first studies on the application of HPLC to the analysis of wines appeared at the end of the 1970s for the analysis of polyphenols. Since then, HPLC has been applied to the separation, characterization and determination of a large number of wine compounds

or groups of compounds. The literature concerning the application of HPLC in wine and must analysis is very extensive, but it is important to emphasize the particular interest of this technique in the study of polyphenols, amino acids, biogenic amines, organic acids and sugars.

The use of HPLC is rarely recommended in the official methods. However, carboxylic acids, saccharose, hydroxymethylfurfural and some additives such as sweeteners can be determined by official HPLC methods.

As mentioned above, one of the main problems when dealing with wines is the complexity of the matrix. Although HPLC offers the possibility to choose columns, solvents, detectors and derivatizing reagents, many of the chromatographic procedures developed for HPLC determinations in wines involve some kind of sample pretreatment. These procedures generally make use of either ion exchange

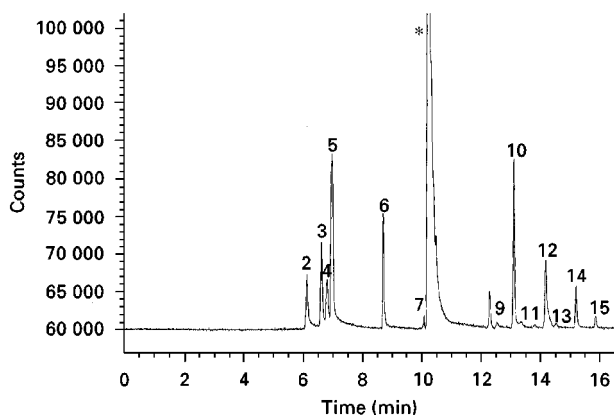


Figure 3 Sulfur compounds found in the headspace of a cryogenically trapped wine (GC-FPD). Key: 1, hydrogen sulfide; 2, methanethiol; 3, carbon disulfide; 4, ethanethiol; 5, dimethyl sulfide; 6, methyl ethyl sulfide (internal standard); 7, diethyl sulfide; 8, methyl propyl sulfide; 9, ethanol; 10, tiophene (internal standard); 11, methyl thioacetate; 12, dimethyl disulfide; 13, ethyl thioacetate; 14, ethyl methyl disulfide; 15, diethyl disulfide. (Reproduced with permission from Mestres M, Busto O and Guasch J (1997) Chromatographic analysis of volatile sulfur compounds in wines using the static headspace technique with flame photometric detection. *Journal of Chromatography A* 773: 261–269. Copyright 1997, Elsevier Science.)

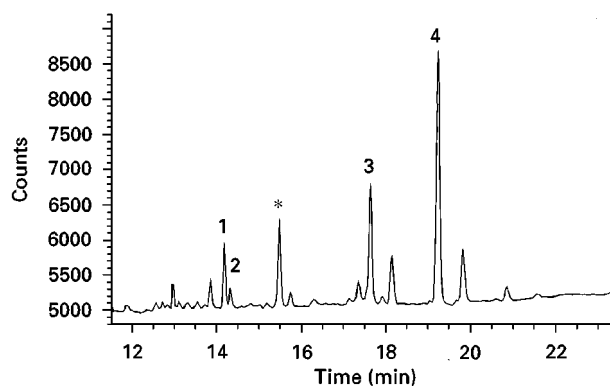


Figure 4 Pyrazines found in the headspace of a wine after SPME (GC-NPD). Key: 1, 3-isopropyl-2-methoxypyrazine; 2, 3-ethyl-2-methoxypyrazine; 3, 3-sec-butyl-2-methoxypyrazine; 4, 3-isobutyl-2-methoxypyrazine; *, 3-isopropyl-2-ethoxy-pyrazine (internal standard).

chromatography and/or solvent of solid-phase extraction.

Sample Preparation

Filtration of samples through a 0.45 μm membrane is always recommended before injecting wines into the HPLC system. This process can be before or at the same time as more complex pretreatments.

One of the methods for avoiding the presence of interfering substances is eluting wine through a low pressure liquid chromatographic column. Polyvinylpyrrolidone (PVP), polyvinylpolypyrrolidone (PVPP) and polyamide adsorbents are used to eliminate polyphenolic substances and silica is used to retain proteins. Ion exchangers are commonly used either to clean up samples or to isolate ionized amines and organic acids from wines.

The most common method used to pretreat samples is solvent extraction with ether or ethyl acetate, although many researchers use more selective solvents.

Solvent extraction has generally been replaced by SPE and SPME. Although there are some applications of carbon and ion exchange cartridges, octadecylsilane (C_{18}) is the most commonly used adsorbent. Many of the analytes whose determination in wines is of interest (such as polyphenols, amino and aroma compounds) can be selectively retained or eluted with slight modifications of matrix conditions (such as pH or addition of ion pair reagents) or by transforming the analytes by derivatization.

Chromatographic Separation

Reversed stationary phase (RP) are the most popular in the HPLC analysis of wines, although it is fully recognized that they are not capable of separating all kinds of analytes in wine. Apart from some special applications, silica is utilized almost exclusively as the support material and C_{18} as the bonded phase.

Since wines are constituted of analytes spanning a wide range of polarities, linear solvent strength gradients are preferred for analysis. Mobile phases normally consist of binary mixtures of either methanol or acetonitrile and slightly acidified water.

The variable UV-visible (UV-vis) wavelength detector is the most popular, although fluorescence and refractive index detectors are also common. Photodiode array detection has also found some application.

Selected Applications

In contrast to GC, the analysis of wines by HPLC has focused on determining compounds with similar chemical functionality.

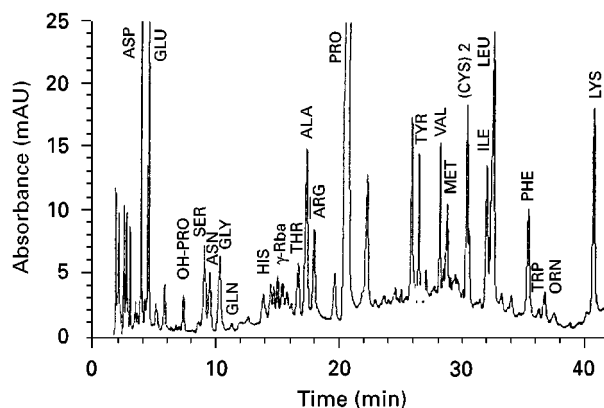


Figure 5 Chromatogram of free amino acids in white wine after derivatization with PITC and DAD detection. (Reproduced with permission from Calull M, Fàbregas J, Marcé RM and Borrull F (1991) Determination of free amino acids by precolumn derivatization with phenylisothiocyanate. Application to wine samples. *Chromatographia* 31: 272–276.)

Ion exchange chromatography has become the most popular technique for the determination of amino acids due to the use of autoanalysers. After chromatographic separation, the analytes are derivatized with ninhydrin, fluorescamine or *o*-phthalaldehyde and detected by spectrophotometry. Amino acids can also be determined by RP-HPLC, which is faster than ion exchange chromatography. The stationary phases are based on amino and, especially, C_{18} chemical groups. Although isocratic elution is used in some applications, gradient elution is preferred because it enables the simultaneous determination of amino acids of different polarities. Mobile phases are normally of binary composition (methanol or acetonitrile and an aqueous buffer solution). As in ion chromatography methods, the amino acids are derivatized, but this time dansyl chloride or phenylisothiocyanate (Figure 5) are used for UV-vis detection and *o*-phthalaldehyde for fluorimetric detection.

Amines are also determined by HPLC, either by direct injection or, more commonly, by derivatization. When they are directly injected, they are separated by ion pair chromatography on a C_{18} column and detected by conductimetry or spectrophotometry. The main limitation of these procedures is that mobile phases shorten the life of the column, so procedures involving the separation of derivatized amines are preferred. Ninhydrin is one of the reagents commonly used in post-column derivatization. The separation is done either by RP-HPLC or by ion exchange chromatography. However, these methods are very time-consuming and so pre-column derivatizations are preferred. The derivatizing reagents used in this case are the same as when dealing with

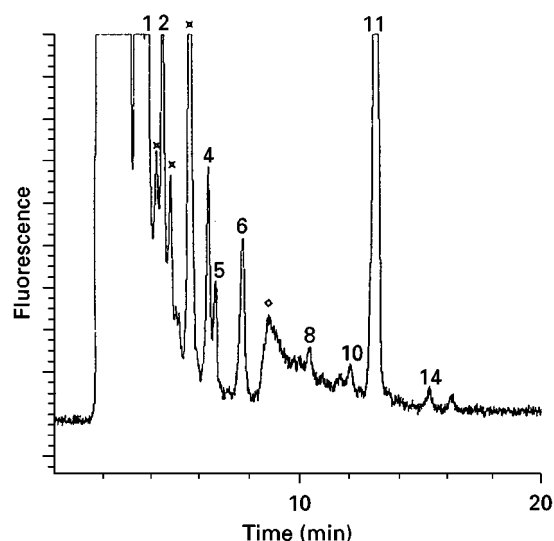


Figure 6 OPA-derivatives of biogenic amines in red wine after SPE and fluorescence detection. Key: 1, ethanolamine; 2, histamine; 4, ethylamine; 5, tyramine; 6, isopropylamine; 8, tryptamine; 10, phenethylamine; 11, putrescine; 14, cadaverine; ◇, peak corresponding to the excess of OPA; x, unknown. (Reproduced with permission from Busto O, Guasch J and Borrull F (1995) Improvement of a solid-phase extraction method for determining biogenic amines in wines. *Journal of Chromatography A* 718: 309–317. Copyright 1995, Elsevier Science.)

amino acids, *o*-phthalaldehyde being the most used (Figure 6). The derivatives are separated by RP-HPLC and detected by spectrophotometry or fluorimetry.

Although carboxylic acids can be determined by GC, after suitable derivatization, the OIV proposes the use of HPLC for determining carboxylic acids in wines, as an alternative to the usual enzymatic procedures. RP-HPLC is used either by direct injection of the wine or by derivatization of the acids before separation. Direct injection of carboxylic acids is a simple method, but the use of mobile phases at low acidic pH (to avoid acid ionization) considerably reduces the life of the analytical column, hence derivatization is recommended. Furthermore, when acids are transformed into their corresponding esters, detection is more sensitive. The different derivatization methods reported so far for the determination of organic acids with spectrophotometric detection and which are worthy of special mention are those which use organic compounds containing the chromophore groups phenacyl, naphthacyl and *p*-nitrobenzyl. The organic groups containing coumarin and anthracene groups, on the other hand, are used for fluorimetric detection. Mobile phases are of binary solvents (normally methanol and water) and the elution is done isocratically or with a linear gradient.

Anion exchange chromatography is an alternative to RP-HPLC, using mobile phases made of organic

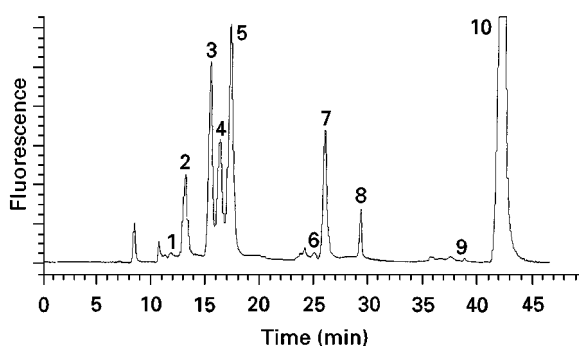


Figure 7 Chromatogram of a wine obtained by high resolution ion exclusion chromatography and refractometric detection. Key: 1, citric acid; 2, tartaric acid; 3, glucose; 4, malic acid; 5, fructose; 6, acetic acid; 7, glycerol; 8, lactic acid; 9, methanol; 10, ethanol.

solvents buffered at a pH close to 8 and with conductimetric or refractometry detection. Although good results are obtained by this method, ion exclusion chromatography using strong cation exchange phases has become the best technique. There are stationary phases specifically developed for determining carboxylic acids in fermented products, which permit the simultaneous determination of sugars, ethanol, methanol and glycerol in a single run. Mobile phases consist of slightly acidic water solutions and the detectors used are either UV or refractive index. Figure 7 shows an example of the chromatogram that is obtained when wine is directly injected under these conditions.

Some papers have reported the separation of carboxylic acids by NP-HPLC and ion pair chromatography, but the results are not comparable to those obtained from the methods described above.

Although the official methods of analysis of sugars are based on enzymatic techniques, sugars can also be determined by HPLC. The preferred methods are based on the use of specific ion exclusion polymeric columns because they enable the simultaneous determination of carbohydrates and other analytes, as already mentioned. The mobile phase used is dilute sulfuric acid and the detection is carried out by spectrophotometry or refractometry. RP-HPLC of sugar benzoylated derivatives followed by spectrophotometric detection has also been used to determine carbohydrates in wines (Figure 7).

According to the OIV methods, saccharose is analysed by HPLC. In this case, the column used is based on 3-aminopropylsiloxane-bonded phases and the mobile phase is acetonitrile and water with refractive index detection.

There are classical methods for estimating the total phenol content of wines, but HPLC is necessary for the determination of individual polyphenolic

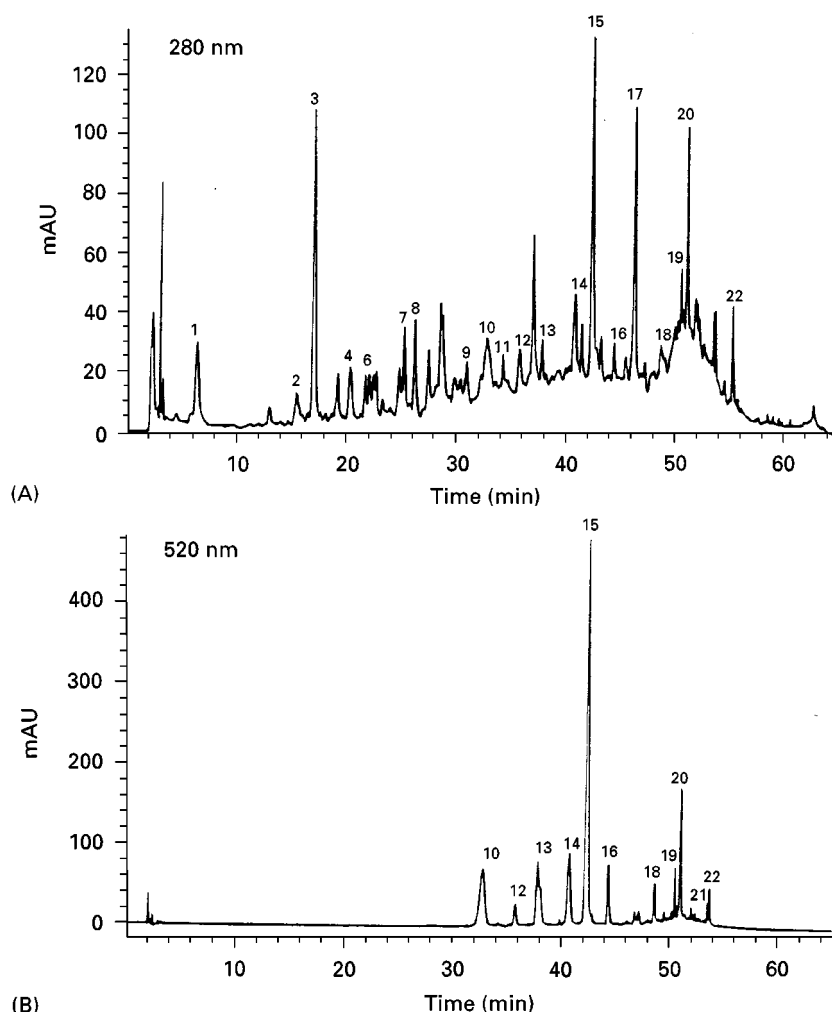


Figure 8 HPLC chromatograms of a must monitored (A) at 280 nm for all phenolic compounds, and (B) at 520 nm to selectively detect anthocyanins. Key: 1, gallic acid; 2, *cis*-caffeoyltartaric; 3, *trans*-caffeoyltartaric; 4, *S*-glutathionylcaftaric; 5, *cis*-coumaroyltartaric; 6, *trans*-coumaroyltartaric; 7, procyanidin B1; 8, catechin; 9, procyanidin B2; 10, delphinidin-3-glucoside; 11, epicatechin; 12, cyanidin-3-glucoside; 13, petunidin-3-glucoside; 14, peonidin-3-glucoside; 15, malvidin-3-glucoside; 16, cyanidin-3-glucoside acetate; 17, rutin; 18, petunidin-3-glucoside acetate; 19, peonidin-3-glucoside acetate; 20, malvidin-3-glucoside acetate; 21, peonidin-3-glucoside acetate (*p*-coumarate); 22, malvidin-3-glucoside acetate (*p*-coumarate). (Reproduced with permission from Lamuela RM and Waterhouse AL (1994) A direct HPLC separation of wine phenolics. *American Journal of Enology and Viticulture* 45: 1–5.)

compounds. Chromatographic procedures are conditioned by the lack of suitable standards and the complexity of chromatograms. Thus, the determination is tackled from the point of view of the two different families of phenolic compounds: flavonoids (anthocyanins, flavanols and procyanidins), and non-flavonoids (hydroxycinnamic and hydroxybenzoic derivatives). Nevertheless, only the pretreatment of samples is different depending on the fraction that has to be isolated. HPLC on reversed-phase columns is almost universally used for anthocyanin separation. The most common used support is C_{18} . Extremely acid solvents are required to suppress ionization of the analytes. Solvents such as methanol/water and acetonitrile/water (in varying propor-

tions), acidified at low pH with phosphoric, perchloric or formic acid, have been used with different solvent programmes. When dealing with flavonols and procyanidins, extraction and purification of wines prior to HPLC is needed. HPLC analysis of flavonols is achieved on C_{18} columns with binary solvent systems consisting of acetonitrile and acetic acid in water and using gradient elution programmes. Procyanidins are chromatographed on C_{18} , C_8 or cyano columns and dilute acid is normally required as a component of the solvent to obtain satisfactory peak shapes. Hydroxycinnamic acids are also analysed by HPLC, by using C_{18} columns and methanol/water eluents slightly acidified with acetic acid. In all cases, detection is carried out spectrophotometrically (Figure 8).

Other substances which are present in wine but which are not determined as frequently as the ones discussed above can also be determined by HPLC. These include additives such as sorbic, salicylic, benzoic and ascorbic acids, which can be determined, according to OIV methods, by RP-HPLC coupled with either spectrophotometric or refractive index detectors.

Future Trends

Both GC and HPLC techniques are widely used in wine analysis. Although the methodologies are normally based on traditional separations, multidimensional chromatographic methods (with or without chiral phases) are increasingly being introduced, frequently coupled online with other analytical devices. More recently, capillary electrophoresis and supercritical fluid chromatography have also been used for wine determinations, but they are still in an early stage of application.

At present, most of the chemical compounds present in wine can be determined by means of a great variety of chromatographic methods described in the literature. Future trends, however, will focus more on internal method validation rather than on development of new methodologies. Future official methods of analysis will then include the minimum requirements (accuracy, precision, limit of detection, robustness, and so on) that an analytical method must fulfil in order to guarantee the validity of the results obtained.

See Colour Plate 128.

See also: II/Chromatography. Extraction. II/Chromatography: Gas: Headspace Gas Chromatography. III/Amines: Gas Chromatography. Amino Acids: Gas

Chromatography; Liquid Chromatography. Phenols: Gas Chromatography; Liquid Chromatography; Solid-Phase Extraction.

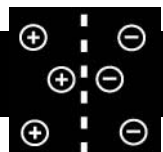
Further Reading

- Acree TE and Teranishi R (eds) (1993) *Flavor Science. Sensible Principles and Techniques*, ACS Professional Reference Book. Washington, DC: American Chemical Society.
- Doneche B (ed.) (1993) *Les Acquisitions Récentes en Chromatographie du Vin*. Paris: Lavoisier.
- Gordon MH (ed.) (1990) *Principles and Applications of Gas Chromatography in Food Analysis*. Chichester: Ellis Horwood.
- Horwitz W (ed.) (1990) *Official Methods of the Association Official of Analytical Chemistry*, 15th edn. Arlington, VA: AOAC.
- Linskens HF and Jackson JF (eds) (1988) *Wine Analysis*. Berlin: Springer.
- Maarse H (ed.) (1991) *Volatile Compounds in Foods and Beverages*. New York: Dekker.
- Maarse H and Beltz R (eds) (1985) *Isolation, Separation and Identification of Volatile Compounds in Aroma Research*. Dordrecht: D. Reidel.
- Morton ID and MacLeod AJ (eds) (1982) *Food Flavours*. Amsterdam: Elsevier.
- Nollet LML (ed.) (1992) *Food Analysis by HPLC*. New York: Dekker.
- Nykänen L and Suomalainen H (1983) *Aroma of Beer, Wine and Distilled Alcoholic Beverages*. Dordrecht: D. Reidel.
- OIV (1990) *Recueil des Méthodes Internationales d'Analyse des Vins et des Moûts*. Paris: Office International de la Vigne et du Vin.
- OIV (1994) *Recueil des Méthodes Internationales d'Analyse des Boissons Spiritueuses, des Alcohols et de la Fraction Aromatique des Boissons*. Paris: Office International de la Vigne et du Vin.

XENOBIOTICS: MAGNETIC AFFINITY SEPARATIONS

See III/BIOLOGICALLY ACTIVE COMPOUNDS AND XENOBIOTICS: MAGNETIC AFFINITY SEPARATIONS

ZEOLITES: ION EXCHANGERS



C. D. Williams, University of Wolverhampton, Wolverhampton, UK

The ion exchange properties of zeolites have been known since 1858, when Eichhorn studied the use of chabazite as an ion exchanger. In the 1920s and 1930s several ion exchange studies were reported.

Table 1 Phosphate based molecular sieve characteristics

Number	Structure type	Porosity	Pore size (μm)	Saturation H_2O capacity ($\text{cm}^3 \text{g}^{-1}$)
<i>Structure fully determined</i>				
5	Novel	Large	0.80	0.31
11	Novel	Medium	0.60	0.16
14	Novel	Small	0.40	0.19
15	Leucophosphate			
16	Zuvnite	Very small	0.30	0.30
17	Erionite	Small	0.43	0.28
20	Sodalite	Very small	0.30	0.24
25	Novel	Very small	0.30	0.17
46	Novel			
<i>Structures inferred from X-ray powder patterns</i>				
37	Faujasite	Large	0.80	0.35
34	Chabazite	Small	0.43	0.30
35	Levynite	Small	0.43	0.30
42	[A]	Small	0.43	0.30
43	Gismondine	Small	0.43	0.34
44	Chabazite	Small	0.43	0.3–0.34
47	Chabazite	Small	0.43	0.3–0.34
<i>Unknown structures</i>				
36	Novel	Large	0.80	0.31
40	Novel	Large	0.70	0.33
31	Novel	Medium	0.65	0.17
41	Novel	Medium	0.60	0.22
18	Novel	Small	0.43	0.35
26	Novel	Small	0.43	0.23
33	Novel	Small	0.40	0.23
39	Novel	Small	0.40	0.23
28	Novel	Very small	0.30	0.21

During the 1960s many groups studied the ion exchange behaviour of the new synthetic zeolites then being produced. Due to the enormous commercial potential of zeolites, many research groups worldwide began serious efforts to synthesize new microporous zeolites and zeotype materials. The first major breakthrough was made by workers at Union Carbide, who in 1982 produced the aluminophosphate molecular sieves (Table 1). Although these materials are electrically neutral and have no intrinsic ion exchange properties, they did lead to the development

of other substituted aluminophosphates that do have ion exchange properties (Table 2).

Since the early 1980s several new zeotypes, based on oxoanion frameworks, have been developed. The major group of materials of interest as far as ion exchange properties are concerned are the layered group IV acid salts. These include phosphates, arsenates, molybdates, tungstates, antimonates, silicates and silicophosphates. Most of these materials act as cation exchangers. Early attempts at synthesis mimicked zeolite preparations using reactive amorphous gels crystallized at temperatures between 120 and 200°C. This crystallization produced a variety of materials, which have been classified by their structure type: α -layered exchangers, γ -layered exchangers, fibrous exchangers, 3-D net exchangers and unsolved structure exchangers. Table 3 lists some of the more important α -layered ion exchangers.

The structure of αZrP was determined by Clearfield in 1969. The inorganic layers are formed by a plane of octahedral Zr atoms that are linked together alternatively above and below via phosphite groups. Three oxygen atoms of the phosphite group are coordinated in this way and the fourth bears a hydrogen atom (Figure 1).

Table 2 Phosphate based molecular sieves with ion exchange character

Number	Structure types
40	Novel
41	Novel
34, 44	Chabazite
35	Levynite
37	Faujasite
42	A
17	Erionite
20	Sodalite
5, 11, 16, 31	AlPO_4

Table 3 Important α layered ion exchangers

Compound	Formula	Interlayer distance (\AA)	Ion exchange capacity (mmol g^{-1})
Titanium phosphate	$\text{Ti}(\text{HPO}_4)_2 \cdot \text{H}_2\text{O}$	7.56	7.76
Zirconium phosphate	$\text{Zr}(\text{HPO}_4)_2 \cdot \text{H}_2\text{O}$	7.56	6.64
Hafnium phosphate	$\text{Hf}(\text{HPO}_4)_2 \cdot \text{H}_2\text{O}$	7.56	4.17
Germanium phosphate	$\text{Ge}(\text{HPO}_4)_2 \cdot \text{H}_2\text{O}$	7.6	7.08
Tin(IV) phosphate	$\text{Sn}(\text{HPO}_4)_2 \cdot \text{H}_2\text{O}$	7.76	6.08
Lead(IV) phosphate	$\text{Pb}(\text{HPO}_4)_2 \cdot \text{H}_2\text{O}$	7.8	4.79
Titanium arsenate	$\text{Ti}(\text{HAsO}_4)_2 \cdot \text{H}_2\text{O}$	7.77	5.78
Zirconium arsenate	$\text{Zr}(\text{HAsO}_4)_2 \cdot \text{H}_2\text{O}$	7.78	5.14
Tin(IV) arsenate	$\text{Sn}(\text{HAsO}_4)_2 \cdot \text{H}_2\text{O}$	7.8	4.80

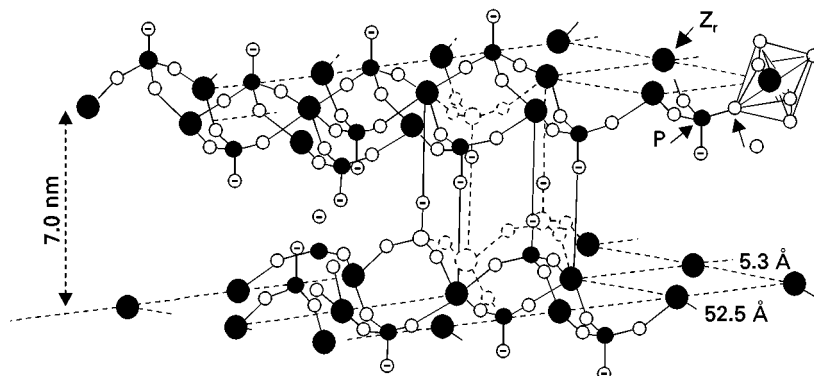
The α ZrP exchangers have been characterized by carrying out potentiometric titrations against MCl and MOH solution mixtures. X-ray analysis of the solid phases shows that α ZrP is initially converted to $\text{ZrMH}(\text{PO}_4)_2 \cdot n\text{H}_2\text{O}$ then on further exchange is converted to $\text{Zr}(\text{MPO}_4)_2 \cdot n\text{H}_2\text{O}$. At any point during the ion exchange process these two phases coexist together with the solution phase. The interlayer distance is large enough to accommodate unhydrated Li^+ , Na^+ and K^+ ; however Rb^+ and Cs^+ are too large to enter without lattice expansion. The energy to expand the lattice is supplied by a base, neutralizing the lattice protons and allowing larger cations to enter.

The γ -layered compounds are far less common than the α compounds. Both $\gamma\text{ZrPZr}(\text{HPO}_4)_2 \cdot 2\text{H}_2\text{O}$ and $\gamma\text{TiTi}(\text{HPO}_4)_2$ are known, but both suffer from hydration at high exchange levels. Both materials have large interlayer distances and as a consequence can accept large cations such as Cs^+ .

Pastor *et al.* have reviewed the synthesis, characterization and ion exchange, ion transport, sorptive and catalytic properties of inorganically pillared layered metal(IV) phosphates, typified by $\text{Zr}(\text{BPO}_4)_2 \cdot \text{H}_2\text{O}$. Porous nanostructures are generally prepared from metal(IV) phosphates either by ion exchange of polynuclear species or by intercalation from solutions of

condensed species obtained by the hydrolysis of organometallic precursors using sol-gel methods. Thermal treatment is used to eliminate organic moieties, condense hydroxyl groups, eliminate water and consolidate the structure by grafting the pillar to the layer. The different strategies devised to overcome the problem presented by the high layer charge density of α - and γ -structured phosphates in obtaining porous solids are described, including exfoliation and local surface growth of pillaring ions, and modification of the zirconium phosphate matrix in order to reduce the cation exchange capacity. Structural and textural characteristics of Al, Cr, mixed Al-Cr, Fe-Cr, Ga-Al and of Si-pillared phosphates obtained from X-ray analysis by fine structure (XAFS), X-ray photoelectron spectroscopy (XPS), and magic angle spinning nuclear magnetic resonance (MAS-NMR) are presented, and the perspectives of nanocomposite pillared layered solids in general are discussed in the current context of mesoporous solids synthesized using templates.

The fibrous materials are exemplified by cerium and thorium(IV) phosphates. Their fibrous nature allows them to be fabricated into papers that allow fast separation of cations. The precise structure of these phosphates is unclear but is probably $\text{M}(\text{HPO}_4)_2 \cdot \text{H}_2\text{O}$, where $\text{M} = \text{Ce}$ or Th .

**Figure 1** Structure of α Zr-P.

The three-dimensional materials have the general formula $NM_2(IV)(XO_4)_3$, where M(IV) is Ti, Zr, Th or Ge; X is P or As and N is a univalent cation. The structures consist of XO_4 tetrahedra and $M(IV)O_6$ octahedral linked by corner sharing to form 3-D networks; this linking forms cavities, occupied by N^+ . If phosphate is progressively replaced by silicate the cavities open up, allowing free movement of the N^+ cations and leading to the cation exchange properties. Numerous specific examples of these materials can be found in the literature, particularly the gallium phosphate-derived materials.

A more recent series of exchangers are those of the titanosilicate type, which have zeolite type pores/cavities. The materials have a formula $Na_2Ti_2O_3SiO_4 \cdot 2H_2O$ and are synthesized from an alkaline medium under similar conditions to those used to crystallize zeolites. The structure has been solved using Rietveld refinement and shows titanium atoms in clusters of four, octahedrally coordinated by oxygen atoms. The silicate groups link the titanium clusters into a square which then shares corners with other titanium cluster squares to form a 3-D network. Half of the sodiums are linked into the framework while the other half are labile and available for ion exchange.

In 1991 a zincosilicate containing three-, four- and five-member rings connected together to form a porous eight- and intersecting nine-member ring channel was reported. Initial studies indicate that the labile monovalent cations can be exchanged.

A great deal of synthetic work has been directed at replacing the aluminium in various zeolites with other metals/nonmetals, including the crystallization of ferrisilicates, borosilicates, gallosilicates, vanadosilicates and titanosilicates. In 1992 the synthesis of a zincophosphate anionic eight-ring three-dimensional framework was reported. During the synthesis the anionic framework was stabilized by cationic, protonated diazabicyclo[2.2.2.]octane or dabco $[(H_2N_2C_6H_{12})^{2+}]$ molecules and water. These materials, although chemically similar to Clearfield's layered phosphates/phosphites, benefit from having a stable open 3-D structure. No ion exchange data has been given but thermal analysis shows that the framework is stable even after the organic dabco has been removed. This calcined material has potential as a cation exchanger. In 1991 the synthesis of sodium zirconium phosphate with a zeolite-type framework was reported. The synthesis followed typical aluminophosphate preparations using triethylamine as a template. The synthesis was carried out in an acidic medium, resulting in the template becoming protonated. Once crystalline, the sample had the template removed by calcination and the adsorption properties of the new material were studied. The

material remained microporous after calcination; however, no ion exchange studies were carried out. Initial studies suggest that this material would act as a cation exchanger.

However, although an enormous number of new materials have been synthesized since 1990, there are few reports on the ion exchange characteristics of these materials.

Future Developments

Over the past five years increasing emphasis has been placed on the investigation into microporous materials based on oxoanion networks other than the aluminosilicates (zeolites). The vast array of microporous materials with potential ion exchange properties is enormous. The number of reported nonzeolite molecular sieves now tops 130. The range of materials includes gallosilicates, borosilicates, ferrosilicates, germanium aluminates, titanosilicates, silico alumino phosphate (SAPO) and metal alumino phosphate (MeAPO) molecular sieves. Most of these new materials have not yet been characterized for their ion exchange properties. The potential of these materials is as yet unrealized but, with increasing environmental demands, it is only a matter of time before these materials are explored.

See also: II/Ion Exchange: Historical Development; Inorganic Ion Exchangers; Novel Layered Materials: Phosphates; Novel Layered Materials: Non-Phosphates; Theory of Ion Exchange.

Further Reading

- Annen MJ, Davis ME, Higgins JB and Schlenker JL (1991) The physicochemical properties of VPI-7: a microporous zinco-silicate with three membered rings. *Materials Research Society Symposium Proceedings* 233: 245-253.
- Breck DW (1974) *Zeolite Molecular Sieves*. New York: Wiley.
- Dongare MK, Singh P and Suryavanshi PM (1992) Hydrothermal synthesis and characterisation of crystalline sodium zirconium phosphates. *Materials Research Bulletin* 27: 637-645.
- Dyer A, Hudson MJ and Williams PA (eds) (1997) *Progress in Ion Exchange, Advances and Applications*. Cambridge: Royal Society of Chemistry.
- Harrison WTA, Martin TE, Thurman EG and Stucky GD (1992) Tetrahedral atom zincophosphate structures: synthesis and structural characterisation of two novel anionic eight ring frameworks containing cationic 1,4 diazabicyclo[2.2.2.]octane guests. *Journal of Materials Chemistry* 2: 175-181.
- Notari B (1993) Titanium silicates. *Catalysis Today* 18: 163-172.

- Pastor PO, Torres PM, Castellon ER *et al.* (1996) *Chemistry of Materials* 8: 1758–1769.
- Poojary DM, Cahill RA and Clearfield A (1994) Synthesis, crystal structure, and ion exchange properties of a novel porous titano-silicate. *Chemical Materials* 6: 2364–2368.
- Ratnasami P and Kumar R (1991) Ferri-silicate analogues of zeolites. *Catalysis Today* 9.
- Szostak R (1989) *Molecular Sieves: Principles of Synthesis and Identification*. New York: Von Nostrand Reinold.
- Szostak R (1992) *Handbook of Molecular Sieves*. New York: Von Nostrand Reinold.
- Wilson ST, Lok BM, Messina CA and Flanigen EM (1984) *Synthesis of AlPO₄ Molecular Sieves*. Proceedings of the 6th International Zeolite Conference (Reno Conference). Guildford: Butterworth Scientific, pp. 97–109.

ZINC ORES: FLOTATION

See **III/LEAD AND ZINC ORES: FLOTATION**

ZONE REFINING COUNTERCURRENT CHROMATOGRAPHY

See **III/PH-ZONE REFINING COUNTERCURRENT CHROMATOGRAPHY**

ESSENTIAL GUIDES FOR ISOLATION/PURIFICATION OF CELLS

J. Bauer, Max-Planck-Institut für Biochemie,
Martinsried, Germany

Copyright © 2000 Academic Press

In cell-separation technology the term 'component' of a mixture corresponds to a group of cells, which is usually called a cell population and shares a number of common features. How many common features a group of cells has to share in order to be called a cell population depends on the interest of the 'separator'. For example, a T-cell population may be a group of mononuclear white blood cells bearing CD3 antigens, while a helper cell population usually comprises mononuclear white blood cells bearing CD3 and CD4 antigens.

Cells metabolize as long as they live independently, whether they remain in an actual state of activation or differentiation or they proceed to another one. This means that a whole cell must not change its appearance or functions, but some cell components are chemically modified either anabolically or catabolically. So for discussing cell separation the term 'chemical modification' should be converted to 'biological modification' and in this chapter the expression 'without biological modification' will be defined as purification of cells without changes or signals for changes of cellular states of activation and/or differentiation.

No technology has been developed so far which allows picking of cell populations directly out of pieces of plant or animal tissues. So a 'mixture' which will be separated is normally a suspension of single cells prepared from parts of plants, from organs or body fluids of animals and humans or from two- or three-dimensional *in vitro* cell cultures. These cell sources already contain preselected groups of cells, the so-called organ or fluid (e.g. blood) specific cells. Still, a series of populations differing in important features are present in most plant or animal body compartments. In these instances, it may be of interest to separate cells for studying their biology or for using some of their capabilities in medicine or biotechnology.

Thus the following reflections on essential guides for separation/purification of cells are based on separations defined as processes of any scale by which cell populations of single-cell suspensions are separated from each other without biological modification.

Methods for Cell Separation without Biological Modification

The above definition rules out some technologies, frequently used to prepare homogeneous cell populations, because they include biological modifications of cells. For example, the enrichment of cell types of interest by establishing cell lines or cell clones will not be considered as a subject in this chapter. Cell lines or cell clones may be very useful sources of important genes and gene products. However, their cells are transformed in unnaturally fast growing states, in order to separate them from unwanted accompanying cells. Also cell separation/purification techniques using different capabilities of various kinds of cells to adhere to surfaces of, for example, culture dishes or fibres or to bind antibodies or macromolecules labelled by fluorescence dyes or magnetic beads, will not be described, because cell interactions with foreign components or antibody binding sites very often induce biological modifications. Of course, cell-purification methods like those mentioned above are very useful in research and biotechnology. The reader may find more informations regarding these techniques in the Further Reading.

This chapter focuses on application of counter-current centrifugal elutriation (CCE) and free-flow electrophoresis (FFE). These methods use differences of physical cell parameters such as specific cell density, cell size or negative surface charge density but do not include steps of cell labelling or cell transformation. They have the advantage that cells can be purified within a short time while they are kept suspended in biocompatible fluids or even culture media. Cell contacts to foreign surfaces and/or biologically active substances are thereby minimized and signals of activation and differentiation are delivered to cells during the isolation procedure to a minimal extent. Both methods may help to obtain sufficient numbers of identical cells with a high degree of purity and vitality for studying the biological role, which a defined cell population may play within an organism or for transplantation of cells with states of activation and differentiation suitable to fit in the new organism of a recipient.

Single-Cell Suspensions

Up to the present, cell separation by physical methods has required single-cell suspensions. Some cell

compartments such as peripheral blood, ascites, lymph or other body fluids already contain single cells. Cells of organs such as bone marrow, spleen or thymus can easily be removed, for example with the help of needles. The dissociation of single cells from two- or three-dimensional tissue cultures and from solid body tissues needs more rigorous methods. These cells not only adhere to each other, but are also more or less firmly attached to the extracellular matrix, a complex network of collagen, proteoglycans and cross-linking proteins such as laminin and fibronectin. Mechanical dissociation by scraping cell monolayers from their surfaces or by forcing tissue pieces or cell aggregates through orifices or syringes or pipettes very often damages the cells and results in a poor yield. An enzymatic treatment or pretreatment of cell cultures or organs is thus often applied in order to digest the extracellular matrix and/or to weaken the cell-cell attachment sites. The selection of the enzymes, their concentration and their time and temperature of application depend on the type of organ and its originating organism. Enzymes frequently used for animal cell preparation are collagenase, trypsin, pronase, dispase, papain, chymotrypsin, hyaluronidase, lysozyme and DNase, while cellulase is a typical enzyme for plant tissue dissociation. Sometimes the action of the enzymes is supported by the presence of EDTA (ethylenediaminetetraacetic acid), which destroys binding sites mediated by Ca^{2+} ions. Details regarding techniques of preparing single cells may be found in books quoted in the Further Reading. In general, the enzymatic treatment has to be optimized for each cell-separation process, because the enzymes may not only attack cell membrane components which keep the cells within the tissue but may also destroy important cell-membrane functions.

If neither mechanical nor enzymatic methods lead to satisfactory results, an alternative way may be to incubate pieces of tissue on surfaces which challenge the cells to move out of the tissue and to form monolayers surrounding the tissue. For example, cells of human prostate tumour sections, which cannot be dissociated in viable single cells by a number of mechanical and enzymatic techniques, migrate out of the tissue and form a monolayer, when incubated in culture dishes for a few weeks. After removal of the tissue, the cells can easily be scraped off the plastic dish surface.

Pre-Separation

As soon as single cells are available, countercurrent centrifugal elutriation or cell electrophoresis may be applied. However, some cell-separation tasks need pre-enrichment of the cells of interest. Especially

where an investigator is interested in a peripheral blood leukocyte population such as a lymphocyte, granulocyte, monocyte or even reticulocyte population, the erythrocytes comprising more than 99% of the blood cells have to be removed before one of these white blood cell populations may be purified. In these instances, it has proved useful to perform a first step of density-gradient centrifugation, which does not need pre-labelling of cells. The method allows the separation of mononuclear leukocytes consisting mainly of lymphocytes and monocytes from granulocytes and erythrocytes. The separation principle is based on different specific densities of the various cell populations. In practice, a tube is filled with a biocompatible isotonic medium with a specific density adjusted between the specific densities of the cells to be separated and the cell mixture is layered on the top of this medium. Then the whole sample is exposed to a few hundred g by centrifugation. The forces cause mononuclear leukocytes with a density lower than the separation medium to remain at the top, while those with higher density sediment to the bottom. The specific density of the medium is adjusted by silica colloids, which are coated with an inert material and have low osmolality. Although modern commercially available density-gradient separation media are very inert and direct damage of the cells is seldom observed, the silica colloids are pinocytosed by some cells.

If this is a problem, prolonged centrifugation of whole blood may be an alternative route. During such a centrifugation procedure, a layer of white blood cells is formed above the erythrocytes. This layer, called a buffy coat, contains mononuclear as well as polymorphonuclear leukocytes and lies directly on the erythrocytes. The white cells may be collected. Although co-collection of a considerable number of red cells is usually unavoidable, a degree of white blood cell pre-enrichment can be achieved which allows reasonable further separation by, e.g. CCE.

Countercurrent Centrifugal Elutriation (CCE)

The method of CCE and the equipment required for cell separation according to cell size have already been described so they are summarized only brief here. Cells loaded into the elutriation chamber are subjected to centrifugal sedimentation forces generated by rotation in an outward direction and to counterflow fluid forces pumped into the separation chamber in an inward direction. As long as sedimentation forces are balanced by the opposite fluid forces, different cell populations take different chamber positions depending mainly on their sizes

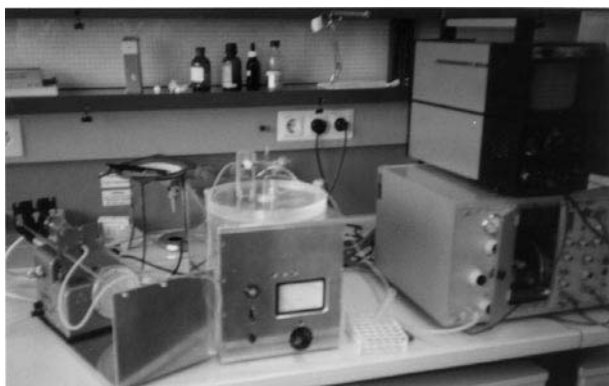


Figure 1 Table-top elutriator (middle) together with an infusion pump driving the counterflow (left) and a volume analyser (right).

and to a lesser extent on their specific densities. If the counterflow rate is increased by speeding up a pump and/or the sedimentation forces are decreased by reducing centrifugation velocity, the various cell populations are washed out sequentially with increasing size ranges.

Commercially, small elutriation chambers with 5 mL separation volume and large ones with 40 mL are available together with suitable centrifuges and rotors from Beckman Instruments (Palo Alto, USA). They can accommodate up to 10^9 and 10^{10} cells, respectively. A laboratory device has also been constructed; it consists of a table-top centrifuge with a small rotor which has a separation chamber with a volume of 0.5 mL to which 10^6 tissue cells or 2×10^7 mononuclear leukocytes may be loaded (Figure 1).

In order to fractionate cells with different sizes into different fractions, counterflow rates and rotor speeds have to be adjusted depending on rotor size, chamber volume and the size of the cells to be separated. The result of each separation should be controlled by recording volume distributions of the cells of each fraction with the help of cell size analysers. Beckman

rotors are frequently operated at speeds ranging from 1000 to 4000 rpm. Dependent on the actual rotor speed, the counterflow through small chambers may be started at rates between 8 and 20 mL min⁻¹ and increased for fractional elution stepwise up to 100 mL min⁻¹ (Table 1); counterflow rates through large separation chambers may start at 50 mL min⁻¹. The table-top centrifuge is operated at counterflow rates between 1 and 6 mL min⁻¹, while the rotation speeds are between 500 and 2200 rpm for tissue cell separation and between 1500 and 2800 rpm for leukocyte separation (Table 2). Using any of the instruments, separation times are short and the cells may be kept suspended in culture medium. Thus unwanted exposure of the cells to stimulatory environments are minimized so that characteristics of separated populations will rather closely reflect the status of the original cells before fractionation.

Because of these advantages, CCE has proved most useful, if applied for the separation tasks listed below:

- For cell cycle analyses, the cellular DNA content is normally determined. However, cells have to be killed in order to make their DNA accessible for intercalating fluorescence molecules. If living cells in different steps of the cell cycle need to be separated, an increase of cell size during passage through the cell cycle may be used as a separation parameter. With the help of CCE the small cells, which are in G1 phase can be separated from S-phase cells which have intermediary size and from the G2/M-phase cells which have the largest size of the cell population. Many flow cytometric analyses of the DNA content of separated cells have already proved that CCE enables the separation of cells of cell lines in fractions, which have up to 100% G1 phase cells, up to 80% S-phase cells and up to 80% G2/M phase cells, respectively.
- A number of different kinds of cells such as mononuclear phagocytes recognize very non-specifically

Table 1 Examples of counterflow and rotor speed adjustments using a Beckman elutriator equipped with JE-6 rotor (small separation chamber)

Cell mixtures:	sheep erythrocytes/reticulocytes	human mononuclear leukocytes	cultured human lymphocytes/macrophages
Pre-enrichment:	buffy coat	density-gradient centrifugation	none
Cell size range:	28–42 μm^3	180–400 μm^3	180–2000 μm^3
Rotor speed:	3000 rpm	2460 rpm	2460 rpm
Counterflow:	9–24 mL min ⁻¹	16.5–40 mL min ⁻¹	16.5–81 mL min ⁻¹
Desired cells:	reticulocytes	lymphocytes/monocytes	macrophages
Eluted at:	24 mL min ⁻¹	22 mL min ⁻¹ /40 mL min ⁻¹	80 mL min ⁻¹
Use:	analysis of volume regulation	further enrichment, immunological tests	surface charge analysis

For details, see: Lauf PK and Bauer J (1987) *Biochemical and Biophysical Research Communications* 144: 849–855 and Bauer J and Hannig K (1984) *Electrophoresis* 5: 269–274.

Table 2 Examples of counterflow and rotor speed adjustments using the self-made table-top elutriator

Cell mixture:	cultured human mononuclear leukocytes	human erythrocytes/granulocytes	cultured human tissue cells
Pre-enrichment:	none	buffy coat	none
Cell size range:	180–2000 μm^3	90–400 μm^3	1000–3000 μm^3
Rotor speed:	2800, 500 rpm	2800, 1500 rpm	2200–500 rpm
Counterflow:	2.5, 4, 6 mL min^{-1}	4–6 mL min^{-1}	4–6 mL min^{-1}
Desired cells:	antibody-producing cells	granulocytes	hyperdiploid cells
Eluted at:	6 mL min^{-1} /500 rpm	6 mL min^{-1} /1500 rpm	6 mL min^{-1} /500 rpm
Use:	antibody secretion	analysis	analysis

For details, see: Bauer J and Hannig K (1988) *Journal of immunological Methods* 112: 213–218 and Bauer J, Grimm D, Hofstaedter F and Wieland W (1992) *Biotechnological Progress* 8: 494–500.

foreign molecules and particles entering an organism. So despite many alternative methods such as antibody-dependent sorting or panning, CCE, which does not involve cell adhesion to matrices or to antibodies, is often preferred, to separate monocytes from peripheral blood or bone marrow and to purify macrophages from alveolar tissues or Kupffer cells from liver and to enrich mast cells, if contacts to stimulatory surfaces and substances must be avoided.

- Problems still exist in the detailed study of the biological and physiological features of healthy and malignant animal tissue cells and plant protoplasts. These cells have not yet been characterized, as well as, for example, lymphoid cells. Antibodies against the surface epitopes of such cells are not isolated in great abundance, so fractionation of single-cell populations, obtained from tissues of various organisms, by CCE, is a competitive way to provide important homogeneous cell populations for biological, toxicological and pharmacological studies.
- CD34-positive hematopoietic stem cells are very helpful to restore hematopoiesis of patients, who have to undergo whole-body radiation or rigorous chemotherapy. In the past, CD34-positive cells were separated either by panning, immunomagnetic sorting or fluorescence-activated cell sorting. All these techniques include expensive time-consuming steps of labelling cells by antibodies and generate problems of removing the antibodies/ligands from the surface of the purified cells. CCE thus appears to be an alternative method for CD34-positive stem cell purification as the stem cells have a similar volume as mononuclear leukocytes. However, resolution improvements still seem to be necessary.

Free-Flow Cell Electrophoresis (FFE)

Another method for purifying cell populations without antibody tagging or cell adherence is free-flow

electrophoresis. Its basic principle has already been described and is repeated briefly here. A laminar buffer stream flows between two narrowly spaced parallel glass plates forming a separation chamber. Near one end of the chamber, a cell suspension is injected as a narrow band into the fluid flow which carries the cells through an electric field applied perpendicularly to the carrier fluid flow. Cells exposed to the electric field migrate laterally towards the positively charged electrode with velocities depending on their negative surface charge densities. Thus cells with different negative surface charge densities migrate at different speeds, arrive at different points along the opposite edge line and can be collected for preparative isolation.

This principle is called ‘free-flow zone electrophoresis’ (FFZE) and is still the only electrophoresis mode applicable to cell separation, although it has poorer resolution than other electrophoresis modes such as isoelectric focusing (IEF) and isotachopheresis (ITP), because it is a non-focusing process. In addition, most whole cells do not tolerate a fluid pH below 6.9 and above 7.5 and need media which allow reasonable electrophoretic mobilities, but are simultaneously biocompatible. So for quite a long time, cell electrophoresis was rarely applied, particularly as resolution was often not high enough to purify cell populations with different mean electrophoretic mobilities but overlapping distribution curves and this second drawback negatively influenced cell vitality. Cells had to be suspended in media lacking NaCl or other physiologically important ions, because too many ions in the chamber medium caused problems of performance such as overheating of the medium and short electromigration distances, as long as only conventional devices with homogeneous chamber media were available.

Recently, a new type of FFE was developed which opened new possibilities of electrophoretic cell separation. It is called Octopus and is commercially available from the Dr. Weber GmbH, Kirchheim, Germany (Figure 2). It is quite suitable to perform

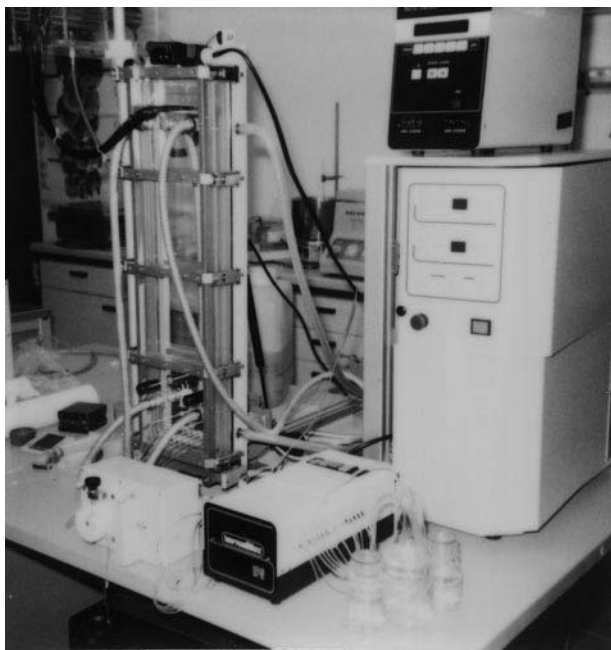


Figure 2 An Octopus free-flow electrophoresis apparatus with the electrophoresis chamber in vertical position (left) and implements such as a power supply, a pump and the control unit (right). (A generous gift of the Dr. Weber GmbH, D-85551 Kirchheim, Germany. More information about the machine may be found at <http://members.aol.com/ffeweber/default.htm>.)

preparative cell electrophoresis but can easily be adjusted to IEF and ITP of sub-cellular particles or molecular substances. Its electrophoresis chamber has a length of 500 mm and a width of 100 mm and can be fixed in a vertical or a horizontal position, as long as specimen sedimentation does not play a role. The thickness is variable, between 0.4 mm and 0.2 mm, so that heat-removal efficiency may be enhanced, if ions are required in cell suspension media and the application of high electric fields is necessary. An optical particle detection system allows control of process stability.

The major advantage of the new system is that various media may flow through the chamber adjacent to each other and the sample may be introduced at the optimal site (Figure 3). This means for cell electrophoresis, that one central cell suspension medium, which may contain up to 50 mmol L^{-1} NaCl is pumped between two margin media with elevated quantities of ions flowing at both edges (Table 3). They cover the electrode membranes, protect the separation medium from detrimental influences of the electrodes, prevent diminution of Na^+ and Cl^- ion concentrations within the central chamber area and conduct the electric current to this area of cell transport with minimal voltage drop.

Like CCE, FFE is most advantageous if antibodies coupled to fluorescent dyes or magnetic beads are not

available or must not be applied. So the method is quite useful, when cells are separated by CCE because of the reasons explained above and the resulting fractions still contain cells which belong to different populations, but have equal size, while their electrophoretic mobilities are different. For example, cell fractions are routinely obtained, which contain more than 90% monocytes, if pre-enriched mononuclear leukocytes are elutriated. In such fractions, up to 0.2% antibody-producing cells with equal size as monocytes but different electrophoretic mobilities (EPM) are often co-collected. The antibody-producing cells can be further enriched by FFE. Similarly, T-cell fractions obtained by CCE contaminated by accessory cells, of equal size have been submitted to a following step of FFE purification. T-cells of individual blood donors were obtained, which did not respond to concanavalin A unless accessory cells were re-added.

A cell feature, which cannot be defined by antibodies is the negative surface charge density. Its biological role is still very poorly understood. Observations made during recent cell electrophoretic studies appear currently like very scattered mosaic stones which do not allow the whole picture to be revealed. For example, erythrocytes change their EPM in patients suffering various kinds of diseases, monocytes change their EPM when maturing to non-activated macrophages, B-cells change their EPM when developing to antibody-producing cells *in vivo* but not *in vitro*, and mice with different erythrocyte EPM have different sensitivities to malaria infection (see Further Reading). These accumulating data suggest that further efforts in studying the biological relevance of the negative surface charge density by FFE will be worthwhile.

Since electrophoresis media with $20\text{--}50 \text{ mmol L}^{-1}$ NaCl can be used for cell separation, tissue cells can be processed without clotting. Now it is possible to electrophorese cell suspensions obtained from tissues directly or indirectly after a few passages of culture. The separations performed so far have revealed quite interesting new tissue cell sub-populations. Hence, future application of FFE to fractionation of viable tissue cells appears promising.

Conclusions

Essential guides for separation/purification of cells have been described in this chapter following a definition of cell separations as processes of any scale by which cell populations are separated from each other without biological modification, i.e. without changes of their actual states of activation and differentiation. As explained above and shown in Figure 4 single cells

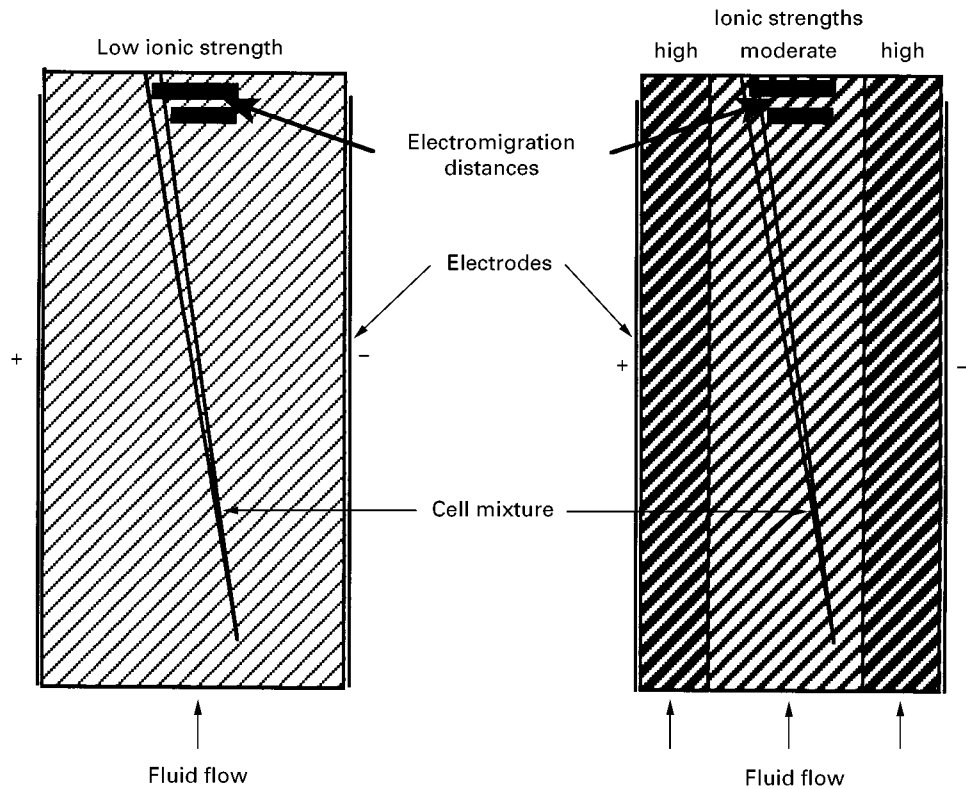


Figure 3 Scheme of free flow electrophoresis chambers working with homogeneous (left) and segmented (right) carrier fluids.

suspended in suitable media after preparation from human or animal body fluids, from human, animal or plant tissues or from *in vitro* cultures are prerequisites of such processes. If a cell suspension with a reasonable number of desired cells is available, methods such as countercurrent centrifugal elutriation and free-flow electrophoresis may be applied, either each

of them alone or in combination. As both cell-separation methods are rapid and work while cells are kept in suspensions with minimal contact with foreign surfaces but do not require labelling of cell surfaces by antibodies or other macromolecules, a fair chance can be expected to obtain homogeneous cell populations retaining their original states of activation and

Table 3 Examples of buffer systems for homogeneous and segmented FFE chamber fluids

Cell-suspension medium	Margin buffers	Electrode buffer(s)
<i>Homogeneous</i> 27 mmol L ⁻¹ triethanolamine 4 mmol L ⁻¹ potassium acetate 27 mmol L ⁻¹ sucrose 1 mmol L ⁻¹ glucose 216 mmol L ⁻¹ glycine pH 7.2 adjusted by acetic acid		342 mmol L ⁻¹ triethanolamine 40 mmol L ⁻¹ potassium acetate pH 7.2 adjusted by acetic acid
<i>Segmented</i> central: 10 mmol L ⁻¹ triethanolamine 2 mmol L ⁻¹ sodium acetate 50 mmol L ⁻¹ NaCl 2 mmol L ⁻¹ glucose 180 mmol L ⁻¹ sucrose pH 7.2 adjusted by acetic acid	anodal: 50 mmol L ⁻¹ triethanolamine 250 mmol L ⁻¹ Na ₂ SO ₃ pH 7.2 adjusted by acetic acid cathodal: 50 mmol L ⁻¹ triethanolamine 250 mmol L ⁻¹ NaCl 75 mmol L ⁻¹ sucrose pH 7.2 adjusted by acetic acid	anodal: 200 mmol L ⁻¹ sodium acetate cathodal: 100 mmol L ⁻¹ HCl 100 mmol L ⁻¹ NaCl 200 mmol L ⁻¹ imidazole

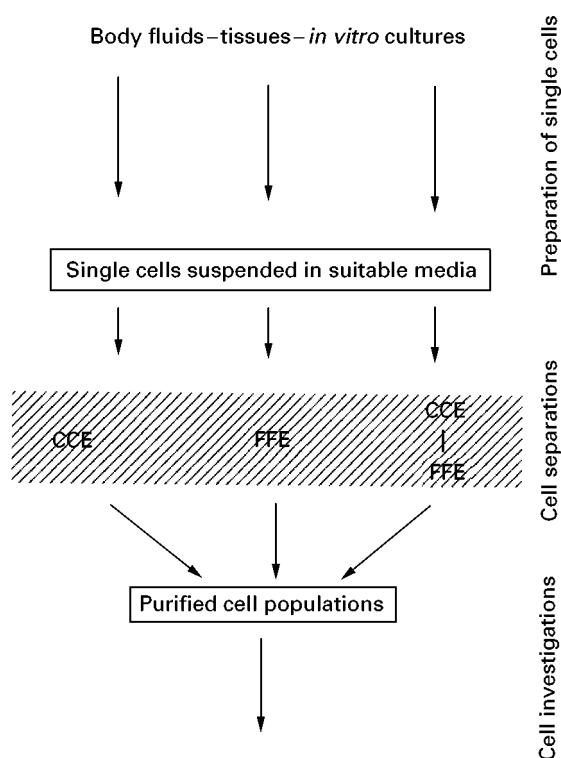


Figure 4 Flow diagram showing a survey of the processes of cell purification described in this article.

differentiation, even if appropriate antibodies are not available.

Cells purified without biological modifications may be especially useful if it is of interest to study their original *in vivo* status or to use them for transplantation purposes and if size or surface charge-related phenomena are to be investigated. As knowledge of possible cellular characteristics and components is continuously accumulating, questions on their actual

expression under normal and pathological conditions will frequently arise. For studying such questions, homogeneous cell populations retaining their original *in vivo* status may become so important that techniques and instruments required for their purification will be further improved.

See also: **Cells and Cell Organelles: Field Flow Fractionation.**

Further Reading

- Bauer J (1987) Electrophoretic separation of cells. *Journal of Chromatography* 418: 359-383.
- Bauer J (1994) *Cell Electrophoresis*. Boca Raton: CRC Press.
- Bauer J (1998) Advances in cell separation: recent developments in counterflow centrifugal elutriation and continuous flow cell separation. Carrier free electrophoresis. *Electrophoresis* 19: Special issue.
- Bauer J (1999) *Journal of Chromatography* 722: 55-69.
- Coleman R, Wilton JC, Stone V and Chipman JK (1995) *General Pharmacology* 26: 1445-1453.
- Dixon RA and Gonzales RA (1994) *Plant Cell Culture: A Practical Approach*. Oxford: Oxford University Press.
- Merrill GF (1998) In: Mather JP and Barnes D (eds) *Methods in Cell Biology*, vol. 57, pp. 229-249. San Diego: Academic Press.
- Pretlow TG and Pretlow TP (1982) *Cell Separation: Methods and Applications*. New York: Academic Press.
- Shapiro HM (1995) *Practical Flow Cytometry*, 3rd edn. New York: Wiley-Liss.
- Specto DL, Goldmann RD and Leinwand LA (1998) *Cells. A Laboratory Manual*, vol 1: *Culture and Biochemical Analysis of Cells*. New York: Cold Spring Harbor Laboratory Press.

ESSENTIAL GUIDES FOR ISOLATION/PURIFICATION OF DRUG METABOLITES

I. P. Nnane and A. J. Hutt, Kings' College London, UK
L. A. Damani, Chinese University of Hong Kong, Hong Kong

This article is reproduced from *Encyclopedia of Analytical Science*, Copyright © 1995 Academic Press

Metabolite Isolation and Identification

Following the administration of drugs to either animals or man, very few of the drugs are excreted

unchanged. The majority undergo biotransformations by interaction with a complex series of enzymes. This process, known as drug metabolism, is not restricted to drugs but occurs with all chemicals that are taken in by living systems, including food additives, pesticides, carcinogens, etc. These chemicals are termed exogenous compounds, as opposed to endogenous, or naturally present, compounds.

Metabolic studies have made, and continue to make, fundamental contributions to the drug

discovery process and also to the elucidation of mechanisms of both drug action and toxicity. During the early stages of drug development, an evaluation of the metabolic dispositional profile of a compound may yield valuable information and significantly contribute to the drug candidate selection procedure. In addition, drug metabolism has a central role in the safety evaluation of novel drug substances, and the regulatory authority guidelines for toxicity testing all make reference to metabolic and pharmacokinetic data.

The reactions of drug metabolism may be divided into two groups, the phase I or functionalization reactions and the phase II or conjugation reactions. The phase I reactions involve either the introduction or unmasking of a functional group, e.g. hydroxyl, carboxyl or amino group, within a molecule by the processes of oxidation, reduction or hydrolysis. The groups introduced generally result in an increase in the polarity, and therefore the aqueous solubility, of the metabolite compared with the parent compound. Depending on the reaction type, the change in physicochemical properties may be relatively minor, e.g. dealkylation of a tertiary to a secondary amine, or substantial, e.g. hydrolysis of an ester or amide.

The phase II reactions are biosynthetic and involve the addition of an endogenous molecule to the drug, or a phase I metabolite of the drug, by reaction with a suitable functional group, e.g. carboxyl, hydroxyl, amino, etc. The products of these reactions are generally polar, hydrophilic molecules that are ionized under physiological conditions, and hence the excretion of the foreign compound into urine or bile is facilitated. Examples of reaction types include conjugation with glucuronic acid, sulfate, glutathione and amino acids, all of which result in an increase in the polarity of the product compared to the drug. Some conjugation reactions, namely methylation and acetylation, may result in an increase in the lipid solubility of the metabolite compared that of the drug; however, this depends very much on the nature of the substrate. The two phases of drug metabolism are intimately linked, as shown in Figure 1.

As a result of the metabolic transformations outlined here, and analytical sample of biological origin may contain several substances which vary markedly in their physicochemical properties. For example metabolic products may be acidic, basic, neutral or zwitterionic and relatively hydrophilic or hydrophobic. The examination of such samples therefore presents the bioanalyst with a considerable challenge as the sample will contain relatively small quantities of structurally related materials dispersed in an extreme-

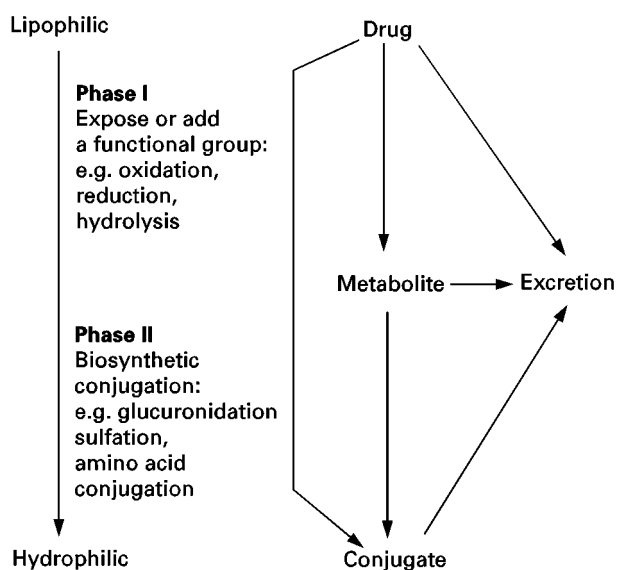


Figure 1 Relationships between phase I and phase II metabolic transformations.

ly complex matrix containing numerous potentially interfering endogenous materials. The isolation and characterization of metabolic products therefore requires a range of analytical methodologies, primarily in the areas of separation and spectroscopic techniques.

Sample Types

The range of techniques used to investigate the metabolism of drugs is relatively wide (Table 1) and the bioanalyst may therefore be presented with samples which vary markedly in terms of both their nature and origin. In *in vivo* metabolic studies, following the administration of a drug to either animals or humans, the major sample types examined include blood, plasma, urine, faeces and less commonly bile and milk. In *in vitro* methodology, sample types may

Table 1 Biological techniques used in drug metabolism

Methodology	Example
Administration of the drug to whole animals	Human or standard laboratory species, e.g. rat, dog, etc.
Isolated perfused organs	Liver, kidney, lung, intestine
Tissue slices	Liver, kidney
Isolated cells	Hepatocytes, renal cells, lung cells, enterocytes, blood cells
Subcellular fractions	Whole tissue homogenates, postmitochondrial supernatant, microsomal fractions, cytosol
Purified enzymes	Cytochrome P-450 and flavin monooxygenases

range from relatively clean perfusion fluids to complex tissue homogenates. Thus the bioanalyst may be presented with liquid, semisolid and solid samples for evaluation, each of which presents different problems. Plasma, for example, contains relatively high concentrations of proteins which may interfere with the chromatographic separation of metabolites or damage chromatographic stationary phases. The samples therefore require deproteination prior to analysis. Samples which are solids, or semisolids, may affect the separation characteristics of solid-phase extraction cartridges and it is frequently the case that such samples are homogenized prior to analysis.

Preliminary Sample Pretreatment

Because of the nature of the sample types and the potential range of physicochemical properties of the analytes, the samples encountered in metabolic studies generally require extensive pretreatment prior to instrumental analysis. It is essential that any manipulations carried out on the sample do not result in *ex vivo* changes to the analytes. A general approach to sample treatment is presented in Figure 2. Preliminary sample preparation plays an important role in the specificity of an analytical procedure. The initial step involves sample clean-up to remove potentially interfering substances, fractionation of the metabolic products according to their physicochemical properties, concentration of the sample for analysis and possible hydrolysis of conjugated metabolites. Having obtained a primary extract, the analytes are further purified, generally by a chromatographic procedure, prior to characterization by conventional spectroscopic techniques.

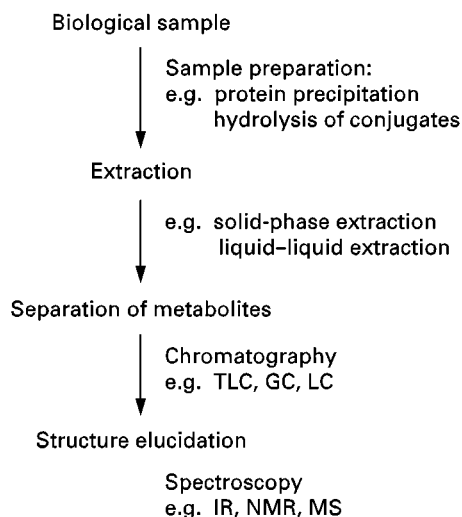


Figure 2 General approach for the isolation and characterization of metabolic products.

Hydrolysis of Conjugates

One of the most frequently encountered phase II pathways is conjugation with glucuronic acid. Several functionalities undergo this reaction, yielding a variety of bond types between the sugar moiety and the aglycone, e.g. carboxyl groups yield acyl glucuronides, phenolic and alcoholic hydroxyl groups yield ether linkages, thiols and amino functions yield S- and N-glucuronides respectively, and examples of carbon glucuronides are also known. The stability of these various linkages varies considerably, as does their susceptibility to hydrolytic treatments, the common methods of hydrolysis being mild alkali, acid or treatment with the enzyme β -glucuronidase.

A number of problems may occur during sample pretreatment; acyl glucuronides for example are relatively labile under mild alkaline conditions and may undergo hydrolysis in samples which are not stored with care. An additional problem with compounds of this type is that they also undergo facile intramolecular rearrangement at mild alkaline pH giving rise to mixtures of the corresponding 2-, 3- and 4-O-acyl esters of glucuronic acid. Such glucuronic acid esters are resistant to hydrolysis by β -glucuronidase but may be hydrolysed by treatment with mild alkali. Thus the amount of aglycone liberated by treatment of the conjugate with the enzyme may be lower than that found following treatment with alkali. Etheral glucuronides are stable to treatment with mild alkali, but may be hydrolysed with acid or β -glucuronidase. The stability of both N- and S-glucuronides to either chemical or enzymatic treatment is highly dependent on the nature of the aglycone and the bond type. Carbon-linked glucuronide conjugates are resistant to β -glucuronidase.

The liberation of an aglycone upon incubation of a conjugate with β -glucuronidase may only be taken as presumptive evidence that the conjugate is a glucuronide if adequate controls have been carried out, e.g. inhibition of hydrolysis by the specific β -glucuronidase inhibitor, saccharo-1,4-lactone, identification of the carbohydrate moiety by chromatography and detection with naphthoresorcinol.

Sulfation is a relatively common conjugation reaction for phenolic hydroxyls, alcohols and some amino compounds. Sulfate conjugates may be hydrolysed by aryl sulfatases. However, the commercially available preparations may be contaminated with β -glucuronidase, which should be inhibited by the addition of saccharo 1,4-lactone. Acid hydrolysis of solvolysis may also be employed but the reactivity of the conjugates may vary considerably.

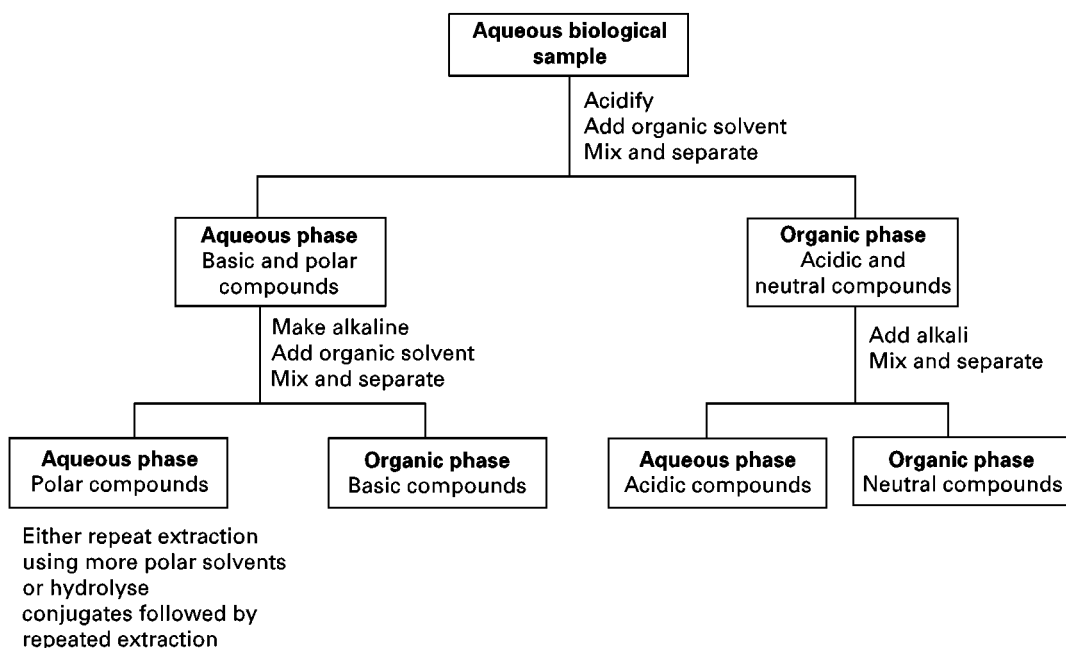


Figure 3 General scheme for the fractionation of drug metabolites using solvent extraction.

In contrast, amino acid conjugates of carboxylic acids are relatively stable and may be isolated and characterized by conventional methodology.

Methods of Isolation – Extraction Techniques

Extraction techniques may be used for the preliminary purification and fractionation of metabolic products from the biological matrix. Further purification of the individual metabolites may be achieved using chromatographic techniques.

Liquid–Liquid Extraction

As pointed out previously, drug metabolites vary greatly in terms of their physicochemical properties. Selective isolation of material may be achieved by extraction from the aqueous-based biological samples, after appropriate adjustment of pH, using an immiscible solvent. The choice of solvent is critical and it may be possible to fractionate the analytes by sequential extraction using solvents of different polarities, with or without adjustment of sample pH. Having obtained an organic extract of the compounds of interest the sample may be cleaned up further by ‘back-extraction’ into an aqueous phase with appropriate pH adjustment. A general scheme for the extraction of a drug and metabolites is presented in **Figure 3** and examples of commonly used solvents. Used either alone or in combination, are

presented in **Table 2**. Thus a particular drug or its metabolites can be selectively isolated from a biological matrix by a consideration of the physicochemical properties of the material, careful choice of solvent and adjustment of the pH of the aqueous medium. Ideally the solvent should completely extract the drug and its metabolites in a single extraction while keeping the amount of coextracted endogenous compounds to a minimum. However, the efficiency of the extraction procedure must be investigated and a double or triple extraction coupled with a ‘salting out’ procedure may be necessary.

Solvents for extraction should be of high purity grade and it is frequently important that they are distilled prior to use. This distillation will ensure that the solvents are free of trace quantities of solutes which on sample concentration may be present in

Table 2 Examples of commonly used solvents for extraction of biological fluids

<i>Solvent</i>	<i>Dielectric constant</i>	<i>Boiling point (°C)</i>
<i>n</i> -Hexane	1.9	68.7
<i>n</i> -Heptane	2.0	98.4
Carbon tetrachloride	2.2	76.8
Toluene	2.4	111.0
Diethyl ether	4.3	34.5
Chloroform	4.8	61.2
Ethyl acetate	6.0	77.1
Dichloromethane	9.1	40.2

concentrations greater than that of the analytes and may therefore interfere with the subsequent analysis. Phthalates for example are universal contaminants and are frequently observed in the mass spectra of metabolic products. Solvents such as diethyl ether frequently contain aldehydic impurities which may react with the analyte, e.g. (–)-ephedrine reacts with the acetaldehyde, propionaldehyde or formaldehyde present in ether to yield a series of oxazolidine derivatives during isolation. Chlorinated solvents should be used with caution in the presence of basic compounds; several analgesic agents, e.g. dextromethorphan, pethidine and methadone, have been shown to undergo alkylation during the concentration of dichloromethane extracts of the drugs. Traces of peroxides rapidly form in diethyl ether and may oxidize drugs, or their metabolites. The products of such reactions may then be erroneously identified as metabolites. Additional problems may also arise during concentration of extracts because of the degradation of thermolabile compounds and the loss of volatile compounds. Evaporation under reduced pressure and/or freeze-drying are useful alternative approaches.

Ion Pair Extraction

Highly polar metabolites cannot usually be extracted efficiently using solvents. In this case the metabolites, in their ionized state, can be paired with a counterion of opposite charge. Isolation of several biogenic amines, together with some of their metabolites, has been achieved by this approach. Catecholamines and their derivatives, for example, have been extracted from biological samples using di(2-ethylhexyl)phosphoric acid as a counterion.

Liquid–Solid Extraction

The isolation of drugs and their metabolites by adsorption methods offers an alternative approach to the traditional solvent extraction. Liquid–solid extraction, also known as solid-phase extraction (SPE) employs a wide range of materials including coated charcoal, silica, alumina and ion exchange resins. The biological fluid is passed through a column packed with the adsorbent and the materials of interest are separated from the components of the matrix by elution with an appropriate solvent. The success of the technique depends on the affinity of the analytes for the adsorbent and the strength of the eluting solvent.

In recent years the development of chemically bonded silica stationary phases for liquid chromatography (LC) has resulted in cartridge forms of these materials for liquid–solid extraction and SPE. The use

of these packings for extraction is based on the principles of LC; the packing materials however are of larger particle size (50 μm) than those used in LC. Thus analytes with a greater affinity for the stationary phase are retained and highly polar endogenous components of the matrix may be eluted with polar solvents. The retained materials may then be selectively eluted from the packing depending on their physicochemical properties, the nature of the adsorbent and the elution solvent. The range of phases for SPE is fairly extensive and includes C_2 , C_8 and C_{18} alkyl, phenyl, cyclohexyl, amino, diol and cyano, in addition to a variety of ion exchange phases. This range allows considerable versatility in terms of both selectivity and specificity for analyte isolation. SPE is superior in many respects to solvent extraction; it is highly reproducible, efficient and easier to automate, it generates less waste solvent and the only major drawback is the relatively high cost of the cartridges.

Methods of Isolation – Chromatographic Techniques

Chromatographic techniques are extensively used in bioanalysis for the separation, isolation and purification of drugs and their metabolites from biological fluids. Such techniques can provide useful preliminary information concerning the physicochemical properties of the metabolites in relation to those of the drug. Although they give little information concerning specific chemical structures, comparison of the chromatographic properties of an analyte with those of an authentic reference compound may provide sufficient information to establish the identity of a particular metabolic product.

Thin-Layer Chromatography

Thin-layer chromatography (TLC) is relatively cheap, easy to use, rapid and robust. These features account for the widespread use of the technique in metabolic studies, particularly for the isolation and purification of analytes prior to their characterization by spectroscopic techniques. A wide variety of stationary phases is available; these include silica gel, alumina and a number of bonded hydrocarbon phases (e.g. C_2 , C_8 , C_{18}) for reversed-phase and ion exchange separations. Such phases are coated onto plastic, aluminium foil or glass supports. A recent innovation in TLC stationary phase technology involves the introduction of high performance thin-layer chromatographic (HPTLC) plates which are coated with a layer (200 μm) of 5- μm particle size silica which offers improved performance in terms of resolution and

speed of chromatographic development. A number of chiral TLC phases have also been introduced. However the application of these phases in bioanalytical studies has been limited.

The chromatographic phases can be prepared with fluorescent indicators which facilitate the detection of ultraviolet absorbing analytes. The visualization of analytes may also be achieved by the use of a wide range of chromogenic spray reagents. The colour reactions observed with appropriate reagents may be of assistance in the determination of class of metabolite, e.g. glycine conjugates yield characteristic red-orange colours on treatment with *p*-dimethylaminobenzaldehyde, naphthoresorcinol is used for the detection of glucuronides, potassium dichromate–silver nitrate for sulphur(II) and ninhydrin for glutathione conjugates.

The main application of TLC in metabolic studies is in the isolation of metabolites, for subsequent identification by spectroscopic techniques. However, it can also be used quantitatively if radiolabelled drugs are used, or by the application of scanning densitometry.

Gas Chromatography

Gas chromatography (GC) is the technique of choice for the separation and determination of volatile, thermally stable and relatively low relative-molecular-mass drugs and metabolites. GC separation may be carried out using either packed or capillary columns. GC columns are usually made of glass, stainless-steel, copper, aluminium or PTFE (polytetrafluoroethylene). However in metabolic studies glass columns are preferred to minimize the potential thermal breakdown of metabolites during analysis. For example, the decomposition of primary and secondary hydroxylamines, formed on metabolic *N*-oxidation of the corresponding amines, takes place readily on the heated surfaces of metal columns.

A wide range of stationary phases is available for GC separation and a variety of solid support materials for packed columns is encountered. The amount of loading of the stationary phase on the support may also vary considerably, thus the number of possible combinations of phase and support are essentially unlimited. Liquid phases based on polymers of poly(ethylene glycol) and dimethylsilicone have been widely used in bioanalysis. The poly(ethylene glycols) are polar and Carbowax 20M is frequently used, both with and without potassium hydroxide, as a stationary phase. Carbowax 20M is a particularly useful phase for analysis of low relative-molecular-mass amines and their metabolites, e.g. amphetamine and related compounds. Problems arise with compounds of greater molecular mass because of the maximum

operating temperature of 200°C for Carbowax 20M. In contrast the silicon phases may be used up to c. 350°C, and common phases encountered in metabolic studies include OV1 and OV101 polymers and the more polar phenylmethylsilicones OV17 and OV25. The most commonly used support materials in bioanalysis include Chromosorb G and W, Gas Chrom Q, Haloport F and Chromosorb 750. These support materials are not entirely inert and are frequently washed with acid or silanized prior to being coated with the stationary phase. Glass beads may also be used as support material for GC because of their inert nature and they may also be coated with low loadings of stationary phase. *N*-Hydroxyamphetamine, a thermolabile metabolite of amphetamine, was first chromatographed successfully without prior derivatization using a column containing Carbowax 20M (0.2%) coated onto a glass bead support.

Several GC detector systems have been described. However only four types are commonly used in bioanalysis, the flame ionization detector, the electron capture detector, the nitrogen–phosphorus detector, and the mass spectrometer. Of these the mass spectrometer is the most specific and can provide information on the structural features of compounds. The flame ionization detector is the most widely used in metabolic studies, and sample quantities as low as 1 ng can be determined depending on detector design. Electron capture detectors respond to halogenated compounds, and compounds containing nitro groups or conjugated carbonyls, etc., and thus the suitability of this detector for metabolic studies depends on the structure of the analyte. This selectivity, together with sensitivity (detection of 1 pg of material is possible) increases the utility of this system. Derivatization of compounds that do not contain halogens with appropriate reagents frequently yields volatile products which are ideal for analysis by GC using this detector system, e.g. the analysis of debrisoquine and its 4-hydroxy metabolite following derivatization with hexafluoroacetylacetone to yield the corresponding bis(trifluoromethyl)pyrimidine derivatives. Nitrogen–phosphorus detectors are extremely sensitive and are 20 000–40 000 times more sensitive to nitrogen than to carbon. In bioanalysis such detectors are useful particularly for heterocyclic compounds, which are less likely to lose nitrogen via metabolic deamination than are acyclic compounds.

The products of metabolism are generally more polar than the drug, have less volatility, long GC retention times and produce tailing peaks. Thus metabolites are frequently derivatized prior to analysis to increase volatility, modify chromatographic properties and increase detector response. The most common techniques are: silylation, the replacement

of active hydrogen by trimethylsilyl groups (e.g. OH, SH, NH₂); alkylation using diazomethane, dimethylformamide, dialkyl acetals, or boron trifluoride and an alcohol; and acylation using perfluoroacyl reagents to yield trifluoroacetyl, heptafluorobutyl, etc. derivatives.

Liquid Chromatography

LC is an extremely versatile technique and has a number of advantages over GC in terms of bioanalysis. For example, highly polar compounds which are difficult to extract from aqueous solutions, e.g. glucuronide and sulfate conjugates and quaternary ammonium derivatives, may be analysed directly without the necessity for extraction; the technique is normally carried out at room temperature and therefore thermolability of analytes is not a major consideration; and the technique is nondestructive so that the eluent containing the analytes may be collected and used for additional offline characterization.

A variety of different stationary phases is available for LC, but the reversed-phase packings (e.g. C₂, C₈, C₁₈, phenyl) are the most commonly used in metabolic studies. The mobile phases utilized with such columns are based on aqueous solvents containing variable quantities of organic modifiers. Such systems allow analyte sample preparation to be simplified, reducing the preanalysis manipulation steps. Provided the chromatographic system has sufficient resolving power, it may be possible to inject directly either a dilute sample or a plasma sample following precipitation of plasma proteins with an organic solvent compatible with the LC mobile phase. This approach has the obvious advantages of reduction of tedious sample manipulation steps and also in the reduction of human exposure to samples of clinical origin. A disadvantage of the direct injection approach is that protein precipitation may occur on injection of plasma samples into the chromatograph. However, the use of precolumns can protect the analytical column and the instrument.

The most frequently used detection systems in LC analysis are either fixed- or variable-wavelength ultraviolet (UV) detectors, fluorescence detectors or electrochemical detectors. While analyte derivatization is not as commonly used with LC, as with GC, derivatives may be used to enhance the detector sensitivity, particularly if fluorescence is used. Multiple-wavelength UV detectors and the diode array detector are particularly useful in metabolic studies. The use of such detectors in analysis provides a three-dimensional chromatographic retention and the entire spectrum of a sample may be determined in a single chromatographic run. The main applications of these

detector systems in bioanalysis are to ensure chromatographic peak purity and to provide initial spectroscopic data for metabolite identification. If the compound under investigation is radiolabelled then a suitable LC radiodetector may also be used to facilitate the detection of metabolites.

Capillary Electrophoresis

A technique that is likely to make an impact on bioanalysis in the near future is capillary electrophoresis (CE). This technique, and its variants, offers a number of advantages over conventional chromatographic techniques, e.g. high column efficiencies and short analysis times, particularly where samples are complex mixtures. At present CE instruments are limited in terms of sample size, but this may be an advantage when working with biological fluids as it minimizes potential contaminants. An additional advantage of the technique is that by manipulation of the analytical conditions the nature of the components entering the capillary may be controlled and interference effects reduced. A variety of detector systems has been described for CE, including fluorescence, electrochemical and mass spectrometry systems, but the majority of commercially available instruments incorporate a sensitive UV detector system. Bioanalytical applications of CE have been described for the determination of cefpiramide and anticancer agents in human plasma.

Methods of Identification

The elucidation of metabolite structure is dependent on the use of spectroscopic techniques, either directly linked to chromatographic systems (the so-called 'hyphenated': techniques, GC-MS, LC-MS), or used offline following the isolation and purification of analytes. The main techniques used in bioanalysis are ultraviolet (UV), infrared (IR) and nuclear magnetic resonance (NMR) spectroscopy and mass spectrometry (MS). However, the technique or combination of techniques finally adopted will be dependent on the complexity of the problem and the amount of pure isolated material available.

Ultraviolet Spectroscopy

This technique is widely used for the quantitative analysis of drugs and metabolites in biological samples. However, the amount of structural information which can be obtained from a UV spectrum of a metabolite is limited. If the site of metabolism in a molecule is at, or adjacent to, a chromophore then the UV spectrum is likely to yield useful structural information, e.g. oxidation of an aromatic ring to

yield a phenol, the spectrum of which can be influenced by alteration of pH, reduction of an aromatic nitro group to yield an amine, and reactions which result in the introduction of conjugated double bonds, e.g. aromatization.

Infrared Spectroscopy

IR spectra are highly diagnostic and the examination of an IR spectrum provides a simple, rapid and often reliable method of assigning metabolite structure. Until relatively recently the sensitivity of IR spectrometers restricted their application in metabolic studies but the development of Fourier transform infrared (FTIR) and the application of these instruments as detector systems for both GC and supercritical fluid chromatography has increased the potential of the technique in bioanalysis significantly.

Nuclear Magnetic Resonance Spectroscopy

NMR spectroscopy has been routinely used in metabolic studies as a means of structure elucidation for a number of years. The major limitation of the technique has been sensitivity. However instrumental developments, with improvements in resolution, analytical power and sensitivity, have changed the way the technique is used in bioanalysis.

There are now a number of reports of direct NMR examination of biological samples with minimal or no preliminary sample clean-up processes and biological fluids have been placed directly in the NMR sample tube. It has also been possible, using NMR techniques, to examine metabolism and distribution in cells and organs.

Proton NMR is the most widely used technique in drug metabolism because of its high sensitivity and the large number of observable protons in most drugs and their metabolites. As bioanalytical samples are initially obtained in aqueous solution the intense water signal present must be either eliminated, suppressed or edited out of the spectrum. Signals from endogenous materials may also obscure signals of interest because of overlap resulting from the narrow chemical shift range in proton NMR. Direct proton NMR has been used to examine the urinary disposition of paracetamol following the oral administration of the drug to humans. Using this approach it was possible to examine the urinary metabolite profile following both therapeutic doses and overdoses of the drug.

Other nuclei of interest in bioanalysis include ^{19}F , ^{31}P , ^{15}N and ^{13}C , although sensitivity may be a problem with some of these nuclei (e.g. ^{15}N). An approach which may yield useful information with these nuclei is to use compounds appropriately labelled with

stable isotopes. This approach may be particularly useful if the label is introduced at a site which undergoes transformation. For example the fate of [carboxyl- ^{13}C]phenylacetic acid has been examined following administration to a horse. This compound undergoes both amino acid and glucuronic acid conjugation and the major metabolites could readily be distinguished following direct NMR examination of urine samples and observation of the ^{13}C -carbonyl resonances. NMR has also been used directly linked with HPLC for metabolite work.

Mass Spectrometry

As a result of its extreme sensitivity and ability to provide diagnostic information, MS is the standard technique for the identification of metabolic products. All the major MS techniques have been utilized in metabolic investigations and thus it is relatively easy to find publications detailing applications of electron impact, chemical ionization, field desorption and fast atom bombardment in drug metabolism. The major advantage of MS is the ability to use the technique in combination with either GC or LC. Such hyphenated techniques, particularly GC-MS, have been extensively used in metabolic studies and the development of thermospray ionization for LC-MS has enabled spectra of nonvolatile hydrophilic analytes, e.g. metabolic conjugates, to be determined directly. As a result of the variety of ionization modes available, and the ability to link the technique to GC or LC, there are few bioanalytical problems to which MS cannot make a valuable contribution.

There are essentially three main applications of MS, particularly the hyphenated techniques, in metabolic studies.

1. The characterization and structure elucidation of metabolic products.
2. Quantitative analysis using the mass spectrometer as a sensitive chromatographic detector for selected single or multiple ion monitoring, using for example compounds labelled with stable isotopes as internal standards. An alternative approach involves the administration of a labelled compound to a patient who is at steady state, and use of the nonlabelled material to examine the pharmacokinetics of what is effectively a 'single' drug dose under these conditions.
3. Mechanistic investigations, e.g. the source of oxygen in a metabolite may be determined by carrying out appropriate experiments using $^{18}\text{O}_2$ or H_2^{18}O ; the use of compounds labelled with stable isotopes, e.g. replacement of hydrogen with deuterium to determine kinetic isotope effects on metabolism.

MS has made a number of important contributions to drug metabolism and the further development of the technique, together with advances in instrumentation, will enhance its application in this area.

See also: **II/Chromatography: Gas:** Column Technology; Detectors: Mass Spectrometry. **Chromatography: Liquid:** Detectors: Ultraviolet and visible Detection; Nuclear Magnetic Resonance Detectors. **Chromatography: Thin-Layer (planar):** Layers. **Electrophoresis:** Capillary Electrophoresis; Capillary Electrophoresis Detection; Capillary Electrophoresis-Mass Spectrometry; Capillary Electrophoresis-Nuclear Magnetic Resonance. **Extraction:** Analytical Extractions; Solid-Phase Extraction; Solvent Based Separation; **III/Drugs of Abuse:** **Solid-Phase Extraction. Drugs and Metabolites:** Liquid

Chromatography-Mass Spectrometry; Liquid Chromatography-Nuclear Magnetic Resonance-Mass Spectrometry.

Further Reading

- Gibson GG, ed. (1993) *Progress in Drug Metabolism*, vol. 13. London: Taylor & Francis.
- Moffat AC, Jackson JV, Moss MS and Windopp B, eds (1986) *Clarke's Isolation and identification of Drugs in Pharmaceuticals, Body Fluids and Post-Mortem Material*. London: The Pharmaceutical Press.
- Reid E and Wilson ID (1992) *Methodological Surveys in Biochemistry and Analysis*, vol. 22. London: Royal Society of Chemistry.

ESSENTIAL GUIDES FOR ISOLATION/PURIFICATION OF ENZYMES AND PROTEINS

S. Doonan, University of East London, UK

Copyright © 2000 Academic Press

Nature of the Problem

The purification of proteins presents a unique challenge in the field of separation science. Typically, the particular protein to be isolated will constitute 1% or less (sometimes much less) of the material in the original extract and all of the contaminants will have basically the same chemical characteristics, i.e. they are all proteins. There is the added complication that for most purposes it is necessary to retain the biological activity of the protein, and the inherent instability of protein structures restricts the range of temperatures and solvent compositions that can be used during purification.

Tools for its Solution

Clearly, methods for the separation of proteins must be based on those characteristics in which they differ from one another. The most important of these are listed in Table 1 along with the separation techniques that exploit those differences. These various properties are not of equal generality or of equal utility for purification purposes.

By far the most widely used technique for protein isolation is ion exchange chromatography. The generality of the method arises from the fact that proteins contain ionizable amino acids and hence carry a net

charge at all pH values except the unique pH (the isoelectric point) at which the positive and negative charges are equal. Moreover, two proteins that have the same charge at a particular pH are likely to differ in charge at some other pH. Ion exchange chromatography is technically simple and can be adopted for use over a very large range of scales. Chromatofocusing and isoelectric focusing are methods that depend on the differences in isoelectric points between proteins but are less widely used for preparative work than is ion exchange chromatography because of increased cost, restrictions of scale and technical difficulty.

Electrophoresis is a special case. Electrophoretic methods are of central importance in analytical protein chemistry but, until recently, have not proved

Table 1 Properties of proteins that can be exploited for purification and associated experimental methods

Electrical charge	Ion exchange chromatography Chromatofocusing Isoelectric focusing (Electrophoresis)
Hydrophobic surface regions	Hydrophobic chromatography
General surface properties	Salt fractionation
Size	Size-exclusion chromatography Membrane filtration
Specific binding site	Affinity chromatography Dye-binding chromatography Lectin chromatography
Surface carbohydrate	Metal chelate chromatography
Metal-binding site	Immunoaffinity chromatography
Antigenic determinants	

useful for purification purposes. The reason for the change has been the development of ultra high sensitivity techniques for structural analysis that has blurred the distinction between analytical and preparative methods. Hence the inclusion of electrophoresis in Table 1 as a preparative method, although it serves that purpose for a limited range of applications (see later).

Although the surfaces of most soluble proteins are predominantly polar, many of them have patches of hydrophobic amino acids that, under appropriate conditions (usually at high salt concentrations), can bind to hydrophobic matrices. This provides a method for separation provided that elution from the matrix can be achieved under conditions that do not lead to loss of biological activity.

Proteins differ from one another in their solubilities in salt solutions. Clearly, in a complex mixture of proteins the solubilities of the components will overlap and hence fractional precipitation with salt, usually ammonium sulfate, provides only a crude separation method. However, it is widely used as a first step in purification procedures, particularly when working on a large scale. Occasionally, fractional precipitation with an organic solvent (ethanol, acetone) is used but there is a possibility of protein denaturation at high solvent concentrations.

Proteins also differ from one another in size and this can be exploited in size-exclusion chromatography. This is inherently a method of low resolution and can rarely achieve more than separation of mixtures of proteins into broad size classes. However, a very important application of size-exclusion chromatography is for changing the composition (e.g. the pH) of the solvent between steps in a purification procedure. Dialysis can also be used for this purpose but is much slower. The same restriction of low resolution applies to separations using membrane filtration, but this technique is of enormous utility at various stages in a purification schedule for reducing the volume of protein solutions: the single major 'contaminant' in a protein solution is water.

Whereas the methods above depend on differences in structures of proteins there is also a set of procedures that depend essentially on differences in biological activity. In the vast majority of cases, biological activity of a protein depends on it recognizing and binding to a ligand. For example, enzymes bind to substrates and inhibitors, hormones bind to receptors, antibodies bind to antigens and so on. This specific biological activity can be exploited by construction of a matrix to which the appropriate ligand is (usually covalently) attached. Passage of a protein mixture through the resulting affinity matrix should result in binding of one or a small number of

proteins that recognize the ligand. Subsequent elution can be achieved by passage of a solution of the ligand, or a suitable analogue, through the column. This method has seen widespread application in the purification of enzymes and is in principle capable of very high selectivity because of the specificity of enzyme/substrate or enzyme/inhibitor binding. The selectivity achieved is, however, often limited by the fact that the ligand may be charged and hence gives rise to ion exchange effects, or it may be hydrophobic and give rise to nonspecific hydrophobic interactions. Despite this, affinity chromatography is a very powerful method and its use is restricted more by the fact that it is often necessary to design and synthesize the affinity matrix oneself rather than by inherent limitations.

Dye binding chromatography is a variant of affinity chromatography and relies on the fact that a variety of chlorotriazine textile dyes interact moderately specifically with enzymes that have nucleotide (ATP, NAD(H), coenzyme A (CoA)) binding sites. The ability of dye-containing matrices to recognize nucleotide-dependent enzymes is not a purely affinity effect – indeed the structural similarity between the dyes used and the cofactors is not obvious – and includes elements of ion exchange and hydrophobic effects. Nevertheless, these methods often work remarkably well for isolation of groups of nucleotide-dependent enzymes or even of individual members when biospecific elution methods are used.

Lectin chromatography and metal chelate chromatography are available when the protein of interest has either surface carbohydrate or a metal-binding site, respectively. The former method depends on the fact that various plants produce proteins (lectins) that bind specifically to particular classes of carbohydrate. If the lectin is coupled to an appropriate support then the product matrix will specifically bind glycoproteins from a mixture of proteins. Elution can be effected by passage of a solution of the appropriate monosaccharide through the column. In metal chelate chromatography the matrix has a chelating agent covalently attached and loaded with an appropriate metal ion. On passage of a mixture of proteins through the column those with a binding site for the metal will be retained and subsequently can be eluted by passage of a solution of metal ions through the column.

Immunoaffinity chromatography is in principle the most specific method available for protein isolation. It involves raising an antibody to the target protein, attaching the antibody to a supporting material and then using this as an affinity matrix. The extreme specificity of antigen-antibody interactions should ensure high selectivity in binding the

target protein. However, there are two problems. Clearly, the protein has to have been isolated previously in order for an antibody to be produced. A highly purified protein will be required to raise polyclonal antibodies. Alternatively, a partly purified antigen can be used to produce monoclonal antibodies but this adds an extensive new dimension to a purification procedure. The major restriction on the application of the method, however, is the difficulty of elution of proteins from the immunoaffinity matrix once bound. The tightness of binding often requires extreme conditions for efficient elution (very high or low pH, presence of chaotropic agents) such that many protein molecules become denatured during the elution process.

Putting them Together

Faced with the variety of methods available for the separation of proteins the question arises as to which of them to use and in which order for development of a purification schedule for a particular protein. The answer to this depends on a whole host of issues such as:

- how much protein is required?
- what sources of the protein are available?
- has the gene for the protein been cloned?
- is the protein required to be completely pure?
- is it necessary to retain biological activity?
- has it been done before?

If the answer to the last question is positive, the obvious approach is to try to reproduce the reported purification procedure. It may not work exactly as described – small variations in procedures between laboratories can give rise to significant differences in the behaviour of proteins during purification – but it should be relatively easy to adjust conditions to get it right. Development of a new protocol is time-consuming and not usually worthwhile unless it is to be used repeatedly and an existing method appears to be unnecessarily cumbersome; even then the published method should provide a valuable guide on how to make improvements.

What follows are descriptions of the sorts of schedules of methods that might be used in a variety of situations.

Large-Scale Isolation of an Active Protein

Large-scale here is taken to mean a laboratory-scale purification of a few tens of milligrams of protein. Industrial scale purification might well follow the same general pattern but there would be engineering problems associated with scaling up that will not be dealt with here. In the case of a protein to

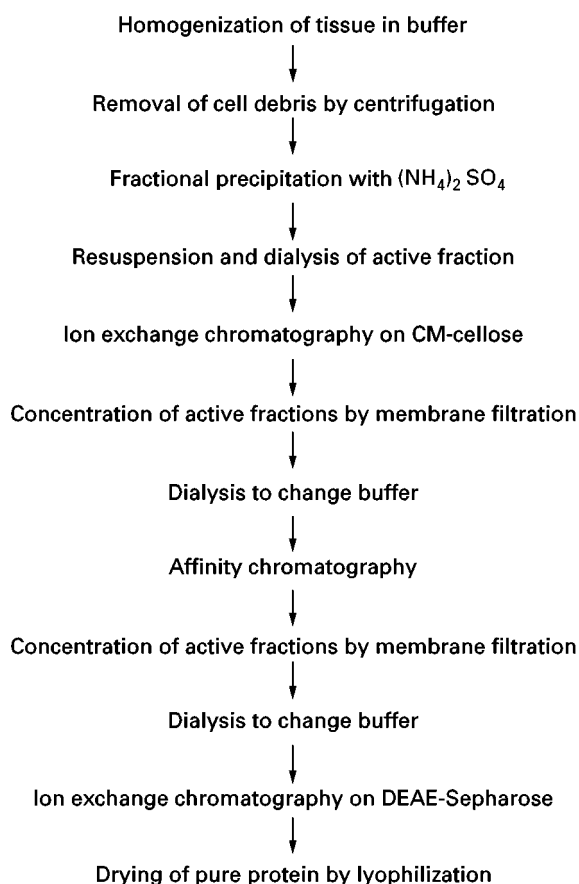


Figure 1 Flow chart for the purification of an enzyme.

be used for therapeutic purposes there would also be specific requirements imposed by regulatory agencies that are beyond the scope of the present discussion.

The flow chart in **Figure 1** outlines steps in the protocol for purification of an enzyme developed in the author's laboratory. The starting material was 5 kg of pig liver. If the source of the enzyme or other protein is not of importance for the purpose of the investigation then the best choice is to use an animal tissue that can be obtained in quantity from a commercial abattoir. Animal tissues are generally easy to homogenize in a domestic food blender. Other sources such as fungi, bacteria and plants present difficulties in disruption of the tissue and are best avoided unless the source is constrained by the problem in hand.

Ten litres of buffer was used for homogenization and, after removal of debris, the volume of protein solution was 8.5 L. This volume of solution is difficult to handle and hence fractional precipitation with ammonium sulfate was used both to obtain an initial crude purification and, more importantly,

reduce the volume. After centrifugation of the active fraction, resuspension of the pellet and dialysis the volume was reduced to 500 mL.

The next step was ion exchange chromatography. There were choices to be made of whether to use a cation or anion exchanger, and as to which of the various available supporting materials (cellulose, Sepharose, Superose) was to be preferred. In the present case, a cellulose-based matrix was chosen. This was essentially because the amount of protein in the sample (about 100 g) made it necessary to use a large amount of exchanger and correspondingly a large column. Cellulose-based exchangers are much cheaper than other varieties and, in addition, large columns of cellulose exchangers have better flow characteristics than do those of other materials. The choice of carboxymethyl (CM) cellulose rather than the anion exchanger diethylaminoethyl (DEAE) cellulose was dictated by previous experience of the behaviour of the two materials for the separation of crude protein mixtures.

The protein of interest was retained by the CM-cellulose and was eluted by application of a gradient of increasing sodium chloride. This is to be preferred over the other possibility of using conditions where the protein is not retained on the column since a higher degree of purification is likely to be achieved on gradient elution. After combination and concentration of the active fractions the volume of the sample had been reduced to about 50 mL and the amount of protein to about 1 g. These amounts were suitable for the application of a variety of small-scale but more highly resolving techniques. For example, had the enzyme of interest been a glycoprotein then lectin affinity chromatography would have been a good choice. Similarly, hydrophobic chromatography could have been used. An advantage of using the latter technique would have been that it would not have been necessary to remove the sodium chloride from the sample after gradient elution from CM-cellulose given that in hydrophobic chromatography the sample is applied in a solution of high salt content to promote interaction with the matrix.

In practise it was relatively easy in the present case to develop an affinity matrix for the enzyme based on an analogue of the substrate. It was worthwhile to do this because it was intended to repeat the purification frequently so that the time involved in preparing the affinity matrix was subsequently recovered. If a purification is essentially one-off then this is unlikely to be the case.

After affinity chromatography the product was examined by electrophoresis and found to contain

two minor contaminants, both more basic than the target enzyme. Hence, a final step using an anion exchanger under conditions where the protein of interest was absorbed but the contaminants were not, or were bound more weakly, suggested itself. The exchanger chosen was DEAE-Sepharose, which has a greater resolving power than cellulose-based products.

The final product of the purification procedure was 28 mg of protein that was homogeneous, as judged by the usual criterion of producing a single band after sodium dodecyl sulfate–polyacrylamide gel electrophoresis (SDS-PAGE). The enzyme had been purified 6000-fold compared with the original homogenate and the yield was about 50%.

Small-Scale Isolation of an Active Protein

Isolation of a few milligrams of active protein follows the same general principles as outlined above but can often be achieved in a smaller number of steps. For example it is not necessary to carry out fractional precipitation with salt because the small volume of protein solution will allow direct use of ion exchange chromatography as the first purification step. In addition, because of the small scale of the procedure, the high resolving power of ion exchange chromatography or of hydrophobic chromatography in fast protein liquid chromatography (FPLC) mode can be exploited, which may allow a reduction in the number of chromatographic steps required. FPLC differs from conventional column chromatography in that it employs very fine particle size matrices that offer greater resolving power for protein mixtures. Fully automated equipment is also available that allows for greater reproducibility between runs than do conventional methods. Capacity is, however, limited.

Proteins from Sub-Cellular Organelles

Many proteins in higher organisms exist in discrete subcellular organelles such as mitochondria, chloroplasts and lysosomes. If the target protein is one of these it may be advantageous to make a preparation of the organelle and isolate the protein from that rather than from a total tissue homogenate. Isolation of subcellular organelles is usually carried out by preparative differential centrifugation. Proteins can subsequently be extracted from the organelles and purified by standard techniques.

The advantage of this approach is obvious. Given that the organelles contain a more restricted range of proteins than does the parent cell then the purification procedure is likely to be much simpler. The downside is that the isolation of subcellular structures is time-consuming and, except on a relatively small

scale, there may not be a net saving of time in adopting this approach.

Membrane Proteins

Integral membrane proteins present special problems because of their location within membranes and because they are not soluble in aqueous buffer solutions. The first step will be to obtain a preparation of the membrane of interest, usually by differential centrifugation. Next, the protein has to be extracted from the membrane preparation, most commonly by using solutions of detergents such as Triton X-100, Lubrol PX, digitonin, sodium cholate, etc. This is a crucial step and the best detergent to use to obtain optimum release of the protein from the membrane fragments can be determined only by trial and error.

Once a soluble extract of the protein has been obtained its purification can be achieved using the usual chromatographic techniques except that, because of solubility problems, it will be necessary to maintain a standing concentration of detergent in the buffers. This frequently adversely affects the performance of ion exchange materials and more success in isolation of membrane proteins has been achieved by exploiting their binding properties, that is, by using various forms of affinity chromatography.

A final problem, once the protein has been purified, will usually be to remove the detergent from the preparation or to change the detergent type. This can be achieved by a variety of methods, including equilibrium dialysis, gel filtration and a variety of chromatographic methods.

Peripheral membrane proteins, that is, those that are only loosely associated with the membrane, do not usually present special problems. They can be released from membrane preparations by salt extraction or by changes in pH, are usually soluble in aqueous buffers, and are amenable to the usual purification methods.

Products from Cloned Genes

As a result of the rapid developments in genetic technology in recent years it is now relatively easy to clone the gene for any protein of interest and express it in a suitable bacterial host. This does not change the methods that are available for purification but it does allow for simplification of the purification procedure. An obvious example is that expression of the gene can be manipulated so that its protein product represents a very high percentage of the protein in the host cell. Values of up to 50% have been achieved, which obviously simplifies the subsequent purification. Similarly, some success has

been achieved in modifying genes by the attachment of an export signal so that the host organism excretes the protein product into the culture medium.

Other approaches to facilitating purification of cloned gene products involve the construction of fusion proteins. One example of this is where a tail of basic residues (lysine or arginine) is engineered onto the protein. This tail will make the protein very basic and hence increase its affinity for ion exchangers such as CM-Sephadex. If, after elution from the exchanger, further purification is required then the tail can be removed (by digestion with carboxypeptidase B) followed by further chromatography under the same conditions. The decreased basicity consequent on removal of the tail will ensure that the protein now behaves differently compared with any contaminants whose properties will not have been modified.

Other approaches involve engineering affinity labels onto the protein. For example, fusion products between a target protein and maltose-binding protein from *Escherichia coli* can be very readily purified by amylose affinity chromatography. Similarly, antibodies to certain small peptide sequences, referred to as flags, have been raised so that fusion proteins bearing these flag sequences can be readily purified by immunoaffinity chromatography.

Obviously, in any particular case the question needs to be asked as to whether the time and cost involved in genetic engineering of the desired protein product is justified in terms of the time saved in subsequent purification. The answer is likely to be positive only if the purification is to be repeated frequently.

Special Cases

The procedures described above should be used when it is important to retain the biological activity of the protein of interest. Essentially, this means using experimental conditions under which the native three-dimensional structure of the protein is preserved. There are some situations where this is not necessary and all that is important is that the primary structure of the protein remains unchanged. An important example of this is where the protein is required for amino acid sequence analysis. In this case additional techniques can be used for purification. For example reverse-phase HPLC using hydrocarbon (C_4 – C_{18}) stationary phases provides for high-resolution separation of proteins but elution often requires the use of organic solvents such as acetonitrile, which frequently leads to denaturation. The method is, however, extremely powerful for final

separation of partly purified proteins for sequence analysis.

For a variety of applications, including *N*-terminal sequence analysis using modern high-sensitivity techniques, only very small amounts of protein (a few micrograms) are required. For these applications the resolving power of SDS-PAGE can be exploited to separate even relatively crude mixtures. The protein of interest is then removed from the acrylamide gel, for example by using an appropriate blotting technique, and the blot subjected to analysis.

More recently this approach has been extended to the identification of proteins in cell homogenates. The total cell extract is separated by two-dimensional electrophoresis, most commonly using isoelectric focusing in the first dimension and SDS-PAGE in the second dimension. Individual spots are excised from the gel, the protein subjected to digestion with trypsin, and the trypsin fragments analysed by mass spectrometry. The set of peptide masses obtained is then scanned against a data bank of the masses of tryptic peptides from all known proteins. In most cases this allows unique identification of the protein in the gel spot, provided that its sequence is known either from direct analysis or by translation of a DNA sequence.

Detection and Quantification

It is clearly of central importance in any purification procedure that a method is available for detecting the presence of the protein of interest in the fractions from the various separation steps. In the case of enzymes this is easy because they possess catalytic activity that can be measured by some appropriate analytical technique. Other proteins might require the use of a bioassay, or an immunoassay, or perhaps the identification of the protein as a particular band produced on analytical electrophoresis.

What might not be so obvious is the importance of quantification of the recovery of the protein at each stage of the purification procedure – that is, of keeping an inventory. Unless this is done it is very easy to end up with a disappearing yield of the protein of interest and not to know at which step or steps it disappeared. At each step it is important to measure the total protein content and the amount of the

protein of interest. This allows not only the recovery but also the degree of enrichment of the protein to be determined. Any step for which either of these is low should be abandoned.

In the case of enzymes, keeping this inventory is straightforward; it is simply necessary to measure the catalytic activity of a known volume of the fractions. In other cases it is much more difficult. Bioassays can be very time consuming. Immunoassays are not usually too difficult, but in this case it is necessary to bear in mind that immunological reactivity of a protein may be retained even though biological activity has been lost. In the case of a protein with no known biological activity, or where the activity is very difficult to measure, then recovery can be assessed from the measurements of the intensity of the appropriate band produced by analytical electrophoresis. Whatever the difficulties, however, keeping a score card is essential if a successful purification protocol is to be developed.

See also: **I/Affinity Separation. Centrifugation. II/Affinity Separation:** Hydrophobic Interaction, Chromatography; Immobilised Boronates and Lectins; Immunoaffinity Chromatography. **Chromatography:** Protein Separation; Size Exclusion Chromatography of Polymers. **Chromatography: Liquid:** Mechanisms: Size Exclusion Chromatography. **Electrophoresis:** Isoelectric Focusing; Two-dimensional Electrophoresis. **Membrane Separations:** Membrane Bioseparations. **III/Proteins:** Centrifugation; Electrophoresis; Field Flow Fractionation; High-Speed Countercurrent Chromatography; Ion Exchange.

Further Reading

- Deutscher MP (ed.) (1990) *Guide to Protein Purification*. San Diego: Academic Press.
- Doonan S (ed.) (1996) *Protein Purification Protocols*. Totowa, Humana.
- Harris ELV and Angal S (eds) (1989) *Protein Purification Methods*. Oxford: IRL Press.
- Harris ELV and Angal S (eds) (1990) *Protein Purification Applications*. Oxford: IRL Press.
- Kenney A and Fowell S (eds) (1992) *Practical Protein Chromatography*. Totowa: Humana.
- Walker JM (ed.) (1998) *Protein Protocols on CD-Rom*. Totowa: Humana.

ESSENTIAL GUIDES FOR ISOLATION/PURIFICATION OF IMMUNOGLOBULINS

A. Layer, P. Schneider, J.-D. Tissot and M. A. Duchosal, Service Régional Vaudois de Transfusion Sanguine, Lausanne, Switzerland

Copyright © 2000 Academic Press

Introduction

The immunoglobulins (Igs), proteins produced by B lymphocytes, have been extensively studied both at molecular and genetic levels. They consist of two identical heavy chains and two identical light chains having therefore the same isotype and the same type, respectively. Igs are purified for three main purposes. (i) as therapeutic injections to patients; (ii) for use as a tool in research or clinical diagnosis; and (iii) for their biochemical analysis (specificity, isotype or clonal diversity). Most of these applications require that the binding activity of Igs be retained throughout all the purification procedures.

Purification of Igs can be performed according to their physicochemical properties, their biological activities or a combination of both. The technique used will depend on the desired degree of purity and the amount and nature of the starting material. The methods that have been described are generally directly applicable to crude materials such as serum, ascitic fluid or cell culture supernatant. Two-dimensional polyacrylamide gel electrophoresis (2D-PAGE) affords an efficient way of evaluating the degree of purity reached in affinity purifications. Several aspects of 2D-PAGE analysis are described in detail in two other articles 'Electrophoresis/Two-dimensional PAGE' and 'Clinical Applications of Electrophoresis/Electrophoresis' in this Encyclopedia.

As a general rule, and independently of the technique used, the starting material should always be devoid of any insoluble substances and the purification be preceded by centrifugation or filtration. Viscous fluids, such as serum, may be diluted before use, especially for chromatographic procedures. The solutions should contain a bacteriostatic agent, such as 0.02% sodium azide (NaN_3), and be kept on ice. Ig solutions should be handled gently, avoiding bubbling or frothing, because such manipulations may be

accompanied by denaturing effects, and may lead to protein precipitation.

Purification by Precipitation

Solubility of the proteins, particularly Igs, in water relies mainly on the ability to make hydrogen bonds between polar or ionic groups with water molecules (hydrophilic interactions), and on the capacity to maintain hydrophobic groups that cannot interact with water molecules buried inside the proteins. In addition, the solubility of Igs is temperature-dependent. Any external factor capable of modifying hydrogen bonds or decreasing the medium hydrophilicity will decrease the solubility of the proteins and may eventually lead to their precipitation. Each protein has its own physicochemical characteristic, including solubility. For this reason, several differential precipitation procedures can be developed to isolate Igs from various fluids. These procedures are presented below.

Differential Ethanol Precipitation

The first fractionation of plasma proteins for therapeutic use was described in 1949 by E.J. Cohn. The basic procedure, with few modifications, is still widely used in industrial fractionation centres. Basically, ethanol is added progressively to the medium to a final concentration varying from 8 to 40%. Subsequently, the temperature is decreased to -3°C and then to -5°C . Finally, the pH is decreased from 7.3 to 4.8. These steps yield precipitation fractions, called Cohn's fractions I-V. Fraction II contains the γ -globulins or Igs. The treatment of this fraction with caprylic acid (see below) allows the preparation of Igs that are enriched in IgA and IgM. This approach is used when large amounts of Igs are needed, i.e. for therapeutic purposes (from up to 5000 L plasma) and will not be detailed further.

Ammonium Sulfate Precipitation

Small and highly charged ions, such as ammonium ions, replace bound water molecules when present at a sufficient concentration. This decreases protein

solubility and, when the ammonium sulfate concentration is increased stepwise, a sequential precipitation of proteins may be obtained.

Practically, a saturated solution of ammonium sulfate (761 g L^{-1} ; 4.1 mol L^{-1}) is slowly added to a stirred (in order to avoid local over-increase in concentration) solution of Igs, until the final desired concentration, usually expressed as a percentage of ammonium sulfate saturation, is reached. Although some interspecies variability is observed for Ig solubility, a 50% ammonium sulfate saturation is usually appropriate for most Ig precipitation procedures. Pre-precipitation at 40% ammonium sulfate saturation may be useful to remove large protein aggregates and proteins that may precipitate at low ammonium ion concentration. The precipitation is allowed to occur at 4°C for 6–12 h. The precipitate is recovered by centrifugation at 2000–5000 g for 20–30 min. In general, the pellet is then gently solubilized in a minimal volume of a physiological buffer, and dialysed to remove the residual ammonium sulfate. Alternatively, Ig purity can be increased by washing the pellet with a 50% saturated solution and solubilization in PBS, followed by another round of ammonium sulfate Ig precipitation. When starting with serum or cell supernatant containing serum, this method allows the removal of most albumin and haemoglobin, but the precipitated fraction still contains several serum proteins in addition to Igs. In this case this approach must be coupled with another purification technique if pure material is needed. When starting with a serum-free cell culture supernatant, this method is convenient to isolate, and to concentrate, monoclonal Igs in one step. In addition, the method is easy, cheap and can be applied to large volumes.

Caprylic Acid Precipitation

The solubility of proteins is altered by the presence of some short chain fatty acids, such as octanoic acid (caprylic acid) at mildly acidic pH. Basically, caprylic acid increases medium hydrophobicity. In practice the pH of the starting solution must be adjusted to 4 by the addition of about 2 vol of a 60 mmol L^{-1} sodium acetate buffer. Then, 0.04–0.07 vol of caprylic acid (depending on the starting material as well as on the animal species of the Igs) is added drop by drop while stirring, and the solution is incubated at room temperature for 30 min. Under these conditions, most of the serum proteins are precipitated, with the exception of IgG, which is recovered in the supernatant after centrifugation at 5000 g for 10 min. This method bears similarities with that of ammonium sulfate precipitation. In particular, it needs to be coupled with another one to yield highly purified Ig fractions.

Chromatographic Methods

In chromatographic procedures, compounds in solution are separated by allowing them to flow through a selective medium poured in a column. Differential interactions between molecules and matrix are responsible for them migrating at various speeds, or even completely immobilizing them. Separated molecules are recovered in the effluent of the column. Several commercially available preparations allow separation of proteins according to their various physicochemical properties. Detailed information about the use of such media is furnished by the manufacturers or can be found in the literature for particular applications.

Ion Exchange Chromatography

An ion exchanger consists of a positively or negatively charged group covalently bound to an insoluble matrix. Charged molecules with complementary polarity to that of the immobilized groups bind to the matrix through electrostatic interactions, whereas uncharged or similarly charged molecules pass freely through the matrix. Since the net charge of a protein depends on the pH, the starting experimental conditions must be carefully chosen. The bound proteins may be desorbed either by change in pH, or by change in the ionic strength. The former modifies the charge of the protein, whereas salts compete with the binding of the protein to the resin. Addition of NaCl is most frequently used for elution. As the strength of the protein–matrix interaction depends on the net protein charge, a sequential elution can be performed by gradually increasing salt concentration. Because Igs have a more basic isoelectric point than most other serum proteins, ion exchange chromatography can be used for their purification. Practically, the matrix should be extensively washed with 0.5 mol L^{-1} HCl or 0.5 mol L^{-1} NaOH before use, and then equilibrated with the binding buffer. In addition, the sample must be dialysed against the binding buffer before being loaded on the resin.

At pH 6.5 (5 mmol L^{-1} phosphate), Igs will not bear negative charges, and therefore will not bind to a positively charged matrix such as diethylaminoethyl (DEAE) matrix, which is not the case for other serum proteins. A bulk Ig fraction can therefore be recovered in the flow-through. In contrast, Igs will bear a negative net charge at pH 8.5 (10 mmol L^{-1} Tris), and thus will bind to a positively charged matrix (DEAE). Sequential elution of proteins bound to the matrix can be performed by increasing the concentration of NaCl from 0.05 to 1 mol L^{-1} . Igs are among the first serum proteins to be eluted, at salt concentrations usually below 0.5 mol L^{-1} . Ig isotypes can be

differentially purified using this method. Relatively pure IgG is usually recovered in the first eluted fraction; IgM, the last eluted Ig isotype, may also be recovered in quite a pure form, whereas IgD and IgA, with intermediate elution properties, are only poorly resolved with this method. Ion exchange chromatography can yield sufficiently pure antibodies if the starting material is a cell culture supernatant or an ascitic fluid, but it must be coupled to an additional purification step when samples such as serum are used. The method is also cheap and is convenient for large initial volumes.

Hydroxyapatite Chromatography

Immobilized hydroxyapatite (calcium phosphate hydroxide) is used for another kind of adsorption chromatography. At pH 6.8, Igs bind to the matrix, and are eluted when a linear gradient of phosphate buffer from 120 to 300 mmol L⁻¹ is applied. When highly purified Ig fractions are needed, this technique must be coupled to another one, again depending on the starting material.

Gel Filtration Chromatography

A gel filtration matrix consists of beads containing pores of various sizes. As the sample flows through the matrix, the largest molecules are excluded from the beads. They stay only in the mobile phase, and move fast. The smaller molecules, depending principally on their sizes but also on their shapes, diffuse more or less inside the pores, and move more slowly within the column. Thus, this system allows the separation of the proteins according to their sizes and shapes. Various matrices with particular structures, pore sizes and excluding limits (the M_r at which the proteins are no more able to enter into the beads) are available commercially. Gel filtration can be used within broad pH ranges, with or without detergents such as 1% sodium dodecyl sulfate (SDS), or dissociating agents such as urea or guanidine. Ig purification is usually performed without sophisticated conditions, and allows the separation of IgM molecules that are considerably larger than IgG as well as many other serum proteins. Using an exclusion limit of 300–500 kDa, and a column volume of at least 20 times larger than that of the starting solution, IgM is easily recovered in the excluded peak. Due to the time needed to allow a complete passage, the use of a fraction collector is highly recommended. Fractions corresponding to 1–3 initial volumes should be collected. Gel filtration must usually be coupled with other methods to yield sufficient Ig purity, and is mainly limited to the purification of IgM.

Precipitation of Immune Complexes

The Precipitin Reaction

When antigens are added in adequate proportions to a mixture of antibodies, specific Igs and antigens will form a lattice which is susceptible to precipitate (the precipitin reaction). This macromolecular complex can then be easily recovered by centrifugation. The required amount of antigens to be added must be determined by establishing a precipitation curve. This implies that one should also have a procedure allowing the precipitate to be quantified. The use of radiolabelled antigens is particularly suitable for this when restricted amounts of antigens are available. Complement activation, which occurs in normal fresh serum, is able to inhibit the precipitation strongly. Therefore, it is necessary to make either a pre-purification of the Igs or to inhibit the complement cascade by the addition of ethylenediaminetetraacetic acid before performing a precipitin reaction. The precipitated lattice is subsequently re-solubilized either by incubation with serum or with an excess of free antigen, or by digestion with papain, which generates Fc fragments.

Polyethylene Glycol Precipitation

Soluble (nonlattice) immune complexes, either present naturally, or generated by adding a corresponding antigen, precipitate from serum in the presence of 3–4% polyethylene glycol (PEG; M_r 6000) after 2–12 h incubation at 4°C. This method has been widely used to isolate circulating immune complexes in various pathological situations. Other high molecular weight proteins, as well as aggregated Igs, can also precipitate using above-mentioned conditions. Therefore, additional steps of purification, using protein G or A (see below), are generally warranted before sufficiently pure material can be used. Solubilization of most PEG-precipitated immune complexes can easily be performed using most buffers that do not contain PEG. In contrast, dissociation of immune complexes requires quite harsh conditions, that are frequently not compatible with techniques allowing the further purification of free Igs devoid of antigens. Immunoprecipitation of specific antibodies is therefore mainly limited to analytical purposes that do not need biological activity. Ig light and heavy chains from immune complexes are easily solubilized in buffers containing SDS, and can be analysed by SDS-PAGE or 2D-PAGE.

Affinity Chromatography

In affinity chromatography, samples containing Igs are incubated in the presence of a matrix consist-

ing of an Ig-binding molecule covalently coupled to a bead support. Unbound molecules are removed by washing, and specifically bound Igs are then eluted using an appropriate buffer. The method is highly specific and high Ig purity is usually reached in a single step. Ig-binding molecules belong to three major groups: (i) bacterial protein A or protein G; (ii) specific antigens; and (iii) monospecific antibodies directed to epitopes on Igs (such as goat anti-human Ig antibody). Various bead supports and coupling procedures have been studied. The use of commercially available activated beads has now allowed preparation of affinity media within most laboratories. In particular cyanogen bromide (CNBr)-activated Sepharose beads can easily be used for most applications and detailed instructions are furnished by the manufacturers. After coupling, the resin should be extensively washed to remove all uncoupled Ig-binding molecule, and equilibrated in binding buffer. The binding capacity of each resin should be determined experimentally before use. If sample binding is indifferently performed in a container (batch procedure) fixed on a rotating wheel or through a column, washing and elution are best performed through a column. The use of a peristaltic pump is highly recommended to ensure a fixed flow.

Washing and elution steps are best followed online with a UV detector set to monitor at 280 nm. Alternatively, fractions may be collected and tested individually using either UV absorption or more specific procedures. When necessary (see elution conditions below), the eluate has to be collected in a neutralizing solution, and the resin immediately re-equilibrated in the binding buffer. Unused resins should be stored at 4°C in the presence of a bacteriostatic agent, such as 0.02% sodium azide or 20% ethanol.

Affinity Chromatography using Immobilized Protein G and A

Protein A and protein G are present within the bacterial cell walls of *Staphylococcus aureus* and of group G streptococci, respectively. Both proteins have high affinity for the Fc region of IgG, but bind differentially IgG subclasses from various species. Whereas protein G bind all human and mouse IgG subclasses, protein A presents only low binding capacity for human IgG₃ and mouse IgG₁. Ready-to-use matrix-immobilized protein G or A is commercially available, and detailed information about the binding properties of these two proteins can be found in the literature or furnished by the manufacturers. Binding buffers usually contain 100 mmol L⁻¹ Tris or 10 mmol L⁻¹ phosphate with 0.15 mol L⁻¹ NaCl, at pH 8 for protein A and pH 7 for protein G. After Ig

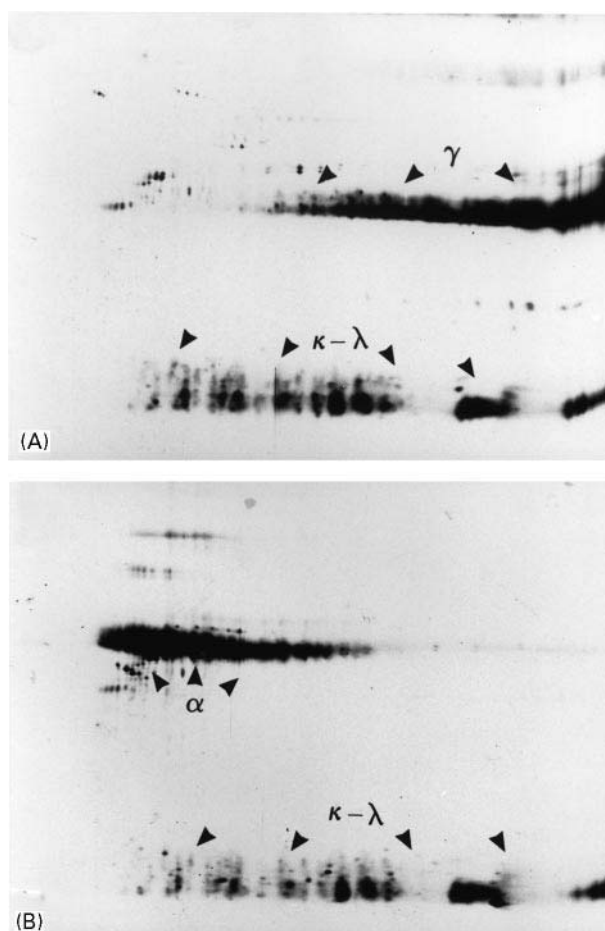


Figure 1 (A) 2D pattern of IgG purified over protein G-Sepharose. Human serum was incubated with commercially available protein G-Sepharose (Pharmacia), and IgG eluted as indicated in the text. γ heavy chains migrate within pIs ranging from 6 to more than 10, with a size of about 50 kDa. Light chains display pIs ranging from 5 to 10 and size between 21 and 26 kDa. γ , IgG heavy chain; κ , λ , light chains. (B) 2D pattern of IgA affinity purified over a homemade anti- α chain-Sepharose resin. The affinity resin was prepared from commercially available CNBr-activated Sepharose (Pharmacia), according to the manufacturer's recommendations, and commercially available goat anti-human α chain antibodies. α chains migrate with a pI ranging from 4.9 to 6.1 and a size of about 58 kDa. α , IgA heavy chain; κ , λ , light chains.

binding to samples, the resin is washed with about 20 vol of the binding buffer until online UV absorption of the flow-through medium gives an optical density back to zero. Elution of IgG is best performed by addition of 100 mmol L⁻¹ glycine pH 2–3 in tubes containing a suitable amount of a neutralizing buffer such as 1 mol L⁻¹ Tris, pH 8 or 1 mol L⁻¹ phosphate, pH 7. As illustrated in **Figure 1**, IgG is highly purified after a single-step procedure over protein G column, with no other heavy chain class detectable. The strength of the protein A(G)–Ig interaction, which is mainly based on hydrophobic

interactions, can be increased by raising salt concentrations of the binding and washing buffers to 3.3 and 3 mol L⁻¹, respectively. This high salt concentration method was initially described for the purification of mouse IgG₁ on protein A, but is now obsolete, due to the availability of protein G. The use of an excess of protein A allows IgG₁, IgG₂ and IgG₄ to be depleted from samples and IgG₃ to be purified using protein G in a second step. A sequential elution of all four IgG subclasses from protein A using a pH gradient has been described, but the resolution is quite low and subclass-specific purification of IgG₁₋₄ is now best performed using immobilized monospecific anti-Ig raised against either γ_1 , γ_2 , γ_3 or γ_4 heavy chains of the IgG molecule.

The elution yield from protein G or A using standard procedures is never 100% (see below) and residual IgG can be eluted during a second run procedure and may contaminate the new IgG being purified with IgG from the previous run. In order to avoid any Ig contamination from a previous experiment, it is therefore highly advisable to use either the same batch of protein G or A for the same initial IgG preparation or to use a new batch of resin for each procedure.

Affinity Chromatography using Immobilized anti-Igs

In this method, the immobilized binding molecules are Igs (mouse, rabbit, goat, sheep) directed against Ig heavy and/or light chains. Using antibodies of various specificities, it is possible to isolate either total Igs (using anti- κ and - λ chains), particular Ig isotopes (using anti- μ , - γ , - δ , - α or - ϵ chain) or IgG subclasses (using anti- γ_1 , - γ_2 , - γ_3 or - γ_4 chains). The interaction between immobilized and targeted immunoglobulins is just a particular type of antibody-antigen interaction. Binding and elution are therefore basically performed using the same conditions as those used for immobilized antigen supports (see below). Figure 1B shows that IgA purified from a human serum sample over an anti- α chain resin does not display any other heavy but α chain isotope. The resolution obtained by 2D-PAGE in separating various Ig heavy chains is illustrated in Figure 2.

IgG subclasses can be purified using two different procedures named positive and negative isolations. In positive isolation, the desired subclass is immobilized on a resin, washed and recovered by elution, whereas in the negative isolation, all unwanted subclasses are bound on resin and the desired subclass is recovered in the flow-through. The advantage of this latter approach is that the final preparation is not exposed to strong nonphysiological conditions which may denature the purified IgG sub-

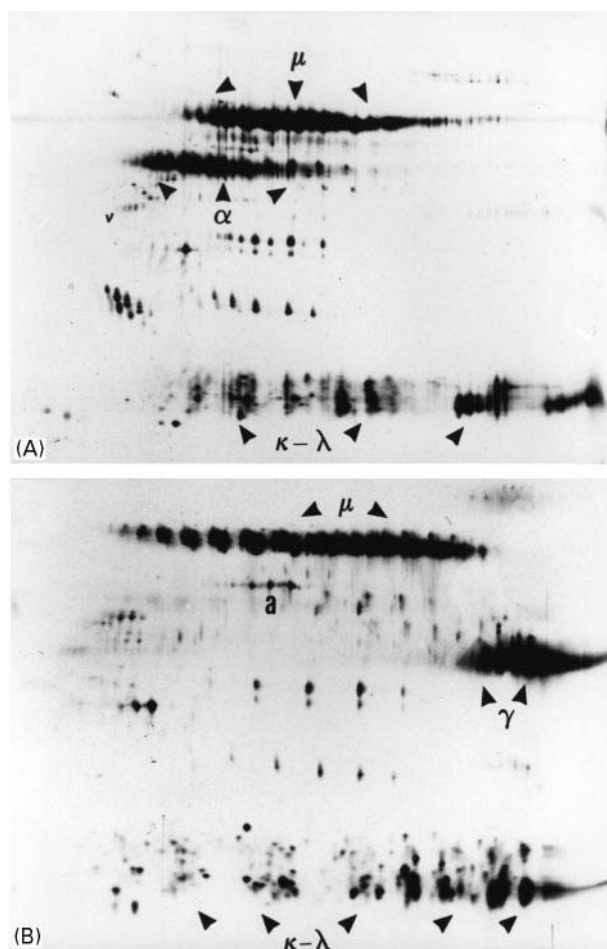


Figure 2 (A) 2D pattern of a mixture of affinity purified IgM and IgA; (B) 2D pattern of a mixture of affinity purified IgM and IgG. Immunoglobulins were purified over homemade anti- μ chain-Sepharose resin, anti- α -chain-Sepharose resin and anti- γ -chain-Sepharose resin and mixed as indicated before electrophoresis. Resins were prepared according to the manufacturer's instructions, from CNBr-activated Sepharose and commercially available goat anti-human μ , α and γ chains. Immunoglobulins were prepared from serum as indicated in the text. μ chains migrate with pIs between 5.6 and 6.4, and size of 72 kDa. μ , IgM heavy chain; α , IgA heavy chain; γ , IgG heavy chain; κ , λ , light chains.

class. Disadvantages are that the methodology requires larger amounts of resin and several immobilized antibodies and that, when biological fluids are processed, the final preparation still contains proteins other than IgG.

Affinity Chromatography using Immobilized Antigens

A commonly used method for purifying and recovering antigen-specific, and antigen-free, Igs from a polyclonal mixture of antibodies involves the use of matrix-bound antigens that bind specific, antibodies at physiological pH and salt concentration

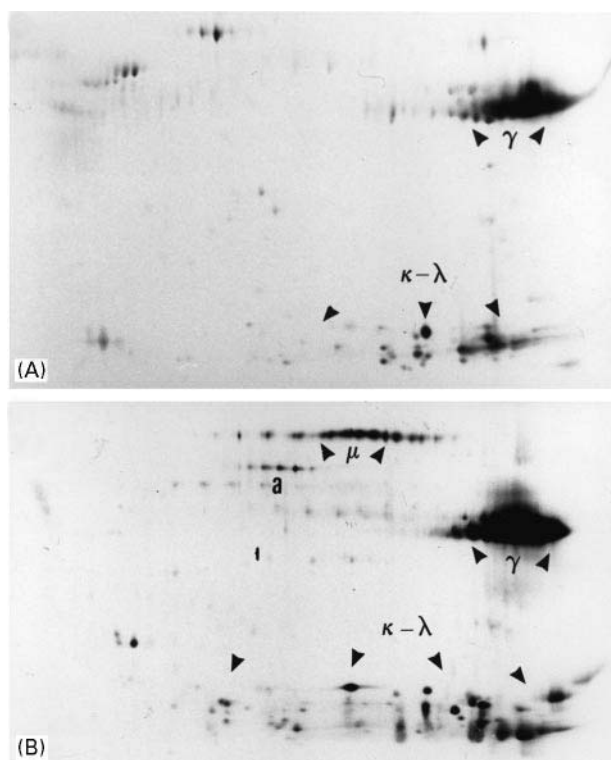


Figure 3 2D patterns of affinity purified anti-tetanus toxoid antibodies. Immunoglobulins were purified from two severe combined immunodeficient (SCID) mice (A and B) previously injected with human lymphocytes and boosted with tetanus toxoid. Homemade tetanus toxoid-Sepharose resin was prepared according to manufacturer's recommendations, from commercially available (Pharmacia) CNBr-activated Sepharose and a home preparation of tetanus toxoid. Igs were SDS-eluted, as indicated in the text. γ , IgG heavy chain; μ , IgM heavy chain; κ , λ , light chains, a, albumin.

(10 mmol L⁻¹ Tris or phosphate buffer saline (PBS) 0.15 mol L⁻¹ NaCl, pH 7.5). The unbound material is washed away with about 20 resin-volumes of binding buffer. Elution of bound antibodies is commonly performed by successive washes with 100 mmol L⁻¹ glycine, pH 2–3 and 100 mmol L⁻¹ triethylamine, pH 11–12. The eluted fractions are subsequently recovered into tubes containing neutralizing buffer. Elution solutions such as 5 mol L⁻¹ LiCl/PBS, 3.5 mol L⁻¹ MgCl₂/PBS, 1% SDS, 2–8 mol L⁻¹ urea, 3 mol L⁻¹ thiocyanate, 10% dioxane, or 50% ethylene glycol can also be used.

The purification of anti-tetanus toxoid Igs over a toxoid-coated resin is presented in Figure 3. Both 2D-PAGE light chain patterns shown depict a limited number of easily distinguishable spots, typical of oligoclonal Igs. These patterns are clearly different from that of total Igs (and purified total IgG, not shown) from the same serum, indicating that a subpopulation of Igs was purified. Whereas the anti-tetanus toxoid antibodies shown in Figure 3A

consist only of IgG, some IgM anti-tetanus toxoid antibodies were also present in the case shown in Figure 3B.

Affinity Chromatography Using Jacalin or Complement

Jacalin (a carbohydrate-binding molecule) allows the separation of both subclasses of pre-purified IgA (jacalin binds IgA₁ but not IgA₂). Complement C1q will bind antigen-complexed Igs. Anti-complement Igs will bind immune complexes bound to components of the complement system.

Recovery from Affinity Resins

As already mentioned, elution from protein G or A-Sepharose may be incomplete. In our hands, purification of 6–12 mg batches of IgG from various sources resulted in a recovery of about 50%, using acidic elution. Similar recovery yields have also been reported by others, using similar elution. Purification of anti-tetanus toxoid antibodies on tetanus toxoid-Sepharose resulted likewise in a 50% loss of antibody activity. We further investigated antibody recovery yield using affinity-purified radiolabelled antibodies. When purification was scaled down to 10 μ g Ig (an amount that allows enzyme-linked immunosorbent assay or electrophoresis techniques), recovery of bound material from protein G or tetanus toxoid-Sepharose was only about 10%. The percentage of lost Igs was roughly inversely proportional to the initial Ig amount. Some loss is acceptable when purifying large batches of monoclonal antibodies. On the other hand, when purifying antibodies for analytical purposes, one should keep in mind that antibody losses may skew the final results; the composition (isotype, subclass and diversity) of the eluted fraction may indeed no longer reflect the composition of Igs that were initially loaded on the resin. The problem of low recovery could be solved by heating Ig-loaded protein G- or tetanus toxoid-Sepharose in the presence of SDS and dithioerythritol; more than 97% of bound Igs could be recovered by this way. Of course, such treatment does limit further analysis to methods that do not require biological activity of Igs, such as electrophoresis, since Igs are denatured under such conditions.

Conclusion

Many different methods have been described over the years to purify Igs, and the most important have been briefly presented in this article. Of course, we have made a choice between the many methods available, and the list is not exhaustive. Numerous

Table 1 Summary of the major approaches for purifying immunoglobulins

Starting material	Methods	Purposes
Plasma, ascitis	Affinity chromatography on protein G or A	Isolation of pure IgG
Plasma, ascitis, pre-purified immunoglobulin fractions	Affinity chromatography on purified antigens	Purification of monospecific antibodies
Plasma, ascitis, pre-purified immunoglobulin fractions	Affinity chromatography using mono-specific antibodies (anti- α , - γ , - μ , - κ or - λ)	Isolation of immunoglobulins of a single isotype
Plasma, ascitis, pre-purified immunoglobulin fractions	(NH ₄) ₂ SO ₄ /DEAE Sepharose	Preparation of large amounts of relatively pure immunoglobulin fractions
Plasma, ascitis, pre-purified immunoglobulin fractions	(NH ₄) ₂ SO ₄ -Hydroxyapatite	Preparation of large amounts of relatively pure immunoglobulin fractions
Plasma, ascitis, pre-purified immunoglobulin fractions	Gel filtration/DEAE Sepharose	Preparation of relatively pure IgM fractions

variations and/or combinations of methods may be used to satisfy a particular need, depending on the starting material, as well as for the purpose of the purification. However, for most current applications, affinity purification procedures appear to be the most elegant and selective methods. The binding capacities of affinity resins are usually high (up to 20 mg of immunoglobulins per mL resin), and their reusability allows the purification of quite large amounts of pure immunoglobulins in relatively short times.

Table 1 summarizes the most efficient methods of purifying Igs.

Further Reading

- Akerström B and Björck L (1986) A physicochemical study of protein G: a molecule with unique immunoglobulin G-binding properties. *Journal of Biological Chemistry* 261: 10240–10247.
- Akerström B, Brodin T, Reis K and Björck L (1985) Protein G: a powerful tool for binding and detection of monoclonal and polyclonal antibodies. *Journal of Immunology* 135: 2589–2592.
- Bukovsky J and Kennett RH (1987) Simple and rapid purification of monoclonal antibodies from cell culture supernatants and ascites fluids by hydroxyapatite chromatography on analytical and preparative scales. *Hybridoma* 6: 219–228.
- Burnouf T (1994) New trends in plasma fractionation and plasma products (review). *Vox Sanguinis* 67 (suppl 3): 251–253.
- Crowley-Nowick PA, Campbell E, Schrohenloher RE *et al.* (1996) Polyethylene glycol precipitates of serum contains large proportion of uncomplexed immunoglobulins and C3. *Immunological Investigations* 25: 91–101.
- Harlow E and Lane D (1988) *Antibodies: A Laboratory Manual*, pp. 283–318. Cold Spring: Cold Spring Harbor Laboratories.
- Labrou N and Clonis YD (1994) The affinity technology in downstream processing. *Journal of Biotechnology* 36: 95–119.
- Langone JJ (1982) Applications of immobilized protein A in immunochemical techniques. *Journal of Immunological Methods* 55: 277–296.
- Langone JJ (1982) Protein A of *Staphylococcus aureus* and related immunoglobulin receptors produced by streptococci and pneumococci. *Advances in Immunology* 32: 157–252.
- Page M, Baines MG and Thorpe R (1994) Preparation of purified immunoglobulin G (IgG). *Methods in Molecular Biology* 32: 407–432.
- Perosa F, Carbone R, Ferrone S and Dammacco F (1990) Purification of human immunoglobulins by sequential precipitation with caprylic acid and ammonium sulfate. *Journal of Immunological Methods* 128: 9–16.
- Rojas G, Jimenez JM and Gutierrez JM (1994) Caprylic acid fractionation of hyperimmune horse plasma: description of a simple procedure for antivenom production. *Toxicon* 32: 351–363.
- Scholz GH, Vieweg S, Leistner S *et al.* (1998) A simplified procedure for the isolation of immunoglobulins from human serum using a novel type of thiophilic gel at low salt concentration. *Journal of Immunological Methods* 219: 109–118.

ESSENTIAL GUIDES FOR ISOLATION/ PURIFICATION OF NUCLEIC ACIDS

**G. A. Monteiro, J. M. S. Cabral and
D. M. F. Prazeres**, Centro de Engenharia
Biológica e Química, Instituto Superior Técnico,
Lisboa, Portugal

Copyright © 2000 Academic Press

Introduction

Isolation/purification of nucleic acids (NAs – dsDNA, ssDNA, tRNA, mRNA, etc.) is a common and crucial step in most molecular biology, biomolecule engineering, cancer research, recombinant DNA, forensic analysis, gene therapy, DNA vaccines and diagnostics (e.g. DNA chips) applications. Most often, NAs are isolated and purified merely as a way of obtaining quantitative and qualitative information about a certain sample (e.g. paternity testing, screening for viruses in clinical samples, etc.). Several purification methods have been developed by laboratories and companies involved in the above-mentioned areas. These protocols and processes are based on the same general principles, and follow three main stages: obtaining the NA source (cell growth, tissue isolation,

chemical or enzymatic reaction), primary isolation and purification. Different techniques exist that can be used alone or in combination within each step of the isolation/purification scheme (Figure 1).

When choosing an isolation/purification protocol or process, NA researchers and manufacturers should take into account several aspects. Especially important are the nature of the target NA, the final application, cost and availability of the technique (Table 1). The final application will determine which specifications (yield, purity, safety, efficacy, identity) the final NA preparation should follow.

Nucleic Acids

The success of NA purification relies on a minimal understanding of the molecular composition and structure of the target molecule. NAs are linear polymers of nucleotides (adenylate, guanylate, cytidylate and uridylate in RNA and deoxyadenylate, deoxyguanylate, deoxycytidylate and thymidylate in DNA) linked by phosphodiester bonds. The presence of negatively charged phosphate groups in the backbone of the molecule confers a polyanionic

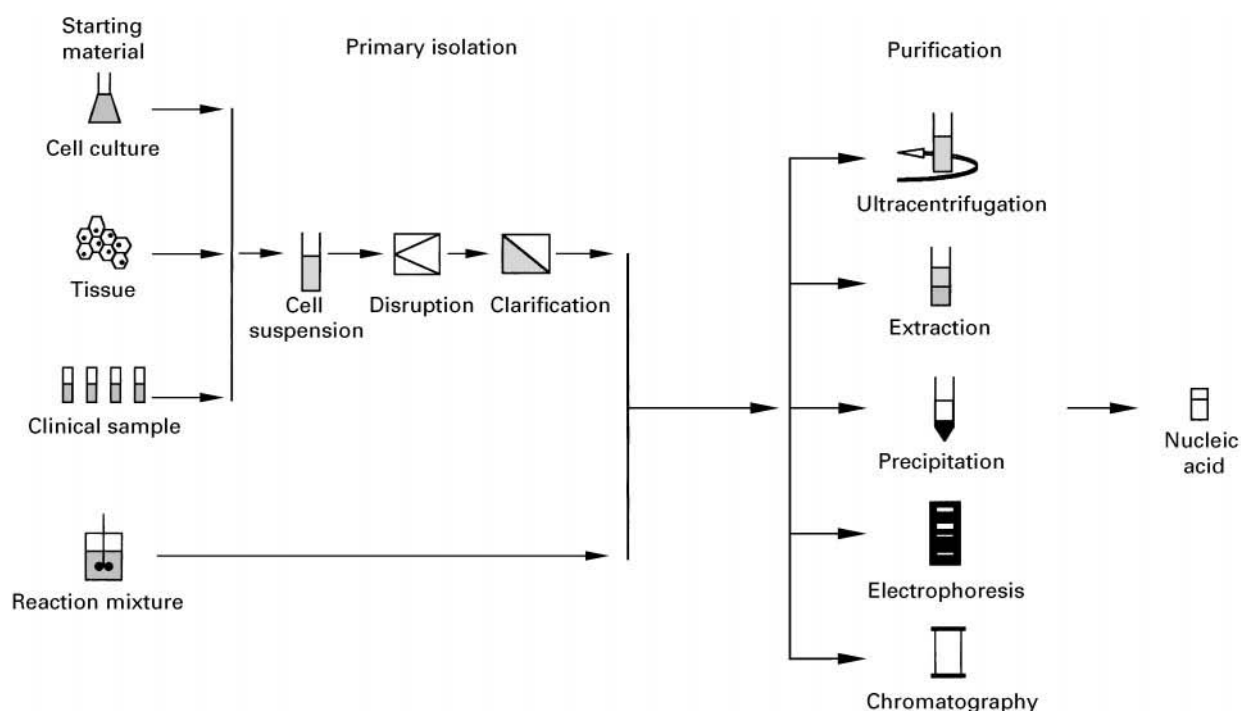


Figure 1 Strategies for the isolation/purification of nucleic acids.

Table 1 Relevant aspects to the choice of a nucleic acid isolation/purification protocol or process*Target nucleic acid*

DNA or RNA

Size (from a few base pairs to 100 kb or more)

Base composition (e.g. poly(A)⁺ segments)

Structure (single/double strand, secondary and tertiary structure, supercoiling)

*Application*Material for research (cloning, sequencing, *in vitro* translation, etc.)

Material for therapeutic use (gene therapy, gene marking, DNA vaccines, antisense)

Material for identification and quantification (diagnostics, forensics, medicine)

Specifications

Purity

Yield

Potency

Safety

Identity

Source

Cells

Prokaryotic (bacteria)

Eukaryotic (plant, animal, fungi including yeast)

Viruses (M13, phage λ , human immunodeficiency virus, hepatitis)

Chemical and enzymatic mixture

Oligonucleotides from solid-phase synthesis

Restriction digests

Polymerase chain reaction mixtures

Labelling and modifying reaction mixtures

Type of processing

Single sample

High-throughput

Parallel, *n* samples with the same target NAParallel, *n* samples with different target NASequential, *n* samples with same target NASequential, *n* samples with different target NA*Cost*

Per number of isolation (diagnostics)

Per amount of target DNA (large scale manufacture)

Other

Time

Scaleability of process

Environmental issues

Safety of protocol

Robustness

Automation

nature to NAs. DNA molecules are often double-helix structures formed by two strands winding around each other and around a common axis. These structures are stabilized by hydrogen bonds and mainly by stacking forces. The helix axis can also be coiled, forming a higher order structure, named supercoiling. RNA can take on the same configurations as DNA, having secondary and tertiary structures; it can be single-stranded (more often) or double-stranded, linear (more often) or circular, and it can also form hybrid helices with DNA. Double-

stranded NAs melt to single strands fairly sharply as condition (temperature, OH⁻, denaturants like formaldehyde or formamide) becomes more denaturing. Renaturation is achieved when the reversible denaturation condition is removed. However, if the denaturation condition is quickly removed, the process is irreversible. The stability of double strands increases with the mole fraction of GC pairs and decreases as the pH is varied towards either side of neutrality. RNA is particularly sensitive to alkaline conditions.

Primary Isolation

Cell Disruption

Cells from the source organism are first recovered from the starting material, whether it is a cell culture, tissue or clinical sample, and resuspended in an appropriate buffer. The isolation of the target NA then starts with the disruption or lysis of the cells. There are several cell disruption methods that can be used alone or in combination (Table 2).

The choice of disruption method should consider factors such as the effect on the final NA, the cell type (animal or plant culture or tissues; fungi or Gram-negative or -positive bacteria spheres or filaments; viruses), the scale (laboratory- or industrial-scale), sample volume and number of samples, associated costs, duration and final application.

Usually, cell disruption is combined with a chemical or an enzymatic step for the inactivation of intracellular nucleases, which can degrade the target NA if a controlled method is not properly adopted. The physical and chemical conditions present during cell lysis are a key step in NA isolation. Temperature should be kept around 4°C to avoid nuclease activities that degrade the NAs. When an enzymatic step is included (performed at around 25–35°C), for instance by adding proteinase K or RNase to hydrolyse proteins or contaminating RNAs, caution should be taken with the presence of endogenous DNases that are active in the same temperature range.

The release of NAs during lysis significantly increases the viscosity of the solution, making mixing a difficult task. The lysates show non-Newtonian properties, exhibiting a rheological behaviour that makes flow and handling of the material very difficult. This issue is particularly troublesome on a large scale. The mixing at this stage should be very gentle to avoid shearing of the target NA. In certain proto-

cols and processes it is important to maintain the contaminating NAs with the highest molecular weight possible, in order to facilitate their removal in the subsequent steps. Glucose or sucrose is often included in the lysis buffer or after disruption, in order to protect NAs against shearing. Sensitivity to shear increases with molecular weight, and a single-stranded NA is more sensitive than a double-stranded one with the same length. Special care should thus be taken when handling (pipetting, pouring, mixing) NA solutions of high molecular weight.

The lysis buffer usually contains a chelating agent such as ethylenediaminetetraacetic acid (EDTA). The removal of divalent cations (mainly Ca²⁺ and Mg²⁺) from biological membranes and cell walls (when present) destabilizes their structure, facilitating lysis, and reduces the activity of endogenous Mg²⁺-dependent nucleases, preventing NA degradation. Protein-denaturing agents (e.g. detergents, phenol, guanidinium hydrochloride) are commonly added. The detergents denature proteins, including the ones associated with NAs, and solubilize lipids from membranes, facilitating cell disruption. Finally, the lysis buffer pH must be tightly controlled and local pH extremes avoided, since low pH values promote the hydrolysis of DNA, and alkaline pH favours the cleavage of RNA and the irreversible denaturation of chromosomal DNA. Moreover, very low pH values lead to depyrimidation and depurination.

RNA is notoriously susceptible to degradation and special care is required in its purification. The presence of endogenous and/or exogenous RNases is a major concern, since RNases can recover activity even after harsh denaturation treatments (e.g. boiling). High concentrations of strong chaotropic agents (e.g. guanidinium hydrochloride, guanidinium thiocyanate, caesium trifluoroacetate) is often used to inactivate RNases irreversibly and simultaneously promote the disruption of cellular membranes.

Table 2 Summary of cell disruption methods

<i>Physical</i>	<i>Chemical</i>	<i>Biological</i>
Pressure	Detergents	Enzymes
Ultrasound	SDS	RNase
Blades	Triton	Lysozyme
Grinding	Acid	Proteinase K
Freeze–thaw	Alkali	Viruses
Osmotic shock	Organic solvents	
Dehydration	Phenol	
	Chaotropic salts	
	Urea	
	Guanidinium hydrochloride	
	Guanidinium thiocyanate	
	Caesium trifluoroacetate	
	Thiol reduction	

Clarification of Lysates

After cell lysis and inactivation of endogenous nucleases, cellular debris, proteins and other precipitated molecules must be removed. This is usually achieved by means of centrifugation or filtration steps. During this operation, certain amounts of NAs can be lost in the liquid entrained in the solid phase. Extensive removal of water from the solid phase can be performed to increase the yield, but this operation usually also increases the amount of impurities. Minimum shear should be exerted in order to preserve the integrity of the target NA. The solution obtained after clarification is more or less rich in several impurities. Small molecules such as nucleotides, nucleosides,

amino acids, sugars and inorganic ions are easily removed, but DNA, RNA, polysaccharides and proteins are difficult to remove because these macromolecules have some common physical and chemical characteristics. The impurity profile and amount in a clarified lysate depend not only on the cell type, but also on factors such as phase growth and growth conditions (carbon and nitrogen sources, media richness, dissolved CO₂ and O₂, pH, etc), as well as on the method used for disruption (Table 2).

Purification

After the primary isolation steps, most impurities in solution are comprised of NAs from the source organism, denatured forms of the target NA, proteins and endotoxins (Gram-negative bacteria). The similarities between these molecules and their wide molecular weight range make purification difficult. Several methods are available to purify NAs, depending on the amount, yield and purity needed, and also on the availability of methods and associated costs.

Gradient Centrifugation

A classical method for separating DNA or RNA from each other, and from proteins and polysaccharides, uses equilibrium-density gradient (or isopycnic) centrifugation, which is based on differences in particle density. The density gradients can be self-forming or pre-formed continuous gradients, prepared with caesium salts (e.g. CsCl, Cs₂SO₄) or iodinated compounds (e.g. metrizoate, metrizamide, nycodenz). Equilibrium-density gradient centrifugation is one of the most efficient methods available for the purification of NAs. The major drawbacks are its dependence on high cost reagents and equipment (the ultracentrifuge) and the fact that it is a time-consuming operation (typically at least 48 h of centrifugation). When using this method, it should be kept in mind that centrifugal conditions may affect the native characteristics of the sample. For instance, the presence of endogenous and/or exogenous nucleases during a long-term process can lead to NA degradation. In addition, the chemical constituents of the solutions can affect the integrity of NAs. Physical degradation as a result of shear stress should be avoided, too.

The position of NAs in the gradient is usually located by measuring the absorbance at 260 nm. However, in a CsCl isopycnic separation, the DNA molecules band at approximately the same density. An alternative approach in this case is to band DNA in CsCl gradients in the presence of ethidium bromide or propidium iodide, which intercalate differentially between the bases of DNA, resulting in dif-

ferent molecule buoyant densities. This technique allows the separation of supercoiled plasmids, nicked or relaxed plasmid forms, genomic DNA, RNA and proteins.

Liquid-Liquid Extraction

Solvent extraction is often used to remove proteins and lipids from NAs. The pH values of the extractant organic phase and of the starting aqueous phase are very important because partition coefficients of NAs are pH-dependent. A classical system for solvent extraction uses a sequential extraction with phenol:chloroform (1:1). Although phenol is an efficient denaturant of proteins, it does not completely inactivate RNases, and it solubilizes RNA with long poly(A)⁺ tails. These problems can be partially overcome by introducing isoamyl alcohol in the phenol/chloroform mixture.

In spite of the efficiency of solvent extraction, residual contaminants still remain in solution. Furthermore, solvents like phenol and chloroform are extremely toxic for both the operator and the environment. Even small amounts in the final NA preparation are potentially toxic to live recipient cells and can interfere in downstream experiments. This makes solvent extraction an unacceptable method when preparing NA for therapeutic use.

Extraction of NAs has also been performed with aqueous two-phase systems. This technique relies on the fact that concentrated aqueous solutions of polysaccharides, such as dextran and polyethylene glycol (PEG), are immiscible. Many biological components (polymers, cells, cell organelles) including NAs show different solubility in the two phases formed, and will therefore separate by partitioning. By manipulating the system conditions (e.g. buffer, polymer and salt concentration) it may be possible to separate DNA from RNA, native from denatured DNA and single from double or triple strands. The technique, however, has not been studied in depth, and therefore is not commonly used.

Precipitation

Precipitation with ethanol or isopropanol is commonly used to concentrate NAs. Typically, 2 vol of ethanol or 0.7 (v/v) isopropanol is added to the NA solution. The process is more efficient if performed in the presence of moderate concentrations of monovalent cations and at low temperatures (below 4°C). The concentration and type of salt (cation: ammonium, lithium, sodium, potassium; anion: acetate, chloride) used in precipitation should be optimized for the target NA. The duration and speed of the centrifugation step used to recover the precipitate

material are also important, and should be adjusted according to the concentration of NA (longer and faster centrifugation for lower concentrations). If the amount of target NA is low, an inert carrier such as glycogen can be added to the mixture to increase precipitation efficiency. After draining liquid from the precipitated material, an appropriate buffer is added to redissolve the NAs.

Another method for precipitation of NA uses PEG/salt (NaCl, MgCl₂) systems. The method is based on the fact that the size of the DNA molecule precipitated by PEG is dependent on the concentration and molecular weight of PEG. It can thus be used either to fractionate DNA according to molecular mass, or simply to precipitate the total DNA content. The method is rapid and inexpensive but consistent yields are difficult to obtain.

The precipitation methodology, although generally used to concentrate NAs, is also effective as a purification step. Selective precipitation could be achieved, for instance, with high concentrations of different salts or changes in pH to precipitate proteins or nontarget DNA or RNA. For example, ammonium sulfate is often used to precipitate contaminating proteins. Lithium chloride precipitation has also been used in the preparation of large RNA. It takes advantage of the fact that small RNAs (tRNAs and 5S RNA) are soluble in solutions of high ionic strength, whereas large RNAs (rRNAs and mRNAs) are insoluble and precipitate out. After centrifugation, the high molecular weight RNA is redissolved in water or buffer.

Gel Electrophoresis

Gel electrophoresis on agarose or polyacrylamide gels is a powerful technique commonly used to separate, identify and purify NAs. Under the effect of an electrical field, NA molecules migrate through the gel matrix at a rate that is inversely proportional to their size. The resolving power of gel electrophoresis is extremely high, enabling the separation of molecules that differ in size by as little as 1 bp. The position of the individual molecules in the gel can be determined by staining with a fluorescent intercalating dye such as ethidium bromide. By using a number of techniques, such as electroelution or low-melting agarose gels, it is possible to recover DNA of high purity from the gels. However, the scale associated with electrophoresis is generally small.

Chromatography

Chromatography has been increasingly used to purify NAs. The technique is powerful, rapid and simple to perform, while avoiding the use of toxic compounds

common to competing technologies like ultracentrifugation and phenol/chloroform extraction.

Disposable column cartridges packed with particles of a stationary phase, and operating in the gravity flow format, often constitute an essential part of commercial isolation kits for lab-scale applications. In many cases, centrifugation is combined with disposable spin columns to enhance and speed the isolation. High-throughput and automated formats using these column cartridges are increasingly available that enable the processing of several samples at the same time, minimize hands-on preparation time, and reduce the risk of sample mix-ups. Purification using high pressure liquid chromatography (HPLC) has also been performed as a preparative step to isolate small quantities of NAs. In large scale applications, column chromatography is a central process step. For large scale applications, economic constraints demand regeneration and re-use of the expensive chromatographic media. Furthermore, if material is being produced for clinical use, validation of the cleaning is indispensable.

Different types of chromatography, such as gel filtration, ion exchange, hydrophobic interaction, reversed-phase, adsorption and affinity, have been used for the purification of NAs (Table 3).

Except in the case of gel filtration, the mode of operation of the chromatographic columns, whether small or large, is similar. Two possibilities exist:

1. Interaction of the target NA with the chromatographic support: column feed, binding of the target NA to the stationary phase, removal of impurities by washing and selective elution and, finally, elution of the target NA (Figure 2A).
2. No interaction of the target NA with the chromatographic support: column feed, collection of the target nucleic in the flow-through, binding of impurities to the stationary phase and, finally, column disposal or removal of the impurities by selective elution (Figure 2B).

A chromatographic column can also be used in conjunction with an enzyme process in order to improve the selectivity of the method. For instance, DNase (RNase) treatment of bound NAs will remove DNA (RNA), while leaving RNA (DNA) behind.

Purification by anion exchange takes advantage of the interaction between negatively charged phosphate groups in the DNA or RNA backbone and positively charged ligands on the surface of the particles that constitute the stationary phase. A salt gradient is usually used to displace the different NA species, which in principle should elute in order of increasing overall net charge, which in turn is a function of chain

Table 3 Purification of nucleic acids by chromatography

<i>Chromatography</i>	<i>Basis of separation</i>	<i>Examples and applications</i>
Anion exchange	Charge, charge density	Plasmid purification Plasmid copy number analysis Fractionation of restriction fragments
Hydrophobic interaction	Hydrophobic interaction	Separation of polymerase chain reaction products Separation of dsDNA from ssDNA and RNA Fractionation of supercoiled and relaxed plasmids
Reversed-phase	Hydrophobic interaction	Separation of dsDNA from ssDNA and RNA Separation of supercoiled and relaxed plasmid Purification of oligonucleotides (chemical synthesis)
Adsorption	Selective adsorption	Capture of nucleic acids by silica (glass powder, diatomaceous earth) Separation of dsDNA from ssDNA by hydroxyapatite Separation of RNA from DNA with boronic acids
Affinity	Structure recognition	Triple helix formation Hybridization of poly(A) ⁺ tails to oligo(dT) ligands Plasmid purification with acridine dye ligands
Gel filtration	Size, shape	Buffer exchange Salt and oligonucleotide removal Fractionation of supercoiled and relaxed plasmids Removal of endotoxins

length. When column cartridges are used, the salt gradient is always a step for convenience, while in process applications linear gradients can improve selectivity.

Anion exchange chromatography can also be used as a nonsize-based NA purification tool. In some cases, base sequence and composition affect the elution pattern of NAs in anion exchangers. The shape and size of the molecules may also play an important role. This is the case, for example, in the purification of plasmid variants. In some anion exchangers, the more compact supercoiled plasmid forms, which have a higher charge density, elute later than the open circular forms, which have a lower overall charge density.

Since many of the NAs being isolated are normally very large molecules, their binding to most of the existent anion exchangers is likely to occur only at the surface. This constitutes an important capacity limitation, especially in large scale applications. Different types of stationary phases have been used for anion exchange chromatography of NAs. Typical examples include weak ligands such as diethylaminoethyl and dimethylamino coupled to silica, polymeric or composite (inorganic + polymeric) matrices and strong ligands such as quaternary amines coupled to polymeric matrices.

Hydrophobic interaction chromatography has not been described for the purification of NAs, but recent results indicate that matrices derivatized with mildly hydrophobic residues are able to separate double-stranded DNA from RNA and single-stranded DNA under nondenaturing conditions.

In reversed-phase chromatography, NAs are also retained by the hydrophobic interaction of the bases with the chromatographic resin, but here, the density of ligands is much higher. Separation of single- and double-stranded DNA has been accomplished in C₁₈ columns and differentiation between DNA and RNA due to the effect of ribose and deoxyribose has also been reported. In reversed-phase chromatography, the binding is stronger than in hydrophobic interaction chromatography due to the higher ligand density. This requires elution to be carried out under more severe conditions, for instance, by using eluents with organic solvents, which can have a deleterious effect on the structure of the target molecule. For this reason, reversed-phase chromatography is more suited for the purification of smaller NAs that are less prone to denaturation. This is the case with synthetic oligonucleotides, used as primers or as blocking agents in antisense technologies, that are synthesized by solid-phase chemistry and purified by reversed-phase chromatography.

In adsorption chromatography, a stationary phase is used that selectively binds NAs in the presence of chaotropic salts, which remove water from hydrated molecules in solution, ensuring separation from complex biological mixtures. For instance, NAs adsorb to silica (glass) in the presence of sodium iodide or guanidinium hydrochloride, and to hydroxyapatite in the presence of urea. Polysaccharides and proteins do not adsorb and are removed by washing. Elution is performed using a low salt buffer. Hydroxyapatite further displays an ability to separate

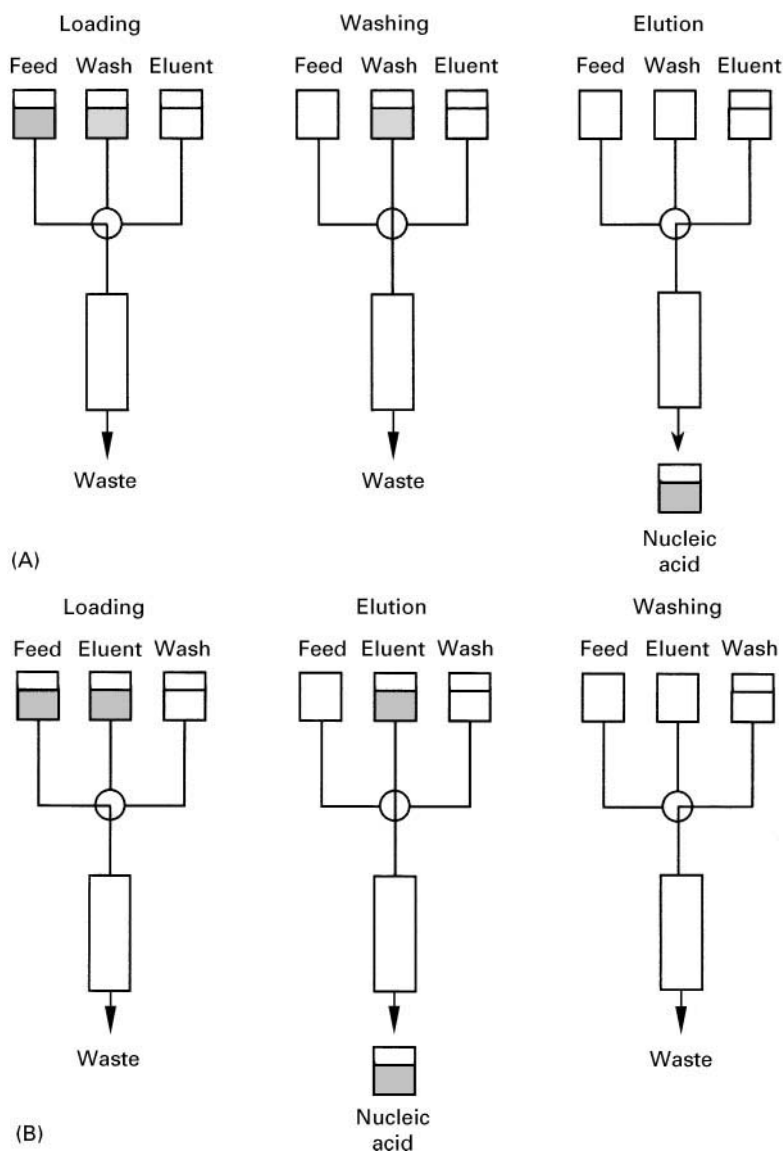


Figure 2 Mode of operation of chromatographic columns in nucleic acid purification: (A) interaction of the target nucleic acid with the chromatographic support; (B) no interaction of the target nucleic acid with the chromatographic support.

single-stranded NAs that bind less tightly from double-stranded NAs.

A method for the selective adsorption of RNA in the presence of DNA employs immobilized boronic acid derivatives which, above their pK_a values, form cyclic complexes with vicinal diols. Since the deoxyribose sugars lack the vicinal diol of ribose sugars in RNA, DNA is poorly adsorbed and can be washed away easily.

Affinity chromatography is based on the recognition of a particular structure in the target NA molecule by an immobilized ligand. In triple-helix affinity chromatography, the formation of triple helices between oligonucleotides linked to a chromatographic matrix and duplex sequences present on

dsDNA is explored. The affinity of poly(A)⁺ tails of mRNA to oligo(dT) probes has also been explored as a way of capturing and purifying mRNA. The combination of affinity ligands with magnetic particles is another recent development that avoids the use of packed columns. It allows the binding of the target molecule directly from solution, with the particle complex being recovered with a magnet. The high selectivity of affinity chromatography makes it a powerful tool for the one-step purification of NAs. However, since each ligand targets a specific base sequence, the versatility of the technique is low and the associated cost high.

Size exclusion or gel filtration chromatography has been used to fractionate NA molecules on the basis of

their relative size. By selecting a gel with an appropriate selectivity for the size range in question it is possible, for example, to isolate supercoiled plasmid DNA from microbial contaminants such as genomic DNA, RNA, proteins and endotoxins. Another feature of size exclusion chromatography, often explored when purifying NAs, is the possibility of exchanging buffers and removing salts, nucleotides, excess primers and other small molecules. This type of column is commercially available in the cartridge format for the clean-up of NA solutions.

Quality Control of Final Nucleic Acid

The final NA quality criteria will vary with the NA inherent complexity, its intended use and the method and complexity of manufacture. The researcher and/or producer will select several quality control tests that depend on their own application. NAs can be quantitatively and qualitatively analysed by a number of chemical, biochemical and physical assays. Some quality controls of NA preparations are summarized in Table 4.

A method used widely to estimate the amount of RNA or DNA is spectrophotometric analysis. The absorbance at 260 nm is relatively accurate (depending on base composition) and reproducible when applied to purified samples without significant amounts of contaminants (e.g. proteins, other NAs, phenol), and to moderately diluted or concentrated prepara-

tions. Spectrophotometric scans between 220 and 320 nm are also used to detect salt and organic contaminations. The purity of NAs based on the absorbance ratio 260 nm/280 nm is commonly used. A 260 nm/280 nm ratio between 1.8 and 2.0 is usually considered to be a good estimation of purity. This method was initially developed to quantify the contaminating NAs in protein preparations. For this reason, it often fails when used for NA purity assessment. Therefore, when a high level of purity is critical, care should be taken while using this method, and it should be complemented by other purity analysis. HPLC, capillary electrophoresis or methods using specific fluorescent dyes, quantitative DNA or RNA hybridization and quantitative polymerase chain reaction are preferable.

Conclusions

Isolation/purification of nucleic acids is becoming more and more important with the emergence of areas such as genomics, gene therapy and DNA vaccination and the growing importance of clinical diagnostics and forensics. The general strategies and technologies commonly used in the purification and isolation of NAs have been reviewed in this article. Critical issues and bottlenecks that still hamper the purification of nucleic acids have also been highlighted. Although the future will certainly bring more efficient isolation/purification methodologies, designed for high-throughput and automated preparation/analysis, the core technologies and strategies described here will most likely retain their importance.

Further Reading

- Harwood AJ (1996) *Basic DNA and RNA Protocols. Methods in Molecular Biology*, vol. 58. New Jersey: Humana Press.
- Muller W (1985) Partitioning of nucleic acids. In: Walter H, Brooks DE and Fisher D (eds) *Partitioning in Aqueous Two-Phase Systems: Theory, Methods, Uses and Application to Biotechnology*, pp. 227–266. Orlando, FL: Academic Press.
- Prazeres DMF, Ferreira GNM *et al.* (1999) Large scale production of pharmaceutical grade plasmid DNA for gene therapy: problems and bottlenecks. *Trends Biotechnology* 17: 169–174.
- Rickwood D (1984) *Centrifugation, A Practical Approach*, 2nd edn. Oxford: IRL Press.
- Sambrook J, Fritsch EF and Maniatis T (1989) *Molecular Cloning*, 2nd edn., Cold Spring Harbor, FL: CSH Laboratory Press.
- Sinden RR (1994) *DNA Structure and Function*. San Diego, CA: Academic Press.

Table 4 Quality control tests for DNA or RNA preparations

Test	Method
Appearance	Visual inspection
Identity	Restriction enzyme analysis
	Gel and capillary electrophoresis
Concentration	Sequencing
	Spectrophotometry A260 nm
Other nucleic acids	HPLC
	Gel and capillary electrophoresis
	DNA or RNA hybridization
	HPLC
Proteins	Colorimetric assay (e.g. BCA)
	Sodium dodecyl sulfate-polyacrylamide gel electrophoresis
	Immunoassays
Polysaccharides	Specific assays (e.g. HPLC, enzymatic assays, LAL)
Lipopolysaccharides	Nuclease-specific assays
Nucleases	Cytopathic effects
Sterility	Reverse transcriptase assay
	Electron microscopy
	Bioburden assay

Sofer G and Hagel L (1997) *Handbook of Process Chromatography: A Guide to Optimization, Scale-up, and Validation*. San Diego, CA: Academic Press.

Thompson JA (1986) A review of high-performance liquid chromatography in nucleic acids research III. Isolation,

purification, and analysis of supercoiled plasmid DNA. *BioChromatography*, 1: 68–80.

US FDA (1991) *Points to Consider in Human Somatic Cell Therapy and Gene Therapy*. Rockville, MD: FDA.

ESSENTIAL GUIDES FOR ISOLATION/PURIFICATION OF POLYSACCHARIDES

R.-C. Sun and J. Tomkinson,
University College of Wales, Bangor, UK
Copyright © 2000 Academic Press

Introduction

The isolation of polysaccharides from biological sources represents an important source of these valuable materials. Biomass such as cereal straws and grasses, are an enormous underutilized energy resource as raw materials in the production of paper, panel products, chemicals and other industrial products. On a dry-weight basis, the straws and grasses contain 65–85% of polysaccharides, with hemicelluloses ranked second to cellulose in abundance; however, it must be noted that the chemical content of the hemicellulose, with respect to saccharide ratios changes with plant growth and maturity (Table 1).

At the present time, there is widespread interest in the use of hemicelluloses, particularly arabinoxylan-rich hemicelluloses as precursors in food gums. More recently, water-soluble xylans from corn cobs have shown biological activity as immuno-modulating compounds. Other potential industrial applications of hemicelluloses are to be found in the fields of

adhesives, thickeners in foods, stabilizers, biodegradable film formers and emulsifiers. They can also be easily converted to primary chemicals such as xylose, xylitol, furfural, hydroxymethylfurfural and levulinic acid.

Hemicelluloses, however, are the most complex components in the cell wall of straws and grasses. They form hydrogen bonds with cellulose, covalent bonds (mainly α -benzyl ether linkages) with lignins and ester linkages with acetyl units and hydroxycinnamic acids. To investigate the potential utilizations of polysaccharides from straws and grasses, a thorough study of the isolation procedures is necessary. Details of the method are reviewed as follows.

Cell Wall Preparation

The straw or grass is cut into 1–2-cm lengths, air-dried, and ground to pass through a 0.5–0.8-mm screen. The ground sample is then further dried in a cabinet oven with air circulation at 50–60°C for 12–16 h. Dried material is dewaxed by refluxing with toluene–EtOH (2 : 1, v/v) or defatted with chloroform–methanol (2 : 1, v/v) for 6 h in a Soxhlet apparatus. The dewaxed sample is treated with α -amylase to degrade the starch or extracted with phenol–acetic

Table 1 Chemical composition of agricultural residues (per cent dry matter)

Species	Water-solubles	Cellulose	Hemicelluloses	Lignin	Extract	Ash
Wheat straw	4.7	38.6	32.6	14.1	1.7	5.9
Rice straw	6.1	36.5	27.7	12.3	3.8	13.3
Rye straw	4.1	37.9	32.8	17.6	2.0	3.0
Barley straw	6.8	34.8	27.9	14.6	1.9	5.7
Oat straw	4.6	38.5	31.7	16.8	2.2	6.1
Maize stems	5.6	38.5	28.0	15.0	3.6	4.2
Corn cobs	4.2	43.2	31.8	14.6	3.9	2.2
Esparto	6.1	35.8	28.7	17.8	3.4	6.5
Sugar beet pulp	(pectin 27.1) 5.9	18.4	14.8	5.9	1.4	3.7
Bagasse	4.0	39.2	28.7	19.4	1.6	5.1
Oil palm fibre	5.0	40.2	32.1	18.7	0.5	3.4
Abaca fibre	3.7	60.4	20.8	12.4	0.8	2.5

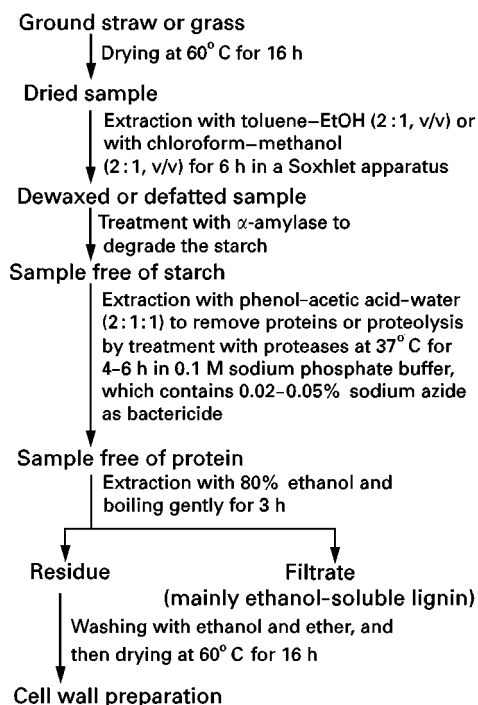


Figure 1 Scheme for procedures in cell wall preparation from straw or grass.

acid-water (2 : 1 : 1) to remove proteins. The proteins can also be extracted from the residue with sodium dodecyl sulfate solution containing 10 mM 1,4-dithiothreitol at room temperature for 3 h. To degrade the proteins, proteolysis is started by addition of proteases at 37°C for 4–6 h in 0.1 M sodium phosphate buffer, pH 7.5, containing 0.02–0.05% sodium azide as bactericide. The cell walls are recovered by filtration, extensively washed with water, and then treated with 80% ethanol to release the ethanol-water-soluble components. These consist mainly of free phenols and ethanol-soluble lignins together with small amounts of low-molecular-weight polysaccharides (~10% w/w of ethanol extract). After filtration, the cell wall preparations are dried by solvent exchange through ethanol and diethyl ether. Figure 1 summarizes the procedures for cell wall preparation.

Fractional Extraction of Cell Wall Polysaccharides

Water-Soluble Polysaccharides

The scheme for fractional extraction of cell wall polysaccharides is illustrated in Figure 2. The prepared cell walls are stirred with distilled water at 75–80°C for 2 h. The residue is filtered off on a nylon cloth, washed with ethanol and ether, and dried in an

oven at 60°C for 16 h. Water-soluble polysaccharides are isolated by precipitation of the concentrated supernatant with 4 volumes of 95% ethanol and recovered by centrifugation. The resultant solid is subsequently purified by extensive washing with 75% ethanol and then freeze-dried. As shown in Table 1, water-soluble polysaccharides obtained from various straws and grasses account for 3.7–6.8% of the dry matter and have much lower weight-average molecular weights ($\bar{M}_w = \sim 8000 \text{ g mol}^{-1}$) when compared to those of hemicellulosic fractions. Neutral sugar analysis shows that arabinose and galactose are the major sugar constituents, whereas xylose and glucose are present in only small amounts in this fraction. Detailed studies of water-soluble polysaccharides from rapeseed meal, sorghum stalk, and dehulled legume seeds and their hulls have been reported.

Pectic Polysaccharides

The pectic polysaccharides are restricted to the primary cell wall and middle lamella of higher plant tissues and growth zones. They are most abundant in soft tissues, such as rinds of citrus fruit (~30%), sugar beet pulp (~25%), and apple peels (~15%), but are present in only small proportions in woody

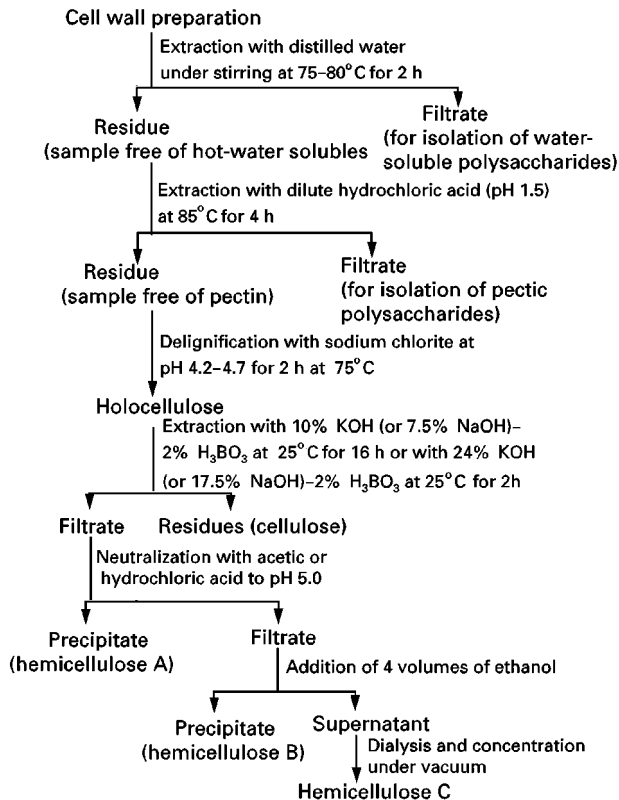


Figure 2 Scheme for fractional extraction of polysaccharides from straw or grass.

tissue such as straw and grass (0.5–1.5% dry matter). The term ‘pectins’ or ‘pectic substances’ is associated with acidic polysaccharides consisting of a backbone of mainly (1 → 4)- α -bound D-galacturonic acid residues interrupted by the insertion of α -linked L-rhamnose residues. Other constituent sugars such as L-arabinose, D-galactose, D-xylose, L-fucose, and traces of 2-O-methyl-D-xylose and 2-O-methyl-L-fucose are attached in the side chains. The pectins can be extracted with dilute acid, e.g. HCl solution at pH 1.5 or with chelating agents such as 0.2% aqueous ammonium oxalate, disodium ethylenediaminetetraacetic acid (EDTA), and sodium hexametaphosphate (SHP) solution at pH 3–4 for 4 h at 85°C. After extraction, the filtrates are adjusted to pH 4.0 with 1 M NaOH. The pectic polysaccharides are isolated by precipitation of the filtrates in 4 volumes of 95% ethanol and recovered by centrifugation. Crude pectins are extensively washed with 70% acidified ethanol and fractionated by ion exchange chromatography on a column (550 mm × 15 mm) of DEAE Sepharose Fast Flow (Pharmacia, Sweden), initially equilibrated in 0.005 M NaAc–buffer pH 5.0 or on a QAE Sephadex A-25 column (80 × 1.5 cm i.d.; Pharmacia, Sweden) equilibrated with 10 mM imidazole-HCl buffer (pH 7.0). Other columns used to fractionate the pectic polysaccharides include a DEAE-Sepharose CL6B column (23 × 5 cm; Pharmacia, Sweden) equilibrated with 0.005 M sodium succinate buffer at pH 4.8, and a DEAE-Sephadex A-50 column (20 × 2 cm; Pharmacia, Sweden) previously equilibrated with 10 mM potassium phosphate buffer (pH 6.0). The neutral and acidic pectic polymers are hydrolysed with 2 M trifluoroacetic acid at 120°C for 2 h in sealed ampoules or with pectinase. In comparison, treatment by pectinase has a significant effect on the hydrolysis of the pectic polymers, while the reverse trend is observed during the treatment of the neutral pectic polysaccharides by acid hydrolysis, since galacturonic acid residues in polysaccharides are known to be resistant to acid hydrolysis. For example, endo-1,4- α -polygalacturonase, pectin and pectate lyases can substantially cleave the α -(1 → 4)-GalpA glycosidic bonds between contiguous galacturonic residues. Previous studies have shown that extraction of the cell wall preparation of sugar beet pulp with water followed by treatment with HCl at pH 1.5, 0.2% ammonium oxalate, 0.2% EDTA, and 0.2% SHP at pH 3.3 for 4 h at 85°C yielded 32.1%, 26.1%, 29.3%, and 30.0% (percent dry cell wall preparation) of pectic polysaccharides, respectively. An optimum extraction procedure was found to be treatment with dilute HCl at pH 1.5 for 4 h at 85°C, in which the pectin contained 84.6% anhydrogalacturonic acid

and only 2.7% ash. Xylose-rich pectic polysaccharides (1.1% of dry matter) can be obtained from wheat straw by extraction with dilute HCl at pH 1.6 for 4 h at 85°C, which contain 44.8% galacturonic acid (released by pectolyase), and 28.4% neutral sugars (released by acid hydrolysis).

Hemicelluloses

The cell wall components that are readily hydrolysed by hot dilute mineral acids, or dissolved by hot dilute alkalis or cold 5% sodium hydroxide solutions have been termed ‘hemicelluloses’. Hemicelluloses belong to a group of heterogeneous polysaccharides which are formed through biosynthetic routes different to the glucose-UDP route of cellulose (a homopolysaccharide). Hemicelluloses of Gramineae such as cereal straws have a backbone of (1 → 4)-linked β -D-xylopyranosyl units. The chain may be linear, but is often branched and usually has other glycosidically bound sugar units. Some xylan chains have D-glucopyranosyluronic acid units attached, but the most important acidic hemicelluloses are O-acetyl-4-O-methyl-D-glucuronoxylans and L-arabino(4-O-methyl-D-glucurono)xylans. In dicots, where the hemicelluloses are mostly xyloglucan, hydroxyproline-rich glycoproteins also comprise a substantial amount of the cell wall and cross-link the carbohydrate polymers to form a rigid matrix. In cereal straws of grasses, these proteins have been replaced by esterified and etherified phenolic compounds. The xylans present in the hemicellulosic backbone can be substituted by arabinose, galactose, glucuronic acid, and methyl glucuronic acid. The arabinoxylan can be isolated directly from fully lignified straws or grasses by extraction with aqueous potassium hydroxide or sodium hydroxide. Usually 80–95% of the total xylan present in straw and grass contains a relatively high percentage of associated lignin (5–10%). This high lignin percentage considerably darkens the polysaccharide limiting their industrial application.

Xylans undergo only partial hydrolysis in alkaline solution at room temperature under an atmosphere of nitrogen. The product obtained – except for the fact that acetyl-, feruloyl-, and *p*-coumaroyl appendices have been partially or completely saponified – is quite similar to the native polysaccharide. The hemicelluloses which have a light brown colour contain a relatively small amount of bound lignin (1–2%), and can be quantitatively isolated from the holocellulose by extraction with aqueous alkali. Delignification of the depectinated cell wall preparations obtained from straws or grasses has been performed with sodium chlorite at 75°C for 2 h in acidic solution

(pH 4.2–4.7) adjusted by 10% acetic acid. The acetylated xylans are soluble in water and in solvents such as dimethylsulfoxide (DMSO), formamide, and *N,N*-dimethylformamide. Although only a part of the xylan can be extracted, the advantage is that no chemical changes take place. Aqueous solutions of potassium and sodium hydroxide are mostly used as the alkaline solvent of choice for the extraction of hemicelluloses. The preferred hydroxide is potassium, mainly because the subsequent potassium acetate formed during the neutralization is more soluble in the alcohol used for precipitation than is sodium acetate. Comparison of the extraction ability of 1 M solutions of potassium, sodium, and lithium hydroxide on wheat straw, shows an approximately equal effect in the rate and yield of solubilization of hemicellulose. However, it has been found that sodium hydroxide and lithium hydroxide are more powerful than potassium hydroxide in removing hemicelluloses, especially mannans from wood samples. The yield of hemicelluloses obtained using calcium hydroxide and liquid ammonia was markedly lower than for the respective alkali metal hydroxide solutions. Liquid ammonia, in general, can be used for pre-swelling prior to an alkaline extraction. Moreover, the yield of hemicelluloses strongly depends on a number of important factors, e.g. type of alkali, concentration, temperature and time of extraction. Addition of sodium borate to the alkali facilitates the dissolution of galactoglucomannans and glucomannans. However, any ester groups present are simultaneously saponified during the alkali extractions.

Hemicelluloses obtained by alkali can be subfractionated into hemicellulose A, B, and C. Hemicellulose A, the more linear and less acidic fraction, is isolated from the supernatant by acidifying to pH 5.0 with acetic acid followed by centrifugation. Hemicellulose B, the more acidic or branched fraction, is obtained from the mother liquor by precipitation with 4 volumes of 95% ethanol, then filtered and

washed with 70% ethanol. The resultant solid is redissolved in water (after the residual salts were dialysed against water until free from salts), and the hemicellulose B recovered by evaporation under reduced pressure at 45°C or by lyophilization. The fraction that remains soluble in aqueous ethanol is named 'hemicellulosic fraction C' and is isolated by dialysis with water and ethanol until free from salts (Figure 2). The yield and neutral sugar composition as well as content of uronic acids of hemicellulosic subfractions of DMSO-solubles, A, B, and C extracted sequentially by DMSO at 80°C for 2 h and 10% KOH–2% H₃BO₃ at 25°C for 16 h from wheat straw holocellulose, are given in Table 2.

Precipitation of the polysaccharide fractions by addition of miscible organic solvents to aqueous solutions is one of the main methods of recovery and purification. Ethanol is the solvent most commonly used, but methanol, acetone, and other organic solvents have also been applied for fractionation of hemicelluloses. In ethanol–water (80:20, v/v) the major portion of the polysaccharides are precipitated and only a small amount of short-chain material is left in solution. In addition to the neutral organic solvents, some more specific precipitation agents are also known, e.g. barium hydroxide for glucomannans and cetyltrimethylammonium bromide or hydroxide for glucuronoxylans. Fehling's solution or other copper salts can be used for precipitation of both glucomannans and glucuronoxylans. Hemicellulosic complexes precipitated by iodine in calcium chloride appear to be relatively unsubstituted by non-xylose residues, whereas the material remaining in solution is more highly substituted by such residues. The methods used to fractionate the hemicelluloses of straws and grasses are similar to those used to fractionate hemicelluloses from woods. The hemicelluloses may be fractionated as their acetates by precipitation from solution by ammonium sulfate, or by chromatography on DEAE-cellulose. The

Table 2 The yield and neutral sugar composition as well as content of uronic acids of hemicellulosic subfractions of DMSO-solubles, A, B, and C extracted sequentially by DMSO at 80°C for 2 h and 10% KOH–2% H₃BO₃ at 25°C for 16 h from wheat straw holocellulose

Hemicellulosic subfractions	Yield (%) [*]	Neutral sugar composition (%) ^{**}					Uronic acids (%) ^{**}	Acetyl content (%) ^{**}
		Ara	Xyl	Man	Gal	Glc		
DMSO-solubles	4.8	8.5	68.1	Trace	3.8	6.5	5.2	7.3
A	7.2	5.2	86.3	0.4	2.4	2.4	2.6	ND ^{***}
B	18.5	11.0	70.0	1.2	5.0	5.3	6.8	ND
C	2.7	12.2	80.3	0.5	3.5	2.0	0.6	ND

^{*}Percent dry matter (w/w).

^{**}Percent hemicellulosic subfractions (w/w).

^{***}ND = not detectable.

precipitated hemicellulose preparations can if desired be further purified by column chromatography.

Gel permeation chromatography is one of the most useful tools for determining the average molecular weights of the isolated hemicellulosic fractions. Ion exchangers based on cellulose, dextran or agarose such as diethylaminoethyl cellulose in different ionic forms can also be used to separate hemicelluloses from each other. Chromatography (in its various forms) is routinely used for the characterization of the acidic hydrolysis products of isolated hemicelluloses. Dialysis of aqueous solutions often removes inorganic salts and other low-molecular-weight impurities prior to chromatography. Alternatively, salt may be removed by electrodialysis, by treatment of solutions with ion-exchange resins, or by gel filtration, using Sephadex, a cross-linked dextran column.

More recently, it has been reported that alkaline peroxide is an effective agent for both delignification and solubilization of hemicelluloses from straws and grasses. This was first proposed in 1984 in studies on the alkaline peroxide delignification of agricultural residues to enhance enzymatic saccharification. Hydrogen peroxide is widely used in the pulp and paper industry to bleach lignin-rich pulps. It has been generally accepted that the bleaching action of hydrogen peroxide is attributable to the hydroperoxide ion (HOO^-), formed in alkaline media, which is the principal active species in hydrogen peroxide bleaching systems. This anion is a strong nucleophile that preferentially attacks ethylenic and carbonyl groups present in lignin. On the other hand, hydrogen peroxide is unstable in alkaline conditions and readily decomposes, particularly in the presence of certain transition metals such as manganese, iron, and copper. This metal-catalysed decomposition of hydrogen peroxide is undesirable in the bleaching operation. However, this decomposition generates more active radicals, such as hydroxyl radicals (HO^\bullet) and

superoxide anion radicals ($\text{O}_2^{\bullet-}$), participating in degradation reaction of lignin and solubilization of hemicelluloses, which therefore, results in significant solubility of the lignin and hemicelluloses. The advantages of hemicellulose extraction with alkaline peroxides are low investment cost, accompanying strong bleaching effect, lower biological and chemical oxygen demand (BOD and COD) effluents as well as the recovery of the solubilized macromolecular hemicelluloses with a minimal degradation. Results show that more than 80% of the original hemicelluloses and over 90% of the original lignin is solubilized during the treatment of cereal straws such as wheat, barley, rice, oat, and rye straw, and maize stems with 2% H_2O_2 at 48°C for 16 h at pH 12.0–12.5 (Table 3). These hemicellulose preparations are white in colour and contain very small amounts of associated lignin (3–5%).

To gain maximum dissolution of the hemicelluloses, it is not necessary to continuously regulate the reaction pH, even though over the course of the treatment (48°C, 16 h) the reaction pH rises from 12.0 to 12.5 and from 12.9 to 13.1, respectively. As the reaction pH becomes more alkaline, increasing amounts of hemicelluloses are solubilized, and the yield of the residue decreases. Incremental increase of the initial reaction pH from 11.5 to 12.5 results in an increase of hemicellulose dissolution of about 20%. During the initial stages of stirring, oxygen evolution is active, and substantial frothing occurs, requiring extractions to be conducted in vessels with volumes two to three times those of the extraction mixtures. After treatment, the cellulose-rich insoluble residue is collected by filtration, washed with distilled water until the pH of the filtrate is neutral, and then dried at 60°C. The supernatant fluid is adjusted to pH 5.5 with 10% HCl and then concentrated. The solubilized hemicelluloses are precipitated by pouring the concentrated supernatant into 4 volumes of

Table 3 The yield, neutral sugar composition, and content of uronic acid and lignin of hemicelluloses obtained by treatment of wheat, rice, rye, barley, and oat straw, and maize stems respectively with 2% H_2O_2 at 48°C for 16 h at pH 12.2

Cereal straw/stems	Yield (%) [*]	Neutral sugar composition (%) ^{**}							Uronic acids (%) ^{**}	Lignin content (%) ^{**}
		Rha	Fuc	Ara	Xyl	Man	Glc	Gal		
Wheat	29.6	0.8	ND ^{***}	13.8	60.5	0.4	9.8	4.5	4.9	5.1
Rice	22.3	0.6	0.3	14.9	56.3	ND	22.3	4.8	4.3	4.7
Rye	26.6	0.5	ND	11.2	65.3	0.3	6.1	3.3	8.1	4.8
Oat	25.6	0.4	ND	10.8	68.3	0.3	6.4	3.6	5.5	4.3
Barley	23.3	0.4	ND	10.6	66.1	0.5	7.6	3.7	5.8	4.5
Maize	22.7	0.5	0.3	15.2	62.7	0.8	6.3	4.7	5.3	3.7

^{*}Percent dry matter (w/w).

^{**}Percent hemicelluloses (w/w).

^{***}ND = not detectable.

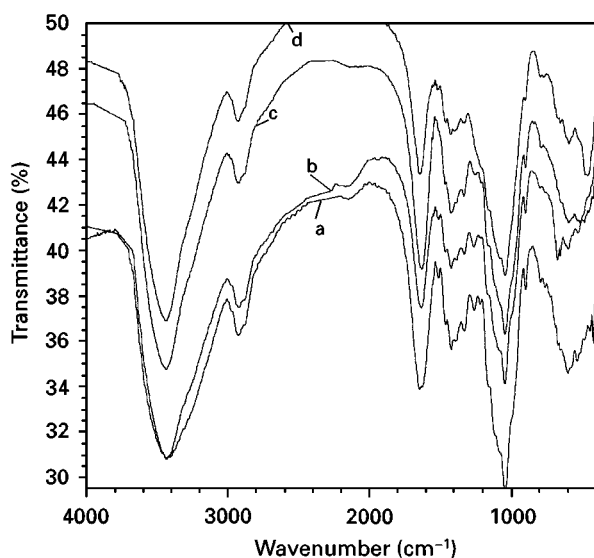


Figure 3 FT-IR spectra of 2% aqueous hydrogen peroxide-soluble hemicellulosic preparations extracted with 2% H_2O_2 at 50°C for 12 h at pH 11.5 from wheat straw (spectrum a), rye straw (spectrum b), maize stem (spectrum c), and rice straw (spectrum d).

ethanol, from which they settle out as a white flocculent precipitate which is freeze-dried. The Fourier transform infrared (FT-IR) spectra of 2% aqueous hydrogen peroxide-soluble hemicellulosic preparations extracted with 2% H_2O_2 at 50°C for 12 h at pH 11.5 are shown in **Figure 3**: wheat straw (spectrum a), rye straw (spectrum b), maize stem (spectrum c), and rice straw (spectrum d). **Figure 4** illustrates the ^{13}C -NMR spectrum of the hemicelluloses extracted with 2% H_2O_2 at 45°C for 12 h at pH 12.0 from maize stems. Obviously, both FT-IR spectra and ^{13}C -NMR spectrum of the hemicelluloses appear to be those of the typical hemicelluloses such as xylan from cereal straws and grasses. These observations reveal

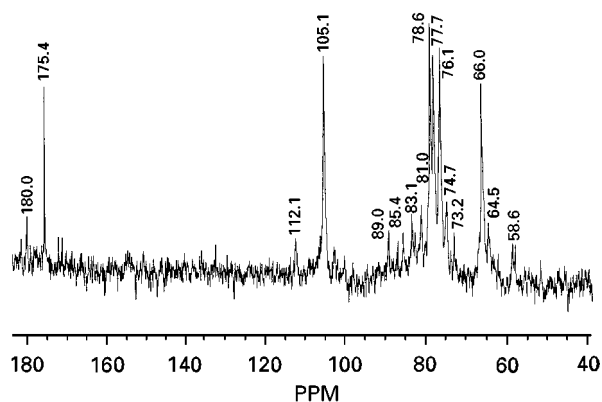


Figure 4 ^{13}C -NMR spectrum of the hemicelluloses extracted with 2% H_2O_2 at 45°C for 12 h at pH 12.0 from maize stems.

that the alkaline peroxide treatments under the conditions given do not affect the overall structure of the macromolecular hemicelluloses. This effective and convenient method of alkaline peroxide treatment may be used for most isolation of hemicelluloses from straws and grasses.

Steam treatment enables the lignocellulosic materials present in straws and grasses to be separated into hemicelluloses, lignin, and cellulose in reasonable yields and purity. Steam-explosion treatments or other steam treatments have the advantage of using a widely-available solvent without significant cost or environmental impact. It is generally agreed that the steaming process is basically an acid-catalysed autohydrolysis due to the small amounts of acetic acid liberated early in the process through cleavage of the hemicellulosic acetyl groups. A portion of the starting material, mainly hemicellulose, is converted into water-soluble products through this acid-catalysed hydrolysis process. The cellulose is not significantly solubilized but undergoes a change in its crystallinity or is partially depolymerized. During this process, the lignocellulosic substrate is steam treated at temperatures ranging from 140 to 240°C for 1–10 min followed by a rapid pressure release (i.e. explosion) through a discharge valve. The hemicelluloses solubilized during the steam or steam-explosion process, are isolated after extraction in water. They comprise mainly acetyl- and 4-O-methylglucuronosyl-substituted xylans, and contain 15–25% and 5–10% bound lignin, respectively. The associated lignins can be removed by treatment of the crude hemicelluloses with 1 M NaOH at 20°C for 2–4 h. All the hemicellulosic preparations have a lower degree of polymerization (40–65), with \bar{M}_w ranging between 5000 and 10 000 g mol^{-1} .

Cellulose

Cellulose is the main constituent of agricultural residues. Approximately 35–45% of the dry substance in most straw and grass species is cellulose, located predominantly in the secondary cell wall. The term ‘ α -cellulose’ is given to the residue remaining after delignification by sodium chlorite in acidic solution and separation of hemicelluloses by extraction of the holocellulose with 24% KOH (or 17.5% NaOH) at 25°C for 2 h or 10% KOH (or 7.5% NaOH) at 25°C for 16 h. This term was originally coined for wood cellulose which is insoluble in strong sodium hydroxide solution. The portion which is soluble in the alkaline medium but precipitated from the neutralized solution was called ‘ β -cellulose’. ‘ γ -Cellulose’ is the name for the portion which remains soluble even in the neutralized solution. This method was

modified in various ways and is now established as the standard method for the determination of α -, β -, and γ -cellulose from straws and grasses. The cellulose-rich residues remaining after alkaline peroxide treatment under the conditions given earlier contain 80–90% cellulose and 10–20% hemicelluloses as well as approximately 5% bound lignin. During steam treatment, cellulose undergoes a change in its crystallinity and can also partially depolymerize, depending on the treatment conditions. The cellulose-rich fibres generated by the steam treatment/explosion process are generally more accessible to chemicals and enzymes under derivatization conditions.

Further Developments

The current views on the fractional isolation of polysaccharides from cereal straws and grasses are based on the culmination of information gained over the past thirty years. In spite of the many studies on the polysaccharides of straws and grasses, little is known about (a) isolation of pectic polysaccharides, (b) isolation of the polysaccharide fraction present in delignification liquors, and (c) isolation of non-glucosyl residues and residual lignins in α -cellulose. Procedures designed to extract pectic substances may extract material that might otherwise be described as partly hemicellulosic, and the converse may also happen. Many procedures used in the isolation of polysaccharides from straws and grasses would lead to the loss of any such polysaccharides present. During delignification of wheat straw with sodium chlorite in acidified solution, 1.2–2.4% of the total hemicelluloses passes into solution. It is also more difficult to isolate pure cellulose without degradation since the hemicelluloses and lignin are strongly associated with cellulose; many of the solubilized hemicelluloses are irreversibly absorbed on the cellulose. In addition, drying straw and grasses in an oven at 60°C may cause autohydrolysis or other changes in polysaccharide morphology. Furthermore, the various procedures used prior to the exhaustive extraction of hemicelluloses may affect quantitative or structural conclusions about the hemicelluloses as they

occur in nature. It is also of interest to note that the hemicellulosic materials extracted by alkali are, only in part, precipitated in ethanol after neutralization of the extract. Under these conditions, a small part of the hemicellulosic materials remains in solution, and is commonly not recovered. All of these points require further investigation to obtain a more reliable standard method for fractional isolation of polysaccharides from cereal straws and grasses.

Further Reading

- Aspinall GO (1970) *Polysaccharides*. Oxford: Pergamon Press.
- Browning BL (1967) *Methods of Wood Chemistry*, Volume II. New York: John Wiley.
- Coughlan MP and Hazlewood GP (1993) *Hemicellulose and Hemicellulases*. London: Portland Press.
- Fengel D and Wegener G (1989) *Wood Chemistry, Ultrastructure, Reactions*. Berlin: Walter de Gruyter.
- Gould JM (1984) Alkaline peroxide delignification of agricultural residues to enhance enzymatic saccharification. *Biotechnology and Bioengineer* 26: 46–52.
- Lawther JM, Sun RC and Banks WB (1995) Extraction, fractionation, and characterization of structural polysaccharides from wheat straw. *Journal of Agricultural and Food Chemistry* 43: 667–675.
- Montane D, Farriol X, Salvado J, Jollez P and Chornet E (1998) Application of stem explosion to the fractionation and rapid vapour-phase alkaline pulping of wheat straw. *Biomass and Bioenergy* 14: 261–276.
- Sjöström E (1981) *Wood Chemistry – Fundamentals and Applications*. New York: Academic Press.
- Steinforth AR (1979) *Cereal Straw*. Oxford: Clarendon Press.
- Sun RC, Fang JM, Mott L and Bolton J (1999) Fractional isolation and characterization of polysaccharides from oil palm trunk and empty fruit bunch fibres. *Holzfor-schung* 53: 253–260.
- Theander O and Åman P (1978) Chemical composition of some Swedish cereal straws. *Swedish Journal of Agricultural Research* 8: 189–194.
- Water RH (1991) *The Chemistry and Technology of Pectin*. San Diego: Academic Press.
- Wilkie KCB (1979) The hemicelluloses of grasses and cereals. *Advances in Carbohydrate Chemistry and Biochemistry* 50: 215–264.

ESSENTIAL GUIDES TO METHOD DEVELOPMENT IN AFFINITY CHROMATOGRAPHY

B. J. Sines and W. H. Velander, Virginia Polytechnic Institute and State University, VA, USA

Copyright © 2000 Academic Press

Introduction

Highly selective affinity-based separations have evolved considerably over the past two decades to improve characteristics related to target specificity, dynamic adsorptive capacity and chemical robustness of the affinity matrix. These separation matrices are used as screening devices for molecular interactions as well as for the purification of complex mixtures at the analytical, preparative and large scale. Affinity adsorptive phases can be synthesized by the attachment of structures called ligands to immiscible polymeric fluids, solvated gels and porous solids. Ligands are selected for their affinity to a soluble or colloidal target species. Advances in technology have been associated with the synthetic and biosynthetic design of affinity ligands and matrices. These advances have been made through a better understanding of phenomena associated with the transport of the target species to the ligand and the nature of molecular interactions between target and ligand. Specialized processing equipment for large and small scale applications has also improved affinity separations.

Matrix Materials and Processing Geometries

Separations achieved by the selective capture of a target from a fluid phase by an affinity ligand confined to an adsorptive phase are most often done in aqueous systems. Therefore, the adsorptive phase for a hydrophilic target species is often a hydrophilic material. More hydrophobic targets require matrices which offer a more hydrophobic environment. In some cases, the adsorptive phase can be a separate fluid phase or soluble component having affinity ligands which will capture and concentrate the target species from complex aqueous mixtures.

Mattiasson demonstrated that heterobifunctional ligands could be used for selective isolation of proteins by affinity precipitation. Heterobifunctional ligands can bind the target and are also covalently coupled to a polymer which can be used to induce precipitation of a target/ligand complex. Alternatively,

multiple but identical binding sites can be occupied on the target by homobifunctional ligands. This results in a cross-linked network between targets which can be precipitated. Polymers used for affinity precipitation applications include chitosan, alginate, polyethyleneimine, and Eudragit S-100 (a copolymer of methyl methacrylate and methacrylic acid). By manipulating such parameters as the pH or temperature, the polymer/ligand/target complex can be reversibly rendered soluble and insoluble. Lactate dehydrogenase and alcohol dehydrogenase have been precipitated using Cibracron Blue 3GA coupled with EudragitTM S-100.

A significant advance in the field of bioseparations is the coupling of affinity ligands to aqueous two-phase systems of water-soluble polymers. Affinity partitioning is the selective extraction of target proteins from crude mixtures using affinity ligands immobilized on to either of two incompatible, water-soluble polymer phases. Mattiasson used triazine dyes coupled to immiscible polymer fluids to purify proteins by affinity partitioning. Reactive triazine dyes have been widely exploited using this separation technique. In comparison to classical chromatographic systems, affinity equilibrium is attained more rapidly in aqueous two-phase partitioning. In addition, high affinity binding capacities and protein recoveries have been achieved. Alternatively to two-phase aqueous polymer partitioning, McCreath and Chase immobilized human immunoglobulin G on to perfluorocarbon emulsions for the selective adsorption of *Staphylococcus aureus* cells containing membrane-bound protein A. These liquid emulsion droplets were comprised of a perfluorocarbon oil cross-linked with poly(vinyl alcohol).

Most of the applications for affinity-based separations are developed for chromatographic processing of aqueous systems. Thus, the ligand is immobilized on a porous bed of solids packed in a column through which liquid can be pumped. Most of the matrices are made of hydrogels composed of cellulose, agarose and dextran. A chief advantage of hydrogel matrices is the combination of an easily derivatized, hydrophilic environment that provides molecular accessibility that can be extended to 10⁶ Da. Other semi-synthetic and synthetic polymeric matrices, such as copolymers of vinyl dimethyl azlactone and methylene-bis-acrylamide, can also provide similar

intraparticle transport features. Coleman immobilized protein A at high density on to azlactone-functionalized polymeric matrices. These affinity matrices demonstrated high throughput capacity combined with low operating pressures. As an alternative to the use of pellicular matrices or matrices comprised of reduced bead particle diameter, Rodriguez and Liapis described the mechanism of perfusion chromatography in which intraparticle mass transfer resistance is reduced by increasing the particle permeability. Velander optimized the molecular accessibility and mechanical stability of uncross-linked cellulose adsorbents by using large diameter beads (>0.3 mm) which operate at low pressures even at high flow rates. These hydrogel matrices had a solids content of only 3% or less and were shown to provide fast intraparticle transport, apparently through a mixed mode of both diffusion and convection. Larsson demonstrated the use of superporous agarose matrices. The agarose beads contained a typical internal porous network in addition to larger pores. These larger pores constituted a significant portion of the bead, up to one-third to one-tenth of the bead particle diameter. Mass transfer characteristics were improved since the larger pores allowed a considerable fraction of the bulk chromatographic flow to penetrate and flow through the individual bead particles. Affinity matrices were prepared using these superporous agarose beads containing immobilized NAD^+ analogue for the isolation of bovine lactate dehydrogenase and protein A for the isolation of rabbit immunoglobulin G. These affinity matrices operated under much higher processing flow rates compared to conventional homogeneous bead columns. The protein A and NAD^+ analogue matrices had processing throughputs five and three times higher, respectively, in comparison to processing throughputs demonstrated by conventional affinity matrices. Thus, a significant improvement to affinity technology is the design of matrices having greater intraparticle accessibility and transport of the target species.

Advances in transport phenomena needed for target contacting with the affinity adsorbent have resulted in matrix designs having large or small particulate as well as membrane geometries. Smaller particles, having mean diameters of about 0.1 mm or less, yield a greater surface area to volume for improved target mixture contacting, but higher drops when operated in a packed bed mode. Thus, specialized affinity separations using high pressure liquid chromatography have been developed for small and large scale. However, these media require pre-clarification of the feed stream before chromatographic processing to prevent column fouling. Alternatively, small diameter particles having a higher density than water can be

fluidized to achieve both filtration and affinity adsorption in a single step using expanded bed chromatography. Expanded bed adsorption chromatography has been developed to provide single stage operation for the isolation of target proteins from crude mixtures such as milk, hybridoma cell culture fluid and fermentation broth. For example, humanized IgG4 antibody was isolated from myeloma cell culture fluid by expanded bed adsorption using recombinant protein A immobilized on to Pharmacia StreamlineTM media.

Planar membranes are often used for affinity separations in analytical assays but some cross-flow, stacked sheet geometries have been developed for large scale applications. Affinity membranes for large scale work can also be cast in tubular hollow fibres. One example of planar membranes was made of a gel formed from two dispersed liquid phases. The chief advantages of affinity membrane systems are the low pressure operation and fast intraparticle transport due to the short diffusion distances in thin membranes. Thus, the kinetics of ligand/target interactions can become rate limiting to affinity separations using thin membranes. Etzel showed that limitations in membrane performance can arise due to variations in porosity and thickness which can result in diffuse breakthrough loading profiles. The stacking of planar membranes can sharpen affinity breakthrough profiles at higher loading flow rates.

Affinity Ligand Selection and Design

Affinity ligands have evolved from antibodies, enzymatic substrates, co-factors, nucleic acids, coenzymes, hormones, immunoglobulin, lectins, effectors and inhibitors to a great diversity of small, low molecular weight peptides, polypeptides and other organic structures. These newer classes of ligands can be made using biosynthetic and wholly synthetic methods. Common to all selection strategies is the need to begin with a diversity of structures from which to discover candidate affinity ligands. The chance discovery of a ligand with desirable properties has been enhanced through the use of phage display and synthetic combinatorial libraries which contain many orders of randomized structural permutations. The structural permutations within a library rely on the polymeric assembly of bi- or multifunctional monomeric molecules into compounds which are typically greater than 10^3 Da in molecular mass. In the case of biosynthetic libraries, the assembled structures are necessarily polypeptides and the subunits are amino acids. In the case of wholly synthetic structures, a variety of bi- and multifunctional organic

subunits that provide high selectivity and yield reactions have been sequentially assembled using soluble or solid-phase linked chemistries. For example, various perturbations of bifunctional molecules having reactive oxazoline chemistry have been used to create assembled combinatorial chemical libraries having 10^3 or more structures. In addition, some wholly synthetic libraries have used amino acids and novel branched chain peptide linkages as core structural platforms.

In 1985, Smith demonstrated the use of phage technology to display candidate polypeptide ligands from a bacterial virus particle which also contains the DNA encoding the polypeptide sequence. The polypeptide is displayed from the virus particle surface in a manner that also enables affinity interactions with a targeted species. Thus, candidate ligands can be screened by the specific adsorption of phage to target species which have been immobilized either to a microtitre assay plate or to a chromatographic matrix. Nonspecifically adsorbed material is then washed away and the specifically adsorbed phage particles are eluted. The eluted phage particles are cultured using microbiological plate-streaking techniques. Candidate phages from the first affinity screening are passed through a second affinity screening and reculturing. Phages obtained from the two affinity and culture selection processes are subjected to DNA sequencing. The DNA sequence of the displayed polypeptide is readily determined because of specific endonuclease restriction sites engineered into the phage genome. The polypeptide ligand DNA sequence then is readily used to create ligands in mass quantity through recombinant fermentation technology. About 10^8 polypeptides can be created within a single phage display library where about 10^1 to 10^2 candidate ligands typically result after a sequence of two affinity and culture screenings. Thus, the chief advantage of the biosynthetic phage display libraries is the large number of library members and facile screening due to the coupled nature of the encoding DNA and displayed polypeptide ligand of the phage particle. The chief disadvantage is the inherent limitation to structures which are polypeptides. However, as a further improvement of phage library technology, Ladner demonstrated that the use of random permutations about a core polypeptide ligand sequence can greatly enhance the affinity of initial ligand candidates. The chemical robustness of polypeptides is typically limited to moderate pH and aqueous environments.

Examples of the use of phage-display libraries in the development of affinity ligands are found throughout the recent literature. Ladner generated a series of libraries comprised of variants of the first

Kunitz domain of human lipoprotein-associated coagulation inhibitor (tissue-factor pathway inhibitor-I). A typical human Kunitz domain was chosen as the parental protein since immunogenicity would be minimal due to its human origin and lack of glycosylation which would facilitate the use of phage-display technology. The library was screened against human plasmin, which is a serine protease that participates in the fibrinolytic process. This study synthesized a protease inhibitor exhibiting a high affinity and specificity for plasmin. Small (~ 58 amino acid residues), stable Kunitz domains, which lack glycosylation, and containing nearly human sequences were selected and determined to have high affinity and specificity towards plasmin. The same phage-display library and screening methodology has been used to select high affinity and high specificity ligands for human plasma kallikrein and human thrombin. Markland demonstrated that certain constraints may be imposed upon primary and tertiary structures to increase specificity relative to more simple linear peptide ligands directed towards the same target. For example, a phage-display library was constructed that displayed an 18 amino acid residue peptide containing two fixed cysteine residues to allow disulfide bond formation. In addition, several variable residue positions between and adjacent to the two cysteine residues were included in the peptide sequence. This library was screened against streptavidin and an anti- β -endorphin monoclonal antibody. The screening yielded phage displaying disulfide-constrained microproteins. The selected phage clones required a disulfide bond for the high affinity binding to both target proteins. Other core peptide motifs have resulted in phage-display libraries displaying protease inhibitory domains derived from wild-type bovine pancreatic trypsin inhibitor. In one case, Ladner selected a ligand which was an inhibitor of human neutrophil elastase that had a 3.6 million-fold higher affinity than that for the parental protein and was reported to exceed the highest affinity cited for any human neutrophil elastase inhibitor by 50-fold.

Wholly synthetic combinatorial libraries typically use a robotic assembly of structures. The robotic equipment used to generate orders of structural permutations essentially consists of a miniaturized chemical factory. These multifunction automated work stations perform sequences of sample mixing, thermostatic reactions, volume reduction and purification of the reaction masses. The identity of individual reaction masses is catalogued. Identification of the newly created chemical structures is deduced from automated combinations of liquid chromatography and mass spectrometry. Libraries having 10^3 to 10^4 distinct members have been synthesized and

characterized in this way. The screening of wholly synthetic libraries is laborious due to the need to putatively identify ligand/target complexes and subsequently to test the ligand structure in an immobilized state. In summary, a chief disadvantage of these libraries is the many order fewer library members that can be generated using the current robotic methods. Another disadvantage is cumbersome information acquisition and management associated with both the characterization of the ligand structure and target affinity. Unlike phage display, the primary molecular structure is not encoded and coupled to the wholly synthetic ligand as enabled by DNA of the phage particle. However, the diversity of chemically robust structures that can be produced from wholly synthetic molecules is an important advantage. In addition, rational design models can greatly decrease the number of permutations necessary from the initial discovery of ligands having lower affinity to the design of high affinity ligand candidates based upon initially discovered, ligand structural motifs. If combined with rapid and sophisticated assay screening methods, combinatorial methodologies provide an efficient process for the development of novel drug leads and affinity ligands. Future improvements in the efficiency of screening combinatorial ligands will likely be made using automated chemical sensor technology.

Affinity peptide ligands can be made using solid-phase chemistry. Houghten showed that the solid-phase-linked chemistries have advantages of separation/wash cycling between reaction sequences as well as being able to provide information about the base structure of the candidate ligands. Independent studies by Pingali and Fassina have demonstrated the use of affinity peptide ligands generated from solid-phase peptide synthesis. Pingali produced an affinity peptide that bound human fibrinogen and a peptide of chromochrome c containing haem that captured human serum albumin (HSA). The anti-fibrinogen tetrapeptide was made using standard Fmoc (*N*-fluorenylmethoxycarbonyl) chemistry. The affinity matrix made from this peptide was highly specific as purified fibrinogen was obtained directly from crude human plasma. Frontal analysis determined that the dynamic binding capacity of the antifibrinogen column was 10.2 mg fibrinogen per millilitre of gel. Similarly, by frontal analysis, an HSA-affinity peptide column was found to have a dynamic binding capacity of 19 mg HSA per millilitre of gel. Fassina used a core motif consisting of a small branched-chain peptide to discover a protein A mimetic affinity ligand. This peptide recognized the Fc fragment of immunoglobulin G from rabbit, goat, sheep and mouse and provided a one-step isolation method for

highly purified immunoglobulin G directly from crude sera. Frontal analysis determined that the dynamic binding capacity was 2 mg rabbit immunoglobulin per millilitre of gel. The peptide also exhibited stability towards sanitization reagents such as 0.1 mol L⁻¹ sodium hydroxide and ethanol. Both of the above-mentioned studies show that peptide-based affinity columns derived from standard solid-phase peptide synthesis can provide a viable alternative to the use of immunoaffinity chromatography.

Molecular modelling is used to deduce likely interactions between the target and affinity ligand, and is frequently used as a basis for further rational design of both biosynthetic and wholly synthetic combinatorial libraries. Once certain nominal affinity motifs have been identified from initial ligand screening, rational design has been used to enhance affinity by creating permutations which build upon structural motifs having lower affinity for the target species. In addition, recent studies have been conducted which attempt to develop 'peptidomimetic' structural compounds, such as aminimides, which have core structures similar to that of peptides, but with improved characteristics. Aminimides are much more chemically stable, have enhanced solubility characteristics and are resistant to enzymatic degradation. Ringe formulated a method for structure-based design involving aminimides in which complete binding surfaces of the targets are mapped. Combinatorial chemistry is then used to identify and improve structural specifications in lead candidates targeted at the corresponding binding sites. Ringe developed a peptidomimetic aminide inhibitor or porcine pancreatic elastase based upon crystal structures of an aminimide analogue.

Affinity dyes are another class of wholly synthetic affinity ligands which are not derived from combinatorial libraries. Reactive synthetic textile dyes are resistant to chemical and biological degradation and can bind selectively and reversibly to a wide range of enzymes and proteins. These ligands evolved from ligands which were first classified as enzyme co-factor mimetics. Many of these co-factor mimetics were members of reactive dyes used for staining textiles and paper. Since the mid-1950s, these reactive textile dyes have been used in the affinity purification of proteins. The use of commercial textile dyes as ligands in the large scale processing of diagnostic, therapeutic and genetically engineered proteins is documented throughout the literature. Since that time, many variations of original dye ligand structures, such as reactive Cibacron Blue, have been synthesized. These new structure-function motifs are no longer considered a simple co-factor mimetic relationship as was recognized between nicotinamide

and Cibacron Blue. Cibacron Blue F3G-A, the most thoroughly studied dye ligand, binds with a variety of proteins such as adenine coenzyme-dependent oxidoreductases, phosphokinases, hydrolases, transferases, nucleases, polymerases, synthetases, lyases, decarboxylases, in addition to glycolytic enzymes and plasma proteins. Lowe has shown that the triazine dye structure binds to clefts of proteins which have no known co-factor binding domains, but have much more subtle, yet specific interactions with triazine dye derivatives. Molecular modelling has also improved the rational affinity design of triazine derivatives through the addition of various chemical moieties to the core triazine structure. Lowe demonstrated the use of computer-aided molecular modelling and design in the development of structurally modified biomimetic dyes based on Cibacron Blue F3G-A and Procion Blue MX-R. A dye ligand was engineered specifically for the capture of horse liver alcohol dehydrogenase.

There are several advantages to the purification of pharmaceutical products using synthetic affinity ligands. A major advantage is that they are not derived from biological sources. Therefore they impart less of a product contamination risk. Hence, regulatory issues concerning the presence of unknown contamination and infectious agents in the final product are circumvented. Other major advantages of these ligands include: lower manufacturing cost; they can be readily immobilized under a wide variety of coupling chemistries to an extensive range of commercially available supports; they can be modified to enhance specificity or stability; and they are more stable and less susceptible towards denaturation. In addition, ligands derived from combinatorial libraries may contain a diversity of novel molecular structures such as organically derived or non-natural amino acid residues such as L-amino acids (D-optical isomers). Well-characterized affinity ligands may ultimately dictate decreased final product costs associated with less expensive process costs (i.e. more robust affinity matrices and less expensive ligands) and higher throughput due to a decrease in number of required chromatographic steps (i.e. decreased buffer usage). Affinity separation of pathogens may be better, enabled by the increased accessibility of small ligands to subtle, yet conserved domains of viruses.

Installation of Affinity Ligands

The covalent installation of the affinity ligand into a chromatographic or membrane-based matrix can profoundly affect the ligand/target binding efficiency. Matrix coupling chemistries usually covalently attach ligands through highly reactive groups such as α -

amino groups. Common activation methods for polysaccharide matrices are cyanogen bromide, divinylsulfone, epoxy, organic sulfonyl chlorides, carbonyl diimidazole, and *N*-hydroxysuccinimide. Polyacrylamide matrices are commonly activated by using glutaraldehyde or hydrazine. Isothiocyanate and γ -glycidoxypropylsilane activation methods are commonly used for silica-based matrices.

Ligands which contain amino acids can be coupled through the ϵ -amino group of lysine, carboxyl groups of aspartate and glutamate, and the phenolic group of tyrosine. Chemistries which randomly couple these residues also result in random orientation and spacing of the immobilized ligand. Some of the most thorough studies of ligand coupling chemistries have been done with proteins, especially antibodies. For example, Velander demonstrated that antibodies used as affinity ligands exhibit best performance characteristics when the binding conformation of the antibody is protected during covalent coupling to the adsorbent phase. A conformationally related effect is the orientation of the immobilized ligand. The use of orientated immobilization methods for antibodies is also applicable to synthetic and biosynthetic affinity ligands that have asymmetric structure due to the presence of both target binding and nonbinding domains. The nonbinding domain is best used for covalent coupling. Coupling of ligands to the support matrix through reactive moieties present within the binding domain can be detrimental from both orientation and non-native conformational effects acting upon the ligand. However, masking or shielding of the binding domain prior to immobilization can be employed to circumvent these effects. Velander used synthetic antigens consisting of water-soluble adducts of poly(2-methyloxazoline) polymers and a synthetic peptide epitope for the masking of monoclonal antibody during immobilization. The mask was then removed from the immobilized antibody. A loss of as much as 50% of the theoretical binding capacity of an immobilized antibody was attributed to orientation effects based upon anti-Fc and anti-Fab probing of immunosorbents made using masked and unmasked antibodies.

Activated matrices which preferentially couple through specific functional groups on ligands can aid in the site-directed, orientated immobilization of affinity ligands. For example, Domen developed several activated matrices in which each couple antibodies through different functional groups. Iodoacetyl groups on SulfoLink™ gel are designed to couple through sulfhydryl groups found predominantly in the hinge region of antibodies. CarboLink™ activated gels couple through aldehyde groups. The aldehyde groups on antibodies can be formed by the

oxidation of carbohydrate found primarily in the Fc region of antibodies. The site-directed method of coupling for a bivalent antibody through the oxidized carbohydrate groups using hydrazide chemistry resulted in the theoretical maximum of two antigen molecules for every antibody immobilized. However, Velander and Orthner found some antibodies immobilized on to matrices using hydrazide chemistry, which couple through the carbohydrate groups, produced no significant differences in immunosorbent antigen binding efficiency in comparison to immunosorbents prepared using random coupling chemistries such as cyanogen bromide. These antibodies were found to have carbohydrate in the binding domain.

The covalent attachment of the ligand through spacer arms becomes necessary when the nonbinding domain of the ligand does not offer sufficient molecular spacing between the molecular structure of the adsorbent and the binding domain to enable unencumbered binding of the target. The use of spacer arms is well documented throughout the literature. For example, Cuatrecasas demonstrated that extension of the ligand from the matrix through a hydrocarbon spacer arm can considerably increase ligand/target binding efficiency. Cuatrecasas prepared specific staphylococcal nuclease affinity matrices by immobilizing the competitive inhibitor, pDTP-aminophenyl, using spacer arms of varying length on to agarose and polyacrylamide matrices. Affinity matrices prepared with the ligand attached directly to cyanogen-bromide-activated Sepharose™ yielded a binding capacity of 2 mg nuclease per millilitre of gel whereas affinity matrices, prepared using a ligand attached to the support through a 3,3'-diaminodipropylamine spacer arm, yielded a binding capacity of 10 mg nuclease per millilitre of gel. In addition to ligand proximity to the support surface, the proximal spatial positioning of adjacent ligands within the support influences binding efficiency as well.

A high local ligand density can also encumber target binding between proximally immobilized ligands. Velander also demonstrated that antibodies immobilized with a low, local density gave as much as 50% of theoretical capacity based on a 2:1 target/antibody, molar stoichiometry. Thus, the majority of activity loss associated with the installation of antibodies into matrices can be attributed to local density and orientation effects. As mentioned above, intramatrix transport phenomena can also affect affinity sorbent performance, particularly for large target molecules. Thus, ligands are best installed into domains with rapid target accessibility. However, orientation, spacer arm and local spatial ligand density

effects must be evaluated at any location within the adsorptive matrix as part of the affinity sorbent optimization process.

Future Developments

A diversity of new wholly synthetic affinity ligands will be synthesized by microfluidic devices which will essentially be 'micro-chemical factories on a chip'. Engineering affinity matrices for optimum performance will also include evaluating different immobilization environments to enhance ligand/target interactions. Since many different target binding environments may need to be screened for a given ligand, miniaturized matrices installed on sensors will likely replace the inefficient batch and chromatographic analysis of optimal immobilization environments. Older pharmaceutical processes, such as blood plasma fractionation, will eventually be supplanted by affinity separation processes.

See also: **II/Affinity Separation:** Affinity Membranes; Affinity Partitioning in Aqueous Two-Phase Systems; Covalent Chromatography; Dye Ligands; Hydrophobic Interaction Chromatography; Immobilised Boronates and Lectins; Immobilised Metal Ion Chromatography; Immunoaffinity Chromatography; Imprint Polymers; Rational Design, Synthesis and Evaluation: Affinity Ligands; Theory and Development of Affinity Chromatography; **Chromatography:** Protein Separation. **Appendix: 1/Essential Guides for Isolation/Purification of Enzymes and Proteins. Essential Guides for Isolation/Purification of Immunoglobulins.**

Further Reading

- Baumbach GA and Hammond DJ (1992) Protein purification using affinity ligands deduced from peptide libraries. *BioPharmacology* 5: 24-29.
- Cannon LE, Ladner RC and McCoy D (1996) Phage-display technology. *IVD Technology* 2 (6).
- Coleman PL, Walker MM, Milbrath DS, Stauffer DM, Rasmussen JK, Krepski LR and Heilmann SM (1990) Immobilization of protein A at high density on azlactone-functional polymeric beads and their use in affinity chromatography. *Journal of Chromatography* 512: 345-363.
- Domen PL, Nevens JR, Mallia AK, Hermanson GT and Klenk DC (1990) Site-directed immobilization of proteins. *Journal of Chromatography* 510: 293-302.
- Fassina G, Verdoliva A, Odierna MR, Ruvo M and Cassani G (1997) Protein A mimetic peptide ligand for affinity purification of antibodies. *Journal of Molecular Recognition* 9: 564-569.
- Garg N, Yu I and Mattiasson B (1996) Dye-affinity techniques for bioprocessing: recent developments. *Journal of Molecular Recognition* 9: 259-274.

- Gupta MN, Kaul D, Guoqiang D, Dissing U and Mattiasson B (1996) Affinity precipitation of proteins. *Journal of Molecular Recognition* 9: 356–359.
- Hogan Jr, JC (1996) Directed combinatorial chemistry. *Nature* 384: 17–19.
- Kaster JA, de Oliveira W, Glasser W and Velander WH (1993) Optimization of pressure-flow limits, strength, intraparticle transport and dynamic capacity by hydrogel solids content and bead size in cellulose immunosorbents. *Journal of Chromatography A* 648: 79–90.
- Lowe CR, Burton SJ, Burton NP, Alderton WK, Pitts JM and Thomas JA (1992) Designer dyes: 'biomimetic' ligands for the purification of pharmaceutical proteins by affinity chromatography. *Tibtech* 10: 442–448.
- McCreath GE and Chase HA (1996) Applications of perfluorocarbon affinity emulsions for the rapid isolation of *Staphylococcus aureus*. *Biotechnology Progress* 12: 77–83.
- Markland W, Ley AC and Ladner RC (1996) Iterative optimization of high-affinity protease inhibitors using phage-display. 2. Plasma kallikrein, and thrombin. *Biochemistry* 35: 8045–8057.
- Orthner CL, Highsmith FA, Tharakan J, Madurawe RD, Morcol T and Velander WH (1991) Comparison of the performance of immunosorbents prepared by site-directed or random coupling of monoclonal antibodies. *Journal of Chromatography* 558: 55–70.
- Pingali A, McGuinness B, Keshishian H, Fei-Wu J, Varady L and Regnier F (1996) Peptides as affinity surfaces for protein purification. *Journal of Molecular Recognition* 9: 426–432.
- Roberts BL, Markland W, Ley AC, Kent RB, White DW, Guterman SK and Ladner RC (1992) Directed evolution of a protein: Selection of potent neutrophil elastase inhibitors displayed on M13 fusion phage. *Proceedings of the National Academy of Sciences USA* 89: 2429–2433.
- Velander WH, Subramanian A, Madurawe RD and Orthner CL (1991) The use of Fab-masking antigens to enhance the activity of immobilized antibodies. *Biotechnology Bioengineering* 39: 1013–1023.

ESSENTIAL GUIDES TO METHOD DEVELOPMENT IN CAPILLARY ELECTROPHORESIS

S. K. Poole, Parke-Davis Pharmaceutical Research, Division of Warner-Lambert Company, Ann Arbor, MI, USA

C. F. Poole, Wayne State University, Detroit, MI, USA

Copyright © 2000 Academic Press

Introduction

Capillary electrophoresis encompasses a number of related separation approaches, some of which are adapted to the requirements of specific applications (Figure 1). They share in common the use of electrolyte solutions as mobile phase, the use of capillary tubes as the separation column, and the use of an electric field to induce sample and mobile phase transport. This allows a similar instrument platform to service all capillary electrophoretic separation techniques with only minor modifications for specific applications. Detection is usually by UV-visible absorption through the fused silica capillary wall, or occasionally by fluorescence, electrochemical or mass spectrometric detection. Contemporary instruments are also highly automated for ease of use and improved control of critical experimental variables.

Classification of capillary electrophoretic techniques according to their usual applications is given in Table 1. These techniques can be considered as

general, sample-type specific, in an early development phase, or of minor importance. Such a broad range of descriptive terms requires further elaboration to indicate how we propose to treat these techniques in this article. Capillary zone electrophoresis (CZE), or simply capillary electrophoresis, and micellar electrokinetic chromatography (MEKC) are widely used and complementary techniques for the separation of ionic and neutral molecules. They are the most important and general in terms of the number of applications and frequency of use. Capillary electrochromatography (CEC) is a relatively new and promising technique with a range of applications similar to liquid chromatography. Since electro-driven flow has been shown to provide both theoretical and practical advantages over pneumatic-driven flow, it has the potential to become a major separation technique. At present, too little is known about the technique to provide a definitive guide to method development, especially as in the future it is likely that new column materials will be developed specifically for capillary electrochromatography with properties different to those currently used. Capillary gel electrophoresis (CGE) is an important technique for the separation of biopolymers but is little used outside of laboratories that perform this type of analysis. Capillary isoelectric focusing (CIEF) is a specialized technique within the field of macromolecule zwitterion separations,

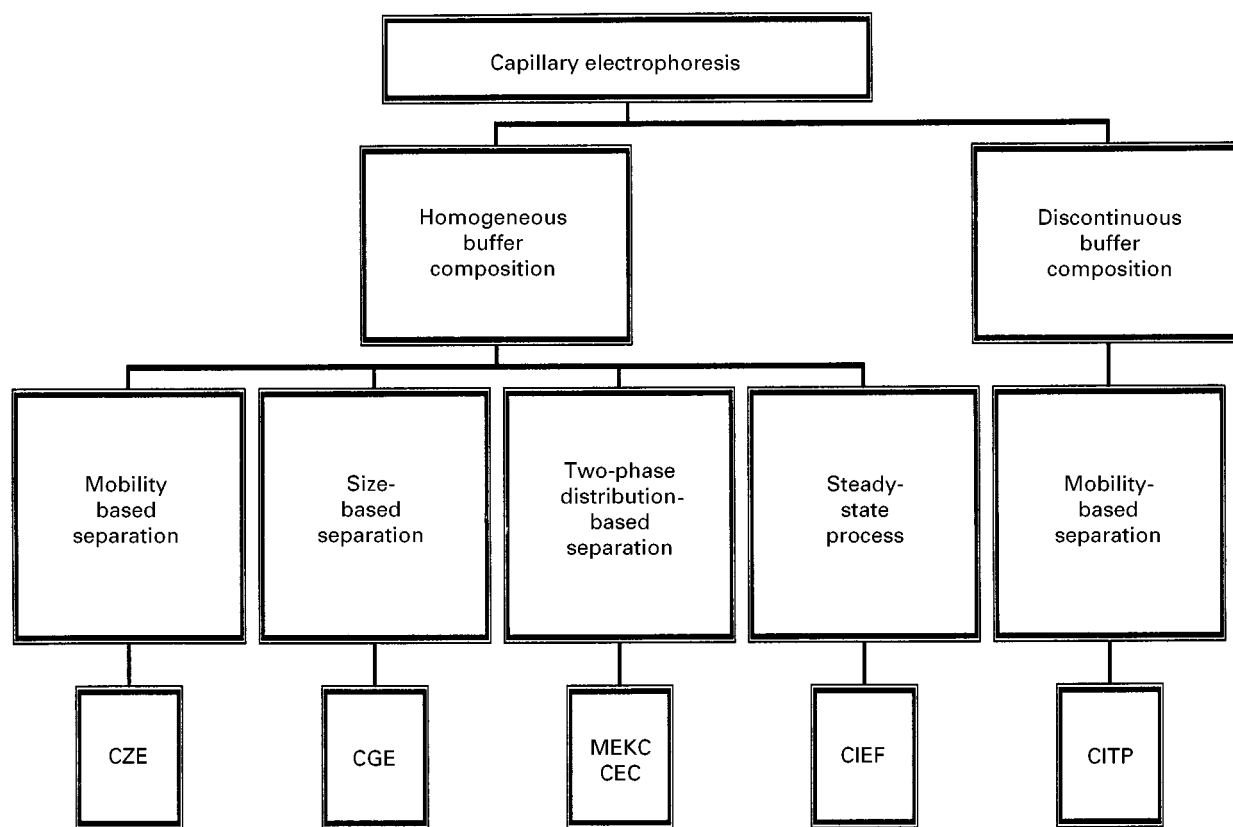


Figure 1 Classification of capillary electrophoretic separation methods based on buffer type and mechanism. CZE = capillary zone electrophoresis; CGE = capillary gel electrophoresis; MEKC = micellar electrokinetic chromatography; CEC = capillary electrochromatography; CIEF = capillary isoelectric focusing; and CITP = capillary isotachopheresis.

largely proteins, requiring special buffers to generate a continuous pH gradient. Capillary isotachopheresis (CITP) is not widely used for separations, it can be rather difficult and tedious to optimize, and yields an integral signal that is different to other separation techniques. Many samples that can be separated by capillary isotachopheresis can also be separated by other electrophoretic techniques more familiar to separation chemists. It is finding increasing use to preconcentrate ions for separation by capillary zone electrophoresis. With this framework in mind we propose to provide general guidelines for method development in capillary zone electrophoresis, micellar electrokinetic chromatography, and gel electrophoresis with only comments and brief instructions applicable to the other capillary electrophoretic techniques.

Sample Suitability

Table 1 provides a general guide to method selection by analogy to established applications. For biopolymers capillary electrophoretic techniques often select themselves, for other compounds the capillary

electrophoretic techniques have to be considered in terms of suitability drawn against other existing chromatographic methods. Reasonable solubility in aqueous solution is required for most separation modes. Non-aqueous capillary electrophoresis is little developed (although promising) and techniques such as micellar electrokinetic chromatography can separate hydrophobic compounds but provide little selectivity. Gas chromatography is usually a better choice for the separation of volatile hydrophobic compounds. High pressure liquid chromatography is often a better choice when low level detection, structural elucidation by mass spectrometry or preparative-scale separations are required. The concentration sensitivity of the capillary electrophoretic techniques using UV-visible absorption detection is limited by the small cross column pathlength and small injection volumes to solutions containing at least $1\text{--}10\ \mu\text{g mL}^{-1}$ and for ease of operation $0.1\ \text{mg mL}^{-1}$ or above is preferred. Various stacking and preconcentration techniques may improve detection limits but these require additional effort and time for optimization that may not be justifiable if another technique is suitable for the separation. Within these

Table 1 Common separation methods using capillary electrophoretic techniques

<i>Technique</i>	<i>Separation mechanism</i>	<i>Applications</i>
Zone electrophoresis	Differences in charge-to-size ratios	Inorganic and organic ions Ionizable compounds Zwitterions Biopolymers
Micellar electrokinetic chromatography	Distribution of neutral and partially ionized compounds between charged micelles and electrolyte solution	Water-soluble neutral compounds Weak acids and bases
Gel electrophoresis	Differences in size and charge (but not size-to-charge ratio) by migration through a gel matrix or entangled polymer network with a range of pore sizes	DNA fragments SDS proteins Macromolecules
Electrochromatography	Distribution between a solid stationary phase and mobile electrolyte solution	Neutral compounds Weak acids and bases Ions
Isoelectric focusing	Differences in isoelectric points in a continuous pH gradient	Proteins Zwitterionic compounds
Isotachopheresis	Differences in electrophoretic mobility of ions sandwiched between two buffers containing ions of greater (leading) and lower (trailing) mobility	Preconcentration of ions

restrictions it is obvious that many sample types and problems can be handled by capillary electrophoretic techniques accounting for its expanding use in analytical chemistry.

Selecting System Variables

Virtually all separations are carried out in fused silica capillary columns 50–100 μm internal diameter and up to 1-m long. Large-bore capillaries provide greater loading capacity and a higher detector response because of the longer pathlength (on-column detection) but generate larger currents and are less efficient at heat dissipation. Small-diameter columns show increased adsorption character due to their larger inner surface area-to-volume ratio but provide more efficient heat dissipation. If detection limits are not a problem, then a small inner diameter column should be used. The choice of capillary length is a compromise between speed (short columns) and separation capacity (long columns). Unless the separation is unusually complicated capillaries should be short (25–50 cm). When a new capillary is put into use or is suspected of being contaminated, a conditioning procedure is required. Washing with a solution of sodium hydroxide, water, and buffer as indicated in Table 2 is normally sufficient. Capillaries with an interior coating are used to alter electroosmotic flow or to minimize analyte ad-

sorption by the capillary wall, particularly for macromolecules. Electroosmotic flow is optimized to obtain useful separations in MEKC and CEC, is often used to improve separations and total sample detection for ions of opposite charge in CZE, but is usually undesirable in CGE, CIEF and CITP. So it is in the later techniques that capillaries with chemically bonded or physically adsorbed coatings are used.

Separations are usually performed with a voltage of 10–30 kV. High voltages provide faster separations with higher efficiency provided that the heat generated is effectively dissipated. A plot of current against applied voltage can be used to optimize operating conditions. The fastest and most efficient separations are obtained at the upper end of the linear portion of the plot. A positive deviation in the plot indicates that the heat removal capacity of the system is being exceeded. Capillary electrophoretic separations are usually performed at or close to room temperature (25°C). Temperature control, however, is important and separation capillaries are thermostated in an air or liquid bath. Thermostating is used to remove heat and to establish a constant temperature. Poor thermostating results in lower efficiency and poor reproducibility of migration times. Temperature is a useful operating variable, which can be used to modify migration times and selectivity, but is generally considered only suitable for fine tuning

Table 2 A guide for selecting initial conditions in capillary electrophoretic separations

Parameter	Setting
Column	Initial experiments use a fused silica capillary 30–50-cm long and 50- or 75- μ m internal diameter. Short columns are appropriate for trial experiments. The complexity of the sample dictates the length. For 2–10 analytes use 35–40 cm; 11–50 analytes 50–60 cm; 50–80 analytes 70–80 cm; and > 80 analytes 90–100 cm. Smaller diameter columns (25 or 50 μ m) provide higher efficiency but lower sample loading capacity.
Initial conditioning	Rinse with 0.1 M sodium hydroxide for 30 min. Flush with water for 15 min followed by the separation buffer for 15 min.
Voltage	Usual range is 10–30 kV. High voltages provide faster separations and greater separation efficiency. The method employed to dissipate heat, the column internal diameter, and buffer type and concentration all affect this decision. Use the highest voltage that does not exceed 100 μ A current as a rough guide. Otherwise plot current against voltage (2.5-kV increments) and operate at a voltage towards the upper portion of the linear plot.
Temperature	Initial experiments use 20–25°C. Selectivity and separation speed varies with temperature, which is optimized to fine-tune a separation (vary from 20 to 60°C in 5°C increments).
Injection	Hydrodynamic (e.g. 3 s at 0.5 p.s.i.) or electrokinetic (2–5 nL)
Detection	Absorption maximum of the analyte of interest, for which the weakest signal is expected because of low concentration or low absorbance. If analyte detection properties are unknown try 200–230 nm.

nearly acceptable separations. Subambient temperatures are not commonly used, as they are less convenient and result in poorer kinetic separation properties.

In general, the sample should be prepared such that the analytes of interest are present in a suitable solution, free from interferences, and at an appropriate concentration for detection. The ionic strength of the sample should be no greater than that of the buffer, with a more or less similar pH to the buffer, and free of matrix problems associated with column wall adsorbing materials and particle matter. For the best peak shapes and resolution the concentration of the injected sample should be about 100 times lower than the concentration of the buffer. Syringe filters for particle removal and ion exchange membrane filtration devices to reduce excessive concentrations of common matrix ions are available. Proteins and similar macromolecules, if not of interest to the analysis, should be precipitated prior to separation to minimize column fouling. Analytes of low water solubility may have to be dissolved in a water-miscible organic solvent or mixture of organic solvent and separation buffer. For other samples it is common practice to dissolve the sample in the run buffer, a diluted solution of the run buffer, or water. Samples are introduced into the separation capillary by hydrodynamic or electrokinetic injection. Both methods provide reproducible injection volumes but sampling bias is associated with electrokinetic injection, which injects increasing amounts of sample components in proportion to their mobility. Hydrodynamic injection is not suitable for CEC and CGE because of the high flow resistance of packed columns.

Capillary Zone Electrophoresis

Once the system variables are set within reasonable ranges the parameters that have most effect on migration times and selectivity are the composition, concentration and pH of the run buffer and the presence of additives, if used, to provide additional selectivity optimization. For a good separation by CZE four features are important: (i) the individual mobilities of the analytes must be different; (ii) the background electrolyte must be homogeneous and the field strength uniform along the column; (iii) neither analytes nor matrix components must interact with the column wall; and (iv) the conductivity of the buffer must substantially exceed the total conductivity of the sample components. Suitable common buffer recipes for a wide pH range are given in Table 3. Additional buffers with their pK_a and anion mobility values are given in Table 4.

Ionic strength and pH greatly affect selectivity and separation time and should be course tuned in initial screening experiments. Low pH is favourable for separating anions (all anions are less mobile) and a high pH is preferred for cation separations. The practical pH range is limited roughly to between 2 and 12. If the pK_a of the sample components is known or can be reasonably estimated, pH optimization should start with a $pH \approx pK_a$. Weak acids and bases change from the neutral form to the fully ionized form over about 4 pH units. In the neutral form their electrophoretic mobility is zero and they all migrate at a fixed velocity due to the electroosmotic flow in common with all neutral species. When totally ionized the ion moves with a constant electrophoretic velocity and may be separated from other

Table 3 Recipes for preparing some common electrophoretic buffers (100 mL of 60 mM buffer)

<i>pH</i>	<i>Buffer system</i>	<i>Acid</i>	<i>Base</i>
	Phosphate	85% Phosphoric acid	Potassium dihydrogenphosphate
2		395.3 mg	349.9 mg
2.5		205.3 mg	574.3 mg
3.0		81.4 mg	720.5 mg
	Acetate	1.0 M Acetic acid	Sodium acetate
3.5		5.67 mL	26.6 mg
4.0		5.08 mL	75.8 mg
4.5		3.81 mL	174.6 mg
5.0		2.13 mL	317.6 mg
5.5		0.89 mL	419.1 mg
	Phosphate	Sodium dihydrogenphosphate (1H ₂ O)	Disodium hydrogenphosphate (2H ₂ O)
6.0		779.2 mg	61.9 mg
6.5		692.8 mg	174.3 mg
7.0		512.2 mg	407.2 mg
7.5		280.7 mg	705.9 mg
8.0		115.5 mg	919.0 mg
	Borate	Boric acid	Disodium tetraborate (10H ₂ O)
8.0		320.9 mg	77.3 mg
8.5		232.7 mg	213.2 mg
9.0		59.3 mg	480.6 mg
	Borate	Disodium tetraborate (10H ₂ O)	0.1 M Sodium hydroxide
9.5		371.0 mg	41.77 mL
10.0		371.0 mg	52.72 mL

ions based on differences in their charge-to-size ratio. When partially ionized the ions migrate with an effective mobility that changes between the two extreme values in a sigmoid fashion as the pH is varied (Figure 2). Ions may be separated in their fully ionized form or partial ionized form as a matter of circumstance; that is, at those conditions that maximizes the difference in charge-to-size ratios. Because changes in mobility tend to be large for partially ionized solutes small pH changes (0.1–0.5 pH units, or smaller for complex mixtures) are used to optimize the separation.

If the pK_a values for a sample are unknown, conduct initial separations in a series of buffers at or near pH 2.5, 4.0, 5.5, 7.0, 8.5 and 10 (see Table 3 for appropriate buffers). To obtain reproducible results over the pH range 4 to 7, careful column conditioning is important. From the plot of the effective mobility against pH identify the most promising pH range for the separation. Optimization then proceeds in smaller changes in pH units as before.

To optimize the buffer concentration initial experiments are performed with a concentration of 30–100 mM for 50- μ m internal diameter columns and 20–50 mM with 75- μ m internal diameter columns. Lower ionic strength buffers are used to obtain faster separations, when selectivity is high, and to separate simple mixtures containing a few

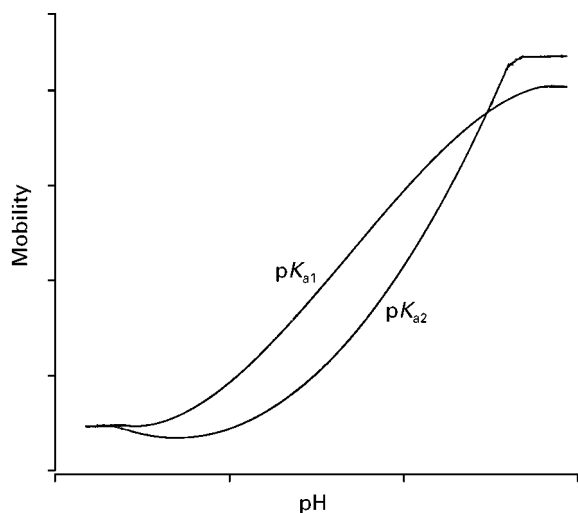
analytes. Higher ionic strength buffers are used for the separation of complex mixtures or to separate analytes with small differences in their electrophoretic mobility. If stacking is used to enhance analyte detectability then the difference in ionic strength between the buffer (high ionic strength) and the sample should be maximized. From Table 4 inorganic buffers are likely to provide better peak shapes for high mobility ions and Good-type (zwitterionic) buffers for low mobility ions. Zwitterionic buffers are useful for many applications where a high concentration and buffering capacity is desirable because of their low specific conductivity, which allows more favourable kinetic separation conditions to be employed.

For difficult separations the selectivity can be further modified by employing secondary chemical equilibria and solvation effects by adding appropriate reagents or solvents to the electrolyte system (Table 5). Increasing the ionic strength of the electrolyte by adding salts such as potassium sulfate modifies the charge and/or conformation of proteins and reduces wall interactions. Metal cations such as Cu^{2+} , Zn^{2+} , Ca^{2+} coordinate to proteins and peptides modifying the net charge. Also, alkanesulfonic acids bind selectively to proteins and peptides through hydrophobic interactions modifying the surface charge as well as reducing wall interactions. Slow

Table 4 Suitable buffers for capillary electrophoresis. Mobility values are at zero ionic strength and 25°C (in $10^{-9} \text{ m}^2 \text{ V}^{-1} \text{ s}^{-1}$)

Buffer	pK_a	Mobility
Phosphoric acid	2.12 (pK_1)	– 35.10
	7.21 (pK_2)	– 58.30
	12.32 (pK_3)	– 71.50
Malonic acid	2.90 (pK_1)	
	5.70 (pK_2)	
Citric acid	3.13 (pK_1)	– 28.70
	4.76 (pK_2)	– 54.30
	6.40 (pK_3)	– 70.80
Lactic acid	3.85	– 35.80
Hydroxyisobutyric acid	3.97	– 33.50
Glutamic acid	4.38	– 28.90
Acetic acid	4.76	– 42.40
MES [2-(<i>N</i> -morpholine)ethanesulfonic acid]	6.13	– 26.80
MOPS [3-(<i>N</i> -morpholine)propanesulfonic acid]	7.20	– 24.40
MOPSO [2-hydroxy-4-morpholinepropanesulfonic acid]	6.79	– 23.80
ACES [<i>N</i> -2-acetamido-2-aminoethanesulfonic acid]	6.84	– 31.30
Imidazole	7.17	52.00
BES [2-(bis(2-hydroxyethyl)amino)ethanesulfonic acid]	7.16	– 24.00
HEPES [<i>N</i> -2-hydroxyethylpiperazine- <i>N'</i> -2-ethanesulfonic acid]	7.51	– 21.80
TRICINE [<i>N</i> -{tris(hydroxymethyl)methyl}glycine]	8.15	
TRIS [tris(hydroxymethyl)aminoethane]	8.08	29.50
TAPS [3-{tris(hydroxymethyl)methyl}aminopropanesulfonic acid]	8.30	– 25.00
BICINE [<i>N,N</i> -bis(2-hydroxyethyl)glycine]	8.35	
Glycylglycine	8.40	
Ammonia	9.26	
Ethanolamine	9.50	44.3
CHES [2-(cyclohexylamino)ethanesulfonic acid]	9.50	
Triethylamine	9.87	
CAPS [3-(Cyclohexylamino)propanesulfonic acid]	10.40	
Diethylammonium	11.40	37.9

adsorption/desorption interactions with the column wall cause peak broadening and tailing and irreversible adsorption leads to modification of the capillary wall. These problems are caused by electrostatic or hydrophobic interactions between macromolecules

**Figure 2** Separation of two hypothetical weak acids as a function of pH by capillary zone electrophoresis.

(usually) and the column wall. Solutions to this problem include using extreme pH buffers, high ionic strength electrolytes, and by using dynamic or chemically bonded wall-coated capillaries. There are no universal solutions and effective methods have to be tailored to the properties of the analyte. Buffer additives are usually used at concentrations of 5–60 mM except for modification of the ionic strength of the electrolyte where much higher concentrations are often required (e.g. 50–250 mM). Urea, which forms hydrogen-bond complexes with proteins and peptides, but is nonionic, is often used at concentrations of 7 M. The separation of metal cations (alkaline earths, transition metals and lanthanides) is difficult because of their similar ionic conductance. In this case complexing agents, such as α -hydroxyisobutyric acid or citrate are required. Since many cations lack a chromophore complexation is an effective method of introducing a chromophore for convenient detection. There is now considerable literature on the separation of anions by capillary electrophoresis. For fast separations it is necessary to reverse the direction of the electro-osmotic flow by adding cationic surfactants below their critical micelle concentration to the buffer

Table 5 Secondary equilibria used to optimize selectivity in capillary electrophoresis

Additives	Function
<i>General considerations</i>	
Inorganic salts	Minimize wall interactions, induce protein conformation changes
Crown ethers	Modify mobility by selective formation of inclusion complexes
Organic solvents	Modify electroosmotic flow, increase solubility of organic ions, modify ion solvation, reduce wall interactions
Urea	Modifies the mobility of proteins by hydrogen-bond complexation
Metal ions	Modify mobility of anions and electroosmotic flow
Alkanesulfonic acids	Modify mobility by ion pair formation, wall adsorption leads to changes in surface properties
Cellulose polymers	Mask active sites on the capillary wall, modify electroosmotic flow
Cationic surfactants	Use to reverse the polarity of the fused silica capillary wall
Organic acids	Modify mobility by ion pair formation
<i>Ion complexation</i>	
Chelate formation (metals)	Polycarboxylic acids (lactate, tartrate, hydroxyisobutyric acid) Ethylene-1,2-diaminetetraacetic acid Dihydroxyazobenzene-5, 5'-disulfonate
Ion pairing	Ionic surfactants (<critical micelle concentration) Cetyltrimethylammonium bromide, tetradecyltrimethylammonium bromide Polyvalent metal cations (Ca^{2+} , Al^{3+} , etc.) CHES and other alkanesulfonic acids, perchlorate
Ion inclusion	Crown ethers (15-crown-6, 18-crown-6, etc.)
<i>Solvent effects</i>	
Organic solvents	Acetonitrile, methanol, 2-propanol, tetrahydrofuran, etc.
Electrolyte	Ionic strength, concentration of the probe (co-ion)

system. The electroosmotic flow and electrophoretic migration now occur in the same direction. For difficult to separate anions normal (counterflow) operation may be the better option at the expense of longer separation times. To reduce peak broadening the mobility of the sample anions should be matched to those of the background electrolyte. For UV-visible detection indirect detection is frequently employed. This requires the addition of a probe (co-ion) of high molar absorption, in low concentration, with the same charge as the analytes. Examples include chromate (most popular), benzoate, salicylate, phthalate, etc.

Micellar Electrokinetic Chromatography

The addition of an ionic surfactant above its critical micelle concentration to the buffer provides an additional separation mechanism based on distribution of the analytes between the micelles and electrolyte. The velocity with which the micelles migrate to the detector is usually different to the velocity of the bulk electrolyte allowing separations based purely on differences in the analyte distribution constants for neutral compounds. For ions differences in both distribution constants and electrophoretic mobility are important. An acceptable separation also requires

favourable kinetic properties (efficiency), provision of an adequate migration window (peak capacity) and a reasonable total separation time. Normally, the experimental conditions are set to establish an acceptable separation time and migration window under conditions where the efficiency is not compromised and the outcome of the experiment controlled by selectivity optimization. Selectivity is influenced largely by the identity of the surfactant and the addition of complexing agents and/or organic solvents to the buffer.

Some common surfactants and their relative solvation properties are summarized in Table 6. Method development usually begins with sodium dodecyl sulfate because of its favourable kinetic and chromatographic properties. (Table 7). Other surfactants are selected based on their complementary properties to sodium dodecyl sulfate using the system constants of the solvation parameter model as a guide (Table 6). For example, sodium cholate (representative of the bile salts) is a stronger hydrogen-bond base and weaker hydrogen-bond acid than sodium dodecyl sulfate. By similar reasoning a working list of surfactants for selectivity optimization would include sodium dodecyl sulfate, sodium cholate, lithium perfluorooctanesulfonate, sodium *N*-dodeconyl-*N*-methyltaurine and tetradecyltrimethylammonium bromide. Table 6 also provides a framework to identify new surfactants

Table 6 Characteristic properties of common surfactants for micellar electrokinetic chromatography

Surfactant	Critical micelle concentration (mM)	Aggregation number	Solvation parameter model system constants*				
			<i>m</i>	<i>r</i>	<i>s</i>	<i>a</i>	<i>b</i>
Sodium dodecyl sulfate	8.2	62	2.99	0.46	− 0.44	− 0.30	− 1.88
Tris(hydroxymethyl)aminoethane dodecyl sulfate			2.56	0.57	− 0.66	− 0.33	− 1.56
Sodium dodecyl sulfonate	9.8	54	2.51	0.51	− 0.70	− 0.14	− 1.51
Sodium cholate	13–15	2–4	2.45	0.63	− 0.47	0	− 2.29
Sodium taurocholate	2.8	4	2.43	0.60	− 0.34	0	− 2.06
Sodium deoxycholate	4–6	4	2.67	0.66	− 0.47	0	− 2.47
Sodium taurodeoxycholate	2–4	8	2.62	0.67	− 0.45	0	− 2.17
Sodium <i>N</i> -dodecanoyl- <i>N</i> -methyltaurine	8.7		3.07	0.72	− 0.50	0.22	− 2.58
Lithium perfluorooctanesulfonate			2.30	− 0.52	0.34	− 0.82	− 0.53
Tetradecyltrimethylammonium bromide	4.4	64	2.82	0.36	− 0.29	0.90	− 2.67
Hexadecyltrimethylammonium bromide	0.026	169	3.40	0.61	− 0.55	0.58	− 3.08
Microemulsion**			3.05	0.28	− 0.69	− 0.06	− 2.81

*The *m* system constant is a measure of the difference in cohesive energy and dispersion interactions for the micelles and electrolyte; the *r* system constant the difference in interactions with lone pair electrons; the *s* system constant the difference in interactions of a dipole type; the *a* and *b* system constants the difference in hydrogen-bond base and hydrogen-bond acid interactions, respectively. The sign of the constant indicates whether the interaction favours distribution to the micelles (positive) or electrolyte system (negative). **Microemulsion consisting of 1.4%wt. sodium dodecyl sulfate, 6.49% wt. butan-1-ol and 0.82%wt. heptane.

with complementary properties to those available at present and to avoid unnecessary experiments with surfactants with different structures but nearly identical selectivity properties.

When selectivity optimization using different surfactant types is exhausted further optimization is achieved by the use of additives (see Table 7). For this purpose the common approaches are the use of mixed

Table 7 Starting conditions for method development in micellar electrokinetic chromatography

Parameter	Setting
Sample	1–2 mg mL ^{−1} dissolved in methanol or water
Column	Fused silica capillary 30–50-cm long with an internal diameter of 50 μm
Initial conditioning	Flush with 0.1 M sodium hydroxide for 3 min and rinse with the run buffer for 5 min. These conditions will have to be varied depending on the previous use (if any) of the column. It is preferable to reserve individual capillaries for each surfactant.
Buffer	20 mM sodium phosphate–sodium tetraborate pH 8 buffer (or see Table 3 for suitable single buffers) containing 50 mM sodium dodecyl sulfate
Voltage	20–25 kV
Temperature	25°C
Injection	50 mbar 1–2 s (hydrodynamic)
Detection	210 nm (or absorption maximum for analyte with lowest absorbance)
<i>Course tuning selectivity</i>	
Surfactant	Choose surfactants of different selectivity (see Table 6) Sodium cholate (72 mM) Sodium <i>N</i> -dodecanoyl- <i>N</i> -methyltaurine (50 mM) Tetradecyltrimethylammonium bromide (50 mM) with reverse polarity Other suitable surfactants
pH	Optimize migration window and separation time (lower pH to extend and raise pH to lower) for neutral compounds. Weak acids and bases may show significant changes in electrophoretic behaviour
Additives	Mixed surfactants formed with neutral and ionic surfactants. For example, Brij 35 (polyoxyethylene[23] dodecyl ether) 1–25 mM Organic solvents methanol, 2-propanol, acetonitrile, tetrahydrofuran 1–25% (v/v) Higher molecular mass solvents of low water solubility 1–5% (v/v) Complexing additives such as α-, β-, γ-cyclodextrins, hydroxypropyl-β-cyclodextrin and heptakis-(2,3,6-tri-O-methyl)-β-cyclodextrin (5–20 mM)
<i>Fine tuning selectivity</i>	
Modify system properties such as column length, temperature, voltage, buffer type and ionic strength.	
Surfactant concentration changes the phase ratio but has little effect on selectivity	

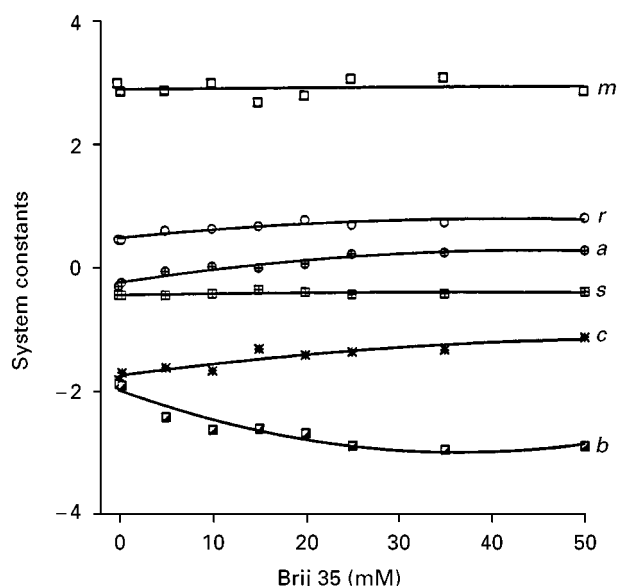


Figure 3 Change in the system constants obtained from the solvation parameter model as a function of the composition of the mixed micelles formed with the neutral surfactant Brij 35 (1–50 mM) and 50 mM sodium dodecyl sulfate. See Table 6. (Reproduced with permission from Poole SK and Poole CF (1997) Variation of selectivity with composition for a mixed-micellar buffer in micellar electrokinetic chromatography. *Journal of High Resolution Chromatography* 20: 174–178.)

surfactant micelles, organic solvents and inclusion complexing agents. A large number of mixed micelles can be employed without any certain prospects of

success. Neutral surfactants such as Brij 35 are often chosen first to adjust selectivity and/or the size of the migration window. **Figure 3** shows an example of the use of Brij 35 to change the selectivity of sodium dodecyl sulfate micelles. The solvation properties of the mixed micelles are not changed radically, even at high concentrations of the neutral surfactant, in agreement with predictions made by the interphase retention model. The main change is the gradual decrease in the hydrogen-bond acidity of the mixed micelles, which should provide a useful change of selectivity for the separation of hydrogen-bond bases. Selectivity modification by addition of organic solvent to the buffer is by no means as useful as in reversed-phase liquid chromatography. At low concentrations modifier effects are small and not strongly dependent on solvent identity, and at higher concentrations they lead to deleterious effects on system efficiency and the separation time. By contrast, the use of complexing additives, such as urea and cyclodextrins has to be considered one of the success stories of MEKC for achieving the separation of isomers, enantiomers, and other difficult to separate compounds capable of forming suitable inclusion complexes. **Figure 4** provides an example of the separation of pharmaceutically important estrogens that were only adequately separated in the system containing the complexing additive. The incorporation of low molecular mass organic solvents and cyclodextrins in the micelles is very low. Their main effect on the distribution properties of the system

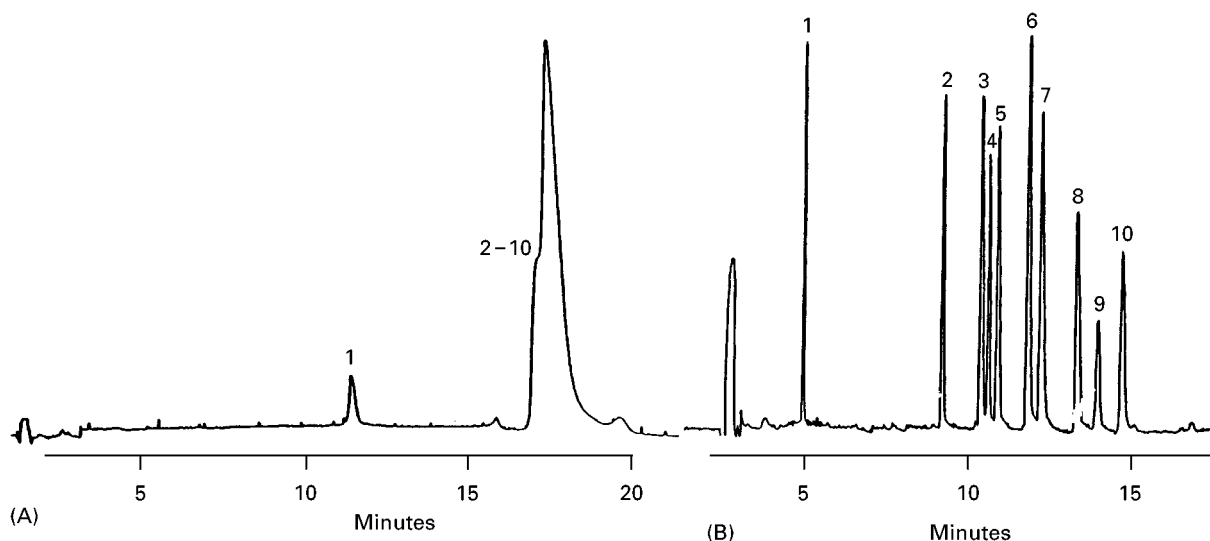


Figure 4 Separation of estrogens by MEKC using a 20 mM sodium phosphate-borate pH 8 buffer containing 50 mM sodium dodecyl sulfate (A) and the same buffer containing 20 mM γ -cyclodextrin (B). Separation conditions: capillary 48.5 cm (effective length 40 cm), internal diameter 50 μ m, temperature 25°C, and field strength 20 kV. Compounds: 1 = estriol; 2 = 17 β -estradiol; 3 = 17 α -estradiol; 4 = 17 β -dihydroequilenin; 5 = 17 β -dihydroequilenin; 6 = 17 α -dihydroequilenin; 7 = 17 α -dihydroequilin; 8 = estrone; 9 = equilenin; and 10 = equilin. (Modified from Poole SK and Poole CF (1996) Separation of pharmaceutically important estrogens by micellar electrokinetic chromatography. *Journal of Chromatography A* 749: 247–225, with permission from Elsevier Science.)

is due to changes in the relative solubility of the analytes in the electrolyte.

Capillary Gel Electrophoresis

Capillary gel electrophoresis is used for the separation of macromolecules such as proteins and nucleic acids, whose mass-to-charge ratios do not vary much with size. Separation requires a sieving medium made up of a crosslinked gel or an entangled polymer network. The capillaries are often wall-coated or chemically bonded to minimize electroosmotic flow that tends to destabilize the columns. Columns filled with rigid crosslinked gels, usually polyacrylamide, are characterized by the total amount of monomer and crosslinking agent (%T) and the ratio of crosslinking agent to total amount of monomer and crosslinking agent (%C) used to prepare the column. Larger pore size gels (lower %T) are used for separating DNA sequencing reaction products whereas the narrow-pore media are best for proteins and small oligonucleotides. Entangled polymer networks of linear polyacrylamide, methylcellulose or dextran have the advantage that they can be forced into the capillary as a solution and replaced when needed. Unlike gels, columns are easily prepared in the laboratory and tend to be more robust. Electrokinetic injection is used for sample introduction. The buffer pH is selected such that the analytes of interest are ionized. TRIS/borate and TRIS/phosphate buffers in the pH range 7.5 to 8.5 (50–200 mM) are fairly general conditions. Sometimes urea (7–8 M) or ethylene glycol (1.5–3.0 M) is added to the buffer as a nonionic denaturing or solubilizing agent and EDTA (about 2 mM) to protect against cation interferences. When SDS-proteins are separated sodium dodecyl sulfate (0.1% w/v) is added to the run buffer. For many practical applications of capillary gel electrophoresis the column materials and reagents required can be purchased in kit form.

Capillary Isoelectric Focusing and Isotachopheresis

Capillary isoelectric focusing is used to separate polypeptides based on differences in their isoelectric points (pI) in wall-coated fused silica capillaries to eliminate electroosmotic flow and nonspecific adsorption of the sample with the capillary wall. The capillary is filled with the sample and a mixture of ampholytes capable of producing a pH gradient that covers the pI values of the proteins. Ampholytes are a mixture of hundreds to thousands of amphoteric compounds, generated by the random addition of acrylic acid to a mixture of linear and branched

oligoamines, providing pI values are fairly well distributed along the pH scale from 3 to 10. In practice about 94% of proteins can be separated in the pH range 3–8.5. This allows a single capillary to be used for hundreds of separations by minimizing alteration to the capillary wall coating. When a voltage is applied (e.g. 15 kV for 4 min) the sample components focus into narrow zones according to their pI values. The zones are then mobilized by hydraulic, electroosmotic or ion addition (by adding 80 mM sodium chloride to either the source or destination vial and applying an electric field) to move them past the detector. The destination vial contains a buffer (catholyte) at a pH higher than the pI of the most basic ampholyte (40 mM sodium hydroxide) and the source vial contains a buffer (anolyte) at a pH lower than the pI of the most acidic ampholyte (20 mM phosphoric acid). To avoid protein precipitation in the focused zones a surfactant or urea can be added to the buffer, the sample diluted, or gel-filled capillaries can be used.

In capillary isotachopheresis sample ions are separated by differences in their mobility in a heterogeneous buffer system created by sandwiching the sample between a leading and terminating buffer with different and specified compositions. It is general practice to separate mixtures in the constant current mode using chemically bonded or dynamically coated capillaries to eliminate electroosmotic flow. As well as fused silica capillaries of standard dimensions wide-bore Teflon (0.5–0.8 mm) tubes have been used in purpose-built apparatus for isotachopheresis. Before commencing the separation both the capillary and destination buffer vial is filled with the leading electrolyte (assuming suppression of the electroosmotic flow). The leading electrolyte ion must have a higher mobility than any of the analytes to be separated and the counterion must be able to set the pH for the separation by ensuring sufficient (but generally not complete) dissociation of weak acids and bases in their own zones. Either sample cations or anions can be determined in the separation but not both simultaneously. The terminating electrolyte is placed in the source vial and should have a lower mobility than any of the analyte ions. Recommendations for buffer selection and operating conditions are summarized in Table 8. If solubility is a problem nonionic or zwitterionic surfactants or urea can be added to both the leading electrolyte and the sample. When fused silica capillaries are used hydroxypropylmethylcellulose, polyethylene glycol or polyvinyl alcohol can be added to the buffers to suppress electroosmotic flow through dynamic coating of the column wall. Detection of

Table 8 Composition of some common capillary isotachopheresis buffers*

Property	pH				
	2.0	3.3	4.5	6.0	8.8
Separation	Cations	Anions	Cations	Anions	Anions
Leading ion	10 mM HCl	10 mM HCl	10 mM KOAc	10 mM HCl	10 mM HCl
Leading counterion		β -Alanine	HOAc	Histidine	Ammediol
Leading additive		0.2% HPMC		0.2% HPMC	0.2% HPMC
Terminating ion	10 mM TRIS	10 mM caproic acid	10 mM HOAc	10 mM MES	10 mM β -Alanine
Terminating counterion	HCl			TRIS	Ba(OH) ₂
Terminating pH	8.5			6.0	9.0
Recommendations					
Leading ion	Cations			Anions	
(20–30 mM)	K ⁺ , NH ₄ ⁺ , Na ⁺			Cl ⁻	
Terminating ion	H ⁺ , or weak base (mobility > H ⁺)			OH ⁻ , or weak acid (mobility > OH ⁻)	
Terminating counterion	Weak acid, pK = pH _L ± 0.5			Weak base, pK = pH _L ± 0.5	
Typical counterions	pH _L				pH _L
Formate	3.2–4.2			β -Alanine	3.1–4.1
Acetate	4.2–5.2			Histidine	5.5–6.5
MES	5.7–6.7			Imidazole	6.6–7.6
Glycine	9.1–10.1			TRIS	7.6–8.6
				Ethanolamine	9.0–10.0

See Table 4 for buffer abbreviations; Ammediol = 2-amino-2-methyl-1,3-propanediol; HPMC = hydroxypropylmethylcellulose; and OAc = acetate.

the separated zones is usually by conductivity or UV-visible absorption. The method has high peak capacity since separated zone boundaries are sharp and close to each other to maintain continuity of the current. When the experimental conditions are correct a steady state is reached in which all zones are migrating at the same speed and the detector output is a series of steps, the length of which corresponds to the concentration of the ion. At first sight the data presentation may be confusing and this combined with the complex method development has suppressed interest in capillary isotachopheresis in favour of other chromatographic methods. The compelling advantage of isotachopheresis is its ability to trace enriched dilute samples, by 100-fold or more, and as a preconcentration or pre-separation technique for capillary zone electrophoresis it is enjoying something of a renaissance.

Conclusions

The capillary electrophoretic methods are sufficiently established to ensure their continued laboratory use but not so mature that significant developments are unexpected in the near future. These developments are likely to be application driven and will impact on the method development process. New systems for separation of biopolymers using gels and

entangled polymers, a wider range of surfactants for selectivity optimization in micellar electrokinetic chromatography, and tailor-made sorbents for selectivity optimization and control of electroosmotic flow in electrochromatography are just some expected improvements. Better models for predicting sample migration should aid computer-aided method development strategies and experimental design approaches for multiparameter optimization of complex mixtures should grow in popularity.

Further Reading

- Baker DR (1995) *Capillary Electrophoresis*. New York: Wiley-Interscience.
- Bossi A, Olivieri E, Castelletti L, Gelfi C *et al.* (1999) General experimental aspects of the use of isoelectric buffers in capillary electrophoresis. *Journal of Chromatography A* 853: 71–82.
- Doble P and Haddad PR (1999) Indirect photometric detection of anions in capillary electrophoresis. *Journal of Chromatography A* 834: 189–212.
- Jimidar M, Yang Q, Smeyers-Verbeke J and Massart DL (1996) Method development and optimization for small ion capillary electrophoresis. *Trends in Analytical Chemistry* 15: 91–102.
- Kaniansky D, Nasar M, Marak J and Bodor R. (1999) Capillary electrophoresis of inorganic ions. *Journal of Chromatography A* 834: 133–178.

- Krivankova L and Bocek P (1997) Synergism of capillary isotachopheresis and capillary zone electrophoresis. *Journal of Chromatography B* 689: 13–34.
- McLaughlin GM, Weston A and Hauße KD (1996) Capillary electrophoresis methods development and sensitivity enhancement strategies for the separation of industrial and environmental chemicals. *Journal of Chromatography A* 744: 123–134.
- Muijselaar PG, Otusuka K and Terabe S (1997) Micelles as pseudo-stationary phases in micellar electrokinetic chromatography. *Journal of Chromatography A* 780: 41–61.
- Poole CF and Poole SK (1997) Interphase model for retention and selectivity in micellar electrokinetic chromatography. *Journal of Chromatography A* 792: 89–104.
- Reijenga JC, Verheggen TPEM, Martens JHPA and Everaerts FM (1996) Buffer capacity, ionic strength and heat dissipation in capillary electrophoresis. *Journal of Chromatography A* 744: 147–153.
- Rodriguez-Diaz R, Zhu M and Wehr T (1997) Strategies to improve performance of capillary isoelectric focusing. *Journal of Chromatography A* 772: 145–160.
- Watzig H, Matthias D and Kunkel A (1998) Strategies for capillary electrophoresis: method development and validation for pharmaceutical and biological applications. *Electrophoresis* 19: 2695–2752.

ESSENTIAL GUIDES TO METHOD DEVELOPMENT IN EXTRACTION

J. R. Dean, University of Northumbria at Newcastle, Newcastle upon Tyne, UK

Copyright © 2000 Academic Press

Introduction

Samples for extraction can be broadly categorized as solid, liquid or gaseous matrices. It is obvious that the different methods of extraction of analytes from

these matrices will also vary. This guide provides an overview of the different approaches for extraction of analytes from these different matrices.

It is important to consider that extraction is only one part of the sample preparation protocol. Other steps are highlighted in Figure 1. A typical solid sample is most likely to be heterogeneous. This is a problem in the analysis, if appropriate steps have not been taken to remove a representative sample using a statistical approach. Failure to do so can make any subsequent extraction and analysis results meaningless.

Also of relevance to any subsequent extraction and analysis is whether the sample has been stored (and preserved, if necessary) in the appropriate manner to prevent losses of the analyte due to degradation and/or adsorption. It is necessary to consider, in the

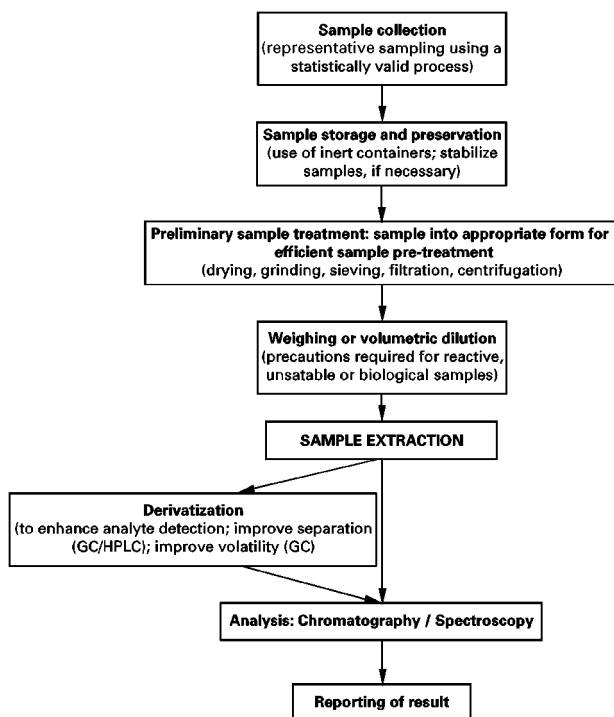


Figure 1 Sample preparation protocol.

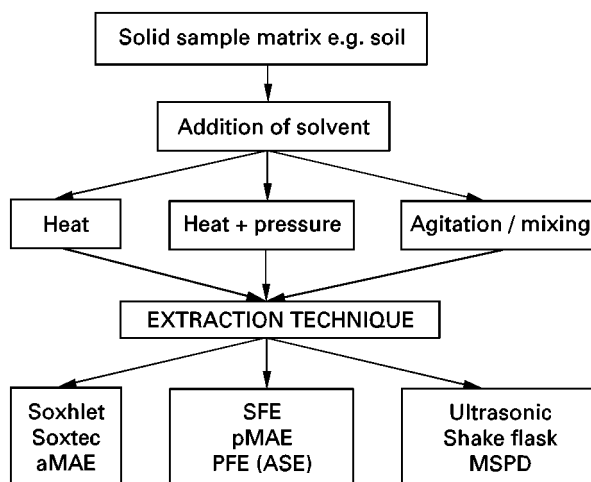


Figure 2 Extraction of analytes from solid matrices.

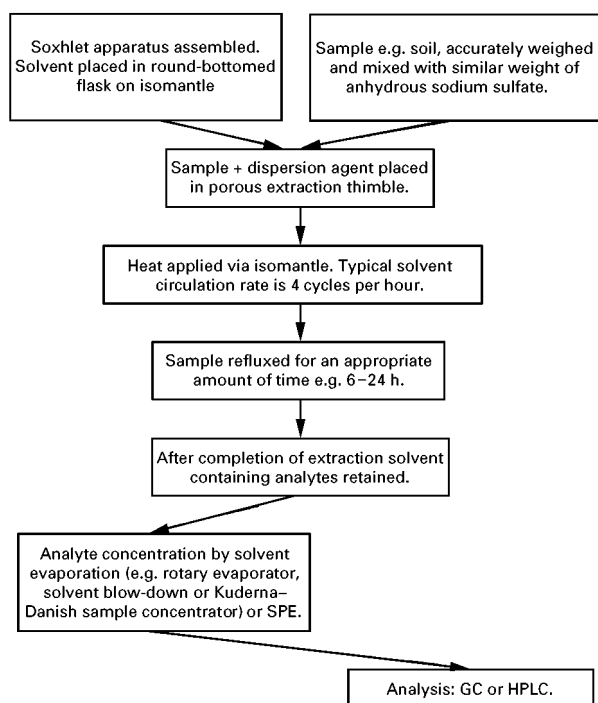


Figure 3 Soxhlet extraction.

case of a soil sample, whether it should be dried (volatile analytes may be lost) or extracted in the unadulterated state. If possible, drying is favoured, as the subsequent matrix can be ground and sieved to increase its surface area (smaller particle size).

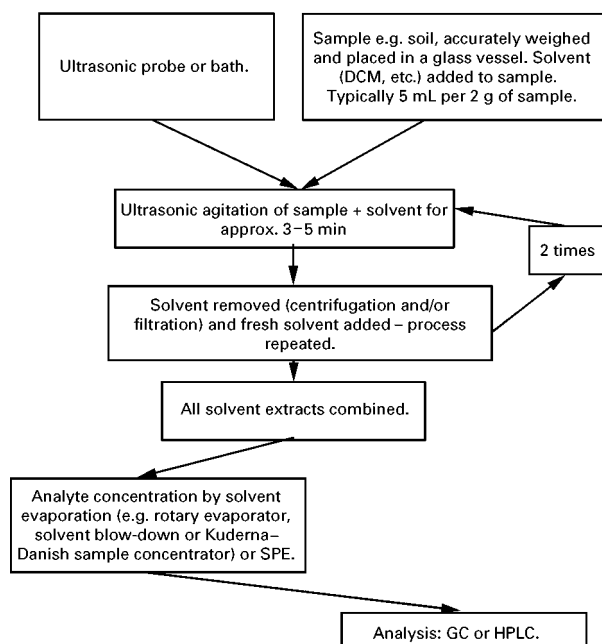


Figure 4 Ultrasonic extraction.

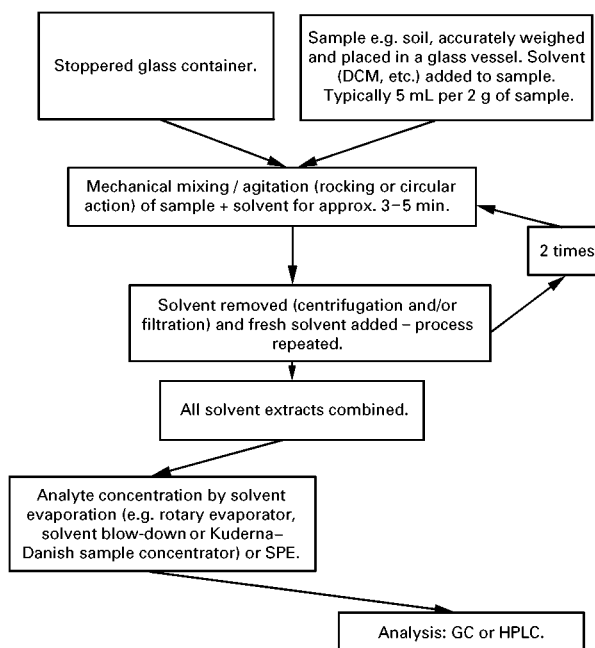


Figure 5 Shake-flask extraction.

Solid Matrices

Extraction of analytes from solid matrices can be classified according to the scheme shown in Figure 2. The main extraction techniques are Soxhlet extraction, soxtec extraction, supercritical fluid extraction

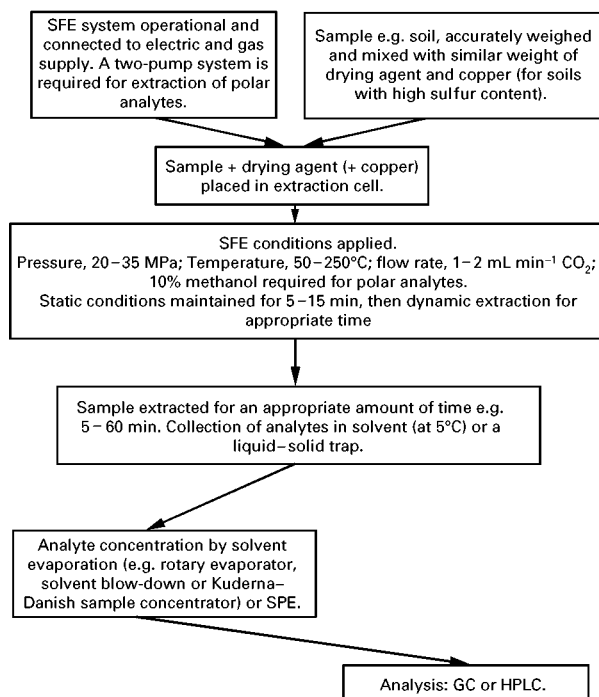


Figure 6 Supercritical fluid extraction.

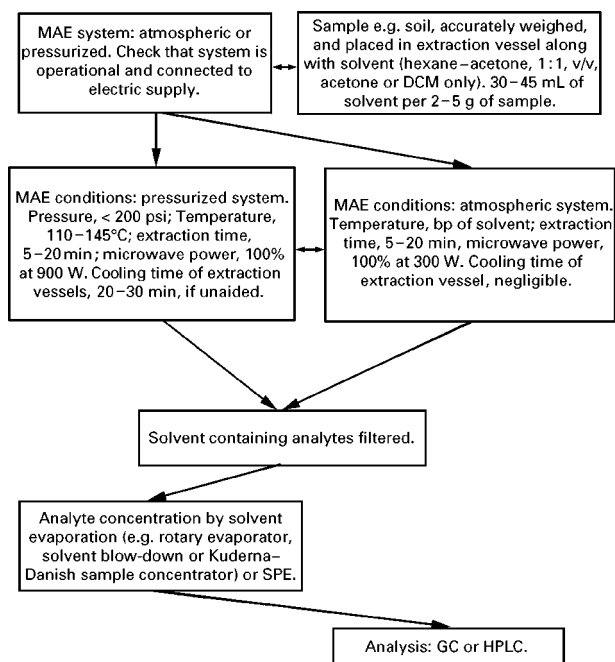


Figure 7 Microwave-assisted extraction.

(SFE), pressurized microwave-assisted extraction (pMAE), atmospheric microwave-assisted extraction (aMAE), pressurized fluid extraction (PFE) or accelerated solvent extraction (ASE), ultrasonic ex-

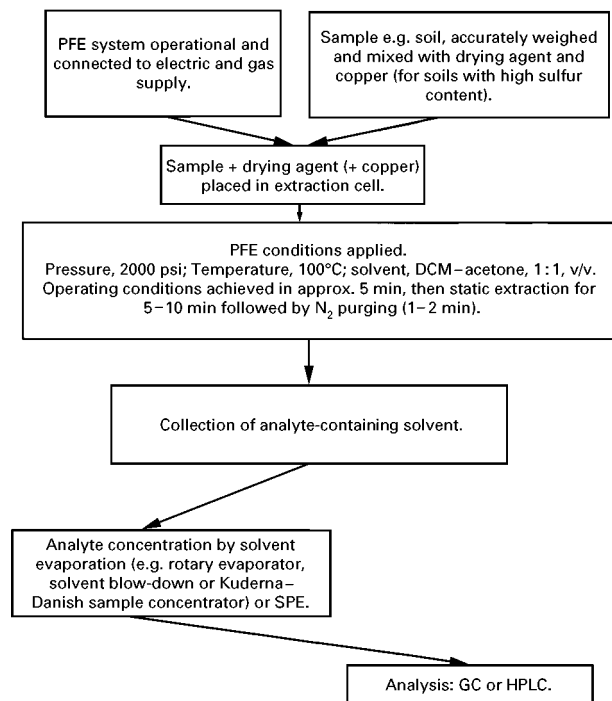


Figure 8 Pressurized fluid extraction (or accelerated solvent extraction).

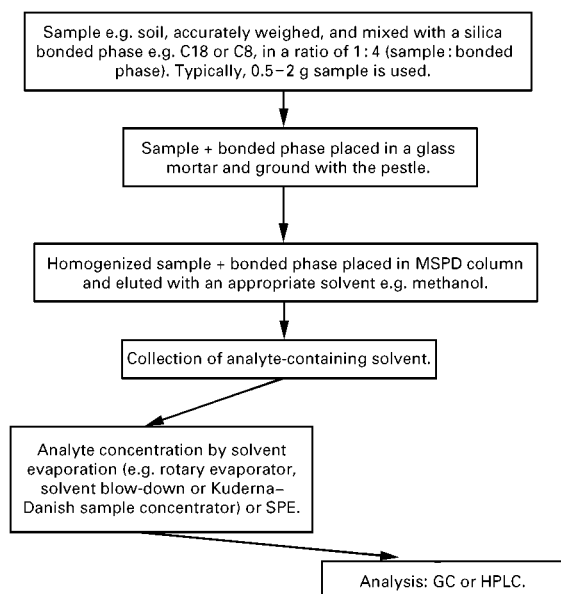


Figure 9 Matrix solid-phase dispersion.

traction, shake-flask extraction and matrix solid phase dispersion (MSPD). Method development approaches for each extraction technique are shown in Figures 3–10.

Liquid Matrices

Liquid extraction approaches are essentially centred around methods of preconcentration. Typically, this involves the use of sorbent and/or an organic solvent. The choice of solvent/organic solvent depending upon the nature of the analyte, e.g. polar/nonpolar. The main extraction approaches are liquid–liquid

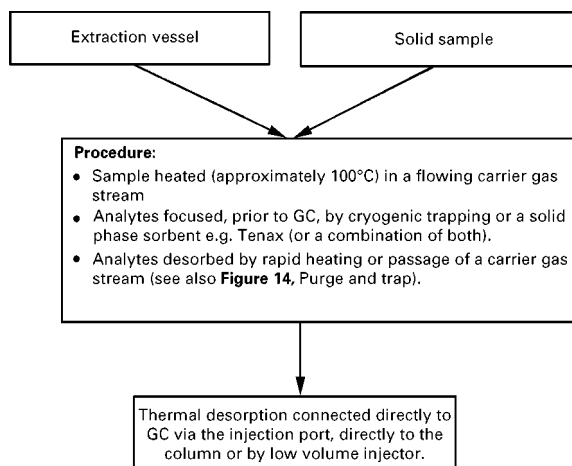


Figure 10 Thermal desorption.

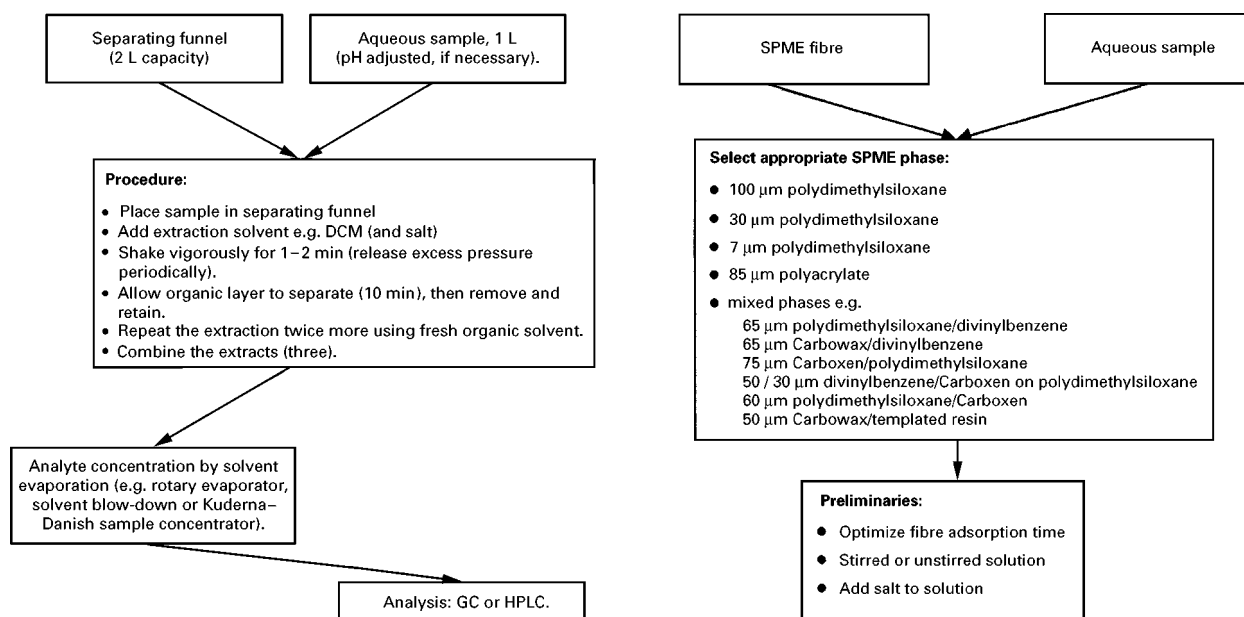


Figure 11 Separating funnel liquid–liquid extraction.

extraction (LLE), solid-phase extraction (SPE) and solid-phase microextraction (SPME). A guide to method development for each extraction technique is shown in Figures 11–14.

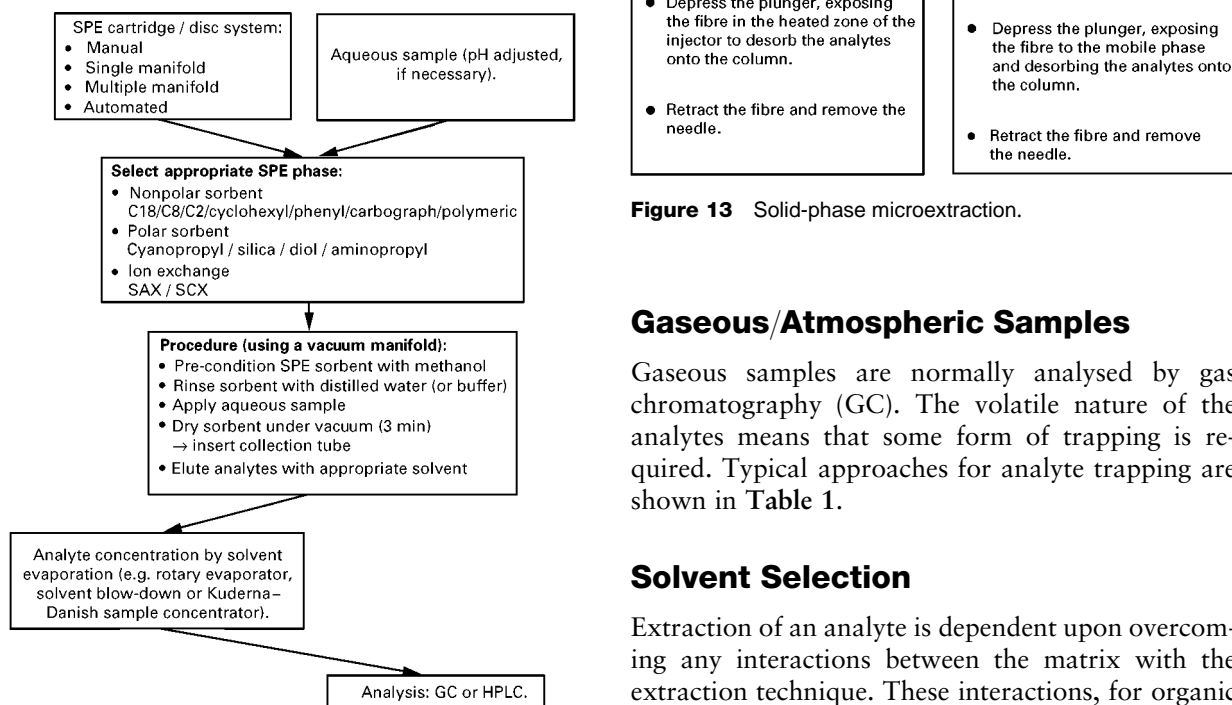


Figure 12 Solid-phase extraction.

Figure 13 Solid-phase microextraction.

Gaseous/Atmospheric Samples

Gaseous samples are normally analysed by gas chromatography (GC). The volatile nature of the analytes means that some form of trapping is required. Typical approaches for analyte trapping are shown in Table 1.

Solvent Selection

Extraction of an analyte is dependent upon overcoming any interactions between the matrix with the extraction technique. These interactions, for organic molecules, are predominantly based on weak forces of attraction between the analyte and the matrix, e.g.

Table 1 Common approaches for gaseous samples

Technique	Comments
Solid phase trapping	Gaseous sample passed through a sorbent, e.g. Tenax, activated charcoal, etc. Trapped analytes are eluted with a suitable solvent.
Liquid trapping	Gaseous sample is bubbled through a suitable trapping solvent. To improve trapping efficiency it is important to minimize the flow rate and/or lower the temperature. The use of multiple traps or impingers may be necessary.
Headspace sampling	Solid or liquid sample placed in a sealed glass vial until equilibrium is reached. Volatile analytes sampled from the headspace using a gas-tight syringe or solid-phase microextraction.
Purge and trap	See Figure 14.
Solid-phase microextraction	See Figure 14 and Headspace sampling, above.

Table 2 Calculation of individual group contributions for a solvent (methanol) and the analyte, DDT

Molecule	Group	Group contribution to dispersion (F_d) $J^{1/2} \text{ cm}^{3/2} \text{ mol}^{-1}$	Group contribution to polarity (F_p) $J^{1/2} \text{ cm}^2 \text{ mol}^{-1}$	Group contribution to hydrogen bonding (U_h) $J \text{ mol}^{-1}$	Molar volume (V) $\text{cm}^3 \text{ mol}^{-1}$
Methanol	CH ₃	420	0	0	33.5
	OH	210	500	20 000	10.0
	Total	630	500	20 000	43.5
DDT	2 × -Ph-	2540	220	0	104.8
	2 × Cl-CH=	900	1100	800	48
	3 × Cl	1350	1650	1200	72
	1 × CH	80	0	0	- 1.0
	> C <	- 70	0	0	- 19.2
	Total	4800	2970	2000	204.6

Table 3 Total Hildebrand solubility parameter and its individual components

Solvent/analyte	Dispersion coefficient, $\delta_d \text{ (MPa}^{1/2}\text{)}$	Polarity, $\delta_p \text{ (MPa}^{1/2}\text{)}$	Hydrogen bonding, $\delta_h \text{ (MPa}^{1/2}\text{)}$	Total Hildebrand solubility parameter, $\delta_t \text{ (MPa}^{1/2}\text{)}$
Methanol	14.48	11.49	21.44	28.31
Acetonitrile	14.78	19.13	6.59	25.06
Acetone	14.52	9.90	5.07	18.29
Dichloromethane	18.25	8.58	3.53	20.48
iso-Hexane	14.27	0.00	0.00	14.27
DDT	23.46	9.75	3.13	25.60

Van der Waal's, hydrogen bonding, etc. While the choice of extraction technique is important, often for economic and environmental concerns, its physical/chemical properties are largely influenced by the choice of solvent (in most cases). This is not to say that the effects of heat, pressure, agitation and sorbent are negligible, but that these on their own are largely unimportant without the presence of an organic solvent and that the choice of solvent is critical. Apart from general rule of thumb guidelines for sol-

vent selection, i.e. like extracts such as a nonpolar analyte can be extracted by a nonpolar solvent, little attempt has been made to offer a scientific approach.

The solvent prediction scheme used is based on the Hildebrand solubility parameter (δ_t). The solubility parameter is a measure of the internal energy of cohesion in the solvent/solute. Solvents with similar solubility parameter form mixtures, hence an analyte and a solvent that have similar solubility parameters, should also form mixtures.

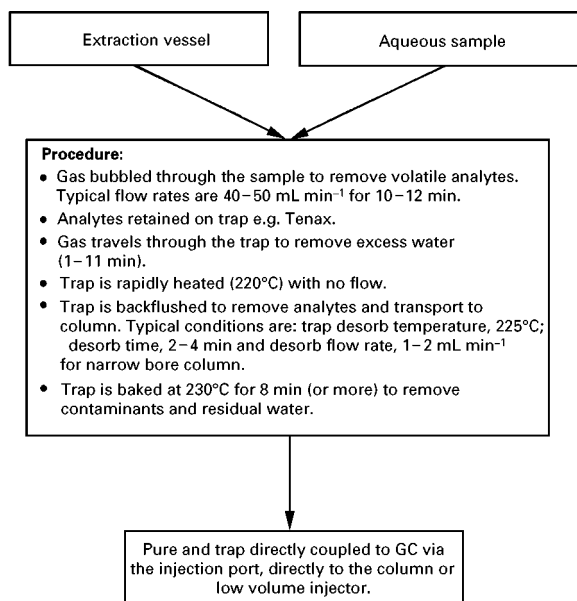


Figure 14 Purge and trap.

δ_t is defined as the square root of the cohesive energy density or:

$$\delta_t = (\Delta E_v / V)^{1/2} \quad [1]$$

where δ_t = total Hildebrand solubility parameter, ΔE_v = energy of vaporization at a given temperature and V = molar volume of the molecule.

Hansen (1967) took this work further and assumed that the total cohesive energy is a linear addition of

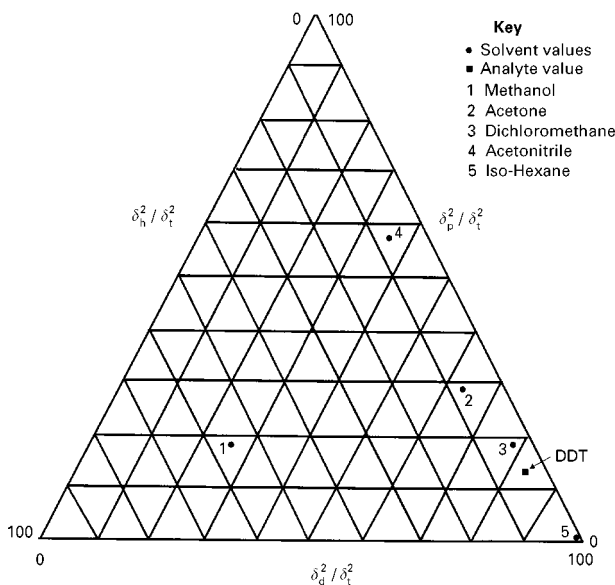


Figure 15 Comparison of calculated solvent and analyte fractional parameters.

Table 4 Pressurized fluid extraction of DDT from contaminated soil followed by GC-MSD quantitation, $n = 6^a$

Solvent	Mean $\mu\text{g g}^{-1}$	SD
Methanol	89	10.1
Acetone	163	7.4
Dichloromethane	220	13.9
Acetonitrile	65	2.9
Iso-Hexane	120	4.4

^aExtraction conditions: sample size 2 g; temperature, 100°C; pressure 2000 psi; static extraction time 10 min; one static/flush cycle.

three components: δ_h , hydrogen bonding ability contribution; δ_d , dispersion co-efficient contribution; and, δ_p , polarity contribution. They are linked by the following equation:

$$\delta_t^2 = \delta_h^2 + \delta_p^2 + \delta_d^2 \quad [2]$$

The individual components of δ_t can be determined using a group contribution additive method. The data available allows each group's contribution to polarity, dispersion and hydrogen bonding (F_p , F_d , and U_h , respectively) to be calculated using the following equations δ_p , δ_h , and δ_d :

$$\delta_d = (z \Sigma F_d) / V \quad [3]$$

$$\delta_p = (z \Sigma F_p) / V \quad [4]$$

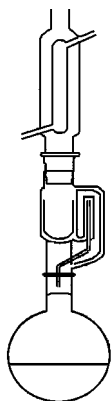
$$\delta_p = (z \Sigma F_p^2)^{1/2} / V \quad [5]$$

$$\delta_h = ((z \Sigma U_h) / V)^{1/2} \quad [6]$$

For molecules with more than one polar group present, then eqn [5] must be used instead of eqn [4] to take into account the interactions between the polar groups.

An example calculation of the individual components of the solubility parameter for a solvent (methanol) and an analyte (1,1,1-trichloro-2,2-bis(p-chlorophenyl)ethane (DDT)) are shown in Table 2. The individual Hansen parameters for a range of solvents and an analyte (DDT) are shown in Table 3. As an example, the calculated total Hildebrand solubility parameter, δ_t , for methanol (28.3 MPa^{1/2}) compared favourably with the literature value of 29.6 MPa^{1/2}.

In order to normalize the data, fractional parameters of the Hildebrand solubility parameter can be calculated and plotted on a triangular graph in order to give a visual representation of the extent of contribution from the three components (polarity,

Box 1 Soxhlet extraction of polycyclic aromatic hydrocarbons from contaminated soil.**Extraction conditions**

Sample size: 10 g plus 10 g anhydrous sodium sulfate

Solvent: 150 mL dichloromethane

Extraction time: 24 h

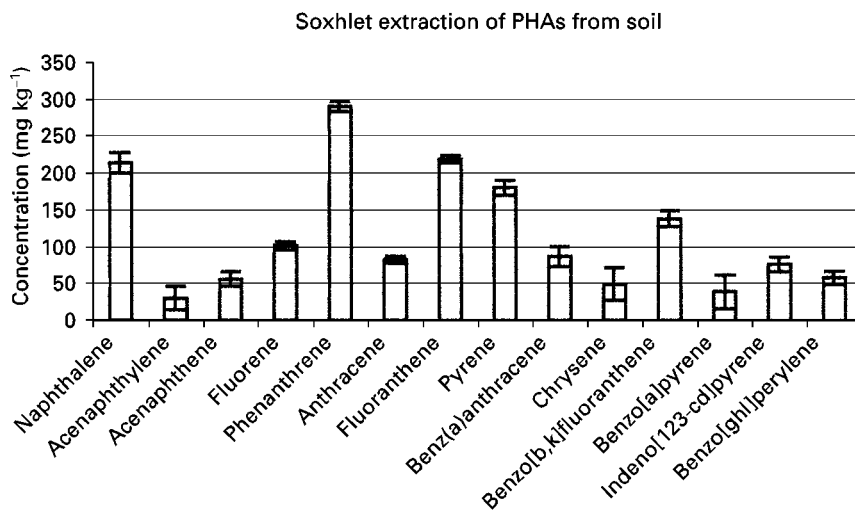
Comments: sample heated using an isomantle. Typically, refluxing of solvent occurs at the rate of 4 h^{-1} .

Extracts were concentrated to 10 mL using rotary evaporator and then diluted twofold before addition of the internal standards.

Analysis of extracts by GC

Separation and identification of individual PAHs was done on a HP 5890 series II + GC fitted with a HP 5972A mass spectrometer. A $30 \text{ m} \times 0.25 \text{ mm i.d.} \times 0.25 \mu\text{m}$ film thickness DB-5 capillary column was used with temperature programming from an initial temperature held at 85°C for 2 min before commencing a 6°C min^{-1} to 300°C , with a final time of 7 min. The split/splitless injector was held at 300°C and operated in splitless mode with the split value closed for 1 min following sample injection. The split flow was set at 40 mL min^{-1} , and the mass spectrometer transfer line was maintained at 270°C . Electron impact ionization at 70 eV with an electron multiplier voltage set at 1500 V was used while operating in single-ion monitoring (SIM) mode.

Typical results: Saim N, Dean JR, Abdullah MP and Zakaria Z (1997) *Journal of Chromatography* 791A: 361.



dispersion and hydrogen bonding). A plot of selected solvents and DDT is shown in Figure 15. Using this plot, it can be seen that dichloromethane (DCM) is predicted to be the optimum solvent for extraction of DDT. Table 4 shows results for the extraction of DDT contaminated soil for selected solvents using accelerated solvent extraction (ASE). It is clearly shown that DCM gives the highest recovery of DDT. Similarly, it is also predicted and confirmed that both isohexane and acetone would remove significantly more of the DDT than methanol and acetonitrile. Work is on-going to identify whether the model can be applied to other systems.

Selected Examples of Extraction of Analytes from Environmental Matrices

In order to provide specific details on particular extraction techniques selected examples are provided from the author's own laboratory. In particular, the following techniques are covered: **Box 1**, Soxhlet extraction of polyaromatic hydrocarbons (PAHs) from contaminated soil; **Box 2**, shake flask extraction of four phenols from soil; **Box 3**, SFE of OCPs from soil and Celite; **Box 4**, pressurized microwave-assisted extraction of PAHs from soil; **Box 5**, atmospheric microwave-assisted extraction of PAHs from

Box 2 Shake flask extraction of phenols from soil**Extraction conditions**

Sample size: 1 g

Solvent: 50 mL methanol–water (60–40% v/v)

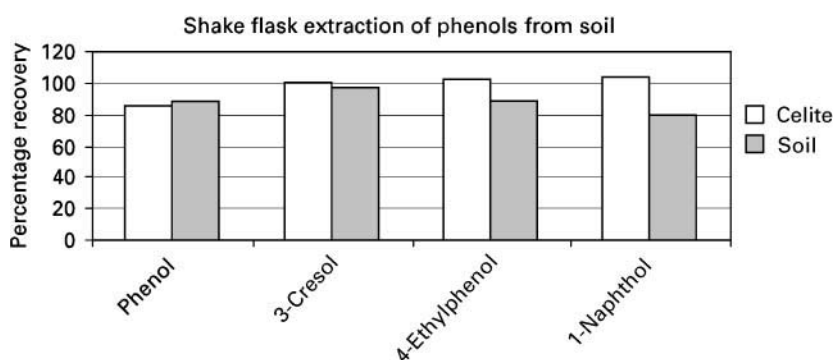
Extraction time: 30 min

Comments: Sample and solvent placed in a 100 mL screw-capped bottle and extracted on a rotating disc Warburg mixer. Resultant sample/solvent was filtered under vacuum. Sample extracted filtered through a 0.45 μm membrane Acrodisc prior to analysis.

Analysis by HPLC

Separation and quantification was achieved using a 25 cm \times 4.6 mm i.d. ODS2 column with UV detection at 275 nm. The mobile phase was operated under isocratic conditions acetonitrile–H₂O–acetic acid (40 + 59 + 1) at a flow rate of 1 mL min⁻¹. A 20 μL Rheodyne injection loop was used to introduce samples and standards on to the column (30°C).

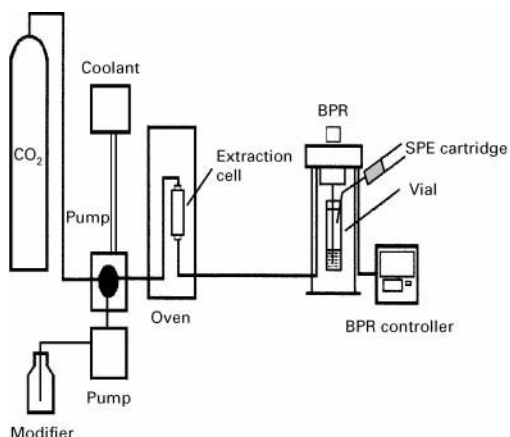
Typical results: Hancock P and Dean JR (1997) *Analytical Communications* 34: 377.



soil; **Box 6**, pressurized fluid extraction of DDT, 1,1-dichloro-2,2-bis(p-chlorophenyl)ethane (DDD) and 1,1-dichloro-2,2-bis(p-chlorophenyl)ethylene (DDE) from soil; **Box 7**, liquid–liquid extraction of PAHs from water; **Box 8**, SPE of phenols from water; **Box 9**, solid-phase microextraction of benzene,

toluene, ethyl benzene and xylene (BTEX) from water; and, **Box 10**, purge and trap of BTEX from water.

Further details on the theoretical and technical aspects of these and other extraction techniques can be found in the relevant entries in the Encyclopedia.

Box 3 Supercritical fluid extraction of organochlorine pesticides from soil and Celite**Extraction conditions**

Sample size: 1 g

SFE conditions: pressure, 250 kg cm⁻²; temperature, 50°C; static extraction time, 15 min followed by 40 min dynamic extraction time; and a flow rate of liquid CO₂, 2 mL min⁻¹.

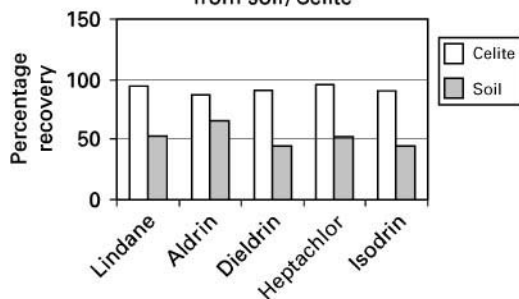
Comments: Extracts collected in a vial containing 3–4 mL DCM. Escaping CO₂ and analytes vented through a C18 SPE cartridge which was back-flushed with 1–2 mL methanol after each extraction.

Analysis by GC

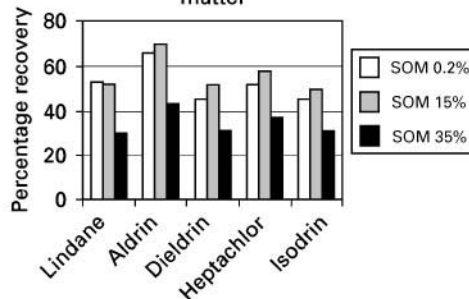
Separation and identification of individual OCPs was done on a HP 5890 series II + GC fitted with a HP 5972A mass spectrometer. A 30 m × 0.25 mm i.d. × 0.25 μm film thickness DB-5 capillary column was used with temperature programming from an initial temperature held at 85°C for 0.75 min before commencing a 16°C min⁻¹ to 285°C, with a final time of 2 min. The split/splitless injector was held at 280°C and operated in splitless mode with the split valve closed for 1 min following sample injection. The split flow was set at 40 mL min⁻¹, and the mass spectrometer transfer line was maintained at 290°C. Electron impact ionization at 70 eV with an electron multiplier voltage set at 1500 V was used while operating in single-ion monitoring (SIM) mode.

Typical results: Dean JR, Barnabas IJ and Owen SP 1996 *Analyst* 121: 465.

Supercritical fluid extraction of OCPs from soil/ Celite

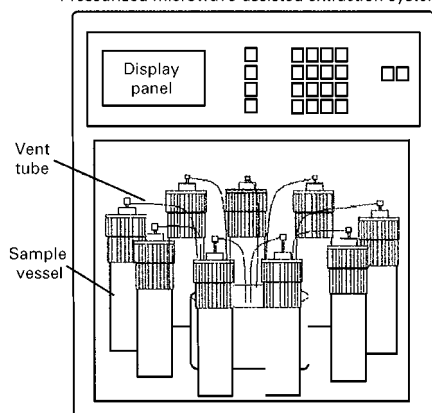


Supercritical fluid extraction of OCPs from soil: Influence of soil organic matter



Box 4 Pressurized microwave-assisted extraction of polycyclic aromatic hydrocarbons (PAHs) from soil.

Pressurized microwave-assisted extraction system

**Extraction conditions**

Sample size: 2 g

Solvent: 40 mL acetone

pMAE conditions: power, 30% (for a 950 W system); temperature, 120°C; extraction time, 20 min.

Comments: After extraction, extraction vessels allowed to cool.

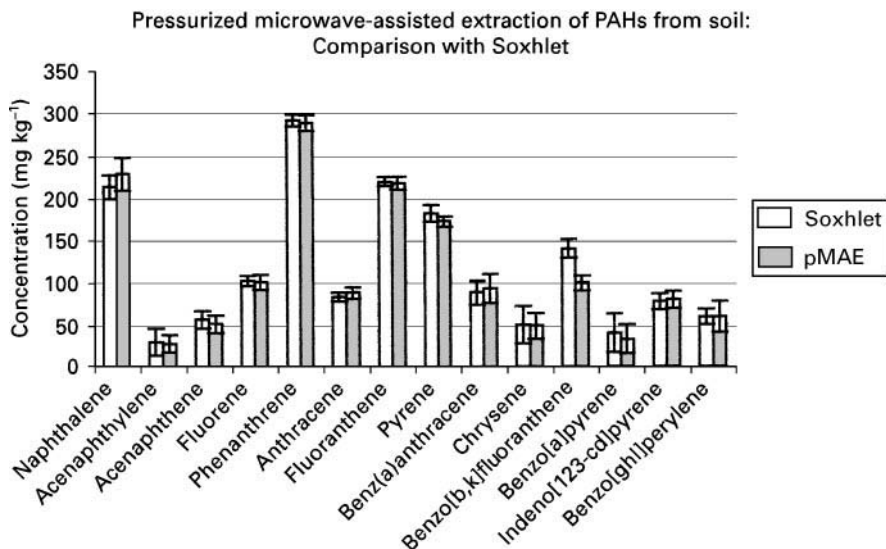
Contents of vessels were then filtered through a GF/A glass microbore filter.

Extracts were concentrated to 5 mL using a rotary evaporator before addition of internal standards.

Analysis by GC

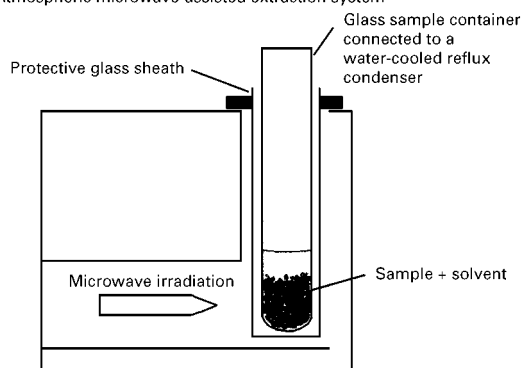
Separation and identification of individual PAHs was done on a Carlo Erba HRGC 5300 Mega Series with on-column injection and flame ionization detection. A 30 m × 0.32 mm i.d. × 0.1 μm film thickness DB-5 HT capillary column was used with temperature programming from an initial temperature held at 50°C for 2 min before commencing a 15°C min⁻¹ to 90°C; hold for 2 min; increase at 6°C min⁻¹ to 300°C with a final hold time of 8 min. The detector temperature was set at 290°C.

Typical results: Saim N, Dean JR, Abdullah MP and Zakaria Z (1997) *Journal of Chromatography* 791A: 361, with permission from Elsevier Science.



Box 5 Atmospheric microwave-assisted extraction of polycyclic aromatic hydrocarbons (PAHs) from soil.

Atmospheric microwave-assisted extraction system

**Extraction conditions**

Sample size: 2 g

Solvent: 70 mL DCM

pMAE conditions: power, 99% (for a 300 W system); extraction time, 20 min.

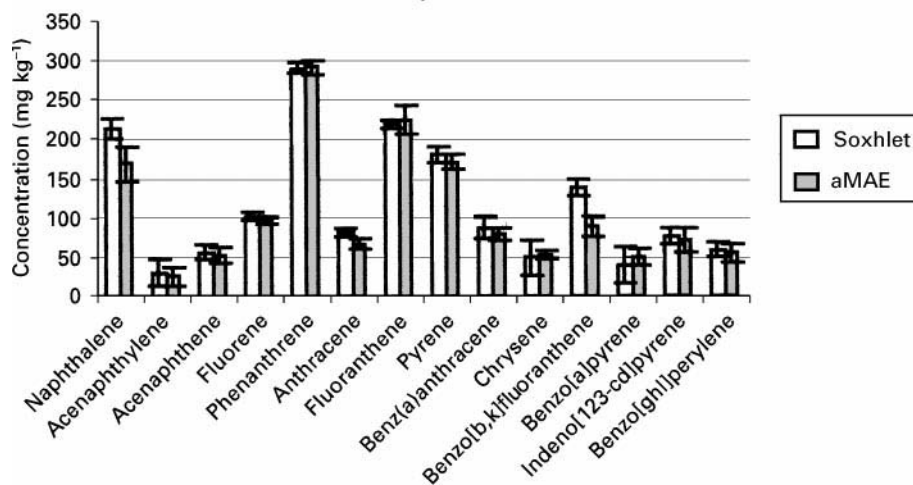
Comments: Contents of extraction vessel was then filtered through a GF/A glass microbore filter. Extracts were concentrated to 5 mL using a rotary evaporator before addition of internal standards.

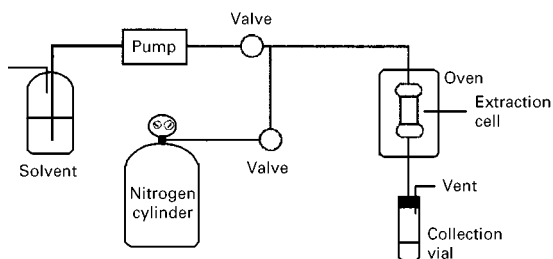
Analysis by GC

Separation and identification of individual PAHs was done on a Carlo Erba HRGC 5300 Mega Series with on-column injection and flame ionization detection. A 30 m × 0.32 mm i.d. × 0.1 μm film thickness DB-5 HT capillary column was used with temperature programming from an initial temperature held at 50°C for 2 min before commencing a 15°C min⁻¹ to 90°C; hold for 2 min; increase at 6°C min⁻¹ to 300°C with a final hold time of 8 min. The detector temperature was set at 290°C.

Typical results: Saim N, Dean JR, Abdullah MP and Zakaria Z (1997) *Journal of Chromatography* 791A: 361, with permission from Elsevier Science.

Atmospheric microwave-assisted extraction of
PAHs from soil: Comparison with Soxhlet



Box 6 Pressurized fluid extraction of DDT, DDD and DDE from soil.**Extraction conditions**

Sample size: 2 g

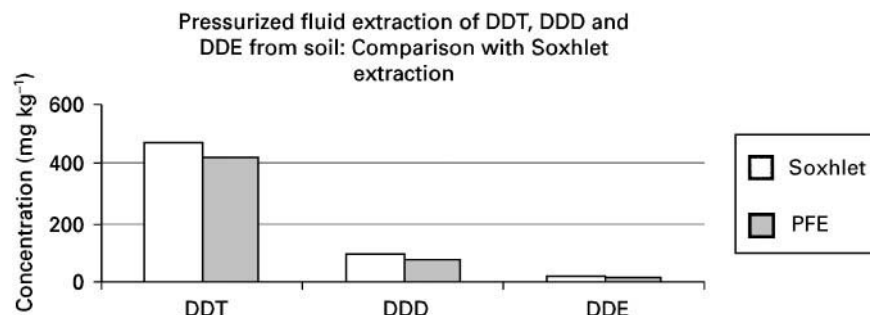
PFE conditions: pressure, 2000 psi; temperature, 100°C; static extraction time, 10 min; and three static/flush cycles.

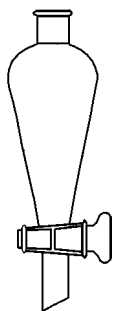
Comments: Sample placed in stainless steel extraction cell on top of a filter to prevent cell frit blockage. Hydromatrix was used to fill the headspace to reduce solvent consumption.

Analysis by GC

Separation and identification of DDT, DDD and DDE was done on a HP 5890 series II + GC fitted with a HP 5972A mass spectrometer. A 30 m × 0.25 mm i.d. × 0.25 μm film thickness DB-5ms capillary column was used with temperature programming from an initial temperature held at 120°C for 2 min before commencing at 5°C min⁻¹ to 290°C, with a final time of 2 min. The split/splitless injector was held at 280°C and operated in splitless mode. The mass spectrometer transfer line was maintained at 280°C. Electron impact ionization at 70 eV with an electron multiplier voltage set at 1500 V was used while operating in single-ion monitoring (SIM) mode.

Typical results: Fitzpatrick LJ and Dean JR (2000) *Journal of Chromatography*, in press.



Box 7 Liquid-liquid extraction of polycyclic aromatic hydrocarbons (PAHs) from water**Extraction conditions**

Sample volume: 25 mL

LLE conditions: sample extracted with 2×3 mL of DCM plus 1 g salt (NaCl). Each extract was shaken for 5 min each.

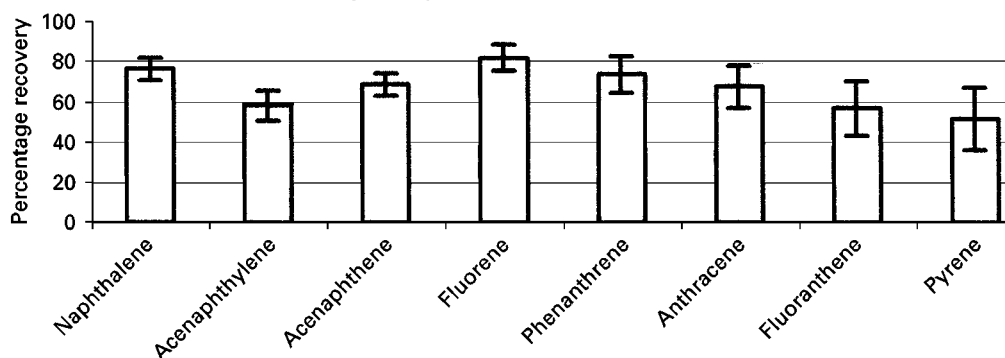
Comments: Combined extracts placed in a volumetric flask, internal standard added, prior to analysis.

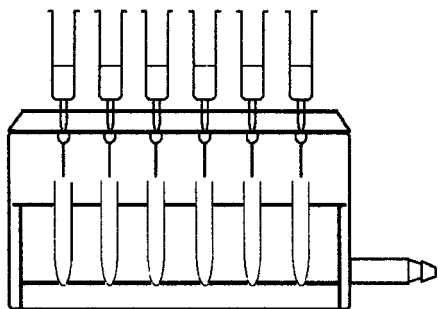
Analysis by GC

Separation and identification of individual PAHs was done on a HP 5890 series II GC fitted with a HP 5971A mass spectrometer. A $30 \text{ m} \times 0.25 \text{ mm i.d.} \times 0.25 \mu\text{m}$ film thickness HP-5ms capillary column was used with temperature programming from an initial temperature held at 90°C for 2 min before commencing a 7°C min^{-1} to 285°C , with a final time of 20 min. The split/splitless injector was held at 280°C and operated in splitless mode with the split valve closed for 1 min following sample injection. The split flow was set at 40 mL min^{-1} , and the mass spectrometer transfer line was maintained at 280°C . Electron impact ionization at 70 eV with an electron multiplier voltage set at 1500 V was used while operating in single-ion monitoring (SIM) mode.

Typical results: Arenaz-Laborda MP (1998) MSc dissertation, University of Northumbria at Newcastle, UK.

Liquid-liquid extraction of PAHs from water



Box 8 Solid phase extraction of phenols from water.**Extraction conditions**

Sample volume: 25 mL

SPE sorbent: PS-DVB, 230 mg

SPE conditions: conditioning, 5 mL of acetonitrile followed by 5 mL of water; sample loading; interference elution, 2 mL of water; and analyte elution, 4 mL of acetonitrile.

Comments: sample extract made up to 10 mL with water.

Analysis by HPLC

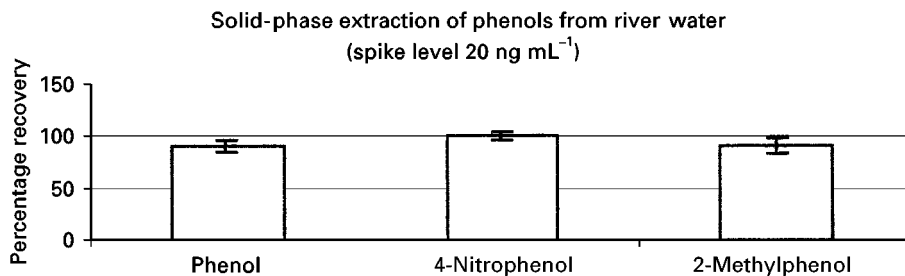
Separation and quantitation was achieved using a 25 cm \times 4.6 mm id ODS2 column with UV detection at 275 nm. The mobile phase was operated under isocratic conditions acetonitrile–H₂O–acetic acid (40 + 59 + 1) at a flow rate of 1 mL min⁻¹. A 100 μ L Rheodyne injection loop was used to introduce samples and standards on to the column (35°C).

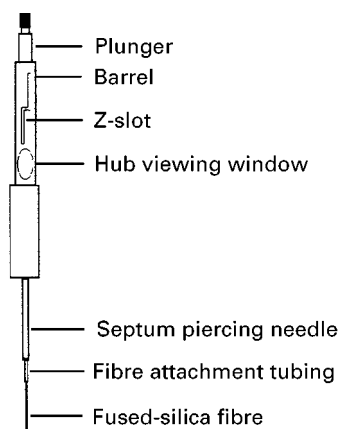
Typical results: Madier C (1997) BSc project, UNN, Newcastle upon Tyne, UK.

Analysis of phenol, 4-nitrophenol and 2-methylphenol.

Calibration range: 0–400 ng mL⁻¹

Correlation coefficients: 0.9993–0.9979.



Box 9 Solid phase microextraction of BTEX from water.**Extraction conditions**

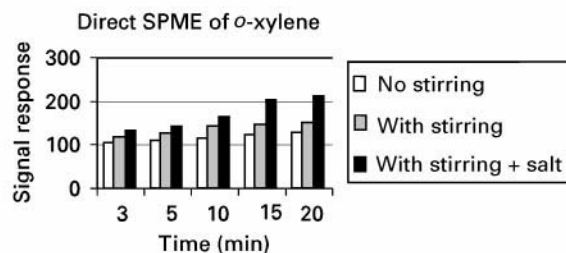
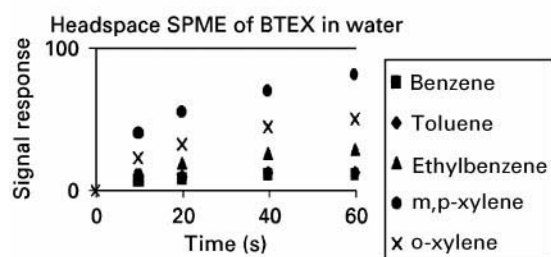
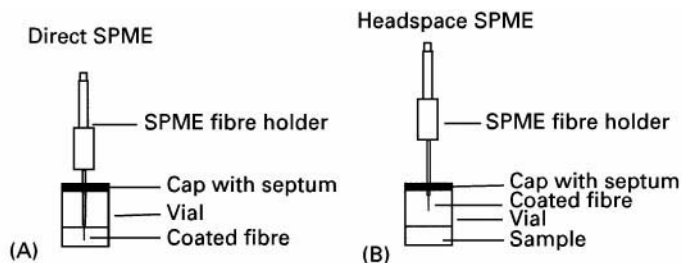
Sample volume: 10 mL
 Fibre: 100 μm polydimethylsiloxane

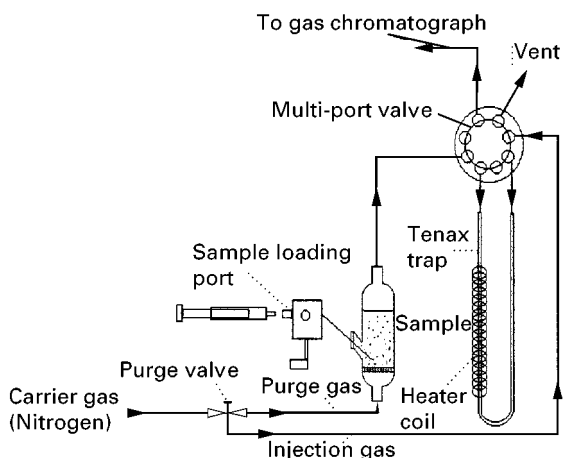
Conditions: SPME: fibre inserted into either the sample or headspace above the sample (with/without stirring; with/without salt) for varying amounts of time.

Analysis by GC

Separation and identification of BTEX was done on a Carlo Erba HRGC 5300 Mega Series with split/splitless injection and flame ionization detection. A 30 m \times 0.25 mm i.d. \times 0.1 μm film thickness DB-5 capillary column was used with temperature programming from an initial temperature held at 50°C for 3 min before commencing a 16°C min⁻¹ to 120°C with a final hold time of 7 min. The detector temperature was set at 250°C.

Typical results: Ahmed HK (1996) MSc dissertation, University of Northumbria at Newcastle, UK.



Box 10 Purge and trap (P&T) of BTEX from water.**Extraction conditions**

Sample volume: 2–10 mL

P&T conditions: Sample sparged for 2–5 min using N_2 .

BTEXs trapped on Tenax trap maintained at 20°C for 1–5 min.

Analytes desorbed by rapid heating to 260°C for 1 min.

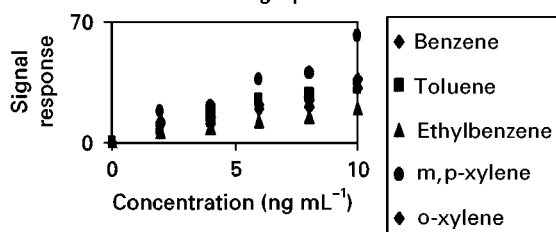
Comments: GC column initially maintained at 50°C to concentrate analytes.

Analysis by GC

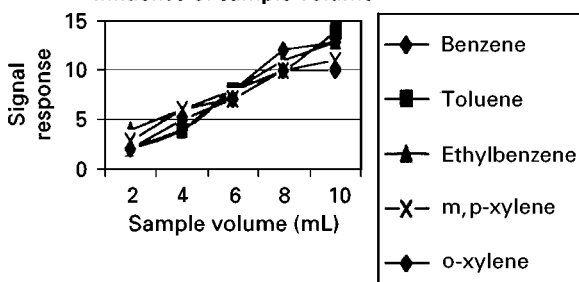
Separation and identification of BTEX was done on a Carlo Erba HRGC 5300 Mega Series with split/splitless injection and flame ionization detection. A 30 m \times 0.25 mm i.d. \times 0.1 μ m film thickness DB-5 capillary column was used with temperature programming from an initial temperature held at 50°C for 3 min before commencing a 16°C min⁻¹ to 120°C with a final hold time of 7 min. The detector temperature was set at 250°C.

Typical results: Ahmed HK (1996), MSc dissertation, University of Northumbria at Newcastle, UK.

Purge and Trap of BTEX from water:
Calibration graphs



Purge and Trap of BTEX from water:
Influence of sample volume



See also: **I/Extraction; Chromatography: Thin-Layer (Planar):** Theory of Thin-Layer (Planar) Chromatography. **Extraction:** Analytical Extractions; Analytical Inorganic Extractions; Microwave-Assisted Extraction; Solid-Phase Extraction; Solid-Phase Microextraction; Solvent Based Separation; Steam Distillation; Supercritical Fluid Extraction; Ultrasound Extractions. **III/Airborne Samples:** Solid-Phase Extraction. **Bioanalytical Applications:** Solid-Phase Extraction. **Drugs of Abuse:** Solid-Phase Extraction. **Environmental Applications:** Solid-Phase Microextraction; Soxhlet Extraction; Supercritical Fluid Extraction. **Herbicides:** Solid-Phase Extraction. **Immobilised Boronic Acids:** Extraction. **Immunoaffinity Extraction.** **Molecular Imprints for Solid-Phase Extraction.** **Multiresidue Methods:** Extraction. **On-line**

Sample Preparation: Supercritical Fluid Extraction. **Pesticides:** Extraction from Water. **Phenols:** Solid-Phase Extraction. **Pressurized Fluid Extraction: Non-Environmental Applications.** **Solid-Phase Extraction with Discs.** **Sorbent Selection for Solid-Phase Extraction.** **Appendix: 2/Essential Guides to Method Development in Solid-Phase Extraction.**

Further Reading

Barton AFM (1983) *The Handbook of Solubility Parameters and other Cohesion Parameters*. Boca Raton: CRC Press Inc.

- Dean JR (1998) *Extraction Methods for Environmental Analysis*. Chichester. John Wiley and Sons.
- Handley AJ (ed.) (1999) *Extraction Methods in Organic Analysis*. Sheffield: Sheffield Academic Press.
- Hansen CM (1967) *Journal of Paint Technology* 39: 104.
- Pawliszyn J (1997) *Solid Phase Microextraction: Theory and Practice*. New York: Wiley-VCH.
- Pawliszyn J (1999) *Applications of Solid Phase Microextraction*. Cambridge: Royal Society of Chemistry, Cambridge.
- Ramsey ED (1998) *Analytical Supercritical Fluid Extraction Techniques*. London: Kluwer Academic Publishers.
- Thurman EM and Mills MS (1998) *Solid Phase Extraction: Principles and Practice*. New York: Wiley-Interscience.
- van Krevelen DW and Hoftzyer PJ (1976) *Properties of Polymers; Their Estimation and Correlation with Chemical Structure*. Amsterdam: Elsevier.

ESSENTIAL GUIDES TO METHOD DEVELOPMENT IN FLOTATION

E. Woodburn, UMIST, Manchester, UK

Copyright © 2000 Academic Press

General

This article is designed to develop methods for an interested non-specialist, by showing how they can be used as a basis for a Chemical Engineering Unit Operations course.

Flotation is practised extensively in industry. The technique requires a detailed knowledge in physical metallurgy, the physical chemistry of surfaces, a competence both in mathematics and practical hydrodynamics.

The operation is based simply on the attachment of an air bubble to either a small or low-density particle, or to a liquid droplet.

Method 1: Selective Separation

Mineral flotation has by far the greatest usage, processing 20 billion tons per year; however the process of delinking newsprint is currently at about 25 million tons per year and is expected to grow significantly in the next decade. In these operations the selective attachment of a bubble to the valuable or an unwanted component of a particle is required. In de-inking, this refers to the removal of ink particles from cellulosic fibres. For mineral processing, a higher degree of selectivity is required, to recover a valuable particle from a suspension of waste particles. This operation is very seldom used on its own but is part of a flowsheet in which, after pretreatment which includes size reduction, a solid suspension in water is fed to the flotation circuit.

In the circuit, cells may be arranged in sequence with each successive cell treating the concentrate

from the previous one to improve its purity; this is, called 'roughing'. The final concentrate from the rougher bank is fed to a bank of 'cleaning' cells. The reject stream from the last of the cleaning cells is itself recycled to improve the final recovery and is called 'scavenging'. The concentrate from the final scavenger stream is recirculated to the feed of the first of the rougher cells. The waste from the final scavenging cell is discharged as the overall plant waste. This may be recycled, or treated to minimize its environmental impact. The final cleaner concentrate is essentially the plant product, although it may also have to be processed possibly by recleaning and drying.

In waste paper, de-inking the ink-rich stream tailings appears in what in mineral processing is the concentrate and the de-inked paper in what is usually the mineral processing tailings.

Method 2: Non-Selective Separations

The other class of operations require only the non-selective attachment of air bubbles to a particle/droplet, producing an aggregate of high buoyancy, so that the attached material can be withdrawn from the top of the flotation vessel. Processes of this type include the off-shore recovery of crude oil which may be 5–50% oil by volume, containing dispersed oil in the form of 10–50 µm oil droplets in water. After processing, virtually all the oil is recovered containing only 0–5% water. Other processing operations of this class include water treatment, in which the rate of setting of the flocculants on their own is very slow while the buoyancy of the air bubble/flocculant is high. Also the separation of rejected plastics from general wastes is economically attractive, with polyethylene terephthalate (PET), polyethylene (PE),

polyvinyl chloride (PVC) and polypropylene (PP) being recoverable.

The effectiveness of any flotation separation is described by the fractional recovery of the desired material, R , in the concentrate stream and its purity, the Grade G . The practical application of this is a principle more honoured in the breach than the observance, and is an area where significant economic improvements are possible.

Method 3: Measures of Separation Efficiency Potentially Achievable

In mineral processing, it is convenient to represent both quantities on a plot $0 \leq R, G \leq 1$. The Grade G is defined as $1 - (1 - x_C)/(1 - x_F)$ where x_F and x_C are the mass fractions of the desired component in the feed and concentrate streams respectively, and the fractional recovery of the desired component $R = (Cx_C)/(Fx_F)$. A perfect separation is therefore one in which $R = G = 1$.

Actual simulations lie on the upper boundary of the Grade-Recovery plot and describe the best R at a defined Grade. The area on the plot whose upper boundary represents optimum operation is called the attainable region. The function of the research worker ultimately is to devise techniques whereby the attainable region may be expanded. The Grade-Recovery plot should also be used by operators to monitor and control plant performance. The applications of automatic feed back control is attractive, but the requirements of online instrumentation, such as image processing and chemical analysis detectors, are still in the development stage. This is particularly so with the control actions which are necessary to be able to compensate for deviations from optimum operations. These include changing in air flow rates and the addition of chemicals. It is in this latter area that there is a large measure of uncertainty, which should be addressed as it again offers the possibility of significant economic improvements. The treated tailings which are usually in great bulk still have to be disposed of, at a significant cost, sometimes requiring slime dams to be built or as landfill. This is an environmental factor which may be very costly, both in the operation of existing plants, and in assessing the viability of new projects. Recycling the waste is environmentally acceptable and may also be profitable.

Method 4: Macro Dry Separations

It is significant that siliceous materials can be floated as they may well be the source of gangue contamination in metallic ore flotation. These gangues are in general disadvantageous to the separation and may

have to be depressed. However the recycling of simple oxide materials such as corundum, haematite and goethite may well be valuable although floated at lower rates.

Ore-dressing – although this is not strictly a flotation operation – effectiveness determines the limiting separation achievable in the flotation circuit. In the first ore-dressing step, separation is based on size reduction and primary mechanical classification. Once again, the details of the circuit depend on the nature and throughput of the raw material to be processed. The general principles involve crushing followed by dry separation in spirals (which are in fact of a helical design). Crushing and dry separations such as screening are relatively cheap and their use should be maximized to achieve the cheapest possible separation of high value materials from those which are exclusively gangue. Of these dry separation methods, the spirals depend on the difference in density between the waste rock and the valuable material. Vibratory screens may follow or be operated in parallel with the spirals. These are only useful if the fines are largely gangue. The valuable-rich stream from the dry separations is then fed to rod and wet or dry ball mills, the product of which goes to hydrocyclones whose underflow is a solid suspension in water whose solids lie in the size range 50–500 μm . This is a size range at which the subsequent flotation operations will function satisfactorily. The fine product from the mills is aimed at producing two separate powder streams in which there is a sharp change in the valuable material content; this process is referred as the liberation of the valuable material. The power costs of milling are extremely high. The overflow from the cyclones are called slimes and go to settling tanks from which the final solids and liquid wastes may be recycled or discharged. These streams are the primary source of environmental pollution and are vulnerable to objections which may require new treatment techniques.

Method 5: The Characterization of the Solid Material

In flotation, the complete characterization of the solid material to be floated, which varies considerably for different materials, is fundamental to the separation. In paper de-inking the type of ink used and its method of attachment to the waste fibre, determines the nature of the process required. This again is an area in which the technology is still developing. In mineral separations for example, the chemical type of both the valuable material and the gangue have to be identified, and it is also crucial to be able to identify and determine the distribution of individual minerals,

throughout the solid matrix of the primary ore. A mineral may be present as individual grains whose boundaries are a source of mechanical weakness in the solid. This facilitates breakage at the grains following impact and also most interestingly, breakage at the grains following differential thermal effects generated in a microwave field. Alternatively, the mineral may be distributed uniformly throughout the solid matrix. The initial characterization is usually done by microscope examination which, in the hands of an experienced operator, is extremely informative, but which usually has to be supplemented by X-ray fluorescence (XRF) analysis.

Method 6: Wet Processing – Hydrodynamics of Cell Design

The practice of mineral beneficiation by flotation is based on the production of an aqueous suspension of particles in the micron-size range and a dispersion of bubbles in a millimetre-size range. It is the objective within this suspension to achieve particle–bubble collision which will be followed by a selective attachment of the particles. In terms of the method of interception/attachment there are two basic types of cell.

Mechanical Cells

In mechanical cells there is a relatively small inner turbulent region enclosed by a larger diameter quiescent zone. The turbulent region is generated by an impeller which in addition has to disperse air into the solid suspension, and then pump the aerated suspension into the quiescent zone. There are a plethora of designs available which have to be carefully evaluated. The design variations should be related to the achievement of a desired interception/attachment efficiency as a function of particle size. These cells are the most commonly encountered in industrial practice principally because they can have very high capacities, with single cells of up to 300 m³.

In the inner region the suspension is exposed to a high level of turbulence, in which particle–bubble interception depends on the different paths between the water eddies and the particle trajectories. Although there are no theoretical calculations to provide a basis for these effects, it is assumed that the interception efficiency is determined by the local turbulent intensity and is increased for large particle sizes with a large differential density between the particle and water. Unfortunately, there is a probability that large particles which have been attached to the bubbles, following the turbulent interception may subsequently become detached from the bubble surface. The detachment will be associated

with the overall strength of the attachment forces; as these forces are surface effects and the specific surface is low, their detachment probability is high. For the small particles with a high specific surface with an overall high attachment force, the detachment probability is low. It is however, also apparent that these smaller lighter particles, as they follow the eddies closely, will have lower interception efficiencies. The net degree of attachment of particles to bubbles will depend on the design of the agitators (impellers).

Cylindrical Vertical Column Cells

The second cell type takes the form of a cylindrical vertical column in which the suspension is dilute, typically containing 5% solids. In these cells the attachment of a desired particle is more specific than in the mechanical cells. These cells may be between 3 m in diameter and 15 m high. The cells are described by the collection and froth zones. There is also an intermediate zone between the top of the collection zone and the froth. This zone functions very similarly to the top of the collection zone. The solid suspension from the milling circuit is added to the top of the collection zone and the air as bubbles through a sparger at the bottom. The bubbles and particles move countercurrently through the relatively quiescent collection zone. The hydrodynamics of the collection zone are relatively easy to describe. Originally the probability P_c of interception was given by $P_c = 3/2 (r_p/r_b)^2$ where r_p and r_b are the spherical radii of the particle and bubble, respectively. The original equations have been approximately corrected to allow for gravitational effects in terms of a parameter $K = 2 (\rho_p r_p^2 U) / (9 \mu_f r_b)$ where U is the bubble rise velocity in water of viscosity μ_f and ρ_p is the particle density. P_c indicates some interesting dependencies on K , e.g. (i) there is a K_c which is approximately 1, below which no collision will occur; the smallest size galena particle that can collide with a 1.5-mm bubble is 30 μm ; (ii) from the definition of K , when it is $> K_c$, an increase in bubble size will increase the collision efficiency and; (iii) very fine particles follow the streamlines exactly and will only collide if the streamline brings them within 1 particle radius of the bubble. Maximum velocities of 0.9, 1.5, 2.2 and 2.7 mm bubbles have been observed to be respectively 25.0, 36.5, 3.47 and 32.0 cm s⁻¹. However caution has to be used using predictions based on K as anomalies have been observed, and more accurate equations are now available. Surface-active chemical frothers, e.g. Dowfroth 250 and methyl isobutyl ketone (MIBK), are normally added at concentrations of the order of 30 ppm, these are to stabilize the final froth. The effect of the presence of these frothers

is to reduce the bubble rise velocity by about 50%. The effect of the surfactants is to adsorb on the bubble surface, increasing the surface viscosity of the water near the bubble, and the bubble rigidity.

Method 7: The Recovery of a Specific Particle Size

The effect of particle size is dependent on interactions with various factors. The ultimate objective is to remove particles of size d_{lib} which is the size at which maximum liberation occurs. Even if the dry separation gives material with a perfect size distribution as the mill feed, there will be a distribution of sizes in the product from the mills, which is the feed to the flotation circuit. If this particle size distribution is $f(d_p)$, the fractional mass of the size d_p , as characterized by their valuable content, then the flotation circuit should aim to maximize the recovery of particles of this size and sizes close to it. Clearly $f(d_{lib})$ should have a maximum and a small standard deviation. Ideally this could take the form of a delta function giving $f(d_{lib}) = \delta(d_{lib}) = 1.0$. The following step is to ensure what spread in the size distribution in the removal of these valuable particles occurs in the flotation circuit. This will depend on the specificity of the interception/attachment efficiency achievable for these particles, with an $f(d)$ size distribution, in a flotation circuit.

The calculation for a specific circuit will depend on the performance of its cells. Consider the specificity of removal of particles in a single mechanical cell. In addition to the interception/attachment in the turbulent zone which has a spread of efficiencies, there is also attachment of particles in the quiescent (pulp) zone which may have a different distribution. There is also a restriction on the new upflow rate through the pulp; if it is too high, non-attached particles may be entrained, and if too low the bubble-particle aggregates may settle. The design problem for the cells is firstly to design an impeller which will produce to the optimum size range of valuable particles, while pumping water at a sufficient rate into the pulp for the necessary upflow in the quiescent zone, which as an optimum bubble size distribution, to maximize the recovery of $f(d_{lib})$.

The bubble-particle contact in mechanical cells is sensitive to variations in the size of both, and the cell has to be designed for optimal removal of particle sizes with a high degree of liberation. It is clear that the requirement of the maximum removal of valuable material is not easily met. The mill product will have a distribution of particle sizes, each size with a varying valuable content. The flotation circuit separation

should also separate the most valuable particles of a size close to d_{lib} . The design challenge is to design milling and flotation circuits capable of producing and removing a specific size. It is also the responsibility of the operators to ensure that the system is operated continuously at its optimum level. These are realistic objectives.

The separations achievable in columns is potentially far more selective than that of the mechanical cells but are restricted by a narrow operating range. The most effective particle size in a column is of the order of 75 μm with bubble sizes varying from about 0.8 to 2.5 mm. This size range may not be consistent with the peak liberation size. The height of the columns is determined by the need for bubbles to accelerate from the bottom to their terminal velocity, where interception is a maximum. At these conditions the loaded bubbles will entrain into the froth significant amounts of solution containing gangue. The most effective feature of the columns is the removal of these waste solids by adding wash water to the top of the deep froth column. The froth at its top surface will overflow with a maximum grade. In industrial practice, columns are used to upgrade (clean) the froth concentrate from the primary cells (roughers).

Method 8: Pulp Microprocesses

Attachment following the interception of a particle by a bubble depends on the magnitude of the surface forces between them. The characterization of these forces to generate selective attachment is possibly the key factor in the separation.

The particles are always dispersed in water and the nature of the wetting of their surfaces determines the effectiveness of air bubble attachment. For hydrophobic surfaces, the water film is weakly bound and would fail easily after impact, thus causing attachment. The selectivity of the separation can be enhanced by the adsorption of a surface-active agent, a conditioner. These have a polar end which attaches to the solid surface, and a non-polar end which sticks into the water making the surface hydrophobic. In a bubble-particle interception, the particle has a time of contact, the sliding time after the initial interception during which the particle and the bubble will be separated by a thin water film. The sliding time will depend on the initial displacement of the particle from the line of centres of the rising bubble and the settling particle. The rate of thinning will depend on the kinetic energy dissipation after impact and London-van der Waals dispersive forces, electrostatic interactions and capillary forces following distortion of the bubble surface during impact. If the film thins

to a critical thickness, it will fail, which results in a successful attachment. Both the thinning process and the critical thickness depend on the interaction energy at the particle–water interface.

The requirement of hydrophobicity as a basis for attachment is justified by the following theoretical treatment. The dispersion energy $\varepsilon(h_x) = -(1/12\pi)A/h_x^2$. The attraction stress between the two surfaces is then $(\partial\varepsilon(h_x)/\partial h_x) = A/(6\pi h_x^3)$ dynes cm^{-2} . A is the Hamaker constant which is of the order of 10^{-12} ergs. For a condensed system to describe the interaction stress, A is replaced by A_{132} which is a linear combination of two surface interactions only. A_{12} represent the interfacial energy between a particle 1 and a bubble 2 separated by a vacuum, A_{13} and A_{23} are the Hamaker constants representing the particle–water and bubble–water interaction energies respectively. A_{33} is the interaction energy between water molecules. The linear combination $A_{132} = A_{12} - (A_{13} + A_{23} - A_{33})$. If A_{13} and A_{23} representing the particle–water and the bubble–water interactions are low, then A_{132} will be greater than A_{12} . The enhanced attraction between particle and air bubble in the presence of water represents hydrophobic bonding.

Experimental characterization of hydrophobicity can be done using the contact angle. If a liquid droplet is placed on a solid surface at the three-phase point of contact, it will form a definite angle θ between the liquid and solid surfaces, which is called the contact angle. If ΔG^0 is the change in free energy of the three-phase contact, following a small change ΔA_s in the area of contact, then $\Delta G^0 = \Delta A_s(\gamma_{SL} - \gamma_{SV}^0) + \gamma_{LV} \cos(\theta - \Delta\theta)$ at equilibrium; this leads to the Young equation, $\gamma_{SL} - \gamma_{SV}^0 + \gamma_{LV} \cos \theta = 0$. Since γ_{SV}^0 is the energy of contact of a solid with a saturated vapour of partial pressure p^0 there is also present on the surface a film of condensed vapour with its own surface energy π^0 . Then the total surface energy of the solid surface is $\gamma_s = \gamma_{SV}^0 + \pi^0$. Substituting in the Young equation for γ_{SL} gives $\gamma_{LV} \cos \theta = \gamma_s - \gamma_{SL} - \pi^0$ in the Dupre equation, the work of adhesion $w_{SLV} = \gamma_{LV}(1 + \cos \theta) + \pi^0$. This relates an increase in θ to a reduction in adhesion energy or alternatively an increase in the surface hydrophobicity.

Electrical Effects

The charge on a solid surface can vary from mineral to mineral and forms a basis for selective separation. The charge is strongly bound close to the surface in the Stern layer while further from the surface the layer is diffuse. If the particle moves in an applied electrical field, a lower potential will be observed which is that at the border of the Stern and the diffuse layers. This is an electrodynamic effect

called the ζ potential. The ζ potential is a strong function of pH; the point where the ζ potential is zero is called the PZC (point of zero charge). For goethite (FeOOH) the PZC is 6.7 and at acid pH the zeta potential is positive. Using RSO_3 which has a negative polar group, the recovery of goethite is 100% below pH 4.5 and 0% above pH 6.7, while if dodecylammonium chloride which has a positive polar group is used, the recovery of goethite in acid solution is 0% while above pH 9.5 the recovery is 100%.

The attachment of bubbles to charged electrical surfaces is underresearched. The bubbles are stabilized by surfactants (frothers) whose polar end may be anionic, cationic or non-ionic. The hydrophobic end of their molecule will be inside the bubble while the polar end is in the water. After impact, the previous treatment suggests that if the electrical forces between the bubble and the particle surface are attractive then A_{132} will increase and conversely, if the two surfaces repel each other, A_{132} will decrease. This is mere speculation as experimental confirmation is held up by the extremely small frother concentrations on the bubble surface, and the difficulty in the determination of the bubble's charge.

Method 9: Froth Microprocesses

As the particle–bubble aggregates rise to the top of the pulp they entrain with them in their boundary layers a small but significant amount of the pulp suspension which contains both unattached valuable and waste particles. The bubbles loaded with valuable solids pass through the upper level of the pulp and form a froth. As they pass into the froth, they entrain with them pulp water. In the froth the void volume of the pulp suspension is reduced from that in the pulp, owing to closer packing of the loaded bubbles. This forms the interface between the pulp and the froth which is readily observable (Figure 1). The sharp reduction of water in the froth at the point is a preliminary drainage effect. Bubbles will rise through the froth until they either burst at the top surface or, as unbroken bubbles loaded with valuable particles, overflow the concentrate weir. This is the final product of a single cell; the unfloated waste product will settle to the bottom of the quiescent region and leave the cell in the tailings stream.

The performance of the froth depends on the stability of the bubble passing through it. This in turn depends on the amount of frother added. At high levels of frother, the individual bubbles will remain as small spheres and will leave over the concentrate weir essentially unchanged from their condition at the bottom of the froth. Their water content will therefore be unchanged and there will be no upgrading of

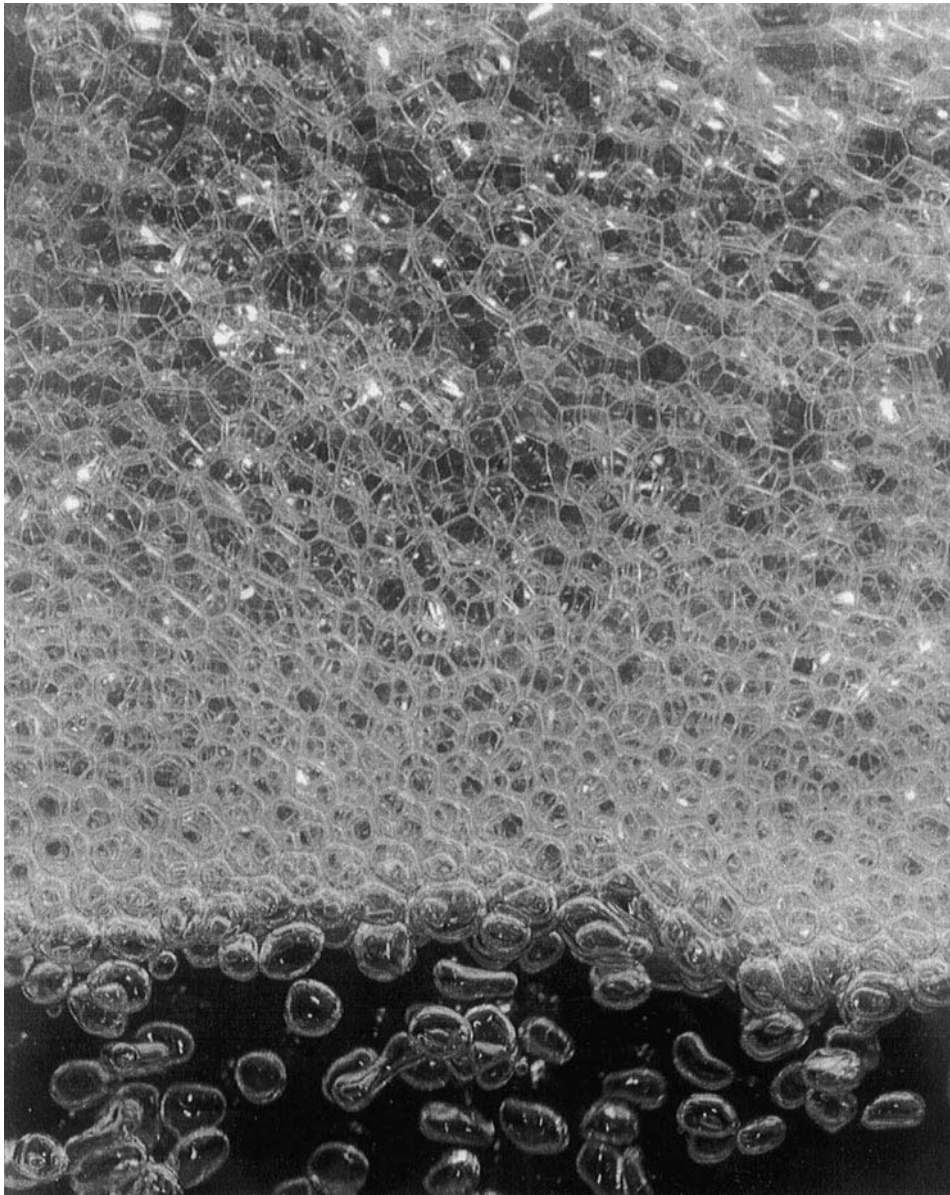


Figure 1 Pulp-froth interface.

the solid product. They will not burst at the top surface of the froth and will flow easily over the weir. With a lower level of frother addition, the spherical bubbles will deform to non-coalescing dodecahedra. The flat faces of the bubbles will be separated by lamellae with a size in microns (**Figure 2**). Water squeezed down the lamellae, flows into plateau borders which are of millimetre size; the three plateau borders at their ends join to form nodes down a network of which the entrained froth water drains back to the pulp. It has been reported that for two-phase foams, that the volumetric water content of the foam will fall from 0.26, at 5 mm from the pulp-foam

interface to 0.016, at 12 cm from the bottom of the foam. After that the value of 0.016 will remain constant through the foam. For coalescing foams the bubbles moving towards the weir will continue to grow, giving a lower volumetric water contents of < 0.01 . The effect of coalescence in a three-phase froth, will therefore be to increase the Grade, G , but with a decrease in fractional recovery, R , because of bubble breakage at the top surface of the froth.

Finally it may be observed that cells may potentially be controlled automatically with online image processing cameras.

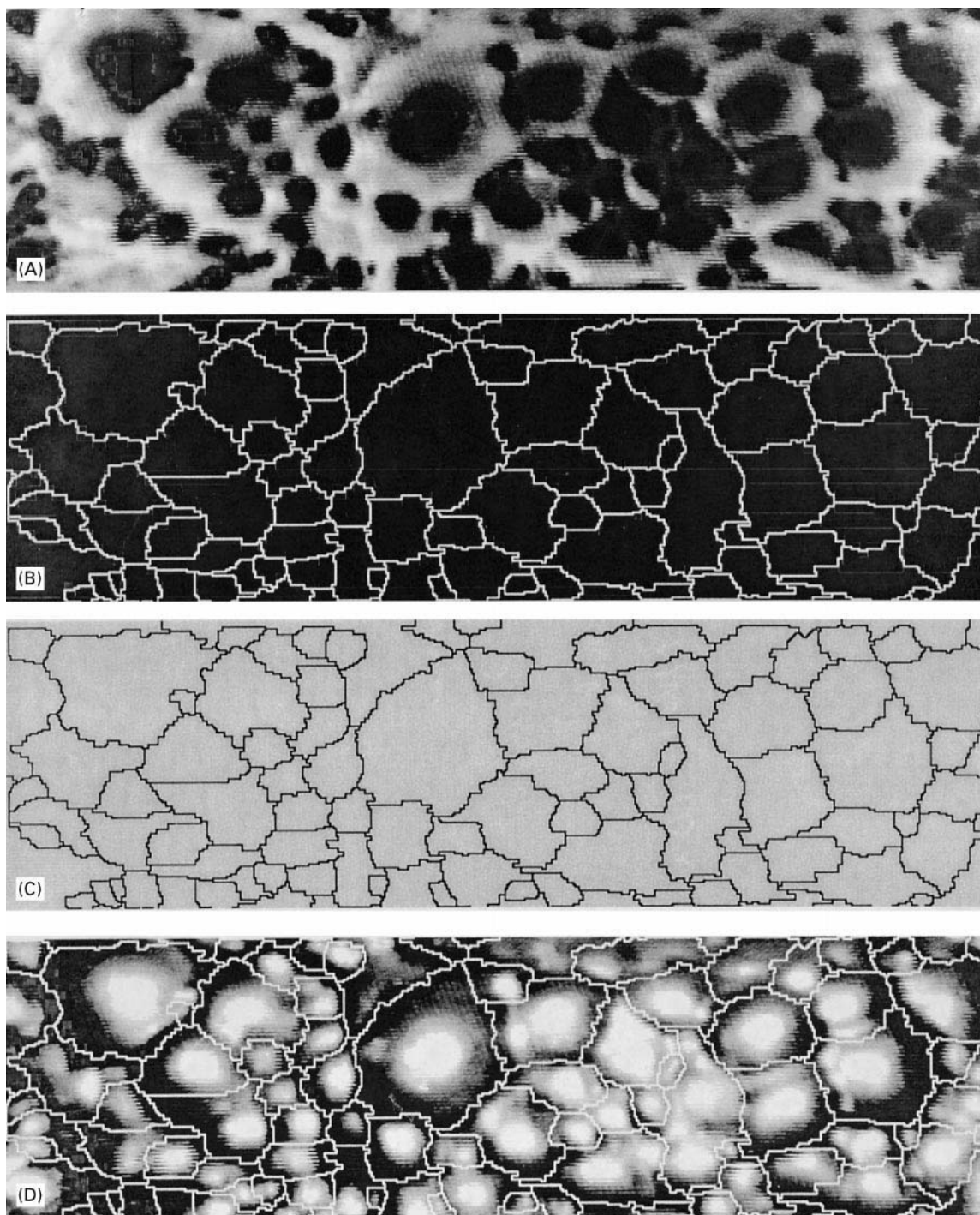


Figure 2 Control of flotation cells by image processing the upper surface of their froths. (A) The bubble structure in inverted light and the same structure with bubble boundaries sharply demarcated. (B) and (C) A comparison between the image-processed bubble structures, in inverted and reflected light, respectively. (D) The bubble structure in reflected light with image-processed boundaries superimposed.

See also: **I/Flotation.** **II/Flotation:** Bubble-Particle Adherence: Synergistic effect of Reagents; Bubble-Particle Capture; Column Cells; Cyclones for Oil/Water Separations; Dissolved Air; Foam Fractionation; Froth Processes and the Design of Column Flotation Cells;

Historical Development; Hydrophobic Surface State Flotation; Intensive Cells: Design; Oil and Water Separation; Reagent Adsorption on Phosphates. **III/De-inking of Waste Paper: Flotation.**

ESSENTIAL GUIDES TO METHOD DEVELOPMENT IN GAS CHROMATOGRAPHY

C. F. Poole, Wayne State University,
Detroit, MI, USA

Copyright © 2000 Academic Press

Introduction

Separations are possible in gas chromatography if the solutes differ in their vapour pressure and/or intensity of solute-stationary-phase interactions. As a minimum requirement the sample, or some convenient derivative of it, must be thermally stable at the temperature required for vaporization. The fundamental limit for sample suitability is established by the thermal stability of the sample and system suitability by the thermal stability of column materials. In contemporary practice an upper temperature limit of about 425°C and a sample molecular weight less than 1250 is indicated with only minor exceptions. A large number of general and selective derivatizing reagents are available for sample modification to enhance compound thermal stability, improve sample separation properties, and to provide compound-selective detection.

Column Types

Wall-coated open tubular columns (WCOT columns), or simply capillary columns, and classical packed columns dominate the practice of gas-liquid chromatography. Porous layer open tubular columns (PLOT columns) and classical packed columns dominate the practice of gas-solid chromatography. Classical packed columns are usually 0.5–3 m long with an internal diameter greater than 2 mm packed with adsorbent or liquid-coated support particles of 100–250 µm diameter. WCOT columns are typically up to 100 m long with internal diameters of capillary dimensions coated with a thin, and usually immobilized, film of stationary phase leaving an open interior passageway down the centre of the column. PLOT columns are identical to WCOT columns with the liquid phase replaced by a layer of fine adsorbent particles. WCOT and PLOT columns are the first choice for analytical separations because of their superior peak capacity and greater chemical inertness. Packed columns offer a lower cost choice for some applications, are easier to use, are relatively tolerant of thermally unstable and involatile sample components and are better suited to isolating prep-

arative-scale quantities of materials. Only a limited number of poly(siloxane) and poly(ethylene glycol) stationary phases have been successfully immobilized in WCOT columns compared to the larger number and variety of stationary phases available for use in packed columns.

Column Properties

The high permeability of WCOT columns allows long columns to be used to provide very high total plate numbers, as indicated in Table 1. Narrow-bore and thin-film columns are intrinsically the most efficient and are selected for fast chromatography. Since resolution increases only as the square root of the plate number, and also the column length, large values for the plate number are required for difficult separations. Such large numbers are available in gas chromatography, albeit at the expense of separation time, allowing separations to be achieved with only minimal differences in selectivity. In contrast to other chromatographic methods, separations in gas chromatography are often achieved through kinetic optimization, allowing many separations to be obtained on a limited number of stationary phases. A favourable feature of kinetic optimization is that the outcome is readily predictable from simple arithmetic calculations once some information of peak order has been established in a trial separation.

At a given temperature the partition coefficient is constant and the observed retention factor will depend on the phase ratio. The phase ratio is given by the column volume accessible to the mobile phase divided by the volume of stationary phase. Columns with a large phase ratio provide small retention factors for volatile compounds and require inconveniently large plate numbers to provide adequate resolution. Columns with a low phase ratio, that is, thick film columns, have a lower intrinsic efficiency than thin film columns, but provide better resolution of volatile compounds, because they provide more favourable retention factors. They also allow separations of volatile compounds at a higher and more convenient temperature range than is possible with thin film columns. For volatile compounds this often means at temperatures above room temperature as opposed to cryogenic temperatures. For high boiling compounds, columns with a low phase ratio are not

Table 1 Characteristic properties of some representative columns

Column type	Length (m)	Internal diameter (mm)	Film thickness (μm)	Phase ratio	Column plate number	Plates per metre
Classical packed	2	2.16	10%(w/w)	12	3 640	1 820
	2	2.16	5%(w/w)	26	4 000	2 000
WCOT	30	0.10	0.10	249	480 000	16 000
	30	0.10	0.25	99	368 550	12 285
	25	0.25	0.25	249	160 000	6 400
	50	0.25	0.25	249	320 000	6 400
	100	0.25	0.25	249	640 000	6 400
	30	0.32	0.32	249	150 000	5 000
	30	0.32	0.50	159	131 330	4 380
	30	0.32	1.00	79	102 080	3 400
	100	0.32	1.00	79	304 200	3 400
	30	0.32	5.00	15	68 970	2 300
	10	0.53	1.00	132	23 500	2 340
	30	0.53	1.00	132	70 420	2 340
	10	0.53	5.00	26	14 700	1 470
	30	0.53	5.00	26	43 940	1 470
	50	0.53	5.00	26	73 200	1 470

useful because they lead to long separation times. Increasing the phase ratio by reducing the film thickness lowers the retention factors to a value within the optimum range so that there is little deterioration in resolution and faster separations are obtained. Packed columns have low phase ratios compared to most WCOT columns. For compounds of moderate and low volatility, separation times on packed columns are generally longer. Since several combinations of film thickness and column radius can be used to generate the same phase ratio, there are other factors that need to be considered for selecting these variables for a particular separation.

Mobile-Phase Selection

Nearly all separations are achieved with hydrogen, helium or nitrogen as the carrier gas. At temperatures and pressures typical of normal operation in gas chromatography these gases behave almost ideally, providing a transport mechanism for the sample without influencing selectivity. The exception is gas-solid chromatography where the carrier gas participates in the retention process through competition with the sample for stationary-phase adsorption sites. Differences between hydrogen, helium and nitrogen are not usually large but absolute retention and retention order can change as a function of the carrier gas type and average carrier gas pressure. Heavier carrier gases, such as carbon dioxide, are more effective at influencing retention in gas-solid chromatography than the common carrier gases.

Although the choice of carrier gas does not significantly influence selectivity in gas-liquid chromatography,

it can still influence resolution through its effect on efficiency. This results from differences in gas diffusivity. The separation time is also affected because the optimum carrier gas velocity decreases with solute diffusion rates. In pressure-limiting conditions, gas viscosity differences are important as well. Nitrogen provides lower plate heights but at a lower optimum velocity (Figure 1), leading to long separation times. Close to the optimum plate height region, the ascending portions of the curves are shallower for hydrogen and helium. Thus, for separations at mobile-phase velocities higher than the optimum velocity, hydrogen and, to a lesser extent, helium provide faster separations than nitrogen with little loss in efficiency. For thick-film columns ($> 0.5 \mu\text{m}$), diffusion in the stationary phase is a significant factor in zone broadening and the relative contribution of the carrier gas to separation performance and time are not as great. Thick-film columns should be operated close to the optimum velocity, with the choice of carrier gas being less significant. Nitrogen is often the preferred carrier gas for these columns. For packed columns nitrogen provides (slightly) higher efficiency at low temperatures and flow rates, while hydrogen is superior at higher temperatures and at above optimum velocities. Hydrogen is preferred in pressure-limited conditions because of its lower viscosity. A considerable difference in the relative cost of helium in the USA and Europe has resulted in different preferences on the two continents. For WCOT columns, helium is widely used in the USA for safety rather than theoretical considerations, while hydrogen is commonly used in Europe.

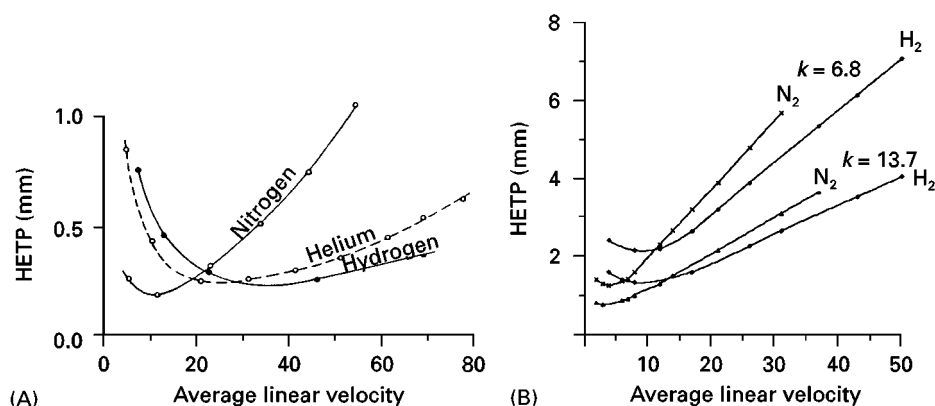


Figure 1 Influence of the choice of carrier gas on the efficiency of (A) a thin-film and (B) a thick-film WCOT column (k is the retention factor).

Stationary-Phase Selection

Given the nonsolvating properties of the mobile phase in gas chromatography, selectivity optimization is a matter of stationary-phase selection. Over the years thousands of substances have been evaluated as stationary phases and most abandoned in favour of a smaller number of liquids and adsorbents with favourable temperature operating ranges, kinetic properties and possibility of immobilization if used in WCOT columns.

Packed-column liquid phases can be roughly categorized into four groups:

1. hydrocarbon and perfluorocarbon liquid phases
2. ether and ester liquid phases

3. liquid organic salts
4. poly(siloxane) liquid phases

Representative examples and their useful temperature operating range are summarized in **Tables 2** and **3**. Most can be considered useful for general applications, except for the perfluorocarbon liquid phases that are used for the speciation of perfluorocarbon compounds or the separation of reactive compounds (metal fluorides, interhalogen compounds and non-metal halides) that tend to destroy conventional phases. The family of poly(siloxanes) provides the widest range of favourable stationary-phase properties and variation in selectivity. They are the most widely used stationary phases for packed-column

Table 2 Characteristic properties of some liquid phases used in packed-column gas chromatography

Name	Structure	Temperature range (°C)	
		Minimum	Maximum
Hexadecane	$C_{16}H_{34}$	< 20	50
Squalane	2,6,10,15,19,23-hexamethyltetracosane	< 20	120
Apolane-87	$(C_{18}H_{37})_2CH(CH_2)_4C(C_2H_5)_2(CH_2)_4CH(C_{18}H_{37})_2$	30	280
Fomblin YR	$-[OCF(CF_3)CF_2]_n[OCF_2]_m-$	30	< 255
PPE-5	$C_6H_5O(C_6H_5O)_3C_6H_5$	20	200
Dioctyl phthalate	$C_8H_4(COOC_8H_{17})_2$	< 20	160
EGS	$HO(CH_2)_2[OOCCH_2CH_2COO(CH_2)_2]_nOH$	100	210
DEGS	$HO(CH_2)_2O(CH_2)_2[OOCCH_2CH_2COO(CH_2)_2O(CH_2)_2]_nOH$	20	200
Carbowax 20M	$HO(CH_2CH_2O)_nCH_2CH_2OH$	60	225
FFAP		50	250
1,2,3-Tris(2-cyanoethoxy)propane	$(CH_2OCH_2CH_2CN)_3$	20	170
Tetrabutylammonium perfluorooctanesulfonate		< 20	220
Tetrabutylammonium 4-toluenesulfonate		55	200
Tetrabutylammonium tetrafluoroborate		162	290
Ethylammonium 4-toluenesulfonate		121	220
Tetrabutylphosphonium chloride		83	230

PPE-5, Poly(phenyl ether); EGS, poly(ethylene glycol succinate); DEGS, poly(diethylene glycol succinate); Carbowax 20M, poly(ethylene glycol); FFAP, Carbowax 20M treated with 2-nitroterephthalic acid.

Table 3 Characteristic properties of some poly(siloxane) liquid phases used for packed-column gas chromatography

Name	Structure	Temperature operating range (°C)	
		Minimum	Maximum
OV-1	Dimethylsiloxane (gum, molecular weight $> 10^6$)	100	350
OV-101	Dimethylsiloxane (oil, molecular weight 3×10^4)	< 20	350
OV-7	Phenylmethyldimethylsiloxane 80% methyl and 20% phenyl	< 20	350
OV-17	Phenylmethylsiloxane 50% methyl and 50% phenyl	< 20	350
OV-25	Phenylmethyldiphenylsiloxane 25% methyl and 75% phenyl	< 20	300
OV-210	Trifluoropropylmethylsiloxane 50% methyl and 50% 3,3,3-trifluoropropyl	< 20	275
OV-225	Cyanopropylmethylphenylmethylsiloxane 50% methyl, 25% phenyl and 25% 3-cyanopropyl	< 20	250
Silar 7CP	Cyanopropylphenylsiloxane 75% 3-cyanopropyl and 25% phenyl	50	250
OV-275	Di(cyanoalkyl)siloxane 70% 3 cyanopropyl and 30% 2-cyanoethyl		250
Silar 10CP	Di(3-Cyanopropyl)siloxane	50	250

gas-liquid chromatography and, because of their ease of immobilization, are the dominant stationary phases used to prepare WCOT columns (Table 4). With today's technology the only other family of stationary phases that can be immobilized for WCOT columns are the poly(ethylene glycols).

The selectivity of the stationary phases is of more interest than their chemical structure for method development. Liquid stationary phases have been classified based on their solvent strength (polarity) and selectivity. Classification based on the idea of polarity has had to be abandoned because of the lack of a working definition. Selectivity is defined as the relative capacity of a stationary phase for specific intermolecular interactions, such as dispersion, induction,

orientation and complexation (including hydrogen bond formation). Unlike solvent strength (polarity) it should be feasible to devise experimental scales of stationary-phase selectivity. Modern approaches to stationary-phase classification by selectivity are based on the cavity model of solvation. This model assumes that the transfer of a solute from the gas phase to solution in the stationary phase involves three steps. Initially a cavity is formed in the stationary phase of the same size as the solute. The solute is then transferred to the cavity with reorganization of solvent molecules around the cavity and the set-up of solute-solvent interactions. Retention in gas-liquid chromatography, therefore, will depend on the cohesive energy of the stationary phase, represented by the

Table 4 Rough guide to the temperature operating range for bonded poly(siloxane) liquid phases in open tubular columns

Type	Temperature range (°C)		High temperature version
	Minimum	Maximum	
Dimethylsiloxane	– 60	325	420
Dimethyldiphenylsiloxane (5% diphenyl)	– 60	325	420
Dimethyldiphenylsiloxane (35% diphenyl)	40	300	340
Dimethyldiphenylsiloxane (50% diphenyl)	40	325	390
Methylphenylsiloxane	0	280	
Dimethyldiphenylsiloxane (65% diphenyl)	50	260	370
3,3,3-Trifluoropropylmethylsiloxane (50% trifluoropropyl)	45	240	300
3-Cyanopropylphenyldimethylsiloxane (6% cyanopropylphenyl and 84% dimethyl)	20	280	
3-Cyanopropylphenyldimethylsiloxane (25% cyanopropylphenyl and 75% dimethyl)	40	240	
3-Cyanopropylphenyldimethylsiloxane (50% cyanopropylphenyl and 50% dimethyl)	40	230	
3-Cyanopropyl-silphenylene co-polymer (equivalent to 70% dicyanopropyl)			290
Poly(ethylene glycol)	20	250	280
FFAP	40	250	

FFAP, Poly(ethylene glycol) treated with 2-nitroterephthalic acid.

free energy required for cavity formation, the formation of additional dispersion interactions of a solute-solvent type, and on selective solute-solvent polar interactions dependent on the complementary character of the polar properties of the solute and stationary phase. Quantitatively, these interactions are described by the solvation parameter model set out below in the form suitable for stationary-phase classification:

$$\log k = c + rR_2 + s\pi_2^H + a\Sigma\alpha_2^H + b\Sigma\beta_2^H + l \log L^{16} \quad [1]$$

where k is the retention factor. The remainder of the equations is made up of product terms called system constants (r, s, a, b, l) and solute descriptors ($R_2, \pi_2^H, \Sigma\alpha_2^H, \Sigma\beta_2^H, \log L^{16}$). Each product term represents a contribution from a defined intermolecular interaction to the solute property. The solute descriptors are free energy-related solute properties known for about 4000 compounds with others available by estimation or from experiment. They are not of immediate interest to us here except to note that once the system constants are established, the retention property of any solute with known or easily estimated solute descriptors can be estimated for that system by simple arithmetic calculation using the model described. The system constants (also called phase constants in gas chromatography) contain the information of the stationary-phase properties and provide an unambiguous means of classification. The r phase constant refers to the ability of the stationary phase to interact with solute n - or π -electron pairs. The s phase constant to the ability of the stationary phase to take part in dipole-type interactions. The a phase constant is a measure of stationary-phase hydrogen bond basicity and the b phase constant a measure of stationary-phase hydrogen bond acidity. The l phase constant describes (in part) the contribution of cavity formation and dispersion interactions to retention and, more specifically, indicates the ability of the stationary phase to separate members of a homologous series. The phase constants for any stationary phase can be determined through the method of multiple linear regression analysis by measurement of a retention property for a series of varied solutes with known solute descriptors.

The stationary phase constants for a number of common liquid phases at a reference temperature of 121°C are summarized in Table 5. The system constants in Table 5 are only loosely scaled to each other so that changes in magnitude in any column can be read directly, but changes in magnitude along rows must be interpreted more cautiously. Most stationary

phases possess some capacity for lone-pair electron interactions (r constant), but selectivity for this interaction is all but nonexistent among common stationary phases. Fluorine-containing stationary phases have negative values of the r constant representing the tighter binding of electron pairs in fluorocarbon compared to hydrocarbon groups. Lone pair electron interactions do not usually make a significant contribution to retention in gas-liquid chromatography and are not considered a primary means of selectivity optimization. The most striking feature of Table 5 is the paucity of stationary phases with significant hydrogen bond acidity (b constant). In the case of EGAD, DEGS and TCEP, the small b phase constants indicated in Table 5 are probably a product of impurities and thermal modification of the stationary phases during use rather than a fundamental property of the stationary phases themselves.

A few novel stationary phases with strong hydrogen bond acid properties have been synthesized recently, but none of these are commercially available. Stationary-phase hydrogen bond acid interactions, therefore, do not contribute significantly to method development strategies for the commonly used stationary phases. The only practical exception seems to be the poly(trifluoropropylmethylsiloxane) WCOT column stationary-phase DB-210, which exhibits some weak hydrogen bond acidity, presumably acquired through the immobilization process that is absent from the structurally similar packed-column stationary phase QF-1. That leaves the most important stationary-phase properties for selectivity optimization as their cohesive energy and capacity for dipole-type and hydrogen bond base interactions.

Cluster analysis provides a visual picture of the difference in selectivity for different stationary phases and a classification of their properties into groups of similar selectivity (Figure 2). The stationary phases most similar to each other are next to each other and are connected. Connections at the extreme left-hand side of the dendrogram occur for phases with similar properties and those towards the right-hand side with greater degrees of difference. Stationary phases with no paired descendents are singular phases with properties that cannot be duplicated by the other phases. The stationary phases are classified into five groups with three phases behaving independently. Group 1 contains squalane, Apolane-87, OV-3, OV-7, SE-30 and OV-105. These are phases of low cohesive energy with minimal capacity for polar interactions. The second group of stationary phases contains OV-22, OV-25, OV-11, OV-17, PPE-5 and DDP. These phases have low cohesive energy and are weakly dipolar and hydrogen bond basic. QF-1 is loosely connected to this group but is significantly

Table 5 System constants derived from the solvation parameter model for common stationary phases at 121°C

Stationary phase	System constant				
	<i>r</i>	<i>s</i>	<i>a</i>	<i>b</i>	<i>l</i>
<i>Hydrocarbon phases</i>					
Squalane	0.13	0.01	0	0	0.58
Apolane-87	0.17	0	0	0	0.56
<i>Ether and ester phases</i>					
Poly(phenyl ether) 5 rings (PPE-5)	0.23	0.83	0.34	0	0.53
Carbowax 20M (CW20M)	0.32	1.26	1.88	0	0.45
Poly(ethylene glycol) Ucon 50 HB 660	0.37	0.63	1.28	0	0.50
Nitroterephthalic acid modified poly(ethylene glycol) (DB-FFAP)	0.21	1.42	2.08	0	0.43
1,2,3-Tris(2-cyanoethoxypropane) (TCEP)	0.12	2.09	2.10	0.26	0.37
Didecylphthalate (DDP)	0	0.75	0.77	0	0.56
Poly(ethylene glycol adipate) (EGAD)	0.13	1.39	1.82	0.21	0.43
Poly(diethylene glycol succinate) (DEGS)	0.23	1.57	2.11	0.17	0.41
<i>Liquid organic salts</i>					
Tetrabutylammonium 4-toluenesulfonate (QBApTS)	0.16	1.58	3.30	0	0.46
Tetrabutylammonium tris(hydroxymethyl)methyl-amino-2-hydroxy-1-propanesulfonate (QBATAPSO)	0.27	1.96	3.06	0	0.32
Tetrabutylammonium 4-morpholinepropanesulfonate (QBAMPS)	0	1.75	3.54	0	0.55
Tetrabutylammonium methanesulfonate (QBAMES)	0.33	1.45	3.76	0	0.44
<i>Poly(siloxane) phases</i>					
Poly(dimethylsiloxane) (SE-30)	0.02	0.19	0.13	0	0.50
Poly(dimethyldiphenylsiloxane) (DB-5) (5 mol% diphenylsiloxane)	0	0.28	0.19	0	0.51
Poly(dimethylmethylphenylsiloxane) (OV-3) (10 mol% phenyl)	0.03	0.33	0.15	0	0.50
Poly(dimethylmethylphenylsiloxane) (OV-7)	0.06	0.43	0.17	0	0.51
Poly(dimethylmethylphenylsiloxane) (OV-11) (35 mol% phenyl)	0.10	0.54	0.17	0	0.52
Poly(methylphenylsiloxane) (OV-17)	0.07	0.65	0.26	0	0.52
Poly(dimethyldiphenylsiloxane) (HP-50) (50 mol% diphenylsiloxane)	0.16	0.62	0.28	0	0.47
Poly(methylphenyldiphenylsiloxane) (OV-22) (65 mol% phenyl)	0.20	0.66	0.19	0	0.48
Poly(methylphenyldiphenylsiloxane) (OV-25)	0.28	0.64	0.18	0	0.47
Poly(cyanopropylmethyltrimethylsiloxane) (10 mol% cyanopropylmethylsiloxane) (OV-105)	0	0.36	0.41	0	0.50
Poly(cyanopropylmethylphenylmethylsiloxane) (OV-225)	0	1.23	1.07	0	0.47
Poly(cyanopropylphenyldimethylsiloxane) (50 mol% cyanopropylphenylsiloxane) (DB-225)	0	1.21	1.18	0	0.44
Poly(dicyanoalkylsiloxane) (OV-275)	0.21	2.08	1.99	0	0.29
Poly(trifluoropropylmethylsiloxane) (QF-1)	−0.45	1.16	0.19	0	0.42
Poly(trifluoropropylmethylsiloxane) (DB-210)	−0.27	1.15	0	0.19	0.43
Poly(dimethylsiloxane)-poly(ethylene glycol) copolymer (OV-330)	0.10	1.06	1.42	0	0.48

more dipolar and has a more significant and opposite capacity for lone pair electron interactions. The third group contains OV-330 and OV-225 with UH50B loosely connected to this group. Compared to the second group these stationary phases are more dipolar and hydrogen bond basic and slightly more cohesive. They represent an increase in the intensity of the same range of interactions as the group 2 stationary phases. The fourth group contains the liquid organic salts with QBATAPSO distinguished within this group by its greater cohesive energy. Phases in this group are dipolar and the strongest hydrogen bond bases. The fifth group of solvents is divided into two subgroups. TCEP and OV-275 are strongly dipolar, hydrogen bond basic and have high cohesive energy.

EGAD, CW20M and DEGS have a similar range of polar interactions, but not quite as intense, and have a lower cohesive energy. For selectivity optimization in packed-column gas chromatography, a single phase is initially selected from each group. Subsequently, for fine-tuning additional phases are selected from within the group, identified as possessing the desired separation properties.

For historical reasons stationary phases are classified at a common reference temperature of about 120°C. The capacity of a stationary phase for specific intermolecular interactions determined at one temperature can be misleading for selectivity optimization at other distant temperatures. The broad outlines in Table 5 and Figure 2 remain true but changes in

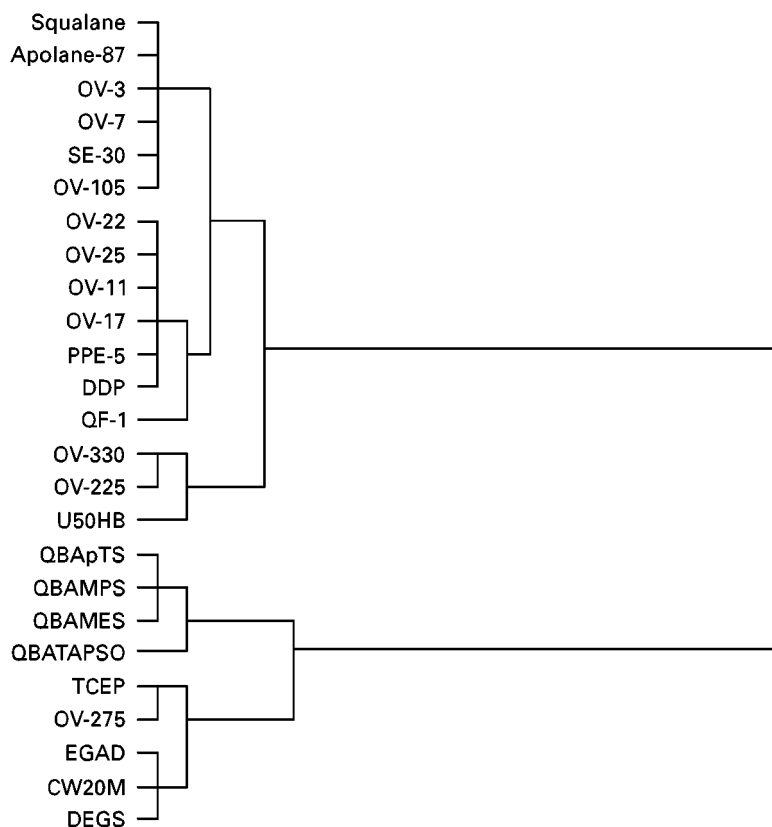


Figure 2 Nearest neighbour complete link cluster dendrogram for some common stationary phases. The abbreviations for the stationary phases are identified in Tables 2, 3 and 5.

rank order due to cross-overs occur at different temperatures. Also, selectivity differences between individual stationary phases are enhanced at low temperatures with phases becoming more alike at higher temperatures. Information on the contribution of polar interactions to retention at high temperatures is scarce. These contributions could be small and stationary-phase selectivity differences rather limited at high temperatures.

Gas-solid chromatography is used for a narrower range of separations than gas-liquid chromatography. Because of higher retention, typical applications are the separation of fixed gases, volatile hydrocarbons, halocarbons, organic solvents and sulfur gases. The presence of immobilized active centres enhances the separation of isomers and isotopes. These separations are often difficult or impossible with liquid phases. A rough guide to the selection of sorbents for particular applications is given in Table 6. PLOT columns provide higher efficiency, faster separations and faster column regeneration compared to packed columns. Surface coating with inorganic salts and small amounts of liquid phase are used to extend the molecular weight separation range with inorganic oxide and carbon sorbents and to optimize selectivity.

PLOT columns generally require greater care in their use than WCOT columns. Other features include lower efficiency than WCOT columns, limited sample capacity and high activity.

General Elution Problem

In gas chromatography there is an approximate exponential relationship between retention time and solute boiling point at a constant (isothermal) column temperature. Consequently, it is impossible to establish a suitable compromise temperature for the separation of mixtures with a boiling point range exceeding about 100°C. This is generically referred to as 'the general elution problem' and is characterized by long separation times, poor separations of early eluting peaks and poor detectability of late eluting peaks due to zone broadening. The general solution to this problem is the use of programmed temperature and flow separation modes. Neither constant nor programmed modes are superior to each other. They are complementary, with the properties of the sample deciding which approach is adopted.

Temperature programming is the most popular programmed separation mode in gas chromatography.

Table 6 General applications of PLOT columns in gas chromatography

Stationary phase	Maximum operating temperature (°C)	Typical applications
Alumina oxide	200	Alkanes, alkenes, alkynes and aromatic hydrocarbons from C ₁ to C ₁₀ . C ₁ and C ₂ halocarbons
Silica gel	250	Hydrocarbons (C ₁ to C ₄), inorganic gases, volatile ethers, esters and ketones
Carbon	350	Inorganic gases and hydrocarbons (C ₁ to C ₅)
Carbosieves	150	C ₁ to C ₆ compounds
Molecular sieves (5A and 13X)	350	Hydrogen, oxygen, nitrogen, methane and noble gases Hydrocarbons (C ₁ to C ₃) on 5A with higher alkanes on 13X (up to C ₁₂) but not isomer separations
Porous polymers		
Q	310	Hydrocarbons (C ₁ to C ₁₄), halocarbons (C ₁ and C ₂), volatile oxygenated solvents
S	250	(C ₁ to C ₆), thiols, amines, nitro compounds, nitriles, water and inorganic gases
U	190	

Q, Poly(divinylbenzene-styrene); S, poly(divinylbenzene-vinylpyridine); U, poly(divinylbenzene-ethylene glycol dimethacrylate).

Stationary phases of high thermal stability allow wide temperature ranges to be used and temperature is easily adjusted and controlled. Temperature programme techniques are the most useful approach for scouting the properties of an unknown sample and are compatible with the large volume injection modes employing low temperature solute refocusing used in trace analysis. Flow programming is easily achieved with instruments fitted with electronic pressure control but is limited by the narrow pressure range which is usually available. It can be used to separate thermally labile compounds at a lower temperature than required for temperature-programmed separations. On the other hand, flow programming results in a loss of efficiency for late eluting peaks and presents difficulties in calibrating flow-sensitive detectors.

A temperature programme consists of a series of changes in the oven temperature and includes isothermal and controlled temperature rise segments. In essence, most programmes are simple, consisting of an initial isothermal period, a linear temperature rise segment, final isothermal period at the temperature reached at the end of the rise segment, and a cool-down period to return the oven to the starting temperature. The initial and final isothermal periods are optional, the temperature rise segment can be selected over a wide range (0.1 to *c.* 100°C min⁻¹), nonlinear changes in temperature may be used (extremely rare) and for complex mixtures, several linear programmes may be used in sequence to optimize the separation. The initial oven temperature is selected with due consideration to the resolution of the earliest eluting peaks in the chromatogram. If the temperature chosen is too high, the resolution of the initial peaks may be inadequate and, if it is too low, resolution may be acceptable but the separation time will be extended needlessly. The final temperature should be

selected so that the termination of the temperature rise segment and elution of the last sample component coincide unless the last few eluting peaks are particularly difficult to separate and require an isothermal period. Peaks eluting after completion of the temperature rise segment will be wider than those eluted during the programme. The selection of the heating rate represents a compromise between the necessity of maintaining a minimum acceptable resolution for the sample and the desire to reduce the separation time. This is governed largely by the complexity of the sample and its boiling point range. For samples containing components of different polarity temperature-induced changes in selectivity make the prediction of the resolution of closely spaced peaks a problem. Certain generalities can be made however. For the most difficult separations a slow heating rate will usually provide the optimum resolution. The separation time of weakly retained solutes is more readily adjusted by changing the flow rate of the carrier gas than the heating rate. For strongly retained solutes increasing the heating rate causes a proportional decrease in the separation time at a constant carrier gas flow rate. The retention time of well-retained solutes are less affected by changing flow rates in temperature-programmed gas chromatography.

The lack of an exact mathematical model to describe temperature-programmed separations makes computer simulation for their rapid optimization difficult. Simplex optimization of experimental variables and a model based on the linear elution strength approximation have been used with some success. The linear elution strength approach has the advantage that it only requires experimental data from two temperature-programmed separations of a sample using different programme rates. A series

of empirical equations are then employed to predict optimum separation conditions using relative resolution maps.

Generic Method Development

Method development commences with a definition of the problem and a review of available resources. Some pointers are given in Table 7. The separation of enantiomers requires special stationary phases and some separations of isomers use liquid crystal stationary phases that are not common laboratory items. Fast separations require special equipment and truly fast separations are only possible for simple mixtures. The separation of complex mixtures can be speed-optimized but not necessarily performed quickly on the same timescale used for simple mixtures. Preparative separations are usually performed with packed columns unless only a small amount of material

is to be isolated. Most analytical separations are performed using WCOT and PLOT columns, except for reasons noted earlier. A general guide to the selection of column types and dimensions is given in Table 8. For a sample of unknown composition a generic method for sample evaluation is provided in Table 9. These instruction sets will work for most simple mixtures and provide a starting point for difficult samples.

Injection and Detection Considerations

The choice of sample inlet depends on the injection volume, concentration of analytes, thermal stability of the analytes, concentration of involatile matrix components, volatility range of the analytes, relative volatility difference between the analytes and

Table 7 Defining the problem and utilizing available resources to formulate a solution

Problem definition

How many detectable compounds are present in the sample?

This is the only way to know that a separation is complete. It indicates the complexity of the problem, if only because, statistically, as the number of components requiring separation increases, so does the difficulty of achieving the separation. Fast separations are not easy for complex mixtures

Are all components equally relevant?

The only separation required is that of the compounds of interest from each other and all other compounds in the sample. The latter compounds can be considered as matrix components and need not be individually separated. This reduces the difficulty of providing a separation fit for the defined purpose

Are standards available for the compounds of interest?

This enables peaks to be tracked through initial trial separations and links difficult-to-separate compound pairs to their structure so that informed changes to the separation system can be made. It is required for calibration if quantification is needed

What is the concentration range of relevant compounds?

Trace components may initially be missed because of inadequate dynamic range if only the major components are considered. Particular injection techniques and selective detectors may be required to detect some compounds at anticipated concentrations

Is identification of unknowns required?

If unknown compounds are to be identified, retention information alone will be inadequate in most cases. Coupling to mass or infrared spectroscopic detectors is usually required to achieve the desired level of confidence in the result

Resources

Literature describing similar separations

Substantial databases of the chromatographic literature in an electronic searchable form are available. Column manufacturers' catalogues contain information on the separation of common sample types and certified columns may be available for mixtures subject to routine analysis. Official methods controlled by regulatory agencies usually specify appropriate columns for the separation

Past experience with similar samples

Life is a learning experience and there is no substitute for a good memory. What worked in a previous case for a similar sample is probably a good starting point for the new sample. Colleagues may have an informed opinion based on a different lifetime experience

Availability of certain columns and equipment

Resources are restricted to available columns and equipment and an evaluation of whether they will provide the information required is performed. Additional resources may have to be purchased or informed decisions made of the suitability of substituting available for desired resources

Compound information from handbooks

Structures, molecular weight, boiling point (or vapour pressure), solubility in common solvents is useful information that can be found in handbooks for many compounds which are identical or similar to the compounds of interest. This is useful for stationary-phase selection, derivatization strategies and detector selection

Table 8 Guide to the selection of WCOT columns*Column internal diameter*

- Use 0.25 mm i.d. columns for normal split and splitless injection unless sample overloading is a problem
- Use 0.32 mm i.d. columns for splitless and on-column injection, especially when injecting large sample amounts
- Use 0.53 mm i.d. columns as a replacement for packed columns, for the separation of samples containing < 30 components, or samples with components spanning a wide concentration range
- Use 0.18 mm i.d. (or less) columns when the maximum efficiency is required and for high speed separations (modifications to standard instruments may be needed)

Film thickness

- Standard film thicknesses are used for most applications (0.25 μm for 0.25 and 0.32 i.d. columns)
- Use thin film columns (0.1–0.25 μm) for solutes of low volatility (e.g. waxes, triglycerides, steroids, etc.)
- Use thick film columns (1–5 μm) for volatile solutes (e.g. solvents, gas-purgeable compounds)
- Choose columns with a similar phase ratio to obtain similar retention (larger phase ratios reduce retention)

Stationary phase

- If the sample composition is unknown, begin with a nonpolar stationary phase such as a poly(dimethylsiloxane) or poly(dimethyldiphenylsiloxane) with a low mol fraction of diphenylsiloxane groups that separate mainly by differences in volatility
- To improve selectivity, choose a stationary phase whose polarity best matches that of the solutes (similar dipolarity or complementary hydrogen bond interactions). See Figure 2 for the systematic identification of suitable stationary phases
- Consider using a PLOT column for the separation of light hydrocarbons and gases (other applications are indicated in Table 6)

Set-up conditions

Internal diameter (mm)	0.18	0.25	0.32	0.53
Flow rate (mL min ⁻¹)				
Hydrogen, $u = 40 \text{ cm s}^{-1}$	0.6	1.4	2.4	5.2
Helium, $u = 20 \text{ cm s}^{-1}$	0.3	0.7	1.2	2.6
Sample capacity (μg)	< 0.05	0.05–0.1	0.4–0.5	1.2
Separation number	40	30	25	15
Separation efficiency ($n \text{ m}^{-1}$)	5300	3300	2700	1600

solvent, and the required accuracy and precision. Split injection is commonly used for evaluating separation conditions, even if a different injection technique is used for routine applications. Split injection involves offline vaporization and mixing of the sample vapours with the gas phase, a portion of which is the carrier gas flow for the column and is

responsible for transporting a fraction of the sample into the column. Sample bands are narrow, preserving the resolving power of the column. Split injection can handle samples containing involatile matrix components and is the preferred method for injecting gases and volatile samples such as solvents. Accuracy and precision are often poor compared to

Table 9 Generic exploratory conditions for the separation of a sample of unknown composition

Stationary phase	Nonpolar poly(dimethylsiloxane) or poly(dimethyldiphenylsiloxane) with 5 mol% diphenylsiloxane groups
Column	Length 10–30 m Internal diameter 0.25 or 0.32 mm Film thickness 0.25 μm (1.0 μm for volatile compounds)
Flow rate	u_{opt}
Temperature	Programme from 50 to 300°C at 20°C min ⁻¹ (or to temperature limit for phase) Note the elution temperature (T_{E}) and range of T_{E} values T_{E} range < 25°C isothermal analysis T_{E} range > 25°C programmed analysis
Isothermal	Optimize range of retention factors (k). T_{opt} found from plot of $\log k$ versus $1/T$
Programmed	From original programme: 1 Select T initial ($T_{\text{E}} - 20$ for first component) 2 Select T final ($T_{\text{E}} + 20$ for last component) 3 Programme rate selected based on complexity. Simple mixture 10°C min ⁻¹ or higher and complex mixture 1–2°C min ⁻¹
Injector/detector	Initially high (c. 350°C). Reset, based on findings in trial chromatograms
Temperature	c. 25°C higher than the final column temperature
Injector	Split with a split ratio 1 : 50 to 1 : 100
Detector	Universal (flame ionization detector)

Table 10 Characteristic properties of common detectors

Detector	Minimum detectable amount	Linear response range	Selectivity
Thermal conductivity	$3 \times 10^{-9} \text{ g mL}^{-1}$	10^4	
Flame ionization	$10^{-12} \text{ g s}^{-1}$	10^6	
Thermionic ionization	$10^{-13} \text{ g s}^{-1}(\text{N})$ $10^{-14} \text{ g s}^{-1}(\text{P})$	10^4	$4 \times 10^4 \text{ gC/gN}$ $7 \times 10^4 \text{ gC/gP}$ 0.5 gN/gP
Photoionization	$10^{-12} \text{ g mL}^{-1}$	10^7	
Helium ionization	$4 \times 10^{-14} \text{ g s}^{-1}$	10^4	
Electron capture	$10^{-13} \text{ g mL}^{-1}$	10^4	
Flame photometric	$10^{-11} \text{ g s}^{-1}(\text{S})$ $10^{-12} \text{ g s}^{-1}(\text{P})$	Nonlinear 10^5	$10^3\text{--}10^6 \text{ gC/gS}$ $5 \times 10^5 \text{ gC/gP}$
Sulfur chemiluminescence	$4 \times 10^{-13} \text{ g s}^{-1}(\text{S})$	$10^3\text{--}10^4$	$10^6\text{--}10^7 \text{ gC/gS}$
Microwave plasma	$1\text{--}75 \times 10^{-13} \text{ g s}^{-1}$	10^4	Large
Electrolytic conductivity	$10^{-12} \text{ g s}^{-1}(\text{N})$ $10^{-13} \text{ g s}^{-1}(\text{Cl})$ $5 \times 10^{-13} \text{ g s}^{-1}(\text{S})$	$10^3\text{--}10^5$	$10^4\text{--}10^9 \text{ gC/g(N, Cl or S)}$

other injection techniques and sample information is not preserved for mixtures of a wide volatility range. Splitless injection allows larger sample volumes to be injected for trace analysis but requires an effective refocusing mechanism using cold trapping or solvent effects. Optimization of injection conditions is relatively complicated and time-consuming but accuracy and precision are good for favourable cases. On-column injection is the most accurate and precise injection technique but is limited to small sample volumes and requires relatively clean extracts. Programmed temperature vaporization injection is able to emulate all of the above injection methods as well as allowing large volume injections in the solvent-venting mode. Injection techniques using flash vaporization place the greatest thermal stress on the sample and are unsuitable for labile compounds. All methods can be automated, resulting in improved accuracy and precision compared to manual injection techniques.

Gas chromatography is blessed by a number of reliable and near universal and selective detectors (Table 10). Interfacing of gas chromatography to spectroscopic detectors for structural elucidation as well as quantification is straightforward and reduced to routine practice. For general applications the flame ionization detector is difficult to eclipse. It is sensitive, rugged, has a wide linear range, and it has a near universal response to carbon-containing compounds. It has a poor response to the noble gases and certain simple organic compounds containing a single carbon atom bonded to nitrogen, oxygen or sulfur. Thermal conductivity or helium ionization detection can be used for these compounds. A wide range of element-selective detectors and structure-selective de-

tectors has been developed for particular applications demanding matrix discrimination, low sample detectability, or for portable instruments. There are few situations encountered in gas chromatography where the identification of a suitable detector is the limit to progress.

Further Reading

- Abraham MH, Poole CF and Poole SK (1999) Classification of stationary phases and other materials by gas chromatography. *Journal of Chromatography A* 842: 79–114.
- Bautz DE, Dolan JW and Snyder LR (1991) Computer simulation as an aid in method development for gas chromatography. I. The accurate prediction of separation as a function of experimental conditions. *Journal of Chromatography* 541: 1–20.
- Jayatilaka A and Poole CF (1993) Computer-assisted optimization of the gas chromatographic separation of equine estrogens. *Journal of Chromatography* 617: 19–27.
- Jennings W, Mittlefehldt E and Stremple P (1997) *Analytical Gas Chromatography*. San Diego: Academic Press.
- Ji Z, Majors RE and Guthrie EJ (1999) Porous layer open-tubular capillary columns: preparations, applications and future directions. *Journal of Chromatography A* 842: 115–142.
- Poole CF and Poole SK (1991) *Chromatography Today*. Amsterdam: Elsevier.
- Rotzsche H (1991) *Stationary Phases in Gas Chromatography*. Amsterdam: Elsevier.
- Villalobos R and Annino R (1991) Computer-aided design and optimization of an on-line gas chromatographic procedure for the analysis of purgeable compounds in waste water. *Journal of High Resolution Chromatography* 14: 681–685.

ESSENTIAL GUIDES TO METHOD DEVELOPMENT IN LIQUID CHROMATOGRAPHY

J. W. Dolan and L. R. Snyder, LC Resources Inc.,
CA, USA

Copyright © 2000 Academic Press

Introduction: Steps in Method Development

Development of a method for a high performance liquid chromatography (HPLC) separation can be a major undertaking. Before the separation can be made, the sample must be in a suitable form to inject, and pretreatment steps are often required to remove major interferences or materials that might shorten the column life. After conditions for adequate separation are determined, some level of method validation is usually performed. Sample pretreatment and method validation are beyond the scope of the present discussion, which concentrates on achieving separation. This article describes only the major steps that are required for most samples. For additional information, the reader is urged to consult the reference by Snyder *et al.* (see Further Reading) which covers HPLC method development in detail. Additional method development information can be found in the other monographs listed.

General Approach

There are different approaches to HPLC method development, but we will follow the steps outlined in Table 1 and discussed below. For most samples, this approach provides the highest probability of success with the minimum investment in time and effort.

The first step in HPLC method development is to choose a chromatographic mode or method type. The most common modes are reversed-phase, normal-phase, ion exchange and size exclusion. User surveys over the last 10 years consistently show that most separations are performed using reversed-phase col-

umns. For the present discussion, reversed-phase separation is assumed. The following section gives a brief description of the use of alternative HPLC modes for special samples.

Once a mode is selected, the next step is to find conditions that will provide a separation of most of the sample components. When this has been achieved, it is then possible to estimate the effort that will be required to obtain an adequate separation of all components. This first step can be accomplished using either gradient or isocratic elution. We favour an initial gradient run, because all peaks are likely to elute in a defined time with reasonable separation of both early and late peaks. Usually several isocratic runs are required to achieve a similar result, and often no isocratic conditions will provide an acceptable separation. From the initial gradient run it is possible to estimate whether isocratic elution is possible. If this is the case, it is also possible to estimate conditions that give reasonable separation of most sample components.

As soon as this minimal separation is obtained, the chromatogram should be examined for problems related to peak shape. Most obvious are peak tailing problems. Although perfectly symmetrical peaks are preferred, many separations (usually for samples that contain basic compounds) will have one or more peaks that exhibit tailing. Most workers will accept peaks with asymmetry factors, $A_s \leq 2.0$ (United States Pharmacopeia (USP) tailing factor, $T_f \leq 1.7$). More severe tailing suggests the presence of unwanted sample interactions with the stationary phase. The most common fixes for tailing bands, in order of decreasing usefulness, are:

1. the use of columns designed for the separation of basic samples (based on very pure, type B silica);
2. adjustment of pH;
3. addition of triethylamine as a tailing suppressor;
4. use of ion pairing;
5. switching to a nonsilica (e.g. polymeric) column.

Symmetrical peaks that are too broad can also signal poor chromatographic behaviour; e.g. when column plate numbers, N , for the sample are $< 60\%$ of the column manufacturer's test report. Broad peaks can result from the use of too strong a sample solvent, injection volumes that are too large, column overload or column problems. Usually it is advisable

Table 1 General approach to HPLC method development

Select HPLC method
Obtain minimal separation
Check for and correct peak shape and width problems
Fine-tune primary variable
Change additional variables
Adjust column conditions

first to repeat the separation on a new column, to be sure that the problem is caused by a bad column. Reducing the injection volume to $< 25 \mu\text{L}$, keeping the injected mass $< 10 \mu\text{g}$, matching the injection solvent with the mobile phase and increasing the column temperature are some possible approaches to sharpening broad peaks.

Once acceptable peak shape is obtained, the next step is to fine-tune the primary variable: the percentage of organic solvent in the mobile phase, %B, for isocratic separations, or gradient time, t_G , for gradient elution. In general, weaker (lower %B) isocratic mobile phases or shallower (larger t_G) gradients will increase resolution at the expense of longer run times and broader peaks (with lower detection sensitivity). The best separation depends on the relative importance of peak resolution, run time and detection sensitivity, and will usually correspond to an intermediate value of %B or t_G .

An example of the effect of isocratic solvent strength (%B) on retention and selectivity is seen in **Figure 1** for the simulated separations of eight aromatic compounds. It is seen that retention and bandwidth increase inversely with %B. In general, R_s also increases, but not for every peak pair – only seven out of the eight peaks are visible at 70% and 50%B. Note the relative forward movement of benzene from 70%B, where it co-elutes with 2-nitrotoluene to 50%B, where it co-elutes with 2,6-dinitrotoluene; at intermediate solvent strengths it is resolved from neighbouring peaks.

Figure 2 shows the effect of gradient time (t_G) on retention and selectivity for simulated separations of a proprietary mixture of 11 herbicides. Retention and bandwidth increase with increasing t_G . The overall resolution increases with longer gradients, but note that peak 7, which elutes after peak 6 in the 20 min gradient, moves ahead of peak 7 with longer gradient times.

When satisfactory separation cannot be obtained by adjustment of the primary variable (%B or t_G), the usual problem is one of overlapping bands or selectivity. In the latter case, other conditions (mobile phase, column packing, temperature) can be varied. For example, we recommend starting with acetonitrile as the B solvent. Changes in selectivity are often observed if methanol or tetrahydrofuran is used instead of acetonitrile. Other variables worth examining are column temperature, pH (for ionic samples), use of ion-pairing reagents (ionic samples) and different types of stationary phase (e.g. change from C_{18} to a cyano or phenyl phase).

The final step in method development is to adjust so-called column conditions: flow rate, column dimensions and/or packing particle size. Typically,

sample resolution increases only slowly with decrease in flow rate or increase in column length, while run time increases much faster. If resolution is greater than required, this means that an increase in flow rate and/or decrease in column length can be used for a significant decrease in run time with acceptable loss in resolution. Smaller particle columns are typically used in shorter lengths; these small particle columns can provide shorter run times without loss in resolution or increase in column pressure. The column pressure drop (or system pressure) increases with higher flow rates, longer columns and smaller particles. Since it is desirable to maintain a system pressure $< 200 \text{ atm}$, this places a further constraint on the latter column conditions.

The simulated chromatograms of **Figure 3** show the effect of changes in column conditions on the aromatic sample of **Figure 1**. The lower run is the same as the middle run of **Figure 1**, using a 250 mm, $5 \mu\text{m}$ particle column with a flow rate of 2 mL min^{-1} , generating $R_s = 2.0$ in 11 min with 100 bar back pressure. By changing to a 150 mm, $3.5 \mu\text{m}$ column at the same flow rate, the run time is reduced to 6 min. For many applications, the narrower peaks (and thus lower detection limits) and shorter run time will be worth the minimal loss in resolution and increase in pressure ($R_s = 1.85$, 120 bar back pressure). If lower resolution is acceptable, a shorter column (75 mm, $3.5 \mu\text{m}$) at a higher flow rate (4 mL min^{-1}) will reduce the run time to $< 2 \text{ min}$, as shown in **Figure 3C** ($R_s = 1.15$, 120 bar back pressure).

Choice of HPLC Mode

Reversed-phase HPLC will prove adequate for most samples. Sample types requiring other chromatographic methods are summarized in **Table 2**. For samples that fall in one of these categories, consult the Further Reading section for detailed instructions.

Choice of Starting Conditions

A recommended set of starting conditions is summarized in **Table 3**. A C_8 or C_{18} column is chosen, with no particular preference for either phase. The $150 \times 4.6 \text{ mm}$ column size packed with $5 \mu\text{m}$ particles is capable of achieving most separations; with flow rates of $1\text{--}2 \text{ mL min}^{-1}$, run times are usually $< 15 \text{ min}$. One of the newer type B (low metal) silicas is strongly recommended for optimum peak shape and better column-to-column reproducibility.

Acetonitrile–water is recommended as mobile phase, because of its lower viscosity (and lower pressure drop), as well as its ability to be used with low

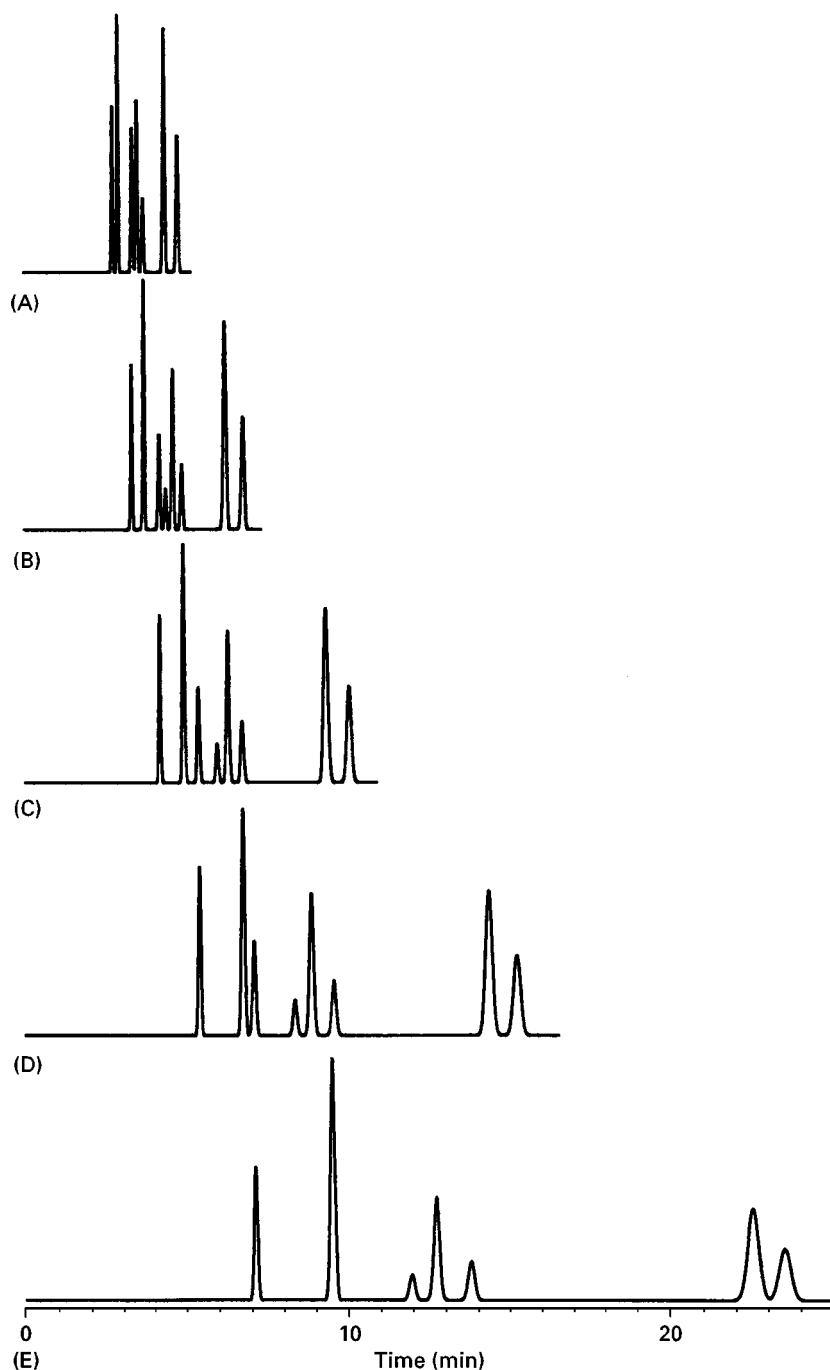


Figure 1 Simulated chromatograms for isocratic separations of aromatic compounds on a C_{18} column using water–acetonitrile mobile phases. (A) 70%; (B) 65%; (C) 60%; (D) 55%; (E) 50% acetonitrile. Samples: nitrobenzene, 2,6-dinitrotoluene, benzene, 2-nitrotoluene, 4-nitrotoluene, 3-nitrotoluene, 2-nitro-1,3-xylene, and 4-nitro-1,2-xylene (in retention order).

wavelength UV detection (≥ 190 nm; required for assay of some samples). If ionizable compounds are present in the sample, a buffer should be used. Phosphate at pH 2.5 is recommended for the initial separation, but note its reduced solubility for $> 80\%$ acetonitrile–buffer. When a volatile buffer is needed for liquid chromatography–mass spectrometry (LC-

MS) applications, 0.1% trifluoroacetic acid (pH 1.9), formic acid or ammonium acetate can be used.

The column should be thermostatted to maintain constant temperature and retention times; 5–15°C above room temperature is recommended for the initial separation. Temperature can be further adjusted to change selectivity if necessary. A sufficient

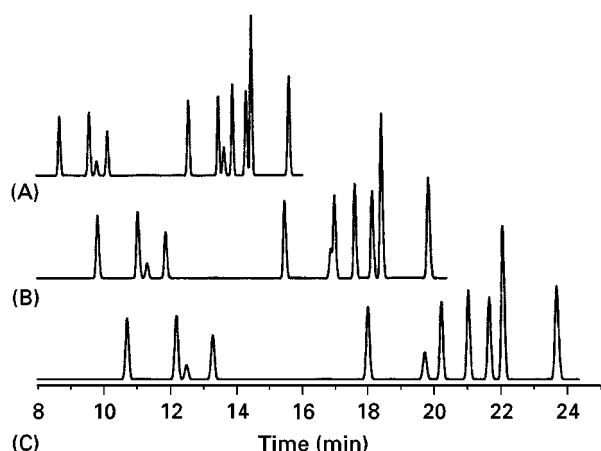


Figure 2 Simulated chromatograms for gradient separations of a proprietary herbicide mixture with a buffer–acetonitrile mobile phase. 5–80% acetonitrile in (A) 20; (B) 30; (C) 40 min.

weight of sample must be injected to obtain adequate detection sensitivity, but weights $> 10 \mu\text{g}$ should be avoided initially. Similarly, sample volume should be $< 50 \mu\text{L}$ to avoid excess band broadening.

Control of the Separation: Selection of Conditions

The selection of conditions for an HPLC method is expedited by a systematic approach. Because the goal of most separation development is to establish resolution for some or all peaks in a chromatographic run, we will use the fundamental resolution equation (eqn [1]) as a guideline:

$$R_s = \frac{1}{4}(N^{0.5})(\alpha - 1)(k/(1 + k)) \quad [1]$$

i ii iii

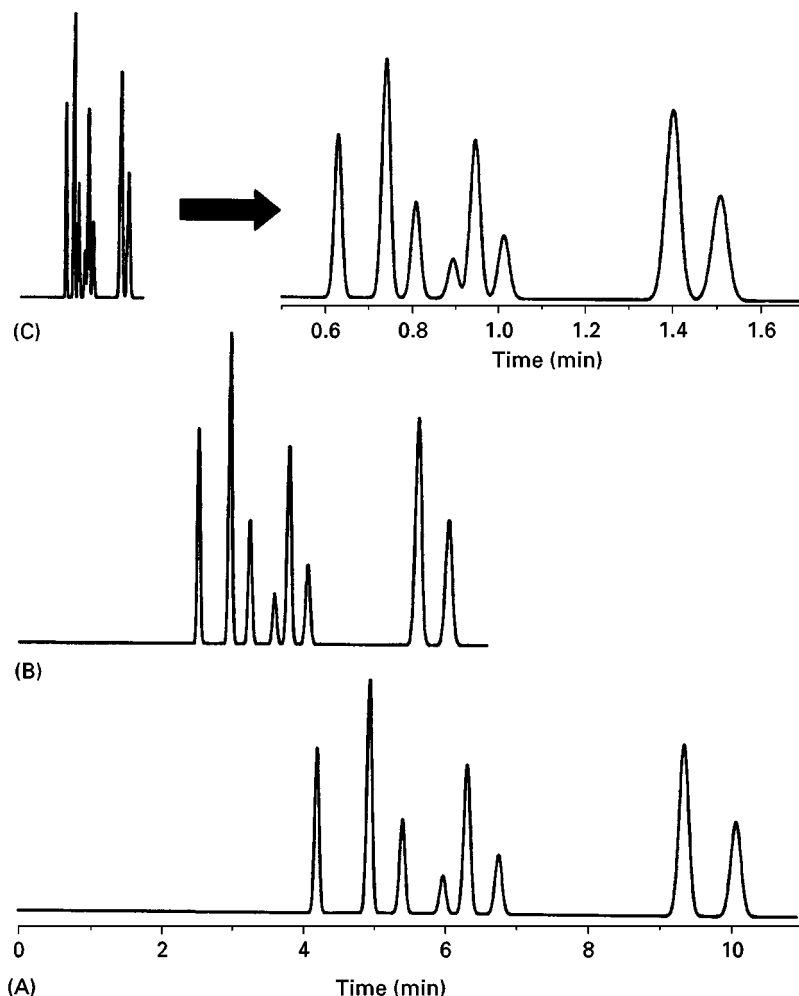


Figure 3 Simulated chromatograms for the sample shown in Figure 1 (60% acetonitrile) when column conditions are varied. (A) 250 mm, $5 \mu\text{m}$ particle column at a flow rate of 2 mL min^{-1} ; (B) 150 mm, $3.5 \mu\text{m}$ at 2 mL min^{-1} ; (C) 75 mm, $3.5 \mu\text{m}$ at 4 mL min^{-1} (expanded scale in upper right).

Table 2 Preferred HPLC methods and columns for different samples

Sample characteristics	Preferred HPLC method/column
High molecular weight	Special columns usually required Size exclusion and ion exchange HPLC often preferred
Optical isomers (enantiomers) present	Special chiral columns required
Other isomers (stereo-, position, etc.)	Normal-phase often best, especially with unmodified silica
Mixtures of inorganic salts	Ion chromatography
Carbohydrates	Amino-bonded phase columns with reversed-phase conditions; ion exchange resins
Biological samples	Special conditions often required for life science samples; may not require different approach
Hydrocarbon mixtures	Normal-phase with unmodified silica

where R_s is the resolution, N is the column plate number, α is the separation factor (selectivity), and k is the retention factor. The influence of each of these variables on the separation is discussed below.

Control of Retention

Term iii of eqn [1] varies with solvent strength. For reversed-phase separations, increased % B increases solvent strength, reduces sample retention (values of k), and reduces the size of term iii (and the value of R_s). The retention factor, k , is calculated using eqn [2]:

$$k = (t_R - t_0)/t_0 \quad [2]$$

where t_R is the retention time and t_0 is the column dead time. In general, as k increases, resolution and run time increase while bandwidth increases and peak height (sensitivity) decreases. For the best chromato-

graphic performance, separations in which $0.5 < k < 20$, or better $1 < k < 10$, are preferred. If k is too small (low retention), resolution is often poor because peaks tend to bunch at t_0 , while interferences from unretained sample components can also be a problem. When k is too large, run times are excessive, and detection sensitivity suffers because of wide peaks. Because of the major effect of solvent strength on separation, the selection of an acceptable value of % B should be the first priority. As will be seen in the following section, separation selectivity may also be affected by % B . Examples of the effect of % B on the separation were discussed earlier in conjunction with the chromatograms of Figure 1.

For isocratic method development, the rule of three can be used as a guideline to adjust retention by varying % B . The rule of three states that retention (or k) changes about threefold for a 10% change in mobile-phase % B . Thus, a change from 50% methanol to 60% methanol will reduce retention times by about three times. Similarly, a 20% B change will cause a 3×3 or about 10-fold change in retention. A convenient way to select a value of % B for isocratic separations is to start at 90% or 100% B and reduce % B in 10% steps until retention is in a reasonable range, then carry out final small adjustments in this variable.

Control of Selectivity

The selectivity term, ii, of eqn [1] is based on the separation factor α , defined in eqn [3]:

$$\alpha = k_2/k_1 \quad [3]$$

where k_1 and k_2 are values of k for the first and second peaks of interest, respectively. Because α is related to k , changing k by varying % B often results in changes in selectivity as well. Because the optimization of term iii of eqn [1] depends on the adjustment of % B , corresponding changes in selectivity (term ii) are conveniently made at the same time (by small further adjustments in % B). Note that acceptable values of

Table 3 Experimental conditions for initial isocratic HPLC separation

Separation variable	Preferred initial choice
<i>Column</i>	
Dimensions (length, i.d.)	150 \times 4.6 mm
Particle size	5 μ m
Stationary phase	C ₈ or C ₁₈
<i>Mobile phase</i>	
Solvents A/B	Water–acetonitrile
% B	Variable
Buffer	25 mmol L ⁻¹ phosphate, pH 2.5 or 0.1% trifluoroacetic acid
Additives ^a (e.g. ion pair reagents, amines)	As necessary
Flow rate	1–2 mL min ⁻¹
Temperature	40°C
<i>Sample size</i>	
Volume ^b	< 50 μ L
Mass ^b	< 100 μ g

^aMainly affecting separation of ionized compounds.

^bAssumes 150 \times 4.6 mm reversed-phase column.

term iii can often be achieved by any value of %B within a 5–10% range. The ease of changing %B is a further reason for using this variable to vary selectivity.

Although selectivity is influenced by %B, changes in other conditions can have a much larger effect on values of α . Changes in the organic solvent type, pH, or use of additives are usually the next choice, once mobile-phase %B is optimized in terms of both k and α . For simplicity, we recommend changes in organic solvent first for neutral compounds. After starting with acetonitrile, change next to methanol, while reserving tetrahydrofuran as a last choice for solvent type. Changes in temperature can provide further changes in selectivity, especially for acid and base samples. If the sample contains acids and/or bases, changes in mobile-phase pH can be the most powerful means to control selectivity. If none of these approaches is successful, mobile-phase additives, such as ion-pairing reagents may be helpful, or a different kind of column (C₁₈, cyano, phenyl) can be tried.

Control of Column Efficiency

We have noted that sample resolution is not much increased by changes in column conditions (except for a large increase in run time). For the same reason, the column plate number N and term i of eqn [1] usually cannot provide a large increase in resolution, once terms ii and iii have been optimized. This means that it is important to select initial conditions which provide a value of N that will be sufficient for most separations. For most samples, we recommend one of the newer columns based on a low metal silica, often termed type B or base-deactivated silica. These columns reduce unwanted chemical interactions that cause peak tailing and column-to-column variations. Columns packed with spherical 5, 3.5 or 3 μm particles are preferable. We favour either (a) 150 \times 4.6 mm, 5 μm or (b) 75 \times 4.6 mm, 3.5 μm columns as a starting point. Column (a) is the first choice of many users because it is robust and has sufficiently low back pressure to allow operation at 2 mL min⁻¹, resulting in short run times. Smaller particles give a better compromise of plate number versus run time (for the same column pressure drop), but are more prone to problems such as blockage by particulates in the sample or mobile phase.

If the adjustment of conditions for optimization of terms ii (α) and iii (k) in eqn [1] has been successful, not infrequently sample resolution will be greater than required. In this case, run time can often be substantially reduced by increasing flow rate while decreasing column length. The latter represents the

most profitable use of term i (by change in column conditions).

Gradient Elution

Most workers prefer isocratic methods for routine use. If an isocratic separation is not feasible because of too broad a sample retention range ($0.5 < k < 20$ not possible for all peaks), gradient elution is required. Even where a final isocratic method is possible, it is still advantageous to begin the method development process with a gradient run. Thus, a single gradient run can be carried out which will provide an attractive value of term iii for every sample peak, thus avoiding problems in isocratic elution that are caused by values of %B that are too large or too small (poor resolution, long run times, wide peaks and poor detection sensitivity). With isocratic separation, several runs (and several hours) may be required to find conditions for which $0.5 < k < 20$ for the sample. In contrast, equivalent conditions for gradient elution can be determined in advance and the first run can generate a reasonable separation. Furthermore, by using method development software with gradient input runs, it is easy to convert a gradient method to an isocratic one and to evaluate the trade-offs between an isocratic and gradient final method.

Typical starting conditions for gradient elution are given in Table 4. In general, longer gradient times (smaller %B min⁻¹ changes) will give the same results (increased resolution and run time, broader and

Table 4 Recommended gradient elution starting conditions

<i>Separation variable</i>	<i>Preferred initial choice</i>
<i>Column</i>	
Dimensions (length, i.d.)	150 \times 4.6 mm
Particle size	5 μm
Stationary phase	C ₈ or C ₁₈
<i>Mobile phase</i>	
Solvents A/B	Water–acetonitrile
%B	5–100% B in 20 min ^a
Buffer	25 mmol L ⁻¹ phosphate, pH 2.5 or 0.1% trifluoroacetic acid
Additives ^b (e.g. ion pair reagents, amines)	As necessary
Flow rate	1–2 mL min ⁻¹
<i>Temperature</i>	40°C
<i>Sample size</i>	
Volume ^c	< 50 μL
Mass ^b	< 100 μg

^aWith phosphate buffers and acetonitrile, use 5–80% B in 15 min.

^bMainly affecting separation of ionized compounds.

^cAssumes 150 \times 4.6 mm reversed-phase column.

shorter peaks) as using a weaker mobile phase (lower %B) in isocratic separations. The earlier discussion of the chromatograms of Figure 2 illustrated the effect of gradient time on the separation. For more detailed instructions in the use of gradient elution, consult the Further Reading section.

Method Development Strategies

The goal for method development is to obtain a robust method with acceptable resolution and run time. The strategy to reach this goal has two components. First, selectivity variables should be chosen for testing in an order that is most likely to give a successful separation in the minimum amount of development time. Second, for robustness in routine use and method transfer, the separation conditions should be as simple as possible and avoid potentially unstable parameters.

Most neutral or ionic samples can be separated successfully with reversed-phase columns and simple binary mobile phases of water or buffer in combination with one of the three primary organic solvents – acetonitrile, methanol or tetrahydrofuran. A choice of conditions should be made by investigating the parameter most likely to succeed, then moving to the next most likely, and so forth. If a satisfactory separation cannot be obtained by single-parameter optimization, the use of (simultaneous) two-parameter optimization can be explored.

Choice of Selectivity Variables

Selectivity variables should be examined one at a time in a systematic manner. Starting conditions generally will correspond to those listed in Table 3 or 4. Systematic method development can be approached by proceeding in order through the variables listed in Table 5, as described below.

Optimize %B First adjust the mobile-phase %B for reasonable *k* values and fine-tune for selectivity, as described previously. Acetonitrile is generally the first choice for organic solvent, but methanol is an accept-

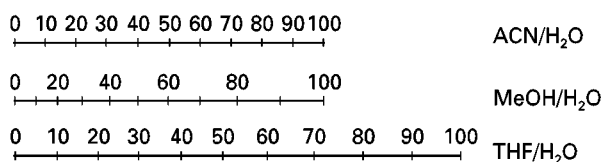


Figure 4 Solvent nomograms for reversed-phase separations. Convert percentage acetonitrile (ACN) to percentage methanol (MeOH) or percentage tetrahydrofuran (THF) by moving vertically between scales.

able alternative. Use water as the A solvent for neutrals or a low pH buffer for ionics.

Solvent type If a separation cannot be obtained with acetonitrile, change to methanol and repeat the optimization experiments. A mobile phase that gives approximately the same retention time can be selected with the help of the nomogram shown in Figure 4. For example, 60% acetonitrile–water is roughly equivalent to 70% methanol–water. If neither solvent provides satisfactory separations, some workers will try tetrahydrofuran at this point, but we recommend delaying the use of this solvent until later. Tetrahydrofuran readily forms peroxides and is less desirable for other reasons.

Figure 5 illustrates both the use of the nomogram of Figure 4 and the selectivity that may be obtained with different organic solvents using simulated chromatograms of a 10-component steroid mixture on a C₁₈ column. Figure 5A shows the best separation with acetonitrile (50%); the resolution of the critical pairs is shown. Figure 4 indicates that 50% acetonitrile is equivalent to about 60% methanol, and the methanol separation is shown in Figure 5B. The separation in methanol is significantly improved, but still unsatisfactory, so tetrahydrofuran is tried next. Figure 5C shows the 40% tetrahydrofuran separation, with baseline resolution of all peaks. Note that the nomogram is not perfect – the indicated tetrahydrofuran concentration resulted in a longer run time than for acetonitrile or methanol.

Temperature Column temperature should be controlled so that retention times do not drift. In general, a 1–2% change in retention will be observed for a 1°C change in temperature, but many workers do not appreciate that selectivity also often changes with temperature. A second experiment run at 20–30°C higher temperature will indicate if improved selectivity can be obtained by varying column temperature. While changes in α as a result of a change in temperature are smaller than for other changes in conditions, this disadvantage is offset by the greater

Table 5 Choice of selectivity variables

Optimize %B using acetonitrile or methanol
Solvent type (acetonitrile versus methanol)
Temperature
pH (ionics)
Column type (C ₈ = C ₁₈ > CN > amide > phenyl)
Additives
Tetrahydrofuran
Separation mode

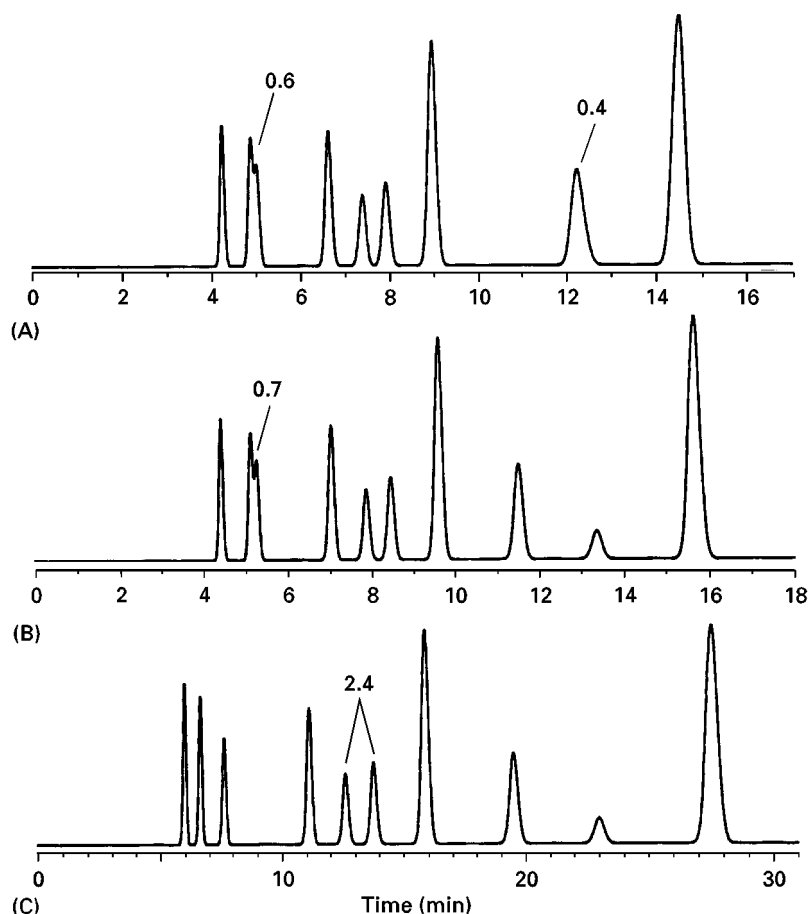


Figure 5 Comparison of selectivity changes with different organic solvents using an 11-component steroid sample and a C_{18} column (simulated chromatograms); resolution of critical peak pair(s) shown as call-outs. (A) 50% acetonitrile; (B) 60% methanol; (C) 40% tetrahydrofuran.

convenience of a change in temperature, without any offsetting disadvantages.

Mobile-phase pH If the sample contains ionizable compounds (acids or bases), mobile-phase pH represents a powerful variable for changing selectivity. Thus, values of k for ionized species will generally be much smaller than for the nonionized compound. As a result, both absolute and relative retention for acids or bases can change dramatically with small changes in pH, when the pK_a value of the compound is within 1–1.5 units of the mobile-phase pH. Be sure to use buffers within their effective buffering range (± 1 unit from the buffer pK_a). When optimizing pH, changes in steps no more than about 0.5 pH units are recommended. Note that silica-based columns are generally limited for use at $2 < \text{pH} < 8$.

On the other hand, the choice of a $\text{pH} < 3$ is advantageous for several reasons: first, the pK_a values of both acids and bases will differ from the

mobile phase pH by > 2 units, so that sample retention will not vary with small changes in pH; i.e., the method will be more robust. Second, bases are usually best separated at low pH, because undesirable interactions between sample molecules and the column packing (i.e. silanols) are suppressed, thereby minimizing peak tailing and maximizing column plate numbers. However, the choice of a $\text{pH} < 3$ means that very little change in selectivity can be expected as a result of intentional changes in pH (e.g. for $2 < \text{pH} < 3$).

Column type The initial separation will usually be done on a C_8 or C_{18} column. For changes in selectivity, it is seldom fruitful to change the bonded-phase chain length (e.g. C_8 to C_{18} or C_4). Similarly, although changes in selectivity may be observed with the same phase obtained from different manufacturers, the magnitude of such changes is generally small. Rather, if the column is to be changed in order to change selectivity, it is recommended to change

to a stationary phase with significantly different chemistry.

After a C_8 or C_{18} column has been tried, a cyano (CN) phase is usually the next choice. Because cyano columns are more polar, similar retention requires the use of 10–20% less organic solvent; e.g. similar retention might be obtained with 35%B on a cyano column as with 50%B on a C_8 column.

A phenyl column is usually the next choice, if a cyano phase does not work. However, recently developed columns with an amide or carbamate function (e.g. Symmetry Shield, Zorbax Bonus RP or Discovery Amide) have proven to have unique selectivity that is also worth exploring when examining column-type effects. Additional information regarding column selection and chemistry can be found in the Further Reading section.

Additives Mobile-phase additives (in addition to buffers) can be used to enhance selectivity with some sample types. For example, ion pairing may be used to advantage when the sample contains both acidic and basic components. While large changes in selectivity are possible by varying the concentration of an ion pair reagent, ion pairing often results in long equilibration times when changing the mobile phase, as well as other problems. Optimization of additives is beyond the scope of the present discussion.

Tetrahydrofuran Tetrahydrofuran as the B solvent often gives significant selectivity changes when compared to acetonitrile or methanol. Problems related to slow equilibration, equipment memory effects, excessive UV background at low wavelengths, instability and unpleasant odour make most workers delay the use of tetrahydrofuran until it is unavoidable. In spite of these potential problems, tetrahydrofuran does have unique selectivity characteristics and will often provide separations when acetonitrile or methanol have failed. If tetrahydrofuran is to be used, use Figure 4 to select starting mobile-phase conditions based on previous experiments with acetonitrile or methanol.

Separation mode When efforts at obtaining a successful reversed-phase separation prove unsuccessful, one should consider other separation modes. Several other separation modes are shown in Table 2.

Single-Variable Optimization

Traditionally, a single variable is optimized at a time during HPLC method development. In most cases, one can proceed through the list of variables in

Table 5 in order, stopping when an adequate separation is achieved. A convenient procedure is to optimize the first variable, then hold that condition constant while changing the next parameter. This sequential optimization of parameters is a straightforward approach. Once all the desired variables have been optimized, it is a good idea to make small and reasonable changes around the final conditions to check robustness. For example, change ± 3 –5%B, ± 0.5 pH units, $\pm 5^\circ\text{C}$, and so forth to make sure the separation is not adversely affected by such changes.

Multi-Variable Optimization

An alternate approach to single-variable optimization is to change two or more parameters at once. Two different approaches are suggested: the method development triangle and the simultaneous optimization of solvent strength (or gradient time) with a second variable. In both of these cases, one should choose variables that change selectivity in different ways, ideally orthogonal to each other in terms of their selectivity effects.

Method development triangle The method development triangle shown in Figure 6 is a widely used approach for selecting the optimum organic solvent or mixture of organic solvents. This is a logical next step when acetonitrile, methanol and tetrahydrofuran have been optimized individually, and the least resolved peak pairs are different for at least two solvents. Each corner of Figure 6 represents a binary-solvent mobile phase with a %B value (for each of these three B solvents) that gives acceptable isocratic

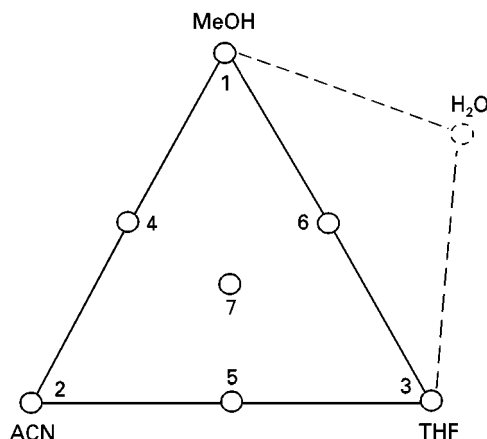


Figure 6 Solvent selectivity optimization for reversed-phase HPLC. Experiments 1, 2 and 3 are binary (water and one organic) mobile phases; 4, 5 and 6 are 1:1 ternary (water and two organics) blends of corner compositions, and 7 is 1:1:1 quaternary (water plus three organics) blend of corner compositions.

separation; e.g. so as to give $k \approx 10$ for the last peak in each separation. These mobile phases (1, 2 and 3 in Figure 6) then are blended 1:1 or 1:1:1 for the remaining experiments. Once all seven experiments are run, the chromatograms can be spread out in the same grid pattern and examined for changes in selectivity between conditions. Further adjustments in solvent blends may be beneficial. For simplicity and robustness, mobile phases with fewer solvents are preferred (binary > ternary > quaternary). As with other optimization strategies, the final conditions should be varied in a systematic manner to determine the robustness of the chosen mobile phase.

Two-variable optimization The method development triangle approach (shown in Figure 6) is one example of the simultaneous variation of two variables. Other two-variable optimization procedures are now possible with the recent availability of appropriate computer simulation software. This new software (DryLab version 3.0, LC Resources) facilitates the simultaneous optimization of either isocratic %B or gradient time and any second variable (e.g. temperature, pH, additive concentration). The combination of two variables having different selectivity actions can help identify separation conditions that are unlikely to be found using more traditional approaches. With the use of optimization software, four to six input runs allow the user to model the separation under any combination of the two variables.

An example of the results of a two-variable optimization is shown in Figure 7 using a 150 mm C_{18} col-

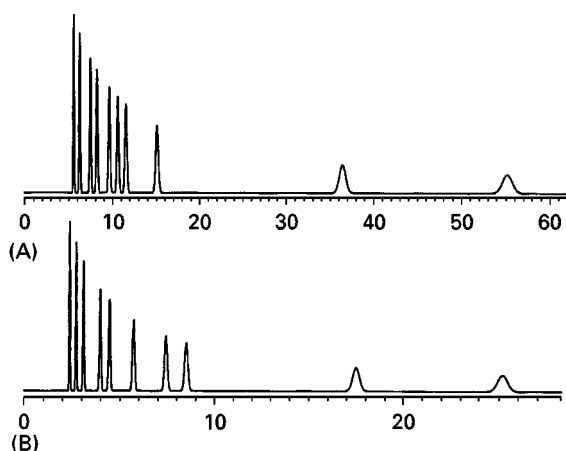


Figure 7 Simulated chromatograms for separation of 10 benzoic acids and anilines using a 150 mm, 5 μ m particle C_{18} column with acetonitrile–buffer mobile phases. (A) Optimum separation at pH 3.0 (15% acetonitrile); (B) optimized %B–pH conditions (pH 3.4, 25% acetonitrile) using computer-assisted method development (DryLab).

Table 6 DryLab® software optimization modes

Parameter	Input experiments
Isocratic %B	2 or 3
Gradient time	2
Normal phase	3
pH	3
Ternary solvent	3
Ionic strength	3
Additive concentration	3
Temperature	2
Gradient time versus temperature	4
Isocratic %B or gradient time versus any variable	4–9

umn with buffered acetonitrile to separate a 10-component mixture of benzoic acids and anilines. The best single-variable separation (at an arbitrary starting pH of 3.0) is shown in Figure 7A with $R_s > 2$, but the %B must be held within $\pm 1\%$ and the pH within ± 0.05 units to maintain $R_s > 1.5$, so the method is not robust. Using six experimental runs and computer optimization, the lower chromatogram (Figure 7B) was obtained, offering $R_s > 2$ for $\pm 5\%$ B and ± 0.1 pH units in half the run time.

Computer-Assisted Method Development

Many of the above changes in separation as a function of conditions can be described in theoretical or empirical equations. The fundamental relationships defined in eqn [1] form the basis of algorithms used to predict resolution. For example, term i of eqn [1] can be calculated from first principles, term ii is defined in eqn [3], and $\log(k)$ is linearly related to %B (term iii). This means that two experiments differing only in %B can be used to predict resolution at any other %B. Similarly, basic theory can relate isocratic and gradient separations in terms of the same retention relationships. A computer program (software) can therefore be used to predict separation as a function of isocratic %B, gradient conditions, and/or column conditions, using two gradient runs to calibrate the sample and initial conditions. The example of Figure 7 required six runs (3 pH values at each of two gradient times) for optimization of isocratic %B and pH. Some of the other variables available for optimization with one of these programs (DryLab® software) are shown in Table 6 along with the number of input experiments required. The use of optimization software is strongly recommended in order to reduce method development time, achieve more robust separations, and gain a better understanding of the separation.

Table 7 Common HPLC separation problems

Observation	Problem source	Solution
Poor peak shape	Wrong silica type Blocked frit or column void Silanol interactions	Use type B silica Replace frit, backflush column Use amine additives, change pH, use end-capped stationary phase
Excessive peak width	Bad column Column overload High molecular weight Unresolved peaks	Replace column Reduce injection volume or mass Normal
Inadequate retention	Mobile phase too strong Column too weak Samples ionized Samples too polar Gradient starting too strong	Improve separation Use lower %B Switch to C ₁₈ Change pH Change to normal phase Start at lower %B
Excessive retention	Mobile phase too weak Column too retentive Samples too hydrophobic Gradient stops too soon	Use higher %B Switch to C ₈ , C ₄ or CN Change to normal phase Stop at higher %B
Excessive retention range	Acids and bases or bases and neutrals in sample Too broad of polarity for isocratic method	Use ion pairing Use gradient elution
Inadequate resolution	Retention too short Poor selectivity Plate number too low	Increase <i>k</i> Change α Use longer column or smaller particle size

Troubleshooting Common Problems

Table 7 highlights some of the commonest causes of chromatographic problems likely to be encountered in the HPLC method development.

Further Reading

Dolan JW and Snyder LR (1989) *Troubleshooting HPLC Systems*. Clifton, NJ: Humana Press.

Horváth Cs (ed.) (1980–86) *High Performance Liquid Chromatography. Advances and Perspectives*, vols 1–4. New York: Academic Press.

Neue UD (1997) *HPLC Columns. Theory, Technology and Practice*. New York: Wiley-VCH.

Snyder LR, Kirkland JJ and Glajch JL (1997) *Practical HPLC Method Development*, 2nd edn. New York: Wiley-Interscience.

ESSENTIAL GUIDES TO METHOD DEVELOPMENT IN SOLID-PHASE EXTRACTION

M. J. M. Wells, Tennessee Technological University, Cookeville, TN, USA

Copyright © 2000 Academic Press

Solid-phase extraction (SPE) is a sample preparation technique combining nonlinear modes of chromatography for the separation, purification, concentration and/or solvent exchange of analytes of

interest. SPE is the removal of chemical constituents from a flowing liquid sample via retention on a solid sorbent, and the subsequent recovery of selected constituents by elution from the sorbent. SPE was developed as an heterogeneous (two-phase) alternative to homogeneous (one-phase) liquid–liquid extraction (LLE) for the isolation of solutes from solution.

Background

The modern era of SPE began in October 1977 when prepackaged, disposable cartridges/columns containing bonded silica sorbents were introduced by Waters Associates. This technique was featured on the cover of *Laboratory Equipment* in May 1978 and the first peer-reviewed method was published in the *Journal of Chromatography* that same year. The term solid-phase extraction wasn't actually popularized until the early 1980s.

Unlike the meagre resources available to early SPE researchers, there are currently thousands of publications for analytes of pharmaceutical and environmental interest that may be consulted for examples of developed SPE methods. Many manufacturers publish bibliographies of methods developed using their products that are available in print or via the Internet. However, it is sometimes difficult to recognize the process used to arrive at published protocol, and, it is still common that an SPE method for the solute-matrix combination required has not been previously developed. Even if an appropriate method exists, it is advisable to understand thoroughly the principles of SPE method development in order to evaluate properly published methods.

Elsewhere in this volume, there are articles dealing with specific SPE topics (Table 1) that should be consulted for detailed descriptions. This contribution addresses method development issues in SPE.

Principles

SPE method development requires exploitation of analyte properties, selection of the appropriate

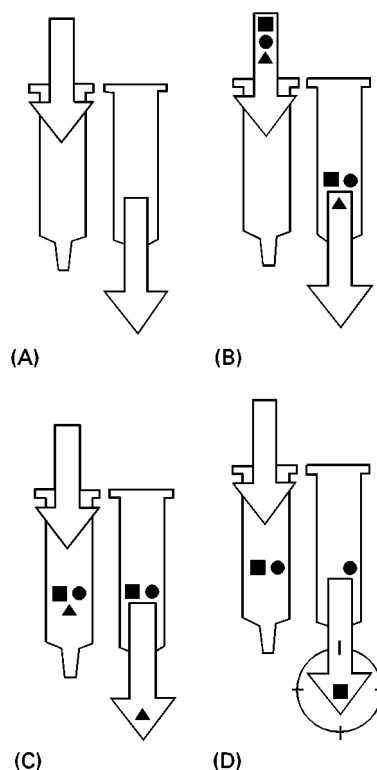


Figure 1 Solid-phase extraction consists of four basic steps: (A) conditioning, (B) retention, (C) rinsing and (D) elution. (A) Conditioning the sorbent prior to sample application ensures reproducible retention of the compound of interest (the isolate). (B) Squares, adsorbed isolate; circles, undesired matrix constituents; triangles, other undesired matrix components. (C) Triangles, rinse the columns to remove undesired matrix components. (D) Circles, undesired components remain; squares, purified and concentrated isolate is ready for analysis. (Reproduced with permission from <http://www.varianinc.com/spp/shared/4step.jpg> at <http://www.varianinc.com/spp/solphase.html> Copyright 1999 Varian, Inc.)

Table 1 Articles on solid-phase extraction appearing in the *Encyclopedia of Separation Science*

Article

Extraction

Solid-phase extraction (SPE)
Automation of SPE
Bioanalytical applications of SPE (excluding drugs of abuse)
Classical SPE
Covalent SPE using immobilized boronic acids
Disk approach to SPE
Drugs of abuse
Herbicides
Insecticides
Medical applications (treatment of blood): SPE
Mixed-mode SPE
Molecular imprints for SPE
Polycyclic aromatic hydrocarbons
Phenols
Restricted-access media (SPE)
Sorbent selection for SPE

sorbent and recognition of limitations imposed on the analysis by the sample matrix. The distribution of the analyte between the sample matrix and the sorbent in SPE is determined by physical and chemical properties of the analyte and the sorbent. The sample matrix can be manipulated to influence the distribution. In SPE method development, identification of the characteristic properties of the analytes of interest is a necessary first step before the sorbent can be selected or the sample matrix can be modified to effect the recovery.

SPE consists of a basic four-step approach (Figure 1):

1. Sorbent preparation or pre-wash: stationary phase conditioning;
2. Retention: analyte adsorption;
3. Sorbent post-wash: removing undesirable contaminants;
4. Elution: analyte desorption.

The four-step process can be as simple as this or may become more involved as one or more of these stages includes additional phases, such as selective adsorption or selective desorption. SPE method development can be tedious because the retention and recovery processes are interdependent. Retention and elution are confounded during method development because the overall analyte recovery is dependent upon both the retention efficiency and the elution efficiency. If the analyte is only recovered in part by an SPE technique, it will be initially unclear whether the problem lies with the retention process or with the elution process.

Because of this quandary, SPE method development can be approached in two ways. An iterative approach to protocol development emulating the classical analytical approach to change one variable at a time can be used. Retention parameters are held constant at selected values while optimizing the elution process (Table 2). Once elution is optimized, then the most favourable conditions for retention are determined. The procedure is repeated until the desired results are obtained.

Alternatively, a factorial experimental design approach to determine extraction efficiency is an efficient method development technique. Parameters important to SPE, such as sample pH, elution solvent strength, ionic strength of the sample, addition of organic modifier to the sample, elution by gravity or vacuum, sorbent retentivity, selection of sorbent mass, sample volume, elution volume and sample concentration, representing effects on both retention and elution, may be selected as factors that influence analyte recovery. The factors are usually tested at two or three levels. As a screening procedure, the factorial design can quickly pinpoint significant effects important to SPE. The objective of the factorial design approach is to obtain as much information as possible from few analyses.

Table 2 Factors affecting SPE retention and elution

Retention

Analyte character
Sorbent type
Matrix additives
Sample volume
Sorbent mass

Elution

Eluting solvent identity
Eluting solvent volume
Elution rate

Table 3 SPE sorbent-analyte interaction mechanisms

<i>Primary mechanism</i>	<i>Sorbents</i>
Van der Waals	Octadecyl, octyl, ethyl, phenyl, cyclohexyl, styrene-divinylbenzene
Polar-dipole/dipole	Cyano, silica, alumina, Florisil
Hydrogen-bonding	Amino, diol
Electrostatic	Cation exchange, anion exchange

Fundamentals

Stationary-phase Conditioning

Each different SPE sorbent requires conditioning or pretreatment in order to activate or prepare the sorbent to retain the analyte. Conditioning of hydrophobic stationary phases requires a two-step process of treatment with organic solvent followed by an aqueous wash. The conditioning solvent is prepared to mimic the chemistry of the sample matrix, that is, matching the pH and/or the ionic strength of the matrix. The volume of each conditioning solvent passed through the sorbent is usually about five times the dead volume of the sorbent. In addition to activating the sorbent, the conditioning solvent(s) also removes undesirable contamination potentially remaining in the sorbent during manufacture.

Retention

Originally, hydrophobic bonded-silica sorbents were the first materials introduced specifically for SPE, but currently, a suite of sorbents in varying formats are available with nonpolar, intermediate nonpolar/polar, polar, strong and weak anion and cation exchange, and steric exclusion (restricted access) properties. SPE sorbents are designed to retain analytes by a primary mechanism (Table 3) but often exhibit a secondary mechanism as well. For example, bonded-phase ion exchange sorbents primarily exhibit anionic or cationic exchange mechanisms but the analyte also experiences nonpolar interactions with the bonded ligand. Also, nonpolar bonded silicas exhibit a secondary polar interaction due to the silica backbone and unreacted surface silanol groups. Knowledge of the dual retention mechanisms encountered in SPE can work to the analyst's advantage. Mixed-mode sorbents (different ligands on the same sorbent) capitalize on dual retention mechanisms by design.

Understanding the mechanism(s) of retention and the selection of an appropriate sorbent depends on a thorough understanding of the character of the analyte. The solute properties of principal importance to retention by SPE are hydrophobicity, polarity and ionogenicity.

Unionized chemicals Many organic compounds are not ionized in water. An unionized organic compound is formed entirely of covalent bonds. SPE sorbent selection and recovery of unionized compounds is known generally to depend on the hydrophobicity of the analyte. The most widely measured parameter used to represent solute hydrophobicity is the octanol/water partition coefficient (K_{ow}), which is the ratio of the analyte concentration in octanol (o) relative to its concentration in an aqueous (w) phase. The logarithm of K_{ow} , also referred to as $\log P$, ranges from -3 to 7 for organic chemicals. Analytes with $\log K_{ow}$ values less than 1 are hydrophilic; analytes with $\log K_{ow}$ values greater than 4 are highly hydrophobic; analytes with $\log K_{ow}$ s between 1 and 4 are intermediate in hydrophobicity/hydrophilicity.

Aliphatic hydrocarbons and mono- and polycyclic aromatic hydrocarbons (PAHs) are nonpolar compounds that tend to increase in hydrophobicity ($\log K_{ow}$) with increasing molecular weight; that is, they tend to be more distributed in the organic, octanol phase, rather than in the aqueous phase. As oxygen- and/or nitrogen-containing functional groups are added to these compounds, they may (but not always) become more polar relative to the parent compound and would distribute more equally between the octanol and water phases, or even prefer to exist in the aqueous phase, thereby decreasing the value of $\log K_{ow}$.

Sorbents for extraction of unionized compounds fall into two general categories: nonpolar extraction sorbents and polar extraction sorbents, depending on the polarity of the functional groups present. Commercially available reversed-phase bonded-silica sorbents for SPE are produced in ranging polarities. The identity of the hydrocarbon covalently bonded to the silica gel backbone may be varied. Common nonpolar ligands bonded on the silica gel surface include aliphatic hydrocarbons of one, two, eight, or 18 methylene, cyclohexyl or phenyl groups. The greater the number of methylene groups in the aliphatic chain, the greater the hydrophobicity of the sorbent generated, i.e. $C_{18} > C_8 > C_2$. For nonionized compounds, the hydrophobicity of the analyte and the hydrophobicity of the sorbent selected for SPE are inversely related; that is, less hydrophobic sorbents are used for highly hydrophobic analytes; conversely, the most hydrophobic sorbents should be used for more polar analytes.

Bonded-phase silica sorbents are known to exhibit mixed-mode retention mechanisms due to silanolphilic (silanol) sites that remain on the sorbent after the initial hydrocarbon is bonded to the surface. The presence of silanol groups reduces the hydrophobic

character of the surface. Silanol groups on the surface of bonded silicas interact with electron-rich hydroxyl, carbonyl, nitrile and nitro functional groups in analytes. Some of the silanol groups on the surface may be masked by a subsequent reaction with a short chain hydrocarbon in a manufacturing process termed end-capping. Consequently, reversed-phase sorbents that are end-capped are more hydrophobic in character than those that are not end-capped. When a less retentive, less hydrophobic sorbent is desired, a nonend-capped product should be tested. Other polar sorbents are produced by adding oxygen- or nitrogen-containing functional groups such as cyano, hydroxyl or amino to the hydrocarbon bonded phase, or functionalized polymeric phases are produced to enhance polarity. Unmodified silica, alumina and Florisil sorbents are polar extraction sorbents.

Matrix additives influence retention in SPE. For many nonionized chemical compounds, increasing the ionic strength of the sample matrix by the addition of sodium chloride decreases analyte solubility in the sample matrix and increases adsorption on to the nonpolar sorbent via a 'salting-out' effect. Increased salt content in the sample matrix may also produce silanol masking. Silanol groups remaining on the surface can also be deactivated through ion pairing by the addition of masking reagents such as tetrabutylammonium hydrogen sulfate to the sample matrix.

Adding water-miscible organic solvents such as methanol or acetonitrile to the sample matrix reduces the surface tension of the sample matrix, thereby decreasing the retentiveness of highly hydrophobic compounds. The addition of salt to increase the ionic strength of the sample matrix and the concomitant addition of methanol to decrease surface tension can be useful in developing methods for samples having multiple compounds that vary widely in their hydrophobic character.

Ionized chemicals Organic chemical compounds that undergo ionization are comprised of derivatives of acidic organic alcohols, carboxylic acids or basic amine functional groups. Substances that ionize dissociate into their conjugate acid or base in aqueous solution. Ionizable compounds, including organic acids such as acetic acid or benzoic acid, and organic bases such as ethylamine or aniline, are weak electrolytes and are incompletely dissociated in water. The acid dissociation constant, K_a , expresses the ratio of ionized to unionized analyte; therefore, the greater the value of K_a (or the logarithm of K_a , the pK_a) the more ionized material is present. Just as in LLE, the dependence of SPE

recovery on sample pH is a function of the pK_a of the analyte.

The relative per cent of unionized analyte to that in the ionized form exhibits a pH-dependent dissociation that can be exploited by SPE methodology. The relative concentrations of dissociated and non-dissociated forms of ionizable analytes in aqueous solution are equal when the solution pH is equal to the pK_a . Therefore, in aqueous solution an organic acid is 99% unionized when the pH of the sample is two log units below the pK_a ; and it is 99% ionized when the pH of the sample is two log units above the pK_a . Two log units is a good rule of thumb for considering retention of ionizable compounds. However, if the sorbent (whether nonpolar, polar or ion exchange) exhibits primary or secondary, nonpolar van der Waals-type interactions, the overall hydrophobicity and size of the ionized form of the analyte can also have an effect upon recovery and influence the two log units generalization.

In SPE method development for ionogenic compounds, the decision to be made is whether to retain the analyte as the dissociated or the undissociated form. If a compound is ionizable, the extraction may be performed using ion exchange of the dissociated form. Alternatively, if the analyte can be converted to an undissociated form by ion suppression or ion pairing, then SPE can be conducted on nonpolar sorbents, as described in the earlier section on unionized chemicals.

Organic acids lose protons in aqueous solution, ionizing to form anions, and are retained on cation exchange sorbents. Organic bases gain protons in aqueous solution, ionizing to form cations, and are retained on anion exchange sorbents. Strong and weak ion exchange sorbents are available for SPE. Ion exchange sorbents developed for SPE retain analytes not only by ionic (electrostatic) attraction, but also through secondary van der Waals (nonpolar) interactions between the analyte and the atoms comprising the bridge that links the charged functional group to the silica gel backbone.

Ion suppression refers to adjusting the pH of the sample matrix to influence the chemistry of the analyte of interest. If the ionizability of the analyte is suppressed by controlling the pH of the sample matrix relative to the pK_a of the analyte, then the analyte can be retained in the unionized form and nonpolar or polar extraction sorbents are used instead of ion exchange sorbents.

Ion pairing involves using a reagent added to the mobile phase to accomplish two objectives: to neutralize the analyte charge by combining with an oppositely charged counterionic solute; and to use a hydrophobic, bulky group on the counterion to

form an ion pair that is hydrophobic enough to be retained on nonpolar extraction sorbents. The ion-pairing strategy applies to ionized organics as well as metal cations.

Ionizable and nonionizable compounds may co-exist in the same sample to be analysed. Selective adsorption of either type of chemical in the presence of the other can be accomplished by controlling the sorbent through a mixed-mode approach or by chromatographic mode sequencing (the use of differing SPE sorbents in tandem), such as using both ion exchange and nonpolar mechanisms to extract the analytes. The use of selective adsorption can be applied to compounds differing in hydrophobicity, charge and structure.

In tandem mode, ionizable and nonionizable compounds may be fractionated by adsorbing nonionizable analytes on nonpolar extraction sorbents and ionized analytes on ion exchange sorbents. Once retained on different sorbents in tandem, they can be physically separated and eluted individually, thereby separating the compounds. Such fractionation often improves the ease of subsequent chromatographic analyses.

Selective adsorption of nonionized compounds in the presence of ionogenic compounds can also be accomplished with pH control of the sample matrix. By selecting a sample pH at which ionogenic compounds exist in the ionized form, it may be possible selectively to retain either the ionized or the nonionized components depending on the type of sorbent selected.

Values for hydrophobic parameters ($\log P$) and acid dissociation constants (pK_a) can often be obtained from the analyte's manufacturer. Alternatively, they can be measured in the laboratory or predicted by numerical estimation methods.

Sample volume and sorbent mass SPE retention is dependent on the relationship between sorbent mass and sample size. The strength of the interaction (whether nonpolar/polar or ion exchange) between the analyte and the sorbent, as influenced by the sample matrix solvent strength, determines the amount of the sample that may be passed through the sorbent before analyte breakthrough occurs. As the strength of the interaction increases and as the sorbent amount increases, the breakthrough volume increases. Breakthrough can be controlled and monitored by attaching a second check cartridge in tandem with the primary extraction cartridge, and eluting them separately.

To establish the dependence of retention on sample loading volume, variable volume samples (each of which comprises a constant molar amount loaded)

are passed through a constant sorbent mass and per cent recovery is plotted as a function of sample loading volume. Repeating this procedure for different sorbent masses will establish the dependence of retention on sorbent mass. Factorial design experiments can also be used to screen for the sorbent mass required relative to sample size. Optimizing the amount of sorbent necessary for the analysis will control analytical costs.

Adsorbed Contaminant Removal

During the retention process, undesirable contaminants in the sample matrix may become associated with the sorbent, or may remain behind in the interstitial spaces between sorbent particles. When the post-wash solvent is identical to the conditioning solvent and to the sample matrix, adsorbed contaminants are not likely to be removed. However, matrix components remaining in the interstitial spaces between sorbent particles will be flushed from the sorbent. The volume of the post-wash solvent should be at least equal to or preferably twice the void volume of the sorbent to ensure that the pore space is entirely replaced with the desired solvent.

If a blank, i.e. uncontaminated, sample matrix is available, it can be used to screen for potential column post-wash solvents. To remove undesirable contaminants in the sample matrix that became associated with the sorbent during the retention process, solvents of greater eluotropic or eluting solvent strength than the conditioning solvent must be used. Even a small amount of the elution solvent can be a post-wash solvent if the effects on the retained analytes of interest are monitored.

Elution

Elution solvent strength and volume The ability of a solvent to overcome the interaction between the analyte and a chromatographic sorbent, thereby causing elution to occur, is known as the solvent's eluotropic strength. Charts of eluotropic series can be consulted to determine relative solvent strength, which is roughly equivalent to polarity. The eluotropic strength of elution solvents on a non-polar adsorbent (e.g. reversed-phase) increases in reverse order to that measured on polar sorbents such as silica or alumina. On reversed-phase sorbents, the eluting power increases as the solvent polarity decreases.

Many different solvents are used for elution of the analytes from sorbents in SPE. Elution by acetic acid, methanol, acetonitrile, acetone, ethyl acetate, diethyl ether, methyl-*tert*-butyl ether, methylene

chloride, benzene and hexane, and aqueous buffers containing appropriate counterions have been reported. Miscible solvent mixtures produce elution solvents of intermediate eluotropic strength.

After candidate elution solvents are selected, an elution solvent screen is conducted. Elution solvents tested at a constant volume are compared for potential to elute the analytes of interest. When selecting a desorption solvent, the effect it will have upon contaminants adsorbed from the sample matrix must be considered. A control sample matrix should also be screened if possible. The solvent demonstrating the most desirable results in the elution screen is further examined for the variation of recovery as a function of the volume of eluting solvent. Generally, the elution solvent selected is the one for which the smallest volume produces acceptable recovery. However, elution with a larger volume of lower eluting strength solvent can have the advantage of leaving strongly retained contaminants on the sorbent as the analyte of interest is desorbed. Solvent selection must also be compatible with the analytical instrumentation used for final analysis.

The elution solvent screen may reveal that selective desorption is possible for an analysis. Selective desorption uses differences in the eluotropic strength of the elution solvents to produce serial desorption. Class separation or distinct fractionation of analytes may be possible if the chemical properties of the analytes differ enough that they respond differently to weak and strong elution solvents.

Elution rate The rate of elution can affect the SPE recovery of solutes from the sorbent. Particularly for highly hydrophobic compounds, there can be slow mass transfer from the stationary phase into the mobile phase. The problem can be overcome by reducing the flow rate during elution, even to the point of allowing elution to occur by gravity if necessary.

Sample concentration independence Finally, any protocol developed must be independent of sample concentration in the range of samples to be analysed. Care must be taken not to exceed the maximum loadability of the sorbent, but that is generally not a problem since SPE is primarily used for trace enrichment.

Applications

Early in SPE history, a series of simple yet ingenious experiments were developed by Bidlingmeyer and Warren that illustrate the principles of SPE. This author has used these experiments as practical demonstrations to introduce SPE method development to

Table 4 SPE isolation of food colours in grape drink

	A	B	C	D	E	F
Sorbent	C ₁₈	C ₁₈	C ₁₈	Silica	Silica	Silica
Mechanism	Van der Waals isocratic separation	Van der Waals selective desorption	Van der Waals ion pairing/silanol masking	Polar-dipole/dipole isocratic separation	Polar-dipole/dipole ion suppression isocratic separation	Polar-dipole/dipole selective desorption
Pre-wash	1) IPA (70%) 2) Water	1) IPA (70%) 2) Water	1) IPA (70%) 2) Cetylpyridinium chloride	Water	Distilled white vinegar	Water
Retention	Drink mix ^a	Drink mix	Drink mix	Drink mix	Drink mix	Drink mix
Post-wash	Water	Water	Cetylpyridinium chloride	Water	Distilled white vinegar	Water
Elution	IPA (18%)	1) IPA (5%) 2) IPA (25%) 3) IPA (70%)	1) IPA (18%) 2) IPA (70%)	IPA (18%)	IPA (16% in vinegar)	1) Water 2) IPA (15%)

IPA, isopropyl alcohol.

^aMixture of FD&C Blue 1 and FD&C Red 40.

new users from elementary school students to adult analysts. These experiments are outlined here (Table 4) as practical applications of the foregoing discussion. They are a useful method development learning aid for novice users because:

1. they demonstrate the four-step process of SPE;
2. the dyes concentrated and separated in these experiments can be observed by the naked eye, clearly revealing extraction and recovery processes;
3. the stepwise recovery of dyes from the sorbent demonstrates the ability of SPE selectively to fractionate samples.

The experiments, A–F in Table 4, demonstrate the use of SPE to isolate food colours using inexpensive reagents. The analytes in these experiments are the dyes FD&C Blue 1 and FD&C Red 40 prepared in an aqueous mixture by dissolving grape-flavoured drink mix (Kool-Aid®), in distilled water. Other reagents necessary for these experiments include vinegar, rubbing alcohol and mouthwash. The original source (Bidlemyer and Warren) should be consulted for details.

The types of sorbents used for the experiments are a hydrophobic, reversed-phase sorbent, C₁₈ (experiments A–C), and a polar sorbent, silica (experiments D–F). The same two analyte dyes are retained in each experiment, albeit via different mechanisms depending on the sorbent: by van der Waals forces on the C₁₈ sorbent and polar dipole–dipole interactions with the silica sorbent.

On the reversed-phase sorbent (C₁₈), conditioning involves exposure of the sorbent to a water-miscible

organic solvent followed by an aqueous wash (experiments A–C). The preparation of the sorbent surface to accept the analyte must be done in this order. Measuring exact amounts of solvents is not necessary during the pre-wash step. The sorbent is not allowed to dry between column preparation steps and the sample loading step. If it does dry out during column preparation, before the sample has begun to be loaded, the process should begin again. The silica sorbent is activated by a single aqueous pre-wash of water (experiments D and F) or distilled white vinegar (experiment E).

As the sample is loaded on to the sorbent, the organic dyes extracted are observed to become concentrated at the leading edge of the sorbent. After the sample is loaded, drying of the column is not crucial, and in fact it is useful in some analyses to dry the sorbent with vacuum before eluting the analytes.

FD&C Blue 1 (Brilliant Blue FCF, CAS # 3844-45-9) and FD&C Red 40 (Allura Red AC, CAS # 25956-17-6) are large dye molecules (formula weights of approximately 800 and 500, respectively) that have negatively charged sulfonate groups in aqueous solution. Although ionogenic, the molecular size and hydrophobicity of the dyes permit retention on the C₁₈ sorbent even without pH control (experiments A and B).

Two of the experiments demonstrate the effect of matrix additives on retention (experiments C and E). In experiment E, distilled white vinegar is used for ion suppression by reducing the pH and its addition results in reversal of the elution order of the dyes. In experiment C, an ion-pairing reagent, cetylpyridinium chloride (Cepacol® mouthwash), is added as

a bulky, hydrophobic, positively charged counterion to pair with the negatively charged sulfonate groups of the dyes. In this case, cetylpyridinium chloride also behaves as a silanol masking agent.

Post-washes flush any remaining sample matrix from the interstitial pores of the sorbent, and in each experiment the post-wash solvent is the same as the last pre-wash solvent. Additives in the drink mix that are not retained (sugars, acids) will elute during sample loading and during the post-wash.

Elution is accomplished by varying the concentration of isopropyl alcohol (commercially available rubbing alcohol is approximately 70% isopropyl alcohol in water). The isopropyl alcohol is mixed with either water (experiments A, B, C, D or F) or vinegar (experiment E). Sample desorption volumes are measured for quantitative purposes. The volume recovered is always less than the volume added. The desorption can be done in one isocratic separation process (experiments A, D and E). Performed in stages, experiments B, C and F are examples of selective desorption. SPE columns generate around 20–200 theoretical plates and this is sufficient in many cases to produce a fractionation of components and chemical classes.

Future Developments

The history of SPE has already been marked by continuous advances in sorbents and the formats in which SPE sorbents are utilized. So, it's a fairly safe prediction that in the future there will be continued development of new SPE sorbents and modes of delivery. Along that trend, recent developments of molecularly imprinted sorbents for SPE and the 96-well plate format for SPE are gaining attention and are expected to be actively developed in the near future. Molecularly imprinted sorbents for SPE are polymeric phases formed with the analyte of interest as a print molecule. The template thus formed exhibits selectivity for the imprinted molecule. The 96-well microassay plate collection format is designed to utilize robotics for simultaneous extraction of 96 samples.

In addition to continued development of specialty-phase sorbents and formats, advances in performing more sophisticated chemistry associated with extraction are predicted. Applications of analyte derivatization in conjunction with SPE are already reported, with the chemical reaction occurring at the sorbent surface. Methods apply either to solid-supported reactants or solid-supported analytes. Selective adsorption schemes that utilize tandem chromatographic mode sequencing approaches will be used to solve complex multiclass/multiresidue extractions. More intricate mixed-mode adsorption mechanisms that

mimic analyte–receptor ‘lock-and-key’ approaches to extraction are expected.

See also: **I/Extraction.** **II/Extraction:** Analytical Extractions; Solid-Phase Extraction; Solid-Phase Microextraction. **III/Airborne Samples: Solid-Phase Extraction.** **Bioanalytical Applications: Solid-Phase Extraction.** **Drugs of Abuse: Solid-Phase Extraction.** **Environmental Applications:** Solid-Phase Microextraction. **Herbicides:** Solid-Phase Extraction. **Immobilised Boronic Acids: Extraction.** **Immunoaffinity Extraction.** **Insecticides:** Solid-Phase Extraction. **Molecular Imprints for Solid-Phase Extraction.** **Solid-Phase Extraction with Cartridges.** **Solid-Phase Extraction with Discs.** **Solid-Phase Matrix Dispersion: Extraction.** **Solid-Phase Microextraction:** Biomedical Applications; Environmental Applications; Food Technology Applications; Overview. **Sorbent Selection for Solid-Phase Extraction.** **Appendix 2: Essential Guides to Method Development in Extraction.**

Further Reading

- Bidlingmeyer BA and Warren FV (1984) An inexpensive experiment for the introduction of high performance liquid chromatography. *Journal of Chemistry Education* 61: 716.
- Hansch C and Leo A (1995) *Exploring QSAR: [1]. Fundamentals and Applications in Chemistry and Biology*. Washington, DC: American Chemical Society.
- Hansch C, Leo A and Hoekman DH (1995) *Exploring QSAR: [2] Hydrophobic, Electronic, and Steric Constants*. Washington, DC: American Chemical Society.
- Lyman WJ, Reehl WF and Rosenblatt DH (1990) *Handbook of Chemical Property Estimation Methods: Environmental Behavior of Organic Compounds*. Washington, DC: American Chemical Society.
- Nakamura M, Nakamura M and Yamada S (1996) Conditions for solid-phase extraction of agricultural chemicals in waters by using *n*-octanol–water partition coefficients. *Analyst* 121: 469
- Simpson NJK (ed.) (2000) *Solid-Phase Extraction: Principles, Strategies, and Applications*. New York: Marcel Dekker.
- Simpson NKJ and Van Horne KC (1993) *Handbook of Sorbent Extraction Technology*, 2nd edn. Palo Alto, CA: Varian Associates.
- Subden RE, Brown RG and Noble AC (1978) Determination of histamines in wines and musts by reversed-phase high-performance liquid chromatography. *Journal of Chromatography* 166: 310.
- Thurman EM and Mills MS (1998) *Solid-Phase Extraction: Principles and Practice*. New York: John Wiley.
- Zief M, Crane LJ and Horvath J (1982) Preparation of steroid samples by solid-phase extraction. *American Laboratory* 14: 120.
- Zief M, Crane LJ and Horvath J (1982) Preparation of steroid samples by solid-phase extraction. *International Laboratory* 12: 102.

ESSENTIAL GUIDES TO METHOD DEVELOPMENT IN SUPERCRITICAL FLUID CHROMATOGRAPHY

P. Schoenmakers, Shell Research and Technology Centre (SRTCA), Amsterdam, The Netherlands and University of Amsterdam, Amsterdam, The Netherlands

Copyright © 2000 Academic Press

Introduction

Supercritical-fluid chromatography (SFC) is defined as a mode of chromatography in which both the temperature and the pressure in the column exceed the critical values of the mobile phase. This definition is exact, but rather arbitrary, as there is no phase transition between gases (or liquids) and supercritical fluids. Technically, a gas chromatograph operated above 2.24 atm with He as the carrier gas, is an SFC instrument according to this definition. We normally speak of gas chromatography when retention is largely controlled by the oven temperature (and largely determined by analyte volatility). We speak of SFC when retention is largely controlled by the mobile-phase density (and largely determined by analyte interaction with the mobile phase). Supercritical-fluid chromatography (another name for it is dense-gas

chromatography) was first developed in the 1960s by Klesper in Aachen, shortly followed by Sie and Rijnders in Amsterdam. The technique subsided into oblivion during the rapid advent of modern high pressure liquid chromatography (HPLC) in the 1970s. It experienced a second youth in the 1980s. During this period, some researchers optimistically claimed that SFC combined the advantages of gas chromatography (GC) and HPLC. Although statements of this kind still appear in the literature today, the chromatographic community as a whole has come to accept that SFC holds a position somewhere in between, rather than above GC and LC. SFC offers an – occasionally favourable – compromise between the two mainstream chromatographic techniques (see Table 1).

Why opt for SFC?

Although this article deals specifically with SFC, we are treating it as a niche technique. In real life, GC and HPLC are more commonly available. When GC can readily be used, SFC offers few advantages other than a lower operating temperature. When

Table 1 General considerations when considering SFC as a possible chromatographic separation method*

Parameter	GC	SFC	LC
(Most) suitable application range	Gases and volatile materials All but the most polar analytes	Low to marginally volatile materials Low to moderately polar analytes	Low-volatile and non-volatile materials All polarities (non-polar to ionic)
Operating temperature	High (related to analyte boiling point)	Low to moderate	Low
Suitable columns	Packed columns (10–50 μm particle diameters) <i>Open-tubular columns (100–500 μm internal diameter)</i>	<i>Packed columns (3–10 μm particle diameters)</i> Open-tubular columns (10–50 μm internal diameter)	<i>Packed columns (1–5 μm particle diameters)**</i> Open-tubular columns (1–5 μm internal diameter)
Suitable detectors	<i>Vacuum detectors (MS)**</i> <i>Gas-phase detectors (FID, NPD, ECD, etc.)†</i>	<i>Vacuum detectors (MS)***</i> <i>Gas-phase detectors (FID, NPD, ECD, etc.)†</i> <i>Liquid-phase detectors (UV, fluorescence)</i>	<i>Vacuum detectors (MS)***</i> <i>Liquid-phase detectors (UV, fluorescence, refractive index, etc.)</i>

*The most suitable technique is given in italics.

**Monolithic columns are an emerging alternative to packed columns.

***MS = mass spectrometry.

†FID = flame-ionization detector; NPD = nitrogen-phosphorus or thermionic detector; ECD = electron-capture detector.

Table 2 Possible mobile phases for SFC and their compatibility with different detection principles

Mobile phase	Polarity	T_c (°C)	p_c (atm)	Detection compatibility			
				FID	UV	MS	IR
Carbon dioxide*	Low	31.05	72.9	++	++	+	±
with modifier:							
Methanol	High	239.4	79.9	—	++	+	—
Formic acid	High			+	+	—	—
Nitrous oxide	Low	36.4	71.5	±	+	+	±
Sulfur hexafluoride	Low	45.5	37.1	± **	+	±	±
n-Butane	Low	152.0	37.5	—	++	±	—
Xenon	Very low	16.6	57.6	+	++	+	++
Ammonia***	High	132.4	111.3	+	+	+	—
Water***	Very high	374.1	217.6	+	+	+	—

*Most suitable mobile phase for most applications.

**Feasible, but highly corrosive.

***Highly corrosive and hardly feasible.

HPLC may readily be used, SFC – when applicable – may offer shorter analysis times and a greater choice of detectors. HPLC can be applied to a much greater variety of samples and analytes than SFC.

Table 1 lists some general considerations for considering or discarding SFC as a possible (analytical) separation technique. The most important reasons for selecting SFC are described below in more detail.

Universal detection When using carbon dioxide (CO₂) as the mobile phase, SFC allows the use of flame-based detectors (see Table 2). The flame-ionization detector can be applied almost universally. Even more importantly, it shows an approximately equal response within a class of analytes. As a result, reference standards within each class (rather than for each individual compound) suffice for calibrating a quantitative method.

Because universal detectors are available in GC, but not in LC, there are potentially, two directions in which relevant SFC–FID methods can be developed:

- analysis of non-volatile materials, that cannot be analysed by GC (including the high-temperature version, HT-GC); and
- achieving separations with a (type of) selectivity that cannot be achieved in GC.

Applications in the former direction are quite rare. Some thermally labile components, such as explosives and peroxides, have been analysed by SFC. However, due to the highly inert nature of GC mobile phases (e.g. helium), the increased inertness of modern GC columns, and the increased flexibility of injection systems (e.g. cold on-column injection), such components can often be analysed with good integrity by GC.

Some components that are not sufficiently volatile for analysis by HT-GC may be amenable to analysis by SFC. However, in the author's experience this is limited to highly apolar materials, such as saturated hydrocarbons. For moderately polar analytes, such as aromatic hydrocarbons, HT-GC appears to allow materials with higher boiling points (lower volatility) to be eluted in comparison with SFC.

The most successful SFC–FID methods follow the second approach, using a unique kind of selectivity. In GC, retention is determined by two factors, viz. the pure-analyte vapour pressure and the interactions of the analyte with the stationary phase. In SFC the effect of the vapour pressure can be minimized by working with high-density mobile phases, while the interaction with the stationary phase can be maximized by using stationary phases with large, active surface areas. This allows a so-called 'group-type selectivity' to be achieved, in which the sample is separated (or classified) into a limited number of distinct groups (or classes) of analytes. Within a class, the size (and thus volatility) of the analyte molecules varies, but the chemical structure (functional groups) remains similar. Examples of such methods include the following.

- Separation of complex hydrocarbon mixtures, for example the separation of middle-distillate fuels (diesel or kerosene) into saturates, mono-aromatics and di-aromatics; the determination of the total amount of olefins in gasoline-type fuels. Both these examples concern highly successful applications of SFC. A group-type separation method for middle distillates is standardized as ASTM D-5186. An ASTM standard method for olefins in

gasoline by SFC is expected to be approved by June 2000.

- Separation of (low-molecular-mass) polymers into fractions representing different end-groups.

In both cases, we try to achieve retention that is affected by the chemical structure of the molecules (the *functionality*) but irrespective of their size (molecular mass). This type of chromatography is – somewhat confusingly – referred to as ‘critical chromatography’, or as ‘supercritical-fluid chromatography at the critical conditions’.

Difficult separations SFC possesses some favourable fundamental characteristics, especially in comparison with liquid chromatography. The molecular diffusion is about an order of magnitude greater than in liquids (but three orders worse than in gases) and the viscosity is about a factor hundred lower than that of a typical liquid. Thus, SFC has advantages in terms of mass transfer and column pressure drop. This may result in higher efficiencies per unit length of column, while longer columns may sometimes be used. Therefore, SFC may be attractive for some difficult separations.

SFC has proved a rather attractive alternative to normal-phase LC for the separation of stereoisomers. Like in normal phase LC, CO₂-based SFC features a polar stationary phase and a non-polar mobile phase. Organic modifiers may be added to modify the mobile-phase polarity and detergent-like molecules have been added to help create adequate selectivities. The advantages of SFC in this context are summarized in Table 3.

SFC is seen to score well in all categories, except its flexibility in dealing with a variety of samples. Reverse-phase LC (RPLC) also scores well in the table. SFC appears to be more attractive as an alternative to normal-phase LC (NPLC) than to RPLC. The latter technique is compatible with almost all sample sol-

vents, ranging from water to quite non-polar organic solvents, such as tetrahydrofuran. NPLC on unmodified silica surfaces can be used in combination with solvents of low-to-medium polarity. When using polar-bonded phases, again a great variety of sample solvents may be introduced on the column. In both cases (RPLC and NPLC), strongly acidic and strongly basic samples cause problems. SFC is typically restricted to solvents and analytes of low to moderate polarity, especially in case FID detection is to be used.

Preparative separations Carbon dioxide is an outstanding solvent for preparative chromatography. It is available in high purities at a relatively low cost and it can easily be removed from the effluent by evaporation. In fact, the latter characteristic implies that it is somewhat more difficult to collect fractions than is the case in preparative LC.

The main disadvantage of CO₂ for preparative chromatography is its low polarity, which seriously limits its applicability as a chromatographic eluent. Packed columns, with large surface areas and thus high sample capacities, are desirable for preparative separations. Without organic modifiers, only components of little or no polarity can be eluted from such columns using CO₂. When substantial amounts of modifiers need to be used, the advantages of using CO₂ diminish.

Hyphenated systems

SFC–MS Although it would seem that the use of CO₂ is also advantageous when coupling a dense-phase chromatograph to a mass spectrometer (MS), successful SFC–MS systems have hardly materialized. In what are now the most common LC–MS interfaces (electrospray, ESI; and atmospheric-pressure chemical ionization, APCI), a high mobile-phase polarity is preferable. Only a small niche remains where

Table 3 General advantages of (packed-column) SFC in comparison with reversed-phase (RPLC) and normal-phase (NPLC) liquid chromatography*

Property	Related to:	RPLC	SFC	NPLC
Efficiency per unit time	Mass transfer (D_m , η)	Second	First	Last
Maximum efficiency	Eluent viscosity (η)	Second	First**	Second
Sample capacity	Surface homogeneity	First	Second	Last
Equilibration time	Eluent strength			
	Surface activity	First	Second	Last
Flexibility (range of samples)	Mass transfer			
	Mobile phase	First	Last	Second
	Surface activity			

*Most important effects are in italics.

**Very high plate numbers have been reached in SFC but operating conditions close to the critical point must be avoided.

SFC-MS may compete with LC-MS, i.e. components of low volatility and low polarity. This implies that there is little incentive for the further development of SFC-MS.

SFC-NMR CO₂ is a perfect eluent when ¹H-NMR is to be coupled with a chromatographic separation device. LC-NMR has received a good deal of attention in recent years and some workers have extended this work to include SFC-NMR. The main instrumental difference is that a high-pressure flow-cell (or 'probe') is required. However, the inherent sensitivity of NMR is so low that fractionation followed by offline spectroscopy is usually the preferred approach.

SFE-SFC Very elegant hyphenated systems may arise from a combination of two separation techniques that both involve supercritical fluids. Such systems include SFC-SFC and SFE-SFC. The latter approach, where the extraction serves as an online sample-preparation technique, has been especially investigated by several groups. Unfortunately, the high expectations surrounding SFE around 1990 have not quite materialized. Current interest in SFE-SFC has waned.

Types of SFC Columns

There are traditionally two approaches to SFC. One involves packed columns, the other open-tubular (capillary) columns. This situation is not different from that experienced in GC and LC. In the former technique, open columns are strongly preferred. In the latter, open columns are ideal in theory, but virtually impossible to use in practice. The optimum internal diameter of open columns used in chromatography is essentially determined by the diffusion coefficients of the analytes in the mobile phase. As a rule of thumb, the required analysis time is given by

$$t_R = \frac{N_{\text{req}} b d^2}{v D_m} (1 + k)$$

where t_R is the required analysis time for a separation with N_{req} theoretical plates and a solute retention factor of k , b is the reduced plate height, d the column diameter, v the reduced (average) velocity and D_m is the diffusion coefficient of the analyte(s) in the mobile phase. Both N_{req} and k are essentially determined by the retention of the analytes. The greater the selectivity (differences in retention), the lower the required number of plates. Neither

N_{req} nor k are affected by the dimensions (length and diameter) of the column. The reduced plate height (b) and the reduced (average) linear velocity (v) have typical values for packed and open-tubular columns. Typically, for packed columns $b = 3$ and $v = 10$, so that $b/v = 0.3$. For open-tubular columns $b = 4.5$ and $v = 45$ are good values, so that $b/v = 0.1$. All things being equal, open-tubular columns are expected to be about three times faster than packed columns.

D_m is the parameter that suggests SFC may allow faster separations than HPLC. However, the diffusion coefficient must be balanced against the characteristic dimension (d) of the column. For packed columns, d is the particle diameter (d_p), while for capillary columns it is the internal diameter of the column (d_c). It follows from the equation that similar performance (in terms of analysis times) can be expected in different forms of open-tubular chromatography when the ratio d_c^2/D_m is kept constant. With $D_{m,\text{gas}} \approx 1000 \times D_{m,\text{SF}} \approx 10^4 \times D_{m,\text{liquid}}$ we find for the optimum diameters of open tubular columns $d_{c,\text{GC}} \approx 30 \times d_{c,\text{SFC}} \approx 100 \times d_{c,\text{LC}}$. Since GC columns have internal diameters between 100 and 500 μm , we anticipate optimal internal diameters for SFC columns to be of the order of 10 μm and for LC columns to be 1–5 μm . Because very many practical problems are associated with the use of such extremely small columns, open-tubular SFC (OT-SFC) has typically been performed with somewhat larger columns (50 or 100 μm). However, this has led to a modest efficiency and speed.

Table 4 provides a summary of some of the advantages and disadvantages of using packed and capillary columns in GC and LC, with a more extensive summary of the characteristics of packed and open-tubular SFC. In SFC, open-tubular columns with optimal diameters are difficult to use. As a result, packed-column SFC is the more robust and more practical technique.

Most Important Parameters

The parameters that are most important in the development of SFC methods are as follows.

Mobile-Phase Density

The outstanding parameter in SFC is the mobile-phase density. This factor plays a role similar to the temperature in GC and the solvent strength in LC. Density gradients (typically increasing density linearly with time) in SFC are the common equivalent of temperature gradients in GC and mobile-phase composition gradients in LC. When the density increases,

Table 4 Advantages (↑) and disadvantages (↓) of packed and open-tubular (capillary) columns in GC, SFC and LC

	GC	SFC	LC
<i>Packed columns</i>	↑ Fast analysis ↑ Large sample capacity ↑ Broad dynamic range ↑ Reliable and robust ↑ Allows preparative separations ⇌ Perceived to be old-fashioned ↓ Low permeability ↓ Limited maximum efficiency	↑ Compatible with back-pressure regulators ↑ Broad range of optimum k values ↑ Programming often not needed ↑ Fast analysis ↑ Large sample capacity ↑ Broad dynamic range ↑ Reliable and robust ↑ Easy online solvent mixing ↑ Routine loop injections ↑ Allows preparative separations ⇌ Columns optimized for LC ↓ Low permeability ↓ Limited maximum efficiency ↓ High pressure drop ↓ Active stationary-phase surface ↓ Modifiers often required ↓ FID often not possible	↑ Compatible with many detectors ↑ Fast analysis ↑ Large sample capacity ↑ Broad dynamic range ↑ Reliable and robust ↑ Allows preparative separations ⇌ Columns still not perfect ↓ Very small particles required ↓ Low permeability ↓ Limited maximum efficiency ↓ High pressure drop
<i>Open-tubular columns</i>	↑ High permeability ↑ High maximum efficiency ↑ Inert surface for polar analytes ⇌ Many different injectors ↓ Limited sample capacity ↓ Limited dynamic range ↓ Sensitive to (large volumes of) solvents ↓ Sensitive to (liquid) water	↑ Inert surface for polar analytes ↑ Modifiers not often needed ↑ FID can usually be used ↑ High permeability ↑ Low column pressure drop ↑ High theoretical efficiency* ⇌ Very low mobile-phase flow rates ↓ Very small diameters required ↓ Sub-optimal (too large) columns commonly used ↓ Little tolerance for extra-column dispersion ↓ Very small sample volumes ↓ Proper injections are difficult (very small volumes and time splitting) ↓ Rather high detection limits ↓ Very small dynamic range ↓ Hard to combine with MS ↓ Narrow range of optimum k values ↓ Sensitive to (large volumes of) solvents ↓ Programming usually required ↓ Requires fixed restrictor (no adequate flow control)	↓ High permeability ↑ High maximum efficiency ⇌ Extremely low flow rates ↓ Very few detection options ↓ Extremely small diameters required ↓ Extremely small sample volumes ↓ High detection limits ↓ Extremely small dynamic range ↓ No tolerance for extra-column dispersion

*In practice, the efficiencies obtained in open-tubular SFC are well below the theoretically expected values.

interactions between the mobile phase and the analytes increase. The analytes are better dissolved in the mobile phase. Retention typically decreases exponentially with increasing density.

The column inlet and outlet pressures are significant parameters, but their effect on retention is indirect, as the pressure affects the density. In this context, the pressure closest to the critical value is most important. In SFC this is the column-outlet pressure.

Pressure, temperature and density are connected through an equation of state. Different equations can be used that provide good estimates for the density of pure supercritical fluids. However, when mixed eluents are used (e.g. CO₂ with a modifier such as methanol), no reliable equation is available that provides the density as a function of pressure and temperature. Nevertheless, when the latter two parameters and the composition of the eluent are established, the density is in principle defined.

Temperature

The second most important parameter is the temperature. Like the pressure, the temperature has a significant effect through its effect on the density. However, at constant density, an increased temperature may lead to a lower retention, especially for relatively volatile analytes. Apart from the temperature of the column oven, the temperature of the injector or injection valve can also be quite significant. In order to test the feasibility of eluting certain analytes by SFC, it is worthwhile to perform some experiments at an increased injector temperature.

Stationary Phase

The stationary phase. The column used plays a major role in SFC, especially when using non-polar mobile phases, such as carbon dioxide. The stationary phase has a large effect on the retention and an often prevailing effect on the selectivity. In addition, the stationary phase has a very large effect on peak shape and peak width (efficiency). Again, this effect is strongest when using non-polar eluents (CO₂).

Studying the effects of different stationary phases can be (very) expensive and time consuming. There are often practical limitations and when the option to use modifiers is available, this may be attempted first, provided UV detection is adequate.

Mobile-Phase Composition

The mobile-phase composition may have dramatic effects on retention, selectivity, efficiency and peak shape in SFC. However, adding modifiers has some significant disadvantages, especially with regard to detector compatibility. Therefore, changing the mobile-phase composition is not the first option in developing an SFC method. There are two modifiers that allow FID detection to be used, i.e. water and formic acid. Both have been investigated, but neither has found many applications in practice. The effect of a modifier tends to be greatest at low concentrations. In this range, the modifier mainly acts by competing with the analytes for strong adsorption sites on the stationary-phase surface. A small amount of modifier (often well below 1%) may lead to a much reduced analysis time and a much increased column efficiency. The use of modifiers often leads to much sharper and much more symmetrical peaks. At higher concentrations, modifiers may still affect retention and selectivity, through increasing the polarity and the density of the mobile phase. However, these effects are much smaller and the variations become more gradual. At these high concentrations it is more likely that different modi-

fiers give rise to substantially different selectivities.

Method Development

The flow chart for developing an SFC method shown as Figure 1 follows logically from the discussion on different types of columns and the overview of main parameters given in previous sections above.

Carbon dioxide will almost always be the eluent of choice. This is assumed to be the case in Figures 1 and 2. Instrument availability is the obvious first consideration. It greatly affects all the other decisions taken. Selecting packed columns is very attractive (see Table 4), but this requires a compatible instrument, with a pumping system capable of delivering substantial flow rates. It is quite possible to use microbore (1-mm i.d.) and packed-capillary (≤ 0.5 mm i.d.) in SFC, but some of the advantages of packed-column SFC are then lost. Most importantly, miniaturized columns do not allow the use of controllable back-pressure regulators. In this case, there is no adequate flow control, a problem that is especially serious when the mobile-phase density (in practice the pressure and/or the temperature) is programmed during the run.

When a novel sample is being subjected to SFC, the recommended strategy is to rapidly establish

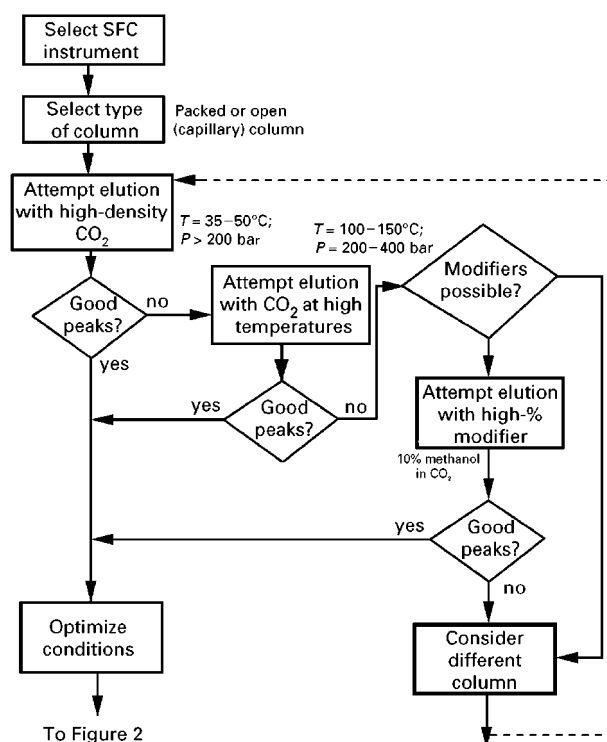


Figure 1 Flow chart for the development of an SFC method.

whether the analytes can be eluted. Because retention decreases with increasing density, high densities must be tried first. Once sharp peaks have been obtained for the analytes it will be easy to increase the retention by lowering the density. In open-tubular SFC a mobile-phase density gradient with a high final density will typically be used. In packed-column SFC, where retention times are typically of the order of minutes, constant elution conditions (isobaric, isothermal, isochoric and isocratic) will be preferred for initial scanning experiments.

Despite the high praise for FID, it is extremely valuable to have an informative detector available at this stage. A UV detector, especially a multichannel diode-array (DAD) instrument, will provide much on-line information on the progress of the method development. It is very much easier to know the whereabouts of different analyte peaks in the chromatogram if DAD and FID data are obtained simultaneously. In open-tubular SFC, a DAD cannot be used and SFC-MS is the obvious choice. However, SFC-MS is not an easily accessible practical tool.

If the analytes cannot be eluted at the highest possible (or highest practical) CO₂ density, it may yet be worthwhile to attempt elution at elevated temperatures. Increasing the temperature may lead to lower densities, but this may be compensated by an increased analyte volatility, especially for analytes with a significant vapour pressure. In addition, adsorption effects (including analyte-stationary-phase interactions) may be reduced. The temperature of the injector plays a different role. Sometimes it has proven beneficial to inject at temperatures well above the column temperature. In many cases, the sample (or sample solvent) is a limiting factor. When loop injection is used, the temperature must usually be kept well below the boiling point of the solvent.

If the analytes are not eluted as sharp, symmetrical peaks at high densities, nor at increased temperatures, then the use of modifiers may be attempted if this is an option. Using pre-mixed CO₂-based mobile phases is not attractive for reasons of accuracy and reproducibility as the composition in the cylinder will vary with time. Also, the flexibility regarding the possible concentrations is very limited. However, this is often the only choice in miniaturized (open-tubular) systems. In some cases, mixtures have been prepared inside the pump head of a syringe pump, which is preferred in terms of accuracy and flexibility. Many packed-column SFC systems allow more convenient online mixing, which makes it relatively easy to investigate the possible advantages of using modifiers. Unless experiments are performed with water or formic acid as a modifier (neither being very practical), the

use of FID is not feasible at this point. It may be useful to attempt a few different modifiers. However, the chances of obtaining good peaks become very small once the addition of 10% methanol has proven inadequate for the purpose.

The scanning experiments suggested so far can typically be performed within one or two days. This is what is referred to when it is claimed that method development in SFC can be very rapid. If at this stage the results are unsatisfactory, an important decision needs to be made. It is quite possible that better results will be obtained on a different column. However, when it is decided to investigate the use of different columns the amount of work needed will be multiplied. If there are still good reasons to opt for SFC, then it is most realistic to identify the column with the most inert surface (for example, a column packed with polysiloxane-coated particles) and repeat the sequence outlined above. If this attempt is not successful, then an alternative separation technique must be seriously considered.

Method Improvement and Troubleshooting

If at any stage during the method development rapidly eluting, sharp peaks have been obtained for the analytes, then the separation can be optimized. The actions that may be taken are summarized in Figure 2.

From the initial results it may be concluded whether the retention should be increased. The appropriate action depends on the stage at which success was obtained. If high-density CO₂ at a low temperature proved successful, then reducing the density will suffice. When elevated temperatures were

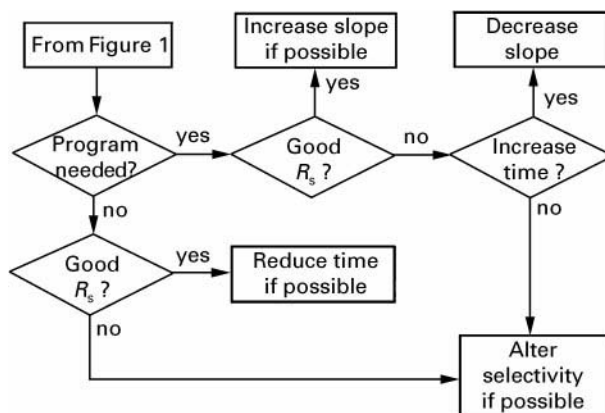


Figure 2 Flow chart for the optimization of an SFC method. R_s denotes resolution (i.e. ratio of distance between two peaks and their average base width).

used, the temperature may be lowered and/or the pressure may be decreased to achieve optimal elution conditions. If a modifier was used then the concentration of modifier may be lowered or the mobile-phase density may be decreased.

When moving the retention of the analytes into the optimum range, it will become apparent whether or not programmed elution is needed. In packed-column SFC this will only be the case if the last analyte has a high retention factor (say $k > 15$) when the first eluting analyte has $k = 1$. In marginal cases, it may be possible to use a different (less selective) stationary phase to avoid programmed analysis. In open-tubular SFC, programmed analysis is often needed just to deal with the excess of solvent introduced with the analytes. Resolution in programmed analysis can typically be increased by lowering the eluent strength (in SFC typically the density) at the start of the program and by lowering the slope (increasing the duration of the gradient segment of the program). In either case, this leads to a longer analysis time. In open-tubular SFC (or when using a fixed restrictor in packed-column SFC) the flow rate may be relatively high, especially in later parts of the program. In this case lowering the flow rate (by preparing a smaller restrictor) may be more rewarding, either by itself, or in combination with lowering the gradient slope.

If a separation under non-programmed conditions leads to abundant resolution between the relevant analytes, it may be possible to decrease the retention time. In order of decreasing rewards, this may be achieved by decreasing the column length, increasing the flow rate, or increasing the eluent strength (increasing the density or the modifier concentration). In the more important case in which the achieved resolution is inadequate, the pressure and/or temperature may be altered, but this often affects retention much more than selectivity (i.e. the retention factors of the various analytes tend to be affected in the same way). If modifiers are being used, different modifiers may lead to different selectivities. However, the most likely road to success is to attempt different stationary phases at this stage.

When we considered the use of different stationary phases at the end of the method-development stage, this was thought not to be very promising. However, in the present situation, at the method-optimization stage, it has already been demonstrated that SFC is a feasible technique for eluting the analytes, but not yet for separating them. Trying different stationary phases with greatly different selectivities may be a rewarding option at this stage.

The actions outlined here may also be relevant when the separation deteriorates at some stage during the development or application of an SFC method.

When this is the case, proper functioning of the equipment should first be verified. The mobile-phase density (pressure and temperature), flow rate and composition may all be verified. If variation in either of these parameters is excluded, then a change in the stationary-phase surface is a probable diagnosis. The column may be simply replaced at this stage, but a few other options are open. These are listed below.

- It is possible that the column is contaminated with very 'heavy' (high molecular weight) or very polar material from the sample or the solvent, that cannot be eluted under SFC conditions. In this case it may be possible to wash the column with a liquid solvent such as 2-propanol, to recondition it in the SFC instrument (without the FID connected), and to use it again for the application.
- It is possible that the column is 'irreversibly' altered by the presence of sample or solvent components. Water on a silica column is the most obvious example. Water may be removed by drying a column overnight at a high temperature (e.g. 250°C) under a small flow of an inert gas (N₂, H₂ or He). A GC oven is very useful for this purpose.
- In case non-programmed conditions are used, it may be advantageous to program the column to different conditions at the end of each analysis, each series of samples, or each working day to avoid column contamination.
- Some columns may change gradually in a truly irreversible manner. The use of amino-derivatized columns is not recommended in combination with CO₂, due to the anticipated formation of carbamates. If such a column is to be used, a gradual change of the stationary phase may necessitate gradual adaptation of the mobile-phase density or composition to maintain adequate resolution. Less dramatic changes of the surface may occur with different stationary phases (e.g. a gradual loss of some chemically bonded ligands from the surface) and these may also be counteracted by small changes in the conditions, rather than by frequently replacing the column.

See also: II/Chromatography: Supercritical Fluid: Historical Development; Instrumentation; Large-Scale Supercritical Fluid Chromatography; Theory of Supercritical Fluid Chromatography.

Further Reading

Anton K and Berger C (eds) (1998) *Supercritical-Fluid Chromatography in Packed Columns: Techniques and Applications*. New York: Marcel Dekker.

- Berger TA (1995) *Packed-Column SFC*, pp. 102–136. London: Royal Society of Chemistry.
- Berger TA (1997) Separation of polar solutes by packed column supercritical-fluid chromatography. *Journal of Chromatography A* 785: 3–33.
- Jinno K (1992) *Hyphenated Techniques in Supercritical-Fluid Chromatography and Extraction*. Amsterdam: Elsevier.
- Markides KE, Lee ML and Later DW (1989) Capillary supercritical-fluid chromatography: practical aspects. In: Yang FJ (ed.) *Microbore Column Chromatography: A Unified Approach to Chromatography*, pp. 239–266. New York: Marcel Dekker.
- Mulcahey LJ, Rankin CL and McNally MP (1994) Environmental applications of supercritical-fluid chromatography. *Advances in Chromatography* 34: 251–308.
- Petersson P and Markides KE (1994) Chiral separations performed by supercritical-fluid chromatography. *Journal of Chromatography A* 666: 381–394.
- Schoenmakers PJ (1988) Supercritical-fluid chromatography: open columns vs. packed columns. In: Smith RM (ed.) *Supercritical-Fluid Chromatography*, pp. 102–136. London: Royal Society of Chemistry.
- Schoenmakers PJ and Uunk LGM (1989) Mobile and stationary phases for supercritical-fluid chromatography. *Advances in Chromatography* 30: 1–80.
- Smith RM (ed.) (1988) *Supercritical-fluid Chromatography*. London: Royal Society of Chemistry.
- Smith RM and Hawthorne SB (eds) (1997) *Supercritical Fluids in Chromatography and Extraction*. Oxford: Elsevier.
- White CM (ed.) (1988) *Modern Supercritical-Fluid Chromatography*. Heidelberg: Hüthig.
- Wilson ID and Davis RJ (1993) Supercritical-fluid chromatography and extraction of pharmaceuticals. In: Dean J (ed.) *Application of Supercritical Fluids in Industrial Analysis*, pp. 74–103. Glasgow: Blackie.

ESSENTIAL GUIDES TO METHOD DEVELOPMENT IN THIN-LAYER (PLANAR) CHROMATOGRAPHY

S. Nyiredy, Research Institute for Medicinal Plants, Budakalász, Hungary

Copyright © 2000 Academic Press

Introduction

One of the most critical steps of qualitative and quantitative planar (thin-layer) chromatographic (TLC) analysis is development of a method resulting in sufficient separation. The main steps of method development are summarized in **Figure 1**. The first stage is selection of the stationary phase, the vapour phase, and suitable solvents. This stage is the *sine qua non* of method development, and the selection of these can occasionally immediately result in a suitable separation. For most real separation problems the second stage, optimization of the mobile phase is also necessary. The third part of method development is selection of the final conditions, for example the mode of development, transfer of the mobile phase to an appropriate forced-flow method, and last but not least, the selection of suitable operating parameters. This paper gives essential guides to method development in planar chromatography and draws attention to the most important considerations.

Stationary Phase Selection

TLC separations can be performed on modified, unmodified, and impregnated stationary phases, because of differences between the chemical properties of the sorbent material and those of compounds present in the sample to be separated. Different types of chromatographic process (normal-phase, reversed-phase, partition, and ion exchange chromatography) can be distinguished on the basis of the types of interactions involved. Although more than 90% of TLC separations are performed on silica, chemically bonded phases have recently become increasingly popular for solving special separation problems.

In normal-phase chromatography the hydroxyl groups on the surface of the silica are the polar, active centres which result in the interactions leading to the retention of the compounds to be separated. These interactions are mainly hydrogen-bonding and induced dipole–dipole interactions. The stationary phase can generally be characterized in terms of its specific surface area, specific pore volume, and mean pore diameter.

Unmodified stationary phases include silicas, aluminas, kieselguhr, silicates, controlled-porosity glass, cellulose, starch, gypsum, polyamides, and

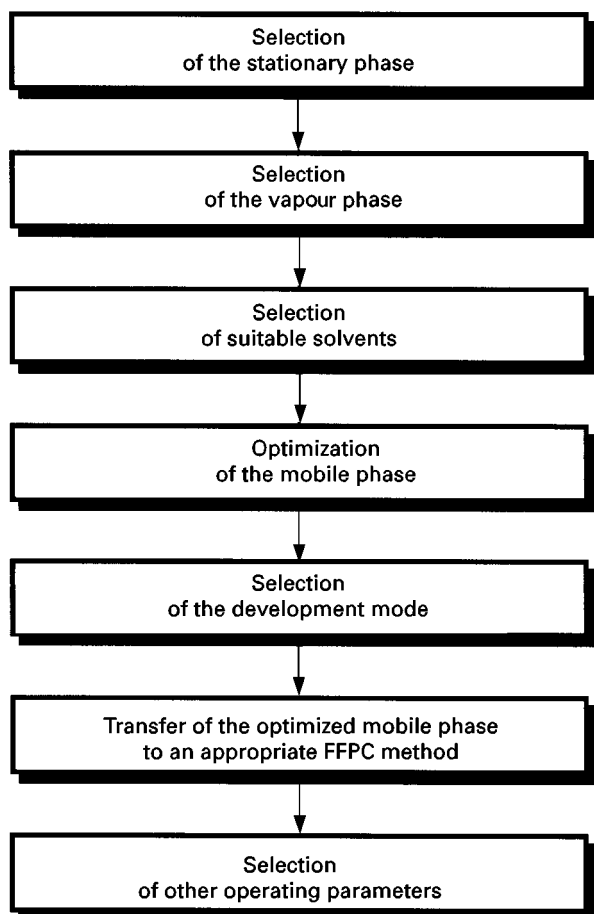


Figure 1 Schematic diagram of method development.

chitin. For TLC separations silica is manufactured by spontaneous polymerization and dehydration of aqueous silicic acid, which is prepared by adding acid to a solution of sodium silicate. The product of this process is an amorphous, porous solid, the specific surface area of which can vary over a wide range (200 to more than $100 \text{ m}^2 \text{ g}^{-1}$, as can the average pore diameter (10–1500 Å).

Modified silicas can be nonpolar or polar adsorbents. The former include silicas bearing alkane or alkene chains or phenyl groups, whereas the polar modified silicas contain cyano, diol, amino, or thiol groups or substance-specific complexing ligands. The structures of some chemically modified silicas are shown in Figure 2.

Almost all the stationary phases used in normal- and reversed-phase column liquid chromatography are also available for TLC. The dimensions of commercially available analytical thin-layer plates are 10×10 , 10×20 or 20×20 cm; the layer thickness is 20 or 25 μm . It is generally accepted that better resolution is obtained on thinner layers (10 μm), depending on the mode of detection. The silica materials commonly used for precoated plates have an average particle size of ca. 11 μm , the size range is from 3 to 18 μm ; for analytical layers prepared in the user's laboratory the average particle size is 15 μm and the range of particle sizes is much greater. The average particle size of precoated high-performance TLC (HPTLC) plates is now 5–6 μm and the range of particle sizes is very small.

	R	Name of stationary phase
	-OH	Silica
	-C ₈ H ₁₇	C ₈ or octyl
	-C ₁₂ H ₂₅	C ₁₂ or dodecyl
	-C ₁₈ H ₃₇	C ₁₈ or octadecyl
	-C ₃ H ₆ -CN	Cyanopropyl
	-C ₃ H ₆ -NH ₂	Aminopropyl
	-C ₃ H ₆ -O-CH ₂ -CHOH-CH ₂ OH	Diol
	-C ₄ H ₈ -chiral layer	Chiral

Figure 2 The structures of some commercially available surface-modified silicas.

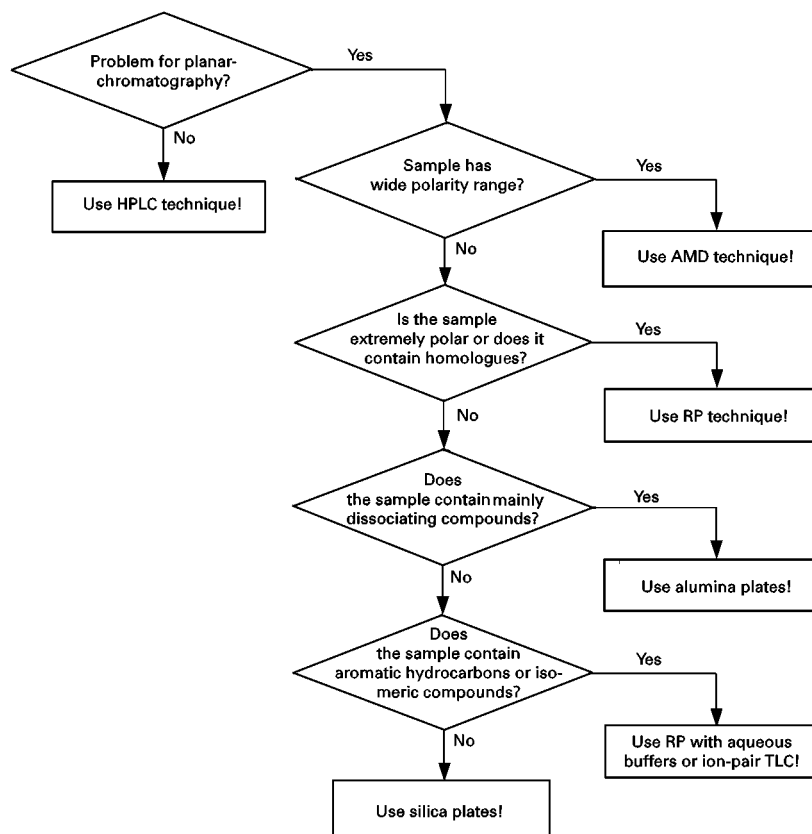


Figure 3 Flow chart illustrating a systematic approach for the selection of the appropriate separation technique and stationary phase.

Precoated analytical layers with a preadsorbent zone are also commercially available for linear development. This zone serves to hold the sample until development begins. Compounds soluble in the solvent system pass through the preadsorbent zone and are concentrated in a narrow band on entering the chromatographic layer; this improves resolution. **Figure 3** gives a decision flow chart for the systematic selection of the appropriate separation technique and stationary phase.

Vapour Phase Selection

In planar chromatography the separation process occurs in a three-phase system of stationary, mobile, and vapour phases, all of which interact both with each other and with the operating conditions. Selection of chamber type and vapour space is a variable offered only by planar chromatography as the third dimension of the chromatographic parameters. The role of the vapour phase in TLC is well known, although little attention is given to this in practice.

In planar chromatography two basic types of chromatographic chamber must be distinguished. In the common normal (N) chamber the distance

between the layer and the wall of the chromatographic tank is more than 3 mm. If this distance is smaller, the chamber is said to have the S configuration. Both types of chamber can be used for unsaturated or saturated systems. As a rule of thumb, if the sample contains fewer than seven compounds to be quantitatively determined, saturated N chambers must be selected for method development. If the sample contains more than seven substances, or the separation is very difficult, S chambers must be selected which enable transfer of the optimized mobile phase by forced-flow.

Often the separation problem cannot be solved by use of conventional TLC with solvent migration by capillary action, because of the relatively modest separating power of the method. In such circumstances use of one of the different forced-flow techniques is necessary; this must be considered during selection of the vapour phase. The chambers used for forced-flow planar separations can be also assigned to the above two categories. The chambers used for overpressured layer chromatography (OPLC) are unsaturated S chambers, theoretically and practically devoid of any vapour space. This must be considered in the selection of appropriate solvents and during the

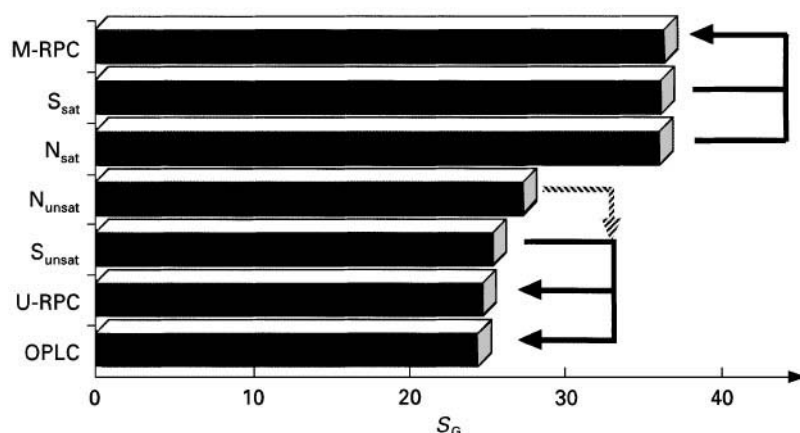


Figure 4 The saturation grade of different forced-flow methods, in comparison with the N and S chambers.

optimization of the solvent system. In rotation planar chromatography (RPC) the size, and thus the extent of saturation, of the vapour phase can be varied. In RPC the micro and ultramicro chambers belong to the S-chamber type. Because in microchamber RPC the plate rotates with the small chromatographic chamber, and the distance between the layer and the lid of the chamber is less than 2 mm, the vapour space is rapidly saturated. In ultramicrochamber RPC the lid of the chamber is placed directly on the plate and so in practice there is no vapour space, as in OPLC.

When a mobile phase is transferred from a chromatographic tank separation to a forced-flow technique, the vapour phase can be characterized on the basis of the saturation grade (S_G). The S_G value of

a given chromatographic chamber can be calculated by dividing the sum of the hR_F values of the three furthest-migrating substances by the sum of the hR_F values of all the components, subtracting the result from 1, and multiplying the answer by 100. The saturation grade can be used as a measure of the reproducibility of separations with given stationary and mobile phases and at different temperatures and humidity; this enables transfer of the mobile phase to other vapour-phase conditions. **Figure 4** shows the saturation grade of the different chromatographic chambers. The lines indicate suggested mobile phase transfer possibilities; the dotted line indicates other mobile phases which might be used, but with less probability of success.

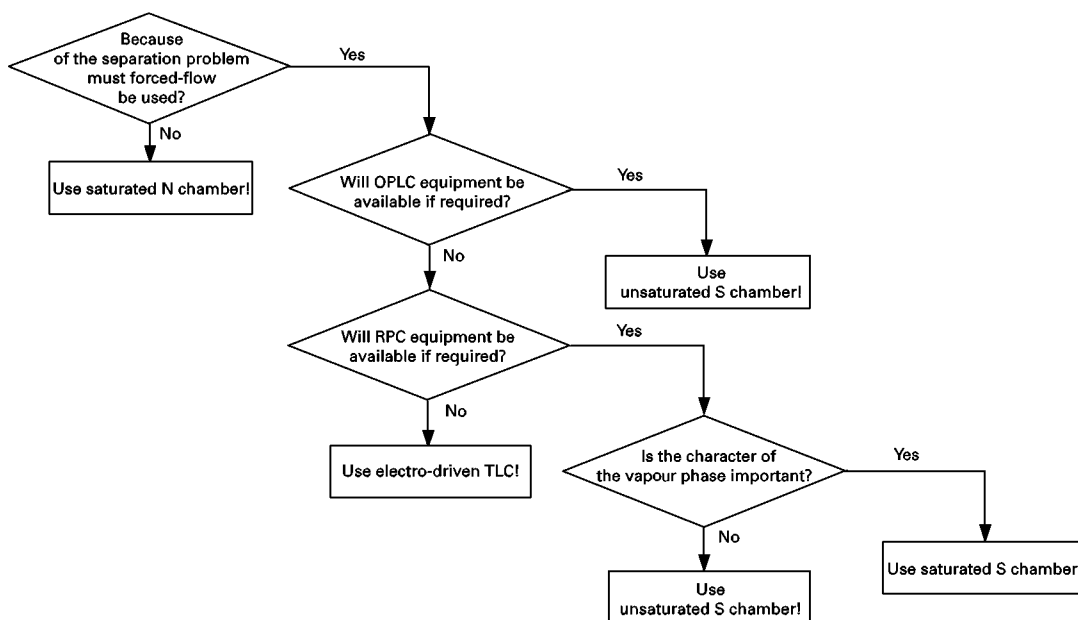


Figure 5 Flow chart illustrating a systematic approach for the selection of the appropriate chromatographic chamber and vapour phase.

Among the forced-flow methods the highest separating power is obtained with OPLC, because of the optimum mobile phase velocity on the HPTLC plate and the greater separation distance. If, therefore, the quality of the final separation is likely to be determined by the separation distance, OPLC and, for the preassay, the unsaturated S chamber must be selected. If RPC equipment is available for improving the efficiency of the final separation, the choice of chromatographic tank for the preassay depends on the types of compound to be separated. If the acidic or basic character of the vapour phase is important for the separation, a saturated S-chamber (micro-chamber) should be used; if this is not available, a saturated N chamber is the right selection for the TLC pre-assay. If the mobile phase is to be transferred

to a U-RPC separation, an unsaturated S chamber (ultramicro chamber) must be chosen. These considerations are summarized in Figure 5.

Selection of Suitable Solvents

The modern strategy of solvent selection is based on the solvent classification by Snyder, who classified more than 80 solvents into eight groups for normal-phase chromatography according to their properties as proton acceptors (x_a) and proton donors (x_d), and their dipole-dipole interactions (x_n).

For, selection of suitable solvents, preliminary experiments are performed on silica TLC plates with the nine solvents indicated by stars in Table 1, which lists the solvents commonly used in planar chromatography.

Table 1 Solvent classification based on solvent strength and selectivity values

Group	Solvent	Solvent strength (S_i)	X_e	X_d	$S_v = \frac{X_e}{X_d}$
–	<i>n</i> -Hexane	0	–	–	0.10*
I	<i>n</i> -Butyl ether	2.1	0.44	0.18	2.44
	Diisopropyl ether	2.4	0.48	0.14	3.43
	Methyl- <i>t</i> -butyl ether	2.7	0.49	0.14	3.50
	Diethyl ether*	2.8	0.53	0.13	4.08
II	<i>i</i> -Pentanol	3.7	0.56	0.19	2.95
	<i>n</i> -Butanol	3.9	0.56	0.19	2.95
	<i>i</i> -Propanol	3.9	0.55	0.19	2.89
	<i>n</i> -Propanol	4.0	0.54	0.19	2.84
	Ethanol*	4.3	0.52	0.19	2.74
	Methanol	5.1	0.48	0.22	2.18
III	Tetrahydrofuran*	4.0	0.38	0.20	1.90
	Pyridine	5.3	0.41	0.22	1.86
	Methoxyethanol	5.5	0.38	0.24	1.58
	Methylformamide	6.0	0.41	0.23	1.78
	Dimethylformamide	6.4	0.39	0.21	1.86
	Dimethylsulfoxide	7.2	0.39	0.23	1.70
IV	Acetic acid*	6.0	0.39	0.31	1.26
	Formamide	9.6	0.36	0.23	1.57
V	Dichloromethane*	3.1	0.29	0.18	1.61
	1,1-Dichloroethane	3.5	0.30	0.21	1.43
	Benzyl alcohol	5.7	0.40	0.30	1.33
VI	Ethyl acetate*	4.4	0.34	0.23	1.48
	Methyl ethyl ketone	4.7	0.35	0.22	1.59
	Dioxane	4.8	0.36	0.24	1.50
	Acetone	5.1	0.35	0.23	1.52
	Acetonitrile	5.8	0.31	0.27	1.15
VII	Toluene*	2.4	0.25	0.28	0.89
	Benzene	2.7	0.23	0.32	0.72
	Nitrobenzene	4.4	0.26	0.30	0.87
	Nitromethane	6.0	0.28	0.31	0.90
VIII	Chloroform*	4.1	0.25	0.41	0.61
	Dodecafluoroheptanol	8.8	0.33	0.40	0.83
	Water	10.2	0.37	0.37	1.00

*Approximate value.

After these initial TLC experiments with the neat solvents, the solvent strength (S_i) must either be reduced or increased so that the substance zones are distributed between R_F 20 and 80. The two theoretical situations are depicted in Figure 6 (A and P in Figure 6). If the compounds to be separated migrate in the upper third of the plate (A-a in Figure 6) the solvent strength must be reduced by dilution with hexane. If the neat solvents do not cause migration of

the substances, the solvent strength must be increased (P-a in Figure 6) by the addition of water. In both circumstances the solvent strength should be varied so that better distribution of the substance zones is obtained. Consequently, the structures and properties of the compounds to be separated do not have to be known. Their classification as apolar (A) or polar (P) compounds can be made in accordance with their behaviour in these TLC experiments.

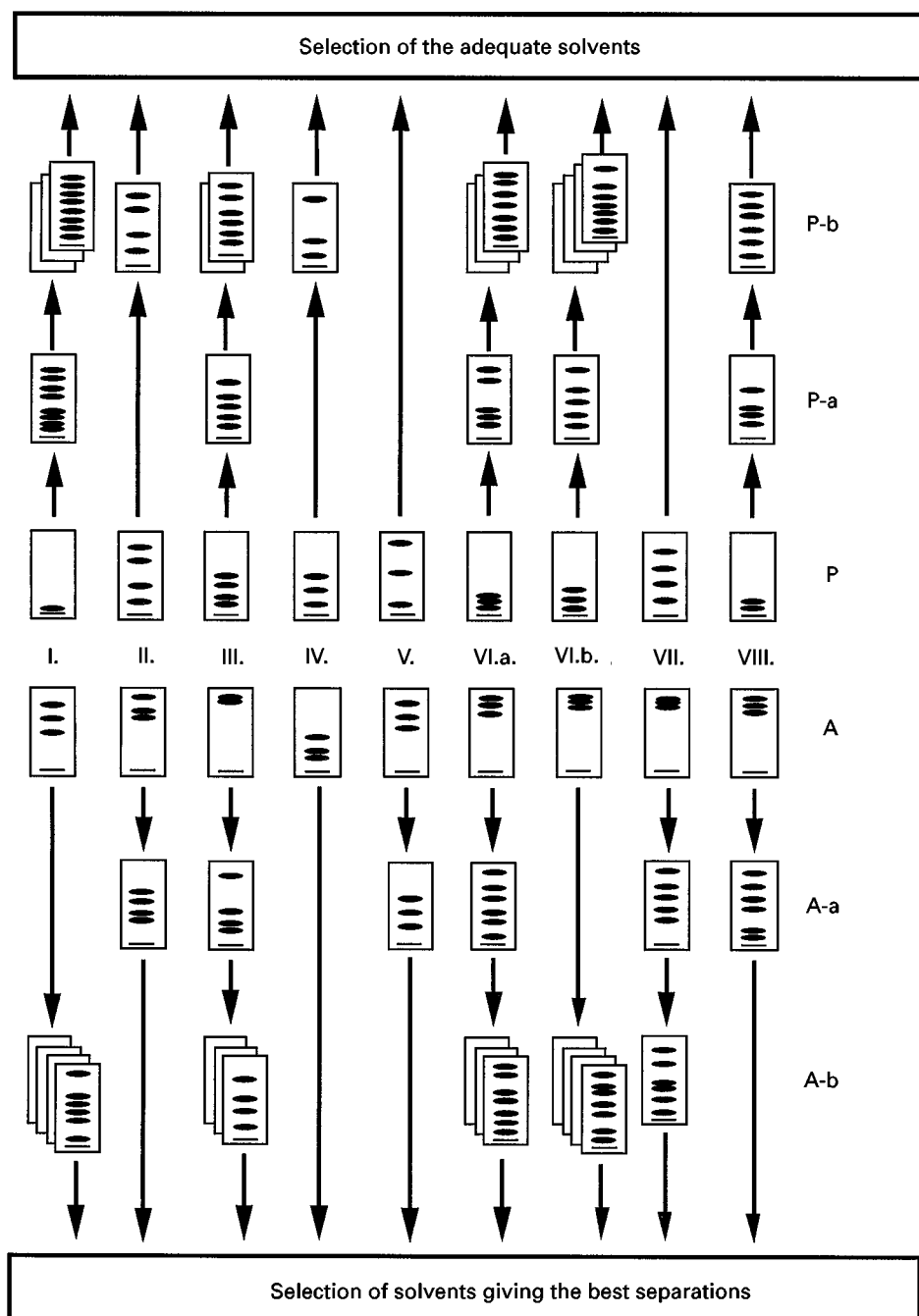


Figure 6 Strategy for the selection of a suitable TLC solvent.

If solvents result in good separation, their homologues or other solvents of the same group can also be tested, as indicated by A-b and P-b in Figure 6. After these experiments the solvents giving the best separations are chosen for further optimization of the separation of apolar compounds. For optimization of the mobile phase for separation of polar compounds, suitable solvents are again selected; the solvent mixture should contain one solvent in which the compounds do not migrate; this is necessary for the transfer of the mobile phase to certain forced-flow techniques. In certain circumstances a suitable separation can be achieved with this solvent-selection strategy. The individual steps of this method of solvent selection are depicted in a flow chart in Figure 7.

Thus the structures and properties of the compounds to be separated do not have to be known for these experiments. After these experiments, the solvents giving adequate separations are chosen for optimization of the mobile phase.

Mobile Phase Optimization

Mobile phase optimization is based both on modification of published data, on experience with the analytes, and on intuition. As sample composition becomes more complex, however, systematic solvent optimization becomes increasingly important. For systematic mobile phase optimization four methods are generally used in planar chromatography:

- window diagram
- sequential simplex method
- Geiss's structural approach
- the 'PRISMA' model.

Because only the 'PRISMA' model is currently suitable for both manual and automatic mobile phase optimization, this method is summarized below.

After the selection of suitable solvents the construction of the actual 'PRISMA' model is begun. In general between two and five solvents might be selected for the construction of the model; modifiers might

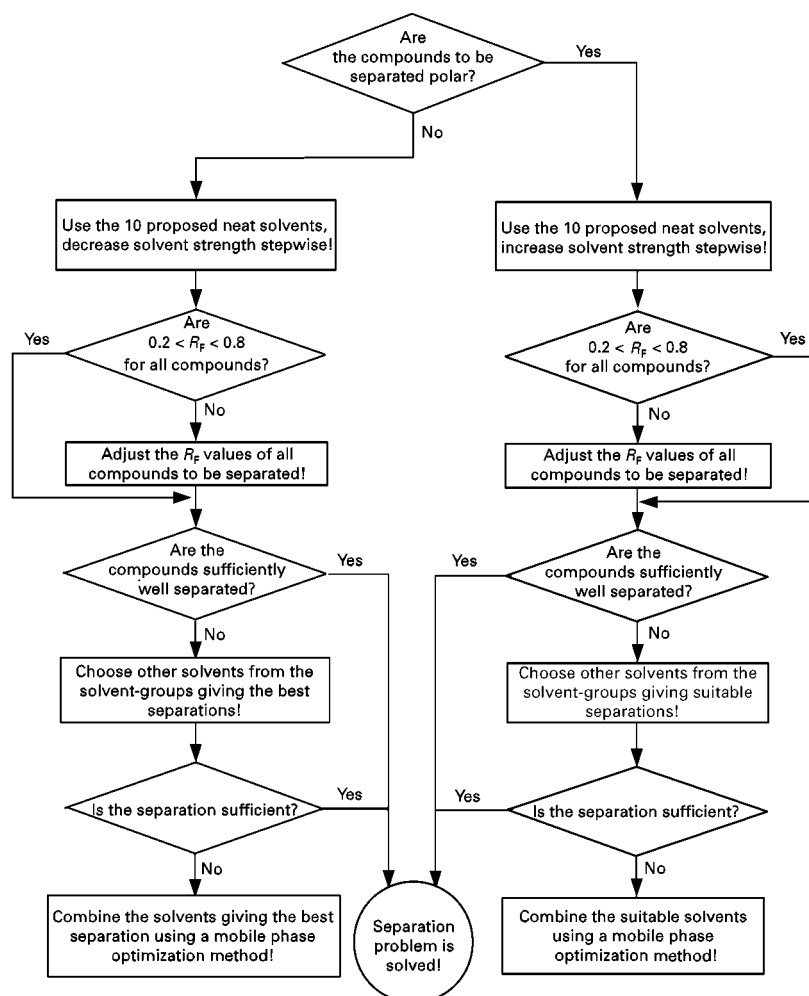


Figure 7 Flow chart illustrating a systematic approach for the selection of suitable solvents.

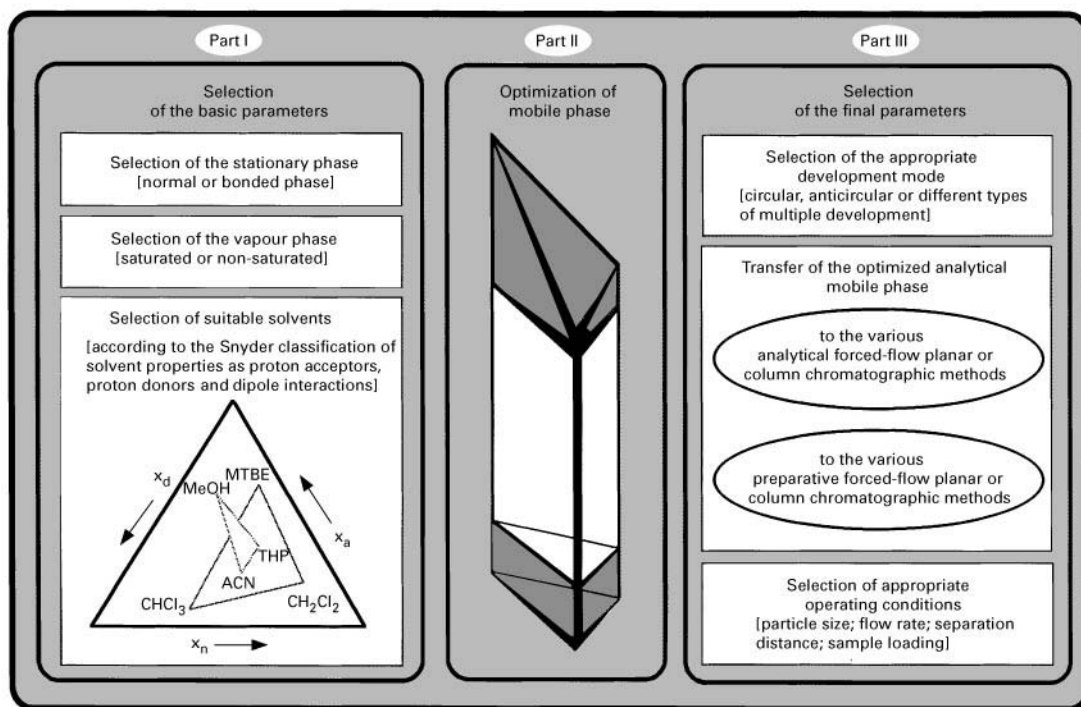


Figure 8 The 'PRISMA' system for the systematic optimization of a planar chromatographic method.

also be added. The actual 'PRISMA' model is a three dimensional geometrical design which correlates the solvent strength with the selectivity value of the mobile phase. The tripartite model (see the central part of **Figure 8**) consists of an irregular top part (light grey), a regular middle part (white) and the lower part (dark grey) symbolizing the modifier(s). When working with silica as the stationary phase, the upper frustum is generally used for the optimization of mobile phases, with or without modifier, for the separation of polar compounds. The regular centre portion of the prism is used for the optimization of mobile phases, with or without modifier, for the separation of apolar compounds. The construction of the model, the role of solvent strength, and the characterization of the selectivity points (P_s) are described extensively in the literature.

The selectivity points on the vertical planes of the regular part of the prism can be obtained by diluting the solvent mixtures with a solvent-strength regulator. Solvent-strength (S_T) values decrease from top to bottom; at the base of the prism S_T is zero. If sections are taken across the regular prism parallel to the base, triangles of different S_T levels are obtained. Obviously, the solvent strength is identical at all points on one of these triangles, and all points on a vertical straight line correspond to the same selectivity point.

For normal-phase chromatography hexane ($S_i = 0$) is the regulator. If reversed-phase plates must be used

for the separation, the regular part of the model is used for the separation, irrespective of the polarity of the compounds to be separated. In these circumstances water, rather than hexane, must be used as the solvent-strength regulator.

The solvent-strength values of the modifier(s) are treated by the 'PRISMA' model as additive terms. For the sake of simplicity, the solvent-strength values of the modifiers are neglected, because they are usually present at low, constant concentrations (generally between 0.1 and 3%, e.g. acids, ion pairs).

Manual Optimization Procedure

The four basic selectivity points within the regular part of the prism ($P_s = 333, 811, 181, 118$) for four solvent mixtures and the three basic selectivity points on the side of the prism ($P_s = 550, 75-25, 25-75$) for three solvent mixtures are emphasized in **Figure 9**. The black points symbolize mixtures of one solvent and the solvent strength regulator (binary systems); the dark grey points symbolize mixtures of two solvents and the regulator (ternary systems); and the three-digit numbers symbolize mixtures of three solvents and the regulator (quaternary systems).

If three solvents were selected for the separation of apolar compounds, optimization is performed within the regular part of the model with the help of the four basic selectivity points. The steps for optimizing the solvent combination for apolar compounds are

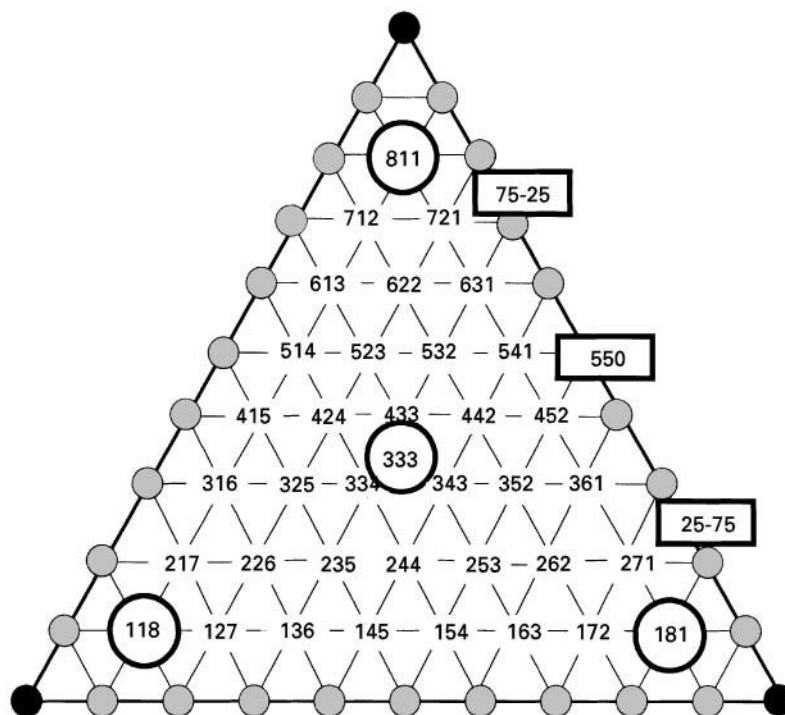


Figure 9 Favoured selectivity points for mobile phase optimization.

depicted in a flow chart in **Figure 10**. If two solvents were selected, the optimization is performed along the side of the prism. In both circumstances the solvent strength is adjusted and then different selectivity points are tested. If three to five solvents are selected as best, the number of solvents is reduced on the basis of criteria such as the number of compounds separated and the ΔR_F values obtained. If the solvent combinations tested with this strategy do not result in a sufficient separation, or at least the beginnings of a separation, of important pairs of substances, other solvents must be selected and the process must be repeated, as indicated in the flow chart.

For the separation of apolar compounds the optimization is generally a rapid process because a few experiments are sufficient to evaluate the optimum mobile-phase composition.

For polar compounds, the optimization is always started on the top irregular triangle of the model, either within the triangle, when three solvents were selected, or along one side, when two solvents were selected. Water is usually used as a modifier to increase solvent strength and reduce tailing; if water is used, several selectivity points cannot be tested because of immiscibility problems (especially near $P_s = 811$).

Changing the selectivity points on the top triangle also changes the solvent strength; thus a small change in the selectivity point might result in a large difference in resolution, especially when the solvent

strength of the selected solvents differs substantially. The subsequent procedure is similar to that for the apolar compounds, but the solvent strength must be adjusted after a suitable selectivity is found. The flow chart for the optimization of the solvent combination for polar compounds is shown in **Figure 11**.

In contrast to the separation of apolar compounds, optimization is a longer process for polar substances because of the simultaneous change in solvent strength and selectivity. When water, in particular, is one of the solvents selected for the construction of the triangle, a small change in selectivity results in extreme changes in resolution. More chromatographic experience is, therefore, necessary if the separation problem is to be solved rapidly.

Manual optimization of the mobile phase must be performed until at least the beginnings of a separation of the compounds is obtained. This can usually be achieved with the first 'PRISMA' combination, assuming the individual solvents were selected correctly.

Automatic Optimization Procedure

The basis of automatic mobile-phase optimization, the correlation between mobile-phase composition and resolution for saturated TLC systems, can be described by mathematical functions. The correlation between bR_F values and the selectivity points at a constant solvent strength level can be expressed by

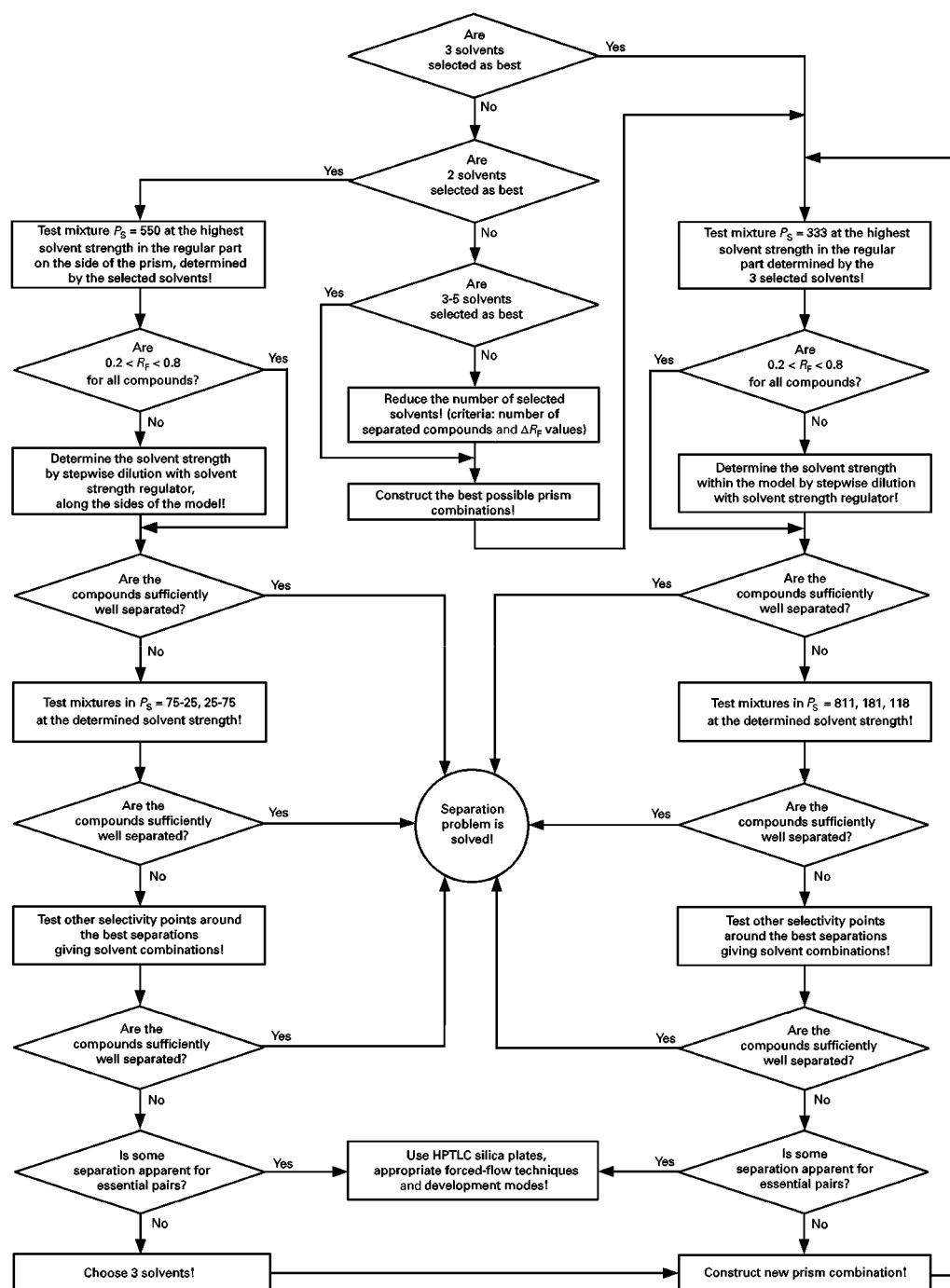


Figure 10 Flow chart illustrating a systematic approach for the optimization of the mobile phase for the separation of nonplanar compounds.

the function:

$$bR_F = a(P_S)^2 + b(P_S) + c$$

For quaternary solvent systems, the correlation between bR_F values and solvent strength at a constant selectivity point can be expressed by the function:

$$\ln bR_F = d(S_T) + e$$

Because the vertical correlation can be linearized, measurements on three solvent-strength levels are needed to calculate the bR_F values for all selectivity points in the spatial design. These correlations are also relevant when modifiers are used in constant amounts, for different classes of substance. From these correlations of bR_F values with the selectivity of the mobile phase, the chromatographic behaviour of

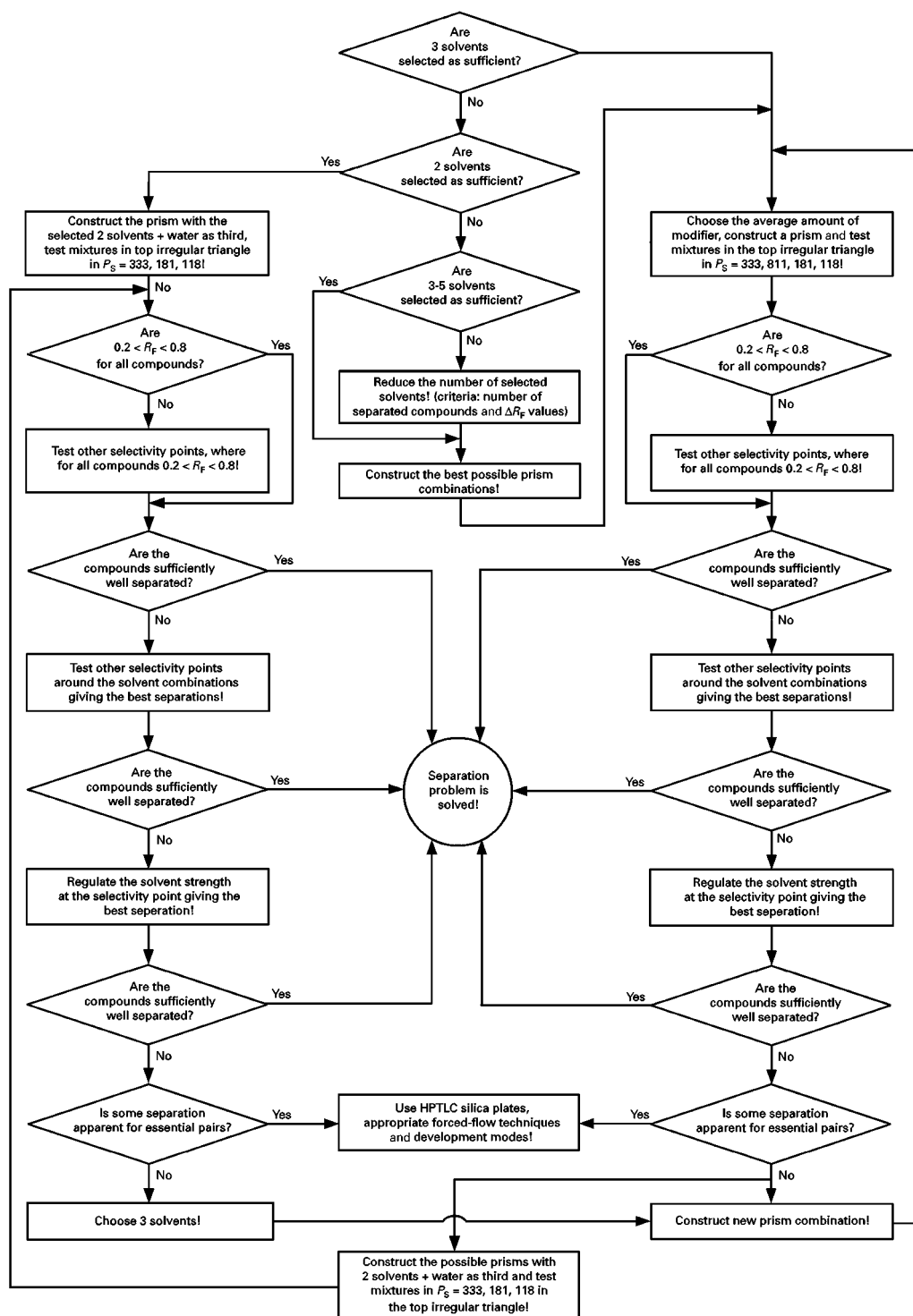


Figure 11 Flow chart illustrating a systematic approach for the optimization of the mobile phase for the separation of polar compounds.

substances to be separated can be predicted for all selectivity values in saturated chromatographic chambers.

The separation quality of predicted chromatograms can be assessed by use of a chromatographic

response function (CRF). The optimum composition can be found by a simple mathematical procedure which maximizes the CRF by monitoring its dependence upon mobile-phase composition. Twelve measurements are necessary to discover a local opti-

Table 2 Required measurements for automatic mobile phase optimization to achieve the global optimum

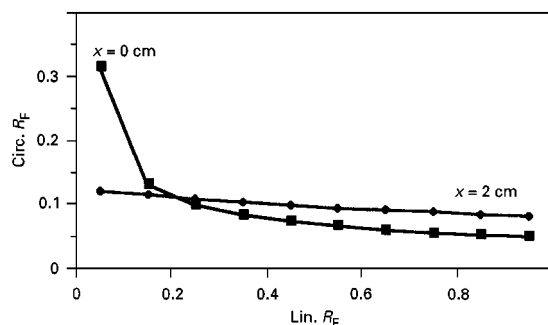
Solvent strength	Selectivity points					
S_{T1}	811	631	118	343	136	181
S_{T2}	811	433	118	316	361	181
S_{T3}	811	613	118	334	163	181

num, and fifteen for the global optimum. To increase the accuracy, six measurements at three different solvent strength levels (18 experiments) are necessary, as is seen in Table 2.

Selection of the Mode of Development

Planar chromatography differs from all other chromatographic methods in that it enables selection of the optimum mode of development; the linear mode of development is used most frequently. Because ascending development has no theoretical advantage over horizontal development, the latter, being more adaptable, has become increasingly common in recent years.

The advantage of circular development, where the solvent system migrates radially from the centre of the plate to the periphery, is well known for the separation of compounds in the lower R_F range. Working with the same mobile phase, the resolution is about 4–5 times higher in circular than in linear development mode, as is seen in Figure 12. This statement is only valid if the samples are spotted exactly at the centre ($x = 0$ cm). If the distance between the sample and the mobile phase inlet is, e.g. 2 cm, there is no significant difference in the lower R_F range between circular and linear development (see Figure 12). Development can, however, be started at a point displaced from the centre if a filter-paper ring is used to achieve higher mobile-phase velocity. Under these conditions many samples can be applied and the advantages of circular development can be exploited.

**Figure 12** Effect on the ΔR_F value of the distance between mobile phase inlet and sample.

In anticircular development the mobile phase is applied to the layer as a circle and flows towards the centre. Because the solvent flow velocity decreases with the square of the distance, but the area wetted also decreases with the square of the distance travelled, the speed of mobile-phase migration is practically constant. Although anticircular development is rarely used, it is an accepted approach in TLC if resolution must be increased in the higher R_F range.

The multiple development (MD) techniques, UMD (unidimensional MD) and IMD (incremental MD) can also be used to increase separating power in the lower R_F range. UMD is the repeated development of the plate over the same development distance with mobile phase of the same composition; between development steps the mobile phase is removed from the layer by careful drying and the dried plate is returned to the development chamber for development under the same chromatographic conditions as previously. IMD is an alternative version of this technique in which successive chromatographic developments are performed over increasing development distances with mobile phase of the same composition. In the IMD first development distance is the shortest and subsequent development steps are over longer distances; the development distance usually increases by equal increments. The last migration distance, the longest, corresponds to the useful development length of the plate (but can depend on the mobile phase employed).

The advantages of the different modes of development can be summarized as follows:

- circular development increases resolution in the lower R_F range
- anticircular development increases resolution in the higher R_F range
- UMD is most effective at improving separation in the lower R_F range
- IMD improves zone-centre separation.

A comparison of these modes of development is presented in Figure 13.

Mobile Phase Transfer

There are two reasons for transferring the optimized TLC mobile phase. The first is that the separation is not sufficiently good and better resolution might be achieved by use of forced-flow methods. The optimized TLC mobile phase is, therefore, transferred without alteration to the U-RPC or OPLC technique. When the latter is used, a prerun must be performed. For separation of nonpolar compounds the prerun can be performed with hexane; for separation of polar

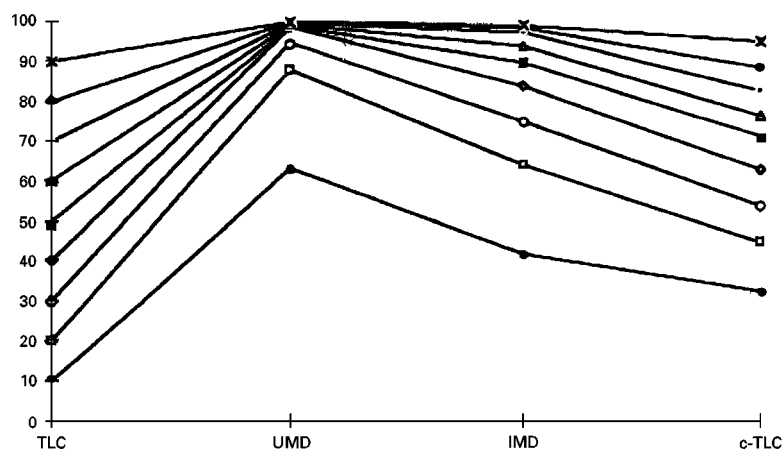


Figure 13 Effect of linear, circular, UMD, and IMD development modes on R_F values in the lower R_F range.

substances the prerun can be performed with any component of the mobile phase in which the components do not migrate. The selection of this solvent

might be considered during optimization of the mobile phase. Highly effective separation can be achieved by use of HPTLC plates and forced-flow techniques.

The second reason for transferring an optimized TLC mobile phase is when scaling up to the various preparative chromatographic systems. As a result of the characterization of the different saturation grade of chromatographic chambers (see **Figure 4**), excellent mobile phase transfer between analytical and preparative planar chromatographic methods and analytical HPLC can be achieved. The transfer can be performed on the basis of the chromatographic conditions used. Dry-filled preparative columns (for flash, low-pressure liquid, and medium-pressure liquid chromatography) can be equilibrated with the solvent used for the prerun in analytical OPLC, whereas if the column is filled by the slurry technique, the slurry must be prepared from the same solvent as was used for the OPLC prerun. In both of these, air bubbles can be eliminated by passage of an appropriate amount of the solvent used for the prerun; preparative separation can then be started with the optimized unsaturated TLC mobile phase.

The possibilities of mobile-phase transfer between the different solid-liquid chromatographic methods are comprehensively summarized in **Figure 14**, which demonstrates the possibilities of direct transfer. Different lines show those applicable to the different methods; dotted lines and thin lines are indicative of offline and online methods, respectively, whereas thick lines indicate the possibility of transfer of the optimized mobile phase without change between different solid-liquid planar and column chromatographic techniques, both offline and online.

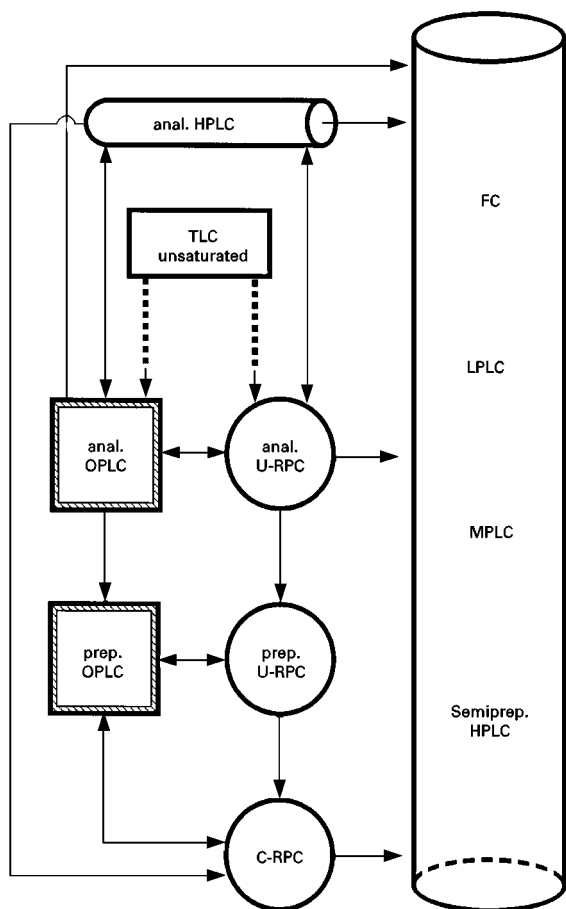


Figure 14 Possibilities of transferring the optimized TLC mobile phase to the different forced-flow planar chromatographic methods, and to preparative column liquid chromatographic techniques.

the migration of the mobile phase. The local mobile-phase velocity can be influenced by the mode of development selected.

In TLC separation efficiency improves with the square root of the separation distance. The optimum, however, depends on the quality of the plate (average particle size and size distribution of the stationary phase), the vapour space, the mode of development, and the properties of the compounds to be separated. The first of these cannot be influenced by the user of precoated plates. The maximum length of commercially available precoated plates is 20 cm. Thus, the maximum separation distance in linear development is 18 cm. The efficiency and rapidity of planar chromatography can be increased by the use of a novel category of multilayer OPLC, long-distance OPLC, by use of which the separation efficiency is increased significantly. In this technique the end of the first plate has a slit-like perforation through which the mobile phase is transferred to a second layer. Clearly, on this basis, a very long separation distance can be achieved by combining one plate with another.

Sample application is one of the most important stages of successful planar chromatography. The amount of applied sample depends on the determination method. Generally, μg and ng quantities of sample can be determined, but even less than 100 pmol substance per chromatogram zone has been reported.

During method development, the separation distance always depends on the mode of development and the forced-flow technique used, and on the development distance; this is summarized in **Figure 15** in the form of a flow-chart.

In normal circumstances alteration of temperature is not an effective means of modifying selectivity and maximizing resolution. If two compounds are unresolved at a given temperature, they normally remain unseparated at other temperatures, irrespective of whether N- or S-chambers are used. It can generally be stated that in saturated chromatographic chambers, which are most commonly used, the temperature does not have a great influence on separations. A change of $\pm 5^\circ\text{C}$ results in a change in hR_F of less than 3. Nevertheless, in the interest of reproducibility in duplicate separations it is important to note the working temperature. Remarkably, temperature is now being found to play an important role in the selectivity and efficiency of OPLC separations.

Strategy of Method Development

The 'PRISMA' optimization system is a strategy for method development in liquid chromatography. Fig-

ure 8, which shows the 'PRISMA' system for planar chromatography, consists of three parts. The first part is the selection of the basic parameters; stationary and vapour phases and suitable solvents, the last according to the Snyder classification. The second part is the optimization of the mobile phase, using the 'PRISMA' optimization model. The third part is the selection of the final parameters; the mode of development, transfer of the mobile phase to the appropriate forced-flow method and, last but not least, the selection of suitable operating conditions. The 'PRISMA' system enables the combination of the appropriate mode of development with the appropriate forced-flow technique by the use of a mobile phase of optimized composition; this offers special possibilities for solving difficult separation problems. This system provides guidelines for method development in planar chromatography.

See also: II/Chromatography: Thin-Layer (Planar) Chromatography: Historical Development; Instrumentation; Layers; Modes of Development; Conventional; Modes of Development; Forced Flow Overpressured Layer and Centrifugal Chromatography.

Further Reading

- Geiss F (1987) *Fundamentals of Thin Layer Chromatography (Planar Chromatography)*. Heidelberg: Hüthig.
- Nyiredy Sz (1992) Planar chromatography. In: Heftmann E (ed.) *Chromatography*, 5th edition, pp. A109–150. Amsterdam: Elsevier.
- Nyiredy Sz (1997) Solvent classification for liquid chromatography. In: Kaiser O, Kaiser RE, Gunz H and Günter W (eds) *Chromatography*, pp. 231–239. Düsseldorf: InCom Sonderband.
- Nyiredy Sz, Botz L, Sticher O (1989) ROTACHROM®. A new instrument for rotation planar chromatography (RPC). *Journal of Planar Chromatography* 2: 53–61.
- Nyiredy Sz, Dallenbach-Toelke K and Sticher O (1988) The 'PRISMA' optimization system in planar chromatography. *Journal Planar Chromatography* 1: 336–342.
- Nyiredy Sz, Fatér Zs, Botz L and Sticher O (1992) The role of chamber saturation in the optimization and transfer of the mobile phase. *Journal Planar Chromatography* 5: 308–315.
- Schoenmakers PJ (1986) *Optimization of Chromatographic Selectivity*. Amsterdam: Elsevier.
- Sherma J and Fried B (eds) (1995) *Handbook of Thin-Layer Chromatography*. New York: Dekker.
- Szepesi G and Nyiredy Sz (1995) Pharmaceuticals and drugs. In: Fried B and Sherma J (eds) *Handbook of Thin Layer Chromatography*, pp. 819–876. Marcel Dekker: New York.
- Tyihák E and Mincsovics E (1988) Forced-flow planar liquid chromatographic techniques. *Journal of Planar Chromatography* 1: 6–19.

ESSENTIAL GUIDES TO METHOD DEVELOPMENT IN TWO-DIMENSIONAL ELECTROPHORESIS

M. J. Dunn, Imperial College School of Medicine,
Harefield Hospital, Middlesex, UK

Copyright © 2000 Academic Press

Introduction

Most one-dimensional (1-D) methods of polyacrylamide gel electrophoresis are limited to the resolution of 100 or so protein zones. These techniques are therefore not suitable for the analysis of complex mixtures containing several thousands of proteins, such as total protein homogenates of whole cells and tissue. In addition, they are only able to separate proteins on the basis of a single physico-chemical property. For example, the observation of a particular zone following SDS-PAGE does not imply protein heterogeneity, but simply indicates that any proteins present in that zone have nearly identical size properties, while their charge (and other) properties could be very different.

The best approach to this problem is to combine two different 1-D methods into a 2-D procedure. Ideally, the methods used for each dimension should be selected by their ability to separate proteins according to different properties in each dimension. Thus, if each method when used alone is able to resolve 100 protein zones, it would be expected that up to 10 000 proteins might be resolved when these methods are used orthogonally. This level of resolution has rarely been achieved in practice, but nevertheless 2-D has become the method of choice for the analysis of patterns of protein expression in whole cells, tissues and organisms; the area now known as proteomics.

History of 2-D

The first protein separation by 2-D is attributed to Smithies and Poulik who in 1956 described a combination of paper and starch gel electrophoresis for the separation of serum proteins. Since that time, subsequent advances in electrophoresis, such as the use of polyacrylamide gels, discontinuous buffer systems, gradient gels, SDS-PAGE, and isoelectric focusing (IEF) have all resulted in the development of improved methods of 2-D. These developments cul-

minated in the 1970s with publications from several independent groups describing a combination of a first-dimension separation by IEF under denaturing conditions with a second dimension separation by SDS-PAGE. This coupling of IEF with SDS-PAGE resulted in a method of 2-D which separates proteins according to two independent parameters, charge and size.

The O'Farrell Method of 2-D

The method described by O'Farrell in 1975 has formed the basis of almost all subsequent developments in 2-D, and several thousand papers have been published using this technique in the 25 years following its publication. This method was optimized for the separation of the proteins of *Escherichia coli* (*E. coli*) and used a combination of IEF in cylindrical gels (cast in glass capillary tubes) containing 8 M urea and 2% w/v of the non-ionic detergent, Nonidet P-40 (NP-40), with the SDS-PAGE system of Laemmli. This method was able to resolve around 500 proteins from *E. coli*. It has subsequently been applied to a wide variety of samples.

Limitations of the O'Farrell Method

The main problem with the 2-D method of O'Farrell is associated with the synthetic carrier ampholytes (SCA) which are used to generate the pH gradient in the IEF dimension. SCA are produced by a complex synthetic process which is difficult to control reproducibly. This results in considerable batch-to-batch variability and limits the reproducibility and consistency of 2-D separations. Perhaps more importantly SCA are relatively small molecules, which are not fixed within the IEF gel. As a consequence, the electroendosmotic flow of water that occurs during IEF results in migration of the SCA molecules towards the cathode.

This process, known as 'cathodic drift', results in pH gradient instability and is exacerbated using tube gels due to the negatively charged groups present on the walls of the glass capillaries. In practice, pH gradients using the O'Farrell method of 2-D rarely extend far beyond pH 7, with the resultant loss of the basic proteins. This problem was recognized by O'Farrell, who developed an alternative procedure,

known as non-equilibrium pH gradient electrophoresis (NEPHGE), for the 2-D separation of basic proteins. In this method, separation occurs on the basis of protein mobility in the presence of a rapidly forming pH gradient, but reproducibility is extremely difficult to control. Fortunately, this problem was solved with the development of immobilized pH gradient (IPG) IEF.

2-D Using IPG IEF

IPG IEF gels are prepared using Immoblines (Amersham Pharmacia Biotech), a series of eight acrylamide derivatives with the structure $\text{CH}_2=\text{CH}-\text{CO}-\text{NH}-\text{R}$, where R contains either a carboxyl or tertiary amino group. These form a series of buffers with different pK values distributed through-

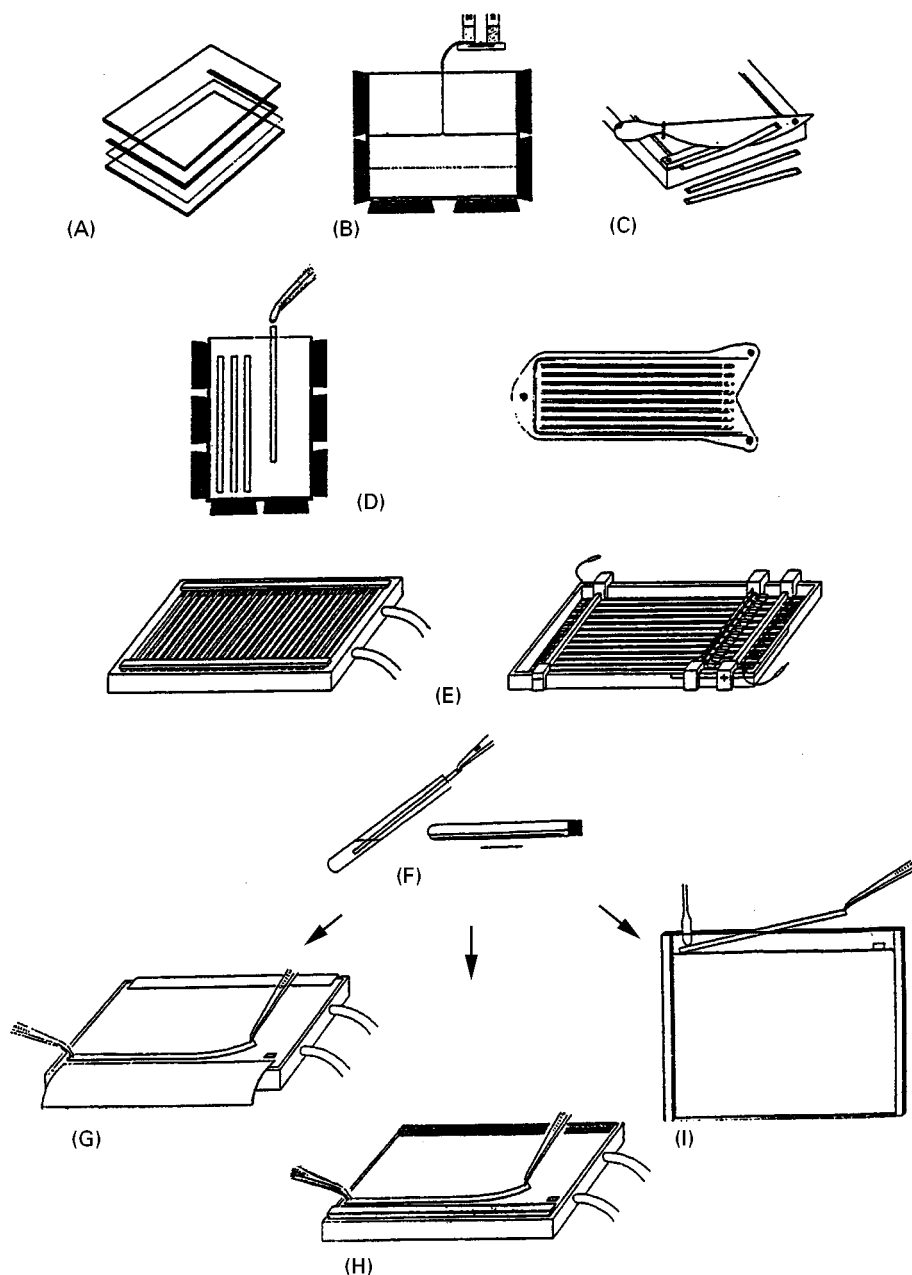


Figure 1 Schematic diagram of the procedure of 2-D using IPG IEF. (A) Assembly of the polymerization cassette for the preparation of IPG and SDS gels cast on plastic backings, (B) casting of IPG and gradient SDS gels, (C) cutting of washed and dried IPG gels into individual IPG strips, (D) rehydration of IPG strips, (E) IEF in individual IPG strips, (F) equilibration of IPG strips prior to SDS-PAGE, (G) transfer of IPG strip onto surface of laboratory-made horizontal SDS gel along cathodic wick, (H) transfer of IPG strip onto surface of commercial horizontal SDS gel along cathodic buffer strip, (I) loading of IPG strip onto the surface of a vertical SDS gel. (Courtesy of A. Görg, Technical University, Munich, Germany).

out the pH range 3 to 10. The appropriate IPG reagents, calculated according to published recipes, are added to the mixture used for gel polymerization. Thus, during polymerization, the buffering groups which will form the pH gradient are covalently attached via vinyl bonds to the polyacrylamide backbone. IPG generated in this way are, therefore, immune to the effects of electroendosmosis, so that they provide the opportunity to carry out IEF separations which are extremely stable, allowing the true equilibrium state to be attained.

Initial attempts to implement the IPG technology to 2-D separations encountered several problems. Fortunately, largely due to the work of Görg and her colleagues, these problems have been solved and IPG IEF has become the method of choice for the first dimension separation of 2-D. The method is shown schematically in **Figure 1**. Briefly, IPG slab gels of the desired pH range are cast (**Figure 1(B)**) according to the extensive library of published recipes. After polymerization, the gels are washed, dried and stored at -20°C . The required number of gel strips (3–5 mm wide) for 2-D are cut off of the slab using a paper cutter (**Figure 1(C)**). Alternatively, a range of ready-made strips is available commercially from Amersham Pharmacia Biotech. IPG strips of any desired

length can be used, but it should be remembered that, in general, the larger the separation area of a 2-D gel, the more proteins can be resolved. Strips of 18 cm are usually employed for high-resolution separations, while shorter strips (7 or 11 cm) are used for rapid screening applications.

A choice of a linear pH gradient from 3.5 to 10 is often useful for the initial analysis of a new type of sample. However, for many samples this can result in loss of resolution in the region of pH 4 to 7, in which the pI values of many proteins occur. This problem can be overcome to some extent with the use of a non-linear pH 3.5–pH 10 IPG IEF gel, in which the pH 4–7 region contains a much flatter gradient than in the pH 7–10.5 region. This allows good separation in the pH 4–7 region while still resolving the majority of the more basic species (**Figure 2**). However, use of a pH 4–7 IPG IEF gel will result in even better protein separation (**Figure 3**). Commercial IPG strips are available for these pH ranges (Amersham Pharmacia Biotech). Laboratory-made IPG strips with either very narrow pH gradients (spanning 1 pH or less) can be useful for separating components with very similar pI values, while very basic pH gradients can be used to advantage for certain types of sample, such as ribosomal proteins and nuclear proteins.

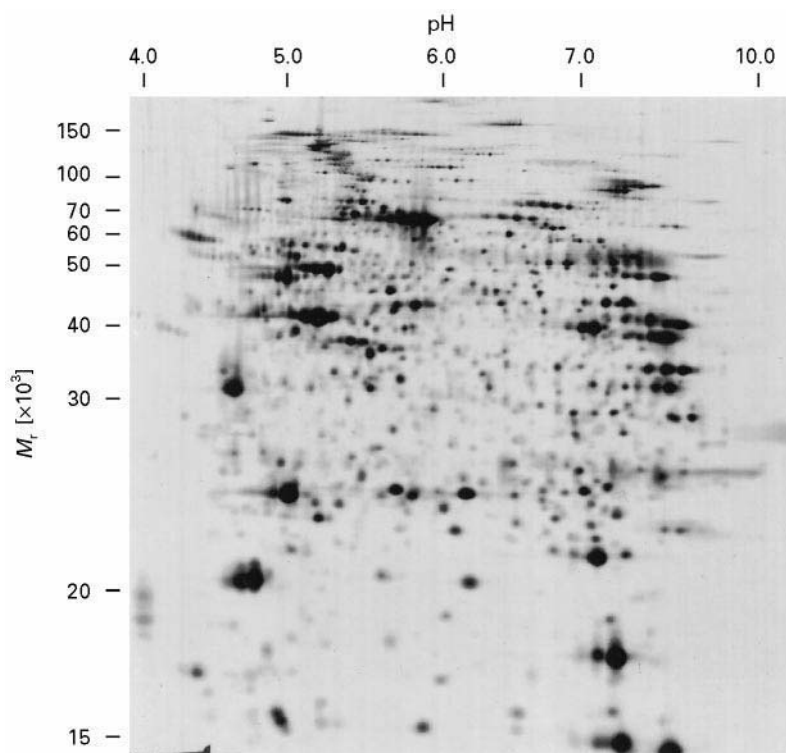


Figure 2 A 2-D separation of 100 μg heart proteins using a nonlinear pH 3.5 to 10 IPG IEF gel in the first dimension. The protein pattern was visualized by silver staining. The scale at the top indicates the nonlinear pH gradient obtained using an IPG 3-10 NL strip for the first dimension IEF separation. The scale at the left indicates the size separation in the range 15 to 150 kDa using a 15% SDS-PAGE gel in the second dimension.

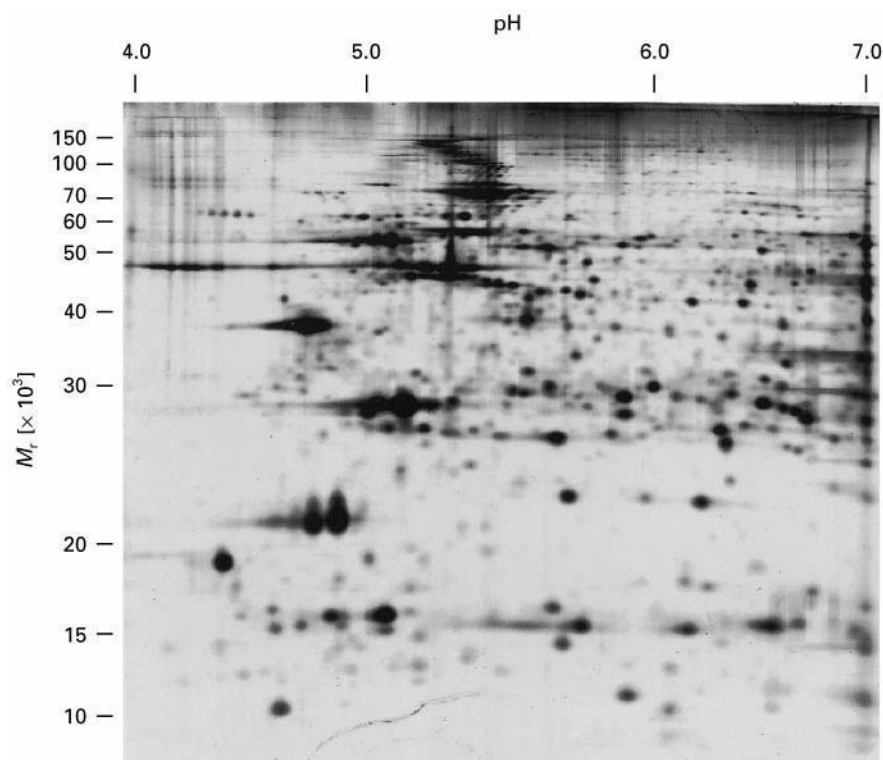


Figure 3 A 2-D separation of 100 µg heart proteins using a linear pH 4 to 7 IPG IEF gel in the first dimension. The protein pattern was visualized by silver staining. The scale at the top indicates the linear pH gradient obtained using an IPG 4-7 strip for the first dimension IEF separation. The scale at the left indicates the size separation in the range 10 to 150 kDa using a 10% SDS-PAGE gel in the second dimension.

For use in 2-D, the strips are rehydrated in a re-swelling cassette (**Figure 1(D)**) in a solution containing 8 M urea, 0.5% non-ionic (e.g. NP-40, Triton X-100) or zwitterionic (CHAPS) detergent (3-[(cholamidopropyl)dimethylammonio]-1-propanesulfonate), 15 mM DTT and 0.2% synthetic carrier ampholyte (SCA) of the appropriate pH range. The strips are then placed directly on the surface of the cooling plate of a horizontal flat-bed electrophoresis apparatus (**Figure 1(E)**). A convenient alternative is to use the special strip tray available from Pharmacia (**Figure 1(E)**). This tray is fitted with a corrugated plastic plate which contains grooves allowing easy alignment of the IPG strips. In addition, the tray is fitted with bars carrying the electrodes and a bar fitted with sample cups allowing the application of samples at any desired point on the gel surface. This tray is filled with silicone oil which protects the gel from the effects of the atmosphere during IEF. Horizontal streaking can often be observed at the basic end of 2-D protein profiles, particularly when IPG 6-10 is used for the first dimension. This problem can be resolved by applying an extra electrode strip soaked in 15 mM DTT on the surface of the IPG strip alongside the cathodic electrode strip. This has the advantage

that the DTT within the gel, which migrates towards the anode during IEF, is replenished by the DTT released from the strip at the anode. An alternative approach is to use the non-charged reducing agent, tributyl phosphine (TBP), which does not migrate during IEF and has been found to greatly improve protein solubility during IEF.

Sample Preparation

There is no universal method of sample preparation for 2-D due to the diverse nature of samples which can be analysed. Whatever method is used, it is essential to minimize protein modifications which can result in artefactual spots on 2-D protein patterns. In particular, samples containing urea should not be heated as this will lead to charge heterogeneity as a result of protein carbamylation by isocyanate ions formed from the decomposition of urea. Proteases present within samples can also readily result in artefactual spots, so that samples should be subjected to minimal handling and kept cold at all times. Protease inhibitors can also be added.

Liquid samples containing a relatively high protein concentration (e.g. serum, plasma) require little or no

pre-treatment prior to 2-D. However, less concentrated solutions (e.g. urine, cerebrospinal fluid (CSF), amniotic fluid) often require concentration by methods such as lyophilization, or precipitation with trichloroacetic acid (TCA) or acetone. Solid tissue samples must usually be disrupted in the presence of solubilization solution. For small samples this is readily achieved by crushing the sample in liquid nitrogen using a pestle and mortar, while larger tissue samples must be homogenized using a suitable device. Cell suspensions can be readily harvested by centrifugation, while cells adherent to a substrate, such as a tissue culture flask or dish, should be collected by scraping (the use of proteases should be avoided to prevent possible sample degradation). Alternatively, the cells can be detached by lysis directly in a small volume of sample solubilization solution.

Sample Solubilization

The most popular method for protein solubilization for 2-D is that originally described by O'Farrell, using a mixture of 9.5 M urea, 4% w/v NP-40, 1% w/v DTT and 2% w/v SCA. While this method works well for the majority of samples, it is not universally applicable, with membrane proteins representing a particular challenge. The zwitterionic detergent, CHAPS has been found to be effective for the solubilization of membrane proteins, particularly when used at a concentration of 4% w/v in combination with a mixture of 2 M thiourea and 8 M urea. Linear sulfobetaine detergents, such as SB 3-10 or 3-12, are also effective solubilizing agents, but these are not compatible with high concentrations of urea. This can be overcome by using these reagents at 2% w/v in combination with 5 M urea, 2 M thiourea and 2% CHAPS.

The presence of nucleic acids can be problematic during IEF. This is due to an increase in the viscosity of the sample and in some cases formation of complexes with the sample proteins, leading to artefactual migration and streaking. If problems of this type are suspected, it is best to degrade the nucleic acid by the addition of a suitable pure (i.e. protease free) endonuclease to the sample solubilization solution.

Sample Reduction

Protein disulfide bonds are normally reduced with free thiol-containing reagents such as DTT or β -mercaptoethanol. However, reagents such as DTT are charged so that they migrate out of the gel during IEF, leading to reoxidation of the sample proteins which can result in loss of sample solubility. It has recently been reported that replacing the thiol-containing re-

ducing agents with a non-charged reducing agent such as tributyl phosphine (TBP) can greatly increase protein solubility during the IEF dimension and result in increased transfer to the second dimension gel.

Sample Application and Running Conditions

Samples are usually applied into silicone rubber frames or special sample cups (Figure 1(E)) placed either at the anodic or cathodic end of the IPG strips, the optimum position being determined empirically for each type of sample. The initial voltage should be limited to 150 V for 30 min to allow maximal sample entry and then progressively increased until 3500 V is attained. The time required for the run depends on several factors, including the type of sample, the amount of protein applied, the length of the IPG strips, and the pH gradient. The IEF run should be performed at 20°C, as at lower temperatures there is a risk of urea crystallization and higher temperatures have been found to result in alterations in the relative positions of some proteins on the final 2-D patterns. Some typical running conditions are given in Table 1.

This method of sample application can result in protein precipitation and the effect is more pronounced when high protein loadings (1 mg or more) are used. The problem can be overcome by reswelling the IPG strips directly in the solution containing the protein sample to be analysed. Very high protein loads (>10 mg) have been successfully separated using this method, but there can be a selective loss of high molecular weight, very basic and membrane proteins. Recently a new integrated instrument, named the IPGPhor (Amersham Pharmacia Biotech), has been developed to simplify the IPG IEF dimension 2-D. This instrument features a strip holder that provides for the rehydration of individual IPG strips with or without sample, optional separate sample loading, and subsequent IEF, all without handling the strip after it is placed in the ceramic strip holder. The

Table 1 Suggested running conditions for 18 cm IPG strips for the first, IEF dimension of 2-D. The strips should be run at 0.05 mA per strip (2 mA maximum total), 0.5 W maximum, 20°C

Voltage (maximum)	IPG strip (pH range)	Time
150	All	30 min
300	All	60 min
1500	All	60 min
3500	4-7	42 000 Vh
	4-8	35 000 Vh
	4-9	30 000 Vh
	6-10	35 000 Vh
	3-10.5	25 000 Vh

instrument can accommodate up to 12 individual strip holders and incorporates Peltier solid-state cooling and a programmable 8000 V, 1.5 mA power supply.

Equilibration Between Dimensions

After the IPG IEF dimension, strips can be used immediately for the second dimension. Alternatively, strips can be stored between two sheets of plastic film at -80°C for periods of several months. Prior to the second-dimension separation, it is essential that the IEF gels are equilibrated to allow the separated proteins to interact fully with sodium dodecyl sulfate (SDS) so that they will migrate properly during SDS-PAGE (Figure 1(F)). The recommended protocol is to incubate the IPG IEF gel strips for 15 min in 50 mM Tris buffer, pH 8.8 containing 2% w/v SDS, 1% w/v DTT, 6 M urea and 30% w/v glycerol. The urea and glycerol are used to reduce electroosmotic effects which otherwise result in reduced protein transfer from the first to the second dimension. This is followed by a further 15 min equilibration in the same solution containing 5% w/v iodoacetamide in place of DTT. The latter step is used to alkylate any free DTT, as otherwise this migrates through the second-dimension SDS-PAGE gel, resulting in an artefact known as 'point-streaking' which can be observed after silver staining. An alternative procedure, allowing equilibration to be achieved in a single step, is to replace the DTT in the equilibration buffer with 5 mM TBP, which is uncharged and so does not migrate during SDS-PAGE.

The Second Dimension

After equilibration, the first dimension IEF gels are applied directly to the surface of the second-dimension SDS-PAGE gels. The SDS-PAGE gels can be of any appropriate single or gradient polyacrylamide, and can be used either in a vertical (Figure 1(I)) or horizontal format (Figure 1(G), 1(H)). The use of vertical formats enables multiple gels to be run simultaneously, which improves reproducibility, while the use of horizontal, 0.5 mm thin SDS gels cast on plastic supports improves the ease of handling the gels and gives rapid separations.

Resolution of 2-D

The resolving capacity of 2-D gels is usually considered to be proportional to the total gel area available for the separation. Using 18 cm long IPG IEF gels in combination with 20 cm long second-dimension SDS-PAGE gels, around 2000 proteins can be readily

resolved. Only a few hundred proteins can be separated using mini-gel formats, but these are much quicker to run and can be useful for rapid screening purposes. For maximum resolution of very complex mixtures, very large format gels (>30 cm in each dimension) can be used. These are reported to be able to separate as many as 5000 to 10 000 proteins from whole cell lysates, but this is achieved at the expense of the ease of gel handling and processing.

Reproducibility of 2-D

Until recently reproducibility was a major problem limiting the more widespread application of 2-D. Using the tube gel technique of O'Farrell, it was often difficult to obtain reproducible separations of a particular type of sample even within a single laboratory, while comparison of 2-D separation patterns generated in different laboratories was often considered to be impossible. The use of dedicated equipment for 2-D, such as the ISO-DALT (Amersham Pharmacia Biotech) and the Investigator (ESA Inc) systems, helps in this regard as it allows the simultaneous electrophoresis of large numbers (between 5 and 20) of 2-D gels under reproducibly controlled conditions. More importantly, inter-laboratory studies of various types of sample (heart, barley, yeast) have unequivocally demonstrated that 2-D using IPG IEF results in 2-D protein separations with very high spatial and quantitative reproducibility.

Proteomics

2-D separation has now matured into a technique which is capable of separating reproducibly thousands of proteins present in samples such as cells, tissues and even whole organisms. Recent developments in methods for the microchemical characterization of proteins, particularly techniques for the analysis of proteins and peptides by mass spectrometry, now make it possible to identify and characterize proteins spots directly from 2-D gels. This has made 2-D separation an ideal tool to use in studies designed to determine the nature and function of the large number of structural genes being identified in various genome initiatives. This area has become known as 'proteomics' and is the subject of a separate article.

Further Reading

Blomberg A, Blomberg L, Norbeck J *et al.* (1995) Inter-laboratory reproducibility of yeast protein patterns analyzed by immobilized pH gradient two-dimensional gel electrophoresis. *Electrophoresis* 16: 1935–1945.

- Corbett JM, Dunn MJ, Posch A and Görg A (1994) Positional reproducibility of protein spots in two-dimensional polyacrylamide gel electrophoresis using immobilised pH gradient isoelectric focusing in the first dimension: An interlaboratory study. *Electrophoresis* 15: 1205–1211.
- Dunn MJ (1987) Two-dimensional polyacrylamide gel electrophoresis. In: Chrambach A, Dunn MJ and Radola BJ (eds) *Advances in Electrophoresis*, Vol. 1, pp. 1–109. Weinheim: VCH.
- Dunn MJ (1993) *Gel Electrophoresis: Proteins*. Oxford: BIOS Scientific.
- Görg A, Postel W and Günther S (1988) The current state of two-dimensional electrophoresis with immobilized pH gradients. *Electrophoresis* 9: 531–546.
- Görg A, Boguth G, Obermaier C, Posch A and Weiss W (1995) Two-dimensional polyacrylamide gel electrophoresis with immobilized pH gradients in the first dimension (IPG-Dalt): The state of the art and the controversy of vertical versus horizontal systems. *Electrophoresis* 16: 1079–1086.
- Görg A, Obermaier C, Boguth G *et al.* (1997) Very alkaline immobilized pH gradients for two-dimensional electrophoresis of ribosomal and nuclear proteins. *Electrophoresis* 18: 328–337.
- Herbert BR, Sanchez JC and Bini L (1997) Two-dimensional electrophoresis: The state of the art and future directions. In: Wilkins MR, Williams KL, Appel RD and Hochstrasser DF (eds) *Proteome Research: New Frontiers in Functional Genomics*, pp. 13–33. Berlin: Springer.
- Humphery-Smith I, Cordwell SJ and Blackstock WP (1997) Proteome research: Complementarity and limitations with respect to the RNA and DNA worlds. *Electrophoresis* 18: 1217–1242.
- Klose J and Kobalz U (1995) Two-dimensional electrophoresis of proteins: An updated protocol and implications for a functional analysis of the genome. *Electrophoresis* 16: 1034–1059.
- O'Farrell PH (1975) High resolution two-dimensional electrophoresis of proteins. *Journal of Biological Chemistry* 250: 4007–4021.
- Pennington SR, Wilkins MR, Hochstrasser DF and Dunn MJ. Proteome analysis: From protein characterization to biological function. *Trends in Cell Biology* 7: 168–173.
- Rabilloud T, Adessi C, Giraudel A and Lunnardi J (1997) Improvement of the solubilization of proteins in two-dimensional electrophoresis with immobilized pH gradients. *Electrophoresis* 18: 307–316.
- Wilkins MR, Williams KL, Appel RD and Hochstrasser DF (eds) (1997) *Proteome Research: New Frontiers in Functional Genomics*. Berlin: Springer.

3. ABBREVIATIONS

2,3,4,6-TeCP	2,3,4,6-tetrachlorophenol
2,3-DMP	2,3-dimethylpentane
2,4,5-T	2,4,5-trichlorophenoxyacetic acid
2,4,5-TP	2-(2,4,5-trichlorophenoxy)propionic acid
2,4,6-TCP	2,4,6-trichlorophenol
2,4-D	2,4-dichlorophenoxyacetic acid
2,4-DCP	2,4-dichlorophenol
2,4-DMP	2,4-dimethylphenol
2-CP	2-chlorophenol
2-DNP	2-dinitrophenol
2-M-4,6-DNP	2-methyl-4,6-dinitrophenol
2-NP	2-nitrophenol
4-NP	4-nitrophenol
AA	amino acid
AAA	amino acid compositional analysis
AAS	atomic absorption spectrometry
ACN	acetonitrile
ADAM	9-anthryldiazomethane
ADC	analog-to-digital converter
AD-CSP	amylose <i>tris</i> -(3,5-dimethylphenylcarbamate) CSP
AE	alcohol ethoxylates
AEDA	aroma extract dilution analysis
AFM	atomic force microscopy
AGP	α_1 -acid glycoprotein

AMD	automated multiple development
AMW	acidic mine waters
ANN	artificial neural network
APCI	atmospheric pressure chemical ionization
APE	alkylphenol ethoxylates
API	atmospheric pressure ionization
AQC	6-aminoquinolyl-N-hydroxysuccinimidyl carbamate
ASE	accelerated solvent extraction
ASE	Archimedean screw effect
ASP	amnesic poisoning
ASPEC	automated SPE clean-up
ASTM	American Society for Testing and Materials
b.p.	boiling point
BE	benzoylecgonine
BF	batch factor
BF	Best Foods
BGE	background electrolyte
BOD	biological oxygen demand
BPR	back-pressure regulator
BSA	bovine serum albumin
BSTFA	<i>N,O</i> -bis-(trimethylsilyl)trifluoroacetamide
BTEX	benzene, toluene, ethylbenzene, xylene
BTX	benzene, toluene, xylene
C(GC) ²	comprehensive gas chromatography
c.m.c.	critical micellar concentration
CB	Contaminants Branch
CBH I	cellobiohydrolase I
CCC	countercurrent chromatography
CCDs	charged coupled devices
CCP	chiral coated phase
CD	cyclodextrin
CDCCC	centrifugal droplet countercurrent chromatography
CDR	chiral derivatization reagent
CE	capillary electrophoresis
CEC	capillary electrochromatography
CF-FAB	continuous flow – fast atom bombardment
CI	chemical ionization
CID	collision-induced dissociation
CLA	conjugated linoleic acid
CLD	chemiluminescence detector
CMA	chiral mobile-phase additive
CMP	chiral mobile phase
CMR	continuous membrane reactor
CoMFA	comparative molecular field analysis
CPC	coil planet centrifuges
CPF	co-current permeate flow
CPT	cone penetrometer
cSFC	supercritical fluid chromatography with a capillary column
CSP	chiral stationary phase
CTA	cellulose triacetate
CTAB	cetyltrimethylammonium bromide
CV	coefficient of variation
CXC	cation exchange chromatography
CZE	capillary zone electrophoresis
DA	domoic acid

DABITC	dimethylaminoazobenzene isothiocyanate
DABS	dimethylaminonaphthalene-5-sulfonyl
DAG	diacetonegluonic acid
DANS	1-N, N'-dimethylaminonaphthalene-5-sulfonyl
DB-5	5% poly(diphenyldimethylsiloxane)
DBT	dibenzothiophene(s)
DBV	divinylbenzene
DCCC	droplet countercurrent chromatography
DCTFA	1,2-dichlorotetrafluoroacetone
DEHPA	di(2-ethylhexyl)phosphoric acid
DETA	diethylenetriamine
DIA	deisopropylatrazine
DIC	diisopropylcarbodiimide
DIGE	difference gel electrophoresis
DMAPA	dimethylaminopropylamine
DMCS	dimethylchlorosilane
DME	α,ω -dicarboxylic acid methyl esters
DMOX	4,4-dimethyloxazoline
DNP	dinitrophenyl
DNPH	2,4-dinitrophenylhydrazine
DNPU	3,5-dinitrophenyl urethane
DP	degree of polymerization
DRI	differential refractive index
DRIFT	diffuse reflectance Fourier transform infrared
DSC	N,N'-disuccinimidylcarbonate
DSP	diarrhoeic poisoning
DTX	dinophysistoxins
ECD	electron-capture detector
ECF	ethyl chloroformate
ECL	equivalent chain length
ECN	equivalent carbon number
ED	electrodialysis
ED	extractive distillation
EDMA	ethylene glycol dimethacrylate
EDTA	ethylenediaminetetraacetic acid
ee	enantiomer excess
EG	ethylene glycol
EGA	ethylene glycol adipate
EHPA	mono-2-ethylhexyl ester
EI	electron ionization
ELCD	electrolytic conductivity detector
ELSD	evaporative light-scattering detector
EOF	electroosmotic flow
EPA	Environmental Protection Agency
ESCA	electron spectroscopy for chemical analysis
ESI	electrospray ionization
EtG	ethyl glucuronide
FAB	fast atom bombardment
FAEE	fatty acid ethyl ester
FAME	fatty acid methyl ester
FDA	Food and Drug Administration
FDNB	1-fluoro-2,4-dinitrobenzene
FFA	free fatty acid
FFPPC	forced flow PPC
FID	flame ionization detector

FMOc	fluoronylmethyl chloroformate
FPD	flame photometric detector
FTD	flame thermionic detector
FT-IR	Fourier transform infrared spectrometry
FT-Raman	Fourier transform Raman
GC	gas chromatography
GC-FTIR	gas chromatography – Fourier transform infrared spectrometry
GC-IRMS	gas chromatography – isotope ratio mass spectrometry
GC-MS	gas chromatography – mass spectrometry
GC-MS/MS	GC with coupled or tandem MS
GFAA	graphite furnace atomic absorption
GFC	gel filtration chromatography
GLP	Good Laboratory Practice
GPC	gel permeation chromatography
HAS	human serum albumin
HDC	hydrodynamic chromatography
HDEHP	di-(2-ethylhexyl)orthophosphoric acid
HETEs	hydroxyeicosatetraenes
HETP	height equivalent to one theoretical plate
HFB	heptafluorobutryl
HI	hydrophobic interaction
HIC	hydrophilic interaction chromatography
HIC-CXC	hydrophilic interaction – cation exchange chromatography
HMDS	hexamethyldisilazine
HOM	humic organic matter
HOMO	highest occupied molecular orbital
HPA	heteropolyacid
HPALC	high performance affinity liquid chromatography
HPIC	high performance ion chromatography
HPLC	high performance liquid chromatography
HPLC-CSP	HPLC-chiral stationary phases
HPTLC	high performance thin-layer chromatography
HRGC	high resolution gas chromatography
HS	humic substances
HSCCC	high speed countercurrent chromatography
HSES	hydrostatic equilibrium system
HS-GC	headspace-gas chromatography
HSSI	N-hydroxysulfosuccinimide
HS-SPME	headspace-solid-phase microextraction
HTGC	high temperature gas chromatography
HVS	high volume sampling
i.d.	internal diameter
IAM	immobilized artificial membrane
IBCF	isobutyl chloroformate
IBOC	N-isobutyloxycarbonyl
ICP-AES	inductively coupled plasma-atomic emission spectroscopy
ICP-MS	inductively coupled plasma-mass spectrometry
ICR	ion cyclotron resonance
IE	ion exchange
IEC	ion exchange chromatography
IEF	isoelectric focusing
IIR	ion interaction reagent
IP-TLC	ion pair-thin-layer chromatography
IR	infrared
IS	internal standard

ITD	ion trap detector/detection
IXISS	ion exchange isothermal supersaturation
JT	Joule-Thompson
L/B	length-to-breadth
LAS	linear alkylbenzenesulfonate
LC	liquid chromatography
LDH	lactic acid dehydrogenase
LD-OPLC	long-distance overpressured-layer chromatography
LEC	liquid exclusion chromatography
LFER	linear free-energy relationship
LLE	liquid-liquid extraction
LOD	limit of detection
LOX	liquid oxygen
LSC	liquid-solid chromatography
LSER	linear solvation energy relationship
LSIMS	liquid secondary ion mass spectrometry
LTB ₄	leukotriene B ₄
LUMO	lowest unoccupied molecular orbital
LVS	low volume sampling
MA	macrocyclic antibiotic
MAC	multistage air compressor
MAGIC	monodisperse aerosol generator interface for chromatography
MALDI	matrix-assisted laser desorption ionization
MALDI-MS	matrix-assisted laser desorption ionization-mass spectrometer
MASE	microwave-assisted solvent extraction
MBTH	3-methyl-2-benzothiazolinone hydrazone-HCl
MCF	methyl chloroformate
MCTA	microcrystalline cellulose triacetate
MDGC	multidimensional gas chromatography
MDMA	3,4-methylenedioxymethamphetamine
ME	methyl ester
MEKC	micellar electrokinetic chromatography
MF	microfiltration
MIBK	methylisobutylketone
MID	multiple ion detection
MIPs	molecular imprinted polymers
MLL	mean list length
ML-OPLC	multi-layer overpressured-layer chromatography
MP	mobile phase
MPA	mobile phase additive
MPA	3-mercaptopropionic acid
MPLC	medium pressure liquid chromatography
MS	mass spectrometry
MSD	mass selective detector/detection
MS-MS	tandem mass spectrometry
MSPD	matrix solid phase dispersion
MSTFA	<i>N</i> -methyl- <i>N</i> -trimethylsilyltrifluoroacetamide
MTBSTFA	<i>N</i> - <i>t</i> -butyldimethylsilyl- <i>N</i> -methyltrifluoroacetamide
MWD	molecular weight distribution
MWPC	multiwire proportional counters
NAC	<i>N</i> -acetyl-L-cysteine
NBP	4-(<i>p</i> -nitrobenzyl)pyridine
NCA	National Council on Alcoholism
NCI-GC-MS	negative ion chemical ionization-GC-MS
nd	not determined

NF	nanofiltration
NFM	N-formylmorpholine
NHYD	ninhydrin
NIR	near-infrared spectroscopy
NMP	N-methylpyrrolidone
NMR	nuclear magnetic resonance
NN	neural network
NP	normal phase
NPD	nitrogen-phosphorus detector
NQS	1,2-naphthoquinone-4-sulfonate
NRTL	nonrandom two liquids
NSAID	nonsteroidal anti-inflammatory drugs
o.d.	outer diameter
OA	okadaic acid
ODS	octadecylsilica
ODS-1	commercial octadecylsilica phase
OGCHI	ovoglycoprotein from chicken egg whites
OMCHI	chicken ovomucoid
OMCTS	octamethylcyclotetrasiloxane
OMTKY	turkey ovomucoid
OPA/MCE	<i>o</i> -phthalaldehyde/ β -mercaptoethanol
O-PFBO	O-pentafluorobenzoyloxime
OPLC	overpressured-layer liquid chromatography
OPTLC	overpressured TLC
OV-225	commercial phase
oxo-ETEs	oxo-eicosatetraene
P & T	purge-and-trap
PA	photoacoustic
PA	polyacrylate
PAD	pulsed amphoteric detector/detection
PAH	polyaromatic hydrocarbons
PAR	4-(2-pyridylazo)resorcinol
PAS	photoacoustic spectroscopy
PB	particle beam
PCA	principal component analysis
PCB	polychlorinated biphenyl
PCDD	polychlorinated dibenzo- <i>p</i> -dioxin
PCDF	polychlorinated dibenzofuran
PCP	pentachlorophenol
PDB	Pee Dee Belimnite
PDCA	pyridine-2,6-dicarboxylate
PDMS	poly(dimethylsiloxane)
PED	pulsed electrochemical detection
PEEK	polyetheretherketone
PEG	poly(ethylene glycol)
PEI	poly(ethyleneimine)
PEO	poly(ethylene oxide)
PETRA	pentaerythritol triacrylate
PFB	pentafluorobenzyl
PFBBBr	pentafluorobenzyl bromide
PFBOA	pentafluorobenzoyloxime
PFP	pentafluoropropionyl
PFPH	pentafluorophenylhydrazine
PGC	porous graphitic carbon
PGM	platinum group metals

PHDC	packed column hydrodynamic chromatography
PLOT	porous-layer open-tubular
PLS	partial least squares
PMMA	poly(methyl methacrylate)
PNBX	potassium <i>n</i> -butylxanthate
PNP	purine nucleoside phosphorylase
PPC	preparative planar thin-layer chromatography
PPO	2,5-diphenyloxazole
PS	poly(styrene)
PSD	particle size distribution
PS-DVB	poly(styrene-divinylbenzene)
PSFC	packed-column supercritical fluid chromatography
PSP	paralytic poisoning
PTFE	poly(tetrafluoroethylene)
PTH	phenylthiohydantoin
PV	pervaporation
QSAR	quantitative structure-activity relationship
QSERR	quantitative structure enantioselective retention relationship
QSRR	quantitative structure-retention relationship
R/D	reflux-to-overhead ratio
RI	refractive index
RIA	radioimmunoassay
RLCCC	rotation locular countercurrent chromatography
RMM	relative molar mass
RO	reverse osmosis
RP	reversed-phase
RPC	reversed-phase chromatography
RS	Raman scattering
RSD	relative standard deviation
S/F	solvent-to-feed ratio
S/N	signal-to-noise ratio
SAC	strong acid cation
SARA	saturates, aromatics, resins and asphaltenes
SB/CD	short bed/continuous development
SBC	strong base anion
SBF	separation by flow
SCA	synthetic carrier ampholyte
SCOT	support-coated open-tubular
SD	standard deviation
SDE	simultaneous distillation-extraction
SDGlu	<i>N</i> -dodecanoyl-L-glutamate
SDS	sodium dodecyl sulfate
SDS-PAGE	sodium dodecyl sulfate-polyacrylamide gel electrophoresis
SDVal	sodium <i>N</i> -dodecanoyl-L-valinate
SDVB	styrene-divinylbenzene
SEC	size exclusion chromatography
SERRS	surface-enhanced resonance Raman scattering
SERS	surface-enhanced Raman scattering
SF	solvent front
SF ₆	sulfur hexafluoride
SFC	supercritical fluid chromatography
SFE	supercritical fluid extraction
SIM	selected ion monitoring
SIM	single ion monitoring
SMB	simulated moving bed

SN	separation number
SP	stationary phase
SPE	solid-phase extraction
SPM	simultaneous pyrolysis/methylation
SPME	solid-phase microextraction
SRB	sulfate-reducing bacteria
SS	supersaturated solution
STC	sodium taurocholate
STDC	sodium taurodeoxycholate
STX	saxitoxin
TA	time-to-amplitude
TAA	tetraalkylammonium
TAB	<i>N</i> -trifluoroacetyl- <i>n</i> -butyl ester
TBDMS	<i>t</i> -butyldimethylsilyl
TCD	thermal conductivity detector
TDS	total dissolved solids
TEA	thermal energy analyser
TEAA	triethylammonium acetate
TEAP	triethylammonium phosphate
TEG	triethylene glycol
TEPA	tetraethylenepentamine
TFA	trifluoroacetyl/trifluoroacetic acid
TGA	thermogravimetric analyser
THBC	1,2,3,4-tetrahydro- β -carboline
THCA	11-nor- Δ^9 -tetrahydrocannabinol-9-carboxylic acid
THF	tetrahydrofuran
TIQ	1,2,3,4-tetrahydroisoquinoline
TLC	thin-layer chromatography
TLC-MS	thin-layer chromatography-mass spectrometry
TLRC	thin-layer radiochromatography
TLV	threshold limit value
TMAH	tetramethylammonium hydroxide
TMCS	trimethylchlorosilane
TPMA	trimethylphenylammonium hydroxide
TMS	trimethylsilyl
TOC	total organic carbon
TOEDA	tetraoctylethylenediamine
TRIM	trimethylolpropane trimethacrylate
TSI	thermospray ionization
TTF	tetrathiafulvalene
UF	ultrafiltration
UHP	ultrahigh purity
UNIQUEAC	universal quasichemical
UrdPase	uridine phosphorylase
UTP	uniform transmembrane pressure
UV/Vis	ultraviolet-visible
V _C	total column capacity
VFA	volatile fatty acids
VLDL	very low-density lipoproteins
VLE	vapour-liquid equilibrium
VOCs	volatile organic chemicals
VPO	vapour pressure osmometry
V _R	retention volume of the solute
V _{SF}	retention volume of solvent front
WAC	weak acid cation

WBA	weak base anion
WCOT	wall-coated open-tubular
WPC	whey protein concentrates
XE-60	commercial phase
XRF	X-ray fluorescence
ZDDP	zinc dialkyldithiophosphate
β -CD	β -cyclodextrin

4. ANALYTICAL CHIRAL SEPARATION METHODS (IUPAC RECOMMENDATIONS 1997)

Prepared for publication by

V. A. Davankov, Russian Academy of Sciences, Moscow, Russia

© 1997 IUPAC

Abstract

In recent years there has been considerable interest in the synthesis and separation of enantiomers of organic compounds especially because of their importance in the biochemistry and pharmaceutical industry. Frequently the methods used for the separations, for monitoring the progress of an asymmetric synthesis or optical purity of the products are chromatographic with either liquids, gases, or supercritical fluids as the mobile phase. More recently capillary electrophoresis has been added as an analytical chiral separation method.

These applications have led to a number of terms and expressions in addition to those commonly used or recently recommended for the chemistry and physical properties of chiral compounds. This Nomenclature provides the descriptions and definitions for additional terms particularly related to analytical separation methods, and to the formation and enantiomeric purity of chiral products

Introduction

Enantiomers are two chemically identical molecular species which differ from each other as non-superposable mirror images. The most simple and vivid model for enantiomeric structures is the two hands, left and right. Enantiomers, in addition to diastereomers and *cis-trans*-isomers, are thus a special case of stereoisomers.

The chirality (handedness) of enantiomeric molecules is caused by the presence of one or more chirality elements (chirality axis, chirality plane, or chirality centre, e.g. asymmetric carbon atom) in their structure. The chirality sense and optical activity of the enantiomers are determined by their absolute configuration, i.e. the spatial arrangement of the atoms in the molecule. In contrast to their conformation, the configuration of enantiomers cannot be changed without a change in the connectivity of constituent atoms. Designation of the configuration of enantiomers should be made in accordance with the Cahn-Ingold-Prelog *R, S*-system. The Δ - Λ designations for enantiomers of octahedral complexes and the *D, L* Fischer-Rosanoff designations for amino acids and sugars are also in use.

Conventional chemical synthesis, in contrast to asymmetric synthesis, deals mostly with the transformations of achiral compounds. If these reactions result in the formation of a chirality element in the molecule, the reaction product appears to be an equivalent mixture of a pair of enantiomers, a racemate, which is optically inactive. Racemates are also formed through racemisation of chiral compounds. Racemates crystallize in the form of a racemic compound or, less frequently, as a conglomerate.

Separation of the enantiomers comprising the racemate, i.e. the resolution of the racemate, is a common problem in stereochemical research as well as in the preparation of biologically active compounds, in particular, drugs. The problem is that in contrast to diastereomers and all the other types of isomeric species,

enantiomers, in an achiral environment, display identical physical and chemical properties. (Energetic inequivalence of enantiomeric species, which can arise from the violation of parity by the weak interactions [1], is negligibly small- of the order of 10^{-14} J mol⁻¹).

One approach to separate enantiomers, sometimes referred to as indirect enantiomeric resolution, involves the coupling of the enantiomers with an auxiliary chiral reagent to convert them into diastereomers. The diastereomers can then be separated by any achiral separation technique.

Nowadays, direct separation methods are commonly used in which the enantiomers are placed in a chiral environment. As a matter of principle, only chiral selectors or chiral irradiation (e.g. a polarized light beam which consists of two chiral circular-polarised components) can distinguish between two enantiomers. Chiral selectors can be an appropriate chiral molecule or a chiral surface (e.g. a chiral seed crystal). Due to the enantioselectivity (a special case of stereoselectivity) of the interaction with the two enantiomers, the chiral selector either transforms the enantiomers at a different rate into new chemical entities (kinetic enantioselectivity) or forms labile molecular adducts of differing stability with the enantiomers (thermodynamic enantioselectivity). Enzymic selective transformation of L-enantiomers of racemic D,L-amino acids is a typical example of a kinetically enantioselective process (kinetic resolution). Enantioselective (chiral) chromatography does not modify the enantiomeric species to be separated and thus represents an example of a thermodynamically enantioselective process.

Direct enantiomeric resolutions are only feasible in chromatographic systems which contain an appropriate chiral selector. The latter can be incorporated into the stationary phase (chiral stationary phase) or be permanently bonded to or coated onto the surface of the column packing material (chiral bonded and chiral coated stationary phases). In all these cases it is appropriate to refer to the chromatographic column as an enantioselective (chiral) column. Enantioselective chromatography can also be performed on achiral chromatographic columns using the required chiral selector as a chiral mobile phase or a chiral mobile phase additive. Combinations of several chiral selectors in the mobile phase [2] as well as mobile and stationary phases [3] are also feasible.

In the case of chiral stationary phases, the enantiomer that forms the more stable association with the chiral selector will be the more strongly retained species of the racemate. The enantioselectivity of the chiral chromatographic system is then expressed as the ratio of the retention factors of the two enantiomers. This ratio may approach the value of the thermodynamic enantioselectivity of the association of the chiral selector with the enantiomers. This situation occurs when the association with the chiral selector governs the retention of the enantiomers in the chromatographic system and other, non-selective types of solute-sorbent interactions are negligible. On other hand, a chiral mobile phase reduces the retention of the solute enantiomer which forms a stronger association with the chiral selector. Here again, the limit for the enantioselectivity of the chiral chromatographic system is set by the enantioselectivity of the selector-solute association (in the mobile phase). However, in the majority of chiral mobile phase systems, the chiral selector as well as its associates with the solute enantiomers are distributed between the mobile and stationary phases. The effective enantioselectivity of the chromatographic system will therefore be proportional to the ratio of the enantioselectivities of the association processes in the stationary and mobile phases [4].

Interaction of the chiral selector of the system with the enantiomers of the solute results in the formation of two labile diastereomers. These differ in their thermodynamic stability, provided that at least three active points of the selector participate in the interaction with corresponding sites of the solute molecule. This three-point interaction rule is generally valid for enantioselective chromatography, with the extension to the rule, stating that one of the required interactions may be mediated by the adsorption of the two components of the interacting pair onto the sorbent surface [5].

Because of the multiplicity and complexity of the interactions of the enantiomers to be separated with the chiral selector, sorbent surface and other components of the chromatographic system, the total enantioselectivity can depend strongly on the composition, pH and temperature of the mobile phase. Therefore, in papers on enantioselective chromatography, it is important to define these parameters.

Enantioselective chromatography and capillary electrophoresis are extensively employed in the analysis of the enantiomeric composition (enantiomeric excess, optical purity) of chiral compounds. Liquid and supercritical fluid chromatography are also used for the isolation of chiral compounds from racemic mixtures on a preparative scale.

Enantioselective separations have been realised in all possible separation techniques, including gas chromatography, column liquid chromatography, thin-layer chromatography, supercritical fluid chromatography, as well as electromigration methods, countercurrent liquid chromatography and liquid-liquid extractions.

Numerous review papers and special monographs [6–15] describe the technical details as well as the achievements and potential of these important modern separation techniques.

In the following glossary of definitions and terms related to the chromatographic and capillary-electrophoretic separation of chiral compounds some terms (those marked with asterisks) were defined in the Basic Terminology of Stereochemistry, recently published by the IUPAC Joint Working Party on Stereochemical Terminology [16]. Some of these definitions contain further cross references which are to be found in the original paper.

Terms and Definitions

General Terms Related to Chirality

***Chirality** The geometric property of a rigid object (or spatial arrangement of points or atoms) of being non-superposable on its mirror image; such an object has no symmetry elements of the second kind (a mirror plane, $\sigma = S_1$, a centre of inversion, $i = S_2$, a rotation-reflection axis, S_{2n}). If the object is superposable on its mirror image the object is described as being achiral. *See also* handedness.

Diastereoisomers (Diastereomers) *see* diastereoisomerism

Diastereoisomerism *Stereoisomerism* other than enantiomerism and *cis-trans* isomerism. Diastereoisomers (or diastereomers) are stereoisomers not related as mirror images. Diastereoisomers are characterised by differences in physical properties, and by differences in chemical behaviour towards achiral as well as chiral reagents.

***Enantiomer** One of a pair of molecular entities which are mirror images of each other and non-superposable. *See also* enantiomorph.

***Stereoisomers** Isomers that possess identical constitution but which differ in the arrangement of their atoms in space. *See* enantiomer, diastereomer, *cis-trans*-isomers.

Terms Related to the Separated Process

Chiral additive The *chiral selector* which has been added as a component of a mobile phase or electrophoretic medium.

Chiral mobile phase A mobile phase containing a *chiral selector*.

Chiral selector The *chiral* component of the separation system capable of interacting *enantioselectively* with the *enantiomers* to be separated.

Chiral stationary phase A stationary phase which incorporates a *chiral selector*. In not a constituent of the stationary phase as a whole, the chiral selector can be chemically bonded to (*chiral bonded stationary phase*) or immobilized onto the surface of a solid support or column wall (*chiral coated stationary phase*), or simply dissolved in the liquid stationary phase.

Enantioselective chromatography (electrophoresis) The separation of *enantiomeric* species due to the *enantioselectivity* of their interaction with the *chiral selector(s)* of a chromatographic (electrophoretic) system. Also called *Chiral chromatography (electrophoresis)*.

Enantioselective column A chromatographic column containing a *chiral stationary phase*. Also called a *chiral column*.

Enantioselectivity (in chiral separations) The preferential interaction with the chiral selector of one enantiomer over the other.

Enantioselectivity of a chromatographic (electrophoretic) system The ratio of the retention factors of two solute enantiomers in a chiral chromatographic (electrophoretic) system.

Terms Related to the Chiral Purity of the Sample

***Diastereoisomer excess/Diastereoisomeric excess** This is defined by analogy with *enantiomer excess*, as $D_1 - D_2$ [and the percent diastereoisomer excess as $100(D_1 - D_2)$], where the mole fractions of the two diastereoisomers in a mixture or the fractional yields of two diastereoisomers formed in a reaction are D_1 and D_2 ($D_1 + D_2 = 1$). The term is not applicable if more than two diastereoisomers are present. Frequently this term is abbreviated to d.e. *See* stereoselectivity; diastereoisomerism.

***Enantiomer excess/Enantiomeric excess** For a mixture of (+) and (-) enantiomers, with composition given as the mole or weight fractions $F_{(+)}$ and $F_{(-)}$ (where $F_{(+)} + F_{(-)} = 1$) the enantiomeric excess is defined as $|F_{(+)} - F_{(-)}|$ (and the percent enantiomer excess by $100|F_{(+)} - F_{(-)}|$). Frequently this term is abbreviated as e.e. *See* optical purity.

***Enantiomeric purity** *see* Enantiomer excess

***Optical purity** The ratio of the observed optical rotation of a sample consisting of a mixture of enantiomers to the optical rotation of one pure enantiomer. *See* enantiomeric excess.

References

1. S. F. Mason and G. E. Tranter, The electroweak origin of bimolecular handedness, *Proc. R. Soc. London, A* **397**, 45–65 (1985).
2. D. Sybilska, A. Bielejewska, R. Nowakowski, K. Duszczuk and J. Jurczak, Improved chiral recognition of some compounds via the simultaneous use of beta-cyclodextrin and its permethylated derivative in a reversed-phase high-performance liquid chromatographic system, *J. Chromatogr.*, **625**, 349–352 (1992).
3. K. J. Duff, H. L. Gray, R. J. Gray and C. C. Bahler, Chiral stationary phases in concert with homologous chiral mobile phase additives: Push/pull model, *Chirality*, **5**, 201–206 (1993).
4. V. A. Davankov, A. A. Kurganov and T. M. Ponomareva, Enantioselectivity of complex formation in ligand-exchange chromatographic systems with chiral stationary and/or chiral mobile phases, *J. Chromatogr.*, **452**, 309–316 (1988).
5. V. A. Davankov, V. R. Meyer and M. Rais, A vivid model illustrating chiral recognition induced by achiral structures, *Chirality*, **2**, 208–210 (1990).
6. A. M. Krstulovic, Editor, *Chiral Separations by HPLC, Applications to Pharmaceutical Compounds*, Ellis Horwood, 1989, 548 pp.
7. V. A. Davankov, A. A. Kurganov and A.S. Bochkov, Resolution of racemates by high-performance liquid chromatography, *Adv. Chromatogr.*, **22**, 71–116 (1983).
8. P. Schreier, A. Bernreuther and M. Huffer, *Analysis of Chiral Organic Molecules*, Walter de Gruyter & Co., 1995, 331 pp.
9. D. W. Armstrong and S. M. Han, Enantiomeric Separations in Chromatography, *CRC Critical Reviews in Analytical Chemistry*, **19**, 175–224 (1988).
10. W. H. Pirkle and T. C. Pochapsky, Consideration of chiral recognition relevant to the liquid chromatographic separation of enantiomers, *Chem. Rev.*, **89**, 347–362 (1989).
11. *Chiral Separations by Liquid Chromatography* (ACS Symposium Series, No. 471), ed. by S. Ahuja, American Chemical Society, Washington, DC, 1991, 239 pp.
12. W. A. Koenig, *Gas Chromatographic Enantiomer Separation with Modified Cyclodextrins*, Hüthig, Heidelberg, 1992, 168 pp.
13. *A Practical Approach to Chiral Separations by Liquid Chromatography*, ed. by G. Subramanian, VCH, Weinheim (FRG), 1994.
14. S. Allenmark, *Chromatographic Enantioseparation*, Ellis Horwood, New York, 2nd ed./1991.
15. E. Francotte, Contribution of preparative chromatographic resolution to the investigation of chiral phenomena, *J. Chromatogr. A*, **666**, 565–601 (1994).
16. G. P. Moss, Basic Terminology of Stereochemistry (IUPAC Recommendations 1996), *Pure Appl. Chem.*, **68**, 2193–2222 (1996).

5. BIOLOGICAL BUFFERS

Table 1 This table of frequently used buffers gives the pK_a value at 25°C and the useful pH range of each buffer. The buffers are listed in order of increasing pH

Acronym	Name	Mol. wt.	pK_a	Useful pH range
MES	2-(<i>N</i> -Morpholino)ethanesulphonic acid	195.2	6.1	5.5–6.7
BIS TRIS	<i>Bis</i> (2-hydroxyethyl)iminotris(hydroxymethyl)methane	209.2	6.5	5.8–7.2
ADA	<i>N</i> -(2-Acetamido)-2-iminodiacetic acid	190.2	6.6	6.0–7.2
ACES	2-[(2-Amino-2-oxoethyl)amino]ethanesulphonic acid	182.2	6.8	6.1–7.5
PIPES	Piperazine- <i>N,N'</i> - <i>bis</i> (2-ethanesulphonic acid)	302.4	6.8	6.1–7.5
MOPSO	3-(<i>N</i> -Morpholino)-2-hydroxypropanesulphonic acid	225.3	6.9	6.2–7.6
BIS TRIS PROPANE	1,3- <i>Bis</i> [<i>tris</i> (hydroxymethyl)methylamino]propane	282.3	6.8 ^a	6.3–9.5
BES	<i>N,N</i> - <i>Bis</i> (2-hydroxyethyl)-2-aminoethanesulphonic acid	213.2	7.1	6.4–7.8
MOPS	3-(<i>N</i> -Morpholino)propanesulphonic acid	209.3	7.2	6.5–7.9
HEPES	<i>N</i> -(2-Hydroxyethyl)piperazine- <i>N'</i> -(2-ethanesulphonic acid)	238.3	7.5	6.8–8.2
TES	<i>N</i> - <i>Tris</i> (hydroxymethyl)methyl-2-aminoethanesulphonic acid	229.2	7.5	6.8–8.2
DIPSO	3-[<i>N,N</i> - <i>Bis</i> (2-hydroxyethyl)amino]-2-hydroxypropanesulphonic acid	243.3	7.6	7.0–8.2
TAPSO	3-[<i>N</i> - <i>Tris</i> (hydroxymethyl)methylamino]-2-hydroxypropanesulphonic acid	259.3	7.6	7.0–8.2
TRIZMA	<i>Tris</i> (hydroxymethyl)aminomethane			
HEPPSO	<i>N</i> -(2-hydroxyethyl)piperazine- <i>N'</i> -(2-hydroxypropanesulphonic acid)	121.1	8.1	7.0–9.1
POPSO	Piperazine- <i>N,N'</i> - <i>bis</i> (2-hydroxypropanesulphonic acid)	268.3	7.8	7.1–8.5
EPPS	<i>N</i> -(2-Hydroxyethyl)piperazine- <i>N'</i> -(3-propanesulphonic acid)	362.4	7.8	7.2–8.5
TEA	Triethanolamine	252.3	8.0	7.3–8.7
TRICINE	<i>N</i> - <i>Tris</i> (hydroxymethyl)methylglycine	149.2	7.8	7.3–8.3
BICINE	<i>N,N</i> - <i>Bis</i> (2-hydroxyethyl)glycine	179.2	8.1	7.4–8.8
TAPS	<i>N</i> - <i>Tris</i> (hydroxymethyl)methyl-3-aminopropanesulphonic acid	163.2	8.3	7.6–9.0
AMPSO	3-[(1,1-Dimethyl-2-hydroxyethyl)amino]-2-hydroxypropanesulphonic acid	243.3	8.4	7.7–9.1
		227.3	9.0	8.3–9.7
CHES	2-(<i>N</i> -Cyclohexylamino)ethanesulphonic acid	207.3	9.3	8.6–10.0
CAPSO	3-(Cyclohexylamino)-2-hydroxy-1-propanesulphonic acid	237.3	9.6	8.9–10.3
AMP	2-Amino-2-methyl-1-propanol	89.1	9.7	9.0–10.5
CAPS	3-(Cyclohexylamino)-1-propanesulphonic acid	221.3	10.4	9.7–11.1

^a $pK_a = 9.0$ for the second dissociation stage.

The table is reprinted with permission of Sigma Chemical Company, St. Louis, Mo.

6A. CLASSIFICATION AND CHARACTERIZATION OF STATIONARY PHASES FOR LIQUID CHROMATOGRAPHY (IUPAC RECOMMENDATIONS 1997)

Descriptive Terminology

Prepared for publication by

R. M. Smith, Loughborough University, Loughborough, Leicestershire, UK

A. Marton, University of Veszprém, Veszprém, Hungary

© 1997 IUPAC

Abstract

A wide range of stationary phases and column packing materials have been developed over the years for liquid chromatography and these need to be described accurately and unambiguously. The present paper, which is the first of a series planned for this area, recommends terms for the description of the stationary phase materials and their properties and expands the list of terms given in Nomenclature of Chromatography [PAC, 1993, 65, 819–872.]. It concentrates on the chemical properties and chromatographic role of the materials. Many of the terms to describe their physical properties as particles have been discussed in a recent paper on the characterization of porous solids [PAC, 1994, 66, 1739–1758].

Index

Introduction

General descriptive terms for the stationary phase

Terms for the nature of the stationary phase material

Modes of application of stationary phase materials

Physical properties of the stationary phase materials

References

Appendix. Terms from the Nomenclature for Chromatography [1] which have been redefined

Introduction

One of the major problems throughout analytical liquid (and supercritical fluid) chromatography has been in reproducibly transferring methods between columns and systems. One of the main factors is that there are large differences in the chemical and physical properties of stationary phase materials, even between those which are nominally the same, such as octadecylsilyl (ODS)-bonded silicas. In addition, the methods used to describe the physical and chemical properties of these stationary phase materials are not standardized and even the terms used have not been agreed. In the laboratory, the behaviour of the stationary phases is also dependent on the nature of the interaction of specific mobile phases and analytes with the stationary phase.

The present discussions will concentrate on chromatographic applications of stationary phases. The standardization of analytical stationary phase materials falls into two areas.

- a) Terms needed to describe the physical and chemical properties of the stationary phase materials.
- b) Methods and tests needed to describe the operational properties of these materials. This is an important area but one where research is still active and as yet no consensus of approaches and techniques has been reached. This topic still requires much experimental work and was considered inappropriate for the Commission to consider at this time. It is also the subject of work by ASTM committees and others who are in a better position to carry out experimental work and to organise comparative studies.

The present paper considers the first of these areas and recommends a number of terms for the description of stationary phase materials and their chemical and physical properties. Some descriptive terms for the stationary phase have already been defined in the Nomenclature of Chromatography (NC) [1] and in the recently published Nomenclature for Analytical Chiral Separation methods (CS) [2]. In addition many of the Recommendations for the Characterization of Porous Solids published by the Physical Chemistry Division [3] are relevant to the physical description of stationary phase materials.

Amended and expanded definitions are now recommended for a number of the terms. The original versions are included in the Appendix.

General Descriptive Terms for the Stationary Phase

A number of these terms are generally applicable throughout chromatography and were defined previously in the Nomenclature for Chromatography (NC) [1]. However, in a number of cases, an inappropriate capitalization was used in NC, particularly of the second word in terms and these have been corrected in the definitions reproduced here.

Stationary Phase [Replaces NC 1.1.05]

One of the two phases forming a chromatographic system. It is the part of a chromatographic system responsible for the retention of the analytes, which are being carried through the system by the *mobile phase*. It may be a solid, a gel or a liquid. If a liquid, it may be distributed on a *solid support*. This *solid support* may or may not contribute to the separation process. The liquid may also be chemically bonded to the solid (*bonded phase*) or immobilized onto it (*immobilized phase*).

The expression *chromatographic bed* or *sorbent* may be used as a general term to denote any of the different forms in which the stationary phase is used.

Note: Particularly in gas chromatography where the stationary phase is most often a liquid, the term *liquid phase* is used for it as compared to the *gas phase*, i.e. the mobile phase. However, particularly in the early development of liquid chromatography, the term ‘liquid phase’ had also been used to characterize the mobile phase as compared to the ‘solid phase’ i.e. the stationary phase. Due to this ambiguity the use of the term ‘liquid phase’ is discouraged. If the physical state of the stationary phase is to be expressed, the use of the adjective forms, such as *liquid stationary phase* and *solid stationary phase*, *bonded stationary phase* or *immobilized stationary phase*, are recommended.

Packing Material, Stationary Phase Material [Replaces NC 3.1.07]

The *packing* is the active solid, stationary phase plus solid support or swollen gel which is contained in the chromatographic column. In liquid chromatography the usage of the terms *packing material* and *stationary phase material* are often synonymous. The term *packing material* is preferred as a general term for a loose, usually particulate, material intended for chromatographic use before it is packed into the column. Once it is packed and in contact with the mobile phase, it becomes the *stationary phase* as one of the two chromatographic phases. The *stationary phase* usually consists of a specific *stationary phase material*, which has been packed into a column. Both are typically given the same description.

Solid Support (NC 3.1.03)

A solid that holds the stationary phase but, ideally, does not contribute to the separation process.

Continuous Bed Packing

A column packing, which is a single entity, rather than being composed of individual particles.

Carbon Loading (of the Packing Material)

Mass fraction of the packing material which is carbon. Usually taken as a guide to the extent of alkyl substitution on the surface. Usually reported as percentage carbon determined using elemental analysis.

Terms for the Nature of the Stationary Phase Material**Immobilized Stationary Phase (Material) [Replaces, NC 1.1.05.2]**

A stationary phase which has been immobilized on the support particles, or on the inner wall of the column tubing, e.g. by either a physical attraction (*coated stationary phase*), by chemical bonding (*bonded stationary phase*), or by *in situ* polymerisation (*cross-linked stationary phase*) after coating.

Coated stationary phase (material) A material in which a stationary phase is immobilized by a physical attraction to the surface of the solid support.

Filled stationary phase (material) An immobilized stationary phase (*material*) in which a liquid fills the pores of the solid phase.

Bonded stationary phase (material) [Replaces NC 1.1.05.1] A stationary phase which is covalently bonded to solid support particles or to the inside wall of the column tubing. Sometimes referred to as a *bonded phase (material)*. The bonded stationary phase (*material*) may be *monomeric*, *polymeric* or *polymer-grafted phase (material)* and the *stationary phase (material)* can also receive additional treatment to give a *capped (end-capped) stationary phase (material)*.

Bonded phase See *Bonded stationary phase* [Replaces NC 1.1.05.1]

Monomeric-bonded stationary phase (material) Bonded stationary phase (material) prepared using a reagent, usually monofunctional, which reacts with single sites on the surface of the solid support.

Polymeric-bonded stationary phase (material) Bonded stationary phase (material) prepared using a polyfunctional reagent which can react both with the surface of the solid support and/or with additional reagent molecules.

Polymer-grafted stationary phase (material) Bonded stationary phase (material) in which a pre-formed polymer has been bound to the surface by a chemical bond.

Capped stationary phase (material) (also known as end-capped stationary phase (material)) Bonded stationary phase (material) which has been treated with a second (usually less bulky) reagent, which is intended to react with remaining functional (e.g. silanol) groups which have not been substituted by the original reagent because of steric hindrance.

Alkyl-bonded stationary phase (material) Bonded stationary phase (material) in which the group bound to the surface contains an alkyl chain (usually between C₁ and C₁₈).

Phenyl-bonded stationary phase (material) Bonded stationary phase (material) in which the group bound to the surface contains a phenyl group.

Cyano-bonded stationary phase (material) Bonded stationary phase in which the group bound to the surface contains a cyanoalkyl-($-\text{[CH}_2\text{]}_n\text{-CN}$) group.

Diol-bonded stationary phase (material) Bonded stationary phase in which the group bound to the surface contains a vicinal dihydroxyalkyl ($-\text{[CH}_2\text{]}_n\text{-CHOH-CH}_2\text{OH}$) group.

Amino-bonded stationary phase (material) Bonded stationary phase in which the group bound to the surface contains an aminoalkyl- (usually a $-\text{[CH}_2\text{]}_n\text{-NH}_2$) group.

Internal surface reversed-phase (ISRP) materials Bonded stationary phase in which the external surface of the solid support carries different bonded groups from the internal pores (usually an external hydrophilic layer with a more hydrophobic internal layer). Examples include *restricted-access stationary phase (material)* in which polar macromolecules are excluded from the internal pores.

Cross-linked Stationary Phase (Material) A stationary phase (material) in which the liquid phase coating on a solid support has been polymerized or cross-linked after coating to make it insoluble in the mobile phase.

Polymeric Stationary Phase (Material)

Stationary phase (material) based on particles of a cross-linked organic polymeric material. Typical materials are *polystyrene divinylbenzene copolymers* (PS-DVB) and modified PS-DVB materials.

Liquid-coated Stationary Phase (Material)

A material in which a liquid stationary phase is coated on the surface of the solid support.

Modes of Application of Stationary Phase Materials

Stationary phases are often defined in terms of the mode of chromatography being employed in the separation.

Size Exclusion Chromatographic Phases

These phases are described in *Compendium of macromolecular nomenclature* [4] (term 3.4.6). or in the Nomenclature for Chromatography section 6 [1].

Ion-exchange Stationary Phases

The principle terms have already been defined in NC (section 5) and are included here for comparison.

Cation exchanger (NC 5.302) Ion-exchanger with cations as counter-ions. The term *cation-exchange resin* may be used in the case of solid organic polymers.

Anion exchanger (NC 5.3.03) Ion-exchanger with anions as counter-ions. The term *anion-exchange resin* may be used in the case of solid organic polymers.

Chiral Stationary Phase (CS 2.4 [2])

A stationary phase which incorporates a *chiral selector*. If not constituent of the stationary phase as a whole, the chiral selector can be chemically bonded to (*chiral bonded stationary phase*) or immobilized onto the surface of a solid support or column wall (*chiral coated stationary phase*), or simply dissolved in the liquid stationary phase.

Affinity Stationary Phase (Material)

Bonded stationary phase (material) containing attached (adsorbed or covalently bonded) ligand molecules with a specific biological interaction for a particular molecule or small group of related molecules.

Perfusion Stationary Phase (Material)

Stationary phase in which the mobile phase primarily travels through the pores of the stationary phase.

Physical Properties of the Stationary Phase Material

Recommendations for the characterization of porous solids have recently been published by the Commission on Colloid and Surface Chemistry [3] and many of these are relevant to the characterization of stationary phase materials. In particular the conclusions presented in that paper should be noted, **especially, that in many cases absolute values of the parameters such as pore diameter and surface area cannot be obtained.** The measured value frequently depends on the method of measurement (and this should always be stated) and the selection of a method of characterization starts from the intended use of the material. These comments would also apply to the determination of particle diameter. In addition, the calculation methods for average particle diameters, such as number average or weight average, must be reported.

Previously Defined General Terms

Particle diameter (d_p) (NC 3.1.08) The average diameter of the solid particles.

Pore radius (r_p) (NC 3.1.09) The average radius of the pores within the solid particles.

References

1. L. S. Ettre, 'Nomenclature for chromatography (IUPAC Recommendations 1993)', *Pure Appl. Chem.*, 1993, **65**, 819–872.
2. V. A. Davankov, 'Analytical Chiral Separation Methods. (IUPAC Recommendations 1997)', *Pure Appl. Chem.*, 1997, **69**, 1469–1474.
3. J. Rouquerol, D. Avnir, C. W. Fairbridge, D. H. Everett, J. H. Haynes, N. Pernicone, J. D. F. Ramsay, K. S. W. Sing and K. K. Unger, 'Recommendations for the Characterization of Porous Solids', *Pure Appl. Chem.*, 1994, **66**, 1739–1758.
4. W. V. Metanowski, *Compendium of Macromolecular Nomenclature*, Blackwell, Oxford, 1991.

Appendix 1.

Terms from the 'Nomenclature for Chromatography' [1] which have been Redefined.

1.1.05. Stationary phase

One of the two phases forming a chromatographic system. It may be a solid, a gel or a liquid. If a liquid it may be distributed on a solid. This solid may or may not contribute to the separation process. The liquid may also be chemically bonded to the solid (*bonded phase*) or immobilized onto it (*immobilized phase*).

The expression *chromatographic* bed or sorbent may be used as a general term to denote any of the different forms in which the stationary phase is used.

Note: Particularly in gas chromatography where the stationary phase is most often a liquid, the term *liquid phase* is used for it as compared to the *gas phase*, i.e., the mobile phase. However, particularly in the early development of liquid chromatography, the term ‘liquid phase’ had also been used to characterize the mobile phase as compared to the ‘solid phase’, i.e. the stationary phase. Due to this ambiguity the use of the term ‘liquid phase’ is discouraged. If the physical state of the stationary phase is to be expressed the use of the adjective forms, such as *liquid stationary phase* and *solid stationary phase*, *bonded phase* or *immobilized phase*, are recommended.

1.1.05.1. Bonded phase

A stationary phase which is covalently bonded to the support particles or to the inside wall of the column tubing.

1.1.05.2. Immobilized phase

A stationary phase which immobilized on the support particles, or on the inner wall of the column tubing, e.g. by *in situ* polymerization (cross-linking) after coating.

3.1.07. Packing

The active solid, stationary phase plus solid support or swollen gel contained in a tube.

6B. Characterization of Ion Exchange Chromatographic Stationary Phases

Prepared for publication by

A. Marton, University of Veszprém, Veszprém, Hungary

© 1997 IUPAC

Abstract

In order to characterize ion exchange chromatographic stationary phases the thermodynamic exchange constant and the free energy interaction parameters are recommended. These parameters are calculated from the experimentally available corrected selectivity coefficient *vs.* exchanger phase composition functions. The equations used for the calculations have been obtained by introducing the Friedman equation (developed for the calculation of the excess free energy change) into the thermodynamic derivation. The suggested parameters also make possible the estimation of the value of the selectivity coefficient at an arbitrary exchanger phase composition. The characteristic parameters of the ion exchange resins and the equations in a directly suitable form for the estimation of the selectivity coefficient are calculated and presented for several systems.

Introduction

Parameters for the physical and chemical characterization of chromatographic stationary phases including ion exchangers have already been defined [1]. The purpose of this paper is to introduce sensitive numerical parameters for the comparison of operation ion exchange chromatographic stationary phases based on their selectivity coefficient exhibited in a particular ion exchange equilibria. For two competing counter ions (e.g. A^+ and B^{z+}) the problem arises not only because various selectivity coefficients may be assigned to the various commercially available products, but also because the exact value of the selectivity coefficient

may vary considerably with the degree of conversion of the exchanger phase as the ion exchange reaction (1) proceeds.



Here R represents the (usually monovalent) functional group covalently bond to a solid phase. The so-called corrected selectivity coefficient (K') is an experimentally available parameter defined for the above equilibria as:

$$K' = \frac{\bar{x}_B \cdot a_A^z}{\bar{x}_A^z \cdot a_B} \quad (2)$$

Throughout this article, symbols with overbars refer to the resin phase where the standard and reference states of RA and R_zB are taken to the respective mono-ionic forms of the exchanger in equilibrium with water. Symbols without a bar refer to the solution phase where the Henryan standard and reference states are accepted in accordance with conventional practice [2]. \bar{x} denotes mole or, if $z > 1$, equivalent fraction (in general $\bar{x}_i = z_i \cdot \bar{m}_i / \sum z_i \cdot \bar{m}_i$ and the summation is carried out over all counterion molalities \bar{m}_i), a and the parameter \bar{a} (see below) are the activities in the solution and resin phases respectively. For the ultimate characterization and comparison of the selectivity of the exchange reactions the more exactly defined thermodynamic exchange constant, K^T is recommended [2,3]:

$$K^T = \frac{\bar{a}_B \cdot a_A^z}{\bar{a}_A^z \cdot a_B} \quad (3)$$

An extensive compilation of the K^T data for the various ion exchange equilibria has been made in an earlier report of the IUPAC [4]. Since the ion exchange equilibrium constant is directly related to the distribution coefficient of the ion studied its knowledge in the calculation of the retention volume, or generally in the design of ion exchange separations, is indispensable. Considering however, that in the majority of analytical ion exchange separations practically either one or the other end to the mole fraction scale is utilized ($\bar{x}_A \approx 1$ or $\bar{x}_B \approx 1$), the thermodynamic constant could be quite far from the actual (operational) value of the selectivity coefficient. The suggested characterization method is meant to provide a solution for these seemingly conflicting aspects.

Using the concentrated electrolyte solution model of the ion exchange resins, equations were derived for the composition dependence of the selectivity coefficient (see equations on pages 104 and 105 of reference [5]). From the experimentally available functions $\ln K'$ vs. \bar{x}_B the derived relationships make possible both the calculation of the thermodynamic exchange constant and the so-called free energy interaction parameters which, in turn, could be used to calculate the selectivity coefficient at any value of \bar{x}_B . It was proved that the free energy interaction parameters are related to the selectivity controlling properties of the ion exchanger phase, such as the crosslinking of the polymer matrix, the type of the functional group and the size of the exchanging counter ions [5]. The purpose of the suggested method is to characterize the ion exchangers with these parameters in connection with their actual ion exchange reaction. It may also be considered as an operational characterization which uses both the thermodynamic constant and the above mentioned free energy interaction parameters to estimate the value of the corrected selectivity coefficient at an arbitrary exchanger phase composition.

Theoretical Background

When reaction (1) takes place a mixture of the concentrated electrolytes is always formed. The composition of this mixture (\bar{x}_B) varies as the resin is converted from A^+ and B^{z+} form. According to H.L. Friedman [6] the excess free energy change (ΔG^E) accompanying the formation of a two component electrolyte solution mixture at constant ionic strength I (containing a common cation or anion) can be approximated by the equation:

$$\Delta G^E = R \cdot T \cdot I^2 \cdot x_A \cdot x_B \cdot [g_0 + g_1 \cdot (x_A - x_B)] \quad (4)$$

Here x_A and x_B are the mole fractions of the components (e.g. RA and R_zB) and g_0 and g_1 are the so called free energy interaction parameters independent of the composition. These terms have been introduced by

Table 1 Summary of the equations used for the calculations

$\ln K' = a_0 + a_1 \cdot \bar{x}_B + a_2 \cdot \bar{x}_B^2$ (5)	
$a_2 < 0$	$a_2 > 0$
$\bar{g}_0 = \frac{a_1 + a_2}{2 \cdot z}$ (6)	$\bar{g}_0 = \frac{a_1 + a_2}{2 \cdot z}$ (9)
$\bar{g}_1 = \frac{-a_2}{6 \cdot z}$ (7)	$\bar{g}_1 = \frac{a_2}{6 \cdot z}$ (10)
$\ln K^T = a_0 + z \cdot \bar{g}_0 + z \cdot \bar{g}_1$ (8)	$\ln K^T = a_0 + z \cdot \bar{g}_0 - z \cdot \bar{g}_1$ (11)

Friedman to account for the strength of pair and triplet interactions respectively in a concentrated two component electrolyte solution mixture. The existence of a similar mixture of concentrated electrolyte solutions is supposed to be present in the exchanger phase too. It has been pointed out [5] that by introducing eqn. (4) into the thermodynamic derivation the composition dependence of the selectivity coefficient can be expressed conveniently by these free energy interaction parameters. Equations suggested for the calculation of the characteristic ion exchange parameters (\bar{g}_0 , \bar{g}_1 and $\ln K^T$) were taken from reference [5] and are summarized for our purpose in Table 1.

Although a direct, *a priori*, calculation of the free energy interaction parameters for the concentrated electrolyte solution of the exchanger phase is still not feasible a detailed analysis of several literature data proved that their value is dramatically influenced by the crosslinking of the inert (polymer) matrix, by the type and density of the active group of the resin and by the type of the counter ion [5]. Consequently, these parameters by themselves are characteristic for the ion exchange chromatographic stationary phase *i.e.* a difference in their values for the two compared stationary phases indicate differences in relevant structural parameters governing ion exchange selectivity.

Source of Experimental Data and Examples for the Suggested Ion Exchange Stationary Phase Characterization

An important criteria for the application of the equations shown in Table 1 is that the exchange reaction should be completely reversible, where the exchange capacity is freely accessible to the competing counter ions. The exchange equilibrium should be studied at a constant temperature and ionic strength in the full range of mole fraction scale and the corrected selectivity coefficient, K' defined by eqn. (2) should be calculated at each exchanger phase composition. As an application of the above equations, we can consider the following experimental data obtained by Bonner [7] for the Na^+/H^+ exchange reaction on a strongly acidic Dowex 50 \times 8 resin:

\bar{x}_{Na^+} :	0.12	0.22	0.32	0.42	0.58	0.70	0.75	0.86
$\ln K'$:	0.470	0.438	0.438	0.439	0.451	0.405	0.343	0.270

When eqn. (5) of Table 1 is fitted to the above $\ln K'$ vs. \bar{x}_{Na^+} data pairs then the following coefficients are obtained: $a_0 = 0.400$, $a_1 = 0.398$, $a_2 = -0.624$ (the curve fitting program used for the calculation is given in reference [8]). Since $a_2 < 0$ eqns. (6, 7 and 8) of Table 1 can be used for the calculation of the characteristic parameters of the studied exchange equilibria. The obtained values are: $\bar{g}_0 = -0.113$, $\bar{g}_1 = 0.104$, $\ln K^T = 0.39$.

The function describing the dependence of $\ln K'$ on the exchanger phase composition can therefore be given by the so-called selectivity polynomial:

$$\ln K' = 0.400 + 0.398 \cdot \bar{x}_{\text{Na}^+} - 0.624 \cdot \bar{x}_{\text{Na}^+}^2 \quad (12)$$

If in the actual exchange process the estimated value of the stationary phase loading is e.g. 0.1 (or at the other extreme end of the mole fraction scale is e.g. 0.9) then the calculated $\ln K'$ value is 0.433 (or 0.253)

which are certainly more realistic values for the design of an ion exchange separation process than the value of $\ln K^T$ (0.39).

If the experimentally obtained ($\ln K'$ vs. \bar{x}_B) function is concave i.e. $a_2 > 0$ then eqns. (9, 10 and 11) of Table 1 should be used for the calculation of the above parameters. It may also happen that the experimental data fits well with a straight line. In this case the above equations are also valid but, of course, now $a_2 = 0$. The choice between the linear or the quadratic fitting procedures can be made by the comparison of the goodness of fit parameters. It is, in fact, automatically calculated by the referred curve fitting program and the improvement in the goodness of fit can be seen immediately when the degree of the polynomial is changed (e.g. from one to two).

In order to illustrate the wide scope of applicability of the suggested characterization method Tables 2 and 3 show the calculated values of the above discussed equilibrium parameters for a set of systems. The equilibria

Table 2 Free energy interaction parameters (\bar{g}_0 and \bar{g}_1) and the selectivity polynomial for some ion exchange equilibria

B ⁺	DVB%	\bar{g}_0	\bar{g}_1	$\ln K^T$	$\ln K'$	Ref.
$RH + B^+ \leftrightarrow RB + H^+$						
Li ⁺	4	0.020	0.061	0.263	$0.304 - 0.327 \bar{x}_B + 0.368 \bar{x}_B^2$	9
	8	-0.030	0.101	0.222	$0.353 - 0.669 \bar{x}_B + 0.608 \bar{x}_B^2$	9
	16	-0.242	0.142	0.353	$0.737 - 1.338 \bar{x}_B + 0.854 \bar{x}_B^2$	9
Na ⁺	4	0.01	0.088	0.139	$0.041 + 0.548 \bar{x}_B - 0.528 \bar{x}_B^2$	9
	8	-0.113	0.104	0.390	$0.400 + 0.398 \bar{x}_B - 0.624 \bar{x}_B^2$	9
	16	-0.423	0.215	0.445	$0.653 + 0.444 \bar{x}_B - 1.290 \bar{x}_B^2$	9
K ⁺	4	-0.612	0.102	0.474	$0.534 + 0.289 \bar{x}_B - 0.613 \bar{x}_B^2$	9
	8	-0.314	0.144	0.729	$0.899 + 0.235 \bar{x}_B - 0.863 \bar{x}_B^2$	9
	16	-1.039	0.106	1.019	$1.952 - 1.439 \bar{x}_B - 0.640 \bar{x}_B^2$	9
Rb ⁺	4	0.354	0.073	0.494	$0.775 - 0.270 \bar{x}_B - 0.439 \bar{x}_B^2$	10
	8	-0.607	0.035	0.856	$1.458 - 1.423 \bar{x}_B + 0.209 \bar{x}_B^2$	10
	16	-1.196	0.241	1.059	$2.014 - 0.946 \bar{x}_B - 1.446 \bar{x}_B^2$	10
Cs ⁺	4	-0.398	0.083	0.587	$0.893 - 0.282 \bar{x}_B - 0.496 \bar{x}_B^2$	10
	8	-0.891	0.006	0.832	$1.717 - 1.746 \bar{x}_B - 0.035 \bar{x}_B^2$	10
	16	-1.487	0.093	1.082	$2.476 - 2.417 \bar{x}_B - 0.557 \bar{x}_B^2$	10
NH ₄ ⁺	4	-0.156	—	0.303	$0.460 - 0.313 \bar{x}_B$	9
	8	-0.333	—	0.576	$0.909 - 0.667 \bar{x}_B$	9
	16	-0.647	—	-0.763	$1.411 - 1.295 \bar{x}_B$	9
N(Me) ₄ ⁺	7	-0.649	—	0.081	$0.730 - 1.298 \bar{x}_B$	11
N(Et) ₄ ⁺	7	-4.245	—	-0.489	$3.756 - 8.491 \bar{x}_B$	11
N(Pr) ₄ ⁺	7	-5.565	—	-0.870	$4.695 - 11.130 \bar{x}_B$	11
N(Bu) ₄ ⁺	7	-9.371	—	-0.785	$8.586 - 18.742 \bar{x}_B$	11
$RNa + B^- \leftrightarrow RB + Na^+$						
Cs ⁺	8	-0.094	0.003	0.813	$0.445 - 0.173 \bar{x}_B - 0.016 \bar{x}_B^2$	12
Ag ⁺	8	-0.184	0.033	1.308	$0.720 - 0.173 \bar{x}_B - 0.196 \bar{x}_B^2$	12
Tl ⁺	8	-0.154	0.045	1.660	$0.810 - 0.081 \bar{x}_B - 0.389 \bar{x}_B^2$	12
$RCl + B^- \leftrightarrow RB + Cl^-$						
Br ⁻	2	-0.048	—	0.896	$0.945 - 0.097 \bar{x}_B$	13
	4	-0.085	—	1.028	$1.114 - 0.171 \bar{x}_B$	13
	8	-0.123	—	1.118	$1.311 - 0.245 \bar{x}_B$	13
	10	-0.214	—	1.411	$1.625 - 0.427 \bar{x}_B$	13
I ⁻	2	-0.087	—	1.219	$1.327 - 0.278 \bar{x}_B + 0.213 \bar{x}_B^2$	14
	4	-0.121	—	1.487	$1.567 - 0.004 \bar{x}_B - 0.246 \bar{x}_B^2$	14
	8	-0.197	—	2.297	$2.549 - 0.724 \bar{x}_B + 0.329 \bar{x}_B^2$	14
	10	-0.287	—	2.946	$3.143 - 0.029 \bar{x}_B - 0.546 \bar{x}_B^2$	14
NO ₃ ⁻	2	-0.084	0	0.643	$0.727 - 0.168 \bar{x}_B$	14
	4	-0.061	0	0.841	$0.903 - 0.123 \bar{x}_B$	14
	8	-0.149	0	1.171	$1.321 - 0.299 \bar{x}_B$	14
	10	-0.169	0	1.456	$1.653 - 0.393 \bar{x}_B$	14
ClO ₄ ⁻	8	0.698	0.409	3.924	$5.033 - 3.855 \bar{x}_B + 2.458 \bar{x}_B^2$	15
ClO ₃ ⁻	8	0.195	0	0.891	$0.694 + 0.393 \bar{x}_B$	15
BrO ₃ ⁻	8	-0.077	0	0.354	$0.431 + 0.154 \bar{x}_B$	15
IO ₃ ⁻	8	-0.093	0.054	-1.272	$-1.233 + 0.136 \bar{x}_B - 0.323 \bar{x}_B^2$	15
HCO ₃ ⁻	8	-0.073	0.100	-1.010	$-0.840 - 0.751 \bar{x}_B + 0.605 \bar{x}_B^2$	15
OH ⁻	8	-0.315	0.118	-2.371	$-2.174 + 0.077 \bar{x}_B - 0.708 \bar{x}_B^2$	15
SCN ⁻	8	-0.481	0.142	3.29	$3.91 - 1.816 \bar{x}_B + 0.854 \bar{x}_B^2$	15

Table 3 Free energy interaction parameters (\bar{g}_0 and \bar{g}_1) and the selectivity polynomial for some anion exchange equilibria

B^{2-}	F.G.	\bar{g}_0	\bar{g}_1	$\ln K^T$	$\ln K'$	Ref.
$2RCl + B^{2-} \leftrightarrow R_2B + 2Cl^-$						
Ox^{2-}	TMA ⁺	0.187	1.012	-2.290	$-0.644 - 11.4 \bar{x}_B + 12.15 \bar{x}_B^2$	16
Ma^{2-}		0.460	0.565	-3.048	$-2.838 - 4.942 \bar{x}_B + 6.782 \bar{x}_B^2$	16
Su^{2-}		0.288	0.017	-3.760	$-4.303 + 0.945 \bar{x}_B + 0.207 \bar{x}_B^2$	16
Gl^{2-}		0.07	0.44	-4.050	$5.07 + 5.00 \bar{x}_B - 5.28 \bar{x}_B^2$	16
Ad^{2-}		-0.562	0.956	-4.975	$-5.763 + 9.233 \bar{x}_B - 11.47 \bar{x}_B^2$	16
Pi^{2-}		-0.922	0.102	-5.384	$-5.58 + 8.590 \bar{x}_B - 12.28 \bar{x}_B^2$	16
Ox^{2-}		-2.09	1.52	-7.10	$-5.96 + 9.90 \bar{x}_B - 18.29 \bar{x}_B^2$	16
Ma^{2-}		-0.845	0.81	-5.46	$5.39 + 6.30 \bar{x}_B - 9.68 \bar{x}_B^2$	16
Su^{2-}		+0.097	0.17	-4.05	$-4.59 + 2.44 \bar{x}_B - 2.05 \bar{x}_B^2$	16
Gl^{2-}		+0.387	0.32	-3.29	$-3.43 - 2.29 \bar{x}_B + 3.89 \bar{x}_B^2$	16
Ad^{2-}	TEA ⁺	+0.006	0.07	-4.25	$-4.42 - 0.95 \bar{x}_B - 0.926 \bar{x}_B^2$	16
Pi^{2-}		-0.515	0.438	-4.96	$-4.81 + 3.20 \bar{x}_B - 5.26 \bar{x}_B^2$	16

B^{2-} : Ox^{2-} = Oxalic, Ma^{2-} = Malonic, Su^{2-} = Succinic, Gl^{2-} = Glutaric, Ad^{2-} = Adipic, Pi^{2-} = Heptanedioic (Pimelic) acid anion F.G.: functionalities of the Amberlite resin, tetramethyl and tetraethylammonium groups (TMA⁺, TEA⁺).

selected, mostly from the 'classics' of the ion exchange literature are meant to represent both inorganic and organic cation and anion exchange reactions, where the crosslinking of the polymer matrix, the size of the active group and the size of the counter ion varies considerably.

Conclusion

The nonideal behaviour of the exchanger phase is recognized to be highly characteristic for the ion exchanger as a chromatographic stationary phase. As a quantitative measure of this nonideality the free energy interaction parameters are calculated from the data of equilibrium measurements. These data are then applied to construct the so-called selectivity polynomial which, in turn, can be used to estimate the selectivity coefficient at any required composition of the exchanger phase. Beyond the highly specific, numerically sensitive feature of these parameters their recommendation for the characterization of ion exchange chromatographic stationary phases is further supported by their connection with thermodynamic equilibrium constant of the exchange reaction.

References

1. R. M. Smith, A. Marton, 'Classification and characterization of stationary phases for liquid chromatography Part I. Descriptive Terminology', *Pure and Appl. Chem.* (under publication).
2. F. Helfferich, *Ion Exchange*, McGraw Hill, New York, 1962, p.95.
3. H. M. N. H. Irving, 'Recommendations on Ion Exchange Nomenclature', *Pure and Appl. Chem.*, **29**, 619-623 (1972).
4. Y. Marcus, D. H. Howerly, 'Ion Exchange Equilibrium Constants', *IUPAC Commission V/6 Equilibrium Data*, (1972).
5. A. Marton, J. Inczédy, 'Application of the concentrated electrolyte solution model in the evaluation of ion exchange equilibria' *Reaction Polymers*, **7**, 101-109 (1988).
6. H. L. Friedman, *Ionic Solution Theory*, Interscience, New York, 1962, p.225.
7. O. D. Bonner, 'A selectivity scale for some monovalent cations on Dowex 50', *J. Phys. Chem.*, **58**, 318-320 (1954).
8. J. D. Lee, T. D. Lee, *Statistics and Computer Methods in BASIC*, Van Nostrand Reinhold, Wokingham, 1982, p.121.
9. O. D. Bonner, 'A selectivity scale for some monovalent cations on Dowex 50', *J. Phys. Chem.*, **58**, 318-320 (1954).
10. O. D. Bonner, 'Ion exchange equilibria involving rubidium, cesium and thallous ions', *J. Phys. Chem.*, **59**, 719-721 (1955).
11. J. R. Millar, D. G. Smith, W. E. Marr, T. R. E. Kressman, 'Solvent modified polymer networks. Part III', *J. Chem. Soc.*, 2740-2746 (1964).
12. A. Jász, T. Lengyel, 'Investigation of binary ion exchange equilibria with radioisotopes' (in Hungarian), *Magy. Kém. Foly.*, **67**, 351-369 (1961).
13. B. Soldano, D. Chesnut, 'Osmotic approach to ion exchange equilibrium', *J. Am. Chem. Soc.*, **77**, 1334-1339 (1955).
14. H. P. Gregor, G. J. Belle, R. A. Marcus, 'Studies on ion exchange resins XIII', *J. Am. Chem. Soc.*, **77**, 2713-2719 (1955).
15. A. Marton, 'Relation of the free energy interaction parameters to some structural properties of ion exchange resins', *Talanta*, **41**, 1127-1132 (1994).
16. S. Subramonian, D. Clifford, 'Monovalent/divalent selectivity and the charge separation concept', *Reactive Polymers*, **9**, 195-209 (1988).

7. CONVERSION OF UNITS

The table below gives conversion factors from a variety of units to the corresponding SI unit. For each physical quantity the name is given, followed by the recommended symbol(s). Then the SI unit is given, followed by the esu, emu, Gaussian unit (Gau), atomic unit (au), and other units in common use, with their conversion factors to SI. The constant ζ which occurs in some of the electromagnetic conversion factors is the (exact) pure number $2.997\,924\,58 \times 10^{10} = c_0/(\text{cms}^{-1})$.

The inclusion of non-SI units in this table should not be taken to imply that their use is to be encouraged. With some exceptions, SI units are always to be preferred to non-SI units. However, since many of the units below are to be found in the scientific literature, it is convenient to tabulate their relation to the SI.

For convenience units in the esu and Gaussian systems are quoted in terms of the four dimensions *length*, *mass*, *time*, and *electric charge*, by including the franklin (Fr) as an abbreviation for the electrostatic unit of charge and $4\pi\epsilon_0$ as a constant with dimensions $(\text{charge})^2/(\text{energy} \times \text{length})$. This gives each physical quantity the same dimensions in all systems, so that all conversion factors are pure numbers. The factors $4\pi\epsilon_0$ and the Fr may be eliminated by writing $\text{Fr} = \text{esu of charge} = \text{erg}^{1/2}\text{cm}^{1/2} = \text{cm}^{3/2}\text{g}^{1/2}\text{s}^{-1}$, $4\pi\epsilon_0 = \epsilon_0^{(\text{ir})} = 1 \text{ Fr}^2 \text{ erg}^{-1} \text{ cm}^{-1} = 1$, to recover esu expressions in terms of three base units. The symbol Fr should be regarded as a compact representation of (esu of charge).

Conversion factors are either given exactly (when the = sign is used), or they are given to the approximation that the corresponding physical constants are known (when the \approx sign is used). In the latter case the uncertainty is always less than ± 5 in the last digit quoted.

Name	Symbol	Relation to SI
<i>Length, l</i>		
metre (SI unit)	m	
centimetre (cgs unit)	cm	$= 10^{-2} \text{ m}$
bohr (au)	a_0 , b	$= 4\pi\epsilon_0\hbar^2/m_e e^2 \approx 5.291\,77 \times 10^{-11} \text{ m}$
ångström	Å	$= 10^{-10} \text{ m}$
micron	μ	$= \mu\text{m} = 10^{-6} \text{ m}$
x unit	X	$\approx 1.002 \times 10^{-13} \text{ m}$
fermi	f, fm	$= \text{fm} = 10^{-15} \text{ m}$
inch	in	$= 2.54 \times 10^{-2} \text{ m}$
foot	ft	$= 12 \text{ in} = 0.3048 \text{ m}$
yard	yd	$= 3 \text{ ft} = 0.9144 \text{ m}$
mile	mi	$= 1760 \text{ yd} = 1609.344 \text{ m}$
nautical mile		$= 1852 \text{ m}$
<i>Area, A</i>		
square metre (SI unit)	m^2	
barn	b	$= 10^{-28} \text{ m}^2$
acre		$\approx 4046.856 \text{ m}^2$
are	a	$= 100 \text{ m}^2$
hectare	ha	$= 10^4 \text{ m}^2$
<i>Volume, V</i>		
cubic metre (SI unit)	m^3	
litre	l, L	$= \text{dm}^3 = 10^{-3} \text{ m}^3$
lambda	λ	$= \mu\text{l} = 10^{-6} \text{ dm}^3$
barrel (US)		$\approx 158.987 \text{ dm}^3$
gallon (US)	gal (US)	$= 3.785\,41 \text{ dm}^3$
gallon (UK)	gal (UK)	$= 4.546\,09 \text{ dm}^3$

Name	Symbol	Relation to SI
<i>Mass, m</i>		
kilogram (SI unit)	kg	
gram (cgs unit)	g	$= 10^{-3} \text{ kg}$
electron mass (au)	m_e	$\approx 9.109\,39 \times 10^{-31} \text{ kg}$
unified atomic mass unit, dalton	u, Da	$= m_a(^{12}\text{C})/12 \approx 1.660\,540 \times 10^{-27} \text{ kg}$
tonne	t	$= \text{Mg} = 10^3 \text{ kg}$
pound (avoirdupois)	lb	$= 0.453\,592\,37 \text{ kg}$
ounce (avoirdupois)	oz	$\approx 28.3495 \text{ g}$
ounce (troy)	oz (troy)	$\approx 31.1035 \text{ g}$
agrain	gr	$= 64.798\,91 \text{ mg}$
<i>Time, t</i>		
second (SI, cgs unit)	s	
au of time	\hbar/E_h	$\approx 2.41888 \times 10^{-17} \text{ s}$
minute	min	$= 60 \text{ s}$
hour	h	$= 3600 \text{ s}$
day ^a	d	$= 86\,400 \text{ s}$
year ^b	a	$\approx 31\,556\,952 \text{ s}$
svedberg	Sv	$= 10^{-13} \text{ s}$
<i>Acceleration, a</i>		
SI unit	m s^{-2}	$= 9.806\,65 \text{ m s}^{-2}$
standard acceleration of free fall	g_n	
gal, galileo	Gal	$= 10^{-2} \text{ m s}^{-2}$
<i>Force, F</i>		
newton (SI unit) ^c	N	$= \text{kg m s}^{-2}$
dyne (cgs unit)	dyn	$= \text{g cm s}^{-2} = 10^{-5} \text{ N}$
au of force	E_h/a_0	$\approx 8.238\,73 \times 10^{-8} \text{ N}$
kilogram-force	kgf	$= 9.806\,65 \text{ N}$
<i>Energy, U</i>		
joule (SI unit)	J	$= \text{kg m}^2 \text{ s}^{-2}$
erg (cgs unit)	erg	$= \text{g cm}^2 \text{ s}^{-2} = 10^{-7} \text{ J}$
hartree (au)	E_h	$= \hbar^2/m_e a_0^2 \approx 4.359\,75 \times 10^{-18} \text{ J}$
rydberg	Ry	$= E_h/2 \approx 2.179\,87 \times 10^{-18} \text{ J}$
electronvolt	eV	$= e \times \text{V} \approx 1.602\,18 \times 10^{-19} \text{ J}$
calorie, thermochemical	cal _{th}	$= 4.184 \text{ J}$
calorie, international	cal _{IT}	$= 4.1868 \text{ J}$
15°C calorie	cal ₁₅	$\approx 4.1855 \text{ J}$
litre atmosphere	1 atm	$= 101.325 \text{ J}$
British thermal unit	Btu	$= 1055.06 \text{ J}$
<i>Pressure, p</i>		
pascal (SI unit)	Pa	$= \text{N m}^{-2} = \text{kg m}^{-1} \text{ s}^{-2}$
atmosphere	atm	$= 101\,325 \text{ Pa}$
bar	bar	$= 10^5 \text{ Pa}$
torr	Torr	$= (101\,325/760) \text{ Pa} \approx 133.322 \text{ Pa}$
millimetre of mercury (conventional)	mmHg	$= 13.5951 \times 980.665 \times 10^{-2} \text{ Pa} \approx 133.322 \text{ Pa}$
pounds per square inch	psi	$\approx 6.894\,757 \times 10^3 \text{ Pa}$

Name	Symbol	Relation to SI
<i>Power, P</i>		
watt (SI unit)	W	$= \text{kg m}^2 \text{s}^{-3}$
horse power	hp	$= 745.7 \text{ W}$
<i>Action, L, J (angular momentum)</i>		
SI unit	J s	$= \text{kg m}^2 \text{s}^{-1}$
cgs unit	erg s	$= 10^{-7} \text{ J s}$
au of action	\hbar	$= \hbar/2\pi \approx 1.054 \times 10^{-34} \text{ J s}$
<i>Dynamic viscosity, η</i>		
SI unit	Pa s	$= \text{kg m}^{-1} \text{s}^{-1}$
poise	P	$= 10^{-1} \text{ Pa s}$
centipoise	cP	$= \text{mPa s}$
<i>Kinematic viscosity, ν</i>		
SI unit	$\text{m}^2 \text{s}^{-1}$	$= 10^{-4} \text{ m}^2 \text{s}^{-1}$
stokes	St	
<i>Thermodynamic temperature, T</i>		
kelvin (SI unit)	K	
degree Rankine ^d	°R	$= (5/9) \text{ K}$
<i>Entropy, S</i>		
<i>Heat capacity, C</i>		
SI unit	J K^{-1}	
clausius	Cl	$= \text{cal}_{\text{th}}/\text{K} = 4.184 \text{ J K}^{-1}$
<i>Molar entropy, S_{m}</i>		
<i>Molar heat capacity, C_{m}</i>		
SI unit	$\text{J K}^{-1} \text{mol}^{-1}$	
entropy unit	e.u.	$= \text{cal}_{\text{th}} \text{ K}^{-1} \text{mol}^{-1} = 4.184 \text{ J K}^{-1} \text{mol}^{-1}$
<i>Molar volume, V_{m}</i>		
SI unit	$\text{m}^3 \text{mol}^{-1}$	
amagat ⁵	amagat	$= V_{\text{m}} \text{ of real gas at 1 atm and 273.15 K}$ $\approx 22.4 \times 10^{-3} \text{ m}^3 \text{mol}^{-1}$
<i>Amount density, $1/V_{\text{m}}$</i>		
SI unit	mol m^{-3}	
amagat ^e	amagat	$= 1/V_{\text{m}} \text{ of a real gas at 1 atm and 273.15 K}$ $\approx 44.6 \text{ mol m}^{-3}$
<i>Plane angle, α</i>		
radian (SI unit)	rad	
degree	°	$= \text{rad} \times 2\pi/360 \approx (1/57.295\,78) \text{ rad}$
minute	'	$= \text{degree}/60$
second	"	$= \text{degree}/3600$
grade	grad	$= \text{rad} \times 2\pi/400 \approx (1/63.661\,98) \text{ rad}$

Name	Symbol	Relation to SI
<i>Radioactivity, A</i>		
becquerel (SI unit)	Bq	$= \text{s}^{-1}$
curie	Ci	$= 3.7 \times 10^{10} \text{ Bq}$
<i>Absorbed dose of radiation^f</i>		
gray (SI unit)	Gy	$= \text{J kg}^{-1}$
rad	rad	$= 0.01 \text{ Gy}$
<i>Dose equivalent</i>		
sievert (SI unit)	Sv	$= \text{J kg}^{-1}$
rem	rem	$\approx 0.01 \text{ Sv}$
<i>Electric current, I</i>		
ampere (SI unit)	A	
esu, Gau	$(10/\zeta)\text{A}$	$\approx 3.335\,64 \times 10^{-10} \text{ A}$
biot (emu)	Bi	$= 10 \text{ A}$
au	eE_{h}/\hbar	$\approx 6.623\,62 \times 10^{-3} \text{ A}$
<i>Electric charge, Q</i>		
coulomb (SI unit)	C	$= \text{A s}$
franklin (esu, Gau)	Fr	$= (10/\zeta)\text{C} \approx 3.335\,64 \times 10^{-10} \text{ C}$
emu (abcoulomb)		$= 10 \text{ C}$
proton charge (au)	e	$\approx 1.602\,18 \times 10^{-19} \text{ C} \approx 4.803\,21 \times 10^{-10} \text{ Fr}$
<i>Charge density, ρ</i>		
SI unit	C m^{-3}	
esu, Gau	Fr cm^{-3}	$= 10^7 \zeta^{-1} \text{C m}^{-3} \approx 3.33564 \times 10^{-4} \text{ C m}^{-3}$
au	ea_0^{-3}	$\approx 1.081\,20 \times 10^{-12} \text{ C m}^{-3}$
<i>Electric potential, V, ϕ</i>		
volt (SI unit)	V	$= \text{JC}^{-1} = \text{J A}^{-1} \text{s}^{-1}$
esu, Gau	erg Fr^{-1}	$= \text{Fr cm}^{-1}/4\pi\epsilon_0 = 299.792\,458 \text{ V}$
$\text{'cm}^{-1}\text{g}$	$e \text{ cm}^{-1}/4\pi\epsilon_0$	$\approx 1.439\,97 \times 10^{-7} \text{ V}$
au	$e/4\pi\epsilon_0 a_0$	$= E_{\text{h}}/e \approx 27.2114 \text{ V}$
mean international volt		$= 1.000\,34 \text{ V}$
US international volt		$= 1.000\,330 \text{ V}$
<i>Electric resistance, R</i>		
ohm (SI unit)	Ω	$= \text{V A}^{-1} = \text{m}^2 \text{kg s}^{-3} \text{A}^{-2}$
mean international ohm		$= 1.1000\,49 \Omega$
US international ohm		$= 1.000\,495 \Omega$
<i>Electric field, E</i>		
SI unit	V m^{-1}	$= \text{J C}^{-1} \text{m}^{-1}$
esu, Gau	$\text{Fr cm}^{-2}/4\pi\epsilon_0$	$= 2.997\,924\,58 \times 10^4 \text{ V m}^{-1}$
$\text{'cm}^{-2}\text{g}$	$e \text{ cm}^{-2}/4\pi\epsilon_0$	$\approx 1.439\,97 \times 10^{-5} \text{ V m}^{-1}$
au	$e/4\pi\epsilon_0 a_0^2$	$= 5.142\,21 \times 10^{11} \text{ V m}^{-1}$
<i>Electric field gradient, $E'_{\alpha\beta}$, $q_{\alpha\beta}$</i>		
SI unit	V m^{-2}	$= \text{J C}^{-1} \text{m}^{-2}$
esu, Gau	$\text{Fr cm}^{-3}/4\pi\epsilon_0$	$= 2.997\,924\,58 \times 10^6 \text{ V m}^{-2}$

Name	Symbol	Relation to SI
'cm' ⁻³ , g	$e \text{ cm}^{-3}/4\pi\epsilon_0$	$\approx 1.439\,97 \times 10^{-3} \text{ V m}^{-2}$
au	$e/4\pi\epsilon_0 a_0^3$	$\approx 9.717\,36 \times 10^{21} \text{ V m}^{-2}$
<i>Electric dipole moment, p, μ</i>		
SI unit	C m	
esu, Gau	Fr cm	$\approx 3.335\,64 \times 10^{-12} \text{ C m}$
debye	D	$= 10^{-18} \text{ Fr cm} \approx 3.335\,64 \times 10^{-30} \text{ C m}$
'cm' dipole length ^g	$e \text{ cm}$	$\approx 1.602\,18 \times 10^{-21} \text{ C m}$
au	ea_0	$\approx 8.478\,36 \times 10^{-30} \text{ C m}$
<i>Electric quadrupole moment, $Q_{\alpha\beta}$, $\Theta_{\alpha\beta}$, eQ</i>		
SI unit	C m ²	
esu, Gau	Fr cm ²	$\approx 3.335\,64 \times 10^{-14} \text{ C m}^{-2}$
'cm ² ',	$e \text{ cm}^2$	$\approx 1.602\,18 \times 10^{-23} \text{ C m}^2$
quadrupole area ^g		
au	ea_0^2	$\approx 4.486\,55 \times 10^{-40} \text{ C m}^2$
<i>Polarizability, α</i>		
SI unit	J ⁻¹ C ² m ²	= F m ²
esu, Gau, 'cm ³ '	$4\pi\epsilon_0 \text{ cm}^3$	$\approx 1.112\,65 \times 10^{-16} \text{ J}^{-1} \text{ C}^2 \text{ m}^2$
polarizability volume ^g		
'Å ³ ', ^g	$4\pi\epsilon_0 \text{ Å}^3$	$\approx 1.112\,65 \times 10^{-40} \text{ J}^{-1} \text{ C}^2 \text{ m}^2$
au	$4\pi\epsilon_0 a_0^3$	$\approx 1.648\,78 \times 10^{-41} \text{ J}^{-1} \text{ C}^2 \text{ m}^2$
<i>Electric displacement, D</i> <i>(Volume) polarization, P</i>		
SI unit	C m ⁻²	
esu, Gau	Fr cm ⁻²	$= (10^5/9) \text{ C m}^{-2} \approx 3.33564 \times 10^{-6} \text{ C m}^{-2}$
(But note: the use of the esu or Gaussian unit for electric displacement usually implies that the irrational displacement is being quoted, $D^{(\text{ir})} = 4\pi D$.)		
<i>Magnetic flux density, B</i> <i>(magnetic field)</i>		
tesla (SI unit)	T	$= \text{J A}^{-1} \text{ m}^{-2} = \text{V s m}^{-2} = \text{Wb m}^{-2}$
gauss (emu, Gau)	G	$= 10^{-4} \text{ T}$
au	\hbar/ea_0^2	$\approx 2.350\,52 \times 10^5 \text{ T}$
<i>Magnetic flux, ϕ</i>		
weber (SI unit)	Wb	$= \text{J A}^{-1} = \text{V s}$
maxwell (emu, Gau)	Mx	$= \text{G cm}^{-2} = 10^{-8} \text{ Wb}$
<i>Magnetic field, H</i> <i>(Volume) magnetization, M</i>		
SI unit	A m ⁻¹	$= \text{C s}^{-1} \text{ m}^{-1}$
oersted (emu, Gau)	Oe	$= 10^3 \text{ A m}^{-1}$
(But note: in practice the oersted, Oe, is only used as a unit for $H^{(\text{ir})} = 4\pi H$; thus when $H^{(\text{ir})} = 1 \text{ Oe}$, $H = (10^3/4\pi) \text{ A m}^{-1}$.)		

Name	Symbol	Relation to SI
<i>Magnetic dipole moment, m, μ</i>		
SI unit	A m^2	$= \text{J T}^{-1}$
emu, Gau	erg G^{-1}	$= 10 \text{ A cm}^2 = 10^{-3} \text{ J T}^{-1}$
Bohr magneton ^b	μ_{B}	$= e\hbar/2m_{\text{e}} \approx 9.274\,02 \times 10^{-24} \text{ J T}^{-1}$
au	$e\hbar/m_{\text{e}}$	$= 2\mu_{\text{B}} \approx 1.854\,80 \times 10^{-23} \text{ J T}^{-1}$
nuclear magneton	μ_{N}	$= (m_{\text{e}}/m_{\text{p}})\mu_{\text{B}} \approx 5.050\,79 \times 10^{-27} \text{ J T}^{-1}$
<i>Magnetizability, ξ</i>		
SI unit	J T^{-2}	$= \text{C}^2 \text{ m}^2 \text{ kg}^{-1}$
au	$e^2 a_0^2 / m_{\text{e}}$	$\approx 7.891\,04 \times 10^{-29} \text{ J T}^{-2}$
<i>Magnetic susceptibility, χ, κ</i>		
SI unit	1	
emu, Gau	1	
(But note: in practice susceptibilities quoted in the context of emu or Gaussian units are always values for $\chi^{(\text{ir})} = \chi/4\pi$; thus when $\chi^{(\text{ir})} = 10^{-6}$, $\chi = 4\pi \times 10^6$)		
<i>Molar magnetic susceptibility, χ^{m}</i>		
SI unit	$\text{m}^3 \text{ mol}^{-1}$	
emu, Gau	$\text{cm}^3 \text{ mol}^{-1}$	$= 10^{-6} \text{ cm}^3 \text{ mol}^{-1}$
(But note: in practice the units $\text{cm}^3 \text{ mol}^{-1}$ usually imply that the irrational molar susceptibility is being quoted, $\chi_{\text{m}}^{(\text{ir})} = \chi_{\text{m}}/4\pi$; for example if $\chi_{\text{m}}^{(\text{ir})} = -15 \times 10^{-6} \text{ cm}^3 \text{ mol}^{-1}$, which is often written as ‘ -15 cgs ppm ’, then $\chi_{\text{m}} = -1.88 \times 10^{-10} \text{ m}^3 \text{ mol}^{-1}$.)		

^aNote that the day is not exactly defined in terms of the second since so-called leap-seconds are added or subtracted from the day semiannually in order to keep the annual average occurrence of midnight at 24:00 on the clock.

^bThe year is not commensurable with the date and not a constant. Prior to 1967, when the atomic standard was introduced, the tropical year 1900 served as the basis for the definition of the second. For the epoch 1900.0, it amounted to $365.242\,198\,79 \text{ d} \approx 31\,556\,925.975 \text{ s}$ and it decreases by 0.530 seconds per century. The calendar years are exactly defined in terms of the day:

Julian year = 365.25 d

Gregorian year = 365.2425 d.

The definition in the table corresponds to the Gregorian year. This is an average based on a year of length 365 days, with leap years of 366 days; leap years are taken *either* when the year is divisible by 4 but is not divisible by 100, *or* when the year is divisible by 400.

^c1 N is approximately the force exerted by the earth upon an apple.

^d $T/^{\circ}\text{R} = (9/5)T/\text{K}$. Also, Celsius temperature θ is related to thermodynamic temperature T by the equation:

$$\theta/^{\circ}\text{C} = T/\text{K} - 273.15$$

Similarly Fahrenheit temperature θ_{F} is related to Celsius temperature θ by the equation:

$$\theta_{\text{F}}/^{\circ}\text{F} = (9/5)(\theta/^{\circ}\text{C}) + 32$$

^eThe name ‘amagat’ is unfortunately used as a unit for both molar volume and amount density. Its value is slightly different for different gases, reflecting the deviation from ideal behaviour for the gas being considered.

^fThe unit röntgen, employed to express exposure to X or γ radiations, is equal to: $\text{R} = 2.58 \times 10^{-4} \text{ C kg}^{-1}$.

^gThe units in quotation marks for electric potential through polarizability may be found in the literature, although they are strictly incorrect; they should be replaced in each case by the units given in the symbol column. Thus, for example, when a quadrupole moment is quoted in ‘ cm^2 ’, the correct unit is $e \text{ cm}^2$; and when a polarizability is quoted in ‘ \AA^3 ’, the correct unit is $4\pi\epsilon_0 \text{\AA}^3$.

^hThe Bohr magneton μ_{B} is sometimes denoted BM (or B.M.), but this is not recommended.

(Reprinted with permission from Mills I *et al.* (1993) *Quantities, Units and Symbols in Physical Chemistry*, 2nd edn. Oxford: Blackwell Scientific Publications.)

8. DEFINITIONS AND SYMBOLS FOR UNITS

The International System of Units (SI)

The International System of units (SI) was adopted by the 11th General Conference on Weights and Measures (CGPM) in 1960. It is a coherent system of units built from seven *SI base units*, one for each of the seven dimensionally independent base quantities: they are the metre, kilogram, second, ampere, kelvin, mole, and candela, for the dimensions length, mass, time, electric current, thermodynamic temperature, amount of substance, and luminous intensity, respectively. The *SI derived units* are expressed as products of powers of the base units, analogous to the corresponding relations between physical quantities but with numerical factors equal to unity.

In the International System there is only one SI unit for each physical quantity. This is either the appropriate SI base unit itself or the appropriate SI derived unit. However, any of the approved decimal prefixes, called *SI prefixes*, may be used to construct decimal multiples or submultiples of SI units.

It is recommended that only SI units be used in science and technology (with SI prefixes where appropriate). Where there are special reasons for making an exception to this rule, it is recommended always to define the units used in terms of SI units.

Definitions of the SI Base Units

Metre: The metre is the length of path travelled by light in vacuum during a time interval of $1/299\,792\,458$ of a second (17th CGPM, 1983).

Kilogram: The kilogram is the unit of mass; it is equal to the mass of the international prototype of the kilogram (3rd CGPM, 1901).

Second: The second is the duration of $9\,192\,631\,770$ periods of the radiation corresponding to the transition between the two hyperfine levels of the ground state of the caesium-133 atom (13th CGPM, 1967).

Ampere: The ampere is that constant current which, if maintained in two straight parallel conductors of infinite length, of negligible circular cross-section, and placed 1 metre apart in vacuum, would produce between these conductors a force equal to 2×10^{-7} newton per metre of length (9th CGPM, 1948).

Kelvin: The kelvin, unit of thermodynamic temperature, is the fraction $1/273.16$ of the thermodynamic temperature of the triple point of water (13th CGPM, 1967).

Mole: The mole is the amount of substance of a system which contains as many elementary entities as there are atoms in 0.012 kilogram of carbon-12. When the mole is used, the elementary entities must be specified and may be atoms, molecules, ions, electrons, other particles, or specified groups of such particles (14th CGPM, 1971).

Examples of the use of the mole

1 mol of H_2 contains about 6.022×10^{23} H_2 molecules, or 12.044×10^{23} H atoms

1 mol of HgCl has a mass of 236.04 g

1 mol of Hg_2Cl_2 has a mass of 472.08 g

1 mol of Hg_2^{2+} has a mass of 401.18 g and a charge of 192.97 kC

1 mol of $\text{Fe}_{0.91}\text{S}$ has a mass of 82.88 g

1 mol of e^- has a mass of 548.60 μm and a charge of -96.49 kC

1 mol of photons whose frequency is 5×10^{14} Hz has energy of about 199.5 kJ

Candela: The candela is the luminous intensity, in a given direction, of a source that emits monochromatic radiation of frequency 540×10^{12} hertz and that has a radiant intensity in that direction of $(1/683)$ watt per steradian (16th CGPM, 1979).

Names and Symbols for the SI Base Units

The symbols listed here are internationally agreed and should not be changed in other languages or scripts.

Physical quantity	Name of SI unit	Symbol for SI unit
Length	metre	m
Mass	kilogram	kg
Time	second	s
Electric current	ampere	A
Thermodynamic temperature	kelvin	K
Amount of substance	mole	mol
Luminous intensity	candela	cd

(Reprinted with permission from Mills I *et al.* (1993) *Quantities, Units and Symbols in Physical Chemistry*, 2nd edn. Oxford: Blackwell Scientific Publications.)

SI Derived Units with Special Names and Symbols

Physical quantity	Name of SI unit	Symbol for SI unit	Expression in terms of SI base units
Frequency ^a	hertz	Hz	s^{-1}
Force	newton	N	$m\ kg\ s^{-2}$
Pressure, stress	pascal	Pa	$N\ m^{-2} = m^{-1}\ kg\ s^{-2}$
Energy, work, heat	joule	J	$N\ m = m^2\ kg\ s^{-2}$
Power, radiant flux	watt	W	$J\ s^{-1} = m^2\ kg\ s^{-3}$
Electric charge	coulomb	C	As
Electric potential, electromotive force	volt	V	$J\ C^{-1} = m^2\ kg\ s^{-3}\ A^{-1}$
Electric resistance	ohm	Ω	$V\ A^{-1} = m^2\ kg\ s^{-3}\ A^{-2}$
Electric conductance	siemens	S	$\Omega^{-1} = m^{-2}\ kg^{-1}\ s^3\ A^2$
Electric capacitance	farad	F	$C\ V^{-1} = m^{-2}\ kg^{-1}\ s^4\ A^2$
Magnetic flux density	tesla	T	$V\ s\ m^{-2} = kg\ s^{-2}\ A^{-1}$
Magnetic flux	weber	Wb	$V\ s = m^2\ kg\ s^{-2}\ A^{-1}$
Inductance	henry	H	$V\ A^{-1}\ s = m^2\ kg\ s^{-2}\ A^{-2}$
Celsius temperature ^b	degree Celsius	$^{\circ}C$	K
Luminous flux	lumen	lm	cd sr
Illuminance	lux	lx	cd sr m^{-2}
Activity ^c (radioactive)	becquerel	Bq	s^{-1}
Absorbed dose ^c (of radiation)	gray	Gy	$J\ kg^{-1} = m^2\ s^{-2}$
Dose equivalent ^c (dose equivalent index)	sievert	Sv	$J\ kg^{-1} = m^2\ s^{-2}$
Plane angle ^d	radian	rad	1 $= m\ m^{-1}$
Solid angle ^d	steradian	sr	1 $= m^2\ m^{-2}$

^aFor radial (angular) frequency and for angular velocity the unit $rad\ s^{-1}$, or simply s^{-1} , should be used, and this may *not* be simplified to Hz. The unit Hz should be used *only* for frequency in the sense of cycles per second.

^bThe Celsius temperature θ is defined by the equation $\theta/^{\circ}C = T/K - 273.15$.

The SI unit of Celsius temperature is the degree Celsius, $^{\circ}C$, which is equal to the kelvin, K. $^{\circ}C$ should be treated as a single symbol, with no space between the $^{\circ}$ sign and the letter C. (The symbol $^{\circ}K$, and the symbol $^{\circ}$, should no longer be used).

^cThe units becquerel, gray and sievert are admitted for reasons of safeguarding human health.

^dThe units radian and steradian are described as 'SI supplementary units'. However, in chemistry, as well as in physics, they are usually treated as dimensionless derived units, and this was recognized by CIPM in 1980. Since they are then of dimension 1, this leaves open the possibility of including them or omitting them in expressions of SI derived units. In practice this means that rad and sr may be used when appropriate and may be omitted if clarity is not lost thereby.

(Reprinted with permission from Mills I *et al.* (1993) *Quantities, Units and Symbols in Physical Chemistry*, 2nd edn. Oxford: Blackwell Scientific Publications.)

SI Derived Units for Other Quantities

This table gives examples of other SI derived units; the list is merely illustrative.

Physical quantity	Expression in terms of SI base units	
Area	m^2	
volume	m^3	
Speed, velocity	m s^{-1}	
Angular velocity	s^{-1} , rad s^{-1}	
Acceleration	m s^{-2}	
Moment of force	N m	$= \text{m}^2 \text{kg s}^{-2}$
Wavenumber	m^{-1}	
Density, mass density	kg m^{-3}	
Specific volume	$\text{m}^3 \text{kg}^{-1}$	
Amount concentraion ^a	mol m^{-3}	
Molar volume	$\text{m}^3 \text{mol}^{-1}$	
Heat capacity, entropy	J K^{-1}	$= \text{m}^2 \text{kg s}^{-2} \text{K}^{-1}$
Molar heat capacity, molar entropy	$\text{J K}^{-1} \text{mol}^{-1}$	$= \text{m}^2 \text{kg s}^{-2} \text{K}^{-1} \text{mol}^{-1}$
Specific heat capacity, specific entropy	$\text{J K}^{-1} \text{kg}^{-1}$	$= \text{m}^2 \text{s}^{-2} \text{K}^{-1}$
Molar energy	J mol^{-1}	$= \text{m}^2 \text{kg s}^{-2} \text{mol}^{-1}$
Specific energy	J Kg^{-1}	$= \text{m}^2 \text{s}^{-2}$
Energy density	J m^{-3}	$= \text{m}^{-1} \text{kg s}^{-2}$
Surface tension	$\text{N m}^{-1} = \text{J m}^{-2}$	$= \text{kg s}^{-2}$
Heat flux density, irradiance	W m^{-2}	$= \text{kg s}^{-3}$
Thermal conductivity	$\text{W m}^{-1} \text{K}^{-1}$	$= \text{m kg s}^{-3} \text{K}^{-1}$
Kinematic viscosity, diffusion coefficient	$\text{m}^2 \text{s}^{-1}$	
Dynamic viscosity	$\text{N s m}^{-2} = \text{Pa s}$	$= \text{m}^{-1} \text{kg s}^{-1}$
Electric charge density	C m^{-3}	$= \text{m}^{-3} \text{s A}$
Electric current density	A m^{-2}	
Conductivity	S m^{-1}	$= \text{m}^{-3} \text{kg}^{-1} \text{s}^3 \text{A}^2$
Molar conductivity	$\text{S m}^2 \text{mol}^{-1}$	$= \text{kg}^{-1} \text{mol}^{-1} \text{s}^3 \text{A}^2$
Permittivity	F m^{-1}	$= \text{m}^{-3} \text{kg}^{-1} \text{s}^{-4} \text{A}^2$
Permeability	H m^{-1}	$= \text{m kg s}^{-2} \text{A}^{-2}$
Electric field strength	V m^{-1}	$= \text{m kg s}^{-3} \text{A}^{-1}$
Magnetic field strength	A m^{-1}	
Luminance	cd m^{-2}	
Exposure (X and γ rays)	C kg^{-1}	$= \text{kg}^{-1} \text{s A}$
Absorbed dose rate	Gy s^{-1}	$= \text{m}^2 \text{s}^{-3}$

^aThe words ‘amount concentration’ are an abbreviation for ‘amount-of-substance concentration’. When there is not likely to be any ambiguity this quantity may be called simply ‘concentration’.

(Reprinted with permission from Mills I *et al.* (1993) *Quantities, Units and Symbols in Physical Chemistry*, 2nd edn. Oxford: Blackwell Scientific Publications.)

SI Prefixes

To signify decimal multiples and submultiples of SI units the following prefixes may be used.

Submultiple	Prefix	Symbol	Multiple	Prefix	Symbol
10^{-1}	deci	d	10	deca	da
10^{-2}	centi	c	10^2	hecto	h
10^{-3}	milli	m	10^3	kilo	k
10^{-6}	micro	μ	10^6	mega	M
10^{-9}	nano	n	10^9	giga	G
10^{-12}	pico	p	10^{12}	tera	T

Submultiple	Prefix	Symbol	Multiple	Prefix	Symbol
10^{-15}	femto	f	10^{15}	peta	P
10^{-18}	atto	a	10^{18}	exa	E
10^{-21}	zepto	z	10^{21}	zetta	Z
10^{-24}	yocto	y	10^{24}	yotta	Y

(Reprinted with permission from Mills I *et al.* (1993) *Quantities, Units and Symbols in Physical Chemistry*, 2nd edn. Oxford: Blackwell Scientific Publications.)

Prefix symbols should be printed in roman (upright) type with no space between the prefix and the unit symbol.

Example kilometre, km

When a prefix is used with a unit symbol, the combination is taken as a new symbol that can be raised to any power without the use of parentheses.

Examples $1 \text{ cm}^3 = (0.01 \text{ m})^3 = 10^{-6} \text{ m}^3$
 $1 \mu\text{s}^{-1} = (10^{-6} \text{ s})^{-1} = 10^{-6} \text{ s}^{-1}$
 $1 \text{ V/cm} = 100 \text{ V/m}$
 $1 \text{ mmol/dm}^3 = 1 \text{ mol m}^{-3}$

A prefix should never be used on its own, and prefixes are not to be combined into compound prefixes.

Example pm, not $\mu\mu\text{m}$

The names and symbols of decimal multiples and submultiples of the SI base unit of mass, the kg, which already contains a prefix, are constructed by adding the appropriate prefix to the word gram and symbol g.

Examples mg, not μkg ; Mg, not kkg

The SI prefixes are not to be used with $^{\circ}\text{C}$.

ISO has recommended standard representations of the prefix symbols for use with limited character sets.

Units in Use Together with the SI

These units are not part of the SI, but it is recognized that they will continue to be used in appropriate contexts. SI prefixes may be attached to some of these units, such as millilitre, ml; millibar, mbar; megaelectronvolt, MeV; kilotonne, kt. A more extensive list of non-SI units, with conversion factors to the corresponding SI units, is given in the appendix, Conversion of Units.

Physical quantity	Name of unit	Symbol for unit	Value in SI units
Time	minute	min	60 s
Time	hour	h	3600 s
Time	day	d	86 400 s
Plane angle	degree	$^{\circ}$	$(\pi/180) \text{ rad}$
Plane angle	minute	'	$(\pi/10\,800) \text{ rad}$
Plane angle	second	"	$(\pi/648\,000) \text{ rad}$
Length	ångström ^a	Å	10^{-10} m
Area	barn	b	10^{-28} m^2
Volume	litre	l, L	$\text{dm}^3 = 10^{-3} \text{ m}^3$
Mass	tonne	t	$\text{Mg} = 10^3 \text{ kg}$
Pressure	bar ^a	bar	$10^5 \text{ Pa} = 10^5 \text{ N m}^{-2}$
Energy	electronvolt ^b	eV(= $e \times \text{V}$)	$\approx 1.60218 \times 10^{-19} \text{ J}$
Mass	unified atomic mass unit ^{b,c}	u(= $m_a(^{12}\text{C})/12$)	$\approx 1.66054 \times 10^{-27} \text{ kg}$

^aThe ångström and the bar are approved by CIPM for 'temporary use with SI units', until CIPM makes a further recommendation. However, they should not be introduced where they are not used at present.

^bThe values of these units in terms of the corresponding SI units are not exact, since they depend on the values of the physical constants e (for the electronvolt) and N_A (for the unified atomic mass unit), which are determined by experiment. See appendix, Fundamental Constants.

^cThe unified atomic mass unit is also sometimes called the dalton, with symbol Da, although the name and symbol have not been approved by CGPM.

(Reprinted with permission from Mills I *et al.* (1993) *Quantities, Units and Symbols in Physical Chemistry*, 2nd edn. Oxford: Blackwell Scientific Publications.)

Atomic Units

For the purposes of quantum mechanical calculations of electronic wavefunctions, it is convenient to regard certain fundamental constants (and combinations of such constants) as though they were units. They are customarily called *atomic units* (abbreviated: au), and they may be regarded as forming a coherent system of units for the calculation of electronic properties in theoretical chemistry, although there is no authority from CGPM for treating them as units. The first five atomic units in the table below have special names and symbols. Only four of these are independent; all others may be derived by multiplication and division in the usual way, and the table includes a number of examples.

The relation of atomic units to the corresponding SI units involves the values of the fundamental physical constants, and is therefore not exact. The numerical values in the table are based on the estimates of the appendix, Fundamental Constants. The numerical results of calculations in theoretical chemistry are frequently quoted in atomic units, or as numerical values in the form (*physical quantity*)/(*atomic unit*), so that the reader may make the conversion using the current best estimates of the physical constants.

Physical quantity	Name of unit	Symbol for unit	Value of unit in SI
mass	electron rest mass	m_e	$9.109\,3897\,(54) \times 10^{-31} \text{ kg}$
charge	elementary charge	e	$1.602\,177\,33\,(49) \times 10^{-19} \text{ C}$
action	Planck constant/ $2\pi^a$	\hbar	$1.054\,572\,66\,(63) \times 10^{-34} \text{ J s}$
length	bohr ^a	a_0	$5.291\,772\,49\,(24) \times 10^{-11} \text{ m}$
energy	hartree ^a	E_h	$4.359\,7482\,(26) \times 10^{-18} \text{ J}$
time		\hbar/E_h	$2.418\,884\,3341\,(29) \times 10^{-17} \text{ s}$
velocity ^b		$a_0 E_h/\hbar$	$2.187\,691\,42\,(10) \times 10^6 \text{ m s}^{-1}$
force		E_h/a_0	$8.238\,7295\,(25) \times 10^{-8} \text{ N}$
momentum, linear		\hbar/a_0	$1.992\,8534\,(12) \times 10^{-24} \text{ N s}$
electric current		$e E_h/\hbar$	$6.623\,6211\,(20) \times 10^{-3} \text{ A}$
electric field		E_h/ea_0	$5.142\,2082\,(15) \times 10^{11} \text{ V m}^{-1}$
electric dipole moment		ea_0	$8.478\,3579\,(26) \times 10^{-30} \text{ C m}$
magnetic flux density		\hbar/ea_0^2	$2.350\,518\,08\,(71) \times 10^5 \text{ T}$
magnetic dipole moment ^c		$e\hbar/m_e$	$1.854\,803\,08\,(62) \times 10^{-23} \text{ J T}^{-1}$

^a $\hbar = h/2\pi$; $a_0 = 4\pi\epsilon_0\hbar^2/m_e e^2$; $E_h = \hbar^2/m_e a_0^2$.

^bThe numerical value of the speed of light, when expressed in atomic units, is equal to the reciprocal of the fine structure constant α ; $c/(\text{au of velocity}) = \hbar/a_0 E_h = \alpha^{-1} \approx 137.035\,9895\,(61)$.

^cThe atomic unit of magnetic dipole moment is twice the Bohr magneton, μ_B .

(Reprinted with permission from Mills I *et al.* (1993) *Quantities, Units and Symbols in Physical Chemistry*, 2nd edn. Oxford: Blackwell Scientific Publications.)

Dimensionless Quantities

Values of dimensionless physical quantities, more properly called 'quantities of dimension one', are often expressed in terms of mathematically exactly defined values denoted by special symbols or abbreviations, such as % (per cent) and ppm (part per million). These symbols are then treated as units, and are used as such in calculations.

Fractions (Relative Values, Yields, Efficiencies)

Fractions such as relative uncertainty, mole fraction x (also called amount fraction, or number fraction), mass fraction w , and volume fraction ϕ , are sometimes expressed in terms of the symbols summarized in the table below.

Name	Symbol	Value	Examples
percent	%	10^{-2}	The isotopic abundance of carbon-13 expressed as a mole fraction is $x = 1.1\%$
part per million	ppm	10^{-6}	The relative uncertainty in the Planck constant $h (= 6.626\,0755(40) \times 10^{-34} \text{ J s})$ is 0.60 ppm The mass fraction of impurities in a sample of copper was found to be less than 3 ppm, $w < 3\text{ppm}$

(Reprinted with permission from Mills I *et al.* (1993) *Quantities, Units and Symbols in Physical Chemistry*, 2nd edn. Oxford: Blackwell Scientific Publications.)

These multiples of the unit one are not part of the SI and ISO recommends that these symbols should never be used. They are also frequently used as units of ‘concentration’ without a clear indication of the type of fraction implied (e.g. mole fraction, mass fraction or volume fraction). To avoid ambiguity they should only be used in a context where the meaning of the quantity is carefully defined. Even then, the use of an appropriate SI unit ratio may be preferred.

Deprecated Usage

Adding extra labels to ppm and similar symbols, such as ppmv (meaning ppm by volume) should be avoided. Qualifying labels may be added to symbols for physical quantities, but never to units.

The symbols % and ppm should not be used in combination with other units. In table headings and in labelling the axes of graphs the use of % and ppm in the denominator is to be avoided. Although one would write $x(^{13}\text{C}) = 1.1\%$, the notation $100x$ is to be preferred to $x/\%$ in tables and graphs.

The further symbols listed in the table below are also to be found in the literature, but their use is to be deprecated. Note that the names and symbols for 10^{-9} and 10^{-12} in this table are based on the American system of names. In other parts of the world a billion sometimes stands for 10^{12} and a trillion for 10^{18} . Note also that the symbol ppt is sometimes used for part per thousand, and sometimes for part per trillion.

To avoid ambiguity the symbols ppb, ppt and pphm should not be used.

Name	Symbol	Value	Examples
part per hundred	pph	10^{-2}	(Exactly equivalent to percent, %)
part per thousand	ppt	10^{-3}	Atmospheric carbon dioxide is depleted in carbon-13 mass fraction by 7‰ (or 7 ppt) relative to ocean water
permille ^a	‰	10^{-3}	
part per hundred million	pphm	10^{-8}	The mass fraction of impurity in the metal was less than 5 pphm
part per billion	ppb	10^{-9}	The air quality standard for ozone is a volume fraction of $\phi = 120 \text{ ppb}$
part per trillion	ppt	10^{-12}	The natural background volume fraction of NO in air was found to be $\phi = 140 \text{ ppt}$
part per quadrillion	ppq	10^{-15}	

^aThe permille is also spelled per mille, per mill, permil or pro mille.

(Reprinted with permission from Mills I *et al.* (1993) *Quantities, Units and Symbols in Physical Chemistry*, 2nd edn. Oxford: Blackwell Scientific Publications.)

9. FUNDAMENTAL PHYSICAL CONSTANTS

The following values were recommended by the CODATA Task Group on Fundamental Constants in 1986. For each constant the standard deviation uncertainty in the least significant digits is given in parentheses.

Quantity	Symbol	Value
Permeability of vacuum ^a	μ_0	$4\pi \times 10^{-7} \text{ H m}^{-1}$ (defined)
Speed of light in vacuum	c_0	$299\,792\,458 \text{ m s}^{-1}$ (defined)
Permittivity of vacuum ^a	$\varepsilon_0 = 1/\mu_0 c_0^2$	$8.854\,187\,816 \dots \times 10^{-12} \text{ F m}^{-1}$
Plank constant	h $\hbar = h/2\pi$	$6.626\,075\,5(40) \times 10^{-34} \text{ J s}$ $1.054\,572\,66(63) \times 10^{-34} \text{ J s}$
Elementary charge	e	$1.602\,177\,33(49) \times 10^{-19} \text{ C}$
Electron rest mass	m_e	$9.109\,389\,7(54) \times 10^{-31} \text{ kg}$
Proton rest mass	m_p	$1.672\,623\,1(10) \times 10^{-27} \text{ kg}$
Neutron rest mass	m_n	$1.674\,928\,6(10) \times 10^{-27} \text{ kg}$
Atomic mass constant, (unified atomic mass unit)	$m_u = 1 \text{ u}$	$1.660\,540\,2(10) \times 10^{-27} \text{ kg}$
Avogadro constant	L, N_A	$6.022\,136\,7(36) \times 10^{23} \text{ mol}^{-1}$
Boltzmann constant	K	$1.380\,658(12) \times 10^{-23} \text{ J K}^{-1}$
Faraday constant	F	$9.648\,530\,9(29) \times 10^4 \text{ C mol}^{-1}$
Gas constant	R	$8.314\,510(70) \text{ J K}^{-1} \text{ mol}^{-1}$
Zero of the Celsius scale		273.15 K (defined)
Molar volume, ideal gas, $p = 1 \text{ bar}$, $\theta = 0^\circ \text{C}$		$22.711\,08(19) \text{ l mol}^{-1}$
Standard atmosphere	atm	$101\,325 \text{ Pa}$ (defined)
Fine structure constant	$\alpha = \mu_0 e^2 c_0 / 2\hbar$ α^{-1}	$7.297\,353\,08(33) \times 10^{-3}$ $137.035\,989\,5(61)$
Bohr radius	$a_0 = 4\pi\varepsilon_0 \hbar^2 / m_e e^2$	$5.291\,772\,49(24) \times 10^{-11} \text{ m}$
Hartree energy	$E_h = \hbar^2 / m_e a_0^2$	$4.359\,748\,2(26) \times 10^{-18} \text{ J}$
Rydberg constant	$R_\infty = E_h / 2\hbar c_0$	$1.097\,373\,153\,4(13) \times 10^7 \text{ m}^{-1}$
Bohr magneton	$\mu_B = e\hbar / 2m_e$	$9.274\,0154(31) \times 10^{-24} \text{ J T}^{-1}$
Electron magnetic moment	μ_e	$9.284\,770\,1(31) \times 10^{-24} \text{ J T}^{-1}$
Landé g-factor for free electron	$g_e = 2\mu_e / \mu_B$	$2.002\,319\,304\,386(20)$
Nuclear magneton	$\mu_N = (m_e / m_p) \mu_B$	$5.050\,786\,6(17) \times 10^{-27} \text{ J T}^{-1}$
Proton magnetic moment	μ_p	$1.410\,607\,61(47) \times 10^{-26} \text{ J T}^{-1}$
Proton magnetogyric ratio	γ_p	$2.675\,221\,28(81) \times 10^8 \text{ s}^{-1} \text{ T}^{-1}$
Magnetic moment of protons in H_2O , μ'_p	μ'_p / μ_B	$1.520\,993\,129(17) \times 10^{-3}$
Proton resonance frequency per field in H_2O	$\gamma'_p / 2\pi$	$42.576\,375(13) \text{ MHz T}^{-1}$
Stefan-Boltzmann constant	$\sigma = 2\pi^5 k^4 / 15\hbar^3 c_0^2$	$5.670\,51(19) \times 10^{-8} \text{ W m}^{-2} \text{ K}^{-4}$
First radiation constant	$c_1 = 2\pi\hbar c_0^2$	$3.741\,7749(22) \times 10^{-16} \text{ W m}^2$
Second radiation constant	$c_2 = \hbar c_0 / k$	$1.438\,769(12) \times 10^{-2} \text{ m K}$
Gravitational constant	G	$6.672\,59(85) \times 10^{-11} \text{ m}^3 \text{ kg}^{-1} \text{ s}^{-2}$
Standard acceleration of free fall	g_n	$9.806\,65 \text{ m s}^{-2}$ (defined)

^a $\text{H m}^{-1} = \text{N A}^{-2} = \text{N s}^2 \text{ C}^{-2}$; $\text{F m}^{-1} = \text{C}^2 \text{ J}^{-1} \text{ m}^{-1}$; ε_0 may be calculated exactly from the defined values of μ_0 and c_0 .

(Reprinted with permission from Mills I *et al.* (1993) *Quantities, Units and Symbols in Physical Chemistry*, 2nd edn. Oxford: Blackwell Scientific Publications.)

Values of Common Mathematical Constants

Mathematical constant	Symbol	Value
Ratio of circumference to diameter of a circle	π	3.141 592 653 59
Base of natural logarithms	e	2.718 281 828 46
Natural logarithm of 10	ln 10	2.302 585 092 99

(Reprinted with permission from Mills I *et al.* (1993) *Quantities, Units and Symbols in Physical Chemistry*, 2nd edn. Oxford: Blackwell Scientific Publications.)

10. IMPORTANT PEAKS IN THE MASS SPECTRA OF COMMON SOLVENTS

The following table gives the most important peaks that appear in the mass spectra of the most common solvents which might occur as an impurity in organic samples. The solvents are classified in ascending order of their M^+ peaks. The highest intensity peaks are indicated with (100%).¹⁻³

Important peaks in the mass spectra of common solvents

Solvents	Formula	M^+	Important peaks (m/z)
Water	H ₂ O	18 (100%)	17
Methanol	CH ₃ OH	32	31 (100%), 29, 15
Acetonitrile	CH ₃ CN	41 (100%)	40, 39, 38, 28, 15
Ethanol	CH ₃ CH ₂ OH	46	45, 31 (100%), 27, 15
Dimethyl ether	CH ₃ OCH ₃	46 (100%)	45, 29, 15
Acetone	CH ₃ COCH ₃	58	43 (100%), 42, 39, 27, 15
Acetic acid	CH ₃ CO ₂ H	60	45, 43, 18, 15
Ethylene glycol	HOCH ₂ CH ₂ OH	62	43, 33, 31 (100%), 29, 18, 15
Furan	C ₄ H ₄ O	68 (100%)	42, 39, 38, 37, 29, 18
Tetrahydrofuran	C ₄ H ₈ O	72	71, 43, 42 (100%), 41, 40, 39, 27, 18, 15
<i>n</i> -Pentane	C ₅ H ₁₂	72	57, 43 (100%), 42, 41, 39, 29, 28, 27, 15
Dimethylformamide (DMF)	HCON(CH ₃) ₂	73 (100%)	58, 44, 42, 30, 29, 28, 18, 15
Diethyl ether	(C ₂ H ₅) ₂ O	74	59, 45, 41, 31 (100%), 29, 27, 15
Methyl acetate	CH ₃ CO ₂ CH ₃	74	59, 43 (100%), 42, 32, 29, 28, 15
Carbon disulphide	CS ₂	76 (100%)	64, 44, 38, 32
Benzene	C ₆ H ₆	78 (100%)	77, 52, 51, 50, 39, 28
Pyridine	C ₅ H ₅ N	79 (100%)	80, 78, 53, 52, 51, 50, 39, 26
Dichloromethane	CH ₂ Cl ₂	84	86, 51, 49 (100%), 48, 47, 35, 28
Cyclohexane	C ₆ H ₁₂	84	69, 56, 55, 43, 42, 41, 39, 27
<i>n</i> -Hexane	C ₆ H ₁₄	86	85, 71, 69, 57 (100%), 43, 42, 41, 39, 29, 28, 27
<i>p</i> -Dioxane	C ₄ H ₈ O ₂	88 (100%)	87, 58, 57, 45, 43, 31, 30, 29, 28
Tetramethylsilane (TMS)	(CH ₃) ₄ Si	88	74, 73, 55, 45, 43, 29
1,2-Dimethoxyethane	(CH ₃ OCH ₂) ₂	90	60, 58, 45 (100%), 31, 29
Toluene	C ₆ H ₅ CH ₃	92	91 (100%), 65, 51, 39, 28
Chloroform	CHCl ₃	118	120, 83, 81, (100%), 47, 35, 28
Chloroform-d ₁	CDCl ₃	119	121, 84, 82 (100%), 48, 47, 35, 28
Carbon tetrachloride	CCl ₄	152 (not seen)	121, 119, 117 (100%), 84, 82, 58.5, 47, 35, 28
Tetrachloroethene	CCl ₂ =CCl ₂	164 (not seen)	168, 166 (100%), 165, 164, 131, 128, 129, 95, 94, 82, 69, 59, 47, 31, 24

Reprinted from T.J. Bruno and P.D.N. Svoronos, *CRC Handbook of Basic Tables for Chemical Analysis*, CRC Press, Boca Raton, FL, 1989, p. 357.

References

1. Clerce, J. T., Pretsch, E., and Seibl, J., *Studies in Analytical Chemistry*, Vol. I. *Structural Analysis of Organic Compounds by Combined Application of Spectroscopic Methods*, Elsevier, Amsterdam, 1981.
2. McLafferty, F. W., *Interpretation of Mass Spectra*, University Science Books, Mill Valley, CA, 1980.
3. Pasto, D. J. and Johnson, C. R., *Organic Structure Determination*, Prentice-Hall, Englewood Cliffs, NJ, 1969.

11. NOMENCLATURE AND TERMINOLOGY FOR ANALYTICAL PYROLYSIS (IUPAC RECOMMENDATIONS 1993)

Prepared for publication by

P. C. Uden, University of Massachusetts, Amherst, MA, USA

© 1993 IUPAC

Abstract

This paper defines terms and definitions used in analytical methods of pyrolysis and includes expressions for coupled systems and for the description of the temperature profiles and the products that are obtained.

Introduction

Thermal degradation under controlled conditions is often used as part of an analytical procedure, either to render a sample into a suitable form for subsequent analysis by gas chromatography, mass spectrometry or infrared spectroscopy or by direct monitoring as an analytical technique in its own right. A range of terms and expression have been used in the field and this nomenclature brings these together in a systematic manner and assigns each a specific meaning.

Analytical Pyrolysis

Analytical Pyrolysis

The characterization, in an inert atmosphere, of a material or a chemical process by a chemical degradation reaction(s) induced by thermal energy.

Catalytic Pyrolysis

A pyrolysis that is influenced by the addition of a catalyst.

Char

A solid carbonaceous pyrolysis residue.

Coil Pyrolyser

A pyrolyser in which the sample (sometimes located in a tubular vessel) is placed in a metal coil that is heated to cause pyrolysis.

Continuous Mode (Furnace) Pyrolyser

A pyrolyser in which the sample is introduced into a furnace preheated to the final temperature.

Curie-Point Pyrolyser

A pyrolyser in which a ferromagnetic sample carrier is inductively heated to its Curie point.

Filament (Ribbon) Pyrolyser

A pyrolyser in which the sample is placed on a metal filament (ribbon) that is resistively heated to cause pyrolysis.

Final Pyrolysis Temperature ($T_{(f,Py)}$)

The final (steady state) temperature which is attained by a pyrolyser. (The terms 'equilibrium temperature' and 'pyrolysis temperature' may be used when referring to an isothermal pyrolysis; they are not recommended for use with a non-isothermal pyrolysis.)

Flash Pyrolysis

A pyrolysis that is carried out with a fast rate of temperature increase, of the order of 10 000 K/s.

Fractionated Pyrolysis

A pyrolysis in which the same sample is pyrolysed at different temperatures for different times in order to study special fractions of the sample.

In-Source Pyrolysis

A pyrolysis in which the reactor is located within the ion source of a mass spectrometer.

IR-Pyrogram

Chromatogram of a pyrolysate detected by infrared spectrometry.

Isothermal Pyrolysis

A pyrolysis during which the temperature is essentially constant.

Maximum Pyrolysis Temperature ($T_{(max,Py)}$)

The highest temperature in a temperature/time profile.

MS-Pyrogram

Chromatogram of a pyrolysate detected by mass spectrometry.

Off-Line Pyrolysis

A pyrolysis in which the products are trapped before analysis.

Oxidative Pyrolysis

A pyrolysis that occurs in the presence of an oxidative atmosphere.

Pressure Monitored Pyrolysis

A pyrolysis technique in which the pressure of the volatile pyrolysates is recorded as the sample is heated.

Pulse Mode Pyrolyser

A pyrolyser in which the sample is introduced into a cold furnace which is then heated rapidly.

Pyrogram

A chromatogram of a pyrolysate.

Pyrolysate (Pyrolyzate)

The products of pyrolysis.

Pyrolyser (Pyrolyzer)

A device for performing pyrolysis.

Pyrolysis

A chemical degradation reaction that is caused by thermal energy. The term *pyrolysis* generally refers to an inert environment.)

Pyrolysis-Gas Chromatography (Py-GC)

A pyrolysis technique in which the volatile pyrolysates are directly conducted into a gas chromatograph for separation and detection.

Pyrolysis-Gas Chromatograph-Mass Spectrometry (Py-GC-MS)

A pyrolysis technique in which the volatile pyrolysates are separated and analysed by on-line gas chromatography-mass spectrometry.

Pyrolysis-Gas Chromatography-Infrared Spectroscopy (Py-GC-IR)

A pyrolysis technique in which the volatile pyrolysates are separated and analysed by on-line gas chromatography-infrared spectroscopy.

Pyrolysis-Infrared Spectroscopy (Py-IR)

A pyrolysis technique in which the pyrolysates are detected and analysed by on-line infrared spectroscopy.

Pyrolysis-Infrared Spectrum

Infrared spectrum obtained from *pyrolysis-infrared spectroscopy*.

Pyrolysis-Mass Spectrometry (Py-MS)

A pyrolysis technique in which the volatile pyrolysates are detected and analysed by on-line mass spectrometry.

Pyrolysis-Mass Spectrum

Mass spectrum obtained from *pyrolysis-mass spectrometry*.

Pyrolysis Reactor

That portion of the pyrolyser in which the pyrolysis takes place.

Pyrolysis Residue

That portion of the pyrolysate that does not leave the reactor.

Pyrolysis Thermogram

The result of a temperature programmed pyrolysis in which the detector signals, e.g. total ion current or single ions, total absorbance or a GC-detector, are plotted against time or temperature.

Reductive Pyrolysis

A pyrolysis which occurs in the presence of a reducing atmosphere.

Sequential Pyrolysis

A pyrolysis in which the same initial sample is repetitively pyrolysed under identical conditions (final pyrolysis temperature, temperature rise time and total heating time).

Stepwise Pyrolysis

A pyrolysis in which the sample temperature is raised stepwise. The pyrolysis products are recorded between each step.

Tar

A liquid pyrolysis residue.

Temperature-Programmed Pyrolysis

A pyrolysis during which the sample is heated at a controlled rate within a temperature range in which pyrolysis occurs.

Temperature Rise Time (TRT)

The time required for a pyrolyser temperature to be increased from its initial to its final temperature.

Temperature Time Profile (TTP)

A graphical representation of temperature *versus* time for a particular pyrolysis experiment or pyrolyser.

Total heating time (THT)

The time between the onset and conclusion of the sample heating in a pyrolysis experiment.

Volatile Pyrolyzate

That portion of the pyrolystate which has adequate vapour pressure to reach the detector.

List of Symbols

$T_{(f,Py)}$	Final pyrolysis temperature
$T_{(max,Py)}$	Maximum pyrolysis temperature

Index of Acronyms

Py-GC	Pyrolysis-gas chromatography
Py-GC-IR	Pyrolysis-gas chromatography-infrared spectroscopy
Py-GC-MS	Pyrolysis-gas chromatography-mass spectrometry
Py-IR	Pyrolysis-infrared spectroscopy
Py-MS	Pyrolysis-mass spectrometry
THT	Total heating time
TRT	Temperature rise time
TTP	Temperature time profile

12A. NOMENCLATURE

Chromatography (IUPAC Recommendations 1993)

Prepared for publication by

L. S. Ettre, Yale University, New Haven, CT, USA

© 1993 IUPAC

Abstract

This report presents definitions of terms and symbols used in all chromatographic separations. The reports covers gas, liquid, size-exclusion, ion-exchange and supercritical-fluid chromatography and both column and planar modes of separation. Definitions are included for the description of the separation process, the chromatographic system and equipment and the properties of detectors.

Introduction

The Commission on Analytical Nomenclature of IUPAC has been active for a long time in establishing nomenclatures for chromatography. After proposing suitable nomenclatures for gas chromatography [1–2] and ion exchange [3–4] the Commission developed a unified nomenclature for chromatography [5–6]. Parallel to these activities other standardization bodies and scientists have also dealt with nomenclatures on gas chromatography [7–15], supercritical-fluid chromatography [16], liquid chromatography [17–20], exclusion chromatography [21–23] and planar chromatography [24].

The original activities of the IUPAC Commission on Analytical Nomenclature aimed to create a unified nomenclature applicable to all forms of chromatography, took place over 20 years ago. Since that time chromatographic techniques have advanced significantly. Based on these developments it was decided to prepare a new, up-to-date universal chromatography nomenclature, which also considers the recommendations incorporated in the various other nomenclatures developed since the original work of IUPAC.

The present nomenclature was prepared by Dr. L. S. Ettre originally for the Commission on Analytical Nomenclature. Following the reorganization of the Commissions of the Analytical Division at the General Assembly in Lund in 1989, this project became the responsibility of the Commission on Chromatography and Other Analytical Separations (LLTC). The Nomenclature considers all the previous nomenclatures referenced above as well as the four publications dealing with these nomenclatures [25–27].

The present nomenclature deals with all chromatographic terms and definitions used in the major chromatographic techniques such as gas, liquid and supercritical-fluid chromatography, column and planar chromatography, partition, adsorption, ion-exchange and exclusion chromatography. However, it does not include terms related to the results calculated from chromatography data such as e.g. the various molecular weight terms computed from the primary data obtained by exclusion chromatography. Also it does not deal with detailed information related to detection and detectors or the relationships between chemical structure and chromatographic retention.

General Rules

In developing the unified nomenclature the rules and recommendations set up by IUPAC's Division of Physical Chemistry [28] were followed. According to these, the following symbols should be used for major physical and physico-chemical quantities and units:

area	A
density	ρ
diameter	d
diffusion coefficient	D
equilibrium constant	K
mass (weight)	W
pressure	p or P
radius	r
rate constant	k
temperature (kelvin)	T
time	t
velocity	u
viscosity	η
volume	V

The only deviation from the rules set by the Division of Physical Chemistry of IUPAC is the use of L (instead of l) for length. The reason for this is the easy interchangeability in a printed, and particularly typed, text of the

letter l with the numeral 'one'. Additional basic symbols accepted were F for the volumetric flow rates and w for the peak widths. Also, differentiation has been made between p (for pressures) and P (for relative pressure).

In addition to these basic rules the following additional rules are followed in the present proposal:

- (a) Except for a few superscripts further differentiation is always made by using subscripts and never composite symbols.
- (b) Superscripts are used for various retention times and volumes and to specifically indicate data obtained in programmed-temperature conditions.
- (c) Subscripts referring to the physical conditions or the phase are capitalized, e.g. M and S for the mobile and stationary phases respectively, or, in gas chromatography, G for the gas and L for the liquid phase. Thus, e.g. the diffusion coefficient in the mobile phase is D_M and not D_m .
- (d) In addition to those mentioned above, a few capitalized subscripts are used such as R for 'retention' (as in t_R and V_R), N for 'net' (as in t_N and V_N) and F in R_F , the retardation factor used in planar chromatography.
- (e) Compound subscripts are avoided. If a given compound is indicated and there is already a subscript, and if the compound is characterized by more than a simple number or letter, then the new subscript should be in parentheses. Thus, while it is $t_{R,i}$, it should be $t_{R(st)}$ or $t_{R(z+1)}$.
- (f) In addition to reference to the outlet of a column, subscript 'o' is also used in a number of terms to describe some fundamental values. Similarly subscript 'i' has various meanings, depending on the term in which it is used.
- (g) Physical parts of the system are generally characterized by lower-case subscripts such as, c for column, p for particles or pores, and f for film.

Three tables follow the nomenclature, listing alphabetically the terms, symbols and acronyms included in the text.

Contents

1. General Terminology

- 1.1. Basic Definitions
- 1.2. Principal Methods
- 1.3. Classification According to the Shape of the Chromatographic Bed
- 1.4. Classification According to the Physical State of the Mobile Phase
- 1.5. Classification According to the Mechanism of Separation
- 1.6. Special Techniques

2. Terms Related to the Chromatographic System

- 2.1. Apparatus in Column Chromatography
- 2.2. Apparatus in Planar Chromatography

3. Terms Related to the Chromatographic Process and the Theory of Chromatography

- 3.1. The Chromatographic Medium
- 3.2. The Column
- 3.3. The Chromatogram
- 3.4. Diffusion
- 3.5. Temperatures
- 3.6. The Mobile Phase
- 3.7. Retention Parameters in Column Chromatography
- 3.8. Retention Parameters in Planar Chromatography
- 3.9. Distribution Constants
- 3.10. Terms Expressing the Efficiency of Separation

4. Terms Related to Detection

- 4.1. Classification of Detectors
- 4.2. Detector Response

- 4.3. Noise and Drift
- 4.4. Minimum Detectability
- 4.5. Linear and Dynamic Ranges

5. Special Terminology Used in Ion-exchange Chromatography

- 5.1. Basic Definitions
- 5.2. The Mobile Phase
- 5.3. The Chromatographic Medium
- 5.4. Capacity Values
- 5.5. Diffusion, Selectivity and Separation
- 5.6. Distribution Constants

6. Special Terminology Used in Exclusion Chromatography

- 6.1. The Column
- 6.2. Retention Parameters
- 6.3. Efficiency Terms

Tables

- 1. Index of Terms
- 2. List of Symbols
- 3. List of Acronyms Used in Chromatography

Figures

- 1. Typical Chromatograms
- 2. Typical Plane Chromatogram
- 3. Widths of the Gaussian Peak at Various Heights as a Function of the Standard Deviation of the Peak
- 4. Measurement of the Noise and Drift of a Chromatographic Detector
- 5. Linearity Plot of a Chromatographic Detector
- 6. Determination of the Linear and Dynamic Ranges of a Chromatographic Detector
- 7. Retention Characteristics in Exclusion Chromatography

1. General Terminology

1.1. Basic Definitions

1.1.01. Chromatography Chromatography is a physical method of separation in which the components to be separated are distributed between two phases, one of which is stationary (stationary phase) while the other (the mobile phase) moves in a definite direction.

1.1.02. Chromatogram A graphical or other presentation of detector response, concentration of analyte in the effluent or other quantity used as a measure of effluent concentration versus effluent volume or time. In planar chromatography “chromatogram” may refer to the paper or layer with the separated zones.

1.1.03. Chromatograph (verb) To separate by chromatography.

1.1.04. Chromatograph (noun) The assembly of apparatus for carrying out chromatographic separation.

1.1.05. Stationary phase The stationary phase is one of the two phases forming a chromatographic system. It may be a solid, a gel or a liquid. If a liquid, it may be distributed on a solid. This solid may or may not contribute to the separation process. The liquid may also be chemically bonded to the solid (*Bonded Phase*) or immobilized onto it (*Immobilized Phase*).

The expression *Chromatographic Bed* or *Sorbent* may be used as a general term to denote any of the different forms in which the stationary phase is used.

Note: Particularly in gas chromatography where the stationary phase is most often a liquid, the term *Liquid Phase* is used for it as compared to the *Gas Phase*, i.e. the mobile phase. However, particularly in the

early development of liquid chromatography, the term 'liquid phase' had also been used to characterize the mobile phase as compared to the 'solid phase' i.e. the stationary phase. Due to this ambiguity, the use of the term 'liquid phase' is discouraged. If the physical state of the stationary phase is to be expressed, the use of the adjective forms such as *Liquid Stationary Phase* and *Solid Stationary Phase*, *Bonded Phase* or *Immobilized Phase* is proposed.

1.1.05.1. Bonded phase A stationary phase which is covalently bonded to the support particles or to the inside wall of the column tubing.

1.1.05.2. Immobilized phase A stationary phase which is immobilized on the support particles, or on the inner wall of the column tubing, e.g. by *in situ* polymerization (cross-linking) after coating.

1.1.06. Mobile phase A fluid which percolates through or along the stationary bed, in a definite direction. It may be a liquid (*Liquid Chromatography*) or a gas (*Gas Chromatography*) or a supercritical fluid (*Supercritical-Fluid Chromatography*). In gas chromatography the expression *Carrier Gas* may be used for the mobile phase. In elution chromatography the expression *Eluent* is also used for the mobile phase.

1.1.07. Elute (verb) To chromatograph by elution chromatograph. The process of elution may be stopped while all the sample components are still on the chromatographic bed or continued until the components have left the chromatographic bed.

Note: The term 'elute' is preferred to the term *Develop* used in former nomenclatures of planar chromatography.

1.1.08. Effluent The mobile phase leaving the column.

1.1.09. Sample The mixture consisting of a number of components the separation of which is attempted on the chromatographic bed as they are carried or eluted by the mobile phase.

1.1.10. Sample components The chemically pure constituents of the sample. They may be unretained (i.e. not delayed) by the stationary phase, partially retained (i.e. eluted at different times) or retained permanently. The terms *Elute* or *Analyte* are also acceptable for a sample component.

1.1.11. Solute A term referring to the sample components in partition chromatography.

1.1.12. Solvent A term sometimes referring to the liquid stationary phase in partition chromatography.

Note: In liquid chromatography the term 'solvent' has been often used for the mobile phase. This usage is not recommended.

1.1.13. Zone A region in the chromatographic bed where one or more components of the sample are located. The term *Band* may also be used for it.

1.2. Principal Methods

1.2.01. Frontal chromatography A procedure in which the sample (liquid or gas) is fed continuously into the chromatographic bed. In frontal chromatography no additional mobile phase is used.

1.2.02. Displacement chromatography A procedure in which the mobile phase contains a compound (*the Displacer*) more strongly retained than the components of the sample under examination. The sample is fed into the system as a finite slug.

1.2.03. Elution chromatography A procedure in which the mobile phase is continuously passed through or along the chromatographic bed and the sample is fed into the system as a finite slug.

1.3. Classification According to the Shape of the Chromatographic Bed

1.3.01. Column chromatography A separation technique in which the stationary bed is within a tube. The particles of the solid stationary phase or the support coated with a liquid stationary phase may fill the whole inside volume of the tube (*Packed Column*) or be concentrated on or along the inside tube wall leaving an open, unrestricted path for the mobile phase in the middle part of the tube (*Open-Tubular Column*).

1.3.02. Planar chromatography A separation technique in which the stationary phase is present as or on a plane. The plane can be a paper, serving as such or impregnated by a substance as the stationary bed (*Paper Chromatography*, PC) or a layer of solid particles spread on a support, e.g. a glass plate (*Thin-Layer Chromatography*, TLC). Sometimes planar chromatography is also termed *Open-Bed Chromatography*.

1.4. Classification According to the Physical State of the Mobile Phase

1.4.01. Chromatographic techniques are often classified by specifying the physical state of *both* phases used. Accordingly, the following terms are in use:

Gas-liquid chromatography (GLC)
 Gas-solid chromatography (GSC)
 Liquid-Liquid chromatography (LLC)
 Liquid-solid chromatography (LSC)

The term *Gas-Liquid Partition Chromatography* (GLPC) can also be found in the literature. However, often distinction between these modes is not easy. For example, in GC, a liquid may be used to modify an adsorbent-type solid stationary phase.

1.4.02. Gas chromatography (GC) A separation technique in which the mobile phase is a gas. Gas chromatography is always carried out in a column.

1.4.03. Liquid chromatography (LC) A separation technique in which the mobile phase is a liquid. Liquid chromatography can be carried out either in a column or on a plane.

Note: Present-day liquid chromatography generally utilizing very small particles and a relatively high inlet pressure is often characterized by the term *High-Performance* (or *High-Pressure*) *Liquid Chromatography*, and the acronym HPLC.

1.4.04. Supercritical-fluid chromatography (SFC) A separation technique in which the mobile phase is a fluid above and relatively close to its critical temperature and pressure.

Note: In general the terms and definitions used in gas or liquid chromatography are equally applicable to supercritical-fluid chromatography.

1.5. Classification According to the Mechanism of Separation

1.5.01. Adsorption chromatography Separation is based mainly on differences between the adsorption affinities of the sample components for the surface of an active solid.

1.5.02. Partition chromatography Separation is based mainly on differences between the solubilities of the sample components in the stationary phase (gas chromatography), or on differences between the solubilities of the components in the mobile and stationary phases (liquid chromatography).

1.5.03. Ion-exchange chromatography Separation is based mainly on differences in the ion exchange affinities of the sample components.

Note: Present day ion-exchange chromatography on small particle high efficiency columns and usually utilising conductometric or spectroscopic detectors is often referred to as *Ion Chromatography* (IC).

1.5.04. Exclusion chromatography Separation is based mainly on exclusion effects, such as differences in molecular size and/or shape or in charge. The term *Size-Exclusion Chromatography* may also be used when separation is based on molecular size. The terms *Gel Filtration* and *Gel-Permeation Chromatography* (GPC) were used earlier to describe this process when the stationary phase is a swollen gel. The term *Ion-Exclusion Chromatography* is specifically used for the separation of ions in an aqueous phase.

1.5.05. Affinity chromatography This expression characterizes the particular variant of chromatography in which the unique biological specificity of the analyte and ligand interaction is utilized for the separation.

1.6. Special Techniques

1.6.01. Reversed-phase chromatography An elution procedure used in liquid chromatography in which the mobile phase is significantly more polar than the stationary phase, e.g. a microporous silica-based material with chemically bonded alkyl chains.

Note: The term “reverse phase” is an incorrect expression to be avoided.

1.6.02. Normal-phase chromatography An elution procedure in which the stationary phase is more polar than the mobile phase. This term is used in liquid chromatography to emphasize the contrast to reversed-phase chromatography.

1.6.03. Isocratic analysis The procedure in which the composition of the mobile phase remains constant during the elution process.

1.6.04. Gradient elution The procedure in which the composition of the mobile phase is changed continuously or stepwise during the elution process.

1.6.05. Stepwise elution The elution process in which the composition of the mobile phase is changed in steps during a single chromatographic run.

1.6.06. Two-dimensional chromatography A procedure in which parts or all of the separated sample components are subjected to additional separation steps. This can be done, e.g. by conducting a particular fraction eluting from the column into another column (system) having different separation characteristics. When combined with additional separation steps, this may be described as *Multi-Dimensional Chromatography*.

In planar chromatography two-dimensional chromatography refers to the chromatographic process in which the components are caused to migrate first in one direction and subsequently in a direction at right angles to the first one; the two elutions are carried out with different eluents.

1.6.07. Isothermal chromatography A procedure in which the temperature of the column is kept constant during the separation.

1.6.08. Programmed-temperature chromatography (temperature programming) A procedure in which the temperature of the column is changed systematically during a part or the whole of the separation.

1.6.09. Programmed-flow chromatography (flow programming) A procedure in which the rate of flow of the mobile phase is changed systematically during a part or the whole of the separation.

1.6.10. Programmed-pressure chromatography (pressure programming) A procedure in which the inlet pressure of the mobile phase is changed systematically during a part or whole of the separation.

1.6.11. Reaction chromatography A technique in which the identities of the sample components are intentionally changed between sample introduction and detection. The reaction can take place upstream of the column when the chemical identity of the individual components passing through the column differs from that of the original sample, or between the column and the detector when the original sample components are separated in the column but their identity is changed prior to entering the detection device.

1.6.11.1. Pyrolysis-gas chromatography A version of reaction chromatography in which a sample is thermally decomposed to simpler fragments before entering the column.

1.6.11.2. Post-column derivatization A version of reaction chromatography in which the separated sample components eluting from the column are derivatized prior to entering the detector. The derivatization process is generally carried out “on-the-fly”, i.e. during transfer of the sample components from the column to the detector. Derivatization may also be carried out before the sample enters the column or the planar medium; this is *pre-column (preliminary) derivatization*.

2. Terms Related to the Chromatographic System

2.1. Apparatus in Column Chromatography

2.1.01. Pump A device designed to deliver the mobile phase at a controlled flow-rate to the separation system. Pumps are generally used in liquid chromatography.

2.1.01.1. Syringe pumps Pumps with a piston, which advances at a controlled rate within a smooth cylinder to displace the mobile phase.

2.1.01.2. Reciprocating pumps Pumps with a single or multiple chamber, from which the mobile phase is displaced by reciprocating piston(s) or diaphragm(s).

2.1.01.3. Pneumatic pumps Pumps which employ a gas to displace the liquid mobile phase either directly or via a piston.

2.1.02. Sample injector A device by which a liquid, solid or gaseous sample is introduced into the mobile phase of the chromatographic bed.

2.1.02.1. Direct injector A device which directly introduces the sample into the mobile-phase stream.

2.1.02.2. Bypass injector A device in which the sample is first introduced into a chamber (loop), temporarily isolated from the mobile phase system by valves, which can be switched to make an instantaneous diversion of the mobile phase stream through the chamber to carry the sample to the column. A bypass injector may also be known as a *Valve Injector* or *Sampling Valve* (see 2.1.02.7).

2.1.02.3. On-column injector A device in which the sample is directly introduced into the column. In gas chromatography the on-column injector permits the introduction of the liquid sample into the column without prior evaporation.

2.1.02.4. Flash vaporizer A heated device used in gas chromatography. Here the liquid sample is introduced into the carrier gas stream with simultaneous evaporation and mixing with the carrier gas prior to entering the column.

2.1.02.5. Split injection A sample introduction technique used in gas chromatography. The sample is flash vaporized and after thorough mixing of the sample with carrier gas, the stream is split into two portions, one being conducted to the column and the other being discarded.

2.1.02.6. Programmed temperature vaporizer (PTV) A sample introduction device used in gas chromatography. The liquid sample is introduced, usually with a syringe, into a device similar to a flash vaporizer, the temperature of which is kept low, below the boiling point of the sample components. After withdrawal of the syringe, the device is heated up very rapidly in a controlled fashion to evaporate the sample into the continuously flowing carrier gas stream. The PTV may also be used in the split mode: in this case, the carrier gas stream containing the evaporated sample components is split into two portions, one of which is conducted into the column while the other is discarded.

2.1.02.7. Gas sampling valve A bypass injector permitting the introduction of a gaseous sample of a given volume into a gas chromatograph.

2.1.03. Column oven A thermostatically controlled oven containing the column, the temperature of which (*Separation Temperature* or *Column Temperature*) can be varied within a wide range.

2.1.04. Fraction collector A device for recovering fractional volumes of the column effluent.

2.1.05. Detector A device that measures the change in the composition of the eluent by measuring physical or chemical properties.

2.2. Apparatus in Planar Chromatography

2.2.01. Spotting device The syringe or micropipet used to deliver a fixed volume of sample as a spot or streak to the paper or thin-layer media at the origin.

2.2.02. Elution chamber (developing chamber) A closed container, the purpose of which is to enclose the media used as well as the mobile phase to maintain a constant environment in the vapor phase.

2.2.02.1. Sandwich chamber A chamber in which the walls are close enough to the paper or plate to provide a relatively fast equilibration.

2.2.02.2. Ascending elution (ascending development) A mode of operation in which the paper or plate is in a vertical or slanted position and the mobile phase is supplied to its lower edge; the upward movement depends on capillary action.

2.2.02.3. Horizontal elution (horizontal development) A mode of operation in which the paper or plate is in a horizontal position and the mobile-phase movement along the plane depends on capillary action.

2.2.02.4. Descending elution (descending development) A mode of operation in which the mobile phase is supplied to the upper edge of the paper or plate and the downward movement is governed mainly by gravity.

2.2.02.5. Radial elution (radial development) or circular elution (circular development) A mode of operation in which the sample is spotted at a point source at or near the middle of the plane and is carried outward in a circle by the mobile phase, also applied at that place.

2.2.02.6. Anticircular elution (anticircular development) The opposite of 2.2.02.5. Here the sample as well as the mobile phase is applied at the periphery of a circle and both move towards the center.

2.2.02.7. Chamber saturation (saturated development) This expression refers to the uniform distribution of the mobile phase vapor through the elution chamber prior to chromatography.

2.2.02.8. Unsaturated elution (unsaturated development) This expression refers to chromatography in an elution chamber without attaining chamber saturation.

2.2.02.9. Equilibration The expression refers to the level of saturation of the chromatographic bed by the mobile-phase vapor prior to chromatography.

2.2.03. Visualization chamber A device in which the planar media may be viewed under controlled-wavelength light, perhaps after spraying with chemical reagents to render the separated components as visible spots under specified conditions.

2.2.04. Densitometer A device which allows portions of the developed paper or thin-layer media to be scanned with a beam of light of a specified wavelength for measurements of UV or visible light absorption or fluorescence, providing values which can be used for the quantisation of the separated compounds.

3. Terms Related to the Chromatographic Process and the Theory of Chromatography

3.1. The Chromatographic Medium

3.1.01. **Active solid** A solid with sorptive properties.

3.1.02. **Modified active solid** An active solid the sorptive properties of which have been changed by some treatment.

3.1.03. **Solid support** A solid that holds the stationary phase but, ideally, does not contribute to the separation process.

3.1.04. **Binders** Additives used to hold the solid stationary phase to the inactive plate or sheet in thin-layer chromatography.

3.1.05. **Gradient layer** The chromatographic bed used in thin-layer chromatography in which there is a gradual transition in some property.

3.1.06. **Impregnation** The modification of the separation properties of the chromatographic bed used in planar chromatography by appropriate additives.

3.1.07. **Packing** The active solid, stationary liquid plus solid support, or swollen gel contained in a tube.

3.1.07.1. *Totally porous packing* Here the stationary phase permeates each porous particle.

3.1.07.2. *Pellicular packing* In this case the stationary phase forms a porous outer shell on an impermeable particle.

3.1.08. **Particle diameter (d_p)** The average diameter of the solid particles.

3.1.09. **Pore radius (r_p)** The average radius of the pores within the solid particles.

3.1.10. **Liquid-phase loading** A term used in partition chromatography to express the relative amount of the liquid stationary phase in the column packing. It is equal to the mass fraction (%) of liquid stationary phase in the total packing (liquid stationary phase plus support).

3.2. The Column

3.2.01. **Column** The tube and the stationary phase contained within, through which the mobile phase passes.

3.2.02. **Packed column** A tube containing a solid packing.

3.2.03. **Open-tubular column** A column, usually having a small diameter in which either the inner tube wall, or a liquid or active solid held stationary on the tube wall acts as the stationary phase and there is an open, unrestricted path for the mobile phase.

3.2.03.1. *Wall-coated open-tubular (WCOT) column* In these columns the liquid stationary phase is coated on the essentially unmodified smooth inner wall of the tube.

3.2.03.2. *Porous-layer open-tubular (PLOT) column* In these columns there is a porous layer on the inner wall. Porosity can be achieved by either chemical means (e.g. etching) or by the deposition of porous particles on the wall from a suspension. The porous layer may serve as a support for a liquid stationary phase or as the stationary phase itself.

3.2.03.3. Support-coated open-tubular (SCOT) column A version of a PLOT column in which the porous layer consists of support particles and was deposited from a suspension.

3.2.04. Capillary column A general term for columns having a small diameter. A capillary column may contain a packing or have the stationary phase supported on its inside wall. The former case corresponds to a *Packed Capillary Column* while the latter case corresponds to an *Open-Tubular Column*. Due to the ambiguity of this term its use without an adjective is discouraged.

3.2.05. Column volume (V_c) The geometric volume of the part of the tube that contains the packing:

$$V_c = A_c L$$

where A_c is the internal cross-sectional area of the tube and L is the length of the packed part of the column.

In the case of wall-coated open-tubular columns the column volume corresponds to the geometric volume of the whole tube having a liquid or a solid stationary phase on its wall.

3.2.06. Bed volume Synonymous with *Column Volume* for a packed column.

3.2.07. Column diameter (d_c) The inner diameter of the tubing.

3.2.08. Column radius (r_c) The inside radius of the tubing.

3.2.09. Column length (L) The length of that part of the tube which contains the stationary phase.

3.2.10. Cross-sectional area of the column (A_c) The cross-sectional area of the empty tube:

$$A_c = \pi r_c^2 = \pi (d_c/2)^2$$

3.2.11. Interparticle volume of the column (V_o) The volume occupied by the mobile phase between the particles in the packed section of a column. It is also called the *Interstitial Volume* or the *Void Volume* of the column.

3.2.11.1. In liquid chromatography, the interparticle volume is equal to the mobile-phase hold-up volume (V_M) in the ideal case, neglecting any extra-column volume.

3.2.11.2. In gas chromatography, the symbol V_G may be used for the interparticle volume of the column. In the ideal case, neglecting any extra-column volume, V_G is equal to the corrected gas hold-up volume (V_M^o) (see 3.6.03 and 3.7.04):

$$V_G = V_M^o = V_M \cdot j$$

3.2.12. Interparticle porosity (ε) The interparticle volume of a packed column per unit column volume:

$$\varepsilon = V_o/V_c$$

It is also called the *Interstitial Fraction* of the column.

3.2.13. Extra-column volume The volume between the effective injection point and the effective detection point, excluding the part of the column containing the stationary phase. It is composed of the volumes of the injector, connecting lines and detector.

3.2.13.1. Dead-volume This term is also used to express the extra-column volume. Strictly speaking, the term “dead-volume” refers to volumes within the chromatographic system which are not swept by the mobile phase. On the other hand, mobile phase is flowing through most of the extra-column volumes. Due to this ambiguity the use of the term “dead-volume” is discouraged.

3.2.14. Liquid-phase film thickness (d_f) A term used in connection with open-tubular columns to express the average thickness of the liquid stationary phase film coated on the inside wall of the tubing.

3.2.15. Stationary-phase volume (V_s) The volume of the liquid stationary phase or the active solid in the column. The volume of any solid support is not included. In the case of partition chromatography with a liquid stationary phase, it is identical to the *Liquid-Phase Volume* (V_L).

3.2.16. Mass (weight) of the stationary phase (W_s) The mass (weight) of the liquid stationary phase or the active solid in the column. The mass (weight) of any solid support is not included. In the case of partition chromatography with a liquid stationary phase it is identical to the *Liquid Phase Mass (Weight)* (W_L).

3.2.17. Phase ratio (β) The ratio of the volume of the mobile phase to that of the stationary phase in a column:

$$\beta = V_o/V_s$$

In the case of open-tubular columns the geometric internal volume of the tube (V_c) is to be substituted for V_o .

3.2.18. Specific permeability (B_o) A term expressing the resistance of an empty tube or packed column to the flow of a fluid (the mobile phase). In the case of a packed column

$$B_o = \frac{d_p^2 \varepsilon^3}{180(1 - \varepsilon)^2} \approx \frac{d_p^2}{1000}$$

In the case of an open-tubular column

$$B_o = \frac{r_c^2}{8}$$

3.2.19. Flow resistance parameter (Φ) This term is used to compare packing density and permeability of columns packed with different particles; it is dimensionless.

$$\Phi = d_p^2/B_o$$

where d_p is the average particle diameter. In open-tubular columns $\Phi = 32$.

3.3. The Chromatogram

3.3.01. Differential chromatogram A chromatogram obtained with a differential detector (see Figure 1A).

3.3.02. Integral chromatogram A chromatogram obtained with an integral detector (see Figure 1B).

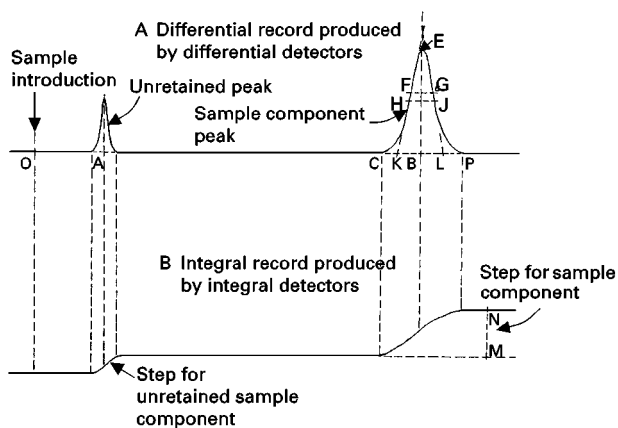


Figure 1 Typical chromatogram: A, differential record produced by differential detector; B, integral record produced by integral detector.

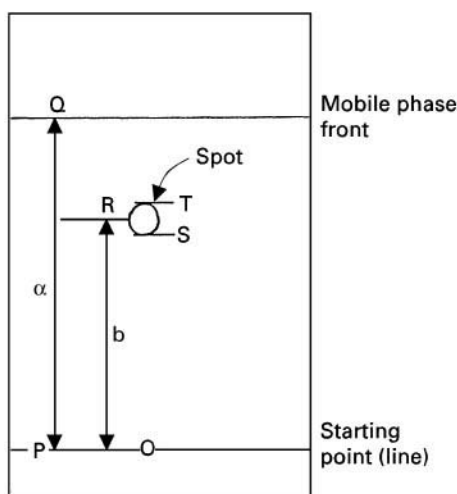


Figure 2 Typical planar chromatogram.

3.3.03. Starting point or line The point or line on a chromatographic paper or layer where the substance to be chromatographed is applied (P in Figure 2).

3.3.04. Spot A zone in paper and thin-layer chromatography of approximately circular appearance.

3.3.04.1. Spot diameter (ST in Figure 2) The width of the sample component spot before or after chromatography.

3.3.05. Baseline The portion of the chromatogram recording the detector response when only the mobile phase emerges from the column.

3.3.06. Peak The portion of a differential chromatogram recording the detector response when a single component is eluted from the column (see Figure 1A). If separation is incomplete, two or more components may be eluted as one *Unresolved Peak*.

3.3.06.1. Peak base (CP in Figure 1A) The interpolation of the baseline between the extremities of the peak.

3.3.06.2. Peak area (CHFEGJP in Figure 1A) The area enclosed between the peak and the peak base.

3.3.06.3. Peak maximum (E in Figure 1A) The point on the peak at which the distance to the peak base, measured in a direction parallel to the axis representing detector response, is a maximum.

3.3.06.4. Peak height (EB in Figure 1A) The distance between the peak maximum and the peak base, measured in a direction parallel to the axis representing detector response.

3.3.06.5. Standard deviation (σ) The term in the exponent of the equation relating the width and height of a Gaussian peak:

$$y = y_o \cdot \exp. - \left[\frac{x^2}{2\sigma^2} \right]$$

where y is the peak height at any point on the peak, y_o is the peak height at maximum, x is the distance from the ordinate (i.e. half of the width at that point), and σ is the standard deviation of the peak. In practice, the standard deviation can be calculated from one of the peak-width values specified below.

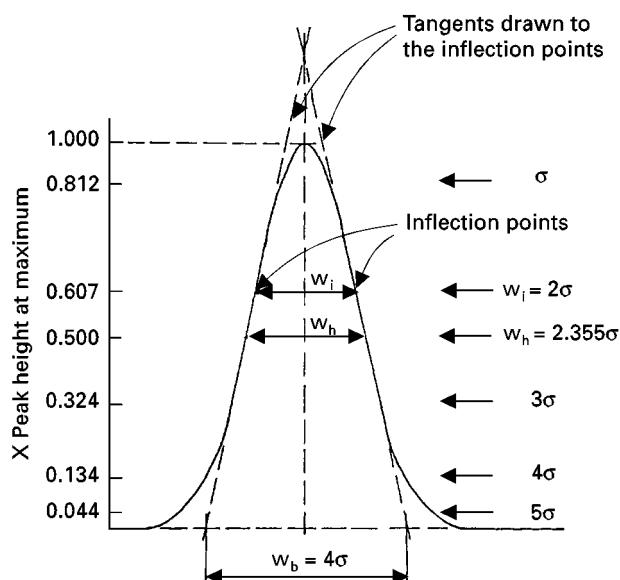


Figure 3 Widths of a Gaussian peak at various heights, as a function of the standard deviation of the peak.

3.3.06.6. *Variance of the peak* The square of the standard deviation (σ^2).

3.3.07. **Peak-widths** Peak-widths represent retention dimensions (time or volume) parallel to the baseline. If the baseline is not parallel to the axis representing time or volume, then the peak-widths are to be drawn parallel to this axis. Three peak-width values are commonly used in chromatography (see Figure 1A and Figure 3).

3.3.07.1. *Peak-width at base (w_b)* (KL in Figure 1A and Figure 3) The segment of the peak base intercepted by the tangents drawn to the inflection points on either side of the peak.

3.3.07.2. *Peak-width at half height (w_h)* (HJ in Figure 1A and Figure 3) The length of the line parallel to the peak base at 50% of the peak height that terminates at the intersection with the two limbs of the peak

Note: The peak-width at base (w_b) may be called the 'base width'. However, the peak width at half height (w_h) must never be called the 'half width' because that has a completely different meaning. Also, the symbol $w_{1/2}$ should never be used instead of w_h .

3.3.07.3. *Peak-width at inflection points (w_i)* (FG in Figure 1A and Figure 3) The length of the line drawn between the inflection points parallel to the peak base.

3.3.07.4. In the case of Gaussian (symmetrical) peaks, the peak-widths are related to the standard deviation (σ) of the peak according to the following equations:

$$w_b = 4\sigma$$

$$w_h = 2\sigma\sqrt{(2 \ln 2)} = 2.355\sigma$$

$$w_i = 2\sigma$$

3.3.08. **Tailing** Asymmetry of a peak such that, relative to the baseline, the front is steeper than the rear. In paper chromatography and thin-layer chromatography, it refers to the distortion of a spot showing a diffuse region behind the spot in the direction of flow.

3.3.09. Fronting Asymmetry of a peak such that, relative to the baseline, the front is less steep than the rear. In paper chromatography and thin-layer chromatography, it refers to the distortion of a spot, showing a diffuse region in front of the spot in the direction of flow.

3.3.10. Step The portion of an integral chromatogram recording the amount of a component, or the corresponding change in the signal from the detector as the component emerges from the column (see Figure 1B).

3.3.10.1. Step height (NM in Figure 1B) The distance, measured in the direction of detector response, between straight-line extensions of the baselines on both sides of a step.

3.3.11. Internal standard A compound added to a sample in known concentration to facilitate the qualitative identification and/or quantitative determination of the sample components.

3.3.12. External standard A compound present in a standard sample of known concentration and volume which is analysed separately from the unknown sample under identical conditions. It is used to facilitate the qualitative identification and/or quantitative determination of the sample components. The volume of the external standard (standard sample) need not to be known if it is identical to that of the unknown sample.

3.3.13. Marker A reference substance chromatographed with the sample to assist in identifying the components.

3.4. Diffusion

3.4.01. The diffusion coefficient (D) is the amount of a particular substance that diffuses across a unit area in 1 s under the influence of a gradient of one unit.

It is usually expressed in the units $\text{cm}^2 \text{s}^{-1}$.

3.4.02. Diffusion coefficient in the stationary phase (D_s or D_L) The diffusion coefficient characterizing the diffusion in the stationary phase. In partition chromatography with a liquid stationary phase, the symbol D_L may be used to express this term.

3.4.03. Diffusion coefficient in the mobile phase (D_M or D_G) The diffusion coefficient characterizing the diffusion in the mobile phase. In gas chromatography where the mobile phase is a gas, the symbol D_G may be used to express this term.

3.4.04. Diffusion velocity (u_D) This term is used in liquid chromatography in the expression of the reduced mobile-phase velocity (see 3.6.05.3). The diffusion velocity expresses the speed of diffusion into the pores of the particles:

$$u_D = D_M/d_p$$

3.5. Temperatures

3.5.01. Ambient temperature (T_a) The temperature outside the chromatographic system.

3.5.02. Injection temperature The temperature within the injection device.

3.5.03. Separation temperature (T_c) The temperature of the chromatographic bed under isothermal operation. In column chromatography it is called the *Column Temperature*.

3.5.04. Temperatures during programmed-temperature analysis

3.5.04.1. Initial temperature The temperature of the chromatographic bed (column) at the start of the analysis. Temperature programming might start immediately upon sample introduction or it can be preceded by a short isothermal period (*Initial Isothermal Temperature*). In the case, the time of the *Initial Isothermal Period* must also be specified.

3.5.04.2. *Program rate* The rate of increase of column temperature. The rate of temperature increase is usually linear ($^{\circ}\text{C}.\text{min}^{-1}$) but it may also be non-linear. During one analysis the temperature rate may be changed and/or the temperature programming may be interrupted by an isothermal period. In this case one is speaking about *Multiple Programming*. In multiple programming each program must be specified by its initial and final temperatures and program rate.

3.5.04.3. *Mid-analysis isothermal temperature* The temperature of the column in an isothermal period during elution. The corresponding time (*Mid-Analysis Isothermal Period*) must also be specified.

3.5.04.4. *Final temperature* The highest temperature to which the column is programmed.

3.5.04.5. *Final isothermal temperature* The final temperature of the program if it is followed by an isothermal period. The time corresponding to the *Final Isothermal Period* must also be specified.

3.5.04.6. *Retention temperature* The column temperature corresponding to the peak maximum.

3.5.05. **Detector temperature** The temperature of the detector cell. In the case of a detector incorporating a flame, it refers to the temperature of the detector base.

3.6. The Mobile Phase

3.6.01. **Mobile phase viscosity (η)** The viscosity of the mobile phase at the temperature of the chromatographic bed.

3.6.02. Pressures

3.6.02.1. *Inlet pressure (p_i)* The *absolute* pressure at the inlet of a chromatographic column.

3.6.02.2. *Outlet pressure (p_o)* The absolute pressure at the exit of a chromatographic column. It is usually but not necessarily equal to the *Ambient Pressure (p_a)*, the atmospheric pressure outside the chromatographic system.

3.6.02.3. *Pressure drop (Δp)* The difference between the inlet and outlet pressures:

$$\Delta p = p_i - p_o$$

3.6.02.4. *Relative pressure (P)* The ratio of the inlet and outlet pressures:

$$P = p_i/p_o$$

3.6.03. **Mobile phase compressibility correction factor (j)** A factor, applying to a homogeneously filled column of uniform diameter, that corrects for the compressibility of the mobile phase in the column. It is also called the *Compressibility Correction Factor*. In gas chromatography, the correction factor can be calculated as:

$$j = \frac{3}{2} \frac{p^2 - 1}{p^3 - 1} = \frac{3}{2} \frac{(p_i/p_o)^2 - 1}{(p_i/p_o)^3 - 1}$$

In liquid chromatography the compressibility of the mobile phase is negligible.

Note: In former nomenclatures the term 'pressure gradient correction factor' was sometimes used to express the same term. This is, however, an incorrect name, because it is not the pressure gradient but the compression of the mobile phase which necessitates the use of this factor. In liquid chromatography, where mobile phase compression is negligible, no correction factor has to be applied to the mobile phase velocity; however, there is still a pressure gradient along the column.

3.6.04. Flow rate The volume of mobile phase passing through the column in unit time.

3.6.04.1. The flow rate is usually measured at the column outlet, at ambient pressure (p_a) and temperature (T_a , in K); this value is indicated with the symbol F . If a water-containing flowmeter was used for the measurement (e.g. the so-called soap bubble flowmeter) then F must be corrected to dry gas conditions in order to obtain the *Mobile Phase Flow Rate at Ambient Temperature* (F_a):

$$F_a = F(1 - p_w/p_a)$$

where p_w is the partial pressure of water vapor at ambient temperature.

3.6.04.2. In order to specify chromatographic conditions in column chromatography, the flow-rate (*Mobile Phase Flow Rate at Column Temperature*, F_c) must be expressed at T_c (kelvin), the column temperature:

$$F_c = F_a(T_c/T_a)$$

3.6.05. Velocities

3.6.05.1. Mobile-phase velocity (u) The linear velocity of the mobile phase across the average cross-section of the chromatographic bed or column. It can be calculated from the column flow-rate at column temperature (F_c), the cross-sectional area of the column (A_c) and the interparticle porosity (ϵ):

$$u = F_c/(\epsilon A_c)$$

In practice the mobile phase velocity is usually calculated by dividing the column length (L) by the retention time of an unretained compound (t_M ; see 3.7.03):

$$u = L/t_M$$

3.6.05.2. In gas chromatography, due to the compressibility of the carrier gas, the linear velocity will be different at different longitudinal positions in the column. Therefore two terms must be distinguished:

The *Carrier Gas Velocity at the Column Outlet* (u_o) can be obtained as above, from the carrier gas flow rate measured at column outlet:

$$u_o = F_c/(\epsilon A_c)$$

The *Average Linear Carrier Gas Velocity* (\bar{u}) is obtained from u_o , by correcting it for gas compressibility:

$$\bar{u} = u_o j$$

The average linear carrier gas velocity can also be obtained by dividing the column length (L) by the retention time of an unretained compound (t_M):

$$\bar{u} = L/t_M$$

In liquid chromatography where mobile phase compression is negligible, $\bar{u} = u$.

3.6.05.3. Reduced mobile phase velocity (v) A term used mainly in liquid chromatography. It compares the mobile phase velocity with the velocity of diffusion into the pores of the particles (the so-called diffusion velocity, u_D ; see 3.4.04):

$$v = \bar{u}/u_D = \bar{u}d_p/D_M$$

In open-tubular chromatography:

$$v = \bar{u}d_c/D_M$$

3.7. Retention Parameters in Column Chromatography

3.7.01. Retention parameters may be measured in terms of chart distances or times, as well as mobile phase volumes; e.g., t'_R (time) is analogous to V'_R (volume). If recorder speed is constant, the chart distances are directly proportional to the times; similarly if the flow rate is constant, the volumes are directly proportional to the times.

Note: In gas chromatography, or in any chromatography where the mobile phase expands in the column, V_M , V_R and V'_R represent volumes under column outlet pressure. If F_c , the carrier gas flow rate at the column outlet and corrected to column temperature (see 3.6.04.2), is used in calculating the retention volumes from the retention time values, these correspond to volumes at column temperatures.

3.7.02. The various conditions under which retention volumes (times) are expressed are indicated by superscripts: thus, a prime ('; as in V'_R) refers to correction for the hold-up volume (and time) while a circle ($^\circ$; as in V_R°) refers to correction for mobile-phase compression. In the case of the net retention volume (time) both corrections should be applied: however, in order not to confuse the symbol by the use of a double superscript, a new symbol (V_N , t_N) is used for the net retention volume (time).

3.7.03. Hold-up volume (time) (V_M , t_M) The volume of the mobile phase (or the corresponding time) required to elute a component the concentration of which in the stationary phase is negligible compared to that in the mobile phase. In other words, this component is not retained at all by the stationary phase. Thus, the hold-up volume (time) is equal to the *Retention Volume (Time) of an Unretained Compound*. The hold-up volume (time) corresponds to the distance OA in Figure 1A and it includes any volumes contributed by the sample injector, the detector, and connectors.

$$t_M = V_M/F_c$$

In gas chromatography this term is also called the *Gas Hold-up Volume (Time)*.

3.7.04. Corrected gas hold-up (volume (V_M°)) The gas hold-up volume multiplied by the compression (compressibility) correction factor (j):

$$V_M^\circ = V_M \cdot j$$

Assuming that the influence of extracolumn volume on V_M is negligible,

$$V_M^\circ = V_G$$

(see 3.2.11.2)

3.7.05. Total retention volume (time) (V_R , t_R) The volume of mobile phase entering the column between sample injection and the emergence of the peak maximum of the sample component of interest (OB in Figure 1a), or the corresponding time. It includes the hold-up volume (time):

$$t_R = V_R/F_c$$

3.7.06. Peak elution volume (time) (\bar{V}_R , \bar{t}_R) The volume of mobile phase entering the column between the start of the elution and the emergence of the peak maximum, or the corresponding time. In most of the cases, this is equal to the total retention volume (time). There are, however, cases when the elution process does not start immediately at sample introduction. For example, in liquid chromatography, sometimes the column is washed with a liquid after the application of the sample to displace certain components which are of no interest and during this treatment the sample does not move along the column. In gas chromatography, there are also cases when a liquid sample is applied to the top of the column but its elution starts only after a given period. This term is useful in such cases.

3.7.07. Adjusted retention volume (time) (V'_R , t'_R) The total elution volume (time) minus the hold-up volume (time). It corresponds to the distance AB in Figure 1a:

$$V'_R = V_R - V_M$$

$$t'_R = t_R - t_M = (V_R - V_M)/F_c = V'_R/F_c$$

3.7.08. Corrected retention volume (time) (V_R° , t_R°) The total retention volume (time) multiplied by the compression correction factor (j):

$$V_R^\circ = V_R \cdot j$$

$$t_R^\circ = V_R \cdot j/F_c = V_R^\circ/F_c$$

3.7.09. Net retention volume (time) (V_N , t_N) The adjustment retention volume (time) multiplied by the compression correction factor (j):

$$V_N = V'_R \cdot j$$

$$t_N = V'_R \cdot j/F_c = V_N/F_c$$

3.7.10. In liquid chromatography, the compression of the mobile phase is negligible and thus, the compression correction factor does not apply. For this reason, the total and corrected retention volumes (times) are identical ($V_R = V_R^\circ$; $t_R = t_R^\circ$) and so are the adjusted and net retention volumes (times) ($V'_R = V_N$; $t'_R = t_N$).

3.7.11. Specific retention volumes

3.7.11.1. The specific retention volume at column temperature (V_g^θ) The net retention volume per gram of stationary phase (stationary liquid, active solid or solvent-free gel (W_s)):

$$V_g^\theta = V_N/W_s$$

3.7.11.2. Specific retention volume at 0°C (V_g) The value of V_g^θ corrected to 0°C:

$$V_g = V_g^\theta \frac{273.15 \text{ K}}{T_c} = \frac{V_N}{W_s} \frac{273.15 \text{ K}}{T_c}$$

where T_c is the column temperature (in kelvin).

3.7.12. Retention factor (k) The retention factor is a measure of the time the sample component resides in the stationary phase relative to the time it resides in the mobile phase: it expresses how much longer a sample component is retarded by the stationary phase than it would take to travel through the column with the velocity of the mobile phase. Mathematically, it is the ratio of the adjusted retention volume (time) and the hold-up volume (time):

$$k = V'_R/V_M = t'_R/t_M$$

If the distribution constant (see 3.9) is independent of sample component concentration, then the retention factor is also equal to the ratio of the amounts of a sample component in the stationary and mobile phases respectively, at equilibrium:

$$k = \frac{\text{amount of component in stationary phase}}{\text{amount of component in mobile phase}}$$

If the fraction of the sample component in the mobile phase is R (see 3.7.13), then the fraction in the stationary phase is $(1 - R)$; thus

$$k = (1 - R)/R$$

Note: In former nomenclatures and in the literature one may find the expressions *Partition Ratio*, *Capacity Ratio*, *Capacity Factor* or *Mass Distribution Ratio* to describe this term.

In the literature the symbol k' is often used for the retention factor, particularly in liquid chromatography. The original reason for this was to clearly distinguish it from the partition coefficient (distribution constant) for which the symbol K had been utilized. Since, however, the distribution constants are all identified with a subscript, there is no reason to add the prime sign to this symbol. It should be emphasized that all the recognized nomenclatures (IUPAC, BS, ASTM) have always clearly identified the capacity factor with the symbol k and not k' .

3.7.12.1. Logarithm of the retention factor This term is equivalent to the R_M value used in planar chromatography (see 3.8.05). The symbol κ is suggested to express $\log k$:

$$\kappa = \log k = \log[(1 - R)/R].$$

3.7.13. Retardation factor (R) The fraction of the sample component in the mobile phase at equilibrium; it is related to the retention factor and other fundamental chromatography terms:

$$R = 1/(k + 1)$$

3.7.14. Relative retention values

3.7.14.1. Relative retention (r) The ratio of the adjusted or net retention volume (time) or retention factor of a component relative to that of a standard, obtained under identical conditions:

$$r = V'_{Ri}/V'_{R(st)} = V_{Ni}/V_{N(st)} = t'_{Ri}/t'_{R(st)} = k_i/k_{st}$$

Depending on the relative position of the peak corresponding to the standard compound in the chromatogram, the value of r may be smaller, larger or identical to unity.

3.7.14.2. Separation factor (α) The relative retention value calculated for two adjacent peaks ($V'_{R2} > V'_{R1}$):

$$\alpha = V'_{R2}/V'_{R1} = V_{N2}/V_{N1} = t'_{R2}/t'_{R1} = k_2/k_1$$

By definition, the value of the separation factor is always greater than unity.

The separation factor is also identical to the ratio of the corresponding distribution constants.

Note: The separation factor is sometimes also called the 'selectivity'. The use of this expression is discouraged.

3.7.14.3. Unadjusted relative retention (r_G or α_G) Relative retention calculated by using the total retention volumes (times) instead of the adjusted or net retention volumes (times):

$$r_G = V_{Ri}/V_{R(st)} = t_{Ri}/t_{R(st)} = \frac{k_i + 1}{k_{st} + 1}$$

Subscript G commemorates E. Glueckauf, who first used this expression.

3.7.14.4. Relative retention (r) and separation factor (α) values must always be measured under isothermal conditions. On the other hand, the unadjusted relative retention (r_G or α_G) values may also be obtained in

programmed-temperature or gradient-elution conditions. Under such conditions, the symbol RRT (for *Relative Retention Time*) has also been used to describe the unadjusted relative retention values.

Using the same stationary and mobile phases and temperature, the relative retention and separation factor values are reproducible between chromatographic systems. On the other hand, the unadjusted relative retention (and 'relative retention time') values are only reproducible within a single chromatographic system.

3.7.15. Retention index; Kováts (retention) index (I) The retention index of a sample component is a number, obtained by interpolation (usually logarithmic), relating the adjusted retention volume (time) or the retention factor of the sample component to the adjusted retention volumes (times) of two standards eluted before and after the peak of the sample component.

In the *Kováts Index* or *Kováts Retention Index* used in gas chromatography, n -alkanes serve as the standards and logarithmic interpolation is utilized:

$$I = 100 \left[\frac{\log X_i - \log X_z}{\log X_{(z+1)} - \log X_z} + z \right]$$

where X refers to the adjusted retention volumes or times, z is the number of carbon atoms of the n -alkane eluting before, and $(z + 1)$ is the number of carbon atoms of the n -alkane eluting after the peak of interest:

$$V'_{Rz} < V'_{Ri} < V_{R(z+1)}$$

The *Kováts (Retention) Index* expresses the number of carbon atoms (multiplied by 100) of a hypothetical normal alkane which would have an adjusted retention volume (time) identical to that of the peak of interest when analyzed under identical conditions.

The *Kováts Retention Index* is always measured under isothermal conditions. In the case of *temperature-programmed gas chromatography* a similar value can be calculated utilizing direct numbers instead of their logarithm. Since both the numerator and denominator contain the difference of two values, here we can use the total retention volumes (times). Sometimes this value is called the *Linear Retention Index*:

$$I^T = 100 \left[\frac{t_{Ri}^T - t_{Rz}^T}{t_{R(z+1)}^T - t_{Rz}^T} + z \right]$$

where t_R^T refers to the total retention times (chart distances) measured under the conditions of temperature programming. The value of I^T will usually differ from the value of I measured for the same compound under isothermal conditions, using the same two phases.

3.8. Retention Parameters in Planar Chromatography

3.8.01. Mobile-phase front The leading edge of the mobile phase as it traverses the planar media. In all forms of development except radial, the mobile phase front is essentially a straight line parallel to the mobile phase surface. It is also called the *Liquid Front* or *Solvent Front*.

3.8.02. Mobile-phase distance The distance travelled by the mobile phase travelling along the medium from the starting (application) front or line to the mobile phase front. It is the distance a in Figure 2.

3.8.03. Solute distance The distance travelled by the solute along the medium from the starting (application) point or line to the center of the solute spot. If the solute spot is not circular, an imaginary circle is used whose diameter is the smallest axis of the spot. It is the distance b in Figure 2.

3.8.04. Retardation Factor (R_F) Ratio of the distance travelled by the center of the spot to the distance simultaneously travelled by the mobile phase. Using the symbols of Figure 2:

$$R_F = b/a$$

By definition the R_F values are always less than unity. They are usually given to two decimal places. In order to simplify this presentation the hR_F Values may be used: they correspond to the R_F values multiplied by 100.

Ideally, the R_F values are identical to the R values (see 3.7.13).

3.8.05. R_M value A logarithmic function of the R_F value:

$$R_M = \log \frac{1 - R_F}{R_F} = \log \left[\frac{1}{R_F} - 1 \right]$$

3.8.06. Relative retardation (R_{rel}) This term is equivalent to relative retention used in column chromatography: it is the ratio of the R_F value of a component to the R_F value of a standard (reference) substance. Since the mobile phase front is common for the two components, the R_{rel} value can be expressed directly as the ratio of the distances travelled by the spot of the compound of interest (b_i) and the reference substance (b_{st}) respectively:

$$R_{rel} = R_{F(i)}/R_{F(st)} = b_i/b_{st}$$

Note: In former nomenclatures the symbol R_s was used to express relative retardation in planar chromatography. Because of its identity with the symbol for peak resolution (see 3.10.01) the symbol R_{rel} is suggested for relative retardation in planar chromatography.

3.9. Distribution Constants

The distribution constant is the concentration of a component in or on the stationary phase divided by the concentration of the component in the mobile phase. Since in chromatography a component may be present in more than one form (e.g. associated and dissociated forms), the analytical condition used here refers to the total amount present without regard to the existence of various forms.

These terms are also called the *Distribution Coefficients*. However, the present term conforms more closely to the general usage in science.

The concentration in the mobile phase is always calculated per unit volume of the phase. Depending on the way the concentration in the stationary phase is expressed various forms of the distribution constants may exist.

3.9.01. Distribution Constant (K_c) In the general case, the concentration in the stationary phase is expressed *per unit volume of the phase*. This term is mainly applicable to partition chromatography with a liquid stationary phase but can also be used with a solid stationary phase:

$$K_c = \frac{W_{i(S)}/V_S}{W_{i(M)}/V_M}$$

where $W_{i(S)}$ and $W_{i(M)}$ are the amounts of component i in the stationary and mobile phases, while V_S and V_M are the volumes of the stationary and mobile phases, respectively.

The term *Distribution Constant* and the symbol K_c are recommended in preference to the term *Partition Coefficient* which has been in use in partition chromatography with a liquid stationary phase.

The value of K_c is related to the retention volume (V_R) of a sample component and the volumes of the stationary (V_S) and mobile phases (V_M) in the column:

$$V_R = V_M + K_c V_S$$

In gas chromatography both V_R and V_M have to be corrected for gas compressibility: therefore V_R° (see 3.7.08) is to be used for V_R , and $V_G = V_M^\circ$ (see 3.2.11.2) is to be used for V_M .

$$V_R^\circ = V_G + K_c V_S$$

3.9.02. Distribution constant (K_g) In the case of a solid stationary phase, the distribution constant may be expressed *per mass (weight) of the dry solid phase*:

$$K_g = \frac{W_{i(S)}/W_s}{W_{i(M)}/V_M}$$

where $W_{i(st)}$ and $W_{i(M)}$ are the amounts (masses) of the component i in the stationary and mobile phases, respectively, W_{st} is the mass (weight) of the dry stationary phase, and V_M is the volume of the mobile phase in the column.

3.9.03. Distribution constant (K_s) In the case of adsorption chromatography with a well characterized adsorbent of known surface area, the concentration in the stationary phase may be expressed *per unit surface area*:

$$K_s = \frac{W_{i(S)}/A_s}{W_{i(M)}/V_M}$$

where $W_{i(S)}$ and $W_{i(M)}$ are the amounts (masses) of the component i in the stationary and mobile phases, respectively, A_s is the surface area of the stationary phase, and V_M is the volume of the mobile phase in the column.

Note: The symbols used in 3.9.01 through 3.9.03 are generalized.

3.10. Terms Expressing the Efficiency of Separation

3.10.01. Peak resolution (R_s) The separation of two peaks in terms of their average peak width at base ($t_{R2} > t_{R1}$):

$$R_s = \frac{(t_{R2} - t_{R1})}{(w_{b1} + w_{b2})/2} = \frac{2(t_{R2} - t_{R1})}{w_{b1} + w_{b2}}$$

In the case of two adjacent peaks it may be assumed that $w_{b1} \approx w_{b2}$, and thus, the width of the second peak may be substituted for the average value:

$$R_s \approx (t_{R2} - t_{R1})/w_{b2}$$

3.10.02. Separation number (SN) This expresses the number of peaks which can be resolved in a given part of the chromatogram between the peaks of two consecutive n -alkanes with z and $(z + 1)$ carbon atoms in their molecules:

$$SN = \frac{t_{R(z+1)} - t_{Rz}}{w_{hz} + w_{h(z+1)}} - 1$$

In the German literature the symbol TZ (*Trennzahl*) is commonly used to express the separation number.

As the separation number depends on the n -alkanes used for the calculation, they always must be specified with any given SN value.

3.10.03. Plate number (N) A number indicative of column performance, calculated from the following equations which depend on the selection of the peak width expression (see 3.3.07):

$$N = (V_R'/\sigma)^2 = (t_R/\sigma)^2$$

$$N = 16(V_R'/w_b)^2 = 16(t_R/w_b)^2$$

$$N = 5.545(V_R'/w_h)^2 = 5.545(t_R/w_h)^2$$

The value of 5.545 stands for $8 \ln 2$ (see 3.3.07.4). These expressions assume a Gaussian (symmetrical) peak.

In these expressions the units for the quantities inside the brackets must be consistent so that their ratio is dimensionless: i.e., if the numerator is a volume, then peak width must also be expressed in terms of volume.

Note: In former nomenclatures the expressions ‘Number of Theoretical Plates’ or ‘Theoretical Plate Number’ were used for the same term. For simplification, the present name is suggested.

3.10.04. Effective plate number (N_{eff}) A number indicative of column performance calculated by using the adjusted retention volume (time) instead of the total retention volume (time). It is also called the *Number of Effective Plates*:

$$N_{\text{eff}} = (V'_R/\sigma)^2 = (t'_R/\sigma)^2$$

$$N_{\text{eff}} = 16(V'_R/w_b)^2 = 16(t'_R/w_b)^2$$

$$N_{\text{eff}} = 5.545(V'_R/w_h)^2 = 5.545(t'_R/w_h)^2$$

The plate number and effective plate number are related to each other:

$$N = N_{\text{eff}} \left[\frac{k+1}{k} \right]^2$$

Where k is the retention factor (see 3.7.12).

Notes: In the former literature the expression ‘number of effective theoretical plates’ had been used to express this term. This is incorrect since the plate number is either theoretical or effective, but cannot be both. In former nomenclatures the respective symbols n and N have been used for the plate number and the effective plate number. However, there was often a confusion in the proper selection of lower case and capital letters; therefore, the present usage, characterizing the effective plate number by a subscript, is suggested.

3.10.05. Plate height (H) The column length (L) divided by the plate number:

$$H = L/N$$

It is also called the *Height Equivalent to One Theoretical Plate* (HETP).

3.10.06. Effective plate height (H_{eff}) The column length divided by the effective plate number:

$$H_{\text{eff}} = L/N_{\text{eff}}$$

It is also called the *Height Equivalent to One Effective Plate*.

Notes: In the former literature the expression ‘height equivalent to one effective theoretical plate’ had been used to express this term. This is incorrect, since the plate height is either theoretical or effective (see 3.10.04), but cannot be both.

In former nomenclatures the respective symbols h and H have been used for the plate height and the effective plate height, respectively. However, there was often a confusion in the proper selection of lower case and capital letters and also due to the fact that h (lower case letter) is also used to express the reduced plate height (see 3.10.07). The present usage is suggested in order to avoid any confusion.

3.10.07. Reduced plate height (h) A term used in liquid chromatography. It is the ratio of the plate height to the average particle diameter:

$$h = H/d_p$$

For open-tubular columns:

$$h = H/d_c$$

4. Terms Related to Detection

4.1. Classification of Detectors

4.1.01. Classification according to the form of response

4.1.01.1. *Differential detectors* These measure the instantaneous difference in the composition of the column effluent.

4.1.01.2. *Integral detectors* These measure the accumulated quantity of sample component(s) reaching the detector.

4.1.02. Classification according to the basis of response

4.1.02.1. *Concentration-sensitive detector* A device the response of which is proportional to the concentration of a sample component in the eluent.

4.1.02.2. *Mass-flow sensitive detector* A device the response of which is proportional to the amount of sample component reaching the detector in unit time.

4.1.03. Classification according to Detector selectivity

4.1.03.1. *Universal detector* A detector which responds to every component in the column effluent except the mobile phase.

4.1.03.2. *Selective detector* A detector which responds to a related group of sample components in the column effluent.

4.1.03.3. *Specific detector* A detector which responds to a single sample component or to a limited number of components having similar chemical characteristics.

4.2. Detector Response

4.2.01. **Detector sensitivity (S)** The signal output per unit concentration or unit mass of a substance in the mobile phase entering the detector.

4.2.01.1. In the calculation of detector sensitivity the signal output of the detector is given as peak area in mV.min, A.s or AU.min (AU = absorbance unit). These values are obtained from the *integrated* peak area converted to the units specified.

Alternately, the peak area can also be obtained by multiplying the peak height at maximum (in mV, A or AU) by the peak-width at half height (in time units). The peak area calculated in this way will be 6% less than the true integrated peak area, assuming that peak is Gaussian.

4.2.01.2. In the case of *concentration-sensitive detectors*, sensitivity is calculated per unit concentration in the mobile phase:

$$S = A_i F_c / W_i = E / C_i$$

where A_i is the integrated peak area (in mV.min or AU.min), E is the peak height (in mV or AU), C_i is the concentration of the particular substance in the mobile phase at the detector (in g.cm⁻³), F_c is the mobile phase flow rate corrected to column temperature (in cm³.min⁻¹) and W_i is the mass (amount) of the substance present (in mg). The dimensions of detector sensitivity are mV.cm³.mg⁻¹ or AU.cm³.mg⁻¹.

4.2.01.3. In the case of thermal-conductivity detectors, this sensitivity value is also called the *Dimbat-Porter-Stross Sensitivity* of the detector.

In the case of *mass-flow sensitive detectors*, sensitivity is calculated per unit mass of the test substance in the mobile phase entering the detector:

$$S = A_i / W_i = E_i / M_i$$

where A_i is the integrated peak area (in A.s), E_i is the peak height (in A), M_i is the mass rate of the test substance entering the detector (in g.s⁻¹), and W_i is the mass (amount) of test substance present (in g). The dimension of detector sensitivity is A.s.g⁻¹ or C.g⁻¹.

4.2.02. Relative detector response factor (f) The relative detector response factor expresses the sensitivity of a detector relative to a standard substance. It can be expressed on an equal mole, equal volume or equal mass (weight) basis:

$$f_i = (A_i/A_{st})f_{st}$$

where A refers to the peak area of the compound of interest (subscript i) and standard (subscript st) respectively, and f_{st} is the response factor of the standard compound. Usually, an arbitrary value (e.g. 1 or 100) is assigned to f_{st} . Expressing the relative molar responses and using n -alkanes as the standards, the assigned value of f_{st} is usually the number of carbon atoms of the n -alkanes multiplied by 100 (e.g. 600 for n -hexane).

If the relative detector response factor is expressed on an equal mass (weight) basis, the determined sensitivity values can be substituted for the peak area.

4.3. Noise and Drift

4.3.01. Noise (N) (see Figure 4) The amplitude expressed in volts, amperes, or absorbance units of the envelope of the baseline which includes all random variations of the detector signal the frequency of which is in the order of one or more cycles per minute. In the case of photometric detectors the amplitude may be expressed in absorbance units per unit cell length.

4.3.02. Drift (see Figure 4) The average slope of the noise envelope, expressed in volts, amperes, or absorbance units per hour. It may be actually measured for 0.5 hour and extrapolated to one hour.

4.4. Minimum Detectability

The concentration or mass flow of a sample components in the mobile phase gives a detector signal equal to twice the noise level. It can be calculated from the measured sensitivity (S) and noise (N):

$$D = 2N/S$$

where D is the minimum detectability, expressed either as concentration or mass-flow of the substance of interest in the mobile phase at the detector. Both sensitivity and minimum detectability must be determined for the same substance.

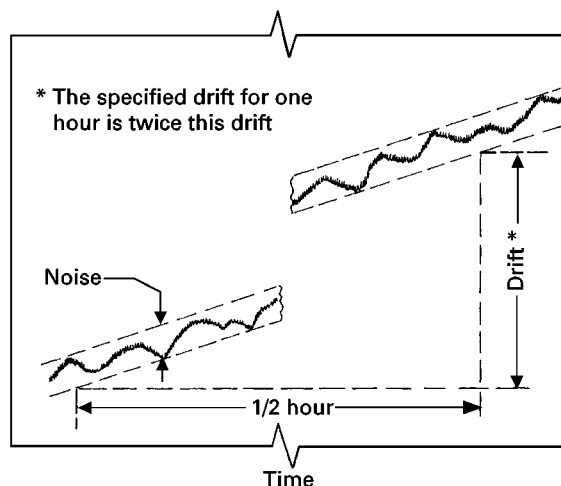


Figure 4 Measurement of the noise and drift of a chromatographic detector.

4.5. Linear and Dynamic Ranges

4.5.01. Linear range The linear range of a chromatographic detector represents the range of concentrations or mass flows of a substance in the mobile phase at the detector over which the sensitivity of the detector is constant within a specified variation, usually ± 5 percent.

4.5.01.1. The best way to present detector linear range is the *Linearity Plot* (see Figure 5) plotting detector sensitivity against amount injected, concentration or mass flow-rate. Here, the upper limit of linearity can be graphically established as the amount, concentration, or mass flow-rate) at which the deviation exceeds the specified value ($\pm x\%$ window around the plot). The lower limit of linearity is always the minimum detectable amount determined separately for the same compound.

4.5.01.2. Alternatively, the linear range of a detector may be presented as the plot of peak area (height) against concentration or mass flow-rate of the test substance in the column effluent at the detector (see Figure 6). This plot may be either linear or log/log. The upper limit of linearity is that concentration (mass flow-rate) at which the deviation from an ideal linearity plot is greater than the specified percentage deviation ($\pm x\%$ window).

4.5.01.3. Numerically, the linear range can be expressed as the ratio of the upper limit of linearity obtained from the linearity plot and the minimum detectability, both measured for the same substance.

4.5.01.4. When presenting the linear range of a detector, either as a plot as a numerical value, the test substance, the minimum detectability, and the specified deviation must be stated.

4.5.02.

4.5.02.1. Dynamic range The dynamic range of detector is that range of concentration or mass flow-rates of a substance over which an incremental change in concentration or mass flow-rate produced an incremental change in detector signal. Figure 6 Presents a plot used for the determination of the dynamic range of a detector.

4.5.02.2. The lower limit of the dynamic range is the minimum detectability. The upper limit is the highest concentration at which a further increase in concentration (mass flow-rate) will still give an observable

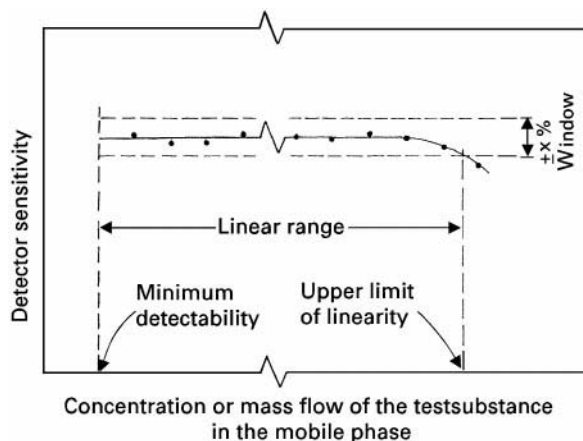


Figure 5 Linearity plot of a chromatographic detector. The scale of the ordinate is linear: the scale of the abscissa may be either linear or logarithmic.

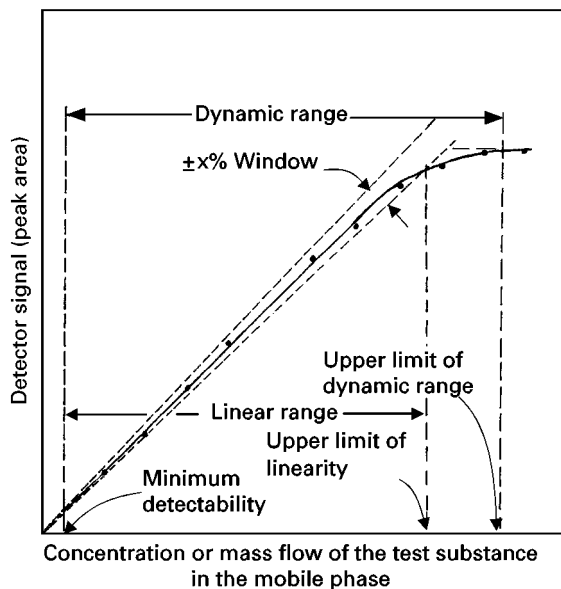


Figure 6 Determination of the linear and dynamic ranges of a chromatographic detector. Such a plot is usually in a log-log scale.

increase in detector signal, and the dynamic range is the ratio of the upper and lower limits. The dynamic range is greater than the linear range.

4.5.02.3. Numerically the dynamic range can be expressed as the ratio of the upper limit of the dynamic range obtained from the plot and the minimum detectability, both measured for the same substance.

4.5.02.4. When expressing the dynamic range of a detector, the test substance and the minimum detectability must be stated.

Table 1 Index of terms

Compound terms are generally listed at two places: under the main term and also under the full name. Exception was made when both the main term and its adjective start with same letter. For example, ion-exchange chromatography is listed as 'ion-exchange chromatography' and 'chromatography, ion-exchange'; on the other hand, column chromatography is listed only as 'chromatography, column.' The numbers refer to the relevant sections. Terms specifically used in planar chromatography (PC), ion-exchange chromatography (IEC) and exclusion chromatography (EC) are indicated by the corresponding acronyms.

A		Chamber saturation	(PC) 2.2.02.7
Active solid	3.1.01	Chromatogram	1.1.02
Adjusted retention time	3.7.07; (EC) 6.2.03	- differential	3.3.01
Adjusted retention volume	3.7.07; (EC) 6.2.03	- integral	3.3.02
Adsorption chromatography	1.5.01	Chromatograph	1.1.03; 1.1.04
Affinity chromatography	1.5.05	Chromatographic bed	1.1.05
Ambient pressure	3.6.02.2	Chromatography	1.1.01
Ambient temperature	3.5.01	- adsorption	1.5.01
Anion exchange	(IEC) 5.1.10	- affinity	1.5.05
Anion-exchange membrane	(IEC) 5.3.04	- column	1.3.01
Anion exchanger	(IEC) 5.3.03	- displacement	1.2.02
- basic form	5.3.03.1	- elution	1.2.03
Anion-exchange resin	(IEC) 5.3.03	- exclusion	1.5.04
Anticircular development	(PC) 2.2.02.6	- frontal	1.2.01
Application point (line)	(PC) 3.3.03	- gas	1.1.06; 1.4.02
Ascending elution (development)	(PC) 2.2.02.2	- gas-liquid	1.4.01
		- gas-solid	1.4.01
B		- gel-permeation	1.5.04
Band	3.3.05	- ion	1.5.03
Baseline	3.3.05	- ion-exchange	1.5.03
Bed density	(IEC) 5.6.03	- ion-exclusion	1.5.04
Bed volume	3.2.06	- isothermal	1.6.07
Bed volume capacity	(IEC) 5.4.03	- liquid	1.1.06; 1.4.03
Bifunctional ion exchanger	(IEC) 5.3.01.3	- liquid-liquid	1.4.01
Binder	(PC) 3.1.04	- liquid-solid	1.4.01
Bonded phase	1.1.05.1	- normal-phase	1.6.02
Break-through capacity	(IEC) 5.4.05	- open-bed	1.3.02
Bypass injector	2.1.02.2	- paper	1.3.02
C		- partition	1.5.02
Capacity	(IEC)	- planar	1.3.02
- bed-volume	5.4.03	- programmed-flow	1.6.09
- break-through	5.4.05	- programmed-temperature	1.6.08
- practical specific	5.4.04	- pyrolysis-gas	1.6.11.1
- theoretical specific	5.4.01	- reaction	1.6.11
- volume	5.4.02	- reversed-phase	1.6.01
Capacity factor	3.7.12; (EC) 6.2.05	- supercritical-fluid	1.4.04
Capacity ratio	3.7.12	- thin-layer	1.3.02
Capillary column	3.2.04	- two-dimensional	1.6.06
- open-tubular	3.2.03	Circular elution (development)	(PC) 2.2.02.5
- packed	3.2.04	Co-ions	(IEC) 5.1.08
Carrier gas	1.1.06	Column	3.2
- velocities	3.6.05.2	- capillary	3.2.04
Cation exchange	(IEC) 5.1.09	- cross-sectional area	3.2.10
Cation-exchange membrane	(IEC) 5.3.04	- diameter	3.2.07
Cation exchanger	(IEC) 5.3.02	- interparticle porosity	3.2.12
- acid form	5.3.02.1	- interparticle volume	3.2.11; (EC) 6.1.01
		- interstitial fraction	3.2.12

Table 1 Continued

Column	3.2	Distribution constants	3.9; (IEC) 5.6; (EC) 6.2.06
- interstitial volume	3.2.11; (EC) 6.1.01	Drift	4.3.02
- intraparticle volume	(EC) 6.1.02	Dynamic range (of detector)	4.5.02
- intrastitial volume	(EC) 6.1.02		
- length	3.2.02	E	
- open-tubular	3.2.03	Effective plate height	3.10.06; (EC) 6.3.04
- packed	3.2.02	Effective plate number	3.10.04; (EC) 6.3.04
- radius	3.2.08	Effluent	1.1.08
- temperature	2.1.03	Electron exchanger	(IEC) 5.3.01.7
- void volume	3.2.11	Elute	1.1.07
- volume	3.2.05	Eluent	1.1.06
Column oven	2.1.03	Elution	
Compression (Compressibility)		- anticircular	2.2.02.6
correction factor	3.6.03	- ascending	2.2.02.2
Concentration-sensitive detectors	4.1.02.1	- chamber	2.2.02
Corrected gas hold-up volume (time)	3.7.04	- circular	2.2.02.5
Corrected retention volume (time)	3.7.08	- descending	2.2.02.4
Corrected selectivity coefficient	(IEC) 5.5.03	- horizontal	2.2.02.3
Counter-ions	(IEC) 5.1.02	- radial	2.2.02.5
		- unsaturated	2.2.02.8
D		Elution chromatography	1.2.03
Dead volume	3.2.13.1	Equilibration	(PC) 2.2.02.9
Densitometer	(PC) 2.2.04	Exclusion chromatography	1.5.04
Derivatisation		External solution	(IEC) 5.2.02
- post-column	1.6.11.2	External standard	3.3.12
- pre-column	1.6.11.2	Extracolumn volume	3.2.13
Descending elution (development)	(PC) 2.2.02.4		
Detector	2.1.05	F	
- concentration-sensitive	4.1.02.1	Film thickness (of the liquid phase)	3.2.14
- differential	4.1.01.1	Final isothermal period	3.5.04.5
- dynamic range	4.5.02	Final isothermal temperature	3.5.04.5
- integral	4.1.01.2	Final temperature	3.5.04.4
- linearity plot	4.5.01.2	Fixed ions	(IEC) 5.1.03
- linear range	4.5.01	Flash vaporizer	2.1.02.4
- mass-sensitive	4.1.02.2	Flow programming	1.6.09
- minimum detectability	4.4	Flow-rates	3.6.04
- relative response factor	4.2.02	Flow-resistance parameter	3.2.19
- selective	4.1.03.2	Fraction collector	2.1.04
- sensitivity	4.2.01	Frontal chromatography	1.2.01
- specific	4.1.03.3	Fronting	3.3.09
- universal	4.1.03.1		
Develop	(PC) 1.1.07	G	
Developing chamber	(PC) 2.2.02	Gas chromatography	1.4.02
Development (PC)		Gas hold-up time	3.7.03
- anticircular	2.2.02.6	Gas hold-up volume	3.7.03
- ascending	2.2.02.2	- corrected	3.7.04
- circular	2.2.05.5	Gas-liquid chromatography	1.4.01
- descending	2.2.02.4	Gas phase	1.1.05
- horizontal	2.2.02.3	Gas sampling valve	2.1.02.7
- radial	2.2.02.5	Gas-solid chromatography	1.4.01
- saturated	2.2.02.7	Gel-permeation chromatography	1.5.04
- unsaturated	2.2.02.8	Gradient elution	1.6.04
Differential chromatogram	3.3.01	Gradient layer	3.1.05
Diffusion	3.4		
Diffusion coefficient		H	
- in ion exchanger	(IEC) 5.5.01	Height equivalent to one effective plate	3.10.06; (EC) 6.3.04
- in mobile phase	3.4.03	Height equivalent to one theoretical plate	3.10.05; (EC) 6.3.03
- in stationary phase	3.4.02	Heterogeneous ion-exchange membrane	(IEC) 5.3.04
Diffusion velocity	3.4.04	High-performance liquid chromatography	1.4.03
Dimbat-Porter-Stross sensitivity	4.2.01.2	- - thin-layer chromatography	1.4.03
Direct injector	2.1.02.1		
Displacement chromatography	1.2.02		
Displacer	1.2.02		

Table 1 *Continued*

Hold-up time	3.7.03	Liquid chromatography	1.4.03
Hold-up volume	3.7.03	Liquid-liquid chromatography	1.4.01
- corrected	3.7.04	Liquid phase	1.1.05
Homogeneous ion-exchange membrane	(IEC) 5.3.04	- film thickness	3.2.14
Horizontal elution (development)	(PC) 2.2.02.3	- loading	3.1.10
		- mass (weight)	3.2.16
		- volume	3.2.15
I		Liquid-solid chromatography	1.4.01
Immobilized phase	1.1.05.2	Liquid stationary phase	1.1.05
Impregnation	(PC) 3.1.06		
Initial isothermal period	3.5.04.1	M	
Initial isothermal temperature	3.5.04.1	Macroporous ion exchanger	5.3.01.5
Initial temperature	3.5.04.1	Marker	3.3.13
Injection temperature	3.5.02	Mass distribution ratio	3.7.12
Injector	2.1.02	Mass-flow sensitive detectors	4.1.02.2
- bypass	2.1.02.2	Mid-analysis isothermal period	3.5.04.3
- direct	2.1.02.1	Mid-analysis isothermal temperature	3.5.04.3
- flash vaporizer	2.1.02.4	Minimum detectability	4.4
- on-column	2.1.02.3	Mobile phase	1.1.06
- programmed-temperature vaporizer	2.1.02.6	- compression correction factor	3.6.03
- split	2.1.02.5	- distance	(PC) 3.8.02
- valve	2.1.02.2	- flow-rates	3.6.04
Inlet pressure	3.6.02.1	- front	(PC) 3.8.01
Integral chromatogram	3.3.02	- reduced	3.6.05.3
Integral detector	4.1.01.2	- velocities	3.6.05.1; 3.6.05.2
Internal standard	3.3.1	- viscosity	3.6.01
Interparticle porosity	3.2.1.2	Modified active solid	3.1.02
Interparticle volume	3.2.11; (EC) 5.1.01	Monofunctional ion exchanger	5.3.01.2
Interstitial fraction	3.2.12	Multi-dimensional chromatography	1.6.06
Interstitial volume	3.2.11; (EC) 6.1.01	Multiple programming	3.5.04.2
Intraparticle volume	(EC) 6.1.02		
Intrastitial volume	(EC) 6.1.02	N	
Ion chromatography	1.5.03	Net retention volume (time)	3.7.09
Ion-exchange chromatography	1.5.03	Noise	4.3.01
ion exchange	(IEC) 5.1.01	Normal-phase chromatography	1.6.02
- isotherm	5.1.04	Number of effective plates	3.10.04; (EC) 6.3.04
Ion-exchange membrane	(IEC) 5.3.04	Number of theoretical plates	3.10.03; (EC) 6.3.03
Ion exchanger	(IEC) 5.3.01		
- anion	5.3.03	O	
- bifunctional	5.3.01.3	On-column injector	2.1.02.3
- cation	5.3.02	Open-bed chromatography	1.3.02
- macroporous	5.3.01.5	Open-tubular column	3.2.03
- monofunctional	5.3.01.2	- porous-layer	3.2.03.2
- polyfunctional	5.3.01.4	- support-coated	3.2.03.3
- redox	5.3.01.8	- wall-coated	3.2.04.1
- salt form	5.3.01.6	Outlet pressure	3.6.02.2
Ion-exclusion chromatography	1.5.04	Oven	2.1.03
Ionogenic group	5.1.07		
Isocratic analysis	1.6.03	P	
Isothermal chromatography	1.6.07	Packing	3.1.07
Isothermal period		- pellicular	3.1.07.2
- final	3.5.04.5	- totally porous	3.1.07.1
- initial	3.5.04.1	Packed capillary column	3.2.04
- mid-analysis	3.5.04.3	Packed column	3.2.02
K		Paper chromatography	(PC) 1.3.02
Kováts Retention Index	3.7.15	Particle diameter	3.1.08
		Partition chromatography	1.5.02
L		Partition coefficient	3.9.01
Linearity plot (of detector)	4.5.01.2	Partition ratio	3.7.12
Linear range (of detector)	4.5.01	Peak	3.3.06
Linear retention index	3.7.15	- area	3.3.06.2
		- base	3.3.06.1
		- fronting	3.3.09

Table 1 Continued

Peak	3.3.06	Relative retention	3.7.14
- height	3.3.06.4	- unadjusted	3.7.14.3
- maximum	3.3.06.3	Relative retention time	3.7.14.4
- resolution	3.10.01; (EC) 6.3.01	R_M value	(PC) 3.8.05
- standard deviation	3.3.06.5	Resin matrix	(IEC) 5.3.01.1
- tailing	3.3.08	Resolution	3.10.01; (EC) 6.3.01
- variance	3.3.06.6	Retardation factor	3.7.13; (PC) 3.8.04
- widths	3.3.07	Retention factor	3.7.12; (EC) 6.2.05
Peak elution volume (time)	3.7.06	- logarithm	3.7.12.1
Pellicular packing	3.1.07.2	Retention index	3.7.15
Permeability, specific	3.2.18	Retention parameters	3.7; (PC) 3.8
Perm-selectivity	(IEC) 5.3.04.1	Retention temperature	3.5.04.6
Phase		Retention times	
- immobilized	1.6.02	- adjusted	3.7.07; (EC) 6.2.03
- mobile	1.1.06; 3.6	- corrected	3.7.08
- stationary	1.1.05	- net	3.7.09
Phase ratio	3.2.17	- peak elution	3.7.06
Planar chromatography	1.3.02	- total	3.7.05; (EC) 6.2.02
Plate height	3.10.05; (EC) 6.3.03	- total mobile-phase	6.2.04
- effective	3.10.06; (EC) 6.3.04	- unretained compound	3.7.03; (EC) 6.2.02
- reduced	3.10.07; (EC) 6.3.05	Retention volumes	
- theoretical	3.10.05; (EC) 6.3.03	- adjusted	3.7.07; (EC) 6.2.03
Plate number	3.10.03; (EC) 6.3.03	- corrected	3.7.08
- effective	3.10.04; (EC) 6.3.04	- net	3.7.09
- theoretical	3.10.03; (EC) 6.3.03	- peak elution	3.7.06
Pneumatic pump	2.1.01.3	- specific	3.7.11
Pore radius	3.1.09	- total	3.7.05; (EC) 6.2.02
Porous-layer open-tubular column	3.2.03.2	- total mobile phase	(EC) 6.2.04
Post-column derivatization	1.6.11.2	- unretained compound	3.7.03; (EC) 6.2.01
Practical specific capacity	(IEC) 5.4.04	Reversed-phase chromatography	1.6.01
Pre-column derivatization	1.6.11.2		
Pressure	3.6.02	S	
- ambient	3.6.02.2	Salt form of ion exchanger	(IEC) 5.3.01.6
- drop	3.6.02.3	Sample	1.1.09
- inlet	3.6.02.1	- component	1.1.10
- outlet	3.6.02.2	- injector	2.1.02
- programming	3.6.11	Sampling valve	2.1.02.2
- relative	3.6.02.4	Selective detectors	4.1.03.2
Programmed-flow chromatography	1.6.09	Selectivity coefficient	(IEC) 5.5.02
Programmed pressure		- corrected	5.5.03
chromatography	1.6.10	Sensitivity of detectors	4.2.01
Programmed-temperature		- Dimbat-Porter-Stross	4.2.01.2
chromatography	1.6.08	Separation factor	3.7.14.2; (IEC) 5.5.04
Programmed-temperature vaporizer	2.1.02.6	Separation number	3.10.02
Program rate	3.5.04.2	Separation temperature	2.1.03
Pumps	2.1.01	Solid stationary phase	1.1.05
- pneumatic	2.1.01.3	Solid support	3.1.03
- reciprocating	2.1.01.2	Solute	1.1.11
- syringe	2.1.01.1	Solute distance	(PC) 3.8.03
Pyrolysis-gas chromatography	1.6.11.1	Solvent	1.1.12; (IEC) 5.2.01
		Sorption	(IEC) 5.1.05
		- isotherm	(IEC) 5.1.06
R		Specific capacity (IEC)	
Radial elution (development)	(PC) 2.2.02.5	- practical	5.4.04
Reaction chromatography	1.6.11	- theoretical	5.4.01
Reciprocating pump	2.1.01.2	Specific detectors	4.1.03.3
Redox ion exchanger	(IEC) 5.3.01.8	Specific permeability	3.2.18
Redox polymers	(IEC) 5.3.01.7	Specific resolution	(EC) 6.3.02
Reduced plate height	3.10.07; (EC) 6.3.05	Specific retention volume	3.7.11
Reduced velocity (of mobile phase)	3.6.05.3	Split injection	2.1.02.5
Relative pressure	3.6.02.4	Spot	(PC) 3.3.04
Relative response factor (of detector)	4.2.02	- diameter	3.3.04.1
Relative retardation	(PC) 3.8.06	Spotting device	(PC) 2.2.01

Table 1 *Continued*

Standard deviation	3.3.06.5	Theoretical plate number	3.10.03; (EC) 6.3.03
Starting point	(PC) 3.3.03	Theoretical specific capacity	(IEC) 5.4.01
Stationary mobile-phase volume	(EC) 6.1.03	Thin-layer chromatography	1.3.02
Stationary phase	1.1.05	Total mobile-phase time	(EC) 6.2.04
- volume	3.2.15	Total mobile-phase volume	(EC) 6.1.03; 6.2.04
- mass (weight)	3.2.16	Totally porous packing	3.1.07.1
Step	3.3.10	Trennzahl	3.10.02
- height	3.3.10.1	Two-dimensional chromatography	1.6.06
Stepwise elution	1.6.05		
Supercritical-fluid chromatography	1.4.04	U	
Support	3.1.03	Unadjusted relative retention	3.7.14.3
Support-coated open-tubular column	3.2.03.2	Universal detectors	4.1.03.1
Syringe pump	2.1.01.1	Unsaturated elution (development)	(PC) 2.2.02.8
T		V	
Tailing	3.3.08	Valve injector	2.1.02.2
Temperature		Variance	3.3.06.6
- ambient	3.5.01	Velocities (of mobile phase)	3.6.05.1
- column	2.1.03; 3.5.03	Viscosity (of mobile phase)	3.6.01
- detector	3.5.05	Visualization chamber	(PC) 2.2.03
- final	3.5.04.4	Void volume	3.2.11
- final isothermal	3.5.04.5	Volume capacity	(IEC) 5.4.02
- initial	3.5.04.1	Volume swelling ratio	(IEC) 5.3.06
- initial isothermal	3.5.04.1		
- injection	3.5.02	W	
- mid-analysis isothermal	3.5.04.3	Wall-coated open tubular column	3.2.03.1
- program rate	3.5.04.2	Weight-swelling ratio in solvent	(IEC) 5.3.05
- retention	3.5.04.6		
- separation	2.1.03; 3.5.03	Z	
Theoretical plate height	3.10.05; (EC) 6.3.03	Zone	1.1.13

Table 2 List of symbols

The numbers in parentheses refer to the relevant sections. Symbols used specifically in planar chromatography (PC), ion-exchange chromatography (IEC) or exclusion-chromatography (EC) are indicated by the corresponding acronyms.

<i>a</i>	Mobile phase-distance in PC (3.8.02)
<i>A</i>	Peak area (4.2.01)
<i>A_c</i>	Cross-sectional area of a column (3.2.10)
<i>A_s</i>	Surface area of stationary phase in column (3.9.03)
<i>b</i>	Solute distance in PC (3.8.03)
<i>B₀</i>	Specific permeability (3.2.18)
<i>C_i</i>	Concentration of a test substance in the mobile phase at the detector (4.2.01.2)
<i>d_c</i>	Column inside diameter (3.2.07)
<i>d_f</i>	Thickness of liquid phase film (3.2.14)
<i>d_p</i>	Particle diameter (3.1.08)
<i>D</i>	Minimum detectability of a detector (4.4)
<i>D</i>	Diffusion coefficient in general (3.4)
<i>D_{ex}</i>	Diffusion coefficient in an ion exchanger (5.5.01)
<i>D_G</i>	Diffusion coefficient in the gas phase (3.4.03)
<i>D_L</i>	Diffusion coefficient in the liquid stationary phase (3.4.02)
<i>D_M</i>	Diffusion coefficient in the mobile phase (3.4.03)
<i>D_S</i>	Diffusion coefficient in the stationary phase (3.4.02)
<i>E</i>	Peak height (4.2.01.2)
<i>f</i>	Relative detector response factor (4.2.02)
<i>F</i>	Mobile-phase flow-rate, measured at column outlet under ambient conditions with a wet flowmeter (3.6.04.1)
<i>F_a</i>	Mobile-phase flow-rate at ambient temperature (3.6.04.1)
<i>F_c</i>	Mobile-phase flow-rate, corrected to column temperature (3.6.04.2)
<i>h</i>	Reduced plate height (3.10.07)
<i>hR_F</i>	RF × 100 (3.8.04)
<i>H</i>	Plate height (height equivalent to one theoretical plate) (3.10.05)
<i>H_{eff}</i>	Effective plate height (height equivalent to one effective plate) (3.10.06; in EC: 6.3.04)

Table 2 Continued

I	Retention index; Kováts (retention) index (3.7.15)
I^T	Retention index obtained in programmed temperature analysis; Linear retention index (3.7.15)
j	Mobile phase compression (compressibility) correction factor (3.6.03)
k	Retention factor (capacity factor) (3.7.12)
k_e	Retention factor (capacity factor) in EC (6.2.05)
$k_{A,B}$	Selectivity coefficient in IEC (5.5.02)
$k_{A,B}^a$	Corrected selectivity coefficient (IEC) (5.5.03)
K	Distribution constants in general (3.9)
K_c	Distribution constant in which the concentration in the stationary phase is expressed as mass of substance per volume of the phase (3.9.01). In IEC, it refers to unit volume of the swollen ion exchanger (5.6.01)
K_g	Distribution constant in which the concentration in the stationary phase is expressed as mass of substance per mass of the solid phase (3.9.02). In IEC, it refers to unit mass of the dry ion exchanger (5.6.02)
K_s	Distribution constant in which the concentration in the stationary phase is expressed as mass of substance per surface area of the solid phase (3.9.03)
K_v	Distribution constant used in IEC, in which the concentration in the stationary phase is expressed as volume of substance per volume of the dry ion exchanger (5.6.03)
K_o	Distribution constant in EC (6.2.06)
L	Column length (3.2.09)
M	in EC: molecular mass (6.3.01 & 6.3.02)
M_i	Mass rate of the test substance entering the detector (4.2.01.3)
N	Noise of a detector (4.3.01)
N	Plate number (number of theoretical plates) (3.10.03)
N_{eff}	Effective plate number (number of effective plates) (3.10.04; in EC: 6.3.04)
p	Pressure in general (3.6.02)
p_a	Ambient pressure (3.6.02.2)
p_i	Inlet pressure (3.6.02.1)
p_o	Outlet pressure (3.6.02.2)
p_w	Partial pressure of water at ambient temperature (3.6.04.1)
Δp	Pressure drop (3.6.02.3)
P	Relative pressure (3.6.02.4)
Q_A	Practical specific capacity of an ion exchanger (5.4.04)
Q_B	Break-through capacity of an ion-exchange bed (5.4.05)
Q_V	Volume capacity of an ion exchanger (5.4.02)
r	Relative retention (3.7.14.1)
r_c	Inside column radius (3.2.08)
r_G	Unadjusted relative retention (3.7.14.3)
r_p	Pore radius (3.1.09)
R	Retardation factor in column chromatography; fraction of a sample component in the mobile phase (3.7.12 & 3.7.13)
$(R - 1)$	Fraction of a sample component in the stationary phase in column chromatography (3.7.12)
R_F	Retardation factor in PC (3.8.04)
R_M	Logarithmic function of R_F (PC) (3.8.05)
R_{rel}	Relative retardation in PC (3.8.06)
R_s	Peak resolution (3.10.01)
R_{sp}	Specific resolution in EC (6.3.02)
$R_{1/2}$	Peak resolution in EC (6.3.02)
S	Detector sensitivity (4.2.01)
SN	Separation number
t	Time in general
t_i	Retention time corresponding to the interparticle volume (V_i) of the column (EC) (6.1.02)
t_t	Retention time corresponding to the total mobile phase volume (V_t) in the column (EC) (6.2.04)
t_o	Retention time of an unretained compound in EC (6.2.01)
t_M	Mobile-phase hold-up time; except in EC (see 6.1.01) it is also equal to the retention time of an unretained compound (3.7.03)
t_N	Net retention time (3.7.09)
t_R	Total retention time (3.7.05; in EC: 6.2.02)
t_R^T	Total retention time in temperature-programmed analysis (3.7.05 & 3.7.15)
\bar{t}_R	Peak elution time (3.7.06)
t'_R	Adjusted retention time (3.7.07; in EC: 6.2.03)
t_R^c	Corrected retention time (3.7.08)
T	Temperature in general (always in kelvin) (3.5)
T_a	Ambient temperature (3.5.01)
T_c	Column temperature (3.5.03)
TZ	Trennzahl number (separation number) (3.10.02)
u	Mobile-phase velocity (3.6.05.1)

Table 2 *Continued*

\bar{u}	Average linear carrier gas velocity (3.6.05.2)
u_D	Diffusion velocity (3.4.04)
u_o	Carrier gas velocity at column outlet (3.6.05.2)
V	Volume in general
V_c	Column volume (3.2.05)
$V_{(DIE)}$	Volume of dry ion exchanger (5.6)
V_{ext}	Extra-column volume (6.1.03)
V_g	Specific retention volume at 0°C (3.7.11.2)
V_g^θ	Specific retention volume at column temperature (3.7.11.1)
V_i	Intraparticle volume of column in EC (6.1.02)
V_G	Interparticle volume of column in GC (3.2.11.2)
V_L	Liquid-phase volume (3.2.15)
V_M	Mobile-phase hold-up volume; except in EC (see 6.1.01) it is also equal to the retention volume of an unretained compound (3.7.03)
V_M^o	Corrected gas hold-up volume (3.7.04)
V_M	Volume of mobile phase in column (3.9.01)
V_N	Net retention volume (3.7.09)
V_o	Interparticle volume of column (3.2.11); in EC, it is also equal to the retention volume of an unretained compound (6.2.01)
V_R	Total retention volume (3.7.05; in EC: 6.2.02)
\bar{V}_R	Peak elution volume (3.7.06)
V'_R	Adjusted retention volume (3.7.07; in EC: 6.2.03)
V_R^o	Corrected retention volume (3.7.08)
V_S	Volume of stationary phase in column (3.2.15, 3.9.01)
$V_{(SIE)}$	Volume of swollen ion-exchanger (5.6)
$V_t^{(sol)}$	Total mobile-phase volume in the column (the mobile phase hold-up volume in EC) (6.1.03 and 6.2.04)
w_b	Peak width at base (3.3.07.1)
w_h	Peak width at half height (3.3.07.2)
w_i	Peak width at the inflection points (3.3.07.3)
W	Amount (mass) in general
W_i	Amount (mass) of a test substance present (4.2.01.2)
$W_{(IE)}$	Amount of the component i in the ion exchanger (5.6)
$W_{(M)}$	Amount of component i in the mobile phase (3.9)
$W_{(S)}$	Amount of the component i in the stationary phase (3.9)
W_L	Amount (mass) of the liquid phase in the column (3.2.16)
W_S	Amount (mass) of the stationary phase in the column (3.2.16)
z	Number of carbon atoms of a n -alkane eluted before the peak of interest (3.7.15)
$(z + 1)$	Number of carbon atoms of a n -alkane eluted after the peak of interest (3.7.15)

Greek symbols

α	Separation factor (relative retardation) (3.7.4.2)
α	Separation factor in IEC (5.5.04)
α_G	Unadjusted separation factor (relative retention) (3.7.14.3)
β	Phase ratio (3.2.17)
ε	Interparticle porosity (3.2.12)
η	Mobile phase viscosity (3.6.01)
θ	superscript in V_g^θ (3.7.11.1)
κ	$\log k$ (3.7.12.1)
ν	Reduced mobile phase velocity (3.6.05.3)
ρ	Bed density in IEC (5.6.03)
σ	Standard deviation of a Gaussian peak (3.3.06.5)
σ^2	Variance of a Gaussian peak (3.3.06.5)
Φ	Flow resistance parameter (3.2.19)

Subscripts

The generally used subscripts are listed. There are a few specific subscripts not listed here.

a	Ambient
c	Column
eff	Effective
f	Film of liquid phase
i	Compound of interest
o	Outlet of column
p	Particle
st	Standard

Table 2 *Continued**Subscripts*

G	Gas phase
L	Liquid stationary phase
M	Mobile phase; also external solution in IEC
N	Net (as in net retention time or volume; correction for both the holdup time (volume) and gas compressibility)
R	Retention (as in retention time or volume)
S	Stationary phase; in IEC: ion exchanger
1,2	Two adjacent ($t_{R2} > t_{R1}$ except in EC where $M_2 > M_1$ and thus $t_{R1} > t_{R2}$)

Superscripts

T	Indication that value was obtained in programmed-temperature analysis
'	Adjusted (as in adjusted retention time or volume)
°	Corrected (as in corrected retention time or volume)

Table 3 List of acronyms used in chromatography

EC	Exclusion chromatography
GC	Gas chromatography
GLC	Gas-liquid chromatography
GLPC	Gas-liquid partition chromatography
GPC	Gel-permeation chromatography
GSC	Gas-solid chromatography
HETP	Height equivalent to one theoretical plate
HPLC	High-performance liquid chromatography
IC	Ion chromatography
IEC	Ion-exchange chromatography
LC	Liquid chromatography
LLC	Liquid-liquid chromatography
LSC	Liquid-solid chromatography
PC	Paper chromatography or Planar chromatography
PLOT	Porous-layer open-tubular (column)
PTV	Programmed-temperature vaporizer
RRT	Relative retention time
SCOT	Support-coated open-tubular (column)
SFC	Supercritical-fluid chromatography
TLC	Thin-layer chromatography
WCOT	Wall-coated open-tubular (column)

References

1. Preliminary Recommendations on Nomenclature and Presentation of Data in Gas Chromatography. *Pure. Appl. Chem.* **1**, 177–186 (1960).
2. Recommendations on Nomenclature and Presentation of Data in Gas Chromatography. *Pure Appl. Chem.* **8**, 553–562 (1964).
3. Recommendations on Nomenclature for Ion Exchange. Information Bulletin Appendices on Tentative Nomenclature, Symbols, Units and Standards, No. 5, IUPAC Secretariat, Oxford, January 1970.
4. Recommendations on Ion-Exchange Nomenclature. *Pure Appl. Chem.* **29**, 619–624 (1972).
5. Recommendations on Nomenclature for Chromatography. Information Bulletin Appendices on Tentative Nomenclature, Symbols, Units and Standards, No. 15, IUPAC Secretariat, Oxford, February 1972.
6. Recommendations on Nomenclature for Chromatography. *Pure Appl. Chem.* **37**, 447–462 (1974).
7. Glossary of Terms of Gas Chromatography. British Standard 3382. British Standards Institution, London. First published: 1963; latest revision 1969.
8. Gas Chromatography Terms and Relationships. ASTM E 355. American Society for Testing & Materials, Philadelphia, PA; originally published in 1968, latest revision: 1989.
9. Packed Column Gas Chromatography. ASTM E 260. American Society for Testing & Materials, Philadelphia, PA; originally published in 1965, latest revision: 1991.
10. Calculation of Gas Chromatography Response Factors. ASTM D 4626. American Society for Testing & Materials, Philadelphia, PA; originally published in 1986, latest revision: 1990.
11. Thermal Conductivity Detectors Used in Gas Chromatography. ASTM E 516. American Society for Testing & Materials, Philadelphia, PA; originally published in 1974, latest revision: 1991.

12. Flame Ionization Detectors Used in Gas Chromatography. ASTM E 594. American Society for Testing & Materials, Philadelphia, PA; originally published in 1977.
13. Electron Capture Detectors Used in gas Chromatography. ASTM E 697. American Society for Testing & Materials, Philadelphia, PA; originally published in 1979, latest revision: 1991.
14. Nitrogen/Phosphorus Thermionic Ionization Detectors for Use in Gas Chromatography. ASTM E 1140. American Society for Testing & Materials, Philadelphia, PA; originally published in 1986.
15. Flame Photometric Detectors Used in Gas Chromatography, ASTM E 840. American Society for Testing & Materials, Philadelphia, PA; originally published in 1981, latest revision: 1991.
16. Supercritical-Fluid Chromatography Terms and Relationships. ASTM E 1449. American Society for Testing & Materials, Philadelphia, PA; originally published in 1992.
17. Liquid Chromatography Terms and Relationships. ASTM E 682. American Society for Testing & Materials, Philadelphia, PA; Originally published in 1979.
18. Refractive Index Detectors Used in Liquid Chromatography. ASTM E 1303. American Society for Testing & Materials, Philadelphia, PA; originally published in 1989.
19. Fixed-Wavelength Photometric Detectors Used in Liquid Chromatography. ASTM E 685. American Society for Testing & Materials, Philadelphia, PA; originally published in 1979.
20. Ion Chromatography Terms and relationships. ASTM 1151. American Society for Testing & Materials, Philadelphia, PA; originally published in 1987.
21. Use of Liquid Exclusion Chromatography Terms and Relationships. ASTM D 3536. American Society for Testing & Materials, Philadelphia, PA; originally published in 1978, latest revision: 1986.
22. Molecular Weight Averages and Molecular Weight Distribution by Liquid Exclusion Chromatography (Gel-Permeation Chromatography GPC) ASTM D 3536. American Society for Testing & Materials, Philadelphia, PA; originally published in 1976, latest revision: 1991.
23. Molecular Weight Averages and Molecular Weight Distribution by Certain Polymers by Liquid Size Exclusion Chromatography (Gel-Permeation Chromatography GPC) Using Universal Calibration. ASTM D 3593. American Society for Testing & Materials, Philadelphia, PA; originally published in 1977, latest revision: 1986.
24. E. Stahl: Nomenclature in Chromatography. *Chromatographia* 1, 338–342 (1968).
25. L. S. Ettre: The Nomenclature of Chromatography. I. Gas Chromatography. *J. Chromatogr.* 165, 235–256 (1979).
26. L. S. Ettre: The Nomenclature of Chromatography. II. Liquid Chromatography. *J. Chromatogr.* 220, 29–63 (1981).
27. L. S. Ettre: The Nomenclature of Chromatography, III. General Rules for Future Revisions. *J. Chromatogr.* 220, 65–69 (1981).
28. I. Mills, T. Cvitaš, K. Homann, N. Kalley, and K. Kuchitsu, Quantities, Units and Symbols in Physical Chemistry, Blackwell Scientific Publications, Oxford, UK, 1988.

5. Special Terminology Used in Ion-exchange Chromatography

The general terms and definitions discussed in the previous chapters are also valid in ion-exchange chromatography. In addition, the following terms and definitions refer specifically to this variant of the technique.

5.1. Basic Definitions

- 5.1.01. **Ion exchange** The process of exchanging ions between a solution and an ion exchanger.
- 5.1.02. **Counter-ions** In an ion exchanger, the mobile exchangeable ions.
- 5.1.03. **Fixed ions** In an ion exchanger, the non-exchangeable ions which have a charge opposite to that of the counter-ions.
- 5.1.04. **Ion-exchange isotherm** The concentration of a counter-ion in the ion exchanger expressed as a function of its concentration in the external solution under specified conditions and at constant temperature.
- 5.1.05. **Sorption** Uptake of electrolytes or non-electrolytes by the ion exchanger through mechanisms other than pure ion exchange.
- 5.1.06. **Sorption isotherm** The concentration of a sorbed species in the ion exchanger, expressed as a function of its concentration in the external solution under specified conditions and at constant temperature.

5.1.07. Ionogenic groups The fixed groupings in an ion exchanger which are either ionized or capable of dissociation into fixed ions and mobile counter-ions

5.1.08. Co-ions The mobile ionic species in an ion exchanger with a charge of the same sign as the fixed ions.

5.1.09. Cation exchange The process of exchanging cations between a solution and a cation exchanger.

5.1.10. Anion exchange The process of exchanging anions between a solution and an anion exchanger.

5.2. The Mobile Phase

5.2.01. Solvent The term used in classical ion exchange to express the mobile phase.

5.2.02. External solution The solution in contact with the ion exchanger which contains the ionized species before and after exchange with the ion exchanger.

5.3. The Chromatographic Medium

5.3.01. Ion exchangers A solid or liquid, inorganic or organic substance containing ions exchangeable with others of the same charge, present in a solution in which the ion exchanger is considered to be insoluble.

Note: It is recognized that there are cases where liquid exchangers are employed and where it may be difficult to distinguish between the separation process as belonging to ion exchange or liquid-liquid distribution, but the broad definition given here is regarded as that which is most appropriate.

5.3.01.1. Resin matrix The molecular network of an ion exchanger which carries the ionogenic groups.

5.3.01.2. Monofunctional ion exchanger An ion exchanger containing only one type of ionogenic group.

5.3.01.3. Bifunctional ion exchanger An ion exchanger containing two types of ionogenic groups.

5.3.01.4. Polyfunctional ion exchanger An ion exchanger containing more than one type of ionogenic groups.

5.3.01.5. Macroporous ion exchanger An ion exchanger with pores that are large compared to atomic dimensions.

5.3.01.6. Salt form of an ion exchanger The ionic form of an ion exchanger in which the counter-ions are neither hydrogen nor hydroxide ions. When only one valence is possible for the counter-ion, or its exact form or charge is not known, the symbol or the name of the counter-ion without charge is used, e.g., sodium-form or Na-form, tetramethylammonium-form, orthophosphate-form. When one of two or more possible forms is exclusively present, the oxidation state may be indicated by a Roman numeral, e.g. Fe^{II}-form, Fe^{III}-form.

5.3.01.7. Redox polymers Polymers containing functional groups which can be reversibly reduced or oxidized. *Electron Exchanger* may be used as a synonym.

5.3.01.8. Redox ion exchangers Conventional ion exchangers in which reversible redox couples have been introduced as counter-ions either by sorption or complex formation. They closely resemble redox polymers in their behavior.

5.3.02. Cation exchanger Ion exchanger with cations as counter-ions. The term *Cation-Exchange Resin* may be used in the case of solid organic polymers.

5.3.02.1. Acid form of a cation exchanger The ionic form of a cation exchanger in which the counter-ions are hydrogen ions (H-form) or the ionogenic groups have added a proton forming an undissociated acid.

5.3.03. Anion exchanger Ion exchanger with anions as counter-ions. The term *Anion-Exchange Resin* may be used in the case of solid organic polymers.

5.3.03.1. Base form of an anion exchanger The ionic form of an anion exchanger in which the counter-ions are hydroxide groups (OH-form) or the ionogenic groups form an uncharged base, e.g. $-\text{NH}_2$.

5.3.04. Ion-exchange membrane A thin sheet or film of ion-exchange material which may be used to separate ions by allowing the preferential transport of either cations (in the case of a *Cation-Exchange Membrane*) or anions (in the case of an *Anion-Exchange Membrane*). If the membrane material is made from only ion-exchanging material, it is called a *Homogeneous Ion-Exchange Membrane*. If the ion-exchange material is embedded in an inert binder, it is called a *Heterogeneous Ion-Exchange Membrane*.

5.3.04.1. Perm-selectivity A term used to define the preferential permeation of certain ionic species through ion-exchange membranes.

5.3.05. Weight-swelling ratio in solvent Mass of solvent taken up by unit mass of the dry ion exchanger. The solvent must always be specified.

5.3.06. Volume-swelling ratio Ratio of the dry swollen volume to the true dry volume of the ion exchanger.

5.4. Capacity Values

5.4.01. Theoretical specific capacity Amount (mmol) of ionogenic group per mass (g) of dry ion exchanger. If not otherwise stated, the capacity should be reported per mass (g) of the H-form of a cation exchanger and of the Cl-form of an anion exchanger.

5.4.02. Volume capacity (Q_v) Amount (mmol) of ionogenic group per volume (cm^3) of swollen ion exchanger. The ionic form of the ion exchanger and the medium should be stated.

5.4.03. Bed volume capacity Amount (mmol) of ionogenic group per bed volume (cm^3) (see 3.2.06) determined under specified conditions. The conditions should always be specified.

5.4.04. Practical specific capacity (Q_A) Total amount of ions (mmole) taken up per mass (g) of dry ion exchanger under specified conditions. The conditions should always be specified.

5.4.05. Break-through capacity of ion-exchange bed (Q_B) The practical capacity of an ion exchanger bed, obtained experimentally by passing a solution containing a particular ionic or molecular species through a column containing the ion exchanger. This is under specified conditions and is determined by measuring the amount of species which has been taken up when the species is first detected in the effluent or when the concentration in the effluent reaches some arbitrarily defined value. The break-through capacity may be expressed in millimoles or milligrams taken up per gram of dry ion exchanger or per cm^3 of bed volume.

5.5. Diffusion, Selectivity and Separation

5.5.01. Diffusion coefficient in the ion exchanger (D_{ex}) The meaning of this term is the same as the specified in 3.4.01-3.4.02.

5.5.02. Selectivity coefficient ($k_{A/B}$) The equilibrium coefficient obtained by application of the law of mass action to ion exchange and characterizing quantitatively the ability of an ion exchanger to select one of two ions present in the same solution. The ions involved in the exchange should be specified as subscripts. Examples:

Exchange: $\text{Mg}^{2+} - \text{Ca}^{2+}$

$$k_{\text{Mg/Ca}} = \frac{[\text{Mg}]_s/[\text{Ca}]_s}{[\text{Mg}]_s/[\text{Ca}]_s}$$

Exchange: $\text{SO}_4^{2+} - \text{Cl}^-$

$$k_{\text{SO}_4/\text{Cl}} = \frac{[\text{SO}_4]_S/[\text{Cl}]_S^2}{[\text{SO}_4]_M/[\text{Cl}]_M^2}$$

In the above equations subscript S refers to the ion exchanger ('stationary phase') and M to the external solution ('mobile phase'). For exchanges involving counter-ions differing in their charges, the numerical value of $k_{A/B}$ depends on the choice of the concentration scales in the ion exchanger and the external solution (molal scale, molar scale, mole fraction scale, etc.). Concentration units must be clearly stated for an exchange of ions of differing charges.

5.5.03. Corrected selectivity coefficient ($k_{A/B}^a$) This is calculated in a way identical to the selectivity coefficient except that the concentrations in the external solutions are replaced by activities.

5.5.04. Separation factor ($\alpha_{A/B}$) The definition of this term is identical to the definition given in 3.7.14.2. In an exchange of counter-ions of equal charge the separation factor is equal to the selectivity coefficient (see 5.5.01), provided that only one type of ion represents the analytical concentration (e.g. in exchanges of K^+ and Na^+) but not in systems where several individual species are included in the analytical concentrations.

5.6. Distribution constants

A *Distribution Constant* is the concentration of a component in the ion exchanger (the stationary phase) divided by its concentration in the external solution (the mobile phase). The concentration in the external solution is always calculated per unit volume. Depending on the way the concentration in the ion exchanger is expressed three forms of the distribution constant may exist.

In 5.6.01-5.6.03, $W_{i(\text{IE})}$ and $W_{i(\text{sol})}$ are the amounts of the component i in the ion exchanger and in the external solution; V_{SIE} and V_{DIE} are the volumes of the swollen and dry ion exchanger, respectively; $V_{(\text{sol})}$ is the volume of the external solution.

5.6.01. Distribution constant (K_c) In this case, the concentration in the ion exchanger is calculated as mass (weight)/volume and it refers to the swollen ion exchanger:

$$K_c = \frac{W_{i(\text{IE})}/V_{(\text{SIE})}}{W_{i(\text{sol})}/V_{(\text{sol})}}$$

5.6.02. Distribution constant (K_g) In this case, the concentration in the ion exchanger is calculated as mass/mass (weight/weight) and it refers to dry ion exchanger:

$$K_g = \frac{W_{i(\text{IE})}/V_{(\text{DIE})}}{W_{i(\text{sol})}/V_{(\text{sol})}}$$

5.6.03. Distribution constant (K_v) In this case, the concentration in the ion exchanger is calculated as volume/volume and it refers to the dry ion exchanger:

$$K_v = \frac{V_{i(\text{IE})}/V_{(\text{DIE})}}{W_{i(\text{sol})}/V_{(\text{sol})}}$$

If the *Bed Density* is ρ , expressed in grams of dry resin per cm^3 of bed, then

$$K_v = K_g \rho$$

6. Special Terminology Used in Exclusion Chromatography

Besides the terms and definitions used in general in chromatography, a number of special terms exist in exclusion chromatography. In addition, due to the different nature of the chromatographic separation, some

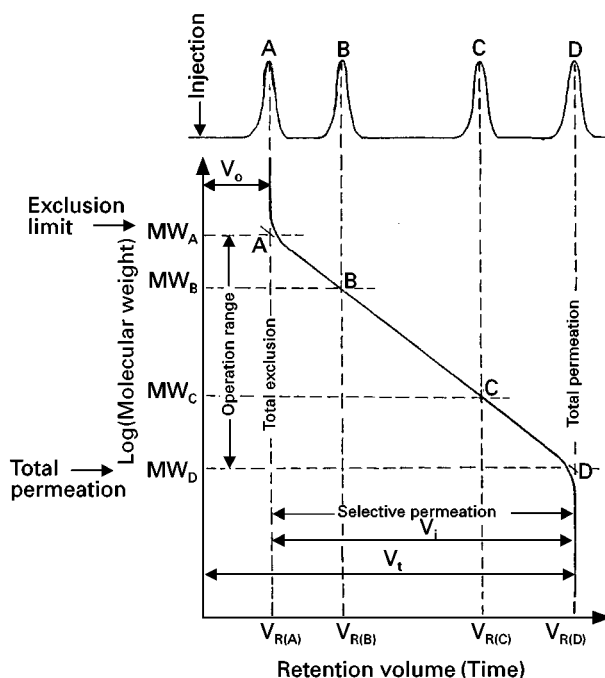


Figure 7 Retention characteristics in exclusion chromatography. A standard sample is analysed (top); subsequently, the retention volumes (times) are plotted against the logarithms of the corresponding molecular weights. Peak A corresponds to a non-retained sample component the molecules of which are larger than the largest pores in the gel particles (total exclusion); peak D corresponds to a sample component the molecules of which are smaller than the smallest pores in the gel particles (total penetration).

of the general chromatographic terms have a different meaning here. For further explanation of some of the terms, see Figure 7.

Below, only the *chromatography* terms are listed. For a discussion of the molecular weight terms calculated from the chromatographic data see the specialized nomenclatures (e.g. refs. 15–18).

6.1. The Column

6.1.01. Interparticle volume of the column (V_0) The volume of the mobile phase in the interstices between the gel particles. It is also called the *Interstitial Volume* of the column.

In exclusion chromatography, the interparticle volume of the column is equal to the retention volume of an unretained compound; however, it is *not* equal to the mobile phase hold-up volume (V_t). The reason for this is that in practice the mobile phase molecules are always smaller than the smallest pores of the column packing. Thus, they will enter all the pores available in the packing and therefore, will be eluted last. As a contrast, in general liquid chromatography, the mobile-phase hold-up volume (see 3.7.03) and the retention volume of a non-retained compound are practically equal.

6.1.02. Intraparticle volume of the column (V_i) The volume of the mobile phase within the pores of the gel particles. It is also called the *Intrastitial Volume* of the column or the *Stationary Mobile-Phase Volume*.

The retention time equivalent to V_i is t_i :

$$t_i = V_i / F_c$$

6.1.03. Total mobile-phase volume in column (V_t) The sum of the interparticle and intraparticle volumes:

$$V_t = V_0 + V_i$$

In the definition of V_t the extra-column volume of the system (V_{ext} ; see 3.2.13) is neglected. If it is not negligible, it must also be added:

$$V_t = V_0 + V_i + V_{ext}$$

6.2. Retention Parameters

6.2.01. Retention volume (time) of an unretained compound (V_o , t_o) The retention volume of a sample component the molecules of which are larger than the largest pores of the gel particles. These will be eluted first from the column. The corresponding retention time is t_o :

$$t_o = V_o/F_c$$

Ignoring any extra-column volume, V_o is equal to the interparticle volume of the column (see 6.1.01).

6.2.02. Retention volume (time) (V_R , t_R) The retention volume (time) of a sample component the molecules of which are smaller than the largest pores of the gel particles but larger than the smallest pores. The corresponding retention time is t_R :

$$t_R = V_R/F_c$$

6.2.03. Adjusted retention volume (time) (V'_R , t'_R) The total retention volume less the retention volume of an unretained compound:

$$V'_R = V_R - V_o$$

The corresponding retention time is t'_R :

$$t'_R = t_R - t_o = V'_R/F_c = (V_R - V_o)/F_c$$

6.2.04. Total mobile phase volume (time) (V_t , t_t) The retention volume (time) of a sample component the molecules of which are smaller than the smallest pores of the gel particles. The corresponding retention times is t_t :

$$t_t = V_t/F_c$$

6.2.05. Retention factor (k_e) The ratio of the adjusted retention volume (time) and the retention volume (time) of an unretained compound:

$$k_e = \frac{V_R - V_o}{V_o} = \frac{t_R - t_o}{t_o}$$

It may also be called the *Capacity Factor*. However, the suggested expression better defines its real meaning (see also 3.7.12).

6.2.06. Distribution constant in exclusion chromatography (K_o) The fraction of the intraparticle volume (the volume of the pores) available to the molecules of a particular sample component for diffusion:

$$K_o = \frac{V_R - V_o}{V_i}$$

For an unretained compound, $V_R = V_o$ and thus, $K_o = 0$. On the other hand, for a compound the molecules of which are smaller than the smallest pores, $V_R = V_t$ and thus, $K_o = 1$. In other words, the value of K_o varies between zero and unity.

In exclusion chromatography, K_o is related to the retention volume of a sample component and the inter- and intraparticle volumes of the column (V_o and V_i , respectively) in a manner analogous to the relationship in general liquid chromatography:

$$V_R = V_o + K_o V_i$$

6.3. Efficiency Terms

6.3.01. Peak resolution ($R_{1/2}$) The definition of this term is identical to that given in 3.10.01.

$$R_{1/2} = \frac{V_{R1} - V_{R2}}{(w_{b1} + w_{b2})/2}$$

Here V_{R1} and V_{R2} represent the peaks corresponding to compounds with molecular masses M_1 and M_2 respectively: by definition $M_2 > M_1$. In exclusion chromatography, larger molecules are eluted first, therefore, $V_{R1} > V_{R2}$.

Because of the addition of a new term, the specific resolution (see 6.3.02), the symbol $R_{1/2}$ is suggested for peak resolution in exclusion chromatography.

6.3.02. Specific resolution (R_{sp}) Peak resolution also considering the molecular masses of the two test compounds:

$$R_{sp} = \frac{V_{R1} - V_{R2}}{(w_{b1} + w_{b2})/2} \frac{1}{\log(M_2/M_1)}$$

The test compounds used for the determination of the specific resolution should have a narrow molecular-mass distribution (the ratio of the mass-average and number-average molecular masses should be equal to or less than about 1.1) and differ by a factor of about 10 in their molecular masses.

Note: In some nomenclatures, the symbol R_s is used for the specific resolution. Due to the possibility of confusing it with the general resolution term (see 3.10.01), the symbol R_{sp} is suggested here.

6.3.03. Plate number and plate height (N, H) The definitions of these terms are identical to those given in 3.10.03 and 3.10.05.

6.3.04. Effective plate number and effective plate height (N_{eff}, H_{eff}) The definitions of these terms are identical to those given in 3.10.04 and 3.10.06, except that the retention volume of a non-retained compound (V_o ; see 6.2.01) is used in the calculations:

$$N_{eff} = 16 \left[\frac{V_R - V_o}{w_b} \right]^2 = 5.545 \left[\frac{(V_R - V_o)}{w_h} \right]^2$$

$$N_{eff} = 16 \left[\frac{t_R - t_o}{w_b} \right]^2 = 5.545 \left[\frac{(t_R - t_o)}{w_h} \right]^2$$

$$H_{eff} = L/N_{eff}$$

6.3.05. Reduced plate height (h) The definition of this term is identical to that given in 3.10.07.

12B. Liquid-Liquid Distribution (Solvent Extraction) (IUPAC Recommendations 1993)

Prepared for publication by

N. M. Rice, H. M. N. H. Irving (1980) and M. A. Leonard* (1987)

*The Queens University of Belfast, Belfast, UK

© 1993 IUPAC

Abstract

The widespread use of liquid-liquid distribution, ranging from an analytical chemical technique to a unit operation in various fields of chemical technology (e.g. petroleum refining, nuclear fuel reprocessing, hydrometallurgy, food technology, biochemistry) has led to a proliferation of terminology. This paper extends the scope of the definitions beyond those previously recommended (*Pure Appl. Chem.* 1970, **21**, 111–113) and a list of terms, including those previously published, is presented under the following general headings: general definitions of phenomena, operations and relationships; components of the solvent phase; fundamental parameters for quantitative description of liquid-liquid distribution systems; process terminology applicable to large scale continuous operations.

Introduction

In 1970 IUPAC published 'Recommended Nomenclature for Liquid-Liquid Distribution' [1] which represented the work of several generations of the Nomenclature Commission V.3 of the International Union of Pure and Applied Chemistry, assisted by the work of an *ad hoc* working party which considered the whole of the nomenclature of separation processes. The choice of terms selected for definition was somewhat arbitrarily restricted to those commonly used in what might be termed small scale batch or laboratory analytical procedures. Many requests were received to extend the range of terms defined and the need for a complete revision was emphasized by the publication independently of other nomenclature proposals [2–5].

The wide variation [6] in the choice of symbols and in nomenclature adopted by authors of papers published in the Proceedings of the International Conferences on Solvent Extraction in Gothenburg (1966) and in Scheveningen (1971) convinced the organizing committee of the next conference at Lyons (ISEC-1974) of the desirability of providing authors with an extensive set of recommendations in order to aim at consistency in nomenclature and symbols in the published proceedings. These were drawn up by a working party of the Solvent Extraction and Ion Exchange Group of the Society of Chemical Industry (SCI), after meetings at Bradford and Birmingham (England) attended by representatives of all aspects of the field. Their report, drawn up by Dr Rice (as Secretary) formed the basis of discussions at the IUPAC General Assembly held in Munich during August 1973. This led to a new set of recommendations which were made available for comment at ISEC-74. After further discussions at a meeting of Commission V.3 of IUPAC in London in November 1974 and at the IUPAC General Assembly in Madrid in 1975, a tentative document was issued as an Information Bulletin [7] by IUPAC in July 1977 and further discussed at the IUPAC General Assembly in Warsaw in August 1977. At almost the same time the Solvent Extraction and Ion Exchange Group of the SCI authorized publication of their considered proposals for Recommended Nomenclature for Solvent Extraction in *Chemistry in Industry* to coincide with the International Solvent Extraction Conference (ISEC-77) in Toronto [8]. A synthesis of all these proposals including the comments received on the tentative IUPAC proposals was discussed at the IUPAC General Assembly in Davos in September 1979, and circulated in draft form at ISEC-80 in Liege in September 1980, where some minor amendments to process terminology were proposed. Further discussion took place at Commission meetings in London in December 1980 and Leuven in September 1981.

These revised recommendations have been drawn up in collaboration with the Committee of the Solvent Extraction and Ion Exchange Group of the Society of Chemical Industry and have been discussed at several International Solvent Extraction Conferences.

Following the rearrangement of Commissions at the 35th IUPAC General Assembly in Lund in 1989, this project became the responsibility of the Limited Life Time Commission on Chromatography and Other Analytical Separations.

Since automated methods of analysis frequently simulate many of the features of large-scale industrial practice – not least in that the attainment of distribution equilibrium or quantitative extraction is not always achieved or even necessary – it seemed important in revising the original nomenclature to increase the scope of the terms previously defined so as to provide chemical engineers, clinical biochemists, food technologists, hydrometallurgists, nuclear technologists, petrochemists and physical as well as analytical chemists with a comprehensive set of symbols and nomenclature. In order to distinguish what might be termed 'processing' nomenclature, from that of a more fundamental nature, the recommendations have been placed in separate sections. However, the importance of achieving consistent usage and a common language for all users of

liquid-liquid extraction cannot be overstressed. The distinction between the two sets of terms is merely one of convenience and does not imply any real difference in their importance. In many instances, it is difficult to decide the appropriate category for a certain term so that the classification is somewhat arbitrary. Furthermore, some additional terms commonly used in the metallurgical industry have been added since publication of the tentative proposals [7].

In order to keep the definitions as general as possible the liquid phases involved have been designated as 'extract' or 'solvent' rather than 'organic phase' and 'other phase' or 'feed' rather than 'aqueous phase'. The need clearly to label and specify the relevant phase in any equations or graphs is emphasized. Symbols are recommended for a few of the more important parameters. The clear designation of the extract phase components is stressed; the term 'solvent' should be reserved for the composite phase rather than any individual component although it may be the only component in that phase. Terms which have become jargon in particular industrial situations or which may be confusing because of ambiguity have been listed as "not recommended". No attempt has been made to define standard chemical engineering terms, e.g. mass transfer coefficient, but certain terms, e.g. 'equilibrium constant' are discussed in relation to their usage in liquid-liquid distribution.

When the nomenclature is applied to other types of extraction systems (e.g. two immiscible aqueous phases, such as a concentrated salt solution and a concentrated aqueous solution of poly(ethylene glycol), two immiscible non-aqueous liquids or two immiscible molten salts), the two immiscible phases should be clearly specified and can equally well be distinguished and denoted by the general terms, Phase I and Phase II. It is also recognized that in the petrochemical and food-processing industries the extractant phase may well be an inorganic liquid (e.g. liquid sulfur dioxide, supercritical carbon dioxide). This situation can be described by using the terms "epi-phase" and "hypo-phase" for the less dense and more dense phases, respectively, recognizing that mass transfer could be in either direction. Occasionally, cases arise where metals are partitioned among three liquid phases, such as concentrated KCl, acetonitrile and hexane. The application of the recommended nomenclature to any situation is clearly a matter of common sense. What is important is that in a given situation the phases used should be completely specified.

Since the 'organic phase' is commonly quite a complex solution of one or more organic liquids containing one or more extractants and possibly 'modifiers' of various sorts as well as a 'diluent', particular care has been taken over the definitions applicable to these various components.

'Concentration' is frequently used in the list of definitions. In general any suitable concentration units may be employed but the *same* units should be used for each phase and should be clearly specified in the text.

Following normal convention, 'activities' rather than 'concentrations' should be used where thermodynamic equilibrium quantities are implied. However, use of the appropriate 'concentration quotient' as an approximation for the equilibrium constant in the limiting case of dilute solutions or in conjunction with the appropriate activity coefficients follows logically.

One semantic problem is the occurrence of three English terms – 'extraction', 'distribution' and 'partition' – to describe the transfer of a solute between phases whereas in many other languages only one suitable term exists (e.g. Verteilung). An attempt has been made to obviate this difficulty in the present work but its complete avoidance is not possible owing to established usage. The terms and symbols, which have been defined are listed in Tables 1 and 2, respectively. In some cases these represent changes, clarifications, or specific usages of previously defined terms [9], in particular those related to chromatographic separations [10], and the differences are not in Appendix 1.

The current reviser (MAL) suggests use of the term 'distribution' when referring to the total concentration of related species and 'partition' when referring to a single species. The term 'constant' should be reserved for fixed thermodynamic true constants, otherwise 'ratio' should be used. A survey of the literature shows reasonable agreement over the symbol and title of *partition constant* and *distribution ratio* but nomenclature for the *partition ratio* is a nightmare. Appendix 2 summarizes past usage.

1. General Definitions

1.1 Antagonism

The converse to *synergism* (1.23).

Note: The terms *anti-synergism*, *antisynergic* and *anti-synergistic* should not be used.

1.2 Coextraction

Formation of mixed-species aggregates in a low-polarity organic phase.

1.3 Conditioning

A synonym for *pre-equilibration* (1.16).

1.4 Distribution

The apportionment of a solute between two phases.

Note: the term *partition* (1.15) or *extraction* (1.9) may also be used in this sense where appropriate.

1.5 Distribution Isotherm

The relationship (algebraic or graphical) between the concentration of a solute in the *extract* (2.7) and the corresponding concentration of the same solute in the other phase at equilibrium at a specified temperature.

Note: Alternative terms in common use are *equilibrium line* (1.7) and in the appropriate contexts: *extraction isotherm*, *scrubbing isotherm* and *stripping isotherm*. *Partition isotherm* is not normal usage.

1.6 Equilibration

The operation by which a system of two or more phases is brought to a condition where further changes with time do not occur.

Note: This term is not synonymous with *pre-equilibration* (1.16) and should not be used in that sense.

1.7 Equilibrium Line

A plot of the distribution isotherm (1.5).

1.8 Extract (Verb)

To transfer a solute from a liquid phase to another immiscible or partially miscible liquid phase in contact with it.

Notes:

- (i) The term is also applied to the dissolution of material from a solid phase with a liquid in which it is not wholly soluble (i.e. *leaching*). See *solvent extraction* (1.19).
- (ii) For usage as a noun see under '2 Components of the Solvent Phase'.

1.9 Extraction (in Liquid-liquid Distribution)

See *liquid-liquid extraction*.

Notes:

- (i) See under '4 Process Terminology' for a more specific usage of *extraction*.
- (ii) *Distribution* (1.4) and *partition* (1.15) are often used as synonyms for the general phenomenon of *extraction* where appropriate.

1.10 Liquid Ion Exchange

A term used to describe a liquid-liquid extraction process that involves a transfer of ionic species from the extractant to the aqueous phase in exchange for ions from the aqueous phase.

Notes:

- (i) The term does not imply anything concerning the nature of the bonding in the extracted complex.
- (ii) The term "*Solvent Ion Exchange*" (SIX) is not recommended.

1.11 Liquid-liquid Distribution (Extraction) (Partition)

The process of transferring a dissolved substance from one liquid phase to another (immiscible or partially miscible) liquid phase in contact with it.

Note: Although *extraction*, *partition* and *distribution* are not synonymous, *extraction* may replace *distribution* where appropriate.

1.12 Macro-element See *Main Solute*.

Notes:

- (i) This term is vague and is not recommended.
- (ii) Macroelement has a different meaning in analytical chemistry and the term *major component*, the meaning of which is obvious, is preferable.

1.13 Main (extractable) solute.

That (or those) species transferred which is of greatest economic or chemical interest.

Note: It is not necessarily the species present at greatest concentration.

1.14 Micro-element

This term should *not* be used in the sense of a minor component or a *contaminant* in the feed to a liquid-liquid distribution system.

Note: Microelement has a different meaning in analytical chemistry and the terms *minor component*, *impurity* or *contaminant* the meaning of which are obvious, are preferable.

1.15 Partition

This term is often used as a synonym for *distribution* (1.4) and *extraction* (1.9). However, an essential difference exists by definition between *distribution constant* or *partition ratio* (3.17) and *partition constant* (3.16).

Note: This term should be, but is not invariably, applied to the distribution of a single definite chemical species between the two phases.

1.16 Pre-equilibration

- (i) Preliminary treatment of a solvent in order to convert the extractants into a suitable chemical form.
- (ii) Preliminary treatment of either phase with a suitable solution of the other phase (in the absence of *main extractable solute(s)* (1.13)) so that when the subsequent *equilibration* (1.6)) is carried out changes in the (volume) *phase ratio* (3.19) or in the concentrations of other components are minimised.

Notes:

- (i) The use of *equilibration* (1.6) in this sense is confusing and should be avoided.
- (ii) The term *conditioning* may be used as a synonym for *pre-equilibration*.

1.17 Re-extraction

Since the prefix 're-' can signify 'back' as well as 'again' this term is ambiguous and *should be avoided*, except where the process of extraction (e.g. from aqueous solution to an organic phase) in a single direction is repeated (following stripping). It should not be used as a synonym for *stripping* (4.3) or *back-extraction* (4.1).

1.18 Salting Out

The addition of particular electrolytes to an aqueous phase in order to increase the *distribution ratio* (3.5) of a particular solute.

Notes:

- (i) The addition of electrolytes to improve phase separation behaviour should not be referred to as salting out.
- (ii) The term is also used for the addition of electrolytes to reduce the mutual partial miscibility of two liquids.
- (iii) It has no connection with *synergism* (1.23).

1.19 Solvent Extraction

The process of transferring a substance from any matrix to an appropriate liquid phase. If the substance is initially present as a solute in an immiscible liquid phase the process is synonymous with *liquid-liquid extraction* (1.11).

Notes:

- (i) If the extractable material is present in a solid (such as a crushed mineral or an ore) the term *leaching* may be more appropriate. The extractable material may also be a liquid entrapped within or adsorbed on a solid phase.
- (ii) Common usage has established this term as a synonym for *liquid-liquid distribution* (1.11). This is acceptable provided that no danger of confusion with extraction from solid phases exists in a given context.

1.20 Solvent Ion Exchange (SIX)

This term is not recommended (see *liquid ion exchange*) (1.10).

1.21 Sublation

A flotation process in which the material of interest, adsorbed on the surface of gas bubbles in a liquid, is collected on an upper layer of immiscible liquid.

Notes: There is no liquid-phase mixing in the bulk of the system; as a result recoveries can approach 100%.

1.22 Substoichiometric Extraction

Here the amount of reagent used is lower than that dictated by stoichiometry. If the constants of formation and extraction of the complexes are high, the amount of extracted metal is dictated by the amount of extractant introduced.

1.23 Synergism

A term describing the co-operative effect of two (or more) *extractants* (2.8) where the *distribution ratio* (3.5) for the combination is greater than the largest individual *distribution ratio* (measured under comparable conditions)

Notes:

- (i) The corresponding adjective is *synergic* and the term *synergistic* should not be used.
- (ii) No standard method for quantification of the phenomenon has been agreed and any approach should be clearly defined in a given situation.

2. Components of the Solvent Phase

2.1 Accelerator See *Catalyst* (2.3), *Kinetic Synergist* (2.10), *Modifier* (2.11)

Note: This term may be used as a synonym for catalyst.

2.2 Carrier See *Diluent* (2.5)

This term is not recommended.

2.3 Catalyst (in Liquid-liquid Distribution)

A substance included in the *solvent* (2.12) to increase the rate of transfer without affecting the position of equilibrium.

Notes: The term *accelerator* may also be used but *kinetic synergist* is not recommended.

2.4 Cosolvent See *Diluent* (2.5)

2.5 Diluent

The liquid or homogeneous mixture of liquids in which *extractant(s)* (2.8) and possible *modifier(s)* (2.11) may be dissolved to form the *solvent* (2.12) phase.

Notes:

- (i) The term *carrier*, which implied an inert diluent is not recommended.
- (ii) Although the diluent may well be a single liquid or even the major portion of the extracting phase, the term *solvent* (2.12) should not be used in this sense as it has a much wider meaning in the context of liquid-liquid extraction, although the term *cosolvent* may be used in certain circumstances.
- (iii) The diluent by itself does not extract the *main (extractable) solute* appreciably

2.6 Epi-Phase

The less dense phase in a distribution system.

Note: The term is often used when two non-aqueous phases are present or when the *solvent* (2.12) is an aqueous solution. See also *hypo-phase* (2.9).

2.7 Extract (Noun)

The separated phase (often but not necessarily organic) that contains the material extracted from the other phase.

Notes:

- (i) Where appropriate the term “*loaded solvent*” (4.15) may be used, but is not recommended.
- (ii) For usage as a verb see 1.8.

2.8 Extractant

The active component(s) primarily responsible for transfer of a solute from one phase to the other.

Notes:

- (i) The term *extracting agent* is a synonym but *solvent* (2.12) and *ligand* should not be used in this context.
- (ii) Certain *extractants* that consist of liquids immiscible with water (e.g. Tributyl phosphate or certain ketones) might comprise the only component of the initial organic phase but *extractant(s)* can also be dissolved in *diluent* (2.5).

2.9 Hypo-Phase

The denser phase in an extraction system.

Note: The term is often used when two non-aqueous phases are present or when the *solvent* (2.12) is an aqueous phase. See also *epi-phase* (2.6).

2.10 Kinetic Synergist

This term is not recommended as a synonym for *catalyst* (2.3) or *accelerator* (2.1).

2.11 Modifier

A substance added to a *solvent* (2.12) to improve its properties e.g. by increasing the solubility of an *extractant* (2.8), changing interfacial parameters, or reducing adsorption losses.

Note: Additives used to enhance extraction rates should be called *accelerators* (2.1) or *catalysts* (2.3).

2.12 Solvent (in Liquid-liquid Distribution)

The term applied to the whole initial liquid phase containing the *extractant* (2.8).

Notes:

- (i) The solvent may contain only *extractant* or it may be a composite homogeneous mixture of *extractant(s)* (2.8) with *diluent(s)* (2.5) and also sometimes *modifiers* (2.11) and *accelerators* (2.1).
- (ii) The term *solvent* must not be used as a synonym for any of the individual components of a composite liquid phase even where, in the case of a single component (e.g. 3-methylbutan-2-one or tributyl phosphate), it becomes identical with the *extractant*.
- (iii) The term may be qualified to denote the *extract* from a given processing *step* (4.41), e.g. *loaded solvent* (4.15).

3. Fundamental Parameters

3.1 Concentration Factor

Not recommended. See *extraction factor* (3.10).

3.2 Decontamination Factor

The ratio of the proportion of contaminant to product before treatment to the proportion after treatment. It is the reciprocal of the *enrichment factor* (3.6).

3.3 Distribution Coefficient

This term is not recommended as a synonym for *distribution ratio* (3.5).

3.4 Distribution Constant

A synonym for *partition ratio* (3.17).

3.5 Distribution Ratio (in Liquid-liquid Distribution) (*D*)

The ratio of the total analytical concentration of a solute in the *extract* (2.7) (regardless of its chemical form) to its total analytical concentration in the other phase.

Notes:

- (i) If there is possible confusion with the *extraction factor* or (*mass*) *distribution ratio* (3.13), the term *concentration distribution ratio* (symbol D_C) should be used, but this is not common usage. This is reasonably compatible with chromatographic nomenclature.
- (ii) The terms *distribution coefficient*, *extraction coefficient* and, where appropriate, *scrubbing coefficient*, *stripping coefficient* are widely used alternatives but are not recommended. If they must be used in a given situation the term *ratio* is preferable to *coefficient*.
- (iii) In equations relating to aqueous/organic systems the organic phase concentration is, by convention, the numerator and the aqueous phase concentration the denominator. In the case of *stripping ratio* the opposite convention is sometimes used but should then be clearly specified.
- (iv) In the past there has been much confusion between the *distribution ratio* as defined above, the value of which varies with experimental conditions, e.g. pH, presence of complexing agents, extent of achievement of equilibrium, etc. and the true *partition constant* (3.16) which is by definition invariable or the *partition coefficient* or *distribution constant* which apply to a particular chemical species under specified conditions. For this reason the terms *distribution constant* (3.4), *partition constant* (3.16), *partition coefficient* (3.15), *partition ratio* (3.17) and *extraction constant* (3.9) should not be used in this context.
- (v) The use of the ratio: *light phase concentration to heavy phase concentration* is ambiguous and is not recommended.
- (vi) The *distribution ratio* is an experimental parameter and its value does not necessarily imply that distribution equilibrium between the phases has been achieved.

3.6 Enrichment Factor (in Liquid-liquid Distribution) (*S*)

The factor by which the ratio of the amounts of two substances in the *feed* (4.11) must be multiplied to give their ratio after treatment.

$Q_A/Q_B = S_{A,B}(Q'_A/Q'_B)$ where Q_A and Q'_A are the final and initial amounts of species A and Q_B and Q'_B are the final initial amounts of species B. Hence $S_{A,B} = E_A/E_B$ where E is the *fraction extracted* (3.11). In terms of D , n , r (where n is the number of stages and r the *phase ratio* (3.19))

$$S_{A,B} = \frac{1 - (1 + rD_A)^{-n}}{1 - (1 + rD_B)^{-n}}$$

3.7 Extractability

A property which qualitatively indicates the degree to which a substance is extracted.

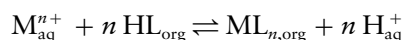
Note: This term is imprecise and generally used in a qualitative sense. It is not a synonym for *fraction extracted* (3.11).

3.8 Extraction Coefficient

This term is not recommended as a synonym for *distribution ratio* (3.5).

3.9 Extraction (Equilibrium) Constant at Zero Ionic Strength (K_{ex}°)

The equilibrium constant of the distribution reaction expressed in terms of the reacting species. Thus, for the gross reaction:



in which the reagent HL initially dissolved in an organic phase reacts with a metal ion M^{n+} in aqueous solution to form a product ML_n which is more soluble in the organic phase than in water,

$$K_{\text{ex}}^{\circ} = \frac{a_{\text{ML}_n,\text{org}} \times a_{\text{H}^{+},\text{aq}}^n}{a_{M^{n+},\text{aq}} \times a_{\text{HL},\text{org}}^n}$$

Notes:

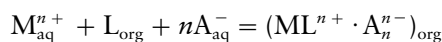
- (i) When concentrations are used instead of activities or mixed terms are employed as when H^{+} and/or M^{n+} are measured with an electrode, the appropriate name is *extraction constant*, symbol K_{ex} , accompanied by a careful definition. K_{ex}° may be termed the *thermodynamic extraction constant*.
- (ii) The extraction constant is related to other terms relevant to such systems by:

$$K_{\text{ex}} = \frac{D_{\text{ML}_n} \beta_n K_a^n}{D_{\text{HL}}^n}$$

where β_n is the overall formation constant of ML_n and K_a is the dissociation constant of HL. When the reagent HL is more soluble in water than the other immiscible phase it may be more convenient to define a special equilibrium constant in terms of HL_{aq} :

$$K_{\text{ex}} = D_{\text{ML}_n} \beta_n K_a^n$$

- (iii) In distribution equilibria involving non-aqueous systems, e.g. liquid SO_2 , molten salts and metals, the mass action equilibrium constant for the relevant extraction process can be identified with K_{ex} which should be explicitly defined in this context.
- (iv) In actual practice, it may be necessary to include other terms to take into account other complexes formed by auxiliary reagents and the solvation and/or polymerization of the various species. In such cases, K_{ex} must be defined with reference to the relevant explicit chemical equation. An example is complex formation between the metal ion and an uncharged crown ether or cryptand molecule followed by ion-pair extraction:



$$K_{\text{ex}} = \frac{[\text{ML}^{n+} A_n^{n-}]_{\text{org}}}{[M^{n+}]_{\text{aq}} [L]_{\text{org}} [A^{-}]_{\text{aq}}^n}$$

- (v) Use of Ringbom's "conditional extraction constant",

$$K_{\text{ex}}^{\text{eff}} = \frac{a_{\text{H}^{+}}^n \cdot [\text{ML}'_n]_{\text{org}}}{[M']_{\text{aq}} [\text{HL}'_n]_{\text{org}}^n}$$

in conjunction with alpha coefficients is useful [11].

- (vi) The phases can also be specified by the formula of the solvent or by other symbols (preferably Roman numerals) or by overlining formulae referring to one phase, usually the less polar one. The subscript aq (or w) is often omitted; aq is preferable to w as the latter is appropriate only in English and German.
- (vii) The qualification "Equilibrium" is often omitted.
- (viii) The terms *partition constant* and *distribution constant* **must not** be used in this sense.

3.10 Extraction Factor (D_m)

The ratio of the total mass of a solute in the extract to that in the other phase.

Notes:

- (i) It is the product of the (*concentration*) *distribution ratio* and the appropriate *phase ratio*.
- (ii) It is synonymous with the *concentration factor* or *mass distribution ratio*, this latter term being particularly apt.
- (iii) The term *concentration factor* is often employed for the overall *extraction factor* in a process or process step.

3.11 Fraction Extracted (E)

The fraction of the total quantity of a substance extracted (usually by the solvent) under specified conditions, i.e. $E_A = Q_A/Q'_A$ where Q_A is the mass of A extracted and Q'_A is the total mass of A present at the start.

Notes:

- (i) E may be expressed as a percentage, % E .
- (ii) The term *extractability* is qualitative and should not be used as a synonym for *fraction extracted*.
- (iii) If the aqueous phase is extracted with n successive portions of solvent, the phase volume ratio (solvent/feed) being r each time, the fraction extracted is given by:

$$E_n = 1 - (rD + 1)^{-n}$$

If $n = r = 1$, $E_1 = D/(1 + D)$ this expression is a concept of value in chromatography theory.

- (iv) The fraction extracted is also known as the *recovery factor*, especially for a multistage process.

3.12 Loading Capacity

The maximum concentration of solute(s) that a *solvent* (2.12) can contain under specified conditions.

Notes:

- (i) The terms *maximum loading*, *saturation capacity* and *saturation loading* are synonymous.
- (ii) All the above terms should clearly be distinguished from *ultimate capacity* (3.29)

3.13 Mass Distribution Ratio See Extraction Factor (3.10)**3.14 Maximum Loading See Loading Capacity (3.12)****3.15 Partition Coefficient**

This term is not recommended and should not be used as a synonym for *partition constant* (3.16), *partition ratio* or *distribution ratio* (3.5).

3.16 Partition Constant (K_D°)

The ratio of activity of a given species A in the extract to its activity in the other phase with which it is in equilibrium, thus

$$(K_D^\circ)_A = a_{A,org}/a_{A,aq}$$

Its value should not vary with composition but depends on the choice of standard states and on the temperature (and eventually the pressure).

Note: See *transfer activity coefficient* (3.28).

3.17 Partition Ratio (K_D)

The ratio of the concentration of a substance in a single definite form, A, in the *extract* (4.8) to its concentration in the same form in the other phase at equilibrium, e.g. for an aqueous/organic system

$$(K_D)_A = [A]_{org}/[A]_{aq}$$

Notes:

- (i) K_D is sometimes called the *distribution constant*; this is a good synonym. The terms *distribution coefficient*, *distribution ratio* (3.5), *partition constant* (3.16) and *extraction constant* (3.9) should not be used as synonyms for *partition ratio*.
- (ii) The use of the inverse ratio (aqueous/organic) may be appropriate in certain cases, e.g. where the organic phase forms the *feed* (4.11) but its use in such cases should be clearly specified. The ratio of the concentration in the denser phase to the less dense phase is not recommended as it can be ambiguous.
- (iii) If the pure *solvent* and infinitely dilute feed are taken as the standard state, $K_D \rightarrow K_D^\circ$ as the total concentration of dissolved materials decreases.

3.18 $pH_{0.5}$ or $pH_{1/2}$

That value of pH in an aqueous phase at which the *distribution ratio* (3.5) is unity at equilibrium.

Note: 50% of the solute is extracted ($E = 0.5$) *only* when the *phase ratio* (3.19) is unity.

3.19 Phase Ratio (in Liquid-liquid Distribution) (r)

The ratio of the quantity of the solvent (2.12) to that of the other phase.

Notes:

- (i) Unless otherwise specified the phase ratio refers to the *phase volume ratio*.
- (ii) If other aspects of the phase ratio are employed viz. *phase mass ratio*, *phase flow ratio*, these should be specified.

3.20 Recovery Factor

This term is not recommended. *Fraction extracted* (3.11) should be used.

3.21 Saturation Capacity See *Loading Capacity* (3.12)

3.22 Saturation Loading See *Loading Capacity* (3.12)

3.23 Selectivity Coefficient

This term should not be used as a synonym for *separation factor* (3.26).

Note: This term has a specific meaning in relation to ion exchange by solid exchangers.

3.24 Selectivity Ratio

Synonym for *selectivity coefficient* (3.23). It should not be used as a synonym for *separation factor* (3.26).

3.25 Separation Coefficient

This term is not recommended. A synonym for *separation factor* (3.26).

3.26 Separation Factor (in Liquid-liquid Distribution) ($\alpha_{A,B}$)

The ratio of the respective *distribution ratios* (3.5) of two extractable solutes measured under the same conditions.

$$\alpha_{A,B} = D_A/D_B$$

Notes:

- (i) By convention the solutes designated as A and B in the above are chosen so as to make $\alpha > 1$.
- (ii) The term *separation coefficient* is not recommended.
- (iii) The terms *selectivity coefficient* (3.23) and *selectivity ratio* (3.24) are not synonymous and should not be used.

3.27 Stoichiometric Capacity See *Ultimate Capacity* (3.29)**3.28 Transfer Activity Coefficient (γ_t)**

A term used to quantify the difference in the free energy of a solute ion in two different standard states often in two different liquid phases. The relationship is $\Delta_t G^\circ = v RT \ln \gamma_t$ where $\Delta_t G^\circ$ is the transfer Gibbs energy and v is the number of ions in the solute. See *partition constant*.

Notes:

- (i) See *IUPAC Information Bulletin* No. 34 (1974) [12] for full details.
- (ii) It should not be confused with the *mass transfer coefficient* which represents the specific rate of transfer of a species from one phase to another.
- (iii) It does not necessarily imply the physical transfer of a solute between two liquid phases.

3.29 Ultimate Capacity

The theoretical maximum capacity of a *solvent* (2.12) containing a given concentration of *extractant* (2.8) for a solute under any conditions.

Note: Where appropriate the term *stoichiometric capacity* can be used.

4. Process Terminology**4.1 Back Extraction**

A synonym for *stripping* (by extraction) (4.43).

4.2 Back Washing

Often used as a synonym for *stripping* (4.43). This term is not recommended.

4.3 Continuity Inversion

A change in the mutual dispersion of two phases in contact. See *inversion* (4.13).

4.4 Crowding

The displacement of an impurity from an extract phase by contact with a solution containing the main extractable solute. See *scrubbing* (4.23), *exchange extraction* (4.8).

Note: The main solute need not be present in a pure solution but should have a higher *distribution ratio* (3.5) than the impurities present.

4.5 Crud

A deposit or emulsion at the interface between two partially settled phases.

Notes:

- (i) The phenomenon of crud formation arises from many causes and this definition does not imply any single one.
- (ii) Other terms – some unprintable – have been used but *crud* is the generally accepted term.

4.6 Density Inversion

The interchange of the denser and less dense phases due to changes in solute concentration. See *inversion* (4.13).

Note: *Phase inversion* (4.20) is often used in this context but is ambiguous.

4.7 Differential Contactor

A type of continuous multistage extraction equipment in which there is only one interface at which phase separation by settling occurs. See *theoretical stage* (4.52).

4.8 Exchange Extraction

An extraction operation or process in which a metal from one phase is exchanged with the equivalent amount of a second metal from the other phase. See *crowding* (4.4).

Note:

- (i) This term may be used in connection with any step (e.g. *loading*, (4.16), *scrubbing* (4.23) or *stripping* (4.43) in a process).
- (ii) This applies also to organic or molecular species.

4.9 Extraction (in Process Liquid-liquid Distribution)

In connection with processes, this term often refers to the initial transfer step whereby the *main solute* (1.13), often together with impurities, is transferred from *feed* to *solvent* (2.12). See *loading* (4.16).

Notes:

- (i) *Partition and distribution* (1.4) are not synonyms in this specific instance.
- (ii) The term *extraction* may be used in a more general sense. See under “General Definitions” (1.9).

4.10 Extraction Isotherm See Distribution Isotherm (1.5)**4.11 Feed**

A solution introduced into an *extraction* system.

Note: It should be clearly identified (e.g. *scrub feed*) but, if used without qualification, it may be taken to designate the initial liquid phase containing the main solute to be transferred.

4.12 Height Equivalent to a Theoretical Stage (HETS)

See explanation of *Theoretical Stage* (4.52).

4.13 Inversion (or Phase Inversion)

This term is used in two senses which should be specified.

- (i) *density inversion* (4.6)
- (ii) *continuity inversion* (4.3)

4.14 Load (in Liquid-liquid Distribution) (Verb)

To transfer solute from a *feed* (4.11) to another liquid phase.

4.15 Loaded Solvent See Extract (2.7)

Note: This term is usually used to denote the *extract* (2.7) after completion of a particular step, e.g. *extraction* or *scrubbing* (4.23)

4.16 Loading (Noun)

The concentration of an extracted solute in the *extract* (2.7).

4.17 Loading (Verb) See Load (4.14)

Note: Used in this sense the term normally refers to the operation of transferring the *main solute* (1.13)), often with impurities from the *feed* to the *solvent* (2.12).

4.18 O.K. Liquor

Sometimes used as a synonym for *strip product solution* (4.48) or *strip liquor* (4.42)

Note: This term is confusing and **should not** be used.

4.19 Operating Line

A graphical representation of the mass balance relationship of a solute across an extraction process *step* (4.41) or *stage* (4.38).

4.20 Phase Inversion See *Density Inversion* (4.6)**4.21 Raffinate**

The phase remaining after extraction of some specified solute(s). *When necessary* it should be further specified, e.g. *scrub raffinate* (4.30).

Note: The original meaning of *raffinate* as a “refined product” has become extended and changed by common usage.

The term should normally be applied only to waste streams but the latter may form the feed to a further extraction process for another solute.

4.22 Regeneration See *Solvent Regeneration* (4.37)**4.23 Scrubbing See *Crowding* (4.2) and *Selective Stripping* (4.33)**

The process of selectively removing contaminating solutes (impurities) from an *extract* (2.7) that contains these as well as the *main extractable solute* (1.13) by treatment with a new immiscible liquid phase.

Note: The term *stripping* (4.43) has a different meaning and should not be used in this sense although this usage has been customary in certain industries.

4.24 Scrubbing Agent

The chemical reagent used to effect *scrubbing* (4.23).

Note: Often used as a synonym for its solution.

4.25 Scrubbing Agent Solution

The solution used to effect *scrubbing* (4.23)

Note: The term *scrub solution* is ambiguous and is not recommended.

4.26 Scrubbing Isotherm See *Distribution Isotherm* (1.5)**4.27 Scrub Feed**

The *extract* (2.7) to be scrubbed.

4.28 Scrub Liquor See *Scrub Raffinate* (4.30)

Note: This term is ambiguous and is not recommended.

4.29 Scrub Product Solution

The solution that results from the *scrubbing* of impurities from an extract phase.

Note: The term *scrub liquor* is also used but can be confused with the *scrubbing agent solution* (4.25) and is not recommended. See *scrub raffinate* (4.30).

4.30 Scrub Raffinate

This term should only be used where the product solution from scrubbing is discharged to waste. *Scrub product solution* (4.29) is better where this stream is combined with *feed* (4.11) to the loading section.

4.31 Scrubbing Ratio See *Distribution Ratio* (3.5)

Note: The term *scrubbing coefficient* is not recommended. This term is not common.

4.32 Scrub Solution See *Scrubbing Agent Solution* (4.25)

Note: This term should not be used as it is ambiguous and can be confused with *scrub raffinate* (4.30) or *scrub product solution* (4.29).

4.33 Selective Scrubbing See *stripping* (4.43)**4.34 Solvent Inventory**

The total quantity of solvent present in the process.

4.35 Solvent Loss

The total quantity of solvent lost during the operation of a process.

Note: There are a number of ways currently in use to express both *solvent inventory* and *solvent loss* and authors should carefully define how they are using the terms until a generally agreed procedure can be recommended.

4.36 Solvent Purification

See *solvent regeneration*. The description *solvent purification* naturally applies also to the purification of fresh solvent (2.12).

4.37 Solvent Regeneration

Treatment of the solvent for re-cycling, e.g. by removal of degradation products or non-strippable solutes.

Note: The term *solvent purification* is synonymous, but the terms *scrubbing* (4.23), *stripping* (4.31) and *washing* should not be used in this context.

4.38 Stage

That physically distinct part of an extraction process in which transfer of solute(s) occurs, followed by phase separation. See *theoretical stage* (4.52).

Notes:

- (i) For certain types of equipment with a single phase separation interface, the term *theoretical stage* (4.52) is more appropriate.
- (ii) Equilibrium need not necessarily be established in a stage.

4.39 Stagewise Contactor

A type of continuous multi-stage liquid-liquid contactor in which each stage has a physically distinct cycle of interphase contact and separation.

Note: There will be the same number of phase separation interfaces as there are stages.

4.40 Steady State (in Liquid-liquid Distribution)

The state of a continuous process when it is operating in such a way that the concentration of solutes in exit streams remains constants with respect to time for constant feed concentrations, even though the two phases are not necessarily in thermodynamic equilibrium in any part of the process.

Note: The term *equilibrium* should not be used to describe this situation.

4.41 Step (in Liquid-liquid Distribution)

That operation in an overall extraction process in which transfer of solute(s) occurs in a particular direction, e.g. *Loading* (4.16), *stripping* (4.43), *scrubbing* (4.23).

4.42 Strip Liquor

A liquid phase resulting from the operation of *stripping* (4.43). See *strip solution* (4.50) and *strip raffinate* (4.49).

Notes:

- (i) This term is ambiguous and should be used carefully. *Strip raffinate* (4.49) is more appropriate.
- (ii) The term O.K. *Liquor* (4.18) is not recommended.

4.43 Stripping

The process of removing solute(s) from a *loaded solvent* or *extract* (2.7). Generally this refers to the main solute(s) present.

Notes:

- (i) Where appropriate, e.g. when liquid-liquid distribution is used for *stripping*, the term *back-extraction* can be used. The terms *back-washing* and *re-extraction* (1.17) are not recommended.
- (ii) The recent application of *selective stripping* of solutes as a separation method leads to some confusion between the terms *stripping* and *scrubbing* (4.23). It is recommended that the term *scrubbing* be reserved for the operation of removing contaminants (impurities) from an *extract* (2.7) (where the *scrub raffinate* (4.30) is often recycled to the loading step) and the term *selective stripping* be used where two or more main solutes are stripped successively from an *extract*, usually with different *stripping agents* (4.44), with a view to their subsequent separate recovery from solution for analysis.

4.44 Stripping Agent

The active substance effective in *stripping* (4.43).

4.45 Stripping Agent Solution

The liquid phase used to accomplish *stripping* (4.43).

4.46 Stripping Ratio See *Distribution Ratio* (3.5)

Notes:

- (i) This term is usually defined as the inverse ratio to the *distribution ratio* (3.5, comment iii), i.e. in aqueous-organic systems the aqueous phase concentration of solute is the numerator and the organic phase concentration the denominator. Their usage should be clearly defined.
- (ii) The term *stripping coefficient* is not recommended.

4.47 Stripping Ratio See *Distribution Isotherm* (1.5), *Equilibrium Line* (1.7)

Note: In the graphical representation of *stripping isotherms*, the axes are often interchanged from those used to represent the phases for *extraction isotherms*. It is essential that the axes be clearly labelled.

4.48 Strip Product Solution

The liquid phase resulting from *stripping* (4.43) of a *solvent* (2.12). See *stripping liquor* (4.42), *strip solution* (4.50), *strip raffinate* (4.30), *O.K. liquor* (4.18).

Note: The last four terms are not recommended.

4.49 Strip Raffinate

This term is not recommended. *Raffinate* (4.21) should be reserved for waste streams and the liquid phase resulting from stripping normally contains the desired product.

4.50 Strip Solution

The liquid phase used for *stripping* (4.43).

Note: There is some ambiguity between the terms *strip liquor* and *strip solution*. Perhaps *strip product solution* (4.48) would be more appropriate to the former and *stripping agent solution* (4.45) for the latter. See *stripping agent* (4.44).

4.51 Tenor

A term sometimes used to denote the concentration levels of various solutes in the *feed* (4.11). It is not recommended.

4.52 Theoretical Stage

That part of a continuous multi-stage contactor in which the amount of solute transferred from one phase to the other is equivalent to that which would be transferred in an actual stage at equilibrium under comparable conditions of solute concentration in each phase as determined from the *distribution isotherm* (1.5) and *operating line* (4.19) for the system.

Note: Thus from the number of theoretical stages so determined and the height of the contactor the *height equivalent to a theoretical stage* (HETS) may be calculated.

4.53 Washing See solvent regeneration (4.37)

Note: This term is vague and is not recommended.

Table 1 Index of terms

Accelerator	2.1	Partition coefficient	3.15
Antagonism	1.1	Partition constant	3.16
Back extraction	4.1	Partition ratio	3.17
Back washing	4.2	pH _{0.5} or pH _{1/2}	3.18
Carrier	2.2	Phase inversion	4.13, 4.20
Catalyst (in liquid-liquid distribution)	2.3	Phase ratio (in liquid-liquid distribution)	3.19
Coextraction	1.2	Pre-equilibration	1.16
Concentration factor	3.1	Raffinate	4.21
Conditioning	1.3	Regeneration	4.22
Continuity inversion	4.3	Recovery factor	3.20
Cosolvent	2.4	Re-extraction	1.17
Crowding	4.4	Salting out	1.18
Crud	4.5	Saturation capacity	3.21
Decontamination factor	3.2	Saturation loading	3.22
Density inversion	4.6	Scrubbing	4.23
Differential contactor	4.7	Scrubbing agent	4.24
Diluent	2.5	Scrubbing agent solution	4.25
Distribution	1.4	Scrubbing isotherm	4.26
Distribution coefficient	3.3	Scrub feed	4.27
Distribution constant	3.4	Scrub liquor	4.28
Distribution isotherm	1.5	Scrub product solution	4.29
Distribution ratio (in liquid-liquid distribution)	3.5	Scrub raffinate	4.30
Enrichment factor (in liquid-liquid distribution)	3.6	Scrubbing ratio	4.31
Epi-phase	2.6	Scrub solution	4.32
Equilibration	1.6	Selectivity coefficient	3.23
Equilibrium line	1.7	Selectivity ratio	3.24
Exchange extraction	4.8	Selective stripping	4.33
Extract (noun)	2.7	Separation coefficient	3.25
Extract (verb)	1.8	Separation factor (in liquid-liquid distribution)	3.26
Extractability	3.7	Solvent	2.12
Extractant	2.8	Solvent extraction	1.19
Extraction	1.9	Solvent inventory	4.34
Extraction (in process liquid-liquid distribution)	4.9	Solvent ion exchange (six)	1.20
Extraction coefficient	3.8	Solvent loss	4.35
Extraction factor	3.10	Solvent purification	4.36
Extraction isotherm	4.10	Solvent regeneration	4.37
Feed	4.11	Stage	4.38
Fraction extracted	3.11	Stagewise contactor	4.39
Height equivalent to a theoretical stage (HETS)	4.12	Steady state (in liquid-liquid distribution)	4.40
Hypo-phase	2.9	Step (in liquid-liquid distribution)	4.41
Inversion	4.13	Stoichiometric capacity	3.27
Kinetic synergist	2.10	Strip liquor	4.42
Liquid ion exchange	1.10	Stripping	4.43
Liquid-liquid distribution (extraction) (partition)	1.11	Stripping agent	4.44
Load (in liquid-liquid distribution) (verb)	4.14	Stripping agent solution	4.45
Loaded solvent	4.15	Stripping ratio	4.46
Loading (noun)	4.16	Stripping isotherm	4.47
Loading (verb)	4.17	Strip product solution	4.48
Loading capacity	3.12	Strip raffinate	4.49
Macro-element	1.12	Strip solution	4.50
Main (extractable) solute	1.13	Sublation	1.21
Mass distribution ratio	3.13	Substoichiometric extraction	1.22
Maximum loading	3.14	Synergism	1.23
Micro-element	1.14	Tenor	4.51
Modifier	2.11	Theoretical stage	4.52
O.K. Liquor	4.18	Transfer activity coefficient	3.28
Operating line	4.19	Ultimate capacity	3.29
Partition	1.15	Washing	4.53

Table 2 Index of symbols

D	Distribution ratio (in liquid-liquid distribution)	3.5
S	Enrichment factor (in liquid-liquid distribution)	3.6
D_m	Extraction factor	3.10
K_{ex}^o	Extraction (equilibrium) constant at zero ionic strength	3.9
E	Fraction extracted	3.11
K_d^o	Partition constant	3.16
K_d	Partition ratio	3.17
r	Phase ratio (in liquid-liquid distribution)	3.19
$\alpha_{A,B}$	Separation factor (in liquid-liquid distribution)	3.26
γ_t	Transfer activity coefficient	3.28

Appendix 1. Comparison of Nomenclature With Previously Defined Terms

(OB, Orange Book [9]; Chrom, Nomenclature for Chromatography [10])

Carrier (2.12) This term is not recommended in this area (OB p54)

Catalyst (in liquid-liquid distribution) (2.3) Defined as a specific use of *catalyst* (OB p56).

Diluent (2.5) Redefined from OB 9.2.4 and 9.2.10 in a more general sense

Distribution (1.4) Now defined – only mentioned in OB 9.2.6

Distribution coefficient (3.3) Not recommended in this area (OB 9.4.10)

Distribution constant (3.4) Matches uses in Chrom 3.9 and 5.6.

Distribution ratio (in liquid-liquid distribution) (3.5) Slight clarification of usage from OB 9.2.6

Enrichment factor (in liquid-liquid distribution) (3.6) Rewording of OB 9.2.8 to make more general.

Extractant (2.8) Redefined compared to OB 9.2.11

Extraction (in liquid-liquid distribution) (1.9) See more precise term OB 9.2.4

Extraction coefficient (3.8) Not recommended (OB 9.2.6)

Extraction constant (3.9) Slightly amended from OB 9.2.5

Liquid-liquid distribution (1.11) Redefined from OB 9.2.4

Mass distribution ratio (3.13) Unchanged from OB 9.4.10. Not recommended in Chrom 3.7.12.

Modifier (2.11) Term now defined (see OB 9.2.4)

Partition (1.15) Term now defined (OB 9.2.1)

Partition coefficient (3.15) and *partition constant* (3.16) Not recommended (OB 9.2.6) agrees 3.9.01

Recovery factor (3.20) Now not recommended (OB 9.2.7)

Salting out (1.18) Definition broadened from OB 9.2.15

Selectivity coefficient (3.23) Not recommended in this area (used in Chrom 5.5.02)

Separation factor (in liquid-liquid distribution) (3.25) Specifically defined for this area to distinguish from Chrom 3.7.14.2 and 5.5.04

Solvent (in liquid-liquid distribution) (2.12) Specific definition provided for this area more limited than OB 9.1.2 and redefines 9.2.9. Differs from Chrom 1.1.11 and 5.2.01

Appendix 2. Survey of Partition Terminology Used by Authors of Books

Term: Activities of a single species $\frac{a_{A,org}}{a_{A,aq}}$

Symbol	Name	Reference
K_D°	Partition constant	9
P°	Activity partition constant	13
P	Partition coefficient or Distribution coefficient	14, 15
K_p	Thermodynamic partition constant	16
p° or K_p°	Thermodynamic partition constant	17
P	Thermodynamic partition coefficient or Partition coefficient	18
K_D	Distribution coefficient	19
K	Distribution coefficient	15

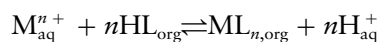
Term: Total concentration of related species $\frac{(C_A)_{org}}{(C_A)_{aq}}$

Symbol	Name	Reference
D_c	Concentration distribution ratio	9, 16, 31
D	Distribution ratio	14, 19, 20, 22, 23, 25, 26, 27, 31, 33, 34, 37
D	Distribution coefficient	17, 18, 37, 38
D^{Total}	Distribution coefficient	34
q	Distribution coefficient	11
Q	Extraction coefficient	39
E	Extraction coefficient	36
E	Distribution ratio	17, 35

Term: Concentration distribution of $\frac{[A]_{org}}{[A]_{aq}}$ a single species

Symbol	Name	Reference
K_D	Distribution constant	9, 20, 21
K_D	Distribution coefficient	21, 22, 23, 24
K_D	Distribution or partition coefficient	25
K_D	Partition coefficient	26
K_D	Partition constant	27
K	Partition coefficient	14, 28, 29
K or λ	Partition ratio	30
K	Partition or Distribution coefficient	31
K	Distribution coefficient	15
K_p	Partition coefficient	16
P	Partition constant or coefficient	32
P	Partition coefficient or distribution constant	33
P	Partition ratio	17, 18
D	Distribution ratio	11, 34
Q	Partition ratio	35
Q_c	Molar partition constant	36

Term: Equilibrium constant for:



$$\text{i.e.} = \frac{[ML_n]_{org} \times [H^+]_{aq}^n}{[M]_{aq}^n \times [HL]_{org}^n}$$

Symbol	Name	Reference
K_{ex}°	Extraction constant at zero ionic strength (activities in above)	9
K_{ex}	Extraction constant or Overall extraction constant	9, 19, 20
K_{ext}	Extraction equilibrium constant	32
K	Extraction constant	39
K'_{ex}	Conditional extraction constant	11

References

1. Recommended Nomenclature for Liquid-Liquid Distribution, *Pure Appl. Chem.*, **21**, 111–113 (1970).
2. Y. Marcus, *Rev. Pure Appl. Chem.*, **18**, 460–464 (1969).
3. A. W. Ashbrook and G. M. Ritcey, *Canad. Mining J.*, 70–72 (May 1972).
4. D. W. Bridges and J. B. Rosenbaum, *U.S. Bureau of Mines Information Circular*, IC 7139, (1962).
5. W. Fischer, K. Biesenberger, J. Happner and U. Noltz, "Old and New Processes for Multiplicative Distribution (liquid-liquid extraction)" *Angew. Chem. Internat. Edn.*, **3**, 791–800 (1964).
6. Proceedings ISEC-71, Society of Chemical Industry, London, **2**, 25–27 (1971).
7. H. M. N. H. Irving and N. M. Rice, *IUPAC Inform. Bull.* No. 63. (July 1977).
8. N. M. Rice, *Chem. Ind.*, 718–723 (1977).
9. H. Freiser and G. H. Nancollas, *Compendium of Analytical Nomenclature*, Blackwell Scientific Publications, Oxford, 2nd Ed., (1987).
10. Recommendations on Nomenclature for Chromatography, *Pure Appl. Chem.*, **65**, 819–872 (1993).
11. A. Ringbom, *Complexation in analytical chemistry*, Interscience, New York, 1963.
12. *IUPAC Inform. Bull.* **34**, (1974).
13. I. M. Kolthoff, E. B. Sandell, E. J. Meehan and S. Bruckenstein, *Quantitative chemical analysis*, 4th Ed., Macmillan, London, 1969.
14. M. S. Cresser, *Solvent extraction in flame spectroscopic analysis*, Butterworths, London, 1978.
15. E. W. Berg, *Physical and chemical methods of separation*, McGraw Hill, New York, 1963.
16. D. G. Peters, J. M. Hayes and G. M. Hieftje, *Chemical Separations and measurements, theory and practice of analytical chemistry*, Saunders, New York, 1974.
17. E. B. Sandell and H. Onishi, *Photometric determination of traces of metals (General aspects)*, 4th Ed., Part 1., Wiley Interscience, New York, 1978.
18. Y. Marcus and A. S. Kertes, *Ion-exchange and solvent extraction of metal complexes*, Wiley, Chichester, 1969.
19. R. A. Day and A. L. Underwood, *Quantitative analysis*, Prentice-Hall, Engelwood Cliffs, NJ, 1980.
20. H. A. Laitinen and W. E. Harris, *Chemical analysis*, 2nd Ed., McGraw Hill, New York, 1975.
21. J. S. Fritz and G. H. Shenk, *Quantitative analytical chemistry*, Allyn and Bacon, Boston, 1969.
22. G. H. Morrison and H. Freiser, *Solvent extraction in analytical chemistry*, Wiley, Chichester, 1957.
23. G. D. Christian and J. E. O'Reilly, *Instrumental analysis*, Allyn and Bacon, Boston, 1986.
24. D. A. Skoog and D. M. West, *Fundamentals of analytical chemistry*, Holt, Rinehart and Winston, New York, 1976.
25. A. I. Vogel, *Quantitative inorganic analysis*, 3rd Ed., Longmans, London, 1961.
26. F. W. Fifield and D. Kealy, *Principles and practice of analytical chemistry*, International Textbook, London, 1983.
27. A. S. Kertes and Y. Marcus (Eds), *Solvent extraction chemistry* 1968, Wiley InterScience, New York, 1969.
28. Cumming and Kay, Revised by R. A. Chalmers, *Quantitative chemical analysis*, 11th Ed. Oliver and Boyd, Edinburgh, 1956.
29. R. U. Brumblay, *A first course in quantitative analysis*, Addison Welsey, Reading, MA, 1970.
30. H. F. Walton, *Principles and methods of chemical analysis*, 2nd Ed., Prentice Hall, London, 1964.
31. D. J. Pietrzyk and C. W. Frank, *Analytical chemistry*, Academic, New York, 1979.
32. I. M. Kolthoff and E. B. Sandell, *Textbook of quantitative inorganic analysis*, Macmillan, London, 1950.
33. H. A. Flaschka, A. J. Barnard, and P. E. Sturrock, *Quantitative analytical chemistry*, 2nd Ed., Willard Grant/Wadsworth, Belmont CA 1980.
34. G. H. Brown and E. M. Sallee, *Quantitative chemistry*, Prentice Hall, London, 1963.
35. R. A. Chalmers, *Aspects of analytical chemistry*, Oliver and Boyd, Edinburgh, 1968.
36. L. Sucha and S. Kotryl, *Solution equilibria in analytical chemistry*, Van Nostrand/Reinhold, New York, 1972.
37. H. A. C. McKay, T. V. Healy, I. L. Jenkins and A. Naylor, *Solvent extraction of metals*, Macmillan, London, 1966.
38. Z. Marczenko, *Separation and spectrophotometric determination of elements*, Ellis Horwood, Chichester, 1986.
39. J. Stary, *Solvent extraction of metal chelates*, Pergamon, Oxford, 1974.

12C. Non-Linear Chromatography (IUPAC Recommendations 1996)

Prepared for publication by

J. Å. Jönsson, University of Lund, Lund, Sweden

© 1996 IUPAC

Synopsis

This report summarizes and comments on terms and symbols used for the description of non-linear chromatography.

Introduction

In the IUPAC recommendations *Nomenclature for Chromatography* [1], the conditions of linear chromatography are tacitly assumed. In all versions of chromatography, however, non-linear effects are common. These are seen as concentration-dependent retention times and asymmetric (e.g. tailing or fronting) peaks. Asymmetric peaks can result from a number of other causes as well, i.e. large extra-column volumes. In many applications, non-linear effects are disadvantageous as they decrease peak resolution and disturb quantitative evaluation. However, in preparative chromatography, heavy overloading is employed in order to increase material throughput, leading to prominent non-linear effects. A comprehensive text on non-linear chromatography has recently been published [2].

In this paper, some of the concepts and terms used for non-linear chromatography are described. It is to read as a complement to the *Nomenclature for Chromatography* (CN) [1], to which numerous references are given.

1. Terms Related to Isotherms

1.1 Distribution Isotherm (in Chromatography)

The equilibrium relation between the concentration of a sample component in the stationary phase c_s , and in the mobile phase c_M , expressed as a function $c_s = f(c_M)$.

Note: The relation can be influenced also by concentrations of other sample components. c_s and c_M are usually expressed *per unit volume of the phase*; c_s may also be expressed *per mass of the dry solid phase* or *per unit surface area*. This is discussed in CN, section 3.9.

In some versions of chromatography, a distribution isotherm can be seen as a *partition isotherm*, an *adsorption isotherm*, or a combination of these, depending on the mechanism of separation (cf. CN 1.5).

1.1.1 Partition isotherm (in chromatography) Isotherm describing partition of the sample component between the bulk of a liquid stationary phase and a liquid, gaseous or supercritical mobile phase.

1.1.2 Adsorption isotherm Isotherm describing adsorption of the sample component on the surface of the stationary phase from the mobile phase.

Note: Adsorption isotherms can be described by Langmuir, Freundlich and other adsorption isotherm equations. See [3], p. 13.

1.2 Linear Distribution Isotherm

A distribution isotherm which can be approximated as $c_s = K_C c_M$, where K_C is a constant.

Note: At low concentrations, all distribution isotherms tend towards being linear. K_C is the *distribution constant* (cf. CN 3.9 and 3.4 in ref. 4).

1.3 Non-linear Distribution Isotherm

A distribution isotherm which is not linear.

Note: A non-linear isotherm can have several shapes, as classified by Brunauer *et al.* [5]. In chromatography convex or concave shapes are common, as well as combinations.

1.3.1 Convex isotherm Distribution isotherm, the slope of which is continuously decreasing (see Figure 1A).

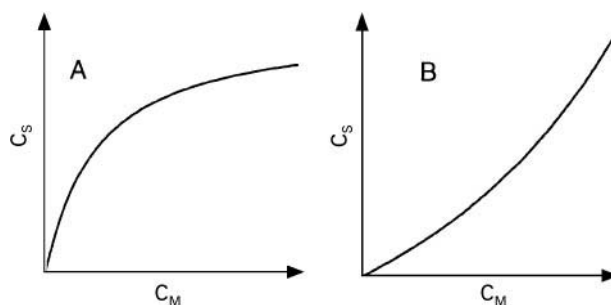


Figure 1 Different types of distribution isotherms for the concentrations of a compound in the stationary (C_s) and mobile (C_M) phases: (A) convex isotherm, (B) concave isotherm.

Note: The resulting chromatographic peak is tailing (CN 3.3.08). Adsorption isotherms are often of this type. A special case is the Langmuir adsorption isotherm.

1.3.2 Concave isotherm Distribution isotherm, the slope of which is continuously increasing (see Figure 1B).

Note: The resulting chromatographic peak is fronting (CN 3.3.09). In gas-liquid chromatography, overloading often results in a concave isotherm.

2. Types of Chromatographic Processes

2.1 Linear Chromatography

Chromatographic process, where the retention is governed by a linear distribution isotherm.

2.2 Non-linear Chromatography

Chromatographic process, where the retention is governed by a non-linear distribution isotherm.

2.3 Ideal Chromatography

Chromatographic process, where no peak-broadening effects (such as diffusion, slow mass transfer, etc.) operate.

Note: This is a hypothetical case, implying that the plate number (CN 3.10.03) is infinite.

2.4 Non-ideal Chromatography

Chromatographic process with normal peak-broadening effects.

2.5 Non-ideal, Linear Chromatography

Chromatographic process, where the retention is governed by a linear distribution isotherm and normal peak-broadening take place.

Note: This case is commonly assumed in analytical chromatography, as described in ref. 1.

2.6 Ideal, Non-linear Chromatography

Chromatographic process, where only the curvature of the distribution isotherm determines the shape of the peaks while other peak-broadening processes are neglected.

Note: The assumption of ideal, non-linear (INL) chromatography is often made in order to facilitate theoretical treatments. It can be justified in cases of efficient columns and distribution isotherms with prominent non-linearity.

2.7 Non-ideal, Non-linear Chromatography

Chromatographic process, where both isotherm curvature and other peak-broadening processes (such as diffusion) contribute to the peak shape.

Note: This case comprises most peaks in common practice that are characterized as ‘tailing’ or ‘fronting’.

3. Retention Parameters in Non-Linear Chromatography

3.1 Total Retention Volume (Time) in Ideal, Non-linear Chromatography ($V_{R(INL)}$, $t_{R(INL)}$)

The volume of mobile phase entering the column between sample introduction and the emergence of a certain concentration of the sample component at the column outlet; or the corresponding time.

Note: This volume (time) can be measured to the peak maximum or to other points on the peak. Under the conditions of ideal, non-linear chromatography, the total retention volume is given by:

$$V_{R(INL)} = V_M + \frac{\partial c_s}{\partial c_M} \cdot V_s \quad (1)$$

With a constant flow rate F_c through the column, the *total retention time in ideal, non-linear chromatography* is given by $t_{R(INL)} = V_{R(INL)}/F_c$ as in CN 37.05. If appropriate, V_s in equation (1) may be exchanged for the surface area of the stationary phase or the mass of the stationary phase, depending on the definition of c_s (cf. 1.1 and CN 3.9). In the case of a linear distribution isotherm, equation (1) is in agreement with corresponding equation in CN 3.9.01. Note that the retention is determined by the *slope* of the isotherm, not by the *ratio* c_s/c_M . This particular point was discussed by Helfferich [6].

Typical peaks in ideal, non-linear chromatography are shown in **Figure 2**. The curved (‘diffuse’) flanks are described by equation (1) and the area of the peak (determined by the total amount of the sample component) gives the position of the vertical flank.

The retention volume in ideal, non-linear chromatography is thus a function of the mobile phase concentration of the sample component. The retention volume to the maximum of the peak (cf. CN 3.7.05) is related the value of the slope of the distribution isotherm at the maximum value of the mobile phase concentration of the sample component at the column outlet.

The broadening of the peaks in Figure 2 is totally caused by the isotherm non-linearity. As the derivation of equation (1) implies that the plate number N is infinite, it is obviously meaningless to apply equations such as those described in CN 3.10.03 and 3.10.04 to characterize peaks of this kind.

3.2 Total Retention Volume (Time) in Non-ideal, Non-linear Chromatography ($V_{R(NINL)}$, $t_{R(NINL)}$)

The definition is analogous to that in 3.1 above.

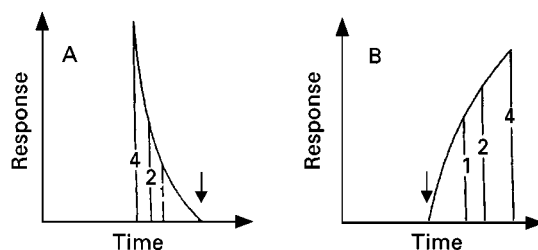


Figure 2 Typical peak shapes in ideal, non-linear chromatography. Peaks A and B are generated by equation (1) from the distribution isotherms in Figures 1A and 1B, respectively. The numbers 1, 2, 4 signify the relative amounts of the sample component. The retention time at low sample concentration, i.e. in the case that the curvature of the distribution isotherm is negligible, is indicated with an arrow.

Note: In the general case of non-ideal, non-linear (NINL) chromatography, only numerical solutions to the applicable non-linear partial differential equations involved can be found. Several examples are found ref 2, where simulated NINL peaks are compared with INL peaks with the same parameters, except for the diffusion term. It is seen that the NINL peaks are lower, wider and more tailing than the INL peak. With a reasonably efficient column ($N > 5000$ for symmetric peaks), the difference might be neglected for practical purposes.

Thus, even if no explicit equation for the retention volume in the NINL case can be given, Equation (1) is approximately valid also for a NINL peak, the discrepancy depending on the column efficiency.

To measure distribution isotherms by chromatography, the so-called *Elution by Characteristic Point (ECP)* method has been suggested. Retention volumes to several points on the curved flank of an experimental peak are measured and related to the solute concentration at those points. The distribution isotherm can then be calculated using Equation (1). The validity of the method depends on the efficiency of the column used for these measurements.

There is no known general way of calculating meaningful peak broadening parameters, such as plate numbers from NINL peaks. As the NINL case in practice is common, this observation is important: The usual equations for the calculation of plate numbers (such as those described in CN 3.10.03) should only be applied to effectively symmetrical peaks.

References

1. Recommendations for Nomenclature for Chromatography. *Pure Appl. Chem.* **65**, 819–872 (1993).
2. G. Guiochon, S. Golshan Shirazi and A. M. Katti, *Fundamentals of Preparative and Non-linear Chromatography*. Academic Press. Inc. Boston (1994).
3. V. Gold, K. L. Loeming, A. D. McNaught and P. Sehl. *Compendium of Chemical Terminology*. Blackwell Science Publishers. Oxford, UK. 1987.
4. Recommendations for Nomenclature for Liquid-Liquid Distribution (Solvent Extraction). *Pure. Appl. Chem.* **65**, 2372–2396 (1993).
5. S. Brunauer, L. S. Deming, W. E. Deming and E. Teller, *J. Amer. Chem. Soc.* **62**, 1723 (1940)
6. F. Helfferich. *J. Chem. Educ.* **41**, 410 (1964).

12D. Supercritical Fluid Chromatography and Extraction (IUPAC Recommendations 1993)

Prepared for publication by

R. M. Smith, Loughborough University of Technology, Loughborough, Leicestershire, UK

© 1993 IUPAC

Abstract

The report present definitions for the terms and symbols used when supercritical fluids are employed as the liquid phase in chromatography and allied areas including sample extraction. The terms supplement those in the general Nomenclature for Chromatography and includes additional more specific terms.

Introduction

Following the General Assembly Meeting in 1989 the Limited Life Time Commission for Chromatography and Other Analytical Separations took over the work on the nomenclature for chromatography that had previously been undertaken by the Commission for Analytical Nomenclature. A major part of the work was the Nomenclature for Chromatography which had been developed over a number of years by L. S. Ettre and has recently been published [1]. This work was comprehensive and included all the major areas of chromatography. Specialist chapters covered the specific areas of size exclusion chromatography and ion-exchange

chromatography. However, it was clear that as further new areas of separation science were developed specific terminologies of further additional terms and definitions would be needed.

Over the last few years the use of a supercritical fluid as the mobile phase in chromatography has become an accepted routine method. In the Nomenclature for Chromatography Ettre noted (1.4.04) "In general, the terms and definitions used for gas or liquid chromatography are equally applicable to supercritical-fluid chromatography". However, supercritical fluid chromatography has also lead to the use in the literature of a number of new terms whose meanings have been generally adopted by workers in the field. These new terms are formalized in the present Supplement to the general nomenclature of chromatography. Supercritical fluids have also been used for the extraction of samples and frequently similar equipment and operating conditions have been employed and many of the terms are also applicable in this field.

This nomenclature is designed to be used as a supplement to the principal nomenclature paper and is written as Section 7 of that paper [1]. It therefore omits any terms which have already been defined unless a new or additional definition has been necessary. The paper is also complementary to the definitions and terms for supercritical fluid chromatography recently published by ASTM [2].

*7. Special Terminology Used in Supercritical-Fluid Chromatography and Extraction

7.1 Basic Definitions

7.1.1 Critical temperature (T_c) The maximum temperature at which a gas can be converted into a liquid by an increase in pressure.

7.1.2 Critical pressure (p_c) The minimum pressure which would suffice to liquefy a substance at its critical temperature. Above the critical pressure, increasing the temperature will not cause a fluid to vaporize to give a two-phase system.

7.1.3 Critical point The characteristic temperature (T_c) and pressure (p_c) above which a gas cannot be liquefied.

7.1.4 Supercritical fluid The defined state of a compound, mixture or element above its critical pressure (p_c) and critical temperature (T_c).

7.1.5 Reduced temperature (T_r) The ratio of the temperature (T) in the system to the critical temperature (T_c)

$$T_r = T/T_c$$

7.1.6 Reduced pressure (p_r) The ratio of the pressure in the system (p) to the critical pressure (p_c).

$$p_r = p/p_c$$

7.2 The Mobile Phase

7.2.1 The *mobile phase* was defined previously in 1.1.06

7.2.2 Mobile-phase pressure

7.2.2.1 Outlet pressure (p_o) Defined as in 3.6.02.2. However, unlike gas and liquid chromatography the outlet pressure in supercritical-fluid chromatography has to be maintained above ambient pressure by a flow restrictor (7.3.1) or back-pressure regulator (7.3.2).

7.2.2.2 Pressure drop across the column (Δp) Defined as 3.6.02.3.

*For Sections 1–6 see *Pure & Appl. Chem.*, Vol. 65, No. 4, pp. 819–872, 1993.

7.2.3 Mobile-phase volume flow rate. Defined as 3.6.04. In supercritical-fluid chromatography this is usually quoted as the rate of delivery of the pumping system.

7.2.4 Mobile-phase mass flow rate The rate of mass flow through the column. It is usually determined by measuring the gas-flow rate (or liquid-flow rate) at ambient conditions after the mobile phase has been depressurized. If liquid modifiers are present in the mobile phase, corrections will be needed.

7.2.5 Mobile-phase composition The composition of the mobile-phase which is delivered to the column. This should be described in such a way that it can be reproduced in different laboratories. It can be expressed on a mass, volume, or mole fraction basis but in each case the temperature and pressure must also be defined.

If the individual components are pumped separately, the relative delivery flow rates should be defined.

Premixed eluents are often used and can be defined by their mass composition as recorded by the manufacturer. However, the delivered composition may depend on the relative volatility of the components and can change as a function of syringe pump volume and time.

7.2.5.1 Mobile-phase modifier Modifiers are materials (usually organic compounds such as methanol or acetonitrile) added to the supercritical fluid being used as the mobile phase to alter the elution properties.

7.3 Instrumentation

Most of the components of the instrumentation for supercritical-fluid chromatography are in common with liquid and gas chromatography and are defined in **Section 2.1 Apparatus for Column Chromatography**.

7.3.1 Flow restrictor This is a device which restricts the flow of the mobile phase leaving the column and is used to maintain the pressure in the chromatographic column.

7.3.1.1 Capillary restrictor This is a capillary tube which may be tapered or constricted and acts as a mass-flow controller. The column pressure is controlled by adjusting the pump flow rate.

7.3.1.2 Frit restrictor A frit placed at the end of an open-tubular column to act as a flow restrictor. Sometimes referred to as an *integral frit restrictor*.

7.3.2 Back-pressure regulator This is a device which is placed after the column and is used to regulate the pressure in the column by a pressure-adjustable diaphragm or controlled nozzle so that the same column-outlet pressure is maintained irrespective of the mobile-phase pump flow rate.

7.3.3 Sample injector as defined in 2.1.02. The most common form in supercritical-fluid chromatography is the *bypass injector* (see 2.1.02.2). In capillary supercritical-fluid chromatography a *timed injector* is often used.

7.3.3.1 Timed injector This is a form of *bypass injector* in which the rotation of the valve is timed so that only a portion of the contents of the sample loop can pass to the column.

7.3.4 High-pressure flow cell A flow-through cell (usually spectroscopic) designed for use at high pressures so that the sample remains dissolved in the mobile phase during detection.

7.4 The Chromatographic Medium

Supercritical-fluid chromatographic separations are carried out using capillary columns or packed columns similar to those used in gas or liquid chromatography (see **Section 3.1**). Stationary phases are usually chemically bonded to the support. Non-chemically bonded phases are often unsuitable as the stationary phase may be soluble in the mobile phase.

7.5 Terms Related to the Chromatographic Process

7.5.1 Isobaric separation Chromatographic separation carried out using constant inlet and outlet pressure conditions.

7.5.2 Isopycnic separation Chromatographic separations carried out using constant density conditions. The temperature and pressure may be altered during the run (originally the term *isoconfertic separation* was used but this term is not recommended).

7.5.3 Programmed elution A procedure in which the conditions of the separation are changed in a programmed manner. Unlike gas or liquid chromatography both the pressure and temperature can be programmed.

The term “*gradient elution*” should be restricted to changes in composition of the mobile phase with time (see 1.6.04).

7.5.3.1 Density-programmed elution A separation carried out using a pressure and/or temperature programme so that the density of the mobile phase changes with time in a pre-determined manner during the separation.

7.5.3.2 Pressure-programmed elution A separation carried out using a programmed increasing pressure with time.

7.5.3.3 Pressure/temperature-programmed elution A separation carried out using conditions where the pressure and temperature are programmed simultaneously. The temperature may be programmed to increase or decrease.

7.6 Coupled-systems

As well as discrete chromatographic detectors, supercritical-fluid chromatography has been coupled to more complex detectors and to other separation techniques and the most widely used are listed here.

7.6.1 Coupled supercritical-fluid chromatography-mass spectrometry (SFC-MS) Separation system in which the column effluent from a supercritical-fluid chromatograph is passed directly to the inlet chamber of a mass spectrometer.

7.6.2 Coupled supercritical-fluid chromatography-Fourier-transform infrared spectrometry (SFC-FTIR) Separation system in which the column effluent from a supercritical-fluid chromatograph is passed directly through a Fourier-transform infrared spectrometer.

7.6.3 Coupled supercritical-fluid chromatography-gas chromatography (SFC-GC) Separation system in which a fraction from the supercritical-fluid chromatograph effluent is transferred directly to the inlet port or column of a gas chromatograph system.

7.7 Supercritical-fluid Extraction

7.7.1 Supercritical-fluid extraction (SFE) Extraction of a material using a supercritical fluid. The extracted material is usually recovered by reducing the temperature or pressure of the extraction fluid and allowing the volatile components of the mobile phase to evaporate. Instrumentally supercritical-fluid extraction can use many of the components of a supercritical-fluid chromatographic system. It can be used either as an on-line sample introduction method for a chromatographic separation or as an off-line sample preparation method.

7.7.2 Coupled supercritical-fluid extraction-supercritical-fluid chromatography (SFE-SFC) System in which a sample is extracted with a supercritical-fluid which then places the extracted material in the inlet port of a supercritical-fluid-chromatographic system. The extract is then chromatographed directly using a supercritical fluid.

7.7.3 Coupled supercritical-fluid extraction-gas chromatography (SFE-GC) and Coupled supercritical-fluid chromatography-liquid chromatography (SFE-LC) System in which a sample is extracted using a supercritical fluid which is then depressurized to deposit the extracted material in the inlet port or column of a gas or liquid chromatographic system, respectively. The extract is then chromatographed directly.

Table 1 Index of additional terms

Back-pressure regulators	7.3.2
Capillary restrictors	7.3.1.1
Coupled supercritical-fluid chromatography-mass spectrometry	7.6.1
Coupled supercritical-fluid extraction-Fourier-transform infrared spectroscopy	7.6.2
Coupled supercritical-fluid chromatography-gas chromatography	7.6.3
Coupled supercritical-fluid extraction-gas chromatography	7.7.3
Coupled supercritical-fluid extraction-liquid chromatography	7.7.3
Coupled supercritical-fluid extraction-supercritical-fluid chromatography	7.7.2
Critical point	7.1.3
Critical pressure	7.1.2
Critical temperature	7.1.1
Density-programmed elution	7.5.3.1
Flow restrictors	7.3.1
Frit restrictor	7.3.1.2
High-pressure flow cell	7.3.4
Integral frit restrictor	7.3.1.2
Isobaric separation	7.5.1
Isopycnic separation	7.5.2
Mobile-phase composition	7.2.5
Mobile-phase modifiers	7.2.5.1
Mobile-phase mass flow rate	7.2.4
Mobile-phase volume flow rate	7.2.3
Pressure programmed elution	7.5.3.2
Pressure/temperature-programmed elution	7.5.3.3
Programmed elution	7.5.3
Reduced temperature	7.1.5
Reduced pressure	7.1.6
Supercritical fluid	7.1.4
Supercritical-fluid extraction (SFE)	7.7.1
Timed injector	7.3.3.1

Table 2 List of symbols

p_c	Critical pressure	7.1.2
T_c	Critical temperature	7.1.1
p_r	Reduced pressure	7.1.6
T_r	Reduced temperature	7.1.5

Table 3 List of acronyms

SFE	Supercritical-fluid extraction
SFC-FTIR	Supercritical-fluid chromatography-Fourier transform infrared spectroscopy
SFC-GC	Supercritical-fluid chromatography-gas chromatography
SFC-LC	Supercritical-fluid chromatography-liquid chromatography
SFC-MS	Supercritical-fluid chromatography-mass spectrometry
SFE-GC	Supercritical-fluid extraction-gas chromatography
SFE-LC	Supercritical-fluid extraction-liquid chromatography
SFE-SFC	Supercritical-fluid extraction-supercritical-fluid chromatography

References

1. Recommendations for Nomenclature for Chromatography, *Pure and Applied Chemistry*, **65**, 819–872 (1993).
2. 'Standard Guide for Supercritical Fluid Chromatography terms and relationships', ASTM E 1449, American Society for Testing and Materials, Philadelphia, PA, 1992.

13. pH SCALE FOR AQUEOUS SOLUTIONS

Values of pH For Primary Standard Reference Solutions

Primary ref. standard	Temperature (°C)															
	0	5	10	15	20	25	30	35	37	40	50	60	70	80	90	95
Saturated (at 25°C) potassium hydrogentartrate 0.1 mol kg ^{−1} Potassium dihydrogencitrate 0.025 mol kg ^{−1} Disodium hydro- genphosphate + 0.025 mol kg ^{−1} potassium dihydro- gen phosphate 0.03043 mol kg ^{−1} Disodium hydro- genphosphate + 0.008695 mol kg ^{−1} potassium dihydrogen phosphate 0.01 mol kg ^{−1} Disodium tetraborate 0.025 mol kg ^{−1} Sodium hydro- gencarbonate + 0.025 mol kg ^{−1} sodium carbonate	—	—	—	—	—	3.557	3.552	3.549	3.548	3.547	3.549	3.560	3.580	3.610	3.650	3.674
	3.863	3.840	3.820	3.802	3.788	3.776	3.766	3.759	3.756	3.754	3.749	—	—	—	—	—
	6.984	6.951	6.923	6.900	6.881	6.865	6.853	6.844	6.841	6.838	6.833	6.836	6.845	6.859	6.876	6.886
	7.534	7.500	7.472	7.448	7.429	7.413	7.400	7.389	7.386	7.380	7.367	—	—	—	—	—
	9.464	9.395	9.332	9.276	9.225	9.180	9.139	9.102	9.088	9.068	9.011	8.962	8.921	8.884	8.850	8.833
	10.317	10.245	10.179	10.118	10.062	10.012	9.966	9.926	9.910	9.889	9.828	—	—	—	—	—

Note: Based on an uncertainty of ± 0.2 mV in determined ($E - E^0$), the uncertainty is ± 0.003 in pH in the range 0–50°C.

pH Values of Operational Reference Solutions

Operational standard ref. solution	Temperature (°C)															
	0	5	10	15	20	25	30	37	40	50	60	70	80	90	95	
0.1 mol kg ^{−1} Potassium tetroxalate ^a	—	—	—	—	1.475	1.479	1.483	1.490	1.493	1.503	1.513	1.52	1.53	1.53	1.53	
0.05 mol kg ^{−1} Potassium tetroxalate ^a	—	—	1.638	1.642	1.644	1.646	1.648	1.649	1.650	1.653	1.660	1.671	1.689	1.72	1.73	
0.05 mol kg ^{−1} Sodium hydrogendiglycolate ^b	—	3.466	3.470	3.476	3.484	3.492	3.502	3.519	3.527	3.558	3.595	—	—	—	—	
Saturated (at 25°C) Potassium hydrogen-tartrate	—	—	—	—	—	3.556	3.549	3.544	3.542	3.544	3.553	3.570	3.596	3.627	3.649	
0.05 mol kg ^{−1} Potassium hydrogenphthalate (RVS)	4.000	3.998	3.997	3.998	4.000	4.005	4.011	4.022	4.027	4.050	4.080	4.115	4.159	4.21	4.24	
0.1 mol dm ^{−3} Acetic acid + 0.1 mol dm ^{−3} sodium acetate	4.664	4.657	4.652	4.647	4.645	4.644	4.643	4.647	4.650	4.663	4.684	4.713	4.75	4.80	4.83	
0.01 mol dm ^{−3} Acetic acid + 0.1 mol dm ^{−3} sodium acetate	4.729	4.722	4.717	4.714	4.712	4.713	4.715	4.722	4.726	4.743	4.768	4.800	4.839	4.88	4.91	
0.02 mol kg ^{−1} Piperazine phosphate ^c	—	6.477	6.419	6.364	6.310	6.259	6.209	6.143	6.116	6.030	5.952	—	—	—	—	
0.025 mol kg ^{−1} Disodium hydrogen-phosphate + 0.025 mol kg ^{−1} potassium dihydrogen phosphate	6.961	6.935	6.912	6.891	6.873	6.857	6.843	6.828	6.823	6.814	6.817	6.830	6.85	6.90	6.92	
0.03043 mol kg ^{−1} Disodium hydrogen-phosphate + 0.008695 mol kg ^{−1} potassium disodium phosphate	7.506	7.482	7.460	7.441	7.423	7.406	7.390	7.369	—	—	—	—	—	—	—	
0.04 mol kg ^{−1} Disodium hydrogen-phosphate + 0.01 mol kg ^{−1} potassium dihydrogen phosphate	—	7.512	7.488	7.466	7.445	7.428	7.414	7.404	—	—	—	—	—	—	—	
0.05 mol kg ^{−1} Tris hydrochloride + 0.01667 mol kg ^{−1} Tris ^d	8.399	8.238	8.083	7.933	7.788	7.648	7.513	7.332	7.257	7.018	6.794	—	—	—	—	
0.05 mol kg ^{−1} Disodium tetraborate (Na ₂ B ₄ O ₇)	9.475	9.409	9.347	9.288	9.233	9.182	9.134	9.074	9.051	8.983	8.932	8.898	8.88	8.84	8.89	
0.01 mol kg ^{−1} Disodium tetraborate (Na ₂ B ₄ O ₇)	9.451	9.388	9.329	9.275	9.225	9.179	9.138	9.086	9.066	9.009	8.965	8.932	8.91	8.90	8.89	
0.025 mol kg ^{−1} Sodium hydrogencarbonate + 0.025 mol kg ^{−1} sodium carbonate	10.273	10.212	10.154	10.098	10.045	9.995	9.948	9.889	9.866	9.800	9.753	9.728	9.725	9.75	9.77	
Saturated (at 20°C) calcium hydroxide	13.360	13.159	12.965	12.780	12.602	12.431	12.267	12.049	11.959	11.678	11.423	11.192	10.984	10.80	10.71	

Note: Uncertainty is ± 0.003 in pH between 0 and 60°C rising to ± 0.01 above 70°C.

^aPotassium trihydrogen dioxalate (KH₃C₄O₈).

^bSodium hydrogen 2,2'-oxydiethanoate.

^cC₄H₁₀N₂ · H₃PO₄.

^d2-Amino-2(hydroxymethyl)-1,3 propanediol or tris(hydroxymethyl)aminomethane.

Useful Data on Some Standard Buffer Solutions

	Molecular formula	Molarity (mol kg ⁻¹)	Relative molar mass	Density at 20°C (g cm ⁻³)	Molarity at 20°C (mol l ⁻¹)	Mass of 1 l at 20°C (g)	Mass tolerance for ± 0.001 pH ^a (g)	Mass tolerance expressed as a percentage (%)
Potassium tetraoxalate	KH ₃ C ₄ O ₈ · 2H ₂ O	0.1	254.1913	1.0091	0.09875	25.1017	0.07	0.27
Potassium tetraoxalate	KH ₃ C ₄ O ₈ · 2H ₂ O	0.05	254.1913	1.0038	0.04965	12.6202	0.034	0.26
Disodium hydrogen orthophosphate	Na ₂ HPO ₄	0.025	141.9588	1.0038	0.02492	3.5379	0.02	0.56
Potassium dihydrogen orthophosphate	KH ₂ PO ₄	0.025	136.0852			3.3912	0.02	0.58
Disodium tetraborate	Na ₂ B ₄ O ₇ · 10H ₂ O	0.05	381.367	1.0075	0.04985	19.0117	0.9	4.73
Disodium tetraborate	Na ₂ B ₄ O ₇ · 10H ₂ O	0.01	381.367	1.0001	0.009981	3.8064	0.19	0.49
Sodium carbonate	Na ₂ CO ₃	0.025	105.9887	1.0021	0.02494	2.6428	0.017	0.064
Sodium hydrogencarbonate	NaHCO ₃	0.025	84.0069			2.0947	0.013	0.62

^aCalculated from known dilution value of solution.

(Reprinted with permission from Mills I *et al.* (1993) *Quantities, Units and Symbols in Physical Chemistry*, 2nd edn. Oxford: Blackwell Scientific Publications.)

14. PROPERTIES OF PARTICLES, ELEMENTS AND NUCLIDES

Properties of Some Particles

Name	Symbol ^a	Spin <i>I</i>	Charge number <i>z</i>	Rest mass		Magnetic moment μ/μ_N	Meanlife τ/s
				<i>m/u</i>	<i>mc</i> ² /MeV		
Photon	γ	1	0	0	0		
Neutrino	ν_e	1/2	0	0	0		
Electron ^b	<i>e</i>	1/2	− 1	5.485 799 03 (13) × 10 ^{−4}	0.510 999 06 (15)	1.001 159 652 193 (10) ^c	
Muon	μ^\pm	1/2	± 1	0.113 428 913 (17)	105.658 389 (34)	1.001 165 923 (8) ^d	2.197 3 (4) × 10 ^{−6}
Pion	π^\pm	1	± 1	0.149 832 3 (8)	139.5679 (7)		2.6030 (24) × 10 ^{−8}
Pion	π^0	1	0	0.144 9008 (9)	134.9743 (8)		8.4 (6) × 10 ^{−17}
Proton	<i>p</i>	1/2	1	1.007 276 470 (12)	938.272 31 (28)	2.792 847 386 (63)	
Neutron	<i>n</i>	1/2	0	1.008 664 904 (14)	939.565 63 (28)	− 1.913 042 75 (45)	889.1 (21)
Deuteron	<i>d</i>	1	1	2.013 553 214 (24)	1875.613 39 (53)	0.857 437 6 (1)	
Triton	<i>t</i>	1/2	1	3.015 500 71 (4)	2808.921 78 (85)	2.978 960 (1)	
Helion	<i>h</i>	1/2	2	3.014 932 23 (4)	2808.392 25 (85)	− 2.127 624 (1)	
α-Particle	α	0	2	4.001 506 170 (50)	3727.380 3 (11)	0	

^aThe Particle Data Group recommends the use of italic symbols for particles and this has been adopted by many physicists.

^bThe electron as β -particle is sometimes denoted by β .

^cThe value is given in Bohr magnetons μ/μ_B , $\mu_B = eh/2m_e$.

^dThe value is given as μ/μ_μ , where $\mu_\mu = eh/2m_\mu$.

(Reprinted with permission from Mills I *et al.* (1993) *Quantities, Units and Symbols in Physical Chemistry*, 2nd edn. Oxford: Blackwell Scientific Publications.)

In nuclear physics and chemistry the masses of particles are often quoted as their energy equivalents (usually in mega electronvolts). The unified atomic mass unit corresponds to 931.494 32 (28) MeV.

Atom-like pairs of a positive particle and an electron are sometimes sufficiently stable to be treated as individual entities with special names.

*Examples*positronium (e^+e^-) $m(e^+e^-) = 1.097\,152\,503(26) \times 10^{-3}u$ muonium (μ^+e^- ; Mu) $m(\text{Mu}) = 0.113\,977\,478(17)u$

The positive or negative sign for the magnetic moment of a particle implies that the orientation of the magnetic dipole with respect to the angular momentum corresponds to the rotation of a positive or negative charge respectively.

Standard Atomic Weights of the Elements 1991

As agreed by the IUPAC Commission on Atomic Weights and Isotopic Abundances in 1979 the relative atomic mass (atomic weight) of an element, E , can be defined for any specified sample. It is the average mass of its atoms in the sample divided by the unified atomic mass unit* or alternatively the molar mass of its atoms divided by the standard molar mass $M^\theta = Lm_u = 1\text{ g mol}^{-1}$:

$$A_r(E) = \bar{m}_a(E)/u = M(E)M^\theta$$

The variations in isotopic composition of many elements in samples of different origin limit the precision to which a relative atomic mass can be given. The standard atomic weights revised biennially by the IUPAC Commission on Atomic Weights and Isotopic Abundances are meant to be applicable for normal materials. This means that to a high level of confidence the relative atomic mass of an element in any normal sample will be within the uncertainty limits of the tabulated value. By 'normal' it is meant here that the material is a reasonably possible source of the element or its compounds in commerce for industry and science and that it has not been subject to significant modification of isotopic composition within a geologically brief period. This, of course, excludes materials studied themselves for very anomalous isotopic composition.

The relative atomic masses of many elements depend on the origin and treatment of the materials. The notes to this table explain the types of variation to be expected for individual elements.

A value in brackets denotes the mass number of the most stable isotope. ρ denotes density, $\theta_{c,m}$ denotes melting temperature, $\theta_{c,b}$ denotes boiling temperature and c_p denotes specific heat capacity. subl. denotes sublimes.

Element	Symbol	Atomic number	Relative atomic mass	ρ (g cm ⁻³)	$\theta_{c,m}$ (°C)	$\theta_{c,b}$ (°C)	c_p (J kg ⁻¹ K ⁻¹)	Oxidation states	Note
Actinium	Ac	89	(227)	10.1	1050	3200		3	A
Aluminium	Al	13	26.9815	2.70	660	2470	900	3	
Americium	Am	95	(243)	11.7	(1200)	(2600)	140	3,4,5,6	A
Antimony	Sb	51	121.75	6.62	630	1380	209	3,5	g
Argon	Ar	18	39.948	1.40(87 K)	– 189	– 186	519		g,r
Arsenic (α , grey)	As	33	74.9216	5.72		613 subl.	326	3,5	
Astatine	At	85	(210)		(302)				A
Barium	Ba	56	137.34	3.51	714	1640'		2	
Berkelium	Bk	97	(247)					3,4	A
Beryllium	Be	4	9.01218	1.85	1280	2477	1.82×10^3	2	
Bismuth	Bi	83	208.9806	9.80	271	1560	121	3,5	
Boron	B	5	10.81	2.34	2300	3930	1.03×10^3	3	g,m,r
Bromine	Br	35	79.904	3.12	– 7.2	58.8	448	1,3,4,5,6	
Cadmium	Cd	48	112.40	8.64	321	765	230	2	g
Caesium	Cs	55	132.9055	1.90	28.7	690	234	1	
Calcium	Ca	20	40.08	1.54	850	1487	653	2	g
Californium	Cf	98	(251)					3	A
Carbon (graphite)	C	6	12.011	2.25 (graphite) 3.51 (diamond)	3730 subl.	4830	711 (graphite) 519 (diamond)	2,4	r

*Note that the atomic mass constant, m_u , is equal to the unified atomic mass unit, u , and is defined in terms of the mass of the carbon-12 atom: $m_u = 1u = m_a(^{12}\text{C})/12$.

Element	Symbol	Atomic number	Relative atomic mass	ρ (g cm ⁻³)	$\theta_{C,m}$ (°C)	$\theta_{C,b}$ (°C)	c_p (J kg ⁻¹ K ⁻¹)	Oxidation states	Note
Cerium	Ce	58	140.12	6.78	795	3470	184	3,4	g
Chlorine	Cl	17	35.453	1.56(238 K)	− 101	34.7	477	1,3,4,5,6,7	m
Chromium	Cr	24	51.996	7.19	1890	2482	448	2,3,6	
Cobalt	Co	27	58.9332	8.90	1492	2900	435	2,3	
Copper	Cu	29	63.546	8.92	1083	2595	385	1,2	r
Curium	Cm	96	(247)					3	A
Dysprosium	Dy	66	162.50	8.56	1410	2600	172	3	g
Einsteinium	Es	99	(254)					3	A
Erbium	Er	68	167.26	9.16	1500	2900	167	3	g
Europium	Eu	63	151.96	5.24	826	1440	138	2,3	g
Fermium	Fm	100	(253)					3	A
Fluorine	F	9	18.9984	1.11 (85 K)	− 220	− 188	824	1	
Francium	Fr	87	(223)		(27)			1	A
Gadolinium	Gd	64	157.25	7.95	1310	3000	234	3	g
Gallium	Ga	31	69.72	5.91	29.8	2400	381	3	
Germanium	Ge	32	72.59	5.35	937	2830	322	4	
Gold	Au	79	196.9665	19.3	1063	2970	130	1,3	
Hafnium	Hf	72	178.49	13.3	2220	5400	146	4	
Helium	He	2	4.00260	0.147 (4 K)	− 270	− 269	5.19 × 10 ³		g,r
Holmium	Ho	67	164.9303	8.80	1460	2600	163	3	
Hydrogen	H	1	1.0080	0.070 (20 K)	− 259	− 252	1.43 × 10 ⁴	1	g,m,r
Indium	In	49	114.82	7.30	157	2000	238	1,3	
Iodine	I	53	126.9045	4.93	114	184	218	1,3,5,7	
Iridium	Ir	77	192.22	22.5	2440	5300	134	2,3,4,6	
Iron	Fe	26	55.847	7.86	1535	3000	448	2,3,6	
Krypton	Kr	36	83.80	2.16 (121 K)	− 157	− 152	247	2	g,m
Lanthanum	La	57	138.9055	6.19	920	3470	201	3	g
Lawrencium	Lr	103	(257)						A
Lead	Pb	82	207.2	11.3	327	1744	130	2,4	g,r
Lithium	Li	3	6.941	0.53	180	1330	3.39 × 10 ³	1	g,m,r,
Lutetium	Lu	71	174.97	9.84	1650	3330	155	3	g
Magnesium	Mg	12	24.305	1.74	650	1110	1.03 × 10 ³	2	
Manganese	Mn	25	54.9380	7.20	1240	2100	477	2,3,4,6,7	
Mendelevium	Md	101	(256)					3	A
Mercury	Hg	80	200.59	13.6	− 38.9	357	138	1,2	
Molybdenum	Mo	42	95.94	10.2	2610	5560	251	2,3,4,5,6	g
Neodymium	Nd	60	144.24	7.00	1020	3030	188	3	g
Neon	Ne	10	20.179	1.20 (27 K)	− 249	− 246	1.03 × 10 ³		g,m
Neptunium	Np	93	(237)	20.4	640			3,4,5,6	A
Nickel	Ni	28	58.71	8.90	1453	2730	439	2,3	
Niobium	Nb	41	92.9064	8.57	2470	3300	264	3,5	
Nitrogen	N	7	14.0067	0.808 (77 K)	− 210	− 196	1.04 × 10 ³	1,2,3,4,5	g,r
Nobelium	No	102	(254)						A
Osmium	Os	76	190.2	22.5	3000	5000	130	2,3,4,6,8	g
Oxygen	O	8	15.9994	1.15 (90 K)	− 218	− 183	916	2	g,r
Palladium	Pd	46	106.4	12.0	1550	3980	243	2,4	g
Phosphorus	P	15	30.9738	1.82 (white) 2.34 (red)	44.2 (white) 590 (red)	280 (white)	757 (white) 670 (red)	3,5	
Platinum	Pt	78	195.09	21.4	1769	4530	134	2,4,6	
Plutonium	Pu	94	(242)	19.8	640	3240		3,4,5,6	A
Polonium	Po	84	(210)	9.4	254	960	126	2,4	A
Potassium	K	19	39.102	0.86	63.7	774	753	1	
Praseodymium	Pr	59	140.9077	6.78	935	3130	192	3,4	
Promethium	Pm	61	(147)		1030	2730	184	3	A
Protoactinium	Pa	91	(231)	15.4	1230		121	4,5	Z
Radium	Ra	88	(226)	5.0	700	1140	121	2	A
Radon	Rn	86	(222)	4.4 (211 K)	− 71	− 61.8	92		A
Rhenium	Re	75	186.2	20.5	3180	5630	138	2,4,5,6,7	
Rhodium	Rh	45	102.9055	12.4	1970	4500	243	2,3,4	
Rubidium	Rb	37	85.4678	1.53	38.9	688	360	1	g
Ruthenium	Ru	44	101.07	12.3	2500	4900	238	3,4,5,6,8	g

Element	Symbol	Atomic number	Relative atomic mass	ρ (g cm ⁻³)	$\theta_{C,m}$ (°C)	$\theta_{C,b}$ (°C)	c_p (J kg ⁻¹ K ⁻¹)	Oxidation states	Note
Samarium	Sm	62	150.4	7.54	1070	1900	197	2,3	g
Scandium	Sc	21	44.9559	2.99	1540	2730	556	3	
Selenium	Se	34	78.96	4.81	217	685	322	2,4,6	
Silicon	Si	14	28.086	2.33	1410	2360	711	4	r
Silver	Ag	47	107.868	10.5	961	2210	234	1	g
Sodium	Na	11	22.9898	0.97	97.8	890	1.23×10^3	1	
Strontium	Sr	38	87.62	2.62	768	1380	284	2	g,r
Sulphur (α, rhombic)	S	16	32.06	2.07 (α)	113 (α)	445	732	2,4,6	g,r
				1.96 (β)	119 (β)				
Tantalum	Ta	73	180.9479	16.6	3000	5420	138	5	
Technetium	Tc	43	(99)	11.5	2200	3500	243	7	A
Tellurium	Te	52	127.60	6.25	450	990	201	2,4,6	g
Terbium	Tb	65	158.9254	8.27	1360	2800	184	3,4	
Thallium	Tl	81	204.37	11.8	304	1460	130	1,3	
Thorium	Th	90	232.0381	11.7	1750	3850	113	3,4	g,Z
Thulium	Tm	69	168.9342	9.33	1540	1730	159	2,3	
Tin (white)	Sn	50	118.69	7.28 (white)	232	2270	218	2,4	g
				5.75 (grey)					
Titanium	Ti	22	47.90	4.54	1675	3260	523	2,3,4	
Tungsten	W	74	183.85	19.4	3410	5930	134	2,4,5,6	
Unnilennium	Une	109							A,U
Unnilhexium	Unh	106							A,U
Unniloctium	Uno	108							A,U
Unnilpentium	Unp	105							A,U
Unnilquadium	Unq	104							A,U
Unnilseptium	Uns	107							A,U
Uranium	U	92	238.029	19.1	1130	3820	117	3,4,5,6	g,m,Z
Vanadium	V	23	50.9414	5.96	1900	3000	481	2,3,4,5	
Xenon	Xe	54	131.30	3.52 (165 K)	− 112	− 108	159	2,4,6,8	g,m
Ytterbium	Yb	70	173.04	6.98	824	1430	146	2,3	g
Yttrium	Y	39	88.9059	4.34	1500	2930	297	3	
Zinc	Zn	30	65.37	7.14	420	907	385	2	
Zirconium	Zr	40	91.22	6.49	1850	3580	276	2,3,4	g

(g) geologically exceptional specimens are known in which the element has an isotopic composition outside the limits for normal material. The difference between the average relative atomic mass of the element in such specimens and that given in the table may exceed considerably the implied uncertainty.

(m) modified isotopic compositions may be found in commercially available material because it has been subjected to an undisclosed or inadvertent isotopic separation. Substantial deviations in relative atomic mass of the element from that given in the table can occur.

(r) range in isotopic composition of normal terrestrial material prevents a more precise relative atomic mass being given; the tabulated $A_r(E)$ value should be applicable to any normal material.

(A) Radioactive element that lacks a characteristic terrestrial isotopic composition.

(Z) An element without stable nuclide(s), exhibiting a range of characteristic terrestrial compositions of long-lived radionuclide(s) such that a meaningful relative atomic mass can be given.

(U) The names and symbols given here are systematic and based on the atomic numbers of the elements as recommended by the IUPAC Commission on the Nomenclature of Inorganic Chemistry. The names are composed of the following roots representing digits of the atomic number:

1 un,	2 bi,	3 tri,	4 quad,	5 pent,
6 hex,	7 sept,	8 oct,	9 enn,	0 nil

The ending -ium is then added to the three roots. The three-letter symbols are derived from the first letters of the corresponding roots. (Reprinted with permission from Mills *et al.* (1993) *Quantities, Units and Symbols in Physical Chemistry*, 2nd edn. Oxford Scientific Publications.)

Electronic Configurations of the Elements (Ground States)

Atomic number	Element	Shell													
		K		L		M			N						
		1s	2s	2p	3s	3p	3d	4s	4p	4d	4f				
1	Hydrogen	1													
2	Helium	2													
3	Lithium	2	1												
4	Beryllium	2	2												
5	Boron	2	2	1											
6	Carbon	2	2	2											
7	Nitrogen	2	2	3											
8	Oxygen	2	2	4											
9	Fluorine	2	2	5											
10	Neon	2	2	6											
11	Sodium	2	2	6	1										
12	Magnesium	2	2	6	2										
13	Aluminium	2	2	6	2	1									
14	Silicon	2	2	6	2	2									
15	Phosphorus	2	2	6	2	3									
16	Sulphur	2	2	6	2	4									
17	Chlorine	2	2	6	2	5									
18	Argon	2	2	6	2	6									
19	Potassium	2	2	6	2	6		1							
20	Calcium	2	2	6	2	6		2							
21	Scandium	2	2	6	2	6	1	2							
22	Titanium	2	2	6	2	6	2	2							
23	Vanadium	2	2	6	2	6	3	2							
24	Chromium	2	2	6	2	6	5	1							
25	Manganese	2	2	6	2	6	5	2							
26	Iron	2	2	6	2	6	6	2							
27	Cobalt	2	2	6	2	6	7	2							
28	Nickel		2	6	2	6	8	2							
29	Copper	2	2	6	2	6	10	1							
30	Zinc	2	2	6	2	6	10	2							
31	Gallium	2	2	6	2	6	10	2	1						
32	Germanium	2	2	6	2	6	10	2	2						
33	Arsenic	2	2	6	2	6	10	2	3						
34	Selenium	2	2	6	2	6	10	2	4						
35	Bromine	2	2	6	2	6	10	2	5						
36	Krypton	2	2	6	2	6	10	2	6						
Atomic number	Element	Shell													
		K		L	M	N		O				P			
					4s	4p	4d	4f	5s	5p	5d	5f	6s	6p	6d
37	Rubidium	2	8	18	2	6		1							
38	Strontium	2	8	18	2	6		2							
39	Yttrium	2	8	18	2	6	1	2							
40	Zirconium	2	8	18	2	6	2	2							
41	Niobium	2	8	18	2	6	4	1							
42	Molybdenum	2	8	18	2	6	5	1							
43	Technetium	2	8	18	2	6	6	1							
44	Ruthenium	2	8	18	2	6	7	1							
45	Rhodium	2	8	18	2	6	8	1							
46	Palladium	2	8	18	2	6	10								

Atomic number	Element	Shell														
		K	L	M	N	O					P					
						4s	4p	4d	4f	5s	5p	5d	5f	6s	6p	6d
47	Silver	2	8	18	2	6	10	1								
48	Cadmium	2	8	18	2	6	10	2								
49	Indium	2	8	18	2	6	10	2	1							
50	Tin	2	8	18	2	6	10	2	2							
51	Antimony	2	8	18	2	6	10	2	3							
52	Tellurium	2	8	18	2	6	10	2	4							
53	Iodine	2	8	18	2	6	10	2	5							
54	Xenon	2	8	18	2	6	10	2	6							
55	Caesium	2	8	18	2	6	10		2	6		1				
56	Barium	2	8	18	2	6	10		2	6		2				
57	Lanthanum	2	8	18	2	6	10		2	6	1	2				
58	Cerium	2	8	18	2	6	10	2	2	6		2				
59	Praseodymium	2	8	18	2	6	10	3	2	6		2				
60	Neodymium	2	8	18	2	6	10	4	2	6		2				
61	Promethium	2	8	18	2	6	10	5	2	6		2				
62	Samarium	2	8	18	2	6	10	6	2	6		2				
63	Europium	2	8	18	2	6	10	7	2	6		2				
64	Gadolinium	2	8	18	2	6	10	7	2	6	1	2				
65	Terbium	2	8	18	2	6	10	9	2	6		2				
66	Dysprosium	2	8	18	2	6	10	10	2	6		2				
67	Holmium	2	8	18	2	6	10	11	2	6		2				
68	Erbium	2	8	18	2	6	10	12	2	6		2				
69	Thulium	2	8	18	2	6	10	13	2	6		2				
70	Ytterbium	2	8	18	2	6	10	14	2	6		2				
71	Lutetium	2	8	18	2	6	10	14	2	6	1	2				
72	Hafnium	2	8	18	2	6	10	14	2	6	2	2				
73	Tantalum	2	8	18	2	6	10	14	2	6	3	2				
74	Tungsten	2	8	18	2	6	10	14	2	6	4	2				
75	Rhenium	2	8	18	2	6	10	14	2	6	5	2				
76	Osmium	2	8	18	2	6	10	14	2	6	6	2				
77	Iridium	2	8	18	2	6	10	14	2	6	9					
78	Platinum	2	8	18	2	6	10	14	2	6	9	1				
79	Gold	2	8	18	2	6	10	14	2	6	10	1				
80	Mercury	2	8	18	2	6	10	14	2	6	10	2				
81	Thallium	2	8	18	2	6	10	14	2	6	10	2	1			
82	Lead	2	8	18	2	6	10	14	2	6	10	2	2			
83	Bismuth	2	8	18	2	6	10	14	2	6	10	2	3			
84	Polonium	2	8	18	2	6	10	14	2	6	10	2	4			
85	Astatine	2	8	18	2	6	10	14	2	6	10	2	5			
86	Radon	2	8	18	2	6	10	14	2	6	10	2	6			
Atomic number	Element	Shell														
		K	L	M	N	O					p			Q		
						5s	5p	5d	5f	6s	6p	6d	7s			
87	Francium	2	8	18	32	2	6	10			2	6				1
88	Radium	2	8	18	32	2	6	10			2	6				2
89	Actinium	2	8	18	32	2	6	10			2	6	1			2
90	Thorium	2	8	18	32	2	6	10			2	6	2			2
91	Protoactinium	2	8	18	32	2	6	10		2	2	6	1			2
92	Uranium	2	8	18	32	2	6	10	3	2	6	6	1			2
93	Neptunium	2	8	18	32	2	6	10	4	2	6	6	1			2
94	Plutonium	2	8	18	32	2	6	10	6	2	6					2
95	Americium	2	8	18	32	2	6	10	7	2	6					2

Atomic number	Element	Shell											
		K	L	M	N	O	p					Q	
						5s	5p	5d	5f	6s	6p	6d	7s
96	Curium	2	8	18	32	2	6	10	7	2	6	1	2
97	Berkelium	2	8	18	32	2	6	10	8	2	6	1	2
98	Californium	2	8	18	32	2	6	10	10	2	6		2
99	Einsteinium	2	8	18	32	2	6	10	11	2	6		2
100	Fermium	2	8	18	32	2	6	10	12	2	6		2
101	Mendelevium	2	8	18	32	2	6	10	13	2	6		2
102	Nobelium	2	8	18	32	2	6	10	14	2	6		2
103	Lawrencium	2	8	18	32	2	6	10	14	2	6	1	2

(Reprinted with permission from Mills I *et al.* (1993) *Quantities, Units and Symbols in Physical Chemistry*, 2nd edn. Oxford: Blackwell Scientific Publications.)

Properties of Nuclides

The table contains the following properties of naturally occurring and some unstable nuclides:

Column

1. Z is the atomic number (number of protons) of the nuclide.
2. Symbol of the element.
3. A is the mass number of the nuclide. The * sign denotes an unstable nuclide (for elements without naturally occurring isotopes it is the most stable nuclide) and the # sign a nuclide of sufficiently long lifetime to enable the determination of its isotopic abundance.
4. The atomic mass is given in unified atomic mass units, $u = m_a(^{12}\text{C})/12$, together with the standard errors in parentheses and applicable to the last digit quoted.
5. Isotopic abundances are given as mole fractions, x , of the corresponding atoms in percents. They were recommended in 1989 by the IUPAC Commission on Atomic Weights and Isotopic Abundances. The uncertainties given in parentheses are applicable to the last digits quoted and cover the range of probable variations in the materials as well as experimental errors.
6. I is the nuclear spin quantum number.
7. Under magnetic moment the maximum z -component expectation value of the magnetic dipole moment, m , in nuclear magnetons is given. The positive or negative sign implies that the orientation of the magnetic dipole with respect to the angular momentum corresponds to the rotation of a positive or negative charge, respectively. An asterisk * indicates that more than one value is given in the original compilation. The value of highest precision or most recent data is given here.
8. Under quadrupole moment, the electric quadrupole moment area is given in units of square femtometres, $\text{fm}^2 = 10^{-30} \text{ m}^2$, although most of the tables quote them in barns ($1 \text{ barn} = 10^{-28} \text{ m}^2 = 100 \text{ fm}^2$). The positive sign implies a prolate nucleus, the negative sign an oblate nucleus. The data for $Z \leq 20$ were taken from the compilation by P. Pykkö with values for Cl and Ca corrected by D. Sundholm (private communication), and the others from P. Raghavan. An asterisk* indicates that more than one value is given in the original compilation.

Z	Symbol	A	Atomic mass, m_a (u)	Isotopic abundance, 100 x	Nuclear spin, I	Magnetic moment, m (μ_N)	Quadrupole moment, Q (fm^2)
1	H	1	1.007 825 035 (12)	99.985 (1)	1/2	+ 2.792 847 386 (63)	+ 0.2860 (15)
		2	2.014 101 779 (24)	0.015 (1)	1	+ 0.857 438 230 (24)	
		3*	3.016 049 27 (4)		1/2	+ 2.978 962 479 (68)	
2	He	3	3.016 029 31 (4)	0.000 137 (3)	1/2	− 2.127 624 848 (66)	
		4	4.002 603 24 (5)	99.999 863 (3)	0	0	
3	Li	6	6.015 1214 (7)	7.5 (2)	1	+ 0.822 056 67 (26)*	− 0.082 (4)
		7	7.016 0030 (9)	92.5 (2)	3/2	+ 3.256 462 53 (40)*	− 4.01

Z	Symbol	A	Atomic mass, m_a (u)	Isotopic abundance, 100 x	Nuclear spin, I	Magnetic moment, m (μ_N)	Quadrupole moment, Q (fm ²)
4	Be	9	9.012 1822 (4)	100	3/2	− 1.177 492 (17)*	+ 5.288 (38)
5	B	10	10.012 936 9 (3)	19.9 (2)	3	+ 1.800 644 75 (57)	+ 8.459 (24)
		11	11.009 3054 (4)	80.1 (2)	3/2	+ 2.688 6489 (10)	+ 4.059 (10)
6	C	12	12 (by definition)	98.90 (3)	0	0	
		13	13.003 354 826 (17)	1.10 (3)	1/2	+ 0.702 4118 (14)	
		14*	14.003 241 982 (27)		0	0	
7	N	14	14.003 074 002 (26)	99.634 (9)	1	+ 0.403 761 00 (6)	+ 2.01 (2)
		15	15.000 108 97 (4)	0.366 (9)	1/2	− 0.283 188 842 (45)	
8	O	16	15.994 914 63 (5)	99.762 (15)	0	0	
		17	16.999 1312 (4)	0.038 (3)	5/2	− 1.893 80	− 2.558 (22)
		18	17.999 1603 (9)	0.200 (12)	0	0	
9	F	19	18.998 403 22 (15)	100	1/2	+ 2.628 868 (8)	
10	Ne	20	19.992 4356 (22)	90.48 (3)	0	0	
		21	20.993 8428 (21)	0.27 (1)	3/2	− 0.661 797 (5)	+ 10.155 (75)
		22	21.991 3831 (18)	9.25 (3)	0	0	
11	Na	23	22.989 7677 (10)	100	3/2	+ 2.217 6556 (6)*	+ 10.06 (20)
12	Mg	24	23.985 0423 (8)	78.99 (3)	0	0	
		25	24.985 8374 (8)	10.00 (1)	5/2	− 0.855 465 (8)	+ 19.94 (20)
		26	25.982 5937 (8)	11.01 (2)	0	0	
13	Al	27	26.981 5386 (8)	100	5/2	+ 3.641 504 687 (65)	+ 14.03 (10)
14	Si	28	27.976 9271 (7)	92.23 (1)	0	0	
		29	28.976 4949 (7)	4.67 (1)	1/2	− 0.555 29 (3)	
		30	29.973 7707 (7)	3.10 (1)	0	0	
15	P	31	30.973 7620 (6)	100	1/2	+ 1.131 60 (3)	
16	S	32	31.972 070 70 (25)	95.02 (9)	0	0	
		33	32.971 458 43 (23)	0.75 (1)	3/2	+ 0.643 8212 (14)	− 6.78 (13)
		34	33.967 866 65 (22)	4.21 (8)	0	0	
		36	35.967 080 62 (27)	0.02 (1)	0	0	
17	Cl	35	34.968 852 721 (69)	75.77 (5)	3/2	+ 0.821 8743 (4)	− 8.11 (8)
		37	36.965 902 62 (11)	24.23 (5)	3/2	+ 0.684 1236 (4)	− 6.39 (6)
18	Ar	36	35.967 545 52 (29)	0.337 (3)	0	0	
		38	37.962 7325 (9)	0.063 (1)	0	0	
		40	39.962 3837 (14)	99.600 (3)	0	0	
19	K	39	38.963 7074 (12)	93.2581 (44)	3/2	+ 0.391 507 31 (12)*	+ 5.9 (6)
		40	39.963 9992 (12)	0.0117 (1)	4	− 1.298 1003 (34)	− 7.3 (7)
		41	40.961 8254 (12)	6.7302 (44)	3/2	+ 0.214 870 09 (22)	+ 7.2 (7)
20	Ca	40	39.962 5906 (13)	96.941 (18)	0	0	
		42	41.958 6176 (13)	0.647 (9)	0	0	
		43	42.958 7662 (13)	0.135 (6)	7/2	− 1.317 643 (7)	− 4.09 (8)
		44	43.955 4806 (14)	2.086 (12)	0	0	
		46	45.953 689 (4)	0.004 (4)	0	0	
		48	47.952 533 (4)	0.187 (4)	0	0	
21	Sc	45	44.955 9100 (14)	100	7/2	+ 4.756 4866 (18)	− 22 (1)*

Z	Symbol	A	Atomic mass, m_a (u)	Isotopic abundance, 100 x	Nuclear spin, I	Magnetic moment, m (μ_N)	Quadrupole moment, Q (fm ²)
22	Ti	46	45.952 6294 (14)	8.0 (1)	0	0	
		47	46.951 7640 (11)	7.3 (1)	5/2	− 0.788 48 (1)	+ 29 (1)
		48	47.947 9473 (11)	73.8 (1)	0	0	
		49	48.947 8711 (11)	5.5 (1)	7/2	− 1.104 17 (1)	+ 24 (1)
		50	49.944 7921 (12)	5.4 (1)	0	0	
23	V	50 #	49.947 1609 (17)	0.250 (2)	6	+ 3.345 6889 (14)	20.9 (40)*
		51	50.943 9617 (17)	99.750 (2)	7/2	+ 5.148 705 73 (18)	− 5.2 (10)*
24	Cr	50	49.946 0464 (17)	4.345 (13)	0	0	
		52	51.940 5098 (17)	83.789 (18)	0	0	
		53	52.940 6513 (17)	9.501 (17)	3/2	− 0.474 54 (3)	− 15 (5)*
		54	53.938 8825 (17)	2.365 (7)	0	0	
25	Mn	55	54.938 047 1 (16)	100	5/2	+ 3.468 7190 (9)	+ 33 (1)*
26	Fe	54	53.939 6127 (15)	5.8 (1)	0	0	
		56	55.934 9393 (16)	91.72 (30)	0	0	
		57	56.935 3958 (16)	2.2 (1)	1/2	+ 0.090 623 00 (9)*	
		58	57.933 2773 (16)	0.28 (1)	0	0	
27	Co	59	58.933 1976 (16)	100	7/2	+ 4.627 (9)	+ 40.4 (40)*
28	Ni	58	57.935 3462 (16)	68.077 (9)	0	0	
		60	59.930 7884 (16)	26.223 (8)	0	0	
		61	60.931 0579 (16)	1.140 (1)	3/2	− 0.750 02 (4)	+ 16.2 (15)
		62	61.928 3461 (16)	3.634 (2)	0	0	
		64	63.927 9679 (17)	0.926 (1)	0	0	
29	Cu	63	62.929 5989 (17)	69.17 (3)	3/2	+ 2.2227 3456 (14)*	− 21.1 (4)*
		65	64.927 7959 (20)	30.83 (3)	3/2	+ 2.381 61 (19)*	− 19.5 (4)
30	Zn	64	63.929 1448 (19)	48.6 (3)	0	0	
		66	65.926 0347 (17)	27.9 (2)	0	0	
		67	66.927 1291 (17)	4.1 (1)	5/2	+ 0.875 2049 (11)*	+ 15.0 (15)
		68	67.924 8459 (18)	18.8 (4)	0	0	
		70	69.925 325 (4)	0.6 (1)	0	0	
31	Ga	69	68.925 580 (3)	60.108 (9)	3/2	+ 2.016 589 (44)	+ 16.8*
		71	70.924 7005 (25)	39.892 (9)	3/2	+ 2.562 266 (18)	+ 10.6*
32	Ge	70	69.924 2497 (16)	21.23 (4)	0	0	
		72	71.992 0789 (16)	27.66 (3)	0	0	
		73	72.923 4626 (16)	7.73 (1)	9/2	− 0.879 4677 (2)	− 17.3 (26)
		74	73.921 1774 (15)	35.94 (2)	0	0	
		76	75.921 4016 (17)	7.44 (2)	0	0	
33	As	75	74.921 5942 (17)	100	3/2	+ 1.439 475 (65)	+ 31.4 (6)*
34	Se	74	73.922 4746 (16)	0.89 (2)	0	0	
		76	75.919 2120 (16)	9.36 (1)	0	0	
		77	76.919 9125 (16)	7.63 (6)	1/2	+ 0.535 074 24 (28)*	
		78	77.917 3076 (16)	23.78 (9)	0	0	
		80	79.916 5196 (19)	49.61 (10)	0	0	
		82	81.916 6978 (23)	8.73 (6)	0	0	
35	Br	79	78.918 3361 (26)	50.69 (7)	3/2	+ 2.106 400 (4)	+ 33.1 (4)
		81	80.916 289 (6)	49.31 (7)	3/2	+ 2.270 562 (4)	+ 27.6 (4)
36	Kr	78	77.920 396 (9)	0.35 (2)	0	0	
		80	79.916 380 (9)	2.25 (2)	0	0	
		82	81.913 482 (6)	11.6 (1)	0	0	
		83	82.914 135 (4)	11.5 (1)	9/2	− 0.970 669 (3)	+ 25.3 (5)
		84	83.911 507 (4)	57.0 (3)	0	0	
		86	85.910 616 (5)	17.3 (2)	0	0	

Z	Symbol	A	Atomic mass, m_a (u)	Isotopic abundance, 100 x	Nuclear spin, I	Magnetic moment, m (μ_N)	Quadrupole moment, Q (fm ²)
37	Rb	85	84.911 794 (3)	72.165 (20)	5/2	+ 1.353 3515 (8)*	+ 22.8 (43)*
		87 #	86.909 187 (3)	27.835 (20)	3/2	+ 2.751 818 (2)	+ 13.2 (1)
38	Sr	84	83.913 430 (4)	0.56 (1)	0	0	
		86	85.909 2672 (28)	9.86 (1)	0	0	
		87	86.908 8841 (28)	7.00 (1)	9/2	− 1.093 6030 (13)*	+ 33.5 (20)
		88	87.905 6188 (28)	82.58 (1)	0	0	
39	Y	89	88.905 849 (3)	100	1/2	− 0.137 415 42 (34)*	
40	Zr	90	89.904 7026 (26)	51.45 (3)	0	0	
		91	90.905 6439 (26)	11.22 (4)	5/2	− 1.303 62 (2)	− 20.6 (10)
		92	91.905 0386 (26)	17.15 (2)	0	0	
		94	93.906 3148 (28)	17.38 (4)	0	0	
		96	95.908 275 (4)	2.80 (2)	0	0	
41	Nb	93	92.906 3772 (27)	100	9/2	+ 6.1705 (3)	− 32 (2)*
42	Mo	92	91.906 809 (4)	14.84 (4)	0	0	
		94	93.905 0853 (26)	9.25 (3)	0	0	
		95	94.905 8411 (22)	15.92 (5)	5/2	− 0.9142 (1)	− 2.2 (1)*
		96	95.904 6785 (22)	16.68 (5)	0	0	
		97	96.906 0205 (22)	9.55 (3)	5/2	− 0.9335 (1)	+ 25.5 (13)*
		98	97.905 4073 (22)	24.13 (7)	0	0	
		100	99.907 477 (6)	9.63 (3)	0	0	
43	Tc	98*	97.907 215 (4)		6		
44	Ru	96	95.907 599 (8)	5.52 (6)	0	0	
		98	97.905 287 (7)	1.88 (6)	0	0	
		99	98.905 9389 (23)	12.7 (1)	5/2	− 0.6413 (51)*	+ 7.9 (4)
		100	99.904 2192 (24)	12.6 (1)	0	0	
		101	100.905 5819 (24)	17.0 (1)	5/2	− 0.7188 (60)*	+ 45.7 (23)
		102	101.904 3485 (25)	31.6 (2)	0	0	
		104	103.905 424 (6)	18.7 (2)	0	0	
45	Rh	103	102.905 500 (4)	100	1/2	− 0.088 40 (2)	
46	Pd	102	101.905 634 (5)	1.02 (1)	0	0	
		104	103.904 029 (6)	11.14 (8)	0	0	
		105	104.905 079 (6)	22.33 (8)	5/2	− 0.642 (3)	+ 66.0 (11)*
		106	105.903 478 (6)	27.33 (3)	0	0	
		108	107.903 895 (4)	26.46 (9)	0	0	
		110	109.905 167 (20)	11.72 (9)	0	0	
47	Ag	107	106.905 092 (6)	51.839 (7)	1/2	− 0.113 679 65 (15)*	
		109	108.904 756 (4)	48.161 (7)	1/2	− 0.130 690 62 (22)*	
48	Cd	106	105.906 461 (7)	1.25 (4)	0	0	
		108	107.904 176 (6)	0.89 (2)	0	0	
		110	109.903 005 (4)	12.49 (12)	0	0	
		111	110.904 182 (3)	12.80 (8)	1/2	− 0.594 886 07 (84)*	
		112	111.902 757 (3)	24.13 (28)	0	0	
		113 #	112.904 400 (3)	12.22 (8)	1/2	− 0.622 300 92 (87)	
		114	113.903 357 (3)	28.73 (28)	0	0	
		116	115.904 755 (4)	7.49 (12)	0	0	
49	In	113	112.904 061 (4)	4.3 (2)	9/2	+ 5.5289 (2)	+ 79.9
		115 #	114.903 882 (4)	95.7 (2)	9/2	+ 5.5408 (2)	+ 81.0*
50	Sn	112	111.904 826 (5)	0.97 (1)	0	0	
		114	113.902 784 (4)	0.65 (1)	0	0	
		115	114.903 348 (3)	0.34 (1)	1/2	− 0.918 83 (7)	

Z	Symbol	A	Atomic mass, m_a (u)	Isotopic abundance, 100 x	Nuclear spin, I	Magnetic moment, m (μ_N)	Quadrupole moment, Q (fm ²)
50	Sn	116	115.901 747 (3)	14.53 (11)	0	0	
		117	116.902 956 (3)	7.68 (7)	1/2	− 1.001 04 (7)	
		118	117.901 609 (3)	24.23 (11)	0	0	
		119	118.903 311 (3)	8.59 (4)	1/2	− 1.047 28 (7)	
		120	119.902 1991 (29)	32.59 (10)	0	0	
		122	121.903 4404 (30)	4.63 (3)	0	0	
		124	123.905 2743 (17)	5.79 (5)	0	0	
51	Sb	121	120.903 8212 (29)	57.36 (8)	5/2	+ 3.3634 (3)	− 36 (4)*
		123	122.904 2160 (24)	42.64 (8)	7/2	+ 2.5498 (2)	− 49 (5)
52	Te	120	119.904 048 (21)	0.096 (2)	0	0	
		122	121.903 050 (3)	2.603 (4)	0	0	
		123	122.904 2710 (22)	0.908 (2)	1/2	− 0.736 9478 (8)	
		124	123.902 8180 (18)	4.816 (6)	0	0	
		125	124.904 4285 (25)	7.139 (6)	1/2	− 0.888 505 13 (43)*	
		126	125.903 3095 (25)	18.95 (1)	0	0	
		128	127.904 463 (4)	31.69 (1)	0	0	
		130	129.906 229 (5)	33.80 (1)	0	0	
53	I	127	126.904 473 (5)	100	5/2	+ 2.813 273 (84)	− 78.9
54	Xe	124	123.905 8942 (22)	0.10 (1)	0	0	
		126	125.904 281 (8)	0.09 (1)	0	0	
		128	127.903 5312 (17)	1.91 (3)	0	0	
		129	128.904 7801 (21)	26.4 (6)	1/2	− 0.777 9763 (84)	
		130	129.903 5094 (17)	4.1 (1)	0	0	
		131	130.905 072 (5)	21.2 (4)	3/2	+ 0.691 8619 (39)	− 12.0 (12)
		132	131.904 144 (5)	26.9 (5)	0	0	
		134	133.905 395 (8)	10.4 (2)	0	0	
		136	135.907 214 (8)	8.9 (1)	0	0	
55	Cs	133	132.905 429 (7)	100	7/2	+ 2.582 0246 (34)*	− 0.371 (14)*
56	Ba	130	129.906 282 (8)	0.106 (2)	0	0	
		132	131.905 042 (9)	0.101 (2)	0	0	
		134	133.904 486 (7)	2.417 (27)	0	0	
		135	134.905 665 (7)	6.592 (18)	3/2	+ 0.837 943 (17)*	+ 16.0 (3)*
		136	135.904 553 (7)	7.854 (36)	0	0	
		137	136.905 812 (6)	11.23 (4)	3/2	+ 0.937 365 (20)*	+ 24.5 (4)*
		138	137.905 232 (6)	71.70 (7)	0	0	
57	La	138#	137.907 105 (6)	0.0902 (2)	5	+ 3.713 646 (7)	+ 45 (2)*
		139	138.906 347 (5)	99.9098 (2)	7/2	+ 2.783 0455 (9)	+ 20 (1)
58	Ce	136	135.907 140 (50)	0.19 (1)	0	0	
		138	137.905 985 (12)	0.25 (1)	0	0	
		140	139.905 433 (4)	88.48 (10)	0	0	
		142	141.909 241 (4)	11.08 (10)	0	0	
59	Pr	141	140.907 647 (4)	100	5/2	+ 4.2754 (5)	− 5.89 (42)
60	Nd	142	141.907 719 (4)	27.13 (12)	0	0	
		143	142.909 810 (4)	12.18 (6)	7/2	− 1.065 (5)	− 63 (6)
		144	143.910 083 (4)	23.80 (12)	0	0	
		145	144.912 570 (4)	8.30 (6)	7/2	− 0.656 (4)	− 33 (3)
		146	145.013 113 (4)	17.19 (9)	0	0	
		148	147.916 889 (4)	5.76 (3)	0	0	
		150	149.920 887 (4)	5.64 (3)	0	0	
61	Pm	145*	144.912 743 (4)		5/2		

Z	Symbol	A	Atomic mass, m_a (u)	Isotopic abundance, 100 x	Nuclear spin, I	Magnetic moment, m (μ_N)	Quadrupole moment, Q (fm ²)
62	Sm	144	143.911 998 (4)	3.1 (1)	0	0	
		147 #	146.914 894 (4)	15.0 (2)	7/2	− 0.8148 (7)	− 25.9 (26)
		148	147.914 819 (4)	11.3 (1)	0	0	
		149	148.917 180 (4)	13.8 (1)	7/2	− 0.6717 (7)*	+ 7.5 (8)*
		150	149.917 273 (4)	7.4 (1)	0	0	
		152	151.919 728 (4)	26.7 (2)	0	0	
		154	153.922 205 (4)	22.7 (2)	0	0	
63	Eu	151	150.919 702 (8)	47.8 (15)	5/2	+ 3.4717 (6)	+ 90.3 (10)*
		153	152.921 225 (4)	52.2 (15)	5/2	+ 1.5330 (8)*	+ 241.2 (21)*
64	Gd	152	151.919 786 (4)	0.20 (1)	0	0	
		154	153.920 861 (4)	2.18 (3)	0	0	
		155	154.922 618 (4)	14.80 (5)	3/2	− 0.257 23 (35)*	+ 130 (2)*
		156	155.922 118 (4)	20.47 (4)	0	0	
		157	156.923 956 (4)	15.65 (3)	3/2	− 0.337 26 (55)*	+ 136 (2)*
		158	157.924 019 (4)	24.84 (12)	0	0	
		160	159.927 049 (4)	21.86 (4)	0	0	
65	Tb	159	158.925 342 (4)	100	3/2	+ 2.014 (4)	+ 143.2 (8)
66	Dy	156	155.924 277 (8)	0.06 (1)	0	0	
		158	157.924 403 (5)	0.10 (1)	0	0	
		160	159.925 193 (4)	2.34 (6)	0	0	
		161	160.926 930 (4)	18.9 (2)	5/2	− 0.4803 (25)*	+ 250.7 (20)*
		162	161.926 795 (4)	25.5 (2)	0	0	
		163	162.928 728 (4)	24.9 (2)	5/2	+ 0.6726 (35)	+ 264.8 (21)
		164	163.929 171 (4)	28.2 (2)	0	0	
67	Ho	165	164.930 319 (4)	100	7/2	+ 4.173 (27)	+ 349 (3)*
68	Er	162	161.928 775 (4)	0.14 (1)	0	0	
		164	163.929 198 (4)	1.61 (1)	0	0	
		166	165.930 290 (4)	33.6 (2)	0	0	
		167	166.932 046 (4)	22.95 (15)	7/2	− 0.563 85 (12)	+ 356.5 (29)
		168	167.932 368 (4)	26.8 (2)	0	0	
		170	169.935 461 (4)	14.9 (2)	0	0	
69	Tm	169	168.934 212 (4)	100	1/2	− 0.2316 (15)	
70	Yb	168	167.933 894 (5)	0.13 (1)	0	0	
		170	169.934 759 (4)	3.05 (6)	0	0	
		171	170.936 323 (3)	14.3 (2)	1/2	+ 0.493 67 (1)*	
		172	171.936 378 (3)	21.9 (3)	0	0	
		173	172.938 208 (3)	16.12 (21)	5/2	− 0.679 89 (3)*	+ 280 (4)
		174	173.938 859 (3)	31.8 (4)	0	0	
		176	175.942 564 (4)	12.7 (2)	0	0	
71	Lu	175	174.940 770 (3)	97.41 (2)	7/2	+ 2.2327 (11)*	+ 349 (2)*
		176 #	175.942 679 (3)	2.59 (2)	7	+ 3.1692 (45)*	+ 492 (3)*
72	Hf	174	173.940 044 (4)	0.162 (3)	0	0	
		176	175.941 406 (4)	5.206 (5)	0	0	
		177	176.943 217 (3)	18.606 (4)	7/2	+ 0.7935 (6)	+ 336.5 (29)*
		178	177.943 696 (3)	27.297 (4)	0	0	
		179	178.945 8122 (29)	13.629 (6)	9/2	− 0.6409 (13)	+ 379.3 (33)*
		180	179.946 5457 (30)	35.100 (7)	0	0	
73	Ta	180	179.947 462 (4)	0.012 (2)	8		
		181	180.947 992 (3)	99.988 (2)	7/2	+ 2.3705 (7)	+ 328 (6)*

Z	Symbol	A	Atomic mass, m_a (u)	Isotopic abundance, 100 x	Nuclear spin, I	Magnetic moment, m (μ_N)	Quadrupole moment, Q (fm ²)
74	W	180	179.946 701 (5)	0.13 (4)	0	0	
		182	181.948 202 (3)	26.3 (2)	0	0	
		183	182.950 220 (3)	14.3 (1)	1/2	+ 0.117 784 76 (9)	
		184	183.950 928 (3)	30.67 (15)	0	0	
		186	185.954 357 (4)	28.6 (2)	0	0	
75	Re	185	184.952 951 (3)	37.40 (2)	5/2	+ 3.1871 (3)	+ 218 (2)*
		187 #	186.955 744 (3)	62.60 (2)	5/2	+ 3.2197 (3)	+ 207 (2)*
76	Os	184	183.952 488 (4)	0.02 (1)	0	0	
		186	185.953 830 (4)	1.58 (30)	0	0	
		187	186.955 741 (3)	1.6 (3)	1/2	+ 0.064 651 89 (6)	
		188	187.955 830 (3)	13.3 (7)	0	0	
		189	188.958 137 (4)	16.1 (8)	3/2	+ 0.659 933 (4)	+ 85.6 (28)
		190	189.958 436 (4)	26.4 (12)	0	0	
		192	191.961 467 (4)	41.0 (8)	0	0	
77	Ir	191	190.960 584 (4)	37.3 (5)	3/2	+ 0.1507 (6)*	+ 81.6 (9)*
		193	192.962 917 (4)	62.7 (5)	3/2	+ 0.1637 (6)*	+ 75.1 (9)*
78	Pt	190	189.959 917 (7)	0.01 (1)	0	0	
		192	191.961 019 (5)	0.79 (6)	0	0	
		194	193.962 655 (4)	32.9 (6)	0	0	
		195	194.964 766 (4)	33.8 (6)	1/2	+ 0.609 52 (6)	
		196	195.964 926 (4)	25.3 (6)	0	0	
		198	197.967 869 (6)	7.2 (2)	0	0	
79	Au	197	196.966 543 (4)	100	3/2	+ 0.148 158 (8)*	+ 54.7 (16)*
80	Hg	196	195.965 807 (5)	0.15 (1)	0	0	
		198	197.966 743 (4)	9.97 (8)	0	0	
		199	198.968 254 (4)	16.87 (10)	1/2	+ 0.505 885 49 (85)	
		200	199.968 300 (4)	23.10 (16)	0	0	
		201	200.970 277 (4)	13.18 (8)	3/2	− 0.560 2257 (14)*	+ 38.5 (40)*
		202	201.970 617 (4)	29.86 (20)	0	0	
		204	203.973 467 (5)	6.87 (4)	0	0	
81	Tl	203	202.972 320 (5)	29.524 (14)	1/2	+ 1.622 257 87 (12)	
		205	204.974 401 (5)	70.476 (14)	1/2	+ 1.638 214 61 (12)	
82	Pb	204	203.973 020 (5)	1.4 (1)	0	0	
		206	205.974 440 (4)	24.1 (1)	0	0	
		207	206.975 872 (4)	22.1 (1)	1/2	+ 0.582 583 (9)*	
		208	207.976 627 (4)	52.4 (1)	0	0	
83	Bi	209	208.980 374 (5)	100	9/2	+ 4.1106 (2)	− 37.0 (26)*
84	Po	209*	208.982 404 (5)		1/2		
85	At	210*	209.987 126 (12)				
86	Rn	222*	222.017 571 (3)		0	0	
87	Fr	223*	223.019 733 (4)		3/2	+ 1.17 (2)	+ 117 (1)
88	Ra	226*	226.025 403 (3)		0	0	
89	Ac	227*	227.027 750 (3)		3/2	+ 1.1 (1)	+ 170 (20)
90	Th	232 #	232.038 0508 (23)	100	0	0	
91	Pa	231*	231.035 880 (3)		3/2	2.01 (2)	− 172 (5)

Z	Symbol	A	Atomic mass, m_a (u)	Isotopic abundance, 100 x	Nuclear spin, I	Magnetic moment, m (μ_N)	Quadrupole moment, Q (fm ²)
92	U	233*	233.039 628 (3)		5/2	0.59 (5)	+ 366.3 (8)
		234#	234.040 9468 (24)	0.0055 (5)	0	0	
		235#	235.043 9242 (24)	0.7200 (12)	7/2	− 0.38 (3)*	+ 455 (9)*
		238#	238.050 7847 (23)	99.2745 (60)	0	0	
93	Np	237*	237.048 1678 (23)		5/2	+ 3.14 (4)	+ 388.6 (6)
94	Pu	244*	244.064 199 (5)		0		
95	Am	243*	243.061 375 (3)		5/2	+ 1.61 (4)	+ 420 (130)
96	Cm	247*	247.070 347 (5)				
97	Bk	247*	247.070 300 (6)				
98	Cf	251*	251.079 580 (5)				
99	Es	252*	252.082 944 (23)				
100	Fm	257*	257.095 099 (8)				
101	Md	258*	258.098 57 (22)				
102	No	259*	259.100 931 (12)				
103	Lr	260*	260.105 320 (60)				
104	Unq	261*	261.108 69 (22)				
105	Unp	262*	262.113 76 (16)				
106	Unh	263*	263.118 22 (13)				
107	Uns	262*	263.122 93 (45)				
108	Uno	265*	265.130 16 (99)				
109	Une	266*	266.137 64 (45)				

(Reprinted with permission from Mills I *et al.* (1993) *Quantities, Uses and Symbols in Physical Chemistry*, 2nd edn. Oxford: Blackwell Scientific Publications.)

15. SOLVENTS FOR ULTRAVIOLET SPECTROPHOTOMETRY

Solvent	Cutoff wavelength (nm)	Dielectric constant (20°C)	
Acetic acid	260	6.15	
Acetone	330	20.7	(25°C)
Acetonitrile	190	37.5	
Benzene	280	2.284	
2-Butanol	260	15.8	(25°C)
<i>n</i> -Butyl acetate	254		
Carbon disulphide	380	2.641	
Carbon tetrachloride	265	2.238	
1-Chlorobutane	220	7.39	(25°C)
Chloroform ^a	245	4.806	
Cyclohexane	210	2.023	
1,2-Dichloroethane	226	10.19	(25°C)
1,2-Dimethoxyethane	240		
<i>N,N</i> -Dimethylacetamide	268	59	(83°C)
<i>N,N</i> -Dimethylformamide	270	36.7	
Dimethyl sulphoxide	265	4.7	
1,4-Dioxane	215	2.209	(25°C)
Diethyl ether	218	4.335	
Ethanol	210	24.30	(25°C)
2-Ethoxyethanol	210		
Ethyl acetate	255	6.02	(25°C)
Glycerol	207	42.5	(25°C)
<i>n</i> -Hexadecane	200	2.06	(25°C)
<i>n</i> -Hexane	210	1.890	
Methanol	210	32.63	(25°C)
2-Methoxyethanol	210	16.9	
Methyl cyclohexane	210	2.02	(25°C)
Methyl ethyl ketone	330	18.5	
Methyl isobutyl ketone	335		
2-Methyl-1-propanol	230	1	
<i>N</i> -Methyl-2-pyrrolidone	285	32.0	
Pentane	210	1.844	
<i>n</i> -Pentyl acetate	212		
1-Propanol	210	20.1	(25°C)
2-Propanol	210	18.3	(25°C)
Pyridine	330	12.3	(25°C)
Tetrachloroethylene ^b	290		
Tetrahydrofuran	220	7.6	
Toluene	286	2.379	(25°C)
1,1,2-Trichloro-1,2,2-trifluoroethane	231		
2,2,4-Trimethylpentane	215	1.936	(25°C)
<i>o</i> -Xylene	290	2.568	
<i>m</i> -Xylene	290	2.374	
<i>p</i> -Xylene	290	2.270	
Water		78.54	(25°C)

^a Stabilized with ethanol to avoid phosgene formation.

^b Stabilized with thymol (isopropyl meta-cresol).

Reprinted from T. J. Bruno and P. D. N. Svoronos, *CRC Handbook of Basic Tables for Chemical Analysis*, CRC Press, Boca Raton, FL, 1989, p. 212.

16. STATISTICAL TABLES

The following tables are presented in a format that is compatible with the needs of analytical chemists: the significance level $P = 0.05$ has been used in most cases, and it has been assumed that the number of measurements available is fairly small. Except where stated otherwise, these abbreviated tables have been taken, with permission, from *Elementary Statistics Tables* by Henry R. Neave, published by George Allen & Unwin Ltd. (Tables 1–3, 5–6, and 7–11). The reader requiring statistical data corresponding to significance levels and/or numbers of measurements not covered in the tables is referred to these sources.

Table 1 The t -distribution

Value of $ t $ for a confidence interval of: Critical value of t for P values of: Number of degrees of freedom	90% 0.10	95% 0.05	98% 0.02	99% 0.01
1	6.31	12.71	31.82	63.66
2	2.92	4.30	6.96	9.92
3	2.35	3.18	4.54	5.84
4	2.13	2.78	3.75	4.60
5	2.02	2.57	3.36	4.03
6	1.94	2.45	3.14	3.71
7	1.89	2.36	3.00	3.50
8	1.86	2.31	2.90	3.36
9	1.83	2.26	2.82	3.25
10	1.81	2.23	2.76	3.17
12	1.78	2.18	2.68	3.05
14	1.76	2.14	2.62	2.98
16	1.75	2.12	2.58	2.92
18	1.73	2.10	2.55	2.88
20	1.72	2.09	2.53	2.85
30	1.70	2.04	2.46	2.75
50	1.68	2.01	2.40	2.68
∞	1.64	1.96	2.33	2.58

The critical values of $|t|$ are appropriate for a *two*-tailed test. For a *one*-tailed test the value is taken from the column for *twice* the desired P -value, e.g. for a one-tailed test, $P = 0.05$, 5 degrees of freedom, the critical value is read from the $P = 0.10$ column and is equal to 2.02.

Table 2 Critical values of F for a one-tailed test ($P = 0.05$)

v_1 : v_2	1	2	3	4	5	6	7	8	9	10	12	15	20
1	161.4	199.5	215.7	224.6	230.2	234.0	236.8	238.9	240.5	241.9	243.9	245.9	248.0
2	18.51	19.00	19.16	19.25	19.30	19.33	19.35	19.37	19.38	19.40	19.41	19.43	19.45
3	10.13	9.552	9.277	9.117	9.013	8.941	8.887	8.845	8.812	8.786	8.745	8.703	8.660
4	7.709	6.944	6.591	6.388	6.256	6.163	6.094	6.041	5.999	5.964	5.912	5.858	5.803
5	6.608	5.786	5.409	5.192	5.050	4.950	4.876	4.818	4.772	4.735	4.678	4.619	4.558
6	5.987	5.143	4.757	4.534	4.387	4.284	4.207	4.147	4.099	4.060	4.000	3.938	3.874
7	5.591	4.737	4.347	4.120	3.972	3.866	3.787	3.726	3.677	3.637	3.575	3.511	3.445
8	5.318	4.459	4.066	3.838	3.687	3.581	3.500	3.438	3.388	3.347	3.284	3.218	3.150
9	5.117	4.256	3.863	3.633	3.482	3.374	3.293	3.230	3.179	3.137	3.073	3.006	2.936
10	4.965	4.103	3.708	3.478	3.326	3.217	3.135	3.072	3.020	2.978	2.913	2.845	2.774
11	4.844	3.982	3.587	3.357	3.204	3.095	3.012	2.948	2.896	2.854	2.788	2.719	2.646
12	4.747	3.885	3.490	3.259	3.106	2.996	2.913	2.849	2.796	2.753	2.687	2.617	2.544
13	4.667	3.806	3.411	3.179	3.025	2.915	2.832	2.767	2.714	2.671	2.604	2.533	2.459
14	4.600	3.739	3.344	3.112	2.958	2.848	2.764	2.699	2.646	2.602	2.534	2.463	2.388
15	4.543	3.682	3.287	3.056	2.901	2.790	2.707	2.641	2.588	2.544	2.475	2.403	2.328
16	4.494	3.634	3.239	3.007	2.852	2.741	2.657	2.591	2.538	2.494	2.425	2.352	2.276
17	4.451	3.592	3.197	2.965	2.810	2.699	2.614	2.548	2.494	2.450	2.381	2.308	2.230
18	4.414	3.555	3.160	2.928	2.773	2.661	2.577	2.510	2.456	2.412	2.342	2.269	2.191
19	4.381	3.522	3.127	2.895	2.740	2.628	2.544	2.477	2.423	2.378	2.308	2.234	2.155
20	4.351	3.493	3.098	2.866	2.711	2.599	2.514	2.447	2.393	2.348	2.278	2.203	2.124

v_1 = number of degrees of freedom of the numerator and v_2 = number of degrees of freedom of the denominator.

Table 3 Critical values of F for a two-tailed test ($P = 0.05$)

v_1 : v_2	1	2	3	4	5	6	7	8	9	10	12	15	20
1	647.8	799.5	864.2	899.6	921.8	937.1	948.2	956.7	963.3	968.6	976.7	984.9	993.1
2	38.51	39.00	39.17	39.25	39.30	39.33	39.36	39.37	39.39	39.40	39.41	39.43	39.45
3	17.44	16.04	15.44	15.10	14.88	14.73	14.62	14.54	14.47	14.42	14.34	14.25	14.17
4	12.22	10.65	9.979	9.605	9.364	9.197	9.074	8.980	8.905	8.844	8.751	8.657	8.560
5	10.01	8.434	7.764	7.388	7.146	6.978	6.853	6.757	6.681	6.619	6.525	6.428	6.329
6	8.813	7.260	6.599	6.227	5.988	5.820	5.695	5.600	5.523	5.461	5.366	5.269	5.168
7	8.073	6.542	5.890	5.523	5.285	5.119	4.995	4.899	4.823	4.761	4.666	4.568	4.467
8	7.571	6.059	5.416	5.053	4.817	4.652	4.529	4.433	4.357	4.295	4.200	4.101	3.999
9	7.209	5.715	5.078	4.718	4.484	4.320	4.197	4.102	4.026	3.964	3.868	3.769	3.667
10	6.937	5.456	4.826	4.468	4.236	4.072	3.950	3.855	3.779	3.717	3.621	3.522	3.419
11	6.724	5.256	4.630	4.275	4.044	3.881	3.759	3.664	3.588	3.526	3.430	3.330	3.226
12	6.554	5.096	4.474	4.121	3.891	3.728	3.607	3.512	3.436	3.374	3.277	3.177	3.073
13	6.414	4.965	4.347	3.996	3.767	3.604	3.483	3.388	3.312	3.250	3.153	3.053	2.948
14	6.298	4.857	4.242	3.892	3.663	3.501	3.380	3.285	3.209	3.147	3.050	2.949	2.844
15	6.200	4.765	4.153	3.804	3.576	3.415	3.293	3.199	3.123	3.060	2.963	2.862	2.756
16	6.115	4.687	4.077	3.729	3.502	3.341	3.219	3.125	3.049	2.986	2.889	2.788	2.681
17	6.042	4.619	4.011	3.665	3.438	3.277	3.156	3.061	2.985	2.922	2.825	2.723	2.616
18	5.978	4.560	3.954	3.608	3.382	3.221	3.100	3.005	2.929	2.866	2.769	2.667	2.559
19	5.922	4.508	3.903	3.559	3.333	3.172	3.051	2.956	2.880	2.817	2.720	2.617	2.509
20	5.871	4.461	3.859	3.515	3.289	3.128	3.007	2.913	2.837	2.774	2.676	2.573	2.464

v_1 = number of degrees of freedom of the numerator and v_2 = number of degrees of freedom of the denominator.

Table 4 Critical values of Q ($P = 0.05$)

Sample size	Critical value
4	0.831
5	0.717
6	0.621
7	0.570
8	0.524
9	0.492
10	0.464

Taken from E.P. King, *J. Am. Statist. Assoc.*, 1958, **48**, 531, by permission of the American Statistical Association.

Table 5 Critical values of χ^2 ($P = 0.05$)

Number of degrees of freedom	Critical value
1	3.84
2	5.99
3	7.81
4	9.49
5	11.07
6	12.59
7	14.07
8	15.51
9	16.92
10	18.31

Table 6 The sign test

n	$r = 0$	1	2	3	4	5	6	7
4	0.063	0.313	0.688					
5	0.031	0.188	0.500					
6	0.016	0.109	0.344	0.656				
7	0.008	0.063	0.227	0.500				
8	0.004	0.035	0.144	0.363	0.637			
9	0.002	0.020	0.090	0.254	0.500			
10	0.001	0.011	0.055	0.172	0.377	0.623		
11	0.001	0.006	0.033	0.113	0.274	0.500		
12	0.000	0.003	0.019	0.073	0.194	0.387	0.613	
13	0.000	0.002	0.011	0.046	0.133	0.290	0.500	
14	0.000	0.001	0.006	0.029	0.090	0.212	0.395	0.605
15	0.000	0.000	0.004	0.018	0.059	0.151	0.304	0.500

The table uses the binomial distribution with $P = 0.5$ to give the probabilities of r or less successes for $n = 4$ –15. These values correspond to a one-tailed sign test and should be doubled for a two-tailed test.

Table 7 Wilcoxon signed rank test. Critical values for the test statistic at $P = 0.05$

n	One-tailed test	Two-tailed test
5	0	NA
6	2	0
7	3	2
8	5	3
9	8	5
10	10	8
11	13	10
12	17	13
13	21	17
14	25	21
15	30	25

The null hypothesis can be rejected when the test statistic is \leq the tabulated value. NA indicates that the test cannot be applied.

Table 8 Wilcoxon rank sum test; Mann-Whitney U -test. Critical values for U or the lower of T_1 and T_2 at $P = 0.05$

n_1	n_2	One-tailed test	Two-tailed test
3	3	0	NA
3	4	0	NA
3	5	1	0
3	6	2	1
4	4	1	0
4	5	2	1
4	6	3	2
4	7	4	3
5	5	4	2
5	6	5	3
5	7	6	5
6	6	7	5
6	7	8	6
7	7	11	8

The null hypothesis can be rejected when U or the lower T value is \leq the tabulated value. NA indicates that the test cannot be applied.

Table 9 The Spearman rank correlation coefficient. Critical values for ρ at $P = 0.05$

<i>n</i>	<i>One-tailed test</i>	<i>Two-tailed test</i>
5	0.900	1.000
6	0.829	0.886
7	0.714	0.786
8	0.643	0.738
9	0.600	0.700
10	0.564	0.649
11	0.536	0.618
12	0.504	0.587
13	0.483	0.560
14	0.464	0.538
15	0.446	0.521
16	0.429	0.503
17	0.414	0.488
18	0.401	0.472
19	0.391	0.460
20	0.380	0.447

Table 10 The Kolmogorov goodness of fit test

<i>n</i>	<i>One-tailed test</i>	<i>Two-tailed test</i>
1	0.950	0.975
2	0.776	0.842
3	0.636	0.708
4	0.565	0.624
5	0.509	0.563
6	0.468	0.519
7	0.436	0.483
8	0.410	0.454
9	0.388	0.430
10	0.369	0.409
11	0.352	0.392
12	0.338	0.375
13	0.326	0.361
14	0.314	0.349
15	0.304	0.338
16	0.295	0.327
17	0.286	0.318
18	0.278	0.309
19	0.271	0.301
20	0.265	0.294

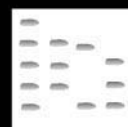
Critical values for one-tailed and two-tailed tests at $P = 0.05$. The appropriate value is compared with the maximum difference between the experimental and theoretical cumulative frequency curves.

Table 11 The Kolmogorov test for normality

<i>n</i>	<i>One-tailed test</i>	<i>Two-tailed test</i>
3	0.367	0.376
4	0.345	0.375
5	0.319	0.343
6	0.297	0.323
7	0.280	0.304
8	0.265	0.288
9	0.252	0.274
10	0.241	0.262
11	0.231	0.251
12	0.222	0.242
13	0.215	0.234
14	0.208	0.226
15	0.201	0.219
16	0.195	0.213
17	0.190	0.207
18	0.185	0.202
19	0.181	0.197
20	0.176	0.192

Critical values for one-tailed and two-tailed tests at $P = 0.05$. The appropriate value is compared with the maximum difference between the experimental and theoretical cumulative frequency curves.

17. THIN LAYER (PLANAR) CHROMATOGRAPHY: DETECTION



A. Misra, Bareilly, India

Copyright © 2000 Academic Press

The following tables list detection methods and reagents suitable for detecting and identifying substances separated by thin-layer (planar) chromatography.

Table 1.1 Methods of detection on TLC plates (aluminium oxide) by heating (Types 150/T or 60/E)

<i>Substances</i>	<i>Temperature/time</i>	<i>Remarks</i>
Pesticides, e.g. aminocarb, captan, difolatan, landrin, rotenone	200°C, 45 min	Induction of fluorescence in weakly fluorescent or nonfluorescent pesticides and amplification of natural fluorescence. There are some differences between basic and acidic aluminium oxide layers
Δ^4 -3-Ketosteroids, e.g. testosterone and <i>epi</i> -testosterone in urine	180°C, 20 min	Pale blue induced fluorescence ($\lambda_{fl} = 440$ nm) for Δ^4 -3-ketosteroids, detection limit: 5 ng
Δ^4 -3-Ketosteroids, e.g. trimethylsilyl-testosterone	180°C, 20 min or 150°C, 20 min	Conversion of Δ^4 -3-ketosteroids or their trimethylsilyl or acetyl derivatives in fluorescent components, whereby the detection limits were improved by 65% for the acetates. Δ^5 -3-keto- and Δ^5 -3-OH-steroids also react with the same sensitivity
Testosterone	180°C, 20 min	Induced fluorescence ($\lambda_{fl} > 430$ nm, cut off filter) by thermal treatment of the chromatogram, the fluorescence increased by a factor of 2.5 by dipping in a solution of Triton X-100 – chloroform (1 + 4). Working range: 2–50 ng substance per chromatogram zone. Prewashing the layers with methanol-ammonia solution (25%) (50 + 50) increased the precision
Testosterone	180°C, 20 min	Induced fluorescence and fluorescence amplification by a factor of 25 by dipping the chromatogram in a solution of Triton X-100 – chloroform (1 + 4)
Δ^4 -3-Ketosteroids, e.g. progesterone in plasma	150°C, 20 min	Conversion of Δ^4 -3-ketosteroids into fluorescent derivatives ($\lambda_{fl} = 440$ nm). Relatively selective for progesterone at 150°C detection limit: 2–5 ng

Table 1.2 Methods of fluorimetric detection on TLC plates (silica gel) by heating

<i>Substances</i>	<i>Temperature/time</i>	<i>Remarks</i>
Essential oil components	800–900°C	Induction of fluorescence in a special apparatus
Steroids, e.g. cholesterol, triolein, androsterone; sugars, e.g. fructose, glucose, ribose; amino acids, pyrimidines, purines, alkaloids	110–150°C, 2–12 h	Conversion to fluorescent derivatives by heating
Alkaloids, e.g. raubasine and its metabolites in plasma, urine and bile	120°C, 1 h	Amplification of the natural fluorescence of raubasine ($\lambda_{fl} = 482$ nm), detection limit 20 ng
Alkaloids, e.g. reserpine, rescinnamine	105°C, 2 h	Induced fluorescence ($\lambda_{fl} > 500$ nm, cut off filter). Possibly formation of 3-dehydro derivatives
Alkaloids, e.g. reserpine, ajmaline, rescinnamine	105°C, 2 h or 105°C, 15 h	Induction of stable fluorescence ($\lambda_{fl} > 480$ nm, cut off filter), detection limits 5–20 ng
Alkaloids, e.g. cocaine, ecgonine, benzoylecgonine, ecgonine methyl ester	280°C, 8 min or 260°C, 10–30 min	Pale blue induced fluorescence ($\lambda_{fl} > 390$ nm, cut off filter), fluorescence amplification by a factor of 2 on dipping in liquid paraffin solution; detection limits: < 10 ng
Alkaloids, e.g. lupanine, angustifoline, sparteine, lupinine, hydroxylupanine	130°C, 17–35 h	Induced blue fluorescence ($\lambda_{fl} = 400$ nm), detection limits: 10 ng
Pesticides, e.g. dursban, azinphos-methyl, menazon, imidan, phosalone, zinophos	200–225°C, 20–120 min	Induced fluorescence or amplification of natural fluorescence; detection limits: 10–300 ng
Organophosphorus pesticides, e.g. coumaphos, menazon, maretin, dursban	200°C, 45 min	Induced fluorescence or amplification of natural fluorescence, detection limits: 1–80 ng
Pesticides, e.g. fuberidazol	200°C, 45 min	Amplification of the natural fluorescence of some pesticides and bathochromic shift of the excitation and emission maxima; detection limits: 5–100 ng
Pesticides, e.g. coumatetralyl, methabenzthiazuron, propylisom, naptalam, thioquinox, warfarin etc.	200°C, 45 min	Induced fluorescence ($\lambda_{fl} > 430$ nm, cut off filter); detection limits: 6–600 ng
Coumaphos	200°C, 20 min	Residue analysis; induced fluorescence on heating ($\lambda_{fl} > 400$ nm); detection limit: 1 ng
Potasan, coumaphos, coroxon	200°C, 20 min	Induced blue fluorescence ($\lambda_{fl} = 430$ nm or 450 nm), identification of the fluorescent derivatives as chlorferon or 4-methylumbelliferone
Coumaphos	200°C, 20 min	Residue determination in honey, induced fluorescence ($\lambda_{fl} > 400$ nm, cut off filter); detection limit: 0.5 ng
Rubratoxin B	200°C, 10 min	Induced fluorescence that can be intensified by gassing the previously heated chromatogram plates with ammonia vapours (10 min). This also alters the colour of the emitted light to pale blue
Glucose or methylglucosides	135°C, 3 min or 140°C, 10 min	Induced yellow fluorescence
Sugar derivatives	'Mild heating over a Bunsen burner'	No details of whether fluorescence was produced or if a carbonization reaction occurred
Sugars, e.g. glucose, fructose, galactose, mannose etc.	160°C, 10 min	Production of fluorescence by heating the chromatogram after covering it with a glass plate. Sugar alcohols and C ₁ –C ₁ bonded oligosaccharides do not react; detection limit: 10 ng

Table 1.2 *Continued*

<i>Substances</i>	<i>Temperature/time</i>	<i>Remarks</i>
Sugars, e.g. glucose, glucosamine, fucose, raffinose, cellobiose, methylated sugars	80 → 260°C, gradient or 200°C, 5 min	Production of fluorescence by temperature gradients (10°C/30 s) to determine the optimum heating temperature for the individual substances. Oligosaccharides require higher temperatures than monosaccharides. Detection limit: 1 nMol. The fluorescence colours are characteristic particularly for the methylated sugars
Lipids, e.g. β -sitosterol, geraniol, dolichol, squalene, cholesterol	200°C, 15 min	Induced fluorescence; detection limits: < 1 μ g cholesterol
C-Nucleosides	Moderate heating on a hot plate	No details of whether fluorescence or carbonization was produced
Nomifensine and metabolites	70°C, 2 h + UV ₂₅₄	Heating and simultaneous UV irradiation produced intense yellow fluorescence ($\lambda_{fl} > 460$ nm, cut off filter)

Reproduced with permission from, Jork H, Funk W, Fisher W and Wimmer H (1994). *Thin Layer Chromatography: Regents and Detection Methods*, volume 1B. Weinheim: Wiley VCH.

Table 1.3 Examples of fluorimetric detection after thermal treatment of layer after chromatography

<i>Substances</i>	<i>Temperature/time</i>	<i>Remarks</i>
Sugars, e.g. lactose, glucose, fructose	120°C, 15 min	Violet fluorescence on a dark blue background
Sugars, e.g. lactose, glucose, fructose	120°C, 15 min	Induced fluorescence; detection limits in nanogram range
Glucose, fructose	Infrared lamp or 170°C each for 3 min	Heating produced stable bluish-white fluorescence ($\lambda_{exe} = 365$ nm and $\lambda_{fl} > 400$ nm, cut off filter K 400), detection limits; 5–10 ng
Sugars, e.g. glucose, rhamnose, xylose etc.	160°C, 3–4 min or infrared lamp	Induction of brilliant stable fluorescence $\lambda_{exe} = 365$ nm and $\lambda_{fl} > 400$ nm (cut off filter K 400), sugar alcohols do not fluoresce; detection limits; 5–10 ng
Creatine, creatinine, uric acid in urine and serum	150°C, 3–4 min	Stable fluorescence $\lambda_{exe} = 365$ nm and $\lambda_{fl} > 400$ nm (cut off filter K 400)
Sugars, e.g. sucrose, ribose, xylose	150°C, 3–4 min	Induced fluorescence $\lambda_{exe} = 365$ nm and $\lambda_{fl} > 400$ nm (cut off filter K 400)

Reproduced with permission from, Jork H, Funk W, Fisher W and Wimmer H (1994). *Thin Layer Chromatography: Regents and Detection Methods*, volume 1B. Weinheim: Wiley VCH.

Table 2 Some substances that produce intense fluorescence when treated with ionized nitrogen after they have been chromatographed

<i>Substance</i>	<i>Exposure time [s]</i>	<i>Substance</i>	<i>Exposure time [s]</i>
Cholesterol	60	Oleic acid	180
Cholesteryl pelargonate	60	Morphine	180
Progesterone	60	Codeine	180
Testosterone	60	Cocaine	180
Dieldrin	60	Dimerol	180
Tetrahydrocannabinol	60	Phenobarbital	180
Inositol	60	Chlorpromazine	180
Lauryl alcohol	180	d-Amphetamine sulfate	180
<i>n</i> -C ₂₂ H ₄₆	180	Methadone	180
Phenol	180		

Reproduced with permission from Jork H, Funk W, Fisher W and Wimmer H (1994). *Thin Layer Chromatography: Regents and Detection Methods*, volume 1B. Weinheim: Wiley VCH.

Table 3 Reagents suitable for the recognition of functional groups

<i>Functional group</i>	<i>Reagent</i>	<i>Remarks</i>
Acetylene compounds	Dicobaltoctacarbonyl	Formation of coloured complexes. After the reagent excess has been washed out, reaction with bromine vapour yields cobalt bromide, which reacts with α -nitroso- β -naphthol to yield red chromatogram zones on an almost colourless background
Aldehydes	4-Amino-3-hydrazino-5-mercapto-1,2,4-triazole (Purpald reagent)	Aldehydes yield violet chromatogram zones on a whitish-yellow background. Some alcohols form yellow to orange-coloured chromatogram zones
Aldehydes	2,4-Dinitrophenylhydrazine	Formation of coloured hydrazones or osazones. It is possible to distinguish between saturated and unsaturated hydrazones using potassium hexacyanoferrate (III)
Aldehydes	Hydrazine sulfate + hydrochloric acid	Aromatic aldehydes yield coloured hydrazones
Alcohols	4-(4-Nitrobenzyl)pyridine	Amino compounds, esters and ethers do not interfere, but phenols and acids as well as epoxides, olefins and substances containing labile halogen probably do
Alcohols (diols, polyols, sugars)	Lead(IV) acetate – dichlorofluorescein	Diol cleavage of vicinal diols, e.g. sugars, sugar alcohols. The lead tetraacetate consumed is no longer available to decompose the fluorescent dichlorofluorescein
Amines (primary)	Ninhydrin	Reddish or bluish chromatogram zones are produced, amino sugars and amino acids also react. Unexpectedly ascorbic acid also reacts
Amines (primary aliphatic and aromatic)	Diphenylboric anhydride + salicylaldehyde (DOOB)	Fluorescent reaction products are produced
Amines (primary)	α -Phthalaldehyde (OPA)	In the presence of mercaptoethanol α -phthalaldehyde reacts with primary amines and amino acids to yield fluorescent isoindole derivatives

Table 3 *Continued*

<i>Functional group</i>	<i>Reagent</i>	<i>Remarks</i>
Amines (primary)	Trinitrobenzenesulfonic acid (TNBS)	On heating primary amines react with TNBS to yield intensely coloured Meisenheimer complexes. Amino acids also react
Amines (primary)	Fluorescamine	Primary aliphatic and aromatic amines yield fluorescent derivatives. Primary aromatic amines yield stable yellow-coloured derivatives that can be eluted from the TLC layer
Amines (primary aromatic)	Sodium nitrite + α -naphthol or Bratton-Marshall reagent	Diazotization of the primary amine followed by coupling with α -naphthol or N-(L-naphthyl)ethylenediamine. Sulfonamides also react
Amines (primary aromatic)	4-(Dimethylamino)benzaldehyde + acid	Alkaloids and indole derivatives also react
Amines (capable of coupling)	Fast blue salt B, fast blue salt BB, fast black salt K, diazotized sulfanilic acid (Pauly's reagent), diazotized sulfanilamide or 4-nitroaniline	Intensely coloured azo dyes are produced. Catecholamines, imidazoles and phenols also react
Amines (primary and secondary)	7-Chloro-4-nitrobenzo-2-oxa-1,3-diazole (NBD chloride)	Fluorescent 4-nitrobenzofurazan derivatives are produced. Phenols and thiols also react
Amines (primary and secondary aromatic)	<i>p</i> -Chloranil	The reaction depends on the catalytic effect of silica gel. Monochlorobenzene as solvent for the reagent, also contributes. There is no reaction on cellulose layers
Amines (secondary aliphatic and alicyclic)	Sodium nitroprusside + acetaldehyde	Secondary aliphatic and alicyclic amines yield blue-coloured chromatogram zones (e.g. morpholine, diethanol amine)
Amines (long-chain primary, secondary and tertiary plus quaternary ammonium salts)	Cobalt(II) thiocyanate	Long-chain primary, secondary and tertiary amines and long-chain quaternary ammonium salts yield blue chromatogram zones on a pink background
Carboxyl groups (carboxylic acids)	Indicators, e.g. bromocresol green, bromocresol green + bromophenol blue + potassium permanganate, bromocresol purple, methyl red + bromothymol blue	Detection depends on the colour change of the indicator in acid medium. Quaternary ammonium salts give a colour change in some cases
Carboxyl groups (carboxylic acids)	2,6-Dichlorophenol-indophenol (Tillmann's reagent)	Organic acids release the red undissociated acid from the blue mesomerically stabilized phenolate anion. Reductones reduce the reagent to a colourless compound
Carboxyl groups (carboxylic acids)	Aniline + aldose (e.g. glucose)	The action of acid causes glucose to be converted to furfural which reacts with aniline to yield a coloured product
Halogen derivatives	Silver nitrate, ammoniacal (Dedonder's, Tollens' or Zaffaroni's reagent)	Halogen compounds yield black chromatogram zones on a pale grey background
Ketones	2,4-Dinitrophenylhydrazine	Formation of coloured hydrazones or osazones. It is possible to distinguish between saturated and unsaturated hydrazones using potassium hexacyanoferrate (III)

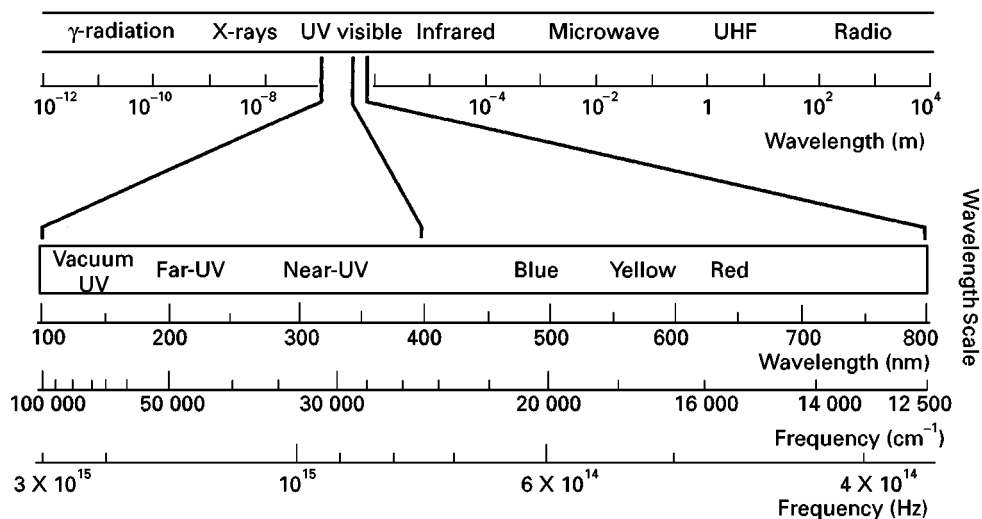
Table 3 *Continued*

<i>Functional group</i>	<i>Reagent</i>	<i>Remarks</i>
Nitro derivatives	Benzylcyanide + benzyl-trimethylammonium hydroxide	Nitro compounds, e.g. explosives, or pesticides containing nitro groups yield gray to bluish-green chromatogram zones on a brownish background
Peroxides	1-Naphthol + N ⁴ -ethyl-N ⁴ - (2-methanesulfonamidoethyl)-2-methyl-1,4-phenylenediamine (peroxide reagent)	A quinonimine dyestuff is produced on reaction with peroxides
Peroxides	Iron(II) sulfate + ammonium thiocyanate	Peroxides rapidly oxidize iron(II) to iron(III) ions which react to yield brown-red iron(III) thiocyanate complexes
Peroxides	Potassium iodide + starch	Peroxides release free iodine which forms a blue complex with the starch
Peroxides	N,N-Dimethyl-1,4-phenylenediamine (N,N-DPDD), N,N,N',N'-tetra-methyl-1,4-phenylene-diamine (TPDD)	Peroxides, e.g. alkyl hydroperoxides, oxidize N,N-DPDD to Wurster's red and TPDD to Wurster's blue
Phenols	7-Chloro-4-nitrobenzo-2-oxa-1,3-diazole (NBD chloride)	Fluorescent 4-nitrobenzofuran derivatives are produced. Primary and secondary aromatic amines and thiols also react
Phenols (capable of coupling)	Fast blue salt B, fast blue salt BB, fast black salt K, diazotized sulfanilic acid (Pauly's reagent) diazotized sulfanilamide or 4-nitroaniline	Intensely coloured azo dyes are formed. Catecholamines, imidazoles and amines capable of coupling also react
Thiols, thioethers, disulfides	Sodium metaperiodate + benzidine	Substances with divalent sulfur yield white chromatogram zones on a blue background
Thiols	7-Chloro-4-nitrobenzo-2-oxa-1,3-diazole (NBD chloride)	Fluorescent 4-nitrobenzofuran derivatives are formed. Primary and secondary aromatic amines and phenols also react

Reproduced with permission from Jork H, Funk W, Fisher W and Wimmer H (1994). *Thin Layer Chromatography: Regents and Detection Methods*, volume 1B. Weinheim: Wiley VCH.

See also: **II/Chromatography: Thin-Layer (Planar):** Densitometry and Image Analysis; Spray Reagents.

18. WAVELENGTH SCALE



The range of electromagnetic radiation. The lower part is an enlargement of the UV-visible region

Colour Plate 1

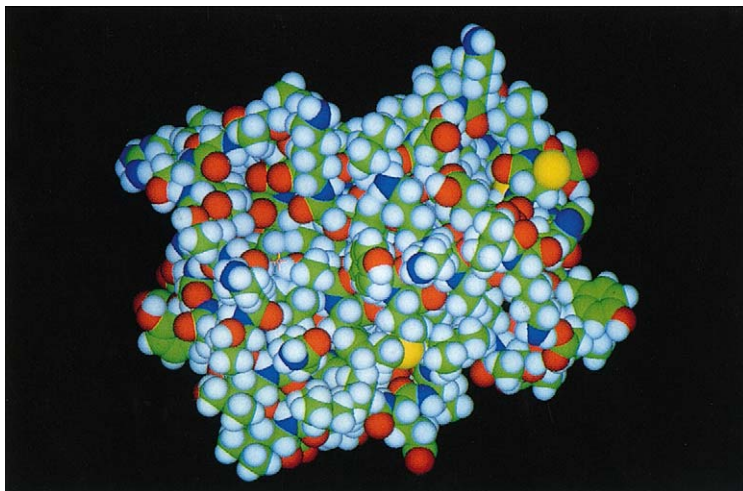


Plate 1 Affinity Separation Computer-generated model of the molecular structure of Interleukin-2 (IL-2), created using data from crystallographic studies. IL-2 is used to artificially boost the immune response against certain human cancers. It is released by certain key cells of the immune system (T-lymphocytes) that have been activated by foreign antigens. IL-2 amplifies the proliferation of other types of T-cells - particularly the “killer” T-cells that attack cancer cells directly. In one immunotherapy technique, blood is removed from a cancer victim, doped with IL-2 and cultured *in vitro* to raise the population of T-cells. The product is then reinjected into the patient. (With permission from J. C. Revy / Science Photo Library.)

Colour Plate 2



Plate 2 Centrifugation The Swedish physical chemist, Theodor Svedberg, 1884-1971. Svedberg studied at Uppsala and stayed at this university for life. Chiefly interested in the chemistry of colloids (a suspension of large particles) and how best to separate out floating giant molecules, he developed the ultracentrifuge. Spinning at high speed a powerful enough centrifugal force will affect large molecules and purify out proteins. Svedberg, in this way, calculated the relative molecular mass of haemoglobin. For this technique and for his other work on colloids, Svedberg was awarded the Nobel Prize for chemistry in 1926. The unit of sedimentation velocity, the *svedberg* (S) is named after him. (With permission from Science Photo Library.)

Colour Plate 3

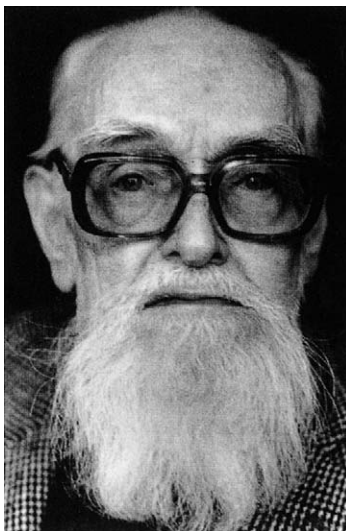


Plate 3 Chromatography Archer Martin (b.1910), British chemist and Nobel Laureate. Martin studied at Cambridge, gaining his doctorate in 1938 before performing research on vitamins. He later joined the staff of the Wool Industries Research Association where he met R.L.M Synge. Whilst looking into the problem of separating complex mixtures of amino acids, Martin and Synge developed partition Chromatography. By 1944, Martin had advanced the technique to combine both partition and absorption methods – and discovered paper Chromatography. This powerful analytical method won Martin and Synge the 1952 Nobel Prize for Chemistry. Photographed in 1993. (With permission from Nick Sinclair / Science Photo Library.)

Colour Plate 4

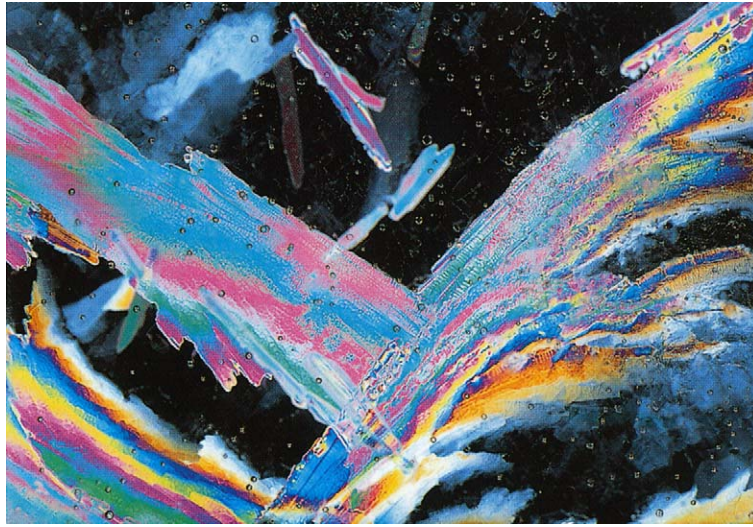


Plate 4 Crystallization Ice Crystals. Polarised light micrograph of a thin sheet of ice. The ice appears to have many colours within it. These are *birefringence* patterns due to different wavelengths of plane polarised light being rotated by different amounts. These colours indicate strong internal tensions in the ice, a result of the outer layers of ice freezing before the inner regions and therefore introducing stress into the crystal structure. Magnifications: unknown. (With permission from Adrienne Hart-Davis / Science Photo Library.)

Colour Plate 5

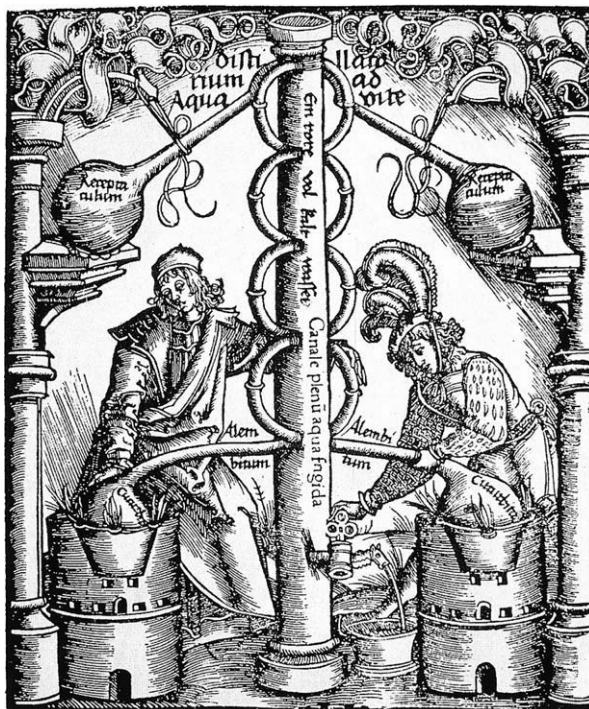


Plate 5 Distillation Illustration of a sixteenth century alcohol distillation set up showing two boiling vessels (bottom), the central column, or rectifying column, containing cold water & two receiving vessels (top). The illustration was produced by one Ulstadius in 1526. There is no further information on him or the publication. (With permission from Dr Jeremy Burgess / Science Photo Library.)

Colour Plate 6

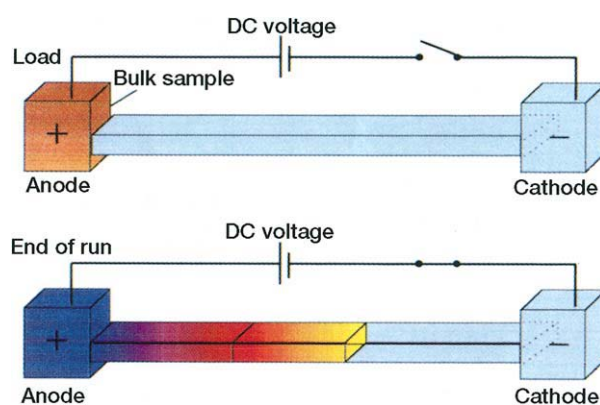


Plate 6 Electrophoresis The principle of moving boundary electrophoresis.

Colour Plate 7

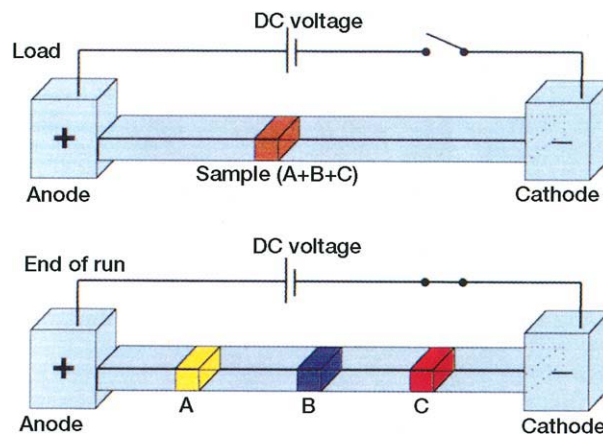


Plate 7 Electrophoresis The principle of zone electrophoresis.

Colour Plate 8

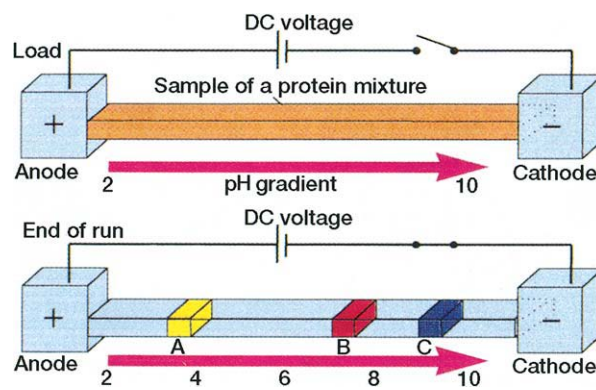


Plate 8 Electrophoresis The principle of isoelectric focussing.

Colour Plate 9

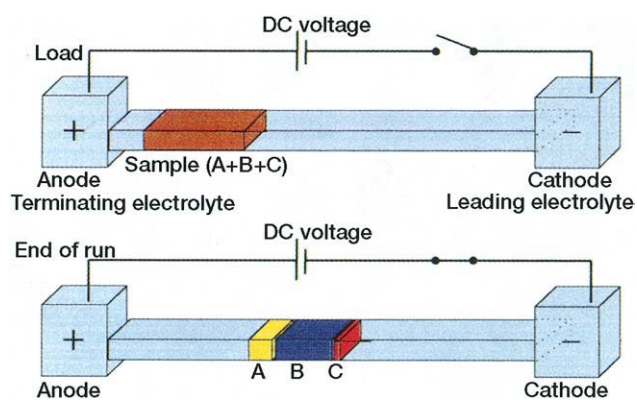


Plate 9 Electrophoresis. The principle of isotachopheresis.

Colour Plate 10



Plate 10 Flotation Gold nuggets panned from a riverbed on the Pacific slopes of the Andes mountains near the Colombian border. (With permission from Dr Merely Read / Science Photo Library.)

Colour Plate 11

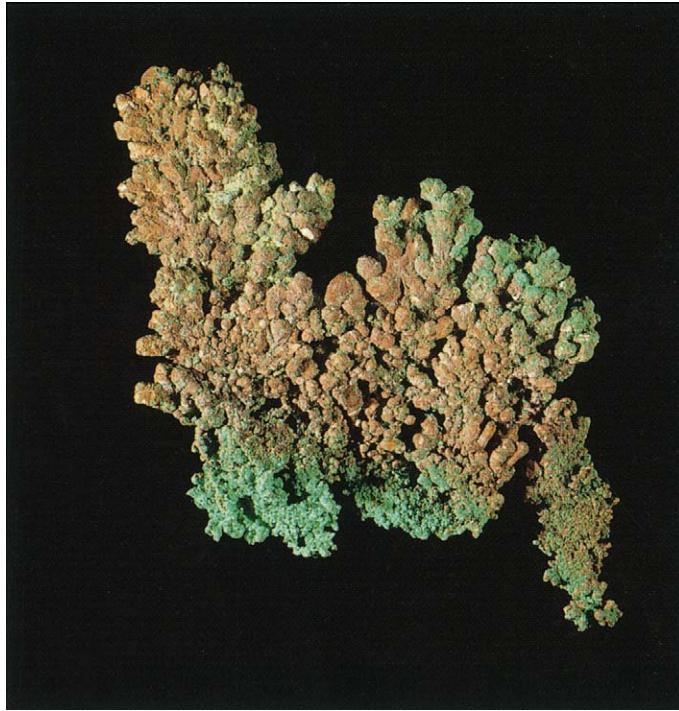


Plate 11 Flotation A sample of native (naturally occurring) copper. Native copper usually occurs in compact, filiform or dendritic masses, although tetrahedral or octahedral crystals are occasionally found. (With permission from J. C. Revy / Science Photo Library.)

Colour Plate 12

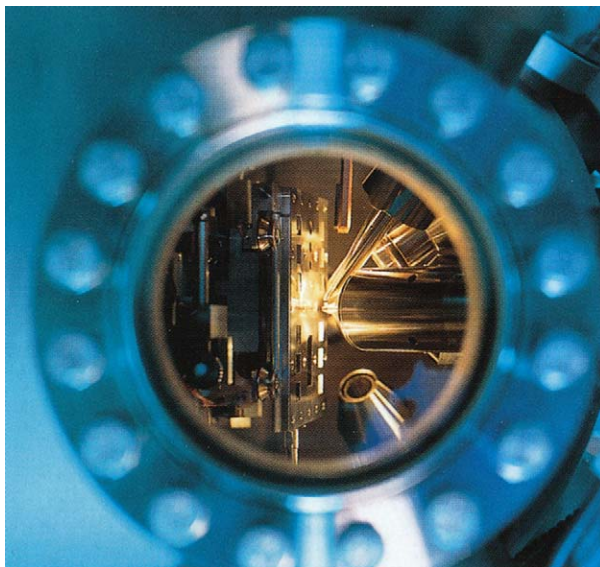


Plate 12 Mass Spectrometry Time-of-flight secondary ion mass spectrometer. View of a sample tray of a time-of-flight secondary ion mass spectrometer (TOF SIMS). This mass spectrometer analyses the surface of a sample. A pulsed ion beam is used to remove molecules from the outermost surface of the sample and convert them to ions. This is done at low intensity so that large or “macro” molecules, such as polymers, stay intact. The ions are taken up into a flight tube and accelerated toward a detector. The time taken to reach the detector determines the mass of the ion. This mass spectrometer helps to accurately determine the chemical composition of a sample’s surface. (With permission from Tek Image / Science Photo Library.)

Colour Plate 13

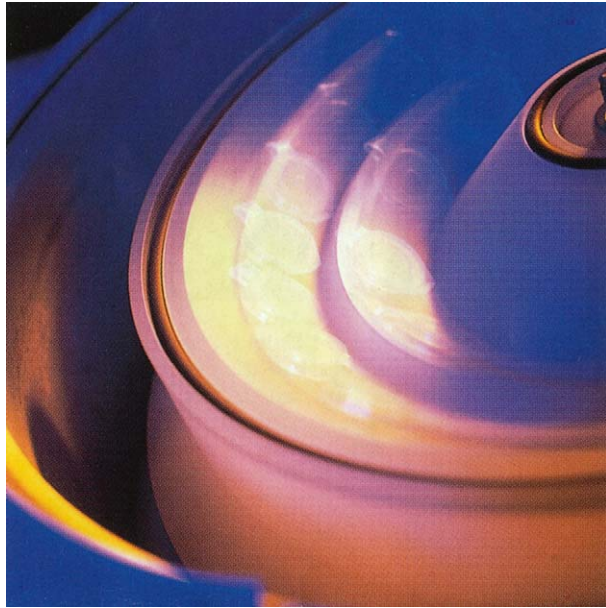


Plate 13 Centrifugation View of a centrifuge in operation. Centrifuges separate samples into their components by spinning them in tubes at high speed. The force of spinning pushes the densest matter to the very bottom of the tube. (With permission from Tek Image / Science Photo Library.)

Colour Plate 14



Plate 14 Centrifugation A centrifuge used to separate the various components in the blood. The liquid is placed into a container that is spun at high speed around a central axis; the centrifugal force separates groups of particles with different densities. Blood is separated into red cells, white cells and plasma. (With permission from Chris Priest / Science Photo Library.)

Colour Plate 15

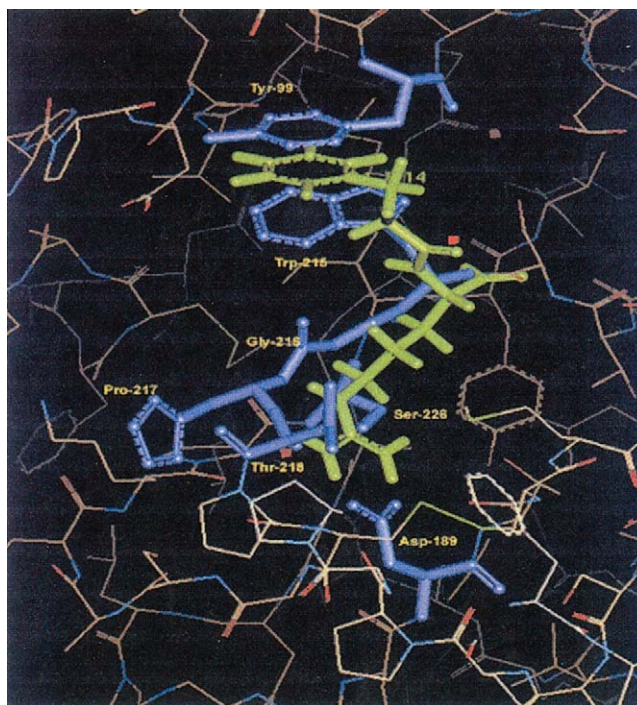


Plate 15 Affinity Separation: Rational Design, Synthesis and Evaluation Illustration of the molecular model of porcine pancreatic kallikrein with the dipeptidyl motif Arg-Phe occurring in the natural kallikrein substrate, kinioge complex using Quanta 97. The residues in the BPTI inhibitor not involved in the complex were deleted, leaving residues Lys-15 and Cys-14, which were substituted with arginine and phenylalanine respectively. The dipeptide was energy-minimized and its side chains were adjusted to interact with the primary and secondary binding sites, as the Lys-Cys dipeptide does in the BPTI-porcine pancreatic kallikrein complex.

Colour Plate 16

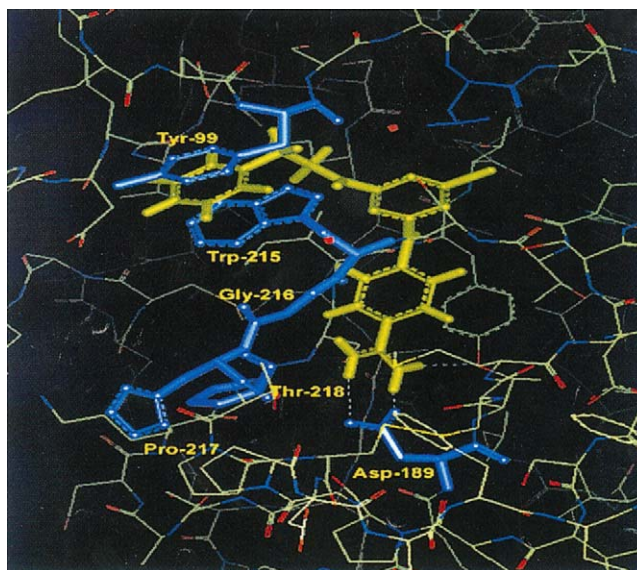


Plate 16 Affinity Separation: Rational Design, Synthesis and Evaluation Illustration of the synthetic ligand docked in the substrate-binding site of porcine pancreatic kallikrein. The ligand is an analogue of the Arg-Phe dipeptide that occurs in the natural substrate of kallikrein, kininogen, and is responsible for the enzyme-substrate complex. The benzamidine and phenethylamine moieties substituted on a triazine framework mimic the Arg-Phe dipeptide. The ligand was designed and energy-minimized in Quanta 97 and moved in the vicinity of the substrate-binding site, whence the side chains were adjusted to fit in the primary and secondary binding sites in porcine kallikrein. The aromatic ring of phenethylamine stacks in the primary binding site between Tyr-99 and Trp-215 and the benzamidine group forms several interactions with Asp-189, Ser-226, Gly-216, Pro-217 and Thr-218, forming the secondary binding site.

Colour Plate 17

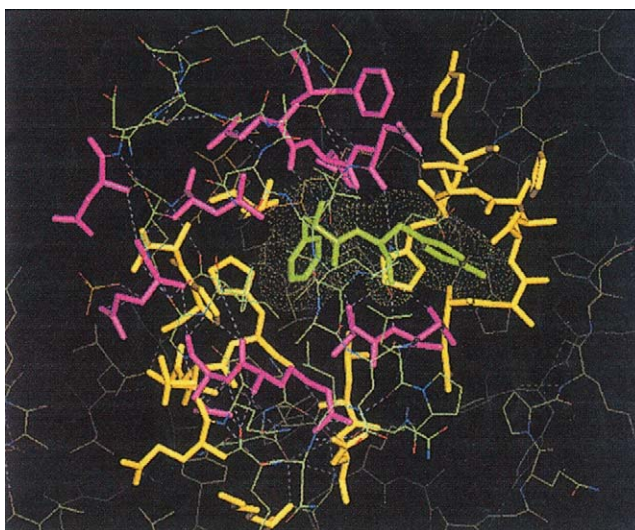


Plate 17 Affinity Separation: Rational Design, Synthesis and Evaluation. The complex between the Fb fragment of SpA and Fc fragment of IgG. The residues in pink represent amino acids in SpA interacting with the residues inter- and intramolecular hydrogen bonding. The interaction involves a total of 32 amino acids spanning an intersurface area corresponding to 40nm^2 . The interaction is predominantly characterized by hydrophobic interactions as well as some hydrogen bonding and two salt bridges.

Colour Plate 18

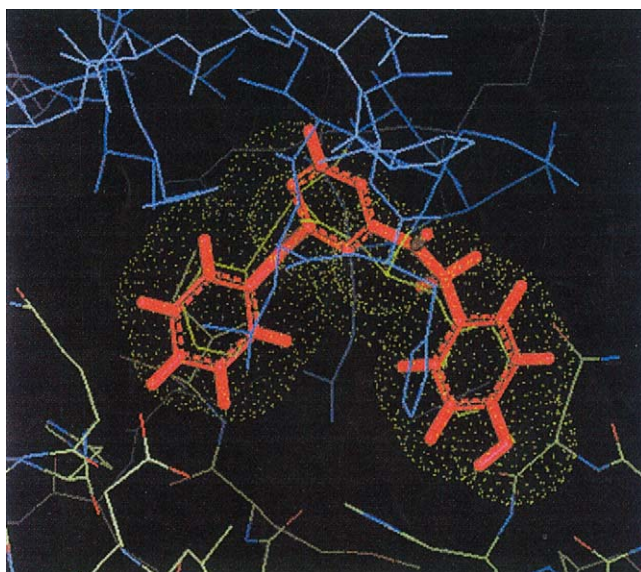


Plate 18 Affinity Separation: Rational Design, Synthesis and Evaluation Molecular model between the Fc fragment of IgA and the synthetic ligand ApA. The ligand, in red, is a mimic of the key dipeptide Phe-Tyr, in green, in SpA and comprises anrfino and tyramino moieties substituted on a triazinyl framework. ApA is located at the putative binding site among the amino acid residues involved in the interaction between the Fc part of IgG and fragment of SpA.

Colour Plate 19

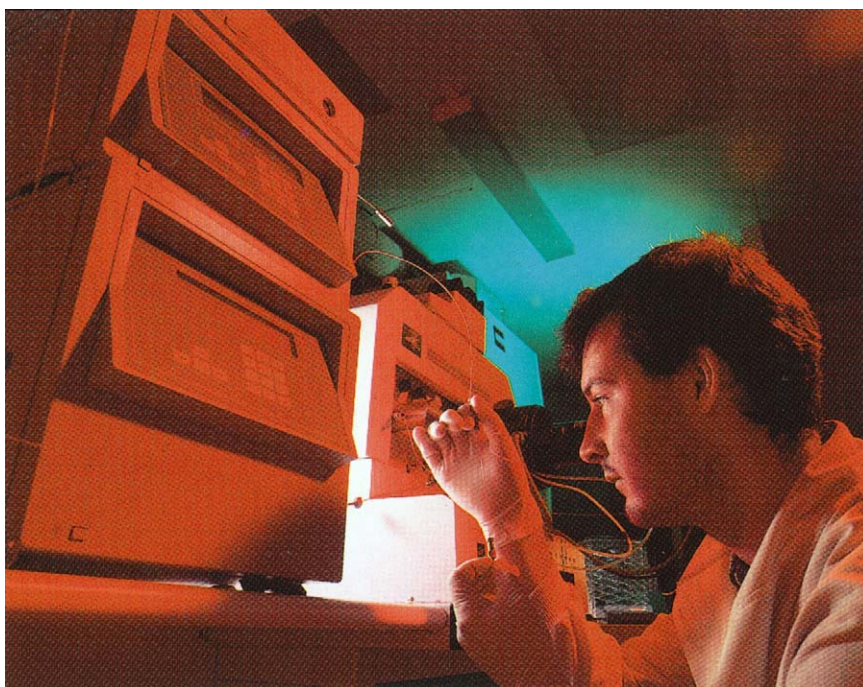


Plate 19 Chromatography: Gas Chromatography column. Technician examining a chromatography column leading into a mass spectrometer. The column is packed with small beads which separate the sample into different fractions. The fractions are then run into the mass spectrometer, which ionises and fragments the molecules. The amount the fragments deviate is indicative of their mass and charge. This can provide detailed information on the fractions' structures. This technique can be used to study many volatile molecules. (With permission from James King-Holmes / Science Photo Library).

Colour Plate 20

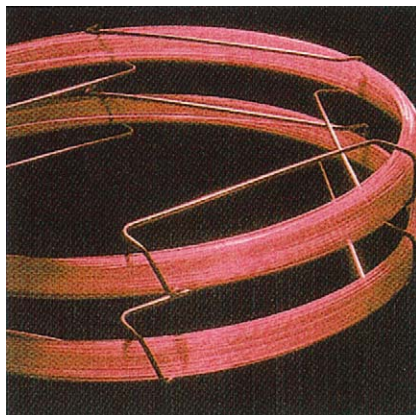


Plate 20 Chromatography: Gas Fused silica capillary column. (Reproduced with permission of Supelco Inc, Bellafonte, PA, USA)

Colour Plate 21



Plate 21 Chromatography: Liquid Radial compression column cartridge. Radial compression is a technique used in high pressure liquid Chromatography whereby an external pressure is applied to the outside of the column. This ensures that the column walls remain in intimate contact with the particles of stationary phase contained within the column. This prevents the formation of voids that would reduce the chromatographic performance of the system.

Colour Plate 22

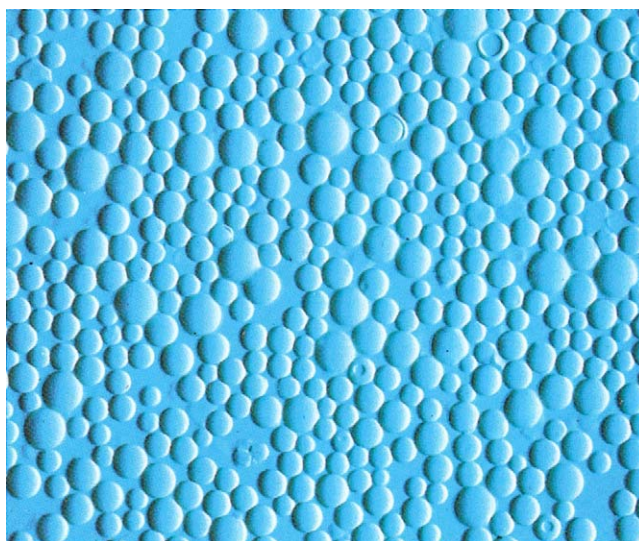


Plate 22 Chromatography: Liquid Light micrograph in interference contrast illumination of particles used in a high-pressure liquid Chromatography (HPLC) column. These tiny particles use strong anionic exchange (SAX) to cause the change in movement rates of the liquid's components through the HPLC column. SAX involves the exchange of a negative ion of a component in the liquid with a similarly charged ion in the column particles. Non-ionic components, or those with ionic charges different to that of the particles, are unaffected. Magnification x200 at 35mm size. (With permission from Andrew Syred / Science Photo Library).

Colour Plate 23



Plate 23 Chromatography: Liquid Large-Scale Liquid Chromatography. Scientist with column Chromatography equipment. Column Chromatography is used to separate the various components from a mixture of chemicals. During this process the mixture is put in the top of the column. The mixture passes through a porous substance, which selectively hinders the movement of each of the components. This means that some components will travel further in a given time than others, allowing each of them to be individually collected. Photograph of equipment used to isolate chemicals produced by microorganisms, including genetically engineered varieties. (With permission from Maximilian Stock Ltd / Science Photo Library).

Colour Plate 24

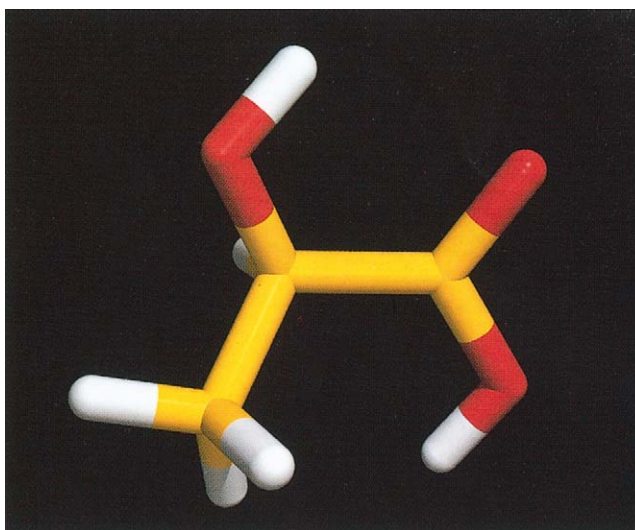


Plate 24 Chromatography: Liquid Chromatography is used to separate enantiomers. (R) – lactic acid. Computer illustration of a molecule of (R) – lactic acid (formula: $C_3H_6O_3$). Atoms are represented as cylinders and are colour-coded: carbon (yellow), hydrogen (white) and oxygen (red). Four different groups are joined to the central carbon atom here, a property known as chirality. The groups are given priorities based on their atomic number, and the molecule is viewed along the line of the bond to the lowest priority group. The order of the other groups decreasing priorities determines whether the isomer is classified as R (clockwise as here) or S (anti-clockwise). (With permission from Prof. K. Seddon / Science Photo Library).

Colour Plate 25

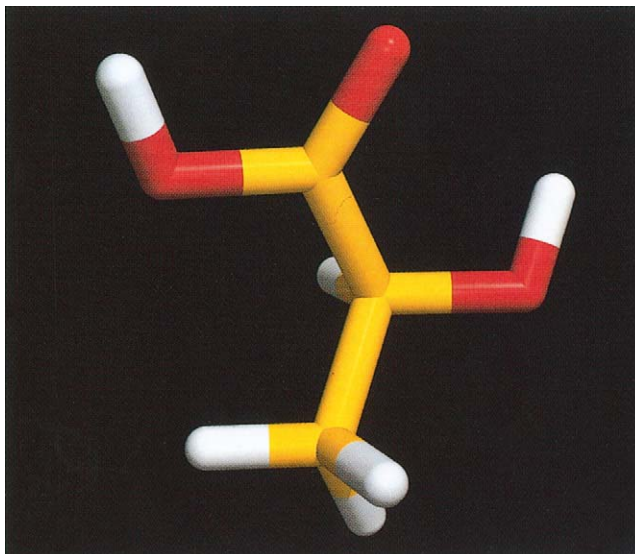


Plate 25 Chromatography: Liquid Chromatography is used to separate enantiomers. (S) – lactic acid. Computer illustration of a molecule of (S) – lactic acid (formula: $C_3H_6O_3$). Atoms are represented as cylinders and are colour-coded: carbon (yellow), hydrogen (white) and oxygen (red). Four different groups are joined to the central carbon atom here, a property known as chirality. The groups are given priorities based on their atomic number, and the molecule is viewed along the line of the bond to the lowest priority group. The order of the other groups decreasing priorities determines whether the isomer is classified as S (anti-clockwise, as here) or R (clockwise). (With permission from Prof. K. Seddon / Science Photo Library).

Colour Plate 26

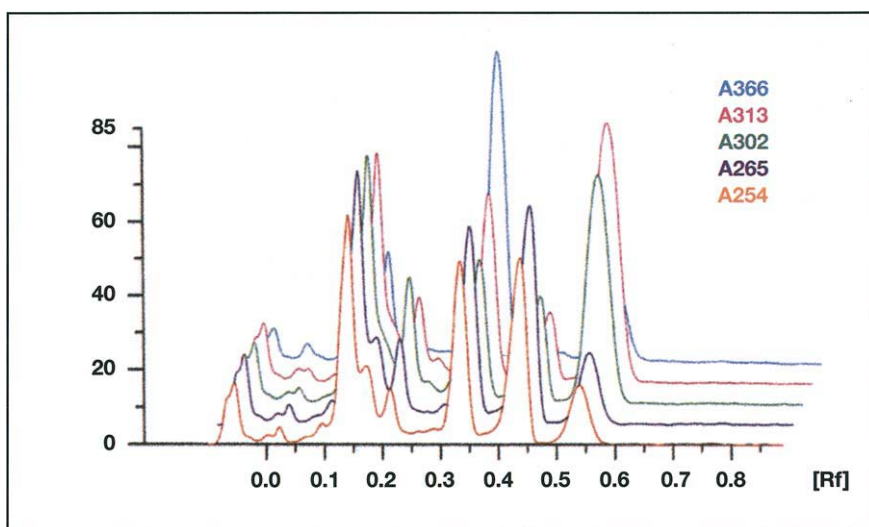


Plate 26 Chromatography: Thin-Layer (Planar) Separation of sulfonamides in a complex animal feed matrix on an HPTLC silica gel 60 plate. The plate has been scanned at five different wavelengths and the chromatogram overlaid in a three-dimensional presentation. (Reprinted from Camag literature, CAMAG, Muttens, Switzerland.)

Colour Plate 27

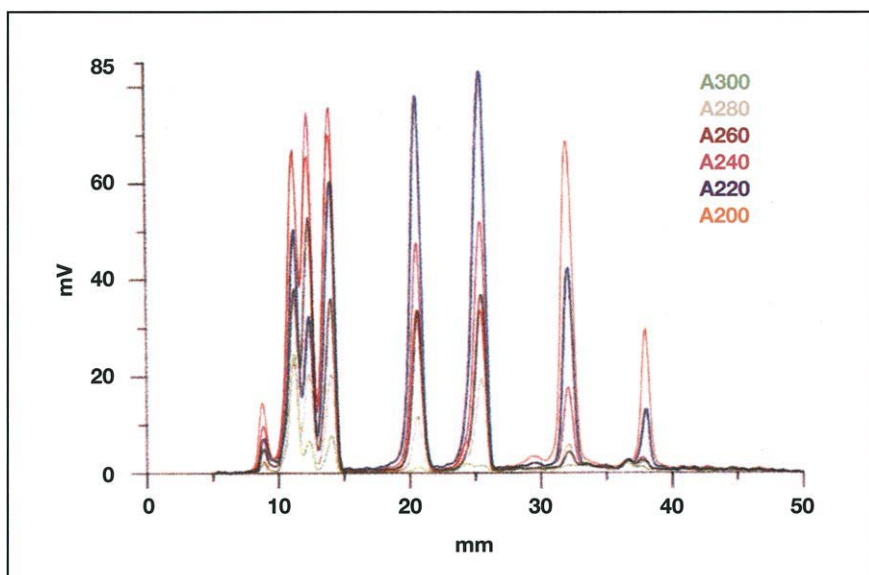


Plate 27 Chromatography: Thin-Layer (Planar) Separation of pesticides in tap water on an HPTLC silica gel 60 plate by AMD. Multi-wavelength (six wavelengths) evaluation permits resolution by optical means of fractions insufficiently separated. (Reprinted from Camag literature, CAMAG, Muttens, Switzerland.)

Colour Plate 28

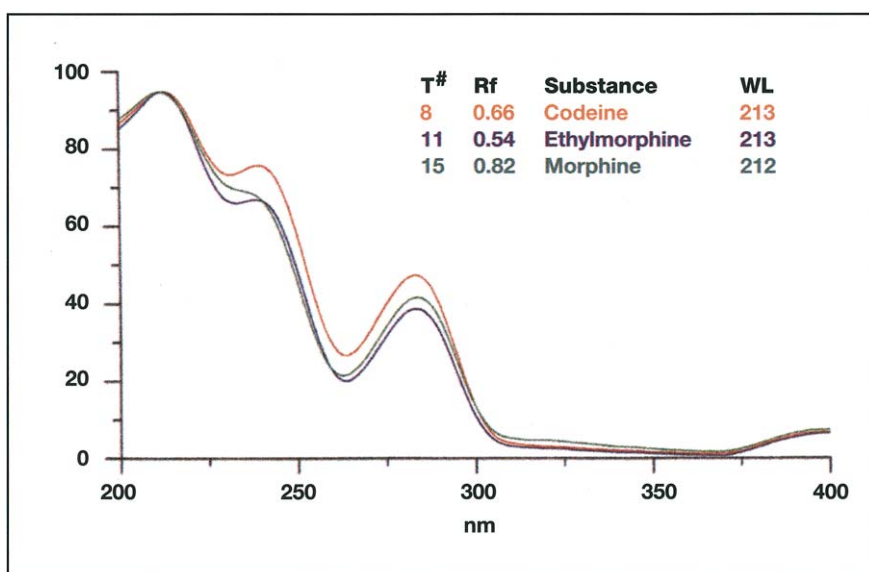


Plate 28 Chromatography: Thin-Layer (Planar) UV spectra of codeine, ethylmorphine and unknown (morphine) overlaid. Spectra of codeine and ethylmorphine taken from spectral library. Spectrum of morphine taken from chromatogram. (Reprinted from Camag literature, CAMAG, Muttens, Switzerland.)

Correlation of spectrea without R_F value

<i>Substance</i>	<i>Correlation</i>
Ethylmorphine	0.9924
Codeine	0.9905
Nalorphine	0.9848
Morphine	0.9839

Correlation of spectrea with R_F value

<i>Substance</i>	<i>Correlation</i>
Morphine	0.9839
Atenolol	0.9223
Salbutamol	0.9174
Solalol	0.8939

Colour Plate 29



Plate 29 Chromatography: Thin-Layer (Planar) CAMAG U-chamber (1976) developed by Kaiser.

Colour Plate 30



Plate 30 Chromatography: Thin-Layer (Planar) Camag automated multiple development chamber AMD 2.

Colour Plate 31

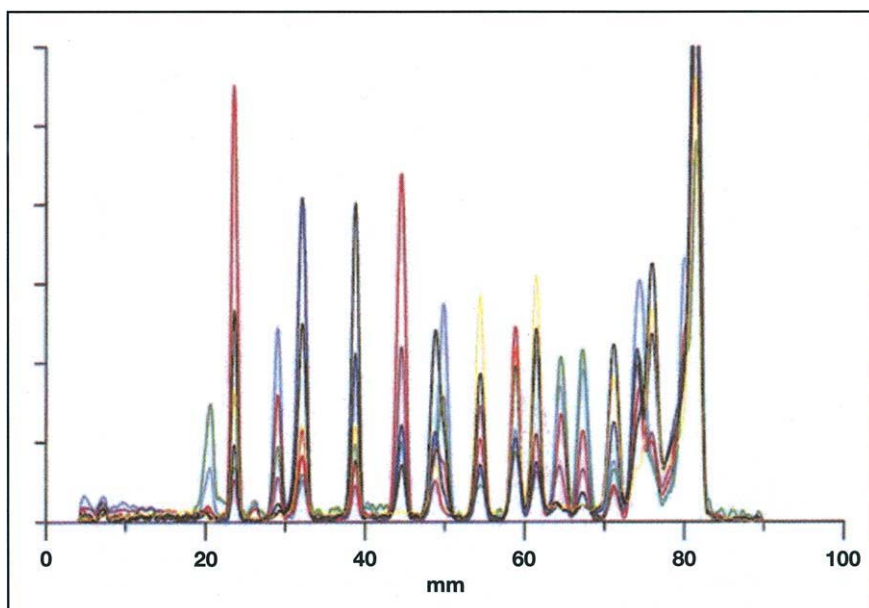


Plate 31 Chromatography: Thin-Layer (Planar) Multiwavelength scan of a pesticide mixture after AMD separation.

Colour Plate 32



Plate 32 Chromatography: Thin-Layer (Planar) An electropneumatically operated spray system for TLC. (Reproduced with the permission of Merck Ltd., UK.)

Colour Plate 33

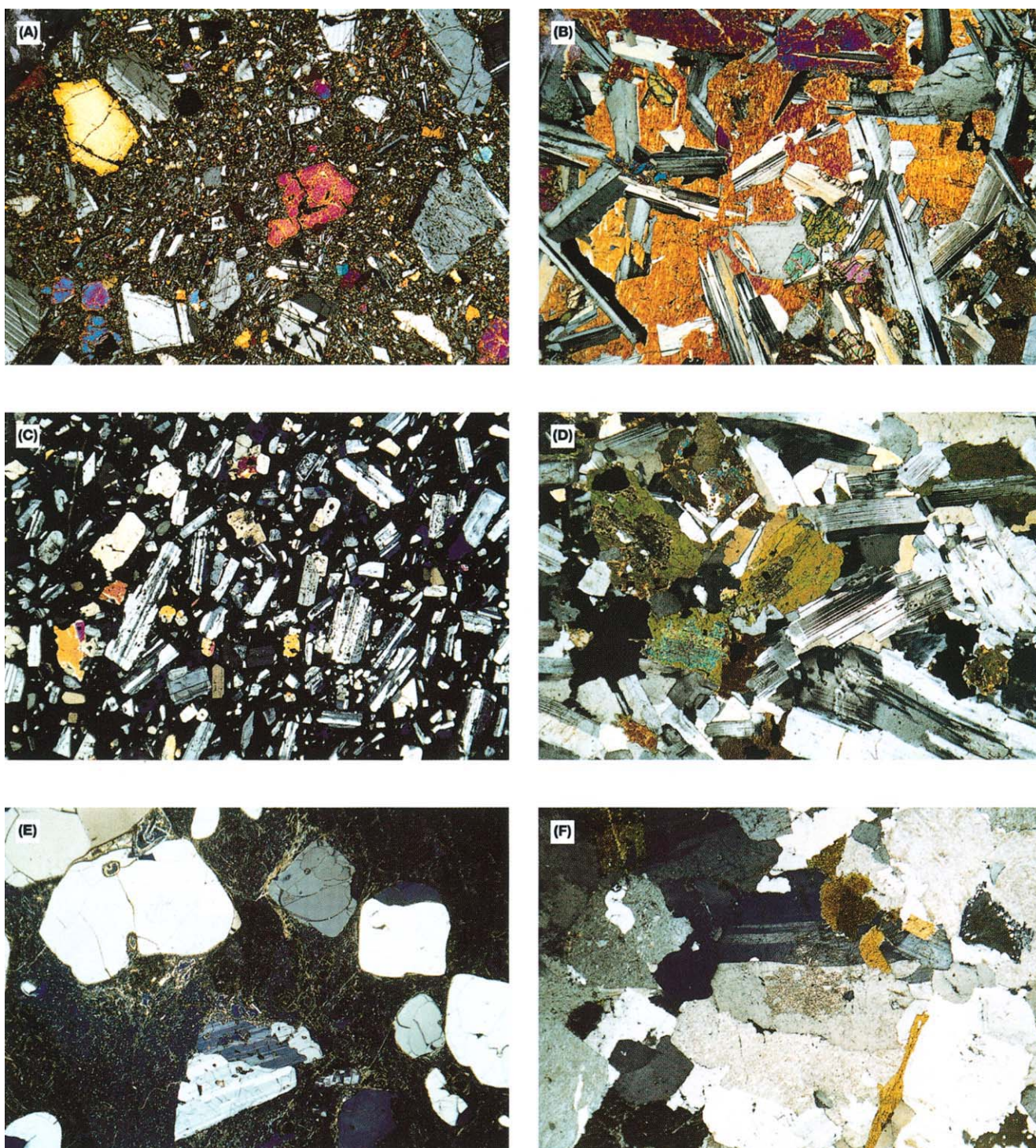


Plate 33 Crystallization: Geocrystallization Crossed polarizer photomicrographs of (A) a glassy basalt, (B) a gabbro, (C) an andesite, (D) a diorite, (E) a rhyolite and (F) a granite. Each of these photographs was taken at the same magnification (horizontal field is 10mm across). The bulk composition of the magma forming the basalt and gabbro are broadly similar, as is the bulk composition for the andesite and diorite and the rhyolite and granite. The clearly observable differences in texture result from differences in crystal growth and nucleation rates. (A) Basalt showing large crystals (phenocrysts) of plagioclase feldspar (grey), Ca-rich pyroxene (purple, at centre) and olivine (yellow, top left) in a finer grained groundmass of these minerals. (B) Gabbro showing crystals of Ca-rich pyroxene (red-orange) enclosing plagioclase (grey-white with multiple twinning) and olivine (blue, green and red grains right of centre). (C) Andesite showing phenocrysts of plagioclase (grey-white with multiple twinning) and pyroxene (yellow-orange-red) set in a fine-grained glassy ground mass. (D) Diorite showing a rock comprised of plagioclase feldspar (grey-white multiply twinned crystals), pyroxene, amphibole (green) and interstitial quartz (yellow-grey). Note how the amphibole crystals form a jacket or coating on the pyroxene (centre). (E) Rhyolite showing perlitic cracking in glassy ground mass and phenocrysts of quartz and plagioclase (twinned). Note the corroded and resorbed grain boundaries of the phenocrysts. (F) Granite showing interlocking crystals of plagioclase (twinned), alkali feldspar (turbid, dusty appearance), quartz (clear) and biotite (speckly orange).

Colour Plate 34



Plate 34 Crystallization: Geocrystallization Quartz Outcrop, Marble Bar, West Australia. (Reproduced with permission from Spectrum Colour Library.)

Colour Plate 35



Plate 35 Crystallization: Geocrystallization Mineral layering in the Rum Igneous Intrusion, NW Scotland. This photograph shows spectacular centimeter-scale mineral layering in Unit 14 of the Eastern Layered Series of the Rum Layered Igneous Intrusion. The Rum Intrusion forms one of a number of layered intrusions, including Skaergaard in East Greenland and The Cullins, on Skye, NW Scotland, which are part of the North Atlantic Tertiary Igneous Province. Now exhumed by the combined effects of erosion and uplift, these intrusions mark the site of crystallizing magma chambers 60 million years ago, during the early rifting stages of the North Atlantic Ocean. The near horizontal layers were formed by sequential precipitation of crystals of different composition (principally plagioclase, pyroxene, olivine and spinel) on the floor of a magma chamber. The darker layers are rich in the minerals olivine and pyroxene, the lighter layers richer in plagioclase. Mimicking sedimentary rocks where the principal hydraulic agent of sorting is a water column, in layered intrusions magma was the hydraulic agent and dense minerals, like spinel and olivine, settled more rapidly than plagioclase, leading to units which are graded from spinel and olivine-rich bases to plagioclase-rich tops.

Colour Plate 36



Plate 36 Crystallization: Melt Crystallization Sulphur deposits. View of yellow sulphur deposits around vents on the crater floor of the Mutnovsky volcano on the Kamchatka peninsula, Russia. These deposits are formed when hot sulphurous gases from the volcano condense and solidify when they meet the cooler air and rocks. The main gases involved are gaseous sulphur itself and hydrogen sulphide, which is oxidised by the air to sulphur and water. (Reproduced with permission from Science Photo Library.)

Colour Plate 37



Plate 37 Distillation: Freeze-Drying Isolator, Class 100, for filling, transportation and loading of vials into the freeze-drying plant. Decontamination of the isolator and the equipment therein is accomplished by vaporized hydrogen peroxide (VHP). The VHP 100® generator can be seen in the centre in front of the isolator. (Courtesy of Steris GmbH, Hürth, Germany.)

Colour Plate 38



Plate 38 Distillation: Historical Development Oil refinery. Oil refinery with towers and chimneys. In an oil refinery, crude oil is heated and passed through catalytic cracking towers to break up the heavy crude oil hydrocarbon molecules into lighter fragments. The resulting components, from heavy industrial oils and tars through to light fuels (like petrol and kerosene) and gas, are separated out. The components, called fractions, may then be processed. Photograph of the refinery at Milford Haven, Wales. (Reproduced with permission from Science Photo Library.)

Colour Plate 39

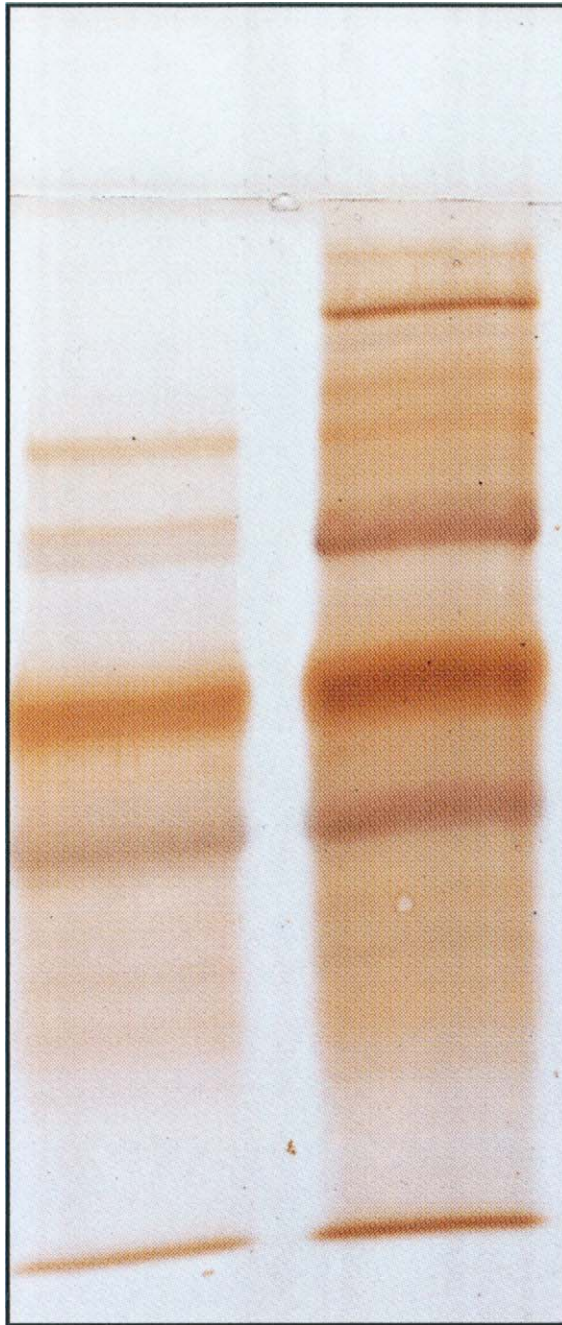


Plate 39 Electrophoresis: Agarose Gels *Direct dual* immunostaining of polyacrylamide/glyoxyl-agarose composite gel to profile fibrinogen g-chain (grey), c/g-chain (umber) cross-linking by plasma transglutaminase (right lane), and the chain composition of plasma fibrinogen. The illustration depicts sieving equivalent to a regular polyacrylamide gel, and subsequent rendering of the gel for antibody permeation by removing the polyacrylamide. (Reproduced with permission from Shainoff et al., 1991, Journal of Biological Chemistry 266: 6429.)

Colour Plate 40

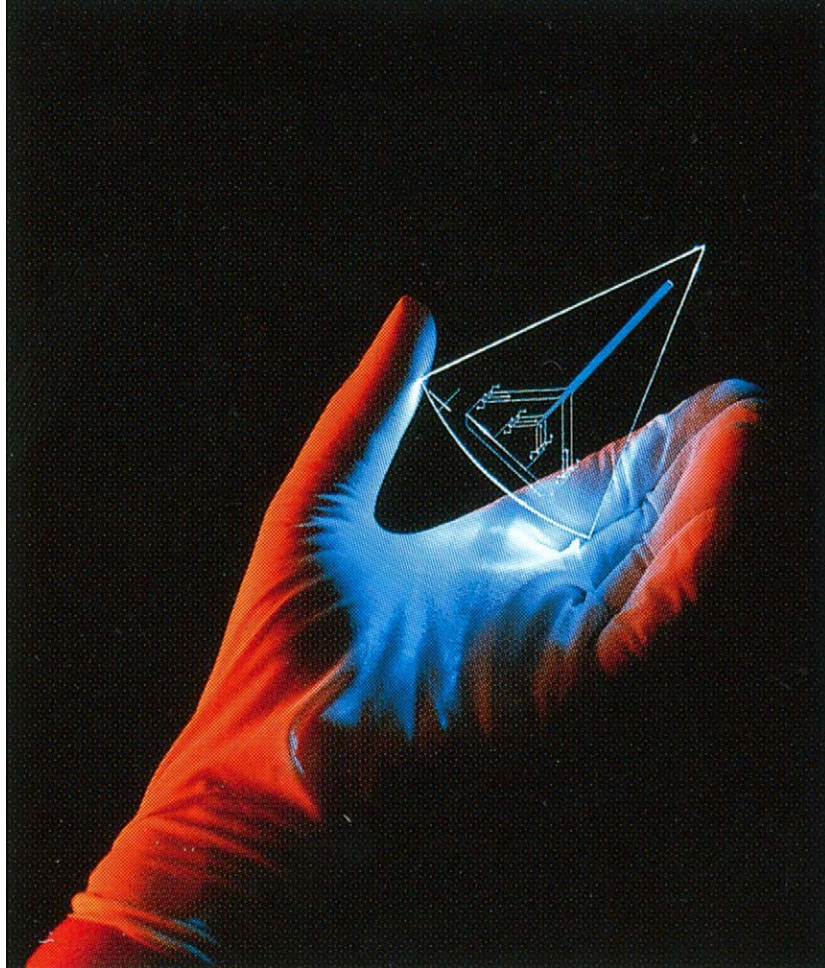


Plate 40 Electrophoresis: Deoxyribonucleic Acid, Theory of Techniques for Separation DNA chip. Gloved hand holding a device for rapidly analysing samples of DNA (Deoxyribonucleic Acid) at the scene of a crime. The device (the “DNA chip”) is made of clear plastic. Narrow channels have been etched on the plastic by techniques similar to those used to make electronic microchips. Samples containing fragments of DNA are put in the channels. The fragments move apart when an electric current is applied (electrophoresis), allowing the DNA’s composition to be analysed. This device is suitable for genetic linkage studies and clinical diagnostics as well as forensic investigation. It was developed at the Massachusetts Institute of Technology (MIT), USA. (Reproduced with permission from Science Photo Library.)

Colour Plate 41

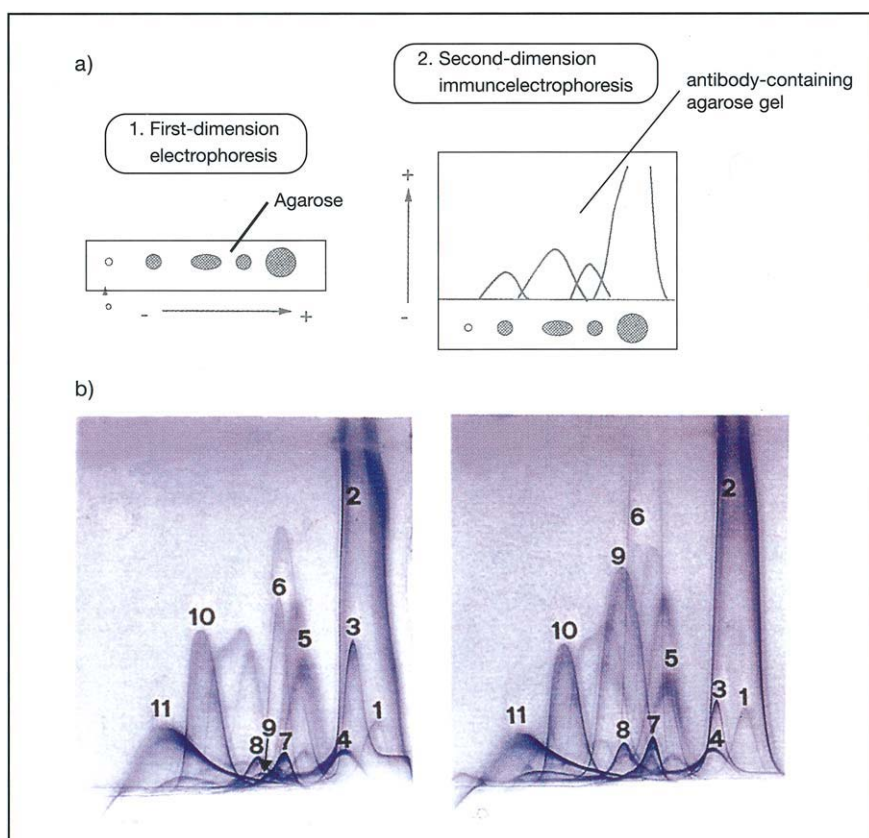


Plate 41 Electrophoresis: Immunelectrophoresis (A) Schematic illustration of crossed IE. 1, Agarose electrophoresis of the sample (O = origin, corresponding to the well where the sample is applied); 2, a longitudinal strip of the first-dimensional gel is transferred into a second-dimension gel containing a polyvalent antiserum. The second-dimension IE is performed perpendicularly to the first-dimension run. (B) Example of use of the crossed IE technique. The blood serum from the same pig is analysed (left) before and (right) 48h after turpentine injection. The changes in the protein concentrations, induced by inflammation, can easily be studied by analysing the area (or height) of the different-numbered peaks. (Reproduced with permission from Science Photo Library.)

Colour Plate 42

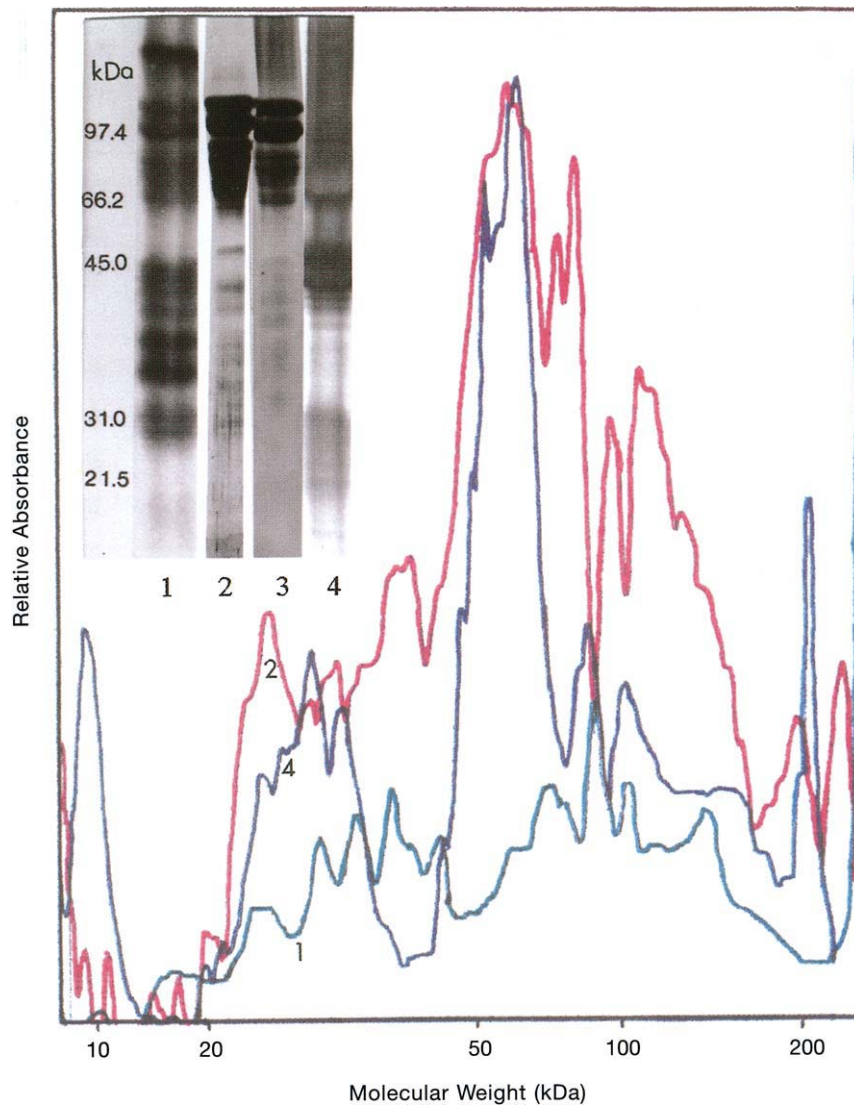


Plate 42 Electrophoresis: Gel Electrophoresis The inset shows the separation of human head hair proteins using 12 % sodium dodecyl sulfate-polyacrylamide gel electrophoresis with the point of migration of standard proteins to the left under the heading kDa: lanes 1 -3 *S*-carboxymethylated proteins; lane 4 reduced non-*S*-carboxymethylated proteins; lane 1 ^{14}C Autoradiograph; lanes 2 and 4, silver stain; lane 3, Coomassie stain. The main body of the figure shows a densitometric profile of the separated lane 1 (autoradiograph ^{14}C -*S*-carboxymethylated, green). Lane 2 (silver stain, *S*-carboxymethylated, red); lane 4 (silver stain, non-*S*-carboxymethylated). Molecular weights were extrapolated from a plot of log MWt vs. relative migration of standard proteins.

Colour Plate 43

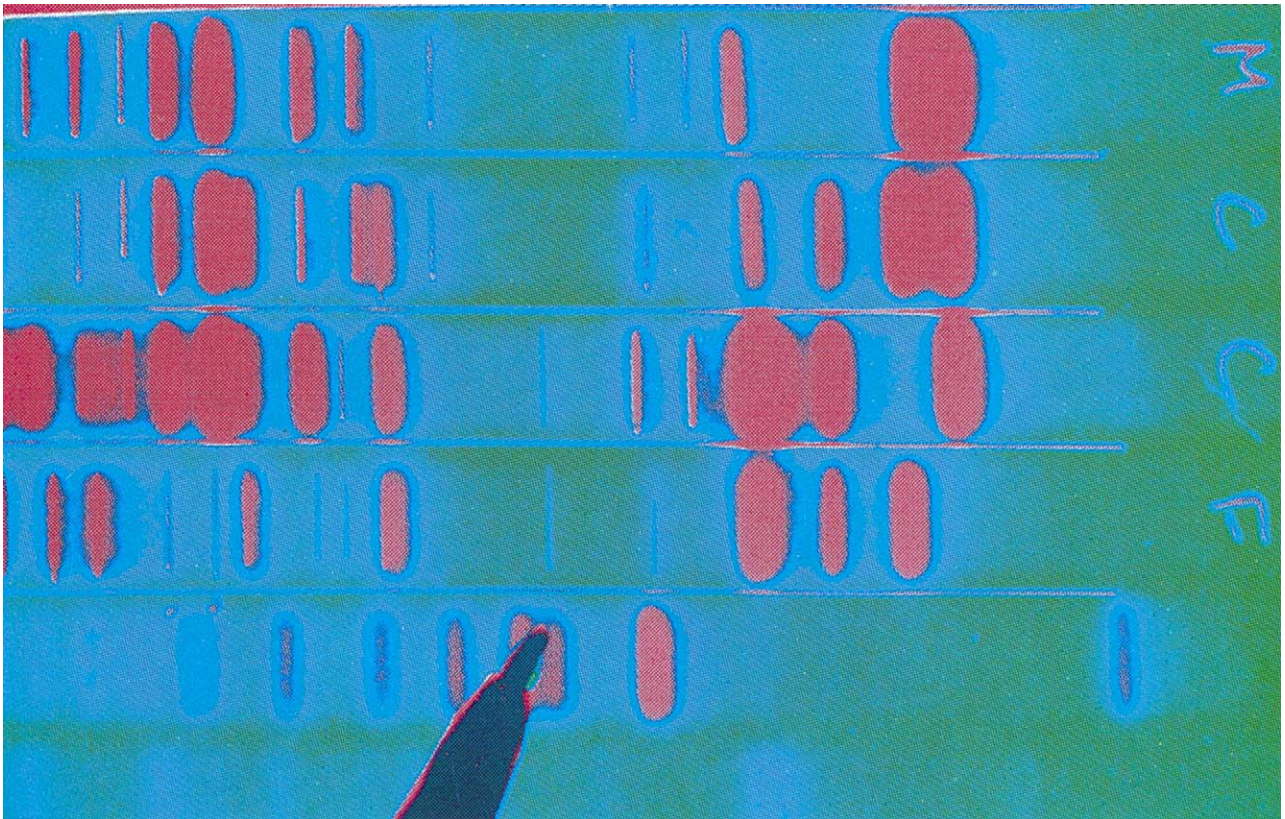


Plate 43 Electrophoresis: Two-dimensional Electrophoresis DNA fingerprints prove family relationships. (Reproduced with permission from Custom Medical Stock.)

Colour Plate 44



Plate 44 Extraction: Supercritical Fluid Extraction Extraction of taxol. A researcher loading a supercritical fluid extractor with crushed bark. The bark contains the anti-cancer drug taxol, and is from the Pacific Yew (*Taxus brevifolia*). Taxol has been shown to be effective in restricting various types of cancers, particularly of the breast, ovary, skin and colon. Laboratories are looking into ways of synthesising this natural drug, as the tree has become a protected species. Photographed at the institute for the Chemistry of Natural Substances (ICSN), Gif-sur-Yvette, France.

Colour Plate 45



Plate 45 Flotation: Oil and Water Separation Oil-water separators. Gullfaks 'A' Platform with Flotel POLYCASTLE and Sikorsky S61n Helicopter inbound. Norway, Block-34. May 1987. Oil-water separators may have to operate under harsh environmental conditions. (Reproduced with permission from Eye Ubiquitous.)

Colour Plate 46

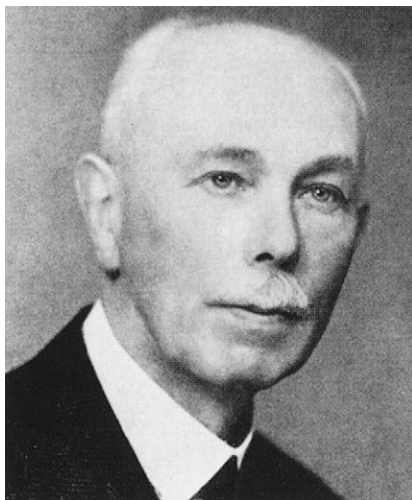


Plate 46 Mass Spectrometry Portrait of Francis Aston (1877-1945), British physicist and Nobel Laureate. After WW1, Aston helped Thomson in his studies of the deflection of ions in magnetic fields. He went on to improve Thomson's apparatus, designing it so as to make all atoms of a given mass fall on the same part of a photographic plate. Working with neon, he found that two lines were observed, indicating the presence of two isotopes. He repeated this with chlorine with similar results. The device, called the mass spectrometer, showed that most stable elements had isotopes. His work earned him the 1922 Nobel Prize for Chemistry, and introduced a powerful new analytical tool to science. (Reproduced with permission from Science Photo Library.)

Colour Plate 47



Plate 47 Membrane Separations: Dialysis in Medical Separations Kidney (haemodialysis) machine, used for the removal of waste materials from the bloodstream of a person whose kidneys function insufficiently. A stream of blood from an artery is circulated through the machine on one side of a semipermeable membrane, while a solution of comparable electrolytic concentration circulates on the other side. Water & waste products pass across the membrane but blood cells & proteins are too large to do so. Purified blood is returned to the body through a vein. Circulating blood is visible inside the plastic tubing. (Reproduced with permission from Science Photo Library.)

Colour Plate 48



Plate 48 Membrane Separations: Diffusion Dialysis Chemical dialysis. Glassware used for purifying solutions by separating them from *colloid* chemicals using dialysis. During dialysis an impure solution is placed in a semi-permeable membrane (spheres) which is immersed in a pure solvent. Some of the chemicals within the membrane may pass out into the solvent by diffusion. The chemicals that remain trapped within the membrane are called *colloids*. *Colloids* usually consist of large molecules & tiny particles, although their exact composition depends upon the nature of the membrane. (Reproduced with permission from Science Photo Library.)

Colour Plate 49



Plate 49 Membrane Separations: Filtration Pall Ultipor® VF[®] Grade DV50 virus filters for high protein-transmissible virus filtration. (Photo courtesy of Pall Corporation, East Hills, NY.)

Colour Plate 50



Plate 50 Membrane Separations: Filtration Pall Ultiplex[™] high flow filters, providing efficient and economical high-flow filtration with reduced waste disposal costs. (Photo courtesy of Pall Corporation, East Hills, NY.)

Colour Plate 51



Plate 51 Membrane Separations: Pervaporation Vapour permeation unit for recovering ink solvent.

Colour Plate 52

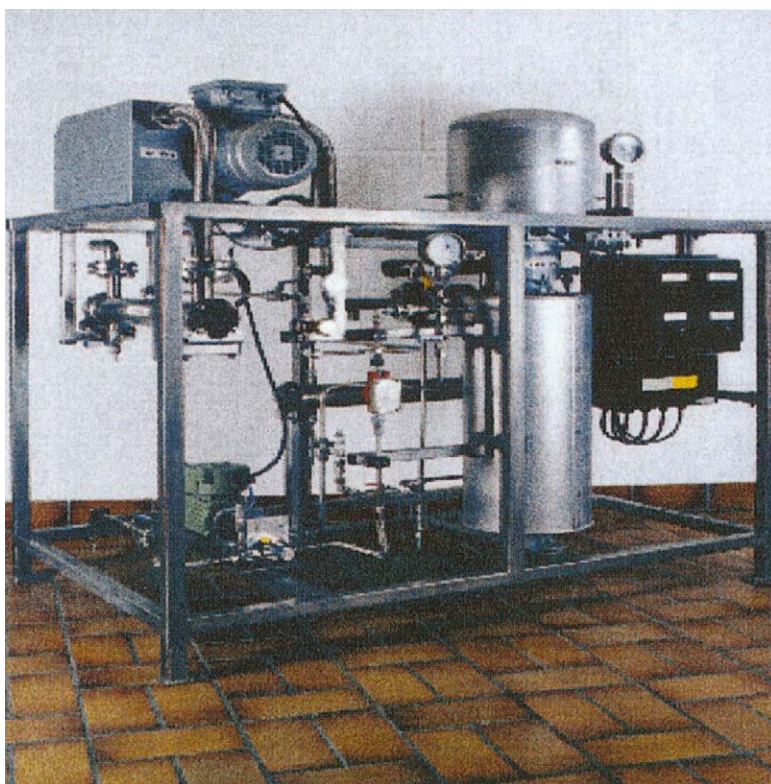


Plate 52 Membrane Separations: Pervaporation Standard unit for batch dehydration of rinse alcohol.

Colour Plate 53

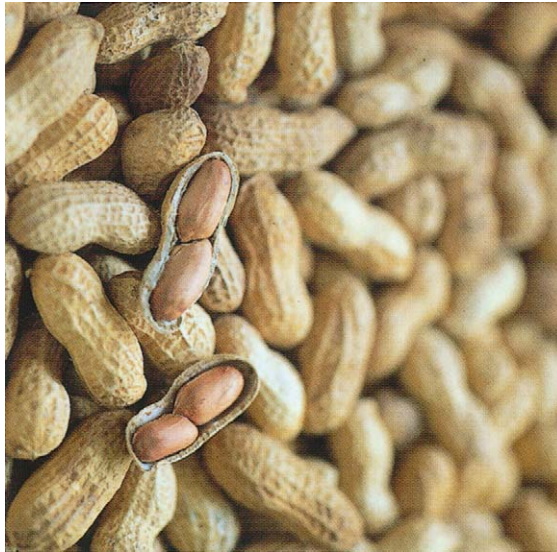


Plate 53 Aflatoxins and other Mycotoxins Aflatoxins are found in mouldy peanuts and are very toxic. Exposure to mycotoxins can produce both acute and chronic toxic effects ranging from death to deleterious effects on the central nervous, cardiovascular and pulmonary systems, and on the alimentary tract. (Reproduced with permission from Spectrum Colour Library.)

Colour Plate 54

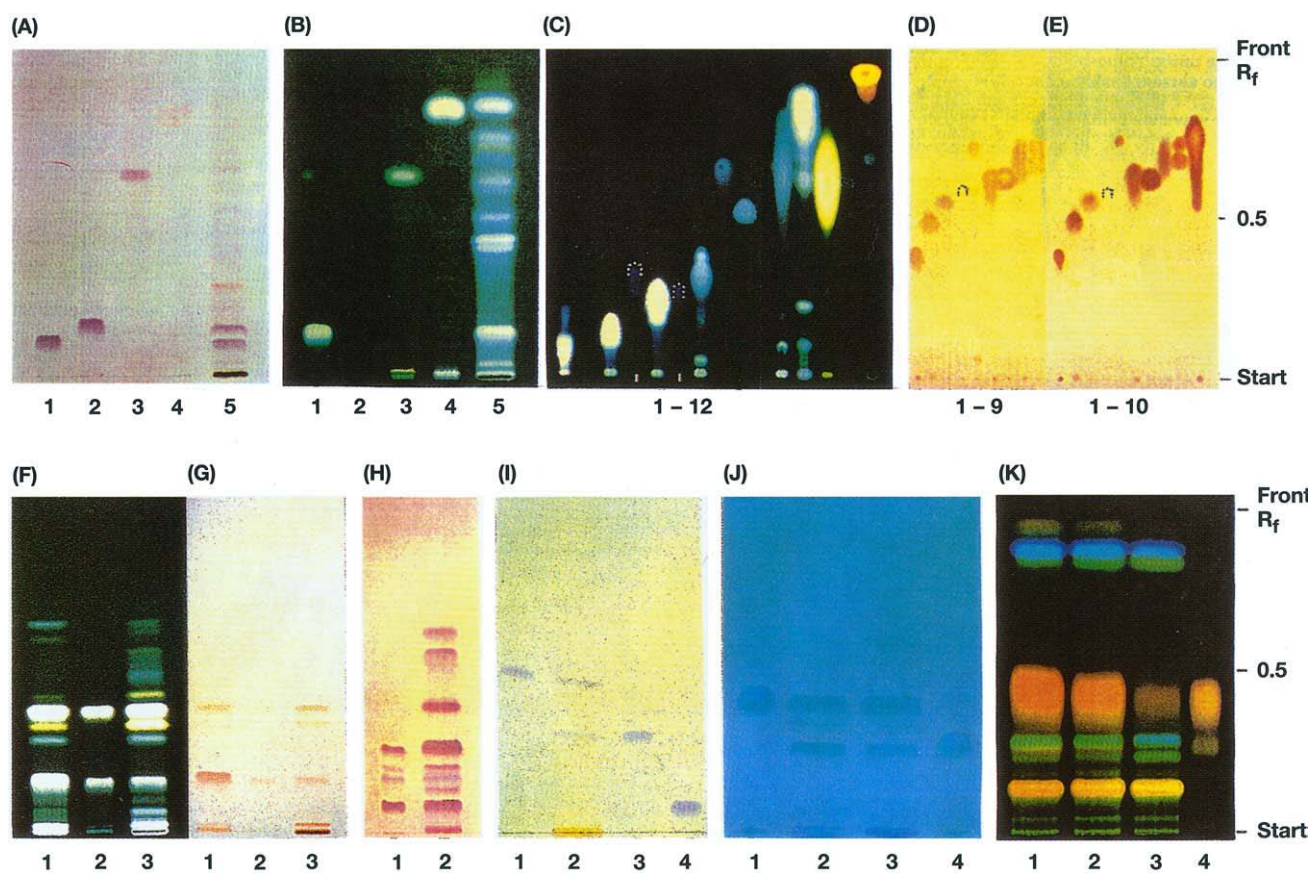


Plate 54 Alkaloids: Thin-Layer (Planar) Chromatography The chromatograms of the separated alkaloids developed on silica gel or alumina in solvent systems 1–4, detected with different reagents. Solvent systems: 1, toluene–ethyl acetate–diethylamine (70 : 20 : 10); 2, chloroform–diethylamine (90 : 10); 3, toluene–chloroform–ethanol (28.5 : 57 : 14.5); 4, 1-propanol–water–formic acid (90 : 9 : 1). (Reproduced with permission from Wagner H and Bladt S (1996) *Plant Drug Analysis. Thin-layer Chromatography Atlas*. Berlin: Springer.)

Colour Plate 55



Plate 55 Archaeology Mummified human remains. Recent developments in instrumental chromatographic techniques have enabled trace amounts of organic residues to be detected. Examples of organic residues include the balms in the wrappings of mummified bodies and traces of colouring dyes impregnated in ancient textiles. (Reproduced with permission from Frank Spooner Pictures.)

Colour Plate 56

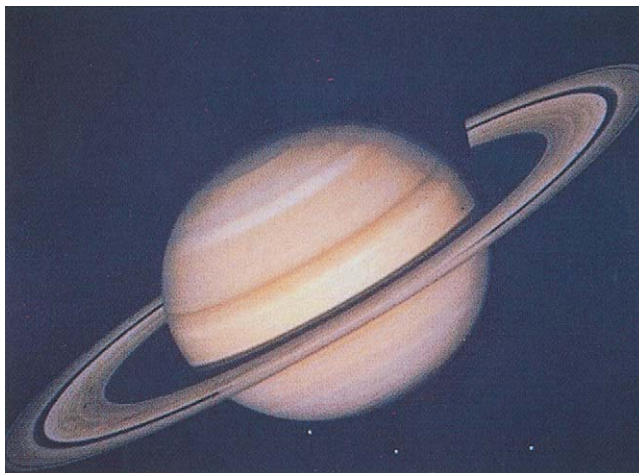


Plate 56 Atmospheric Analysis A photograph of the gas giant Saturn and its ring system. Analysis of the composition of the atmospheres of this and the other planets in the solar system represents a significant future challenge for separation science. Saturn ring system Galileo 1996-1997 © 1998 NASA/Custom Medical Stock, all rights reserved. (Reproduced with permission from Custom Medical Stock.)

Colour Plate 57



Plate 57 Atmospheric Analysis Air pollution monitor. The initial step of sample acquisition is a far from trivial task in atmospheric measurements. (Reproduced with permission from Eye Ubiquitous.)

Colour Plate 58

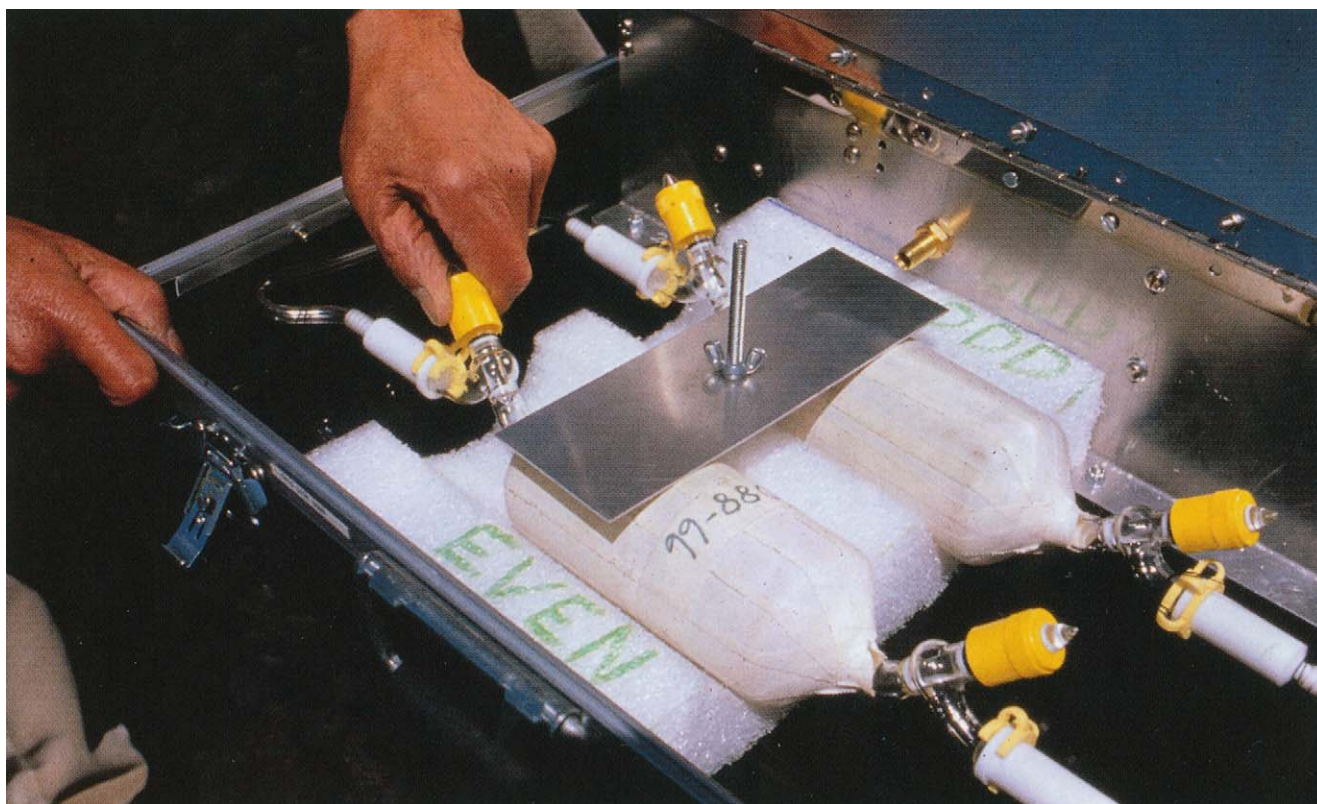


Plate 58 Atmospheric Analysis Atmospheric monitoring. A climate physicist using portable air sampling equipment. The suitcase-sized container holds two vacuum flasks. These are connected to a 6 meter-long mast at the top of which is a sampling probe. To take a sample, a valve is opened on one of the flasks. Air is drawn in and the flask resealed, allowing the air sample to be stored for later analysis. This equipment was designed by the Climate Monitoring and Diagnostic Laboratory of the US National Oceanic and Atmospheric Administration (NOAA), Hawaii. (Reproduced with permission from Science Photo Library.)

Colour Plate 59

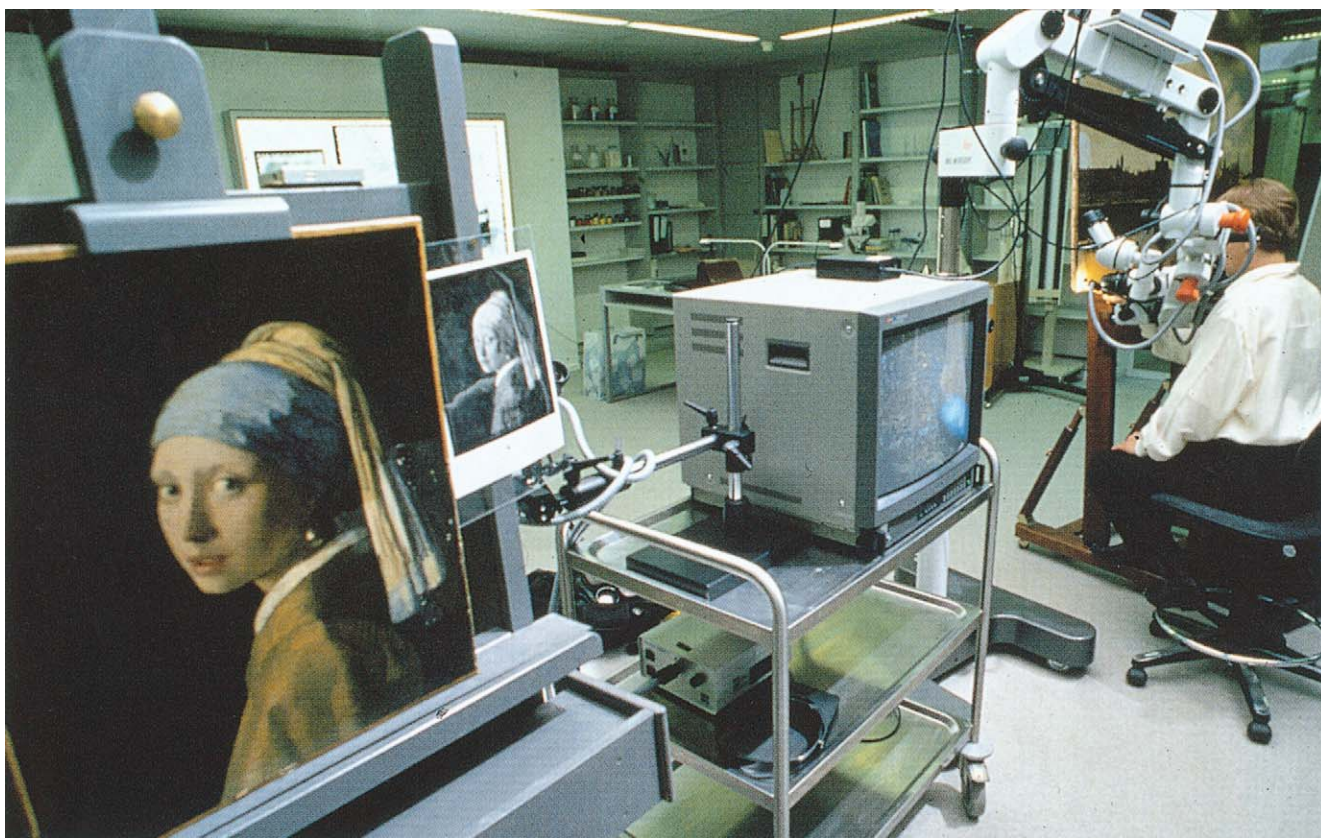


Plate 59 Art Conservation In order to design the optimum safe conservation/restoration treatment plan, which takes account of the original materials used by the artist, conservators require a detailed knowledge of the materials used. (Reproduced with permission from Frank Spooner Pictures.)

Colour Plate 60

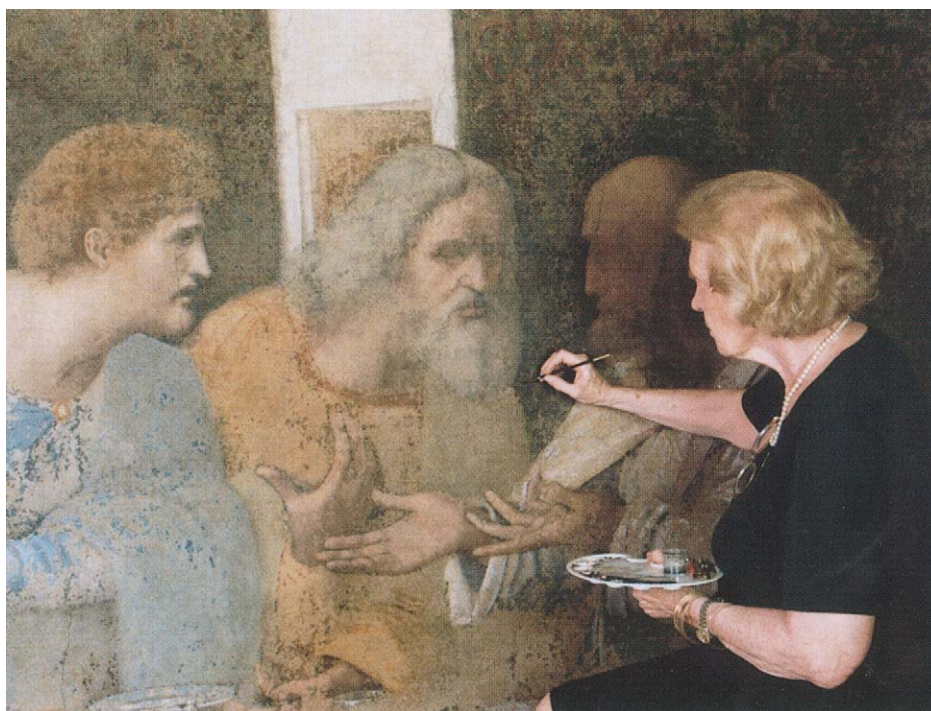


Plate 60 Art Conservation A knowledge of the composition of the materials used by artists, derived in part using analytical methods based on separation science, enables restoration to be undertaken with confidence. (Reproduced with permission from Frank Spooner Pictures.)

Colour Plate 61

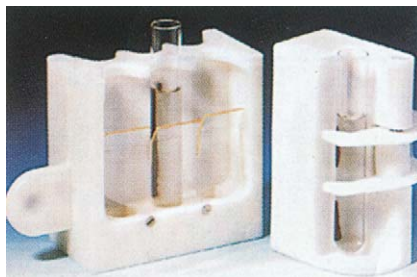


Plate 61 Biologically Active Compounds and Xenobiotics Examples of test-tube magnetic separators (Dynal, Norway). Left, Dynal MPC-6; right, Dynal MPC-1. (Courtesy of Dynal, Oslo, Norway.)

Colour Plate 62

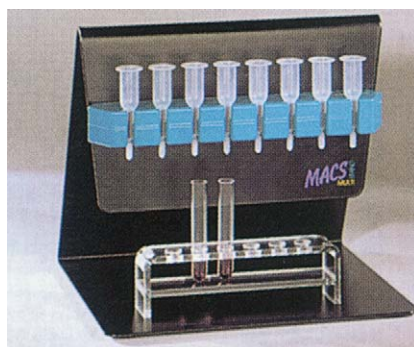


Plate 62 Biologically Active Compounds and Xenobiotics A typical example of laboratory-scale high gradient magnetic separators. OctoMACS Separator (Miltenyi Biotec, Germany) can be used for simultaneous isolation of mRNA. (Courtesy of Miltenyi Biotec, Germany.)

Colour Plate 63

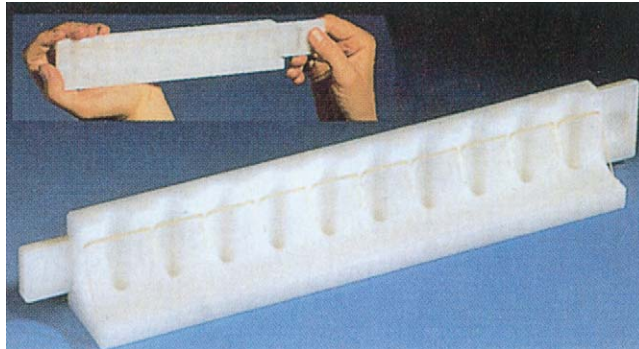


Plate 63 Cells: Isolation Example of a magnetic separator (Dynal MPC-M) for work with microcentrifuge tubes of the Eppendorf type, with a removable magnet plate to facilitate easy washing of magnetic particles. (Courtesy of Dynal, Oslo, Norway.)

Colour Plate 64

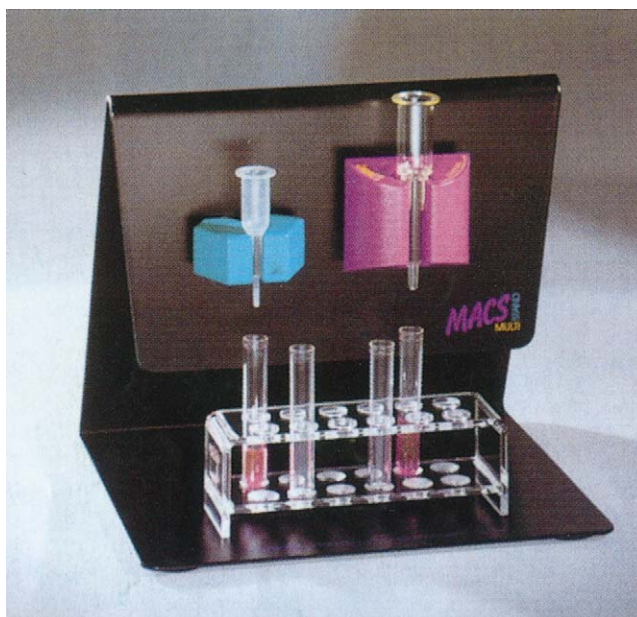


Plate 64 Cells: Isolation Examples of laboratory-scale high gradient magnetic separators. Left: MiniMACS separation unit; right: MidiMACS separation unit, both with inserted columns. (Courtesy of Miltenyi Biotec, Germany.)

Colour Plate 65

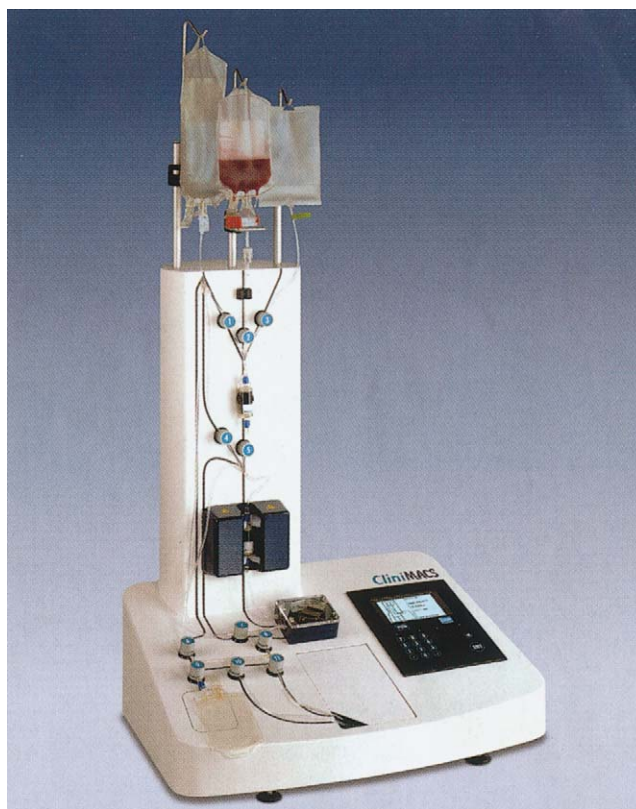


Plate 65 Cells: Isolation Computer-controlled magnetic cell sorter CliniMACS. (Courtesy of Miltenyi Biotec, Germany.)

Colour Plate 66

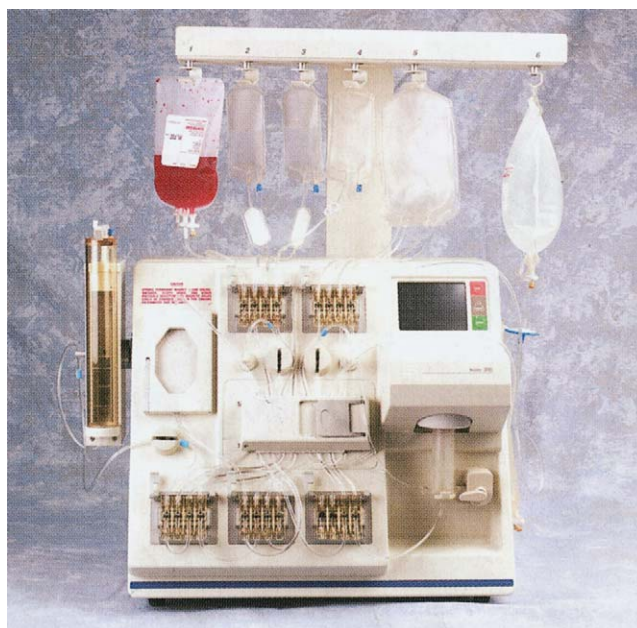


Plate 66 Cells: Isolation The Isolex 300i Cell Selection System. (Courtesy of Nexell Therapeutics, USA.)

Colour Plate 67



Plate 67 Chiral Separations: Crystallization Crystallization remains an important method for the resolution and purification of enantiomers, as first used by Pasteur for D and I tartaric acid. (Reproduced with permission from Science Photo Library.)

Colour Plate 68

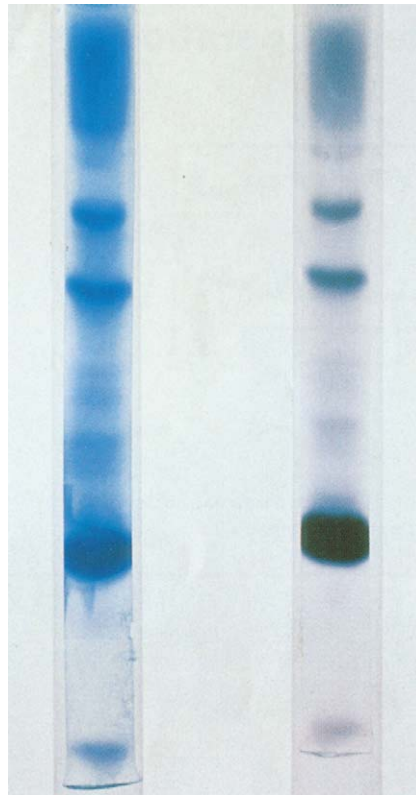


Plate 68 Clinical Applications: Electrophoresis Multiple sclerosis test. Electrophoresis test result performed on cerebrospinal fluids (CSF) of a patient with *multiple sclerosis*. Two traces are seen, black (right) and blue of the same patient. Dark bands in each trace are produced by migration and separation of particles in CSF through a gel; the large band (lower frame) shows albumin protein; two smaller protein bands are at upper frame; at the top is a long band containing smaller bands that include gamma globulin (immunoglobulin). Gamma globulin in CSF confirms *multiple sclerosis*. *Multiple sclerosis* is a nervous system disease which produces symptoms such as slurred speech, muscle weakness, disability and paralysis. (Reproduced with permission from James Stevenson/Science Photo Library.)

Colour Plate 69

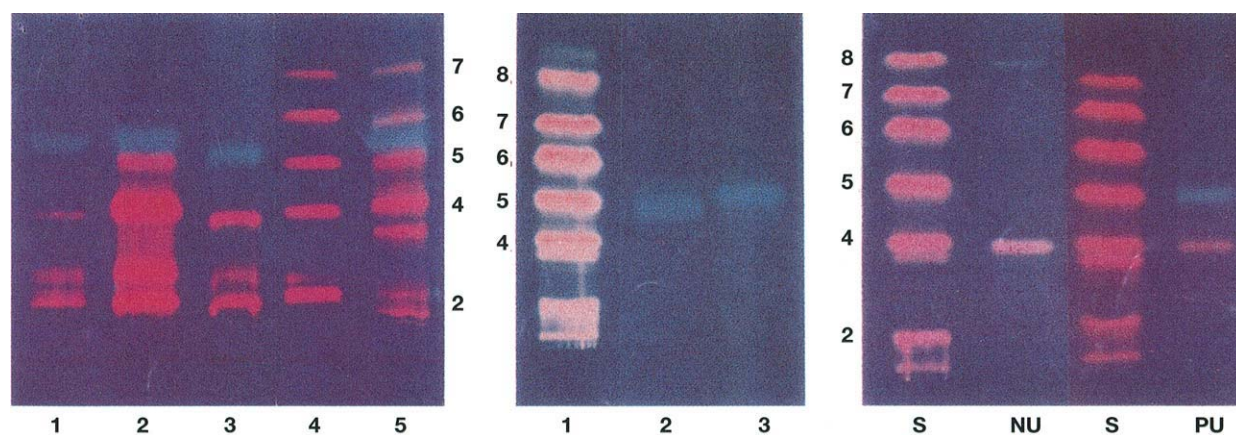


Plate 69 Clinical Chemistry: Thin Layer Chromatography RP-HPTLC chromatograms of fecal porphyrins to porphyria cutanea tarda (PCT) and variegate porphyria (VP) patients. Left panel: lane 1, VP feces of patient 1; lane 2, VP feces of patient 2; lane 3, external quality control sample of VP; lane 4, mixed calibrators of free porphyrins; lane 5, PCT feces; d, deuteroporphyrin. Middle panel: lane 1, mixed calibrators of free porphyrins; lane 2, i-urobilin standard; lane 3, stecobilin standard. Right panel: S, mixed calibrators of free porphyrins; NU, commercial urine control with a negative Urobilistix result; PU, urine obtained from a patient with hepatitis and a positive Urobilistix result; 8, uroporphyrin; 7, heptacarboxylic porphyrin; 6, hexacarboxylic porphyrin; 5, pentacarboxylic porphyrin; 4, coproporphyrin; 3, tricarboxylic porphyrin; 2, protoporphyrin. Reprinted from Lam C-W, Lai C-K and Chan Y-W (1998) *Clinical Chemistry* 44 (2): 345-346, with permission.

Colour Plate 70

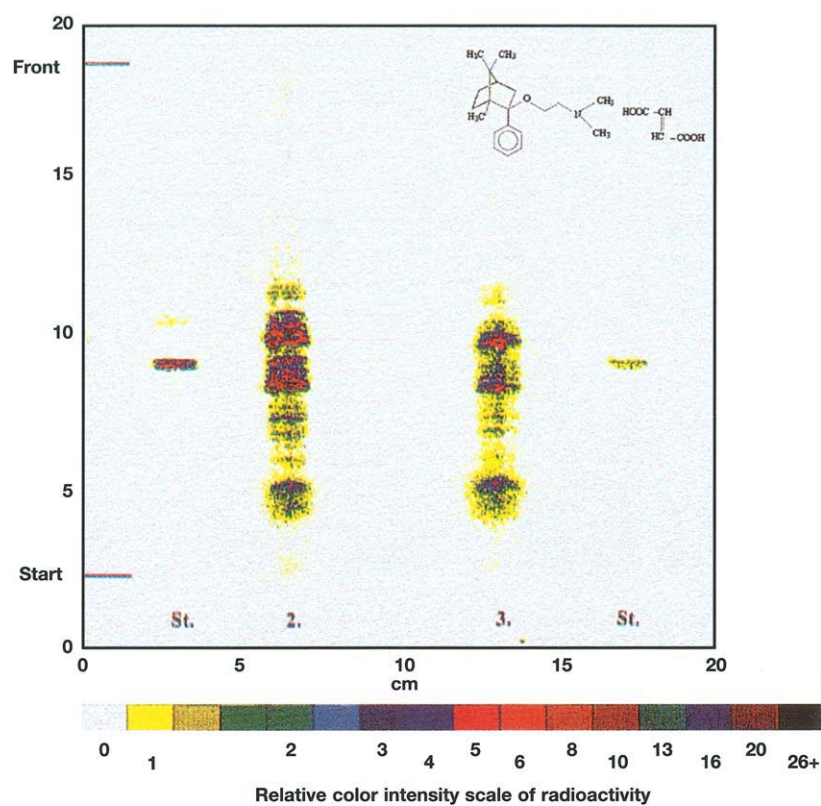


Plate 70 Clinical Chemistry: Thin Layer Chromatography OPLC-DAR profile of dog urine extracts. Sample, dog urine samples after 10mg kg⁻¹ oral dosing of ¹⁴C-daramcidlane. The first and fourth tracks are standards (St); tracks 2 and 3, 0-24-h and 24-48-h urine fractions, respectively. Single OPLC development eluent A; external pressure, 5.0 Mpa; flow rate, 250 mL; eluent volume, 4100 mL; time, 994 s; DAR run time, 60 min. Reprinted from Szúnyog J, Mincesovics E, Hazai I and Dlebovich I (1998) *Journal of Planar Chromatography-Modern TLC* 11 (1): 25-29, with permission.

Colour Plate 71

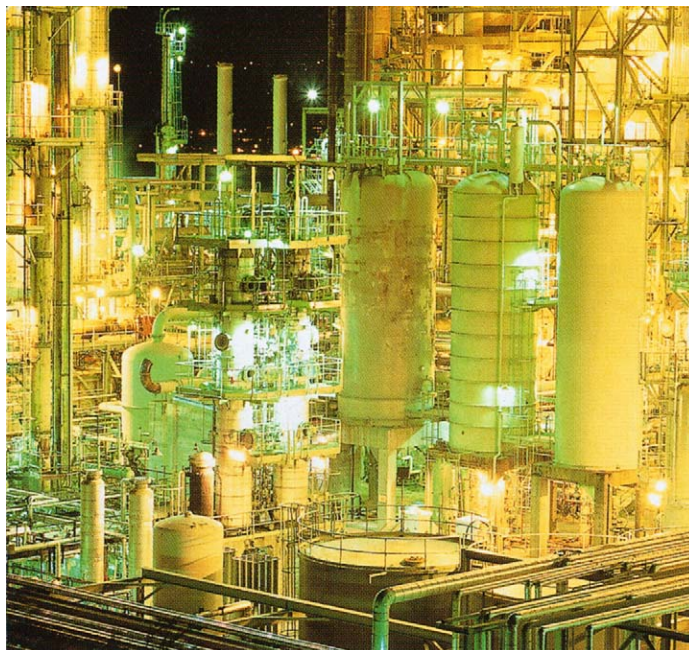


Plate 71 Crude Oil Oil refinery at night. At the refinery, crude oil is heated and passed through catalytic cracking towers. These are used to break up the heavy crude oil hydrocarbon molecules into lighter fragments. The resulting components, from heavy industrial oils and tars through to light fuels (such as petrol and kerosene) and gas, are separated out. The various components, called fractions, may then be collected and shipped separately. Photographed in British Columbia, Canada. (Reproduced with permission from Science Photo Library.)

Colour Plate 72

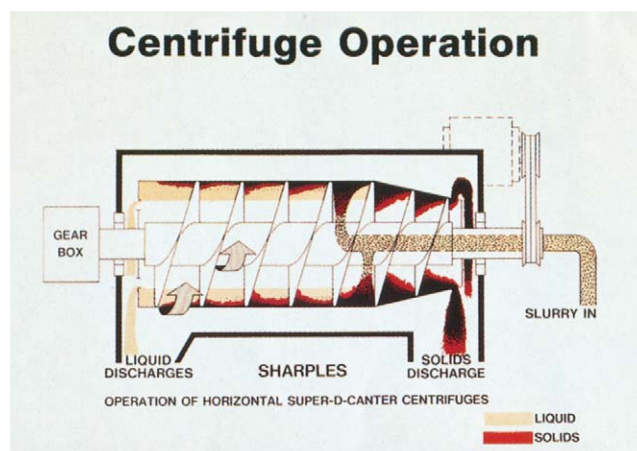


Plate 72 Decanter Centrifuges in Pharmaceutical Applications General Decanter Operation.

Colour Plate 73

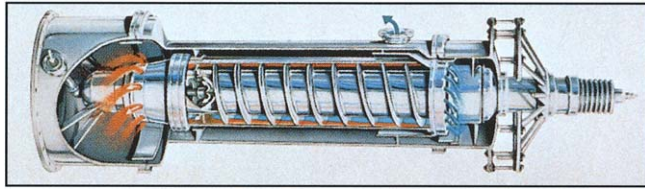


Plate 73 Decanter Centrifuges in Pharmaceutical Applications Vertical Decanter.

Colour Plate 74

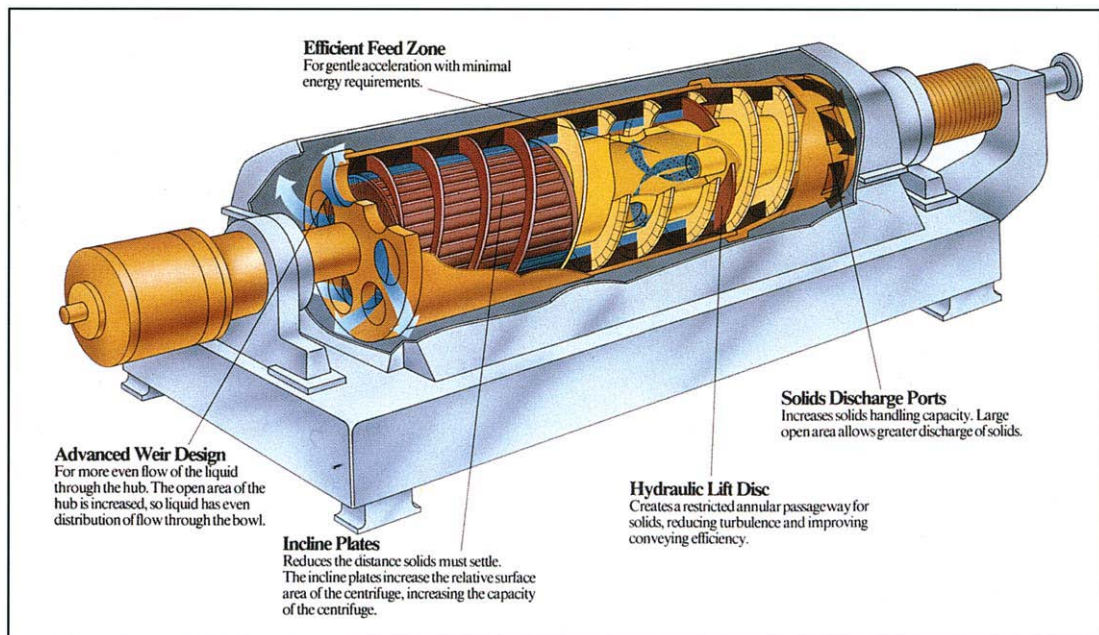


Plate 74 Decanter Centrifuges in Pharmaceutical Applications Performance enhancing features of a decanter centrifuge.

Colour Plate 75



Plate 75 Deoxyribonucleic Acid Profiling Gene mapping. A scientist studies a series of DNA sequencing autoradiograms or “genetic fingerprints” through a magnifying glass. He is determining the sequence of base pairs (cytosine, guanine, adenine, thymine) that form the code for a section of DNA. A sample of DNA has been cut into fragments by an enzyme and marked with a radioactive tag for sequencing. The DNA fragments are then separated by electrophoresis in an agarose gel, moving different distances along the gel according to their size. The resulting banding pattern, as seen here, is visualized by applying a radiographic film to produce these autoradiograms. (Reproduced with permission from Geoff Tomkinson/Science Photo Library.)

Colour Plate 76

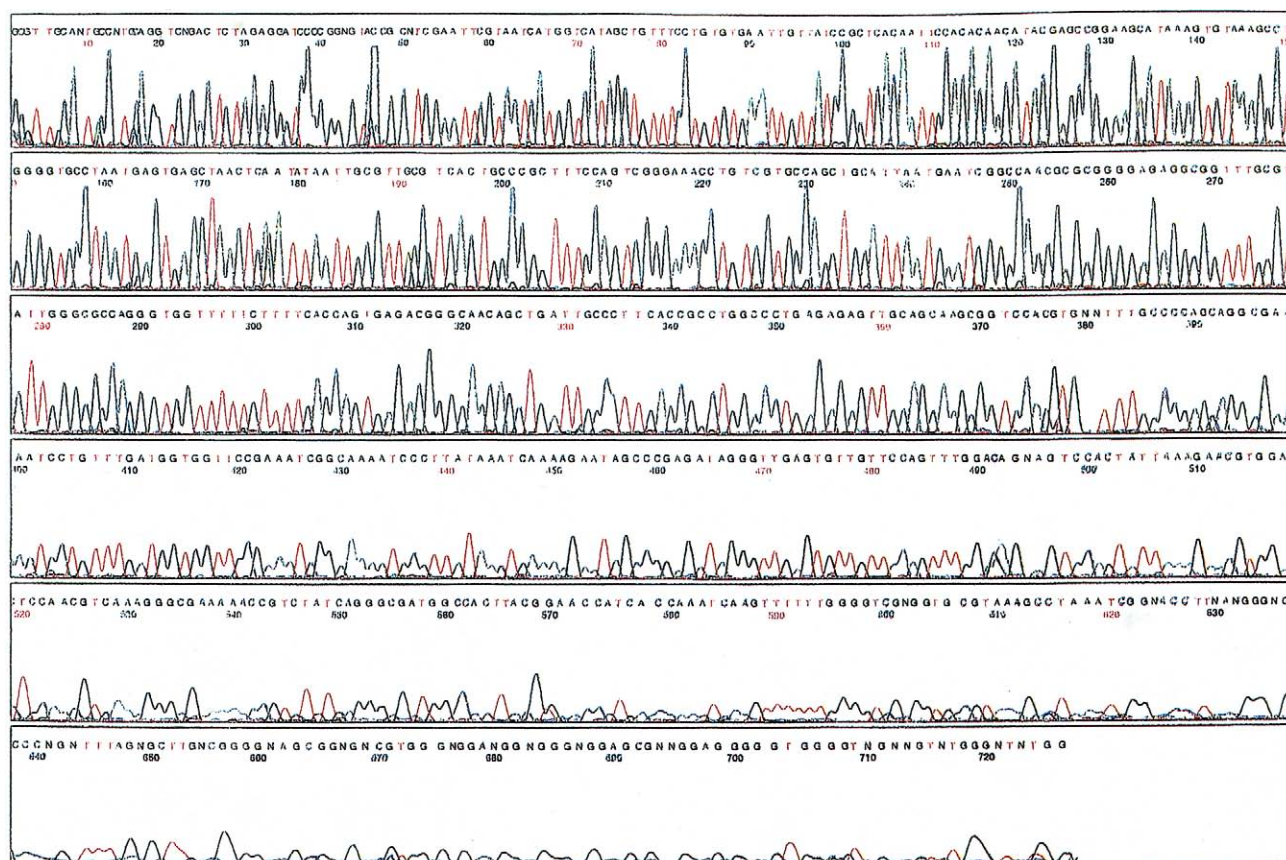


Plate 76 Deoxyribonucleic Acid Profiling: Capillary Electrophoresis Four-colour M13mp 18 sequencing separation at 42C. the separation of DNA sequencing fragments was performed in a 6.5% poly(dimethylacrylamide) (98kDa) solution (75cP) in 100 mmol L⁻¹ TAPS buffer (pH 8.0) containing 8 mol L⁻¹ urea. A 50mm i.d. fused silica capillary, 51cm long (40cm to the window) was used. DNA was electrokinetically injected for 20s at 60 V cm⁻¹, and the fragments were separated for 125 min at 160 V cm⁻¹. (Reproduced with permission from Madabhushi (1998), *Electrophoresis* 19: 224 - 230.)

Colour Plate 77



Plate 77 Dyes: Chromatography A scientist studying a selection of circular paper chromatograms of industrial dyes. Paper chromatography involves placing a small amount of the substance under investigation on a piece of filter paper, then slowly dripping a solvent into the centre of the paper. The solvent spreads out, over the paper by capillary action, carrying with it the components of the substance at differing rates. The distance travelled along the paper by each component during the time of the experiment is a measure of this characteristic transport rate and may be used to identify each component. (Reproduced with permission from Geoff Tompkinson/Science Photo Library.)

Colour Plate 78

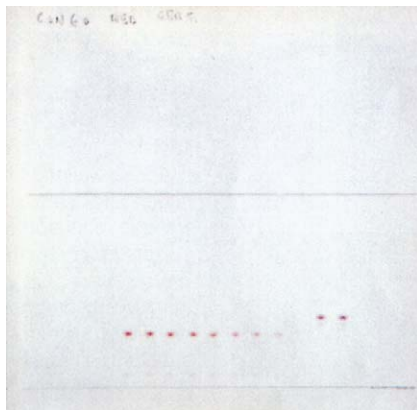


Plate 78 Dyes: Thin-Layer (Planar) Chromatography Set of certified Congo red standards developed on a silica gel 60 HPTLC layer. Mobile phase: ethyl acetate-methanol-ammonia solution (0.88)-water (35 + 11 + 5 + 5 v/v). A minor impurity is visible at R_f value 0.07. The two dye substances alongside these are a dye that was claimed to be Congo red.

Colour Plate 79

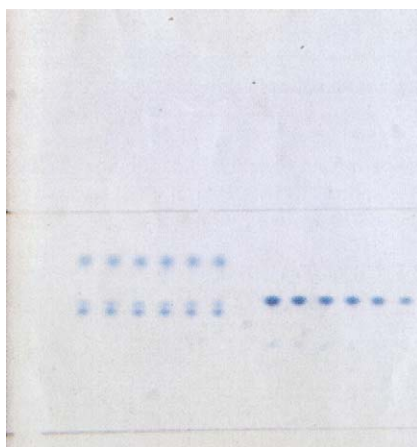


Plate 79 Dyes: Thin-Layer (Planar) Chromatography Separation of brilliant cresyl blue on silica gel 60 HPTLC plate. Mobile phase ethyl acetate-methanol-ammonia solution (0.88)-water (35 + 11 + 5 + 5 v/v), saturated tank. Six standards applied at increasing concentration (from 50 ng) on the right side of the plate. The six samples developed on the left, all of equal concentration, were claimed to be brilliant cresyl blue, but in fact were a mixture of toluidine blue and Nile sulfate.

Colour Plate 80

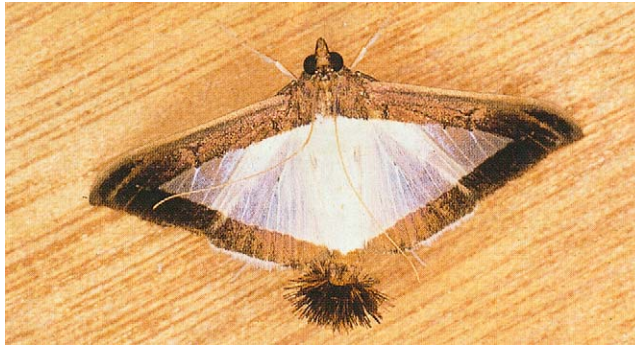


Plate 80 An Adult Moth The development of insects from eggs through the larval stages to adults is under endocrine control. One of the groups of developmental hormones which control this process are the ecdysteroids. These compounds can be isolated from insects by a variety of separation techniques and chromatographic methods are used widely for their analysis. (Reproduced with permission from Sinclair Stammers/Science Photo Library.)

Colour Plate 81



Plate 81 Essential Oils A field of lavender, *Lavandula spica*. The name comes from the Latin for wash (lavare), referring to the plant's use in toilet preparations. It flowers between midsummer and early autumn, and it is harvested just before the flowers are fully open. It is a favourite plant of bees. Lavender has antitussive and antispasmodic properties. The essential oil obtained from the flowers is an excellent antiseptic and insecticide, and is reputed to neutralise a viper's venom. Photographed in Provence, France. (Reproduced with permission from Science Photo Library.)

Colour Plate 82



Plate 82 Essential Oils: Distillation Lavender oil is evaporated by steam in the still, condensed, and collected in a Florentine Flask. Jersey. (Reproduced with permission from Eye Ubiquitous.)

Colour Plate 83



Plate 83 Explosives Ammonium nitrate burning. An explosion of flames leaps out of a dish containing burning ammonium nitrate (NH_4NO_3). Ammonium nitrate is used in the manufacture of explosives and fertilisers. It was first used as an explosive by Alfred Nobel, founder of the Nobel Prize, who used it in his dynamite mixtures in 1875. Separations, particularly chromatographic, are important for the characterization of explosives, particularly in forensic contexts. (Reproduced with permission from Science Photo Library.)

Colour Plate 84

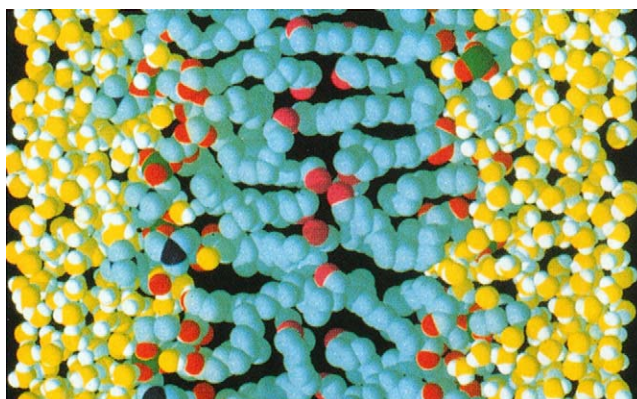


Plate 84 Fats Phospholipid bilayer. Molecular graphic of the phospholipid bilayer that forms the membrane around all living cells. There are many chromatographic methods for the separation and characterisation of lipids. The cell membrane is made of phospholipid molecules, each of which has a hydrophilic (soluble in water) and hydrophobic (insoluble in water) end. The hydrophobic part of the phospholipid is a fatty acid chain, shown here in blue. The molecules line up in two sheets, with the fatty acid chains forming a hydrophobic layer in the middle. The hydrophilic surface on both sides of the membrane, shown here in yellow and white, is the point of contact for molecules leaving or entering the cell. (Reproduced with permission from National Institutes of Health/Science Photo Library.)

Colour Plate 85



Plate 85 Herbicides: Gas Chromatography Scientist spraying part of an unripe grain field during a herbicide experiment. Residues of herbicides will persist in the plant or in the soil for a variable time, depending on their physiochemical properties and on the environmental conditions. Analysis of herbicide residues in these matrices is important, not only from the point of view of the efficacy of the application, but also to know the distribution and persistence of these compounds in food and the environment. (Reproduced with permission from Rosenfeld Images Ltd/Science Photo Library.)

Colour Plate 86

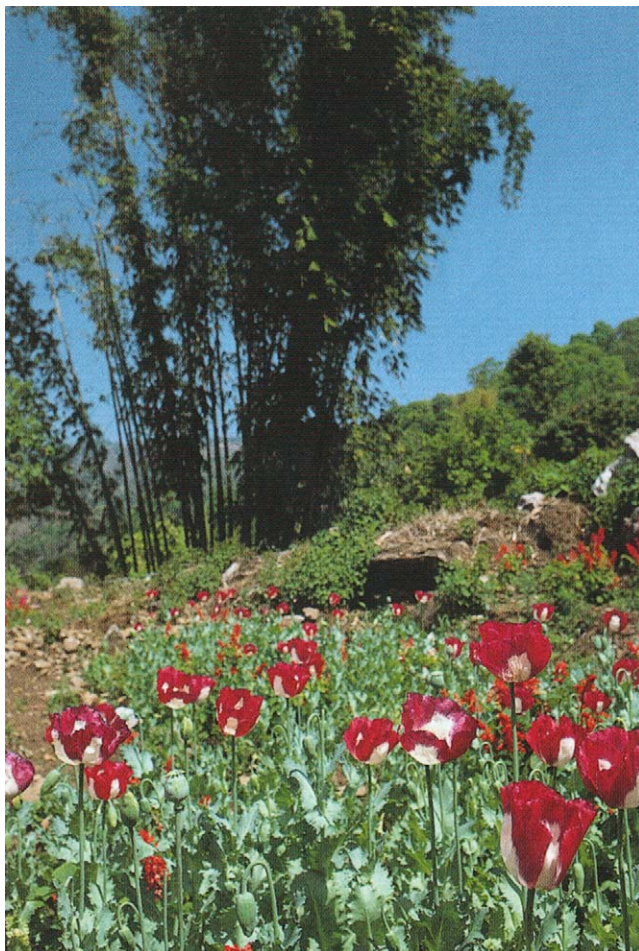


Plate 86 Heroin: Liquid Chromatography and Capillary Electrophoresis Poppy field in the Far East. The separation and quantitative determination of opiates is required for a wide variety of purposes and applications. (Reproduced with permission from Eye Ubiquitous.)

Colour Plate 87

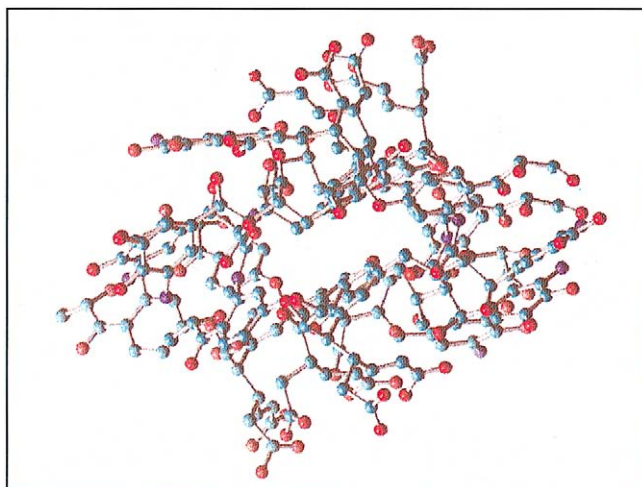


Plate 87 Humic Substances: Liquid Chromatography Molecular model of the lowest energy conformations of humic acid building blocks linked to form a hexamer. Carbon atoms are green, oxygen atoms are red, nitrogen atoms are purple and hydrogen atoms are not shown. (Reproduced with permission from Davies and Ghabbour, 1999.)

Colour Plate 88

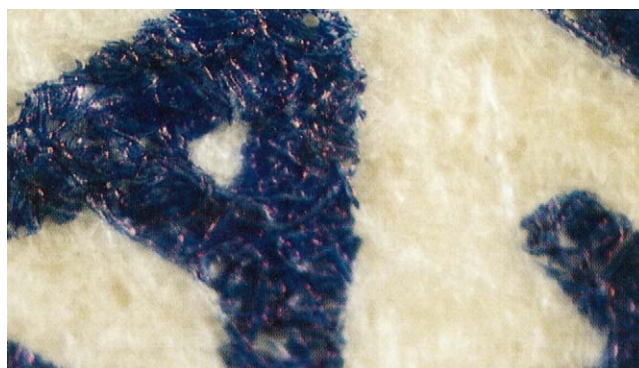


Plate 88 Inks: Forensic Analysis by Thin-Layer (Planar) Chromatography Offset lithography photographed at 27X.

Colour Plate 89

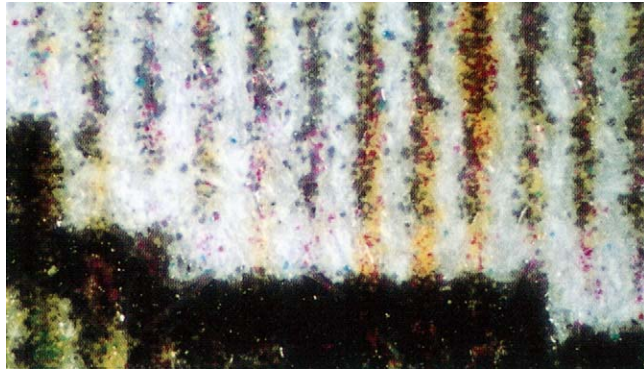


Plate 89 Inks: Forensic Analysis by Thin-Layer (Planar) Chromatography Full colour toner photographed at 27X.

Colour Plate 90

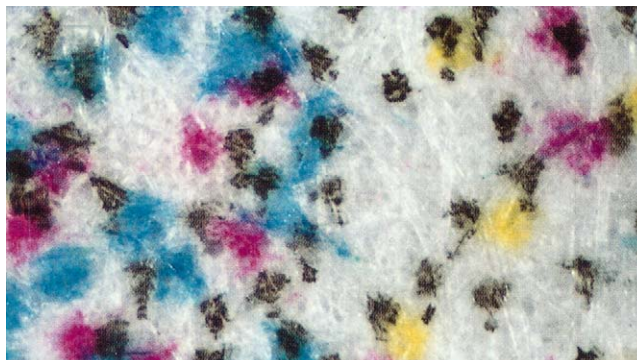


Plate 90 Inks: Forensic Analysis by Thin-Layer (Planar) Chromatography Full colour ink jet photographed at 27X.

Colour Plate 91

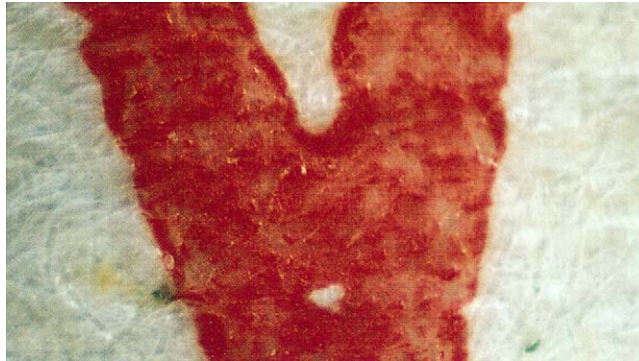


Plate 91 Inks: Forensic Analysis by Thin-Layer (Planar) Chromatography Letterpress ink photographed at 27X.

Colour Plate 92

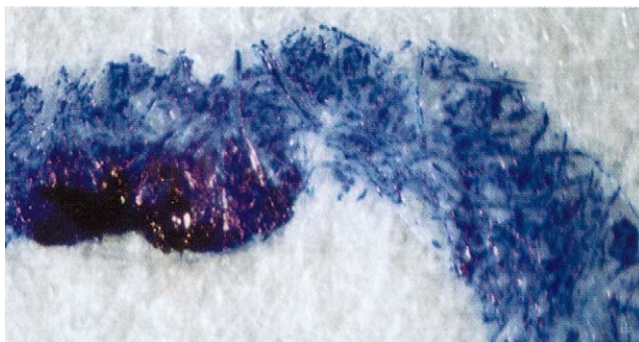


Plate 92 Inks: Forensic Analysis by Thin-Layer (Planar) Chromatography Writing ink photographed at 27X.

Colour Plate 93

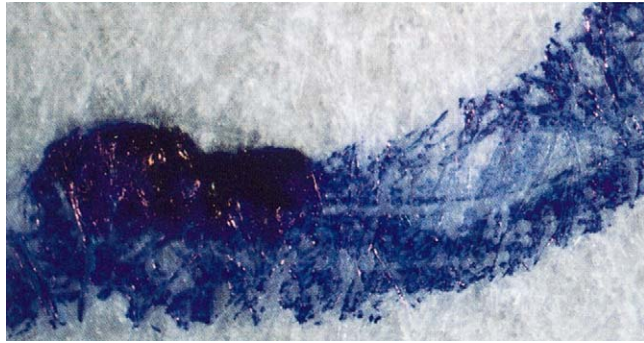


Plate 93 Inks: Forensic Analysis by Thin-Layer (Planar) Chromatography Ballpoint writing ink photographed at 27X.

Colour Plate 94



Plate 94 Inks: Forensic Analysis by Thin-Layer (Planar) Chromatography Non-ballpoint writing ink (solvent-based) photographed at 27X.

Colour Plate 95

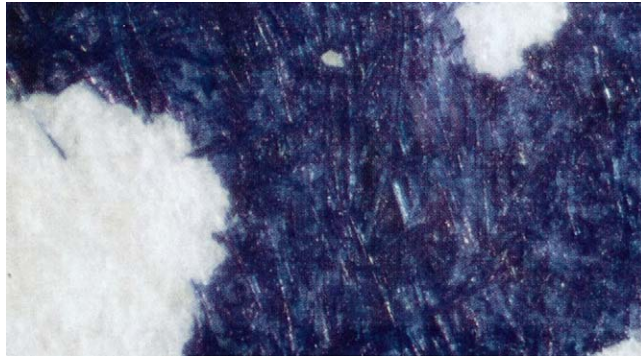


Plate 95 Inks: Forensic Analysis by Thin-Layer (Planar) Chromatography Non-ballpoint writing ink (fountain pen) photographed at 27X.

Colour Plate 96

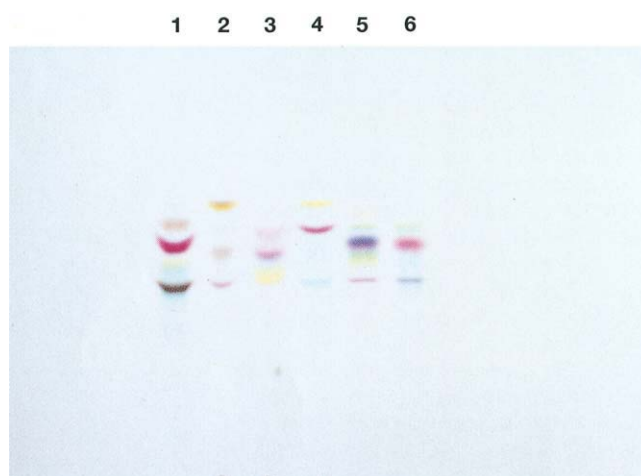


Plate 96 Inks: Forensic Analysis by Thin-Layer (Planar) Chromatography Thin-layer chromatogram of full colour jet inks, solvent system I.

Colour Plate 97

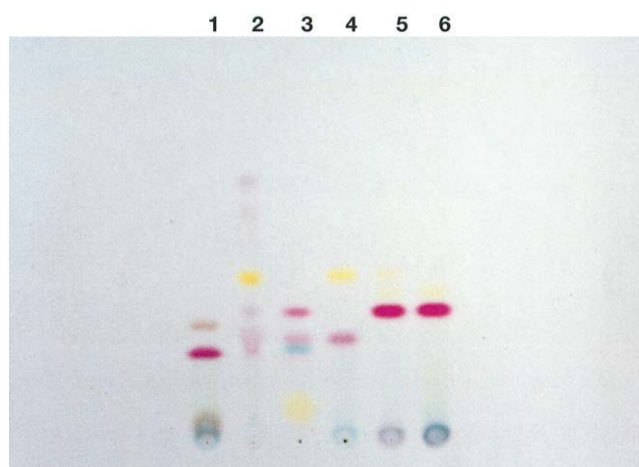


Plate 97 Inks: Forensic Analysis by Thin-Layer (Planar) Chromatography Thin-layer chromatogram of full colour jet inks, solvent system V.

Colour Plate 98

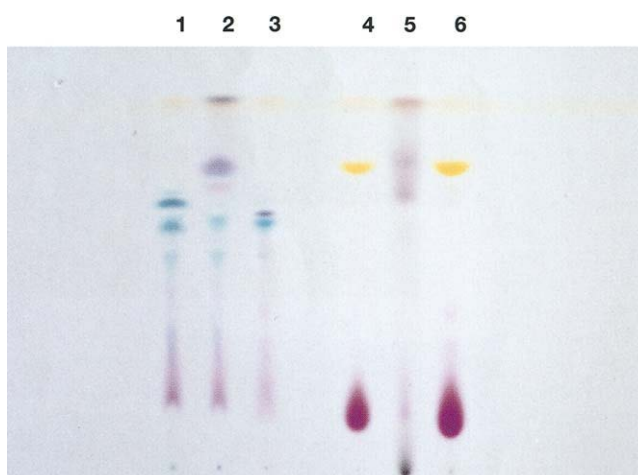


Plate 98 Inks: Forensic Analysis by Thin-Layer (Planar) Chromatography Thin-layer chromatogram of ballpoint inks, solvent system I.

Colour Plate 99

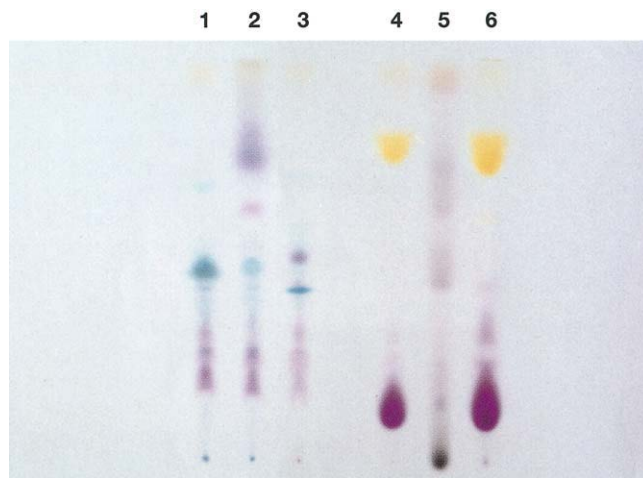


Plate 99 Inks: Forensic Analysis by Thin-Layer (Planar) Chromatography Thin-layer chromatogram of ballpoint inks, solvent system II.

Colour Plate 100

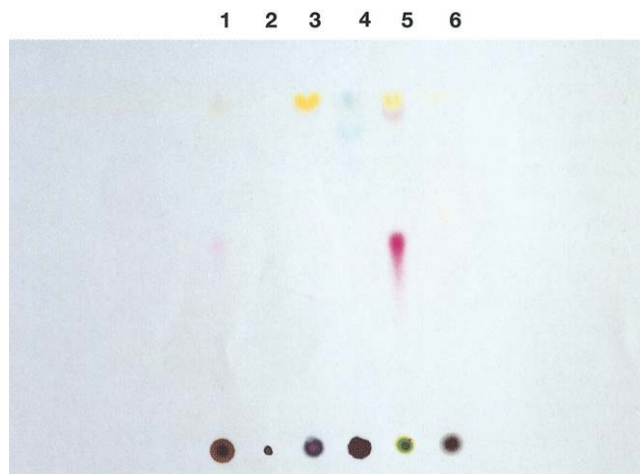


Plate 100 Inks: Forensic Analysis by Thin-Layer (Planar) Chromatography Thin-layer chromatogram of full colour toner, solvent system I.

Colour Plate 101



Plate 101 Inks: Forensic Analysis by Thin-Layer (Planar) Chromatography Thin-layer chromatogram of full colour toner, solvent system IV.

Colour Plate 102



Plate 102 Isotope Separations: Gas Centrifugation Nuclear explosion. Aerial view of the nuclear explosion, code-named Seminole, at Enewetak Atoll in the Pacific Ocean on 6 June 1956. This atomic bomb was detonated at ground level and had the same explosive force of 13.7 thousand tonnes (kilotonnes) of TNT. It was detonated as part of Operation Redwing, an American programme, which tested systems for atomic bombs. (Reproduced with permission from Science Photo Library.)

Colour Plate 103

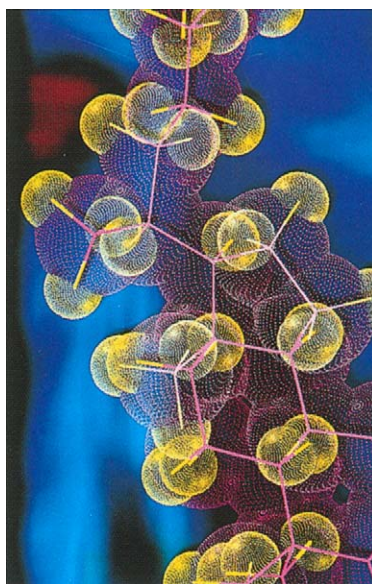


Plate 103 Lipids Computer graphic of part of a cholesterol molecule. Pink spheres represent carbon atoms, yellow spheres represent hydrogen and the lines represent the bonds between them. Cholesterol is an important constituent of cells, playing a crucial role in the synthesis of hormones and bile salts. It also helps to transport fats in the bloodstream to tissues throughout the body. (Reproduced with permission from US Department of Energy/Science Photo Library.)

Colour Plate 104



Plate 104 Marine Toxins: Chromatography Shuttle photograph of a phytoplankton, or algal bloom (a colouring of water arising from a high concentration of plankton) in a northwest Coral Sea off the Queensland Coast, Australia. Plankton drift more or less passively with the water flow, hence orbital photographs of plankton colonies can provide information on the prevailing currents. Here, the leading edge of a probable concentration of plankton is seen as a light irregular line and sheen in the sea at top right. Reports from ships in this area refer to floating mats of algae up to 2 metres thick. The discolouration of the water in and around the bay is due to the sediment load present in the rivers feeding into it. (Reproduced with permission from NASA/Science Photo Library.)

Colour Plate 105

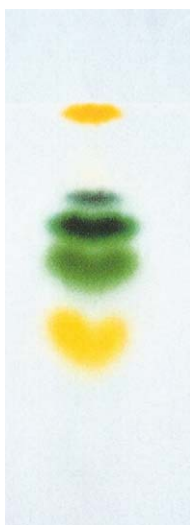


Plate 105 Natural Products: Thin-Layer (Planar) Chromatography Thin Layer Chromatogram (TLC) of an extract of thylakoid membranes from the leaf of annual meadow grass *Poa annua*. TLC plastic sheets are coated with a 60 F254 silica gel that measures 0.2 millimetres thick. The extract was placed just above the solvent level at the bottom of the lane used to separate the sample. The picture shows the components of the extract separated according to their relative migration distance in the separation system. Six bands are seen; top (orange) is carotene; 2 (green) pheophytin; 3 (green) chlorophyll A; 4 (green) chlorophyll B; 5 (yellow) & 6 (mere trace) are carotenoids. The line across the top of the image is the solvent front. (Reproduced with permission from Science Photo Library.)

Colour Plate 106

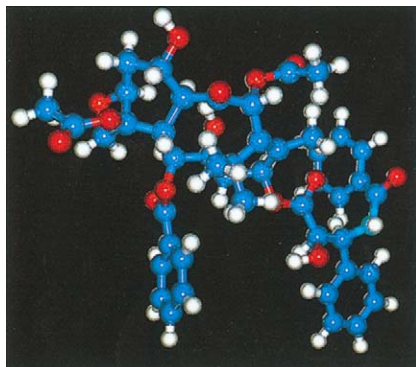


Plate 106 Natural Products: Thin-Layer (Planar) Chromatography Taxol. Computer graphic of a molecule of taxol, an anti-cancer drug. The atoms and their bonds are colour-coded: carbon (C, dark blue); hydrogen (H, white); oxygen (O, red); nitrogen (N, light blue). Taxol has a chemical formula $C_{47}H_{51}NO_{14}$. It is found in the bark of the Pacific Yew tree, *Taxus brevifolia*, and can also be artificially synthesised. Taxol is particularly effective against advanced breast cancer and ovarian cancer. The drug works by inhibiting the protein *tubulin* to form microtubules, important structures involved in cell division (mitosis). The presence of taxol stabilises the microtubules, disrupting mitosis in the rapidly dividing cancer cells. (Reproduced with permission from Science Photo Library.)

Colour Plate 107



Plate 107 Neurotoxins: Chromatography Prairie rattlesnake's mouth. View of the open mouth and fangs of the northern Pacific prairie rattlesnake (*Crotalus viridis oreganus*). This is a subspecies of the prairie rattlesnake that lives in the north-western parts of North America. The fangs are seen enclosed by a membrane at the tip of the snake's upper jaw. These snakes feed mainly on small rodents, which they kill by injecting venom with these fangs. The prairie rattlesnake is widely distributed throughout western North America, with many subspecies existing. Their venom is dangerous and potentially fatal to humans. (Reproduced with permission from Science Photo Library.)

Colour Plate 108



Plate 108 Centrifugation Titanium belt driven and air driven rotors used in the arrayable flow-through centrifuge. A penny is shown for scale.

Colour Plate 109

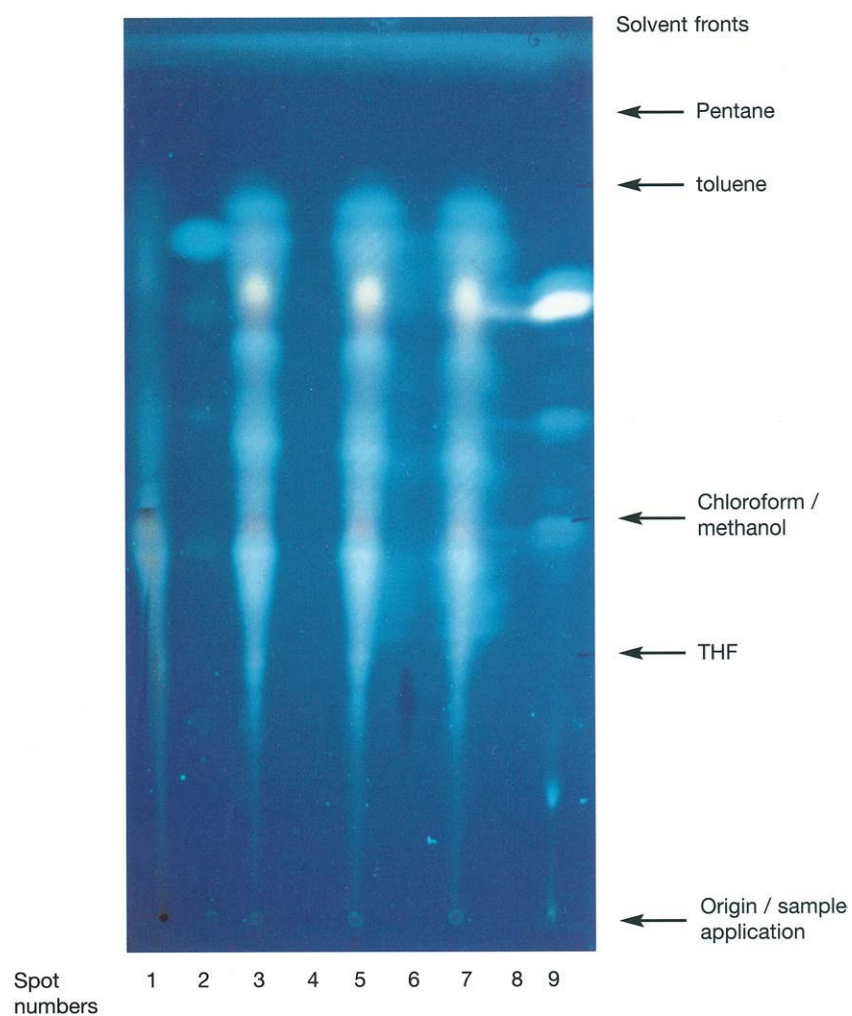


Plate 109 Petroleum Products: Thin-Layer (Planar) Chromatography Analytical separation of coal tar pitch, tetrahydrofuran solubles, on silica developed sequentially in tetrahydrofuran, chloroform/methanol (4 : 1 v/v), toluene and pentane. Pitch at lanes 3, 5 and 7; perylene at lane 2; rubrene at lane 9; pyrogallol at lane 6; coal extract at lane 1. Whatman K6 silica; solvent fronts THF 55 mm, chloroform/methanol 83 mm, toluene 153 mm and pentane 178 mm.

Colour Plate 110

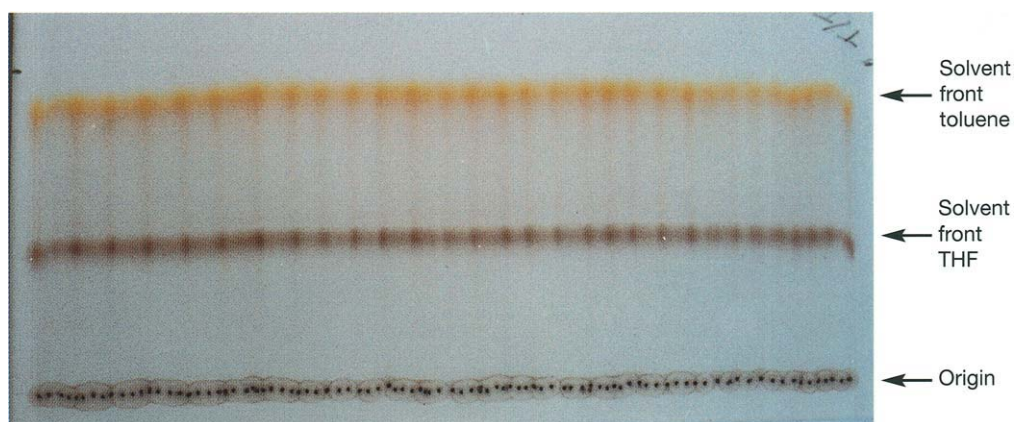


Plate 110 Petroleum Products: Thin-Layer (Planar) Chromatography Preparative development of a synthetic naphthalene mesophase pitch applied in pyridine slurry and developed in tetrahydrofuran and toluene.

Colour Plate 111

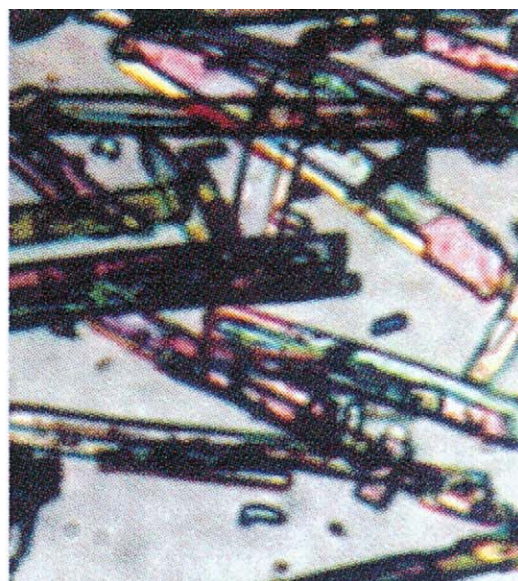
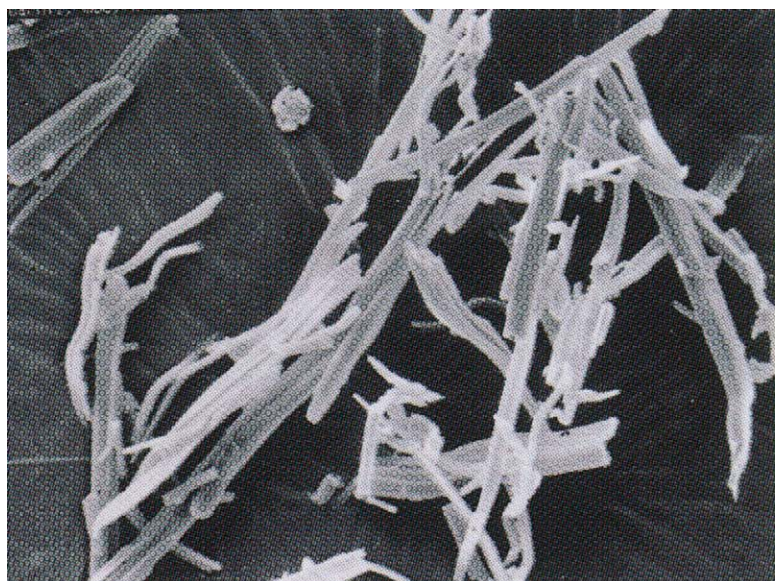
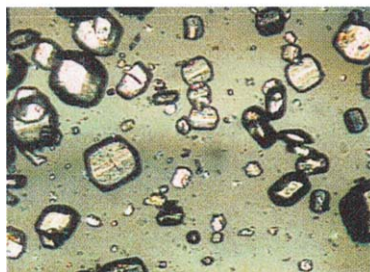


Plate 111 Pharmaceuticals: Crystallization Habit of Abecarnil grown from methanol after spontaneous nucleation at relatively high supersaturations (left) and grown at moderately low supersaturations after the addition of seeds (right).

Colour Plate 112

Solvent I



Solvent II



Plate 112 Pharmaceutical: Crystallization Habit of a steroid crystallized from two different solvents.

Colour Plate 113



Plate 113 Pharmaceuticals: Crystallization Shape of particles obtained via spray drying. The left micrograph shows well-separated spherical particles typically obtained. Note the indentations on one side. The right micrograph shows felted needles that are in addition interwoven. Both products are fully crystalline.

Colour Plate 114

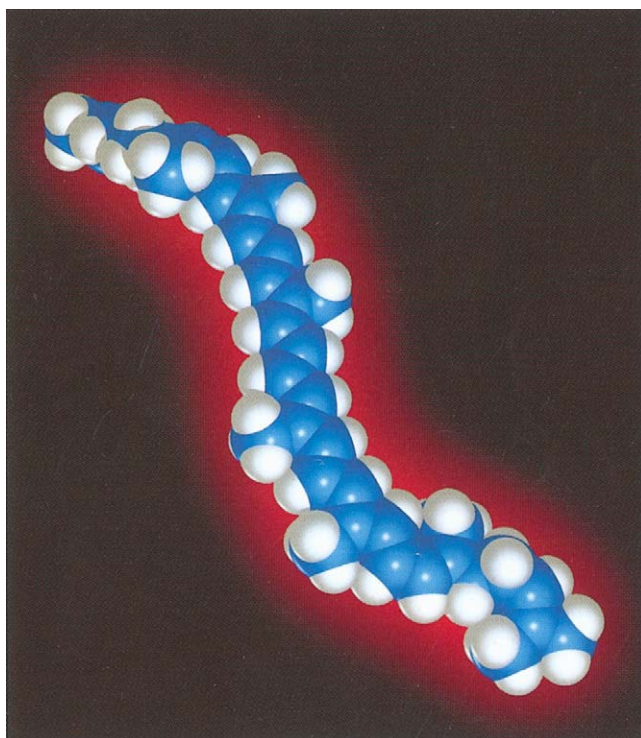


Plate 114 Pigments Lycopene. Computer graphic of lycopene, the red carotenoid pigment of tomatoes, rose hips and many other berries, and flowers of the pot marigold, *Calendula officinalis*. This hydrocarbon molecule contains two types of atoms: carbon (C, blue) and hydrogen (H, white). It has the chemical formula $C_{40}H_{56}$ (With permission from Science Photo Library.)

Colour Plate 115

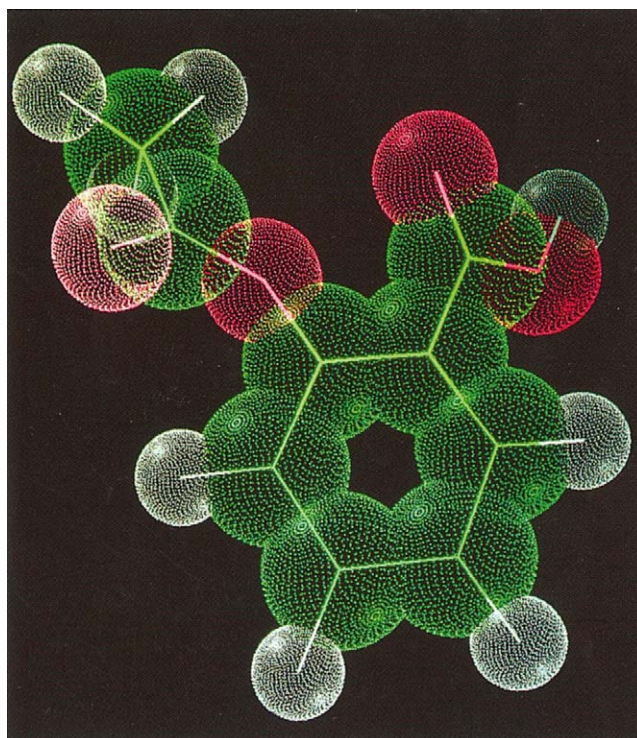


Plate 115 Prostaglandins Aspirin. Computer graphic of a molecule of aspirin or acetylsalicylic acid, a pain killing (analgesic), anti-inflammatory drug used to treat fever, injuries, arthritis and heart disease. The lines represent the bonds between atoms, which are shown as colour-coded spheres: carbon is green, oxygen is red and hydrogen is white. Aspirin works by blocking the action of the *cyclooxygenase* enzymes, which produce hormone-like *prostaglandin* fatty acids. Some of these *prostaglandins* sensitise nerve endings and dilate blood vessels after an injury. Large doses of aspirin over long periods can lead to stomach and intestinal ulcers. (With permission from Science Photo Library.)

Colour Plate 116

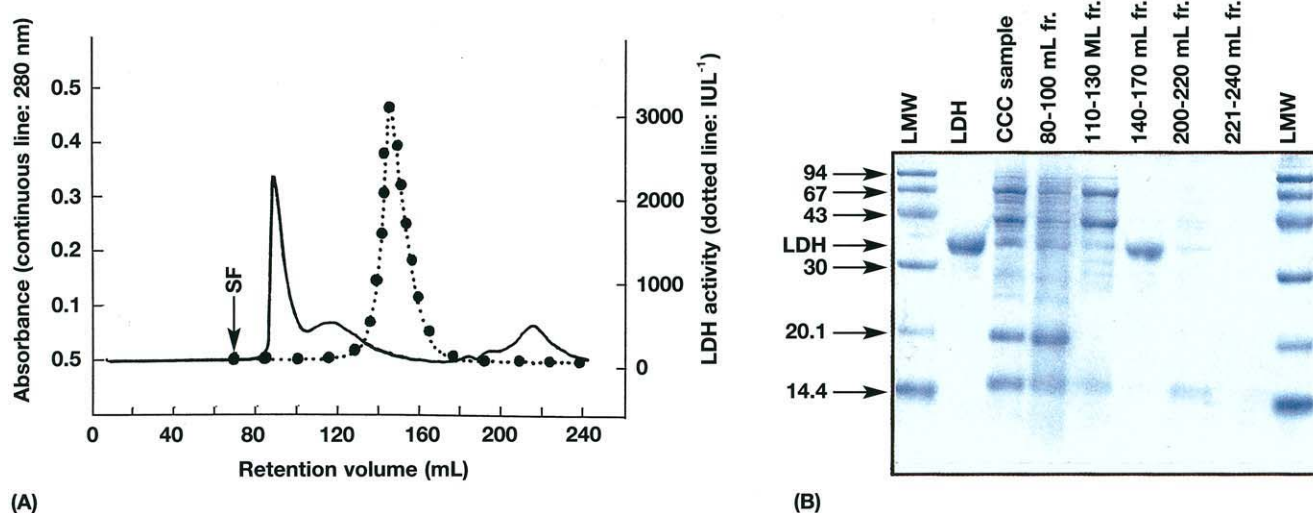


Plate 116 Proteins: High Speed Countercurrent Chromatography (A) Countercurrent chromatography of bovine heart homogenate and (B) SDS-PAGE profile of the fractions. Experimental conditions: column is a 2.6 mm i.d. PTFE multilayer coil, $\beta = 0.50-0.60$, 165 ml capacity; sample is a mixture of 3 ml bovine heart crude extract, 3 ml solvent system (1.5 ml each phase); solvent system consists of 16% (w/w) PEG 1000 12.5 % (w/w) potassium phosphate (pH 7.3); mobile phase is the lower phase; flow rate 2.0 ml min⁻¹; revolution: 500 rpm; SF, solvent front. LMW, low molecular weight protein markers.

Colour Plate 117

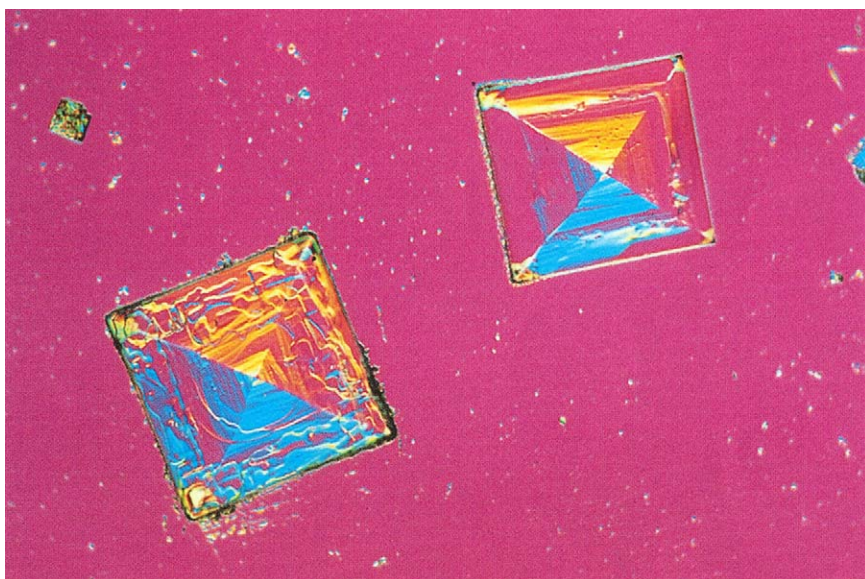


Plate 117 Sodium Chloride: Crystallization Polarised light micrograph of crystals of salt (sodium chloride). Salt crystals are built up from a cubic lattice of sodium and chlorine ions. In the absence of impurities an exact cubic crystal is formed. In practice the basic cube is often disrupted by dislocations giving rise to crystals with a variety of shapes, although they retain the underlying cubic symmetry. Magnification: x50 at 3mm size. (With permission from Science Photo Library.)

Colour Plate 118



Plate 118 Sugar Derivatives Dextrose. Polarised light micrograph of dextrose (glucose) sugar crystals. Magnification: x5 at 33mm size. (With permission from Science Photo Library.)

Colour Plate 119



Plate 119 Sulfur Compounds Garlic cloves and bulbs. View of several cloves and bulbs of garlic (*Allium sativum*). Garlic is a herb that is extensively used in cooking for its strong, distinctive taste. As well as its culinary uses, it is also a remarkable medicinal herb. It has powerful antibiotic properties when the juice is applied to wounds. It can also be used as an insect repellent. In common with other members of the onion family, it can help to reduce blood cholesterol levels and hypertension (high blood pressure). Oil of garlic is available in capsules for those who desire beneficial properties but dislike the taste. (With permission from Science Photo Library.)

Colour Plate 120

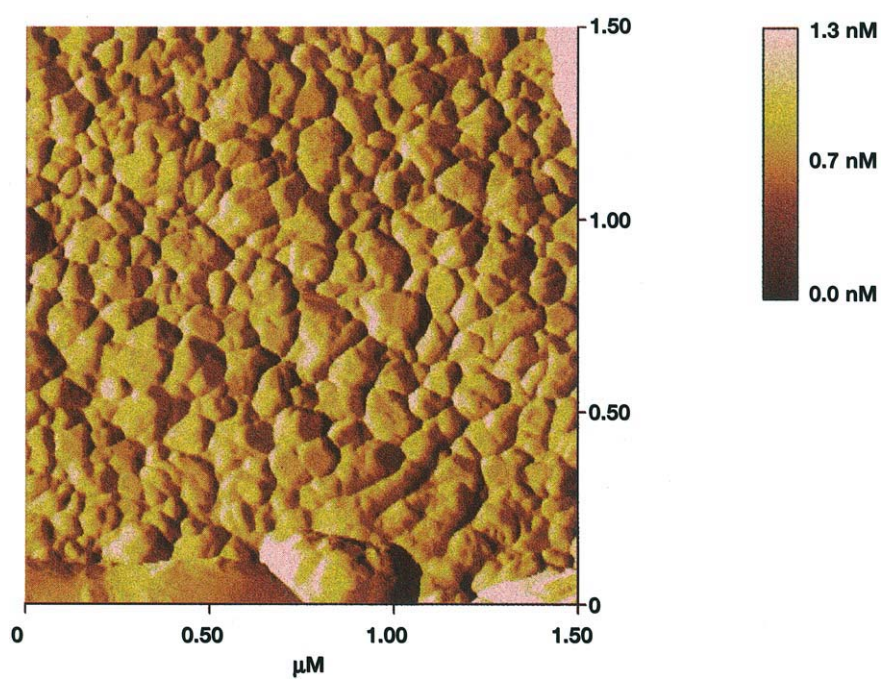


Plate 120 Thin-Layer Chromatography-Vibration Spectroscopy AFM photograph of a silver-coated HPTLC silica gel KG60 plate (post-overlayer SERS activation). NanoScope III; tapping mode.

Colour Plate 121

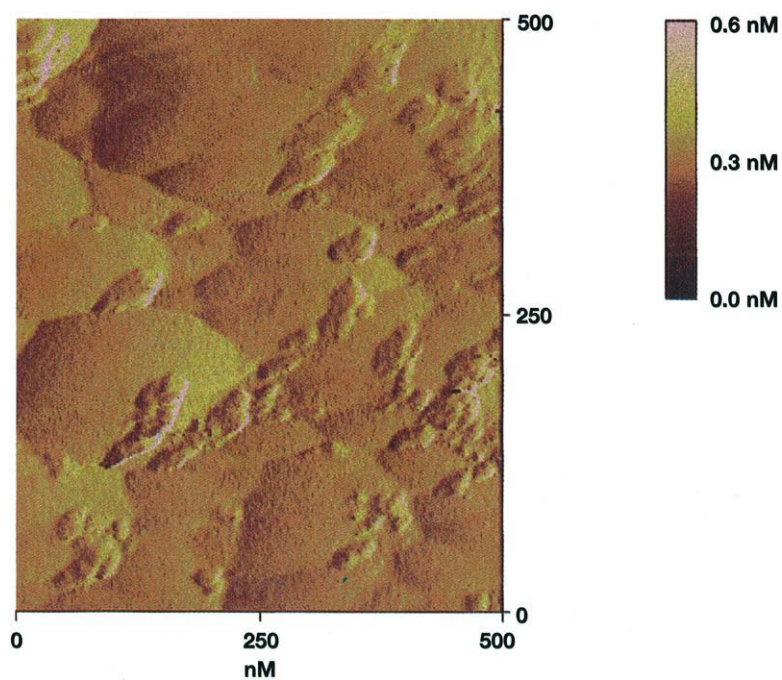


Plate 121 Thin-Layer Chromatography-Vibratlon Spectroscopy AFM (tapping mode) surface plot of a silver colloidal SERRS activated silica gel plate (KG60, Merck). A selected $X = Y = 500$ nm spot area of a $1\mu\text{l}$ of 10^{-10} M rhodamine 6G spotted on the plate. The silver hydrosol marker has a diameter of between 10 and 60 nm.

Colour Plate 122



Plate 122 Tobacco Volatiles Cigarette testing. Cigarettes being tested for the nicotine and tar content of their smoke during either medical research or as part of quality control in the tobacco industry. The cigarettes are being held vertically and having air sucked through them into the tubes in which their butts (brown) have been placed. The air will be analysed for its tar and nicotine content. Nicotine acts as a stimulant on the central nervous system and is the chemical that causes cigarette addiction. The tar is one of the numerous toxic by-products released by the burning of the cigarette. (With permission from Science Photo Library.)

Colour Plate 123



Plate 123 Triglycerides Olive harvesting. Orchard of olive trees *Olea europaea*, with nets laid around each tree to catch falling olives. Although this is a traditional way of harvesting olives, once the fruit is picked it is graded mechanically by size for pressing. Small olives have a higher oil content. The principal product of the cultivation of the tree is olive oil. *Olea europaea* has evergreen leaves and oval fruit coloured green, then black. This small tree is distributed around the Mediterranean region. Photographed in Apulia, Italy. (With permission from Science Photo Library.)

Colour Plate 124



Plate 124 Veterinary Drugs The demands for specificity, reliability, speed and turnover in residue analysis of veterinary drugs are continuously increasing. (With permission from Eye Ubiquitous.)

Colour Plate 125

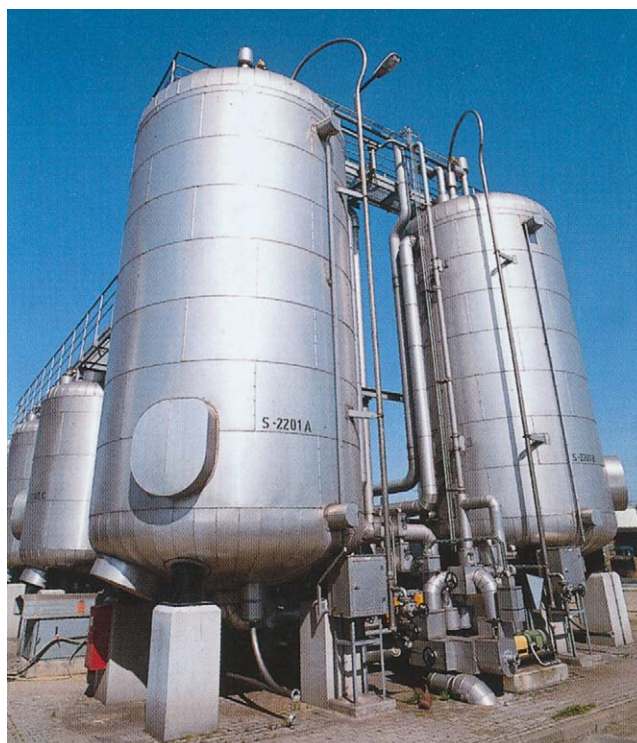


Plate 125 Water Treatment Waste water treatment. Clarifying tanks used in the last stage of treating industrial waste water. In these tanks, water is passed through filters made of activated charcoal. Activated charcoal can be used to remove solid particles as well as soluble organic chemicals such as pesticides. (With permission from Science Photo Library.)

Colour Plate 126



Plate 126 Water Treatment Waste water treatment. View of waste water entering a pool at water treatment plant. The water is undergoing a preliminary flotation separation process. Detergent foam (lower centre) floats on the surface of the water. This allows the waste water to be drained off and treated separately. Photographed in England. (With permission from Science Photo Library.)

Colour Plate 127



Plate 127 Whisky: Distillation Whisky distillery, Glenfiddich. In general, during distillation of completely miscible liquids, the component with the higher boiling point moves towards the bottom of the still while the component with the lower boiling point moves towards the top. In whisky production, water boils at a higher temperature while ethyl alcohol boils at a lower temperature. As a result, the grain residue is naturally carried to the bottom of the still along with the water. (With permission from Spectrum Colour Library.)

Colour Plate 128

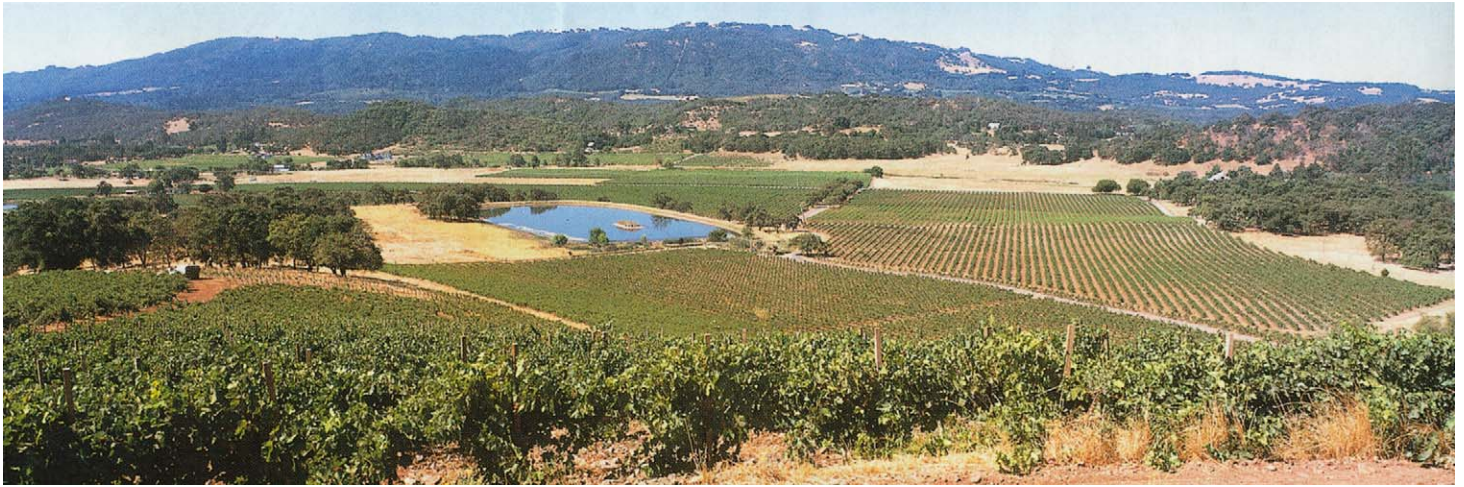


Plate 128 Wine View of grapevines, *Vitis vinifera*, in a wine vineyard. The grapevines are growing in ordered rows for ease of harvesting. The type of wine varies according to the soil, climate, variety of grape and the particular winemaking technique. Photographed at the Kunde Estate Winery, Sonoma County, California, USA. (With permission from Science Photo Library.)